1,8-Dioxa[8](2,7)pyrenophane, a Severely Distorted Polycyclic Aromatic Hydrocarbon**

Graham J. Bodwell,* John N. Bridson, Tom J. Houghton, Jason W. J. Kennedy, and Michael R. Mannion

One of the distinguishing features of the smaller cyclophanes is the presence of nonplanar aromatic rings. The introduced distortions often lead to unusual spectroscopic properties as well as unusual chemical behavior. The extent to which an isolated benzene ring can be bent and still remain stable has been investigated thoroughly (for example, for [*n*]paracyclophanes[1, 2] and [*n*]metacyclophanes[2]) both from an experimental and a theoretical point of view. Although several [*n*]cyclophanes that contain polycyclic aromatic hydrocarbons have been reported, most of these (for example, [*n*](1,3)-[3] and [*n*](1,4)naphthalenophanes,[4] and [*n*](9,10)anthracenophanes[5]) can be viewed as benzannelated [*n*]paracyclophanes and [*n*]metacyclophanes. That is, the distortions from planarity are primarily localized to one ring. We are aware of no instance in which the tolerance of any polycyclic aromatic hydrocarbon to bending over its entire aromatic surface has been systematically investigated (by, for instance, pushing it to the limit).[6] Since a variety of nonplanar polycyclic aromatic hydrocarbons are subunits in the surfaces of the fullerenes (Fig. 1), we became interested in preparing and studying such compounds. We now report our initial results of this work, namely the tolerance of pyrene (a subunit of D_{5h} C_{70} (Scheme 1) and D_{6h} C_{84}, among others) towards distortions from planarity.

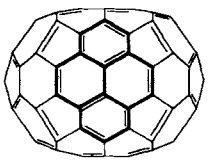

Scheme 1. The pyrene subunit of D_{5h} C_{70}.

In order to impart nonplanarity over the entire pyrene framework, our first choice of targets were the [*n*](2,7)-pyrenophanes. The synthetic approach is based upon the well-known valence isomerization of [2.2]metacyclophane-1,9-dienes to 10b,10c-dihydropyrenes, which normally occurs under mild conditions.[7] Theoretical and experimental studies have concluded that the dihydropyrene is usually the energetically more favorable valence isomer.[8] When the cyclophanediene bears internal hydrogen substituents, loss of hydrogen from the dihydropyrene to give a pyrene derivative often takes place readily.[9]

The title compound **9** was prepared as shown in Scheme 2.[10] Readily available 5-hydroxyisophthalic acid (**1**) was esterified and then converted into the tetraester **3** by reaction with sodium hydride/1,6-dibromohexane/TBAI (tetra-*n*-butylammonium iodide). Reduction of **3** with $LiAlH_4$ afforded tetraol **4**, which was brominated crude with a mixture of HBr and H_2SO_4 (2/1) to yield tetrabromide **5**. Reaction of **5** with Na_2S/Al_2O_3[11] readily furnished the [8.3.3](1,3,5)dioxadithiacyclophane ("tethered *syn*-dithia[3.3]metacyclophane") **6** (67%). In its 300 MHz ^{1}H NMR spectrum, the internal and external protons of **6** (*para* and *ortho* to the ether oxygen) appear as broad singlets at $\delta = 6.71$ and 6.39, respectively. Since **6** cannot undergo a *syn* to *syn'* conformational flip, it is not surprising that the thioether

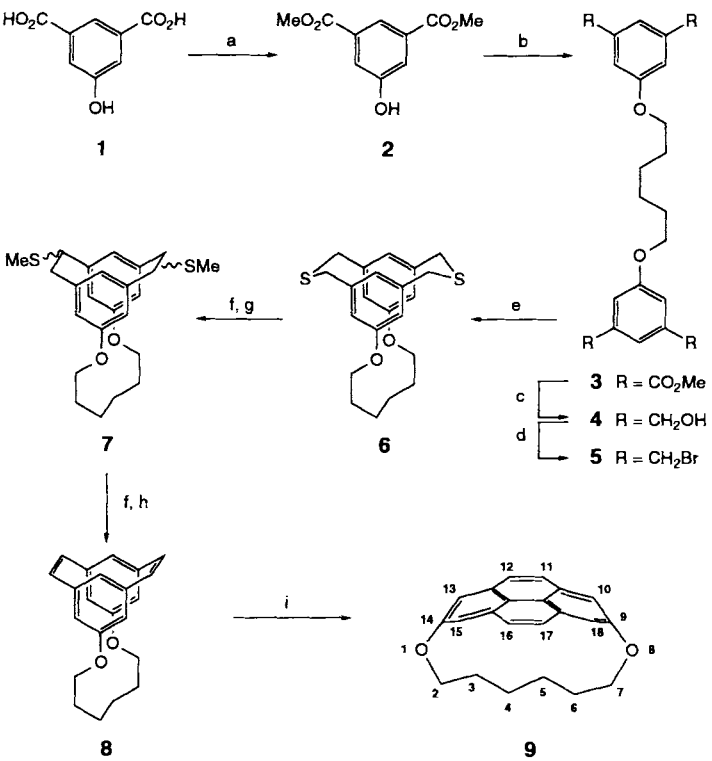

Scheme 2. Reagents and conditions: a) MeOH, H_2SO_4, Δ, 3 h, 94%; b) $Br(CH_2)_6Br$, NaH, TBAI, THF, Δ, 3 h, 80%; c) $LiAlH_4$, THF, room temperature (RT), 16 h; d) HBr/H_2SO_4 2/1, RT, 1 h, 46% based on **3**; e) Na_2S/Al_2O_3, 18% $EtOH/CH_2Cl_2$, RT, 24 h, 67%; f) $(MeO)_3CHBF_4$, CH_2Cl_2, RT, 2 h; g) *t*BuOK, THF, Δ, 3 h, 66% based on **6**; h) *t*BuOK, *t*BuOH/THF 1/1, RT, 3 h, 83% based on **7**; i) DDQ, benzene, Δ, 12 h, 67% (and 26% of **8**).

bridge protons appear as an AB system ($J = 14.7$ Hz) at $\delta = 3.79$ and 3.75. Methylation of **6** with Borch reagent followed by Stevens rearrangement gave the bridge-contracted cyclophane **7** as a mixture of isomers. Methylation of **7** with Borch reagent followed by Hofmann elimination cleanly afforded tethered [2.2]metacyclophanediene **8**. The internal and external protons are observed at $\delta = 6.95$ and 6.11, respectively. The bridge alkene protons appear at $\delta = 7.15$, which is closely comparable with other etheno-bridged cyclophanes.[12] Diene **8** can be stored on the bench in air for at least three months without significant decomposition, although considerable decomposition occurs in solution ($CDCl_3$) in the space of a day. Treatment of **8** with DDQ (2,3-dichloro-5,6-dicyanobenzoquinone) in benzene at reflux resulted in smooth conversion into 1,8-dioxa[8](2,7)pyrenophane **9**.[13] Some unchanged starting material was also recovered. This reaction proceeds very slowly in the absence of DDQ under the same conditions. The aromatic region of the ^{1}H NMR spectrum of **9** contains singlets at $\delta = 7.84$ (H11, H12, H16, H17) and 7.44 (H10, H13, H15, H18).[14] The corresponding signals of 2,7-dimethoxypyrene are observed at $\delta = 7.97$ and 7.69.[14, 15] The bridge protons are observed as symmetrical multiplets centered at $\delta = 3.58$ (H2, H7), 0.10 (H3, H6) and −1.47 (H4, H5). This suggests that the bridge undergoes a rapid pseudorotation at room temperature. Relative to the signals of cyclophane precursor **5** as reference, $\Delta\delta$ is 0.40 for H2/H7, 1.72 for H3/H6, and 3.02 for H4/H5. By comparison, the highest field protons in [6]paracyclophane (the smallest isolable [*n*]paracyclophane) appear at $\delta = -0.6$.[16] Pyrenophane **9** exhibits similar stability to **8**.

A single crystal X-ray structure analysis of **9**[17] revealed a number of unusual structural features (Fig. 1). The distortions

[*] Dr. G. J. Bodwell, Dr. J. N. Bridson, T. J. Houghton, J. W. J. Kennedy, M. R. Mannion
Department of Chemistry, Memorial University of Newfoundland
St. John's, NF, A1B 3X7 (Canada)
Fax: Int. code +(709)737-3702
e-mail: gbodwell@kean.ucs.mun.ca

[**] Curved Aromatic Compounds, Part 1. Support of this work from the Natural Sciences and Engineering Research Council (NSERC) of Canada and Xerox Research Centre of Canada (XRCC) is gratefully acknowledged.

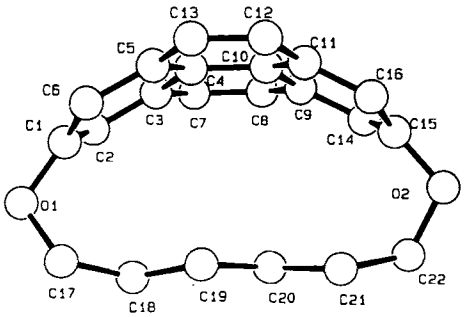

Fig. 1. Molecular structure of **9** in the crystal (ORTEP plot) [17]. Note: The crystallographic numbering differs from the systematic numbering. Selected bond lengths [Å]: C1 - C2 1.377(7), C2 - C3 1.399(6), C3 - C4 1.419(6), C4 - C10 1.420(6), C3 - C7 1.439(7), C7 - C8 1.346, O1 - C1 1.394(6), O1 - C17 1.457(6), C17 - C18 1.518(7), C18 - C19 1.506(6), C19 - C20 1.520(6).

Table 1. Bend angles [ ] between planes in the pyrene moiety of **9**.

Planes defined by [a]		Angle
C1, C2, C6	C2, C3, C5, C6	16.2
C2, C3, C5, C6	C3, C4, C5	13.3
C3, C4, C5	C3, C5, C9, C11	15.6
C3, C5, C9, C11	C9, C10, C11	15.4
C9, C10, C11	C9, C11, C14, C16	13.1
C9, C11, C14, C16	C14, C15, C16	14.3
C1, C2, C6	C14, C15, C16	87.8

[a] The crystallographic numbering shown in Fig. 1 is employed.

in the pyrene moiety are spread out more or less equally over the entire carbon skeleton. Angles formed by adjacent planes of carbon atoms are between 13.1° and 16.2° and average 14.6° (Table 1). The corresponding angles in D_{5h} C_{70}[18] and D_{6h} C_{84} should average 18° and 15°, respectively. The pyrene unit in **9** can thus be viewed as a close approximation of part of the surface of D_{6h} C_{84}. Further distortions are observed at the termini of the pyrene unit, where the two C_{aryl}–O bonds are bent out of the planes defined by C1, C2, C6 and C14, C15, C16 by 8.8°. The total bend of the pyrene unit (angle between the C1-C2-C6 and C14-C15-C16 planes) is 87.8°. There is also a fair correlation between the aromatic C–C bond lengths in **9** with those observed[18] and calculated[19] for D_{5h} C_{70}. The severe bend of the aromatic portion of the molecule is accompanied by stretching of the aliphatic chain. The C-C-C bond angles are between 115.0° and 119.4°, whereas the bond angles at oxygen are 110.5° and 110.6°. Given that arene bends of over 20° and aliphatic C-C-C bond angles of up to 126.5° have been observed in derivatives of [6]paracyclophane,[20] we are optimistic that even more distorted [*n*](2,7)pyrenophanes are obtainable.

Received: November 29, 1995 [Z 8601 IE]
German version: *Angew. Chem.* **1996**, *108*, 1418–1420

Keywords: cyclophanes · fullerene fragments · strained rings · pyrenes

[1] B. Ma, H. M. Sulzbach, R. B. Remington, H. F. Schaefer III, *J. Am. Chem. Soc.* **1995**, *117*, 8392–8400, and refs. [1–11] therein.
[2] V. V. Kane, W. H. de Wolf, F. Bickelhaupt, *Tetrahedron* **1994**, *50*, 4575–4622.
[3] P. Grice, C. B. Reese, *J. Chem. Soc. Chem. Commun.* **1980**, 424–425, and references therein.
[4] Y. Tobe, S. Saiki, K. Naemura, *Tetrahedron Lett.* **1995**, *36*, 939–942, and references therein; D. S. van Es, F. J. J. de Kanter, W. H. de Wolf, F. Bickelhaupt, *Angew. Chem.* **1995**, *107*, 2728–2730; *Angew. Chem. Int. Ed. Engl.* **1995**, *34*, 2553–2555.
[5] Y. Tobe, N. Utsumi, S. Saiki, K. Naemura, *J. Org. Chem.* **1994**, *59*, 5516–5517, and references therein.
[6] For some isolated examples of cyclophanes containing polycyclic aromatic hydrocarbons that are bent over their entire aromatic surfaces, see J. A. Reiss in *Cyclophanes, Vol II* (Eds.: P. M. Keehn, S. M. Rosenfeld), Academic Press, New York, **1983**, pp. 443–484; P. Schuchmann, K. Hafner, *Tetrahedron Lett.* **1995**, *36*, 2603–2606.
[7] Overview: R. H. Mitchell in *Advances in Theoretically Interesting Molecules, Vol. 1* (Ed.: R. P. Thummel), JAI Press, London, **1989**, p. 135–199.
[8] H.-R. Blattmann, W. Schmidt, *Tetrahedron* **1970**, *26*, 5885–5899; W. Schmidt, *Helv. Chim. Acta* **1971**, *54*, 862–868; and *Tetrahedron Lett.* **1972**, *13*, 581–584.
[9] R. H. Mitchell, V. Boekelheide, *J. Am. Chem. Soc.* **1970**, *92*, 3510–3512.
[10] Several higher homologues of **9** have also been prepared by this route. Details of this work will be published elsewhere along with full experimental details of the synthesis described in this paper. Attempts to prepare the next lower homologue of **9** have so far been unsuccessful.
[11] G. J. Bodwell, T. J. Houghton, H. E. Koury, B. Yarlagadda, *Synlett* **1995**, 751–752.
[12] V. Boekelheide, R. A. Hollins, *J. Am. Chem. Soc.* **1970**, *92*, 3512–3513; R. H. Mitchell, V. Boekelheide, *ibid.* **1974**, *96*, 1547–1557; J. R. Davy, J. A. Reiss, *Aust. J. Chem.* **1976**, *29*, 163–171; T. Otsubo, V. Boekelheide, *J. Org. Chem.* **1977**, *42*, 1085–1087.
[13] **9**: ^{13}C NMR (75 MHz, $CDCl_3$): δ = 153.6, 132.6, 127.4, 126.9, 123.2, 77.7, 27.9, 26.7; IR ($CHCl_3$): $\tilde{\nu}$ = 3040 (w), 2975 (m), 2940 (s), 2880 (m), 1460 (m), 1430 (s), 1290 (m), 1270 (s), 1110 (s), 905 (s) cm^{-1}; MS (EI, 70 eV): *m/z* (%) = 316 (M^+, 100), 234 (57), 206 (49), 205 (61), 188 (56), 176 (70); HRMS: calcd 316.14622, found 316.1451. We have prepared about 1 g of material in a single run so far.
[14] Assignments are based on NOE difference experiments.
[15] This compound was prepared by a route analogous to that in Scheme 1.
[16] V. V. Kane, A. D. Wolf, M. Jones Jr., *J. Am. Chem. Soc.* **1974**, *96*, 2643–2644.
[17] Crystal data for **9**: straw colored single crystal (regular polygon), 0.40 × 0.30 × 0.20 mm from heptane/xylenes, $C_{22}H_{20}O_2$, M_r = 316.40, monoclinic, $P2_1/c$ (No. 14), a = 9.247(6), b = 23.106(8), c = 8.568(5) Å, b = 115.29(5)°, V = 1655(3) Å^3, Z = 4, ρ_{calcd} = 1.270 g cm^{-3}, $F(000)$ = 672 $\mu(Mo_{K\alpha})$ = 0.74 cm^{-1}, T = 299 K, Rigaku AFC6S diffractometer, graphite monochromated $Mo_{K\alpha}$ radiation (λ = 0.71069 Å), $\omega - 2\theta$ scan type with ω scan width = 1.31 + 0.35 tanθ, ω scan speed 4.0 min^{-1} (up to 3 rescans for weak reflections), 3215 reflections measured, 3013 unique (R_{int} = 0.080), Lorentz-polarization and secondary extinction (coefficient = 0.31078 × 10^{-5}) corrections. Solution by direct methods, refinement by full-matrix least-squares methods (1556 reflections with $I > 2\sigma(I)$) with 219 variables led to R = 0.065 and R_w = 0.065, GOF = 2.79. All calculations used the TEXSAN package (Molecular Structure Corporation). All non-hydrogen atoms refined anisotropically; hydrogens included in calculated positions but not refined. Crystallographic data (excluding structure factors) for the structure(s) reported in this paper have been deposited with the Cambridge Crystallographic Data Centre as supplementary publication no. CCDC-179-34. Copies of the data can be obtained free of charge on application to The Director, CCDC, 12 Union Road, Cambridge CB2 1EZ, UK (fax: Int. code +(1223)336-033; e-mail: teched@chemcrys.cam.ac.uk).
[18] A. V. Nikolaev, T. J. S. Dennis, K. Prassides, A. K. Soper, *Chem. Phys. Lett.* **1994**, *223*, 143–148; S. van Smaalen, V. Petricek, J. L. de Boer, M. Dusek, M. A. Verheijen, G. Meijer, *ibid.* **1994**, *223*, 323–328.
[19] G. E. Scuseria, *Chem. Phys. Lett.* **1991**, *180*, 451–456; F. Negri, G. Orlandi, F. Zerbetto, *J. Am. Chem. Soc.* **1991**, *113*, 6037–6040; K. Raghavachari, C. M. Rohlfing, *J. Phys. Chem.* **1991**, *95*, 5768–5773; J. Baker, P. W. Fowler, P. Lazzeretti, M. Malagoli, R. Zanasi, *Chem. Phys. Lett.* **1991**, *184*, 182–186; W. Andreoni, F. Gygi, M. Parrinello, *Chem. Phys. Lett.* **1992**, *189*, 241–244; C. Z. Wang, C. T. Chan, K. M. Ho, *Phys. Rev. B* **1992**, *46*, 9761–9767.
[20] Y. Tobe, K.-I. Ueda, K. Kakiuchi, Y. Odaira, Y. Kai, N. Kasai, *Tetrahedron* **1986** *42*, 1851–1858; J. L. Jessen, G. Schröder, W. Tochtermann, *Chem. Ber.* **1985** *118*, 3287–3298; J. Liebe, C. Wolff, C. Krieger, J. Weiss, W. Tochtermann, *ibid.* **1985** *118*, 4144–4178.

A Triple Anion Complex Containing Enolate, Amide, and Halide—A New Structural Type in Lithium Chemistry**

Kenneth W. Henderson, Andrea E. Dorigo, Paul G. Williard,* and Peter R. Bernstein

The growing use of lithium bases as reagents for organic and organometallic transformations has led to a realization of the role that aggregation plays in their reactivity and selectivity.[1-3] Complexes of lithium bases, including mixed anion and mixed cation combinations, have been intensely investigated in solution and in the solid state.[2] An important example of altering aggregation to tailor reactivity and stereoselectivity is the use of lithium halide additives in enolization and addition reactions.[3] Combining crystal structure data with theoretical calculations, we recently investigated a reaction sequence for enolization and subsequent aldol addition involving halide-containing mixed anion complexes.[4] As further support for the involvement of halides in organolithium aggregates we now provide the structure of an aggregate containing lithiated amide, enolate, and halide ligands. This compound has several unique features leading to a new structural category for a tetranuclear lithium compound containing mixed anions.

Complex **1** crystallized from a solution containing a 1:1:1:2 ratio of LiBr, $LiN(SiMe_3)_2$, $LiOC(tBu)=CH_2$ and $Me_2NCH_2CH_2NMe_2$ (TMEDA). An X-ray crystallographic study revealed that **1** consists of four lithium cations, one amide anion, one bromide ion, and two enolate residues (Fig. 1).[5] Formation of complexes that do not reflect the ratio of reactants used is commonplace for reactions involving lithium.[2,6] A feature of the structure is a novel "butterfly" arrangement, in which all four metal atoms lie in the same plane (Li1 and Li2 are 0.180 Å and 0.234 Å, respectively, out of the plane formed by all ligating atoms of the anions and the cations). Alternative tetrameric frameworks that have been observed are mostly cubanes (stacks) or edge-to-edge ladders,[2] although open octagons[7] and a bicyclo[2.4.0]octane system[8] have also been reported (Fig. 2). Complex **1** can be viewed as a three rung ladder trimer of lithium bromide, lithium pinacolate, and lithium hexamethyldisilazide in which a second lithium pinacolate residue is complexed 'side-on' to the ladder. Another bromide-containing tetranuclear aggregate (**2**) has been identified.[9] In this instance the structure is a cubane.

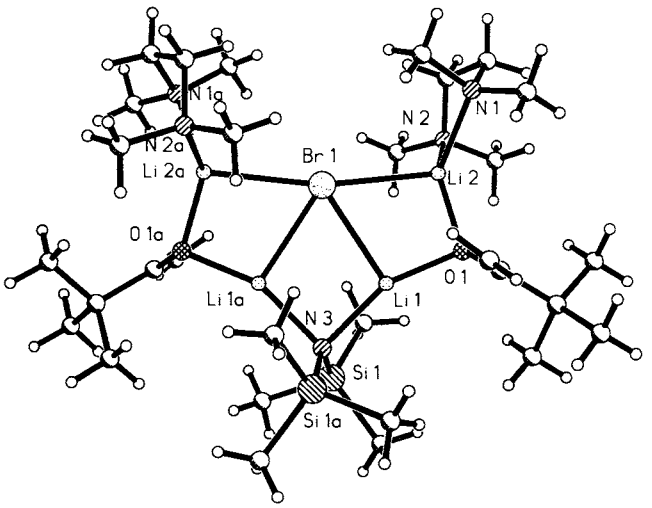

Fig. 1. Molecular structure of **1** with hydrogen atoms omitted for clarity. Key bond lengths [Å] and angles [°]: Li1–Br1 2.604(7), Li1–O1 1.845(7), Li1–N3 2.001(7), Li2–Br1 2.613(6), Li2–O1 1.843(7), Li2–N1 2.094(7), Li2–N2 2.084(7), Li2-Br1-Li2a 167.8(3), Li1-Br1-Li2 64.3(2), Li1-Br1-Li1a 65.2(3), Br1-Li1-N3 102.9(3), Br1-Li1-O1 98.9(3), Br1-Li2-O1 98.6(3), Li1-O1-Li2 97.7(3), Li1-N3-Li1a 89.1(4).

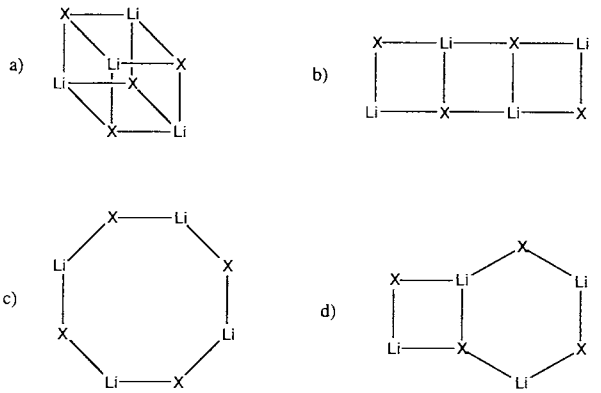

Fig. 2. Known structural types for lithium tetramers. a) Cubane, b) ladder, c) octagon, and d) bicyclo[2.4.0]octane system.

$[LiBr \cdot LiN(SiMe_3)_2 \cdot \{LiOC(tBu)=CH_2\}_2 \cdot (TMEDA)_2]$ **1**

$[LiBr \cdot (PhLi)_3 \cdot (Et_2O)_3]$ **2**

Another unique feature of **1** is that it contains three different types of anion in the aggregate. To our knowledge, **1** is the only crystallographically characterized example of an alkali metal complex that is composed of three distinct anions. This is remarkable, since over 1500 crystal structures containing lithium are reported in the Cambridge Structural Database. In part, the lack of information on such systems is due to the experimental difficulty in preparing mixed anion complexes.[4]

There are two distinct types of lithium atom present in the structure of **1**. Li1 and Li1a are three-coordinate and trigonal planar, bridging three anion types, whereas Li2 and Li2a are four-coordinate and tetrahedral, bonding to the bromine ion, an enolate ion, and a TMEDA molecule. However, the Li–O and Li–Br bond lengths are almost identical for both types of metal coordination (Li1–Br1 2.604 Å and Li2–Br1 2.613 Å; Li1–O1 1.845 Å and Li2–O1 1.843 Å). There is also a short contact distance between the three-coordinate lithium center and the α-carbon of the enolate (Li1–C8 2.586 Å, whereas Li1–C7, the distance to the β-carbon, is 3.016 Å).

Ladder structures are common in organolithium chemistry;[2] however, no reports on structures such as **1**, in which an anionic center bridges four *in-plane* lithium atoms, have been published. Clearly, this is a consequence of the nature of the electronegative center, bromine, but the bulk of the substituents and ligands present also plays a part. To demonstrate this, we performed semi-empirical PM3[10] calculations on two isomers—"ladder"-shaped and "butterfly"-shaped—of the model systems **I**–**III** (Fig. 3). We found that both factors influence the

[*] Prof. P. G. Williard, Dr. K. W. Henderson, Dr. A. E. Dorigo
Department of Chemistry
Brown University
Providence, RI, 02912 (USA)
Fax: Int. code +(401)863-2594
Dr. P. R. Bernstein
Zeneca Pharmaceuticals,
Wilmington, DE 19897 (USA)

[**] This work was funded in part by Zeneca Pharmaceuticals (grant no. 235). P. G. W. and A. E. D. wish to thank the N.I.H. for support (grant no. GM-35982).

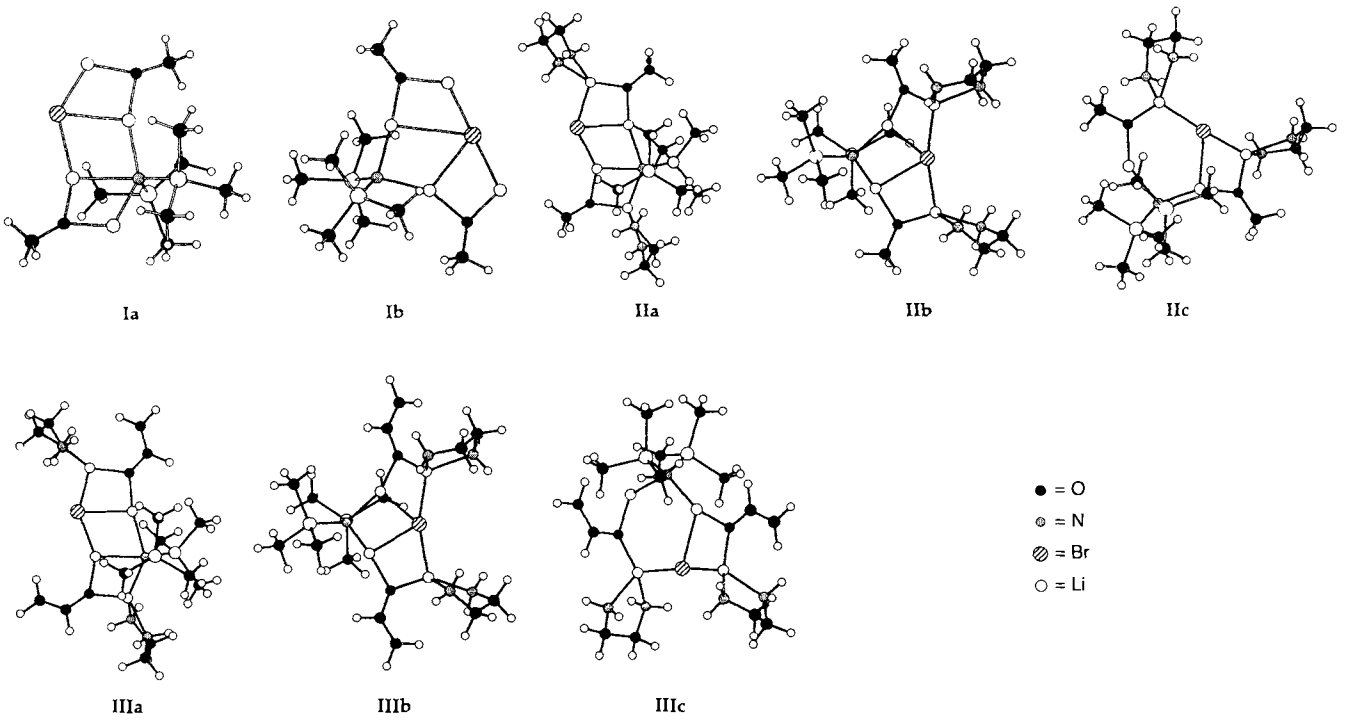

Fig. 3. PM3-optimized structures **I**–**III**. Calculated heats of formation [kcal mol^{-1}]: **Ia** −361.8, **Ib** −354.7, **IIa** −411.2, **IIb** −414.6, **IIc** −416.7, **IIIa** −377.8, **IIIb** −382.9, **IIIc** −385.7. Absolute HF/LANL2DZ energies [Hartree]: **Ia** −571.62484, **Ib** −571.63637, **IIa** −950.12458, **IIb** −950.15169, **IIc** −950.12620.

relative energies of the two isomers. Thus, the ladder structure **Ia**, in which the substituent on oxygen is a methyl group and neither lithium center has a ligand, is 7.1 kcal mol^{-1} more stable than the butterfly form **Ib**. However, coordination of two lithium centers with diaminoethane renders **IIa** less stable than **IIb** by 3.4 kcal mol^{-1}. Remarkably, a third structure, **IIc**, is even more stable than **IIb**, by 2.1 kcal mol^{-1}. This structure is best described as a bicyclic system formed by the fusion of a four-membered and a six-membered ring. A tetramer of LiCl solvated by TMEDA was recently found to have a similar structure.[8] Finally, replacement of the methoxy groups with acetaldehyde enolate residues gives a 2.8 kcal mol^{-1} preference for **IIIc** over **IIIb** and a 7.9 kcal mol^{-1} preference for **IIIc** over **IIIa**.

In all models (except for the simplest structures **Ia** and **Ib**) the ladder structure is clearly disfavored. It is still not clear why PM3 gives a lower energy for the bicyclic structure. To clarify the issue regarding the relative energies of the two systems, we performed single-point ab initio calculations[11] on **Ia**, **Ib**, **IIa**, **IIb**, and **IIc** at the HF/LANL2DZ[12] level using the PM3 geometries. At this level, **Ib** becomes favored over **Ia** by 7.2 kcal mol^{-1}. Structure **IIb** is favored by 16.0 and 17.0 kcal mol^{-1} over **IIc** and **IIa**, respectively. The large discrepancy between the relative stabilities determined with PM3 and ab initio calculations of the butterfly forms is probably due to the use of minimal basis sets in PM3, which are not flexible enough to describe the bonding of the tetracoordinate bromine center in **Ib** and **IIb** properly. It therefore appears that, at the highest level of theory, the butterfly-shaped structures are more stable than alternative geometries.

The crucial element in the stabilities of the butterfly and ladder forms is the nature of the amido nitrogen. We have formerly established that, due to a combination of electronic and steric factors, hexamethyldisilazide ions are poor μ_3-bridging anions.[13] As a consequence, the second lithium enolate group prefers to bond to bromine, leaving the amido nitrogen tetracoodinate.

We previously theorized that complexes similar to **1** may be involved during enolization reactions and will affect selectivity (Scheme 1).[4] In fact, **1** is very similar to complex **D** in Scheme 1, which supports this hypothesis (compounds

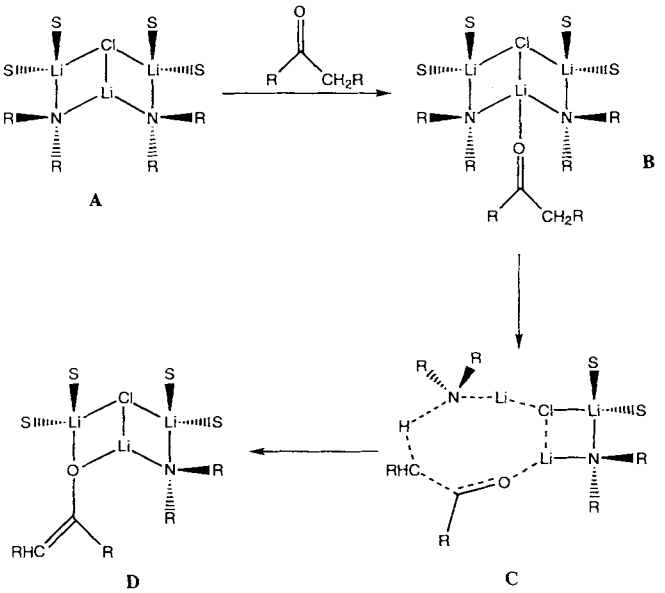

Scheme 1. Postulated mechanism of enolization in the presence of lithium complexes. For details, see text.

analogous to **A** are known, and transition state **C** is energetically viable according to ab initio calculations). Interestingly, the enolization of 3-pentanone gives an optimium *E*/*Z* selectivity when 0.3–0.4 equivalents of LiCl per lithium amide are present.[14] Such a ratio is consistent with the structure of **1**. Complex **1** also demonstrates the important fact that triple anion aggregates of lithium are stable species.

 © VCH Verlagsgesellschaft mbH, D-69451 Weinheim, 1996 0570-0833/96/3512-1323 $ 15.00+.25/0

Experimental Procedure

To a cooled mixture (approx. 0 °C under an argon atmosphere) containing *n*BuBr (2 mmol), hexamethyldisilazane (4 mmol), and TMEDA (4 mmol) in 2 mL of pentane was added *n*BuLi (6 mmol, from a 2 M solution in pentane). The mixture was stirred for five minutes, after which pinacolone (2 mmol) was added over a period of one minute. The opaque solution was warmed to 20 °C and concentrated to half volume in vacuo. After gentle heating, the clear colorless solution was kept at −20 °C. Upon standing for several weeks, a small crop of crystalline **1** was deposited. Although the yield of these crystals varied with the crystallization conditions, it was reproducible and not insignificant.

Received: October 30, 1995 [Z.8511IE]
German version: *Angew. Chem.* **1996**, *108*, 1420–1422

Keywords: ab initio calculations · enolizations · lithium compounds · stereoselectivity

[1] a) P. G. Williard, Q. Y. Liu, *J. Am. Chem. Soc.* **1993**, *115*, 3380; b) D. B. Collum, *Acc. Chem. Res.* **1993**, *26*, 227; c) L. M. Jackman, B. C. Lange, *Tetrahedron* **1977**, *33*, 2737; d) G. Boche, *Angew. Chem.* **1989**, *101*, 286; *Angew. Chem. Int. Ed. Engl.* **1989**, *28*, 277; e) D. Seebach, *ibid.* **1988**, *100*, 1685 and **1988**, *27*, 1624; f) S. C. Ball, I. Cragg-Hine, M. G. Davidson, R. P. Davies, A. J. Edwards, I. Lopez-Solera, P. R. Raithby, R. Snaith, *ibid.* **1995**, *107*, 1002 and **1995**, *34*, 921; g) B. J. Wakefield, *Organolithium Methods*, Academic Press, London, **1988**.

[2] Reviews on lithium structural chemistry: a) E. Weiss, *Angew. Chem.* **1993**, *105*, 1565; *Angew. Chem. Int. Ed. Engl.* **1993**, *32*, 1501; b) K. Gregory, P. von R. Schleyer, R. Snaith, *Adv. in Inorg. Chem.* **1991**, *37*, 47; c) R. E. Mulvey, *Chem. Soc. Rev.* **1991**, *20*, 167.

[3] a) A. Loupy, B. Tchoubar, *Salt effects in Organic and Organometallic Chemistry*, VCH, New York, **1991**, Chapters 4 and 5, and references therein; b) C. H. Heathcock in *Asymmetric Synthesis, Vol. 3* (Ed.: J. D. Morrison), Academic Press, New York, **1984**; c) E. Juaristi, A. K. Beck, J. Hansen, T. Matt, T. Mukhopadhyay, M. Simson, D. Seebach, *Synthesis* **1993**, 1271; d) D. Seebach, A. K. Beck, A. Studer in *Modern Synthetic Methods, Vol. 7* (Eds: B. Ernst, C. Leumann), VCH, Weinheim, **1995**, p. 1.

[4] K. W. Henderson, A. E. Dorigo, P. G. Williard, P. R. Bernstein, P. von R. Schleyer, *J. Am. Chem. Soc.* **1996**, in press.

[5] Crystal data for **1**: $C_{15}H_{36}Br_{0.3}Li_2N_{2.5}O_1Si_1$, monoclinic, $C2/c$, $a = 27.431(2)$, $b = 11.8250(10)$, $c = 17.649(3)$ Å, $\beta = 127.79$°, $V = 4524(9)$ Å^3, $\rho_{calcd} = 1.026$ g cm^{-3}, $2\theta_{max} = 50$°, $Z = 8$, $Mo_{K\alpha}$ radiation, $\lambda = 0.71073$ Å, scan mode $\theta - 2\theta$, $T = 195$ K, 4641 measured reflections, 3937 independent reflections, 3937 used in the refinement, no σ limits, no absorption corrections, Lp corrections, structure solved by direct methods using SHELXTL, all nonhydrogen atoms anisotropic, 204 parameters, H atoms were refined in idealized positions, $R = 5.45$, $wR = 12.79$, full-matrix least-squares on F^2 using SHELXL-93, largest peak and hole in the final difference map 0.317 and −0.392 e Å^{-3}; crystallographic data (excluding structure factors) for the structure(s) reported in this paper have been deposited with the Cambridge Crystallographic Data Centre as supplementary publication no. CCDC-179-33. Copies of the data can be obtained free of charge on application to The Director, CCDC, 12 Union Road, Cambridge CB2 1EZ, UK (fax: int. code +(1223) 336-033; e-mail: teched@chemcrys.cam.ac.uk).

[6] a) K. W. Henderson, P. G. Williard, P. R. Bernstein, *Angew. Chem.* **1995**, *107*, 1218; *Angew. Chem. Int. Ed. Engl.* **1995**, *34*, 1117; b) W. Clegg, K. W. Henderson, R. E. Mulvey, P. A. O'Neil, *J. Chem. Soc. Chem. Commun.* **1994**, 769.

[7] a) M. F. Lappert, M. J. Slade, A. Singh, J. L. Atwood, R. D. Rodgers, R. Shakir, *J. Am. Chem. Soc.* **1983**, *105*, 302; b) D. M. Anderson, P. B. Hitchcock, M. F. Lappert, *Inorg. Chim. Acta* **1988**, *141*, 157; c) J. A. Brandy, A. Berry, M. L. H. Green, K. Prout, *J. Chem. Soc. Chem. Commun.* **1985**, 1462; d) R. A. Forder, K. Prout, *Acta Crystallogr. Sect. B* **1974**, *30*, 2318.

[8] D. Hoffman, A. Dorigo, P. von R. Schleyer, H. Reif, D. Stalke, G. M. Sheldrick, E. Weiss, M. Geissler, *Inorg. Chem.* **1995**, *34*, 262.

[9] H. Hope, P. P. Power, *J. Am. Chem. Soc.* **1983**, *105*, 5320.

[10] Semiempirical calculations were performed using the *MOPAC* program package: J. J. P. Stewart, *MOPAC*, Version 6.00. For the PM3 parameterization of lithium, see: E. Anders, R. Koch, P. Freunscht, *J. Comp. Chem.* **1993**, *14*, 1301.

[11] *Gaussian 94* (Revision B.3), M. J. Frisch, G. W. Trucks, H. B. Schlegel, P. W. M. Gill, B. G. Johnson, M. A. Robb, J. R. Cheeseman, T. A. Keith, G. A. Petersson, J. A. Montgomery, K. Raghavachari, M. A. Al-Laham, V. G. Zakrewski, J. V. Ortiz, J. B. Foresman, J. Cioslowski, B. B. Stefanov, A. Nanyakkara, M. Challacombe, C. Y. Peng, P. Y. Ayala, W. Chen, M. W. Wong, J. L. Andres, E. S. Replogle, R. Gomperts, R. L. Martin, D. J. Fox, J. S. Binkley, D. J. Defrees, J. Baker, J. J. P. Stewart, M. Head-Gordon, C. Gonzalez, J. A. Pople, Gaussian, Inc., Pittsburgh, PA, **1995**.

[12] a) P. J. Hay, W. R. Wadt, *J. Chem. Phys.* **1985**, *82*, 270; b) P. J. Hay, W. R. Wadt, *ibid.* **1985**, *82*, 284.

[13] K. W. Henderson, A. E. Dorigo, P. G. Williard, P. v. R. Schleyer, R. E. Mulvey, *J. Am. Chem. Soc.*, submitted.

[14] P. L. Hall, J. H. Gilchrist, D. B. Collum, *J. Am. Chem. Soc.* **1991**, *113*, 9571.

Novel X-ray Method for In Situ Determination of Gelator Strand Structure: Polymorphism of Cholesteryl Anthraquinone-2-carboxylate**

Emanuele Ostuni, Peter Kamaras, and Richard G. Weiss*

We report a novel method to discern the packing of molecules within fibers, and demonstrate its application to thermally reversible gels that employ cholesteryl anthraquinone-2-carboxylate (CAQ[1–3]) (**1**) as gelator. It is shown that the morph responsible for the fibers in this case is not the one obtained by "normal" crystallization. Although the method may not be applicable to all gels, it offers the possibility for determining in situ the molecular packing arrangement of gelator fibers and other assemblies of this generic type.

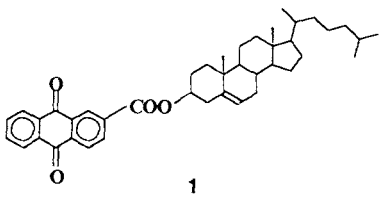

1

CAQ (**1**) and many structurally related gelators form thermotropic liquid-crystalline phases[1, 4, 5] and, in some cases, the gels are birefringent like lyotropic phases.[1a, 5] The length and thickness of the gelator fibers can be influenced strongly by solvent properties[1b, 2, 6, 7] and by the rate of formation of the fiber networks.[5, 7] Terech et al. have exploited elegantly small angle neutron scattering (SANS) and small angle X-ray scattering (SAXS) data to deduce information about the dimensions of fibers and the types of junctions between them in various gel phases.[3, 8, 9] Yet, some important structural questions remain unanswered. For instance 1) how do molecules pack within a fiber? and 2) what, if any, is the relationship between bulk crystals and "fiber crystals"?

Our method addresses these questions by relating structural information from powder and single-crystal X-ray diffraction data from different sample phases without losing the correlation among them.[10] First, the X-ray powder diffraction pattern of a gel is subtracted from that of the neat liquid component measured under identical conditions.[11] The difference is thus the diffraction from the solid-like fibers that are composed primarily of gelator molecules since virtually all of the liquid component of the gel is disordered (as it is in its neat state).[1, 8, 9] If the subtracted diffraction pattern and the powder diffractogram from a crystalline form of the neat gelator are virtually the same, molecular packing in gelator fibers can be related to that in bulk single crystals.

Differential scanning calorimetry (DSC) thermograms of neat CAQ and its X-ray powder diffractograms (vide infra) show that the solid obtained upon cooling from the mesophase is different from that from the crystals from solution (solvent:

[*] Prof. R. G. Weiss, E. Ostuni, Dr. P. Kamaras
Department of Chemistry, Georgetown University
Box 571227, Washington, DC 20057-1227 (USA)
Fax: Int. code +(202)687-6209
e-mail: weissr@gusun.georgetown.edu

[**] We are indebted to Prof. Timothy Swager and Mr. Bing Xu of the University of Pennsylvania for their generosity in allowing us to use their powder diffractometer and for helpful discussions. The National Science Foundation is gratefully acknowledged for its support of this work (CHE-9422560) and for its partial support of the purchase of the single-crystal diffractometer (CHE-9115394).

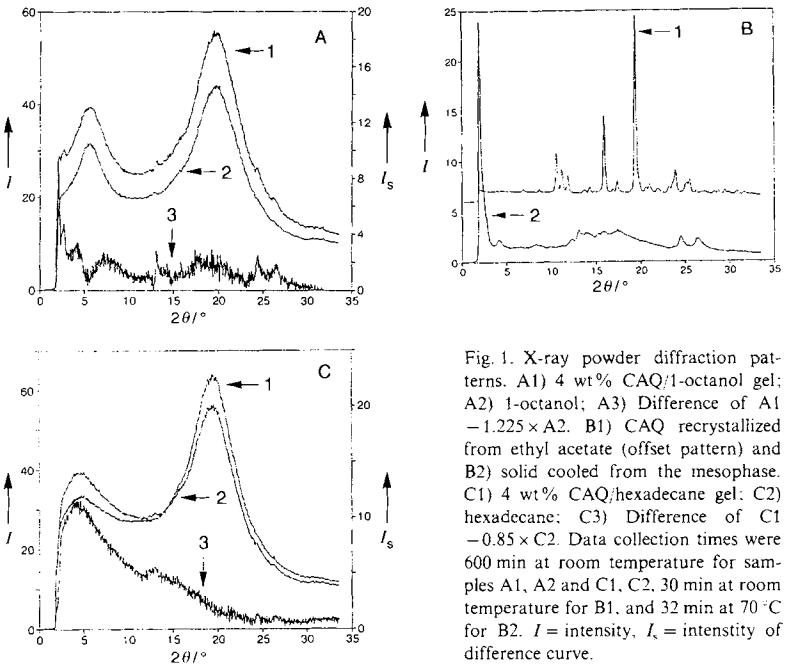

Fig. 1. X-ray powder diffraction patterns. A1) 4 wt% CAQ/1-octanol gel; A2) 1-octanol; A3) Difference of A1 $-1.225 \times$ A2. B1) CAQ recrystallized from ethyl acetate (offset pattern) and B2) solid cooled from the mesophase. C1) 4 wt% CAQ/hexadecane gel; C2) hexadecane; C3) Difference of C1 $-0.85 \times$ C2. Data collection times were 600 min at room temperature for samples A1, A2 and C1, C2, 30 min at room temperature for B1, and 32 min at 70 °C for B2. I = intensity, I_s = intenstity of difference curve.

ethyl acetate or 1-butanol/toluene)—CAQ is a polymorphous solid, like several other gelators we have studied.[1, 4, 12] Thus, the melting temperature and heat of transition for the first heating thermogram (166 °C and 55 $J g^{-1}$) are different from those of all subsequent heating cycles (169.7 °C and 25.9 $J g^{-1}$). Fibers are apparent in electron micrographs of CAQ/silicone oil gels[2] and they offer the best explanation for SANS and SAXS data derived from CAQ/1-alkanol and CAQ/alkane gels.[3] The diffraction pattern of a CAQ/1-octanol gel (Fig. 1 A1) is, as expected, very similar to that of the neat liquid component (Fig. 1 A2), since it is isotropic on a mesoscopic scale.[1] However, it includes barely discernible peaks whose intensity can be amplified by subtracting the diffraction pattern of a capillary filled with 1-octanol from that of the corresponding CAQ/1-octanol gel. The resultant pattern (Fig. 1 A3) is very similar to that of solid CAQ cooled from its mesophase (Fig. 1 B2), but not to that of recrystallized CAQ (Fig. 1 B1). The pattern for the liquid phase was multiplied by 1.225, an empirical factor, before subtraction since the ability of the liquid to diffract is different from that of the gel. These data provide compelling evidence that the strands of the gelator network in 1-octanol consist primarily of CAQ molecules packed like those in the neat solid cooled from the mesophase.

An analogous treatment of diffraction data from a CAQ/hexadecane gel results in a pattern that cannot be related as easily to one of the gelator dimorphs (Fig. 1C). Nevertheless, the peaks at about 13° and those at 24–28°, characteristic only of CAQ cooled from the mesophase, are evident; thus, CAQ/hexadecane gels may consist of fibers whose molecular packing is also like that of neat solid CAQ cooled from its mesophase.

The presence of broad diffuse features in subtracted patterns from both gels, corresponding to diffraction of the isotropic liquids, is consistent with the conclusions from SANS and SAXS analyses[3] that some liquid-component molecules are incorporated in or anisotropically associated with the fibers near junction zones. As yet, our technique is not capable of assessing quantitatively the degree of liquid participation.

Although the dimorph from the mesophase has not been obtained yet in a form amenable to single-crystal diffraction, we assume (on the basis of the low-angle peak in the powder pattern and the parallel arrangement of molecules in the mesophase) that the fibers contain CAQ molecules in lamellar-like arrays.

The packing arrangement of CAQ molecules in a single crystal[13] (obtained from 1-butanol/toluene) was determined by an X-ray structural analysis (Fig. 2). Its powder diffraction pattern simulated from the single-crystal packing information[14] is virtually superimposable with that in Figure 1 B1, providing further evidence that recrystallization from ethyl acetate and 1-butanol/toluene produces the same dimorph. The molecular packing displays none of the characteristics expected of gelator fibers. There are no apparent (strongly) attractive interactions. Individual molecules have neighbors whose long axes are parallel, but each is staggered so that there are no lamellae. Also, π-π interactions[1, 5] between anthraquinonyl groups and steroidal–steroidal interactions[15] are not apparent: neighboring aromatic groups are canted with respect to each other by 19°; the nearest approach (3.14 Å) is between an oxygen atom of an anthraquinonyl group of one molecule and the carbonyl oxygen atom of the ester group of a neighboring molecule; all other intermolecular distances are at least 3.9 Å. Within a molecule, the angle between the non-weighted least-squares plane defined by the carbon atoms of the aromatic ring nearer the steroidal group and by the carbon atoms at the 1, 3, and 5 positions in the steroidal A-ring is about 55°. Whatever layering does exist is not expected to impart the mechanical strength necessary to construct a colloidal network of fibers.

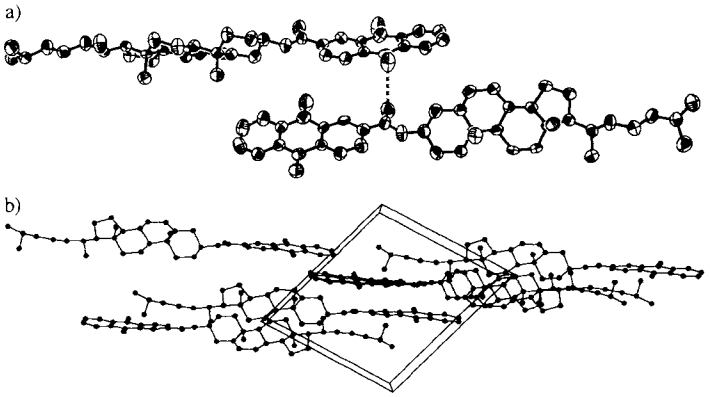

Fig. 2. Molecular packing of CAQ in crystals obtained from 1-butanol/toluene. a) ORTEP plot (50% probability; hydrogen atoms removed for clarity); the dashed line shows the shortest intermolecular interaction. b) Molecular packing within the unit cell.

In summary, we have described a methodology for ascertaining the molecular packing of gelator molecules in strands constituting colloidal networks in physical gels and have presented examples of its application using CAQ. The method takes into consideration the potential polymorphous character of many gelator molecules and, for that reason, it maintains direct relationships among data sets derived from the various states of matter. The fact that the CAQ morph in the gel fibers is *not* the one obtained upon a "normal" crystallization indicates the caution necessary in relating molecular packing in gel and neat phases.

Received: December 4, 1995 [Z8610IE]
German version: *Angew. Chem.* **1996**, *108*, 1423–1425

Keywords: gels · mesophases · structure elucidation

[1] a) Y.-C. Lin, Ph.D. Thesis, Georgetown University, Washington, DC, **1987**; b) Y.-C. Lin, B. Kachar, R. G. Weiss, *J. Am. Chem. Soc.* **1989**, *111*, 5542; c) Y.-C. Lin, R. G. Weiss, *Macromolecules* **1987**, *20*, 414.

[2] V. J. Bujanowski, D. E. Katsoulis, M. J. Ziemelis, *J. Mater. Chem.* **1994**, *4*, 1181.

[3] P. Terech, E. Ostuni, R. G. Weiss, *J. Phys. Chem.*, **1996**, *100*, 3759.

[4] a) R. Mukkamala, R. G. Weiss, *J. Chem. Soc. Chem. Comm.* **1995**, 375; b) R. Mukkamala, R. G. Weiss, *Langmuir*, **1996**, *12*, 1474.

[5] a) E. Ostuni, M. S. Thesis, Georgetown University, Washington, D. C., **1995**; b) E. Ostuni, R. G. Weiss, 29th ACS Middle Atlantic Regional Meeting, May 1995, Washington, D. C., Abstract 238.

[6] C. Fee, R. G. Weiss, unpublished results.

[7] I. Furman, R. G. Weiss, *Langmuir* **1993**, 9, 2084.

[8] P. Terech, I. Furman, R. G. Weiss, *J. Phys. Chem.* **1995**, *99*, 9558.

[9] a) P. Terech, F. Volino, R. Ramasseul, *J. Phys. (Paris)*, **1985**, *46*, 895; b) P. Terech, *J. Phys. II*, **1992**, *2*, 2181; c) P. Terech, I. Furman, H. Bouas-Laurent, R. Ramasseul, R. G. Weiss, *Faraday Discuss. Chem. Soc.* **1996**, in press; d) P. Terech, V. Schaffhauser, P. Maldivi, J. M. Guenet, *Europhys. Lett.* **1992**, *17*, 515; e) P. Terech, *Croat. Chem. Acta* **1992**, *65*, 425; f) R. H. Wade, P. Terech, E. A. Hewat, R. Ramasseul, F. Volino, *J. Colloid Interface Sci.* **1986**, *114*, 442.

[10] Recently, Menger et al. made the guarded claim in this journal [10a] to have determined for the first time the packing arrangement of molecules at the atomic level in a self-assembled gel fiber. They attempted to examine fibers of gels from dibenzoyl-L-cystine (DBC) in mixtures of water and ethanol. Unfortunately, their molecular packing arguments are based upon single-crystal diffraction data from a *related* molecule, di(*p*-toluoyl)-L-cystine (DTC), that precipitated from water/ethanol mixtures, and then was recrystallized from yet a *different* solvent (methanol ethyl acetate) before being analyzed! Considering that polymorphism of gelator molecules is common (contrary to assumption [10a]), that different strand types can be found in gels of one gelator and different liquid components [1b,6–8], and that subtle structural changes (such as addition or subtraction of even one carbon atom on a chain) can have drastic consequences on molecular packing in crystals [10b] and gelation ability [7], we consider the extrapolation from DBC gels to DTC recrystallized from a different solvent to be compromising in the best scenario and a source of erroneous conclusions in the worst one. a) F. M. Menger, Y. Yamasaki, K. K. Catlin, T. Nishimi, *Angew. Chem.* **1995**, *107*, 616; *Angew. Chem. Int. Ed. Engl.* **1995**, *34*, 585; b) B. M. Sheikh-Ali, M. Rapta, G. B. Jameson, R. G. Weiss, *Acta Crystallogr. Sect. B* **1995**, *51*, 823.

[11] Powder diffraction data were collected on an Inel CPS 120 diffractometer with a XRG 3000 X-ray generator using $Cu_{K\alpha}$ radiation; temperature was controlled with a Minco CT 137 temperature controller connected to a custom-made oven.

[12] L. Lu, R. G. Weiss, *Langmuir* **1995**, *11*, 3630.

[13] Single-crystal structure data for **1** ($C_{42}H_{52}O_4$): Determination of the lattice parameters and measurement of the intensities were carried out with a Siemens P4/RA diffractometer ($Mo_{K\alpha}$ radiation) at room temperature. Structure determination and refinement were done with SHELXTL-5 package. Full-matrix least squares refinement was done on F^2. Hydrogen atoms of CH_3 groups were located by using difference Fourier synthesis with toroidal averaging and refined as a group with idealized tetrahedral geometry riding on the methyl carbon atom with isotropic temperature factors of 1.5 times U_{eq}. Single-crystal structure data: monoclinic space group $P2_1$, $a = 11.973(4)$, $b = 11.087(5)$, $c = 13.523(4)$ Å, $\beta = 107.89(3)°$, $V = 1708.3(11)$ Å^3, $Z = 2$. 3087 reflections were collected of which 2646 were symmetry independent with $R_{int} = 0.0645$, 420 parameters, $R1 = 0.0474$, $wR2 = 0.1147$. Crystallographic data (excluding structure factors) for the structure(s) reported in this paper have been deposited with the Cambridge Crystallographic Data Centre as supplementary publication no. CCDC-179-35. Copies of the data can be obtained free of charge on application to The Director, CCDC, 12 Union Road, Cambridge CB2 1EZ, UK (fax: Int. code +(1223) 336-033; e-mail: teched@chemcrys.cam.ac.uk).

[14] The powder pattern was simulated from the single-crystal data file (.hkl format) using the SHELXTL-5 (version 5.03) program package. The intensities were merged and corrected for Lorenzian polarization and multiplicity.

[15] K. Murata, M. Aoki, T. Suzuki, T. Harada, H. Kawabata, T. Komori, F. Ohseto, K. Ueda, S. Shinkai, *J. Am. Chem Soc.* **1994**, *116*, 6664.

Reversible Encapsulation of Guest Molecules in a Calixarene Dimer**

Blake C. Hamann, Ken D. Shimizu, and Julius Rebek, Jr.*

Dedicated to Professor C. David Gutsche on the occasion of his 75th birthday

A molecular capsule[1] based on the hemispherical substructure of a calix[4]arene was recently described.[2] Urea functions placed on the "upper" rim of the calix[4]arene permit dimerization to occur through a head-to-tail hydrogen bonding pattern (Fig. 1), a pattern which is remniscent of those observed for

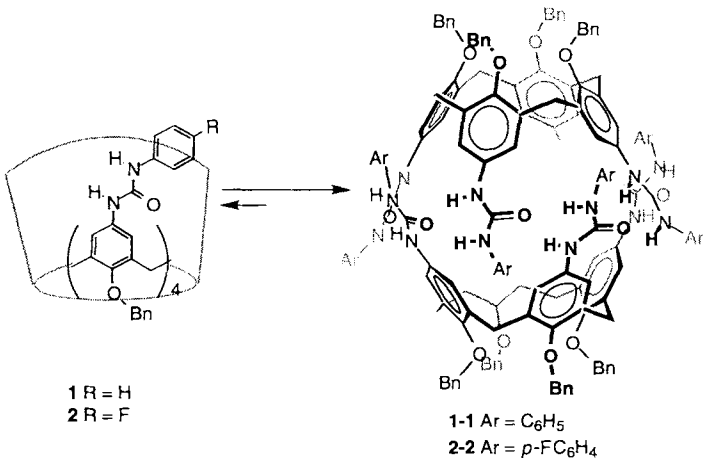

Fig. 1. The dimerization of the urea-substituted calix[4]arene through the formation of intermolecular hydrogen bonds. Bn = benzyl.

diaryl ureas in the solid state.[3] The direct observation of guests within the capsule has now been achieved, and permits a measure of the stoichiometries and exchange rates of guests into and out of the capsule. We report here on these developments and apply a computational method to estimate the interior volume of the capsule.

The capsule **2-2** was prepared from the appropriate tetraamine as previously described[1, 4] for **1-1** but using *p*-fluorophenyl isocyanate as the electrophile in the final step of the synthesis. The signals of the fluorine atoms in **2-2** serve as an internal standard for ^{19}F NMR spectroscopy. The compound is monomeric in [D_6]DMSO but a well-behaved dimer in [D_{10}]-*p*-xylene solution, and its ^1H NMR spectra are recorded in Figure 2. The characteristic features of the spectrum—two different calixarene proton resonances at $\delta = 5.78$ and 7.95, the meta coupling between them ($J = 2.4$ Hz), the widely separated AB system for the methylene protons of the calixarene (characteristic of a cone conformation),[5] and the AB quartet for the benzyl protons (which reflects the asymmetry imparted by the "direction" of the circle of urea functions)—leave little doubt that the structure is the dimeric **2-2** shown in Figure 1.[6]

[*] Prof. J. Rebek, Jr.,[+] B. C. Hamann, K. D. Shimizu
Department of Chemistry
Massachusetts Institute of Technology
Cambridge, MA 02139 (USA)
Fax: Int. code +(617)253-7929

[**] We thank Professors David Reinhoudt, George Whitesides, and Volker Böhmer for suggestions and advice, and Professor Philip Eaton for a sample of cubane. The National Institutes of Health provided financial support.

[+] Address after July 1, 1996: Institute for Chemical Biology, The Scripps Research Institute, 10550 N. Torrey Pines Road, La Jolla, CA 92037 (USA).

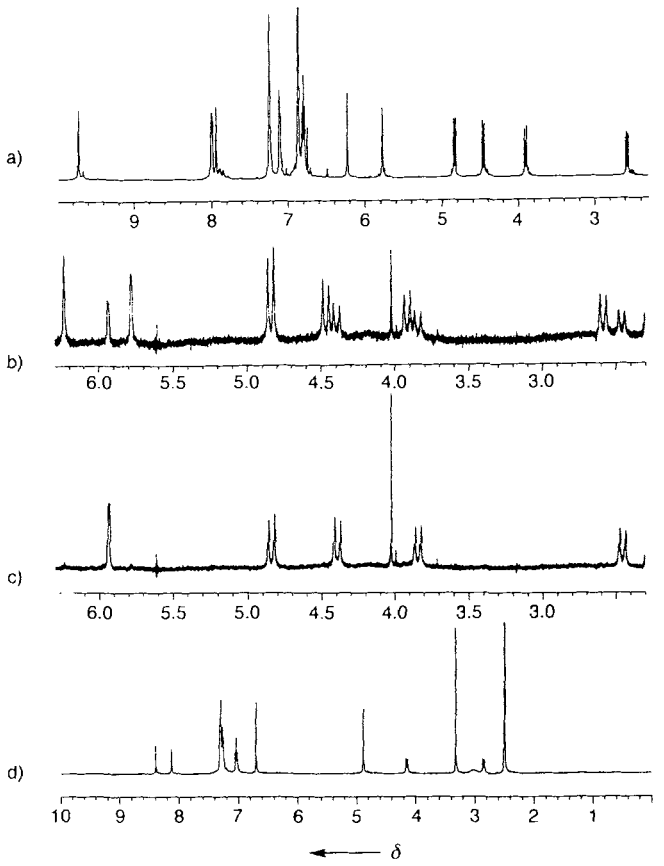

Fig. 2. ^{1}H NMR spectra of **2-2** in [D_{10}]*p*-xylene. a) Without addition of benzene. b) 4 minutes after the addition of 5 μL benzene, and c) 40 minutes after the addition of 5 μL benzene. d) ^{1}H NMR spectrum of **2** in [D_6]DMSO.

When fluorobenzene is added to the solution of **2-2**, a new signal emerges upfield in the ^{19}F NMR spectrum. The integration indicates an approximately 1:1 stoichiometry, and implies that encapsulation of fluorobenzene has occurred.[7] On addition of other ureas such as the phenyl-α-phenylethyl derivative **3** to the latter solution, the fluorobenzene is liberated and the signals of a new calixarene species appear in the ^{1}H NMR spectrum. This most likely results from the "denaturation" of the calixarene dimer **4** by the urea derivative through competitive hydrogen bonding (Fig. 3), a process analogous to the denaturation of proteins with urea. One of the many posssible structures for the denatured product is **5** (Fig. 3).

Direct observation of the encapsulated guests by ^{1}H NMR spectroscopy is also possible, given some time. For example, when excess benzene is added to the solution of **2-2** (Fig. 2a), a new singlet appears at $\delta = 4.02$ and grows over the course of about 40 minutes (Fig. 2b and 2c). Integration again indicates an approximately 1:1 ratio of benzene to the capsule **2-2**, and the half-life for the uptake is about eight minutes. Equilibrated solutions of benzene and the dimeric calixarene in [D_{10}]*p*-xylene indicate an association constant K of 230 M^{-1} for benzene encapsulation.[8]

The encapsulation of other guests such as fluorobenzene, *p*-difluorobenzene, and pyrazine has also been directly monitored by NMR spectroscopy (Fig. 4a–c). Particularly striking

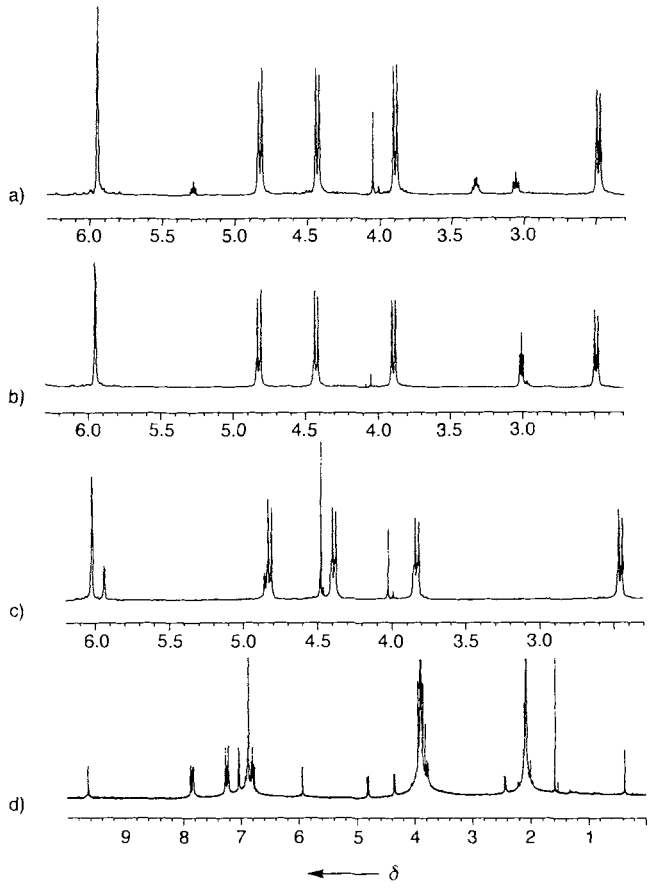

Fig. 4. ^{1}H NMR spectra of solutions of **2-2** in [D_{10}]*p*-xylene (2.94×10^{-3} M) with benzene (22×10^{-3} M) and a) fluorobenzene, b) *p*-difluorobenzene, and c) pyrazine (each 22×10^{-3} M); d) ^{1}H NMR spectrum in [D_{10}]*p*-xylene with excess cubane.

are the different chemical shifts observed for the *ortho*-, *meta*-, and *para*-hydrogen atoms of encapsulated fluorobenzene; the *para*- and *ortho*-hydrogen atoms are separated by more than 2 ppm! This is evidence that a particular orientation is favored by this guest within the cavity. The orientation of fluorobenzene in **4** shown is consistent with the chemical shifts observed. The *ortho*- and *meta*-hydrogen atoms are directed at the π-electron systems of the phenyl rings of the calixarene, while the *para*-hydrogen atom and the fluorine atom are directed at the encircling urea groups. Competition studies of other guests were undertaken and the affinity of the calixarene dimer for these (relative to benzene) is given in Table 1. The high affinity observed for pyrazine also hints at

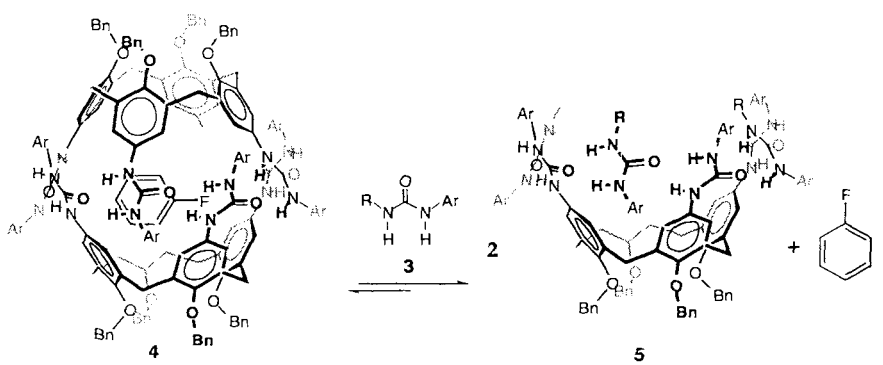

Fig. 3. The "denaturation" of capsule **4** on addition of urea derivative **3**, resulting in the liberation of *p*-fluorobenzene.

Table 1. Relative affinities of **2-2** for guests in competition with benzene [a]

Guest	Affinity	
	$T = 25\,^{\circ}C$	$T = 50\,^{\circ}C$
C_6H_6	1.0	0.82
C_6H_5F	2.6	2.5
p-$C_6H_4F_2$	5.8	6.9
C_6H_5Cl	0.30	0.55
$C_6H_5CH_3$	< 0.1	< 0.1
C_6H_5OH	0.83	1.2 [b]
$C_6H_5NH_2$	0.32	0.39
pyrazine	3.2	3.0
pyridine	1.2	1.1

[a] Concentration of dimer is 2.936×10^{-3} M; guest and benzene concentrations are 21.94×10^{-3} M each. [b] A precipitate formed after several hours.

a conformation that directs the lone pairs of electrons on the nitrogen atom toward the urea hydrogen atoms in the complex.[9]

Determination of "negative volume", the cavity size inside of a molecule, has been particularly **difficult.**[10] Low-tech methods, such as physically building a space-filling model and measuring the amount of plaster that can be pressed into its interior, have been used with practical results.[11] We have found that the modeling program MacroModel can measure the negative volume of a cavity through a simple series of calculations. MacroModel calculates the positive volume of a molecule and does so without calculating overlapping volumes twice. For the case of **2-2**, the volume that the host occupies was calculated. Next, the cavity was "stuffed" with smaller overlapping arbitrary molecules in a way that no unoccupied space remained inside the cavity. Care was taken to avoid ruptures, that is, penetration of the stuffing through the outer van der Waals (VDW) surface of the dimeric capsule. The calculation was repeated on the filled capsule, and subtraction of the first volume from the second gives the volume of the cavity.

In this manner, the volume of **1-1** was calculated to be ≈ 210 Å^3. In addition, the volumes of several guests were measured for comparison (Table 2). These measurements show that most guests appear to fill $\approx 50\%$ or less of the available space in the cavity. By comparison, in a liquid 70% of space is filled.

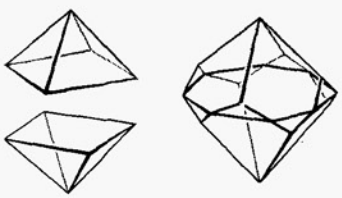

Fig. 5. Schematic representations of the cavity formed by the dimerization of **2**. The two square pyramids (left) represent the separate calix[4]arenes and the geometric figure (right) the assembled cavity.

The shape of the cavity within **2-2** is not easy to visualize. A geometric simplification is shown in Figure 5. Each calix[4]arene is represented by a square pyramid with its triangular facets corresponding to the phenyl rings of the macrocycle. In the dimer, the pyramids are offset by 45°, and the corners are cut off to simulate the eight interleaved urea groups that mark the equator of the structure.

A horizontal slice through the plane of the urea group yields an octagonal cavity, a vertical slice gives a diamond-shaped cavity, having different angles and lengths for the top and bottom sections. Overall the cavity has a height of ≈ 10 Å and a width of 7–8 Å, measured from VDW surface to VDW surface (Fig. 6). Modeling shows that guests such as benzene, cyclohexane, and chloroform can be easily accommodated.

As the cross sections in Figure 6 show, cubane would fit well in the cavity. The energy-minimized structures for the complexes with cubane are shown in Figure 7, in which the cavity walls

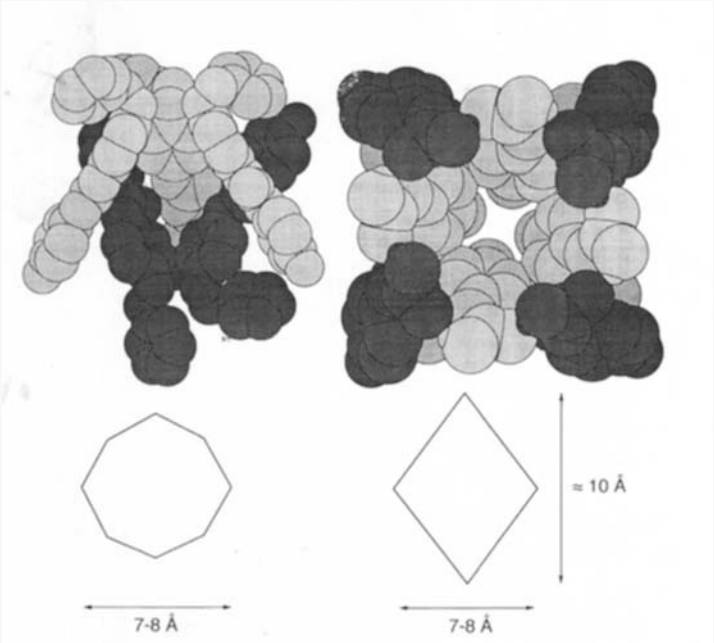

Fig. 6. Horizontal and vertical cross sections of van der Waals surfaces of **2-2**. In each view half of the dimer has been cut away.

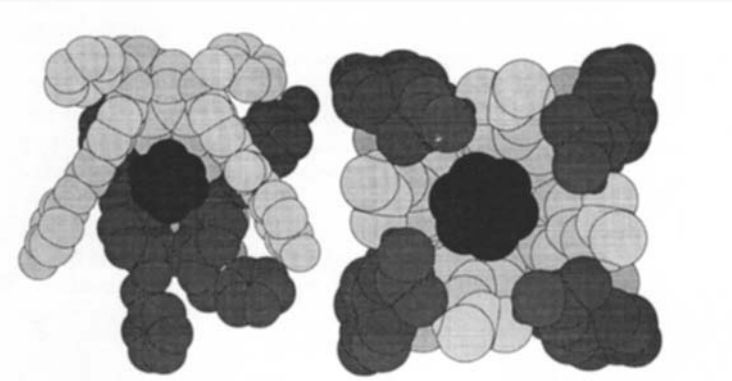

Fig. 7. Views of CPK representations of **2-2** with encapsulated cubane from side and top views. Only half of the dimer is shown in each case

Table 2. Volume V [Å^3] and length of the longest axis L of various guests [a]

Guest	V	L
benzene	83	7.4
chloroform	77	6.4
dichlormethane	61	6.4
toluene	99	8.3
m-xylene	118	8.3
p-xylene	117	9.2
o-xylene	118	8.3

[a] The longest axis was measured from VDW surface to VDW surface [Å]

have been cut away for ease of visualization. In the experiment, when cubane was added to a solution of **2-2** in [D_{10}]p-xylene, a 1:1 complex was formed, as shown by the ^{1}H NMR spectrum (Fig. 4d). We are currently exploring the limits of shape-selectivity of these dimeric capsules.

Received: January 8, 1996 [Z 8707 1E]
German version: *Angew. Chem.* **1996**, *108*, 1425–1427

Keywords: calixarenes · host–guest chemistry · inclusion compounds

[1] K. D. Shimizu, J. Rebek, Jr., *Proc. Nat. Acad. Sci. USA* **1995**, *92*, 12403–12407.
[2] For recent reviews of calixarene chemistry see: V. Böhmer, *Angew. Chem.* **1995**, *107*, 785–818; *Angew. Chem. Int. Ed. Engl.* **1995**, *34*, 713–745; P. Linnane, S. Shinkai, *Chem. Ind. (London)* **1994**, 811–814; C. D. Gutsche, *Aldrichimica Acta* **1995**, *28*, 3–9; S. Shinkai, *Tetrahedron* **1993**, *49*, 8933-8968.
[3] M. C. Etter, T. W. Panunto, *J. Am. Chem. Soc.* **1988**, *110*, 5896–5897; M. C. Etter, Z. Urbańczyk-Lipkowska, M. Zia-Ebrahimi, T. W. Panunto, *J. Am. Chem. Soc.* **1990**, *112*, 8415–8426.
[4] C. D. Gutsche, P. F. Pagoria, *J. Org. Chem.* **1985**, *50*, 5795–5802.
[5] P. Timmerman, W. Verboom, D. N. Reinhoudt, A. Arduini, S. Grandi, A. R. Sicuri, A. Pochini, R. Ungaro, *Synthesis* **1994**, 185–189; P. Timmerman, K. G. A. Nierop, E. A. Brinks, W. Verboom, C. J. M. van Veggel, W. P. van Hoorn, D. N. Reinhoudt, *Chem. Eur. J.* **1995**, *1*, 132–143.
[6] For other host–guest compounds with calixarenes see: J. D. van Loon, R. G. Janssen, W. Verboom, D. N. Reinhoudt, *Tetrahedron Lett.* **1992**, *33*, 5125–5128; K. Koh, K. Araki, S. Shinkai, *ibid.* **1994**, *35*, 8255–8258.
[7] The ^{19}F NMR spectrum of fluorobenzene in [D_{10}]*p*-xylene showed a resonance at $\delta = -113.1$; upon encapsulation with **2-2** a new resonance appeared at $\delta = -118.5$. The resonance for **2-2** appeared at $\delta = -119.4$ and remained unchanged upon encapsulation of fluorobenzene.
[8] For examples of encapsulation in covalently linked hemispheres see: T. A. Robbins, C. B. Knobler, D. R. Bellow, D. J. Cram, *J. Am. Chem. Soc.* **1994**, *116*, 111–122; A. Ikeda, S. Shinkai, *J. Chem. Soc. Perkin Trans. 1* **1993**, 2671–2673; L. Garel, J. P. Dutasta, A. Collet, *Angew. Chem.* **1993**, *105*, 1249–1251; *Angew. Chem. Int. Ed. Engl.* **1993**, *32*, 1169–1171. For encapsulation in noncovalent assemblies see: N. Branda, R. Wyler, J. Rebek, Jr., *Science* **1994**, *263*, 1267–1268; R. Meissner, J. de Mendoza, J. Rebek, Jr., *ibid.* **1995**, *270*, 1485–1488.
[9] A recent study of encapsulation using hydrogen-bonded assemblies also finds pyrazine a welcome guest: R. G. Chapman, J. C. Sherman, *J. Am. Chem. Soc.* **1995**, *117*, 9081–9082.
[10] N. Branda, Ph.D. Thesis, Massachusetts Institute of Technology, **1994**; G. J. Kleywegt, T. A. Jones, *Acta Crystallogr. Sect. D* **1994**, 50, 178.
[11] C. N. Eid, Jr., D. J. Cram, *J. Chem. Educ.* **1993**, *70*, 1993.

Heterogeneous Palladium-Catalyzed Regioselective Hydrostannation of Alkenes**

Mark Lautens,* Sophie Kumanovic, and Christophe Meyer

Hydrometalation of carbon–carbon multiple bonds is a powerful method for the generation of useful organometallic compounds.[1] We have previously described the nickel-catalyzed hydroalumination and ring opening of oxabicyclic systems such as **1** leading to the cycloalkenol **2** (Scheme 1).[2] Recently we reported the palladium-catalyzed hydrostannation of **1**,[3] leading to the organostannane **3** in which the tin occupies a distal position. Transmetalation of the latter with methyllithium afforded the regioisomeric ring-opened product **4**.

We were interested in extending the scope of the hydrostannation reaction to a wider variety of alkenes. It is well-known that palladium complexes catalyze the hydrostannation of alkynes to yield vinylstannanes.[4] However, the corresponding reaction of unactivated alkenes has not been reported to our knowledge. This reaction should, in principle, lead to tetraalkylstannanes. Although simple tetraalkylstannanes fail to undergo efficient tin–lithium exchange, an appropriately located heteroatom shifts the equilibrium due to coordination to the newly formed organolithium compound, thus allowing the exchange

[*] Prof. M. Lautens, Dr. S. Kumanovic, Dr. C. Meyer
Department of Chemistry
University of Toronto
Toronto, Ontario M5S 1A1 (Canada)
Fax: Int. code +(416)978-6083
e-mail: mlautens@alchemy.chem.utoronto.ca

[**] M. L. thanks NSERC Canada for support of this work in the form of an E. W. R. Steacie Fellowship. S. K. thanks the NSERC for a postdoctoral fellowship. C. M. thanks the Ministère des Affaires Etrangères Français for a Lavoisier grant.

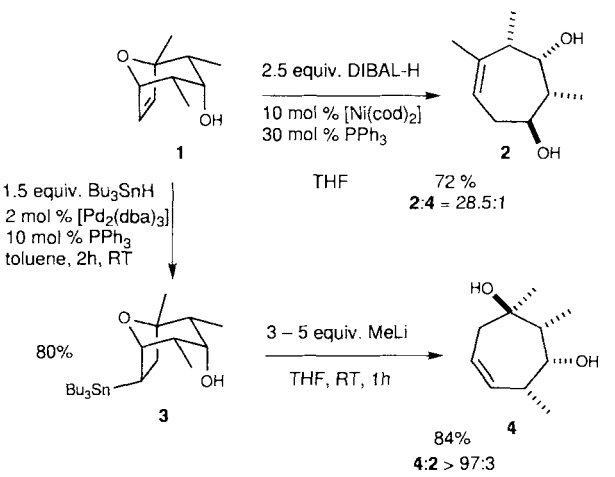

Scheme 1. Hydrometalation–ring opening sequences of oxabicyclic compound **1**. RT = room temperature, DIBAL-H = diisobutylaluminum hydride.

to proceed.[5] Interestingly, 3-tributylstannyl-1-propanol has been shown by Seebach and Meyer to be transmetalated to 3-lithioalkoxypropyllithium,[6a] and the dramatic influence of the alkoxy moiety in a related process has been nicely illustrated by Carpenter and Newman-Evans.[6b] More recently, Knochel et al. have applied this tin–lithium exchange reaction to the synthesis of chiral, γ-functionalized secondary alcohols.[6c]

Hydrostannation of double bonds has mostly been achieved under radical conditions by heating the compounds in neat tin hydrides, sometimes in the presence of a radical initiator.[7] Activated alkenes including styrene react rapidly, but this reaction lacks generality. Since addition of stannyl radicals onto a carbon–carbon double bond is reversible,[7b] a high concentration of tin hydride is required to achieve an efficient quench of the initially formed β-stannyl radical. Alternatively, ultrasound-promoted radical hydro- and hydroxystannations of activated double bonds have also been described.[7e]

When we attempted to perform the hydrostannation of allyl alcohol [Eq. (a)] with the homogeneous Pd catalyst that worked

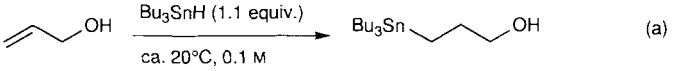

(a)

efficiently for the conversion of **1** to **3**, the corresponding 3-tributylstannyl-1-propanol was produced in no more than 5% yield (Table 1, entry 1). Similarly, other allylic alcohols failed to give high yields of hydrostannated products in the presence of the commonly used soluble catalyst [$Pd(PPh_3)_4$].

However, we have found that this reaction can be performed in high yield under heterogeneous catalysis. Pd/C was the first

Table 1. Hydrostannation of allyl alcohol according to Equation (a).

Entry	Catalyst	Solvent	Time [a]	Yield [%] [b]
1	[$Pd_2(dba)_3$] 2.5 mol % PPh_3 10 mol %	THF	ca. 12 h	4
2	·	EtOH abs.	ca. 12 h	23 [c]
3	Pd/C 10 mol %	AcOEt	ca. 12 h	35
4	[$Pd(OH)_2$]/C [d, e]	EtOH abs.	2 h	50
5	[$Pd(OH)_2$]/C [d]	THF	1 h	82

[a] Total time elapsed before workup. [b] Yield of isolated product. [c] No reaction occurs if the solvent is degassed, or if galvinoxyl is added. Galvinoxyl = 2,6-di-*tert*-butyl-α-(3,5-di-*tert*-butyl-4-oxo-2,5-cyclohexadien-1-ylidene)-*p*-tolyloxy (free radical). [d] 10 mol % Pd from Pearlman's catalyst (dry weight basis). [e] Addition of galvinoxyl has no effect on this reaction.

catalyst we examined (entry 3), but $[Pd(OH)_2]/C$ (Pearlman's catalyst, entries 4 and 5) was more efficient at promoting the hydrostannation of a variety of alkenes, provided that Bu_3SnH was added slowly over one or more hours. Transition metals are known to catalyze the decomposition of tributyltin hydride to hexabutyldistannane and molecular hydrogen,[7a] and this was the main side reaction we had to overcome. The major side product of the reaction is Bu_6Sn_2, which is easily removed by column chromatography.

The catalytic influence of palladium hydroxide is demonstrated by the fact that in its absence, 3-tributylstannyl-1-propanol is produced in only 23% yield, because of an inefficient radical pathway (entry 2). The latter pathway can be completely inhibited by degassing the solvent or by adding radical scavengers such as galvinoxyl. THF was the optimum solvent for this heterogeneously catalyzed hydrostannation (entry 5), although ethanol gave good yields as well.

The reaction has been successfully applied to a wide variety of alkenes (Table 2). The allylic alcohols can be either secondary or tertiary (entries 1 and 2). The presence of a coordinating group located at the allylic position is not required for the reaction to proceed, since 3-buten-1-ol, 10-undecen-1-ol (entry 3), acrolein diethyl acetal (entry 4), and vinylacetic acid (entry 5) are regioselectively hydrostannated in good yields. In the case of acrylonitrile (entry 6), both heterogeneously and previously reported homogeneously catalyzed hydrostannations afford the α adduct,[8] confirming that the reaction follows a polar pathway. *N*-Vinylphthalimide (entry 6) is hydrostannated in acceptable yield, and the resulting compound is of significant interest, since α-phthalimidostannanes can function as α-aminostannane equivalents in Stille-type coupling reactions.[9]

Allyl amine derivatives (entry 7) are also hydrostannated in excellent yields under the same conditions, which provides an efficient route to γ-aminostannanes.

1,1-Disubstituted alkenes react efficiently (entry 8), but unactivated 1,2-dialkyl-substituted alkenes give low yields of hydrostannated products under these conditions. However, aryl substituted alkenes react smoothly, leading to benzylstannanes (entries 9 and 10). Interestingly, in the case of 1,2-dihydronaphthalene, we have found that radical-initiated addition of Bu_3SnH proceeds with the opposite regiochemistry in 88% yield.

In conclusion, we have shown that a wide variety of alkenes can be efficiently hydrostannated under heterogeneous conditions, providing easy access to organostannanes that are not easily prepared by other routes. This reaction can also be complementary to the radical-based hydrostannation reactions in terms of the regioselectivity of the addition. Further developments on this reaction, especially in the design of diastereo- and enantioselective hydrostannations, are currently underway.

Table 2. Heterogeneously catalyzed hydrostannation of substituted alkenes.

Entry	Alkene	Product [a]		Yield [%] [b]
1	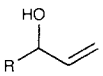	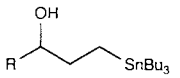	R = Ph R = 2-furyl	96 92
2	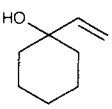	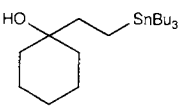		94 [c]
3	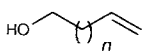	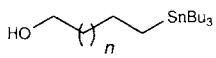	$n = 1$ $n = 8$	91 [d] 80
4	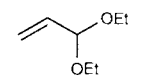	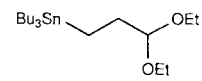		85
5	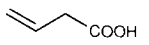	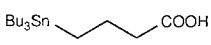		78
6	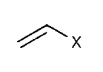	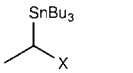	X = CN X = *N*-phthaloyl	84 60
7	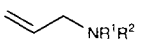	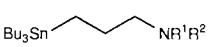	$R^1 = H$, $R^2 = CO_2tBu$ $R^1 = H$, $R^2 = Bn$ $R^1 = R^2 = Bn$ $R^1 = H$, $R^2 = COPh$	89 81 80 88
8	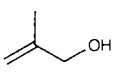	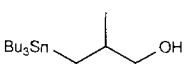		90
9	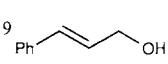	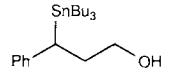		94
10	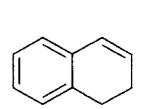	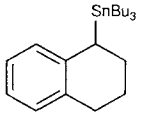		90

[a] Conditions: 1.5 equiv Bu_3SnH, 10 mol% Pd from Pearlman's catalyst, THF (0.1 M), room temperature, 1 h. [b] Yields of isolated products. [c] Reaction performed in absolute ethanol. [d] An 84:1 ratio of the linear and branched isomers was observed.

Experimental Procedure

General procedure for the heterogeneous, palladium-catalyzed hydrostannations of alkenes: Tributyltin hydride (1.5 mmol) was added over 1 hour by syringe pump to a well-stirred mixture of the alkene (1 mmol) and $[Pd(OH)_2]/C$ (Pearlman's catalyst, 53 mg, 0.1 mmol of Pd) in THF (10 mL). The reaction mixture was stirred for an additional hour and then filtered through a pad of celite. Flash chromatography on silica gel (hexanes:ethyl acetate mixtures as eluent) gave the product.

1-Phenyl-3-(tributylstannyl)propan-1-ol (entry 1): Purified by flash chromatography (hexanes:ethyl acetate 100:0 to 10:1), colorless oil (yield 96%). ^1H NMR (400 MHz, $CDCl_3$) $\delta = 7.36-7.24$ (m, 5H), 4.53 (m, 1H), 1.96–1.83 (m, 3H), 1.52–1.20 (m, 12H), 0.89–0.59 (m, 17H); ^{13}C NMR (100 MHz, $CDCl_3$) $\delta = 144.5$, 128.3, 127.4, 125.9, 77.7, 36.2, 29.2, 27.4, 13.7, 8.80, 4.20.

Received: December 19, 1995 [Z8662IE]
German version: *Angew. Chem.* **1996**, *108*, 1428–1429

Keywords: allylic alcohols · heterogeneous catalysis · hydrostannation · regioselectivity · tin compounds

[1] J. A. Labinger, K. Smith, A. Pelter, J. J. Eisch, T. Hiyama, T. Kusumoto in *Comprehensive Organic Synthesis, Vol. 8* (Eds.: B. M. Trost, I. Fleming), Pergamon Press, Oxford, **1991**, p. 667–792.
[2] M. Lautens, P. Chiu, S. Ma, T. Rovis, *J. Am. Chem. Soc.* **1995**, *117*, 532.
[3] M. Lautens, W. Klute, *Angew. Chem.* **1996**, *108*, 472; *Angew. Chem. Int. Ed. Engl.* **1996**, *35*, 442.
[4] a) T. N. Mitchell, *J. Organomet. Chem.* **1986**, *304*, 1; b) Y. Ichinose, H. Oda, K. Oshima, K. Utimoto, *Bull. Chem. Soc. Jpn.* **1987**, *60*, 3468; c) K. Kikukawa, H. Umekawa, F. Wada, T. Matsuda, *Chem. Lett.* **1988**, 881; d) H. X. Zhang, F. Guibé, G. Balavoine, *J. Org. Chem.* **1990**, *55*, 1857; e) S. Casson, P. Kocienski, *Synthesis* **1993**, 1133.
[5] M. Pereyre, J. P. Quintard, A. Rahm, *Tin in Organic Synthesis*, Butterworths, London, **1986**.
[6] a) N. Meyer, D. Seebach, *Chem. Ber.* **1980**, *113*, 1290; b) R. H. Newman-Evans, B. K. Carpenter, *Tetrahedron Lett.* **1985**, *26*, 1141; c) W. Brieden, R. Ostwald, P. Knochel, *Angew. Chem.* **1993**, *105*, 629; *Angew. Chem. Int. Ed. Engl.* **1993**, *32*, 582.
[7] a) W. P. Neumann, *The Organic Chemistry of Tin*, Wiley, New York, **1970**, and references therein; b) H. G. Kuivila, R. Sommer, *J. Am. Chem. Soc.* **1967**, *89*, 5616; c) D. D. Davis, R. L. Chambers, H. T. Johnson, *J. Organomet. Chem.* **1970**, *25*, C13; d) W. P. Neumann, *Synthesis* **1987**, 665; e) E. Nakamura, Y. Imanishi, D. Machii, *J. Org. Chem.* **1994**, *59*, 8178.
[8] P. Four, F. Guibé, *Tetrahedron Lett.* **1982**, 1825.
[9] J. Ye, R. K. Bhatt, J. R. Falck, *J. Am. Chem. Soc.* **1994**, *116*, 1.

Molecular Structure of $[Pd_6Cl_{12}]$ in Single Crystals Chemically Grown at Room Temperature**

Daniela Belli Dell'Amico,* Fausto Calderazzo,* Fabio Marchetti, and Stefano Ramello

$[Pd_2Cl_4(CO)_2]$, which according to spectroscopic data is a centrosymmetric chloro-bridged dimer ($\tilde{\nu}_{CO} = 2163\ cm^{-1}$ in thionyl chloride(solv.)), can be prepared by carbonylation of palladium(II) chloride.[1] The thermodynamic data of the equilibrium (a) were established as $\Delta H^0 = -(56.9 \pm 1)\ kJ\,mol^{-1}$ and $\Delta S^0 = -(128.7 \pm 3)\ J\,mol^{-1}\,K^{-1}$).

$$2\,PdCl_{2(s)} + 2\,CO_{(solv.)} \rightleftharpoons [Pd_2Cl_4(CO)_2]_{(solv.)} \qquad (a)$$

We reckoned that slow decrease of the partial pressure of CO over a solution of the dimer could give single crystals of palladium(II) chloride. This experiment could be of interest for many reasons. It should provide a) information about the crystal phase in equilibrium with the carbonyl compound; b) the possibility of adjusting our earlier estimate of the bond dissociation energy (BDE) for the Pd^{II}–CO bond;[1] and c) the possibility of growing single crystals of $PdCl_2$ at room temperature, an experiment which had no precedent in the literature. Furthermore, as both α-[2] and β-$PdCl_2$[3] are reported to sublime as $[Pd_6Cl_{12}]$, as confirmed by mass spectrometric experiments,[3, 4] growing crystals from the experimental setup based on Equation (a) would exploit a well-established dinuclear precursor, different from that operating in the $Pd_{(s)} + Cl_2$ experiments at high temperature[1, 5] (in the range 400–600 °C). Further points of interest are that the bonding parameters of $[Pd_6Cl_{12}]$ are still unknown, since the original structural assignment[3] was based on a Guinier data collection on a microcrystalline sample. Moreover, the data of the α-modification, reported by A. F. Wells[2] to be composed of infinite, linear chains of chloro-bridged square-planar palladium atoms, were collected with a less sophisticated X-ray diffractometer than those available nowadays.[6]

A solution of $[Pd_2Cl_4(CO)_2]$ (about 3×10^{-2} M) in thionyl chloride in a Schlenk tube open to the atmosphere over several days at room temperature, deposited well-formed single crystals of $PdCl_2$ (elemental analysis), which were only sparingly soluble in thionyl chloride.[8] The single-crystal X-ray structure analysis showed the compound to be the hexanuclear $[Pd_6Cl_{12}]$ compound, described by H. Schäfer and co-workers[3] and classified as the β-modification, to distinguish it from the α-one.[2] The molecular structure (Fig. 1) is similar, but not identical, to that of $[Pd_6Cl_{12}]$, prepared by G. Thiele and co-workers[9] by vapor-phase recrystallization of microcrystalline $PtCl_2$ at 550 °C in the presence of dichlorine.[10]

The hexanuclear $[Pd_6Cl_{12}]$ molecule can be described as a cube whose edges are approximately 4.62 Å long; the central points of faces and edges are occupied by the palladium atoms and by the chlorine atoms, respectively. The coordination around the palladium atoms is almost exactly square-planar; the most notable deviations are the short Pd–Cl(1) distance of 2.304(1) Å and the distance of the palladium atom from the plane Cl(1)-Cl(1′)-Cl(2)-Cl(2″) (0.028(1) Å). The bond angles at the chloro ligands range between 90.70(5) and 92.04(5)°. The average Pd–Cl distance of 2.310(4) Å, which is the same as that observed in α-$PdCl_2$[2] (2.31 Å), corresponds to a rather strong palladium–chlorine bond, taking into consideration that for a considerable number of known crystal structures the average Pd^{II}–Cl distance is 2.43(6) Å (for bridging chloro ligands with bond angles at palladium of approximately 90°).[12] A value of 2.36 Å was reported for $[Pt_6Cl_{12}]$, alias β-$PtCl_2$,[9] as expected for metal cations with very similar ionic radii.[13] The six palladium atoms define an octahedron, whose tetragonal planes contain four bridging chloro ligands each; the shortest intramolecular Pd···Pd distances of 3.283(1) and 3.329(2) Å are considerably longer than the distance in palladium metal (2.750 Å).[14]

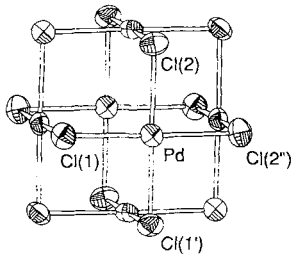

Fig. 1. The molecular structure of $[Pd_6Cl_{12}]$. The ellipsoids are represented at 50% probability. ′ = y, z, x; ″ = $-z, -x, -y$; ‴ = z, x, y; ⁗ = $-y, -z, -x$. Bond lengths [Å] and angles [°]: Pd–Cl(1) 2.304(1), Pd–Cl(1′) 2.310(1), Pd–Cl(2) 2.314(1), Pd–Cl(2″) 2.312(1); Cl(1)-Pd-Cl(1′) 90.26(9), Cl(1′)-Pd-Cl(2) 178.40(3), Cl(1)-Pd-Cl(2) 90.37(5), Cl(1′)-Pd-Cl(2″) 90.13(5), Cl(1)-Pd-Cl(2″) 178.65(3), Cl(2)-Pd-Cl(2″) 89.18(3), Pd″-Cl(1)-Pd 90.70(5), Pd-Cl(2)-Pd⁗, 92.04(5).

Polycrystalline samples of the palladium(II) chloride that had been prepared from the carbonyl derivative were subjected to X-ray diffraction experiments with a Gandolfi camera: the diffraction pattern corresponded satisfactorily to that calculated[15] from the single-crystal structure (Table 1), thus showing that the bulk of the palladium chloride in equilibrium with the carbonyl-chloropalladium complex is $[Pd_6Cl_{12}]$.

On the basis of these new findings on the nature of the palladium(II) chloride involved in equilibrium (a), a ΔH_f^0 value of $-(478 \pm 10)\ kJ\,mol^{-1}$ was calculated[17] for $[Pd_2Cl_4(CO)_2]_{(g)}$; the Pd^{II}–CO BDE in the dinuclear carbonyl derivative was estimated as $104 \pm 4\ kJ\,mol^{-1}$, thus confirming the earlier results.[1]

In conclusion, we have confirmed that palladium(II) chloride, which plays a role as a precursor in several catalytic processes,[19] if prepared at room temperature is the hexanuclear compound $[Pd_6Cl_{12}]$, regardless of the method of preparation.[4] Furthermore we have established its metrical parameters. The best method for preparing $[Pd_6Cl_{12}]$ appears to be equilibration of palladium(II) chloride suspended in thionyl chloride with CO at atmospheric pressure and room temperature. The result is, of course, independent of the nature of the chloride initially used. The Pd–CO bond is confirmed as atypical[20] and is characterized by a moderate bond strength and by a high $\tilde{\nu}_{CO}$ stretching frequency, comparable to that of $[BH_3(CO)]$[21] ($\tilde{\nu}_{CO} = 2165\ cm^{-1}$ in the gas phase) and $[CaCp^*_2(CO)]$[22] ($\tilde{\nu}_{CO} = 2158\ cm^{-1}$, toluene), suggestive of a predominant σ-contribution.

Experimental Procedure

In a Schlenk tube, $PdCl_2$ (1.06 g, 6.0 mmol) [as obtained by evaporation under reduced pressure of an aqueous acidic solution of $[PdCl_4]^{2-}$ followed by treatment of the resulting solid with $SOCl_2$ at room temperature (satisfactory Pd, Cl analyses)] was suspended in $SOCl_2$ (100 mL) and stirred under CO at atmospheric pressure at 18 °C for 70 h. This resulted in a red solution of $[Pd_2Cl_4(CO)_2]$. The container was

[*] Prof. D. Belli Dell'Amico, Prof. F. Calderazzo, Dr. F. Marchetti, S. Ramello
Dipartimento di Chimica e Chimica Industriale, Università di Pisa
Via Risorgimento 35, I-56126 Pisa (Italy)
Fax: Int. code +(50)20-237

[**] This work was supported by the Consiglio Nazionale delle Ricerche (CNR), Progetto Strategico Tecnologie Chimiche Innovative. We thank Chimet S.p.A., Badia al Pino, (Italy) for a loan of palladium.

Table 1. Calculated and observed X-ray powder diffraction patterns of $[Pd_6Cl_{12}]$ [a].

hkl	d (calcd.) [Å]	$I_{rel.}$	d (exp.) [Å]	I
0 1 0	6.844	100	6.85	vs
1 1 0	6.524	50	6.46	s
1 1 1	4.722	9	4.72	mw
1 1 0	4.020	27	4.01	m
1 2 0	3.825	2		
2 1 1	3.766	16	3.76	mw
0 2 0	3.422	1		
2 2 0	3.262	27	3.25	m
1 2 1	3.030	17	3.04	w
2 2 1	2.944	20	2.94	w
1 1 1	2.867	2		
3 1 1	2.684	16	2.68	w
1 2 0	2.625	11	2.62	w
1 3 0	2.533	80	2.54	vs
2 3 0	2.482	2		
3 2 1	2.466	8	2.46	vw
2 2 2	2.361	4	2.36	vw
0 3 0	2.281	9	2.28	w
2 3 1	2.220	6		
3 2 2	2.186	4		
3 3 0	2.175	2		
3 1 1	2.154	1		
1 2 1	2.113	5	2.12	vw
3 3 1	2.072	2		
2 2 0, 4 1 1	2.000	22	2.00	m
1 3 0	1.921	3		
2 4 0	1.913	2	1.915	vw
4 2 2	1.883	4		
1 4 0	1.870	11	1.869	w
3 2 3	1.835	4		
3 4 0	1.816	5		
4 3 1	1.809	11	1.811	vw
3 2 1	1.773	32	1.771	w
2 4 1	1.733	3		
0 4 0	1.711	1		
3 4 1, 2 2 1	1.705	4		
1 4 1	1.655	2		
1 3 1	1.646	1		
4 4 0	1.631	22	1.633	w
5 2 1, 2 3 0	1.599	3		

[a] Similar results were obtained on a microcrystalline sample sealed in a glass capillary, or on a small polycrystalline aggregate of almost spherical shape glued at the end of a glass fiber. The sample for the X-ray powder diffraction experiment should not be milled. Although crystalline palladium(II) chloride is apparently stable in air over extended periods of time, milling in air resulted in the appearance of spurious lines, similar to those attributed in the literature to commercial palladium chloride [16], alias the low-temperature form [5], alias γ-$PdCl_2$ [11c,4].

left open to the atmosphere for 22 days; the red-brown crystalline deposit of $[Pd_6Cl_{12}]$ was collected by filtration and dried in vacuo (0.52 g, 49% yield). The crystals of $[Pd_6Cl_{12}]$ were small reddish-black rhombohedra bounded by six faces of the form $\{100\}$. A crystal of approximate dimensions $0.14 \times 0.14 \times 0.072$ mm was glued at the end of a glass fiber and its X-ray diffraction pattern was studied with a Weissenberg camera. It showed trigonal symmetry without systematic absences. Cell parameters were measured and intensity data were collected on a Siemens P4 single-crystal automatic diffractometer equipped with graphite-monochromatized $Mo_{K\alpha}$ radiation ($\lambda = 0.71069$ Å). Cell parameters were calculated based on the accurately centered setting angles of 21 strong reflections with $12.6 \leq \theta \leq 19.2°$. Crystal data: Pd_6Cl_{12}, $M_r = 1063.9$, $T = 296(2)$ K, space group $R\bar{3}$ (no. 148), $a = 8.0600(9)$ Å, $\alpha = 108.07(2)°$, $V = 422.63(8)$ Å^3, $Z = 1$, $\rho_{calcd} = 4.180$ g cm^{-3}, $\mu(Mo_{K\alpha}) = 8.115$ mm^{-1}, $F(000) = 480$. The collected intensities of 1477 reflections with $3 \leq \theta \leq 35°$, on merging the equivalent ones and after correction for Lorentz and polarization effects, resulted in an internal R value of 0.16; the application of a Gaussian absorption correction [23] based on crystal shape and size reduced it to 0.025. The diffraction symmetry indicated the space groups $R\bar{3}$ or $R3$. We placed the Pd and Cl atoms in the positions the appropriate atoms have in $[Pt_6Cl_{12}]$ [9], and first tried to refine the structure in the $R\bar{3}m$ space group, that is the same as that for $[Pt_6Cl_{12}]$. The R factor decreased to 0.192; then the mirror planes were removed, refinement was continued in the $R\bar{3}$ space group, and anisotropy in the thermal motion was introduced: the R value dropped to 0.022; 29 parameters were refined based on 806 independent reflections $\{R_1 = 0.022 = \Sigma||F_o| - |F_c||.\Sigma|F_o|; wR_2 = 0.055 = [\Sigma w(F_o^2 - F_c^2)^2/\Sigma w(F_o^2)^2]^{1/2}; w = 1/[\sigma^2(F_o^2) + (0.0164P)^2 + 0.33P]$ where $P = [MAX(F_o^2, 0) + 2F_c^2]$, $S = 1.143 = [\Sigma w(F_o^2 - F_c^2)^2/(N - P)]^{1/2}\}$ [23]. All calculations and drawings were performed by using the SHELXTL [24a] and ORTEPII [24b] programs, respectively. For the X-ray diffraction experiments on polycrystalline samples (Table 1) a small polycrystalline aggregate of $[Pd_6Cl_{12}]$ of almost spherical shape was glued at the end of a glass fiber and the diffraction pattern was measured with a Gandolfi camera (114.6 mm) and Ni-filtered $Cu_{K\alpha}$ ($\lambda = 1.54178$ Å) radiation. The positions of the lines were measured with a precision caliper equipped with an optical alignment device [25].

Received: January 15, 1996 [Z 8722 IE]
German version: *Angew. Chem.* **1996**, *108*, 1430–1432

Keywords: chlorine compounds · palladium compounds · structure elucidation

[1] D. Belli Dell' Amico, F. Calderazzo, N. Zandonà, *Inorg. Chem.* **1984**, *23*, 137.
[2] A. F. Wells, *Z. Kristallogr.* **1938**, *100*, 189; L. Pauling, *The Nature of the Chemical Bond*, 3rd ed., Cornell University Press, Ithaca, NY, 1960, p. 157.
[3] H. Schäfer, U. Wiese, K. Rinke, K. Brendel, *Angew. Chem.* **1967**, *79*, 244; *Angew. Chem. Int. Ed. Engl.* **1967**, *6*, 253.
[4] A. Yatsimirski, R. Ugo, *Inorg. Chem.* **1983**, *22*, 1395.
[5] J. R. Soulen, W. H. Chappell, Jr., *J. Phys. Chem.* **1965**, *69*, 3669.
[6] Some of the reported experiments with $PdCl_2$ have been carried out on samples that had been prepared in an external laboratory [2,5,7] or by an unspecified procedure [3].
[7] W. van Bronswyk, R. Nyholm, *J. Chem. Soc.* **1968**, 2084.
[8] Although it may appear so, this is not a fortuitous experiment: slow diffusion of moisture in the air into the reactor has the beneficial effect of decreasing the partial pressure of CO on the solution due to the formation of SO_2 and HCl from the solvent. The preparation has been repeated several times successfully. Depending on the rate of admission of air into the reactor single crystals or microcrystalline samples can be obtained.
[9] a) K. Brodersen, G. Thiele, H. G. Schnering, *Z. Anorg. Allg. Chem.* **1965**, *337*, 120; b) G. Thiele, K. Brodersen, *Fortsch. Chem. Forsch.* **1968**, *10*, 631.
[10] Another modification of $PtCl_2$, a polynuclear compound, classified as α-$PtCl_2$, was identified on the basis of both Guinier data on a microcrystalline sample [11c] and X-ray diffraction data on a single crystal [11c]; this substance was obtained [11] by heating $[Pt_6Cl_{12}]$ for 1–2 days at 500 °C or by treating platinum metal with dichlorine (3 atm) in several temperature gradients ranging between 520 and 440 °C and 800 and 780 °C. The α-modifications of palladium(II) and platinum(II) chlorides were reported [11c] not to be isotypic.
[11] a) U. Wiese, H. Schäfer, H. G. von Schnering, C. Brendel, K. Rinke, *Angew. Chem.* **1970**, *82*, 135; *Angew. Chem. Int. Ed. Engl.* **1970**, *9*, 158; b) H. Schäfer, U. Wosiewitz, *Z. Anorg. Allg. Chem.* **1975**, *415*, 202; c) B. Krebs, C. Brendel, H. Schäfer, *ibid.* **1988**, *561*, 119.
[12] A. G. Orpen, L. Brammer, F. H. Allen, O. Kennard, D. G. Watson, R. Taylor, *J. Chem. Soc. Dalton Trans.* **1989**, S1–S83.
[13] R. D. Shannon, *Acta Crystallogr. Sect. A* **1976**, *32*, 751.
[14] a) K. L. Shelton, P. A. Merewether, B. J. Skinner, *Can. Mineral.* **1981**, *19*, 599; b) A. F. Wells, *Structural Inorganic Chemistry*, 5th ed., Clarendon Press, Oxford, **1986**, p. 1288.
[15] W. Kraus, G. Nolze: POWDER CELL, Program for X-ray powder patterns calculation, Federal Institute for Materials Research and Test, Berlin, Germany, **1995**; we thank Dr. G. Nolze for providing a copy of the program prior to publication.
[16] a) JCPDS, Joint Committee on Powder Diffraction Standards, 1601 Park Lane, Swarthmore, PA, USA, card No. 1–228; b) J. D. Hanawalt, H. W. Rinn, L. K. Frevel, *Ind. Eng. Chem. Anal. Ed.* **1938**, *10*, 457, Table XII; [*Chem. Abstr.* **1938**, *32*, 7841]. This is a collection of powder diffraction data for 1000 chemical substances; the data referring to $PdCl_2$ were collected on a sample of unspecified origin.
[17] The calculation requires the following data from the literature: $\Delta H_f^0 = -167$ kJ mol^{-1} for $PdCl_2$ as 1:6 of $[Pd_6Cl_{12}]$ [18]; BDE values for terminal and bridging Pd–Cl bonds [3], 259 and 194 kJ mol^{-1}, respectively. Other data are from ref. [1].
[18] a) W. E. Bell, U. Merten, M. Tagami, *J. Phys. Chem.* **1961**, *65*, 510; b) H. Schäfer, *Z. Anorg. Allg. Chem.* **1975**, *415*, 217.
[19] P. M. Maitlis, *The Organic Chemistry of Palladium, Vol. 1, 2*, Academic Press, London, **1971**.
[20] D. Belli Dell' Amico, F. Calderazzo, *Pure Appl. Chem.* **1986**, *58*, 561. This article pointed out the atypical nature of metal–CO bonds for palladium(II), platinum(II), and gold(I), due to a largely predominant σ contribution. Systems with similar properties have been more recently described for silver(I), palladium(II), and mercury, all characterized by extremely high $\tilde{\nu}_{CO}$ values. Relevant references on this subject are: P. K. Hurlburt, O. P. Anderson, S. H. Strauss, *J. Am. Chem. Soc.* **1991**, *113*, 6277; C. Wang, H. Willner, M. Bodenbinder, R. J. Batchelor, F. W. B. Einstein, F. Aubke, *Inorg. Chem.* **1994**, *33*, 3521; M. Bodenbinder, G. Balzer-Jöllenbeck, H. Willner, R. J. Batchelor, F. W. B. Einstein, C. Wang, F. Aubke, *Inorg. Chem.* **1996**, *35*, 82.
[21] G. W. Bethke, M. K. Wilson, *J. Chem Phys.* **1957**, *26*, 1118.

[22] P. Selg, H. H. Brintzinger, R. A. Andersen, I. Horváth, *Angew. Chem.* **1995**, *107*, 877; *Angew. Chem. Int. Ed. Engl.* **1995**, *34*, 791.
[23] Further details of the crystal structure investigation are available on request from the Fachinformationszentrum Karlsruhe, D-76344 Eggenstein-Leopoldshafen (Germany), on quoting the depository number CSD-404624.
[24] a) G. M. Sheldrick, SHELXTL-Plus, Rel. 5.03, Siemens Analytical X-ray Instruments Inc., Madison, Wisconsin, **1995**; b) C. K. Johnson, ORTEP II: a Fortran Thermal-Ellipsoid Plot Program for Crystal Structure Illustrations, ORNL-5138, Oak Ridge National Laboratory, Oak Ridge, TN, USA, March **1976**.
[25] After submission of this paper, we learned that Prof. G. Thiele, Universität Freiburg, Germany, and his group had obtained complementary crystallographic data on single crystals of solvated (benzene or chloroform) $[Pd_6Cl_{12}]$, grown at room temperature from the corresponding solutions. Satisfactory agreement has been found between the sets of data obtained independently in the two laboratories. We thank Prof. G. Thiele for communicating his results prior to publication.

Tetrakis(tri-*tert*-butylsilyl)-*tetrahedro*-tetragermane $(t\mathrm{Bu_3Si})_4\mathrm{Ge_4}$—The First Molecular Germanium Compound with a $\mathrm{Ge_4}$ Tetrahedron**

Nils Wiberg,* Walter Hochmuth, Heinrich Nöth, Andrea Appel, and Martin Schmidt-Amelunxen

According to ab initio calculations,[1, 2] the strain energy of $(EH)_n$ polyhedra (E = Si, Ge) increases with the number of the three-membered rings in the framework of the polyhedron, thus in the order *hexahedro*-octasilane (-germane) **A**, *triprismo*-hexasilane (-germane) **B**, and *tetrahedro*-tetrasilane (-germane) **C**.[3]

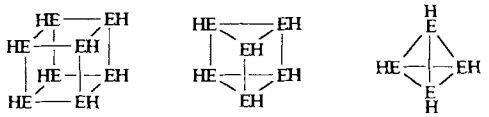

A **B** **C**

Consequently, initially the hexahedranes $(ER)_8$ (E/R = Si/$SiMe_2t$Bu,[4a] Si/CMe_2iPr,[4b] Si/2,6-$C_6H_3Et_2$,[4c] Ge/$CMeEt_2$,[4c] Ge/2,6-$C_6H_3Et_2$[4c]) and triprismanes $(ER)_6$ (E/R = Si/2,6-$C_6H_3i\mathrm{Pr}_2$,[4e] Ge/$CH(SiMe_3)_2$,[4d] Ge/2,6-$C_6H_3i\mathrm{Pr}_2$[4e]) were obtained. We synthesized the first molecular silicon compound **1** with a Si_4 tetrahedron[5, 6] by the reaction of tetrabromo-1,2-bis(supersilyl)disilane $t\mathrm{Bu_3Si-SiBr_2-SiBr_2-Si}t\mathrm{Bu_3}$ (**3**) with supersilylsodium $t\mathrm{Bu_3SiNa}$ in tetrahydrofuran (THF) [Eq. (a); supersilyl = $Si t\mathrm{Bu_3}$[7]].

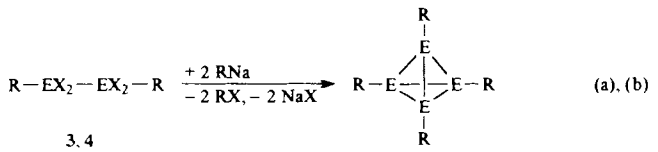

(a) E = Si; X = Br
(b) E = Ge; X = Cl

R = $Si t\mathrm{Bu_3}$

1, E = Si
2, E = Ge

(a), (b)

[*] Prof. Dr. N. Wiberg, Dipl.-Chem. W. Hochmuth, Prof. Dr. H. Nöth, Dipl.-Chem. A. Appel, Dr. M. Schmidt-Amelunxen
Institut für Anorganische Chemie der Universität
Meiserstrasse 1, D-80333 München (Germany)
Fax: Int. code +(89)5902-578

[**] Compounds of Silicon and Its Group Analogues Part 108; Sterically Overloaded Supersilyl Compounds, Part 10. This work was supported by the Deutsche Forschungsgemeinschaft. Part 107 and 9: Ref. [3].

In an effort to obtain a molecular germanium compound with a Ge_4 tetrahedron by an analogous route, we treated tetrachloro-1,2-bis(supersilyl)digermane $t\mathrm{Bu_3Si-GeCl_2-GeCl_2-Si}t\mathrm{Bu_3}$ (**4**), which formed from $GeCl_4$ and $t\mathrm{Bu_3SiNa}$ in THF at room temperature along with other products ($t\mathrm{Bu_3SiGeCl_3}$, $(t\mathrm{Bu_3Si})_2GeCl_2$, $(t\mathrm{Bu_3Si})_2$, $t\mathrm{Bu_3SiCl}$), and was characterized by X-ray crystallography, with $t\mathrm{Bu_3SiNa}$ in THF at −78 °C. This reaction led to the *tetrahedro*-tetragermane **2** in low yield [Eq. (b)] together with other products containing supersilyl groups that are also formed in the reaction of $GeCl_2 \cdot C_4H_8O_2$ and $t\mathrm{Bu_3SiNa}$ (see below). Compound **4** reacts with sodium in C_6D_6 at room temperature initially to give the tetrahedrane **2**, which is, however, attacked by sodium; one of the resulting products, namely $t\mathrm{Bu_3SiNa}$, reacts as described with unconverted **4**.[8] $t\mathrm{Bu_3SiNa}$ reacts with $GeCl_2 \cdot C_4H_8O_2$ in THF via a series of—in part isolable—intermediates[9] likewise to give **2** and additional products [Eq. (c)].

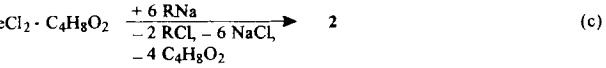

(c)

The tetragermane **2** forms intense red crystals, which are hydrolyzed slowly by water, and are rapidly oxidized by air. Compound **2** can be reduced with sodium; among the products of the reaction is $t\mathrm{Bu_3SiNa}$, which can be identified by conversion with Me_3SnCl into $t\mathrm{Bu_3Si-SnMe_3}$.

So far we have only been able to obtain crystals suitable for X-ray diffraction[12] from solutions prepared according to Equation (c) after exchanging THF by pentane. However, in addition to **2** these contain superdisilane $t\mathrm{Bu_3Si-Si}t\mathrm{Bu_3}$,[11] which fills the large holes between the almost spherical molecules of **2** in the crystal, and thereby stabilizes the structure of the crystal. The monoclinic unit cell of the crystals with the composition $2(t\mathrm{Bu_3Si})_4Ge_4 \cdot (t\mathrm{Bu_3Si})_2$ (**2a**) contains four molecules of **2** and—in the cavities—two molecules of $t\mathrm{Bu_3Si-Si}t\mathrm{Bu_3}$ (Fig. 1). The building unit **2** in the crystal of **2a** contains almost regular Ge_4 tetrahedra (Fig. 2). The Ge–Ge (av. 2.44 Å) and Ge–Si (2.38 Å) distances are slightly longer than those in $H_3Ge-GeH_3$ (2.41 Å[13]) and $H_3Ge-SiH_3$ (2.36 Å[13]), respectively; for comparison Si–Si distances in **1** are 2.35 (*endo*) and 2.37 Å (*exo*),[3] in $H_3Si-SiH_3$ and $Me_3Si-SiMe_3$ 2.331 and 2.338 Å, respectively[13]. The fact that $t\mathrm{Bu_3Si-Si}t\mathrm{Bu_3}$ in crystals

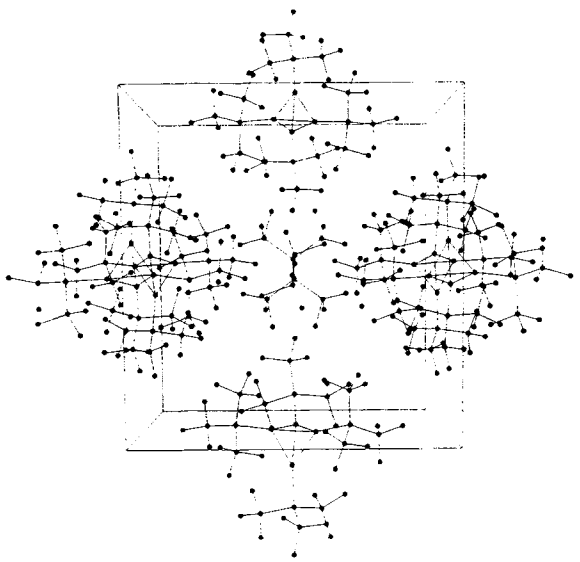

Fig. 1. Perspective view of the monoclinic unit cell of **2a** along the *c* axis.

 © VCH Verlagsgesellschaft mbH, D-69451 Weinheim, 1996 0570-0833/96/3512-1333 $ 15.00+.25/0

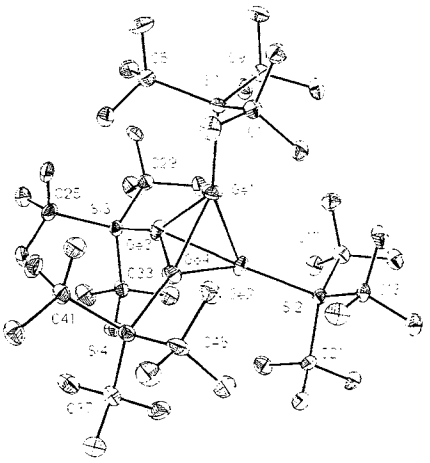

Fig. 2. Structure of **2** in the crystal **2a** (ORTEP plot). Selected bond lengths [Å] and angles [°]: Ge1-Ge2 2.447(2), Ge2-Ge3 2.446(2), Ge3-Ge4 2.443(3), Ge1-Ge4 2.431(2), Ge1-Ge3 2.447(2), Ge2-Ge4 2.435(2), Ge1-Si1 2.385(4), Ge2-Si2 2.385(4), Ge3-Si3 2.378(4), Ge4-Si4 2.383(4), Si-C (av) 1.94; Ge-Ge-Ge 59.62(7)–60.10(7), Si1-Ge1-Ge4 142.3(1), Si2-Ge2-Ge4 141.4(1), Si1-Ge1-Ge2 155.8(1), Si1-Ge1-Ge3 132.9(1), Si2-Ge2-Ge3 156.7(1), Si2-Ge2-Ge1 132.5(1), Si3-Ge3-Ge4 145.6(1), Si4-Ge4-Ge1 144.9(1), Si3-Ge3-Ge2 131.0(1), Si3-Ge3-Ge1 153.7(1), Si4-Ge4-Ge2 146.1(1), Si4-Ge4-Ge3 142.7(1), C-Si-C (av) 112.8.

of **2a** has a slightly larger Si–Si distance (2.719(8) Å) than that in superdisilane crystals (2.697(2) Å[11]) is possibly attributed to van der Waals attractions between supersilane and **2** in **2a** (see below). Although the Ge_4 tetrahedron suggests a symmetrical (radial) arrangement of the supersilyl groups, they are slightly bent; the Si-Ge4-Ge bond angles differ by up to only 3.4°, the Si-Ge2-Ge angles by up to 24.2°. The reason for this might be the proximity of tBu$_3$Si–SitBu$_3$; the center of the Si–Si bond lies on a crystallographic inversion center.

Experimental Procedure

tBu$_3$SiNa (0.69 mmol) [11] in THF (1.3 mL) was added dropwise to a solution of $GeCl_2 \cdot C_4H_8O_2$ (0.050 g, 0.22 mmol) in THF (1 mL) at room temperature. After 12 h, the THF was removed under vacuum from the resulting red-brown suspension, the oily residue was taken up in pentane (2 mL), and filtered to remove insoluble material. Intense red crystals of the composition $2(t\text{Bu}_3\text{Si})_4\text{Ge}_4 \cdot (t\text{Bu}_3\text{Si})_2$ (**2a**) (0.008 g, 11 % yield) crystallized from the filtrate at −25 °C over a long period. M.p. >360 °C (above 280°C slow decomposition). ^{1}H NMR (C_6D_6, TMS, internal): $\delta = 1.374$ (4 SitBu$_3$); ^{13}C{^{1}H} NMR (C_6D_6, TMS, internal): $\delta = 31.87$ (12 CMe_3), 26.17 (12 CMe_3); ^{29}Si{^{1}H} NMR (C_6D_6, INEPT, TMS, external): $\delta = 59.0$ (4 SitBu$_3$); UV (heptane): $\lambda_{max} = 501$ nm.

Received: February 16, 1996 [Z 8828 IE]
German version: *Angew. Chem.* **1996**, *108*, 1437–1438

Keywords: germanium compounds · tetrahedranes

[1] S. Nagase, *Angew. Chem.* **1989**, *101*, 340; *Angew. Chem. Int. Ed. Engl.* **1989**, *28*, 329; *Polyhedron* **1991**, *10*, 1299.

[2] According to calculations (N. Matsunaga, M. S. Gordon, *J. Am. Chem. Soc.* **1994**, *116*, 11407) *triprismo*-hexasilane and -hexagermane $(EH)_6$ are considerably more stable than their isomers, hexasila- and hexagermabenzene. *tetrahedro*-Tetrasilane and -tetragermane [1] $(EH)_4$ are more stable than their isomers, planar tetrasila- and tetragermacyclobutadiene, but slightly less stable than $(EH)_4$ compounds with puckered E_4 rings. Of course, sterically demanding substituents contribute to the stabilization of the tetrahedrane structure.

[3] N. Wiberg, C. M. M. Finger, H. Auer, K. Polborn, *J. Organomet. Chem.* **1996**, in press.

[4] Hexahedranes $(SiR)_8$ and $(GeR)_8$: a) H. Matsumoto, K. Higuchi, Y. Hoshino, H. Koike, Y. Naoi, Y. Nagai, *J. Chem. Soc. Chem. Commun.* **1988**, 1083; b) H. Matsumoto, K. Higuchi, S. Kyushin, M. Goto, *Angew. Chem.* **1992**, *104*, 1410; *Angew. Chem. Int. Ed. Engl.* **1992**, *31*, 1354; c) A. Sekiguchi, T. Yatabe, H. Kamatani, C. Kabuto, H. Sakurai, *J. Am. Chem. Soc.* **1992**, *114*, 6260; Triprismanes $(SiR)_6$ and $(GeR)_6$: d) A. Sekiguchi, C. Kabuto, H. Sakurai, *Angew. Chem.* **1989**, *101*, 97; *Angew. Chem. Int. Ed. Engl.* **1989**, *28*, 55; e) A. Sekiguchi, T. Yatabe, C. Kabuto, H. Sakurai, *J. Am. Chem. Soc.* **1993**, *115*, 5853.

[5] N. Wiberg, C. M. M. Finger, K. Polborn, *Angew. Chem.* **1993**, *105*, 1140; *Angew. Chem. Int. Ed. Engl.* **1993**, *32*, 1054.

[6] $(SiR)_8$, $(SiR)_6$, and $(SiR)_4$ were first synthesized in 1988 [4a], 1993 [4e], and 1993 [5], respectively, $(GeR)_8$, $(GeR)_6$, and $(GeR)_4$ in 1992 [4c], 1989 [4d], and 1996 [this publication].

[7] N. Wiberg in *Frontiers of Organosilicon Chemistry* (Eds.: A. R. Bassindale, P. P. Gaspar), Royal Society of Chemistry, Cambridge, **1991**, p. 263.

[8] N. Wiberg, W. Hochmuth, K. Polborn, unpublished results.

[9] Initially, only *cis,trans*-1,2,3-trichloro-1,2,3-tris(supersilyl)cyclotrigermane $(t\text{Bu}_3\text{SiGeCl})_3$ forms together with $(t\text{Bu}_3\text{Si})_2\text{GeCl}_2$ as a pale yellow oxidation-sensitive, hydrolysis-stable powder (crystals from MeOH/tBuOMe 85/15) [8] (reported in part at the DFG colloquium "Aufbau und Funktionalisierung von Polyedergerüsten aus Hauptgruppenelementen" in Kochel, near München, **1995**): ^{1}H NMR (C_6D_6, TMS, internal): $\delta = 1.386$ (s, 2 SitBu$_3$), 1.376 (s, SitBu$_3$); ^{13}C{^{1}H} NMR (C_6D_6, TMS, internal): $\delta = 31.76/31.86$ (6 CMe_3/3 CMe_3), 25.62/21.06 (6 CMe_3/3 CMe_3); ^{29}Si NMR (C_6D_6, TMS, external): $\delta = 46.33$ (2 SitBu$_3$), 48.28 (SitBu$_3$). In the further course of the reaction tBu$_3$SiX (X = H, Cl, SitBu$_3$) and a substance, whose NMR shifts resemble those of a recently described cyclotrigermene [10], are formed as well as an unidentifiable compound and the *tetrahedro*-tetragermane **2**.

[10] A. Sekiguchi, H. Yamazaki, C. Kabuto, H. Sakurai, *J. Am. Chem. Soc.* **1995**, *117*, 8025.

[11] N. Wiberg, H. Schuster, A. Simon, K. Peters, *Angew. Chem.* **1986**, *98*, 100; *Angew. Chem. Int. Ed. Engl.* **1986**, *25*, 79.

[12] Crystal structure analysis of **2a**: A single crystal (0.4 × 0.3 × 0.25 mm) was mounted in perfluoroether oil under argon, placed in a Lindemann capillary, and centered on a Siemens P4 diffractometer at −70 °C. The data was collected with a Siemens SMART area detector, the monoclinic unit cell calculated by using reflections ≥10 $I/\sigma(I)$. After reduction of the data, the structure was solved by direct methods (SHELXTL). Whereas the molecular structure of $(t\text{Bu}_3\text{SiGe})_4$ was refined without difficulty, tBu$_3$Si–SitBu$_3$ showed rotational disorder within the tBu$_3$ groups. As a result some of the anisotropic temperature parameters of these C atoms are very large and the bond lengths not meaningful. All non-hydrogen atoms were included in the refinement with anisotropic temperature parameters, the H atoms in calculated positions with a riding model. Nevertheless, a comparatively high residual electron density remains for three atoms (1.816, 1.39, 0.96 e Å^{-3}) in the space between two $(t\text{Bu}_3\text{SiGe})_4$ molecules. The following weighting scheme was applied: $w^{-1} = \sigma^2 F_o^2 + (xP)^2 + yP$ with $P = (F_o^2 + 2F_c^2)/3$. Crystallographic data: $C_{60}H_{135}Ge_4Si_5$, $M_r = 1027.34$, $a = 18.1997(2)$, $b = 16.8809(2)$, $c = 25.0074(4)$ Å, $\beta = 97.949(1)°$, $V = 7609.1(2)$ Å^3, $Z = 8$, $\rho_{calcd} = 1.124$ Mg m^{-3}, $\mu = 1.674$ mm^{-1}. Data collection: $2\theta \leq 46.6°$, $-18 \leq h \leq 17$; $-18 \leq k \leq 18$, $-12 \leq l \leq 27$; measurement rate: 10 s per setting, 11463 measured relections, 8256 of which symmetry-independent. Refinement with 8248 reflections and 601 variables, weighting scheme: $x/y = 0.0753/138.2605$, GOF = 1.193, $R1$ (4σ) = 0.0927, $wR2 = 0.2676$. Further details of the crystal structure investigation may be obtained from the Fachinformationszentrum Karlsruhe, D-76344 Eggenstein-Leopoldshafen (Germany) on quoting the depository number CSD-405202.

[13] Data from Comprehensive Organometallic Chemistry (Eds.: G. Wilkinson, F. G. A. Stone, E. W. Abel), Pergamon, Oxford, **1982**.

Formation of Macrocyclic Lactones by Enantioselective Intramolecular Cyclopropanation of Diazoacetates Catalyzed by Chiral Cu^{I} and Rh^{II} Compounds**

Michael P. Doyle,* Chad S. Peterson, and Dann L. Parker, Jr.

Macrocyclization is an essential synthetic element in the preparation of large ring compounds, and a variety of transformations have been reported for this process.[1] Only one, however, the macrocyclization of an ω-alkynal in the synthesis of the

[*] Prof. M. P. Doyle, Dr. C. S. Peterson, D. L. Parker, Jr.
Department of Chemistry, Trinity University
San Antonio, TX 78212-7200 (USA)
Fax: Int. code +(210)736-7569
e-mail: mdoyle@trinity.edu

[**] This work was supported by grants from the Robert A. Welch Foundation and the National Science Foundation.

16-membered ring of (*R*)-(−)-muscone, has been reported to occur with high levels of asymmetric induction in a catalytic process.[2] With unlimited chain length between reacting partners, enantio- and diastereoselectivity for a specific macrocyclization should be the same as that in the corresponding intermolecular process. However, at least in metal carbene catalyzed transformations, there is ordinarily a dramatic fall-off in stereocontrol with increasing ring size.[3] We recently reported that catalytic intramolecular cyclopropanation of diazoacetates is an effective methodology for macrocyclization in select cases, promoted by electrophilic dirhodium(II) catalysts, even when placed in direct competition with the normally favored allylic cyclopropanation.[4] We now report that high stereocontrol (enantioselectivity and diastereodifferentiation) has been achieved in catalytic intramolecular cyclopropanations, leading to the formation of macrocycles.

The reaction of conveniently handled and prepared[5] $[Cu(MeCN)_4](PF_6)$ and Evans's chiral bis(dihydrooxazole) (**1**)[6] with diazoacetate **2a** in refluxing dichloromethane led to a single macrocyclic cyclopropane, identified as **3a**, with 90% *ee* in 82% yield. For comparison, intramolecular cyclopropanation of 2-methyl-2-propen-1-yl diazoacetate under the same conditions gave **5** with 87% *ee* in 82% yield. By using the chiral complex $[Rh_2(5S\text{-mepy})_4]$ (**4**) (5*S*-mepy = methyl (5*S*)-2-pyrrolidone 5-carboxylate anion), which for 2-methyl-2-propen-1-yl diazoacetate resulted in **5** with only 7% *ee*,[7] diazo decomposition of **2a** produced the macrocycle **3a** with 47% *ee* (77% yield). Similar results were obtained with allyl diazoacetate **2b** by using $[Cu(MeCN)_4](PF_6)$/**1** (**3b**: 80% *ee*, 71% yield). In contrast to intermolecular reactions of diazo esters, in which the predominant product is generally the *trans* diastereoisomer,[8] these macrocyclizations provide only the *cis* isomer (NOE NMR experiments). All reactions were performed under standard conditions[7] without high dilution. The yields given are those of the purified products, and enantiomeric excesses were determined by GC with baseline resolution.

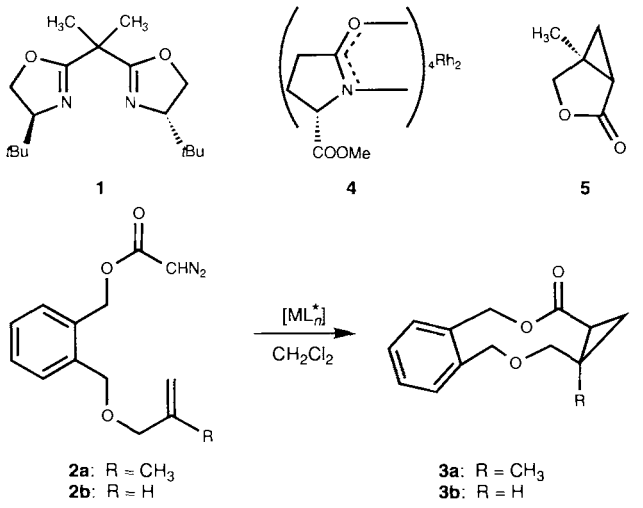

With the (*Z*)-2-buten-1,4-diyl diazoacetate derivative **6**, macrocycle formation was the predominant intramolecular reaction with $[Cu(MeCN)_4](PF_6)$/**1** (**7**: 87% *ee*, 43% yield; **8**: 41% *ee*, 19% yield), whereas allylic cyclopropanation was the sole result of the $[Rh_2(5S\text{-mepy})_4]$-catalyzed reaction (**8**: 96% *ee*, 84% yield).[9]

To determine if macrocycle formation is due primarily to conformational restrictions placed on the metal carbene intermediate formed from **2** or **6**, the saturated derivative **9** was also subjected to diazo decomposition. Surprisingly, use of $[Cu(MeCN)_4](PF_6)$/**1** resulted in the formation of the macrocycle **10** as the only isolable product with 91% *ee* in 43% yield.

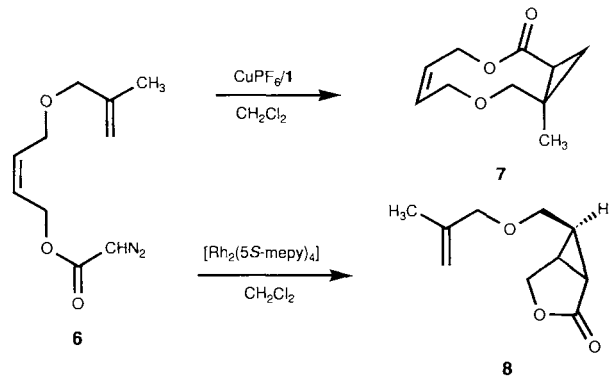

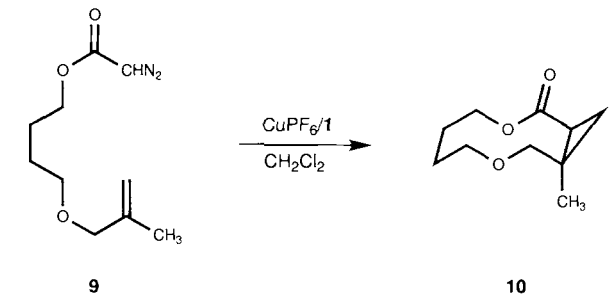

Thus the restricted degrees of conformational freedom afforded by **2** and **6** are not the a priori cause of these facile macrocyclizations, although the relative rigidity of **2** and **6** may account for increased reactivity in intramolecular cyclopropanations.

With the diazoacetate **11** there is a competition between the intramolecular cyclopropanations to give the bicyclo[10.1.0] and bicyclo[15.1.0] ring systems, but in reactions catalyzed by $[Cu(MeCN)_4](PF_6)$/**1** the bicyclo[15.1.0] product **12** (90% *ee*, 61% yield) was formed with greater than 25:1 regiochemical preference for the larger macrocycle. With $[Cu(MeCN)_4](PF_6)$ alone, **12** was formed with a 6:1 regiochemical preference. The ability of diazo esters to undergo macrocyclization, even to form 15-membered rings, with high enantioselectivity and diastereocontrol suggests the amazing versatility of this methodology.

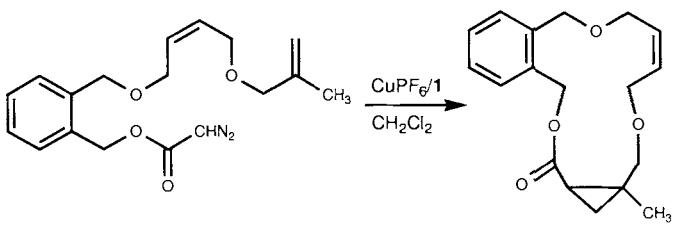

Experimental Procedure

In a typical procedure, $[Cu(CH_3CN)_4](PF_6)$(3.6 mg, 9.6 mmol) and ligand **1** (3.4 mg, 11.5 μmol) were added to an oven-dried two-neck round-bottom flask fitted with a reflux condenser and a rubber septum. To this flask was added freshly distilled CH_2Cl_2 (10 mL), and the homogeneous solution was stirred at reflux for 5 min. Diazoacetate **2a** (250 mg, 960 mmol) was dissolved in CH_2Cl_2 (10 mL) and added over 5 h by syringe pump to the clear catalyst solution. Upon completion of addition, the entire solution was passed through a plug of silica gel, and the solvent

was removed under reduced pressure. The resulting solid material was purifed by flash chromatography on silica gel (5:1 hexanes:ethyl acetate) to yield pure **3a** (183 mg, 82%) as a white solid (90% *ee*, GC analysis, 145 °C, Chiraldex G-DA (Alltech and Assoc., Inc.); $[\alpha]_D^{25} = -9.2$ ($c = 1.0$ in MeOH)).

Received: January 29, 1996 [Z 8758 IE]
German version: *Angew. Chem.* **1996**, *108*, 1439–1440

Keywords: asymmetric catalysis · copper compounds · cyclopropanations · diazo compounds · macrocycles

[1] Reviews: C. J. Roxburgh, *Tetrahedron* **1995**, *51*, 9767–9822; H. Stach, M. Hesse, *ibid.* **1988**, *44*, 1573–1590; I. Paterson, M. M. Mansuri, *ibid.* **1985**, *41*, 3569–3624; K. C. Nicolaou, *ibid.* **1977**, *33*, 683–710; M. A. Titus, *Chem. Rev.* **1988**, *88*, 719–732; G. R. Newkome, J. D. Sauer, J. M. Roper, D. C. Hager, *ibid.* **1977**, *77*, 513–597.

[2] W. Oppolzer, R. N. Radinov, *J. Am. Chem. Soc.* **1993**, *115*, 1593–1594.

[3] Reviews: M. P. Doyle in *Comprehensive Organometallic Chemistry, Vol. 12* (Ed.: L. S. Hegedus), Pergamon, New York, **1995**, Chapter 5.1; H.-U. Reissig in *Stereoselective Synthesis of Organic Compounds/ Methods of Organic Chemistry* (Houben-Weyl), *4th ed., 1952-, Vol. 21c*, pp. 3179–3270; T. Ye, M. A. McKervey, *Chem. Rev.* **1994**, *94*, 857–1160; A. Padwa, K. E. Krumpe, *Tetrahedron* **1992**, *48*, 5385–5453. Recent developments in catalytic asymmetric intramolecular metal carbene cyclizations: M. P. Doyle, A. B. Dyatkin, M. N. Protopopova, C. I. Yang, C. S. Miertschin, W. R. Winchester, *Rec. Trav. Chim. Pays-Bas* **1995**, *114*, 163–170; T. G. Gant, M. C. Noe, E. J. Corey, *Tetrahedron Lett.* **1995**, *36*, 8745–8748; C. Piqué, B. Fähndrich, A. Pfaltz, *Synlett* **1995**, 491–492.

[4] M. P. Doyle, M. N. Protopopova, C. D. Poulter, D. H. Rogers, *J. Am. Chem. Soc.* **1995**, *117*, 7281–7282.

[5] G. J. Kubas, *Inorg. Synth.* **1979**, *19*, 90–92.

[6] D. A. Evans, K. A. Woerpel, M. M. Hinman, M. M. Faul, *J. Am. Chem. Soc.* **1991**, *113*, 726–728; D. A. Evans, K. A. Woerpel, M. J. Scott, *Angew. Chem.* **1992**, *104*, 439–441; *Angew. Chem. Int. Ed. Engl.* **1992**, *31*, 430–432.

[7] M. P. Doyle, R. E. Austin, A. S. Bailey, M. P. Dwyer, A. B. Dyatkin, A. V. Kalinin, M. M. Y. Kwan, S. Liras, C. J. Oalmann, R. J. Pieters, M. N. Protopopova, C. E. Raab, G. H. P. Roos, Q.-L. Zhou, S. F. Martin, *J. Am. Chem. Soc.* **1995**, *117*, 5763–5775.

[8] A. Pfaltz, *Acc. Chem. Res.* **1993**, *26*, 339–345; P. Müller, C. Baud, D. Ene, S. Motallebi, M. P. Doyle, B. D. Brandes, A. B. Dyatkin, M. M. See, *Helv. Chim. Acta* **1995**, *78*, 459–470; H. Nishiyama, Y. Itoh, Y. Sugawara, H. Matsumoto, K. Aoki, K. Itoh, *Bull. Chem. Soc. Jpn.* **1995**, *68*, 1247–1262.

[9] Product control in $[Rh_2(5S\text{-mepy})_4]$-catalyzed reactions of **2** and **6** is consistent with the relative reactivities of olefins and arenes for intramolecular cyclizations catalyzed by dirhodium(II) carboxamidates: A. Padwa, D. J. Austin, A. T. Price, M. A. Semones, M. P. Doyle, M. N. Protopopova, W. R. Winchester, A. Tran, *J. Am. Chem. Soc.* **1993**, *115*, 8669–8680.

What is the Structure of the Calmodulin Antagonist Konbamide from *Theonella* sp.? Synthesis of Two Isomers by Direct Biomimetic Introduction of Bromine in Hydroxytryptophan-Containing Cyclic Peptides**

Ulrich Schmidt* and Steffen Weinbrenner

Many marine plants and animals store halogens. Their peptidic components often include halogenated tyrosine[1] and tryptophan. For example, the nonribosomal amino acid 6-bromotryptophan is incorporated into clionamide[2] and celenamide,[3] which are isolated from algae. Similarly, the cyclic natural product jaspamide[4] contains 2-bromo-*N*-methyltryptophan as a ring element. 2-Bromo-5-hydroxytryptophan is a component of the cyclic peptides konbamide,[5] orbiculamide A,[6] and keramamides B–D,[7] which are isolated from the sea sponge *Theonella*, and we have synthesized the halogenated compound by direct bromination of hydroxytryptophan derivatives.[9] Both the amino acid and its *N*-acyl derivatives are unstable and therefore cannot be used in natural product synthesis.

In the biosynthesis of bromine-containing peptides the bromination of the peptide in the last step is a subject of debate; even electrophilic, nonenzymatic substitution by bromine (formed from oxidation of Br^- ions, perhaps by symbiotic algae) seems plausible. In the following, we describe our experiments on the biomimetic synthesis of konbamide by electrophilic bromination of a preformed cyclic peptide. Konbamide has structural characteristics (Scheme 1) that complicate its synthesis: the sensitive 2-bromo-5-hydroxytryptophan, lysine in which the ε-amino group is a ring member, and the urea side chain.

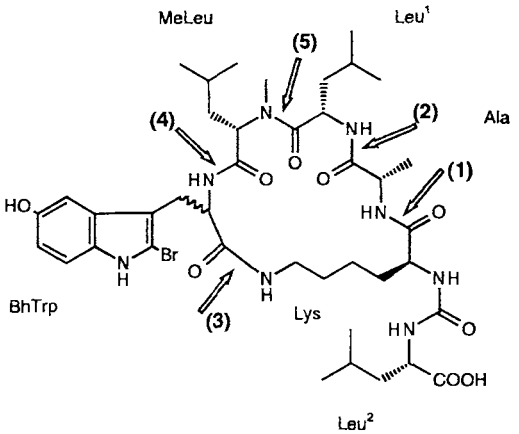

Scheme 1. Postulated structure of konbamide. Strategic bonds in retrosynthetic analysis are marked with arrows.

Intramolecular acylation at the alanine (position 1) or leucine (position 2) nitrogen atoms were both possibilities for the ring closure. Both positions seem to be unhindered and both activated alanine and lysine are quite configurationally stable. Based on our experience in the synthesis of glidobaktin,[9] ring closure at the ε-amino group of lysine (position 3) is not promising. Ring closure at the hydroxytryptophan (position 4) or *N*-methylleucine (position 5) nitrogen atoms was ruled out because of the difficulty in acylating secondary nitrogen centers and the facile racemization of activated *N*-methylleucine.

The linear pentapeptide **5**, which could undergo ring closure at the alanine nitrogen atom, was obtained by straightforward reaction of **2** and **4** (Scheme 2). From this point on, all protective groups had to be compatible with 2-bromo-5-tryptophan, which was to be formed after ring closure. For protection of the phenolic OH group we chose a pivaloyl ester, which had already been used successfully in synthesis of 2-bromo-5-hydroxytryptophan. It prevents 4- and 6-substitution of hydroxytryptophan during bromination, is conserved during hydrolysis of the methyl ester **6**, and can be cleaved from **11** without destruction of the sensitive tryptophan functionality.

Ring closure of **8** at position 1 was achieved with the pentafluorophenyl (PFP) ester method, which we developed, in a biphasic system to produce **9** in 63% yield. The corresponding ring closure at the leucine nitrogen atom proceeded in 60% yield. The ring closure could be performed by the same method without protection of the phenolic group, but this had a yield of

[*] Prof. Dr. U. Schmidt, Dr. S. Weinbrenner
Institut für Organische Chemie und Isotopenforschung der Universität
Pfaffenwaldring 55, D-70569 Stuttgart (Germany)
Fax: Int. code +(711)685-4321

[**] Amino Acids and Peptides, Part 101. This work was supported by the Deutsche Forschungsgemeinschaft and by the Fonds der Chemischen Industrie. Part 100: U. Schmidt, C. Braun, H. Sutoris, *Synthesis* **1995**, 223.

 © VCH Verlagsgesellschaft mbH, D-69451 Weinheim, 1996 0570-0833/96/3512-1336 $ 15.00+.25/0

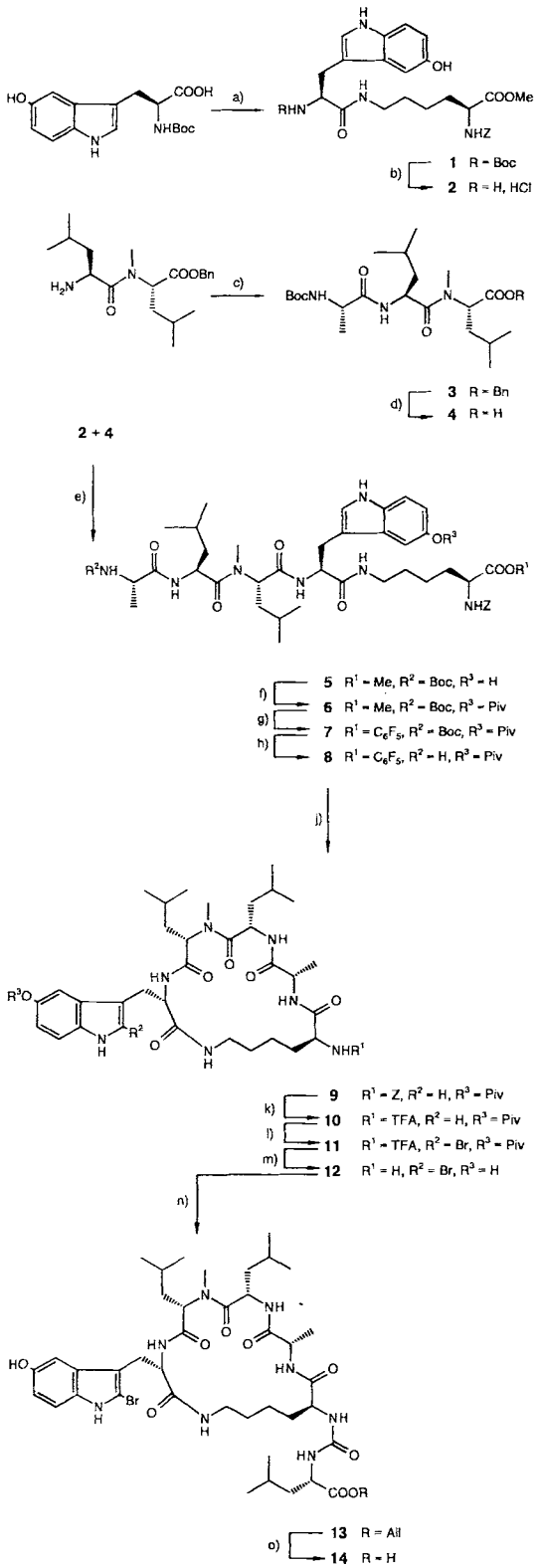

Scheme 2. Synthesis of "konbamide" **14**. a) THF, Z(H, HCl)-(*S*)-Lys-OMe, Bop-Cl, Et_2NH, 0 °C, 16 h, 80%; b) HCl, dioxane, room temperature (RT); 2 h; c) CH_2Cl_2, Boc-(*S*)-Ala-OH, TBTU, Et_2NH, 0 °C, 3 h, 88%; d) MeOH, Pd/C/H_2, RT, 3 h, 98%; e) DMF, 2-(diphenylphosphoryl)azide, −20 °C, 48 h, 86%; f) CH_2Cl_2, PivOCl, Et_3N, RT, 3 h, 97%; g) dioxane, H_2O, NaOH, RT, 97%; CH_2Cl_2, 1-ethyl-3-(3-dimethylaminopropyl)carbodiimide (EDC), PFP, −20 °C → RT, 16 h; h) HCl, dioxane, RT, 2 h; j) $CHCl_3$, $NaHCO_3$, RT, 5 h; g)–h): 63%; k) MeOH, Pd/C/H_2, RT, 16 h; THF, TFA anhydride, RT, 16 h, 93%; l) CH_2Cl_2, NBS, RT, 30 min, 75%; m) MeOH, H_2O, NaOH, RT, 24 h; n) THF, allyl (*S*)-2-isocyanato-4-methylpentanoate, RT, 24 h; m)–n): 40%; o) THF, $[Pd(PPh_3)_4]$, RT, 5 h; 75%.

only 30%. Exchange of the Z-protective group for a trifluoroacetyl (TFA) protective group gave substrate **10**, which was brominated with *N*-bromosuccinimide (NBS) without a radical starter or light in a straightforward reaction. The TFA and pivaloyl protective groups were removed from the resultant bromide **11** by careful alkaline hydrolysis to produce **12**. The urea side chain was formed by using allyl (*S*)-2-isocyanato-4-methylpentanoate[10] (from leucine). Finally, the allyl ester **13** was cleaved with Pd^0[11] to afford the acid **14**.

Minor differences between the synthetic product and the natural compound were evident by HPLC.[12] Similarly the optical rotation and the NMR spectra of the synthetic product and the natural substance were not completely identical. In particular, there were noticeable differences in the α-H and NH signal regions (Table 1). In contrast, the mass spectra were the same.[13]

Table 1. Comparison of characteristic NMR data for natural konbamide [5] and **14**.

14	Konbamide	Assignment [5]
4.01–4.08 (m, 1H)	3.93 (m, 1H)	Lys-α-NH
4.10–4.18 (m, 1H)	4.03 (dd, J = 9.0, 5.0 Hz, 1H)	Leu^2-α-H
4.28–4.30 (m, 1H)	4.18 (m, 1H)	Ala-α-H
4.61–4.65 (m, 1H)	4.61 (ddd, J = 11.3, 9.0, 3.5 Hz, 1H)	BhTrp-α-H
4.71–4.78 (m, 2H)	4.72 (m, 2H)	MeLeu-α-H Leu^1-α-H
6.20 (d, J = 7.9 Hz, 1H)	6.26 (d, J = 9.0 Hz, 1H)	Leu^2-NH
6.33 (d, J = 8.3 Hz, 1H)	6.42 (d, J = 7.4 Hz, 1H)	Lys-α-NH
7.41 (d, br., 1H)	7.44 (dd, J = 7.8, 3.3 Hz, 1H)	Lys-ε-NH
8.26 (d, J = 5.6 Hz, 1H)	6.99 (d, J = 5.7 Hz, 1H)	Ala-NH
8.43 (d, J = 9.0 Hz, 1H)	8.29 (d, J = 9.0 Hz, 1H)	BhTrp-NH
8.84 (d, J = 5.9 Hz, 1H)	8.74 (d, J = 6.2 Hz, 1H)	Leu^1-NH

One possible explanation is that the natural compound and the synthetic product are diastereomers. During their investigation of the natural substance by 2D-NMR, FAB-MS analysis, and total hydrolysis, the Japanese authors[5] determined that the amino acids are L-configurated after the hydrolysis, by using GC and HPLC on chiral phases. Bromohydroxytryptophan decomposes during hydrolysis and thus its configuration was left open.

The amino acids resulting from hydrolysis of the synthetic product also proved to be L-configurated. To exclude a different configuration at bromohydroxytryptophan as the reason for the difference between the synthetic product and the natural substance, we also synthesized the diastereomer of **14** with D-bromohydroxytryptophan. However, the HPLC retention time of this product also deviated from that of the natural substance. Thus the proposed structure of konbamide cannot be correct.

Received: February 21, 1996 [Z8844IE]
German version: *Angew. Chem.* **1996**, *108*, 1432–1433

Keywords: configuration elucidation · konbamide · natural products · peptides

[1] W. R. Chan, W. F. Tinto, P. S. Mauchaud, L. J. Todaro, *J. Org. Chem.* **1987**, *52*, 3091; N. K. Gulavita, A. E. Wright, P. J. McCarthy, S. A. Pomponi, M. Kelly-Borges, *J. Nat. Prod.* **1993**, *56*, 1613.

[2] Isolation and structure determination: R. J. Andersen, R. J. Stonard, *Can. J. Chem.* **1979**, *57*, 2325; Synthesis: U. Schmidt, A. Lieberknecht, H. Griesser, H. Bökens, *Tetrahedron Lett.* **1982**, *23*, 4911.

[3] Isolation and structure determination: R. J. Andersen, R. J. Stonard, *Can. J. Chem.* **1980**, *58*, 2121; Synthesis: U. Schmidt, J. Wild, *Angew. Chem.* **1984**, *96*, 996; *Angew. Chem. Int. Ed. Engl.* **1984**, *23*, 991.

[4] Isolation and structure determination: T. M. Zabrisky, J. A. Klocke, C. M. Ireland, A. H. Marens, T. F. Molinsky, D. J. Faulkner, C. Xu, J. C. Clardy, *J. Am. Chem. Soc.* **1986**, *108*, 3123; P. Crews, L. V. Manes, M. Boehler, *Tetrahedron Lett.* **1986**, *27*, 2797; Synthesis: P. A. Grieco, Y. S. Hon, A. J. Perez-

Medrano, *J. Am. Chem. Soc.* **1988**, *110*, 1630; K. S. Chu, G. R. Negrete, J. P. Konopelsky, *ibid.* **1991**, *113*, 5196; R. Rao, M. K. Gujar, B. R. Nallagandu, A. Bhandari, *Tetrahedron Lett.* **1993**, *34*, 7085.
[5] J. Kobayashi, M. Sato, T. Murayama, M. Ishibashi, M. R. Wälchi, M. Kanai, J. Shoji, Y. Ohizumi, *J. Chem. Soc. Chem. Commun.* **1991**, 1050.
[6] N. Fusetani, T. Sugawara, S. Matsunaga, *J. Am. Chem. Soc.* **1991**, *113*, 7811.
[7] J. Kobayashi, F. Itagaki, H. Shigemori, M. Ishabashi, K. Takahashi, M. Ogura, S. Nagasawa, T. Nakamura, H. Hirota, T. Ohta, S. Nozoe, *J. Am. Chem. Soc.* **1991**, *113*, 7812.
[8] U. Schmidt, S. Weinbrenner, *Synthesis* **1996**, 28.
[9] U. Schmidt, A. Kleefeldt, R. Mangold, *J. Chem. Soc. Chem. Commun.* **1992**, 1687.
[10] Synthesis analogous to that of the methyl ester: J. S. Nowick, N. A. Powell, T. M. Nguyen, G. Noronha, *J. Org. Chem.* **1992**, *57*, 7364.
[11] H. Kunz, H. Waldmann, *Angew. Chem.* **1984**, *96*, 49; *Angew. Chem. Int. Ed. Engl.* **1984**, *23*, 71.
[12] We thank Prof. J. Kobayashi for providing a sample of the natural substance.
[13] The measurements were kindly performed by Dr. K. Eckart at the Max-Planck-Institut für experimentelle Medizin in Göttingen.

A Chelate-Amidozirconium Fragment as Building Block for Unsupported Trinuclear ZrM_2 Heterobimetallic Complexes (M = Fe, Ru, Co)**

Stefan Friedrich, Lutz H. Gade,* Ian J. Scowen, and Mary McPartlin

With the recent development of halide complexes with tripodal amido ligands, monofunctional building blocks for the generation of directly metal–metal bonded M′–M heterobimetallic compounds (M′ = Ti, Zr, Hf; M = late transition metal) of unprecedented stability have been made available[1, 2] and have enabled a systematic investigation into their chemical reactivity.[3] We have now extended this strategy to the development of difunctional building blocks (Scheme 1), which may be employed in the synthesis of stable trinuclear complexes containing two equivalent Zr–M bonds, thus opening up the possibility of extending the cooperative reactivity of early–late heterobimetallic compounds to involve three complex fragments.

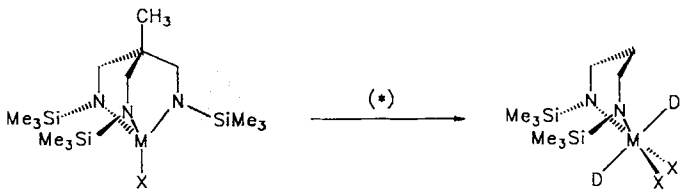

Scheme 1. Relationship between monofunctional and difunctional amidohalide complexes of the metals of the titanium triad used as building blocks for heteronuclear compounds. (*): Formal removal of an anionic "amido-arm" in a tridentate ligand.

[*] Dr. L. H. Gade, S. Friedrich
Institut für Anorganische Chemie der Universität
Am Hubland, D-97074 Würzburg (Germany)
Fax: Int. code +(931)888-4605
Dr. I. J. Scowen, Prof. M. McPartlin
School of Applied Chemistry, University of North London
Holloway Road, London N7 8DB (UK)

[**] This work was supported by the Deutsche Forschungsgemeinschaft (L. H. G., S. F.), the Engineering and Physical Science Research Council (M. McP., I. J. S), the Deutscher Akademischer Austauschdienst, and the British Council (ARC grant). We thank Professor Werner for his support and Degussa AG for a gift of basic chemicals.

This type of trinuclear complex possessing two highly polar metal–metal bonds is particularly rare; the only fully characterized and studied example is Casey's $ZrRu_2$ complex $[Cp_2Zr\{Ru(CO)_2Cp\}_2]$ ($Cp = C_5H_5$).[4] More recently, Pályi et al. have given a preliminary account of the generation of $[Cp_2Zr\{Co(CO)_4\}_2]$ by salt metathesis or alkane elimination.[5] Based on early work by Bürger et al.[6] we synthesized the difunctional amidozirconium complexes of the type $[CH_2(CH_2NSiMe_3)_2ZrCl_2(D)_2]$ (D = thf, pyridine),[7] which have proved to be ideally suited for the synthesis of such trinuclear complexes. Reaction of the complex $[CH_2(CH_2NSiMe_3)_2ZrCl_2(thf)_2]$ **1** with two molar equivalents of the carbonyl metalates $K[CpM(CO)_2]$ (M = Fe, Ru) and $Na[Co(CO)_3(PPh_3)]$ yields the corresponding trinuclear $ZrFe_2$, $ZrRu_2$, and $ZrCo_2$ compounds **2**–**4** (Scheme 2). While both **2** and **3** are stable in

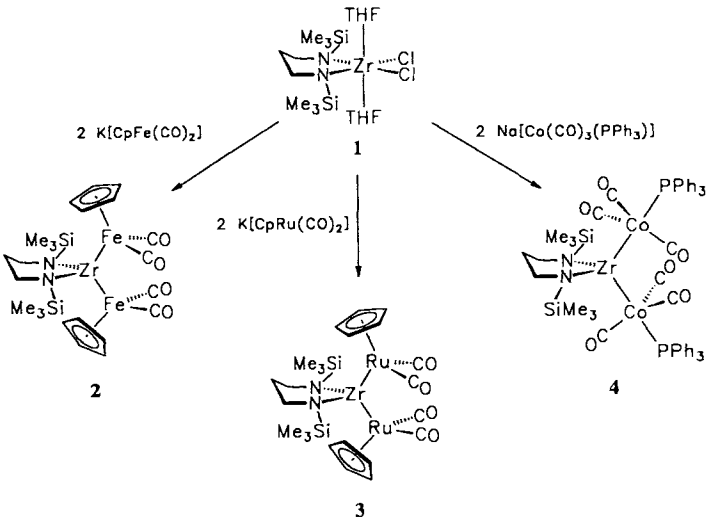

Scheme 2. Synthesis of the ZrM_2 heterobimetallic complexes **2**–**4**.

solution, the $ZrCo_2$ complex **4** slowly decomposes generating $[Co(CO)_3(PPh_3)]_2$ and an intractable Zr-containing material. The existence of metal–metal bonds in **2**–**4** was initially deduced from the IR spectra, in which the ν(CO) bands are shifted to higher wavenumbers relative to those of the alkali metal salts of the anions (Table 1). It is interesting to compare the position of the asymmetric ^{12}CO stretching vibration of **3** with that of $[Cp_2Zr\{Ru(CO)_2Cp\}_2]$.[4] For **3** $\Delta\tilde{\nu}(\nu(CO)_{as})$ was found to be 97 cm^{-1} relative to the free carbonyl metalate [$\tilde{\nu}(\nu(CO_{as}))$ = 1896, 1811 cm^{-1}], while the value for Casey's $ZrRu_2$ compound is only 71 cm^{-1}.[8] The greater Lewis acidity of the amidozirconium fragment in comparison to that of the Cp_2Zr unit apparently induces a higher degree of charge redistribution from the late transition metal to the early transition metal through the metal–metal bond, which therefore assumes a more covalent character.

This difference in the IR spectroscopic data should be reflected in the molecular structures of the compounds. To establish such a relationship, and in order to structurally characterize a $ZrFe_2$ species for the first time, single-crystal X-ray structure analyses of **2** and **3** were carried out (Fig. 1).[9] The compounds are isomorphous and their gross features are identical. In each, the central Zr atom adopts a distorted terahedral coordination geometry (**2**: N(1)-Zr-N(2) = 97.5(3), Fe(1)-Zr-Fe(2) = 116.2(1)°; **3**: N(1)-Zr-N(2) = 97.6(2), Ru(1)-Zr-Ru(2) = 115.84(2)°) and links to iron or ruthenium complex fragments through direct unsupported metal–metal bonds.

Table 1. Selected spectroscopic data [a].

2: ^{1}H NMR: δ = 0.43 (s, 18H, Si(CH$_3$)$_3$), 1.31 (m, 2H, CH$_2$), 3.32 (m, 4H, CH$_2$N), 4.56 (s, 10H, Cp); ^{13}C NMR: δ = 1.6 (Si(CH$_3$)$_3$), 33.0 (CH$_2$), 43.4 (CH$_2$N), 82.8 (Cp), 216.3 (CO); IR: $\tilde{\nu}$(ν(CO)) = 2005 (s), 1941 (vs), 1888 (vs) cm^{-1}

3: ^{1}H NMR: δ = 0.48 (s, 18H, Si(CH$_3$)$_3$), 1.34 (m, 2H, CH$_2$), 3.17 (m, 4H, CH$_2$N), 4.91 (s, 10H, Cp); ^{13}C NMR: δ = 1.8 (Si(CH$_3$)$_3$), 35.5 (CH$_2$), 45.6 (CH$_2$N), 85.7 (Cp), 205.1 (CO); IR: $\tilde{\nu}$(ν(CO)) = 1968 (s), 1908 (s) cm^{-1}

4: ^{1}H NMR: δ = 0.37 (s, 18H, Si(CH$_3$)$_3$), 1.22 (m, 2H, CH$_2$), 3.39 (m, 4H, CH$_2$N), 6.93–7.02, 7.52–7.69 (m, 30H, PPh$_3$); ^{13}C NMR: δ = 0.9 (Si(CH$_3$)$_3$), 30.2 (CH$_2$), 43.3 (CH$_2$N), 128.9 (d, C^3, ^3J(P,C) = 10.2 Hz), 130.0 (C^4), 133.5 (d, C^2, ^2J(P,C) = 11.6 Hz), 135.7 (d, C^1, ^1J(P,C) = 41.4 Hz), 206.6 (br., CO); ^{31}P NMR: δ = 60.0; IR: $\tilde{\nu}$(ν(CO)) = 2042 (vw), 1962 (s), 1925 (vs), 1915 (vs) cm^{-1}

5: ^{1}H NMR: δ = 0.37 (s, 18H, Si(CH$_3$)$_3$), 1.40 (m, 1H, H^c, CHH), 2.05 (m, 1H, H$^{c'}$, CHH), 3.23 (ddd, 2H, H^a, CHHN, ^2J(H^a,H^b) = 13.7 Hz, ^3J(H^a,H$^{c/c'}$) = 7.0 Hz, ^3J(H^a,H$^{c/c'}$) = 2.9 Hz), 3.44 (ddd, 2H, H^b, CHHN, ^3J(H^b,H$^{c/c'}$) = 8.8 Hz, ^3J(H^b,H$^{c/c'}$) = 2.5 Hz), 4.47 (s, 5H, Cp); ^{13}C NMR: δ = 0.4 (Si(CH$_3$)$_3$), 38.4 (CH$_2$), 51.8 (CH$_2$N), 81.8 (Cp), 215.7 (CO); IR: $\tilde{\nu}$(ν(CO)) = 2007 (w), 1947 (s), 1895 (s) cm^{-1}

6: ^{1}H NMR: δ = 0.39 (s, 18H, Si(CH$_3$)$_3$), 1.52 (m, 1H, H^c, CHH), 2.07 (m, 1H, H$^{c'}$, CHH), 3.21 (ddd, 2H, H^a, CHHN, ^2J(H^a,H^b) = 13.0 Hz, ^3J(H^a,H$^{c/c'}$) = 7.7 Hz, ^3J(H^a,H$^{c/c'}$) = 2.8 Hz), 3.40 (ddd, 2H, H^b, CHHN, ^3J(H^b,H$^{c/c'}$) = 8.0 Hz, ^3J(H^b,H$^{c/c'}$) = 2.7 Hz), 4.94 (s, 5H, Cp); ^{13}C NMR: δ = 0.4 (Si(CH$_3$)$_3$), 38.5 (CH$_2$), 52.1 (CH$_2$N), 84.8 (Cp), 204.9 (CO); IR: $\tilde{\nu}$(ν(CO)) = 2017 (m), 1968 (vs), 1908 (vs) cm^{-1}

7: ^{1}H NMR: δ = 0.07 (s, 18H, Si(CH$_3$)$_3$), 1.43 (m, 1H, H^c), 2.31 (m, 1H, H$^{c'}$), 3.38 (ddd, 2H, H^a, ^2J(H^a,H^b) = 14.2 Hz, ^3J(H^a,H$^{c/c'}$) = 5.1 Hz, ^3J(H^a,H$^{c/c'}$) = 3.0 Hz), 3.64 (ddd, 2H, H^b, ^3J(H^b,H$^{c/c'}$) = 10.8 Hz, ^3J(H^b,H$^{c/c'}$) = 1.9 Hz), 3.95 (s, 3H, NCH$_3$), 4.50 (s, 5H, CpFeZr), 4.54 (s, 5H, CpFeC); ^{13}C NMR: δ = 0.5 (Si(CH$_3$)$_3$), 41.2 (CH$_2$), 47.0 (NCH$_3$), 50.4 (CH$_2$N), 80.9 (CpFeZr), 90.2 (*Cp*FeC), 215.0 ((*CO*)$_2$FeC), 220.1 ((CO)$_2$FeZr), 283.2 (C=N); IR: $\tilde{\nu}$(ν(CO)) = 2005 (s), 1951 (s), 1924 (s), 1862 (s) cm^{-1}

8: ^{1}H NMR: δ = 0.04 (s, 18H, Si(CH$_3$)$_3$), 1.47 (m, 1H, H^c, CHH), 2.39 (m, 1H, H$^{c'}$, CHH), 3.34 (ddd, 2H, H^a, CHHN, ^2J(H^a,H^b) = 14.0 Hz, ^3J(H^a,H$^{c/c'}$) = 5.7 Hz, ^3J(H^a,H$^{c/c'}$) = 2.9 Hz), 3.64 (ddd, 2H, H^b, CHHN, ^3J(H^b,H$^{c/c'}$) = 10.4 Hz, ^3J(H^b,H$^{c/c'}$) = 2.0 Hz), 3.89 (s, 3H, NCH$_3$), 4.99 (s, 5H, CpRuZr), 5.01 (s, 5H, CpRuC); ^{13}C NMR: δ = 0.4 (Si(CH$_3$)$_3$), 40.8 (CH$_2$), 48.9 (NCH$_3$), 50.0 (CH$_2$N), 84.1 (CpRuZr), 93.3 (*Cp*RuC), 200.0 ((*CO*)$_2$RuC), 208.4 ((CO)$_2$RuZr), 271.6 (C=N); IR: $\tilde{\nu}$(ν(CO)) = 2015 (s), 1955 (s), 1942 (s), 1876 (s) cm^{-1}

[a] NMR spectra recorded at 200.13 MHz (^{1}H), 50.32 MHz (^{13}C), and 81.03 MHz (^{31}P) in C$_6$D$_6$. IR spectra were recorded in toluene. Correct elemental analyses obtained for all compounds.

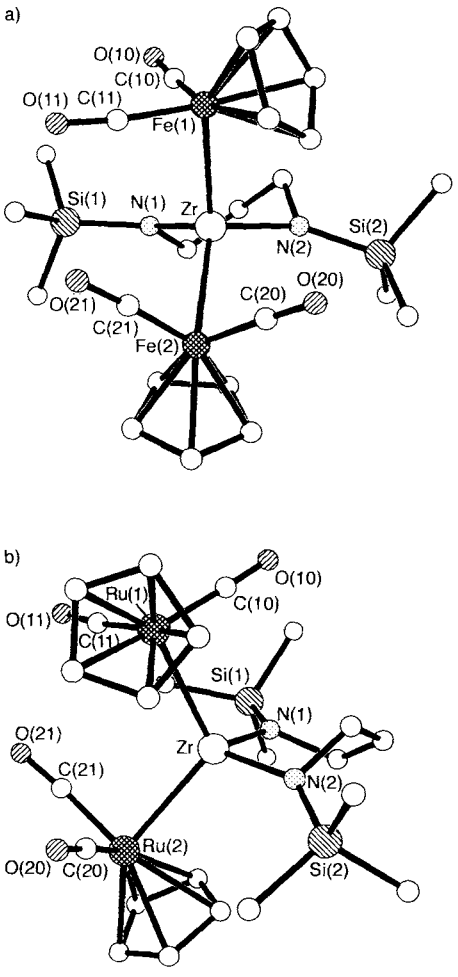

Fig. 1. Crystal structures of the nearly isostructural complexes [CH$_2$(CH$_2$NSiMe$_3$)$_2$Zr{M(CO)$_2$Cp}$_2$]. a) **2** (M = Fe). Selected bond lengths [Å]: Zr–Fe(1) 2.665(2), Zr–Fe(2) 2.664(2), Zr–N(1) 2.036(7), Zr–N(2) 2.040(7), Fe(1)–C(10) 1.720(11), Fe(1)–C(11) 1.720(11), Fe(1)–Cp 2.095(10)–2.111(11), Fe(2)–C(20) 1.722(12), Fe(2)–C(21) 1.712(12), Fe(2)–Cp 2.086(9)–2.121(11). b) **3** (M = Ru). Selected bond lengths [Å]: Zr–Ru(1) 2.7372(7), Zr–Ru(2) 2.7452(7), Zr–N(1) 2.042(5), Zr–N(2) 2.025(5), Ru(1)–C(10) 1.851(8), Ru(1)–C(11) 1.857(9), Ru(1)–Cp 2.258(7)–2.296(8), Ru(2)–C(20) 1.841(8), Ru(2)–C(21) 1.846(7), Ru(2)–Cp 2.255(7)–2.305(7).

The Zr–Fe distances in **2** of d[Zr–Fe(1)] = 2.665(2) and d[Zr–Fe(2)] = 2.664(2) Å lie in the range between those found in [MeSi{SiMe$_2$N(4-CH$_3$C$_6$H$_4$)}Zr–Fe(CO)$_2$Cp][3] and [CH$_2$(CH$_2$NSiMe$_3$)$_2$(Cp)Zr–Fe(CO)$_2$Cp][7] [d(Fe–Zr) = 2.605(2) and 2.745(1) Å, respectively]. The Zr–Ru bonds in **3** (d[Zr–Ru(1)] = 2.7372(7), d[Zr–Ru(2)] = 2.7452(7) Å) are by far the shortest found in unsupported Zr–Ru complexes. The corresponding bonds in [Cp$_2$Zr{Ru(CO)$_2$Cp}$_2$] (d[Zr–Ru(1)] 2.938(1), d[Zr–Ru(2)] = 2.948(1) Å)[4] and [Cp$_2$Zr(O*t*Bu)-Zr–Ru(CO)$_2$Cp] (d(Zr–Ru) = 2.910(1) Å)[10] are significantly longer. In a theoretical study on the metal–metal bonding in Zr–M complexes Wolczanski et al. have pointed out that the Zr–M bond length critically determines the degree of metal–metal π-bonding and thus the degree of charge relocalization between the two metal centers.[11] The different positions of the $\tilde{\nu}$(CO) IR bands in the amido complexes and the Cp$_2$Zr derivatives is thus manifested in their structural data. The comparatively "open" coordination of the Zr centers in **2** and **3** and, consequently, the reduced steric interaction between the {CpM(CO)$_2$} fragments in both compounds is particularly remarkable and is reflected in the rapid internal rotation around the Zr–M bonds, which is not frozen out even upon cooling NMR samples to 180 K.[12]

Upon reaction of **2** and **3** with **1** in a molar ratio of 1:1, a quantitative complex fragment redistribution is observed that generates the dinuclear compounds **5** and **6**, respectively.[13]

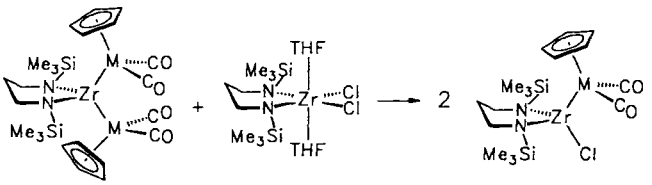

2, M = Fe; **3**, M = Ru — **1** — **5**, M = Fe; **6**, M = Ru

Attempts to generate a ZrFeRu heterotrimetallic complex by reacting **5** with [CpRu(CO)$_2$]$^-$ or **6** with [CpFe(CO)$_2$]$^-$ led to product mixtures in which the target compound could not be unambiguously identified. The facility of the Zr-bonded {CpM(CO)$_2$} fragment to be displaced by a nucleophile, thus

 © VCH Verlagsgesellschaft mbH, D-69451 Weinheim, 1996 0570-0833/96/3512-1339 $ 15.00+.25/0

competing with Cl^-, is the underlying reason for this observation. That this is indeed a kinetic phenomenon and not a consequence of a redistribution equilibrium of the trinuclear complexes is inferred from the unsuccessful attempts to generate a trimetallic species through conproportionation of **2** and **3** even upon heating such mixtures.

The stability of **2** and **3** enables the systematic investigation of the reactivity of systems containing two symmetry-related Zr–M bonds. In view of our previous studies on insertion reactions of polar unsaturated molecules into the Zr–M bonds of dinuclear systems[3] it was of particular interest to assess how the transformation at one Zr–M bond would affect the other. Since in contrast to $[Cp_2Zr\{Ru(CO)_2Cp\}_2]$,[4] both **2** and **3** proved to be completely inert to CO (1 atm), we chose methyl isocyanide as substrate. Compounds **2** and **3** react with one molar equivalent of CH_3NC to yield the mono-insertion products **7** and **8**, respectively, which proved to be inert towards a further equivalent of the substrate or even a large excess of it.

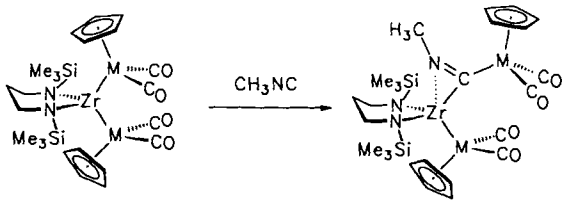

2, M = Fe
3, M = Ru

7, M = Fe
8, M = Ru

The IR spectra of **7** and **8** display a significant shift of the ν(CO) bands in comparison to those of the starting materials (Table 1): the C-bonded $\{CpM(CO)_2\}$ fragments are shifted to higher wavenumbers and the Zr-bound $\{CpM(CO)_2\}$ unit is shifted to significantly lower wavenumbers. The latter is particularly interesting since it indicates that insertion into one Zr–M bond influences the second Zr–M bond. The charge redistribution between the directly metal–metal bonded donor and acceptor complex fragments in **7** and **8** appears to be significantly reduced and thus the residual electron density at the $\{CpM(CO)_2\}$ fragment greater, as reflected in the IR data.

In order to obtain detailed information of the structural consequences of the isocyanide insertion a crystal structure analysis of **8** was carried out (Fig. 2).[14] Similar to the structures of **2** and **3** the central zirconium atom in **8** adopts a distorted tetrahedral coordination with the η^2-"metallaiminoacyl ligand" occupying one coordination site. The most remarkable feature is the increased length of the remaining Zr–Ru bond (d[Zr–Ru(2)] = 2.8639(6) Å) compared to those in the starting material. The resulting reduction of the π-donor–acceptor interaction between the two metal centers is probably responsible for the higher remaining electron density at Ru(1), as manifested in the position of the ν(CO) bands in the IR spectrum. An increase in the metal–metal bond length should imply an enhanced reactivity towards a second equivalent of the substrate, a notion which apparently contradicts the observed reactive behavior. Since **7** and **8** are sterically less crowded than **2** and **3** this situation must be due to changes in the electronic structure of the compounds, an aspect we are currently investigating.

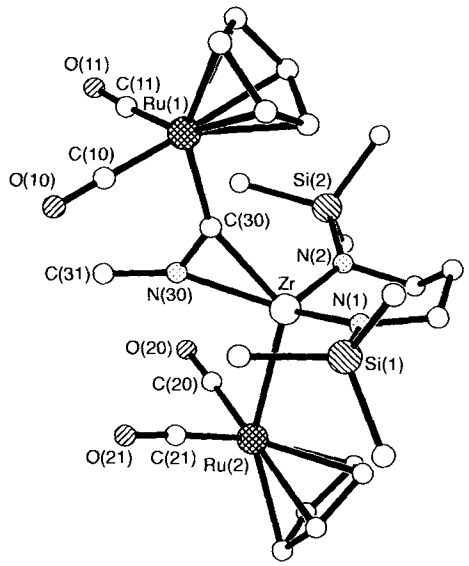

Fig. 2. Crystal structure of **8**, the isocyanide insertion product of $[CH_2(CH_2NSiMe_3)_2Zr\{Ru(CO)_2Cp\}_2]$. Selected bond lengths [Å]: Zr–Ru(1) 2.8639(6), Zr–N(1) 2.066(4), Zr–N(2) 2.025(4), Zr–N(30) 2.185(4), Zr–C(30) 2.237(4), Ru(1)–C(10) 1.858(6), Ru(1)–C(11) 1.835(6), Ru(1)–Cp 2.274(5)–2.309(5), Ru(2)–C(20) 1.866(6), Ru(2)–C(21) 1.865(6), Ru(2)–Cp 2.264(14)–2.303(8), Ru(2)–C(30) 2.040(4).

Experimental Procedure

2–4: To a mixture of solid $[CH_2(CH_2NSiMe_3)_2ZrCl_2(thf)_2]$ (**1**) (550 mg, 1.05 mmol) and solid alkali metal carbonylate [15] toluene (20 mL) and THF (2 mL) were added at ambient temperature. After the mixture had been stirred for 1 h, Na powder (20 mg) was added to the reaction mixture. The mixture was stirred for another 2 h, the solvent was then removed in vacuo, and the residue extracted with pentane (25 mL). After filtration, the solvent of the filtrate was again removed in vacuo, and the residue recrystallized from diethyl ether (4 mL) at −78 °C. Compounds **2–4** were obtained as yellow crystalline solids in yields of 37, 65, and 31%, respectively.

5, **6**: Solid **2** or **3** (0.5 mmol) and **1** (260 mg, 0.5 mmol) was dissolved in C_6H_6 (10 mL) and stirred for 24 h after which the conversion to **5** and **6**, respectively, was complete. The solid products were isolated in almost quantitative yields after removal of the solvent in vacuo and washing of the residue with cold pentane.

7, **8**: To a solution of $[CH_2(CH_2NSiMe_3)_2Zr\{M(CO)_2Cp\}_2]$ (M = Fe: **2**, Ru: **3**; 0.29 mmol) in toluene (5 mL) was added CH_3NC (16.5 μL, 0.29 mmol). After the mixture had been stirred at room temperature for 5 min, the solvent was removed in vacuo and the solid residue extracted with diethyl ether (5 mL). Upon filtration the solution was concentrated to 3 mL and stored at −60 °C. Compounds **7** and **8** were obtained as yellow crystalline solids in yields of 62 and 67%, respectively. The same materials were isolated in the presence of an excess of CH_3NC.

Received: January 24, 1996 [Z8748IE]
German version: *Angew. Chem.* **1996**, *108*, 1440–1443

Keywords: heterobimetallic complexes · zirconium compounds

[1] S. Friedrich, H. Memmler, L. H. Gade, W.-S. Li, M. McPartlin, *Angew. Chem.* **1994**, *106*, 705; *Angew. Chem. Int. Ed. Engl.* **1994**, *33*, 676.
[2] a) M. Herberhold, G.-X. Jin, *Angew. Chem.* **1994**, *106*, 1016; *Angew. Chem. Int. Ed. Engl.* **1994**, *33*, 964; b) D. W. Stephan, *Coord. Chem. Rev.* **1989**, *95*, 41.
[3] B. Findeis, M. Schubart, C. Platzek, L. H. Gade, I. J. Scowen, M. McPartlin, *Chem. Commun.* **1996**, 219.
[4] C. P. Casey, R. F. Jordan, A. L. Rheingold, *Organometallics* **1984**, *3*, 504. See also C. P. Casey, *J. Organomet. Chem.* **1990**, *400*, 205.
[5] T. Bartik, H. Windisch, A. Sorkau, K.-H. Thiele, C. Kriebel, A. Herfurth, M. Tschoerner, G. Zucchi, G. Pályi, *Inorg. Chim. Acta* **1994**, *227*, 201.
[6] a) H. Bürger, D. Beiersdorf, *Z. Anorg. Allg. Chem.* **1979**, *459*, 111; b) K. Wiegel, H. Bürger, *ibid.* **1976**, *426*, 301; c) D. J. Brauer, H. Bürger, E. Essig, W. Gschwandtner, *J. Organomet. Chem.* **1980**, *190*, 343; d) H. Bürger, W. Gschwandtner, G. R. Liewald, *ibid.* **1983**, *259*, 145.
[7] S. Friedrich, L. H. Gade, I. J. Scowen, M. McPartlin, *Organometallics* **1995**, *14*, 5344.
[8] Fischer has pointed out that the shift of the asymmetric ^{12}CO stretching frequency may be viewed as a measure of the acceptor strength of the Lewis acidic metal fragment relative to the base $\{CpM(CO)_2\}^-$: R. A. Fischer, T. Priermeier, *Organometallics* **1994**, *13*, 4306 and references therein.
[9] Crystal data for **2**: $C_{23}H_{34}Fe_2N_2O_4Si_2Zr$, M = 661.67, monoclinic, space group $P2_1/n$, a = 11.333(3), b = 13.001(3), c = 19.364(4) Å, β = 96.58(3)°, V = 2834.30 Å^3, Z = 4, ρ_{calcd} = 1.551 g cm^{-3}, $F(000)$ = 1352, $\mu(Mo_{K\alpha})$ = 1.42 mm^{-1}. Yellow block-shaped crystal (0.37 × 0.32 × 0.32 mm^3) in Linde-

 © VCH Verlagsgesellschaft mbH, D-69451 Weinheim, 1996 0570-0833/96/3512-1340 $ 15.00+.25/0

mann tube under Ar. The structure was determined by heavy atom method and refined on F for 2725 absorption-corrected data with $I/\sigma(I) > 3$ from a total of 5394 reflections (θ_{max} 25°) scanned on a Philips PW1100 four-circle diffractometer at 295 K. Anisotropic displacement parameters applied to all non-hydrogen atoms apart from the twofold disordered methylene group at C(9) (60:40); hydrogen atoms on Cp rings were located in difference-Fourier maps and remaining hydrogen atoms were included in idealized positions and assigned common $U_{iso} = 0.11$ and 0.08 Å^2, respectively. At final convergence $R = 0.0559$, $R_w = 0.0554$ for 308 parameters. Programs: ref. [16a–c]. Crystal data for **3**: $C_{23}H_{34}N_2O_4Ru_2Si_2Zr$, $M = 752.06$, monoclinic, space group $P2_1/n$, $a = 11.3944(9)$, $b = 13.196(2)$, $c = 19.5280(14)$ Å, $\beta = 96.191(5)°$, $V = 2919.1(6)$ Å^3, $Z = 4$, $\rho_{calcd} = 1.711$ g cm^{-3}, $F(000) = 1496$, $\mu(Cu_{K\alpha}) = 12.181$ mm^{-1}. Yellow block-shaped crystal (0.48 × 0.40 × 0.40 mm^3) in Lindemann tube under Ar. The structure was determined by direct methods and refined on F^2 for 3907 independent, absorption-corrected reflections from a total of 4138 collected ($R_{int} = 0.0610$, T_{max} 0.386, T_{min} 0.125) using a Siemens P4 diffractometer (θ_{max} 56.74°) at 293 K. Anisotropic displacement parameters were assigned for all non-hydrogen atoms apart from the twofold disordered methylene group at C(9) (60:40); hydrogen atoms of methylene and methyl carbon atoms were included in idealized positions and assigned $U_{iso} = 1.2$ and 1.5 times U_{eq} of the parent carbon, respectively. At final convergence $R_1 = 0.0379$, $wR_2 = 0.0961$ [$I/\sigma(I) > 2$] and $R_1 = 0.0432$, $wR_2 = 0.2808$ (all data), goodness-of-fit on F^2 1.113 for 316 parameters. Programs: ref. [16d]. See also ref. [14b].

[10] C. P. Casey, R. F. Jordan, A. L. Rheingold, *J. Am. Chem. Soc.* **1983**, *105*, 665.

[11] G. S. Ferguson, P. T. Wolczanski, L. Parkanyi, M. Zonnevylle, *Organometallics* **1988**, *7*, 1967.

[12] This is in contrast to Casey's observations for $[Cp_2Zr\{Ru(CO)_2Cp\}_2]$ in which the internal rotations around the Zr–Ru bonds could be frozen out at 180 K [4].

[13] The dinuclear compounds **5** and **6** may also be synthesized by reaction of **1** with one molar equivalent of $K[CpM(CO)_2]$.

[14] Crystal data for **8**: $C_{25}H_{37}N_3O_4Ru_2Si_2Zr$, $M = 793.12$, monoclinic, space group $P2_1/c$, $a = 10.8252(9)$, $b = 13.0511(9)$, $c = 23.089(2)$ Å, $\beta = 95.720(6)°$, $V = 3245.8(4)$ Å^3, $Z = 4$, $\rho_{calcd} = 1.623$ g cm^{-3}, $F(000) = 1584$, $\mu(Mo_{K\alpha}) = 1.340$ mm^{-1}. Yellow block-shaped crystal (0.50 × 0.40 × 0.38 mm^3) in Lindemann tube under Ar. The structure was determined by direct methods and refined on F^2 for 5665 independent, absorption corrected reflections from a total of 7245 collected ($R_{int} = 0.0212$, T_{max} 0.300, T_{min} 0.233) using a Siemens P4 diffractometer (θ_{max} 25°) at 293 K. Anisotropic displacement parameters were assigned for all non-hydrogen atoms apart from carbon atoms of the twofold disordered Cp ring (70:30) attached to Ru(2); hydrogen atoms of methylene and methyl carbon atoms were included in idealized positions and assigned $U_{iso} = 1.2$ and 1.5 times U_{eq} of the parent carbon, respectively. At final convergence $R_1 = 0.0335$, $wR_2 = 0.0765$ [$I/\sigma(I) > 2$] and $R_1 = 0.0531$, $wR_2 = 0.0882$ (all data), goodness-of-fit on F^2 1.050 for 328 parameters. Programs: ref. [16d]. b) Crystallographic data (excluding structure factors) for the structure(s) reported in this paper have been deposited with the Cambridge Crystallographic Data Centre as supplementary publication no. CCDC-179-36. Copies of the data can be obtained free of charge on application to The Director, CCDC, 12 Union Road, Cambridge CB2 1EZ, UK (fax: int. code +(1223) 336-033; e-mail: teched@chemcrys.cam.ac.uk).

[15] a) M. Brookhart, W. B. Studabaker, R. Husk, *Organometallics* **1987**, *6*, 1141; b) K. Noak, *Helv. Chim. Acta* **1964**, *47*, 1555; c) A. R. Manning, *J. Chem. Soc. A* **1968**, 1135; d) D. Seyferth, M. D. Millar, *J. Organomet. Chem.* **1972**, *38*, 373.

[16] a) SHELX76: G. M. Sheldrick, University of Cambridge, **1976**; b) SHELX86: G. M. Sheldrick, University of Göttingen, **1986**; c) DIFABS, N. Walker, D. Stuart, *Acta Crystallogr. Sect. A* **1983**, *39*, 158; d) SHELXTL, Siemens Analytical X-Ray Instruments Inc., Madison, WI, USA, **1994**.

A Flavo-Thiazolio-Cyclophane as a Functional Model for Pyruvate Oxidase**

Patrizio Mattei and François Diederich*

Pyruvate oxidase is a flavin adenine dinucleotide (FAD) and thiamine diphosphate (ThDP) dependent enzyme found in lactobacteria,[2] whose X-ray crystal structure has recently been determined.[3] The enzyme catalyzes the reaction from pyruvate to acetyl phosphate (Scheme 1, pathway I). ThDP-mediated decarboxylation of pyruvate generates an active aldehyde, which is oxidized by FAD. The resulting reduced flavin ($FADH_2$) is reoxidized by dioxygen under formation of H_2O_2. Finally, the 2-acetylthiazolium intermediate produced by oxidation of the active aldehyde reacts with inorganic phosphate producing the energy storage metabolite acetyl phosphate and regenerating the thiazolium ylide.

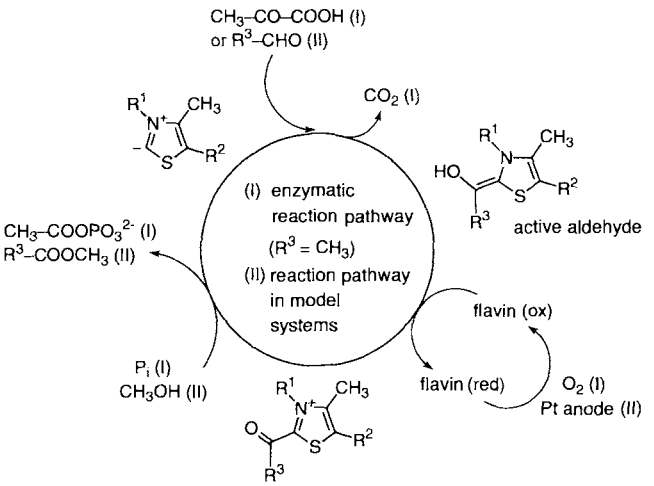

Scheme 1. Catalytic cycles in the conversion of pyruvate to acetyl phosphate catalyzed by pyruvate oxidase (pathway I) and in the oxidation of a carboxaldehyde to a methyl ester in model systems (pathway II).

In a similar reaction sequence, aldehydes are oxidized in water or alcohols to carboxylic acids and esters, respectively (Scheme 1, pathway II). These conversions have been catalyzed by simple thiazolium ions,[4] thiazolium micelles,[5] and thiazolio-cyclodextrins[6] in the presence of oxidizing agents such as nitrobenzene,[4a–d] ferricyanide,[6] and flavins.[4e, 5] We recently reported the catalytic use of thiazolio-cyclophane **1**, which con-

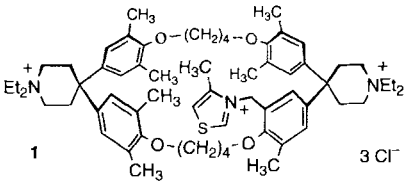

1

[*] Prof. F. Diederich, Dipl.-Chem. P. Mattei
Laboratorium für Organische Chemie
ETH-Zentrum
Universitätstrasse 16, CH-8092, Zürich (Switzerland)
Fax: Int. code +(1)632-1109

[**] Catalytic Cyclophanes, Part 10. This work was supported by the Stipendienfonds der Basler Chemischen Industrie and Hoffmann-La Roche. We thank E. Martinborough and B. Brandenberg for help with the NMR studies. Part 9: [1].

tains a binding site for aromatic substrates.[1] In basic methanolic solution, a bound aromatic aldehyde reacts to give the active aldehyde,[7] which subsequently is oxidized, by transfer of a hydride equivalent to a flavin derivative,[8] to an acylthiazolium intermediate. This intermediate rapidly reacts with the solvent to afford a methyl ester, while the thiazolium ylide is regenerated. The dihydroflavin formed is reoxidized electrochemically at low anodic potential (-300 mV vs. Ag/AgCl). This catalytic cycle is a mild preparation of aromatic esters with high turnover rates. We felt that these rates could be further enhanced by incorporating the flavin directly into the receptor molecule, since CPK model examinations suggested that the active aldehyde intermediate encapsulated in the cavity was not easily accessible for intermolecular oxidation by an external flavin molecule. Efficient trapping of the active aldehyde by the oxidizing agent helps prevent side reactions such as the benzoin condensation and prevents the oxidation step from becoming rate-limiting.[1]

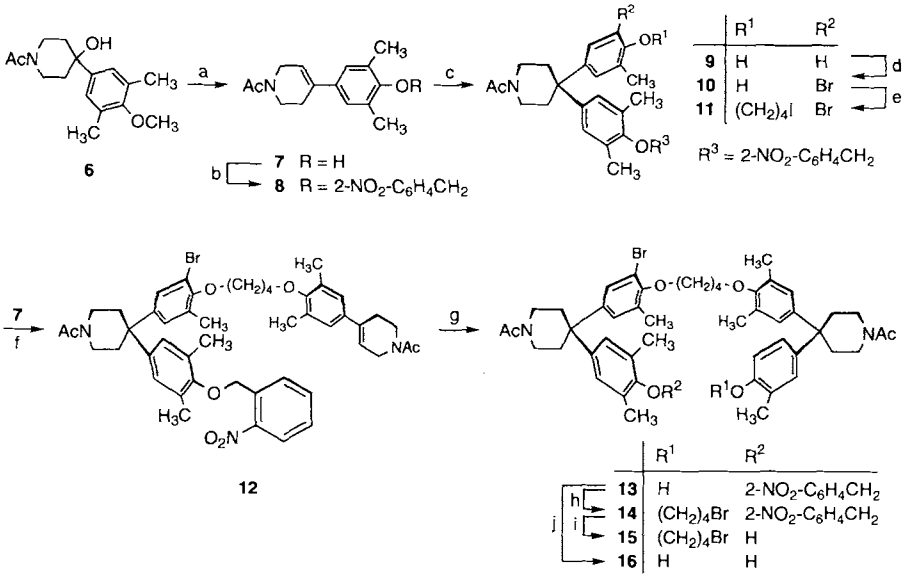

Scheme 2. Synthesis of the cyclization precursors **15** and **16**. a) BBr_3, CH_2Cl_2, reflux, 93%; b) 2-nitrobenzyl chloride, K_2CO_3, CH_3CN, reflux, 98%; c) *o*-cresol, $BF_3 \cdot OEt_2$, CH_2Cl_2, 50 °C, 93%; d) Br_2, CH_2Cl_2, 0 °C, 92%; e) 1,4-diiodobutane, K_2CO_3, 2,6-di-*tert*-butyl-*p*-cresol, acetone, reflux, 91%; f) Cs_2CO_3, acetone, 40 °C, 80%; g) *o*-cresol, $BF_3 \cdot OEt_2$, CH_2Cl_2, 50 °C, 96%; h) 1,4-dibromobutane, K_2CO_3, CH_3CN, reflux, 91%; i) *hv*, 2,6-di-*tert*-butyl-*p*-cresol, THF, 20 °C, 96%; j) *hv*, THF, 20 °C, 87%.

We describe herein the synthesis and preliminary evaluation of the catalytic performance of the novel cyclophane **2**, the first functional model of pyruvate oxidase that combines a well-defined binding site with flavin and thiazolium prosthetic groups. The flavo-thiazolio-cyclophane **2** will be compared to our previously published system {**1** + external flavin},[1] the non-macrocyclic bis(coenzyme) derivative **3**, and the simple system {*N*-benzylthiazolium ion **4** + flavin **5**}.

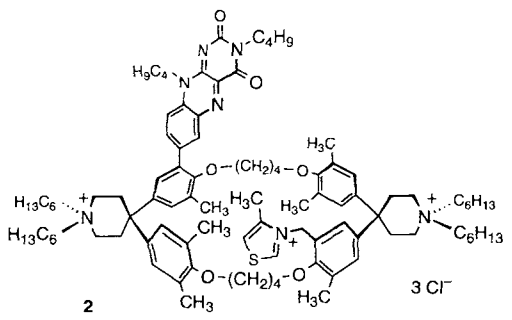

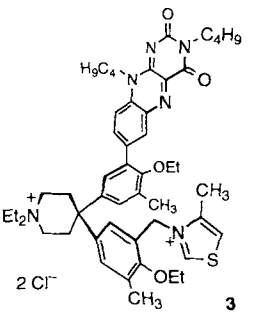

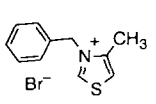

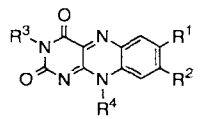

	R^1	R^2	R^3	R^4
5	2-CH_3O-C_6H_4	H	C_4H_9	C_4H_9
22	Br	H	C_4H_9	C_4H_9
26	CH_3	CH_3	CH_3	Tetra-*O*-acetylribityl

Unlike earlier tetraoxa[*n*.1.*n*.1]paracyclophane receptors,[1, 9] **2** is nonsymmetric, that is the four benzene rings have three different substitution patterns; as a result a novel synthetic approach had to be developed. The cyclization precursors **15** and **16** were prepared from the tertiary alcohol **6**[11] (Scheme 2).[10] The 2-nitrobenzyl ether was selected as a phenol protecting group in compounds **8**–**14** because of its excellent stability towards $BF_3 \cdot OEt_2$ needed in the construction of the two diphenylmethane units in **15** and **16** (steps c and g in Scheme 2). Simple benzyl ethers are cleaved under similar Friedel–Crafts reaction conditions.[11] Photolytic deprotection[12] of **13** and **14** succeeded without affecting the sensitive C–Br bonds.

The formation of target compound **2** from cyclization precursors **15** or **16** is shown in Scheme 3. The ω-bromoalkylated phenol **15** underwent an intramolecular macrocyclization to give **17** in 83% yield! Alternatively, cyclophane **17** was obtained in 41% yield in a bimolecular macrocyclization of bis(phenol) **16** with 1,4-dibromobutane. Hydrolysis of **17** to the bis(secondary amine) **18**, followed by acylation with hexanoyl chloride gave **19**, which was reduced with $BH_3 \cdot THF$ to afford the bis-(tertiary amine) **20**. The boronic acid **21** was prepared from bromocyclophane **20** by metalation with *n*BuLi/TMEDA, followed by treatment with excess trimethylborate and aqueous workup. Suzuki-coupling[13] of **21** with the 7-bromoflavin **22**[14] afforded **23** in 56% yield (from **20**). This key step in the preparation of **2** is general and provides a convenient access to 7-arylflavins. Quaternization of **23** followed by ion exchange led to the flavo-cyclophane **24**. Chloromethylation of **24** with CH_2O/HCl in AcOH/conc. aq. HCl[1] yielded the benzyl chloride **25** which, upon heating in 4-methylthiazole and chromatography on reversed-phase silica gel (C_{18}), furnished the water-soluble flavo-thiazolio-cyclophane **2**.

The complexation of 2-naphthaldehyde with flavo-cyclophane **24** and flavo-thiazolio-cyclophane **2** was investigated in ^1H NMR binding titrations in D_2O/CD_3OD (3:2) at 300 K (Table 1). The binding free energy measured for the complex of **24** was in the same range as that determined for a similar cyclophane lacking the flavin moiety.[1] The stability of the com-

 © VCH Verlagsgesellschaft mbH, D-69451 Weinheim, 1996 0570-0833/96/3512-1342 $ 15.00+.25/0

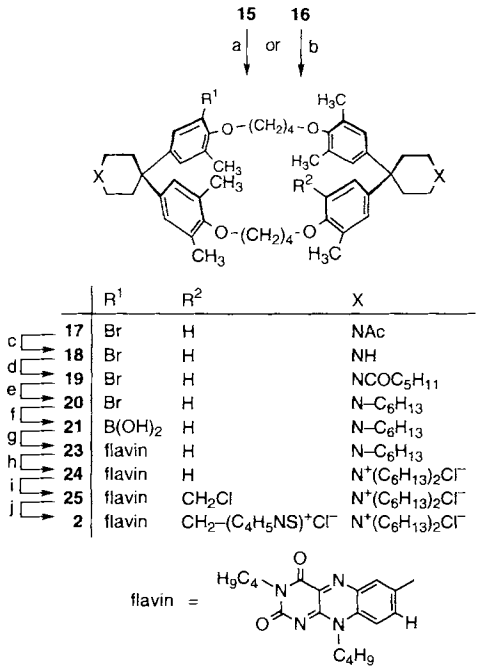

		R^1	R^2	X
c	**17**	Br	H	NAc
d	**18**	Br	H	NH
e	**19**	Br	H	$NCOC_5H_{11}$
f	**20**	Br	H	$N{-}C_6H_{13}$
g	**21**	$B(OH)_2$	H	$N{-}C_6H_{13}$
h	**23**	flavin	H	$N{-}C_6H_{13}$
i	**24**	flavin	H	$N^+(C_6H_{13})_2Cl^-$
j	**25**	flavin	CH_2Cl	$N^+(C_6H_{13})_2Cl^-$
	2	flavin	$CH_2{-}(C_4H_5NS)^+Cl^-$	$N^+(C_6H_{13})_2Cl^-$

Scheme 3. Synthesis of the flavo-thiazolio-cyclophane **2**. a) Cs_2CO_3, CH_3CN, reflux, 83%; b) 1,4-dibromobutane, Cs_2CO_3, CH_3CN, reflux, 41%; c) KOH, 2-methoxyethanol, reflux, 95%; d) hexanoyl chloride, Et_3N, THF, 20 °C, 95%; e) BH_3·THF, THF, reflux, 93%; f) *n*BuLi, *N,N,N',N'*-tetramethylethylenediamine (TMEDA), THF, −78 °C, then $B(OCH_3)_3$, then H^+/H_2O; g) **22**, $[PdCl_2(PPh_3)_2]$, aq. Na_2CO_3, PhH:EtOH, reflux, 56%; h) 1-iodohexane, CH_3CN, reflux, then ion exchange (Cl^-), 88%; i) aq. CH_2O, HCl (g), AcOH/conc. aq. HCl, 40 °C, 75%; j) 4-methylthiazole, 80 °C, 67%.

Table 1. Association constants K_a and binding free energies $-\Delta G^\circ$ from ^{1}H NMR spectroscopy (binding titrations) for 1:1 complexes of 2-naphthaldehyde at $T = 300$ K [a].

Host	K_a [L mol^{-1}]	$-\Delta G$ [kcal mol^{-1}]	Solvent	Degree of saturation [%]
24	5300	5.1	D_2O/CD_3OD (3:2)	93
2	2900	4.8	D_2O/CD_3OD (3:2)	88
2	26	1.9	CD_3OD	71
3	- [b]	-	CD_3OD	-

[a] For titrations in D_2O/CD_3OD, [2-naphthaldehyde] = 0.5 mM, [cyclophane] varied. For titrations in CD_3OD, [host] = 10 mM, [2-naphthaldehyde] varied. The association constants were obtained by nonlinear least-squares curve fitting of the titration data. Accuracy of the K_a values about ±15%. Also shown is the degree of saturation reached in the titrations. [b] No appreciable complexation detected.

plex with **2** is somewhat lower, presumably owing to self-complexation of the thiazolium ring within the cavity as was found for **1**.[1]

The oxidation of 2-naphthaldehyde in methanol to methyl 2-naphthoate is catalyzed by **2** in the presence of Et_3N. The reaction was initiated by adding Et_3N (50 mM) to a degassed solution of **2** (0.5 mM) and 2-naphthaldehyde (2–50 mM) in MeOH under argon. The course of the reaction was followed by monitoring the decrease in absorbance of the flavin chromophore upon reduction to the colorless dihydro form. Initial velocities were determined by standard linear regression analysis of the linear portion of the plot of absorbance versus time. For comparison, this oxidation was also studied under similar conditions with **3** and {**4** +**5**}.[15]

Saturation kinetics was observed with cyclophane **2** (Fig. 1, Table 2). A Lineweaver–Burk plot ($1/v$ vs. 1/[2-naphthaldehyde])[15] gave $v_{max} = 1.2 \times 10^{-4}$ M s^{-1} and $K_M = 23$ mM. The

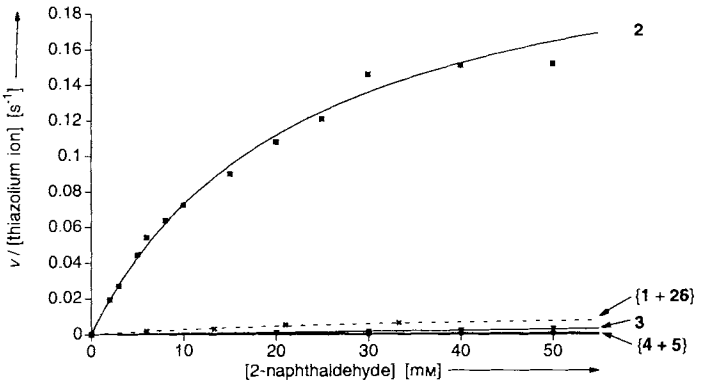

Fig. 1. Plot of relative initial rates versus substrate concentrations for the oxidation of 2-naphthaldehyde to methyl 2-naphthoate catalyzed by **2**, **3**, and {**4** +**5**} [15] as well as {**1** +**26**} [1]. For meaningful comparison, v/[thiazolium ion] rather than v is plotted, since experimental conditions required different concentrations of the various catalysts [15].

Table 2. Oxidation of 2-naphthaldehyde to methyl 2-naphthoate in the presence of Et_3N in methanol.

Catalyst	Second-order rate constant [M^{-1} s^{-1}]
flavo-thiazolio-cyclophane **2**	$k_{cat}/K_M = 10$ [a]
thiazolio-cyclophane **1** and flavin **26**	$k_{cat}/K_M = 0.36$ [b]
flavo-thiazolio-cleft **3**	$k_2 = 0.058$
thiazolium ion **4** and 7-arylflavin **5**	$k_2 = 0.015$

[a] $k_{cat} = 0.24$ s^{-1}, $K_M = 23$ mM. [b] $k_{cat} = 0.013$ s^{-1}, $K_M = 36$ mM.

Michaelis constant is slightly lower than the dissociation constant (K_a^{-1}) measured by ^{1}H NMR titration (38 mM), which can be attributed to unproductive conformations of the host–guest complex.[16] The turnover number $k_{cat} = v_{max}/[\mathbf{2}]$ was calculated to be 0.24 s^{-1}; this value represents approximately a twentyfold acceleration in comparison to the reaction with the bimolecular system {**1** +**26**},[1] and is one of the highest turnover numbers reported for artificial enzymes.[17] Since the bimolecular reaction is already zero order in the oxidizing agent,[1, 5, 6] the acceleration obtained with **2** cannot be expressed in terms of an effective molarity. Although we actually measured the disappearance of the oxidized flavin and thus the initial formation rate of the 2-acylthiazolium intermediate, we can equate its appearance to the formation of the methyl ester, since the reaction of this intermediate with MeOH is fast under basic conditions.[18] In contrast, rates in the presence of **3** and {**4** +**5**} increased in a linear fashion with increasing substrate concentration (Fig. 1).

A comparison of the apparent rate constant k_{cat}/K_M for **2** with the calculated second-order rate constants for the catalyst systems **3** and {**4** +**5**}, which lack the macrocyclic binding site revealed that the reaction with **2** is 170-fold and 670-fold, respectively, faster than with **3** and {**4** +**5**}. The large increase in the reaction rate with **2** is a result of the intramolecularity of all key steps in the catalytic cycle. The formation of the methyl ester was confirmed by ^{1}H NMR spectroscopy. Comparison with authentic samples of 2-naphthaldehyde and methyl 2-naphthoate showed that no by-product was formed.

Unfortunately, attempts to run the reaction under aerobic conditions in order to reoxidize the flavin (as is the case for the reaction with pyruvate oxidase, Scheme 1) largely led to the oxidative destruction of the thiazolium catalyst **2**, and no more than 1.1 equivalents of methyl ester were formed with one equivalent of catalyst.[19] A higher number of catalytic cycles was observed with the more reactive 4-cyanobenzaldehyde. There-

fore, in our future preparative-scale studies with **2**, we will apply the electrochemical regeneration of the oxidized flavin under anaerobic conditions[1] in order to complete the catalytic cycle. These studies with **2**, which has been prepared in gram quantities, will also explore the interesting catalytic oxidation of aldehydes into carboxamides. In parallel, we are investigating the monooxygenase activity of the novel flavo-cyclophane **24** in the hydroxylation of phenolic compounds.[20]

Received: January 31, 1996 [Z8711IE]
German version: *Angew. Chem.* **1996**, *108*, 1434–1437

Keywords: cyclophanes · enzyme mimetics · pyruvate oxidase

[1] S.-W. Tam-Chang, L. Jimenez, F. Diederich, *Helv. Chim. Acta* **1993**, *76*, 2616–2639.
[2] a) B. Sedewitz, K. H. Schleifer, F. Götz, *J. Bacteriol.* **1984**, *160*, 273–278; b) F. Götz, B. Sedewitz in *Biochemistry and Physiology of Thiamine Diphosphate Enzymes*, (Eds.: H. Bisswanger, J. Ullrich), VCH, Weinheim, **1991**, pp. 286–293.
[3] a) Y. A. Muller, G. E. Schulz, *Science (Washington, D. C.)* **1993**, *259*, 965–967; b) Y. A. Muller, G. Schumacher, R. Rudolph, G. E. Schulz, *J. Mol. Biol.* **1994**, *237*, 315–335.
[4] a) J. Castells, H. Llitjós, M. Moreno-Mañas, *Tetrahedron Lett.* **1977**, 205–206; b) J. Castells, F. Pujol, H. Llitjós, M. Moreno-Mañas, *Tetrahedron* **1982**, *38*, 337–346; c) H. Inoue, K. Higashiura, *J. Chem. Soc. Chem. Commun.* **1980**, 549–550; d) H. Inoue, S. Tamura, *ibid.* **1985**, 141–142; e) Y. Yano, Y. Tsukagoshi, *J. Chem. Res. (S)* **1984**, 406–407.
[5] a) Y. Yano, Y. Hoshino, W. Tagaki, *Chem. Lett.* **1980**, 749–752; b) S. Shinkai, T. Yamashita, Y. Kusano, O. Manabe, *Tetrahedron Lett.* **1980**, *21*, 2543–2546; c) S. Shinkai, T. Yamashita, Y. Kusano, O. Manabe, *J. Org. Chem.* **1980**, *45*, 4947–4952; d) *J. Am. Chem. Soc.* **1982**, *104*, 563–568.
[6] D. Hilvert, R. Breslow, *Bioorg. Chem.* **1984**, *12*, 206–220.
[7] a) For a discussion of the reaction of thiazolium salts with benzaldehyde see: Y.-T. Chen, G. L. Barletta, K. Hagjoo, J. T. Cheng, F. Jordan, *J. Org. Chem.* **1994**, *59*, 7714–7722; b) R. Breslow, *J. Am. Chem. Soc.* **1957**, *79*, 1762–1763; c) *ibid.* **1958**, *80*, 3719–3726.
[8] This redox reaction has been investigated in detail on a model system: C. C. Chiu, K. Pan, F. Jordan, *J. Am. Chem. Soc.* **1995**, *117*, 7027–7028.
[9] a) F. Diederich, *Cyclophanes*, The Royal Society of Chemistry, Cambridge, **1991**; b) F. Diederich, K. Dick, D. Griebel, *Chem. Ber.* **1985**, *118*, 3588–3619; c) D. R. Carcanague, F. Diederich, *Angew. Chem.* **1990**, *102*, 836–838; *Angew. Chem. Int. Ed. Engl.* **1990**, *29*, 769–771.
[10] All new compounds described were fully characterized by ^1H and ^{13}C NMR, FT-IR, UV/VIS, and fluorescence spectroscopy, mass spectrometry (FAB$^+$ or EI), and elemental analysis or high-resolution mass spectrometry.
[11] D. R. Carcanague, Ph.D. Thesis, University of California, Los Angeles, **1991**.
[12] B. Amit, E. Hazum, M. Fridkin, A. Patchornik, *Int. J. Pept. Protein Res.* **1977**, *9*, 91–96.
[13] a) N. Miyaura, T. Yanagi, A. Suzuki, *Synth. Commun.* **1981**, *11*, 513–519; b) N. Miyaura, A. Suzuki, *Chem. Rev.* **1995**, *95*, 2457–2483.
[14] a) F. Yoneda, Y. Sakuma, M. Ichiba, K. Shinomura, *J. Am. Chem. Soc.* **1976**, *98*, 830–835; b) F. Yoneda, Y. Sakuma, K. Shinomura, *J. Chem. Soc. Perkin Trans 1* **1978**, 348–351; c) F. Yoneda, K. Shinozuka, K. Hiromatsu, R. Matsushita, Y. Sakuma, M. Hamana, *Chem. Pharm. Bull.* **1980**, *28*, 3576–3583.
[15] Experiments were run in triplicate in a 0.2 cm UV cuvette at $T = 300$ K and $[Et_3N] = 50$ mM. Eadie–Hofstee plots (v vs. v/[2-naphthaldehyde]) and nonlinear least-squares curve-fitting of the saturation kinetics data gave k_{cat} and K_M values identical to those determined in the Lineweaver–Burk plot. The wavelength λ for the monitoring of the disappearance of the visible flavin absorption was chosen in such a manner that the initial absorbance was $A_0 = 1.0$: **[2]** = 0.5 mM, $\lambda = 455.0$ nm; **[3]** = 2 mM, $\lambda = 505.2$ nm; **[4]** = 10 mM, and **[5]** = 2 mM, $\lambda = 510.4$ nm. In the reaction with {**4** + **5**}, k_2 was found to be zero order in **[5]**. The reaction velocity for the catalyst system {**1** + **26**} had been measured under similar conditions at $T = 303$ K; L. S. Jimenez, Ph.D. Thesis, University of California, Los Angeles, **1989** [1].
[16] A. Fersht, *Enzyme Structure and Mechanism*, 2nd ed., Freeman, New York, **1985**.
[17] H. Dugas, *Bioorganic Chemistry*, 3rd ed., Springer, New York, **1995**, and references therein.
[18] T. C. Bruice, N. G. Kundu, *J. Am. Chem. Soc.* **1966**, *88*, 4097–4098.
[19] Reactions were run for 1 h at room temperature and $[Et_3N] = 50$ mM, [aldehyde] = 50 mM, and **[2]** = 5 mM.
[20] A widely studied enzyme performing this reaction is the FAD-dependent monooxygenase 4-hydroxybenzoate hydroxylase, see B. Entsch, W. J. H. van Berkel, *FASEB J.* **1995**, *9*, 476–483.

Determination of the Enantiomeric Ratio of Unprotected Amino Acids by NMR Spectroscopy with C_2-Chiral Palladium Compounds

Bernd Staubach and Joachim Buddrus*

α-Amino acids are important compounds in chemistry and biochemistry. Current syntheses focus on compounds with *S*- or *R*-configuration and with additional substituents in α- or other positions.[1–3] In most cases, for the determination of the enantiomeric ratio the chiral amino acid is chemically modified and subjected to NMR spectroscopy or chromatography. NMR analysis[4] is carried out by reacting the amino acid with chiral carboxylic acid chlorides under Schotten–Baumann conditions[5] or with chiral phosphonates;[6] in each case a workup procedure of the diastereomeric mixture is necessary prior to NMR analysis. NMR analysis is also feasible with water-soluble chiral lanthanoid shift reagents, however, line broadening due to paramagnetic relaxation is often observed.[7] For gas chromatographic analysis the amino acid is converted in two steps to its corresponding N-acyl ester and investigated on a chiral stationary phase.[8,9] Liquid chromatographic analysis is carried out with diastereomeric derivatives (from chiral isothiocyanate[10]) under normal phase conditions on an achiral stationary phase, or with free amino acids under reversed-phase conditions in the presence of chiral auxiliaries either in the mobile[11] or in the stationary phase;[12] analysis with free amino acids by liquid chromatography may suffer from problems concerning UV detection.[11b] Analysis by capillary electrophoresis is accomplished after derivatization with *o*-phthaldialdehyde/cysteine.[13] Here we report on a NMR spectroscopic method that permits determination of the enantiomeric ratio of the unprotected amino acid by using chiral palladium compounds.[14]

$[Pd(H_2NCH_2CH_2NH_2)(H_2O)_2(NO_3)_2]$ (**1a**) is known to react with α-amino acids **2** in water to yield the square-planar bicyclic compounds **3a**.[15] Starting from optically active C_2-chiral 1,2-diamines, we prepared aqueous solutions of the chiral palladium compounds **1b–e** and subsequently treated them with amino acids to give the diastereomeric palladium complexes **3b–e** (*cis*/*trans* isomers). The NMR analysis of the diastereomeric complexes yielded the enantiomeric ratio of the amino acid directly.

The equilibrium (a) lies predominantly but not completely to the right, and is slow on the NMR time scale, as indicated by NMR signals of both the free and the complexed amino acid. However, complexation is completed by adding NaOD (ca. 0.75 equiv). The addition of larger amounts was avoided to

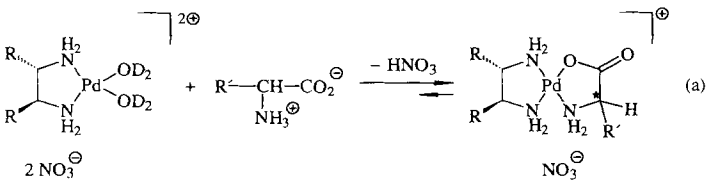

(a)

1	R
a	H
b	CH_3
c	C_6H_5
d	CH_2CH_2-
e	CD_2OCH_3

2 **3a–e**

[*] Prof. Dr. J. Buddrus, Dipl.-Chem. B. Staubach
Institut für Spektrochemie und Angewandte Spektroskopie an der Universität
Postfach 101352, D-44013 Dortmund (Germany)
Fax: Int. code + (231)1392-120

prevent dimerization of **1**[16] or ring opening of **3**[17] in alkaline solution. The NMR signals of the two diastereomers are separated both in the ^1H and ^{13}C NMR spectra. The amino acid residue yields two sets of NMR signals, whereas the diamine residue leads to four sets of signals (two pairs of diastereomeric atoms). Figure 1a and 1b show the ^{13}C and ^1H NMR spectrum of **3d**, which is obtained from DL-alanine and **1d**. To test the ability of the chiral palladium compounds **1** as suitable auxiliaries, alanine with different *R*/*S* ratios was prepared by weighing the pure enantiomers and examining the products of the reaction with **1d**. NMR spectroscopic analysis gives the same ratio within the experimental error (±1%; Fig. 1c). Evidently, kinetic resolution (if any) is below the NMR detection limit.

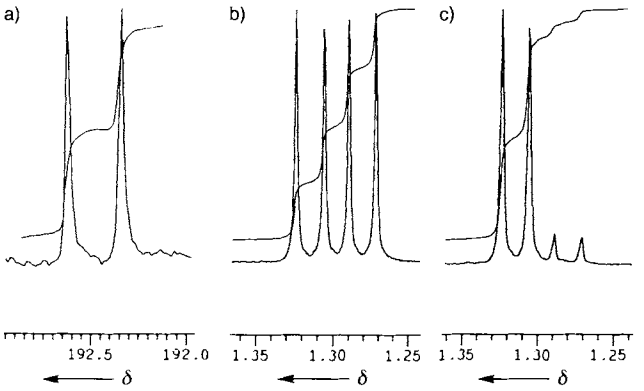

Fig. 1. NMR spectra of **3d** (R′ = CH_3) in D_2O; a) ^{13}C NMR spectrum (100 MHz, carbonyl region); b) and c) ^1H NMR spectrum (400 MHz, methyl region) from DL-alanine and L-alanine with 80% *ee*, respectively.

To investigate the influence of the substituent R in **3b–e** on the magnitude of the NMR signal separation, several optically active 1,2-diamines were tested:[18] (2*S*,3*S*)-2,3-diaminobutane, (1*R*,2*R*)-1,2-diphenylethylenediamine, (1*R*,2*R*)-1,2-diaminocyclohexane, (2*R*,3*R*)-2,3-diamino-1,1,4,4-tetradeuterio-1,4-dimethoxybutane, and in addition to these C_2-chiral diamines (*R*)-1,2-propylenediamine. The results obtained with DL-alanine as analyte are presented in Table 1. The largest signal separation

Table 1. ^1H NMR signal separation of the diastereomeric mixture of type **3**, obtained from the auxiliaries **1b–f** and DL-alanine.

Auxiliary	**1c**	**1d**	**1b**	**1e**	**1f** [b]
$\Delta\delta$ [Hz][a]	22.4	14.0	10.8	8.2	7.0

[a] Separation of the CH_3 signals in the alanine residue at 400 MHz. [b] Obtained from (*R*)-1,2-diaminopropane [19].

was observed with **1c** (R = phenyl), which can be explained by the magnetic anisotropy of the benzene ring. Unfortunately, compound **1c** is only sparingly soluble in D_2O, necessating longer NMR measuring time. Most experiments were performed with the auxiliary **1b**, because this compound is sufficiently water-soluble and gives simple ^1H NMR spectra. Several natural α-amino acids, three artificial α-amino acids (one of them alkylated in α-position), and one β-amino acid, all of them unprotected, were investigated; selected ^1H and ^{13}C NMR signal separations are given in Scheme 1.

In summary, the enantiomeric ratio of a chiral α- or β-amino acid can be easily determined: The free amino acid is simply added to an aqueous solution of one of the optically active palladium compounds **1b–e**, and the diastereomeric mixture is

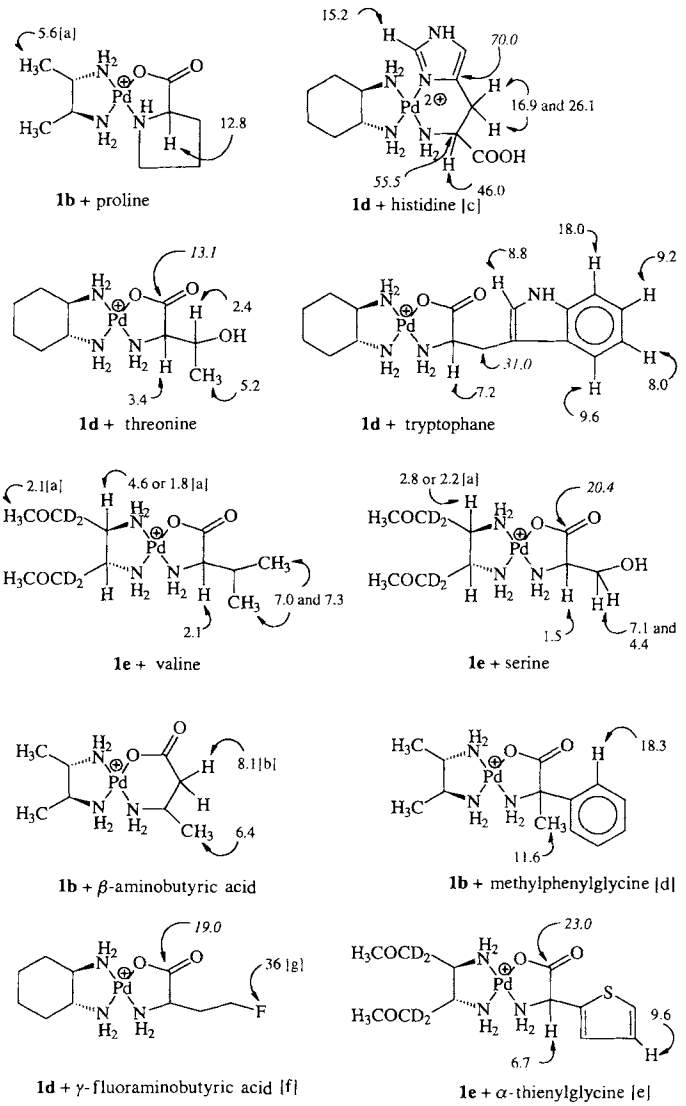

Scheme 1. Diastereomeric ^1H (400 MHz) and ^{13}C (100 MHz) signal separations (in Hz) of some palladium/DL-amino acid complexes (^{13}C NMR signal separations in italics). a) Separation arbitrarily assigned to one of the two constitutopic groups; b) separation arbitrariliy assigned to one of the diastereomeric protons; c) structure proposed according to ref. [20]; d)–f) compounds kindly provided by Prof. M. Schneider, Prof. H. J. Altenbach, Wuppertal, and Prof. G. Haufe, Münster, respectively; g) ^{19}F NMR at 360 MHz.

directly analyzed by ^1H or ^{13}C NMR spectroscopy. In contrast to line widths obtained with paramagnetic lanthanoid shift reagents, the line width of all compounds of type **3** is less than 1 Hz. We are currently preparing further auxiliaries of type **1** with a view to increasing the magnitude of the separations of the NMR signals. Even larger separation of the NMR signals are obtained with the C_2-chiral compound **1a** (NH_2 replaced by (*R*)-$NHCH(CH_3)C_6H_5$): 98 Hz (400 MHz) for the protons of the methyl group in DL-alanine.

Experimental Procedure

The chiral diamines [18] were treated with $[K_2PdCl_4]$ to give the corresponding $[Pd(diamine)Cl_2]$ complexes [21]. $[Pd(diamine)Cl_2]$ (0.02 mmol) and $AgNO_3$ (0.04 mmol) were suspended in D_2O (1 mL) and stirred for 30 minutes. After removal of the precipitated AgCl by centrifugation, a clear yellow solution of $[Pd(diamine)(D_2O)_2(NO_3)_2]$ (**1**), which is stable at room temperature for several months, was obtained [16]. Free amino acid **2** (0.017 mmol) and NaOD (0.015 mmol) were added and the mixture was stirred until it became clear (1 to 10 minutes). The solution was analyzed by ^1H NMR spectroscopy. For analysis by ^{13}C NMR

spectroscopy the concentrations of the reactants were chosen 15 times higher (about 0.3 M), which is the upper limit of solubility for the compounds **1b**, **1d**, and **1e**.

Received: December 15, 1995 [Z8648IE]
German version: *Angew. Chem.* **1996**, *108*, 1443–1445

Keywords: amino acids · chiral auxiliaries · NMR spectroscopy · palladium compounds

[1] a) R. M. Williams, *Synthesis of Optically Active α-Amino Acids*, Pergamon, Oxford, **1989**; b) J. Mulzer, H. J. Altenbach, M. Braun, K. Krohn, H. U. Reissig *Organic Synthesis Highlights*, VCH, Weinheim, **1991**, p. 300.
[2] J. Kamphuis, W. H. J. Boesten, B. Kaptein, H. F. M. Hermes, T. Sonke, Q. B. Broxterman, W. J. J. van den Tweel, H. E. Schoemaker in *Chirality in Industry* (Eds.: A. N. Collins, G. N. Sheldrake, J. Crosby), Wiley, **1992**, p. 187.
[3] J. W. Scott, *Top. Stereochem.* **1989**, *19*, 209.
[4] For reviews concerning NMR spectroscopic determination of enantiomeric purity of organic compounds including amino acids see: a) D. Parker, *Chem. Rev.* **1991**, *91*, 1441; b) R. Hulst, R. M. Kellogg, B. L. Feringa, *Recl. Trav. Chim. Pays-Bas* **1995**, *114*, 115.
[5] a) W. H. Kruizinga, J. Bolder, R. M. Kellogg, *J. Org. Chem.* **1988**, *53*, 1826; b) W. Breuer, I. Ugi, *J. Chem. Res. Miniprint* **1982**, 2901.
[6] a) R. Hulst, R. W. J. Zijlstra, N. Koen de Vries, B. L. Feringa, *Tetrahedron: Asymmetry* **1994**, *5*, 1701; b) R. Hulst, N. Koen de Vries, B. L. Feringa, *Angew. Chem.* **1992**, *104*, 1089; *Angew. Chem. Int. Ed. Engl.* **1992**, *31*, 1092.
[7] a) K. Kabuto, Y. Sasaki, *J. Chem. Soc. Chem. Comm.* **1984**, 316; b) R. Hulst, N. K. de Vries, B. L. Feringa, *J. Org. Chem.* **1994**, *59*, 7453; c) J. Kido, Y. Okamoto, H. G. Brittain, *J. Org. Chem.* **1991**, *56*, 1412; d) J. A. Peters, C. A. M. Vijverberg, A. P. G. Kieboom, H. van Bekkum, *Tetrahedron Lett.* **1983**, *24*, 3141.
[8] E. Gil-Av, B. Feibush, R. Charles-Sigler, *Tetrahedron Lett.* **1966**, 1009.
[9] V. Schurig, *Asymmetric Synth.* **1983**, *1*, 59.
[10] M. Lobell, M. P. Schneider, *J. Chromatogr.* **1993**, *633*, 287.
[11] a) V. Davanakov, Y. Zolototarev, A. Kurganov, *J. Liq. Chromatography* **1979**, *2*, 1191; b) W. H. Pirkle, *Asymmetric Synth.* **1983**, *1*, 87.
[12] a) T. Shinbo, T. Yamaguchi, K. Nishimura, M. Sugiura, *J. Chromatograph.* **1987**, *405*, 145; b) A. Shibukawa, T. Nakagawa in *Chiral Separations by HPLC* (Ed.: A. M. Krstulovic), Wiley, **1989**, p. 476.
[13] H. J. Issaq, K. C. Chan, *Electrophoresis* **1995**, *16*, 467.
[14] For NMR analysis of chiral aminophosphonic acids with $[K_2PdCl_4]$ see: Z. Głowacki, M. Topolski, E. Matczak-Jon, M. Hoffmann, *Magn. Res. Chem.* **1989**, *27*, 922.
[15] M. C. Lim, *J. Chem. Soc. Dalton Trans.* **1978**, 726.
[16] M. C. Lim, R. B. Martin, *J. Inorg. Nucl. Chem.* **1976**, *38*, 1911.
[17] T. G. Appleton, A. J. Bailey, D. R. Bedgood, Jr., J. R. Hall, *Inorg. Chem.* **1994**, *33*, 217.
[18] (1*R*,2*R*)-1,2-diphenylethylenediamine and (1*R*,2*R*)-1,2-diaminocyclohexane were purchased from Fluka, Buchs, Switzerland. (*R*)-1,2-diaminopropane was prepared according to ref. [19]. (2*S*,3*S*)-2,3-diaminobutane was prepared starting from (2*R*,3*R*)-2,3-butandiol [22]. (2*R*,3*R*)-2,3-diamino-1,1,4,4-tetradeuterio-1,4-dimethoxybutane was prepared according to the corresponding undeuterated compound [23] starting from (2*R*,3*R*)-dimethyltartrate acetonide, total yield over six steps 21%. ^{1}H NMR (as bishydrochloride in [D$_6$]DMSO): δ = 8.74 (s, 6H, 2NH$_3$), 3.67 (s, 2H, CH), 3.53 (s, 6H, 2OCH$_3$); ^{13}C{^{1}H} NMR ([D$_6$]DMSO): δ = 66.1 (quint., CD$_2$; J(C,D) = 22 Hz), 58.5 (OCH$_3$), 49.8 (CH).
[19] F. P. Dwyer, F. L. Grawan, A. Shulman, *J. Am. Chem. Soc.* **1959**, *81*, 290.
[20] N. N. Chernova, V. V. Strukov, G. B. Avetikyan, V. N. Chernonozhkin, *Russ. J. Inorg. Chem.* **1980**, *25*, 872.
[21] B. J. McCornick E. N. Jaynes, Jr., R. I. Kaplan, *Inorg. Synth.* **1972**, *13*, 216.
[22] S. Y. M. Chooi, P.-H. Leung, S.-C. Ng, G. H. Quek, K. Y. Sim, *Tetrahedron: Asymmetry* **1991**, *2*, 981.
[23] D. Seebach, H. O. Kalinowski, B. Bastani, G. Crass, H. Daum, H. Dörr, N. P. DuPreez, V. Ehrig, W. Langer, C. Nüssler, H.-A. Oei, M. Schmidt, *Helv. Chim. Acta* **1977**, *60*, 301.

Chiral Catalytic Membranes**

Ivo F. J. Vankelecom,* Diedrik Tas, Rudy F. Parton, Valérie Van de Vyver, and Pierre A. Jacobs

The easy separation of a solid catalyst from the reaction mixture is one of the main advantages offered by heterogeneous catalysts and an essential prerequisite for their regeneration. Since the cost of most chiral homogeneous catalysts is very high, their heterogenization is highly desirable. Chiral complexes are the most important class of homogeneous enantioselective catalysts.[1] Typical examples are the Ru-BINAP complex [2,2′-bis(diphenylphosphanyl-1,1′-binaphtyl]chloro(*p*-cymene)-ruthenium[2] (**1**) and the Jacobsen catalyst *N*,*N*′-bis(3,5-di-*tert*-butylsalicylidene)chloro-1,2-cyclohexanediaminemanganese[3] (**2**), which catalyze hydrogenation and epoxidation reactions, respectively. For the Jacobsen catalyst (**2**), no successful hetero-

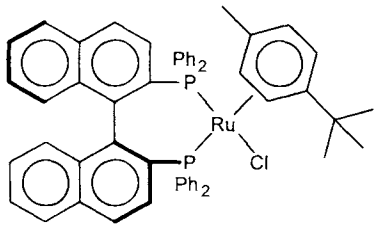

1

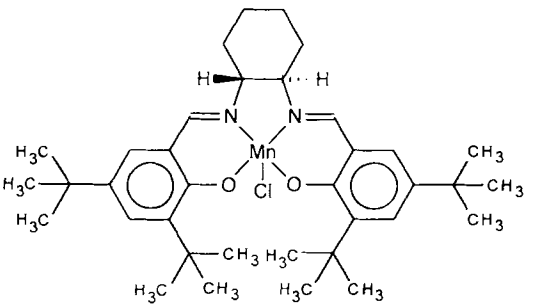

2

genization procedure has been published, and regeneration does not seem possible. In only one case was a homogeneous chromium-containing Jacobsen catalyst successfully recycled 5 times.[4] However, this was in the enantioselective ring opening of epoxides, a reaction that involves no oxidants and thus avoids oxidative destruction of the complex, a major deactivation route for salen complexes. In the case of BINAP-based catalysts, only a triphasic system consisting of a solid support, the sulfonated form of the complex dissolved in an ethyleneglycol phase, and an immiscible phase containing the substrate has been reported.[5]

Here we present the preparation, catalytic characterization, and regeneration of the heterogeneous chiral catalysts by means of a new, versatile, and generally applicable method for complex immobilization. The above-mentioned BINAP complex **1** and

[*] Dr. I. F. J. Vankelecom, D. Tas, Dr. R. F. Parton, V. Van de Vyver, Prof. P. A. Jacobs
Centrum voor Oppervlaktechemie en Katalyse
Katholieke Universiteit Leuven
Kardinaal Mercierlaan 92, B-3001 Leuven (Belgium)
Fax: Int. code +(16)321998
e-mail: ivo.vankelecom@agr.kuleuven.ac.be

[**] This work was supported by the Belgian Federal Government (IUAP-PAI grant on Supramolecular Catalysis). I. F. J. V. acknowledges a post-doctoral fellowship from the Katholieke Universiteit Leuven. D. T. and R. F. P. thank the Belgian National Fonds voor Wetenschappelijk Onderzoek (N. F. W. O.) for research grants.

chiral Schiff base complexes **2** were occluded in an elastomeric type polydimethylsiloxane (PDMS) membrane. In both cases, a perfectly regenerable catalytically active membrane was obtained that provided essentially the same catalytic activity, product, and enantiomeric selectivity as the homogeneous case. In contrast to earlier polymer-supported catalysts in which complexes were immobilized through electrostatic interactions,[6] covalent bonds,[7] or coordinative[8] bonds, the complex is captured here in the elastomer network merely by steric restrictions. In the epoxidations the bimolecular oxidation between active Jacobsen complexes is prevented here by the reduced diffusivity of the immobilized complexes in the membrane matrix.

The complexes **1** and **2** were occluded in a PDMS membrane (see Experimental Procedure), and the activity of the resulting catalytic membranes was tested in the hydrogenation of methyl acetylacetate (for **1**) or in the epoxidation of olefins (for **2**). The results of catalysis with free Jacobsen catalysts and those occluded in membranes are summarized in Table 1. Our experimental results for activities, product selectivities, and enantiomeric selectivities with the homogeneous catalysts agree well with published data (entries 1 and 5).[3, 9–13] No significant differences are obtained with the catalytic membranes (entries 2 and 6), apart from a reduced selectivity in entry 2. This is attributed to the formation of phenylacetaldehyde and 1-phenyl-1,2-ethanediol, probably formed at the membrane edges. The (*S*,*S*) form of the salen complex gives the same results as its (*R*,*R*) form (compare entry 8 with 9). Moreover, the catalytic membranes are regenerable by a simple washing procedure (entries 3, 4, and 7). The reaction mixture was analyzed by atomic absorption spectrometry (AAS) after evaporating the organics and subsequently redissolving the Mn complexes in water. Of a total amount of 112 ppm Mn in the original membrane, negligible concentrations of 1.2 and 0.8 ppm Mn were obtained in the solution after the epoxidation of cyclooctadiene and styrene, respectively. As the catalytic results obtained do not vary significantly with membrane thickness, it is not very probable that diffusion in the membrane is controlling the rate of the catalytic reaction (entries 6 and 10). It should be stressed that the homogeneous complex is a much more selective catalyst for epoxidation of *cis*-alkenes than for the epoxidation of *trans*-alkenes, giving very high *ee* values for the former olefins. Preliminary work seems to indicate that the same is true for the corresponding chiral catalytic membrane.

Table 1. Epoxidation of olefins with NaOCl at 4 °C with a PDMS-occluded (*S*,*S*)-salen complex **2**.

No.	Olefin	*x* [%] [a]	*s* [%] [b]	TOF [c]	*ee* [%] [d]
1	styrene [e]	78	100	0.0406	57
2	styrene	84	80	0.0438	52
3	styrene [f]	84	80	0.0438	52
4	styrene [g]	84	80	0.0438	52
5	*trans*-β-methylstyrene [e]	17	77	0.0088	20
6	*trans*-β-methylstyrene	13	80	0.0067	18
7	*trans*-β-methylstyrene [f]	13	80	0.0067	18
8	*cis,cis*-1,3-cyclooctadiene	5	64	0.0026	50
9	*cis,cis*-1,3-cyclooctadiene [h]	8	71	0.0042	50
10	*trans*-β-methylstyrene [i]	13	80	0.0065	18

[a] Conversion after 8 h. [b] Product selectivity epoxide/aldehyde. [c] Turnover frequency, based on conversions after 8 h. [d] Enantiomeric excesses were obtained with gas chromatography on a Chiraldex G-TA column (Alltech) with γ-cyclodextrin as active phase. [e] Reference experiment under homogeneous conditions. [f] After one regeneration consisting of washing with acetone and air-drying of the membrane at 60 °C. [g] After a second regeneration of the membrane. [h] With the (*R*,*R*)-salen complex. [i] Using a membrane 0.4 mm thick.

The hydrogenation of methyl acetoacetate was chosen as a test reaction in the case of the membrane-occluded Ru-BINAP complex. Until recently, the catalytic asymmetric hydrogenation of ketones suffered from low activity and/or enantioselectivity. However, Noyori and co-workers performed the enantioselective hydrogenation of β-ketoesters in an efficient manner (more than 98% *ee*) using Ru^{II}-BINAP complexes. This opens opportunities for producing functionalized alcohols in synthetically useful enantiomeric excesses.[14, 15] Regeneration of the expensive catalyst requires a complex procedure though. Therefore, a membrane occluded Ru-BINAP complex was assayed here for the hydrogenation of methyl acetoacetate. Results on the hydrogenation of methyl acetoacetate with a membrane-occluded Ru-BINAP catalyst are summarized in Table 2. Complex leaching was absent in all cases. The ruthenium content in the reaction mixture was below the AAS detection limit (0.16 ppm), indicating less than 0.2% leaching. In agreement with earlier reports, very low activity and enantiomeric selectivity results when the solvent is water (entry 1).[5] With ethyleneglycol, polyethyleneglycol, or glycerol as solvent, the activity and enantioselectivity can be improved (entries 2–4). Conversions could be increased further at higher temperatures (entry 5) with only a slight loss in *ee* (still without leaching). After regeneration the catalytic activity of the chiral membrane was almost unchanged (entry 6).

Table 2. Results of the hydrogenation of methyl acetoacetate with a PDMS-occluded Ru-(*S*)-BINAP catalyst (**1**) in different solvents at 60 or 80 °C.

Entry	Solvent	*T* [°C]	TOF [a]	ee [%]
1	water	60	0.03	22
2	ethyleneglycol	60	0.16	61
3	polyethyleneglycol	60	0.16	70
4	glycerol	60	0.09	63
5	glycerol	80	0.17	61
6	glycerol[b]	80	0.15	60

[a] Turnover frequency [min^{-1}], based on conversions after 48 hours. [b] After regeneration by air drying at 60 °C.

In conclusion, a new versatile and general way of immobilizing complexes is presented, which can be applied to a broad variety of catalysts. The method is interesting, especially for chiral complexes, becauses the chirality of the catalyst is kept intact by occlusion in a dense polymer in the absence of any supplementary chemical bonding. The chiral catalytic membranes remain heterogeneous under a wide range of conditions and show good to excellent activity and enantioselectivity in hydrogenation as well as in partial oxidation reactions. It is clear that the present two-phase system is more generally applicable and versatile than any three-phase system.[5] Further improvement of activity by systematically changing the membrane thickness, its degree of cross-linking, and the nature of functional groups is within the scope of our future research.

Experimental Procedure

Immobilization of the chiral complexes **1** and **2** by occlusion in a PDMS membrane: A 20 vol% solution in chloroform of a 10/1 weight ratio of prepolymer (RTV-615A, linear polydimethylsiloxane chains with terminal vinyl groups) and crosslinker (RTV-615B, linear polydimethylsiloxane chains carrying several hydride groups) from General Electric was stirred in an oil bath at 70 °C for 1 hour. The chiral complex (obtained from Aldrich) was then added (0.5 wt% for **1** and 2 wt% for **2**), and the mixture was further stirred at room temperature for another 2 hours. The solvent was then allowed to evaporate. Finally, the membrane was cured under vacuum at 150 °C for 1 h. For catalyst **1**, the whole procedure took place in a nitrogen atmosphere. The average thickness of the catalyst membrane was 0.2 mm.

which corresponds to a loading of approximately 0.108 μmol cm^{-2} for **1** and of 0.629 μmol cm^{-2} for **2**. Before use, the catalytic membranes were washed with toluene.

Hydrogenation of methyl acetoacetate (MAA) (molar ratio MAA/catalyst/solvent = 5000/1/40000) with occluded complex **1** was performed in a 100 mL modified Parr autoclave equipped with a turbine-type stirring device rotated at 600 rpm. Hydrogen was admitted just below the turbine at 6 MPa at 60 °C. The membrane was fixed between the turbine and the hydrogen outlet to provide optimum gas transfer to the membrane.

Epoxidation of olefins was performed in a countercurrent membrane reactor, with separate streams of oxidant and substrate (as a 0.6 vol% solution in heptane) on each side of the catalytic membrane (diameter of approximately 15 cm). An aqueous solution of NaOCl was used as oxidant. The olefin/metal complex/oxidant molar ratio was 25/1/100.

Received: September 20, 1995
Revised: March 13, 1996 [Z8413IE]
German version: *Angew. Chem.* **1996**, *108*, 1445–1447

Keywords: catalysis · chirality · membranes

[1] A. N. Collins, G. N. Sheldrake, J. Crosby, *Chirality in Industry*, 1st ed., Wiley, Chichester, **1992**.
[2] R. Noyori, H. Takaya, *Acc. Chem. Res.* **1990**, *23*, 345; S. Akutagawa, *Appl. Catal.* **1995**, *128*, 171.
[3] E. N. Jacobsen in *Catalytic Asymmetric Synthesis*, 1st ed. (Ed.: I. Ojima), VCH, New York, **1993**, pp. 159–202.
[4] L. E. Martínez, J. L. Leighton, D. H. Carsten, E. N. Jacobsen, *J. Am. Chem. Soc.* **1995**, *117*, 5897–5898.
[5] K. T. Wan, M. E. Davis, *Nature* **1994**, *370*, 449.
[6] D. R. Leanord, J. R. L. Smith, *J. Chem. Soc. Perkin Trans. 2*, **1990**, 1917–1923.
[7] P. R. Cooke, J. R. L. Smith, *J. Chem. Soc. Perkin Trans. 1* **1990**, 1913–1923.
[8] P. Anzenbacher, V. Král, *J. Mol. Catal.* **1995**, *96*, 311–315.
[9] J. F. Larrow, E. N. Jacobsen, Y. Gao, Y. Hong, X. Nie, C. M. Zepp, *J. Org. Chem.* **1994**, *59*, 1939
[10] M. Palucki, P. J. Pospisil, W. Zhang, E. N. Jacobsen, *J. Am. Chem. Soc.* **1994**, *116*, 9333–9334
[11] E. N. Jacobsen, W. Zhang, A. R. Muci, J. R. Ecer, L. Deng, *J. Am. Chem. Soc.* **1991**, *113*, 7063–7064
[12] H. Alper, N. Hamel, *J. Am. Chem. Soc.* **1990**, *112*, 2803–2804
[13] T. Katsuki, *Coord. Chem. Rev.* **1995**, *140*, 185–214.
[14] R. Noyori, T. Ohkuma, M. Kitamura, H. Takaya, *J. Am. Chem. Soc.* **1987**, *109*, 5856–5858.
[15] M. Kitamura, T. Ohkuma, S. Inoue, N. Sayo, H. Kumobayashi, S. Akutagwa, T. Ohta, H. Takaya, R. Noyori, *J. Am. Chem. Soc.* **1988**, *110*, 629–631.

Corrigendum

In the communication "Bridgehead Functionalization of Non-Enolizable Ketones: the First Preparatively Useful Methods" by U. P. Spitz and P. E. Eaton (*Angew. Chemie Int. Ed. Engl.* **1994**, *33*, 2220) the structure of compound **11** is not at shown but is rather the isomeric bicyclo[3.3.0]octane-1-carboxylic acid. We are grateful to Prof. Kiyomi Kakiuchi for this information. At present it is not known when the Favorskii contraction that connects the two ring systems occurs (cf. A. C. Cope, E. S. Graham, *J. Am. Chem. Soc.* **1951**, *73*, 4702–4706).

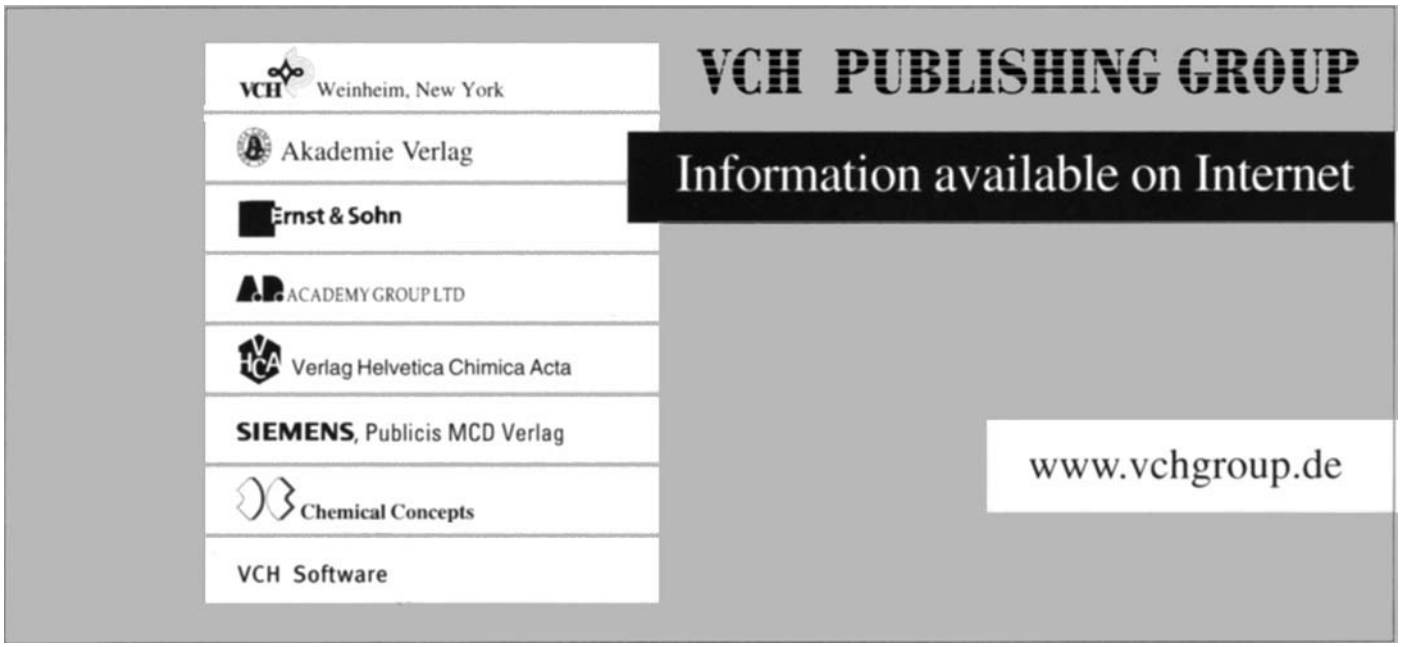

 © VCH Verlagsgesellschaft mbH, D-69451 Weinheim, 1996 0570-0833/96/3512-1348 $ 15.00+.25/0

The Shape of Things to Come

Molecular Modeling of Inorganic Compounds. By *P. Comba* and *T. W. Hambley*. VCH Verlagsgesellschaft, Weinheim, 1995. 197 pp., hardcover DM 188.00.—ISBN 3-527-29076-1

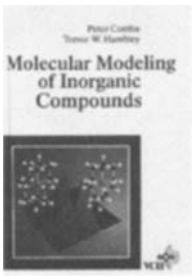

If the maturity of a subject can be judged by the number of textbooks describing it, then this contribution by Comba and Hambley certainly marks a most distinguished start for inorganic molecular modeling. It is a nicely produced, extensive, and readable account of empirically based computational approaches to the structure and energetics of inorganic species although, by their own definition, the title should have been "Molecular Mechanics for Inorganic Compounds", since there is no coverage of electronic structure methods whether semi-empirical or ab-initio.

The text is essentially divided into three sections. After a general introduction, Part I (Chapters 1–5) deals with the theoretical/mathematical basis of molecular mechanics (MM), Part II (Chapters 6–14) with various applications, and Part III (Chapters 15–17) with a series of practical tips and guidelines for doing calculations and interpreting results. References are collated independently for each part and are comprehensive, although the layout leads to repetition and Refs. 288 and 289 from Part II are missing.

The material in Part I is reasonably straightforward but is nicely presented, well organized and absolutely necessary for a text which assumes no prior knowledge of the subject. Probably the most salient point which emerges in Part I (and is consistently repeated throughout) is that individual force field (FF) parameters need bear no relationship to their spectroscopically determined counterparts. The FF parameters need to be taken as a whole and judged on their ability to reproduce global quantities such as molecular structure. The individual 'ideal' bond lengths, 'ideal' angles, force constants, etc. are not physically meaningful in themselves.

The real meat of the text is contained in Part II where an astonishing diversity of applications is sampled, ranging from computing structures for molecular visualization, through to estimating enantioselectivities; from racemate separations and stereoselective synthesis to metal ion selectivity; from combining MM calculations with spectroscopic measurements to electron transfer reactions; from the Jahn–Teller effect to bioinorganic chemistry, organometallics, and s-, p-, and f-block systems.

The applications naturally focus on the authors' own contributions, mainly in transition metal chemistry, but this still gives a remarkably wide and varied coverage—a testimony to their pioneering role in this area. Together with selected examples from organometallic, main group and f-block chemistry, the reader can certainly get a feel for the kinds of systems and properties which can be modeled.

In many ways most of Part III becomes almost self-evident from reading Parts I and II, but the authors take the time to discuss some of the practical pitfalls encountered when attempting to apply MM to inorganic molecules, especially transition metal systems, and while not being an out-and-out plug for their program system MOMEC, one assumes it would be a good vehicle for putting their philosophy into practice.

The ultimate message is clear and definitely upbeat. MM can work even within the richness and diversity of inorganic chemistry provided you recognize its interpolative nature and work within this constraint. This may be restrictive and may also require the user to develop a force field if none already exists for the systems of interest. While this may not always be for the faint-hearted, the authors make a compelling justification for the success of MM and it is encouraging to see just what can be achieved.

Overall, this book will appeal both to the active research scientist and to the intellectually curious and is required reading for all those with an interest in theoretical approaches to inorganic systems.

Robert J. Deeth
Inorganic Computational Chemistry Group
Department of Chemistry
University of Warwick
Coventry (UK)

On Being a Scientist: Responsible Conduct in Research. *Committee on Science, Engineering, and Public Policy; National Academy of Sciences; National Academy of Engineering; Institute of Medicine.* National Academy Press, Washington, D.C., 1995. VIII, 27 pp., paperback $ 5.00 (single copy); $ 4.00 each (2–9 copies); $ 2.50 each (10 or more copies) plus $ 4.00 for shipping and handling.—ISBN 0-309-05196-7

According to Frank Press, past president of the U.S. National Academy of Sciences: "Traditionally, young scientists have learned about the methods and values of scientific research from personal contact with more experienced scientists, and such interactions remain the best way for researchers to absorb what is still a largely tacit code of professional conduct". Recently, however, the increasing size of research teams and the accelerating pace of research have rendered such informal transmission of values insufficient.

Furthermore, the familiar "mad scientist" image is a false stereotype fostered and encouraged by films, television, literature, and the sensation-seeking mass media. From the unrealistically optimistic view of science and scientists as purveyors of unlimited "better things for better living" (the motto of E. I. du Pont de Nemours and Company), a backlash against science has come to pass with a

This section contains book reviews and a list of new books received by the editor. Book reviews are written by invitation from the editor. Suggestions for books to be reviewed and for book reviewers are welcome. Publishers should send brochures or (better) books to Dr. Illenora Beckmann, Redaktion Angewandte Chemie, Postfach 101161, D-69451 Weinheim, Germany. The editor reserves the right of selecting which books will be reviewed. Uninvited books not chosen for review will not be returned.

vengeance, as scientists are blamed for technological disasters such as Three Mile Island, Bhopal, Chernobyl, and current environmental problems such as pollution, the greenhouse effect, acid rain, the erosion of the ozone layer by CFCs, oil spills, and the proliferation of pesticides and nuclear weapons and nuclear wastes. In addition to all the above negative views, recent allegations of fraud in scientific disputes at the highest levels have provoked a questioning of the ethics of scientists and technologists, as what the public regards as their presumptuous curiosity and search for scientific truth lead to disaster, when scientists allegedly fail to foresee and take responsibility for the results of their research and development.

To deal with these problems, in 1989 the U.S. National Academy of Sciences published a short but important booklet, *On Being a Scientist*, prepared by the academy's Committee on the Conduct of Science. Written primarily for beginning graduate and undergraduate research students and printed in a run of more than 200000 copies, the largest ever commissioned by the academy, it sought "to describe some of the basic features of a life in contemporary research and some of the personal and professional issues that researchers will encounter in their work".

In order to incorporate the important developments in science ethics during the past half dozen years, such as new policies and procedures established by research institutions and government agencies for dealing with unethical behavior, a new, updated version of the original booklet has been prepared. For example, it includes new material on guidelines for research conduct and related matters taken from *Responsible Science: Ensuring the Integrity of the Research Process* (National Academy Press, Washington, D.C., Vol. 1, **1992**, Vol. 2, **1993**), a thorough analysis of scientific misconduct prepared by the Panel on Scientific Responsibility and the Conduct of Research under the Committee on Science, Engineering, and Public Policy of the National Academy of Sciences, National Academy of Engineering, and Institute of Medicine. It reflects suggestions from readers of the first booklet, instructors who used it in classes and seminars, and graduate students and professors who commented on drafts of the revision.

This booklet of practical advice answers questions that are fundamental, but usually neglected in courses, such as: how should anomalous data be treated? how much confidence must a researcher have in the results of a particular experiment before publishing a paper? how much of a contribution should a researcher or faculty adviser make before being listed as coauthor? how can scientists avoid self-delusion in making observations? how should errors in papers be corrected? what are the borderlines between honest error, negligent error, and misconduct? what should a researcher do when he or she suspects a colleague of scientific misconduct?

Among the topics discussed are scientific method, treatment of data, the relation between hypotheses and observations, peer review, recognition and priority in discovery, replication and the openness of communication, scientific progress, the social foundations of science, experimental techniques, values in science, publication and openness, allocation of credit, authorship practices, error and negligence, misconduct, responding to violations of ethical standards, the scientist in society, and patent procedures. To be sure, these topics are dealt with in greater detail in specialized monographs, such as those listed in the booklet's three-page annotated bibliography, but rarely are they found in a general pamphlet short enough to be read from cover to cover in an hour or two. Science is depicted throughout as a human endeavor with all its virtues and defects; historical examples abound—from Galileo to scientists who release their results directly to the public through a press conference (cold fusion is discussed, although Pons and Fleischmann are not mentioned by name).

A very useful, provocative, and effective means of illustrating research ethics that was lacking in the first version is the inclusion of nine hypothetical scenarios, ranging in length from one to three paragraphs. These deal with conflicts arising when the black-and-white, clear-cut areas of science meet the gray, more ambiguous areas of human values and biases. Each scenario is followed by three questions on how to deal with the problems and issues portrayed, viz., selection of data, conflict of interest, industrial sponsorship of academic research, sharing of research materials, allocation of credit, publication practices, fabrication in grant applications, plagiarism, and informing on a colleague ("whistle-blowing"). A three-page appendix at the end of the booklet offers guidance in thinking about, discussing, or debating the scenarios, but the scenarios remain open-ended, and no definitive answers or specific ways of dealing with the situations are given. This stance is in accordance with the authors' belief that "research ethics is not a complete and finalized body of knowledge. These issues are still being discussed, explored, and debated, and all researchers have a responsibility to move the discussion forward".

This attractive and well-planned booklet deals with fields of science from astronomy to zoology and abounds with provocative case studies such as the discovery of pulsars, the location of spiral nebulae, eugenics, the rejection of Mendelian genetics in the USSR, and polywater. Pertinent quotations from scientific authorities such as Albert Einstein, Barbara McClintock, Peter Medawar, Alvin Weinberg, and John Ziman are included, usually in sidebars. The booklet's contents will undoubtedly be used as a basis for discussion and debate in undergraduate or graduate classes or seminars on research ethics, research methods or statistics, and the history, sociology, or philosophy of science as well as in meetings of scientific societies in general, or those that aim to develop ethics policies or guidelines.

Although this booklet was written largely with an American audience in mind, it deals with matters of vital concern to the global scientific community. Moreover, in addition to being a *sine qua non* for scientific novices, it provides lessons of great value to all scientists at all stages of their scientific careers. As the preface points out, "in particular, senior scientists have a special responsibility in upholding the highest standards for conduct, serving as role models for students and young scientists, designing educational programs, and responding to alleged violations of ethical norms. Senior scientists can themselves gain a new appreciation for the importance of ethical issues by discussing with their students what had previously been largely tacit knowledge". Furthermore, in view of the current prevalence of anti-scientific prejudice among citizens who are increasingly called upon to vote on issues with a considerable scientific or technological component, the general public could certainly benefit from the booklet's lucid explanation of the nature of science as process as well as product and the limitations of science and the provisional nature of its findings.

In the past, our department has presented our graduating chemistry majors with a year's subscription to a scientific periodical. This booklet should make a gift of equal or even greater value.

George B. Kauffman
Department of Chemistry
California State University
Fresno, CA (USA)

 © VCH Verlagsgesellschaft mbH, D-69451 Weinheim, 1996 0570-0833/96/3512-1350 $ 15.00+.25/0

Enzyme Catalysis in Organic Synthesis. A Comprehensive Handbook. Volumes 1 and 2. Edited by *K. Drauz* and *H. Waldmann*. VCH Verlagsgesellschaft, Weinheim, 1995. 1050 pp., hardcover DM 498.00, $ 475.00.— ISBN 3-527-28479-6

Enzyme-catalyzed reactions are now an important part of the armory of modern organic synthesis. These reactions proceed under mild conditions, with high substrate specificity and with high stereo-, regio-, and chemoselectivity. The main area of application of enzymatic reactions is in the synthesis of enantiomerically pure and polyfunctional compounds. Because of the enormous developments that have occurred in this area during the past decade, it seemed an appropriate time to bring together the current state of knowledge in the form of this substantial multiauthor work. The articles in this handbook have been written by 53 recognized international experts. They cover the literature up to the beginning of 1994, with over 4000 references, and the subject index of more than 70 pages serves as a very effective key to the contents.

The work is divided into three parts. The first, consisting of about 160 pages, contains an introduction followed by chapters on the production and isolation of enzymes, their immobilization, process engineering for enzyme-catalyzed biotransformations, and microbiological transformations using growing and resting cells. This part of the book introduces the basic principles of enzyme-catalyzed reactions, including enzyme kinetics and the standard techniques for preparing, purifying and using enzymes.

The second part (about 800 pages) begins with eight chapters that are essentially devoted to different types of enzyme-catalyzed reactions that can be used in synthesis. These are followed by four shorter chapters dealing with special applications of enzymes. The first chapter (about 200 pages) covers the hydrolysis and formation of CO bonds. This includes esterase- and lipase-catalyzed kinetic racemate separation processes based on the hydrolysis of carboxylic acids and the esterification of alcohols. Asymmetrization reactions of *meso* and prostereogenic carboxylic acid derivatives and alcohols are also treated in detail. This chapter also deals with the hydrolysis of epoxides by epoxide-hydrolases and the use of glycosidases and glycosyl-transferases for forming and breaking glycosidic bonds. The following chapter (240 pages) is concerned with the formation and hydrolysis of CN bonds including, for example, the hydrolysis of nitriles using nitrilases, and the use of nitrile-hydratase to catalyze amide formation followed by the protease-catalyzed hydrolysis of the amides. The use of proteases for the hydrolysis and formation of peptide bonds is treated in detail, and considerable space is devoted to the synthesis of amino acids and peptides using proteases. Next is a chapter of 40 pages on the formation and breaking of PO bonds. This is followed by a chapter of about 50 pages on the formation of CC bonds using aldolases, transketolases, or transaldolases, or by addition of hydrogen cyanide to aldehydes and ketones using oxynitrilases. The following chapter (about 70 pages) deals with the application of dehydrogenases to the reduction of aldehydes, ketones, carboxylic acids, C=N bonds, and C=C bonds. A chapter of over 130 pages is devoted to a survey of oxidation reactions, including hydroxylations, epoxidations, *cis*-dihydroxylations of arenes, oxidations of alcohols, Baeyer–Villiger oxidations, oxidations of sulfides, and halogenations, using mono- and dioxygenases, oxidoreductases, and peroxidases. A 40-page chapter then covers enzyme-catalyzed isomerizations such as the racemization of amino acids by racemases. Next is a chapter discussing numerous examples where enzyme-catalyzed reactions have played a valuable role in the use of protecting groups. These methods achieve selective protection of amino, thiol, carboxyl, and hydroxyl groups, mainly in polyfunctional molecules. The next chapter reviews the use of catalytic antibodies in organic synthesis. This second part ends with three shorter chapters on enzymatic analysis and biosensors, protein engineering, and enzymes derived from highly thermophilic and hyperthermophilic archaeabacteria and eubacteria. The third part contains tables giving information about commercially available enzymes and suppliers.

This handbook is an indispensable source of information about all types of enzyme-catalyzed reactions that can be used in syntheses. The many examples of the use of enzymes in organic synthesis are in themselves enough to make this two-volume work an enormously valuable resource. The wealth of information is presented in a very clear form; in particular the presentation of results in tables enables the reader to quickly find the essential data, and also provides stimulating ideas for following up. The work is intended for synthetic chemists in academic and industrial research, and for biochemists, microbiologists, and biotechnologists whose work involves biotransformations. It is very clearly set out, easy to read, and sturdily bound. It should be in every library.

Fritz Theil
Institut für Angewandte Chemie
Berlin-Adlershof (Germany)

Glycal Assembly

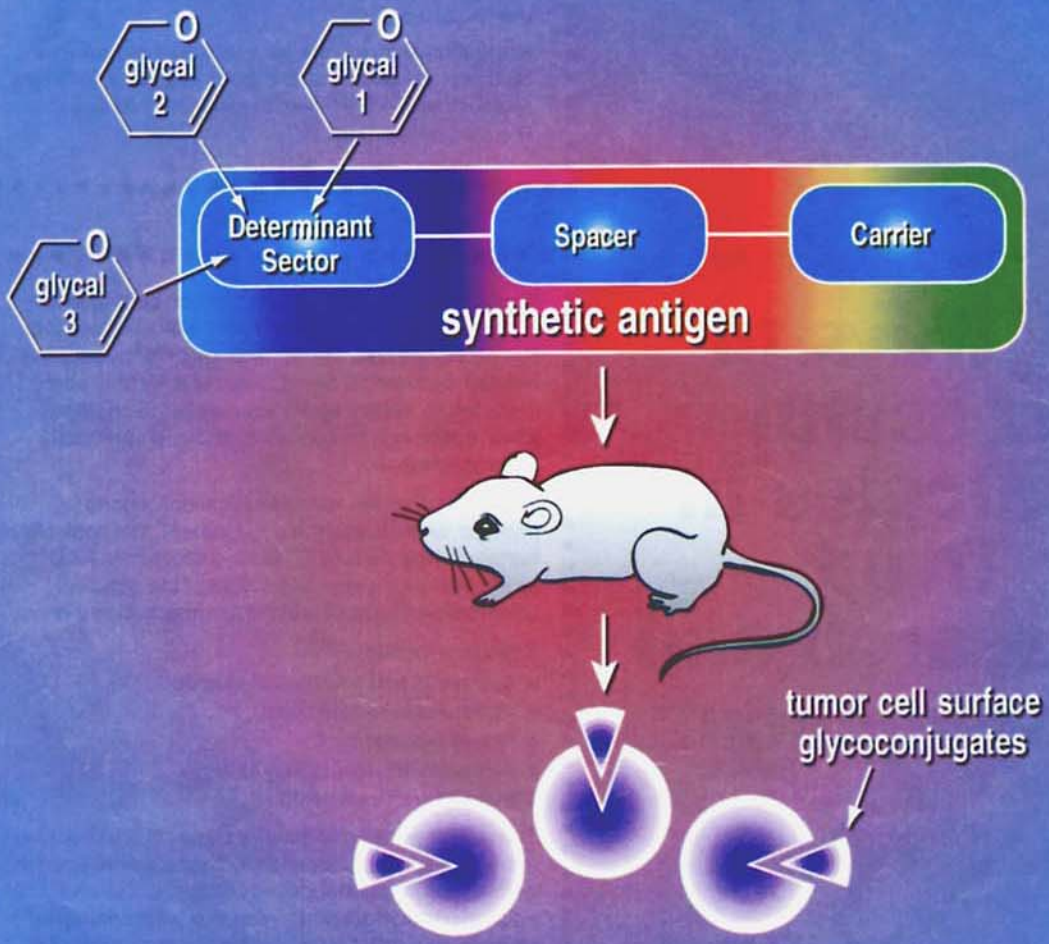

mouse antibodies bind to tumor transformed cell lines

Glycals in Organic Synthesis: The Evolution of Comprehensive Strategies for the Assembly of Oligosaccharides and Glycoconjugates of Biological Consequence

Samuel J. Danishefsky and Mark T. Bilodeau

This review provides a personal account of the explorations of a research group in oligosaccharide and glycoconjugate construction. The journey began twenty years ago with the study of Diels–Alder reactions of complex dienes. By extending this methodology to aldehydo-type heterodienophile equivalents, access to unnatural glycals was gained (LACDAC reaction). From this point a broad-ranging investigation of the use of glycals in the synthesis of oligosaccharides and other glycoconjugates was begun. Mobilization of glycals both as glycosyl donors and glycosyl acceptors led to the strategy of glycal assembly. Several new glycosylation techniques were developed to provide practical underpinning for this logic of glycal assembly. Glycal-based paradigms have been shown to be nicely adaptable to solid phase supported synthesis. Moreover, glycal assembly—both in solution and on solid phases—has been used to gain relatively concise and efficient entry to a variety of biologically interesting and potentially valuable constructs. Some of these syntheses, particularly in the field of tumor antigens, have led to novel compounds which are in the final stages of preclinical assessment. This review presents an account of the chemical reasoning at the center of the program.

Keywords: glycals · glycoconjugates · glycosylations · oligosaccharides · synthetic methods

1. Background and Settings

The synthesis of carbohydrate-based structures is emerging as a major frontier area for organic chemistry. In addition to their well-appreciated roles in supporting structural matrices, in energy storage, and as biosynthetic starting materials, carbohydrates are cast in a variety of interesting settings as glycoconjugates, for example as antibiotics,[1] antitumor agents,[2] and cardiotonic glycosides.[3] The gangliosides are being increasingly implicated as tumor antigens and cellular differentiation markers.[4] The importance of the carbohydrate domains in glycoproteins and glycolipids as elements in cell surface recognition is manifested by their role in cellular adhesion[5, 6] and as determinants in blood group typing.[7] Another incentive for focusing on carbohydrates is their usefulness as enantiomerically pure starting materials for the synthesis of various natural products and other types of target molecules.[8]

Our first encounter with carbohydrate chemistry arose from happenstance rather than through careful planning. A slight digression may be appropriate. From 1974 to 1981 we had been investigating the synthetic potential of the uncatalyzed Diels–Alder reaction of siloxydienes with electrophilic dienophiles.[9, 10] Actually the problem that triggered those studies was a proposed synthesis of vernolepin.[11] For that purpose we thought that intermediate **4** might be useful (Scheme 1). It seemed to have all of the functionality necessary to allow for a plausible route to our target (the dotted arrows highlight transformations that were eventually achieved). At the time, however, there was no known route to efficiently introduce the $\Delta^{1,2}$ conjugated double bond via a saturated 3-ketone in the *cis*-fused series of compounds.

This problem prompted the idea of using the parent version of diene **1** (R^1, $R^2 = H$) in a Diels–Alder reaction with dienophile **3** (itself the product of the Diels–Alder reaction of 1,3-butadiene with methyl propiolate). The synergism of the 1,3-substituents on **1** (R^1, $R^2 = H$) facilitated reaction with the sluggish dienophile **3**. Furthermore the adduct could be easily transformed into the desired **4**.

The matching of electronically complementary Diels–Alder components did indeed favor many otherwise difficult cycloadditions. By taking advantage of functional groups in the diene component at the points of linkage (for example in **3**, Scheme 1), we were able to realize the total synthesis of a variety of natural products, including vernolepin. Some of the other targets were also quite challenging, and their total syntheses were not without instructional value (cf. prephenic acid (Scheme 1), pentalenolactone, and griseofulvin).

[*] Prof. S. J. Danishefsky, Dr. M. T. Bilodeau
Laboratory for Bioorganic Chemistry
The Sloan-Kettering Institute for Cancer Research
1275 York Avenue, Box 106, New York, NY 10021 (USA)
Fax: Int. code +(212) 772-8691
and
Department of Chemistry, Columbia University
Havemeyer Hall, New York, NY 10027 (USA)

 © VCH Verlagsgesellschaft mbH, D-69451 Weinheim, 1996 0570-0833/96/3513-1381 $ 15.00+.25/0

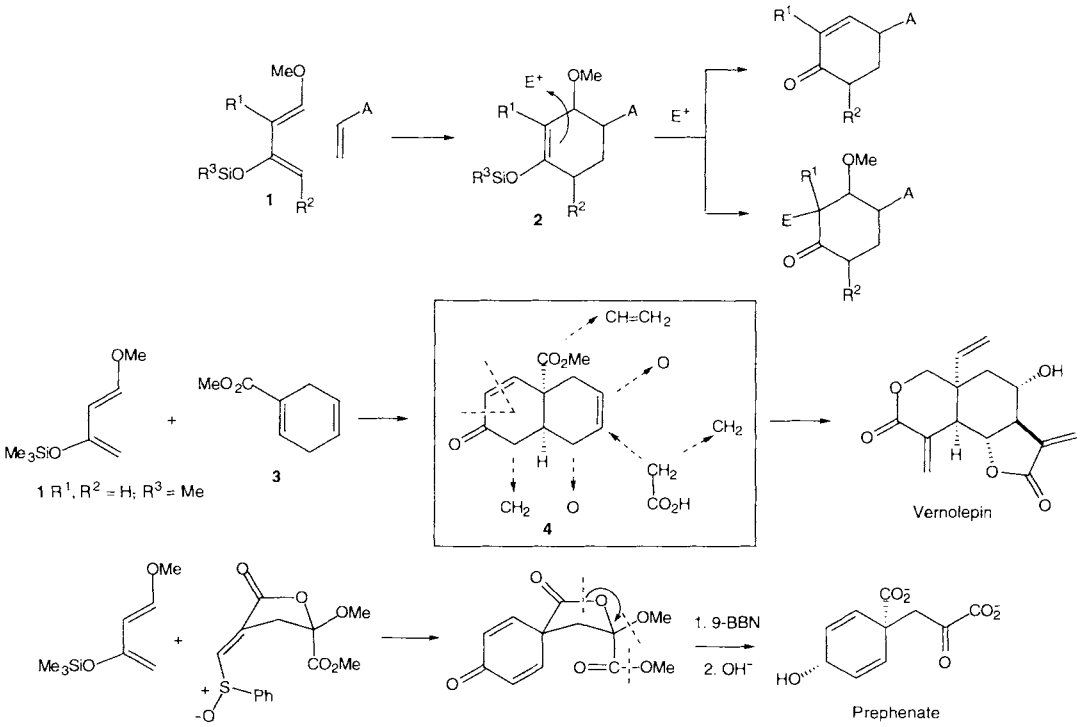

Scheme 1. Diels–Alder reactions of siloxydienes with electrophilic dienophiles (A = electron-withdrawing substituent, E^+ = electrophile, including H^+).

Perhaps the most enduring aspect of this early work in Pittsburgh was the interest it spawned in diene **1**, in the broad class of siloxydienes and, more generally, in the concept of heavily functionalized dienes in the Diels–Alder reaction. While these ideas are now taken for granted, much follow-through work was needed for them to gain wide acceptance and usage.[12]

As the use of functionalized dienes in all-carbon Diels–Alder reactions was developing in many other laboratories,[13] we cast our attentions toward a new departure. We came to wonder about the possibility of the cycloaddition of siloxydienes with aldehydes. Elsewhere we have related the early history of this reaction.[14] While it was known that aldehydes especially activated by adjacent electron-withdrawing groups (e.g. α-dicarbonyl systems or α-polyhaloaldehydes) would undergo cycloaddition with "nucleophilic" dienes,[15] analogous processes were not realizable with typical aldehydes under thermal conditions. It remained for James Kerwin, then a graduate student in our laboratory at Yale University, to discover that under appropri-

Samuel J. Danishefsky received a Bachelor of Science degree from the Yeshiva University, New York, NY (USA), and a Ph.D. from Harvard University, Cambridge, MA, under the direction of Peter Yates. He did a postdoctoral tour with Gilbert Stork as an NIH Fellow at Columbia University, New York, NY. He began his independent career at the University of Pittsburgh, Pittsburgh, PA, from 1964 to 1979. He was Professor of Chemistry at Yale University, New Haven, CT, from 1980 to 1993. At Yale he was Chairman of the Department from 1981 to 1987 and was named Sterling Professor in 1990. He is currently the Director of the Laboratory for Bioorganic Chemistry at the Sloan-Kettering Institute for Cancer Research. He returned to Columbia University as Professor of Chemistry in 1993. He is a member of the National Academy of Science and co-recipient of the 1996 Wolf Prize in Chemistry.

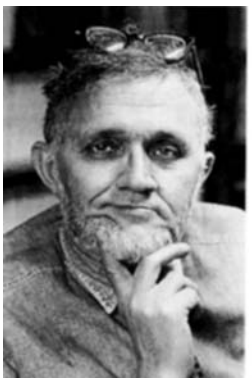

S. J. Danishefsky

M. T. Bilodeau

Mark T. Bilodeau received his B. S. degree in chemistry in 1988 from Boston College, Chestnut Hill, MA, where he worked in the laboratory of T. Ross Kelly. In 1993 he earned his Ph.D. in organic chemistry from Harvard University under the guidance of David A. Evans. After receiving his degree he moved to the Sloan-Kettering Institute for Cancer Research, where he was an NIH postdoctoral fellow with Samuel J. Danishefsky. While at the Sloan-Kettering Institute he focused on the synthesis of a human breast tumor antigen and the carbohydrate domain of asparagine-linked glycopeptides. He has since assumed a position in the Medicinal Chemistry Department of Merck & Co. in West Point, PA.

ate Lewis acid catalysis, cyclocondensation between suitable siloxydienes and aldehydes was in fact a general and reliable reaction.[16] After several years of investigation the cyclocondensation reaction emerged as a central element in a new strategy for the synthesis of polyoxygenated natural products.[17]

2. The Synthesis of Enantiomerically Enriched Artificial Glycals and Applications to Total Synthesis

The Lewis acid catalyzed diene–aldehyde cyclocondensation (LACDAC) reaction provided a rapid route to novel dihydropyrones of the type **5** (Scheme 2). It was subsequently shown, first

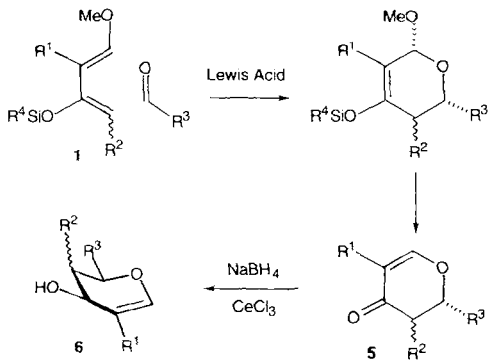

Scheme 2. Synthesis of glycals by the LACDAC reaction (β-R^2: gluco series; α-R^2: galacto series).

by Toby Sommer, that 1,2-reduction of such dihydropyrones with sodium borohydride mediated by cerium(III) chloride gave alcohols such as **6** in which the hydroxyl group is in equatorial position (Scheme 2).[18] We began to refer to such compounds as "glycals." The term had been reserved by carbohydrate chemists for naturally derived pyranose or furanose systems bearing a C1–C2 double bond. The possibility that racemic compounds such as **6**, derived by purely synthetic means, might be described as "glycals" was greeted not surprisingly with reservation by some in the community of traditional carbohydrate chemists, but to us, the connection seemed obvious.

Four pathways have subsequently been followed to produce enantiomerically enriched or enantiomerically pure dihydropyrones and glycals by means of the LACDAC reaction.[14] We review them here chronologically.

Early, but only modest success was achieved by using enantiomerically pure oxophilic lanthanide complexes as Lewis acid catalysts in the cyclocondensation reaction.[19] Lanthanides bearing chiral ligands had, of course, previously been used as chemical shift reagents. It is often overlooked but perhaps worth remembering that the experiments of Mark Bednarski, wherein [Eu(hfc)$_3$] imparted enantioselectivity in the LACDAC reaction, were among the first examples of decent enantiotopic induction in the metal-catalyzed formation of carbon–carbon bonds (hfc = 3-(heptafluoropropyl(hydroxymethylene)-D-camphorato).

In the next phase we investigated the effects of mounting an enantiomerically pure auxiliary on the diene component. Here, only painfully modest seletivities were realized. However, dramatic diastereomeric excesses were obtained by combining the use of a chiral auxiliary with an enantiomerically pure lanthanide complex.[20] After separation of the diastereomeric products, enantiomerically pure versions of dihydropyrones were available. This strategy was used in the synthesis of L-glucose (**7**)[21] and in the construction of the carbohydrate fragment of avermectin A_{1a} (**8**, Scheme 3).[22] An interesting feature here is that the effects of the catalyst and auxiliary are nonmultiplicative. Indeed, Bednarski's best results were obtained when the enantioselective tendencies of the auxiliary and catalyst components of the "*ee* enrichment package" veered in opposite directions.

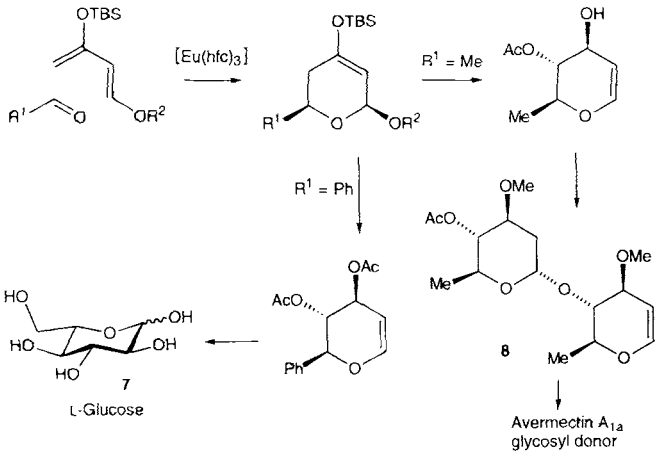

Scheme 3. Enantioselective LACDAC reactions (R^2 = L-8-phenylmenthyl).

It is well to note that H. Yamamoto and co-workers have pioneered the use of enantiomerically pure BINAP-based Lewis acid catalysts (BINAP = 1,1'-binaphthalene-2,2'-diylbis(diphenylphosphane), which confer high enantioselectivity on the LACDAC reaction.[14, 23] This chemistry, in conjunction with the stereoselective reduction of dihydropyrones by the Luche system ($NaBH_4/CeCl_3$), constitutes an excellent route for the formation of novel enantiomerically pure artificial glycals.

Unlike these methods, in which the de novo induction of chirality in the dihydropyrone was attempted, the third approach started with enantiomerically pure aldehydes. The proximal stereogenic center in these aldehyde heterodienophiles imparted face selectivity to the LACDAC reaction. In this way various complex optically pure glycals were obtained from precursors that were formed in high diastereomeric excesses. This chemistry allowed us to achieve synthetic routes to the higher order monosaccharides[24] including lincosamine,[25] *N*-acetylneuraminic acid,[26] *rac*-3-deoxy-*manno*-2-octulosonic acid (KDO),[26] hikosamine,[27] and octosyl acid A.[28] In some cases (**11** → α-methylhikosanamide and **14** → octosyl acid, Scheme 4) the pyrone substructure served as a temporary locus for establishing configurational relationships which were unveiled upon opening of the ring.

Most of our advances in systems bearing resident chirality were achieved with aldehydes in which the stereogenic centers contain electron-withdrawing groups α to the formyl function (cf. **9** + **10** → **11**; **12** + **13** → **14**, Scheme 4). However, some striking successes were realized even when the resident chirality was more remote from the site of induction. In our syntheses of tunicaminyluracil (Scheme 4)[29] and compactin (Scheme 5)[30]

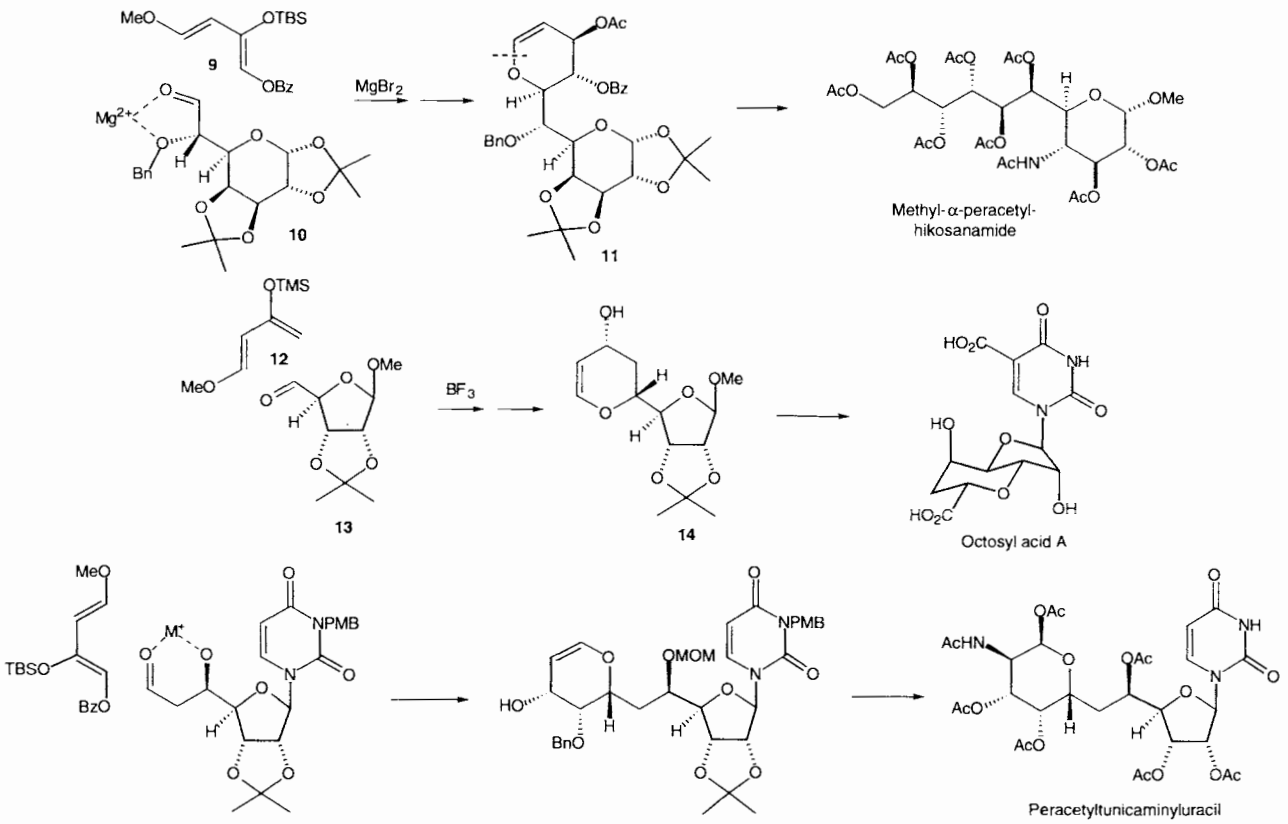

Scheme 4. Applications of the LACDAC reaction to total synthesis.

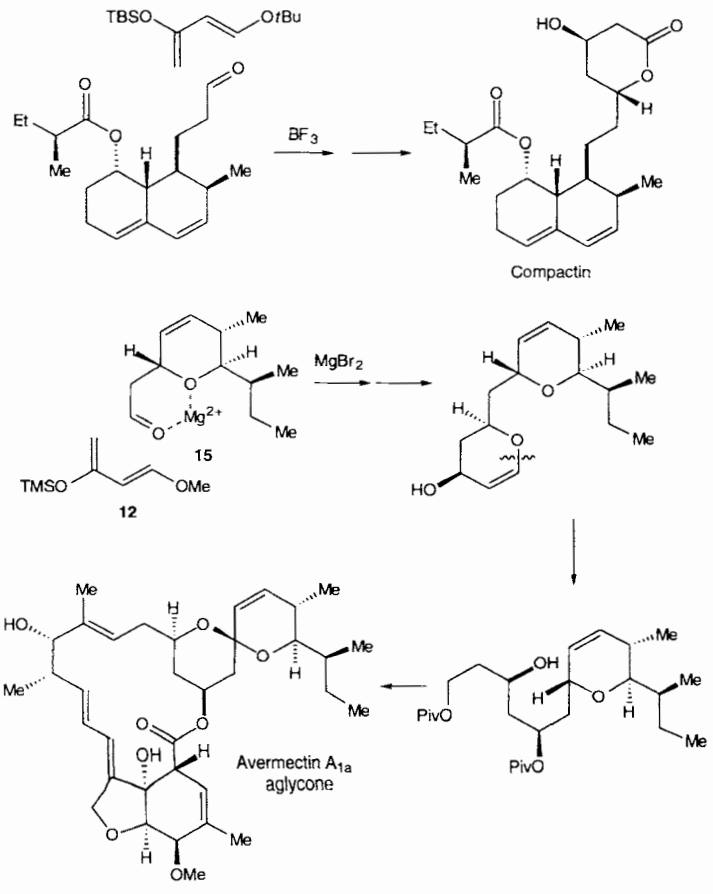

Scheme 5. Applications of the LACDAC reaction to total synthesis.

significant diastereoselectivities were attained in the absence of an α-directing function. Another important case of strong selectivity, involving resident chirality at some distance from the site of bond formation, arose during the LACDAC reaction of **12** and **15**. This was an important step en route to our total synthesis of the aglycone of avermectin A_{1a} (Scheme 5).[22] Another particularly important demonstration was realized during our synthesis of 6-deoxyerythronolide B (**16** + **17** → **18**, Scheme 6),

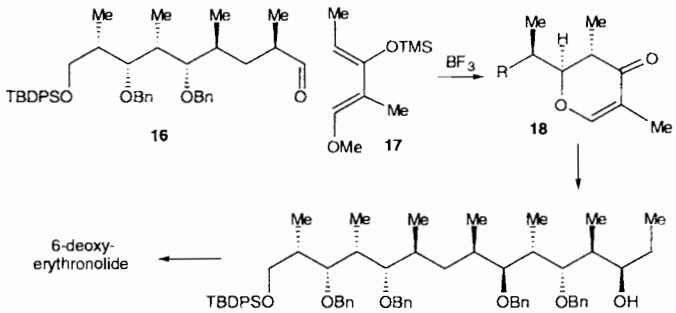

Scheme 6. Application of the LACDAC reaction to the synthesis of 6-deoxyerythronolide.

wherein the stereogenicity seems to be enhanced by stereocenters remote from the aldehyde.[31] It appears probable that new potentials for face selectivity in the LACDAC reaction still remain to be identified and tapped.

As previously mentioned, Sommer had demonstrated that reduction of dihydropyrones with the Luche system ($NaBH_4$/$CeCl_3$) is quite selective for formation of an equatorial hydroxyl

group at C3 and is not significantly complicated by 1,4-addition.[18] This chemistry paved the way for the fourth and most general route to enantiomerically pure artificial glycals.[32, 33] Thus, David Berkowitz found that racemic compounds of the type **19** could be kinetically resolved by enantioselective acetylation exploiting the Wong method (lipase PS-30 and vinyl acetate as the acylating agent, Scheme 7).[34]

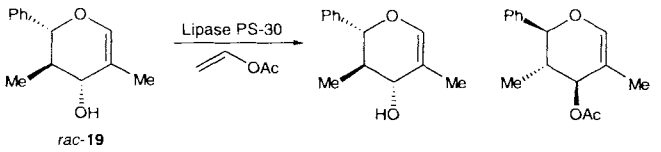

rac-**19**

Scheme 7. Enzymatic resolution of a racemic glycal.

Our enthusiasm for the LACDAC methodology notwithstanding, naturally occurring sugars are still the best source of glycals bearing the usual hexose functionality at C3, C4, and C6. In particular, glycals closely related to D-glucal, D-galactal, and D- or L-fucal are readily accessible from commercially available precursors. It is only when the required functionality of the target glycal is not reasonably accessible from carbohydrates that total synthesis by means of LACDAC chemistry can be superior to partial synthesis.

The synthesis of glycals from carbohydrate precursors bearing a axial hydroxyl group at C3 (for example D-allal and D-gulal) can be achieved by reductive elimination of hetero groups at C1 and C2.[35] However, in several important instances the starting hexoses bearing axial hydroxyl groups at C3 were themselves accessible only with extreme difficulty. A route was devised to deal with this type of situation. Our method exploits a form of the Ferrier-type displacement of glycals.[36, 37] As will be seen, the classical Ferrier rearrangement leading to pseudoglycals was valuable to our developing program (Scheme 8).

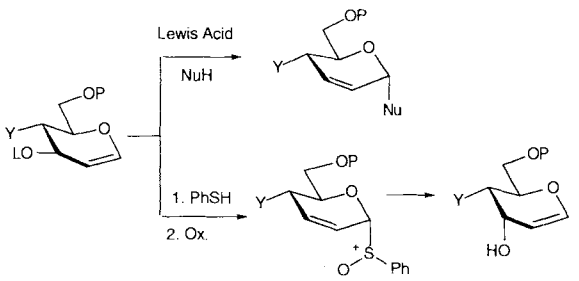

Scheme 8. Ferrier rearrangements of glycals and utilization of subsequent sulfoxide rearrangements (LO = leaving group, Y = α-OR for allals, Y = β-OR for gulals).

For the case at hand, reaction of a C3 equatorial glycal with thiophenol gives rise to an axial thiophenyl "pseudoglycal," which is converted by oxidation into a C3 axial glycal, presumably by rearrangement of its sulfoxide.[38, 39] While the scope, limitations, and mechanism of this reaction have not been fully defined, it has already found application in our total synthesis of the trisaccharide sector of esperamicin and the aryltetrasaccharide sector of calicheamicin (see Schemes 59 and 60, respectively).

As access to glycals was being significantly improved, and as our syntheses of many of the higher order monosaccharides were being concluded, we began to explore new options for using glycals as synthetic building blocks in the construction of various glyconjugates. Before turning to the main theme of this report, we will review the application of glycals to the stereoselective synthesis of C-glycosides. A key reaction developed can be regarded as a Lewis acid promoted "carbon-Ferrier" process.[40] Thus reactions of allyltrimethylsilane with activated glucal or galactal derivatives afforded C-glycosides bearing axial allyl functions (**20**, Scheme 9).

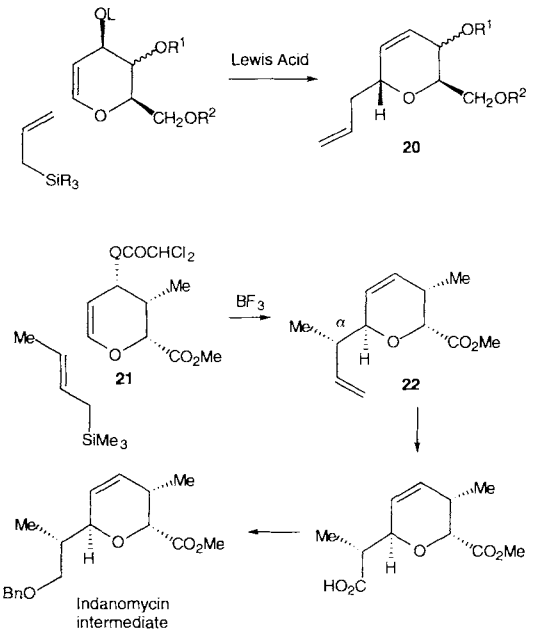

Scheme 9. Allylsilanes employed in the Ferrier rearrangement (OL = leaving group, α-OR^1: gluco series, β-OR^1: galacto series).

Subsequently, it was found that reaction of various glycals with *cis*- and *trans*-crotylsilanes affords methallylated glycosides with good stereoselectivitiy at C_α. The resulting configuration is a function of the geometry of the crotyl group. This capability was used to good effect in our syntheses of indanomycin,[41] zincophorin,[42] and avermectin A_{1a}.[22] Thus, reaction of *trans*-crotylsilane with glycals **21** (Scheme 9) and **23** (Scheme 10) gave rise to **22** and **24** as the major products, respectively. However, triphenyl(*cis*-crotyl)silane reacted with glycal **25** to give rise to **26** (Scheme 10). The latter was reduced then treated with lithium dimethylcuprate to provide **27**, from which we were able to reach the avermectin aglycone via **15**.

3. Glycals in the Synthesis of Oligosaccharides—Some Early Notions

We now turn to the use of glycals in the general construction of oligosaccharides and other glyconjugates. To facilitate discourse, we make reference to a useful terminological distinction that has evolved to describe the two components entering into a glycosylation reaction. Thus, the component that contributes

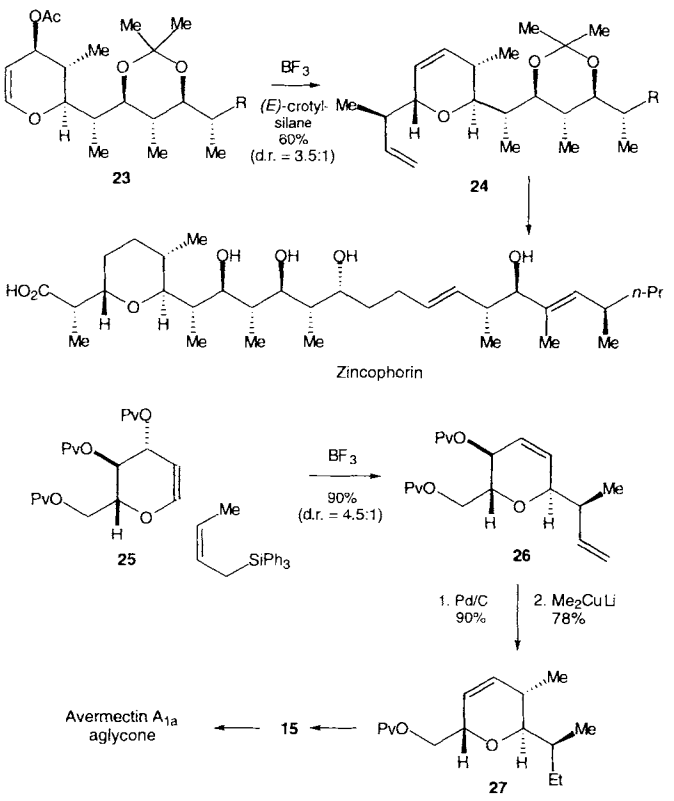

Scheme 10. The use of the allylsilane Ferrier rearrangement in total synthesis.

the anomeric carbon of the resultant glycoside is described as the glycosyl donor (Scheme 11). The donor reacts with a glycosyl acceptor to establish a glycoside. In the overwhelming majority of glycosylation reactions, the acceptor is a nucleophile that furnishes the oxygen of the resultant glycoside by replacement of a leaving group at the anomeric carbon of the electrophilic glycosyl donor. However, the novel glycosylations of Schmidt,[43] David and Lubineau,[44] Vasella,[45] and Kahne[46] attest to the need to decouple the terms "glycosyl donor" and "glycosyl acceptor" from mechanistic descriptors such as "nucleophile" and "electrophile".

It is also well to distinguish two modalities by which glycals can function as glycosyl donors (Scheme 11). In one motif the glycal is first converted, through a reaction or sequence of reactions, into an isolable or at least identifiable glycosyl donor (for

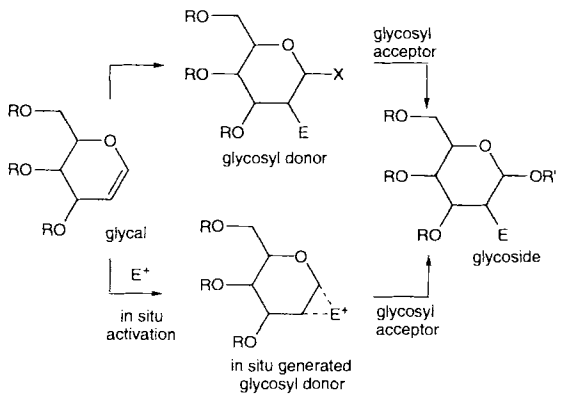

Scheme 11. Glycals as glycosyl donors.

instance, by epoxidation, azidonitration,[47] or sulfonamidoglycosylation, vide infra). In essence the glycal is a precursor to a structurally defined glycosyl donor. Alternatively, in situ electrophilic activation might mobilize the glycal to function as the donor in the form of a substoichiometric nonisolable intermediate rather than as a defined reaction component.

The possibility of utilizing glycals as glycosyl donors in disaccharide synthesis had been demonstrated in the pioneering research of Lemieux[48] and Thiem[49] by halonium-mediated coupling to suitably disposed acceptors. These particular reactions had been shown by Thiem[49] to have a high proclivity for *trans*-diaxial addition and provided a crucial route to α-linked disaccharides bearing an axial 2-iodo function on the nonreducing end. Owing to the difficulty in effecting nucleophilic displacement of the iodine in such systems,[50] the Thiem chemistry has thus far found its most useful application in the synthesis of 2-deoxyglycosides.[49, 51]

Our chemistry, directed toward assembly of glycoconjugates and oligosaccharides, came to be organized around four questions: 1) Could a glycal linkage at the terminating end of a di- or oligosaccharide serve as a useful glycosyl donor (by either of the modalities discussed above)? 2) Could glycals also function as glycosyl acceptors? Surprisingly, prior to our investigation this question had not been examined. 3) Could unnatural glycals available through LACDAC chemistry serve as stereoselective glycosyl donors and acceptors? 4) Would the glycal-based methodology be of sufficient scope to find useful application in the total synthesis of complex multifunctional targets? The translatability of advances from the relatively sheltered world of "synthetic demonstrations" to the often harsh and more demanding realities of the total synthesis of complex targets cannot be assumed as a matter of course!

If glycals could serve both as glycosyl donors and as glycosyl acceptors in a broad range of couplings, a reiterative strategy for the syntheses of complex glycoconjugates, including oligosaccharides, could be contemplated. A potentially important advantage of glycal-based glycosylations was to be the simplification of achieving differentiated hydroxyl protection and presentation. This is readily appreciated by comparison of Schemes 12 and 13.

Scheme 12 portrays the classical strategy of glycosylation[52] using fully oxygenated pyranose donors and acceptors. In the very simple case of coupling hexoses D (donor) and A (acceptor) to produce the protected DA disaccharide, several challenges must be overcome. The anomeric hydroxyl function in the eventual donor sugar must be distinguished as a leaving group from the other four hydroxyls. In the eventual acceptor, a particular free hydroxyl (one of five such groups) must be identified for glycosylation, while the anomeric area of the "acceptor" system is properly protected. If one is to proceed toward the DAA′ trisaccharide, the "*exo*" glycoside moiety of the DA disaccharide must be distinguished from its "*endo*" counterpart. With this accomplished, a leaving group (a glycosyl-donating function) is installed on the erstwhile A sugar, and this ensemble must be appended to glycosyl acceptor A′, in which one of five hydroxyls has been identified as the acceptor for the glycosylation.

We contrast this situation with the projected formation of the DAA′ trisaccharide by reiterative coupling of glycals

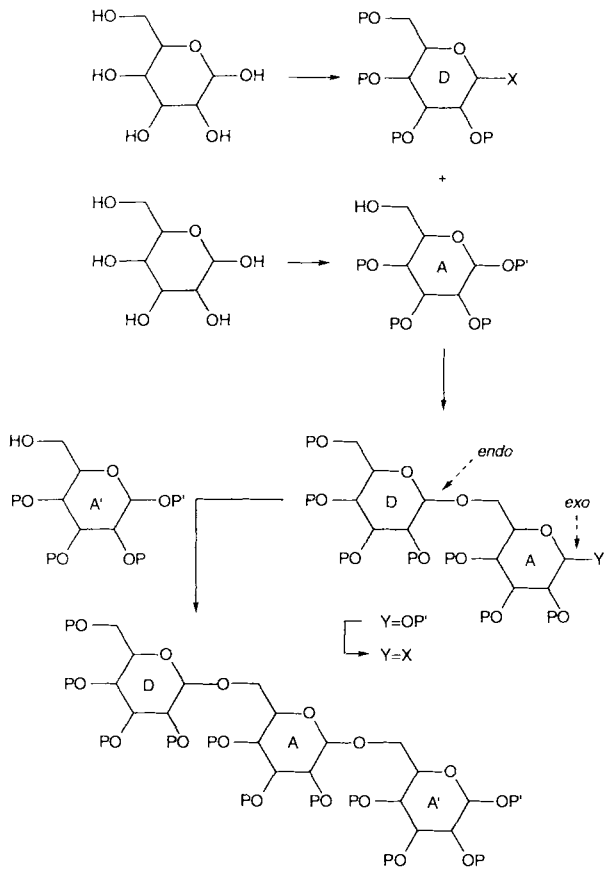

Scheme 12. Synthesis of a trisaccharide (DAA') by conventional methods. (The stereochemistry of glycosidic linkages is not implied.) A, A' = acceptor unit, D = donor unit, P = protecting group, X = leaving group.

(Scheme 13). The activatable olefinic linkage of uniformly protected glycal D functions as the donor. One of three hydroxyls of acceptor glycal A is to be presented for glycosylation to give the DA disaccharide. After coupling, the glycal linkage of DA is

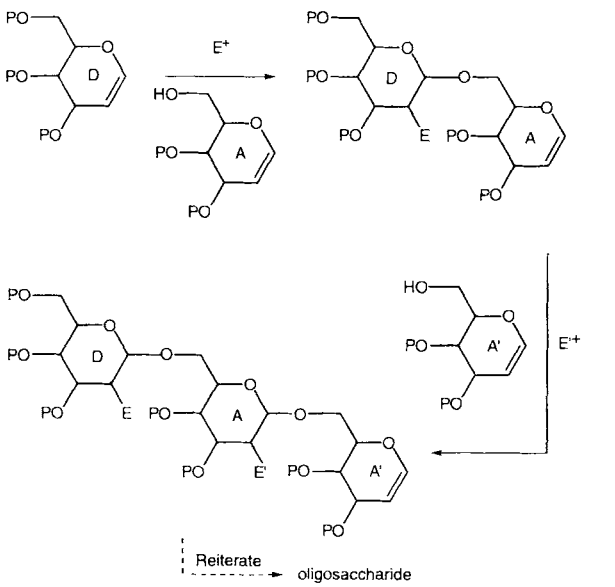

Scheme 13. Synthesis of a trisaccharide (DAA') by a glycal assembly strategy. (The stereochemistry of glycosidic linkages is not implied.) Reiteration of the glycosylation sequence leads to oligosaccharides.

activated (either in situ or in a discrete process) to produce a DA donor vis à vis a new acceptor glycal, A'. In this way, trisaccharide DAA' is obtained. It can be readied for elongation by priming the glycal in the A' sector en route to tetrasaccharide or higher oligomers.

For the reiterative method described in Scheme 13 to be viable and widely applicable, glycals must also function as glycosyl acceptors. Furthermore, for the sorts of extended applications we had begun to contemplate, it would be necessary for glycal linkages at the putative reducing end of larger oligosaccharides to also function as viable donors. For maximum applicability, it would be necessary to fashion a menu of coupling methods in which glycals serve both as donors and as acceptors. To use these concepts in the construction of unnatural glyconjugates and oligosaccharides, unnatural glycals, obtained by synthesis, must be amenable to the methodology being developed.

4. Haloglycosylation

The iodoglycosylation reaction developed by Lemieux[48] and Thiem[49] seemed to represent a particularly difficult challenge to the concurrent use of glycals as acceptors and donors. Classically, iodoglycosylation is carried out with a glycal serving as a donor. The glycal linkage is attacked by an "I^+ equivalent" reagent, for example *N*-iodosuccinimide or *sym*-collidine iodonium perchlorate. In the ordinary case, the presumed substoichiometric intermediate **28** (Scheme 14), arising from the attack of I^+ on the glycal, is attacked by coexisting non-glycal acceptor, in which the reducing end is suitably capped. The stereochemistry of glycosylation is governed by *trans*-diaxial addition and the α-linked disaccharide **29** is produced.

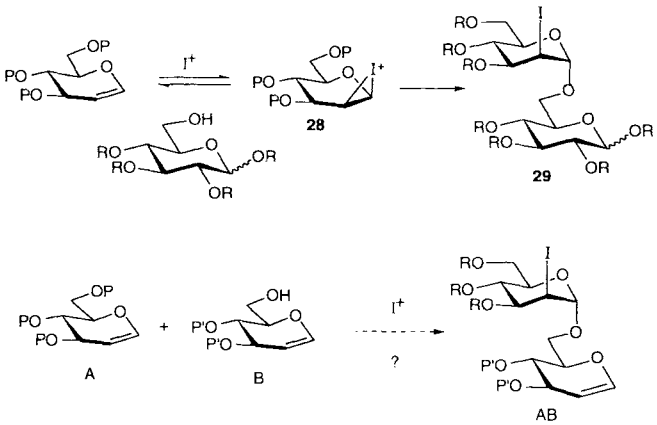

Scheme 14. Iodonium salt mediated coupling of glycals.

We first considered the coupling of two glycals through iodoglycosylation. Such a coupling had apparently not been previously attempted. The problem is controlling the roles of the glycals. Since species **28** is generated as a fleeting intermediate, it seemed very unlikely that the sequential introduction of the two nonidentical glycals (A and B, Scheme 14) and the iodinating agent would control the outcome. Indeed the order of addition of glycals does not determine which one serves as the donor and which as the acceptor en route to the desired AB glycal.

In the case of nonidentical glycals, a particular glycal can be prevented from functioning as a glycosyl acceptor by blocking all of its hydroxyl functions. However, owing to the presence of glycal functionality in the putative acceptor, it can serve as glycosyl donor (see Scheme 14). Therefore, even if one of the two glycals were ineligible as a glycosyl acceptor, significant problems (symmetrical coupling and polymerization) could be encountered in regulating the glycosyl acceptor.

An interesting possible solution presented itself. The thought was that the pattern of protecting groups of the glycal might be used to direct the reaction. While it had long been known that acyl protecting groups lower the reactivity of glycosyl donors,[53a] the idea of exploiting this effect in the coupling of two glycosyl donors had not been conceptualized until the seminal experiments of Fraser-Reid et al.[53b, 54] For the case at hand, consider the two glycals, projected donor **30** and projected acceptor **32** (Scheme 15). The oxygen atoms of **32** are acylated, while those of **30** are alkylated (or silylated). It seemed likely that **30** would be more nucleophilic than **32** towards the iodonium electrophile. Hence, I^+ will attack **30**, thereby generating the mechanistically operative glycosyl donor **31**. Furthermore, as **30** does not have a free hydroxyl group, it cannot act as an acceptor. Glycal **32**, which is equipped with a hydroxyl group, can function as the glycosyl acceptor, giving rise to iodoglycoside **33**. For reduction of this concept to practice, it is necessary that the rate of formation and the effective concentration of **31** be much greater than that of the corresponding species derived from **32** or from the disaccharide product **33.**

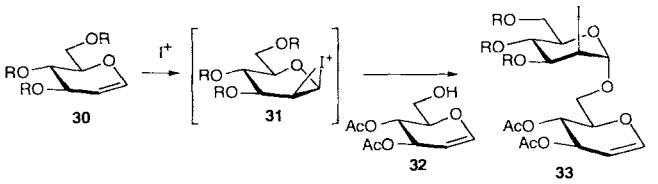

Scheme 15. The use of glycal donors and acceptors in iodoglycosylations (R = alkyl).

The realization of this possibility was achieved by Richard Friesen (**34** + **35** → **36**, Scheme 16).[55] To reiterate the strategy, it was necessary to enhance the nucleophilicity of the disaccharide glycal toward I^+ so that it would function as a glycosyl donor to the next acceptor, hydroxy diester **35**. For this purpose, **36a** was converted to **36b**. Indeed, iodinative coupling of **36b** with **35** gave rise to **37**. The analogous coupling of glycal **36a** with the capped (non-glycal) acceptor diisopropylidenegalactose was of interest. This case, which led smoothly to **38**, again demonstrated (as was already well known from earlier studies) that glycals bearing acyl protecting groups are certainly competent donors in iodoglycosylation reactions with non-glycal acceptors. The essence of Friesen's finding was that the otherwise active 1,2-double bond of the diester-protected glycal substrate does not compete with the analogous double bond in the triether for attack by the iodonium species.

We have not yet elucidated in detail the quantitative effects of the glycal substituents on the iodonium-mediated coupling. The most obvious position where the electronic difference between

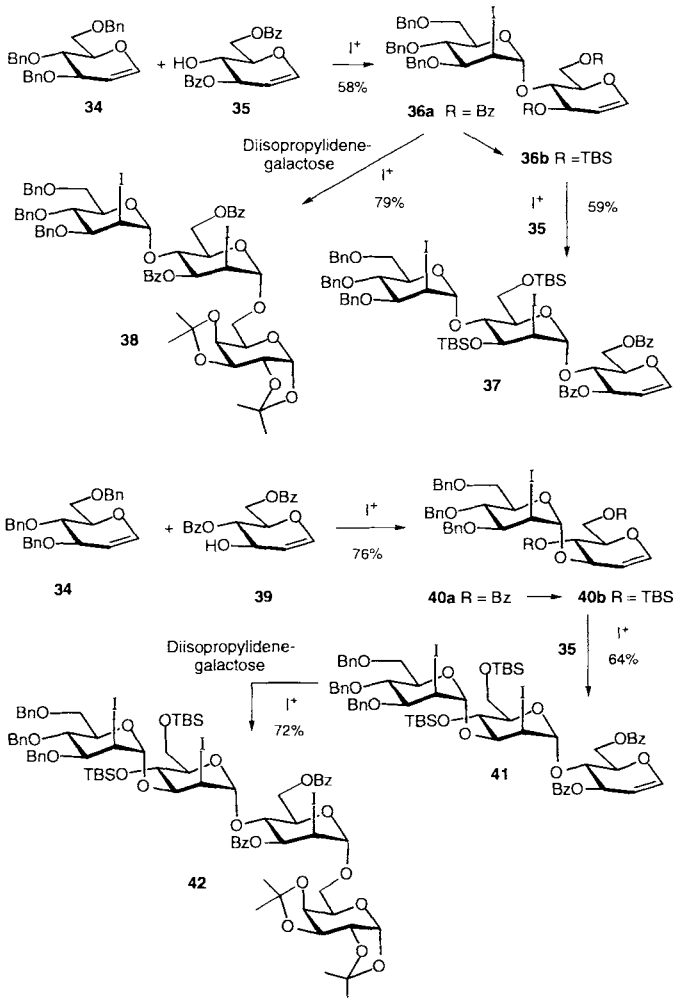

Scheme 16. Polysaccharide assembly employing the iodoglycosylation reaction.

an acyloxy and an alkoxy group would be likely to be decisive would seem to be at the C3 center allylic to the double bond. However, the clean and successful coupling of **34** and **39** to give **40a** (Scheme 16) indicates that even without an acyloxy group at C3, subtle effects can be exploited to bring about an orderly progression leading to glycosylation. The disaccharide thus obtained was subjected to the aforementioned procedure (**40a** → **40b** → **41**) to provide trisaccharide glycal **41**. The trisaccharide **41** was also extended by reaction with diisopropylidenegalactose to give rise to the tetrasaccharide **42**.

We were then in a position to exploit this control of glycal-glycal coupling in a synthesis of ciclamycin 0 (Scheme 17).[56, 57] The key coupling steps to prepare trisaccharide glycal **48** are shown. Fortunately, it was feasible to use **48** to iodoglycosylate the ciclamycin 0 aglycone (ε-pyrromycinone), leading after a few steps, to the natural product itself (**49**). Also, iodonium-mediated coupling of **48** and daunomycinone afforded, after deiodination, the hybrid anthracyclinone **50**.

The synthesis of novel anthracyclines using unnatural glycals **51** and **52** (by the LACDAC reaction) has been developed further (Scheme 18).[33] The handedness of the sugar domain (e.g. in **53** and **54**) has a profound effect on the DNA binding properties of the modified daunomycinone. This experiment provid-

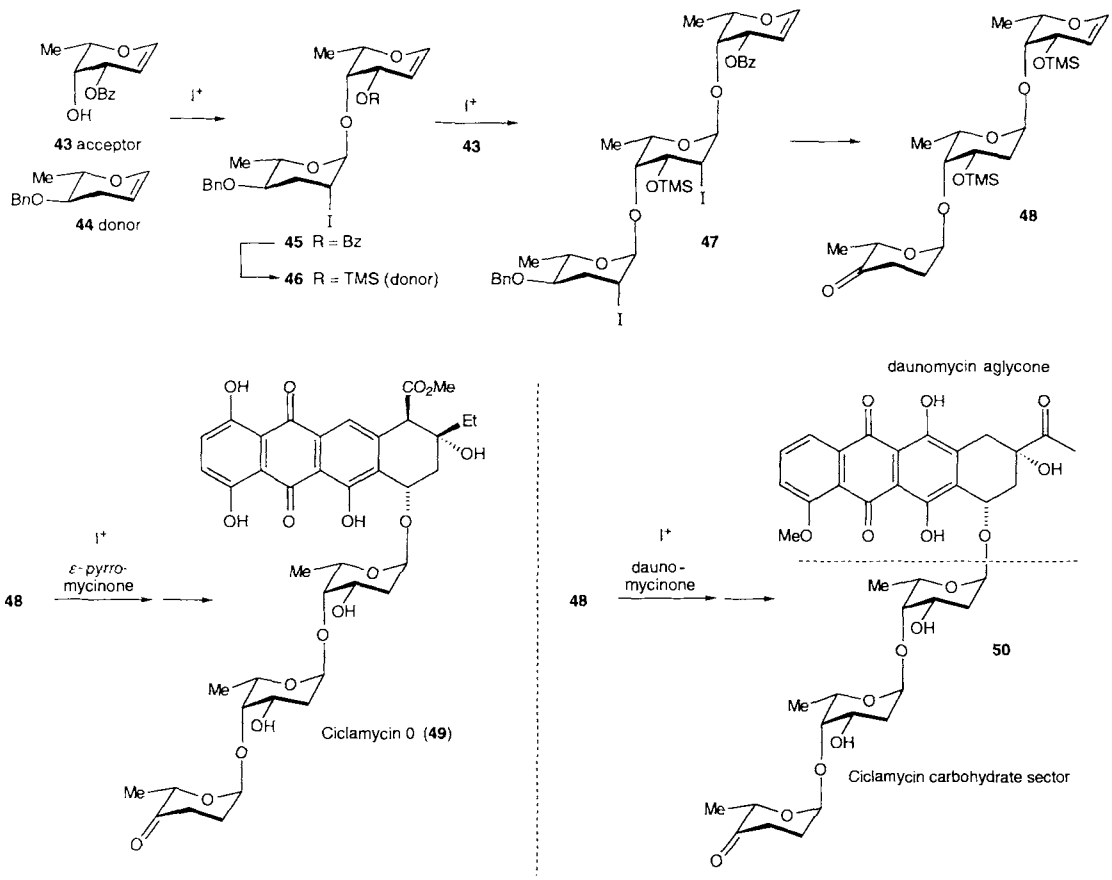

Scheme 17. Synthesis of ciclamicin 0.

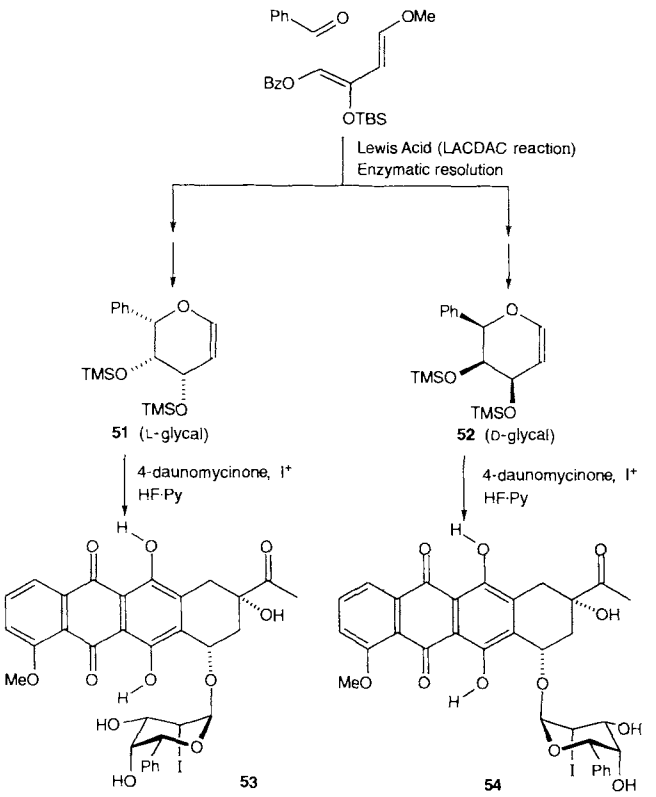

Scheme 18. Enzymatically resolved glycals attached to the daunomycin aglycone. The carbohydrate domain of **53** exhibits the "natural" configuration and is strongly bound to DNA, that of **54** has the opposite configuration and is weakly bound to DNA. Py = pyridine.

ed us with the first sense of the potentially important role of the carbohydrate sector in mediating interactions in the DNA–drug effector region. This critical lesson was not forgotten when we worked in the calicheamicin series (see Section 9).

By combining access to unnatural glycals in optically pure form (in either enantiomeric series), with the capacity for iodoglycosylation, it will be possible to explore in detail the role of the carbohydrate sector in DNA recognition and in the cytotoxicity of the anthracycline antitumor agents. Work in this general direction is now in progress in our laboratory.

5. Azaglycosylation of Glycals

Given the excellent access to natural and unnatural glycals by either total synthesis or partial synthesis (see Section 2), it seemed appropriate to investigate the possibility of their use as precursors to glycosides of 2-acylaminosugars. Of course, in the light of the iodoglycosidation chemistry discussed in Section 4, the most obvious approach to introduce an equatorially disposed nitrogen at C2 would entail displacement of the axial iodo substituent (**55** → **56**, Scheme 19). However, S_N2 reactions at centers with (axial) leaving groups in a 1,2-*anti* relationship to an axial glycoside bond tend to be low yielding. A different approach to this problem for the case of an *N*-acetylmannosamine glycoside, developed in our laboratory, involved exploiting an intramolecular hydroxy nucleophile at C3 (**57** → **58**).[55] While interesting, this method is rather lengthy and, in any case does not address the critical series of glycosides

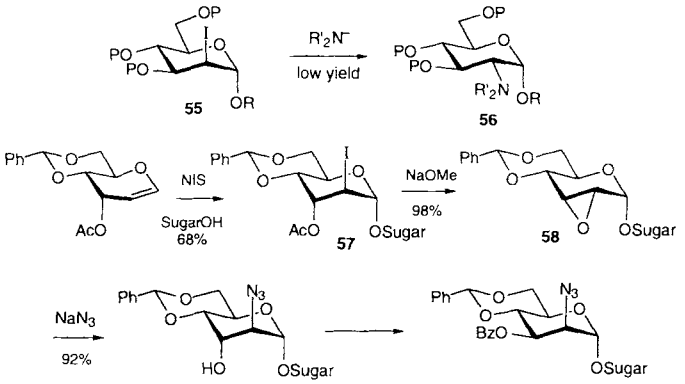

Scheme 19. Synthesis of an α-mannosamine from a glycal.

corresponding to *N*-acetylglucosamine. Such glycosides appear, for instance, in asparagine-linked glycoproteins (see Section 10).[58]

Two methods for introducing a nitrogen at C2 via a glycal had been studied earlier by Lemieux. An important first advance employed nitrosochlorination of glycals.[59] While this route constituted significant progress at the time, the methods to convert the oximino products to desired goal structures were not fully optimal as regards to yield and stereoselectivity. Better results were achieved by azidonitration (**59** → **60**, Scheme 20).[47] Indeed, this method led to the synthesis of various goal systems. For instance, in our first synthesis of tunicaminyluracil, we made recourse to azidonitration of glycal **61**, which had been derived from the LACDAC methodology.[29a]

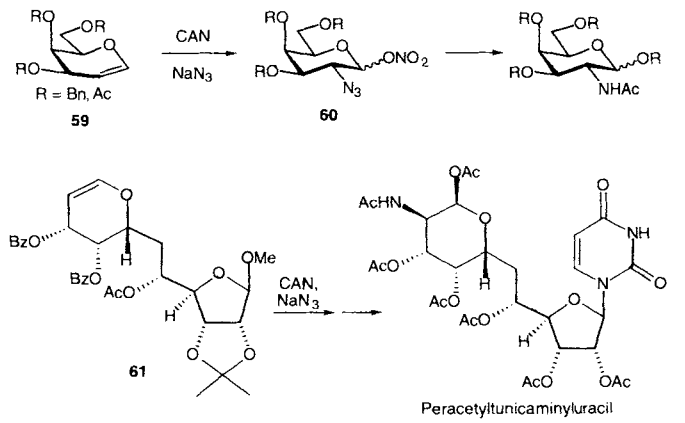

Scheme 20. Azidonitration of glycals. CAN = cerium ammonium nitrate.

A very interesting solution to the problem of converting glycals to such goal systems was developed by Fitzsimmons, Le Blanc, and co-workers.[60] It starts with the cycloaddition of azodicarboxylates with glycals, giving **62** (Scheme 21). Under various forms of acidic mediation, systems such as **62** can function as glycosyl donors (**62** → **63**). Several protocols were developed such that the hydrazodicarboxylate linkage can be reductively cleaved and the resulting products converted to desired 2-acetamido targets. Indeed, we took advantage of this chemistry in our second and more effective synthesis of tunicaminyluracil (Scheme 21).[29b]

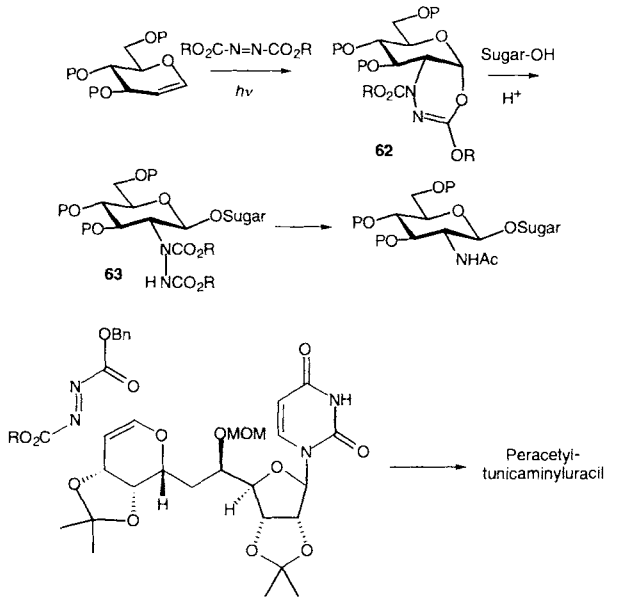

Scheme 21. Cycloaddition of azodicarboxylates with glycals.

For reasons that will become clear when we discuss the total synthesis of allosamidin,[61] we sought a new method to reach glycal **66** (Scheme 22). The condition was that stereoelectronic factors rather than issues of local steric hindrance should govern product formation. In other words, application of the method to be developed to either a glucal or an allal bearing a C3 axial hydroxyl, or protected hydroxyl group, should result in the C2-α-acetamido product.

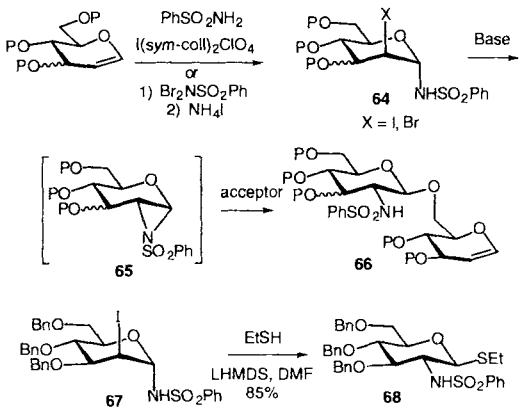

Scheme 22. Iodosulfonamidation of glycals. P = protecting group or sugar, LHMDS = lithium hexamethyldisilazide.

The key reaction developed by David Griffith to deal with this problem was that of sulfonamidoglycosylation.[62] The method, which involves *trans*-diaxial addition of an *N*-halobenzenesulfonamide to a glycal, leads to **64**. Under appropriate conditions, a range of nucleophiles can be used to convert **64** to glycosides of 2-α-benzenesulfonylglycosamine derivatives. The incoming acceptor can be a pyranose with a suitably differentiated hydroxyl group, or it can be a glycal (e.g. **66**) thus allowing for reiteration of the process. Also, the donor can be a di- or oligosaccharide terminating in a glycal linkage to undergo sulfonamidoglycosylation.

While we have not succeeded in properly characterizing the intermediate between the 2β-halo-1α-sulfonamidopyranosides (e.g. **64**), and the product **66**, we have reason to believe that the 1,2-sulfonylaziridine **65** is, in fact, the active glycosylating entity. This moiety functions as a very powerful electrophile, prompting clean β-attack by the nucleophile at the anomeric carbon. Several protocols have been developed for liberating the amino system from its 2-sulfonamide precursor (see Section 10). Furthermore, an iodosulfonamide can be readily converted to the corresponding ethyl thioglycoside (see **67** → **68**, Scheme 22). The latter can subsequently be employed as an azaglycosyl donor to some advantage. This conversion has been proven to be very useful in several important cases where the direct glycosylation of iodosulfoamides fails (see Schemes 53 and 54).

Below we describe three of the early applications of the sulfonamidoglycosylation of glycals. The first application of this new chemistry was in the total synthesis of the very powerful chitinase inhibitor allosamidin.[51] The route to allosamidin exploited sulfonamidoglycosylation at two stages. In the first application, the allal-type glycal **70** was used (Scheme 23). This glycal is available either from allose or, more interestingly, by rearrangement of the α-thiophenyl derivative **69** (in turn available by a sequence starting with the Ferrier transformation of D-glucal triacetate).[36] Bromosulfonamidation of **70** afforded **71**, which was coupled to glycal **72** in the presence of potassium hexamethyldisilazide (KHMDS) to give **73**. The latter then functioned as an azaglycosyl donor. Bromosulfonamidation of **73** afforded **74**. Reaction of **74** with aglycone derivative **76** afforded, after several steps, allosamidin (**77**). Incidentally, the synthesis of **76** was accomplished by enantioselective desymmetrization of the *meso* compound **75**,[64] thus enabling a pleasing route to the natural enantiomer.

A second early application came in the important field of sialyl Le^x glycosides.[64-66] The sialyl Le^x substructure at the nonreducing end of glycoproteins on the cell surface is the key recognition element in E-selectin and P-selectin mediated adhesion.[67] This discovery has spurred interest in the field of sialyl Le^x chemistry.[68] The goals, as we defined them from a combined chemistry–biology perspective, focused on the synthesis of an intermediate that could serve as a launching point to reach various glycosides of sialyl Le^x. Such glycosides could be screened as potential inhibitors of the natural ligand.

Toward this end, we identified sialyl Le^x glycal derivative **85** as a suitable target (Scheme 24). We also hoped to study the

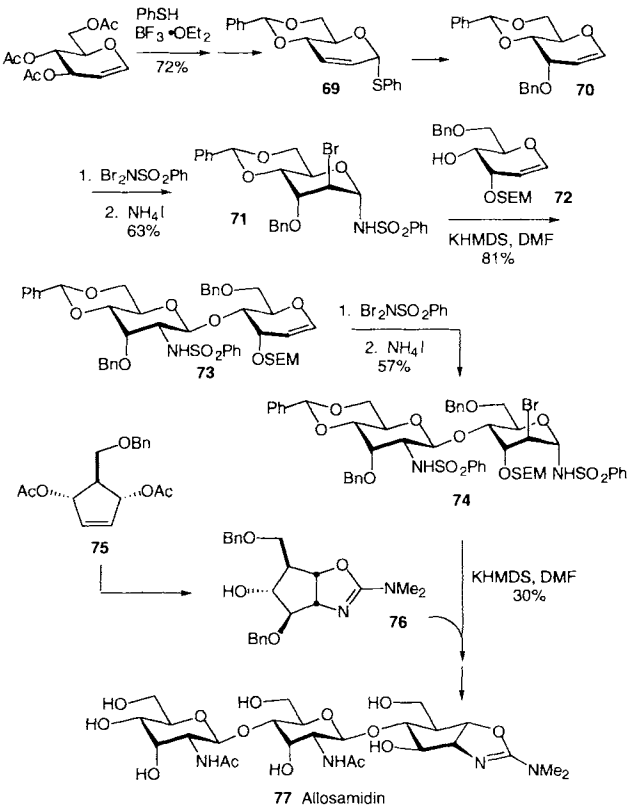

Scheme 23. The synthesis of allosamidin. SEM = trimethylsilylethoxymethyl.

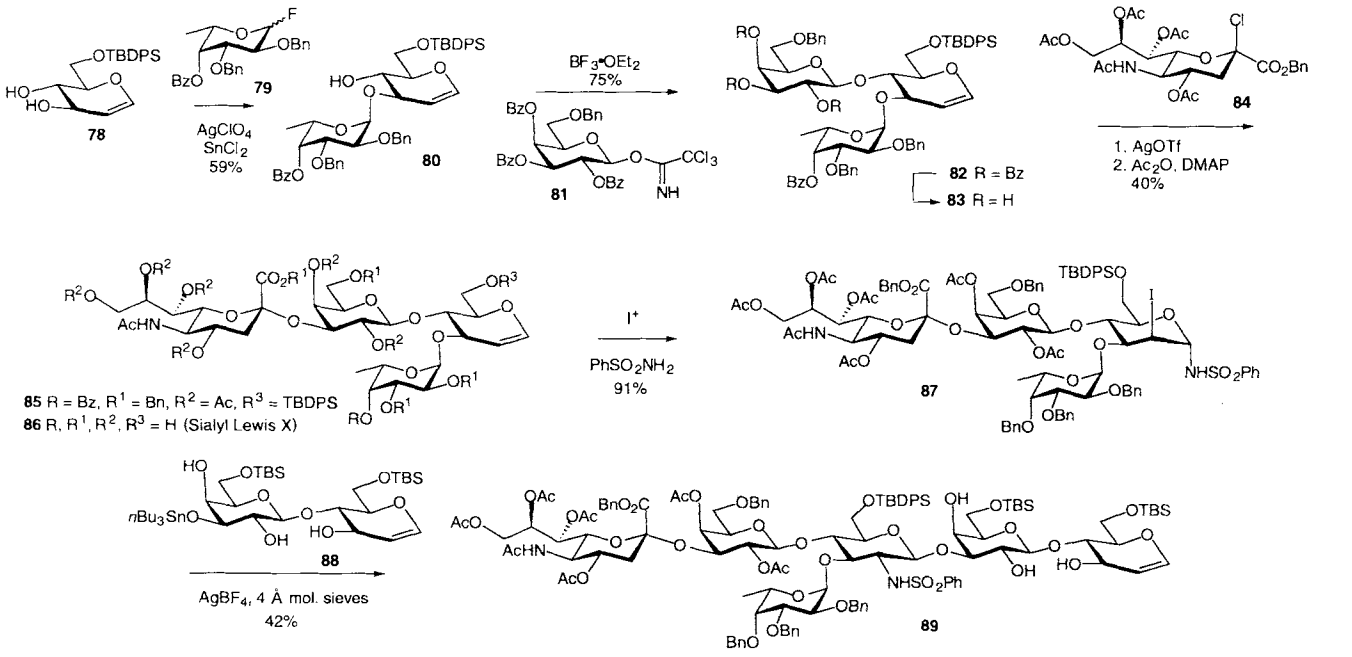

Scheme 24. Synthesis of a sialyl Le^x glycal.

properties of the fully deprotected derived glycal **86** in an ELAM binding assay. Moreover, if the azaglycosylation chemistry described above could be extended to the protected system **85**, we could gain access to a range of more extended oligomers from a late stage in the synthesis. In this way we would obviate the need for a separate lengthy synthesis for each assay candidate.

A key discovery in this regard, first registered by Jacquelyn Gervay and John Peterson, was that glycal **78**, containing silyl protection only at the primary (C6) hydroxyl group, undergoes selective fucosylation with **79** at the allylic alcohol center (C3) (Scheme 24). Conveniently, after fucosylation, the C4 hydroxyl was available to serve as the acceptor toward the galactosyl trichloroacetimidate donor **81**, thus affording Le^x derivative **82** (and, after deprotection, **83**). Sialylation of **83** with the known sialyl donor **84** and acetylation led to protected product **85**, and eventually to the deprotected sialyl Le^x glycal **86**.

Furthermore, **85** underwent iodosulfonamidation to afford **87** (Scheme 24). This compound served as an *N*-sulfonylglucosaminyl donor toward stannyl-activated glycosyl acceptors (e.g. **87** + **88** → **89**). The prospect of exploiting the glycal linkage for still further derivatization is obvious. A further simplification in reaching the Le^x glycal series employing a 1,2-anhydrogalactose derivative has been achieved, and this is described later in this review (see Scheme 50).[56]

The possibility of using a glycal linkage in the construction of glycopeptides by sulfonamidoglycosylation presented itself. In the event, iodosulfonamide **90** was treated with sodium azide to produce, cleanly, the anomeric β-azide **91**, which was converted to **92** (Scheme 25).[69] The anomeric amine was acylated by

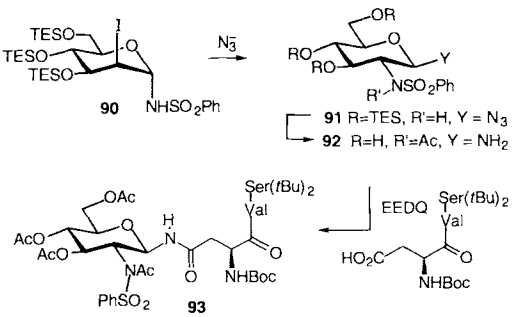

Scheme 25. Synthesis of N-linked glycopeptides from iodosulfonamides. TES = triethylsilyl.

suitable aspartate residues, including that of a tripeptide, using 2-ethoxy-*N*-ethoxycarbonyl-1,2-dihydroquinoline (EEDQ) to afford **93**. At that stage, deprotection of the sulfonamide in the presence of the sensitive glycopeptide bond, even at the level of a monosaccharide tripeptide was problematic. Given our rapidly developing methodology for the synthesis of oligosaccharides terminating in glycals (see Section 6), the ability to convert such compounds to asparagine-linked glycopeptides was seen to constitute an important goal in synthesis of large complex oligosaccharide–peptides. We shall return to the dramatic progress achieved in this area after addressing the matter of solid-phase oligosaccharide synthesis (see Schemes 73 and 74).

6. Applications of 1,2-Anhydrosugars to Glycoside Synthesis

While iodoglycosylation and sulfonamidoglycosylation provide valuable capabilities for the conversion of glycals to various glycosides, there was a need for a very general route to convert glycals into common glycosides of glucose, galactose, and mannose. Ideally the new methodology would embrace both α- and β-glycosides. In search of this type of method, we considered the possibility of directly converting glycals **94** to glycal epoxides **95** (Scheme 26). At the time we undertook this

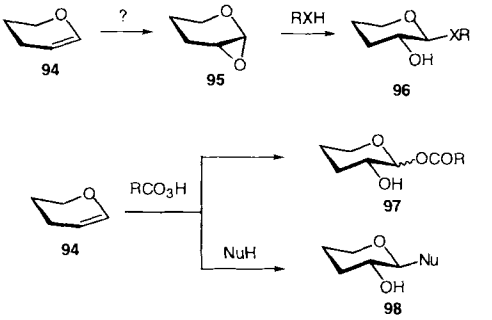

Scheme 26. Direct epoxidation of glycals.

investigation, two serious impediments to the broad applicability of 1,2-anhydrosugars presented themselves. First, there had been no reported methodology for the direct conversion of a glycal to its 1,2-oxirane derivative. While such systems were well known for 60 years (for example Brigl's anhydride),[70] they had hitherto been prepared only after somewhat lengthy protocols from hexose derivatives. However, given our focus on glycals, we considered the possibility that such epoxides might be readily obtained directly from glycals. Previous attempts to prepare 1,2-anhydro systems from the reactions of various peracids with glycals led, not to the 1,2-oxiranes, but to products of their heterolysis (**97** and **98**).[71] Certainly, the indications were that glycal epoxides were exceedingly sensitive to opening of the oxirane ring by nucleophilic attack at the anomeric carbon.

Also, the record of using α-epoxides such as **95** as stereoselective β-glycosylating agents for the formation of compounds such as **96** was none too promising.[72] Previous attempts to prepare disaccharides by employing a 1,2-oxirane as a glycosyl donor with various acceptors often resulted in nonstereoselective glycoside formation, although the application of such a donor in the historic Lemieux construction of sucrose[73] was certainly a milestone accomplishment in synthetic organic chemistry.

Owing to the difficulties associated with synthesizing 1,2-oxiranes, in most of their applications as glycosylating agents the systems contain acyl protecting groups at positions 2, 3 and 4. We wondered whether such resident groups might participate in the ring opening of the epoxide, thereby compromising clean inversion in the glycosidation reaction. In this connection, we were struck by reports from the laboratories of Schuerch and co-workers,[74] wherein perbenzylated 1,2-anhydroglucose underwent stereoregular polymerization under the influence of protic acids. It was recognized that in principle epoxy polymer-

ization of a 1,2-anhydrosugar corresponds to a reiterative glycosidation. If the polymer were indeed being produced in a stereodefined fashion with regular 1β linkages, it seemed that, at least in the polymerization case, the glycosylation reactions were stereospecific.

We therefore focused on several tasks. We sought a general method for the conversion of a glycal to a 1,2-anhydrosugar. The second emphasis was investigating whether glycals, which do not bear potential neighboring group participants of their resident functionalities, might serve as more stereoselective and efficacious donors in the formation of β-glycosides. Furthermore, we would investigate whether suitably differentiated glycals could function as glycosyl acceptors in glycosylations using glycal epoxide donors. We were not unmindful that should such a step be accomplished, the product would itself be a candidate for further elongation through reiteration of the sequence of epoxidation and coupling.

A major advance in our technology was contributed by Randall Halcomb. He found that a variety of glycals react smoothly with 2,2-dimethyldioxirane (**99**, DMDO),[75] prepared as a solution in dichloromethane according to the protocol of Murray.[76] For instance, glucal derivative **34** reacted smoothly with **99** to afford **100** in near-quantitative yield (Scheme 27). Solvolysis of **100** with neat methanol provided methyl glycoside **101**, whose structure was confirmed unequivocally by NMR analysis. Based on configuration of the methanolysis products, we estimate the stereoselectivity of epoxidation to be at least 20:1 in favor of the α-isomer. We emphasize, however, that with resident acetyl protecting groups, the stereoselectivity of epoxidation is much reduced (cf. Scheme 46). Epoxidation of galactal derivative **102** provided **103**.

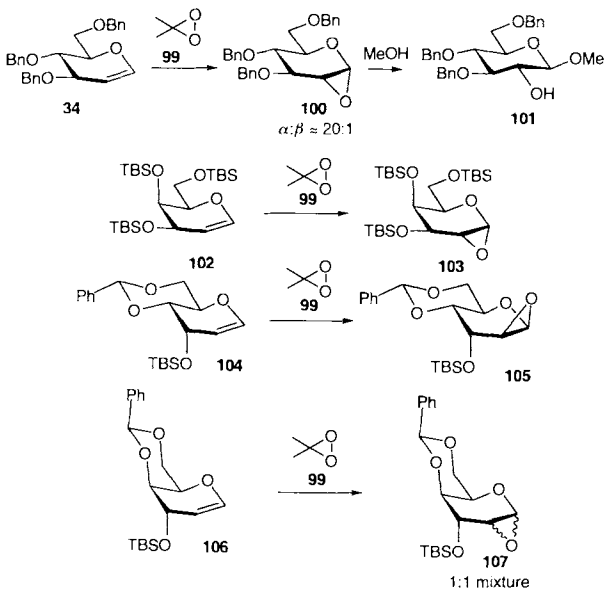

Scheme 27. Epoxidation of glycals by 2,2-dimethyldioxirane (**99**).

It was of interest to probe the allal series. In the event, glycal **104** bearing the axial 3-TBSO function undergoes quite selective epoxidation from its β-face, providing **105**. On the other hand, the gulal derivative **106**, with hindering substituents on both faces of the double bond, gave a 1:1 mixture of epoxides **107**.

Armed with these results, we investigated the glycosyl-donating properties of these epoxides, particularly those derived from glucose and galactose. We soon discovered that the glycosylation of acceptors more complex than methanol and present to a roughly stoichiometric degree was slow and required promotion. A universal promoter has not been discovered. With moderately acidic acceptors such as phenols[77] and indoles[78] (vide infra) best results were obtained under basic conditions. Presumably under these conditions the kinetically active form of the acceptor is the alkoxide. With ordinary alcohol acceptors, including those in which the hydroxyl group is part of a saccharide, the most widely used promoter has been anhydrous zinc chloride. In some special applications (for example the synthesis of gangliosides) stannyl derivatives generated in situ gave the best results (vide infra).

Our earliest results with **100** as a donor are summarized in Scheme 28. Subsequent to these experiments, it was found that this particular oxirane is among the poorest of the donors[79, 80]

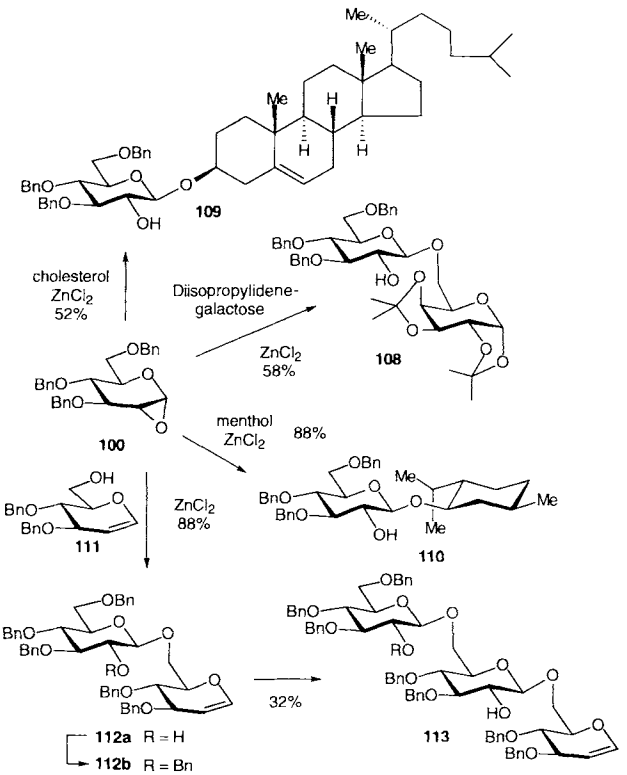

Scheme 28. Coupling of an anhydrosugar with representative acceptors.

and, depending on the case, some α-glycoside is produced. It has since been learned that glycosylation yields can be improved by constraining the C3 and C4 or C4 and C6 oxygen functions into a cyclic motif (see Schemes 37 and 80). Nonetheless, the method had already enabled an easily executed two-step pathway from glucal derivatives to β-glycosides. That these products are fashioned with a uniquely distinguished free hydroxyl group adjacent to the β-glycosidic bond became a crucial element in our synthesis of complex branched saponins and the blood group determinants (vide infra). Also, the finding that the glycosyl acceptor for the glycal epoxide can itself be a glycal (see formation of **112**) had indeed established the basis for a reiterative

strategy for the synthesis of repeating β-glycosides such as **113**. This type of reiterability was in turn a central component of our solid-phase synthesis of oligosaccharides, in which the glycosyl donor is mounted to a solid matrix (see Section 10).

We also demonstrated the applicability of the glycal epoxide method to the synthesis of 2-deoxy-β-glycosides.[77, 81a] Here we took advantage of the uniquely placed free hydroxyl group at C2 as a target for deoxygenation. This was accomplished by free radical reduction of the derived pentafluorophenylthiocarbonate (Scheme 29).[81b] This demonstrates the feasibility of

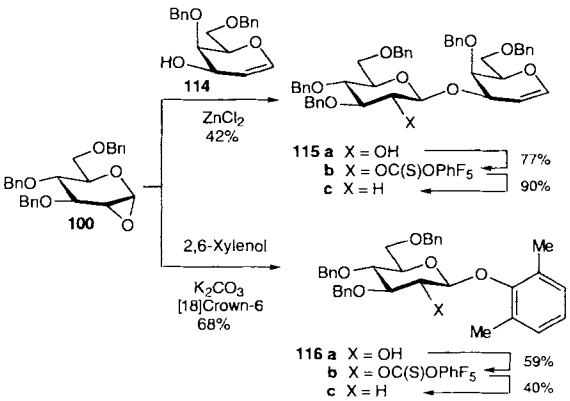

Scheme 29. Coupling of epoxides with secondary alcohols and phenols as acceptors.

a Barton deoxygenation in the presence of a glycal linkage. Again, the basis for ready reiterability of the sequence is seen in the progression **100** + **114** → **115**. The glycosylation of 2,6-xylenol by donor **100** leading to **116a** set the stage for the synthesis of β-aryloxyglucosides and, following deoxygenation, the corresponding 2-deoxyaryloxyglucosides such as **116c**.

The uniquely generated 2′-hydroxyl group arising from opening of the 1,2-epoxide donor has also been exploited in the synthesis of β-mannosides by means of the Garegg oxidation/reduction protocol (Scheme 30).[82] Thus, oxidation of **112a** with acetic anhydride and DMSO followed by reduction of the unpurified product with $NaBH_4$ and acetylation provided selectively the β-mannoside **117** in 89% yield.

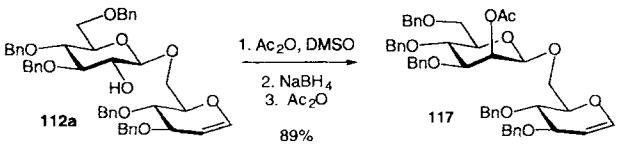

Scheme 30. Creation of β-mannosides by oxidation/reduction.

In addition, we have shown that in certain cases an α-glucoside can be obtained directly from a glucal epoxide (Scheme 31).[83] Reaction of the epoxide **100** with stannylether **118**, promoted by $AgBF_4$, followed by acetylation afforded the α-glycoside **119**. The process was readily reiterated to provide the trisaccharide **120**. Reactions with secondary acceptors proceeded in lower yields and exhibited sharply diminished stereoselectivities. This method is presently limited to primary

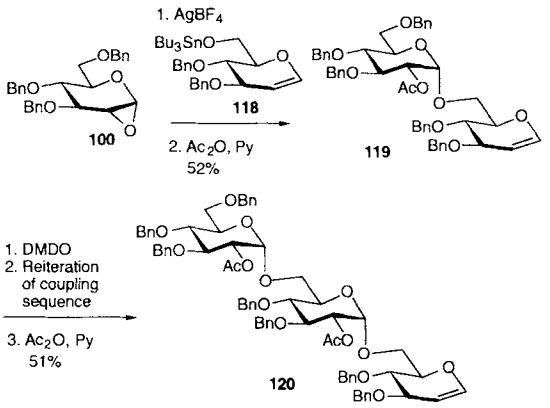

Scheme 31. Direct formation of α-linked glucose linkages. Py = pyridine, DMDO = dimethyldioxirane (**99**).

hydroxyl acceptors and certainly does not constitute a comprehensive solution to the challenging problem of generating α-glycosides. A solution to the conversion of glucals to α-glucosides was attained by transformation of the α-epoxides to known α-glucoside donors (see Scheme 40).

In Scheme 32 we demonstrate the applicability of the glycal epoxide method to the facile construction of a complex 2-branched β-aryl glycoside.[84] Compound **121** was constructed from **100** and 2,6-dimethoxyphenol. In the original approach **123** was to be prepared by iodinative glycosylation of **121** and **122** followed by reduction. As matters transpired the one-step

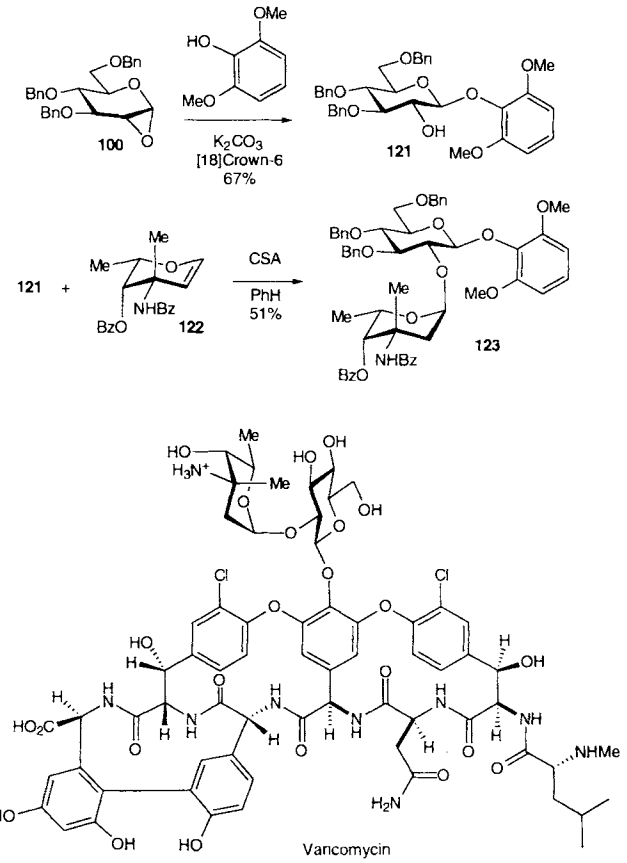

Scheme 32. Synthesis of a branched β-aryl disaccharide. CSA = 1-(*S*)-(+)-camphorsulfonic acid.

proton-mediated coupling of **121** and **122** proceeded stereospecifically. We note that product **122** encapsulates the salient features of the branched aryl glycoside domain of the potent antibiotic vancomycin.

It was of interest to attempt to extend these ideas to the synthesis of β-glycosides of furanose derivatives. Russel Dushin took up this possibility in the context of the first total synthesis of the calmodulin-dependent phosphodiesterase inhibitor KS 502 (**127**, Scheme 33).[85] The salicylate glycosyl acceptor **124** was assembled in a straightforward way. The furanoid 1,2-glycal epoxide **125** was synthesized from D-talonic acid via the corresponding glycal. Coupling of **124** and **125** gave **126** with high stereoselectivity. The steps from **126** to KS 502 (**127**), while not trivial, proved to be manageable.

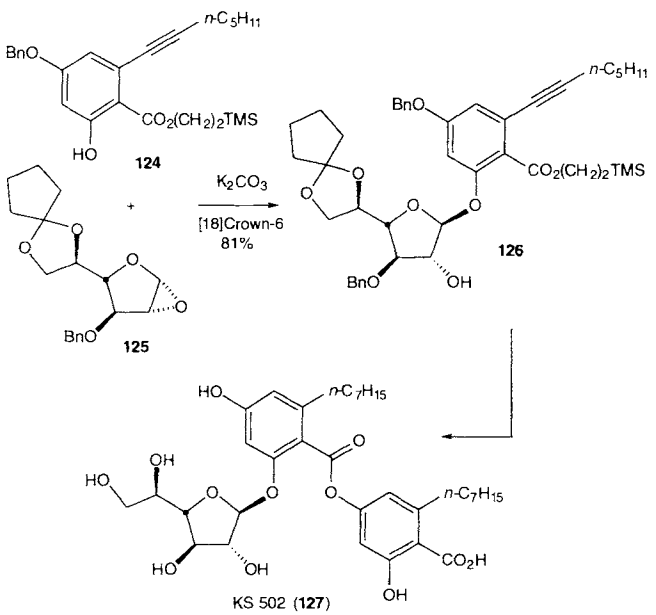

Scheme 33. Synthesis of KS 502 (**127**).

The possibility of utilizing 1,2-oxiranes derived from furanoid epoxides in the synthesis of nucleosides was briefly examined.[86] Interestingly, the furanoid glycal **128** underwent smooth epoxidation with dimethyldioxirane to produce, in 9:1 selectivity, the α-epoxide **129** (Scheme 34). Thus, at least in the furanoid glycal series, "hydroxyl direction" in the epoxidation seems to be operative. Interesting in this regard is the recent report of Murray which demonstrates that in nonpolar solvents the epoxidation of 2-cyclohexen-1-ol with 2,2-dimethyldioxirane does exhibit directivity.[87] In our case, the labile **129** was used as a glycosyl donor in a Vorbrüggen-type reaction[88] with pyrimidine derivative **130** to give stereospecifically **131**. The yield for fashioning of the nucleoside bond is somewhat disappointing and has not yet been improved.

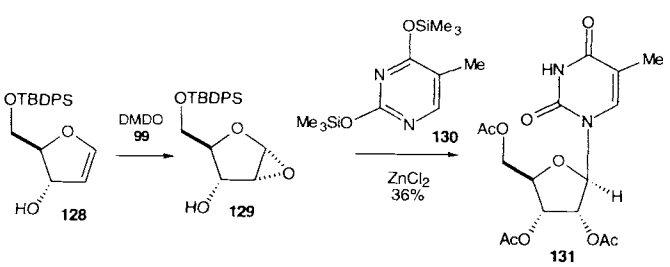

Scheme 34. Synthesis of nucleoside **131** (d.r. = 4:1).

Another area of inquiry was the possibility of using glycal epoxides to glycosylate indoles. Michel Gallant took up this problem. He found that deprotonation of **132** with sodium hydride followed by glycosylation with **100** and acetylation gave rise to model system **133** (Scheme 35).[78] Our motivation in studying the N-glycosylation of indoles with such oxiranes was the potential application of such reactions to the synthesis of natural products. Gallant and J. T. Link first brought our newfound capability to bear in the synthesis of the antitumor agent rebeccamycin (**136**). They took recourse to differentiated secoimide **134** as the acceptor and the differentiated oxirane **135** as the donor.

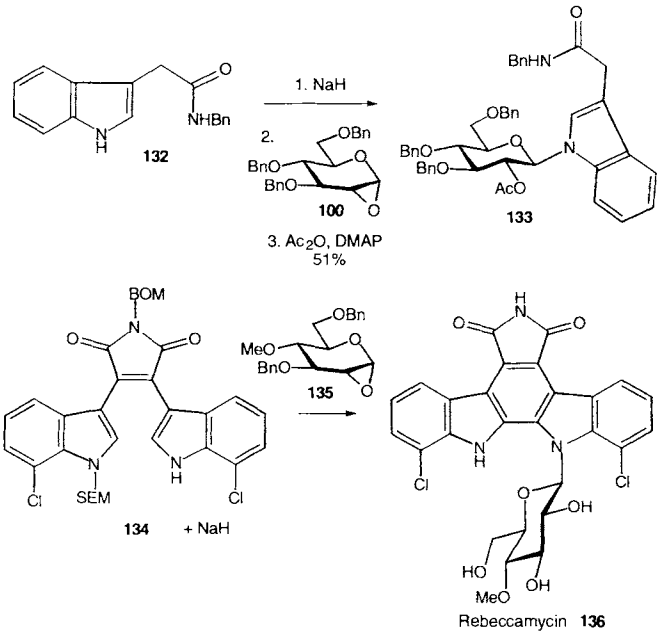

Scheme 35. Indole glycosylation by anhydrosugars. DMAP = 4-dimethylaminopyridine.

A more adventurous, yet related project was apparent: a total synthesis of the premier protein kinase-C inhibitor, staurosporine. Link, Subha Raghavan, and Gallant rose to the challenge. They noted the possibility that staurosporine might be constructed by formation of two indolyl glycoside bonds. Accordingly, the aglycone **137** and glycosylating agent **139** were assembled (Scheme 36).[89, 90] The former was assembled from *N*-benzyloxymethyl 3,4-dibromomalemide and indolylmagnesium bromide through the modular motif previously used in the rebeccamycin effort. The synthesis of the hexose portion started with the mono(triisopropylsilyl) (mono-TIPS) protected L-glucal, which was converted to bis(trichloroacetimidate) **138**. A rather interesting vinylogous Schmidt glycosylation was employed, in which the "leaving group" is the trichloroacetimidate function at C3 "donor" carbon. This led, eventually, to the 1,2-epoxy donor **139**. Coupling of the sodium salt of **137** with

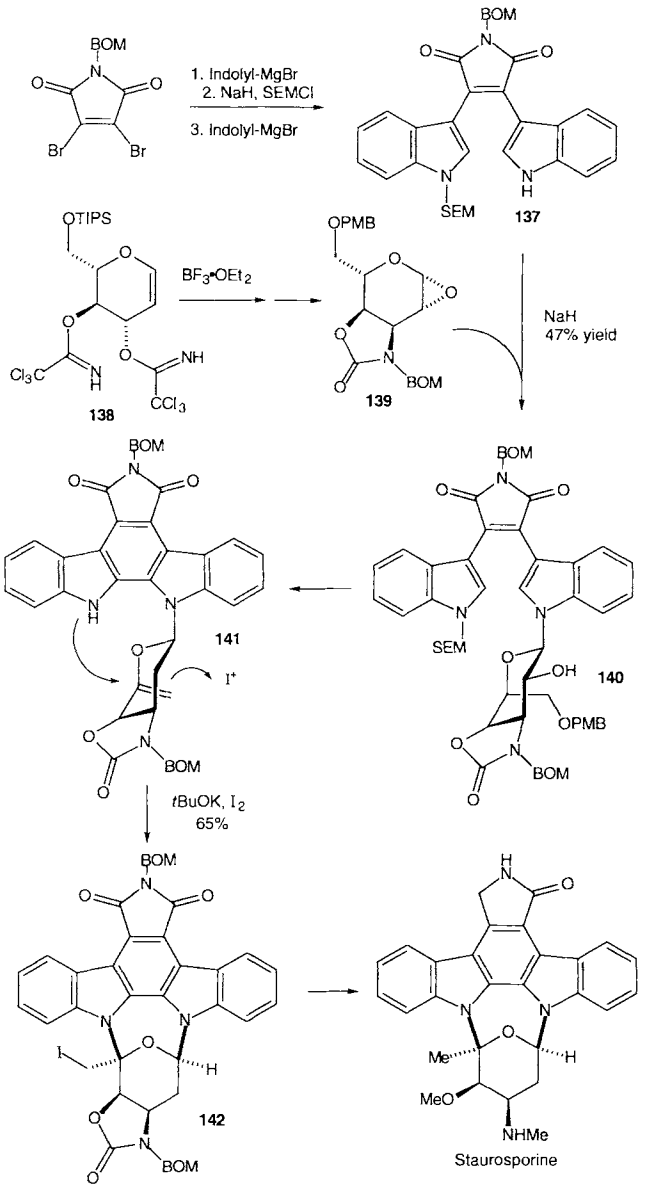

Scheme 36. The synthesis of staurosporine. BOM = benzyloxymethyl.

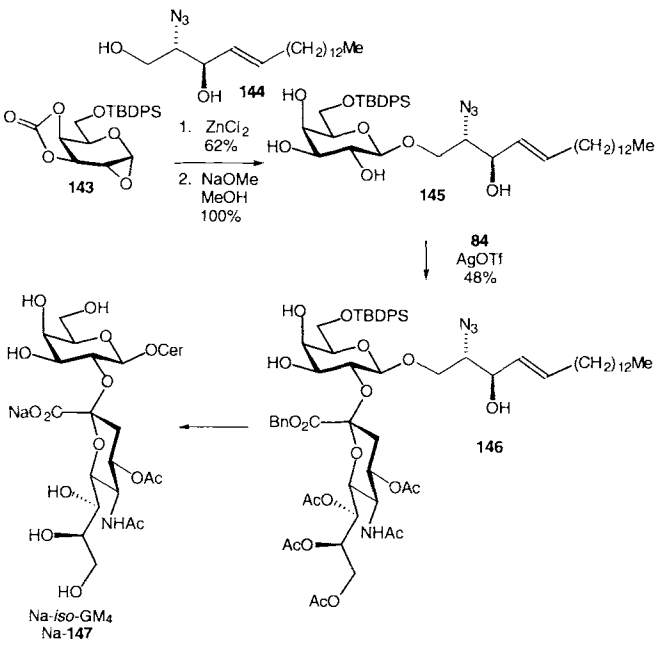

Scheme 37. Synthesis of "iso-GM_4." Cer = ceramidyl.

139 afforded **140**. Several further steps yielded **141**, the potassium salt of which underwent smooth intramolecular "indolo"-N-glycosylation to afford **142** and, after a number of steps, staurosporine was obtained.

The possibility of using glycal epoxides in the construction of gangliosides was examined.[91,92] An important advance in this area relied on the use of galactal-derived epoxide **143** (Scheme 37). Previously, in many cases, galactal-derived epoxides did not function well as stereospecific β-galactoside donors. The use of a cyclic carbonate protecting group engaging the C3 and C4 oxygens (see structure **143**) can lead to favored β-galactosylation in a variety of situations. In the event, reaction of Schmidt construct **144** with **143** resulted in a high degree of selectivity for β-glycoside formation at the primary alcohol. Cleavage of the carbonate gave rise to tetraol **145**. Contrary to many apparent precedents, **145** underwent sialylation at the C2 rather than the C3 hydroxyl group. This surprise was uncovered when the product, later known to be **146**, was carried through several steps to produce **147**, whose spectroscopic properties were inconsistent with formulation as GM_4. We have referred to **147** as "iso-GM_4."

Even today we are unable to explain this remarkable departure from the precedents of Hasegawa et al.[93] and our own experience in the sialyl Le^x series (see Scheme 24, formation of **85**).[66] It must be a special consequence of the presence of the pre-ceramide side chain, although the particular functional group responsible for an apparent activation at C2 cannot be specified.

Fortunately, however, a straightforward way of circumventing this difficulty presented itself to Gervay and Peterson. Thus, glycal **148** was directly submitted to sialylation with **84** (Scheme 38). Coupling occurred smoothly at the allylic hydroxyl group, generating a 3-sialylated galactal derivative which, upon treatment with 1,8-diazabicyclo[5.4.0.]undec-7-ene

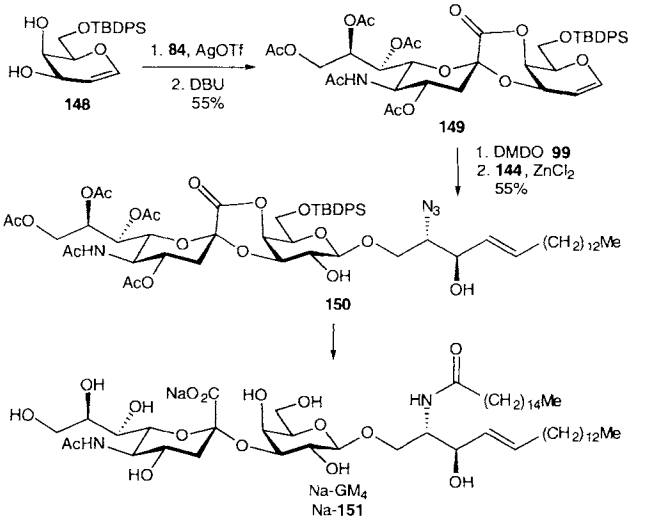

Scheme 38. Synthesis of GM_4.

(DBU), provided the 3,4-spirolactone, glycal **149**. Epoxidation with dimethyldioxirane and glycosylation with ceramide precursor **144** produced glycoside **150**. This compound was, indeed, converted to the pure sodium salt of GM_4 (**151**).

A combination of chemical and biological methods was used by Kevin K. C. Liu in a particularly straightforward synthesis of the important ganglioside GM_3 (**156**).[91] Thus, lactal was uniformly protected with triethylsilyl groups to produce **152** (Scheme 39). The latter underwent epoxidation and coupling

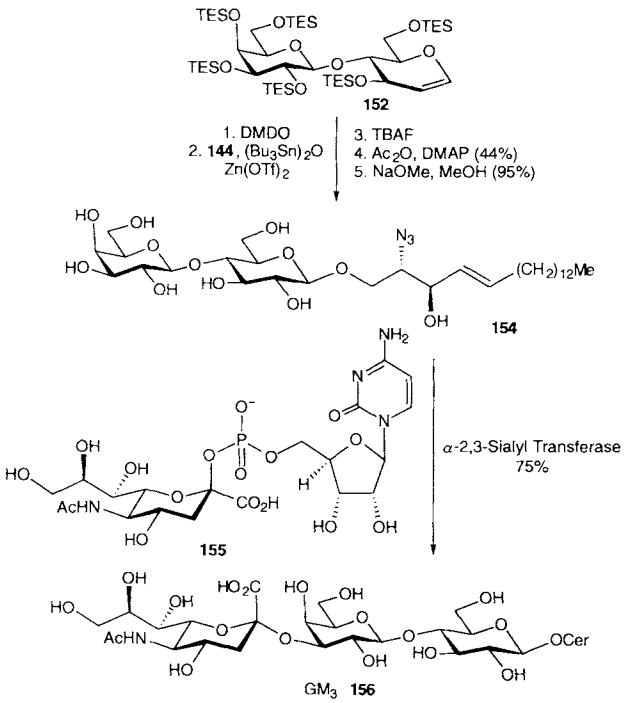

Scheme 39. Synthesis of GM_3.

with the stannylated version of the Schmidt diol **144**, followed by desilylation to produce, in high yield and high specificity, compound **154**. This compound responded to enzymatic sialylation with cytidine monophosphate (CMP) sialic acid (**155**) under mediation by a 2,3-sialyl transferase. After total deprotection, GM_3 (**156**) was in hand. Though cofactors were not regenerated in our experiments, this chemoenzymatic approach provides the most direct route to GM_3.

Thus far we have focused on the use of glycal epoxides in the synthesis of β-glycosides. It is also possible to convert such epoxides to other glycosylating agents (Scheme 40).[94] For instance, Dana Gordon found that compound **100** could be converted to the thiophenyl glycoside **157**, the pentenyl glycoside **158**, the benzylaminoglucoside **159**, and fluoroglycoside **160**. Compound **160a**, upon benzylation of the single free hydroxyl group at C2, gave rise to **160b**, which served as a glycosyl donor in a conventional Mukaiyama reaction[95] to produce α-glycoside **161**. The route from glycals to α-glycosides found important application in Gordon's synthesis of the cyanobacterial sulfolipid, a compound alleged to have anti-HIV activity (Scheme 40).[96] Still another application arose during our synthesis of the carbohydrate section of acarbose.[97]

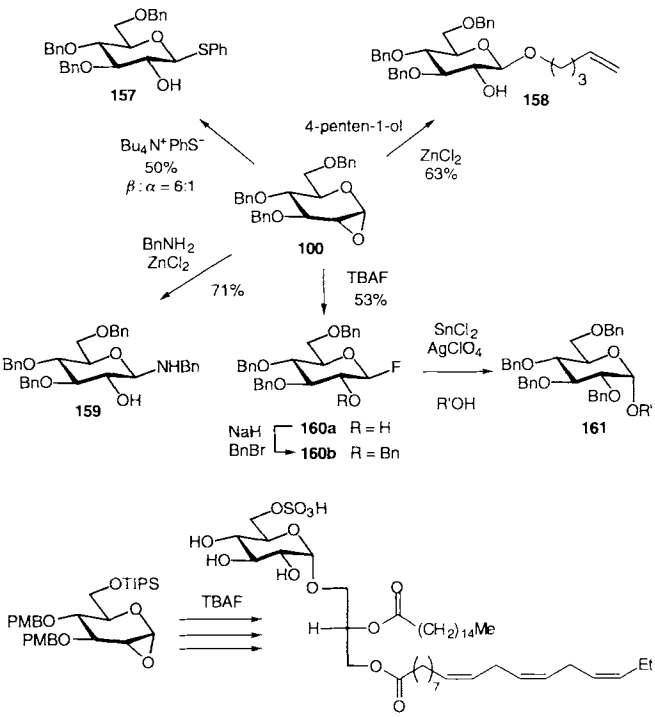

Scheme 40. Conversion of anhydrosugars to other donors, and synthesis of a cyanobacterial sulfolipid.

At this stage we could perceive the emergence of a comprehensive strategy for oligosaccharide construction based on glycal acceptors and glycal-derived donors. We began to field-test the concepts of glycal assembly in the context of specific biologically active and important goal systems. It is almost indisputable that the "combat worthiness" of new concepts in synthesis and new synthetic methodology are best evaluated in the context of multifaceted target structures (for example natural products), where unanticipated difficulties are apt to arise.

An advance in the development of the logic of glycal assembly was achieved in our synthesis of the complex saponin, desgalactotigonin (Schemes 41 and 42).[98, 99] John Randolph took note of the collection of β-glycoside linkages in this target. In particular, we focused on the branched glucose ring in the carbohydrate sector, which is β-linked to the axial hydroxyl group at C4 of a galactose. Particularly intriguing is the branching of this glucose: its C2-hydroxyl is β-linked to another glucose, while at C3 it is β-linked to a xylose. The introduction of this central glucose ring in the form of glycal derivative **163** brought forth major simplifications in protecting group strategy. The free hydroxyl at C3 served as an acceptor toward the xylal-derived epoxide **162** to afford, after benzylation, **164b**. The acceptor for coupling to this donor was fashioned from galactal cyclic carbonate derivative **165**. Epoxidation of **165** followed by coupling to the tigogenin aglycone afforded **166**. Once again this type of epoxide had served us very well as a β-galactosylating agent (cf. **143** in Scheme 37). Several steps were required on the resultant glycoside: 1) cleavage of the cyclic carbonate, 2) engagement of the 4- and 6-hydroxyls in a benzylidene protecting group, 3) benzylation at C2, 4) cleavage of the benzylidene linkage, and 5) rebenzylation at C6 and stannylation at C4 to produce acceptor **167b**. Coupling of **167b** with the epoxide of **164b** under

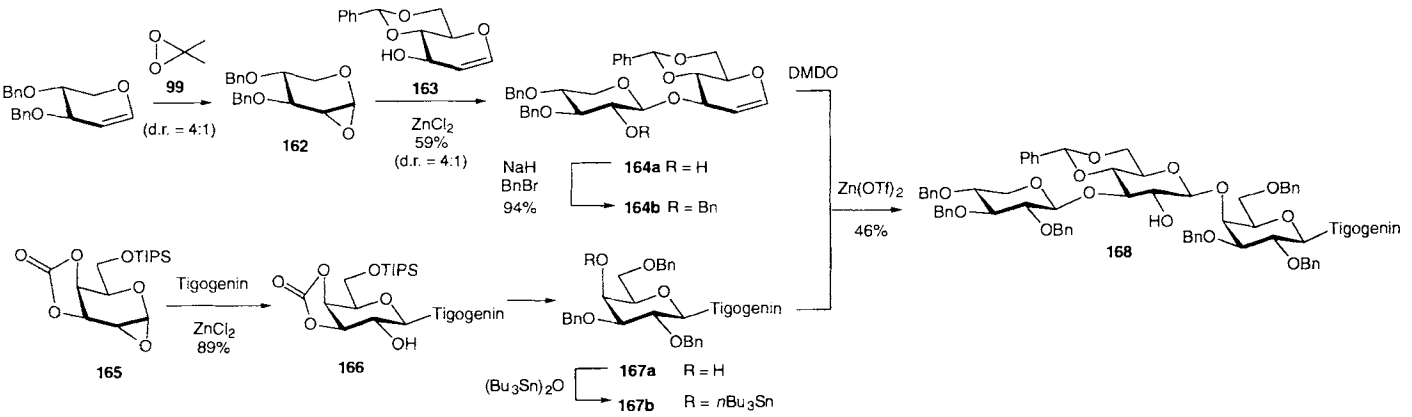

Scheme 41. Synthesis of desgalactotigonin (part 1).

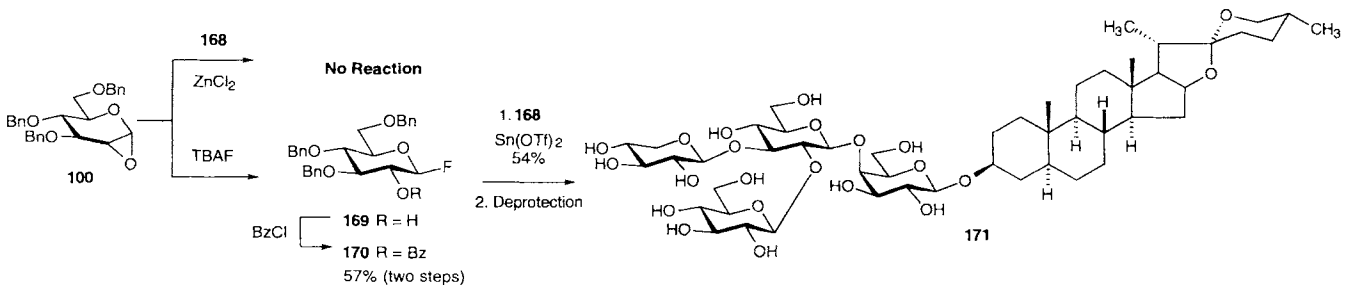

Scheme 42. Synthesis of desgalactotigonin (part 2).

mediation by zinc triflate afforded, albeit in only 46% yield, the steroidal trisaccharide **168**. The glycal epoxide coupling method had targeted a unique hydroxyl group at C2 of the central glucose for branching.

At this stage, however, the free hydroxyl group in **168**, flanked as it was by glycosidic bonds at C1 and C3, did not lend itself to glycosylation with epoxide donors (cf. **100**, Scheme 42). However, we were readily able to fashion a competent donor from **100**. Thus, fluoridolysis[94] afforded **169**, which was converted to its benzoate **170**. The latter functioned with apparent α-face participation to heavily favor β-glycoside formation. Indeed, coupling of **170** with **168** was smoothly accomplished, and was followed by deprotection to provide desgalactotigonin (**171**).

In summary, the logic of glycal assembly had allowed for a high degree of convergence in assembling the complex branched target system. Glycal epoxide opening had been used to expose a unique hydroxyl group to function as a glycoside acceptor (see **169**) and to install a participating neighboring group in a regiospecific fashion. The participating group could be used to direct a fluoroglycosyl donor toward β-glycoside formation (en route to **171**).

7. Lewis Determinants, Blood Group Determinants, and Tumor Antigens

The grounds seemed to be sufficiently secure to apply the glycal assembly logic to the synthesis of Lewis and blood group determinants. In so doing we would be drawing from glycal epoxides and halosulfonamides in the same synthesis. The glycal epoxide methodology would be used to install β-glycosidic linkages and the azaglycosylation methodology would be used to incorporate the *N*-acetyl glucosamine substructure. John Randolph and Victor Behar took up this problem in earnest. In the synthesis of the first target, the Le^y determinant,[100,101] the objective was not only to prepare the carbohydrate sector of the determinant, but also to conjugate it to a carrier protein such that it would more closely approximate the realities in biological systems. The Le^y determinant was of particular interest to us because it had been previously identified as an important epitope for eliciting antibodies against colon and liver adenocarcinoma cell lines.[102] It has recently been implicated as a marker in metastatic prostate cancer.[103] We hoped to simulate this capacity with fully synthetically derived antigen. For this purpose it would be necessary to conjugate this synthetic product to a carrier of the type used to stimulate immune response. To preserve the integrity of the core epitope sector, it would be insulated from the carrier through a spacer domain.

Inspection of the Le^y structure points toward the possibility of building from a central lactose core for this purpose. Given our preference for exploring the chemistry of glycals, lactal (**172**) was identified as the lactose equivalent (Scheme 43). The two primary hydroxyl groups were silylated to produce the bis-TBDPS derivative **173** (TBDPS = *tert*-butyldiphenylsilyl). At this point we took advantage of the *cis* relationship of C3′ and C4′ of **173** by engaging these hydroxyl substituents in the form of cyclic carbonate **174**. Thus, the required two hydroxyl groups at C3 and C2′ of the galactose moiety were readily designated in two steps to function as glycosyl acceptor sites. Fluorosugar **79** was employed as the glycosyl donor. It bears a nonparticipatory benzyl ether at C2 and a potentially participating benzoate

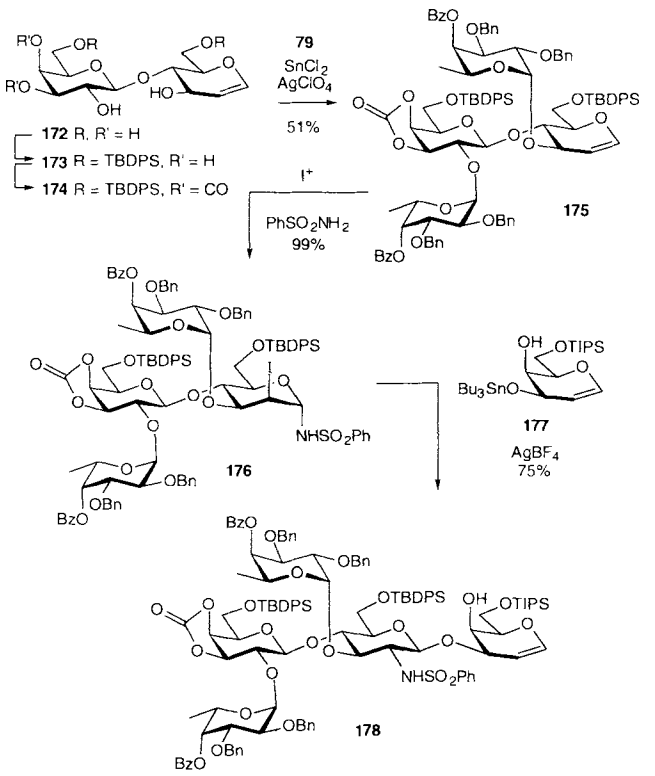

Scheme 43. Synthesis of a Le^y glycal.

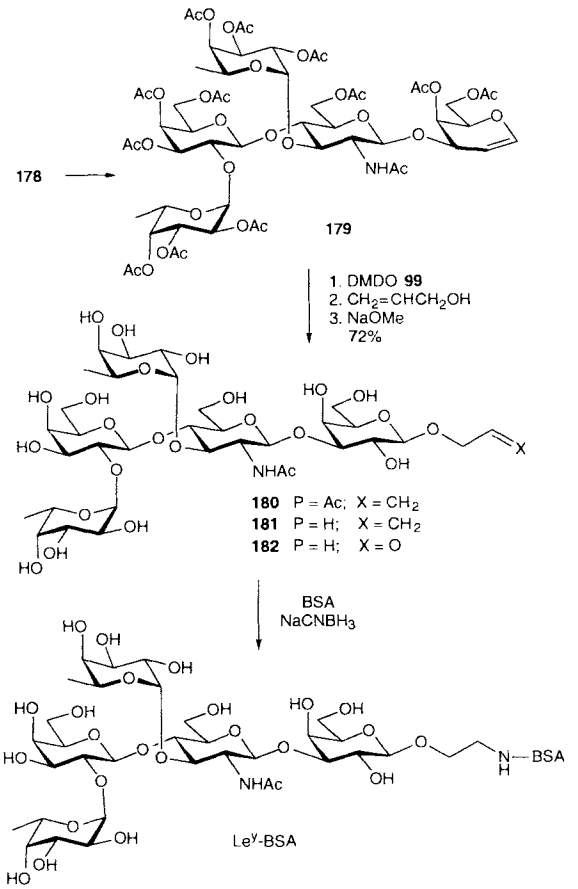

Scheme 44. Conjugation of Le^y to a protein carrier.

at C4. In the event, treatment of **174** with **79** under suitable conditions results in clean incorporation of two fucose residues with formation of compound **175**. The glycal double bond was then subjected to iodosulfonamidation under the usual conditions to give rise to **176**, which functioned as a masked azoglycosyl donor. The critical coupling of **176** with the mono-TIPS stannylated galactal derivative **177** gave the bisfucosylated compound **178** in 75% yield. Thus the tetrasaccharide determinant was efficiently constructed such that it still contained an exploitable double bond.

Before we proceeded to the final glycosylation, it was strategically useful to convert the benzenesulfonamide function to an acetamido group as well as to regularize all of the protecting groups as acetates (Scheme 44). This goal was accomplished and led to compound **179**, which was subjected to the action of dimethyldioxirane. The epoxide thus produced functioned as a competent donor with allyl alcohol as the acceptor to provide **180**. Removal of all acetate groups, affording **181**, was accomplished by the action of sodium methoxide. Thus the logic of glycal assembly combined with the powerful technologies of azaglycosylation and of glycosylation via glycal-derived 1,2-anhydrosugars allowed for a highly concise and convergent synthesis of **181**. We were then ready for the conjugation phase and relied on the reductive amination method developed Bernstein and Hall in a much simpler context.[104] In practice, the double bond of the allyl group of **181** was cleaved to give the uncharacterized aldehyde **182**. The latter was conjugated to bovine serum albumin (BSA) through the action of sodium cyanoborohydride. Amino acid and carbohydrate analysis of the pseudo-glycoprotein indicated the incorporation of approximately 15 pentasaccharide units into the 38 lysine residues theoretically available. Immunization studies of conjugates of **182** in mice are currently in progress, and the earliest results are promising.

It is possible that oligosaccharide domains will someday be synthesized from non-carbohydrate building blocks. At the present time, however, this prospect is virtually unimaginable. Therefore, the basic challenges of synthetic design lie in selecting the molecular components of the synthesis in such a fashion that their assembly in the desired sense is least complicated. Conciseness is the goal in the orchestration of the diverse functionalities and in chemically identifying those loci destined to serve as the glycosyl acceptors and donors in the coupling steps. In both the syntheses of **171** and **181** the use of glycals toward these goals had been demonstrated.

John Randolph accomplished the synthesis of the Le^b determinant, again in bioconjugatable form.[101, 105] This determinant is more challenging from the synthetic standpoint than the Le^y target, because lactal (**172**), trivially available from lactose, cannot serve as a starting material. We proceeded as follows: the TIPS galactal derivative **165** was converted to its epoxide through the agency of dimethyldioxirane (Scheme 45). The acceptor **183** was readily fashioned from glucal itself. Here we could take advantage of another enormous simplification of the glycal method. Coupling of **183** with the epoxide of **165** occurred exclusively at the C3 hydroxyl of **183** to provide **184**, in which the particular hydroxyls to be fucosylated (at C4 of the glucose and C2′ of the galactose) have been smoothly distin-

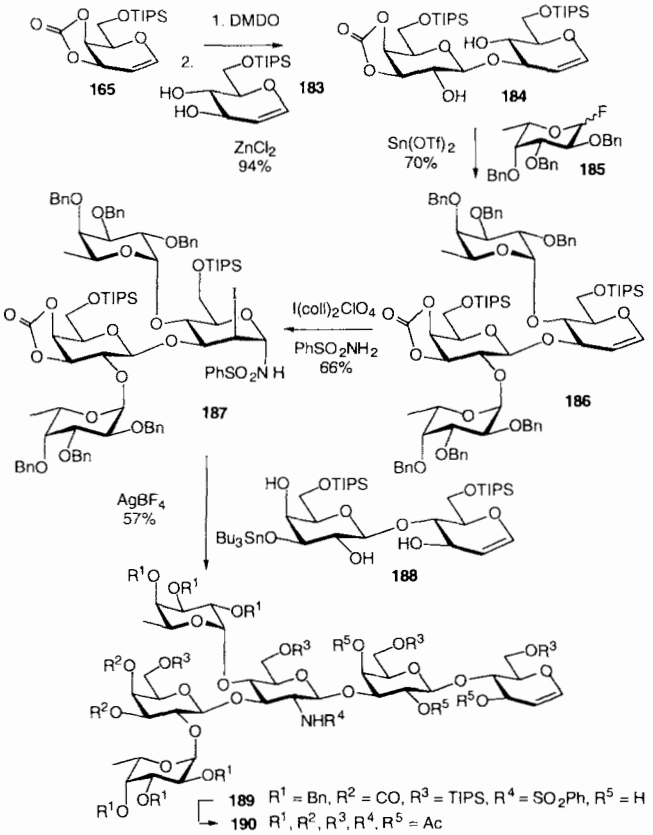

Scheme 45. Synthesis of a Le^b glycal.

guished from other functions. Twofold fucosylation did, indeed, occur using the readily available donor **185** and the tetrasaccharide glycal **186** was efficiently obtained. Compound **186** was prepared for azaglycosylation through iodobenzenesulfonamidation to afford **187**. The latter reacted with lactal derivative **188**, which was prepared from lactal (**172**) in two steps. Coupling of **188** and **187** provided **189**. Thus, the critical tetrasaccharide recognition domain of the Le^b determinant had been assembled in a highly convergent fashion and insulated, through a disaccharide spacer, from the implement to be used in bioconjugation. For this purpose, all silyl groups were removed through the action of tetra-*n*-butylammonium fluoride (TBAF) and the benzyl groups were cleaved by sodium in ammonia. The crude product was peracetylated to give **190**, which was converted to its 1,2-anhydrosugar derivative, as a mixture of isomers, and thence to the corresponding allyl glycosides (Scheme 46). This serious breakdown in the stereochemistry of epoxidation arose from the presence of a resident acetate protecting group in the terminal glucose residue. As described earlier (see Scheme 26), triacetyl glucal is also a poor substrate for stereoselective epoxidation. Since conjugation occurs at some distance from the epitope domain, it is not clear that the stereochemistry of the glycoside bond leading to the carrier domain is of consequence at the biological level.

Cleavage of all acetate groups gave rise to **191** and **192**. These oligosaccharides were separately ozonolized and the resultant glycolic aldehyde products were reductively coupled to human serum albumin (HSA) by the Bernstein–Hall protocol[104] to provide adducts **193** and **194**.

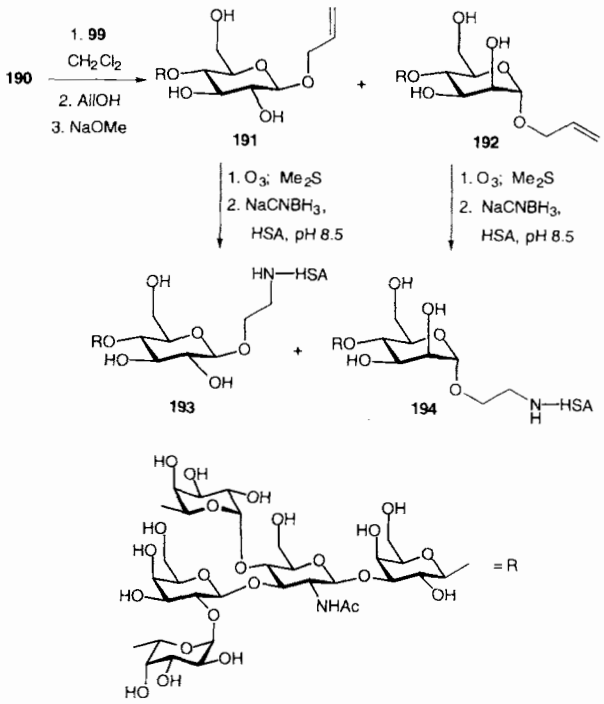

Scheme 46. Conjugation of Le^b to a carrier protein. All = allyl.

Approximately 33 carbohydrate hexamer units were incorporated, presumably by linkage to side chain amino groups of lysine. This construct is of particular interest to us because it incorporates the recognition domain implicated in the binding of *Helicobacter pylori* to gastric epithelial cells.[106] This form of infection is claimed to be one of the major causative elements of gastric ulcer and possibly gastric cancer. The possibility of synthesizing soluble binding agents for *H. pylori* constitutes an exciting goal for the glycal assembly methodology.

The chemistry described here can readily be accommodated into a synthesis of an H-type I tetrasaccharide as well.[101] This is accomplished by a selective α-fucosylation of the disaccharide unit **184** (Scheme 47). Fucosylation with donor **185**, as before, occured with a 5.5:1 selectivity at the 2′-hydroxyl in preference to reaction at the 4-hydroxyl, providing **195**.

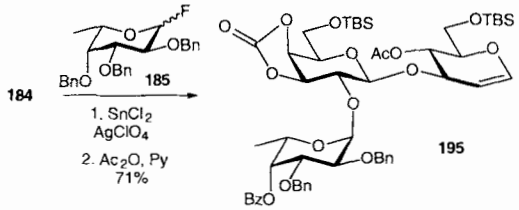

Scheme 47. Synthesis of an H-type I glycal.

Furthermore, we have synthesized a tetrasaccharide having the H-type II structural domain (Scheme 48).[101] Reaction of epoxide **196** (derived from **165**) with the glucal **197** provided the differentiated lactal **198**, in which the newly presented C2′-hydroxyl is available for the requisite fucosylation. $Sn(OTf)_2$-promoted coupling yielded trisaccharide **199** bearing the H-type II domain. We further demonstrated that the structure

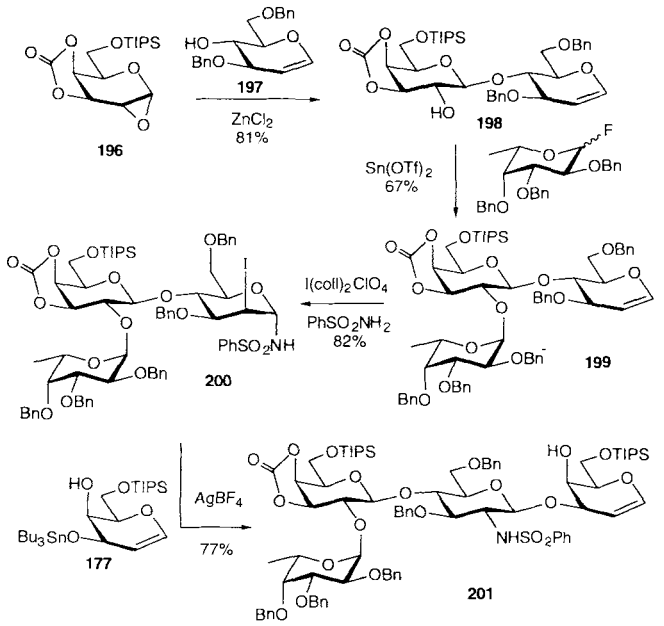

Scheme 48. Synthesis of an H-type II glycal.

can be extended to a tetrasaccharide, employing the standard iodosulfonamide chemistry, to provide **200**. The latter, upon reaction with **177**, afforded **201**.

We have extended glycal chemistry toward the synthesis of the human A and B blood group determinants, which govern the ABO typing system. The synthesis of the core structure of the B determinant is shown in Scheme 49.[107] In the described case, trisaccharide **199** (Scheme 48) with the H-type II domain was used as the starting point. The carbonate was cleaved and the resulting diol was glycosylated with fluorosugar **202** to provide tetrasaccharide **203** containing the B-type domain. After acetylation, standard iodosulfonamide chemistry was employed to provide **205**. This B-type II structure was extended to the pentasaccharide **206** by utilizing the standard coupling conditions with acceptor **177**. The pentasaccharide **206** was readily deblocked to provide the unprotected version of the compound. Considerable progress in the A group series has also been accomplished at this writing, but the project is not yet complete (see Section 11).[107]

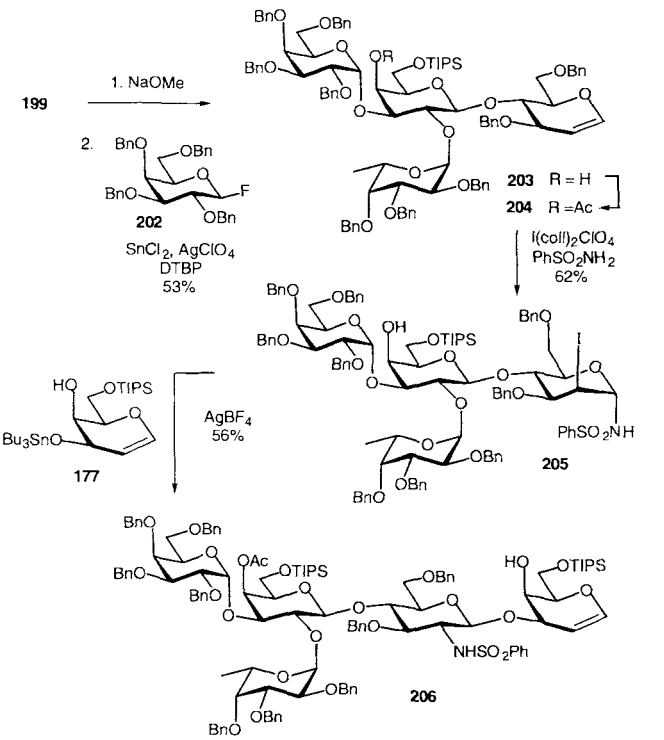

Scheme 49. Synthesis of a B-type II glycal. DTBP = di-*tert*-butylperoxide.

Returning to the series of Lewis determinants, our synthesis of the Le^x domain, previously described in Scheme 24, was greatly simplified by the use of a 1,2-anhydrosugar donor (Scheme 50).[66] Fucosylation of monoprotected glucal **207** afforded the disaccharide **208**, which is analogous to the acceptor employed in the earlier synthesis (cf. **80** in Scheme 24). In this later case, however, the acceptor was found to react under optimized conditions with the epoxide **196** to give Le^x trisaccharide **209** in 81% yield. Epoxide **196** is far more accessible than donor **81** was in the earlier work.

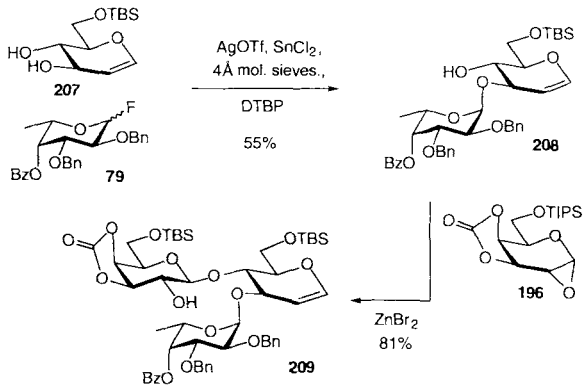

Scheme 50. A concise synthesis of the Le^x domain (cf. Scheme 24, compound **82**).

8. Total Synthesis of the Breast Tumor Antigen: Challenges and Solutions

The glycal assembly method has culminated in the recently completed synthesis of a hexasaccharide glycosphingolipid, which is a breast tumor associated antigen of potential clinical importance. Compound **210** was isolated from breast cancer cell line MCF-7 and was immunocharacterized by the monoclonal antibody MBr1 (Scheme 51).[108] Our synthesis of **210** involved the construction of two trisaccharide domains, which were then brought together to provide the hexasaccharide.[109] Galactal **211** was converted into the fluorosugar **212** (Scheme 52). The desired acceptor **213** was fashioned from disaccharide **190** (itself

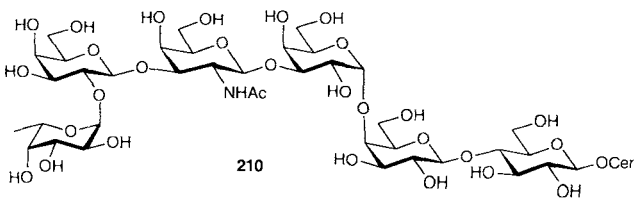

Scheme 51. Structure of the MBr1 carbohydrate antigen.

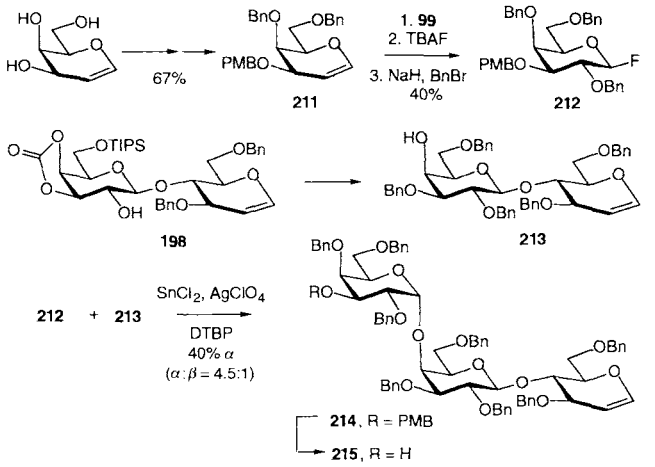

Scheme 52. Synthesis of a trisaccharide acceptor.

obtained by glycal coupling, see Scheme 49) after protecting group manipulations. Coupling of **212** and **213** afforded the trisaccharide **214**. Deprotection of the PMB ether provided **215**, setting the stage for merger with a suitable trisaccharide donor.

Construction of the donor began with **196**, which was glycosylated with acceptor **216** to afford the disaccharide **217** with excellent selectivity (Scheme 53). Regioselective fucosylation of the equatorial hydroxyl of **217** with donor **185** provided the trisaccharide **218**. This trisaccharide was acetylated to produce **219** which, after now standard treatments, was transformed to iodosulfonamide **221**. Unfortunately, iodosulfonamide donors of this type were not competent in the desired direct coupling reaction (see Scheme 22) with various trisaccharide acceptors. A large excess of difficultly available acceptor would be necessary, and this requirement is certainly not appropriate. We therefore

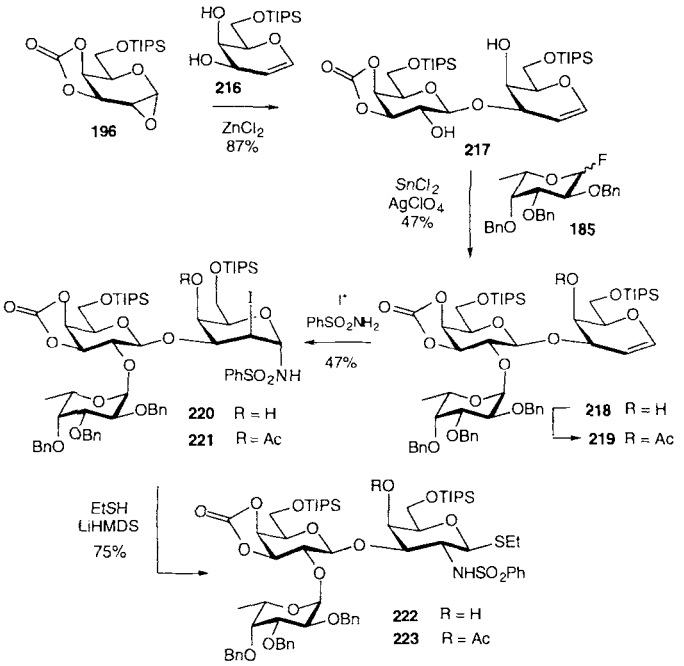

Scheme 53. Synthesis of a trisaccharide donor. LiHDMS = lithium hexamethyldisilazide.

examined the conversion of **221** to thioglycosides donors (see Scheme 22). Treatment of iodosulfonamide **221** with lithium ethanethiolate indeed afforded exclusively the β-ethyl thioglycoside **223**. Such compounds, under promotion by methyl triflate, function as azaglycosyl donors in coupling reactons with even complex donors. (In Section 11 we discuss some limitations in the projected merger of highly hindered partners.)

Precedent established in our program had suggested that, in coupling reactions, donors of this type would give the β-configurated product, presumably due to sulfonamide participation.[110] In the event, the reaction of **223** with the acceptor **215** afforded a hexasaccharide, which was advanced through the remaining manipulations in the synthesis (Scheme 54). However, the spectral properties of the ultimate product **226** did not

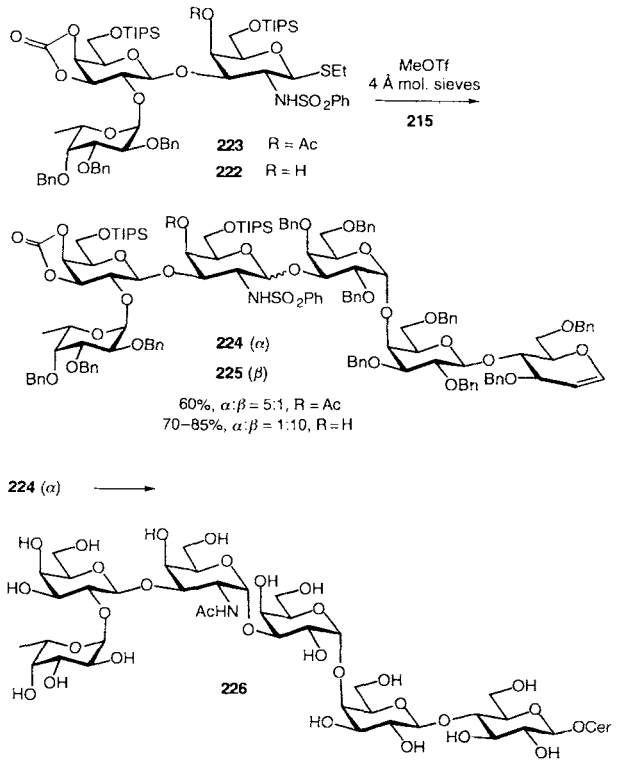

Scheme 54. Synthesis of the hexasaccharide glycal **226**.

correspond to those reported by Hakomori for the natural antigen, assumed to be properly represented by structure **210**. On this basis, and on the basis of self-consistent spectral analysis, we concluded that the material obtained from the coupling of the two trisaccharides had arisen from selective formation of the unexpected (and undesired) α-linked product **224**. We subsequently found that when the trisaccharide donor **222** (obtained by the sequence **218** → **220** → **222**) was employed in the key coupling reaction, the desired β-configurated product **225** was indeed obtained with high selectivity. Thus, there may be an unsuspected electronic or participatory effect biasing the system towards formation of the α-linked product when the 4-hydroxyl group is substituted . Alternatively, there may be a positive β-directing effect exerted by the 4-hydroxyl group of the donor. We emphasize that the occurrence of α-glycosylation and the remarkable turnover in selectivity has not yet been fully general-

ized, though it has been observed in several other cases (see synthesis of asialo-GM_1 in Section 11). This matter is being currently investigated and should be codified in due course. It does serve to once again underline the subtlety of the influences on the stereochemistry of glycosylation. The outcome is not merely a function of the type of donor and the type of reaction conditions employed. In complicated cases it can be much influenced by specific molecular interactions between donor and acceptor.

The properly configured hexasaccharide **225** was epoxidized and coupled with ceramide precursor **227** to provide **228** (Scheme 55). This ceramide attachment can be conducted more

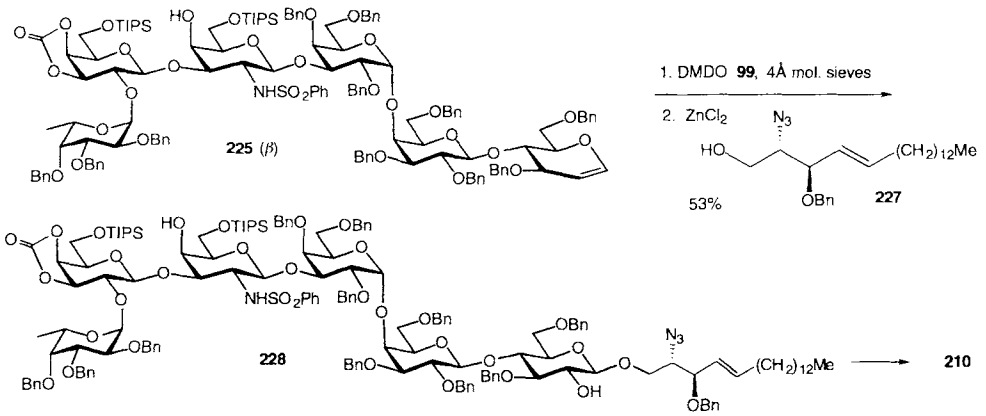

Scheme 55. Completion of the synthesis of the MBr1 antigen.

efficiently on trisaccharide **214**. For reasons that are not yet clear, this alternate route, which is being investigated, presently gives a lower β/α ratio in the (3 + 3) coupling when the acceptor already contains the lipid fragment at the reducing end.

Compound **228** was elaborated and deprotected to afford the natural material **210**. The fully synthetic antigen **210** has been shown to bind to monoclonal antibody MBr1 in the enzyme linked immunosorbent assay (ELISA) and in immune thin layer chromatography assays, while the unnatural isomer **226** exhibits very weak binding in the same assays. Also, MBr1 is strongly reactive with human breast cancer cell line MCF-7 by flow cytometry. Preincubation of MBr1 with glycosphingolipid **210** completely inhibits this reactivity with MCF-7.

Hexasaccharide **225** was also converted to the corresponding allyl glycoside **229** and through this to protein conjugates, as described previously for Le^b and Le^y (Scheme 56). Early studies indicate that our synthetic constructs are immunogenic in vivo. The usefulnesss of the antibodies thus produced against cancer

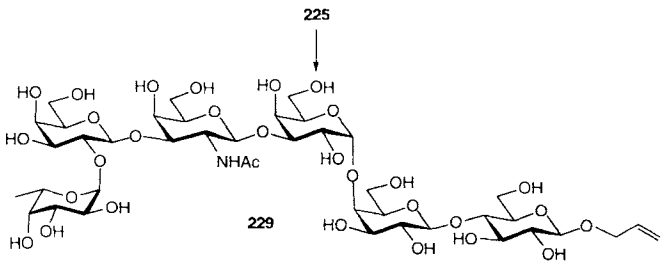

Scheme 56. Formation of an MBr1 allyl glycoside for protein conjugation.

cells is currently being evaluated (see Section 11). The ultimate goal is to develop compounds suited for vaccinelike applications in cancer treatment.

9. The Calicheamicin Problem

In the examples of glycal assembly discussed thus far ensembles were created from familiar carbohydrate building blocks. One of the large advantages of the glycal assembly method has been a reduction in the number of protecting group manipulations necessary to bring about the synthesis of complex target structures. A challenging extension of the glycal assembly method, in which several of the building blocks were far from conventional, was in the construction of the carbohydrate domains of the enediyne antibiotics calicheamicin (**230**, Scheme 57) and esperamicin (**231**).[111-115]

These investigations had several goals. First, we wanted to synthesize these sugar domains so that their biological properties could be examined in the absence of the effector feature of the drugs. Since the intact carbohydrate domains had not been successfully retrieved by degradation of the drugs, this objective seemed to be attainable only by synthesis. The realization of this synthesis through glycal assembly chemistry would confront us with some fresh challenges not encountered with conventional carbohydrate domains.

Moreover, we hoped to accomplish a total synthesis of calicheamicin γ_1^I itself. We had previously synthesized the aglycone domain, calicheamicinone, in racemic as well as enantiomerically pure form.[116] For a total synthesis it was our goal to deliver a fully synthetic carbohydrate domain, as a glycosyl donor, to an appropriate aglycone construct functioning as the acceptor. It seemed likely that the viability of the glycosyl donor would require extensive protecting group manipulations for the hydroxyl, alkylamino, and hydroxylamino functions. Thus, it would be crucial that deprotection of the carbohydrate domain be feasible with survival of this and the aglycone domain. Correspondingly, it would be desirable if the aglycone sector were in a maximally advanced state when functioning as the acceptor. In that way, the burden of dealing with the myriad of sensitive functionality subsequent to coupling would be minimized.

With these goals in mind, we started work on the core carbohydrate domain of esperamicin (**231**). Chemists at Bristol Myers Squibb with access to the drug had found that treatment of **231** with sodium borohydride led to **233a**, in addition to uncharacterized aglycone product (Scheme 57).[117] This reaction implied that reduction of the drug was producing **232** en route to **233a**, which was characterized as methyl glycoside **233b**. Obviously, a perception of the approximate rate of this rearrangement was of great interest to us. Presumably, our eventual car-

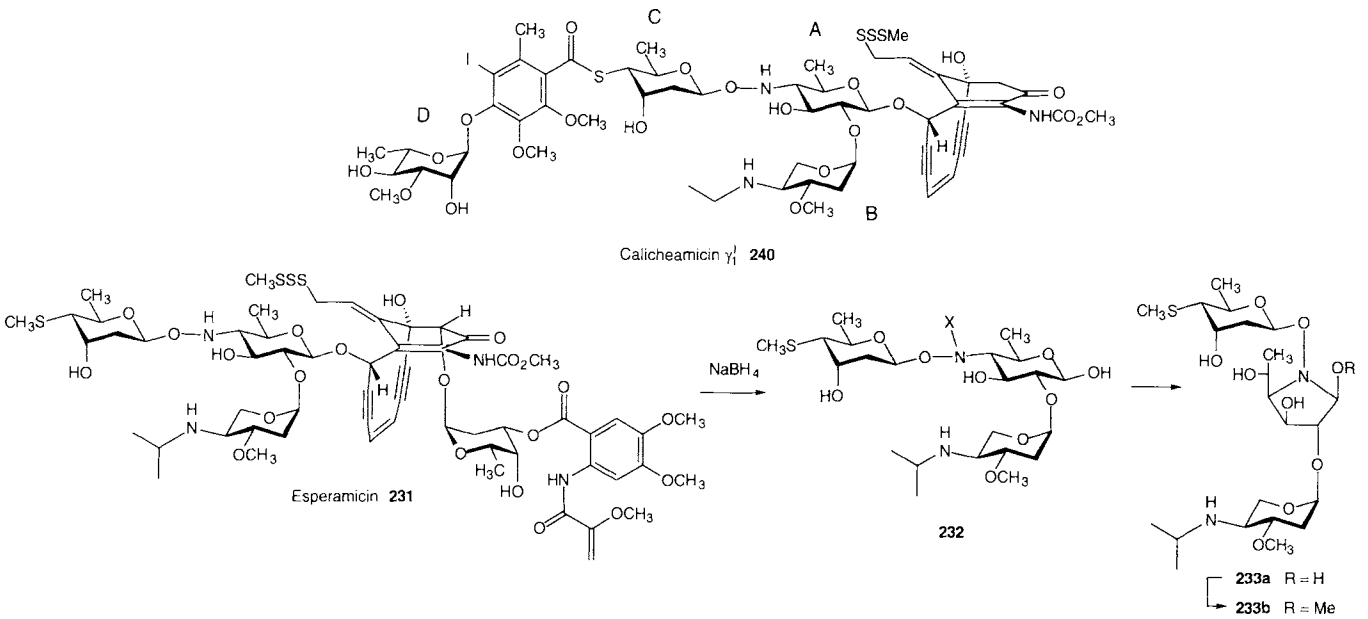

Scheme 57. Structures of calicheamicin and esperamicin.

bohydrate sector glycosyl donor (in the calicheamicin series) would be fashioned from **233a** through manipulations at a free hydroxyl group at the anomeric carbon of its reducing end. The Bristol Myers result suggested that the concurrent presence of a free reducing end and a free NH group on the hydroxylamino spacer might well be incompatible. If this restriction were indeed the case, protection of the latter would be necessary as we passed through a construct with a free reducing end.

For the synthesis of the esperamicin carbohydrate domain, three glycals were mobilized (Scheme 58). Thus, D-fucal (**234**) was readily converted to **235**. The second glycal, **240**, was prepared from the previously reported methyl glycoside **238** via the anomeric thiophenyl compound **239** by pyrolysis of its derived sulfoxide.

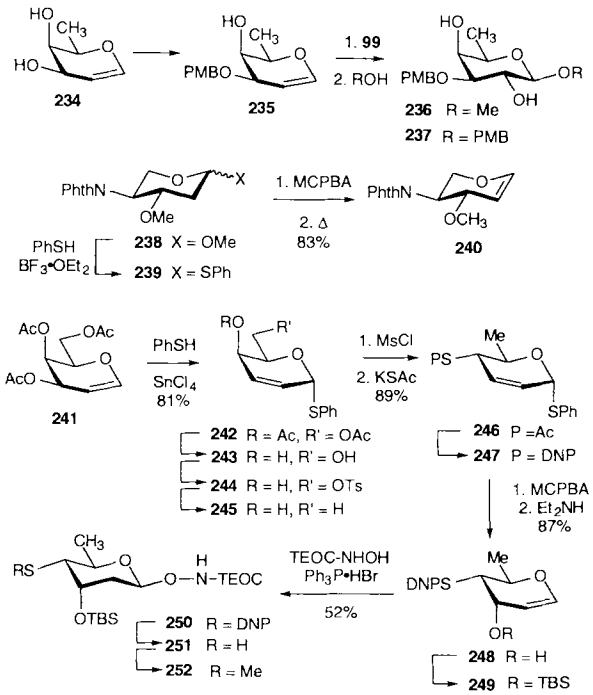

Scheme 58. Synthesis of the esperamicin carbohydrate domain (part 1). MCPBA = *m*-chloroperbenzoic acid, Ms = methanesulfonyl, Phth = phthaloyl, Ts = toluenesulfonyl.

The fashioning of the required thiosugar-containing glycal was challenging. D-galactal triacetate **241** was converted to **242** by thiophenyl Ferrier rearrangement.[36] After formation of diol **243** and thence tosylate **244**, reduction afforded **245** and soon thereafter **246** and **247**. Following rearrangement of the derived sulfoxide and suitable protection, **249** was in hand. This compound served as a donor with *N*-trimethylsilylethyloxycarbonyl (TEOC) hydroxylamine to afford **250**. The chemoselectivity of the addition reaction was only 1.5:1 (the minor product was the *N*-glycoside). The stereoselectivity, however, was very high in favor of the β-glycoside. Presumably this exclusive β-face attack is a consequence of the resident α-axial-OTBS function (TBS = *tert*-butyldimethylsilyl). Removal of the dinitrophenyl (DNP) group and methylation provided **252**.

The assembly process started with epoxidation of **235** along conventional lines. Reaction of the resultant anhydrosugar with methanol and alternatively *p*-methoxybenzyl alcohol afforded **236** and **237**, respectively (Scheme 59). Iodoglycosylation of **240** with **236** and **237** occurred quite selectively at the C2 (equatorial) hydroxyl to afford, after deiodination, disaccharides **253** and **255**, respectively. Thus, the epoxide opening and iodoglycosylation strategies had been choreographed to provide rapid routes to the unusual disaccharides **253** and **255**. These compounds were in turn converted to triflates **254** and **256**, which were smoothly coupled to the carbamate sodium salt derived by deprotonation of **252**.[118] In this way, tricyclic compounds **257** and **258** were in hand.

In the methyl glycoside series (**257**) the phthalimide was cleaved and an *N*-isopropylamine linkage fashioned by reductive amination with acetone. Cleavage of the TEOC and TBS protecting groups afforded methyl glycoside **259** (Scheme 60).

Similarly, in the *p*-methoxybenzyl (PMB) case (**258**), once again the phthalimide was cleaved and the *N*-isopropyl group introduced. We next exposed the free reducing end by cleaving

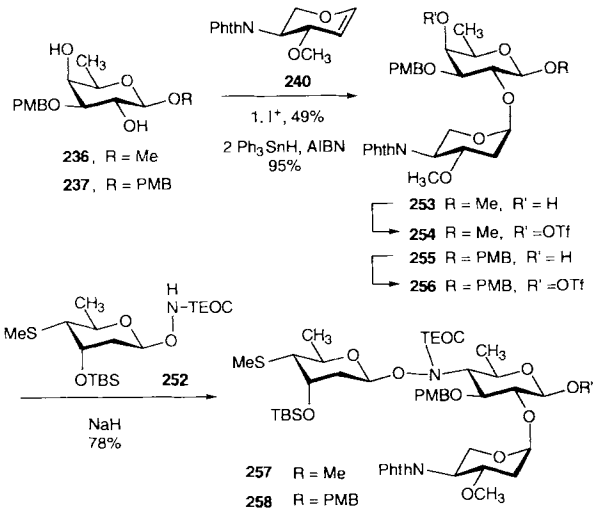

Scheme 59. Synthesis of the esperamicin carbohydrate domain (part 2). AIBN = 2,2'-azobisisobutyronitrile, Tf = trifluoromethanesulfonyl.

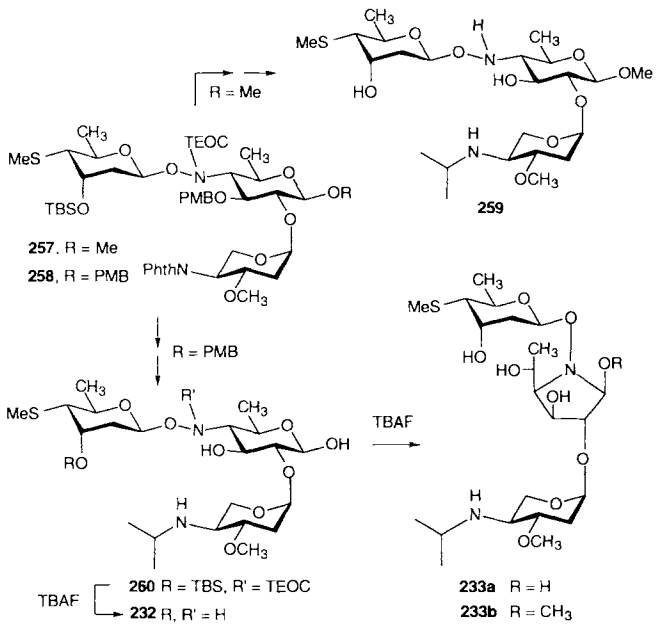

Scheme 60. Synthesis of the esperamicin carbohydrate domain (part 3).

the PMB groups. At this point, compound **260** was in hand. The *N*-TEOC group at the hydroxylamine linkage prevented the ensemble from rearranging to an azafuranose. Indeed, when construct **260** was exposed to the action of TBAF all silyl-based protecting groups were cleaved. However, compound **232**, which would correspond to the fully deprotected core trisaccharide domain of esperamicin, was not isolated or observed. Rather, the isolated product was the azafuranose **233a** and was best characterized as the methyl glycoside **233b**. This compound proved to be identical with a sample that had been derived from esperamicin by the chemists at Bristol Myers (vide supra).

At this stage, it was clear that for the core trisaccharide to maintain viability either the spacer hydroxylamine or the anomeric center at the reducing end must be protected. Since preparation of a glycosyl donor to serve as a calicheamicin-directed construct would probably require the intermediacy of a construct with a free reducing end, it would be necessary to maintain protection of the NH group of the hydroxylamine spacer center during this fashioning stage.

Our attention was next directed to the aryltetrasaccharide domain of calicheamicin. Of course, the synthesis of the ABC sector of **230** would be closely patterned after the program followed in the esperamicin series. Thus, we focused on the CD sector of the domain (Scheme 61). We started with glycal **261**,

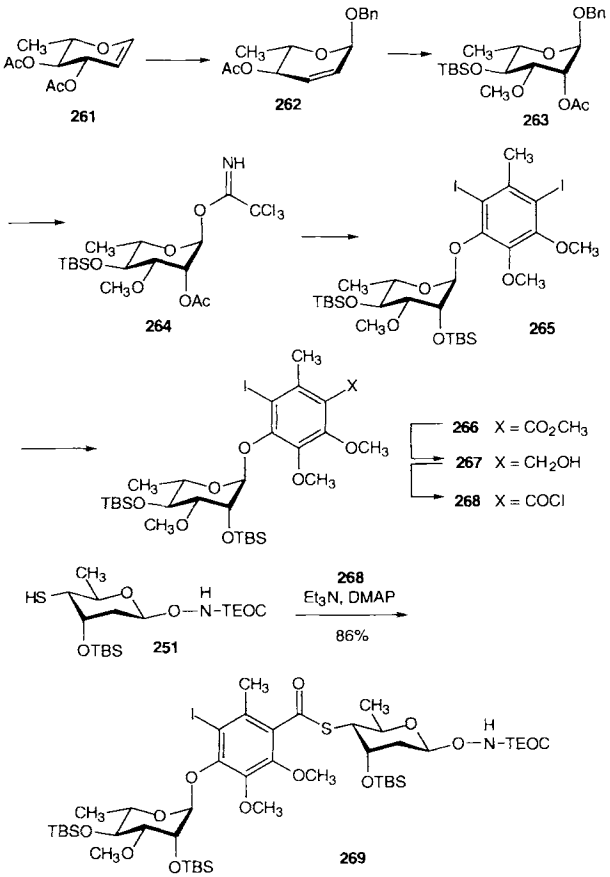

Scheme 61. Synthesis of the calicheamicin carbohydate domain (part 1).

which was available from L-rhamnal. Ferrier rearrangement with benzyl alcohol afforded **262**, which was converted by osmylation, monomethylation (of the derived stannylene), and silylation to provide **263**. After debenzylation, the trichloroacetimidate donor function was introduced, affording **264**. Schmidt coupling of **264** to 2,4-diiodo-5,6-dimethoxy-3-methylphenol afforded **265**. Regioselective palladium-mediated carbonylation furnished **266**, which upon reduction (to **267**), followed by oxidation and formation of the acid chloride, provided **268**.[119] The previously described C-ring thiol-containing glycal **251** underwent acylation with **268** to afford aryl disaccharide **269**.

Kahne coupling[118] of the anion of **269** with the triflate **254** produced the aryl tetrasaccharide **270** (Scheme 62). Removal of the phthalamide group was followed by reductive ethylation and cleavage of all silyl-based blocking groups and the PMB ether to provide **272**. A variety of independent investigations by our group[120-122] and by Nicolaou et al.,[123, 124] who had earlier synthesized the carbohydrate domain,[125] revealed that

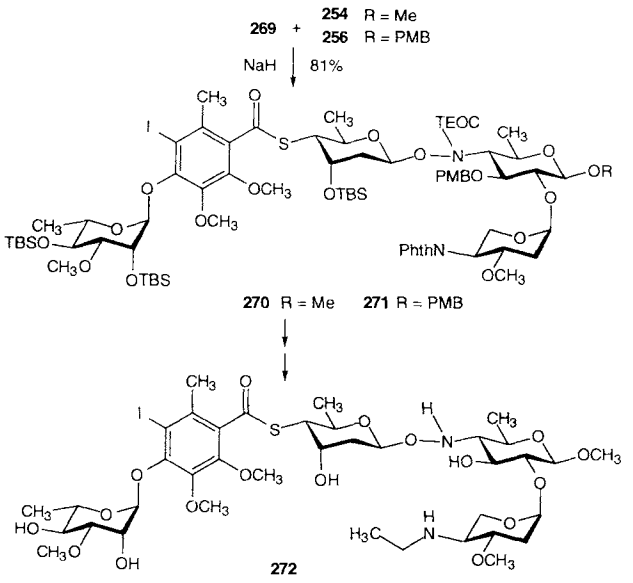

Scheme 62. Synthesis of the calicheamicin carbohydrate domain (part 2).

the recognition attribute of calicheamicin is, in fact, vested in the aryltetrasaccharide domain embodied in **272**.

Our next goal was to demonstrate that a competent glycosyl donor could be fashioned from **272** and, above all, delivered to a reasonably advanced version of the aglycone domain. For this purpose, **269** and **256** were coupled to provide aryl tetrasaccharide **271** (Scheme 62). Deprotection of **271** with 2,3-dichloro-5,6-dicyanobenzoquinone (DDQ) afforded **273**, which was converted to the trichloroacetimidate donor **274**. Among the aglycone acceptors screened was **275**. Schmidt coupling of **274** and **275** indeed gave rise to a 3:1 mixture of **276** and the corresponding α-glycoside, which were readily separable (Scheme 63). This was the first such demonstrated glycoside coupling of two fully synthetic domains in the calicheamicin series.[126]

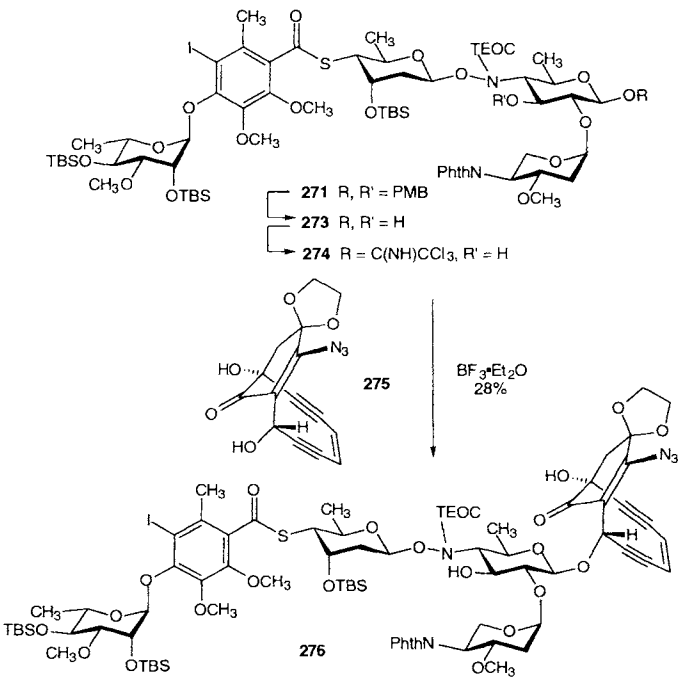

Scheme 63. Coupling of the carbohydrate sector to an enediyne core.

While the result was certainly pleasing, it soon became clear that compound **276** was insufficiently developed for advancement to fully synthetic calicheamicin. During this era of the program, several valuable insights were garnered. A key finding was that hydrazine-induced cleavage of the phthalimide group was not possible in the presence of the cyclic enediyne functionality. Under various conditions, destruction of the enediyne network (albeit in an uncharacterizable way) occurred far more rapidly than liberation of the amine from the phthalimide. Similarly to be taken to heart, was the finding that cleavage of the axial TBS protecting groups with TBAF was a problematic step. When the final deprotection was conducted on various constructs containing these protecting groups, the rhamnose D ring was seriously damaged or lost. This loss could be minimized at low temperatures (−10 °C), but under these conditions deprotection of the axial TBS groups took roughly seven days. Based on the results of experiments in which the "survival times" of these functional groups were determined, it seemed unlikely that an enediyne moiety could withstand the action of these conditions for the period of time required for freeing of the alcohol from its TBS derivative.

In response to these problems, and taking cognizance of the first total synthesis of calicheamicin by Nicolaou and colleagues,[111] we changed our pattern of protecting groups to that shown in Scheme 64. In preparing for the final push toward calicheamicin γ_1^I, several processes were improved. The route to

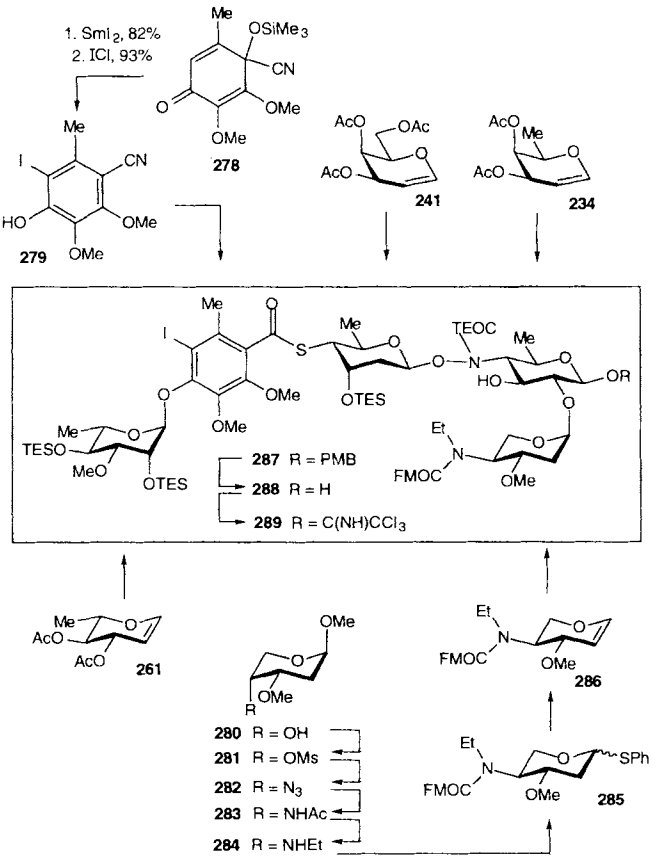

Scheme 64. Improved synthesis of the calicheamicin carbohydrate domain. FMOC = 9-fluorenylmethyloxycarbonyl.

the aromatic sector was totally revamped and streamlined. A key finding, per se unrelated to carbohydrate chemistry, was registered by Steven Olson. He found that mono-TMS cyanohydrin derivatives of quinones (e.g. **278**) are converted to *p*-hydroxybenzonitriles (e.g. **279**) through the action of samarium(II) iodide.[127] D-fucal (**234**), D-galactal triacetate (**241**), and L-rhamnal diacetate (**261**) were the building blocks for the A, C, and D rings, essentially as before, with the exception that triethylsilyl groups were employed instead of TBS functions as the protecting groups for the hydroxyl groups.

The starting material for the 9-fluorenylmethyloxycarbonyl (FMOC)-containing glycal was mesylate **281**, derived from differentiated methylglycoside **280**. Serge Boyer found that azide displacement upon **281** afforded **282** and, in seriatum, the acetamide **283** and then the *N*-ethyl derivative **284** were fashioned. Thiophenol displacement at the anomeric center provided **285**, which upon oxidation and thermolysis afforded **286**. Glycal assembly in analogy to our first calicheamicin synthesis used **237** for the iodoglycosylation with **286**, en route to the AB section. Continuation of the sequence led to tetrasaccharide **287**, thence to **288**, and finally to **289**.

At this stage Steven Hitchcock was able to investigate a most exciting possibility. Glycosylation could be conducted with **289** as the projected donor and **290** as the acceptor (Scheme 65). The feasibility of employing such a structurally advanced acceptor arose from the use of donor **289**. Since no oxidations or reductions would be necessary to bring the projected product to the state required in the drug, one would hope to use the otherwise vulnerable acceptor **290**, in which the allylic trisulfide functionality is already present. Fortunately, reaction under particularly mild conditions (AgOTf, 4Å molecular sieves)[128] allowed for glycosylation. All blocking groups were discharged in two steps, and calicheamicin γ_1^I (**230**) was in hand. Thus, an ultimately convergent synthesis had been accomplished.

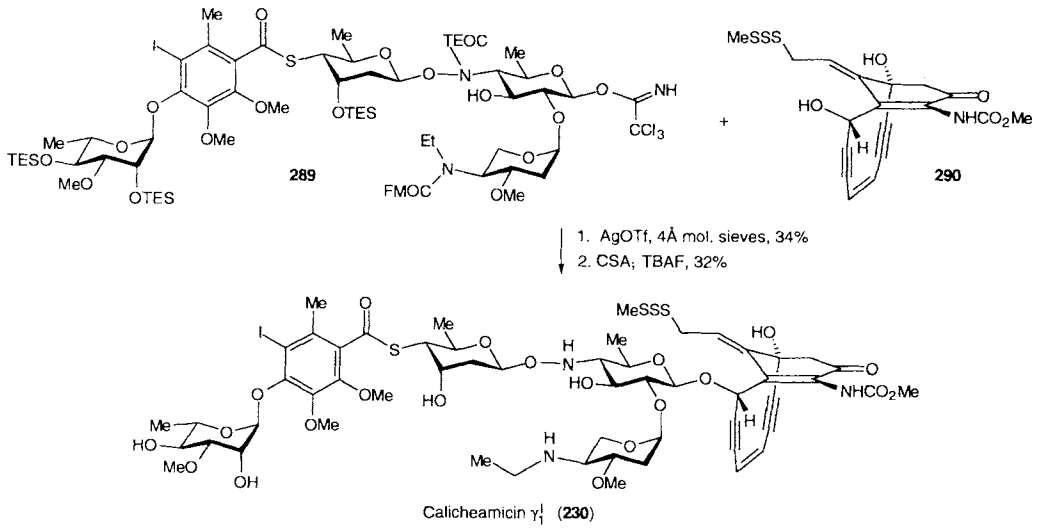

Scheme 65. The ultimately convergent synthesis of calicheamicin.

10. Solid-Phase Oligosaccharide Synthesis

Progress in the synthesis of oligosaccharides and glycoconjugates by the solution-based methodology described in the previous sections was certainly reassuring. Yet because of the importance of this field, these advances prodded us to seek still greater levels of simplicity and efficiency. It was instructive to think about this problem in the broader context of biooligomer synthesis, thus inviting analogies between oligosaccharide synthesis and the synthesis of oligonucleotides and peptides. Of course, impressive advances had been registered in the solution-phase synthesis of these latter biooligomers. However, it is clear that the major upsurge in their synthesis arose only after solution-based coupling methods were adapted to the solid phase. While polymer-supported synthesis of oligopeptides[129] and oligonucleotides[130] is not a panacea, it has certainly been of enormous benefit in improving yields, simplifying procedures, and obviating the need for purification at each stage. Obviously, in solid-phase methodology the potential advantage of such purification after each elongation is substantially forfeited. Hence the chemistry of the various reiterations must be sufficiently efficient that a single purification at the final stage affords product of the required homogeneity.

In polypeptide and oligonucleotide synthesis, it is the high yields in the individual coupling steps that seem to render the final-stage purification strategy viable. Excellent yields arise from the inherent quality of the coupling steps and are further "amplified" by the capacity to employ excess solution-based coupling partner, which is removed from the solid phase by filtration.

By contrast, solid-phase synthesis of oligosaccharides is much less developed.[131] This assessment is in no sense intended as a critique of the practitioners of the field; rather it reflects the fact that the problem of oligosaccharide synthesis is intrinsically far more complicated than the corresponding problem in oligonucleotide and oligopeptide synthesis (Scheme 66).

Consider the synthesis of oligonucleotides, particularly oligo-2-deoxynucleotides (Scheme 66). Assuming the availability of the individual nucleosides, each elongation involves the fashioning of an internucleotide phosphate bond. For this purpose it is necessary to distinguish between the 5′- and 3′-hydroxyl groups and to discover a high-yielding coupling step. The fashioning of the internucleotide bond does not create a new chiral center. Similarly, in fashioning a peptide the α-amino and α-carboxyl groups must be distinguished from any such or related functionality (for example thiol and hydroxyl groups) present on various side chains. An efficient coupling is necessary for amide bond forma-

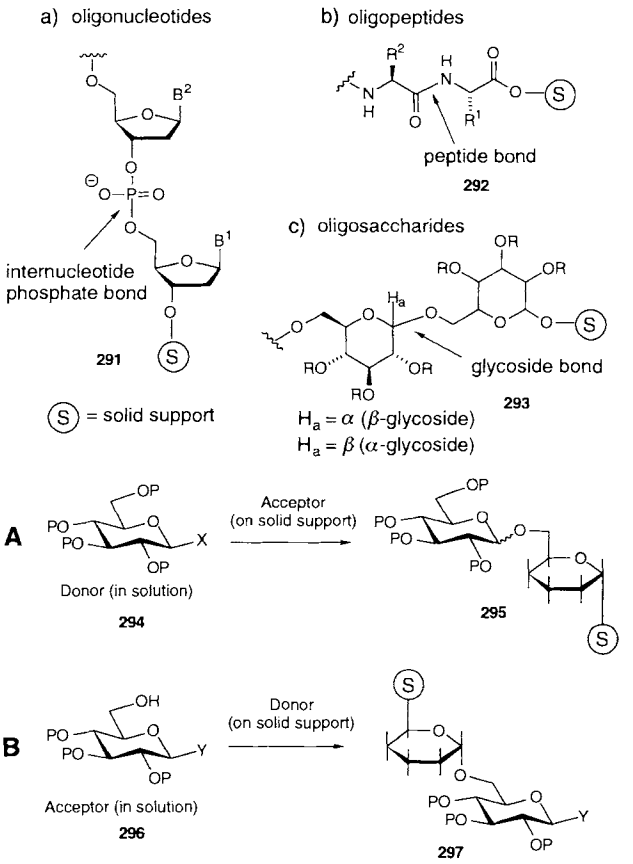

Scheme 66. Solid-phase synthesis of biopolymers. B^1, B^2 = nucleobases.

tion. Once again, no new chirality arises in the elongation of the oligopeptide. The two strategies for elongation of these biopolymers on solid supports are implied in structures **291** and **292** in Scheme 66. Clearly, in contemplating the synthesis of an oligosaccharide on solid support (cf. **293**) the complexity level rises markedly.

Thus, in fashioning the repeating units from an aldohexose, one must distinguish the anomeric region of one of the components to serve as the donor region (see **294**). In the case of combining hexose units, one must also differentiate one of five rather closely related hydroxyls to serve as the glycosyl acceptor center (see **296**). Most demanding is the need to control the configuration at each newly emerging glycosidic bond. Unlike the synthesis of the other biooligomers, the linkage of saccharide monomers through formation of a glycoside bond has serious stereochemical consequences. Given the enormously more complicated nature of the problem of oligosaccharide synthesis on a solid support, the dramatic progress that has been registered is indeed amazing and speaks eloquently for the creativity and tenacity of its founding practitioners.

In contemplating the syntheses of oligosaccharides on a solid support, two overall strategies can be entertained. In one instance (Case A) a glycosyl acceptor is mounted to a support, and solution-based donor (**294**) as well as promoter are administered for the coupling step leading to glycoside **295**. To reiterate the process, a new acceptor must be fashioned on the support. This would generally involve cleavage of a specific protecting group (P) to generate a new acceptor center in a defined position.

In the alternative strategy (Case B) the polymer-bound glycosyl donor reacts with the solution-based acceptor (**296**). For reiteration, the donor functionality must be unveiled from the terminal anomeric functionality (Y) on the support-bound structure (**297**). Also, positionally defined glycosyl acceptors must be synthesized for each iteration such that acceptor character is manifested at a particular hydroxyl center and donor character can be fashioned at the anomeric center of the product. The incremental complexities of oligosaccharide synthesis on a solid support relative to that associated with the other classes of biooligomers is virtually palpable upon analysis of the problem.

It was in dealing with the problem of solid-phase carbohydrate synthesis that we felt that glycal-based constructions might prove to be particularly valuable.[132, 133] The guiding paradigm was that shown in Scheme 67. Polymer-bound glycal

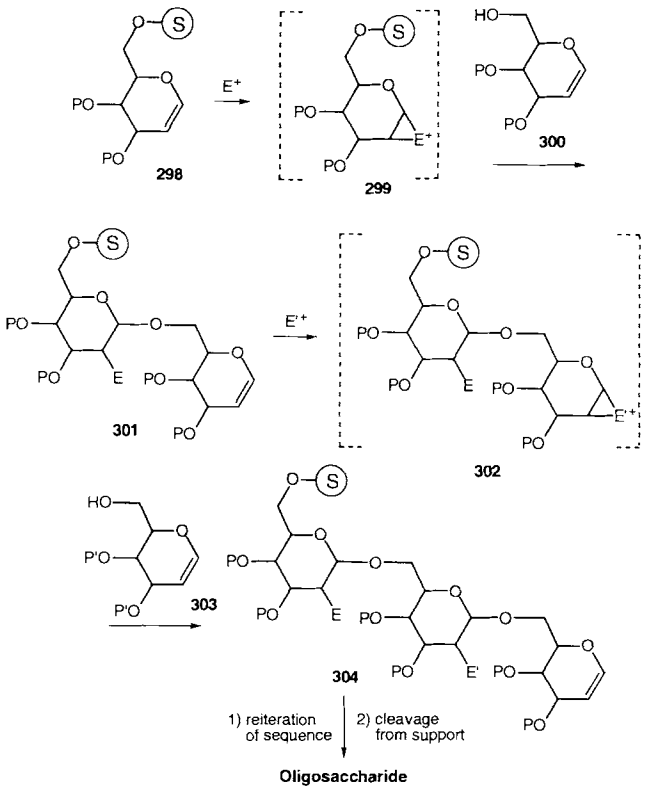

Scheme 67. Solid-phase carbohydrate synthesis employing glycals. P, P′ = protecting groups; E^+, E'^+ = electrophiles.

298 would be synthesized by attaching the requisite glycal to a suitable solid support. The system would be activated by unspecified electrophile E^+ to furnish polymer-bound donor **299**. In principle **299** can be a substoichiometric intermediate (cf. iodoglycosylation) or a characterizable chemical entity (cf. 1,2-epoxide). Coupling of **299** with solution-based glycal acceptor **300** would give rise to the elongated polymer-bound glycal **301**. Reiteration of the process generates **304** via new polymer-bound donor **302** and solution-based acceptor **303** (which may or may not be identical to **300**).

Several decisions, starting with the choice of polymer, were necessary to study the implementability of the scheme. We elect-

ed a silicon-based attachment of the growing carbohydrate domain to the solid support and turned to commercially available polystyrene (cross-linked with 1% divinylbenzene). Fortunately, we were able to take good advantage of the findings of Chan[134] registered in a totally different context. Thus, metalation of the polymer leads to formation of the aryllithium species. When exchange is followed by silylation with a difunctional silane of the type R_2SiCl_2, a silyl chloride functionalized resin is obtained (Scheme 68).

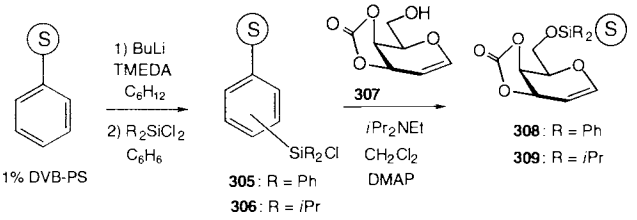

Scheme 68. Preparation of a polymer-linked glycal. TMEDA = tetramethylethylenediamine. 1% DVB-PS = polystyrene cross-linked with 1% divinylbenzene.

In our initial explorations[132] we silylated with diphenyldichlorosilane and attached the first glycal (**307**) through a conventional silylether forming reaction to provide **308**. Subsequent studies revealed that the spacer in the products arising from elongation of **308** lacked the needed hydrolytic stability. Accordingly, we turned to the use of diisopropyldichlorosilane as the silylating agent, which led us to **309** as our support-bound donor of choice. We determined the loading of carbohydrate to be in excess of 0.9 mmol per gram of **307**. The activation method we developed at first was that of glycal epoxidation using 2,2-dimethyldioxirane as the oxidant. Of course, from this point on the support-bound compounds (e.g. **310**) were generally not fully characterizable (Scheme 69). Reaction of **310** with glycal acceptor **307** mediated by zinc chloride afforded **311**. We could establish the actual presence of **311** by treatment with tetra-*n*-butylammonium fluoride (TBAF), which provided **312** in roughly 90% yield. Reiteration of the sequence, twice more, using acceptors **307** and **111** in sequence followed by removal from the polymer with TBAF led to tetrasaccharide **315** in 74% overall yield (approximately 90% average yield per coupling step). The reader will recognize that in these early forays we relied heavily on galactose epoxide donors of the type **310**. These tend to offer high margins of β-product formation (see Scheme 37). That galactosylation is also an important capability in fashioning biologically important oligosaccharides had not escaped our attention.

Several features of the method should be emphasized. First, the polymer-bound donors in which the C3 and C-4 hydroxyl groups are engaged as a cyclic carbonate are, in fact, highly stereoselective galactosylating agents. Single purification at the tetrasaccharide stage was a straightforward matter. Another feature was the "self-policing" nature of failed couplings. While the average coupling yields are only about 90%, the uncoupled epoxide is apparently destroyed by hydrolysis. Thus, we do not encounter entities with deletions in the interior of the chain.

Glycosyl acceptors with secondary hydroxyl groups are also accommodated by this method (Scheme 70). Compound **313**,

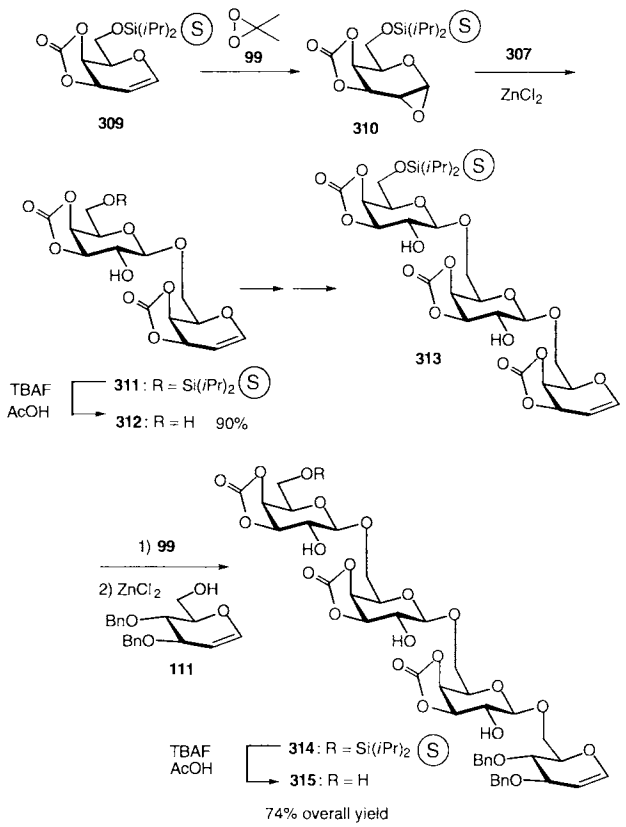

Scheme 69. Solid-phase synthesis of 1,6-linked polysaccharide residues.

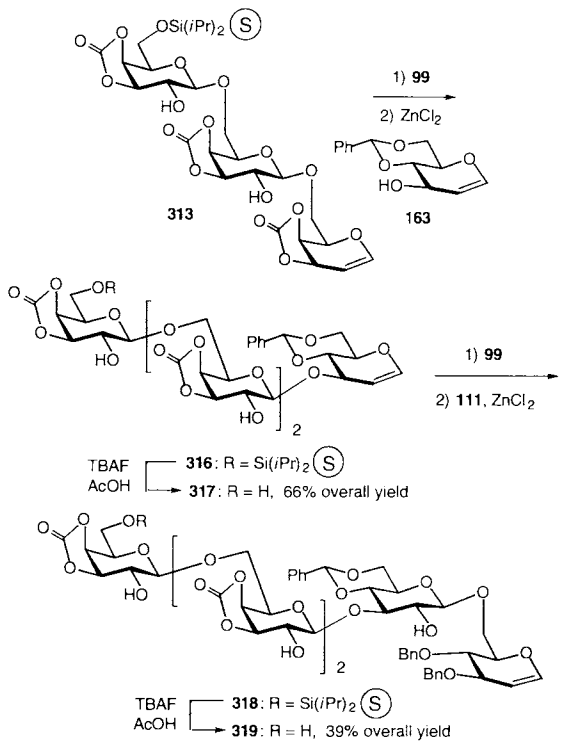

Scheme 70. Synthesis of a pentasaccharide on a solid support.

following epoxidation with **99**, reacted with D-glucal derivative **163** to give **316**. Tetrasaccharide **317** was retrieved from the support by the action of TBAF in a 66% overall yield based on **309**. Assuming 90% yield per coupling in the synthesis of **313**,

glycosidation of **163** had occurred in roughly 80% yield. An additional example demonstrating the use of glycals with secondary hydroxyl groups is the coupling of solution-based 3,6-dibenzylglucal with **310** to give the corresponding 1,4-linked disaccharide product.

Compound **316** was oxidized with **99** to give a polymer-bound glucosyl donor. This epoxide reacted with $ZnCl_2$ and a solution of **111** in THF to provide **318**, which was cleaved from the support to give pentasaccharide **319** in 39% overall yield from **309**. This glycosylation, which had been achieved in approximately 60% yield based upon **316**, also occurred with a high degree of stereoselectivity. However, in this particular case, a minor component, believed to be the α-glycoside, was detected in the ^{1}H NMR spectrum. The ratio of the desired all-β-glycoside product to this unknown component was in excess of 10:1. This apparent erosion from strict β selectivity using this glucal-derived donor can perhaps be controlled by appropriate modification of the as yet unoptimized conditions.

The scheme can be rendered more convergent through recourse to disaccharide and higher oligomer acceptors (Scheme 71). Thus, epoxidation of polymer-bound tetrasaccharide glycal **316** followed by zinc chloride mediated coupling with disaccharide acceptor glycal **320** and retrieval from the support (TBAF) afforded **322** in a 58% overall yield (29% overall from **309**, 45% yield from **316**).

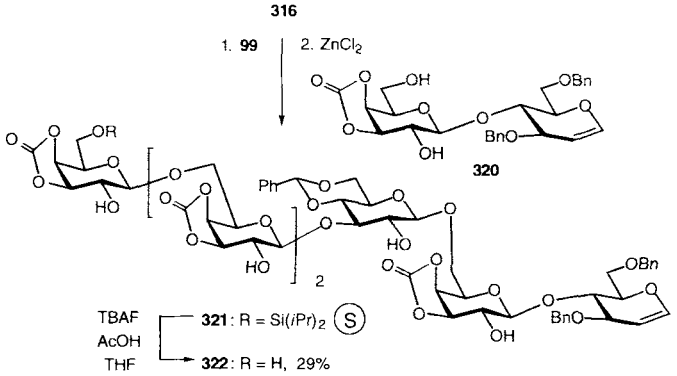

Scheme 71. Synthesis of a hexasaccharide on a solid support.

It should be noted that this last coupling involves the regioselective glycosylation of a diol acceptor. This element of "site direction" in the use of polymer-bound donors with solution-based acceptors can be a significant advantage since protecting group manipulations can be minimized.

The solid-phase method is also applicable to the synthesis of branched structures through the logic of glycal assembly (see Schemes 41 and 42). We demonstrated the principle with support-bound glycal **309**, which was epoxidized and coupled to acceptor **183** to afford disaccharide **323** (Scheme 72). The latter served as a polymer-bound glycosyl acceptor in a reaction with fluorosugar **185** mediated by stannous triflate. Tetrasaccharide **324** was retrieved from the polymer with TBAF to afford **325**, a glycal precursor of Lewis b. Thus, it was demonstrated that branching at the C2 hydroxyl could be achieved in a growing chain by exploiting the hydroxyl group unveiled in the epoxide donor based glycosylation.

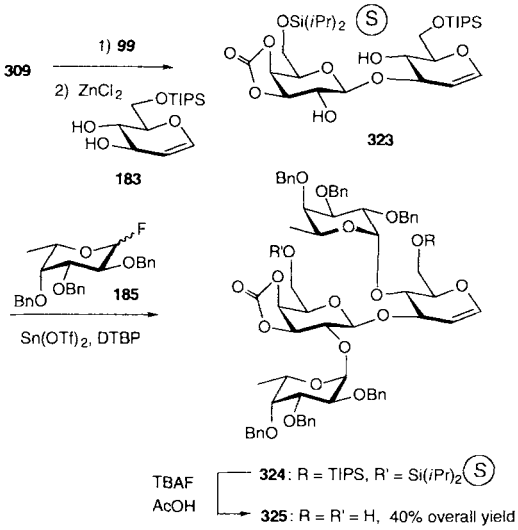

Scheme 72. Synthesis of branched sugars on a solid support. DTBP = di-*tert*-butylperoxide.

We note that at this stage direct sulfonamidoglycosylation of solution-phase carbohydrate acceptors with polymer-bound donors (cf. Scheme 22) was not possible. While halosulfonamide adducts of glycals can be formed on supports, the glycosidation failed. Thus, we were unable to make our way from polymer-bound **324** to the full Lewis b determinant. Instead, we had to revert to solution-phase methods (see **325**) and complete the Lewis b synthesis by the previously discussed procedure. More recently we have developed a two-stage protocol for conducting sulfonamidoglycosylation on support-bound substrates (see Scheme 81).

Another of our goals was to build upon the capabilities attained in glycal assembly to synthesize glycopeptides. Our first objective was to reach asparagine-linked glycopeptides. Brilliant advances in glycopeptide synthesis have been achieved by many researchers,[135] including notably, Paulsen, Kunz,[135e] Meldal, and Lansbury.[135c] The strategy we hoped to implement would be radically different and maximally convergent.

It was envisioned that a terminal glycal of a synthetic oligosaccharide domain would be subjected to iodosulfonamidation. As demonstrated earlier in a simpler model (see **90** → **91**, Scheme 25), treatment of such an intermediate with azide results in formation of β-anomeric azide with suprafacial movement of the α-sulfonamide from C1 to C2. Reduction of the azide and acylation of the resultant anomerically pure β-aminosugar provided a protected glycopeptide (**93**, Scheme 25). Fortunately, this capability was tranferable to the solid phase (vide infra).

This was to serve as the cornerstone of our strategy. First, however, a cautionary note is appropriate. While the synthesis of glycopeptide ensembles is a complex undertaking, the most difficult part of the enterprise may actually be the final maneuvers required to produce the fully deprotected entity. Thoughtful planning and corresponding care must be exercised since the *N*-asparagine-linked glycopeptide can be a rather vulnerable construct.

Jacques Roberge took up the problem in great detail and was subsequently joined by Xenia Beebe. In this presentation we spare the reader the description of the many setbacks encoun-

tered in implementing the seemingly straightforward design with provision for full deprotection. We will first present the solution synthesis of glycopeptides by this method[136] and then demonstrate its compatibility with synthesis on solid supports.

In synthesizing the carbohydrate domain of the glycopeptide we focused on a target structure amenable to the most straightforward methodology we had developed. For this purpose, we relied on the galactal epoxide **196**, which reacted with **307** to give, after acetylation, disaccharide **326** (Scheme 73). Epoxidation of **326** followed by reaction with acceptor **111** furnished, after acetylation, the trisaccharide glycal **327**. This set the stage for functionalization of the glycal linkage with a view to glycopeptide formation. In pursuit thereof, we eventually settled on the use of 9-anthracenylsulfonamide (**328**) in the iodosulfonamidation reaction. We have demonstrated that this protecting group can be readily removed under a variety of mild reducing conditions.

Treatment of **327** with **328** and di-*sym*-collidine iodonium perchlorate gave rise to **329**. Reaction of the latter with tetra-*n*-butylammonium azide triggered the expected relocation of the sulfonamide. The resulting azidotrisaccharide was then acetylated. Azide reduction and reductive cleavage of the sulfonamide was accomplished with aluminum amalgam to afford **330**. Acylation of the β-amine was conducted with the ω-carboxyl group of the tripeptide TrocAspLeuThrOAll in the presence of IIDQ, giving rise to **331**. Deprotection was accomplished by desilylation, removal of the allyl group, reductive removal of the Troc group, and hydrogenolysis of the benzyl groups. Lastly, the two cyclic carbonate linkages were cleaved by KCN/ethanol and the free N-linked glycopeptide **332** was in hand. We view this synthesis of the trisaccharide tripeptide ensemble as an important plateau in aspiring to the synthesis of glycopeptides.

Having demonstrated the feasibility of the synthesis in solution, we next turned to conducting it on the solid support (Scheme 74).[137] Polymer-supported disaccharide **311** was extended by epoxidation, reaction with **111**, and acetylation to provide trisaccharide **333**. After treatment of **333** with anthracenesulfonamide and I(*sym*-coll)$_2$ClO$_4$, the clean formation of **334** was inferred from subsequent steps. Reaction of this material with tetra-*n*-butylammonium azide followed by acetylation provided the anomeric azide **335**. This success is in contrast to our inability to achieve polymer-based sulfonamidoglycosylation of carbohydrate acceptors (see Scheme 71).

The principal advantage in using the anthracenesulfonamide linkage is that it can be cleaved by a variety of mild methods. For instance, we developed the use of thiophenol or 1,3-propanedithiol and Hünig's base for the removal of the anthracenesulfonyl group. These protocols are compatible with synthesis on solid supports. Also, anthracenesulfonamide itself is more soluble than benzenesulfonamide in THF, which is a good swelling solvent for the polymer. Thus, the use of the anthracene-based agent results in a more efficient and complete iodosulfonamidation reaction. Treatment of **335** with 1,3-propanedithiol and iPr$_2$NEt effected both the reduction of the azide and removal of the sulfonamide. The resulting amine was coupled with tripeptide **336** and alternatively with pentapeptide **337** in the presence of IIDQ to afford the protected glycopeptides **338** and **339**, respectively. Removal from the solid support with HF·pyridine provided the glycopeptides **340** and **341** in overall yields of 30 and 37%, respectively. For the synthesis of **341** this constitutes an average yield of approximately 90% per step over the ten steps from polymer-bound glycal **309**. Chromatography on a short column of reversed-phase silica gel (C-18) was sufficient to obtain **340** and **341** in pure form. This ready purification can be attributed to the previously described "self-policing" feature of the solid-phase glycal assembly method (see Scheme 70) and illustrates the efficiency in the conversion of the terminal glycal to the terminal glucosylamine.

The remaining protecting groups in both **340** and **341** were cleaved under standard conditions to provide the completely deblocked glycopeptides, **342** and **343**, in yields of 61 and 48% (from **340** and **341**), respectively. Structural characterization of the glycopeptides by NMR spectroscopy confirmed the β-con-

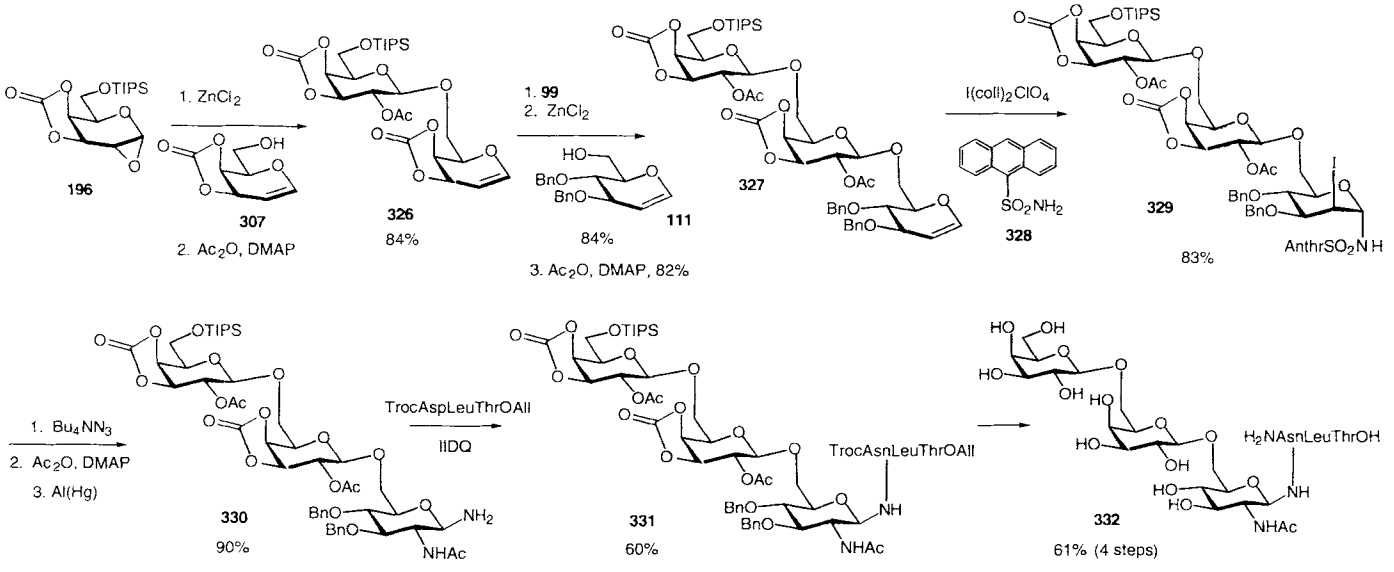

Scheme 73. Synthesis of N-linked glycopeptides. All = allyl, Anthr = anthracenyl, Troc = trichloroethoxycarbonyl, IIDQ = 2-isobutoxy-1-isobutoxycarbonyl-1,2-dihydroquinoline.

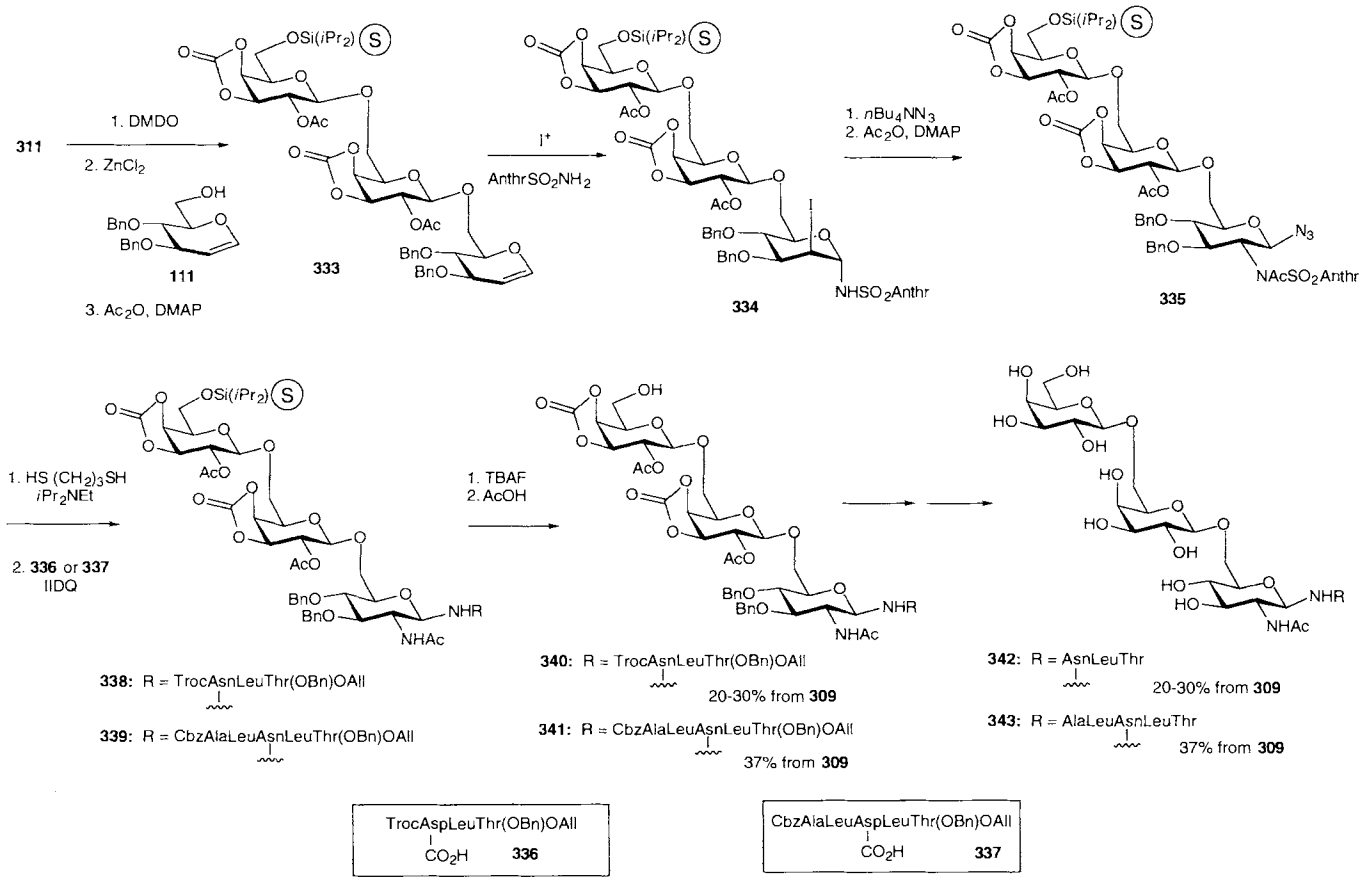

Scheme 74. Synthesis of N-linked glycopeptides on a solid support. Cbz = benzyloxycarbonyl.

figuration of all the anomeric linkages. The structures were further corroborated by mass spectroscopy.

The presence of orthogonal protecting groups on the C- and N-termini of the peptide provides the opportunity to extend the peptide chain while the ensemble is bound to the solid support. Alternatively, after removal from the support, the liberated peptide terminus may provide a functionality for linking to a carrier molecule to generate other glycoconjugates. Scheme 75 shows how the peptide portion of the glycopeptide was extended while still bound to the polymer support. The solid phase bound trisaccharide pentapeptide **345** was assembled as previously described from **335** by employing pentasaccharide **344** in the coupling reaction. The C-terminus of **345** was deprotected to give acid **346**, which was then coupled to tripeptide **347** with a free N-terminus to give glycopeptide **348**. Retrieval from the solid support afforded the trisaccharide–octapeptide **349** in an 18% overall yield from polymer-bound galactal carbonate.

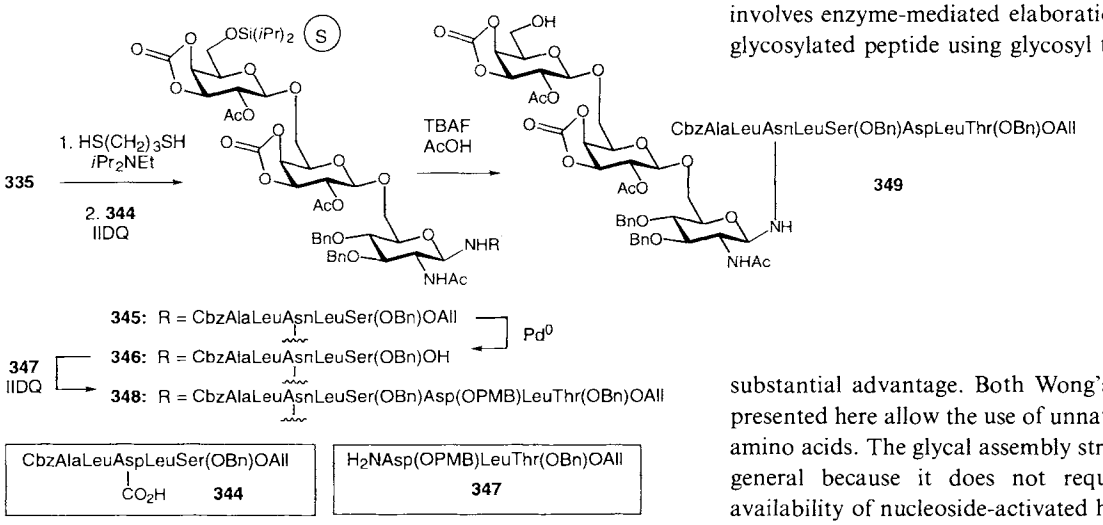

Scheme 75. Synthesis of N-linked glycopeptides on a solid support.

In contemplating the future of glycopeptide synthesis, one should take particular note of the method of Wong,[138] which involves enzyme-mediated elaboration of a solid phase bound glycosylated peptide using glycosyl transferases to append unprotected nucleoside phosphate activated monosaccharides in the elongation phase. The conjugate is retrieved from the solid support by protease action. Protecting group manipulations are not necessary in enzymatically mediated chemistry, which can be a substantial advantage. Both Wong's method and the method presented here allow the use of unnatural amino acids and non-amino acids. The glycal assembly strategy is in principle totally general because it does not require transferases and the availability of nucleoside-activated hexoses. It can also accommodate the inclusion of unnatural (artificial) sugars in the

construction. Such building blocks are available from the Lewis acid catalyzed diene–aldehyde cyclocondensation reaction (Scheme 2). All workable approaches, whether purely chemical or chemo-enzymatic, are complementary for reaching the common goal of carefully designed, fully synthetic glycopeptides.

11. Studies in Progress

Thus far we have confined ourselves to a review of programs that have been completed and published. It is well to bring the reader up to date on current efforts in our laboratory. This update will help to underscore the sorts of chemical and biological problems we are addressing through the strategy of glycal assembly.

11.1. Synthesis of Blood Group A (Type 2) Determinant

We have been continuing our work in the total synthesis of human blood group determinants using glycal assembly. An important recent target has been the blood group A (type 2) determinant.[7] While we have not yet reached this goal, in the sense of producing a fully deprotected, suitably conjugated blood group A substructure, the substantial progress realized[139] suggests that this will be achieved shortly. The synthesis started with previously described compound **199**, which was converted to glycal **350** such that the C3′-hydroxyl of the galactose moiety could subsequently function as the glycosyl acceptor site (Scheme 76). Fortunately, this coupling could be accomplished by using the anomerically pure C2-azido chloride **351**, as pioneered by Paulsen.[140] The resulting **352** has now been converted by our standard protocols to the pentacyclic glycal **353**. The latter awaits suitable conjugation to provide the synthetic human blood group A determinant and immunological investigation.

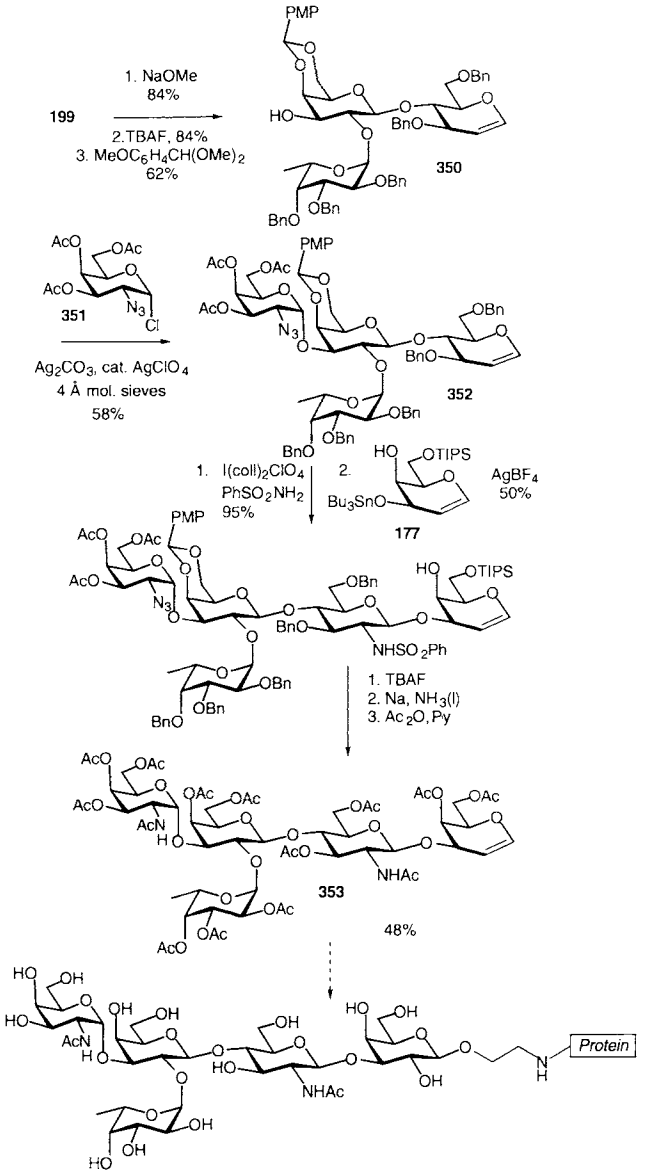

Scheme 76. Synthesis of a glycal of the blood group A (type 2) determinant.

11.2. An Approach to the N3 Antigen

Our synthesis of the N3 antigen is now nearing completion. We, as well as others,[141] have high hopes that a suitably conjugated version of this antigen can be used to detect even minuscule amounts of the N3 antibody, which appears to be specifically produced in response to gastrointestinal cancer.

The realization of this synthetic goal by glycal assembly methodology turned out to be more complicated than might have been expected. The exercise has been valuable in exposing some limits of the technology described earlier in this report. It was found that sulfonamidoglycosylation, either directly (cf. Scheme 22) or by the two-stage protocol employing a saccharide having an ethylsulfanyl substituent at the anomeric center (cf. Scheme 54), can be undermined if the combined steric demands of the donor and acceptor are too high. At the present time we have developed a sense as to when such coupling reactions may fail, but we do not have firm guidelines for predicting what levels of congestion may be tolerated for specific combinations of donors and acceptors. Clearly, such insight will be necessary if this already powerful method is to reach full fruition in applications to complex settings.

For the synthesis of the N3 antigen, we proceeded as described in Schemes 77 and 78.[142] Glycal **355** was used to construct the key building block **356**, which was further converted to the complex azaglycosylation donor **357**. The acceptor triol **358** bearing a levulinoyl protecting group was assembled from glucal and galactal. Fortunately, the 3′,4′,5′-triol in **358** was sufficiently noncongested that the coupling with **357** by direct "rollover" of the sulfonamido group was possible. Upon unveiling of the primary hydroxyl by hydrazine-induced cleavage of levulinoyl protecting group, acceptor **359** was in hand. Starting with D-glucal, following conversions that the reader will at this stage anticipate, donor **360** bearing a strategic *p*-methoxybenzyl protecting group at C4 of the GlcNAc ring was assembled (Scheme 78). The components met the anticipated requirements for coupling at the relatively unhindered primary acceptor site in **359** flanked by a free hydroxyl at C4′. Successful coupling was followed by acetylation of the axial C4′ hydroxyl site on the galactose. We then exposed a unique acceptor site by cleavage of the PMB group (see asterisk **361**). We had recog-

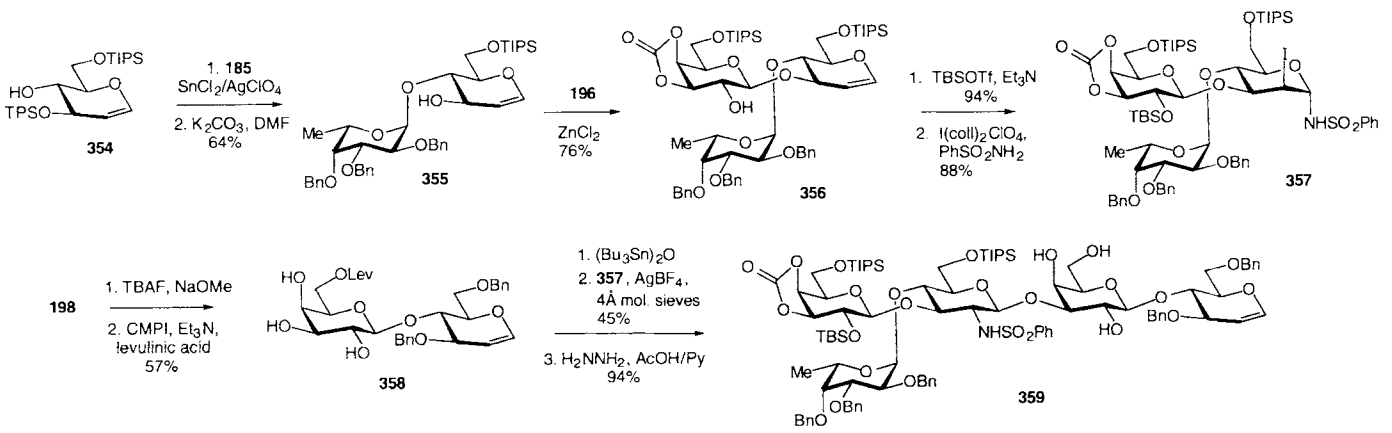

Scheme 77. Synthesis of the N3 antigen (part 1). CMPI = 2-chloro-1-methylpyridinium iodide, Lev = levulinoyl.

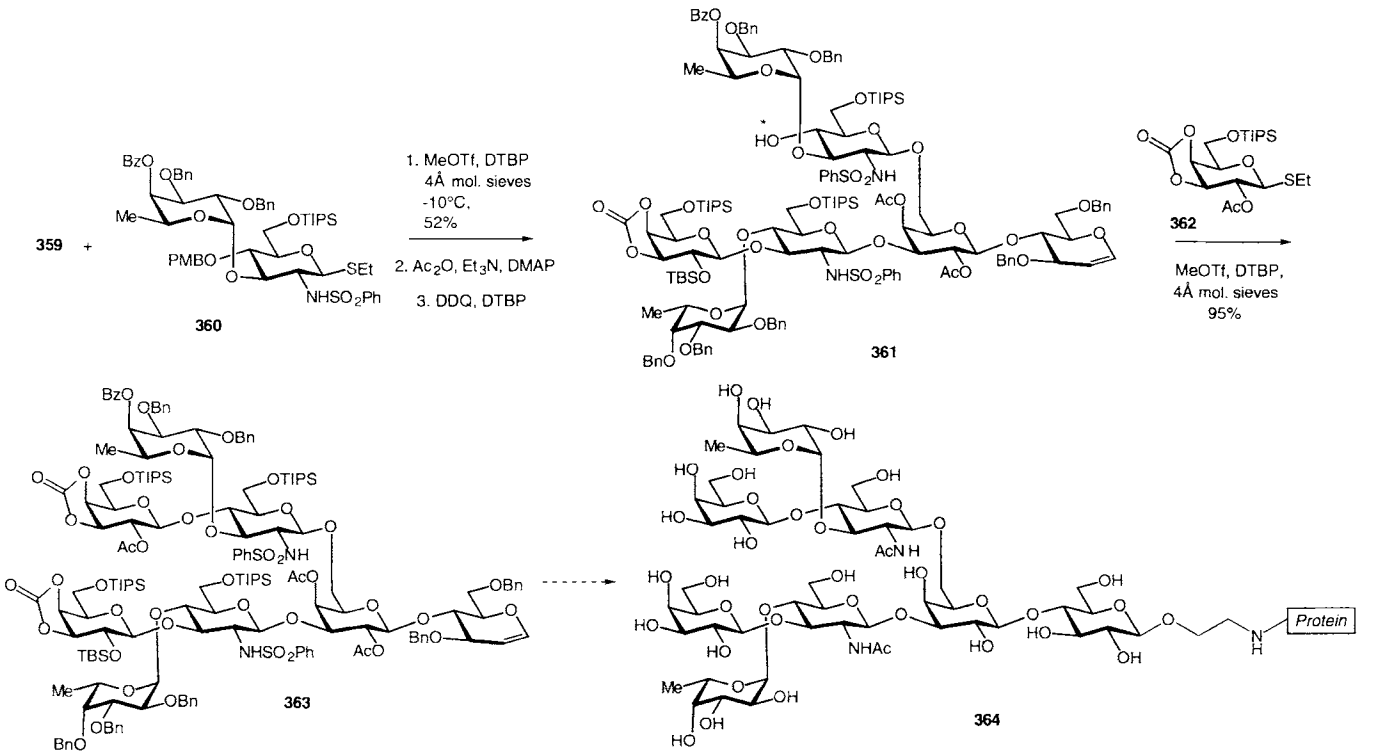

Scheme 78. Synthesis of the N3 antigen (part 2).

nized the steric congestion at this acceptor site and had accordingly simplified the demands on the coupling process through the use of a more reactive thioethyl donor. Indeed, **361** underwent successful coupling with donor **362**, fashioned from D-galactal, to produce the N3 glycal precursor **363** in 95% yield. We are currently completing the total synthesis of the N3 antigen and preparing useful N3 conjugates, which may find use as immunostimulants or as diagnostic agents.

This successful preparation of the protected N3 glycal **363** emphasizes an important dimension to the synthesis complex oligosaccharides not often recognized by students of general organic chemistry. Although the basic building blocks are in a broad sense generally defined in advance, there are many opportunities for ingenuity and creativity in how they are brought together. The problems can be quite challenging in the synthesis of compounds with increasing degrees of branching.

Note that in compound **361** one out of 19 potential hydroxyl groups[143] has been identified as the acceptor site. Moreover, it is located in a sterically congested region of the molecule. Yet coupling occurs smoothly because the acceptor center is being merged with a rather reactive donor (**362**). For those who are willing to labor at mastering the "grammar" of complex oligosaccharide synthesis, there is ample opportunity to author a new "literature" of large proportions.

11.3. Synthesis of Asialo-GM_1

In this vein we turn to our recently completed total synthesis of asialo-GM_1.[144] The biological rationale for conducting this project is clear: Al-Awqati and co-workers have implicated membrane-bound asialo-GM_1 as a primary infection site of cys-

tic fibrosis associated pathogens.[145] Indeed, the interior GalNAc-Gal sector of asialo-GM_1 had earlier been claimed to be a general carbohydrate bioligand for pathogenic association in a variety of other infections.[146] Our hope is to generate soluble, cell-permeable versions of these substructures to study their potential as infection decoys.

The full power of azaglycosylation methodology has been brought to bear on the synthesis.[147] Our route started with the previously described **217**, which was suitably upgraded to produce the azaglycosyl donor **365** featuring a free axial hydroxyl in the donor ring (Scheme 79). As noted in the synthesis of the human breast tumor antigen (see Scheme 54), this arrangement tends to favor β-glycoside formation in the sulfonamidoglycosylation reaction. In the case at hand, **365** was coupled to the suitably differentiated and previously described glycosyl acceptor **213** to give **366**. This reaction constituted a severe challenge to our technology, as it required linkage at the very hindered axial bond of the lactal-derived construct. From this achievement, the steps to asialo-GM_1(**368**) followed the protocols that had been well worked out in previous demonstrations. Synthetic **368**, as well as other constructs derived from the terminal glycosidic sites does, indeed, bind to cystic fibrosis associated pathogens.[148]

11.4. Synthesis of the Polysaccharide Core of a Glycopeptide

Our long-term program of synthesizing a natural-type (high mannose containing), fully competent and deprotected asparagine-linked glycopeptide has been progressing well (Scheme 80).[149] Thus, dibenzylglucal epoxide **34** was converted to the ethylsulfanyl-substituted **369** and further to the mannosyl donor **370** (cf. Scheme 30). The azaglycosyl donor **372** was fashioned from **371** as shown and successfully coupled to **197** to produce **373**.

A key element of our strategy was the use of the epoxide derived from glycal **374** protected at C4 and C6 by a *p*-methoxybenzylidene group. This compound was derived from D-glucal in the usual way. The epoxide derived from **374** was transformed to the ethylsulfanylglycoside **375**, which was coupled smoothly with **373** and **375**. Glycal **376** was eventually obtained. Reductive opening of the benzylidene linkage and desilylation pin-

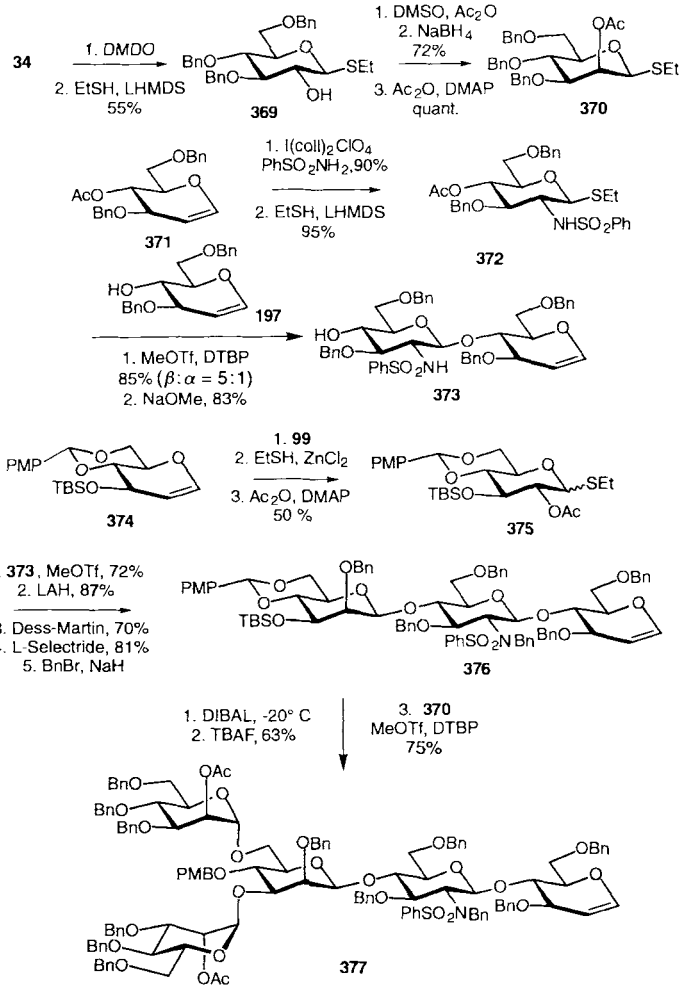

Scheme 80. Synthesis of the polysaccharide core of a glycopeptide. LAH = lithium aluminum hydride, DIBAL = diisobutylaluminum hydride.

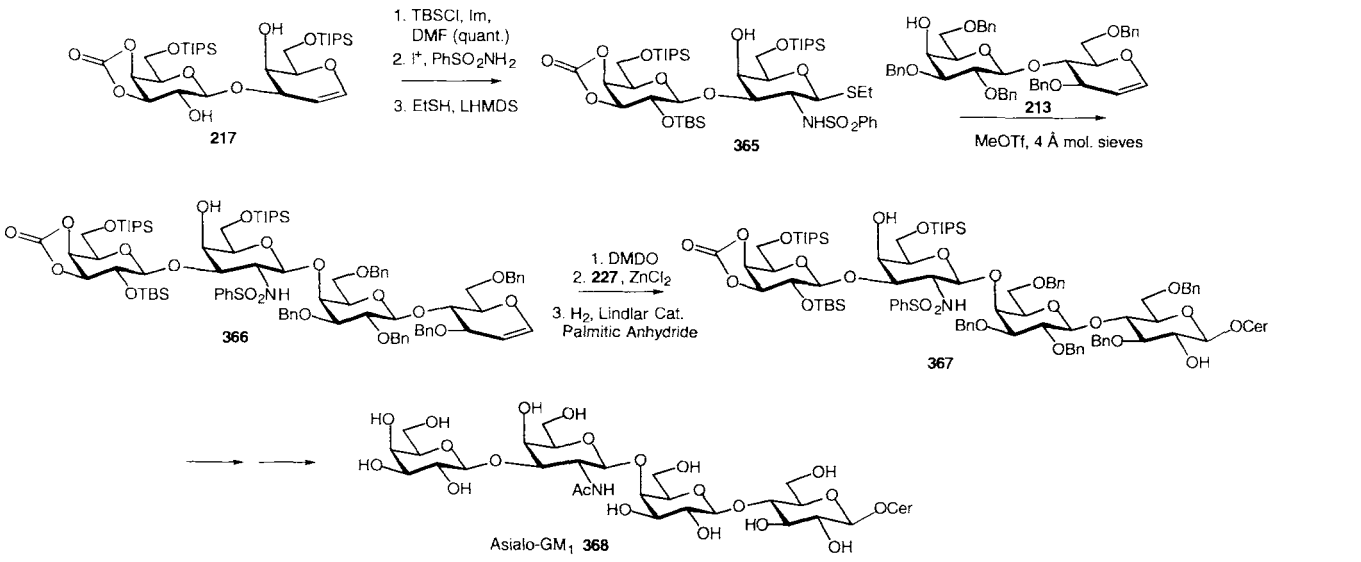

Scheme 79. Synthesis of asialo-GM_1. Im = imidazole.

pointed the α-mannosyl acceptor sites en route to the "high mannose region glycal" **377**. The assembly of the full mannose region in the construct containing an explotiable glycal constitutes a significant advance. Upon refinement of this technology, the stage will be set for introduction of the asparagine-linked peptide by previously described methods (see Scheme 75).

11.5. Solid-Phase Synthesis of a 2-Sulfonamido-2-Deoxyglycoside

Of course, our long-term goal is to synthesize the entire glycopeptide, including the mannose-rich region, on a solid support. The carbohydrate section of the glycopeptide would, eventually, culminate in presentation of blood group or tumor antigen epitopes at the nonreducing end of the construct. Previously, we had noted that azaglycosylation was not successful in our solid-phase protocols, save for introduction of an azido group at the anomeric center (see discussions associated with Schemes 72 and 73).

A significant advance in our technology has now arisen from the demonstration that the polymer-bound **378**, prepared from the previously described **309** in the usual way, can be used to furnish a competent azaglycosyl donor (Scheme 81).[150] Thus,

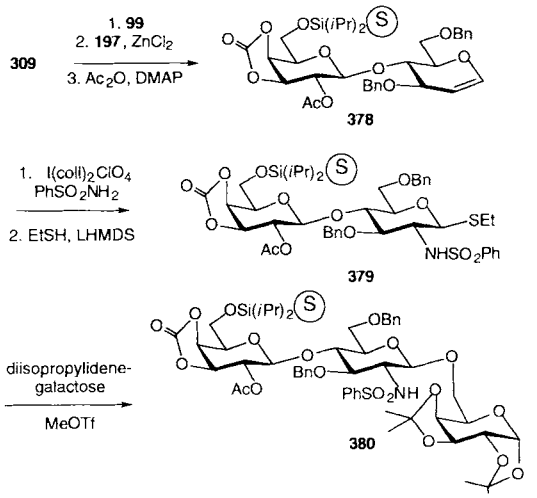

Scheme 81. Lactosamine synthesis on a solid support.

378 was converted to the polymer-bound donor **379**, which reacted with solution-phase diisopropylidenegalactose to produce **380**. Thus, though the generality of azaglycosidation of polymer-bound donors is not yet fully established, certainly the prospects for achieving a strictly solid-phase synthesis of glycopeptide-linked tumor antigens are now quite promising.

11.6. Preclinical Assessments

At present we are focusing on protein conjugates of the human breast tumor (MBr1) and Le^y antigens. In each case, synthetic conjugates bind to appropriate antibodies. These studies clearly implicate the carbohydrate sectors as the key immunological recognition sites. Mapping efforts are well underway to ascertain the key contributions to binding in the carbohydrate domain.

Most encouraging is the fact that our fully synthetic constructs in both series, when injected in mice, generate antibodies that bind in vitro to target cell lines (Scheme 82). These promising findings invite the next question, whether such constructs will provide clinically useful immunological protection or even regression in a human setting. The protocols needed to put such large and important questions to the test are now being developed.

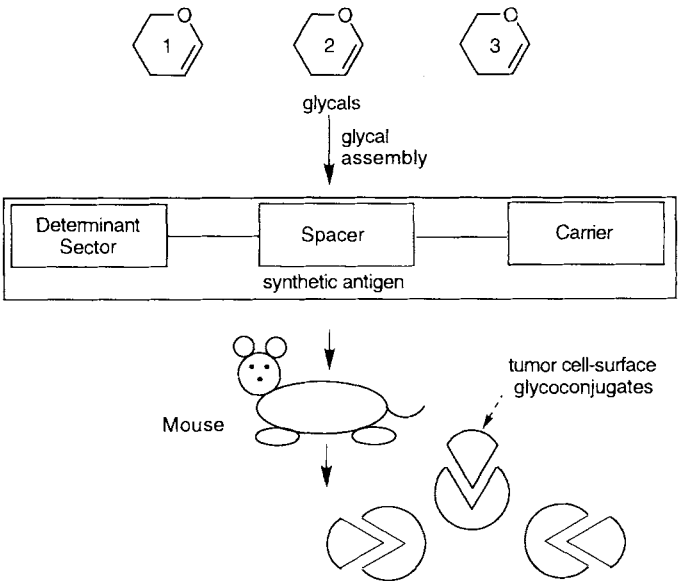

Scheme 82. Inoculation of mice with synthetic antigens. Mouse antibodies bind to tumor-transformed cell lines.

12. Conclusions and Futuristic Perceptions

In this article we have shown, by example, the power of glycal assembly. Of course, ours is only one of several laboratories addressing the synthesis of complex oligosaccharides. We cannot claim these methods to be indispensable; all of the target molecules described in this review could probably have been reached by other coupling methods or assembly strategies. A fair number of the syntheses shown here have in fact been achieved through more conventional carbohydrate chemistry. We do, however, feel that glycal assembly may offer large advantages in synthetic conciseness. These stategies may obviate many of the onerous protecting group manipulations that have dominated this field. Glycal assembly has stimulated the development of new coupling technologies, and the methods are constantly improving. Those who maintain an open mind about carbohydrate technology would be well advised to consider ways in which glycals might be useful for their purposes.

We are confident that solid-phase oligosaccharide synthesis, our methods and others,[138] will be expanded, and that substantial progress in this regard is in the offing. We expect major new advances in glycopeptide synthesis to be realized by our methods, by other chemical methods, and, indeed, by enzymatically assisted methods. Certainly, the goal of adapting solid-phase methodology to include assembly of the mannose-rich regions of glycopeptides is high on our list of priorities.

Ultimately, the test of the success at the chemical level will be whether complex oligosaccharides and glycoconjugates can be synthesized effectively by even nonspecialists. Despite the success of the methods described here, this is currently far from the case and further developments are needed. The challenges and the opportunities of oligosaccharide synthesis are immense and many solutions are possible, including some which await creative formulation by future practitioners.

We venture the opinion that even as progress is made on the chemical issues, the "really decisive" terrain may be shifting. In the past chemists have lavished a great deal of time and energy in developing a host of glycosylation methods and strategies. These advances have spawned a new and very serious challenge – the conceptualization of valuable targets. Though many unsolved chemical problems continue to arise, the time is already at hand to prepare and evaluate new constructs to test important possibilities in structural biology, immunology, and medicine. In our own work it is only in the last year that our glycal methodology has produced ample amounts of carrier protein conjugated carbohydrate-based tumor antigens for preclinical and, hopefully, clinical evaluation. At this time no one can safely predict the full impact of such carbohydrate–protein constructs on either the diagnosis or the treatment of cancer. The most we can safely assert is that this clinical issue will be probed in detail. Thus, the largest challenges may now lie in choosing synthetic targets and in marshaling the multidisciplinary resources for systematic evaluation of the products of such efforts.

We close this review with some thoughts concerning life on the chemistry–biology frontier. In this account we have shown by historical progression how our laboratory, starting with fascinating problems in the field of "small molecule" natural products, has become involved in issues of tumor expression and tumor immunology. One of the singular contributions which we and like-oriented research groups bring to such coalitions is a sensitivity for precisely defined structures. When collaborating with biologists in identifying bioactive compounds and charting their functions, the chemist insists that the compounds in question be demonstrably pure and that the structural assignments, down to each stereogenic center, be corroborated. But chemistry's contribution to the enterprise is certainly more than restraints arising from insistence on thoroughness and intellectual exactitude. Methodical building upon the principles of our science leads to the magic of synthesis—with its unique capability to prepare molecules of virtually any shape and juxtaposition of functional groups. Creative synthesis is the indispensable talent that the chemist will bring to the many exciting struggles and opportunities in the future.

The research reviewed in this paper was possible only through the dedication, enthusiasm, and creativity of scores of co-workers, whose names are acknowledged on the publications cited from our laboratory. In a few instances we identified individual colleagues who were involved at particularly sensitive points of the journey. However, it is to all our associates on these papers, and to other members of the laboratory (who were available for the extensive discussions that helped to fashion these experiments) to whom the program is lastingly indebted.

Needless to say, external funding was also necessary! This support was provided largely by the National Institutes of Health (AI 16943, CA 28824, HL 25848). In addition, M. T. B. gratefully acknowledges the NIH for a Postdoctoral Research Fellowship (GM 16291). We also note and express our thankfulness for generous inputs over these twenty years from various public-spirited supporters in the pharmaceutical industry, particularly the Merck Corporation and, more recently the Pfizer Foundation for Graduate Fellowships.

Received: August 14, 1995 [A130IE]
German version: *Angew. Chem.* **1996**, *108*, 1482–1522

[1] See inter alia: "The Carbohydrate-Containing Antibiotics": A. K. Mallams in *Carbohydrate Chemistry* (Ed.: J. F. Kennedy), Oxford Science Publications, Oxford, UK, **1988**, Chapter 3, pp. 73–170; "Aminocyclitol Antibiotics": K. L. Rinehart, T. Suami, *ACS Symp. Ser.* **1980**, *125*; "Nucleotide Analogues as Antiviral Agents": J. C. Martin, *ibid.* **1988**, *401*.

[2] See inter alia: *The Chemistry of Antitumor Antibiotics* (Ed.: W. A. Remers), Wiley, New York, **1978**; *Anthracycline and Anthracenedione Based Anticancer Agents* (Ed.: J. W. Lown), Elsevier, Amsterdam, **1988**; *Lectins and Glycoconjugates in Oncology* (Eds.: H. J. Gabius, G. A. Nagel), Springer, New York, **1988**.

[3] T. W. Smith, *N. Engl. J. Med.* **1988**, *318*, 358.

[4] a) H. F. Oettgen, *Gangliosides and Cancer*, VCH, Weinheim, **1989**; b) K. Toshima, K. Tatsuta, *Chem. Rev.* **1993**, *93*, 1503; c) R. R. Schmidt in *Comprehensive Organic Synthesis, Vol. 6* (Eds.: B. M. Trost, I. Fleming, E. Winterfeldt), Pergamon, Oxford, **1991**, p. 33.

[5] A. Varki, *Proc. Natl. Acad. Sci. USA* **1994**, *91*, 7390.

[6] D. E. Levy, P. C. Tang, J. H. Musser in *Annual Reports in Medicinal Chemistry* (Ed.: W. K. Hagmann), Academic Press, San Diego, **1994**, p. 215.

[7] J. B. Lowe in *The Molecular Basis of Blood Diseases* (Eds.: G. Stamatoyannopoulos, A. W. Nienhuis, P. W. Majerus, H. Varmus), Saunders, Philadelphia, **1987**, Chapter 8, p. 293.

[8] S. Hannessian, *Total Synthesis of Natural Products: The Chiron Approach*, Pergamon, **1983**.

[9] S. J. Danishefsky, *Acc. Chem. Res.* **1981**, *14*, 400.

[10] For a general review of functionalized dienes in Diels–Alder reactions see: M. Petrzilka, J. I. Grayson, *Synthesis* **1981**, 753.

[11] S. J. Danishefsky, P. F. Schuda, T. Kitahara, S. J. Etheredge, *J. Am. Chem. Soc.* **1977**, *99*, 6066.

[12] S. J. Danishefsky, M. Hirama, N. Fritsch, J. Clardy, *J. Am. Chem. Soc.* **1979**, *101*, 7013. For a full account of these early explorations see: S. J. Danishefsky, *Acc. Chem. Res.* **1981**, 14, 1981.

[13] F. Fringuelli, A. Taticchi, *Dienes in the Diels–Alder Reaction*, Wiley, New York, **1990**.

[14] S. J. Danishefsky, *Chemtracts Org. Chem.* **1989**, *2*, 273.

[15] S. David, J. Eustache, A. Lubineau, *J. Chem. Soc. Perkin Trans. 1* **1979**, 1795; J. Jurczak, A. Golebiowski, T. Bauer, *Synthesis* **1985**, 928; H. C. J. G. van Balen, A. A. Brockius, J. W. Scheeren, R. J. F. Niviad, *Recl. Trav. Chim. Pays-Bas* **1979**, *98*, 36; R. W. Aben, J. W. Scheeren, *J. Chem. Soc. Perkin Trans. 1* **1979**, 3132. This last paper mentions the use of $ZnCl_2$ to promote the cycloaddition of **1** (R^1, R^2 = H) with aldehydes to provide γ-dihydropyrones. No examples are given. Insofar as the unspecified finding may have included unactivated aldehydes, this report would be the first disclosure of the concept of the LACDAC reaction.

[16] S. J. Danishefsky, J. F. Kerwin, S. Kobayashi, *J. Am. Chem. Soc.* **1982**, *104*, 358; S. J. Danishefsky, J. F. Kerwin, *J. Org. Chem.* **1982**, *47*, 3183.

[17] S. J. Danishefsky, *Aldrichimica Acta* **1986**, *19*, 59.

[18] T. Sommer, Yale University, **1981**, unpublished results of studies towards the synthesis of chalcose.

[19] M. Bednarski, C. Maring, S. J. Danishefsky, *Tetrahedron Lett.* **1983**, *24*, 3451.

[20] M. Bednarski, S. J. Danishefsky, *J. Am. Chem. Soc.* **1983**, *105*, 6968.

[21] M. Bednarski, S. J. Danishefsky, *J. Am. Chem. Soc.* **1986**, *108*, 7060.

[22] a) S. J. Danishefsky, D. M. Armistead, F. E. Wincott, H. G. Selnick, R. Hungate, *J. Am. Chem. Soc.* **1989**, *111*, 2967; b) *ibid.* **1987**, *109*, 8117; c) S. J. Danishefsky, H. G. Selnick, D. M. Armistead, F. E. Wincott, *ibid.* **1987**, *109*, 8119.

[23] K. Marouka, T. Itoh, T. Shirasaka, H. Yamamoto, *J. Am. Chem. Soc.* **1988**, *110*, 310.

[24] S. J. Danishefsky, M. P. DeNinno, *Angew. Chem.* **1987**, *99*, 15; *Angew. Chem. Int. Ed. Engl.* **1987**, *26*, 15.

[25] S. J. Danishefsky,, E. Larson, J. Springer, *J. Am. Chem. Soc.* **1985**, *107*, 1274.

[26] S. J. Danishefsky, M. P. DeNinno, S.-H. Chen, *J. Am. Chem. Soc.* **1988**, *110*, 929.

[27] S. J. Danishefsky, C. Maring, *J. Am. Chem. Soc.* **1989**, *111*, 2193.

[28] S. J. Danishefsky, R. Hungate, G. Shulte, *J. Am. Chem. Soc.* **1988**, *110*, 7434.

[29] a) S. J. Danishefsky, M. Barbachyn, *J. Am. Chem. Soc.* **1985**, *107*, 6647; b) S. J. Danishefsky, S. L. DeNinno, S.-H. Chen, L. Boisvert, M. Barbachyn, *ibid.* **1989**, *111*, 5810.

[30] S. J. Danishefsky, B. Simoneau, *J. Am. Chem. Soc.* **1989**, *111*, 2599.
[31] D. C. Myles, S. J. Danishefsky, *Pure Appl. Chem.* **1989**, *61*, 1235; D. C. Myles, S. J. Danishefsky, *J. Org. Chem.* **1990**, *55*, 1636.
[32] D. B. Berkowitz, S. J. Danishefsky, *Tetrahedron Lett.* **1991**, *32*, 5497.
[33] D. B. Berkowitz, S. J. Danishefsky, G. K. Schulte, *J. Am. Chem. Soc.* **1992**, *114*, 4518.
[34] H. M. Sweers, C.-H. Wong, *J. Am. Chem. Soc.* **1986**, *108*, 7060; Y.-F. Wang, C.-H. Wong, *J. Org. Chem.* **1988**, *53*, 3127.
[35] a) M. Sharma, R. K. Brown, *Can. J. Chem.* **1966**, *44*, 2825; b) R. U. Lemieux, E. Fraga, K. A. Watanabe, *ibid.* **1968**, *46*, 61.
[36] M. D. Wittman, R. L. Halcomb, S. J. Danishefsky, *J. Org. Chem.* **1990**, *55*, 1979.
[37] R. J. Ferrier, N. Prasad, *J. Chem. Soc. C* **1969**, 570; R. J. Ferrier, *Adv. Carbohydr. Chem. Biochem.* **1969**, *24*, 199.
[38] a) P. Bickart, F. W. Carson, J. Jacobus, E. G. Miller, K. Mislow, *J. Am. Chem. Soc.* **1968**, *90*, 4869; b) R. Tang, K. Mislow, *ibid.* **1970**, *92*, 2100.
[39] a) D. A. Evans, G. C. Andrews, C. L. Sims, *J. Am. Chem. Soc.* **1971**, *93*, 4956; b) D. A. Evans, C. A. Bryan, C. L. Sims, *ibid.* **1972**, *94*, 2891; c) D. A. Evans, G. C. Andrews, *Acc. Chem. Res.* **1974**, *7*, 147.
[40] S. J. Danishefsky, J. F. Kerwin, *J. Org. Chem.* **1982**, *47*, 3803.
[41] S. J. Danishefsky, S. DeNinno, P. Lartey, *J. Am. Chem. Soc.* **1987**, *109*, 2082.
[42] S. J. Danishefsky, H. G. Selnick, R. E. Zelle, M. P. DeNinno, *J. Am. Chem. Soc.* **1988**, *110*, 4368.
[43] R. R. Schmidt, *Angew. Chem.* **1986**, *98*, 213; *Angew. Chem. Int. Ed. Engl.* **1986**, *25*, 212.
[44] S. David, A. Lubineau, J.-M. Vatele, *J. Chem. Soc. Chem. Commun.* **1978**, 535.
[45] A. Vasella, *Pure Appl. Chem.* **1991**, *63*, 507.
[46] D. Kahne, D. Yang, J. J. Lim, R. Miller, E. Paguaga, *J. Am. Chem. Soc.* **1988**, *110*, 8716.
[47] R. U. Lemieux, R. M. Ratcliffe, *Can. J. Chem.* **1979**, *57*, 1244.
[48] R. U. Lemieux, S. Levine, *Can. J. Chem.* **1964**, *42*, 1473; R. U. Lemieux, A. R. Morgan, *ibid.* **1965**, *43*, 2190.
[49] J. Thiem, H. Karl, J. Schwentner, *Synthesis* **1978**, 696; J. Thiem, H. Karl, *Tetrahedron Lett.* **1978**, 4999; J. Thiem, P. J. Ossowowski, *Carbohydr. Chem.* **1984**, *3*, 287; J. Thiem, A. Prahst, T. Wendt, *Liebigs Ann. Chem.* **1986**, 1044; J. Thiem, W. Klaffke, *J. Org. Chem.* **1989**, *54*, 2006; J. Thiem, *ACS Symp. Ser.* **1989**, *396*, Kap. 8.
[50] For examples of attempted displacement of corresponding sulfonates see: W. Karpiesiuk, A. Banaszek, A. Zamojski, *Carbohydr. Res.* **1989**, *186*, 156; A. C. Richardson, *ibid.* **1969**, *10*, 395.
[51] R. U. Lemieux, B. Fraser-Reid, *Can. J. Chem.* **1965**, *43*, 1460.
[52] For recent review of available methods see: a) ref. [4b]; b) J. Banoub, P. Boullanger, D. Lafont, *Chem. Rev.* **1992**, *92*, 1167.
[53] a) H. Paulsen, *Angew. Chem.* **1982**, *94*, 184; *Angew. Chem. Int. Ed. Engl.* **1982**, *21*, 155; b) D. R. Mootoo, P. Kondradsson, U. Udodong, B. Fraser-Reid, *J. Am. Chem. Soc.* **1988**, *110*, 5583. This paper introduced the concept of "armed" and "disarmed" *n*-pentenylglycosides. In the work of Friessen [55], which was virtually complete before this landmark paper was published, there is no analog to the disarmed substrate. Glycals bearing acyloxy groups function perfectly well as glycoxyl donors. Such donors simply react with acceptors slower than their triether counterparts do.
[54] For additional examples see: R. Roy, F. O. Anderson, M. Letellier, *Tetrahedron Lett.* **1992**, *33*, 6053; L. A. J. M. Sliedregt, K. Zegelaar-Jaarsvald, G. A. van der Marel, J. H. van Boom, *Synlett* **1993**, 335.
[55] a) R. W. Friesen, S. J. Danishefsky, *J. Am. Chem. Soc.* **1989**, *111*, 6656; b) *Tetrahedron* **1990**, *46*, 103.
[56] K. Suzuki, G. A. Sulikowski, R. W. Friesen, S. J. Danishefsky, *J. Am. Chem. Soc.* **1990**, *112*, 8895.
[57] For an even more concise synthesis of cicamycin 0 see: S. Raghavan, D. Kahne, *J. Am. Chem. Soc.* **1993**, *115*, 1580.
[58] A. Kobata, *Eur. J. Biochem.* **1992**, *209*, 483.
[59] R. U. Lemieux, T. L. Nagabhushan, *Can. J. Chem.* **1968**, *46*, 401.
[60] B. J. Fitzsimmons, Y. Leblanc, N. Chan, J. Rokach, *J. Am. Chem. Soc.* **1988**, *110*, 5229; Y. Leblanc, B. J. Fitzsimmons, *Tetrahedron Lett.* **1989**, *30*, 2889.
[61] D. A. Griffith, S. J. Danishefsky, *J. Am. Chem. Soc.* **1991**, *113*, 5863.
[62] D. A. Griffith, S. J. Danishefsky, *J. Am. Chem. Soc.* **1990**, *112*, 5811.
[63] D. R. Deardorf, A. J. Matthews, D. S. McMeekin, C. L. Craney, *Tetrahedron Lett.* **1986**, *27*, 1255.
[64] S. J. Danishefsky, K. Koseki, D. A. Griffith, J. Gervay, J. M. Peterson, F. E. McDonald, T. Oriyama, *J. Am. Chem. Soc.* **1992**, *114*, 8329.
[65] S. J. Danishefsky, J. Gervay, J. M. Peterson, F. E. McDonald, K. Koseki, T. Oriyama, D. A. Griffith, C.-H. Wong, D. P. Dumas, *J. Am. Chem. Soc.* **1992**, *114*, 8331.
[66] S. J. Danishefsky, J. Gervay, J. M. Peterson, F. E. McDonald, K. Koseki, D. A. Griffith, T. Oriyama, S. Marsden, *J. Am. Chem. Soc.* **1995**, *117*, 1940.
[67] a) M. L. Phillips, E. Nudelman, F. C. A. Gaeta, M. Perez, A. K. Singhal, S. Hakamori, J. C. Paulson, *Science* **1990**, *250*, 1130; b) G. Walz, A. Aruffo, W. Kolanus, M. Bevilacqua, B. Seed, *Science* **1990**, *250*, 1132; c) J. B. Lowe, L. M. Stoolman, R. P. Nair, R. D. Larsen, T. L. Berhend, R. M. Marks, *Cell* **1990**, *63*, 475; d) M. Tiemyer, S. J. Swiedler, M. Ishihara, M. Moreland, H. Schweingruber, P. Hirtzer, B. K. Brandley, *Proc. Natl. Acad. Sci. USA* **1991**, *88*, 1138; e) M. J. Polley, M. L. Phillips, E. Wayner, E. Nudelman, A. K. Singhal, S. Hakamori, J. C. Paulson, *ibid.* **1991**, *88*, 6224.
[68] a) M. M. Palcic, A. P. Venot, R. M. Ratcliffe, O. Hindsgaul, *Carbohydr. Res.* **1989**, *190*, 1; b) A. Kameyama, H. Ishida, M. Kiso, A. Hasegawa, *ibid.* **1991**, *209*, C1; c) A. Kameyama, H. Ishida, M. Kiso, A. Hasegawa, *J. Carbohydr. Chem.* **1991**, *10*, 549; d) K. C. Nicolaou, C. W. Hummel, N. J. Bockovich, C.-H. Wong, *J. Chem. Soc. Chem. Commun.* **1991**, 870; e) D. P. Dumas, Y. Ichikawa, C.-H. Wong, J. B. Lowe, P. N. Rajan, *Bioorg. Med. Chem. Lett.* **1991**, *1*, 425; f) K. C. Nicolaou, C. W. Hummel, Y. Iwabuchi, *J. Am. Chem. Soc.* **1992**, *114*, 3126; g) G. E. Ball, R. A. O'Neill, J. E. Schultz, J. B. Lowe, B. W. Weston, J. O. Nagy, E. G. Brown, C. J. Hobbs, M. D. Bednarski, *J. Am. Chem. Soc.* **1992**, *114*, 5449; h) Y. Ichikawa, Y.-C. Lin, D. P. Dumas, G.-J. Shen, E. Garcia-Juncenda, M. A. Williams, R. Bayer, C. Ketcham, L. E. Walker, J. C. Paulson, C.-H. Wong, *J. Am. Chem. Soc.* **1992**, *114*, 9283.
[69] F. E. McDonald, S. J. Danishefsky, *J. Org. Chem.* **1992**, *57*, 7001.
[70] P. Z. Brigl, *Z. Physiol. Chem.* **1922**, *122*, 245.
[71] F. Sweet, R. K. Brown, *Can. J. Chem.* **1966**, *44*, 1571.
[72] a) W. J. Hickenbottom, *J. Chem. Soc.* **1928**, 3140; b) E. Hardegger, J. de Pascual, *Helv. Chim. Acta* **1948**, *31*, 221; c) L. L. Klein, W. W. McWhorter, Jr., S. S. Ko, K.-P. Pfaff, Y. Kishi, *J. Am. Chem. Soc.* **1982**, *104*, 7362; d) V. Bellosta, S. Czernecki, *J. Chem. Soc. Chem. Commun.* **1989**, 199.
[73] R. U. Lemieux, G. Huber, *J. Am. Chem. Soc.* **1953**, *75*, 4118.
[74] D. L. Trumbo, C. Schuerch, *Carbohydr. Res.* **1985**, *135*, 195.
[75] S. J. Danishefsky, R. L. Halcomb, *J. Am. Chem. Soc.* **1989**, *111*, 6661.
[76] R. W. Murray, R. Jeyaraman, *J. Org. Chem.* **1985**, *50*, 2847.
[77] J. Gervay, S. J. Danishefsky, *J. Org. Chem.* **1991**, *56*, 5448.
[78] M. Gallant, J. T. Link, S. J. Danishefsky, *J. Org. Chem.* **1993**, *58*, 343.
[79] In some cases the α-glycoside produced coeluted with excess acceptor and thus went unnoticed [80].
[80] C. M. Timmers, G. A. van der Marel, J. H. van Boom, *Recl. Trav. Chim. Pays-Bas* **1993**, *112*, 609; C. A. Timmers, G. A. van der Marel, J. H. van Boom, *Chem. Eur. J.* **1995**, *1*, 159.
[81] a) A direct methods for the formation of 2-deoxy-β-glycosides from glycals employing $Ph_3P{\cdot}HBr$ has been developed: V. Bolitt, C. Mioskowski, S.-G. Lee, J. R. Falck, *J. Org. Chem.* **1990**, *55*, 5812; b) D. H. R. Barton, J. C. Jaszberenyi, *Tetrahedron Lett.* **1989**, *30*, 2619.
[82] a) K. K.-C. Liu, S. J. Danishefsky, *J. Org. Chem.* **1994**, *59*, 1892; b) H. B. Boren, G. Ekborg, K. Eklind, P. J. Garegg, Å. Pilotti, C.-G. Swahn, *Acta Chem. Scand.* **1973**, *27*, 2639.
[83] K. K.-C. Liu, S. J. Danishefsky, *J. Org. Chem.* **1994**, *59*, 1895.
[84] R. G. Dushin, S. J. Danishefsky, *J. Am. Chem. Soc.* **1992**, *114*, 3472.
[85] R. Dushin, S. J. Danishefsky, *J. Am. Chem. Soc.* **1991**, *113*, 655.
[86] K. Chow, S. J. Danishefsky, *J. Org. Chem.* **1990**, *55*, 4211.
[87] R. W. Murray, M. Singh, B. L. Williams, H. M. Moncrieff, *Tetrahedron Lett.* **1995**, *36*, 2437.
[88] U. Niedballa, H. Vorbrüggen, *J. Org. Chem.* **1974**, *39*, 3654.
[89] J. T. Link, M. Gallant, S. Huber, S. J. Danishefsky, *J. Am. Chem. Soc.* **1993**, *115*, 3782.
[90] J. T. Link, S. Raghavan, S. J. Danishefsky, *J. Am. Chem. Soc.* **1995**, *117*, 552; J. T. Link, S. Raghavan, M. Gallant, S. J. Danishefsky, T. C. Chou, M. Ballas, *ibid.*, **1996**, *118*, 2825.
[91] K. K.-C. Liu, S. J. Danishefsky, *J. Am. Chem. Soc.* **1993**, *115*, 4933.
[92] J. Gervay, J. M. Peterson, T. Oriyama, S. J. Danishefsky, *J. Org. Chem.* **1993**, *58*, 5465.
[93] T. Murase, A. Kameyama, K. P. R. Kartha, H. Ishida, M. Kiso, A. Hasegawa, *J. Carbohydr. Chem.* **1989**, *8*, 265.
[94] D. Gordon, S. J. Danishefsky, *Carbohydr. Res.* **1990**, *206*, 361.
[95] T. Mukaiyama, Y. Murai, S. Shoda, *Chem. Lett.* **1981**, 431.
[96] D. M. Gordon, S. J. Danishefsky, *J. Am. Chem. Soc.* **1992**, *114*, 657.
[97] T. K. Park, S. J. Danishefsky, *Tetrahedron Lett.* **1994**, *35*, 2671.
[98] J. T. Randolph, S. J. Danishefsky, *J. Am. Chem. Soc.* **1993**, *115*, 8473.
[99] J. T. Randolph, S. J. Danishefsky, *J. Am. Chem. Soc.* **1995**, *117*, 5693.
[100] V. Behar, S. J. Danishfefsky, *Angew. Chem.* **1994**, *106*, 1534; *Angew. Chem. Int. Ed. Engl.* **1994**, *33*, 1468.
[101] S. J. Danishefsky, V. Behar, J. T. Randolph, K. O. Lloyd, *J. Am. Chem. Soc.* **1995**, *117*, 5701.
[102] a) T. Kaizu, S. B. Levery, E. Nudelman, R. E. Stenkamp, S. Hakomori, *J. Biol. Chem.* **1986**, *261*, 11254; b) S. B. Levery, E. Nudelman, N. H. Anderson, S. Hakomori, *Carbohydr. Res.* **1986**, *151*, 311; c) S. Hakomori, E. Nudelman, S. B. Levery, R. Kannagi, *J. Biol. Chem.* **1984**, *259*, 4672; d) Y. Fukushi, S. Hakomori, E. Nudelman, N. Cochran, *ibid.* **1984**, *259*, 4681; e) Y. Fukushi, E. Nudelman, S. B. Levery, S. Hakomori, H. Rauvala, *ibid.* **1984**, *259*, 10511; f) J. Sakamoto, K. Furukawas, C. Cardon-Dardo, B. W. T. Lin, W. J. Rettig, H. F. Oettgen, L. J. Old, K. O. Lloyd, *Cancer Res.* **1986**, *46*, 1553.
[103] R. B. Myers, S. Srivastava, W. E. Grizzle, *J. Urol. (Baltimore)* **1995**, *153*, 1572.
[104] a) M. A. Bernstein, L. D. Hall, *Carbohydr. Res.* **1980**, *78*, C1; b) R. U. Lemieux, *Chem. Soc. Rev.* **1978**, *7*, 423; c) R. U. Lemieux, D. R. Bundle, D. A. Baker, *J. Am. Chem. Soc.* **1975**, *97*, 4076, and references therein.
[105] J. T. Randolph, S. J. Danishefsky, *Angew. Chem.* **1994**, *106*, 1538; *Angew. Chem. Int. Ed. Engl.* **1994**, *33*, 1470.

[106] T. Boren, P. Falk, K. A. Roth, G. Larson, S. Normark, *Science* **1993**, *262*, 1892.
[107] P. F. Cirillo, unpublished results.
[108] E. G. Bremer, S. B. Levery, S. Sonnino, R. Ghidoni, S. Canevari, R. Kannagi, S. Hakomori, *J. Biol. Chem.* **1984**, *259*, 14773; S. Menard, E. Tagliabue, S. Canevari, G. Fossati, M. I. Colnaghi, *Cancer Res.* **1983**, *43*, 1295.
[109] M. T. Bilodeau, T. K. Park, S. Hu, J. T. Randolph, S. J. Danishefsky, P. O. Livingston, S. Zhang, *J. Am. Chem. Soc.* **1995**, *117*, 7840.
[110] D. A. Griffith, Dissertation, Yale University, **1992**.
[111] For the first total synthesis of calicheamicin see: a) K. C. Nicolaou, C. W. Hummel, E. N. Pitsinos, M. Nakada, A. L. Smith, K. Shibayama, H. Saimoto, *J. Am. Chem. Soc.* **1992**, *114*, 10082; b) K. C. Nicolaou, C. W. Hummel, M. Nakada, K. Shibayama, E. N. Pitsinos, H. Saimoto, Y. Mizuno, K.-U. Baldenius, A. L. Smith, *ibid.* **1993**, *115*, 7625.
[112] S. Hitchcock, S. Boyer, M. Y. Chu Moyer, S. Olson, S. J. Danishefsky, *Angew. Chem.* **1994**, *106*, 928; *Angew. Chem. Int. Ed. Engl.* **1994**, *33*, 858.
[113] R. Halcomb, S. Boyer, M. Wittman, S. Olson, D. Denhardt, K. K. C. Liu, S. J. Danishefsky, *J. Am. Chem. Soc.* **1995**, *117*, 5720.
[114] S. Hitchcock, M. M. Chu Moyer, S. J. Danishefsky, *J. Am. Chem. Soc.* **1995**, *117*, 5750.
[115] R. L. Halcomb, M. D. Wittman, S. Olson, S. J. Danishefsky, J. Golik, H. Wong, D. Vyas, *J. Am. Chem. Soc.* **1991**, *113*, 5080.
[116] a) J. N. Haseltine, M. P. Cabal, N. B. Mantlo, N. Iwasawa, D. S. Yamashita, R. S. Coleman, G. M. Schulte, S. J. Danishefsky, *J. Am. Chem. Soc.* **1991**, *113*, 3856; b) D. S. Yamashita, V. P. Rocco, S. J. Danishefsky, *Tetrahedron Lett.* **1991**, *32*, 6667; c) V. P. Rocco, S. J. Danishefsky, G. K. Schulte, *ibid.* **1991**, *32*, 6671.
[117] J. Golik, H. Wong, B. Krishnan, D. Vyas, T. W. Doyle, *Tetrahedron Lett.* **1991**, *32*, 1851.
[118] D. Yang, S.-H. Kim, D. Kahne, *J. Am. Chem. Soc.* **1991**, *113*, 4715.
[119] K. C. Nicolaou, T. Li, N. Masahisa, C. W. Hummel, A. Hiatt, W. Wrasidlo, *Angew. Chem.* **1988**, *100*, 1138; *Angew. Chem. Int. Ed. Engl.* **1988**, *27*, 1097.
[120] J. Drak, N. Iwasawa, D. M. Crothers, S. J. Danishefsky, *Proc. Natl. Acad. Sci. USA* **1991**, *88*, 7464.
[121] J. Aiyar, S. A. Hitchcock, D. Denhart, K. K.-C. Liu, S. J. Danishefsky, D. M. Crothers, *Angew. Chem.* **1994**, *106*, 925; *Angew. Chem. Int. Ed. Eng.* **1994**, *33*, 855.
[122] J. Aiyar, S. J. Danishefsky, D. M. Crothers, *J. Am. Chem. Soc.* **1992**, *114*, 7552.
[123] K. C. Nicolaou, S.-C. Tsay, T. Suzuki, G. F. Joyce, *J. Am. Chem. Soc.* **1992**, *114*, 7555.
[124] T. Li, V. A. Estevez, K. U. Baldenius, K. C. Nicolaou, G. F. Joyce, *J. Am. Chem. Soc.* **1994**, *116*, 3709.
[125] For the first synthesis of the full carbohydrate domain see: K. C. Nicolaou, R. D. Bromeberg, T. Miryazaki, N. A. Stylianides, T. J. Schulze, W. Stahl, *J. Am. Chem. Soc.* **1990**, *112*, 8193.
[126] R. L. Halcomb, S. H. Boyer, S. J. Danishefsky, *Angew. Chem.* **1992**, *104*, 314; *Angew. Chem. Int. Ed. Engl.* **1992**, *31*, 338.
[127] S. H. Olson, S. J. Danishefsky, *Tetrahedron Lett.* **1994**, *43*, 7901.
[128] S. P. Douglas, D. M. Whitfield, J. J. Krepinsky, *J. Carbohydr. Chem.* **1993**, *12*, 131.
[129] J. Jones, *The Chemical Synthesis of Peptides*, Clarendon, Oxford, **1991**.
[130] G. M. Blackburn, M. J. Gait in *Nucleic Acids in Chemistry and Biology* (Eds.: G. M. Blackburn, M. J. Gait), IRL, Oxford University Press, Oxford, **1990**, p. 73.
[131] a) J. M. J. Fréchet in *Polymer-Supported Synthesis of Oligosaccharides* (Eds.: P. Hodge, D. C. Sherrington), Wiley, Chichester, **1980**, pp. 407–434; b) S. J. Danishefsky, J. Y. Roberge in *Glycopeptides and Related Compounds: Synthesis, Analysis and Applications* (Eds.: D. G. Large, D. G. Warren), Marcell Dekker, in press.
[132] K. F. McClure, J. T. Randolph, R. Ruggeri, S. J. Danishefsky, *Science* **1993**, *260*, 1307.
[133] J. T. Randolph, K. F. McClure, S. J. Danishefsky, *J. Am. Chem. Soc.* **1995**, *117*, 5712.
[134] T.-H. Chan, W.-Q. Huang, *J. Chem. Soc. Chem. Commun.* **1985**, 909.
[135] a) Ref. [131b]; b) M. Meldal, *Curr. Opin. Struct. Biol.* **1994**, *4*, 710. For selected recent examples see: c) S. T. Cohen-Anisfeld, P. T. Lansbury, Jr., *J. Am. Chem. Soc.* **1993**, *115*, 10531; d) D. Vetter, D. Tumelty, S. K. Singh, M. A. Gallop, *Angew. Chem.* **1995**, *107*, 94; *Angew. Chem. Int. Ed. Engl.* **1995**, *34*, 60; e) U. Sprengard, G. Kretzschmar, E. Bartnik, C. Hüls, H. Kunz, *Angew. Chem.* **1995**, *107*, 1104; *Angew. Chem. Int. Ed. Engl.* **1995**, *34*, 990.
[136] S. J. Danishefsky, J. Y. Roberge, *Pure Appl. Chem.* **1995**, *67*, 1647.
[137] J. Y. Roberge, X. Beebe, S. J. Danishefsky, *Science* **1995**, *269*, 202.
[138] M. Schuster, P. Wang, J. C. Paulson, C.-H. Wong, *J. Am. Chem. Soc.* **1994**, *116*, 1135.
[139] P. F. Cirillo, unpublished results.
[140] H. Paulsen, W. Stenzel, *Chem. Ber.* **1978**, *111*, 2334.
[141] B. E. Anderson, M. Grove, L. E. Davis (Northwestern University) US-A 5376531, **1994** [*Chem. Abstr.* **1994**, *121*, 705].
[142] I. J. Kim, T. K. Park, unpublished results.
[143] There are 17 actual O-protected hydroxyl groups and two latent hydroxyl groups inherent in the glycal double bond.
[144] O. Kwon, unpublished results.
[145] L. Imundo, J. Barasch, A. Prince, Q. Al-Awqati, *Proc. Natl. Acad. Sci. USA* **1995**, *92*, 3019.
[146] H. C. Krivan, D. D. Roberts, V. Ginsburg, *Proc. Natl. Acad. Sci. USA* **1988**, *85*, 6157.
[147] O. Kwon, unpublished results.
[148] Q. Al-Awqati, personal communication.
[149] X. Beebe, S. Hu, M. T. Bilodeau, P. Seeberger, P. F. Cirillo, unpublished results.
[150] S. Hu, P. Seeberger, unpublished results.

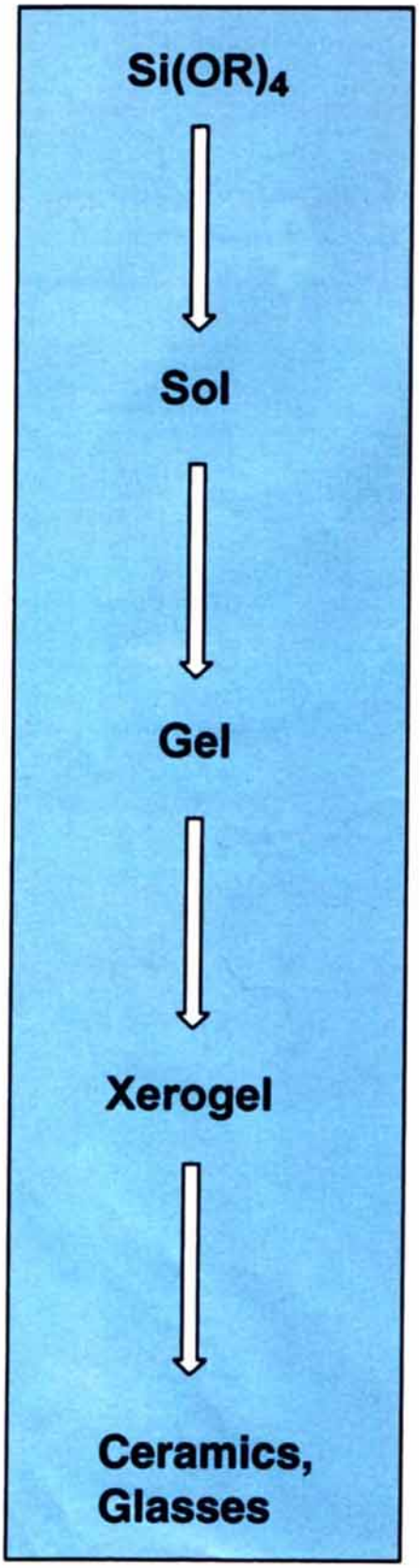

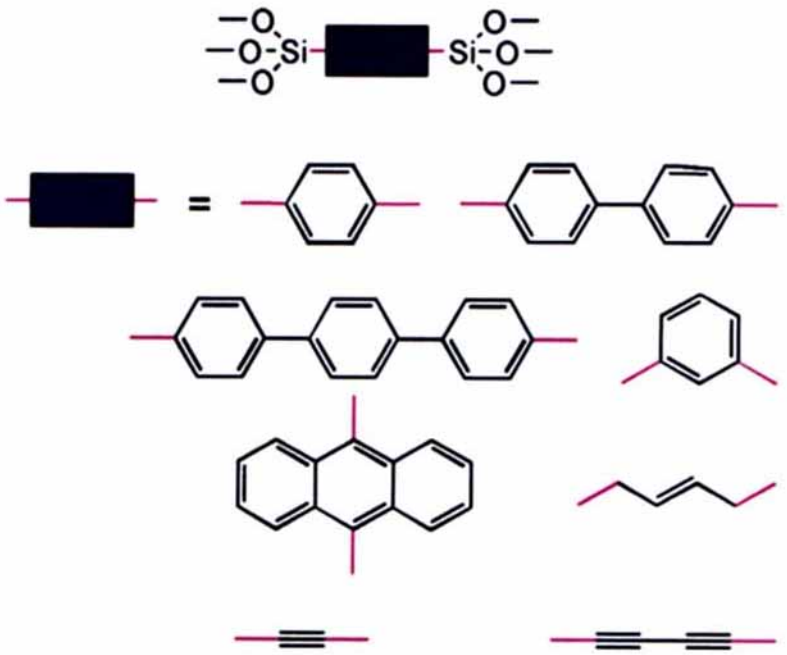

How ceramics and glasses can be synthesized by new procedures and which organic building blocks and transition metal fragments these can contain, is described by herein.

Recent Developments of Molecular Chemistry for Sol–Gel Processes

Robert J. P. Corriu* and Dominique Leclercq

This review focuses on some aspects of the chemistry involved in the preparation of oxides by sol–gel methods. This field is opening interesting possibilities for molecular chemistry and among those presented herein are: 1) the use of precursors containing functional groups for the preparation of solids with specific chemical reactivity; 2) the non-hydrolytic gelation (NHG) route, a new general method for the synthesis of oxides that allows the use of oxygen donors (ethers, alcohols, alkoxides) other than water; the mechanism is based on oxygen–carbon bond cleavage; 3) organic–inorganic hybrid solids containing covalent bonds for which the chemical reactivity is used to demonstrate the presence of substructure in the globally amorphous solid; the substructure greatly depends on the geometry of the organic moiety.

Keywords: materials design · molecular chemistry · organic–inorganic hybrid composites · sol–gel process

1. Introduction

Organic and inorganic molecular chemistry has made great progress during the last few decades. Nowadays, chemists can construct almost every conceivable structure. The next goals for chemistry are the synthesis of biomolecules and planned synthesis of solids with specific properties.

Apart from polymer materials, most ceramic and glass materials are prepared by solid-state reactions. The main exceptions, in which the synthetic methods are based on a molecular chemistry approach, are the synthesis of ceramics by pyrolysis of organometallic polymers, for example the preparation of silicon carbide fibers from the Yajima process,[1] and the preparation of oxides by sol–gel processes.[2]

Clearly, the planned synthesis of solids whose properties can be controlled at the molecular scale is one of the challenges of molecular chemistry. From this viewpoint, organosilicon chemistry has a very great future, since it is an ideal link between molecular and solid-state chemistry. Silicon–carbon bonds are very stable and silicon-containing moieties can be included in many different sites in organic molecules; they can induce the formation of many kinds of polymers and can also lead to a wide variety of solid materials including oxides, silicides, and thermomechanical ceramics.

For these reasons, since 1986 we have been interested in organosilicon compounds as potential precursors for the synthesis of solids. This review will focus mainly on the chemistry and not on the physics and materials science of sol–gel processing. The molecular chemical aspect is emphasized by the presentation of new precursors, a new chemical route in the sol–gel process, and the report of hybrid organic–inorganic materials, which are a new class of materials.

[*] Prof. Dr. R. J. P. Corriu, Dr. D. Leclercq
Laboratoire des précurseurs moléculaires de matériaux
UMR 44/ case 007, Université Montpellier II
Place E. Bataillon, F-34095 Montpellier cédex 5 (France)
Fax: Int. code +67143888

2. Sol–Gel Chemistry: General Remarks

Sol–gel processes have been well studied and developed in materials science since they are well-suited to preparing materials and to designing devices with very specific properties.[2] The sol–gel processes may be divided into two classes depending on the nature of the precursors; inorganic precursors (chlorides, nitrates, sulfides, etc.) and alkoxide precursors. The route that involves the use of alkoxide precursors appears as the more versatile one.[3] The most important step in this route is the formation of an inorganic polymer by hydrolysis reactions, during which the molecular precursor is transformed into a highly crosslinked solid in a one-pot procedure (Scheme 1).

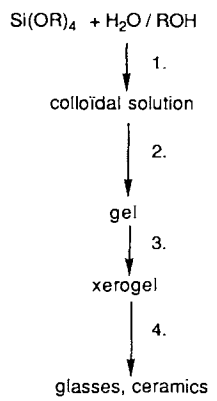

Scheme 1. Sol–gel process. 1. Hydrolysis/condensation, 2. Sol–gel transition. 3. Drying. 4. Densification.

Hydrolysis of a solution of tetraalkoxysilanes in an organic solvent such as alcohol leads to the formation of products with silanol functions, which form a sol (colloidal dispersion of particles in a liquid) by condensation polymerization.[2] The continuation of the process gives a gel (continuous solid skeleton enclosing a continuous liquid phase). This transformation is designated the sol–gel

transition. Gels may exhibit spontaneous shrinkage, called syneresis, on ageing. The network is initially supple and allows further condensation and bond formation induces contraction of the network and expulsion of liquid from pores. Drying of the gel by evaporation under normal conditions gives a dried gel, called a xerogel. Xerogels are interesting materials because of their porosity and high surface area, which make them useful as catalyst substrates, filters, etc. They are also useful in the preparation of dense ceramics by sintering (the densification is driven by the interfacial energy).[2] The advantage of the molecular approach to the synthesis of materials is based on the fact that the precursors can be obtained in the form of monoliths, films, fibers, and monosized powders directly from the gel state. The transformation from xerogel to ceramic is mainly the concern of material scientists, whereas the transformation of the molecular precursors to gels is the domain of molecular chemists.

Metal alkoxides are very sensitive to hydrolysis.[4] Thus, because of the low reactivity of tetraalkoxysilanes, their hydrolysis, which is usually catalyzed, has been more extensively studied. At this point, it is important to point out that in aquo-organic solvents, the pH value is not well defined. It is merely a measured value and not the exact one of the acidity (or basicity) of the mixture. The H_0 function introduced by Hammet[5] is the only true value of the proton activity that depends strongly on the water/organic solvent ratio. Since we have discussed this in detail elsewhere it will not be developed here.[6]

Even in the case of alkoxysilanes, only the mechanism of the first steps of the sol–gel process are well known.[7] It involves a nucleophilic attack by water at the silicon center. The detailed mechanism, however, is dependent on the catalyst used. Three kinds of catalysis are possible: acid, basic (OH^-), and nucleophililic (F^-, *N*-methylimidazole, hexamethyl phosphoramide (HMPA), etc.)

1) Acid catalysis: The first step is the reversible protonation of the alkoxy group which confers to it a better leaving character (Scheme 2). Nucleophilic substitution by water (or by silanol) occurs via a pentacoordinate intermediate.

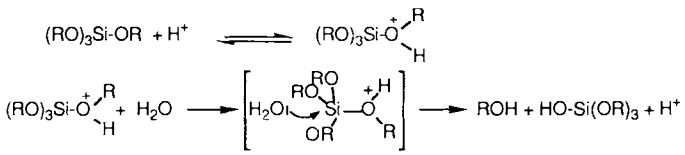

Scheme 2.

2) Basic catalysis: The nucleophilic hydroxide ion reacts with the alkoxysilane by nucleophilic substitution via the formation of a pentacoordinate intermediate and elimination of the alkoxide RO^- (Scheme 3). The catalyst re-forms by reaction with water. However, this mechanism has been recently questioned, since bases could act as nucleophilic catalysts [see 3].[8]

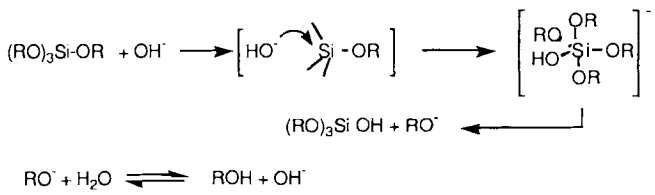

Scheme 3.

3) Nucleophilic catalysis: The nucleophilic catalyst (F^-, HMPA, *N*-methylimidazole, *N*,*N*-dimethylaminopyridine) coordinates to the alkoxysilane giving rise to a pentacoordinate silicon intermediate that is more reactive toward nucleophilic

R. J. P. Corriu

D. Leclercq

Robert Corriu, born in 1934 in Port-Vendres, France, obtained his Docteur es Sciences Physiques in 1961 from the Université de Montpellier. He became Assistant Professor at the Université de Perpignan in 1963, Associate Professor at the Université de Poitiers in 1964, and Professor at the Université de Montpellier in 1969. His research interests in organometallic chemistry are focused on organosilicon, organogermanium, and organophosphorus compounds, transition metal complexes, and hypercoordinate silicon and phosphorus compounds. He is currently concentrating his research efforts into the chemistry of organometallic polymers as precursors to materials. He has obtained awards from the French Chemical Society (Prix Sue in 1969 and Prix Lebel in 1985), from the CNRS (silver medal in 1982), and from the American Chemical Society (Kipping Award in 1984). He was elected to the French Academy of Sciences in 1991 and obtained the Alexander von Humboldt Research Award in 1992, and the Max Planck Research Award in 1993.

Dominique Leclercq, born in 1952 in Fourmies, France, obtained his Docteur es Sciences Physiques in 1984 from the Université de Montpellier II with a thesis on the mechanisms of nucleophilic substitution on organophosphorus compounds. After a postdoctoral position at the Centre de Recherche Rhône-Poulenc, Aubervilliers, he studied the chemistry of organometallic compounds as precursors to materials. He is currently interested in the preparation of non-oxide ceramics by pyrolysis of polycarbosilanes and polysilazanes as well as in synthesis of oxide ceramics by the sol–gel process.

substitutions (by water or silanol) than the tetracoordinate one (Scheme 4). The nucleophile coordinates to this pentacoordinate intermediate, leading to a hexacoordinate intermediate or transition state, which subsequently gives rise to the formation

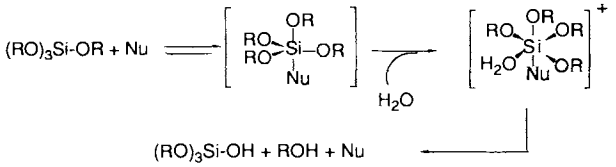

Scheme 4. Nu = nucleophile.

of alcohol and silanol and re-formation of the catalyst. The mechanism of this reaction has been evidenced by kinetic and stereochemical studies[9] and is supported by theoretical calculations.[10] The hydoxide ion could also act as nucleophilic catalyst.[8]

These mechanisms, however, address only the first step of a very complex process. Many kinetic studies have been devoted to the first stage of the sol–gel process. Kinetic analyses were performed by using a functional group model, which allows the evaluation of global rate constants.[11] The only study on the determination of the rate constants of individual component reactions of the acid-catalyzed hydrolysis of silicates was reported by Chojnowski et al.[12] This work emphasizes the role of alcoholysis reactions in the overall process. Many simulations have been done, based on different hypotheses, permitting an explanation of the shape of the solids formed under some experimental conditions.[13] However, these are only empirical procedures for the synthesis of solids with defined structures. Every small change in the experimental conditions (temperature, solvent, concentrations, nature and concentration of catalyst, and external factors such as sonication or pressure, etc.) modifies drastically the texture (specific surface area, size and distribution of pores, density, processibility, etc.) of the solid obtained. A detailed knowledge of the chemical mechanisms, which permits prediction and control of the properties of the final amorphous material at the molecular scale, is an exciting challenge for molecular chemists.

In this review, we will not give a detailed account of the chemistry of building blocks[14] or mechanistic studies of the sol–gel transition.[2] Instead, we focus on 1) new precursors, 2) new chemical routes for the sol–gel process, and 3) hybrid organic–inorganic solids.

3. New Precursors

3.1. $HSi(OR)_3$

The hydrolysis of $HSi(OR)_3$ (R = Me, Et, *i*Pr) performed under acid conditions avoids the hydrolysis of the Si–H bonds and leads to a gel of composition $HSiO_{1.5}$.[15] Under nucleophilic or basic conditions silica is formed with evolution of H_2 (Scheme 5).[15] Indeed, nucleophilic substitution of hydridosilicates $[HSi(OR)_4]^-$ leads only to cleavage of the Si–H bond.[16] This reaction parallels the nucleophilic activation of the Si–H bond, which permits selective and efficient reduction.[17]

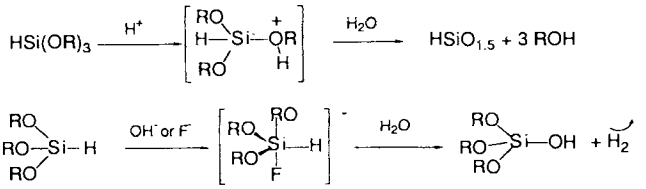

Scheme 5. Hydrolysis of trialkoxysilanes.

The $HSiO_{1.5}$ gel shows spectroscopic features similar to those of the crystalline octahydrosilsesquioxane $[HSiO_{3/2}]_8$ ($\tilde{\nu}_{Si-H}$ = 2250 cm^{-1}, $\delta_{Si} = -85$).[18] In contrast to silica gels, these gels are not hydrophilic. This is easily explained by the absence of silanol groups in the gel and by the presence of the hydrophobic Si–H groups at the surface of the gel, instead of hydrophilic Si–OH groups in the case of silica.

The thermal treatment of these solids is interesting. Under an oxidizing atmosphere, as expected, the Si–H bonds are oxidized leading to an increase in weight (10%) due to the formation of silica.[15, 19] Under an NH_3 atmosphere silicon oxynitrides are formed with a high content of nitrogen (3 wt%).[20] The mechanism of nitridation, which was determined by IR and NMR spectroscopy and by thermogravimetric analysis coupled with mass spectrometry (TGA/MS), is a three-step process (Scheme 6).[19, 20] The first step is the formation of silylamine

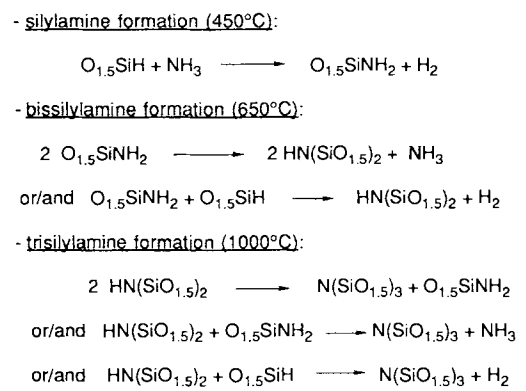

Scheme 6. Mechanism of nitridation of $HSiO_{1.5}$.

functions at about 450 °C as a result of the reaction of the Si–H bond with ammonia. Condensation of silylamine functions with each other or with Si–H functions above 650 °C leads to the formation of silazane groups. These then undergo condensation reactions with each other and/or with silylamine and/or with Si–H at 1000 °C, leading to the formation trisilylamines. This illustrates that the Si–H group can be considered as a functional group.

Other interesting reactions take place upon heating under argon. At 350 °C, a very unexpected rearrangement takes place that leads to the evolution of SiH_4, which was detected by a mass spectrometer coupled with the TGA apparatus.[19, 21] The solid-state MAS ^{29}Si NMR spectrum of the gel heated at 400 °C under argon shows two additional peaks at $\delta = -50$ and $\delta = -110$ corresponding to H_2SiO_2 and SiO_4 units, respectively (Fig. 1). On heating to a higher temperature (570 °C), the signal

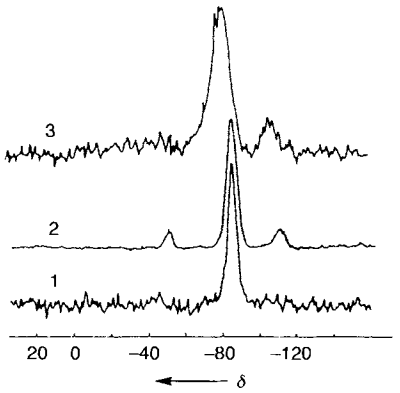

Fig. 1. ^{29}Si CP/MAS NMR spectra of a $HSiO_{1.5}$ gel heat treated at 1) 150 °C, 2) 405 °C, and 3) 565 °C.

for the H_2SiO_2 structural unit disappears. The formation of SiH_4 arises from redistribution reactions that occur in the solid (Scheme 7), regardless of the atmosphere under which the reactions were performed (air, ammonia, or argon).[19] Nitridation of the gel begins at 450 °C, following the loss of silane at 350 °C.

$$2\ HSiO_{1.5} \rightleftharpoons H_2SiO + SiO_2$$
$$H_2SiO + HSiO_{1.5} \rightleftharpoons H_3SiO_{0.5} + SiO_2$$
$$H_3SiO_{0.5} + HSiO_{1.5} \rightleftharpoons SiH_4 + SiO_2$$

Scheme 7. Redistribution of the Si–H and Si–O bonds in $HSiO_{1.5}$.

On heating in air, the formation of silane is not observed. However, the dissymmetrical exothermic peak observed by differential thermal analysis (DTA), as well as the presence of water detected by mass spectrometry indicate that SiH_4 is formed, but that it is rapidly oxidized in an exothermic reaction.[22]

At temperatures between 450 and 900 °C, evolution of H_2 is detected. Taking into account what would be expected in solution, the formation of Si–Si bonds leading to silicon sesquioxide Si_2O_3 has been proposed (Scheme 8).[23] Furthermore, X-ray diffraction showed the formation of cristobalite and crystalline silicon at 1600 °C, which was attributed to disproportionation of Si_2O_3 (Scheme 9).[23]

$$O_{1.5}Si\text{-}H \longrightarrow O_{1.5}Si^{\cdot} + H^{\cdot}$$
$$2\,H^{\cdot} \longrightarrow H_2$$
$$2\,O_{1.5}Si^{\cdot} \longrightarrow O_{1.5}Si\text{-}SiO_{1.5}$$

Scheme 8. Formation of Si_2O_3 by dehydrogenation of $HSiO_{1.5}$.

$$2\,Si_2O_3 \longrightarrow Si + 3\,SiO_2$$

Scheme 9. Disproportionation of silicon sesquioxide.

ESR spectra between 400 and 1200 °C show that the pyrolyzed gel contains $O_3Si^{\cdot}$, $O_2SiSi^{\cdot}$, $OSi_2Si^{\cdot}$, $Si_3Si^{\cdot}$ radicals (10^{17} unpaired electrons per g gel).[18] Furthermore, an X-ray absorption near-edge structure (XANES) spectroscopic study reveals that the product obtained by heating at 500 °C contains predominantly regions with Si–Si bonds and those with Si–O. Thus, during the thermal dehydrogenation of $HSiO_{1.5}$ between 400 and 900 °C, Si–Si bond formation competes with a formal redistribution of Si–Si and Si–O bonds. The ESR signals can thus be assigned to the resulting tetrahedral $Si(Si_xO_{4-x})$ units.

The Si–Si bond formation can be interpreted according to the mechanism of the thermolysis of alkoxydisilane in solution, in which a redistribution of Si–Si and Si–O bonds occurs via silylene intermediates.[24] Indeed, due to the restricted mobility of the $O_3Si^{\cdot}$ radicals in the solid state, a recombination reaction is less likely than a reaction with an oxygen atom of the neighboring $HSiO_{1.5}$ network (Scheme 10). The resulting silylene reacts to form Si–Si bonds by insertion into Si–H, Si–O, or Si–Si bonds (Scheme 11).

$$HSiO_{1.5} \longrightarrow H^{\cdot} + {}^{\cdot}SiO_{1.5}$$

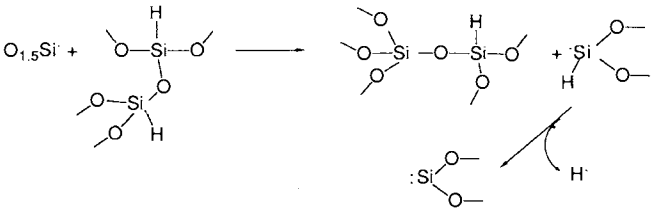

Scheme 10. Formation of silylenes.

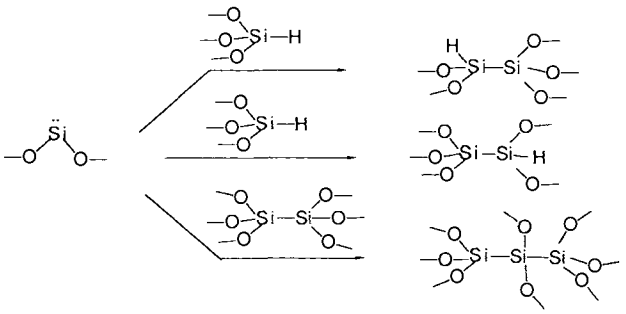

Scheme 11. Insertion reactions of silylene.

The thermal dehydrogenation of hydrosilsesquioxide gels does not lead directly to the formation of the stable silicon and silica phases but to the silicon sesquioxide phase that consists of a mixture of tetrahedral $Si(Si_zO_{4-z})$ units.[18]

3.2. Si_2Cl_6

The synthesis of a definite compound Si_2O_3 with only one tetrahedral $Si(Si_3O)$ site necessitates formation of Si–Si bonds at low temperature. A simple method has been proposed that employs hexachlorodisilane as a precursor (Scheme 12).[25]

$$Cl_3Si\text{-}SiCl_3 \xrightarrow[-95°C]{3\,H_2O\,/\,Et_2O} Si_2O_3 + 6\,HCl$$

Scheme 12. Synthesis of Si_2O_3.

Neutral or acid hydrolysis does not cleave the Si–Si bonds.[25] The hydrolysis of Si_2Cl_6 gives rise to an evolution of HCl, which provides acidic conditions. The reaction affords a white amorphous powder (with a specific surface area of 600 m^2g^{-1}) in which most of the Si–Si bonds are preserved (more than 90% of the theoretical ones). The silicon sesquioxide product has been characterized by IR spectroscopy (very weak Si–H stretching band at 2265 cm^{-1}, $\tilde{\nu}(SiO_{1.5}) =$ 875 cm^{-1}), ^{29}Si MAS NMR spectroscopy ($\delta = -71$, half

height width 954 Hz), and X-ray absorption spectroscopy (absorption edge at 1840.5 eV, those of silicon and silica are at 1836 eV and 1844 eV, respectively).[25] The representation of the average interatomic distances in Si_2O_3 in the bulk material obtained by extended X-ray absorption fine structure (EXAFS) spectroscopy is given in Figure 2. Thus, Si_2O_3, prepared in this

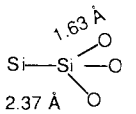

Fig. 2. Average environment determined by EXAFS spectroscopy of the silicon atoms in Si_2O_3 in the bulk material.

way is a defined compound in which each silicon atom is bonded to three oxygen atoms and one silicon atom rather than a random mixture of Si-like and SiO_2-like tetrahedra.[25] However, this product contains quite a few absorbed water molecules as shown by IR spectroscopy.

The thermal evolution of this compound was studied by TGA/MS and by ^{29}Si MAS NMR spectroscopy. Above 200 °C water and hydrogen are evolved. The presence of water arises from desorption and from condensation of silanol groups, which are formed by hydrolysis of the Si–Si bonds (see below). The formation of H_2 is attributed to the hydrolysis of Si–Si and Si–H bonds (Scheme 13). The NMR spectrum of the remaining

$$O_{1.5}Si{-}SiO_{1.5} \xrightarrow{H_2O} O_{1.5}Si{-}OH + O_{1.5}Si{-}H$$

$$2\,O_{1.5}Si{-}OH \longrightarrow 2\,SiO_2 + H_2O$$

$$O_{1.5}Si{-}OH + O_{1.5}Si{-}H \longrightarrow 2\,SiO_2 + H_2$$

Scheme 13. Hydrolysis of the Si–Si bond in Si_2O_3.

solid corresponds to hydrated silica. Hydrolysis of the Si–Si bonds, which leads to the formation of silica, occurs during heating due to absorbed water in the gel. Similar cleavage of Si–Si bonds by adsorbed NH_3 was encountered in the synthesis of triimidodisilane by ammonolysis of Si_2Cl_6.[26] The hydrophilic character of silicon sesquioxide Si_2O_3 does not allow its metastability to be studied.

3.3. Organosilicon Precursors

Silicon oxycarbide species have been characterized by X-ray photoelectron spectroscopy (XPS) [27, 28] and by high-resolution solid-state ^{29}Si MAS NMR.[28–38] The system may be described as a composite material formed by a silicon oxycarbide phase of the composition $SiC_xO_{(1-x/2)}$, and free carbon (arising from an excess carbon phase). In this phase the carbon atoms are only linked to silicon atoms under the formation of $C(Si_4)$ sites, and the oxygen atoms are involved in Si-O-Si bridges.

Silicon oxycarbides were reported at the interface between silicon carbide substrates and the silica surface layers formed by oxidation.[34] Nicalon ceramic fibers, which are obtained by pyrolysis of a polycarbosilane crosslinked by oxidation, consist of β-silicon carbide and graphite crystallites embedded in a continuous phase of glassy silicon oxycarbide.[35] The pyrolysis of polysiloxane gels, which were obtained by hydrolysis of organosilanes, appears to be a versatile route to silicon oxycarbide glasses or silicon carbide, because of the carbothermal reduction that takes place above 1400 °C.[31, 33, 42, 43]

A great variety of polysiloxane precursors with varied compositions and structures has been prepared by hydrolysis/condensation (or co-hydrolysis/condensation) of alkoxy- or chlorosilane monomers (or co-monomers) bearing non-hydrolyzable substituents such as methyl, ethyl, vinyl, phenyl, or hydro groups (Scheme 14). However, in the case of alkyl groups, carbon is lost during the pyrolysis by β-elimination; thus, the final carbon content is the same as obtained by starting from methyl precursors. The use of precursors with unsaturated substituents such as phenyl and vinyl groups leads to a high final carbon content but as a free carbon phase.

$$n\,R_{4-x}SiX_x + n\,(x/2)\,H_2O \longrightarrow (R_{4-x}SiO_{x/2})_n + nx\,HX$$

X= MeO, EtO, Cl ; R= Me, Et, Vi, Ph, H....

Scheme 14. Preparation of polysiloxane precursors. Vi = vinyl.

To date, only the composition of one oxycarbide has been studied in detail. It does not depend on the C/Si ratio in the precursors, since a large fraction of the carbon atoms belongs to a phase formed from excess carbon. The O/Si ratio in the oxycarbide, however, is always slightly higher than that in the gel, since in addition to the formation of Si-O-Si bridges, thermal redistribution reactions between Si–C and Si–O bonds take place, leading to the formation of volatile organosilicon species and SiO_4 groups (Scheme 15).[20, 39] Most of the polysiloxane precursors described have O/Si ratios close to 1.5; they give rise, after pyrolysis in argon at about 1000 °C, to silicon oxycarbide phases with O/Si ratios between 1.5 and 1.8.

$$2\,CH_3SiO_{1.5} \rightleftharpoons (CH_3)_2SiO + SiO_2$$

$$CH_3SiO_{1.5} + (CH_3)_2SiO \rightleftharpoons (CH_3)_3SiO_{0.5} + SiO_2$$

$$2\,(CH_3)_3SiO_{0.5} \rightleftharpoons (CH_3)_3SiOSi(CH_3)_3$$

Scheme 15. Redistribution of Si–C and Si–O bonds.

A change in the composition of the silicon oxycarbide phase may be achieved by simply decreasing the O/Si ratio. However, a decrease of the O/Si ratio entails a decrease in the number of siloxane bridges; thus, the level of crosslinking in the precursor decreases, which favors the formation of volatile organosilicon compounds during pyrolysis. This, in turn, may change the composition of the gel and lead to a low pyrolysis yield. For instance, linear polysiloxanes (O/Si = 1) such as polydimethylsiloxane $(Me_2SiO)_n$ give a negligible ceramic yield, because of the loss of volatile cyclic oligomers. Thus, to prepare good precursors with low O/Si ratios, the Si-O-Si bridges have to be replaced by other bridges in order to decrease the O/Si ratio without decreasing the level of crosslinking in the precursor.[28, 31]

This approach has been developed starting from precursors containing Si–Si bonds such as dimethyltetrachlorodisilane

$MeCl_2SiSiCl_2Me$, or "disilane residue" ("S" mixture), $(CH_3)_xCl_{6-x}Si_2$, a product arising from the direct synthesis of methylchlorosilanes (reaction of methyl chloride with copper/silicon),[31] and bridging alkyl groups such as polydichlorosilylethylene $(Cl_2SiCH_2CH_2SiCl_2)_n$, obtained by hydrosilylation of vinyldichlorosilane ($ViHSiCl_2$).[28] Starting from $ViHSiCl_2$, two precursors of unknown composition **A** and **B** have been prepared: hydrosilylation followed by hydrolysis/condensation led to **A**, whereas hydrolysis followed by hydrosilylation led to **B** (Scheme 16). In this way, silicon oxycarbide phases have been

$$n\ ViHSiCl_2 \xrightarrow{\varepsilon\text{-}H_2PtCl_6} (Cl_2SiCH_2CH_2SiCl_2)_{n/2} \xrightarrow{H_2O} \mathbf{A}$$

$$ViHSiCl_2 \xrightarrow{H_2O} (ViHSiO)_n \xrightarrow{\varepsilon\text{-}H_2PtCl_6} \mathbf{B}$$

Scheme 16. Preparation of precursors **A** and **B**. Vi = vinyl.

prepared with compositions in the range O/Si = 1.3 to 1.14. The higher oxygen content of the oxycarbide glass that was obtained from the disilane precursors is due to partial hydrolysis of the Si–Si bonds and chiefly to redistribution reactions, which lead to the formation of silica and volatile carbon-rich oligomeric silanes. Indeed the loss of silicon compounds during pyrolysis is in the range 2 to 20%.[31] Thus the composition of the oxycarbide phases may be varied depending on the nature of the precursors (Table 1).

Table 1. Composition of oxycarbide phases synthesized from different precursors.

Precursor	T [°C] [a]	Composition of the gel	Composition of the oxycarbide phase
$MeSiO_{1.5}$	900	$SiO_{1.69}C_{0.8}$	$SiO_{1.69}C_{0.15}$ (+ 0.65 C)
SiO_2/Me_2SiO	970	$SiO_{1.75}C_{0.37}$	$SiO_{1.75}C_{0.12}$ (+ 0.25 C)
$MeSiO_{1.5}/Me_2SiO$	970	$SiO_{1.57}C_{0.66}$	$SiO_{1.57}C_{0.21}$ (+ 0.45 C)
$Me_2Si_2O_2$	1000	$SiO_{1.29}C_{0.77}$	$SiO_{1.29}C_{0.36}$ (+ 0.41 C)
"S" [b]	1000	$SiO_{1.26}C_{0.76}$	$SiO_{1.26}C_{0.37}$ (+ 0.39 C)
A [c]	900	$SiO_{1.29}C_{1.42}$	$SiO_{1.29}C_{0.36}$ (+1.06 C)
B [c]	900	$SiO_{1.14}C_{1.74}$	$SiO_{1.14}C_{0.43}$ (+1.31 C)

[a] T = Pyrolysis temperature. [b] "S" = disilane residue. [c] For **A** and **B** see Scheme 16.

The ^{29}Si MAS NMR and XPS spectra show that the distribution of the five tetrahedral SiO_xC_{4-x} sites changes with the composition of the oxycarbide phase.[28, 40] As the O/Si ratio decreases, the relative amount of Si–C rich tetrahedra increases. A comparison of the measured and calculated spectra (Fig. 3) revealed that in fact the silicon oxycarbide phase may be described as a purely random distribution of Si–O and Si–C bonds that forms an independent single phase regardless of the composition.[38] The nature of the precursor governs the composition of the glass; however, the environment of the silicon atoms depends only on the O/Si ratio and is not related to the structure of the precursor.

On heating the sample, the distribution of the SiO_xC_{4-x} sites of the oxycarbide glasses is greatly altered; the ^{29}Si NMR spectra show that the intensity of the peaks corresponding to SiO_4 and SiC_4 sites increases between 1200 and 1350 °C, immediately prior to the occurrence of the carbothermal reduction.[40] This behavior underlines the metastability of silicon oxycarbide

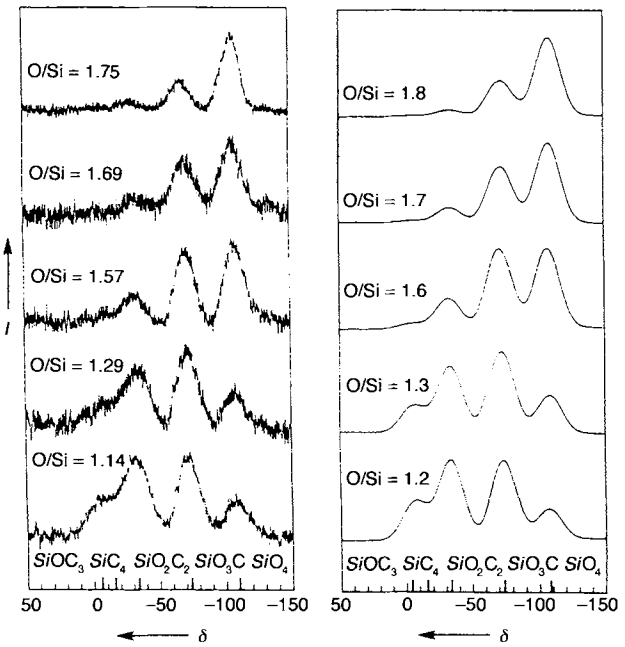

Fig. 3. ^{29}Si MAS NMR spectra of silicon oxycarbide glasses with various O/Si ratios; left: experimentally determined spectra; right: simulated spectra for a purely random distribution of Si–O and Si–C bonds.

phases, which tend to give the thermodynamically stable silicon carbide and silica phases. This phase separation has been ascribed to a continuation of the redistribution reactions of Si–O and Si–C bonds. This rearrangement to a mixture of silicon carbide and silica shows that the formation of silicon carbide by carbothermal reduction above 1400 °C involves the reduction of silica by the excess carbon rather than the reduction of the silicon oxycarbide phase. It has been reported that gaseous silicon monoxide SiO is the intermediate species of the reaction (Scheme 17).[41, 42]

$$SiO_2(s) + C(s) \longrightarrow SiO(g) + CO(g)$$
$$SiO(g) + 2\,C(s) \longrightarrow SiC(s) + CO(g)$$
$$SiO_2 + 3\,C \longrightarrow SiC + 2\,CO$$

Scheme 17. Carboreduction of SiO_2.

For silicon glasses containing an excess of carbon (more than 1.5 C per O), SiO_2 is converted to silicon carbide and the excess carbon remains in the residue.[33] That means that the reaction of gaseous SiO with carbon is very fast. When the excess of carbon is very low (less than 0.2 C), the carboreduction reaction does not occur; the pure silicon oxycarbide phase is thermally stable up to 1500 °C.[43] When the carbon excess is too low to allow the total conversion of SiO into SiC, a large amount of silicon monoxide is lost during this reaction.[38]

4. New Chemical Routes in Sol–Gel Processing

Hydrolysis and condensation of tetraalkoxysilanes $(RO)_4Si$ readily gives monolithic gels (that is, gels formed from one piece that do not exhibit internal cleavage). However, metal alkoxides

are much more reactive toward hydrolysis and condensation, and generally lead to the formation of precipitates.[3] Sophisticated processes based on decreasing the reactivity of the metal alkoxide precursors by chemical modification (alcohol exchange, addition of carboxylic acids or β-diketones) or on controlling the local concentration of water (alcohol dehydration, esterification, micelles microemulsions) have been developed to achieve monolithic gels.[3, 44, 45]

Furthermore, the different reactivities of alkoxysilanes and transition metal alkoxides toward hydrolysis and condensation also make it difficult to control the composition and the homogeneity of binary oxides by the sol–gel process.[46]

To counter the extreme hydrolytic reactivity of metal alkoxides, new condensation reactions have to be developed that permit the formation of metal-oxygen-metal (M-O-M) bridges without hydrolysis. One such method is based on the reaction of acetone with a zinc alkoxide, which results in the formation of a gel, via the decomposition of the intermediate ketolate complex, followed by liberation of zinc oxide, the alcohol, and mesityl oxide (Scheme 18).[47] This reaction is restricted to basic metal alkoxides that are capable of inducing ketolization of ketone.

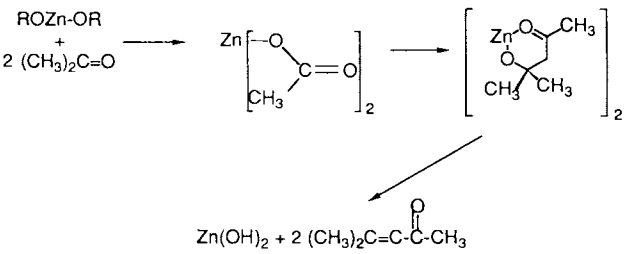

Scheme 18. Reaction of ketone with zinc alkoxides.

The condensation reaction of an acetoxysilane with metal alkoxides under liberation of ester molecules likewise leads to M-O-M bridges (Scheme 19).[48]

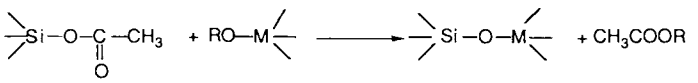

Scheme 19. Synthesis of Si-O-M units by ester elimination.

A third method has been developed that is based on well-established organic chemistry; that is, ethers are cleaved by iodotrimethylsilane to give alkyl iodide and hexamethyldisiloxane (Scheme 20).[49] In this reaction, the alkoxysilane formed

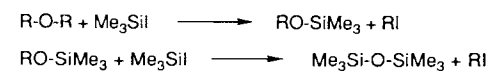

Scheme 20. Cleavage of ethers by Me_3SiI.

from the ether and iodosilane reacts with further iodosilane to give a siloxane. This reaction has already been reported by Gerrard et al, who showed that silica can be formed by heating tetrachlorosilane with tetrabenzyloxysilane (Scheme 21).[50] The alkoxy groups may also be formed in situ by reaction of metal halides with benzaldehyde (Scheme 22).[51]

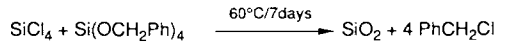

Scheme 21. Formation of silica from tetrachlorosilane and tetrabenzyloxysilane.

Scheme 22. Reaction of metal halides with benzaldehyde.

These reactions show that products containing M-O-M bridges may be synthesized starting from metal halides and different oxygen donors such as alkoxides, ethers, or benzaldehyde. The mechanism of the condensation reaction involves the coordination of the oxygen atom of the metal alkoxide to the metal center of the metal chloride. This complex reacts further to give M-O-M bridges (Scheme 23). The general principle of

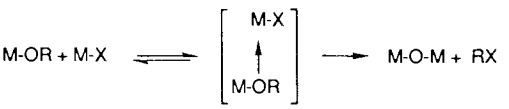

Scheme 23. Condensation of metal alkoxides with metal halides.

this nonhydrolytic process is to induce cleavage of the carbon–oxygen bond instead of the metal–oxygen one. This nonhydrolytic route has been applied to the preparation of monocomponent as well as bicomponent gels.[52]

4.1. Monocomponent Gels

4.1.1. Silica Gels

Silicon tetrachloride does not react with tetraethoxysilane (TEOS), diethyl ether, or diisopropyl ether, but with oxygen donors in which the alkyl group has a greater electron-releasing capacity.[50, 53, 54] Silica nonhydrolytic gels (NHG) can be obtained from silicon tetrachloride and dibenzyl ether, benzaldehyde, or tetrabenzyloxysilane (Table 2).

Table 2. Specific BET surface areas S [$m^2 g^{-1}$] of silica obtained by the NHG process by treating tetrachlorosilane with organic oxygen donors at 110 °C in sealed tubes.

Oxygen donor	t [a]	S
$PhCH_2OCH_2Ph$	15	731
PhCHO	2	265
$Si(OCH_2Ph)_4$	8	500

[a] t = gel time [d].

The main drawback of this NHG process is the large weight loss during calcination, which can be attributed to the large proportion of residual organic components. For example, the weight loss observed during the calcination of the gel derived from $SiCl_4$ and $Si(OCH_2Ph)_4$ was 73%. However, this process may be improved by using a Lewis acid as catalyst. In this way, commercially available materials such as tetraethoxysilane (TEOS) and diethyl ether can be used as starting materials in the

nonhydrolytic condensations.[55] In the presence of $FeCl_3$ as catalyst, silica NHG were obtained by reacting silicon tetrachloride with tetraisopropoxysilane, tetraethoxysilane, diisopropyl ether, or diethyl ether as oxygen donors.[55]

4.1.2. *Alumina Gels*

When a solution of aluminum chloride and either aluminum triisopropoxide (in stoichiometric amounts), or diisopropyl ether (1.5 equiv) is heated, monolithic alumina gels are formed (Scheme 24).[56] Aluminum chloride was solubilized by formation of an addition complex with ether. It is noteworthy that gelation occurs faster with diisopropyl ether than with aluminum triisopropoxide (Table 3).

$$AlCl_3 + Al(OiPr)_3 \xrightarrow[110\,^\circ C,\ 24\,h]{Et_2O/CCl_4} \text{Monolithic gel} \xrightarrow{\text{calcination}} \text{Alumina NHG}$$

$$AlCl_3 + 1.5\,iPrO \xrightarrow[110\,^\circ C,\ 2\,h]{CH_2Cl_2} \text{Monolithic gel} \xrightarrow{\text{calcination}} \text{Alumina NHG}$$

Scheme 24. Preparation of nonhydrolytic alumina.

Table 3. Specific BET surface areas S [$m^2 g^{-1}$] of alumina obtained by the NHG process by treating $AlCl_3$ with oxygen donors.

Oxygen donor	t [a]	$\Delta m/m$ [%] 200–1000 °C	Yield [%]	XRD	S [b]
$Al(OiPr)_3$	24	35	86	amorphous	370
$1.5\,iPr_2O$	2	45	92	amorphous	400

[a] t = gel time [h]. [b] Determined at 650 °C. XRD = X-ray powder diffraction pattern of samples calcined at 500 °C.

The weight loss during calcination measured by TGA and the yields of alumina are similar regardless of the oxygen donor used. More interesting is the amorphous character of the resulting alumina. Hydrated crystalline alumina gels are formed when the hydrolytic sol–gel process is used.[57] Under the conditions employed by ourselves, the crystallization of hydrated phases such as boehmite (AlO(OH)) is not possible. The alumina remained amorphous even after 5 h calcination at 750 °C; at this temperature the specific surface area of calcined samples is quite high, around 300 $m^2 g^{-1}$. The formation of crystalline γ-Al_2O_3 was observed after heating samples at 850 °C for 5 h. For comparison, hydrated alumina gels obtained by hydrolysis of alkoxide precursors usually crystallize to give γ-Al_2O_3 below 500 °C.[57]

Another difference to the hydrated alumina is the presence of a high proportion of pentacoordinate aluminum atoms in alumina gels prepared from $AlCl_3$ and aluminum triisopropoxide, as determined by ^{27}Al NMR spectroscopy.[58] In most cases the aluminas contain tetracoordinate or hexacoordinate Al atoms, whereas pentacoordinate Al atoms have been found in only a very few examples.[59] The regions with pentacoordinate Al atoms are retained in the calcined samples up to the crystallization of γ-Al_2O_3 above 750 °C. The pentacoordination is attributed to the fact that aluminum chloride and aluminum triisopropoxide form a trinuclear aluminum complex in which one aluminum atom is pentacoordinate and the other two are tetracoordinate (Fig. 4).[60] This structure is maintained in solution even after heating for up to 3/4 of the gelation time.[58]

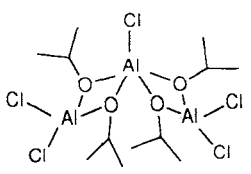

Fig. 4. Stucture of the trinuclear complex obtained from aluminum chloride and aluminum triisopropoxide.

4.1.3. *Titania Gels*

The role of the oxygen donor in the nonhydrolytic gel process was investigated by reacting titanium tetrachloride with titanium tetraisopropoxide or with a stoichiometric amount of an ether such as tetrahydrofuran (THF), di(*n*-propyl) ether, di(isopropyl) ether, diethyl ether, and dimethoxyethane (DME) without solvent.[61] The addition of oxygen donors to $TiCl_4$ gives solids of the composition $ROTiCl_3$ (Scheme 25), which melt below 110 °C; thus, the reactions took place in the homogeneous liquid phase.

$$TiCl_4 + ROR \longrightarrow Cl_3TiOR + RCl$$

Scheme 25.

Gelation occurs in all cases at much longer times than under hydrolytic conditions (Table 4). The gel time is dependent on the oxygen donor and increases in the order: $Ti(OiPr)_4 \approx iPr_2O < Et_2O < THF < nPr_2O < DME$. The analysis of the syneresis liquid confirms the formation of alkyl chlorides as the by-product (with isomerization of the propyl chloride in the case of di-*n*-propyl) ether).

Table 4. Properties of titania obtained from $TiCl_4$ and ethers at 110 °C in a sealed tube.

Oxygen donor	t [b]	Alkyl chloride	$\Delta m/m$ [%]	Yield [%]	XRD [c]	XRD [d] %A	XRD [d] %R
THF	60	$Cl(CH_2)_4Cl$	18	89	A	57	43
nPr_2O	70	*n*PrCl (86%) *i*PrCl (14%)	16	81	A	89	11
iPr_2O	12	*i*PrCl	16	95	A	86	14
Et_2O	17	EtCl	22	74	A	42	58
DME	85	-	47	80	A	0	100
$Ti(OiPr)_4$	12	*i*PrCl	14	90	A	100	0

[a] A: anatase, R: rutile. [b] t = gel time [h]. [c] Samples calcined at 500 °C. [d] Samples calcined at 1000 °C.

The absence of dichloro-1,2-ethane as syneresis liquid (methyl chloride is too volatile to be isolated) in the gel formed with DME and the weight loss ($\Delta m/m$ = 47%) during calcination is attributed to the fact that $TiCl_4$ reacts only with the end groups of DME, leading to a hybrid organic–inorganic gel (ethylene-bridged TiO_2) (Scheme 26).

$$2\,M\text{-}Cl + CH_3\text{-}O\text{-}CH_2CH_2\text{-}O\text{-}CH_3 \longrightarrow M\text{-}O\text{-}CH_2CH_2\text{-}O\text{-}M + 2\,CH_3Cl$$

Scheme 26. Preparation of a hybrid organic–inorganic gel.

The titania yields after calcination (above 500 °C) were large (74–95%). Titania calcined at 500 °C crystallizes in the anatase form. By heating to 1000 °C (without holding time), a proportion of anatase was transformed to rutile; complete transformation was only observed for the sample prepared from DME, whereas the transformation had not yet begun at this temperature for the sample derived from $Ti(OiPr)_4$. This result is of particular interest because the transformation of anatase to rutile is crucial for the porosity and the surface area of the material.[62] For example, in membrane applications the anatase–rutile transformation is inhibited by doping.[62]

Table 6. Properties of aluminosilicate gels obtained by the NHG process, and specific BET surface areas S [$m^2 g^{-1}$] of the calcined gels.

No.	t [a]	Al/Si [b]	Al/Si [c]	$\Delta m/m$ [d] [%]	Yield [%]	S [e]
1	<18 h (RT)	0.39	0.46±0.005 (700)	29	100	706 (700)
2	<20 min (110 °C) [f]	2.5	2.2±0.02 (900)	41	92	237 (900)
3	<2 h (110 °C) [f]	3.0	3.17±0.03 (900)	28	100	234 (900)
4	<2 h (110 °C) [f]	10.5		33	100	367 (800)

[a] t = gel time, RT: room temperature. [b] Molar ratio in the initial solution. [c] Molar ratio in the oxide after calcination, determined from EDX spectroscopy. Values in parentheses are the calcination temperatures [°C]. [d] Weight loss from TGA in air. [e] Values in parentheses are the calcination temperatures [°C]. [f] Gelation in sealed tube.

4.2. Bicomponent Gels

4.2.1. General Aspects

In the synthesis of bicomponent gels problems arise with respect to the composition and the homonegeity of gels because of the difference in the rates of hydrolysis and condensation of the various metal alkoxides used.[63]

Owing to the mechanism of its mode of condensation, the nonhydrolytic sol–gel process appears well suited to the preparation of binary oxides.[64] Furthermore, any composition is theoretically attainable by several chemical combinations, provided that the number of chloride substiuents is equal to the number of alkyl groups R (in the alkoxides $M(OR)_n$ or in the ether R_2O). However, redistribution reactions between metal chlorides and metal alkoxides could give rise to heterogeneous gels, the compositions of which may be difficult to control.

4.2.2. SiO_2/Al_2O_3 System

SiO_2/Al_2O_3 gels with different compositions, in which the Al/Si ratio varied from 0.39 to 10.52, were prepared from metal chlorides and an ether or from a metal chloride and a metal alkoxide (Table 5).

Table 5. Molar composition of aluminum- and silicon-containing solutions that were used for the gelation.

No.	$AlCl_3$	$Al(OiPr)_3$	$SiCl_4$	$Si(OiPr)_4$	iPr_2O	Solvent
1	2	0	1.86	3.31	0	CH_2Cl_2
2	6	0	2.4	0	12.7	CCl_4/Et_2O
3	3	3	1.04	0.99	0	CCl_4/Et_2O
4	10.5	0	1	0	17.8	CH_2Cl_2

Monolithic gels were obtained for all the compositions (Table 6). The overall yields of binary oxide, determined after calcination in air, were very large (92–100%) (Table 6). Based on X-ray diffraction patterns, the gels remained amorphous after calcination up to 700 °C. Their specific surface areas in the amorphous state were determined by the Brunauer–Emmet–Teller (BET) method. As expected from the high yields, the compositions of the calcined gels, determined by energy-dispersive X-ray spectroscopy (EDX), are rather close to those of the initial solution. Thus, in the NHG process, the composition of the binary oxides can be controlled by the stoichiometry of the starting solution.

The homogeneity of the binary oxides has been investigated by ^{29}Si solid-state MAS NMR spectroscopy. The ^{29}Si chemical shifts of the silicon atom of a given SiO_4 tetrahedron are quite sensitive to the number of further silicon atoms attached at the vertices. Thus, a downfield shift of the signal of $\Delta\delta = 5$ is observed for each substitution of a Si atom by an Al atom, generating the five possible local environments of silicon Si[4Si], Si[Al, 3Si], Si[2Al, 2Si], Si[3Al,Si], and Si[4Al].[65]

The ^{29}Si NMR spectra of various silicoaluminates prepared reveal a large distribution of chemical shifts (Fig. 5). A comparison of the ^{29}Si chemical shift observed for the Si-rich oxide (gel 1, signal centered at $\delta = -102$) with that of the Al-rich oxide (gel 4, signal centered at $\delta = -84$), reveals a regular downfield shift, which is attributed to the formation of Si-O-Al bonds. This downfield shift reflects the increase in the number of Si-O-Al bridges; however, the distribution of Si and Al atoms in the oxides is purely random.

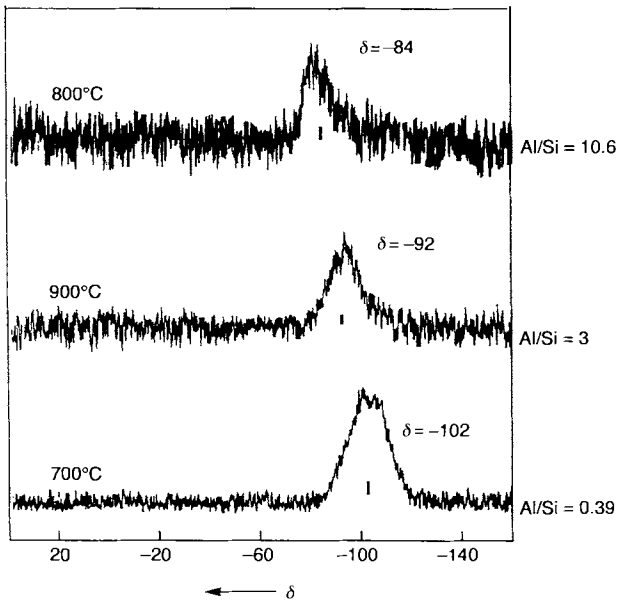

Fig. 5. ^{29}Si MAS NMR spectra of silicoaluminates with various Al/Si ratios.

Another way to determine the homogeneity of bicomponent gels is to study their crystallization. The crystallization tem-

perature of a binary oxide of known composition strongly depends on the homogeneity of the starting gel. For example, in the Al_2O_3/SiO_2 system, mullite, $3Al_2O_3 \cdot 2SiO_2$, is the only compound with a stoichiometric composition. The crystallization of pre-mullite gels is known to be influenced by ultrastructure, giving a clear insight into the scale of mixing between aluminum and silicon.[66] Indeed, when the homogeneity is achieved at the atomic level, crystallization of tetragonal mullite occurs at 980 °C. When the gel is homogeneous only on the namometer scale, a spinnel phase crystallizes at the same temperature (980 °C), whereas mullite is obtained at 1200 °C.

In order to study the homogeneity of nonhydrolytic gels with stoichiometric mullite composition,[67] two gels were prepared in which diisopropyl ether or aluminum triisopropoxide were used as oxygen donor (Scheme 27). Their conversion to mullite

$$6\,AlCl_3 + 2\,SiCl_4 + 13\,iPr_2O \xrightarrow[110°C]{CH_2Cl_2} \text{Gel} + 13\,iPrCl$$

$$5/3\,AlCl_3 + 13/3\,Al(OiPr)_3 + 2\,SiCl_4 \xrightarrow[110°C]{Et_2O/\,CCl_4} \text{Gel} + 13\,iPrCl$$

Scheme 27. Preparation of premullite gels for the synthesis of mullite.

was followed by DTA, X-ray diffraction (XRD), and MAS NMR spectroscopy. The DTA curves indicated a sharp exothermic peak near 1000 °C for the gel prepared with the ether, corresponding to the crystallization of tetragonal mullite. The other gel showed a broad peak near the same temperature due to the appearance of spinel. The ^{29}Si MAS NMR spectra of both samples calcined at 900 °C are very similar. The broad signal centered at about $\delta = -92$ corresponds to that expected for a random distribution of Al and Si in the oxides. Thus, DTA appears a more accurate probe for homogeneity of premullite gels than solid-state NMR spectroscopy.

The nonhydrolytic sol–gel process, in which the metal chloride reacts under condensation with oxygen donors, is a quite general procedure, which is only limited by the insolubility of some metal chlorides in organic solvents.

The main advantages expected from this route are: 1) the preparation of non-hydrated oxides and oxides with a low number of hydroxyl groups at low temperatures; 2) improved control over the molecular level homogeneity and stoichiometry of multicomponent oxides; 3) access to new structures by retaining the complex molecular framework of precursors in solution.

5. Organic–Inorganic Hybrid Materials

Organic–inorganic hybrid materials are a very wide field of growing interest.[68, 69] They encompass inorganic oxides that function as fillers in organic polymers, and also solids consisting of polymers or organic molecules included in inorganic oxide networks.

The preparation of hybrid materials in which organic molecules are covalently bound to silica is opening interesting perspectives for chemists. The organic moieties can be located inside the solid or only at its surface.[70–72] When only one organic substituent in the silicon alkoxide precursor is linked by C–Si bond, the hydrolysis of the $Si(OR)_3$ group leads to a crosslinked solid in which most of the organic groups are located at the surface. A review on this kind of hybrid polymer was recently published.[69e] The incorporation of an organic spacer inside an inorganic matrix can be performed when at least two covalent bonds are formed between the organic molecule and the solid. The organic spacers used are given in Scheme 28.

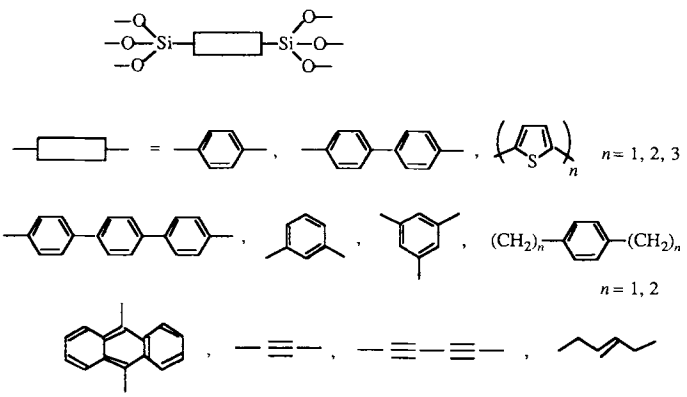

Scheme 28. Organic spacers in polysiloxane hybrid gels.

In most cases the gels were obtained by hydrolysis of $Si(OMe)_3$ or $Si(OEt)_3$ groups; however, SiH_3 groups, which were hydrolyzed with fluoride ions or $[(Ph_3P)_3RhCl]$ as catalyst, have also been used (Scheme 29).[71b] The solid was identified

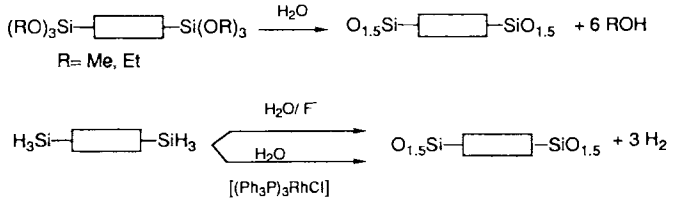

Scheme 29. Gelation of bridged bissilyl precursors.

by cross polarization magic angle spinning (CP-MAS) NMR spectroscopy: ^{13}C NMR spectroscopy showed that the organic groups remain intact in the gel. ^{29}Si NMR spectroscopy showed that the Si–C bonds are still present, since the cleavage of these bonds would lead to the formation of easily detectable $RO\text{-}Si(OSi)_3$ and $Si(OSi)_4$ units. These units are named in conformity with usage in silicone chemistry; thus, the names used are based on the functionality of the precursor (Me_3SiOR [M], $Me_2Si(OR)_2$ [D], $MeSi(OR)_3$ [T] and $Si(OR)_4$ [Q]) and on the number of Si-O-Si bonds ($T^2 = CSi(OSi)_2OR$).[39] The degree of condensation has been quantitatively determined by ^{29}Si CP-MAS NMR spectroscopy, [70b] and is largely dependent on the catalyst used for polycondensation. The use of an acid catalyst leads to a lower degree of condensation (65–75%) than a basic one (89–90%). As previously pointed out, the specific surface area of the solid is highly dependent on the experimental conditions (solvent, concentration of reagents, catalyst, functionality

Table 7. Gelation conditions for the various hybrid precursors and specific BET surface areas S [$m^2 g^{-1}$] of the calcined gels.

No.	Precursor	c [a]	Solv. [b]	Catalyst [c]	t [min] [d]	S
1		3	MeOH	NH_4F (10^{-3})	10^{-1}	1030
2		1	MeOH	NH_4F (10^{-3})	10	516
3		1	THF	NH_4F (10^{-3})	1	493
4		0.5	THF	NH_4OH (2.6)	45	1260
5		0.5	THF	NH_4OH (10^{-2})	95	380
6		0.5	THF	HCl (5×10^{-3})	600	129
7		0.5	MeOH	HCl (10^{-2})	95	770
8	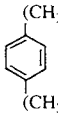	0.5	MeOH	NH_4F (10^{-2})	45	5
9		0.5	MeOH	NH_4OH (10^{-2})	8×10^4	4
10		0.5	THF	NH_4F (10^{-2})	3900	7
11		0.5	THF	NH_4OH (10^{-2})	360	0
12		0.5	THF	HCl (10^{-2})	30	8
13	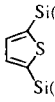	1	MeOH	NH_4F (10^{-3})	15	685
14		1	THF	NH_4F (10^{-3})	15	19
15	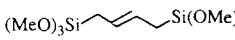	3	MeOH	NH_4F (10^{-3})	60	325
16		1	MeOH	NH_4F (10^{-3})	2×10^4	0
17		0.1	MeOH	NH_4OH (2.6)	30	977
18	$(MeO)_3Si(CH_2)_6Si(OMe)_3$	1	MeOH	NH_4F (10^{-3})	3	433
19	$(MeO)_3Si(CH_2)_8Si(OMe)_3$	1	MeOH	NH_4F (10^{-3})	20	0
20	$(MeO)_3Si(CH_2)_{12}Si(OMe)_3$	1	MeOH	NH_4F (10^{-3})	1	0
21	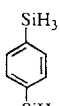	0.5	THF	Bu_4NF (10^{-3})	300	1000
22		0.5	THF	$(Ph_3P)_3RhCl$ (10^{-3})	10^4	54
23		0.5	THF	Bu_4NF (10^{-3})	35	0
24		0.5	THF	$(Ph_3P)_3RhCl$ (10^{-3})	30	100

[a] c = concentration [mol L^{-1}]. [b] Solv. = solvent. [c] Value in parentheses is the concentration of the catalyst [mol L^{-1}]. [d] t = Gel time.

of the silane precursor).[71] In the case of hybrid solids (e.g. organo-bridged polysiloxanes), the nature of the organic moiety becomes an important parameter. The influence of the organic moiety on the specific surface area is illustrated in Table 7.

Some of these solids behave as highly porous materials with very high specific surface areas (up to 1260 $m^2 g^{-1}$). For precursors with an aliphatic chain, the specific surface area and the porosities are highly dependent on the length of the chain. Long chains (more than ten CH_2 groups) lead to solids that behave as resins with no specific surface area or porosity. Under specific conditions, shorter chains (less than ten CH_2 groups) lead to mesoporous solids. However, it is impossible to predict the porosity of the resulting solid from the nature of the organosilane precursor. All the parameters capable of modifying the kinetics of the substitution reactions taking place at the silicon center during the polycondensation process control the formation of the solid and are of importance for the porosity of the material. These include concentrations of reagents, solvent, functionality at silicon, catalyst, external parameters (sonication, pressure etc...), and nature and geometry of the organic moiety, etc. The influence of the experimental conditions on the structure (texture) of the polycondensate is evident from Table 7.

5.1. Potential Applications

Since the field of organic–inorganic hybrid materials is very new, only a few possible applications have been explored up until now. Porous hybrid solids such as polysiloxanes with phenylene bridges have been used as the confinement matrix for inclusion of semiconductor particles of CdS: nanosized CdS particules have been deposited uniformly in the hybrid matrix. Likewise by complexation of $Cr(CO)_3$ groups on the phenylene-bridged groups included in the hybrid matrix, followed by thermal treatment, it is possible to produce a gel that includes Cr^0 crystalline nanoclusters.[70c]

Fluorescent xerogels have been prepared starting from terphenylene- and anthracene-bridging organosilanes.[70b] Films exhibiting interesting nonlinear optical (NLO) properties have been prepared starting from precursors containing organic dye molecules as bridging units.[70f]

The hydrolysis of a mixture of 1.1-bistrimethoxysilylferrocene with tetramethoxysilane has led to the formation of a gel containing ferrocene bridge units.[72a] This material was used as an electrode that is stable toward various solvents under aerobic conditions.

5.2. Short-Range Order in Organic–Inorganic Hybrid Materials

Besides the intrinsic physical properties (electronic, optical, magnetic, etc.) that are possibly afforded by the organic molecules embedded in the solid, there is one interesting question that concerns the structure of the amorphous solid: Does the molecular structure give rise to some short-range order in the amorphous solid?

At present, it is difficult to answer this question since there are not many tools available that permit characterization of amorphous systems. Multinuclear NMR and X-ray absorption spectroscopy (XANES, EXAFS) provide information about only the basic unit and whether the basic unit is present or not in the solid; however, they do not provide any information about the medium-range structure of the solid. Similarly, the X-ray diffraction method is useful only for long-range structured solids that are crystalline. The small angle X-ray scattering (SAXS) method allows the study of medium-range structure (or substructure); however, up until now, this method has been used only for studies on the fractal dimensions of hybrid solids.[69d,g]

To circumvent the lack of physical methods, the chemical reactivity of the organic moiety of hybrid solids has been used to obtain some chemical evidence of short-range order in the amorphous hybrid silica network for hybrid solids having a substructure (a structure intermediate between an amorphous one and one with long-range crystalline order).[71,72,82,85,86] To achieve this goal, hybrid organic–inorganic solids containing organic moieties covalently bonded to at least two $Si(OMe)_3$ groups have been prepared. The organic moieties undergo a specific and selective reaction with each other or with external reagents, which may be easily evidenced by spectroscopic means. In all the cases considered, the general procedure involves the preparation of precursors with selected organic moi-

eties and their gelation by hydrolysis. The presence of the organic component in the hybrid solid without chemical transformation or Si-C bond cleavage has been determined by ^{13}C and ^{29}Si CP MAS NMR spectroscopy.

5.2.1. *Crosslinkage of Diynes in the Gel*

Diyne units have been chosen as functional bridges because of their very selective reactivity. The polymerization of the diacetylene groups occurs topochemically,[73-75] that is a particular arrangement of the triple bonds to one another is required. As illustrated in Scheme 30, the 1-4 addition, leading to enyne formation, requires the diacetylene units to be parallel to each other.[76]

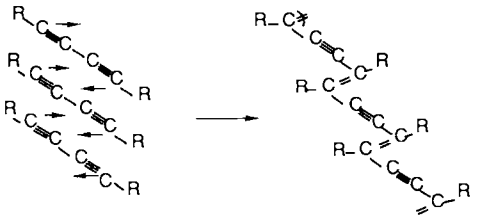

Scheme 30. Topochemical polymerization of diacetylene units.

A gel containing diacetylene units has been prepared from 1,4-bis(trimethoxysilyl)buta-1,3-diyne (^{13}C NMR: $\delta = 79.4$, and 87.8 (C-*C*≡*C*-Si), IR: $\tilde{\nu} = 2202$ and 2091 cm^{-1}). After the mixture had been heated at 200 °C under argon, the formation of enynes, and the associated crosslinking in the solid was detected by spectroscopy (^{13}C NMR: $\delta = 133$, ^{29}Si NMR: $\delta = -74$, IR: $\tilde{\nu} = 2169$ cm^{-1}).[77] Moreover, the same spectroscopic features have been found regardless of whether gelation is performed before the crosslinking (route A) or whether the crosslinking is induced by irradiation before the gelation (route B) (Scheme 31).

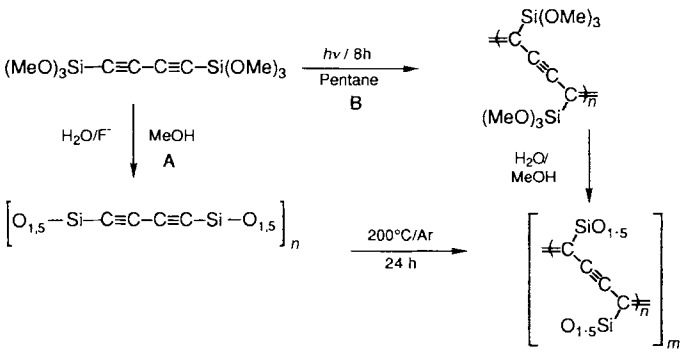

Scheme 31. Sythesis of gels containing acetylene units.

It is interesting to compare this polymerization with the crosslinkage observed in the case of polymers [-SiR_2-C≡C-C≡C-]$_n$ for which the DTA curve is highly dependent on the organization in the solid.[76] In the DTA curve of crystalline polymers of this type (R = Me,Et), a sharp peak occurs at 200 °C that can be attributed to the crosslinking reaction. In contrast, the poorly crystalline (R = Ph) or noncrystalline polymers (R = $SiMe_3$) are crosslinked only between 250 °C and 350 °C. In the case of gels the crosslinking reaction starts at lower temperatures as shown in Figure 6: The DTA curve exhibits an exothermic transformation between 120 and 350 °C with a maximum at 250 °C.

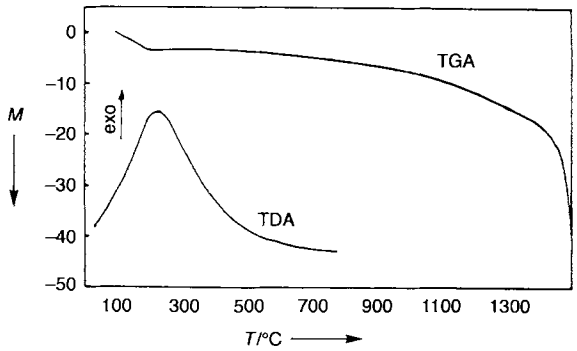

Fig. 6. TGA and TDA curves of a gel containing diyne units. M = loss of mass [%].

The facile reaction between the diyne fragments at a relatively low temperature within the amorphous gel may be indicative of a favorable arrangement of the diyne moieties. The enyne formation involves parallelism between several diacetylene units inside the solid. These results suggest the formation of "substructures" in the silica network that permit the 1-4 addition between the organic units.

5.2.2. *Polymerization of Thiophene Units Inside the Matrix*

Polythiophenes are obtained by electropolymerization,[78] and silylated thiophenes have been shown to be very efficient precursors for this polymerization,[79, 80] leading to polymers in which the thiophene units are bonded to each other mainly in the α position.[84] Gels containing bissilylated mono-, bis-, and terthiophene have been prepared.[82] ^{13}C and ^{29}Si CP MAS NMR spectra show that the structure of the precursor remains intact in the solid without cleavage of the Si–thiophene bond. The electrochemical oxidation of the gels deposited as films at the electrode leads to a fast polymerization reaction of the thiophene units included in the hybrid matrix (Scheme 32).[82] The

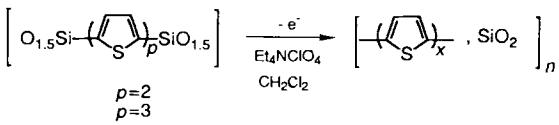

Scheme 32. Electropolymerization of gels containing silylated thiophenes.

same reaction is also possible by chemical oxydation using $FeCl_3/CHCl_3$ as oxidising agent.[82] The polythiophene formed in situ cannot be separated from the solid; it was identified in the film by Raman spectroscopy ($\tilde{\nu} = 1458$, 1220, 1171, 1047, 700, 682, and 652 cm^{-1}).[82]

The mechanism of oxidative polymerization known for silylated thiophenes requires the thiophene units to be close to each

other.[81] Thus, the fast polymerization inside the gels suggests the formation of thiophene aggregates with some regular geometry. Furthermore, it is impossible to separate the polymer from the solid, which is attributed to the presence of $O_{1.5}Si$ end groups in the polymer. The thiophene units are present in the gel in a more or less aggregated state, and oxidation leads to the formation of polymeric segments by coupling of proximal thiophene units.

Since the mobility in the solid is restricted, and since the polymerization is known to take place by coupling of two radicals with precise steric requirements, it has been concluded that the polymer formation occurs only because of the presence of thiophene aggregates with some regular geometry, which are formed during the gelation process.[82]

5.2.3. Complexation of Aromatic Groups Bound to Silica

Aromatic organosilanes react readily with $Cr(CO)_6$ to form $Cr(CO)_3$ complexes.[83, 84] This reaction was used to test the reactivity of phenyl groups attached to a silica network.[85] In the case of monosilylated phenyl systems, the introduction of $Cr(CO)_3$ in gels, which had been prepared from monosilylated phenyl compounds, is possible (Scheme 33) since most of the

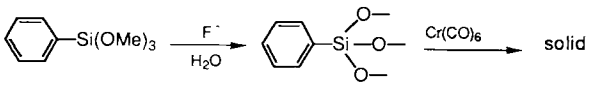

Scheme 33. $Cr(CO)_3$-containing phenylsilasesquioxane.

phenyl groups are accessible because they are located at the surface of silica.[85] The presence of the phenyl groups at the surface also explains the high hydrophobicity of these solids. The complexation has been monitored by IR and NMR spectroscopy and quantitatively determined by TGA and EDX investigations.[85]

On the other hand it is possible to prepare gels containing $Cr(CO)_3$-complexed phenylene groups from bis-silylated phenylene compounds,[70, 71] but the complexation must take place prior to gelation (Scheme 34).[85] However, the operation is not commutative: when the gelation is performed first, it is impossible to introduce the $Cr(CO)_3$ moieties to the phenylene

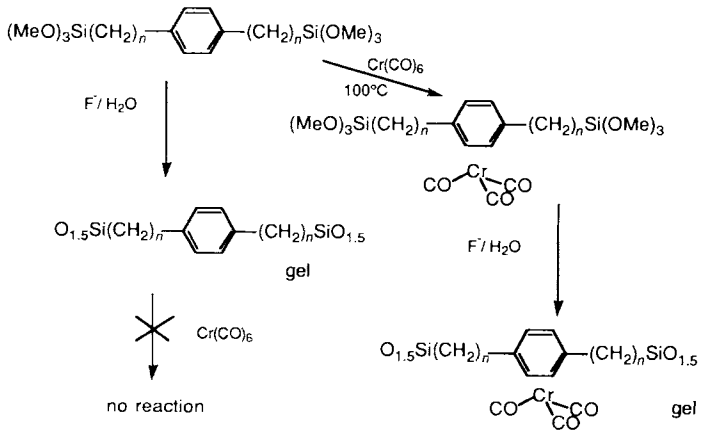

Scheme 34. Reactions of gels containing bissilylated phenylene groups.

ring. It has been concluded that most of the phenylene groups are located in the core of the solid and are thus not accessible for chemical reactions. This is consistent with the high hydrophilicity observed for gels containing *p*-phenylene units.[85]

However, the chemical behavior of these gels is highly dependent on the nature of the precursor. When the precursor contains rigid phenylene units, the resulting solid is hydrophilic (Si–OH at the surface), and the organic units, located in the core of the solid, are not accessible for chemical reactions. When more flexible organic groups such as phenylene-1,4-bis(ethylene) are introduced, the properties of the product are completely different: The solid is hydrophobic and reacts with $Cr(CO)_6$ since the phenylene groups are present at the surface.

The constitution of the starting materials influences the spatial arrangement of the organic units in the resulting condensation polymers.

5.2.4. Solids Containing Charge Transfer Complexes

The importance of the interactions between the organic units on the structure of the solid obtained during the gelation process is illustrated by the inclusion of charge transfer complexes in gels.[82] Scheme 35 shows the inclusion in silica of the charge transfer complexes formed between bissilylated terthiophenes

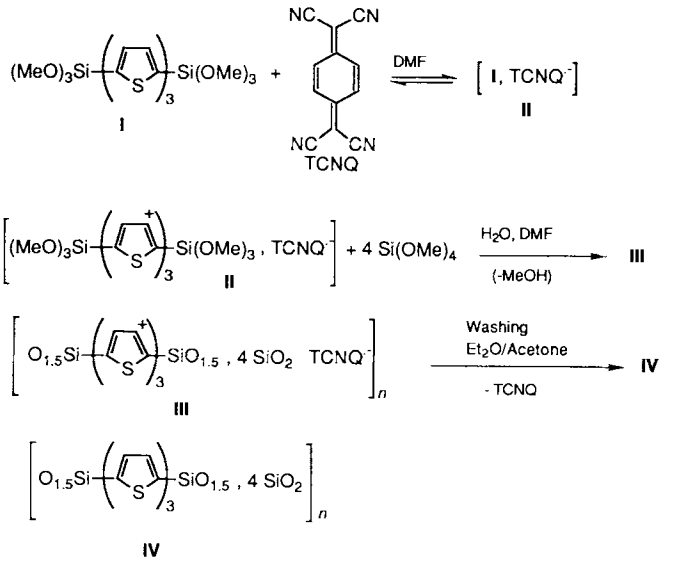

Scheme 35. Charge transfer complex from terthiophene and TCNQ in a polysiloxane gel.

and 7,7,8,8-tetracyano-*p*-quinodimethane (TCNQ). These complexes remain unchanged after gelation as shown by absorption spectroscopy (λ = 855, 752, 684 nm) and by conductivity measurements ($\varkappa = 10^{-6}\,S\,cm^{-1}$). Even though these interactions are very weak, they are evidently strong enough to control the structure in the amorphous solid.

5.2.5. Control of Solid Formation by Intermolecular Interactions

All the factors capable of modifying the course of polycondensation reactions are of importance. In order to illustrate

the drastic effect of the kinetic factors on the formation of the solid, the influences of a template effect on the rate of gelation and on the structure of the solid obtained have been investigated.

The polycondensation of an olefinic trialkoxysilane $(MeO)_3Si\text{-}(CH_2)_n\text{-}CH{=}CH\text{-}(CH_2)_n\text{-}Si(OMe)_3$ ($n = 1,2$) by the sol–gel process has been studied in the presence of Pd^{II} complexes (Scheme 36).[71, 86] This system was chosen because of the

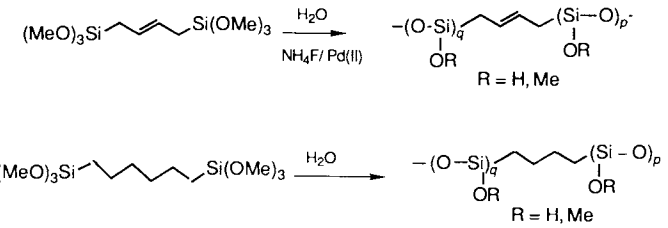

Scheme 36. Gelation with unsaturated and saturated trialkoxysilanes.

pronounced ability of C–C double bonds to coordinate around Pd centers[87] (template effect) and the behavior was compared to that of the corresponding saturated precursors $(MeO)_3Si\text{-}(CH_2)_6Si(OMe)_3$.

In all cases, a transparent gel was formed, and ^{13}C and ^{29}Si NMR spectroscopic analysis clearly established that the Si–C bond is retained in the solid. Whereas differences in the experimental conditions did not produce significant changes in the hybrid network at the molecular level, drastic differences appeared in the kinetics of gelation. In the presence of Pd^{II} compounds the gel time was reduced by almost two orders of magnitude (Table 8). In contrast, the reaction of the saturated

Table 8. Preparation of gels with unsaturated and saturated bis(trimethoxysilyl) precursors.

Precursor	Additive	Amount [a]	t [min] [b]
$(MeO)_3Si$–⁄\⁄–$Si(OMe)_3$	NH_4F	10^{-3}	29×10^3
	NH_4F/Li_2PdCl_4	$10^{-3}/5 \times 10^{-2}$	90
	Li_2PdCl_4	5×10^{-2}	75
	NH_4F/LiCl	$10^{-3}/10^{-1}$	50×10^3
	$NH_4F/(CH_3CN)_2PdCl_2$	$10^{-3}/5 \times 10^{-2}$	30
$(MeO)_3Si$–⁄\⁄\–$Si(OMe)_3$	NH_4F	10^{-3}	1×10^4
	NH_4F/Li_2PdCl_4	$10^{-3}/5 \times 10^{-2}$	120
$(MeO)_3Si$–⁄\⁄\⁄\–$Si(OMe)_3$	NH_4F	10^{-3}	2.9×10^3
	NH_4F/Li_2PdCl_4	$10^{-3}/5 \times 10^{-2}$	2.9×10^3

[a] Added amount of additive [mol] based on amount of precursor used. [b] t = gel time.

precursor is totally insensitive to the presence of Pd^{II} compounds. Most probably Pd^{II} activation proceeds by a template effect of the metal. As shown in Scheme 37, the formation of an η^2-olefin complex with unsaturated units allows an intramolecular condensation within the coordination sphere of the Pd center. While held in the complex, the monomer is ideally positioned for condensation and siloxane bridge formation. The

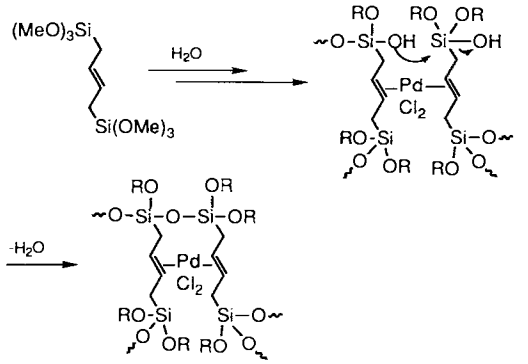

Scheme 37. Pd^{II}-activated gelation.

acceleration of the polycondensation can thus be attributed to the template effect of the palladium center.

The influence of Pd on the composition and properties of the resulting gel has been described.[86] For the gel prepared from unsaturated monomer, 80–100% of Pd was trapped in the hybrid network and remained in the xerogel. Conversely only a few Pd centers were retained in the gel prepared from the saturated C_6 monomers.

The gels containing Pd revealed no catalytic activity in hydrogenations, since the Pd center is not accessible but rather is completely embedded inside the network (Scheme 38 compound

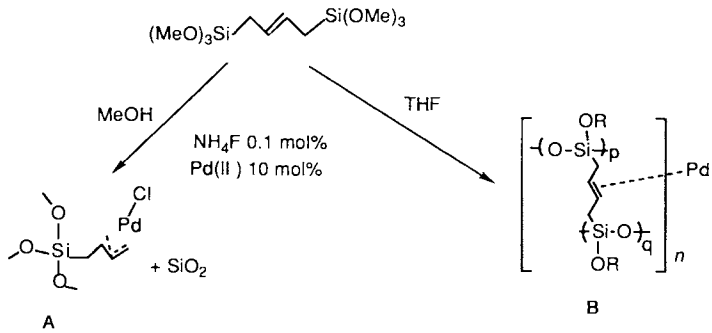

Scheme 38. Influence of the solvent on the catalytic activity of Pd^{II} catalysts. For A and B see text.

B). The condensation proceeded quite differently in MeOH than in THF. In methanol, the Si–C bond was cleaved and η^3-allylpalladium species were formed.[88] The resulting solid with η^3-allylpalladium complexes at the surface behaves as a very efficient catalyst for hydrogenation reactions (Scheme 38 compound **A**)

In conclusion, the results observed illustrate that the structure of the solid obtained during the gelation of hybrids of organosilanes with at least two $C\text{–}Si(OR)_3$ bonds depends greatly on the nature of the organic moieties included. These organic units can be located at the surface or in the core, and can lead to the formation of a substructure in the amorphous network. Furthermore, the chemical reactivity of the organic components appears as a very useful tool for the study of these systems, D. which show a degree of order.

6. Summary and Outlook

The field of research opened by the chemistry associated with the sol–gel process, which can be considered as sol–gel chemistry, is very wide. The chemistry of building blocks or new oxide synthesis with a particular attention to the chemistry of hybrid organic–inorganic solids are only two of the many research areas that have opened up for molecular chemists working in this field.

In this review we have focused on three main topics: 1) We have described the possibilities opened by new functional precursors, which allow the introduction of reactive centers in a solid at moderate temperature (300–450 °C). The polycondensates synthesized in this way undergo subsequent reactions which involve the same mechanisms as in solution; however, the restricted mobility of reactive centers in the solid changes dramatically the progress of the reaction. Metastable phases, silicon sesquioxide Si_2O_3, silicon oxynitride, and siliconoxycarbide have been obtained by this route. 2) A new general route for the synthesis of oxides has been described. In this sol–gel process, instead of H_2O, which is usually used in the inorganic polymerization, other oxygen donors such as ethers R_2O are employed. This method seems particularly attractive for the synthesis of multicomponent oxides homogeneous in the atomic region. 3) The field of hybrid organic–inorganic solids was considered with the aim of studying the possible organization in the solid, induced by the structure of the organic component of the hybrid precursor. Investigations into the chemical reactivity revealed the presence of aggregates between the organic components in the core of the solid. The structure and the texture of the products obtained are also highly dependent on the nature of the organic moiety.

Received: July 10, 1995 [A 122IE]
German version: *Angew. Chem.* **1996**, *108*, 1524–1540

[1] a) S. Yajima, J. Hayashi, M. Omori, *Chem. Lett.* **1975**, 931; b) S. Yajima, K. Okamura, J. Hayashi, *ibid.* **1975**, 1209.
[2] S. Sakka, K. Kamiya, *J. Non-Cryst. Solids*, **1980**, *42*, 403; C. J. Brinker, G. W. Scherer, *Sol Gel Science: the Physics and Chemistry of Sol–Gel Processing*, Academic Press, San Diego, **1990**; L. C. Klein, *Ann. Rev. Sci.* **1985**, 227; *Sol–Gel Technologgy for Thin Films, Fibers, Preforms, Electronics and Speciality Shapes*, Noyes, Park Ridge, NJ, **1988**; L. L. Hench, J. K. West, *Chem. Rev.* **1990**, *90*, 33; C. D. Chandler, C. Roger, M. J. Hampden-Smith, *ibid.* **1993**, *93*, 1205.
[3] J. Livage, M. Henry, C. Sanchez, *Progr. Solid State Chem.* **1988**, *18*, 259.
[4] D. C. Bradley, R. C. Mehrotra, D. P. Gaur, *Metal Alkoxides*, Academic Press, New York, **1978**, and references therein.
[5] L. P. Hammett, A. J. Deyrup, *J. Am. Chem. Soc.* **1932**, *54*, 2721.
[6] R. J. P. Corriu, D. Leclercq, A. Vioux, M. Pauthe, J. Phalippou, in *Ultrastructure Processing of Advanced Ceramics* (Eds.: J. D. Mackenzie, D. R. Ulrich), Wiley, Chichester, **1988**, 113.
[7] R. Aelion, A. Loebel, F. Eirich, *Rec. Trav. Chim*, **1950**, *69*, 61; *J. Am. Chem. Soc.* **1950**, *72*, 5705; W. T. Grubb, *ibid.* **1954**, *76*, 3408; C. Eaborn, *Organosilicon Compounds*, Butterworth, London, **1960**.
[8] R. J. P. Corriu, C. Guerin, B. J. L. Henner, Q. Wang, *Organometallics* **1991**, *10*, 3200.
[9] R. J. P. Corriu, G. Dabosi, M. Martineau, *J. Organomet. Chem.*, **1978**, *150*, 27; *ibid.*, **1978**, *154*, 33; *ibid.* **1980**, *186*, 25.
[10] D. Schomburg, R. Krebs, *Inorg. Chem.* **1984**, *23*, 1378; J. J. Harland, J. S. Payne, R. O. Day, R. R. Holmes, *ibid.* **1987**, *26*, 760; R. Damrauer, L. W. Burggraf, L. P. Davis, M. S. Gordon, *J. Am. Chem. Soc.* **1988**, *110*, 6601; L. P. Davis, L. W. Burggraf, M. S. Gordon, *ibid.* **1988**, *110*, 3056; J. A. Deiters, R. R. Holmes, *ibid.* **1990**, *112*, 7197.
[11] R. A. Assink, B. D. Kay, *J. Non-Cryst. Solids* **1988**, *99*, 359; **1988**, *107*, 35; B. D. Kay, R. A. Assink, *ibid.* **1988**, *104*, 112.
[12] J. Chojnowski, M. Cypryk, K. Kazmierski, K. Rozga, *J. Non-Cryst. Solids* **1990**, *125*, 40.
[13] R. K. Iler, *Chemistry of Silica*, Wiley, New York **1979**.
[14] a) V. W. Day, W. G. Klemperer, V. V. Mainz, D. M. Millar, *J. Am. Chem. Soc*, **1985**, *107*, 8262; W. G. Klemperer, V. V. Mainz, D. M. Millar, *Mat. Res. Soc. Symp. Proc.* **1986**, *73*, 3; W. G. Klemperer, S. D. Ramamurthi, *ibid.* **1988**, *121*, 1; P. C. Cagle, W. G. Klemperer, C. A. Simmons, *ibid.* **1990**, *180*, 29; b) F. J. Feher, K. J. Weller, *Inorg. Chem.*, **1991**, *30*, 880; F. J. Feher, K. J. Weller, J. W. Ziller, *J. Am. Chem. Soc*, **1992**, *114*, 9686, F. J. Feher, K. J. Weller, *Chem. Mater.* **1994**, *6*, 7; c) P. A. Agaskar, *J. Am. Chem. Soc.* **1989**, *111*, 6858; *Inorg. Chem.*, **1990**, *29*, 1603; *Colloids Surf.* **1992**, *63*, 131; *J. Chem. Soc. Chem. Commun.* **1992**, 1024.
[15] M. Pauthe, J. Phalippou, R. J. P. Corriu, D. Leclercq, A. Vioux, *J. Non-Cryst. Solids*, **1989**, *113*, 21.
[16] R. Corriu, C. Guerin, B. Henner, Q. Wang, *Inorg. Chim. Acta*, **1992**, *198–200*, 705.
[17] R. Corriu, R. Perz, C. Reyé, *Tetrahedron*, **1983**, *39*, 999.
[18] V. Belot, R. Corriu, D. Leclercq, P. Lefèvre, P. H. Mutin, A. Vioux, A. M. Flanck in *Chemical Processing of Advanced Materials* (Eds.: L. L. Hench, J. K. West), Wiley, **1992**, p. 143; V. Belot, R. Corriu, A. M. Flanck, D. Leclercq, P. Lefèvre, P. H. Mutin, A. Vioux in *Eurogel'91* (Ed. : S. Vilminot, R. Nass, H. Schmidt), Elsevier, Saarbrücken, **1992**, p. 77.
[19] V. Belot, R. Corriu, D. Leclercq, P. H. Mutin, A. Vioux, *Chem. Mater.* **1991**, *3*, 127.
[20] M. Pauthe, J. Phalippou, R. J. P. Corriu, D. Leclercq, A. Vioux, *J. Non-Cryst. Solids* **1990**, *125*, 187, 195.
[21] V. Belot, R. Corriu, D. Leclercq, P. H. Mutin, A. Vioux, *J. Mater. Sci. Lett.* **1990**, *9*, 1052.
[22] H. J. Emeleus, K. J. Stewart, *J. Chem. Soc.* **1935**, 1182.
[23] G. H. Wagner, A. N. Pines, *Ind. Eng. Chem.* **1952**, *44*, 321.
[24] W. H. Atwell, D. R. Weyenberg, *Angew. Chem.* **1969**, *81*, 485; *Angew. Chem. Int. Ed. Engl.* **1969**, *8*, 469.
[25] V. Belot, R. Corriu, D. Leclercq, P. Lefèvre, P. H. Mutin, A. Vioux, A. M. Flanck, *J. Non-Cryst. Solids* **1991**, *127*, 207.
[26] M. Billy, *Bull. Soc. Fr.* **1961**, 1550.
[27] L. Porte, A. Sartre, *J. Mater. Sci.* **1989**, *24*, 271; P. Schreck, C. Vix-Guterl, P. Ehrburger, J. Lahaye, *ibid.* **1992**, *27*, 4243.
[28] R. J. P. Corriu, D. Leclercq, P. H. Mutin, A. Vioux, *Mat. Res. Symp. Proc.* **1994**, *346*, 351.
[29] H. Zhang, C. G. Pantano, *J. Am. Ceram. Soc.* **1990**, *73*, 958; *Mater. Res. Soc. Symp. Ser.* **1992**, *271*, 795.
[30] F. Babonneau, K. Thorne, J. D. Mackenzie, *Chem. Mater.* **1989**, *1*, 554.
[31] V. Belot, R. J. P. Corriu, D. Leclercq, P. H. Mutin, A. Vioux, *J. Non-Cryst. Solids* **1992**, *144*, 287, and **1992**, *147,148*, 52.
[32] F. Babonneau, L. Bois, J. Livage, *J. Non-Cryst. Solids* **1992**, *147,148*, 280.
[33] G. T. Burns, R. B. Taylor, Y. Xu, A. Zangvil, G. Zank, *Chem. Mater.* **1992**, *4*, 1313.
[34] F. Babonneau, G. D. Soraru, G. D'Andrea, S. Dire, L. Bois, *Mater. Res. Soc. Symp. Ser.* **1992**, *271*, 789.
[35] R. Pampuch, W. S. Ptak, S. Jonas, J. Stoch, *Mater. Sci. Monogr.* **1980**, *6*, 435.
[36] J. Lipowitz, H. A. Freeman, R. T. Chen, E. R. Prack, *Adv. Ceram. Mater.* **1987**, *2*, 121.
[37] G. M. Renlund, S. Prochazka, R. H. Doremus, *J. Mater. Res.* **1991**, *6*, 2716, 2723.
[38] R. J. P. Corriu, D. Leclercq, P. H. Mutin, A. Vioux, *J. Mater. Sci.* **1995**, *30*, 2313.
[39] V. Belot, R. J. P. Corriu, D. Leclercq, P. H. Mutin, A. Vioux, *J. Polym. Sci. A* **1992**, *30*, 613.
[40] V. Belot, R. J. P. Corriu, D. Leclercq, P. H. Mutin, A. Vioux, *J. Non-Cryst. Solids* **1994**, *176*, 33.
[41] J. J. Biernacki, G. P. Wotzak, *J. Am. Ceram. Soc.* **1989**, *72*, 122.
[42] N. Klinger, E. L. Strauss, K. L. Komarek, *J. Am. Ceram. Soc.* **1966**, *49*, 369.
[43] G. D. Soraru, G. D'Andrea, R. Campostrini, F. Babonneau, G. Mariotto, *J. Am. Ceram. Soc.* **1995**, *78*, 379.
[44] A. Léaustic, R. E. Riman, *J. Non-Cryst. Solids* **1991**, *135*, 259.
[45] C. Guizard, M. Stitou, A. Larbot, L. Cot, J. Rouvière, *Mat. Res. Soc. Proc. Ser.* **1988**, *121*, 115.
[46] K. Kamiya, S. Sakka, Y. Tatemichi, *J. Mater. Sci.* **1980**, *15*, 1765.
[47] S. C. Goel, M. Y. Chiang, P. C. Gibbons, W. E. Buhro, *Mat. Res. Soc. Proc. Ser.* **1992**, *271*, 3.
[48] J. Caruso, M. J. Hampden-Smith, A. L. Rheingold, G. Yap, *J. Chem. Soc. Chem. Commun.* **1995**, 157; J. Caruso, M. J. Hampden-Smith, E. N. Duesler, *J. Chem. Soc. Chem. Commun.* **1995**, 1041; M. Iwasaki, A. Yasumori, S. Shibata, M. Yamane, *J. Sol–Gel Sci. Technol.* **1994**, *2*, 25; M. Jansen, E. Guenther, *Chem. Mater.* **1995**, 2110.
[49] T. L. Ho, G. A. Olah, *Synthesis* **1977**, 417; M. E. Jung, M. A. Lyster, *J. Org. Chem.* **1977**, *42*, 3761.
[50] W. Gerrard, J. V. Jones, *J. Chem. Soc.* **1952**, 1690.
[51] M. E. Jung, A. B. Mossman, M. A. Lyster, *J. Org. Chem.* **1978**, *43*, 3698.
[52] R. J. P. Corriu, D. Leclercq, P. Lefèvre, P. H. Mutin, A. Vioux, *J. Non-Cryst. Solids* **1992**, *146*, 301; *J. Mater. Chem.* **1992**, *2*, 673; *Chem. Mater.* **1992**, *4*, 961.
[53] R. Schwartz, W. Kucher, *Chem. Ber.* **1956**, *89*, 169.
[54] W. Gerrard, K. D. Kilburn, *J. Chem. Soc.* **1956**, 307.

[55] L. Bourget, R. J. P. Corriu, D. Leclercq, P. H. Mutin, A. Vioux, unpublished results.
[56] S. Acosta, R. J. P. Corriu, D. Leclercq, P. Lefèvre, P. H. Mutin, A. Vioux, *J. Non-Cryst. Solids* **1994**, *170*, 234.
[57] K. Wafers, C. Misra in *Oxides and Hydroxides of Aluminum*, Alcoa Technol., Alcoa, PA, **1987** Paper 19.
[58] S. Acosta, R. J. P. Corriu, D. Leclercq, P. H. Mutin, A. Vioux, *J. Sol–Gel Sci. Techol.* **1994**, *2*, 25.
[59] a) R. C. T. Slade, J. C. Southern, I. M. Thompson, *J. Mater. Chem.* **1991**, *1*, 563; b) F. R. Chen, J. G. Davis, J. J. Fripiat, *J. Catal.* **1992**, *133*, 263; c) T. E. Wood, A. R. Siedle, J. R. Hill, R. P. Skarjune, C. J. Goodbrake, *Mater. Res. Soc. Symp. Proc.* **1990**; *180*, 97.
[60] A. I. Yanovskii, V. A. Kozunov, N. Ya. Turova, N. G. Furmanova, Yu. T. Stuchkov, *Dokl. Chem. Engl. Transl.* **1979**, *244*, 119.
[61] P. Arnal, R. J. P. Corriu, D. Leclercq, P. H. Mutin, A. Vioux, *Mat. Res. Soc. Symp. Proc.* **1994**, *346*, 339.
[62] K. P. Kumar, K. Keizer, A. J. Burggraaf, *J. Mater. Chem.* **1993**, *3*, 1141.
[63] S. Sakka, K. Kamiya, *J. Non-Cryst. Solids* **1980**, *42*, 403.
[64] S. Acosta, P. Arnal, R. J. P. Corriu, D. Leclercq, P. H. Mutin, A. Vioux, *Mat. Res. Soc. Symp. Proc.* **1994**; *346*, 43.
[65] C. Engelhart, D. Michel in *High-Resolution Solid-State NMR of Silicates and Zeolites*, Wiley, New York, **1987**, pp 147–149.
[66] B. E. Yoldas, *J. Mater. Sci.* **1992**, *27*, 6667, and references therein.
[67] S. Acosta, R. J. P. Corriu, D. Leclercq, P. H. Mutin, A. Vioux, *Mat. Res. Soc. Symp. Proc.* **1994**, *346*, 345.
[68] For a general survey see *Hybrid Organic–inorganic Composites*, *ACS Symp. Ser.* **1994**, *585*; *New J. Chem.* **1994**, *18*, 989–1117.
[69] a) H. K. Schmidt, *Mater. Res. Soc. Symp. Proc.* **1984**, *32*, 327; b) H. K. Schmidt *Inorganic and Organometallic Polymers*, *ACS Symp. Ser.* **1988**, *360*, p 333; c) H. K. Schmidt, *Mater. Res. Soc. Symp. Proc.* **1990**, *180*, 961, and references therein; d) J. D. Mackenzie, *J. Sol–Gel Sci. Technol.* **1994**, *2*, 81, and references therein; e) U. Schubert, N. Hüsing, A. Lorenz, *Chem. Mater.* **1995**, *7*, 2010; f) D. A. Loy, K. J. Shea, *Chem. Rev.* **1995**, *95*, 1431; g) the fractal dimension of an object is the factor that connects the mass m of the object to its radius r according to $m \propto r^{df}$. df is called the fractal dimension. For dense spheroidal particles (euclidean object) $df = 3$; for fractal object $2 < df < 3$.
[70] a) K. J. Shea, D. A. Loy, O. W. Webster, *Chem. Mater.* **1989**, *1*, 574; b) *J. Am. Chem. Soc.* **1992**, *114*, 6700, and references therein; c) K. M. Choi, K. J. Shea, *ibid*, **1994**, *116*, 9052; d) *J. Phys. Chem.* **1994**, *98*, 3207; e) K. M. Choi, J. C. Hemminger, K. J. Shea, *ibid*, **1995**, *99*, 4720; f) H. W. Oviatt, K. J. Shea, S. Kalluri, Y. Shi, W. H. Steier, L. R. Dalton, *Chem. Mater.* **1995**, *7*, 493.
[71] a) R. J. P. Corriu, J. J. E. Moreau, P. Thepot, M. Wong Chi Man, *Chem. Mater.* **1992**, *4*, 1217–1224; b) *J. Sol–Gel Sci. Technol.* **1994**, *2*, 87.
[72] a) P. Audebert, P. Calas, G. Cerveau, R. J. P. Corriu, N. Costa; *J. Electroanal. Chem.* **1994**, *372*, 275; b) G. Cerveau, R. J. P. Corriu, N. Costa, *J. Non-Cryst. Solids* **1993**, *163*, 226.
[73] J. L. Brefort, R. J. P. Corriu, P. Gerbier, C. Guerin, B. J. L. Henner, A. Jean, T. Kuhlman, F. Garnier, A. Yassar, *Organometallics* **1992**, *11*, 2500.
[74] a) H. Bässler, V. Enkelmann, H. Sixl, *Adv. Polym. Sci.* **1984**, 63; b) R. R. Chance, G. N. Pattel, *J. Polym. Sci. Polym. Phys. Ed.* **1978**, *16*, 859; c) R. R. Chance, G. N. Pattel, E. A. Turi, Y. P. Khanna, *J. Am. Chem. Soc.* **1978**, *100*, 1307; d) A. O. Patil, D. D. Desmpande, S. S. Talwar, A. B. Biswas, *J. Polym. Sci. Polym. Chem. Ed.* **1981**, *19*, 1155; e) J. Kato, K. Nakamura, S. Yamazakis, T. Amano, *J. Polym. Sci. Part A Polym. Chem.* **1989**, *27*, 1853.
[75] a) R. J. P. Corriu, C. Guerin, B. J. L. Henner, A. Jean, P. H. Mutin, *J. Organomet. Chem.* **1990**, *396*, C3; b) R. J. P. Corriu, P. Gerbier, C. Guerin, B. J. L. Henner, A. Jean, P. H. Mutin, *Organometallics* **1992**, *11*, 2507.
[76] R. J. P. Corriu, P. Gerbier, C. Guerin, B. J. L. Henner, R. J. Fourcade, *J. Organomet. Chem.* **1993**, *449*, 111.
[77] A. J. Melreyer, R. H. Baughmann, *J. Polymer Sci. Polymer Phys. Ed.* **1989**, *27*, 1853, and references therein.
[78] a) F. Garnier, *Angew. Chem.* **1989**, *101*, 529; *Angew. Chem. Int. Ed. Engl.* **1989**, *28*, 513; b) F. Roncali, *Chem. Rev.* **1992**, *92*, 711, and references therein.
[79] a) M. Lemaire, W. Büchner, R. Garreau, H. Hoa, A. Guy, J. Roncali, *J. Electroanal. Chem.* **1991**, *312*, 547; b) *ibid.* **1990**, *281*, 293; c) J. Roncali, A. Guy, M. Lemaire, R. Garreau, H. Hoa, *ibid.* **1991**, *312*, 277.
[80] a) S. K. Ritter, R. E. Noftle, *Chem. Mater.* **1992**, *4*, 872; b) H. Matsuda, Y. Taniki, K. Kaeriyama, *J. Polym. Sci. A*, **1992**, *30*, 1667; c) J. Guay, A. Diaz, R. Wu, J. M. Tour, L. H. Dao, *Chem. Mater.* **1992**, *4*, 254.
[81] J. L. Sauvajol, C. Chorro, J. P. Lère-Porte, R. J. P. Corriu, J. J. E. Moreau, P. Thépot, M. Wong Chi Man, *Synth. Met.*, **1994**, *62*, 233.
[82] R. J. P. Corriu, J. J. E. Moreau, P. Thépot, M. Wong Chi Man, C. Chorro, J. P. Lère-Porte, J. L. Sauvajol, *Chem. Mater.* **1994**, *6*, 15.
[83] M. Moran, I. Cuadrado, M. C. Pascual, C. M. Casado, J. Losada, *Organometallics* **1992**, *11*, 1210.
[84] K. M. Choi, K. J. Shea, *Chem. Mater.* **1993**, *5*, 1067.
[85] G. Cerveau, R. J. P. Corriu, C. Lepeytre, *J. Mater. Chem.* **1995**, *5*, 793.
[86] R. J. P. Corriu, J. J. E. Moreau, P. Thépot, M. Wong Chi Man, *J. Mater. Chem.* **1994**, *4*, 987.
[87] a) G. N. Schrauzer, S. Eichler, *Chem. Ber.* **1962**, *95*, 550; b) G. N. Schrauzer, P. Glockner, S. Eichler, *Angew. Chem.* **1964**, *76*, 28; *Angew. Chem. Int. Ed.* **1964**, *3*, 185; c) J. S. Ward, R. Pettit, *J. Am. Chem. Soc.* **1971**, *93*, 262; d) A. P. Humphries, S. A. R. Knox, *J. Chem. Soc. Dalton Trans.* **1978**, 1514; e) J. K. Kochi, *Organometallics Mechanism and Catalysis*, Academic Press, London **1978**, p 429.
[88] a) J. M. Kliegman, *J. Organomet. Chem.* **1971**, *29*, 73; b) T. Hayashi, H. Ito, M. Kumada, *Tetrahedron Lett.* **1982**, *23*, 4605; c) T. Hayashi, M. Konishi, M. Kumada, *J. Chem. Soc. Chem. Commun.* **1983**, 736; d) R. J. P. Corriu, N. Escudie, C. Guérin, *J. Organomet. Chem.* **1984**, *271*, C7; e) T. Hayashi, A. Yamamoto, T. Iwata, Y. Ito, *J. Chem. Soc. Chem. Commun.* **1987**, 398; f) K. Fugani, K. Ohsima, K. Utimoto, H. Nozaki, *Bull. Chem. Soc. Jpn.* **1987**, *60*, 2509; g) S. Ogoshi, W. Yoshida, K. Ohe, S. Murai, *Organometallics* **1992**, *12*, 578.

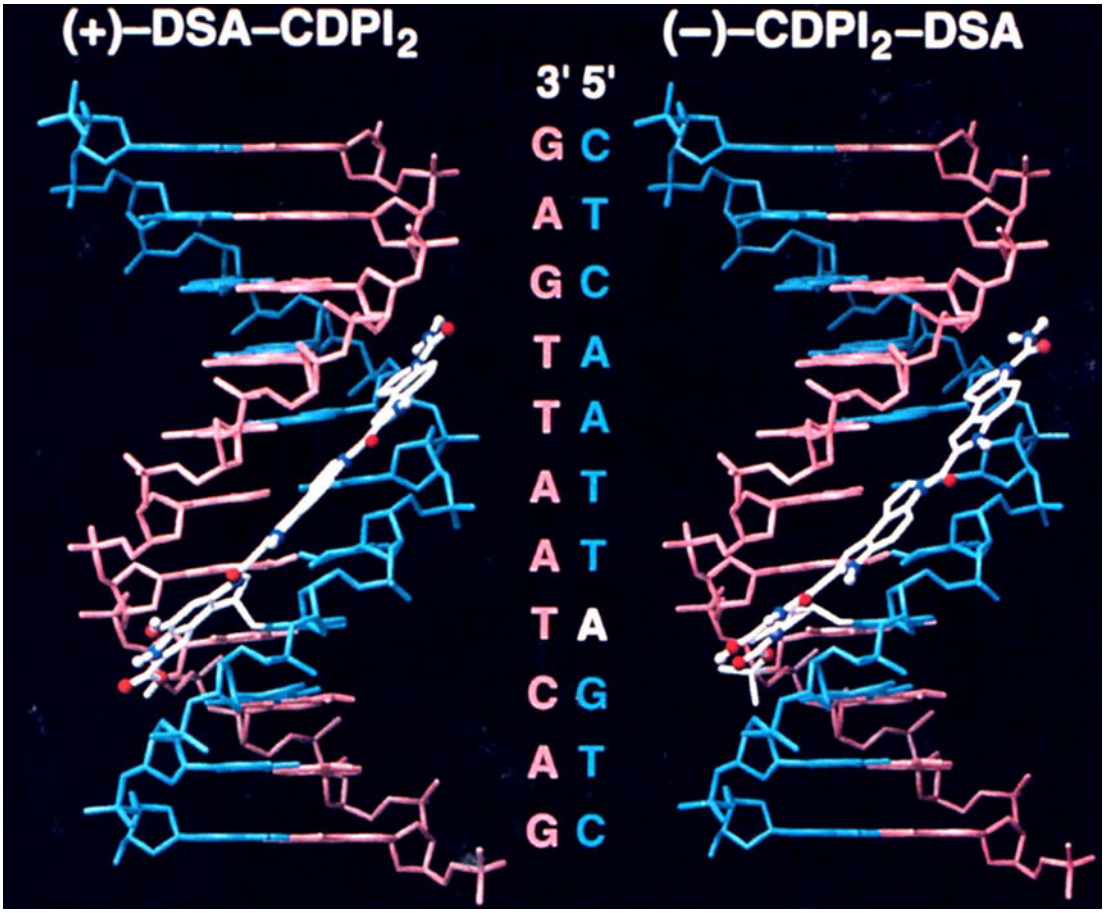

Merely reversing the arrangement of the DNA-binding structural elements (DSA-$CDPI_2$→$CDPI_2$-DSA) causes a DNA alkylating agent to behave like the enantiomer of the natural product, although the alkylation unit has the configuration found in nature. Model studies on the binding of the enantiomers to DNA provide an explanation.

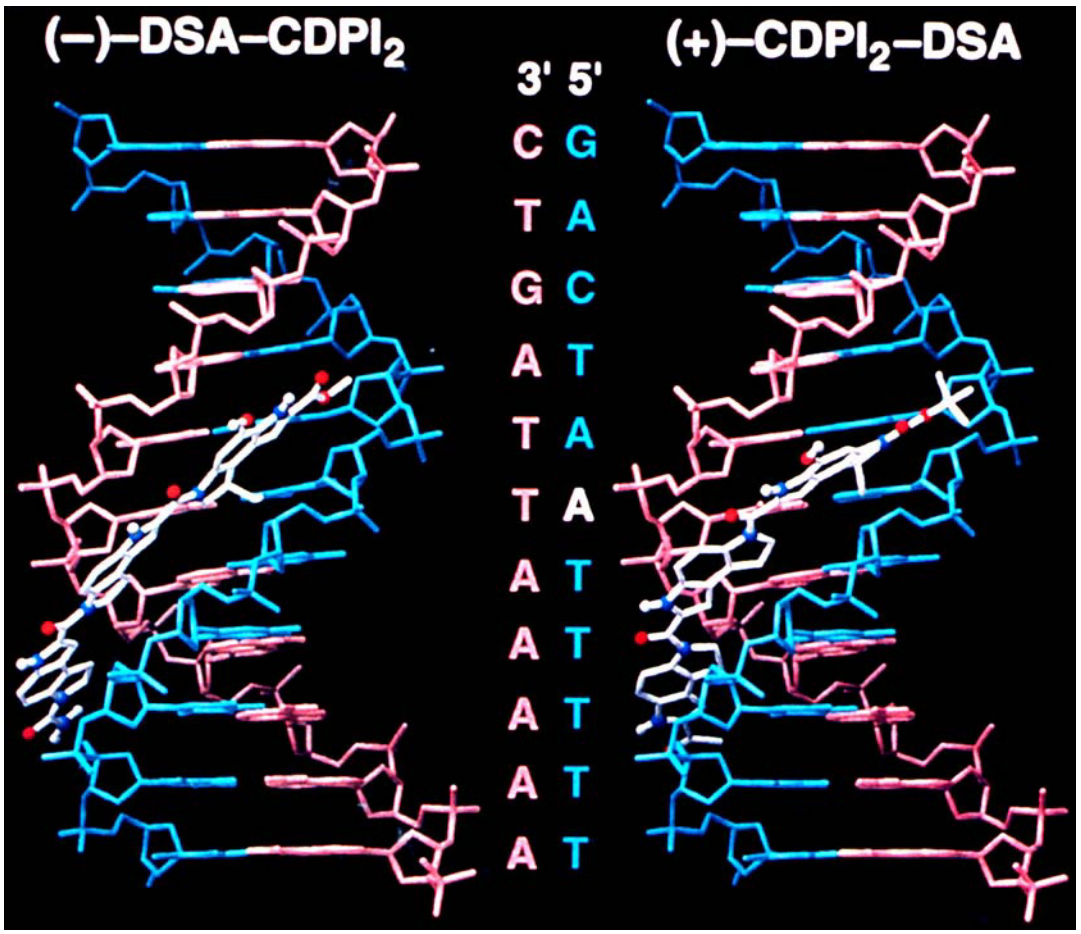

CC-1065 and the Duocarmycins: Understanding their Biological Function through Mechanistic Studies**

Dale L. Boger* and Douglas S. Johnson

We review here studies defining the DNA alkylation properties of a class of potent antitumor antibiotics that includes CC-1065 and the duocarmycins, as well as investigations that delineate fundamental relationships between their structure, functional reactivity, and biological properties. In conjunction with the study of the natural products themselves, the examination of synthetic agents containing deep-seated structural changes, the unnatural enantiomers of the natural products, and related analogs has defined the structural basis for the sequence selective alkylation of duplex DNA and proved to be the key to understanding the fundamental relationships between chemical structure, functional reactivity, and biological properties. The characteristic DNA alkylation proceeds by reversible, stereoelectronically controlled adenine-N3 addition to the least substituted carbon of the activated cyclopropane within AT-rich minor groove sites. Both the natural and unnatural enantiomers alkylate DNA, and the sequence selectivity of both is controlled and dominated by the preferential noncovalent binding of the agents within the narrower, deeper, AT-rich minor groove and the steric accessibility to the alkylation site on penetration of this groove. Among the fundamental relationships between structure and properties, the most striking is the direct relationship between chemical or functional stability and biological potency. Within a short time, simplified and readily accessible synthetic agents rationally based on the natural product leads have been developed, which exhibit comparable and exceptional biological potency (IC_{50} = 50 to 51 pM) and improved efficacy. The fundamental relationships that have been defined to date can be expected to provide the foundation for future developments and advances.

Keywords: antibiotics · antitumor agents · DNA alkylation · duocarmycins

1. Introduction

Substantial progress has been made toward understanding the origin of the sequence-selective recognition of duplex DNA by small organic molecules[1-5] including a wide range of naturally occurring antitumor antibiotics. Major factors contributing to the interest include the desire to define the basis for the therapeutic properties of the naturally occurring antitumor antibiotics that have been shown to bind DNA, to define the nature of DNA lesions induced by toxic, mutagenic, or carcinogenic materials,[6] and to alter transcription, translation, or protein expression and exploit the ramifications for therapeutic purposes.

Three fundamental issues to be addressed in the examination of DNA binding agents are the origin of binding affinity, binding selectivity, and reaction selectivity including DNA alkylation or cleavage. Each can independently exert control on the apparent sequence-selective recognition of DNA, and the relative importance and origin of these effects remain an important objective of most investigations. The emergence of experimental techniques for the rapid sequencing of DNA,[7-10] for the determination of DNA binding selectivity and affinity including footprinting and affinity cleavage techniques,[11,12] and for the determination of sites of DNA modification[13] coupled with the structural characterization of DNA complexes at defined sites by X-ray crystallography,[14,15] NMR spectroscopy,[16,17] and molecular modeling[18,19] has advanced the understanding of the molecular interactions responsible for the sequence-selective recognition of DNA.

A powerful complement to such tools in the examination of naturally derived DNA binding agents is the preparation and subsequent examination of key partial structures, agents containing deep-seated structural modifications in the natural product, and their corresponding unnatural enantiomers. Well-conceived, deep-seated structural modifications may be used to directly address and define both the structural basis for the sequence-selective recognition of DNA and fundamental relationships between structure, functional reactivity, and biological properties. This is especially important in the case of natural products that are identified by directed screening efforts. In contrast to the study of the biological role of primary metabo-

[*] Prof. D. L. Boger, D. S. Johnson
Department of Chemistry, The Scripps Research Institute
10550 North Torrey Pines Road, La Jolla, CA 92037 (USA)
Fax: Int. code +(619) 784-7550

[**] An appendix contains all important abbreviations used in this review.
e-mail: boger@scripps.edu

 © VCH Verlagsgesellschaft mbH, D-69451 Weinheim, 1996 0570-0833/96/3513-1439 $ 15.00+.25/0

lites, the presence of secondary metabolites and the perceived origin of the identified lead is often misrepresented. Nature, with its vast array of secondary metabolites, provides a diverse library of small organic molecules for random screening. Not always, and perhaps only rarely, is the role of the identified natural products related to the biological basis of the screening efforts responsible for their detection and identification. Consequently, it may be a mistake to assume that nature has optimized or even devised the agent for purposes related to the biological process for which the screening assay was set up. Rather, it is more accurate to recognize that nature has only provided a novel lead or solution that has not yet been optimized. A challenging problem remains: to understand the beautiful solutions and subtle design elements that nature has provided in the form of a natural product and to extend this solution through rational design elements to provide more selective, more efficacious, or more potent agents designed specifically for the problem or target under investigation.

One of the newest class of agents shown to alkylate DNA includes (+)-CC-1065 (**1**),[20–23] (+)-duocarmycin A (**2**),[24–29] and (+)-duocarmycin SA (**3**)[30–33] (Fig. 1). Because of their remarkable cytotoxic potency, substantial efforts have been devoted to defining their properties.[34–50] These studies show that the agents exert their biological effects through a sequence-selective alkylation of DNA. The reversible, stereoelectronically controlled adenine-N3 addition to the least substituted cyclopropane carbon has been found to occur within selected AT-rich sites in the minor groove, and extensive efforts have been devoted to determining the origin of the DNA alkylation selectivity, to establishing the link between DNA alkylation and the ensuing biological properties,[51] and to defining the fundamental principles underlying the relationships between structure, chemical reactivity, and biological activity. The initial limited studies conducted with naturally derived duocarmycin SA (**3**), the most recent addition to this class of agents, revealed a combination of properties that make it the most exciting of the natural products identified to date. In addition to lacking the characteristic of delayed toxicity of (+)-CC-

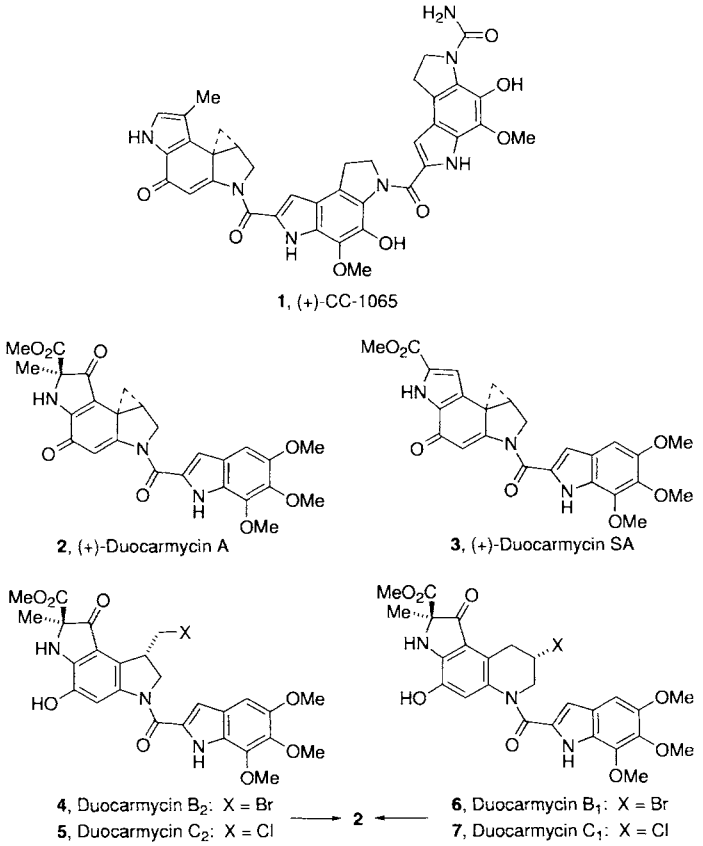

Fig. 1. Structures of CC-1065 and the duocarmycins.

D. L. Boger

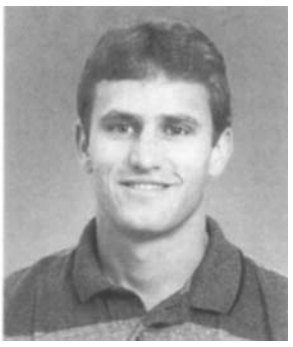
D. S. Johnson

Born August 22, 1953 in Hutchinson, Kansas, Dale L. Boger received his BSc in chemistry from the University of Kansas (1975, with highest distinction and honors in chemistry) and Ph.D. in chemistry from Harvard University (1980). He immediately returned to the University of Kansas as a member of the faculty in the Department of Medicinal Chemistry till 1985, when he moved to the Department of Chemistry at Purdue University. In 1991 he joined the faculty at The Scripps Research Institute as the Richard and Alice Cramer Professor of Chemistry. His research interests span the fields of organic and bioorganic chemistry and include the development of synthetic methodology, the total synthesis of natural products, heterocyclic chemistry, bioorganic chemistry, medicinal chemistry, the study of DNA–agent and protein–ligand interactions, and antitumor agents.

Douglas S. Johnson was born August 24, 1969 in Roseville, Minnesota. He received his BSc in chemistry from the University of Minnesota (1991, summa cum laude), where he conducted research in the laboratory of Professor T. R. Hoye. He is presently a graduate student in chemistry at The Scripps Research Institute, where he is studying the synthesis and evaluation of antitumor and DNA binding agents under the direction of Professor D. L. Boger. His research interests include the synthesis of biologically important molecules as well as designed analogs to study their mechanism of action.

1065,[52] it is the most stable and most potent member of this class of agents. In fact, the name duocarmycin SA is an abbreviation of its original name, duocarmycin Stable A, which was introduced before its structure was established. As detailed herein, this combination of properties is not fortuitous, but rather the enhanced functional stability of duocarmycin SA is directly responsible for its increased biological potency. The studies complement those conducted on other DNA alkylating agents including the nitrogen mustards, the mitomycins, aflatoxin, epoxides of polyaromatic hydrocarbon diols, azinomycin, saframycin, anthramycin and related agents, and dichloroplatinum and related agents.[1-6]

2. DNA Alkylation Properties

2.1. DNA Alkylation Selectivity of the Natural Products

The event, sequence selectivity, quantitation, reversibility, and structure determination of the predominant DNA alkylation by **1**–**3** have been defined.[53-72] The identification of the alkylation site and the assessment of relative selectivity were achieved by thermally induced depurination and strand cleavage of labeled DNA after exposure to the agents (Scheme 1). The selectivity in alkylations by (+)-duocarmycin A (**2**) and (+)-duocarmycin SA (**3**) proved nearly indistinguishable.[54, 56] In each case alkylation took place at an adenine residue that was flanked by two 5′-A or -T bases, and the preferred order of these three-base sequences proved to be 5′-AAA > 5′-TTA > 5′-TAA > 5′-ATA. In addition, A or T dominated over G or C as a fourth 5′ base, and this feature distinguished high-affinity sites from low-affinity sites. An additional weak preference for a purine (Pu) over pyrimidine (Py) at the 3′ base preceding the adenine alkylation site was detected, which was more prominent in the low-affinity sites. Table 1 summarizes the consensus sequence derived from the evaluation of alkylations with **2**[56] and **3**.[54] Although these agents alkylated the same sites, two important distinctions were defined. The least reactive of the agents, (+)-duocarmycin SA (**3**), alkylated DNA with a greater efficiency (10–100×) and a greater selectivity among the available sites. In addition, the selectivity of the related naturally occurring agents **4**–**7** (see Fig. 1) was indistinguishable from that of **2**, which may be attributed to their facile cyclopropane ring closure under the conditions of assay.[54, 56] This behavior of **6**–**7** requires that they first close to form **2** prior to alkylating DNA, and that this is the biologically relevant and more potent form of the agent. These observations with **4**–**7** are general throughout the set of agents examined to date. In fact, not only are the selectivities in DNA alkylation of such seco agents indistinguishable, but often the DNA alkylation efficiencies and biological potencies are also the same, which indicates that the cyclopropane ring closure is not a limiting factor. Only in the cases of the more difficult or slower spirocyclizations have distinguishing features in DNA alkylation efficiency or biological potency been observed.[33, 56]

The preceding studies of (+)-CC-1065 (**1**) revealed a selectivity for a similar, but more extended five-base-pair, AT-rich alkylation site.[53, 64-72] Table 1 summarizes the consensus sequence derived from our evaluation of (+)-CC-1065.[53, 71-72] Each site of alkylation proved to be an adenine residue flanked by two

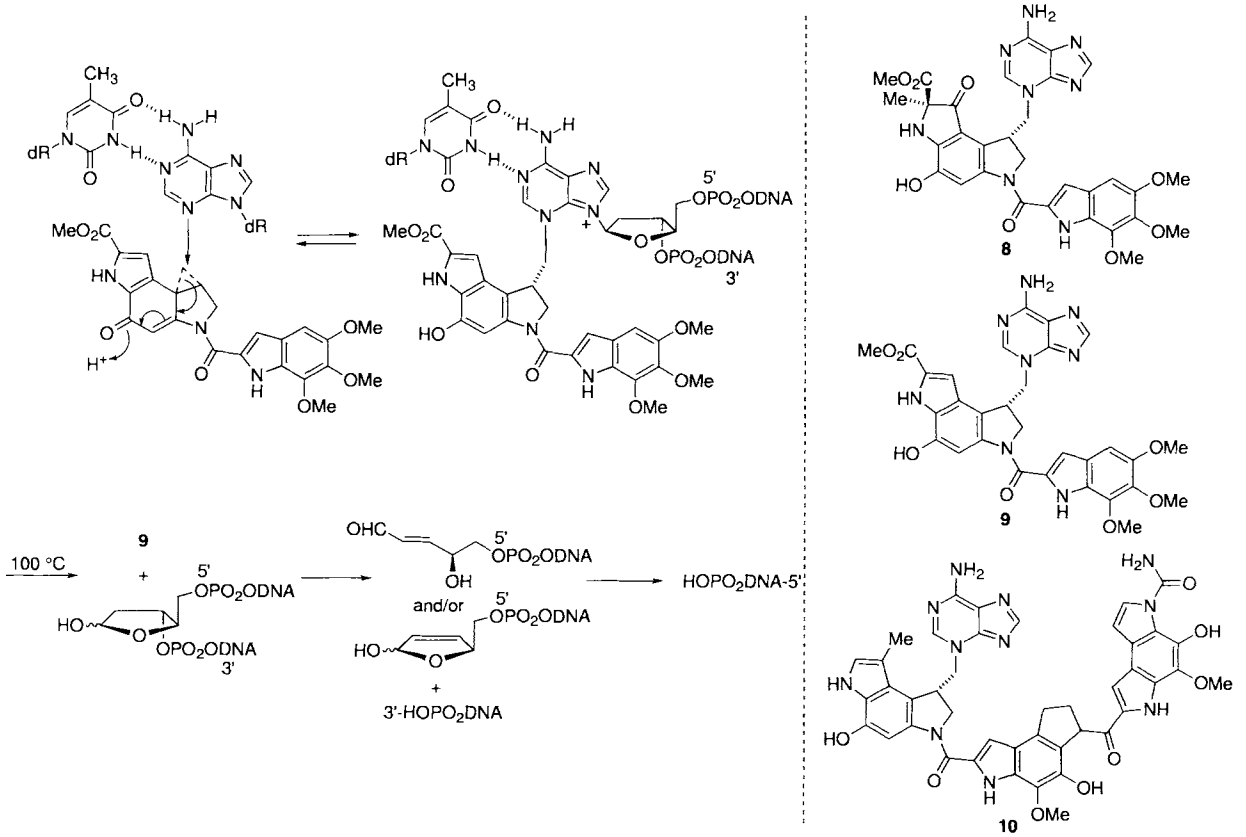

Scheme 1. Course of the DNA alkylation by **3** and structures of the characterized adenine adducts of **1** (**10**), **2** (**8**), and **3** (**9**).

Table 1. Consensus sequences for the DNA alkylation reactions of the natural products and their unnatural enantiomers [a].

Agent	Base [b]	5′	4	3	2	1	0	−1	−2	−3	−4	3′
1	A/T (56)		67	78	94	98	100	55	–	–	–	
	consensus		A/T ≥ G/C	A/T > G/C	A/T	A/T	A	Pu ≥ Py	–	–	–	
2 and **3**	A/T (56)		58	79	100	100	100	69	–	–	–	
	consensus		N	A/T > G/C	A/T	A/T	A	Pu > Py	–	–	–	
ent-**3**	A/T (56)		–	–	–	93	100	96	73	56	–	
	consensus		–	–	–	A/T	A	A/T	A/T > G/C	N	–	
ent-**1**	A/T (56)		–	–	–	88	100	93	82	73	56	
	consensus		–	–	–	A/T	A	A/T	A/T > G/C	A/T > G/C	N	

[a] The numbers listed in the table give the percentage of the indicated base located at the designated position relative to the adenine-N3 alkylation site. [b] The numbers in parentheses give the percentage composition within the DNA examined.

5′-A or -T bases. The sequence preference for the three-base, AT-rich alkylation site followed a similar order: 5′-AA<u>A</u> = 5′-TT<u>A</u> > 5′-TA<u>A</u> > 5′-AT<u>A</u>. In addition, the agent exhibited a strong preference for the fourth 5′ base to be A or T, a weaker preference for the fifth 5′ base to be A or T, and a weak preference for the 3′ base preceding the alkylation site to be a purine. These preferences for the fourth and fifth 5′ bases distinguished the high- from the low-affinity sites, and the preference for a 3′ purine over pyrimidine was more prominent in the lower affinity sites. The strict AT requirement within the first three base pairs represents a combination of the initial 3′ adenine-N3 alkylation site and an adjacent 5′ two-base AT site required to accommodate the central subunit binding. The weaker preferences for A or T as the fourth and fifth 5′ bases reflect, as observed with the high-affinity sites, a preferential AT-rich site for the third subunit also bound in the minor groove. A study of shorter and more extended analogs of CC-1065 revealed that this selectivity for AT-rich sites corresponds nicely to the length of the agent and, hence, the size of binding site required to accommodate the agent.[53, 71]

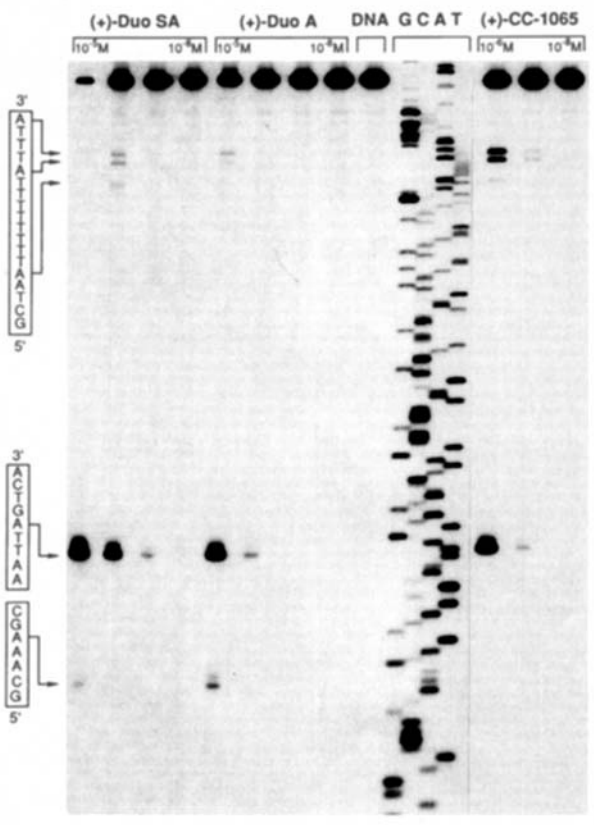

Fig. 2. Thermally induced strand cleavage (by heating to 100 °C for 30 min) of double-stranded DNA (SV40 DNA fragment, 144 base pairs, nucleotide no. 5238-138, clone w794) after 24 h incubation of DNA with the agent at 25 °C and removal of unbound agent by EtOH precipitation followed by denaturing PAGE (8%) and autoradiography. Lanes 1–4: **3** (1×10^{-5} M–1×10^{-8} M); lanes 5–8: **2** (1×10^{-5} M–1×10^{-8} M); lane 9: control DNA; lanes 10–13: Sanger G, C, A, and T reactions; lanes 14–16: **1** (1×10^{-6} M–1×10^{-8} M).

Figure 2 illustrates the similarities of **2** and **3** and their subtle distinctions from **1** in their behavior toward DNA. According to the concentrations required to detect alkylation, (+)-duocarmycin SA (**3**) is approximately ten times more efficient at alkylating the DNA than (+)-duocarmycin A (**2**) and subtly more efficient than (+)-C-1065 (**1**). Although **3** and **2** alkylate the same sites, **3** exhibits a greater degree of discrimination among the available sites. This is evident from the relative concentrations required to detect the minor and major alkylation sites for the two agents. Similarly, while CC-1065 and the duocarmycins both alkylate the same high-affinity site in this segment of DNA, distinctions in the alkylation of the minor sites are apparent, including the lack of alkylation by (+)-CC-1065 at the shorter three-base AT-rich site 5′-GCAA<u>A</u>.

The sequence selectivity observed with intracellular SV40 DNA is essentially identical to that observed with purified SV40 DNA except that higher concentrations of **1** are required.[74–76] Thus, in vitro analyses with purified DNA reflect the sequence-selective reactivity of **1** with intracellular DNA.

2.2. DNA Alkylation Selectivity of the Unnatural Enantiomers

One of the more revealing discoveries that was made possible through use of synthetic materials was that the unnatural enantiomers may also constitute effective DNA alkylating agents and potent cytotoxic agents.[53, 54, 68, 71] Moreover, the ability to compare the behavior of the two enantiomers proved to be the key to understanding the structural origin of the sequence selectivity in DNA alkylations. Consistent with its relative cytotoxic potency, *ent*-(−)-duocarmycin SA was found to alkylate DNA at concentrations approximately ten times that required for the natural enantiomer;[54] Table 1 summarizes its consensus alkylation sequence. Each alkylation site detected was an adenine residue, and essentially each alkylation site was flanked by a 5′- and 3′-A or -T base and exhibited the following sequence preference: 5′-A<u>A</u>A > 5′-A<u>A</u>T > 5′-T<u>A</u>A > 5′-T<u>A</u>T. An additional strong preference for A or T as the second 3′ base from the alkylation site was observed. In this regard, the (−)-duocarmycin SA alkylation was analogous to the natural enan-

tiomer with the exception that the binding orientation is reversed (5′ → 3′) over an AT-rich, 3.5-base-pair site. However, whereas the bound natural (+)-enantiomer covers an AT-rich, 3.5-base-pair site extending from the adenine-N3 alkylation site in the 3′ → 5′ direction across the adjacent two to three 5′ bases (that is, 5′-AAAA), the AT-rich, 3.5-base-pair site for the unnatural (−)-enantiomer extends in the reverse 5′ → 3′ direction starting at the first 5′ base site preceding the adenine-N3 alkylation site and extending across the alkylation site to the first and second adjacent 3′ bases (that is, 5′-AAAA). The reversed binding orientation is required to permit adenine addition to the least substituted cyclopropane carbon, and the alkylation selectivity for an offset AT-rich site is the natural consequence of the diastereomeric relationship of the adducts.

Similarly, preceding studies had shown that (−)-CC-1065 alkylates DNA with an efficiency equivalent to that of the natural enantiomer, but the alkylation rate is slower.[68, 71] Consistent with these observations, the unnatural and natural enantiomers of CC-1065 have been found to exhibit indistinguishable cytotoxic potency and in vivo antitumor activity.[68, 71] Table 1 summarizes the consensus alkylation sequence for (−)-CC-1065, which proved similar to (−)-duocarmycin SA but which exhibits an AT selectivity that extends across five base pairs.[53, 68] Each alkylation site proved consistent with 5′-adenine-N3 alkylation and agent binding in the minor groove in the 5′ → 3′ direction from the alkylation site covering five base pairs across an AT-rich region. All alkylation sites detected in the sequencing studies proved to be adenine, and nearly all of the 3′ and 5′ bases flanking the adenine-N3 alkylation site proved to be A or T. The preferred order for the sequence of these bases is as follows: 5′-AAA > 5′-TAA > 5′-AAT, 5′-TAT. There also proved to be a substantial preference for A or T as the second and third 3′ base.

Unlike duocarmycin SA, the unnatural enantiomer of duocarmycin A proved to be 100 or more times less effective than the natural enantiomer at alkylating DNA and 100 or more times less potent in cytotoxic assays.[59] Although these observations initially appeared confusing, they could be attributed to well-defined differences in the diastereomeric adducts derived from the two enantiomers, for which duocarmycin A is especially sensitive.[54, 73] Inversion of the configuration at C6 of **2**, which leads to **11** (Fig. 3), had no effect on the DNA alkylation

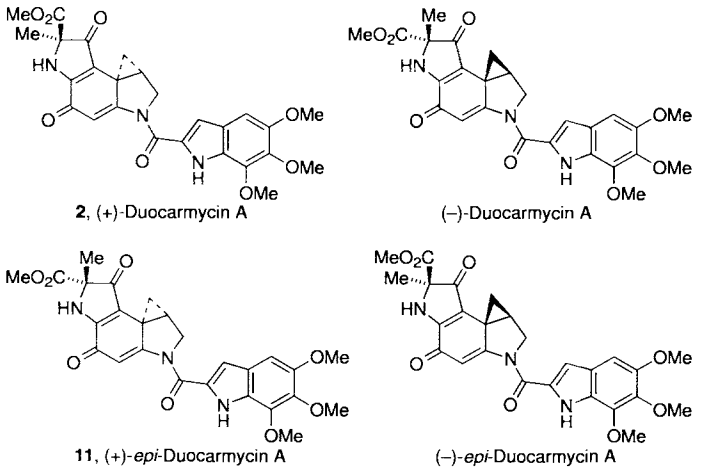

Fig. 3. Stereoisomers of (+)-duocarmycin A (**2**).

Table 2. Cytotoxic potencies of **1**–**3** and their isomers and the relative DNA alkylation efficiencies.

Agent	IC_{50}, L1210 [pM]	Rel. Alkylation Efficiency
(+)-**3**, (+)-duocarmycin SA	10	1
(−)-**3**, *ent*-(−)-duocarmycin SA	100	0.1
(+)-**2**, (+)-duocarmycin A	200	0.05
(−)-**2**, *ent*-(−)-duocarmycin A	>22000	<0.0005
(+)-**11**, *epi*-(+)-duocarmycin A	1600	0.01
(−)-**11**, *ent*,*epi*-(−)-duocarmycin A	>24000	<0.0005
(+)-**1**, (+)-CC-1065	20	0.5
(−)-**1**, *ent*-(−)-CC-1065	20	0.5

sequence selectivity and only a small impact on the DNA alkylation efficiency and cytotoxic potency of the agent (Table 2).

As detailed in the following sections, the DNA alkylation properties and selectivity of the unnatural enantiomers have proven uniquely valuable in establishing the key recognition elements and structural features responsible for polynucleotide recognition. Ultimately their preparation and subsequent evaluation alongside the natural enantiomers provided deeper insights into the behavior of the natural products themselves and led to the evolution of models that clearly delineate the requirements for DNA alkylation and the origin of the selectivity.

2.3. Adenine-N3 Alkylation

Since the thermally induced cleavage of DNA employed to identify the alkylation sites only detects adducts susceptible to thermal glycosidic bond cleavage (adenine-N3 and guanine-N3 or -N7 alkylation), the occurrence of additional alkylation reactions would not be detected under such conditions. Thus, the quantitation of the adenine-N3 alkylation, confirmation of its structure through isolation and characterization of the thermally released adducts, and the search for undetected alkylation sites have been conducted. In these studies, the adenine-N3 alkylation of DNA present in excess by (+)-duocarmycin A (**2**), (+)-duocarmycin SA (**3**), (−)-duocarmycin SA, and (+)-CC-1065 (**1**) accounts for 86–92%,[57] 90–100%,[54] 86–92%,[54] and 80–90%,[66] respectively, of their consumption and constitutes the virtually exclusive alkylation event (Scheme 1, p. 1441). The full characterization of the adducts led to the unambiguous assignment of the structures **8**–**10** (see Scheme 1) in which addition of the adenine-N3 atom to the unsubstituted cyclopropane carbon of the agents was established. The demonstration that **6** and **7** also provide the adduct **8**[56, 57] requires that they first convert to **2** prior to alkylating DNA.

2.4. Adenine-N3 and Trace Guanine-N3 Alkylation

All three agents and their corresponding seco precursors provide predominantly or exclusively adenine-N3 adducts (>90%). However, a minor guanine-N3 alkylation has been detected with **2** and to a lesser extent with **1**, but only upon isolation of the thermally released adduct following treatment of DNA with excess agent,[61, 62] within oligodeoxynucleotides lacking a high-affinity adenine-N3 alkylation site,[62] or when the adenine alkylation sites within AT-rich regions of DNA were

protected from alkylation with agents (including distamycin) that bind with high affinity in the AT-rich minor groove.[63] A study of this minor guanine-N3 alkylation with **2** revealed that as the agent-to-base-pair ratio in the reaction mixture was varied from 1:10 to 1:160, the ratio of adenine-N3 to guanine-N3 alkylation steadily increased from 1.4:1 to 11:1 (92:8),[61] which clearly indicates that adenine-N3 alkylation is preferred when available.[57] In contrast, duocarmycin SA showed no evidence of guanine-N3 alkylation when subjected to similar or more forcing reaction conditions.[54] Even under vigorous conditions, unchanged agent was recovered, and the selectivity (adenine-N3/guanine-N3 alkylation) was greater than 25:1. This enhanced selectivity of **3** may be attributed to its decreased reactivity. Notably, under the relevant conditions of limiting agent even **2** provided nearly exclusive adenine-N3 alkylation.[57] Since **3** is much more potent than **2**, the minor guanine-N3 alkylation cannot be uniquely important to the biological properties of the agents and may represent a nonproductive competitive event.

Thus, the relative reactivity of the agents may influence the DNA alkylation selectivity. Under the conditions of limiting agent and excess DNA, where little or no guanine-N3 alkylation is detected, the studies have illustrated that the more stable and less reactive agents are both more efficient and more selective among the available alkylation sites. These distinctions would appear to be most important to exploit.

2.5. Reversibility of the DNA Alkylation Reaction: Binding-Driven Bonding

Although the duocarmycin DNA alkylations have proven similar to those of CC-1065, one important feature distinguishes the agents. Unlike **1**, which irreversibly alkylates DNA, duocarmycins **2** and **3** alkylate DNA reversibly.[54, 58] The ease of reversibility proved dependent upon the relative reactivity of the agent and hence the stability of the adduct, as well as on the extent of the noncovalent binding interactions (Fig. 4). Consistent with the relative reactivity of the agents and the expected stability of the adducts, the (+)-duocarmycin A (**2**) retroalkylation reaction was slower than that of (+)-duocarmycin SA (**3**). In addition, the rate of retroalkylation was faster, and the adduct was much less stable with N-BOC-DSA (**12**) (see Fig. 5) than with **3**, which may be attributed to the lack of stabilization from the trimethoxyindole binding. (+)-CC-1065 (**1**) is less reactive than **2** but more reactive than **3**. The lack of detection of a reversible alkylation by **1** under comparable conditions may be taken as a further indication of the dependence of reversibility on the extent of the noncovalent binding stabilization. Consistent with this interpretation, analogs of CC-1065 possessing the same alkylation subunit but simpler and smaller binding subunits were the first such agents shown to alkylate DNA reversibly.[70]

Thus, dominant forces stabilizing the DNA alkylation reaction are not only the covalent bond but also the stabilizing noncovalent interactions derived from hydrophobic binding and van der Waals contacts. That is, the alkylation reaction is rendered less reversible or irreversible by noncovalent binding stabilization. The importance of these observations becomes clear when the properties of the agents are compared. The exceptionally potent cytotoxic activity of the natural products relative to that of the simple derivatives of the alkylation subunits themselves (Fig. 5) may be attributed in part to the simple event of noncovalent binding stabilization of the inherently reversible DNA alkylation reaction.

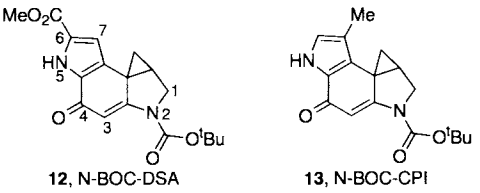

12, N-BOC-DSA **13**, N-BOC-CPI

Fig. 5. Structures of derivatives of the alkylation subunits.

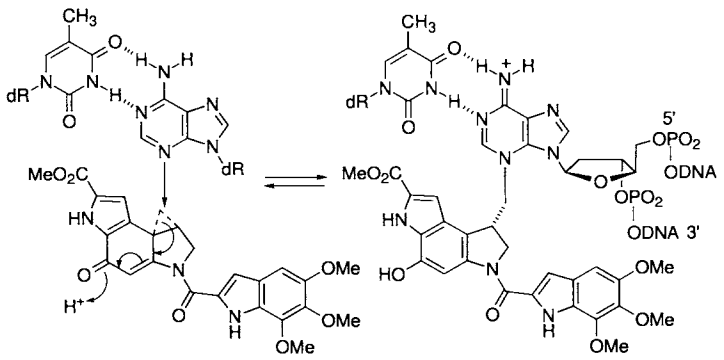

Fig. 4. Reversible DNA alkylation reaction, exemplified with **3**. The characteristics of the reversible reaction are as follows: The rate of the reverse reaction increases with increasing pH, temperature, and ionic strength. It is greater for duocarmycin SA than for duocarmycin A, showing the general decrease with increasing stability of the adduct and increasing agent reactivity. It is greater for the duocarmycins than for CC-1065 and even larger for N-BOC-DSA indicating a general decrease with increasing stabilization provided by the noncovalent binding interactions.

This reversible nature of the alkylation reaction itself along with the equilibrium binding requires that four rate constants be addressed in assessing the sequence-selective alkylation [Eq. (a)]. The large differences in the extent of reversibility sug-

$$\text{substrate} + \text{DNA} \underset{k_d}{\overset{k_a}{\rightleftharpoons}} \text{substrate}\cdot\cdot\text{DNA} \underset{k_{retroalk.}}{\overset{k_{alk}}{\rightleftharpoons}} \text{substrate-DNA} \qquad \text{(a)}$$

gest that treatments to date have neglected two of the more important rate constants,[43, 46] namely the relative rates of retroalkylation at competing or potentially nonobserved sites and the dissociation rates (off rates) for the available binding sites. The off rates for some noncovalent adducts have been shown qualitatively to be quite slow.[82]

These observations coupled with studies indicating that the noncovalent binding equilibrium is established through decomplexation, not through procession along the minor groove, suggest that dissociation rates and not simply association rates or $K_b (= k_a/k_d)$ may be especially important.[96] Defined oligonucleotides that contain sites capable of noncovalent binding but incapable of alkylation have been shown to inhibit the rates of

DNA alkylation. This would suggest that the rates of equilibrium binding may be slow and that the dissociation rate or relative K_b, not the association rate or rate of alkylation, may be rate-determining. Moreover, this inhibition of DNA alkylation was the same whether the competitive site for noncovalent binding was inter- or intramolecular. These studies would seem to demonstrate that the first binding equilibration in Equation (a) may be slow relative to alkylation and that the off rates or relative K_b are significant and should not be neglected.

2.6. Models of the DNA Alkylation for Enantiomeric Agents

The examination of the natural products, their synthetic unnatural enantiomers, and key partial structures not only resulted in the unusual observation that the unnatural enantiomers constitute effective DNA alkylating agents and potent antitumor antibiotics, but has also led to the emergence of a detailed model[53, 54] of the structural features responsible for their selective alkylation of DNA. The characterization of **8**–**10**, the unambiguously established absolute configuration of the agents, and the definition of the alkylation consensus sequences for both enantiomers of **1**–**3** provided the necessary information for the construction of accurate models of the adenine-N3 alkylation. Figure 6 illustrates models of the (+)- and (−)-duocarmycin SA alkylation at a common site in w794 DNA (5′-CTAATT), which is a high-affinity site for the unnatural enantiomer, and a minor site for the natural enantiomer.[54]

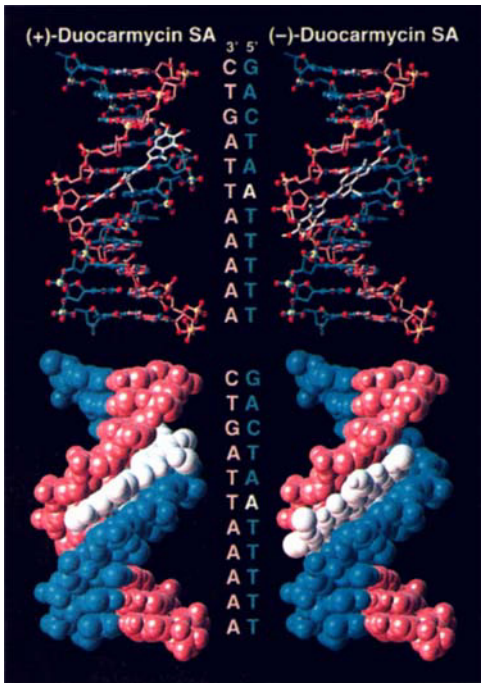

Fig. 6. Stick and space-filling models illustrating the alkylation at the same site within w794 DNA (duplex 5′-d(GACTAATTTTT)) by (+)-duocarmycin SA (left) and (−)-duocarmycin SA (right). The binding of the natural enantiomer extends in the 3′ → 5′ direction from the adenine-N3 alkylation site across the sequence 5′-CTAA, that of the unnatural enantiomer in the reverse 5′ → 3′ direction across the site 5′-AATT.

Similar models of the (+)- and (−)-CC-1065 alkylations may be found in Figure 7.[53] For both the duocarmycins and CC-1065 the hydrophobic face of the agent is imbedded deeply in the minor groove, the polar functionality lies on the outer face of the complex, and the bound helical conformation of the agent complements the topological curvature and pitch of the minor

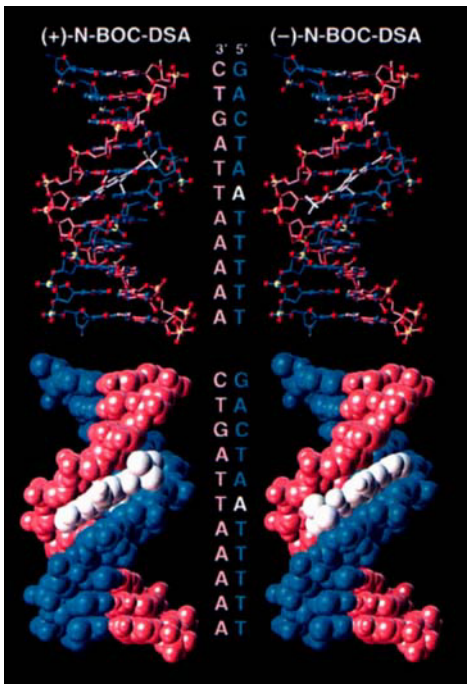

Fig. 7. Stick and space-filling models illustrating the alkylation at the same site within w794 DNA (duplex 5′-d(GACTAATTTTT)) by (+)-CC-1065 (left) and (−)-CC-1065 (right). The binding of the natural enantiomer extends in the 3′ → 5′ direction from the adenine-N3 alkylation site across the sequence 5′-ACTAA, that of the unnatural enantiomer in the reverse 5′ → 3′ direction across the site 5′-AATTT.

groove spanning an AT-rich, 3.5- or 5-base-pair site, respectively. For (+)-duocarmycin SA, the binding spans 3.5 base pairs starting with the 3′-adenine alkylation site and extends in the 3′ → 5′ direction over two to three adjacent 5′ base pairs (5′-CTAA). For the enantiomer, the binding similarly spans a 3.5-base-pair, AT-rich site, but one which necessarily starts at the 5′ base adjacent to the alkylation site and extends in the 5′ → 3′ direction over the alkylation site and one to two adjacent 3′ base pairs (5′-AATT). This alkylation selectivity within an offset AT-rich site is the natural consequence of the diastereomeric relationship of the adducts, and the reversed binding orientation (with respect to the alkylation site) in the minor groove is required to permit addition of the adenine-N3 atom to the least substituted carbon of the electrophilic cyclopropane. The importance of the fourth base (A/T > G/C) in the binding sequences is the reason why this site constitutes a high-affinity site for the unnatural enantiomer but only a minor site for the natural enantiomer. Similarly, the CC-1065 models[53] accommodate the larger size of the more extended five-base-pair, AT-rich binding site of the enantiomeric agents, their reversed binding orientation in the minor groove, and their AT-rich selectivity offset relative to the alkylation site.

The apparently confusing distinctions in the relative efficiency of DNA alkylations by the natural and unnatural enantiomers were found to correlate with the extent of the stabilization of the inherently reversible noncovalent binding in the adducts, as well as with the degree of steric bulk surrounding the C7 center of the agent. Consistent with expectations based on the models, the unnatural enantiomers are especially sensitive to the steric bulk around this C7 center.[53, 54, 73]

3. Key Partial Structures

3.1. N-BOC-DSA: A DNA Alkylating Agent Whose Selectivity and Efficiency Are Independent of Its Absolute Configuration

The accuracy of the models were revealed when they were found to provide a beautiful explanation for the unusual observation that both enantiomers of simple derivatives of the alkylation subunit, for example N-BOC-DSA (**12**)[54] or N-BOC-CPI (**13**, see Fig. 5),[53, 68] alkylate the same sites in DNA. In addition to illustrating that the DNA alkylation reactions of (+)- and (−)-**12** are both substantially less efficient (about $10^4\times$) and less selective (selectivity: 5′-A<u>A</u> > 5′-T<u>A</u>), and proceed with a different profile from that of (+)- or (−)-duocarmycin SA or CC-1065, the studies have shown that both enantiomers of **12** alkylate the same sites with essentially the same efficiency independent of the absolute configuration.[54] This feature of such simple agents is general, and the *N*-acetyl derivatives have been shown to behave similarly. Figure 8 illustrates these features nicely, and the consensus alkylation selectivity for both (+)- and (−)-N-BOC-DSA and -N-BOC-CPI is summarized in Table 3. Although these observations may appear unusual, they are a natural consequence of the diastereomeric relationship of the adducts. The natural enantiomer binds in the 3′ → 5′ direction from the site of alkylation extending over the adjacent 5′ base. The unnatural enantiomer binds in the reverse 5′ → 3′ orientation but with binding that also covers the same adjacent 5′ base. These alkylation site models,[53, 54] which are illustrated in Figure 9, nicely accommodate the observed selectivity of 5′-A<u>A</u> > 5′-T<u>A</u> for both enantiomers. The apparent preference of 5′-A<u>A</u> over 5′-T<u>A</u> (about 2:1) observed when examining one strand of single end-labeled DNA at a time is statistical rather than structural in nature. The unlabeled complementary partner strand of a 5′-TA sequence contains an identical competitive site, whose alkylation diminishes the apparent alkylation efficiency of the labeled strand. The factor controlling alkylation is simply the depth of penetration into the minor groove achieved by the agent, which is essential for the adenine-N3 alkylation of the electrophilic cyclopropane. For simple agents such as **12** and **13**, it is sufficient when the adjacent 5′ base is A or T, and models of an unobserved 5′-G<u>A</u> alkylation support this proposal.[53, 54] For **3** or **1**, a larger 3.5- or 5-base-pair, AT-rich region surrounding the alkylation site is required to permit sufficient groove penetration for alkylation, which is further facilitated by the preferential noncovalent binding of the agents within the narrower, deeper, AT-rich minor groove.[82]

These distinctions are important but not uniformly accepted in the work conducted to date. Whereas our studies revealed

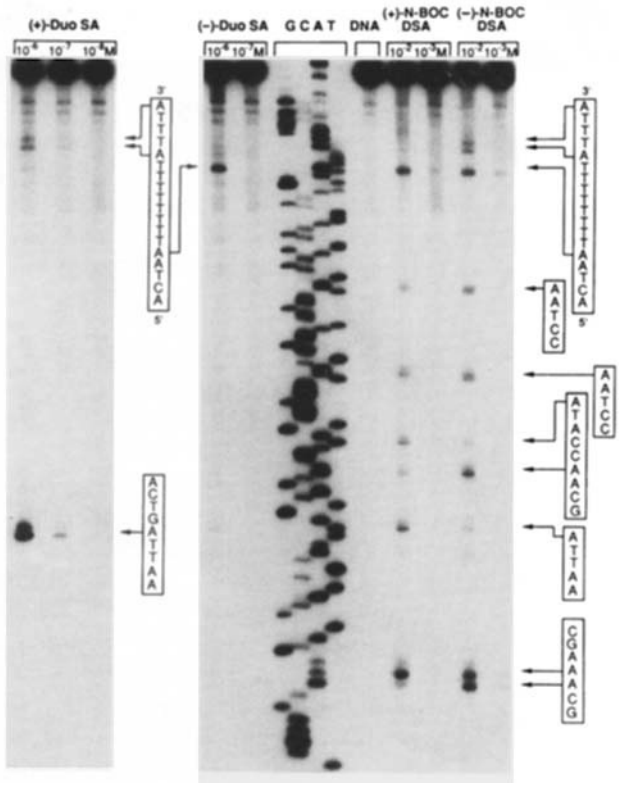

Fig. 8. Thermally induced strand cleavage (by heating to 100 °C for 30 min) of w794 DNA (SV40 DNA segment, 144 base pairs, nucleotide no. 5238-138) after 24 h incubation of DNA with (+)- or (−)-duocarmycin SA at 25 °C and with (+)- or (−)-N-BOC-DSA at 37 °C and removal of unbound agent by EtOH precipitation followed by denaturing PAGE (8%) and autoradiography. Lanes 1–3: **3** (1×10^{-6}–1×10^{-8} M); lanes 4 and 5: ***ent*-3** (1×10^{-6}–1×10^{-7} M); lanes 6–9: Sanger G, C, A, and T reactions; lane 10: control DNA; lanes 11 and 12: (+)-**12** (1×10^{-2}–1×10^{-3} M); lanes 13 and 14: (−)-**12** (1×10^{-2}–1×10^{-3} M).

distinctions between the natural products and simple derivatives of the alkylation subunit in the extent of the alkylation selectivity, the collaborative efforts of the Hurley and Upjohn groups with CPI-derivatives report an indistinguishable or subtly distinguishable alkylation selectivity between (+)-CC-1065 and (+)-N-acetyl-CPI.[43, 46, 47, 67, 68] This premise has led them to the conclusion that all the structural requirements for observation of the alkylation selectivity by (+)-CC-1065 are embodied in the CPI alkylation subunit.

Despite the similarities in the behavior of N-BOC-DSA (**12**) and N-BOC-CPI (**13**), two important differences were observed. First, both the natural and unnatural enantiomers of **12** are more efficient at alkylating DNA and are biologically more potent than the corresponding enantiomers of **13**. These differences may be attributed to the enhanced stability of **12**, which leads to more productive DNA alkylation. Secondly, while little or no distinction was observed in the DNA alkylation efficiencies of the natural and unnatural enantiomers of **12**, the natural enantiomer of **13** was found to be both more efficient and more cytotoxic than its unnatural enantiomer by a factor of between 10 and 100. As detailed later, this apparently confusing behavior of enantiomeric pairs may be attributed to the degree of steric bulk surrounding the C7 center, for which the diastereomeric adducts derived from the unnatural enantiomers are especially sensitive.

Table 3. Consensus sequences for DNA alkylation by key substructures and analogs of CC-1065 and the duocarmycins [a].

Agent	Base [b] 5′	6	5	4	3	2	1	0	−1	−2	−3	−4	−5	3′
natural enantiomers														
(+)-CPI-CDPI$_3$	A/T (56)	72	77	69	69	100	100	100	54	–	-			
(+)-**17**	consensus	A/T > G/C	A/T > G/C	A/T > G/C	A/T > G/C	A/T	A/T	A	N					
(+)-CC-1065	A/T (56)	–	–	67	78	94	98	100	55	-	–	-		
1	consensus			A/T ≥ G/C	A/T > G/C	A/T	A/T	A	Pu ≥ Py					
(+)-CPI-CDPI$_2$	A/T (56)	–	–	67	78	94	98	100	55	–	–	–	–	
(+)-**16**	consensus			A/T ≥ G/C	A/T > G/C	A/T	A/T	A	Pu ≥ Py					
(+)-CPI-PDE-I$_1$	A/T (56)	–	–	–	65	100	100	100	58	–	–	–	–	
(+)-**14**	consensus				A/T ≥ G/C	A/T	A/T	A	Pu ≥ Py					
(+)-CPI-CDPI$_1$	A/T (56)	–	–	–	65	100	100	100	58	–	-			
(+)-**15**	consensus				A/T ≥ G/C	A/T	A/T	A	Pu ≥ Py					
(+)-duocarmycin SA	A/T (56)	–		-	79	100	100	100	69	–	-			
3	consensus				A/T > G/C	A/T	A/T	A	Pu > Py					
(+)-N-BOC-CPI	A/T (56)	-	-	–	–	-	97	100	66	-	–	-	-	
(+)-**13**	consensus						A/T	A	Pu > Py					
(+)-N-BOC-DSA	A/T (56)	-	–	–	–	–	95	100	65	-	–	-	-	
(+)-**12**	consensus						A/T	A	Pu > Py					
unnatural enantiomers														
(−)-N-BOC-DSA	A/T (56)	–	–	-	-	–	95	100	65	–	-			–
(−)-**12**	consensus						A/T	A	Pu > Py					
(−)-N-BOC-CPI	A/T (56)	–	-	-	-	–	97	100	66	–				–
(−)-**13**	consensus						A/T	A	Pu > Py					
(−)-duocarmycin SA	A/T (56)	–	–	–	–	-	93	100	96	73	56			-
ent-**3**	consensus						A/T	A	A/T	A/T > G/C	N			
(−)-CPI-CDPI$_2$	A/T (56)	-	–	-	-	–	88	100	93	82	73	56		
(−)-**16**	consensus						A/T	A	A/T	A/T > G/C	A/T > G/C	N		
(−)-CC-1065	A/T (56)	–	-	–	–	-	88	100	93	82	73	56	-	
ent-**1**	consensus						A/T	A	A/T	A/T > G/C	A/T > G/C	N		
(−)-CPI-CDPI$_3$	A/T (56)	-	–	-	-	–	100	100	100	100	86	86	57	
(−)-**17**	consensus						A/T	A	A/T	A/T	A/T > G/C	A/T > G/C	N	

[a] The numbers listed in the table give the percentage of the indicated base located at the designated position relative to the adenine-N3 alkylation site. [b] The numbers in parentheses give the percentage composition within the DNA examined.

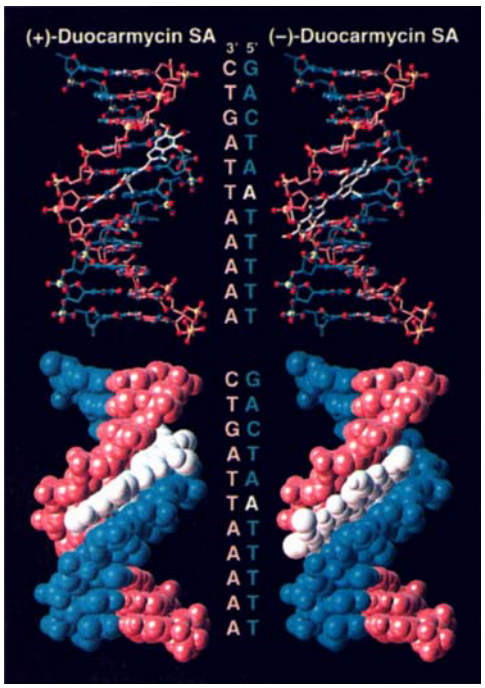

Fig. 9. Stick and space-filling models illustrating the alkylation of the same site within w794 DNA (duplex 5′-d(GACTAATTTTT)) by (+)-**12** (left) and (−)-**12** (right). The binding of the natural enantiomer extends in the 3′ → 5′ direction from the adenine-N3 alkylation site across the site 5′-AA, that of the unnatural enantiomer in the reverse 5′ → 3′ direction but across the same 5′-AA site.

3.2. CPI-PDE-I$_1$: A Key Substructure of CC-1065

In early efforts to establish the role of each of the subunits of CC-1065, both enantiomers of CPI-PDE-I$_1$ (**14**, Fig. 10) were prepared for evaluation.[71] Although a number of interesting

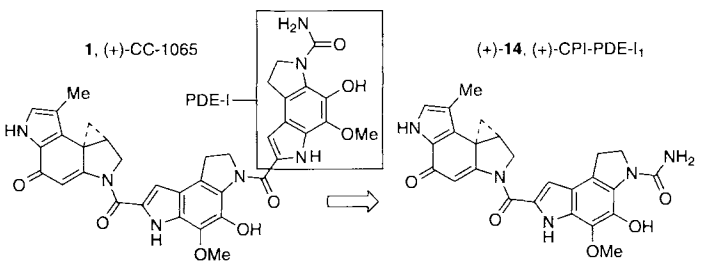

Fig. 10. CPI-PDE-I$_1$ (**14**), a key substructure of CC-1065.

observations were made in this early study, only two of the more seminal are described below. First, (+)-CPI-PDE-I$_1$ displayed in vitro cytotoxic activity indistinguishable from (+)-CC-1065, indicating that the entire righthand subunit framed in Figure 10 was unnecessary for observation of the full biological potency of the natural product. The subsequent discovery of the duocarmycins, which also lack this third subunit, provided indepen-

dent confirmation of its relative unimportance to the biological properties of the natural enantiomers. In addition, the natural enantiomer of **14** exhibited a similar, although perceptibly altered DNA alkylation selectivity from that observed with (+)-CC-1065. Table 3 (Section 3.1) summarizes the consensus alkylation sequence found for (+)-**14**. Like (+)-CC-1065, each alkylation site detected proved to be adenine, and each site was flanked by two 5′-A or -T bases. The same order of preference as in the case of **1** was observed for this three-base, AT-rich alkylation region: 5′-AA<u>A</u>≈5′-TT<u>A</u>>5′-TA<u>A</u>>5′-AT<u>A</u>. The distinctions between (+)-**14** and (+)-CC-1065 were found to lie in the AT preference extended to the fourth and fifth 5′ bases. With (+)-**14**, a weaker preference for the fourth 5′-A or -T base was observed, and unlike (+)-CC-1065, no preference for the fifth 5′ base was observed. Thus, like the subsequent observations made with duocarmycin A and SA, (+)-**14** exhibits alkylation selectivity for a shorter 3.5-base-pair, AT-rich site. Consequently, the presence of the DNA binding subunits were found to influence the sequence selectivity of DNA alkylation, and a full study of shorter and more extended analogs of CC-1065 revealed that this AT-rich selectivity corresponds nicely to the length of the agent and the size of the region surrounding the alkylation site required to bind the agent (see Table 3).[53, 71]

The relative cytotoxic potencies of related agents, including those that lack the DNA binding subunits altogether, suggested an additional important functional role for the DNA binding subunits. (+)-N-BOC-CPI and (+)-N-acetyl-CPI, which lack an attached DNA binding subunit, proved to be approximately 1000 to 10000 times less potent than (+)-CC-1065. In contrast, the natural enantiomers of the agents **14**–**17** (see Figs. 10 and 12), which possess one to three DNA binding subunits, proved equipotent with the natural product (Table 4). Similarly, (+)-N-BOC-CPI and (+)-N-acetyl-CPI were substantially less efficient (1000–10000×) at alkylating DNA, whereas **14**–**17** and **1** exhibited comparable efficiencies but different DNA alkylation rates and subtly distinguishable selectivities for AT-rich alkylation sites, corresponding to their relative sizes. This, in conjunction with computational studies, quantitative molecular modeling studies, and an appreciation of the intrinsic stability of the agents, suggested to us that the DNA alkylation was inherently reversible but stabilized by the noncovalent interactions provided by the DNA binding subunits. Furthermore, it suggested that a single DNA binding subunit would provide this stabilization for the natural enantiomers and that it was the simple event of the stabilization that provided the full potentiation of the biological properties. At this time the reversible nature of the DNA alkylation was not recognized, and the Hurley and Upjohn groups, in their complementary efforts, proposed that the distinctions were due to the rates of DNA alkylation and the kinetic aspects of the formation of the DNA adducts.[46] These varying proposals led to the subsequent discovery that the DNA alkylation reactions are indeed reversible and that the adducts are increasingly stabilized by the presence and size of the DNA binding subunits.[58, 70]

Table 4. In vitro cytotoxic activity of key partial structures of CC-1065 and the duocarmycins.

Agent	IC_{50}, L1210 [pM]
natural enantiomers	
(+)-**12**, (+)-N-BOC-DSA	6000
(+)-**13**, (+)-N-BOC-CPI	300000
3, (+)-duocarmycin SA	10
1, (+)-CC-1065	20
(+)-**14**, (+)-CPI-PDE-I_1	20
(+)-**15**, (+)-CPI-$CDPI_1$	40
(+)-**16**, (+)-CPI-$CDPI_2$	20
(+)-**17**, (+)-CPI-$CDPI_3$	20
unnatural enantiomers	
(−)-**12**, (−)-N-BOC-DSA	60000
ent-**3**, (−)-duocarmycin SA	100
ent-**1**, (−)-CC-1065	20
(−)-**14**, (−)-CPI-PDE-I_1	≥2400
(−)-**15**, (−)-CPI-$CDPI_1$	≥6300
(−)-**16**, (−)-CPI-$CDPI_2$	20
(−)-**17**, (−)-CPI-$CDPI_3$	50

3.3. CPI-$CDPI_2$: A Precise Functional Analog of CC-1065

Among the first analogs of CC-1065 examined, that which was derived from removal of the methoxy and hydroxy substituents from the central and righthand subunits proved especially revealing (Fig. 11). CPI-$CDPI_2$ proved particularly important to examine because of the growing perception at the time that the polar functionality on CC-1065 was contributing significantly to the properties of the agents. Its examination addressed three important questions. The first was the contribution that the substituents may make to DNA binding, the resulting alkylation properties of the natural product, and their contribution to the biological properties. Although the substituents were initially expected to influence the DNA alkylation properties significantly, extensive molecular modeling studies did not support such a role.[38, 41] Secondly, the C4 hydroxy group had been suggested to facilitate DNA binding by hydrogen bonding to the carbonyl group of the linking subunit, thereby stabilizing

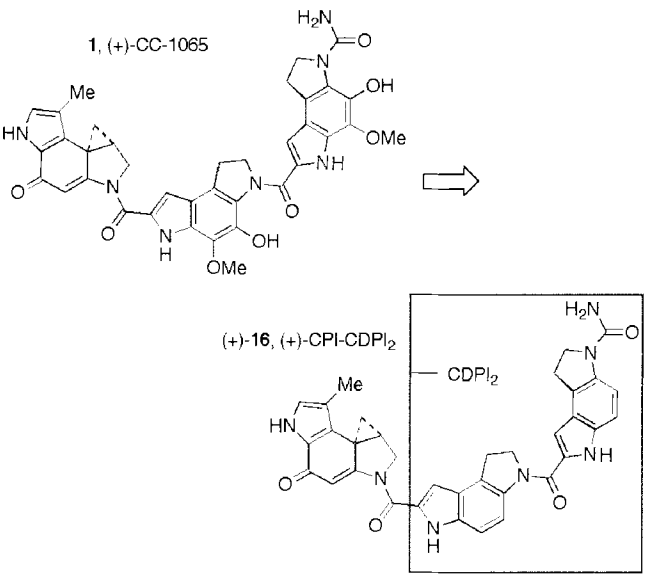

Fig. 11. CPI-$CDPI_2$ (**16**), a precise functional analog of CC-1065.

a curved and helical conformation required for groove binding. However, this intramolecular hydrogen bonding introduced an exaggerated pitch to the helical conformation of CC-1065, and the less pronounced inherent pitch of the helical conformation of (+)-**16** more closely followed that required for minor groove binding.[38, 77, 78] Finally, oxidation of the central and righthand subunits to an extended *para*-quinone imine was thought potentially to contribute to the delayed toxicity of (+)-CC-1065.[80]

The preparation of both enantiomers of CPI-$CDPI_2$[77] and their comparison with the enantiomers of CC-1065 revealed that the two agents were indistinguishable.[71] The cytotoxic activity, in vivo antitumor activity, and DNA alkylation efficiencies and selectivities of both enantiomers of CPI-$CDPI_2$ were identical to those of the corresponding CC-1065 enantiomer. Moreover, (+)-CPI-$CDPI_2$ exhibited the delayed toxicity characteristic of (+)-CC-1065, whereas both the unnatural enantiomers lacked this property.[79] Thus, the examination of **16** established that the hydroxy and methoxy substituents on the central and righthand subunits of CC-1065 do not contribute to the properties of the natural product. Some of the conclusions drawn from a complementary and concurrent study were initially distinct from this[79] but later revised.[46]

The indistinguishable profiles of DNA alkylation proved particularly revealing when compared to those of the series of structurally related agents detailed in the next section. The studies were facilitated through introduction of a useful protocol for rapidly securing substantial quantities of DNA labeled at one end with ^{32}P.[72]

3.4. CPI-$CDPI_n$: Extended and Shortened Analogs of CC-1065

In initial efforts to establish the functional roles of each of the CC-1065 subunits, the full set of shortened and extended agents **15**–**17** were prepared for comparative examination (Fig. 12).[71] In these studies, CPI-$CDPI_1$ and CPI-PDE-I_1 proved indistinguishable, and the natural enantiomers of CPI-$CDPI_n$ ($n = 1-3$) and CPI-PDE-I_n ($n = 1-2$) exhibited the same cytotoxic potency. Pertinent to defining the origin of the DNA alkylation selectivity of (+)-CC-1065 is the observation that the natural enantiomers of (+)-CPI-$CDPI_1$ and (+)-CPI-PDE-I_1, as well as (+)-CPI-$CDPI_3$, were distinguishable from natural product and (+)-CPI-$CDPI_2$. The former exhibited a selectivity for shorter 3.5-base-pair, AT-rich alkylation sites, while the latter favored a more extended, 6.5–7-base-pair, AT-rich site.[53] Table 3 summarizes the consensus alkylation sequences for both the natural and unnatural enantiomers of these key substructures of CC-1065.

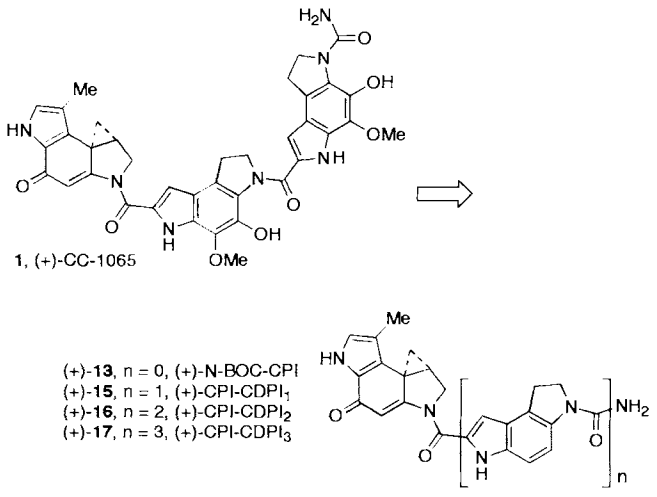

Fig. 12. CPI-$CDPI_n$, extended and shortened analogs of CC-1065.

One of the initially confusing observations was that the unnatural enantiomers of CPI-$CDPI_1$ and CPI-PDE-I_1, unlike (−)-CC-1065, failed to alkylate DNA productively and were relatively nonpotent cytotoxic agents (Table 4). Although this was not easily rationalized at the time the observations were made, it now can be attributed to the extent of stabilization provided by the noncovalent contacts and the degree of steric bulk surrounding the C7 center of the CPI or DSA alkylation subunit (**12** or **13**, respectively). For the unnatural enantiomer, this results from destabilizing steric interactions with the 5′ base preceding the alkylated adenine residue on the alkylated strand of DNA, which decelerate the rate of DNA alkylation and destabilize reversible adduct formation. A single DNA binding subunit is necessary to stabilize reversible adduct formation for the natural CPI alkylation subunit, whereas the unnatural CPI enantiomer requires two such DNA binding subunits. In sharp contrast, a single DNA binding subunit is required for both the natural and unnatural enantiomers of DSA, since the destabilizing steric interactions at C7 unique to the unnatural enantiomer adducts have been reduced.

Further simplifications in the DNA binding subunits have been accomplished and studies with agents containing deep-seated modifications in this region have been described. These are discussed in more detail in Section 10.

4. Noncovalent Binding Affinity and Selectivity

4.1 PDE-I_n, $CDPI_n$, $ACDPI_n$, and $TACDPI_n$

Important early insights into the structural origin of the sequence-selective DNA alkylation were derived from the examination of the characteristics of the noncovalent binding to DNA of **18**–**21**, key partial structures of **1**–**3** that were not capable of the covalent bond formation (Fig. 13). Although the studies have been conducted with a range of agents and various DNA,[81–84] only the seminal aspects of the studies are summarized in Figure 13. Both relative and absolute DNA binding constants have been established, and the agents exhibited a substantial selectivity for binding to the AT-rich minor groove (Table 5).[82, 83] In addition, $CDPI_3$ was the optimum binding agent within the $CDPI_n$ series (Fig. 13, bottom). The minor groove binding of $CDPI_3$ spans five base pairs or half a helix turn, which constitutes the largest site accessible for synchronous binding of both ends of the rigid agent. Partially bound forms of the larger agents, for instance $CDPI_4$ bound through a $CDPI_2$ subunit only, constitute productive and stable noncovalent complexes, and $CDPI_4$ and $CDPI_5$ were not as effective as $CDPI_3$. The removal of the hydroxy and methoxy substituents (PDE-$I_n \rightarrow CDPI_n$) had only a small impact on the

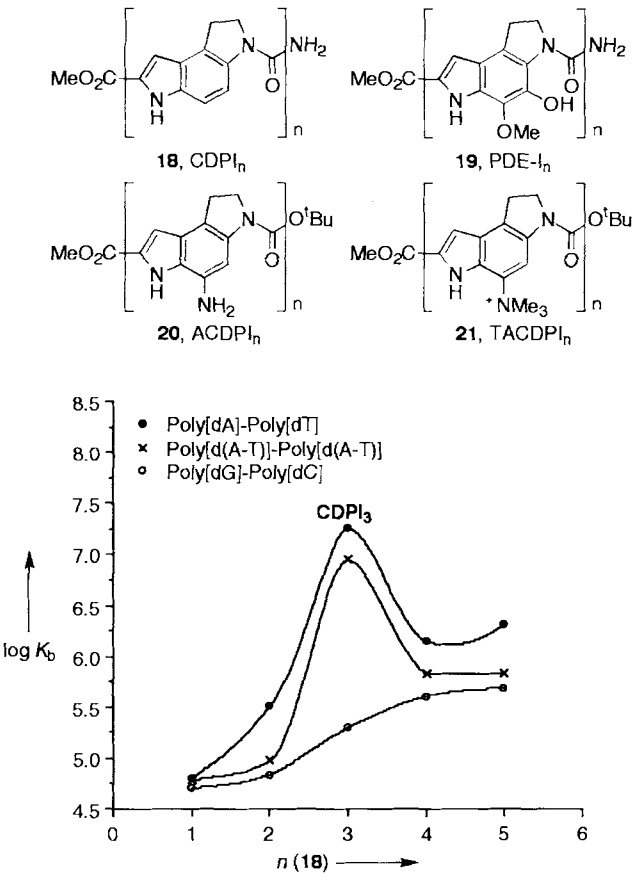

Fig. 13. Structures (top) and binding constants (bottom) of substrates that bind noncovalently to DNA.

binding affinity and no apparent impact on the selectivity for AT-rich binding sites.[82] Since there is no CDPI$_n$ functionality that would provide hydrogen bonding or electrostatic stabilization, the affinity is derived principally from stabilizing van der Waals contacts. The preference for AT-rich minor-groove binding is probably due to the deeper penetration of the agents into the narrower, AT-rich minor groove, where the stabilizing contacts are maximized.

Consequently, the studies suggested that (+)-CC-1065 is best represented as a selective alkylating group superimposed upon the rigid CDPI$_3$ skeleton[82] rather than as a reactive alkylating agent (CPI) attached to a DNA binding agent (PDE-I$_2$). The agents exhibit a substantial preference for noncovalent binding at AT-rich regions in the minor groove, which is optimal with the rigid trimer. Among features that contribute to minor-groove binding selectivity, at least two structural characteristics of an A-T base pair and of a run of A-T base pairs are important to agents that rely on stabilizing van der Waals contacts and hydrophobic binding. First, the amino substituent of a G-C base pair that extends into the minor groove has no counterpart in an A-T base pair (Fig. 14). This results in a sterically more accessible region adjacent to an A-T base pair that permits the deeper penetration of an agent into the minor groove and enhances the stabilization derived from van der Waals contacts. In addition, X-ray crystallographic studies of oligodeoxynucleotides that contain a run of A-T base pairs in the center of their structure have revealed characteristic features including the constricted width of the AT-rich minor groove.[14, 15] Illustrated in Figure 14 (bottom) is a plot of the effective width of the minor groove of four such oligodeoxynucleotides that highlights this

Table 5. Binding constants and free energies of binding for the noncovalent binding to three DNA sequences.

Agent	K_b [M^{-1}]	ΔG°_{298} [kcal mol^{-1}]	Agent	K_b [M^{-1}]	ΔG°_{298} [kcal mol^{-1}]	Agent	K_b [M^{-1}]	ΔG°_{298} [kcal mol^{-1}]
Poly[dA]-Poly[dT]								
CDPI$_1$	6.4×10^4	−6.6	ACDPI$_1$	5.7×10^3	−5.1	TACDPI$_1$	3.8×10^5	−7.6
CDPI$_2$	3.2×10^5	−7.5	ACDPI$_2$	2.8×10^4	−6.1	TACDPI$_2$	1.4×10^7	−9.8
CDPI$_3$	1.8×10^7	−9.9	ACDPI$_3$	9.6×10^5	−8.2	TACDPI$_3$	1.3×10^8	−11.1
CDPI$_4$	1.4×10^6	−8.4	ACDPI$_4$	5.6×10^5	−7.8			
CDPI$_5$	2.1×10^6	−8.6						
CDPI$_3$-O*t*Bu	1.5×10^7	−9.8						
PDE-I$_2$	1.6×10^7	−9.8						
PDE-I$_3$	$>4.8\times10^7$	–						
distamycin	$>1.1\times10^8$	(−11.4)						
Poly[d(A-T)]-Poly[d(A-T)]								
CDPI$_1$	6.1×10^4	−6.5	ACDPI$_1$	4.3×10^3	−5.0	TACDPI$_1$	4.5×10^5	−7.7
CDPI$_2$	9.6×10^4	−6.8	ACDPI$_2$	2.1×10^4	−5.9	TACDPI$_2$	2.1×10^7	−10.0
CDPI$_3$	8.9×10^6	−9.5	ACDPI$_3$	1.4×10^5	−8.4	TACDPI$_3$	5.4×10^8	−11.9
CDPI$_4$	6.7×10^5	−8.0	ACDPI$_4$	2.2×10^5	−7.3			
CDPI$_5$	6.7×10^5	−8.0						
CDPI$_3$-O*t*Bu	7.3×10^6	−9.3						
PDE-I$_2$	4.6×10^6	−9.1						
PDE-I$_3$	$>2.6\times10^7$	–						
distamycin	$>7.2\times10^7$	(−12.6)						
Poly[dG]-Poly[dC]								
CDPI$_1$	5.1×10^4	−6.4	ACDPI$_1$	3.2×10^3	−4.8	TACDPI$_1$	2.1×10^4	−5.9
CDPI$_2$	6.9×10^4	−6.6	ACDPI$_2$	4.3×10^3	−5.0	TACDPI$_2$	1.0×10^6	−8.2
CDPI$_3$	2.0×10^5	−7.2	ACDPI$_3$	1.4×10^5	−7.0	TACDPI$_3$	1.6×10^6	−8.4
CDPI$_4$	4.1×10^5	−7.7	ACDPI$_4$	1.0×10^5	−6.8			
CDPI$_5$	4.9×10^5	−7.8						
CDPI$_3$-O*t*Bu	2.1×10^5	−7.3						
PDE-I$_2$	–	–						
PDE-I$_3$	$>7.7\times10^5$	−8.0						
distamycin	$>2.9\times10^6$	–						

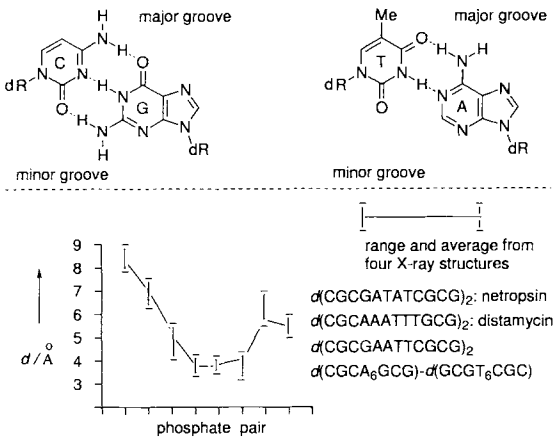

Fig. 14. GC and AT base pairs illustrating the resulting difference in width of the DNA groove. d = effective width of the minor groove.

narrower, AT-rich minor groove. This important conformational feature of DNA possessing runs of A-T base pairs contributes prominently to the selectivity of the agents that depend on stabilizing van der Waals contacts for noncovalent binding. The noncovalent complexes of such agents may be expected to form preferentially within the narrower, sterically more accessible, AT-rich minor groove, where the stabilizing van der Waals contacts are most effectively provided.

More recently the DNA binding properties of ACDPI$_n$ (**20**, $n = 1-4$) and TACDPI$_n$ (**21**, $n = 1-3$) have been described.[83] As with the CDPI$_n$ series, ACDPI$_3$ proved to be the optimal minor groove binding agent and exhibited a selectivity for AT- rather than GC-rich DNA. Similarly, TACDPI$_n$ exhibited a substantial selectivity for AT-rich DNA binding sites ($n = 3$, $\Delta\Delta G = -2.7$ to -3.5 kcal mol^{-1}). The comparison of CDPI$_n$ substrates with ACDPI$_n$ substrates illustrated that the introduction of a strong electronegative substituent onto the outer face of the agent reduced the binding affinity through introduction of destabilizing electrostatic interactions with the phosphate backbone. In contrast, the behavior of TACDPI$_n$ substrates revealed that the introduction of a C5 quaternary amine substantially enhanced the binding affinity through introduction of stabilizing electrostatic interactions with the phosphate backbone (Fig. 15).

Finally, the terminal urethane of CC-1065 was found not to contribute to the minor-groove binding affinity or selectivity.[82]

4.2. Affinity Cleavage: The Sites for Noncovalent Binding and for Alkylation Coincide

A study of the efficiency and selectivity of DNA cleavage by the Fe^{III} complex of the affinity cleavage agent **22**[85] (Fig. 16)

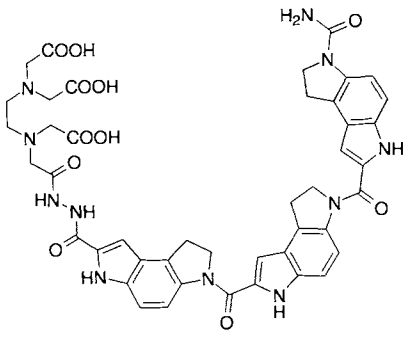

22

Fig. 16. Structure of the affinity cleavage agent **22**.

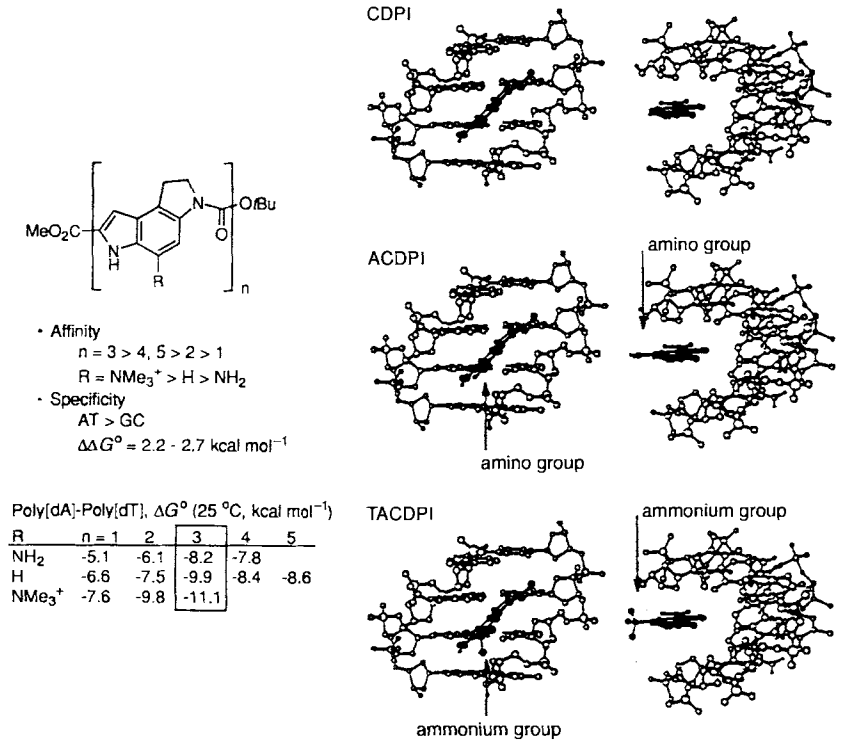

Poly[dA]-Poly[dT], $\Delta G°$ (25 °C, kcal mol^{-1})

R	n = 1	2	3	4	5
NH_2	-5.1	-6.1	-8.2	-7.8	
H	-6.6	-7.5	-9.9	-8.4	-8.6
NMe_3^+	-7.6	-9.8	-11.1		

Fig. 15. Influence of the C5 substituent of the agent binding in the minor groove of DNA on binding affinity and selectivity.

has provided further direct evidence that for both (+)- and (−)-CC-1065 all DNA alkylation sites coincide with AT-rich regions suitable for noncovalent binding.[86] Importantly, no DNA alkylation sites were observed to lie outside such preferred noncovalent binding regions. To a first approximation, the relative alkylation efficiencies between sites paralleled the relative cleavage efficiencies of Fe^{III}-**22** at the competing sites. As the affinity cleavage agent **22** provided clean cleavage at both ends of a five-base-pair binding site, it must bind in both orientations in the site. The offset H-abstraction sites leading to DNA cleavage confirm minor-groove binding. This relationship of the DNA cleavage sites for **22** surrounding the w794 five-base-pair, AT-rich, high-affinity alkylation site for CC-1065 is illustrated in Figure 17. Notably, (+)-CC-1065 can only alkylate one site and strand in this sequence, since in its reversed bound orientation the activated cyclopropane is placed adjacent to the two 3′ T bases on the left strand.

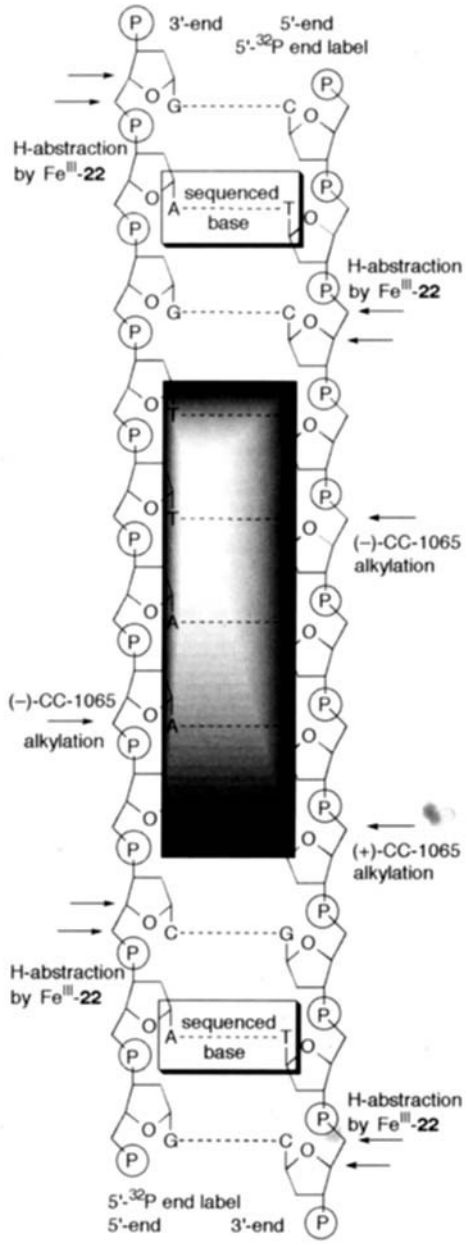

Fig. 17. Model illustrating the relationships between the sequenced cleavage sites for Fe^{III}-**22**, its C4′ and C5′ H-abstraction sites, the five-base-pair, AT-rich site for noncovalent binding, and the sites of adenine-N3 alkylation by (+)- and (−)-CC-1065 in w794 DNA.

4.3. Circular Dichroism Studies

Difference circular dichroism studies initially demonstrated that CC-1065 binds in the AT-rich regions of the minor groove in double-stranded B DNA.[87–97] This technique has also shown that (+)-CC-1065 forms a stable noncovalent complex with the Dickerson dodecamer d(CGCGAATTCGCG)$_2$.[91, 92, 96] In fact, all adenine-containing duplex deoxyoligonucleotides initially bind (+)-CC-1065 noncovalently, as evidenced by a transient absorption at 390 nm, and then react to produce a covalent adduct, which shows a maximum ellipticity at 370 nm.[89–97] In the exceptions, which bind but do not react with CC-1065, the binding sites do not contain an adenine properly positioned to permit alkylation. For example, the activated cyclopropane of (+)-CC-1065 is placed proximal to the two 3′-T bases of the Dickerson dodecamer in both bound orientations, and thus no accessible nucleophilic site is available for alkylation. Contrary to assertions of the uniqueness of the alkylation reaction, the positioning of this nucleophilic adenine-N3 site need not be exquisite but must be on the right end of the binding site. Consistent with this, the unnatural enantiomer of CC-1065 readily alkylates the Dickerson dodecamer, and its activated cyclopropane is oriented toward the opposite strand proximal to the two 5′-A bases. It is misleading to suggest that such studies illustrate that noncovalent binding cannot dominate or control DNA alkylation, if only a single mismatched binding site is examined.[46, 96] As the studies with the affinity cleavage agent **22** illustrate, noncovalent binding at an AT-rich site in the minor groove may not guarantee alkylation, but it is a prerequisite to the observation of DNA alkylation.

5. Proposals for the Origin of Polynucleotide Recognition

In the course of studies on CC-1065 and the duocarmycins, the alkylation selectivity of the natural enantiomers has been attributed to a sequence-dependent activation of the reaction through C4 carbonyl protonation by a strategically positioned phosphate in the DNA backbone,[43–47, 67–69] to the conformational variability of DNA and alkylation at junctions of bent DNA,[98–103] or to preferential noncovalent binding and subsequent alkylation within the narrower, deeper, AT-rich minor groove of DNA (Scheme 2).[34–42] Central to the different interpretations are the perceived similarities[43–48, 64–68] or dis-

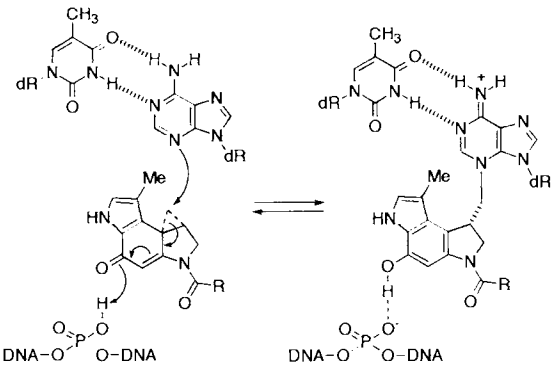

Alkylation Model:
- (+)-CPI and (+)-CC-1065 alkylation selectivities are identical
  - selectivity is inherent in the CPI alkylation subunit and the alkylation reaction
- Alkylation selectivity is independent of binding selectivity
- Different features control the (−)-CC-1065 alkylation
- Conformational flexibility of DNA with alkylation at junctions of bent DNA
- Sequence-dependent activation by C4 carbonyl protonation by the phospate backbone
  - C4 carbonyl is required for activation and alkylation selectivity

Noncovalent Binding Model:
- (+)-CPI and (+)-CC-1065 alkylation selectivities are different
  - CPI is a modest electrophile superimposed on a five-base-pair, AT-rich binding agent
- Alkylation selectivity is controlled by binding selectivity and steric accessibility to the alkylation site
- Same features control the (−)-CC-1065 alkylation
- Alkylation within appropriate AT-rich binding sequences
- Phosphate activation does not control the alkylation selectivity
  - C4 carbonyl is not required

Scheme 2. Summary of the key features of the proposed models.

tinctions[34-42, 53, 54] in the alkylation selectivity of simple derivatives, including **12** and **13** and the natural products **1**–**3**. The former two proposals advocated by the Hurley and Upjohn groups are based on the premise that (+)-**13** and (+)-**1** alkylate the same sites and that the alkylation subunit or alkylation reaction controls the selectivity irrespective of noncovalent binding. In contrast, the latter proposal advocated in our studies requires that the selectivity of the agents for AT-rich noncovalent binding sites and their steric accessibility to the alkylation site that accompanies deep penetration into the AT-rich minor groove control the sequence selectivity. This latter model accommodates nicely the reverse and offset 3.5- (for **3**) or 5-base-pair (for **5**), AT-rich, adenine-N3 alkylation selectivities of the natural and unnatural enantiomers of **3** and **1** and requires that **12** and **13** and **1**–**3** exhibit distinct alkylation selectivities (see Fig. 8 and Table 3).[53, 54, 71]

All groups have concluded that the DNA alkylation selectivity displayed by the unnatural enantiomer is dominated by the selectivity of the agents for AT-rich noncovalent binding, as advanced in our studies.[45, 53, 54, 68] However, the Hurley–Upjohn proposal for the natural enantiomers requires that different fundamental polynucleotide recognition elements are operative for the natural and unnatural enantiomers.[68] Because of such distinct interpretations, we set out to unambiguously test the proposed models with the intention of establishing the origin of the DNA alkylation selectivity. This has proven to be especially important to address at this juncture, since the (+)-CC-1065 alkylation of duplex DNA has been suggested to be, and is often cited as, a prototypical example of sequence-dependent DNA reactivity.[43, 46, 47] Before such a proposal should be widely accepted, experimental support and verification should be provided.

5.1 Definitive Tests of Proposed Models for the Origin of the CC-1065 and Duocarmycin DNA Alkylation Selectivity

5.1.1. Test of the Importance of C4-Carbonyl Protonation for Sequence-Selective DNA Alkylation

Although the proposal that a sequence-dependent activation through C4 carbonyl protonation by a strategically placed phosphate in the DNA backbone is attractive, a direct test of its viability indicates it cannot be the source of the DNA alkylation sequence selectivity. In the key study[104, 105] it was shown that **23**–**26** (Fig. 18) exhibited identical alkylation selectivities (5′-AA > 5′-TA) irrespective of their absolute configuration, and the selectivities were identical to those of both enantiomers of **12** and **13**. In addition, the natural enantiomers of **27**–**30** exhibited DNA alkylation selectivities identical to (+)-CC-1065 (Fig. 19)[104] and were much more selective and efficient than **23**–**26**. Because **25**/**26** and **29**/**30**, which lack the C4 carbonyl, alkylate the same sites as **23** or **27**, respectively, a sequence-dependent phosphate protonation and activation cannot be the event that determines the alkylation selectivity. In addition, the much more selective DNA alkylation by **27**–**30**/**1**–**3** than by **23**–**26**/**12**–**13**—independent of the nature of the electrophile—is not consistent with the assertions that the alkylation reaction

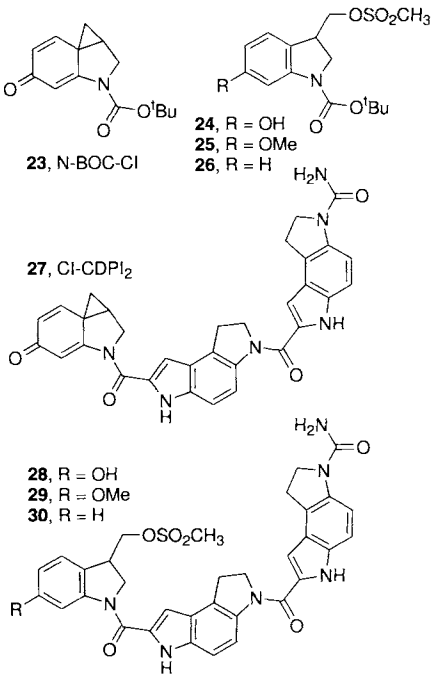

Fig. 18. Structures of the agents **23**–**30**.

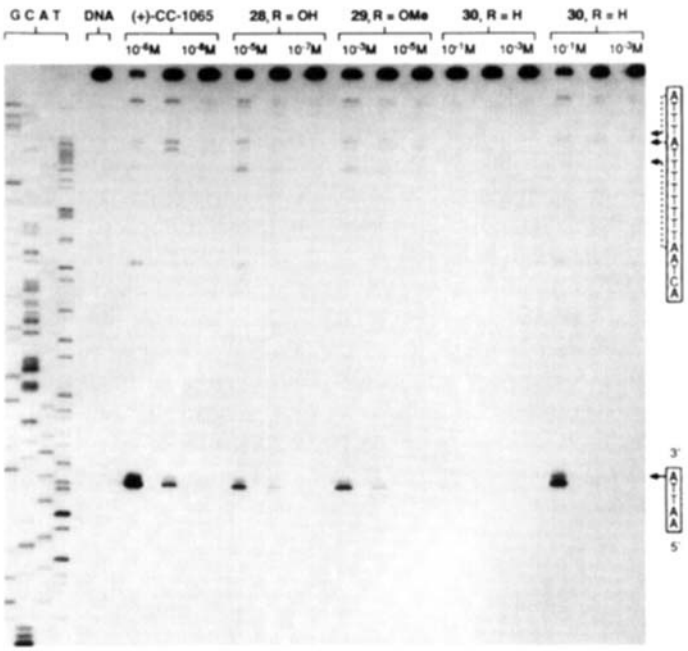

Fig. 19. Thermally induced strand cleavage (by heating to 100 °C for 30 min) of double-stranded DNA (SV40 DNA fragment, 144 base pairs; nucleotide no. 138-5238, clone w794) after 24 h incubation at 4 °C or 37 °C and removal of unbound agent by EtOH precipitation followed by denaturing PAGE (8%) and autoradiography. Lanes 1–4: Sanger G, C, A, and T reactions; lane 5: control DNA; lanes 6–8, (+)-CC-1065 (**1**, 2.5×10^{-6}–2.5×10^{-8} M, 4 °C); lanes 9–11: **28** (2.5×10^{-5}–2.5×10^{-7} M, 4 °C); lanes 12–14: **29** (2.5×10^{-3}–2.5×10^{-5} M, 4 °C); lanes 15–17: **30**, (2.5×10^{-1}–2.5×10^{-3} M, 4 °C); lanes 18–20: **30** (2.5×10^{-1}–2.5×10^{-3} M, 37 °C). The results shown here for the racemates of **28**–**30** are identical to those under analogous conditions for the pure natural enantiomers.

and nature of the alkylation subunit control the alkylation selectivity, but are consistent with the noncovalent binding model.

In addition, the DNA alkylation reaction is not likely to be acid catalyzed at pH 7–7.6 as advocated by Warpehoski,[106]

but rather Lewis acid catalyzed by virtue of metal cations associated with the deprotonated phosphate backbone. Attempts to derive rate accelerations for the DNA alkylation reaction must be tempered by this consideration of a Lewis acid or Brønstedt acid catalyzed reaction.

5.1.2. A Switch in the Inherent Alkylation Selectivity of an Enantiomer by Reversal of the Agent Orientation: A Definitive Demonstration of the Origin of the DNA Alkylation Selectivity

Key to the second and definitive study[108] was the disclosure that both the natural and unnatural enantiomer of duocarmycin SA alkylate DNA efficiently.[54] One unique feature of **3** is the methyl ester at C6 on the lefthand side of the alkylation subunit that complements the righthand side linking amide. This provides the ability to introduce DNA binding subunits on either side of the duocarmycin SA alkylation subunit. In the studies, both the natural and unnatural enantiomers of the extended and reversed duocarmycin SA analogs **31** and **32** (Fig. 20) were examined. We anticipated that (+)- and (−)-DSA-$CDPI_2$ (**31**) would, in general, exhibit alkylation selectivity for a more extended (five-base-pair) site than the site favored by **3** and, in particular, behave identically to (+)-CC-1065 (that is, 5′-AAAAA selectivity) and (−)-CC-1065 (that is, 5′-AAAAA selectivity), respectively.[53] From the noncovalent binding model, the reversed agents (+)- and (−)-$CDPI_2$-DSA (**32**) were projected to exhibit a similar five-base-pair, AT-rich alkylation selectivity, but one that extends in the atypical reverse direction from an alkylation site. Moreover, the alkylation sites for the natural enantiomer of the reversed agent (+)-**32** should coincide with those of *ent*-**1** and (−)-**31**, and analogously those of the unnatural enantiomer (−)-**32** with (+)-CC-1065 or (+)-DSA-$CDPI_2$ (**31**). In contrast, the alkylation site model, in which the natural enantiomer alkylation selectivity is embodied in the alkylation subunit and the DNA alkylation reaction is independent of binding selectivity, would require that the two natural enantiomers (+)-**31** and (+)-**32** alkylate the same sites. Thus, the examination of the DNA alkylation selectivities of both enantiomers of **31** and **32** provided an unambiguous test of the models with a definitive resolution.

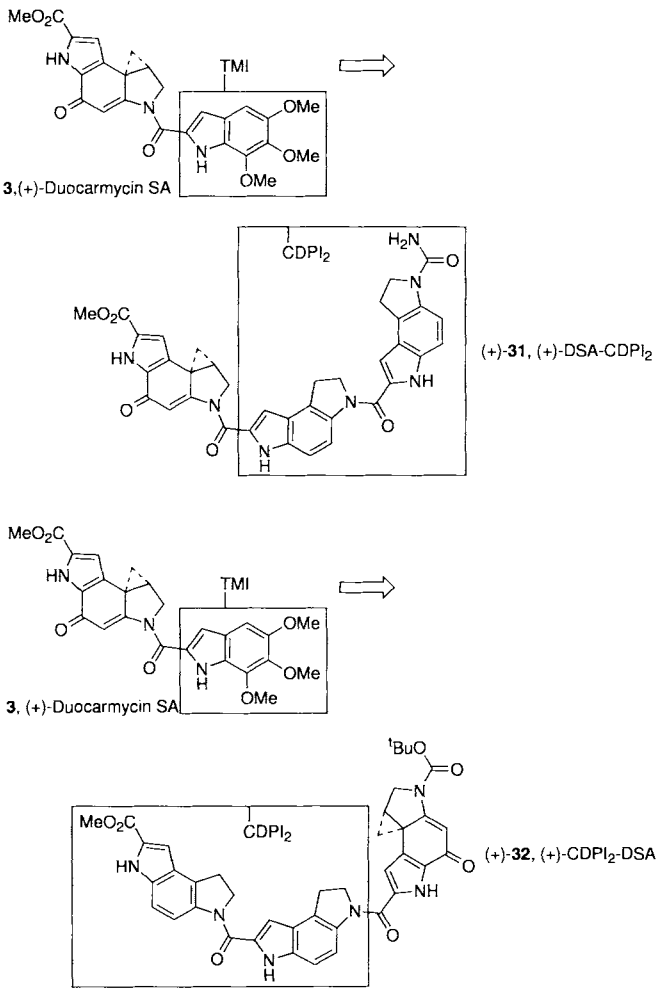

Fig. 20. Extended (top) and reversed (bottom) analogs of (+)-duocarmycin SA (**3**).

Both (+)- and (−)-**31** were found to alkylate DNA with the same selectivity as (+)- and (−)-**1**, respectively (Table 6).[109] The natural enantiomer of the reversed agent (+)-**32** alkylated DNA with the same selectivity as (−)-**31** and *ent*-**1**.[108, 109] This is illustrated beautifully in Figure 21, which highlights the comparisons between the alkylation selectivities not only of the typ-

Table 6. Consensus sequences for the DNA alkylation by extended (**31**) and reversed duocarmycin SA analogs (**32**) [a].

Agent	Base [b] 5′	4	3	2	1	0	−1	−2	−3	−4	3′
natural enantiomers											
(+)-CC-1065 (**1**)	A/T (56)	67	78	94	98	100	55				
	consensus	A/T > G/C	A/T > G/C	A/T	A/T	A	Pu ≥ Py	–	–	–	
(+)-DSA-$CDPI_2$ ((+)-**31**)	A/T (56)	71	85	100	100	100	63	–	–	–	
	consensus	A/T > G/C	A/T > G/C	A/T	A/T	A	Pu > Py	–	–	–	
(+)-$CDPI_2$-DSA ((+)-**32**)	A/T (56)	–	–	–	95	100	98	85	70	55	
	consensus	–	–	–	A/T	A	A/T	A/T > G/C	A/T > G/C	N	
unnatural enantiomers											
(−)-DSA-$CDPI_2$ ((−)-**31**)	A/T (56)	–	–	–	100	100	100	90	73	58	
	consensus	–	–	–	A/T	A	A/T	A/T	A/T > G/C	N	
(−)-$CDPI_2$-DSA ((−)-**32**)	A/T (56)	69	81	98	98	100	59	–	–	–	
	consensus	A/T > G/C	A/T > G/C	A/T	A/T	A	Pu > Py	–	–	–	
(−)-CC-1065 (*ent*-**1**)	A/T (56)	–	–	–	88	100	93	82	73	56	
	consensus	–	–	–	A/T	A	A/T	A/T > G/C	A/T > G/C	N	

[a] The numbers listed in the table give the percentage of the indicated base located at the designated position relative to the adenine-N3 alkylation site. [b] The numbers in parentheses give the percentage composition within the DNA examined.

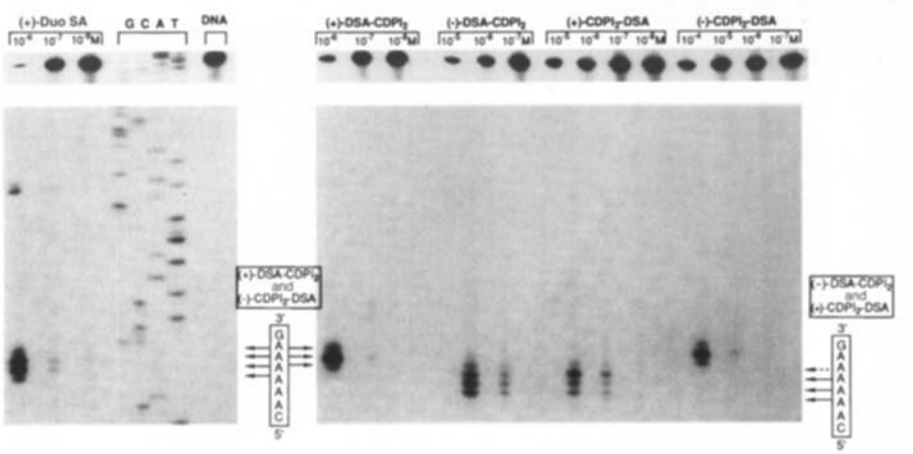

Fig. 21. Thermally induced strand cleavage (by heating to 100 °C for 30 min) of w836 DNA (146 base pairs, nucleotide no. 5189-91) after incubation at 25 °C, removal of unbound agent by EtOH precipitation followed by denaturing 8% PAGE and autoradiography. Lanes 1–3: (+)-**3**, 1×10^{-6}–1×10^{-8} M; lanes 4–7: Sanger G, C, A, and T sequencing standards; lane 8: control DNA; lanes 9–11: (+)-**31**, 1×10^{-6}–1×10^{-8} M); lanes 12–14: (−)-**31**, 1×10^{-5}–1×10^{-7} M; lanes 15–18: (+)-**32**, 1×10^{-5}–1×10^{-8} M; lanes 19–22: (−)-**32**, 1×10^{-4}–1×10^{-7} M.

ical natural and unnatural enantiomers of **31** but also of the two enantiomers of the reversed agents **32**. This incorporation and conversion of a natural enantiomer of the duocarmycin SA alkylation subunit into an agent that exhibits the DNA alkylation selectivity of a typical unnatural enantiomer by simple reversal of the orientation of the DNA binding subunits is only consistent with a model in which the binding selectivity and the depth of minor groove penetration in the vicinity of the alkylation site is controlling the sites of alkylation. Moreover, the observations are definitively inconsistent with alternative models based on the premise that the natural enantiomer's alkylation subunit controls the alkylation selectivity. Similarly, the unnatural enantiomer of the reversed agent (−)-**32** was found to alkylate the same sites as (+)-**31** and **1**, typical natural enantiomers. Thus, this switch in the inherent enantiomeric alkylation selectivity that accompanies the simple reversal of agent orientation is general and confirms that the same fundamental recognition features are operative for both the natural and unnatural enantiomers (Fig. 22).

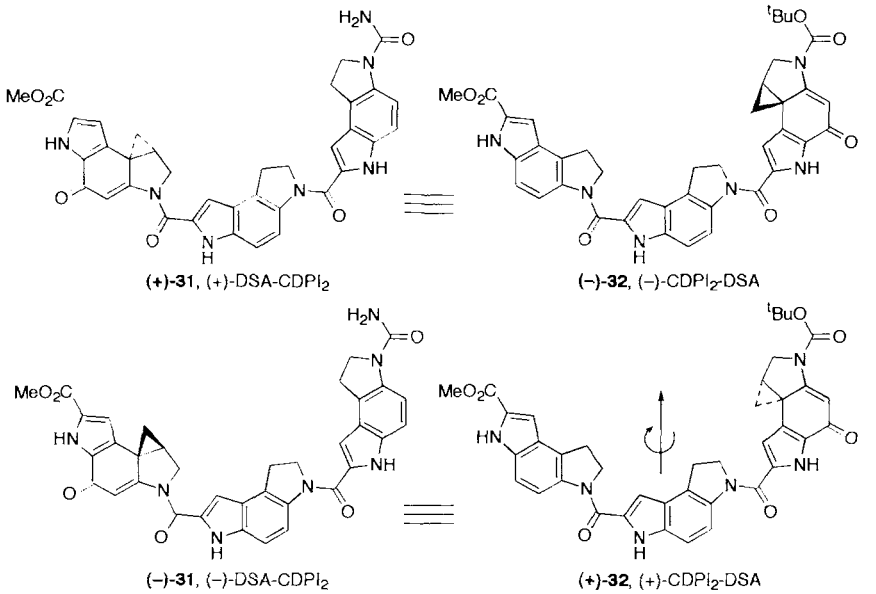

Fig. 22. Representations of the enantiomers of **31** and **32** that highlight the similarities in their experimental behavior. The arrow indicates the rotation of 180° in the horizontal plane (see text).

Although this behavior of the agents may not be obvious from the two dimensional representations of **31** and **32**, a simple rotation of **32** in the horizontal plane reveals the remarkable structural similarities between the two classes of agents and illustrates that it is the pairs of natural and unnatural enantiomers of different substrates **31** and **32** that orient the cyclopropane in comparable directions relative to the DNA binding subunits. Illustrated in Figure 23 are models of the alkylation by (+)-**31** and (−)-**32** at the high-affinity site 5′-AATTA and in Figure 24, models of the alkylation by (−)-**31** and (+)-**32** at the high-affinity site 5′-AATTT. The significance of these comparisons should not be underestimated. The results not only require that the same recognition features are affecting both enantiomers, but also represent an unambiguous demonstration that noncovalent binding in an AT-rich region is controlling and determining the sites of DNA alkylation for both the natural and unnatural enantiomers. In addition, since the DNA alkylation selectivities of (+)-**31**/(−)-**32** or (−)-**31**/(+)-**32** are identical despite the distinctions in the positioning of the cyclopropane, the positionings need not be precise, just accessible.

5.1.3. "Sandwiched" Analogs of Duocarmycin SA: A Class of Agents Whose DNA Alkylation Selectivity Is Independent of Absolute Stereochemistry

In a subsequent and further elegant verification of these observations, the natural and unnatural enantiomers of **33** were prepared by attaching a single DNA binding subunit to both sides of the duocarmycin SA alkylation subunit (Fig. 25) and subjected to examination.[109] Consistent with the noncovalent binding model, both (+)- and (−)-**33** exhibited identical DNA alkylation selectivities, which were distinct either from the natural or from the unnatural enantiomers of the extended or reversed agents **31** and **32** (Table 7).

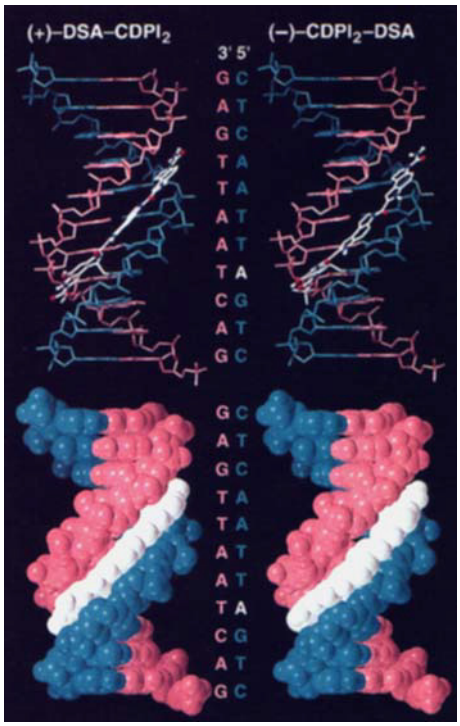

Fig. 23. Stick and space-filling models of the alkylation at a high-affinity site in w794 DNA (5′-CTCAATTAGTC) by (+)-**31** (left) and (−)-**32** (right). The natural enantiomer extends in the 3′ → 5′ direction from the adenine N3 alkylation site across the five-base, AT-rich site 5′-AATTA. The unnatural enantiomer of the reversed agent binds in the same 3′ → 5′ direction across the identical five-base, AT-rich site 5′-AATTA.

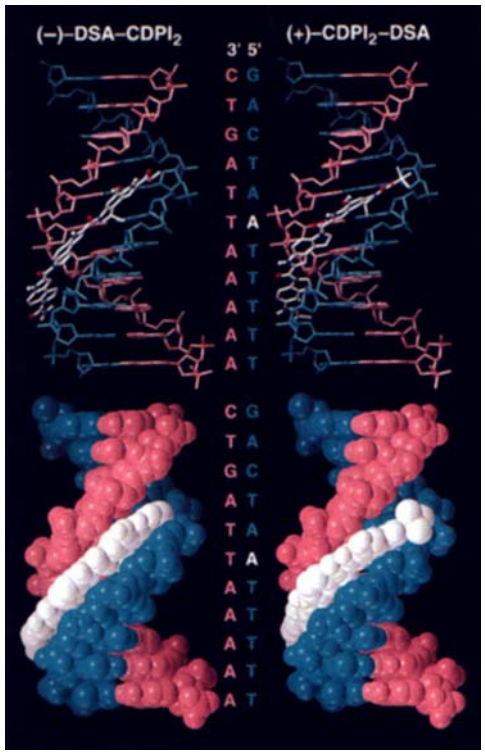

Fig. 24. Stick and space-filling models of the alkylation at a high-affinity site in w794 DNA (5′-GACTAATTTTT-3′) by (−)-**31** (left) and (+)-**32** (right). The unnatural enantiomer binds in the 5′ → 3′ direction across the five-base, AT-rich site 5′-AATTT. The natural enantiomer of the reversed agent binds in the same 5′ → 3′ direction across the identical five-base, AT-rich site 5′-AATTT.

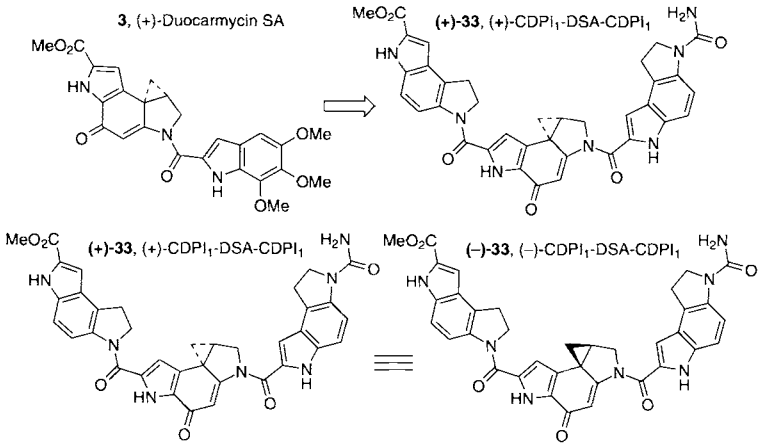

Fig. 25. Sandwich analogs of duocarmycin SA.

6. Structural Characterization of Oligo-Agent Complexes

Spectroscopic studies of complexes of the agents within defined sites of deoxyoligonucleotides have established the accuracy of the models and have begun to reveal subtle elements present in the structures. Most prominent is the confirmation of the binding orientation within the minor groove of the natural and unnatural enantiomers relative to the alkylated strand and the offset nature (relative to the alkylation site) of the binding site occupied by the agent.

A detailed NMR study of the complex formed between the duplex d(GACTAATTGAC)·d(GTCAATTAGTC), which contains the sequence of the high-affinity

Table 7. Consensus sequences for the DNA alkylation by the natural and unnatural enantiomers of sandwich analogs of duocarmycin SA. [a].

Agent	Base [b] 5′	4	3	2	1	0	−1	−2	−3	−4	3′
natural enantiomers											
(+)-CC-1065 (**1**)	A/T (56)	67	78	94	98	100	55	-	–	–	
	consensus	A/T > G/C	A/T > G/C	A/T	A/T	A	Pu ≥ Py	-		–	
(+)-CDPI$_1$-DSA-CDPI$_1$ ((+)-**33**)	A/T (56)		68	87	95	100	95	74	68	–	
	consensus	–	N	A/T > G/C	A/T	A	A/T	A/T > G/C	N	–	
unnatural enantiomers											
(−)-CDPI$_1$-DSA-CDPI$_2$ ((−)-**33**)	A/T (56)	–	64	86	94	100	94	78	68	–	
	consensus	–	N	A/T > G/C	A/T	A	A/T	A/T > G/C	N	–	
(−)-CC-1065 (*ent*-**1**)	A/T (56)		–		88	100	93	82	73	56	
	consensus		–		A/T	A	A/T	A/T > G/C	A/T > G/C	N	

[a] The numbers listed in the table give the percentage of the indicated base located at the designated position relative to the adenine-N3 alkylation site. [b] The numbers in parentheses give the percentage composition within the DNA examined.

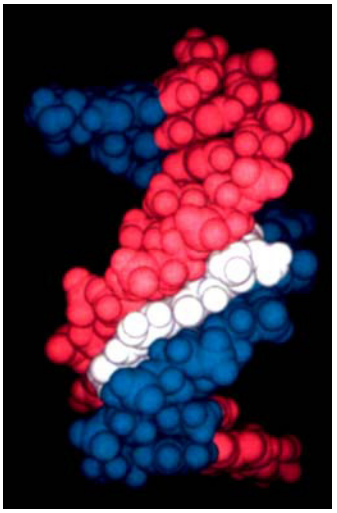

Fig. 26. Space-filling model of the covalent complex between (+)-duocarmycin SA and d(GACTAATTGAC)·d(GTCAATTAGTC) produced by molecular dynamics simulations restrained by NMR-derived distance constraints [110].

alkylation site found in w794 DNA, and (+)-duocarmycin SA has been conducted.[110] The studies, which have provided a high-resolution solution structure of the covalent complex, confirm the accuracy of the original models by disclosing the adenine-N3 alkylation and 3′ → 5′ binding in the minor groove across the 5′-ATTA site (Fig. 26).

A complex of (+)-CC-1065 with d(CGATTAGC)·d(GCTAATCG) has been studied by NMR.[111] The agent is covalently attached to the N3 atom of the A6 residue and binds in the 3′ → 5′ direction across five base pairs in the minor groove. A complex of (+)-CC-1065 with d(GGCGGAGTTAGG)·d(CCTAACTCCGCC) has also been characterized.[69, 112] In these studies, the alkylated adenine was shown to exist in the protonated form in which the two hydrogens were located on the exocyclic C6-amino group.[112] Since no phosphate in the backbone lies close enough to have protonated the C4 carbonyl, it was suggested that an intervening water molecule mediates this protonation by bridging the phenolic proton of CPI and the phosphate between A16 and A17. A very small ^{17}O (H_2O^{17}) isotope effect on line broadening of this phenolic proton NMR signal was observed and used to support this proposal[69] and the suggestion that this interaction may provide a molecular basis for the DNA alkylation sequence selectivity of (+)-CC-1065 and its analogs. However, it was later shown that the results of the ^{17}O experiments cannot be simply attributed to a purported tightly bound water molecule as earlier proposed.[47] Following adduct formation, the 12-mer duplex becomes bent (17–22°) about a locus lying between T8 and T9, which leads to a narrowing of the minor groove in this region.

A complex of (+)-CPI-$CDPI_2$ with $d(CGCTTAAGCG)_2$ has also been studied.[113] The NMR data support formation of a major adduct at A7 in which the agent binding is oriented toward the 5′ end of the alkylated strand.

A site-specific covalent adduct of duocarmycin A with an intramolecular DNA triple helix has been examined.[114] In this complex, duocarmycin A was found to bind and alkylate in the minor groove at a single adenine in the sequence 5′-AAAA-3′ in a manner analogous to duplex DNA alkylation. The bound duocarmycin A in the minor groove does not expel the third pyrimidine strand from the major groove of the triplex at low temperature and acidic pH. However, it did lower the pK_a for protonation of the third strand cytidines in the major groove by 1.8 pH units.

7. Modified Alkylation Subunits

As distinctions in the importance of the alkylation subunits of **1**–**3** and their contribution to the DNA alkylation profile surfaced, studies of modified alkylation subunits were initiated to address the problem directly. Agents containing deep-seated modifications in the alkylation subunit not accessible by simple derivatization could be anticipated to define the structural features contributing to functional reactivity and regioselectivity, to define the extent and contributing structural features effecting DNA alkylation selectivity or efficiency, and to delineate key fundamental relationships between structure, functional reactivity, and biological properties.

7.1. CI: Minimum Potent Pharmacophore of the Alkylation Subunits and Common Pharmacophore in the Natural Products

One of the first class of agents examined incorporated the parent alkylation subunit 1,2,7,7a- tetrahydrocyclopropa-[*c*]indol-4-one (CI, Fig. 27). Consistent with expectations, the CI-based agents proved to be exceptionally reactive electrophiles. In spite of this large change in the structure and relative reactivity of the alkylation subunit, the DNA alkylation selectivities of the agents **27** and **34** were remarkably similar to the natural products **1** and **2**/**3**, respectively, and their examina-

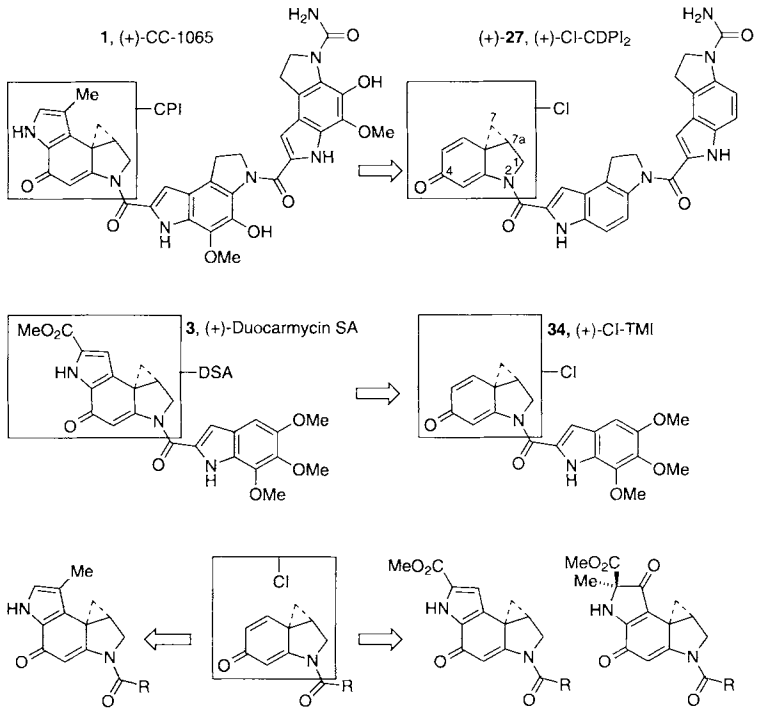

Fig. 27. CI: the minimum potent pharmacophore of the alkylation units of CC-1065 (top, including the atomic numbering for CI) and duocarmycin (center) and thus the common pharmacophore of CC-1065 and the duocarmycins (bottom).

tion provided more insight into the relative importance and role of the alkylation subunit than anticipated.[55, 56, 72, 115, 116] At the time the studies were conducted, the purported importance of the alkylation subunit was so heavily emphasized that the simple removal of the CPI C7 methyl group, much less the entire pyrrole segment, was arguably considered detrimental to the DNA alkylation selectivity.

The CI alkylation subunit was shown to constitute the minimum potent pharmacophore of the natural products' alkylation subunits and the common pharmacophore of CC-1065 and the duocarmycins. The exceptionally reactive CI-based agents alkylated the same sites as the corresponding CPI- or duocarmycin-based agents, but did so with lower efficiency and less selectivity among the available sites. Importantly, no new adenine-N3 alkylation sites were detected despite a 1000 × increase in reactivity. This observation provided the initial indication that the nature of the alkylation reaction was not as critical to DNA alkylation selectivity as suggested by others.[46] Consistent with their instability the CI agents alkylated DNA less efficiently and exhibited a pronounced decrease in cytotoxic potency.

7.2. CBI: A Simplified and Improved Alkylation Subunit

Similarly, the examination of the class of agents containing the 1,2,9,9a-tetrahydrocyclopropa[*c*]benz[*e*]indol-4-one (CBI) alkylation subunit, in which the deep-seated change is the replacement of the fused pyrrole with a fused benzene ring (Fig. 28), proved important and timely.[115–125] The anticipated release of strain that accompanies the ring expansion of the fused aromatic ring led to decreased reactivity and increased stability relative to the CPI alkylation subunit (4 ×) and increased cytotoxic potency (4 ×) without affecting the DNA alkylation selectivity. The CBI-based agents alkylated the same sites as the corresponding CPI or DSA-based agents and with an efficiency and relative selectivity consistent with their reactivity. They were more efficient and more selective among the available alkylation sites than the corresponding CPI-based or DA-based agents and comparable to the DSA-based agents. Despite their diminished reactivity, the CBI-based agents alkylated DNA at a faster rate than the corresponding CPI-based agent[119, 120] and at a rate comparable to that observed with the corresponding DSA-based agent.[73] This has suggested that the degree of steric bulk surrounding the C7 center of CPI or DSA may affect both the rate and relative efficiency of DNA alkylation and that the CPI C7 methyl group, once projected as important, may actually diminish the inherent properties of the CPI-based agents.

An examination of the CBI- and CI-based agents led to the proposal that a direct relationship exists between cytotoxic potency and functional stability. At the time these observations were made, the prevailing expectation was that the reverse relationship between functional reactivity (not stability) and cytotoxic potency was important[46, 159] and that even modest changes in the alkylation subunits would adversely, not productively, influence the DNA alkylation and biological properties of the agents. Consequently, the results from the CBI-based agents led to a shift in the paradigms of the field. Most importantly, it also revealed that in vivo antitumor efficacy[121, 166] may be observed in agents containing deep-seated and simplifying structural changes in the alkylation subunit and that the potency of the naturally derived materials may be enhanced by simply enhancing chemical stability. Although the sites of DNA alkylation are not altered, the rate and efficiency are increased, and the inherent selectivity among the available sites may be increased by increasing the functional stability of the agent.

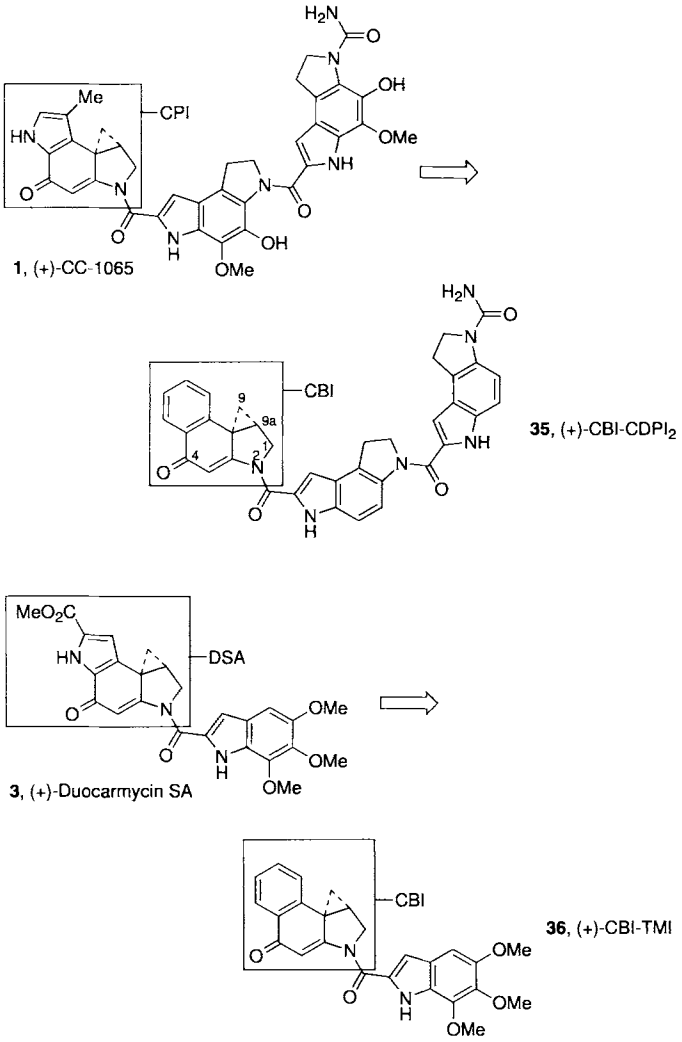

Fig. 28. CBI analogs of CC-1065 (top) and duocarmycin SA (bottom). The atomic numbering for CBI is shown in **35**.

7.3. MCBI and CCBI: Electronic Effects on Functional Reactivity

In the continued examination of the structural features that affect reactivity, the substituted CBI derivatives, MCBI (**37**)[126] and CCBI (**38**),[127] in which a C7 methoxy or cyano substituent has been placed *para* to the C4 carbonyl, have been recently prepared (Fig. 29). Their preliminary and ongoing examination has revealed an important and surprisingly small impact of the C7 substituent on the functional reactivity of the agents. This is discussed in detail in Section 8.

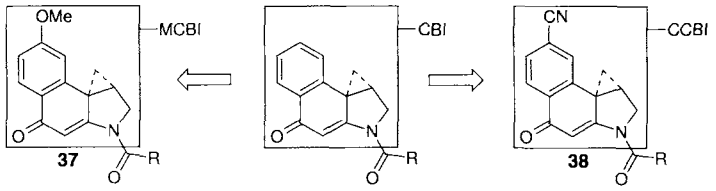

Fig. 29. MCBI and CCBI: structural elements used in the study of the electronic effects on the functional reactivity.

7.4. CBQ: An Exceptionally Reactive Alkylation Subunit

The ring expanded 2,3,10,10a-tetrahydrocyclopropa[*d*]-benzo[*f*]quinol-5-one (CBQ) alkylation subunit was prepared and incorporated into analogs of the natural products (Fig. 30).[128–130] Their examination revealed a surprising but

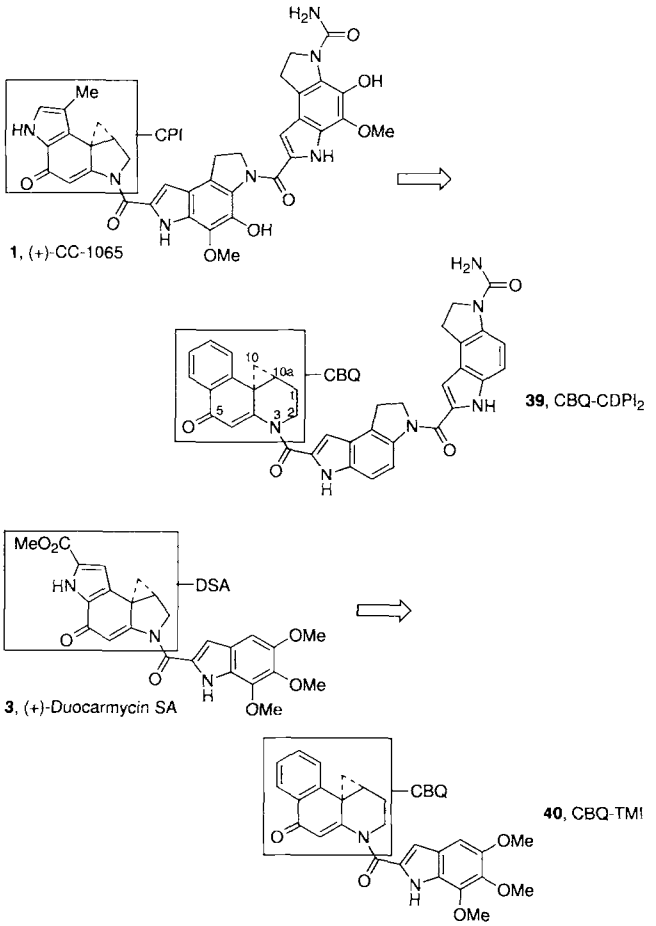

Fig. 30. CBQ-CDPI$_2$ (**39**) and CBQ-TMI (**40**): an alkylation unit showing exceptional reactivity.

normal level of functional reactivity and a number of subtle structural features that impact this reactivity,[128, 129] reaction regioselectivity,[129] and mechanism of acid catalyzed solvolysis and nucleophilic addition,[129] as well as subtle factors contributing to the adenine-N3 alkylation regioselectivity.[130] These are discussed in detail in Section 8.

7.5. C_2BI-CDPI$_2$ and C_2BI-TMI: Exquisitely Designed Adenine–Adenine Cross-Linking Agents

The core structure of C_2BI-CDPI$_2$ and C_2BI-TMI and their achiral precursors **41** and **42** (Fig. 31) was taken from the CBI-based agents, which are exceptionally stable and synthetically more accessible than the core structures of the natural alkylation subunits.[131, 132] In addition, the acyclic agents **41** and **42** lacking the preformed cyclopropane ring could be expected to

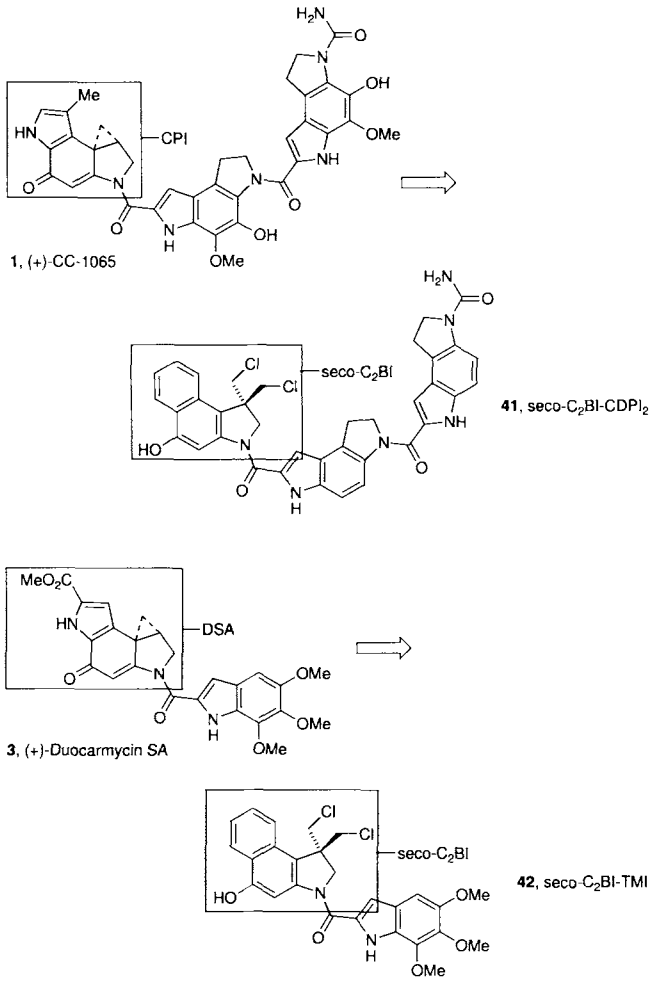

Fig. 31. Achiral precursors of C_2BI-CDPI$_2$ (**41**) and C_2BI-TMI (**42**): DNA cross-linking agents.

display properties identical to C_2BI-CDPI$_2$ and C_2BI-TMI, but are achiral. This simple feature of **41** and **42** not only provided attractive synthetic candidates that did not require resolution or asymmetric synthesis, but also a single agent for biological evaluation free of the necessity of documenting the behavior of both enantiomers.

In addition, the bis-alkylating capabilities of **41** and **42** provided the opportunity to cross-link DNA in which their two alkylating groups act independently as the individual enantiomers. When this occurs within a sequence such as d(AT-TA)·d(TAAT), the adenine-N3 alkylation by the natural enantiomer component of **42** occurs at its high-affinity site of 5′-ATTA-3′ with agent binding in the 3′ → 5′ direction relative to

the strand it alkylates, across a 3.5 base, AT-rich site. The alkylation by the unnatural enantiomer component of **42** is directed to the complementary strand, leading to cross-linking with adenine-N3 alkylation at its high-affinity site of 3′-TAAT-5′ with agent binding in the reversed 5′ → 3′ direction relative to the strand it alkylates, across a 3.5 base AT-rich site (Fig. 32).

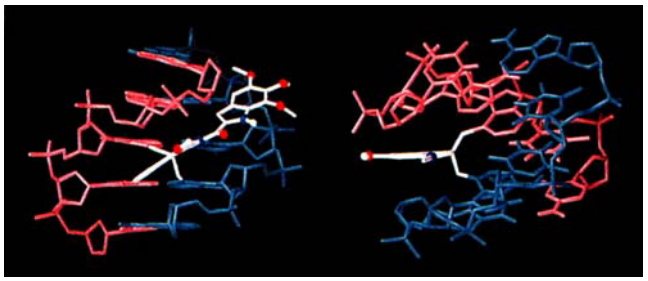

Fig. 32. View from the front and from the groove of the product of the cross-linking reaction of C_2BI-TMI in the w794 DNA high-affinity site (5′-(ATTAG)·5′-(CTAAT)). For details, see text.

Consistent with the fact that the reversed binding orientation and the offset AT-rich binding sites relative to the alkylated adenine of both enantiomers coincide in a single binding and cross-linking site, **41** and **42** were found to be efficient cross-linking agents.[131, 132] Figure 32 gives an alternative depiction of DNA alkylations by the natural and unnatural enantiomers, where complementary strand reactions occur from one binding orientation.

Additional cross-linking agents have been disclosed, including **43**, which is based on the CC-1065 structure and constructed by linking two CPI units together (Fig. 33).[133–142]

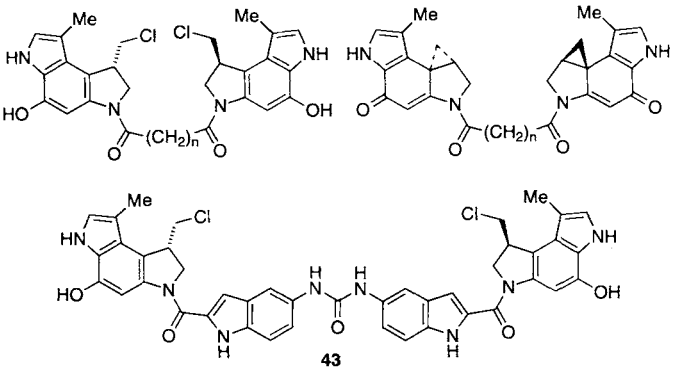

43

Fig. 33. Structures of additional DNA cross-linking agents.

7.6. Other Modifications in the DNA Alkylation Subunits

A number of agents incorporating additional modifications in the DNA alkylation subunits are shown in Figure 34. These include agents with alteration of the duocarmycin A and B_2 alkylation subunits,[143] furan analogs of CC-1065[144] and duocarmycin SA,[143] substituted CI analogs,[145] a simplified cyclopropyl derivative,[146] a gramine analog related to the CPI unit,[147] the 9,9-difluoro-CBI derivative,[148] and an isomeric cyclopropacyclohexadienone that combines the features of both CC-1065 and the mitomycins.[149]

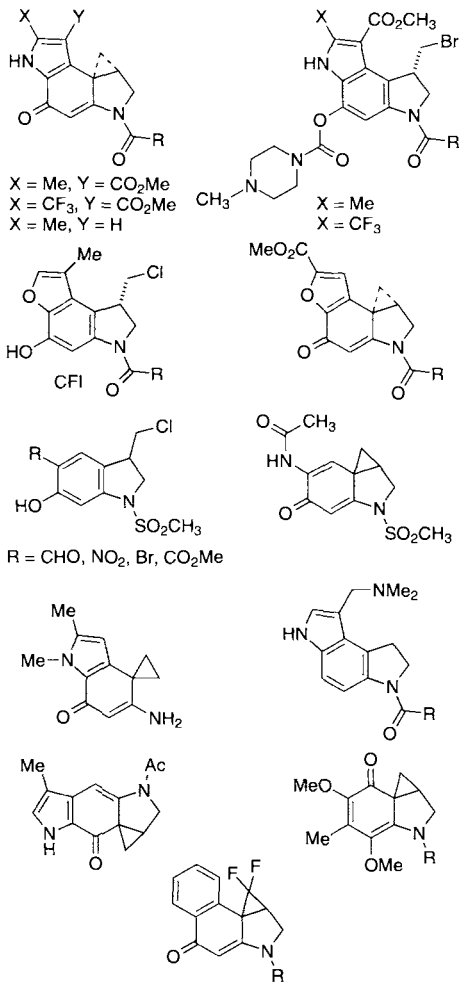

Fig. 34. Other modifications in the DNA alkylation subunits of CC-1065 and the duocarmycins.

8. Fundamental Relationships Between Structure, Functional Reactivity, and Biological Properties

In addition to the total synthesis of the natural products (CC-1065 (**1**),[77, 150–152] duocarmycin A (**2**),[153, 154] and duocarmycin SA (**3**),[155–157]) and the extensive number of investigations directed at the authentic subunits of the natural products[41, 50] and their analogs,[158–162] studies that have provided agents containing deep-seated structural modifications have proven valuable in defining the relationships between structure, functional reactivity, and biological properties.[34–38]

8.1. Definition of a Fundamental Relationship Between Functional Reactivity and Biological Activity

The proposed acid catalyzed activation of the DNA alkylation reaction led to the expectation that a direct relationship may exist between the reactivity and cytotoxic activity of the

agents and to the proposal that the biological potency may be enhanced as the electrophilic reactivity is increased.[159] However, studies conducted with the agents **44**–**51** revealed the reverse relationship and that the most stable agents may be expected to exhibit the most potent cytotoxic activity (Fig. 35). Moreover, a well-defined, direct relationship between stability toward solvolysis and biological potency (IC_{50}, L1210) has been observed and proved to be general with both simple and full analogs of the natural products.[118–121, 126, 129, 163, 166]

	k [s^{-1}]	$t_{1/2}$ [h] (pH 3)	IC_{50} [nM]
N-BOC-DSA	1.08×10^{-6}	177	6
N-BOC-CBI	1.45×10^{-6}	133	80
N-BOC-MCBI	1.75×10^{-6}	110	100
N-BOC-CPI	5.26×10^{-6}	37	330
N-BOC-DA	1.75×10^{-5}	11	1000
N-BOC-CBQ	9.07×10^{-5}	2.1	2000
N-BOC-Cl	1.98×10^{-2}	0.01	18000

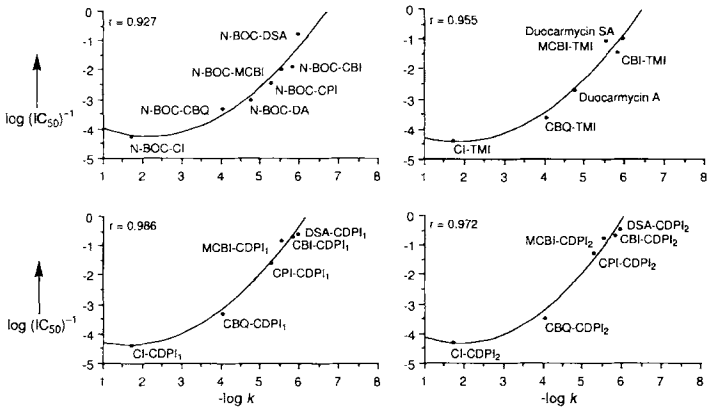

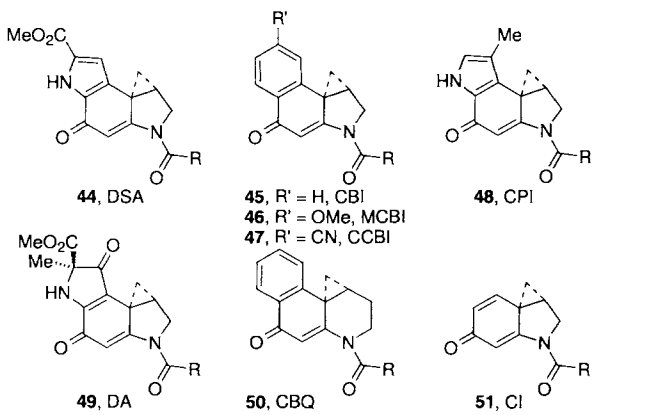

Fig. 35. Direct correlation between chemical or functional stability and cytotoxic potency of analogs of the natural products. R represents BOC, TMI, CDPI, or $CDPI_2$ shown in the graphs. N-BOC-**44** is identical to **12**. The unit for IC_{50} in the top right plot is nM; in all the other plots it is pM.

8.2. Establishment and Verification of a Fundamental Relationship between Functional Reactivity and Biological Activity

Examination of the properties of **52**–**55**,[163] simple derivatives of CBI, led to the validation of this direct relationship between solvolysis stability and cytotoxic potency (Fig. 36). Their examination revealed a direct, linear relationship between

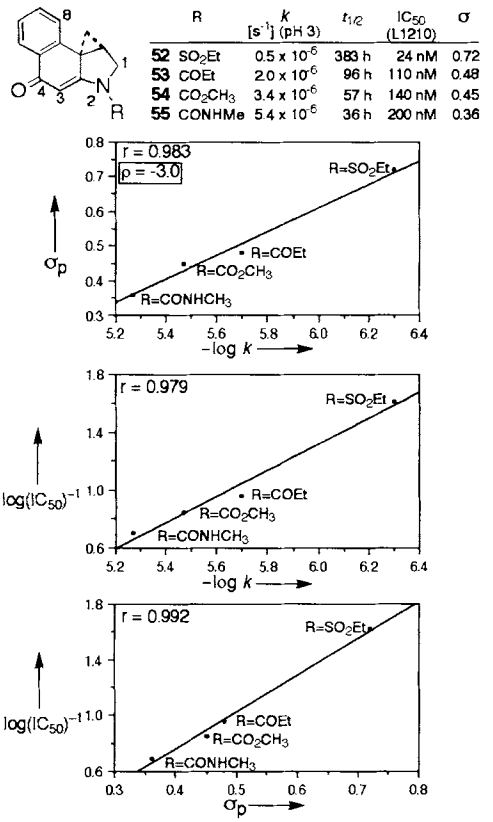

Fig. 36. Effect of the N2 substituent on the cytotoxic activity and the rate of solvolysis.

the cytotoxic potency (L1210, $\log 1/IC_{50}$) and the solvolytic stability ($-\log k$, pH 3) within the reactivity range examined. Similarly, a linear relationship was found between the electron-withdrawing properties of the N2 substituents (Hammet σ_p constant) and the solvolysis reactivity ($-\log k$, pH 3) in which the strongest electron-withdrawing substituents provide the most stable agents. This latter relationship reflects the influence of the N2 substituent on the ease of C4 carbonyl protonation required for catalysis of solvolysis, and those with the stronger electron-withdrawing substituents exhibit the slower solvolysis rates. Moreover, the slope of the plot of σ_p versus $\log k$ revealed a remarkably large ρ value of -3.0. This large negative ρ value is indicative of the strong vinylogous amide conjugation and suggests that the reactivity may be greatly influenced by the nature of the N2 substituent and its interaction with the cyclopropylcyclohexadienone. Less obvious but more fundamental, the observations follow a predictable linear relationship between the cytotoxic potency (L1210, $\log 1/IC_{50}$) and the electron-withdrawing properties of the N^2 substituent (σ_p). The agents with the strongest electron-withdrawing substituents proved to be the most potent agents (Fig. 36).

These fundamental correlations between the functional reactivity of the agents and their biological potency should prove useful in designing new analogs. For agents that possess sufficient reactivity to alkylate duplex DNA, the chemically more stable agents are predicted to be the biologically more potent agents. Presumably this may be attributed to the more effective delivery of the more stable agents to their intracellular target.

8.3. Substituted CBI substrates: Magnitude of Electronic Effects on Functional Reactivity and the Verification of the Fundamental Relationship between Functional Reactivity and Biological Activity

In efforts to address the structural features of **1**–**3** that contribute to their functional reactivity, the substituted CBI agents **46** and **47** (see Fig. 35) and a full set of analogs of the natural products that incorporate these modified alkylation subunits have been prepared.[126, 127] Against expectations, the nature of the C7 substituent, which is *para* to the C4 carbonyl, had only a very modest effect on the functional reactivity of the agents. On using acid catalyzed solvolysis as a measure of their relative reactivity, **46** was found to be only 1.2 to 1.05 times more reactive than the parent **45**, and **47** less than twice as stable at pH = 3 or 2 (Fig. 37). These studies provided a clear validation of the direct relationship between functional stability and cytotoxic potency and revealed a predictable direct relationship between the electronic properties of the C7 substituent (σ_p constant) and the functional reactivity ($-\log k$, pH 3), a direct relationship between the cytotoxic potency (L1210, $\log 1/IC_{50}$) and functional stability ($-\log k$, pH 3), and a fundamental, direct relationship between cytotoxic potency (L1210, $\log 1/IC_{50}$) and the electronic properties of the C7 substituent (σ_p constant); again the strongest electron-withdrawing substituent provided the most potent agent (Fig. 37). Importantly, the very modest effect of the C7 substituent on the functional reactivity was reflected in the determination of the exceptionally small ρ value of -0.3.

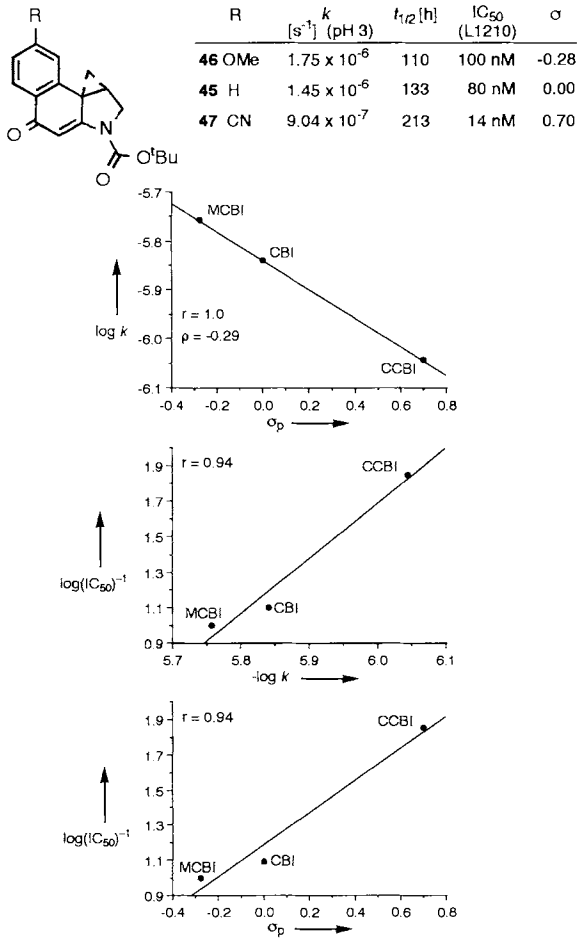

R	k [s^{-1}] (pH 3)	$t_{1/2}$ [h]	IC_{50} (L1210)	σ
46 OMe	1.75×10^{-6}	110	100 nM	-0.28
45 H	1.45×10^{-6}	133	80 nM	0.00
47 CN	9.04×10^{-7}	213	14 nM	0.70

Fig. 37. Electronic effects of the substituted CBI analogs **45**–**47**.

This surprisingly modest effect of the *para* C7 substituent suggests that protonation of the C4 carbonyl may not be the rate-limiting step of solvolysis or acid catalyzed nucleophilic addition and that little charge buildup at the substitution site occurs in the transition state ($\rho = -0.3$). Further study with these agents (Section 8.6) also supports the proposal that the cyclopropane ring opening requires the presence and assistance of a nucleophile (S_N2 mechanism). No doubt this contributes to the DNA alkylation selectivity and is consistent with the expectation that the positioning of the nucleophile (adenine-N3) and not C4–O protonation is the rate-determining event. This remarkably small electronic effect on the solvolysis rate had no impact on the solvolysis regioselectivity, and stereoelectronically controlled nucleophilic addition to the least substituted cyclopropane carbon was observed exclusively.

8.4. Stereoelectronic Control

Two characteristics of the alkylation subunits **44**–**51** have proven important in the studies to date. The first is the stereoelectronically controlled, acid catalyzed opening of the cyclopropane, which dictates addition of a nucleophile to the least substituted carbon. The second is the rate of acid catalyzed solvolysis and the demonstration of a direct relationship between solvolysis stability and cytotoxic potency. A recent comparison of the chemical and structural properties of N-BOC-**50** and N-BOC-**45** confirmed the stereoelectronic control of the solvolysis or alkylation reactions of **44**–**51** and revealed an unappreciated but fundamentally important stability for the duocarmycin and CC-1065 alkylation subunits and its structural origin.[128, 129] The solvolysis reactivity of **50** along with that of **44**–**51** are summarized in Figure 35. In addition to the increased reactivity of **50** (63 ×) relative to that of N-BOC-**45**, the solvolysis of **50** occurs with nucleophilic addition to both C10 and C10a, while that of **45** occurs exclusively at the least substituted cyclopropane carbon atom (Scheme 3).[129]

The X-ray structure of N-BOC-**50**[128, 129] provided the structural insights into this difference in solvolysis reactivity and regioselectivity (Scheme 3). It is clear from the X-ray structure of CBI[118, 128] that the bent orbital of the cyclopropane bond extending to the least substituted carbon is nearly perpendicular to the plane of the cyclohexadienone and consequently overlaps nicely with the developing π system of the solvolysis product phenol (Fig. 38), whereas the cyclopropane bond extending to the tertiary carbon is nearly in the plane of the cyclohexadienone, and its orbital is nearly orthogonal to the π system of the product phenol. Thus, opening of the cyclopropane occurs with addition of a nucleophile to the least substituted carbon, and the stereoelectronic control responsible for this addition selectivity overrides the intrinsic electronic preference for ring-expansion ring opening. In contrast, N-BOC-CBQ exhibits different characteristics. The cyclopropane is ideally conjugated with the cyclohexadienone π system, the plane defined by the

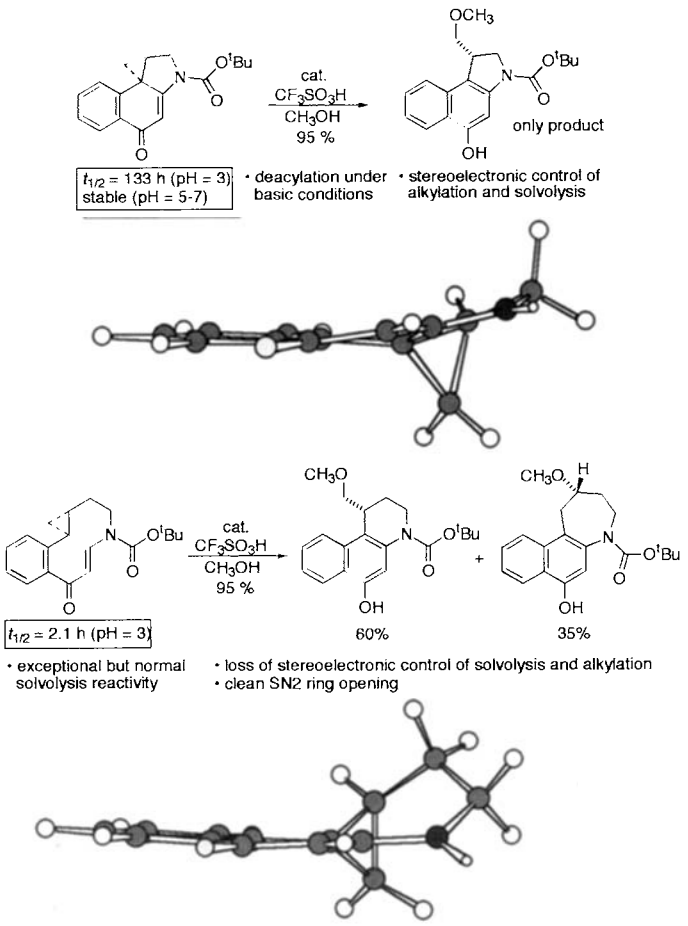

Scheme 3. Comparison of the solvolysis reactivity and X-ray structures of N-BOC-**45** (top) and N-BOC-**50** (bottom).

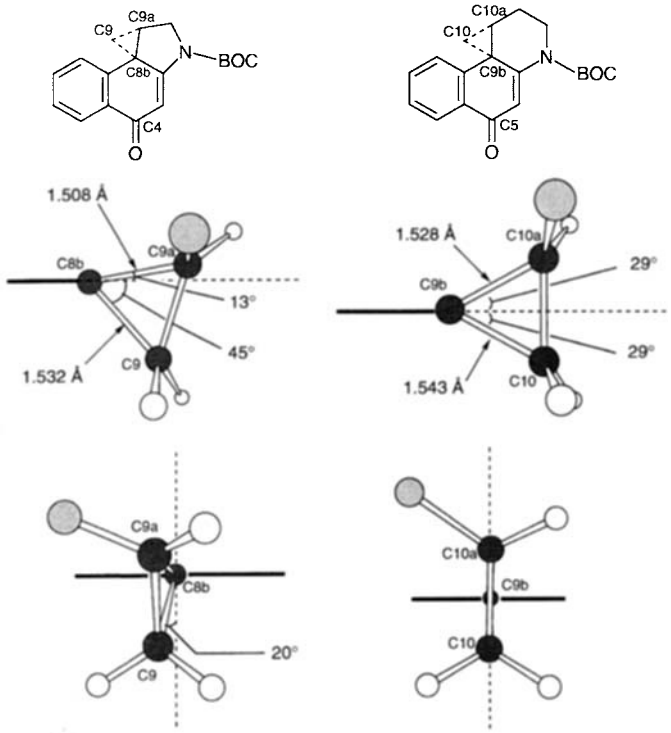

Fig. 38. Side and rear views of the activated cyclopropane rings of **45** and N-BOC-**50**, illustrating data taken from the X-ray crystal structures and highlighting the idealized overlap and alignment of the cyclopropane ring of N-BOC-**50** with the cyclohexadienone π-system.

cyclohexadienone ideally bisects the cyclopropane, and the bonds extending to the secondary and tertiary cyclopropane carbon atoms are equally aligned with the π system. Thus, the two available cyclopropane bonds are equally aligned for cleavage, and addition to both occurs.[129] The subtle differences in the relative amounts of the ring-expanded solvolysis product may be attributed to destabilizing torsional strain that accompanies nucleophilic attack at the more substituted center.

In contrast to the CBI-based agents, which react regiospecifically to provide exclusively one acid catalyzed addition product under a wide variety of reaction conditions, both N-acyl-CPI and N-acyl-DA agents (including duocarmycin A) have been shown to provide variable amounts of the abnormal ring expansion solvolysis products depending on the reaction conditions. To date, this has not been investigated in detail, and the structural origin of the minor ring expansion reaction with CPI or DA has not been established. It may be related to their increased reactivity or different degrees of stereoelectronic alignment derived from subtly altered cyclopropane conjugation. The delineation of the structural origin of these distinctions may, no doubt, be derived from comparative crystallographic studies of the respective alkylation subunits, and such detailed studies are in progress.

8.5. Structural Origin of an Unappreciated but Productive Stability of the Natural Alkylation Subunits: Extent of Cyclopropane Conjugation and Activation

The rapid solvolysis of N-BOC-CBQ was initially surprising; however, important insights into this enhanced reactivity are clear from the X-ray structures. Although they reside in a cyclopropane fused to a six- rather than a five-membered ring, the lengths of the CBQ C9b–C10a (1.528 Å) and C9b–C10 (1.543 Å) bonds are greater than those found in CBI (1.508 and 1.532 Å, respectively) and nicely reflect the enhanced cleavage reactivity[128] (Fig. 38). This lengthening of the cyclopropane bonds may be attributed to the idealized conjugation or π delocalization of both the C9b–C10a and C9b–C10 cyclopropane bonds with the cyclohexadienone π-system. Contributing to this enhanced conjugation is the ideal geometrical alignment of C10 and C10a with C9b, C5, and the carbonyl oxygen atom. For CBI, the constraints of the fused five-membered ring place its C9 and C9a at a 20° angle off this plane and prevent ideal alignment and overlap of either the C8b–C9a or C8b–C9 bond with the cyclohexadienone π system. This idealized cyclopropane conjugation with the cyclohexadienone π system in N-BOC-**50** results in the observed longer and weaker bonds and higher solvolysis reactivity.

Thus, the geometrical constraints of the fused five-membered ring found in the CC-1065 or duocarmycin alkylation subunits impose stereoelectronic control on the nucleophilic cleavage of the cyclopropane dictating addition to the least substituted carbon atom. In addition, the nonideal alignment and overlap of the cyclopropane with the cyclohexadienone π system found in the naturally occurring alkylation subunits result in diminished electrophilic reactivity. The fundamental insight derived from these comparisons is not the solvolysis reactivity of N-BOC-**50**, but rather the surprising stability of the CBI, DSA, and CPI

alkylation subunits. In spite of structural features that intuitively suggest high reactivity, the latter agents are uncharacteristically stable. This unusual stability is imposed by fusion of the cyclopropane to the five-membered ring, which constrains it to a nonideal alignment and overlap with the cyclohexadienone π system.

8.6. Mechanism of Acid Catalyzed Solvolysis and Nucleophilic Addition

Studies with N-BOC-CBQ (**50**) also resulted in an unambiguous determination of the mechanistic course of the acid catalyzed solvolysis reaction. Both the racemate and the pure (+) isomer of **50** were subjected to acid catalyzed methanolysis (0.1 equiv CF_3SO_3H, CH_3OH, 25 °C, 1 h, 95%). The abnormal, ring-expanded solvolysis product derived from optically active **50** was formed with exclusive inversion of the configuration at the reacting center, which indicates an S_N2 ring-opening reaction.[129] The demonstration was unambiguous and contrasts the conclusions of Warpehoski and Harper[107] in which a free carbocation and an S_N1 mechanism has been invoked to account for the minor CPI ring expansion solvolysis products. These and related studies[127] with the CBI-based agents have also shown that the acid catalzyed nucleophilic addition displays a first-order dependence on both the acid and nucleophile concentration. Together, these studies illustrate that the slow step is not C4 carbonyl protonation, but rather nucleophilic addition to the activated cyclopropane following rapid and reversible protonation of the C4 carbonyl oxygen atom [Eq. (b)].

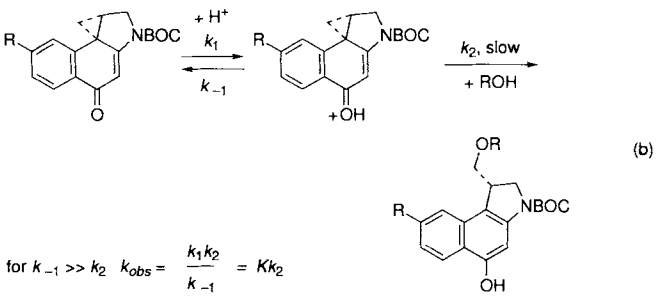

These studies have significant implications on the rate-determining step of the DNA alkylation reaction and, thus, the origin of the DNA alkylation sequence selectivity. Even though both of the CBQ cyclopropane bonds are equally aligned for cleavage, the acid catalyzed cyclopropane ring-opening reaction still occurs with a slight preference for normal rather than ring-expansion solvolysis. This latter pathway would be strongly preferred if substantial positive charge were to develop at the reacting cyclopropane carbon atom (secondary rather than primary carbocation character). The fact that it is not preferred and that reaction at the more substituted center occurs with full inversion of configuration by a strict S_N2 reaction mechanism further supports the prior kinetic evidence that the slow step of the reaction is not carbonyl protonation but rather the attack (or positioning) of the nucleophile, which preferentially occurs at the least hindered cyclopropane carbon.

8.7. Additional Subtle Features Contributing to the DNA Alkylation Regioselectivity

The examination of the DNA alkylation properties of CBQ-TMI (**40**) and related agents showed that they alkylated the same sites as the corresponding enantiomers of the agents incorporating the DSA, DA, CPI, CBI, or CI alkylation subunits.[130] Consistent with their reactivity, they exhibited less selectivity among the available sites and alkylated DNA with a lower efficiency. Importantly, only adducts derived from adenine-N3 addition to the least substituted cyclopropane carbon atom were detected under the relevant conditions of limiting agent concentrations. The adenine-N3 adduct obtained by thermal depurination was isolated, characterized, and shown to be derived only from addition to the least substituted cyclopropane carbon atom of CBQ-TMI (**40**). Since the CBQ-based agents exhibit nonselective solvolysis regioselectivity with cleavage of both the usual external and unusual internal cyclopropane bonds, the observations suggest that the clean regiochemical course of the characteristic adenine-N3 alkylation may benefit not only from stereoelectronic effects, but from additional features that complement the normal addition as well. These include the preferential adoption of binding orientations that favor the normal adenine-N3 addition (proximity effects), destabilizing torsional strain and steric interactions that accompany the abnormal adenine-N3 addition (Fig. 39), and a potential binding-induced conformational change in CBQ that imposes the stereoelectronic preference for adenine-N3 addition to the least substituted cyclopropane carbon (Fig. 40). Of these, the destabilizing torsional and steric interactions that accompany the abnormal adenine-N3 addition might be most significant and contribute similarly to the regioselectivity of the DNA alkylation reactions of **1**–**3** and related agents.[130]

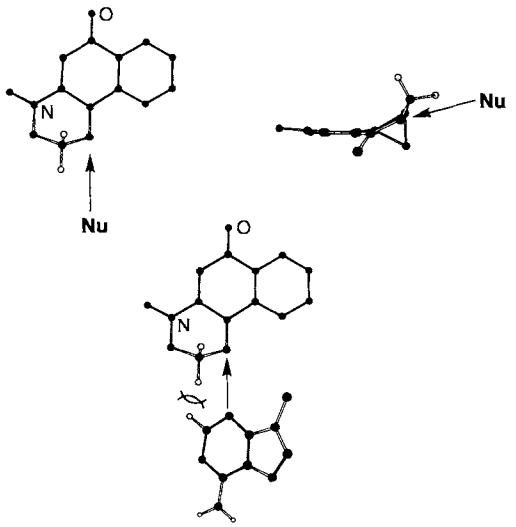

Fig. 39. Top and side views of the atypical nucleophilic addition to the most substituted cyclopropane carbon of CBQ. Top: Illustration of the eclipsing interaction between a nucleophile Nu and the C1-H^a, and the torsional strain that results from it. Bottom: The relative orientation of the reactants in the adenine-N3 addition taken from a model of a noncovalent complex of DNA and CBQ-TMI[130] when constrained in the minor groove. The diagram highlights the additional destabilizing steric interaction between Ad-C2-H and C1-H^a. The other hydrogen atoms and the trimethoxyindole subunit have been removed for clarity. In some formulas the cyclopropane ring is obscured.

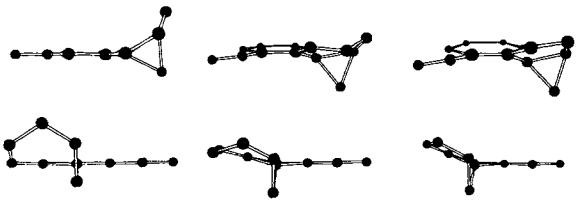

Fig. 40. Side and rear views of the CBQ boat (left, X-ray structure analysis [128,129]), CBQ half chair (middle), and CBI (right, X-ray structure analysis [118]) conformations, illustrating the relative orientations of the cyclopropane ring. Like in the case of CBI, the higher energy half-chair conformation of CBQ ($\Delta E = 1.0-1.5$ kcal mol^{-1}) would impose stereoelectronic control of the addition to the least substituted cyclopropane carbon atom. (Hydrogen atoms have been removed for clarity.)

8.8. Experimental Verification of Vinylogous Amide Stabilization: A Stable, Isolable *para*-Quinomethide

Because of the significant contribution of the vinylogous amide stabilization of the structures **44**–**51**, the *para*-quinomethide **56** and its stable precursors were prepared and examined (Fig. 41).[164] Unlike *para*-naphthoquinomethides, which are

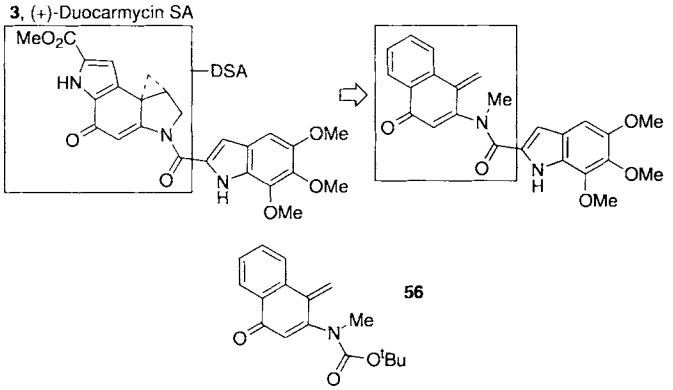

Fig. 41. *para*-Quinomethide (**56**) rendered isolable by vinylogous amide stabilization. For further information on **56**, see text.

not sufficiently stable for isolation, characterization, or detection and are inferred reaction intermediates, the *para*-quinomethide **56** was isolated (with SiO_2 chromatography!) and characterized. Although **56** is still exceptionally reactive and substantially more reactive than **44**–**51**, the unusual stability that permits its isolation may be attributed to this key vinylogous amide stabilization, which is lost upon aromatization.

8.9. Additional Key Features

A number of additional unique structural features of **44**–**51** also contribute to their stability. The stability ordering **44**–**48** > **49** > **51** can be attributed to the diminished gain in delocalization energy that accompanies aromatization in a system that bears a fused aromatic ring.[116,156] The increased stability ordering **44** > **48**, **47** > **45** and **49** > **51** can be attributed to the conjugated electron-withdrawing group which diminishes C4 carbonyl protonation required of solvolysis and alkylation.[126,127,156] The increased stability of **45** > **48** can be attributed in part to the release of strain that accompanies the substitution of a fused six-membered for a fused five-membered arene ring.[118,122] Finally, the vinylogous amide stabilization of the cyclohexadienone structure, which is lost upon aromatization, contributes significantly to the stability of **44**–**51**.[164]

8.10. Relationship Between Alkylation Subunit Structure and DNA Alkylation Selectivity

The agents containing the natural (CPI, DSA, or DA) or modified (CI, CBI, CBQ, CFI) alkylation subunits attached to the same DNA binding subunits have been found to alkylate the same sites. Notably, no new or unique sites or alterations in the DNA alkylation sequence selectivity attributable to structural changes in the alkylation sites have been disclosed. In such sequencing studies, the alkylations are conducted with a large excess of DNA and limiting agent concentrations, and consequently, minor or forced additional reactions are not observed (for instance, minor guanine-N3 alkylation). These selectivities, which have been experimentally derived and summarized elsewhere,[56,71,105,122,130,144] can also be extrapolated from the data presented in Tables 1, 3, and 6 for the DSA, DA, or CPI-based agents. The distinctions between the agents lie in the greater selectivity among the available sites observed with the chemically more stable agents (DSA ≥ CBI > CPI > DA > CBQ > CI). In addition, it is notable that the corresponding precursor agents lacking the cyclopropane (i.e., **4**–**7**) also alkylate the same sites. Although in most cases this may be attributed to their facile closure to the cyclopropane-containing agents under the conditions of the assay, important and key studies have shown that this is not necessarily required.[55,56,104,105]

8.11. Relationship Between Functional Reactivity, DNA Alkylation Rate or Efficiency, and Biological Properties

To date, the relative efficiency of DNA alkylation follows closely the relative cytotoxic potencies observed with the agents. As the alkylation subunit reactivity diminishes, the relative efficiency of DNA alkylation increases. This was presumed to be attributable to the nonproductive consumption of the more reactive agents. The assumption was confirmed in the initial[56] studies with duocarmycin A and reestablished in more recent investigations with duocarmycin A[61,62] and CBQ-TMI (**40**).[130] Similarly, as the size of the DNA binding subunits increase, the relative efficiencies of DNA alkylation increase to a maximum and then level off for agents that possess the same alkylation subunit. This is consistent with the expectation that an increase in the noncovalent binding affinity within the minor groove provided by the DNA binding subunits increases both the rate and efficiency of DNA alkylation. The maximum plateau in cytotoxic potency occurs at approximately the same point at which the relative efficiencies in DNA alkylation also reach a plateau, even though the DNA alkylation rates vary widely. Thus, although the relative cytotoxic potencies have been suggested to be directly related to the relative rates of DNA alkylation,[46] we have suggested that the cytotoxic potencies may more closely follow the trends in relative DNA alkylation

efficiencies.[71, 120] Since the DNA alkylation reactions are inherently reversible, it is attractive to suggest that the maximum plateau in the DNA alkylation efficiency and cytotoxic activity may be achieved only when the inherently reversible adduct formation is fully stabilized by a sufficiently strong noncovalent binding. This would seem to be validated in the recent studies with the 7-MCBI derivatives.[126]

Although the careful comparisons are limited in the studies conducted to date, the chemically more stable agents have not only been determined to alkylate DNA more efficiently but also to do so more rapidly. It is not intuitively obvious that this would be expected for a Brønsted acid or Lewis acid catalyzed reaction and may be a consequence of the limited number of agents examined to date. For example, the most reactive of the agents carefully examined to date are the CBQ-based agents, which have been shown qualitatively to alkylate DNA slower than the CPI-, CBI-, or DSA-based agents. Similarly, the CPI-based agents alkylate DNA with both a lower efficiency and lower rate than the CBI-based agents even though they are four times more reactive (Fig. 42). In contrast, the CBI-based agents alkylate DNA with efficiencies and rates that are both only slightly lower than those of the exceptionally stable DSA-based agents (Fig. 42). Thus, the chemically most stable class of agents examined to date also alkylate DNA at the fastest rate. It is also the class of agents that possess the smallest degree of inherent steric bulk on the inside concave face of the alkylation subunit especially surrounding the DSA C7 position. Thus, it may be that steric bulk surrounding this C7 center diminishes the inherent rate of DNA alkylation, and the agents examined carefully to date follow this trend (DSA > CBI > CPI).

9. Structural Origin of the Distinctions between Enantiomers: Sensitivity to C7 Steric Interactions

The studies have suggested an attractive explanation for the sometimes confusing behavior (relative DNA alkylation efficiency and relative biological potency) of pairs of enantiomeric agents that may be traced to a single structural feature: the degree of steric bulk surrounding the CPI or DSA C7 center within the alkylation subunit for which the unnatural enantiomers are especially sensitive. The distinctions between enantiomers have proven readily detectable with the simple alkylation subunits themselves (that is, N-BOC-DSA (**12**), -CI (N-BOC-**51**), -CPI (**13**), and -CBI (N-BOC-**45**)), are most prominent with the dimer-based agents (like duocarmycin SA, duocarmycin A, CBI-CDPI$_1$, CPI-CDPI$_1$ (**15**), and CPI-PDE-I$_1$ (**14**), Table 8, Fig. 43), and are less prominent with the larger trimer- or tetramer-based agents (CC-1065, CPI-CDPI$_2$ (**16**), CBI-CDPI$_2$, and CPI-CDPI$_3$ (**17**)).[54, 73] In general, less distinction in the biological potency and relative DNA alkylation efficiency has been observed with the CI and duocarmycin SA enantiomeric pairs, both of which lack substituents or steric bulk at this position within the alkylation subunit. Moreover, the distinctions among enantiomeric CI-based agents, which lack the pyrrole ring altogether, are generally smaller than those observed with the duocarmycin SA-derived agents (DSA > CI). In contrast, the CPI-, CBI-, and duocarmycin A-based agents generally exhibit more pronounced distinctions within enantiomeric pairs (CPI > duocarmycin A > CBI). This suggests that the behavior of the unnatural enan-

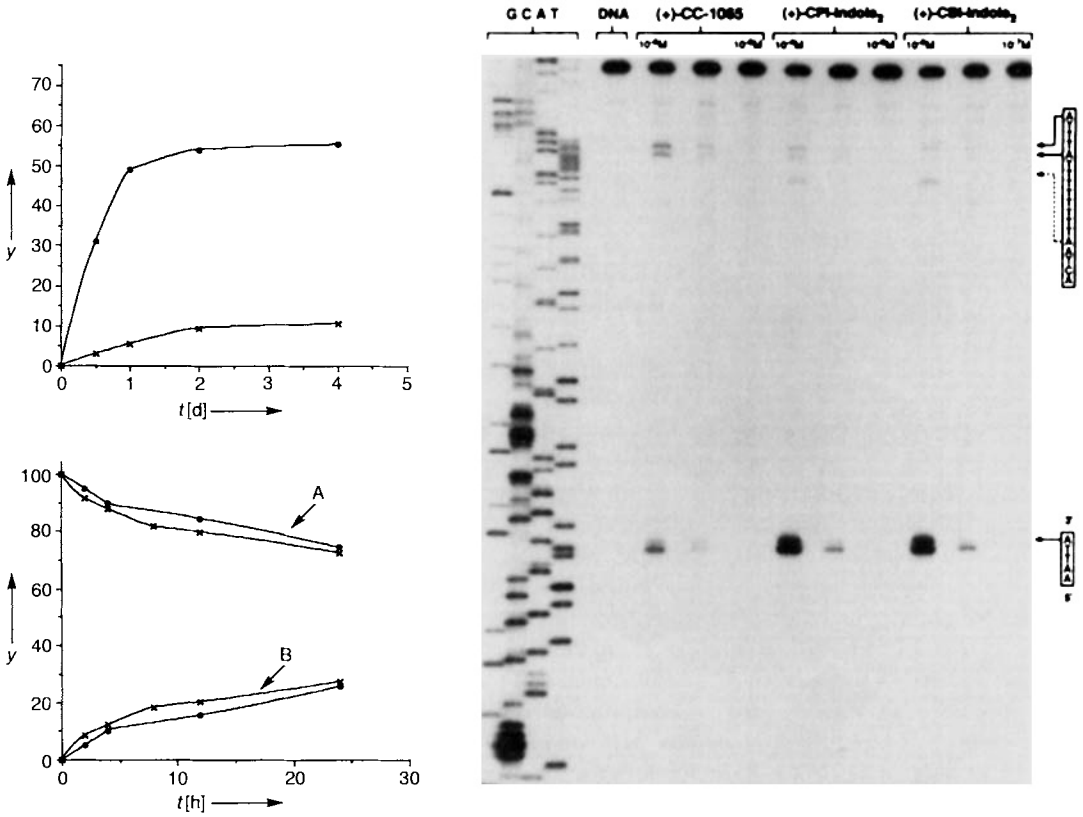

Fig. 42. Top left: Plot of percentage of integrated optical density (y) versus time, established through autoradiography of 5'-^{32}P end-labeled DNA and used to monitor the relative rate of w794 alkylation at the 5'-AATTA high-affinity binding site for (+)-CBI(indole)$_2$ (●) and (+)-CPI(indole)$_2$ (×); 37 °C, 0–5 days, 1×10^{-5} M agent. Bottom, left: Plot of percentage of integrated optical density (y) versus time, established through autoradiography of 5'-^{32}P end-labeled DNA and used to monitor the relative rate of w794 alkylation at the 5'-AATTA high-affinity binding site for (+)-duocarmycin SA (**3**, ×) and (+)-CBI-TMI (**36**, ●); 4 °C, 0–24 h, 1×10^{-6} M agent. A = unchanged DNA, B = alkylation/cleavage. Right: Thermally induced strand cleavage (by heating to 100 °C for 30 min) of double-stranded DNA (SV40 DNA fragment, 144 base pairs; nucleotide no. 138-5238, clone w794) after 24 h incubation of DNA with the agent at 4 °C, followed by removal of unbound agent with denaturing PAGE (8%) and autoradiography. Lanes 1–4, Sanger G, C, A, and T reactions; lane 5, control DNA; lanes 6–8, **1** (1×10^{-6}–1×10^{-8} M); lanes 9–11, (+)-CPI(indole)$_2$ (1×10^{-4}–1×10^{-6} M); lanes 12–14, (+)-CBI(indole)$_2$ (1×10^{-5}–1×10^{-7} M).

Table 8. Comparison of the natural and unnatural enantiomers of the agents.

Agent	Configuration	IC_{50}, L1210 [ng mL^{-1}]	rel. IC_{50}	[a]
(+)-CI-TMI	natural	10	1	0.5–2.0
(−)-CI-TMI	unnatural	10	1	
(+)-duocarmycin SA	natural	0.006	1	10
(−)-duocarmycin SA	unnatural	0.06	0.1	
(+)-CBI-TMI	natural	0.01	1	100
(−)-CBI-TMI	unnatural	0.9	0.01	
(+)-duocarmycin A	natural	0.1	1	>100
(−)-duocarmycin A	unnatural	>10	<0.001	
(+)-CI-CDPI$_1$	natural	10	1	0.5–2.0
(−)-CI-CDPI$_1$	unnatural	20	0.5	
(+)-DSA-CDPI$_1$	natural	0.002	1	10–100
(−)-DSA-CDPI$_1$	unnatural	0.06	0.03	
(+)-CBI-CDPI$_1$	natural	0.002	1	>100
(−)-CBI-CDPI$_1$	unnatural	>2	<0.001	
(+)-CPI-CDPI$_1$	natural	0.02	1	>100
(−)-CPI-CDPI$_1$	unnatural	>3	<0.006	

[a] The relative concentrations of the (unnatural/natural) enantiomers required to detect DNA alkylation.

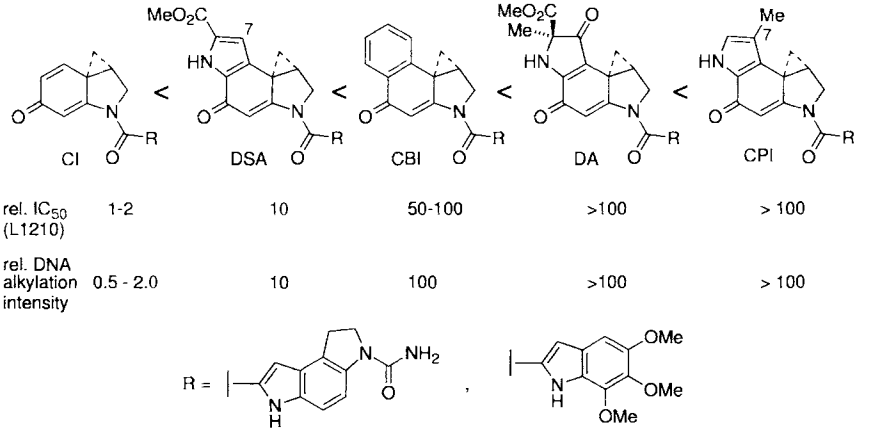

Fig. 43. Origin of the distinctions between the behavior of pairs of enantiomers toward DNA alkylation: steric bulk surrounding the DSA and CPI C7 center.

tiomer of duocarmycin SA as well as that of all agents studied to date is derived from a pronounced steric interaction of the C7 center with the 5′ base adjacent to the adenine N3 alkylation site necessarily present with the 5′ → 3′ binding of the unnatural enantiomer. The 3′ → 5′ binding model for the natural enantiomers benefits from a less substantial but still potentially significant sensitivity to steric bulk at this same C7 position.

Consistent with the empirical observations to date and in agreement with models of the alkylation adducts, the studies suggest that agents lacking steric bulk surrounding the position occupied by a CPI or duocarmycin SA C7 substituent are predictably more effective at alkylating DNA, that the unnatural enantiomers of such agents are especially sensitive to steric bulk at this position, and that as this steric bulk is reduced, the distinctions between the enantiomers diminish. The only exception to these generalizations was observed with the MCBI-based agents, where the properties of the two enantiomers are more similar than those of the enantiomers of the CBI-based agents.[126] This has suggested that such distinctions may be reduced or overcome by the introduction of additional noncovalent binding stabilization into the alkylation subunit itself.

10. Modified DNA Binding Subunits

One of the earliest and easiest structural features of the agents subjected to examination was the DNA binding subunits attached by an amide linkage to the naturally occurring alkylation subunits. These studies confirmed that hydrophobic righthand subunits convey binding affinity for the DNA minor groove, confer selectivity for binding at an AT-rich site in the minor groove, stabilize covalent adduct formation, accelerate the rate of DNA alkylation, contribute to and/or dominate the sequence selectivity of DNA alkylation,[108,109] and affect the physiochemical properties of the naturally occurring agents. Many of these issues are discussed in the context of the key analogs of CC-1065 and the duocarmycins described in Sections 2–5.

10.1. Systematic Substructure Examination of the CC-1065 DNA Binding Subunits

Early studies defined the degree of simplification and the optimum DNA binding subunits for analogs of CC-1065 that maintain the full potency of the natural product but improve in vivo antitumor efficacy. The PDE-I_2 subunits of CC-1065 could be reduced to $(indole)_2$ with full maintenance of cytotoxic potency and with significant enhancements in the in vivo antitumor activity (Fig. 44).[158–162] Further simplifications or reductions in the size of the DNA binding subunits (for example, $(indole)_1$) resulted in diminished properties, although the attachment of the trimethoxyindole (TMI) subunit of the duocarmycins has provided a potent agent.[165] This suggests that an appropriately substituted, single DNA binding subunit (for example, TMI or CDPI$_1$) may provide fully potent cytotoxic agents. Similar studies with the CBI-based agents have been conducted and have extended these observations (Fig. 44).[73,117–127,166]

Notably, this latter class of agents incorporating the synthetic and simplified CBI alkylation subunit and the simplified, synthetic $(indole)_2$ (**57**, Fig. 45) or TMI DNA binding subunits constitute synthetic, designed analogs of the natural products that possess potent and efficacious antitumor activity.[73,121,166] Consequently, a large degree of variation may be tolerated in this portion of the structure for optimization of the biological and physiochemical properties of the agents (Fig. 45).

We have advanced the proposal that it is not the kinetic rates of DNA alkylation[46] that are responsible for the difference in the cytotoxic potencies of the agents bearing a common alkylation subunit, but rather the relative efficiency of DNA alkylation and thermodynamic stability of the adducts.[38] Consistent with this proposal the cytotoxic potencies plateau for agents bearing a common alkylation subunit when sufficient noncovalent binding provides stable adducts. Moreover, this maximum potency is directly related to the functional stability of the agents. The chemically more stable agents provide the greatest

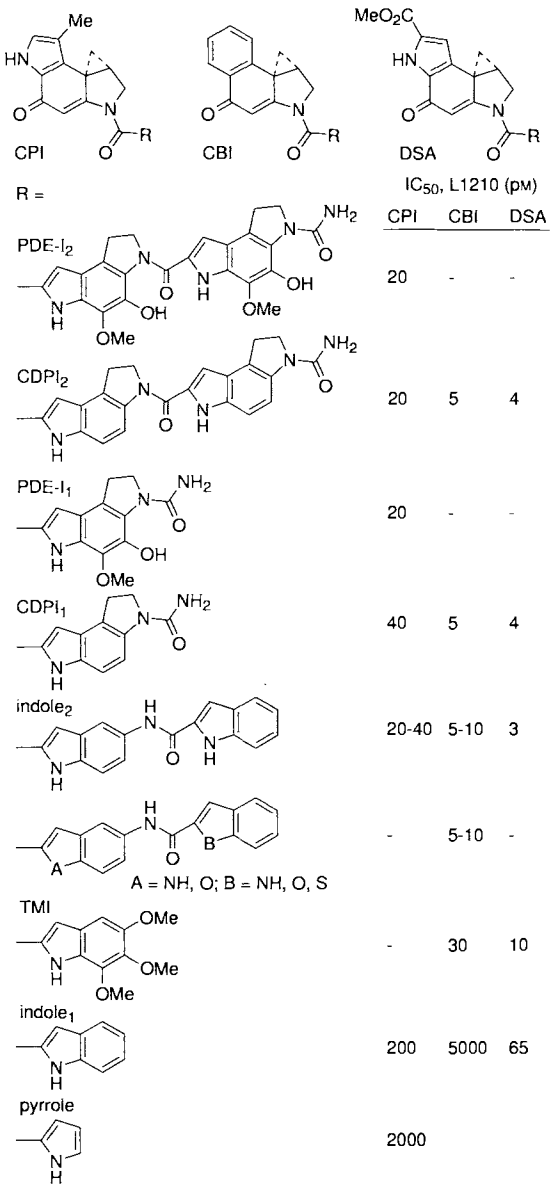

Fig. 44. Influence of the structure of the DNA binding subunits on the cytotoxic activity of CPI, CBI, and DSA analogous. The numbers on the right are the IC_{50} values (L1210) in pM.

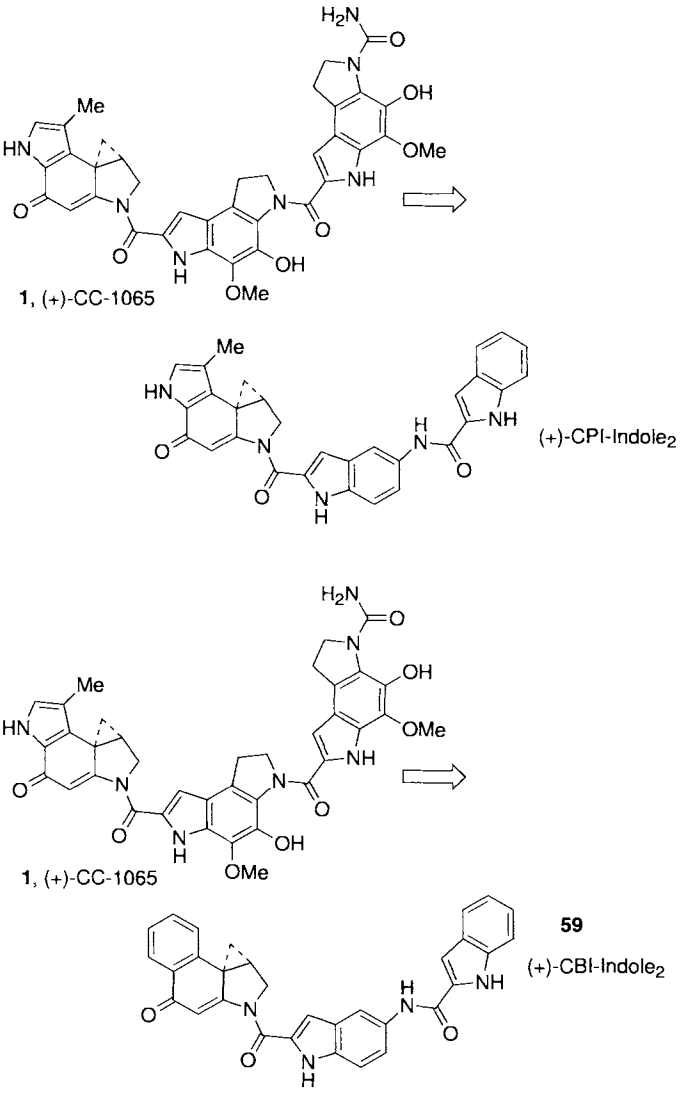

Fig. 45. (+)-CPI(indole)$_2$ and (+)-CBI(indole)$_2$: potent antitumor agents.

potency (CPI: 20pM, CBI: 5pM, DSA: 3–4pM). This is presumably because the chemically more stable agents reach their intracellular target more effectively.

10.2. Systematic Substructure Examination of the Duocarmycin DNA Binding Subunit

More recent studies systematically examined the role of the three methoxy substituents on the trimethoxyindole DNA binding subunit of duocarmycin SA.[109] The C6 and C7 methoxy substituents, which lie on the outer or peripheral face of the DNA–agent complexes, individually contribute only a small or no enhancement to cytotoxic potency and the relative efficiency of DNA alkylation (C6>C7), while the C5 methoxy substituent, which is deeply imbedded in the minor groove, contributes fully to such properties (Fig. 46). In fact, the agent with a single C5 methoxy substituent proved indistinguishable from the natural product indicating that it alone is sufficient for full potentiation of the properties. Consistent with the results of modeling studies detailed in early studies on CC-1065,[41] this may be attributed to the additional noncovalent binding stabilization provided by the C5 methoxy substituent imbedded in the minor groove.[82]

Importantly, the studies provided further key evidence supporting the proposal that the full potentiation of the cytotoxic potency of the agents is derived from noncovalent binding stabilization of an inherently reversible DNA alkylation rather than differences in the relative rates of DNA alkylation.[109]

10.3. Deep-Seated Modifications in the DNA Binding Subunits

Two interesting deep-seated modifications in the DNA binding subunits of the natural products have been detailed. The first was based on the disclosure that electropositive substituents placed on the outer face of the DNA binding subunits substan-

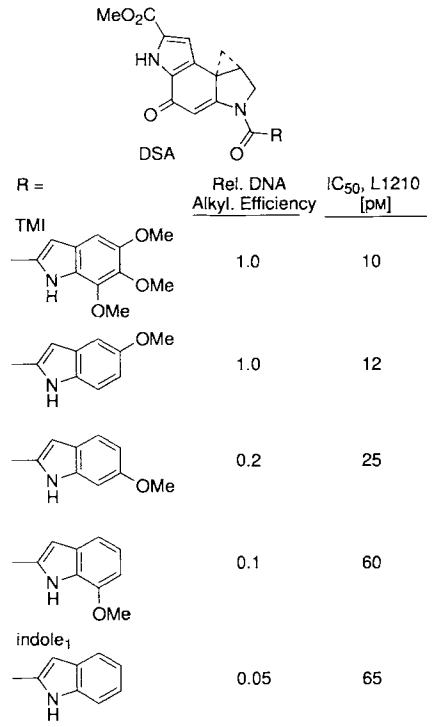

Fig. 46. The effect of methoxy substituents on the activity of duocarmycin SA analogs. Eff_{rel} = relative efficiency of the DNA alkylation.

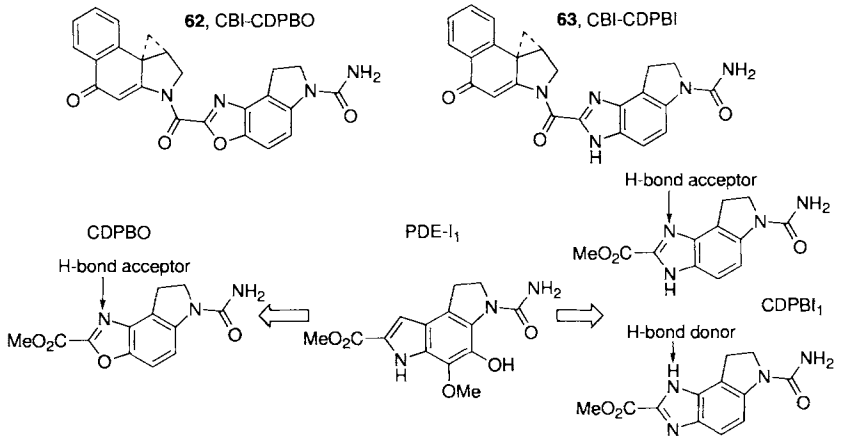

Fig. 48. CBI-CDPBO and CBI-CDPBI: model compounds with modified structural elements for DNA binding.

tially increase DNA binding affinity without affecting DNA binding selectivity and simultaneously increase water solubility. This may be attributed to a spatially well-defined stabilizing electrostatic interaction with the negatively charged DNA phosphate backbone.[83] These studies have been extended to **59–61** (Fig. 47) containing a quaternary ammonium salt on a single indole DNA binding subunit capable of providing this same strong electrostatic binding stabilization.[84] Consistent with expectations, the water soluble agents **59–61** alkylated DNA with the same efficiency as **1** or **3** and were one hundred times more effective than **58**, which lacks the positively charged group.

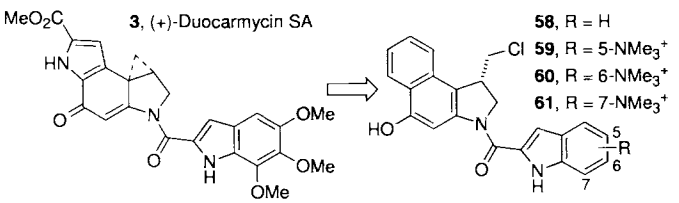

Fig. 47. Structures of **59–61**, the ammonium derivatives of **58**, as analogs of **3**.

The second important modification was based on the observations of Dervan[12, 167] and Lown[168] that the AT-rich, noncovalent binding selectivity of distamycin could be altered to accommodate a G-C base pair through introduction of a nitrogen into the backbone structure to serve as a hydrogen bond acceptor from a guanine C2-amine.[169] In analogy to such studies, the agents **62** and **63** were designed and prepared (Fig. 48).[170] They contain deep-seated modifications in the DNA binding subunits with incorporation of a nitrogen capable of serving as a hydrogen bond acceptor (CDPBO, CDPBI) or hydrogen bond donor (CDPBI) on their inside concave face, which is in intimate contact with the minor groove floor. The DNA alkylation selectivities of **62** and **63** are identical to those of CBI-CDPI$_1$ but with a substantially diminished efficiency (100×). Thus, the introduction of a single nitrogen atom had a pronounced and detrimental effect on the relative efficiency of DNA alkylation, but no apparent effect on DNA alkylation selectivity.

11. Biochemical Studies: Mechanism of Action

11.1. Apoptosis: A Link Between DNA Alkylation, Cytotoxic Activity, and Antitumor Properties

The first step in defining the link between DNA alkylation and effective antitumor activity was detailed in studies demonstrating that sensitive tumor-cell lines including L1210 and Molt-4 are triggered to undergo apoptotic cell death at agent concentrations (100 pM) below that required for typical cell death by necrosis observed in nonsensitive cell lines.[51] Apoptosis is a specific mechanism of cell death different from necrosis: cells undergo morphological changes including a characteristic heterochromatin condensation, degradation of genomic DNA, nuclear disintegration, and packaging of cell remains into apoptotic bodies that are removed by macrophages.

11.2. Cell Cycle Effects

The fundamental features of the cell cycle include growth, DNA replication, mitosis, and cell division. The cell cycle is divided into two parts—interphase and mitosis (M). The S phase (DNA synthesis) occurs in the middle of interphase and is preceded by G_1, the gap between mitosis (M) and DNA synthesis (S) and followed by G_2, the gap between replication and mitosis. The extent to which an antitumor agent affects these events has important implications on its mechanism of action. (+)-CC-1065 blocks progression of cells at G_2 and M.[49, 171–173] No effect was observed in the transitions

from M to G_1 or G_1 to S. At agent concentrations low enough to arrest the cell cycle at G_2 and M, cells were able to pass slowly through S phase even though CC-1065 inhibits DNA synthesis. Similarly, adozelesin (**65**, see Fig. 49) was found to cause G_2 arrest.[174, 175]

11.3. DNA Processing Enzymes

The alkylation of duplex DNA by CC-1065 and related agents inhibits many DNA processing enzymes[176] (including the S1 nuclease responsible for digestion of single strand DNA,[88] T4 ligase,[177] helicase[178–181]) and terminates DNA polymerase catalyzed DNA synthesis (replication) at the adduct sites.[182] The CC-1065 adenine-N3 adduct produces a pronounced inhibition and enhancement patterns of DNA cleavage upon DNase I or MPE-Fe^{II} footprinting.[183] Attempts to correlate agent structure with the extent of both the mutagenic effects of the adenine-N3 alkylation [184–191] and resistance[192–194] have been disclosed.

12. Delayed Toxicity

A serious limitation in the use of agents related to (+)-CC-1065 (**1**) is the characteristic, delayed fatal toxicity of the natural product.[52] When the toxicity of **1** was examined in non-tumor-bearing mice, an unusual form of lethal, delayed hepatoxicity was observed at therapeutic antineoplastic doses. At single dose levels of 12.5 $\mu g\,kg^{-1}$ administered intravenously (iv), delayed deaths were observed at 50 days, and at 10 $\mu g\,kg^{-1}$ single dose (ip) administration, delayed deaths were observed at 70 days. The mouse LD_{50} value (iv) was determined to be 9 $\mu g\,kg^{-1}$ single dose and 0.3 $\mu g\,kg^{-1}$ per day, five daily doses. These delayed deaths were accompanied by dramatic changes in the morphology of hepatic mitochondria. Animal pretreatment with agents that induce cytochrome P-450 metabolism was unsuccessful in preventing the toxicity of **1**. Importantly, the unnatural enantiomer of CC-1065, which is equally potent in vitro and equally efficacious in vivo, does not embody this property suggesting it is not inherent in the structure or a required consequence of the mechanism of action responsible for the productive antitumor activity. Similarly, most but not all CC-1065 analogs do not display this delayed toxicity nor do the duocarmycins and their analogs reported to date. Much speculation on the origin of this unusual property has been detailed.[47, 97, 176] Among the more intriguing is the suggestion that the delayed toxicity may be related to the degree of DNA alkylation reversibility and consequently the extent of the noncovalent binding stabilization of the reversible adduct.[37, 58] The agents whose absolute configuration (adducts of the natural enantiomers are more stable than those of unnatural enantiomers) and extent of noncovalent binding render the alkylation irreversible may be prone to this delayed toxicity. This suggests that the optimal agents may be those that form stable but not irreversible adducts. Regardless of whether this impacts on the delayed toxicity, this proposal implies that there may be inherent benefits to the use of the chemically most stable alkylation subunits whose degree of reversibility is greatest and whose nondiscriminant alkylation reactivity is diminished coupled with their attachment to an appropriately sized DNA binding subunit capable of providing stable but not irreversible adduct formation.

13. Clinical Candidates

Four agents that are analogs of **1** and contain the authentic CPI alkylation subunit or a seco precursor have been put forward as clinical candidates.[195, 196] The first two, **64** (U-71,184) and **65** (adozelesin), were derived from the first stage of studies on analogs of **1** in which systematic modifications, simplifications, and optimization of the DNA binding subunits were conducted (Fig. 49).[197–199] Carzelesin (**66**) is a prodrug that after

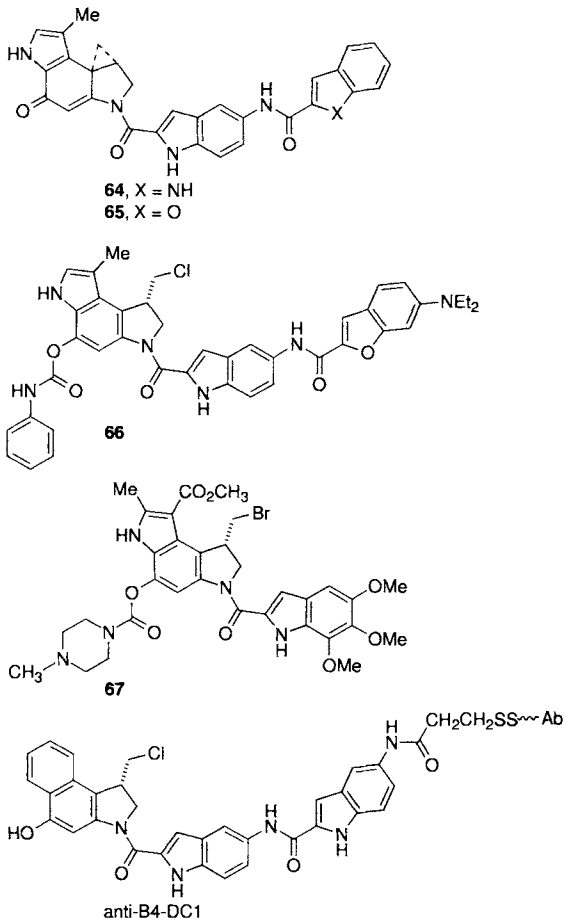

Fig. 49. Candidates for clinical trials.

releasing the free phenol upon carbamate hydrolysis ($t_{1/2}$ = 18–52 min in plasma; $t_{1/2}$ = 40 min in cell culture) readily cyclizes to the corresponding agent containing the cyclopropane.[200] Bizelesin (**43**) is a DNA cross-linking agent incorporating two CPI alkylation subunit precursors and is approximately 20 to 30 times more potent than **1** (IC_{50}(L1210) = 1 pM vs 20 pM).[201]

From the duocarmycin class of agents, KW-2189 (**67**) has been selected for clinical trials in Japan.[202–205] It is a semisynthetic duocarmycin B_2 derivative, which possesses improved antitumor activity, water solubility, and stability.

When conjugates of (+)-CBI-(indole)$_2$ (Fig. 45) that were first prepared with materials from our laboratory were linked by a cleavable disulfide to humanized versions of the antibodies (mAbs) anti-B4 and N901 and directed against the tumor-associated antigens CD19 and CD56, respectively, they proved to be extremely potent and antigen-selective in killing target cells in culture.[206] The anti-B4 disulfide conjugate with (+)-CBI-(indole)$_2$ showed antitumor efficacy in an aggressive, in vivo, metastatic, human B-cell lymphoma model and completely cured animals bearing large tumor burdens. It was shown to be considerably more effective than doxorubicin, cyclophosphamide, etoposide, or vincristine at their maximum tolerated doses. Such tumor-selective targeting of the potent cytotoxic agents related to **1** and the duocarmycins by reversible linkage to tumor-directed antibodies thus improved their inherent selectivity. Because of the potentially low delivery of the antibody-linked agents, which is limited by the number of cell surface cognate antigens, such approaches require that the linked cytotoxic agent be exceptionally potent. Only a limited number of agents including **1**–**3** and their synthetic analogs possess such required potencies.

14. Summary and Future Prospects

In a remarkably short period the definition of the DNA alkylation properties and the basis for the sequence-selective recognition and alkylation of DNA by this new class of antitumor antibiotics have been described. This may well represent the best understood and most thoroughly investigated class of sequence-selective DNA alkylating agents examined to date. Major issues in understanding the polynucleotide recognition and functional reactivity of the agents and their potential utility have been detailed. Nonetheless, several fundamental unresolved issues remain, including a consensual agreement on the origin of the DNA alkylation selectivity, the importance of the rates or efficiencies of DNA alkylation relative to the thermodynamic stability of the reversible adducts, the origin of the characteristic but unique delayed toxicity of **1**, the extent and origin of catalysis of the DNA alkylation reaction, and the link between DNA alkylation and selective antineoplastic activity. Importantly, the present understanding of the origin of the properties of the natural products emerged principally through the design and evaluation of synthetic substructures and agents containing deep-seated structural changes (as well as their unnatural enantiomers), rather than through extensive studies conducted solely on the natural products themselves. Speculation on the origin of properties, which may result in misconceptions or misrepresentations, may and should be addressed by direct and often unambiguous tests employing well-devised synthetic agents. Some such agents have also proven much more efficacious than the natural products themselves, which illustrates that their productive properties may be enhanced by well-founded and designed structural changes. The fact that such structural changes may also often simplify the target analog suggest that it will be a synthetically designed rather than naturally derived agent in this class that will ultimately become clinically significant. No doubt, the fundamental principles defined in the studies conducted to date may provide the foundation for such future developments and advances.

Abbreviations

DSA: duocarmycin SA alkylation subunit
DA: duocarmycin A alkylation subunit
CPI: 1,2,8,8a-tetrahydro-7-methylcyclopropa[*c*]pyrrolo[3,2-*e*]indol-4-one
CBI: 1,2,9,9a-tetrahydrocyclopropa[*c*]benz[*e*]indol-4-one
MCBI: 1,2,9,9a-tetrahydro-7-methoxycyclopropa[*c*]benz[*e*]indol-4-one
CCBI: 1,2,9,9a-tetrahydro-7-cyanocyclopropa[*c*]benz[*e*]indol-4-one
CI: 1,2,7,7a-tetrahydrocyclopropa[1,2-*c*]indol-4-one
CBQ: 2,3,10,10a-tetrahydro-1*H*-cyclopropa[*d*]benz[*f*]quinol-5-one
C_2BI: 9a-(chloromethyl)-1,2,9,9a-tetrahydrocyclopropa[*c*]benz[*e*]indol-4-one
CDPI: 3-carbamoyl-1,2-dihydro-3*H*-pyrrolo[3,2-*e*]indole-7-carboxylate
TMI: 5,6,7-trimethoxyindole-2-carboxylate
CDPBO: 3-carbamoyl-1,2-dihydro-3*H*-pyrrolo[3,2-*e*]-benzoxazole-7-carboxylate
CDPBI: 3-carbamoyl-1,2,-dihydro-3*H*-pyrrolo[3,2-*e*]benzimidazole-7-carboxylate
TACDPI: 5-trimethylammonio-3-carbamoyl-1,2-dihydro-3*H*-pyrrolo[3,2-*e*]indole-7-carboxylate
ACDPI: 5-amino-3-carbamoyl-1,2-dihydro-3*H*-pyrrolo-[3,2-*e*]indole-7-carboxylate
IC_{50}: the concentration of agent required to inhibit by 50% the growth of the indicated cell line (L1210) in a 72 h assay.

Received: May 30, 1995 [A 116 IE]
German version: *Angew. Chem.* **1996**, *108*, 1542–1580

[1] *Molecular Basis of Specificity in Nucleic Acid-Drug Interactions* (Eds.: B. Pullman, J. Jortner), Kluwer, Dordrecht, **1990**.
[2] *Nucleic Acid Targeted Drug Design* (Eds.: C. L. Propst, T. J. Perun), Marcel Dekker, New York, NY, **1992**.
[3] *Molecular Aspects of Anticancer Drug-DNA Interactions, Vol. 1* (Eds.: S. Neidle, M. Waring), CRC, Boca Raton, FL, **1993**.
[4] *Molecular Aspects of Anticancer Drug-DNA Interactions, Vol. 2* (Eds.: S. Neidle, M. Waring), CRC, Boca Raton, FL, **1994**.
[5] D. S. Johnson, D. L. Boger in *Comprehensive Supramolecular Chemistry, Vol. 4* (Ed.: J.-M. Lehn), Pergamon, New York, NY, **1996**, in press.
[6] *DNA Adducts: Identification and Biological Significance* (Eds.: K. Hemminki, A. Dipple, D. E. G. Shuker, F. F. Kadlubar, D. Segerbäck, H. Bartsch), Oxford University Press, New York, **1994**.
[7] A. M. Maxam, W. Gilbert, *Proc. Natl. Acad. Sci. USA* **1977**, *74*, 560–564; A. M. Maxam, W. Gilbert, *Methods Enzymol.* **1980**, *65*, 499–560.
[8] F. Sanger, S. Nicklen, A. R. Coulsen, *Proc. Natl. Acad. Sci. USA* **1977**, *74*, 5463–5467.
[9] B. J. B. Ambrose, R. C. Pless, *Methods Enzymol.* **1987**, *152*, 522–538.
[10] W. M. Barnes, *Methods Enzymol.* **1987**, *152*, 538–556.
[11] J. C. Dabrowiak, A. A. Stankus, J. Goodisman in Ref. [2], pp. 93–149.
[12] P. B. Dervan, *Science* **1986**, *232*, 464–471.
[13] J. W. Lown in *Molecular Aspects of Anticancer Drug Action* (Eds.: S. Neidle, M. J. Waring), VCH, Weinheim, **1983**, pp. 283–314.
[14] R. E. Dickerson in *Structure and Methods: DNA and RNA, Vol. 3* (Eds.: R. H. Sarma, M. H. Sarma), Adenine, Schenectady, NY, **1990**, pp. 1–38.
[15] O. Kennard, W. N. Hunter, *Angew. Chem.* **1991**, *103*, 1280–1303; *Angew. Chem. Int. Ed. Engl.* **1991**, *30*, 1254–1277.
[16] J. Feigon, V. Sklenar, E. Wang, D. E. Gilbert, R. F. Macaya, P. Schultze, *Methods Enzymol.* **1992**, *211*, 235–253.
[17] M. S. Searle, *Prog. Nucl. Magn. Reson. Spectrosc.* **1993**, *25*, 403–480.
[18] C. E. Bugg, S. E. Ealick, *Crystallographic and Modeling Methods in Molecular Design*, Springer, New York, **1990**.
[19] S. N. Rao in Ref. [2], pp. 65–91.
[20] L. J. Hanka, A. Dietz, S. A. Gerpheide, S. L. Kuentzel, D. G. Martin, *J. Antibiot.* **1978**, *31*, 1211–1217.

[21] D. G. Martin, C. G. Chidester, D. J. Duchamp, S. A. Mizsak, *J. Antibiot.* **1980**, *33*, 902–903.
[22] D. G. Martin, C. Biles, S. A. Gerpheide, L. J. Hanka, W. C. Krueger, J. P. McGovren, S. A. Mizsak, G. L. Neil, J. C. Stewart, J. Visser, *J. Antibiot.* **1981**, *34*, 1119–1125.
[23] C. G. Chidester, W. C. Krueger, S. A. Mizsak, D. J. Duchamp, D. G. Martin, *J. Am. Chem. Soc.* **1981**, *103*, 7629–7635.
[24] I. Takahashi, K. Takahashi, M. Ichimura, M. Morimoto, K. Asano, I. Kawamoto, F. Tomita, H. Nakano, *J. Antibiot.* **1988**, *41*, 1915–1917.
[25] T. Yasuzawa, T. Iida, K. Muroi, M. Ichimura, K. Takahashi, H. Sano, *Chem. Pharm. Bull.* **1988**, *36*, 3728–3731.
[26] M. Ichimura, K. Muroi, K. Asano, I. Kawamoto, F. Tomita, M. Morimoto, H. Nakano, *J. Antibiot.* **1988**, *41*, 1285–1288.
[27] K. Ohba, H. Watabe, T. Sasaki, Y. Takeuchi, Y. Kodama, T. Nakazawa, H. Yamamoto, T. Shomura, M. Sezaki, S. Kondo, *J. Antibiot.* **1988**, *41*, 1515–1519.
[28] T. Ogawa, M. Ichimura, S. Katsumata, M. Morimoto, K. Takahashi, *J. Antibiot.* **1989**, *42*, 1299–1301.
[29] S. Ishii, M. Nagasawa, Y. Kariya, H. Yamamoto, S. Inouye, S. Kondo, *J. Antibiot.* **1989**, *42*, 1713–1717.
[30] M. Ichimura, T. Ogawa, K. Takahashi, E. Kobayashi, I. Kawamoto, T. Yasuzawa, I. Takahashi, H. Nakano, *J. Antibiot.* **1990**, *43*, 1037–1038.
[31] T. Yasuzawa, Y. Saitoh, M. Ichimura, I. Takahashi, H. Sano, *J. Antibiot.* **1991**, *44*, 445–447.
[32] M. Ichimura, T. Ogawa, S. Katsumata, K. Takahashi, I. Takahashi, H. Nakano, *J. Antibiot.* **1991**, *44*, 1045–1053.
[33] T. Yasuzawa, K. Muroi, M. Ichimura, I. Takahashi, T. Ogawa, K. Takahashi, H. Sano, Y. Saitoh, *Chem. Pharm. Bull.* **1995**, *43*, 378–391; M. Ichimura, T. Ogawa, K. Takahashi, A. Mihara, I. Takahashi, H. Nakano, *Oncol. Res.* **1993**, *5*, 165–171.
[34] D. L. Boger, D. S. Johnson, *Proc. Natl. Acad. Sci. USA* **1995**, *92*, 3642–3649.
[35] D. L. Boger, *Acc. Chem. Res.* **1995**, *28*, 20–29.
[36] D. L. Boger, *Chemtracts: Org. Chem.* **1991**, *4*, 329–349.
[37] D. L. Boger in *Proc. Robert A. Welch Found. Conf. Chem. Res.* **1991**, *35*, 137–179.
[38] D. L. Boger, *Adv. Heterocycl. Nat. Prod. Synth.* **1992**, *2*, 1–188.
[39] D. L. Boger, *Pure Appl. Chem.* **1993**, *65*, 1123–1132.
[40] D. L. Boger, *Pure Appl. Chem.* **1994**, *66*, 837–844.
[41] R. S. Coleman, D. L. Boger, *Stud. Nat. Prod. Chem.* **1989**, *3*, 301–383.
[42] D. L. Boger in *Heterocycles in Bioorganic Chemistry* (Eds.: J. Bergman, H. C. van der Plas, M. Simonyl), Royal Society of Chemistry, Cambridge, **1991**, pp. 103–129.
[43] M. A. Warpehoski, *Adv. DNA Sequence Specific Agents* **1992**, *1*, 217–245.
[44] M. A. Warpehoski, *Drugs Fut.* **1991**, *16*, 131–141.
[45] M. A. Warpehoski, J. P. McGovren, M. A. Mitchell, L. H. Hurley in *Molecular Basis of Specificity in Nucleic Acid-Drug Interactions* (Eds.: B. Pullman, J. Jortner), Kluwer, Dordrecht, **1990**, pp. 531–550.
[46] M. A. Warpehoski, L. H. Hurley, *Chem. Res. Toxicol.* **1988**, *1*, 315–333.
[47] L. H. Hurley, P. H. Draves in Ref. [3], pp. 89–133.
[48] L. H. Hurley, D. R. Needham-VanDevanter, *Acc. Chem. Res.* **1986**, *19*, 230–237.
[49] V. L. Reynolds, J. P. McGovren, L. H. Hurley, *J. Antibiot.* **1986**, *39*, 319–334.
[50] P. A. Aristoff, *Adv. Med. Chem.* **1993**, *2*, 67–110.
[51] D. L. Boger, D. S. Johnson, W. Wrasidlo, *Bioorg. Med. Chem. Lett.* **1994**, *4*, 631–636.
[52] J. P. McGovren, G. L. Clarke, E. A. Pratt, T. F. DeKoning, *J. Antibiot.* **1984**, *37*, 63–70.
[53] D. L. Boger, D. S. Johnson, W. Yun, C. M. Tarby, *Bioorg. Med. Chem.* **1994**, *2*, 115–135.
[54] D. L. Boger, D. S. Johnson, W. Yun, *J. Am. Chem. Soc.* **1994**, *116*, 1635–1656.
[55] D. L. Boger, T. Ishizaki, H. Zarrinmayeh, P. A. Kitos, O. Suntornwat, *J. Org. Chem.* **1990**, *55*, 4499–4502.
[56] D. L. Boger, T. Ishizaki, H. Zarrinmayeh, S. A. Munk, P. A. Kitos, O. Suntornwat, *J. Am. Chem. Soc.* **1990**, *112*, 8961–8971.
[57] D. L. Boger, T. Ishizaki, H. Zarrinmayeh, *J. Am. Chem. Soc.* **1991**, *113*, 6645–6649.
[58] D. L. Boger, W. Yun, *J. Am. Chem. Soc.* **1993**, *115*, 9872–9873.
[59] D. L. Boger, W. Yun, S. Terashima, Y. Fukuda, K. Nakatani, P. A. Kitos, Q. Jin, *Bioorg. Med. Chem. Lett.* **1992**, *2*, 759–765.
[60] H. Sugiyama, M. Hosoda, I. Saito, A. Asai, H. Saito, *Tetrahedron Lett.* **1990**, *31*, 7197–7200.
[61] A. Asai, S. Nagamura, H. Saito, *J. Am. Chem. Soc.* **1994**, *116*, 4171–4177.
[62] H. Sugiyama, K. Ohmori, K. L. Chan, M. Hosoda, A. Asai, H. Saito, I. Saito, *Tetrahedron Lett.* **1993**, *34*, 2179–2182.
[63] K. Yamamoto, H. Sugiyama, S. Kawanishi, *Biochemistry* **1993**, *32*, 1059–1066.
[64] L. H. Hurley, V. L. Reynolds, D. H. Swenson, G. L. Petzold, T. A. Scahill, *Science* **1984**, *226*, 843–844.
[65] D. R. Needham-VanDevanter, L. H. Hurley, V. L. Reynolds, N. Y. Theriault, W. C. Krueger, W. Wierenga, *Nucl. Acids Res.* **1984**, *12*, 6159–6168.
[66] V. L. Reynolds, I. J. Molineux, D. J. Kaplan, D. H. Swenson, L. H. Hurley, *Biochemistry* **1985**, *24*, 6228–6237.
[67] L. H. Hurley, C.-S. Lee, J. P. McGovren, M. A. Warpehoski, M. A. Mitchell, R. C. Kelly, P. A. Aristoff, *Biochemistry* **1988**, *27*, 3886–3892.
[68] L. H. Hurley, M. A. Warpehoski, C.-S. Lee, J. P. McGovren, T. A. Scahill, R. C. Kelly, M. A. Mitchell, N. A. Wicnienski, I. Gebhard, P. D. Johnson, V. S. Bradford, *J. Am. Chem. Soc.* **1990**, *112*, 4633–4649.
[69] C. H. Lin, J. M. Beale, L. H. Hurley, *Biochemistry* **1991**, *30*, 3597–3602.
[70] M. A. Warpehoski, D. E. Harper, M. A. Mitchell, T. J. Monroe, *Biochemistry* **1992**, *31*, 2502–2508.
[71] D. L. Boger, R. S. Coleman, B. J. Invergo, S. M. Sakya, T. Ishizaki, S. A. Munk, H. Zarrinmayeh, P. A. Kitos, S. C. Thompson, *J. Am. Chem. Soc.* **1990**, *112*, 4623–4632.
[72] D. L. Boger, S. A. Munk, H. Zarrinmayeh, T. Ishizaki, J. Haught, M. Bina, *Tetrahedron* **1991**, *47*, 2661–2682.
[73] D. L. Boger, W. Yun, *J. Am. Chem. Soc.* **1994**, *116*, 7996–8006.
[74] T. J. Zsido, J. M. Woynarowski, R. M. Baker, L. S. Gawron, T. A. Beerman, *Biochemistry* **1991**, *30*, 3733–3738.
[75] K. L. Weiland, T. P. Dooley, *Biochemistry* **1991**, *30*, 7559–7565.
[76] M. M. McHugh, J. M. Woynarowski, M. A. Mitchell, L. S. Gawron, K. L. Weiland, T. A. Beerman, *Biochemistry* **1994**, *33*, 9158–9168.
[77] D. L. Boger, R. S. Coleman, *J. Am. Chem. Soc.* **1988**, *110*, 1321–1323 und 4796–4807. D. L. Boger, R. S. Coleman, *J. Org. Chem.* **1988**, *53*, 695–698.
[78] Consistent with this proposal, the observed induced circular dichroism upon DNA binding and alkylation by (+)-CC-1065 is much larger than that of (+)-**16**, indicating a greater conformational change upon binding for CC-1065. This larger induced circular dichroism for CC-1065 was mistakenly attributed to a higher binding and alkylation efficiency in early studies [79].
[79] M. A. Warpehoski, V. S. Bradford, *Tetrahedron Lett.* **1988**, *29*, 131–134.
[80] D. L. Boger, L. R. Cerbone, D. Yohannes, *J. Org. Chem.* **1988**, *53*, 5163–5166.
[81] D. L. Boger, R. S. Coleman, *J. Org. Chem.* **1984**, *49*, 2240–2245; D. L. Boger, R. S. Coleman, B. J. Invergo, *J. Org. Chem.* **1987**, *52*, 1521–1530.
[82] D. L. Boger, B. J. Invergo, R. S. Coleman, H. Zarrinmayeh, P. A. Kitos, S. C. Thompson, T. Leong, L. W. McLaughlin, *Chem. Biol. Interact.* **1990**, *73*, 29–52.
[83] D. L. Boger, S. M. Sakya, *J. Org. Chem.* **1992**, *57*, 1277–1284.
[84] D. L. Boger, W. Yun, N. Han, D. S. Johnson, *Bioorg. Med. Chem.* **1995**, *3*, 611–621.
[85] D. L. Boger, J. Zhou, *J. Org. Chem.* **1993**, *58*, 3018–3024.
[86] D. L. Boger, J. Zhou, H. Cai, *Bioorg. Med. Chem.* **1996**, *4*, 859–868.
[87] L. H. Li, D. H. Swenson, S. L. F. Schpok, S. L. Kuentzel, B. D. Dayton, W. C. Krueger, *Cancer Res.* **1982**, *42*, 999–1004.
[88] D. H. Swenson, L. H. Li, L. H. Hurley, J. S. Rokem, G. L. Petzold, B. D. Dayton, T. L. Wallace, A. H. Lin, W. C. Krueger, *Cancer Res.* **1982**, *42*, 2821–2828.
[89] W. C. Krueger, L. H. Li, A. Moscowitz, M. D. Prairie, G. Petzold, D. H. Swenson, *Biopolymers* **1985**, *24*, 1549–1572.
[90] W. C. Krueger, D. J. Duchamp, L. H. Li, A. Moscowitz, G. L. Petzold, M. D. Prairie, D. H. Swenson, *Chem. Biol. Interact.* **1986**, *59*, 55–72.
[91] W. C. Krueger, M. D. Prairie, *Chem. Biol. Interact.* **1987**, *62*, 281–295.
[92] N. Y. Theriault, W. C. Krueger, M. D. Prairie, *Chem. Biol. Interact.* **1988**, *65*, 187–201.
[93] D. H. Swenson, G. L. Petzold, M. G. Williams, L. H. Li, M. D. Prairie, W. C. Krueger, *Chem. Biol. Interact.* **1988**, *67*, 199–213.
[94] B. C. Moy, M. D. Prairie, W. C. Krueger, B. K. Bhuyan, *Cancer Res.* **1989**, *49*, 1983–1988.
[95] W. C. Krueger, M. D. Prairie, *Chem. Biol. Interact.* **1991**, *79*, 137–149.
[96] W. C. Krueger, N. T. Hatzenbuhler, M. D. Prairie, M. H. Shea, *Chem. Biol. Interact.* **1991**, *79*, 265–286.
[97] W. C. Krueger, M. D. Prairie, *Chem. Biol. Interact.* **1992**, *82*, 31–46.
[98] C. H. Lin, D. Sun, L. H. Hurley, *Chem. Res. Toxicol.* **1991**, *4*, 21–26.
[99] C.-S. Lee, D. Sun, R. Kizu, L. H. Hurley, *Chem. Res. Toxicol.* **1991**, *4*, 203–213.
[100] C. H. Lin, G. C. Hill, L. H. Hurley, *Chem. Res. Toxicol.* **1992**, *5*, 167–182.
[101] Z.-M. Ding, R. M. Harshey, L. H. Hurley, *Nucl. Acids Res.* **1993**, *21*, 4281–4287.
[102] D. Sun, C. H. Lin, L. H. Hurley, *Biochemistry* **1993**, *32*, 4487–4495.
[103] A. S. Thompson, D. Sun, L. H. Hurley, *J. Am. Chem. Soc.* **1995**, *117*, 2371–2372.
[104] D. L. Boger, S. A. Munk, H. Zarrinmayeh, *J. Am. Chem. Soc.* **1991**, *113*, 3980–3983.
[105] D. L. Boger, H. Zarrinmayeh, S. A. Munk, P. A. Kitos, O. Suntornwat, *Proc. Natl. Acad. Sci. USA* **1991**, *88*, 1431–1435.
[106] M. A. Warpehoski, D. E. Harper, *J. Am. Chem. Soc.* **1994**, *116*, 7573–7580.
[107] M. A. Warpehoski, D. E. Harper, *J. Am. Chem. Soc.* **1995**, *117*, 2951–2952.
[108] D. L. Boger, D. S. Johnson, *J. Am. Chem. Soc.* **1995**, *117*, 1443–1444.
[109] D. L. Boger, D. Hertzog, B. Bollinger, D. S. Johnson, H. Cai, unpublished results; D. L. Boger, D. Hertzog, B. Bollinger, P. Mèsini, H. Cai, unpublished results.

[110] P. S. Eis, J. Rydzewski, J. Smith, D. A. Case, D. L. Boger, W. J. Chazin, unpublished results.

[111] T. A. Scahill, R. M. Jensen, D. H. Swenson, N. T. Hatzenbuhler, G. Petzold, W. Wierenga, N. D. Brahme, *Biochemistry* **1990**, *29*, 2852–2860.

[112] C. H. Lin, L. H. Hurley, *Biochemistry* **1990**, *29*, 9503–9507.

[113] R. Powers, D. G. Gorenstein, *Biochemistry* **1990**, *29*, 9994–10008.

[114] C. H. Lin, D. J. Patel, *J. Am. Chem. Soc.* **1992**, *114*, 10658–10660; *J. Mol. Biol.* **1995**, *248*, 162–179.

[115] D. L. Boger, R. J. Wysocki, Jr., *J. Org. Chem.* **1989**, *54*, 1238–1240.

[116] D. L. Boger, R. J. Wysocki, Jr., T. Ishizaki, *J. Am. Chem. Soc.* **1990**, *112*, 5230–5240.

[117] D. L. Boger, T. Ishizaki, R. J. Wysocki, Jr., S. A. Munk, P. A. Kitos, O. Suntornwat, *J. Am. Chem. Soc.* **1989**, *111*, 6461–6463.

[118] D. L. Boger, T. Ishizaki, P. A. Kitos, O. Suntornwat, *J. Org. Chem.* **1990**, *55*, 5823–5832.

[119] D. L. Boger, T. Ishizaki, *Tetrahedron Lett.* **1990**, *31*, 793–796.

[120] D. L. Boger, S. A. Munk, T. Ishizaki, *J. Am. Chem. Soc.* **1991**, *113*, 2779–2780.

[121] D. L. Boger, T. Ishizaki, S. M. Sakya, S. A. Munk, P. A. Kitos, Q. Jin, J. M. Besterman, *Bioorg. Med. Chem. Lett.* **1991**, *1*, 115–120.

[122] D. L. Boger, S. A. Munk, *J. Am. Chem. Soc.* **1992**, *114*, 5487–5496.

[123] D. L. Boger, W. Yun, B. R. Teegarden, *J. Org. Chem.* **1992**, *57*, 2873–2876.

[124] D. L. Boger, J. A. McKie, *J. Org. Chem.* **1995**, *60*, 1271–1275.

[125] P. A. Aristoff, P. D. Johnson, D. Sun, *J. Med. Chem.* **1993**, *36*, 1956–1963; P. A. Aristoff, P. D. Johnson, *J. Org. Chem.* **1992**, *57*, 6234–6239; K. J. Drost, M. P. Cava, *J. Org. Chem.* **1991**, *56*, 2240–2244.

[126] D. L. Boger, J. A. McKie, H. Cai, B. Cacciari, P. G. Baraldi, *J. Org. Chem.* **1996**, *61*, 1710–1729.

[127] D. L. Boger, N. Han, C. M. Tarby, C. W. Boyce, H. Cai, Q. Jin, P. A. Kitos, *J. Org. Chem.*, im Druck; D. L. Boger, J. A. McKie, N. Han, C. M. Tarby, H. W. Riggs, P. A. Kitos, *Bioorg. Med. Chem. Lett.* **1996**, *6*, 659–664.

[128] D. L. Boger, P. Mèsini, C. M. Tarby, *J. Am. Chem. Soc.* **1994**, *116*, 6461–6462.

[129] D. L. Boger, P. Mèsini, *J. Am. Chem. Soc.* **1994**, *116*, 11335–11348.

[130] D. L. Boger, P. Mèsini, *J. Am. Chem. Soc.* **1995**, *117*, 11647–11655.

[131] D. L. Boger, M. S. S. Palanki, *J. Am. Chem. Soc.* **1992**, *114*, 9318–9327.

[132] D. L. Boger, D. S. Johnson, M. S. S. Palanki, P. A. Kitos, J. Chang, P. Dowell, *Bioorg. Med. Chem.* **1993**, *1*, 27–38.

[133] M. A. Mitchell, P. D. Johnson, M. G. Williams, P. A. Aristoff, *J. Am. Chem. Soc.* **1989**, *111*, 6428–6429.

[134] M. A. Mitchell, R. C. Kelly, N. A. Wicnienski, N. T. Hatzenbuhler, M. G. Williams, G. L. Petzold, J. L. Slightom, D. R. Siemieniak, *J. Am. Chem. Soc.* **1991**, *113*, 8994–8995.

[135] C.-S. Lee, N. W. Gibson, *Cancer Res.* **1991**, *51*, 6586–6591.

[136] C.-S. Lee, N. W. Gibson, *Biochemistry* **1993**, *32*, 2592–2600.

[137] C.-S. Lee, N. W. Gibson, *Biochemistry* **1993**, *32*, 9108–9114.

[138] C.-S. Lee, G. P. Pfeifer, N. W. Gibson, *Biochemistry* **1994**, *33*, 6024–6030.

[139] Z.-M. Ding, L. H. Hurley, *Anti Cancer Drug Des.* **1991**, *6*, 427–452.

[140] D. Sun, L. H. Hurley, *J. Am. Chem. Soc.* **1993**, *115*, 5925–5933.

[141] F. C. Seaman, L. Hurley, *Biochemistry* **1993**, *32*, 12577–12585.

[142] D. Sun, H.-J. Park, L. H. Hurley, *Chem. Res. Toxicol.* **1993**, *6*, 889–894.

[143] a) K. Okabe, M. Takahashi, H. Muratake, M. Natsume, Ref. [143c], pp. 64; b) Y. Fukuda, K. Fuluta, Y. Ohmori, S. Terashima, Ref. [143c], pp. 266; c) *Abstr. Pap. 115th Annu. Meet. Pharm. Soc. Jpn. (Sendai)*, **1995**.

[144] F. Mohamadi, M. M. Spees, G. S. Staten, P. Marder, J. K. Kipka, D. A. Johnson, D. L. Boger, H. Zarrinmayeh, *J. Med. Chem.* **1994**, *37*, 232–239.

[145] R. J. Sundberg, E. W. Baxter, *Tetrahedron Lett.* **1986**, *27*, 2687–2690; R. J. Sundberg, T. Nishiguchi, *Tetrahedron Lett.* **1983**, *24*, 4773–4776; R. J. Sundberg, E. W. Baxter, W. J. Pitts, R. Ahmed-Schofield, T. Nishiguchi, *J. Org. Chem.* **1988**, *53*, 5097–5107; R. J. Sundberg, W. J. Pitts, *J. Org. Chem.* **1991**, *56*, 3048–3054; K. J. Drost, R. J. Jones, M. P. Cava, *J. Org. Chem.* **1989**, *54*, 5985–5988; J. H. Tidwell, S. L. Buchwald, *J. Org. Chem.* **1992**, *57*, 6380–6382; L. F. Tietze, T. Grote, *Chem. Ber.* **1993**, *126*, 2733–2737; T. Sakamoto, Y. Kondo, M. Uchiyama, H. Yamanaka, *J. Chem. Soc. Perkin Trans. 1* **1993**, 1941–1942; Y. Wang, R. Gupta, L. Huang, J. W. Lown, *J. Med. Chem.* **1993**, *36*, 4172–4182; Y. Wang, J. W. Lown, *Heterocycles* **1993**, *36*, 1399–1410.

[146] T. A. Bryson, G. A. Roth, *Tetrahedron Lett.* **1988**, *29*, 2167–2170.

[147] S. Rajeswari, A. A. Adesomoju, M. P. Cava, *J. Heterocycl. Chem.* **1989**, *26*, 557–564.

[148] D. L. Boger, T. J. Jenkins, *J. Am. Chem. Soc.*, submitted.

[149] D. L. Boger, R. M. Garbaccio, unpublished results.

[150] R. C. Kelly, I. Gebhard, N. Wicnienski, P. A. Aristoff, P. D. Johnson, D. G. Martin, *J. Am. Chem. Soc.* **1987**, *109*, 6837–6838; W. Wierenga, *J. Am. Chem. Soc.* **1981**, *103*, 5621–5623.

[151] P. Magnus, T. Gallagher, J. Schultz, Y.-S. Or, T. P. Ananthanarayan, *J. Am. Chem. Soc.* **1987**, *109*, 2706–2711.

[152] R. E. Bolton, C. J. Moody, M. Pass, C. W. Rees, G. Tojo, *J. Chem. Soc. Perkin Trans. 1* **1988**, 2491–2499.

[153] Y. Fukuda, Y. Itoh, K. Nakatani, S. Terashima, *Tetrahedron* **1994**, *50*, 2793–2808; *ibid.* **1994**, *50*, 2809–2820.

[154] D. Boger, T. Nishi, J. A. McKie, T. Ogiku, *J. Am. Chem. Soc.* **1996**, *118*, 2301–2302.

[155] D. L. Boger, K. Machiya, *J. Am. Chem. Soc.* **1992**, *114*, 10056–10058.

[156] D. L. Boger, K. Machiya, D. L. Hertzog, P. A. Kitos, D. Holmes, *J. Am. Chem. Soc.* **1993**, *115*, 9025–9036. Review: D. L. Boger in *Advances in Nitrogen Heterocycles, Vol. 1* (Ed.: C. J. Moody), JAI, Greenwich, CT, **1995**, pp. 229–247.

[157] H. Muratake, I. Abe, M. Natsume, *Tetrahedron Lett.* **1994**, *35*, 2573–2576; *Chem. Pharm. Bull.* **1996**, *44*, 67–79; H. Muratake, N. Matsumura, M. Natsume, *ibid.* **1995**, *43*, 1064–1066.

[158] W. Wierenga, B. K. Bhuyan, R. C. Kelly, W. C. Krueger, L. H. Li, J. P. McGovren, D. H. Swenson, M. A. Warpehoski, *Adv. Enzyme Regul.* **1986**, *25*, 141–155.

[159] M. A. Warpehoski, I. Gebhard, R. C. Kelly, W. C. Krueger, L. H. Li, J. P. McGovren, M. D. Prairie, N. Wicnienski, W. Wierenga, *J. Med. Chem.* **1988**, *31*, 590–603.

[160] M. A. Warpehoski, *Tetrahedron Lett.* **1986**, *27*, 4103–4106.

[161] L. H. Li, T. L. Wallace, T. F. DeKoning, M. A. Warpehoski, R. C. Kelly, M. D. Prairie, W. C. Krueger, *Invest. New Drugs* **1987**, *5*, 329–337.

[162] L. H. Li, R. C. Kelly, M. A. Warpehoski, J. P. McGovren, I. Gebhard, T. F. DeKoning, *Invest. New Drugs* **1991**, *9*, 137–148.

[163] D. L. Boger, W. Yun, *J. Am. Chem. Soc.* **1994**, *116*, 5523–5524.

[164] D. L. Boger, T. Nishi, B. R. Teegarden, *J. Org. Chem.* **1994**, *59*, 4943–4949.

[165] M. A. Mitchell, K. L. Weiland, P. A. Aristoff, P. D. Johnson, T. P. Dooley, *Chem. Res. Toxicol.* **1993**, *6*, 421–424.

[166] D. L. Boger, W. Yun, N. Han, *Bioorg. Med. Chem.* **1995**, *3*, 1429–1453.

[167] W. S. Wade, P. B. Dervan, *J. Am. Chem. Soc.* **1987**, *109*, 1574–1575.

[168] J. W. Lown, *Chemtracts: Org. Chem.* **1993**, *6*, 205–237.

[169] M. Lee, A. L. Rhodes, M. D. Wyatt, S. Forrow, J. A. Hartley, *Biochemistry* **1993**, *32*, 4237–4245.

[170] D. L. Boger, W. Yun, H. Cai, N. Han, *Bioorg. Med. Chem.* **1995**, *3*, 761–775.

[171] B. K. Bhuyan, K. A. Newell, S. L. Crampton, D. D. Von Hoff, *Cancer Res.* **1982**, *42*, 3532–3537.

[172] B. K. Bhuyan, S. L. Crampton, E. G. Adams, *Cancer Res.* **1983**, *43*, 4227–4232.

[173] E. G. Adams, G. J. Badiner, B. K. Bhuyan, *Cancer Res.* **1988**, *48*, 109–116.

[174] B. K. Bhuyan, K. S. Smith, E. G. Adams, G. L. Petzold, J. P. McGovren, *Cancer Res.* **1992**, *52*, 5687–5692.

[175] H. N. Nguyen, B.-U. Sevin, H. Averette, J. Perras, R. Ramos, D. Donato, *J. Cancer Res. Clin. Oncol.* **1992**, *118*, 515–522.

[176] L. H. Hurley, D. Sun in *Perspectives in Medicinal Chemistry* (Eds.: B. Testa, E. Kyburg, W. Fuhrer, R. Giger), VCH, New York, **1993**, pp. 299–313.

[177] D. Sun, L. H. Hurley, *Anti Cancer Drug Des.* **1992**, *7*, 15–36.

[178] D. Sun, L. H. Hurley, *J. Med. Chem.* **1992**, *35*, 1773–1782.

[179] I. P. Maine, D. Sun, L. H. Hurley, T. Kodadek, *Biochemistry* **1992**, *31*, 3968–3975.

[180] H. Naegeli, L. Bardwell, E. C. Friedberg, *Biochemistry* **1993**, *32*, 613–621.

[181] P. Houston, T. Kodadek, *Proc. Natl. Acad. Sci. USA* **1994**, *91*, 5471–5474.

[182] D. Sun, L. H. Hurley, *Biochemistry* **1992**, *31*, 2822–2829.

[183] D. R. Needham-VanDevanter, L. H. Hurley, *Biochemistry* **1986**, *25*, 8430–8436; L. H. Hurley, D. R. Needham-VanDevanter, C.-S. Lee, *Proc. Natl. Acad. Sci. USA* **1987**, *84*, 6412–6416.

[184] M. K. Jacobson, D. Twehous, L. H. Hurley, *Biochemistry* **1986**, *25*, 5929–5932.

[185] M.-S. Tang, C.-S. Lee, R. Doisy, L. Ross, D. R. Needham-VanDevanter, L. H. Hurley, *Biochemistry* **1988**, *27*, 893–901.

[186] C. P. Selby, A. Sancar, *Biochemistry* **1988**, *27*, 7184–7188.

[187] M.-S. Tang, M. Qian, A. Pao, *Biochemistry* **1994**, *33*, 2726–2732.

[188] P. R. Harbach, R. J. Trzos, J. H. Mazurek, D. M. Zimmer, G. L. Petzold, B. K. Bhuyan, *Mutagenesis* **1986**, *1*, 407–410.

[189] P. R. Harbach, D. M. Zimmer, J. H. Mazurek, B. K. Bhuyan, *Cancer Res.* **1988**, *48*, 32–36.

[190] T. J. Monroe, M. A. Mitchell, *Cancer Res.* **1993**, *53*, 5690–5696.

[191] L. Imperatori, G. Damia, P. Taverna, E. Garattini, L. Citti, L. Boldrini, M. D'Incalci, *Carcinogenesis* **1994**, *15*, 533–537.

[192] B. C. Moy, G. L. Petzold, G. J. Badiner, R. C. Kelly, P. A. Aristoff, E. G. Adams, L. H. Li, B. K. Bhuyan, *Cancer Res.* **1990**, *50*, 2485–2492.

[193] T. J. Zsido, T. A. Beerman, R. L. Meegan, J. M. Woynarowski, R. M. Baker, *Biochem. Pharmacol.* **1992**, *43*, 1817–1822.

[194] B. K. Bhuyan, K. S. Smith, R. C. Kelly, E. G. Adams, I. Abraham, K. E. Sampson, *Cancer Res.* **1993**, *53*, 1354–1359.

[195] W. Wierenga, *Drugs Fut.* **1991**, *16*, 741–750.

[196] R. D. Hightower, B.-U. Sevin, J. Perras, H. Nguyen, R. Angioli, M. Untch, H. Averette, *Cancer Invest.* **1993**, *11*, 276–282.

[197] R. D. Hightower, B.-U. Sevin, J. P. Perras, M. Untch, R. Angioli, R. Ramos, H. Averette, *Gynecol. Oncol.* **1992**, *47*, 186–190.

[198] S. Côté, R. L. Momparler, *Anti Cancer Drugs* **1993**, *4*, 327–333.

[199] G. F. Fleming, M. J. Ratain, S. M. O'Brien, R. L. Schilsky, P. C. Hoffman, J. M. Richards, N. J. Vogelzang, D. A. Kasunic, R. H. Earhart, *J. Natl. Cancer Inst.* **1994**, *86*, 368–372.

[200] L. H. Li, T. F. DeKoning, R. C. Kelly, W. C. Krueger, J. P. McGovren, G. E. Padbury, G. L. Petzold, T. L. Wallace, R. J. Ouding, M. D. Prairie, I. Gebhard, *Cancer Res.* **1992**, *52*, 4904–4913.
[201] D. L. Walker, J. M. Reid, M. M. Ames, *Cancer Chemother. Pharmacol.* **1994**, *34*, 317–322.
[202] K. Gomi, E. Kobayashi, K. Miyoshi, T. Ashizawa, A. Okamoto, T. Ogawa, S. Katsumata, A. Mihara, M. Okabe, T. Hirata, *Jpn. J. Cancer Res.* **1992**, *83*, 113–120.
[203] A. Okamoto, M. Okabe, K. Gomi, *Jpn. J. Cancer Res.* **1993**, *84*, 93–98.
[204] E. Kobayashi, A. Okamoto, M. Asada, M. Okabe, S. Nagamura, A. Asai, H. Saito, K. Gomi, T. Hirata, *Cancer Res.* **1994**, *54*, 2404–2410.
[205] H. Ogasawara, K. Nishio, Y. Takeda, T. Ohmori, N. Kubota, Y. Funayama, T. Ohira, Y. Kuraishi, Y. Isogai, N. Saijo, *Jpn. J. Cancer Res.* **1994**, *85*, 418–425.
[206] R. V. J. Chari, K. A. Jackel, L. A. Bourret, S. J. Derr, B. M. Tadayoni, K. M. Mattocks, S. A. Shah, C. Liu, W. A. Blattler, V. S. Goldmacher, *Cancer Res.* **1995**, *55*, 4079–4085.

VCH Weinheim, New York
Akademie Verlag
Ernst & Sohn
ACADEMY GROUP LTD
Verlag Helvetica Chimica Acta
SIEMENS, Publicis MCD Verlag
Chemical Concepts
VCH Software

VCH PUBLISHING GROUP
Information available on Internet
www.vchgroup.de

Planar-Chiral Ferrocenes: Synthetic Methods and Applications

Antonio Togni*

Since its discovery, and because of its stability and the wealth of methods for its derivatization, ferrocene has played an important role in many areas of synthetic and materials chemistry. Thus ferrocene has been incorporated into more complex structures, which then displayed, for example, nonlinear optical, liquid crystalline, or ferromagnetic properties.[1] From a stereochemical point of view, however, one of the most important attributes of, for example, 1,2- or 1,3-disubstituted ferrocenes such as **1** and **2** is that they are planar-chiral, and thus potentially available in enantiomerically pure form.[2]

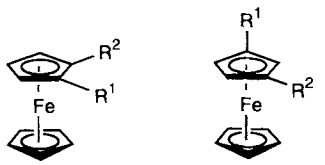

1 **2**

So far, the most important method for preparing enantiopure (or enantiomerically enriched) planar-chiral ferrocene derivatives relies upon a diastereoselective *ortho*-lithiation and subsequent reaction with an appropriate electrophile. The most prominent example of this methodology is based on the pioneering work of Ugi and co-workers (Scheme 1).[3]

Thus, lithiation of ferrocenylamine (*R*)-**3** with BuLi generates the two possible diastereoisomers of **4** (for simplicity formulated here as monomeric, nonsolvated species) in a ratio of 96 to 4. Following the reaction with the electrophile, the diastereoisomeric side-product is usually easily separated by crystallization and/or chromatography. This strategy, which involves the use of stereogenic *ortho*-directing groups, has been further developed in more recent years by several research groups. Thus, the sulfoxide **6**,[4] the acetal **7**,[5] and the oxazoline **8**[6] have been found to afford high diastereoselectivities. These functional groups, however, are not necessarily those one may want to incorporate into the final planar-chiral product; that is, they may need to be removed or modified. An exception to this observation is the oxazoline fragment in compound **8** that has been demonstrated to fulfill both the role of a diastereoselective *ortho*-directing functionality and of a ligand for transition metals in homogeneous-catalyzed reactions (see below).

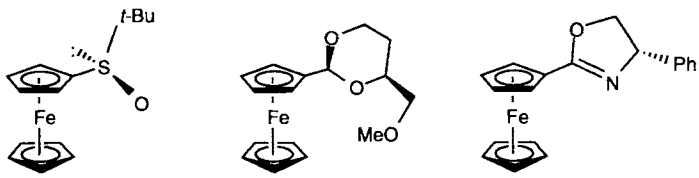

6 **7** **8**

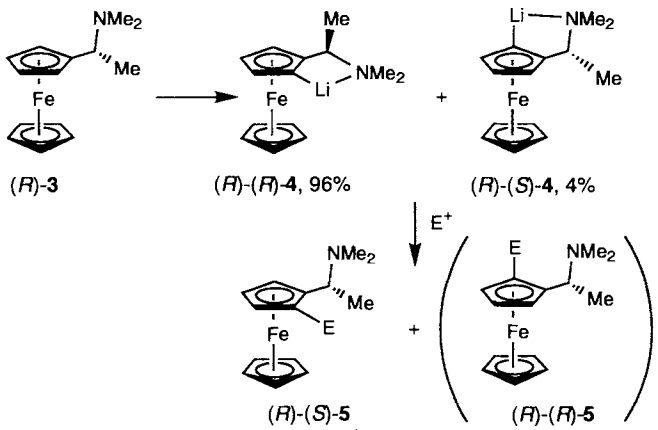

Scheme 1. Diastereoselective *ortho*-lithiation of (*R*)-**3**.

Since amines of type **3** (or the corresponding alcohols as synthetic equivalents) still remain the most versatile starting materials for diastereoselective lithiation processes, and because the amino group can easily be substituted in a stereoretentive process,[3a] methods have been developed for their enantioselective preparation. Recent work includes the amino alcohol catalyzed addition of dialkylzinc reagents to ferrocene-carbaldehyde,[7] and the 1,2-addition of organolithium compounds to the corresponding SAMP-hydrazone,[8] as illustrated in Scheme 2. Further methods involve the enantioselective reduction of ferrocenyl ketones using chiral oxazaborolidine boranes[9] and lipase-mediated desymmetrization of acetoxymethyl derivatives.[10] All these procedures make use of chiral auxiliaries (or catalysts) for the generation of the α-stereogenic center bearing a heteroatom functionality. Among these methods those starting from ferrocenyl ketones are more straightforward and do not involve, for example, cumbersome operations for the removal of chiral auxiliaries, or complex work-up and separation procedures. Therefore, they are anticipated to become even more significant in the near future.

[*] Prof. Dr. A. Togni
Laboratorium für Anorganische Chemie
der Eidgenössischen Technischen Hochschule
ETH-Zentrum, Universitätstrasse 6, CH-8092 Zürich (Switzerland)
Fax: Int. code + (1)632-1090
e-mail: togni@inorg.chem.ethz.ch

 © VCH Verlagsgesellschaft mbH, D-69451 Weinheim, 1996 0570-0833/96/3513-1475 $ 15.00+.25/0

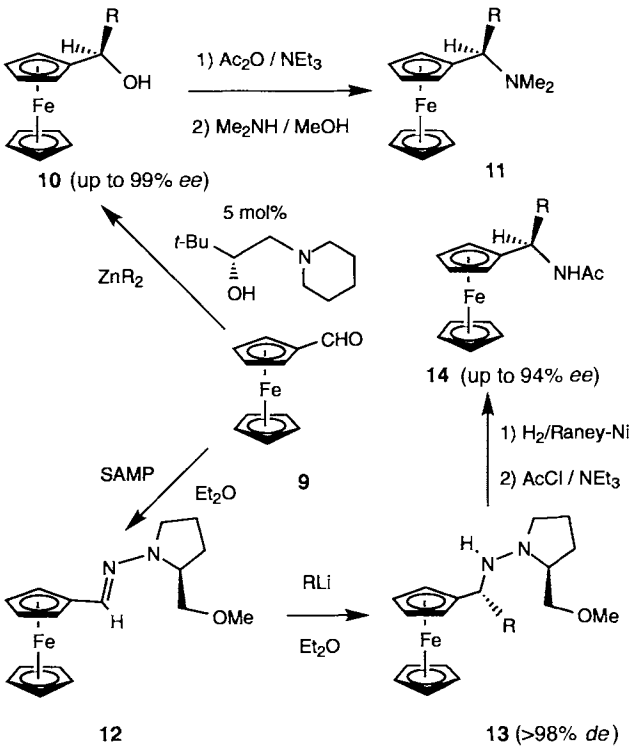

Scheme 2. New syntheses of chiral ferrocenylamines. SAMP = (*S*)-1-amino-2-(methoxymethyl)pyrrolidine.

A completely different approach for the preparation of planar-chiral ferrocenes, which represents an important development in this area, was reported recently by Snieckus and co-workers.[11] Indeed it was shown that the enantioselective *ortho*-lithiation of ferrocenylamides of type **14** is effectively achieved by utilizing the alkaloid (−)-sparteine as a chiral inducing agent (see example in Scheme 3). The novelty of the

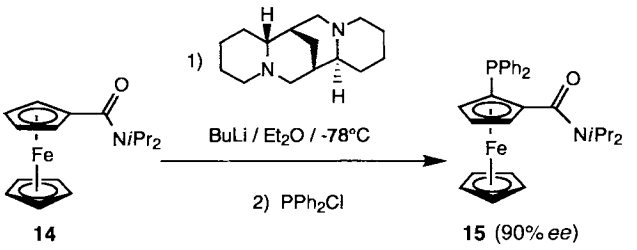

Scheme 3. Sparteine-mediated enantioselective synthesis of **15**.

method lies in the fact that for the first time planar-chiral ferrocenes have been generated highly selectively and without the need of introducing a stereogenic directing group. The application of the reagent BuLi/sparteine in ferrocene chemistry is a welcome extension of the concept of enantioselective deprotonation developed inter alia by Hoppe and co-workers in recent years.[12] Despite the impressive results (the phosphane **15** can be obtained in 90% *ee* and in 82% yield, whereas other electrophiles, for example TMSCl or benzophenone afford optical yields up to 98% and 99% *ee*, respectively), it remains to be seen whether or not the method may be applied so successfully also to ferrocenes bearing substituents other than amides. Furthermore, will there be a chance to overcome the disadvantage of the single enantiomeric form of (−)sparteine?[13]

Probably the most important class of planar-chiral ferrocenes accessible by the techniques delineated above is that of chelating ligands for transition metal catalyzed asymmetric reactions.[1] Progress in this area is characterized, among others, by ligands of type **16**,[14] **17**,[15] and **18**.[16]

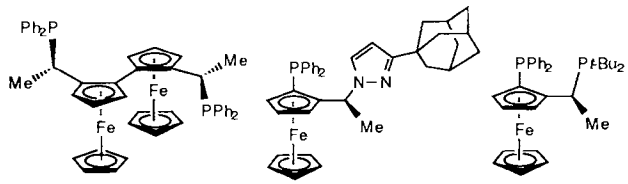

The C_2-symmetric biferrocene **16** has been reported by Ito and co-workers to behave as a *trans*-spanning chelating ligand. The combination of C_2-symmetry and *trans* coordination geometry is conceptually new in the field and is promising for future development. TRAP (the abbreviation for this kind of compounds) affords high enantioselectivities in the Rh-catalyzed asymmetric Michael reaction of 2-cyanopropionates, the hydrosilylation of simple ketones, and the hydrogenation of β,β-disubstituted *N*-acetylaminoacrylic acid derivatives.

The P,N ligand **17** represents a class of chiral auxiliaries that are amenable to easy steric and electronic tuning, an aspect that is anticipated to play an important role in the further development of asymmetric catalysis. Thus, ligands of this type have been shown to afford the highest enantioselectivities reported so far for the Rh-catalyzed hydroboration of styrenes with catecholborane (up to 98.5% *ee*) and for the Pd-catalyzed substitution of allylic acetates and carbonates with benzylamine (up to >99% *ee*). The advantage offered by these ligands is the ease of their synthetic modification, which relies upon the simple idea of a construction kit. The latter comprises 1) the carrier of the chiral information (the amine **3**), 2) a set of chlorophosphanes (for the generation of the planar-chiral phosphane-amine intermediate), and 3) a series of substituted pyrazoles to be used as nucleophiles. The assembly of these three fragments occurs in two consecutive synthetic steps, and allows the ligand to be adapted to the needs of a particular reaction in an unprecedented way.

The same type of considerations apply to diphosphanes of the Josiphos type such as **18**.[16] This specific compound, containing the bulky $t\mathrm{Bu}_2\mathrm{P}$ group, has been found to be the only ligand that affords a very high diastereoface selectivity in the hydrogenation of compound **19** to give **20**, an intermediate in a new synthesis of (+)-biotin[17] (Scheme 4). The analogous achiral starting material containing a benzyl protecting group, instead of a stereogenic phenethyl group, affords under the same reaction conditions 90% *ee*. This quite remarkable process, which involves the hydrogenation of a fully substituted C=C bond, is currently being applied on a commercial scale by Lonza AG.

A second and probably more important technical application of this type of ligands has recently been disclosed by Ciba-Geigy. Derivative **21** constitutes the chiral component of the excep-

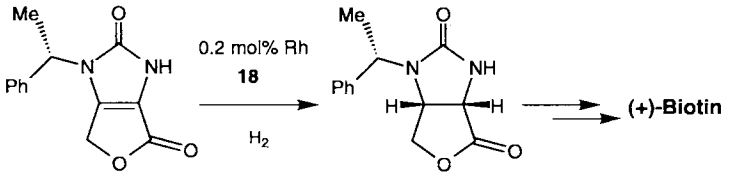

19 20 (99% ds)

Scheme 4. Asymmetric hydrogenation of **19** to give **20**, which is used for the preparation of (+)-biotin.

tionally highly active iridium catalyst used for the enantioselective hydrogenation of imine **22**, an intermediate in the synthesis of the herbicide (*S*)-Metolachlor (**24**)[18] (Scheme 5).

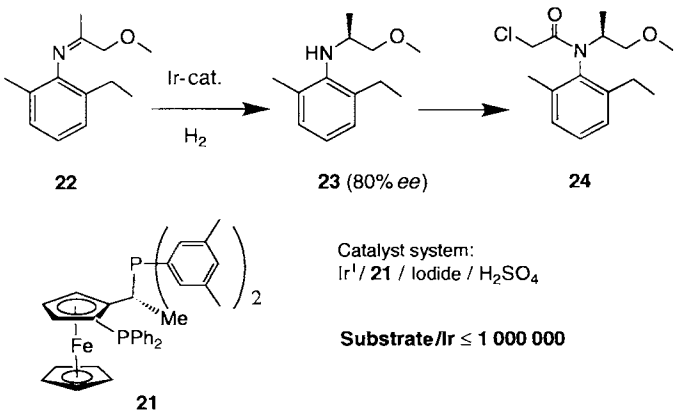

Scheme 5. Asymmetric imine hydrogenation in the production process of the herbicide (*S*)-Metolachlor (**24**).

The relatively low selectivity obtained in this catalytic reaction (80% *ee*) is tolerable for an agrochemical product. Much more important in this specific case are the activity and productivity of the catalyst. Besides a decisive co-catalytic effect of added acids (the exact role of the added iodide salt and of the acid are still unclear), one of the key features of this large industrial process is the use of ferrocenyl ligand **21**, which turns out to be superior to all commercially available chiral chelating diphosphanes with respect to a combination of several important aspects.

To our knowledge, the latter two examples constitute the first industrial applications of chiral ferrocenyl ligands and are a clear demonstration of the potential of this class of compounds. Any improvement of their synthetic versatility will mirror not only their fundamental interest, but shall be welcome also by the practitioner in the fine-chemical industry who is willing to extend the scope of homogeneous catalysis as a powerful synthetic method.

German version: *Angew. Chem.* **1996**, *108*, 1581–1583

Keywords: asymmetric syntheses · ferrocenes · ferrocenyl ligands · metalations

[1] For a recent overview, see: *Ferrocenes. Homogeneous Catalysis. Organic Synthesis. Materials Science* (Eds.: A. Togni, T. Hayashi), VCH, Weinheim, **1995**.

[2] For a discussion of ferrocene chemistry from a stereochemical point of view, see the classical: K. Schlögl, *Top. Stereochem.* **1967**, *1*, 39.

[3] a) D. Marquarding, H. Klusacek, G. W. Gokel, P. Hoffmann, I. K. Ugi, *J. Am. Chem. Soc.* **1970**, *92*, 5389; b) G. W. Gokel, I. K. Ugi, *J. Chem. Educ.* **1972**, *49*, 294.

[4] F. Rebière, O. Riant, L. Ricard, H. B. Kagan, *Angew. Chem.* **1993**, *105*, 644; *Angew. Chem. Int. Ed. Engl.* **1993**, *32*, 568.

[5] O. Riant, O. Samuel, H. B. Kagan, *J. Am. Chem. Soc.* **1993**, *115*, 5835.

[6] Y. Nishibayashi, K. Segawa, K. Ohe, S. Uemura, *Organometallics* **1995**, *14*, 5486, and references therein.

[7] a) Y. Matsumoto, A. Ohno, S. Lu, T. Hayashi, N. Oguni, M. Hayashi, *Tetrahedron: Asymmetry* **1993**, *4*, 1763; b) L. Schwink, S. Vettel, P. Knochel, *Organometallics* **1995**, *14*, 5000.

[8] D. Enders, R. Lochtman, G. Raabe, *Synlett* **1996**, 126. For a second approach that utilizes SAMP derivatives see: C. Ganter, T. Wagner, *Chem. Ber.* **1995**, *128*, 1157.

[9] a) A. Ohno, M. Yamane, T. Hayashi, N. Oguni, M. Hayashi, *Tetrahedron: Asymmetry* **1995**, *6*, 2495; b) L. Schwink, P. Knochel, *Tetrahedron Lett.* **1996**, *37*, 25.

[10] See for example: G. Nicolosi, R. Morrone, A. Patti, M. Piattelli, *Tetrahedron: Asymmetry* **1992**, *3*, 753.

[11] M. Tsukazaki, M. Tinkl, A. Roglans, B. J. Chapell, N. J. Taylor, V. Snieckus, *J. Am. Chem. Soc.* **1996**, *118*, 685.

[12] D. Hoppe, F. Hintze, P. Tebben, M. Paetow, H. Ahrens, J. Schwerdtfeger, P. Sommerfeld, J. Haller, W. Guarnieri, S. Kolczewski, T. Hense, I. Hoppe, *Pure Appl. Chem.* **1994**, *66*, 1479, and references therein.

[13] Chiral amines for which both enantiomers are readily available have recently been used in analogous reactions. However, they afforded significantly lower enantioselectivities. See: a) D. Price, N. S. Simpkins, *Tetrahedron Lett.* **1995**, *36*, 6135. b) Y. Nishibayashi, Y. Arikawa, K. Ohe, S. Uemura, *J. Org. Chem.* **1996**, *61*, 1172.

[14] M. Sawamura, H. Hamashima, M. Sugawara, R. Kuwano, Y. Ito, *Organometallics* **1995**, *14*, 4549, and references therein.

[15] A. Togni, U. Burckhardt, V. Gramlich, P. S. Pregosin, R. Salzmann, *J. Am. Chem. Soc.* **1996**, *118*, 1031.

[16] A. Togni, C. Breutel, A. Schnyder, F. Spindler, H. Landert, A. Tijani, *J. Am. Chem. Soc.* **1994**, *116*, 4062.

[17] J. McGarrity, F. Spindler, R. Fuchs, M. Eyer, (LONZA AG), EP-A 624 587 A2, **1995** [*Chem. Abstr.* **1995**, *122*, P81369q].

[18] For an account of the successful development of this process, see: F. Spindler, B. Pugin, H.-P. Jalett, H.-P. Buser, U. Pittelkow, H.-U. Blaser, *Proceedings of the Conference on Catalysis of Organic Reactions*, Atlanta. **1996**; *Chem. Ind. (Dekker)*, **1996**, *63*, in press.

 © VCH Verlagsgesellschaft mbH, D-69451 Weinheim, 1996 0570-0833/96/3513-1477 $ 15.00+.25/0

Design of Diradical-based Hydrogen Abstraction Agents**

Peter Chen*

Interest in the chemistry of diradicals has undergone a vigorous resurgence over the last decade, in large part due to the putative intermediacy of arene diradicals in the DNA-cleaving activity of the enediyne family of antitumor antibiotics. There were early indications from the Masamune[1] and Sondheimer[2] groups, but the first unambiguous demonstration of the presence of arene diradicals produced by the cyclization of enediynes was reported by Bergman and co-workers.[3] The field lay fallow for many years until the discovery of the remarkable polyunsaturated ring structures for esperamicin, dynemicin, and calicheamicin.[4]

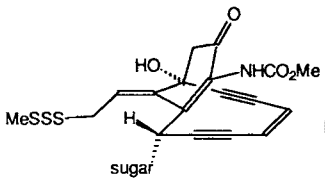

calicheamicin

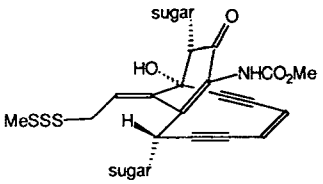

esperamicin

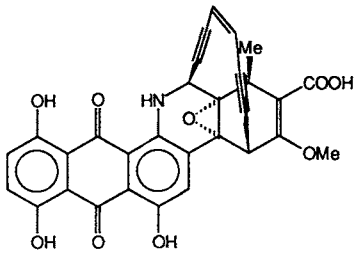

dynemicin

It became evident that the enediyne antitumor antibiotics cycloaromatized to form a substituted 1,4-didehydrobenzene (*p*-benzyne) diradical, which could initiate DNA cleavage by hydrogen abstraction from the sugar phosphate backbone of duplex DNA. Further studies have elucidated the design principles behind the various functional domains of the natural products: the triggering by the trisulfide moieties[4] in calicheamicin and esperamicin, the DNA recognition function of the pendant oligosaccharide chains,[5] the control of cycloaromatization through complexation by the apoprotein in kedarcidin[6] and neocarzinostatin,[7] etc. One marvels at the elegance and modular design of the natural products. Nevertheless, it is almost a truism to state that the natural products are highly optimized under some set of constraints for some biological function, which may or may not bear much relationship to the constraints or function that the enediynes find as therapeutic agents. It is therefore highly desirable to understand the ways in which organic chemists may re-engineer the functionalities of the natural products to effect a rational modification in properties.[8] The modular design of the enediyne series of compounds makes this enterprise particularly attractive. In this report, perspectives on the redesign of the "warhead" part of the enediyne drugs are discussed with an emphasis on recent developments in the field of arene diradicals that provide handles for alteration of function.

The diradicals that form from the natural products are all 1,4-diradicals: either substituted *p*-benzynes or 3,7-dehydroindenes. The functional significance of this restricted range of structures is not altogether clear, although suggestions (see below) can be made. Arene diradicals for which spectroscopic, thermochemical, and/or kinetic data have recently appeared include *p*-benzyne,[9, 10] 9,10-dehydroanthracene,[11, 12] and the larger condensed species, which form by tandem cyclizations.[13, 14]

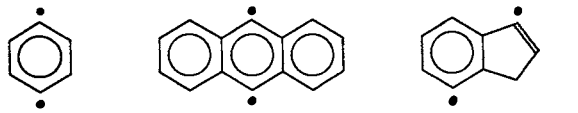

p-benzyne 9,10-dehydroanthracene 3,7-dehydroindene

In the older literature, there are also structures such as the presumed cyclization product of Sondheimer's tetrayne.[2] While there are many reasons to study diradicals, the key questions in the present context are: What would happen if one were to use one of the nonnaturally occurring diradicals in a DNA-cleaving agent? What would the advantages and disadvantages be relative to *p*-benzyne, for example? What handles does one have, from an engineering point-of-view, to modify the chemistry?

In this light, the preparation and characterization of arene diradicals with connectivity or substitution different from those occurring in the natural products is of high interest. The recent report of the clean preparation, under matrix-isolation conditions, of 1,3-didehydrobenzene (*m*-benzyne),[15] opens the way to the physical characterization of an arene diradical which, while never implicated in the activity of a natural product, may have desirable properties from the engineering point-of-view.

A comparison of the results obtained by IR spectroscopy with those from ab initio calculations confirms the identity of the common product that is formed from different precursors by flash vacuum pyrolysis (FVP) and photolysis (Scheme 1). Noteworthy is the survival of *m*-benzyne under the conditions employed for FVP, which is in marked contrast to *p*-benzyne, which has been trapped, but never isolated. The earlier reports that pyrolysis of 1,3-diiodobenzene[16] or isophthaloyl diiodide[17] produced hex-3-ene-1,5-diyne do indicate that there

[*] Prof. Dr. P. Chen
Laboratorium für Organische Chemie
der Eidgenössischen Technischen Hochschule
Universitätstrasse 16, CH-8092 Zürich (Switzerland)
Fax: Int. code +(1)632-1280
e-mail: peter@chen2.ethz.ch

[**] This work was supported financially by the ETH Zürich and the Kontaktgruppe für Forschungsfragen (Basel).

 © VCH Verlagsgesellschaft mbH, D-69451 Weinheim, 1996 0570-0833/96/3513-1478 $ 15.00+.25/0

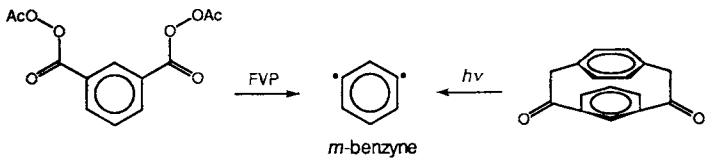

Scheme 1. Formation of *m*-benzyne.

is a rearrangement/ring-opening pathway, but with an activation energy that must be higher than the barrier of 19.8 kcal mol^{-1}[10] for the ring-opening of *p*-benzyne. One can write plausible mechanisms, based on carbene isomers of the enediyne, which rationalize the rearrangement (Scheme 2).

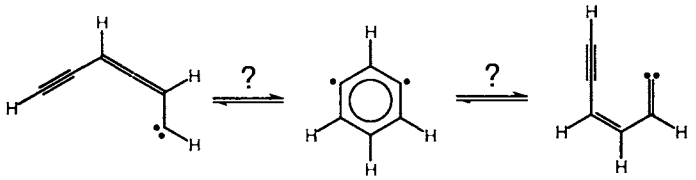

Scheme 2.

However, given that *m*-benzyne has a heat of formation 15 kcal mol^{-1} lower[9] than *p*-benzyne, and the vinylidene isomer of the enediyne, for example, should lie perhaps 40 kcal mol^{-1} above the enediyne, the greater kinetic stability of *m*- versus *p*-benzyne is not difficult to understand. With information gleaned from the experiment, one is almost in a position to make a prediction as to the effect of replacing *p*-benzyne by *m*-benzyne as a hydrogen abstraction agent. To close the argument, one needs only to know something about 1,4-diradicals as abstraction agents.

We have reported the absolute rates of hydrogen abstraction from acetonitrile and isopropyl alcohol by the 9,10-dehydroanthracene diradical[12] as a model for the reaction by *p*-benzyne or any other 1,4-arene diradical. The second-order rate constants for the hydrogen abstraction obtained at room temperature by measuring the transient absorption after flash photolysis and trapping of the reactive intermediate are $k_{MeCN} = (1.1 \pm 0.2) \times 10^3\,M^{-1}s^{-1}$ and $k_{iPrOH} = (6.5 \pm 0.6) \times 10^3\,M^{-1}s^{-1}$, and thus 100–200 times lower than the corresponding rate constants for the phenyl radical[18] or the 9-anthryl radical.[19] A reduced rate in hydrogen abstraction reactions for *p*-benzyne relative to that for the phenyl radical was also found by ab initio calculations at the CASPT2N/6-31G** level.[20] The lowered reactivity of a singlet ground-state diradical relative to that of a reference monoradical was rationalized by a valence-bond promotion energy argument that correlated the singlet–triplet splitting in the diradical to the magnitude of rate reduction. The singlet–triplet splitting in the arene diradicals, in turn, is determined primarily by the extent of through-bond coupling between the two radical sites. Accordingly, by choosing a diradical whose structure favors or disfavors through-bond coupling, or by tuning the energies of the σ and/or σ^* orbitals by way of substituents on the σ-framework, it should be possible to tune the rate of hydrogen abstraction to optimize the process for a particular set of constraints. The heats of formation for *o*-, *m*-, and *p*-benzyne, determined experimentally within the last two years,[9, 10] indicate a much larger coupling in *m*-benzyne than in *p*-benzyne. Ab initio calculations confirm the effect as manifested by a larger singlet–triplet splitting.[21] One would expect, therefore, that the rate of hydrogen abstraction by *m*-benzyne should be even lower than that by *p*-benzyne. Conversely, the diradicals formed by tandem cyclizations, by virtue of greater separation of the two radical centers, should be more reactive than *p*-benzyne.

Accordingly, the substantial stabilization from the 1,3-through-bond interaction in *m*-benzyne should impose both thermodynamic and kinetic barriers to hydrogen abstraction which could be very useful. From the heat of formation,[9] it is clear that abstraction of hydrogen by *m*-benzyne from donors with C–H bonds stronger than 94 kcal mol^{-1} would be endothermic. Even for those donors with a weak enough C–H bond, the promotion energy argument above suggests that there should be a substantial additional component to the activation energy which would nevertheless slow the hydrogen abstraction. The diradical should be long-lived, and presumably, selective in its attack.

It remains only to consider the possible functional significance of arene diradicals in the natural products, given their rather low rate of hydrogen abstraction, and the possible modification in that function upon replacement by a different diradical. Of course, it is conceivable that there is no special reason at all for the occurrence of such diradicals in Nature, but given that there are now many examples of radical-based biological processes,[22] one can imagine that, if it were to be advantageous to have a better abstraction agent, it would have been possible to have one. Greater selectivity, associated in general with lower reactivity, is one possible reason for the choice of a diradical agent versus a monoradical one. A more interesting possibility comes from the differential reactivity between an arene diradical and the phenyl radical. The first hydrogen abstraction by a *p*-benzyne-type diradical proceeds rather slowly (and presumably selectively) and yields the two-hundredfold more reactive phenyl radical. Reaction at the same target site is then likely, in this case meaning that two hydrogen atoms are abstracted from closely spaced positions, rather than from widely separated locations. For DNA cleavage, one would presume that this would lead to more double-stranded breaks, as has been shown to be the case in DNA cleavage by calicheamicin.[23] The exploitation of the differential rates of hydrogen abstraction between diradicals and monoradicals to enhance the likelihood for double-stranded breaks represents an elegant use of intrinsic reactivity to achieve a functional goal. The differential is further enhanced if *m*-benzyne is substituted for *p*-benzyne. While the former should be even slower and more selective than the latter in the first hydrogen abstraction, both diradicals produce the same phenyl radical for the second abstraction. DNA need not even be the target. The general motif associated with diradical-based hydrogen abstractions would be the use of an activated C–H bond, for example benzylic, allylic, etc., to direct the attack on a neighboring, unactivated C–H bond.

Some consequences of recent studies of the chemistry of arene diradicals have been discussed with an view to identifying the factors responsible for the particular choice of diradicals in natural products, and the advantages and disadvantages that

would be incurred if an alternative structure were to be substituted. Important structural features for rational modification of the diradical "warhead" have been suggested.

German version: *Angew. Chem.* **1996**, *108*, 1584–1586

Keywords: diradicals · DNA cleavage · enediynes

[1] N. Darby, C. U. Kim, J. A. Salaün, K. W. Shelton, S. Takada, S. Masamune, *J. Chem. Soc. Chem. Commun.* **1971**, 1516.
[2] J. Mayer, F. Sondheimer, *J. Am. Chem. Soc.* **1966**, *88*, 602; H. N. C. Wong, F. Sondheimer, *Tetrahedron Lett.* **1980**, *21*, 217.
[3] R. G. Bergman, *Acc. Chem. Res.* **1973**, *6*, 25.
[4] K. C. Nicolaou, W. M. Dai, *Angew. Chem.* **1991**, *103*, 1453; *Angew. Chem. Int. Ed. Engl.* **1991**, *30*, 1387.
[5] J. Drak, N. Iwasawa, S. J. Danishefsky, D. M. Crothers, *Proc. Natl. Acad. Sci. USA* **1991**, *88*, 7464; S. Walker, R. Landowitz, W.-D. Ding, G. A. Ellestad, D. Kahne, *ibid.* **1992**, *89*, 4608; J. Aiyer, S. J. Danishefsky, D. M. Crothers, *J. Am. Chem. Soc.* **1992**, *114*, 7552; K. C. Nicolaou, S.-C. Tsay, T. Suzuki, G. F. Joyce, *ibid.* **1992**, *114*, 7555; S. C. Mah, C. A. Townsend, T. D. Tullius, *Biochemistry* **1994**, *33*, 614.
[6] K. Iida, M. Hirama, *J. Am. Chem. Soc.* **1995**, *117*, 8875.
[7] H. Sugiyama, K. Yamashita, T. Fujiwara, I. Saito, *Tetrahedron* **1994**, *50*, 1311.
[8] J. Wang, P. J. DeClercq, *Angew. Chem.* **1995**, *107*, 1898; *Angew. Chem. Int. Ed. Engl.* **1995**, *34*, 1749; D. P. Arya, D. J. Jebaratam, *Tetrahedron Lett.* **1995**, *36*, 4369; L. Banfi, G. Guanti, *Angew. Chem.* **1995**, *107*, 2613; *Angew. Chem. Int. Ed. Engl.* **1995**, *34*, 2393; Y.-F. Lu, C. W. Harwig, A. G. Fallis, *J. Org. Chem.* **1993**, *58*, 4202.
[9] P. G. Wenthold, R. R. Squires, *J. Am. Chem. Soc.* **1994**, *116*, 6401.
[10] W. R. Roth, H. Hopf, C. Horn, *Chem. Ber.* **1994**, *127*, 1765.
[11] O. L. Chapman, C. C. Chang, J. Kolc, *J. Am. Chem. Soc.* **1976**, *98*, 5703.
[12] M. J. Schottelius, P. Chen, *J. Am. Chem. Soc.* **1996**, *118*, 4896.
[13] K. M. Barucha, R. M. Marsh, R. E. Minto, R. G. Bergman, *J. Am. Chem. Soc.* **1992**, *114*, 3120.
[14] J. W. Grissom, T. L. Calkins, H. A. McMillen, Y. Jiang, *J. Org. Chem.* **1994**, *59*, 5833.
[15] R. Marquardt, W. Sander, E. Kraka, *Angew. Chem.* **1996**, *108*, 825; *Angew. Chem. Int. Ed. Engl.* **1996**, *35*, 746.
[16] I. P. Fischer, F. P. Lossing, *J. Am. Chem. Soc.* **1963**, *85*, 1018.
[17] R. Marquardt, Diplomarbeit, Technische Universität, Braunschweig, **1993**.
[18] J. C. Scaiano, L. C. Stewart, *J. Am. Chem. Soc.* **1983**, *105*, 3609.
[19] F. M'Halla, J. Pinson, J. M. Savéant, *J. Am. Chem. Soc.* **1980**, *102*, 4120.
[20] C. F. Logan, P. Chen, *J. Am. Chem. Soc.* **1996**, *118*, 2113.
[21] W. T. Borden, A. Nicolaides, *J. Am. Chem. Soc.* **1993**, *115*, 11951; S. G. Wierschke, J. J. Nash, R. R. Squires, *ibid.* **1993**, *115*, 11958.
[22] P. A. Frey, *Chem. Rev.* **1990**, *90*, 1343.
[23] N. Zein, W. J. McGahren, G. O. Morton, J. Ashcroft, G. A. Ellestad, *J. Am. Chem. Soc.* **1989**, *111*, 6888.

Time is money...

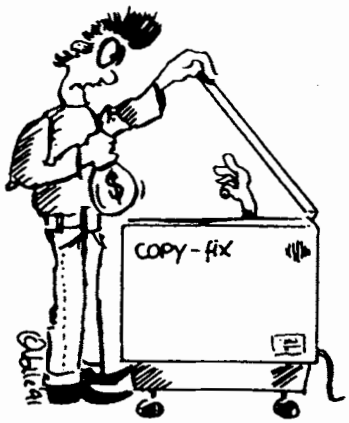

Save both by starting a personal subscription to *Angewandte Chemie* (now with *Chemistry - A European Journal*). At 9¢ per page you can't go wrong. With your own private copy you can read the "hot" articles before they cool, and waste less time in front of the copier.

Order now!
An order form can be found on the last page of this issue.

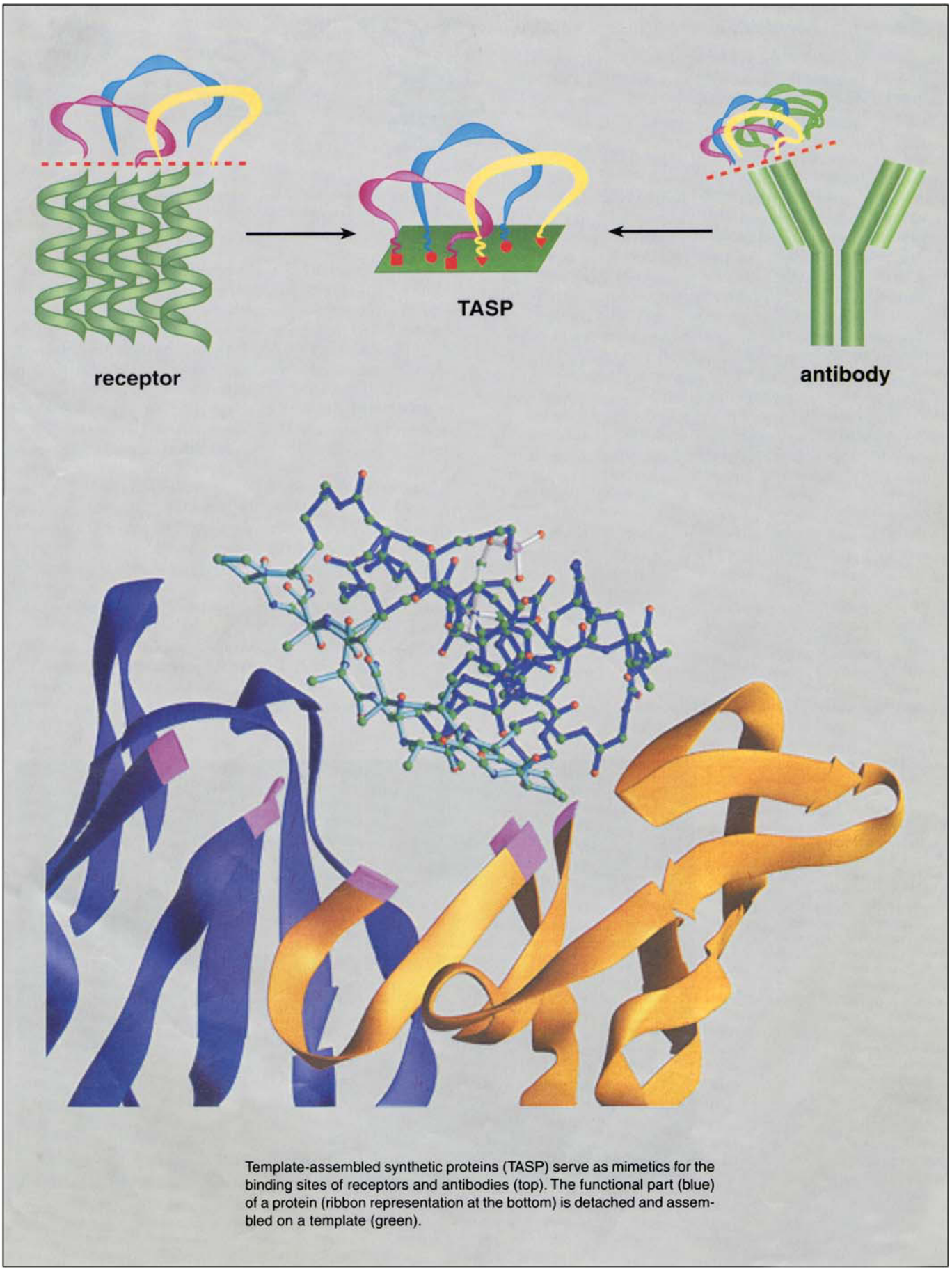

Template-assembled synthetic proteins (TASP) serve as mimetics for the binding sites of receptors and antibodies (top). The functional part (blue) of a protein (ribbon representation at the bottom) is detached and assembled on a template (green).

 © VCH Verlagsgesellschaft mbH, D-69451 Weinheim, 1996 0570-0833/96/3513-1481 $ 15.00+.25/0

Template Assembled Synthetic Proteins (TASP) as Functional Mimetics of Proteins**

Manfred Mutter,* Pascal Dumy, Patrick Garrouste, Christian Lehmann, Marc Mathieu, Cristina Peggion, Stéphane Peluso, Alain Razaname, and Gabriele Tuchscherer

The use of peptidomimetics and topological templates has become an important tool in protein design and mimicry.[1-4] By introducing these elements in the design process, the synthetic chemist aims to unravel the complex interplay between protein structure and function. In order to avoid the well-known protein folding problem, we have introduced the concept of template assembled synthetic proteins (TASP); here, templates serve as built-in devices for directing the intramolecular assembly of covalently attached peptide blocks into characteristic folding topologies.[5-8] So far, problems with the synthesis have prevented the development of the full potential of this approach.[5] According to the TASP approach, the functional part of a protein, for example the antigen binding site of an antibody or the ligand binding site of a receptor, is detached from the rest of the molecule and assembled on a topological template, which mimics the loop supporting structural framework of the native protein (Fig. 1). Here, we elaborate the methodologies for the synthesis of this novel generation of functional TASP compounds.

The approach comprises two key elements: 1) peptide sequences (loops) containing C- and N-terminal functional-

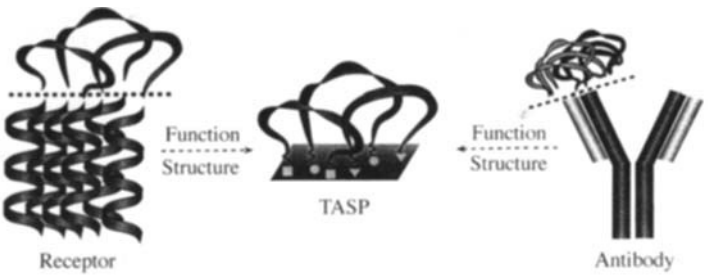

Fig. 1. Concept of template assembled synthetic proteins as mimetics of the binding region of receptors and antibodies.

groups (sticky ends) for chemoselective ligation[9-12] and 2) topological templates for the regioselective assembly of the loops. A prototype template consists of two antiparallel β-sheet peptides linked through β-turn-inducing dipeptides or nonpeptidic β-turn mimetics.[13-15] NMR spectroscopic investigations and molecular dynamics calculations confirm the preferred conformations of the TASP templates shown in Figures 2a and b; the attachment sites, for example the ε-amino groups of the lysine side chains, are all directed to one side of the β-sheet plane.Choosing from a variety of orthogonal protecting groups for peptide synthesis, we have developed a set of cyclic peptides as templates for the selective attachment of loop sequences.[13-15] In tailoring the flexibility of the backbone and side chains, this template motif may dispose any desired number and geometry of attachment sites.

The stepwise condensation of peptide sequences (loops, $\mathbf{L}^i$) onto these topological templates $\mathbf{T}^i$ (Table 1) is achieved by amide, oxime, and thioether formation[9-12] or combinations thereof.

In strategy A (Scheme 1), the C-terminally activated (step 1) fully protected loop $\mathbf{L}^i$ is fixed to the template $\mathbf{T}$, which contains one single reactive attachment site after removal of the protecting group Y^i (step 2, amide 1). Selective deprotection of the

[*] Prof. Dr. M. Mutter, Dr. P. Dumy, Dr. P. Garrouste, Dr. C. Lehmann, Dipl.-Chem. M. Mathieu, Dipl.-Chem. C. Peggion, Dipl.-Chem. S. Peluso, Dr. A. Razaname, Dr. G. Tuchscherer
Institute for Organic Chemistry, University of Lausanne
BCH-Dorigny, CH-1015 Lausanne (Switzerland)
Fax: Int. code +(21)692-4015
e-mail: mmutter@ulys.unil.ch

[**] This work was supported by the Swiss National Science Foundation.

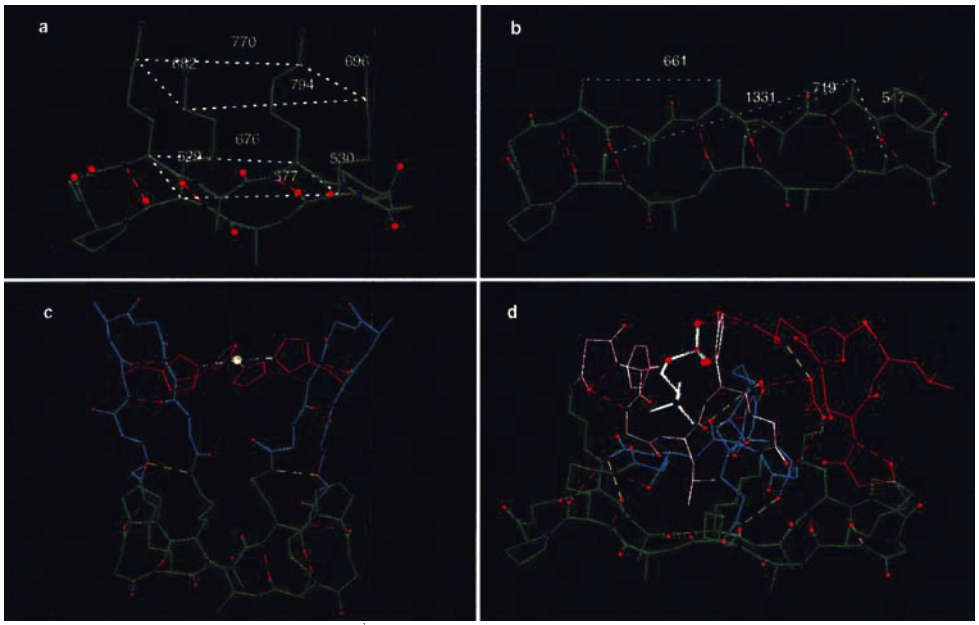

Fig. 2. Design of TASP compounds as functional protein mimetics. a) A cyclic $(ProGlyLysAlaLys)_2$ β-sheet mimetic (template $\mathbf{T}^2$) generated as a full structure from a regularized protein Cα-trace by using the program MOLOC [23,24]. Recent NMR/RMD investigations [15] reveal that the cyclopeptide adopts an antiparallel β-sheet structure spanned between two β-turns of type II. The given idealized $C_\alpha - C_\alpha$ distances [pm] indicate that the mean longitudinal distances are approximately 1.4 Å larger than the transannular ones, whereas the distances on the level of the attachment sites $C_\varepsilon - C_\varepsilon$ may adjust through a type of "crankshaft" motion along the $C_\gamma - C_\delta$ bond into distances suitable to accommodate a structural unit as exemplified below [25]. b) The extension of the chain of a cyclic peptide to a 14-mer unit $(ProGlyLysAlaLysAlaLys)_2$ ($\mathbf{T}^1$) increases the number of potential attachment sites and range of accessible distances. Thus larger distances become accessible to span functional loops that may even mimic an enzymatic binding cavity. c) Two-loop TASP **TASP II** with a square-planar metal binding site that is formed by condensation of two identical HisAlaGlyHisGly sequences on an 10-mer template ($\mathbf{T}^2$). The conformation was optimized by MAB force field calculations [24]; the metal binding geometry was deduced by weighted superposition of the histidine side chains onto the X-ray crystal structure of tetrakis(imidazole)copper(II) sulfate [26]. d) Representation of one of the eight possible directional isomers of a three-loop TASP as a mimetic for the antigen binding site of the phosphorylcholine specific antibody McPC603 [18,19]. In this model selected side chains were considered to be flexible; zero-distance and weak hydrogen bond constraints are sufficient to retain the shape of the binding cavity to enable it to host the amphiphilic zwitterionic species.

Table 1. Template $\mathbf{T}^i$ and loop sequences $\mathbf{L}^i$ for the synthesis of TASP compounds [a].

$\mathbf{T}^1$: c[K(Y^1)C(Acm)K(Y^1)PGK(Y^2)AK(Y^2)AK(Y^3)PGK(Y^3)A]
$\mathbf{T}^2$: c[K(Y^4)PGK(Y^1)AK(Y^2)PGK(Y^3)A]
$\mathbf{T}^3$: c[K(Y^5)PGK(Y^6)AK(Y^2)PGK(Y^3)A]
$\mathbf{T}^4$: c[K(Y^6)PGCDRKK(Y^6)PGFACA]

$\mathbf{L}^1$: Suc-K(Boc)GY(*t*Bu)NG-OH
$\mathbf{L}^2$: Suc-FGLY(*t*Bu)G-OH
$\mathbf{L}^3$: Suc-E(*t*Bu)LGR(Pmc)G-OH
$\mathbf{L}^4$: Boc-S(*t*Bu)H(Trt)AGH(Trt)G-OH
$\mathbf{L}^5$: Alloc-S(*t*Bu)H(Trt)AGH(Trt)G-OH
$\mathbf{L}^6$: X^1-HPGHK(X^2)G-NH_2
$\mathbf{L}^7$: X^2-FSRSDELTRHIRIHTGK(X^2)G-OH

[a] Abbreviations: Y^1: Boc = *tert*-butoxycarbonyl; Y^2: Dde = 1-(4,4-dimethyl-2,6-dioxocyclohexylidene)ethyl; Y^3: Alloc = allyloxycarbonyl; Y^4: Fmoc = 9-fluorenylmethoxycarbonyl; Y^5: $COCH_2CH_2S$-Trt; Y^6: H_2NOCH_2CO; Suc: $HOOC(CH_2)_2CO$; X^1: maleoyl-β-Ala; X^2: OCHCO; A: Ala; C: Cys; D: Asp; E: Glu; F: Phe; G: Gly; H: His; I: Ile; K: Lys; L: Leu; N: Asn; P: Pro; R: Arg; S: Ser; Y: Tyr; Acm: acetamidomethyl; Trt: trityl; Pmc: 2,2,5,7,8-pentamethylchroman-6-sulfonyl.

N-terminal amino group of the loop $\mathbf{L}^i$ (step 3) and activation of the carboxyl group on the template (step 4) completes the cyclization of the loop (amide 2). Alternatively, the selective attachment of the N-terminal end may proceed by the formation of an oxime bond after the aminooxy group on the template has been deprotected (step 2 in strategy B). The condensation of peptides containing the same functional groups at both chain ends (for example carboxyl or aldehyde groups, strategies A′ and D, respectively) proceeds in one step and results in a mixture of two isomers with differently oriented loops. These strategies are very suitable for preparing TASP compound libraries for functional screening.[16] Chemoselective ligation procedures[9–12] allow for the condensation of completely unprotected peptides in aqueous solution or solvent mixtures (strategies C and D). Here, the regioselective attachment of a loop peptide to the template in one single condensation step (strategy C) can be achieved by the combination of two orthogonal ligation techniques (e.g. oxime and thioether formation).

The individual strategies (Scheme 1) were evaluated by fixing peptide loops $\mathbf{L}^i$ of different chain length and sequence to cyclic peptides (see Fig. 2a and b) as regioselectively addressable templates $\mathbf{T}^i$ (Table 1). The kinetics of the reaction were monitored by analytical HPLC (Fig. 3) and the target molecules were characterized mainly by ES mass spectrometry, amino acid analysis, and NMR spectroscopy. Typically, the condensation proceeds

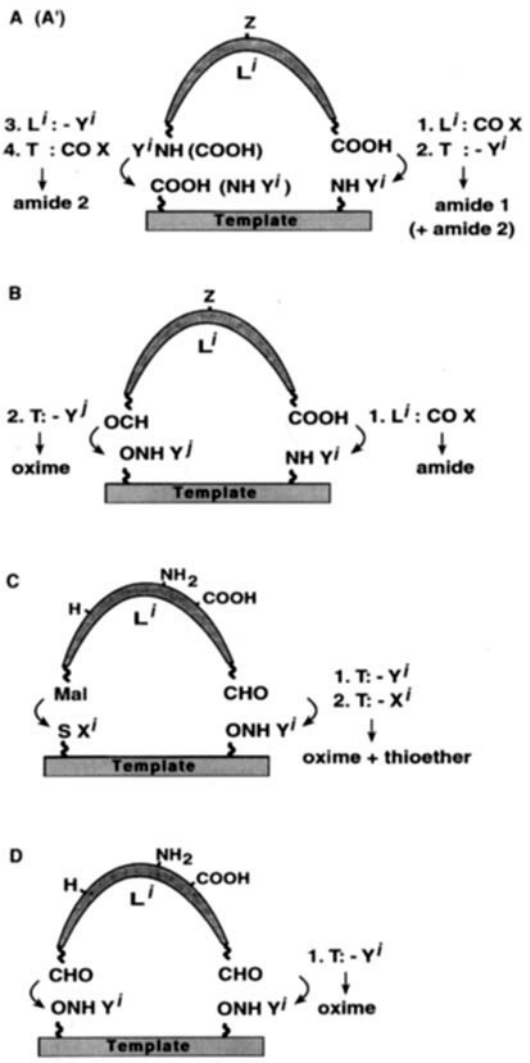

Scheme 1. Strategies A - D for the attachment of peptide loop sequences ($\mathbf{L}^i$) to topological templates $\mathbf{T}^i$ (Table 1); Y^i and Y^j: amino protecting groups of the attachment sites; Z: side chain protecting groups of $\mathbf{L}^i$. A/A′: $\mathbf{L}^1$–$\mathbf{L}^3$, $\mathbf{T}^1$; B: $\mathbf{L}^4$, $\mathbf{L}^5$, $\mathbf{T}^2$; C: $\mathbf{L}^6$, $\mathbf{T}^3$; D: $\mathbf{L}^7$, $\mathbf{T}^4$.

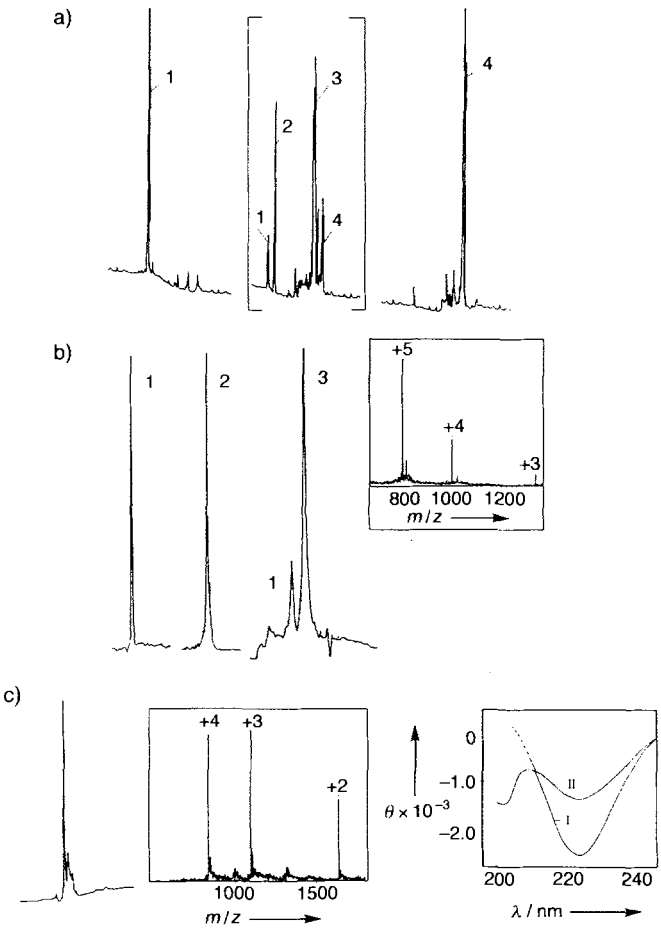

Fig. 3. a) Typical HPL chromatograms of a loop condensation reaction according to strategy A′. 1: $\mathbf{T}^1$ after removal of Y^i (Table 1); 2: PyBop; 3: Noncyclized product after fixation of one chain end (only observed by in situ activation of $\mathbf{L}^1$ at high dilution); 4: Crude product (two isomers) after ligation of $\mathbf{L}^1$ to $\mathbf{T}^1$ (reaction time: 1 h). b) HPL chromatogram of the condensation reaction of the 18-mer peptide $\mathbf{L}^7$ with $\mathbf{T}^4$ (strategy D). 1: $\mathbf{T}^4$; 2: $\mathbf{L}^7$; 3: Crude ligation product (two isomers; reaction time 1 h); insert: ES-MS (m/z_{calcd}: 4003 [M^+]. c) Synthesis of **TASP 1**. Left: HPL chromatogram of crude product; middle: ES-MS (m/z_{calcd}: 3280 [M^+]); right: CD spectra in trifluoroethanol (TFE) (I) and TFE/H_2O (1/1) (II); $c = 1$ mg mL^{-1}

to completion within less than two hours by applying equimolar amounts of L^i and **T** (Fig. 3a, b). In strategy A′ and D, the reaction between L^i and **T** is performed at high dilution ($<10^{-3}$ M) in order to enhance intramolecular loop cyclization. Under these conditions, we observe a pronounced difference in the reaction kinetics of the first and second attachment step: after fixation of one chain end of the loop L^i to the template, the loop cyclization reaction proceeds very fast, as indicated by the absence of the intermediate noncyclized molecule. Apart from the selective fixation of the C- and N-terminal end of a loop L^i as in strategies A–C, the noncyclic intermediate (Fig. 3a in brackets) is only detected when the cyclization is sterically hindered due to the presence of several loops on the template. However, even the condensation of a designed 18-mer peptide to a bifunctional template by oxime bond formation (L^7, strategy D) proceeded without detectable amounts of the intermediate species (Fig. 3b). The increased tendency for loop cyclization on topological templates compared to the regular head-to-tail cyclization reactions is in accord with the theory of peptide macrocyclization.[17]

Starting from a pool of *n* orthogonal amino or carboxyl protecting groups, up to *n* different loops can be selectively fixed according to the individual strategies depicted in Scheme 1. By extending the palette of orthogonal protecting groups and by combining various ligation techniques, TASP compounds of higher structural and functional complexity (including TASP compound libraries) become accessible.

As a first example of a potentially ligand (metal, substrate, antigen, transition state analogue) binding TASP compound, peptides derived from the CDR (complementarity-determining region) loop sequences of the phosphorylcholine binding monoclonal antibody McPC603[18, 19] were covalently attached to a topological template (Fig. 2d, **TASP I** in Scheme 2). Starting from a cyclic peptide with pairs of selectively addressable reactive sites, the stepwise condensation of three peptides (L^1–L^3) by amide bond formation according to strategy A′ provided **TASP I** in high yield and purity (Fig. 3c, left). It is noteworthy that even in the presence of two loops on the template, the condensation of the third loop proceeded smoothly as shown by the HPL chromatogram. Interestingly, the isomers (exhibiting the same molecular mass, Fig. 3c, center) with differently oriented loops were obtained in nonequimolar amounts, indicating an energetic nonequivalence of the different loop orientations. The CD spectra (Fig. 3c, right) show the characteristic features of a loop cluster conformation.[15, 20]

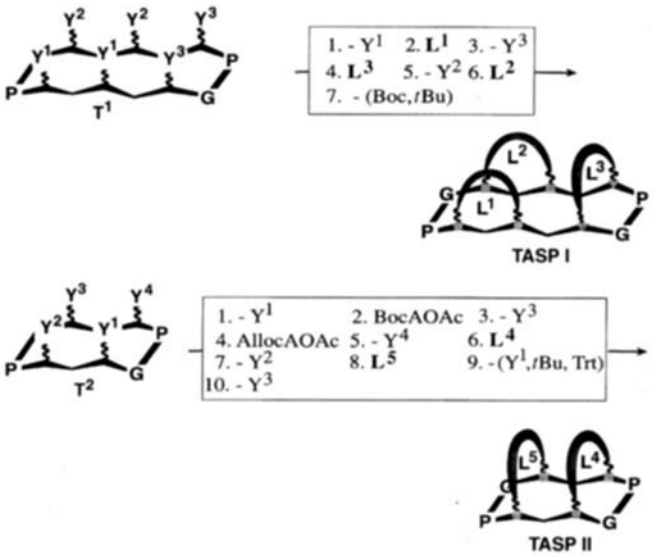

Scheme 2 Synthetic strategies for the assembly of **TASP I** (Fig. 2d) and **TASP II** (Fig. 2c). **TASP I**: L^1–L^3, T^1; **TASP II**: L^4, L^5, T^2 (Table 1).

The regioselective fixation of loops (strategy B) for TASP compounds with defined chain topology was illustrated by the design and synthesis of a potentially metal binding 2-loop TASP (Fig. 2c, **TASP II** in Scheme 2). To this end, two amino groups of the template T^2 were transformed into aminooxy groups as chemoselectively addressable attachment sites (steps 2 and 4 in Scheme 2). Subsequently, two peptides, each containing two histidine residues as metal binding sites (L^5, L^6), were fixed step by step by C-terminal amide and N-terminal oxime bond formation according to strategy B.

These prototype TASP compounds proved to be readily soluble in aqueous buffer solutions and polar organic solvents, and thus allowed a variety of biochemical investigations of the structure. Preliminary investigations on the conformational and binding properties support the hypothetical structures of T^2 suggested by molecular modeling studies (Fig. 2c, d).[21]

In summary, the presented strategies provide a synthetic entry to a new generation of TASP compounds, thereby extending the template concept[5] in protein design and mimicry. Most notably, the stepwise condensation of peptide loops to regioselectively addressable templates may be performed in aqueous solution and proceeds to completion within hours. The envisaged reattachment of the topological templates to the solid support will further simplify the multistep synthesis of differential loop cyclizations for generating TASP compound libraries. The state-of-the-art in chemoselective ligation and orthogonal protecting techniques determines the number of selectively attachable loops and thus the complexity of the TASP compounds. However, by exploiting the immense repertoire of synthetic organic chemistry for the incorporation of functional groups (sticky ends) into peptide chains, the scope of the present approach will be rapidly expanded. For example, ligand-directed assembly of helices, β-sheets, and loops onto tailor-made templates represents a new tool for studying supramolecular assembly and molecular recognition processes. Furthermore, this novel concept opens the way for a new generation of functional protein mimetics with a pivotal role in drug design.

Experimental Procedure

The templates and loop sequences (Table 1) were synthesized according to standard procedures in solid-phase peptide synthesis [22] by using orthogonally protected Lys, Glu, and Cys residues in the template sequence **T** as selectively addressable attachment sites for the loops. The N-terminal carboxyl group of L^1–L^3 was introduced by treating the resin-bound peptide with succinic anhydride. The aminooxyacetyl group (Y^6 in T^4) was introduced by coupling Y^iHNOCH_2COOH to the ε-NH_2 group of the lysine residue [9,11]. The aldehyde function in the loop sequences (**L**) was generated by mild oxidation ($NaIO_4$) of a serine residue attached either at the N-terminus (L^4, L^5, strategy B) or at the side chain of a lysine residue (L^6, L^7, strategies C, D). Coupling of maleoyl-β-alanine (Mal) with PyBop (PyBop = benzotriazol-1-yloxytris(pyrrolidino)phosphonium hexafluorophosphate) at the N-terminus (L^6) provided the functional group Mal applied in strategy C [12]. For the condensation of the loops L^i to the templates T^i, 1.1 equivalents of L^i were added to a 1 mM solution of T^i. Amide bond formation (A, B) was achieved by using PyBop as coupling reagent in DMF, oxime formation in acetate buffer, pH 4.5 (C,D), and thioether formation in buffer pH 7 (in combination with oxime pH 4; C). In general, the condensation reaction proceeded to completion within less than two hours at room temperature.

TASP I was synthesized by sequential removal of the Boc (TFA), Alloc ($[(Ph_3P)_2PdCl_2]/Bu_3SnH$), and Dde (2% $H_2NNH_2 \cdot H_2O$ in DMF) amino protecting groups in the template T^1 and subsequent ligation of L^1–L^3 in DMF through the activated N- and C-terminal carboxyl groups (1 equiv PyBop; strategy A′). After the final deprotection step (TFA), the target molecules were purified by reversed-phase HPLC (Vydac, C18) and characterized by ES-MS (Fig. 3c).

For the synthesis of **TASP II** (Scheme 2), the Boc amino protecting group in the template T^2 was removed (TFA) and the amine coupled with $BocHNOCH_2COOH$ (PyBop, DMF). In the second step, the Alloc group of T^2 was removed with

[$(Ph_3P)_2PdCl_2$]/Bu_3SnH] and AllocHNOCH$_2$COOH coupled to the ε-NH_2 group of the lysine residue (PyBop, DMF). After removal of the Fmoc group with 20% piperidine in DMF, L^4 was ligated through its C-terminal carboxyl group to the free ε-NH_2 group of lysine in T^2 (PyBop, 1 equiv); after removal of the Dde protecting group with 2% $H_2NNH_2 \cdot H_2O$ in DMF, L^5 was attached in the same manner. Subsequently, all acid-labile protecting groups were removed with TFA, the N-terminal serine residue in L^4 was oxidized with $NaIO_4$, and the first oxime bond was formed. Finally, Aloc was cleaved with [$(Ph_3P)_2PdCl_2$]/Bu_3SnH and the N-terminal serine residue in L^5 transformed to an aldehyde ($NaIO_4$), which readily formed the second oxime bond. The target molecules were characterized by ES-MS and amino acid analysis.

Received: February 8, 1996 [Z87971E]
German version: *Angew. Chem.* **1996**, *108*, 1587–1591

Keywords: protein mimetics · template syntheses

[1] G. Tuchscherer, M. Mutter, *J. Biotechnol.* **1995**, *41*, 197.
[2] G. Tuchscherer, B. Dörner, U. Sila, B. Kamber, M. Mutter, *Tetrahedron* **1993**, *49*, 3559.
[3] J. W. Bryson, S. F. Betz, H. S. Lu, D. J. Suich, H. X. Zhou, K. T. O'Neil, W. F. DeGrado, *Science* **1995**, *270*, 935.
[4] J. P. Schneider, J. W. Kelly, *Chem. Rev.* **1995**, *95*, 2169.
[5] M. Mutter, S. Vuilleumier, *Angew. Chem.* **1989**, *101*, 551; *Angew. Chem. Int. Ed. Engl.* **1989**, *28*, 535.
[6] M. Mutter, G. Tuchscherer, C. Miller, K. H. Altmann, R. I. Carey, D. F. Wyss, A. M. Labhardt, J. E. Rivier, *J. Am. Chem. Soc.* **1992**, *114*, 1463.
[7] G. Tuchscherer, M. Mutter, *J. Peptide Sci.* **1995**, *1*, 3.
[8] G. Tuchscherer, C. Servis, G. Corradin, U. Blum, J. Rivier, M. Mutter, *Protein Sci.* **1992**, *1*, 1377.
[9] K. Rose, *J. Am. Chem. Soc.* **1994**, *116*, 30.
[10] P. E. Dawson, S. B. H. Kent, *J. Am. Chem. Soc.* **1993**, 115, 7263.
[11] G. Tuchscherer, *Tetrahedron Lett.* **1993**, *34*, 8419.
[12] A. Nefzi, X. Sun, M. Mutter, *Tetrahedron Lett.* **1994**, *36*, 229.
[13] I. Ernest, J. Kalvoda, C. Sigel, G. Rihs, H. Fritz, M. J. J. Blommers, F. Raschdorf, E. Francotte, M. Mutter, *Helv. Chim. Acta* **1993**, *76*, 1539.
[14] P. Dumy, I. M. Eggleston, S. E. Cervigni, U. Sila, X. Sun, M. Mutter, *Tetrahedron Lett.* **1995**, *36*, 1255.
[15] P. Dumy, I. M. Eggleston, G. Esposito, S. Nicula, M. Mutter, *Biopolymers* **1996**, in press.
[16] R. A. Houghten, C. Pinilla, S. E. Blondelle, J. R. Appel, C. T. Dooley, J. H. Cuervo, *Nature* **1991**, *354*, 84.
[17] According to cyclization theory, the cyclization equilibrium constant K is proportional to the volume density $W(r)$ of the head to tail vectors $\langle r \rangle$ (where $\langle\ \rangle$ denotes the statistical mechanical average of r over all accessible loop conformations). Assuming in a first approximation a random coil conformation of the flexible loop sequence and a Gaussian distribution of $\langle r \rangle$, $W(r)$ at a fixed distance r_1 of the reacting chain ends (r_1 corresponds to the distance between the loop attachment sites on the template) approaches a maximal value for $r_1 \approx \langle r \rangle$. Consequently, the tendency for ring closure in loop condensation reactions (where $r_1 \rightarrow \langle r \rangle$) is predicted to be higher than in regular cyclization reactions (where $r_1 \rightarrow 0$). see: M. Mutter, *J. Am. Chem. Soc.* **1977**, *99*, 8307.
[18] Y. Satow, G. H. Cohen, E. A. Padlan, D. R. Davies, *J. Mol. Biol.* **1986**, *593*, 190.
[19] G. B. Bloomberg, D. Askin, A. R. Gargaro, M. J. A. Tanner, *Tetrahedron Lett.* **1993**, *34*, 4709.
[20] R. W. Woody, *Peptides, (NY)* **1985**, *7*, 15.
[21] These studies will be subject of a separate publication.
[22] J. M. Stewart, J. D. Young, *Solid Phase Peptide Synthesis*, 2nd ed., Pierce Chemical, Rockford, IL, **1984**.
[23] P. R. Gerber, *Biopolymers* **1992**, *32*, 1003.
[24] P. R. Gerber, K. Müller, *J. Comput. Aided Mol. Design* **1995**, *9*, 251.
[25] P. J. Flory, *Statistical Mechanics of Chain Molecules*, Interscience, New York, NY, **1969**.
[26] G. Fransson, B. K. S. Lundberg, *Acta Chem. Scand.* **1972**, 26, 3969.

Synthesis, Crystal Structure, and Magnetic Properties of an Octanuclear Nickel(II) Complex with a *hexahedro*-Ni_8 Core**

Juan Faus,* Francisco Lloret, Miguel Julve, Juan M. Clemente-Juan, M. Carmen Muñoz, Xavier Solans, and Mercedes Font-Bardía

There is currently great interest in polynuclear complexes of transition metals, a large and structurally diverse class of compounds.[1] Polynuclear high-spin nickel(II) complexes have been isolated with a large number of ligands, and much attention has been devoted to the study of their magnetic properties.[2] Most of them are dinuclear, but several trinuclear and cubane-like tetranuclear species have been studied.[2–4] Complexes of higher nuclearity are very scarce, although a few pentanuclear aggregates are known.[5] Very recently, a undecanuclear and a cyclic dodecanuclear species have been characterized.[4, 6]

The violurate anion H_2vi^- (H_3vi = violuric acid or 5-(hydroxyimino)-2,4,6-(1*H*,3*H*,5*H*)-pyrimidinetrione) is a strong-field, bidentate ligand, which coordinates to transition metal ions through the oxime-N atom and the O atom of a vicinal carbonyl group to form a five-membered chelate ring (Fig. 1).[7] Potentially, H_2vi^- is an ambidentate ligand, since it might bind the metal ions through the oxime-O atom and the O atom of the other vicinal carbonyl group to form in this case a six-membered chelate ring; it therefore might also be a bis(bidentate) bridging ligand (Fig. 1). However, these coordination modes have not been characterized up to now.

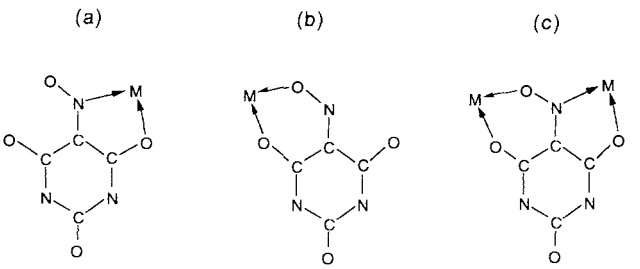

Fig. 1. Possible coordination modes of the violurato ligand (hydrogen atoms are not shown): a) bidentate-*N*,*O*; b) bidentate-*O*,*O* (unknown); c) bis(bidentate), bridging (this work).

Metal ion coordination increases the acidity of H_2vi^- considerably, which undergoes deprotonation much more easily than as a free acid.[8] The resulting Hvi^{2-} anion should exhibit a greater tendency to act as a bridging ligand, but although the deprotonation of some violurato complexes was investigated,[8] no polynuclear species is known.

[*] Prof. Dr. J. Faus, Dr. F. Lloret, Prof. Dr. M. Julve, J. M. Clemente-Juan
Departamento de Química Inorgánica, Facultad de Química
Universidad de Valencia
Dr. Moliner 50, E-46100-Burjassot, Valencia (Spain)
Fax: Int. code +(6)3864322
e-mail: juan.faus@uv.es
Dr. M. C. Muñoz
Departamento de Física Aplicada, Universidad Politécnica de Valencia
Prof. Dr. X. Solans, Dr. M. Font-Bardía
Departament de Cristal.lografia, Mineralogia i Dipòsits Minerals
Universidad de Barcelona

[**] This work was supported by the Spanish Dirección General de Investigación Científica y Técnica (DGICYT) (Projects PB94-1002 and PB94-0998) and the Human Capital and Mobility Program (Network on Magnetic Molecular Materials from EECC) through Grant ERBCHRX-CT920080.

Studies of complex formation between Ni^{2+} and H_2vi^- in a mixture of dimethylsulfoxide (DMSO) and water (80/20) as solvent showed the stepwise formation of mononuclear 1:1, 1:2, and 1:3 complexes.[9] The neutral 1:2 species is insoluble in water and precipitates quantitatively as $[Ni(H_2vi)_2(H_2O)_2]\cdot 3H_2O$; the anionic complex $[Ni(H_2vi)_3]^-$ has been isolated from ethanolic solutions as a sodium salt.[10] Although deprotonation products of these complexes were also reported,[9, 10] their molecular structures remain unknown.

We report here the synthesis, crystal structure, and magnetic properties of **1**, a compound that contains an octanuclear Ni^{II}

$K_4[Ni(H_2O)_6][Ni_8(Hvi)_{10}(H_2vi)_2]\cdot 20H_2O$ **1**

complex ion consisting of a cubic aggregate of nickel atoms linked by twelve μ-violurato ligands. A planar, octagonal, diamagnetic thiolatonickel(II) complex was characterized some years ago,[11] but **1** is the first paramagnetic octanuclear Ni^{II} complex. As far as we know, the only precedent for a *hexahedro*-Ni_8 geometry is found in the compounds $[Ni_8(\mu_4\text{-}PPh)_6(CO)_8]$, $[Ni_8(\mu_4\text{-}PPh)_6(CO)_4(PPh_3)_4]$, and $[Ni_8(\mu_4\text{-}PPh)_6Cl_4(PPh_3)_4]$, three closely related metal clusters with Ni–Ni bonds along the edges of the cube.[12]

Beautiful, black prisms of **1** are obtained in high yield in a one pot synthesis by slow precipitation of aqueous solutions of potassium acetate containing Ni^{2+} and H_2vi^- in a ligand-to-metal ratio of less than 2. Its formula could not be established by elemental analysis, but was determined by crystal structure analysis by X-ray diffraction.

Crystals of **1** consist of octanuclear $[Ni_8(Hvi)_{10}(H_2vi)_2]^{6-}$ complex anions, $[Ni(H_2O)_6]^{2+}$ and K^+ cations, and many molecules of water of crystallization. Each anion is formed by eight Ni^{2+} ions arranged at the vertices of a cube (edge length 4.8 Å) and linked through twelve bis(bidentate) violurato ligands (Fig. 2). There are no terminal ligands. Two ligands are coplanar with each face of the cube in such a way that the oximato bridges span two opposite edges in opposite directions. The N–O bonds cut the edges with angles varying between 23° and 53°, connecting two nickel atoms in a *trans* conformation. As far as we know, this is a new coordination mode for a μ-oximato ligand and causes a much longer metal–metal distance than the usual *cis* conformation.[13] The electric charge on the anion of 6 – is defined by the number of countercations, namely one $[Ni(H_2O)_6]^{2+}$ and four K^+ ions, which implies that ten of the twelve violurato ligands are Hvi^{2-} and two are H_2vi^- ions. Most likely, crystal packing effects dictate the incomplete deprotonation of the ligands. Each nickel(II) ion is coordinated to three ligands to give an octahedral geometry. Two different metal environments (NiN_3O_3 and NiO_6) alternate at the vertices of the cube. However, the complex unit has only a ternary axis and no twofold axis, with the result that four metal ions and four ligands are nonequivalent by symmetry.

We can rationalize the formation of this polynuclear complex as the result of the interaction between monomeric complexes $[Ni(Hvi)_3]^{4-}$ and Ni^{2+}. $[Ni(Hvi)_3]^{4-}$ can act as a tris(bidentate) O-donor ligand (μ_3-ligand) binding three Ni^{2+} cations. In this tetranuclear fragment the lines joining the central metal ion with the peripheral ones are mutually perpendicular, defining the corner of a cube. On the other hand, one Ni^{2+} can bind three of ligand complexes with the same Ni_4 geometry as above. Thus, the formation of a discrete *hexahedro*-Ni_8 species is a natural consequence of the spatial arrangement of three bidentate ligands around the metal ion in an octahedral complex and the relative position of the two pairs of donor atoms in a violurato bridge. It should be possible to synthesize similar homo- or even heterometallic cubic complexes with other metal ions.

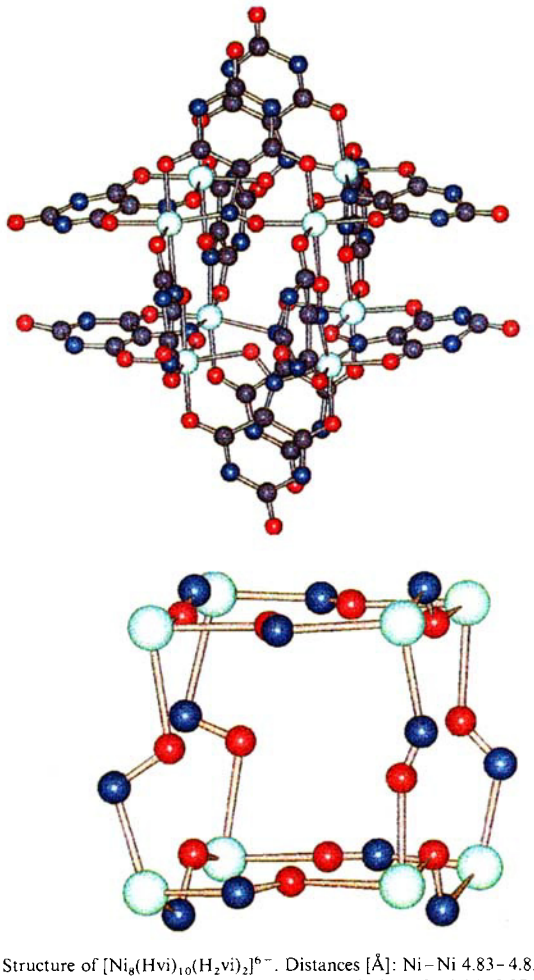

Fig. 2. Top: Structure of $[Ni_8(Hvi)_{10}(H_2vi)_2]^{6-}$. Distances [Å]: Ni–Ni 4.83–4.85, Ni–O 1.97–2.22, Ni–N 2.01–2.30. The nickel atoms are displaced by 0.06–0.07 Å above and below the mean planes of the square faces, which form dihedral angles of 90°. The dihedral angles between the mean planes of the violurato ligands and the faces of the cube vary between 4 and 7°. Bottom: A detail of the structure of $[Ni_8(Hvi)_{10}(H_2vi)_2]^{6-}$ showing only the nickel ions and the oximato groups of the violurato ligands.

The magnetic properties of **1** are shown in Figure 3. The product of the molar magnetic susceptibility by the absolute temperature (χT) decreases quickly on cooling, and a plot of this product against temperature gives a smooth sigmoidal curve. The value of χT at room temperature (7.5 $cm^3 mol^{-1} K$) is significantly smaller than that calculated for nine noninteracting Ni^{II} ions. This decrease reveals that a strong antiferromagnetic coupling is occurring among nickel(II) centers at distances of 4.8 Å. The value of χT at 4 K of 1 $cm^3 mol^{-1} K$ is due exclusively to the isolated $[Ni(H_2O)_6]^{2+}$ countercation; the cubic octanuclear complex has become diamagnetic.

Magnetic data have been analyzed with the spin Hamiltonian $\hat{H} = -J\sum S_i S_j$ ($i<j$, $i=1-8$). Calculations have been performed with a general program that takes into account the isotropic exchange interactions between the eight magnetic centers with the same spin, $S=1$. The effective Hamiltonian has been written in terms of irreducible tensors by applying the Wigner-Eckart theorem and the usual method of successive couplings. The theoretical curve fits the experimental data very well with $J = -60\ cm^{-1}$ and $g = 2.27$. A fixed χT contribution of 1.2 $cm^3 mol^{-1} K$ has been considered for the $[Ni(H_2O)_6]^{2+}$ ion. The limiting value at infinite temperature with uncoupled

 © VCH Verlagsgesellschaft mbH, D-69451 Weinheim, 1996 0570-0833/96/3513-1486 $ 15.00+.25/0

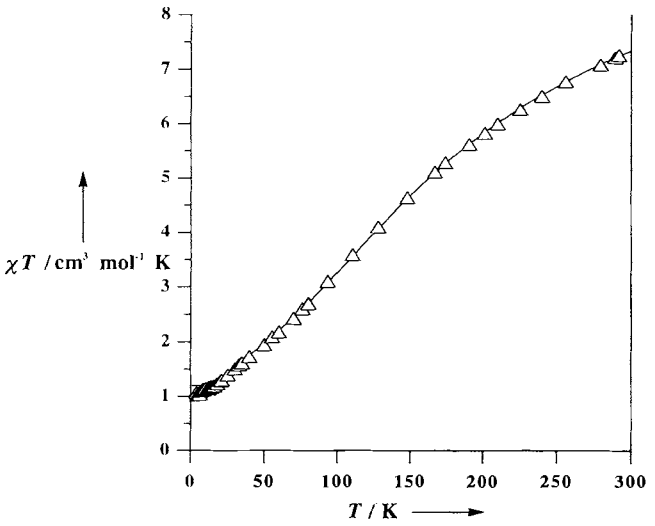

Fig. 3. Temperature dependence of χT for **1**. Triangles represent experimental points and the continuous line is the theoretical curve.

magnetic centers is 11.3 $cm^3 mol^{-1}$ K. This strong coupling is in agreement with the magnetic behavior of other oximato ligands[13] and clearly shows the special ability of a *trans* μ-oximato group to transmit electronic effects between distant metal ions.

The energy level diagram is complicated. It consists of 1107 different spin states associated with nine different values of total spin, from $S = 0$ to $S = 8$. The ground state is a singlet, the most excited state the only one with $S = 8$, and the energy gap between them about 1600 cm^{-1}.

Experimental Procedure

Synthesis of **1**: Potassium acetate (10 g) and nickel(II) acetate tetrahydrate (249 mg, 1 mmol) were dissolved in water (100 mL) under gentle heating. Violuric acid monohydrate (232.75 mg, 1.33 mmol) and LiOH (55.86 mg, 1.33 mmol) dissolved in water (50 mL) were then added. On standing, a black crystalline solid separated from the resulting dark solution. Precipitation began in a few hours and was complete in about two days. The solid was filtered, washed with water, and dried in the air (yield 85%). Anal.: C 18.7, N 16.39, H 1.95%; calcd: C 19.12, N 16.7, H 2.18%. The crystals obtained were suitable for X-ray diffraction studies.

Crystal structure analysis: Prismatic crystal, $0.1 \times 0.1 \times 0.2$ mm, crystal system trigonal, space group $R\bar{3}$, with $a = b = 16.007(2)$, $c = 36.284$ Å, $\alpha = \beta = 90°$, $\gamma = 120°$, $V = 8051(2)$ Å^3, $Z = 3$, $\rho_{calcd} = 1.840$ g cm^{-3}, $1.57° < \theta < 27°$, $Mo_{K\alpha}$ radiation ($\lambda = 0.71069$ Å), $T = 293(2)$ K. Of 4351 independent reflections measured ($\omega/2\theta$ scan), 2691 were assumed as observed ($I > 2\sigma(I)$). Lorentz polarization corrections but no absorption corrections were made. Absorption coefficient $\mu = 1.826$ mm^{-1}. The structure was solved by direct methods with the SHELXS computer program [14], 518 parameters refined by full-matrix least-squares method with the SHELXL-93 program [15], 3349 reflections used (very negative intensities not included). Hydrogen atoms were not found. $R = 0.0709$, $wR = 0.175$ (on $|F|^2$). Max./min. peaks in final difference synthesis 0.820/ − 0.580 e Å^{-3}, respectively. Crystallographic data (excluding structure factors) for the structure reported in this paper have been deposited with the Cambridge Crystallographic Data Centre as supplementary publication no. CCDC-179-61. Copies of the data can be obtained free of charge on application to The Director, CCDC, 12 Union Road, Cambridge CB21EZ, UK (Fax: Int. code +(1223) 336-033; e-mail: teched@chemcrys.cam.ac.uk.)

Received: February 7, 1996 [Z8793IE]
German version: *Angew. Chem.* **1996**, *108*, 1591–1593

Keywords: complexes with nitrogen ligands · magnetic properties · nickel compounds

[1] I. G. Dance in *Comprehensive Coordination Chemistry, Vol.1*, (Eds.: G. Wilkinson, R. D. Gillard, J. A. McCleverty), Pergamon, Oxford, **1987**, p. 135.
[2] L. Sacconi, F. Mani A. Bencini in *Comprehensive Coordination Chemistry, Vol.5* (Eds.: G. Wilkinson, R. D. Gillard, J. A. McCleverty), Pergamon, Oxford, **1987**, pp. 276–287.
[3] a) M. A. Halcrow, J. C. Huffman, G. Christou, *Angew. Chem.* **1995**, *107*, 971; *Angew. Chem. Int. Ed. Engl.* **1995**, *34*, 889; b) M. A. Halcrow, J. Sun, J. C. Huffman, G. Christou, *Inorg. Chem.* **1995**, *34*, 4167–4177.
[4] A. J. Blake, E. K. Brechin, A. Codron, R. O. Gould, C. M. Grant, S. Parsons, J. M. Rawson, R. E. P. Winpenny, *J. Chem. Soc. Chem. Commun.* **1995**, 1983.
[5] E. G. Bakalbassis, E. Diamantopoulou, S. P. Perlepes, C. P. Raptopoulou, V. Tangoulis, A. Terzis, T. F. Zafiropulos, *J. Chem. Soc. Chem. Commun.* **1995**, 1347, and references therein.
[6] A. J. Blake, C. M. Grant, S. Parsons, J. M. Rawson, R. E. P. Winpenny, *J. Chem. Soc. Chem. Commun.* **1994**, 2363.
[7] a) J. Faus, M. Julve, F. Lloret, M. C. Muñoz, *Inorg. Chem.* **1993**, *32*, 2013; b) J. Faus, M. Julve, F. Lloret, J. A. Real, J. Sletten, *ibid.* **1994**, *33*, 5535.
[8] a) F. Almazán, E. García-España, M. Mollar, F. Lloret, M. Julve, J. Faus, X. Solans, N. Alins, *J. Chem. Soc. Dalton Trans.* **1990**, 2565; b) C. Bremard, G. Nowogrocki, S. Sueur, *ibid.* **1981**, 1856; c) J. M. Moratal, J. Faus, *Inorg. Chim. Acta* **1977**, *25*, L1.
[9] E. García-España, J. M. Moratal, J. Faus, *Transition Met. Chem.* **1986**, *11*, 1.
[10] J. Moratal, J. Faus, *Rev. Chim. Miner.* **1979**, *16*, 203.
[11] I. G. Dance, M. L. Scudder, R. Secomb, *Inorg. Chem.* **1985**, *24*, 1201.
[12] a) L. D. Lower, L. F. Dahl, *J. Am. Chem. Soc.* **1976**, *98*, 5046; b) D. Fenske, R. Basoglu, J. Hachgenei, F. Rogel, *Angew. Chem.* **1984**, *96*, 160; *Angew. Chem. Int. Ed. Engl.* **1984**, *23*, 160.
[13] R. Ruiz, J. Sanz, B. Cervera, F. Lloret, M. Julve, C. Bois, J. Faus, M. C. Muñoz, *J. Chem. Soc. Dalton Trans.* **1993**, 1623; *ibid.* **1993**, 3035.
[14] G. M. Sheldrick, *Acta Crystallogr. Sect. A* **1990**, 467.
[15] G. M. Sheldrick, *SHELXL-93, A program for crystal structure refinement*, University of Gottingen, **1993**.

Sequence-Specific Recognition of DNA by a Major and Minor Groove Binding Ligand**

Jason W. Szewczyk, Eldon E. Baird, and Peter B. Dervan*

Two nonbiological approaches for the sequence-specific recognition of double helical DNA that target a broad repertoire of sequences are oligonucleotide-directed triple helix formation[1] and pyrrole/imidazole polyamide–DNA complexes.[2] For recognition of the major groove of DNA, a pyrimidine oligonucleotide binds parallel to the purine Watson–Crick strand.[1] Specificity is derived from thymine (T) recognition of adenine–thymine base pairs (T·AT base triplets) and protonated cytosine (C^+) recognition of guanine–cytosine base pairs (C^+·GC base triplets).[1] For recognition of the minor groove of DNA, polyamides containing *N*-methylimidazole (Im) and *N*-methylpyrrole (Py) amino acids are combined side-by-side and the DNA sequence-specificity is controlled by the linear sequence of pyrrole and imidazole amino acids.[2–4] Antiparallel pairing of imidazole (Im) opposite pyrrolecarboxamide (Py) targets a GC base pair, while pyrrolecarboxamide opposite imidazole targets a CG base pair.[2] A pyrrole/pyrrole pairing combination is partially degenerate and targets both TA and AT base pairs.[2, 3] A pyrrole/imidazole polyamide "hairpin" with γ-aminobutyric acid (γ) serving as a "turn monomer" provides a versatile motif for high-affinity recognition of a wide variety of sequences in the minor groove of DNA.[5] A key issue is to determine if the models of both major and minor groove binding

[*] Prof. P. B. Dervan, J. W. Szewczyk, E. E. Baird
Arnold and Mabel Beckman Laboratories of Chemical Synthesis
California Institute of Technology
Pasadena, CA 91125 (USA)
Fax: Int. code +(818)683-8753

[**] We are grateful to the National Institutes of Health for support (GM-27681) and to the Howard Hughes Medical Institute for a Predoctoral Fellowship to E. E. B.

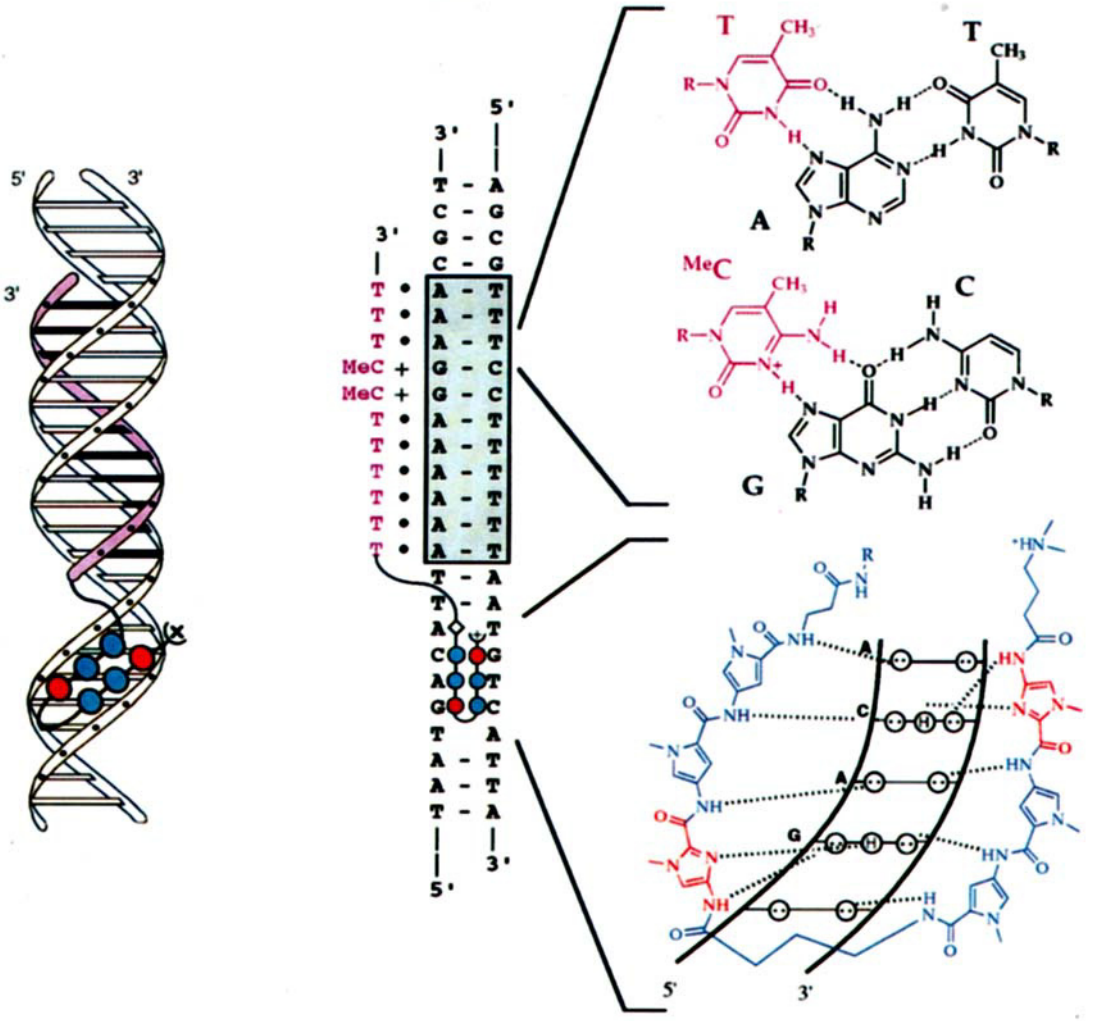

Fig. 1. Left: A ribbon model depicting a hairpin pyrrole/imidazole polyamide–oligonucleotide simultaneously binding the major and minor grooves of double helical DNA. The red and blue circles represent *N*-methylimidazole and *N*-methylpyrrole rings, respectively, and the diamond represents β-alanine. Right: Two-dimensional models depicting the molecular interactions responsible for sequence-specific recognition. Top right: The TAT and CGC base triplets formed by Hoogsteen hydrogen bonding of T to a Watson–Crick AT base pair and protonated ^{Me}C to a Watson–Crick GC base pair, respectively. The bases in the third strand are depicted in lavender, the bases in the Watson–Crick strand are depicted in black. Bottom right: Expected complex of ImPyPyγImPyPyβ with the binding site 5′-TGACA-3′. Circles with dots represent lone pairs on N3 of purines and O2 of pyrimidines, and circles containing an H represent the N2 hydrogen on guanine. Putative hydrogen bonds are illustrated by dashed lines.

recognition can be combined within a single molecule without compromising the sequence specificity of either recognition domain.

We report that a hairpin polyamide linked to an 11-mer oligonucleotide specifically and simultaneously binds the major and minor grooves of DNA at subnanomolar concentration. A pyrimidine oligonucleotide, 5′-TTTTTT^{Me}C^{Me}CTTT-3, covalently tethered by a twelve-atom linker to the polyamide of sequence composition ImPyPyγImPyPyβ (β = β-alanine) binds to 16 base pairs of double helical DNA by formation of a specific hairpin pyrrole/imidazole polyamide–DNA complex in the minor groove and a specific triple helix in the major groove (Fig. 1). According to the two binding models, the hybrid ligand–DNA complex affords 10 discrete hydrogen bonds for recognition of 5 base pairs in the minor groove (5′-TGACA-3′) and 22 discrete hydrogen bonds for recognition of 11 base pairs in the major groove (5′-AAAAAAGGAAA-3′).

The polyamide ImPyPyγImPyPyβ, modified with a free primary amino group at the C terminus, was prepared by solid-phase methods[6, 7] and allowed to react with either acetic anhydride to provide control hairpin **1**, or with a support-bound *N*-hydroxysuccinimide ester of a suitably 5′-modified 11-mer oligonucleotide 5′-TTTTTT^{Me}C^{Me}CTTT-3′ to provide the conjugate, ImPyPyγImPyPyβ-(linker)-TTTTTT^{Me}C^{Me}CTTT-3′ **3** upon deprotection.[8] Similarly, a control conjugate **4** was synthesized with a "reverse" polyamide sequence composition PyPyImγPyPyImβ. Polyamide–oligonucleotides **3** and **4** were purified by reverse-phase HPLC and the molecular composition

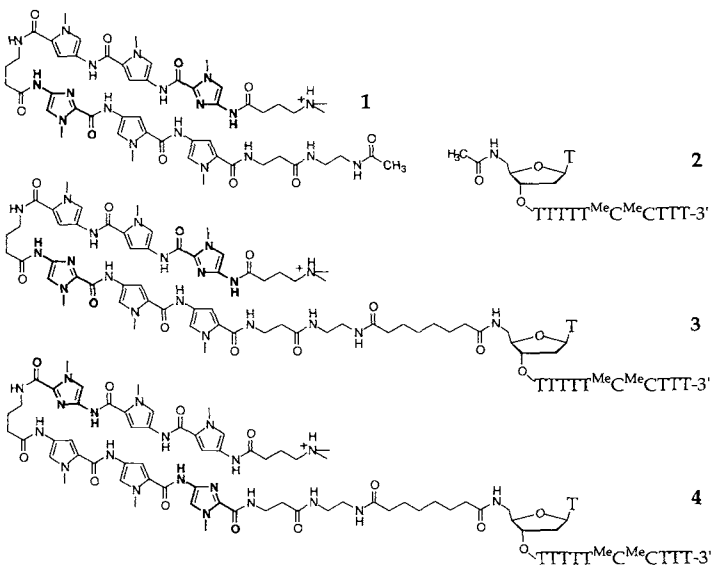

was verified by MALDI-TOF mass spectrometry,[9] UV spectroscopy,[10] and HPLC analysis of the products of enzymatic phosphodiester hydrolysis. A DNA fragment was constructed that contains the 18 base pair site 5′-*TGACA*T-*TAAAAAAGGAAA*-3′ composed of a 5 base pair polyamide binding site separated by two base pairs from an 11 base pair triple helix site. For controls, isolated 5 base pair polyamide and

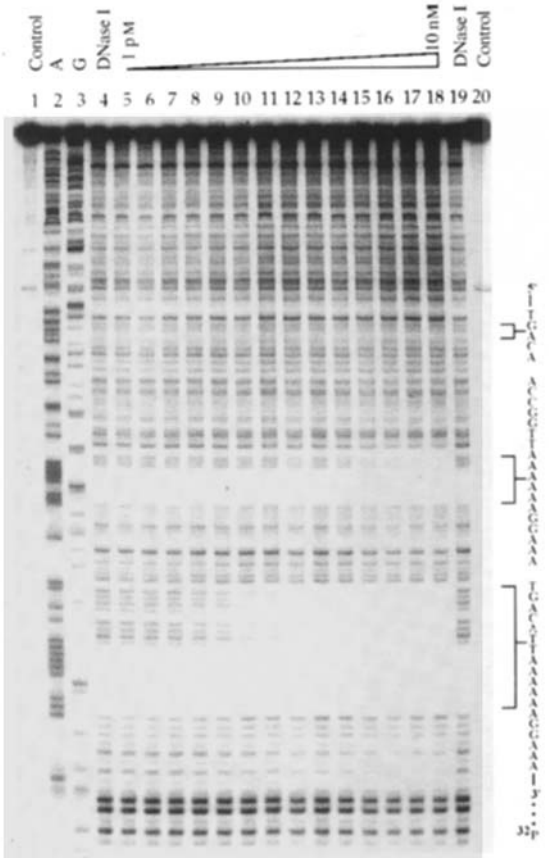

Fig. 2. DNaseI footprinting titration of pyrrole/imidazole polyamide–oligonucleotide **3** with a ^{32}P end-labeled 302 base pair restriction fragment. Gray scale representation of a storage phosphor autoradiogram of a 8% denaturing polyacrylamide gel representing a tenfold change in the signal from the lowest (5 arbitrary units, white) to highest (50 arbitrary units, black) intensities. The binding site is shown to the right of the autoradiogram. Lanes 1 and 20: intact DNA; lane 2: A reaction; lane 3: G reaction; lanes 4 and 19: DNaseI standard; lanes 5–18: 1, 5, 10, 20, 50, 100, 150, 250, 400, and 650 pM, and 1.5, 2.5, 6.5, and 10 nM polyamide–oligonucleotide **3**, respectively.

11 base pair triple helix binding sites were also present on the fragment.[11]

Quantitative DNaseI footprint titration experiments[12] on a 302 base pair restriction fragment afford the binding affinities of the designed ligands (Fig. 2). Polyamide **1** binds to five base pairs of the target site 5′-TGACATTAAAAAAGGAAA-3′ with an equilibrium association constant, $K_a = (1.3 \pm 0.3) \times 10^8\ M^{-1}$. Unmodified oligonucleotide **2** binds eleven base pairs 5′-TGACATTAAAAAAGGAAA-3′ with an equilibrium association constant, $K_a = (2.5 \pm 0.8) \times 10^5\ M^{-1}$. The hybrid polyamide–oligonucleotide **3** binds the designated target site 5′-TGACATTAAAAAAGGAAA-3′ with an apparent first-order equilibrium association constant, $K_a > 2 \times 10^{10}\ M^{-1}$,[13] representing at least a 150-fold increase in binding affinity relative to the unlinked subunits. In controls, the binding affinity of **3** at either the five base pair polyamide binding site, 5′-TGACATTAGCTCGTAATG-3′, ($K_a < 1.0 \times 10^5\ M^{-1}$) or the oligonucleotide eleven base pair site, 5′-ACCGGTTAAAAAAGGAAA-3′, ($K_a = 1.9 \times 10^9\ M^{-1}$) is reduced by approximately tenfold relative to binding at the designated match site. Mismatch polyamide–oligonucleotide **4**, binds the 18 base pair target, 5′-TGACATTAAAAAAGGAAA-3′, ($K_a = (6.1 \pm 0.2) \times 10^7\ M^{-1}$) with 300-fold reduced affinity relative to the match conjugate **3**.

Polyamide–oligonucleotide **3** binds with subnanomolar affinity only at the designated target site, indicating that the 3.0 kcal mol^{-1} binding enhancement results from *simultaneous* expand the repertoire of sequences targeted by artificial methods and create a new motif for the design of molecules for the sequence-specific recognition of both grooves of the DNA double helix.

Received: March 25, 1996 [Z 8974 IE]
German version: *Angew. Chem.* **1996**, *108*, 1596–1598

Keywords: DNA · polyamides · triple helices

[1] a) H. E. Moser, P. B. Dervan, *Science* **1987**, *238*, 645; b) T. Le Doan, L. Perrouault, D. Praseuth, N. Habhoub, J. L. Decout, N. T. Thoung, J. Lhomme, C. Helene, *Nucleic Acids Res.* **1987**, *15*, 7749.

[2] a) W. S. Wade, M. Mrksich, P. B. Dervan, *J. Am. Chem. Soc.* **1992**, *114*, 8783; b) M. Mrksich, W. S. Wade, T. J. Dwyer, B. H. Geierstanger, D. E. Wemmer, P. B. Dervan, *Proc. Natl. Acad. Sci. USA* **1992**, *89*, 7586; c) W. S. Wade, M. Mrksich, P. B. Dervan, *Biochemistry* **1993**, *32*, 11385.

[3] a) J. G. Pelton, D. E. Wemmer, *Proc. Natl. Acad. Sci. USA* **1989**, *86*, 5723; b) *J. Am. Chem. Soc.* **1990**, *112*, 1393.

[4] a) M. Mrksich, P. B. Dervan, *J. Am. Chem. Soc.* **1993**, *115*, 2572; b) B. H. Geierstanger, T. J. Dwyer, Y. Bathini, J. W. Lown, D. E. Wemmer, *ibid.* **1993**, *115*, 4474; c) M. Mrksich, P. B. Dervan, *ibid.* **1993**, *115*, 9892; d) T. J. Dwyer, B. H. Geierstanger, M. Mrksich, P. B. Dervan, D. E. Wemmer, *ibid.* **1993**, *115*, 9900; e) B. H. Geierstanger, J. P. Jacobsen, M. Mrksich, P. B. Dervan, D. E. Wemmer, *Biochemistry* **1994**, *33*, 3055; f) M. Mrksich, P. B. Dervan, *J. Am. Chem. Soc.* **1994**, *116*, 3663; g) B. H. Geierstanger, M. Mrksich, P. B. Dervan, D. E. Wemmer, *Science* **1994**, *266*, 646; h) M. Mrksich, P. B. Dervan, *J. Am. Chem. Soc.* **1995**, *117*, 3325.

[5] a) M. Mrksich, M. E. Parks, P. B. Dervan, *J. Am. Chem. Soc.* **1994**, *116*, 7983; b) M. E. Parks, E. E. Baird, P. B. Dervan, *ibid.*, in press.

[6] E. E. Baird, P. B. Dervan, *J. Am. Chem. Soc.*, in press.

[7] Pyrrole/imidazole polyamides were prepared by solid-phase methods [6], cleaved from the support with ethylenediamine, and purified by preparative HPLC. **1**: MALDI-TOF MS (M + H): found 1065.0, calcd 1065.1.

[8] The oligonucleotide was cleaved from the support and deprotected by treatment with 0.1 M NaOH (55 C, 18 h). For other synthetic methodology see A. N. Sinyakov, S. G. Lokhov, I. V. Kutyavin, H. B. Gamper, R. B. Meyer, *J. Am. Chem. Soc.* **1995**, *117*, 4995.

[9] **3**: MALDI-TOF MS (M − H): obsd 4487, calcd 4483; **4**: MALDI-TOF MS (M − H): obsd 4484, calcd 4483.

[10] The UV spectrum of the polyamide–oligonucleotide is a summantion of the spectra of the individual components: λ_{max} (ε) [H_2O] = 260 nm (138000), 310 nm (54000).

[11] The plasmid pCON1 was prepared by hybridization of two complementary sets of synthetic oligonucleotides 5′-d(CCGGGAACGTAATGACATTAGCTCG-TAATGTTATTAGCTCGCTAAGGT-CATTACCGGTTAAAAAAGGAA-ACGCTCGA)-3′,5′-d(GGCGTCGAGCGTTT-CCTTTTTTAACCGGTA-ATGACCTTAGCGAGCTAATAACATTACGAGCTAATGTC-ATTACG-TTC)-3′ and 5′-d(CGCCGCTAATGACATTAAAAAAGGAAACGCTC-GAGCTCGTGGGCCCTAGCGTCGTAGCTAGCGTCGTCTTAAG)-3′,5′-(TCGA-CTTAAGACGACGCTAGCTACGACGCTAGGGCCCACGAGC-TCGAGCGTTTCCTTTT-TTAATGTCATTAGC)-3′, which were subsequently ligated into pUC19 previously cleaved with *Ava*I and *Sal*I. The plasmid was digested with *Afl*II, labeled at the 3′ end, and digested with *Fsp*I. The 302 base pair restriction fragment was isolated by nondenaturing gel electrophoresis and used in all experiments described here.

[12] The quantitative footprint titration experiments were executed in a total volume of 400 μL with a final concentration of each species as indicated. The ligands were added to solutions of radio-labeled restriction fragment, NaCl (10 mM), Bis Tris·HCl (10 mM, pH 7.0), and spermine (250 μM), and incubated for 24 h at 22 C. Footprinting reactions were initiated by addition of 10 mL stock solution of DNaseI (2.4 units mL^{-1}) containing $MgCl_2$ (200 mM), $CaCl_2$ (200 mM), Bis Tris·HCl (10 mM), and glycerol (20%), and allowed to proceed for 6 min at 22 C. The reactions were quenched by addition of 50 μL of a solution made up of 107 μL of water, 788 μL of NaCl (4 M), 425 μL of EDTA (0.5 M, pH 8.0), 40 μL of calf thymus DNA (1 mM base pairs), 40 μL of glycogen (20 mg mL^{-1}). The DNA was precipitated by addition of ethanol, resuspended in 80% formamide loading buffer, and analyzed by electrophoresis on an 8% polyacrylamide denaturing gel at 2000 V for 1 h. Data analysis were performed as previously described [5a].

[13] Equilibrium association constants. $K_a > 1 \times 10^{10}\ M^{-1}$ determined by quantitative DNaseI footprint titration experiments represent lower estimates.

[14] a) J. P. Sluka, S. J. Horvath, M. F. Bruist, M. I. Simon, P. B. Dervan, *Science* **1987**, *238*, 1129; b) J. P. Sluka, S. J. Horvath, A. C. Glasgow, M. I. Simon, P. B. Dervan, *Biochemistry* **1990**, *29*, 6551; c) J. Feng, R. C. Johnson, R. E. Dickerson, *Science* **1994**, *263*, 348.

Selective Binding of the Dipeptides L-Phe-D-Pro and D-Phe-L-Pro to β-Cyclodextrin**

Milana Maletic,* Helma Wennemers,* D. Quentin McDonald, Ronald Breslow, and W. Clark Still

Over the past three decades inclusion complexes of cyclodextrins have emerged as one of the paradigms of host–guest chemistry.[1] The hydrophobic effect, which determines the binding of substrates to enzymes and antibodies to antigens, also drives the binding of hydrophobic molecules to cyclodextrins.[2] Although it is known that many biologically important molecules form stable inclusion complexes with cyclodextrins in water, the search for new substrates is continuing. Among the known cyclodextrin substrates are the hydrophobic amino acid residues: phenylalanine, tyrosine, and tryptophan. Their complexes with cyclodextrins have been exploited in enzyme modeling,[3] in drug delivery,[4] and in peptide separations.[5] However, cyclodextrin binding to small peptide fragments is still not well understood. In this report we study the binding of β-cyclodextrin to di- and tripeptides using a combinatorial chemistry approach.

In recent years combinatorial chemistry has become a major tool in the search for suitable substrates for a given receptor and vice versa.[6] By using such methods it has become possible to detect subtle differences in host–guest association, including binding selectivities that could not have been predicted by modeling or easily detected by conventional experiments.[7]

The orange-colored nickel salophen complexes **1** and **2** having two and one β-cyclodextrin substituents, respectively, were screened against a tripeptide library on hydrophilic poly(ethyleneglycol)polystyrene (TentaGel)[8] in water. The library was prepared by encoded split synthesis and had the general structure AA3-AA2-AA1-NH$(CH_2)_2$-Tent aGel.[9] At each position 29 different amino acids were used. Thus, the library contained maximally 29^3 (24389) different tripeptides.[10]

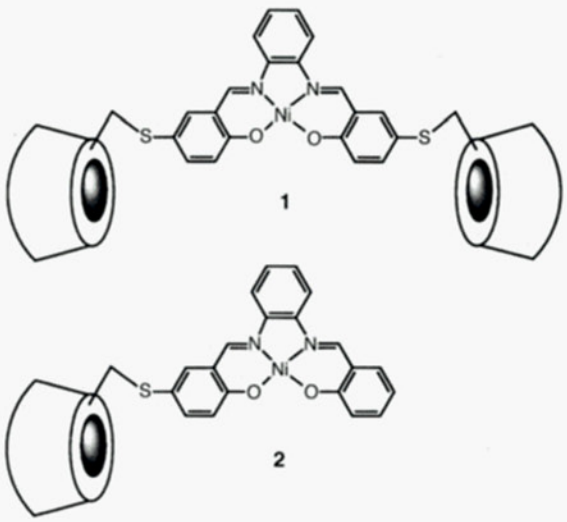

The bis(cyclodextrin) receptor **1** showed remarkably selective binding when screened against the tripeptide library in water at pH 7. After equilibration for 24 h, about 1 out of every 200 beads picked up the orange color of the receptors at a receptor concentration of roughly 2 mM. The same observation was made with the mono(cyclodextrin) receptor (Fig. 1), indicating that a single cyclodextrin unit is sufficient for the observed binding. Addition of sodium 4-*tert*-butylbenzoate as a competitive inhibitor for cyclodextrin caused desorption of the dye from the beads, suggesting the cyclodextrin to be the major locus of peptide binding.

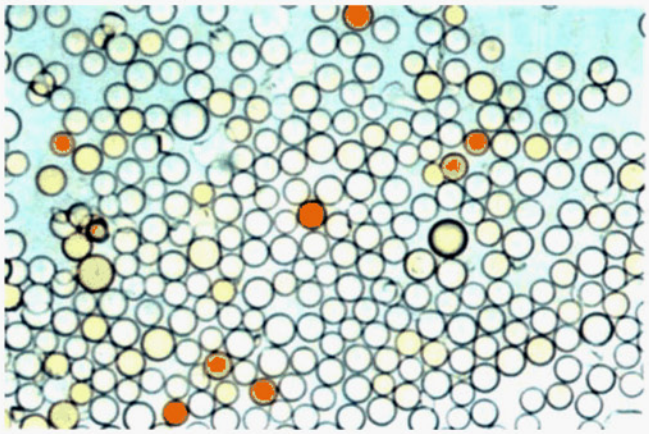

Fig. 1. Picture of a typical binding assay of receptor **2** to the described peptide library.

Decoding the tripeptides on the colored beads by using electron capture gas chromatography revealed a remarkable selectivity: *all* of the selected beads when receptor **1** was used and most of the selected beads when receptor **2** was used bore a sequence containing either L-Phe-D-Pro or D-Phe-L-Pro (Table 1). None of the other possible phenylalanine-containing dipeptides were found, and more interestingly, the diastereomeric, homochiral dipeptides L-Phe-L-Pro or D-Phe-D-Pro were not selected.

Table 1. Sequences selected by receptors **1** and **2** in the assay of the tripeptide library[a].

AA3	AA2	AA1	Frequency of occurrence [%] with 1	2
L-Phe	D-Pro	X	36	46
X	L-Phe	D-Pro	16	8
D-Phe	L-Pro	X	28	31
X	D-Phe	L-Pro	20	0

[a] X represents the third amino acid of the tripeptide.

In order to study this highly selective binding we synthesized the two dipeptides **3** and **4** and determined their binding energies

TFA·H_2N-L-Phe-D-Pro-CONHCH$_3$ **3**

TFA·H_2N-L-Phe-L-Pro-CONHCH$_3$ **4**

to β-cyclodextrin in aqueous solution by NMR-monitored titration. All binding studies were carried out at a constant concen-

[*] M. Maletic, Dipl.-Chem. H. Wennemers, Dr. D. Q. McDonald, Prof. R. Breslow, Prof. W. C. Still
Department of Chemistry, Columbia University
New York, NY 10027 (USA)
Fax: Int. code +(212)854-5429
e-mail: clark@still3.chem.columbia.edu

[**] We acknowledge the support of National Science Foundation (Grant CHE 9544253) (W. C. S.), the National Institute of Health, the Office of Naval Research (R. B.), and the Fonds der Chemischen Industrie (Kékulé Fellowship for H. W.). M. M. and H. W. contributed equally to the presented work.

tration of 2.0 mM of the dipeptide and with eight different amounts of β-cyclodextrin (0.0–13 mM) in D_2O. The binding curves were fit using KaleidaGraph and the standard iteration procedure.[11]

In the ^1H NMR spectrum of L-Phe-D-Pro mainly (>95%) one conformer, the *s-trans* conformer,[12] is visible and the signals of several protons shift significantly upon addition of β-cyclodextrin. The binding constant was found to be $180 \pm 20\ M^{-1}$ ($\Delta G = -3.0 \pm 0.1$ kcal mol^{-1}). Large upfield shifts are observed for three protons (H3′, H4′, H5′) of proline from one face of the pyrrolidine ring, whereas the three alkyl protons (H3, H4, H5) on the other proline ring face do not shift measurably. This finding is consistent with a binding mode where one face of proline fits over cyclodextrin as a "cap" and the phenyl ring of phenylalanine is fully inserted into the hydrophobic β-cyclodextrin cavity, allowing the more hydrophilic functional groups of the dipeptide to reside in water (see Fig. 2). Both the hydrophobic interaction between the pyrrolidine ring and the cyclodextrin cavity, and the encapsulation of the phenyl ring by the cavity account for the high stability of this complex. The binding constant of the *s-cis* conformer could not be determined due to its small population (< 5%).

The ^1H NMR spectrum of L-Phe-L-Pro shows that two conformers are present in a ratio of 5:1 in favor of the *s-trans* conformer.[12] In contrast to the D-L heteroisomer, the *s-trans* conformer of L-Phe-L-Pro binds to β-cyclodextrin only with low affinity. However, several peaks of the minor *s-cis* conformer exhibit large shifts when β-cyclodextrin is added, accounting for a binding constant of $120 \pm 5\ M^{-1}$ ($\Delta G = -2.8 \pm 0.1$ kcal mol^{-1}). During the binding titration the *s-trans*:*s-cis* ratio changes from 5:1 to 3:1, which is in agreement with the observed binding constant. The binding mode of the minor *s-cis* conformer to β-cyclodextrin seems to be analogous to that of the major *s-trans* conformer of the heterochiral dipeptide; all hydrophilic functional groups are exposed to the solvent. In contrast, the major *s-trans* L-Phe-L-Pro conformer binds more weakly to β-cyclodextrin because some of its hydrophilic functional groups cannot escape exposure to the hydrophobic cyclodextrin cavity. Its binding constant was estimated by NMR to be $20 \pm 5\ M^{-1}$ (saturation ca. 20%), which is on the same order of magnitude as the binding constant of phenylalanine alone to β-cyclodextrin.[4]

As the more tightly binding conformer of L-Phe-L-Pro is present at only 21%, it is not surprising that beads carrying L-Phe-L-Pro never picked up the deep orange color in the solid-phase binding assay.

To further investigate the structure of the dipeptide complexes with β-cyclodextrin, we performed extensive conformational searches using the MacroModel 5.0 program. The calculations used the united atom AMBER* force field[13] and the GB/SA model for water.[14] Searching was performed using the MCMM[15] method in blocks of 5000 steps and was continued until no further low-energy structures (<3 kcal mol^{-1} higher in energy than the global minimum) were located in any block (giving a total of 15000 steps for each complex). The search took account of all rotatable bonds in the peptide as well as rotation and translation of the peptide relative to β-cyclodextrin. The starting geometry of β-cyclodextrin was taken from its X-ray crystal structure.[16]

The conformational searches yielded low-energy structures that support the binding modes of the two dipeptides suggested by our NMR experiments. In the lowest energy structures of L-Phe-D-Pro and β-cyclodextrin, the phenyl and pyrrolidine rings are in close proximity and form a hydrophobic plug that is able to associate strongly with the cavity of the β-cyclodextrin (Fig. 2).

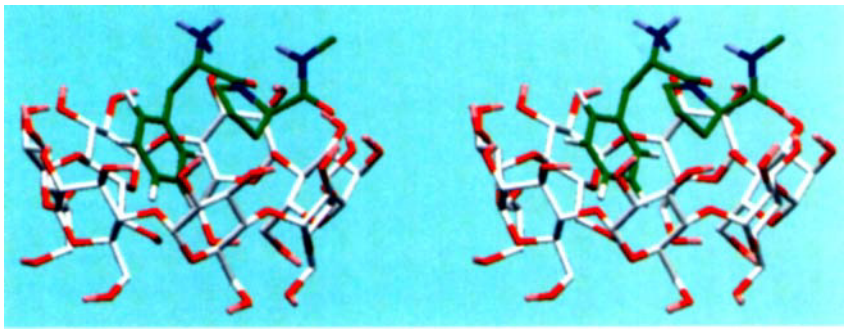

Fig. 2. Stereoview of the lowest energy structure of the complex between L-Phe-D-Pro and β-cyclodextrin as calculated with MacroModel 5.0.

The conformational search of L-Phe-L-Pro and β-cyclodextrin yields a similar structure for the *s-cis* conformer, but there are additional lower energy structures in which only the phenyl ring is included in the cavity and the hydrophobic proline ring is partially exposed to solvent at the cavity entrance.

In summary, by combinatorial means a remarkable binding selectivity of β-cyclodextrin to the enantiomeric dipeptides L-Phe-D-Pro and D-Phe-L-Pro was discovered. With the help of NMR spectroscopy it was possible to propose a binding mechanism. This selectivity could be exploited for the design of novel sequence-specific peptide-cleaving catalysts based on β-cyclodextrin.

Experimental Procedure

3: D-Pro-$NHCH_3$ (90 mg, 0.70 mmol) and *N*-Boc-L-Phe (186 mg, 0.70 mmol) were dissolved in 3 mL of CH_2Cl_2 and coupled with EDC (372 mg, 1.40 mmol). The *N*-Boc protected dipeptide was purified by flash chromatography on silica gel (CH_2Cl_2:acetone 5:1 then 2:1) and crystallization (Et_2O/hexanes). TFA (1 mL) was added to a solution of the *N*-Boc protected dipeptide (200 mg, 0.32 mmol) in 4 mL of CH_2Cl_2. Removal of all volatiles at reduced pressure after 1.5 h afforded 210 mg (80%) of TFA·L-Phe-D-Pro-$NHCH_3$ as a colorless solid. (TFA·L-Phe-D-Pro-$NHCH_3$ **4** was obtained analogously.)

3: TFA·L-Phe-D-Pro-$NHCH_3$ (*trans* conformer): ^1H NMR (500 MHz, D_2O, 25 C, CH_3CN): δ = 1.40 (m, 1H; Pro-H4′), 1.68 (m, 2H; Pro-H3 and Pro-H4), 1.90 (m, 1H; Pro-H3′), 2.60 (m, 1H; Pro-H5′), 2.61 (s, 3H; CH_3), 3.02 (dd, J = 13.4, 9.0 Hz, 1H; Phe-βH), 3.11 (dd, J = 13.4, 6.3 Hz, 1H; Phe-βH′), 3.38 (m, 1H; Pro-H5), 4.14 (dd, J = 4.6, 8.3 Hz, 1H; Pro-αH), 4.41 (dd, J = 6.3, 9.0 Hz, 1H; Phe-αH), 7.21 (m, 2H; arom.), 7.32 (m, 3H; arom.); ^{13}C NMR (75.4 MHz, CD_3OD, 25 C): δ = 25.24, 26.35, 30.78, 38.29, 48.45, 54.19, 61.65, 129.05, 130.07, 130.24, 130.37, 130.61, 135.44, 168.53, 174.55; high-resolution MS calcd for $C_{15}H_{21}N_3O_2$ (M^+): m/z: 275.1534; found: 275.1644.

4: TFA·L-Phe-L-Pro-$NHCH_3$: ^1H NMR (500 MHz, D_2O, 25 C, CH_3CN): *trans* conformer: δ = 1.77 (m, 1H; Pro-H3′), 1.85 (m, 2H; Pro-H4 and Pro-H4′), 2.13 (m, 1H; Pro-H3), 2.64 (s, 3H; CH_3), 2.99 (dd, J = 14.5, 7.5 Hz, 1H; Phe-βH′), 3.21 (dd, J = 14.5, 6.2 Hz, 1H; Phe-βH), 3.25 (m, 1H; Pro-H5′), 3.61 (m, 1H, Pro-H5), 4.27 (dd, J = 6.3, 8.1 Hz, 1H; Pro-αH), 4.43 (pseudo-t, J = 7.3 Hz, 1H; Phe-αH), 7.24 (m, 2H; arom.), 7.30 (m, 3H; arom.); *cis* conformer: δ = 1.56 (m, 3H; Pro-H3, Pro-H3′ and Pro-H4), 1.70 (m, 1H; Pro-H4), 2.60 (s, 3H; CH_3), 2.90 (dd, J = 13.2, 9.8 Hz, 1H; Phe-βH), 3.05 (dd, J = 13.2, 5.4 Hz, 1H; Phe-βH′), 3.29 (m, 1H; Pro-αH), 3.33 (m, 1H; Pro-H5), 3.42 (m, 1H; Pro-H5′), 3.80 (dd, J = 9.8, 5.4 Hz, 1H; Phe-αH), 7.13 (m, 2H; arom.), 7.27 (m, 3H; arom.); ^{13}C NMR (75.4 MHz, CD_3OD, 25 C): δ = 23.08, 26.00, 26.36, 26.66, 30.45, 32.62, 37.70, 38.90, 54.41, 61.38, 61.85, 128.89, 129.11, 130.13, 130.51, 130.81, 135.36, 135.43, 168.65, 174.15; high-resolution MS: calcd for $C_{15}H_{21}N_3O_2$ (M^+): m/z: 275.1534; found: 275.1633.

Compound **1** was prepared in analogy to known procedures [17]. ^{1}H NMR (400 MHz, [D$_6$]DMSO, 25 °C): δ = 8.98 (s, 2H; CH), 8.09 (m, 2H; CH), 7.74 (s, 2H; CH), 7.39 (m, 4H; CH), 6.87 (d, J = 8.8 Hz, 2H; CH), 5.74 (m, 28H; OH), 4.82 (m, 14H; CH), 4.48 (m, 12H; OH), 3.65 (m, 56H; 4CH, 2CH$_2$), 3.30 (m, 28H; CH). ^{13}C NMR (75.4 MHz, [D$_6$]DMSO, 25 °C): δ = 164.6, 156.2, 142.2, 139.3, 137.3, 128.0, 121.7, 120.7, 120.5, 116.3, 102.5, 102.0, 101.7, 84.9, 81.6, 81.4, 73.1, 72.9, 72.4, 72.1, 70.1, 60.0, 59.6. FAB-MS calcd for $C_{104}H_{151}N_2O_{70}S_2Ni$ ([M + H]$^+$): m/z: 2671.7; found: 2672; UV/Vis (H_2O): λ_{max} (ε) = 374 (20000), 273 (55000) nm.

Received: January 22, 1996 [Z8743IE]
German version: *Angew. Chem.* **1996**, *106*, 1594–1596

Keywords: combinatorial chemistry · cyclodextrins · molecular recognition · peptides

[1] M. L. Bender, M. Komiyama, *Cyclodextrin Chemistry*, Springer, New York, **1978**; W. Saenger, *Angew. Chem.* **1980**, *92*, 343–361; *Angew. Chem. Int. Ed. Engl.* **1980**, *19*, 344–362; J. Szejtli, *Cyclodextrins and Their Inclusion Complexes*, Akademiai Kiado, Budapest, **1982**.
[2] R. Breslow, *Acc. Chem. Res.* **1991**, *24*, 159–164.
[3] For a recent review, see: R. Breslow, *Acc. Chem. Res.* **1995**, *28*, 146–153.
[4] K. Matsuyama, S. El-Gizawy, J. H. Perrin, *Drug Dev. Ind. Pharm.* **1987**, *13*, 2687–2691; J. Horsky, J. Pitha, *J. Inclusion Phenom. Mol. Recognit. Chem.* **1994**, *18*, 291–300.
[5] A. Wutte, G. Gubitz, S. Friebe, G.-J. Krauss, *J. Chromatogr. A* **1994**, *661*, 7–12; *ibid.* **1994**, *677*, 186–191; K. B. Lipkowitz, S. Raghothama, J. Yang, *J. Am. Chem. Soc.* **1992**, *114*, 1554–1562.
[6] For recent reviews, see: M. A. Gallop, R. W. Barrett, W. J. Dower, S. P. A. Fodor, E. M. Gordon, *J. Med. Chem.* **1994**, *37*, 1233–1251, 1385–1401.
[7] A. Borchardt, W. C. Still, *J. Am. Chem. Soc.* **1994**, *116*, 7467–7468; H. Wennemers, S. S. Yoon, W. C. Still, *J. Org. Chem.* **1995**, *60*, 1108–1109.
[8] TentaGel S NH$_2$ from Rapp Polymere. E. Bayer, *Angew. Chem.* **1991**, *103*, 117–133; *Angew. Chem. Int. Ed. Engl.* **1991**, *30*, 113 129.
[9] A total of 15 tag molecules (five tags per AAn) were used to encode the library according to the method reported: M. H. J. Ohlmeyer, R. N. Swanson, L. W. Dillard, J. C. Reader, G. Asouline, R. Kobayashi, M. Wigler, W. C. Still, *Proc. Natl. Acad. Sci. U. S. A.* **1993**, *90*, 10922–10926.
[10] AAn = Gly, D-Ala, L-Ala, D-Val, L-Val, D-Leu, L-Leu, D-Phe, L-Phe, D-Pro, L-Pro, D-Ser, L-Ser, D-Thr, L-Thr, D-Asp, L-Asp, D-Glu, L-Glu, D-Asn, L-Asn, D-Gln, L-Gln, D-His, L-His, D-Lys, L-Lys, D-Arg, L-Arg. Note: tyrosine and tryptophan were not included in the library.
[11] K. A. Connors, *Binding Constants: "The Measurement of Molecular Complex Stability"*, Wiley, New York, **1987**; KaleidaGraph by Abelbeck Software.
[12] NOE difference experiments confirmed the identity of the *s-trans* and *s-cis* conformers of both dipeptides. The *s-trans* conformer shows a strong NOE between the α-H of Phe and the H4 proton of proline; the *s-cis* conformer shows a NOE between the α-H of Phe and the α-H of Pro. All peaks were assigned by ^{1}H,^{1}H-COSY experiments.
[13] D. Q. McDonald, W. C. Still, *Tetrahedron Lett.* **1992**, *33*, 7743–7746; H. Senderowitz, C. Parish, W. C. Still, *J. Am. Chem. Soc.* **1996**, in press.
[14] W. C. Still, A. Tempczyk, R. C. Hawley, T. Hendrickson, *J. Am. Chem. Soc.* **1990**, *112*, 6127–6129.
[15] G. Chang, W. C. Guida, W. C. Still, *J. Am. Chem. Soc.* **1989**, *111*, 4379–4386.
[16] CSD code BCDEXD1, K. Lindner, W. Saenger, *Angew. Chem.* **1978**, *90*, 738–740; *Angew. Chem. Int. Ed. Engl.* **1978**, *17*, 694–695.
[17] W. Zhang, E. N. Jacobsen, *J. Org. Chem.* **1991**, *56*, 2296-2298.

Self-Assembly of a Two-Component Hydrogen-Bonded Network: Comparison of the Two-Dimensional Structure Observed by Scanning Tunneling Microscopy and the Three-Dimensional Crystal Lattice**

Katrin Eichhorst-Gerner, Andreas Stabel, Georg Moessner, Dries Declerq, Suresh Valiyaveettil, Volker Enkelmann, Klaus Müllen,* and Jürgen P. Rabe*

Dedicated to Professor Marianne Baudler on the occasion of her 75th birthday

The self-assembly of molecules to form well-defined supramolecular structures under the influence of weak forces such as hydrogen bonds, electrostatic interactions, and hydrophobic effects in the solid state[1] and in solution[2] has been explored in detail. *Single-component* two-dimensional hydrogen-bonded networks of small molecules[3] and polymers[4] have previously been studied by scanning tunneling microscopy (STM); however, no molecular-scale images of monolayers of *stoichiometric* assemblies with *two or more components* have been reported. Having explored the self-assembly of 5-alkoxy isophthalic acids of the general formula C_nIsA (Scheme 1) in the bulk,[5–7] we

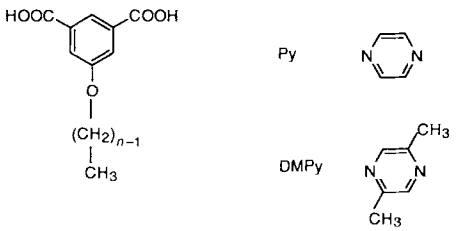

C_nIsA, n = 12, 16

Scheme 1. Left: General formula of the isophthalic acid derivatives discussed in the text. n gives the total number of C atoms of the alkoxy substituents. Right: Py = pyrazine, DMPy = 2,5-dimethylpyrazine.

present here STM images of these molecules and their 2:1 stoichiometric donor–acceptor complexes with the bifunctional bases pyrazine (Py) and 2,5-dimethylpyrazine (DMPy) with submolecular resolution. We compare the structural data obtained on the two-dimensional (2D) crystals by STM with those from X-ray structural analysis of the three-dimensional (3D) crystals.

STM images of highly ordered monolayers of C_{16}IsA (Fig. 1 top), C_{12}IsA · 0.5Py (Fig. 2 top), and C_{16}IsA · 0.5DMPy (Fig. 2 bottom) have been obtained with submolecular resolution.

[*] Prof. Dr. K. Müllen, Dr. A. Stabel, Dipl.-Chem. G. Moessner, Dr. D. Declercq, Dr. S. Valiyaveettil, Priv.-Doz. Dr. V. Enkelmann
Max-Planck-Institut für Polymerforschung
Postfach 3148, D-55021 Mainz (Germany)
Fax: Int. code +(6131)379100
Prof. Dr. J. P. Rabe, Dipl.-Phys. K. Eichhorst-Gerner
Institut für Physik der Humboldt Universität
Invalidenstrasse 110, D-10115 Berlin (Germany)
Fax: Int. code +(30)2803232
e-mail: rabe@physik.hu-berlin.de

[**] This work was supported by the BMBF projekt "Molekulare Elektronik" A. S. thanks the Fonds der chemischen Industrie for a Kekulé scholarship and S. V. acknowledges the Max-Planck-Gesellschaft for a fellowship.

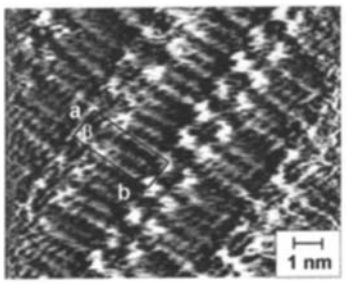

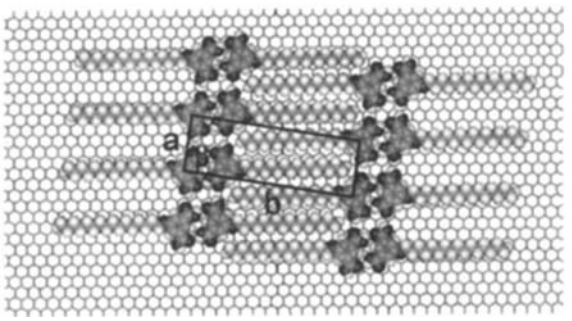

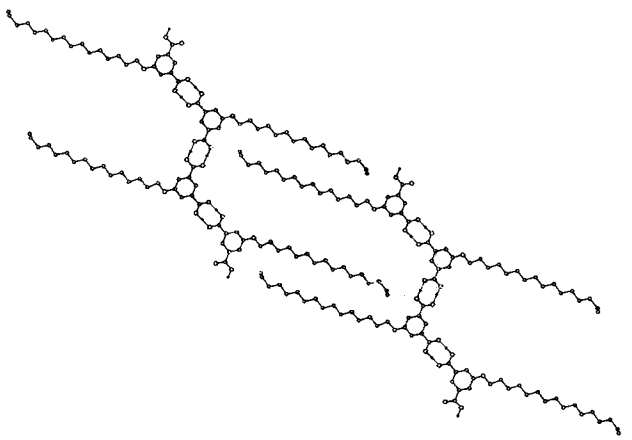

Fig. 1. Top: STM image of an ordered monolayer of C_{16}IsA on graphite with unit cell; $U_T = 0.6$ V, $I_T = 1.5$ nA. Middle: Schematic representation of 2D crystal lattice of C_{16}IsA as deduced from STM images. Bottom: 2D cut through the 3D crystal structure determined by single-crystal X-ray analysis; the hydrogen-bonded strands lie in the plane of the page

The unit cell data for the 2D crystals (see also Fig. 1 bottom) are summarized in Table 1. The 2D data were obtained by in-situ comparison with the underlying graphite lattice, the lattice constants of which are known. Refinement of the data was achieved by evaluating the Moiré pattern.[8] To allow a direct comparision of the 2D and 3D structures, another 2D unit cell with the parameters a, b, and β was defined for a 2D cut through the 3D crystal structure (see also Fig. 1 bottom).

In both the 2D and the 3D structures the pure acid (C_{16}IsA) forms closely packed arrays of interdigitating hydrogen-bonded ribbons. In the 3D structure two sets of planes are of interest: the first is defined by the hydrogen-bonded strands (see the plane of the drawing Fig. 1 bottom), and the second contains the alkyl chains; the two planes form an angle of 51°. However, in the 2D structure, the hydrogen-bonded strands and alkyl chains must lie in one plane. As a result, the hydrogen bonding pattern in the 2D structure is different from the one in the 3D crystal lattice. A proposal for the 2D hydrogen bonding pattern is depicted in Scheme 2.

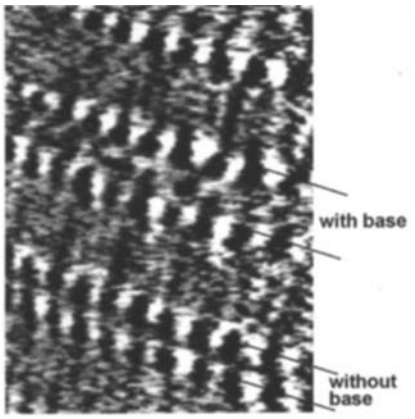

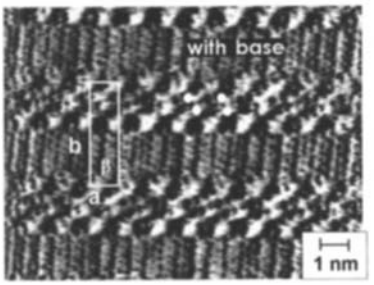

Fig. 2. Top: STM image of C_{12}IsA · 0.5Py on graphite; $U_T = 0.7$ V, $I_T = 1$ nA. No length scale is given because the image is slightly distorted (see text) in the horizontal direction. Bottom: STM image of an ordered monolayer of C_{16}IsA · 0.5DMPy on graphite with unit cell; $U_T = 0.6$ V, $I_T = 0.7$ nA

Table 1. Unit cell data of the 2D and 3D structures of the investigated compounds.

	2D Structure	2D cut through 3D structure [a]
C_{16}IsA		
a	0.93 ± 0.015 nm	1.572 nm [b]
b	3.3 ± 0.2 nm	2.654 nm
β	90 ± 2	104
C_{12}IsA · 0.5Py		
a	0.93 ± 0.015 nm	0.88 nm
b	3.44 ± 0.3 nm	3.36 nm
β	90 ± 2	93
A	3.20 nm²	2.95 nm²
C_{16}IsA · 0.5DMPy		
a	0.93 ± 0.015 nm	[c]
b	3.77 ± 0.2 nm	
β	90 ± 2	

[a] Determined from single-crystal X-ray structure [5] (see Fig. 3 top). [b] The 3D crystal structure of C_{16}IsA does not consist of flat planes, hence no 2D cut through this 3D crystal represents the structure completely. [c] X-ray powder diffractograms show that C_nIsA · 0.5 Py and C_nIsA · 0.5DMPy ($n = 12, 14, 16, 18, \ldots$) form homologous series of structures, in which the lattice parameters change by regular increments for each CH_2. CH_2 unit added [12].

The introduction of a bifunctional aromatic base such as pyrazine leads to strong hydrogen bonding between the COOH group and the N atom of the diazine, which, in turn, changes the self-assembly pattern.[9]

For the system C_{12}IsA · 0.5Py in 3D this results in a hydrogen-bonded network as was previously shown.[5] A cut through the 3D crystal (see Fig. 3 top) reveals a nearly close-packed structure. The STM image of a monolayer (see Fig. 2 top) shows that the structure corresponds closely to this crystal plane (see also Table 1). From the width of the lamellae one must con-

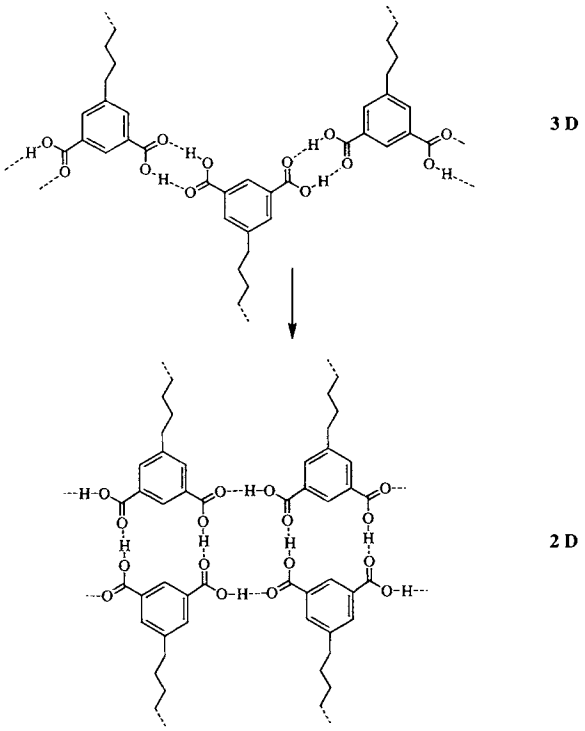

Scheme 2.

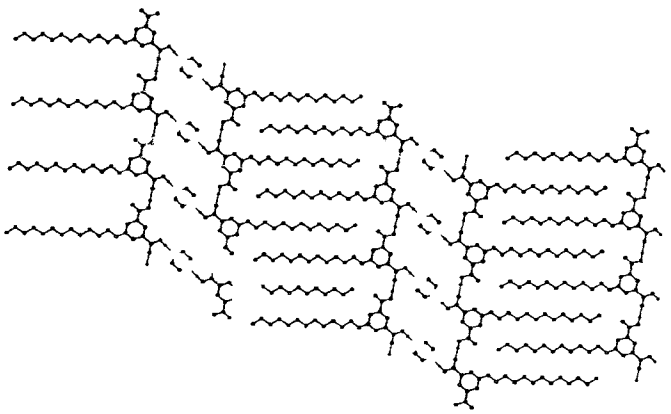

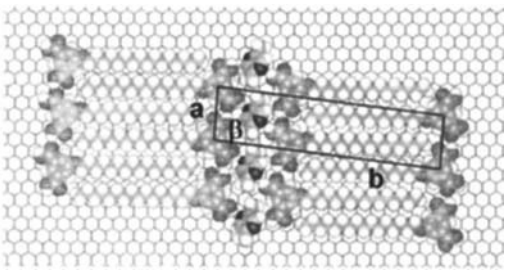

Fig. 3. Top: 2D cut through the 3D crystal structure of C_{12}IsA · 0.5Py. Bottom: Schematic representation of the 2D crystal lattice of C_{16}IsA · 0.5DMPy as deduced from STM images (see Fig. 2 bottom).

clude, however, that not all dimers contain a pyrazine acceptor molecule. This coexistence of two similar 2D crystal structures can be explained by the fact that the monolayer is in a dynamic equilibrium with the supernatant solution, which contains both acid and base. The relatively low resolution of Figure 2 top is attributed to some molecular mobility, which occurs because the plane is not completely close-packed along the row of the pyrazine molecules (see Fig. 3 top). Accordingly, the corresponding 2D packing observed by STM is less stable than a truly close-packed arrangement would be. Hence monolayer formation is not particularly favorable, and therefore almost saturated solutions are required in order to push the equilibrium between solvation and monolayer formation towards the latter. The beginning of bulk precipitation may then cause increased friction for the tip ploughing through, thereby causing some image distortion along the fast scan direction (here from right to left).

From studying the 2D-packing behavior of the complex with CPK models it can be deduced that the use of the 2,5-dimethyl-substituted pyrazine would lead to a more close-packed structure and hence to monolayers of higher stability. Another method for obtaining more stable monolayers of alkyl-substituted molecules at the solution–graphite interface is to increase the length of the alkyl chain.[10, 11] The system meeting these requirements, C_{16}IsA · 0.5DMPy, indeed displayed a greater monolayer stability, and therefore better quality STM images could be obtained (see Fig. 2 middle). It was also observed that the addition of DMPy stabilized the C_{16}IsA monolayer considerably. We attribute this phenomenon to the greater strength of the acid–base hydrogen bond as compared to the acid–acid hydrogen bond, which it replaces.[2c]

The 2D structure of C_{16}IsA 0.5DMPy consists of hydrogen-bonded strands of acid molecules. The alkyl side chains of two neighboring strands interdigitate and the resulting lamellae are cross-linked by diazine molecules. This structure is analogous to a projection plane of the 3D crystal structure of C_{16}IsA · 0.5Py. The 2D structure of C_{16}IsA · 0.5DMPy and a molecular sheet projection plane of the 3D structure of C_{12}IsA · 0.5Py are schematically depicted in Figure 3. They can be compared directly because the powder diffraction X-ray analysis of C_{16}IsA · 0.5Py reveals that it is isostructural to C_{12}IsA · 0.5Py.[12] A similar analogy between 2D and 3D crystal structures has previously been reported for long-chain alkanes,[13] fatty alcohols, and diols.[3c] In the case of C_{16}IsA · 0.5DMPy, the methyl substituents of the base DMPy occupy the existing free volume as anticipated, but leave the structure otherwise unaltered. The methyl groups are visible in the STM images (see Fig. 2 middle) and are highlighted by white dots in four illustrative cases.

In summary, we have presented STM images with submolecular resolution of monolayers of pure 5-alkoxyisophthalic acid and a donor–acceptor complex of the latter. Based on data from the X-ray crystal structure analysis, it has been possible to increase the stability of the monolayer by utilizing a space-filling base as an acceptor. Whereas the 2D structure of the pure acid shows little resemblance to its 3D structure, the 2D molecular sheet of the supramolecular assembly from a 2:1 mixture of the diacid and diazine is identical to a projection plane of the corresponding 3D crystal. We are currently extending the concept of donor–acceptor complex formation on graphite with a view to creating controlled two-dimensional molecular patterns and to designing monolayers that are two-dimensionally cross-linked by hydrogen bonding.

Experimental Procedure

The synthesis of C_nIsA has been described elsewhere [5]. Samples of highly oriented pyrolytic graphite (HOPG) (12 × 12 × 2 mm, quality ZYB) were obtained from Advanced Ceramics, Cleveland, USA.

A drop of solution (2 mM) of C_nIsA in phenyloctane was applied to a vertically placed slab of freshly cleaved HOPG with a Pasteur pipette. The drop slipped off the substrate leaving an approximately 20 μm thick liquid film on the surface [14], into which the tunneling tip was immersed. The physisorbed two-dimensional crystals

were investigated in situ at the solid–liquid interface using a scanning tunneling microscope (STM) constructed in our institute [15]. The tunneling tips were electrochemically etched (2 N KOH + 6 N NaCN) from a 0.25 mm Pt/Ir (80:20) wire. After the investigation of the pure C_nISA solution, a drop of pure Py or DMPy was added. After a few minutes, images of the stoichiometric compound could be recorded. Unless mentioned otherwise, the STM images were obtained in constant height mode under ambient conditions (scan rate: 0.3 Hz per image, positive tip bias, $U_T = 0.1$ to 1.0 V, $I_T = 0.5$ to 1 nA). They were recorded on videotape in real time and digitized later. Data are reported as recorded without digital image processing.

Single crystals suitable for X-ray crystal structure analyses [5, 6] were grown by slow evaporation of THF solutions. Crystal structure analyses were performed on an Enraf–Nonius CAD4 diffractometer, by using graphite-monochromated $Cu_{K\alpha}$ radiation ($\lambda = 1.5405$ Å). The structures were solved by direct methods (SIR 88, Molen) and refined by full-matrix least squares analyses with anisotropic temperature factors for C, N, and O. The H atoms were refined in the riding mode with fixed isotropic temperature factors.

Received: November 23, 1995 [Z 8585IE]
German version: *Angew. Chem.* **1996**, *108*, 1599–1602

Keywords: crystal engineering · hydrogen bonds · isophthalic acid · scanning tunneling microscopy

[1] a) G. R. Desiraju, *Crystal Engineering. The Design of Organic Solids*, Elsevier, Amsterdam, **1989**; b) J.-M. Lehn, *Angew. Chem.* **1990**, *102*, 1347; *Angew. Chem. Int. Ed. Engl.* **1990**, *29*, 1304; c) M. C. Etter, *Acc. Chem. Res.* **1990**, *23*, 120; d) G. F. Persico, J. D. Wuest, *J. Org. Chem.* **1993**, *58*, 95; e) S. C. Zimmerman, B. F. Duerr, *ibid.* **1992**, *57*, 2215; f) G. R. Desiraju, *Angew. Chem.* **1995**, *107*, 2541; *Angew. Chem. Int. Ed. Engl.* **1995**, *34*, 2328.

[2] a) G. M. Whitesides, J.-P. Mathias, C. T. Seto, *Science* **1991**, *254*, 1312; b) J.-P. Mathias, E. E. Simanek, C. T. Seto, G. M. Whitesides, *Macromol. Symp.* **1994**, *77*, 157; c) Y. Ikeura, K. Kurihara, T. Kunitake, *J. Am. Chem. Soc.* **1991**, *113*, 7342.

[3] a) S. Buchholz, J. P. Rabe, *Angew. Chem.* **1992**, *104*, 189; *Angew. Chem. Int. Ed. Engl.* **1992**, *31*, 189; b) R. Heinz, J. P. Rabe, W.-V. Meister, S. Hoffmann, *Thin Solid Films* **1995**, *264*, 246; c) N. J. Tao, Z. J. Shi, *J. Phys. Chem.* **1994**, *98*, 1464; d) R. Heinz, Dissertation, Universität Mainz, **1995**.

[4] M. Sano, M. O. Sandberg, S. Yoshimura, *Langmuir* **1994**, *10*, 3815.

[5] S. Valiyaveettil, V. Enkelmann, K. Müllen, *J. Chem. Soc. Chem. Commun.* **1994**, 2097.

[6] V. Enkelmann, S. Valiyaveettil, G. Moessner, K. Müllen, *Supramolecular Science* **1995**, *2*, 3.

[7] M. Pfaadt, G. Moessner, D. Pressner, S. Valiyaveettil, C. Boeffel, K. Müllen, H. W. Spiess, *J. Mater. Chem.* **1995**, *5*, 2265.

[8] A. Stabel, R. Heinz, F. C. De Schryver, J. P. Rabe, *J. Phys. Chem.* **1995**, *99*, 8690.

[9] a) J. Rebek, Jr., B. Askew, M. Killoran, D. Nemeth, F.-T. Lin, *J. Am. Chem. Soc.* **1987**, *109*, 2426; b) T. Kato, J. M. J. Fréchet, *ibid.* **1989**, *111*, 8533; c) T. Kato, J. M. J. Fréchet, P. G. Wilson, T. Saito, T. Uryu, A. Fujishima, C. Jin, F. Kaneuchi, *Chem. Mater.* **1993**, *5*, 1094.

[10] R. Hentschke, B. L. Schürmann, J. P. Rabe, *J. Chem. Phys.* **1992**, *96*, 6213.

[11] S. Buchholz, Dissertation, Universität Mainz, **1991**.

[12] G. Moessner, S. Valiyaveettil, unpublished results.

[13] J. P. Rabe, S. Buchholz, *Science* **1991**, *253*, 424.

[14] R. Heinz, A. Stabel, J. P. Rabe, G. Wegner, F. C. De Schryver, D. Corens, W. Dehaen, C. Süling, *Angew. Chem.* **1994**, *106*, 2154; *Angew. Chem. Int. Ed. Engl.* **1994**, *33*, 2080.

[15] J. P. Rabe, M. Sano, D. Batchelder, A. A. Kalatchev, *J. Microsc. (Oxford)* **1988**, *152*, 573.

Poly(phenylenesulfidephenylenamine) (PPSA)—the "Compound" of Polyphenylenesulfide with Polyaniline

Li Xiang Wang, Thomas Soczka-Guth, Edsko Havinga, and Klaus Müllen*

Polyphenylenesulfide (PPS) **2**[1] and polyaniline (PAni, pseudo leucoemeraldine form) **3**[2] are two remarkable polymers containing aromatic building blocks. Whereas PPS is notable for its chemical stability, the outstanding characteristic of PAni

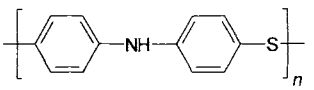

PPSA **1**

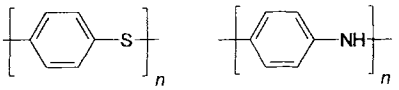

PPS **2** PAni **3**

is its ability to form electrically conducting films. The wide distribution of these two materials is attributed not only to their special properties but also to their ready accessibility: PPS can be prepared from 1,4-dichlorobenzene and sodium sulfide by the Philips process,[1] and PAni by the anodic or chemical oxidation of aniline.[2] We have combined PAni and PPS by the simple synthesis of poly(phenylenesulfidephenylenamine) (PPSA) **1**, which has promising electronic, mechanical, and optical properties.

In principle, **1** can be synthesized by forming either amino bridges or sulfide bridges; the latter method has been found to have certain advantages.[3] However, the condensation of methylsulfoxyarenes with another arene, with intermediate formation of a sulfonium cation, appears to be a particularly attractive method for producing diphenylsulfide units.[4]

We first investigated the suitability of this reaction for the condensation with diphenylamine units by synthesizing the model compound 4,4′-di(4-tolylsulfanyl)diphenylamine **8** (Scheme 1).

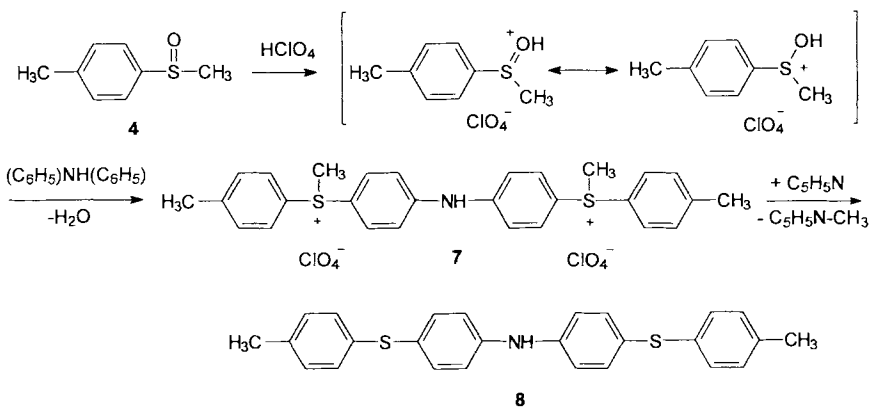

Scheme 1. Synthesis of **8** from **4**.

[*] Prof. Dr. K. Müllen, Dr. L. X. Wang, Dipl.-Chem. T. Soczka-Guth
Max-Planck-Institut für Polymerforschung
Postfach 3148, D-55021 Mainz (Germany)
Fax: Int. code +(6131)379-100
Dr. E. Havinga
Philips Research Laboratories
Prof. Hostlaan 4, NL-5600 AA Eindhoven (The Netherlands)

 © VCH Verlagsgesellschaft mbH, D-69451 Weinheim, 1996 0570-0833/96/3513-1495 $ 15.00+.25/0

The required methyltolyl sulfoxide **4** is prepared in high purity and in yields of 70–80% by the oxidation[5] of 4-methylthioanisole with Ce^{IV} (Scheme 2). The acid-induced condensation of **4** with diphenylamine leads quantitatively to the sulfonium salt **7**, which is demethylated by heating in pyridine to give **8** (95–98% yield).

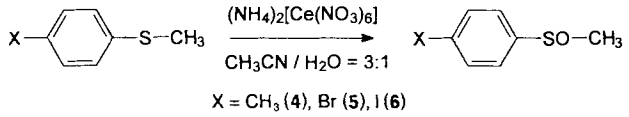

Scheme 2. Synthesis of **4**, **5**, and **6**.

Another model compound 4,4′-di(4′-methyldiphenylamine-4-sulfanyl)diphenylamine **11** can be obtained analogously to **8** by the reaction of 4-methylsulfinyl-4′-methyldiphenylamine **9**[6] with diphenylamine by first forming the sulfonium salt **10** and then demethylating this in 91% yield (Scheme 3). The monomer **12** required for the polymer synthesis can be obtained by the Cu^{I}-catalyzed reaction of 4-iodomethylsulfinylbenzene[5, 7] or of 4-bromomethylsulfinylbenzene[5] with aniline analogously to that with **9** (Scheme 4).[6]

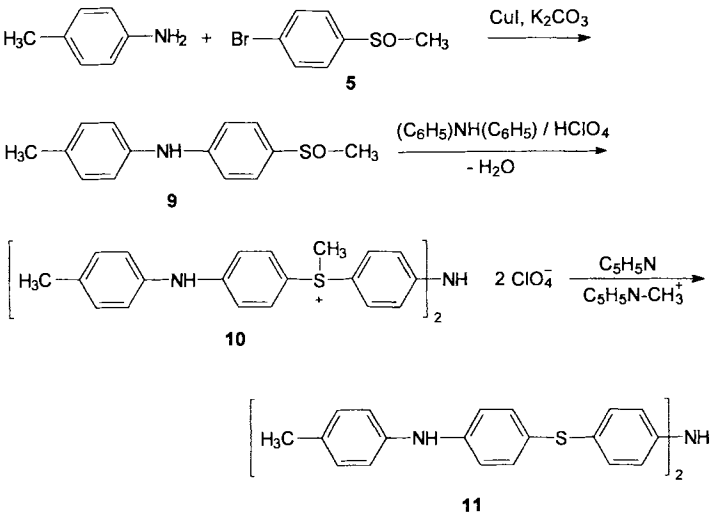

Scheme 3. Synthesis of **11**.

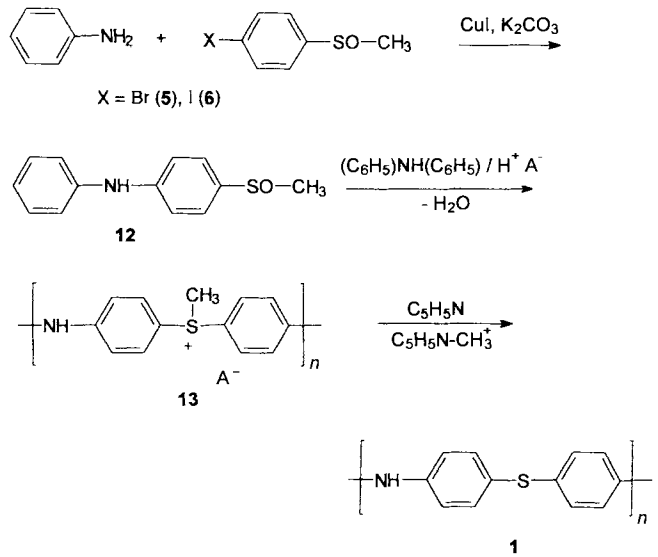

Scheme 4. Synthesis of **1** from the precursors **12** and **13**.

The precursor polymer **13**[8] is obtained in 94% yield by adding **12** to a strong acid. This polysulfonium salt **13** is soluble in pyridine, DMF, and *N*-methylpyrrolidone (NMP) at room temperature. A determination of the molar mass by size-exclusion chromatography was not possible because of interactions with the column material.

The title compound **1**, which is obtained in 98% yield by the demethylation of **13**,[9] is, unlike PPS and PAni, structurally well-defined and very soluble. In the ^{13}C NMR spectrum ([D_6]DMSO, 75 MHz) only the expected four signals (δ = 118.0, 125.7, 132.6, 142.7) were observed (IR (KBr) ν = 820 cm^{-1}; UV (quartz) λ_{max} = 204, 333 nm; fluorescence emission maxima (excitation 350 nm, THF) at 390, 410 nm). The molar mass was determined to be M_n = 109000 and M_w = 206000 by size-exclusion chromatography in THF,[10] and to be M_n = 110000 by membrane-osmometric measurements in DMF.[11] Thermogravimetric analysis showed that **1** is stable up to 380 °C.

The very high solubility of PPSA compared with that of PPS and PAni is surprising. Reasons for this could be the low crystallinity of PPSA and the lack of cross-linking in the structure.

Optically clear, free-standing films can be prepared from the solution of the polymer. The modulus of elasticity E of the polymer film was determined to be 1.3 GPa (PPS: E = 3.8 GPa). It is especially remarkable that films of **1** adhere very well to metals, especially gold.

The structural similarity between **1**, polyaniline, and polyphenylenesulfide raises the question of the electrochemical properties and dopability of the polymer. Investigations by cyclic voltammetry show that **8** is a substituted diphenylamine, since the half-wave potentials lie in the same range as those for 4,4′-disubstituted diphenylamines.[12] The half-wave potentials of **1** ($E_{1/2}$ = 0.67 V, $E_{1/2}$ = 1.17 V) correspond to those of **8**; the increase in current with the number of measured cycles is attributed to the increase in ionic concentration in the polymer film during the measuring process.[13]

Preliminary doping tests were carried out on free-standing films of **1**. Such films doped with $SbCl_5$ had a conductivity of 0.2 $S cm^{-1}$ and those doped with $FeCl_3$ 0.9 $S cm^{-1}$, and retained their flexibility even after doping.[14] The conductivity of the black films remains unchanged for several weeks in dry air. The conductivity, which is low in comparison to that of PPS (up to 200 $S cm^{-1}$)[15] and that of PAni (up to ca. 100 $S cm^{-1}$),[16] is likewise attributable to the low crystallinity of the PPSA.

An important aspect of this is the structural similarity of the dehydrogenation product of **1**, the polyaminyl radical **15** (polyphenylenesulfurnitride, PPSN), to the polysulfazene **14**, which has metallic conductivity properties.[17]

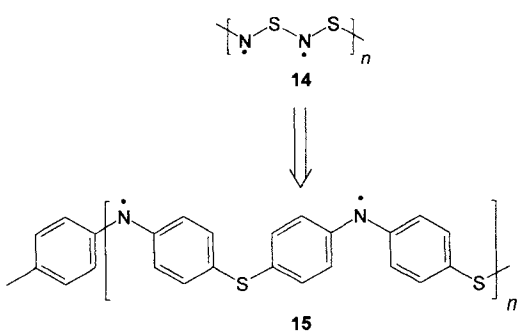

We have prepared the aminyl radical **16** of the model compound **8** by UV irradiation of a solution of **8** in toluene containing dibenzoyl peroxide, and have characterized this by ESR

 © VCH Verlagsgesellschaft mbH, D-69451 Weinheim, 1996 0570-0833/96/3513-1496 $ 15.00+.25/0

spectroscopy. The low g value (2.00374) and the coupling constants ($a_{H_o} = 0.338$ mT, $a_{H_m} = 0.133$ mT, $a_N = 0.802$ mT), which are typical of aminyl radicals, enabled the presence of a nitroxyl radical to be ruled out.[18] The diradical **17** (g = 2.00374) prepared by dehydrogenation of the model compound **11** could be confirmed by ESR spectroscopy. Zero field splitting at 135 K (toluene, glass) was determined to be 1.76 mT. The distance of 1.17 nm found from this by point dipole estimation is in good agreement with the calculated distance between the aminyl centers of 1.02 nm.[19]

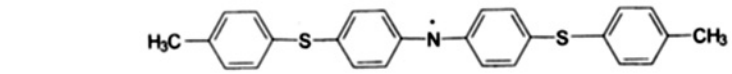

16

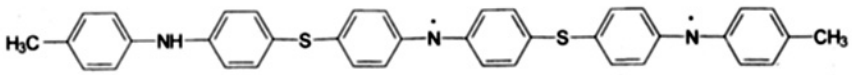

17

The new polymer PPSA has a well-defined structure and a high molecular weight. It is colorless, stable at temperatures up to 380 °C, very soluble in many common organic solvents, and dopable. Continuing investigations into its optical and electronic properties and into the conversion of **1** into the polyradical **15** are in progress.

Received: February 5, 1996 [Z8783IE]
German version: *Angew. Chem.* **1996**, *108*, 1602–1604

Keywords: aminyl radicals · polyphenylenamines · polyphenylenesulfides · polysulfazenes

[1] L. Freund, W. Heitz, *Makromol. Chem.* **1990**, *191*, 815; W. Heitz, M. Peter (Bayer AG), DE-A 4311139 A1 941006, **1993**; H. W. Hill in *High Performance Polymers: Their Origin and Development* (Ed.: R. B. Seymour, G. S. Kirschbaum), Elsevier, New York, **1986**, pp. 135–148; J. T. Edmonds, H. W. Hill (Philips Petroleum Co.), US-A 3 354 129, **1967**.

[2] A. G. MacDiarmid, A. J. Epstein in *Conjugated Polymeric Materials* (Eds.: J. L. Brédas, R. R. Chance), Kluwer, Boston, **1990**, p. 53; F. Lux, *Polymer* **1994**, *14*, 2915.

[3] T. Migita, T. Shimizu, Y. Asami, J. Shiobara, Y. Kato, M. Kosugi, *Bull. Chem. Soc. Jpn.* **1980**, *53*, 1385; J. Lindley, *Tetrahedron* **1984**, *40*, 1439; T. Fujisawa, M. Kakutani, *Polym. Lett.* **1970**, *8*, 511.

[4] E. Shouji, S. Nishimura, K. Yamamoto, E. Tsuchida, *Chem. Lett.* **1994**, 403; K. Yamamoto, E. Shouji, H. Nishide, E. Tsuchida, *J. Am. Chem. Soc.* **1993**, *115*, 5819; T. Fujisawa, M. Kakutani, N. Kobayashi, *Polym. Lett.* **1973**, *11*, 725.

[5] T. Ho, *Synthesis* **1973**, *2*, 347.

[6] **9**: toluidine, 4-bromomethylsulfoxybenzene, potassium carbonate, copper(I) iodide, 1,3-dimethyltetrahydro-2(1H)-pyrimidinone, 190 °C, 18 h, 35–45% yield.

[7] A. Gattermann, *Annalen der Chemie*, **1913**, *393*, 232.

[8] **13**: ^{1}H NMR (200 MHz, [D$_6$]DMSO): 9.58 (s, 1H, NH), 7.95 und 7.41 (d, 4H, J(H,H) = 8.7 Hz), 3.70 (s, 3H, S$^+$-CH$_3$); ^{13}C NMR (50 MHz, [D$_6$]DMSO): 146.6, 131.8, 118.7, 117.4, 117.4, 24.0.

[9] **1**: ^{1}H NMR (200 MHz, [D$_6$]DMSO): 8.41 (s, 1H, NH), 7.03 und 7.21 (d, 4H, J(H,H) = 9.2 Hz).

[10] Columns; SDV gel, 10-μ particles (10^3, 10^5, 10^6 Å), PS calibration.

[11] Abimed-MO-1, membrane-UF-C-10 (RC), DMF.

[12] G. Cauquis, H. Delhomme, D. Serve, *Tetrahedron Lett.* **1971**, *44*, 4113.

[13] R. Bilger, J. Heintze, *Synth. Met.* **1991**, *41–43*, 2893.

[14] Four-point measurements with linear test geometry, direct current.

[15] J. E. Frommer, R. L. Elsenbaum, R. R. Chance, *ACS Symp. Ser.* **1984**, *242*, 447.

[16] A. G. MacDiarmid in *Conjugated Polymers and Related Materials* (Eds.: W. R. Salaneck, I. Lundström, B. Ranby), Oxford University Press, Oxford, **1993**, p. 73, and references therein.

[17] C. M. Mikulski, P. J. Russo, M. S. Saran, A. D. MacDiarmid, A. F. Garito, A. J. Heeger, *J. Am. Chem. Soc.* **1975**, *97*, 6358.

[18] L. Grossi, *J. Chem. Soc. Chem. Commun.* **1989**, 1248; F. Neugebauer, S. Bamberger, *Chem. Ber.* **1974**, *107*, 2363.

[19] Geometry optimization by the AM-1 method; J. J. P. Stewart, *J. Am. Chem. Soc.* **1985**, *107*, 3902.

Synthesis and Structure of a Discrete Hexanuclear Uranium–Phosphate Complex**

Ladd M. Mokry, Norman S. Dean, and Carl J. Carrano*

Multinuclear complexes form a widespread group of inorganic materials that have both theoretical and practical importance.[1] They have added not only to our understanding of chemical bonding but they are also excellent models for many intermediates in heterogeneous catalytic processes.[2] Indeed some complexes have been prepared that are so large that the dividing line between discrete molecules and extended solids has become blurred.[1c, 3] While there are many representatives of this class of compound among both the p- and d-block metals, there seem few if any examples among the heavy f-block elements such as the actinides.[4] In the course of trying to prepare new phosphate-based chelating agents for extraction of the uranyl ion from aqueous waste streams (of importance to the nuclear power industry and environmental chemistry), we have prepared and characterized a novel hexanuclear uranium complex, which we believe to be the first high nuclearity "cluster" of this element ever reported.[5]

Reaction of one equivalent of [TpVCl$_2$(dmf)], where Tp = hydridotris(pyrazolyl)borate, with three equivalents of sodium diphenylphosphate and half an equivalent of uranyl acetate in aqueous acetonitrile under inert atmosphere produced a deep green solution. The deep green color is attributed to the initial formation of the μ-oxo-bis-(μ-acetato)divanadium(III) dimer, as determined by UV/Vis spectroscopy.[6] Over the course of several hours this solution turns light green and deposits a pale green solid (**1**). IR spectroscopic analysis of the product indicated the absence of the uranyl oxo groups and the trispyrazolylborate capping ligand, while demonstrating the presence of diphenylphosphate. Fortunately under high dilution conditions large green crystals of **1** were formed which allowed a detailed X-ray structural determination to be undertaken.[7]

The single-crystal structure of **1** is characterized by an octahedral array of uranium atoms, in which each face is capped by a μ_3-oxo (hydroxo) group (Fig. 1). Each uranium atom is further coordinated by four diphenylphosphate groups, which form bridges with its four nearest uranium neighbors. Thus, the uranium atoms are overall eight coordinate with approximate square anitiprism geometry (Fig. 2). All of the U–O bonds are essentially equivalent in length and lie in a narrow range between 2.30–2.42 Å. The U–U distances of about 3.85 Å are larger than the sum of the covalent radii, hence no metal–metal bonds are evident. Although the X-ray analysis allows an unequivocal determination of the overall structure, it provides no information concerning the protonation state of the capping ligands (i.e. oxo or hydroxo) since hydrogen atoms are not visible on the difference map in the presence of uranium, nor does it give a clue as to the oxidation sate of the uranium atoms. Simple charge

[*] Prof. C. J. Carrano, L. M. Mokry, Dr. N. S. Dean
Department of Chemistry
Southwest Texas State University
San Marcos, TX 78666 (USA)
Fax: Int. code +(512)245-2374
e-mail: cc05@swt.edu

[**] This work was supported by the Robert A. Welch Foundation (Grant AI-1157), the Dreyfus Foundation and the National Science Foundation (NSF-ILI instrumentation grant).

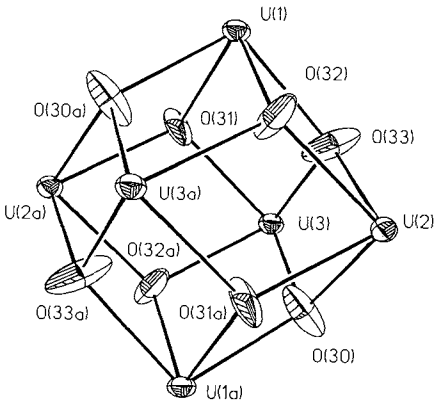

Fig. 1. View of the core structure of **1** (30% probability ellipsoids).

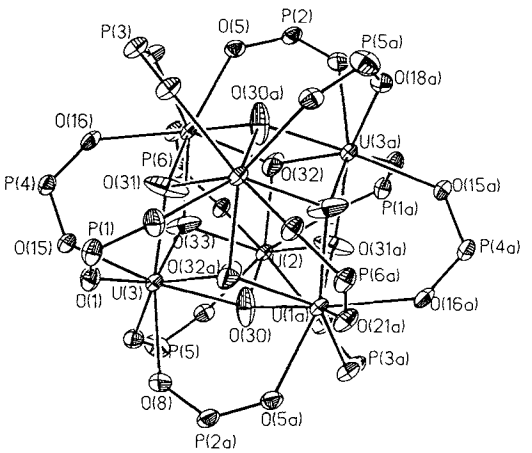

Fig. 2. Structure of **1** in the crystal (30% probability ellipsoids). Phenoxy groups on P and all hydrogen atoms have been omitted for clarity.

considerations predicts an average uranium valence of 4.67 (formally two U^{VI} and four U^{IV}) if one assumes μ_3-oxo capping ligands. For μ_3-hydroxo capping ligands an average valence of 3.33 (formally four U^{III} and two U^{IV}) is expected. In either case the valences appear to be completely delocalized as all the uranium atoms are structurally equivalent. Several lines of evidence led us to favor the the presence of μ_3-hydroxo capping ligands. First, the thermal ellipsoids of the μ_3-oxygen atoms are all elongated normal to the trigonal face such as might be expected if there were unaccounted for electron density due to a bound proton. The analytical data also fit best to a formulation with hydroxo groups, and the presence of a sharp band at 3581 cm^{-1} in the IR spectrum is readily assigned as a non-hydrogen bonded O–H stretching vibration. Finally, we have also undertaken a bond valence sum (BVS) analysis, a procedure that has found widespread utility in assigning ambiguous oxidation states in metal clusters.[9] The BVS analysis gives an average valence of 3.33, a value consistent only with the hydroxo formulation. In any event it is clear that the vanadium(III) must provide the reducing equivalents, as the well-characterized vanadium(IV) complex $[\{TpVO(C_6H_5O)_2PO\}_2]_2$ is the only other identifiable product produced.[10] The room temperature magnetic moment has been measured but appears to be less than that expected for either of the valence formulations, suggesting perhaps some superexchange mediated spin coupling.[11] However, the interpretation of magnetic data for the actinides is very complex and a complete analysis will require a variable temperature study.

The results presented here demonstrate that there is nothing inherently unstable about high nuclearity actinide complexes, and we expect to see the number of such well-characterized complexes grow rapidly because of their potential applications. The emerging chemistry of uranium hydroxides and alkoxides represents, for example, important models for the complexes likely to be present in aqueous solutions of the actinides, which may be environmentally important species involved in transporting these elements in ground waters.[12] In addition these high nuclearity complexes may have useful roles to play as X-ray contrast and protein labeling agents.[13]

Experimental Procedure

1: To a mixture of $[TpVCl_2(dmf)]$ (0.41 g, 1 mmol) and uranyl acetate (0.2 g, 0.5 mmol) dissolved in acetonitrile (30 mL) was added a solution of the sodium salt of diphenylphosphate (0.72 g, 3 mmol) in H_2O (1 mL). After the mixture had been stirred overnight, the pale green precipitate was filtered off and washed with water and acetonitrile to yield 0.21 g (54% based on uranium) of product. Elemental analysis: Found: C 38.06, H 2.89%; calcd: C 38.09, H 2.83%. IR (KBr): $\nu[cm^{-1}]$ = 3581(w), 3071(w), 1591(m), 1491(m), 1213(s), 1095(s), 951(s), 780(m), 683(m), 533(m), 510(m). Magnetic moment at 298 K is 2.3 BM mol^{-1}. UV/Vis (dichloromethane): λ[nm] = 432, 468, 492, 510, 550, 636, 652, 670.

Received: December 22, 1995 [Z8683IE]
German version: *Angew. Chem.* **1996**, *108*, 1676–1677

Keywords: multinuclear complexes · phosphorus compounds uranium compounds

[1] See for example: a) D. M. P. Mingos, T. Sloe, L. Zhenyang, *Chem. Rev.* **1990**, *90*, 383; b) G. Schmid, *Chem. Rev.* **1992**, *92*, 1709; c) *Clusters and Colloids* (Ed.: G. Schmid), VCH, Weinheim, **1994**.
[2] L. N. Lewis, *Chem. Rev.* **1993**, *93*, 2693.
[3] D. Fenske, H. Krautscheid, *Angew. Chem.* **1990**, *102*, 1513; *Angew. Chem. Int. Ed. Engl.* **1990**, *29*, 1452.
[4] Some Th "clusters" are known see for example: a) A. Simon, F. Böttcher, J. K. Cockcroft, *Angew. Chem.* **1991**, *103*, 79; *Angew. Chem. Int. Ed. Engl.* **1991**, *30*, 101; b) T. P. Brown, A. Simon, F. Böttcher, F. Ueno, *Angew. Chem.* **1995**, *107*, 647; *Angew. Chem. Int. Ed. Engl.* **1995**, *34*, 567.
[5] Our search through the literature turned up only a few tetranuclear and no larger structurally characterized complexes of uranium. See *Chem. Rev.* **1994**, *94*, 895, as well as ref. [9].
[6] M. R. Bond, R. S. Czernuszewicz, B. Dave, Q. Yan, M. Mohan, R. Verastegue, C. J. Carrano, *Inorg. Chem.* **1995**, *34*, 5857.
[7] Crystal structure of **1**: $C_{144}H_{128}O_{56}P_{12}U_6$, M_r = 4554.2 $g mol^{-1}$; crystal dimensions 0.5 × 0.8 × 0.25 mm^3, triclinic, space group $P\bar{1}$, a = 16.357(5), b = 16.475(3), c = 16.544(3) Å, α = 107.25(2), β = 101.36(2), γ = 108.06(2)°, Z = 1, V = 3837.6(15) $Å^3$, ρ_{calcd} = 1.967 $mg m^{-3}$, T = 298 K, $2\theta_{max}$ = 45.0°, Siemens P4 diffractometer, $Mo_{K\alpha}$ radiation (λ = 0.71073 Å), 0-2θ scan, 11168 reflections collected, 9598 independent (R_{int} = 0.030), 7409 observed with $F > 4\sigma(F_o)$, heavy atom method, $\sigma w(F_o - F_c)^2$ minimized with $w^{-1} = \sigma^2(F) + 0.0008F^2$, 966 parameters refined, R = 0.0487, wR = 0.0587. Crystallographic data (excluding structure factors) for the structure(s) reported in this paper have been deposited with the Cambridge Crystallographic Data Centre as supplementary publication no. CCDC-179-37. Copies of the data can be obtained free of charge on application to The Director, CCDC, 12 Union Road, Cambridge CB2 1EZ, UK (fax: Int. code +(1223) 336-033; e-mail: teched@chemcrys.cam.ac.uk).
[8] Alternatively of course this may be due to simple oxo/hydroxo group disorder.
[9] I. D. Brown, D. Altermatt, *Acta Crystallogr. B* **1985**, *41*, 244; see also a) V. Soghomoniun, R. C. Haushalter, Q. Chen, J. Zubieta, *Inorg. Chem.* **1994**, *33*, 1700; b) Q. Chen, J. Zubieta, *J. Chem. Soc. Chem. Comm.* **1994**, 2663, for examples of its use.
[10] M. R. Bond, L. M. Mokry, T. Otieno, J. Thompson, C. J. Carrano, *Inorg. Chem.* **1995**, *34*, 1894.
[11] M. Bickel, B. Kanellakopulos, *J. Solid State Chem.* **1993**, 107, 273.
[12] W. G. Van der Sluys, A. P. Sattelberger, *Chem. Rev.* **1990**, *90*, 1027.
[13] E. A. Deutsch, K. F. Deutsch, D. L. Nosco, U. S. pat. no. 91-699848 910805, **1995**.

2-Triaxanemethyl Cation and 2,10-*para*-[3².5⁶]Octahedranedimethyl Dication**

George A. Olah,* Herwig A. Buchholz,* G. K. Surya Prakash,* Golam Rasul, James J. Sosnowski, Roger K. Murray Jr.,* Mikhael A. Kusnetsov, Shelue Liang, and Armin de Meijere*

Dedicated to Professor Ivar Ugi on the occasion of his 65th birthday

Cyclopropylmethyl cations are among the most extensively studied class of carbocations. The rapid interconversions of cyclopropylmethyl, cyclobutyl, and homoallyl derivatives via carbocation intermediates have attracted considerable attention.[1] Historically cyclopropylmethyl cations were the first carbocations to be named "nonclassical",[1, 2] and many interesting and intriguing studies concerning the direct observation of cyclopropylmethyl cations under stable ion conditions by NMR spectroscopy have recently been reviewed.[2g]

The parent primary cyclopropylmethyl cation $C_4H_7^+$ was characterized by ^1H and ^{13}C NMR spectroscopy under stable ion conditions by Olah and co-workers as early as 1970.[3] Subsequent low-temperature NMR evidence on ^{13}C-[4, 5] and ^2H-labeled[6] systems, including solid-state NMR measurements[7a] and high-level ab initio calculations,[7b] excluded classical cyclopropylmethyl or cyclobutyl ion structures. Rather, the cyclopropylmethyl cation is a rapidly equilibrating mixture of nonclassical bicyclobutonium cations (**1** and **3**) and the bisected cyclopropylmethyl cation **2**.[5, 6, 7]

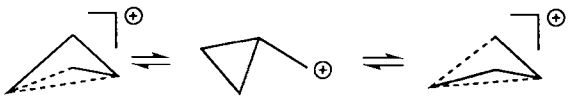

1 **2** **3**

The only known example of a "static" bisected primary cyclopropylmethyl cation was prepared by Schmitz and Sorensen by ionizing 1-nortricyclanemethanol (**4**) with SbF_5 in SO_2ClF at low temperature.[8] In **4** the cyclopropyl moiety is locked in a norbornane framework.

[*] Prof. G. A. Olah, Dr. H. A. Buchholz, Prof. G. K. S. Prakash, Dr. G. Rasul
Loker Hydrocarbon Research Institute and Department of Chemistry
University of Southern California
University Park, Los Angeles, CA 90089-1661 (USA)
Fax: Int. code +(213)740-6679
e-mail: prakash@methyl.usc.edu

Prof. R. K. Murray, Jr., Dr. J. J. Sosnowski
Department of Chemistry and Biochemistry
University of Delaware, Newark, DE 19716 (USA)
Fax: Int. code +(302)831-6335

Prof. Dr. A. de Meijere, Doz. Dr. M. A. Kusnetsov, Dr. S. Liang
Institut für Organische Chemie der Universität
Tammannstrasse 2, D-37077 Göttingen (Germany)
Fax: Int. code +(551)39-9475
e-mail: ameijer1@gwdg.de

[**] Stable Carbocations, Part 298. This work was supported at University of Southern California by the Loker Hydrocarbon Research Institute and the National Science Foundation, at University of Delaware by the University of Delaware Research Foundation, and at the Universität Göttingen by the Fonds der Chemischen Industrie. The systematic name of 2-triaxanemethyl cation and 2,10-*para*-[3².5⁶]octahedranedimethyl dication are 2-tetracyclo[3.3.1.0^{2,4}.0^{3,7}]nonanemethyl cation and 2,10-heptacyclo[6.4.0.0^{2,4}.0^{3,7}.0^{5,12}.0^{9,11}]dodecanedimethyl dication, respectively. The latter skeleton has also been termed ditriaxane [21], but we prefer the more descriptive trivial name *para*-[3².5⁶]octahedrane for the parent hydrocarbon and hence also for its derivatives. For Part 297 see N. J. Head, G. K. S. Prakash, A. B. Hashimi, G. A. Olah, *J. Am. Chem. Soc.* **1995**, *117*, 12005.

The static bisected ion structure **5a** seems to be almost exclusively populated and is the only spectroscopically observable species. This has been rationalized by considering the contribution of a vinyl-bridged 2-norbornyl cation structure (**5b**) to the resonance hybrid.[9] Involvement of an alternative bicyclobutonium ion type structure **6** was ruled out.

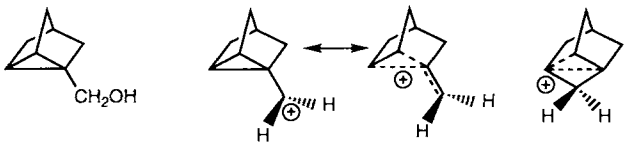

4 **5a** **5b** **6**

In the cyclopropylmethanol derivatives, 2-triaxanemethanol (**7**)[10] and 2,10-ditriaxanedimethanol (**8**),[11] the cyclopropyl moieties are also rigidly locked in oligocyclic hydrocarbon frameworks. We explored under stable ion conditions the behavior of **7** and **8** as potential precursors to related cyclopropylmethyl cations. The observed intriguing mono- and dications were characterized by low-temperature ^{13}C NMR spectroscopy. IGLO calculations (IGLO = Individual Gauge for Localized Orbitals) on density functional theory (DFT)[12] optimized structures helped resolve the nature of the monocation.

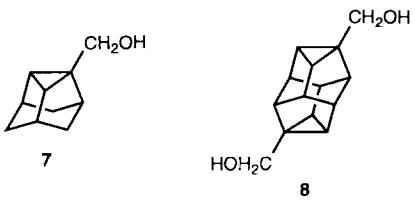

7 **8**

2-Triaxanemethanol (**7**) was ionized at −78 °C in SO_2ClF with SbF_5 and gave an orange solution.[13] The 75 MHz proton-decoupled ^{13}C NMR spectrum[14] of this species at −80 °C shows only seven resonances (assigned on the basis of multiplicities and coupling constants): $\delta^{13}C$ = 147.9 (s), 97.6 (d, $J_{C,H}$ = 187.1 Hz), 52.7 (t, $J_{C,H}$ = 134.7 Hz), 47.3 (t, $J_{C,H}$ = 168.3 Hz), 43.4 (d, $J_{C,H}$ = 151.4 Hz), 38.7 (t, $J_{C,H}$ = 136.5Hz), and 36.6 (d, $J_{C,H}$ = 149.9 Hz) in a ratio of 1:2:1:1:1:2:2. The chemical shifts remain constant over the temperature range of −100 to −40 °C. This is in accordance with either a single ground-state structure for the ion or a set of rapidly equilibrating unsymmetrical bicyclobutonium ion structures. Similar studies on the parent cyclopropylmethyl cation had already established the fast, temperature-dependent, degenerate equilibration of the cyclopropylmethyl cation and bicyclobutonium ion.[4] Since the ion has apparent C_s symmetry, possible structures include the static, classical, bisected cyclopropylmethyl cation **9**, a fast equilibrium of the nonclassical, unsymmetrical, bridged bicyclobutonium ions **10a** and **10b**, or a fast equilibrium of the classical 2,5-dehydro-3-protoadamantyl cations **11a** and **11b**.

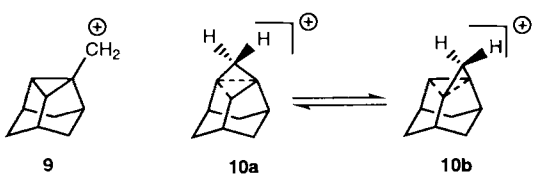

9 **10a** **10b**

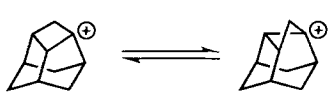

11a **11b**

 © VCH Verlagsgesellschaft mbH, D-69451 Weinheim, 1996 0570-0833/96/3513-1499 $ 15.00+.25/0

Geometry optimizations of the possible ions were carried out at the Becke3LYP/6-31G* level by using the Gaussian 94[12b] program package (Fig. 1). ^{13}C NMR chemical shifts were calculated by IGLO[15] with the standard DZ basis set and the

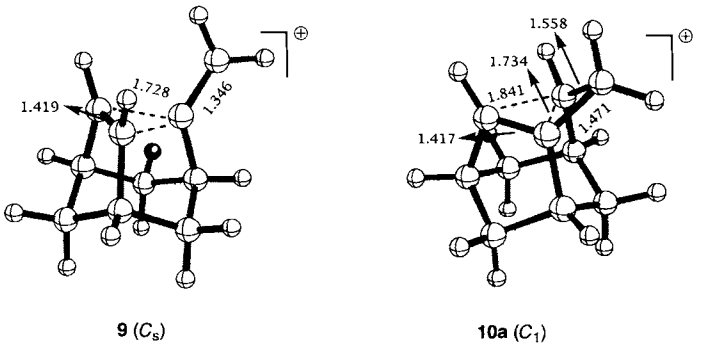

9 (C_s) **10a** (C_1)

Fig. 1. Selected Becke3LYP/6-31G*-optimized parameters [Å] of **9** and **10a**.

Becke3LYP/6-31G* geometries. The calculated chemical shifts for the carbocationic center of the static bisected ion **9** ($\delta^{13}C = 200.7$, Scheme 1) lie in the same range as that for Sorensen's nortricyclylmethyl cation **5** ($\delta^{13}C = 191.4$). Undoubtedly the difference of $\Delta\delta = 153$ between the calculated and

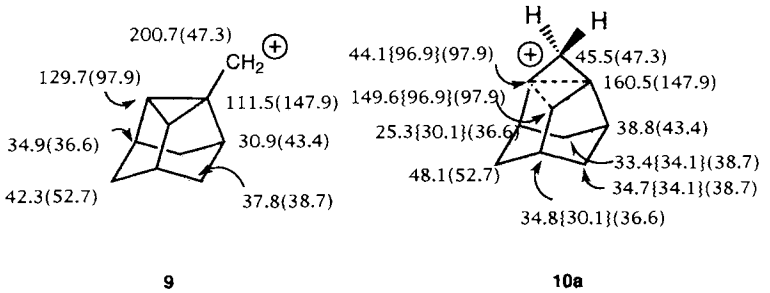

9 **10a**

Scheme 1. Calculated ^{13}C NMR chemical shifts of **9** and **10a**. Experimental values are given within parentheses and averaged values for **10a/b** within braces.

the experimentally measured ^{13}C NMR chemical shift excludes **9** as the major species in the equilibrium. On applying the empirical ^{13}C chemical shift additivity concept[16] the difference of $\Delta\delta^{13}C = 226$ between the total sum of the ^{13}C NMR chemical shifts of the ion ($\sum\delta = 638$) and the total sum of the ^{13}C chemical shifts of the corresponding hydrocarbon ($\sum\delta = 412$[17]) further supports a nonclassical structure. Typically, a difference of 350 or greater indicates a classical carbocationic nature, whereas $\Delta\delta$ values for nonclassical carbocations are significantly smaller.[16] The most likely structure for the cation from **7** is a set of rapidly equilibrating bicyclobutonium ions (**10a/b**) with apparent C_s symmetry.

Since ion **10a** is only 0.6 kcal mol^{-1} more stable than **9** at the B3LYP/6-31G* level, **10a/b** probably lies on a rather flat potential energy surface. Rearrangements of carbocations involving low energy barriers are common.[1e] In fact by taking the average IGLO calculated ^{13}C NMR chemical shifts of the two optimized, degenerate structures **10a** and **10b** a good agreement with the experimental values is obtained (Scheme 1). Thus the ionization product of **7** can be best described as a set of rapidly equilibrating (with a low energy barrier) nonclassical unsymmetrically bridged bicyclobutonium ions **10a/b**.

Structurally similar to **7** is the diol 2,10-*para*-[$3^2.5^6$]octahedranedimethanol (**8**). In **8** two cyclopropylmethanol units are locked into a rigid hydrocarbon framework. Because its geometry resembles that of **7**, similar spectroscopic features to those of **10a/b** for the ionization product derived from **8** can be expected. On the other hand, formation of a distonic[18] primary cyclopropylmethyl dication gives a considerably higher atom-to-charge ratio than the cation from **7**, which could lead to a lower extent of σ delocalization into the strained cyclopropyl moieties.

Ionization of **8** with SbF_5 in SO_2ClF at $-78\,^\circ C$ resulted in a dark yellow solution.[13] The 75 MHz proton-decoupled ^{13}C NMR spectrum of this solution at $-80\,^\circ C$ shows only five absorptions, indicating the presence of a highly symmetric dication: $\delta^{13}C = 135.7$ (s, C_{quat}), 118.9 (t, $J_{C,H} = 174$ Hz, methylene groups), 105.0 (d, $J_{C,H} = 193.2$, four β CHs), 66.4 (d, $J_{C,H} = 148.8$, two belt CHs), and 53.3 (d, $J_{C,H} = 156.1$, four belt CHs) in a ratio of 1:1:2:1:2. Considering the similar geometry and a correlation between charge density and ^{13}C NMR chemical shifts,[19] the downfield shift of the methylenes by $\delta = 71$ relative to that of **10a/b** clearly indicates higher positive charge density on the methylene groups in the dication from **8** and less charge delocalization into the cyclopropylmethyl moieties in the framework. On the other hand, this positively charged carbon atom is still relatively shielded relative to that of Sorenson's nortricyclylmethyl cation **5** (upfield shift for this dication: $\Delta\delta = 72.5$), which indicates still substantial positive charge delocalization into the cyclopropane moiety and clearly rules out the static bisected structure **12** for the ionization product of **8**.

A test for the temperature dependence of the NMR spectrum showed no significant changes in the range from -100 to $-30\,^\circ C$.[20] Application of the empirical ^{13}C NMR chemical shift additivity rule also supports the assignment of a bridged structure for this ion. The difference between the total sum of the ^{13}C NMR chemical shifts for this ion ($\sum\delta = 1275.6$) and the total sum for the structurally closely related parent hydrocarbon 2,9-dimethylditriaxane ($\Delta\delta = 774.6$)[21] is 250 ppm per unit of positive charge. Comparison of this value with related monocharged systems such as the highly delocalized cyclopropylmethyl cation ($\Delta\delta = 283$) and the static, bisected nortricyclylmethyl cation ($\Delta\delta = 470$) supports the bicyclobutonium type nonclassical structures **13a/b/c**[22] for the ionization product of **8**.

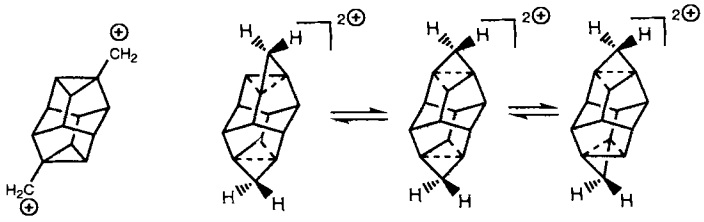

12 **13a** **13b** **13c**

Received: September 6, 1995
Revised version: January 3, 1996 [Z 8371 IE]
German version: *Angew. Chem.* **1996**, *108*, 1623–1626

Keywords: ab initio calculations carbocations nonclassical structures · NMR spectroscopy

[1] P. Ahlberg, G. Jonsall, C. Engdahl, *Adv. Phys. Org. Chem.* **1982**, *19*, 223.

[2] a) P. D. Bartlett in *Nonclassical Ions: Reprints and Commentaries in Frontiers in Chemistry*, W. A. Benjamin, New York, **1965**; b) H. G. Richey, Jr., in *Carbonium Ions, Vol. 3* (Eds.: G. A. Olah, P. von R. Schleyer), Wiley, New York, **1972**, p. 1201; c) K. B. Wiberg, A. B. Hess, Jr., A. J. Ashe in *Carbonijm Ions, Vol. 3* (Ed.: G. A. Olah, P. von R. Schleyer), Wiley, New York, **1972**, p. 1295; d) H. C. Brown in *The Nonclassical Ion Problem*, Plenum Press, New York, **1977**, Chap. 5; e) P. Vogel, *Carbocation Chemistry*, Elsevier, Amsterdam, **1985**, p. 350; f) J. D. Roberts, R. H. Mazur, *J. Am. Chem. Soc.* **1985**, *73*, 3542; g) G. A. Olah, V. P. Reddy, G. K. S. Prakash, *Chem. Rev.* **1992**, *92*, 69.

[3] G. A. Olah, D. P. Kelly, C. L. Juell, R. D. Porter, *J. Am. Chem. Soc.* **1970**, *92*, 2544.

[4] a) G. A. Olah, C. L. Juell, D. P. Kelly, R. D. Porter, *J. Am. Chem. Soc.* **1972**, *94*, 146; b) J. Staral, I. Yavari, J. D. Roberts, G. K. S. Prakash, D. J. Donovan, G. A. Olah, *J. Am. Chem. Soc.* **1978**, *100*, 8016.

[5] a) W. J. Brittain, M. E. Squillacote, J. D. Roberts, *J. Am. Chem. Soc.* **1984**, *106*, 7280; b) M. Saunders, K. E. Laidig, M. Wolfsberg, *ibid.* **1989**, *111*, 8989.

[6] a) M. Saunders, H.-U. Siehl, *J. Am. Chem. Soc.* **1980**, *102*, 6868; b) W. J. Brittain, M. E. Squillacote, J. D. Roberts, *ibid.* **1984**, *106*, 7280.

[7] a) P. C. Myhre, G. G. Webb, C. S. Yannoni, *J. Am. Chem. Soc.* **1990**, *112*, 8992; b) M. Saunders, K. E. Laidig, K. B. Wiberg, P. von R. Schleyer, *ibid.* **1988**, *110*, 7652, and references therein.

[8] T. S. Sorensen, L. R. Schmitz, *J. Am. Chem. Soc.* **1982**, *104*, 2600.

[9] T. S. Sorensen, L. R. Schmitz, *J. Am. Chem. Soc.* **1982**, *104*, 2605.

[10] Alcohol **7** was prepared in 59% yield by the reduction of triaxane-2-carboxylic acid with lithium aluminum hydride. The acid was obtained in 49% yield by the oxidation of 2-acetyltriaxane with sodium hypobromite. For the synthesis of methyl ketone, see: A. Nickon, D. F. Covey, G. D. Pandit, J. J. Frank, *Tetrahedron Lett.* **1975**, 3681.

[11] 2,10-(*para*-[$3^2.5^6$]octahedrane)dimethanol (**8**) was obtained in 74% yield by the reduction of 2,10-(*para*-[$3^2.5^6$]octahedrane)dicarboxylic acid dimethylester with lithium aluminum hydride. For the synthesis of 2,10-*para*-[$3^2.5^6$]octahedrane)dicarboxylic acid dimethylester, see C.-H. Lee, S. Liang, T. Haumann, R. Boese, A. de Meijere, *Angew. Chem.* **1993**, *105*, 611; *Angew. Chem. Int. Ed. Engl.* **1993**, *32*, 559.

[12] a) T. Ziegler, *Chem. Rev.* **1991**, *91*, 651; b) Gaussian 94 (Revision A.1), M. J. Frisch, G. W. Trucks, H. B. Schlegel, P. M. W. Gill, B. G. Johnson, M. A. Robb, J. R. Cheeseman, T. A. Keith, G. A. Peterson, J. A. Montgomery, K. Raghavachari, M. A. Al. Laham, V. G. Zakrzewski, J. V. Ortiz, J. B. Foresman, J. Cioslowski, B. B. Stefanov, A. Nanayakkara, M. Challacombe, C. Y. Peng, P. Y. Ayala, W. Chen, M. W. Wong, J. L. Andres, E. S. Replogle, R. Gomperts, R. L. Martin, D. J. Fox, J. S. Binkley, D. J. Defrees, J. Baker, J. J. P. Stewart, M. Head-Gordon, C. Gonzalez, J. A. Pople, Gaussian, Inc., Pittsburgh PA, 1995.

[13] Preparation of cations: In a 5 mm NMR tube, the appropriate alcohol (15 mg) slurried in SO_2ClF (0.2 mL) at $-78\,^{\circ}C$ (dry ice/acetone bath) is treated with a tenfold excess of precooled SbF_5 in SO_2ClF (0.7 mL) under rapid vortex stirring. Upon dissolution of the alcohol, ionic solutions were obtained.

[14] All absorptions are referred to the CD_3 signal ($\delta^{13}C = 29.8$) of external [D_6]acetone in standard capillaries in the same NMR tube.

[15] (a) M. Schindler, *J. Am. Chem. Soc.* **1987**, *109*, 1020; b) W. Kutzelnigg, U. Fleischer, M. Schindler, *NMR Basic Princ. Prog.*, **1991**, *23*, 165.

[16] P. von R. Schleyer, D. Lenoir, P. Mison, G. Liang, G. K. S. Prakash, G. A. Olah, *J. Am. Chem. Soc.* **1980**, *102*, 683.

[17] The ^{13}C NMR chemical shifts of the parent hydrocarbon 3-methy-[3.3.1.$0^{3,8}$]nonane is not reported; they were estimated based on the data of related compounds or calculated based on the IGLO DZ//HF/3-21G level of theory.

[18] The Greek word distonic (meaning distant) is used to distinguish these dications from gitonic (proximal) dications. For a discussion see G. A. Olah, *Angew. Chem.* **1993**, *105*, 805; *Angew. Chem. Int. Ed. Engl.* **1993**, *32*, 907.

[19] a) G. J. Ray, R. J. Kurland, A. K. Colter, *Tetrahedron* **1971**, *27*, 735; b) P. C. Lauterbur, *J. Am. Chem. Soc.* **1961**, *83*, 1838; c) H. Spiesecke, W. G. Schneider, *Tetrahedron Lett.* **1961**, 468; d) E. W. Lalancette, R. E. Benson, *J. Am. Chem. Soc.* **1965**, *85*, 1941; e) G. A. Olah, M. Bollinger, A. M. White, *ibid.* **1969**, *91*, 3667; f) G. A. Olah, D. Mateescu, *ibid.* **1970**, *92*, 1430; g) R. Ditchfield, D. P. Miller, J. A. Pople, *Chem. Phys. Lett.* **1970**, *6*, 573; h) R. Ditchfield, D. P. Miller, J. A. Pople, *J. Chem. Phys.* **1971**, *54*, 4186; i) D. G. Farnum, *Adv. Phys. Org. Chem.* **1975**, *11*, 123.

[20] Only small changes of up to $\Delta\delta = 2$ were observed in certain peaks in the ^{13}C NMR spectra of the ions over the studied temperature range.

[21] (a) K.-I. Hirao, Y. Ohuchi, O. Yonemitsu, *J. Chem. Soc. Chem. Commun.* **1982**, 99; b) K.-I. Hirao, H. Takahashi, Y. Ohuchi, O. Yonemitsu, *J. Chem. Res. Synop.* **1992**, 319; *J. Chem. Res. Miniporint* **1992**, 2601.

[22] Ions **16a** and **16c** are enatiomeric.

Hexaborylbenzene and Tetraborylethene Derivatives**

Andreas Maderna, Hans Pritzkow, and Walter Siebert*

Dedicated to Professor Marianne Baudler on the occasion of her 75th birthday

Functionalized tetraborylethenes and tetra- and hexaborylbenzene derivatives are potential precursors for new boron heterocycles. Tetraborafulvalenes **A** and benzobis- and benzotris(1,3-diborole) derviatives **B** and **C**, respectively, are suitable for the synthesis of doubly and triply stacked complexes with

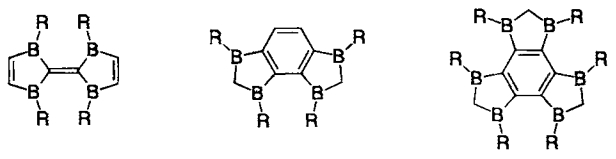

A **B** **C**

1,3-diborolyl bridging ligands. Additionally, tetra- and hexaborylbenzenes can be used for synthesizing band and sheet polymers. In this way a graphite analogue $(C_3B)_n$, in which every boron atom is surrounded by three C atoms, could be made by polycondensation of $C_6(BR_2)_6$ under elimination of BR_3. We report here on the first synthesis of perborylated C–C multiply bonded systems by transition metal catalyzed reactions of bi(1,3,2-benzodioxaborolyl)acetylene (**1**).[1] Cyclotrimerization of **1** provides **2a**, the first example of a hexaborylbenzene derivative. Diboration of **1** with 2,2'-bi(1,3,2-benzodioxaborolyl)-borane (**3**) leads to the tetraborylethene compound **4a**. The boron–oxygen bonds in **2a** and **4a** can be cleaved with methyllithium and trimethylaluminum (Scheme 1).

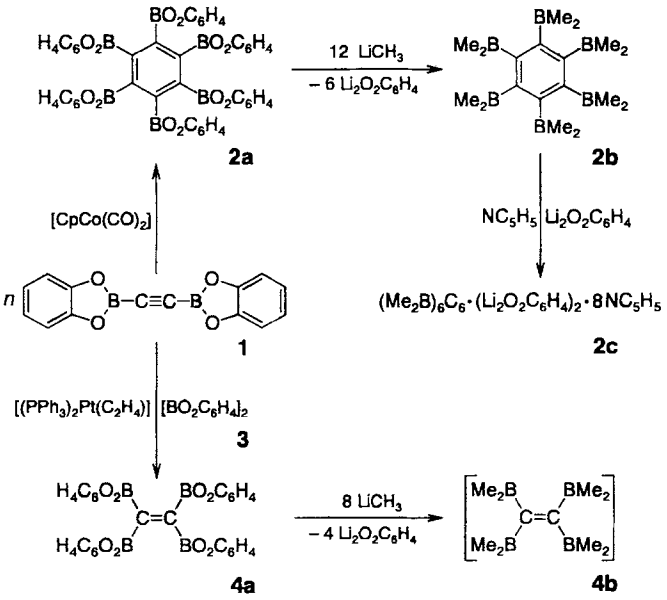

Scheme 1.

[*] Prof. Dr. W. Siebert, A. Maderna, Dr. H. Pritzkow
Anorganisch-chemisches Institut der Universität
Im Neuenheimer Feld 270, D-69120 Heidelberg (Germany)
Fax: Int. code +(6221)545609

[**] This work was supported by the Deutsche Forschungsgemeinschaft (SFB 247) and the Fonds der Chemischen Industrie.

The synthesis of substituted arenes by cobalt-catalyzed trimerization of alkynes is well known and has found broad applications in organic synthesis.[2] In an analogous manner, the diborylacetylene **1**[1] can be cyclotrimerized with (η^5-cyclopentadienyl)dicarbonylcobalt in refluxing toluene to give the hexaborylbenzene **2a** in 67% yield. Compound **2a** is only slightly soluble in most solvents; in methanol a slow reaction takes place leading to the formation of $H_4C_6O_2BOMe$. Purification of **2a** is accomplished by multiple washings with THF and CH_2Cl_2. Subsequent drying provides analytically pure, air-stable **2a**. The ^{11}B NMR spectrum in [D_8]toluene at 372 K shows a broad signal at $\delta = 33$; the chemical shift of the boron-bound C atoms in the ^{13}C NMR spectrum ($\delta = 143$) appears in the range expected for 1,2-diborylbenzene derivatives.[3]

In analogy to the cleavage of the B–O bonds in 2-alkyl-1,3,2-benzodioxaborole derivatives with Grignard reagents,[4] a solution of **2a** in toluene reacts with methyllithium in diethyl ether to form a yellow solution of the methyl derivative **2b**. After separation of the precipitated $C_6H_4O_2Li_2(OEt_2)_n$, **2b** was identified by GC-MS analysis to be the only product. Surprisingly, the ^{11}B NMR spectrum of the yellow solution shows a broad signal at $\delta = 6$, which indicates a donor–acceptor interaction between the oxygen atoms of dissolved $C_6H_4O_2Li_2$ and the boron atoms. Additionally, two signals of lower intensity appear in the highfield region at $\delta = -17.4$ and -20.6, which we assign to the boranates **2b**·$(LiMe)_n$ and $LiBMe_4$.[5] Addition of an excess of pyridine results in an orange-red solution from which a crystalline, lithium-containing product precipitates. NMR and mass spectra indicate a compound based on **2b**, dilithio-1,2-dioxabenzene, and pyridine.

The crystal structure analysis indicated the formation of compound **2c** (Fig. 1), in which two oxygen atoms from two $Li_2O_2C_6H_4$ units each bridge two BMe_2 groups. The boron

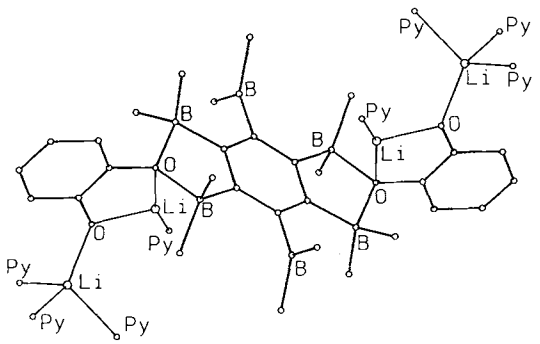

Fig. 1. Structure of **2c** in the crystal. Py = C_5H_5N.

atoms of the other two boryl groups, which are *para*-positioned with respect to one another, are planar coordinated. The BC_2 planes are perpendicular to the central benzene plane. However, no satisfactory refinement of the structure analysis was possible, due to the poor quality of the crystal, resulting from disordered solvent and/or pyridine. The ^{11}B NMR spectrum of **2c** shows a broad signal at $\delta = 0$. No signals for the BMe_2 groups were found in the lowfield region. From this it can be concluded that only four-coordinate boron atoms are present in solution.

Concentration of the yellow toluene/diethyl ether solution of **2b** resulted in the formation of a yellow precipitate. Further removal of solvent provides a yellow, insoluble, air-sensitive powder. The ^{11}B NMR spectrum of a saturated solution of this in CH_2Cl_2 shows a broad signal at $\delta = 85$ as well as a signal at $\delta = 6$, which indicates the presence of **2b**. In the EI mass spectrum of the yellow product, the highest mass appears at 317 (M^+ for **2b**). The reaction of a suspension of **2a** in hexane with trimethylaluminum also results in **2b**; removal of the insoluble components by filtration provides a yellow filtrate whose ^{11}B NMR (only one signal at $\delta = 85$) and EI-MS ($m/z = 317$, M^+) spectra confirm that this product is formed.

According to Suzuki and Miyaura[6] alkynes react catalytically with 2,2'-bi(4,4,5,5-tetramethyl-1,3,2-dioxaborolanyl)-platinum and tetrakis(triphenylphosphane)platinum to give *Z*-1,2-diborylethenes. Heating a solution of the diborylacetylene **1** and the diborane(4) **3** in toluene in the presence of bis(triphenylphosphane)(ethene)platinum[8] for 24 h results in the tetraborylethene derivative **4a** in 50% yield (see Scheme 1). Compound **4a** is an air-stable solid that is very poorly soluble. The first $C_2(BX_2)_4$ compound (X = F) was obtained by gas-phase reaction of carbon with B_2F_4.[13] The ^{11}B NMR spectrum of **4a** in [D_4]methanol shows a broad signal at $\delta = 34$ and a signal of lower intensity at $\delta = 18$ that can be assigned to $C_6H_4O_2BOCD_3$, which is formed by the methanolysis of **4a**. The ^{13}C NMR signal of the boron-bound C atoms could not be detected due to the poor solubility of the compound.

Different reactivity is seen upon the stoichiometric addition of bis(triphenylphosphane)(ethene)platinum. In addition to traces of **4a**, the corresponding substituted 1,1,2,2-tetraborylethene derivative is obtained in 8% yield.[9] Its synthesis is probably due to the intermediate formation[11] of 1,3,2-benzodioxaborole and subsequent double hydroboration of **1**.

The reaction of **4a** with methyllithium already occurs at $-5\,^\circ C$; however, due to the enhanced reactivity of the boryl groups compared to those in **2b**, the resulting **4b** could not be identified by GC-MS analysis. Upon addition of pyridine, the ^{11}B NMR spectrum of the red-brown solution shows, just as for **2c**, a signal at $\delta = 0$ as well as a signal for $LiBMe_4$ ($\delta = -19.5$). We assume that a product analogous to **2c** is formed from **4b**, $Li_2O_2C_6H_4$, and pyridine. The ^{13}C NMR spectrum, like that of **2c**, shows a broad signal for the BMe_2 groups ($\delta = 13$) and a broad signal for the boron-bound, sp^2-hybridized carbon atoms ($\delta = 158$). Attempts to synthesis donor-free **4b** from **4a** and trimethylaluminum provided a yellow solution whose ^{11}B NMR spectrum shows a signal for **4b** at $\delta = 82$ and for trimethylborane at $\delta = 87$. The isolation and characterization of **4b** has not yet been successful.

Electronic as well as steric features of **1** are decisive for the formation of **2a** and **4a**. The Lewis acidity of the boron atoms is reduced due to the donor function of the oxygen atoms. The C–C triple bond is only minimally lengthened[1] to allow the necessary coordination at the metal center during the catalytic cycle. The planar benzodioxaborolyl substitutents are advantageous in that they are able to rotate with respect to one another and allow the approach of several alkynes to the reactive metal center. Transition metal catalyzed cyclotrimerization and diboration of **1** offers a pathway to unsaturated, perborylated compounds, which can be used for the synthesis of new boron heterocycles. These can, in turn, be used for organic synthesis as well as applications as hydride[12] and fluoride acceptors.

Experimental Procedure

2a: **1** (1.234 g, 4.7 mmol) and (η^5-cyclopentadienyl)dicarbonylcobalt (0.042 g, 0.23 mmol, 5 mol%) in toluene (25 mL) were heated under reflux for 24 h. Afterwards, the precipitate was isolated by filtration, washed several times with THF and CH_2Cl_2 and dried in vacuum. Yield: 0.827 g (67%), m.p.: >310 °C, ^1H NMR (200 MHz, [D_8]THF): $\delta = 6.4$–6.8 (m); ^{13}C NMR (50 MHz, [D_4]MeOH): $\delta = 146.2$, 120.8, 116.3 (C_6H_4), 143 (CB, br.); ^{11}B NMR (64 MHz, [D_8]toluene, 373 K): $\delta = 33$ ($\Delta\nu_{1/2} = 580$ Hz); HR-MS (EI): m/z 785.1879 (M^+ calcd. $^{12}C_{42}{}^1H_{24}{}^{10}B_1{}^{11}B_5{}^{16}O_2$: 785.1862); correct C, H analysis.

 © VCH Verlagsgesellschaft mbH, D-69451 Weinheim, 1996 0570-0833/96/3513-1502 $ 15.00+.25/0

4a: **1** (473 mg, 1.8 mmol), **3** (430 mg, 1.8 mmol), and bis(triphenylphosphane)-(ethene)platinum (83 mg, 0.12 mmol, 6.2 mol%) in toluene (15 mL) were heated under reflux for 24 h. Afterwards, the precipitate was isolated by filtration, washed several times with THF and CH_2Cl_2, and dried in vacuum. Yield: 455 mg (50.6%), m.p.: >310 °C, ^{1}H NMR (200 MHz, [D$_4$]MeOH): δ = 6.5–6.9 (m); ^{13}C NMR (50 MHz, [D$_4$]MeOH): δ = 146.3, 120.9, 116.4 (C_6H_4), CB not observed; ^{11}B NMR (64 MHz, [D$_4$]MeOH): δ = 34 ($\Delta\nu_{1/2}$ = 524 Hz), 18 ($\Delta\nu_{1/2}$ = 58 Hz, $C_6H_4O_2BOCD_3$); HR-MS (EI): *m/z* 500.1209 (M^+, calcd $^{12}C_{26}{}^1H_{16}{}^{10}B_4{}^{16}O_8$: 500.1217); correct C, H analysis.

2b, **2c**: A suspension of **2a** (785 mg, 1 mmol) in toluene (15 mL) and methyllithium (8 mL of a 1.5 M solution in diethyl ether, 12 mmol) was first stirred for 1.5 h at −5 °C and then for 8 h at 25 °C. After removing the insoluble components, a yellow solution of **2b** was obtained which contained minor amounts of boranates. ^{11}B NMR (64 MHz): δ = 6 ($\Delta\nu_{1/2}$ = 466 Hz), −17.4 ($\Delta\nu_{1/2}$ = 87 Hz), −20.6 ($\Delta\nu_{1/2}$ = 29 Hz); GC-MS: *m/z* (%) 317 (100) [M^+], 302 (17.4) [M^+ − Me], 41 (92.4) [BMe_2^+]. An excess of pyridine was added to the yellow solution. Crystalline **2c** precipitated from the resulting orange-red solution at room temperature. Yield: 296 mg (33%), m.p.: >250 °C (decomp), ^{1}H NMR (200 MHz, $CDCl_3$): δ = −0.3 to 0.3 (m, BMe), 5.8–6.9 (m, C_6H_4), 7.0 (m, Py), 7.5 (m, Py), 8.2 (m, Py); ^{13}C NMR (50 MHz, $CDCl_3$): δ = 13.0 (BMe, br), 114.6, 116.5, 118.2, 120.0, 153.6, 160.0 (C_6H_4), 123.7, 136.6, 149.6 (Py), 168.0 (CB, br); ^{11}B NMR (64 MHz, $CDCl_3$): δ = 0.3 ($\Delta\nu_{1/2}$ = 204 Hz); MS (FD): *m/z* 982 [M^+ − Py − 4Me].

Received: February 12, 1996 [Z 8807 IE]
German version: *Angew. Chem.* **1996**, *108*, 1664–1666

Keywords: boron compounds · catalysis · diborylacetylenes

[1] H. Schulz, G. Gabbert, H. Pritzkow, W. Siebert, *Chem. Ber.* **1993**, *126*, 1593.
[2] K. P. C. Vollhardt, *Angew. Chem.* **1984**, *96*, 525; *Angew. Chem. Int. Ed. Engl.* **1984**, *23*, 539.
[3] D. E. Kaufmann, R. Boese, A. Scheer, *Chem. Ber.* **1994**, *127*, 2349.
[4] S. Cabiddu, A. Maccioni, M. Secci, *Gazz. Chim. Ital.* **1972**, *102*, 555.
[5] H. Nöth, B. Wrackmeyer, *Nuclear Magnetic Resonance Spectroscopy of Boron Compounds*, Springer Berlin, **1978**.
[6] T. Ishiyama, N. Matsuda, N. Miyaura, A. Suzuki, *J. Am. Chem. Soc.* **1993**, *115*, 11018; T. Ishiyama, N. Matsuda, M. Murata, F. Ozawa, A. Suzuki, N. Miyaura, *Organometallics* **1996**, *15*, 713.
[7] C. N. Welch, S. G. Shore, *Inorg. Chem.* **1968**, *7*, 226.
[8] C. D. Cook, G. S. Jauhal, *J. Am. Chem. Soc.* **1968**, *90*, 1464.
[9] In the EI mass spectrum, only the molecular peak at *m/z* = 502 was observed in the higher mass region. A signal for [$M^+ - H_2$] (**4a**$^+$) was not observed; compare with ref. [10].
[10] P. Frankhauser, F. Kuhlmann, A. Krämer, H. Pritzkow, W. Siebert, *Chem. Ber.* **1993**, *126*, 1291.
[11] C. N. Iverson, M. R. Smith III., *J. Am. Chem. Soc.* **1995**, *117*, 4403.
[12] H. E. Katz, *J. Am. Chem. Soc.* **1985**, *107*, 1420.
[13] J. E. Dobson, P. M. Tucker, F. G. A. Stone, R. Schaeffer, *J. Chem. Soc. A* **1969**, *12*, 1882.

Synthesis of Naturally Occurring, Conformationally Restricted Oxazole- and Thiazole-Containing Di- and Tripeptide Mimetics**

Georgi Videnov, Dietmar Kaiser, Christoph Kempter, and Günther Jung*

Residues that restrict the peptide backbone are synthesized in Nature inter alia by the following modifications: N- and α-alkylations,[1] α,β-didehydroamino acid and sulfide ring formations,[2] and synthesis of aromatic five-membered heterocycles.[3] The unusual amino acids of most peptide antibiotics are incorporated by multienzyme complexes.[1] However, an increasing number of posttranslational modifications originating from enzymatic, ribosomally synthesized precursor proteins has been detected.[2] Thus, the fascinating 43-peptide antibiotic microcin B17, which inhibits DNA-gyrase, contains four oxazole and four thiazole rings,[3b] which arise by cyclizations and dehydrogenations from di- and tripeptide units containing Gly, Ser, and Cys residues of the precursor protein (69 residues) followed by cleavage of a leader peptide (26 residues). A wide variety of oxazole-, thiazole-, and thiazoline-containing natural products has also been isolated from marine organisms[4a–i] and microorganisms.[4j–m] The reported syntheses of oxazole[5,6] and/or thiazole[7] derivatives include only few examples of aminoalkyl- or aminoaryloxazolecarboxylic acids.[6a,g,i]

Substituted five-membered heterocycles are pharmacophores of many natural and synthetic, bioactive compounds. In particular, the amino- and carboxy-functionalized heterocycles found in microcin B17 (Scheme 1) are valuable building blocks for peptidomimetics, which restrict the ω,ψ-conformational freedom in peptides. As a part of our efforts towards the total synthesis of microcin B17,[3] we developed efficient procedures for the preparation of Boc- and Fmoc-protected amino acids derived from oxazole, thiazole, bisthiazole, oxazolyl-thiazole, and thiazolyl-oxazole, which can be considered as di- and tripeptide mimetics. We also discovered a novel, useful procedure for the oxidative conversion of intermediate oxazoline into corresponding oxazole rings with 1,8-diazabicyclo[5.4.0]undec-

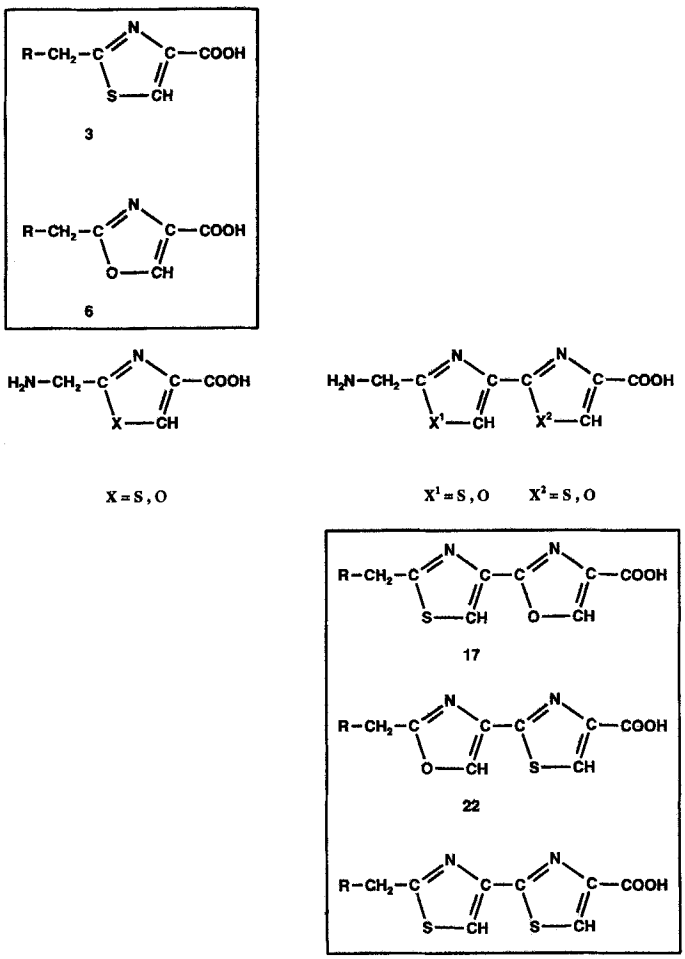

Scheme 1. R = Boc–NH.

[*] Prof. Dr. G. Jung, Dr. G. Videnov, Dipl.-Chem. D. Kaiser, Dipl.-Chem. C. Kempter
Institut für Organische Chemie der Universität
Auf der Morgenstelle 18, D-72076 Tübingen (Germany)
Fax: Int. code +(7071)29-6925
e-mail: guenther.jung@uni-tuebingen.de

[**] This work was supported by the Deutsche Forschungsgemeinschaft (Ju 103/9-1 and 436 BUL-113/68/0).

7-ene (DBU)/CCl_4/acetonitrile/pyridine. This reagent proved to be superior to the known reagent $CuBr_2$/DBU/hexamethylenetetramine (HMTA).

For the synthesis of 2-aminomethylthiazole-4-carboxylic acid (Scheme 2), *N*α-Boc-glycinamide (**1**) was converted into thioamide **2** by Lawesson's reagent.[8] Cyclocondensation of **2** with 3-brom-2-oxo-propionic acid[9] leads to **3** in 74% yield. After

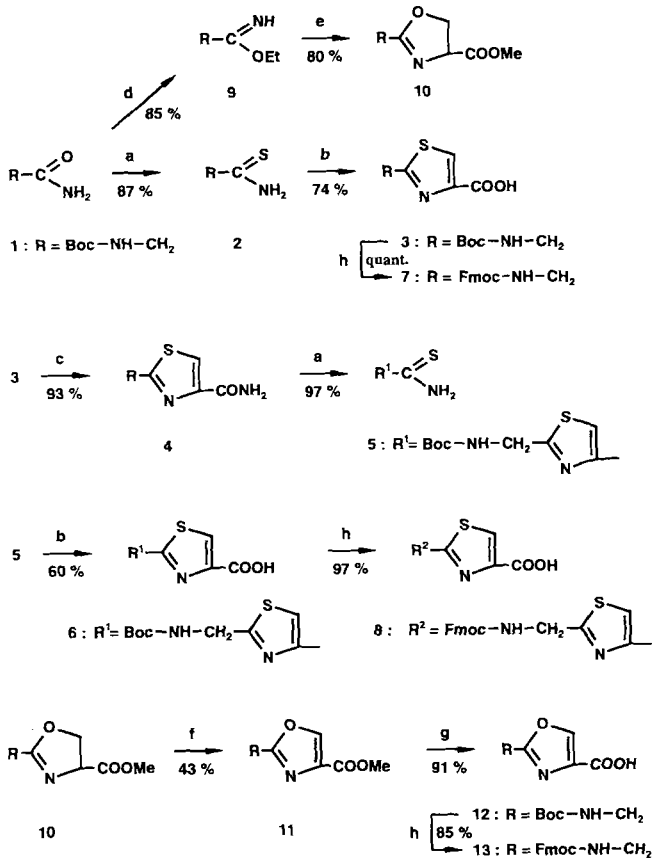

Scheme 2. a) Lawesson's reagent [8] ; b) 3-brom-2-oxo-propionic acid [4a–c,9]; c) *i*BuOCOCl, MeMorph, NH_4OH ; d) Et_3OPF_6 [10]; e) serine-OMe·HCl [11b]; f) DBU, CCl_4, CH_3CN, Py; g) NaOH; h) TFA then Fmoc-OSu.

Boc deprotection (50% trifluoroacetic acid (TFA)/CH_2Cl_2) the Fmoc protecting group was introduced by Fmoc-OSu (9-fluorenylmethoxycarbonyl-*O*-succinimide) to give **7**. The acid **3** was converted via amide **4** into thioamide **5** with isobutyl chloroformate/aqueous ammonia in THF. Reaction of the thioamide **5** with 2-bromopyruvic acid yielded the Boc-bisthiazole **6** (60%), which was converted into the Fmoc compound **8**.

The synthesis of the building block 2-aminomethyloxazole-4-carboxylic acid was accomplished by a novel route (Scheme 2). Treatment of the amide **1** with triethyloxonium hexafluorophosphate gave the imino ether **9**.[10] The intermediate oxazoline **10** was obtained in high yield (80%) by cyclization of the imino ether **9** with serine methyl ester in CH_2Cl_2.[11] Oxidation of **10** with the reagent DBU/CCl_4/acetonitrile/pyridine gave the oxazole **11** (43%), which was saponified to give **12**. Removal of the Boc group and reprotection with Fmoc-OSu afforded **13**.

The Boc- and Fmoc-protected 2-(2′-aminomethylthiazole-4′-yl)oxazole-4-carboxylic acids were synthesized according to Scheme 3. The amide **4** was converted into the imino ether **14** as described for **9**. Formation of the thiazolyloxazoline derivative

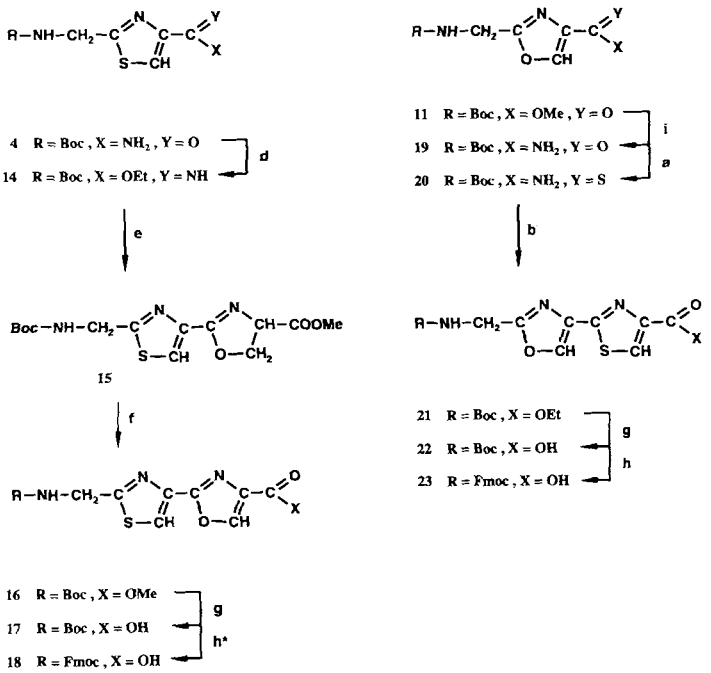

Scheme 3. For a), b), and e)–h) see Scheme 2; i) MeOH–NH_4OH.

15 occurs in high yield (72%). Oxidation of **15** with the novel procedure described for **10** yielded the ester **16**, which was saponified without problems to give **17**. Deprotection of the aminomethyl group and introduction of the Fmoc group afforded **18**.

For the synthesis of Boc- and Fmoc-protected 2-(2′-aminomethyloxazole-4′-yl)thiazole-4-carboxylic acid (Scheme 3) **11** was converted into amide **19** with methanol/ aqueous ammonia and to the thioamide **20**. The condensation of thioamide **20** with ethyl bromopyruvate (modified Hantzsch reaction[4a, b, j]) yielded the ethyl ester **21**. Basic hydrolysis of **21** gave the acid **22**, which was treated successively with 50% TFA/CH_2Cl_2 and Fmoc-OSu to obtain **23**.

The preparation of the oxazole- and/or thiazole-derived amino acids described above enabled us to synthesize fully active microcin B17,[13] and the use of these and related building blocks for the synthesis of further bioactive products is the object of intense research. During our experiments, we developed a novel method for the oxidation of oxazolines to oxazoles, which we hope will prove useful for the synthesis of related heterocycles. A report on X-ray structures, ab initio calculations, NMR spectroscopy studies and molecular dynamics simulation (MDS) studies summarizes the structural properties of the novel amino acids.[14]

Experimental Procedure

Thin-layer chromatography: glass sheets coated with silica gel (E. Merck, Darmstadt); solvent systems: A = $CHCl_3$/MeOH/H_2O (80/30/5); B = $CHCl_3$/MeOH/AcOH (95/5/3); C = $CHCl_3$/MeOH (9/1); D = EtOAc/*n*-hexane (1/1); E = *n*BuOH/AcOH/H_2O (4/1/1). Silica gel for flash chromatography was from J. T. Baker (Deventer, Holland). Instrumentation and conditions: Mass spectrometry: API III triple quadrupole mass spectrometer with an electrospray ion source at atmospheric pressure (Sciex, Thornhill, Canada); electrospray ionization mass spectra (ESI-MS) were taken in the positive mode; samples were dissolved in 10% HCOOH/MeOH (1/1). NMR spectroscopy: Bruker AC 250 spectrometer (Bruker Physics, Karlsruhe, Germany); solutions in $CDCl_3$ and [D_6]DMSO (c = 40 mg mL^{-1}); chemical shifts referenced to the solvent peaks [δ(^{13}C, CDCl3) = 77, δ(^{13}C, [D_6]DMSO) = 39.5 and δ(1H, [D_6]DMSO) = 2.49].

1: Gly-NH_2·HCl (22.0 g, 0.2 mol), triethylamine (28.0 mL, 0.2 mol) and di-*tert*-butyl dicarbonate [12] (48.0 g, 0.22 mol) in THF/water (4/1) (300 mL) were stirred

 © VCH Verlagsgesellschaft mbH, D-69451 Weinheim, 1996 0570-0833/96/3513-1504 $ 15.00+.25/0

at room temperature (RT) until the starting material was consumed (TLC system A). Yield 31.0 g (89%); homogeneous (TLC systems A and C).

2: Lawesson's reagent [8] (30.0 g, 75 mmol) and a solution of **1** (17.4 g, 100 mmol) in dimethoxyethane (400 mL) was stirred at room temperature until **1** was consumed (TLC system C). The solvent was removed in vacuo. A solution of the residue in EtOAc was extracted with 10% $NaHCO_3$, and the aqueous phase reextracted with EtOAc (2×). The combined organic phases were washed with brine and dried. Evaporation and crystallization from EtOAc/*n*-hexane afforded a yellow solid. Yield 17.0 g (89%); homogeneous (TLC systems B and C). ^{1}H NMR ([D$_6$]DMSO): δ = 1.38 (s, 9H; $3CH_3$), 3.81(d, ^3J(H,H) = 6.07 Hz, 2H; CH_2), 7.82 (t, ^3J = 5.92 Hz, 1H; NH), 9.0, 9.66 (br s, 1H; $CONH_2$); ^{13}C NMR ([D$_6$]DMSO): δ = 28.2 (Boc-CH_3), 50.5 (CH_2), 78.3 (Boc-C_q), 155.5 (Boc-CO), 204.0 (C=S).

3: 3-brom-2-oxo-propionic acid (1.93 g, 11.6 mmol), thioamide **2** (1.52 g, 8 mmol), and $CaCO_3$ (2.3 g, 23 mmol) were added to dry ethanol (60 mL) and stirred at room temperature under Ar for 5 h. The reaction mixture was filtered, and the solid washed with ethanol (2×20 mL). The combined filtrate was evaporated, and the residue dissolved in EtOAc (150 mL), the solution washed with 5% $KHSO_4$ and brine, and then dried. After evaporation the solid **3** was crystallized from EtOAc/*n*-hexane. Yield 1.48 g (74%); homogeneous (TLC system A). ^{1}H NMR ([D$_6$]DMSO): δ = 1.41 (s, 9H; $3CH_3$), 4.39 (d, ^3J(H,H) = 5.87 Hz, 2H; CH_2), 7.82 (t, ^3J(H,H) = 5.86 Hz, 1H; NH), 8.34 (s, 1H; CH_{Thz}), 12.94 (br s, 1H; COOH); ^{13}C NMR ([D$_6$]DMSO): δ = 28.6 (Boc-CH_3), 43.1 (CH_2), 80.9 (Boc-C_q), 129.1 (C^5_{Thz}), 148.2 (C^4_{Thz}), 158.2 (Boc-CO), 164.0 (C^2_{Thz}), 173.7 (COOH). ESI-MS: *m/z*: 259 $[M+H]^+$, 276 $[M+NH_4]^+$, 281 $[M+Na]^+$.

4: To **3** (5.2 g, 20 mmol) and *N*-methylmorpholine (2.2 mL, 20 mmol) in THF (100 mL) was added isobutyl chloroformate (5.2 mL, 20 mmol) at −20 °C. After 4 min aqueous ammonia (6 mL, 0.1 M) was added. After 3 h at room temperature and subsequent evaporation, the residue was precipitated with 10% $NaHCO_3$, filtered, and the solid was washed with water, dried, and crystallized from ethanol/ether/*n*-hexane. Yield 4.77 g, (93%); homogeneous (TLC systems A and C); X-ray structure analysis [14]. ^{1}H NMR ([D$_6$]DMSO): δ = 1.41 (s, 9H; $3CH_3$), 4.41 (d, ^3J(H,H) = 6.03, 2H; CH_2), 7.53, 7.65 (s, 1H; $CONH_2$), 7.8 (t, ^3J(H,H) = 5.66, 1H; NH), 8.14 (s, 1H; CH_{Thz}); ^{13}C NMR ([D$_6$]DMSO): δ = 28.1 (Boc-CH_3), 42.0 (CH_2), 78.7 (Boc-C_q), 124.0 (C^5_{Thz}), 150.0 (C^4_{Thz}), 155.8 (Boc-CO), 162.2 (C^2_{Thz}), 171.5 ($CONH_2$). ESI-MS: *m/z*: 258 $[M+H]^+$, 275 $[M+NH_4]^+$, 280 $[M+Na]^+$.

5: Prepared from **4** (4.33 g, 16.85 mmol) as described for **2**. Crystallization from ethanol/*n*-hexane. Yield 4.4 g (97%); homogeneous (TLC systems B and C); X-ray structure analysis [14]. ^{1}H NMR ([D$_6$]DMSO): δ = 1.41 (s, 9H; $3CH_3$), 4.4 (d, ^3J(H,H) = 5.94 Hz, 2H; CH_2), 7.85 (t, ^3J(H,H) = 5.83, 1H; NH), 8.35 (s, 1H; CH_{Thz}), 9.41, 9.94 (br s, 1H; $CONH_2$); ^{13}C NMR ([D$_6$]DMSO): δ = 28.2 (Boc-CH_3), 42.1 (CH_2), 78.8 (Boc-C_q), 127.0 (C^5_{Thz}), 153.4 (C^4_{Thz}), 155.8 (Boc-CO), 171.3 (C^2_{Thz}), 189.2 (C=S). ESI-MS: *m/z*: 274 $[M+H]^+$.

6: Prepared from **5** (2.0 g, 7.3 mmol) as described for **3**. Crystallization from EtOAc/ether. Yield 1.5 g (60%); homogeneous (TLC system A); X-ray structure analysis [14]. ^{1}H NMR ([D$_6$]DMSO): δ = 1.43 (s, 9H; $3CH_3$), 4.46 (d, ^3J(H,H) = 6.05 Hz, 2H; CH_2), 7.86 (t, ^3J(H,H) = 5.9, 1H; NH), 8.25, 8.48 (s, 1H; C^5_{Thz}, $C^{5'}_{Thz}$), 13.11 (br s, 1H; COOH); ^{13}C NMR ([D$_6$]DMSO): δ = 28.2 (Boc-CH_3), 42.0 (CH_2), 78.7 (Boc-C_q), 117.9 ($C^{5'}_{Thz}$), 128.9 (C^5_{Thz}), 147.3 (C^4_{Thz}), 148.2 (C^4_{Thz}), 155.8 (Boc-CO), 162.0 ($C^{2'}_{Thz}$), 162.2 (C^2_{Thz}), 172.8 (COOH). ESI-MS: *m/z*: 342 $[M+H]^+$, 359 $[M+NH_4]^+$, 364 $[M+Na]^+$.

7: **3** (1.3 g, 5 mmol) was deprotected quantitatively in 50% TFA/CH_2Cl_2 (20 mL) for 45 min. Fmoc-OSu (2.0 g, 6 mmol) in THF (30 mL) was added to the TFA salt and Na_2CO_3 (1.0 g, 10 mmol) in water (15 mL). After 12 h at room temperature THF was removed in vacuo, and the aqueous phase was diluted with water, acidified (1 N HCl) to pH 3 and filtered. The solid product was recrystallized from ethanol/ether. Yield 1.9 g (100%); homogeneous (TLC system A). ESI-MS: *m/z*: 381 $[M+H]^+$, 403 $[M+Na]^+$, 425 $[M+2Na]^+$.

8: Prepared from **6** (1.0 g, 2.9 mmol) as described for **7**. Crystallization from ethanol/ether. Yield 1.3 g (97%). ESI-MS: *m/z*: 464 $[M+H]^+$, 486 $[M+Na]^+$, 508 $[M+2Na]^+$.

9: The imino ether **9** was prepared from **1** (3.5 g, 20 mmol) according to ref. [10], obtained as a oil, and used without purification. Yield 3.4 g (85%). IR (Nujol): $\tilde{\nu}$ = 1653 cm^{-1} (C=N); ESI-MS: *m/z*: 203 $[M+H]^+$, 220 $[M+NH^4]^+$, 225 $[M+Na]^+$.

10: Oxazoline **10** was prepared according to ref. [11b] starting from **9** (3.4 g, 17 mmol) and H-Ser-OMe·HCl (3.1 g., 20 mmol) in CH_2Cl_2 (100 mL). Oxazoline **10** was obtained as a oil and used without purification. Yield 3.5 g (80%). ^{13}C NMR ($CDCl_3$): δ = 28.3 (Boc-CH_3), 27.9 (CH_2), 52.7 ($OOCH_3$), 67.7 (C^4_{Oxa}), 70.1 (C^5_{Oxa}), 79.9 (Boc-C_q), 155.5 (Boc-CO), 167.7 (C^2_{Oxa}), 171.2 (COO). ESI-MS: *m/z*: 259 $[M+H]^+$, 281 $[M+Na]^+$, 297 $[M+K]^+$.

11: DBU (3 mL, 30 mmol) was added to **10** (2.0 g, 7.75 mmol, about 80% purity) in a mixture of CCl_4 (10 mL), pyridine (15 mL), and acetonitrile (15 mL). After 3 h at room temperature the solvent was removed in vacuo, the residue dissolved in EtOAc, the solution extracted with 0.5 N HCl and the aqueous phase reextracted with EtOAc (2×). The EtOAc phase was washed with brine, dried, and the solvent evaporated. Chromatography on SiO_2 (EtOAc/*n*-hexane, 1:1) afforded oxazole **11**. Yield 0.85 g (43%). X-ray structure analysis [14]. ^{1}H NMR ([D$_6$]DMSO): δ = 1.4 (s, 9H; $3CH_3$), 3.86 (s, 3H; OCH_3), 4.45 (d, ^3J(H,H) = 5.77, 2H; CH_2), 5.34 (br t, 1H; NH), 8.16 (s, 1H; CH_{Oxa}); ^{13}C NMR ([D$_6$]DMSO): δ = 28.3 (Boc-CH_3) 38.0 (CH_2), 52.2 ($OOCH_3$), 80.4 (Boc-C_q), 133.4 (C^5_{Oxa}), 144.2 (C^4_{Oxa}), 155.1 (Boc-CO), 161.4 (C^2_{Oxa}), 162.3 (COO). ESI-MS: *m/z*: 257 $[M+H]^+$, 274 $[M+NH_4]^+$ 279 $[M+Na]^+$.

12: NaOH (0.24 g in 10 mL of water) was added to ester **11** (0.78 g, 3 mmol) in dioxane (30 mL). After 1 h at room temperature the solution was neutralized with 10% $KHSO_4$ to pH 6. Removal of the dioxane in vacuo was followed by acidification to pH 3 and extraction with EtOAc (3×). The extract was dried, and the solvent removed in vacuo. Crystallization from EtOAc/*n*-hexane. Yield 0.66 g (91%); homogeneous (TLC systems A and C). ^{1}H NMR ([D$_6$]DMSO): δ = 1.37 (s, 9H; $3CH_3$), 4.25 (d, ^3J(H,H) = 5.92 Hz, 2H; CH_2), 7.53 (t, ^3J(H,H) = 5.75 Hz, 1H; NH), 8.66 (s, 1H; CH_{Oxa}), 13.02 (br s, 1H; COOH); ^{13}C NMR ([D$_6$]DMSO): δ = 28.1 (Boc-CH_3), 37.2 (CH_2), 78.5 (Boc-C_q), 133.2 (C^5_{Oxa}), 145.1 (C^4_{Oxa}), 155.6 (Boc-CO), 162.0 (C^2_{Oxa}), 162.4 (COOH). ESI-MS: *m/z*: 243 $[M+H]^+$, 260 $[M+NH_4]^+$, 265 $[M+Na]^+$, 281 $[M+K]^+$.

13: Prepared from **12** (0.27 g, 1.1 mmol) as described for **7**. Crystallization from ethanol/ether/*n*-hexane. Yield 0.34 g (85%); homogeneous (TLC system A); ^{13}C NMR ([D$_6$]DMSO): δ = 37.6 (CH_2), 46.7 (Fmoc-C9), 65.9 (Fmoc-CH_2O), 120.0 (Fmoc-C4,C5), 125.2 (Fmoc-C1, C8), 127.1, 127.6 (Fmoc-C3,C6,C2,C7), 133.7 (C^5_{Oxa}), 140.7 (Fmoc-C4a,C4b), 143.8 (Fmoc-C8a,C9a), 145.0 (C^4_{Oxa}), 156.3 (Fmoc-CO), 162.0 (C^2_{Oxa}), 162.1 (COOH); ESI-MS: *m/z*: 365 $[M+H]^+$, 387 $[M+Na]^+$.

14: The imino ether **14** was prepared from **4** (4.8 g, 18.7 mmol) as described for **9**. The product was obtained as a oil and used without purification. Yield 5.1 g (95%). ESI-MS: *m/z*: 286 $[M+H]^+$.

15: The thiazolyl-oxazoline **15** was obtained from **14** (5.1g, 18 mmol) and Ser-OMe·HCl (1.55 g, 10 mmol) by heating under reflux for 3 h; after additional 12 h at room temperature, work up as described for **10**. Compound **15** was recrystallized from EtOAc/*n*-hexane. Yield 4,4 g (72%). ^{13}C NMR ([D$_6$]DMSO): δ = 28.1 (Boc-CH_3), 41.9 (CH_2), 52.2 ($OOCH_3$), 7.14 (CH_{Oxa}), 69.6 (CH^2_{Oxa}), 78.7 (Boc-C_q), 125.6 (CH_{Thz}), 142.2 (N-C_{Thz}), 155.8 (Boc-CO), 160.3 (C=N_{Oxa}), 171.3 (C=N_{Thz}), 172.2 (COO); ESI-MS: *m/z*: 342 $[M+H]^+$.

16: The thiazolyl-oxazole **16** was prepared from **15** (2.1 g, 6.1 mmol) as described for **11**. After purification on SiO_2 with EtOAc/*n*-hexane (2/1) as eluent, **16** was obtained as a colorless solid and recrystallized from EtOAC/*n*-hexane. Yield 1.1 g (55%); homogeneous (TLC systems B and C). ^{1}H NMR ([D$_6$]DMSO): δ = 1.41 (s, 9H; $3CH_3$), 3.83 (s, 3H; CH_3), 4.44 (br s, 2H; CH_2), 7.88 (br t, 1H; NH), 8.39 (s, 1H; CH_{Oxa}), 8.93 (s, 1H; CH_{Thz}); ^{13}C NMR ([D$_6$]DMSO): δ = 28.1 (Boc-CH_3), 42.0 (CH_2), 78.7 (Boc-C_q), 122.8 (CH_{Thz}), 133.3 (N-C_{Thz}), 141.3 (N-C_{Oxa}), 145.4 (CH_{Oxa}), 155.8 (Boc-CO), 157.2 (CH_{Oxa}), 161.0 (CH_{Thz}), 173.0 (COO); ESI-MS: *m/z*: 340 $[M+H]^+$, 362 $[M+Na]^+$.

17: The acid **17** was obtained from **16** (0.47 g, 1.4 mmol) as described for **12**. Crystallization from EtOAc/ether. Yield 0.42 g (92%); homogeneous (TLC system A). ^{1}H NMR ([D$_6$]DMSO): δ = 1.42 (s, 9H; $3CH_3$), 4.41 (d, ^3J(H,H) = 5.67 Hz, 2H; CH_2), 7.86 (br t, 1H; NH), 8.36 (s, 1H; CH_{Oxa}), 8.82 (s, 1H; CH_{Thz}); ESI-MS: *m/z*: 326 $[M+H]^+$, 348 $[M+Na]^+$.

18: Fmoc derivative **18** was prepared from **17** (0.55 g, 1,7 mmol) as described for **7**. Crystallization from ethanol/ether. Yield 0.7 g (92%); homogeneous (TLC system A); ESI-MS: *m/z*: 448 $[M^+]$, 465 $[M+NH4]^+$, 470 $[M+Na]^+$, 486 $[M+K]^+$.

19: Aqueous ammonia (10 mL) was added in one portion to **11** (0.51 g, 2 mmol) in methanol (30 mL) and stirred at room temperature for 15 h. After evaporation in vacuo 10% $NaHCO_3$ (50 mL) was added to the residue, which was then filtered off and washed with water. The solid was recrystallized from EtOAc/*n*-hexane. Yield 0.46 g (96%); homogeneous (TLC systems B and C); ^{1}H NMR ([D$_6$]DMSO): δ = 1.38 (s, 9H; $3CH_3$), 4.26 (d, ^3J (H,H) = 5.90 Hz, 2H; CH_2), 7.46 (br s, 2H; $CONH_2$), 7.21 (t, ^3J (H,H) = 5.58 Hz, 1H; NH), 8.49 (s, 1H; CH_{Oxa}), ^{13}C NMR ([D$_6$]DMSO): δ = 28.2 (Boc-CH_3), 37.3 (CH_2), 78.5 (Boc-C_q), 136.2 (C^5_{Oxa}), 141.9 (C^4_{Oxa}), 155.5 (Boc-CO), 161.7 (C^2_{Oxa}), 161.8 ($CONH_2$).

20: Prepared from **19** (0.84 g, 3.5 mmol) as described for **2**. The thioamide **20** was crystallized from EtOAc/*n*-hexane. Yield 0.76 g (84%); homogeneous (TLC systems B and C); ^{1}H NMR ([D$_6$]DMSO): δ = 1.37 (s, 9H; $3CH_3$), 4.26 (d, ^3J (H,H) = 5.65 Hz, 2H; CH_2), 7.54 (br t, 1H; NH), 8.57 (s, 1H; CH_{Oxa}), 9.25, 9.79 (br s, 1H; $CSNH_2$); ^{13}C NMR ([D$_6$]DMSO): δ = 28.1 (Boc-CH_3), 37.4 (CH_2), 78.5 (Boc-C_q), 140.9 (C^5_{Oxa}), 143.7 (C^4_{Oxa}), 155.5 (Boc-CO), 161.7 (C^2_{Oxa}), 187.5 (C=S).

21: Ester **21** was prepared from **20** (0.75 g, 2.9 mmol), $KHCO_3$ (1.5 g, 15 mmol) and ethyl bromopyruvate (1.25 mL, 10 mmol) in DME (50 mL) according to refs. [4a,b,j]. After purification on SiO_2 with EtOAc/*n*-hexane (2/1) as eluent **21** was crystallized from EtOAc/*n*-hexane. Yield 0.57 g, (57%); homogeneous (TLC systems B and C); ^{13}C NMR ([D$_6$]DMSO): δ = 14.2 (OCH_3), 28.2 (Boc-CH_3), 37.4 (CH_2), 60.9 (OCH_2), 78.5 (Boc-C_q), 129.1 (C^5_{Thz}), 134.5 (C^5_{Oxa}), 137.2 (C^4_{Oxa}), 147.2 (C^4_{Thz}), 155.7 (Boc-CO), 159.9 (C^2_{Oxa}), 160.6 (C^2_{Thz}), 162.9 (COO); ESI-MS, *m/z*: 354 $[M^+]$.

22: The Boc compound **22** was prepared from **21** (0.42 g, 1.2 mmol) as described for **12**. Crystallization from EtOAc/*n*-hexane. Yield 0.36 g (92%); homogeneous (TLC systems B and C); ^{1}H NMR ([D$_6$]DMSO): δ = 1.4 (s, 9H; $3CH_3$), 4.32 (br d, 2H; CH_2), 7.59 (br t, 1H; NH), 8.49 (s, 1H; CH_{Oxa}), 8.78 (s, 1H; CH_{Thz}); ^{13}C NMR ([D$_6$]DMSO): δ = 28.2 (Boc-CH_3), 37.4 (CH_2), 78.6 (Boc-C_q), 128.6 (C^5_{Thz}), 134.6 (C^5_{Oxa}), 137.0 (C^4_{Oxa}), 148.4 (C^4_{Thz}), 155.7 (Boc-CO), 159.6 (C^2_{Oxa}), 161.9 (C^2_{Thz}), 162.9 (COOH).

23: The Fmoc compound **23** was prepared from **22** (0.32 g, 1 mmol) as described for **7**. Crystallization from ethanol/ether. Yield 0.42 g (93%); homogeneous (TLC system A); ESI-MS: m/z 448 $[M^+]$, 470 $[M + Na]^+$, 492 $[M + 2Na]^+$.

Received: January 31, 1996 [Z 8774 IE]
German version: *Angew. Chem.* **1996**, *108*, 1604–1607

Keywords: amino acids · heterocycles · oxidations · peptide mimetics · synthetic methods

[1] *Biochemistry of peptide antibiotics* (Eds.: H. Kleinkauf, H. von Döhren), de Gruyter, Berlin, **1990**.

[2] a) G. Jung, *Angew. Chem.* **1991**, *103*, 1067–1084; *Angew. Chem. Int. Ed. Engl.* **1991**, *30*, 1051–1068; b) *Nisin and novel lantibiotics* (Eds.: G. Jung, H.-G. Sahl), Escom, Leiden, **1991**; c) R. Jack, F. Götz, G. Jung in *Biotechnology Vol. 7*, 2nd ed., (Eds.: H.-J. Rehm, G. Reed, H. Kleinkauf, H.von Doeren), VCH, Weinheim, **1996**, in press.

[3] a) A. Bayer, S. Stevanovic, S. Freund, J. Metzger, G. Jung in *Peptides 1992* (Eds.: A. C. H. Schneider, A. N. Eberle), Escom, Leiden, **1993**, pp. 117–118; b) A. Bayer, S. Freund, G. N. Nicholson, G. Jung, *Angew. Chem.* **1993**, *105*, 1410–1413; *Angew. Chem. Int. Ed. Engl.* **1993**, *32*, 1336–1339; c) A. Bayer, S. Freund, G. Jung, *Eur. J. Biochem.* **1995**, *234*, 414–426.

[4] a) N. Fusetani, S. Matsunaga, *Chem. Rev.* **1993**, *93*, 1793–1806; b) B. S. Davidson, *ibid.* **1993**, *93*, 1771–1791; c) J. Kobayashi, M. Ishibashi, *ibid.* **1993**, *93*, 1753–1770; d) M. J. Garson, *ibid.* **1993**, *93*, 1699–1733; e) J. P. Michael, G. Pattenden. *Angew. Chem.* **1993**, *105*, 1–24; *Angew. Chem. Int. Ed. Engl.* **1993**, *32*, 1–24; f) G. Pattenden, *J. Heterocyclic Chem.* **1992**, *29*, 607–618; g) J.-R. Lewis, *Nat. Prod. Rep.* **1993**, *10*, 29–50; h) J. R. Lewis, *ibid.* **1992**, *9*, 81–101; i) D. J. Faulkner, *ibid.* **1992**, *9*, 323–364; j) H. Drechsel, H. Stephan, R. Lotz, H. Haag, H. Zähner, K. Hantke, G. Jung, *Liebigs Ann. Chem.* **1995**, 1727–1733; k) H. G. Floss, J. M. Beale, *Angew. Chem.* **1989**, *101*, 147–179; *Angew. Chem. Int. Ed. Engl.* **1989**, *28*, 146–177; l) B. T. Breil, P. W. Ludden, E. W. Triplett, *J. Bacteriol.* **1993**, *175*, 3693–3702; m) further citations [3c].

[5] I. J. Turchi in *Oxazoles*, (Eds.: A. Weissberger, E. C. Taylor), Wiley, New York, **1986**, pp. 1–342, and references therein.

[6] For some recent syntheses of oxazoles, see a) E. Aguilar, A. I. Meyers, *Tetrahedron Lett.* **1994**, *35*, 2477–2480; b) A. I. Meyers, F. Tavares, *ibid.* **1994**, *35*, 2481–2484; c) M. Tiecco, L. Testaferri, M. Tingoli, F. Marini, *J. Org. Chem.* **1993**, *58*, 1349; d) M. Yokoyama, Y. Menjo, M. Watanabe, H. Togo, *Synthesis*, **1994**, 1467–1470; e) H. Vorbrüggen, K. Krolikiewicz, *Tetrahedron*, **1993**, *49*, 9353–9372; f) R. D. Connell, M. Tebbe, A. R. Gangloff, P. Helquist, *ibid.* **1993**, *49*, 5445–5459; g) P. Wipf, C. P. Miller, *J. Org. Chem.* **1993**, *58*, 3604–3606; h) J. C. Barrish, J. Songh, S. H. Spergel, W.-C. Han, T. Kissick, D. R. Kronenthal, R. H. Mueller, *ibid.* **1993**, *58*, 4494–4496; i) G. Li, P. M. Warner, D. J. Jebaratnam, *ibid.* **1996**, *61*, 778–780.

[7] a) U. Schmidt, R. Utz, A. Lieberknecht, H. Griesser, B. Potzolli, J. Bahr, K. Wagner, P. Fischer, *Synthesis*, **1987**, 233–236, 236–241; b) U. Schmidt, P. Gleich, H. Griesser, R. Utz, *ibid.* **1986**, 992–998; c) R. C. Kelly, I. Gebhard, N. Wicnienski, *J. Org. Chem.* **1986**, *51*, 4590–4594; d) U. Schmidt, H. Griesser, *Tetrahedron Lett.* **1986**, *27*, 163–166; e) R. Houssin, M. Lohez, J.-L. Bernier, J.-P. Henichart, *J. Org. Chem.* **1985**, *50*, 2787–2788; f) G. R. Pettit, P. S. Nelson, G. W. Holzapfel,*ibid.* **1985**, *50*, 2654–2659; g) U. Schmidt, R. Utz, P. Gleich, *Tetrahedron Lett.* **1985**, *26*, 4367–4370; h) C. W. Holzapfel, G. R. Pettit, *J. Org. Chem.* **1985**, *50*, 2323–2327; i) M. W. Bredenkamp, C. W. Holzapfel, R. M. Snyman, W. J. van Zyl, *Synth. Commun.* **1992**, *22*, 3029–3039.

[8] S. Scheibye, B. S. Petersen, S. O. Lawesson, *Bull. Soc. Chim. Belg.* **1978**, *87*, 229–238.

[9] R. C. Kelly, I. Gebhard, N. Wicnienski, *J. Org. Chem.* **1986**, *51*, 4590–4594.

[10] R. J. Bergeron, J. S. McManis, J. B. Dionis, J. R. Garlich, *J. Org. Chem.* **1985**, *50*, 2780–2782.

[11] a) M. Reuman, A. I. Meyers, *Tetrahedron* **1985**, *41*, 837–860; b) K. Yonetani, Y. Hirotsu, T. Shiba, *Bull. Chem. Soc. Jpn* **1975**, 3302–3305.

[12] V. Pozdnev, *Bioorg. Khim.* **1977**, *3*, 1605–1610.

[13] G. Videnov, D. Kaiser, M. Brooks, G. Jung, *Angew. Chem.* **1996**, *108*, 1607; *Angew. Chem. Int. Ed. Engl.* **1996**, *35*, 1506.

[14] D. Kaiser, G. Videnov, C. Maichle-Mössmer, J. Strähle, G. Jung, unpublished.

Synthesis of the DNA Gyrase Inhibitor Microcin B17, a 43-Peptide Antibiotic with Eight Aromatic Heterocycles in its Backbone**

Georgi Videnov, Dietmar Kaiser, Marc Brooks, and Günther Jung*

Dedicated to Professor Helmut Zahn on the occasion of his 80th birthday

The complete structure elucidation of the most unusual polypeptide microcin B17 (McB17),[1,2] a DNA gyrase inhibitor, reveals that it contains four oxazole and four thiazole rings within its backbone of 43 amino acids. McB17 inhibits DNA replication with remarkably high biological activity.[3] The glycine-rich peptide antibiotic is ribosomally synthesized by *Escherichia coli* strain LP 17,[4] and posttranslational enzymatic backbone modifications of glycine, serine, and cysteine residues in the 69 amino acid precursor lead to the formation of 2-aminomethylthiazole-4-carboxylic acid [gly(Thz)] and 2-aminomethyloxazole-4-carboxylic acid [gly(Oxa)], as well as the bicyclic 2-[2′-amino-methyloxazole-4′-yl]thiazole-4-carboxylic acid [gly(OxaThz)] and 2-[2′-amino-methylthiazole-4′-yl]-oxazole-4-carboxylic acid [gly(ThzOxa)] (Fig. 1). The synthesis of these novel constraint amino acids and their Boc and Fmoc derivatives is described separately.[6] Here we summarize details of the total synthesis of McB17 that we first reported in 1995.[5]

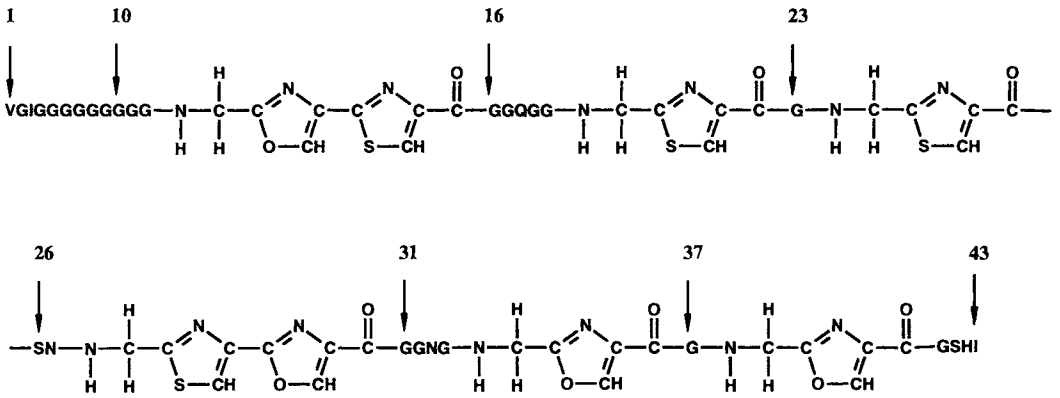

Fig. 1. Formula of the glycine-rich peptide antibiotic microcin B17 containing eight heterocyclic modifications that constrain the backbone [1,2]. Protein amino acids are abbreviated in the one-letter code and numbered according to the unmodified precursor protein.

McB17 was built up by 9-fluorenylmethoxycarbonyl (Fmoc) solid-phase synthesis starting from Fmoc-Ile-Wang resin. Fmoc-protected amino acids were coupled with an equimolar ratio of 2-(1*H*-benzotriazol-1-yl)-1,1,3,3-tetramethyluronium tetrafluoroborate (TBTU), *N*-hydroxybenzotriazole (HOBt), and diisopropylethylamine (DIEA), and the reaction was monitored for completion with ninhydrin. Due to problems in the stepwise synthesis of the glycine-rich N-terminal part, we used Fmoc-Gly-Gly-OH, Fmoc-Gly-Gly-Gly-OH, Fmoc-Ile^3-Gly^4-OH, and Boc-Val^1-Gly^2-OH in the appropriate positions (Fig. 1). In particular, Boc-Val^1-Gly^2-OH, Fmoc-Ile^3-Gly^4-

[*] Prof. Dr. G. Jung, Dr. G. Videnov, Dipl.-Chem. D. Kaiser, Dipl.-Biol. M. Brooks
Institut für Organische Chemie der Universität
Auf der Morgenstelle 18, D-72076 Tübingen (Germany)
Fax: Int. code +(7071)29-6925
e-mail: guenther.jung@uni-tuebingen.de

[**] This work was supported by the Deutsche Forschungsgemeinschaft (SFB 323, project C2-Jung).

OH, and Fmoc-Gly^5-Gly^6-OH had to be coupled twice. The assembled peptide was cleaved from the resin with a 3:3:3:91 mixture of dimethylsulfide, *meta*-cresol, ethanedithiol, and trifluoroacetic acid (TFA) for 1 h at room temperature and precipitated with ether. The raw synthetic McB17 was about 50% pure and was chromatographed to high purity (>95%) by semipreparative HPLC (Nucleosil 300C18 5 μm, 8 × 250 mm; CH_3CN/H_20 containing 0.1% TFA). The structural identity of purified McB17 was confirmed by HPLC (Fig. 2), electrospray mass spectrometry (ESI-MS), and 2D NMR spectroscopy. The mass spectrum of the synthetic microcin B17 shows peaks having the expected mass of doubly and triply charged molecular ions (Fig. 2). The enantiomeric purity of HPLC purified McB17 has been determined by gas chromatography of a derivatized hydrolysate (48 h) on a Chirasil-Val to be within the usually tolerated values (<1%).

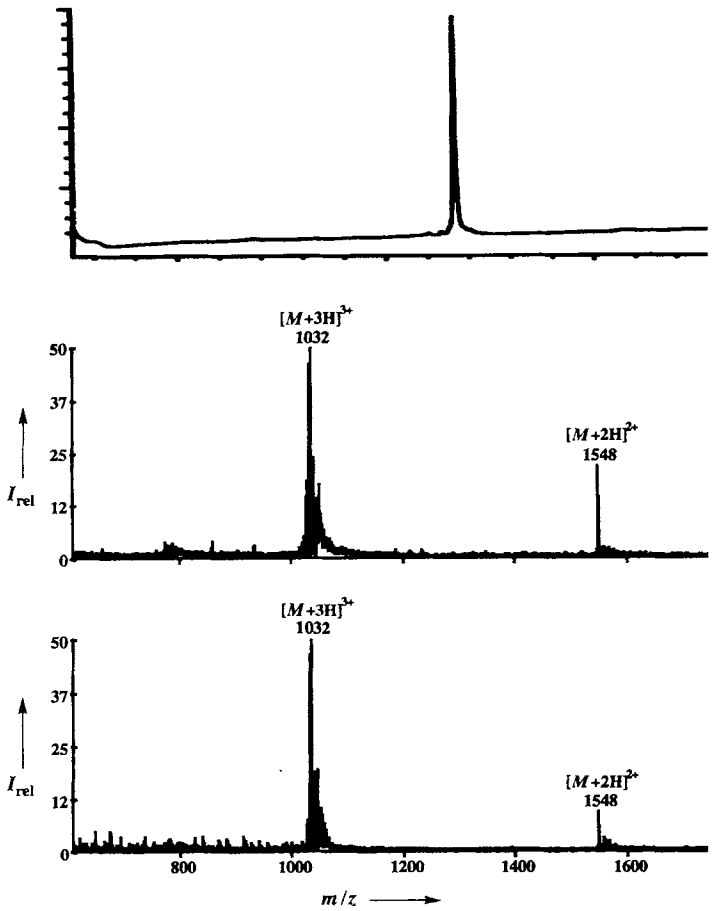

Fig. 2. HPLC chromatogram of purified synthetic microcin B17 (top) and ESI-MS spectra of the synthetic (center) and the purified natural (bottom) microcin B17 (M_r = 3094).

2D $^1H,^{13}C$ HSQC spectra (HSQC = heteronuclear single quantum coherence) were recorded to confirm the structure of the synthetic peptide originating from 43 amino acids, since we could rely on our complete NMR signal assignments of both the ^{15}N- and $^{13}C,^{15}N$-labeled natural McB17.[2] As expected the region for arene protons shows, besides the histidine signals, eight carbon signals that can be assigned to the CH groups of the eight five-membered heteroarenes. Thiazole rings show ^{13}C chemical shifts between δ = 125 and 130 and the oxazole ring between δ = 140 and 146. The spectrum of the synthetic product clearly exhibits the signals of the heteroaromatic modifications, which correspond exactly to those of natural McB17 (Fig. 3). Only the signal of the CH group in position 29 shows small deviations from the corresponding signal of the $^{13}C,^{15}N$-labeled sample, probably due to the strong pH dependence of signals of this moiety. Such a dependence was also observed in the natural sample.[2] The imidazol CH signals are broadened in both the synthetic and natural sample and are not visible in Figure 3 due to the particular level chosen for the illustrated 2D spectrum. The aliphatic signal region is in full agreement with the signals of the natural sample.[2]

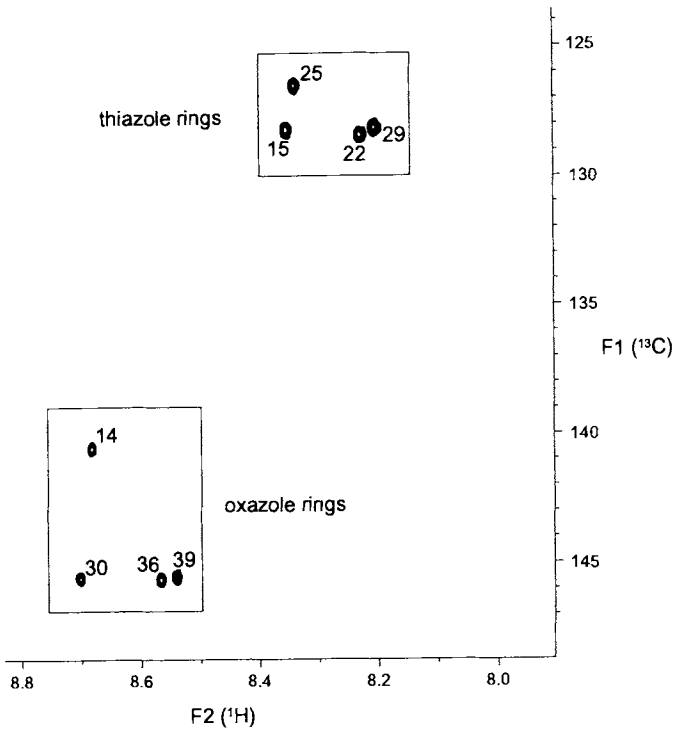

Fig. 3. Arene region of the $^1H,^{13}C$ HSQC spectrum of synthetic microcin B17 (c = 8 mg mL^{-1}, [D_6]DMSO) showing CH signals of the eight heterocycles (see Fig. 1). The signals were assigned according to ref. [2], and the numbering of heterocyclic residues relates to the sequence of the unmodified precursor protein.

An *Escherichia coli* (rec A$^-$) strain was used as a microcin B17 indicator strain in an agar diffusion assay. The lyophilized synthetic microcin was dissolved in urea buffer and spotted on an agar plate. After incubation the inhibition zones revealed the same antibacterial activity as the natural McB17.

The synthesis of McB17 confirms our previously published structure elucidation[1, 2] and represents a solid basis for our ongoing studies of structure–activity relationships of this gyrase inhibitor.

Experimental Procedure

NMR: 2D NMR spectra were taken at 600.13 MHz (^1H) on an AMX-600 (Bruker, Karlsruhe) with an inverse triple resonance probe. McB17 was dissolved in [D_6]DMSO (c = 8 mg mL^{-1}; reference DMSO: ^1H, δ = 2.50; ^{13}C, δ = 43.5; 305 K). For $^1H,^{13}C$ HSQC spectra at natural isotope abundance we used a pulse sequence of enhanced sensitivity applying gradients for coherence selection [7,8]. The offset frequency was set at δ = 135 (arene region) and δ = 45 (aliphatic region) in the ^{13}C dimension, and the experiment was carried out with a spectral band width of δ = 30 and 70, respectively, in the indirect dimension.

Antibacterial assays: The activity of McB17 was tested by the limited dilution assay [9]. The dissolution of the lyophilized sample in a TRIS buffer (pH 8) containing 50% urea and 1 mM EDTA resulted in a concentration of 1 mg McB17 per mL. Samples (each 5 μL) of a dilution series were spotted on M 63 glucose plates that were covered with 3 mL of minimal soft agar freshly seeded with 2×10^7 indicator

bacteria. After overnight incubation at 37 °C, the diameters of the halos were measured. The reciprocal of the minimum mass of McB17 that produced a clear halo of growth inhibition was defined as activity. The indicator strain was *E. coli* K12 16-19 Ufr/recA⁻/B1/T1, T5 sensitive (laboratory collection of the University of Tübingen, Microbiology Department), which is hypersensitive to McB17 due to its mutation in the SOS regulated recA⁻ gene [10].

Received: January 31, 1996 [Z 8775 IE]
German version: *Angew. Chem.* **1996**, *108*, 1607–1609

Keywords: DNA gyrase inhibitor · microcin B17 · natural products · peptide antibiotics · peptide syntheses

[1] A. Bayer, S. Stevanovic, S. Freund, J. Metzger, G. Jung in *Peptides 1992* (Eds.: C. H. Schneider, A. N. Eberle), Escom, Leiden, **1993**, pp. 117–118.
[2] a) A. Bayer, S. Freund, C. N. Nicholson, G. Jung, *Angew. Chem.* **1993**, *105*, 1410–1413; *Angew. Chem. Int. Ed. Engl.* **1993**, *32*, 1336–1339; b) A. Bayer, S. Freund, G. Jung, Eur. *J. Biochem.* **1995**, *234*, 414–426.
[3] F. Baquero, F. Moreno, *FEMS Microbiol. Lett.* **1984**, *23*, 117–124.
[4] J. L. Vizan, C. Hernandez-Chico, I. del Castillo, F. Moreno, *EMBO J.* **1991**, *10*, 467–476.
[5] G. Videnov, D. Kaiser, C. Kempter, G. Jung in *Peptides, Chemistry, Structure and Biology* (Eds.: P. T. P. Kaumaya, R. S. Hodges), Mayflower Scientific, Kingswinford, UK, **1996**.
[6] G. Videnov, D. Kaiser, C. Kempter, G. Jung, *Angew. Chem.* **1996**, *108*, 1604, *Angew. Chem. Int. Ed. Engl.* **1996**, *35*, 1503.
[7] J. Cavanagh, A. G. Palmer III, P. E. Wright, M. Rance, *J. Magn. Reson.* **1991**, *91*, 429–436.
[8] L. E. Kay, P. Keifer, T. Saarinen, *J. Am. Chem. Soc.* **1992**, *114*, 10663–10665.
[9] A. Mayr-Harting, A. J. Hedges, R. C. W. Berkey, *Methods Microbiol.* **1972**, *7A*, 315–422.
[10] M. Herrero, F. Moreno, *J. Gen. Microbiol.* **1986**, *132*, 393–402.

$[Sb_{12}\{(2\text{-MeO})C_6H_4N\}_{18}]\cdot 6THF$; A Twenty-Four Membered Imidoantimony(III) Metallacycle**

Michael A. Beswick, Maxwell K. Davies, Michael A. Paver, Paul R. Raithby, Alexander Steiner, and Dominic S. Wright*

Dimethyl amido complexes of p block metals $[E(NMe_2)_x]$ (E = Sb and Bi, $x = 3$;[1] Sn, $x = 2$[2]) are highly potent deprotonation reagents. Thus, the reactions of $[Sb(NMe_2)_3]$ with primary amines RNH_2 in the molar ratio 1:1 at low temperature give the dimeric imidoantimony(III) complexes $[\{(Me_2N)Sb(\mu\text{-}NR)\}_2]$ in which the amine ligands have been doubly deprotonated.[1b] The further reaction of the terminal Me_2N groups of $[\{(Me_2N)E(\mu\text{-}NR)\}_2]$ with [RNHLi] (E = Sb, Bi; R = C_6H_{11} (Cy), *t*Bu) in the molar ratio 1:2 produce cage complexes containing dianions such as $[E_2(NR)_4]^{2-}$.[1d, e] Such polyimido anions of elements of Group 15,[1c, d] which can be generated by similar "mixed-metallation" reactions, have an interesting coordination chemistry; they undergo both transmetallation[3a] and cocomplexation with metal salts.[3b] Our interests have broadened to encompass the syntheses and coordination chemistry of a range of anionic and neutral p block metallaligands.[4] We report here that the mixed-metallation reaction of $[Sb(NMe_2)_3]$ with the tris(amido)stannate complex **1** (ma = 2-methoxyanilino dianion, $(2\text{-OMe})C_6H_4N^{2-}$) leads to the formation of **2**, an imidoantimony(III) metallacyclic complex.

$[(Hma)Sn(\mu\text{-}Hma)_2Li\cdot 2THF]$ **1**

$[Sb_{12}(ma)_{18}]\cdot 6THF$ **2**

The reaction of **1** with $[Sb(NMe_2)_3]$ (1:1 equiv) was carried out in an attempt to prepare a mixed-metal complex containing the trigonal bipyramidal anion $[Sn(\mu\text{-}ma)_3Sb]^-$. However, the product of this reaction is not the simple species that was originally sought but the imidoantimony(III) metallacyclic complex **2** (Scheme 1). Although the mechanism of this reaction is not clear, the presence of the Sn^{II} reagent appears to be important, since attempts to prepare **2** by direct reaction of $[H_2ma]$ with $[Sb(NMe_2)_3]$ (3:2 equiv) were unsuccessful (see Experimental Procedure).

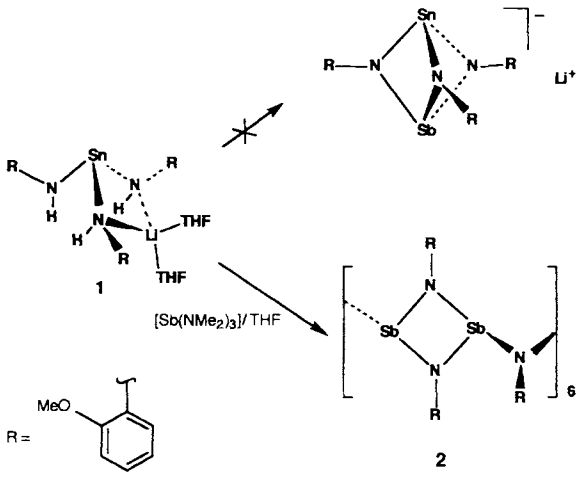

Scheme 1.

The low-temperature X-ray structure analysis of **2** (Fig. 1 top) shows that the reaction of **1** with $[Sb(NMe_2)_3]$ does not follow a simple deprotonation reaction pathway.[5] Molecules of **2** are composed of six Sb_2N_2 rings linked by bridging imido groups into a planar twenty-four membered metallacyclic ring. In addition there are six THF molecules in the lattice. The orientation of the Sb_2N_2 moieties, perpendicular to the macrocyclic core of **2**, produces an overall toroid structure (Fig. 1 bottom). Several metallacyclic complexes containing transition metals linked by O-centered ligands have structural arrangements related to that of **2**.[6] Although metallacyclic complexes containing main group elements are known[7] and other twenty-four membered rings based on phosphorus–nitrogen backbones have been characterized,[8] complex **2** is the largest structurally characterized metal imido complex of Group 15 and the first p block metal metallacyclic imido complex.

The planar Sb_2N_2 units from which the metallacyclic ring is constructed are a distorted rhombic shape (N-Sb-N av 77.2°, Sb-N-Sb 102.8°). There is surprisingly little variation in the Sb–N bond lengths throughout the whole molecule (Sb–N av 2.070 Å within the dimer units; cf. av 2.044 Å for the bridging imido groups connecting them). The angles and bond lengths found within the Sb_2N_2 units are similar to those which have

[*] Dr. D. S. Wright, Dr. M. A. Beswick, M. K. Davies, M. A. Paver, Dr. P. R. Raithby, Dr. A. Steiner
University Chemical Laboratory
Lensfield Road, Cambridge CB2 1EW (UK)
Fax: Int. code +(1223) 336362
e-mail: dsw1000@cus.cam.ac.uk

[**] This work was supported by the Engineering and Physical Sciences Research Council (M. A. B., M. K. D.), The Royal Society (P. R. R., D. S. W.), Jesus College Cambridge (fellowship for M. A. P.), and The European Union (fellowship for A. S.).

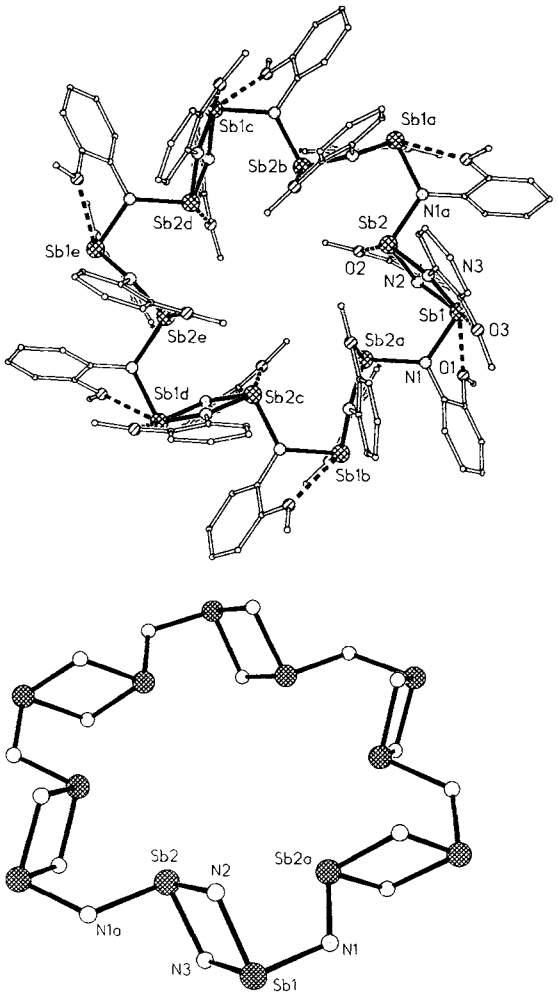

Fig. 1. Top: Structure of **2** in the solid state. Hydrogen atoms and THF lattice solvation have been omitted for clarity. Important bond lengths [Å] and angles [°]: Sb1–N1 2.04(1), Sb1–N2 2.10(1), Sb1–N3 2.07(2), Sb2–N2 2.06(1), Sb2–N3 2.10(1), Sb2a–N1 2.05(1), Sb1–O1 3.08(2), Sb1–O3 2.71(1), Sb2–O2 2.76(2), Sb2···Sb2e ca. 7.8; Sb2a-N1-Sb1 120.2(6), N1-Sb1···Sb2 100.1(4), Sb1···Sb2-N1a 100.3(4). Bottom: Toroid structure of the core of **2**.

been previously observed in the structures of isolated dimeric $Sb^{III,V}$ complexes.[1a, b, f] The formation and stability of the metallacyclic structure, as opposed to the alternative formation of a polymer, may conceivably be due to the presence of strong Sb–O interactions which hold the cyclic framework of **2** together. One of the Sb centers of each Sb_2N_2 unit interacts with a methoxy group from a bridging ma ligand within the Sb_2N_2 unit (Sb–O 2.76 Å), whereas the second Sb has an intra-Sb_2N_2 contact to the other bridging methoxy group (Sb–O 2.71 Å) and an inter-Sb_2N_2 contact to a methoxy group of a bridging ma ligand (Sb–O 3.08 Å). These interactions are well within the sum of the van der Waals radii of Sb and O (3.70 Å) and are considerably shorter than the weak intermolecular Sb···O contacts observed in the structure of $[\{(Me_2N)Sb[\mu\text{-}NC_6H_2\text{-}3,4,5\text{-}(OMe)_3]\}_2]$ (av 3.500 Å). The result of these interactions is a cyclic $Sb_{12}N_{18}$ backbone in which alternating highly distorted four-coordinate and five-coordinate Sb^{III} centers are present.

As a result of the inter-Sb_2N_2 interaction of one of the bridging methoxy groups with the four-coordinate Sb centers of **2**, the associated aromatic ligands are distorted significantly out of the planes of each of the Sb_2N_2 moieties. The six attached methoxy ligands of these are directed towards the center of the metallacycle (three above and three below the $Sb_{12}N_{18}$ ring), giving rise to an almost perfectly octahedral macrocyclic cavity (distance between diametrically opposite Sb centers ca. 7.8 Å; Sb-N-Sb 120.2(6)° and Sb···Sb-N av 100.2°). This arrangement presents the exciting prospect of selective complexation of metal ions by this new type of metallacyclic ligand. In addition, there is also the possibility of anion complexation by the Lewis acidic Sb^{III} centers.

We are currently investigating the syntheses of other Group 15 metallacyclic complexes using a similar synthetic approach to that used in the synthesis of **2** and the applications of **2** as a novel macrocylic ligand to transition and main group metals. The variation in the functionalities of the imido (and potentially phosphido and arsenido) ligands in these species may introduce further possiblities for site-selective metal complexation.

Experimental Procedure

1: H_2ma (0.74 g, 6 mmol) in THF (20 mL) was treated with *n*BuLi (4.0 mL, 1.5M, 6 mmol) at 0 °C. To the yellow solution of the lithiate was added $[Cp_2Sn]$ (2.5 mL, 0.8M in THF, 2 mmol) [9] at room temperature. The reaction mixture was briefly heated to reflux (which resulted in changing the color of the mixture to a more intense yellow) and the solvent was reduced in vacuo to about 8 mL, whereupon a yellow solid precipitated. The solid was redissolved by heating gently, and storage at room temperature (24 h) gave a crop of yellow crystalline blocks of **1**. The low-temperature X-ray structure of **1** shows that the complex has the formula $[(Hma)Sn(\mu\text{-}Hma)_2Li\cdot 2THF]\cdot 0.5\,THF$. The THF in the lattice was removed when the complex was placed under vacuum (ca. 15 min, 10^{-1} atmos) during isolation. The following analytical and spectroscopic data refer to the dry amorphous powder produced; yield 0.98 g (77%); m.p. 226 °C; IR (nujol): $\tilde{\nu}_{max}[cm^{-1}] = 3327$ (w, N–H str), 1588 (m, arene str), 1223 (s, C–O str), 734 (s, *o*-substituted Ph ring); ^1H NMR (+ 25 °C, 250 MHz, $(CD_3)_2SO$): $\delta = 6.67$ (3H, dd, C(3)-H), 6.55 (3H, dd, C(6)-H), 6.46 (3H, td, C(4)-H), 6.09 (3H, td, C(5)-H), 3.72 (3H, s, N-H), 3.64 (9H, s, MeO), 3.57 (24H, m, THF), 1.73 (24H, m, THF); elemental analyses: Calc. C 54.7, H 6.3, N 6.6; found C 53.4, H 6.3, N 6.4.

2: A solution of **1** (1.59 g, 2.5 mmol) in THF (25 mL) was treated with $[Sb(NMe_2)_3]$ (1 mL, 2.5M in THF, 2.5 mmol) at 0 °C. Warming the reaction mixture to room temperature followed by briefly heating to reflux caused the initial yellow solution to intensify in color to give a lemon-yellow solution. The solution was filtered (Celite) and the solvent was reduced in vacuo to about 7 mL, whereupon a yellow solid precipitated. The precipitate was redissolved by warming gently and lemon-yellow crystals of **2** were formed by storage at room temperature (24 h); yield 0.22 g (26%); m.p. decomp 180 °C; IR (nujol): $\tilde{\nu}_{max}[cm^{-1}] = 1586$ (m, arene str), 728 (s, *o*-substituted Ph ring); ^1H NMR (+ 25 °C, 250 MHz, $(CD_3)_2SO$): $\delta = 6.60$ (48H, m, aryl C-H), 3.72 (36H, s, MeO), 3.57 (24H, m, THF), 1.74 (24H, m, THF); elemental analyses: Calc. C 44.2, H 4.3, N 6.2; found C 42.5, H 4.2, N 6.4. The analytical and spectroscopic data confirm that, unlike **1**, the lattice solvation by THF is robust.

Received: January 2, 1996
Revised version: February 26, 1996 [Z8693IE]
German version: *Angew. Chem.* **1996**, *108*, 1660–1662

Keywords: antimony compounds · complexes with nitrogen ligands · imido complexes · metallacycles

[1] a) A. J. Edwards, N. E. Leadbeater, M. A. Paver, P. R. Raithby, C. A. Russell, D. S. Wright, *J. Chem. Soc. Dalton Trans.* **1994**, 1479; b) A. J. Edwards, M. A. Paver, P. R. Raithby, M. Rennie, C. A. Russell, D. S. Wright, *ibid.* **1994**, 2963; c) A. J. Edwards, M. A. Paver, M. Rennie, P. R. Raithby, C. A. Russell, D. S. Wright, *Angew. Chem.* **1994**, *106*, 1334; *Angew. Chem. Int. Ed. Engl.* **1994**, *33*, 1277; d) R. A. Alton, D. Barr, A. J. Edwards, M. A. Paver, P. R. Raithby, M. Rennie, C. A. Russell, D. S. Wright, *J. Chem. Soc. Chem. Commun.* **1994**, 1481; e) A. J. Edwards, M. A. Beswick, J. R. Galsworthy, M. A. Paver, P. R. Raithby, M.-A. Rennie, C. A. Russell, K. L. Verhorevoort, D. S. Wright, *Inorg. Chim. Acta* in press; f) A. J. Edwards, M. A. Paver, P. Pearson, P. R. Raithby, M.-A. Rennie, C. A. Russell, D. S. Wright, *J. Organomet. Chem.* **1995**, *503*, C29.

[2] a) R. E. Allan, M. A. Beswick, A. J. Edwards, M. A. Paver, P. R. Raithby, M.-A. Rennie, D. S. Wright, *J. Chem. Soc. Dalton Trans.* 1995, 1991; b) R. E. Allan, M. A. Paver, P. R. Raithby, A. Steiner, D. S. Wright, *Chem. Commun.* in press.

[3] a) D. Barr, A. J. Edwards, M. A. Paver, S. Pullen, P. R. Raithby, M. Rennie, C. A. Russell, D. S. Wright, *Angew. Chem.* **1994**, *106*, 1960; *Angew. Chem. Int. Ed. Engl.* **1994**, *33*, 1875; b) D. Barr, A. J. Edwards, A. Paver, P. R. Raithby, M.-A. Rennie, C. A. Russell, D. S. Wright, *ibid.* **1995**, *107*, 1088 and **1995**, *34*, 1012.

[4] M. A. Paver, C. A. Russell, D. S. Wright, *Angew. Chem.* **1995**, *107*, 1077; *Angew. Chem. Int. Ed. Engl.* **1995**, *34*, 1545.

[5] X-ray data for **2**: $C_{150}H_{174}H_{18}O_{24}Sb_{12}$, $F_w = 2395.87$, space group rhombohedral $R\bar{3}$ (no. 148), $a = 27.704(8)$, $c = 18.281(6)$ Å, $V = 12151(6)$ Å^3, $Z = 3$, $\lambda = 0.71073$ Å, $\rho_{calc} = 1.670$ Mgm^{-3}, $\mu(Mo_{K\alpha}) = 2.035$ mm^{-1}. Data were collected on a Siemens-Stoe AED diffractometer using an oil-coated [10] crystal of dimensions $0.3 \times 0.2 \times 0.2$ mm using the θ/ω method ($7.14 \leq 2\theta \leq 45.4°$). Of a total of 5484 reflections collected, 3563 were independent. The structure was solved by direct methods and refined by full-matrix least-squares on F^2 to final values of $R1 = 0.077$ (for 3563 data with $F > 4\sigma F$) and $wR2 = 0.231$ (all data) [$R1 = \Sigma||F_o| - |F_c||/\Sigma|F_o|$, $wR2 = \{[\Sigma w(F_o^2 - F_c^2)^2]/\Sigma wF_o^4\}^{0.5}$, $w = 1/[\sigma^2(F_o^2) + (xP)^2 + yP]$, $P = (F_o^2 + 2F_c^2/3)$] [11]. Largest difference between peak and hole in the final difference map, 1.965 and -1.525 e Å^{-3}. Crystallographic data (excluding structure factors) for the structure(s) reported in this paper have been deposited with the Cambridge Crystallographic Data Centre as supplementary publication no. CCDC-179-49. Copies of the data can be obtained free of charge on application to The Director, CCDC, 12 Union Road, Cambridge CB2 1EZ, UK (fax: Int. code +(1223) 336-033; e-mail: teched@chemcrys.cam.ac.uk).

[6] See for example, a) A. J. Blake, C. M. Grant, S. Parsons, J. M. Rawson, R. E. P. Winnpenny, *J. Chem. Soc. Chem. Commun.* **1994**, 2363; b) A. Caneschi, D. Gatteschi, J. Laugier, P. Rey, R. Sessoli, C. Zanchini, *J. Am. Chem. Soc.* **1988**, *110*, 2795; c) A. Müller, W. Plass, E. Krickmeyer, S. Dillinger, H. Bögge, A. Armatage, A. Proust, C. Bengholt, U. Bergmann, *Angew. Chem.* **1994**, *106*, 897; *Angew. Chem. Int. Ed. Engl.* **1994**, *33*, 849; d) A. Müller, E. Krickmeyer, J. Meyer, H. Bögge, F. Peters, W. Plass, E. Diemann, S. Dillinger, F. Nonnenbruch, M. Rauderath, C. Menke, *ibid.* **1995**, *107*, 2293 and **1995**, *34*, 2122; e) K. L. Taft, C. D. Delfs, G. C. Papaefthymiou, S. Foner, D. Gatteschi, S. L. Lippard, *J. Am. Chem. Soc.* **1994**, *116*, 823; f) P. Klüfers, J. Schuhmacher, *Angew. Chem.* **1994**, *106*, 925; *Angew. Chem. Int. Ed. Engl.* **1994**, *33*, 1863.

[7] a) M. T. Blanda, J. H. Horner, M. Newcomb, *J. Org. Chem.* **1989**, *54*, 4626; b) X. Yang, C. B. Knobler, M. F. Hawthorne, *Angew. Chem.* **1991**, *103*, 1519; *Angew. Chem. Int. Ed. Engl.* **1991**, *30*, 1507.

[8] a) Y. Ni, A. J. Laugh, A. L. Rheingold, I. Manners, *Angew. Chem.* **1995**, *107*, 1079; *Angew. Chem. Int. Ed. Engl.* **1995**, *34*, 998; b) R. T. Oakley, S. J. Rettig, N. L. Paddock, J. Trotter, *J. Am. Chem. Soc.* **1995**, *107*, 6923.

[9] See for example, a) M. A. Paver, D. Stalke, D. S. Wright, *Angew. Chem.* **1993**, *105*, 445; *Angew. Chem. Int. Ed. Engl.* **1993**, *32*, 428; b) M. A. Paver, C. A. Russell, D. Stalke, D. S. Wright, *J. Chem. Soc. Chem. Commun.* **1993**, 1350; c) A. J. Edwards, M. A. Paver, P. R. Raithby, C. A. Russell, D. Stalke, A. Steiner, D. S. Wright, *Inorg. Chem.* **1994**, *33*, 2370; d) A. J. Edwards, M. A. Paver, P. R. Raithby, C. A. Russell, D. Stalke, A. Steiner, D. S. Wright, *J. Chem. Soc. Dalton Trans.* **1993**, 1465.

[10] D. Stalke and T. Kottke, *J. Appl. Crystallogr.* **1993**, *26*, 615.

[11] G. M. Sheldrick, SHELXL 93, Universität Göttingen, **1993**.

Metastable Reverse Globular Micelles and Giant Micellar Wires from Block Copolymers**

Joachim P. Spatz, Stefan Mößmer, and Martin Möller*

Amphiphilic molecules such as surfactants and lipids associate in aqueous solution to form rather well-defined globular, rodlike, and platelet micelles, continuous structures, bilayers, and bilayer vesicles. These can partly transform from one to another when the solution conditions such as the ionic strength, the concentration, pH, or temperature are changed.[1] For block copolymers (that is, macromolecular amphiphiles) different structure variations are known in the bulk, depending on the length of the constituent blocks. In solution, however, block copolymers tend to form globular micelles.[2-7] Their size depends on the solvent and on the absolute and relative length of the blocks. In quantitative agreement with theoretical predictions, experimental evidence indicates that the cores are not spherical but have the shape of ellipsoids.[8, 9]

Only recently Eisenberg et al. observed for the first time different morphologies of polystyrene(PS)-*block*-poly(acrylic acid) associates in aqueous solution, namely, spheres, rods, lamellae, vesicles, and complex aggregates of reverse micelles.[8-10] An essential condition for the formation of these structures was that the PS core block was long relative to the outer poly(acrylic acid) block. Dispersion in water was achieved by dissolving the block copolymer in DMF-rich solvent mixtures, followed by addition of water and dialysis. Because of the vitrification of the PS core, the structure can be frozen in a nonequilibrium state.

This work deals with polystyrene-*block*-poly(2-vinylpyridine)s with a poly(2-vinylpyridine) (P2VP) block that is significantly longer than the PS block. In a dilute solution of toluene these block copolymers are expected to form reverse globular micelles, which, however, become unstable as the solvent evaporates, that is, the solution concentration increases. Transmission electron microscopy (TEM) and scanning force microscopy (SFM) is employed to study how preservation or transformation of the metastable structures upon formation of thin films depends on the block lengths and the ionic character of the core block. In a similar study we recently demonstrated that intact globular micelles are deposited from a dilute solution of a symmetrical polystyrene-*block*-poly(2-vinylpyridine) in toluene.[11-16] Transformation of the globular micelles to the lamellar bulk equilibrium structure could be inhibited by neutralization of the poly(2-vinylpyridine) block with $HAuCl_4$, which establishes a stabilizing dipole–dipole interaction.

Two polystyrene-*block*-poly(2-vinylpyridine) samples differing in their absolute molecular weight but having a similar styrene:P2VP ratio (R) were used. Table 1 summarizes the molecular characteristics. The polymers have been treated with different equivalents of $HAuCl_4$ per pyridine group in a dilute solution of toluene. The absolute molecular weight, the R ratio, and the degree of neutralization L ($L = n_{HAuCl_4}/n_{P2VP}$) are the parameters that effect the kinetic stability of a structure formed in dilute solution (in this case, globular micelles) when the solvent is evaporated. The rate of evaporation will also influence the structure transformation, as the stability is only kinetically controlled. The rate of evaporation will be subject of a subsequent paper; in the present work it was kept constant for all investigations.

Table 1. Molecular characteristics of the block copolymers.

Sample	M_n(PS) [a] [g mol^{-1}]	M_n(P2VP) [b] [g mol^{-1}]	M_n (total) [c] [g mol^{-1}]	M_w/M_n [c]
PS80-P2VP320	7.900	34.900	57.600	1.10
PS180-P2VP700	19.000	74.000	108.300	1.19

[a] Molecular weight measured by GPC for the polystyrene block before addition of the second monomer. [b] Molecular weight calculated from the styrene/2-vinylpyridine composition obtained by ^{1}H NMR in relation to the length of the PS block. [c] Molecular weight measured by GPC for the block copolymer according to narrow molecular weight polystyrene standards.

Figure 1 depicts a TEM and a SFM picture of a thin film of the PS80-P2VP320 polymer that had been treated with 0.7 equivalents of $HAuCl_4$ per pyridine unit ($L = 0.7$). Dark areas

[*] Prof. Dr. M. Möller, Dipl.-Phys. J. P. Spatz, Dipl.-Chem. S. Mößmer
Organische Chemie III – Makromolekulare Chemie der Universität
Albert-Einstein-Allee 11, D-89069 Ulm (Germany)
Telefax: Int. code +(731) 502-2883
e-mail: martin.moeller@chemie.uni-ulm.de

[**] This work was supported by the Deutsche Forschungsgemeinschaft (SFB 239) and the Fonds der Chemischen Industrie. We thank the section Elektronenmikroskopie of the University of Ulm for carrying out the electron microscopy measurements.

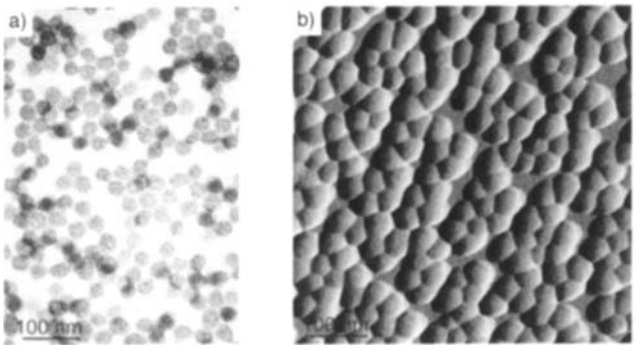

Fig. 1. Transmission electron and scanning force micrographs of spherical micelles formed of PS80-P2VP320, $R = 0.24$, $L = 0.7$. a) TEM reveals the core of the micelles (small black dots). b) SFM depicts the outer contour with the corona of the micelles, which cannot be seen by TEM. a) and b) have the same scale.

in the TEM image represent agglomerations of small gold particles, which form upon irradiation by the electron beam (electron irradiation stimulates reduction of Au^{III} ions).[12, 16] The arrangement of the gold particles indicates that the globular micelles were preserved in the solvent-free state. The gold particles mark the micelle core. The outer contours of the micelles can also be seen in the SFM picture in Figure 1b. Comparison of the TEM picture with the SFM picture reveals that the core remained less affected by the close packing of the micelles within the thin film, whereas the PS shell was significantly deformed and approached a honey comb structure as flat contact areas were formed between the micelles.

Figure 2 shows TEM pictures of a film that was formed under identical conditions from the same block copolymer, which, however, had been treated with a smaller amount of $HAuCl_4$ ($L = 0.3$). In coexistence with the globular micelles a new structure, giant cylindrical micelles, were formed. Again, the gold-loaded core of the micelles is depicted by the black areas in the TEM pictures. The ratio of the length of the cylinder to its diameter (the aspect ratio) exceeded values of 2000. While the diameters of the disks is (32 ± 3) nm, the diameter of the stripes is uniformly (21 ± 3) nm.

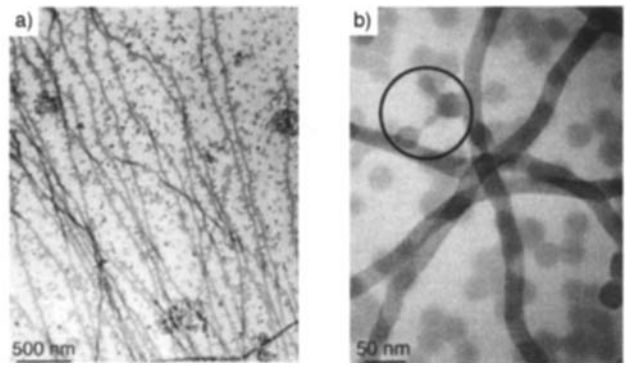

Fig. 2. The TEM images show a) the formation of cylindrical micelles with an aspect ratio a of about 2000 and b) cylindrical micelles in direct contact. The circle marks the initial step of the transformation from cylinders to wires.

Very obviously a number of the spherical micelles coagulated to form the long isolated cylinders, which are known for low molecular weight surfactants,[18] but have only been observed once for block copolymers in solution.[9] As shown in Figure 2b, these micellar wires cross each other without the integrity of the cylinders being affected by the direct contact. The initial step of the transformation from cylinders to wires is marked by the circle in Figure 2b. Apparently the transformation occurs on surface contact of the spherical micelles.

Figure 3 shows a scanning force micrograph of the micellar wires. The image displays the amplitude control signal, emphasizing rather small features in height.[17] Apparently, the corona of the cylinders is still corrugated with a periodic structure similar to the dimensions of globular micelles. Comparison of the contacts between spheres and wires demonstrates that the contour of the latter is less deformed by the contact.

Fig. 3. SFM amplitude control signal (length of one side corresponds to 2 μm) of a monolayer of spherical micelles on top of which cylindrical micelles were formed.

Neither the cylinders nor the globules represent the bulk equilibrium structure for the strongly unsymmetric block copolymers in the solvent-free state.[19] Apparently the formation of the micellar wires is controlled by the decrease in the kinetic stability of the spherical micelles as the degree of ionization of the core block is lowered from 0.7 to 0.3. This is consistent with the observation that no micellar wires were formed when at the same time the R ratio was increased. At $L = 0.3$, a PS110-P2VP280 ($R = 0.39$) did not yield cylindrical structures.

A second, important point is the observed contraction of the core radius upon formation of the micellar cylinders. This is in agreement with expectations and can be regarded as the driving force of the transformation. At the R ratios employed here, the core blocks have to stretch in order to form globular micelles with a minimum total interface area, which depends on the size and the number of micelles.[4, 5, 7] The penalty in entropy for the stretching is balanced by the reduced contacts between the ionic and nonpolar units. As the solvent evaporates, the balance is disturbed and the cylindrical micelles represent a more favorable structure with respect to the free energy. Thus, diminishing L to 0.3 accelerates the transformation kinetics to the more favorable micellar wires.

This is also demonstrated by the comparison of the two block copolymer samples that have the same composition but different absolute molecular weights (Table 2). The obtained decrease in the core diameter can be correlated to the increase in kinetic stability on transforming the globule to cylinders and depends on the absolute molecular weight. The smaller the ratio D of the diameter of the spheres to that of the cylindrical micelles, the smaller the free energy gain by the transformation. A higher molecular weight results in slow relaxation times, which have a direct influence on the transformation kinetics. This argument is consistent with the observation that the aspect ratio of the

Table 2. Dimensions of spherical and cylindrical wires.

Dimensions	PS80-b-P2VP330 $R = 0.24$, $L = 0.3$	PS180-b-P2VP700 $R = 0.26$, $L = 0.3$
D_1 [nm] [a]	32	35
D_2 [nm] [b]	21	27
D [c]	1.52	1.30
a	2×10^3	2×10^2

[a] D_1 = diameter of the spherical micelle. [b] D_2 = diameter of the micellar wire. [c] $D = D_1/D_2$. [d] a = aspect ratio = (micellar length)/(micellar diameter)

molecular wires was reduced considerably as D decreased from 1.52 to 1.30 on changing from PS80-P2VP320 to PS180-P2VP700.

Summarizing, we emphasize the following points (Fig. 4): 1) Coagulation of spherical micelles is explained by the reduced chain stretching. 2) This results in an increased grafting density in the corona and a higher shape stability. 3) The ends of the cylinders are particularly activated because of a reduced grafting density. Points 2) and 3) explain the coexistence of spheres and cylinders and the linear growth of the cylinders.

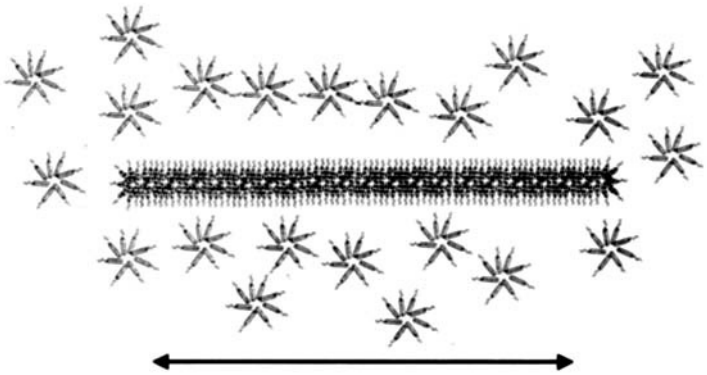

Fig. 4. The formation of micellar cylinders. Globular micelles can only join the ends of a cylinder. The arrow indicates the direction of growth. However, micellar transformations can be blocked by kinetic stabilization of the structure during the evaporation process.

Experimental Procedure

Sample preparation: The polystyrene-*block*-poly(2-vinylpyridine) block copolymers were synthesized by anionic polymerization [20, 21]. A solution of block copolymer (0.5 wt% in toluene) was mixed with different amounts of $HAuCl_4 \cdot H_2O$, depending on the molar concentration of pyridine groups (L = $HAuCl_4$/P2VP). The mixture was stirred for at least 24 h to allow complete dissolution of the gold salt within the cores of the block copolymer micelles. The solutions were diluted to 1–3 mg block copolymer per milliliter. Thin films were prepared by putting a drop of the solution onto an electron microscopy grid coated with a thin layer of carbon, which was in direct contact with a soaking tissue to remove the solution immediately. The film thickness was controlled both in this way and by varying the concentration.

Bright-field TEM images were recorded with a PHILIPS EM400T microscope operated with 80 kV. In order to minimize the destruction of the polymer by the electron beam, the electron beam intensity was kept as low as possible (second condenser lens: 50 Pt, lens: 30 Au). Scanning force microscopy with the same samples (grids) that were used for electron microscopy were performed with a Nanoscope III [17] operating in the tapping mode [22].

Received: January 25, 1996 [Z 8754 IE]
German version: *Angew. Chem.* **1996**, *108*, 1673–1676

Keywords: block copolymers · micelles · scanning force microscopy · thin films

[1] J. Israelachvili, *Intermolecular & Surface Forces*, 2nd. ed., Academic Press, San Diego, **1991**.
[2] Z. Gao, A. Eisenberg, *Macromolecules*, **1993**, *26* 7353.
[3] Z. Gao, X. F. Zhong, A. Eisenberg, *Macromolecules* **1994**, *27*, 794.
[4] D. Nguyen, S. K. Varshney, C. E. Williams, A. Eisenberg, *Macromolecules* **1994**, *27*, 5086.
[5] D. Nguyen, C. E. Williams, A. Eisenberg, *Macromolecules* **1994**, *27*, 5090.
[6] A. Halperin, *Macromolecules* **1990**, *23*, 2724.
[7] L. Leibler, H. Orland, J. C. Wheeler, *J. Chem. Phys.* **1983**, *79*, 3550.
[8] Z. Gao, S. K. Varshney, S. Wong, A. Eisenberg, *J. Chem. Phys.* **1994**, *27*, 7923.
[9] L. Zhang, A. Eisenberg, *Science* **1995**, *268*, 1728.
[10] P.-G. de Gennes in *Solid State Physics* (Ed.: L. Leibert), Academic Press, New York, **1978**; Supplement 14, p. 1.
[11] J. P. Spatz, A. Roescher, S. Sheiko, G. Krausch, M. Möller, *Adv. Mater.* **1995**, *7*, 731.
[12] J. P. Spatz, S. Sheiko, M. Möller, *Macromolecules* **1996**, *29*, 3220.
[13] A. Roescher, Dissertation, University of Twente, Holland, **1995**.
[14] A. Roescher, M. Möller, *Polym. Mater. Sci. Eng.* **1995**, *73*, 156.
[15] A. Roescher, M. Möller, *Polym. Mater. Sci. Eng.* **1995**, *72*, 283.
[16] J. P. Spatz, A. Roescher, M. Möller, *Adv. Mater.* **1996**, *8*, 337.
[17] Digital Instruments, CA, Santa Barbara.
[18] H. Hoffmann, G. Ebert, *Angew. Chem.* **1988**, *100*, 933; *Angew. Chem. Int. Ed. Engl.* **1988**, *27*, 902.
[19] F. S. Bates, *Annu. Rev. Phys. Chem.* **1990**, *41*, 525.
[20] S. Mößmer, Diplomarbeit, Universität Ulm, **1996**.
[21] M. Möller, R. W. Lenz, *Macromol. Chem.* **1989**, *190*, 1153.
[22] J. P. Spatz, S. Sheiko, M. Möller, R. W. Winkler, P. Reineker, O. Marti, *Nanotechnology* **1995**, *6*, 40.

Synthesis, Structure, and Bonding of a Mixed-Valent Tetraphosphete**

Walter Frank,* Volker Petry, Elmar Gerwalin, and Guido J. Reiss

Investigations of compounds of the general formula P_4R_4 have so far been concerned exclusively with cyclotetraphosphane $(PH)_4$ and its derivatives.[1] Neither experimental nor theoretical studies exist that deal with the valence-isomeric $1\lambda^5,3\lambda^5$-tetraphosphete $(H_2PP)_2$ and its derivatives, although two conceptual approaches are possible to such a mixed-valent 4π-electron four-membered ring system (**A**): First, it may be considered an analogue of the diphosphetes **B**[2] and the isovalence-electronic cyclodiphosphazenes **C**;[3] second, it is evidently related to the phosphinylidene-σ^4-phosphoranes[4] and in

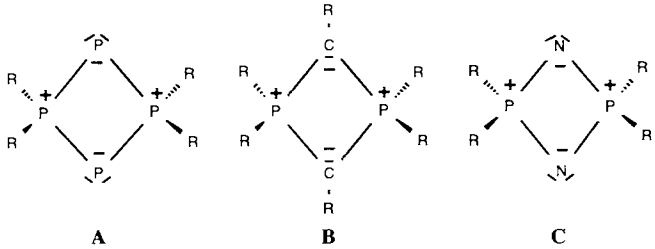

A **B** **C**

[*] Prof. Dr. W. Frank, Dipl.-Chem. V. Petry, Dipl.-Chem. E. Gerwalin, Dr. G. J. Reiss
Fachbereich Chemie der Universität
Postfach 3049, D-67653 Kaiserslautern (Germany)
Fax: Int. code +(631)205-2187
e-mail: walter@chemie.uni-kl.de

[**] This work was supported by the Fonds der Chemischen Industrie and the Bundesland Rheinland-Pfalz (post-graduate grant for V. P. within the Graduiertenkolleg "Phosphorchemie als Bindeglied verschiedener chemischer Disziplinen"). We acknowledge the grant of computing time by the Regionales Hochschulrechenzentrum Kaiserslautern.

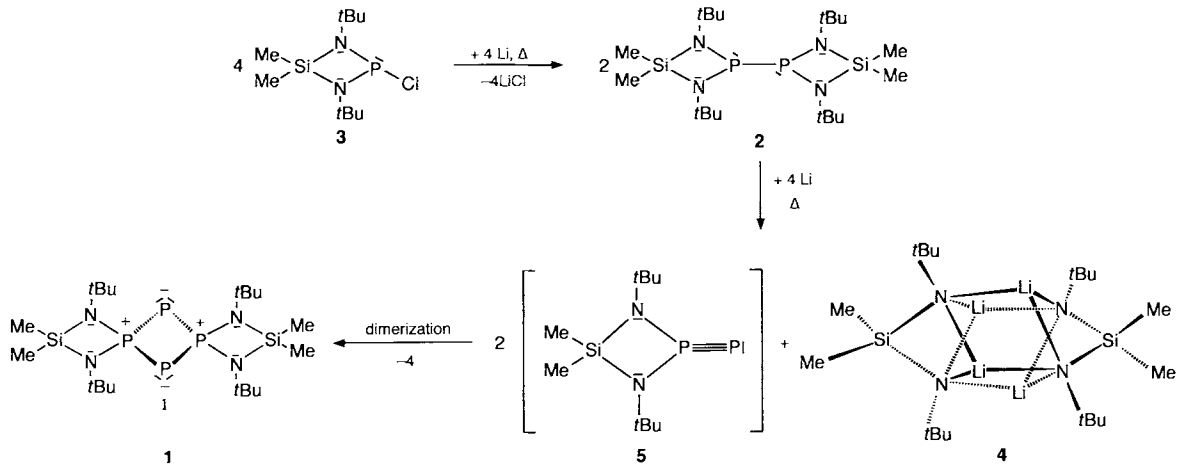

Scheme 1. Postulated mechanism for the formation of 1.

particular to those having acyclic "monounsaturated" λ^5P-λ^3P-λ^5P structural units.[5] Recently we have developed a simple route to compound **1** (see Scheme 1), which contains a $1\lambda^5,3\lambda^5$-tetraphosphete four-membered ring as the central structural unit of a dispirocyclic system.

Compound **1** is formed, in addition to the tetrakis(amino)-diphosphane **2**, in the reduction of the bis(amino)chlorophosphane **3**[6] with lithium. The reaction was monitored by NMR spectroscopy, which suggested that **1** is formed as a secondary product from **2** (Scheme 1). Since more complex mechanisms may also be contemplated under the reaction conditions given, and direct evidence for an intermediary phosphidophosphorane **5** has not been obtained, further investigations will be necessary to show whether or not **1** is actually formed by a "head-to-tail" type dimerization (Scheme 1). The lithium amide **4**[7] was identified by ^{7}Li NMR as well as by ^{1}H NMR spectroscopy and by the molecular ion M^+ in the EI mass spectrum as the only other lithium-containing compound in addition to dissolved lithium chloride.

The intense yellow compound **1**, which can be handled in air for long periods of time without decomposition, has been characterized by elemental analysis, mass spectrometry, ^{1}H NMR and ^{31}P NMR spectroscopy, and by a crystal structure investigation.[8] It is poorly soluble in both nonpolar and polar solvents. Therefore, ^{1}H NMR and ^{31}P NMR spectra could be recorded only in dioxane at elevated temperature. Under such conditions, the spectra are consistent with D_{2h} symmetry of the molecule. While the ^{31}P NMR chemical shift of the σ^4-P atoms is in good agreement with the values found in comparable compounds, that of the σ^2-P atoms has a rather unusual value lying between the ranges usually obtained for phosphinylidene-σ^4-phosphoranes and diphosphenes.

Upon crystallization, the point symmetry of the molecules of **1** is lowered (to C_i), as might be expected, while the D_{2h} symmetry is roughly conserved for the spirocyclic skeleton of Si, N, and P atoms (Fig. 1). The extent of rhombic distortion of the central P_4 ring is remarkable, exhibiting an unusually acute P1-P2-P1a angle of 79.4°. All of the P–P bonds in the ring are approximately equal in length (Table 1); the distances are typical of monounsaturated λ^5P-λ^3P-λ^5P structural units.[5]

In the EI mass spectrum of **1**, M^+ is the peak with the largest m/z observed. In addition to the cyclic $[Me_2Si(NtBu)_2P]^+$ ion and its characteristic fragments, the radical cation of the monomeric phosphidophosphorane **5** and its decomposition products are observed with higher source temperatures.

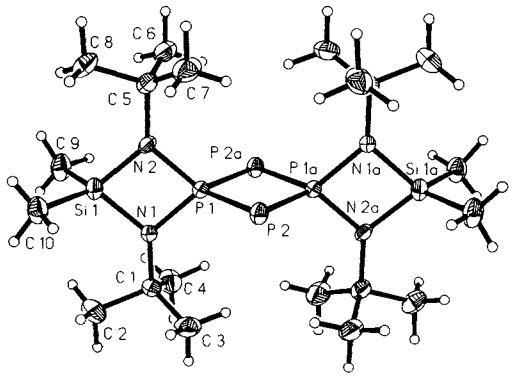

Fig. 1. Molecular structure of 1; 50% probability ellipsoids for anisotropic atomic displacement; hydrogen atoms omitted for clarity. Selected distances [Å] and angles [°] (see also Table 1): a: $-x$, $-y$, $-z$: Si1-C9 1.846(4), Si1-C10 1.860(4), N1-C1 1.483(3), N2-C5 1.483(3), C-C 1.516(5)–1.527(5), C-H 0.91(3) 1.01(4); P2a-P1-N1 118.2(1), P2a-P1-N2 118.2(1), N1-Si1-C9 116.0(2), N1-Si1-C10 115.8(2), N2-Si1-C9 115.4(1), N2-Si1-C10 116.4(1), C9-Si1-C10 108.6(2), Si1-N1-C1 132.5(2), P1-N1-C(1) 131.1(2), Si1-N2-C5 132.0(2), P1-N2-C5 131.3(2).

Table 1. Comparison of selected distances [Å], angles [°], and bond orders s [11] of **1** and the model compounds $[\{PP(NMe)_2SiH_2\}_2]$ (**6**) and $(PPH_2)_2$ (**7**) [a].

	1	**6**	**7**
Symmetrie	C_i	D_{2h}	D_{2h}
P1–P2/P2a	2.139(1)/2.142(1)	2.141	2.170
P1···P1a	2.736(1)	2.733	2.770
P2···P2a	3.293(1)	3.297	3.340
P1–N1/N2	1.711(2)/1.711(2)	1.689	–
P1–H	–	–	1.391
Si1–N1/N2	1.735(2)/1.734(2)	1.735	–
N1/N2–C1/C5	1.483(3)/1.483(3)	1.446	–
P1-P2-P1a	79.4(1)	79.3	79.3
P2-P1-P2a	100.6(1)	100.7	100.7
P2-P1-N1/N2	118.3(1)/118.2(1)	117.9	–
N1-P1-N2	84.5(1)	85.7	–
H-P1-H	–	–	100.3
Si1-N1/N2-P1	96.2(1)/96.2(1)	95.7	–
N1-Si-N2	83.1(1)	82.9	–
s(P1–P2/P2a)	1.29/1.28	1.07	1.04
s(P1–N1/N2)	0.98/0.98	0.71	–
s(P1–H)	–	–	0.91
s(Si1–N1/N2)	0.97/0.97	0.60	–

[a] The structure of **1** was determined by X-ray structure analysis, those of the model compounds **6** and **7** by ab initio calculations (RHF6-31G*).

 © VCH Verlagsgesellschaft mbH, D-69451 Weinheim, 1996 0570-0833/96/3513-1513 $ 15.00+.25/0

Ab initio quantum chemical calculations[9] revealed a very good agreement of the structural parameters of the model compound **6**, in which each of the CH_3 groups is replaced by a H atom (the conformational arrangement of the resulting methyl groups is like that of the *tert*-butyl groups in Fig. 1),[10] with those in **1** obtained by crystal structure investigation (Table 1). The important structural features of **1** (equivalent P1–P2 and P1–P2a distances, rhombic distortion) are basically accounted for by formulations as a bis(ylide) **I** or as a system with delocalized double bonds **II**. From the two canonical π-MOs schematically represented in Figure 2, it can be seen immediately that pπ-pπ bond contributions are considered in **1**, whereas the 3c/2e interactions in comparable cyclodiphosphazenes are formulated in terms of pπ-dπ fractions.[4b] The calculated charge distributions in the P_4 ring of **1** and in the P_2N_2 ring of its phosphazene analogue $[\{NP(NMe)_2SiH_2\}_2]$ **8** show that the ylidic character is predominant in each case (natural charges:[14] **6**: P1 +1.40, P2 −0.45, N −1.34; **8**: P1 +2.49, N_{ring} −1.55, N_{term} −1.38), but is reduced in **1** as compared to **8**. In contrast, the π-bond fraction calculated by Mulliken population analyses and NLMO analyses[14] is significantly higher in **1** than in **8**. According to our MP2/6-31G* calculations,[9] the parent compound $1\lambda^5,3\lambda^5$-tetraphosphete **7** is less stable by 109.2 kJ mol^{-1} than the valence-isomeric cyclotetraphosphane $(PH)_4$ in its most stable conformation (all-*trans*, D_{2d} symmetry).

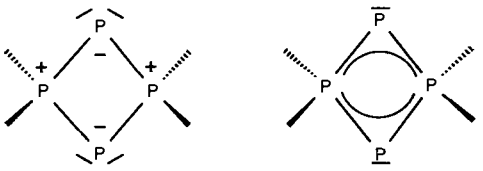

I II

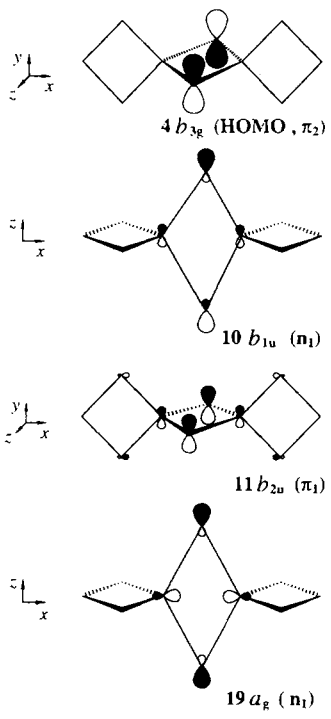

Fig. 2. π and n orbitals relevant for the discussion of the bonding in the P_4 ring of **1**; calculated orbital energies of the nine highest occupied orbitals [eV]: π_2(HOMO) −6.81, n_2 −8.38, π_1 −8.78, $7b_{2g}$ −9.51, $2a_u$ −10.40, $9b_{1u}$ −11.73, $16b_{3u}$ −11.82, n_1 −12.40.

Experimental Procedure

1,3,7,9-Tetra-*tert*-butyl-2,2,8,8-tetramethyl-1,3,7,9-tetraaza-$4\lambda^5$,5,$6\lambda^5$,10-tetraphospha-2,8-disiladispiro[3.1.3.1]deca-4,6(10)-diene (**1**) and 1,3,1′,3′-tetra-*tert*-butyl-4,4,4′,4′-tetramethyl-[2,2′]-bis(1,3,2,4-diazaphosphasiletidinyl) (**2**): Lithium (0.37 g, 53.3 mmol) was suspended in a solution of **3** (10.7 g, 40.0 mmol) [6] in THF (150 mL), and the mixture was heated to reflux. After two days, complete conversion of **3** to yield the diphosphane **2** and the tetraphosphete **1** was established by ^{31}P NMR spectroscopy. From the orange filtrate of the reaction mixture, 1.89 g (18%, based on **3**) of yellow plates of **1** crystallized in the course of two weeks at −35 °C. The solvent was removed from the mother liquor in vacuo, and a yellow oil was distilled at 54 °C/10^{-2} mbar from the highly viscous red residue. The oil congealed almost completely, often only after several days, with crystallization of colorless plates of **2** (5.65 g, 61%, m.p. 30 °C).

1: Elemental analysis (M_r = 524.69): found (calcd) : C 45.3 (45.8), H 8.9 (9.2), N 10.6 (10.7)%; MS (EI, 70 eV, 1.0 mA, source temperature = 240 °C): *m/z* (%): 524 (29) [M^+], 262 (19) [$(M/2)^+$], 247 (61) [$(M/2 - CH_3)^+$], 231 (100) [$(M/2 - P)^+$], 191 (11) [$(CH_3Si(NH)(NC_4H_9)P_2)^+$], 175 (11) [$((CH_3)_2Si(NH)(NC_4H_9)P)^+$], 135 (18) [$(CH_3Si(NH)_2P_2)^+$], 119 (64) [$((CH_3)_2Si(NH)_2P)^+$]; ^{31}P NMR (161.98 MHz, 350 K, dioxane, [D_8]toluene, H_3PO_4 85% ext.): A_2B_2 spin system, 12 lines resolved (ν_3, ν_4, and ν_{11}, ν_{12} superimposed), δ_A(P(2)) = 62.6, δ_B(P(1)) 102.4, ^1J(A,B) = 392 Hz; ^1H NMR (400 MHz, 350 K, dioxane, TMS ext.): δ = 0.45 (s, 12H, $Si(CH_3)_2$), 1.39 (s, 36H, $NC(CH_3)_3$).

2: Elemental analysis (M_r = 462.74): found (calcd): C 52.2 (51.9), H 10.4 (10.5), N 12.4 (12.1)%; MS (CI (iC_4H_{10}), 200 eV, 0.2 mA, source temperature = 200 °C): *m/z* (%): 463 (2) [$(M)H^+$], 462 (4) [M^+], 231 (100) [$(M/2)^+$]; ^{31}P NMR (161.98 MHz, THF, H_3PO_4 85% ext.): δ = 190.0 (s); ^1H NMR (400 MHz, THF, TMS ext.): δ = 0.43 (s, 6H, $SiCH_3$), 0.59 (s, 6H, $SiCH_3$), 1.42 (s, 36H, $NC(CH_3)_3$).

Received: February 9, 1996 [Z 8800 IE]
German version: *Angew. Chem.* **1996**, *108*, 1616–1618

Keywords: low-valent compounds · mixed-valent compounds · phosphetes · phosphorus compounds · silicon compounds

[1] a) H. Schiffer, R. Ahlrichs, M. Häser, *Theor. Chim. Acta* **1989**, *75*, 1; b) W. W. Schoeller, T. Busch, *Chem. Ber.* **1991**, *124*, 1369; c) G. J. Palenik, J. Donohue, *Acta Crystallogr.* **1962**, *15*, 564; d) J. C. J. Bart, *Acta Crystallogr. Sect. B* **1969**, *25*, 762; more crystal structure investigations see references in [1b].

[2] R. Appel, F. Knoll, H.-D. Wihler, *Angew. Chem.* **1977**, *89*, 415; *Angew. Chem. Int. Ed. Engl.* **1977**, 16, 402; J. Weiss, B. Nuber, *Z. Anorg. Allg. Chem.* **1981**, *473*, 101; J. Svara, E. Fluck, H. Riffel, *Z. Naturforsch. B* **1985**, *40*, 1258; H. Keller, G. Maas, M. Regitz, *Tetrahedron Lett.* **1986**, 27, 1903; H. H. Karsch, T. Rupprich, M. Heckel, *Chem. Ber.* **1995**, *128*, 959; recently also a $1\lambda^5,2\lambda^3$-diphosphete was described: R. Armbrust, M. Sanchez, R. Reau, U. Bergsträsser, M. Regitz, G. Bertrand, *J. Am. Chem. Soc.* **1995**, *117*, 10785.

[3] a) A. Baceiredo, G. Bertrand, J. P. Majoral, G. Sicard, J. Jaud, J. Galy, *J. Am. Chem. Soc.* **1984**, *106*, 6088; b) G. Trinquier, *ibid.* **1986**, *108*, 568; R. Ahlrichs, H. Schiffer, *ibid.* **1985**, *107*, 6494.

[4] A. B. Burg, W. Mahler, *J. Am. Chem. Soc.* **1961**, *83*, 2388.

[5] a) A. Schmidpeter in *Multiple Bonds and Low Coordination in Phosphorus Chemistry* (Eds.: M. Regitz, O. J. Scherer), Thieme, Stuttgart, **1990**, p. 338; b) H. H. Karsch, E. Witt, A. Schneider, E. Herdtweck, M. Heckel, *Angew. Chem.* **1995**, *107*, 628; *Angew. Chem. Int. Ed. Engl.* **1995**, *34*, 557.

[6] J. Neemann, U. Klingebiel, *Chem. Ber.* **1981**, *114*, 527; O. J. Scherer, M. Püttmann, C. Krüger, G. Wolmershäuser, *Chem. Ber.* **1982**, *115*, 2078; M. Veith, B. Bertsch, V. Huch, *Z. Anorg. Allg. Chem.* **1988**, *559*, 73.

[7] D. J. Brauer, H. Bürger, G. R. Liewald, *J. Organomet. Chem.* **1986**, *308*, 119.

[8] $C_{20}H_{48}N_4P_4Si_2$, M_r = 524.69; crystal dimensions: 0.30 × 0.30 × 0.05 mm^3, monoclinic, space group $P2_1/n$, a = 6.3876(12), b = 12.189(2), c = 18.599(3) Å, β = 97.072(10), Z = 2, V = 1437.0(4) Å^3, ρ_{calcd} = 1.213 Mgm^{-3}, T = −90 ± 1 °C, $2\theta_{max}$ = 45.0°, four-circle diffractometer, $Mo_{K\alpha}$ radiation (λ = 0.71073 Å), ω scan, 2701 reflections measured, 1759 independent, and 1671 observed ($I > 2\sigma(I)$), LP correction (μ = 0.362 mm^{-1}), structure solution by direct methods and ΔF synthesis, $\Sigma w(F_o^2 - F_c^2)^2$ minimized with $w = \sigma^{-2}$, 169 parameters refined, R_1 = 0.035, wR_2 = 0.048; $\Delta\rho_{max}/\Delta\rho_{min}$ = +0.20/−0.24 e Å^{-3}. Crystallographic data (excluding structure factors) for the structure reported in this paper have been deposited with the Cambridge Crystallographic Data Centre as supplementary publication no. CCDC-179-60. Copies of the data can be obtained free of charge on application to The Director, CCDC, 12 Union Road, Cambridge CB2 1EZ, UK (fax: Int. code +(1223) 336-033; e-mail: teched@chemcrys.cam.ac.uk).

[9] The MO calculations have been performed on an SGI PowerChallenge at the Regionales Hochschulrechenzentrum Kaiserslautern using the program package Gaussian 94, revision B.3. M. J. Frisch, G. W. Trucks, H. B. Schlegel, P. M. W. Gill, B. G. Johnson, M. A. Robb, J. R. Cheeseman, T. Keith, G. A. Petersson, J. A. Montgomery, K. Raghavachari, M. A. Al-Laham, V. G. Zakrzewski, J. V. Ortiz, J. B. Foresman, C. Y. Peng, P. Y. Ayala, W. Chem, M. W. Wong, J. L. Andres, E. S. Replogle, R. Gomperts, R. L. Martin, D. J. Fox, J. S. Binkley, D. J. Defrees, J. Baker, J. P. Stewart, M. Head-Gordon, C. Gonzalez, J. A. Pople, Gaussian, Inc., Pittsburgh PA, **1995**.

[10] The geometries of **6** and all other calculated compounds have been confirmed by frequency analyses to be minima of the corresponding potential energy surfaces.

[11] **1**: Empirical Brown bond orders, I. D. Brown, D. Altermatt, *Acta Crystallogr. Sect. B* **1985**, *41*, 441; for $r_0(\lambda^5P\text{-}\lambda^3P)$, the value 2.232 has been assumed (cf. e.g. [12]); **6** and **7**: Wiberg indices [13] based on natural atomic orbitals [14]).

[12] M. Scheer, P. G. Jones, *J. Organomet. Chem.* **1992**, *434*, 57.

[13] K. Wiberg, *Tetrahedron* **1968**, *24*, 1083.

[14] A. E. Reed, *J. Chem. Phys.* **1983**, *78*, 4066; *ibid.* **1985**, *83*, 1736.

A Mild General Procedure for the One-Pot Conversion of Amides to Aldehydes**

Shelley Bower, Kristina A. Kreutzer, and Stephen L. Buchwald*

Functional group manipulation is fundamental to synthetic organic chemistry and, hence, the development of new transformations remains of great interest. The conversion of an amide to an aldehyde is an underdeveloped transformation; few good general methods are available.[1] Existing techniques usually utilize aluminum or boron hydrides.[2] Many such reactions are substrate specific, the outcome of the reaction being dependent upon the nature of the nitrogen substituents.[3] The high reactivity of some reagents is manifested by low functional group tolerance, overreduction to amines, or the formation of other byproducts.[2b, 4] Herein, we describe a general procedure for the conversion of amides to aldehydes that employs readily available, inexpensive reagents, and operates under mild conditions at room temperature.

Recently we have reported a number of catalytic and stoichiometric titanium-mediated hydrosilylations of carbonyl compounds, including procedures for the reduction of esters[5] and lactones.[6] Herein we describe the reactions of a stoichiometric quantity of $Ti(OiPr)_4$ and Ph_2SiH_2 with amides [Eq. (a)]. In most instances an enamine is the initial product (see below).[7] Subsequent aqueous workup then affords the aldehyde.

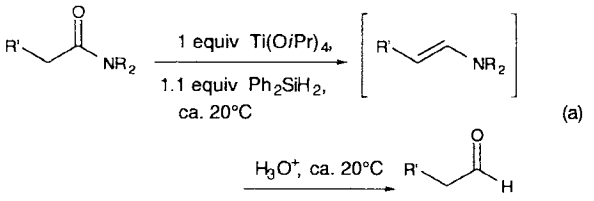

(a)

Typically, the reaction is carried out neat, using 1.0 equivalent $Ti(OiPr)_4$ and 1.1 equivalents Ph_2SiH_2 at room temperature, although the reaction can be carried out in THF or benzene if desired. Examination of the ^1H NMR spectrum of the crude reaction product with anisole as an internal standard shows the yields of enamine to be in the range 80–95%. No overreduction to amine is observed. The enamine may be easily hydrolyzed in situ by using a simple aqueous workup (2:1 THF/1 M HCl or wet silica gel/THF for acid-sensitive compounds) to yield the desired aldehyde, usually in excellent yields.[8] While the reaction does not proceed with any significant catalytic turnover,[9] the cost of $Ti(OiPr)_4$ is insignificant for most applications.

To explore the scope of this method, the reduction of a number of substrates was investigated (Table 1). The results shown in entries 1–4 demonstrate that the reaction can be carried out using both tertiary amides with aliphatic nitrogen substituents of varying steric demands (entries 1–3) or with aromatic substituents (entry 4). In this latter case hydrosilylation afforded a mixture of enamine and a hemiaminal, both of which could be hydrolyzed to the desired aldehyde. In addition, secondary amides with a bulky N-substituent are efficiently processed (entry 5), although, while 1.1 equiv of Ph_2SiH_2 was sufficient for complete conversion to the enamine, an additional equivalent of Ph_2SiH_2 caused the reaction to proceed much faster. The reaction tolerates a number of different functional groups including internal and terminal C–C double bonds (entries 6 and 7), and even terminal C–C triple bonds (entry 8). No competitive reduction of a nitrile moiety (entry 9) was observed. An epoxide

Table 1. Titanium-mediated conversion of amides to aldehydes [a].

Entry	Amide	Product	Work-up [b]	Yield [%] [c]
1	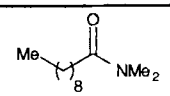	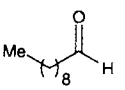	A	74
2	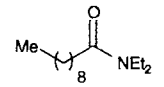	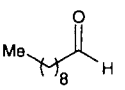	A	90
3	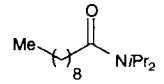	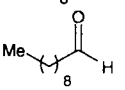	A	78
4	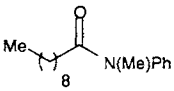	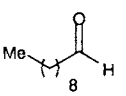	A	83
5 [d]	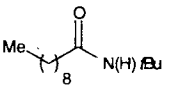	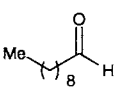	A	90
6	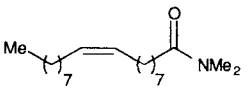	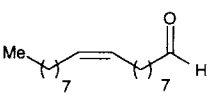	A	86
7	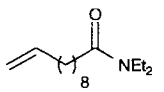	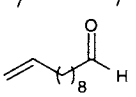	A	90
8	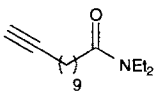	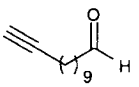	A	71
9 [e]	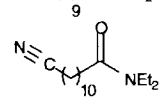	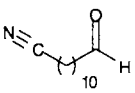	B	80
10	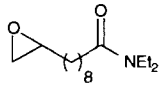	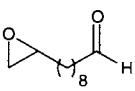	B	50
11	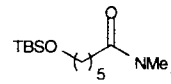	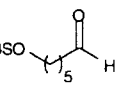	B	87
12	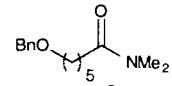	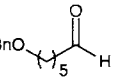	A	81
13 [f]	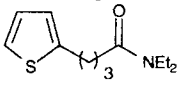	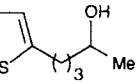	B	65
14 [f]	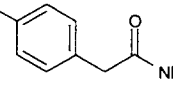	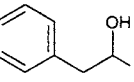	A	80 [g]

[a] All reactions were carried out neat at room temperature using 1.0 equiv $Ti(OiPr)_4$ and 1.1 equiv Ph_2SiH_2 except where indicated. [b] Workup A: 2/1 THF/1 M HCl, room temperature, 30 min to 3 h. Workup B: 2/1 THF/H_2O, excess silica gel, room temperature, 2–5 h. [c] Yields refer to products isolated after column chromatography. All compounds were characterized by ^1H NMR, ^{13}C NMR, and IR spectroscopy, and determined to be >95% pure by ^1H NMR spectroscopy and gas chromatography. [d] 2.5 equiv Ph_2SiH_2 were used. [e] This reaction was performed in THF. [f] Crude aldehyde was treated with excess MeMgBr, Et_2O, 0 °C. [g] Product contaminated with ≈5% $Ph_2Si(OH)_2$.

[*] Prof. Dr. S. L. Buchwald, Dr. S. Bower,[+] Dr. K. A. Kreutzer[++] Department of Chemistry Massachusetts Institute of Technology Cambridge, MA 02139 (USA) Fax: Int. code +(617)253-3297 e-mail: sbuchwal@mit.edu

[+] New address: Rhone-Poulenc-Rorer Limited (UK)

[++] New address: Dupont Central Research and Development, Wilmington, DE (USA)

[**] This work was supported by the National Institutes of Health and Pfizer Inc.

(entry 10) and two ethers (entries 11 and 12) were also successfully transformed under these conditions. The crude aldehydes derived from amides containing a thiophene moiety (entry 13) and from an aromatic bromide (entry 14), while not isolable in pure form,[10] could be treated directly with an excess of MeMgBr to afford secondary alcohols. This demonstrates that isolation of the aldehyde is not necessary for the application of this procedure.[11]

Limitations of this methodology include that aldehydes derived from optically active α-chiral amides, which would be produced via enamine intermediates, would be formed with complete epimerization at the α-stereogenic center. Additionally there is a requirement of an aliphatic α-hydrogen atom in the amide substrate for successful enamine formation; for instance, *N*,*N*-dimethyl cinnamide, upon treatment under our standard conditions, afforded a complex mixture of unidentified products. When no α-hydrogen was present, a mixture of aldehyde and the corresponding alcohol was obtained after aqueous work-up. Primary amides also afforded a mixture of unidentified products.

At present, detailed mechanistic studies have not been undertaken and the exact process of enamine formation is unclear. It has been proposed that a titanium hydride-like complex (**1**), which is obtained by a σ-bond metathesis reaction[12] between Ph_2SiH_2 and $Ti(OiPr)_4$, is the active reductant (Scheme 1). However, the exact structure of this species is not known. Initial insertion of the amide into the titanium–hydrogen bond of **1** affords hemiaminal **2**, which may then convert to the enamine, either directly by elimination or indirectly via an iminium ion (**3**).

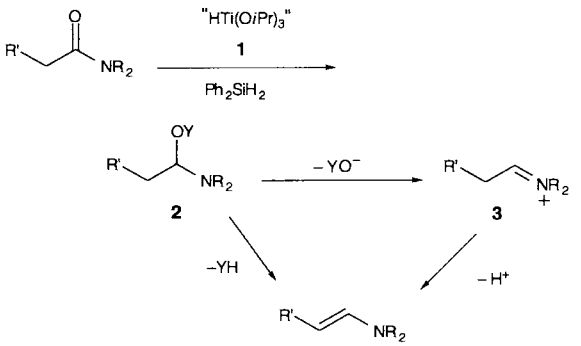

Scheme 1. Proposed mechanism of enamine formation. Y = $Si(H)Ph_2$ or $Ti(OiPr)_3$.

In summary, we have developed a mild and efficient one-pot method for the conversion of amides to aldehydes that proceeds at room temperature and employs readily available, air-stable reagents. The reaction is general for a variety of tertiary and secondary, aliphatic and aromatic amides and tolerates a wide range of different functional groups. The simplicity of this method makes it an attractive new tool to the organic chemist. Studies to further elucidate the scope of this and other related transformations are currently underway.

Experimental Procedure

Undecenal (entry 7 in Table 1): To a dry flask containing neat *N*,*N*-diethyl undecenamide (0.155 mL, 0.65 mmol) under argon was added Ph_2SiH_2 (0.135 mL, 0.72 mmol) and $Ti(OiPr)_4$ (0.196 mL, 0.65 mmol). Initial effervescence was observed **[caution!]** and the reaction mixture was stirred at room temperature until analysis by thin layer chromatography showed complete consumption of the starting material (ca. 5 h). The mixture was diluted with THF (20 mL), treated with 1 M HCl (10 mL), and after stirring for 1 h, poured into ether (80 mL). The organic layer was washed with 1 M HCl (3 × 10 mL), saturated sodium bicarbonate solution (2 × 10 mL), and brine (10 mL), then dried ($MgSO_4$) and concentrated in vacuo. Flash column chromatography on silica gel (15% hexane/ether) afforded 99 mg of undecenal (90%) [CAS registry number 1337-83-3]. An alternative workup for acid-sensitive compounds proceeds as follows: The mixture was treated with THF (20 mL), H_2O (10 mL), and silica gel (ca. 2 g), and stirred for 3–5 h at room temperature, then poured into ether (80 mL). The organic layer was washed with H_2O (3 × 10 mL) and brine (10 mL), dried (Na_2SO_4), and concentrated in vacuo. The residue was purified by flash column chromatography.

Received: January 31, 1996 [Z 8770 IE]
German version: *Angew. Chem.* **1996**, *108*, 1662–1664

Keywords: aldehydes · amides · enamines · hydrosilylations · titanium compounds

[1] a) M. Muraki, T. Mukaiyama, *Chem. Lett.* **1975**, 875–878; b) H. C. Brown, A. Tsukamoto, *J. Am. Chem. Soc.* **1964**, *86*, 1089–1095.
[2] For examples using aluminum hydrides see: a) R. C. Larock, *Comprehensive Organic Transformations: A Guide to Functional Group Preparations*, VCH, New York, **1989**, p. 623–624; b) J. Málek, M. Cerny, *Synthesis* **1972**, 217–234; c) N. M. Yoon, J. H. Ahn, D. K. An, Y. S. Shon, *J. Org. Chem.* **1993**, *58*, 1941–1944; d) S.-C. Tsay, J. A. Robl, J. R. Hwu, *J. Chem. Soc. Perkin Trans. 1* **1990**, 757–759, and references therein; e) for examples using boron hydrides see: H. C. Brown, D. B. Bigley, S. K. Arora, N. M. Yoon, *J. Am. Chem. Soc.* **1970**, *92*, 7161–7167.
[3] For example see: a) S. Nahm, S. M. Weinreb, *Tetrahedron Lett.* **1981**, *22*, 3815–3818; b) D. L. Comins, J. D. Brown, *J. Org. Chem.* **1986**, *51*, 3566–3572.
[4] V. M. Micovic, M. L. J. Mihailovic, *J. Org. Chem.* **1953**, *18*, 1190–1200.
[5] a) S. C. Berk, K. A. Kreutzer, S. L. Buchwald, *J. Am. Chem Soc*, **1991**, *113*, 5093–5095; b) S. C. Berk, S. L. Buchwald, *J. Org. Chem.* **1992**, *57*, 3751–3753; c) K. J. Barr, S. C. Berk, S. L. Buchwald, *ibid.* **1994**, *59*, 4323–4326; d) M. T. Reding, S. L. . Buchwald, *ibid.* **1995**, *60*, 7884–7890.
[6] X. Verdaguer, S. C. Berk, S. L. Buchwald, *J. Am. Chem. Soc*, **1995**, *117*, 12641–12642.
[7] The reduction of lactams to enamines using DIBAL (diisobutyl aluminum hydride) as the reductant has been reported: a) R. V. Stevens, R. K. Mehra, R. L. Zimmerman, *J. Chem. Soc. Chem. Commun.* **1969**, 877–878; b) A. G. Shultz, R. D. Lucci, J. J. Napier, H. Kinoshita, R. Ravichandra, P Shannon, Y. K. Lee, *J. Org. Chem. Soc.* **1985**, *50*, 217–231; c) R. D. Gless, H. Rapoport, *J. Org. Chem.* **1979**, *44*, 1324–1336.
[8] Occasionally, a deep blue color was noted in the reaction mixture but there was no significant correlation with either the rate or efficiency of the reaction.
[9] These reactions were found to be catalytic in $Ti(OiPr)_4$ (5 mol%) with $(EtO)_3SiH$ **[caution!]** K. A. Kreutzer, PhD Thesis, Massachusetts Institute of Technology, **1992**. However, due to the undesirable toxicity of $(EtO)_3SiH$ and the potential to form pyrophoric derivatives under certain conditions (for more details see ref. [5]), this method was not developed further.
[10] Both 2-thiophenebutanal and *para*-bromophenylethanal proved difficult to isolate cleanly from the reaction mixture, either by column chromatography or by kugelrohr distillation. Contamination with silicon-derived impurities was usually observed.
[11] In addition, α-branched amides could also be reduced: *N*,*N*-dimethyl-2,2-diphenylacetamide was reduced cleanly to enamine under the reaction conditions, although purification of the resultant aldehyde in this instance proved problematic.
[12] a) H.-G. Woo, T. D. Tilley, *J. Am. Chem. Soc.* **1989**, *111*, 3757–3758 & 8043–8044; b) T. D. Tilley, *Acc. Chem. Res.* **1993**, *26*, 22.

Reversible Formation of Raftlike Organoimidotetrarhodium Clusters by the Migration of RhL_n^+ Fragments**

Cristina Tejel, You-Mao Shi, Miguel A. Ciriano,* Andrew J. Edwards, Fernando J. Lahoz, and Luis A. Oro*

One of the general methods for the synthesis of clusters is the removal of ligands to create electron-deficient metal centers, which increases their affinity to form metal–metal interac-

[*] Dr. M. A. Ciriano, Prof. L. A. Oro, Dr. C. Tejel, Dr. Y.-M. Shi, Dr. A. J. Edwards, Dr. F. J. Lahoz
Departamento de Química Inorgánica
Instituto de Ciencia de Materiales de Aragón
Universidad de Zaragoza-C. S. I. C., E-50009-Zaragoza (Spain)
Fax: Int. code +(76)761143

[**] We thank the Dirección General de Investigación Cientifica y Técnica (DGICYT) for financial support (Projects PB92-86-C2 and PB94-1186) and a fellowship to Y.-M. S. (on leave from Dalian Institute of Chemical Physics, Chinese Academy of Sciences), and the European Union Human Capital and Mobility Program (CT93-0347) for a fellowship to A. J. E.

tions.[1] Conversely, increasing the electron count of a cluster by the addition of electrons, either by reduction or by addition of a ligand, usually leads to the breaking of metal–metal bonds.[2] Here we describe an unusual reversible reaction in which the addition of an innocent two-electron donor to a metallic center in a tetranuclear complex leads to the formation of three new metal–metal bonds by the migration of a metal fragment. Thus, the metal fragment has a choice of donor sites in a cluster, and hops from one to another by the addition or removal of a two-electron donor.

Recently we described the preparation and structure of the 60-electron clusters **1** (cod = 1,5-cyclooctadiene) and **2** (tfb = tetrafluorobenzobarrelene)

$[Rh_4(\mu\text{-}p\text{-}MeC_6H_4N)_2(\text{diolefin})_4]$

1, diolefin = cod
2, diolefin = tfb

in which the organoimido ligands bridge a metallic triangular core having one nonbonded edge; the fourth metal atom is η^5-coordinated to one arene ring and is not involved in cluster bonding.[3] Reactions of **1** and **2** with carbon monoxide under atmospheric pressure in toluene at 55 °C and room temperature, respectively, unexpectedly give the clusters **3** and **4** (Scheme 1), which were isolated in 85% yield as dark-red crystalline solids. The structure of **4** (Fig. 1) consists of an essentially planar butterfly arrangement of the metal atoms in which two triangles of Rh atoms share a common edge.[4] One of these triangles is bicapped by two *para*-tolylimido ligands, forming a trigonal bipyramid comprising three Rh and two N atoms. The second adjacent triangle of Rh atoms results when the fourth Rh atom bridges a Rh–Rh edge. Each of the Rh atoms in the bicapped triangle has two terminal CO ligands, while the fourth Rh atom completes a distorted trigonal bipyramidal coordination sphere, bonding to a further terminal CO ligand and a chelating tfb ligand. The metal–metal separations of between 2.758(2) and 2.895(2) Å are all clearly within the range expected for metal–metal single bonds. Complex **4** can be considered as a 62-electron system, consistent for a butterfly geometry,[5] and represents the first structurally characterized

$[Rh_4(\mu\text{-}p\text{-}MeC_6H_4N)_2(\text{diolefin})(CO)_7]$

3, diolefin = cod
4, diolefin = tfb

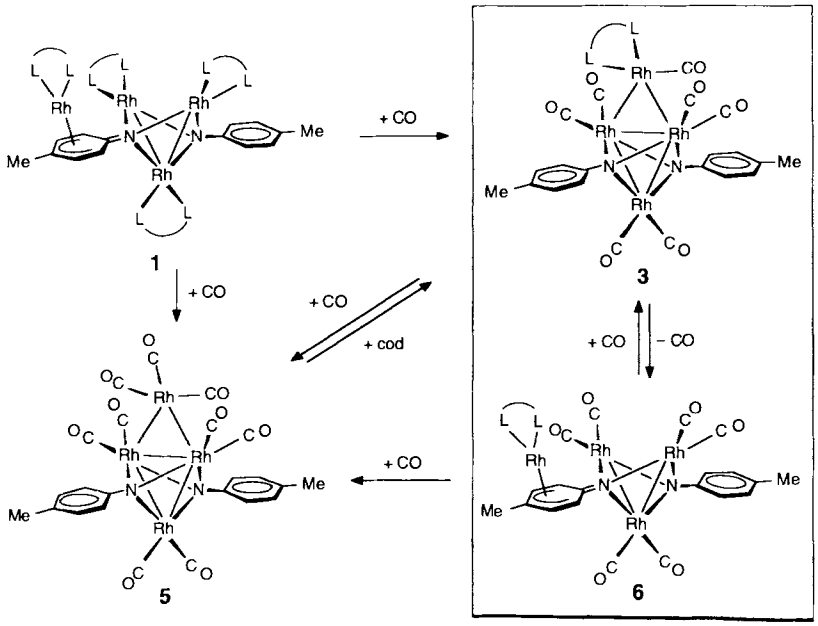

Scheme 1. L L = cod.

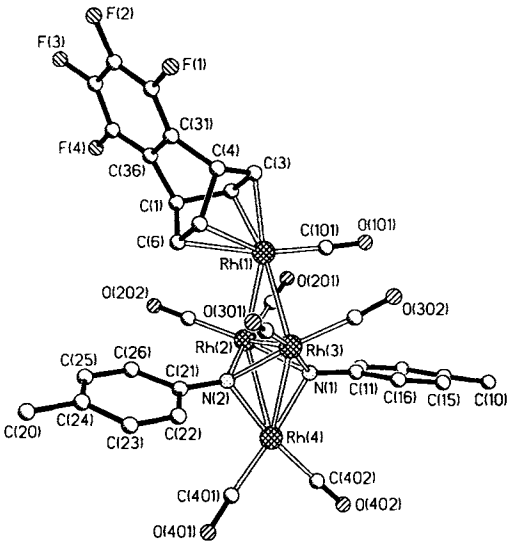

Fig. 1. The molecular structure of **4**. Selected bond lengths [Å] and angles [°]. The values in parentheses represent the equivalent value for the second independent molecule in the asymmetric unit. Rh(1)–Rh(2) 2.864(3) (2.892(3)), Rh(1)–Rh(3) 2.758(2) (2.791(2)), Rh(2)–Rh(3) 2.800(2) (2.812(2)), Rh(2)–Rh(4) 2.895 (2.889(2)), Rh(3)–Rh(4) 2.885(3) (2.849(2)), Rh(2)–N(1) 2.076(14) (2.015(13)), Rh(3)–N(1) 2.057(14) (2.054(14)), Rh(4)–N(1) 2.032(15) (2.051(14), Rh(2)–N(2) 2.089(13) (2.060(13)), Rh(3)–N(2) 2.052(14) (2.040(14)), Rh(4)–N(2) 2.044(14) (2.055(14)), N(1)–C(11) 1.428(21) (1.414(19)), N(2)–C(21) 1.429(20) (1.439(19)); Rh(2)-Rh(1)-Rh(3) 59.70(6) (59.28(6)), Rh(1)-Rh(2)-Rh(3) 58.25(6) (58.57(6)), Rh(1)-Rh(3)-Rh(2) 62.04(6) (62.15(6)), Rh(3)-Rh(2)-Rh(4) 60.85(6) (59.94(6)), Rh(2)-Rh(3)-Rh(4) 61.21(6) (61.38(6)), Rh(2)-Rh(4)-Rh(3) 57.94(6) (58.68(6)). Rh(2)-N(1)-C(11) 128(1) (132(1)), Rh(3)-N(1)-C(11) 128.(1) (119(1), Rh(4)-N(1)-C(11) 123.(1) (124(1)), Rh(2)-N(2)-C(11) 134(1) (127(1)), Rh(3)-N(2)-C(11) 122(1) (127(1)), Rh(4)-N(2)-C(11) 123(1) (125(1)).

planar tetrarhodium cluster with a raftlike structure (dihedral angles of 178.4(1)° and 171.5(1)° for the two independent molecules in the asymmetric unit). Other remarkable features include the coexistence of formally seven-coordinate and five-coordinate rhodium atoms, and the presence of carbonyl and diolefin ligands on the same rhodium center. This structure is maintained in solution, as shown by the $^{13}C\{^1H\}$ and ^1H NMR spectra of **3** and **4** at low temperature; however, complexes **3** and **4** undergo a fluxional process at room temperature that is probably associated with the pentacoordination of one rhodium atom (Table 1). Cooling a hot solution of **3** or **4** under an atmosphere of carbon monoxide leads to the replacement of the diolefin ligand to give **5**. These reactions can be reversed simply by plac-

$[Rh_4(\mu\text{-}p\text{-}MeC_6H_4N)_2(CO)_9]$ **5**

ing complex **5** in the presence of cod or tfb under an inert atmosphere. Complex **5** is a purple solid, which can be isolated in 70% yield. A comparison of the spectroscopic data in the fingerprint regions shows that **5** has a raftlike structure similar to that found for **4**. In addition, complex **3** slowly loses CO on standing in solution in toluene at room temperature to give black crystals of **6**. Complex **6** is a 60-elec-

$[Rh_4(\mu\text{-}p\text{-}MeC_6H_4N)_2(cod)(CO)_6]$ **6**

tron cluster with a structure similar to that described for **1**, according to the $^{13}C\{^1H\}$, ^1H NMR, and IR spectra. Complex **6** com-

 © VCH Verlagsgesellschaft mbH, D-69451 Weinheim, 1996 0570-0833/96/3513-1517 $ 15.00+.25/0

Table 1. Selected spectroscopic data for the new complexes.

3: IR (CH_2Cl_2): $\tilde{\nu}$ = 2062 (w, CO), 2037 (vs, CO), 2017 (sh, CO), 1987 (m) cm^{-1}; ^1H NMR (CD_2Cl_2, 193 K): δ = 7.32 (δ_A, 2H, Ph), 6.91 (δ_B, J(A,B) = 8.3 Hz, 2H, Ph), 7.19 (δ_A, 2H, Ph'), 6.89 (δ_B, J(A,B) = 8.2 Hz, 2H, Ph'), 5.74 (br. s, 2H, =CH), 4.46 (br. s, 2H, =CH), 2.31 (m, 8H, CH_2), 2.24 (s, 3H, Me), 2.22 (s, 3H, Me'); $^{13}C\{^1H\}$ NMR (CD_2Cl_2, 193 K): δ = 187.9 (d, J(Rh,C) = 65 Hz, 2CO), 187.4 (d, J(Rh,C) = 72 Hz, CO), 187.1 (d, J(Rh,C) = 70 Hz, CO), 186.7 (d, J(Rh,C) = 65 Hz, 2CO), 186.5 (d, J(Rh,C) = 69 Hz, CO), 163.9 (q, ^2J(Rh,C) = 1 Hz, *ipso*-C, Ph), 163.8 (q, ^2J(Rh,C) = 1 Hz, *ipso*-C, Ph'), 132.9 (C4, Ph), 132.7 (C4, Ph'), 127.8 (C3, Ph), 127.4 (C3, Ph'), 122.3 (C2, Ph), 121.7 (C2, Ph'), 116.3 (d, J(Rh,C) = 4 Hz, =CH), 74.3 (d, J(Rh,C) = 12 Hz, =CH), 31.9 (CH_2), 27.7 (CH_2), 20.1 (Me and Me'); MS (FAB$^+$): *m/z* (%): 898 (M^+ − CO, 50) 870 (M^+ − 2CO, 100)

4: IR (hexane): $\tilde{\nu}$ = 2067 (w, CO), 2056 (s, CO), 2046 (s, CO), 2035 (vs, CO), 2032 (m, CO), 1996 (m, CO), 1985 (m) cm^{-1}; ^1H NMR (CD_2Cl_2, 193 K): δ = 7.36 (δ_A, 2H, Ph), 6.94 (δ_B, J(A,B) = 8.3 Hz, 2H, Ph), 7.15 (δ_A, 2H, Ph'), 6.86 (δ_B, J(A,B) = 8.2 Hz, 2H, Ph'), 5.51 (br. s, 2H, CH), 5.23 (m, 2H, =CH), 4.42 (m, 2H, =CH), 2.26 (s, 3H, Me), 2.16 (s, 3H, Me'); $^{13}C\{^1H\}$ NMR (CD_2Cl_2, 193 K): δ = 189.3 (d, J(Rh,C) = 70 Hz, CO), 187.9 (d, J(Rh,C) = 64 Hz, 2CO), 187.5 (d, J(Rh,C) = 71 Hz, CO), 187.0 (d, J(Rh,C) = 70 Hz, CO), 186.4 (d, J(Rh,C) = 65 Hz, 2CO), 164.5 (q, ^2J(Rh,C) = 1 Hz, *ipso*-C, Ph), 163.7 (q, ^2J(Rh,C) = 1 Hz, *ipso*-C, Ph'), 133.4 (C4, Ph), 133.3 (C4, Ph'), 128.3 (C3, Ph), 127.8 (C3, Ph'), 122.5 (C2, Ph), 121.7 (C2, Ph'), 99.6 (d, J(Rh,C) = 4 Hz, =CH), 52.3 (d, J(Rh,C) = 11 Hz, =CH), 40.5 (CH), 20.3 (Me), 20.2 (Me'); MS (FAB$^+$): *m/z* (%): 1016 (M^+ − CO, 52), 988 (M^+ − 2CO, 100)

5: IR (CH_2Cl_2): $\tilde{\nu}$ = 2081 (m, CO), 2062 (s, CO), 2048 (vs, CO), 2029 (m, CO), 2008 (m) cm^{-1}; ^1H NMR (CD_2Cl_2, 223 K): δ = 7.30 (δ_A, 4H, Ph), 6.91 (δ_B, J(A,B) = 8.3 Hz, 2H, Ph), 2.25 (s, 6H, Me); $^{13}C\{^1H\}$ NMR (CD_2Cl_2, 223 K): δ = 193.5 (d, J(Rh,C) = 56 Hz, 2CO), 185.5 (d, J(Rh,C) = 63 Hz, 4CO), 185.3 (d, J(Rh,C) = 72 Hz, 2CO), 175.3 (d, J(Rh,C) = 77 Hz, CO), 163.8 (q, ^2J(Rh,C) = 1 Hz, *ipso*-C, Ph), 134.7 (C4, Ph), 128.1 (C3, Ph), 121.9 (C2, Ph), 20.7 (Me); MS (FAB$^+$): *m/z* (%): 846 (M^+ − CO, 35), 818 (M^+ − 2CO, 75), 790 (M^+ − 3CO, 45), 762 (M^+ − 4CO, 40), 734 (M^+ − 5CO, 70), 706 (M^+ − 6CO, 65), 678 (M^+ − 7CO, 60), 622 (M^+ − 9CO, 100)

6: IR (CH_2Cl_2): $\tilde{\nu}$ = 2029 (s, CO), 1973 (s) cm^{-1}; ^1H NMR (CD_2Cl_2, 298 K): δ = 7.27 (δ_A, 2H, Ph), 6.85 (δ_B, J(A,B) = 8.5 Hz, 2H, Ph), 6.52 (δ_A, 2H, Ph[a]) [a], 6.18 (δ_B, J(A,B) = 7.0 Hz, 2H, Ph[a]), 4.29 (br. s, 4H, =CH), 2.44 (m, 4H, CH_2), 2.25 (s, 3H, Me), 2.21 (s, 3H, Me[a]), 2.13 (m, 4H, CH_2); $^{13}C\{^1H\}$ NMR (CD_2Cl_2, 298 K): δ = 189.4 (d, J(Rh,C) = 66 Hz, 3CO), 189.1 (d, J(Rh,C) = 73 Hz, 3CO), 166.5 (q, ^2J(Rh,C) = 1 Hz, *ipso*-C, Ph), 156.6 (m, *ipso*-C, Ph[a]), 131.4 (C4, Ph), 127.9 (C3, Ph), 123.1 (q, ^3J(Rh,C) = 1 Hz, C2, Ph), 111.3 (d, ^1J(Rh,C) = 3 Hz, C4, Ph[a]), 103.8 (d, ^1J(Rh,C) = 3 Hz, C3, Ph[a]), 99.2 (dq, ^1J(Rh,C) = 3 Hz, ^3J(Rh,C) = 1 Hz, C2, Ph[a]), 81.3 (d, J(Rh,C) = 13 Hz, = CH), 31.8 (CH_2), 20.5 (Me), 18.6 (Me[a]); MS (FAB$^+$): *m/z* (%): 898 (M^+, 50), 870 (M^+ − 2CO, 75)

[a] [a] Denotes the [η^5-(*p*-MeC_6H_4N)Rh(cod)] fragment.

pletes the stepwise carbonylation from **1** to **5**, since it reacts with CO to give **3** (or **5** depending on the reaction conditions). The implications of the reversible reaction **3**⇌**6** (Scheme 1) are quite remarkable. On addition of CO to complex **6** the [Rh(cod)(CO)] fragment migrates from the η^5-arene coordination site to the trimetallic core. This metal mobility involves the unprecedented formation of three metal–metal bonds in spite of the increase in the electron count of the cluster by two. Conversely, the loss of a CO ligand, usually associated with an increase in the number of metal–metal interactions, leads to a reformation of the trimetallic core and the η^5-arene site. In this process three metal–metal bonds are broken. These facts can be explained in terms of a recognition of two donor sites in the cluster by the metallic fragment that is controlled by the addition of a two-electron donor ligand. The 12-electron fragment $[Rh(cod)]^+$ prefers to coordinate to the arene ring to achieve electronic saturation. Following the introduction of a CO ligand, however, the resulting 14-electron T-shaped fragment $[Rh(cod)(CO)]^+$ prefers to be coordinated to two Rh atoms of the trimetallic core. This implies the remarkable behavior of two metal atoms of an open-edged trimetallic core as donors. Indeed, the trinuclear imido metal core could be considered as a "ligand" that has two potential donor sites to engage a mononuclear fragment. A different, but related, proposal for the bonding of a Pt_3 face as a donor to the $Re(CO)_3$ fragment in the cluster $[Pt_3\{\mu\text{-}Re(CO)_3\}(\mu\text{-dppm})_3]^+$ has been recently reported.[6] Further work on the reactivity of these organoimido clusters and the extension to higher nuclearity clusters is in progress.

Received: February 23, 1996 [Z8850IE]
German version: *Angew. Chem.* **1996**, *108*, 1614–1616

Keywords: clusters · complexes with nitrogen ligands · imido complexes · rhodium compounds

[1] R. D. Adams, *The Chemistry of Metal Cluster Complexes*, (Eds.: D. F. Shriver, H. D. Kaesz, R. D. Adams) VCH, Weinheim, **1990**.
[2] D. Coughlin, J. Lewis, J. R. Moss, A. J. Edwards, M. McPartlin, *J. Organomet. Chem.* **1994**, *444*, C53
[3] C. Tejel, Y.-M. Shi, M. A. Ciriano, A. J. Edwards, F. J. Lahoz, L. A. Oro, *Angew. Chem.* **1996**, *108*, 707; *Angew. Chem. Int. Ed. Engl.* **1996**, *35*, 633.
[4] Crystal data for **4**: $C_{33}H_{20}F_4N_2O_7Rh_4$, M = 1044.15, monoclinic, space group $P2_1/n$ (no. 14), a = 17.959(6), b = 19.069(6), c = 21.004(7) Å, β = 113.41(5)°, V = 6601(4) Å^3, Z = 8, ρ_{calcd} = 2.101 g cm^{-3}, $F(000)$ = 4032, λ = 0.71073 Å, T = 173.0(2) K, $\mu(Mo_{K\alpha})$ = 2.039 mm^{-1}. Data were collected on a Stoe AED diffractometer by using an oil-coated rapidly cooled crystal of dimensions 0.44 × 0.31 × 0.19 mm mounted directly from solution (T. Kottke, D. Stalke, *J. Appl. Crystallogr.* **1993**, *26*, 615). Of a total of 9646 reflections collected by the $2\theta/\omega$ method ($3.5 \le 2q \le 45.0$), 8641 were unique. Data were corrected for absorption (Ψ scan, XEMP, G. M. Sheldrick, SHELXTL PLUS. Siemens Analytical X-ray Instruments, Inc., Madison, WI **1990**) with min. and max. transmission factors, 0.287 and 0.236, respectively. The structure was solved by direct methods (SHELXTL PLUS), and the two molecules located in the asymmetric unit refined by full-matrix least-squares on F^2 (SHELXL-93; G. M. Sheldrick, Göttingen, **1993**) to R_1 0.0726 [$F > 4s(F)$, for 3382 reflections] and wR_2 0.1392 (all data). All metal, nitrogen, and fluorine atoms were refined anisotropic, the remaining carbon and oxygen atoms were refined isotropic. All hydrogen atoms were fixed in idealized positions with thermal parameters (1.2 times that of the corresponding parent carbon atom). Largest peak and hole in the final difference map 0.857 and −0.984 e Å^{-3}. Crystallographic data (excluding structure factors) for the structure reported in this paper have been deposited with the Cambridge Crystallographic Data Centre as supplementary publication no. CCDC-179-58. Copies of the data can be obtained free of charge on application to The Director, CCDC, 12 Union Road, Cambridge CB2 1EZ, UK (fax: Int. code +(1223) 336-033; e-mail: teched@chemcrys.cam.ac.uk).
[5] D. M. P. Mingos, *Acc. Chem Res.* **1984**, *17*, 311.
[6] J. Xiao, R. J. Puddephatt, *Coord. Chem. Rev.* **1995**, *143*, 457.

$LiCHCl_2 \cdot 3$ Pyridine, Structure of a Carbenoid with a Tetrahedral C Atom**

Achim Müller, Michael Marsch, Klaus Harms, John C. W. Lohrenz, and Gernot Boche*

Recently we described the first X-ray crystal structure of a Li/Cl[1] and a MgBr/Br carbenoid;[2] however, both cases deal with vinyl carbenoids, which are more stable because of their C_{sp^2}–halogen bond[3] (decomposition above − 60 °C) than carbenoids with a tetrahedral carbon atom. For instance, studies by Matteson[4] have shown that dichloromethyllithium $LiCHCl_2$ (**2**)[5] "is not stable much above −100 °C". We were interested in whether it is also possible to obtain single crystals and an X-ray crystal structure analysis even from such extremely labile organolithium compounds. The results of the X-ray crystal

[*] Prof. Dr. G. Boche, Dipl.-Chem. A. Müller, M. Marsch, Dr. K. Harms, Dr. J. C. W. Lohrenz
Fachbereich Chemie der Universität
D-35032 Marburg (Germany)
Fax: Int. code + (6421) 288917

[**] This work was supported by the Deutsche Forschungsgemeinschaft (SFB 260 and Graduiertenkolleg "Metallorganische Chemie") and the Fonds der Chemischen Industrie.

structure determination of $LiCHCl_2 \cdot 3$ pyridine ($2 \cdot 3$py) reported herein reveal that this is possible.

$LiCHCl_2$ (**2**) was generated by deprotonation of dichloromethane (**1**) in a mixture of tetrahydrofuran, *tert*-butyl methyl ether, diethyl ether, and pyridine between $-78\,^{\circ}C$ and $-90\,^{\circ}C$ with *n*-butyllithium (Scheme 1). During the crystallization of the pyridine complex $2 \cdot 3$py, the temperature has to be kept

$$\underset{\mathbf{1}}{CH_2Cl_2} \xrightarrow{n\text{-BuLi, py}} \underset{\mathbf{2} \cdot 3\,py}{LiCHCl_2 \cdot 3\,py}$$

Scheme 1. Synthesis of $2 \cdot 3$py. py = pyridine.

strictly in the range between $-100\,^{\circ}C$ and $-98\,^{\circ}C$. The transfer of crystals by using a cold copper "tongue"[1, 2, 6] to the diffractometer was not always successful because of the extreme thermolability of the crystals, which often decomposed rapidly. Figure 1 shows the solid-state structure of $2 \cdot 3$py determined at $-123\,^{\circ}C$.[7]

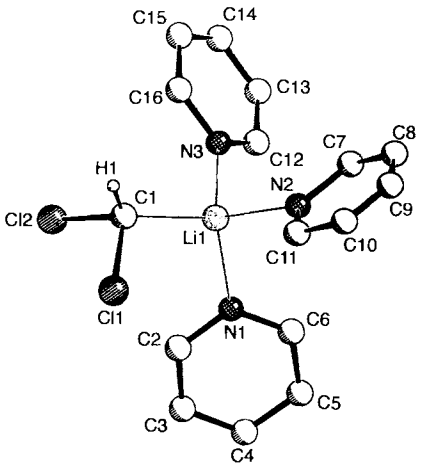

Fig. 1. Crystal structure of $2 \cdot 3$py.

Figure 1 reveals that Li1 coordinates to C1 (Li1–C1 210.5(9) pm) and to the nitrogen atoms of three pyridine molecules (Li1–N1 207.7(8), Li1–N2 201.7(9), Li1–N3 203.3(8) pm). The C–Cl bond lengths (C1–Cl1 185.7(5) pm and C1–Cl2 183.2(5) pm) are especially significant for the carbenoid structure in that *both* C–Cl bonds are approximately 10 pm longer than the C–Cl bonds in **1** (174.6 pm).[14] An elongation of the C–halogen bond was also observed in the vinyl carbenoids mentioned above.[1, 2] This bond lengthening is consistent with the results of calculations[15] and confirms the conclusion drawn by Seebach et al.[16] from NMR investigations, according to which the C–Li bond in carbenoids should have a higher s character and all other bonds a higher p character. The sum of the angles Cl2-C1-Cl1 (105.3(2)°), Cl1-C1-H1 (96(3)°), and Cl2-C1-H1 (107(3)°) of 308°, which is significantly smaller than the tetrahedral value (328°), is in addition to the elongation, further evidence for the increased p character of the C–Cl bonds in $2 \cdot 3$py. This essentially is the reason for the strong electrophilic character of carbenoids, which for a long time was not understood.[3, 15g, h, 17]

How significant is the solvation of the metal cation for the thermal stability and other properties of carbenoids? Model calculations on **2** and on the trihydrate $2 \cdot 3H_2O$ have provided further insight. Figure 2 shows the results of the MP2(fc)/6-31G(d) structure investigations and of the IGLO/II + sp//MP2(fc)/6-31G(d) calculations of the ^{13}C chemical shifts of **2** and $2 \cdot 3H_2O$.

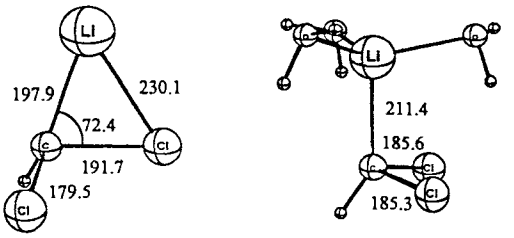

2 $\quad\quad$ **2** · $3H_2O$

$\delta = 62.8$ $\quad\quad$ $\delta = 49.5$

$\delta_{exp} = 50.0$ [16d]

Fig. 2. Calculated structural parameters and NMR shifts of **2** and $2 \cdot 3H_2O$ [18].

In the nonsolvated **2** the bridged structure (like in all other carbenoids[15]) is the most stable one. The Li-bridged C–Cl bond is elongated to 191.7 pm, whereas the other C–Cl bond (179.5 pm) shows only an insignificant elongation compared to the C–Cl bonds in **1** (176.9 pm).[14c] "Bad" external solvation of the Li^+ ion thus supports, through Li-bridging of the C–Cl bond, the Li^+-induced cleavage of this carbenoid bond, which is consistent with experimental observations.[3c] In contrast, if the Li^+ ion is "well" solvated ($2 \cdot 3H_2O$ was chosen as a model for $2 \cdot 3$py) the bond of the Li^+ ion to the Cl atom is broken. The lengths calculated for the C–Cl bonds in $2 \cdot 3H_2O$ (185.3 and 185.6 pm) correspond closely to the values determined in $2 \cdot 3$py (183.2(5) and 185.7(5) pm) as is also the case for the C–Li distance ($2 \cdot 3H_2O$ 211.4 pm; $2 \cdot 3$py 210.5(9) pm). The results of the IGLO calculations are also of particular interest. The calculated ^{13}C chemical shift of the C atom in the Li^+-bridged **2** is $\delta = 62.8$, whereas it is $\delta = 49.5$ in the solvated $2 \cdot 3H_2O$: the Li^+-bridged **2** with the larger downfield ^{13}C chemical shift shows the stronger carbenoid character. Since the measured shift of **2** in THF is $\delta = 50.0$,[16d] the structure of the THF-solvate of **2** should be nearly the same as that of $2 \cdot 3H_2O$ and $2 \cdot 3$py. Thus, investigations of the type shown above even allow conclusions to be drawn on the structure of carbenoids in solution.

Experimental Procedure

Preparation of single crystals of $2 \cdot 3$py: To a mixture of THF (1.70 mL) *tert*-butyl methyl ether (0.80 mL), diethyl ether (0.50 mL), and pyridine (0.50 mL, 489 mg, 6.18 mmol), dichloromethane **1** (0.25 mL) in THF (0.031 M, 0.775 mmol) was added. After the solution had been cooled ($-78\,^{\circ}C$ to $-90\,^{\circ}C$), **1** was deprotonated to **2** with *n*BuLi (0.49 mL, 0.78 mmol, 1.60 M solution in hexane) under constant shaking within 30 min. At $-98\,^{\circ}C$ to $-100\,^{\circ}C$ colorless crystals of $2 \cdot 3$py suitable for X-ray crystal structure analysis had formed after 16 h.

Received: February 16, 1996 [Z 8829 IE]
German version: *Angew. Chem.* **1996**, *108*, 1639–1640

Keywords: ab initio calculations · carbenoids · structure elucidation

[1] G. Boche, M. Marsch, A. Müller, K. Harms, *Angew. Chem.* **1993**, *105*, 1081–1082; *Angew. Chem. Int. Ed. Engl.* **1993**, *32*, 1032–1033; see also A. Maercker, *ibid.* **1993**, *105*, 1072–1074 and **1993**, *32*, 1023.

[2] G. Boche, K. Harms, M. Marsch, A. Müller, *J. Chem. Soc. Chem. Commun.* **1994**, 1393–1394.

[3] Reviews: a) W. Kirmse, *Angew. Chem.* **1965**, *77*, 1–10; *Angew. Chem. Int. Ed. Engl.* **1965**, *4*, 1–10; b) G. Köbrich, *ibid.* **1967**, *79*, 15–27 and **1967**, *6*, 41–52; c) G. Köbrich, *ibid.* **1972**, *84*, 557–570 and **1972**, *11*, 473–485; d) H. Siegel, *Top. Curr. Chem.* **1982**, *106*, 55–78; e) E. V. Dehmlow in *Methoden der Org. Chemie (Houben-Weyl), Supplementary Volume to the 4th ed., Bd. E19b, Vol. 2* (Ed.: M. Regitz), Thieme, Stuttgart **1989**, p. 1505ff.

[4] D. S. Matteson, D. Majumdar, *Organometallics* **1983**, *2*, 1529–1535, ref. [17]. The observations of the authors concerning the thermal lability of **2** is confirmed by our studies. They are in contrast to the report in ref. [5].
[5] G. Köbrich, H. R. Merkle, *Chem. Ber.* **1966**, *99*, 1782–1792; see also G. L. Closs, L. E. Closs, *J. Am. Chem. Soc.* **1960**, *82*, 5723–5728.
[6] a) E. Hahn, Freie Universität Berlin, personal communication; b) M. Veith, H. Bärnighausen, *Acta Crystallogr. Sect. B* **1974**, *30*, 1806–1813.
[7] Crystallographic data for **2** · 3py ($C_{16}H_{16}Cl_2LiN_3$, $M = 328.16$): Monoclinic, space group $P2_1/n$, $a = 1271.3(1)$, $b = 1072.8(5)$, $c = 1273.1(1)$ pm, $\beta = 91.81(1)^\circ$, $V = 1735.5(8) \times 10^{-30}$ m^3, $Z = 4$, $\rho_{calcd} = 1.256$ Mg m^{-3}, $\mu(Cu_{K\alpha}) = 3.331$ mm^{-1}. Data collection on an Enraf-Nonius CAD4 diffractometer with graphite monochromated $Cu_{K\alpha}$-radiation, ω scans, max. 12 s per reflection, $T = 150(2)$ K. 2604 reflections were collected ($4 < \theta < 55^\circ$), of which 2185 were unique ($R_{int} = 0.053$). The structure was solved with direct methods (SHELXTL) and was refined on F^2 with all reflections (SHELXL-93), non-hydrogen atoms anisotropic, hydrogen atoms (without H1) on calculated positions with fixed isotropic temperature factors. The parameters of the weighting scheme calculated by the program were: 0.1150, 2.3053; *wR2* (*R1* for 1949 reflections with $I > 2\sigma(I)$): 0.2051 (0.0740), Goof = 1.033; 204 refined parameters. The data were corrected with the program DIFABS (*R* values without the DIFABS correction: 0.2283, 0.0834). Relatively high temperature factors for the atoms C9 and C10 and "too short" bond lengths C8–C9 and C9–C10 indicate disorder which has not been resolved [13]. All calculations have been performed on an Micro-VAX II and a Dec 3000-300X [8–12].
[8] Siemens SHELXTL (VMS) Vers. 5.04, Siemens-Analytical-X-Ray-Instruments Inc., Madison **1995**.
[9] G. M. Sheldrick, SHELXL-93, Program for the Refinement of Crystal Structures, Göttingen **1993**.
[10] A. L. Spek, Platon 94, Program for Geometrical Analysis of Crystal Structures, Utrecht **1994**.
[11] E. Keller, SCHAKAL-88B, A FORTRAN Program for the Graphic Representation of Molecular and Crystallographic Models, Freiburg **1988**.
[12] N. Walker, D. Stuart, *Acta Crystallogr. Sect. A: Found. Crystallogr.* **1983**, *39*, 158–166.
[13] Crystallographic data (excluding structure factors) for the structure in this paper have been deposited with the Cambridge Crystallographic Data Centre as supplementary publication no. CCDC-179-45. Copies of the data can be obtained without free of charge on application to The Director, CCDC, 12 Union Road, Cambridge CB2 1EZ (fax: Int. code + (1223) 336033; e-mail: teched@chemcrys.cam.ac.uk).
[14] a) Cambridge Structural Database, Update October **1995**, Mean value of 386 structures; searching conditions: 1. no disorder, 2. *R* factor $\leq 10\%$, 3. temperature below $-53\,^\circ$C; b) the measured C–Cl bond length for **1** in the gas phase is 177.2 pm, R. J. Myers, W. D. Gwinn, *J. Chem. Phys.* **1952**, *20*, 1420–1427; c) the C–Cl bond length calculated at the MP2(fc)/6-31G(d) level is 176.9 pm.
[15] a) T. Clark, P. von R. Schleyer, *J. Chem. Soc. Chem. Commun.* **1979**, 883–884; b) T. Clark, P. von R. Schleyer, *Tetrahedron Lett.* **1979**, 4963–4966; c) T. Clark, P. von R. Schleyer, *J. Am. Chem. Soc.* **1979**, *101*, 7747–7748, and references therein; d) P. von R. Schleyer, T. Clark, A. J. Kos, G. W. Spitznagel, C. Rohde, D. Arad, K. N. Houk, N. G. Rondan, *ibid.* **1984**, *106*, 6467–6475, and references therein; e) B. Wang, C. Deng, *Chem. Phys. Lett.* **1988**, *147*, 99–104; f) B. Wang, C. Deng, L. Xu, T. Tao, *ibid.* **1989**, *161*, 388–392; g) G. Boche, A. Opel, M. Marsch, K. Harms, F. Haller, J. C. W. Lohrenz, C. Thümmler, W. Koch, *Chem. Ber.* **1992**, *125*, 2265–2273; h) G. Boche, F. Bosold, J. C. W. Lohrenz, A. Opel, P. Zylauf, *ibid.* **1993**, *126*, 1873–1885.
[16] a) H. Siegel, K. Hiltbrunner, D. Seebach, *Angew. Chem.* **1979**, *91*, 845–846; *Angew. Chem. Int. Ed. Engl.* **1979**, *18*, 785; b) D. Seebach, H. Siegel, K. Müllen, K. Hiltbrunner, *ibid.* **1979**, *91*, 844–845 and **1979**, *18*, 784; c) D. Seebach, H. Siegel, J. Gabriel, R. Hässig, *Helv. Chim. Acta* **1980**, *63*, 2046–2053; d) D. Seebach, R. Hässig, J. Gabriel, *Helv. Chim. Acta* **1983**, *66*, 308–337.
[17] G. Boche, F. Bosold, J. C. W. Lohrenz, *Angew. Chem.* **1994**, *106*, 1228–1230; *Angew. Chem. Int. Ed. Engl.* **1994**, *33*, 1161–1163.
[18] All geometries are optimized at the MP2(fc)/6-31G(d) level with the programs GAUSSIAN92 [19] and TurboMole [20–25]. The nonsolvated species were fully optimized, whereas the solvated ones were optimized on the assumption of local C_3 symmetry for the three water molecules in which the C–Li bond is the rotational axis. The chemical shifts were calculated with the DIGLO program [26–28] using the IGLO/II basis [29] with additional diffuse functions [30] (II + sp).
[19] Gaussian92/DFT M. J. Frisch, G. W. Trucks, H. B. Schlegel, P. M. W. Gill, B. G. Johnson, M. W. Wong, J. B. Foresman, M. A. Robb, M. Head-Gordon, E. S. Replogle, R. Gomperts, J. L. Andres, K. Raghavachari, J. S. Binkley, C. Gonzales, R. L. Martin, D. J. Fox, D. J. Defrees, J. Baker, J. J. P. Stewart, J. A. Pople, **1993**, Pittsburgh PA.
[20] R. Ahlrichs, M. Bär, M. Häser, H. Horn, C. Kölmel, *Chem. Phys. Lett.* **1989**, *162*, 165–169.
[21] M. Häser, R. Ahlrichs, *J. Comput. Chem.* **1989**, *10*, 104–111.
[22] M. Häser, R. Ahlrichs, H. P. Baron, P. Weis, H. Horn, *Theoret. Chim. Acta* **1992**, *83*, 455–470.
[23] H. Horn, H. Weiss, M. Häser, M. Ehrig, R. Ahlrichs, *J. Comput. Chem.* **1991**, *12*, 1058–1064.
[24] A. Schäfer, H. Horn, R. Ahlrichs, *J. Chem. Phys.* **1992**, *97*, 2571–2577.
[25] H. Weiss, M. Ehrig, R. Ahlrichs, *J. Am. Chem. Soc.* **1994**, *116*, 4919–4928.
[26] W. Kutzelnigg, *Isr. J. Chem.* **1980**, *19*, 193–200.
[27] M. Schindler, W. Kutzelnigg, *J. Chem. Phys.* **1982**, *76*, 1919–1933.
[28] W. Kutzelnigg, *J. Mol. Struc. (THEOCHEM)* **1989**, *202*, 11–61.
[29] S. Hutzinaga, *Approximate Atomic Wave Functions*, University of Alberta, Edmonton, **1971**.
[30] T. Clark, J. Chandrasekhar, G. W. Spitznagel, P. von R. Schleyer, *J. Comput. Chem.* **1983**, *4*, 294–301.

Porphyrinoid Macrocycles Based on Thiophene—The Octaethyltetrathiaporphyrin Dication

Emanuel Vogel,* Michael Pohl, Adalbert Herrmann, Torsten Wiss, Christoph König, Johann Lex, Maurice Gross,* and Jean Paul Gisselbrecht

Dedicated to Professor Giorgio Modena on the occasion of his 70th birthday

The aromatic heterocycle thiophene[1] has gained significance as a useful building block for the development of advanced materials (e.g., conducting polymers[2] with possible applications in microelectronics,[3] and electroluminescent[4] and other functional dyes[5]). In that light, porphyrinoid macrocycles based on thiophene become challenging synthetic targets. While mono- and dithiaporphyrins have been known for some time,[6] the true sulfur analogue of porphyrin, the tetrathiaporphyrin dication with thiophene instead of pyrrole units (as its perchlorate), yielded to synthesis by our group only recently.[7] Unfortunately, this dication does not lend itself readily to the desired chemical exploration because of its limited accessibility and poor solubility in common organic solvents. Our efforts, therefore, focused on the preparation of the octaethyltetrathiaporphyrin dication (**1**, as its perchlorate), taking advantage of experience acquired in the porphyrin,[8a] tetraoxaporphyrin,[8b,c] and corrole series,[8d] in which the more soluble octaethyl derivatives serve as versatile model compounds.

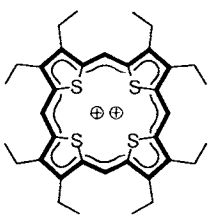

1

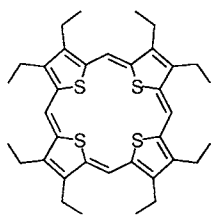

2

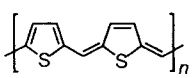

3

[*] Prof. Dr. E. Vogel, Dr. M. Pohl, Dr. A. Herrmann, Dr. T. Wiss, C. König, Dr. J. Lex
Institut für Organische Chemie der Universität
Greinstrasse 4, D-50939 Köln (Germany)
Fax: Int. code +(221)470-5102

Prof. Dr. M. Gross, Dr. J. P. Gisselbrecht
Laboratoire d'Electrochimie et de Chimie Physique du Corps Solide
Université Louis Pasteur
4, rue Blaise Pascal, F-67000 Strasbourg (France)

Among the various chemical transformations the dication **1** might undergo, its two-electron reduction to give the intriguing [20]annulene octaethyltetrathiaisophlorin (**2**)[9] appeared particularly attractive. Due to the presence of a $4n\pi$ conjugation pathway and proper symmetry of the molecule, **2** should possess a small HOMO–LUMO gap and be subject to an isodynamic π-bond shift. Moreover, annulene **2** contains structural features of the intensively studied poly(thienylenemethines) **3**,[10] for which a small gap between the valence (HOMO) and conduction band (LUMO) is predicted.[11] In this communication we report the synthesis of **1** (accompanied by the isolation of a higher order homologue), spectroscopic evidence supporting the formation of octaethyltetrathiaisophlorin (**2**), and the synthesis and characterization of a stable derivative of **2**.

The most obvious approach to the octaethyltetrathiaporphyrin dication **1** is via the previously unknown octaethyltetrathiaporphyrinogen (**5**) (Scheme 1; for selected physical data

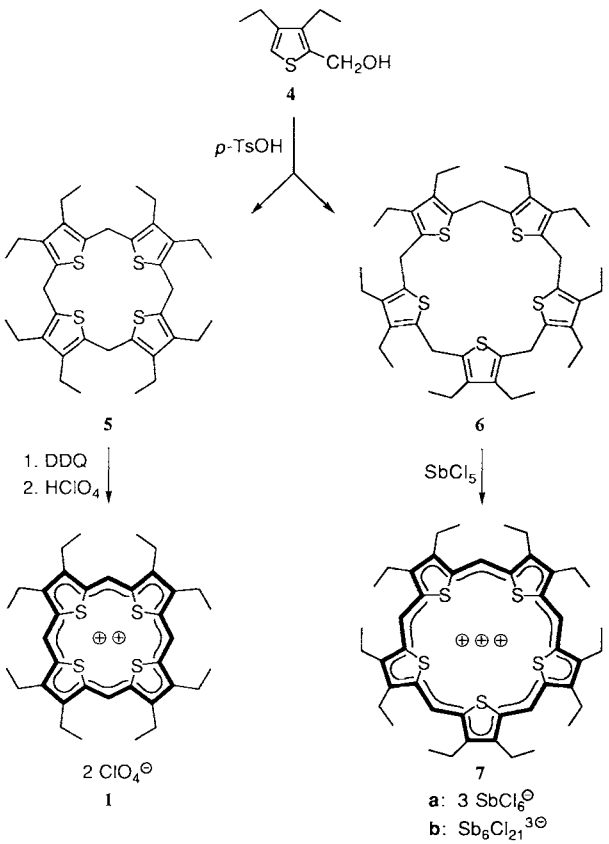

Scheme 1. DDQ = 2,3-dichloro-5,6-dicyano-1,4-benzoquinone.

of this and the other new compounds, see Table 1), that is, by methodology well-established in porphyrin chemistry. Intermediate **5** should be available by either an oxygen–sulfur exchange reaction from octaethyltetraoxaporphyrinogen[8b] under the conditions of the Jurjew reaction,[12] or by a biomimetic, acid-catalyzed cyclocondensation of 3,4-diethyl-2-hydroxymethylthiophene (**4**).[13]

The oxygen–sulfur exchange reaction that was highly successful in the case of unsubstituted tetraoxaporphyrinogen[7] failed completely when applied to the octaethyl derivative, presumably for steric reasons. Furthermore, under typical biomimetic conditions, the cyclocondensation of **4** proved to be unsatisfactory. However, we found that **5** could be obtained in relatively good yield (30%) on treatment of **4** with one equivalent of *para*-toluenesulfonic acid in nitromethane at 100 °C. Under these conditions another interesting compound, the pentacyclocondensation product **6**, was formed in addition to **5** and isolated in 16% yield. Purification of **5** and **6** was achieved by column chromatography on silica gel with a ternary mixture of hexane/toluene/acetonitrile (50/9/1) as the mobile phase. After recrystallization from ethanol, each compound was obtained as colorless needles, with melting points of 196–198 °C and 175–176 °C for **5** and **6**, respectively. The ^{1}H NMR spectra of **5** and **6** are—as expected for such closely related compounds—nearly superimposable, with the result that only mass spectra allowed the correct assignments of their structures.

Table 1. Selected physical data for **1**, **4**–**6**, **10**, and **13**–**15**. ^{1}H NMR: 300 MHz; ^{13}C: 75.5 MHz [a].

1: ^{1}H NMR (CD_3NO_2): δ = 12.53 (s, 4H, H-*meso*), 4.58 (q, 16H, H-2a,3a,7a,8a,12a,13a,17a,18a), 1.98 (t, 24H, H-2b,3b,7b,8b,12b,13b,17b,18b); ^{13}C NMR (CD_3NO_2): δ = 160.53, 160.40, 130.88, 24.35, 18.35; MS (FAB): *m/z* (%) 605 (80), 604 (100) $[M - 2ClO_4]^{\bullet+}$, 603 (30), 589 (10); IR (CsI): $\tilde{\nu}$ = 2970, 2932, 2873, 1519, 1450, 1419, 1373, 1310, 1260, 1192, 1083, 929, 869, 728, 624, 527, 458 cm^{-1}; UV/Vis (CH_2Cl_2, 1% CF_3CO_2H): 266 (15000), 293 (14400), 452 (159000), 613 (11300), λ_{max} (ε) = 667 nm (6700)

4: ^{1}H NMR ($CDCl_3$): δ = 6.85 (t, 1H, H-5), 4.71 (s, 2H, H-2a), 2.59 (q, 2H, H-3a), 2.55 (q, 2H, H-4a), 2.14 (br.s, 1H, H-2b), 1.26 (t, 3H, H-4b), 1.12 (t, 3H, H-3b); ^{13}C NMR ($CDCl_3$): δ = 144.04, 140.48, 137.01, 118.33, 57.99, 21.99, 19.87, 15.31, 13.78; MS (EI, 70 eV): *m/z* (%) 170 (100) $[M]^{\bullet+}$, 153 (94), 141 (75), 137 (47); IR (KBr): $\tilde{\nu}$ = 3240, 3089, 2965, 2932, 2842, 2364, 2345, 1560, 1456, 1429, 1378, 1307, 1253, 1240, 1199, 1167, 1098, 1086, 1054, 1012, 996, 931, 870, 800, 748, 515, 464 cm^{-1}; UV/Vis (cyclohexane): λ_{max} (ε) = 240 (7600), 275 nm (530)

5: ^{1}H NMR ($CDCl_3$): δ = 3.99 (s, 8H, H-5,10,15,20), 2.46 (q, 16H, H-2a,3a,7a,8a,12a,13a,17a,18a), 1.06 (t, 24H, H-2b,3b,7b,8b,12b,13b,17b,18b); ^{13}C NMR ($CDCl_3$): δ = 138.37, 135.71, 26.27, 20.27, 15.25; MS (EI, 70 eV): *m/z* (%) 608 (100) $[M]^{\bullet+}$, 579 (68), 304 (28); IR (KBr): $\tilde{\nu}$ = 2961, 2928, 2869, 1467, 1450, 1370, 1312, 1289, 1223, 1132, 1052, 940, 801, 694 cm^{-1}; UV/Vis (CH_2Cl_2): λ_{max} (ε) = 246 nm (28000)

6: ^{1}H NMR ($CDCl_3$): δ = 4.03 (s, 10H, H-5,10,15,20,25), 2.50 (q, 20H, H-2a,3a,7a,8a,12a,13a,17a,18a,22a,23a), 1.08 (t, 30H, H-2b,3b,7b,8b,12b,13b,17b,18b,22b,23b); ^{13}C NMR ($CDCl_3$): δ = 138.37, 134.50, 26.36, 20.37, 15.28; MS (EI, 70 eV): *m/z* (%) 760 (100) $[M]^{\bullet+}$, 731 (80), 380 (17), 351 (27); IR (KBr): $\tilde{\nu}$ = 2960, 2929, 2870, 1462, 1423, 1373, 1300, 1229, 1145, 1054, 936, 791, 707 cm^{-1}; UV/Vis (CH_2Cl_2): λ_{max} (ε) = 246 nm (37000)

10: ^{1}H NMR ($CDCl_3$): δ = 6.61 (s, 2H, H-15,20), 4.13 (s, 4H, H-5,10), 2.58 (q, 8H, H-2a,3a,12a,13a), 2.48 (q, 4H, H-17a,18a), 2.45 (q, 4H, H-7a,8a), 1.17 (t, 6H, H-3b,12b), 1.13 (t, 6H, H-17b,18b), 1.12 (t, 6H, H-2b,13b), 1.05 (t, 6H, H-7b,8b); ^{13}C NMR ($CDCl_3$): δ = 142.55, 141.66, 141.16, 140.81, 140.31, 137.25, 135.06, 134.48, 107.45, 26.34, 20.63, 20.54, 20.24, 19.59, 15.89, 15.34, 15.17, 14.67; MS (EI, 70 eV): *m/z* (%) 608 (40), 606 (100) $[M]^{\bullet+}$, 604 (25), 579 (8), 303 (20); IR (CsI): $\tilde{\nu}$ = 2965, 2930, 2869, 1560, 1508, 1465, 1391, 1375, 1313, 1284, 1120, 1050, 928, 793, 707 cm^{-1}; UV/Vis (THF): 248 (22900), 323 (17500), 445sh (11300), 469 (15900), 497 (14800), λ_{max} (ε) = 506 nm (13200)

13: ^{1}H NMR ($CDCl_3$): δ = 5.98 (s, 2H, H-10,20), 5.84 (s, 1H, H-15), 2.63 (q, 4H, H-3a,7a), 2.41 (q, 4H, H-2a,8a), 2.26 (q, 4H, H-12a,18a), 2.23 (q, 4H, H-13a,17a), 1.22 (t, 6H, H-3b,7b), 1.13 (t, 6H, H-2b,8b), 1.04 (t, 6H, H-12b,18b), 1.01 (t, 6H, H-13b,17b); ^{13}C NMR (CD_2Cl_2/CF_2Br_2): δ = 151.71, 145.37, 145.26, 144.18, 143.40, 139.73, 118.19, 111.82, 108.30, 89.30, 21.07, 20.49, 20.41, 15.38, 15.23, 15.18; MS (EI, 70 eV): *m/z* (%) 631 (30), 629 (100) $[M]^{\bullet+}$, 614 (4), 314 (18); IR (CsI): $\tilde{\nu}$ = 2966, 2931, 2870, 2179, 1551, 1531, 1471, 1373, 1347, 1314, 1250, 1205, 1167, 1103, 1053, 988, 901, 857, 825, 786, 712 cm^{-1}; UV/Vis (THF): λ_{max} (ε) = 305 (15000), 388 (47000), 622 nm sh (3900)

14: ^{1}H NMR ($CDCl_3$): δ = 6.60 (br.s, 1H, COOH), 3.88 (s, 3H, OCH_3), 2.96 (q, 4H, H-3a,4a), 1.16 (t, 6H, H-3b,4b); ^{13}C NMR ($CDCl_3$): δ = 167.41, 162.32, 153.53, 152.24, 131.79, 129.67, 52.13, 20.99, 20.88, 14.93, 14.87; MS (EI, 70 eV): *m/z* (%) 242 (100) $[M]^{\bullet+}$, 227 (90), 213 (13), 211 (76), 209 (84), 183 (25); IR (KBr): $\tilde{\nu}$ = 2978, 2876, 2630, 1723, 1687, 1659, 1535, 1471, 1427, 1402, 1373, 1320, 1283, 1260, 1232, 1186, 1159, 1091, 1054, 998, 963, 922, 874, 823, 772, 742, 524 cm^{-1}; UV/Vis (cyclohexane): λ_{max} (ε) = 212 (11800), 284 nm (15900)

15: ^{1}H NMR ($CDCl_3$): δ = 7.08 (t, 1H, H-5), 3.83 (s, 3H, OCH_3), 2.95 (q, 2H, H-3a), 2.55 (q, 2H, H-4a), 1.24 (t, 3H, H-4b), 1.13 (t, 3H, H-3b); ^{13}C NMR ($CDCl_3$): δ = 163.02, 151.43, 145.05, 126.46, 125.35, 51.52, 21.76, 20.90, 14.40, 13.89; MS (EI, 70 eV): *m/z* (%): 198 (99) $[M]^{\bullet+}$, 183 (100), 167 (81), 151 (33), 139 (25); IR (film): $\tilde{\nu}$ = 3020, 2969, 2874, 1713, 1543, 1450, 1396, 1317, 1271, 1239, 1190, 1126, 1090, 1064, 1043, 967, 939, 918, 879, 833, 804, 782 cm^{-1}; UV/Vis (CH_2Cl_2): λ_{max} (ε) = 259 (11300), 282 nm sh (6500)

[a] Correct elemental analyses were obtained for all compounds, except for the sensitive compounds **10** and **13**, which gave correct high-resolution mass spectra.

 © VCH Verlagsgesellschaft mbH, D-69451 Weinheim, 1996 0570-0833/96/3513-1521 $ 15.00+.25/0

The remarkably high tendency of **4** to afford the cyclocondensation products **5** and **6** most likely results from a helical effect of the ethyl groups in the 3 and 4 positions of thiophene, as demonstrated by Franck et al.[14] in the porphyrin series. The occurrence of significant amounts of product **6** in the acid-mediated condensation of **4** can best be explained by the fact that thiophene exhibits a wider angle between the exocyclic bonds at the α positions than pyrrole or furan (147° vs. 131° and 126°, respectively[15]). It is interesting to note that the homologues **5** and **6** readily interconvert under the conditons of their formation. For instance, upon heating either pure **5** or **6** to 100 °C in the presence of *para*-toluenesulfonic acid, mixtures of the two compounds in an approximate ratio of 2:1 were obtained. Almost certainly, interconversion between **5** and **6** is initiated by protonation of a thiophene moiety in an α position followed by macrocyclic ring opening.

Oxidation of octaethyltetrathiaporphyrinogen (**5**) to give the octaethyltetrathiaporphyrin dication (**1**, as its perchlorate) could be achieved under conditions similar to those employed in the synthesis of the parent dication,[7] that is, by successive treatment of **5** with 2,3-dichloro-5,6-dicyano-1,4-benzoquinone (DDQ, 3.3 equiv, 2 h, 60 °C) in acetic acid and with 70% perchloric acid (1:10 in acetic acid, 5 equiv, 0.5 h, 80 °C). The intensely colored crystals that separated from the cold reaction mixture were recrystallized from acetic acid, affording blue needles with a metallic luster. As evidenced by the ^{1}H NMR spectrum as well as by elemental analysis, the target compound **1**, which contains 1.5 equivalents of acetic acid enclosed within the crystal lattice, was obtained (70% yield). The acetic acid can be removed by heating this clathrate under vacuum (60 °C, 0.01 mm); the acid-free **1** (as its perchlorate) is left as a green powder.[16] The ethyl groups confer good solubility on **1** in organic acids as well as in dichloromethane, acetonitrile, and nitromethane. On the other hand, when alcohols are used as solvents, instantaneous nucleophilic addition to two adjacent *meso* positions in **1** occurs, resulting in the formation of derivatives of tetrathia-5,10-dihydroisophlorin (**10**).[17]

The ^{1}H NMR spectrum of **1** (in CD_3NO_2), which shows no significant temperature dependence, corresponds to that expected for a dicationic aromatic porphyrinoid, since the *meso* protons (H_m) appear as a singlet at very low field ($\delta = 12.53$). The location of this signal almost coincides with that of the *meso* protons in the unsubstituted dication ($\delta = 12.46$, albeit in 68% $DClO_4/CH_2Cl_2$ int.).[7] When the ^{1}H NMR spectrum of **1** was recorded in the less polar solvent dichloromethane, its resolution decreased (accompanied by a shift of $\Delta\delta = 0.3$ of the signal for the *meso* protons to higher field), an observation indicative of the formation of aggregates.[18]

A comparison of the ^{1}H NMR data of **1** with those of its oxygen analogue **8** (Table 2) reveals that the resonance of the *meso* protons of the thia compound has shifted to lower field ($\Delta\delta = 0.68$). This finding is best explained as arising primarily from a heteroatom effect of the sulfur atoms rather than from an unusually strong diamagnetic ring current in **1**. A similar difference in chemical shift is observed (Table 2) on going from tetrathia-5,10-dihydroisophlorin (**10**) with interrupted cyclic conjugation to its oxygen counterpart **11**. To some extent, the noticeable deshielding of H_m of **1** may also be attributable to the localization of the positive charge at the *meso* carbon atoms, which is more pronounced in **1** than in **8**, as inferred from the relation $\delta^{13}C_m(\mathbf{1}) > \delta^{13}C_m(\mathbf{8})$. The slight puckering of the ring skeleton of **1** (see below) should have only a minor influence on the strength of the aromatic ring current, since even in the starkly nonplanar dication **9** the *meso* protons still resonate at very low field. The UV/Vis spectrum of **1** has experienced the

Table 2. Selected ^{1}H and ^{13}C NMR data (300 MHz and 75.5 MHz, respectively) for the dications **1**, **8**, and **9** as their perchlorates (CD_3NO_2), and the 5,10-dihydroisophlorins **10**–**12** ($CDCl_3$).

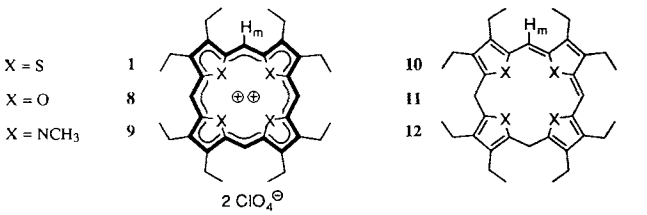

	1	**8**	**9**	**10**	**11**	**12**
δ^1H_m	12.53	11.85	10.39	6.61	5.35	5.28
$\delta^{13}C_m$	130.9	99.2	104.8	107.5	85.5	86.3
Ref.	[a]	[8b]	[7]	[a]	[8c]	[9b]

[a] This report.

anticipated bathochromic shift relative to that of the parent dication[7] [$\Delta\lambda_{max}$(Sôret) ≈ 25 nm].

According to an X-ray crystallographic analysis of the octaethyltetrathiaporphyrin dication (**1**),[19] the steric demand of the sulfur atoms causes the ring skeleton of the molecule to deviate from planarity, albeit slightly (Fig. 1). Dication **1**, like the unsubstituted compound, is centrosymmetric in the crystal, but differs from the latter in conformation. While in the parent dication two diagonal thiophene rings are tilted, in opposite directions, by 23° out of the plane defined by the four *meso* carbon atoms,[7] a *syn,syn,anti,anti* arrangement with twist angles of 19° is found for **1**. Both compounds exhibit distances between adjacent sulfur atoms nearly 1 Å less than the sum of

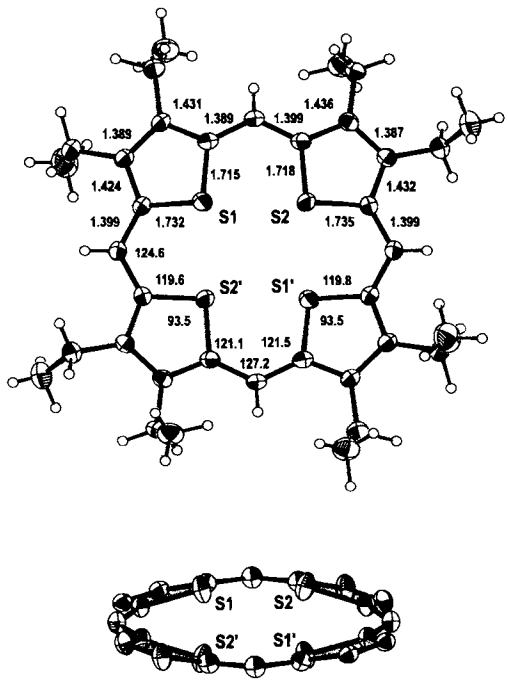

Fig. 1. Structure of octaethyltetrathiaporphyrin dication (**1**, as its perchlorate) in the crystal (top: top view; bottom: perspective view). Vibrational ellipsoids represent 40% probability. With selected bond lengths [Å] and angles [°] (standard deviation approximately 0.009 Å and 0.5°). The thiophene subunits are shaded, and the ethyl groups and hydrogen atoms omitted in the perspective view to visualize the deviation of **1** from planarity better.

 © VCH Verlagsgesellschaft mbH, D-69451 Weinheim, 1996 0570-0833/96/3513-1522 $ 15.00+.25/0

their van der Waals radii. Thus attractive S···S interactions appear to be involved. In solution, the five-membered heterorings of **1** are presumed to exchange sites rapidly by inversion. Indirect evidence in support of this process may be gathered from the ^{1}H NMR spectrum, in which no splitting of the resonances of the diastereotopic CH_2 protons is observed as the temperature is lowered (to $-100\,^\circ C$). Such a splitting is, indeed, found in the case of the conformationally less mobile *N,N',N'',N'''*-tetramethyl compound **9**.[7]

An electrochemical study of the dication **1** was performed with the main purpose of evaluating the possibility of generating the isophlorin **2** by reduction of **1**. This study, carried out in 0.1 M solutions of tetrabutylammonium hexafluorophosphate ($TBAPF_6$, as supporting electrolyte) in dichloromethane at a platinum electrode,[20a] afforded two defined half-wave potentials at $+0.37$ V and $+0.07$ V vs. Ag/AgCl. As confirmed by cyclic voltammetry measurements in the same solvent,[20b] these potentials should be ascribed to two one-electron reductions leading to the radical cation and to tetrathiaisophlorin **2**, respectively. At scan rates $<1\ Vs^{-1}$ the intensity of the second wave decreased with respect to the first, while at the same time an additional reduction wave at -0.32 V appeared. These findings indicate that in the reduction of **1**—in contrast to that of octaethyltetraoxaporphyrin dication (**8**)—the products are not stable under the conditions of the measurements. Further reduction steps that could give rise to the formation of the radical anion or the 22π dianion were not observed up to the cathodic limit of the measurement range. Accordingly, generation of **2** by chemical means seemed feasible.

Attempts to convert **1** into **2** with alkali metals or other conventional reducing agents did not yield defined products. However, when samarium(II) iodide[21] was employed, which is reasonably soluble in organic solvents and possesses a sufficiently negative reduction potential ($\varepsilon_o = -1.5$ V)[21c] without giving rise to overreduction, we were able to record NMR spectra of **2** at low temperatures. Specifically, this was accomplished by adding a solution of SmI_2 in tetrahydrofuran to a suspension of **1** in the same solvent under rigorous exclusion of oxygen at $-40\,^\circ C$. After passing the reaction mixture through a short alumina column (activity grade I) at $-78\,^\circ C$ followed by removal of the solvent, an amorphous solid was obtained. This contained as the major component the tetrathiaisophlorin **2** as an extremely oxygen-sensitive compound, which spontaneously polymerizes at temperatures above $-20\,^\circ C$ (apart from **2**, minor amounts of oligomers were present). The ^{1}H NMR spectrum (300 MHz, [D$_8$]THF, $-50\,^\circ C$) of **2** shows—in accord with the assumption that the compound undergoes an isodynamic π-bond shift that is rapid on the NMR time scale—only one singlet for the *meso* protons ($\delta = 5.26$), one quartet for the methylene protons ($\delta = 2.05$), and one triplet for the methyl protons ($\delta = 0.95$). In parallel herewith, the ^{13}C NMR spectrum (75.5 MHz, [D$_8$]THF, $-50\,^\circ C$) exhibits five signals at $\delta = 145.5$, 142.0, 108.1, 19.9, and 15.1. The presence of a paramagnetic ring current in **2**, though weaker than in tetraoxaisophlorins[8b, 9a] for steric reasons, is evident from the high-field shift of the signal of H_m relative to that of the dihydro compound **10** ($\Delta\delta^1H_m = 1.35$, see also Table 1). Unfortunately, a more detailed spectrosopic characterization of **2** was hampered by the high reactivity of the compound.[22]

Remarkably, replacement of only one of the *meso* hydrogen atoms of **2** by an electron-withdrawing substituent is sufficient to allow the preparation of stable octaethyltetrathiaisophlorins. A case in point is 5-cyanooctaethyltetrathiaisophlorin (**13**), which by analogy to the conversion of **9** into *N,N',N'',N'''*-tetramethyl-5-cyano-octaethylisophlorin,[9b] is produced when a solution of **1** in dry ethanol is treated with sodium cyanide at $-20\,^\circ C$ (Scheme 2). After chromatography on basic alumina (ether/THF 20/1, $-20\,^\circ C$), followed by concentration of the eluate under vacuum and subsequent slow addition of *n*-hexane, **2** is obtained as a blue microcrystalline powder (moderately stable in air when kept in the dark); decomp. above 160 °C, 45% yield.

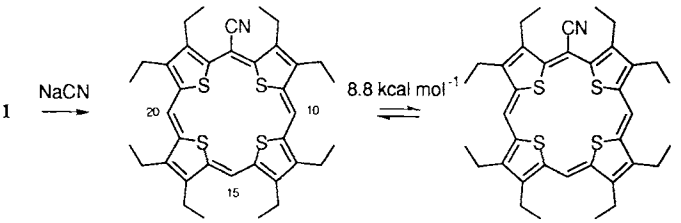

13

Scheme 2.

The ^{1}H NMR spectrum of **13** at room temperature, due to its relative simplicity (effective C_{2v} symmetry), is indicative of a rapid π-bond shift—also isodynamic in this case—and a rapid inversion of the thiophene rings. The *meso* protons give rise to only two singlets at $\delta = 5.98$ (H10,20) and $\delta = 5.84$ (H15), which, owing to the presence of the electronegative nitrile group, are shifted to lower field than the signal of the *meso* protons of **2** ($\Delta\delta = 0.72$ and 0.58, respectively). In order to freeze the π-bond shift of **13** to such an extent that the singlet of the *meso* protons at positions 10 and 20 splits into two signals, it was necessary to cool the sample to $-110\,^\circ C$. From the temperature of coalescence of these signals ($-83\,^\circ C$) a free energy of activation ($\Delta G^{\ddagger}_{190}$) of 8.8 kcal mol^{-1} for the dynamic process was derived. This energy value appears realistic when compared with the corresponding values of the π-bond shifts of the strongly distorted *N,N',N'',N'''*-tetramethyloctaethylisophlorin and the practically planar tetraoxaisophlorin ($\Delta G^{\ddagger}_{298} = 13.2$ kcal mol^{-1}[9b] and $\Delta G^{\ddagger}_{138} < 6$ kcal mol^{-1},[9a] respectively).

The occurrence of the thiaporphyrinogen homologue **6** as a by-product from the cyclocondensation of **4** was anything but an undesired result. On the contrary, compound **6** invited oxidation experiments that ultimately might lead to the decaethylpentathiapentaphyrin trication **7**, a potentially aromatic 22π-electron system.[23] As is evident upon inspection of the resonance structures of **7** (not shown here) with the positive charges located on sulfur, the trication **7** bears the same relationship to pentaphyrin[24] as the tetrathiaporphyrin dication does to porphyrin. In its trisprotonated form, pentaphyrin is in fact isoelectronic with **7**. The first evidence for the formation of **7** was obtained when **6** was treated with DDQ in benzene, and the amorphous precipitate thus produced dissolved in [D$_2$]sulfuric acid. The ^{1}H NMR spectrum of the resulting intensely cherry-red solution proved to be fully consistent with the generation of the obviously highly symmetric aromatic trication **7**, since it contained only three broadened signals at $\delta = 14.66$ (5H, H-*meso*), $\delta = 5.69$ (20H, CH_2), and $\delta = 2.70$ (30H, CH_3). Subsequently, antimony pentachloride ($SbCl_5$) was found to be particularly effective in oxidizing **6** to the trication **7**. On addition of this antimony agent to **6** in dichloromethane, **7** was produced as a mixture of salts from which small amounts of crystals of **7a**, the expected trishexachloroantimonate, and of **7b**—with a polymeric chloroantimonate(III) as the counterion (containing $[Sb_6Cl_{21}]^{3-}$ as repeat unit)—could be separated mechanically.[25] As already revealed by preliminary results of X-ray analyses of

 © VCH Verlagsgesellschaft mbH, D-69451 Weinheim, 1996 0570-0833/96/3513-1523 $ 15.00+.25/0

7a and **7b**, the trication **7** is planar. Further details regarding the structures of **7a** and **7b** will be reported in a forthcoming publication as soon as the as yet unsatisfactory means of isolation can be improved.

Received: July 28, 1995 [Z 8270 IE]
German version: *Angew. Chem.* **1996**, *108*, 1677–1682
Delayed at the authors' request

Keywords: heterocycles · macrocycles · porphyrinoids · thiophenes

[1] *Thiophene and its Derivatives, Part 1–4* (Ed.: S. Gronowitz), Wiley, New York, **1985–1991**.

[2] Review on polythiophenes: J. Roncali, *Chem. Rev.* **1992**, *92*, 711; see also: S. Kozhushkov, T. Haumann, R. Boese, B. Knieriem, S. Scheib, P. Bäuerle, A. de Meijere, *Angew. Chem.* **1995**, *107*, 859; *Angew. Chem. Int. Ed. Engl.* **1995**, *34*, 781.

[3] P. Bäuerle, T. Fischer, B. Bidlingmeier, A. Stabel, J. P. Rabe, *Angew. Chem.* **1995**, *107*, 335; *Angew. Chem. Int. Ed. Engl.* **1995**, *34*, 303; M. J. Marsella, P. J. Carroll, T. M. Swager, *J. Am. Chem. Soc.* **1995**, *117*, 9832; M. J. Marsella, R. J. Newland, P. J. Carroll, T. M. Swager, *ibid.* **1995**, *117*, 9842; J. Guay, A. Diaz, R. Wu, J. M. Tour, *ibid.* **1993**, *115*, 1869; L. F. Lindoy, *Nature* **1993**, *364*, 17; G. Heywang, F. Jonas, *Adv. Mater.* **1992**, *4*, 116; F. Garnier, G. Horowitz, X. Peng, D. Fichou, *ibid.* **1990**, *2*, 592.

[4] P. Dyreklev, M. Berggren, O. Inganäs, M. R. Andersson, O. Wennerström, T. Hjertberg, *Adv. Mater.* **1995**, *7*, 43; R. E. Gill, G. G. Malliaras, J. Wildeman, G. Hadziioannou, *ibid.* **1994**, *6*, 132; F. Geiger, M. Stoldt, H. Schweizer, P. Bäuerle, E. Umbach, *ibid.* **1993**, *5*, 922.

[5] S. Gilmour, S. R. Marder, J. W. Perry, L.-T. Cheng, *Adv. Mater.* **1994**, *6*, 494; F. Effenberger, F. Würthner, *Angew. Chem.* **1993**, *105*, 742; *Angew. Chem. Int. Ed. Engl.* **1993**, *32*, 719.

[6] A. W. Johnson in *Porphyrins and Metalloporphyrins* (Ed.: K. M. Smith), Elsevier, Amsterdam **1975**, p. 729; monothiaporphyrins: R. P. Pandian, T. K. Chandrashekar, *Inorg. Chem.* **1994**, *33*, 3317; P. J. Chmielewski, L. Latos-Grażyński, *ibid.* **1992**, *31*, 5231; L. Latos-Grażyński, J. Lisowski, L. Szterenberg, M. M. Olmstead, A. L. Balch, *J. Org. Chem.* **1991**, *56*, 4043; L. Latos-Grażyński, J. Lisowski, M. M. Olmstead, A. L. Balch, *J. Am. Chem. Soc.* **1987**, *109*, 4428; dithiaporphyrins: R. L. Hill, M. Gouterman, A. Ulman, *Inorg. Chem.* **1982**, *21*, 1450; A. Ulman, J. Manassen, F. Frolow, D. Rabinovich, *J. Am. Chem. Soc.* **1979**, *101*, 7055.

[7] E. Vogel, *Pure Appl. Chem.* **1990**, *62*, 557; E. Vogel, P. Röhrig, M. Sicken, B. Knipp, A. Herrmann, M. Pohl, H. Schmickler, J. Lex, *Angew. Chem.* **1989**, *101*, 1683; *Angew. Chem. Int. Ed. Engl.* **1989**, *28*, 1651.

[8] a) J. L. Sessler, A. Mozaffari, M. R. Johnson, *Org. Synth.* **1992**, *70*, 68, and references therein; b) E. Vogel, J. Dörr, A. Herrmann, J. Lex, H. Schmickler, P. Walgenbach, J. P. Gisselbrecht, M. Gross, *Angew. Chem.* **1993**, *105*, 1667; *Angew. Chem. Int. Ed. Engl.* **1993**, *32*, 1597; c) P. Walgenbach, Dissertation, Universität zu Köln, **1992**; d) E. Vogel, S. Will, A. Schulze Tilling, L. Neumann, J. Lex, E. Bill, A. X. Trautwein, K. Wieghardt, *Angew. Chem.* **1994**, *106*, 771; *Angew. Chem. Int. Ed. Engl.* **1994**, *33*, 731.

[9] Tetraoxaisophlorin: E. Vogel, *Pure Appl. Chem.* **1993**, *65*, 143; R. Bachmann, F. Gerson, G. Gescheidt, E. Vogel, *J. Am. Chem. Soc.* **1992**, *114*, 10855; b) *N,N',N'',N'''*-tetramethyloctaethylisophlorin: M. Pohl, H. Schmickler, J. Lex, E. Vogel, *Angew. Chem.* **1991**, *103*, 1737; *Angew. Chem. Int. Ed. Engl.* **1991**, *30*, 1693; the still hypothetical isophlorin was first mentioned by R. B. Woodward in connection with chlorophyll synthesis: R. B. Woodward, *Angew. Chem.* **1960**, *72*, 651.

[10] W.-C. Chen, S. A. Jenekhe, *Macromolecules* **1995**, *28*, 454; W.-C. Chen, S. A. Jenekhe, *ibid.* **1995**, *28*, 465; M. Hanack, U. Schmid, U. Röhrig, J.-M. Toussaint, C. Adant, J.-L. Brédas, *Chem. Ber.* **1993**, *126*, 1487; G. Hieber, M. Hanack, K. Wurst, J. Strähle, *ibid.* **1991**, *124*, 1597; A. O. Patil, F. Wudl, *Macromolecules*, **1988**, *21*, 540; S. A. Jenekhe, *Nature* **1986**, *322*, 345.

[11] J.-M. Toussaint, B. Thémans, J. M. André, J.-L. Brédas, *Synth. Met.* **1989**, *28*, C205; Y.-S. Lee, M. Kertesz, *J. Chem. Phys.* **1988**, *88*, 2609; M. Kertesz, Y. S. Lee, *J. Phys. Chem.* **1987**, *91*, 2690.

[12] Y. Miyahara, T. Inazu, T. Yoshino, *Chem. Lett.* **1980**, 397; J. K. Jurjew, *Ber. Dtsch. Chem. Ges.* **1936**, *69*, 440.

[13] The previously unknown 3,4-diethyl-2-hydroxymethylthiophene (**4**) was synthesized by the sequence shown below (conditions: a) *t*BuOK in *t*BuOH, 1 h, 25 °C; b) Cu/Δ ca. 300 °C (47%); c) $LiAlH_4$ in THF, 1 h, 25 °C (90%); based on related work by H. Wynberg, D. J. Zwanenburg, *J. Org. Chem.* **1964**, *29*, 1919):

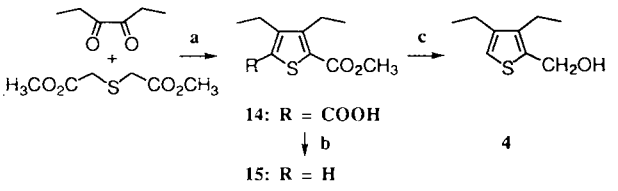

[14] B. Franck, A. Nonn, K. Fuchs, M. Gosmann, *Liebigs Ann. Chem.* **1994**, 503; G. Bringmann, B. Franck, *ibid.* **1982**, 1272; see also: L. F. Tietze, H. Geissler, *Angew. Chem.* **1993**, *105*, 1087; *Angew. Chem. Int. Ed. Engl.* **1993**, *32*, 1038.

[15] Calculated from the values given by C. W. Bird, G. W. H. Cheeseman in *Comprehensive Heterocyclic Chemistry, Volume 4, Part 3* (Eds.: A. R. Katritzky, C. W. Rees), Pergamon, Oxford, **1984**, p. 3.

[16] A crystalline acid-free form of **1** was obtained by crystallization from chloroform/dichloromethane (5/1); blue rods of the composition $\mathbf{1}\cdot 2CHCl_3$.

[17] The UV/Vis spectrum of **1** in dry methanol (λ_{max} = 251, 324, 439sh, 463, 492 nm) is nearly superimposable on that of **10**. The latter compound was obtained on reaction of **1** with either $NaBH_4$ or $LiAlH_4$ in THF; microcrystalline, yellow needles from ethanol, decomp. above 150 °C, 90% yield; for spectroscopic data see Table 1.

[18] For formation of aggregates of **1** with π donors see: A. Mahammed, M. Rabinovitz, I. Willner, E. Vogel, M. Pohl, *J. Phys. Org. Chem.* **1995**, *8*, 647; A. Mahammed, M. Rabinovitz, R. E. Hoffman, I. Willner, E. Vogel, M. Pohl, *ibid* **1995**, *8*, 659.

[19] Data of the crystal structure of $\mathbf{1}\cdot 2CHCl_3$: $C_{36}H_{44}S_4Cl_2O_8\cdot 2CHCl_3$, M_r = 1042.59, crystals from $CHCl_3/CF_3CO_2H$, decomp. above 230 °C; crystal dimensions 0.4 × 0.35 × 0.35 mm, monoclinic, space group $P2_1/n$, a = 8.062(2), b = 21.218(6), c = 13.759(4) Å, β = 102.89(2)°, V = 2294.3 Å^3, Z = 2, ρ_{calcd} = 1.509 g cm^{-3}, $F(000)$ = 1076; μ_{Mo} = 7.22 cm^{-1}; θ_{max} = 27°; 5331 reflections measured; 4989 independant reflections; 3730 reflections observed ($F_o^2 > 2\sigma F_o^2$); $R1$ = 0.0698, $wR2$ = 0.1995. Enraf-Nonius CAD4 diffractometer (room temperature, $Mo_{K\alpha}$ radiation, λ = 0.71069 Å). The structure was solved by direct methods and refined by F^2 with all observed reflections (heavy atoms with anisotropic, H atoms with isotropic temperature factors); $wR2 = [\sum w(F_o^2 - F_c^2)^2/\sum w(F_o^2)^2]^{1/2}$. Programs used: structure determination by MolEN (Enraf Nonius) and refinement by SHELXL-93 (G. M. Sheldrick, University of Göttingen). Calculations were performed at the regional computational center of the University of Cologne. Crystallographic data (excluding structure factors) for the structure reported in this paper have been deposited with the Cambridge Crystallographic Data Centre as supplementary publication no. CCDC-179-41. Copies of the data can be obtained free of charge on application to The Director, CCDC, 12 Union Road, Cambridge CB2 1EZ, UK (fax: Int. code +(1223) 336-033; e-mail: teched@chemcrys.cam.ac.uk).

[20] a) Dichloromethane was dried over CaH_2 and stored under an argon atmosphere. $TBAPF_6$ (Fluka-electrochemical grade) was used as supporting electrolyte. A platinum rotating disc electrode was employed. The logarithmic analysis of the signals resulted in a slope of 0.058 V lg^{-1} for each reduction step. Ferrocene was used as the internal standard at +0.375 V vs. Ag/AgCl. b) Measurements were carried out at scan rates between 0.01 and 20 Vs^{-1} at a platinum electrode. Potentials were measured against an Ag/AgCl electrode as reference.

[21] a) G. A. Molander, *Org. React.* **1994**, *46*, 211; b) G. A. Molander, *Chem. Rev.* **1992**, *92*, 29; c) H. B. Kagan, M. Sasaki, J. Collin, *Pure Appl. Chem.* **1988**, *60*, 1725.

[22] In concentrated solution, compound **2** spontanously polymerizes at temperatures above −20 °C. As inferred from NMR spectroscopy studies, the products arise from intermolecular cycloadditions of **2** and possess phane-type structures.

[23] A neutral 22π thiaporphyrinoid was recently described by M. P. Cava et al.: Z. Hu, M. P. Cava, *Tetrahedron Lett.* **1994**, *35*, 3493; Z. Hu, J. L. Atwood, M. P. Cava, *J. Org. Chem.* **1994**, *59*, 8071.

[24] R. Charrière, T. A. Jenny, H. Rexhausen, A. Gossauer, *Heterocycles* **1993**, *36*, 1561; A. K. Burrell, G. Hemmi, V. Lynch, J. L. Sessler, *J. Am. Chem. Soc.* **1991**, *113*, 4690; H. Rexhausen, A. Gossauer, *J. Chem. Soc. Chem. Commun.* **1983**, 275.

[25] The NMR spectra of the two antimonates **7a** and **7b** in CD_3NO_2 are identical and show sharp signals. Spectroscopic data for **7**: ^{1}H NMR (300 MHz, CD_3NO_2): δ = 14.74 (s, 5H, H-*meso*), 5.73 (q, 20H, CH_2), 2.60 (t, 30H, CH_3); ^{13}C NMR (75.5 MHz, CD_3NO_2): δ = 167.59, 153.15, 130.58, 26.18, 19.52.

 © VCH Verlagsgesellschaft mbH, D-69451 Weinheim, 1996 0570-0833/96/3513-1524 $ 15.00+.25/0

Template-Driven Syntheses of Polymeric Metal Cyanides: A Chiral Nanoporous Host for the nBu$_4$N$^+$ Ion**

Peter Schwarz, Stefan Eller, Eric Siebel, Tarek M. Soliman, R. Dieter Fischer,* David C. Apperley, Nicola A. Davies, and Robin K. Harris*

Dedicated to Professor Erwin Weiss on the occasion of his 70th birthday

Molecular recognition refers to the phenomenon of specific interaction between a receptor and a substrate or a host system and its potential guest.[1] An "intelligent" receptor or host can also adapt structurally to suit different substrates or guests.[2] We have discovered that the guest cations G^{n+} that the anionic 3D network of **1** can accommodate in its lipophilic cavity are as dissimilar as methyl viologen dications (MV^{2+}), cobaltocenium ions ($[CoCp_2]^+$, Cp = η^5-C_5H_5), and Et_4N^+ ions: the topology of the host framework in the host/guest compounds **2**[3a] and **3**,[4] which formally resembles that of **1**, differs significantly depending on the G^{n+} ion used.[3b] Also in the case of compound **4** ($G^+ = Et_4N^+$), which belongs to the same type as **2** and **3**, the results of vibrational[5] and solid-state NMR spec-

$[(Me_3Sn^{IV})_3M^{II}(CN)_6^-] \equiv {}^3_\infty[M^{II}(\mu\text{-}CNSn^{IV}Me_3NC)_3^-]$ (M = Fe, Ru) **1**

${}^3_\infty[(G^{n+})_{1\,n} \subset \mathbf{1}]$ **2**: $G^{2+} = MV^{2+}$; M = Ru
3: $G^- = [CoCp_2]^+$; M = Fe
4: $G^- = Et_4N^+$; M = Fe

troscopy[4] suggest a structurally optimally adapted host system. Here we report that with the larger nBu$_4$N$^+$ ion as the guest the resulting host/guest compound **5** even adopts a different stoichiometry that also has unexpected impact on the structure.

$[(n\text{Bu}_4\text{N})_{0.5}(\text{Me}_3\text{Sn})_{3.5}\text{Fe(CN)}_6 * \text{H}_2\text{O}]$ **5**

Both ion exchange[5] [Eq. (a)] and spontaneous self-assembly[4] [Eq. (b)] afford **5** in virtually quantitative yield (based on the amount of nBu$_4$NCl used).[6] The product is sparingly sol-

$$[(\text{Me}_3\text{Sn})_4\text{Fe(CN)}_6] \xrightarrow[-0.5\,\text{Me}_3\text{SnCl}]{0.5\,n\text{Bu}_4\text{NCl}/\text{H}_2\text{O}} \mathbf{5}\downarrow \quad \text{(a)}$$

$$3.5\,\text{Me}_3\text{SnCl} + 0.5\,n\text{Bu}_4\text{NCl} \xrightarrow[-4\text{KCl}]{\text{K}_4[\text{Fe(CN)}_6]/\text{H}_2\text{O}} \mathbf{5}\downarrow \quad \text{(b)}$$

uble in water as well as in organic solvents. The crystal structure analysis of **5**[7] clearly reveals that the modified composition leads to the formation of a 3D network with a larger cavity than that in **3**.[4] The building blocks are an infinitely long, helical chain A and a 15 atom long chain B (Fig. 1). As in **1**–**4**, all Sn atoms in **5** also have fivefold coordination. Every Fe atom belongs to three discrete strands (A, A', and B); possibly, weak hydrogen bonds between the O atom of every B chain and the

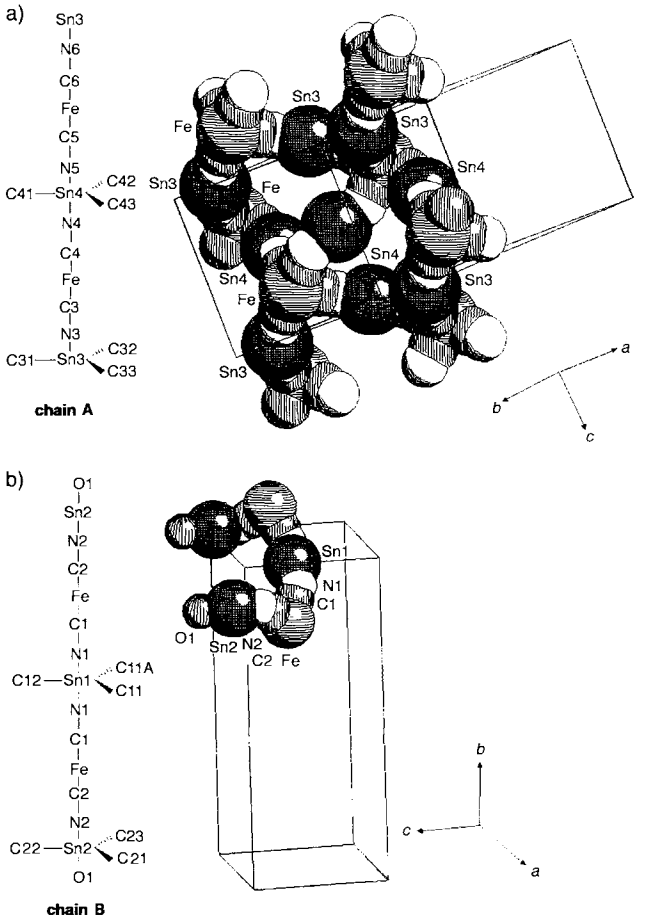

Fig. 1. a) Section of the network of **5**: SCHAKAL representation of the chains of type A only (without CH_3 groups) with complete numbering of the atoms for the vertical A helices. b) SCHAKAL representation and numbering of the atoms of a chain of type B (without CH_3 groups. Interatomic distances [pm] and angles [°] for A: Sn3-N3 229.2(14), Sn3-N6 231.7(14), Sn4-N4 224.8(14), Sn4-N5 248.0(12); C3-N3-Sn3 156.8(11), C6-N6-Sn3 154.8(13), C4-N4-Sn4 156.7(12), C5-N5-Sn4 133.6(11); C4-Fe-C6 89.9(6); C3-Fe-C5 176.9(6); B: Sn1-N1 233.6(13), Sn2-N2 218.7(13), Sn2-O1 266.4(13); C1-N1-Sn1 147.2(12), C2-N2-Sn2 137.6(12), C1-Fe-C2 90.8(6), N2-Sn2-O1 175.3(5); A/B linkage: C1-Fe-C6 178.7(6), C2-Fe-C4 174.9(6).

CN groups[8] of adjacent B' and B'' chains also contribute to the cross-linking (shortest distances [pm]: O1 ··· N1' 320, O1 ··· C1' 323; Fig. 2).

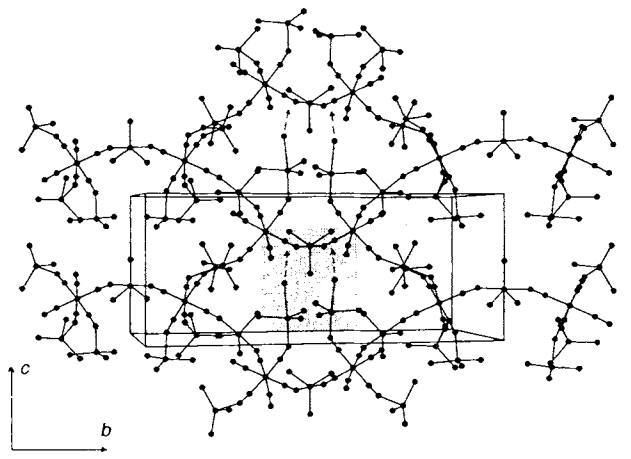

Fig. 2. View of the three-dimensional network of **5** down the a axis. Two adjacent Sn2–O1 ··· (N2–C2) fragments (O–H ··· NC hydrogen bonds) are highlighted by a grey background: nBu$_4$N$^+$ ions and methyl-H atoms have been omitted.

[*] Prof. Dr. R. D. Fischer, Dr. P. Schwarz, Dr. S. Eller, Dipl.-Chem. E. Siebel, T. M. Soliman[+] (MSc)
Institut für Anorganische und Angewandte Chemie der Universität
Martin-Luther-King-Platz 6, D-20146 Hamburg (Germany)
Fax: Int. code +(40)4123-2893
Prof. Dr. R. K. Harris, Dr. D. C. Apperley, N. A. Davies (MSc)
University of Durham, Department of Chemistry
South Road, Durham DH13LE (UK)
Fax: Int. code +(191)386-1127
[+] Deceased

[**] This work was supported by the Deutscher Akademischer Austauschdienst and the British Council (ARC Cooperation), the Deutsche Forschungsgemeinschaft (Program "Nanoporous Crystals"), the Egyptian Ministry of Education ("Channel System"), and the UK EPSRC (through the National Solid-State NMR Service based at Durham).

Figure 3 depicts the approximately rectangular, nanometer-sized channels extending along the *c* axis. The nBu$_4$N$^+$ ions that are located in the channels with an almost perfect fit (C74···C78

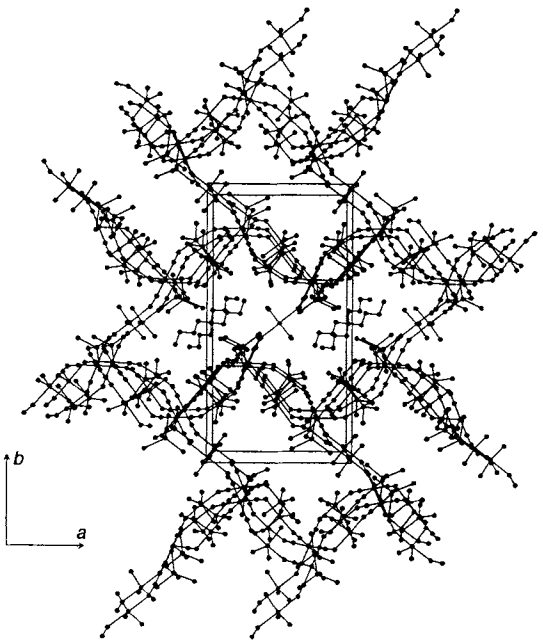

Fig. 3. View of the three-dimensional network of **5** (without methyl-H atoms) down the channels (along the *c* axis). Only in two channels are the nBu$_4$N$^+$ ions depicted.

1.013(4), H741···H781 1.151(4) nm) are not disordered (Fig. 4). The axes of part of the A helices, which are the major constituents of the walls of the channels, also run parallel to the *c* axis (see Fig. 1a). Helical chains in polymeric metal cyanides like **5** (that is, $\{M-CN-E-NC\}_n$ where M = Cu, Mo, W; E = SnR$_3$[9, 10] and $\{M-NC-E-CN\}_n$ where M = Co, Zn: E = Au[11, 12]) are a new structural motif that has only recently attracted increasing attention.[12] In **5** every distorted octahedral Fe(CN)$_6$ unit is, moreover, enantiomorphic, independent of the helicity of the chain.[13] The appearance of six separate ν_{CN} bands in each of the IR and Raman spectra is quite unusual[14] and indicates that different vibrational force constants can be attributed to the six CN ligands, which are at least crystallographically nonequivalent.[15]

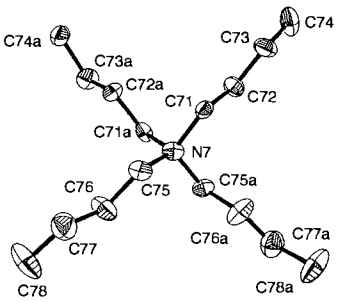

Fig. 4. ORTEP plot of the nBu$_4$N$^+$ ion of **5** (view along the *b* axis; 30% probability).

The CP/MAS NMR spectra (CP = cross polarization, MAS = magic angle spinning) of **5** recorded at 25 °C often display fewer signals or different relative intensities than expected for the number of nonequivalent atoms in the asymmetric unit.[16] Although the four expected ^{119}Sn resonances appear as discrete singlets (Table 1), even after ^{15}N enrichment (to about 50% or 95%[17]) only five (cyanide) ^{15}N and four ^{13}C signals were observed, whereas the asymmetric unit contains six nonequivalent atoms of each. Instead of eleven possible methyl ^{13}C resonances, the spectra show only two (δ = 2.3, 3.5; I_{rel} = 1/2); these split at −115 °C into six singlets δ = −1.9, 0.9, 1.1, 3.1, 3.6, 7.0; I_{rel} = 10, 4, 32, 30, 10, 10). Apparently even then the rapid rotation on the NMR time scale of only one of the four Me$_3$Sn groups about the N-Sn-X axis (X = N, O) is frozen.[18] The α-, β-, and γ-C atoms of the nBu$_4$N$^+$ ion each give rise to a relatively broad ^{13}C NMR signal (δ = 57.4, 25.7, 21.0), whereas two sharper δ-methyl ^{13}C NMR resonances (δ = 16.4, 15.5) appear. In each case, according to the asymmetric unit, two signals are anticipated. The ^{15}N NMR chemical shifts of the guest cations of **4** (δ = −372.6) and **5** (δ = −308.2; one signal predicted from the asymmetric unit) differ significantly. The above discussion of the NMR results seems justified, since the experimentally determined X-ray powder diffraction diagram is in satisfactory agreement with the calculated[7] pattern (Fig. 5).

Table 1. Solid-state NMR data (room temperature) of the {Sn$_{3.5}$Fe(CN)$_6$} skeleton of **5**.

^{119}Sn	δ_{iso}	6	−118	−141	−164	
	I_{rel}	16	30	22	32	
	ζ [a]	−255	−373	−386	−401	
	η [b]	0.47	0.00	0.00	0.00	
^{15}N	δ_{iso}	−101	−118	−121	−132 [c]	−142
	I_{rel}	4.9	4.0	3.6	1	5.6
	J_{SnN}/Hz	112	158	170	–	158
^{13}C	δ_{iso}	196	178	170 [c]	165	
	I_{rel}	2.3	4.2	1	2.1	

[a] $\zeta = \sigma_{zz} - \sigma_{iso}$ (shielding anisotropy). [b] $\eta = (\sigma_{yy} - \sigma_{xx})/\zeta$ (shielding asymmetry). [c] Possibly from an impurity. For technical details and the samples chosen as references, see refs. [9] and [16].

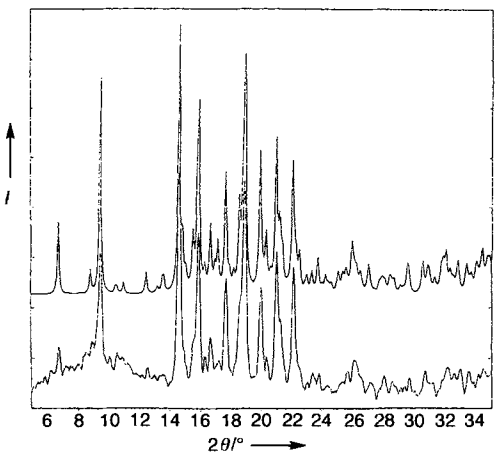

Fig. 5. Calculated (top) and experimental (bottom) X-ray powder diagram of **5**.

A notable feature resulting from the involvement of nBu$_4$N$^+$ is the formation of the {C2-N2-Sn2Me$_3$·OH$_2$} fragment that resembles an only loosely solvated, stanna-isocyanide ligand coordinated to Fe.[19] Striking evidence is a) the relatively short Sn2–N2 contact (218.7 pm), b) in contrast to this, the extremely long Sn2–O1 distance (266.4 pm),[20, 24] c) the nonplanarity of the Me$_3$Sn2 fragment (C21/C22/C23-Sn2-N2 angle: 94.8/97.3/94.4°), d) the ^{119}Sn resonance of δ = +6 (Table 1) that is attributable to a four-coordinate rather than a five-coordinate Sn atom,[25] e) the ^{13}C NMR shift of δ = 196 that displays quite a high frequency for a "classical" cyanide ligand,[26] and f) the ν_{CN} value of 2026 cm^{-1} that is relatively low for a normal Fe–CN → Sn bridge.[14] Complexes with strictly terminal CNER$_3$ ligands (E = Sn, Pb) have not yet been characterized structurally according to our knowledge;[27] thus, for the present the question whether the appearance in **5** of Fe-C2-N2 and C2-N2-

 © VCH Verlagsgesellschaft mbH, D-69451 Weinheim, 1996 0570-0833/96/3513-1526 $ 15.00+.25/0

Sn2 angles that deviate significantly from 180° (171.4 and 137.6°) is mainly attributable to very pronounced Fe→C2 π backbonding must remain open.[28]

The results presented here are specific for the guest (template) ion nBu$_4$N$^+$: with no other $(C_mH_{2m+1})_4N^+$ ion ($m = 1-3,5$) did we obtain a product of the composition $[(R_4N)_x(Me_3Sn)_{4-x}Fe(CN)_6(H_2O)_y]$ with $x = 0.5$ that would be strictly homologous with **5**.[29]

Received: December 5, 1995 [Z 86141E]
German version: *Angew. Chem.* **1996**, *108*, 1611–1614

Keywords: iron compounds · host–guest chemistry · structure elucidation · tin compounds

[1] A. Streitwieser, C. H. Heathcock, E. M. Kosower, *Organische Chemie*, 2nd ed, VCH, Weinheim, **1994**.

[2] For "tunable", pure inorganic hosts, see a) A. Müller, H. Reuter, S. Dillinger, *Angew. Chem.* **1995**, *107*, 2505; *Angew. Chem. Int. Ed. Engl.* **1995**, *34*, 2311, and references therein; b) T. Iwamoto, S.-I. Nishikiori, T. Kitazawa, *Supramol. Chem.* **1995**, *6*, 179.

[3] a) S. Eller, M. Adam, R. D. Fischer, *Angew. Chem.* **1990**, *102*, 1157; *Angew. Chem. Int. Ed. Engl.* **1990**, *29*, 1126. b) A homologue of **2** with the benzyl viologen dication is also known [3a].

[4] P. Schwarz, E. Siebel, R. D. Fischer, D. C. Apperley, N. A. Davies, R. K. Harris, *Angew. Chem.* **1995**, *107*, 1311; *Angew. Chem. Int. Ed. Engl.* **1995**, *34*, 1197.

[5] S. Eller, P. Brandt, A. K. Brimah, P. Schwarz, R. D. Fischer, *Angew. Chem.* **1989**, *101*, 1274; *Angew. Chem. Int. Ed. Engl.* **1989**, *28*, 1263.

[6] Synthesis of **5**: a) A suspension of **6** (450 mg, 0.519 mmol) in a solution of nBu$_4$Cl (273 mg, 1.034 mmol) in water (35 mL) was stirred for about 15 h. Filtration and washing with small portions of water (3×) and drying under vacuum yielded 401 mg (0.442 mmol, 85%) of **5**. Correct C, H, N, O, and Sn analyses, pale green–white, decomp. >260° with darkening. TG/DTA/DTG (in a stream of argon): between 60 and 140 °C a continuous decrease in mass of only about 0.7% (H_2O content of **5**: 1.7%). b) Syntheses of **5** with about 50% [^{15}N]cyanide: To a stirred aqueous solution of $K_4[Fe(CN)_6\cdot 3H_2O]$ (81.3 mg, 0.192 mmol), $K_4[Fe(C^{15}N)_6\cdot 3H_2O]$ (79.0 mg, 0.192 mmol), and nBu$_4$Cl (203 mg, 0.769 mmol) in water (8 mL), a clear solution of Me_3SnCl (306 mg, 1.536 mmol) in water (12 mL) was added dropwise. After workup as above the yield was 320 mg (0.352 mmol, 92%). Single crystal growth of **5** according to Equation (b), but with three- to fivefold more dilute solutions. An analytically and spectroscopically indistinguishable isotopomer of **5** $[(n\text{Bu}_4)_{0.5}(Me_3Sn)_{3.5}Fe(CN)_6\cdot D_2O]$ was obtained in D_2O according to Equation (b).

[7] Crystal structure data of **5**: $C_{24.5}H_{51.5}N_{6.5}OFeSn_{3.5}$, $M_r = 924.48$ g mol^{-1}, orthorhombic, $P2_12_12$ ($h00$ valid only for $h = 2n$, $0k0$ only for $k = 2n$), $a = 1351.4(5)$, $b = 2636.3(10)$, $c = 1096.2(5)$ pm, $V = 3905(3)\times 10^6$ pm^3, $Z = 4$, $\rho_{calcd} = 1.572$ Mg m^{-3}, $F(000) = 1812$. Syntex $P2_1$ four circle diffractometer, $T = 23$ °C, 2θ range: 4–50°. Symmetry independenty reflections: 3880 (total 4049), data/restraints/parameters: 3859/0/333. Direct methods, SHELXTL PLUS (VMS), refinement with SHELXL93 (VMS). $R1 = 0.0554$, $wR2 = 0.1554$, Flack parameter: −0.02(10). Powder diagram calculated with SHELXT/XPOW; 2θ range 0–35°. Further details of the crystal structure investigation may be obtained from the Fachinformationszentrum Karlsruhe, D-76344 Eggenstein-Leopoldshafen (Germany) on quoting the depository number CSD-404541.

[8] a) U. Behrens, A. K. Brimah, R. D. Fischer, *J. Organomet. Chem.* **1991**, *411*, 325; S.-I. Nishikiori, T. Iwamoto, *Chem. Lett.* **1994**, 1199.

[9] A. K. Brimah, E. Siebel, R. D. Fischer, N. A. Davies, D. C. Apperley, R. K. Harris, *J. Organomet. Chem.* **1994**, *475*, 85.

[10] J. Lu, W. T. A. Harrison, A. J. Jacobsen, *Angew. Chem.* **1995**, *107*, 2759; *Angew. Chem. Int. Ed. Engl.* **1995**, *34*, 2557.

[11] S. C. Abrahams, L. E. Zyontz, J. L. Bernstein, *J. Chem. Phys.* **1982**, *76*, 5485.

[12] B. F. Hoskins, R. Robson, N. V. Y. Scarlett, *Angew. Chem.* **1995**, *107*, 1317; *Angew. Chem. Int. Ed. Engl.* **1995**, *34*, 1203.

[13] On rotation of a $Fe(CN)_6$ unit of **5** about its C1-Fe-C6 axis (viewed along C1 → C6) in a clockwise direction, C2 transforms into C3, C3 into C4, and C4 into C5.

[14] $\tilde{\nu}_{CN}$ values [cm^{-1}] of **5** (with C^{14}N-/C^{15}N), IR: 2027 m/1997 s, 2045 m/2014 s, 2065 s/2098 s, 2095 s/2063 s, 2102 sh, 2130 m/2098 s; Raman: 2026 m/1999 m, 2045 s/2020 m, 2065 s/2042 m, 2095 m/2070 s, 2100 s/2070 s, 2130 m/2101 s. Data of **4** for comparison (only C^{14}N), IR: 2052 s, 2065 s; Raman: 2071 m, 2081 s, 2120 s.

[15] The single crystals proved to be too small for CD and NLO studies.

[16] See ref. [4] for previous CP-MAS NMR studies, as well as U. Behrens, A. K. Brimah, T. M. Soliman, R. D. Fischer, D. C. Apperley, N. A. Davies, R. K. Harris, *Organometallics* **1992**, *11*, 1718.

[17] When the enrichment with ^{15}N was over 90%, **5** was prepared only as depicted in Equation (a). In this case, in spite of excellent elemental analyses, a number of surprisingly intense cyanide ^{13}C and ^{15}N NMR signals of the starting material **6** always remained.

[18] a) Cf. ref. [4] as well as R. K. Harris, M. M. Sünnetçioglu, R. D. Fischer, *Spectrochim. Acta* **1994**, *50A*, 2069; b) surprisingly, the position of one signal shifts continuously on cooling from $\delta = 2.2$ (25°) to $\delta = 1.1$ (−115 °C).

[19] Complexes with genuine $CNER_3$ ligands (E = Sn, Pb): M. Moll, H.-J. Seibold, W. Popp, *J. Organomet. Chem.* **1980**, *191*, 193.

[20] So far, the Sn–O distances in trigonal-bipyramidal $\{Me_3SnX(H_2O)\}$ fragments were found to lie between 225.4 pm (X = H_2O [21]) and 245.1 pm (X = NCFe [22]). The large Sn–O bond lengths in the ion-pair-like compound $[\{(Me_3Sn)_2OH\}\{N(SO_2Me)_2\}]$ for Sn–O(H) [211.8(2)/212.6(2) pm] and Sn···O(S) [253.3(2)/268.2(2) pm] [23] seem worth mentioning here.

[21] A. Blaschette, D. Schomburg, E. Wieland, *Z. Anorg. Allg. Chem.* **1989**, *571*, 75.

[22] M. Adam, A. K Brimah, R. D. Fischer, X.-F. Li, *Inorg. Chem.* **1990**, *29*, 1597.

[23] A. Blaschette, E. Wieland, P. G. Jones, I. Hippel, *J. Organomet. Chem.* **1993**, *445*, 55.

[24] Further data for comparison may be found in: L. Jäger, B. Freude, A. Krug, H. Hartung, *J. Organomet. Chem.* **1994**, *467*, 163, and references therein.

[25] The relative abundances of Sn deduced from the asymmetric unit, Sn1:Sn2:Sn3:Sn4 = 0.5:1:1:1, deviate from the data in Table 1.

[26] Chemical shift values of $\delta \approx 190$ have actually been measured in the ^{13}C NMR spectra of some $CNSnR_3$ and $CNPbR_3$ complexes [19].

[27] The principal reason for this is the very attractive coordination number of 5 for many Me_3Sn^{IV} derivatives.

[28] Interestingly it is the Fe-C2 bond that is slightly shorter than the other Fe-C bonds of **5** (Fe–C2 187.6(13) pm, otherwise 189.7(15)–193.2(14) pm).

[29] For $m = 1$ [5] as well as for $m = 3$ and 5 we found x values of between 0.5 and 1; it is also remarkable that no strict Ru homologue of **5** forms with M = Ru instead of Fe.

The Effect of the Surrounding Medium on the Interaction of Nitriles with Boron Trifluoride**

Ian R. Beattie* and Peter J. Jones

In a series of elegant papers, Leopold et al. have examined the interaction of acetonitrile or hydrogen cyanide with boron trifluoride.[1–3] The observations demonstrate a remarkable change in the boron–nitrogen bond length between those bonds in the free molecules (in a pulsed molecular beam of argon) and those in the crystalline solids.[3, 4] In the case of $CH_3CN\cdot BF_3$, the change in bond length was 0.381 ± 0.011 Å. The isolated molecule can be regarded[1] as "structurally quite intermediate between a covalent molecule and a weakly bound complex" although energetically it is much more like a van der Waals molecule.[5] The results of ab initio calculations[6] on the isolated molecule were in good agreement with the microwave data and indeed helped to guide the microwave search initially. Very recently the (calculated) B–N bond length was examined as a function of the dielectric constant of the surrounding medium, by using the self-consistent reaction field (SCRF) method.[7] For $HCN\cdot BF_3$ the critical dielectric constant was approximately 10 D. Media having a dielectric constant higher than this value gave the short B–N distance, as found in the solid. These and related papers[8] have led to a resurgence of interest in such Lewis acid–base complexes.

[*] Prof. I. R. Beattie, P. J. Jones
Geology Department, University of Southampton
Southampton Oceanography Centre
Empress Dock, European Way, Southampton SO14 3HZ (UK)
Fax: Int. code +(1703) 593052

[**] We thank Prof. K. R. Leopold for manuscripts prior to publication, Dr. T. R. Gilson for helpful discussions and gas-phase Raman spectra, Dr. J. S. Ogden for gas-phase IR spectra, and The Leverhulme Trust for a Fellowship to I. R. B.

 © VCH Verlagsgesellschaft mbH, D-69451 Weinheim, 1996 0570-0833/96/3513-1527 $ 15.00+.25/0

The compound $CH_3CN \cdot BF_3$ is well characterized, stable at room temperature, and easily sublimed in a vacuum. Laubengayer and Sears[9] found from vapor density measurements that in the temperature range 50 to 103 °C dissociation is "virtually complete"; however, the photoelectron spectrum of the vapor has been reported.[10, 11] In view of these apparently conflicting results, we examined the IR spectrum of a completely vaporized sample at 50 °C using a long path-length (ca. 90 cm) borosilicate glass cell with sealed-in silicon windows and no taps or joints. The resultant spectrum was a superposition of the spectra due to acetonitrile[12] and boron trifluoride,[13] and no bands due to complex formation were detected. An early study of the IR spectrum of solutions of $CH_3CN \cdot BF_3$ in benzene indicated a solubility of the order of 0.25 M.[14] As benzene has a dielectric constant of only about 2.3 D while that of xenon near the critical point is about 1.8 D,[15] we decided to attempt experiments in liquid and supercritical xenon, since these media have the advantage of being transparent to IR radiation. Unfortunately the solubility was too low to obtain either proton NMR[16] or IR spectra.[17] A redetermination of the solubility in benzene by using ^{19}F NMR spectroscopy with $C_{10}F_8$ as a reference compound gave a value of 0.023 M, an order of magnitude lower than that found previously.

Because of this discrepancy and the importance of studies in media of low dielectric constant, we examined the "CN stretching frequency" of $CD_3CN \cdot BF_3$ in benzene (CD_3CN was used because of problems[18] of Fermi resonance in CH_3CN). Using a borosilicate cell with fused-in silicon windows wedged to give path lengths between 0.0 mm and about 1.0 mm, we were able to verify a new band at 2353 cm^{-1}. Solutions of BF_3, CD_3CN, or $CH_3C^{15}N \cdot BF_3$ did not show this band; however, much of this region is obscured by solvent bands. In nitrobenzene (dielectric constant ca. 35 D), $CH_3CN \cdot BF_3$ showed[19] a "CN stretching frequency" at 2360 cm^{-1}, only a few wave numbers away from that for the corresponding solution in benzene and again close to the solid-state value of 2376 cm^{-1}.[20] Although the observation of a particular frequency does not define a bond length, nonetheless there is considerable evidence that "ν_{CN}" is related to the strength of the interaction of CH_3CN with Lewis acids.[21] Certainly the shift of greater than 100 cm^{-1} from the free ligand in solution in benzene (2248 cm^{-1}) to the complex $CH_3CN \cdot BF_3$ in solution in benzene (2353 cm^{-1}) suggests an interaction in solution comparable to that found in the solid state.

The ^{19}F NMR spectrum of $CH_3CN \cdot BF_3$ in benzene[22] showed one signal at $\delta \approx -139$ relative to $CFCl_3$. (To retain the integrity of the system, no internal standard was used, so δ values are only approximate.) In earlier work[23] in a solution in CH_2Cl_2 (with a dielectric constant of about 9 D), a solution composed of a 1:3:60 mol ratio of BF_3:CH_3CN:CH_2Cl_2 gave a signal at $\delta = -144.2$. The chemical shift value for BF_3 has been reported[24] as $\delta = -125$, and in our experiments[22] we found a solution (ca. 0.2 M) in benzene gave a signal at $\delta = -124$.

All of the above results can be interpreted in terms of the presence of a largely undissociated molecular species in benzene, dichloromethane, or nitrobenzene, whose geometry is similar to that found in the solid state. Attempts to study solutions in *n*-hexane (with a dielectric constant of about 1.9 D) failed due to lack of solubility. It is apparent that the solubility of $CH_3CN \cdot BF_3$ is highly dependent on the dielectric constant of the medium, and we note that the complex is very soluble in excess ligand (CH_3CN).

Matrix isolation is an attractive technique for studying molecular species as solid solutions in a relatively inert environment such as argon (with a dielectric constant of 1.56 D[15]). In order to increase the likelihood of complex formation while minimizing the possible formation of aggregates, we used a bulb containing a 1:10:500 mol ratio of CD_3CN:BF_3:argon, heated to 60 °C to ensure that all the material was in the vapor. The highest product concentration would then be 1:500. The small excess of BF_3, while ensuring that the CD_3CN would "see" the BF_3, has no dipole. Furthermore, the "ν_{CN}" band was expected to be more intense in the complex than in free CD_3CN.[25] Although the resultant IR spectra were inevitably complicated by combination bands of BF_3, there was clear evidence of a product band at 2380 cm^{-1}. It is logical to attribute this band to the $CH_3CN \cdot BF_3$ complex with a structure similar to that found in the solid state, with a band at 2373 cm^{-1}. Figure 1 shows a difference spectrum in the "CN stretching region" between a matrix consisting of a 1:10:500 mol ratio of CD_3CN:BF_3:argon; and a matrix consisting of a 1:50 mol ratio of BF_3:argon.

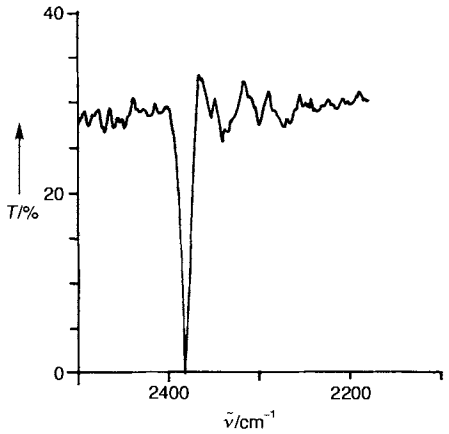

Fig. 1. Difference IR spectrum between a matrix of CD_3CN:BF_3:argon at 1:10:500 and a matrix of BF_3:argon at 1:50 mol ratio. T = transmittance.

The case of $HCN \cdot BF_3$ is complicated by the fact that a) this complex is less stable than $CH_3CN \cdot BF_3$ (HCN is a weaker donor than CH_3CN. Thus the dissociation pressure of $HCN \cdot BF_3$ is 400 Torr at 19 °C,[26] while for $CH_3CN \cdot BF_3$ this pressure is only attained at about 90 °C[9]), and b) there is an acidic proton that can form a hydrogen bond with the fluorine atom or the nitrogen atom of another molecule, or interact with the surrounding medium. A very recent paper[27] discusses the importance of such "a cooperative mechanism" in crystalline $HCN \cdot BF_3$.

When a gas mixture of $HCN \cdot BF_3$ in a 1:1 ratio was condensed at about 12 K and annealed at 100 K, the IR spectrum showed bands [cm^{-1}] at: 3193 (ms), 2209 (s, sharp), ca. 1200 (vs, broad), 863 (s), 803 (w), 653 (s), 512 (ms, sharp). The bands in the region between 3,300 and 1,000 cm^{-1} can reasonably be assigned, in order of decreasing frequency, as ν_{CH}, ν_{CN} and ν_{BF}. They may be compared with ν_{CH} at 3205 and ν_{CN} at 2192 for solid $HCN \cdot AsF_5$[28] and with ν_{BF} of solid $MeCN \cdot BF_3$, "a strong band at about 1200 cm^{-1}".[20]

In a matrix isolation experiment analogous to that for $CH_3CN \cdot BF_3$ (i.e. HCN:BF_3:argon at 1:10:500) product bands appeared at 3246, 2217, and about 1200 cm^{-1}. These correspond closely with those in the solid and identify the matrix-isolated species as $HCN \cdot BF_3$ in the form with short B–N linkage.

 © VCH Verlagsgesellschaft mbH, D-69451 Weinheim, 1996 0570-0833/96/3513-1528 $ 15.00+.25/0

A matrix isolation experiment using an excess of HCN (HCN:BF_3:argon at 10:1:500) gave spectra in which ν_{CN} occurred at 2167 cm^{-1}, with no evidence for a band around 2210 cm^{-1}. Furthermore, condensing a gas mixture of HCN:BF_3 (ca. 5:1) at 12 K showed a strong product band at about 2180 cm^{-1}, together with a broad band at about 1200 cm^{-1}. Annealing at 150 K led to a decrease in intensity of the band at 2180 cm^{-1}, while a band at 2210 cm^{-1}, corresponding to ν_{CN} of solid HCN · BF_3, grew in. Clearly the excess HCN is interacting with the HCN · BF_3. The corresponding solution chemistry is complicated by preferential loss of boron trifluoride. When cold toluene, which contains crystals of HCN · BF_3, is allowed to warm to room temperature, a gas is evolved as the crystals "dissolve". The IR spectrum of the resultant solution shows the presence of free HCN, coupled with a weak broad band at 2167 cm^{-1} analogous to that found in the solid (5 HCN: 1 BF_3) and in the matrix containing excess HCN. A solution in toluene which was about 0.025 M in HCN and had a pressure of approximately two atmospheres of BF_3 above that solution, in addition to free HCN, showed only the 2167 cm^{-1} band, even on cooling to −70 °C.

It is interesting to compare these results with those on gaseous HCN · BF_3, where ν_{CH} is almost unchanged from that of free HCN,[29] showing a very small perturbation of the HCN by the (distant) BF_3. We also note that the van der Waals molecule OC · BF_3 (isoelectronic with HCN · BF_3) shows frequency shifts of the order of 10 cm^{-1} for ν_{CO} and ν_{BF} (antisymmetric stretch).[30, 31] The corresponding ν_{BF} shifts for strong adducts[20] are nearer to 200–250 cm^{-1}, similar to those proposed here for HCN · BF_3. In a matrix isolation experiment, it is always possible for polymerization to occur, notably at the interface with the condensing gas. However, we note: a) that in a separate experiment on HCN in argon at a 1:500 matrix ratio, we found only a trace of dimer, in agreement with a very recent paper by Beichert et al.;[32] b) that to form (RCN · BF_3)$_2$ in a matrix requires two RCN and two BF_3 molecules to come together in the correct orientation. This seems unlikely in our experiments in which the maximum product ratio wuld be 1:1000 and no annealing was carried out after the condensation at 12 K. However, we should emphasize that this does not *exclude* the possibility of polymer formation.

Received: August 7, 1995
Revised version: March 26, 1996 [Z 8281 IE]
German version: *Angew. Chem.* **1996**, *108*, 1656–1658

Keywords: acetonitrile · bond length alternation · boron trifluoride · hydrogen cyanide · matrix isolation

[1] M. A. Dvorak, R. S. Ford, R. D. Suenram, F. J. Lovas, K. R. Leopold, *J. Am. Chem. Soc.* **1992**, *114*, 108–115.
[2] S. W. Reeve, W. A. Burns, F. J. Lovas, R. D. Suenram, K. R. Leopold, *J. Phys. Chem.* **1993**, *97*, 10630–10637.
[3] W. A. Burns, K. R. Leopold, *J. Am. Chem. Soc.* **1993**, *115*, 11622–11623.
[4] B. Swanson, D. F. Shriver, J. A. Ibers, *Inorg. Chem.* **1969**, *8*, 2182–2189.
[5] See also K. R. Leopold, G. T. Fraser, S. E. Novick, W. Klemperer, *Chem. Rev.* **1994**, *94*, 1807–1827.
[6] R. Jurgens, J. Amlöf, *Chem. Phys. Lett.* **1991**, *176*, 263–265.
[7] H. Jiao, P. von R. Schleyer, *J. Am. Chem. Soc.* **1994**, *116*, 7429–7430. In this model, the solute is placed in a spherical cavity in a continuous medium of dielectric constant ε.
[8] V. Jonas, G. Frenking, M. T. Reetz, *J. Am. Chem. Soc.* **1994**, *116*, 8741–8753, and references therein.
[9] A. W. Laubengayer, D. S. Sears, *J. Am. Chem. Soc.* **1945**, *67*, 164–167.
[10] T. Pradeep, C. S. Seekanth, C. N. R. Rao, *J. Chem. Phys.* **1989**, *90*, 4704–4708.
[11] T. Pradeep, C. N. R. Rao, *J. Mol. Struct.* **1989**, *200*, 339–352.
[12] P. Venkateswarlu, *J. Chem. Phys.* **1951**, *19*, 293–298.
[13] J. Vanderryn, *J. Am. Chem. Soc.* **1959**, *30*, 331–332.
[14] H. J. Coerver, C. Curran, *J. Am. Chem. Soc.* **1958**, *80*, 3522–3523.
[15] D. C. J. Marcoux, *Can. J. Phys.* **1970**, *48*, 244–245.
[16] L. Dickinson, G. A. Lawless, personal communication.
[17] S. Kazarian, personal communication.
[18] See for example: G. L. Johnson, L. Andrews, *J. Phys. Chem.* **1983**, *87*, 1852–1859.
[19] J. Miller, M. Onyszchuk, *Can. J. Chem.* **1966**, *44*, 899–902.
[20] B. Swanson, D. F. Shriver, *Inorg. Chem.* **1970**, *9*, 1406–1416. In this article under "unusual temperature and lattice effects" a number of bands are reported which are due to gaseous BF_3.
[21] J. F. Bertrán, E. R. Ruiz, *Spectrochim. Acta.* **1993**, *49A*, 43–46.
[22] J. Street, personal communication.
[23] A. Fratiello, R. E. Schuster, *J. Org. Chem.* **1972**, *37*, 2237–2241. Because of the change in convention for reporting chemical shifts the sign of the δ value was changed.
[24] A. Fox, J. S. Hartmann, *J. Chem. Soc. Dalton Trans.* **1982**, 1275–1283.
[25] V. Z. Gabdrakipov, T. I. Markina, *Zh. Fiz. Khim.* **1979**, *53*, 585–587; *Russ. J. Phys. Chem.* **1979**, *53*, 331–333.
[26] E. Pohland, W. Harlos, *Z. Anorg. Allg. Chem.* **1932**, *207*, 242–245.
[27] E. Iglesias, T. L. Sordo, J. A. Sordo, *Chem. Phys. Lett.* **1996**, *248*, 179–181.
[28] I. C. Tornieporth-Oetting, T. M. Klapötke, T. S. Cameron, J. Valkonen, P. Rademacher, K. Kowski, *J. Chem. Soc. Dalton Trans.* **1992**, 537–543.
[29] E. R. T. Kerstel, B. H. Pate, T. F. Mentel, X. Yang, G. Scotes, *J. Chem. Phys.* **1994**, *101*, 2762–2771.
[30] E. J. Slutys, B. J. van der Veken, *J. Am. Chem. Soc.* **1996**, *118*, 440–445.
[31] J. Gebicki, J. Liang, *J. Mol. Struct.* **1984**, *117*, 283–286.
[32] P. Beichert, D. Pfeiler, E. Knözinger, *Ber. Bunsenges. Phys. Chem.* **1995**, *99*, 1469–1478.

Intramolecular Movements of Lithium in Crystals

Michael Veith,* Michael Zimmer, Kira Fries, Jutta Böhnlein-Maus, and Volker Huch

In certain molecular structures, metal atoms can undergo definite movements without actually leaving the molecule. The lithium atom in the silylamide $(Me_3Si)_4N_4(SiMe_2)_2InLi$, for example, orbits around the central indium atom—its nitrogen coordination changing continually.[1] These movements are accompanied by large framework vibrations of the ligands, however, so that the process is only observed in solution. Model calculations confirm the interpretation of the experimental findings.[2]

We subsequently extended our search to include compounds in which intramolecular movements of lithium atoms can be identified in the *solid state*, and our search proved successful in the case of the lithium salt **1**, which we used as starting material for a series of metal amides.[3, 4] Compound **1** can be prepared according to Scheme 1 with a total yield of 81 %.[5]

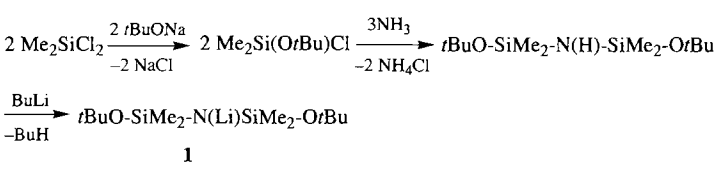

Scheme 1.

[*] Prof. Dr. M. Veith, Dr. M. Zimmer, K. Fries, Dr. J. Böhnlein-Maus, Dr. V. Huch
Institut für Anorganische Chemie der Universität
Postfach 15 11 50, D-66041 Saarbrücken (Germany)
Fax: Int. code +(681)302-3995
e-mail: Veith@sbusol.rz.uni-sb.de

According to molar mass determinations, **1** is dimeric in solution. Depending on the temperature, **1** forms three crystalline phases, in which the symmetry of the crystal lattice increases with increasing temperature. The changes in volume and lattice constants with increasing temperature are depicted in Figure 1;

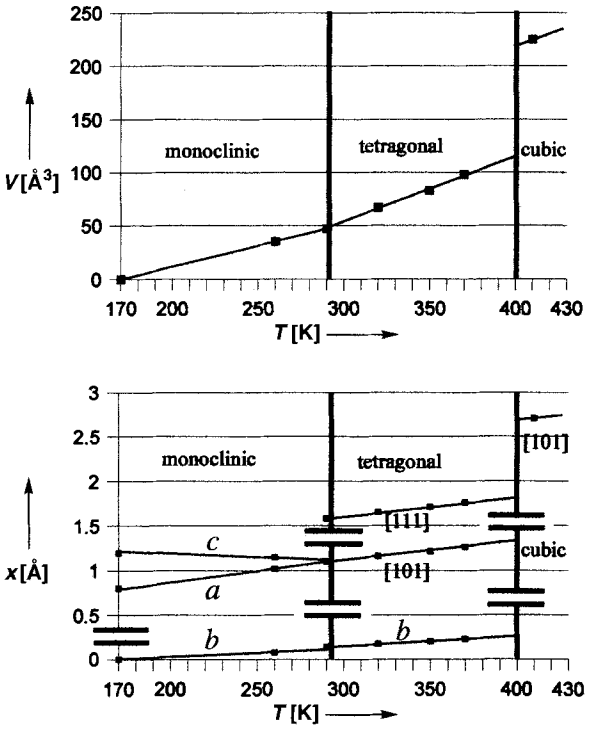

Fig. 1. Change in volume V (top) and lattice constants x (bottom) of crystalline **1** with increasing temperature.

the corresponding space groups and crystal dimensions are listed in Table 1. Whereas the changes in the lattice parameters are only small for the transition from the monoclinic phase to the tetragonal phase (for which a small amount of heat absorption ($\Delta H = +0.45\ \mathrm{kJ\,mol^{-1}}$) was determined by differential scanning calorimetry (DSC) measurements), they are rapid and conspicuous in the second phase transition (tetragonal to cubic), which is accompanied by a considerably higher heat loss

Table 1. Solid-state phases of **1**.

< 293 K (20 °C)
monoclinic crystal system
space group: $P2_1/n$
$a = 16.84(2)$, $b = 13.04(2)$, $c = 17.24(2)$ Å, $\beta = 101.22(8)°$, $V = 3714$ Å^3, $Z = 4$ (183 K)
point symmetry of the molecule: $C_1(1)$
> 293 K (20 °C) to < 405 K (132 °C)
tetragonal crystal system
space group: $P4_2/nmc$
$a = b = 13.239(11)$, $c = 11.042(9)$ Å, $V = 1935$ Å^3, $Z = 2$ (318 K)
point symmetry of the molecule: $\bar{4}m2$ (D_{2d})
$\boldsymbol{a}_t = \boldsymbol{a}_m/2 - \boldsymbol{c}_m/2$; $\boldsymbol{b}_t = \boldsymbol{b}_m$; $\boldsymbol{c}_t = \boldsymbol{a}_m/2 + \boldsymbol{c}_m/2$ [a]
> 405 K (132 °C)
cubic crystal system
fcc (F43*m* or *Fm*3*m*), "plastic phase"
$a = b = c = 16.087(8)$ Å, $V = 4163(1)$ Å^3, $Z = 4$ (415 K)
point symmetry of the molecule: $\bar{4}3m$ (T_d) or $4/m\,\bar{3}2/m$ (O_h)
$[111]_t \approx [110]_k$; shear of the (110) planes in the tetragonal phase to about [0.25 0.25 0]

[a] Subscripted letters: m = monoclinic, t = tetragonal, c = cubic.

($\Delta H = -3.06\ \mathrm{kJ\,mol^{-1}}$). X-ray structure analyses were carried out on single crystals for both the monoclinic and tetragonal phases, but it was only possible to determine the cubic phase by means of powder methods (heatable Guinier camera).[6] The latter phase only leads to few diffraction lines, the intensities of which drastically decrease with increasing diffraction angle, just as is known for *plastic phases*.[7, 8] The phase transitions are reversible; the results of differential thermoanalysis (DTA) studies and temperature-dependent Guinier photographs indicate a small amount of hysteresis.

The results of the X-ray structure analyses are shown as ORTEP diagrams in Figures 2 and 3. In the monoclinic phase

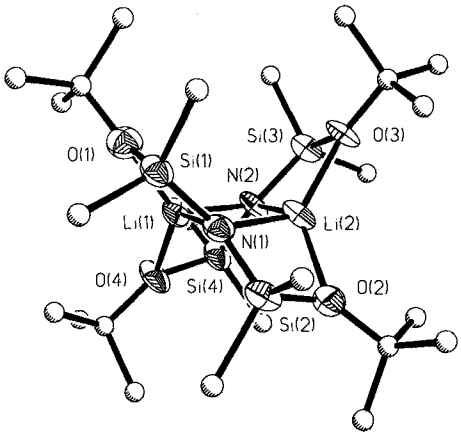

Fig. 2. Structure of **1** in the crystal; low-temperature monoclinic phase [6]. Non-designated atoms are carbon atoms. Selected bond lengths [Å]: Si1-N1 1.670(7), Si1-O1 1.676(6), Si2-N1 1.661(7), Si2-O2 1.676(6), Si3-N2 1.679(6), Si3-O3 1.674(5), Si4-N2 1.667(6), Si4-O4 1.673(6), Li1-O1 1.979(12), Li1-N1 2.067(13), Li1-N2 2.079(13), Li1-O4 1.990(11), Li2-N1 2.077(13), Li2-N2 2.090(13), Li2-O2 1.977(13), Li2-O3 2.000(12).

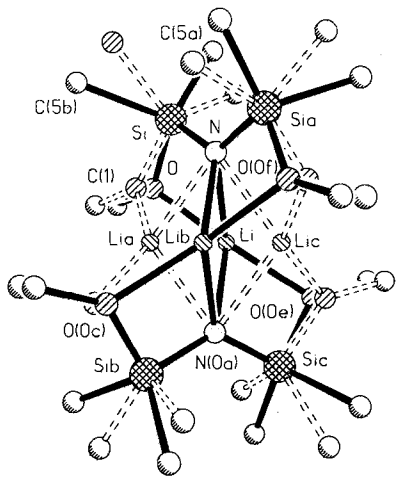

Fig. 3. Atomic split positions in the tetragonal phase of **1**. The partial structure shown with full lines is almost identical to the structure in Figure 2; however, the viewing direction is orthogonal to that in Figure 2.

all atoms occupy an unequivocal position and a typical molecular structure is obtained. The two lithium atoms are each bonded to both alkoxysilazyl ligands, which results in the formation of a central four-membered Li_2N_2 ring. Apart from the two nitrogen atoms, the lithium atoms are each additionally coordinated to the oxygen atoms of the alkoxy groups and thus attain a coordination number (CN) of four. Both *t*BuO–Si(Me)$_2$–N–Si(Me)$_2$–O*t*Bu ligands are largely planar and arranged in such

 © VCH Verlagsgesellschaft mbH, D-69451 Weinheim, 1996 0570-0833/96/3513-1530 $ 15.00+.25/0

a fashion that they almost fulfill an $S_4(\bar{4})$ symmetry operation. Four N_2O_2 coordination polyhedra of almost equal size are thus formed (cf. Fig. 3), of which two are occupied by lithium atoms.

Structure determinations were carried out on the tetragonal phase at three different temperatures (22, 45, and 80 °C; Fig. 3 and the details given in the literature[6] relate to 45 °C). The changes observed in the displacement parameters, and alternative model calculations indicate that the crystal structure is to be interpreted as a superposition of different atomic positions and is not the result of the formation of a twin crystal. It can be deduced from the solid-state NMR spectra (see below) that the cause of the split atomic positions is a special dynamic process in the molecular crystal that becomes more intense after the monoclinic/tetragonal phase transition. The lithium atoms have the largest extreme values for split positions, which give an electron density of Li/2 in the centers of the four N_2O_2 coordination polyhedra described previously. The formal point symmetry of the molecule increases for the monoclinic/tetragonal phase transition from C_1 (one of the three pseudo C_2 axes runs through both nitrogen atoms) to D_{2d} ($\bar{4}2m$). The tetragonal space group of **1**, $P4_2/nmc$, is a higher class (but not a maximum[9]) in the symmetry tree of the monoclinic space group $P2_1/n$, the volume of which is twice as large.

On the transition to the high-temperature phase (that is from tetragonal to cubic) the point symmetry of the molecule **1** increases once more and achieves, depending on the choice of space group, O_h ($m3m$) or T_d ($\bar{4}3m$) symmetry. The amount of exothermic heat energy measured in the DSC experiment is consistent both in size and in sign with an anticipated melting process, which is what the plastic phase represents. The molecules of **1** thus undergo oscillations about their cubic close-packed centers of gravity in the high-temperature phase, which leads to the formation of threefold and fourfold crystallographic axes that are not present in the molecule.

The cause of the phase transition from tetragonal to cubic is thus of a dynamic nature. We have therefore also interpreted the positional disorder in the tetragonal phase as being a direct result of molecular movement. This assumption was in fact confirmed by powder solid-state ^{6}Li, ^{7}Li, ^{13}C, and ^{29}Si MAS NMR (MAS = magic angle spinning) and broad-line NMR spectra, which were recorded at the same temperature intervals as the X-ray experiments.[5, 10] All spectra are consistent with one another and confirm the crystallographically found phase transitions as well as the movements. This is exemplified in the following with the aid of selected spectra.

^{13}C CP/MAS NMR spectra (CP = cross polarization) of **1** were recorded over and above both of the phase transitions (Fig. 4). In the low-temperature monoclinic phase the ^{13}C CP/MAS NMR spectra of **1** has eight signals from methyl groups for the four $SiMe_2$ groups, corresponding to the number expected for the lower molecule symmetry (crystallographically: C_1, pseudo D_2); three of these could not be resolved and are superimposed. The methyl groups of the four crystallographically different *tert*-butyl groups were only split into two signals, whereas the quaternary carbon atoms only gave a single signal corresponding to the low resolution of the chemical shift. At the phase transition monoclinic/tetragonal the group of signals for the eight $SiMe_2$ groups merges to give a singlet. The two signals from the *tert*-butyl groups also degenerate to give a single resonance. The increase in symmetry indicates a reinforced ligand dynamism in the tetragonal phase. The line widths of the *tert*-butyl groups and the $SiMe_2$ group signals increase with increasing temperature and at 343 K the signal from the quaternary carbon atom disappears.[10–12] The attainment of the plastic phase is indicated by the development of new sharp signals in the spectrum at 403 K, the positions of which are different from those in the tetragonal phase. This is in agreement with the crystallographic observation that a completely new lattice build-up is found (immediate surroundings of a particular molecule: tetragonal, CN = 10; cubic, CN = 12).

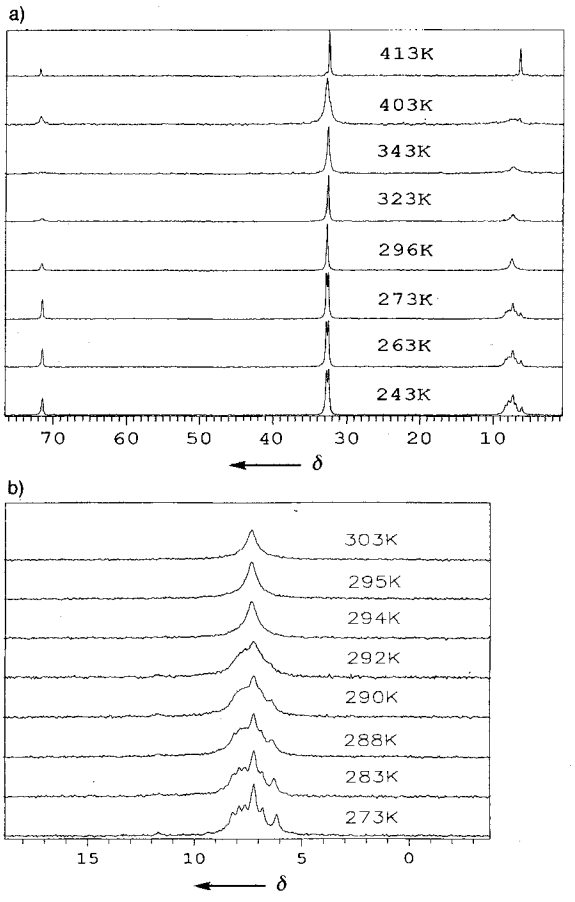

Fig. 4. a) ^{13}C CP/MAS NMR spectra of **1** in the temperature range from 243 K to 413 K. b) The monoclinic/tetragonal phase transition based on the signals of the $SiMe_2$ groups (expanded). Note the abrupt change between 292 and 294 K!

Parallel to the ^{13}C CP/MAS NMR spectra, the temperature-dependent ^{6}Li and ^{7}Li solid-state NMR spectra of **1** show significant changes at the monoclinic/tetragonal phase transition (Fig. 5a). In the low-temperature monoclinic phase, the ^{7}Li MAS NMR spectrum shows the typical line shape resulting from first-order quadrupolar splitting. Comparison with simulated spectra leads to an estimated quadrupolar coupling constant of 100 ± 2 kHz and an asymmetry parameter η of 0.4.[13] The transition to the tetragonal phase is coupled with an immediate disappearance of the rotational side bands of the satellite transitions; only the central line is still observed. The typical line shape with first-order quadrupolar splitting is first registered again at a temperature of about 373 K with the reappearance of the rotational side bands. The distribution of side bands of the satellite transitions at 383 K indicates a quadrupolar coupling constant of 88 ± 2 kHz with an asymmetry parameter $\eta = 0.1$,[13] that is close to cylindrical symmetry.

In agreement with this, the temperature-dependent ^{6}Li CP/MAS NMR spectra of **1**—isotopically enriched to 95 % ^{6}Li—follow an analogous course (Fig. 5b). In the ^{6}Li MAS NMR experiment the line shape also changes considerably and (as in the case of the ^{7}Li MAS NMR experiment) an area with homogeneous line broadening is encountered with corresponding reduced efficiency of the MAS NMR experiment;[14] this is an

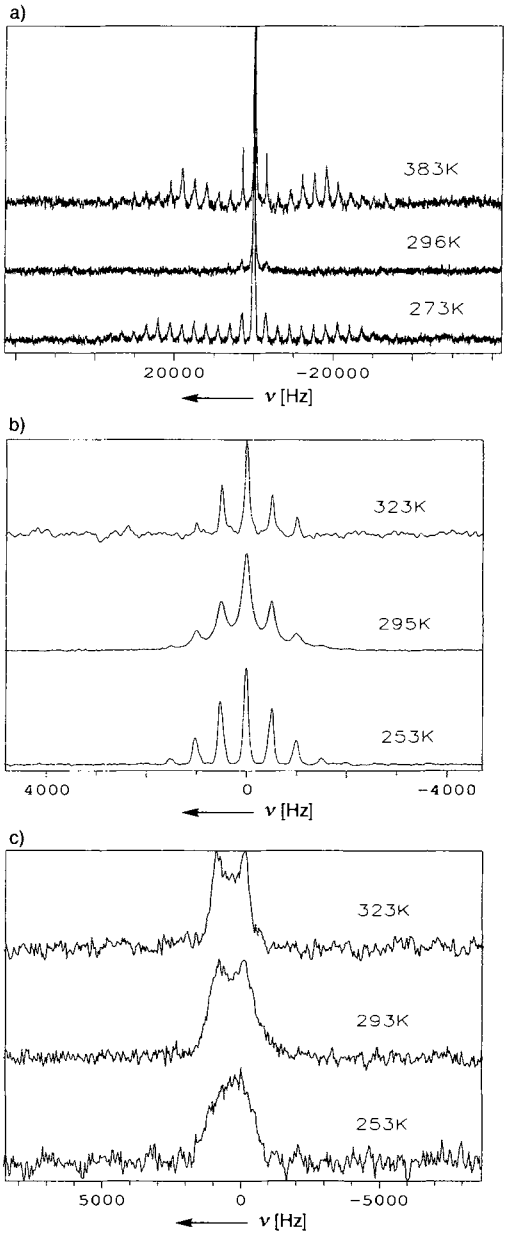

Fig. 5. a) ^{7}Li SPE/MAS NMR spectra (3 kHz) of the monoclinic (273 K) and tetragonal (296, 383 K) phases. b) ^{6}Li CP/MAS NMR spectra (500 Hz) of **1** in the region of the monoclinic/tetragonal phase transition. c) The corresponding ^{6}Li broad line NMR spectra over the same temperature interval.

unequivocal confirmation of dynamic exchange. The simulation of the line shape of the static ^{6}Li broad line NMR spectrum (Fig. 5c) at 323 K in the tetragonal phase suggests a quadrupolar coupling constant of 1.5 kHz and an asymmetry parameter η of 0.1. An effective quadrupolar coupling constant of 87 kHz has thus been calculated for ^{7}Li at 323 K from the ratio of the quadrupolar moments of ^{6}Li and ^{7}Li.[15, 16] This value agrees well with the value of 88 kHz found in the ^{7}Li MAS NMR experiment at 383 K, and thus confirms that the change in the quadrupolar interaction is primarily dependent on the phase transition and not on the temperature. The transition to the high-temperature plastic phase is indicated by the appearance of a sharp peak on the central line of the ^{7}Li solid-state NMR signal, the intensity of which increases with increasing temperature and is activated before the phase transition actually occurs.

The results of our experiments can be summarized as follows. Stronger vibrations of the molecular framework in **1** are stimulated by increases in temperature. The higher amplitudes of the vibrations of the framework atoms are carried over to the two lithium atoms from the tetragonal phase onward. The lithium atoms vibrate out of their distorted tetrahedral N_2O_2 potential minima and, for electrostatic reasons, fall cooperatively into the neighboring potential minima. An alternative movement of the entire molecule around one of the C_2 axes can be excluded on the basis of the data from the X-ray structure analysis. One enantiomer thus changes into its mirror image (in the low-temperature monoclinic phase both enantiomers are present and coupled with one another through inversion centers). Investigations are currently being carried out into how far these movements of the lithium atoms occur chaotically on an intermolecular basis. However, the intramolecular orbital movements of the lithium atoms are coupled to a phase transition, and the positions of the center of gravity of the molecules change only negligibly (Table 1). At very high temperatures the framework vibrations are so large that the molecules then start to slide past one another (a new stacking arrangement of the molecules takes place, Table 1) until more room is available for movement. The molecules begin to sway around their centers of gravity in a disordered fashion and a new plastic phase is formed.

Received: July 21, 1995
Revised version: February 1, 1996 [Z8232IE]
German version: *Angew. Chem.* **1996**, *108*, 1647–1651

Keywords: amides · lithium compounds · NMR spectroscopy · solid-state structures

[1] M. Veith, M. Zimmer, S. Müller-Becker, *Angew. Chem.* **1993**, *105*, 1771; *Angew. Chem. Int. Ed. Engl.* **1993**, *32*, 1731.
[2] F. Maseras, A. Lledos, *J. Chem. Soc. Chem. Commun.* **1995**, 443.
[3] M. Veith, S. Müller-Becker, A. Lengert, N. Engel in *Organosilicon Chemistry* (Eds.: N. Auner, J. Weis), VCH, Weinheim, **1993**.
[4] M. Veith, J. Böhnlein-Maus, A. Lengert, unpublished results.
[5] Synthesis of **1**: Lithium amide (0.04 g, 1.74 mmol) was placed in toluene (10 mL) and $[Me_2Si(OtBu)_2]_2NH$ (0.4 g, 1.44 mmol) was added. The mixture was heated under reflux for 2 h. After filtration to separate excess lithium amide the solvent was removed under reduced pressure. Purification was carried out by recrystallization from toluene to yield 0.33 g (81 %) **1** (colorless, m.p. 240 °C, decomp.). Chemical shifts of **1** in solution (200 MHz [D$_6$] benzene, 296 K, TMS): ^{1}H NMR: $\delta = 0.35$ (s, 24H, $SiMe_2$), 1.31 (s, 36H, CMe_3). ^{13}C NMR: $\delta = 6.8$ (s, 8C, $SiMe_2$), 32.1 (s, 12C, CMe_3), 71.7 (s, 4C, CMe_3); ^{29}Si NMR: $\delta = -11.7$ (s, $SiMe_2$), chemical shifts in the solid state: ^{13}C NMR: (50.3 MHz, δ(TMS) = 0), monoclinic phase (273 K): $\delta = 6.2, 6.8, 7.2, 7.6, 7.9, 8.2$ ($SiMe_2$), 32.4, 32.7 (CMe_3), 71.4 (CMe_3); tetragonal phase (296 K): $\delta = 7.4$ (s, $SiMe_2$), 32.6 (s, CMe_3), 71.4 (s, CMe_3); plastic phase (413 K): $\delta = 6.4$ (s, $SiMe_2$), 32.5 (S, CMe_3), 71.9 (CMe_3); ^{29}Si NMR (39.7 MHz, δ(TMS) = 0); monoclinic phase (273 K): $\delta = -11.3, -11.9, -12.5$ ($SiMe_2$); tetragonal phase (296 K): $\delta = -11.4, -12.1$ (2:1 doublet, quadrupolar splitting = 28 Hz); ^{6}Li NMR (29.4 MHz, δ(ext. LiCl) = 0, 296 K): $\delta = 1.7$ (isotropic shift from MAS (3 kHz) experiment); ^{7}Li NMR: 77.7 MHz, ext. LiCl, 296 K: $\delta = 0.8$ (central line).
[6] Crystal data of the phases of **1** (cf. Table 1). Monoclinic phase: Siemens AED2 diffractometer, ω-θ scan, 3390 reflections of which 820 with $I_o < 2\sigma(I)$; measurement temperature 173 K, structure solved by using direct methods, 325 parameters (all non-hydrogen atoms with anisotropic temperature factors). $R_1 = 0.082$. Maximum and minimum residual electron densities: 0.518 and -0.395 e Å^{-3}, respectively. Tetragonal phase: Measurement conditions as above, measurement temperature: 318 K, 810 independent reflections of which 230 with $I_o < 2\sigma(I)$; structure solved by using direct methods; 78 parameters (all non-hydrogen atoms with anisotropic temperature factors). $R_1 = 0.080$. Maximum and minimum residual electron densities: 0.157 and -0.282 e Å^{-3}, respectively. Programs used: SHELXS-86, SHELXL-93, and SCHAKAL. Further details of the crystal structure investigation may be obtained from the Fachinformationszentrum Karlsruhe, D-76344 Eggenstein-Leopoldshafen (Germany) on quoting the depository number CSD-405028 (monoclinic), 405029 (tetragonal)..
[7] W. J. Dunning, *J. Phys. Chem. Solids* **1961**, *18*, 21.
[8] G. W. Gray, P. A. Winsor, *Liquid Crystals and Plastic Crystals, Vol. 1*, E. Horwood, Chichester, England, **1974**, p. 48.

[9] Symmetry tree and group-subgroup relationships:
$P4_2/nmc \xrightarrow{t2} (Pmmn) \xrightarrow{t2} (P2_1/m) \xrightarrow{k2} P2_1/n\ (a' = a + c;\ b' = c - a)$.

[10] The ^{13}C CP/MAS NMR spectra were recorded at a sample rotation speed of 3 kHz and a contact time of 1 ms. The measurements at higher temperatures (above 50 °C) were carried out by in a single pulse excitation (SPE) experiment. The B_1 field strength of the proton decoupler was varied between 41 and 83 kHz to confirm the line width decoupling strength relationship [11,12]. The best resolution in the ^{29}Si CP/MAS NMR spectra was obtained for the sample enriched to 95 % with the ^6Li isotope. In order to confirm the quadrupolar splitting by ^{14}N [17], the ^{29}Si CP/MAS NMR spectrum was additionally recorded at a field strength of 9.45 T (79.4 MHz). The ^7Li MAS NMR spectra were recorded by using the SPE experiment. In order to avoid saturation, recycle delays of 30 s were used. All ^6Li NMR spectra of the 95 % isotopically enriched compound were recorded by using the cross-polarization method with contact times of 5 to 10 ms. All measurements were performed by using dipolar ^1H decoupling and carried out on a Bruker MSL 200 S spectrometer equipped with a B-VT 2000 temperature control unit. Air-tight Kel-F inserts which fit into 7 mm MAS rotors were used for the preparation of the samples. See ref. [5] for the solid-state NMR data.

[11] W. P. Rothwell, J. S. Waugh, *J. Chem. Phys.* **1981**, *74*, 2721.

[12] J. Kümmerlen, A. Sebald, *Magn. Reson. Chem.* **1994**, *32*, 173.

[13] D. Massiot, H. Thiele, A. Germanus, NMR simulation program WIN-FIT, Bruker-Franzen Analytik, Bremen, **1995**.

[14] J. H. Kristensen, H. Bildsoe, H. J. Jakobsen, N. C. Nielsen, *J. Magn. Reson.* **1992**, *100*, 437.

[15] J. Mason, *Multinuclear NMR*, Plenum Press, New York, **1987**.

[16] T. Pietrass, P. K. Burkert, *Magn. Reson. Chem.* **1993**, *31*, 709.

[17] R. K. Harris, A. C. Olivieri, *Prog. Nucl. Magn. Reson. Spectrosc.* **1992**, *24*, 435.

New Family of Enantiomerically Pure Liquid Crystals Containing a Chiral Biphenyl Core

Guy Solladié,* Philippe Hugelé, Richard Bartsch, and Antoine Skoulios

Many applications of liquid crystals (LC) require chiral and optically active materials. Large-pitch cholesterics obtained by doping nematics with chiral and enantiomerically pure molecules give better response in displays, as shown by Schadt and Helfrich.[1] It is also well known that ferroelectric properties of smectic LC are only observed with chiral mesogenic molecules.[2]

Biphenyls without substituents in the *ortho* position have been used as nematic phases in a huge variety of applications. Most of the time the chirality was obtained by incorporating an asymmetric carbon in a chain linked to the core of the mesomorphic molecule.[2] Although a 2,2',6,6'-tetrachlorobiphenyl derivative in its racemic form was shown to be nonmesomorphic, tetra-*ortho*-substituted biphenyls with axial chirality were found to form cholesteric liquid crystals when they are enantiomerically pure.

For the past several years we have been interested in chirality in liquid crystals.[3] We reported on enantiomerically pure 1-biphenylyl-2-cyclohexylidenethanone derivatives, the first examples of LC with axial chirality in the core of the mesogenic molecules.[4] In that case the presence of a biphenyl substituent was necessary to induce mesomorphic properties, and therefore these compounds can be considered as biphenyl derivatives having axial chirality in the chain. Later on we showed[5a] that racemic substituted *trans*-stilbene epoxides, in which the two aryl groups are in a rigid, nonplanar, and slightly twisted conformation, have mesogenic properties. Recently new examples of this family were reported.[5b] We describe here a new family of enantiomerically pure LC of type **A** and show that molecules containing a rigid twisted biphenyl core with axial chirality can form cholesteric mesophases.

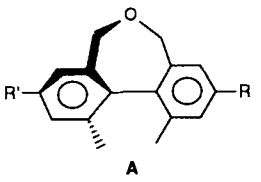

A

The synthesis of the optically active targets (+)-(*R*)-**6** and (−)-(*R*)-**8** started from the chiral dihydrooxazole (+)-(*S*)-**1**, which was dimerized by means of an Ullmann reaction to give a mixture of the two diastereomeric biphenyl derivatives (−)-(*R,S,S*)-**2** and (+)-(*S,S,S*)-**3**, which

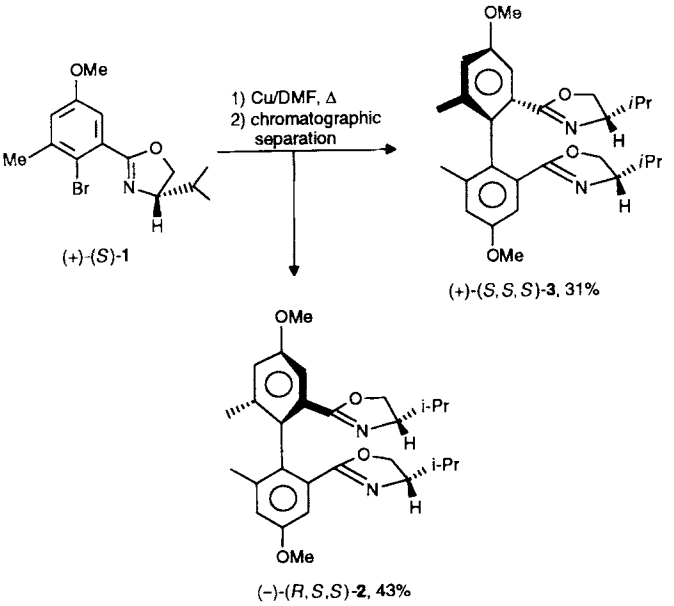

were easily separated by silica gel chromatography. This is the first report of the optical resolution of a biphenyl compound through diastereomeric dihydrooxazole derivatives. The absolute configuration of the biphenyl moiety was established by chemical correlation of (−)-(*R,S,S*)-**2** with the known phenol (+)-(*R*)-**9**[6] (Py = pyridine, DMSO = dimethyl sulfoxide, *m*CPBA = *m*-chloroperbenzoic acid). Comparison of the optical rotation of the sample of (+)-(*R*)-**9** obtained from (−)-(*R,S,S*)-**2** with the literature value[6] attests to the high enantiomeric purity of our synthetic sample.

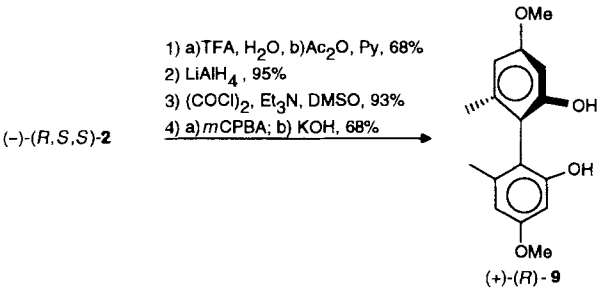

[*] Prof. Dr. G. Solladié, P. Hugelé, Dr. R. Bartsch
Université Louis Pasteur, ECPM
1 rue Blaise Pascal, F-67008 Strasbourg (France)
Fax: Int. code +88 61 65 31
e-mail: Solladie@chimie.u-strasbg.fr
Dr. A. Skoulios
GMO, IPCMS, Strasbourg (France)

The oxepine (−)-(*R*)-**5** was obtained in a few steps from (−)-(*R*,*S*,*S*)-**2**. Opening of the dihydrooxazole rings with trifluoroacetic acid (TFA) to give the corresponding amino esters followed by acetylation of the amino groups, saponification of the esters with *t*BuOK, and hydrolysis of the methoxy groups with BBr_3 furnished the dicarboxylic acid (−)-(*R*)-**4** (m.p. 228 °C; $[\alpha]_D = -20$ ($c = 2$ in ethanol)). Protection of the hydroxyl groups of the phenols with *tert*-butyldimethylsilyl groups, reduction of the carboxyl groups with BH_3·THF (70% yield), and cyclization with triflic anhydride gave the oxepine (−)-(*R*)-**5**. Finally after the silyl groups were removed with tetrabutylammonium fluoride (TBAF), esterification with 4-(octyloxy)-benzoyl chloride afforded the mesogenic chiral biphenyl target (+)-(*R*)-**6**. The enantiomeric purity of the sample was checked by recording its ^{1}H NMR spectrum in presence of tris[3-(trifluoromethylhydroxymethylene)-*d*-camphorato]praseodimium.

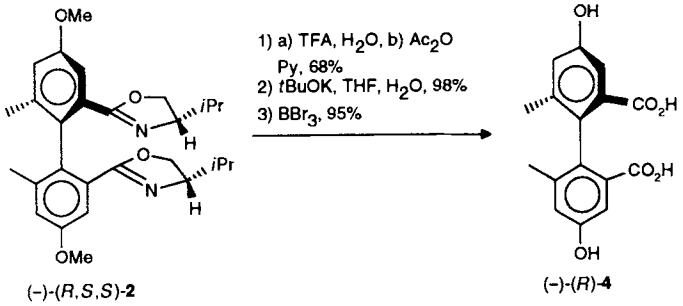

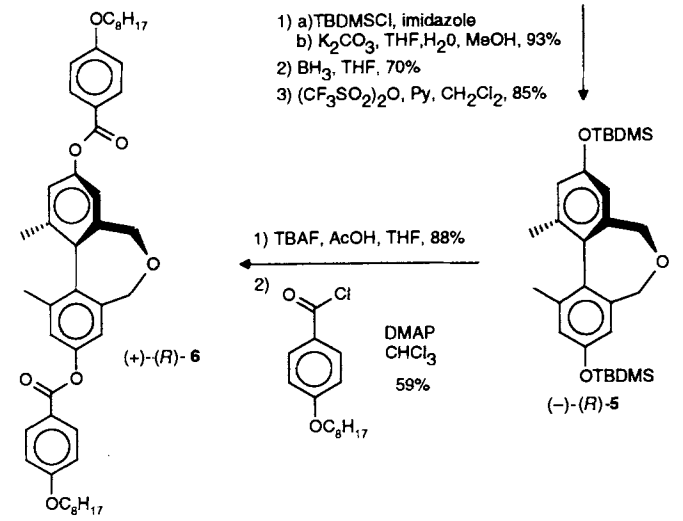

The second mesogenic compound, (−)-(*R*)-**8**, was obtained by deprotecting one phenol group of (−)-(*R*)-**5** and esterifying with 4-(octyloxy)benzoyl chloride to get (−)-(*R*)-**7** (m.p. 76 °C; $[\alpha]_D = 14.8$ ($c = 2$ in acetone). The remaining silyl protecting group in (−)-(R)-**7** was removed by treatment with TBAF, and subsequent etherification 4-(octyloxy)benzyl iodide afforded (−)-(*R*)-**8** (Scheme 1). The configurational stability of compounds **6** and **8** is very high; racemization was not observed at temperatures below 110 °C (determined by the absence of coalescence of the AB systems of the OCH_2 protons).

The liquid crystal behavior of molecules **6** and **8** was briefly investigated by differential scanning calorimetry, polarizing microscopy, and X-ray diffraction. Both molecules were found to produce a cholesteric phase as expected (fluidity; fine schlieren texture; presence of a broad cybotactic ring instead of sharp

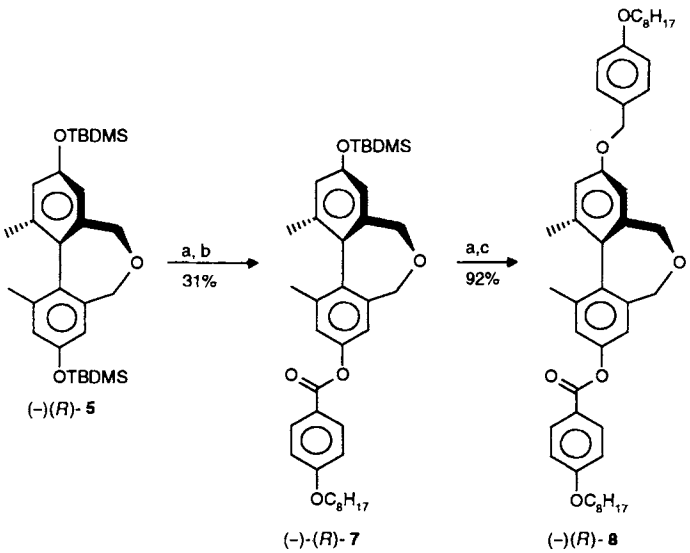

Scheme 1. a) TBAF, AcOH, THF; b) 4-$C_8H_{17}OC_6H_4COCl$, DMAP; c) 4-$C_8H_{17}OC_6H_4CH_2I$.

small-angle Bragg reflections). The phase transition is enantiotropic in nature for **6** (K 75 Ch 105 I) and monotropic for **8** (K (Ch 60) 78 I) (K = crystalline, Ch = cholesteric, I = isotropic). In both cases crystallization proved to be particularly slow, lasting many days when the melt was cooled to room temperature.

Molecular modeling of oxepine **6** (MOPAC software, CAChe work station from Oxford Molecular) showed a dihedral angle of 56° between the aryl rings of the biphenyl. This value is similar to the 57° found by UV analysis for 1,11-dimethyl-5,7-dihydrodibenz[*c*,*e*]oxepine.[7].

These results show for the first time that a rigid, nonplanar, and enantiomerically pure biphenyl derivative can display liquid crystal properties and that the axial chirality of the biphenyl moiety induces a cholesteric mesophase. This is in sharp contrast with the previous studies on racemic noncyclic 2,2′,6,6′-tetrachlorobiphenyl derivatives[8] (torsional angle close to 90°) and on an enantiomerically enriched oxepine[9] very similar to compound **6** with two *ortho*-nitro groups (torsional angle of 58°) in place of the two methyl groups; none of these compounds showed mesogenic properties. We are currently investigating new derivatives of these biphenyl oxepines which may form smectic phases.

Experimental Procedure

2 and **3**: A mixture of **1** (5 g, 16 mmol) and freshly activated copper (5 g) in 30 mL of freshly distilled DMF was heated at reflux for 3 h. After cooling, the mixture was diluted with CH_2Cl_2 and washed with aqueous ammonia until the copper was completely removed. The organic layer was washed with water, dried ($MgSO_4$), and concentrated to give a yellow oil, which was purified by flash chromatography (flow rate = 40 mL min^{-1}, ether/hexane 20/80) over pretreated silica gel. (400 g of silica gel was stirred overnight in 800 mL of ether/hexane (20/80) and 20 mL of Et_3N and the column was filled up with this solution under a small pressure.) 1.6 g (43%) of the atropisomer (−)-(*R*,*S*,*S*)-**2** ($R_f = 0.22$) and 1.1 g (31%) of (+)-(*S*,*S*,*S*)-**3** ($R_f = 0.32$) were obtained.

(−)-(*R*,*S*,*S*)-**2**: ^{1}H NMR (200 MHz, $CDCl_3$): $\delta = 7.14$ (d, $J = 3$ Hz, 2H), 6.86 (d, $J = 3$ Hz, 2H), 4.05–3.6 (m, 6H), 3.84 (s, 6H), 1.54 (oct., $J = 7$ Hz, 2H), 0.74 (d, $J = 7$ Hz, 6H), 0.70 (d, $J = 7$ Hz, 6H); ^{13}C NMR (50 MHz, $CDCl_3$): $\delta = 164.2$, 158.1, 139.4, 132.1, 129.3, 118.0, 110.9, 72.5, 70.0, 55.4, 32.6, 20.6, 18.7, 18.1; $[\alpha]_D = -119.5$ ($c = 1.4$ in ethanol).

(+)-(*S*,*S*,*S*)-**3**: ^{1}H NMR (200 MHz, $CDCl_3$): $\delta = 7.23$ (d, $J = 3$ Hz, 2H), 6.86 (d, $J = 3$ Hz, 2H), 4.02–3.66 (m, 6H), 3.85 (s, 6H), 1.90 (s, 6H), 1.64–1.54 (s, $J = 7$ Hz, 2H), 0.82 (d, $J = 7$ Hz, 6H), 0.75 (d, $J = 7$ Hz, 6H); ^{13}C NMR (50 MHz, $CDCl_3$): $\delta = 164.1$, 157.9, 138.9, 132.5, 129.2, 118.2, 111.1, 72.4, 70.0, 55.3, 32.8,

 © VCH Verlagsgesellschaft mbH, D-69451 Weinheim, 1996 0570-0833/96/3513-1534 $ 15.00+.25/0

20.5, 18.8, 18.2; $[\alpha]_D = +29.5$ ($c = 1.4$ in ethanol). Anal. calcd for $C_{28}H_{36}O_4N_2$: C 72.43, H 7.7, N 6.0; found: C 72.45, H 7.66, N 5.88.

(−)-(*R*)-**5**: M.p. 96 °C, $[\alpha]_D = -15$ ($c = 1.9$ in acetone); ^{1}H NMR (200 MHz, $CDCl_3$): $\delta = 6.79$ (d, $J = 2$ Hz, 2H), 6.70 (d, $J = 2$ Hz, 2H), 4.14 (AB, 4H, $J_{AB} = 11$ Hz, $\Delta\nu = 62$ Hz), 2.14 (s, 6H), 1.01 (s, 18H), 0.24 (d, 12H); ^{13}C NMR (50 MHz, $CDCl_3$): $\delta = 154.8$, 137.4, 136.5, 131.7, 121.6, 118.1, 67.7, 25.8, 20.0, −4.2. Anal. calcd for $C_{28}H_{44}O_3$: C 69.30, H 9.00; found: C 69.27, H 9.02.

(+)-(*R*)-**6**: $[\alpha]_D = +24$ ($c = 1.6$ in acetone); ^{1}H NMR (200 MHz, $CDCl_3$): $\delta = 8.16$ (d, $J = 9$ Hz, 4H), 7.21 (d, $J = 2$ Hz, 2H), 7.12 (d, $J = 2$ Hz, 2H), 6.99 (d, $J = 9$ Hz, 4H), 4.24 (AB, 4H, $J = 11$ Hz, $\Delta\nu = 67$ Hz), 4.05 (t, $J = 7$ Hz, 4H), 2.27 (s, 6H), 1.84 (m, 4H), 1.56–1.21 (m, 20H), 0.90 (t, 6H); ^{13}C NMR (50 MHz, $CDCl_3$): $\delta = 164.9$, 163.6, 150.5, 137.7, 136.5, 135.4, 132.3, 123.5, 121.5, 120.0, 114.4, 68.4, 67.3, 31.8, 29.3, 29.2, 29.1, 26.0, 22.7, 20.0, 14.1. Anal. calcd for $C_{46}H_{56}O_7$: C 76.64, H 7.77; found: C 76.44, H 7.98.

(−)-(*R*)-**8**: $[\alpha]_D = -9.8$ ($c = 2$ in acetone); ^{1}H NMR (200 MHz, $CDCl_3$): $\delta = 8.15$ (d, $J = 9$ Hz, 2H), 7.37 (d, $J = 9$ Hz, 2H), 7.25 (d, $J = 3$ Hz, 1H), 7.18 (d, $J = 2$ Hz, 1H), 7.09 (d, $J = 2$ Hz, 1H), 6.98 (d, $J = 9$ Hz, 2H), 6.93 (d, $J = 9$ Hz, 2H), 6.88 (d, $J = 3$ Hz, 1H), 5.03 (s, 2H), 4.23 (AB, 2H, $J_{AB} = 11$ Hz, $\Delta\nu = 70$ Hz), 4.21 (AB, 2H, $J_{AB} = 11$ Hz, $\Delta\nu = 62$ Hz), 4.05 (t, $J = 6$ Hz, 2H), 3.97 (t, $J = 7$ Hz, 2H), 2.24 (s, 3H), 2.21 (s, 3H), 1.82 (m, 4H), 1.27 (m, 20H), 0.87 (m, 6H); ^{13}C NMR (50 MHz, $CDCl_3$): $\delta = 163.7$, 159.2, 158.6, 150.2, 137.7, 136.6, 136.5, 136.1, 132.4, 130.6, 129.4, 128.8, 123.4, 121.6, 119.9, 116.7, 114.7, 114.4, 112.9, 70.0, 68.4, 68.2, 67.8, 67.5, 31.9, 29.43, 29.35, 29.2, 26.2, 22.8, 20.2, 20.0, 14.2. Anal. calcd. for $C_{48}H_{58}O_6$: C 78.15, H 8.20; found: C 78.31, H 8.46.

Received: January 15, 1996 [Z 8720 IE]
German version: *Angew. Chem.* **1996**, *106*, 1640–1642

Keywords: biphenyls · chirality · liquid crystals

[1] M. Schadt, W. Helfrich, *Appl. Phys. Lett.* **1971**, *18*, 127.
[2] J. W. Goodby, I. Nishiyama, A. J. Stanley, C. J. Booth, W. J. Toyne, *Liq. Cryst.* **1993**, *14*, 37.
[3] G. Solladié, R. G. Zimmermann, *Angew. Chem.* **1984**, *96*, 335; *Angew. Chem. Int. Ed. Engl.* **1984**, *23*, 348.
[4] a) G. Solladié, R. G. Zimmermann, *Angew. Chem.* **1985**, *97*, 70; *Angew. Chem. Int. Ed. Engl.* **1985**, *24*, 64; b) G. Solladié, *J. Org. Chem.* **1985**, *50*, 4062.
[5] a) G. Solladié, R. Bartsch, R. G. Zimmermann, G. Gottarelli, *Israel J. Chem.* **1985**, *25*, 51; b) B. F. Bonini, G. Gottarelli, S. Masiero, G. P. Spada, P. Mariani, B. Yang, *Liq. Cryst.* **1993**, *13*, 13.
[6] a) H. Musso, W. Steckelberg, *Chem. Ber.* **1968**, *101*, 1510; H. Hess, H. Musso, *Liebigs Ann. Chem.* **1979**, 431.
[7] M. Oki, H. Iwamura, N. Hayakawa, *Bull. Chem. Soc. Jpn.* **1964**, *37*, 1865.
[8] D. J. Byron, G. W. Gray, B. M. Worrall, *J. Chem. Soc.* **1965**, 3706.
[9] K. Yang, R. P. Lemieux, *Mol. Cryst. Liq. Cryst.* **1995**, *260*, 247.

An Electroactive Photoisomerizable Monolayer-Electrode: A Command Surface for the Amperometric Transduction of Recorded Optical Signals**

Amihood Doron, Eugenii Katz, Moshe Portnoy, and Itamar Willner*

The development of molecular switching assemblies has attracted extensive research efforts recently, as they provide the basis for molecular electronic and optoelectronic devices.[1, 2] Optical,[3, 4] electrochemical,[5] thermal,[6] and pH[7] triggering signals have been used to activate switchable molecular functions. Electrochemical translocation of molecular components[5] in supramolecular complexes was reported as a mechanism for electroactivated molecular switches. Light-controlled association of ions to photoisomerizable molecular receptors[8] and activation of ion–transport systems[9] represents optical switching at the molecular level. Similarly, light-signaled formation or dissociation of donor–acceptor complexes (like the association of the *cis*-azobenzene 4,4′-bipyridinium salt to the eosin dye, which acts as electron donor) represents an optical molecular switch.[10]

The assembly of molecular switching devices requires the transduction of the molecular switching function by a secondary physical signal. This allows the application of the molecular switching assembly as a Read/Write memory device. Recently, photoisomerizable dithienylethene with two phenol substituents was used for the amperometric transduction of optical signals.[11] In this system one of the photoisomeric states revealed electroactivity that enabled the amperometric transduction of the optical signal and its storage. Similarly, photoisomerizable monolayers assembled on electrodes were applied as optical recording interfaces and command surfaces for electrochemical transduction of the optical signal.[12–14] Specific association (or dissociation) of redox proteins like cytochrome c,[13a] electrically "wired" enzymes like ferrocene-modified glucose oxidase,[13b] and antibodies[14] to the photoisomerizable monolayer electrodes enabled the electrochemical transduction of the optical signals recorded by the photoactive monolayer. Here we wish to report on the assembly of a photoisomerizable electroactive monolayer electrode that enables the amperometric transduction of the optical signals recorded at the monolayer electrode.

Phenoxynaphthacenequinone (**1a**) undergoes reversible photochemical isomerization between the "*trans*"-quinone (**1a**) isomeric state and the "*ana*"-isomer **1b**[15] [Eq. (a)]. Accordingly, 6-[4-(carboxymethyl)phenoxy]-5,12-naphthacenequinone (**2a**)

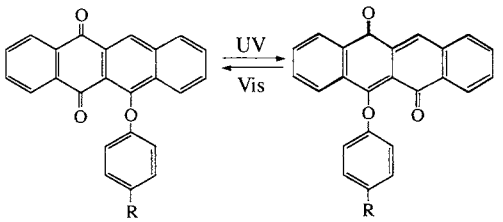

(a)

"*trans*" **1a, 2a** "*ana*" **1b, 2b**

1, R = H
2, R = CH_2CO_2H

was assembled as a monolayer on a gold electrode as outlined in Scheme 1. A cystamine monolayer was assembled on the gold electrode, and **2a** was coupled to this monolayer. Figure 1 (curve a) shows the cyclic voltammogram of the resulting monolayer-electrode. The ill-defined redox-wave is characteristic of a monolayer of the quinone that is not densely packed. Different orientations and configurations of the quinone components (relative to the electrode) in the flexible configuration of the monolayer result in different electron-transfer rates and the ill-defined electrochemical wave.[16] Treatment of the **2a**-modified monolayer electrode with 1-tetradecanethiol results in the association of the thiol to the pinhole defect sites on the electrode surface.[17] This yields a densely packed monolayer with a rigidified orientation of the quinone units in the monolayer assembly. Figure 1 (curve b) shows the cyclic voltammogram of

[*] Prof. I. Willner, A. Doron, Dr. E. Katz, Dr. M. Portnoy
Institute of Chemistry
and
Farkas Center for Light Induced Processes
The Hebrew University of Jerusalem
Jerusalem, 91904 (Israel)
Fax: Int. code +(2)6527715

[**] This research was supported by The Israel Academy of Science and Humanities.

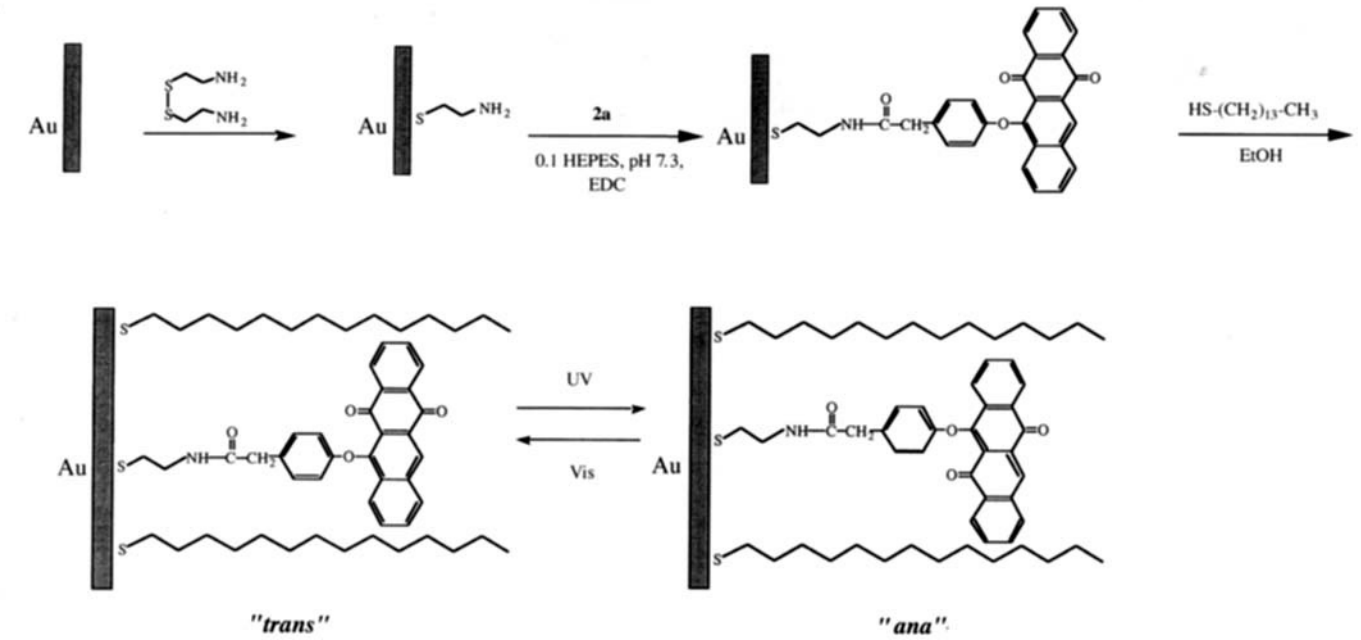

Scheme 1. Assembly of the photoisomerizable quinone **2a** on a gold electrode. EDC = 1-ethyl-3-(3-dimethylaminopropyl)carbodiimide; HEPES = *N*-[2-hydroxyethyl]piperazine-*N'*-[2-ethanesulfonic acid].

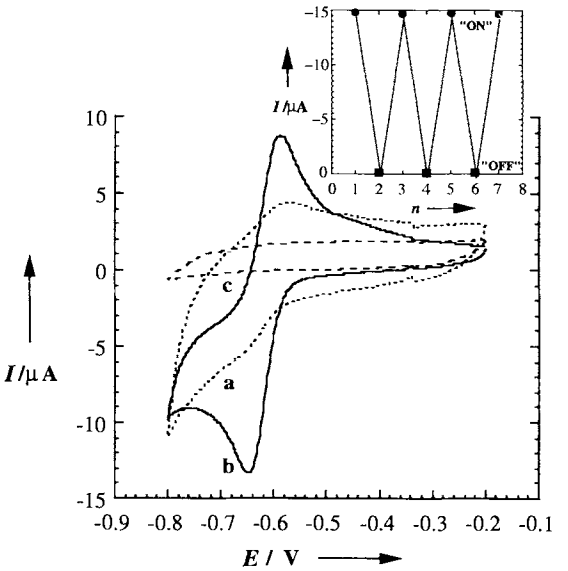

Fig. 1. Cyclic voltammograms of a) **2a**-modified monolayer Au-electrode, b) **2a**-monolayer electrode after treatment of the electrode with an ethanolic solution of $C_{14}H_{29}SH$ (5×10^{-3} M) for 30 min, c) **2b**-monolayer electrode obtained by photoisomerization of the **2a**-monolayer electrode treated with $C_{14}H_{29}SH$ (340 nm $< \lambda <$ 360 nm). All experiments were performed in 0.01 M phosphate buffer and 0.1 M Na_2SO_4, pH 7.0 under Ar, scan rate, 50 mV s^{-1}. Inset: Cyclic amperometric responses at $E = -650$ mV (vs. SCE) of the photoisomerizable monolayer electrode upon reversible optical switching of the monolayer between the *trans*-quinone state **2a** (●), and the *ana*-state **2b**, (■). The transformation of the monolayer-electrodes to the respective isomer states was accomplished by irradiation of the electrode with the appropriate light source for 1 min. n = number of cycles [20].

the **2a**-monolayer electrode after treatment with the long-chain thiol. The quinone is characterized by a well-defined, quasi reversible redox-wave ($E^\circ = -0.62$ V vs. SCE, pH = 7.0). Note that the capacity current of the **2a**-monolayer electrode after treatment with 1-tetradecanethiol is substantially lower than that of the primary **2a**-monolayer electrode, which implies that a densely packed assembly is formed after the treatment of the monolayer with the thiol. Coulometric analysis of the **2a**-monolayer redox wave yields a surface density of the quinone on the electrode surface of 2×10^{-10} mol cm^{-2}. The rate constant for electron transfer from the electrode to the quinone units in the densely packed monolayer configuration was calculated from Laviron's theory[18] to be $k_{et} = 2.5\ s^{-1}$. The *trans*-quinone compound (**1a**) is reduced in a dry dimethylsulfoxide (DMSO) solution at a bare Au electrode with 0.05 M tetrabutylammonium tetrafluoroborate as supporting electrolyte by two successive one-electron reduction processes ($E_1^\circ = -0.91$ and $E_2^\circ \approx -1.46$ V (vs. SCE). In water, **1a** yields an ill-defined redox-wave corresponding to a two-electron reduction process.

Irradiation of the **2a**-monolayer electrode (340 nm $< \lambda <$ 360 nm) in air results in isomerization of the monolayer to the *ana*-state (**2b**). Figure 1, curve (c), shows the cyclic voltammogram of the resulting **2b**-monolayer electrode. The electrode reveals only the background current of the electrolyte. Further illumination of the **2b**-monolayer electrode ($\lambda > 450$ nm) regenerates the **2a**-monolayer electrode, and the voltammetric wave of the *trans*-quinone electroactive monolayer is restored. By cyclic photoisomerization of the monolayer electrode between the *trans*-quinone state **2a** and the *ana*-quinone state **2b**, reversible amperometric transduction of the optical signal recorded by the monolayer-modified electrode is observed (Fig. 1, inset). It should be noted that the absorbance maxima of **2a** in dry dimethylsulfoxide are observed at $\lambda = 245$ and 398 nm, whereas the **2b** shows absorption maxima at $\lambda = 483$, 452, and 248 nm. The photochemical conversion of **2a** to **2b** in a DMSO solution is about 70%. The complete conversion of **2a** to **2b** in the monolayer assembly is attributed to the hydrophobic environment. The photoisomerization of **2a** to **2b** in hydrophobic solutions could not be followed due to limitations in solubility.

The cyclic voltammogram of the **2a**-monolayer electrode is pH-dependent (Fig. 2). As the pH of the electrolyte is increased,

 © VCH Verlagsgesellschaft mbH, D-69451 Weinheim, 1996 0570-0833/96/3513-1536 $ 15.00+.25/0

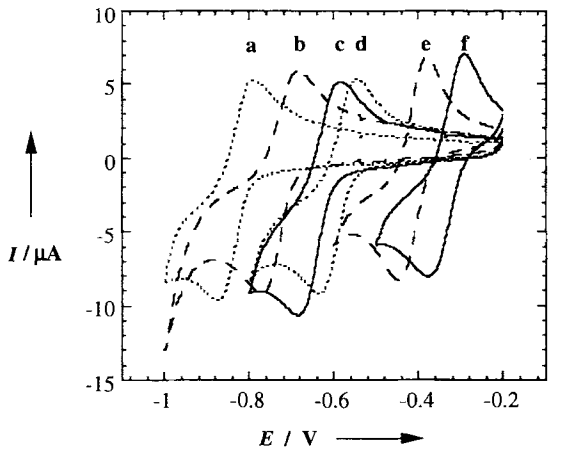

Fig. 2. Cyclic voltammograms of the **2a**-monolayer electrode at different pH values: a) 10.82, b) 8.93, c) 7.27, d) 6.48, e) 3.32, f) 1.93.

a negative shift in the redox potential of the quinone units is observed. The relationship between E° and pH is linear, and the slope of the line is 56 mV per pH unit. This indicates that the reduction of the *trans*-quinone unit involves two electrons and two protons. This pH dependence implies that the quinone units within the monolayer assembly are exposed to the aqueous phase.

We conclude that organization of a photoisomerizable phenoxynaphthacenequinone **2a**-monolayer electrode generates an active surface for optical recording.[19] Photoisomerization of the *ana*-state of the monolayer electrode to the *trans*-state enables the amperometric transduction of the recorded optical signal. Furthermore, reduction of the *trans*-quinone moiety to the hydroquinone form stores the optical signal and reoxidation of the monolayer to the *trans*-quinone state allows the reactivation of the optically recording interface.

Received: January 31, 1996 [Z 8773 IE]
German version: *Angew. Chem.* **1996**, *108*, 1626–1628

Keywords: electrochemistry · naphthocenequinones · optoelectronics · photoswitchable systems

[1] a) J.-M. Lehn, *Angew. Chem.* **1988**, *100*, 91; *Angew. Chem. Int. Ed. Engl.* **1988**, *27*, 90; b) J.-M. Lehn, *ibid.* **1990**, *102*, 1347; and **1990**, *29*, 1304; c) V. Goulle, A. Harriman, J.-M. Lehn, *J. Chem. Soc. Chem. Commun.* **1993**, 1034; d) S. L. Gilat, S. H. Kawai, J.-M. Lehn, *ibid.* **1993**, 1439.

[2] a) T. Iyoda, T. Saika, K. Honda, T. Shimidzu, *Tetrahedron Lett.* **1989**, *30*, 5429; b) J. Daub, J. Salbeck, T. Knöchel, C. Fischer, H. Kunkely, K. M. Rapp, *Angew. Chem.* **1989**, *101*, 1541; *Angew. Chem. Int. Ed. Engl.* **1989**, *28*, 1494; c) J. Daub, C. Fischer, J. Salbeck, K. Ulrich, *Adv. Mater.* **1990**, *3*, 366. d) B. L. Feringa, W. F. Jager, B. de Lange, *J. Am. Chem. Soc.* **1991**, *113*, 5468; e) J. Achatz, C. Fischer, J. Salbeck, J. Daub, *J. Chem. Soc. Chem. Commun.* **1991**, 504.

[3] a) I. Willner, M. Lion-Dagan, S. Marx-Tibbon, E. Katz, *J. Am. Chem. Soc.* **1995**, *117*, 6581; b) E. Katz, M. Lion-Dagan, I. Willner, *J. Electroanal. Chem.* **1995**, *382*, 25.

[4] a) M. Lion-Dagan, S. Marx-Tibbon, E. Katz, I. Willner, *Angew. Chem.* **1995**, *107*, 1730; *Angew. Chem. Int. Ed. Engl.* **1995**, *34*, 1604; b) I. Willner, R. Blonder, E. Katz, A. F. Bückmann, *J. Am. Chem. Soc.*, in press.

[5] R. A. Bissell, E. Córdova, A. E. Kaifer, J. F. Stoddart, *Nature* **1994**, *369*, 133.

[6] E. Katz, I. Willner, *Electroanalysis* **1995**, *7*, 417.

[7] E. Katz, M. Lion-Dagan, I. Willner, *J. Electroanal. Chem.*, in press.

[8] a) S. Shinkai, T. Ogawa, Y. Kusano, O. Manabe, K. Kikukawa, T. Goto, T. Matsuda, *J. Am. Chem. Soc.* **1982**, *104*, 1960; b) S. Shinkai, K. Shigematsu, M. Sato, O. Manabe, *J. Chem. Soc. Perkin Trans. 1* **1982**, 2735; c) S. Shinkai, T. Kouno, Y. Kusano, O. Manabe, *ibid.* **1982**, 2741; d) M. Blank, L. M. Soo, N. H. Wasserman, B. F. Erlanger, *Science* **1981**, *214*, 70.

[9] a) S. Shinkai, T. Minami, T. Kusano, O. Manabe, *J. Am. Chem. Soc.* **1982**, *104*, 1967; b) J. Winkler, K. Deshayes, B. Shao, *ibid.* **1989**, *111*, 769; c) M. Inouye, M. Ueno, T. Kitao, K. Tsuchiya, *ibid.* **1990**, *112*, 8977.

[10] I. Willner, S. Marx, Y. Eichen, *Angew. Chem.* **1992**, *104*, 1255; *Angew. Chem. Int. Ed. Engl.* **1992**, *31*, 1243.

[11] a) S. L. Gilat, S. H. Kawai, J.-M. Lehn, *Chem. Eur. J.* **1995**, *1*, 275; b) S. H. Kawai, S. L. Gilat, R. Ponsinet, J.-M. Lehn, *ibid.* **1995**, *1*, 285.

[12] Z. F. Liu, K. Hashimoto, A. Fujishima, *Nature* **1990**, *347*, 658.

[13] a) M. Lion-Dagan, E. Katz, I. Willner, *J. Chem. Soc. Chem. Commun.* **1994**, 2741; b) I. Willner, A. Doron, E. Katz, S. Levi, A. J. Frank, *Langmuir*, **1996**, *12*, 946.

[14] I. Willner, R. Blonder, A. Dagan, *J. Am. Chem. Soc.* **1994**, *116*, 9365.

[15] a) N. P. Gritsan, L. S. Klimenko, *J. Photochem. Photobiol. A* **1993**, *70*, 103; b) A. Zelichenok, F. Buchholz, E. Fischer, J. Ratner, V. Krongauz, H. Annesez, C. Bräuchle, *ibid.* **1993**, *76*, 135; c) M. Tajima, L. E. Keat, K. Matsunaga, T. Yamashita, M. Tokoro, H. Inoue, *ibid.* **1993**, *74*, 211; d) Z. Fang, S. Wang, Z. Yang, B. Chen, F. Li, J. Wang, S. Xu, Z. Jiang, T. Fang, *ibid.* **1995**, *88*, 23; e) F. Buchholtz, A. Zelichenok, V. Krongauz, *Macromolecules* **1993**, *26*, 906.

[16] M. Sharp, *Electrochim. Acta* **1978**, *23*, 287.

[17] a) E. Katz, N. Itzhak, I. Willner, *J. Electroanal. Chem.* **1992**, *336*, 357; b) E. Katz, H.-L. Schmidt, *ibid.* **1994**, *368*, 87; c) E. Katz, N. Itzhak, I. Willner, *Langmuir* **1993**, *9*, 1392.

[18] E. Laviron, *J. Electroanal. Chem.* **1979**, *101*, 19.

[19] See also the review I. Willner, S. Rubin, *Angew. Chem.* **1996**, *108*, 419; *Angew. Chem. Int. Ed. Engl.* **1996**, *35*, 367.

[20] The cyclic voltammogram does not coincide with that expected for a surface-confined species, where zero peak-to-peak separation is expected. Also, the cathodic wave does not return to the background level due to the cathodic discharge of the solvent at this potential. For similar observations see also K. Weber, S. E. Creager, *Anal. Chem.*, **1994**, *66*, 3164; L.-H. Guo, J. S. Facci, G. McLendon, *J. Phys. Chem.* **1995**, *99*, 8458.

Pyranosyl-RNA: Base Pairing between Homochiral Oligonucleotide Strands of Opposite Sense of Chirality**

Ramanarayanan Krishnamurthy, Stefan Pitsch, Mark Minton, Christian Miculka, Norbert Windhab, and Albert Eschenmoser*

Pyranosyl-RNA (p-RNA) is the structural isomer of RNA[1, 3–5] in which the ribose units exist in the pyranose form and are linked together repetitively by phosphodiester groups between positions C-2′ and C-4′ (Fig. 1). The properties of this *unnatural* oligonucleotide pairing system are considered to be relevant to the problem of the origin of *natural* RNA.[6] Previous investigations[1, 4, 6] have shown that base pairing in p-RNA is not only *stronger* but also *more selective* than in RNA or DNA. The selectivity refers to the pairing mode. So far, only Watson–Crick (WC) pairing and neither Hoogsteen (H) nor

[*] Prof. Dr. A. Eschenmoser, Dr. R. Krishnamurthy, Dr. S. Pitsch, Dr. M. Minton
Laboratorium für Organische Chemie
der Eidgenössischen Technischen Hochschule
Universitätstrasse 16, CH-8092 Zürich (Switzerland)
Fax: Int. code +(1)632-1043
Dr. C. Miculka, Dr. N. Windhab
Institut für Pharmazeutische Chemie der Universität, Biozentrum
Marie-Curie-Strasse 9, D-60439 Frankfurt (Germany)

[**] p-RNA, Part 3, and Chemistry of α-Aminonitriles, Part 18. This work was supported by Ciba-Geigy AG, Basel, by Firmenich & Cie., Geneva, and by the Schulleitung of ETH Zürich. C. M. thanks the Fonds für wissenschaftliche Forschung, Vienna, for a Schrödinger fellowship and the BMBF, Bonn (project no. 0310792), for financial support. N. W. thanks BASF AG, Ludwigshafen, for a research fellowship. A. E. would like to thank Prof. C. R. Noe for generous hospitality to his satellite research group at the Institut für Pharmazeutische Chemie der Universität Frankfurt. Dr. Thomas Carell, ETH-Zürich, translated the German manuscript. Part 2 and Part 17: ref. [1] and ref. [2].

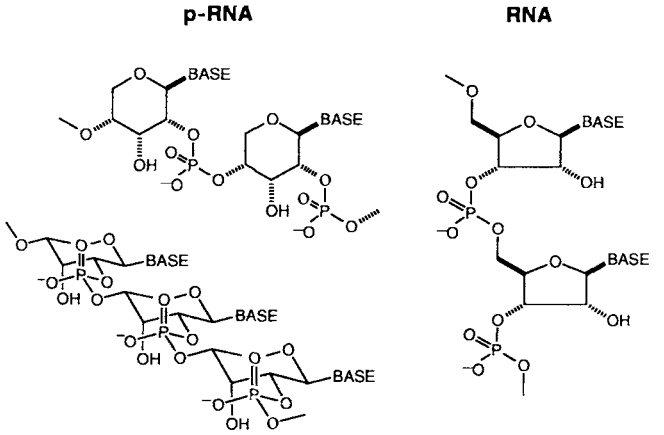

Fig. 1. Constitution of p-RNA and RNA and (idealized) pairing conformation of p-RNA [3, 4].

reverse-Hoogsteen (RH) pairing has been observed. This is in sharp contrast to the behavior of RNA and DNA[7] as well as of synthetic homo-DNA.[11] Probably the most important consequence of the selectivity is the ability of p-RNA to replicate without enzymes.[1] p-RNA oligonucleotides do not suffer from the replication handicap characteristic of RNA-type oligonucleotides caused by the self-deactivation of guanine-rich template strands through guanine self-pairing,[14] as shown by Orgel.[12, 13]

Owing to the constitutional relationship between p-RNA and RNA, the extraordinary pairing properties, and especially the potential of this pairing system for nonenzymatic replication of combinatorial structural information, we are conducting a comprehensive investigation of the chemistry of p-RNA as part of an experimental program directed at a chemical etiology of the structure of the *natural* nucleic acids.[4, 6] In this context the question arises if and how *homochiral* p-RNA strands could be derived from ribopyranosyl mononucleotides, which—from an etiological point of view—would have to be *racemates*. This prompted us to search for the existence of base pairing between homochiral p-RNA strands of opposite sense of chirality.[18]

In p-RNA both purine–pyrimidine and purine–purine WC pairing[21] show high strand enantioselectivity[1] (Fig. 1, see Table 2). WC pairing between *homochiral* oligonucleotides of

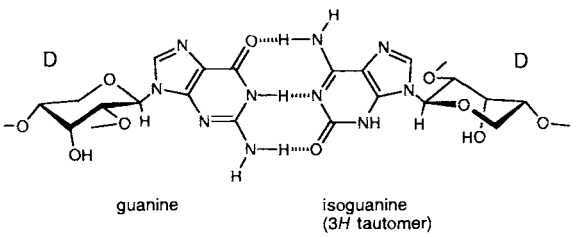

Fig. 2. Constitution of guanine–isoguanine pairing (Watson–Crick mode) [3, 23].

opposite sense of chirality would require either a parallel strand orientation[25] with *anti* conformation of the nucleobases on both sides of a base pair or, in the case of antiparallel strand orientation, *syn* conformation[27] of one of the nucleobases (Table 1). Both types of pairing are "forbidden" in the p-RNA series for reasons analoguous to those put forward to explain the nonoccurrence of H and RH pairing.[1, 4] However, symmetry and model considerations suggest that these restrictions

Table 1. Relationships between pairing mode and strand orientation for homochiral p-RNA strands having the same or the opposite sense of chirality.

Pairing mode	Conformations at the nucleosidic bond	Orientation of homochiral strands with same sense of chirality	opposite sense of chirality
Watson–Crick (WC)	*anti*/*anti* or *syn*/*syn*	antiparallel	parallel
	syn/*anti* or *anti*/*syn*	parallel	antiparallel
Reverse-Watson–Crick (RWC)	*anti*/*anti* or *syn*/*syn*	parallel	antiparallel
	syn/*anti* or *anti*/*syn*	antiparallel	parallel
Hoogsteen (H)	*anti*/*anti* or *syn*/*syn*	parallel	antiparallel
	syn/*anti* or *anti*/*syn*	antiparallel	parallel
Reverse Hoogsten (RH)	*anti*/*anti* or *syn*/*syn*	antiparallel	parallel
	syn/*anti* or *anti*/*syn*	parallel	antiparallel

should vanish with homochiral p-RNA strands of opposite sense chirality, provided that the constitution of the base combinations is such that it corresponds to base pairing in the reverse-Watson–Crick mode (RWC). The topology of the RWC mode allows for a centrosymmetric arrangement of homochiral, but enantiomorphic oligonucleotide backbones and antiparallel strand orientation and *anti* conformation at all nucleosidic bonds. For symmetry reasons such quasi-racemic p-RNA duplexes should have a strictly linear ladder structure, provided that the base pairs, such as purine–purine pairs, are composed of isomorphous bases. Figure 3 features a selection of such quasi-centrosymmetric (tridentate) base combinations in the RWC mode, which are expected to give rise to pairing between homochiral p-RNA strands of opposite sense of chirality.[28] Incidentally, noncanonical base combinations such as isoguanine–cytosine, guanine–isocytosine, and diaminopurine–xan-

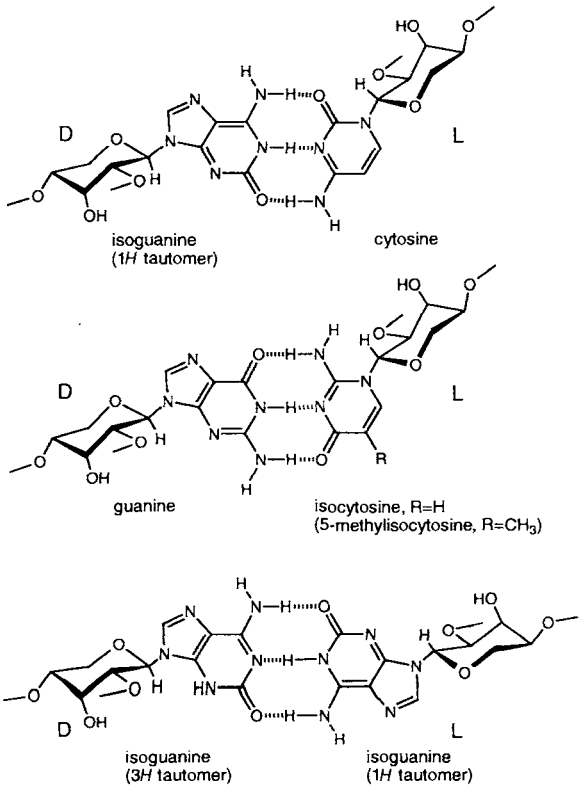

Fig. 3. Purine–pyrimidine and purine–purine pairs in the reverse-Watson–Crick mode in duplexes between homochiral p-RNA strands of opposite sense of chirality.

 © VCH Verlagsgesellschaft mbH, D-69451 Weinheim, 1996 0570-0833/96/3513-1538 $ 15.00+.25/0

thine deserve the same attention as their canonical counterparts in an etiological context.[29] Results of experiments carried out along the expectations delineated above are summarized in Table 2 and documented in Figures 4–7.[30]

Table 2. Melting curves and thermodynamic data of p-RNA pairing complexes. For experimental methods used, see refs. [1,4,11].

Base sequences	T_m [°C] [a] Sense of chirality D/D	L/D	ΔG^{298} [kcal mol^{-1}]	ΔH [kcal mol^{-1}]	$T\Delta S^{298}$ [kcal mol^{-1}]
purine-pyrimidine pairs					
G_6/C_6 [1]	61 [b]	ca. 0	−13.5	−54.3	−40.8 (D/D)
G_8/G_8 [1]	82 [c]	ca. 15			
G_8/(5-methyl-isoC)$_8$	<0	24	−7.5	−32.5	−25.0 (L/D)
$isoG_6/C_6$	<0	29	−7.6	−34.2	−26.6 (L/D)
$isoG_8/C_8$	<0	49	−10.7	−42.0	−31.3 (L/D)
Dp_8/T_8)	50	ca. 0	−12.0	−57.5	−45.5 (L/L)
		8 (25 + 25 μM, 1.5 M NaCl)	−4.8	−31.8	−27.0 (D/L)
purine-purine pairs					
$isoG_6/G_6$ [1]	34	<0			
$isoG_8/G_8$ [1]	56	<0	−12.5	−50.2	−37.7 (D/D)
$isoG_6$/$isoG_6$	<0 [d]	20 [f]			
$isoG_8$/$isoG_8$	~0 [e]	34 [g]	−7.1	−28.0	−20.9 (L/D)
G_8/G_8	<0 [e]	31 (16) [h]			
		51 (25) [i]			

[a] $c \approx 5 + 5$ μM, 0.15 M NaCl; pH 7; 0.01 M Tris. [b] $c = 3.5 + 3.5$ μM. [c] $c = 2.5 + 2.5$ μM. [d] $c = 50$ μM. [e] $c = 10$ μM. [f] $c = 25 + 25$ μM. [g] $50 + 50$ μM. [h] $c = 50 + 50$ μM; the values in parentheses refer to cooling curves. [i] $c = 50 + 50$ μM, 1.5 M NaCl; the values in parentheses refer to cooling curves.

Homochiral strands of pr(isoG$_n$) and pr(C$_n$) ($n = 6$ or 8) with the *same* sense of chirality show neither self-pairing nor pairing in 1:1 mixtures above 0 °C under standard conditions,[1] as determined by temperature-dependent UV and CD spectroscopy. In contrast, L-pr(isoG$_n$) and D-(pr(C$_n$) ($n = 6$ or 8) in equimolar mixtures under otherwise identical conditions, *do* form duplexes. For the octamers the duplex was characterized by temperature-dependent UV and CD spectra (Fig. 4a–c) and by its gel electrophoretic behavior under nondenaturing conditions (Fig. 4d). For the hexamers, the 1:1 stoichiometry of the quasi-racemic complex was established by UV spectroscopy by its mixing curve.[31] Homochiral L-pr(G$_8$) and D-pr[(5-methyl-isoC)$_8$] strands were analoguously shown to form a corresponding purine–pyrimidine duplex which, however, is somewhat less stable than the one formed by L-pr(isoG$_8$) and D-pr(C$_8$) (see Table 2).[32]

Homochiral strands of D- and L-pr(isoG$_n$) ($n = 6$ or 8, Fig. 5), while not showing self-pairing at room temperature, react in equimolar mixtures to form quasi-racemic purine–purine complexes which are easily recognized by their conspicuously strong UV hyperchromicity (Fig. 5a and Table 2). The mixing curve determined for the case $n = 8$ (Fig. 5b)[31] demonstrates the formation of a 1:1 complex; the observed deviation from linearity in the correlation between extinction and composition points to an additional aggregation in which the 1:1 complex associates with either itself, or with one of the (enantiomeric) single strands ($c = 15$ μM, 5 °C, otherwise standard conditions). The pairing of enantiomeric isoguanine strands is also demonstrated by gel electrophoresis under nondenaturing conditions (Fig. 4d).

Homochiral strands of D- and L-pr(G$_8$), neither of which shows self-pairing at room temperature,[1] form a quasi-racemic 1:1 complex (Fig. 6a–c) like that of the isoguanosine strands. However, this complex has an unusually low hyperchromicity and its pairing/depairing curves reproduceably show a hysteresis (Fig. 6a and b). In addition, the mixing curve (5 °C) does not indicate further aggregation of the (1:1) complex (Fig. 6c),

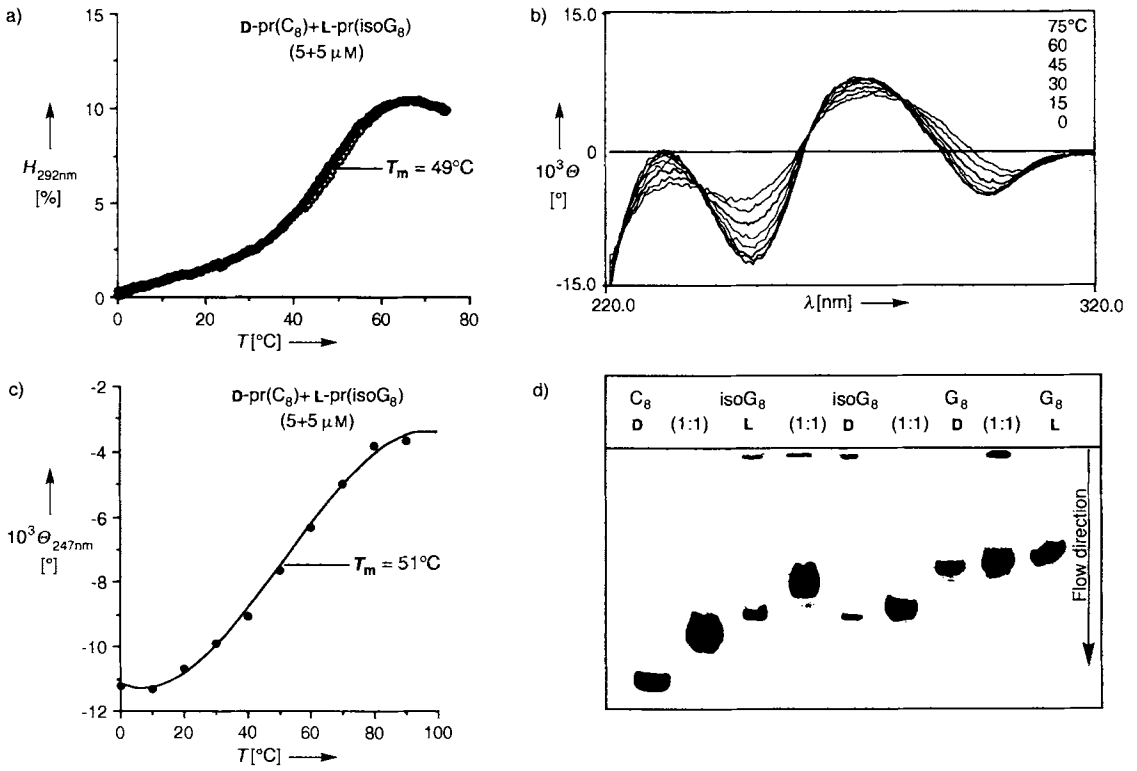

Fig. 4. Pairing between D-pr(C$_8$) and L-pr(isoG$_8$) [30] ($c = 5 + 5$ μM, 0.15 M NaCl, 0.01 M Tris buffer, pH 7). a) UV spectroscopic determination of T_m, $\Delta T = 1$ K min^{-1}, H = hyperchromism; b) temperature dependence of CD spectrum; c) CD spectroscopic determination of T_m; d) gel electrophoresis under nondenaturing conditions (20% acrylamide, 0.09 M Tris·B(OH)$_3$, 0.005 M MgCl$_2$, 6 W, 2 °C, 2.5 h, detection "stains all").

 © VCH Verlagsgesellschaft mbH, D-69451 Weinheim, 1996 0570-0833/96/3513-1539 $ 15.00+.25/0

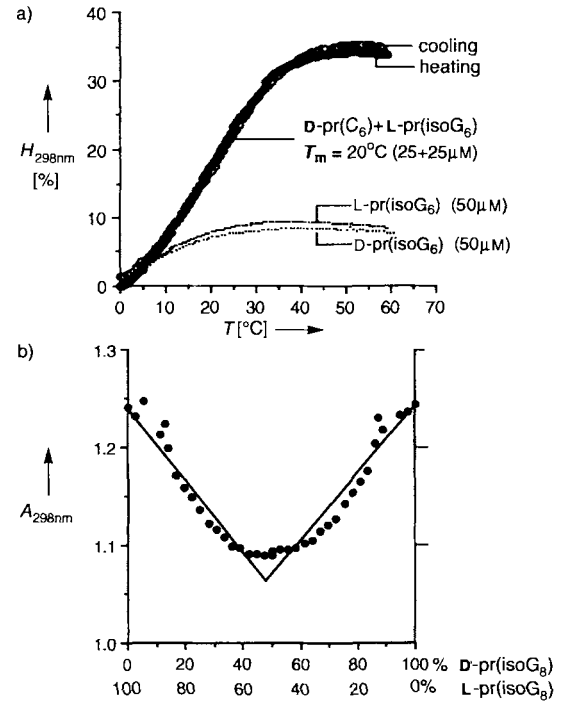

Fig. 5. Pairing between D-pr(isoG$_n$) and L-pr(isoG$_n$) (n = 6 and 8) [30]. a) UV spectroscopic determination of T_m (for conditions see caption of Fig. 4); b) mixing curve [31] of D- + L-pr(isoG$_8$) at 5 °C, c(D + L) = 15 μM (for other conditions see caption of Fig. 4).

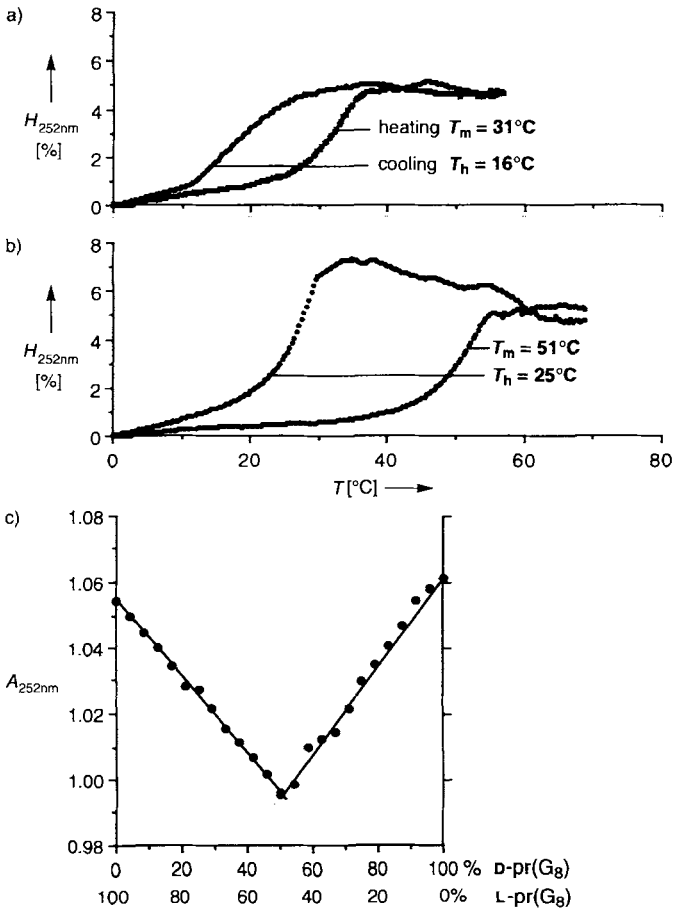

Fig. 6. Pairing between D-pr(G$_8$) and L-pr(G$_8$) [30]. a) UV spectroscopic determination of T_m at normal salt concentration (ΔT = 1 K min^{-1}; b) determination of T_m at high salt concentration; c) mixing curve [31] at 5 °C, c(D + L) = 100 μM (for other conditions see caption of Fig. 4).

in contrast to the isoguanine case. Moreover, the T_m values are more strongly dependent on salt concentration than in the isoguanine series.

Our expectations regarding the pairing of homochiral p-RNA strands of *opposite* sense of chirality (Fig. 3) appear confirmed by observation, at least from a phenomenological point of view: we observe the pairing both of guanine with isocytosine[33] (but not with cytosine), and of isoguanine with cytosine (but not with isocytosine[33]). While neither all-guanosine, nor all-isoguanosine p-RNA strands undergo *isochiral* self-pairing at temperatures above 0 °C,[1] they do feature *heterochiral* pairing. The question must remain open whether the coincidence of expectation and observation is just phenomenological, or whether it also refers to the constitutional assignment of the RWC pairing mode. We think that, at least in the cases of the quasi-racemic purine–pyrimidine duplexes L-pr(isoG$_8$)/D-pr(C$_8$) and L-pr(G$_8$)/D-pr[(5-methyl-isoC)$_8$], the assignment of the RWC pairing mode (Fig. 3 top, middle) is probably correct, simply because we cannot see a *convincing* constitutional alternative.

The proposal of a quasi-centrosymmetric isoguanine–isoguanine pairing in the tridentate RWC mode (Fig. 3 bottom) requires the isoguanine base to engage its 1*H* as well as its 3*H* tautomer in the pairing process. We consider this requirement to be fulfilled, as otherwise no rationale can be offered for the proven occurrence of isochiral guanine–isoguanine pairing in both homo-DNA[22–24] and p-RNA[1] (Table 2) as well as the heterochiral pairing of isoguanine with cytosine in p-RNA (Table 2 and Fig. 3).[34] Nevertheless, the assignment for the D/L isoguanosine pair remains uncertain, since four *didentate* centrosymmetric pairing modes can be considered beside the *tridentate* RWC mode, all formally compatible with the topological constraints of the p-RNA backbone. Of these four, the double-Hoogsteen (DH) mode[35] deserves special attention. It could give rise to a centrosymmetric duplex structure with the potential for further strand aggregation in the RWC mode; this could also be described by saying that the quasi-centrosymmetric RWC duplex has the potential for additional strand aggregation through DH pairing (Fig. 7 top). An alternative aggregation pattern of the RWC duplex is depicted at the bottom of Figure 7.

In contrast to isoguanine there is, to our knowledge, no evidence that tautomers play a role in guanine pairing, as would be required if guanine were to pair with itself in the RWC mode. In fact, the striking differences between the observed properties of the quasi-racemic complexes D/L-pr(G$_8$) and D/L-pr(isoG$_8$) indicate that they quite probably do not have the same pairing mode. Symmetry and model considerations suggest that a quasi-racemic guanine tetrade consisting of alternating D and L strands of pr(G$_8$) in antiparallel orientation (H mode) should be topologically forbidden, for reasons similar to these used to rationalize the strict non-occurrence of H pairing in the isochiral series.[1, 4] On the other hand, duplex formation in the quasi-centrosymmetric RH mode would seem to be topologically allowed; it would require one of the guanines within a (G–G) pair to assume the *syn* conformation at its nucleosidic bond, a requirement that might explain the hysteresis observed for the pairing process. The phenomenon of the quasi-racemic guanine–guanine pairing (and not only this) certainly demands, as well as deserves, further investigation.

The observations described here demonstrate the existence of purine–pyrimidine and purine–purine pairing between homochiral p-RNA strands with opposite sense of chirality. The selection rules for this type of pairing (Table 3) are different from those valid for pairing between homochiral strands of the same sense of chirality (heterochiral versus isochiral pairing).

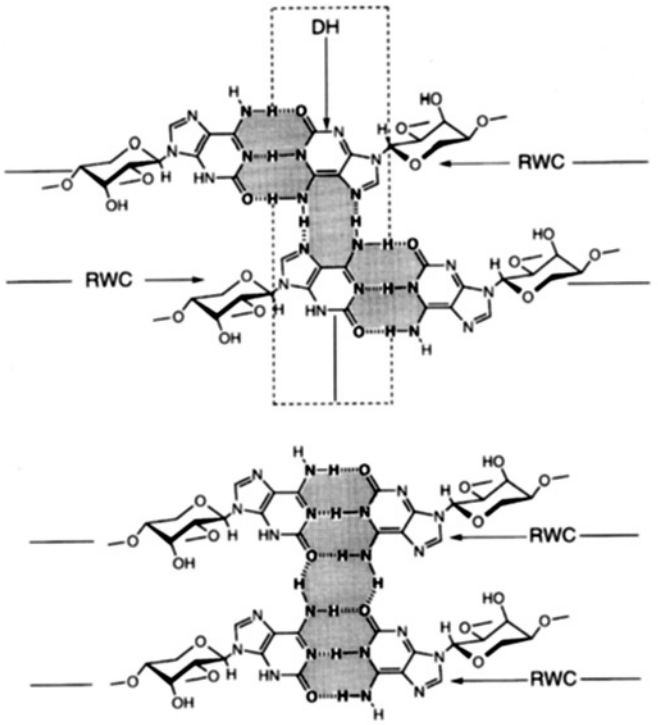

Fig. 7. Hypothetical constitutional models for aggregation of a racemic RWC duplex D-pr(isoG$_8$) + L-pr(isoG$_8$).

Table 3.

Base pairs	Conformations at the nucleosidic bonds [a]	Pairing mode [a]
isoG/isoG	*anti/anti*	RWC and/or DH
G/G	*syn/anti*	RH
isoG/C	*anti/anti*	RWC
G/isoC	*anti/anti*	RWC
Dp/T	*anti/anti*	RWC

[a] Hypothetical.

Observations made so far show that isochiral pairing is uniformly stronger than heterochiral pairing and, in both cases, purine–pyrimidine pairing is stronger than purine–purine pairing. *Of all four variants, the isochiral purine–pyrimidine pairing that dominates pairing in the natural nucleic acids is strongest.* Establishing relationships of this kind would appear to be a prerequisite for the design of conceptual and experimental models of the origin of homochirality in the natural nucleic acids.

Received: February 9, 1996 [Z 8798 IE]
German version: *Angew. Chem.* **1996**, *108*, 1619–1623

Keywords: base pairing · oligonucleotides · RNA

[1] S. Pitsch, R. Krishnamurthy, M. Bolli, S. Wendeborn, A. Holzner, M. Minton, C. Lesueur, I. Schlönvogt, B. Jaun, A. Eschenmoser, *Helv. Chim. Acta* **1995**, *78*, 1621–1635.
[2] P. Lohse, B. Oberhauser, B. Oberhauser-Hofbauer, G. Baschang, A. Eschenmoser, *Croat. Chim. Acta*, in press.
[3] A. Eschenmoser, *Pure Appl. Chem.* **1993**, *65*, 1179–1188.
[4] S. Pitsch, S. Wendeborn, B. Jaun, A. Eschenmoser, *Helv. Chim. Acta* **1993**, *76*, 2161–2183.
[5] S. Pitsch, E. Pombo-Villar, A. Eschenmoser, *Helv. Chim. Acta* **1994**, *77*, 2251–2285.
[6] A. Eschenmoser ("Toward a Chemical Etiology of the Natural Nucleic Acids' Structure") in Proc. R. A. Welch Found., 37. Conf. Chem. Res. 40 Years of the DNA Double Helix, R. A. Welch Foundation, Houston, TX, USA, **1993**, 201–235.
[7] DNA oligonucleotides form triplexes in the WC-H (pyrimidine–purine–pyrimidine) and the WC-RH (pyrimidine–purine–purine) pairing modes, as well as quadruplexes (guanine tetrades) in the H mode; see literature overviews in refs. [8–10].
[8] K. Umemoto, M. H. Sarma, G. Gupta, J. Luo, R. H. Sarma, *J. Am. Chem. Soc.* **1990**, *112*, 4539–4545.
[9] I. Radhakrishnan, D. J. Patel, *Biochemistry* **1994**, *33*, 11405–11416.
[10] C. H. Kang, X. Zhang, R. Ratliff, R. Moyzis, A. Rich, *Nature (London)* **1992**, *356*, 126–131.
[11] J. Hunziker, H.-J. Roth, M. Böhringer, A. Giger, U. Diederichsen, M. Göbel, Ravichandran Krishnan, B. Jaun, C. Leumann, A. Eschenmoser, *Helv. Chim. Acta* **1993**, *76*, 259–352.
[12] G. F. Joyce, L. E. Orgel, *J. Mol. Biol.* **1986**, *188*, 433–441.
[13] L. E. Orgel, *Nature (London)* **1992**, *358*, 203–209.
[14] For examples in which this handicap is circumvented see [15,16] and the work of G. von Kiedrowski et al. [17]
[15] T. Wu, L. E. Orgel, *J. Am. Chem. Soc.* **1992**, *114*, 5496–5501.
[16] H. Rembold, L. E. Orgel, *J. Mol. Evol.* **1994**, *38*, 205–210.
[17] D. Sievers, G. von Kiedrowski, *Nature (London)* **1994**, *369*, 221–224, and references therein.
[18] In a recent paper Garbesi et al. [19] conclude that, in contrast to other reports, L-DNA strands (with all four canonical bases) do not pair in a specific manner either with parallel or antiparallel complementary D-DNA strands. Van Boeckel et al. [20] reported, based on NMR data, that L-d(CAAGG) forms (strongly paired) complexes with D-d(CCUUG) and D-d(GUUCC). These complexes remain constitutionally undefined.
[19] A. Garbesi, M. L. Capobianco, F. P. Colonna, L. Tondelli, F. Arcamone, G. Manzini, C. W. Hilbers, J. M. E. Aelen, M. J. J. Blommers, *Nucleic Acids Res.* **1993**, *21*, 4159–4165, and references therein.
[20] C. A. A. van Boeckel, G. M. Visser, R. A. Hegstrom, J. H. van Boom, *J. Mol. Evol.* **1987**, *25*, 100–105.
[21] In analogy to guanine–isoguanine pairing in the homo-DNA series, see refs. [6, 22–24].
[22] K. Groebke ("Über Purin-Purin-Paarungen bei Hexopyranose-Nukleinsäuren"), Dissertation Nr. 10149, ETH Zürich, **1993**.
[23] K. Groebke, W. Fraser, J. Hunziker, L. Peng, U. Diederichsen, K. Zimmermann, A. Holzner, C. Leumann, A. Eschenmoser, unpublished.
[24] A. Eschenmoser, E. Loewenthal, *Chem. Soc. Rev.* **1992**, *21*, 1–16.
[25] For (homochiral) DNA duplexes with *parallel* strand orientation in which adenine and thymine in *anti* conformation pair in the RWC mode, see ref. [26].
[26] N. Pattabiraman, *Biopolymers* **1986**, *25*, 1603–1606; N. B. Ramsing, T. M. Jovin, *Nucleic Acids Res.* **1988**, *16*, 6659–6676; M. W. Germann, B. W. Kalisch, J. H. van de Sande, *Biochemistry* **1988**, *27*, 8302–8306.
[27] G. F. Joyce, G. M. Visser, C. A. A. van Boeckel, J. H. van Boom, L. E. Orgel, J. van Westrenen, *Nature (London)* **1984**, *310*, 602–604.
[28] The weak complexation observed for the 1:1 mixture of L-pr(G$_8$)/D-pr(C$_8$) (see ref. [1] and Table 2) very probably also corresponds to a RWC mode (didentate guanine (NH, NH$_2$) → cytosine (=O, =N) pairing).
[29] A. Eschenmoser, M. Dobler, *Helv. Chim. Acta* **1992**, *75*, 218–259.
[30] For the synthesis of p-RNA mononucleosides and for the automated synthesis of p-RNA oligonucleotides see ref. [4] and ref. [1]. A detailed description of this work will appear in *Helv. Chim. Acta*.
[31] C. R. Cantor, P. R. Schimmel, *Biophysical Chemistry. Part III: The Behavior of Biological Macromolecules*, Freeman, San Francisco, **1980**, p. 1135–1139.
[32] A sterically induced propeller twist in the duplex L-pr(G$_8$)/D-pr[(5-methyl-isoC)$_8$] could explain why it is less stable than L-pr(isoG$_8$)/D-pr(C$_8$). This may also explain our (surprising) observation that D-pr(isoG$_8$) and D-pr[(5-methyl-isoC)$_8$] do not form a duplex (in contrast to the DNA series [33]).
[33] We did not use isocytosine itself but its 5-methyl derivative for stability reasons. For the (isochiral) pairing between isoguanine with isocytosine in the DNA series see ref. [36] and: A. Rich in *Horizons in Biochemistry* (Eds.: M. Kasha, B. Pullmann), Academic Press, London, **1962**, pp. 103–126; C. Y. Switzer, S. E. Moroney, S. A. Benner, *Biochemistry* **1993**, *32*, 10489–10496.
[34] According to the literature (J. Sepiol, Z. Kazimierczuk, D. Shugar, *Z. Naturforsch. C* **1976**, *31*, 361–370; R. S. Norton, R. P. Gregson, R. J. Quinn, *J. Chem. Soc. Chem. Commun.* **1980**, 339–341), N-9 substituted isoguanine derivatives in aqueous solution exist in, beside the enol form, mainly the 1*H* lactam form (see also F. Seela, C. Wei, Z. Kazimierczuk, *Helv. Chim. Acta* **1995**, *78*, 1843–1854). The pairing behavior of isoguanine in both the homo-DNA and the p-RNA series suggests that the 1*H* and the 3*H* lactam forms are the predominant tautomers present in aqueous medium (see ref. [23]).
[35] Two of the remaining possibilities (which we consider to be less important) would be didentate variants of the tridentate RWC mode, in which two identical isoguanine tautomers could form a base pair. The third possibility would be centrosymmetric didentate self-pairing of the lactam group of the 3*H* tautomer (sterically hindered).
[36] C. Roberts, R. Bandaru, C. Switzer, *Tetrahedron Lett.* **1995**, *36*, 3601–3604; T. Horn, C.-A. Chang, M. L. Collins, *ibid.* **1995**, *36*, 2033–2036.

 © *VCH Verlagsgesellschaft mbH, D-69451 Weinheim, 1996* *0570-0833/96/3513-1541 $ 15.00+.25/0*

Chemical Double-Mutant Cycles for the Measurement of Weak Intermolecular Interactions: Edge-to-Face Aromatic Interactions**

Harry Adams, Fiona J. Carver, Christopher A. Hunter,* Juan Carlos Morales, and Eileen M. Seward

Weak noncovalent interactions are of fundamental importance in determining the three-dimensional structures and functional properties of molecular systems in biology, chemistry, and materials science. If we are to develop the ability to predict and understand the complex behavior of these systems, we will require good models for the forces that control them. One interaction of particular importance is that between two aromatic rings ($\pi-\pi$ interaction).[1-4]

Qualitative models that account for the properties of $\pi-\pi$ interactions have been developed based on simple electrostatic arguments. However, good quantitative computational models for weak interactions of this type require good quantitative experimental data against which the models can be tested.[5, 6]

The quantitative determination of the energies of weak noncovalent interactions is fraught with difficulties. Direct measurement at room temperature in solution is not possible because the interactions are not strong enough to cause intermolecular complexation in a well-defined orientation. They can therefore only be measured as a perturbation of a stronger interaction. However, any changes to a system that affect one interaction are likely to affect other neighboring interactions. A solution to this problem, which has been used to measure interactions between side chains in proteins, is to apply thermodynamic cycles in combination with structure variation (mutagenesis).[7] In this communication we describe the application of the double-mutant cycle concept to a synthetic supramolecular system for the measurement of an intermolecular edge-to-face aromatic interaction.

We recently described a molecular zipper, a 1:1 complex of two amide oligomers held together by hydrogen bonds and edge-to-face $\pi-\pi$ interactions.[8] This structure is ideally suited to the measurement of noncovalent interactions using the double-mutant approach.[9] Since the molecules are essentially rigid, the experiments are not complicated by losses of conformational mobility on complexation.[10] This rigidity also ensures that the $\pi-\pi$ interactions in complex **A** are fixed in edge-to-face orientations by the covalent structures of the molecules and the hydrogen bonds (Scheme 1). The linear array of interaction sites means that chemical mutations at the terminal functional groups can be used to probe the interactions on the ends of the complex without perturbing the structure of the core.

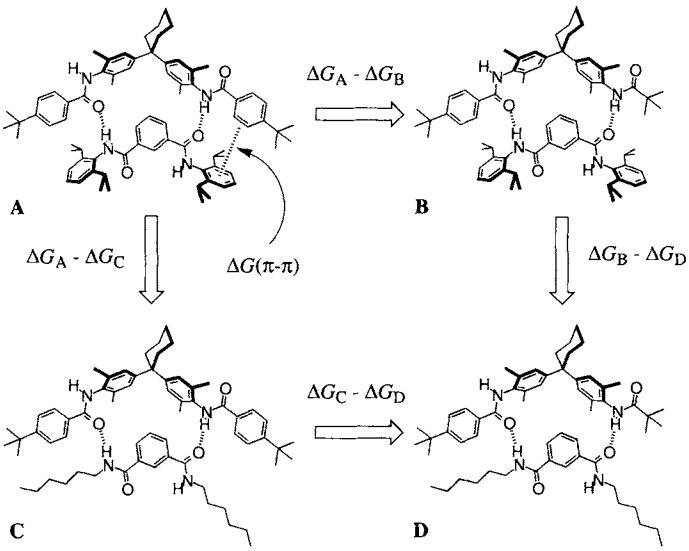

Scheme 1. Chemical double-mutant cycle for measuring the terminal $\pi-\pi$ interaction in complex **A**.

The magnitude of the terminal $\pi-\pi$ interaction in complex **A** could be estimated by removing one of the interacting aryl groups, as in complexes **B** and **C**. However, these single chemical mutations not only remove the interaction of interest, they also remove other secondary interactions, for example those between the amides and the terminal aromatic rings (Scheme 2). The change in the secondary interactions can, however, be quantified by using the double mutant, complex **D**. Comparing complexes **C** and **D** allows us to quantify the change in the secondary interactions that occurs when the **A** → **B** mutation is made. Thus the difference between the two horizontal mutations in Scheme 1, $(\Delta G_A-\Delta G_B)-(\Delta G_C-\Delta G_D)$, gives the magnitude of the terminal $\pi-\pi$ interaction in the absence of secondary effects.[11, 12] Comparing the vertical mutations in Scheme 1 yields the same result [Eq. (a)].

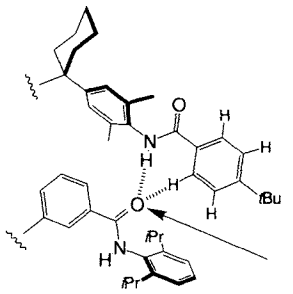

Scheme 2. A possible secondary interaction (marked with an arrow) between the terminal aromatic group and the amide core of complex **A**. A C–H···O hydrogen bond is shown, but other secondary interactions are also possible.

$$\Delta G(\pi-\pi) = \Delta G_A - \Delta G_B - \Delta G_C + \Delta G_D \quad \text{(a)}$$

Compounds **1**–**5** were synthesized in high yield by means of simple amide coupling reactions.[13] The structure of complex **A** in chloroform was determined by ^{1}H NMR spectroscopy. Job's method of continuous variations gave results consistent with a 1:1 stoichiometry.[14] A ROESY experiment on a 1:1 mixture of

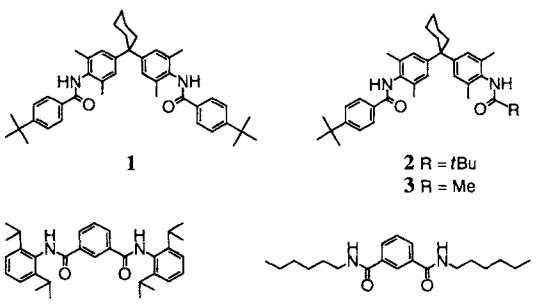

[*] Dr. C. A. Hunter, H. Adams, F. J. Carver
Krebs Institute for Biomolecular Science
Department of Chemistry, University of Sheffield
GB-Sheffield S3 7HF (UK)
Fax: Int. code +(114)273-8673
e-mail: C. Hunter@Sheffield.ac.uk
J. C. Morales
Instituto de Quimica Organica, CSIC, Madrid (Spain)
Dr. E. M. Seward
Merck Sharp & Dohme Research Laboratories (UK)

[**] This work was supported by the EPSRC, Merck Sharp & Dohme (F. J. C.), the Spanish government (J. C. M.), and the Lister Institute (C. A. H).

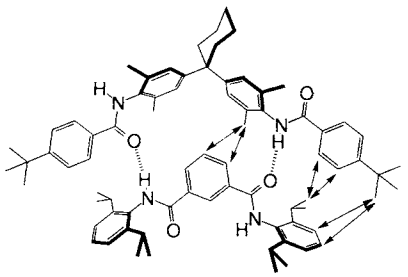

Scheme 3. Intermolecular NOEs observed for a 1:1 mixture of **1** and **4** in a ROESY experiment.

1 and **4** gave the intermolecular NOEs illustrated in Scheme 3, which show that the isophthaloyl group of **4** binds into the aromatic pocket of **1** and that the terminal benzoyl and aniline groups are in close contact. Dilution experiments show that none of the compounds dimerize significantly in chloroform ($K < 1\ \text{M}^{-1}$), and so titrations were analyzed using a simple 1:1 binding isotherm. Titrations were performed using both **1** and **4** as the fixed concentration host, so that accurate limiting complexation-induced changes in chemical shift could be obtained for both components of the complex (Scheme 4). These changes in shift confirm

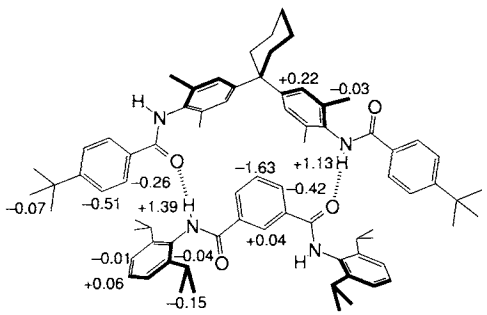

Scheme 4. Limiting complexation-induced changes in ^{1}H NMR chemical shifts for complex **A** in chloroform.

that the $\pi-\pi$ interactions are edge-to-face in the complex: the benzoyl and isophthaloyl protons (with the exception of that at C2) experience large upfield ring current induced shifts, because they lie over the faces of neighboring aromatic rings; the other aromatic protons experience small or downfield shifts, indicating that they sit at the edges of neighboring aromatic rings. The signal due to the isopropyl methyl groups of **4** experiences an upfield shift, because these groups project over the faces of the benzoyl rings of **1**. The large downfield shifts observed for the signals due to the amide NH protons are evidence for the hydrogen-bonding interactions.

Although we have not crystallized the complex formed by **1** and **4**, we have obtained an X-ray crystal structure of the related model compound **6**, which provides strong supporting evidence for the structure of complex **A**.[15] A dimer of **6** is effectively half of complex **A**, and the hydrogen bonds and edge-to-face $\pi-\pi$ interactions proposed for complex **A** are clearly present in the crystal structure of **6**. There are two different edge-to-face $\pi-\pi$ interactions in the structure, and in both, the benzoyl and aniline aromatic rings are in van der Waals contact, oriented at 86° to one another. The distances between the ring centers are 5.02 and 4.94 Å, and the shortest carbon–carbon distances are 3.79 Å in each case.[16]

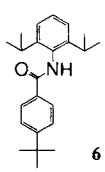

6

Titrations were carried out for the other combinations of compounds **1**–**4** (Table 1). The complexation-induced changes in chemical shift were similar to those observed for complex **A** (Scheme 4), which shows that all four complexes **A**–**D** have

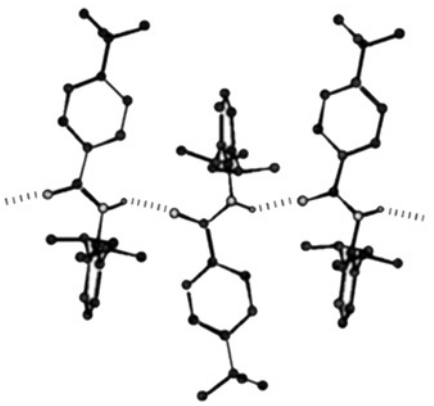

Fig. 1. X-ray crystal structure of **6**. The N–O distances in the hydrogen-bonded amides are 2.83 Å.

essentially the same structure in solution; in other words, the chemical mutations do not perturb the structure of the core of the complex. Table 1 shows the association constants derived from fitting the experimental data to a 1:1 binding isotherm.

Table 1. Association constants K_a in chloroform at 298 K [a].

Complex	Composition	K_a [M^{-1}]	ΔG [kJ mol^{-1}]
A	**1** + **4**	48 ± 2	− 9.6 ± 0.1
B	**2** + **4**	17 ± 2	− 7.1 ± 0.3
C	**1** + **5**	15 ± 3	− 6.8 ± 0.5
D	**2** + **5**	10 ± 2	− 5.7 ± 0.5
B*	**3** + **4**	14 ± 2	− 6.6 ± 0.4
D*	**3** + **5**	8 ± 2	− 5.2 ± 0.5

[a] Average values from at least three experiments. Titration data for four to six different signals were used to determine the association constant in each experiment. Errors are quoted as twice the standard error from the weighted mean (weighting based on the observed change in chemical shift).

Complexes **B**–**D**, which do not contain the terminal $\pi-\pi$ interaction, are clearly less stable than complex **A**. This indicates that this interaction is attractive and makes a significant contribution to the binding energy in chloroform. The results also show that secondary interactions operate in these systems: complex **D**, which does not have these secondary interactions, is less stable than all of the other complexes. Thus the double-mutant cycle is required for accurate quantitation of the edge-to-face $\pi-\pi$ interaction, which according to Equation (a) is -1.4 ± 0.8 kJ mol^{-1}.[17] Chloroform is a competitive solvent for this kind of nonpolar interaction, so the van der Waals and solvophobic contributions to binding are likely to be small, and the interaction measured is probably electrostatic in origin.

Wilcox et al. used a molecular torsion balance to measure an intramolecular edge-to-face $\pi-\pi$ interaction in chloroform, and their estimate (1.0 kJ mol^{-1}) is comparable to ours.[18] However, they also showed that a *tert*-butyl group interacts even more strongly with the face of a π system than an aromatic ring does. This is clearly inconsistent with our results: complex **B** is significantly less stable than complex **A**. To measure the effect of the *tert*-butyl group on our results, we constructed another double-mutant cycle using the methyl mutant **3** in place of the *tert*-butyl mutant **2**, specifically, using complexes **B*** and **D*** in place of complexes **B** and **D** (Scheme 5, Table 1). With this cycle the $\pi-\pi$ interaction is determined to be -1.4 ± 0.8 kJ mol^{-1}. This result is identical to that obtained with the first cycle, and we can detect no significant *tert*-butyl–π interaction in these complexes.

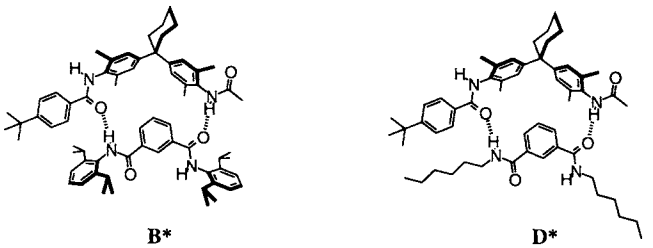

B* D*

Scheme 5. Complexes **B*** and **D***, which use the methyl mutant **3** in place of the *tert*-butyl mutant **2**.

This is consistent with an interaction that is electrostatic in origin, since aromatic protons have a larger net positive charge than alkyl protons.[2] The difference between the torsion balance and the zipper may be due to subtle differences in geometry or solvation.

The double-mutant approach is a powerful method for quantifying weak interaction energies, and the molecular zippers have an ideal structure for exploiting this potential. In principle, the method can be applied to investigate any noncovalent interaction, provided the two interacting functional groups can be attached to the ends of the zippers in an appropriate orientation. The results described here show that very weak interactions can be measured by this method: the edge-to-face $\pi-\pi$ interaction in this system is -1.4 ± 0.8 kJ mol^{-1}. This is not a universal value for edge-to-face $\pi-\pi$ interactions; it is accurate for the particular system we have used and provides an estimate of the likely magnitude of such interactions in other systems. The perceived noncovalent interaction in any system will be affected by secondary interactions and sensitive to solvent and the relative orientation and substitution pattern of the two aromatic rings.

Received: January 11, 1996 [Z 8725 IE]
German version: *Angew. Chem.* **1996**, *108*, 1628–1631

Keywords: hydrogen bonding · $\pi-\pi$ interactions · molecular recognition

[1] S. K. Burley, G. A. Petsko, *Science* **1985**, *229*, 23–28.
[2] C. A. Hunter, *Chem. Soc. Rev.* **1994**, *23*, 101–109.
[3] S. F. Ferguson, E. M. Sanford, E. M. Seward, F. Diederich, *J. Am. Chem. Soc.* **1991**, *113*, 5410–5419; F. Cozzi, M. Cinquini, R. Annuziata, J. S. Siegel, *ibid.* **1993**, *115*, 5330–5331; D. B. Amabilino, P. R. Ashton, C. L. Brown, E. Cordova, L. A. Godinez, T. T. Goodnow, A. E. Kaifer, S. P. Newton, M. Pietraszkiewicz, D. Philp, F. M. Raymo, A. S. Reder, M. T. Rutland, A. M. Z. Slawin, N. Spencer, J. F. Stoddart, D. J. Williams, *ibid.* **1995**, *117*, 1271–1293.
[4] C. A. Hunter, *J. Mol. Biol.* **1993**, *230*, 1025–1054.
[5] W. L. Jorgensen, D. L. Severance, *J. Am. Chem. Soc.* **1990**, *112*, 4768–4774.
[6] J. G. Vinter, *J. Comp. Mol. Des.* **1994**, *8*, 653–668.
[7] L. Serrano, M. Bycroft, A. R. Fersht, *J. Mol. Biol.* **1991**, *218*, 465–475.
[8] A. P. Bisson, F. J. Carver, C. A. Hunter, J. P. Waltho, *J. Am. Chem. Soc.* **1994**, *116*, 10292–10293.
[9] For other examples of the use of thermodynamic cycles to measure weak interactions see: Y. Kato, M. M. Conn, J. Rebek, *J. Am. Chem. Soc.* **1994**, *116*, 3279–3284; Y. Aoyama, M. Asakawa, A. Yamagishi, H. Toi, H. Ogoshi, *ibid.* **1990**, *112*, 3145–3151; Y. Aoyama, M. Asakawa, Y. Matsui, H. Ogoshi, *ibid.* **1991**, *113*, 6233–6240.
[10] M. S. Searle, D. H. Williams, *J. Am. Chem. Soc.* **1992**, *114*, 10690–10697.
[11] One limitation of the approach is that for intermolecular complexes, the entropy of complexation partially compensates the enthalpy of complexation, and the extent to which this occurs may differ in each of the four complexes. It is not clear how significant this effect is in practice, but the implications for our experiments are that the value for the $\pi-\pi$ interaction determined using Equation (a) is a lower limit for the maximum possible interaction that would occur in a system in which all intermolecular modes have been eliminated. See ref. [12] and M. S. Searle, M. S. Westwell, D. H. Williams, *J. Chem. Soc. Perkin Trans. 2* **1995**, 141–151.
[12] A. E. Mark, W. F. Vangunsteren, *J. Mol. Biol.* **1994**, *240*, 167–176.
[13] All new compounds gave satisfactory spectroscopic data.
[14] K. A. Connors, *Binding Constants*, Wiley, New York, **1987**, p. 21–101.
[15] Crystal structure data for **6** ($C_{23}H_{31}NO$): $M_r = 337.49$; crystallizes from dichloromethane as colorless blocks; crystal dimensions $0.54\times0.33\times0.20$ mm. Monoclinic, $a = 10.360(3)$, $b = 9.983(3)$, $c = 21.152(5)$ Å, $\beta = 94.670(10)°$, $V = 2180.4(10)$ Å^3, $Z = 4$, $\rho_{calcd} = 1.028$ g cm^{-3}, space group $P2_1/n$ (a nonstandard setting of $P2_1/c$, C^5_{2h}, No.14), $Mo_{K\alpha}$ radiation ($\lambda = 0.71073$ Å), $\mu(Mo_{K\alpha}) = 0.062$ mm^{-1}, $F(000) = 736$. The data were collected at room temperature in the range $3.5 < 2\theta < 45°$ on a Siemens P4 diffractometer by the Ω scan method. Of the 3875 reflections measured, all of which were corrected for Lorentz and polarizsation effects (but not for absorption), 1564 independent reflections exceeded the significance level $|F|/\sigma(|F|) > 4.0$. The structure was solved by direct methods and refined by full matrix least squares on F^2. Hydrogen atoms were included in calculated positions and refined in the riding mode. Refinement converged at a final $R = 0.0870$ ($wR_2 = 0.2971$, for all 2853 data, 226 parameters, mean and maximum δ/σ 0.000/0.000) with allowance for the thermal anisotropy of all non-hydrogen atoms. Minimum and maximum final electron density: -0.226 and 0.181 e Å^{-3}. A weighting scheme $w = 1/[\sigma^2(F_o^2) + (0.1473P)^2 + 1.4184P]$ where $P = (F_o^2 + 2F_c^2)/3$ was used in the latter stages of refinement. Complex scattering factors were taken from the program package SHELXL93 as implemented on the Viglen 486dx computer. Crystallographic data (excluding structure factors) for the structure reported in this paper have been deposited with the Cambridge Crystallographic Data Centre as supplementary publication no. CCDC-179-47. Copies of the data can be obtained free of charge on application to The Director, CCDC, 12 Union Road, Cambridge CB2 1EZ, UK (fax: Int. code +(1223)336-033; e-mail: teched@chemcrys.cam.ac.uk).
[16] G. Klebe, F. Diederich, *Phil. Trans. R. Soc. London A* **1993**, *345*, 37–48.
[17] The error takes no account of systematic errors inherent in measurements on such weakly binding complexes. Different titration procedures give small but significant changes in the measured association constants, but systematic errors of this type are reduced in a thermodynamic cycle provided all four experiments in the cycle are carried out under identical conditions.
[18] S. Paliwal, S. Geib, C. S. Wilcox, *J. Am. Chem. Soc.* **1994**, *116*, 4497–4498.

μ_3-Imido-Functionalized Chevrel–Sergent-Type Molecular Clusters, a New Class of Inorganic–Organic Hybrid Compounds: Preparations and Alkylation Reactions

Santiago Uriel, Kamal Boubekeur, Patrick Batail,* and Jesús Orduna

In 1995 we reported on the synthesis of chalcogen-enriched, μ_3-heteroatom-substituted hexanuclear chalcohalide cluster dianions $(n\mathrm{Bu_4N})_2[\mathrm{Re_6Q^i_5(\mu_3\text{-}E)Cl^i_2(Cl^a_6)}]$ (Q = S, Se; E = O, S, Se, Te; *i* stands for an inner ligand capping a face of the Re_6 octahedron and *a* for an apical, terminal ligand linked to a single rhenium atom) by reaction of the cluster monoanions $(n\mathrm{Bu_4N})[\mathrm{Re_6Q^i_5Cl^i_3(Cl^a_6)}]$ with silylated reagents $(\mathrm{Me_3Si})_2\mathrm{E}$ at room temperature.[1] We now report efficient reactions in which one face-capping μ_3-chloro core ligand (Cl^i) is displaced by amino substituents upon treatment of the generic cluster monoanions with bis(trimethylsilyl)amine derivatives. Furthermore, and most importantly, it is demonstrated that the μ_3-imido-functionalized cluster cores $[\mathrm{Re_6Q_5(\mu_3\text{-}NR)Cl_2}]^{4+}$, which

[*] Prof. Dr. P. Batail, Dr. S. Uriel, Dr. K. Boubekeur
Institut des Matériaux de Nantes
UMR 110 CNRS-Université de Nantes
2, rue de la Houssinière, F-44072 Nantes (France)
Fax: Int. code +40373995
e-mail: batail@cnrs-imn.fr
Dr. J. Orduna
Instituto de Ciencia de Materiales de Aragón
Universidad de Zaragoza, E-50009 Zaragoza (Spain)

[**] This work was supported by the CNRS, the Région Pays de Loire, the Conseil Général de Loire Atlantique, and the City of Nantes. We thank Siemens S. A. for X-ray diffraction CCD data for one compound.

are isostructural and isoelectronic with the Chevrel–Sergent cluster cores $[Mo_6Q_8]^{4-}$,[2a,b] react with electrophiles—an important and long-cherished goal in this chemistry.[2c–2h]

The reaction of $(n\mathrm{Bu_4N})[Re_6Q_5Cl_9]$ (Q = S, Se) with $(Me_3Si)_2NR$, (R = Me, CH_2Ph), followed by addition of an excess of $n\mathrm{Bu_4NCl}$ affords **1**–**4** in good yields (Scheme 1). As demonstrated earlier in the halide/chalcogenide substitution–functionalization chemistry,[1,3] the driving force of the present substitution reactions, in addition to the formation of Me_3SiCl, is the formation of the cluster dianions, the thermodynamically most stable cluster forms. Thus, besides convincing elemental analysis data, negative liquid secondary ion mass spectrometry[4] (LSIMS data see Table 1) proved extremely valuable in determining the composition, and hence the charge of the new compounds. All fragmentations characteristic of the dianionic clusters in $(n\mathrm{Bu_4N})_2[Re_6Q_5ECl_8]$ (E = O, S, Se, Te)[1] are observed for **1**–**4**. However, several additional peaks are identified, properly assigned, and found to be specific for the amine substituent (R-specific fragmentations, Table 1). Thus, **1**–**4** generate the gas-phase anions, $[Re_6Q_5Cl_6]^-$, $[Re_6Q_5Cl_5]^-$, and $[Re_6Q_5Cl_4]^-$ (Table 1), as a result of the loss of their N-methyl or N-benzyl ligands. Collision-induced dissociation (CID) experiments unambigously demonstrate the formation of these species by gas-phase reactions rather than matrix processes. The precursor-ion spectra of $[Re_6Q_5Cl_6]^-$ ions (m/z = 1489.4 for Q = S; m/z = 1725.1 for Q = Se) show that these species are generated from $[Re_6Q_5(\mu_3\text{-NR})Cl_8]^-$ ions. Likewise, the daughter-ion spectra of $[Re_6Q_5(\mu_3\text{-NR})Cl_8]^-$ ions issued from compounds **1**–**4**, and illustrated in Figure 1 for **3**, indicate the loss of N–R, albeit associated with the concomitant loss of either one or two chlorine atoms.

These results are substantiated further by the X-ray structure determination[5] for **1** (Fig. 2). It should be noted that within the

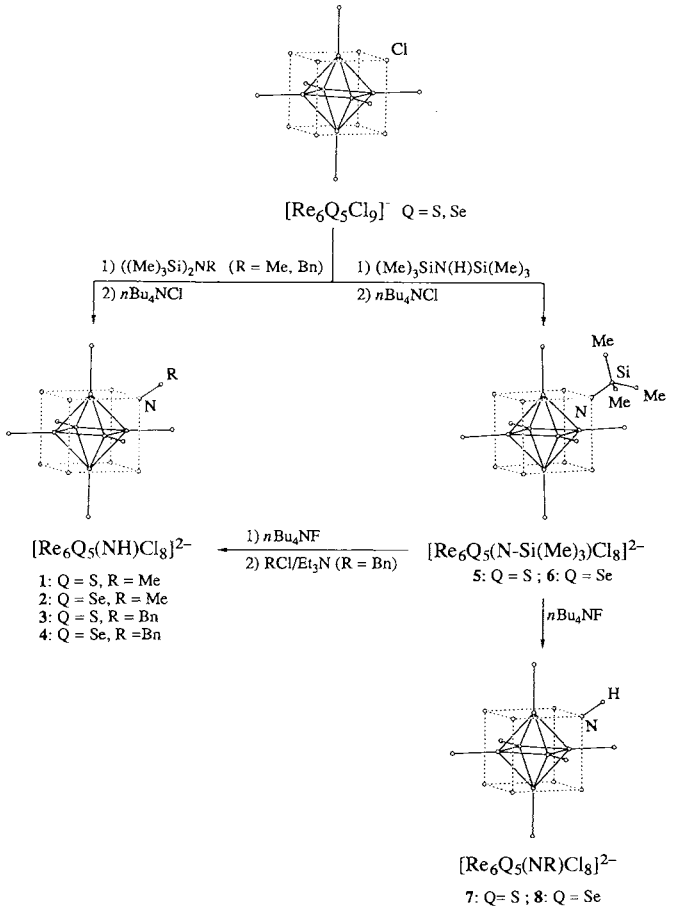

Scheme 1. Reaction scheme for the preparation of **1**–**8**. In each case the counterions of the anionic cluster are $n\mathrm{Bu_4N}$ ions. Bn = benzyl.

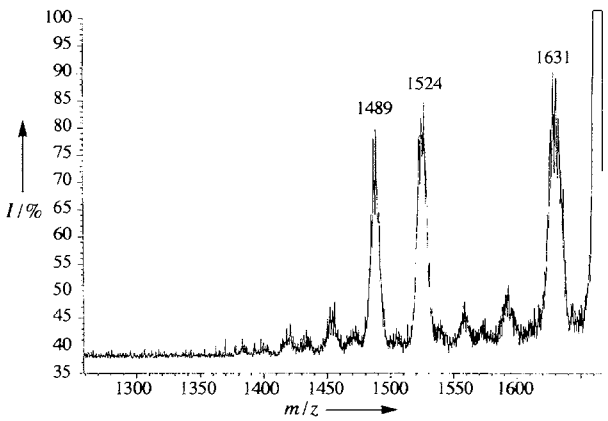

Fig. 1. CID-daughter-ion spectrum of the $[Re_6S_5(\mu_3\text{-}NCH_2Ph)Cl_8]^-$ ion (the off-scale peak on the right-hand side) showing its fragmentation in the gas phase into $[Re_6S_5(\mu_3\text{-}NCH_2Ph)Cl_7]^-$ (m/z = 1631), $[Re_6S_5Cl_7]^-$ (m/z = 1524), and $[Re_6S_5Cl_6]^-$ (m/z = 1489) ions.

Table 1. Negative ion LSIMS data of **1**–**8**, m/z (relative abundance [%]) [a].

Anion	**1**, Q = S R = Me	**3**, Q = S R = $CH_2C_6H_5$	**5**, Q = S R = $Si(Me)_3$	**7**, Q = S R = H	**2**, Q = Se, R = Me	**4**, Q = Se, R = $CH_2C_6H_5$	**6**, Q = Se, R = $Si(Me)_3$	**8**, Q = Se R = H
$[Bu_4NRe_6Q_5NRCl_8]^-$	1832.6 (41)	1908.7 (80)	1890.8 (50)	1818.6 (63)	2068.4 (50)	2144.4 (41)	2126.4 (45)	2054.4 (63)
$[Re_6Q_5NRCl_8]^-$	1590.4 (85)	1666.4 (73)	1648.4 (62)	1576.3 (82)	1826.1 (100)	1902.1 (100)	1884.1 (93)	1812.1 (80)
$[Re_6Q_5NRCl_7]^-$	1555.4 (100)	1631.4 (100)	1613.4 (100)	1541.4 (100)	1791.1 (84)	1867.1 (86)	1849.1 (100)	1777.1 (100)
$[Re_6Q_5NRCl_6]^-$	1518.4 (29)	1594.5 (63)	1576.4 (75)	1504.4 (70)	1754.1 (20)	1830.2 (45)	1812.2 (55)	1740.1 (71)
$[Re_6Q_5NRCl_5]^-$		1559.5 (35)	1541.5 (88)	1469.4 (52)		1795.2 (29)	1777.2 (77)	1705.2 (49)
$[Re_6Q_5NRCl_4]^-$			1506.5 (77)	1434.5 (34)			1742.2 (59)	1670.2 (34)
$[Re_6Q_5NRCl_3]^-$				1399.5 (18)			1707.3 (42)	
$[Re_6Q_5NRCl_8]^{2-}$	795.2 (15)	833.2 (15)	824.2 (7)	788.2 (8)	913.0 (5)	951.1 (20)	942.1 (12)	906.0 (5)
Detailed assignment of R-specific fragmentations								
$[Re_6Q_5NSi(Me)_2Cl_8]^-$			1633.4 (45)				1869.1 (56)	
$[Re_6Q_5NSi(Me)_2Cl_7]^-$			1598.4 (20)				1834.1 (47)	
$[Re_6Q_5NSi(Me)_2Cl_6]^-$			1561.4 (43)				1797.1 (52)	
$[Re_6Q_5NSi(Me)_2Cl_5]^-$			1526.5 (30)				1762.2 (40)	
$[Re_6Q_5NSi(Me)_2Cl_4]^-$			1491.5 (37)					
$[Re_6Q_5Cl_6]^-$	1489.4 (41)	1489.4 (76)			1725.1 (25)	1725.1 (55)		
$[Re_6Q_5Cl_5]^-$	1454.4 (45)	1454.4 (66)			1690.2 (20)	1690.2 (41)		
$[Re_6Q_5Cl_4]^-$	1419.5 (31)	1419.5 (62)			1655.2 (13)	1655.2 (33)		

[a] m/z value of the most abundant ion in the isotopic distribution; peaks above m/z = 300 are included.

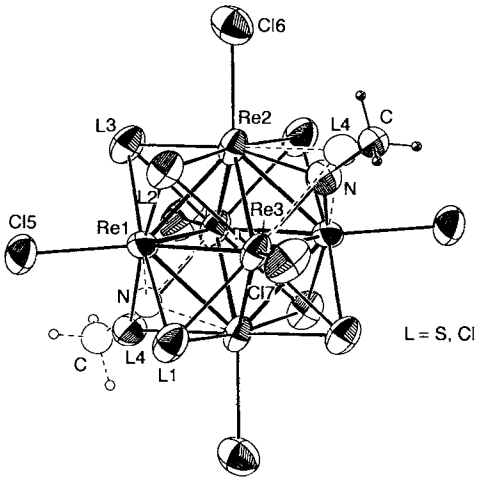

Fig. 2. Crystal structure of the $[Re_6S_5(\mu_3\text{-NMe})Cl_8]^{2-}$ dianion in **1**, showing 50% probability ellipsoids and the atom labeling scheme.

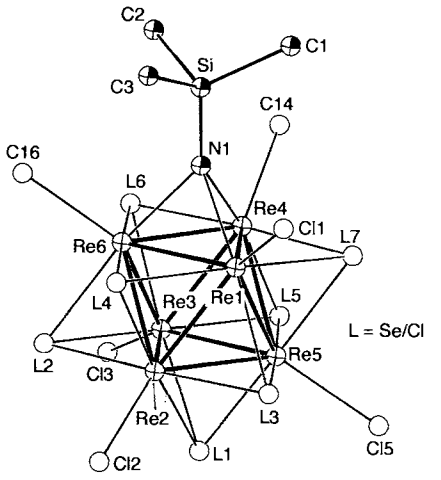

Fig. 3. Representation of the solid-state structure of the $[Re_6SeS_5(\mu_3\text{-}NSiMe_3)Cl_8]^{2-}$ dianion in **6**.

crystal lattice the μ_3-NMe group is found disordered onto two opposite faces of the Re_6 octahedron. There is no apparent distortion of the latter upon coordination by the imido group. On the other hand, the disordered, mixed μ_3-sulfido and μ_3-chloro ligands L4 (Fig. 2) appear to be further away from their Re_3 faces than the other mixed sulfido and chloro ligands L1, L2, and L3. The elevation of the ligands L1–L3 from their respective cluster face is, in fact, comparable to that observed in the structure of $(nBu_4N)_2[Re_6S_6Cl_8]$.[3b] Conversely, the disordered μ^3-N atoms lie closer to their corresponding Re_3 face (av Re–N 2.013(45) Å) than the μ_3-oxygen atom does in the structures of $(nBu_4N)_2[Re_6S_5OCl_8]$[1] (av Re–O 2.087(6) Å) and $(Pr_4N)_2[Re_6Se_4O_2Cl_8]$[3a] (av Re–O 2.083(14) Å and 2.094(19) Å, for the α and β isomers, respectively). However in $(nBu_4N)_2[Re_6S_5OCl_8]$, the Re_3 face capped by an oxygen atom is contracted, while the opposite, sulfur-capped face is expanded. This suggests that the seemingly nondistorted cluster core in **1** in fact corresponds to an average of two distorted opposite cluster faces capped by either a μ_3-N or a μ_3-S atom, that is a contracted and an expanded one, amounting to no apparent net effect. The average Re–Cl^a distance, specific for the charge of the cluster motif, is 2.374(5) Å, as expected for a cluster dianion.[1, 3b]

The trimethylsilylamine-derivatized compounds **5** and **6** were obtained from reactions of $(nBu_4N)[Re_6Q_5Cl_9]$ with $(Me_3Si)_2NH$ (Scheme 1), and were fully characterized by elemental analysis, LSIMS (Table 1), and X-ray diffraction (only for **6**).[6] The structure of the anion of **6** is shown in Figure 3. Remarkably, and in contrast to **1**–**4**, the cluster ions of **5** and **6** do not lose their silylamino ligands under LSIMS conditions. In this case the most characteristic fragmentation is the loss of one methyl radical to give a series of peaks (Table 1) at 15 mass units below those corresponding to successive losses of chlorine atoms. The loss of one methyl group is confirmed by CID experiments.

The trimethylsilyl groups may be removed readily by using fluoride anions as nucleophile.[7] Thus, reaction of **5** and **6** with nBu_4NF affords the long-sought after compounds **7** and **8**, respectively, in high yields. Again the compounds were characterized by elemental analysis and LSIMS (Table 1). Compounds **7** and **8**, as well as **3** and **4** are extremely soluble in organic solvents; thus, good quality single crystals suitable for X-ray diffraction have not yet been obtained.

Finally, we have also been able to demonstrate that the μ_3-NH-functionalized cluster cores readily react with electrophiles. Thus, for example, **5** and **6** react with benzyl chloride and catalytic amounts of triethylamine to give **3** and **4**, respectively. As mentioned earlier **3** and **4** were also obtained independently by the direct substitution–functionalization reactions.

Thus, opportunities are now offered to extend the chemistry of inorganic–organic hybrid compounds. The molecular cores of these compouds are prepared by high-temperature solid-state synthesis only and are subsequently converted to new compounds at room temperature with modern inorganic reactions—in this case, by reactions of imido ligands with electrophiles.

Experimental Procedure

A suspension of $(nBu_4N)[Re_6Q_5Cl_9]$ (Q = S, Se) (100 mg, ca. 50 μmol) [3b] in dry CH_3CN (50 mL) under an argon atmosphere was treated with an excess (ca. 20-fold) of either $(Me_3Si)_2NMe$, $(Me_3Si)_2NCH_2Ph$, or $(Me_3Si)_2NH$. The mixture was stirred at room temperature until complete dissolution of the starting material (5–8 h). An excess of solid $(nBu_4N)Cl$ was then added and the solution was stirred for two hours. The solution was evaporated to dryness in vacuo, the orange residue washed with ethanol and recrystallized from acetonitrile (ca. 15 mL).

1: Yield 68 mg, 60%. Elemental analysis for $C_{33}H_{75}N_3Re_6S_5Cl_8$ (M = 2075.1): Calcd. C 19.1, H 3.64, N 2.02, S 7.72, Cl 13.67; found C 18.75, H 3.32, N 2.26, S 7.83, Cl 13.34.

2: Yield 76 mg, 69%. Elemental analysis for $C_{33}H_{75}N_3Re_6Se_5Cl_8$ (M = 2309.6): Calcd. C 17.16, H 3.27, N 1.82, Cl 12.28; found C 17.01, H 3.05, N 1.96, Cl 12.52.

3: Yield 71 mg, 61%. Elemental analysis for $C_{39}H_{79}N_3Re_6S_5Cl_8$ (M = 2151.2): Calcd. C 21.77, H 3.70, N 1.95, S 7.45, Cl 13.18; found C 22.1, H 3.31, N 2.07, S 7.22, Cl 12.97.

4: Yield 77 mg, 67%. Elemental analysis for $C_{39}H_{79}N_3Re_6Se_5Cl_8$ (M = 2385.7): Calcd. C 19.63, H 3.34, N 1.76, Cl 11.89; found C 20.01, H 3.15, N 1.96, Cl 11.62.

5: Yield 67 mg, 58%. Elemental analysis for $C_{35}H_{81}N_3Re_6S_5Cl_8Si$ (M = 2133.3): Calcd. C 19.71, H 3.83, N 1.97, S 7.51, Cl 13.30; found C 19.35, H 3.47, N 2.04, S 7.69, Cl 13.53.

6: Yield 62 mg, 55%. Elemental analysis for $C_{35}H_{81}N_3Re_6Se_5Cl_8Si$ (M = 2367.8): Calcd. C 17.75, H 3.45, N 1.77, Cl 11.98; found C 17.81, H 3.34, N 1.71, Cl 12.01.

Nucleophilic substitution reactions of the trimethylsilylamine-derivatized cluster cores: A solution of **5** or **6** (100 mg, ca. 50 μmol) in CH_3CN (50 mL) was treated with an excess (ca. 10-fold) of nBu_4NF supported on silica gel 1%. The reaction mixture was stirred for 6 h at room temperature, filtered off, and evaporated to dryness in vacuo. The residue (**7** or **8**, respectively) was washed with ethanol and recrystallized from acetonitrile.

7: Yield 84 mg, 87%. Elemental analysis for $C_{32}H_{73}N_3Re_6S_5Cl_8$ (M = 2061.1): Calcd. C 18.65, H 3.57, N 2.04, S 7.78, Cl 13.76; found C 18.82, H 3.49, N 2.31, S 7.47, Cl 13.42.

8: Yield 86 mg, 89%. Elemental analysis for $C_{32}H_{73}N_3Re_6Se_5Cl_8$ (M = 2295.6): Calcd. C 16.74, H 3.21, N 1.83, Cl 12.36; found C 17.03, H 3.76, N 2.05, Cl 12.48.

Alkylation reactions: A solution of **5** or **6** (50 mg) in CH_2Cl_2 (30 mL) was treated first with nBu_4NF, then with an excess of benzyl chloride and catalytic amounts of

 © VCH Verlagsgesellschaft mbH, D-69451 Weinheim, 1996 0570-0833/96/3513-1546 $ 15.00+.25/0

triethylamine. The reaction mixture was stirred for 18 h and evaporated to dryness in vacuo. The residue was washed with ethanol, dissolved in a 1/1 ethanol/acetonitrile solution and treated with an excess of nBu$_4$NCl in order to ensure complete exchange of any other possible ammonium cations such as Ph(Me)$_3$N$^+$. The solution was evaporated to dryness in vacuo, washed with ethanol and recrystallized from acetonitrile. The LSI mass spectra of the resulting products were identical to those of **3** and **4**.

Received: January 5, 1996 [Z 8709 IE]
German version: *Angew. Chem.* **1996**, *108*, 1631–1634

Keywords: mass spectrometry · organic–inorganic hybrid composite · rhenium compounds

[1] S. Uriel, K. Boubekeur, P. Batail, J. Orduna, E. Canadell, *Inorg. Chem.* **1995**, *34*, 5307–5313.

[2] a) R. Chevrel, M. Sergent, J. Prigent, *J. Solid State Chem.* **1971**, *3*, 515; b) T. Hughbanks, R. Hoffmann, *J. Am. Chem. Soc.* **1983**, *105*, 1150–1162; c) S. C. Lee, R. H. Holm, *Angew. Chem.* **1990**, *102*, 868; *Angew. Chem. Int. Ed. Engl.* **1990**, *29*, 840–856; d) T. Saito, N. Yamamoto, T. Nagase, T. Tsuboi, K. Kobayashi, T. Yamagata, H. Imoto, K. Unoura, *Inorg. Chem.* **1990**, *29*, 764–770; e) D. H. Johnston, D. C. Gaswick, M. C. Lonergan, C. L. Stern, D. F. Shriver, *Inorg. Chem.* **1992**, *31*, 1869–1873; f) N. Perchenek, A. Simon *Z. Anorg. Allg. Chem.* **1993**, *619*, 103–108; g) S. J. Hilsenbeck, V. G. Young, Jr., R. E. McCarley, *Inorg. Chem.* **1994**, *33*, 1822–1832; h) G. M. Ehrlich, C. J. Warren, D. A. Vennos, D. M. Ho, R. C. Haushalter, F. J. DiSalvo, *Inorg. Chem.* **1995**, *34*, 4454–4459.

[3] a) O. M. Yaghi, M. J. Scott, R. H. Holm, *Inorg. Chem.* **1992**, *31*, 4778–4784; b) J.-C. Gabriel, K. Boubekeur, P. Batail, *Inorg. Chem.* **1993**, *32*, 2894–2900.

[4] The LSI mass spectra were recorded as described previously [1]. Helium was used as the collision gas in CID experiments [8] and the pressure was adjusted to reduce the main beam intensity to 50% of its original value. The spectra were recorded by linked scans [9] at constant B/E and B^2/E for daughter-ion and precursor-ion spectra, respectively.

[5] X-ray crystal structure analysis for **1**: $C_{33}H_{75}N_3S_5Cl_8Re_6$, $M_r = 2075.13$, orange crystals, monoclinic, space group $P2_1/n$, $a = 12.895(3)$, $b = 11.468(5)$, $c = 18.365(4)$ Å, $\beta = 90.87(2)°$, $V = 2715.5(1.5)$ Å^3, $Z = 2$, $\rho_{calcd} = 2.54$ g cm^{-3}, $Mo_{K\alpha}$ radiation, empirical absorption corrections ($\mu = 141.2$ cm^{-1}), 5943 independent reflections with ω-2θ scans were measured up to $\theta = 27°$ at 230 K on an Enraf–Nonius CAD4 diffractometer. The structure was solved by the Patterson method. The full matrix least-squares refinements of 266 parameters for 3056 reflections with $I \geq 3\sigma(I)$ converged at $R = 0.036$ and $R_w = 0.045$ (GOF = 1.297). Crystallographic data (excluding structure factors) for the structures reported in this paper have been deposited with the Cambridge Crystallographic Data Centre as supplementary publication no. CCDC-179-51. Copies of the data can be obtained free of charge on application to The Director, CCDC, 12 Union Road, Cambridge CB2 1EZ, UK (fax: Int. code +(1223) 336-033; e-mail: teched@chemcrys.cam.ac.uk).

[6] Preliminary crystallographic data for **6**: $C_{35}H_{81}N_3SiCl_8Se_5Re_6$, $M_r = 2365.78$, orange platelike crystals, monoclinic, space group $P2_1/c$, $a = 24.948(1)$, $b = 11.7636(6)$, $c = 22.279(1)$ Å, $\beta = 111.287(1)°$, $V = 6092(1)$ Å^3, $Z = 4$, $\rho_{calcd} = 2.58$ g cm^{-3}; 20696 reflections were measured with $Mo_{K\alpha}$ radiation up to $\theta = 27°$ at 295 K on a Siemens CCD-area detector based SMART X-ray diffractometer. The structure was solved by direct methods. Experiments to determine the precise structure and its triclinic low-temperature modification, are currently in progress and will be published separately.

[7] a) R. J. P. Corriu, V. Huynh, J. J. E. Moreau, M. Pataud-Sat, *Tetrahedron Lett.* **1982**, *23*, 3257–3260; b) R. J. P. Corriu, V. Huynh, J. J. E. Moreau, *Tetrahedron Lett.* **1984**, *25*, 1887–1890.

[8] a) K. Levsen, H. Schwarz, *Angew. Chem.* **1976**, *88*, 589–599; *Angew. Chem. Int. Ed. Engl.* **1976**, *15*, 509–519; b) F. W. McLafferty, P. F. Bente, R. Kornfeld, S.-C. Tsai, I. Howe, *J. Am. Chem. Soc.* **1973**, *95*, 2120–2129.

[9] R. K. Boyd, *Spectros. Int. J.*, **1982**, *1*, 169–200.

Octakis(3,4-dimethylphenylthio)naphthalene: A Designed Spider Host of Unparalled Versatility**

Gary A. Downing, Christopher S. Frampton, James H. Gall, and David D. MacNicol*

The exactly D_2-symmetric conformation of the spider host[1] octakis(*m*-tolylthio)naphthalene **1** is instrumental in maintaining an open tetragonal host lattice, which, remarkably, is stable even in the absence of a guest.[2] This key conformation is of the *aabbaabb* type[2] where *a* and *b* denote side chains projecting above and below the mean plane of the naphthalene core, respectively. Based on a knowledge of the crystal structure of **1**, we have sought to reproduce this key conformation by judicious modification, with a view to producing related clathrates with larger cavities suitable for versatile storage of guests[3] and lattice-controlled reactivity studies.[4] Salient results from this line of enquiry are now reported.

Initial studies involved replacement of the *meta*-methyl group in the side chains of **1** by the polar methoxy function[5] or the bulky *tert*-butyl group,[6] as in **2** and **3**; however, these changes

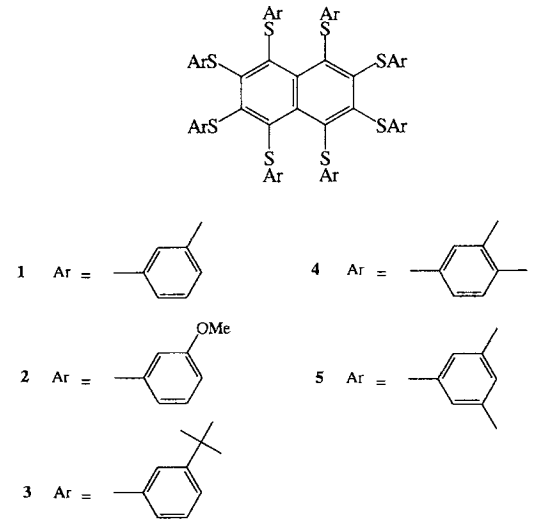

were found to attenuate severely inclusion ability, highlighting the importance of the specific nature of the *meta* substituent in controlling host packing. In view of this, the *meta*-methyl group was retained, and octakis(3,4-dimethylphenylthio)naphthalene **4** and octakis(3,5-dimethylphenylthio)naphthalene **5**, both possessing an additional methyl group in their side chains, were targeted and prepared. Compounds **4** and **5** were found to be at the opposite ends of the inclusion ability spectrum, a direct reflection of their molecular conformations, as described below.

The introduction of a second *meta*-methyl substituent, as in **5**, is incompatible with a D_2 conformation analogous to that of **1**

[*] Dr. D. D. MacNicol, Dr. G. A. Downing, J. H. Gall
Department of Chemistry
University of Glasgow
Glasgow G12 8QQ (UK)
Fax: Int. code +(141)3304888
Dr. C. S. Frampton
Roche Research Centre
P. O. Box 8
Welwyn Garden City
Hertfordshire AL7 3AY (UK)

[**] We thank the EPSRC (UK) for support (to G. A. D.).

 © VCH Verlagsgesellschaft mbH, D-69451 Weinheim, 1996 0570-0833/96/3513-1547 $ 15.00+.25/0

owing to severe *trans*-ring interactions arising from the second methyl group. This leads to the formation of a highly asymmetric *abbaabab* conformation, previously uncategorized,[2] in which two of the *peri*-related side chains have a *syn*-arrangement.[7] Compound **5** has shown no evidence of inclusion compound formation. By contrast, the sterically undemanding introduction of a *para*-methyl substituent as in **4** leaves the parent D_2 host conformation of **1** essentially unperturbed (see below), and the new compound **4** possesses truly versatile inclusion properties.

The first indication of the remarkable inclusion behavior of **4** became apparent during its isolation in the course of which ruby-red cubes containing components of the solvent (40–60° petroleum ether) were obtained on evaporation of chromatographic fractions overnight. Host **4** rapidly revealed an impressive ability to include guest species and these ranged in size from thiophosgene to squalene (Table 1). Moreover, guest classes

Table 1. Representative inclusion compounds formed by **4** [a].

Guest	Host–guest ratio	Guest	Host–guest ratio
thiophosgene	1:2 [b]	methyl ethyl ketone	1:1.2
1,4-dioxane	1:1.9	*m*-xylene	1:1.1
1,4-thioxane	1:1.9	ethyl acetate	1:1.0
trichloroethylene	1:1.8	eugenol	1:1.0
CH_3CCl_3	1:1.6	isobutyrophenone	1:1.0
5-chloropent-1-yne	1:1.6	(*R*)-(+)-1-phenylethylamine	1:1.0
pyridine	1:1.5	eucarvone	1:0.8
DMF	1:1.5	*R*-(+)-limonene	1:0.7
THF	1:1.4	hexamethyldisilazane	1:0.7
benzene	1:1.4	tri-*n*-butylphosphane	1:0.6
toluene	1:1.4	$(CH_3)_3SiC{\equiv}CSi(CH_3)_3$	1:0.6
N-methylmorpholine	1:1.3	$(CH_3)_4Sn$	1:0.3
CCl_4	1:1.3 [c]	$(CH_3CH_2)_4Pb$	1:0.3
benzyl alcohol	1:1.2	HMPA	1:0.3
tert-butyl alcohol	1:1.2	squalene	1:0.3
o-xylene	1:1.2	C_{60}	[d]

[a] Analysis method ^{1}H NMR spectroscopy unless stated otherwise. [b] Thermogravimetric analysis. [c] Microanalysis. [d] See ref. [11].

ranged through hydrocarbons, ethers, alcohols, ketones, amines, amides, and halocarbons, for example. Particularly significant, however, is the propensity of **4** to enclathrate volatile, reactive and toxic materials, such as THF, CCl_4, thiophosgene, tri-*n*-butylphosphane, hexamethylphosphoramide (HMPA), and tetraethyllead. In order to elucidate the origin of the novel properties displayed by **4**, which indicated unusual host packing and void geometry, single-crystal X-ray analyses of the 1,4-dioxane, *t*BuOH, $PbEt_4$, and $(CH_3)_3SiC{\equiv}CSi(CH_3)_3$ adducts were carried out.[8] The adducts of **4** crystallize in the cubic space group $Pn\bar{3}$, a transformation from the tetragonal packing of **1**, which is unique for any pure organic molecular system, as established by reference to the Cambridge Crystallographic Data Base.[9]

The host molecule of **4**, located on a point of 222 symmetry, is constrained to have exact D_2 symmetry, and both enantiomeric conformations are present in the crystal. Figure 1 shows the atomic numbering scheme of the asymmetric unit, and Figure 2 the $PbEt_4$ adduct with a view along one of the twofold rotation axes. The close correspondence of this *aabbaabb* conformation[2] to that of **1** (1,4-dioxane adduct) is indicated by comparison of the related torsion angles [°] (values for **1** in parentheses): C1-C9-C9′-C1′ − 27 (− 27), C9-C1-S1-C11 + 45 (+ 42), C-1-S1-C11-C12 + 49 (+ 50), C1-C2-S2-C22 + 94 (+ 94), and C2-S2-C21-C22 + 11 (+ 11).[9b] There are two large, enantiomerically related, cavities per unit cell; these voids are chiral with symmetry 23(T), and each void is capable of including one bulky guest such as tetraethyllead or up to six[10] medium-sized guests, for example, 1,4-dioxane or 1,4-thioxane.

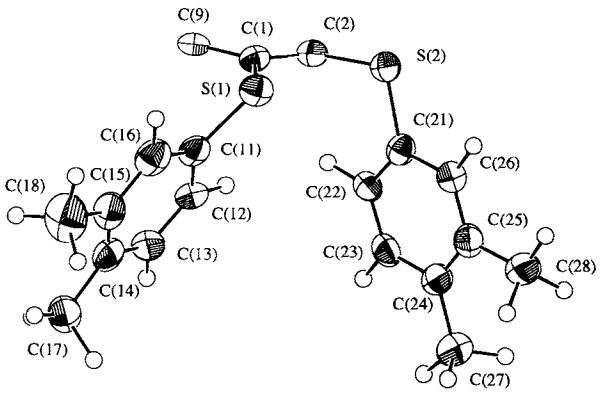

Fig. 1. View of the asymmetric unit in crystals of **4** showing atom numbering scheme. The thermal ellipsoids are drawn at the 50% probability level; hydrogen atoms are drawn as small circles of arbitary radius. Selected bond lengths [Å] and angles [°]: C(1)–C(2) 1.377(8), C(2)–C(2′) 1.42(1), C(1)–C(9) 1.444(7), C(9)–C(9′) 1.44(2); C(2)-C(1)-C(9) 120.4(6), C(1)-C(2)-C(2′) 120.2(4), C(1)-C(9)-C(9′) 116.8(4), C(1)-C(9)-C(1′) 126.3(8), C(9)-C(1)-S(1) 121.0(5) [8b].

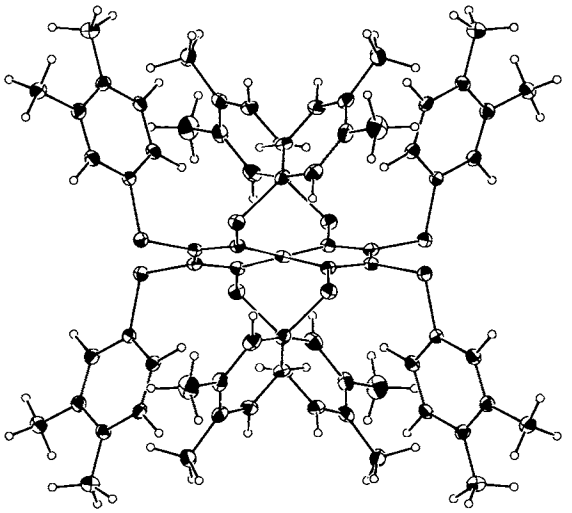

Fig. 2. Structure of **4** in its Et_4Pb clathrate. The view along the twofold rotation axis, which is coincident with the central C–C bond, illustrates the D_2-symmetric conformation of **4**.

The host–guest packing in the $PbEt_4$ adduct of **4** is shown in Figure 3. The six host molecules of **4** shown are centred round a point of $\bar{3}$ symmetry; there are, however, four such equivalent $\bar{3}$ points surrounding each cavity and, as a consequence, guest escape is blocked in all directions. The lead atom of the guest is located on a crystallographic twofold axis, hence, owing to statistical disorder, it appears as an octahedral distribution in Figure 3; the ethyl groups of the guest are highly disordered and are not shown.[11]

Recent work in the literature has described the effective control of reactions involving single molecules as well as dimerizations and polymerizations by the lattice.[4] The availability of discrete nanoscale cavities in **4**, capable of including several guest molecules, opens up the exciting possibility of carrying out controlled oligomerizations and related processes. Work along these lines is currently in progress.

 © VCH Verlagsgesellschaft mbH, D-69451 Weinheim, 1996 0570-0833/96/3513-1548 $ 15.00+.25/0

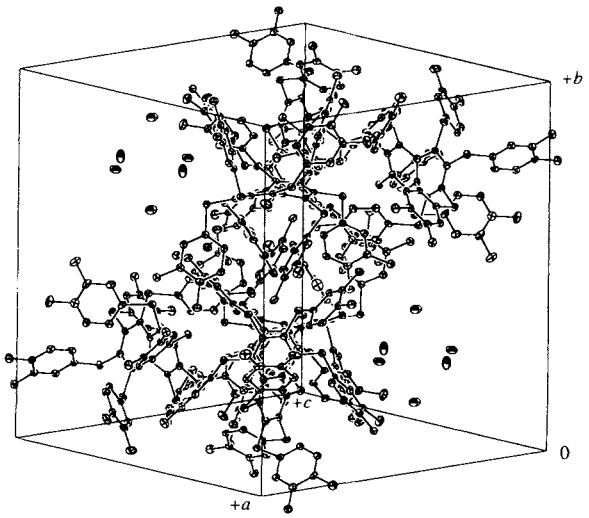

Fig. 3. Host–guest packing in the Et_4Pb clathrate of **4**. The octahedron of (partially occupied) lead atom positions arises from the 23(T) symmetry of the cavity. The highly disordered ethyl groups of the guest are not shown.

Experimental Procedure

4: Perfluoronaphthalene (0.26 g, 0.96 mmol) and sodium 3,4-dimethylbenzenethiolate (2.45 g, 15.3 mmol), prepared from 3,4-dimethylbenzenethiol and sodium in absolute ethanol, were stirred in dry, degassed 1,3-dimethylimidazolidin-2-one (DMEU) (20 mL) for 3 h at ambient temperature, under N_2. The red reaction mixture was then added to toluene (200 mL), washed with water (250 × 10 mL), and evaporation of the solvent gave a red oil which was chromatographed (dry column) on silica gel (60–80° petroleum ether/diethyl ether, 10/1) to afford 0.96 g (82%) of **4** as red cubelike crystals, m.p. 131–133 °C (petroleum ether adduct). ^{1}H NMR (200 MHz, $CDCl_3$): δ = 2.00 (s, 12H), 2.08 (s, 12H), 2.09 (s, 12H), 2.17 (s, 12H), 6.18 (dd, 4H, J = 8.0, 1.9 Hz), 6.44 (dd, 4H, J = 8.0, 1.9 Hz), 6.63 (d, 4H, J = 8.0 Hz), 6.66 (d,4H, J = 1.9 Hz), 6.81 (d, 4H, J = 8.0 Hz), 6.83 (d, 4H, J = 1.9 Hz); ^{13}C NMR (50 MHz, $CDCl_3$): δ = 19.3, 19.5, 19.6, 19.7, 125.0, 125.7, 129.1, 129.7, 129.8, 129.9, 133.8, 134.1, 134.4, 136.1, 136.5, 136.8, 139.9, 140.4, 144.7; FAB MS: m/z: 1216.34 (±0.12) [M^+]; $C_{74}H_{72}S_8$ calculated 1216.34.

5: Perfluoronaphthalene (0.25 g, 0.92 mmol) and sodium 3,5-dimethylbenzenethiolate (2.16 g,13.5 mmol), prepared from 3,5-dimethylbenzenethiol and NaH in THF, were stirred in dry, degassed DMEU (20 mL) for 3 h at ambient temperature, under N_2. The red reaction mixture was then added to toluene (200 mL), washed with water (250 × 10 mL), and evaporation of the solvent gave a red oil, from which compound **5** was obtained on recrystallization from 1,4-dioxane/methanol; yield 0.98g (88%), red crystals, m.p. 180–181 °C. ^{1}H NMR (200 MHz, $CDCl_3$): δ = 2.06 (br. s, 24H), 2.07 (br. s, 24H), 6.37 (m, 8H), 6.47 (m, 8H), 6.62 (m, 4H), 6.64 (m, 4H); ^{13}C NMR (50 MHz, $CDCl_3$): δ = 21.2, 21.3, 124.4, 125.3, 127.3, 127.7, 137.2, 138.0 (overlapping resonances), 138.3, 139.9, 143.3, 146.9; elemental analysis [%]: Calcd for $C_{74}H_{72}S_8$: C 73.02, H 5.92, S 21.06; found C 72.93, H 5.87, S 21.06.

Received: February 12, 1996 [Z 8809 IE]
German version: *Angew. Chem.* **1996**, *108*, 1643–1645

Keywords: arenes · host–guest chemistry · inclusion compounds

[1] See, for example, D. D. MacNicol in *Inclusion Compd.* **1984**, *2*, 123.
[2] D. D. MacNicol, P. R. Mallinson, C. D. Robertson, *J. Chem. Soc. Chem. Commun.* **1985**, 1649.
[3] For examples of storage of toxic guests in high-symmetry ($\bar{3}$) clathrate cages see: A. A. Freer, D. D. MacNicol, P. R. Mallinson, I. Vallance, *Tetrahedron Lett.* **1992**, *33*, 261 (O=CCl_2 in hexakis(*p*-phenoxyphenoxy)benzene); R. J. Cross, J. J. McKendrick, D. D. MacNicol, *Nature (London)* **1973**, *245*, 146 ($Hg(CH_3)_2$ in *p*-hydroxyphenyl-2,2,4-trimethylthiachroman).
[4] For reviews on reaction control by host lattices see, for example, F. Toda, *Inclusion Compd.* **1991**, *4*, 126; M. Farina, *Inclusion Compd*, **1984**, *3*, 297.
[5] C. D. Robertson, Ph.D. Thesis **1990**, Glasgow University.
[6] G. A. Downing, Ph.D. Thesis **1993**, Glasgow University.
[7] G. A. Downing, D. D. MacNicol, P. R. Mallinson, P. K. Milligan, *Acta Crystallogr. Sect. C*, in press.
[8] Crystal data: **4**·0.3(Et_4Pb): $C_{74}H_{72}S_8$·0.3($(CH_3CH_2)_4Pb$), M_r = 1325.03, cubic, space group $Pn\bar{3}$, a = 22.2343(13) Å, V = 10991.8(3) Å^3, Z = 6, ρ_{calcd} = 1.201 g cm^{-3}, $Cu_{K\alpha}$ radiation, λ = 1.54178 Å, cell parameters from 25 reflections, 29.72° ≤ 2θ ≤ 99.32°, μ = 40.04 cm^{-1}, T = 123 K, bright red prism, 0.25 × 0.20 × 0.10 mm. Data Collection: Rigaku AFC7R diffractometer, $2\theta_{max}$ = 139.9°, ω-2θ scans, 5804 reflections collected, 3788 unique, R_{int} = 0.048, 2095 reflections observed, ($I \geq 2\sigma(I)$). Ψ scan absorption correction applied, (transmission factor range 0.65–1.00). The structure was solved by direct methods using SHELXS-86 [12] and refined on F to R = 0.075, R_w = 0.081 and S = 3.56 with $w = 1/\sigma^2(F)$ for the 2095 observed reflections. Hydrogen atoms for the host molecule were placed in calculated positions but not refined. The carbon atoms of the $(Et)_4Pb$ guest molecule were severely disordered and the model is the best fit to the residual electron density. Least-squares refinement was carried out using the teXsan package [13]. Crystal data for **4**·2.0(1,4-dioxane): $C_{74}H_{72}S_8$·2.0($C_4H_8O_2$), M_r = 1394.07, cubic, space group $Pn\bar{3}$, a = 22.5010(38) Å, V = 11392(1) Å^3, Z = 6, ρ_{calcd} = 1.216 g cm^{-3}, $Mo_{K\alpha}$ radiation, λ = 0.71069 Å, μ = 2.83 cm^{-1}, T = 290 K. Crystal data for **4**·1.2(tBuOH): $C_{74}H_{72}S_8$·1.2($(CH_3)_3COH$), M_r = 1306.81, cubic, space group $Pn\bar{3}$, a = 22.2220(24) Å, V = 10973.6(6) Å^3, Z = 6, ρ_{calcd} = 1.186 g cm^{-3}, $Mo_{K\alpha}$ radiation, λ = 0.71069 Å, cell parameters from 25 reflections, 18.78° ≤ 2θ ≤ 21.73°, μ = 2.87 cm^{-1}, T = 123 K, bright red cube, 0.25 × 0.25 × 0.25 mm. Crystal data for **4**·0.6($(CH_3)_3SiC{\equiv}CSi(CH_3)_3$): $C_{74}H_{72}S_8$·0.6($(CH_3)_3SiC{\equiv}CSi(CH_3)_3$), M_r = 1320.10, cubic, space group $Pn\bar{3}$, a = 22.2223(18) Å, V = 10974.1(4) Å^3, Z = 6, ρ_{calcd} = 1.198 g cm^{-3}, $Mo_{K\alpha}$ radiation, λ = 0.71069 Å, cell parameters from 25 reflections, 14.35° ≤ 2θ ≤ 20.69°, μ = 3.05 cm^{-1}, T = 123 K, bright red prism, 0.20 × 0.18 × 0.10 mm. Crystallographic data (excluding structure factors) for the structure(s) reported in this paper have been deposited with the Cambridge Crystallographic Data Centre as supplementary publication no. CCDC-179-43. Copies of the data can be obtained free of charge on application to The Director, CCDC, 12 Union Road, Cambridge CB2 1EZ, UK (Telefax: Int. code Int. Code +(1223) 336-033; e-mail: teched@chemcrys. cam.ac.uk).
[9] a) For an example of a metal-containing system with space group $Pn\bar{3}$, $[Et_4N]_6[Na_{14}Mo_{24}P_{17}O_{97}(OH)_{31}]$·$xH_2O$, see R. C. Haushalter, F. W. Lai, *Angew. Chem. Int. Ed. Engl.* **1989**, *28*, 743; *Angew. Chem.* **1989**, *101*, 802; b) Symmetry transformation used to generate equivalent atoms marked with a ('): $x, 3/2 - y, 1/2 - z$.
[10] Since there are six host molecules of **4** and two cavities per unit cell, uniform occupancy of each cavity by six guest molecules would correspond to a host–guest ratio of 1:2. The 75.4 MHz ^{13}C CP MAS spectrum (for which we thank Dr. D. C. Apperley, Univeristy of Durham) of the 1,4-dioxane adduct of **4** clearly indicates its nonstoichiometric composition (Table 1). Deconvolution of the methyl region reveals that one of the four lattice-symmetry-independent methyl carbon atoms is cleanly split into two components with a ratio close to 2:1; $\delta(CH_3)$ (relative weights in parentheses): 17.7 (1), 18.3 (1), 18.6 (1/3), 19.0 (2/3), and 20.9 (1). This is consistent with sixfold occupancy of two out of each three cages in the crystal, the third containing only five 1,4-dioxane guests, and is in keeping with the observed host–guest ratio of about 1:1.9, measured by ^{1}H NMR spectroscopy for a solution in $CDCl_3$ (see Table 1).
[11] The guest molecules 1,4-dioxane, tBuOH, and $(CH_3)_3SiC{\equiv}CSi(CH_3)_3$ all exhibit a high degree of disorder in their respective inclusion compounds with host **4**. Preliminary experiments have indicated the inclusion of C_{60} (the I_h symmetry of which is compatible with the T cage symmetry) by **4**, though single crystals suitable for X-ray diffraction analysis have not yet been obtained.
[12] G. M. Sheldrick, *Acta Crystallogr. Sect. A* **1990**, *46*, 467.
[13] *teXsan: Single Crystal Structure Analysis Software, Version 1.6*, Molecular Structure Corporation, The Woodlands, TX 77381 (USA) **1993**.

Synthesis and Structure of *ortho*-Phenylenezinc**

Marcel Schreuder Goedheijt, Tom Nijbacker, Otto S. Akkerman, Friedrich Bickelhaupt,* Nora Veldman, and Anthony L. Spek

Dedicated to Professor Erwin Weiss on the occasion of his 70th birthday

In the context of our interest in polymetalated compounds,[1] we had previously prepared *ortho*-phenylenemagnesium (**1**)[2] from *ortho*-phenylenemercury (**2**)[3] (Scheme 1). It turned out

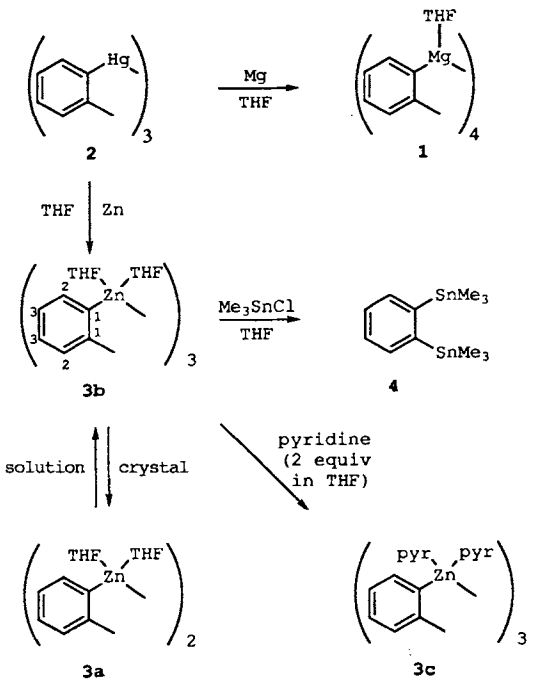

Scheme 1. Synthesis of **1**, **3a–c**, and **4** from **2**.

that **1** has an unusual tetrameric structure in which four magnesium atoms are arranged in the form of a distorted tetrahedron. Similar structures are also observed for the related compounds diphenylvinylenemagnesium and 1,8-naphthalenediylmagnesium,[2] and overall the situation resembles that for tetrameric organolithium clusters. Since **2** has a trimeric structure with linear C-Hg-C bonds[3b] and zinc in many ways assumes a position intermediate between that of magnesium and mercury, it was of interest to investigate the analogous zinc derivative *ortho*-phenylenezinc (**3**). Recently, the corresponding *ortho*-phenylenedizinc diiodide (o-$C_6H_4(ZnI)_2$) was prepared by Tagaki et al. in good yield from *ortho*-diiodobenzene and zinc powder in the presence of *N,N,N',N'*-tetramethyl-1,2-ethylenediamine (TMEDA) and tetramethyl urea (TMU) under irradiation with ultrasound;[4] however, structural information has not been reported.

Analogous to the synthesis of **1**, we prepared **3** by stirring **2** with metallic zinc in THF. The progress of the reaction was monitored by the disappearance of the sparingly soluble **2**. After six hours at room temperature, a clear solution of **3** was obtained; it is remarkable that this process is much faster than the conversion of **2** with magnesium to give **1** which requires two weeks to go to completion.[1] After careful decantation from the resulting amalgam, **3** was obtained in 92% yield (determined by titration after hydrolysis);[5] the compound was further characterized by ^1H and ^{13}C NMR spectroscopy (Table 1) and by derivatization with chlorotrimethylstannane which gave **4**.

Table 1. NMR data (δ, J [Hz]) of **3b,c** [a].

	3b [b]		**3c** [c]	
	δ	J	δ	J
H2	7.37	5.1(d)	7.88	6.3(d)
		3.4(d)		
H3	6.82	5.1(d)	7.37	6.3(d)
		3.4(d)		
Hα	–	–	8.30 [d]	(bs)
Hβ	–	–	6.49 [d]	7.1(d)
				5.8(d)
Hγ	–	–	6.84 [d]	7.6(t)
C1	169.3	(bs)	160.6	(bs)
C2	137.4	151.4(d)	140.2	163.0(d)
				10.0(d)
C3	125.2	151.8(d)	127.1	158.2(d)
Cα [d]	–	–	149.8	170.0(d)
Cβ [d]	–	–	123.7	165.1(d)
Cγ [d]	–	–	137.4	171.0(d)

[a] Numbering: see Scheme 1. [b] In [D_8]THF; ^1H NMR, 200 MHz, 25 °C, standard [D_7]THF $\delta = 1.75$; ^{13}C NMR, 50.3 MHz, standard: [D_8]THF $\delta = 67.4$. [c] In [D_8]toluene; ^1H NMR, 200 MHz, standard [D_7]toluene $\delta = 2.03$; ^{13}C NMR, 50.3 MHz, standard [D_8]toluene $\delta = 19.8$. [d] In pyridine.

Colorless crystals of **3** that were suitable for an X-ray crystal structure determination were obtained by cooling a saturated solution of **3** in THF.[6, 7] Although the crystals were of limited quality, the main features of the structure (**3a**, Fig. 1) could be

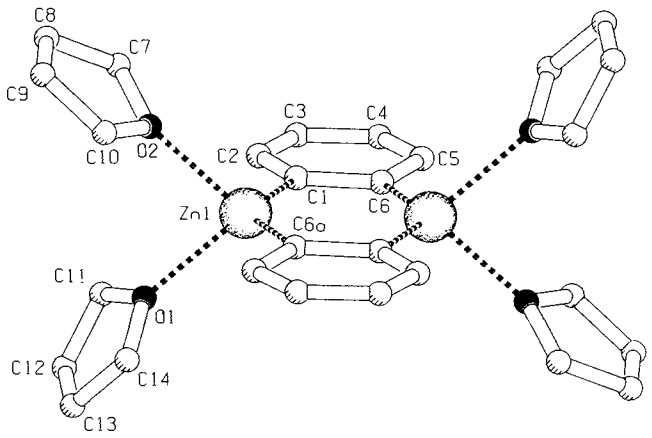

Fig. 1. PLUTON plot of **3a**. Hydrogen atoms are omitted for clarity. Selected bond lengths [Å], bond angles [°], and torsion angles [°]: Zn1–O1 2.272(14), Zn1–O2 2.209(14), Zn1–C1 1.991(16), Zn1–C6 1.963(13), C1–C2 1.39(2), C2–C3 1.34(2), C3–C4 1.37(2), C4–C5 1.38(2), C5–C6 1.43(2), C1–C6 1.41(2), O1-Zn1-O2 85.7(5), O1-Zn1-C1 110.2(6), O1-Zn1-C6a 106.2(5), O2-Zn1-C1 106.8(6), O2-Zn1-C6a 108.6(6), C1-Zn1-C6a 130.3(6), C6-C1-Zn1-C6a 2.4(16), Zn1-C1-C6-Zn1a −2.0(15).

[*] Prof. Dr. Bickelhaupt, Drs. M. Schreuder Goedheijt, Ing. T. Nijbacker, Dr. O. S. Akkerman
Scheikundig Laboratorium, Vrije Universiteit
De Boelelaan 1083, NL-1081 HV Amsterdam (The Netherlands)
Fax: Int. code +(20)4447488
e-mail: bicklhpt@chem.vu.nl
Drs. N. Veldman, Dr. A. L. Spek
Bijvoet Center for Biomolecular Research
Vakgroep Kristal- en Structuurchemie, Universiteit Utrecht
Padualaan 8, NL-3584 CH Utrecht (The Netherlands)
e-mail: spea@xray.chem.ruu.nl

[**] This work was supported by Shell Research B. V. (M. S. G.) and by the Netherlands Foundation for Chemical Research (SON) with financial aid from the Netherlands Organization for Research (NWO) (A. L. S. and N. V.).

derived with sufficient confidence. The solid-state structure of **3** (molecule **3a**) consists of two *ortho*-phenylenezinc units; it is located on a crystallographic inversion center, has approximate D_{2h} symmetry, and may be described as a (practically) planar 9,10-dihydro-9,10-dizincaanthracene in which each zinc atom is surrounded by two aromatic rings and by two THF molecules in a distorted tetrahedral fashion; note that the dimerization is achieved by covalent bonding between each metal and one carbon atom of each of the two phenylene units, and not by electron-deficient two-electron–three-center bonding that has been observed for organozinc compounds only twice,[8] but more often in organomagnesium[2, 9, 10] and especially in organolithium chemistry.[10, 11] The central six-membered ring appears to be slightly distorted, but only seemingly so, as the Zn–C bonds (Zn1–C1 1.991(16) Å, Zn1–C6a 1.963(13)) lie in the expected range and are equalivalent in length within the standard deviation. The molecule is clearly strained because the angle at zinc is unusually small (cf. C1-Zn1-C6a 130.3(6)° versus normal values of about 140–160°[12, 13]), while those at the *ipso* carbon atoms (C2-C1-Zn1 127.9(12)°, C6-C1-Zn1 116.2(11)°) similarly deviate from the usual value of about 122°.[12] Note that a (beneficial) increase of the angle at zinc would lead to a (detrimental) further distortion around the *ipso* carbon atoms. The planarity of the central ring, too, can be understood as a consequence of the large valence angle at zinc: boat-shaped folding as occurs in normal dihydroanthracenes would cause additional reduction of this angle.

Although the solubility of **3** is low (about 0.1 M), it is sufficient to determine the molecular weight by stationary isothermal distillation,[14] which furnished a concentration-independent degree of association of 3.0(±0.1)! Thus, one is confronted with the astounding fact that in the crystalline state, **3** is a dimer (**3a**), but in solution a trimer (**3b**) without discernible tendency towards dissociation. Nevertheless, it is evident that the two forms must be linked by the equilibrium 3 **3a**⇌2 **3b** which is strongly shifted towards **3b** in solution. As a dimer, **3a** is favored over **3b** by entropy, but this is apparently overcompensated by strain. The strain is relieved in **3b** because the C-Zn-C angle can be larger and adopt a normal value without causing angle distortions at the *ipso* carbon atoms; once this is achieved, the driving force for oligomerization is absent, so that entropy protects the system against further association. A similar situation has been encountered for the monomer/dimer equilibrium of magnesacyclohexane in THF.[15]

At present, the exact structure of **3b** is not known. It is unlikely that in analogy to **2** (which also is a trimer),[3b] **3b** has linear carbon-metal-carbon angles. Since zinc is a stronger Lewis acid than mercury, it is assumed that the zinc atom in **3b** will be coordinated by two THF molecules like in **3a** and thus achieve a normal, distorted tetrahedral arrangement. This assumption is supported by the observation that on addition of an excess of pyridine to a solution of **3b** in THF, a yellow precipitate is formed that has the composition of **3c** (^{1}H and ^{13}C NMR spectroscopy); exactly two molecules of pyridine are coordinated to each zinc atom, and the new species **3c**, like **3b**, is trimeric in THF solution according to association measurements.

Surprisingly, **3a** crystallizes from a solution of **3b** although the latter apparently is present in large excess and is thermodynamically more stable. We suggest that in solution, **3a** is present in minute amounts and crystallizes preferentially due to favorable packing effects; it is relevant to point out that the crystallization process at −20 °C took about two weeks.

Finally, one may ask why the *ortho*-phenylene derivatives of zinc (**3a**: dimer; **3b**: trimer; both with a mononuclear metal environment) are so different from that of magnesium (**1**: tetrameric cluster). Of course, the metal–carbon bond is much more polar in the case of magnesium, and apparently, electrostatic contributions to bonding are prominent enough for clustering to become feasible.[2] This is in analogy to organolithium chemistry where high polarity is well-known to favor electron-deficient clusters.[10, 11] In contrast, the Zn–C bonds (as in **3**), and even more so the Hg–C bonds (as in **2**), have sufficient covalent character to facilitate, under the same circumstances, directed bonding.

Experimental Procedure

ortho-Phenylenemercury (**2**) [3] (2.38 g, 8.6 mmol) and zinc (5.23 g, 80 mmol) in THF (50 mL) were stirred for 6 h at room temperature. A light brownish solution with a fine black precipitate was formed. The clear solution was decanted; titration of an aliquot (HCl and EDTA) [5] indicated the formation of **3** in 92% yield. Concentration of this solution and slow cooling (over about 1 day) to −20 °C afforded colorless crystals of **3a** (7.3 mmol, 85%, determined by titration after hydrolysis) after about two weeks.

When an excess of pyridine (1 mL) was added to a solution of **3** (0.42 mmol) in THF (10 mL), the color of the solution changed immediately from colorless to bright yellow. After 3 min, a yellow precipitate of **3c** formed; it was filtered off, dissolved in [D$_8$]toluene and characterized by ^{1}H and ^{13}C NMR spectroscopy.

Received: January 29, 1996 [Z8761IE]
German version: *Angew. Chem.* **1996**, *108*, 1651–1653

Keywords: magnesium compounds · mercury compounds · zinc compounds

[1] F. Bickelhaupt, *J. Organomet. Chem.* **1994**, *475*, 1.
[2] M. A. G. M. Tinga, G. Schat, O. S. Akkerman, F. Bickelhaupt, E. Horn, H. Kooijman, W. J. J. Smeets, A. L. Spek, *J. Am. Chem. Soc.* **1993**, *115*, 2808.
[3] a) L. Vecchiotti, *Ber. dtsch. chem. Ges.* **1930**, *63*, 2275; b) N. A. A. Al-Jabar, A. G. Massey, *J. Organomet. Chem.* **1984**, *275*, 9, and references therein.
[4] K. Takagi, Y. Shimoishi, K. Sasaki, *Chem. Lett.* **1994**, 2055.
[5] A. D. Vreugdenhil, C. Blomberg, *Recl. Trav. Chim. Pays-Bas* **1963**, *82*, 453.
[6] Crystal data for **3a**: $C_{28}H_{40}O_4Zn_2$, M_r = 571.40, colorless, transparent (0.18 × 0.38 × 0.50 mm), triclinic, space group P (no. 2), with a = 8.184(4), b = 8.887(4), c = 10.952(3) Å, α = 93.71(3), β = 112.39(3), γ = 105.34(6)°, V = 697.9(5) Å^3, Z = 1, ρ_{calcd} = 1.360 g cm^{-3}, $F(000)$ = 300, $\mu(Mo_{K\alpha})$ = 17.5 cm^{-1}, 2143 reflections measured, 1970 independent (2.0° < θ < 25.0°, ω scan, $\Delta\omega$ = 1.30 + 0.35 tanθ°, T = 293 K, $Mo_{K\alpha}$ radiation, graphite monochromator, λ = 0.71073 Å) on an Enraf-Nonius CAD4-T diffractometer with rotating anode; 5 h of X-ray exposure time. Data were corrected for Lorentz polarization. The structure was solved by automated Patterson methods (SHELXS86). Refinement on F^2 was carried out by full-matrix least-squares techniques (SHELXL-93); no observance criterion was applied during refinement. Final $R1$ value 0.121, for 979 reflections with $F_o > 4.0\sigma(F_o)$, $wR2$ = 0.297 for 1970 data, $w = 1/[\sigma^2(F_o)^2 + (0.1000P)^2]$, with $P = (\mathrm{Max}(F_o^2, 0) + 2F_c^2)/3$, S = 1.430, for 154 parameters. Mean and maximum shift over error: 0.000 and 0.000. Maximum and minimum residual density: 1.22, −0.73 e Å^{-3}. Crystals invariably showed broad reflection profiles of 3° that even increased to 6° at low temperature. As a result, only data of limited quality could be obtained. All non-hydrogen atoms were refined with anisotropic thermal parameters. The hydrogen atoms were refined riding on their carrier atoms with a fixed isotropic thermal parameter related to the value of the equivalent isotropic thermal parameter of their carrier atoms by a factor of 1.2.
[7] Crystallographic data (excluding structure factors) for the structure reported in this paper have been deposited with the Cambridge Crystallographic Data Centre as supplementary publication no. CCDC-179-59. Copies of the data can be obtained free of charge on application to The Director, CCDC, 12 Union Road, Cambridge CB2 1EZ, UK (fax: Int. code +(1223) 336-033; e-mail: teched@chemcrys.cam.ac.uk).
[8] a) J. G. Noltes, J. W. G. van der Hurk, *J. Organomet. Chem.* **1964**, *1*, 377; b) P. R. Markies, G. Schat, O. S. Akkerman, F. Bickelhaupt, *Organometallics* **1990**, *9*, 2243.
[9] P. R. Markies, O. S. Akkerman, F. Bickelhaupt, W. J. J. Smeets, A. L. Spek, *Adv. Organomet. Chem.* **1991**, *32*, 146.
[10] E. Weiss, *Angew. Chem.* **1993**, *105*, 1565; *Angew. Chem. Int. Ed. Engl.* **1993**, *32*, 1501.
[11] a) J. L. Wardell in *Comprehensive Organometallic Chemistry, Vol. 1* (Eds.: G. Wilkinson, F. G. A. Stone, E. W. Abel), Pergamon, Oxford, England, **1982**, p. 43; b) W. N. Setzer, P. von R. Schleyer, *Adv. Organomet. Chem.* **1985**, *24*, 353; c) A. Maercker, M. Theis, *Top. Curr. Chem.* **1987**, *138*, 1; d) G. W. Klumpp, *Recl. Trav. Chim. Pays-Bas* **1986**, *105*, 1.

[12] a) J. Boersma in *Comprehensive Organometallic Chemistry, Vol. 2* (Eds.: G. Wilkinson, F. G. A. Stone, E. W. Abel) Pergamon, Oxford, England, **1982**, p. 823; b) P. R. Markies, G. Schat, O. S. Akkerman, F. Bickelhaupt, *J. Organomet. Chem.* **1992**, *430*, 1, and references therein.
[13] To our knowledge, only one diarylzinc complex has been described with a small C-Zn-C angle of 132.1(2)°: $[(C_6F_5)_2Zn(thf)_2]$: M. Weidenbruch, M. Herrndorf, A. Schäfer, S. Pohl, W. Saak, *J. Organomet. Chem.* **1989**, 361, 139. However, in this case, the small angle must be caused by the strongly electron-withdrawing aryl groups which increase the p character of the zinc sp^n orbitals involved in bonding to carbon.
[14] A. van Vulpen, J. Coops, *Recl. Trav. Chim. Pays-Bas* **1967**, *85*, 203.
[15] a) H. C. Holtkamp, C. Blomberg, F. Bickelhaupt, *J. Organomet. Chem.* **1969**, *19*, 279; b) F. Bickelhaupt, *Angew. Chem.* **1987**, *99*, 1020; *Angew. Chem. Int. Ed. Engl.* **1987**, *26*, 990.

The $[Mn_2^{IV}(\mu\text{-}O)(\mu\text{-}PhBO_2)_2]^{2+}$ Unit: A New Structural Model for Manganese-Containing Metalloproteins**

Ursula Bossek, Helga Hummel, Thomas Weyhermüller, Karl Wieghardt,* Stephen Russell, Lodewijk van der Wolf, and Uwe Kolb

The structural motif of the μ-oxo(hydroxo)-di-μ-carboxylatodimanganese unit has been discovered in the active centers of some metalloproteins containing manganese. For example, in the catalases from *Lactobacillus plantarum*[1] and *Thermus thermophilus*[2] as well as in a ribonucleotide reductase from *Brevibacterium ammoniagenis*;[3] this structural motif has also been proposed for the tetranuclear manganese cluster in photosystem II (PS II).[4] These proposals were supported by the synthesis of dinuclear model complexes, in which the oxidation state of the two Mn ions was varied in one-electron steps from Mn_2^{II}[5] over $Mn^{II}Mn^{III}$[6] and Mn_2^{III}[7] to $Mn^{III}Mn^{IV}$.[8] The Mn_2^{IV} state was so far not accessible. Complexes of this type are very important for the calibration of the spectroscopic methods that are employed in the characterization of biomolecules. We report here that the corresponding Mn_2^{IV} complexes can be obtained if boronato ligands RBO_2^{2-} are used as bridging ligands instead of carboxylate groups. Surprisingly, the coordination chemistry of boronic acids has aroused little interest to date.[9]

The treatment of 1,4,7-trimethyl-1,4,7-triazacyclononane (L) and phenylboronic acid with $Mn^{II}(ClO_4)_2 \cdot 6H_2O$ in acetone in the presence of air leads to green crystals of **1**. Figure 1 shows

$[LMn^{III}(Ph_2B_2O_3)(ClO_4)]$ **1**

the structure of the octahedral, neutral complex in **1**,[10] which has a monodentate ClO_4^- ion, a cyclic triamine, and the bidentate dianion $[Ph_2B_2O_3]^{2-}$ as ligands; the latter can be regarded as an analog of the pentane-2,4-dionato ion ($acac^-$): In the complex $[LMn^{III}(acac)(OH_2)](ClO_4)_2$[11] the two $Mn^{III}-O_{acac}$ bonds are somewhat longer (1.88 Å) than the corresponding bonds in **1** (1.845 Å).

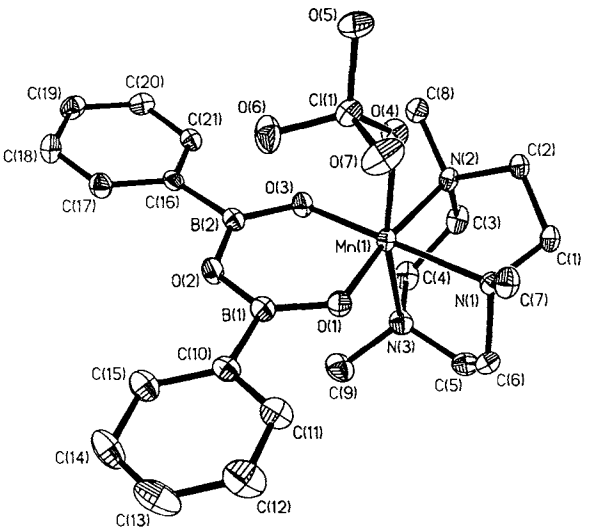

Fig. 1. Structure of the neutral complex in crystals of **1**. Selected bond lengths [Å]: Mn-O1 1.844(3), Mn-O3 1.846(3), Mn-O4 2.354(3), Mn-N1 2.116(3), Mn-N2 2.115(3), Mn-N3 2.272(3), B1-O1 1.348(4), B1-O2 1.386(4), B1-C10 1.574(5), B2-O3 1.348(4), B2-O2 1.382(4), B2-C16 1.572(5).

Hydrolysis of **1** in the presence of air in a mixture of ethanol/water/acetone (3:1:2) to which solid $NaClO_4$ was added gave deep red crystals of **2** after two to three days. The X-ray crystal

$[L_2Mn_2^{IV}(\mu\text{-}O)(\mu\text{-}PhBO_2)_2](ClO_4)_2 \cdot 2Me_2CO$ **2**

structure analysis[10] (Fig. 2) reveals that the dication in **2** consists of two Mn^{IV} ions with octahedral environments; they are linked together by two *syn,syn-O,O'*-coordinated phenylboronic acid dianions and a bent oxo bridge. Thus the structure of **2** corresponds very closely to that found in the μ-oxo-di-μ-carboxylatodimanganese complexes (Table 1).

The missing member of this series, a hydroxo-bridged, mixed-valent $Mn^{II}Mn^{III}$ complex, was also prepared: Treatment of L

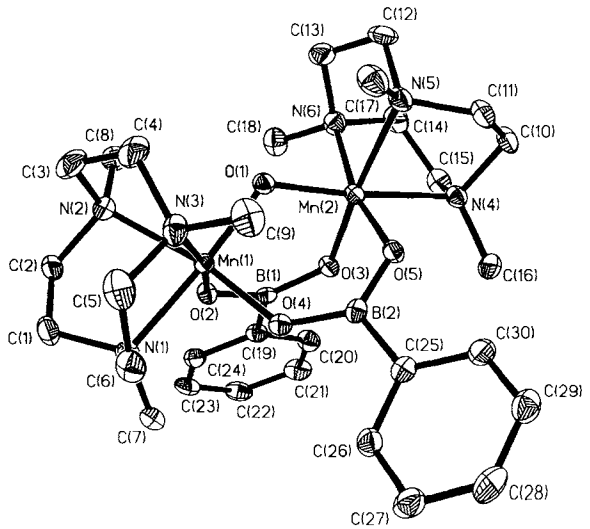

Fig. 2. Structure of the dication in crystals of **2**. Selected bond lengths [Å] and angles [°]: Mn1-N1 2.137(4), Mn1-N2 2.111 (4), Mn1-N3 2.103(4), Mn1-O1 1.823(3), Mn1-O2 1.821(3), Mn1-O4 1.829(3). Die entsprechenden Abstände an Mn2 sind innerhalb der Fehlergrenzen gleich. B1-O2 1.365(6), B1-O3 1.360(6) B2-O4 1.359(6), B2-O5 1.359(7); Mn1 ··· Mn2 3.184(1), Mn1-O1-Mn2 121.9(2).

[*] Prof. Dr. K. Wieghardt, U. Bossek, Dipl.-Chem. H. Hummel, Dr. T. Weyhermüller
Max-Planck-Institut für Strahlenchemie
Stiftstrasse 34–36, D-45470 Mülheim an der Ruhr (Germany)
Fax: Int. code +(208)3063951
Dr. S. Russell, L. van der Wolf
Unilever Research Laboratory Vlaardingen (The Netherlands)
Dr. U. Kolb
Max-Planck-Institut für Kohlenforschung, Mühlheim (Germany)
[**] This work was supported by the Fonds der Chemischen Industrie.

 © VCH Verlagsgesellschaft mbH, D-69451 Weinheim, 1996 0570-0833/96/3513-1552 $ 15.00+.25/0

Table 1. Structural parameters and magnetism of dinuclear $[LMn(\mu\text{-}X)(\mu\text{-}Y)_2MnL]^{n+}$ complexes (X = O, OH; Y = RCO_2^- or RBO_2^{2-}).

Complex	Mn^nMn^m	Mn–X [Å]	Mn–Y [Å]	Mn-X-Mn [°]	Mn···Mn [Å]	J [cm^{-1}] [a]	Ref.
$[L_2Mn_2(\mu\text{-}OH)(\mu\text{-}CH_3CO_2)_2]^+$	Mn_2^{II}	2.053(4)	2.17	109.4(3)	3.351(3)	−9	[5]
3	$Mn^{II}Mn^{III}$	1.932(5)	2.05	119.3(2)	3.449(1)	−9	[b]
		2.065(5)	2.09				
4	Mn_2^{III}	1.83	2.05	121.8(2)	3.193(1)	+5.4	[b]
$[L_2Mn_2(\mu\text{-}O)(\mu\text{-}CH_3CO_2)_2]^{3+}$	$Mn^{III}Mn^{IV}$	1.82	1.97	125.1(3)	3.230(3)	−40	[8]
2	Mn_2^{IV}	1.82	1.83	121.9(2)	3.184(1)	+10	[b]

[a] $H = -2JS_1 \cdot S_2$. [b] This work.

and pivalic acid with $Mn^{II}(ClO_4)\cdot 6H_2O$ in acetone in the presence of air leads to light brown crystals of **3**. The oxidation of **3** by O_2 in a basic medium gave red-violet crystals of **4**. The

$[LMn^{II}(\mu\text{-}OH)(\mu\text{-}(CH_3)_3CCO_2)_2Mn^{III}L](ClO_4)_2$ **3**

$[L_2Mn_2^{III}(\mu\text{-}O)(\mu\text{-}(CH_3)_3CCO_2](ClO_4)_2$ **4**

X-ray structural analyses[10] of **3** and **4** (Fig. 3) show that the valences in **3** are localized and that an OH group forms a bridge between a Mn^{II} and a Mn^{III} ion. In **4** the two Mn^{III} ions are linked by an oxo bridge.

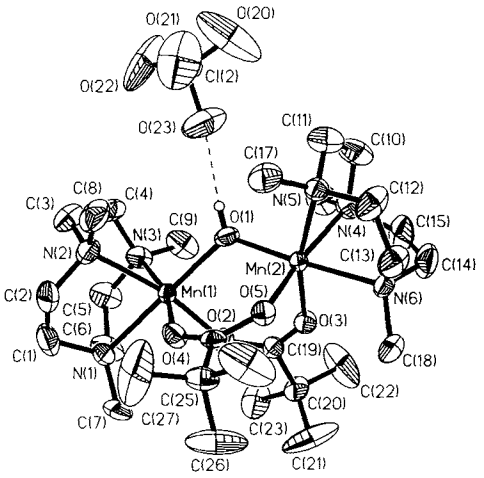

Fig. 3. Structure of the dication in **3** (that of the dication in **4** is very similar and is not shown). Selected bond lengths [Å] and angles [°] (values for **4** are given in parentheses): Mn1···Mn2 3.449(1) (3.193(1)), Mn1-N1 2.262(6) (2.153(4)), Mn1-N2 2.258(7) (2.183(5)), Mn1-N3 2.270(7) (2.268(5)), Mn1-O1 2.065(5) (1.833(3)), Mn1-O2 2.068(5) (2.017(3)), Mn1-O4 2.117(5) (2.090(3)), Mn2-N4 2.169(6) (2.157(4)), Mn2-N5 2.301(5) (2.296(4)), Mn2-N6 2.164(6) (2.141(4)), Mn2-O1 1.932(5) (1.821(3)), Mn2-O3 2.102(4) (2.095(3)), Mn2-O5 1.997(5) (1.997(3)), O1···O23 2.948(9); Mn1-O1-Mn2 119.3(2) (121.8(2)).

The electronic structure of the complexes **1**–**4** was determined from measurements of the temperature dependency of the molar magnetic susceptibility.[12] For **1** a temperature-independent magnetic moment of 4.80 μ_B (40–295 K) was determined, which corresponds to an $S = 2$ ground state for a high-spin Mn^{III} ion (d^4). In contrast, the magnetic moment of **2**, which contains two Mn^{IV} ions (d^3), is temperature-dependent; it increases monotonically from 5.82 μ_B at 300 K to 6.76 μ_B at 4.2 K. Using the formalism of the isotropic Heisenberg–Dirac–van Vleck model ($H = -2JS_1 \cdot S_2$; $S_1 = S_2 = 3/2$) gave a g value of 1.99(2) and a ferromagnetic coupling constant J of $+10(1)$ cm^{-1}. Therefore, the ground state of **2** is $S = 3$. This is surprising, because antiferromagnetic couplings were found for the isostructural and isoelectronic complexes $[L_2Cr_2^{III}(\mu\text{-}O)(\mu\text{-}CH_3CO_2)_2](BPh_4)_2$[13] and $[LCr^{III}(\mu\text{-}O)(\mu\text{-}CH_3CO_2)_2Mn^{IV}(tacn)](PF_6)_3$[14] (tacn = 1,4,7-triazacyclononane).

The exchange couplings in **3** and **4** were calculated analogously. The coupling between the $Mn^{II}(d^5)$ and the $Mn^{III}(d^4)$ ion in **3** is weakly antiferromagnetic, as has been reported for two analogous phenolato-bridged complexes.[6] In **4** the $Mn^{III}(d^4)$ ions are weakly antiferromagnetically coupled—in agreement with earlier observations.[7]

With the complexes $[L_2Mn_2^{II}(\mu\text{-}OH)(\mu\text{-}CH_3CO_2)_2]PF_6\cdot CH_3OH$,[5] **3**, $[L_2Mn_2^{III}(\mu\text{-}O)(\mu\text{-}CH_3CO_2)_2](ClO_4)_2$,[7] $[LMn^{III}(\mu\text{-}O)(\mu\text{-}CH_3CO_2)_2Mn^{IV}L](ClO_4)_3]$,[8] and **2** there is now an "isostructural" series available, in which the oxidation level increases stepwise by one electron per two manganese ions. The energy of the manganese K X-ray absorption edge serves as a measure of the degree of oxidation of the manganese cluster in PS II.[15–17] The present series of complexes can now be used for the experimental verification of the fundamental supposition that the Mn K-edge energy increases linearly with the oxidation level of the Mn ions given that the structure of the complex remains the same. The protonation or deprotonation of the oxo and hydroxo bridge, respectively, does not have any influence on the Mn K-edge energy.[18]

As can be seen from Figure 4, the XANES experiments (*X*-ray *a*bsorption *n*ear *e*dge *s*pectroscopy) carried out on the five

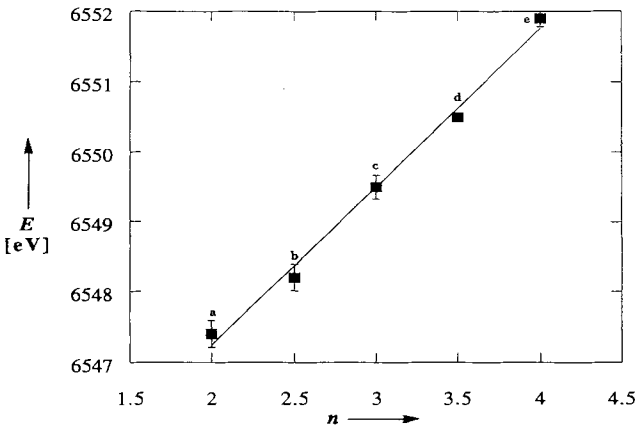

Fig. 4. The Mn K-edge energy E for the complexes a) $[L_2Mn_2^{II}(\mu\text{-}OH)(\mu\text{-}CH_3CO_2)_2]PF_6\cdot CH_3OH$: 6547.4 ±0.4 eV, b) $[L_2Mn_2^{II/III}(\mu\text{-}OH)(\mu\text{-}(CH_3)_3CCO_2)_2](ClO_4)_2$: 6548.2 ±0.4 eV, c) $[L_2Mn_2^{III}(\mu\text{-}O)(\mu\text{-}CH_3CO_2)_2](ClO_4)_2$: 6549.5 ± 0.3 eV, d) $[L_2Mn_2^{III/IV}(\mu\text{-}O)(\mu\text{-}CH_3CO_2)_2](ClO_4)_3$ [19]: 6550.5 eV, e) $[L_2Mn_2^{IV}(\mu\text{-}O)(\mu\text{-}PhBO_2)_2](PF_6)_2$: 6551.9 ±0.2 eV as a function of the average oxidation state n of the Mn ions ((■) measured values; (—) fitted line).

complexes show clearly that, within the error limit, the Mn K-edge energy increases linearly with increasing oxidation level. In particular, the oxidation state of IV is confirmed for the two Mn ions in **2**.

Experimental Procedure

1: 1,4,7-Trimethyl-1,4,7-triazacyclononane (L) (0.50 g) and phenylboronic acid (0.70 g) were dissolved in acetone (40 mL) and treated with $Mn^{II}(ClO_4)_2 \cdot 6H_2O$ (1.0 g). The solution turned green within 60 min on stirring in air. Slow evaporation of the solvent in air gave large green crystals of **1** within one to two days. Yield: 0.81 g (53%). UV/Vis (CH_3CN): λ_{max} (ε [L mol^{-1} cm^{-1}]) 219 (2.26×10^4), 237 (2.0×10^4), 293 (8.7×10^3), 412 (265), 688 nm (19).

2: A solution of **1** (0.50 g) in a mixture of ethanol/water/acetone (3:1:2) (40 mL) was treated with $NaClO_4$ (0.30 g). After the mixture was left to stand in air for two to three days, the solvent was removed and the red-brown residue recrystallized from acetone. Yield: 0.19 g (40%). Alternatively, **2** could also be obtained from the above solution after addition of H_2O_2 (0.5 mL, 30% H_2O_2) and NaOH (0.10 g) in H_2O (2 mL). UV/Vis (CH_3CN) λ_{max} (ε[L mol^{-1} cm^{-1}]) = 222 (3.0×10^4), 274 (1.9×10^4), 370 sh, 693 (137), 710 sh (150), 763 (50), 790 sh (36), 865 nm (21).

3: To a solution of L (0.50 g) and pivalic acid (0.40 g) in acetone (40 mL) was added $Mn^{II}(ClO_4)_2 \cdot 6H_2O$ (1.0 g). The mixture was left to stand in air for about 6 h at 20 °C, during which time the mixture turned brown. After addition of solid $NaClO_4$ (0.90 g) to this solution, brown crystals of **3** precipitated. Recrystallization from acetone. Yield: 0.90 g (70%). UV/Vis (CH_3CN) λ_{max} (ε[L mol^{-1} cm^{-1}]) = 288 (5.8×10^3), 431 (620), 472 nm (517).

4: To a solution of **3** (0.50 g) in acetone (40 mL) in air were added ten drops of triethylamine and solid $NaClO_4$ (0.80 g). On concentration of the red reaction solution, red crystals of **4** formed. Yield: 0.30 g (61%). UV/Vis (CH_3CN) λ_{max} (ε[L mol^{-1} cm^{-1}]) = 312 (1.4×10^4), 400 sh, 485 (719), 522 (691), 730 (136), 990 nm (67).

All new complexes gave satisfactory elemental analyses (C, H, N).

Received: January 22, 1996 [Z 8742 IE]
German version: *Angew. Chem.* **1996**, *108*, 1653–1656

Keywords: boron compounds · EXAFS spectroscopy · magnetic properties · manganese compounds · photosynthesis

[1] a) Y. Kono, I. Fridovich, *J. Biol. Chem.* **1983**, *258*, 6015, 13646; b) W. F. Beyer, Jr., I. Fridovich, *Biochemistry* **1985**, *24*, 6460.

[2] a) V. V. Barynin, A. I. Grebenko, *Dokl. Akad. Nauk. SSR* **1986**, *288*, 1100; b) V. V. Barynin, A. A. Vagin, V. R. Melik-Adamyan, A. I. Grebenko, S. V. Khangulov, A. N. Popov, M. E. Andrianova, B. K. Vainshtein, *ibid.* **1986**, *288*, 877.

[3] A. Willing, H. Follmann, G. Auling, *Eur. J. Biochem.* **1988**, *170*, 603.

[4] V. K. Yachandra, V. J. DeRose, M. J. Latimer, I. Mukerji, K. Sauer, M. P. Klein, *Science* **1993**, *260*, 675.

[5] K. Wieghardt, U. Bossek, B. Nuber, J. Weiss, *Inorg. Chim. Acta* **1989**, *165*, 123.

[6] a) M. Suzuki, S. Murata, A. Uehara, S. Kida, *Chem. Lett.* **1987**, 281; b) M. Suzuki, M. Mikuriya, S. Murata, A. Uehara, H. Oshio, S. Kida, K. Saito, *Bull. Chem. Soc. Jpn.* **1987**, *60*, 4305; c) H. Diril, H.-R. Chang, X. Zhang, S. K. Larsen, J. A. Potenza, C. G. Pierpont, H. J. Schugar, S. S. Isied, D. N. Hendrickson, *J. Am. Chem. Soc.* **1987**, *109*, 6207; d) R. M. Buchanan, K. J. Oberhausen, J. F. Richardson, *Inorg. Chem.* **1988**, *27*, 971; e) H.-R. Chang, H. Diril, M. J. Nilges, X. Zhang, I. A. Potenza, H.-J. Schugar, D. N. Hendrickson, S. S. Isied, *J. Am. Chem. Soc.* **1988**, *110*, 625.

[7] a) K. Wieghardt, U. Bossek, D. Ventur, J. Weiss, *J. Chem. Soc. Chem. Commun.* **1985**, 347; b) J. E. Sheats, R. S. Czernuszewicz, G. C. Dismukes, A. L. Rheingold, V. Petrouleas, J. Stubbe, W. H. Armstrong, R. H. Beer, S. J. Lippard, *J. Am. Chem. Soc.* **1987**, *109*, 1435.

[8] a) K. Wieghardt, U. Bossek, J. Bouvoisin, P. Beauvillain, J.-J. Girerd, B. Nuber, J. Weiss, J. Heinze, *Angew. Chem.* **1986**, *98*, 1026; *Angew. Chem. Int. Ed. Engl.* **1986**, *25*, 1030.

[9] The complex $[(C_6H_5)_4Al_3B_4Cl_5O_6]$, which contains two coordinated $[Ph_2B_2O_3]^{2-}$ ions, has been structurally characterized by X-ray diffraction: R. Köster, K. Angermund, J. Serwatowski, A. Sporzynski, *Chem. Ber.* **1986**, *119*, 1301.

[10] X-ray structural analyses: **1**: $C_{21}H_{31}B_2ClMnN_3O_7$, monoclinic, space group $P2_1/n$, $a = 13.97(1)$, $b = 13.399(8)$, $c = 14.181(9)$ Å, $\beta = 110.69(6)°$, $Z = 4$, $\rho_{calcd} = 1.469$ g cm^{-3}, $\mu(Mo_{K\alpha}) = 0.686$ mm^{-1}, 3338 independent reflections ($I \geq 4.0\sigma(F)$), $T = 213$ K, $R = 0.038$, $wR = 0.041$. **2**: $C_{36}H_{64}B_2Cl_2Mn_2N_6O_{15}$, monoclinic, space group $P2_1/c$, $a = 16.984(1)$, $b = 20.128(1)$, $c = 13.609(1)$ Å, $\beta = 96.56(1)$, $Z = 4$, $\rho_{calcd} = 1.471$ g cm^{-3}, $\mu(Mo_{K\alpha}) = 0.733$ mm^{-1}; 6624 independent reflections, $T = 133$ K, $R = 0.058$. **3**: $C_{28}H_{61}Cl_2Mn_2N_6O_{13}$, monoclinic, space group $P2_1/n$, $a = 11.815(2)$, $b = 16.164(3)$, $c = 21.609(4)$ Å, $\beta = 98.52(2)°$, $Z = 4$, $\rho_{calcd} = 1.417$ g cm^{-3}, $\mu(Mo_{K\alpha}) = 0.831$ mm^{-1}, 6399 independent reflections, $T = 293$ K, $R = 0.067$, $wR = 0.066$. **4**: $C_{28}H_{60}Cl_2Mn_2N_6O_{13}$, monoclinic, space group $P2_1/n$, $a = 11.963(2)$, $b = 15.922(3)$, $c = 21.099(3)$ Å, $\beta = 96.75(1)°$, $Z = 4$, $\rho_{calcd} = 1.447$ g cm^{-3}, $\mu(Mo_{K\alpha}) = 0.831$ mm^{-1}, 5871 independent reflections, $T = 293$ K, $R = 0.059$, $wR = 0.064$. The intensities were measured on a Siemens P4 diffractometer and a Siemens-SMART system (**2**) with monochromatic $Mo_{K\alpha}$ radiation; empirical absorption corrections were carried out by Ψ scans. The structures were solved by Patterson and difference Fourier syntheses and refined against F^2 for all independent reflections; heavy atoms with anisotropic temperature factors; H atoms on calculated positions with isotropic temperature factors. The proton of the OH bridges in **3** was localized in the difference Fourier synthesis and refined without problems. The methyl groups of the pivalato ions are disordered. The Siemens-SHELXTL-PLUS program package of G. M. Sheldrick (Universität Göttingen, Germany) was employed. Further details of the crystal structure investigation may be obtained from the Fachinformationszentrum Karlsruhe, D-76344 Eggenstein-Leopoldshafen (Germany) on quoting the depository number CSD-59407.

[11] K. Wieghardt, K. Pohl, U. Bossek, B. Nuber, J. Weiss, *Z. Naturforsch. B* **1988**, *43*, 1184.

[12] Measurements of the temperature dependence of the magnetic susceptibility (2–300 K) were carried out on a SQUID magnetometer (MPMS Quantum Design) on solid samples of **1**–**4**; the raw data were corrected with the calculated diamagnetic contribution (Pascal constants). Fitting calculations were carried out on the $\chi_M T$ data using a matrix diagonalization procedure and the isotropic Heisenberg–Dirac–van-Vleck model with $H = -2JS_1 \cdot S_2$, additionally, zero field splitting as well as a paramagnetic impurity p were taken into account to give the following parameters: **1**: $g = 1.95$, $|D| = 3.6$ cm^{-1}; **2**: $S_1 = S_2 = 3/2$, $g = 1.99$, $J = +10$ cm^{-1}, $D = 0$, $p = 0$; **3**: $S_1 = 5/2$, $S_2 = 2$; $g_1 = 2.0$, $g_2 = 2.15$, $J = -9.0$ cm^{-1}, $D_1 = 0$ cm^{-1}, $D_2 = 5.0$ cm^{-1}, $p = 6.2\%$ ($S = 2$); **4**: $S_1 = S_2 = 2$, $g = 1.98$, $|D| = 1.3$ cm^{-1}, $J = +5.4$ cm^{-1}, $p = 0$.

[13] L. L. Martin, K. Wieghardt, G. Blondin, J.-J. Girerd, B. Nuber, J. Weiss, *J. Chem. Soc. Chem. Commun.* **1990**, 1767.

[14] K. Wieghardt, U. Bossek, B. Nuber, J. Weiss, J. Bouvoisin, M. Corbella, S. E. Vitols, J.-J. Girerd, *J. Am. Chem. Soc.* **1988**, *110*, 7398.

[15] M:P. Klein, K. Sauer, V. K. Yachandra, *Photosynth. Res.* **1993**, *38*, 265.

[16] T. Ono, T. Noguchi, Y. Inoue, M. Kusunoki, T. Matsushita, H. Oyanagi, *Science* **1992**, *258*, 1335.

[17] K. Sauer, R. D. Guiles, A. E. McDermott, J. L. Cole, V. K. Yachandra, J.-L. Zimmermann, M. P. Klein, S. L. Dexheimer, R. D. Britt, *Chem. Ser.* **1988**, *28A*, 87.

[18] M. J. Baldwin, T. L. Stemmler, P. J. Riggs-Gelasco, M. L. Kirk, J. E. Penner-Hahn, V. L. Pecoraro, *J. Am. Chem. Soc.* **1994**, *116*, 11349.

[19] The XANES experiments were carried out on the Mn-K edge at the experimental station BN3 of the storage ring ELSA at the Universität Bonn. The edge positions were determined by using their first turning points. The experimental error was calculated from the resolution of the monochromator and the reproducibility of the edge positions of a Mn metal foil (6539.0 eV) directly before and after the measurements.

Screw-Sense-Selective Polymerization of Isocyanides by Dinuclear μ-Ethynediyl Complexes**

Fumie Takei, Koichi Yanai, Kiyotaka Onitsuka, and Shigetoshi Takahashi*

Macromolecular asymmetry, which originates from the helical structure of a polymer backbone, has recently attracted a great deal of interest, and some optically active polymers with helical chirality have been synthesized for methacrylates, chloranils, and isocyanates.[1] Such artificial polymers, which contain a stable, single-handed helical conformation, are of special interest in view of their potential as new materials and because of their relation to biomolecules.[2]

Poly(isocyanide)s have a 4_1 helical structure[3] and usually exist in a 1:1 mixture of two conformational isomers with right-handed (*P*) and left-handed (*M*) helices due to the restricted

[*] Prof. Dr. S. Takahashi, F. Takei, K. Yanai, Dr. K. Onitsuka
The Institute of Scientific and Industrial Research
Osaka University, Ibaraki, Osaka 567 (Japan)
Fax: Int. code +(6)879-8459
e-mail: takahashi@sanken.osaka-u.ac.jp

[**] This work was supported by the Grant-in-Aids for Scientific Research on Priority Area of Reactive Organometallics (No. 05236104) from the Ministry of Education, Science, Sports and Culture, Japan.

rotation about the C–C single bond in the polymer backbone. The screw-sense-selective (SSS) polymerization of isocyanides should give optically active poly(isocyanide)s with *P* or *M* helical structure. Indeed, some attempts at the SSS polymerization of isocyanides have been made using transition metal catalysts modified with chiral amine,[4] phosphane,[5] and acetato ligands, [6] as well as by using chiral isocyanides.[7]

Recently we showed[8] that the dinuclear μ-ethynediyl complex **1** undergoes successive multiple insertions of isocyanides exclusively into the Pd–C bond. This leads to a novel living polymerization of aryl isocyanides; however, mononuclear acetylides of the type $[(PR_3)_2PdX(C{\equiv}CR)]$ are inactive to the polymerization. We have now applied the catalytic properties of **1** to the SSS polymerization of isocyanides by utilizing the living nature of the process.

The reaction of **1** with *n* equivalents of phenyl, *p*-tolyl, or 4-*n*-butylphenyl isocyanides [Eq. (a)], led to oligomers **2** (e.g., $n = 10$) as well as polymers **2** (e.g., $n = 100$) in almost quantitative yields. Since these compounds still contain the active end-group $[CPd(PR_3)_2Cl]$, they can be reused as initiators for further polymerization of isocyanides.[8] If a chiral isocyanide is employed, the reaction with **1** may produce chiral oligomer complexes like **3**, which probably can be brought into play for the polymerization of further isocyanide monomers. Our approach to a generally applicable SSS polymerization of isocyanides is based on this characteristic feature of the complexes and the use of a block-copolymerization technique as illustrated in Scheme 1.

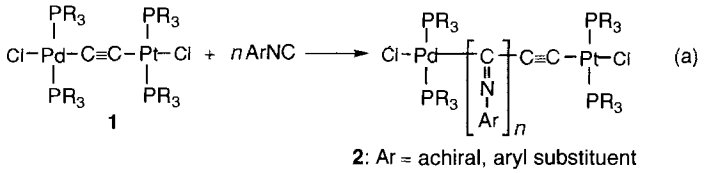

(a)

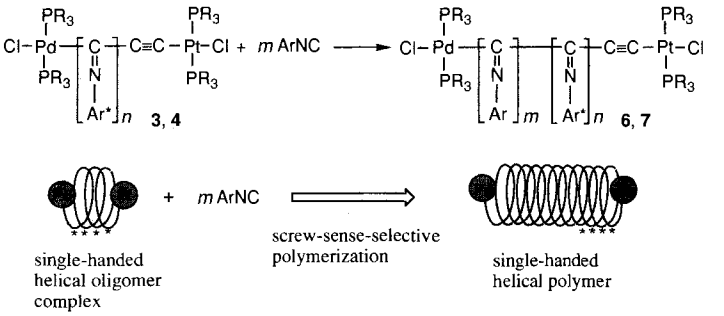

Scheme 1. Screw-sense-selective polymerization of isocyanides.

To prepare the chiral oligomer complex **3**, we treated **1** with 2, 10, 20, and 30 equivalents of the chiral isocyanide *m*-$CNC_6H_4CO_2R^*$ (–)-**5** ($R^* = (-)$-menthyl,[9] $[\alpha]_D^{20} = -83$ ($c = 0.21$ in $CHCl_3$)) and obtained the oligomer complexes **3a** ($n = 2$, $m/z = 1440$, $[\alpha]_D^{20} = +2$), **3b** ($n = 10$, $M_n = 3720$, $[\alpha]_D^{20} = +22$), **3c** ($n = 20$, $M_n = 6580$, $[\alpha]_D^{20} = +176$), and **3d** ($n = 30$, $M_n = 10080$, $[\alpha]_D^{20} = +228$), respectively, which were identified, for example, based on their ^{31}P NMR and circular dichroisum (CD) spectra, and molecular weight measurements.[10] Similarly, the related chiral oligomer complexes **4** were prepared by reactions of **1** with *m*-$CNC_6H_4CO_2R^*$ (+)-**5** ($R^* = (+)$-menthyl, $[\alpha]_D^{20} = +82$ ($c = 0.13$ in $CHCl_3$)).[9] Complex **4d** ($n = 30$) has an $[\alpha]_D^{20}$ value of -225, and the CD spectrum is the same as the mirror image of that of **3d**, indicating that **3d** and **4d** are a pair of enantiomers.

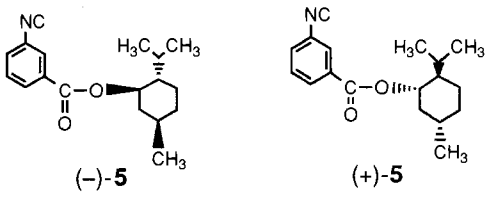

Like **1**, the chiral complexes **3** smoothly polymerized the chiral monomer (–)-**5** in THF under reflux to give polymers with a narrow polydispersity index ($M_w/M_n < 1.08$). Although the monomer shows a negative optical rotation, the polymers and the oligomers exhibit a large positive one. The specific rotation increases proportionally with the increase in the molecular weight of **3** and reaches a constant value of $[\alpha]_D^{20} = +260$ at a molecular weight of more than about 20000, which corresponds to the degree of polymerization P_n of about 70. The large optical rotation clearly arises from macromolecular asymmetry caused by the helical chirality of the polymer backbone and not by the chiral menthyl groups attached to the backbone. Since no appreciable change in the $[\alpha]$ value was observed after heating **3e** ($n = 100$) at reflux in THF for 5 h, the helical structure can be regarded as being stable in solution. Polymers **4** prepared similarly from (+)-**5** exhibit a negative optical rotation; the same relationship as for **3** is observed between the $[\alpha]$ value and the molecular weight. In addition, the CD spectra of, for example, **3e** ($n = 100$) and **4e** ($n = 100$) are mirror images of each other, suggesting that the polymerization of the chiral isocyanide **5** proceeds with a screw-sense selectivity and that polymers **3** and **4** are a pair of enantiomers. The screw sense (*P* or *N*) of the helical enantiomers, however, has not been assigned yet.

Furthermore, we have investigated the SSS polymerization of achiral isocyanides initiated by chiral oligomer complexes **3** and **4**. The screw-sense selectivity of the polymerization has been estimated on the basis of the specific rotation of the resulting polymers. Thus, the oligomer complex **3d** was treated with *m* equivalents of 3-propoxycarbonylphenyl isocyanide to yield polymers **6d-Pr**, the molecular weight and specific rotation of which are listed in Table 1. The relationship between M_w and $[\alpha]$ suggests that a SSS polymerization of the achiral isocyanide occurs at the initial stage of the reaction, but the selectivity

Table 1. Molecular weights $\bar{M}_w$ and optical rotations of polymers **6** and **7** [a].

Initiator [b]	Monomer ArNC	Polymer	$\bar{M}_w \times 10^{-3}$ [c]	$[\alpha]_D^{20}$ [d]
3d	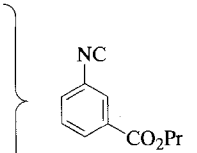	**6d-Pr**	24.0	205
			30.0	157
3b		**6b-diPr**	13.5	126
			21.0	92
3c		**6c-diPr**	14.5	288
			23.5	246
3d	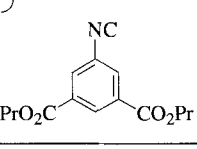	**6d-diPr**	17.5	280
			25.0	272
			29.0	272
4d		**7b-diPr**	18.0	−261
			27.5	−269

[a] See Scheme 1. [b] See text. [c] Determined by GPC analyses calibrated (light scattering method) with the absolute molecular weights of the homopolymers **3**. [d] $c = 0.1$ in $CHCl_3$.

 © VCH Verlagsgesellschaft mbH, D-69451 Weinheim, 1996 0570-0833/96/3513-1555 $ 15.00+.25/0

gradually falls as the degree of polymerization increases. When **3b** and **3c** were used as initiators, the loss of selectivity took place at an early stage of the reactions. Similar results were obtained when *n*-butylphenyl isocyanide was polymerized with **3** as an initiator. The loss of selectivity in the propagation step is probably due to a rather weak steric interaction between the incoming isocyanide monomers and the active site $\{Cl(PEt_3)_2Pd[C(=NAr)]_n\}$ bearing the helical chirality. We therefore chose to investigate the polymerization of the monomer 3,5-dipropoxycarbonylphenyl isocyanide **8**.

Chiral complexes **3** smoothly polymerized the sterically demanding monomer **8** to give polymers **6-diPr** in almost quantitative yields. A summary of the molecular weights and rotation values are given in Table 1. Polymers **6b-diPr** show a rather small specific rotation, indicating the low stereoselectivity of the polymerization. In contrast, polymers **6c-diPr** exhibit a relatively large [α] value, which decreases slightly with increasing molecular weight. The polymers **6d-diPr** maintain very large [α] values even for high molecular weight polymer of at least $M_w = 29000$. As expected, polymers **6**, produced by initiation with **3**, exhibit a negative rotation, while use of **4** as initiator afforded polymers **7-diPr**, which have specific rotations of the opposite sign, but the same absolute values as the corresponding **6-diPr** polymers. These findings suggest that the chiral complexes **3** and **4** are capable of initiating the SSS polymerization of sterically demanding achiral isocyanides with a high stereoselectivity and that the helical chirality of the initiator is preserved during the SSS polymerization. Since the polymerization initiated by **3c** proceeded with a slight decrease of the selectivity, the SSS polymerization of achiral isocyanides seems to require chiral oligomer complexes that possess at least seven turns of single-handed helices as an initiator.[11]

The SSS polymerization of achiral isocyanides described here reveals that chiral transition metal complexes that have been modified by chiral isocyanides can act as effective initiators and provides a new method for preparing poly(isocyanide)s with a single-handed helix.

Received: January 24, 1996 [Z87491E]
German version: *Angew. Chem.* **1996**, *108*, 1634–1636

Keywords: alkyne complexes · chirality · isocyanides · polymerizations

[1] O. Vogl, G. D. Jaycox, *CHEMTECH* **1986**, *16*, 698; Y. Okamoto, T. Nakano, *Chem. Rev.* **1994**, *94*, 349.
[2] See, for example, Y. Okamoto, *CHEMTECH* **1987**, *17*, 176; R. J. M. Nolte, *Chem. Soc. Rev.* **1994**, 11; J. P. Gao, J. P. Chen, Z. Y. Wang, *J. Am. Chem. Soc.* **1995**, *117*, 5377.
[3] O. Vogl, G. D. Jaycox, *Polymer* **1987**, *28*, 2179.
[4] P. C. J. Kamer, R. J. M. Nolte, W. Drenth, *J. Am. Chem. Soc.* **1988**, *110*, 6818, and references therein.
[5] Y. Ito, E. Ihara, M. Murakami, *Angew. Chem.* **1992**, *104*, 1508; *Angew. Chem. Int. Ed. Engl.* **1992**, *31*, 1509; Y. Ito, E. Ihara, M. Murakami, M. Sisido, *Macromolecules* **1992**, *25*, 6810.
[6] T. J. Jeming, B. M. Novak, *J. Am. Chem. Soc.* **1992**, *114*, 7926.
[7] A. J. M. van Beijnen, R. J. M. Nolte, A. J. Naaktgeboren, J. W. Zwikker, W. Drenth, *Macromolecules* **1983**, *16*, 1679.
[8] K. Onitsuka, T. Joh, S. Takahashi, *Angew. Chem.* **1992**, *104*, 893; *Angew. Chem. Int. Ed. Engl.* **1992**, *31*, 851; K. Onitsuka, K. Yanai, F. Takei, T. Joh, S. Takahashi, *Organometallics* **1994**, *13*, 3862.
[9] Starting from *m*-$NO_2C_6H_4CO_2H$ and (−)-menthol (Fluka, [α] = −50) or (+)-menthol (Aldrich, [α] = 48), pale yellow viscous liquids are obtained.
[10] The molecular weight M_w of **3a** (calcd: 1440) was determined by FAB mass spectrometry, that of the other compounds (calcd: **3b**: $m/z = 3719$; **3c**: $m/z = 6569$; **3d** $m/z = 9419$) by a vapor pressure osmometry (VPO) method. The ^{31}P NMR spectra of **3a** showed sharp signals due to PEt_3 groups at $\delta = 16.1$ (bound to Pt, $J(Pt,P) = 2348$ Hz) and 14.0 and 13.3 (bound to Pd, $J(P,P) = 360$ Hz) relative to an external 10% H_3PO_4 reference. Rather broad phosphane signals at $\delta = 15.4$ (bound to Pt) and 13.4 (bound to Pd) were observed for **3b** and **3d**. The absorptions due to $\nu_{C=N}$ in the IR spectra appeared at 1570 cm^{-1} for **3a** and at 1650 cm^{-1} for **3b–d** and **4d**.
[11] T. Nakano, Y. Okamoto, K. Hatada, *J. Am. Chem. Soc.* **1992**, *114*, 1318.

[2.2.2.2]Metacyclophane-1,9,17,25-tetrayne**

Takeshi Kawase, Noriko Ueda, Hossein Reza Darabi, and Masaji Oda*

Although a number of [2.$_n$]metacyclophane-*n*-ynes have been synthesized, the tetrayne **1** has remained unknown.[1, 2] While unsubstituted[1] and substituted[2] compounds are known for the hexayne **3**, only substituted compounds are known for the pentayne **2** and the heptayne **4**.[2] These compounds were synthesized by coupling reactions of acetylenic precursors; however, this method proved unsuitable for synthesizing **1**.[2] We here report the synthesis, properties, and structure of **1**, the smallest member of this class of compounds known to date.

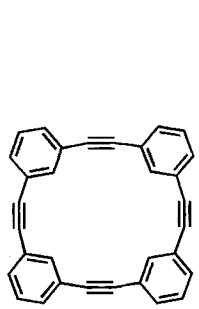

1

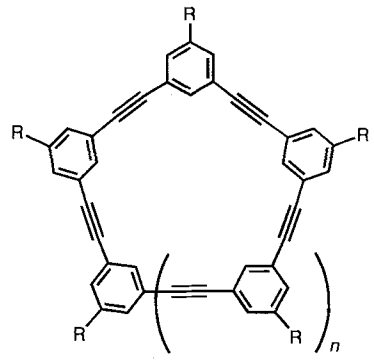

2: $n = 1$ (R = COO*n*Bu)
3a: $n = 2$, R = H
3b: $n = 2$, R = H, *t*Bu alternately
4: $n = 3$ (R = COO*n*Bu)

The strain energy of **1** has been estimated to be about 11 kcal mol^{-1} from a molecular mechanics calculation.[2] This strain energy, though sizable, should be dispersed over the molecule so that each triple bond is only slightly strained. Thus, **1** is expected to be stable enough to avoid undergoing ready addition of nucleophiles, thus allowing the application of the base-promoted dehydrohalogenation method for constructing the triple bonds. Wennerström et al. achieved the synthesis of the (Z^4)- and (Z^3,*E*)-[2.$_4$]metacyclophanetetraenes **6a** and **6b**, respectively, potential precursors to **1**, by a double Wittig reaction.[3] However, the yields of **6a** and **6b** were too low for them to be of use as synthetic intermediates for **1**. We recently reported that the reductive coupling of 4,4′-(*Z*)-stilbenedicarbaldehyde with low-valent titanium reagents affords a mixture of [2.$_4$]paracyclophanetetraenes (including a new *E,Z,E,Z* isomer) in better yields than with the double-Wittig method.[4] We therefore examined the Ti-mediated coupling of the 3,3′-(*Z*)-stilbenedicarbaldehyde (*Z*)-**5**,[5] and obtained the coupling products **6** in improved yields (Scheme 1).

Treatment of (*Z*)-**5** with the low-valent titanium compound, prepared from $TiCl_4$ and Zn in dimethoxyethane (DME),[6] afforded a mixture of **6b**, the new (*E,Z,E,Z*) isomer **6c** (20–50% of the mixture), and a small amount of other isomers in 35–40% yield. The (Z^4)-isomer **6a** and the intramolecular coupling product **7** were not detected. Similar treatment of the (*E*)-isomer

[*] Prof. Dr. M. Oda, Dr. T. Kawase, N. Ueda, Dipl.-Chem. H. R. Darabi
Department of Chemistry, Faculty of Science
Osaka University
Toyonaka, Osaka 560 (Japan)
Fax: Int. code +(6)850-5387

[**] This work was supported by Grants-in-Aid for Scientific Research (06804038 and 05403007) from Ministry of Education, Science and Culture, Japan.

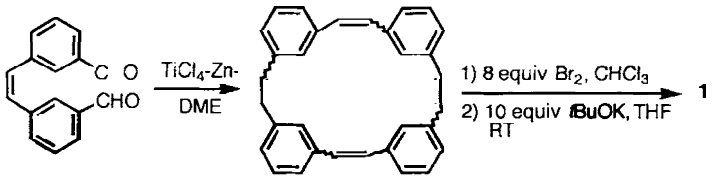

(Z)-5 6

a = (Z⁴); b = (Z³,E),
c = (E,Z,E,Z)

Scheme 1. Synthesis of **1** via **6b** and **6c**.

(*E*)-**5** gave only a trace amount of the cyclic compounds. The new tetraene **6c**, which is the third known member of the six possible stereoisomers, was isolated from the mixture by fractional recrystallization from CH_2Cl_2/hexane. The reaction of the tetraene mixture **6** with bromine and subsequent treatment of the crude octabromide mixture with *t*BuOK gave the tetrayne **1** as a stable crystalline substance in 55% yield (Scheme 1).

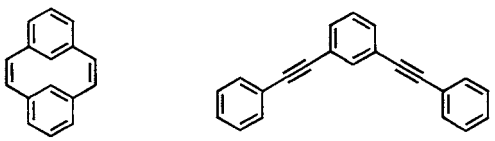

7 **8**

The ^1H and ^{13}C NMR spectra of **1** and **6c** are fairly simple, consistent with the high symmetry of the molecules (see Table 1). The inner protons of **1** are observed at the lowest field ($\delta = 8.07$) among the aromatic protons and at lower field than

Table 1. Physical and spectroscopic data for **1** and **6c**.

1: colorless crystals, decomp >300 °C; MS (FAB): *m/z* 400 (M^+); ^1H NMR (270 MHz, $CDCl_3$): $\delta = 7.35$ (m, 12H), 8.07 (m, 4H); ^{13}C NMR (67.8 MHz, $CDCl_3$): $\delta = 92.20$ (sp-C), 123.78, 128.20, 128.95, 141.85; UV (cyclohexane): λ_{max} (ε) = 214 (50100), 271 (61700 sh), 286 (115000), 303 (67600), 319 (6300), 324 nm (5800 sh); fluorescence (cyclohexane): λ_{max} = 327, 338, 350 nm; Raman (KBr): $\tilde{\nu} = 2202\ cm^{-1}$ (C≡C).

6c: colorless crystals, m.p. 196–197 °C; MS (FAB): *m/z* 408 (M^+); ^1H NMR (270 MHz, $CDCl_3$): $\delta = 6.47$ (s, 4H), 6.50 (s, 4H), 6.99 (dt, $J = 7.6$, 1.7 Hz), 7.10 (dt, $J = 7.6$, 1.7 Hz, 4H), 7.17 (t, $J = 7.6$ Hz, 4H), 7.28 (t, $J = 1.7$ Hz, 4H); ^{13}C NMR (67.8 MHz, $CDCl_3$): δ = 124.80, 127.59, 128.65, 128.84, 130.12, 130.86, 136.73, 137.72.

the corresponding proton of 1,3-di(phenylethynyl)benzene **8** ($\delta = 7.72$[7, 8]), an acyclic homologue of **1**. Since the chemical shifts of the outer protons of **1** are comparable to those of **8**, the low-field shift of the inner protons may be due to greater anisotropic effects from the neighboring triple bonds and benzene rings. The sp carbon atoms of **1** ($\delta = 92.20$) also resonate at slightly lower field than those of diphenylacetylene ($\delta = 89.4$), **2** ($\delta = 89.6$), and **3b** ($\delta = 88.6$ and 89.8), which is consistent with higher ring strain in the molecule; however, the degree of the low-field shift is much smaller than that for strained cycloalkynes.[9, 10]

The absorption spectrum of **1** is similar to those of diphenylacetylene, the *meta*-diyne **8**, and the cyclic hexaynes **3** with the exception of the absorption coefficients which are roughly proportional to the number of diphenylacetylene units. The tetrayne **1** emits remarkably intense fluorescence ($\Phi = 0.16$[11]). The Raman frequency of the triple bonds of **1** ($\tilde{\nu} = 2202\ cm^{-1}$) is a little lower than that of **3a** ($\tilde{\nu} = 2212$ and $2223\ cm^{-1}$)[1], reflecting the deformation of the triple bonds from linearity (more sp^2 character).[9, 10]

The X-ray structure analysis of a single crystal of **1** revealed two important features (Fig. 1).[12] First, the molecule is nearly

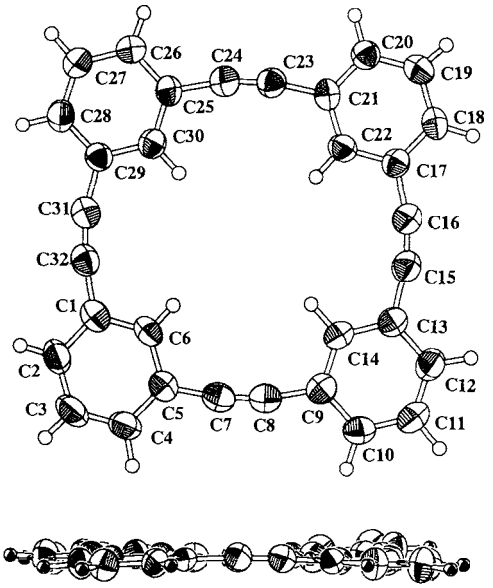

Fig. 1. Crystal structure of **1**. Top: Plan view; bottom: Side view (ORTEP; 50% probability). Selected bond lengths [Å] and angles [°] (standard deviation in parentheses): C5–C7 1.436(7), C7–C8 1.189(6), C8–C9 1.441(6), C13–C15 1.434(6), C15–C16 1.189(6), C16–C17 1.445(6), C21–C23 1.443(6), C23–C24 1.195(5), C24–C25 1.440(6), C29–C31 1.447(6), C31–C32 1.189(6), C32–C1 1.438(6); C5-C7-C8 169.5(6), C7-C8-C9 169.9(6), C13-C15-C16 168.2(5), C15-C16-C17 167.7(5), C21-C23-C24 169.4(5), C23-C24-C25 169.0(5), C29-C31-C32 168.6(5), C31-C32-C1 167.7(5).

planar; the twist angles of the benzene rings from the plane formed by the four triple bonds are less than 2°. Second, the triple bonds are no longer linear but bent (167.7–169.9°), which indicates the strained nature of the molecule. Similar angles occur at the triple bonds in cyclononyne (169.7°)[13] and [2.2](4,4')tolanophane (169°).[14] Although the molecular structure of **1** thus shows some strain around the triple bonds, the molecule is remarkably stable and is inactive towards cyclopentadiene and furan at room temperature.

Received: February 26, 1996 [Z8857IE]
German version: *Angew. Chem.* **1996**, *108*, 1658–1660

Keywords: cycloalkynes · cyclophanes · hydrocarbons · strained rings

[1] H. A. Staab, K. Neunhoeffer, *Synthesis* **1974**, 424.
[2] J. S. Moore, J. Zhang, *Angew. Chem.* **1992**, *104*, 873; *Angew. Chem. Int. Ed. Engl.* **1992**, *31*, 922; J. Zhang, D. J. Pesak, J. L. Ludwick, J. S. Moore, *J. Am. Chem. Soc.* **1994**, *116*, 4227.
[3] B. Thulin, O. Wennerström, I. Somfai, *Acta Chem. Scand.* **1978**, *B 32*, 109.
[4] H. R. Darabi, T. Kawase, M. Oda, *Tetrahedron Lett.* **1995**, *36*, 9525.
[5] (*E*)-**5** and (*Z*)-**5**, were synthesized by a succesive treatment of an isomeric mixture of 3,3'-dibromostilbenes (*E*:*Z* = ca. 2:3) with *n*BuLi and dimethylformamide. The isomers were partially separated in pure form by chromatography on SiO_2, and (*Z*)-**5** of about 85% purity was used for the next reaction: (*E*)-**5**: M.p. 107–108 °C; ^1H NMR (270 MHz, $CDCl_3$): $\delta = 7.21$ (s, 2H, $J(H,H) = 16.5$ Hz, $J(^{13}C,H) = 153.1$ Hz from the ^{13}C satellites), 7.53 (t,

 © VCH Verlagsgesellschaft mbH, D-69451 Weinheim, 1996 0570-0833/96/3513-1557 $ 15.00+.25/0

$J = 7.6$ Hz, 2H), 7.73–7.80 (m, 4H), 8.01 (t, $J = 1.7$ Hz), 10.04 (s, 2H); (*Z*)-**5**: pale yellow oil; ^{1}H NMR: $\delta = 6.75$ (s, 2H· J (H,H) = 12.2 Hz, J (^{13}C,H) = 156.7 Hz from the ^{13}C satellites), 7.34–7.47 (m, 2H), 7.71-7.75 (m, 2H), 9.90 (s, 2H).

[6] T. Mukaiyama, T. Sato, J. Hanna, *Chem. Lett.* **1973**, 1041; J. E. McMurry, *Chem. Rev.* **1989**, *89*, 1513.

[7] The synthesis of **8** has been described without spectral data [8]. The spectral data from our measurements: ^{1}H NMR (270 MHz, $CDCl_3$): $\delta = 7.34$ (m, 6H), 7.38 (dt, $J = 7.2$, 1.7 Hz), 7.46–7.52 (m, 6H), 7.72 (dt, $J = 1.7$, 1.0 Hz); ^{13}C NMR (67.8 MHz, $CDCl_3$): $\delta = 88.59$, 90.03, 123.11, 123.72, 128.41, 128.47, 131.31, 131. 70 (2C), 134.67; UV (cyclohexane): λ_{max} (ε) = 268 (46800), 283 (66100), 301 nm (56200).

[8] H. Zimmer, K. R. Hickey, R. J. Schumacher, *Chimia* **1974**, *28*, 656; C.-J. F. Du, H. Hart, *J. Org. Chem.* **1987**, *52*, 4311.

[9] H. Meier, H. Petersen, H. Kolshorn, *Chem. Ber.* **1980**, *113*, 2398.

[10] Review: H. Meier in *Advances in Strain in Organic Chemistry, Vol.1* (Ed.: B. Halton), JAI Press, London, **1991**, pp. 215–273.

[11] Estimated by use of naphthalene ($\Phi = 0.23$) as a standard; see; D. F. Eaton, *Pure Appl. Chem.* **1988**, *60*, 1107 .

[12] Crystal data for **1**: $C_{32}H_{16}$, crystallized from toluene; $M_r = 400.5$, monoclinic, space group $P2_1/n$ (no. 14), $a = 5.699(4)$, $b = 19.635(4)$, $c = 19.260(2)$ Å, $\beta = 92.12(2)°$, $V = 2153(1)$ Å^3, $Z = 4$, $\rho_{calcd} = 1.235$ g cm^{-3}, $\mu = 0.70$ cm^{-1}, 1423 independent observed reflections with [$F > 3\sigma(F)$, $3° \le 2\theta \le 60°$], refined to $R(Rw) = 0.041(0.042)$. Rigaku AFC5R difractometer with graphite monochromated $Mo_{K\alpha}$ radiation at 295 K. The structure was solved by direct methods (SHELX-86) and refined with the TEXSAN crystallorgraphic software package of Molecular Structure Corporation. All the non-hydrogen atoms were refined anisotropically. Crystallographic data (excluding structure factors) for the structure(s) reported in this paper have been deposited with the Cambridge Crystallographic Data Centre as supplementary publication no. CCDC-179-66. Copies of the data can be obtained free of charge on application to The Director, CCDC, 12 Union Road, Cambridge CB2 1EZ, UK (fax: Int. code +(1223) 336-033; e-mail: teched@chemcrys.cam.ac.uk).

[13] N. L. Allinger, A. Y. Meyer, *Tetrahedron* **1975**, 1807.

[14] M. Bauer, M. Nieger, F. Vögtle, *Chem. Ber.* **1992**, *125*, 2533.

Carbanion-Mediated Heterocyclizations: Regiospecific, General Route to Dibenzo-[*b*,*e*]phosphininones by Synthetic Anionic Equivalents of Friedel–Crafts Reactions and Remote Fries Rearrangement**

Matthew Gray, Brian J. Chapell, Nicholas J. Taylor, and Victor Snieckus*

We report on the first carbanion-mediated synthesis of diverse dibenzo[*b*,*e*]phosphininones **2** and **3** from carbamoyl and carbamoyloxy triarylphosphane oxides, **1a** and **1b** respectively (Scheme 1), which, conceptually, represent synthetic equivalents of anionic Friedel–Crafts and remote Fries rearrangements. This fundamental new chemistry of triarylphosphane oxides, suggested by the Complex Induced Proximity Effect (CIPE),[1] is part of an emerging general class of lithiation-induced regiospecific heterocyclizations,[2] which allows mild and regioselective access to substituted, condensed, and heterocycle-fused phosphininones (Table 1). Moreover, this sparsely investigated class of P-heterocycles,[3] of significance to fundamental

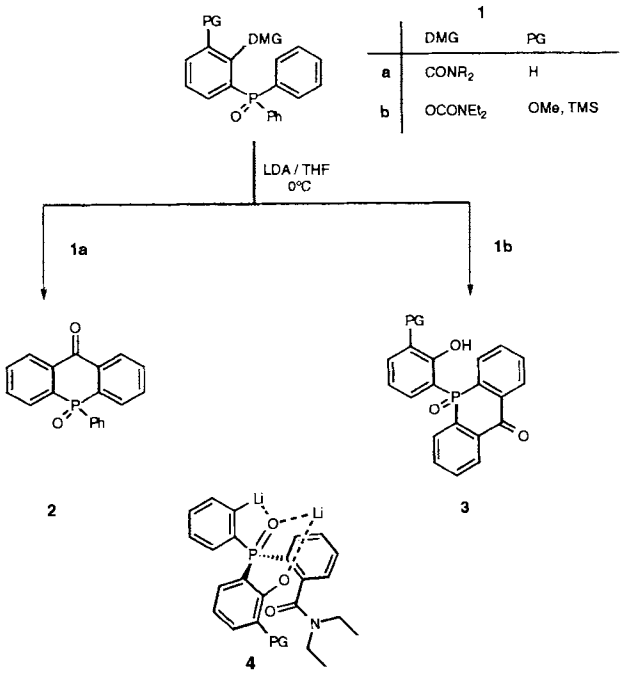

Scheme 1. LDA = lithium diisopropylamide, TMS = trimethylsilyl.

Table 1. Carbanionic route to dibenzo[*b*,*e*]phosphininones. PG = protecting group.

Entry	Substrate	Equiv LDA	Product	Yield [%] [a] (m.p. [°C])
1	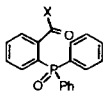	2.2	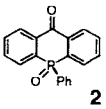	X = NEt2; 81
2		2.2		X = N*i*Pr2; 98[b]
3		3.4	**2**	X = OH; 75 (220-222)[c]
4	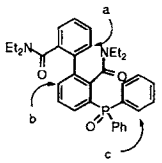	2.9	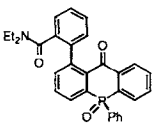	76 (167-167.5)
5	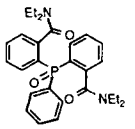	4.0	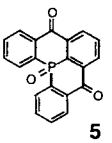 **5**	80 (278-279.5)
6	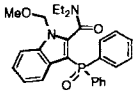	2.2	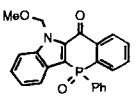	99 (160-161)
7	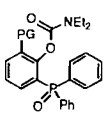	2.2	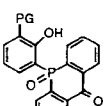 **3**	PG = OMe; 78 (252-253)
8		2.5		PG = TMS; 41[d] (187-187.5)

[a] Yields are of chromatographed material. [b] With Li(tmp) (tmp = 2,2,6,6-tetramethylpiperidin-1-yl), yield = 87%. [c] Published m.p. 220–222 °C [6a], 222–223 °C [7b], 223 °C [7c]. [d] The product of remote carbamoyl migration, (2-diethylcarbamoylphenyl)(2-hydroxy-3-trimethylsilylphenyl)phenylphosphane oxide, was also obtained in ca. 50% yield.

[*] Prof. V. Snieckus, Dr. M. Gray, B. J. Chapell,[+] Dr. N. J. Taylor[+]
Guelph-Waterloo Centre for Graduate Work in Chemistry
University of Waterloo, Waterloo, N2L 3G1, ON (Canada)
Fax: Int. +(519) 746-5884
e-mail: snieckus@buli.uwaterloo.ca

[+] X-ray crystallographic analyses.

[**] We are grateful to NSERC Canada, the NSERC/Monsanto Industrial Chair Award, and the Province of Ontario URIF program (Grant No.2318101) for support of our synthetic programs.

studies of phosphorus bonding,[4] turnstile geometry,[5] and the aromaticity of phosphacycles,[6] has previously been inaccessible, mainly due to limitations inherent in the classical Friedel–Crafts technology.[4–7] Added interest stems from the current popularity of atropisomeric diarylphosphane ligands (e.g. binap) in asymmetric synthesis and homogeneous catalysis.[8]

Encouraged by documentation on the effective properties of $P(O)Ph_2$ in directing metalation [Directed Metalation Group (DMG) properties],[9] we subjected the carbamoyl triarylphosphane oxides **1a** (R = Et, *i*Pr), prepared by $ClP(O)Ph_2$ treatment of the corresponding *ortho*-lithiated benzamide (Table 1),[10] to lithium diisopropylamide (LDA, 2.2 equiv/THF/0 °C) and observed their smooth cyclization to give the parent dibenzo[*b*,*e*]phorphorinone **2** (Table 1, entries 1 and 2). The recent important observation by Mortier[11] suggested cyclization of the corresponding carboxylic acid, which, in the event, led to the same product in somewhat lower yield (entry 3). In entry 4, the potential competition between three sites for metalation and cyclization to form either phosphininone or two types of fluorenone (arrows a, b, and c) is not observed, and only a phosphininone is obtained. The structure was confirmed by X-ray crystallographic analysis.[12a] Double anionic cyclization of a dicarboxamide-substituted triaryl phosphane oxide (entry 5) leads efficiently (47% overall yield based on starting benzamide) to 5*H*,9*H*-phosphinolino[3,2,1-*de*]-14-λ^5-acridophosphine-5,9,14-trione (**5**), a polycyclic system previously prepared by lengthy Friedel–Crafts approaches (overall yield less than 10%).[4] Its X-ray crystal structure (Fig. 1) shows

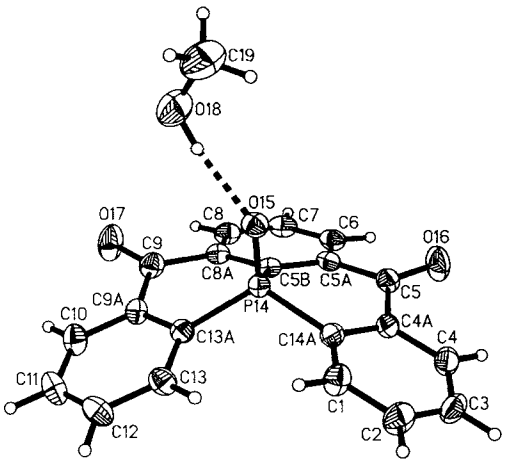

Fig. 1. Structure of **5** in the crystal.

a puckered pentacyclic structure in contrast to the parent **2**, which exhibits only slight deviations from planarity. However, the constraints of the pentacycle reduce pyramidality at phosphorus (sum of C-P-C bond angles, 319.9°; cf. 316.8° in **2**).[12a, b] The scope of this new methodology is illustrated by the preparation in quantitative yield of an indole-fused phosphininone (entry 6), a new ring system.[10, 13]

Tandem remote anionic Fries rearrangement[2a] and anionic Friedel–Crafts reactions are observed on *ortho*-carbamoyloxy triarylphosphane oxides (entries 7,8), leading to hitherto unknown P-phenyl functionalized phosphininones **3** (Scheme 1). The regiochemistry of the second deprotonation leading to intermediate **4** may be dictated by factors of higher electron density in the phenolic ring and OLi ··· O = P coordination effects.

In analogy to observations from other heteroatom-bridged biaryls,[2] the *ortho*-tolyl phosphane oxide **6** (Scheme 2),[14]

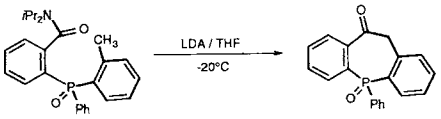

Scheme 2.

when subjected to slightly modified cyclization conditions (2.2 equiv LDA/THF/ − 20 °C), furnished the phosphepine **7** (ca. 50% yield), a ring system with meager literature and potential antidepressant activity.[15]

To probe the potential involvement of CIPE[1] in the anionic Friedel–Crafts reaction, **1a** (R = Et) was subjected to LDA (1.1 equiv; THF/0 °C/40 min) to give a mixture of phosphininone **2** and starting material in 61:39 ratio (by ^1H NMR spectroscopy; respectively, 65% and 27% yields of isolated product). Exposure of **1a** (R = Et) to LDA/TMSCl (2.2 equiv/2.5 equiv; THF/ −70 °C → 0 °C) under in situ conditions[16] provided **2** in 58% yield and only trace amounts of silylated material. Thus cyclization appears to be fast with respect to external electrophile trapping under the assumed thermodynamic conditions, but the relative contributions from amide CIPE and P(O)Ph DMG effects require further investigation.

In summary, a general, convenient, and regiospecific entry into benzo[*b*,*e*]phosphininones, including functionalized, polycyclic, and heterocyclic analogues, has been achieved by directed metalation tactics. The chemistry of this P-heteroatom class,[17] previously inadequately explored because of synthetic inaccessibility, may now be investigated, perhaps with emphasis on development of new phosphane ligands for asymmetric synthesis.[18] Furthermore, this and related studies[2] suggest that carbanion-mediated cyclizations may provide fruitful new methodology for the construction of other dibenzoannelated six- and seven-membered ring heterocycles.

Experimental Procedure

2: *N*,*N*-Diisopropylamine (0.21 mL, 1.52 mmol) in dry THF (12 mL) at temperatures below −70 °C under argon was treated with *n*-butyllithium (0.90 mL, 1.61 M solution in hexanes, 1.45 mmol) by dropwise addition, and the mixture was stirred at 0 °C (20 min). (2-Diethylcarbamoylphenyl)diphenylphosphane oxide (250 mg, 0.66 mmol) in THF (3.5 mL) was added dropwise to this solution at be < 2 °C by cannula over 5 min, and the resulting brown suspension was stirred at 0 °C for 30 min. Saturated aqueous NH_4Cl was added, and the mixture extracted with ethyl acetate, washed with brine, dried ($MgSO_4$), and concentrated in vacuo. Purification by column chromatography (97/3 CH_2Cl_2/MeOH eluent) afforded 10-phenyl-9,10-dihydro-10-λ^5-acridophosphine-9,10-dione (163 mg, 81%): colorless needles, m.p. 220–222 °C (MeOH), (published m.p. 220–222 °C, see Table 1); IR (KBR, cm^{-1}): $\tilde{\nu}$: 3055, 1666, 1200; ^1H NMR (250 MHz, $CDCl_3$): δ = 8.49–8.40 (m, 2H), 8.08–7.96 (m, 2H), 7.78–7.68 (m, 4H), 7.64–7.54 (m, 2H), 7.49–7.33 (m, 3H); ^{31}P NMR (81 MHz, $CDCl_3$, ext. ref. $P(OMe)_3$ in C_6D_6): δ = 4.0; MS (EI): *m*/*z* (%): 304 (44) [M^+]; anal. calcd for $C_{19}H_{13}O_2P$: C 75.00; H 4.31; P 10.18. Found: C 75.26; H 4.46; P 9.96.

Received: December 12, 1995
Revised version: March 18, 1996 [Z 8639 IE]
German version: *Angew. Chem.* **1996**, *108*, 1609–1611

Keywords: Friedel–Crafts reactions · Fries rearrangements · heterocycles · rearrangements · phosphorus compounds

[1] P. Beak, A. I. Meyers, *Acc. Chem. Res.* **1986**, *19*, 356–363.
[2] Cyclizations of a) *ortho*-carbamoyl diaryl sulfone: F. Beaulieu, V. Snieckus, *J. Org. Chem.* **1994**, *59*, 6508–6509; b) corresponding diaryl ethers: O. B. Familoni, I. Ionica, V. Snieckus, *Tetrahedron Lett.*, submitted; c) corresponding diarylamines: J. A. Glänzer, M. Gray, S. MacNeil, V. Snieckus, unpublished results.
[3] L. D. Quin, *The Heterocyclic Chemistry of Phosphorus; Systems based on the Phosphorus–Carbon Bond*, Wiley, New York, **1981**.
[4] C. H. Chen, J. J. Doney, J. L. Fox, H. R. Luss, *J. Org. Chem.* **1985**, *50*, 2914–2917.

[5] D. Hellwinkel, A. Wiel, G. Sattler, B. Nuber, *Angew. Chem.* **1990**, *102*, 677–680; *Angew. Chem. Int. Ed. Engl* **1990**, *29*, 689–692.
[6] a) C. Jongsma, R. Lourens, F. Bickelhaupt, *Tetrahedron* **1976**, *32*, 121–124; b) C. Jongsma, H. Vermeer, F. Bickelhaupt, W. Schäfer, A. Schweig, *ibid.* **1975**, *31*, 2931–2935; c) H. S. Kasmai, J. F. Femia, L. L. Healy, M. R. Lauria, M. E. Lansdown, *J. Org. Chem.* **1987**, *52*, 5461–5466.
[7] a) G. O. Doak, L. D. Freedman, J. B. Levy, *J. Org. Chem.* **1964**, *29*, 2382–2385; b) Y. Segall, I. Granoth, A. Kalir, *J. Chem. Soc. Chem. Commun.* **1974**, 501–502; c) K. A. Petrov, V. A. Chauzov, N. Yu. Mal'kevich, *Zh. Obshch. Khim.* **1977**, *47*, 2516–2522; *J. Gen. Chem. USSR* **1977**, 2299–2304 [*Chem. Abstr.* **1978**, *88*, 89768u].
[8] R. Noyori, *Asymmetric Catalysis in Organic Synthesis*, Wiley, New York, **1994**.
[9] a) R. Schmid, J. Foricher, M. Cereghetti, P. Schönholzer, *Helv. Chim. Acta* **1991**, *74*, 370–389; b) J. M. Brown, S. Woodward, *J. Org. Chem.* **1991**, *55*, 6803–6809; c) N. W. Alcock, J. M. Brown, M. Pearson, S. Woodward, *Tetrahedron Asymmetry* **1991**, *3*, 17–20; d) B. Schaub, J. Titus, M. Schlosser, *Tetrahedron Lett.* **1984**, *37*, 4097–4100. Other P-containing DMGs: e) D. C. Craig, N. K. Roberts, J. L. Tanswell, *Aust. J. Chem.* **1990**, *43*, 1487–1496 (DMG = $P(S)(NMe_2)_2$); f) M. Yoshifuji, T. Ishizuka, Y. J. Choi, N. Inamoto, *Tetrahedron Lett.* **1984**, *25*, 553–556 (DMG = $P(S)Ph(NR_2)$); g) L. Dashan, S. Trippett, *ibid.* **1983**, *24*, 2039–2040 (DMG = $P(O)(NMe_2)_2$); h) C. G. Stuckwisch, *J. Org. Chem.* **1976**, *41*, 1173–1176 (DMG = $P(NPh)Ph_2$).
[10] Reactions were conducted in dilute solutions [12–16 mL THF per mmol except entry 4 (30 mL THF per mmol)]. Yields 59–92%. Standard conditions: entries 1, 7, and 8 (**2**, **3**): a) 1.1–1.15 equiv *s*BuLi/TMEDA (inverse addition), THF, 40–90 min, $< -70\,^{\circ}C$; b) 1.2–1.25 equiv Ph_2POCl, 20–60 min, $< -70\,^{\circ}C$; c) sat. aq. NH_4Cl; entry 2 (**2**): b) 1.2 equiv Ph_2POCl, $< -70\,^{\circ}C \rightarrow$ room temperature (RT); entry 3: prepared according to a known procedure [9d]; entry 4: 2.5 equiv *s*BuLi/TMEDA, 3.0 equiv Ph_2POCl; entry 5 (**5**): b) 0.6 equiv $PhPOCl_2$, 20 min, $< -70\,^{\circ}C$; entry 6: normal addition and b) 1.25 equiv Ph_2POCl, $< -70\,^{\circ}C \rightarrow$ RT.
[11] a) J. Mortier, J. Moyroud, B. Bennetau, P. A. Cain, *J. Org. Chem.* **1994**, *59*, 4042–4044; b) B. Bennetau, J. Mortier, J. Moyroud, J.-L. Guesnet, *J. Chem. Soc. Perkin Trans. 1* **1995**, 1265–1271.
[12] a) Crystallographic data (excluding structure factors) for the structures reported in this paper have been deposited with the Cambridge Crystallographic Data Centre as supplementary publication no. CCDC-179-64. Copies of the data can be obtained free of charge on application to The Director, CCDC, 12 Union Road, Cambridge CB2 1EZ, UK (fax: Int. code +(1223) 336-033; e-mail: teched@chemcrys.cam.ac.uk). b) Crystal data for entry 5: $C_{20}H_{11}O_3P \cdot CH_3OH$, $M_r = 363.33$, colorless needle prism fragment of dimensions (mm) $0.34\{110\} \times 0.84\{001\}$, monoclinic, $I2/a$, $a = 14.204(1)$, $b = 11.015(1)$, $c = 21.617(2)$ Å, $\beta = 99.46(1)^{\circ}$, $V = 3336.0(5)$ Å^3, $Z = 8$, $F(000) = 1504$, $\rho = 1.443$ g cm^{-3}, $4^{\circ} \leq 2\theta \leq 50^{\circ}$, ω scan mode, $T = 200$ K, largest difference peak/hole 0.31/ − 0.28 e Å^{-3}. Data were collected on a Siemens P4 diffractometer with $Mo_{K\alpha}$ radiation ($\lambda = 0.71073$ Å). Of 3074 reflections measured, 2939 were independent. The structure was solved with direct methods (SHELXTL IRIS) and refined by full-matrix least-squares on F (296 parameters), resulting in final R, wR, and GoF values of 0.0308, 0.0352, and 3.03 respectively (for 2476 data with $F > 6.0\sigma(F)$). Absorption correction was face-indexed numerical($\mu(Mo_{K\alpha}) = 1.90$ cm^{-1}, min./max. transmission 0.9275/0.9502). Hydrogen atoms were solved according to a riding model with refined isotropic temperature factors U.
[13] The starting material was prepared by directed metalation: X. Wang, PhD Thesis, University of Waterloo, **1992**.
[14] Prepared by directed *ortho*-metalation with (*o*-Tol)P(Ph)Cl [17a] as electrophile, with subsequent oxidation of the crude phoshane (H_2O_2).
[15] Y. Segall, E. Shirin, I. Granoth, *Phosphorus Sulfur Relat. Elem.* **1980**, *8*, 243–254.
[16] a) T. D. Krizan, J. C. Martin, *J. Am. Chem. Soc.* **1983**, *105*, 6155–6157; b) E. J. Corey, A. W. Gross, *Tetrahedron Lett.* **1984**, *25*, 495–498.
[17] Simple transformations, for example Grignard and alkyllithium additions and reduction to phosphanes have been reported. See refs. [6a, 7b–c] and a) Y. Segall, R. Alkabets, I. Granoth, *J. Chem. Res. Synop.* **1977**, 310–311; *J. Chem. Res. Miniprint* **1977**, 3541–3565; b) I. Granoth, Y. Segall, H. Leader, *J. Chem. Soc. Perkin Trans. 1* **1978**, 465–468; c) K.-C. Chen, S. E. Ealick, D. van der Helm, J. Barycki, K. D. Berlin, *J. Org. Chem.* **1977**, *42*, 1170–1177.
[18] H. Brunner, *Top. Stereochem.* **1988**, p. 129.

The First Synthesis of Enantiopure (−)- and (+)-Isoterrein from Optically Inactive *meso*-Tartaric Acid**

Marian Mikołajczyk,* Maciej Mikina, Michał W. Wieczorek, and Jarosław Błaszczyk

Dedicated to Professor Leopold Horner on the occasion of his 85th birthday

(+)-Terrein (+)-**1**, a metabolite of the mold *Aspergillus terreus*, was first isolated by Raistrick and Smith in 1935.[1] Twenty years later its correct structure was established independently by Grove[2] and by Barton and Miller,[3] who also determined the configuration of the *trans*-diol moiety by conversion of (+)-**1** into a derivative of (+)-tartaric acid. Although the structure of terrein **1** is simple, its synthesis is not trivial because of its sensitivity to acids and bases. Therefore, only after a lapse of twenty years were three synthetic approaches to racemic terrein **1** reported.[4–6] In addition to the synthesis of **1**, Barton and Hulshof[5] also described the preparation of racemic isoterrein **2**, the more stable isomer of **1**, in which the hydroxyl groups are *cis* oriented.

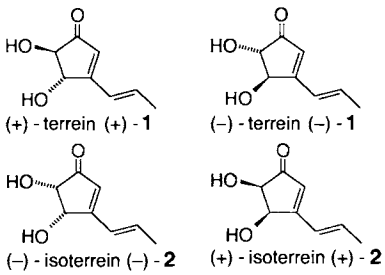

Only recently, two research groups succeeded in synthesizing optically active terrein. Kolb and Hoffmann[7] prepared first racemic terrein **1** by ring contraction of 6-alkoxy-2,3-dihydro-6*H*-pyran-3-one. Then after resolving racemic precursors of **1**, they completed the total synthesis of natural (+)- and unnatural (−)-terrein. Altenbach and Holzapfel[8] devised an elegant and short synthesis of (+)-**1** from L-(+)-tartaric acid utilizing the chemistry of bis(β-oxophosphonates). The synthesis and reactivity of this new class of phosphonates was independently and intensively investigated in our laboratory.[9] As a result of our studies we report here the first synthesis of both enantiopure forms of isoterrein, (−)-**2** and (+)-**2**.[10]

In developing the strategy for the synthesis of both enantiomers of isoterrein we noted that both (+)-terrein and (+)-tartaric acid used in the synthesis of (+)-terrein have the same configuration at the *trans*-diol moiety. Since isoterrein has a *cis*-diol unit, *meso*-tartaric acid would appear to be a suitable starting material; however, it is optically inactive. Therefore, it was necessary to first seek a way to convert *meso*-tartaric acid into an optically active derivative such that the configurational

[*] Prof. Dr. M. Mikołajczyk, M. Mikina
Centre of Molecular and Macromolecular Studies
Polish Academy of Sciences
Sienkiewicza 112, PL-90-363 Łódź (Poland)
Fax: Int. code +(42)847126
Dr. M. W. Wieczorek, Dr. J. Błaszczyk
Institute of Technical Biochemistry, Technical University of Łódź
Stefanowskiego 4/10, PL-90-924 Łódź (Poland)

[**] Financial support by the State Committee of Scientific Research (Grant No. 3/TO9A/08408) and by the Foundation of Polish Science (for J. B.) is gratefully acknowledged.

 © VCH Verlagsgesellschaft mbH, D-69451 Weinheim, 1996 0570-0833/96/3513-1560 $ 15.00+.25/0

relationship at both chiral carbon atoms is preserved. It was gratifying to find that the acid-catalyzed reaction of *meso*-tartaric acid with (+)-camphor and methyl orthoformate in methanol resulted in the formation of a single diastereomer [m.p. 95 °C (hexane), $[\alpha]_{589} = -2.17$ ($c = 20$ in acetone)] of the protected dimethyl *meso*-tartrate **3** in 76% yield (Scheme 1). The X-ray structure determination of **3** (Fig. 1)[11] revealed that this fully diastereoselective desymmetrization reaction led to the diastereomer with *R* and *S* absolute configuration at C11 and C12, respectively.

Starting from **3**, which is easily available in multigram quantities, both enantiomers of isoterrein **2** were obtained as shown in Scheme 1. Thus, treatment of **3** with dimethyl lithiomethanephosphonate produced the protected 3-phosphonomethylcyclopentenone **4** in 59% yield as a mixture of diastereomers **4a** and **4b** in a 55:45 ratio (^{1}H NMR analysis). In accord with our previous studies[9] this one-pot conversion of **3** to **4** involves initial formation of the bis(β-oxophosphonate) **6**, which undergoes fast cyclization to give the kinetically controlled Knoevenagel product **7** (a mixture of two diastereomers) [Eq. (a)]. The latter is transformed then, without isolation, into the Horner–Wittig product **4** by heating in a basic benzene–water mixture at reflux.

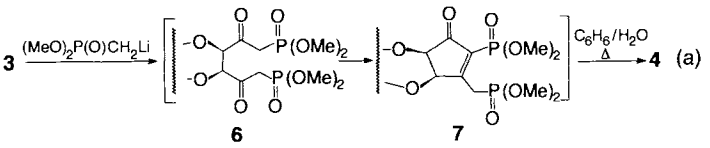

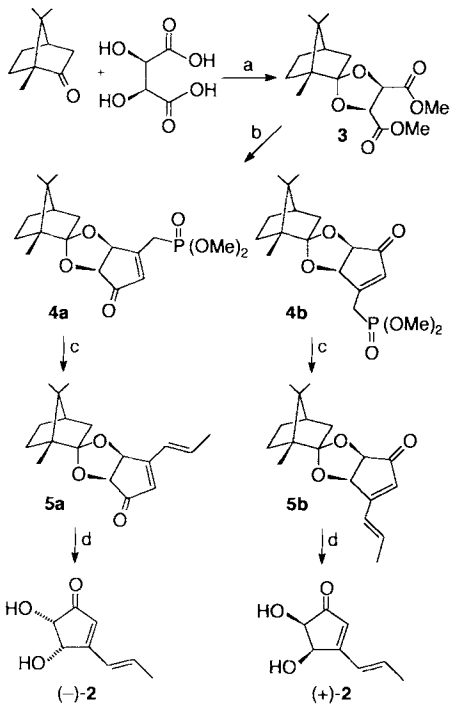

Scheme 1. a) $(MeO)_3CH$, MeOH, H_2SO_4 cat., room temperature (rt), 5 d. b) $(MeO)_2P(O)CH_2Li$ (4 equiv), THF, −78 °C → rt; benzene–H_2O, reflux 3 h, chromatography (silica gel, petroleum ether/acetone 5/1); separation [crystallization from acetone/hexane and chromatography (silica gel, petroleum ether/acetone 5/1)]. c) BuLi, THF, −78 °C, CH_3CHO, rt, 2 h, chromatography (silica gel, petroleum ether/acetone 10/1). d) H_2O/dioxane, aq HCl (36%), 50 °C, 3–4 h, chromatography (silica gel, petroleum ether/acetone 2/1).

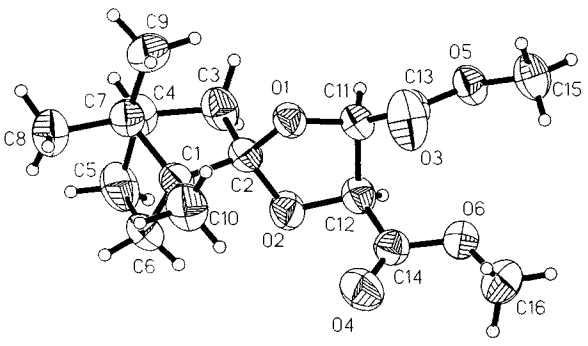

Fig. 1. X-ray crystal structure of **3**. Selected bond lengths [Å] and angles [°]: C2–O1 1.427(3), C2–O2 1.434(4), O1–C11 1.415(4), O2–C12 1.401(4), C11–C12 1.549(3), C11–C13 1.524(4), C12–C14 1.522(3); O1-C2-O2 103.9(2), C2-O1-C11 104.6(2), C2-O2-C12 109,6(2), O1-C11-C12 102.0(2), O2-C12-C11 103.5(2), O1-C11-C13 110.1(2), O2-C12-C14 110.8(2).

Fractional crystallization from hexane/acetone and subsequent column chromatography led to separation of the pure diastereomers **4a** [m.p. 112 °C, $[\alpha]_{589} = -19.7$ ($c = 6$ in acetone)] and **4b** [m.p. 103 °C, $[\alpha]_{589} = +5.4$ ($c = 5.8$ in acetone)]. X-ray crystal structure determinations carried out on single crystals of both **4a** (Fig. 2)[11] and **4b** indicated unequivocally

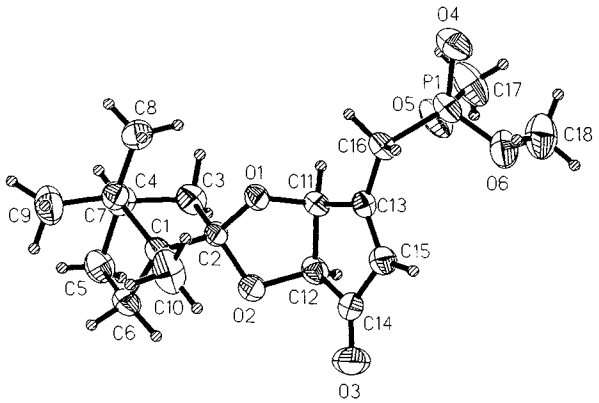

Fig. 2. X-ray crystal structure of **4a**. Selected bond lengths [Å] and angles [°]: C(2)–O1 1.431(3), C2–O2 1.443(4), O1–C11 1.428(4), O2–C12 1.411(3), C11–C12 1.543(3), C11–C13 1.517(3), C12–C14 1.526(4), C13–C15 1.337(4), P1–O4 1.455(3); C12–C14 1.526(4); O1-C2-O2 104.1(2), C2-O1-C11 106.3(2), C2-O2-C12 108.0(2), O1-C11-C12 102.2(2), O2-C12-C11 105.9(2), O1-C11-C13 109.3(2), O2-C12-C14 111.8(2).

that the configurations of the diol moieties in **4a** and **4b** are 11*S*,12*S* and 11*R*,12*R*, respectively. The Horner–Wittig reaction of **4a** with acetaldehyde furnished the protected isoterrein **5a** [m.p. 39–42 °C, $[\alpha]_{589} = -135$ ($c = 5.38$ in hexane)] in 62% yield. Similarly, **3b** afforded the corresponding dienone **5b** [m.p. 144.5–145.5 °C, $[\alpha]_{589} = +142.5$ ($c = 1.19$ in hexane)]. Deprotection of the diol moiety in **5a** and **5b** by acidic hydrolysis afforded in 80% yield both (−)-**2** [m.p. 122–123 °C, $[\alpha]_{589} = -113$ ($c = 2.31$ in acetone)] and (+)-**2** [m.p. 122–122.5 °C, $[\alpha]_{589} = +111$, ($c = 2.19$ in acetone)] in enantiopure form.[12] Since in the last two steps the chiral diol fragment is not affected, (−)-**2** can be assigned the *S*,*S* configuration, and (+)-**2** the *R*,*R* configuration.

It is interesting to note that in the ^{1}H NMR spectra (200 MHz, $CDCl_3$) of the enantiomerically pure isoterreins **2** in addition to the characteristic coupling between the *cis* protons ($J = 5.7$ Hz)[13] further coupling of these protons with the hydroxyl protons is evident visible ($J = 3.1$ and 3.2 Hz). Accordingly, the resonance signals of the hydroxyl protons appear as

 © VCH Verlagsgesellschaft mbH, D-69451 Weinheim, 1996 0570-0833/96/3513-1561 $ 15.00+.25/0

Table 1. Selected spectroscopic data for compounds **2**–**5** [a].

2: ^{1}H NMR (200 MHz, $CDCl_3$): δ = 6.76 (dq, 1H, J = 15.7, 6.7 Hz, =CH(CH_3)), 6.51 (dd, 1H, J = 15.7, 1.4 Hz, =CH), 6.00 (s, 1H, =CH), 5.00 (dd, 1H, J = 5.7, 3.1 Hz, CH), 4.18 (dd, 1H, J = 5.7, 3.2 Hz, CH), 3.09 (d, 1H, J = 3.2 Hz, OH), 2.97 (d, 1H, J = 3.1 Hz, OH), 1.99 (dd, 3H, J = 6.7, 1.4 Hz, CH_3); ^{13}C NMR (50 MHz, $CDCl_3$): δ = 206.1, 170.1, 140.5, 126.3, 126.0, 71.9, 68.2, 19.3

3: ^{1}H NMR ($CDCl_3$, 200 MHz): δ = 4.78 (d, 1H, J = 7.6 Hz, CH), 4.64 (d, 1H, J = 7.6 Hz, CH), 3.73 (s, 3H, CH_3O), 3.72 (s, 3H, CH_3O), 1.9–2.1 (m, 2H), 1.6–1.8 (m, 2H), 1.35–1.55 (m, 2H), 1.1–1.3 (m, 1H), 0.99 (s, 3H, CH_3), 0.91 (s, 3H, CH_3), 0.86 (s, 3H, CH_3); ^{13}C NMR (50 MHz, $CDCl_3$): δ = 171.3, 168.5, 120.5, 75.8, 74.2, 72.9, 52.1, 51.9, 44.9, 44.0, 43.2, 29.6, 26.7, 20.3, 20.0, 9.3

4a: ^{1}H NMR (200 MHz, $CDCl_3$): δ = 6.02 (d, 1H, J = 4.3 Hz, =CH), 5.20 (dd, 1H, J = 5.4, 3.1 Hz, CH), 4.32 (d, 1H, J = 5.4 Hz, CH), 3.79 (d, 6H, J = 11.1 Hz, CH_3O), 3.06 (d, 1H, J = 22.4 Hz, PCH), 3.03 (d, 1H, J = 23.7 Hz, PCH), 1.1–2.1 (m, 7H), 0.95 (s, 3H, CH_3), 0.81 (s, 3H, CH_3), 0.63 (s, 3H, CH_3); ^{13}C NMR (50 MHz, $CDCl_3$): δ = 199.7 (d, J = 2.6 Hz), 166.4 (d, J = 9.9 Hz), 131.0 (d, J = 9.1 Hz), 124.1, 79.8 (d, J = 3.4 Hz), 75.5, 52.8 (d, J = 11.7 Hz), 52.7 (d, J = 11.2 Hz), 49.4 (d, J = 181.1 Hz), 44.8, 44.2, 29.1, 28.4, 26.4, 25.6, 20.0, 19.8, 9.1; ^{31}P NMR (81 MHz, $CDCl_3$): δ = 25.5

4b: ^{1}H NMR (200 MHz, $CDCl_3$): δ = 6.04 (d, 1H, J = 4.3 Hz, =CH), 5.07 (dd, 1H, J = 5.5, 2.9 Hz, CH), 4.46 (d, 1H, J = 5.5 Hz, CH) 3.80 (d, 3H, J = 11.1 Hz, CH_3O), 3.79 (d, 3H, J = 11.1 Hz, CH_3O), 3.07 (d, 1H, J = 22.5 Hz, PCH), 3.05 (d, 1H, J = 23.7 Hz, PCH), 1.10–2.15 (m, 7H), 0.97 (s, 3H, CH_3), 0.82 (s, 3H, CH_3), 0.63 (s, 3H, CH_3); ^{13}C NMR (50 MHz, $CDCl_3$): δ = 199.9, 165.9 (d, J = 10.2 Hz), 131.1 (d, J = 8.8 Hz), 123.9, 77.8 (d, J = 3.7 Hz), 77.1, 52.6 (d, J = 7.4 Hz), 52.5 (d, J = 8.5 Hz), 49.2 (d, J = 188.4 Hz), 44.7, 44.0, 29.3, 28.3, 26.4, 25.5, 19.9, 19.8, 8.8; ^{31}P NMR (81 MHz, $CDCl_3$): δ = 25.5

5a: ^{1}H NMR (200 MHz, $CDCl_3$): δ = 6.70 (dq, 1H, J = 15.7, 6.7 Hz, =CH(CH_3)), 6.45 (d, 1H, J = 15.7 Hz, =CH), 5.79 (s, 1H, =CH), 5.27 (d, 1H, J = 5.8 Hz, CH), 4.33 (d, 1H, J = 5.8 Hz, CH), 1.96 (d, 3H, J = 6.7 Hz, CH_3), 1.1–2.2 (m, 7H), 0.97 (s, 3H, CH_3), 0.82 (s, 3H, CH_3), 0.62 (s, 3H, CH_3); ^{13}C NMR (50 MHz, $CDCl_3$): δ = 200.8, 168.2, 140.3, 126.2, 125.8, 123.6, 77.6, 75.9, 53.6, 51.2, 47.5, 44.8, 44.1, 29.0, 26.5, 20.0, 19.1, 9.0

5b: ^{1}H NMR (200 MHz, $CDCl_3$): δ = 6.68 (dq, 1H, J = 15.7, 6.8 Hz, =CH(CH_3)), 6.47 (dd, 1H, J = 15.7, 1.3 Hz, =CH), 5.81 (s, 1H), 5.13 (d, 1H, J = 5.8 Hz, CH), 4.47 (d, 1H, J = 5.8 Hz, CH), 1.98 (dd, 3H, J = 6.8, 1.3 Hz, CH_3), 1.1–2.15 (m, 7H), 0.99 (s, 3H, CH_3), 0.82 (s, 3H, CH_3), 0.64 (s, 3H, CH_3); ^{13}C NMR (50 MHz, $CDCl_3$): δ = 201.5, 168.1, 140.6, 126.7, 126.1, 124.1, 77.9, 75.9, 51.6, 47.8, 45.2, 44.5, 29.7, 26.9, 20.4, 20.2, 19.3, 9.3

[a] All compounds described here provided correct C,H,P analytical data.

doublets at δ = 2.97 and 3.09. This indicates that the proton exchange in **2** is very slow. Moreover, the ^{1}H NMR spectrum of (−)-**2** measured in the presence of (+)-(*R*)-*tert*-butyl(phenyl)phosphinothioic acid as a chiral solvating agent confirmed its full enantiomeric purity.[14]

In summary, we have developed a short and efficient synthesis of both enantiomers of isoterrein **2** from the easily accessible, optically active derivative of *meso*-tartaric acid **3**. The latter as well as the diastereomeric 3-phosphonomethyl cyclopentenones **4** are promising precursors of other biologically active, chiral, nonracemic cyclopentanoids. Further studies in this direction are in progress.

Received: January 23, 1996 [Z 8744 IE]
German version: *Angew. Chem.* **1996**, *106*, 1645–1647

Keywords: desymmetrization · isoterrein

[1] H. Raistrick, G. Smith, *Biochem. J.* **1935**, *29*, 606.
[2] J. G. Grove, *J. Chem. Soc.* **1954**, 4693.
[3] D. H. R. Barton, E. Miller, *J. Chem. Soc.* **1955**, 1028.
[4] J. Auerbach, S. M. Weinreb, *J. Chem. Soc. Chem. Commun.* **1974**, 298.
[5] D. H. R. Barton, L. A. Hulshof, *J. Chem. Soc. Perkin Trans. 1* **1977**, 1103.
[6] A. J. H. Klunder, W. Bos, B. Zwanenburg, *Tetrahedron Lett.* **1981**, *22*, 4557.
[7] H. C. Kolb, M. R. Hoffmann, *Tetrahedron: Asymmetry* **1990**, *1*, 237.
[8] H.-J. Altenbach, W. Holzapfel, *Angew. Chem.* **1990**, *102*, 64; *Angew. Chem. Int. Ed. Engl.* **1990**, *29*, 67.
[9] M. Mikołajczyk, M. Mikina, *J. Org. Chem.* **1994**, *59*, 6760.
[10] Recently, we briefly reported the synthesis of (+)-**2** from (+)-tartaric acid which, however, afforded a highly racemized product (*ee* ≈ 10%): M. Mikina, M. Mikołajczyk, *Phosphorus Sulfur Silicon*, **1993**, *75*, 39.
[11] Crystal structure determination of **3**: $C_{16}H_{24}O_6$; monoclinic, space group $P2_1$; a = 7.1506(14), b = 9.2308(6), c = 12.4923(7) Å; β = 91.136(9)°, V = 824.4(2) Å^3, Z = 2, ρ_{calcd} = 1.258(2) g cm^{-3}, $\mu(Cu_{K\alpha})$ = 7.6 cm^{-1}, λ = 1.54184 Å, $F(000)$ = 336. Enraf-Nonius CAD4 diffractometer; graphite monochromator; crystal dimensions 0.8 × 0.4 × 0.3 mm. Intensity data collected at room temperature; $\omega/2\theta$ scan mode, scan width (0.74 + 0.14 tanθ). Lattice constants refined by least-squares fit of 25 reflections in θ range 20.0–28.7°; 1804 unique reflections in the scan range $1 \le \theta \le 75°$; *hkl* ranges: *h*: 0 to 8, *k*: −11 to 0, *l*: −15 to 15. Decline in intensities of three standard reflections (2, −3, −4; 2, −1, −6; 2, −1,6) 1.8% during 15.4 hours of exposure; empirical absorption correction applied, transmission minimum = 93.40%, maximum = 97.89%, and average = 94.96%. 1795 observed reflections with $I \ge 3\sigma(I)$ used in structure solution by direct methods and in refinement by full-matrix least-squares on F for 200 parameters; R = 0.038, R_w = 0.046, $w = 1/\sigma^2(F) + 0.00008F^2$, GOF = 1.884. Anisotropic refinement for all non-hydrogen atoms, hydrogen atoms found in a difference Fourier map and set as riding, with fixed isotropic thermal parameters. Residual electron density 0.151/ − 0.183 e Å^{-3}. Crystal structure determination of **4a**: $C_{18}H_{27}O_6P$; orthorhombic, space group $P2_12_12_1$; a = 7.424(1), b = 9.956(2), c = 25.310(5) Å, V = 1870.7(8) Å^3, Z = 4, ρ_{calcd} = 1.315(2) g cm^{-3}, $\mu(Cu_{K\alpha})$ = 15.5 cm^{-1}, λ = 1.54184 Å, $F(000)$ = 792. Enraf-Nonius CAD4 diffractometer; graphite monochromator; crystal dimensions 0.6 × 0.6 × 0.2 mm. Intensity data collected at room temperature; $\omega/2\theta$ scan mode, scan width (0.93 + 0.14 tanθ). Lattice constants refined by least-squares fit of 25 reflections in θ range 21.9–27.7°; 3850 unique reflections in the scan range $1 \le \theta \le 75°$; *hkl* ranges: *h*: 0 to 9, *k*: 0 to 12, *l*: −31 to 31. Decline in intensities of three standard reflections (2,3, −10; 0,3, −11; −1,4, −9) 6.1% during 43.4 hours of exposure. Intensity data corrected using the DECAY program, correction minimum = 1.00003, maximum = 1.03213, and average = 1.01579; empirical absorption correction applied, transmission minimum = 69.81%, maximum = 99.98%, and average = 91.98%. 3823 observed reflections with $I \ge 3\sigma(I)$ used in structure solution by direct methods and in refinement by full-matrix least-squares on F for 228 parameters; R = 0.061, R_w = 0.077, $\omega = 1/\sigma^2(F) + 0.006F^2$, GOF = 1.346. Anisotropic refinement for all non-hydrogen atoms, hydrogen atoms found in a difference Fourier map and set as riding, with fixed isotropic thermal parameters. Residual electron density 1.653/ − 0.700 e Å^{-3} (highest density close to P1: 0.791 Å). Crystallographic data (excluding structure factors) for the structures reported in this paper have been deposited with the Cambridge Crystallographic Data Centre as supplementary publication no. CCDC-179-50. Copies of the data can be obtained free of charge on application to The Director, CCDC, 12 Union Road, Cambridge CB2 1EZ, UK (fax: Int. code +(1223)336-033; e-mail: teched(@chemcrys.cam.ac.uk).
[12] An equimolar mixture of (−)- and (+)-**2** melts at 87–88 °C in agreement with the literature data for (±)-**2** [5].
[13] The value of ^3J(H4,H5) for terrein **1** is 2.5 Hz [5,6].
[14] The application of chiral *tert*-butylphenylphosphinothioic acid for determining the *ee* of diols was presented by Dr. J. Omelańczuk from our laboratory at the International Conference on Phosphorus Chemistry, Jerusalem, **1995** (Abstract Book, p. 122.)

Alkylation of 1-Naphthol with Alcohols over an Iron Oxide Catalyst **

Hanna Grabowska, Włodzimierz Miśta, Ludwik Syper, Józef Wrzyszcz,* and Mirosław Zawadzki

The two naphthol isomers, 1- and 2-naphthol, are commonly used as intermediates in the production of azo dyes, pigments, insecticides, and drugs. The selective alkylation of these compounds is an important reaction in industrial organic chemistry, and there is increasing pressure to find cleaner, more environmentally friendly methods. Heterogeneous catalysis is one possibility.

[*] Prof. Dr. J. Wrzyszcz, H. Grabowska, Dr. W. Miśta, Dr. M. Zawadzki
W. Trzebiatowski Institute of Low Temperature and Structure Research
Polish Academy of Sciences
P. O. Box 937, PL-50-590 Wrocław 2 (Poland)
Fax: Int. code +(71)441029
e-mail: wrzyszcz(@highscreen.int.pan.wroc.pl
Dr. L. Syper
Institute of Organic Chemistry, Biochemistry and Biotechnology
Technical University of Wrocław (Poland)

[**] The research was supported financially by the Polish State Committee for Scientific Research under Grant No. 7S203032 06.

When Brinner et al. and Plüss alkylated naphthols with methanol in the presence of Al_2O_3, they obtained oils containing methylnaphthalenes.[1] When higher alcohols were used longer chain alkyl derivatives of naphthols formed. The alkylation of naphthols with methanol in the presence of Al_2O_3 of varying acidity was systematically investigated by Klemm et al.[2] Depending on reaction temperature, four types of products formed: naphthyl ethers (O-alkylation), methylated naphthols, methylated oxodihydronaphthalenes, and methylnaphthalenes. The complex product mixtures could not be separated or used in further applications.

In studies conducted in the 1970s phenol was methylated to yield *ortho*-cresol and 2,6-dimethylphenol with catalysts consisting mainly of Fe_2O_3 or Cr_2O_3.[3-5] Many other formulations based on these fundamental systems have also been investigated.[6, 7] Inoue and Enomoto[8] employed a Fe_2O_3 catalyst for the alkylation of 1-naphthol with methanol and obtained 2-methyl-1-naphthol in 57% yield and with 100% selectivity. These experiments were carried out in the liquid phase in an autoclave under a pressure of about 100 bar.

We report here that an oxide catalyst composed of mainly iron and additives of chromium, silicon, and potassium can mediate the alkylation of 1-naphthol with methanol carried out in a flow system to provide 2-methyl-1-naphthol in 90% yield. The main component can be separated easily from the product mixture.[9]

During experiments lasting 500 h resin- or tar-type deposits did not form or accumulate on the iron catalyst. When the experiments were interrupted, the reactor allowed to cool, and the system restarted, a stationary equilibrium was again established within roughly one hour and results identical to those recorded previously were obtained. The catalyst can be regenerated repeatedly without loss of activity by passing air through the catalyst bed heated at 743 K. The main component of the catalyst, α-Fe_2O_3, was reduced when the catalyst bed was treated with alcohol vapors or an alcohol solution of 1-naphthol starting at 473 K. During the reduction α-Fe_2O_3 is transformed into magnetite. The oxidative regeneration causes partial oxidation of magnetite into hematite. Owing to the high yield per pass, with liquid hourly space velocities (LHSV) of 1.5–3.0 $L L^{-1} h^{-1}$, 1 L of catalyst can furnish about 250–500 g of products per hour. This indicates the possibility of industrial-scale applications.

The alkylation of 1-naphthol begins at 520 K and accelerates with increased temperature. Up to 570 K the yield of the 2-alkyl-1-naphthol products amounts to more than 50%, and the selectivity of their formation is close to 100%. At higher temperatures 4-alkyl- and 2,4-dialkyl derivatives of 1-naphthol are also formed, albeit in low yield. The products obtained at higher reaction temperatures (640–660 K) also contain trace amounts of compounds having alkyl chains shorter than that of the alcohol used for alkylation.

Figure 1 shows the temperature dependence of the yield of the reaction products and the selectivity of the formation of the main product in the alkylation of 1-naphthol with ethanol. 2-Ethyl-1-naphthol (**1a**) is formed with a yield exceeding 95% and a selectivity of 95–96%. The reaction mixture also contains 4-ethyl-1-naphthol (**2a**) (up to 4%), traces of 2-methyl-1-naphthol (less than 1%), and 2,4-diethyl-1-naphthol (**3a**) in the amounts indicated in the figure. It is interesting that in the presence of the catalyst only C-alkylation occurs. In the whole range of temperatures investigated formation of ethers as a result of O-alkylation was not observed.

Table 1 shows the results of the alkylation of 1-naphthol with ethyl alcohol at different loads and with different molar ratios

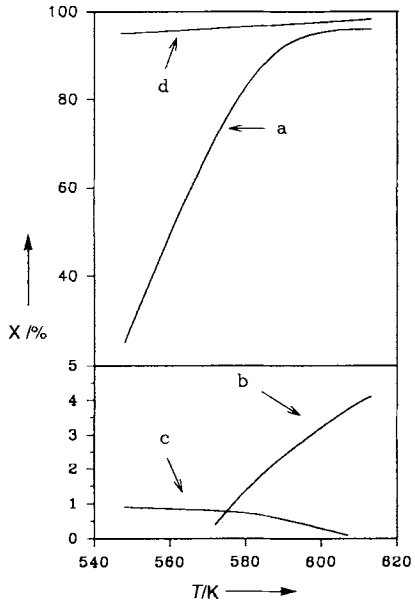

Fig. 1. Alkylation of 1-naphthol with ethyl alcohol. Molar ratio 1-naphthol:alcohol = 1:10, LHSV = 1.5 $L L^{-1} h^{-1}$; X = yields of **1a** (curve a), **2a** (b), **3a** (c), and selectivity for formation of **1a** (d).

Table 1. Results of the alkylation of 1-naphthol with ethyl alcohol at different reaction parameters.

Reaction temp. [K]	608	614	616	616
Molar ratio 1-naphthol:alcohol	1:10	1:10	1:5	1:5
LHSV[$L L^{-1} h^{-1}$]	1.5	3.0	1.5	3.0
Conversion of 1-naphthol[%]	≈100	99.3	99.1	93.1
Selectivity of formation of main product **1a**[%]	96.7	96.8	96.6	97.7
Product components[%]				
2-methyl-1-naphthol	traces	traces	0.4	0.1
2-ethyl-1-naphthol (**1a**)	96.7	96.1	95.7	91.0
4-ethyl-1-naphthol (**2a**)	3.2	3.1	0.4	traces
2,4-diethyl-1-naphthol (**3a**)	traces	–	2.6	1.9
unidentified	0.1	0.1	–	0.1

of reactants. The yield and selectivity of the formation **1a** were not influenced significantly by changes in the load and composition of starting materials. At a molar ratio of 1-naphthol to ethanol of 1:5 the diethyl product **3a** was predominant. The data presented indicate that the selectivity of this reaction can be improved by appropriate choice of parameters.

The product fraction with a boiling point lower than that of 1-naphthol contains mainly unreacted alcohol and traces of aldehydes, ketones, and esters. At reaction temperatures over 620 K naphthalene is also among the products.

1-Naphthol was also alkylated with *n*-propyl and *n*-butyl alcohol in the temperature range of 540–680 K. Table 2 lists the results of experiments carried out under different parameters in which highly selective alkylation was observed in the 2-position. In both cases the corresponding 2-alkyl derivatives **1b** and **1c** were obtained in yields exceeding 85% and with selectivities of about 90%. Small amounts of the 4-alkyl derivatives **2b** and **2c**, the 2,4-dialkyl compounds **3b** and **3c**, 2-methyl-1-naphthol, and **1a** were also detected in the reaction mixture. The last two compounds could have been formed by thermal decomposition

Table 2. Results of the alkylation of 1-naphthol with *n*-propyl and *n*-butyl alcohol at different reaction parameters.

Alcohol	n-C_3H_7OH		n-C_4H_9OH	
Reaction temp. [K]	643	645	634	651
Molar ratio 1-naphthol:alcohol	1:5	1:5	1:10	1:10
LHSV[L L^{-1} h^{-1}]	1.5	4.0	1.5	3.0
Conversion of 1-naphthol[%]	97.3	85.7	98.1	97.2
Selectivity of formation of main product[%]	87.4	89.3	90.7	89.6
Product components[%]				
2-methyl-1-naphthol	2.9	2.0	0.5	1.4
2-ethyl-1-naphthol (**1a**)	2.5	1.8	1.1	2.6
2-*n*-propyl-1-naphthol (**1b**)	85.0	76.5	–	–
4-*n*- propyl-1-naphthol (**2b**)	1.5	1.4	–	–
2,4-di-*n*-propyl-1-naphthol (**3b**)	2.2	2.0	–	–
2-*n*-butyl-1-naphthol (**1c**)	–	–	87.9	87.1
4-*n*-butyl-1-naphthol (**2c**)	–	–	4.0	2.8
2,4-di-*n*-butyl-1-naphthol (**3c**)	–	–	1.9	1.8
unidentified	3.2	2.0	1.5	1.5

of the main products. In analogy to the alkylation of 1-naphthol with ethanol, O-alkylation yielding ethers did not occur. Some products found in trace amounts were not identified.

When higher alcohols were used as alkylating agents, the yield and selectivity of the reaction decreased with increasing chain length. In the case of *n*-pentanol up to 80% yield of 2-*n*-pentyl-1-naphthol (**1d**) was obtained, but the reaction with *n*-hexanol furnished 2-*n*-hexyl-1-naphthol in only 25% yield. The latter reaction also afforded significant amounts of undecanone-6 and the ester $C_6H_{13}CO_2C_5H_{11}$, which formed from alcohol by aldol condensation[10, 11] and Tishchenko reaction,[12, 13] respectively. Since *n*-hexanol and higher alcohols react above all with each other, the amount of alkylated product decreases.

We have also found that 1-naphthol reacts with primary branched alcohols to furnish the *ortho*-alkylated products in low yields and selectivities, and that secondary alcohols are inactive in this reaction.

An explanation of the high activity and selectivity of the iron oxide catalyst in the alkylation of 1-naphthol is that the alcohols are transformed into reactive electrophiles by β-hydride transfer.[14, 15]

In general the selectivity of oxide catalysts is governed by how naphthol is adsorbed on the catalyst surface, which depends on the surface acidity. On more acidic catalysts the naphthols rings take a position parallel to the surface, thus decreasing the likelihood of substitution in the *ortho* position, and as a result many products are formed. In the case of catalysts in which a basic function predominates, the naphthol rings assume a position vertical to the surface. Attack in the *ortho* position is thus preferred and the formation of ethers and others naphthol derivatives is excluded.[16, 17]

Experimental Procedure

The catalyst consisted of iron, silicon, chromium, and potassium oxides in the molar ratio 100:2:1:0.1. Chromium and silicon were used as additives to prevent sintering, and potassium served as an activator [18].

Preparation of catalyst: A solution of 202 g of $Fe(NO_3)_3 \cdot 9H_2O$ in 0.5 L of water and a solution of 2 g of $Cr(NO_3)_3 \cdot 9H_2O$ in 12.5% aqueous ammonia were prepared separately and introduced simultaneously to a vessel containing 0.5 L of water. The mixture was maintained at pH 7 and stirred vigorously at room temperature for ca. 1 h. Then a solution of sodium silicate (3.4 g containing 27% SiO_2) in 100 cm^3 of water was added. After 2 h of stirring the precipitate was filtered off and washed with water to remove nitrate ions. The obtained solid was dried at 383 K for 24 h, powdered, and pelletized with addition of 3 wt%. The pellets were crushed and sieved to give particles with diameters of 0.6–1.2 mm. A 50 g portion of these particles was impregnated with a solution of 0.05 g of K_2CO_3 in 30 cm^3 of water, then dried and calcined at 723 K for 5 h in air. Some of the physico-chemical properties of the catalyst are given in Table 3.

Table 3. Important properties of the catalyst.

	Catalyst		
	Fresh	Used	Regenerated
Iron oxide phases[a]	α-Fe_2O_3	Fe_3O_4	α-Fe_2O_3, Fe_3O_4
Average size of crystallites[nm]	15	26	25
S_{BET}[m^2 g^{-1}]	60	41	42
V_p(0–50 nm)[cm^3 g^{-1}]	0.23	0.18	0.21

[a] From X-ray diffraction and magnetic measurements.

The alkylation reactions were carried out at atmospheric pressure in flow reactors with a fixed bed of 30 g or 3 g of the catalyst. After condensation the reaction products were analyzed chromatographically (FID detector, columns: Silicon Oil DC550 on Chromosorb W and Silicone OV-1 on Chromosorb W-AW-DMCS). Samples were additionally analyzed using a gas chromatograph (HP 5890A) coupled with a mass spectrometer (HP 5971A with a mass-selective detector).

The main products were isolated from the products mixture by middle-pressure column chromatography with silica gel (Kieselgel 60 finer than 230 mesh "Merck") as the adsorbent and mixtures of CH_2Cl_2/petroleum ether 3:7 and 5:5 as eluant. The amounts of isolated main products (**1a–1d**) were in good agreement with the results obtained by GC. The products were further purified by crystallization from hexane. **1a**: M.p. 70–71 °C, **1b**: M.p. 47–48 °C, **1c**: M.p. 73–74 °C, **1d**: M.p. 57–58 °C. The identity of the compounds was confirmed by comparing their melting points and spectroscopic properties (IR, MS, and NMR) with those of authentic samples, which were prepared as follows: 1-Methoxy-naphthalene was *ortho*-lithiated and reacted with appropriate alkyl iodide [19, 20]. The methoxymethyl group was removed by treatment with hydrogen chloride in a methanol–water mixture.

Compounds **2a–c** and **3a–c** were identified by GC using synthetized standards and in addition by means of their MS spectra. Compounds **2a–2c** were obtained from 1-methoxy-4-naphthaldehyde [21], which was reacted with the appropriate alkyl Grignard reagent. The resulting alcohols were reduced with a mixture of $LiAlH_4$ and $AlCl_3$ [22]. The final naphthols were generated by treating suitable methyl ethers with BBr_3 in dichloromethane. Compounds **3a–3c** were obtained from **2a–c** by the procedure described for **1a–c**. 2-Methyl-1-naphthol was obtained earlier [15] by alkylation of 1-naphthol with methanol.

Received: December 1, 1995
Revised version: March 27, 1996 [Z8608IE]
German version: *Angew. Chem.* **1996**, *106*, 1682–1684

Keywords: alkylations · catalysis · iron compounds · naphthols

[1] a) E. Brinner, W. Plüss, H. Paillard, *Helv. Chim. Acta* **1924**, *7*, 1046–1056; b) W. Plüss, *ibid.* **1925**, *8*, 507–512.
[2] a) L. H. Klemm, J. Shabtai, D. R. Taylor, *J. Org. Chem.* **1968**, *33*, 1480–1488; b) L. H. Klemm, C. E. Klopfenstein, J. Shabtai, *ibid.* **1970**, *35*, 1069–1075.
[3] A. Oshima, H. Oshima (Kanegafuchi Chemical Industry Co., Ltd.) GE-A 2124901, **1971**; *Chem. Abstr.* **1972**, *76*, 59196r.
[4] Y. Takami, T. Sato (Agency of Industrial Sciences and Technology), JP-A 7549236, **1973**; *Chem. Abstr.* **1975**, *83*, 96729g.
[5] J. Biały, I. Penczek, N. Kopytowska, J. Wrzyszcz, S. Kulak (Instytut Chemii Przemysłowej) PL-A 105922, **1979**; *Chem. Abstr.* **1980**, *93*, 71286d.
[6] B. E. Leach (Conco Inc.) US-A 4227024, **1980**; *Chem. Abstr.* **1981**, *94*, 712286d.
[7] M. Kawamata, K. Ohshima, A. Kudoh, M. Kotani (Mitsui Toatsu Chemicals Inc.) US-A 4208537, **1980**; *Chem. Abstr.* **1981**, *94*, 30347b.
[8] M. Inoue, S. Enomoto, *Chem. Pharm. Bull.* **1976**, *24*, 2199–2203.
[9] H. Grabowska, W. Mišta, L. Syper, J. Wrzyszcz, M. Zawadzki, EUROPACAT II Congress, September 3–8, 1995, Maastricht, The Netherlands; Book of Abstracts, p. 601.
[10] W. Komarewsky, H. Coley, *J. Am. Chem. Soc.* **1941**, *63*, 700–702, 3269–3270.
[11] a) Kh. M. Minachev, G. A. Loginov, A. M. Markov, *Neftekhimiya* **1969**, *9*, 412–417; b) G. A. Loginov, A. M. Markov, Kh. M. Minachev, *ibid.* **1970**, *10*, 393–399.
[12] D. W. Tishchenko, *Zh. Russ. Fiz-Khim. O-va* **1906**, *38*, 355–482.
[13] H. Tsuji, F. Yagi, H. Hattori, H. Kita, *J. Catal.* **1994**, *148*, 759–770.

 © VCH Verlagsgesellschaft mbH, D-69451 Weinheim, 1996 0570-0833/96/3513-1564 $ 15.00+.25/0

[14] a) A. J. Gellman, Q. Dai, *J. Am. Chem. Soc.* **1993**, *115*, 714–722; b) J. G. Forbes, A. J. Gellman, *ibid.* **1993**, *115*, 6277–6283.
[15] H. Grabowska, W. Mišta, L. Syper, J. Wrzyszcz, M. Zawadzki, *J. Catal.*, in press.
[16] K. Tanabe, T. Nishizaki, in *Proc. Int. Congr. Catal. 6th* **1976** (**1977**), 863–871.
[17] A. Kayo, T. Yamaguchi, K. Tanabe, *J. Catal.* **1983**, *83*, 99–106.
[18] H. Grabowska, W. Kaczmarczyk, J. Wrzyszcz, *Appl. Catal.* **1989**, *47*, 351–355.
[19] C. A. Towsend, L. M. Bloom, *Tetrahedron Lett.* **1981**, *22*, 3923–3924.
[20] T. Kamikawa, I. Kubo, *Synthesis* **1986**, 431–433.
[21] I. N. Godfrey, M. V. Sargent, J. A. Elix, *J. Chem. Soc. Perkin Trans. 1* **1974**, 7, 1353–1354.
[22] J. Blackwell, W. J. Hickinbottom, *J. Chem. Soc.* **1961**, 1405–1407.

Intermolecular Carbene–Carbene Coupling of a Nucleophilic Vinylidene and an Electrophilic 1-Methoxyethylidene Ligand**

Rüdiger Beckhaus,* Jürgen Oster, Rhett Kempe, and Anke Spannenberg

Dedicated to Professor Max Herberhold on the occasion of his 60th birthday

The formation and cleavage of carbon–carbon bonds is one of the basic problems in organometallic chemistry. Experimentally and theoretically intriguing are both intramolecular coupling of carbene ligands forming olefinic species (**1** → **2**) and the possibility of breaking carbon–carbon double bonds in the coordination sphere of transition metals (**2** → **1**).[1–6] Examples for intermolecular C–C coupling (**3** → **4**) on a heterodinuclear complex fragment are still unknown.[7]

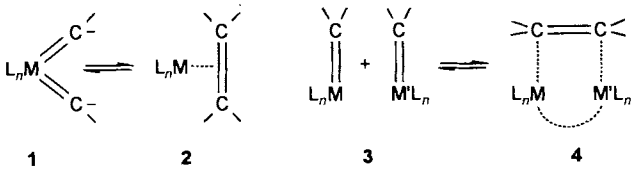

1 **2** **3** **4**

Our investigations concerning the titanaallene species [Cp$^*_2$Ti=C=CH$_2$] (**5**), preferably generated by selective methane elimination from [Cp$^*_2$Ti(CH=CH$_2$)CH$_3$] (**6**) demonstrate the nucleophilic character of the α-carbon atom in **5**, which is responsible for the regiochemistry observed in the preparation of cycloaddition product **7**[8] and for the reactions of **5** with electrophiles.[8e, 9] Here we contrast the reactivity of **5** with that of a classical Fischer-type carbene complex exhibiting an inverse M=C polarity.

[*] Priv.-Doz. Dr. R. Beckhaus, Dipl.-Chem. J. Oster
Institut für Anorganische Chemie der Technischen Hochschule
Professor-Pirlet-Strasse 1, D-52056 Aachen (Germany)
Fax: Int. code +(241)8888-288
e-mail: r.beckhaus@ac.rwth-aachen.de
Dr. R. Kempe, Dr. A. Spannenberg
Arbeitsgruppe Komplexkatalyse der Max-Planck Gesellschaft an der Universität Rostock (Germany)

[**] This work was supported by the Deutsche Forschungsgemeinschaft and the Fonds der Chemischen Industrie. We thank Prof. Dr. G. E. Herberich for his continuing interest and Prof. Dr. U. Rosenthal and his co-workers for the X-ray structure determination. Stimulating remarks from the referees are gratefully acknowledged.

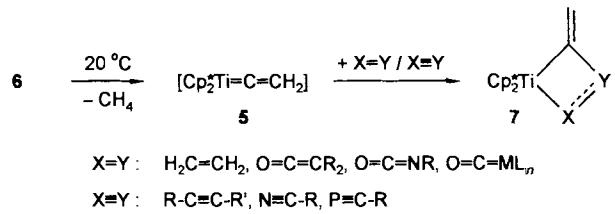

Treatment of [(CO)$_5$Cr=C(OCH$_3$)CH$_3$] (**8**) with **6** in *n*-hexane at a temperature between −30 and 25 °C gives the new heterodinuclear complexes **9** and **10** by an unusual coupling of the Fischer-carbene complex **8** with the intermediate Schrock-carbene complex **5**. The C–C bond formation occurs between carbon atoms of vinylidene, carbene, and carbonyl ligands. After chromatographic workup the separated complexes **9** and **10** can be isolated as air-stable red crystals. Cycloaddition products of type **7**, for example those typical with metal carbonyls,[8c] were not detected.

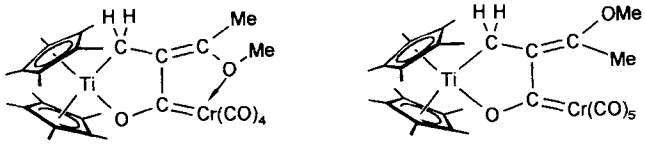

9 **10**

The constitution of **9** and **10** follows from NMR and IR spectroscopic data. The carbene carbon atoms show typical resonances at δ = 336.7 (**9**) and 328.0 (**10**). Characteristic differences can be noted for the substituents of the C=C bond and for the Cr(CO)$_n$ fragment. As a result of the change of configuration at the exocyclic double bond, the methyl resonance shows a remarkable shift from δ = 1.90 (**9**) to 2.89 (**10**) in the ^{1}H NMR spectra. The methoxy coordination is documented by the shift of the OCH$_3$ carbon resonance to lower field (δ = 65.6 (**9**), 54.6 (**10**)). In the infrared spectra of **9** typical signals for a C_{2v} symmetry are observed, whereas a C_{4v} pattern can be detected for the Cr(CO)$_n$ fragment of **10**.

The X-ray structure determination of **9** shows two symmetry-independent molecules (**9**, **9'**) in the asymmetric unit (Fig. 1,

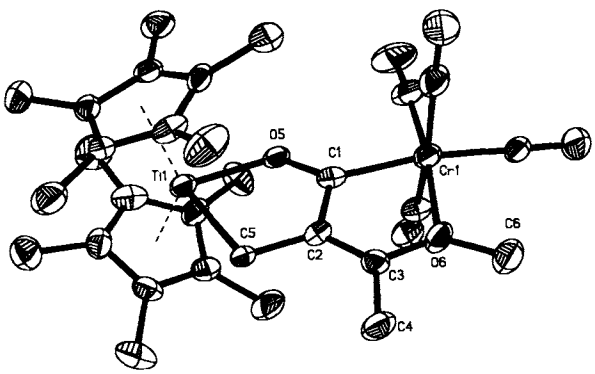

Fig. 1. Molecular crystal of **9**, selected distances [Å] and angles [°] (Cp(1) and Cp(2) represent the centers of the Cp* ligands of the titanocene fragment; in square brackets values of **9'**: Ti–Cp(1) 2.105 [2.114], Ti–Cp(2) 2.090 [2.108], Ti–C5 2.202(7) [2.187(7)], Ti–O5 2.002(5) [2.008(5)], O5–C1 1.299(8) [1.288(8)], C1–C2 1.506(9) [1.465(9)], C5–C2 1.506(9) [1.527(8)], C2–C3 1.337(10) [1.325(9)], C3–C4 1.512(9) [1.483(9)], C3–O6 1.381(8) [1.400(7)], O6–C6 1.470(9) [1.447(8)], O6–Cr 2.204(5) [2.182(5)], C1–Cr1 2.020(8) [2.025(8)]; C5-Ti-O5 78.8(2) [80.1(2)], Ti-O5-C1 125.8(4) [122.6(4)], O5-C1-C2 110.1(7) [113.4(6)], C5-C2-C1 118.4(7) [118.2(6)], C6-O6-C3 121.2(6) [119.1(6)], C4-C3-O6 116.6(7) [118.1(7)].

 © VCH Verlagsgesellschaft mbH, D-69451 Weinheim, 1996 0570-0833/96/3513-1565 $ 15.00+.25/0

data for **9'** are given in brackets).[10] The formation of a chelate ring by OCH_3 coordination leads to a distortion of the octahedral symmetry at the chromium center. Noteworthy in this connection is a small O6-Cr-C1 angle of 76.1(3)°. The Cr–O6 distance of 2.204(5) [2.182(5)] Å is similar to that of bonds in anisyl–carbene complexes[11] and significantly longer than the Cr–O bond in $[(CO)_5Cr(thf)]$ (2.123(3) Å).[12] A Cr–C1 distance of 2.020(8) [2.025(8)] Å can be related to short carbene bonds;[13] acyl resonance forms[14] for **9** can be neglected. In agreement with this, a C1–O5 distance of 1.299(8) [1.288(8)] Å is found. The planes of the bicyclic system are almost coplanar (max. deviation < 0.06 Å).

The formation of the reaction products **9** and **10** is in accordance with a carbene–carbene coupling via the intermediate allene complex **12**.[15] This reaction step can be explained by the

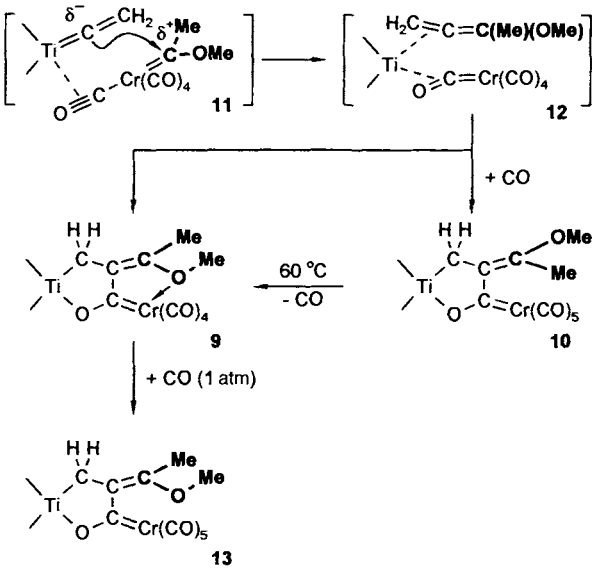

primary interaction of the nucleophilic and the electrophilic carbene carbon atoms shown in **11**, which is supported by coordination of CO to the oxophilic titanium center. Titanium-centerd cycloaddition of the allene molecule with the remaining $Cr(CO)_5$ fragment leads directly to **9** and, after fast CO addition from **8**, to **10**. ^{1}H NMR spectroscopy confirms that **10** is the preferred product rather than **9** (**10**:**9** = 4:1).

Under a CO atmosphere the OCH_3 coordination to the Cr center is reversed, and **13** is formed. In solution **10** can be converted thermally (60 °C) into **9** by elimination of one CO. This reaction is much faster in the presence of PMe_3. No products could be isolated because of the lability of these phosphane adducts. However, the substitution of one CO ligand by PMe_3 is detectable spectroscopically. The formation of an equilibrium between **10** and **12** or the removal of the exocyclic C=C double-bond character by contribution of ionic resonance forms of the vinylcarbene moiety[16] can explain the isomerization of the double-bond system during thermolytic formation of **9** from **10**. The conversion of **13** into **10** is not observed.

The described reaction represents, to our knowledge, the first example of an intermolecular coupling of inversely polarized carbene ligands. The metal-centered coupling of several carbon atoms of different substrates[17] is thereby enlarged by an additional reaction type, which opens up a new potential for synthesis.

Experimental Procedure

9 and **10**: *To a solution of* **6** *(280 mg, 0.778 mmol) in n-hexane (40 mL) was* added **8** (140 mg (0.560 mmol) [18] at −30 °C. After warming to room temperature the reaction mixture was stirred for 3 h. The color changed from yellow to red, and **9**/**10** was obtained as a red-brown precipitate. The solid was dissolved in CH_2Cl_2 (3 mL) and chromatographed on alumina (neutral, 100–125 mesh). With *n*-hexane a yellow solution of unchanged **8** was obtained. Elution with CH_2Cl_2/*n*-hexane (3/1) produced a red solution of **10**. After further elution with tetrahydrofuran a red solution of **9** can be separated. The volume of the solvent was reduced to 2 mL in vacuo. Addition of *n*-hexane (10 mL) gave **9** and **10** as red solids. Crystallization from benzene afforded red crystals of the products.

9: Red crystals, yield 90 mg, 27%, correct elemental analysis. IR (KBr): $\tilde{\nu}$ = 1987 s, 1873 sh, 1865 vs, 1821 s (CO), 1341 cm^{-1} s. IR (CH_2Cl_2): $\tilde{\nu}$ = 1994 s, 1878 vs, 1828 s, 1343 cm^{-1} s. ^{1}H NMR ($CDCl_3$, 500 MHz, 25 °C): δ = 1.87 (s, 2H, CH_2), 1.90 (s, 3H, CH_3), 1.96 [s, 30H, $C_5(CH_3)_5$], 3.97 (s, 3H, OCH_3). ^{1}H NMR (C_6D_6, 500 MHz, 25 °C): δ = 1.26 (s, 3H, CH_3), 1.72 [s, 30H, $C_5(CH_3)_5$], 1.77 (s, 2H, CH_2), 3.34 (s, 3H, OCH_3). ^{13}C{^{1}H} NMR ($CDCl_3$, 125 MHz, 25 °C): δ = 12.1 [$C_5(CH_3)_5$], 13.0 (CH_3), 55.7 (CH_2), 65.3 (OCH_3), 125.7 [$C_5(CH_3)_5$], 145.9 [C=$CCH_3(OCH_3)$], 169.3 [C=$CCH_3(OCH_3)$], 218.8, 230.3, 235.4 [*cis*-$Cr(CO)_4$], 336.7 (C=Cr). MS (70 eV) *m/z* (%): 595 (1) [M^+ + 1], 539 (< 1) [M^+ − 2CO + 1], 496 (< 1) [M^+ − 3CO − CH_3 + 1], 459 (2) [M^+ − Cp*], 318 (21) [$Cp_2^*Ti^+$].

10: Red crystals, yield 120 mg, 34%, m.p. 186–188 °C (decomp.), correct elemental analysis. IR (KBr): $\tilde{\nu}$ = 2043 s, 1963 m, 1926 s, 1899 vs, 1876 s (CO), 1561 m (C=C), 1236 s (OCH_3). IR (CH_2Cl_2): $\tilde{\nu}$ = 2044 s, 1959 sh, 1915 vs, 1564 m, 1232 s. ^{1}H NMR ($CDCl_3$, 500 MHz, 25 °C): δ = 1.92 [s, 30H, $C_5(CH_3)_5$], 2.08 (s, 2H, CH_2), 2.89 (s, 3H, CH_3), 3.77 (s, 3H, OCH_3). ^{13}C{^{1}H} NMR ($CDCl_3$, 125 MHz, 25 °C): δ = 12.0 [$C_5(CH_3)_5$], 17.5 (CH_3), 54.6 (OCH_3), 66.0 (CH_2), 125.1 [$C_5(CH_3)_5$], 153.8 [C=$CCH_3(OCH_3)$], 165.7 [C=$CCH_3(OCH_3)$], 219.1 (*cis*-CO), 224.1 (*trans*-CO), 328.0 (C=Cr). SIMS-MS (Cs^+, 20 kV, 3-nitrobenzyl alcohol): positive ions *m/z* (%): 510 (13) [M^+ − 4CO], 482 (13) [M^+ − 5CO], 318 [$Cp_2^*Ti^+$]; negative ions *m/z* (%): 622 (3) [M^+], 594 (2) [M^+ − CO], 566 (1) [M^+ − 2CO], 459 (40) [M^+ − CO − Cp*].

13: A solution of **9** in $CDCl_3$ (2 mL) is exposed to a CO atmosphere (1 atm) for 30 min (yield 87% by ^{1}H NMR). IR (CH_2Cl_2): = 2042 s, 1958 sh, 1913 vs (CO), 1563 cm^{-1} (C=C). ^{1}H NMR ($CDCl_3$, 500 MHz, 25 °C): δ = 1.93 [s, 30H, $C_5(CH_3)_5$], 2.01 (s, 3H, CH_3), 2.07 (s, 2H, CH_2), 3.85 (s, 3H, OCH_3). ^{13}C{^{1}H} NMR ($CDCl_3$, 125 MHz, 25 °C): δ = 11.9 [$C_5(CH_3)_5$], 15.9 (CH_3), 54.8 (OCH_3), 65.5 (CH_2), 125.0 [$C_5(CH_3)_5$], 146.7 [C=$CCH_3(OCH_3)$], 161.3 [C=$CCH_3(OCH_3)$], 220.0 (*cis*-CO), 225.8 (*trans*-CO), 327.8 (C=Cr).

Received: January 2, 1996
Revised version: March 25, 1996 [Z 8691 IE]
German version: *Angew. Chem.* **1996**, *108*, 1636–1638

Keywords: carbene complexes · carbon–carbon coupling · chromium compounds · titanium compounds · vinylidene complexes

[1] J. M. O'Connor, L. Pu, A. L. Rheingold, *J. Am. Chem. Soc.* **1990**, *112*, 6232–6247.

[2] Early reports describe the liberation of olefins from monocarbene complexes: a) C. P. Casey, R. L. Anderson, *J. Chem. Soc. Chem. Commun.* **1975**, 895–896; b) W. A. Herrmann, *Chem. Ber.* **1975**, *108*, 486–499; c) E. O. Fischer, K. H. Dötz, *J. Organomet. Chem.* **1972**, *36*, C4–C6; d) E. O. Fischer, B. Heckl, K. H. Dötz, J. Müller, H. Werner, *ibid.* **1969**, *16*, P29–P32; e) E. O. Fischer, A. Maasböl, *ibid.* **1968**, *12*, P15–P17.

[3] Isomerization reactions **2** → **1** → **2**: E. L. Weinberg, J. T. Burton, M. C. Baird, M. Herberhold, *Z. Naturforsch. B* **1981**, *36*, 485–487.

[4] Dimerization of carbenes on metal surfaces: a) H. Bock, G. Tschmutowa, H. P. Wolf, *J. Chem. Soc. Chem. Commun.* **1986**, 1068–1069; b) R. C. Brady III, R. Pettit, *J. Am. Chem. Soc.* **1981**, *103*, 1287–1289; c) *ibid.* **1980**, *102*, 6181–6182.

[5] Reactions of the type **2** → **1** are known for electron-rich alkenes: a) M. J. Doyle, M. F. Lappert, P. L. Pye, P. Terreros, *J. Chem. Soc. Dalton Trans.* **1984**, 2355–2364; b) P. B. Hitchcock, M. F. Lappert, P. Terreros, K. P. Wainwright, *J. Chem. Soc. Chem. Commun.* **1980**, 1180–1181; c) M. F. Lappert, P. L. Pye, *J. Chem. Soc. Dalton Trans.* **1978**, 837–844; d) P. B. Hitchcock, M. F. Lappert, P. L. Pye, *ibid.* **1978**, 826–836; e) M. F. Lappert, P. L. Pye, *ibid.* **1977**, 1283–1291; f) M. F. Lappert, P. L. Pye, G. M. McLaughlin, *ibid.* **1977**, 1272–1282; g) M. F. Lappert, P. L. Pye, *ibid.* **1977**, 2172–2180; h) P. B. Hitchcock, M. F. Lappert, P. L. Pye, *ibid.* **1977**, 2160–2172; i) B. Cetinkaya, P. Dixneuf, M. F. Lappert, *ibid.* **1974**, 1827–1833.

[6] a) C. N. Wilker, R. Hoffmann, O. Eisenstein, *New J. Chem.* **1983**, *7*, 535–544; b) R. Hoffmann, C. N. Wilker, O. Eisenstein, *J. Am. Chem. Soc.* **1982**, *104*, 632–634; c) R. Schmidt, *Theoretische Untersuchungen zu Aufbau und Spaltung olefinartiger Bindungen an Übergangsmetallfragmenten*, Dissertation, Technische Universität München, **1988**.

[7] Intermolecular C–C coupling of carbene ligands of the Schrock type during thermolysis or decomposition reactions of homonuclear compounds are formulated via 1,3-dimetallacyclobutanes, in contrast to the transformation

$3 \rightarrow 4$: a) D. H. Berry, T. S. Koloski, P. J. Carroll, *Organometallics* **1990**, *9*, 2952–2962; b) I. M. Saez, N. J. Meanwell, A. Nutton, K. Isobe, A. V. de Miguel, D. W. Bruce, S. Okeya, D. G. Andrews, P. R. Ashton, I. R. Johnstone, P. M. Maitlis, *J. Chem. Soc. Dalton Trans.* **1986**, 1565–1575; c) K. C. Ott, R. H. Grubbs, *J. Am. Chem. Soc.* **1981**, *103*, 5922–5923; d) R. R. Schrock, P. R. Sharp, *ibid.* **1978**, *100*, 2389–2399; e) C. Masters, C. Van der Woude, J. A. Van Dorn, *ibid.* **1979**, *101*, 1633–1634; f) J. H. Merrifield, G.-Y. Lin, W. A. Kiel, J. A. Gladysz, *ibid.* **1983**, *105*, 5811–5819.

[8] a) R. Beckhaus, S. Flatau, S. I. Troyanov, P. Hofmann, *Chem. Ber.* **1992**, *125*, 291–299; b) R. Beckhaus, I. Strauß, T. Wagner, P. Kiprof, *Angew. Chem.* **1993**, *105*, 281–283; *Angew. Chem. Int. Ed. Engl.* **1993**, *32*, 264–266; c) R. Beckhaus, J. Oster, T. Wagner, *Chem. Ber.* **1994**, *127*, 1003–1013; d) R. Beckhaus, J. Oster, *Z. Anorg. Allg. Chem.* **1995**, *621*, 359–364; e) R. Beckhaus, J. Sang, T. Wagner, B. Ganter, *Organometallics* **1996**, *15*, 1176–1187; f) R. Beckhaus, I. Strauß, T. Wagner, *Angew. Chem.* **1995**, *107*, 738–740; *Angew. Chem. Int. Ed. Engl.* **1995**, *34*, 688–690.

[9] a) R. Beckhaus, J. Sang, J. Oster, T. Wagner, *J. Organomet. Chem.* **1994**, *484*, 179–190; b) R. Beckhaus, I. Strauß, T. Wagner, *J. Organomet. Chem.* **1994**, *464*, 155–161.

[10] Crystal structure analysis of **9**: STOE-IPDS diffractometer, graphite monochromated $Mo_{K\alpha}$ radiation, $\lambda = 0.71069$ Å, structure solution direct methods (SHELXS-86: G. M. Sheldrick, *Acta Crystallogr. Sect. A* **1990**, *46*, 467), last square refinement against F^2 (SHELXL-93: G. M. Sheldrick, University of Göttingen, Germany **1993**, unpublished). Structure representation: XP (Siemens). $0.3 \times 0.1 \times 0.05$ mm, dark-red prism (very weak diffracting), space group $P\bar{1}$ (No. 2), triclinic, $a = 10.170(1)$, $b = 17.440(3)$, $c = 18.718(3)$ Å, $\alpha = 63.04(2)$, $\beta = 82.34(2)$, $\gamma = 90.00(2)^\circ$, $V = 2925(1)$ Å^3, $Z = 2$, $\rho_{calcd} = 1.346\ g\,cm^{-3}$, 20421 collected, 8677 unique, 2666 observed ($I = 2\sigma(I)$), $R = 0.057$, wR^2 (all data) = 0.154, 686 parameters. Crystallographic data (excluding structure factors) for the structure(s) reported in this paper have been deposited with the Cambridge Crystallographic Data Centre as supplementary publication no. CCDC-179-48. Copies of the data can be obtained free of charge on application to The Director, CCDC, 12 Union Road, Cambridge CB2 1EZ, UK (fax: Int. code +(1223) 336-033; e-mail: teched@chemcrys.cam.ac.uk).

[11] a) K. H. Dötz, H.-G. Erben, W. Staudacher, K. Harms, G. Müller, J. Riede, *J. Organomet. Chem.* **1988**, *355*, 177–191; b) K. H. Dötz, W. Sturm, M. Popall, J. Riede, *ibid.* **1984**, *277*, 267–275.

[12] U. Schubert, P. Friedrich, O. Orama, *J. Organomet. Chem.* **1978**, *144*, 175–179.

[13] a) U. Schubert, *Coord. Chem. Rev.* **1984**, *55*, 261–286; b) K. H. Dötz, H. Fischer, P. Hofmann, F. R. Kreissl, U. Schubert, K. Weiss, *Transition Metal Carbene Complexes*, VCH, Weinheim, **1983**.

[14] a) M. Sabat, M. F. Gross, M. G. Finn, *Organometallics* **1992**, *11*, 745-751; b) G. Erker, *Angew. Chem.* **1989**, *101*, 411–426; *Angew. Chem. Int. Ed. Engl.* **1989**, *28*, 397–412.

[15] Formation of allenes is observed in reactions of diazocompounds with vinylidene complexes (Fe[15a], Rh[15b]): a) C. P. Casey, G. P. Niccolai, *Organometallics* **1994**, *13*, 2527–2531; b) J. Wolf, R. Zolk, U. Schubert, H. Werner, *J. Organomet. Chem.* **1988**, *340*, 161–178.

[16] Described, for example, for nucleophilic vinylogous reactions: R. Aumann, H. Heinen, *Chem. Ber.* **1987**, *120*, 537–540; compare ionic resonance forms of titanaoxycarbene complexes [14a, 8c].

[17] Examples for complex metal-centered coupling reactions of different carbon atoms: enediolate couplings: a) R. Beckhaus, D. Wilbrandt, S. Flatau, W.-H. Böhmer, *J. Organomet. Chem.* **1992**, *423*, 211–222; b) K. Tatsumi, A. Nakamura, P. Hofmann, R. Hoffmann, K. G. Moloy, T. J. Marks, *J. Am. Chem. Soc.* **1986**, *108*, 4467–4476; c) P. Hofmann, P. Stauffert, M. Frede, K. Tatsumi, *Chem. Ber.* **1989**, *122*, 1559-1577; d) P. Hofmann, M. Frede, P. Stauffert, W. Lasser, U. Thewalt, *Angew. Chem.* **1985**, *97*, 693–694; *Angew. Chem. Int. Ed. Engl.* **1985**, *24*, 712–713; at bimetallic systems: e) D. H. Berry, J. E. Bercaw, A. J. Jircitano, K. B. Mertes, *J. Am. Chem. Soc.* **1982**, *104*, 4712–4715; Dötz reaktion: f) K. H. Dötz, *Angew. Chem.* **1984**, *96*, 573–594; *Angew. Chem. Int. Ed. Engl.* **1984**, *23*, 587–608.

[18] R. Aumann, E. O. Fischer, *Angew. Chem.* **1967**, *79*, 900–901; *Angew. Chem. Int. Ed. Engl.* **1967**, *6*, 879–880.

Epothilone A and B—Novel 16-Membered Macrolides with Cytotoxic Activity: Isolation, Crystal Structure, and Conformation in Solution**

Gerhard Höfle,* Norbert Bedorf, Heinrich Steinmetz, Dietmar Schomburg, Klaus Gerth, and Hans Reichenbach

Myxobacteria of the genus *Sorangium* have proved in the last few years to be extremely versatile producers of biologically active secondary metabolites.[1] This diversity is true both for the basic structures, which are generally new, and for the biological effects and their underlying mechanisms. Sorangia very frequently produce antifungal compounds, which may be explained by the fact that these cellulose-degrading organisms have to compete with fungi for the same ecological niche. Also, the *Sorangium cellulosum* strain So ce90 was identified during screening by its antifungal activity, which guided the isolation of two new, structurally unrelated classes of compounds, the epothilones **1**[2, 3] and the spirangiens.[4] When isolated in the pure form, epothilones A and B (**1a** and **1b**, respectively) showed broad activity against eukaryotic cells; the efficiency of the methyl derivative B was mostly a factor of 2 greater than that of the derivative A.

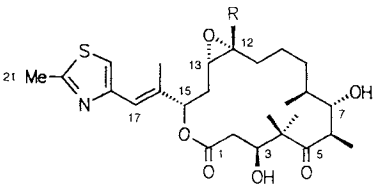

1a R = H

1b R = CH_3

The antifungal activity of **1** against oomycetes (*Plasmopara viticola*, *Phytophthora infestans*), in vitro and in the greenhouse,[5] is noteworthy, as is its cytotoxicity against mouse fibroblasts (cell line L929, **1b**: IC_{50} 2 ng mL^{-1}), which results in disintegration of the cell nucleus and r apoptosis (programmed cell death) within three days.[3] The epothilones also showed noticeable activity and selectivity against breast and colon tumor cell lines in the in vitro antitumor screening program of the National Cancer Institute (NCI).[6, 7] In addition, epothilones were discovered independently by Bollag et al. by a tubulin polymerization assay.[8] This assay, and subsequent detailed studies of their cytotoxicity and inhibition of mitosis show that the epothilones have an almost identical activity and mode of

[*] Prof. Dr. G. Höfle, Dr. N. Bedorf, Ing. I. Steinmetz
Abteilung Naturstoffchemie
Prof. Dr. D. Schomburg
ZWE Molekulare Strukturforschung
Dr. K. Gerth, Prof. Dr. H. Reichenbach
Abteilung Naturstoffbiologie
Gesellschaft für Biotechnologische Forschung
Mascheroder Weg 1, D-38124 Braunschweig (Germany)
Fax: Int. code +(531)6181-461

[**] Antibiotics from Gliding Bacteria, Part 77. Part 76: D. Schummer, E. Forche, V. Wray, T. Domke, H. Reichenbach, G. Höfle, *Liebigs Ann.* **1996**, 971–978. We thank Dr. A. Ross and colleagues at the Bio Pilot Plant of the GBF for help with fermentations, Dr. V. Wray and colleagues from Instrumental Analytics Group for recording the NMR and mass spectra, and B. Pluta, A. Ritter, and K. Schicht for technical assistance. This work was supported by the Fonds der Chemischen Industrie.

action to that of taxol and, according to the results of displacement experiments, apparently compete for the same binding site on microtubules. These discoveries resulted in much interest in the production of epothilones, their three-dimensional structure, and potential homology to taxol, which will be reported herein.

For the synthesis of the epothilones on a gram scale, the extract (46 g) from 230 L of production strain culture[3] is fractionated on Sephadex LH-20 (20 × 100 cm column, 20 mL min^{-1} methanol). Chromatography of the epothilone-containing fractions (R_t = 265–295 min, 12 g) on RP-18 silica gel (Prep-bar system, Merck, 40 × 10 cm column, 180 mL min^{-1} methanol/water 3:1) and rechromatography of the mixed fractions gave a total of 4.8 g epothilone A (**1a**) and 2.1 g epothilone B (**1b**), as colorless oils. Both compounds crystallize on trituration with ethyl acetate.

Elemental analysis and physical data give the empirical formula $C_{26}H_{39}NO_6S$ for **1a** and $C_{27}H_{41}NO_6S$ for **1b**, and ^1H and ^{13}C NMR spectra (Tables 1 and 2) and their 2D correlation are

Table 1 Physical and spectroscopic data for compounds **1a** and **1b**.

1a: Colorles crystals from ethyl acetate/toluene; m.p. 95 °C; solubility in water at 20 °C: 0.7 g L^{-1}; chromatography: R_f = 0.75 (silica gel Si60, dichloromethane/methanol, detection with vanillin/sulfuric acid, blue-gray coloration on heating to 120 °C); HPLC: R_t = 3.5 min (Nucleosil 100, C-18, 5 µ, 125 × 4 mm column, solvent methanol/water 65/35, 1 mL min^{-1}, detection at 254 nm); UV (MeOH): λ_{max} (ε) = 211 (17800), 249 nm (12500); $[\alpha]_D^{21} = -47.1$ (c = 1.0 in methanol); IR (KBr): $\tilde{\nu}$ = 3476, 2974, 2938, 2882, 1738, 1692 cm^{-1}; ^{13}C NMR (150 MHz, [D$_6$]DMSO): δ = 170.3 (C-1), 38.4 (C-2), 71.2 (C-3), 53.1 (C-4), 217.1 (C-5), 45.4 (C-6), 75.9 (C-7), 35.4 (C-8), 29.6 (C-9), 23.6 (C-10), 27.2 (C-11), 56.6 (C-12), 54.4 (C-13), 32.1 (C-14), 76.3 (C-15), 137.3 (C-16), 119.1 (C-17), 152.1 (C-18), 117.7 (C-19), 164.2 (C-20), 18.8 (C-21), 20.8 (C-22), 22.6 (C-23), 16.7 (C-24), 18.4 (C-25), 14.2 (C-27) [a]; EI-MS (70 eV): m/z (%): 493.2485 (22) [Calcd for $C_{26}H_{39}NO_6S$: 493.2498], 421 (20), 306 (70), 166 (50), 165 (84), 164 (100)

1b: colorless crystals form ethyl acetate; m.p. 93–94 °C; chromatography: R_f = 0.75; HPLC: R_t = 4.1 min (conditions see **1a**); UV (MeOH): λ_{max} (ε) = 211 (18600), 249 nm (14100); $[\alpha]_D^{21} = -35.0$ (c = 0.7 in methanol); IR (KBr): $\tilde{\nu}$ = 3487, 2966, 2935, 2880, 1738, 1690 cm^{-1}; ^{13}C NMR (150 MHz, [D$_6$]DMSO): δ = 170.1 (C-1), 38.2 (C-2), 70.5 (C-3), 53.2 (C-4), 217.4 (C-5), 44.9 (C-6), 75.5 (C-7), 35.6 (C-8), 29.6 (C-9), 23.0 (C-10), 32.1 (C-11), 61.0 (C-12), 61.5 (C-13), 33.0 (C-14), 76.6 (C-15), 137.2 (C-16), 119.2 (C-17), 152.1 (C-18), 117.7 (C-19), 164.3 (C-20), 18.9 (C-21), 19.7 (C-22), 22.5 (C-23), 16.4 (C-24), 18.4 (C-25), 22.1 (C-26), 14.1 (C-27); EI-MS (70 eV): m/z (%): 507.2568 (15) [calcd. for $C_{27}H_{41}NO_6S$: 507.2576], 421 (20), 306 (70), 166 (50), 165 (84), 164 (100)

[a] To aid comparison, the methyl group on C-16 in **1a** is also designated C-27.

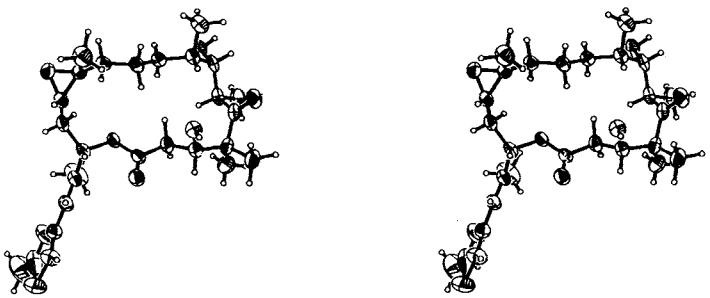

Fig. 1 Stereorepresentation of the crystal structure of **1b**.

Table 2 ^1H NMR data for compounds **1a** and **1b** in [D$_6$]DMSO at 600 MHz.

Atom	**1a** δ	**1a** J [Hz]	**1b** δ	**1b** J [Hz] exp.	**1b** J [Hz] calcd. [b]
2-Ha	2.38	2a,2b = 16.0	2.35	2a,2b = 15.0	
2-Hb	2.50	2a,3 = 11.0	2.38	2a,3 = 9.5	10.9
3-H	3.97	2b,3 = 3.0	4.10	2b,3 = 4.5	1.0
3-OH	5.12	3,3-OH = 6.5	5.08	3,3-OH = 7.0	
6-H	3.07	6,7 = 7.7	3.11	6,7 = 8.4	10.8
7-H	3.49	6,24 = 6.7	3.48	6,24 = 6.8	
7-OH	4.46	7,7-OH = 6.6	4.46	7,7-OH = 6.5	
8-H	1.34	7,8 ≦ 1	1.29	7,8 ≦ 1	0.6
9-Ha	1.15	8,25 = 6.7	1.14	8,25 = 6.8	
9-Hb	1.40		1.38		
10-Ha	1.15 [a]		1.14 [a]		
10-Hb	1.46 [a]		1.43 [a]		
11-Ha	1.35	11a,12 = 9.4	1.31		
11-Hb	1.66	11b,12 = 3.3	1.61		
12-H	2.84	12,13 = 3.5	–		
13-H	3.06	13,14a = 10.0	2.84	13,14a = 9.5	11.6
14-Ha	1.76	13,14b = 3.7	2.05	13,14b = 3.5	2.2
14-Hb	2.10	14a,14b = 14.9	1.84	14a,14b = 15.0	
15-H	5.27	14a,15 = 10.1	5.29	14a,15 = 9.0	9.4
17-H	6.50	14b,15 ≦ 1	6.51	14b,15 = 2.0	1.0
19-H	7.35		7.35		
21-H$_3$	2.65		2.65		
22-H$_3$	0.94		0.90		
23-H$_3$	1.21		1.19		
24-H$_3$	1.06		1.07		
25-H$_3$	0.90		0.91		
26-H$_3$	–		1.19		
27-H$_3$	2.10 [c]		2.11		

[a] Assignment interchangeable. [b] PCMODEL according to the crystal structure. [c] To aid comparison, the methyl group on C-16 in **1a** is also designated C-27.

in agreement with the epothilone structures. This was confirmed by an X-ray structural analysis of **1b**,[9] which also gave the absolute configuration of the eight stereogenic centers (Fig. 1).[10] The crystals obtained from dichloromethane (spatial group $P2_1$) contain two molecules of **1b** and a disordered molecule of dichloromethane in the unit cell. Intermolecular hydrogen bonds are present between 3-OH and the epoxide oxygen atom, and between 7-OH and the C-5 carbonyl group. The carbon backbone of the macrocycle is largely flat, with maximum deviation from the best-fit plane for C-6 (– 0.96 Å) and C-3 (0.85 Å). The methyl groups C-22, C-25, and C-26 adopt an approximately axial position and the side chain with the thiazole ring an equatorial position; 1,3-diaxial interactions are avoided. Only the *cis* configuration of the epoxide[11] produces strain that the molecule cannot avoid.

Information about the conformation in solution was obtained from the vicinal coupling constants of the ring protons, which are compared to the values expected for the crystal structure in Table 2.[12] Since the expected and measured values are consistent, it can be concluded that the conformation of **1a** and **1b** in solution is similar to that in the crystal.[13] Significantly higher values than expected are only found in the spin system 2-H$_2$/3-H with $J_{2b,3}$ = 3.0 (**1a**) and 4.5 Hz (**1b**). Since the neighboring C atoms do not carry protons, it is not possible to give a more exact description of the difference in conformation in this ring segment.

Larger variations can be ruled out, however, since the NOE relations given in Figure 2 are in good agreement with the presumed conformation. There is apparently no preferred conformation for the side chain with the thiazole moiety. In addition, the NOE effects confirm the assignment of the proton signals and indirectly confirm the ^{13}C NMR assignments in Tables 1 and 2. ^1H NMR experiments with **1b** in [D$_4$]methanol and [D$_6$]DMSO with addition of 10 to 50 vol% D$_2$O indicate that the original conformation is maintained in biological media.

A number of structural similarities are apparent on comparison of the epothilones with taxol: both compounds contain a geminal dimethyl group, a β-hydroxyoxo unit, and a small ether ring. Also, the size of the 14-membered perimeter of the diterpene part of taxol corresponds approximately to that of the

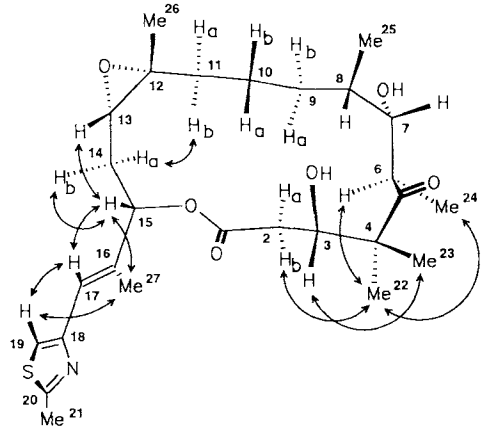

Fig. 2 Selected NOE relations for **1b**.

lactone ring in the epothilones. However, if taxol is reduced to the structural elements required for its biological activity[15] and the spatial orientation of the corresponding functional groups is taken into account, there are no remaining similarities. Furthermore, the spatially distant, essential phenyl residues at the 2- and 13-positions of taxol are only matched by *one* of this type of side chain in the epothilones. From this it has to be concluded that the epothilones and taxol occupy different but possibly overlapping binding sites on microtubules.

Whether the in vivo activity of the epothilones is equivalent or even better than that of taxol has not yet been demonstrated. Advantages which are already apparent are their much higher activity against P-glycoprotein-forming, multiresistant tumor lines,[8] their better solubility in water by a factor of about 30, and their almost unlimited availability by fermentation in a technical culture medium.[3]

Received: 26 March, 1996 [Z8975IE]
German version: *Angew. Chem.* **1996**, *108*, 1671–1673

Keywords: antitumor agents · epothilones · myxobacteria · structure elucidation

[1] a) H. Reichenbach in *Myxobacteria II* (Eds.: M. Dworkin, D. Kaiser), American Society for Microbiology, Washington, DC, **1993**, pp. 13–63; b) H. reichenbach, G. Höfle, *Biotech. Adv.* **1993**, *11*, 219–277; c) G. Höfle, H. Reichenbach in *Sekundärmetabolismus bei Mikroorganismen* (Eds.: W. Kuhn, H.-P. Fiedler), Attempto Verlag, Tübingen, **1995**, pp. 61–78.

[2] G. Höfle, N. Bedorf, K. Gerth, H. Reichenbach (GBF), DE-4138042, **1993** [*Chem. Abstr.* **1993**, *120*, 52841].

[3] K. Gerth, N. Bedorf, G. Höfle, H. Irschik, H. Reichenbach, *J. Antibiot.*, in press; F. Sasse, unpublished results.

[4] G. Höfle, N. bedorf, K. Gerth, H. Reichenbach (GBF), DE-4211055, **1993** [*Chem. Abstr.* **1993**, *119*, 180598].

[5] J. P. Pachlatko, Ciba-Geigy AG, unpublished results.

[6] Developmental Therapeutics Program of the National Cancer Institute, USA: M. R. Grever, S. A. Schepartz, B. A. Chabner, *Semin. Oncol.* **1992**, *19*, 622–638.

[7] The average growth inhibition for 60 human tumor cell lines for a 4:1 mixture of **1a** and **1b** is log(GI50) = − 8.1: A. B. Mauger, NCI, USA, personal communication.

[8] D. M. Bollag, P. A. McQueney, J. Zhu, O. Hensens, L. Koupal, J. Liesch, M. Goetz, E. Lazarides, C. M. Woods, *Cancer Res.* **1995**, *55*, 2325–2333.

[9] $C_{27}H_{41}NO_6S$, crystals from dichloromethane, monoclinic, space group $P2_1$; $a = 1191.9(2)$, $b = 1059.0(2)$, $c = 1375.7(2)$ pm, $\beta = 112.25(2)°$, $Z = 2$, $\rho_{calcd} = 1.196\ g\,cm^{-3}$, $Mo_{K\alpha}$ ($\lambda = 71.073$ pm), θ-2θ measurement, $3° \le 2\theta \le 50°$, $R = 0.059$ ($F \ge 4\sigma(F)$), maximum residual electron density $0.33 \times 10^{-6}\ e\,pm^{-3}$. Software used: Siemens SHELXTL-PLUS (PC version). Further details of the crystal structure investigation can be obtained from the Fachinformationszentrum Karlsruhe, D-76344 Eggenstein-Leopoldshafen (Germany), on quoting the depository number CSD-405210.

[10] The absolute conformation of **1b** was determined according to the method of Flack (H. D. Flack, D. Schwarzenbach, *Acta Crystallogr. Sect. A* **1988**, *44*, 499–506) and confirmed by degradation (O_3/Me_2S, I_2/NaOH, H_2SO_4/H_2O, $NaIO_4$, Ag_2O) to hydroxysuccinic acid, in which the C-15 of the epothilone is converted to the C-2 of hydroxysuccinic acid with retention of configuration. According to the GC comparison of the diisopropyl ester (2-propanol/HCl) with authentic samples on a heptakis(2,6-di-*O*-methyl-3-*O*-pentyl)-β-cyclodextrin phase (W. A. König, B. Gehrcke, *J. High Resolut. Chromatogr.* **1993**, *16*, 175–181), only (2*S*)hydroxysuccinic acid was produced with 8% total yield.

[11] During transposition of the crystallographic results into constitutional formulas, the *trans*-configuration was accidentally given in ref. [2]. We thank Prof. S. J. Danishefsky and Dr. N. Ikemoto for pointing out this mistake.

[12] PCMODEL, Version 368 V 4.0, Serena Software, Bloomington, USA, **1992**.

[13] In a recent preliminary communication by Victory et al. [14] attempts were made to derive the relative configuration and conformation in solution of **1a** on the basis of the ^1H NMR data. The two proposals for the relative configuration are incorrect, and the conformations in solution differ essentially from our own proposal; however, they can first be evaluated conclusively when the spatial assignment of the methylene protons and the atomic coordinates or the dihedral angles of the ring skeleton are known.

[14] S. F. Victory, D. G. Vander Velde, R. K. Jaluri, K. Ravi, G. L. Grunewald, G. I. Georg, *Biorg. Med. Chem. Lett.* **1996**, *6*, 893–898.

[15] D. G. I. Kingston, *Trends Biotechnol.* **1994**, *12*, 222–227.

A Short Enantioselective Synthesis of Carbanucleosides**

Barry M. Trost,* Robert Madsen, Simon G. Guile, and Andrew E. H. Elia

The intense interest in the potential therapeutic applications of carbanucleosides continues to stimulate synthetic efforts.[1, 2] Palladium-catalyzed reactions have become an important tool in their synthesis.[3] A potentially very short asymmetric synthesis of carbanucleosides could evolve by the use of purines (or pyrimidines) as nucleophiles BH in the palladium-catalyzed asymmetric desymmetrization of diesters[4, 5] as illustrated in Scheme 1. In comparison to our first approach for the enantioselective preparation of these compounds such a reaction sequence could reduce the number of steps by a factor of two. In principle, the enantiodiscriminating step in the palladium-catalyzed desymmetrization of *meso*-diesters should be independent of the nucleophile. With simple nucleophiles like malonate,[4] sulfinate,[6a] azide,[6b] and amine,[4] this expectation was fulfilled. Contrary to these results, employment of purines shows a remarkable effect on this enantiodiscriminating step.

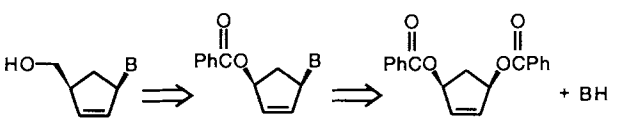

Scheme 1. Retrosynthesis of carbanucleosides. BH = nucleobase (nucleophile).

[*] Prof. Dr. B. M. Trost, Dr. R. Madsen, Dr. S. G. Guile, A. E. H. Elia
Department of Chemistry, Stanford University
Stanford, CA 94305-5080 (USA)
Fax: Int. code +(415)725-0259
e-mail: bmtrost@leland.stanford.edu

[**] We thank the National Science Foundation and the General Medical Sciences Institute of the National Institutes of Health for their support of our programs. R. M. thanks the Thomas B. Thriges and Knud Højgaards Fonds and the Danish Technical Research Council for partial support. Johnson Matthey Alfa Aesar provided a generous loan of palladium salts. Mass spectra were provided by the Mass Spectrometry Facility at the University of California-San Francisco supported by the NIH Division of Research Resources.

Herein we report our results obtained with purines as nucleophiles as well as the application of this strategy in a four-step synthesis of (−)-carbovir.[7]

Previous work established that the diphenylacetate **1a** and the dibenzoate **1b** gave the respective alkylation products with similar *ee* values.[5b] Furthermore, both 1,2-diphenylethyl (e.g., **7**) and cyclohexyl (e.g., **8**) type ligands gave comparable results. Solubility problems with adenine (**2a**) dictated the use of a mixed DMSO/THF solvent system. Reaction of diester **1a** with adenine (**2a**) in the presence of $[Pd_2(dba)_3]\cdot CHCl_3$ **4** and ligand **8** at room temperature led to the desired alkylation product **3a** but in low conversion (Scheme 2). Most disappointingly, hydrolysis (NaOH, CH_3OH, room temperature) and esterification

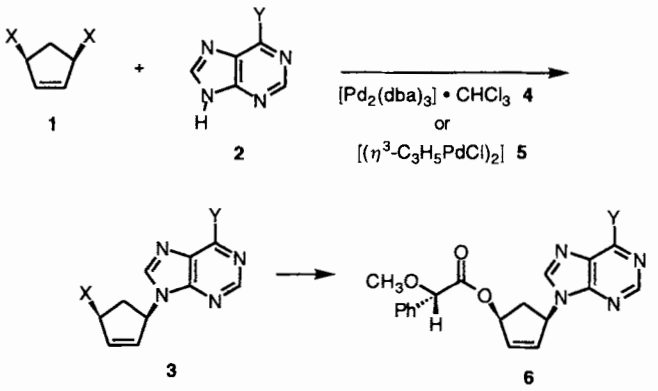

1 2 3 6

Scheme 2. Synthesis of **6**. **1a**: X = Ph_2CHCO_2, **1b**: X = $PhCO_2$, **2a**: Y = NH_2; **2b**: Y = Cl; **3a**: X = Ph_2CHCO_2, Y = NH_2; **3b**: X = $PhCO_2$, Y = Cl; **6a**: Y = NH_2; **6b**: Y = OCH_3.

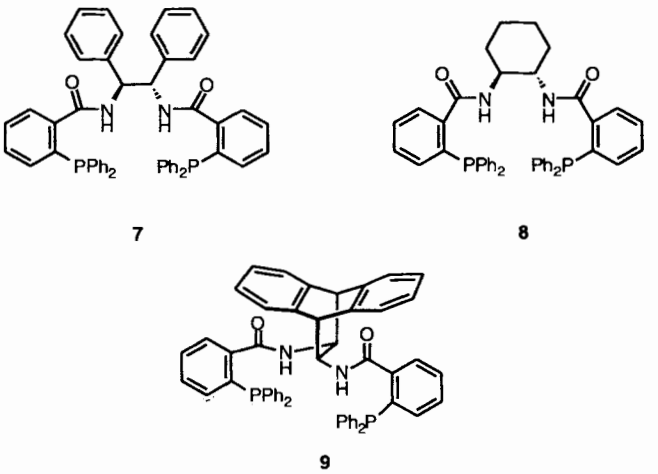

7 8 9

with (*S*)-O-methylmandelic acid (dicyclohexylcarbodiimide (DCC), 4-(dimethylamino)pyridine (DMAP), CH_2Cl_2) to give **6a** indicated the alkylation proceeded only in 9% *ee*. Other work in which N-methylbenzylamine was employed as nucleophile established that use of a DMSO/THF mixture rather than THF alone should not be the reason for such a drastic decrease in enantioselectivity. This observation is further verified herein (see below).

The switch from adenine (**2a**) to 6-chloropurine (**2b**) had a dramatic effect on the reaction. Addition of a tertiary amine such as triethylamine in conjunction with the purine resolves the conversion problem. Thus, the reaction with the 1,2-diphenylethyl ligand **7** and **4** as the palladium(0) source gave better results than that with the cyclohexyl ligand **8** and **5** as the palladium(0) source. When the reaction was performed with 7.6 mol% **7**, 2.5 mol% **4**, and **1b** in THF at room temperature, the crystalline adduct **3b** was obtained in 63% yield[8] (m.p. 90–92°; Table 1). Hydrolysis with sodium hydroxide in methanol gave **3** (X = OH, Y = OCH_3), which was esterified with (*S*)-O-methylmandelic acid (DCC, DMAP, CH_2Cl_2, room temperature) to give **6b**. Examination of the crude product **6b** by NMR spectroscopy revealed the diastereomeric excess to be 97%; the main diastereomer has the absolute configuration depicted in Scheme 2.[9, 10]

Table 1. Physical and spectroscopic data of the compounds **3b**, **11c**, and **14**.

3b: M.p. 90–92 °C; for material of 93% *ee*, $[\alpha]_D^{25} = -106.8$ ($c = 1.71$, CH_2Cl_2). IR ($CHCl_3$): $\tilde{\nu}$ = 1717, 1590, 1561, 1334 cm^{-1}; ^1H NMR (300 MHz, $CDCl_3$): δ = 8.78 (s, 1H), 8.28 (s, 1H), 8.02 (m, 2H), 7.60 (tt, J = 7.4, 1.3 Hz, 1H), 7.46 (m, 2H), 6.57 (dt, J = 5.6, 2.0 Hz, 1H), 6.30 (dd, J = 5.6, 2.4 Hz, 1H), 6.04 (dt, J = 7.4, 2.5 Hz, 1H), 5.87 (m, 1H), 3.25 (ddd, J = 15.3, 8.0, 7.7 Hz, 1H), 2.16 (dt, J = 15.3, 3.0 Hz, 1H); ^{13}C NMR (75 MHz, $CDCl_3$): δ = 165.7, 151.9, 151.2, 150.9, 143.3, 136.4, 133.6, 133.3, 131.6, 129.4, 129.3, 128.5, 77.3, 57.4, 38.5; anal. calcd for $C_{17}H_{13}ClN_4O_2$: C 59.92, H 3.85, N 16.44; found: C 60.16, H 4.00, N 16.67; HR-MS: calcd. 340.0727; found 340.0733.

11c: M.p 156–8 °C. $[\alpha]_D^{25} = -108.8$ ($c = 0.45$, CH_2Cl_2). IR ($CDCl_3$): $\tilde{\nu}$ = 3402, 1737, 1729, 1720, 1621, 1587, 1492, 1269, 1223, 1187 cm^{-1}; ^1H NMR (400 MHz, $CDCl_3$): δ = 8.05–7.99 (m, 4H), 7.57 (t, J = 7.3 Hz, 1H), 7.47–7.34 (m, 11H), 7.25 (m, 1H), 6.48 (dt, J = 1.9, 5.5 Hz, 1H), 6.21 (dd, J = 2.2, 5.5 Hz, 1H), 5.99 (m, 1H), 5.69 (m, 1H), 3.21 (p, J = 7.8 Hz, 1H), 2.55 (s, 3H), 2.13 (dt, J = 3.3, 15.2 Hz, 1H); ^{13}C NMR (101 MHz, $CDCl_3$): δ = 170.6, 165.8, 156.0, 154.5, 152.0, 150.2, 142.1, 135.7, 133.8, 133.2, 129.4, 129.0, 128.4, 127.7–125.3, 120.7, 77.3, 57.3, 38.3, 25.1; anal. calcd for $C_{32}H_{26}N_6O_5$: C 66.89, H 4.56, N 14.63; found: C 67.00, H 4.54, N 14.69

14: M.p. 118–120 °C. $[\alpha]_D^{25} = -61.0$ ($c = 0.5$, CH_2Cl_2): IR ($CDCl_3$): $\tilde{\nu}$ = 3398, 2965, 1737, 1695, 1620, 1589, 1492, 1286, 1205, 1187 cm^{-1}; ^1H NMR (400 MHz, $CDCl_3$): δ = 8.06 (s, 2H), 7.46–7.24 (m, 10H), 6.25 (dt, J = 2.2, 5.5 Hz, 1H), 5.96 (dt, J = 2.3, 5.5 Hz, 1H), 5.74 (m, 1H), 3.79 (m, 1H), 3.77 (s, 3H), 2.91 (dt, J = 9.1, 14.5 Hz, 1H), 2.54 (s, 3H), 2.29 (dt, J = 4.9, 14.5 Hz, 1H); ^{13}C NMR (101 MHz, $CDCl_3$): δ = 173.0, 170.8, 155.9, 154.6, 151.8, 150.3, 142.5, 141.5, 135.2, 132.0, 131.9, 131.8, 130.7, 129.0, 128.4, 128.3, 128.0–125.3, 120.7, 59.0, 52.3, 49.5, 34.0, 25.0; anal. calcd for $C_{27}H_{24}N_6O_5$: C 63.27, H 4.72, N 16.40; found: C 63.09, H 4.93, N 16.13

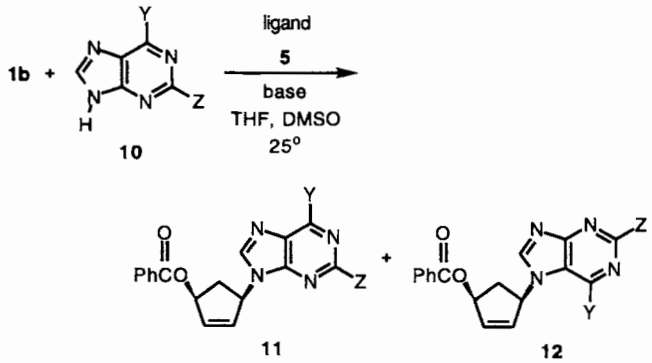

10 11 12

Scheme 3. Synthesis of **11** and **12**. **a**: Y = Cl, Z = NH_2; **b**: Y = $OCH_2CH_2SiMe_3$, Z = NH_2; **c**: Y = $OCONPh_2$, Z = NHAc.

With the aim of finding a guanine equivalent, we turned to 2-amino-6-chloropurine (**10a**) (Scheme 3). In this case, the products of alkylation both at N-9 (i.e. **11a**[8]) and N-7 (i.e. **12a**[8]) were observed, presumably as a result of electronic effects. The choice of the base used played a significant role in this conversion; tertiary amine bases were superior to inorganic bases. In the series triethylamine, dicyclohexylethylamine, diisopropylethylamine, and 1,2,2,6,6-pentamethylpiperidine (pempidine), the yield of the alkylation product increased from 32 to

 © VCH Verlagsgesellschaft mbH, D-69451 Weinheim, 1996 0570-0833/96/3513-1570 $ 15.00+.25/0

73%. With ligand **7** and four equivalents of pempidine as base, a mixture of **11a** and **12a** (3:1 ratio) was isolated in a combined yield of 52% (71% based on recovered starting material (brsm)). The $[\alpha]_D$ value of **11a** was -95.[11] The use of the cyclohexyl ligand **8** instead of **7** led to inferior results on all counts, conversion (only 60%), ratio of **11a**:**12a** (1.4:1), and enantioselectivity ($[\alpha]_D = -48$). On the other hand, with the bicyclic ligand **9**, which presumably has a larger P-Pd-P bite angle, improved results with respect to yield (60%, 66% brsm) and *ee* ($[\alpha]_D = -132$) were achieved, although the selectivity of the N alkylation was still unsatisfactory (**11a**: **12a** = 0.9:1.0). Increasing the steric hindrance associated with the C-6 substituent in an effort to sterically block the N-7 position as in **10b** does lead to a single product but only in 12% yield (21% brsm). If in addition the electron-donating ability of the 2-amino group is reduced by acetylation (as in **10c**[12]), under the same conditions the products **11c**[13] and **12c** were obtained in a combined yield of 62% (71% brsm; **11c**:**12c** = 3.8:1, *ee* 90%). Lowering the temperature from room temperature to 0° increased the ratio of **11c**:**12c** to 8.4:1 and the *ee* to 93–96%.[13] In addition, the doubly alkylated product[8] was obtained in 16% yield.[14] The above-mentioned reaction was carried out as follows: dibenzoate **1b** (1.0 equiv) and purine **10c** (1.2 equiv) in DMSO containing 1,2,2,6,6-pentamethylpiperidine (3 equiv) was added to a solution of 1.5 mol% **5** and 4.5 mol% **9** in THF at 0 °C. After 8 h at 0 °C and the normal work-up, **11c** was isolated in 50–59% yield (54–70% brsm) with 93–96% *ee* (Table 1).[13] Recrystallization from ethyl acetate enhanced the *ee* to >98%.

Access to enantiopure **11c** sets the stage for a short synthesis of (−)-carbovir (**15**). Introduction of the remaining one carbon side chain requires substitution of the benzoate with retention of configuration; this again calls for a Pd(0)-catalyzed reaction. In the event, treatment of **11c** with phenylsulfonylnitromethane (1.2 equiv) and triethylamine (2.5 equiv) in THF at room temperature in the presence of 1.5 mol% **4** and 12 mol% triphenylphosphane gave **13** in 97–99% yield (Scheme 4).

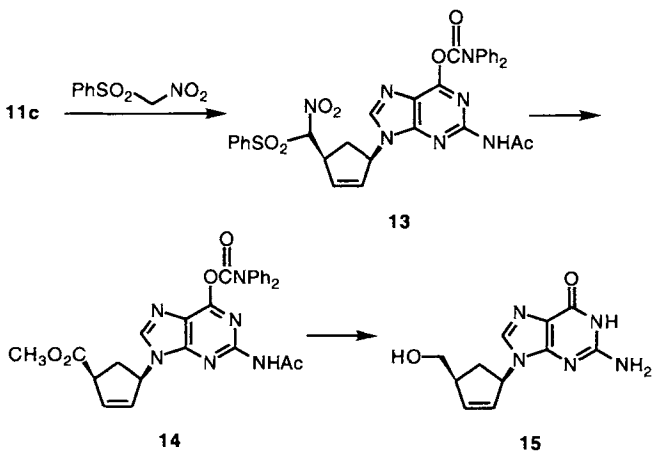

Scheme 4. Synthesis of (−)-carbovir **15**.

Chemoselective oxidative cleavage to give the ester **14** in 71% yield (Table 1) was achieved by treating the tetramethylguanidine salt in methanol/dichloromethane with tetrabutylammonium-oxone[15] buffered with sodium carbonate. Reduction with calcium borohydride[16] in THF followed by an aqueous ammonia work-up generated (−)-carbovir (**15**) in 61% yield (m.p. 255–7 °C, $[\alpha]_D^{25} = -60.1$ ($c = 0.4$, CH_3OH)).[7]

The surprising dependence of the palladium-catalyzed desymmetrization of *meso*-diesters on the nature of the purine base unlike a myriad of other nucleophiles including secondary amines, azides, sulfones, carboxylates, malonates, etc., may derive from their ability to serve as competitive ligands thereby disrupting the normal coordination of the palladium. The requirement for the hindered tertiary amine base may stem from its stabilization of the pronucleophile by hydrogen bonding, thereby disfavoring any equilibrium involving coordination of the pronucleophile or nucleophile to the metal and, at the same time, preventing it from serving as a ligand due to the steric hindrance. Thus, the nature of the nucleophile cannot be totally dismissed in this metal-catalyzed desymmetrization. These results clearly indicate that our normally preferred ligand **8** is not suitable for reactions with these nucleophiles and that better results can be achieved with either **7** or **9**. The ability to use the Pd(0)-catalyzed desymmetrization has resulted in a four-step synthesis of (−)-carbovir from dibenzoate **1b**. Since the first two steps employ Pd(0)-catalyzed alkylations that may be combined into a single event, a three-stage synthesis may evolve. In addition, **3b** was converted analogously in quantitative yield to **16a** (Scheme 5). Ammonolysis gave **16b**, an intermediate in the synthesis of the carbanucleoside (−)-aristeromycin.[3a] This strategy should hold great promise for making carbanucleosides of either enantiomeric series, both of which are of biological interest, more readily available.

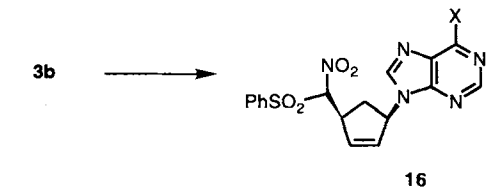

Scheme 5. Synthesis of **16**. **a**: X = Cl; **b**: X = NH_2.

Received: February 19, 1996 [Z8833IE]
German version: *Angew. Chem.* **1996**, *108*, 1666–1668

Keywords: alkylations · asymmetric catalysis · carbanucleosides · palladium compounds

[1] B. M. Trost, D. L. Van Vranken, C. Bingel, *J. Am. Chem. Soc.* **1992**, *114*, 9327.
[2] a) B. M. Trost, M. G. Organ, G. A. O'Doherty, *J. Am. Chem. Soc.* **1995**, *117*, 9662; b) B. M. Trost, D. Stenkamp, S. R. Pulley, *Chem. Eur. J.* **1995**, *1*, 568.
[3] *Nucleosides and Nucleotides as Antitumor and Antiviral Agents* (Eds.: C. K. Chu, D. C. Baker), Plenum, New York, **1993**; J. B. Hobbs in *Comprehensive Medicinal Chemistry, Vol. 2* (Eds.: C. Hansch, P. G. Sammes, J. B. Taylor), Pergamon, Oxford, **1990**, pp. 306–322; J. A. V. Coates, H. I. Ingall, B. A. Pearson, C. R. Penn, R. Storer, C. Williamson, J. M. Cameron, *Antiviral Res.* **1991**, *15*, 161; J. A. Montgomery, *ibid.* **1989**, *12*, 113; K. Isono, *J. Antibiotics* **1988**, *41*, 1711; T. Hovi in *Antiviral Agents: The Development and Assessment of Antiviral Chemotherapy* (Ed.: H. J. Field), CRC Press, Boca Raton, FL, **1988**, Chapter 1, pp. 1–12; M. F. Jones, *Chem. Br.* **1988**, 1122; V. E. Marquez, M. Lim, *Med. Res. Rev.* **1986**, *6*, 1; R. Dolin, *Science* **1985**, *227*, 1296.
[4] L. Agrofoglio, E. Suhas, A. Farese, R. Condom, S. R. Challand, R. A. Earl, R. Guedj, *Tetrahedron* **1994**, *50*, 10611; A. D. Borthwick, K. Biggadike, *ibid.* **1992**, *48*, 571.
[5] For Pd-catalyzed reactions in synthesis of carbanucleosides: a) B. M. Trost, G.-H. Kuo, T. Benneche, *J. Am. Chem. Soc.* **1988**, *110*, 621; b) B. M. Trost, L. Li, S. D. Guile, *ibid.* **1992**, *114*, 8745. Some other examples in which this methodology is employed include: c) A. L. Margolin, D. R. Borcherding, D. Wolf-Kugel, N. Margolin, *J. Org. Chem.* **1994**, *59*, 7215; d) S. Hildbrand, T. Troxler, R. Scheffold, *Helv. Chim. Acta* **1994**, *77*, 1236; e) J. Nokami, H. Matsuura, K. Nakasima, S. Shibata, *Chem. Lett.* **1994**, 1071; f) V. Merlo, S. M. Roberts, R. Storer, R. C. Bethell, *J. Chem. Soc. Perkin 1* **1994**, 1477; g) M. Koga, S. W. Schneller, *J. Org. Chem.* **1993**, *58*, 6471; h) M. E. Jung, H. Rhee, *ibid.* **1994**, *59*, 4719; i) V. Merlo, F. J. Reece, S. M. Roberts, M. Gregson, R. Storer, *J. Chem. Soc. Perkin 1* **1993**, 1717; j) A. D. DaSilva, E. S. Coimbra, J.-L. Fourrey, A. S. Machado, M. R. Geco, *Tetrahedron Lett.* **1993**, *34*, 6745.

 © VCH Verlagsgesellschaft mbH, D-69451 Weinheim, 1996 0570-0833/96/3513-1571 $ 15.00+.25/0

[6] For an enzymatic strategy combined with Pd^0 chemistry: N. B. Dyatkina, F. Thiel, M. von Janta, *Tetrahedron* **1995**, *51*, 761 and 3i.
[7] For other recent syntheses see ref. [3b,d,e,h]; T. Berranger, Y. Langlois, *Tetrahedron Lett.* **1995**, *36*, 5523; M. Legraverend, A. M. Aubertin, G. Obert, C. Huel, E. Bisagni, *Nucleosides, Nucleotides* **1994**, *13*, 915; M. Asami, J. Takahashi, S. Inoue, *Tetrahedron: Asymmetry* **1994**, *5*, 1649; M. Diaz, J. Ibarzo, N. M. Jimenez, R. M. Ortuno, *ibid.* **1994**, *5*, 129; M. E. Jung, H. Rhee, *Tetrahedron Lett* **1993**, *34*, 4449; R. A. Mac Keith, R. Mc Cague, H. F. Olivo, C. F. Palmer, S. M. Roberts, *J. Chem. Soc. Perkin Trans. 1* **1993**, 313; L. Gundersen, T. Benneche, F. Rise, A. Gogoll, K. Undheim, *Acta Chem. Scand.* **1992**, *46*, 761; M. R. Peel, D. D. Sternbach, M. R. Johnson, *J. Org. Chem.* **1991**, *56*, 4990; A. M. Exall, M. F. Jones, C.-L. Mo, P. L. Myers, I. L. Paternoster, H. Singh, R. Storer, G. G. Weingarten, C. Williamson, A. C. Brodie, J. Cook, D. E. Lake, C. A. Meerholz, P. J. Turnbull, R. M. Highcock, *J. Chem. Soc. Perkin Trans. 1* **1991**, 2467.
[8] The proposed structure was confirmed by spectroscopy.
[9] B. M. Trost, J. L. Belletire, S. Godleski, P. G. McDougal, J. M. Balkovec, J. J. Baldwin, M. E. Christy, G. S. Ponticello, S. L. Varga, J. P. Springer, *J. Org. Chem.* **1986**, *51*, 2370.
[10] Notable differences in the ^1H NMR spectra of the *O*-methylmandelates: (*S,S,R*)-diastereomer: $\delta = 1.93$ (dt, $J = 15.3$, 2.5 Hz, 1H), 3.06 (dt, $J = 15.3$, 8.2 Hz, 1H), 3.39 (s, 3H), 6.13 (dd, $J = 5.5$, 2.2 Hz, 1H), 6.24 (dt, $J = 5.5$, 1.9 Hz, 1H), 7.72 (s, 1H), 8.56 (s, 1H); (*S,R,S*)-diastereomer: $\delta = 1.72$ (dt, $J = 15.3$, 3.0 Hz, 1H), 3.00 (dt, $J = 15.3$, 7.6 Hz, 1H), 3.40 (s, 3H), 6.19 (dd, $J = 5.5$, 1.9 Hz, 1H), 6.34 (dt, $J = 5.5$, 1.9 Hz, 1H), 7.79 (s, 1H), 8.54 (s, 1H).
[11] In this case, a comparison of relative *ee* values was only obtained by comparison of rotations. The optical rotation of enantiomerically pure products were not obtained since **10c** proved to be a better guanine equivalent.
[12] Prepared in a one-pot procedure from guanine, see: R. Zou, M. J. Robins, *Can. J. Chem.* **1987**, *65*, 1436.
[13] The *ee* value was determined by NMR spectroscopy by using $[Eu(hfc)_3]$ (hfc = 3-(heptafluoropropylhydroxymethylene)-d-camphorate) as the chiral shift reagent after further transformation to the ester **14**.
[14] The higher *ee* value may arise, in part, from a kinetic resolution of the monoalkylated product superimposed upon the initial asymmetric induction.
[15] B. M. Trost, R. Braslau, *J. Org. Chem.* **1988**, *53*, 532.
[16] S. Daluge, R. Vince, *J. Org. Chem.* **1978**, *43*, 2311.

Directed Synthesis of Nonsymmetrical Bis-Steroidal Pyrazines and the First Biologically Active Cephalostatin Analogues**

Michael Drögemüller, Rolf Jautelat, and Ekkehard Winterfeldt*

Dedicated to Professor Ernst Mutschler on the occasion of his 65th birthday

Cephalostatin 1 (**1**) is the prototype of the cephalostatins and the ritterazins, a family of 30 trisdecacyclic pyrazines, isolated by Pettit and his co-workers since 1988 from the Indian Ocean marine worm *Cephalodiscus gilchristi*[1] and by the group of Fusetani from the tunicate *Riterella tokioka*.[2] The extraordinarily strong cytostatic activity,[1b,3] together with the new and interesting structure and very limited availability,[1a] immediately led to attempts at syntheses in various laboratories.[4–6] Although recently Fuchs et al. reported quite impressive achievements in the total synthesis of cephalostatins and ritterazins, the crucial problem of a direct synthesis of nonsymmetrical bis-steroidal pyrazines was not properly solved. Fuchs and his co-workers prepared the cephalostatins 7 and 12 together with ritterazin K from two precursors in a statistical way and had to separate the three products.[5b] For the first synthesis of nonsymmetrical pyrazines from α-acetoxy ketones and α-amino oximethers, which was not yet been applied to $\Delta^{14,15}$ steroids, Heathcock et al.[4] reported high reaction temperatures (145 °C) paired with low yields and regioselectivity problems.

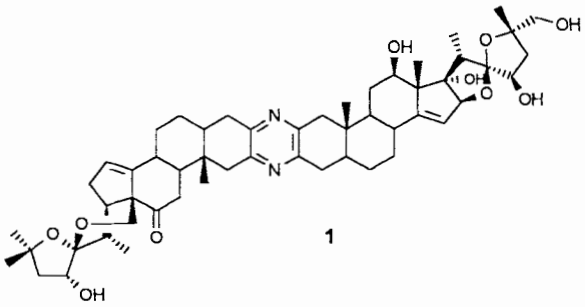

1

Systematic investigations in our laboratories indicated two independent routes to easily accessible cephalostatin analogues, which can provide information on the substructures essential for cytostatic activity. One approach, called the *symmetrical route*, aimed at the straightforward synthesis of symmetrical bis-steroidal pyrazines by dimerization of the usual α-amino ketone precursor.[7] These pyrazines have then to be desymmetrized and further functionalized at a later stage of the synthesis. The other approach, called the *nonsymmetrical route*, called for the direct synthesis of unsymmetrical bis-steroidal pyrazines by coupling of two different steroids.

At the beginning we elaborated the symmetrical route, which afforded in a short and efficient seven-step synthesis the symmetric diketone **3a** from easily available hecogenine acetate **2**.[6] Desymmetrization of this diketone by diastereoselective reduction with L-Selectride afforded the α-hydroxy ketone **4α**, while borohydride reduction provided the β-hydroxy ketone **4β**. These reduction processes under proper conditions also gave rise to the α-diol **5α** and β-diol **5β** (see Scheme 1).

Submitting the selected compounds **3a**, **3b**, **4β**, and **5β** to the U. S. National Cancer Institutes (NCI) in vitro, human-cancer-focused evaluation system,[8] we found that the symmetrical and saturated diketone **3b**[9] (affecting only 4 of 58 cell lines; GI_{50}: MG MID (MG MID = *m*ean *g*raph *mid*point; that is mean activity over all cell lines) > -4.0) showed weak activity. In contrast the symmetrical but unsaturated substances diketone **3a** (affecting 32 of 58 cell lines; GI_{50}: MG MID > -4.3) and β-diol **5β** (affecting 21 of 58 cell lines; GI_{50}: MG MID > -4.2) showed moderate tumor-inhibiting capacity. Finally the nonsymmetrical and unsaturated β-hydroxy ketone **4β** (affecting 58 of 58 cell lines; GI_{50}: MG MID $= -5.3$) revealed significant cytostatic action on all tested tumor cells.[10] Therefore the β-hydroxy ketone **4β** reaches affecting concentrations of standard chemotherapeutics (e.g., cyclophosphamide GI_{50}: MG MID $= -3.7$; 5-fluorouracil GI_{50}: MG MID $= -4.7$; cisplatin GI_{50}: MG MID $= -5.7$; adriamycin GI_{50}: MG MID $= -6.9$).[11] Their activities are similar to those of tamoxifen (GI_{50}: MG MID $= -5.3$)[11] and 4000 times weaker than that of the very potent cephalostatin 1 (**1**) (GI_{50}: MG MID $= -8.9$),[1c] which itself shows a tenfold stronger tumor-inhibiting activity than taxol (GI_{50}: MG MID $= -7.9$).[11]

By comparison to the noncytostatic saturated cephalostatin analogues[4,5a] we recognized that the $\Delta^{14,15}$ double bond is indispensable for the biological activity in general and that the nonsymmetrical structure is of particular importance for the broad scope of this action. Therefore we focused our efforts on

[*] Prof. Dr. E. Winterfeldt, Dipl.-Chem. M. Drögemüller, Dipl.-Chem. R. Jautelat
Institut für Organische Chemie der Universität
Schneiderberg 1b, D-30167 Hannover (Germany)
Fax: Int. code +(511)762-3011
e-mail: winterfeldt@mbox.oci.uni-hannover.de

[**] This work was supported by the Fonds der Chemischen Industrie, the Deutsche Forschungsgemeinschaft, and the Schering AG, Berlin. R. J. thanks the Fonds der Chemischen Industrie for a scholarship.

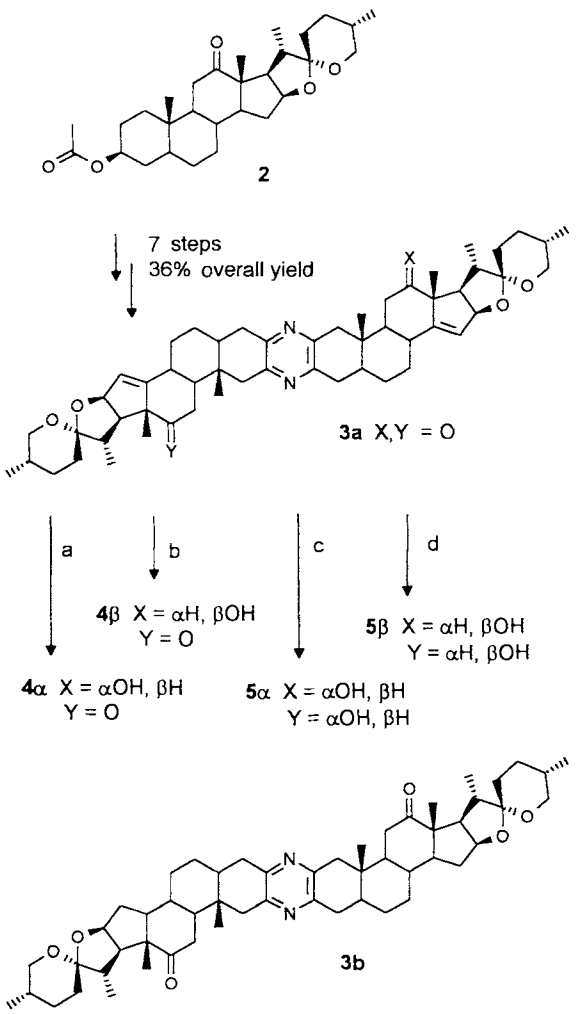

Scheme 1. Synthesis of compounds **4α**, **4β**, **5α**, and **5β**. a) 0.7 equiv L-Selectride, dry toluene, −78 °C, (49% in one step, 82% with recovery of starting material); b) 0.7 equiv $NaBH_4$, CH_2Cl_2/MeOH, −78 °C (47% in one step, 81% with recovery of starting material); c) L-Selectride, dry toluene, −78 °C (96%); d) $NaBH_4$, CH_2Cl_2/MeOH, −78 °C (98%).

a direct formation of nonsymmetrical compounds of this type by the already mentioned nonsymmetrical route.

Having noticed that enamino ketones of type **B** are stable under thermal conditions and do not undergo dimerization, we expected that reaction of **B** with azirines **A** as nondimerizing analogues of α-amino ketones could give an easy access to nonsymmetrical pyrazines **C** (see Scheme 2).

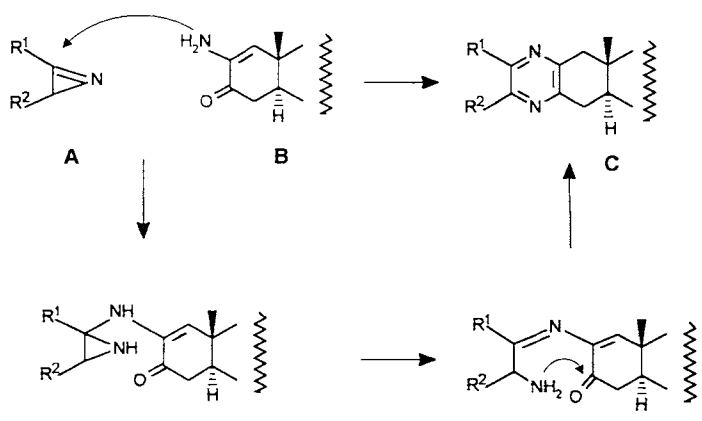

Scheme 2.

As expected treatment of azirine **6**, easily prepared from *trans*-stilbene,[12] with enamino ketone **7** and trifluoracetic acid (TFA) at 0 °C in THF gave pyrazine **8** in 63% yield (see Scheme 3).

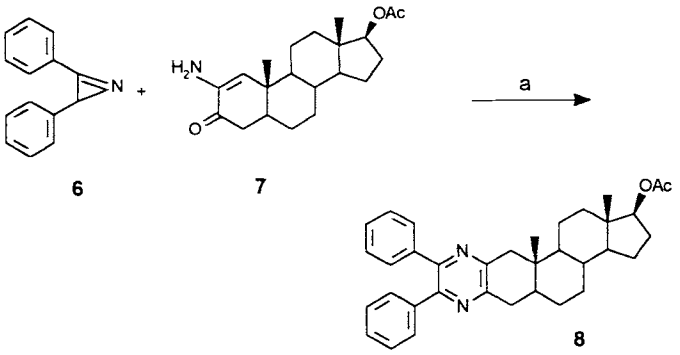

Scheme 3. Preparation of pyrazine **8**. a) THF, TFA, 0 °C, 3 h (63%).

With the intention of combining two steroids we applied—after substantial improvements[13]—Zbiral's[14] method to prepare steroidal vinyl azides as precursors for the corresponding azirines.[15] However, all attempts to generate and isolate these ring-fused azirines failed. When a literature survey[16] confirmed that this kind of compound is indeed highly strained and less stable than monocyclic azirines like **6**, we conducted the azirine formation in the presence of enamino ketone **10** in order to capture in situ the formed azirine. In the event the decomposition of the vinyl azide **9** in refluxing dioxane in the presence of **10** and pyridine-*para*-toluenesulfonate (PPTS) as a mild proton source did generate the unsymmetrical pyrazine **11** in 67% yield (see Scheme 4).

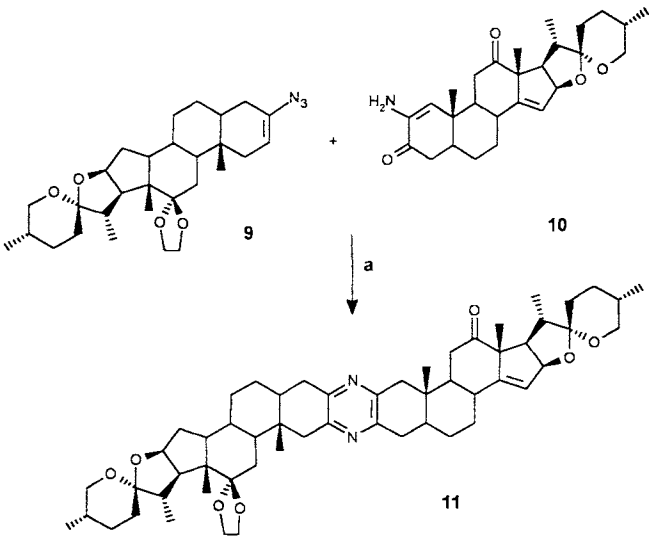

Scheme 4. Synthesis of pyrazine **11**. a) Dioxane, PPTS, 90 min at reflux (67%).

By this method we prepared pyrazine **13** from vinyl azide **12** and enamino ketone **10** in 51% yield and obtained cephalostatin analogues with promising biological activity.[17] Pyrazine **13** was also available independently by the symmetrical route described above, followed by an esterfication of the α-hydroxy ketone **4α** (96% yield). Both products were identical (according

to TLC and IR, ^1H, ^{13}C spectroscopy) and verified the regioselectivity of this new pyrazine-forming reaction. Reduction of pyrazine **13** with sodium borohydride and diisobutylaluminum hydride (DIBAH) gave the α,β-diol **5αβ**, which was also prepared by reduction of α-hydroxy ketone **4α** with sodium borohydride (see Scheme 5).[18]

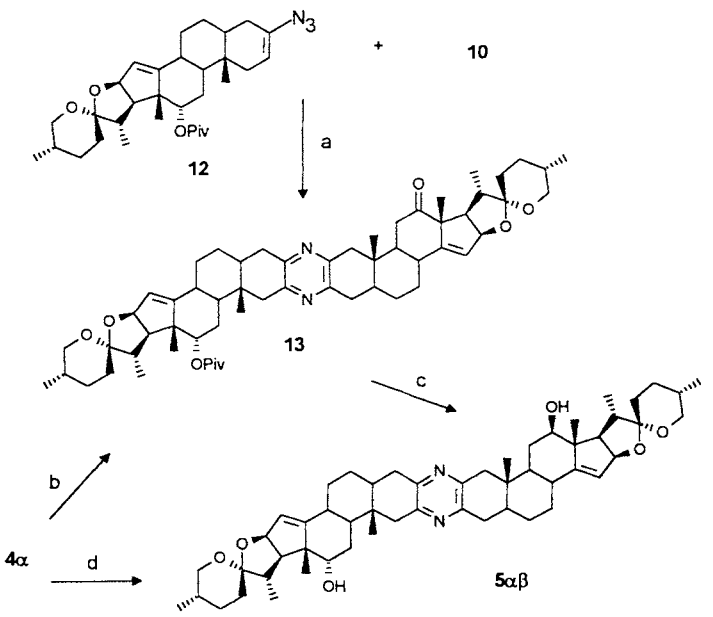

Scheme 5. Synthesis of compounds **13** and **5αβ** a) PPTS, dioxane, 3 Å molecular sieves, reflux (51%); b) pivaloyl chloride, dimethylaminopyridine, pyridine, 100 °C (96%); c) 1) $NaBH_4$, CH_2Cl_2/MeOH, −78 °C; 2. DIBAH, toluene (68%); d) $NaBH_4$, CH_2Cl_2/MeOH, −78 °C (96%).

In conclusion, we were successful in preparing easily accessible, biologically active cephalostatin analogues and in developing a novel method for the directed and flexible synthesis of nonsymmetrical bis-steroidal pyrazines.

Experimental Procedure

13: A degassed solution of **10** (51 mg, 0.11 mmol), **12** (64 mg, 0.12 mmol), PPTS (5 mg), and 3 Å molecular sieves (23 mg) in dry dioxane (2 mL) was heated at reflux under an argon atmosphere for 2 h. After filtration through silica, the solvent was removed and the residue purified by flash chromatography (silica, light petroleum/ethyl acetate = 2/1) to yield 55 mg (51%). White crystals, m.p. 269 °C; UV/Vis (CH_3OH): λ_{max} = 305 (sh), 288, 210 nm; IR (KBr): $\tilde{\nu}$ = 2956, 2932, 2872, 1716(br), 1400, 1376, 1192, 1156, 980, 908 cm^{-1}; ^1H NMR (400 MHz, $CDCl_3$): δ = 0.77–1.03 (m, 24H), 1.18 (s, 9H), 1.20–2.43 (m, 32H), 2.47–2.92 (m, 8H), 3.31–3.53 (m, 4H), 4.78 (dd, J = 8.1 and 2.0 Hz, 1H), 4.90 (dd, J = 7.9 and 2.0 Hz, 1H), 4.93 (s, 1H), 5.49 (s, 1H), 5.52 (s, 1H); ^{13}C NMR (100.6 MHz, $CDCl_3$): δ = 11.52, 11.75, 13.76, 14.10, 17.14, 18.79, 20.75, 26.08, 27.14, 27.85, 27.95, 28.74, 28.77, 30.31, 30.39, 31.09, 31.26, 33.95, 34.20, 35.15, 35.21, 35.68, 36.36, 37.20, 38.91, 41.24, 41.65, 44.21, 44.52, 45.17, 45.75, 49.75, 49.89, 49.92, 53.14, 53.60, 62.29, 67.09, 67.12, 77.71, 83.93, 85.00, 106.64, 107.05, 120.67, 121.56, 148.09, 148.10, 148.58, 148.64, 153.85, 154.28, 177.60, 210.73; FAB-MS (nitrobenzyl alcohol matrix): m/z (%): 932 (100) [MH^+], 818 (27); $C_{59}H_{82}O_7N_2$ (931.31): found C 76.09, H 8.60, N 3.16; calcd C 76.09, H 8.87, N 3.01.

Received: February 19, 1996 [Z 8818 IE]
German version: *Angew. Chem.* **1996**, *108*, 1669–1671

Keywords: azirines · cephalostatins · enamine ketones · pyrazines · synthetic methods

[1] a) G. R. Pettit, M. Inoue, Y. Kamano, D. L. Herald, C. Arm, C. Dufresne, N. D. Christie, J. M. Schmidt, D. L. Doubek, T. S. Krupa, *J. Am. Chem. Soc.* **1988**, *110*, 2006; b) G. R. Pettit, J. Xu, Y. Ichihara, M. D. Williams, M. R. *Can. J. Chem.* **1994**, *72*, 2260; c) G. R. Pettit, J. Xu, M. D. Williams, N. D. Christie, D. L. Doubek, J. M. Schmidt, *J. Nat. Prod.* **1994**, *57*, 52.
[2] S. Fukuzawa, S. Matsunaga, N. Fusetani, *Tetrahedron* **1995**, *51*, 6707.
[3] These series of compounds are among the most potent cytostatics ever screened by the National Cancer Institute (USA). For a short review see A. Ganesan, *Angew. Chem.* **1996**, *108*, 667; *Angew. Chem. Int. Ed. Engl.* **1996**, *35*, 611.
[4] a) S. C. Smith, C. H. Heathcock, *J. Org. Chem.* **1992**, *57*, 6379; b) C. H. Heathcock, S. C. Smith, *ibid.* **1994**, *59*, 6828.
[5] a) Y. Pan, R. L. Merriman, L. R. Tanzer, P. L. Fuchs, *Bioorg. Med. Chem. Lett.* **1992**, *9*, 967; b) J. U. Jeong, S. C. Sutton, S. Kim, P. L. Fuchs, *J. Am. Chem. Soc.* **1995**, *117*, 10157.
[6] A. Kramer, U. Ullmann, E. Winterfeldt, *J. Chem. Soc. Perkin. Trans. 1* **1993**, 2865. The yields of the diketone **3a** synthesis have been substantially improved in the meantime.
[7] Preparation and chemistry of pyrazines: *Comprehensive Heterocyclic Chemistry* (Eds.: A. R. Katritzky, C. W. Rees), 1st ed., Pergamon, Oxford, **1984**, pp. 157–197.
[8] a) M. R. Boyd, K. D. Paull, L. R. Rubinstein in *Antitumor Drug Discovery and Development* (Eds.: F. A. Valeriote, T. Corbett, L. Baker), Kluwer, Amsterdam, **1992**, pp. 11–34; b) K. D. Paull, R. H. Shoemaker, L. Hodes, A. Monks, D. A. Scudiero, L. R. Rubinstein, J. Plowman, M. R. Boyd, *J. Natl. Cancer Inst.* **1989**, *81*, 1088.c) A. Monks, D. A. Scudiero, P. Skehan, R. H. Shoemaker, K. D. Paull, D. Vistica, C. Hose, J. Langley, P. Cronise, A. Vaigro-Wolff, M. Gray-Goodrich, H. Campbell, M. R. Boyd, *ibid.* **1991**, *83*, 757.
[9] S. Flemming, PhD Thesis, Universität Hannover, **1991**.
[10] Substances **3a** (NSC D-674135-O/0-1/55), **3b** (NSC D-674136-P/0-1/56), **5β** (NSC D-674133-M/0-1/53), and **4β** (NSC D-674134-N/0-1/54) were tested by the NCI (Experiment ID 9411MD95). Detailed results will be published elsewhere. We thank the team of Development Therapeutics Program of the NCI fot testing the compounds.
[11] Detailed information about cyclophosphamide (NSC 26271), 5-fluorouracil (NSC 19893), cisplatin (NSC 119875), adriamycin (NSC 123127), tamoxifen (NSC 180973), and taxol (NSC 125973) is available on the World Wide Web: http://epnws1.ncicrf.gov:2345/dis3d/itb/stdagnt tab.html.
[12] F. W. Fowler, A. Hassner, L. A. Levy, *J. Am. Chem. Soc.* **1967**, *89*, 2077.
[13] The vinyl azides were obtained by a sequence of a modified Mitsunobu reaction and an elimination process from the 2β-chloro-3α-hydroxy derivatives in up to 50% yield. Detailed results will be published soon in a full paper.
[14] J. Schweng, E. Zbiral, *Liebigs Ann. Chem.* **1978**, 1089.
[15] V. Nair, K. H. Kim, *Heterocycles* **1977**, *7*, 353.
[16] A. Hassner, F. W. Fowler, *J. Am. Chem. Soc.* **1968**, *90*, 2869.
[17] In this special case the 3 Å molecular sieve is crucial to avoid acid-catalyzed hydrolysis of enamino ketone **10** to the corresponding α-diketone. This seems to be the only annoying side reaction, and its complete suppression leads to even better yields of unsymmetrical pyrazines.
[18] Antitumor-screening of the newly prepared cephalostatin analogues is in progress at the Medizinische Hochschule Hannover (MHH). We especially thank Prof. Dr. W. Beil (MHH).

Chemistry in the Kitchen

Les secrets de la casserole. By *H. This*. Bélin, Paris, 1993. 222 pp., hardcover FF 110.00.—ISBN 2-7011-1585-X. **Révélations gastronomiques.** By *H. This*. Bélin, Paris, 1995. 319 pp., hardcover FF 130.00.—ISBN 2-7011-1756-9. **On Food and Cooking. The Science and Lore of the Kitchen.** By *H. McGee*. Scribner, New York, 1984. 684 pp., hardcover $ 35.00.—ISBN 0-684-18132-0. **The Curious Cook. More Kitchen Science and Lore.** By *H. McGee*. Macmillan, New York, 1990. 339 pp., paperback $ 13.00.—ISBN 0-0200-9801-4

The publication in 1995 of *Révélations gastronomiques* by Hervé This gives one an opportunity to compare it with three other books that are also concerned with the relationships between food preparation and chemistry. These relationships need to be looked into critically, since it is nowadays fashionable to complain that the food we eat is full of chemicals. We are told that pesticides, artificial fertilizers, irradiation, fumigation, artificial aromas, flavor additives, and other "works of the devil" are likely to make us all ill. This sends many people to obscure natural food shops where allegedly "biodynamically grown" products are sold at high prices. However, there are also many, often actually the same people, who buy convenience foods such as soups, sauces, puddings, baking mixtures, etc. which are ready to eat or need only some quick preparation such as adding water and heating. One only needs to look in any supermarket to see the innumerable varieties of joghurts and of sauces made for noodles. Of course there are also simple products such as natural joghurt or curd cheese, and one could buy rice, milk, tomatoes, and onions and make all these concoctions for oneself. The large consumption of ready-prepared meals and pre-processed foods is a social phenomenon that has much to do with "self-fulfillment", leisure activities, and social pressures. However, that is a huge field that has scarcely been studied yet.

The truth is that foodstuffs have never before been so pure, so varied, and so fresh as they are today. Our forebears often used large amounts of salt and pepper to mask the flavor of food that had been spoiled. From medieval times right up to the 18th century it was quite usual for bread, wine, milk, and other commodities to be horribly adulterated. These facts emerge clearly from the chapter on "Food Additives" in the most interesting of the books reviewed here, Harold McGee's *On Food and Cooking – The Science and Lore of the Kitchen*. The book is sturdily bound, although regrettably printed on paper of indifferent quality. It is easily the best of this genre, not only because of the wealth of information provided but also in the arrangement of the material and the thoroughness and soundness of the treatment. It contains a brief introduction followed by Part I, "Foods" (500 pp.), then two shorter parts on "Food and the Body" and "The Principles of Cooking". The first and main part is divided into ten chapters dealing with different types of foods. For example, under "Milk and Milk Products" we learn about the importance of milk in the Bible, and the chemical background relating to casein, whey, cream, and joghurt. On cheese too we find much historical information, but also there are electromicrographs showing its structure and answers to such questions as why mozzarella contains long fibers and why wine is used in making fondue. The chapter on "Eggs" not only answers the perennial question "Which came first, the chicken or the egg?" but also gives a lucid explanation of the very complex chemistry of the cooking of eggs.

History plays an important role throughout McGee's book, and we find this again in the chapters on meat. Domestication of animals, the consumption of meat, the relationship between structure and quality, and the processes of slaughtering, maturing, boiling, and roasting are all treated thoroughly. Here it becomes apparent that the author is an American, as the "cuts" of meat (sirloin, rib, etc.) are quite different from those in Germany. The chapter on "Fruit and Vegetables" mentions many geographical and geohistorical aspects, but also covers topics such as cell structure and the formula of chlorophyll. Here, however, I have to make one of my very few critical comments, as the formulas are poorly drawn, and remind one of the elongated benzene hexagons in old German chemistry textbooks. However, we go on to more excellent stuff, with occasional historical anecdotes such as that concerning the work of Szent-Györgi on vitamin C, and the publication in 1910 of the observations that bananas ripen faster when stored next to oranges and that various green fruits turn red more quickly when near a kerosene stove. Although we now know that these effects are caused by ethylene, its mode of action is still not fully understood.

Everyone knows that eating asparagus causes one's urine to smell foul, and it has long been known that this is due to methyl mercaptan formed by the degradation of methionine. However, until 1960 it was thought that the variation in perception of the intensity of the odor from one individual to another was caused by genetic differences in metabolization. However, we now know that all humans have similar amounts of methyl mercaptan in their urine after eating asparagus, but their perception of it differs widely due to partial anosmia. In the chapter on "Cereals and Nuts" we learn that in "parboiled" rice the vitamin B is completely retained, as the process causes it to move from the husk into the grain itself. Under "Bread" we find much information about baking. The microbiology of the sour dough is discussed in great detail, whereas the history of the noodle is recounted poetically. There is a long chapter on "Sauces". We read about Antoine Carême (1784–1833), who was the greatest cook of his day and invented the excellent sauces or gravies based on meat juices and roux (lightly fried and browned flour), and about Escoffier who by 1910 had a reper-

This section contains book reviews and a list of new books received by the editor. Book reviews are written by invitation from the editor. Suggestions for books to be reviewed and for book reviewers are welcome. Publishers should send brochures or (better) books to the Redaktion Angewandte Chemie, Postfach 101161, D-69451 Weinheim, Federal Republic of Germany. The editor reserves the right of selecting which books will be reviewed. Uninvited books not chosen for review will not be returned.

 © VCH Verlagsgesellschaft mbH, D-69451 Weinheim, 1996 0570-0833/96/3513-1575 $ 15.00+.25/0

toire of about 200 sauces. The action of starch in thickening sauces is explained with simple but informative diagrams showing the hydrogen-bonding of the amylose component. The other group of sauces is based not on starch but on water-in-oil or oil-in-water emulsions stabilized by the lecithin present in egg-yolk or by cholesterol as emulsifying agents. There are detailed references to a debate which took place between 1977 and 1979 in the pages of *Nature* and the *New England Journal of Medicine* on the multiphase colloidal system in sauce béarnaise.

In the chapter on sugar and chocolate the author clears up the widespread misconception that honey, unlike sugar, is "natural" and "healthy". The amounts of vitamins and minerals in honey are negligibly small! Also so-called "raw sugar", or more accurately brown sugar, is not an unrefined and therefore more natural product, but is normal white sugar onto which a film of molasses has been sprayed. With regard to chocolate we learn that the name "praline", dating from about 1650, originates from that of the Duke of Plessis-Praslins, an army commander under Louis XIII and Louis XIV.

In the chapter on wine, beer, and spirits we have some real chemistry. The process of fermentation is treated rather briefly but in a way that is easily understandable by non-chemists. Distillation, a basic operation in chemistry, is then described. However, the formulas given for the various alcohols (p. 486) are not well drawn. Under beer the author mentions the Bavarian purity regulations of 1516 and also the absurdity of the American "light beers", commenting on the latter that "the more closely the beer resembles water the more of it one can drink". On the other hand, Dickens and Hogarth are quoted with regard to the effects of gin.

In Part 2, "Food and the Body", the author describes how, encouraged by advertising and all types of media, people nowadays pay out millions for "organic" and "macrobiotic" foods, for "energy-giving" vitamins, and for special fiber supplements. According to McGee, it is very difficult to persuade people against this kind of nonsense, even though a simple and varied diet tastefully and carefully prepared from good raw food products, enjoyed in moderation, would make all this charlatanism unnecessary.

Part 3 is a comprehensive account of the basic principles of food science. The chemistry and physics of water is clearly explained, including its special characteristics such as the density anomaly and its high specific heat. In discussing carbohydrates the roles of amylose and amylopectin are well described, and the author explains why we differ from many animals in being unable to feed on hay or wood. Under proteins the main emphasis is on their denaturation by the action of salts, acids, or heating. Some important properties of fats are discussed, starting from the structure of the triglycerides. For example, it is explained why cocoa butter, in contrast to all other fats, has a clearly defined melting point, and what causes fats to go rancid.

There is an appendix of a few pages in which some basic principles of chemistry such as atomic models, the Periodic System, bond strengths, and crystal lattices are explained. This seems rather inappropriate and is not really necessary. It is superfluous for the scientist reader, whereas the non-scientist will be unable to make much use of it. The book ends with a very well set out and comprehensive bibliography. Apart from the minor reservations mentioned above the book deserves the highest praise. It contains a clear, competent, thorough, and factual account of all that is worth knowing about this fascinating subject, enlivened by historical information and by simple but informative illustrations. I look forward to the appearance soon of a new edition and, hopefully, a German translation, followed by a wide circulation among all who are interested in cooking.

A few years after the above book the same author wrote *The Curious Cook – More Kitchen Science and Lore*, a very sparsely illustrated paperback forming a kind of supplement to the former book. Its structure follows the pattern of its larger predecessor with three parts, each divided into chapters. Part 1 is called "Playing with Food: Experiments", and begins with a chapter entitled "The Searing Truth". This is a very illuminating description of how one can fry a steak under various experimental conditions such that the juice of the meat does not escape. In precise detail the author dismisses the myth that quick frying on one side "seals the pores" and causes the juice to stay in. This is followed by an examination of why it is that during the frying the fine droplets of oil condense of the *inner* surface of the cook's glasses; the answer is related to the geometry of their trajectories.

The interesting chapter "Green and Brown" explains the well-known but puzzling observations that leaves of basil turn brown so quickly, and why sprinkling vinegar and oil onto lettuce makes it wilt much quicker than it otherwise would. With regard to white butter sauce (beurre blanc) scientific investigations have been carried out to determine the exact ratio of fat to water. It is explained, with reference also to historical precedents, why one cannot use margarine instead of butter for this purpose. In the chapter on fruit ices the author discusses the lowering of the freezing point and the sugar and acid content of fruits. He gives very complicated formulas (not meant to be taken too seriously) for determining the acidity and adjusting it by adding lemon juice; the results must, of course, be evaluated with the help of a computer! We learn that lemons have the lowest ratio of sugar to acid (0.2) and pears have the highest (110). Recipes are given for many different types of ice-cream, including such enticing and exotic kinds as rose ice or avocado-and-pineapple ice. Part 1 ends with a chapter on "The Pleasures of Merely Measuring" which addresses such important problems as how to avoid having the soup burn one's tongue (one has to measure the rate of cooling as a function of viscosity and rate of stirring).

Part 2, "Making the Good Life Better", includes much discussion of the connection between fats and heart disease and of carcinogens in food. The worries about cholesterol, which are especially prevalent in the USA, are put into perspective. The chapter on food and cancer is fascinating. It is emphasized here that grilling meat over wood charcoal, which is nowadays so popular, generates large quantities of carcinogens. The incidence of cancer is certainly very dependent on eating habits. For example, the incidence of intestinal and breast cancer is below average in Japan and among members of certain churches and religious sects in the USA. Bruce Ames, the famous biochemist who has developed well-known tests for carcinogens, claims that with a normal diet one's daily intake of "natural pesticides" present in plants is in the order of grams, about 10^4 times more than the traces of synthetic pesticides we receive! Nevertheless, one should not be afraid to eat fruit or mushrooms. On the whole nature balances things out very well. Cancer can result from changes in the DNA caused by certain compounds such as polycyclic aromatic hydrocarbons, which are present not only in barbecue smoke (and, of course, tobacco smoke), but also in toast and in caramel. However, the body has an inbuilt ability to neutralize such toxins by metabolization. Thus a "cancer-causing" menu made up of beef gravy, grilled steak, and mushrooms can be "detoxified" if it is accompanied by Brussels sprouts, brown rice, a salad with garlic, and apple pie.

 © VCH Verlagsgesellschaft mbH, D-69451 Weinheim, 1996 0570-0833/96/3513-1576 $ 15.00+.25/0

Part 3 seems rather unrelated to the foregoing. However, in the last chapter we again find some useful information under the title "From Raw to Cooked: The Transformation of Flavor". Here we find a discussion of the Maillard reaction, which is difficult to understand even for specialists, but the chapter also deals with aroma-bearing substances such as heterocyclic oxygen, sulfur, and nitrogen compounds. This book can be thoroughly recommended for everyone who wishes to know as much as possible about the processes such as boiling, roasting, and many others that are used in food preparation.

The first of the books by Hervé This is *Les secrets de la casserole*, published in 1993. It is very nicely produced with many instructive illustrations and pretty decorative panels on a pale gray background. The introduction of about 30 pages deals with the main physical and chemical principles involved in food preparation, discusses the relationship between cooking and science, describes the physiology of taste, and considers how color and aroma are related to taste. We learn much that is interesting here, such as why peeled apples quickly turn brown and why lobster meat turns red when boiled.

The main part of the book consists of more than 30 sections of about five pages each, dealing with different foodstuffs such as milk, eggs, meat, vegetables, fruit, bread, etc., and with the various methods of preparation such as boiling, roasting, grilling, and frittering. Each section is subdivided under headings such as "Pineapples which make the food tender", or "Meat from its initial hanging to becoming rotten", or more often under interestingly phrased questions that are then answered briefly or at some length. Examples are: "Why does the crust of the loaf have more flavor than the inside?", "Why is human milk more easily digestible than cows' milk?", "How much mayonnaise can be made from one egg-yolk?", "Why should cauliflower not be boiled too long?", "Why does every little bean produce a little sound?" The answer to the latter question is that beans contain raffinose, a trisaccharide made up of fructose, glucose, and galactose; the last of these passes through the stomach without being absorbed and is digested only in the small intestine by *E. coli*, which breaks it down into carbon dioxide, methane, and hydrogen. Other questions: "Is béarnaise a warm mayonnaise?", "Why must roux be cooked for a long time?", "Why should dough be left to stand?". The answers to all these are expressed clearly, succinctly, and in a form that impresses itself on one's memory, and are illustrated by good diagrams.

In the chapter on wines their evaluation by eye, nose, and tongue is described in clear and thorough detail, as one would naturally expect of a French author. The chemist's attempts at "improving" wines are also discussed. If the wine is too light one can add ethanol. A lack of flavor may be remedied by adding a little vanilla essence or cassis (blackcurrant extract). A wine of recent origin can be "aged" by adding port, and a "vin ordinaire" can be moved a little closer to Bordeaux, as it were, by adding minute quantities of 1-octanol and 3-isobutyl-2-methoxypyrazine. Also the awkward question of why alcohol makes one intoxicated is not avoided. In conclusion the author draws attention to some questions for which there is as yet no answer, and invites his readers to help. For example, why can a mixture of oil and butter be heated to a higher temperature than butter alone? How can apple-juice be prevented from turning dark? Why must one not leave parsley in a marinade for a day or two? Is it true that putting a teaspoon in the neck of a champagne bottle helps to retain its fizz, even after standing for a long time, and if so why? Finally a good index completes this very enjoyable and readable book.

The most recent of these books, *Révélations gastronomiques*, is a particularly handsome work. Like the book described above it is well printed on high quality paper with an excellent binding. Both the chemist who enjoys cooking for pleasure and the cooking enthusiast with an interest in chemistry will find here something quite special, with 55 first-class recipes. It begins with a general introduction and a chapter on good kitchen equipment, in which both the text and the illustrations are very informative. These are followed by five longer chapters containing detailed descriptions of the recipes, each in a separate section with its own logo. The chapters deal separately with aperitifs (5 recipes), starter dishes (16), fish and shellfish (6), meat dishes (13), and desserts (15). Each recipe is treated in five to six pages, beginning with an appropriate vignette, followed by the main title, a suitable quotation from Brillat-Savarin, Verlaine, Racine or some other writer, then a paragraph of introduction giving the ingredients in precise detail, with visual highlighting for clarity. In many cookbooks one finds that the quantities are given with variable and inconsistent precision which makes little sense, as for example in: "take 110 g of flour, 85 g of sugar, and 3 eggs". What exactly does "3 eggs" mean? In contrast, Hervé This keeps consistent precision throughout, as in the experimental section of a report in *Liebigs Annalen* or *Helvetica Chimica Acta*.

The operations are then described in separate steps, varying from 5 to 15 according to the degree of difficulty. Each of these subsections consists of a few lines of clear instructions and a longer commentary, often with diagrams or photographs, describing the chemical processes. All this is presented in a relaxed and witty style. For example, in the recipe for preparing dough we find: "Mix 10 g of yeast with a teaspoonful of sugar and 30 cL of lukewarm water and allow the mixture to stand for a quarter of an hour. – The cube of yeast that you have bought from your baker for a small sum consists of a large number of microorganisms called yeast cells. In the presence of sugar and water these yeast cells begin to develop, multiply themselves by cell division, and release CO_2 which causes the dough to rise. The yeast cells are most active at temperatures of 25–35 °C. If they are too cold their biological machine works more slowly, like that of hibernating marmots in winter. On the other hand, if they are too hot they risk dying. Bear in mind that the yeast cells are not greatly different from the cells that make up your body."

On the whole the recipes are demanding enough to satisfy the enthusiastic amateur cook, but are nevertheless described in sufficient detail to ensure that those with less experience will also succeed. Moreover, they are quite delectable ... goose liver with grapes and apples, poached trout with white butter sauce, roast quail with potato purée, pears with sabayon of Gewürztraminer ...

This excellent book ends with a four-page epilog, an index, and a bibliography. The epilog might be given the rather pompous title "A philosphical view of the art of cooking past and present, in the context of the interaction of art, craft, and science". The essential message of Hervé This is that we should use the opportunity now offered to us by science and technology to reach a better understanding of cooking, so as to do it even better and to increase our enjoyment of life. I have nothing to add to that.

Peter Weyerstahl
Institut für Organische Chemie
der Technischen Universität Berlin
(Germany)

 © VCH Verlagsgesellschaft mbH, D-69451 Weinheim, 1996 0570-0833/96/3513-1577 $ 15.00+.25/0

Encyclopedia of Molecular Biology and Molecular Medicine. Vol. 1. Edited by *R. A. Meyers*. VCH Verlagsgesellschaft, Weinheim, 1996. 462 pp., hardcover DM 460.00 (single vol.)/DM 2550.00 (set).–ISBN 3-527-28471-0/ISBN 3-527-28478-8 (set)

Is there something in molecular biology that you have always wanted to know? Are you familiar with the Achilles cleavage? No? Then do you know of the importance of the plant *Arabidopsis thaliana* in genome research, or of the worm *Caenorhabditis elegans* in the physiology of development? Or would you like to learn more about these two organisms? Are you looking for a quick up-to-date overview of the molecular biological aspects of Alzheimer's disease, of recent developments in the area of therapeutic treatments for AIDS and antisense oligonucleotides, or of chirality?

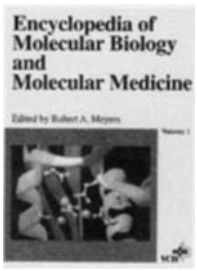

You might go to your library and search, search, search. Or instead you might simply reach for the *Encyclopedia of Molecular Biology and Molecular Medicine* by Robert A. Meyers. Volume 1 of this six-volume work has now appeared, and contains many detailed and expertly written review articles on topics such as those mentioned above. The editorial committee contains many eminent names including seven Nobel laureates (W. Arber, E. J. Corey, R. Huber, A. Klug, L. Pauling†, B. Samuelsson, P. Sharp), and the list of authors of individual articles resembles a hall of fame of modern molecular biology. Consequently the quality of the contributions is everything that one could wish for. Each article contains very useful cross-references to related topics.

In this first volume (A to C) there is a strong emphasis on the fields of molecular biology and genome research. However, all the other related topics within this area are covered under their general headings. Volume 1 contains relatively few articles on molecular medicine, but a glance at the publishers' list of all the keywords covered shows that this is just an accidental consequence of the alphabetical arrangement of topics. Diabetes, Drug Addiction, Drug Synthesis, Drug Targeting, etc. will appear in Volume 2. The literature references given in the individual articles are restricted to a few important ones, and are quite recent in most cases, extending up to 1993 and 1994, and in a few instances even to 1995. With regard to the degree of up-to-dateness it must be borne in mind that the publishers have set themselves the very ambitious goal of completing the six-volume work, with over 300 articles, within one year. Thus, for example, we only have to wait until autumn 1996 for the currently highly topical keyword "Prions", and "Zinc Fingers" will appear in January 1997. The publication of the whole work within a short space of time means that all the articles will be approximately contemporaneous in their coverage, a great advantage in a field that is developing so rapidly.

A work as large as this covering such a wide range of subjects cannot be expected to be absolutely perfect when first published. Nevertheless, it is pleasing to note that errors are comparatively rare. One can excuse the few inconsistencies in formulas (examples: arginine on the inside front cover; NH-*i*Pr instead of NH-*t*Bu in Ro 31-3959, Fig. 5, p. 39–cf. also p. 17; L-Tyr instead of L-Trp in formula 45 on p. 58; missing double bonds in the indoles in Fig. 12, p. 200) and some printing errors in compound names (e.g., "sequinavir" instead of saquinavir on p. 18, and "benzpyrine" instead of benzpyrene on p. 437). The article on Bioorganic Chemistry contains many errors; for example the formulas in Figure 7a on page 164 (explanation of hydrogen-bonding) and in Figure 12 on page 168 (natural substrate, enalapril) contain serious errors, and on pages 168 and 169 (Fig. 13) it is incorrectly stated that acetylsalicylic acid reacts irreversibly with an amino group of the enzyme cyclooxygenase (this should instead be the hydroxy group of Ser-530 in cyclooxygenase). Many structural formulas, such as those of the amino-acids shown on the front jacket flap, are drawn in a rather outdated style, and unfortunately without indicating their stereochemistry. Also, to make it easier to find subject headings in the series later on, it would have been useful to print the letters range A-C on the spine of the volume in addition to "Volume 1". At the price of DM 460 for Volume 1 (or the subscription price of DM 2550 for the entire work, valid until June 30, 1996) the encyclopedia is by no means cheap, but it seems not unreasonable for a work of this size and quality. Within its 462 closely printed large-format pages this first volume contains an enormous wealth of information. A good indication of how useful and interesting the contents are is the fact that after studying it for a short time I was reluctant to put it down; also that I now feel an urgent need for the other five volumes. The rather indifferent quality of the paper seems inappropriate for a book of this price, as also does the annoying practice (now increasingly common with many publishers) of placing all the color figures together in the middle of the book, in this case 13 figures on eight pages. Admittedly this reduces the cost of production, but in a work of this magnitude the small difference would hardly have mattered.

Up to now the *Encyclopedia of Molecular Biology and Molecular Medicine* has no rival to compete with it. It should appeal to a very wide readership, who will find it not only interesting and informative but also an indispensable aid in their everyday work. Chemists, biochemists, molecular biologists, pharmacologists, toxicologists, biologists, geneticists, and medical scientists should all have access to this encyclopedia, as also should everyone whose work is concerned with the molecular basis of diseases or with drug research, whether in universities or in the pharmaceutical industry. I have no hesitation in recommending that one should buy it.

Hugo Kubinyi
BASF AG Ludwigshafen (Germany)

Active Metals. Preparation, Characterization, Applications. Edited by *A. Fürstner*. VCH Verlagsgesellschaft, Weinheim/New York, 1996. 464 pp., hardcover $ 155.00—ISBN 3-527-29207-1

Metals and their derivatives are indispensable auxiliaries in preparative chemistry and catalysis. The book *Active Metals*, edited by Alois Fürstner, contains many examples of organic reactions in which the key step—electron transfer and reduction, cleavage or formation of a chemical bond—is only made possible by the aid of a metal species. Among the various coupling processes that are metal-promoted, special attention has been paid to those of the McMurry type which are immensely useful in organic synthesis; details of their mechanism are presented, as well as their recent applications to the preparation of diols, alkenes, 1,5-dienes and bibenzyls, with emphasis on the large ring and natural products. Not surprisingly we find many examples in this book where the reactions of metals with organic substrates, especially the halides, lead to the formation of well-defined organometallics which are themselves valuable tools in synthetic chemistry. In this context, the preparation and applications of allylic barium reagents and functionalized

 © VCH Verlagsgesellschaft mbH, D-69451 Weinheim, 1996 0570-0833/96/3513-1578 $ 15.00+.25/0

organozinc reagents are treated in more detail. The former, which can be generated stereospecifically, react with a variety of electrophiles with remarkable regio- and stereoselectivity. Organozinc reagents, which have been neglected for a long time because of their low reactivity, can be transformed by transmetallation into unique polyfunctional copper, palladium, or titanium intermediates which, here again, undergo highly selective reactions and are quite interesting in assymetric synthesis.

Active Metals, because of the diversity and wide scope of the reagents and applications described, offers a good entry into the study of organic synthesis by means of metal species, and should convince the reader, if still necessary, of their major importance. It will also satisfy the specialist who will certainly find new information and ideas regarding many transformations. Although obviously not exhaustive—that is not the aim of the monograph—the list of reagents and reactions includes beautiful examples of what is possible by using properly synthesized and defined materials. In fact, it is often a problem for the chemist to control the preparative tricks for obtaining suitable and efficient reagents which will induce successful and reproducible reactions. Undoubtedly, Fürstner's book is without precedent in providing the complete and detailed procedures enabling the chemist to prepare and use active metals. The more conventional route to these is the chemical reduction of metal salts, which can be accomplished by several methods, using alkali metals, manganese-anthracene or magnesium hydride, hydrotriorganoborates, and also electrolysis. Another approach is the physical dispersion of the element, by ultrasonically induced activation or metal evaporation. The principles of each method are clearly presented, as well as the scope and limitations of the different procedures. The details of typical experiments are provided, with essential informations on the handling of specific chemicals, equipment and apparatus.

The active metals thus obtained exist in a variety of physical forms—ultrafine powders, clusters or colloids, intermetallics and alloys—depending, for each preparative method, upon the experimental conditions. Clearly, the symbol M* does not represent a simple real species; moreover, an active metal is often a "living" material which undergoes variations in its physical properties and is not stable enough to be stored indefinitely. These difficulties can be circumvented by immobilizing the active metal on a support. In addition to the improved stability and ease of use, supported metals, especially the metal – graphite combinations, give higher efficiency and selectivity, due to the synergism between the reagent and its carrier. Metal colloids can also be stabilized by tetraalkylammonium or phosphonium salts. It is evident that a reaction will follow a different course depending on the morphology, bulk density, and grain or particle size of the so-called M* species. The contributors to the monograph are leading experts in their special fields, some dealing mainly with the characterization and others with the synthetic applications of the active metals; their diverse approaches brought together in this book are an example of the value and necessity of interdisciplinary studies. Indeed, further significant progress in metal-induced reactions will become possible when the phenomenon of activation and the relationship between the structure of the metal and its reactivity are better understood. The first exciting achievements in this direction open up promising perspectives. Our knowledge of the factors influencing particle growth and the clustering process has been much improved. The characterization of the materials is becoming more accurate, facilitated by the development of suitable techniques (X-ray diffraction and absorption, electron microscopy, scanning tunneling microscopy, and atomic force microscopy), as shown by the elucidation of the morphology of metal – graphite compounds. These studies will attract the attention not only of organic and inorganic chemists but also of materials scientists, who are likely to be interested by the unusual physical properties of these nanostructured materials, such as superparamagnetism. Here again, interdisciplinary collaboration is highly desirable.

Because it is a unique guide to many experiments and an enormous source of valuable information, *Active Metals* should be at the disposal of everyone in a preparative chemistry laboratory. Moreover, as well as practical details and up-to-date references, the book is teeming with stimulating ideas, a lot of new facts and problems that must be known and shared for taking up numerous challenges in various fields of chemistry. I believe that *Active Metals* will have historical importance, since it makes the chemist want to get work in the laboratory and helps him or her to build the science of tomorrow.

Michel Ephritikhine
Service de Chimie Moléculaire
CEA Saclay
Gif-Sur-Yvette Cedex (France)

 © *VCH Verlagsgesellschaft mbH, D-69451 Weinheim, 1996* *0570-0833/96/3513-1579 $ 15.00+.25/0*

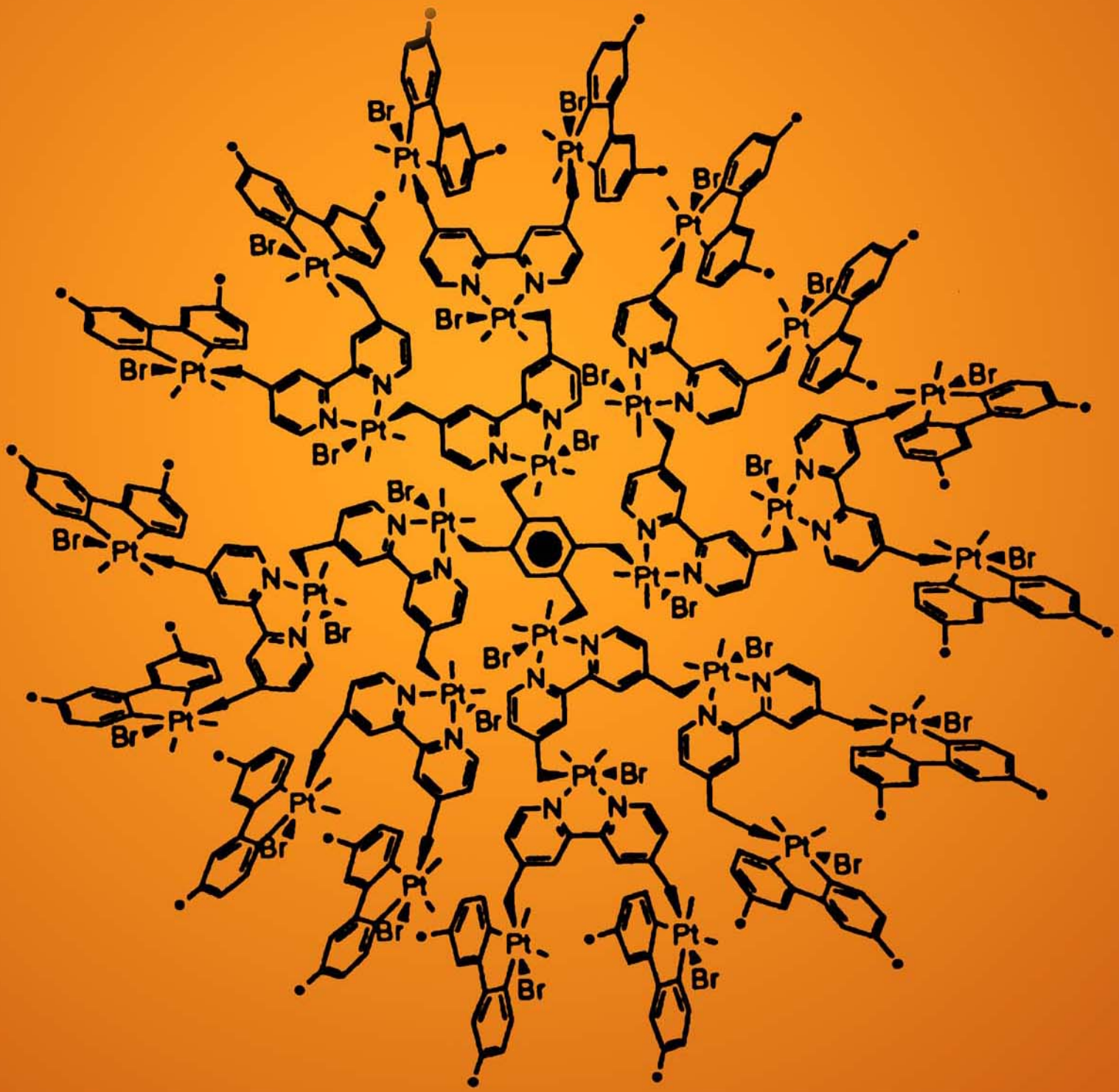

Many fascinating inorganic polymers including dendrimers such as the organoplatinum complex shown here have been recently synthesized

Polymers and the Periodic Table: Recent Developments in Inorganic Polymer Science

Ian Manners*

Dedicated to the memory of Daisy Maud Manners

Polysiloxanes $[-R_2Si-O-]_n$, polyphosphazenes $[-R_2P=N-]_n$, and polysilanes $[-R_2Si-]_n$ illustrate that the incorporation of inorganic elements into a polymer main chain can lead to useful properties. These include low temperature flexibility, high thermal and oxidative stability, flame retardancy, novel forms of chemical reactivity, and intriguing electrical and optical characteristics arising from unusual electronic effects such as the delocalization of σ electrons. However, until recently, the development of inorganic polymer science has been held back by the synthetic problem of finding ways to join atoms of inorganic elements together into long chains. This review surveys many of the exciting advances in the field of inorganic polymers over the past decade and focuses mainly on the new inorganic polymer systems that have been prepared during this period. These include random-network polysilynes, poly(carbophosphazene)s, sulfur–nitrogen phosphorus polymers, poly(organooxothiazene)s, and, very recently, the first examples of polystannanes that possess a main chain of tin atoms. Transition metal based polymer science has also experienced a number of synthetic breakthroughs and new materials include high molecular weight metallocene-based polymers, polymetallaynes incorporating elements such as iron, nickel, and rhodium, liquid crystalline organocobalt and organochromium polymers, and lanthanide-based polymers.

Keywords: inorganic polymers · liquid crystals · main group elements · semiconductors · transition metals

1. Introduction

Despite the fact that carbon is not a particularly abundant terrestrial element, carbon-based or "organic" macromolecules form the basis of life on our planet, and natural or synthetic macromolecules based on carbon chains fill the world around us.[1, 2] Organic polymers are used as plastics and elastomers, films, and fibers in areas as diverse as clothing, car tires, compact discs, packaging materials, and prostheses.[2] Moreover, exciting new applications in electroluminescent and integrated optic devices and sensors are also now under development.[3] The massive growth in the use of organic polymeric materials in the past 50 years can mainly be attributed to their ease of preparation, lightweight nature, and unique ease of fabrication. Their ease of preparation is a consequence of not only the advanced state of organic synthesis, which reflects both the intrinsic logic of this subject and the creativity of scientists interested in the area, but is also due to the accessibility of cheap petroleum-derived monomers.[2]

In contrast to organic chemistry, the chemistry of inorganic elements is generally at a much more primitive state of development. Even seemingly simple small molecules can be surprisingly elusive,[4] and the development of routes to long polymer chains constructed mainly or entirely from inorganic elements has been a particular challenge.

2. The Construction of Long Inorganic Chains: A Synthetic Problem

One might anticipate that application of the techniques that have worked so well for the preparation of organic polymers would allow similarly facile access to inorganic macromolecules. However, consideration of the main synthetic routes to organic polymers (Scheme 1) illustrates the problems associated with this approach. Traditional synthetic protocols that involve a chain-growth mechanism such as addition polymerization (Scheme 1, Route A) are very difficult to use for inorganic polymer synthesis, since suitably reactive but stable multiple bonds involving inorganic elements are generally difficult to prepare. In contrast to the situation for unsaturated organic molecules (α-olefins, acetylenes, nitriles, etc.), the isolation of stable species with multiple bonds between inorganic elements usually requires the presence of sterically demanding, oligomerization-inhibiting ancillary groups.[5] Most of the early attempts to prepare inorganic polymers focused on the use of polycondensations (Scheme 1, Route B). These step-growth routes work well

[*] Prof. I. Manners
Department of Chemistry, University of Toronto
80 St. George Street, Toronto, ON (Canada)
Fax: Int. code + (416)978-8775
e-mail: imanners@alchemy.chem.utoronto.ca

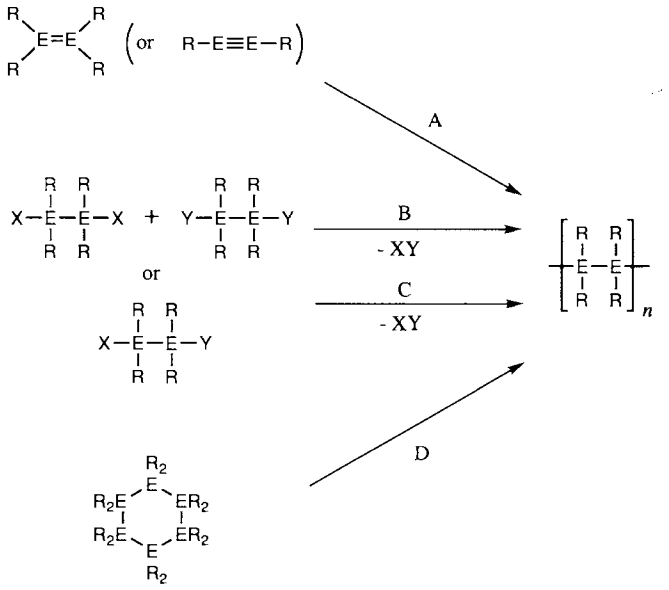

Scheme 1. Syntheses of inorganic polymers (E = inorganic element).

for the synthesis of carbon-based polymers when difunctional organic monomers are used because such species are generally easily accessible in a high degree of purity.[6] This allows the stringent stoichiometry and conversion requirements which need to be fulfilled for the formation of high molecular weight condensation polymers to be satisfied.[7] However, inorganic functional group chemistry is poorly developed and difunctional inorganic monomers (dilithiated species, for example) are often so reactive that they are difficult to prepare and purify. Thus, exact reactant stoichiometries for polycondensation reactions cannot be achieved.[7] This generally results in the formation of low molecular weight oligomeric products, which are well below the critical molar mass (typically M_n = ca. 10000) needed to obtain the necessary interchain entanglement and materials mechanical strength for fabrication into free-standing films, fibers etc. The advantageous processability characteristics associated with macromolecules, which generally constitute the major motivation for making polymers in the first place, cannot therefore be realized.[8] A very promising variant on this type of condensation polymerization is to use monomers that possess groups X and Y, which can be eliminated from the same molecule (Scheme 1, Route C). This circumvents the need for careful control of reaction stoichiometry and, in certain cases, polymerization of monomers of this type can follow a chain-growth-type mechanism, which leads to polymers with high molecular weights much more naturally.[6] Another chain-growth approach that appears very promising is ring-opening polymerization (ROP) (Scheme 1, Route D). Inorganic ring chemistry is very well-developed and thus many potential ROP monomers are available.[9]

As a result of the synthetic difficulties, until recently only three well-characterized inorganic polymer systems existed: polysiloxanes or "silicones" **1**, polyphosphazenes **2**, and polysilanes **3**.[10] Significantly, these materials all possess remarkable properties, which differ substantially from those of conventional organic macromolecules.

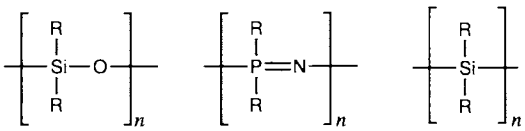

1 **2** **3**

This review aims to provide an overview of the current status of inorganic polymer science[10–14] and will focus mainly on recent developments in the field with particular attention given to the new, well-characterized polymer systems prepared in the last 10 years. Excellent reviews and books have been published that describe the synthesis, properties, applications, and technology of polysiloxanes, polyphosphazenes, and polysilanes in detail. In this article, the main features of these three well-established polymer systems are briefly summarized, as their unique properties help provide the motivation for the further expansion of inorganic polymer science to elements other than Si, P, O, and N in the periodic table. Recent developments concerning new classes of inorganic polymers based on main group elements and transition metals are then described.

Ian Manners was born in London, England in 1961. He received his BSc degree in Chemistry in 1982 at the University of Bristol where he also completed his PhD (in 1985) with Professor Neil Connelly on organotransition metal radicals. From 1986–87 he was a Royal Society European Postdoctoral Fellow at the RWTH, Aachen, Germany working with Professor Peter Paetzold on the chemistry of iminoboranes. Following work as a Research Associate on polyphosphazenes and poly(heterophosphazene)s with Professor Harry R. Allcock at the Pennsylvania State University, USA, he joined the Faculty at the Department of Chemistry, University of Toronto, Canada in July 1990. He became an Associate Professor in 1994 and a Full Professor in 1995 and he is currently a Fellow of the Alfred P. Sloan Foundation (1994–1996) and is the recent recipient of the Rutherford Memorial Medal in Chemistry (1996). His research interests focus on the synthesis, properties, and applications of novel inorganic molecules, polymers, and solid-state materials. He is the author or coauthor of over 120 publications and holds or coholds five patents.

3. Well-Established Inorganic Polymer Systems

3.1. Polysiloxanes or Silicones

Polysiloxanes, which were first developed in the 1930s and 1940s, currently represent the most commercially important inorganic polymer system and comprise a billion dollar global industry.[15,16] Indeed, these materials are now often regarded as commodity polymers rather than specialty products. The main methods of synthesis involve condensation and anion- or cation-induced ring-opening routes and these are illustrated for the synthesis of the most common siloxane polymer, poly(dimethylsiloxane) (**4**) [Eqs. (1) and (2)]. The starting materials

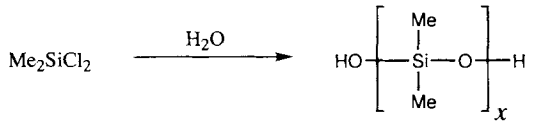

(1)

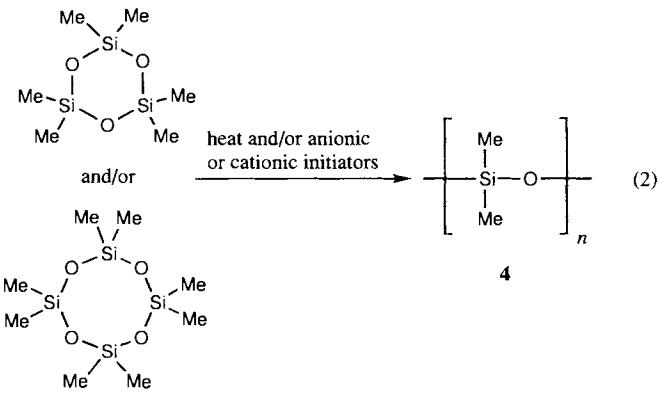

(2)

are organodichlorosilanes of which the most common, Me_2SiCl_2, is readily available by the Rochow–Müller process. The cyclic starting materials used in the ROP route are available by controlled hydrolysis of the corresponding organodichlorosilane.

The exceptional properties of polysiloxanes are a direct result of their inorganic backbone of silicon and oxygen atoms and have resulted in their widespread use as high performance elastomers and fluids, surface modifiers, adhesives, and biomedical materials.[10,15–18] The siloxane backbone, which contains long Si–O bonds (1.64 Å compared to 1.54 Å for a C–C bond), the absence of substituents on every other skeletal atom (oxygen), and a wide bond angle at oxygen (Si-O-Si 143° compared to C-C-C 109°), possesses unique dynamic flexibility. This leads to materials that retain elasticity and do not become brittle even at very low temperatures. For example, poly(dimethylsiloxane), the most common polymer, has a glass transition temperature (T_g) of −123 °C, and for poly(methylhydrosiloxane) the T_g value is even lower (−137 °C). In addition, Si–O bonds are stronger than C–C bonds (bond energies: Si–O ca. 450 kJ mol^{-1}, C–C ca. 348 kJ mol^{-1}) and are more stable to oxidation and UV radiation. This results in higher thermooxidative stability and leads, for example, to the use of polysiloxanes in oil baths found in most chemical laboratories. Poly(dimethylsiloxane) crystallizes at T_m = −40 °C, and for many elastomer applications the introduction of a small percentage of phenyl substituents by random copolymerization is necessary to ensure amorphous character. Crosslinking for elastomer applications can be achieved by a variety of techniques including heating with peroxides or vulcanization at room temperature by which crosslinking can be induced by the transition metal catalyzed hydrosilylations between vinyl substituents and Si–H groups introduced along the polymer chain. In general, the addition of reinforcing agents or fillers such as high surface area silica is also necessary to improve mechanical properties.[10]

Polysiloxanes also have a variety of other useful properties such as hydrophobicity and their exceptionally high permeability to gases. Indeed, snails can live submerged beneath the surface of low molecular weight poly(dimethylsiloxane) fluids for up to 72 h by breathing oxygen that diffuses through the material.[17] Other applications in the biomedical field that take advantage of the high permeability of polysiloxanes include uses as soft contact lenses and artificial skin. However, the leakage of silicone-based materials through polysiloxane membranes in breast implants has raised considerable public concern. Nevertheless, claims of health problems arising from the consequential presence of silicones in the body appear unproven to date.[18]

Although poly(dimethylsiloxane) is the most well-studied example, a wide variety of other polysiloxanes with aliphatic or aromatic side groups are known and these are accessible either by condensation or by cationic- or anionically-induced ROP routes. These other polysiloxanes also have very interesting properties and many have been the subjects of recent studies. For example, the morphology of simple high molecular weight (M_w = ca. 10^5–10^6) *n*-alkyl-substituted polysiloxanes that are available by ROP has been studied in detail.[19] Many, such as poly(di-*n*-pentylsiloxane), poly(di-*n*-hexylsiloxane), and poly(di-*n*-decyl)siloxane, are liquid crystalline and each forms a disordered mesophase. Polysiloxanes with fluoroalkyl substituents (e.g. trifluoropropyl), also known as fluorosilicones, possess novel surface properties and are technologically important with a range of applications.[17] The living anionic ROP of strained cyclic siloxanes such as $(Me_2SiO)_3$ is also important as this permits access to block copolymers with organic monomers.[20]

A very versatile methodology for controlling the properties of polysiloxanes involves hydrosilylation [Eq. (3)]. Reaction of

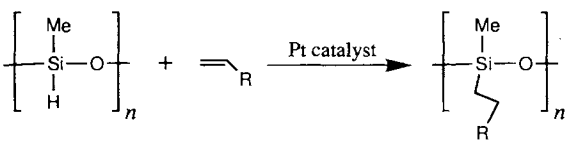

(3)

poly(methylhydrosiloxane) or poly(methylhydrosiloxane)–poly(dimethylsiloxane) copolymers with vinyl-capped species allows the introduction of side groups that give rise to a variety of interesting properties.[21,22]

For example, ferroelectric side-chain liquid crystalline polysiloxanes **5** with short switching times have recently been reported.[23] Another exciting recent development involves the

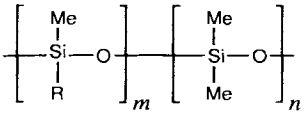

5

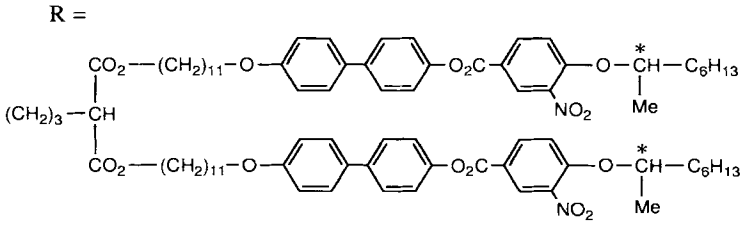

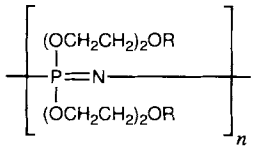

7

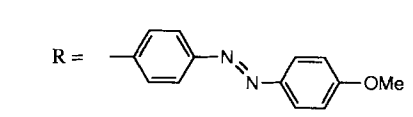

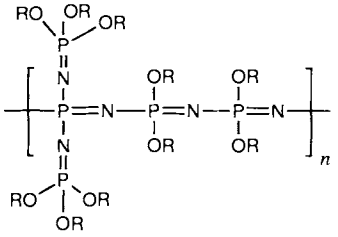

8

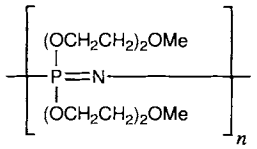

9

use of polysiloxanes functionalized with polar cyanopropyl and crosslinkable methacryloxypropyl groups as the matrices of Na^+ sensing membranes for chemically modified field-effect transistors (CHEMFETs).[24] The advantages of polysiloxanes for this type of application revolve around their high diffusion and permeability coefficients.

3.2. Polyphosphazenes

Polyphosphazenes **2** have a phosphorus–nitrogen backbone. The first example, poly(dichlorophosphazene) (**6**) [Eq. (4)], was prepared in crosslinked form by Stokes at the end of the last century by the thermal ROP of the cyclic trimer $(Cl_2PN)_3$.[10] However, this material, referred to as "inorganic rubber," remained only a chemical curiosity due to its intractability and hydrolytic instability. The key developments concerning this polymer system took place in the mid-1960s when it was shown by Allcock and Kugel that if the ROP of pure $(Cl_2PN)_3$ is carried out carefully, uncrosslinked **6** is formed which is soluble in organic solvents.[25] This permitted replacement of the halogen substituents by reaction with nucleophiles to yield hydrolytically stable poly(organophosphazene)s [Eq. (4)].[10, 26–28]

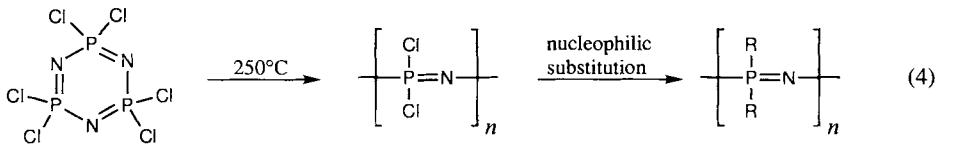

(4)

6

R = OR, OAr, NHR, etc.

The unique reaction sequence comprising ROP followed by nucleophilic substitution with oxygen- or nitrogen-based nucleophiles (generally alkoxides, aryloxides, or primary amines) has been pioneered by Allcock and co-workers, and permits the immense structural diversity of poly(organophosphazene)s and allows the properties to be tuned and specific properties to be introduced.[10] Recent highlights concerning the use of the macromolecular substitution route with **6** and related materials include the introduction of side groups which lead to liquid crystallinity (see polymer **7**),[29] photochromism,[30] photocrosslinkability,[31–33] and the preparation of novel polymers such as **8** with short chain branching.[34]

The phosphazene backbone also inherently possesses a unique range of unusual properties. For example, it is extremely flexible, and poly(alkoxyphosphazene)s such as the *n*-butoxy derivative have glass transitions of below $-100\,^{\circ}C$.[10] Furthermore, it is thermally and oxidatively stable, optically transparent from 220 nm to the near IR region, and it imparts flame-retardant properties. Some of the most important polymers are fluoroalkoxy derivatives and amorphous copolymers are very useful as flame-retardant, hydrocarbon-solvent and oil-resistant elastomers and have found aerospace and automotive applications. Polymers such as the amorphous comb polymer poly[bis(methoxyethoxyethoxy)phosphazene] **9** are of considerable interest as components of polymeric electrolytes in battery technology.[10] Polyphosphazenes are also of interest as biomedical materials, and bioinert, bioactive, membrane-forming, and bioerodable materials and hydrogels have been prepared.[10]

The reaction of poly(dichlorophosphazene) with organometallic reagents such as Grignard or organolithium reagents generally leads to chain cleavage as well as substitution and does not provide a satisfactory route to polymers with only alkyl and aryl side groups bound by direct P–C bonds.[10] In the early 1980s a solution to this problem was provided by the discovery by Neilson and Wisian-Neilson of a condensation route to poly(alkyl/arylphosphazene)s from phosphoranimines [Eq. (5)].[35] The polymerization is in fact a chain-growth reaction, and allows access to high molecular weight polyphosphazenes such as poly(dimethylphosphazene) and poly(methylphenylphosphazene).

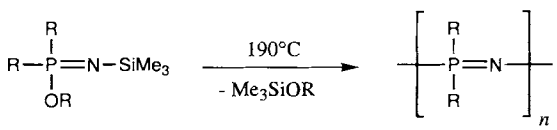

(5)

R = alkyl or aryl

Although several polyphosphazenes have been commercialized, recent work has focused on the development of cheaper and more convenient methods for making these materials. The thermal ROP route requires the synthesis and careful purification of the cyclic trimer $(Cl_2PN)_3$ and the use of elevated temperatures where control of molecular weight is difficult and crosslinking can take place at high conversion which can limit the yield. Recently, condensation reactions have been developed by Matyjaszewski and co-workers that provide an alternative, direct route to fluoroalkoxy phosphazene polymers and aryl derivatives, and also permit access to block copolymers [Eqs. (6) and (7)].[36, 37] The development of condensation routes to poly(dichlorophosphazene) have also been reported. De Jaeger and co-workers have described a promising route that operates at 200 °C [Eq. (8)].[38] Very recently Manners and Allcock and their respective co-workers reported details of a synthesis of poly(dichlorophosphazene) that operates at room temperature and allows molecular weight control [Eq. (9)].[39] These developments offer the prospect of improved routes to phosphazene polymers that may well facilitate more rapid and extensive commercialization.[40]

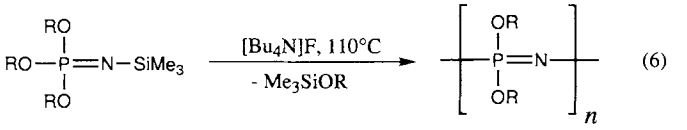
(6)

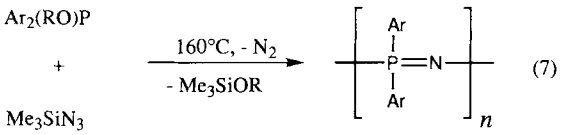
(7)

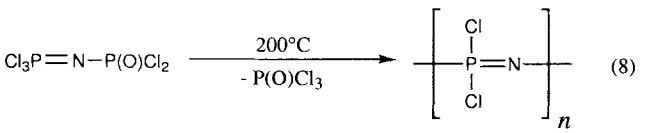
(8)

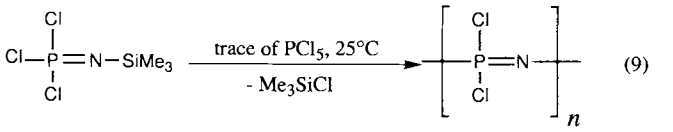
(9)

3.3. Polysilanes

Since the first reports of soluble and processable polysilanes **3** in the late 1970s, these macromolecules have attracted tremendous interest from both a fundamental and an applied perspective.[10, 41–43] The backbone of silicon atoms gives rise to unique electronic and optical properties as a result of the delocalization of σ electrons. Several polysilanes also function as useful thermal precursors to silicon carbide fibers and these materials have also attracted attention with respect to microlithographic applications and as polymerization initiators.[10, 41, 42]

The first report of a soluble polysilane by West and co-workers appeared in 1978, and the material was prepared by the treatment of a mixture of organodichlorosilanes with sodium metal.[44] Instead of only the expected cyclic oligomers, a polymeric product, termed "polysilastyrene" (**10**), was formed [Eq. (10)]. Poly(dimethylsilane) had been previously prepared

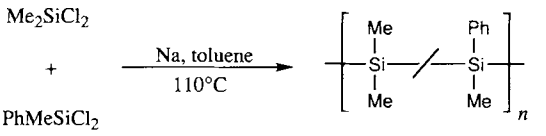
(10)

10

as a highly crystalline insoluble material.[10, 41, 42] The introduction of phenyl groups in the random copolymer reduces the crystallinity and allows the material to be soluble and processable.

The use of this Wurtz coupling route has allowed the preparation of a range of high molecular weight polymers ($M_n > 10^5$) with alkyl or aryl subtituents at silicon. Since 1980 the interest in these polymers has grown tremendously and they have been found to possess a variety of fascinating properties.

One of the most remarkable features of the all-silicon backbone is that it leads to the delocalization of σ electrons, a phenomenon that is virtually unknown in carbon chemistry.[45] This can be understood in terms of the nature of the molecular orbitals associated with the Si–Si σ bonds. These are more diffuse than those associated with C–C σ bonds, since they are constructed from higher energy 3s and 3p atomic orbitals. This leads to significant interactions between the adjacent Si–Si σ bonds along a polysilane chain, a situation analogous to that for the π bonds in π-delocalized polymers such as polyacetylene. Thus a band model rather than a localized model is more appropriate.[10, 42] As a consequence of the delocalization of σ electrons, the σ-σ* transition, which occurs at 220 nm in $Me_3Si-SiMe_3$, moves to lower energy as the number of silicon atoms in the chain increases. In the high polymers the σ-σ* band-gap transitions occur in the near UV region at about 300–400 nm.[46] The electron delocalization also leads to appreciable electrical conductivity following doping. For example, conductivities of up to 0.5 Scm^{-1} have been reported for **10**, after doping with AsF_5.[10] In addition, many of the polymers are thermochromic as the conformations adopted by the polymer change with temperature, which alters the degree of σ delocalization along the main chain. Due to their low energy σ-σ* transitions, polysilanes are photosensitive and have attracted considerable attention as photoresist materials in microlithography.[10, 41, 42]

The main method used to synthesize polysilanes involves the thermally induced Wurtz coupling reaction of organodichlorosilanes with alkali metals [Eq. (11)]. Although improvements in

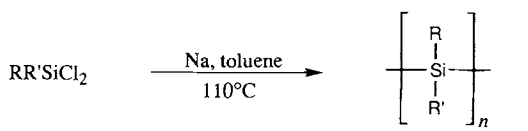
(11)

this process have been reported, for example the use of ultrasound, the harsh conditions for this reaction tend to limit the side groups that can be successfully introduced to nonfunctionalized alkyl and aryl units and makes scale up unattractive.[10]

Because of these limitations, considerable effort has been focused on the development of new synthetic routes to polysilanes. The dehydrogenative coupling process catalyzed by early transition metals, which was discovered by Harrod and co-workers in 1985 [Eq. (12)], is potentially very attractive; however, the

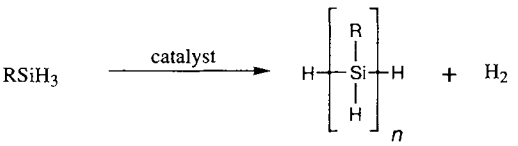

(12)

molecular weights of the polysilanes formed to date are generally quite low ($M_n < 8000$).[47] The catalysts used for these coupling reactions are usually titanocene or zirconocene derivatives.[47,48]

The catalytic dehydrogenation route yields novel polysilanes with Si–H functionalities that are of interest as ceramic precursors.[49] In addition, Waymouth and co-workers have recently shown that a variety of new side groups can be introduced by using a derivatization approach [Eq. (13)].[50]

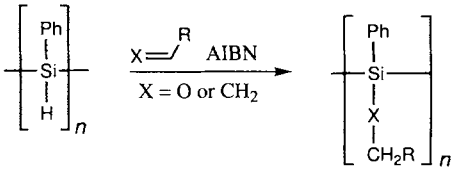

(13)

In 1991 Matyjaszewski and co-workers reported a novel ROP route to polysilanes [Eq. (14)].[51] The key to this approach is to

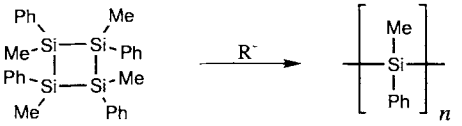

(14)

take readily accessible octaphenylcyclotetrasilane, which is too sterically crowded to undergo ROP, and to replace some of the phenyl groups by smaller methyl substituents (by a two-step process) to make the ring polymerizable.

Sakurai and co-workers have also recently described another novel route to polysilanes that involves the anionic polymerization of disilabicyclooctadienes, which function as masked disilenes [Eq. (15)].[52]

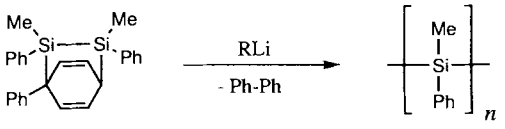

(15)

Recent exciting developments in polysilane research include the use of these materials as hole transport layers in electroluminescent devices.[53] In addition, the photoconductivity of poly(methylphenylsilane) doped with C_{60} is comparable with the best materials currently available.[54] Remarkable, optically active[55] and dendritic polysilanes with extensively σ-delocalized structures[56,57] have also recently been prepared.

4. New Polymers Based on Main Group Elements

Polysiloxanes, polyphosphazenes, and polysilanes illustrate that incorporation of main group elements within a polymer main chain can influence chain flexibility, flame retardancy, and electron delocalization, and can also permit access to new synthetic avenues for the control of polymer microstructure and hence properties. Over the last decade, attention has also focused on the development of a range of new polymer systems based on p-block elements, and these are now reviewed.

4.1. Poly(carbosilane)s

Polymers with a carbon–silicon backbone have been known since the 1960s.[58,59] Thermal and transition metal catalyzed ROP routes were used to prepare these materials. A range of polymers with silicon and unsaturated hydrocarbon linkages in the backbone are also known and several of these materials exhibit significant electrical conductivity upon doping.[60–65] Dendritic poly(carbosilane)s have also been prepared recently.[66,67] Over the past 10 years the main interest in poly(carbosilane)s has focused on their use as precursors to silicon carbide ceramics.[41,42,68–70]

One of the recent highlights of this area is the synthesis and study of the properties of poly(silaethylene) (**11**), a novel analogue of polyethylene, by Interrante and co-workers.[71] This polymer was prepared by the platinum-catalyzed ROP of 1,1,3,3-tetrachlorodisilacyclobutane to yield poly(dichlorosilaethylene), followed by reduction with $LiAlH_4$ [Eq. (16)].[72]

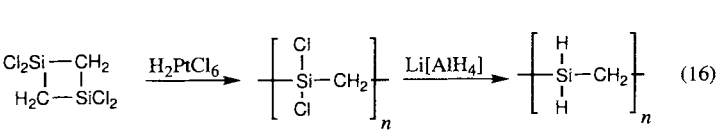

(16)

11

Poly(silaethylene) is air-stable, soluble in organic solvents, and has been well-characterized. In contrast to polyethylene, which is a fairly high melting point solid ($T_m = 138\,°C$), this material is a viscous liquid at room temperature but on cooling to just below room temperature forms a translucent white solid. Below the T_m at about 25 °C the powder X-ray diffraction pattern shows no obvious similarity to that for any of the known forms of polyethylene. The T_g for this material is extremely low (ca. −135 to −140 °C). Significantly, poly(silaethylene) converts to stoichiometric silicon carbide in excellent yield (87%) on pyrolysis to 1000 °C.

Very recent work by Isaka et al. suggests that "saturated" poly(carbosilane)s may possess interesting electronic properties.[73] Periodic poly(carbodisilane)s **12** were prepared by Wurtz coupling and

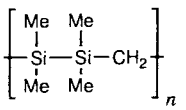

12

show evidence of significant σ conjugation despite the presence of a saturated carbon atom in every repeat unit. Indeed, ab initio calculations for poly(carbodisilane)s indicated that the effective hole masses at the valence band edge were inbetween those in polysilanes and polyethylene.

4.2. Random-Network Polymers of the Group 14 Elements: Polysilynes and Polygermynes

In 1989 Bianconi and Weidman prepared the first members of a class of random-network silicon polymers termed polysilynes $[RSi]_n$.[74] These yellow, film-forming materials (**13**) were synthesized by the Wurtz coupling reaction of organotrichlorosilanes promoted by high intensity ultrasound [Eq. (17)].

$$RSiCl_3 \xrightarrow[\text{THF, ultrasound}]{\text{Na/K}} \left[\begin{array}{c} R \\ | \\ -Si- \end{array}\right]_n \qquad (17)$$

13

Polysilynes **13** are soluble in organic solvents, providing that the organic group R attached to silicon has at least four carbon atoms, and have molecular weights (M_w) of between 10000–15000 by gel permeation chromatography (GPC). Differential scanning calorimetry (DSC) and X-ray powder diffraction studies showed that the materials are amorphous, and NMR studies are consistent with the presence of a randomly constructed rigid network of monosubstituted sp^3-hybridized silicon units (Fig. 1). The electronic properties of these materials are particularly interesting and are significantly different from those of linear polysilanes.[75, 76] Poly(*n*-hexylsilyne), for example, shows an intense near-UV absorption band edge that tails into the visible region up to 450 nm, which is associated with σ conjugation extended in three dimensions (Fig. 2). The three-dimensional structure of these materials leads to additional photostability in comparsion to that for polysilanes. In air, insoluble polysiloxanes are formed by insertion of oxygen atoms into the Si–Si bonds. Potential applications of these materials as photoresists are under investigation; exposure to air or light leads to a pattern that remains after dissolution of unoxidized polymer.

Fig. 1. Random-network structure of the polysilyne **13** (R = *n*-hexyl) (adapted from ref. [75] with permission).

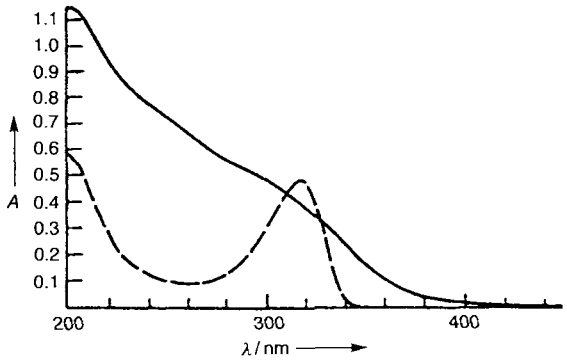

Fig. 2. UV/Vis spectra in cyclohexane of the polysilyne **13** (R = *n*-hexyl) (filled line) compared to that of the polysilane **3** (R = *n*-hexyl) (broken line) (reproduced from ref. [75] with permission). *A* = absorption (arbitrary units).

Very recently random-network polymers have been made for other Group 14 elements.[77] Polygermynes **14** are coffee-colored materials prepared from organotrichlorogermanes by a similar synthetic methodology [Eq. (18)]. These materials have UV/Vis absorptions that tail into the visible region up to 800 nm. Copolymers with polysilynes have also been prepared by using mixtures of $RSiCl_3$ and $RGeCl_3$ and have properties intermediate between those of the homopolymers. For example, $[(n\text{BuSi})_{0.8}(\text{PhGe})_{0.2}]_n$ shows a UV/Vis absorption band that tails up to about 650 nm.[77]

$$RGeCl_3 \xrightarrow[\text{THF, ultrasound}]{\text{Na/K}} \left[\begin{array}{c} R \\ | \\ -Ge- \end{array}\right]_n \qquad (18)$$

14

4.3. Linear Polymers Containing Heavier Group 14 Elements: Polygermanes and Polystannanes

The remarkable properties of polysilanes has led to considerable interest in the development of polymer chains based on the heavier Group 14 elements germanium and tin. Polygermanes were prepared in the mid 1980s by Wurtz coupling techniques similar to those used to prepare the silicon polymers [Eq. (19)].

$$RR'GeCl_2 \xrightarrow[110^\circ C]{\text{Na, toluene}} \left[\begin{array}{c} R \\ | \\ -Ge- \\ | \\ R' \end{array}\right]_n \qquad (19)$$

Studies of these materials indicated that the σ delocalization is even more extensive than for polysilanes and that the σ-σ* band-gap transition for the high polymers is significantly red shifted by about 20 nm in comparison to that for the silicon analogues.[78, 79]

Polystannanes would be expected to have even more σ delocalized structures.[80-82] Indeed, elegant work by Dräger and co-workers in 1987 showed that linear oligostannanes with up to six tin atoms can be prepared and that the σ-σ* transition moves dramatically to lower energy as the chain length is increased. This led to the proposed term "molecular metals" for prospective high molecular weight analogues.[80] However, attempts to generate high polymers by Wurtz coupling of organodichlorostannanes have yielded only low molecular weight oligomers and reduction products. A key breakthrough in this area was reported in 1993 by Tilley and co-workers who showed that transition metal catalyzed dehydrogenative coupling reactions, which had been extensively applied to the synthesis of polysilanes (see Section 3.3), could be applied to secondary stannanes R_2SnH_2 [Eq. (20)].[83] Yellow polystannanes **15** (R = e.g.

$$R_2SnH_2 \xrightarrow[25^\circ C]{\text{Zr catalyst}} \left[\begin{array}{c} R \\ | \\ -Sn- \\ | \\ R \end{array}\right]_n \qquad (20)$$

15

n-butyl, *n*-hexyl, or *n*-octyl) of substantial molecular weight (up to M_w = ca. 96000, M_n = ca. 22000) were prepared by using various zirconocene catalysts. These materials indeed possess σ electrons that are extensively delocalized, as illustrated by the band-gap transition that occurs at 384–388 nm (in THF). In addition, exposure of thin films of the polymers to the oxidant AsF_5 leads to significant electronic conductivities of about 0.01 - 0.3 $S\,cm^{-1}$.[84]

The properties of these remarkable materials are now under detailed scrutiny. They are highly photosensitive and exhibit photobleaching behavior, and on irradiation with UV light depolymerize to yield cyclic oligomers (Fig. 3). The materials are thermally stable to temperatures between 200 and 270 °C in air, and at more elevated temperatures function as interesting precursors to SnO_2.[84]

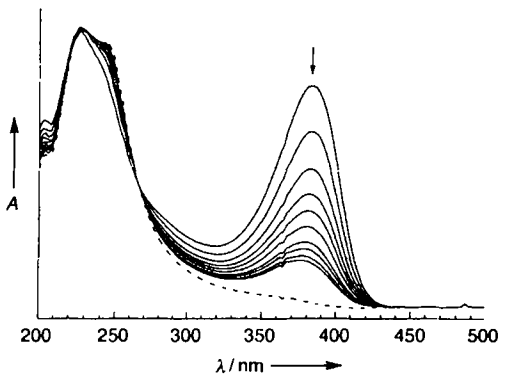

Fig. 3. UV/Vis spectrum of polystannane **15** (R = *n*Bu) illustrating photobleaching behavior in pentane upon irradiation by room light. Measurements were taken every 30 s. The final spectrum is given by the dotted line. (reproduced from ref. [84] with permission). *A* = absorption (arbitrary units).

4.4. Poly(carbophosphazene)s

Poly(carbophosphazene)s have a backbone comprising phosphorus, nitrogen, and carbon atoms and can be regarded as derivatives of classical polyphosphazenes **2** in which every third phosphorus atom is replaced by carbon. The first examples of these materials were discovered in 1989 by Allcock, Nuyken and co-workers.[85] Thermal ROP of a cyclic carbophosphazene was used to prepare the chlorinated polymeric species **16**, which undergoes halogen replacement reactions with nucleophiles such as aryloxides to yield hydrolytically stable poly[(aryloxy)carbophosphazene]s **17** (M_w = ca. 10^5, $M_n = 10^4$) [Eq. (21)].[85-88] The polymer backbone in these materials is

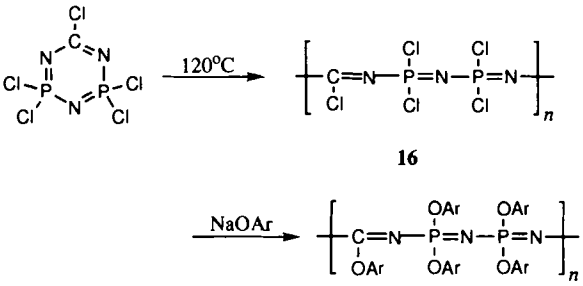

16

(21)

17

less flexible than in classical polyphosphazenes. For example, the halogenated polymer **16** has a T_g value of −21 °C compared to a value of −66 °C for poly(dichlorophosphazene) (**6**).

The reaction of **16** with alkylamines has also been studied.[88] The resulting poly[(alkylamino)carbophosphazene]s are sensitive to hydrolysis. However, arylamino derivatives are moisture-stable, and, in addition, a novel, regioselectively substituted polymer **18** was successfully prepared by the sequential reaction with $NHPh_2$ and trifluoroethoxide anions [Eq. (22)].

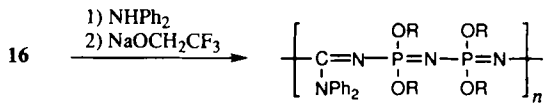

$OR = OCH_2CF_3$

18

(22)

4.5. Sulfur–Nitrogen–Phosphorus Polymers

Sulfur–nitrogen–phosphorus polymers have backbones that can be regarded as compositional hybrids of those present in sulfur–nitrogen polymers, such as the solid-state polymer poly(sulfur nitride) $[SN]_x$ or poly(oxothiazene)s $[RS(O)=N]_n$ (see Section 4.6), and classical polyphosphazenes, $[R_2P=N]_n$ (**2**).[89, 90] The first well-characterized examples of these materials, poly(thiophosphazene)s, were also reported by Allcock, Nuyken and co-workers.[91] These polymers were prepared by the thermal ROP of a cyclothiophosphazene [Eq. (23)]. This yielded the hydrolytically sensitive poly(thiophosphazene) **19** with a backbone comprising three-coordinate sulfur(IV), nitrogen, and phosphorus atoms. Although reaction of **19** with nucleophiles such as aryloxides yielded polymers of the type **20** with improved hydrolytic stability, degradation was still rapid except where very bulky substituents such as *o*-phenylphenoxy were present.

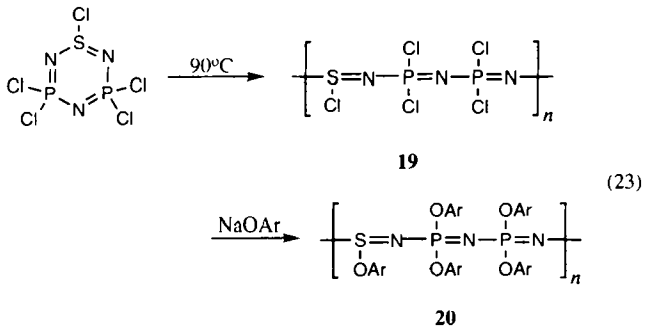

19

20

(23)

Although the backbone of poly(thiophosphazene)s appears to be quite fragile, a particularly interesting feature of the substitution reactions of **19** is that the S–Cl bond is much more reactive than the P–Cl bonds. Regioselective substitution is possible at the sulfur center, yielding macromolecules **22** with different aryloxy substituents at sulfur and phosphorus [Eq. (24)].[91,92]

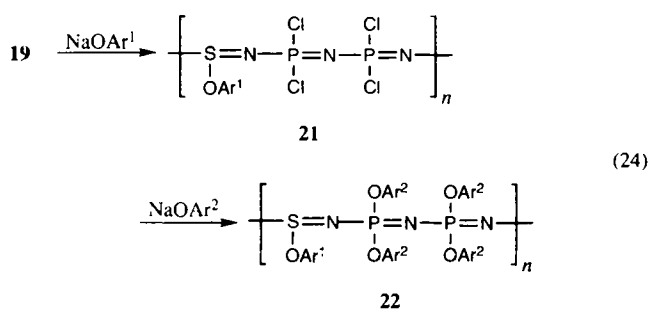

21

22

(24)

In 1991 another class of sulfur–nitrogen–phosphorus polymers, poly(thionylphosphazene)s, were reported by Manners and co-workers.[93,94] These materials, which possess four-coordinate sulfur(VI) atoms in the backbone, have considerably improved stability and were prepared by a thermal ROP of cyclic thionylphosphazenes **23** with either chlorine or fluorine at the sulfur(VI) center [Eq. (25)].[95]

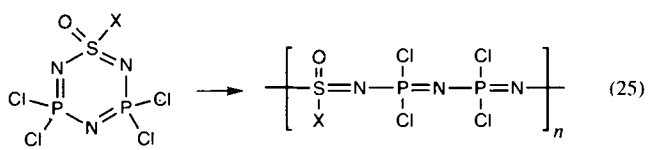

(X = Cl, F) 165°C (X = Cl); 185°C (X = F)

23 24

(25)

The halogenated poly(thionylphosphazene)s **24** that are formed in these ROP reactions (together with small quantities of macrocyclic by-products) are quite sensitive to hydrolysis but a variety of moisture-stable derivatives have been prepared by reaction of this species with aryloxides or amines.[96–98] Mixed-substituent aryloxy–alkoxy polymers have also been prepared.[89] Interestingly, with aryloxides, regioselective substitution at phosphorus is observed and in the resulting polymers (**25**), the sulfur(VI)–halogen bond remains intact. Remarkably, this regioselectivity is the exact reverse of that detected for the poly(thiophosphazene) **19** described above, in which the sulfur(IV) halogen bond is more reactive. In contrast to the reactions with aryloxides, reaction with amine nucleophiles leads to substitution at both the phosphorus and the sulfur(VI) centers to give poly(aminothionylphosphazene)s **26**.[98]

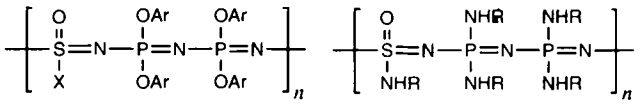

(X = Cl, F) R = Alkyl, Aryl

25 26

Ab initio calculations on isotactic poly(thionylphosphazene)s (**24**; X = Cl or F) indicate a localized electronic structure for the polymer backbone and predict that a *cis*–*trans* helical conformation is the most energetically favorable for isolated macromolecules (Fig. 4).[99] This is in contrast to the analogous classical polyphosphazene **6** in which a *cis*–*trans*-planar conformation is preferred. Studies of the properties of the poly(thionylphosphazene)s also reveal significant differences in thermal transition behavior and polymer morphology compared to that for the classical polyphosphazenes. For example, the polymer $[NSOF\{NP(OPh)_2\}_2]_n$ is an amorphous elastomer (T_g = −15 °C), whereas the analogous classical polyphosphazene $[NP(OPh)_2]_n$ is a microcrystalline thermoplastic (T_m = 390 °C, T_g = −6 °C). The T_g values of the fluorinated poly(thionylphosphazene)s are lower than those of the analogues with chlorine at sulfur. For example, for **24** (X = F) T_g = −56 °C, whereas for **24** (X = Cl) T_g = −46 °C.[97]

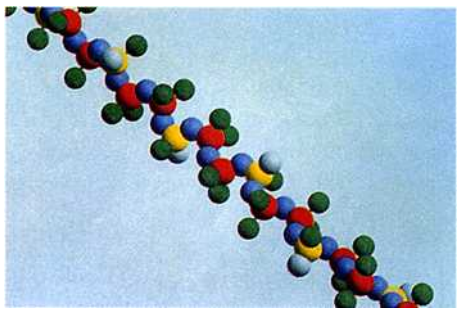

Fig. 4. Helical structure of the poly(thionylphosphazene) **24** (X = Cl) according to ab initio calculations. S: yellow, N: blue, P: red, O: white, Cl: green (picture courtesy of R. Jaeger and G. J. Vancso).

Recently preliminary reports of the first poly(thiazylphosphazene)s **27**, which possess three-coordinate sulfur(III) atoms, have appeared [Eq. (26)].[100] These materials would represent true hybrids of poly(sulfur nitride) and polyphosphazenes and further developments in this area should prove to be particularly interesting.

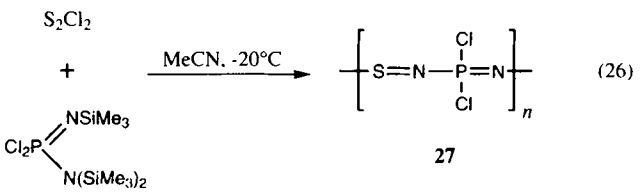

27

(26)

4.6. Poly(oxothiazene)s

Partially characterized poly(oxothiazene)s were briefly reported in the early 1960s.[101] However, in 1992 the first well-characterized examples (**28**) with alkyl or aryl substituents at sulfur were described by Roy.[102] These polymers, which have estimated molecular weights of M_w of about 10^5 and M_n of about 10^4, were synthesized by the condensation polymerization of *N*-silylsulfonimidates at 120–170 °C over two to eight days [Eq. (27)]. These reactions are catalyzed by added Lewis acids

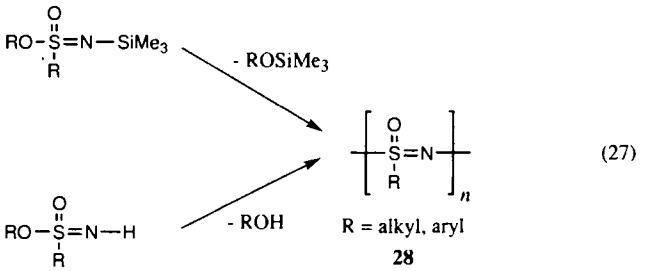

(27)

28

(e.g. $BF_3 \cdot OEt_2$) and bases (e.g. fluoride). By using a mixture of different sulfonimidates, copolymers such as $[MeS(O)=N]_n$-$[PhS(O)=N]_m$ were also successfully prepared. Free sulfonimidates also thermally condense to yield poly(organooxothiazene)s at lower temperatures than their *N*-silyl analogues [Eq. (27)].[102, 103]

Poly(oxothiazene)s appear to be very polar. For example, $[MeS(O)=N]_n$ is soluble in DMF, DMSO, hot water, and concentrated H_2SO_4. Studies of the thermal transition behavior of these materials have indicated that they are amorphous, which is consistent with an atactic structure. Interestingly, the T_g value of $[MeS(O)=N]_n$ is about 60 °C, which is dramatically higher than that for $[Me_2P=N]_n$ ($T_g = -46$ °C). This suggests a much less flexible backbone for poly(oxothiazene)s than for polyphosphazenes, as might be expected from studies on poly(thionylphosphazene)s (see Section 4.5). Thermogravimetric analysis (TGA) showed that the polymers are stable to weight loss up to about 270 °C (at a heating rate of 10 °C min^{-1}). Theoretical studies on $[MeS(O)=N]_n$ have indicated that a *cis-trans* helical conformation is the most stable for this polymer.[103]

4.7. Other Polymers Based on Main Group Elements

The use of new synthetic methodologies has provided access to a range of other polymers incorporating main group elements in the main chain. Examples include interesting 2:1 periodic copolymers **29** prepared by Kobayashi and co-workers by the reaction of cyclic germylenes with *para*-benzoquinones.[104]

Boron-containing polymers are of considerable interest as reactive intermediates and as precursors to boron-based ceramics.[105–110] Sneddon and co-workers have synthesized polyborazines **30** (M_w up to about 7600, M_n up to about 3400) by thermally induced dehydropolymerization of borazines [Eq. (28)].[109] The polymers were isolated as white solids and characterization suggested the presence of a significantly branched structure. Pyrolysis at 1200 °C yielded white boron nitride in 85–93% yield.

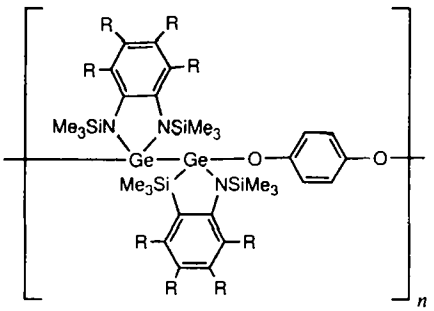

29

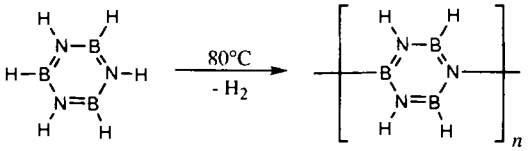

(28)

30

Poly(iminoborane)s **31**, boron–nitrogen analogues of poly(acetylene), have also been briefly reported as white insoluble materials, which swell in certain solvents.[111] These materials are clearly worthy of further investigation. Cyclodiborazane-based polymers have also been prepared and well-characterized.[112] In addition to boron-based systems, polymers with a silicon–nitrogen backbone, polysilazanes **32**, have also attracted considerable attention as precursors to ceramics such as Si_3N_4.[113] Novel, well-characterized polymers with backbones of silasesquioxane cages, which in some cases possess spacer groups containing transition elements such as zirconium, have also been prepared recently by Lichtenhan et al, and these materials have high stability and also exhibit preceramic potential.[114]

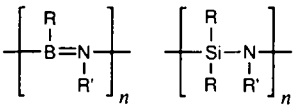

31 **32**

5. Transition Metal Based Polymers

Transition metal complexes and metal-containing solid-state materials display a diverse array of interesting and useful redox, magnetic, optical, electrical, and catalytic properties.[115, 116] The incorporation of transition metals into a polymer main chain therefore clearly offers considerable potential for the preparation of processable materials with properties that differ significantly from those of conventional organic polymers.[117–119] In addition, the diverse range of coordination numbers and geometries that exist for transition elements offer the possibility of accessing polymers with unusual conformational, mechanical, and morphological characteristics. Transition metal based polymers might also be expected to function as convenient and processable thermal or photochemical precursors to metal-containing ceramic films, fibers, and coatings with high stability and desirable and useful physical properties.[120] However, once again the development of this area of inorganic polymer science has been held up by considerable difficulties associated with the synthesis of these materials.

Much of the early work in the field utilized polycondensation routes in which the difunctional precursors were often impure, making low molecular weight, poorly defined materials the logical products. In addition, the resulting products were often insoluble and poorly characterized. Indeed, at the end of a comprehensive review of the field of metallocene-based polymers in 1970 the authors made the critical analysis that many of the structures assigned to the polymers in the article were "hypothetical and need rigorous analytical verification, and the description of experimental procedures and polymer properties more often than not has been superficial or has been lacking altogether".[121]

Over the past five years or so, however, a number of significant synthetic breakthroughs have taken place which have paved the way to the establishment of several examples of soluble, high molecular weight materials that have been well-characterized.

5.1. Metallocene-Based Polymers

5.1.1. Early Work on Ferrocene-Based Polymers

The excellent thermal stability and interesting physical (e.g. redox) properties associated with the ferrocene nucleus have led to extensive efforts aimed at the incorporation of this moiety into polymer structures. The inclusion of this moiety in the side group structure of polymers has been very successful because the synthesis of such materials generally requires only minor modifications of previously established synthetic methodologies. For example, poly(vinylferrocene) (**33**) can be prepared by the free radical addition polymerization of vinylferrocene.[122] The incorporation of ferrocene moieties into the main chains of polymers in which the metal atoms are separated by a considerable distance has also been achieved. Here, by exploiting the extensive organic chemistry of the metallocene nucleus, well-defined difunctional ferrocenes have been prepared, and controlled polycondensation reactions have then been used to yield well-defined products of appreciable molecular weight. Examples of products derived from such reactions include the poly(arylene-siloxane-ferrocene)s (e.g. **34**),[123] ferrocene-containing polyesters,[124] and novel "accordian" type polymers.[125, 126]

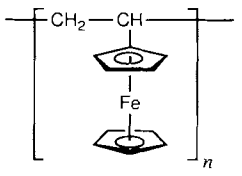

33

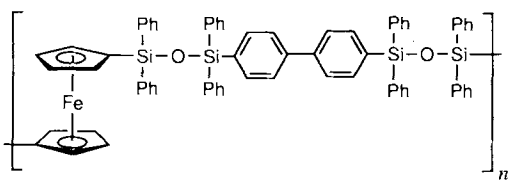

34

In contrast, very few examples of polymers with ferrocene units in close proximity have been prepared. Such materials are desirable if advantage is to be taken of interactions beween the metal atoms. The development of materials with interesting physical (e.g. electronic and/or magnetic) properties might be anticipated based on the properties of molecular species in which two ferrocene units are linked close together. Thus, in such systems the iron atoms can interact and in some cases yield delocalized, mixed-valent species upon one-electron oxidation, even when the metal atoms are up to 7 Å apart.[127, 128] Until recently, work in this field had only yielded materials of low molecular weight ($M_n < 10000$) that were often poorly defined.[121, 129]

5.1.2. Poly(ferrocenylene)s

A typical early route to poly(ferrocenylene)s **35** with $M_n < 5000$ involved polycondensation processes such as the recombination of ferrocene radicals generated by the thermolysis of ferrocene in the presence of peroxides. However, these materials possess other fragments such as CH_2 and O in the main chain.[130] More structurally well-defined poly(ferrocenylene)s such as **35** ($M_n < 4000$) have been prepared by Neuse et al.[131] by the condensation reaction of 1,1-dilithioferrocene·tmeda with 1,1-diiodoferrocene and, significantly, the reaction of 1,1′-dihaloferrocenes with magnesium [Eq. (29)] has

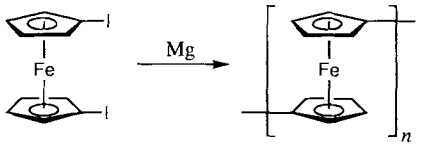

(29)

35

been shown to afford low molecular weight materials (M_n = 4600 for soluble fractions) with appreciable crystallinity.[132] In the latter case, oxidation with 7,7,8,8-tetracyano-*p*-quinodimethane (TCNQ) afforded doped polymers that were delocalized on the Mössbauer timescale (ca. 10^{-7} s) at room temperature and which exhibited electrical conductivities of up to 10^{-2} S cm^{-1}.

5.1.3. Poly(ferrocenylsilane)s Prepared by Ring-Opening Polymerization

Early attempts to prepare macromolecules in which the ferrocene units are separated by an organosilane spacer group also focused on the use of polycondensation reactions.[133, 134] Impure, partially characterized poly(ferrocenylsilane)s were prepared by the reaction of dilithioferrocene with organodichlorosilanes at subambient temperature.[133] The molecular weights of 1400–7000 reported for these materials are characteristic of those obtained from polycondensation processes in which exact reaction stoichiometries are virtually impossible to achieve because one reactant, in this case dilithioferrocene, cannot be readily prepared in pure form.

In 1992 Manners and co-workers reported the first synthesis of high molecular weight poly(ferrocenylsilane)s **37** (M_w = 10^5–10^6, $M_n > 10^5$) by a thermal ROP route.[135] This process involved heating silicon-bridged [1]ferrocenophanes **36** in the melt at 130–220 °C [Eq. (30)]. The presence of a single atom

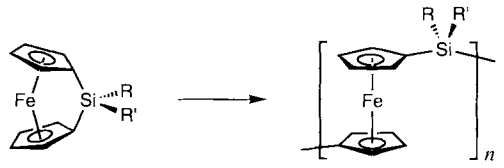

36 R, R' = Alkyl, Aryl, Ferrocenyl 37 (30)

bridging the ferrocene unit in the monomer leads to a strained structure in which the planes of the cyclopentadienyl rings are tilted with respect to one another by an angle of about 21°; in ferrocene the cyclopentadienyl rings are parallel. The presence of strain in the ferrocenophane, which has been measured to be about 80 kJ mol^{-1} for **36** (R = R' = Me), is believed to provide the driving force for the ROP process.

Since this initial discovery, a wide range of silicon-bridged [1]ferrocenophanes with either symmetrically or unsymmetrically substituted silicon atoms have been prepared and similarly polymerized.[136-146] Considerable effort has also been directed towards investigating and understanding the properties of the resulting poly(ferrocenylsilane) materials, the vast majority of which are soluble in organic solvents despite their very high molecular weights.[141] It was initially noted that the electrochemistry of the high polymer **37** (R = R' = Me) showed two reversible oxidation waves in a 1:1 ratio.[135] This provided clear evidence for the existence of interactions between the iron atoms and led to the proposal that initial oxidation occurred at alternating iron sites along the main chain. Recent work on model oligomers has provided clear evidence in support of this postulate.[142] Similar electrochemical behavior has subsequently been detected for a range of other poly(ferrocenylsilane)s.[141, 143-145] The polymers also exhibit interesting morphology and several of the symmetrically substituted derivatives will crystallize. For example, the dimethyl derivative **37** (R = R' = Me) is an amber, film-forming thermoplastic with a T_m of 122 °C and a T_g of 33 °C (see Fig. 5), whereas, the *n*-hexyl analogue **37** (R = R' = *n*-hexyl) is an amber, gummy amorphous material with a T_g of −26 °C.[141, 147]

Poly(ferrocenylsilane)s exhibit excellent thermal stability to weight loss (up to 350–400 °C) and yield interesting ferromagnetic Fe/Si/C ceramic composites at 500–1000 °C.[148-150] Oxidative doping of poly(ferrocenyldimethylsilane) with I_2 yields semiconducting materials (σ = ca. 10^{-7} S cm^{-1}).[141] Significantly, a recent report by Garnier and co-workers indicated that several tetracyanoethylene (TCNE)-oxidized low molecular weight poly(ferrocenylsilane)s (M_w = ca. 1500) show electron delocalization on the Mössbauer timescale (ca. 10^{-7} s) and also ferromagnetic ordering at low temperatures.[151] This discovery should certainly stimulate further research efforts on these materials in the future.

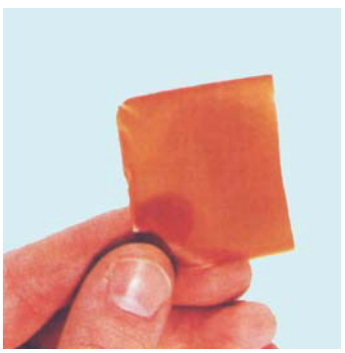

Fig. 5. A solvent-cast film of the poly(ferrocenylsilane) **37** (R = R' = Me).

It was recently shown that silicon-bridged [1]ferrocenophanes undergo "living" anionic ROP at 25 °C by using initiators such as *n*BuLi in THF.[152] This has permitted the synthesis of poly(ferrocenylsilane)s with controlled molecular weights and narrow polydispersities and has also allowed the preparation of the first block copolymers such as **38** containing skeletal transition metal atoms. Very recently the transition metal catalyzed ROP of silicon-bridged [1]ferrocenophanes, which occurs in solution at room temperature, has also been reported.[153, 154]

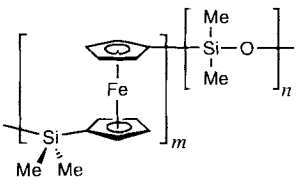

38

Novel random copolymers **39** with oligosilane spacers have been prepared by Matyjaszewski, Manners, and their co-workers by using a thermal copolymerization process.[155] These polymers, which possess backbones containing transition metal atoms together with σ-delocalized polysilane segments, are expected to exhibit interesting photophysical and charge transport properties. Indeed, the materials are photosensitive and the skeletons of the polysilane segments can be selectively cleaved by using UV light.

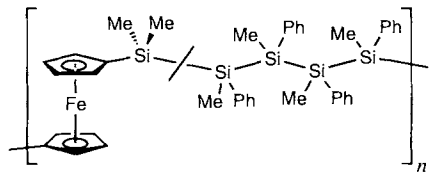

39

Polymerization of a mixture of different silicon-bridged [1]ferrocenophanes also yields random copolymers.[140] In addition, ROP of silicon-bridged [1]ferrocenophanes with silicon-bridged bis(benzene)chromium complexes[156] has very recently been shown to yield unusual bimetallic poly(ferrocenylsilane)–poly(chromarenosilane) copolymers.[157]

5.1.4. *Other Polymetallocenes Prepared by Ring-Opening Polymerization*

The ROP route has also been extended to the synthesis of other polymers from [1]ferrocenophane precursors. Poly(ferrocenylgermane)s **40** were first reported in 1993 and have been well-characterized and exhibit quite similar thermal transition behavior, morphology, and electrochemical behavior to the analogous poly(ferrocenylsilane)s.[158-160]

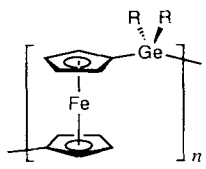

R = Me, Et, *n*Bu, Ph

40

Poly(ferrocenylphosphane)s **41** (and the corresponding phosphane sulfides **42**) are also accessible by the thermal ROP of phosphorus-bridged [1]ferrocenophanes.[161] Polymers of type **41** have been previously prepared by condensation routes and the catalytic potential of some of their transition metal derivatives has already been noted.[162, 163] In addition, very recently the

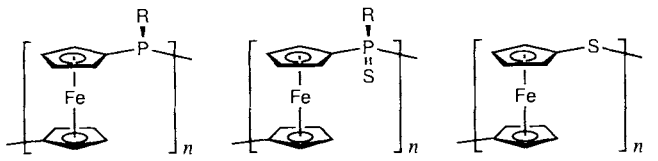

R = alkyl, aryl R = alkyl, aryl

41 **42** **43**

first sulfur-bridged [1]ferrocenophanes have been prepared and polymerized to give poly(ferrocenylsulfide)s such as **43**.[164]

Although disilane-bridged [2]ferrocenophanes have very small ring-tilt angles (ca. 4–5°) and are insufficiently strained to undergo thermal ROP, hydrocarbon-bridged [2]ferrocenophanes **44** have strained ring-tilted structures (tilt-angles = ca. 21°) as a result of the smaller atomic radius of carbon compared to that of silicon.[141] These species yield poly(ferrocenylethylene)s **45** by ROP at 250–300 °C [Eq. (31)].[165] As a

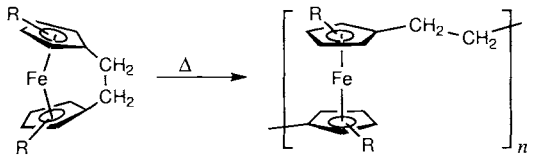

44 **45**

consequence of the presence of a more insulating bridge, the interactions between the iron atoms in these polymers are much smaller than those in poly(ferrocenylsilane)s.[143]

The inclusion of the larger ruthenium atom into a metallocenophane structure gives rise to even more tilted and strained molecules, and hydrocarbon-bridged [2]ruthenocenophanes (tilt-angles = ca. 29–30°) undergo thermal ROP to yield poly(ruthenocenylethylene)s.[166] These materials exhibit significantly different electrochemistry from their iron analogues.

5.1.5. Poly(ferrocenylene persulfide)s Prepared by Atom Abstraction Induced Ring-Opening Polymerization

In early 1992 Rauchfuss and co-workers reported that [3]trithiaferrocenophanes, which are essentially unstrained, function as precursors to poly(ferrocenylene persulfide)s by a novel atom abstraction polymerization route [Eq. (32)].[167] Thus, reaction of [3]trithiaferrocenophanes **46** with PBu_3 led to the formation of the phosphane sulfide, $S{=}PBu_3$, and the polymers **47**.

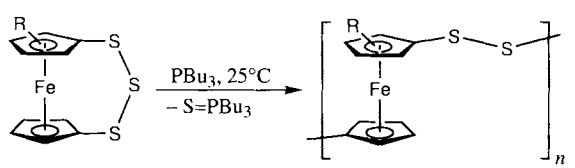

46 **47** (32)

The presence of a butyl substituent on the cyclopentadienyl ring is necessary for the polymer to be soluble. The molecular weights (M_w) of **47** (R = *n*Bu) have been determined to be between 12000 and 359000 (by GPC), depending on the solvent used for the desulfurization reaction. The [3]ferrocenophanes **46** (R = H) and **46** (R = *n*Bu) can be copolymerized to give soluble copolymers with $M_w = 25000$.

Poly(ferrocenylene persulfide)s exhibit a range of very interesting properties.[167–170] They are photosensitive in air, and the S–S bonds can be reversibly reductively cleaved with $Li[BEt_3H]$ and then regenerated upon oxidation with I_2. Their electrochemical behavior is similar to that detected for poly(ferrocenylsilane)s except that the interaction between the iron sites appears to be even greater. The atom abstraction route using PBu_3 as a desulfurization agent has very recently been extended to the preparation of other poly(ferrocenylene persulfide)s with *tert*-butyl substituents, and also to high molecular weight (M_w = 50000–1000000) network polymers by the use of [3]ferrocenophanes with two trisulfido bridges as monomers.[168] Linear poly(ferrocenylene perselenide)s have also been prepared but these materials are of lower molecular weight.[169]

5.1.6. Face-to-Face Metallocene Polymers

The development of rigid-rod metallocene polymers with a multistacked structure has been reported by Rosenblum and co-workers by using condensation routes.[171–175] Palladium-catalyzed coupling of chlorozinc ferrocenes with 1,8-diiodonaphthalene yielded low molecular weight materials ($M_n < 4000$), as the sensitivity of the ferrocene reagent made the accomplishment of exact stoichiometries very difficult. With this in mind, an improved coupling procedure was developed [Eq. (33)] in which treatment of the ferrocene monomers **48** with

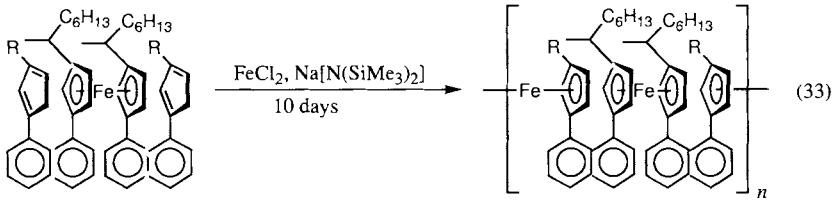

48 **49** (33)

$FeCl_2$ and $Na[N(SiMe_3)_2]$ yielded purple polymers **49** with molecular weights up to $M_n = 18000$; higher molecular components components were also present. Novel mixed-metal copolymers containing Ni and Fe whose soluble fractions were of low molecular weight ($M_n < 3000$) were also obtained by using $[Ni(acac)_2]$ instead of $FeCl_2$.[171] The electrical and magnetic properties of these novel polymers and copolymers have been investigated and conductivities up to $6.7 \times 10^{-3}\ S\,cm^{-1}$ have been determined for I_2-doped materials.[173] Interestingly, structural work on well-defined oligomers suggests that the stacked metallocene units in the polymer form a helical structure.[175]

5.2. Coordination Polymers

In the past, attempts to prepare coordination polymers have been hindered by the insolubility and consequent intractability of the products. These problems arise from the inherent skeletal rigidity of these materials, and the introduction of solubilizing or flexibilizing groups either in the polymer backbone or side group structure is necessary for useful products to be obtained. Recent work has yielded a range of interesting and well-characterized materials with intriguing properties. For example, novel liquid crystalline polymers **50** containing paramagnetic Cu^{II} centers have been prepared by Serrano and co-workers, and soluble, luminescent silver-containing polymers **51** have been reported by Harvey, Michel and co-workers.[176, 177]

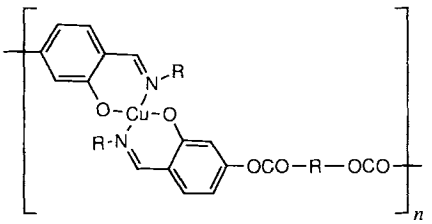

50

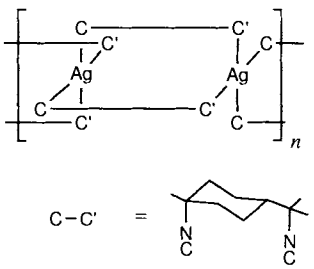

51

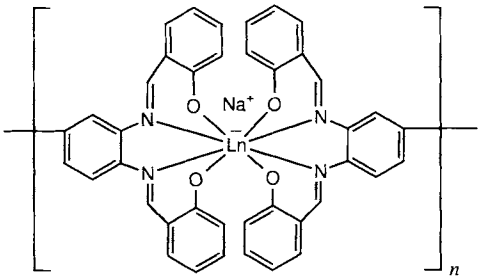

Ln = La, Gd, Y, Yb

52

In addition, well-characterized lanthanide-containing polymers such as **52**, which show polyelectrolyte behavior and which should exhibit interesting photophysical properties, have been reported by Archer and Chen.[178] Several of the polymers are soluble in polar organic solvents such as DMSO, and molecular weights (M_n) up to 18000 have been established. Polymers containing cerium in the main chain possess M_n values up to 30000.[179]

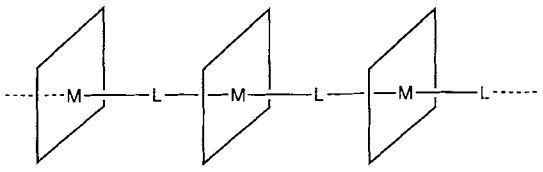

= phthalocyanine L = bipy, CN^-

M = Fe, Ru, Os, Co, Rh, Mn, Cr

53

Phthalocyanine-based polymers, such as the "shish-kebab" polymers **53**, are also of considerable interest and significant electrical conductivities of up to about 0.1 Scm^{-1} have been detected for chemically or electrochemically doped materials.[180, 181] If flexible organic substituents are present on the periphery of the phthalocyanine ring these materials can also be soluble (at least low molecular weight fractions).

The generation of dendrimeric coordination polymers has also been an area of significant recent activity and imaginative routes to novel Ru- or Pt-polypyridyl systems (Fig. 6) have been reported.[182–186] These materials are of interest with respect to their photophysical and electrochemical properties and possibly their catalytic behavior.

5.3. Rigid-Rod Organometallic Polymers

Together with several of the classes of ferrocene-based polymers described above, macromolecules with backbones that contain conjugated C≡C units and transition metal atoms, termed polymetallaynes, represent the best-characterized examples of transition metal based polymers prepared to date.[187] The synthesis and study of these materials is currently an exciting and active area of polymer science.

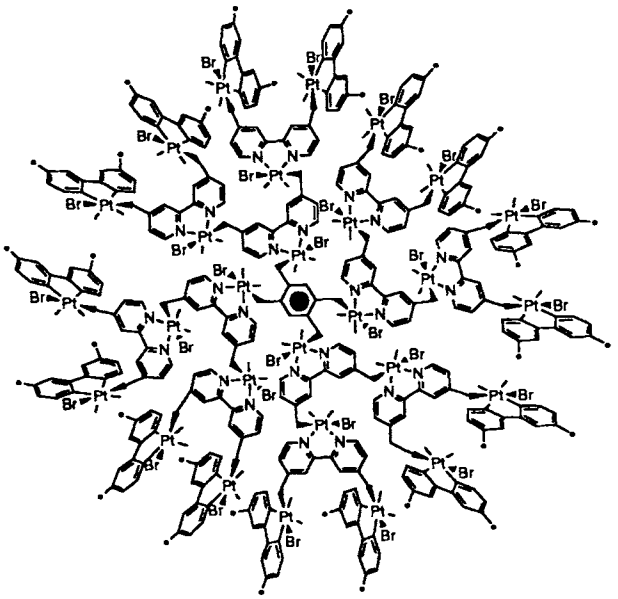

Fig. 6. Structure of a dendrimeric organoplatinum complex (reproduced from ref. [183] with permission).

The first polymetallaynes contained nickel, palladium, or platinum atoms in the main chain and were isolated in 1977 by Sonogashira, Hagihara, and Takahashi as yellow, film-forming materials.[188–190] These were prepared by efficient copper halide catalyzed coupling processes [Eq. (34)] and have estimated molecular weights (M_w) between 13000 and 120000.

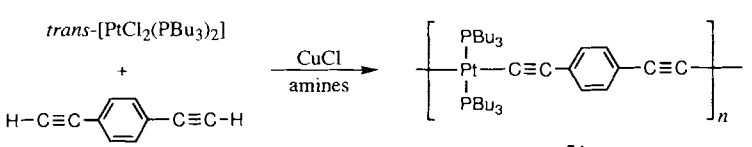

54 (34)

The last few years have seen an important expansion in this area that has yielded a range of new rigid-rod materials by the creative use of a variety of new and well-defined polycondensation strategies. For example, Lewis and co-workers reported a new route to the polyplatinynes **54** based on the reaction of *trans*-$[PtCl_2(PR_3)_2]$ complexes with bis(trimethylstannyl)diynes [Eq. (35)].[191] These rigid-rod polymers possessed estimated weight-average molecular weights up to about 100000 according to GPC measurements.

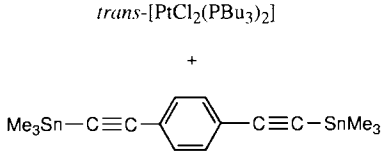

$\xrightarrow{-ClSnMe_3}$ **54** (35)

Lewis and co-workers have also shown that this synthetic procedure could be extended to allow the incorporation of other transition elements such as iron into the polymer main chain (to give **55**) by using $[FeCl_2(Et_2PCH_2CH_2PEt_2)_2]$ as the transition

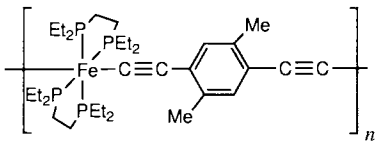

55

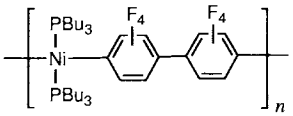

56

metal containing reactant.[192] In addition, Hunter and co-workers have devised condensation routes to the unusual organonickel polymers **56**, and interesting organocobalt and organozirconium polymers containing metallacyclopentadiene moieties in the main chain have been recently reported by the groups of Nishihara and Endo, and by Tilley and co-workers, respectively.[193–196]

In another interesting synthetic development, Marder and co-workers showed that a range of rhodium-containing polyynes **57** are accessible by the reaction of the unsubstituted diynes with $[Rh(PR_3)_4Me]$ in a reaction that involves reductive elimination of methane and the loss of a phosphane ligand [Eq. (36)].[197] In the case where trimethylphosphane ligands are attached to the rhodium center, the polymers are insoluble but the tri(*n*-butyl)phosphane analogues are soluble and yield free-standing solvent-cast films from THF.

Over the past 10 years the physical properties of polymetallaynes have received continued attention because of their novel rigid-rod structures and their conjugated backbones.[198–207] Thus, polyplatinaynes form ordered, liquid crystalline mesophases in solvents in which they are soluble such as trichloroethylene,[198] and these materials also possess novel, third-order nonlinear optical properties,[199] which are of intense current interest for electrooptic device applications. Optical absorption and photoluminescence spectroscopic studies and extended Hückel calculations have shown that polymetallaynes possess a delocalized polymer backbone whose electronic structure is modified by the nature of the transition metal, coligands, and the unsaturated hydrocarbon spacer.[200–202] For example, optical band gaps for a series of polyplatinaynes with platinum centers joined by π-conjugated acetylide–arene linkages of varying length have been measured to be in the range of 2.5–3.1 eV, which is lower than for model complexes and is consistent with conjugation through the metal centers.[201]

Other recent highlights in the area of rigid-rod transition metal based polymers include the synthesis by Bunz and Altmann of a range of interesting thermotropic liquid crystalline organocobalt polymers such as **58** in which the metal is bound to skeletal cyclobutadiene units [Eq. (37)].[208] Novel analogues of such materials in which thiophene units are also incorporated in the polymer main chain have also been prepared and these can form smectic lyotropic liquid crystalline phases.[209]

In addition, the preparation and characterization of novel lyotropic liquid crystalline aramides **59** with complexed chromium (tricarbonyl) units have been reported by Dembek et al.[210] These materials are soluble in organic solvents, which leads to potential processing advantages for the uncomplexed organic

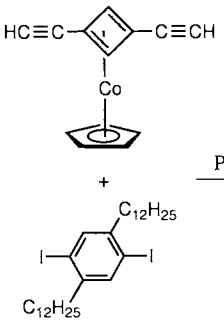

$\xrightarrow{Pd^{II}, CuI}$

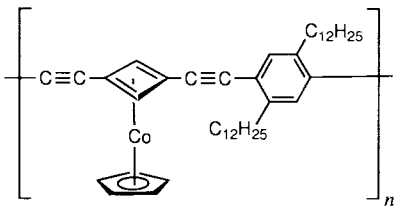

(37)

58

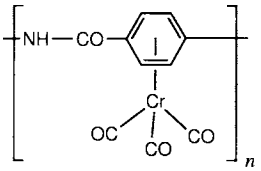

59

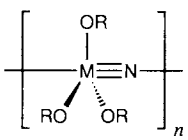

60

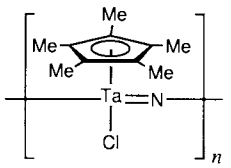

61

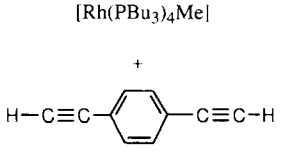

$\xrightarrow{-PBu_3, -CH_4}$

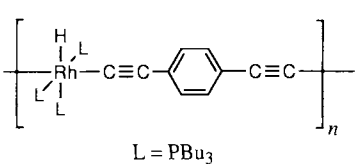

(36)

L = PBu_3

57

polymer, since the $Cr(CO)_3$ groups can be easily added and removed, and poly(*p*-phenyleneterephthalamide) is only soluble in concentated sulfuric acid.[210–212]

Related to polymetallynes are polymeric metal nitrides (e.g. **60** M = Mo or W).[187, 213, 214] Examples of these materials are known in the solid state but these generally dissociate into monomers with M≡N bonds in solvents in which they are soluble. To date, reports of soluble polymers such as **61** and

related species have been very brief[214] but such materials are of considerable interest and warrant further study.

5.4. Polymers with Metal–Metal Bonds in the Main Chain

Polymers containing metal–metal bonds in the polymer backbone might be expected to have novel conductive and photochemical properties.[115] In general, little work has been carried out in this area; however, in 1989 Tyler and co-workers reported polycondensation routes to polyurethanes containing Mo–Mo bonds (**62**) (R = urethane linkage) or $Fe(\mu\text{-}CO)_2Fe$ units (**63**) in the polymer backbone.[215, 216] These polymers

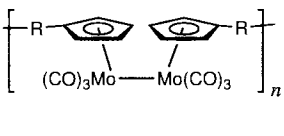

62

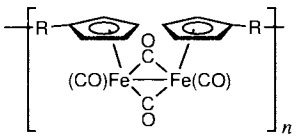

63

have M_n values between 5000 and 20000, and are of interest as photoreactive materials since the metal–metal bonds could be cleaved photochemically by visible light. In contrast, existing polymers generally require ultraviolet light for photodegradation. The quantum yields for the degradation of the polymers were found to decrease with increasing molecular weight.

Interestingly, Morán, Cuadrado, and Mosada and co-workers have recently reported the synthesis of a further class of polymers of structure **63** in which the R group is an oligosiloxane linkage, and these materials display interesting electrochemical properties.[217]

6. Future Prospects

Inorganic polymer science represents an area that until recently has been held back by the synthetic problem of constructing macromolecular chains. Even ten years ago relatively few well-characterized polymer systems were known. Recent advances have led to the preparation of a variety of new polymers that contain main group elements, transition metals, and even lanthanides. In the next few years it will be critical to examine the physical properties of these new materials in detail in both solution and in the solid state. New fundamental science can be expected to emerge as structure–property correlations are established for these novel polymer structures. It is also plausible that some of these new materials with properties that are difficult or impossible to achieve with existing organic materials may fulfill the requirements of niche markets, providing that their synthesis is straightforward and the reactants cheap. Polysiloxanes, and to a lesser extent polyphosphazenes and polysilanes, have already found applications in this way.[10] Ferrocene-based polymers have also attracted significant interest, both as electrode mediators and as materials for the construction of electronic devices.[217–220]

With the whole periodic table available there is clearly almost infinite scope for the design and synthesis of new inorganic polymer materials. For example, preliminary synthetic developments targeting polymers based on metal clusters,[221] metal–metal quadruple bonds,[222] multidecker sandwiches,[223] and metal–carbon multiple bonds[224] illustrate the remarkable potential for inorganic and organometallic chemists to make exciting and important synthetic contributions towards the development of new inorganic macromolecules with unprecedented structures and exciting properties. It is clear that considerable opportunities for both fundamental scientific studies and also applications-oriented work exist for the future.

Received: October 4, 1995 [A 137 IE]
German version: *Angew. Chem.* **1996**, *108*, 1712–1731

[1] Carbon is the 14th most abundant terrestrial element comprising only 0.08 mass % of the earth's crust, oceans, and atmosphere; see S. S. Zumdahl *Chemical Principles* 2nd ed., D. C. Heath, **1995**, p 835.
[2] *Encycl. Polym. Sci. Eng.* [*2nd Revis. Ed.*] **1985**.
[3] a) Q. Zhou, T. M. Swager, *J. Am. Chem. Soc.* **1995**, *117*, 7017; b) W. E. Moerner, *Nature*, **1994**, *371*, 475.
[4] See, for example, "Gallane at Last" A. J. Downs, M. J. Goode, C. R. Pulham, *J. Am. Chem. Soc.* **1989**, *111*, 1936.
[5] For details of isolable, sterically stabilized species with Si=Si and B≡N bonds, inorganic analogues of C=C and C≡C bonds, see a) R. West *Angew. Chem.* **1987**, *99*, 1231; *Angew. Chem. Int. Ed. Engl.* **1987**, *26*, 1201; b) P. Paetzold, *Adv. Inorg. Chem.* **1987**, *31*, 123.
[6] For details of the key differences between chain-growth and step-growth polymerizations see, for example R. J. Young, P. A. Lovell, *Introduction to Polymers*, Chapman & Hall, 2nd ed., New York, **1992**, p. 15–108.
[7] According to Carothers theory of polycondensation reactions, to obtain a polymer with $M_n > 10000$ from a monomer with a molecular weight of 100, even if 100% extent of reaction can be achieved, the ratio of the two difunctional monomers must be better than 0.98:1. See R. J. Young, P. A. Lovell, *Introduction to Polymers*, Chapman & Hall, 2nd ed., New York, **1992**, p 24.
[8] For a discussion of the need for long chains to obtain the valuable properties that are characteristic of polymers see I. M. Campbell, *Introduction to Synthetic Polymers* Oxford University Press, New York, **1994**, pp. 36–39.
[9] *The Chemistry of Inorganic Homo- and Heterocycles, Vol. 1 and 2* (Eds.: I. Haiduc, D. B. Sowerby), Academic Press, Toronto, **1987**.
[10] J. E. Mark, H. R. Allcock, R. West, *Inorganic Polymers*, Prentice Hall, **1992**.
[11] *Inorganic and Organometallic Oligomers and Polymers* (Eds.: R. M. Laine, J. F. Harrod), Kluwer, Amsterdam, **1991**.
[12] a) "Inorganic and Organometallic Polymers": *ACS Symp. Ser.* **1988**, *360*; b) "Inorganic and Organometallic Polymers II": *ACS Symp. Ser.* **1994**, *572*.
[13] For annual reviews of the inorganic polymer literature from 1990 onwards see I. Manners, *Ann. Rep. Prog. Chem. Sect. A Inorg Chem.* **1994**, *91*, 131, and references therein.
[14] "Silicon-Based Polymer Science": *Adv. Chem. Ser.* **1990**, *224*.
[15] *Siloxane Polymers* (Eds.: J. A. Semlyen, S. J. Clarson), Prentice Hall, Englewood Cliffs, NJ, **1991**.
[16] For an entertaining account of the history and applications of polysiloxanes see E. G. Rochow, *Silicon and Silicones*, Springer, Heidelberg, **1987**.
[17] B. Arkles *CHEMTECH*., **1983**, *13*, 542.
[18] For a recent overview of the silicone breast implant controversy see *Chem. Eng. News*, **1995**, December 11, 10–17. See also, for example, a) P. Macdonald, N. Plavac, W. Peters, S. Lugowski, D. Smith, *Anal. Chem.* **1995**, *67*, 3799; b) D. M. Gott, J. J. B. Tinkler, *Silicone Implants and Connective Tissue Disease: Evaluation of Evidence for an Association between the Implantation of Silicones and Connective Tissue Disease* Medical Devices Agency, 14 Russell Square, London, December **1994**.
[19] G. J. J. Out, A. A. Turetskii, M. Möller, D. Oelfin, *Macromolecules* **1994**, *27*, 3310.
[20] J. Chojnowski, *J. Inorg. Organomet. Polym.* **1991**, *1*, 299.
[21] J. Stein, L. N. Lewis, K. A. Smith, K. X. Lettko, *J. Inorg. Organomet. Polym.* **1991**, *1*, 325.
[22] S. Boileau, D. Teyssie, *J. Inorg. Organomet. Polym.* **1991**, *1*, 247.
[23] H. Poths, R. Zentel, *Macromol. Rapid Commun.* **1994**, *15*, 433.
[24] H. Gankema, R. J. W. Lugtenberg, J. F. J. Engbersen, D. N. Reinhoudt, M. Möller, *Adv. Mater.* **1994**, *6*, 944.
[25] H. R. Allcock, R. L. Kugel, *J. Am. Chem. Soc.* **1965**, *87*, 4216.
[26] H. R. Allcock, *J. Inorg. Organomet. Polym.* **1992**, *2*, 197.
[27] H. R. Allcock, *Chem. Mater.* **1994**, *6*, 1476.
[28] H. R. Allcock, *Adv. Mater.* **1994**, *6*, 106.
[29] H. R. Allcock, C. Kim, *Macromolecules* **1989**, *22*, 2596.
[30] H. R. Allcock, C. Kim, *Macromolecules* **1991**, *24*, 2846.

[31] H. R. Allcock, A. A. Dembek, E. H. Klingenberg, *Macromolecules* **1991**, *24*, 5208.
[32] H. R. Allcock, C. G. Cameron, *Macromolecules* **1994**, *27*, 3131.
[33] For other work on the photophysical properties of polyphosphazenes see, for example, G. Facchin, F. Minto, M. Gleria, R. Bertani, P. Bortolus, *J. Inorg. Organomet. Polym.* **1991**, *1*, 389.
[34] D. C. Ngo, J. S. Rutt, H. R. Allcock, *J. Am. Chem. Soc.* **1991**, *113*, 5075; H. R. Allcock, S. E. Kuharcik, C. T. Morrissey, D. C. Ngo, *Macromolecules* **1994**, *27*, 7556.
[35] R. H. Neilson, P. Wisian-Neilson, *Chem. Rev.* **1988**, *88*, 541.
[36] R. A. Montague, K. Matyjaszewski, *J. Am. Chem. Soc.* **1990**, *112*, 6721.
[37] a) K. Matyjaszewski, *J. Inorg. Organomet. Polym.* **1992**, *2*, 5; b) K. Matyjaszewski, R. A. Montague, J. Dauth, O. Nuyken *J. Polym. Sci. Part A: Polym. Chem.* **1992**, *30*, 813; c) K. Matyjaszewski, U. Franz, R. A. Montague, M. L. White *Polymer*, **1994**, *35*, 5005.
[38] G. D'Halluin, R. de Jaeger, J. P. Chambrette, P. Potin *Macromolecules* **1992**, *25*, 1254.
[39] C. H. Honeyman, I. Manners, C. Morrissey, H. R. Allcock, *J. Am. Chem. Soc.* **1995**, *117*, 7035.
[40] Organic polymers with phosphazene side groups also have interesting properties and may also be commercially attractive. See, for example, D. E. Brown, C. W. Allen, *J. Inorg. Organomet. Polym.* **1991**, *1*, 189.
[41] R. West, *J. Organomet. Chem.* **1986**, *300*, 327
[42] R. D. Miller, J. Michl, *Chem. Rev.* **1989**, *89*, 1359
[43] K. Matyjaszewski, *J. Inorg. Organomet. Polym.* **1991**, *1*, 463.
[44] K. S. Madiyasni, R. West, L. D. David, *J. Am. Ceram. Soc.* **1978**, *61*, 504.
[45] For theoretical analyses of the phenomenon of σ delocalization in polysilanes and related materials see, for example: H. Teramae, K. Takeda, *J. Am. Chem. Soc.* **1989**, *111*, 1281; J. Nelson, W. J. Pietro, *J. Phys. Chem.* **1988**, *92*, 1365; A. Savin, O. Jepsen, J. Flad, O. K. Andersen, H. Preuss, H. G. von Schnering, *Angew. Chem* **1992**, *104*, 186; *Angew. Chem. Int. Ed. Engl.* **1992**, *31*, 187.
[46] The lowest absorption bands of polysilanes have also recently been assigned to excitonic rather than interband transitions. See H. Tachibana, M. Matsumoto, Y. Tokura, Y. Moritomo, A. Yamaguchi, S. Koshihara, R. D. Miller, S. Abe, *Phys. Rev. B.* **1993**, *47*, 4363.
[47] a) C. T. Aitken, J. F. Harrod, E. Samuel, *J. Organomet. Chem.* **1985**, *279*, C11; b) C. T. Aitken, J. F. Harrod, E. Samuel, *J. Am. Chem. Soc.* **1986**, *108*, 4059.
[48] T. D. Tilley, *Acc. Chem. Res.* **1993**, *26*, 22, and references therein.
[49] M. Scarlete, S. Brienne, I. S. Butler, J. F. Harrod, *Chem. Mater.* **1994**, *6*, 977.
[50] Y. Hsiao, R. M. Waymouth, *J. Am. Chem. Soc.* **1994**, *116*, 9779.
[51] a) M. Cypryk, Y. Gupta, K. Matyjaszewski, *J. Am. Chem. Soc.* **1991**, *113*, 1046; b) E. Fossum, K. Matyjaszewski, *Macromolecules* **1995**, *28*, 1618.
[52] K. Sakamoto, K. Obata, H. Hirata, M. Nakajima, H. Sakurai, *J. Am. Chem. Soc.* **1989**, *111*, 7641.
[53] H. Suzuki, H. Meyer, J. Simmerer, J. Yang, D. Haarer, *Adv. Mater.* **1993**, *5*, 743.
[54] Y. Wang, R. West, C. H. Yuan, *J. Am. Chem. Soc.* **1993**, *115*, 3844.
[55] H. Frey, M. Möller, K. Matyjaszewski, *Macromolecules* **1994**, *27*, 1814.
[56] J. B. Lambert, J. L Pflug, C. L. Stern, *Angew. Chem.* **1995**, *107*, 106; *Angew. Chem. Int. Ed. Engl.* **1995**, *34*, 98.
[57] A. Sekiguchi, M. Nanjo, C. Kabuto, H. Sakurai, *J. Am. Chem. Soc.* **1995**, *117*, 4195; H. Suzuki, Y. Kimata, S. Satoh, A. Kuriyama, *Chem. Lett.* **1995**, 293.
[58] D. R. Weyenberg, L. E. Nelson, *J. Org. Chem.* **1965**, *30*, 2618; C. S. Cundy, M. F. Lappert, *J. Chem. Soc. Dalton Trans.* **1978**, 665, and references therein.
[59] For some recent work on transition metal catalyzed ROP of silacyclobutanes see H. Yamashita, M. Tanaka, K. Honda, *J. Am. Chem. Soc.* **1995**, *117*, 8873.
[60] R. J. P. Corriu, P. Gerbier, C. Guérin, B. J. L. Henner, A. Jean, P. H. Mutin, *Organometallics*, **1992**, *11*, 2507.
[61] J. L. Bréyfort, R. J. P. Corriu, P. Gerbier, C. Guérin, B. J. L. Henner, A. Jean, T. Kuhlmann, F. Garnier, A. Yassar, *Organometallics* **1992**, *11*, 2500
[62] M. Ishikawa, T. Hatano, Y. Hasegawa, T. Horio, A. Kunai, A. Miyai, T. Ishida, T. Tsukihara, T. Yamanaka, T. Koike, J. Shioya, *Organometallics* **1992**, *11*, 1604.
[63] a) S. J. Sargeant, S. Q. Zhou, G. Manuel, W. P. Weber, *Macromolecules* **1992**, *25*, 2832; b) M. Theurig, S. J. Sargeant, G. Manuel, W. P. Weber, *Macromolecules* **1992**, *25*, 3834.
[64] R. West, S. Hayase and T. Iwahara, *J. Inorg. Organomet. Polym.* **1991**, *1*, 545.
[65] For the use of acyclic diene metathesis polymerization (ADMET) and ring-opening metathesis polymerization (ROMP) to prepare poly(carbosilane)s see, for example, a) K. B. Wagener, D. W. Smith, *Macromolecules* **1991**, *24*, 6073; b) J. T. Anhaus, W. Clegg, S. P. Collingwood, V. C. Gibson, *J. Chem. Soc. Chem. Commun.* **1991**, 1720.
[66] A. W. van der Made, P. W. N. M. van Leeuwen, *J. Chem. Soc. Chem. Commun.* **1992**, 1400.
[67] L. L. Zhou, J. Roovers, *Macromolecules* **1993**, *26*, 963.
[68] R. Laine, F. Babonneau, *Chem. Mater.* **1993**, *5*, 260.
[69] a) J. Bill, F. Aldringer, *Adv. Mater.* **1995**, *7*, 775; b) J. P. Pillot, *Chem. Rev.* **1995**, *95*, 1443.
[70] L. J. Procopio, D. H. Berry, *J. Am. Chem. Soc.* **1991**, *113*, 4039.
[71] L. V. Interrante, H. J. Wu, T. Apple, Q. Shen, B. Ziemann, D. M. Narsavage, K. Smith, *J. Am. Chem. Soc.* **1994**, *116*, 12085.
[72] H. J. Wu, L. V. Interrante, *Macromolecules* **1992**, *25*, 1840; I. L. Rushkin, L. V. Interrante, *Macromolecules* **1995**, *28*, 5160.
[73] H. Isaka, H. Teramae, M. Fujiki, N. Matsumoto, *Macromolecules* **1995**, *28*, 4733.
[74] P. Bianconi, T. W. Weidman, *J. Am. Chem. Soc.* **1988**, *110*, 2342.
[75] P. Bianconi, F. C. Schilling, T. W. Weidman, *Macromolecules* **1989**, *22*, 1697.
[76] T. W. Weidman, P. Bianconi, E. W. Kwock, *Ultrasonics* **1990**, *28*, 310.
[77] W. J. Szymanski, G. T. Visscher, P. A. Bianconi, *Macromolecules* **1993**, *26*, 869.
[78] P. Trefonas III., R. West, *J. Polym. Sci. Polym. Chem. Ed.* **1985**, *23*, 2099.
[79] R. D. Miller, R. Sooriyakumaran, *J. Polym. Sci. Polym. Chem. Ed.* **1987**, *25*, 111.
[80] S. Adams, M. Dräger, *Angew. Chem.* **1987**, *99*, 1280; *Angew. Chem. Int. Ed. Engl.* **1987**, *26*, 1255, and references therein.
[81] L. R. Sita, K. W. Terry, K. Shibata, *J. Am. Chem. Soc.* **1995**, *117*, 8049, and references therein.
[82] K. Takeda, K. Shiraishi, *Chem. Phys. Lett.* **1992**, *195*, 121.
[83] T. Imori, T. D. Tilley, *J. Chem. Soc. Chem. Commun.* **1993**, 1607.
[84] T. Imori, V. Lu, H. Cai, T. D. Tilley, *J. Am. Chem. Soc.*, **1995**, *117*, 9931.
[85] I. Manners, G. Renner, H. R. Allcock, O. Nuyken, *J. Am. Chem. Soc.* **1989**, *111*, 5478.
[86] H. R. Allcock, S. M. Coley , I. Manners, O. Nuyken, G. Renner, *Macromolecules* **1991**, *24*, 2024.
[87] H. R. Allcock, S. M. Coley, I. Manners, K. B. Visscher, M. Parvez, O. Nuyken, G. Renner, *Inorg. Chem.* **1993**, *32*, 5088.
[88] H. R. Allcock, S. M. Coley, C. T. Morrissey, *Macromolecules* **1994**, *27*, 2904.
[89] I. Manners, *Coord. Chem. Revs.* **1994**, *137*, 109.
[90] Poly(sulfur nitride), $[SN]_x$, possesses remarkable properties such as electrical conductivity at room temperature and superconductivity below 0.3 K; see M. M. Labes, P. Love, L. F. Nichols, *Chem. Rev.* **1979**, *79*, 1. $[SN]_x$ is insoluble and has a polymeric structure in the solid state with interchain S···S interactions. As these interactions are crucial to the properties of the material, $[SN]_x$ is best regarded as a solid-state polymer rather than a polymeric material with discrete macromolecular chains of the type discussed in this review article.
[91] J. A. Dodge, I. Manners, G. Renner, H. R. Allcock, O. Nuyken, *J. Am. Chem. Soc.* **1990**, *112*, 1268.
[92] H. R. Allcock, J. A. Dodge, I. Manners, *Macromolecules* **1993**, *26*, 11.
[93] M. Liang, I. Manners, *J. Am. Chem. Soc.* **1991**, *113*, 4044.
[94] M. Liang, I. Manners, *Makromol. Chem. Rapid Commun.* **1991**, *12*, 613.
[95] a) J. C. van de Grampel, *Rev. Inorg. Chem.* **1981**, *3*, 1; b) *Coord. Chem. Rev.* **1992**, *112*, 247.
[96] Y. Ni, A. J. Lough, A. L. Rheingold, I. Manners, *Angew. Chem.* **1995**, *107*, 1079; *Angew. Chem. Int. Ed. Engl.* **1995**, *34*, 998.
[97] Y. Ni, A. Stammer, M. Liang, J. Massey, G. J. Vancso, I. Manners, *Macromolecules* **1992**, *25*, 7119.
[98] Y. Ni, M. Liang, J. Massey, I. Manners, *Macromolecules* **1996**, *29*, 3401.
[99] R. Jaeger, J. Lagowski, I. Manners, G. J. Vancso *Macromolecules* **1995**, *28*, 539.
[100] T. Chivers, D. D. Doxsee, M. Edwards, R. W. Hilts, in *The Chemistry of Inorganic Ring Systems*, (Ed.: R. Steudel) *Studies in Chemistry, Vol. 14*, Elsevier, **1992**, p 291.
[101] a) F. Seel, G. Simon, *Angew. Chem.* **1960**, *72*, 709; b) G. W. Parshall, R. Cramer, R. E. Foster, *Inorg. Chem.* **1962**, *1*, 677.
[102] A. K. Roy, *J. Am. Chem. Soc.* **1992**, *114*, 1530.
[103] A. K. Roy, G. T. Burns, G. C. Lie, S. Grigoras, *J. Am. Chem. Soc.* **1993**, *115*, 2604.
[104] S. Kobayashi, S. Iwata, M. Hiraishi, *J. Am. Chem. Soc.* **1994**, *116*, 6047.
[105] Y. Chujo, N. Takizawa, T. Sakurai, *J. Chem. Soc., Chem. Commun.* **1994**, 227.
[106] Y. Chujo in "Inorganic and Organometallic Polymers II": *ACS Symp. Ser.* **1994**, *572*, 398.
[107] a) R. T. Paine, C. K. Narula, *Chem. Rev.* **1990**, *90*, 73; b) R. T. Paine, *J. Inorg. Organomet. Polym.* **1992**, *2*, 183.
[108] For an excellent overview of recent developments in borazine-based polymers see R. T. Paine, L. G. Sneddon in "Inorganic and Organometallic Polymers II": *ACS Symp. Ser.* **1994**, *572*, 358–374.
[109] P. J. Fazan, J. S. Beck, A. T. Lynch, E. E. Remsen, L. G. Sneddon, *Chem. Mater.* **1990**, *2*, 96.
[110] P. J. Fazan, E. E. Remsen, J. S. Beck, P. J. Carroll, A. R. McGhie, L. G. Sneddon, *Chem. Mater.* **1995**, *7*, 1942.
[111] a) See ref. [5b], pp. 141–143; b) P. Paetzold, T. von Bennigsen-Mackiewicz, *Chem. Ber.* **1981**, *114*, 298.
[112] Y. Chujo, I. Tomita, T. Saegusa, *Macromolecules* **1992**, *25*, 3005.
[113] See ref. [10], pp. 241–243, and references therein; H. N. Han, D. A. Lindquist, J. S. Haggerty, D. Seyferth, *Chem. Mater.* **1992**, *4*, 705.
[114] a) T. S. Haddad, J. D. Lichtenhan *J. Inorg. Organomet. Polym.*, **1995**, *5*, 237; b) J. D. Lichtenhan, N. Q. Vu, J. A. Carter, J. W. Gilman, F. J. Feher, *Macromolecules* **1993**, *26*, 2141; c) J. D. Lichtenhan, Y. A. Otonari, M. J. Carr, *Macromolecules* **1995**, *28*, 8435; d) J. D. Lichtenhan, *Comments Inorg. Chem.* **1995**, *17*, 115.
[115] a) *Inorganic Materials* (Eds.: D. W. Bruce, D. O'Hare), Wiley, **1992**; b) *Extended Linear Chain Compounds, Vols. 1–3*, (Ed.: J. S. Miller), Plenum, New

York, **1982**; c) S. L. Ingham, N. J. Long, *Angew. Chem.* **1994**, *106*, 1847; *Angew. Chem. Int. Ed. Engl.* **1994**, *33*, 1752; d) L. Oriol, J. L. Serrano, *Adv. Mater.* **1995**, *7*, 348.
[116] a) N. G. Connelly, W. E. Geiger, *Adv. Organomet. Chem.* **1984**, *23*, 1; b) N. G. Connelly, W. E. Geiger, *ibid.* **1985**, *24*, 87.
[117] J. E. Sheats, C. E. Carraher, C. U. Pittman, *Metal Containing Polymer Systems*, Plenum, **1985**.
[118] C. U. Pittman, Jr., C. E. Carraher, J. R. Reynolds, "Organometallic Polymers" in *Encyl. Polym. Sci. Eng.* **1987**, *10*, 541.
[119] I. Manners, *Chem. Br.* **1996**, *32*, 46.
[120] See ref. [69]; M. Peuckert, T. Vaahs, M. Brück, *Adv. Mater.* **1990**, *2*, 398.
[121] E. W. Neuse, H. Rosenberg, *J. Macromol. Sci. Rev. Macromol. Chem.* **1970**, *C4(1)*, 1; see p. 130.
[122] C. U. Pittman, J. C. Lai, D. P. Vanderpool, M. Good, R. Prado, *Macromolecules* **1970**, *3*, 746.
[123] W. J. Patterson, S. McManus, C. U. Pittman, *J. Polym. Sci. Part A-1* **1974**, *12*, 837.
[124] K. Gonsalves, L. Zhanru, M. D. Rausch, *J. Am. Chem. Soc.* **1984**, *106*, 3862.
[125] M. E. Wright, M. S. Sigman, *Macromolecules* **1992**, *25*, 6055.
[126] M. E. Wright, E. G. Toplikar, H. S. Lackritz, J. J. Kerney, *Macromolecules* **1994**, *27*, 3016.
[127] U. T. Mueller-Westerhoff, *Angew. Chem.* **1986**, *98*, 700; *Angew. Chem. Int. Ed. Engl.* **1986**, *25*, 702.
[128] a) W. H. Morrison, D. N. Hendrickson, *Inorg. Chem.* **1975**, *14*, 2331; b) J. A. Kramer, D. N. Hendrickson, *ibid.* **1980**, *19*, 3330.
[129] For the recent synthesis of well-characterized polymers (M_n < ca. 11000) with main chains of ferrocene groups and vinylene, divinylene, or oligovinylene units see a) R. Bayer, T. Pöhlmann, O. Nuyken, *Makromol. Chem. Rapid Commun.* **1993**, *14*, 359; b) C. E. Stanton, T. R. Lee, R. H. Grubbs, N. S. Lewis, J. K. Pudelski, M. R. Callstrom, M. S. Erickson, M. L. McLaughlin, *Macromolecules* **1995**, *28*, 8713.
[130] C. U. Pittman, Jr., Y. Sasaki, *Chem. Lett.* **1975**, 383; N. Bilow, A. Landis, H. Rosenberg, *J. Polym. Sci. Part A-1* **1969**, *7*, 2719.
[131] E. W. Neuse, L. Bednarik, *Macromolecules* **1979**, *12*, 187.
[132] T. Yamamoto, K. Sanechika, A. Yamamoto, M. Katada, I. Motoyama, H. Sano, *Inorg. Chim. Acta.* **1983**, *73*, 75, and references therein.
[133] a) H. Rosenberg, U. S. Patent 3426053 (**1969**); b) E. W. Neuse, H. Rosenberg, *J. Macromol. Sci. Revs. Macromol. Chem.* **1970**, *C4(1)*, 110.
[134] a) For an alternative polycondensation procedure to yield poly(ferrocenylsilane)s with M_n = 2200–4100: J. Park, Y. Seo, S. Cho, D. Whang, K. Kim, T. Chang, *J. Organomet. Chem.* **1995**, *489*, 23; b) poly(ferrocenylhexasilane)s with M_w = 3500 have been prepared by a polycondensation route: see M. Tanaka, T. Hayashi, *Bull. Chem. Soc. Jpn.* **1993**, *66*, 334.
[135] D. A. Foucher, B. Z. Tang, I. Manners, *J. Am. Chem. Soc.* **1992**, *114*, 6246.
[136] W. Finckh, R. Ziembinski, B. Z. Tang, D. A. Foucher, D. B. Zamble, A. Lough, I. Manners, *Organometallics* **1993**, *12*, 823.
[137] D. A. Foucher, R. Ziembinski, B. Z. Tang, P. M. Macdonald, J. Massey, R. Jaeger, G. J. Vancso, I. Manners, *Macromolecules* **1993**, *26*, 2878.
[138] D. A. Foucher, R. Ziembinski, R. Petersen, J. Pudelski, M. Edwards, Y. Ni, J. Massey, C. R. Jaeger, G. J. Vancso, I. Manners, *Macromolecules* **1994**, *27*, 3992.
[139] J. K. Pudelski, I. Manners, *J. Am. Chem. Soc.* **1995**, *117*, 7265.
[140] J. K. Pudelski, R. Rulkens, D. A. Foucher, A. J. Lough, P. M. Macdonald, I. Manners, *Macromolecules* **1995**, *28*, 7301.
[141] I. Manners, *Adv. Organomet. Chem.* **1995**, *37*, 131.
[142] R. Rulkens, A. J. Lough, I. Manners, *J. Am. Chem. Soc.* **1994**, *116*, 797.
[143] D. A. Foucher, C. Honeyman, J. M. Nelson, B. Z. Tang, I. Manners, *Angew. Chem.* **1993**, *105*, 1843; *Angew. Chem. Int. Ed. Engl.* **1993**, *32*, 1709
[144] I. Manners, *J. Inorg. Organomet. Polym.* **1993**, *3*, 185.
[145] M. T. Nguyen, A. F. Diaz, V. V. Dement'ev, K. H. Pannell, *Chem. Mater.* **1993**, *5*, 1389.
[146] I. Manners, *Adv. Mater.* **1994**, *6*, 68.
[147] J. Rasburn, R. Petersen, T. Jahr, R. Rulkens, I. Manners, G. J. Vancso, *Chem. Mater.* **1995**, *7*, 871.
[148] B. Z. Tang, R. Petersen, D. A. Foucher, A. Lough, N. Coombs, R. Sodhi, I. Manners, *J. Chem. Soc. Chem. Commun.* **1993**, 523.
[149] R. Petersen, D. A Foucher, B.-Z. Tang, A. J. Lough, N. P. Raju, J. E. Greedan, I. Manners *Chem. Mater.* **1995**, *7*, 2045.
[150] For recent work on the pyrolysis of ferrocene–organosilicon–diacetylene oligomers see R. J. P. Corriu, N. Devylder, C. Guerin, B. Henner, A. Jean, *J. Organomet. Chem.* **1996**, *509*, 249.
[151] M. Hmyene, A. Yassar, M. Escorne, A. Percheron-Guegan, F. Garnier, *Adv. Mater.* **1994**, *6*, 564.
[152] a) R. Rulkens, Y. Ni, I. Manners, *J. Am. Chem. Soc.* **1994**, *116*, 12121; b) Y. Ni, R. Rulkens, I. Manners, *ibid.* **1996**, *118*, 4102.
[153] Y. Ni, R. Rulkens, J. K. Pudelski, I. Manners, *Makromol. Chem. Rapid Commun.* **1995**, *16*, 637.
[154] N. P. Reddy, H. Yamashita, M. Tanaka, *J. Chem. Soc. Chem. Commun.* **1995**, 2263.
[155] E. Fossum, K. Matyjaszewski, R. Rulkens, I. Manners, *Macromolecules* **1995**, *28*, 401.
[156] C. Elschenbroich, J. Hurley, B. Metz, W. Massa, G. Baum, *Organometallics* **1990**, *9*, 889.
[157] K. C. Hultzsch, J. M. Nelson, A. J. Lough, I. Manners *Organometallics* **1995**, *14*, 5496.
[158] D. A. Foucher, I. Manners, *Makromol. Chem. Rapid Commun.* **1993**, *14*, 63.
[159] D. A. Foucher, M. Edwards, R. A. Burrow, A. J. Lough, I. Manners, *Organometallics* **1994**, *13*, 4959.
[160] D. A. Foucher, R. Ziembinski, R. Rulkens, J. M. Nelson, I. Manners in "Inorganic and Organometallic Polymers II": *ACS Symp. Ser.* **1994**, *572*, 449.
[161] C. H. Honeyman, D. A. Foucher, F. Y. Dahmen, R. Rulkens, A. J. Lough, I. Manners, *Organometallics* **1995**, *14*, 5503.
[162] H. P. Withers, D. Seyferth, J. D. Fellmann, P. Garrou, S. Martin, *Organometallics* **1982**, *1*, 1283.
[163] J. D. Fellmann, P. E. Garrou, H. P. Withers, D. Seyferth, D. D. Traficante, *Organometallics* **1983**, *2*, 818.
[164] J. K. Pudelski, R. Rulkens, D. Gates, A. J. Lough, I. Manners, *Angew. Chem.* **1995**, *107*, 1633; *Angew. Chem. Int. Ed. Engl.* **1995** *34*, 1506.
[165] J. M. Nelson, H. Rengel, I. Manners, *J. Am. Chem. Soc.* **1993**, *115*, 7035.
[166] J. M. Nelson, A. J. Lough, I. Manners, *Angew. Chem* **1995**, *106*, 1019; *Angew. Chem. Int. Ed. Engl.* **1994**, *33*, 989.
[167] P. F. Brandt, T. B. Rauchfuss, *J. Am. Chem. Soc.* **1992**, *114*, 1926.
[168] C. P. Galloway, T. B. Rauchfuss, *Angew. Chem* **1993**, *105*, 1407; *Angew Chem. Int. Ed. Engl.* **1993**, *32*, 1319.
[169] a) D. L. Compton, T. B. Rauchfuss, *Organometallics* **1994**, *13*, 4367; b) D. L. Compton, P. F. Brandt, T. B. Rauchfuss, D. F. Rosenbaum, C. F. Zukoski, *Chem. Mater.* **1995**, *7*, 2342.
[170] Ferrocenylsulfido polymers have also been prepared by condensation routes. See: O. Nuyken, T. Pöhlmann, M. Herberhold *Macromol. Rep.* **1992**, *A29(3)*, 211.
[171] H. M. Nugent, M. Rosenblum, P. Klemarczyk, *J. Am. Chem. Soc.* **1993**, *115*, 3848.
[172] M. Rosenblum, *Adv. Mater.* **1994**, *6*, 159.
[173] M. Rosenblum, H. M. Nugent, K.-S. Jang, M. M. Labes, W. Cahalane, P. Klemarczyk, W. M. Reiff, *Macromolecules* **1995**, *28*, 6330.
[174] a) R. Arnold, S. A. Matchett, M. Rosenblum, *Organometallics* **1988**, *7*, 2261; b) B. M. Foxman, M. Rosenblum, *ibid.* **1993**, *12*, 4805.
[175] B. M. Foxman, D. A. Gronbeck, M. Rosenblum, *J. Organomet. Chem.* **1991**, *413*, 287.
[176] M. Marcos, L. Oriol, J. L. Serrano, *Macromolecules* **1992**, *25*, 5362.
[177] D. Perreault, M. Drouin, A. Michel, P. D. Harvey, *Inorg. Chem.* **1992**, *31*, 3688.
[178] H. Chen, R. D. Archer, *Macromolecules* **1995**, *28*, 1609.
[179] H. Chen, J. A. Cronin, R. D. Archer, *Macromolecules* **1994**, *27*, 2174.
[180] M. Hanack, M. Lang, *Adv. Mater.* **1994**, *6*, 819.
[181] T. J. Marks, *Angew. Chem.* **1990**, *102*, 886; *Angew. Chem. Int. Ed. Engl.* **1990**, *29*, 857.
[182] S. Achar, R. J. Puddephatt, *Angew. Chem.* **1994**, *106*, 895; *Angew. Chem. Int. Ed. Engl.* **1994**, *33*, 847.
[183] S. Achar, R. J. Puddephatt, *J. Chem. Soc. Chem. Commun.*, **1994**, 1895.
[184] S. Serroni, G. Denti, S. Campagna, A. Juris, M. Ciano, V. Balzani, *Angew. Chem.* **1992**, *104*, 1540; *Angew. Chem. Int. Ed. Engl.* **1992**, *31*, 1493.
[185] G. R. Newkome, F. Cardullo, E. C. Constable, C. N. Moorefield, A. M. W. Cargill Thompson, *J. Chem. Soc. Chem. Commun.* **1993**, 925.
[186] For some examples of interesting ferrocene-containing organometallic dendrimers see a) B. Alonso, I. Cuadrado, M. Morán, J. Losada, *J. Chem. Soc. Chem. Commun.* **1994**, 2575; b) B. Alonso, M. Morán, C. Casado, F. Lobete, J. Losada, I. Cuadrado, *Chem. Mater.* **1995**, *7*, 1440.
[187] M. H. Chisholm, *Angew. Chem.* **1991**, *103*, 690; *Angew. Chem. Int. Ed. Engl.* **1991**, *30*, 673.
[188] K. Sonogashira S. Takahashi, N. Hagihara, *Macromolecules* **1977**, *10*, 879.
[189] S. Takahashi, N. Hagihara, K. Sonogashira, *Macromolecules* **1978**, *11*, 1063.
[190] N. Hagihara, K. Sonogashira, S. Takahashi, *Adv. Polym. Sci.* **1981**, *41*, 149.
[191] S. J. Davies, B. F. G. Johnson, M. S. Khan, J. Lewis, *J. Chem. Soc. Chem. Commun.* **1991**, 187.
[192] B. F. G. Johnson, A. K. Kakkar M. S. Khan, J. Lewis, *J. Organomet Chem.* **1991**, *409*, C12.
[193] K. C. Sturge, A. D. Hunter, R. McDonald, B. D. Santarsiero, *Organometallics* **1992**, *11*, 3056.
[194] X. A. Guo, K. C. Sturge, A. D. Hunter, M. C. Williams *Macromolecules* **1994**, *27*, 7825.
[195] a) Nishihara, T. Shimura, A. Ohkubo, N. Matsuda, K. Aramaki, *Adv. Mater.* **1993**, *5*, 752; b) I. Tomita, A. Nishio, T. Endo, *Macromolecules* **1994**, *27*, 7009.
[196] S. S. H. Mao, T. D. Tilley, *J. Am. Chem. Soc.* **1995**, *117*, 5365.
[197] H. B. Fyfe, M. Mlekuz, D. Zargarian, N. J. Taylor, T. B. Marder, *J. Chem. Soc. Chem. Commun.* **1991**, 188.
[198] A. Abe, N. Kimura, S. Tabata, *Macromolecules*, **1991**, 24, 6238.
[199] C. C. Frazier, S. Guha, W. P. Chen, M. P. Cockerham, P. L. Porter, E. A. Chauchard, C. H. Lee, *Polymer* **1987**, *28*, 553.
[200] J. Lewis, M. S. Khan, A. K. Kakkar, B. F. G. Johnson, T. B. Marder, H. B. Fyfe, F. Wittmann, R. H. Friend, A. E. Dray, *J. Organomet. Chem.* **1992**, *425*, 165.

[201] M. S. Khan, A. K. Kakkar, N. J. Long, J. Lewis, P. Raithby, P. Nguyen, T. B. Marder, F. Wittmann, R. H. Friend, *J. Mater. Chem.* **1994**, *4*, 1227.
[202] G. Frapper, M. Kertesz *Inorg. Chem.* **1993**, *32*, 732.
[203] W. J. Blau, H. J. Byrne, D. J. Cardin, A. P. Davey, *J. Mater. Chem.* **1991**, *1*, 245.
[204] A. E. Dray, F. Wittmann, R. H. Friend, A. M. Donald, M. S. Khan, J. Lewis, B. F. G. Johnson, *Synthetic Metals* **1991**, *41–43*, 871.
[205] C. W. Faulkner, S. L. Ingham, M. S. Khan, J. Lewis, N. J. Long, P. R. Raithby, *J. Organomet. Chem.* **1994**, *482*, 139.
[206] K. A. Bunten, A. K. Kakkar *J. Mater. Chem.* **1995**, *5*, 2041.
[207] G. Jia, R. J. Puddephatt, J. J. Vittal, N. C. Payne *Organometallics* **1993**, *12*, 263.
[208] M. Altmann, U. H. F. Bunz, *Angew. Chem* **1995**, *107*, 603; *Angew. Chem. Int. Ed. Engl.* **1995**, *34*, 569.
[209] M. Altmann, V. Enkelmann, G. Lieser, U. H. F. Bunz, *Adv. Mater.* **1995**, *7*, 726.
[210] A. A. Dembek, R. R. Burch, A. E. Feiring, *J. Am. Chem. Soc.* **1993**, *115*, 2087.
[211] D. Tanner, J. A. Fitzgerald, B. R. Phillips, *Angew. Chem. Adv. Mater.* **1989**, *101*, 665; *Angew. Chem. Int. Ed. Engl. Adv. Mater.* **1989**, *28*, 649; *Adv. Mater.* **1989**, *1*, 151.
[212] For other recent work on the coordination of transition metal fragments to π-hydrocarbon units see a) A. A. Dembek, P. J. Fagan, M. Marsi, *Macromolecules* **1993**, *26*, 2992; b) A. S. Abd-El-Aziz, C. R. de Denus, *J. Chem. Soc. Chem. Commun.* **1994**, 663.
[213] See, for example, a) S. C. Critchlow, M. E. Lerchen, R. C. Smith, N. M. Doherty, *J. Am. Chem. Soc.* **1988**, *110*, 8071; b) T. P. Pollagi, T. C. Stoner, R. F. Dallinger, T. M. Gilbert, M. D. Hopkins, *ibid.* **1991**, *113*, 703.
[214] a) H. W. Roesky, M. Lücke, *J. Chem. Soc. Chem. Commun*, **1989**, 748; b) *Angew. Chem.* **1989**, *101*, 480; *Angew. Chem. Int. Ed. Engl.* **1989**, *28*, 493.
[215] S. C. Tenhaeff, D. R. Tyler, *Organometallics* **1991**, *10*, 473.
[216] S. C. Tenhaeff, D. R. Tyler, *Organometallics* **1992**, *11*, 1466.
[217] M. Morán, M. C. Pascual, I. Cuadrado, J. Losada, *Organometallics* **1993**, *12*, 811.
[218] S. P. Hendry, M. F. Cardosi, A. P. F. Turner, E. W. Neuse, *Anal. Chim. Acta* **1993**, *281*, 453.
[219] P. D. Hale, L. I. Boguslavsky, T. Inagaki, H. I. Karan, H. S. Lee, T. A. Skotheim, Y. Okamoto, *Anal. Chem.* **1991**, *63*, 677.
[220] G. P. Kittlesen, H. S. White, M. S. Wrighton, *J. Am. Chem. Soc.* **1985**, *107*, 7373.
[221] M. R. Jordan, P. S. White, C. K. Schauer, M. A. Mosley, *J. Am. Chem. Soc.* **1995**, *117*, 5403.
[222] R. H. Cayton, M. H. Chisholm, J. C. Huffman, E. B. Lobkovsky, *J. Am. Chem. Soc.* **1991**, *113*, 8709.
[223] a) X. Meng, M. Sabat, R. N. Grimes, *J. Am. Chem. Soc.* **1993**, *115*, 6143; b) J. R. Pipal, R. N. Grimes, *Organometallics* **1993**, *12*, 4459; c) X. Wang, M. Sabat, R. N. Grimes, *J. Am. Chem. Soc.* **1994**, *116*, 2687.
[224] T. P. Pollagi, S. J. Geib, M. D. Hopkins, *J. Am. Chem. Soc.* **1994**, *116*, 6051.

Time is money...

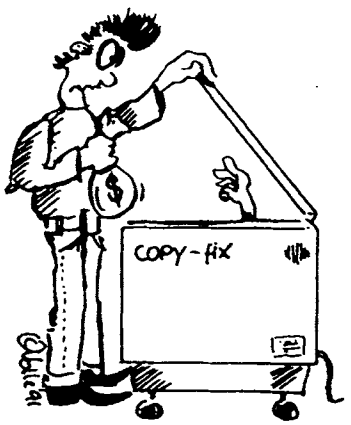

Save both by starting a personal subscription to *Angewandte Chemie* (now with *Chemistry - A European Journal*). At 9¢ per page you can't go wrong. With your own private copy you can read the "hot" articles before they cool, and waste less time in front of the copier.

Order now!
An order form can be found on the last page of this issue.

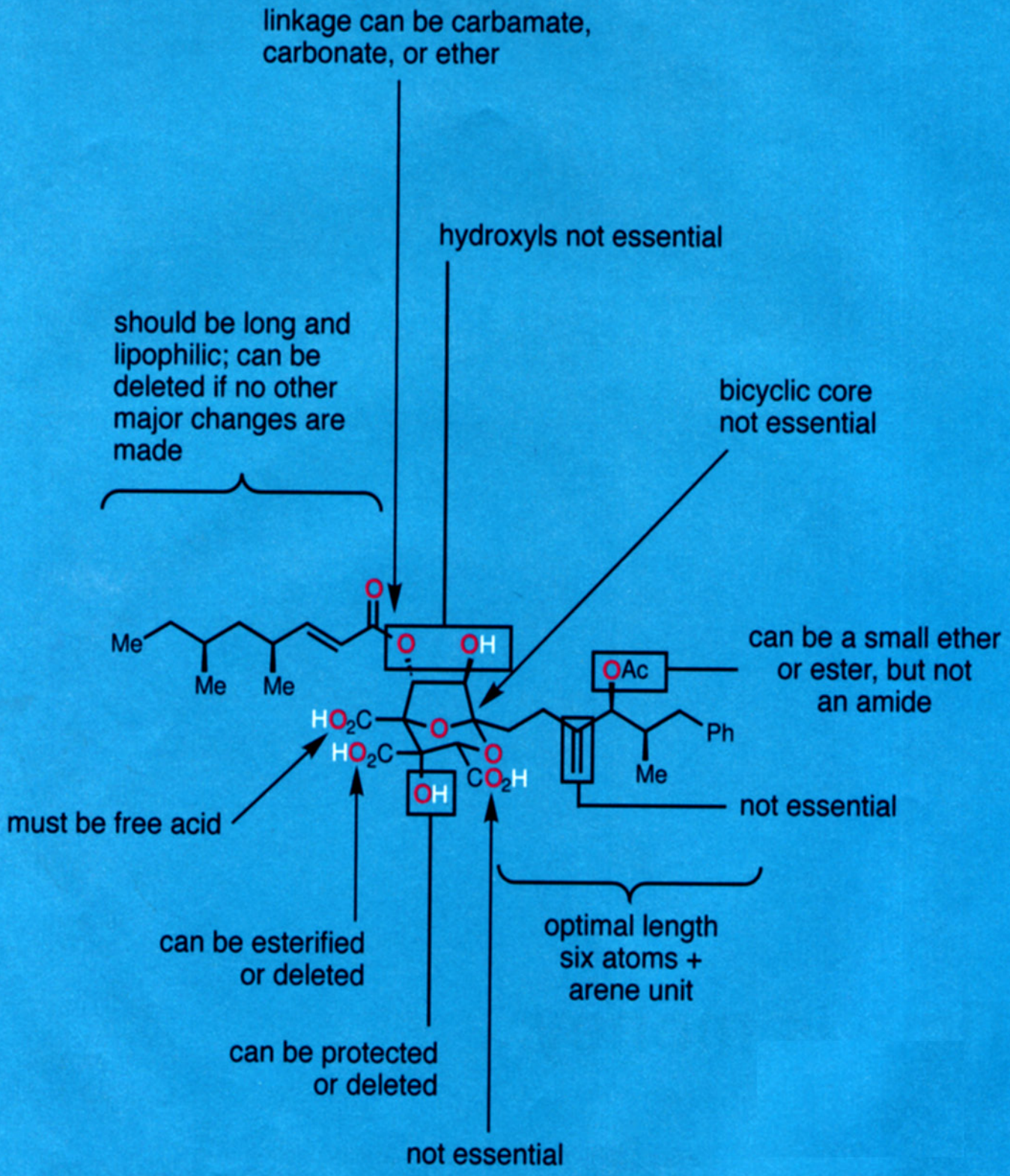

Chemistry and biology are both required in order to determine the importance of individual structure elements in zaragozic acid A.

Chemistry and Biology of the Zaragozic Acids (Squalestatins)**

Alan Nadin and K. C. Nicolaou*

New natural products seldom arouse much excitement. However, with their unprecedented and heavily oxygenated molecular structure, and potentially lucrative biological activity, the zaragozic acids (squalestatins) provoked a flurry of activity among academic and industrial chemists and biologists in the early 1990s. Since they are powerful inhibitors of squalene synthase, the enzyme catalyzing the first committed step on the biosynthetic pathway to cholesterol, hopes were high that the zaragozic acids would follow the huge commercial success of the mevinic acids by becoming second-generation cholesterol-lowering drugs. The unusual and characteristic 2,8-dioxabicyclo[3.2.1]octane-3,4,5-tricarboxylic acid "core" structure of the zaragozic acids stimulated a large number of diverse synthetic studies, ranging from the traditional to the avant garde. In this review we attempt to bring together for the first time the chemistry and biology of this fascinating class of molecules.

Keywords: enzyme inhibitors · natural products · squalestatins · synthetic methods · zaragozic acids

1. Introduction

Cardiovascular disease (CVD) remains the largest cause of human death in industrialized nations. In the U. S. in 1992, 915000 deaths were recorded as resulting from CVD, compared with 521000 from all forms of cancer combined, 86000 from accidents, and 23000 from AIDS.[1] Therefore, even though the relative incidence of CVD has almost halved since the 1950s,[2] there remains keen interest in the pharmaceutical industry for developing better drugs for the treatment of CVD.

The majority of CVD mortalities (79% in 1992)[1] are due to coronary heart disease (CHD) or coronary artery disease (CAD).[3] The main cause of both CHD and CAD is atherosclerosis, a disease colloquially known as "hardening of the arteries". It is characterized by the formation of atherosclerotic plaques composed of cholesterol esters, lipids, and other cellular debris on the inside walls of large and medium-sized arteries.[2] This has the consequence of hardening the artery wall and reducing the cross-sectional area of the lumen, which results in reduced blood flow.[4] Atherosclerosis is also implicated in other mortalities and illnesses, owing to the reduced blood flow to the brain, kidneys, and intestine.[5] Atherosclerosis can be treated in some cases by bypassing the damaged area (coronary bypass surgery), by opening the lumen by balloon angioplasty, or by removing the offending plaques by surgical andarectomy. However, in a landmark ten-year study completed in 1984, the Lipid Research Clinics Program showed that by lowering serum cholesterol levels, the incidence of fatal heart disease could be decreased significantly.[6] This and subsequent studies[7] established abnormal serum cholesterol levels as a major risk factor for heart disease. Today, everyone knows about cholesterol, although there continues to be debate about the issue.[8]

The human body satisfies about half of its requirement for cholesterol by endogenous biosynthesis, which occurs mainly in the liver.[9] The remaining amount is obtained from the diet. Consequently, one often effective way of reducing serum cholesterol levels (and by implication the risk of heart disease) is to reduce the dietary intake of cholesterol.[10] As a result of government-sponsored "healthy eating" campaigns[11] and a greater public awareness of cholesterol, the average dietary consumption of cholesterol in the U. S. has decreased from a peak of about 550 mg per person per day in the 1950s[12] to about 283 mg per person per day in 1988.[13]

However, in many instances dietary regulation is impractical, insufficient, or unpopular. Consequently, extensive efforts have focused on finding effective therapeutic agents for lowering serum cholesterol levels by controlling certain key steps in the cholesterol biosynthetic pathway.[14] Those currently available can be divided into two main classes: bile acid sequestrants and HMG-CoA reductase inhibitors.[15] In response to the search for more effective medicines, emphasis has been placed on finding inhibitors of other key steps in the pathway. These investigations recently led to the isolation of a fascinating class of natural products, named the zaragozic acids or squalestatins. This review gives an overview of the chemistry and biology of these compounds.

[*] Prof. K. C. Nicolaou, Dr. A. Nadin
Department of Chemistry, The Scripps Research Institute
10550 N. Torrey Pines Road, La Jolla, CA 92037 (USA)
Fax: Int. code +(619)784-2103
e-mail: kcn@scripps.edu
and
Department of Chemistry and Biochemistry
University of California, San Diego
9500 Gilman Drive, La Jolla, CA 92093 (USA)

[**] A list of abbreviations frequently used in this review can be found at the end of the article.

In 1991 and 1992 three groups independently and almost simultaneously reported the isolation of the zaragozic acids (squalestatins). The group at Merck[16] refer to them as the zaragozic acids; the groups at Glaxo[17] and Tokyo Noko University/Mitsubishi Kasei Corporation[18] refer to them as squalestatins. We will refer to these compounds as zaragozic acids throughout this review. All three groups isolated zaragozic acid A (squalestatin S1) (**1**, Fig. 1). Merck isolated zaragozic

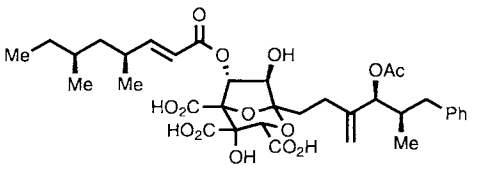

1: zaragozic acid A / squalestatin S1

acid A from the uncharacterized sterile fungus ATCC 20986, isolated from filtrates of the Jalon River in the province of Zaragoza in Spain (hence the name zaragozic acid). Glaxo isolated the same compound from a different fungus, *Phoma* sp. C2932, found in a soil sample from Armacao de Pera, Portugal, and the Japanese group from yet another fungus, *Setosphaeria khartoumensis*. In addition to zaragozic acid A, a number of other zaragozic acids have been found by Merck and Glaxo (Tables 1 and 2).

Glaxo's approach to identifying other naturally occurring zaragozic acids was to extract very minor components from large-scale fermentations of the original producer organism *Phoma*.[19] Besides the three main components (squalestatins S1, H1, and S2), this approach yielded 24 additional squalestatins (Table 1). Each squalestatin can be named by a two-character code, composed of a letter and a number correlated to the structure of the R^1 and R^2 side chains, respectively (Table 1). Some of these minor components could possibly be artifacts from the extraction techniques. It can be seen that with five exceptions (which lack oxygen functions at the C6 and C7 positions, see footnote [b] in Table 1) all the squalestatins and zaragozic acids (Tables 1 and 2) contain the same basic 2,8-dioxabicyclo[3.2.1]octane-3,4,5-tricarboxylic acid "core" with two lipophilic "arms" attached either as an acyl group on the C6 hydroxyl or as an alkyl group on the C1 carbon.

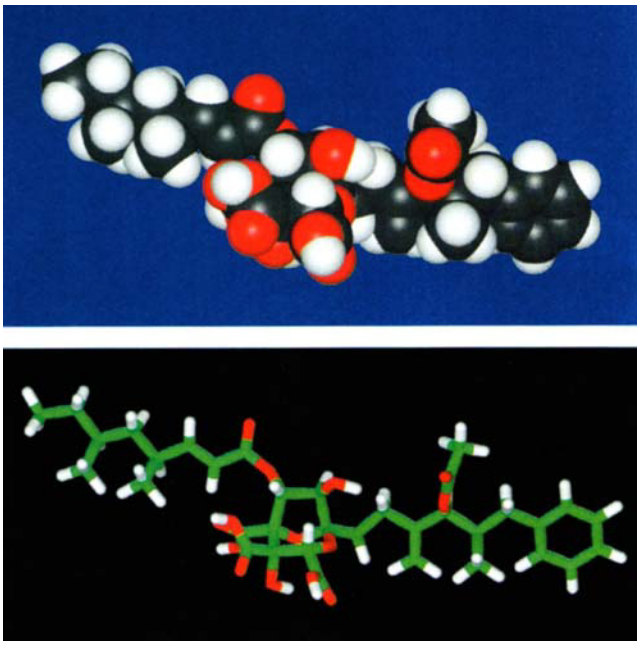

Fig. 1. Space-filling model (top) and ball-and-stick model (bottom) of zaragozic acid A/squalestatin S1 (**1**).

Merck screened a wider variety of fungi from quite different ecosystems (Table 3) and made the remarkable finding that many different fungi (from eleven different taxa of the genus *Ascomycotina*) produce zaragozic acids.[20] The main zaragozic acid produced by each fungus appears to be a characteristic of the particular fungus. For example, *Spororomiella intermedia*, from a variety of ecological sites around the world, produced mainly zaragozic acid B. Zaragozic acid C was produced by *Leptodontidium elatius*,[21] zaragozic acids D and D_2 by *Amauroascus niger*.[22] It is interesting to note that the variety of the side chains in the zaragozic acids (Table 2) is wider than in the squalestatins (Table 1), which might reflect the more diverse origins of the zaragozic acids.

The zaragozic acids appear to be relatively easy to obtain and purify. Glaxo has performed fermentations of *Phoma* on the 5000 L scale;[19] Merck has fermented ATCC 20986 on the 11000 L scale.[107] The unusual tricarboxylic acid function of

K. C. Nicolaou's biography can be found in issue 6/1996 on p. 590. The latest additions to his list of honors include the presentation of this year's Inhoffen lecture sponsored by the Biotechnologische Forschung and the Technische Universität Braunschweig and membership of the U. S. National Academy of Science.

Alan Nadin was born in London, England, in 1968 and received his BA from the University of Cambridge in 1990. He remained there and completed his PhD in 1994 under the direction of Dr. A. B. Holmes on the molecular self-recognition of medium-ring lactams. In 1994 he joined the research group of Professor Nicolaou at The Scripps Research Institute, where he worked on the zaragozic acid and maitotoxin projects. In 1996 he joined Merck, Sharp and Dohme in Harlow, England.

K. C. Nicolaou

A. Nadin

Table 1. Systematic nomenclature for the squalestatins (isolated from *Phoma*) [a, b].

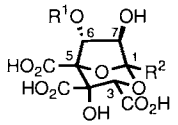

R^1	Code	R^2	Code
H	H	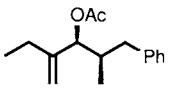	1
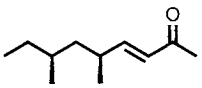	S	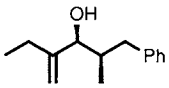	2
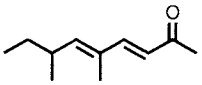	T	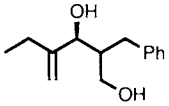	3
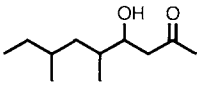	U	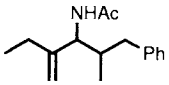	4
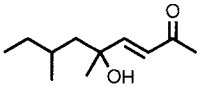	V	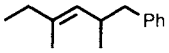	5
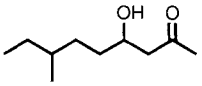	W	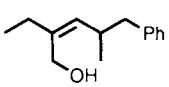	6
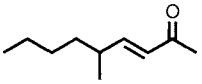	X	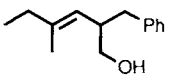	7
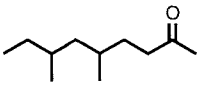	Y	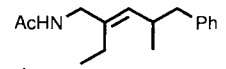	8
		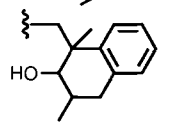	9

[a] Observed combinations: S1, H1, S2, H2, H5, H6, H7, H9, S3, S4, S5, S8, T1, U1, U2, V1a, V1b, V2, W1, W2, X1, Y1. [b] The five deoxysqualestatins: 6-deoxy-H1, 6-deoxy-H5, 7-deoxy-H5, 7-deoxy-S1, 6,7-deoxy-H5.

the zaragozic acids makes initial purification of the crude fermentation extract by ion exchange chromatography relatively easy.

The structure of zaragozic acid A was determined independently by a standard combination of NMR spectroscopy, mass spectrometry, and X-ray structure analysis. Merck established the relative configuration of nine of the ten stereocenters by X-ray analysis of the rearranged derivative **2**; the configuration of the C4′ stereocenter was determined by X-ray analysis of another intermediate.[23] The absolute configuration was determined by circular dichroism measurements on a 6,7-bis(4-bromobenzoate) derivative.

Table 2. Naturally occurring zaragozic acids in addition to **1**.

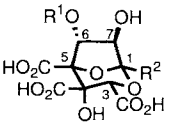

Name	R^1	R^2
B	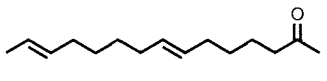	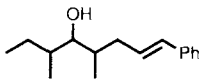
C	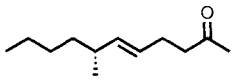	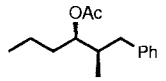
D	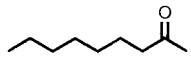	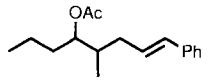
D_2	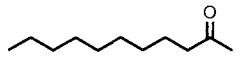	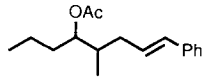
E	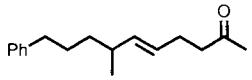	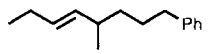
F	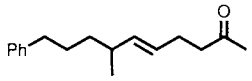	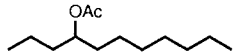

Table 3. Locations where zaragozic acid producing fungi were found.

Compound	Location
zaragozic acid A/ squalestatin S1	Jalon River, Spain tree bark, Philipines tree bark, New Jersey (USA) stem, New Zealand tree bark, Kenya soil, Portugal
zaragozic acid B	cottontail rabbit dung, Arizona (USA) lichen, New Mexico (USA) bighorn sheep dung, Arizona (USA) elk dung, Arizona (USA) goat dung, Greece giraffe dung, Kenya dung of an unidentified herbivore, Kenya
zaragozic acid C	dead wood, North Carolina (USA) basidioma, New Jersey (USA) wood chips, New Jersey (USA)
zaragozic acid D/D_2	soil baited with hair, Spain
zaragozic acid E/F	dead wood, North Carolina (USA)
squalestatins	soil, Portugal

Glaxo determined the relative configuration of the zaragozic acids by X-ray crystal structure analysis of **3**.[17b] The absolute

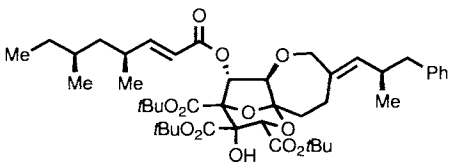

2

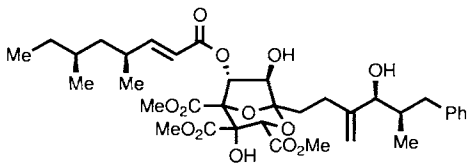

3

configuration was rigorously established by comparing the optical rotation of a derivative of the C6 acyl side chain (obtained by degradation of **1**) with a previously reported value for the same compound. The structure of zaragozic acid A has also been confirmed by three total syntheses.[74c, 81, 92]

The structures of the other zaragozic acids/squalestatins have been established through similar spectroscopic, semisynthetic, and total synthetic methods.[21, 22, 85, 90] However, many of the remote stereocenters in the side chains of the minor squalestatins remain undefined.

The most remarkable feature of the zaragozic acids is the highly oxygenated core structure present in virtually all of the naturally occurring zaragozic acids/squalestatins (see Tables 1 and 2). If the two side chains are replaced by hydrogens, then the resulting "naked" fragment **4** has the molecular composition $C_9H_{10}O_{11}$ and contains 59.8% oxygen by mass. To put this stoichiometry into perspective, this figure should be compared with those of glucose ($C_6H_{12}O_6$, 53.3% oxygen), citric acid ($C_6H_8O_7$, 58.3%), and oxalic acid ($C_2H_2O_4$, 71.1%).

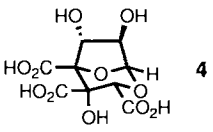

4

The closest relatives to the zaragozic acids appear to be the cinatrins (for example cinatrin A (**5**), Scheme 1), a family of

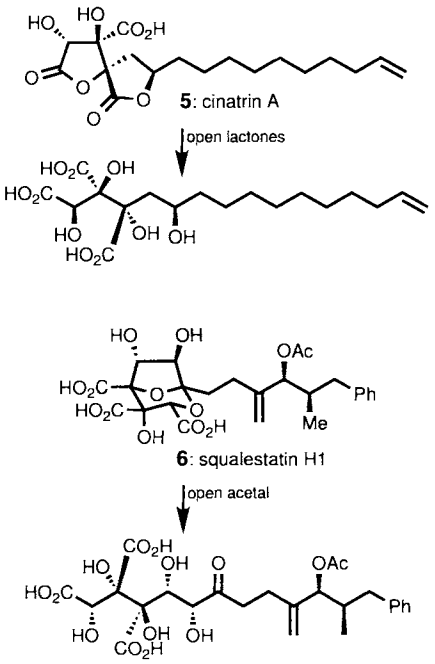

Scheme 1. Structural relationship between the zaragozic acids and the cinatrins.

natural products isolated from the fungus *Circinotrichum falcatisporum* RF-641.[24] These natural products are characterized by a polyoxygenated head attached to a long, linear C_{10} lipophilic tail. The oxygenation pattern of the head bears a very close pseudo-enantiomeric relationship to that of the zaragozic acid core (for example squalestatin H1 (**6**)); if the C_{10} side chain is removed, the "naked" head has the composition $C_8H_{12}O_{10}$ (59.7% oxygen by mass), which is quite comparable to that of the zaragozic acid core. Unfortunately, the cinatrins have received little attention from chemists, which is probably a result of their rather modest biological activity (they are weak inhibitors of phospholipase A_2).

The ring system of the zaragozic acids is officially designated as a 2,8-dioxabicyclo[3.2.1]octane system, and although not unknown, it is decidedly uncommon. It has been found in the alkaloid daphniphylline hydrochloride (**7**),[25] in a family of diarrhetic fish toxins (pectenotoxins 1–3, **8a–c**),[26] and recently in sordinin (**9**), the banana weevil pheromone.[27] It has also

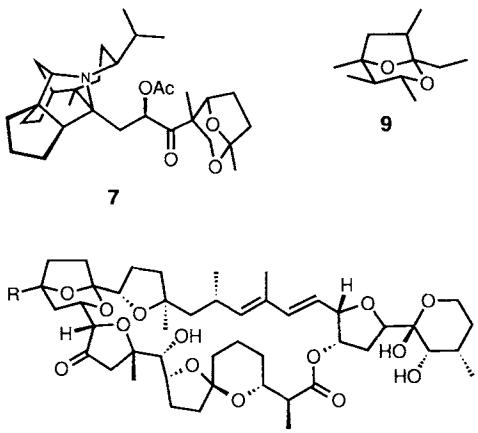

7 **9**

8a: R = CH_2OH PTX1

8b: R = CH_3 PTX2

8c: R = CHO PTX3

been used as a synthetic intermediate en route to other compounds.[28] However, nothing approaching the oxygenated complexity of the zaragozic acid core, which contains six contiguous chiral centers, three of which are quaternary, had ever been seen before.

The role of the zaragozic acids in nature is not clear. However, it is interesting to note that the HMG-CoA reductase inhibitors (see Section 2.1.1) and the HMG-CoA synthase inhibitor L-659699 are all (fungally derived) potent and specific inhibitors of early steps in the sterol synthetic pathway. It has been suggested that because of their antifungal activity (see Section 2.2), the particular zaragozic acid produced by one fungus may be used to defend the colony against an invading colony.[20] This hypothesis suffers from the observation that many producers do not excrete the zaragozic acid they produce. However, the observation that the zaragozic acids are widely found in the fungal kingdom implies that they do serve some general purpose.

2. Biological Role of the Zaragozic Acids

2.1. Background

2.1.1. The Sterol Biosynthetic Pathway

The sterol biosynthetic pathway is one of many catabolic pathways that start from acetyl-coenzyme A (acetyl-CoA), but is unique in being responsible for producing cholesterol and other important terpenes.[29] The main routes are shown in Scheme 2. The pathway starts with acetyl-CoA and acetoacetyl-

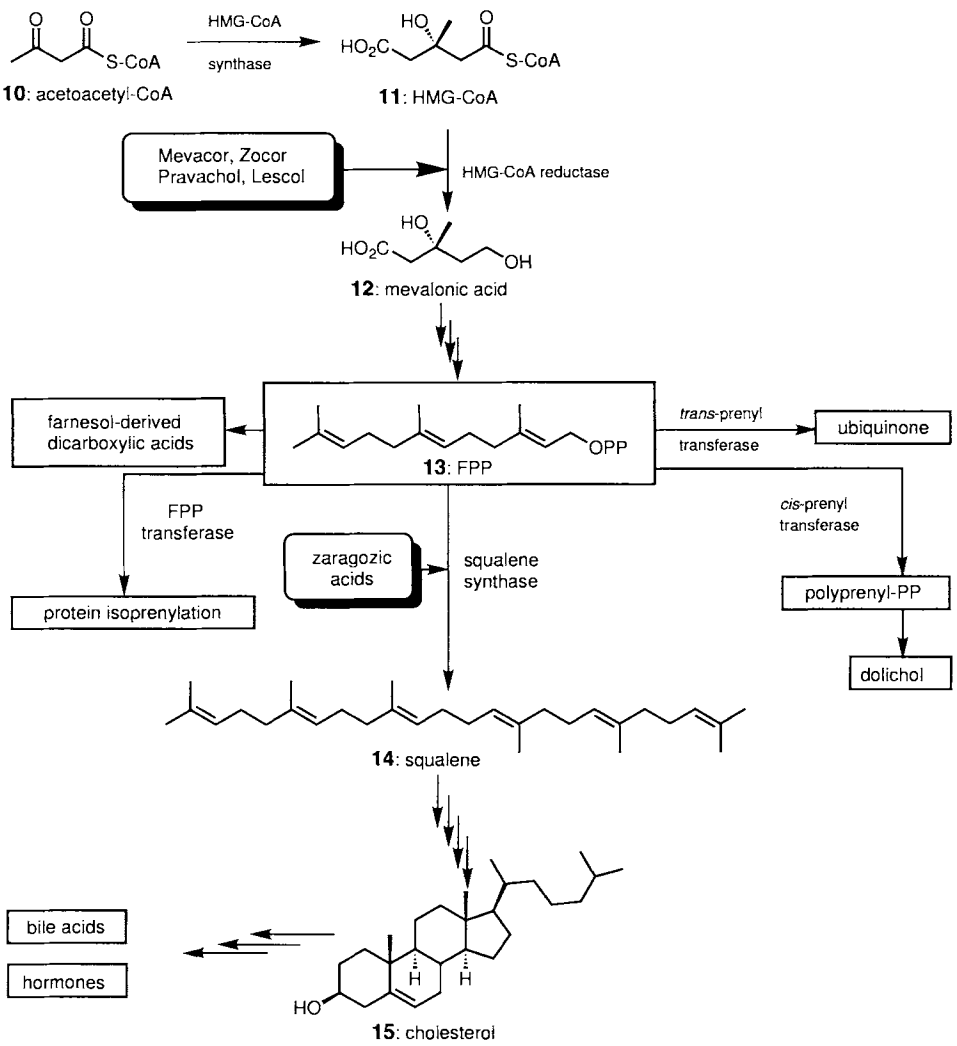

Scheme 2. Simplified sterol biosynthetic pathway. HMG = 3-hydroxy-3-methylglutaryl. FPP = farnesyl pyrophosphate. Mevacor, Zocor, Pravachol, and Lescol are drugs that block mevalonic acid synthesis.

CoA (**10**) (also obtained from acetyl-CoA), which are joined together by HMG-CoA synthase to form hydroxymethylglutaryl-CoA (HMG-CoA) (**11**). HMG-CoA is then reduced under the influence of HMG-CoA reductase to give mevalonic acid (**12**). HMG-CoA reductase is believed to be the major control point for the sterol pathway and accordingly has been the subject of many studies. HMG-CoA reductase is regulated by a number of late-stage products of the sterol pathway, including cholesterol and a hydroxylated derivative, which act at the transcriptional level. A number of steps then convert mevalonic acid into farnesyl pyrophosphate, FPP (**13**). FPP is the last common intermediate for the synthesis of all the end products of the sterol synthetic pathways. Apart from its role in cholesterol biosynthesis, the intracellular pool of FPP is used directly in the synthesis of dozens of other natural products.[30] For example, FPP is used by FPP transferase as the source of farnesyl groups for the farnesylation of certain proteins. This covalent attachment of a farnesyl group is necessary for the biological activity of many of proteins (see Section 2.2). FPP can also be reductively dimerized to give geranylgeranyl pyrophosphate, which plays a similar role in protein isoprenylation. It has been estimated that 2% of all eukaryotic proteins carry isoprenyl units.

FPP is also a substrate for *trans*-prenyl transferase, an enzyme that catalyzes the formation of long-chain all-*trans* polyisoprenes. These are used in the synthesis of ubiquinone, which is the only endogenously synthesized antioxidant, and therefore very important. Similarly, *cis*-prenyl transferase catalyzes the formation of polyprenyl pyrophosphate, a precursor for the biologically important dolichols.

The fourth branch point enzyme, squalene synthase (SS) [E. C. 2.5.1.21], which controls the first committed step en route to cholesterol, is responsible for the synthesis of the sterols. SS catalyzes the reductive head-to-head dimerization of FPP to give squalene (**14**). The few established details of the mechanism of this transformation are given in Section 2.3. A long series of enzyme-catalyzed reactions, involving at least two separate pathways, finally produce cholesterol (**15**). Although important in its own right (it helps to maintain the fluidity of cell membranes), cholesterol is an important building block for the biosynthesis of other sterols such as the fecal steroids, steroid hormones, and bile acids.

2.1.2. Ways of Inhibiting Cholesterol Biosynthesis

In principle, the inhibition of any enzyme in the sterol pathway could lead to a reduction in cholesterol biosynthesis. There have been three main fronts in the search for cholesterol-lowering drugs: a) drug-induced removal of cholesterol from the serum, b) inhibition of the key regulatory enzyme, HMG-CoA reductase, and c) inhibition of squalene synthase. Moderately effective inhibitors of other sterol enzymes are known, for example HMG-CoA synthase,[31] mevalonate pyrophosphate decarboxylase,[32] and acylCoA:cholesterol acyltransferase[33].

If the patient's compliance with dietary restrictions is poor, and if serum cholesterol levels are not satisfactorily lowered, a bile acid sequestrant is often prescribed.[15] Bile acid sequestrants (for example cholestyramine (Bristol-Myers-Squibb) and Cholestipol (Upjohn)) are basic amine anion exchange resins. They work by sequestering sterol-derived bile acid anions, for example glycocholic acid (**16**), in the intestine as an insoluble complex, which

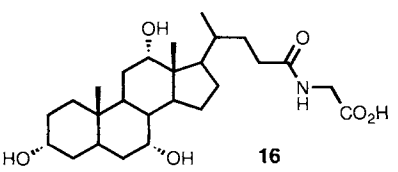

16

is excreted. Although this is often an effective form of treatment, large dosages are required (10–20 g daily), socially unpleasant side effects sometimes arise, and patient response and compliance is often poor and/or attenuates with time.[15]

Shortly after the link between high serum cholesterol levels and atherosclerosis was first proposed, the search for inhibitors of the sterol biosynthetic pathway began. In 1980 Goldstein, Brown, and Faust[34] suggested the "flow diversion hypothesis" for sterol regulation. This model predicted that a decrease in cellular FPP levels would affect only SS, since the other branch point enzymes all have a higher affinity for FPP. Consequently, changes in FPP levels would affect only the pathway leading to cholesterol, and it was therefore hoped that inhibitors of HMG-CoA reductase (which decrease levels of FPP) would not cause serious side effects. These assumptions have largely been proven correct after many years of successful clinical use of HMG-CoA reductase inhibitors. However, there are a few instances of decreased ubiquinone levels in rats and humans[35] treated with high levels of Lovastatin (17) and some other side effects that may have resulted from decreased FPP levels.[36] An excellent review on HMG-CoA reductase inhibitors has been published recently,[37] and we will only outline the main points here. A number of inhibitors of HMG-CoA reductase are known, some of which have become the pharmaceutical industry's best-selling products (Scheme 3). Mevacor (17) (also known as Lovastatin, Mevinacor, Mevlor, Mevinolin, and Monacolin K), first approved by the U. S. Food and Drug Administration (FDA) in 1989, had annual worldwide sales of $1.285 billion in 1992.[38]

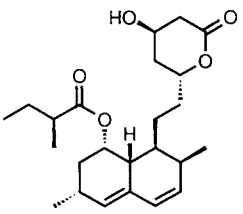

17: Mevacor (Merck)

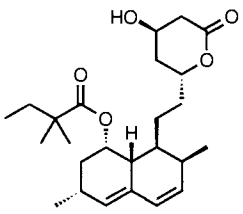

18: Zocor (Merck)

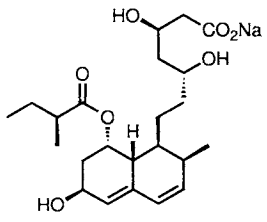

19: Pravachol (Sankyo/Bristol-Myers-Squibb)

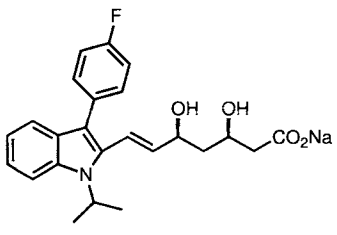

20: Fluvastatin (Sandoz)

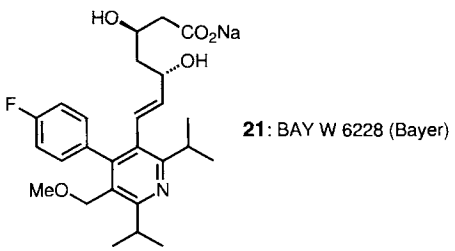

21: BAY W 6228 (Bayer)

Scheme 3. HMG-CoA reductase inhibitors applied as cholesterol-lowering drugs.

The closely related analog Simvastatin (**18**) (Zocor, Zocord, Synvinolin), licensed in 1991, also by Merck, had sales of $475 million in 1992.[38] Pravastatin sodium (**19**) (Mevalotin, Pravachol) from Bristol-Myers-Squibb/Sankyo had sales in 1992 of $824 million.[38] Fluvastatin (Lescol) (**20**) developed by Sandoz was launched in April 1994 at half the price of its competitors, and rapidly captured a substantial portion of the market.[39] Amongst many second-generation analogs of the mevinic acids, Bayer's BAY W 6228 (**21**), currently undergoing clinical trials, looks particularly promising with a potency in dogs some 200 times greater than that of Lovastatin (**17**).[40]

2.2. Biological Activity of the Zaragozic Acids

The biological activity of the zaragozic acids can be grouped into three types. They can be: a) inhibitors of mammalian squalene synthase (cholesterol lowering), b) antifungal agents, and c) farnesyl transferase inhibitors. The first two categories are essentially the same, since the antifungal activity of the zaragozic acids is a result of their inhibition of fungal squalene synthase. However, since cholesterol lowering and antifungal activity are separate therapeutic areas, we will discuss them separately.

The zaragozic acids are the most potent inhibitors of SS known to date. The squalene synthase (cholesterol-lowering) activity of the zaragozic acids has recently been covered in the review by Procopiou and Watson,[41] so we will only outline the main points here. In vitro data has been reported from assays with rat microsomal squalene synthase, Hep-G2 (a human liver cell line) microsomes, and isolated rat hepatocytes (tissue functionally equivalent to liver). In all instances, zaragozic acids were potent and selective inhibitors (Table 4). It should be noted that because of different assay conditions, the IC_{50} values reported by Merck are always lower (apparently more potent) than those given by Glaxo.[41]

Table 4. Biological activities of zaragozic acids/squalestatins.

Compound	IC_{50}[nM] [a]	[b]	MIC[$\mu g mL^{-1}$] [c]
zaragozic acid A/ squalestatin S1	0.5 (Merck) 12 (Glaxo)	250 –	8 –
zaragozic acid B	0.2	1000	–
zaragozic acid C	0.4	150	8–16
zaragozic acid D	6	100	–
zaragozic acid D_2	2	100	–
squalestatin S2	5	–	125
squalestatin H1	26	–	>125

[a] Inhibition of rat squalene synthase. [b] Inhibition of bovine brain farnesyl protein transferase. [c] Minimum inhibitory concentrations against *Candida albicans*.

In vivo studies have also been performed. Glaxo reported that when rats were dosed intravenously with zaragozic acid A (**1**) at levels of 0.1 mg per kg of body weight, cholesterol biosynthesis was reduced by 50%.[42] When marmosets (which apparently have a similar lipoprotein profile to man[43]) were dosed orally with 10 mg per kg per day of zaragozic acid A, serum cholesterol levels fell by up to 75% for eight weeks, with no attenuation of response.[42] Merck reported similar findings with mice.[16a]

Recently other naturally occurring, fungally derived SS inhibitors have been reported. The viridiofungins, for instance **22**,[44] have been isolated by Merck from *Trichoderma viride* (ATCC 74084), and CP-225917 (**23**)[45] has been isolated by

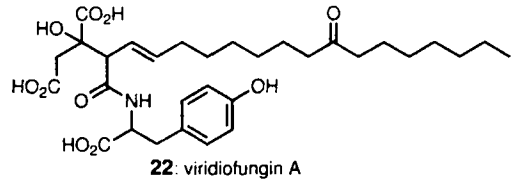

22: viridiofungin A

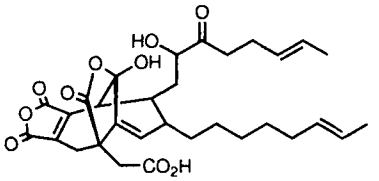

23: CP-225 917

Pfizer from an uncharacterized fungus (ATCC 74256). The viridiofungins (IC_{50} = 0.4–15 μM) are much less potent than the zaragozic acids; the potency of CP-225917 has not been reported. It is interesting to compare the structural similarities between the three families of natural products: both zaragozic acid A and CP-225917 have two lipophilic side chains flanking a polar bicyclic core. Squalestatin H1 (**6**) contains only one side chain attached to a tricarboxylic acid core; the viridiofungins contain a similar tricarboxylate function attached to a lipophilic tail. In addition to the naturally occurring inhibitors, a large number of designed inhibitors have been made (e.g. **24**), most of which are of modest potency.[46]

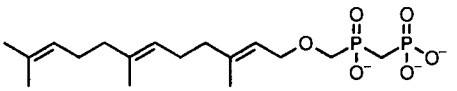

24

Glaxo has reported the antifungal activity of zaragozic acid A against a variety of yeasts and fungi. MICs (minimum inhibitory concentrations) varied between 0.5 and 16 μg mL^{-1} (see Table 4).[41]

The ras proteins are a family of proteins that regulate cell proliferation and differentiation. Ras, the protein of the *ras* oncogene, is implicated in many cancers.[47] It appears, however, that tumorigenesis requires posttranslational modification of ras. This involves attachment of the farnesyl group of FPP to a cysteine residue of ras, which is catalyzed by ras farnesyl:protein transferase (FPTase).[48] There is evidence that inhibitors of FPTase have the potential to be antitumorigenic agents.[49] Scientists at Merck discovered that the zaragozic acids are powerful inhibitors of FPTase (see Table 4),[22] with potency similar to that of other naturally occurring inhibitors.[50] Zaragozic acids D and D_2 are the most potent inhibitors;[22] however, one synthetic analog is the most potent FPTase inhibitor currently known.[50]

2.3. Mechanism of Action of the Zaragozic Acids

Unfortunately, very few papers deal with the interesting question of how the zaragozic acids inhibit SS. This is probably because the mechanism of action of SS is not clearly understood, owing in part to the difficulties in purifying the enzyme and the consequent lack of crystal structure data.[51] As shown in Scheme 4, in the presence of Mg^{2+} and NADPH, SS converts two molecules of FPP (**13**) through two half-reactions into one molecule of squalene (**14**), via presqualene pyrophosphate (PSPP) (**26**). It is now accepted that SS sequentially binds two molecules of FPP, one into a donor site and one into an acceptor site.[52] The order of these events is not known. Reaction of the donor FPP with the acceptor FPP results in the loss of PPi (inorganic pyrophosphate) and the formation of the putative carbocationic intermediate **25**. Loss of a proton then gives PSPP, which can dissociate or remain bound to the enzyme. The second half-reaction (reduction of PSPP to squalene) requires NADPH. It has been shown that NADPH binds to the enzyme after the formation of PSPP.[53] Loss of PPi generates initially carbocation **27**, which is ultimately reduced with NADPH. A stereoelectronic barrier prevents reductive opening of the cyclopropane by NADPH with retention of configuration. It has been suggested that the intermediate **27** undergoes rearrangement to give the tertiary carbenium ion **28**, which can then be reduced by NADPH to give squalene. In the absence of NADPH a number of hydrolysis and elimination products (capable of arising from the carbocation **28**) were isolated.[53] It is still not clear whether the active sites for the two half-reactions overlap or are in the same region on the enzyme.

The first brief suggestion of a mechanism for the inactivation of SS by zaragozic acid A was in the original publication by the

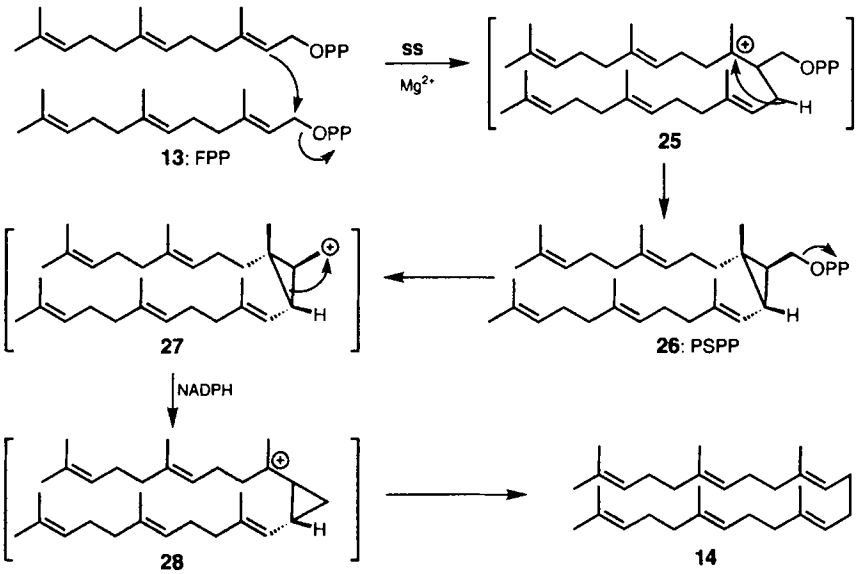

Scheme 4. Proposed steps in the formation of squalene (**14**) catalyzed by squalene synthase (SS)

Merck group.[16] They concluded that zaragozic acids A–C were competitive inhibitors of SS, which worked by possibly acting as PSPP mimics. The structures of zaragozic acid A and PSPP show striking similarities: in both two lipophilic side chains flank a trianionic core.

Glaxo later postulated from medicinal chemistry studies that analogs of zaragozic acid A possessing an acyl side chain at C6 act as FPP mimics, whereas those having both side chains are mimics of PSPP.[54]

Hasumi and co-workers[18] were the first to demonstrate that zaragozic acid A (**1**) inhibits *both* half-reactions of SS: the first (synthesis of PSPP) with a K_i of 14 nM, the second (conversion of PSPP to squalene) with a K_i of 33.4 nM. Under the same conditions the K_i for the overall reaction was 1.6 nM. Merck reported a value of 78 pM for the overall reaction.[16]

The most detailed investigation of the mechanism of action of zaragozic acid A (**1**) was conducted by Harwood and Lindsey at Pfizer.[55] They provided several lines of evidence consistent with inactivation of the enzyme resulting from *competitive inhibition followed by mechanism-based irreversible inactivation*, rather than just strong, reversible competitive inhibition. In other words, zaragozic acid A binds competitively (with respect to FPP) to SS and then reacts covalently with the enzyme to irreversibly inactivate it ("suicide inhibition").[56] It was suggested that the α,β-unsaturated ester of the C6 acyl side chain was the likely site of reaction, presumably by Michael addition of a nucleophilic residue in the active site. This hypothesis was supported by detailed analysis of the kinetics of inhibition of SS by two synthetic analogs. It should be noted, however, that zaragozic acids B and C and many of the potent analogs do not possess an α,β-unsaturated ester. This suggests the intriguing possibility that zaragozic acid A is a mechanism-based irreversible inhibitor of SS, but that other members of the family are simple competitive inhibitors.

2.4. Toxicity of the Zaragozic Acids

Some brief reports on the toxicity of the zaragozic acids have been published. It should be noted that the effect of cholesterol-lowering drugs in vivo can be very species-specific: for example, lovastatin is an effective and nontoxic agent in humans and dogs, but ineffective in rats and mice.[57]

One possible consequence of blocking SS is that FPP accumulates, since it cannot be processed through the cholesterol pathway. It appears that this is the case. It has been shown that in rats treated with zaragozic acid A (**1**), FPP levels increase[58] and HMG-CoA reductase is upregulated.[59] The excess levels of FPP appear to be rapidly catabolized in the liver to a range of farnesyl-derived dicarboxylic acids (FDDCAs) such as **29**, which are excreted in the urine.[60] The same effect can be produced by feeding the rats large quantities of farnesol. When rats were treated with a dosage of 15 mg per kg per day of zaragozic acid A and a bile acid sequestrant, the levels of FDDCAs in the urine rapidly became very high and the animals became very moribund,[59b] which is a symptom of acidosis. Acidosis is a disease associated with abnormal serum pH levels. It was therefore suggested that the toxic effects associated with zaragozic acid A are a result of the acidosis caused by massive overproduction of FDDCAs from an increased pool of FPP.[59b, 61]

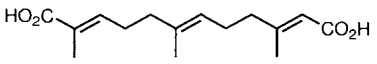

29

When dogs were dosed subcutaneously at 3 mg per kg, both zaragozic acids A and C caused extreme toxicity after one to two weeks.[61] With three other zaragozic acids, the effect depended on the dose and on the potency of the individual zaragozic acid. Even so, little or no lowering of cholesterol levels was observed. However, the toxicity was totally eliminated by co-dosage with a HMG-CoA reductase inhibitor. In the presence of the HMG-CoA reductase inhibitor alone, cholesterol levels were lowered by 50%, and by an additional 20% when both drugs were used. In this case, too, large amounts of FDDCAs were detected. It was suggested that the initially observed toxicity was a result of acidosis. In contrast, rhesus monkeys dosed orally with zaragozic acid A at 10 mg per kg per day for two weeks showed 50–60% lower cholesterol levels and much lower levels of FDDCAs. The reasons for this difference are not clear.

3. Chemistry of the Zaragozic Acids

3.1. Syntheses of Model Systems of the Bicyclic Core

In the last three years a number of research groups have successfully synthesized the zaragozic acids and a number of related model systems. Numerous approaches have been used, and it is very instructive to compare the different strategies and the variety of reactions employed. Table 5 lists the C–C bond connections that each research group has used to synthesize the bicyclic core. For example in the Evans synthesis[90] the C6–C7 bond was made by an aldol reaction, the C4–C5 bond by an enolate addition reaction, and the C1–C1′ bond by an alkyllithium addition—strategies that have all been used in part by

Table 5. Strategic C–C bond connections in syntheses of the bicyclic core of zaragozic acid.

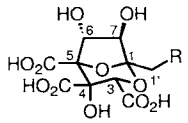

Bond	Research group (method)
C1–C7	Nicolaou (dithiane addition) Armstrong (dithiane addition) Carreira (acetylide addition) Koyama (1,3-dipolar cycloaddition)
C3–C4	Gurjar (Wittig reaction)
C4–C5	Aggarwal (enolate addition) Evans (enolate addition) Roberts (2-lithiofuran addition) Nicolaou (Stille coupling) Armstrong (Stille coupling)
C5–C6	Koyama (1,3-dipolar cycloaddition) Carreira (acetylide addition) Nicolaou (Wittig reaction)
C6–C7	Kraus (modified Mukaiyama reaction) Evans (Evans aldol reaction)
C1–C1′	Evans (alkyllithium addition) Rizzacasa (Grignard addition) Heathcock (organocerium addition)

other research groups. It can also be seen that some retrosynthetic steps are more popular than others. Indeed, every research group except one,[75] has made the bicyclic core by retrosynthetic disconnection of the C1–O8 and O2–C3 bonds, with assembly by an anticipated acid-catalyzed ketalization. To most people, the polyoxygenated core structure looks like a heavily oxidized carbohydrate, and the majority of the syntheses use carbohydrate-based starting materials. Only two syntheses of enantiomerically enriched targets, that by Nicolaou and co-workers[77, 78] and the closely related one by Armstrong and Barsanti,[82] rely on asymmetric catalysis to obtain the core structure.

In the fall of 1993 four groups published successful syntheses of differently functionalized models of the zaragozic acids. The one by Rizzacasa and co-workers[62] is described in Schemes 5

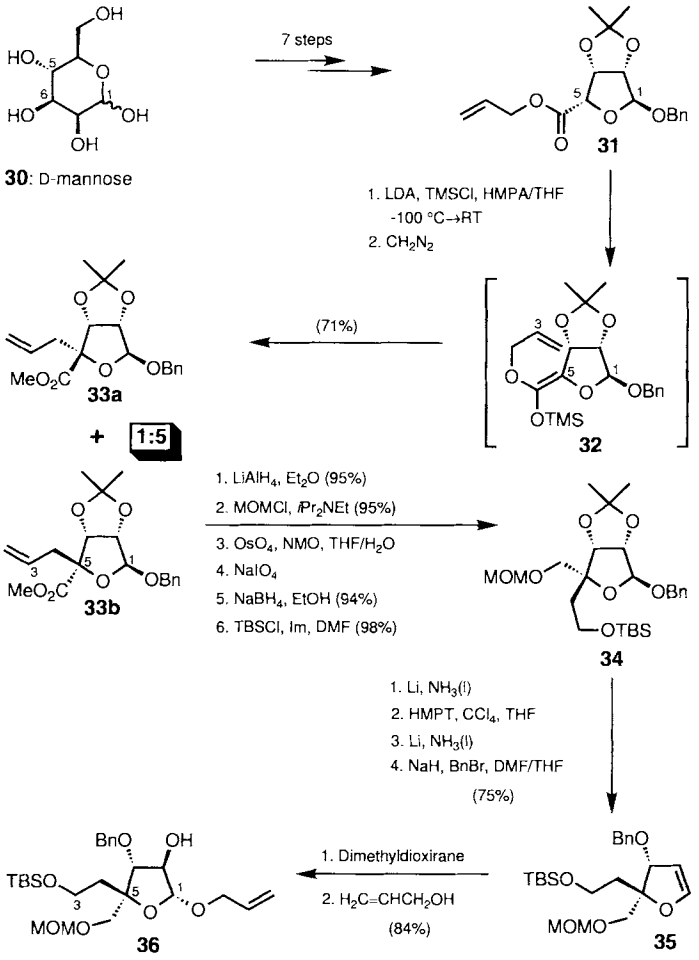

Scheme 5. Early stages of Rizzacasa's synthesis of a zaragozic acid model compound. TMS = trimethylsilyl, RT = room temperature, MOM = methoxymethyl, Im = imidazole, Bn = benzyl.

and 6. Starting with D-mannose (**30**), seven well-precedented steps gave the allyl ester **31**. Note that the "back" five-membered ring has already been constructed. The next few steps establish the correct configuration at the C5 stereocenter and invert the hydroxyl-bearing stereocenter at C7.[*] The C5 quaternary stereocenter was made with an Ireland–Claisen rearrangement,[63] which gave the diastereomers **33a** and **33b** as

[*] Here and in the following discussions the atomic numbering in the synthetic building blocks refers to positions in the final zaragozic acids.

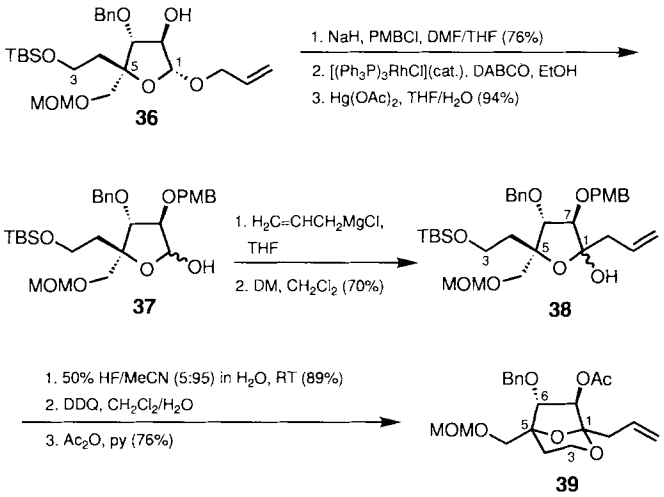

Scheme 6. Final stages of Rizzacasa's synthesis of a zaragozic acid model compound. DABCO = diazabicyclooctane, DDQ = 2,3-dichloro-5,6-dicyano-1,4-benzoquinone.

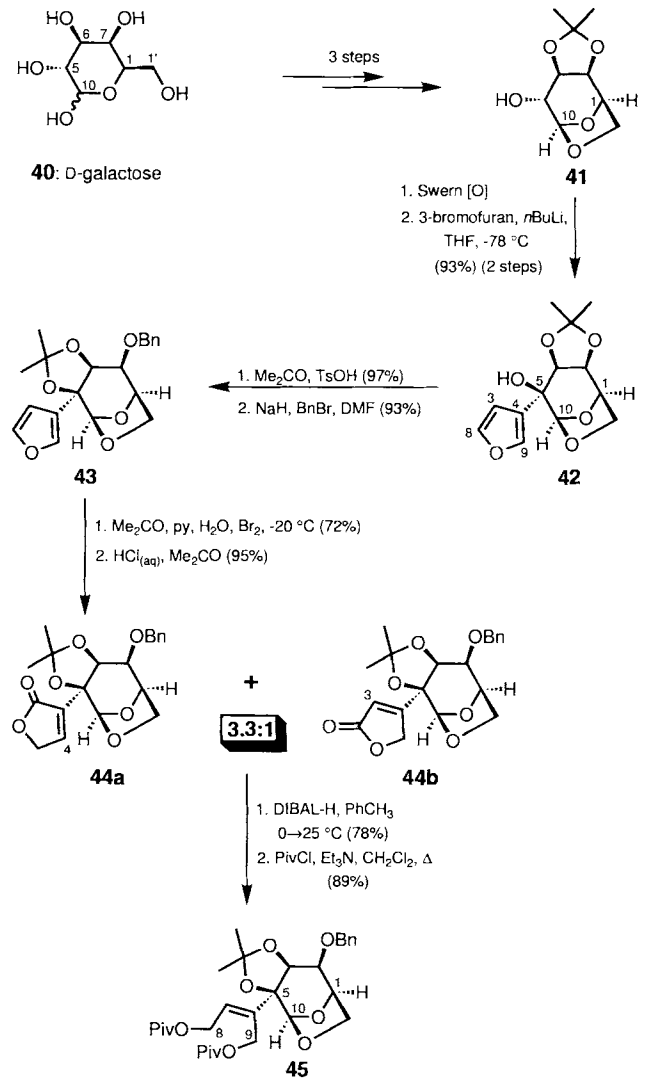

Scheme 7. Early stages of Roberts's synthesis of a zargozic acid model compound. Ts = *para*-toluenesulfonyl. DIBAL-H = diisobutylaluminum hydride.

a 1:5 mixture, via mixed silyl ketene acetal **32**. The major isomer was separated and a series of functional group interconversions furnished the TBS ether **34**. The next six steps were necessary to invert the C7 stereocenter and differentiate the C6 and C7 hydroxyl groups. Reduction of **34** with Li/NH_3 removed the benzyl ether to give a lactol, which was transformed into a glycosyl chloride by treatment with CCl_4 and HMPT. Reductive elimination gave the glycal and freed the C6 hydroxyl group to be protected as a benzyl ether in **35**. Epoxidation with dimethyldioxirane then occurred from the face opposite to the benzyl ether (selectivity >9:1). Regioselective opening of the epoxide with allyl alcohol afforded the allyl ether **36** in 84% yield. The C7 hydroxyl group was protected as a PMB ether and the allyl group was removed to give lactol **37** (Scheme 6). As a model for the C1 side chain, allyl magnesium chloride was added to lactol **37**, and subsequent oxidation yielded the lactol **38**. Note that Evans et al. used the same strategy,[90] but the order of the oxidation and addition steps was reversed in their total synthesis (steps 1 and 2 in the transformation of **196** into **197** in Scheme 40). The key cyclization of **38** to furnish the bicyclo[3.2.1]octane framework was achieved with $HF/MeCN/H_2O$, which removed the silyl protecting group and catalyzed the ketalization. Two protecting group manipulations gave the final derivative **39**.

The Roberts–Glaxo route[64] (Schemes 7 and 8) produced the more highly functionalized derivative **53**. Starting from D-galactose (**40**), three steps gave the anhydropyranose structure **41**. Swern oxidation and addition of 3-lithiofuran to the resulting ketone gave the diastereoisomerically pure alcohol **42** in 93% yield. The C7 and C6 hydroxyl groups were differentiated by shifting the acetonide to C5/C6 with acetone/TsOH and protecting the C7 hydroxyl group as a benzyl ether to give **43**. The furan ring represents the C3/C4 fragment and is essentially a reduced form of the tartrate enolate fragment used by Aggarwal et al.[66] and Evans et al.[90] (Schemes 9 and 40, respectively). Accordingly, the furan ring was oxidized to the dilactol by treatment with bromine, and subsequent acid-catalyzed rearrangement afforded a mixture of the α- and β-substituted butenolides **44a** and **44b**. Although the butenolides could be manipulated further, it was found to be more expedient to homogenize the mixture of regioisomers by reducing both butenolides to the (same) diol with DIBAL-H and protecting the hydroxyl groups as pivaloate esters to give **45**. Acetolysis (cf. **93** → **94** in Scheme 16) afforded a mixture of the desired pyranoside **46** and the novel tricycle **47**, in which the C7 benzyl ether had been removed (Scheme 8). Hydrolysis of the acetate esters then gave the diol **48** after purification. The next four steps (protection of the primary hydroxyl group, reduction of the lactol, protection of the new primary hydroxyl group, and oxidation of the secondary hydroxyl group) gave the protected acyclic ketone **50**. Removal of the C5/C6 acetonide revealed the C5 hydroxyl group, enabling the tetrahydrofuranyl ring of the bicyclic core to form. Formation of another acetonide in a second step gave the spirolactol **51**. The next step was a dihydroxylation of the double bond. This is a crucial step because it generates two stereocenters. Fortunately, Sharpless asymmetric dihydroxylation (AD)[65] with a slightly modified reagent, gave, after 3.5 days, the diol **52** as a single diastereoisomer in 60% yield. Other groups have used asymmetric dihy-

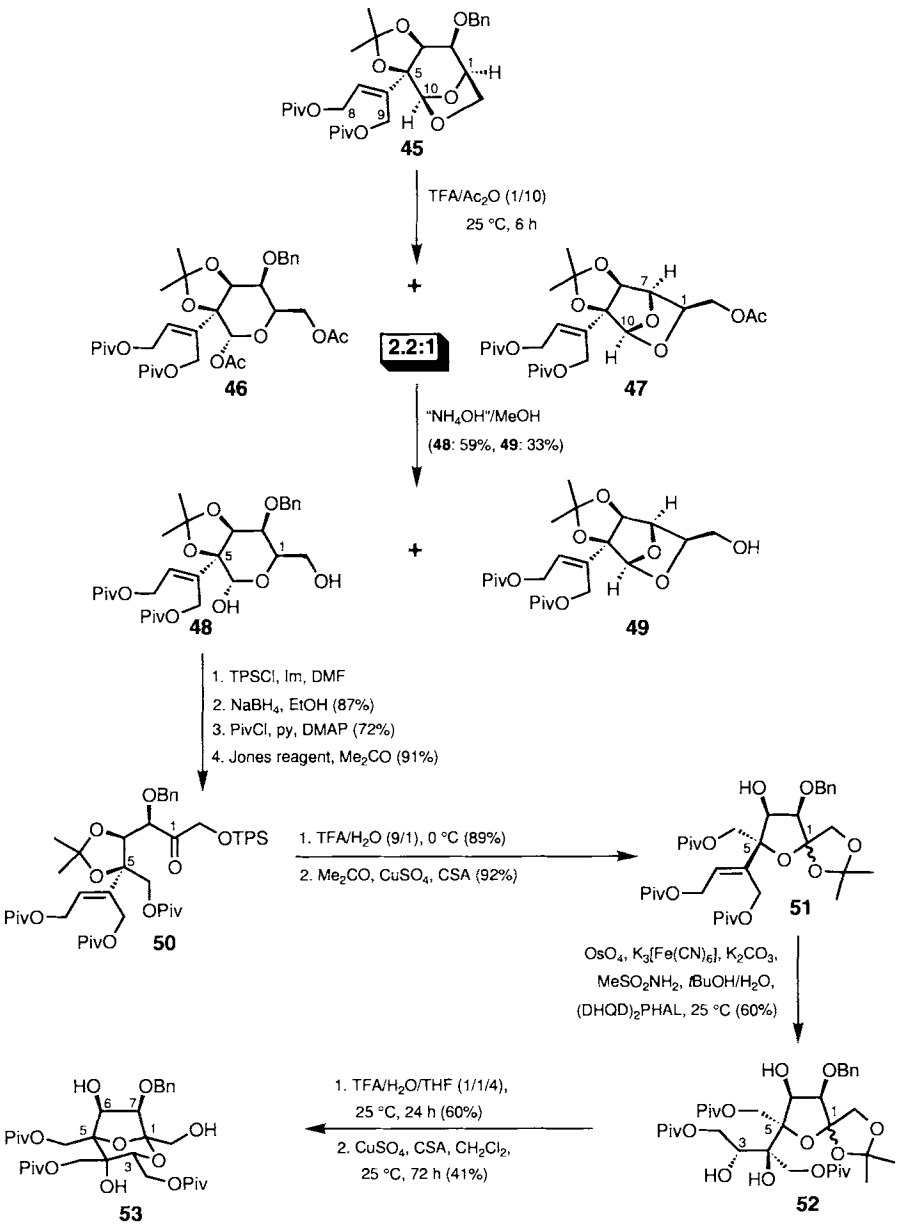

Scheme 8. Final stages of Roberts's synthesis of the zaragozic acid model compound **53**. TFA = trifluoroacetic acid, DMAP = 4-dimethylaminopyridine, $(DHQD)_2PHAL$ = dihydroquinidine 1,4-phthalazinediyl diether (see also Scheme 33).

droxylation to control other stereocenters in the zaragozic acids, with varying degrees of success (see Schemes 22, 29, and 33). Finally, removal of the acetonide and dehydrative ketalization gave the target molecule **53** in 24% overall yield from **52**. The bicyclic structure **53** is a realistically functionalized model system. In principle, correction of the configuration at C6, oxidation of the three pivaloate esters, and introduction of side chains at C1 and C6 should lead to the natural product itself.

The shortest synthesis of a model of the bicyclic core is the two-step preparation described by Aggarwal and co-workers (Scheme 9).[66] By identifying the C3/C4 fragment as an intact

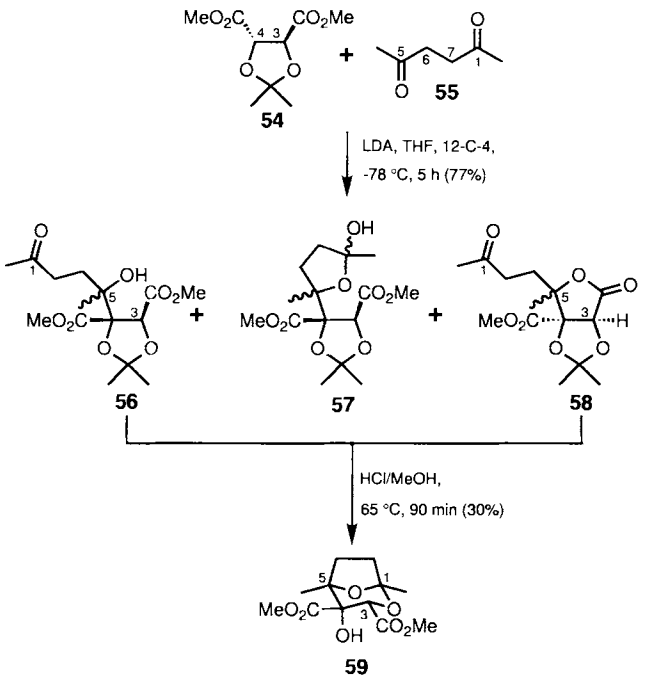

Scheme 9. Aggarwal's synthesis of a model compound. 12-C-4 = [12]crown-4.

tartrate unit, the simple model system **59** was rapidly assembled. Formation of the lithium enolate of **54**, which was derived from (+)-tartaric acid,[67] and condensation with the symmetrical ketone **55**, in the presence of [12]crown-4, gave a mixture of several products in an unselective aldol reaction. Not only were C4 and C5 diastereoisomers produced, but the initial products reacted further to give lactones **57** and lactols **58**. The yield was estimated at 77%, and no attempt was made to purify the reaction mixture. Instead, treatment of the mixture obtained in the first step with refluxing HCl/MeOH for around 90 minutes gave the bicyclic core **59** in an optimal yield of 30%; NMR evidence excludes the alternative structures **60** und **61**. It was suggested that the (5*R*) diastereoisomer **56a** could easily cyclize to afford the desired product **59** (Scheme 10), but that the (5*S*) diastereoisomer would prefer to form bicyclic ketals **62** and **63** rather than the diaxial dimethyl ester **64**, which was assumed to be less stable than **59**. Unfortunately the side products from the reaction were not investigated to support this theory. Although the reactions are low-yielding and unselective, the approach clearly has potential: by using an appropriately functionalized dicarbonyl compound, a strategy for introducing a carboxyl

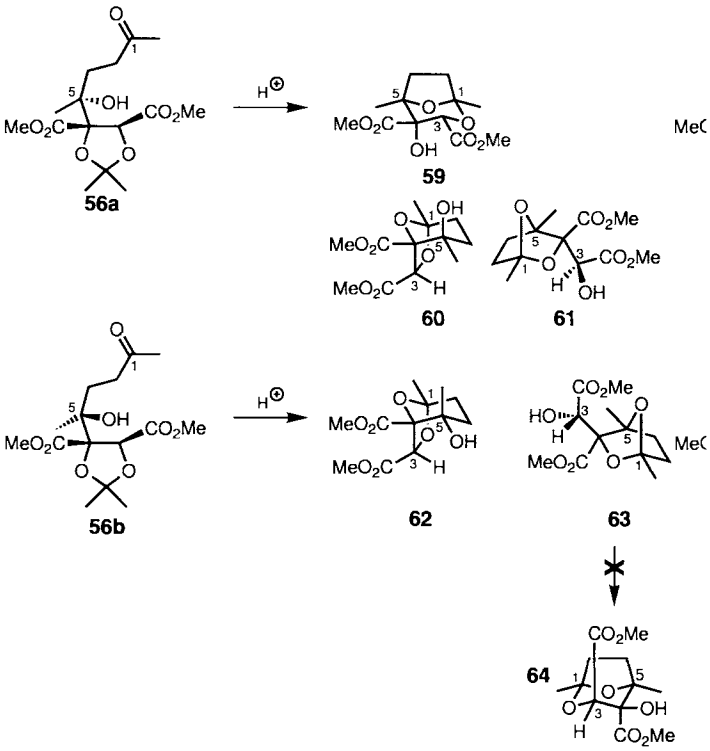

Scheme 10. Proposed intermediates in the rearrangement of **56a** and **56b** (Aggarwal et al.).

substituent at C5, and a method for controlling the aldol reaction, more functionalized zaragozic acid models could be made. Indeed, Evans et al. made use of such improvements in their total synthesis (see Schemes 40 and 41).

Gurjar et al. were the first to discover that the acid-catalyzed ketalization might not be as trivial as initially thought (Scheme 11).[68] Starting with the diacetonide **65**, which was derived from D-glucose, selective hydrolysis of the side chain acetonide, protection of the primary alcohol, and Swern oxidation gave the ketone **66**. A Wittig reaction and protecting group interchange gave the alkene **67**. Dihydroxylation with the Upjohn conditions then gave an inseparable mixture of diols **68a** and **68b** in a 7:3 ratio. It should be noted that because the double bond in **67** is of (*Z*) configuration, one of the stereocenters introduced in the dihydroxylation is destined to be wrong. Moreover, refluxing the mixture of diols with TsOH in chloroform resulted in the formation of not the desired bicyclo[3.2.1]octane skeleton but the bicyclo[2.2.1] systems **69** and **70** in quantitative yield. Unfortunately, it was not shown whether these were kinetic or thermodynamic products. This outcome could be a consequence of the lack of substituents at the C1 center (see Scheme 18), but was suggested to arise from the presence of the ethoxycarbonyl group, which reduced the nucleophilicity of the adjacent C3 hydroxyl group. Accordingly, ester **67** was reduced to give **71** (Scheme 12), and the corresponding diols **72a** and **72b** (with a different protecting group on the C6 hydroxyl group) were submitted to the rearrangement conditions. This time, one diastereoisomer (**72a**) gave the desired bicyclo[3.2.1]octane (anhydrofuran) **73**; the other gave the anhydropyran **74**. This unusual stereochemical dependence was not explained. Note that **73** is pseudo-enantiomeric to the zaragozic acids.

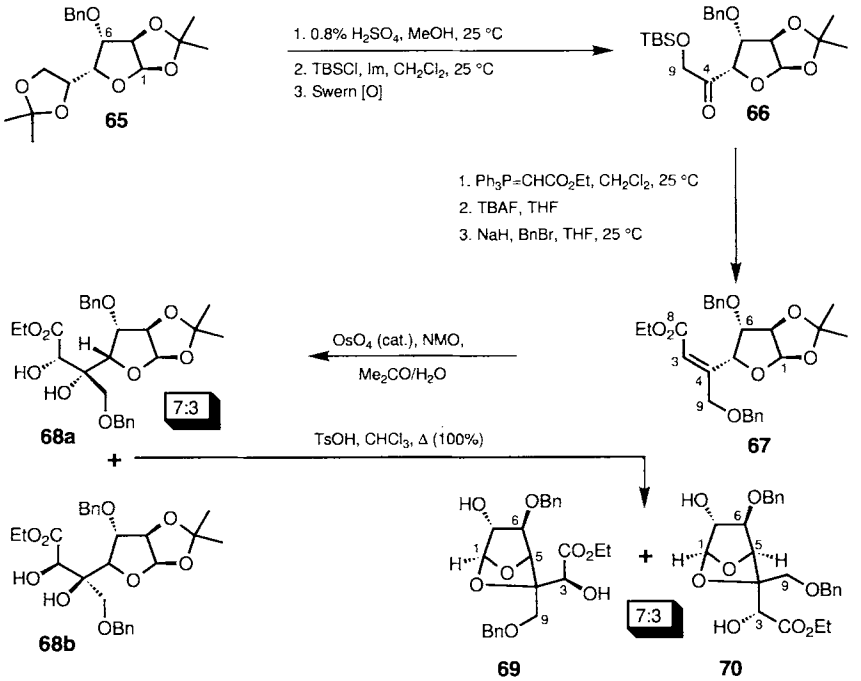

Scheme 11. Gurjar's model study (part 1).

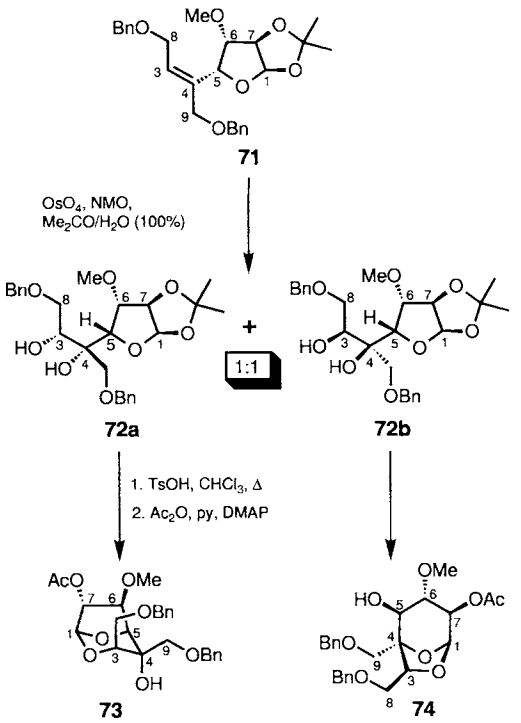

Scheme 12. Gurjar's model study (part 2).

Two later papers[69, 70] described the transformation of a C1-substituted substrate **75** into the vinyl derivative **76** by a standard sequence of reactions (16 steps, Scheme 13). Dihydroxylation gave a 1:1.5 mixture of epimers **77a** and **77b** in quantitative yield. Refluxing this mixture with TsOH in chloroform gave, after acetylation, the two isomers **78** and **79**. It is clear that isomer **77a** forms the [2.2.1] ring system preferentially, while the other affords the [3.2.1] system. Finally, in their most sophisticated model, Gurjar and co-workers found a substrate that yielded only one isomer in the cyclization reaction. Starting with the same acid **75** (Scheme 14), a number of steps gave the ketone **80**. Addition of vinylmagnesium bromide to **80** resulted in one diastereomerically pure alcohol (unfortunately with the wrong relative configuration), which was then protected as a benzyl ether to give **81**. Dihydroxylation gave, also as a single diastereoisomer, diol **82**. As predicted from earlier studies (Scheme 12), acid-catalyzed cyclization and subsequent acetylation then gave the desired bicyclo[3.2.1]octane skeleton **83**. Debenzylation and acetylation furnished the pentaacetate **84**. Note by examination of the enantiomer *ent*-**84** (Scheme 14), it is readily apparent that only two stereocenters (C3 and C4) have the wrong configuration relative to the rest of the molecule. The configuration at C3, which is installed by a dihydroxylation, could probably be easily controlled by using the Sharpless method. The three carboxylic acid functions present in zaragozic acid A are usefully represented by acetoxymethyl groups, and the hydroxyl groups at C6 and C7 are also conveniently differentiated.

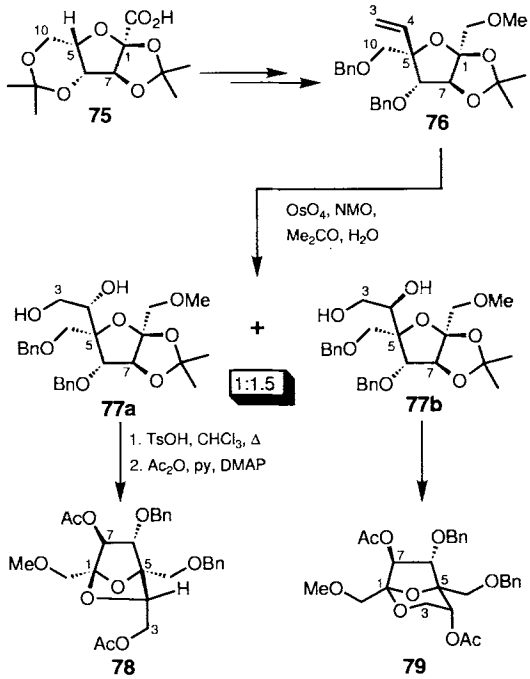

Scheme 13. Gurjar's model study (part 3).

Kraus and Maeda[71] also started their synthesis of a simplified model of the zaragozic acid core from a carbohydrate (Scheme 15). Starting with D-arabinose (**85**), five precedented steps gave the lactol **86**. Treatment of the lactol **86** with ethanethiol and HCl, followed by acetalization with benzaldehyde dimethyl acetal afforded the acetal **87**. They then attempt-

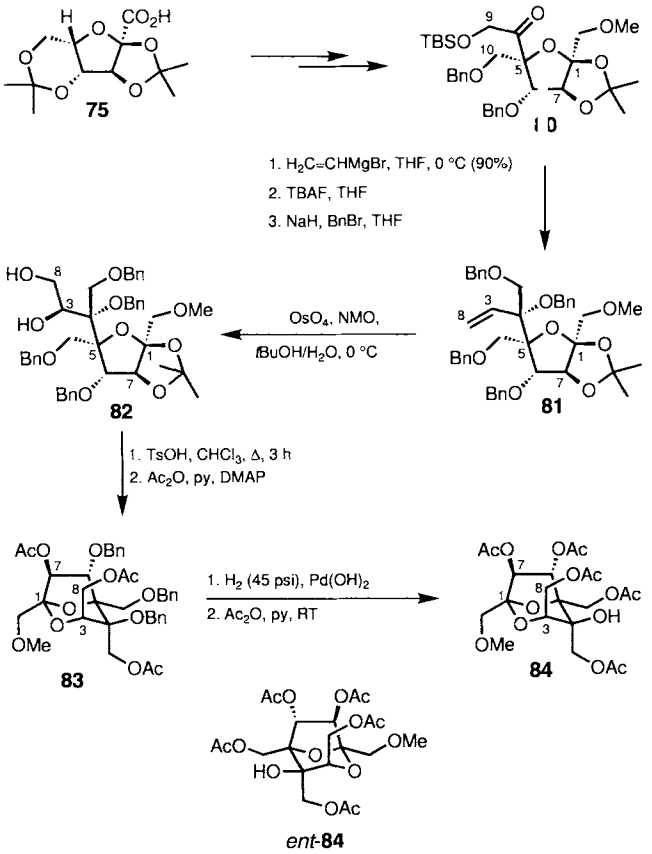

Scheme 14. Gurjar's model study (part 4). 1 psi = 6900 Pa ≈ 52 Torr.

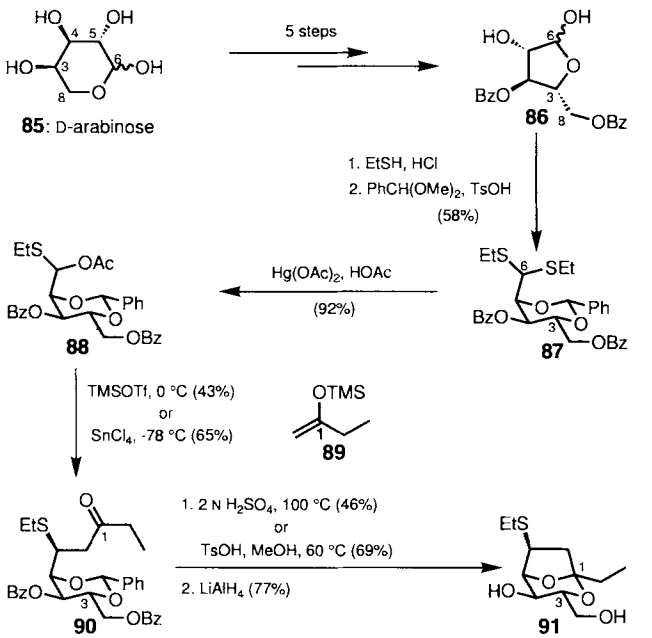

Scheme 15. Synthesis of a zaragozic acid model compound by Kraus and Maeda.

ed to hydrolyze the dithioacetal, but this could not be readily achieved. However, treatment of **87** with mercuric acetate and acetic acid gave the α-acetoxysulfide **88** in 92% yield as a single diastereoisomer, which can, in principle, serve as an aldehyde equivalent. To demonstrate this, a modified Mukaiyama aldol reaction[72] between the silyl enol ether **89** and an appropriate Lewis acid ($SnCl_4$ was found to be the best) was performed. This furnished the sulfide **90** as a single diastereoisomer in 65% yield (but unfortunately with the wrong stereochemistry at C6). Transketalization and reduction of the esters then gave the diol **91** in moderate yield.

Heathcock and co-workers[73] examined in detail the acid-catalyzed ketalization step previously taken for granted by most groups (Scheme 16). In model studies they noticed a substantial

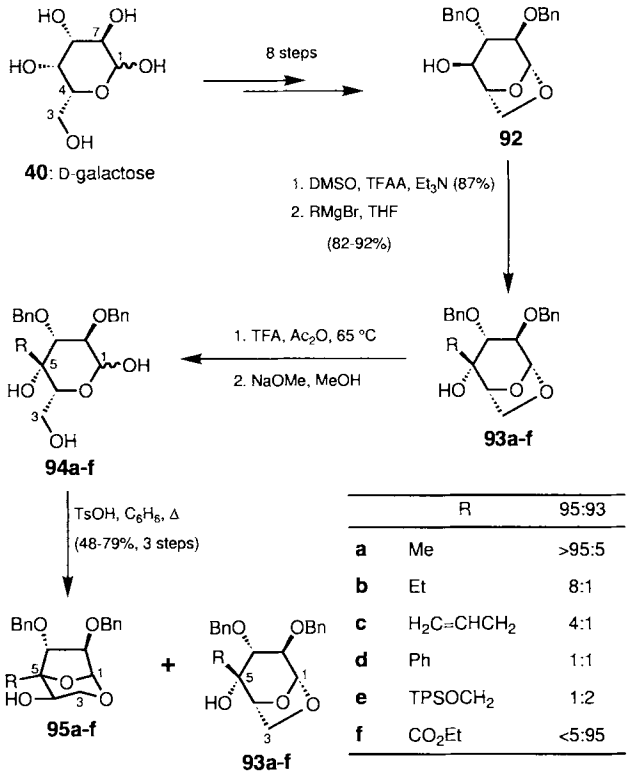

	R	95:93
a	Me	>95:5
b	Et	8:1
c	H_2C=$CHCH_2$	4:1
d	Ph	1:1
e	$TPSOCH_2$	1:2
f	CO_2Et	<5:95

Scheme 16. Early studies by Heathcock et al. on the synthesis of zaragozic acid A. TFAA = trifluoroacetic acid anhydride.

dependence of the outcome of the cyclization of **94** on the nature of the R substituent at C5. Starting from D-galactose (**40**), a series of standard operations gave the anhydropyranose **92**. Oxidation of the C5 hydroxyl group, followed by addition of a variety of Grignard reagents gave, with complete control of diastereoselectivity, alcohols **93a–f**. Acetolysis and solvolysis of the anhydro linkage (see Scheme 8), followed by acid-catalyzed acetalization in refluxing benzene gave mixtures of the desired anhydrofuranoses **95a–f** and starting material (**93a–f**). The ratio was found to be dependent on the C5 substituent; electron-withdrawing groups such as CO_2Et led to preferential formation of the undesired product. Appropriate control experiments established that the observed ratios were subject to kinetic not thermodynamic control. These findings were rationalized by the events shown in Scheme 17. Assuming that the first step in the acid-catalyzed rearrangement is the opening of the acetal to the aldehyde **96**, one of two productive pathways can occur. Path A, attack of the C5 hydroxyl group, gives the five-membered lactol **97**; path B gives the six-membered lactol **98**. Both of these intermediates can eliminate water to form oxonium ions **99** and **100**, respectively. However, it was suggested that the presence of an electron-withdrawing group at C5

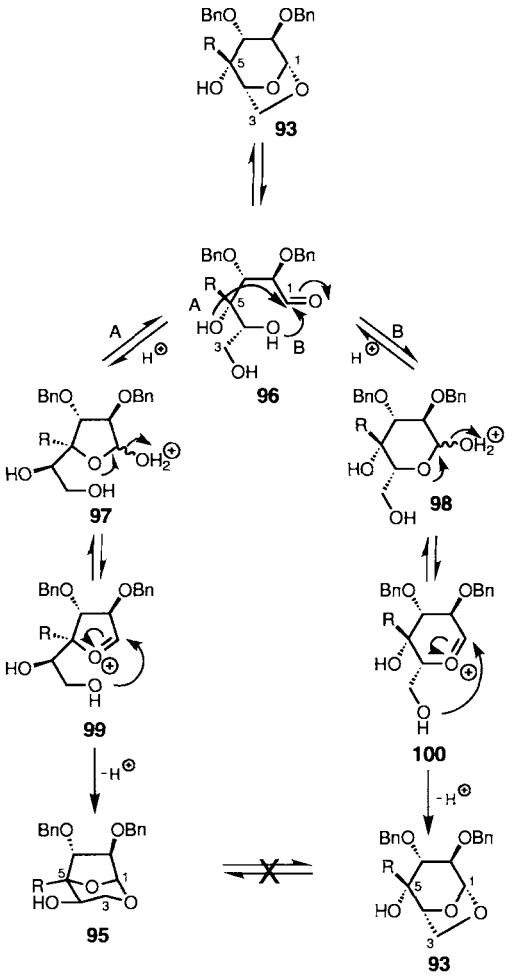

Scheme 17. Rearrangement of C5-substituted anhydrofuranoses (Heathcock et al.). Left: path A; right: path B.

would destabilize the five-membered cyclic oxonium ion **99** relative to **100**, and the reaction would proceed preferentially by path B. Moreover, since the ring closures of each oxonium ion are essentially irreversible under the reaction conditions, the kinetic product cannot equilibrate to yield a thermodynamic mixture of products.

As the zaragozic acids are substituted at C1, the effect of C1 substitution on the acid-catalyzed cyclization was also investigated (Scheme 18). The necessary functionalization of **93c–e** at C1 was achieved efficiently. The six-membered lactols **98c–e** were synthesized and converted into the corresponding lactones **101c–e** by ring opening and formation of the five-membered lactol, introduction of the C3/C4 acetonide, and oxidation. Addition of the organocerium reagent derived from methylmagnesium bromide gave the lactols **102c–e** in good yield. Conventional Grignard reagents caused elimination of the C6 benzyl group. Rearrangement of the lactol then produced a mixture of the two [3.2.1] ring systems, furanoses **103c–e** and pyranoses **104c–e**, but the ratio was less dependent on R and always in favor of the desired furanose form. This time, too, control experiments established that the ratio was subject to kinetic control. After longer reaction times the relative amount of the pyranose form increased until equilibrium was reached, which depended on the nature of R. This was rationalized by the events shown in Scheme 19. Hydrolysis of the acetonide functionality

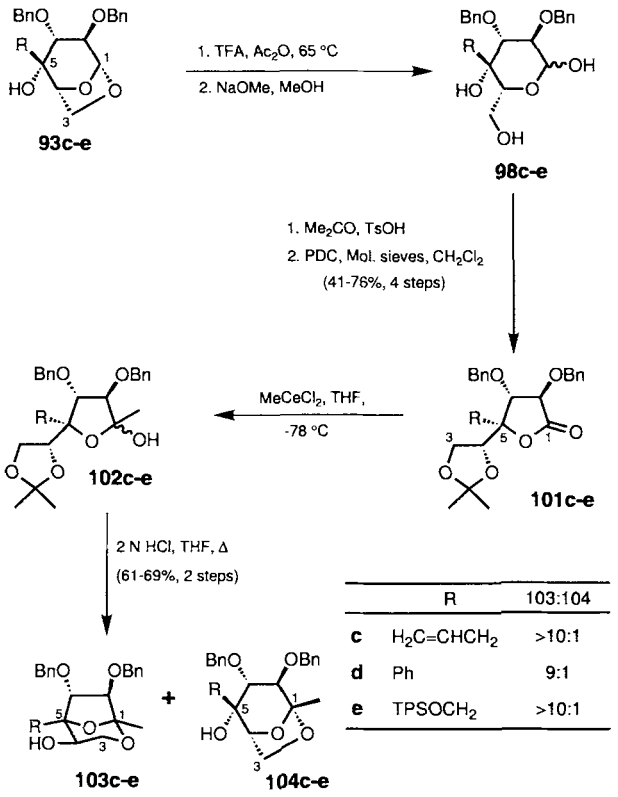

Scheme 18. Introduction of functionality at C1 (Heathcock et al.). PDC = pyridinium dichromate.

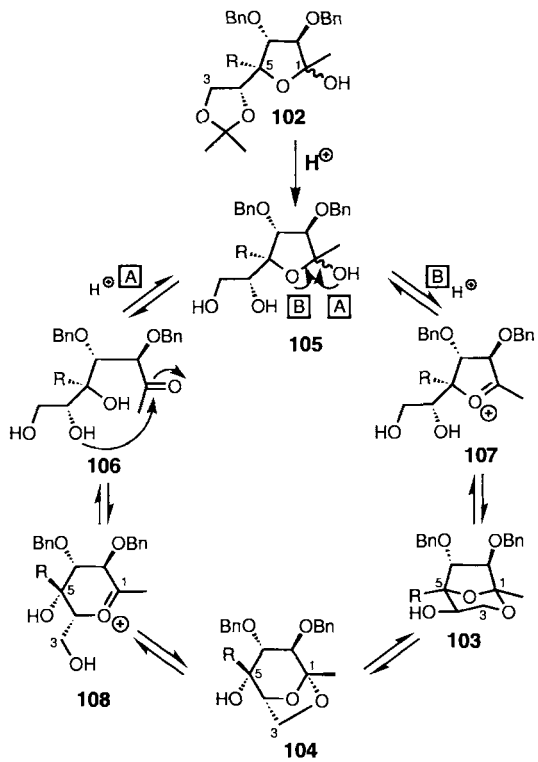

Scheme 19. Rearrangement of lactol **105** (Heathcock et al.).

was assumed to give diol **105**, which could either lead to ketone **106** and oxonium ion **108** (path A) or to the oxonium ion **107** (path B). The facile trapping of oxonium ion **107** to give product **103** is faster than the cyclization of ketone **106** to yield the

oxonium ion **108**, which accounts for the kinetic preference for the furanose form. Oxonium ions **107** and **108** are more stable intermediates (since they are substituted at C1) and the ring-closing steps from each are therefore not irreversible. Thus the two end products can equilibrate via **106** to afford a mixture whose ratio is apparently dependent on the size of R. This methodology was recently used by Heathcock et al. to complete the synthesis of zaragozic acid A,[74] although details have not yet been published.

The most imaginative synthesis of a model of the zaragozic acid core was described by Koyama and coworkers at Merck (Scheme 20).[75] Whereas all the other approaches to the synthesis of the zaragozic acids rely on a ketalization to form the bicyclic core, these researchers used a tandem cyclization–cycloaddition reaction, first developed by Padwa,[76] to assemble the core from two acyclic precursors in a single step. Starting with the diazoketone **109**, rhodium tetraacetate induced decomposition gave the presumed carbonyl ylide **110** by carbene insertion into the C=O bond of the ester. Intermediate **110** then undergoes an intermolecular 1,3-dipolar cycloaddition with an enol ether dipolarophile to give the bicyclic core **111**. The yields, however, are rather modest and the products of course are racemates. In contrast, when ketone **112** was used (Scheme 21), the products **114**, carbocyclic

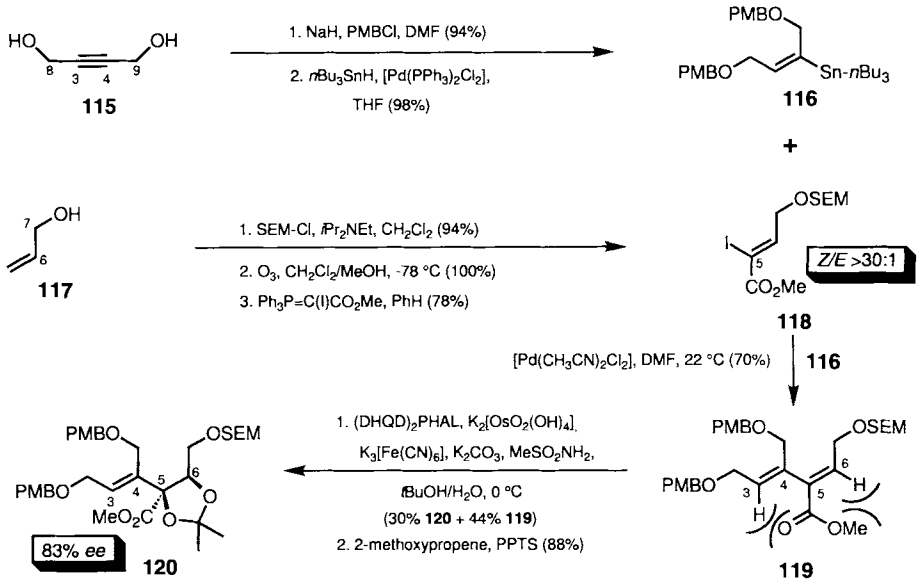

Scheme 22. Early stages of our synthesis of the model compound **130a**. PPTS = pyridinium *para*-toluenesulfonate.

analogs of the zaragozic acids, were obtained in much greater yields.

One of only two syntheses to use asymmetric catalysis to synthesize an enantiomerically enriched model of the core of the zaragozic acids is that by our group (Schemes 22–28).[77, 78] Starting with two readily available starting materials, butyne-1,4-diol (**115**) (an intermediate in the industrial synthesis of THF) and allyl alcohol (**117**), the vinylstannane **116** and the vinyl iodide **118** were synthesized (Scheme 22). Since the alkyne **115** has two identical substituents, the regioselectivity of the *cis*-hydrostannylation was not important. The configuration of the double bond in the vinyl iodide was controlled by a Wittig reaction to give **118** with >30:1 *Z*/*E* selectivity. A Stille coupling[79] of **116** and **118** then formed the diene **119** as a single isomer without any pre-isomerization, a problem that can affect some Stille couplings. It should be noted that the control over the configuration of the double bond was crucial at this stage, since four of the six stereocenters in the core ultimately arise from dihydroxylations of double bonds. The first of two dihydroxylations was conducted under Sharpless conditions,[65] and, remarkably, gave a single regioisomer **120** in around 83% *ee* but only 30% yield. The success of this reaction was found to depend critically on the size of the protecting groups at C7, C8, and C9. The surprising regioselectivity was explained as resulting from a subtle balance of steric and electronic effects.[78] After removal of the PMB protecting groups from **120**, a second dihydroxylation (which was accompanied by spontaneous translactonization) gave triol **123** as a single diastereoisomer in 83% yield (**121** → **123**, Scheme 23). A series of sequential oxidations and protecting group manipulations was then performed to increase the oxidation states at C7, C8, and C9 to the correct levels (**124** → **125**, Scheme 24).

As a model for the alkyl side chain at C1, the anion of 2-methyl-1,3-dithiane (**126**) was added to the aldehyde **125** (Scheme 25). Unfortunately, a (separable) 1:1 mixture of C7 diastereoisomers resulted. The desired diastereoisomer **127a** was desilylated with 2% HCl in MeOH and the dithiane protecting group was removed with $Hg(ClO_4)_2/CaCO_3$ to provide

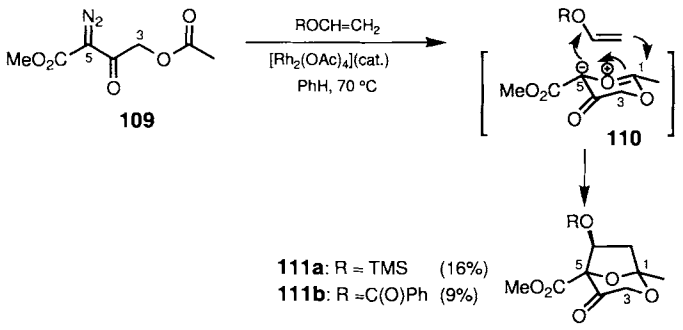

Scheme 20. Approach to the zaragozic acids based on a tandem cyclization–cycloaddition reaction (Koyama et al.).

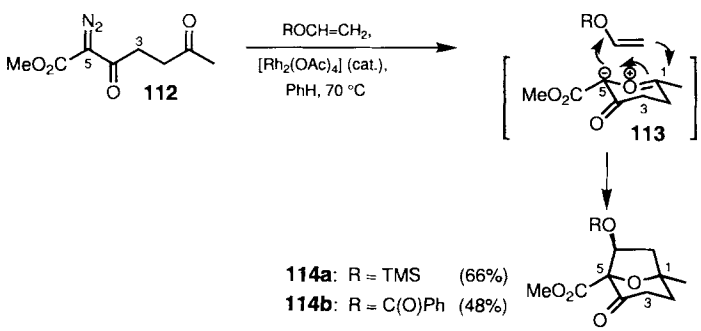

Scheme 21. Synthesis of carbocyclic analogs of zaragozic acid (Koyama et al.).

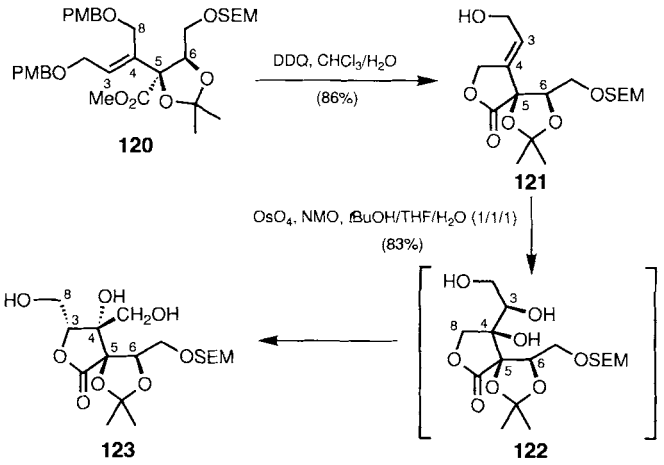

Scheme 23. Synthesis of the model compound **130a**: the second dihydroxylation. **123** is obtained as a single diastereomer.

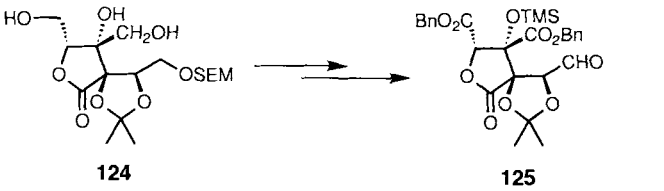

Scheme 24. Synthesis of the model compound **130a**: oxidation of **124** (≙ **123**) to give **125**.

128 in 72% yield. In the tricyclic structure **128a** each carbon atom is at the correct oxidation state, so that an acid-catalyzed removal of the three cyclic protecting groups and subsequent ketalization should give the desired [3.2.1]bicycle **129a**. These predictions proved to be correct, and by refluxing **128a** in 2% HCl in MeOH, **129a** was obtained in 56% yield. The C3 and C5 carboxyl groups had also been usefully differentiated from the C4 benzyl ester in the form of methyl esters. Hydrolysis of the two methyl esters with lithium hydroxide gave the corresponding dicarboxylic acid, which was converted to the tricarboxylic acid **130a** in quantitative yield by hydrogenolysis. The same experiments on the diastereoisomer **127b** (obtained from the dithiane addition reaction) gave the corresponding triacid–triol **130b**, epimeric at C7. The high yield in the rearrangement of **128a** and **128b** is remarkable, particularly in light of Heathcock's studies[73–74] discussed previously and calculations by Evans and co-workers (vide infra).[90]

Two by-products could be isolated from reactions that had not reached completion, methyl glycoside **131** and the alternative [3.2.1] system **132**, both of which could be converted to the desired product **129b** (Scheme 26). This suggested that in this system at least, the desired product was the thermodynamically more stable one.

In an attempt to overcome the poor selectivity obtained in the addition of dithianes to **125**, we replaced the aldehyde derivative **125** with **136**.[78] Starting from intermediate **133** (an analog of **123** with a different protecting group on the C7 hydroxyl group), selective silylation, oxidation, and esterification with DCBI (**137**) gave the ester **134** (Scheme 27). DCBI and its relatives such as DITBI (**176**) have seen widespread use in derivatizing the zaragozic acids.[80] Desilylation of the C8 silyl ether and cleavage of the MEM group with NaI/TMSCl in acetonitrile

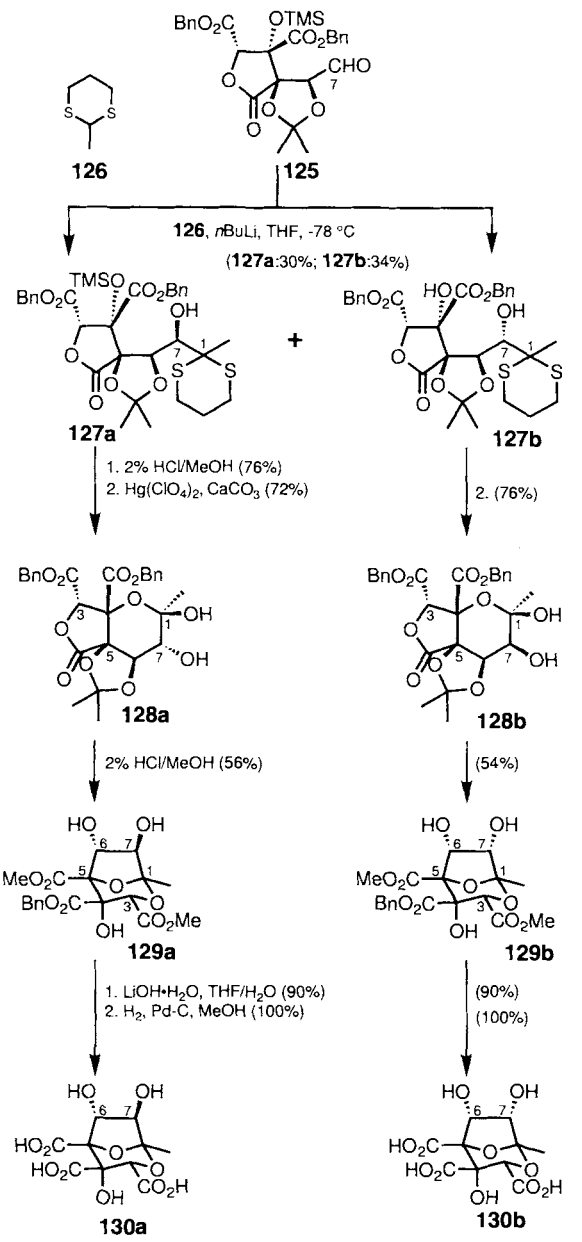

Scheme 25. Synthesis of the model compound **130a**: concluding steps.

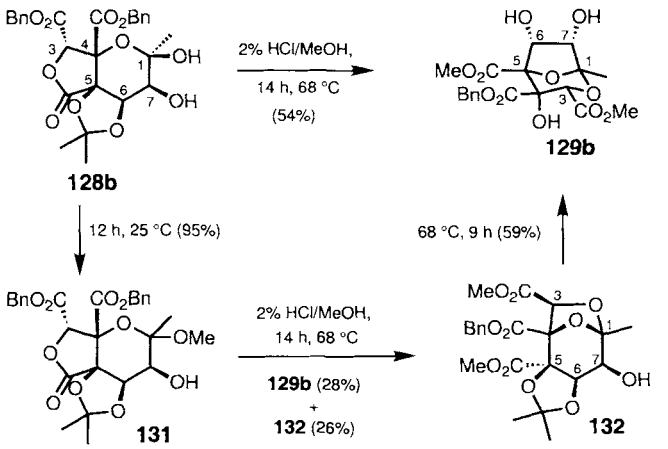

Scheme 26. Rearrangement of the anhydropyran **132**.

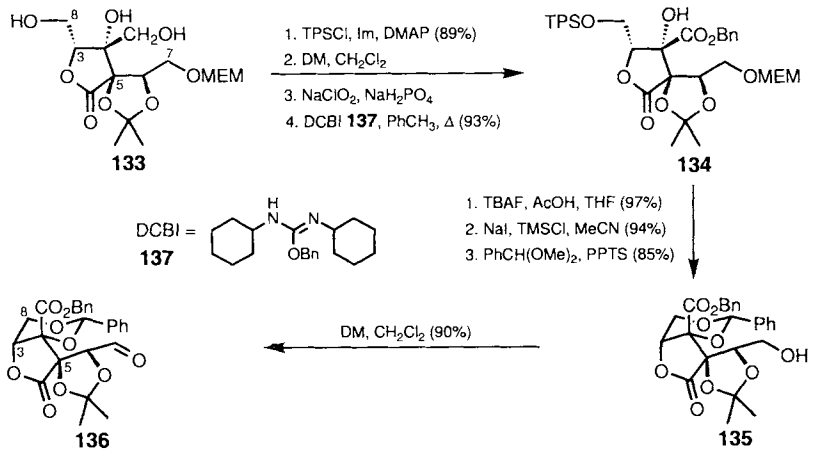

Scheme 27. Synthesis of **136**, an alternative to **125**. MEM = 2-methoxymethyl.

gave the corresponding triol in excellent yield. Subsequent treatment with benzaldehyde dimethyl acetal afforded the benzylidene acetal **135**, and finally, oxidation gave the aldehyde **136**. Addition of the anion of 2-methyl-1,3-dithiane (**126**), the nucleophile used previously, then proceeded with improved diastereoselectivity to give the dithiane **138** as the major product (Scheme 28, ratio of diastereoisomers 3:1). A standard se-

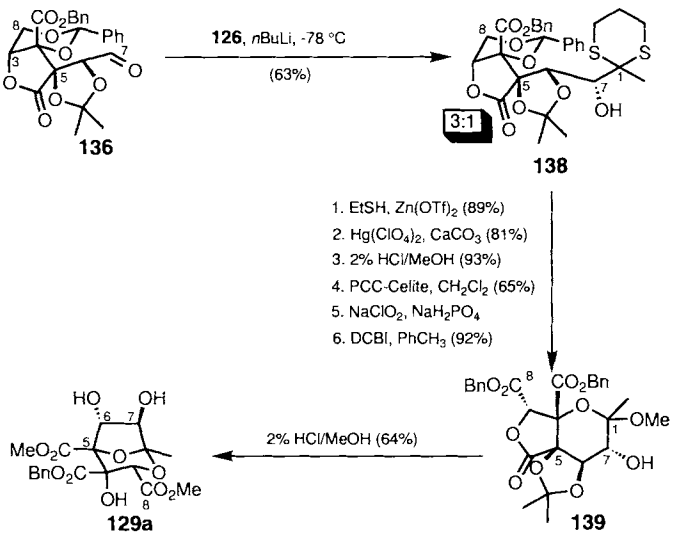

Scheme 28. Final stages of our alternative synthesis of **129a**. PCC = pyridinium chlorochromate.

quence of reactions then provided the methyl glycoside **139**. As before, the methyl glycoside **139** underwent rearrangement to give the previously obtained triester **129a** in 64% yield. Some of these results were later applied in the first synthesis of zaragozic acid A (vide infra).[78, 81]

A very similar approach was described by Armstrong and Barsanti in a recent report (Schemes 29 and 30).[82] Essentially the same strategy was used, but on substrates with lower oxidation states. The same two carbon–carbon bond forming reactions (a Stille coupling and a dithiane–aldehyde coupling) were used to construct the same bonds, and sequential dihydroxylations of a diene were used to introduce the four contiguous hydroxylated stereocenters from C3 to C6. Starting from alkyne **140** (Scheme 29), conjugate addition of lithium iodide gave vinyl iodide **142** in 95% yield. Vinylstannane **141** was synthesized from butyne-1,4-diol (**115**) by sequential *cis*-hydrostannylation and bis(benzylation) reactions. The vinyl iodide and the vinylstannane were then joined together in a Stille reaction employing an exotic mixture of reagents to afford diene **143** in 86% yield. Zinc chloride was added to the reaction mixture to accelerate the transmetalation of the vinylstannane moiety. Reduction of the ethyl ester functionality with DIBAL-H gave the allylic alcohol **144**. This was dihydroxylated under slightly modified Sharpless conditions[65] to afford a mixture of regioisomeric triols. Potassium peroxodisulfate was added to this reaction mixture as an additional stoichiometric re-oxidant. The mixture of triols was then dihydroxylated once more (with the NMO-based version of the AD) to afford pentaol **145** in an overall yield of 45% from **144** and in 76% *ee* as a 9:1 mixture of diastereoisomers. The dihydroxylations could be performed all in one step if the NMO variant was used first, but the *ee* of the resulting pentaol **145** was low (24%), although the yield was good (74%). Protection of the primary hydroxyl group of **145** as a pivaloate ester, bis(acetonide) formation, deprotection of the primary alcohol, and Swern oxidation[83] afforded aldehyde **146**.

As a simple model for the C1 alkyl side chain, the anion of 2-methyl-1,3-dithiane (**126**) was added to aldehyde **146** (Scheme 30). This addition, as in our synthesis (see Scheme 25), was essentially stereorandom. The desired isomer **147b** was separated and the dithiane grouping was removed in 92% yield with $Hg(ClO_4)_2/CaCO_3$. Treatment of the resulting ketone **148** with 2% HCl in MeOH, first at room temperature and then at 50 °C for 5 h, afforded the bicyclic structure **149**, plus an approximately equimolar amount of the anhydropyranose isomer **150**, in a combined yield of 92%. The undesired pyranose form was reported to be the thermodynamically more stable of the two isomers. Clearly, only introduction of the relevant side chains and oxidation of the three benzyloxymethyl groups to carboxyl functions need to be achieved to complete the total synthesis.

The last model study included in this review is that by the late R. E. Shaw and co-workers at Glaxo (Scheme 31).[84] It is included with some license, since they did not attempt to synthesize the bicyclic core. Indeed, the aim was to prepare monocyclic analogs for biological testing. Nevertheless, the synthesis shares some of the features and problems encountered in syntheses of the natural product, and it is included here for completeness. Starting with the bis(acetonide) of D-glucose **151**, three steps gave the cyanohydrin **152**. Oxidation of the cyanohydrin, formation of the methyl ester, hydrolysis of the side chain acetonide, and oxidation of the primary hydroxyl group gave the acid **153** in good overall yield. Standard manipulations then afforded the lactone **154**. Methanolysis of the *para*-nitrobenzyl ester gave the dimethyl ester **155**. Treatment of this with $Ph(CH_2)_6CH(OMe)_2$, a model for the side chain, under acidic dehydrating conditions gave the 1,3-dioxane **156** in 48% yield

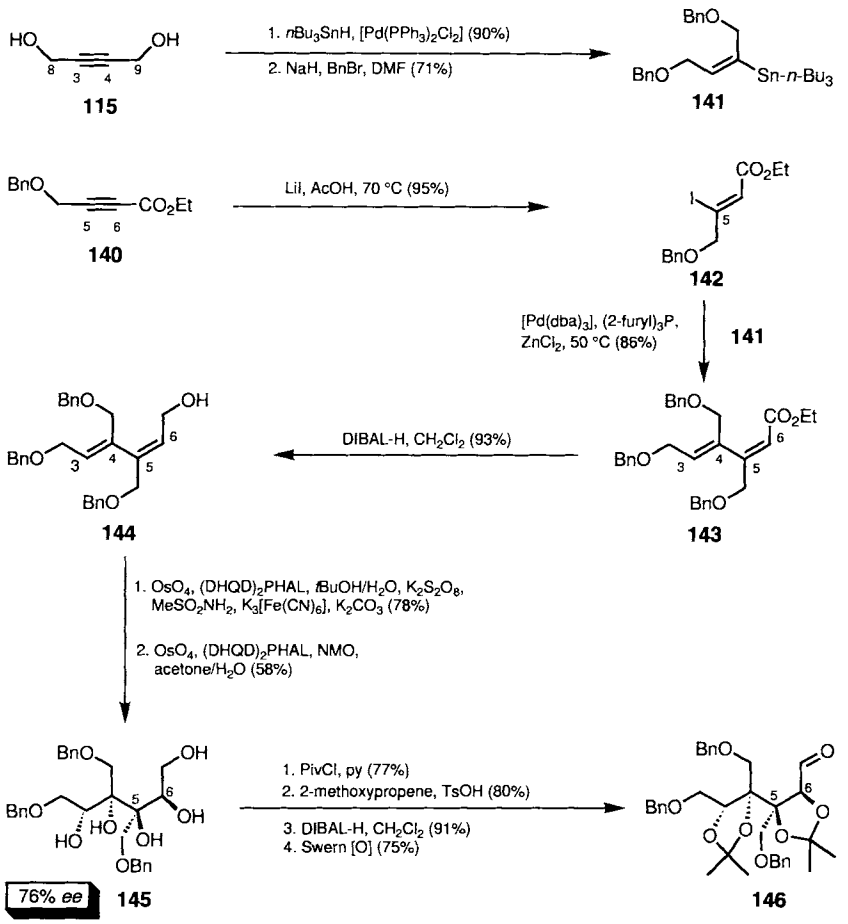

Scheme 29. Armstrong's synthesis of model compound **149** (part 1).

3.2. Total Syntheses of Zaragozic Acids A and C

The first synthesis of zaragozic acid C was reported by Carreira and Du Bois at the end of 1994 (Schemes 32–39).[85, 86] Of the three published syntheses of naturally occurring zaragozic acids, that by Carreira accesses the bicyclic core structure most rapidly. Starting from D-erythro-γ-lactone **162** (which is expensive but can be made readily from ascorbic acid in three steps), three standard reactions gave the amide **163** (Scheme 32). Formation of the C5 stereocenter required the construction of two carbon–carbon bonds and this was achieved in a particularly neat, one-pot reaction. Sequential addition of one equivalent of ethoxyvinyllithium and one equivalent of the Grignard reagent derived from trimethylsilylacetylene afforded an intermediate vinyl ether, which after ozonolysis gave the ester **164** in excellent yield. The diastereoselectivity was >20:1 and was postulated to have arisen through magnesium ion mediated chelation of the intermediate keto group with the neighboring benzyl ether. Reduction of the ethyl ester in **164**, deprotection of the alkyne, and protection of the hydroxyl groups at C10 and C5 with a TBS and a TMS group, respectively, then gave the intermediate **165**.

Unlike the Evans synthesis and our synthesis, Carreira introduces the C1 alkyl side chain at an early stage. Thus the anion of alkyne **165** was added to the aldehyde **166** (see Scheme 46) in the presence of LiBr to form the C1–C7 bond in 93% yield (Scheme 33). Reduction of the alkyne to the necessary *trans* alkene proved difficult, but eventually with a new reagent combination diol **168** could be

and a small amount of the 1,3-dioxolane **157**. However, with the zaragozic acid A side chain equivalent **158** (as a mixture of racemic diastereoisomers) the results were inferior, resulting partly from isomerization of the allylic acetate, and the desired compound **159** could only be isolated in very low yields.

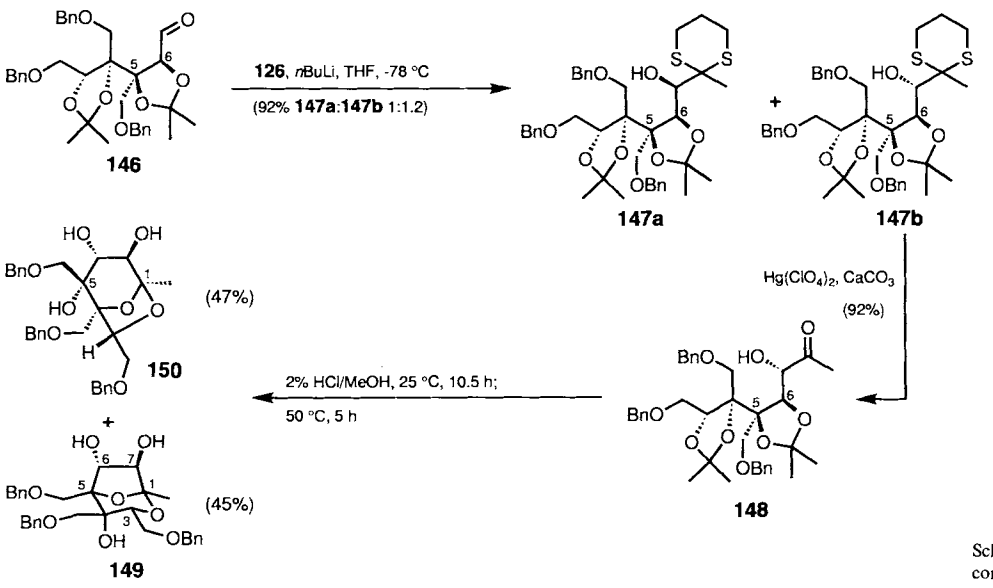

Scheme 30. Armstrong's synthesis of model compound **149** (part 2).

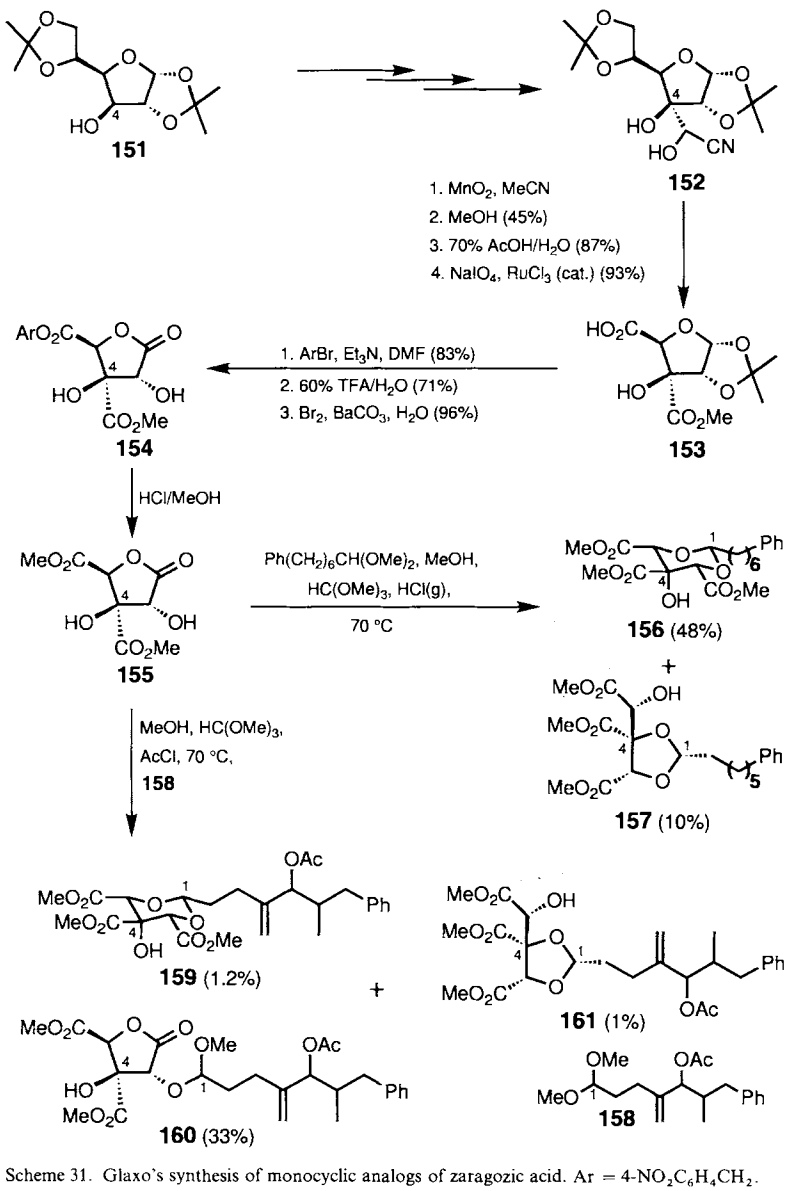

Scheme 31. Glaxo's synthesis of monocyclic analogs of zaragozic acid. Ar = 4-$NO_2C_6H_4CH_2$.

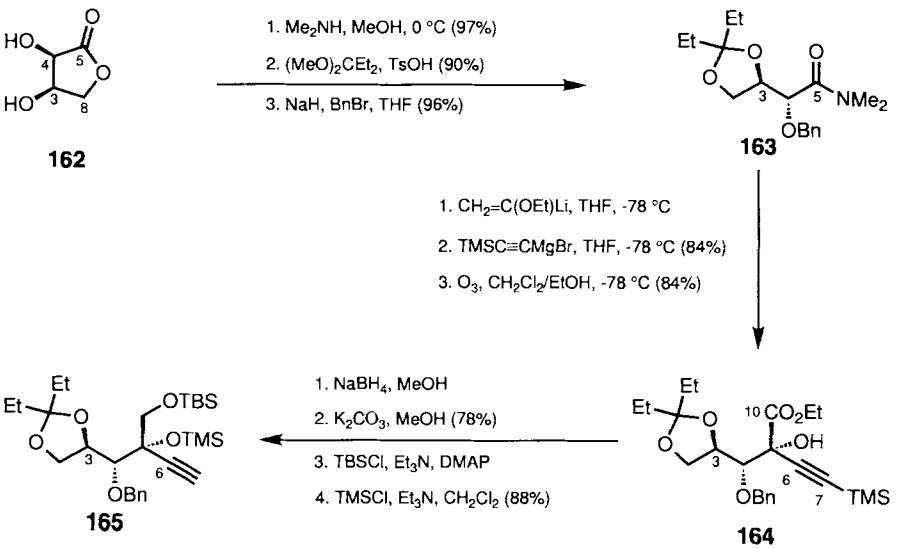

Scheme 32. Early stages of Carreira's synthesis of zaragozic acid C.

obtained in good yield after desilylation. The C6 and C7 stereocenters were then set by a dihydroxylation, which proved more difficult than expected. Under standard catalytic dihydroxylation conditions the substrate favored formation of the undesired diastereoisomer **169b**, and under the standard Sharpless asymmetric dihydroxylation conditions no reaction was observed. However, with a slightly modified set of reagents (NMO instead of $K_2CO_3/K_3[Fe(CN)_6]$ as the stoichiometric oxidant) the desired diastereoisomer **169a** was formed with a slight preference (1.7:1).[65] Remarkably, this ratio was the same regardless of which pseudo-enantiomeric ligand was used in the reaction, a result also encountered recently by Smith and co-workers.[87] The mixture of dihydroxylation products **169a,b** was then treated with HCl in MeOH at room temperature, resulting in the efficient formation of the bicyclic core structure. Protection of the two primary hydroxyl groups as TBS ethers afforded **170**, which was separated from the undesired C7 epimer by chromatography.

The remaining tasks in the synthesis at this point were: a) the introduction of functionality at C4, b) the oxidations, and c) the differentiation of the C6 and C7 hydroxyl groups. To accomplish the first task, the C6 and C7 hydroxyl groups were protected as pivaloate esters, the benzyl ether was removed, and the resulting alcohol was oxidized under Swern conditions to give the C4 ketone **171**. Three different approaches to introduce the C9 carbon atom were tested (Scheme 34). Ultimately, addition of TMSC≡CLi under very carefully optimized conditions gave the best results (→**174**) in terms of yields and selectivity.[88] Other routes (**171** →**172** and **171** →**173**) were less successful.

As in our route, the oxidations initially formed a large part of the synthesis (Scheme 35). Deprotection of alkyne **174**, removal of the pivaloate units and replacement with acetyl groups, selective hydrolysis of the C8 TBS ether, and partial reduction of the alkyne gave the alcohol **175**. Oxidation, esterification, carefully buffered deprotection of the C10 hydroxyl group (to prevent migration of the acetyl group at C6), and a three-step oxidation–esterification of the C10 hydroxyl group gave the diester **177**. Ozonolysis of the double bond in **177** gave the corresponding aldehyde, which was converted into the triester **178**.

Fortunately, this tedious sequence of reactions could be replaced by a more elegant and far more efficient approach, in which the oxidations are performed almost simultaneously (Scheme 36).[86] Starting with the triacetate **179**, hydroly-

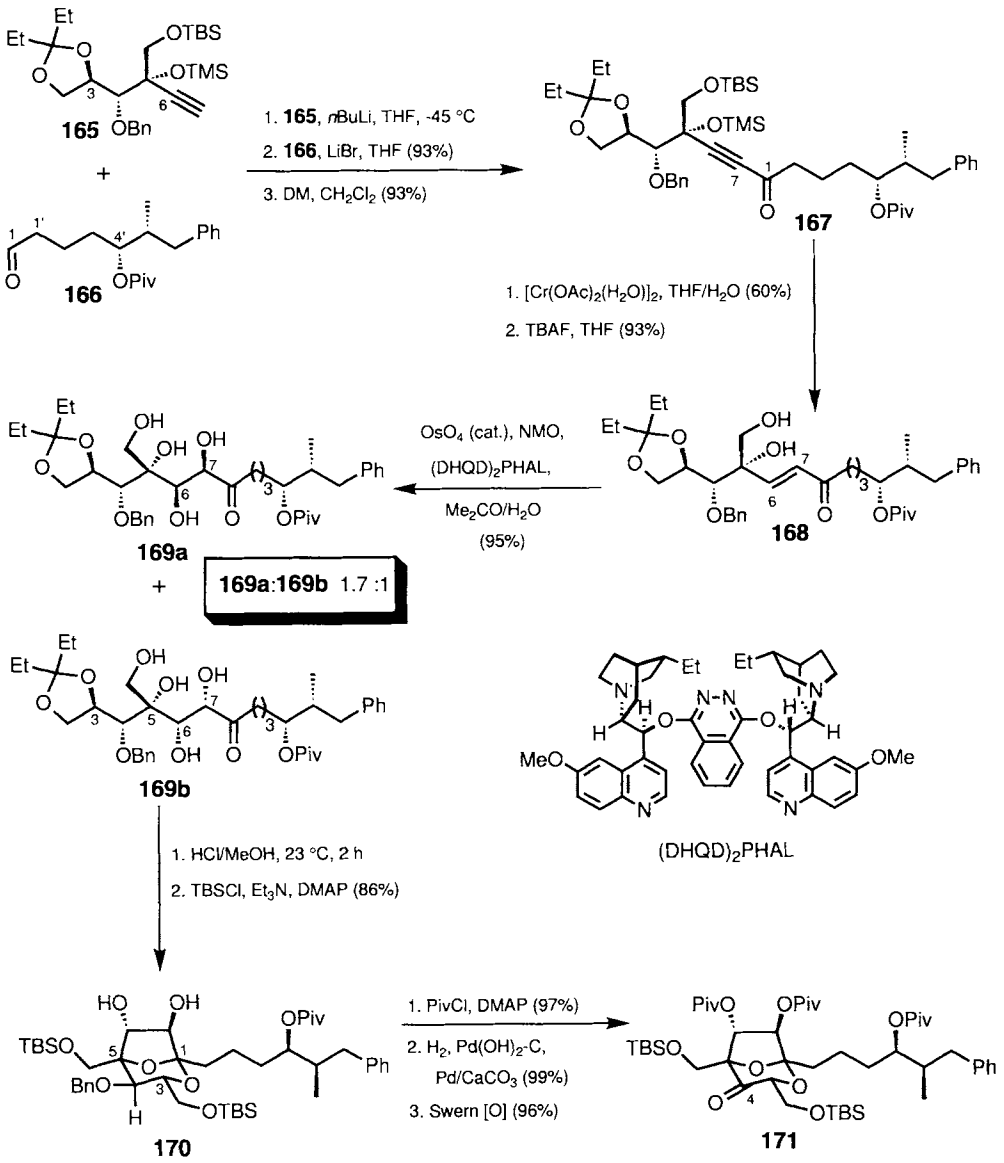

Scheme 33. Formation of the bicyclic core (Carreira et al.).

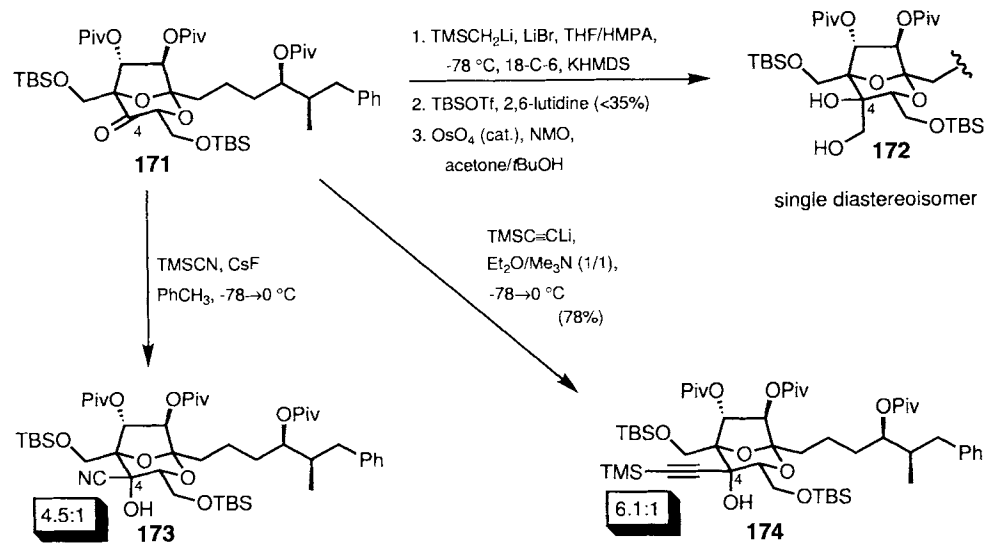

Scheme 34. Introduction of functionality at C4 (Carreira et al.). KHMDS = potassium bis(trimethylsilyl)amide, 18-C-6 = [18]crown-6.

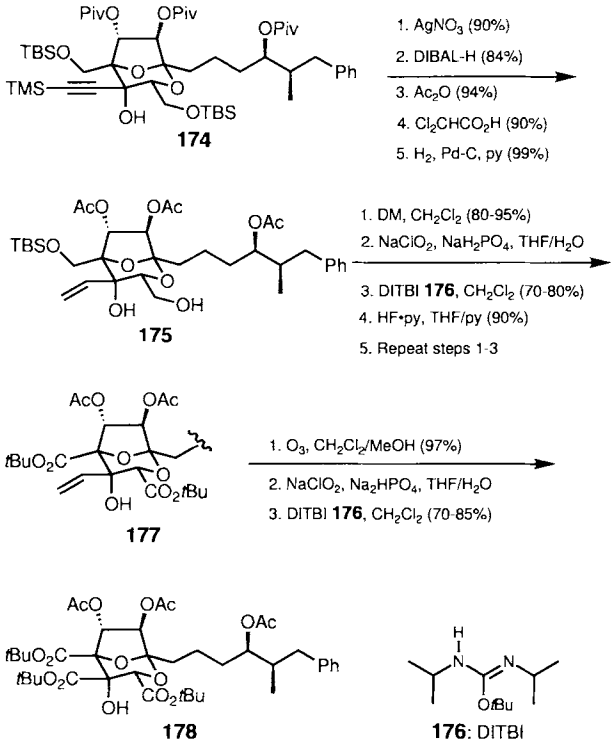

Scheme 35. Stepwise oxidation of the hydroxyl groups of **174** (Carreira et al.).

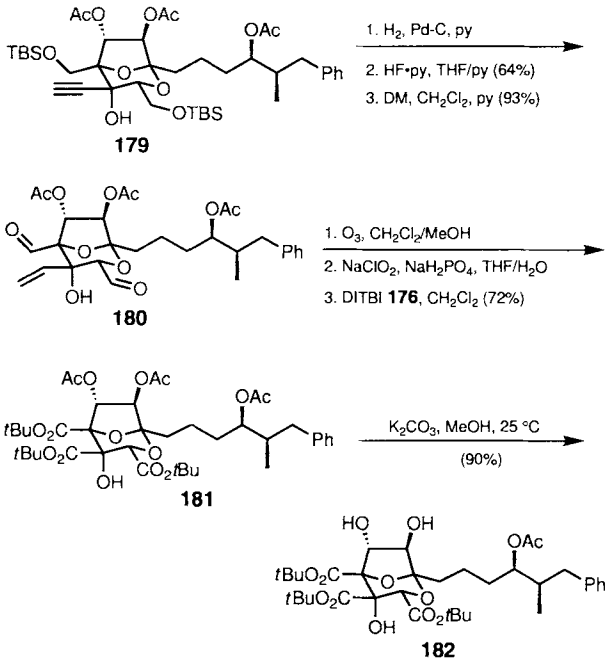

Scheme 36. Simultaneous oxidations to form the tricarboxylate moiety **181** (= **178**) of zaragozic acid C (Carreira et al.).

sis of both TBS ethers, and oxidation with the Dess–Martin reagent[89] gave the dialdehyde **180**. Ozonolysis then gave the trialdehyde (!), which was oxidized further with $NaClO_2$ and esterified as before to give the triester **181**. Finally, a remarkably selective deprotection revealed the C6 and C7 hydroxyl groups and afforded **182**.

Initially, Carreira and Du Bois completed the synthesis of zaragozic acid C (**184**) by esterifying **182** with the acid chloride of the C6 acyl side chain **183** (see Scheme 50), separating the mixture of C6 and C7 regioisomers, and deprotecting the three *tert*-butyl esters (Scheme 37).[85] However, a few model studies

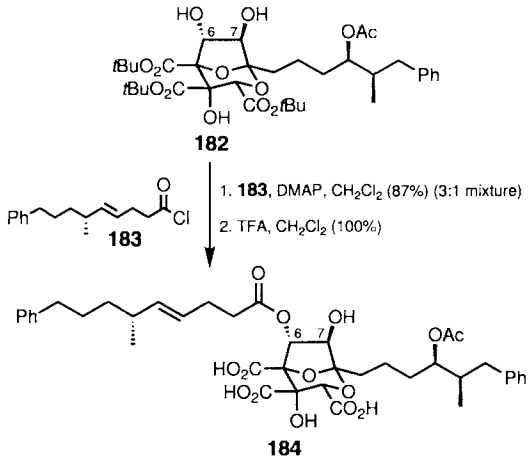

Scheme 37. Conclusion of the synthesis of zaragozic acid C (**184**) (Carreira et al.).

conducted with zaragozic acid A suggested that a much more satisfactory end to the synthesis could be found.[86] Initial studies with **185**, derived from zaragozic acid A (**1**), showed that acylation with hexanoyl chloride in the presence of the exotic phosphorus base **186** gave a mixture of regioisomers **187a** and **187b** in a 10:1 ratio (Scheme 38). This was improved still further by using $(Boc)_2O$ as the acyl source and 4-(1-pyrrolidinyl)pyridine (**189**) as the catalytic base, which afforded **190a**:**190b** in a ratio of >20:1. Remarkably, when the reaction was repeated with DMAP (**188**) in place of **189** the ratio fell to 3:1.

With this procedure to differentiate the C6 and C7 hydroxyl groups, it was a simple matter to introduce the C6 acyl side chain **202** and simultaneously deprotect the three *tert*-butyl esters and the Boc carbonate to give zaragozic acid C (**184**) (Scheme 39).

The synthesis of zargaozic acid C by the Evans group[90] (Schemes 40 and 41) is notable for its efficiency and the complete control exerted over each newly formed chiral center. Two of the key C–C bond forming reactions are coincidentally similar to those reported by other groups: the addition of the C1 alkyl side chain (**198** + **199** → **200**) is similar to the Rizzacasa and Heathcock routes, and the use of a tartrate fragment for the C3/C4 unit is similar to that reported by Aggarwal.

Starting with *N*-acyl oxazolidinone **191**, an Evans aldol reaction[91] with cinnamaldehyde gave the *syn* aldol **192** as a single diastereoisomer, which was converted to the aldehyde **193** in three standard reactions (Scheme 40). The di-*tert*-butyl ester **194** of (+)-tartaric acid was protected as a cyclopentylidene acetal. This protecting group is more labile than the more common acetonide and probably accounted for the mildness of the rearrangement conditions used later in the synthesis (**200** → **201**; Scheme 41). A Mukaiyama aldol reaction between silyl ketene acetal **195** and aldehyde **193** promoted by

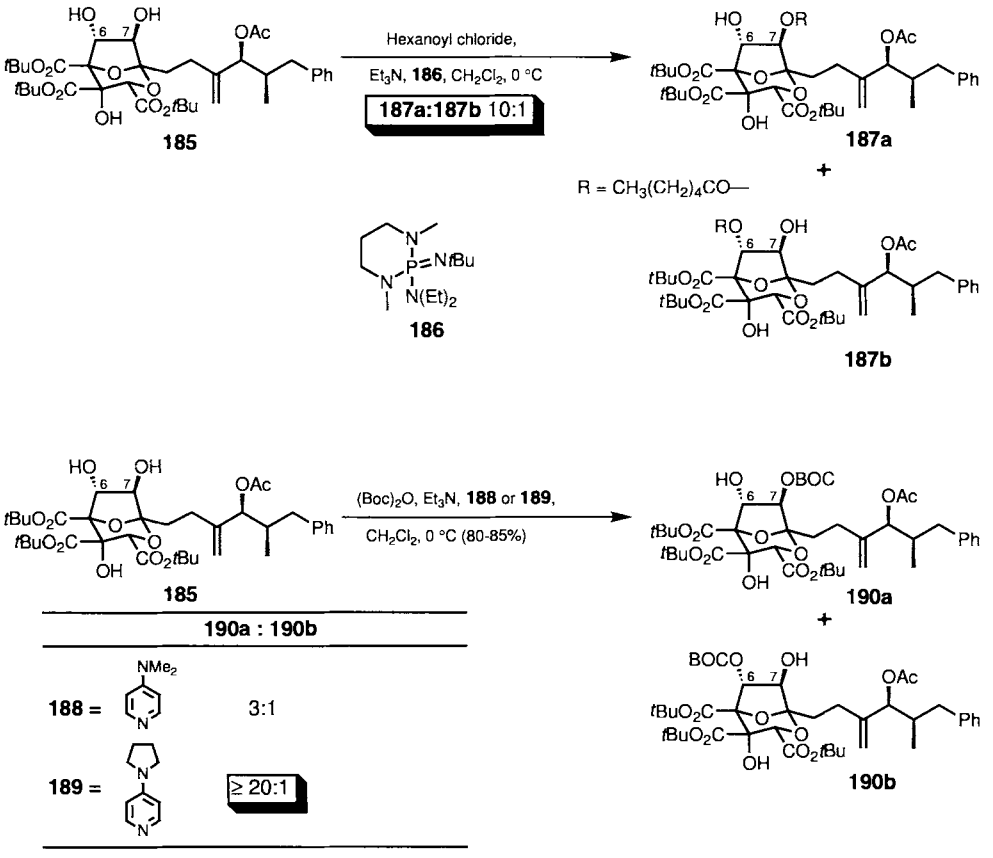

Scheme 38. Selective acylation of the C6 and C7 hydroxyl groups of **185** (Carreira et al.). Boc = benzyloxycarbonyl.

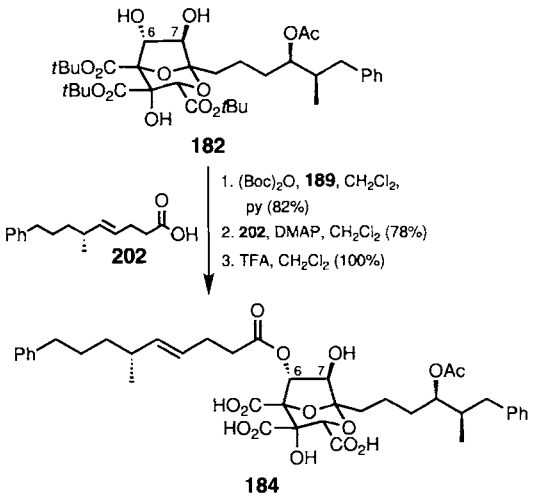

Scheme 39. Selective introduction of the C6 acyl group (Carreira et al.).

(iPrO)$TiCl_3$ gave **196** as a single diastereoisomer. Oxidation of **196** with the Dess–Martin reagent and addition of vinylmagnesium bromide generated the stereocenter at C5 (selectivity >10:1) and introduced the C10 carbon atom. The diastereoselectivity was found to be strongly solvent-dependent. Selective cleavage of the disubstituted double bond gave a lactol, which was oxidized to the lactone **197** with tetra-n-propylammonium perruthenate (TPAP). The tri-*tert*-butyl ester **198** was then obtained by standard methods (Scheme 41). It should be noted that **198** is functionally identical to our aldehyde **125**. Addition of the side chain was achieved by adding the lithio derivative of **199** to the lactone **198**. The PMB protecting group was removed and replaced with an acetyl group to give **200**, which underwent rearrangement at room temperature to yield the bicyclic ketal. Following re-introduction of some of the *tert*-butyl esters and hydrogenolysis of the C6 benzyl ether, alcohol **201** was obtained. Some desilylation of the silyl ether at C7 was encountered during the ketalization step, but this was corrected by resilylating. The final three steps all proceeded without incident: introduction of the C6 acyl side chain (**202**), desilylation of the C7 silyl ether, and deprotection of the three *tert*-butyl esters gave zaragozic acid C (**184**) in an overall yield of 80%. The high degree of convergency of this route owing to the late-stage coupling of the two side chains has also enabled the facile synthesis of zaragozic acid A (**1**).[92]

Our synthesis of zaragozic acid A[81,93] (Schemes 42–44) closely followed the model studies previously described (see Schemes 22–28). Addition of the anion of dithiane **203** to aldehyde **125** gave, as before, an approximate 1:1 mixture of diastereoisomers epimeric at C7 (Scheme 42). The dithiane grouping in the undesired isomer **204** was removed to give the lactol **205**. Unfortunately, during the attempted conversion of lactol **205** to intermediate **206**, the TPS protecting group at C4′ was cleaved and spiroketal **207** was obtained.[78] Interestingly, the spiroketal **207** could not be transformed further to give the bicyclic core **206**.

Accordingly, the more acid-stable di-*tert*-butylmethylsilyl group was used to protect the hydroxyl group at C4′ (**125** + **208** → **209**, Scheme 43). This time the protecting group remained intact during the acid-catalyzed rearrangement, and the bicycle **210** was formed in 40% yield. Removal of the DTBMS

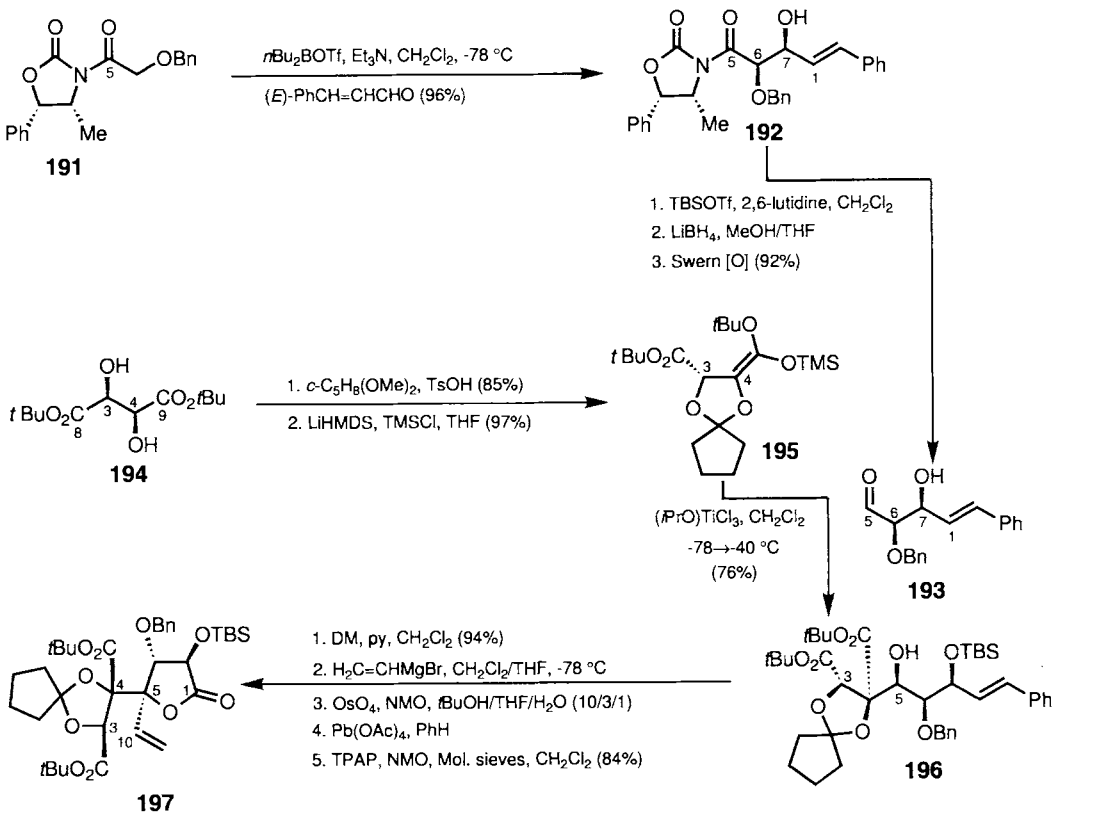

Scheme 40. Early stages of Evans's synthesis of zaragozic acid C (**184**). LiHMDS = lithium bis(trimethylsilyl)-amide.

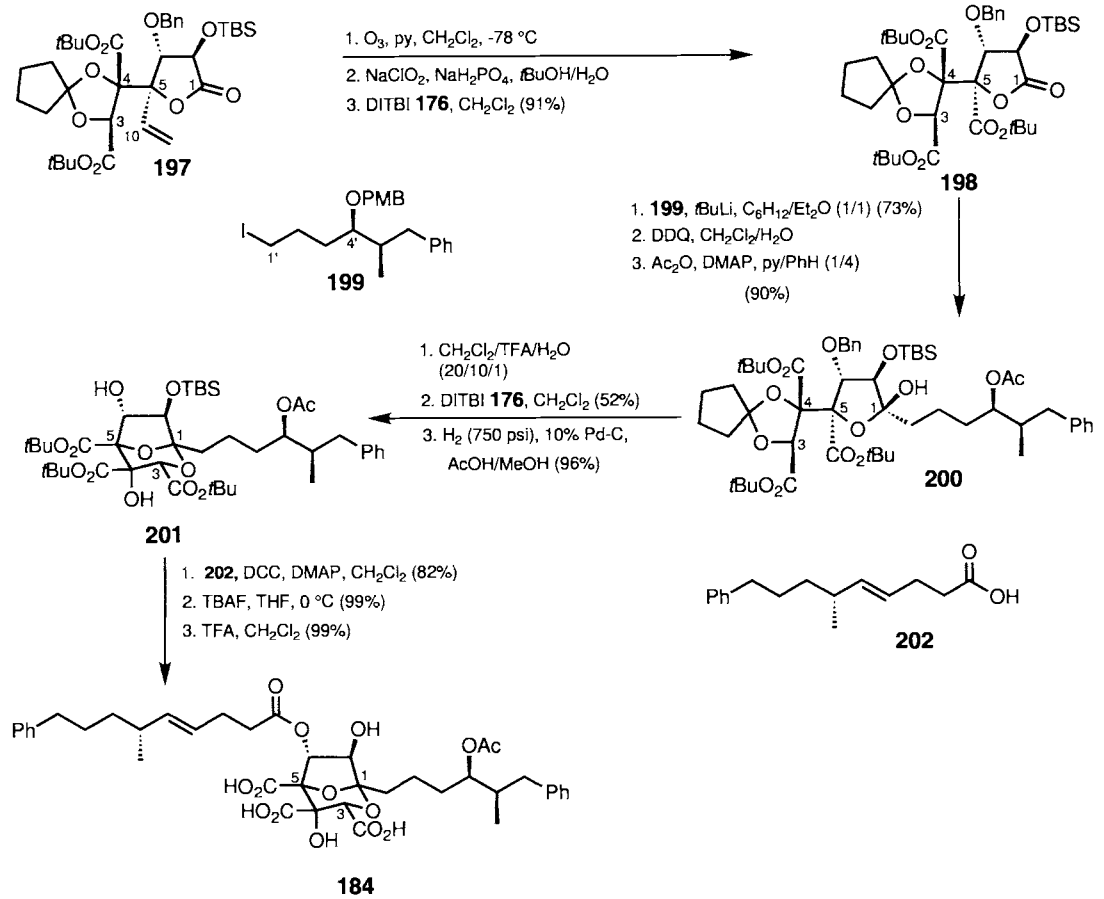

Scheme 41. Final stages of Evans's synthesis of zaragozic acid C (**184**). DCC = *N*,*N*'-dicyclohexylcarbodiimide.

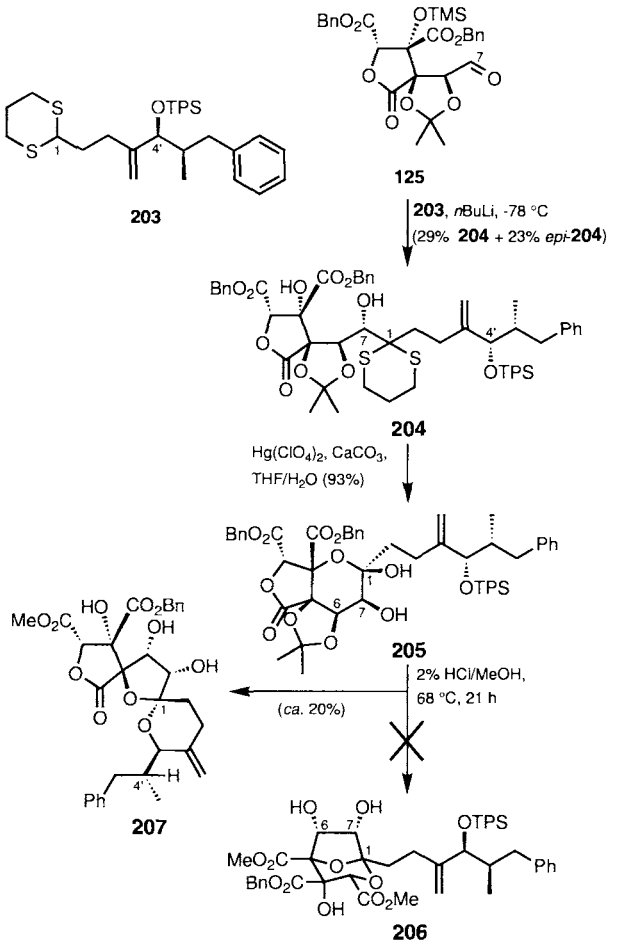

Scheme 42. Attempted synthesis of intermediate **206**.

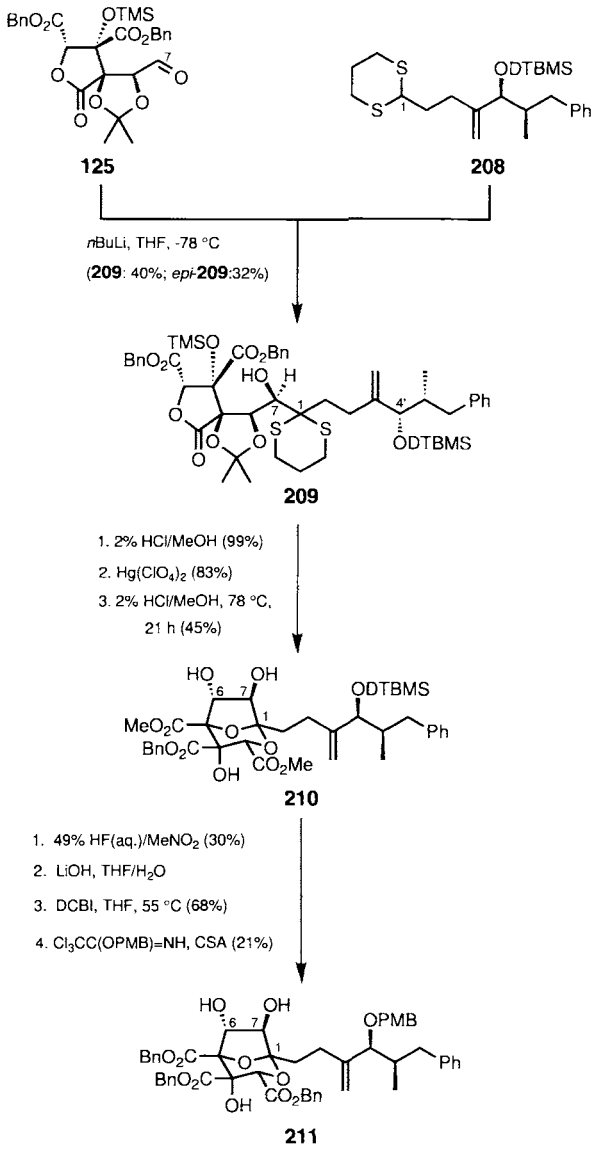

Scheme 43. Our synthesis of intermediate **211**.

protecting group, exchange of the two methyl esters for benzyl esters, and selective protection of the C4′ hydroxyl group as a PMB ether gave the triol **211**, which had been established as an intermediate in earlier degradative studies. The exchange of the methyl esters for benzyl esters was necessary in order to avoid concomitant hydrolysis of the C6 acyl side chain at the end of the synthesis.

Intermediate **211** was converted to zaragozic acid A (**1**) as shown in Scheme 44.[93] Introduction of the C6 acyl side chain (with **214**) was achieved with only modest selectivity (3:2) to give the intermediate **213**. The undesired isomer could be separated by chromatography, hydrolyzed, and recycled. Protection of the C7 hydroxyl group as a TES ether (**215**), deprotection and acetylation of the C4′ hydroxyl group (**216**), and subsequent desilylation gave tribenzyl ester **212** in 77% overall yield. Finally the three benzyl groups were removed, without affecting either the exocyclic double bond or the α,β-unsaturated ester, by transfer hydrogenolysis to give zaragozic acid A (**1**). Furthermore, **211** can be prepared from zaragozic acid A (**1**) by the following route (Scheme 4): a) esterification with DCBI to give the tribenzyl ester **212**, b) selective hydrolysis of the acetate at C4′ under the conditions described by Merck, c) selective protection of the C4′ hydroxyl group with PMB trichloroacetimidate, and d) hydrolysis of the side chain to give (after replacement of some of the benzyl esters) the intermediate **211**.

3.3. Synthesis of the C1 Alkyl Side Chains of Zaragozic Acids A and C

The comparatively simple C6 acyl and C1 alkyl side chains have received less attention than the bicyclic core. Nonetheless, efficient syntheses of both pieces are necessary for total syntheses and for the synthesis of analogs. A common feature of several syntheses of the enantiomerically pure side chains is the use of the Evans oxazolidinone as a chiral auxiliary. In contrast, asymmetric catalysis is used only twice. It should be noted that the exact composition of the C1 alkyl side chain varies slightly. Depending on the synthetic strategy, C1 is sometimes included in the side chain fragment and sometimes in the bicyclic core. The oxidation state of the C1 or C1′ terminal atom also varies with the synthetic plan.

The synthesis of the C1 alkyl side chain of zaragozic acid C by Merck is described in Scheme 45.[94] Starting from *N*-propionyloxazolidinone **217**, an Evans aldol reaction with **218** followed by cleavage of the auxiliary by the Weinreb amide method[95]

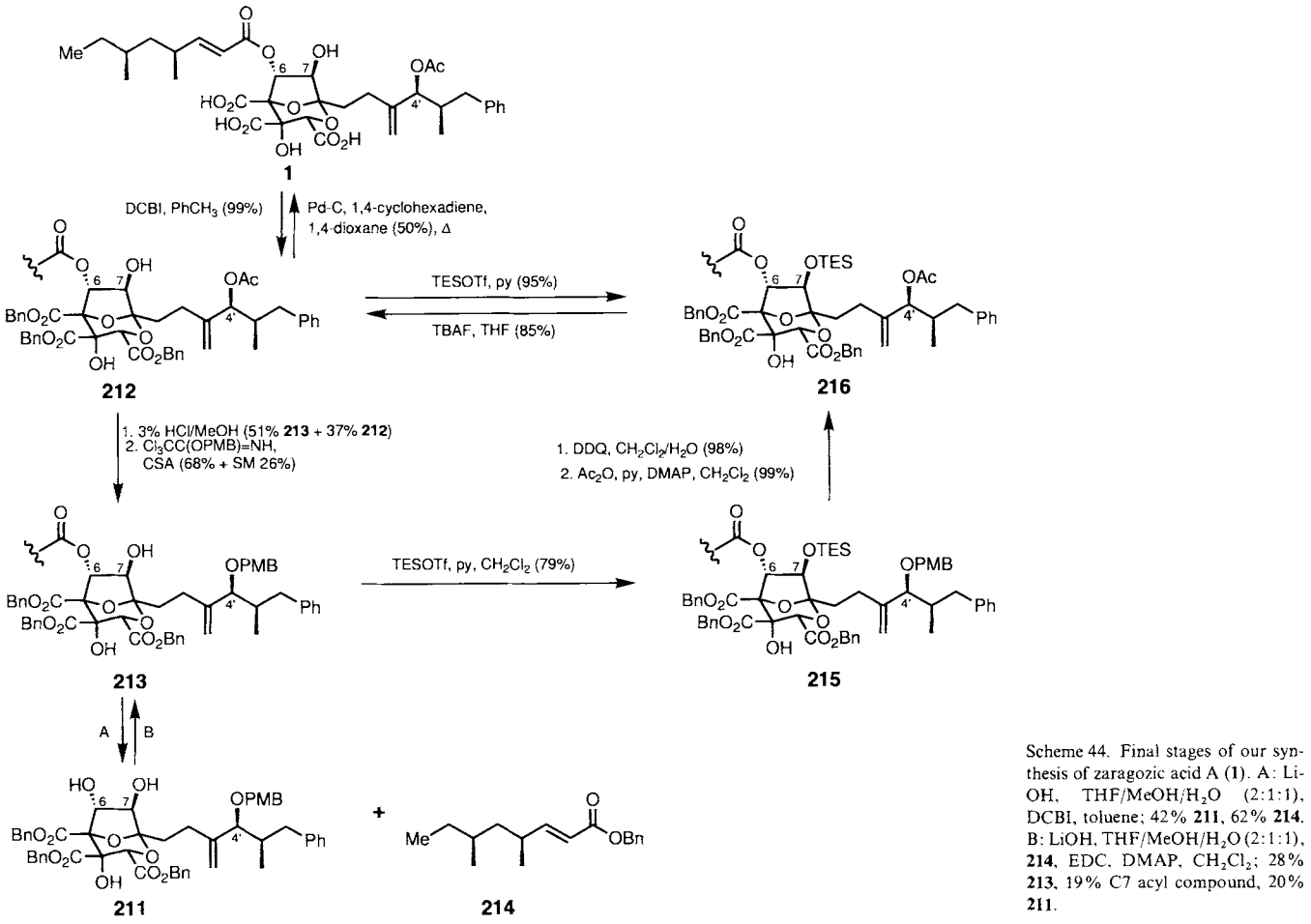

Scheme 44. Final stages of our synthesis of zaragozic acid A (**1**). A: LiOH, THF/MeOH/H_2O (2:1:1), DCBI, toluene; 42% **211**, 62% **214**. B: LiOH, THF/MeOH/H_2O (2:1:1), **214**, EDC, DMAP, CH_2Cl_2; 28% **213**, 19% C7 acyl compound, 20% **211**.

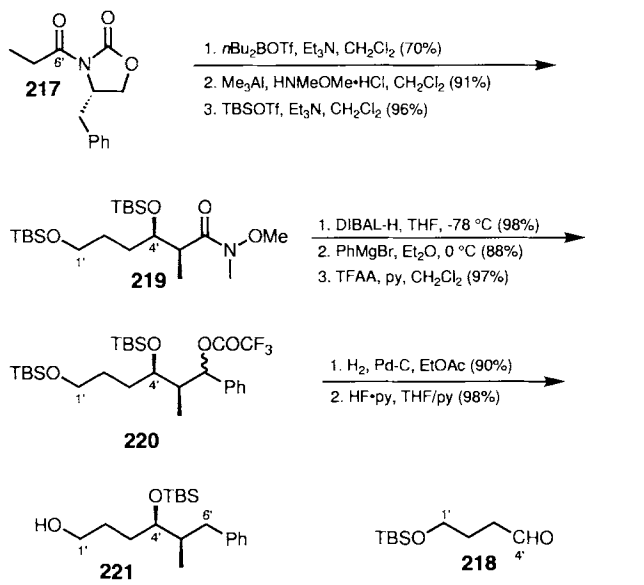

Scheme 45. Synthesis of the C1 alkyl side chain of zaragozic acid C (Merck).

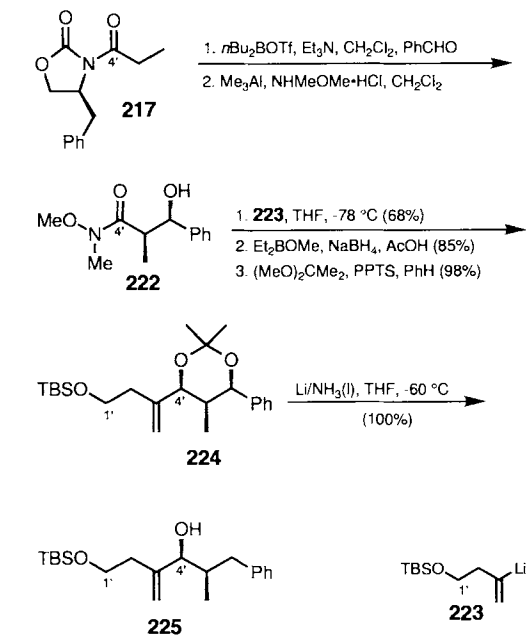

Scheme 46. Synthesis of the C1 alkyl side chain of zaragozic acid A (Merck).

and protection of the resulting hydroxyl group gave the amide **219**. Reduction of the amide, addition of phenylmagnesium bromide, and treatment of the resulting alcohol with trifluoroacetic anhydride gave the trifluoroacetate **220**. Hydrogenolysis removed the benzylic oxygen substituent and selective deprotection with HF in pyridine gave the primary alcohol **221**.

The synthesis of the C1 alkyl side chain of zaragozic acid A is described in Scheme 46.[94] The known Weinreb amide **222** was prepared from **217**. Addition of the vinyllithium derivative **223**, *syn*-selective reduction of the β-hydroxy ketone, and protection

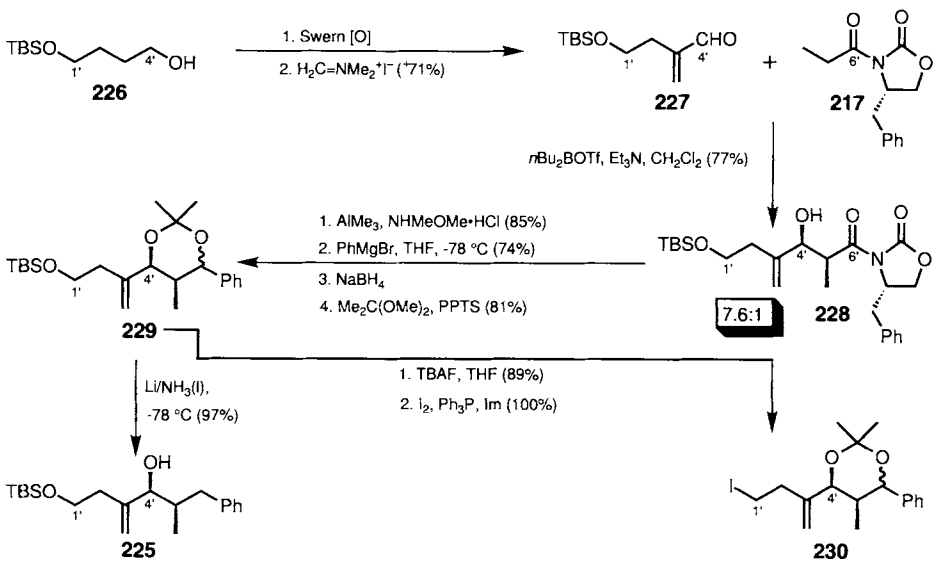

Scheme 47. Synthesis of the C1 alkyl side chain of zaragozic acid C (Rizzacasa et al.).

of the 1,3-diol afforded the acetonide **224**. The benzylic hydroxyl substituent was then efficiently removed by treatment with Li/NH_3 to give the partially protected C1′,C4′ diol **225**.

The same fragment was synthesized independently in a similar fashion by Rizzacasa and co-workers (Scheme 47).[96] The alcohol **226** was oxidized and the resulting aldehyde was treated with Eschenmoser's salt, $H_2C_2{=}NMe_2^{+\ -}$, to yield the α,β-unsaturated aldehyde **227**. This was joined to the C5′/C6′ fragment **217** by an Evans aldol reaction to give the *syn* aldol product **228** as the major component in a 7.6:1 mixture of diastereoisomers.

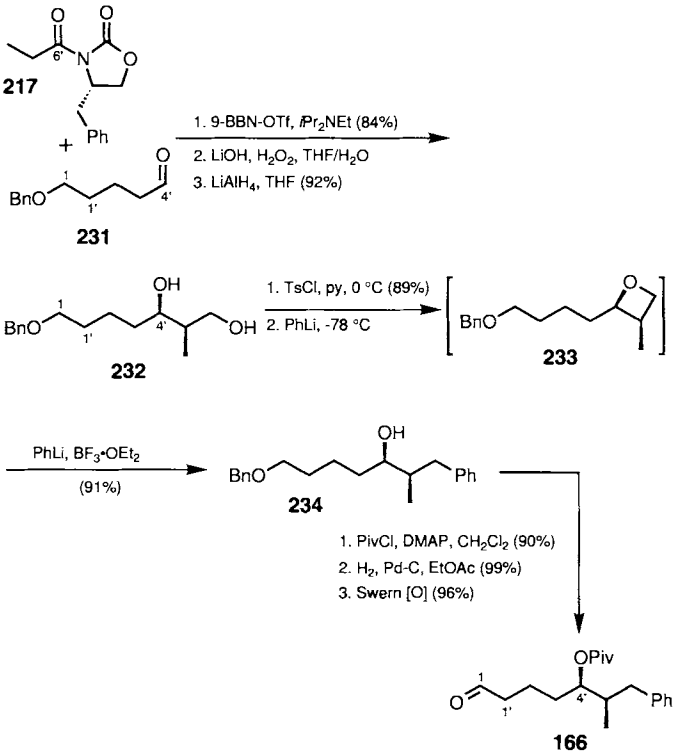

Scheme 48. Synthesis of the C1 alkyl side chain of zaragozic acid C (Carreira et al.). 9-BBN = 9-borabicyclononyl.

Curiously, the Merck group had earlier reported that this route to the alkyl side chain of zaragozic acid A was unsuccessful.[95] Four standard operations then gave the acetonide **229**, which could be converted into the desired iodide derivative **230** of the C1 alkyl side chain fragment or reduced with Li/NH_3 to provide the allylic alcohol **225**.

Carreira's synthesis of the C1 alkyl side chain of zaragozic acid C also relied on an Evans aldol reaction, this time to make the diol **232** (Scheme 48).[86] To introduce the phenyl group, the primary hydroxyl group in **232** was first tosylated selectively. Subsequent treatment with phenyllithium gave the oxetane intermediate **233**. Reaction with a further equivalent of phenyllithium and $BF_3{\cdot}OEt_2$ induced opening of the oxetane at C6′ to furnish intermediate **234**. Three standard manipulations gave the aldehyde **166**.

Our synthesis of the alkyl side chain of zaragozic acid A began with allylic alcohol **235** (Scheme 49).[93] Sharpless asymmetric epoxidation[97] gave the corresponding epoxide (81% *ee*,

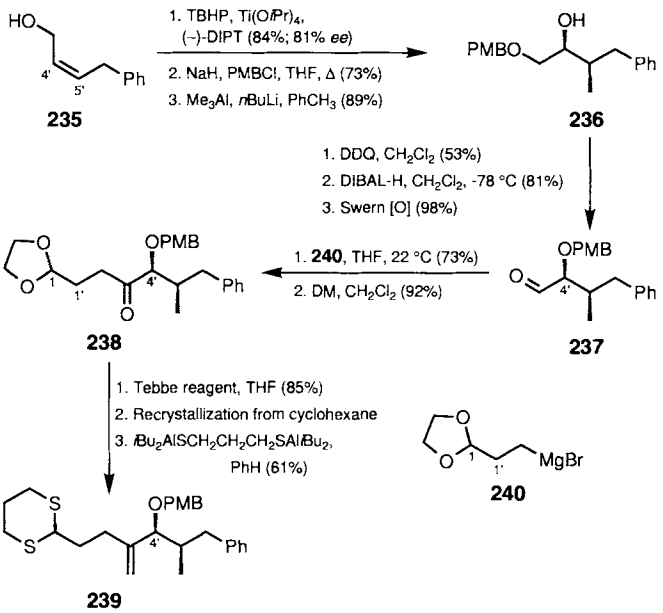

Scheme 49. Our synthesis of the C1 alkyl side chain of zaragozic acid A.

84% yield), which was protected as a PMB ether and opened regioselectively at C5′ with trimethylaluminum to give the alcohol **236** as a single regioisomer. The PMB protecting group was shifted from the primary to the secondary hydroxyl group by oxidation in the absence of water to yield the PMB acetal and then reductive cleavage with DIBAL-H. Swern oxidation then gave aldehyde **237**. Homologation was achieved by addition of the Grignard reagent **240** and oxidation to give the

ketone **238**. Three standard manipulations, including a recrystallization to improve the enantiomeric purity, gave the dithiane **239**.

The shortest synthesis of the alkyl side chain of zaragozic acid A was reported by Shaw and co-workers at Glaxo (Scheme 50).[84] The vinyl bromide **241** was obtained by alkylation of ethyl acetate with 2,3-dibromopropene. Reduction of the ester to the alcohol and silylation gave **242**. Halogen–metal exchange at $-120\,^{\circ}C$ and addition of racemic aldehyde **243** gave **244** as a 1:1 mixture of racemic diastereoisomers. Acetylation and desilylation afforded primary alcohols **245** and **246**, which were separable by preparative HPLC on a cyclodextrin column. Oxidation of the mixture (**245** + **246** ≙ **247**) provided the aldehyde **248**, which was used in the synthesis of monocyclic analogs of zaragozic acid A.

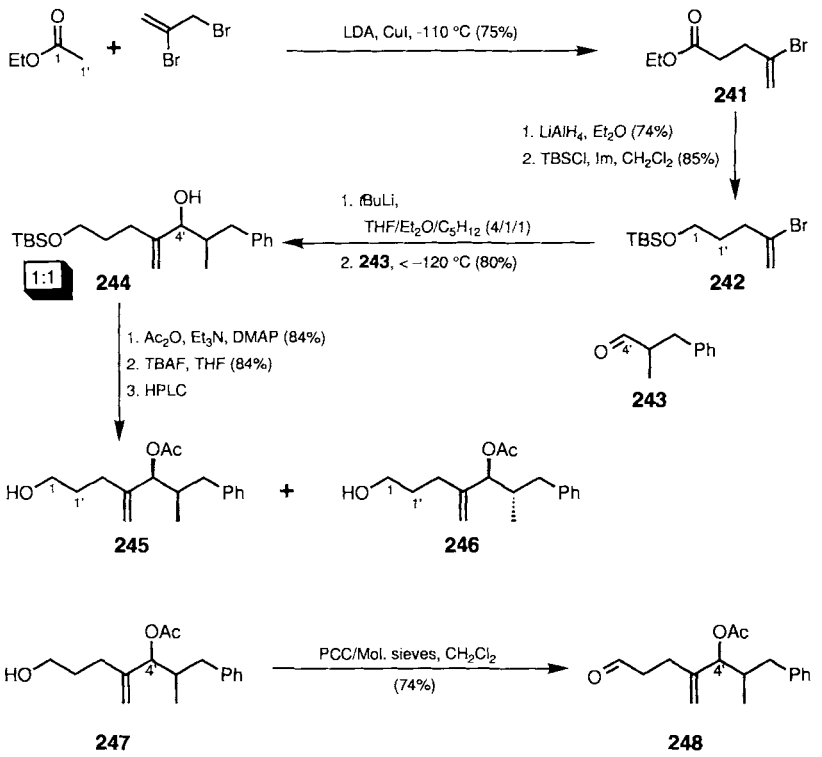

Scheme 50. Synthesis of the C1 alkyl side chain of zaragozic acid A (Glaxo). LDA = lithium diisopropylamide.

diastereoisomers. Heating **251** with triethylorthoacetate in the presence of a catalytic amount of acid effected [3,3]sigmatropic rearrangement to give, after saponification, the carboxylic acid **202**.

The synthesis by Carreira et al. (Scheme 52) generates the same allylic alcohol **251** but by a different sequence.[86] Starting with 5-phenylpentyne (**252**), alkylation with formaldehyde and reduction of the resulting propargylic alcohol gave the allylic alcohol **253**. Sharpless asymmetric epoxidation then provided the epoxide **254** in 98% yield (>95% *ee*). The epoxide was then regioselectively opened at C6″ and the resulting diol was cleaved to afford the aldehyde. Addition of vinylmagnesium bromide then gave allylic alcohol **251**, which was converted to the acid chloride **183**.

The only synthesis of the acyl side chain of zaragozic acid A was conducted by our group (Scheme 53).[93] Owing to the ready availability of zaragozic acid A, supplies of the side chain have been easily obtained by degradation of the natural product. The synthesis, however, is remarkably short and can provide substantial amounts of the side chain **260**. Starting with enantiomerically pure hydrazone **256**,[100] made from propionaldehyde, alkylation with commercially available and optically pure iodide **257** gave **258** (92% *de*). Ozonolysis yielded the aldehyde **259**, which was homologated by a Wittig reaction. Hydrolysis of the ester furnished carboxylic acid **260** in 27% overall yield from **256**.

3.4. Synthesis of the C6 Acyl Side Chains of Zaragozic Acids A and C

The two syntheses of the acyl side chain of zaragozic acid C[86,98] both employ a Johnson–Claisen orthoester rearrangement[99] as the key step. This transformation can be particularly effective at generating a remote chiral center adjacent to a *trans* double bond. The synthesis of the zaragozic acid C side chain by Merck[98] (Scheme 51) provided the first proof of the absolute configuration of zaragozic acid C. Intermediate **250** was synthesized by alkylation of **249** with cinnamyl bromide, followed by hydrogenation. Three standard functional group interconversions gave allylic alcohol **251** as a mixture of

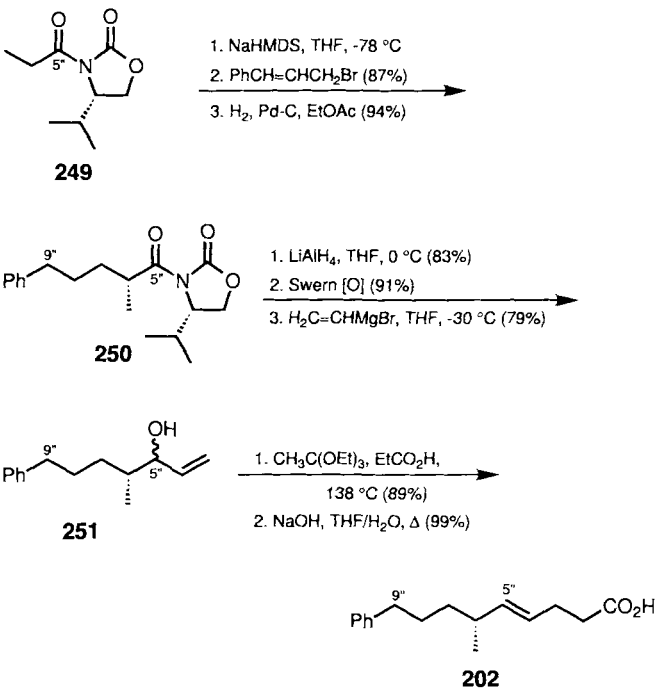

Scheme 51. Synthesis of the C6 acyl side chain of zaragozic acid C (Merck).

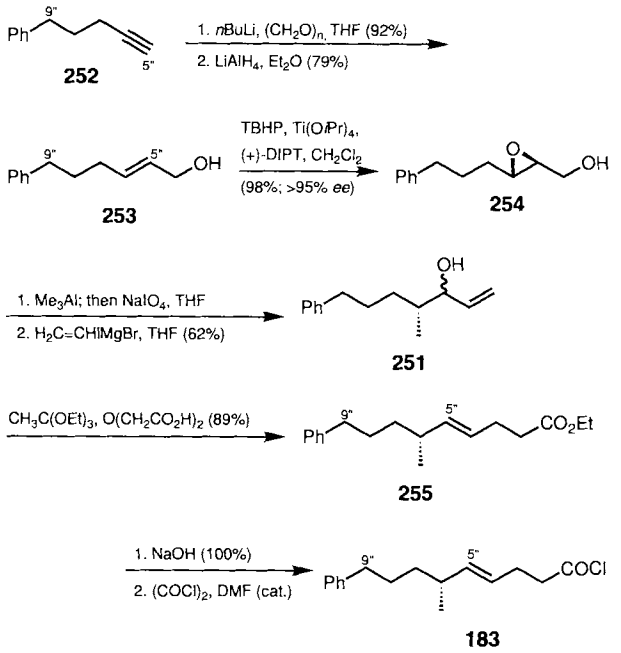

Scheme 52. Synthesis of the C6 acyl side chain of zaragozic acid C (Carreira et al.).

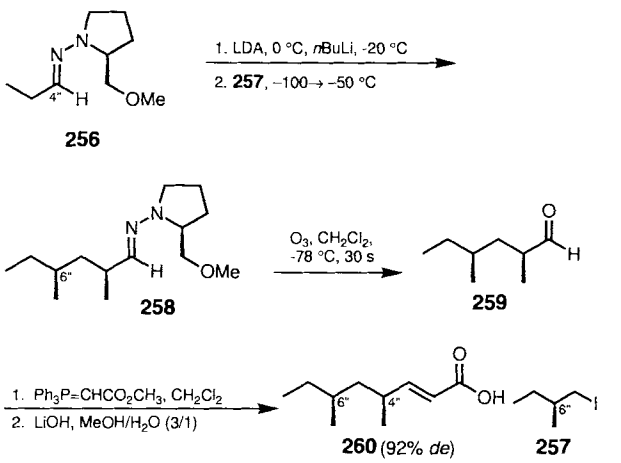

Scheme 53. Our synthesis of the C6 acyl side chain of zaragozic acid A.

3.5. Biosynthesis of the Zaragozic Acids

The biosynthetic origin of zaragozic acid A has been established independently by Merck and Glaxo.[101, 102] The results of standard feeding experiments with isotopically labeled substrates led to the following conclusions regarding the biosynthesis of zaragozic acid A (Scheme 54):

1. Zaragozic acid A is biosynthesized from two polyketide chains (labeled A and B), which comprise the C1 alkyl side chain and the core, and the C6 acyl side chain, respectively.
2. The biosynthesis of the A chain begins with an aromatic nucleus (derived from phenylalanine via benzoic acid). Five intact acetate units are then added in a standard fashion. The final four atoms (C3, C4, C8, and C9) arise from incorporation of an intact succinate unit. However, it was not possible to rule out the possibility that all three carboxyl groups originate from an intact citrate unit.

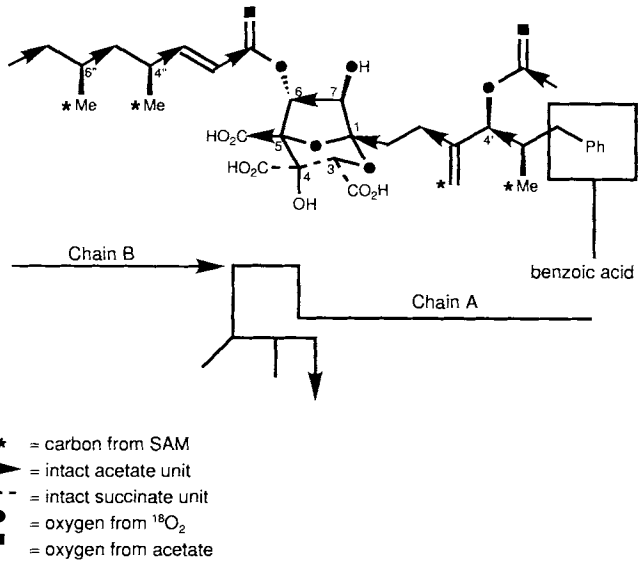

Scheme 54. Biosynthesis of zaragozic acid A (1). SAM = *S*-adenosylmethionine.

3. The C4′ acetyl group stems from an acetate unit.
4. The two one-carbon substituents on the C1 alkyl side chain (C5′-Me and C3′-CH_2) come from *S*-adenosylmethionine (SAM).
5. The B chain is made by successive linkages of four acetate units. The C4″-Me and C6″-Me substituents arise from SAM.
6. The two oxygens attached to C1 and those at C6, C7, and C4′ stem from atmospheric oxygen.
7. The oxygens of the carbonyls of the C4′-acetate and the C6-acyl groups come from acetate.

The elucidation of the biosynthetic origins of the zaragozic acids was not only of academic interest but also necessary in order to design and predict the outcome of feeding experiments aimed at generating analogs biosynthetically.[103–106] A number of minor secondary metabolites, which appear to be precursors of the A chain, have recently been isolated from the fermentation broth of ATCC 20986.[107]

4. Medicinal Chemistry (Structure–Activity Relationships)

A large body of information on structure–activity relationships has been collected by the testing of analogs obtained from the natural product, biosynthetic feeding, biotransformation, and total synthesis. The medicinal chemistry[108–126] has been the subject of an excellent and thorough review by Procopiou and Watson,[41] so we will only outline the main findings here. Figure 2 shows the structure of zaragozic acid A with comments on the importance of various parts of the structure in the assay with rat microsomal squalene synthase. It should be emphasized that many changes are not completely independent. For example, the nature of the C6 acyl side chain influences the effect of many substitutions elsewhere in the molecule. This could result from zaragozic acid A binding either as a PSPP mimic or an FPP mimic (see Section 2.3).

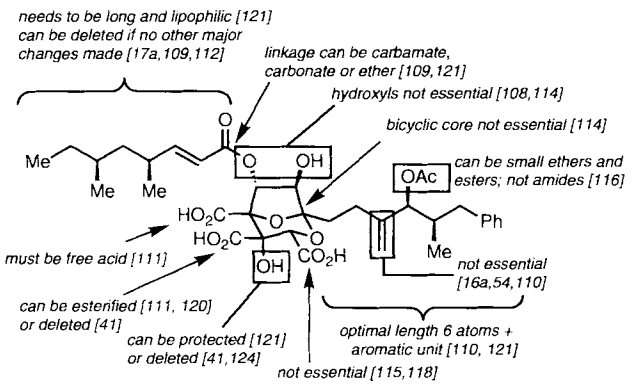

Fig. 2. Important structure–activity relationships of zaragozic acid A and the corresponding references.

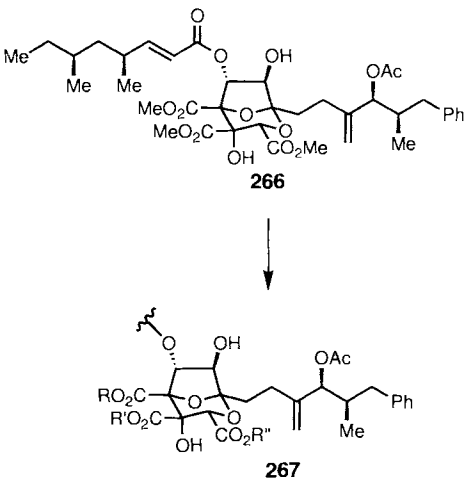

Scheme 56. Selective manipulations of the carboxyl groups of zaragozic acid A (Glaxo).

4.1. Important Manipulations with Zaragozic Acid A

In order to generate analogs efficiently from the natural product, two selective manipulations were required. Firstly, the three carboxyl groups had to be differentially protected, and secondly, methods were needed for the selective manipulation of the C4′-acetyl and C6-ester.

All three carboxyl groups of zaragozic acid A (**1**) can be esterified with a variety of isoureas (e.g. **1** → **261**, Scheme 55)[23, 120] or with *N*,*N*′-dimethylformamide-di-*tert*-butyl acetal.[108] The former method of esterification, originally developed by Mathias,[80] is particularly mild and convenient, particularly for *tert*-butyl esters, and has been used in all of the total syntheses of the zaragozic acids. The C3 carboxyl group can be selectively esterified under Fischer conditions with a variety of alcohols (**1** → **262**, Scheme 55).[111, 120] The benzyl ester derivative was monoesterified further (but only with moderate selectivity) to give a mixture of the C5 monocarboxylic acid **263** and the C4 monocarboxylic acid **264**. Both the C3 and C4 carboxyl groups can be esterified with the isourea method to yield **265**.[120] The benzyl ester function(s) were removed by transfer hydrogenation, and the *tert*-butyl esters with trifluoroacetic acid.[120] By choosing different ester protecting groups, all possible combinations of ester and carboxyl groups are accessible. Alternatively, the trimethyl ester **266** can be selectively deprotected at the C5 carboxyl with LiI/collidine or at the C3 position with one equivalent of sodium hydroxide (Scheme 56).[111]

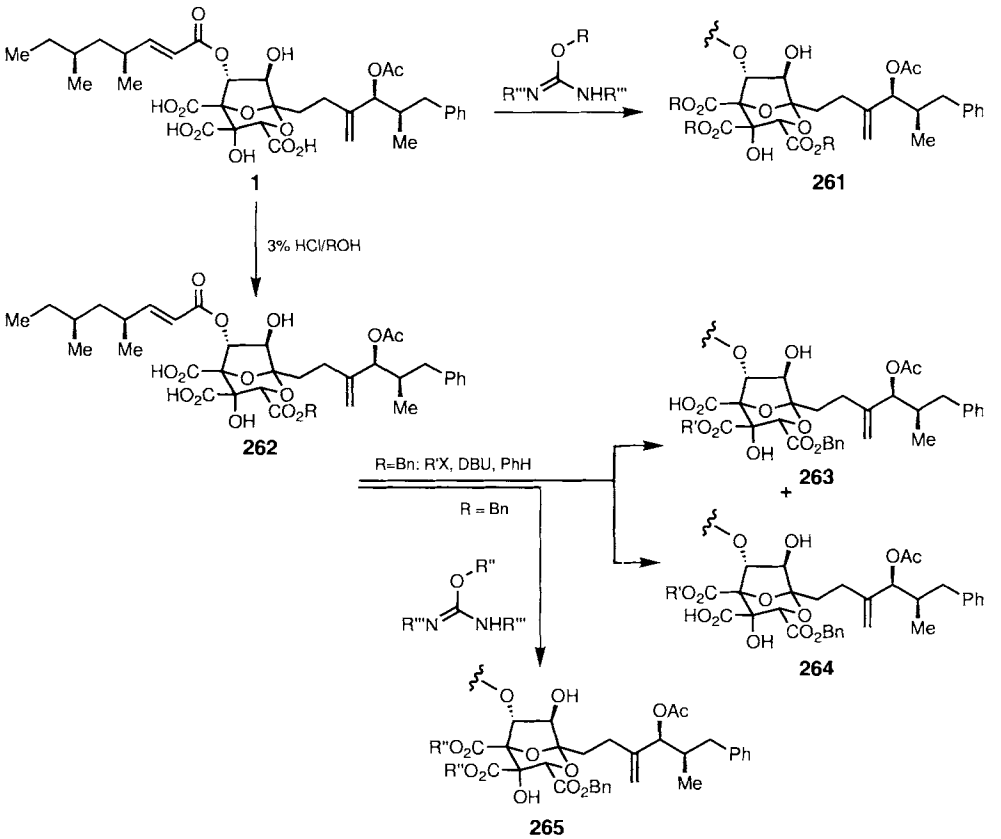

Scheme 55. Selective manipulation of the carboxyl groups of zaragozic acid A (Merck). DBU = 1,5-diazabicyclo[5.4.0]-undec-5-ene. R = R′ = Bn, Me, $Me_3SiCH_2CH_2$, $Me_2CHCH_2CH_2$; R″ = *t*Bu, Me.

The selective cleavage of the α,β-unsaturated C6 acyl side chain can be achieved by treatment with either hydroxylamine[108, 119] or with 0.2% potassium carbonate in methanol[23] (**268** → **269**, **266** → **271**, Scheme 57). The latter reagent causes transesterification of the C3 carboxyl group and therefore is probably not suitable for esters other than *tert*-butyl or methyl. Cleavage of the C4′ acetyl group can be achieved either with EtMgCl/$CeCl_3$[119] or with 3% HCl in MeOH[23] (**268** → **270**, **266** → **272**, Scheme 57).

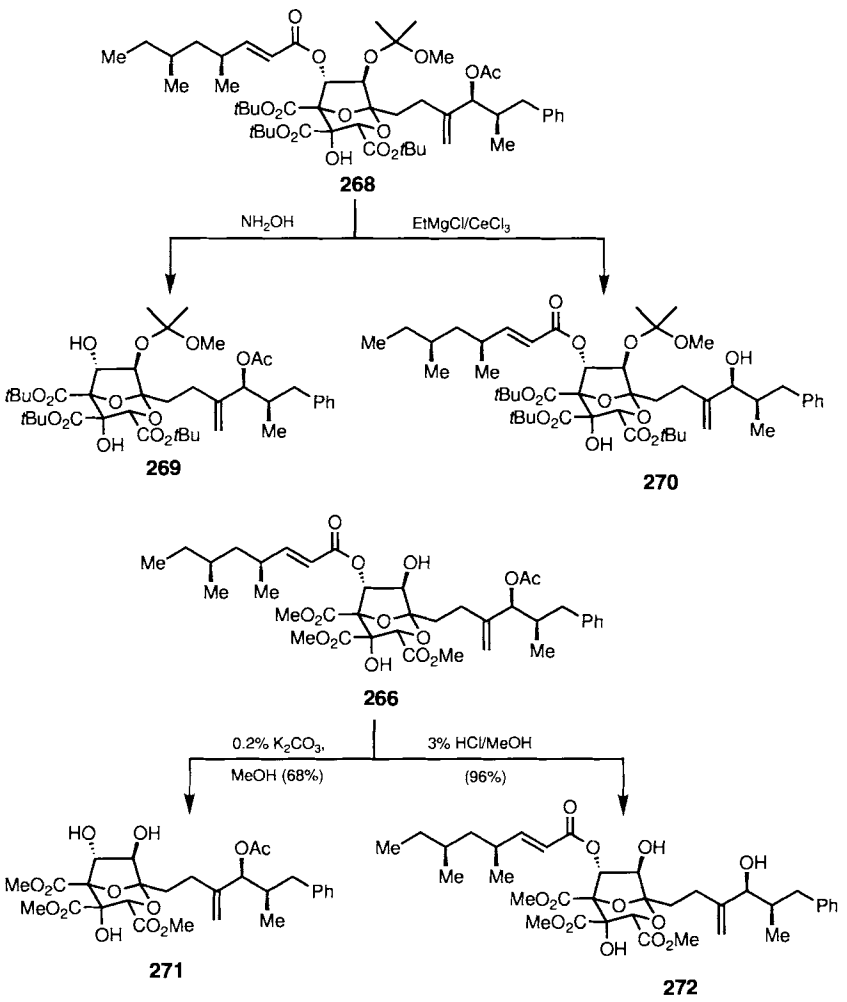

Scheme 57. Selective cleavage of the C4 acetyl and the C6 acyl groups of zaragozic acid A.

4.2. Cleavage of the Bicyclic Core of Zaragozic Acid A

To assess the importance of the bicyclic core for biological activity, and also out of scientific interest, Merck and Glaxo have investigated reactions that break up the bicyclic ketal. It is notable that molecular mechanics calculations and experiments by Evans et al.[90] and others have suggested that the core may be kinetically extremely stable under the conditions used for its formation, but thermodynamically less stable than other alternative structures. Schemes 58–60 show some of the transformations possible once the bicyclic core is opened,[108, 113, 127–128] and provide a challenging set of examples for a problems class in elementary organic chemistry.

5. Summary and Outlook

Of the hundreds of new natural products that are isolated every year, very few cause any excitement. Interest occasionally increases when a natural product is found that contains a functionality or set of functionalities not normally associated with natural products chemistry. Examples from recent years include the brevetoxins,[129] the enediynes,[130] and the manzamines.[131] The excitement is heightened further if these novel structures are accompanied by profound biological activity. The zaragozic acids, with their unprecedented heavily oxygenated core structure and picomolar-level inhibition of squalene synthase, fulfill both conditions. Consequently, in just three years and in around 100 publications,[132] the chemistry, biology, and medicinal potential of the zaragozic acids has been substantially elucidated. The next adventure in natural products chemistry cannot be far away.

A list of frequently used abbreviations:

Bz	benzoyl
CSA	10-camphorsulfonic acid
dba	*trans,trans*-dibenzylidene-acetone
DCBI	*N,N'*-dicyclohexyl-*O*-benzyl-isourea
DET	diethyl tartrate
DHP	3,4-dihydro-2*H*-pyran
DIPT	diisopropyl tartrate
DITBI	*N,N'*-diisopropyl-*O*-*tert*-butylisourea
DM	Dess–Martin periodinane
DTBMS	di-*tert*-butyl-methylsilyl
EDC(I)	1-(3-dimethylaminopropyl)-3-ethylcarbodiimide hydrochloride
HMPA	hexamethylphosphoric triamide
NaHMDS	sodium bis(trimethylsilyl)-amide
NMO	4-methylmorpholine *N*-oxide
Piv	pivaloyl
PMB	4-methoxybenzyl
py	pyridine
SEM	2-(trimethylsilyl)ethoxymethyl
TBAF	tetra-*n*-butylammonium fluoride
TBHP	*tert*-butyl hydroperoxide
TBS	*tert*-butylmethylsilyl
TES	triethylsilyl
Tf	trifluoromethanesulfonate
TPAP	tetra-*n*-propylammonium perruthenate
TPS	*tert*-butyldiphenylsilyl

We wish to thank our collaborators S. La Greca, J. E. Leresche, Z. Yang, and E. W. Yue for useful discussions; Dr. Alan Armstrong (Bristol, UK) and Dr. Panayiotis Procopiou and Dr. Nigel Watson (Glaxo, UK) for preprints of their work; and John Trujillo (Scripps) for the color pictures. We thank the NIH, Merck, Sharp & Dohme, Schering Plough, Pfizer, Hoffman La Roche, Glaxo, Rhône-Poulenc Rorer, and the ALSAM Foundation for financial support.

Received: August 18, 1995 [A133IE]
German version: *Angew. Chem.* **1996**, *108*, 1732–1766

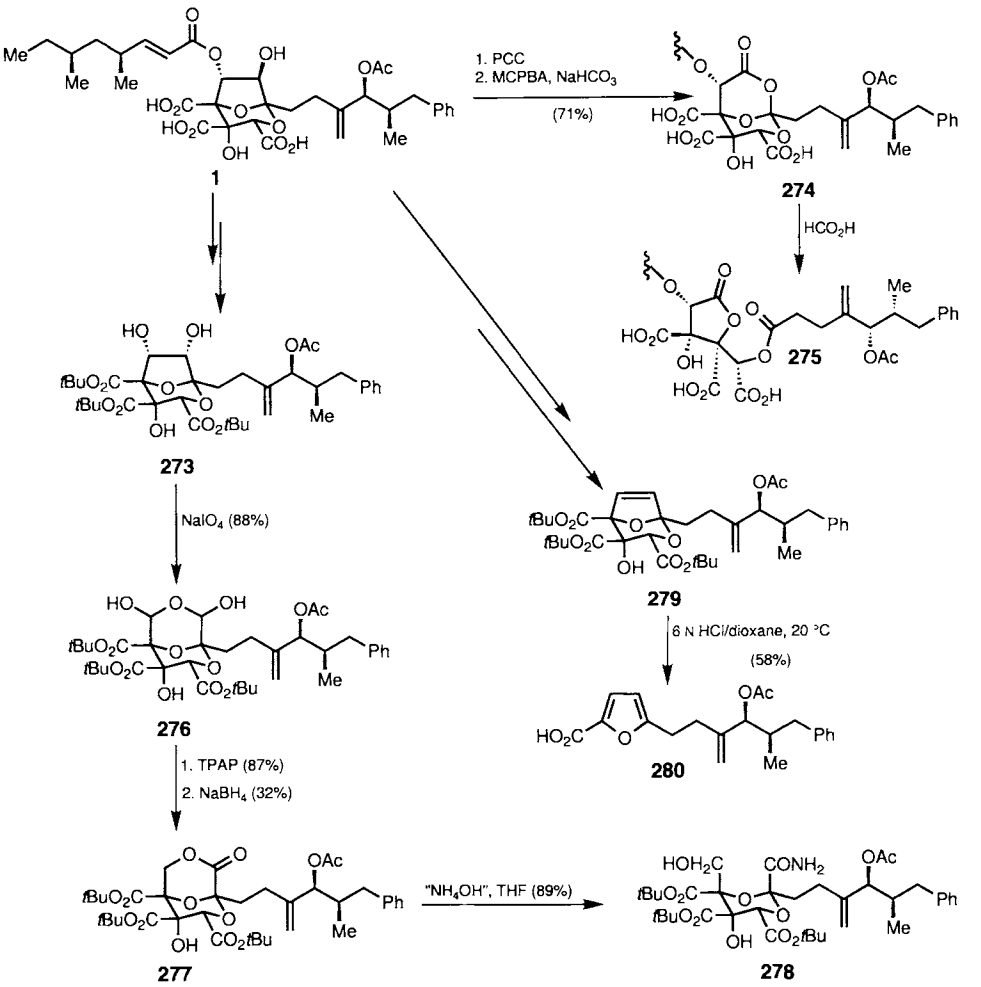

Scheme 58. Three ways to cleave the bicyclic core (Glaxo). MCPBA = *meta*-chloroperbenzoic acid.

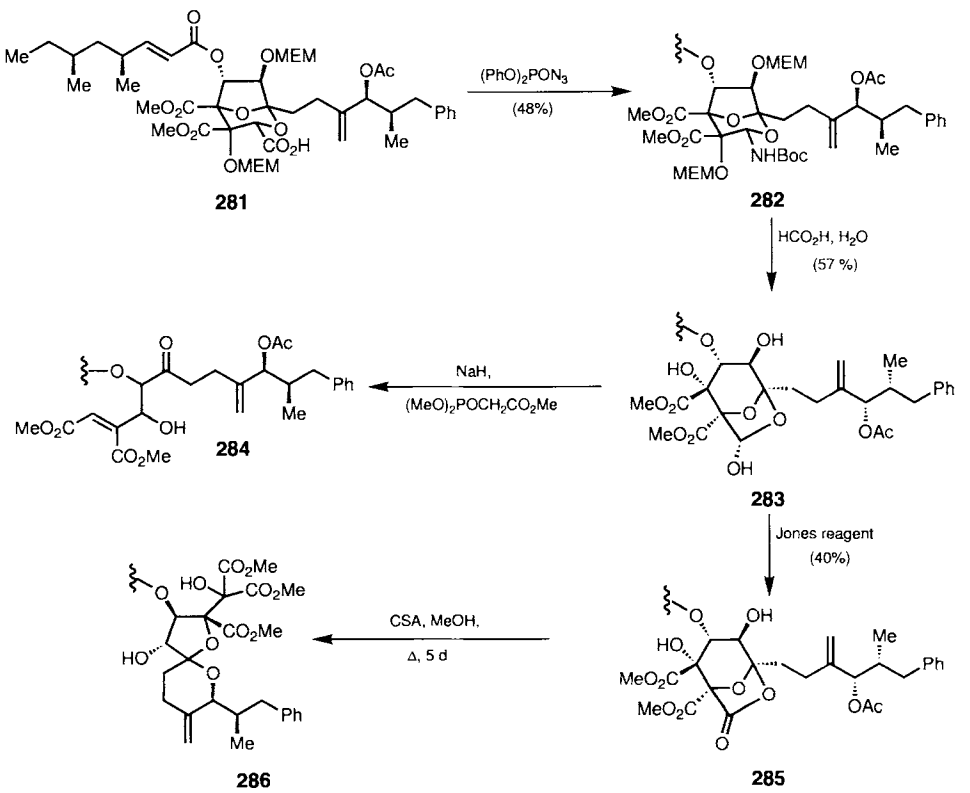

Scheme 59. Further degradation of the bicyclic core (Glaxo). PCC = pyridinium chlorochromate.

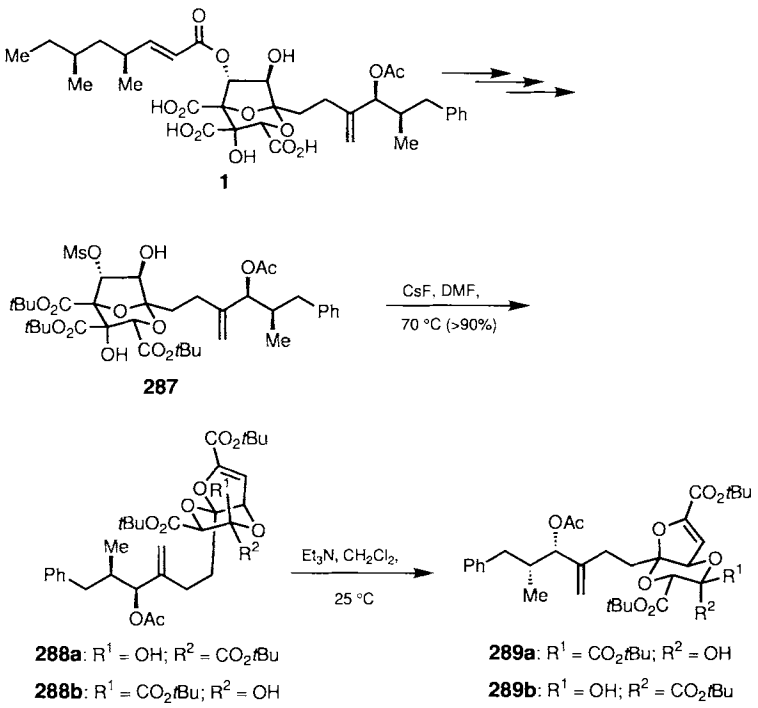

Scheme 60. Degradation of the bicyclic core (Merck).

[1] *Statistical Abstract of the United States: 1994*, 114th ed., U. S. Bureau of Census, Washington, DC, **1994**, Tables 125, 130.

[2] a) *Heart Disease* (Ed.: E. Braunwald), 4th ed., W. B. Saunders, Philadelphia, PA, **1992**; b) J. A. Farmer, A. M. Gotto in ref. [2a], Chapter 37.

[3] *Taber's Cyclopedic Medical Dictionary*, 17th ed., F. A. Davis, Philadelphia, PA, **1994**.

[4] For the pathogenesis of atherosclerosis, see R. Ross in ref. [2a], Chapter 36.

[5] *Encyclopedia of Medicine* (Ed.: C. B. Clayman), American Medical Association, Random House, NY, **1989**.

[6] Lipid Research Clinics Program, *J. Am. Med. Assoc.* **1984**, *251*, 351, 365.

[7] P. H. Jones, J. Patsch, A. M. Gotto in *Hurst's The Heart* (Eds.: R. C. Schlant, R. W. Alexander), 8th ed., McGraw-Hill, New York, **1994**.

[8] M. S. Brown, J. L. Goldstein, *Angew. Chem.* **1986**, *98*, 579; *Angew. Chem. Int. Ed. Engl.* **1986**, *25*, 583.

[9] I. M. Arias, J. L. Boyer, *The Liver: Biology and Pathobiology*, 3rd ed., Raven Press, New York, **1994**.

[10] Report of the National Cholesterol Education Program and Expert Panel on Detection, Evaluation and Treatment of High Blood Cholesterol in Adults: *Arch. Intern. Med.* **1988**, *148*, 36.

[11] A. L. Forbes in *Modern Nutrition in Health and Disease* (Eds.: M. E. Shils, J. A. Olson, M. Shike), 8th ed., Lea and Febiger, Philadelphia, PA, **1994**.

[12] Food Consumption Patterns - U. S. Diet. Proceedings of the Conference on the Decline in CHD Mortality (L. Page, R. M. Marston, *NIH Publ.* **1979**, 79-1610).

[13] *ASI* **1994**, 1356-4.4, Table 4.1.

[14] I. Abe, J. C. Tomesch, S. Wattanasin, G. D. Prestwich, *Nat. Prod. Rep.* **1994**, *11*, 279.

[15] AHFS Drug Information **1995**, Section 24:06.

[16] a) J. D. Bergstrom, M. M. Kurtz, D. J. Rew, A. M. Amend, J. D. Karkas, R. G. Bostedor, V. S. Bansal, C. Dufresne, F. L. VanMiddlesworth, O. D. Hensens, J. M. Liesch, D. L. Zink, K. E. Wilson, J. Onishi, J. A. Milligan, G. Bills, L. Kaplan, M. Nallin-Omstead, R. G. Jenkins, L. Huang, M. S. Meinz, L. Quinn, R. W. Burg, Y. L. Kong, S. Mochales, M. Mojena, I. Martin, F. Pelaez, M. T. Diez, A. W. Alberts, *Proc. Natl. Acad. Sci. USA* **1993**, *90*, 80; b) O. D. Hensens, C. Dufresne, J. M. Liesch, D. L. Zink, R. A. Reamer, F. VanMiddlesworth, *Tetrahedron Lett.* **1993**, *34*, 399.

[17] a) M. J. Dawson, J. E. Farthing, P. S. Marshall, R. F. Middleton, M. J. O'Neill, A. Shuttleworth, C. Stylli, R. M. Tait, P. M. Taylor, H. G. Wildman, A. D. Buss, D. Langley, M. V. Hayes, *J. Antibiot.* **1992**, *45*, 639; b) P. J. Sidebottom, R. M. Highcock, S. J. Lane, P. A. Procopiou, N. S. Watson, *ibid.* **1992**, *45*, 648.

[18] K. Hasumi, K. Tachikawa, K. Sakai, S. Murakawa, N. Yoshikawa, S. Kumazawa, A. Endo, *J. Antibiot.* **1993**, *46*, 689.

[19] W. M. Blows, G. Foster, S. J. Lane, D. Noble, J. E. Piercey, P. J. Sidebottom, G. Webb, *J. Antibiot.* **1994**, *47*, 740.

[20] G. F. Bills, F. Pelaez, J. D. Polishook, M. T. Diez-Matas, G. H. Harris, W. H. Clapp, C. Dufresne, K. M. Byrne, M. Nallin-Omstead, R. G. Jenkins, M. Mojena, L. Huang, J. D. Bergstrom, *Mycol. Res.* **1994**, *98*, 733.

[21] C. Dufresne, K. E. Wilson, D. Zink, J. Smith, J. D. Bergstrom, M. Kurtz, D. Rew, M. Nallin, R. Jenkins, K. Bartizal, C. Trainor, G. Bills, M. Meinz, L. Huang, J. Onishi, J. Milligan, M. Mojena, F. Pelaez, *Tetrahedron* **1992**, *47*, 10221.

[22] C. Dufresne, K. E. Wilson, S. B. Singh, D. L. Zink, J. D. Bergstrom, D. Rew, J. D. Polishook, M. Meinz, L. Huang, K. C. Silverman, R. B. Lingham, M. Mojena, C. Cascales, F. Pelaez, J. B. Gibbs, *J. Nat. Prod.* **1993**, *56*, 1923. [23] K. E. Wilson, R. M. Burk, T. Biftu, R. G. Ball, K. Hoogsteen, *J. Org. Chem.* **1992**, *57*, 7151.

[24] H. Itazaki, K. Nagashima, Y. Kawamura, K. Matsumoto, H. Nakai, Y. Terui, *J. Antibiot.* **1992**, *45*, 38.

[25] N. Sakabe, Y. Hirata, *Tetrahedron Lett.* **1966**, 965.

[26] a) M. Murata, M. Sano, T. Iwashita, H. Naoki, T. Yasumoto, *Agric. Biol. Chem.* **1986**, *50*, 2693; b) T. Yasumoto, M. Murata, Y. Oshima, M. Sano, G. K. Matsumoto, J. Clardy, *Tetrahedron* **1985**, *41*, 1019.

[27] J. Beauhaire, P.-H. Ducrot, C. Malosse, D. Rochat, I. O. Ndiege, D. O. Otieno, *Tetrahedron Lett.* **1995**, *36*, 1043.

[28] For a recent example see: J. K. Crandall, E. Rambo, *Tetrahedron Lett.* **1994**, *35*, 1489.

[29] L. Stryer, *Biochemistry*, W. H. Freeman, New York, **1995**, p. 685 ff.; *Biochemie*, Spektrum Akademischer Verlag, Heidelberg, **1991**, p. 580 ff.; D. Voet, J. G. Voet, *Biochemie*, VCH, Weinheim, **1992**, p. 647 ff.

[30] For a review see: J. Grünler, J. Ericsson, G. Dallner, *Biochim. Biophys. Acta* **1994**, *1212*, 259.

[31] M. D. Greenspan, H. G. Bull, J. B. Yudkovitz, D. P. Hanf, A. W. Alberts, *Biochem. J.* **1993**, *289*, 889.

[32] S. Dhe-Paganon, J. Magrath, R. H. Abeles, *Biochemistry* **1994**, *33*, 13355.

[33] T. Kimura, Y. Takase, K. Hayashi, H. Tanaka, I. Ohtsuka, S. Takao, M. Kogushi, T Yamada, T. Fujimori, I. Saitou, K. Akasaka, *J. Med. Chem.* **1993**, *36*, 1630.

[34] J. R. Faust, M. S. Brown, J. L. Goldstein, *J. Biol. Chem.* **1980**, *255*, 6546.

[35] a) R. A. Wills, K. Folkers, J. L. Tucker, C.-Q. Ye, L.-J. Xia, H. Tamagawa, *Proc. Natl. Acad. Sci. USA* **1990**, *87*, 8928; b) K. Folkers, P. Langsjoen, R. A. Wills, P. Richardson, L.-J. Xia, C.-Q. Ye, H. Tamagawa, *ibid.* **1990**, *87*, 8931.

[36] H. Techelbrahan, J. Olsson, E. Swiezewska, G. Dallner, *J. Biol. Chem.* **1993**, *268*, 23081.

[37] For a review see: A. Endo, K. Hasumi, *Nat. Prod. Rep.* **1993**, *10*, 541.

[38] *Diagnostics Business Matters Incorporating Pharmaceutical Company News*, October **1993**.

[39] *Wall Street Journal*, 16. Juni 1994, p. B7.

[40] G. Thomas, R. Paglia, *XI Int. Symp. Drugs Affecting Lipid Metabolism*, **1992**, Abstracts p. 69.

[41] P. A. Procopiou, N. S. Watson, *Prog. Med. Chem.* **1996**, 331–378.

[42] A. Baxter, B. J. Fitzgerald, J. L. Hutson, A. D. McCarthy, J. M. Motteram, B. C. Ross, M. Sapra, M. A. Snowden, N. S. Watson, R. J. Williams, C. Wright, *J. Biol. Chem.* **1992**, *267*, 11705.

[43] D. Crook, K. H. Weisgraber, S. C. Ball, Jr., R. W. Mahley, *Arterioscleroses* **1990**, *10*, 625.

[44] G. H. Harris, E. T. Turner Jones, M. S. Meinz, M. Nallin-Omstead, G. L. Helms, G. F. Bills, D. Zink, K. E. Wilson, *Tetrahedron Lett.* **1993**, *34*, 5235.

[45] S. Stinson, *Chem. Eng. News* **1995**, *73* (21), p. 29.

[46] a) I. Abe, J. C. Tomesch, S. Wattanasin, G. D. Prestwich, *Nat. Prod. Rep.* **1994**, *11*, 279; b) S. A. Biller, M. J. Sofia, J. W. Abt, B. DeLange, J. K. Dickson, Jr., C. Forster, E. M. Gordon, T. Harrity, D. R. Magnin, J. Marretta, L. C. Rich, C. P. Ciosek, Jr., *ACS Symp. Ser.* **1992**, *497*, 165.

[47] V. Manne, C. S. Ricca, J. G. Brown, A. V. Tuomari, N. Yan, D. Patel, R. Schmidt, M. J. Lynch, C. P. Ciosek, Jr., J. M. Carboni, S. Robinson, E. M. Gordon, M. Barbacid, B. R. Seizinger, S. A. Biller, *Drug Dev. Res.* **1995**, *34*, 121.

[48] For an introduction see: F. Tamanoi, *Trends Biol. Sci.* **1993**, *18*, 349.

[49] J. B. Gibbs, *Cell* **1991**, *65*, 1.

[50] J. B. Gibbs, D. L. Pompliano, S. D. Mosser, E. Rands, R. B. Lingham, S. B. Singh, E. M. Scolnick, N. E. Kohl, A. Oliff, *J. Biol. Chem.* **1993**, *268*, 7617.

[51] G. Kuswik-Rabiega, H. C. Rilling, *J. Biol. Chem.* **1987**, *262*, 1505.

[52] K. A. Mookhtiar, S. S. Kalinowski, D. Zhang, C. D. Poulter, *J. Biol. Chem.* **1994**, *269*, 11201.

[53] D.-L. Zhang, C. D. Poulter, *J. Am. Chem. Soc.* **1995**, *117*, 1641

[54] P. A. Procopiou, E. J. Bailey, M. J. Bamford, A. P. Craven, B. W. Dymock, J. G. Houston, J. L. Hutson, B. E. Kirk, A. D. McCarthy, M. Sareen, J. J. Scicinski, P. J. Sharratt, M. A. Snowden, N. S. Watson, R. J. Williams, *J. Med. Chem.* **1994**, *37*, 3274.

[55] a) S. Lindsey, H. J. Harwood, Jr., *FASEB J.* **1994**, *8*, A1285; b) *J. Biol. Chem.* **1995**, *270*, 9083.
[56] A. Fersht, *Enzyme Structure and Mechanism*, 2nd ed., W. H. Freeman, New York, **1985**.
[57] Y. Tsujita, M. Kuroda, Y. Shimada, K. Tanzawa, M. Arai, I. Kaneko, M. Tanaka, H. Masuda, C. Tarumi, Y. Watanabe, S. Fujii, *Biochim. Biophys. Acta* **1986**, *877*, 50.
[58] a) Ref. [16]; b) P. Bangalore, F. Vilsaint, R. K. Keller, *FASEB J.* **1995**, *9*, A1310; c) V. S. Bansal, S. Vaidya, M. Kurtz, R. Bostedor, J. Karkas, J. D. Bergstrom, *ibid.* **1995**, *9*, A1317.
[59] a) Ref. [16]; b) M. M. Kurtz, V. S. Bansal, R. G. Bostedor, J. I. Germershausen, J. D. Karkas, S. Vaidya, J. D. Bergstrom, *FASEB J.* **1995**, *9*, A1317.
[60] R. G. Bostedor, J. D. Karkas, J. I. Germershausen, M. M. Kurtz, B. H. Arison, V. S. Bansal, S. Vaidya, J. D. Bergstrom, *FASEB J.* **1995**, *9*, A1317.
[61] J. D. Bergstrom, M. M. Kurtz, R. G. Bostedor, J. Karkas, V. S. Bansal, S. Vaidya, G. R. Lankas, C. J. Coiffe, *FASEB J.* **1995**, *9*, A1317.
[62] a) L. M. McVinish, M. A. Rizzacasa, *Tetrahedron Lett.* **1994**, *35*, 923; b) R. W. Gable, L. M. McVinish, M. A. Rizzacasa, *Aust. J. Chem.* **1994**, *47*, 1537.
[63] R. E. Ireland, R. H. Mueller, *J. Am. Chem. Soc.* **1972**, *94*, 5897.
[64] a) H. Abdel-Rahman, J. P. Adams, A. L. Boyes, M. J. Kelly, D. J. Mansfield, P. A. Procopiou, S. M. Roberts, D. H. Slee, N. S. Watson, *J. Chem. Soc. Chem. Commun.* **1993**, 1839; b) H. Abdel-Rahman, J. P. Adams, A. L. Boyes, M. J. Kelly, D. J. Mansfield, P. A. Procopiou, S. M. Roberts, D. H. Slee, P. J. Sidebottom, V. K. Sik, N. S. Watson, *ibid.* **1993**, 1841; c) H. Abdel-Rahman, J. P. Adams, A. L. Boyes, M. J. Kelly, R. B. Lamont, D. J. Mansfield, P. A. Procopiou, S. M. Roberts, D. H. Slee, N. S. Watson, *J. Chem. Soc. Perkin Trans. 1* **1994**, 1259.
[65] H. C. Kolb, M. S. VanNieuwenhze, K. B. Sharpless, *Chem. Rev.* **1994**, *94*, 2483.
[66] V. K. Aggarwal, M. F. Wang, A. Zaparucha, *J. Chem. Soc. Chem. Commun.* **1994**, 87.
[67] D. Seebach, J. D. Aebi, M. Gandercoquoz, R. Naef, *Helv. Chim. Acta* **1987**, *70*, 1194.
[68] M. K. Gurjar, S. K. Das, U. K. Saha, *Tetrahedron Lett.* **1994**, *35*, 2241.
[69] M. K. Gurjar, S. K. Das, K. S. Sadalapure, *Tetrahedron Lett.* **1995**, *36*, 1933.
[70] M. K. Gurjar, S. K. Das, A. C. Kunwar, *Tetrahedron Lett.* **1995**, *36*, 1937.
[71] G. A. Kraus, J. Maeda, *J. Org. Chem.* **1995**, *60*, 2.
[72] M. Ohshima, M. Murakami, T. Mukaiyama, *Chem. Lett.* **1985**, 1871.
[73] S. Caron, A. J. McDonald, C. H. Heathcock, *J. Org. Chem.* **1995**, *60*, 2780.
[74] a) S. Caron, C. H. Heathcock, *208th Natl. Meet. Am. Chem. Soc.*, **1994**, ORGN 299; b) D. Stoermer, C. H. Heathcock, *ibid.*, **1994**, ORGN 300; c) C. H. Heathcock, S. Caron, D. Stoermer, *209th Natl. Meet. Am. Chem. Soc.*, **1995**, ORGN 170.
[75] H. Koyama, R. G. Ball, G. D. Berger, *Tetrahedron Lett.* **1994**, *35*, 9185.
[76] A. Padwa, *Acc. Chem. Res.* **1991**, *24*, 22.
[77] K. C. Nicolaou, A. Nadin, J. E. Leresche, S. La Greca, T. Tsuri, E. W. Yue, Z. Yang, *Angew. Chem.* **1994**, *106*, 2309; *Angew. Chem. Int. Ed. Engl.* **1994**, *33*, 2187.
[78] K. C. Nicolaou, E. W. Yue, S. La Greca, A. Nadin, Z. Yang, J. E. Leresche, T. Tsuri, Y. Naniwa, F. De Riccardis, *Chem. Eur. J.* **1995**, *1*, 467.
[79] J. K. Stille, B. L. Groh, *J. Am. Chem. Soc.* **1987**, *109*, 813.
[80] For a discussion of this undeservedly neglected method of esterification see: L. J. Mathias, *Synthesis* **1979**, *11*, 561.
[81] K. C. Nicolaou, A. Nadin, J. E. Leresche, E. W. Yue, S. La Greca, *Angew. Chem.* **1994**, *106*, 2312; *Angew. Chem. Int. Ed. Engl.* **1994**, *33*, 2190.
[82] A. Armstrong, P. A. Barsanti, *Synlett* **1995**, 903.
[83] A. J. Mancuso, S.-L. Huang, D. Swern, *J. Org. Chem.* **1978**, *43*, 2480.
[84] R. E. Shaw, C. Burgess, R. P. C. Cousins, G. M. P. Giblin, D. G. H. Livermore, A. H. Shingler, C. Smith, P. M. Youds, *Biomed. Chem. Lett.* **1994**, *4*, 2155.
[85] E. M. Carreira, J. Du Bois, *J. Am. Chem. Soc.* **1994**, *116*, 10825.
[86] E. M. Carreira, J. Du Bois, *J. Am. Chem. Soc.* **1995**, *117*, 8106.
[87] M. Iwashima, T. Kinsho, A. B. Smith III, *Tetrahedron Lett.* **1995**, *36*, 2199.
[88] E. M. Carreira, J. Du Bois, *Tetrahedron Lett.* **1995**, *36*, 1209.
[89] a) D. B. Dess, J. C. Martin, *J. Org. Chem.* **1983**, *48*, 4155; b) D. B. Dess, J. C. Martin, *J. Am. Chem. Soc.* **1991**, *113*, 7277; c) R. E. Ireland, L. Liu, *J. Org. Chem.* **1993**, *58*, 2899; d) S. D. Meyer, S. L. Schreiber, *ibid.* **1994**, *59*, 7549.
[90] D. A. Evans, J. C. Barrow, J. L. Leighton, A. J. Robichaud, M. J. Sefkow, *J. Am. Chem. Soc.* **1994**, *116*, 12111.
[91] D. A. Evans, J. V. Nelson, E. Vogel, T. R. Taber, *J. Am. Chem. Soc.* **1981**, *103*, 3099.
[92] D. A. Evans, J. C. Barrow, J. L. Leighton, A. J. Robichaud, M. J. Sefkow, *209th Natl. Meet. Am. Chem. Soc.*, **1995**, ORGN 049.
[93] K. C. Nicolaou, E. W. Yue, Y. Naniwa, F. De Riccardis, A. Nadin, J. E. Leresche, S. La Greca, Z. Yang, *Angew. Chem.* **1994**, *106*, 2306; *Angew. Chem. Int. Ed. Engl.* **1994**, *33*, 2184.
[94] A. J. Robichaud, G. D. Berger, D. A. Evans, *Tetrahedron Lett.* **1993**, *34*, 8403.
[95] D. A. Evans, S. L. Bender, J. Morris, *J. Am. Chem. Soc.* **1988**, *110*, 2506.
[96] J. G. Parsons, M. A. Rizzacasa, *Tetrahedron Lett.* **1994**, *35*, 8263.
[97] a) T. Katsuki, K. B. Sharpless, *J. Am. Chem. Soc.* **1980**, *102*, 5974; b) Y. Gao, R. M. Hanson, J. M. Klunder, S. Y. Ko, H. Masamune, K. B. Sharpless, *ibid.* **1987**, *109*, 5765.
[98] C. Santini, R. G. Ball, G. D. Berger, *J. Org. Chem.* **1994**, *59*, 2261.
[99] W. S. Johnson, *J. Am. Chem. Soc.* **1970**, *92*, 741.
[100] a) D. Enders in *Asymmetric Synthesis, Vol. 3* (Ed.: J. D. Morrison), Academic, Orlando, **1984**, p. 275; b) D. Enders, J. Tiebes, N. DeKimpe, M. Keppens, C. Stevens, G. Smagghe, O. Betz, *J. Org. Chem.* **1993**, *58*, 4881.
[101] K. M. Byrne, B. H. Arison, M. Nallin-Omstead, L. Kaplan, *J. Org. Chem.* **1993**, *58*, 1019.
[102] C. A. Jones, P. J. Sidebottom, R. J. P. Cannell, D. Noble, B. A. M. Rudd, *J. Antibiot.* **1992**, *45*, 1492.
[103] R. J. P. Cannell, M. J. Dawson, R. S. Hale, R. M. Hall, D. Noble, S. Lynn, N. L. Taylor, *J. Antibiot.* **1993**, *46*, 1381.
[104] R. J. P. Cannell, M. J. Dawson, R. S. Hale, R. M. Hall, D. Noble, S. Lynn, N. L. Taylor, *J. Antibiot.* **1994**, *47*, 247.
[105] R. F. Middleton, G. Foster, R. J. P. Cannell, P. J. Sidebottom, N. L. Taylor, D. Noble, M. Todd, M. J. Dawson, G. C. Lawrence, *J. Antibiot.* **1995**, *48*, 311.
[106] T. S. Chen, B. Petuch, J. MacConnell, R. White, G. Dezeny, B. Arison, J. D. Bergstrom, L. Colwell, L. Huang, R. L. Monaghan, *J. Antibiot.* **1994**, *47*, 1290.
[107] G. H. Harris, C. Dufresne, H. Joshua, L. A. Koch, D. L. Zink, P. M. Salmon, K. E. Göklen, M. M. Kurtz, D. J. Rew, J. D. Bergstrom, K. E. Wilson, *Biomed. Chem. Lett.* **1995**, *5*, 2403.
[108] M. G. Lester, G. M. P. Giblin, G. G. A. Inglis, P. A. Procopiou, B. C. Ross, N. S. Watson, *Tetrahedron Lett.* **1993**, *34*, 4357.
[109] G. M. P. Giblin, R. Bell, A. P. Hancock, C. D. Hartley, G. G. A. Inglis, J. J. Payne, P. A. Procopiou, A. H. Shingler, C. Smith, S. J. Spooner, *Biomed. Chem. Lett.* **1993**, *3*, 2605.
[110] P. A. Procopiou, E. J. Bailey, J. L. Hutson, B. E. Kirk, P. J. Sharratt, S. J. Spooner, N. S. Watson, *Biomed. Chem. Lett.* **1993**, *3*, 2527.
[111] N. S. Watson, R. Bell, C. Chan, B. Cox, J. L. Hutson, S. E. Keeling, B. E. Kirk, P. A. Procopiou, I. P. Steeples, J. Widdowson, *Biomed. Chem. Lett.* **1993**, *3*, 2541.
[112] C. Chan, G. G. A. Inglis, P. A. Procopiou, B. C. Ross, A. R. P. Srikantha, *Tetrahedron Lett.* **1993**, *34*, 6143.
[113] D. Andreotti, P. A. Procopiou, N. S. Watson, *Tetrahedron Lett.* **1994**, *35*, 1789.
[114] P. J. Sharratt, J. L. Hutson, G. G. A. Inglis, M. G. Lester, P. A. Procopiou, N. S. Watson, *Biomed. Chem. Lett.* **1994**, *4*, 661.
[115] B. Cox, J. L. Hutson, S. E. Keeling, B. E. Kirk, A. R. P. Srikantha, N. S. Watson, *Biomed. Chem. Lett.* **1994**, *4*, 1931.
[116] M. G. Lester, G. L. Evans, R. A. Henson, P. A. Procopiou, M. Sarcen, M. A. Snowden, S. J. Spooner, A. R. P. Srikantha, N. S. Watson, *Biomed. Chem. Lett.* **1994**, *4*, 2683.
[117] Y. P. Chiang, T. Biftu, G. A. Doss, S. P. Plevyak, R. W. Marquis, J. D. Bergstrom, M. M. Kurtz, D. J. Rew, G. D. Berger, *Biomed. Chem. Lett.* **1993**, *3*, 2029.
[118] C. H. Kuo, S. P. Plevyak, T. Biftu, W. H. Parsons, G. D. Berger, *Tetrahedron Lett.* **1993**, *34*, 6863.
[119] R. M. Burk, G. D. Berger, R. L. Bugianesi, N. N. Girotra, W. H. Parsons, M. M. Ponpipom, *Tetrahedron Lett.* **1993**, *34*, 975.
[120] T. Biftu, J. J. Acton, G. D. Berger, J. D. Bergstrom, C. Dufresne, M. M. Kurtz, R. W. Marquis, W. H. Parsons, D. R. Rew, K. E. Wilson, *J. Med. Chem.* **1994**, *37*, 421.
[121] M. M. Ponpipom, N. N. Girotra, R. L. Bugianesi, C. D. Roberts, G. D. Berger, R. M. Burk, R. W. Marquis, W. H. Parsons, K. F. Bartizal, J. D. Bergstrom, M. M. Kurtz, D. J. Rew, *J. Med. Chem.* **1994**, *37*, 4031.
[122] C. H. Kuo, A. J. Robichaud, D. J. Rew, J. D. Bergstrom, G. D. Berger, *Biomed. Chem. Lett.* **1994**, *4*, 1591.
[123] R. W. Marquis, S. P. Plevyak, G. D. Berger, W. H. Parsons, *Tetrahedron Lett.* **1994**, *35*, 2451.
[124] L. R. Treiber, B. H. Arison, G. A. Doss, L. Huang, J. G. MacConnell, R. R. Miller, R. A. Stearns, *Experientia* **1995**, *51*, 252.
[125] Y.-C. P. Chiang, M. M. Kurtz, J. D. Bergstrom, G. D. Berger, *Biomed. Chem. Lett.* **1995**, *5*, 1643.
[126] M. J. Bamford, C. Chan, A. P. Craven, B. W. Dymock, D. Green, R. A. Henson, B. E. Kirk, M. G. Lester, P. A. Procopiou, M. A. Snowden, S. J. Spooner, A. R. P. Srikantha, N. S. Watson, J. A. Widdowson, *J. Med. Chem.* **1995**, *38*, 3502.
[127] P. A. Procopiou, E. J. Bailey, C. Chan, G. G. A. Inglis, M. G. Lester, A. R. P. Srikantha, P. J. Sidebottom, N. S. Watson, *J. Chem. Soc. Perkin Trans. 1* **1995**, 1341.
[128] N. N. Girotra, R. A. Reamer, M. M. Ponpipom, *Tetrahedron Lett.* **1993**, *34*, 4293.
[129] Y.-Y. Lin, M. Risk, S. M. Ray, D. Van Engen, J. Clardy, J. Golik, J. C. James, K. Nakanishi, *J. Am. Chem. Soc.* **1981**, *103*, 6773.
[130] For a review see: K. C. Nicolaou, W.-M. Dai, *Angew. Chem.* **1991**, *103*, 1453; *Angew. Chem. Int. Ed. Engl.* **1991**, *30*, 1387.
[131] R. Sakai, T. Higa, *J. Am. Chem. Soc.* **1986**, *108*, 6404.

[132] Since this review was submitted a number of important papers on zaragozic acids/squalestatins have appeared; the following were deemed most relevant to this review: a) "The Squalestatins: Inhibitors of Squalene Synthase. Enzyme Inhibitory Activities and in Vivo Evaluation of C3-Modified Analogs": P. A. Procopiou, B. Cox, B. E. Kirk, M. G. Lester, A. D. McCarthy, M. Sareen, P. J. Sharratt, M. A. Snowden, S. J. Spooner, N. S. Watson, J. Widdowson, *J. Med. Chem.* **1996**, *39*, 1413; b) "Inhibitors of Cholesterol Biosynthesis Increase Hepatic Low-Density Lipoprotein Receptor Protein Degradation": G. C. Ness, Z. Zhao, D. Lopez, *Arch. Biochem. Biophys.* **1996**, *325*, 242; c) "The Squalestatins: Decarboxy and 4-Deoxy Analogs as Potent Squalene Synthase Inhibitors": C. Chan, D. Andreotti, B. Cox, B. W. Dymock, J. L. Hutson, S. E. Keeling, A. D. McCarthy, P. A. Procopiou, B. C. Ross, M. Sareen, J. J. Scicinski, P. J. Sharratt, M. A. Snowden, N. S. Watson, *J. Med. Chem.* **1996**, *39*, 207; d) "An Improved Synthesis of 1,6-anhydro-2,3-di-O-benzyl-β-D-xylo-hexopyranos-4-ulose": S. Caron, A. J. McDonald, C. H. Heathcock, *Carbohydr. Res.* **1996**, *281*, 179; e) "Novel Zaragozic Acids from *Leptodontidium elatius*": C. Dufresne, E. T. Turner Jones, M. Nallin-Omstead, J. D. Bergstrom, K. E. Wilson, *J. Nat. Prod.* **1996**, *59*, 52; f) "Characterization of Prenyl Protein Transferase Enzymes in a Human Keratinocyte Cell Line": E. E. MacNulty, N. S. Ryder, *Biochim. Biophys. Acta* **1996**, *1289*, 41; g) "New Fungal Metabolites as Potential Antihypercholesterolemics and Anticancer Agents": L. Huang, R. B. Lingham, G. H. Harris, S. B. Singh, C. Dufresne, M. Nallin-Omstead, G. F. Bills, M. Mojena, M. Sanchez, J. D. Karkas, J. Gibbs, W. H. Clapp, M. S. Meinz, J. D. Bergstrom, *Can. J. Bot.* **1995**, *73*, S898–S906; h) "Synthesis and Biological Activity of J-104,118, a Novel, Potent Inhibitor of Squalene Synthase": Y. Iwasawa, M. Hayashi, T. Nomoto, J. Shibata, M. Mitsuya, K. Hirota, M. Yonemoto, T. Kamei, K. Miura, K. Tomimoto, *Bioorg. Med. Chem. Lett.* **1995**, *5*, 1989; i) "Selective Inhibition of Cholesterol Biosynthesis in Brain Cells by Squalestatin 1": D. C. Crick, J. Suders, C. M. Kluthe, D. A. Andres, C. J. Waechter, *J. Neurochem.* **1995**, *65*, 1365; j) "Regulation of Cholesterol 7α-Hydroxylase Expression by Sterols in Primary Rat Hepatocyte Cultures": K. C. Doerner, E. C. Gurley, Z. R. Vlahcevic, P. B. Hylemon, *J. Lipid Res.* **1995**, *36*, 1168; k) "Discovery, Biosynthesis, and Mechanism of Action of the Zaragozic Acids: Potent Inhibitors of Squalene Synthase": J. D. Bergstrom, C. Dufresne, G. F. Bills, M. Nallin-Omstead, K. Byrne, *Annu. Rev. Microbiol.* **1995**, *49*, 607; l) "Effects of Medium Sterilization on the Production of Zaragozic Acids by the Fungus *Leptodontidium elatius*": N. Connors, R. Prevoznak, T. Brix, A. Seeley, K. Gbewonyo, R. Greasham, P. Salmon, *J. Ind. Microbiol.* **1995**, *15*, 503.

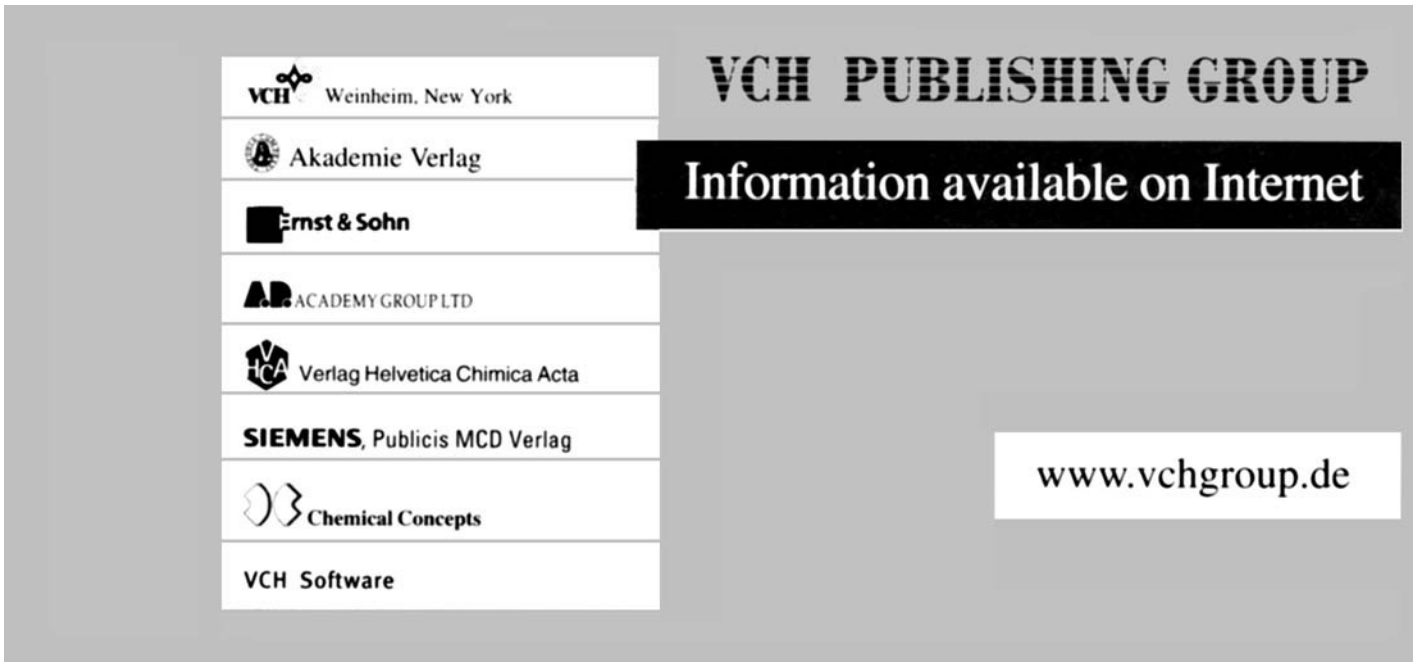

Asymmetric Autocatalysis with Amplification of Chirality**

Carsten Bolm,* Frank Bienewald, and Andreas Seger

Asymmetric metal catalysis has been intensively studied in recent years, and some efficient catalytic methods for the synthesis of enantiomerically pure compounds have been developed.[1] With suitable metal/ligand combinations excellent enantioselectivities and high conversion rates have frequently been achieved. Normally the catalyst must remain unaffected by the continually formed new product in order to achieve a constant, high stereoselectivity. How does it behave, however, when the product itself is a catalyst and, moreover, catalyzes its own asymmetric synthesis? Wynberg recognized very early the great potential of such "asymmetric autocatalysis" for synthesis and as early as 1989 had formulated the challenge that asymmetric autocatalysis could constitute the next generation of asymmetric synthesis.[2] In spite of great efforts the discovery of the first autocatalytic system operating with high enantioselectivity has only recently been made.[3] Two important contributions from Soai et al.[3,4] take pride of place here, but before introducing them we will describe some other fundamental studies.

Seebach, Dunitz et al. first drew attention to the fact that in stereoselective reactions with organometallic reagents differing diastereo- and enantioselectivities could arise because of the formation of various mixed complexes during the course of product formation.[5,6] This led Alberts and Wynberg to investigate the asymmetric additions of organometallic carbon nucleophiles (e.g. ethyllithium) to benzaldehyde (Scheme 1), and they showed that the stereochemical course of both stoichiometric and catalyzed reactions were influenced by metal-containing product molecules (here lithium alcoholates).[7] The product itself is not a catalyst but nevertheless ensures that the newly formed product is optically active. Alberts and Wynberg coined the term "enantioselective autoinduction" for this effect.

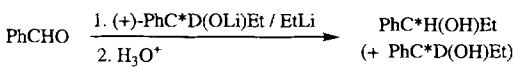

Scheme 1. Asymmetric addition of ethyllithium to benzaldehyde [7]. Chirality centers are identified by a star.

[*] Prof. Dr. C. Bolm,[+] Dr. F. Bienewald, Dipl.-Chem. A. Seger[+]
Fachbereich Chemie der Universität
Hans-Meerwein-Strasse, D-35032 Marburg (Germany)
[+] New Address: Institut für Organische Chemie der RWTH
Professor-Pirlet-Strasse 1, D-52074 Aachen (Germany)
Fax: Int. code +(241)8888-391
e-mail: carsten.bolm@rwth-aachen.de

[**] We wish to thank the DFG (Graduiertenkolleg), BASF AG, and the Volkswagen Stiftung for stipends and financial support.

Danda et al. established that the product powerfully influenced the catalyst in the *metal-free* catalyzed asymmetric hydrocyanation of 3-phenoxybenzaldehyde **1** to (*S*)-**2** by the cyclic dipeptide (*R,R*)-**3**.[8] In the presence of the product the reaction-accelerating effect of the cyclic dipeptide was enhanced. (*R,R*)-**3** alone showed little catalytic activity at first, and with increasing reaction time the enantiomeric excess of (*S*)-**2** increased. If a small amount of (*S*)-**2** was added to the reaction mixture at the start the product was formed with an almost constant, high *ee* value. Here (*S*)-**2** itself is *not* a catalyst and only the interaction between the correct product enantiomer and the cyclic dipeptide leads to better catalysis. In addition asymmetric amplification occurred only in the presence of the product.[9] Thus, 2.2 mol% (*R,R*)-**3** with 2% *ee* at 43% conversion yields the cyanohydrin (*S*)-**2** with 81.6% *ee* when 8.8 mol% (*S*)-**2** with 92% *ee* is added at the start of the reaction. If (*S*)-**2** is not added at the start, the conversion and enantiomeric excess are 4% and 3.4%, respectively. It is also interesting that in this asymmetric amplification the absolute configuration of the product is not determined by the configuration of the catalyst but by that of the added cyanohydrin.

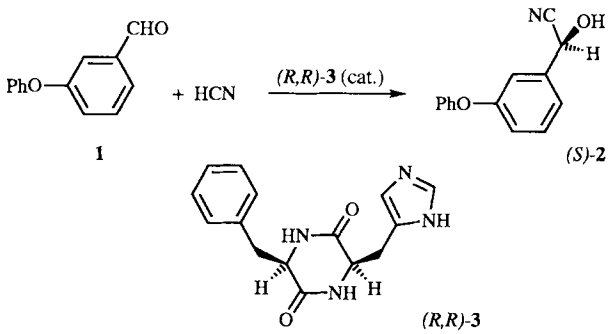

In the examples quoted the product influences stereoselectivity or has a positive effect on an existing catalysis.[10] Things become especially interesting, however, when the chiral product itself is a catalyst for its own formation from achiral precursors. This area of asymmetric autocatalysis was hardly developed for a long time, though in 1953 Frank had already formulated a mathematical model that indicated that "spontaneous asymmetric synthesis", as he called the process, is quite possible.[11] As a natural property of life this could be of fundamental importance in the genesis of asymmetry in nature.[12-14] In the scenar-

io described by Frank two achiral substances, **A** and **B**, react to form optically active products (*R*)-**C** and (*S*)-**C**, each of which can catalyze its own synthesis (Scheme 2a). This corresponds to the working of conventional autocatalysis. If one imagines that the two enantiomeric catalysts mutually reduce (or destroy) their effects (Scheme 2b), the system would show flip-flop

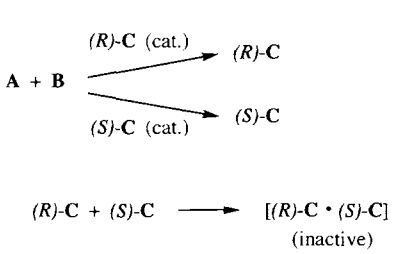

Scheme 2. a) Model for "spontaneous asymmetric synthesis" according to Frank [11]. b) Deactivation of the catalytically active chiral product.

switching properties: even a small statistical fluctuation (for example, if the reaction catalyzed by (*R*)-**C** were preferred for a short time) would have the effect of reducing the catalytic activity of (*S*)-**C** and new (*R*)-**C** would be formed ever more quickly. In such an "aggressive" system a trace of a chiral substance would be enough to ensure its own production in large quantities by autocatalysis. The inductor does not even need to be enantiomerically pure since the model implies the principle of asymmetric amplification. In his article Frank pleaded for the development and testing of simple autocatalytic systems.[11] The first successful reactions with a "chiral autocatalyst" were reported by Soai et al. in 1990.[15] They found that the pyridinyl alcohol **6** catalyzed its own formation from pyridine-3-carbaldehyde (**4**) and diisopropylzinc via the isopropylzinc alcoholate **5**. With 20 mol% (−)-**6** (86% *ee*), workup afforded (−)-**6** in 67% yield with an *ee* of 35%.

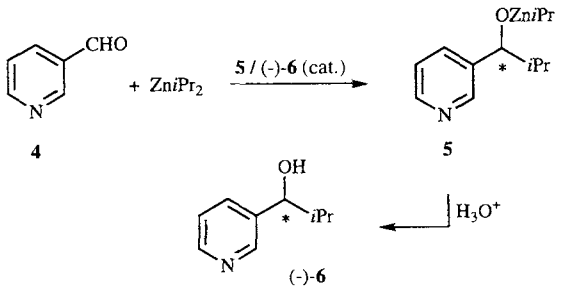

Similarly, in other enantioselective additions of organozinc compounds asymmetric autocatalyses were also demonstrated,[16] though they always gave a product with a much lower *ee* value than that of the catalyst used. Only at the end of 1995 was an important breakthrough achieved[3, 4] when Soai et al. showed that the presence of 20 mol% of the pyrimidyl alcohol (*S*)-**9a** (94.8% *ee*) in the reaction between the corresponding aldehyde **7a** and diisopropylzinc led to the formation of (*S*)-**9a** in 48% yield with an *ee* of 95.7%. The product underwent automultiplication *without* a significant change in the enantiomeric excess.

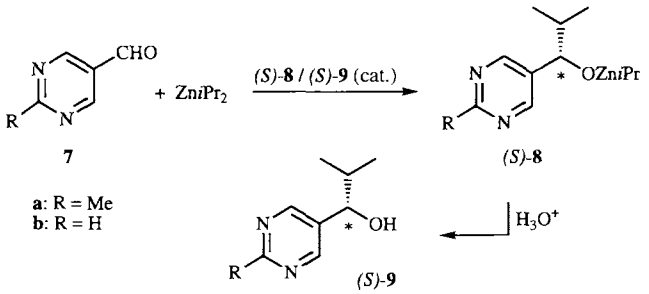

As if this were not enough, Soai et al.[4] also used this system to demonstrate for the first time the asymmetric amplification during autocatalysis that is inherent in the Frank model. Thus, 20 mol% of (*S*)-**9b** with an *ee* of only 2% gave, with autocatalysis, (*S*)-**9b** with an *ee* of 10%. In further reaction cycles the enantiomeric excess rose from 10 through 57 to 81 and finally to 88% (Fig. 1). There was a 942-fold increase in the amount of product after four cycles. The asymmetric amplification shown by this simple self-replicating system behaved, in fact, as predicted by the simple, theoretical Frank model.

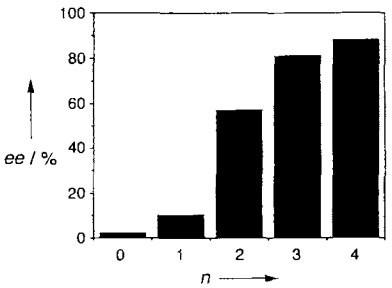

Fig. 1. Increase in the enantiomeric excess of (*S*)-**9b** with the number of reaction cycles *n*.

As the mechanism of the reaction and possible intermediates in solution are still unknown, the phenomenon described here cannot yet be used for the targeted development of further reactions. It is, nevertheless, clear that complex formation with the organometallic reagents is essential to autocatalysis with asymmetric amplification. For this reason a deeper understanding of the behavior of chiral compounds during the formation of complexes would be very useful for the design and discovery of new autocatalytic processes.

German version: *Angew. Chem.* **1996**, *108*, 1767 – 1769

Keywords: asymmetric amplification · asymmetric catalysis · autocatalysis

[1] a) R. Noyori, *Asymmetric Catalysis in Organic Synthesis*, Wiley, New York, **1994**; b) *Catalytic Asymmetric Synthesis* (Ed.: I. Ojima), VCH, Weinheim, **1993**.

[2] H. Wynberg, *Chimia* **1989**, *43*, 150; b) *J. Macromol. Sci. Chem. A* **1989**, *26*, 1033.

[3] T. Shibata, H. Morioka, T. Hayase, K. Choji, K. Saoi, *J. Am. Chem. Soc.* **1996**, *118*, 471.

[4] K. Soai, T. Shibata, H. Morioka, K. Choji, *Nature* **1995**, *378*, 767.

[5] D. Seebach, R. Amstutz, J. D. Dunitz, *Helv. Chim. Acta* **1981**, *64*, 2622.

[6] Review articles: a) D. Seebach, *Proc. Robert A. Welch Found. Conf. Chem. Res.* **1984**, *27*, 93; b) *Angew. Chem.* **1988**, *100*, 1685; *Angew. Chem. Int. Ed. Engl.* **1988**, *27*, 1624.

[7] a) A. H. Alberts, H. Wynberg, *J. Am. Chem. Soc.* **1989**, *111*, 7265; b) *J. Chem. Soc. Chem. Commun.* **1990**, 453.

[8] a) H. Danda, H. Nishikawa, K. Otaka, *J. Org. Chem.* **1991**, *56*, 6740; b) mechanistic interpretation: Y. Shvo, M. Gal, Y. Becker, A. Elgavi, *Tetrahedron Lett.* **1996**, *7*, 911.

[9] a) R. Noyori, M. Kitamura, *Angew. Chem.* **1991**, *103*, 34; *Angew. Chem. Int. Ed. Engl.* **1991**, *30*, 49; b) D. Guillaneux, S.-H. Zhao, O. Samuel, D. Rainford, H. B. Kagan, *J. Am. Chem. Soc.* **1994**, *116*, 9430; c) C. Bolm in *Advanced Asymmetric Synthesis* (Ed.: G. R. Stephenson), Blackie, Glasgow, **1996**, p. 9.

[10] Optically active products can also be formed with racemic metal catalysts. With a chiral additive one of the enantiomeric forms of the catalyst is "poisoned" in situ: a) K. Maruoka, H. Yamamoto, *J. Am. Chem. Soc.* **1989**, *111*, 789; b) J. M. Brown, P. J. Maddox, *Chirality* **1991**, *3*, 345; c) J. W. Faller, J. Parr, *J. Am. Chem. Soc.* **1993**, *115*, 804; d) J. W. Faller, M. Tokunaga, *Tetrahedron Lett.* **1993**, *34*, 7359; e) J. W. Faller, D. W. I. Sams, X. Liu, *J. Am. Chem. Soc.* **1996**, *118*, 1217.
[11] F. C. Frank, *Biochim. Biophys. Acta* **1953**, *11*, 459.
[12] a) J. L. Bada, *Nature* **1995**, *374*, 594; b) W. A. Bonner, *Top. Stereochem.* **1988**, *18*, 1; c) W. J. Meiring, *Nature* **1987**, *329*, 712; d) P. Decker, *Nachr. Chem. Tech. Lab.* **1975**, *23*, 167; e) S. Mason, *Chem. Soc. Rev.* **1988**, *17*, 347; f) W. A. Bonner, *Chem. Ind.* **1992**, 640; g) S. Mason, *Nature* **1985**, *314*, 400.
[13] Nonasymmetric molecular replication and autocatalyses: a) L. E. Orgel, *Nature* **1992**, *358*, 203; b) E. A. Wintner, M. M. Conn, J. Rebek, Jr., *Acc. Chem. Res.* **1994**, *27*, 198; c) *J. Am. Chem. Soc.* **1994**, *116*, 8877; d) G. von Kiedrowski, J. Helbing, B. Wlotzka, S. Jordan, M. Mathen, T. Achilles, D. Sievers, A. Terfort, B. C. Kahrs, *Nachr. Chem. Tech. Lab.* **1992**, *40*, 578; e) T. Achilles, G. von Kiedrowski, *Angew. Chem.* **1993**, *105*, 1225; *Angew. Chem. Int. Ed. Engl.* **1993**, *32*, 1198.
[14] Formation of homochiral crystals from solutions of optically inactive compounds: a) J. Jacques, A. Collet, S. H. Wilen, *Enantiomers, Racemates, and Resolutions*, Wiley, New York, **1981**; b) D. K. Kondepudi, R. J. Kaufman, N. Singh, *Science* **1990**, *250*, 975; c) J. M. McBride, R. L. Carter, *Angew. Chem.* **1991**, *103*, 298; *Angew. Chem. Int. Ed. Engl.* **1991**, *30*, 293, and references therein.
[15] K. Soai, S. Niwa, H. Hori, *J. Chem. Soc. Chem. Commun.* **1990**, 983.
[16] a) K. Soai, T. Hayase, C. Shimada, K. Isobe, *Tetrahedron: Asymmetry* **1994**, *5*, 789; b) K. Soai, T. Hayase, K. Takai, *ibid.* **1995**, *6*, 637; c) C. Bolm, G. Schlingloff, K. Harms, *Chem. Ber.* **1992**, *125*, 1191; d) S. Li, Y. Jiang, A. Mi, G. Yang, *J. Chem. Soc. Perkin Trans 1* **1993**, 885.

Organocyanide Acceptor Molecules as Novel Ligands

Kim R. Dunbar*

Pioneering research carried out at Dupont in the 1950s and 1960s established a wealth of interesting chemistry for conjugated organic molecules with cyanide functionalities.[1] Forty years later, research involving organocyanide molecules continues to flourish, owing to their promise as precursors for molecule-based materials. Among the organocyanide materials demonstrated to exhibit unusual properties is a class of ionic materials that consists of paramagnetic transition metal metallocene cations and radical anions of tetracyanoethylene (TCNE, Scheme 1a).[2] The compounds $[M(Cp)_2^*][TCNE]$ (M = Mn, Fe) crystallize in columns of donors and acceptors,

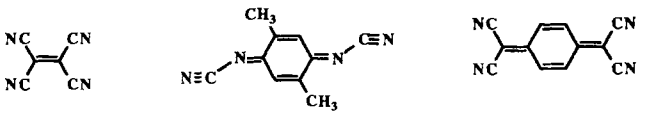

TCNE **DM-DCNQI** **TCNQ**

Scheme 1. Important organocyanide acceptor molecules.

$D^+A^-D^+A^-$, ($D^+ = [M(Cp^*)_2]^+$; $A^- = TCNE^-$) and are remarkable in that they order ferromagnetically at Curie temperatures T_c of 4.8 K (Fe) and 8.8 K (Mn). These results are quite surprising in the context of classical magnets, considering that the materials are not three-dimensional and that the properties are based on spins of organic molecules.

Solids containing transition metals cations σ-bonded to the nitrile groups of polycyano anions are an entirely different category of organocyanide materials than the ionic, stacked systems.[3] A primary motivation for coassembling metal centers and organic radicals in this manner is to achieve new pathways for electronic coupling through $p_\pi - d_\pi$ overlap in addition to the usual p_π overlap of the organic acceptors. With the proper energy match of metal and organic orbitals it may be possible to achieve an interplay between superexchange and charge-transport pathways, perhaps leading to a synergistic state wherein superconductivity and ferromagnetism coexist. At the very least it appears that this strategy holds promise for the design of highly conducting organometallic polymers, as evidenced by the work of Hünig and co-workers, who synthesized a new family of organic acceptors known as dicyanoquinodiimines (DCNQIs, Scheme 1). These DCNQIs form crystalline network solids with copper that exhibit extraordinarily high conductivities that persist to the lowest temperatures.[4] The structures of $[Cu(2,5\text{-}Me_2\text{-}DCNQI)]_2$ (Fig. 1, 2,5-Me_2-DCNQI = DM-DCNQI)

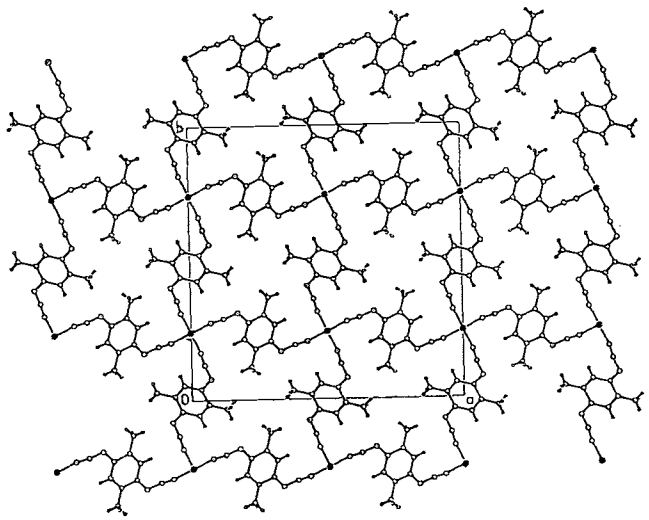

Fig. 1. Pluto representation of a portion of the extended framework structure of $[Cu(DM\text{-}DCNQI)_2]$.

[*] Prof. K. R. Dunbar
Department of Chemistry and
The Center for Fundamental Materials Research
Michigan State University
East Lansing, MI 48824 (USA)
Fax: Int. code +(517)353-1793
e-mail: dunbar@cemvax.cem.msu.edu

consist of an infinite array of tetrahedrally ligated Cu cores bridged by four independent DCNQI ligands, which stack in 1-D columns. The unusual charge-transport properties of these compounds are attributed to the existence of an isotropic 3-D conduction pathway from Robin–Day class III, mixed-valent behavior for the $Cu^{I/II}$ ions bridged by DCNQI in addition to the usual 1-D pathway through stacks of DCNQI radicals.[4b]

In addition to the DCNQI conductors, the most remarkable discovery in the context of polycyano radical chemistry in recent years is that a coordination compound of TCNE formulated as $[V(TCNE)_x]\cdot yCH_2Cl_2$ behaves as a bulk ferromagnet with a T_c above room temperature.[5] Unfortunately, no structural information is available for this fascinating binary TCNE compound. In fact, although they date back several decades,[6] the only structurally characterized example of a *binary* metal/TCNX (X = E or Q) compound is $[Ag(\mu_4\text{-TCNQ})]_n$ (TCNQ = tetracyanoquinodimethane).[7] In the absence of structural information on the simple phases, which are insoluble and therefore quite difficult to crystallize, researchers have turned to mixed-ligand model compounds, whose structures are more easily determined.[3b, 8, 9] In this way, researchers are building the fundamental structure–property relationships that are essential, not only for the full understanding of the physics behind the properties, but for the rational design of new materials with predictable behavior. Among the crystallographically determined TCNE and TCNQ coordination compounds that have been reported in the past few years are novel 1-D and 3-D polymeric structures incorporating μ_2-TCNX and μ_4-TCNX.[8, 9]

In addition to the well-known acceptors depicted in Scheme 1, a number of more exotic organocyanide molecules are also being used as novel ligands for transition metals. Several of these are decomposition products unearthed in the course of investigating the complexation chemistry of TCNE: for example, the unprecedented reductive coupling of TCNE molecules on a metal center to give two pyrrolizinato ligands (L = $[C_{11}N_7H_2]^-$) (Scheme 2a).[10a] The resulting $[ML_2]$ compounds (M = Fe, Ni, Cu, Zn) are of considerable interest in materials applications owing to their similarities to the metal phthalocyanines. The free ligand (LH) was also prepared and crystallized,[10b] as was the free anion, which exists in two tautomeric forms **1** and **2** (Scheme 2b).[10c]

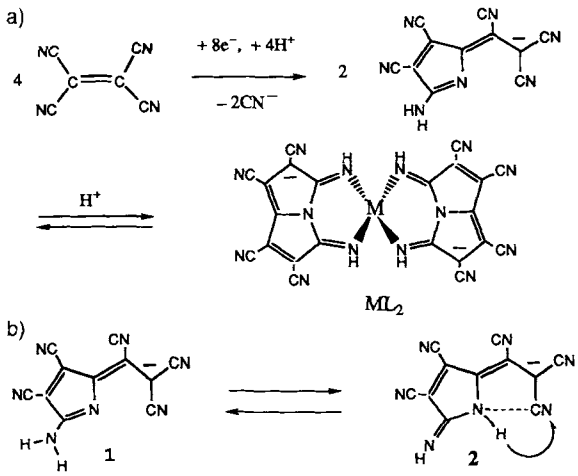

Scheme 2. a) Reductive coupling of TCNE molecules on a metal center to give two pyrrolizinato ligands (L = $[C_{11}N_7H_2]^-$). b) Tautomeric forms **1** and **2** of the free anion $[C_{11}N_7H_2]^-$.

In another report, the new organocyanide $\{C[=C(CN)_2]\text{-}CPh=C(CN)_2\}$ was synthesized from an insertion reaction of TCNE into the acetylide group in $[Ru(\eta^6\text{-}C_6Me_6)\text{-}Cl(C\equiv CPh)(CNR)]$ (Scheme 3).[11] The ligand is bound only through Ru–C bonds, but there are four uncomplexed nitrile groups that are open for possible coordination to other metal centers.

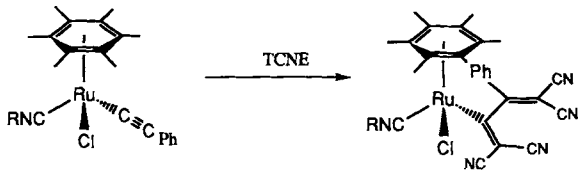

Scheme 3. Insertion of TCNE into the acetylide group in $[Ru(\eta^6\text{-}C_6Me_6)\text{-}Cl(C\equiv CPh)(CNR)]$.

The cyanocarbon ligand $[C_{10}N_7]^-$ (1,1,2,4,5,5-hexacyano-3-azapenta-1,4-dienide) and its 1:1 complex with Ag^I were first reported in 1958[1] but were only recently subjected to X-ray studies by Pala et al., who determined the structures of $[Et_4N][C_{10}N_7]$ and the intriguing coordination polymer $[\{Ag(C_{10}N_7)\}_n]$.[12] In the latter compound, $[C_{10}N_7]^-$ behaves as a tetradentate bridging ligand to two distinctly different types of silver ions, namely with tetrahedral and with a highly unusual square-planar geometry. Figure 2 depicts a single plane in which

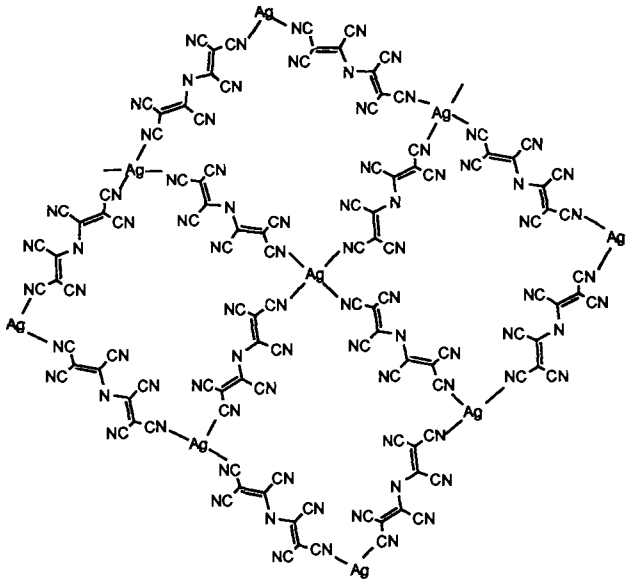

Fig. 2. Schematic representation of polymeric $[\{Ag(C_{10}N_7)\}_n]$ in the (001) plane emphasizing the square-planar Ag sites.

the $[C_{10}N_7]^-$ ions are bonded to square-planar Ag^I ions, which stack along the (001) direction at a distance of 3.15 Å and are linked by the tetrahedral Ag^I ions located between the layers. A comparison of the anion unit in $[Et_4N][C_{10}N_7]$ and $[\{Ag(C_{10}N_7)\}_n]$ reveals that coordination to a metal center does not significantly alter the geometry of the ligand. Electrochemical studies indicate that $[C_{10}N_7]^-$ exhibits two reversible, one-electron reduction processes, the first of which corresponds to the radical species $[C_{10}N_7]^{2-}$, as verified by EPR spectroscopy.

 © VCH Verlagsgesellschaft mbH, D-69451 Weinheim, 1996 0570-0833/96/3515-1660 $ 15.00+.25/0

A recent attempt to prepare $[Mn^{IV}(CN)_6]^{2-}$ from $[Mn^{III}(CN)_6]^{3-}$ led Miller and co-workers to the serendipitous discovery of the novel cyanocarbon {(1,1,2,2-tetracyano-1,2-ethanediyl)bis[imino(cyanomethylene)]}bis[cyanamide] ion $[C_{12}N_{12}]^{2-}$, which was characterized by a single crystal X-ray study.[13] The dianion is centrosymmetric about the central C–C bond and is planar except for the C3 and C3′ cyano groups (Scheme 4). The authors reason that the oxidative decomposition of $[Mn^{III}(CN)_6]^{3-}$ leads to CN^- and $CN^{\bullet}$, which react in a complicated series of reactions that most likely involve cyanogen $(CN)_2$. Cyanide is known to dimerize to cyanogen, which reacts with CN^- to form several products, among them the anion $[C_7N_7]^-$, which can undergo electropolymerization reactions with cyanogen to yield low molecular weight polycyanogen $[C_nN_n]$. Clearly there are many possibilities for the preparation of new cyanocarbons from reactions of cyanogen and CN^- that lead to various combinations of C–C, C–N, and N–N bonds.

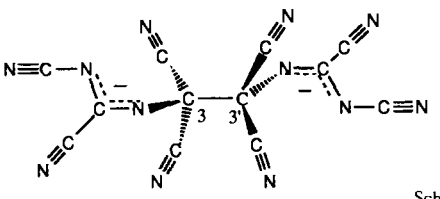

$[C_{12}N_{12}]^{2-}$

Scheme 4. The new cyanocarbon $[C_{12}N_{12}]^{2-}$.

The aforementioned results hint at a wealth of untapped potential for the use of organocyanides as ligands in new complexes and materials. Noncentrosymmetric molecules are of particular interest owing to their potential for exhibiting extensive second-order nonlinear optical effects, as was recently found for the tricyanoguanylidine dianion synthesized by Rasmussen and coworkers (Scheme 5).

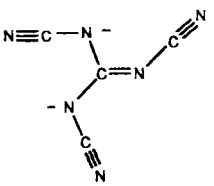

$[C_4N_6]^{2-}$

Scheme 5. Sketch of the new cyanocarbon tricyanoguanylidine depicted as one of the three possible resonance forms.

German version:
Angew. Chem. **1996**, *108*, 1769–1771

Keywords: complexes with nitrogen ligands · cyanides

[1] W. J. Middleton, E. L. Little, D. D. Coffman, V. A. Englehardt, *J. Am. Chem. Soc.* **1958**, *80*, 2795; O. W. Webster, W. Mahler, R. E. Benson, *ibid.* **1962**, *84*, 3678; L. R. Melby, R. J. Harder, W. R. Hertler, W. Mahler, R. E. Benson, W. E. Mochel, *ibid.* **1962**, *84*, 3374.

[2] a) *Extended Linear Chain Compounds* (Ed: J. S. Miller), Plenum, New York, **1982**; b) J. S. Miller, A. J. Epstein, W. M. Reiff, *Chem. Rev.* **1988**, *88*, 201–220; c) *Science* **1988**, *240*, 40–47; d) J. M. Manriquez, M. D. Ward, J. C. Calabrese, P. J. Fagan, A. J. Epstein, J. S. Miller, *Mol. Cryst. Liq. Cryst.* **1989**, *176*, 527–534; e) W. E. Broderick, J. A Thompson, E. P. Day, B. M. Hoffman, *Science* **1990**, *249*, 401–403.

[3] a) R. Gross, W. Kaim, *Angew. Chem.* **1987**, *99*, 257; *Angew. Chem. Int. Ed. Engl.* **1987**, *26*, 251; b) W. Kaim, M. Moscherosch, *Coord. Chem. Rev.* **1994**, *129*, 157–193; c) M. Moscherosch, E. Waldhör, H. Binder, W. Kaim, J. Fiedler, *Inorg. Chem.* **1995**, *34*, 4326–4335.

[4] a) A. Aumüller, S. Hünig, *Liebigs Ann. Chem.* **1986**, 142–164; b) K. Sinzger, S. Hünig, M. Jopp, D. Bauer, W. Bietsch, J. U. von Schütz, H. C. Wolf, R. K. Kremer, T. Metzenthin, R. Bau, S. I. Khan, A. Lindbaum, C. L. Lengauer, E. Tillmanns, *J. Am. Chem. Soc.* **1993**, *115*, 7696; R. Kato, H. Kobayashi, A. Kobayashi, *ibid.* **1989**, *111*, 5224–5232.

[5] J. M. Manriquez, G. T. Yee, R. S. McClean, A. J. Epstein, J. S. Miller, *Science* **1991**, *252*, 1415–1417.

[6] a) A. Rockenbauer, G. Speier, L. Szabo, *Inorg. Chim. Acta.* **1992**, *201*, 5–6; b) E. E. Chain, D. N. Kevill, C. W. Kimball, L. W. Weber, *J. Phys. Chem. Solids* **1976**, *37*, 817–818; c) A. R. Siedle, G. A. Candela, T. F. Finnegan, *Inorg. Chim. Acta* **1979**, *35*, 125–130; d) P. Kathirgamanathan, D. R. Rosseinsky, *J. Chem. Soc. Chem. Commun.* **1980**, 839–840.

[7] L. Shields, *J. Chem. Soc. Faraday Trans. 2* **1985**, *81*, 1.

[8] Polymeric compounds with coordinated TCNQ: a) J. P. Cornelissen, J. H. van Diemen, L. R. Groeneveld, J. G. Haasnoot, A. L. Spek, J. Reedijk, *Inorg. Chem.* **1992**, *31*, 198–202; b) K. R. Dunbar, X. Ouyang, *Chem. Commun.*, submitted.

[9] Polymeric compounds with coordinated TCNE: a) J. S. Miller, J. C. Calabrese, R. S. McLean, A. J. Epstein, *Adv. Mater.* **1992**, *4*, 498; b) A. G. Bunn, P. J. Carroll, B. B. Wayland, *Inorg. Chem.* **1992**, 31, 1297; c) M. M. Olmstead, G. Speier, L. Szabó, *J. Chem. Soc. Chem. Commun.* **1994**, 541; d) J. S. Miller, C. Vazquez, J. C. Calabrese, R. S. McLean, A. J. Epstein, *Adv. Mater.* **1994**, *6*, 217; e) F. A. Cotton, Y. Kim, J. Lu, *Inorg. Chim. Acta* **1994**, *221*, 1; f) F. A. Cotton, Y. Kim, *J. Am. Chem. Soc.* **1993**, *115*, 8511.

[10] a) M. Bonamico, V. Fares, A. Flamini, P. Imperatori, N. Poli, *Angew. Chem.* **1989**, *101*, 1067; *Angew. Chem. Int. Ed. Engl.* **1989**, *28*, 1049; b) V. Fares, A. Flamini, N. Poli, *J. Am. Chem. Soc.* **1995**, *117*, 11580; c) V. Fares, A. Flamini, N. Poli, *J. Chem. Res. (S)* **1995**, 228.

[11] Y. Yamamoto, R. Satoh, T. Tanase, *J. Chem. Soc. Dalton Trans.* **1995**, 307.

[12] M. Decoster, J. E. Guerchais, Y. Le Mest, J. S. Pala, S. Triki, *Polyhedron* **1996**, *15*, 195.

[13] W. E. Buschmann, A. M. Arif, J. S. Miller, *J. Chem. Soc. Dalton Trans.* **1995**, 2343.

[14] R. P. Subrayan, A. H. Francis, J. W. Kampf, P. G. Rasmussen, *Chem. Mater.* **1995**, *7*, 2213.

 © *VCH Verlagsgesellschaft mbH, D-69451 Weinheim, 1996* *0570-0833/96/3515-1661 $ 15.00+.25/0*

Crystallization of Supramolecular Materials: Perhydrotriphenylene (PHTP) Inclusion Compounds with Nonlinear Optical Properties**

Ralf Hoss, Olaf König, Vera Kramer-Hoss, Urs Berger, Peter Rogin, and Jürg Hulliger*

A prerequisite for the design and synthesis of materials with nonlinear optical (NLO) properties is a molecular building block that can be incorporated into a solid in an appropriately functionalized and oriented manner. To obtain new, single-crystal materials that exhibit electrooptical (EO) effects more pronounced than those of the currently known organic NLO crystals,[1-4] stable molecules showing hyperpolarizabilities β_z of up to 10000×10^{-40} $m^4 V^{-1}$ and having dipole moments that can be aligned in a parallel manner within the solid are required. While a large number of target compounds can be envisioned based on these known criteria,[3, 5] the probability is low that during the crystallization of pure NLO compounds a crystal structure with a parallel arrangement of the β_z axes is realized (about 25% for an acentric space group, less than 5% for a nearly parallel packing[1, 3]). Hence, the question of alternatives for the formation of crystalline and structurally optimized EO materials arises. In this study it is shown that perhydrophenylene (PHTP)[6] forms inclusion compounds with electronically optimized NLO species, in which the guest molecules can attain a parallel arrangement; materials with polar properties on a macroscopic level are formed about 90% of the time.

Approaches to incorporating NLO molecules in a parallel fashion into supramolecular host–guest systems have been tried more than ten years ago.[7] Starting with β-cyclodextrin,[8] a number of known clathrate-forming compounds[9, 10] such as urea and thiourea, tri-*o*-thymotide, cyclophosphazene, deoxycholic acid, and PHTP[6] were examined with respect to the formation of inclusion compounds with small organic as well as organometallic species. These host and guest molecules provided a high proportion of polar structures for the inclusion compounds (63–85%) as well.[11] Zeolites have been loaded with NLO compounds with the same goal in mind.[12, 13] The successful incorporation of two strongly hyperpolarizable species (**5**, **8**; see Table 1) into racemic (±)-PHTP was reported only recently.[14] This led to the assumption, that relative to urea, thiourea, and tri-*o*-thymotide, PHTP is particularly well suited to incorporate NLO target molecules of various compositions. The equatorial protons of layered, disk-shaped PHTP molecules form continuous, apolar channels in which the guest molecules are arranged in a parallel fashion (Fig. 1). The formation of inclusion compounds was first studied with the oblong, unbranched, conjugated species **I**–**VI**, which exhibit different patterns of donor (D) and acceptor (A) substituents. These molecular frameworks have already been used to create NLO molecules with large β_z values.[5] In this group, the thiovinyl moiety **IV** was of particular interest due to its strong delocalization of π electrons. Table 1 summarizes the compounds discussed below and some details regarding the synthesis and the detection of polar PHTP-guest materials.

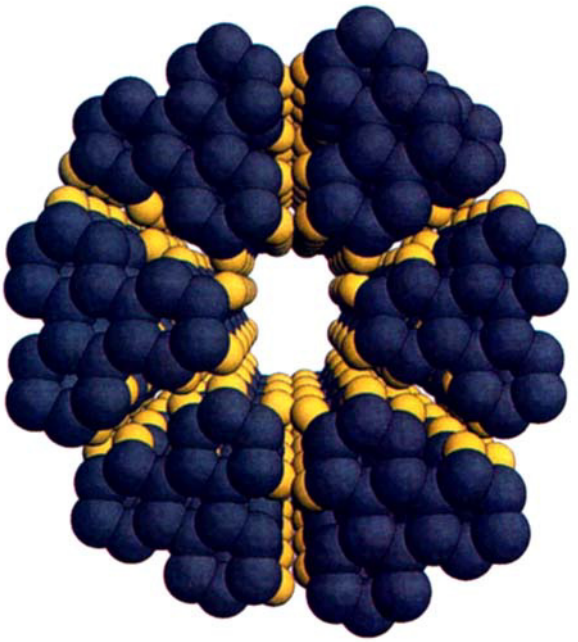

Fig. 1. Van der Waals surface of a PHTP channel (without guest molecules) according to a recent structure elucidation [20]; the van der Waals radii are shown reduced by 30%; carbon grey, hydrogen yellow; computer program employed, ATOMS (Shape Software).

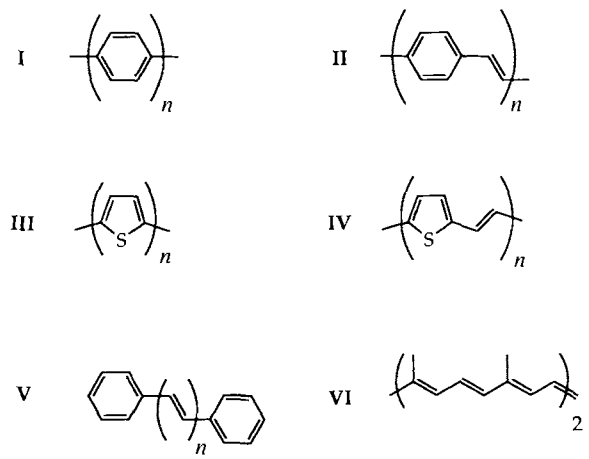

According to the literature,[6] crystals of PHTP–guest complexes can be obtained from solutions as well as from melts. While during crystallizations from solutions the co-inclusion of solvent must be avoided, the formation of crystals from melts is limited to a few, thermally stable NLO guest components. 2-Butanone, in which PHTP is just soluble enough, has been reported as suitable in this context.[6] However, a ^{1}H NMR spectroscopic analysis of the inclusion compounds studied showed co-inclusion of 2-butanone in about ten cases. For a homogeneously colored single crystal of PHTP-**16** that showed no macroscopically visible inclusions, the ratio of **16** to 2-butanone was 1:15. The crystallization of PHTP-**16** and other systems from paraldehyde, on the other hand, yielded solvent-free inclusion complexes. Paraldehyde, with a van der Waals diameter of about 8 Å, is too big to fit into the PHTP channels, which have an inner diameter of about 5 Å. The inclusion compounds could also be prepared, independent of solvents, by solid state reactions and by crystallizations from the gas phase. PHTP-**5**, for example, is formed already during mixing of the powdered starting materials.

[*] Prof. Dr. J. Hulliger, Dr. R. Hoss, O. König, Dr. V. Kramer-Hoss, U. Berger, P. Rogin
Institut für anorganische, analytische und physikalische Chemie
Freiestrasse 3, CH-3012 Berne (Switzerland)
Fax: Int. code +(31)631-3993
e-mail: hulliger@iac.unibe.ch

[**] This work was supported by the Swiss Nationalfonds (projects 2100-037166.93/1, 20-43116.95). We thank H. P. Pfander (University of Berne) and Hoffmann-La-Roche AG for providing 20 g of crocetin dialdehyde, Bayer AG for the hydration to yield PHTP, and C. Bossard (ETH Zurich) as well as K. Krämer (University of Berne) for the use of the lasers.

Table 1. Summary of D-, A-disubstituted NLO compounds, indicating the SHG effects (+ clearly positive, – below the detection limit) after excitation at 1064 (**1**–**6**) or 1300 nm (**7**–**20**), as well as the crystallization conditions (BU, from 2-butanone; PA, from paraldehyde; FR, from solid state reactions; GP, from the gas phase).

Guest Formula	No.	SHG	PHTP inclusion complex, SHG
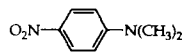	**1**	–	+ FR; + BU
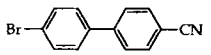	**2**	+	– BU; + PA
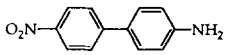	**3**	+	– BU; + PA
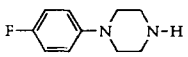	**4**	–	– FR; – BU
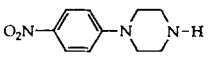	**5**	–	+ FR; + BU; + GP
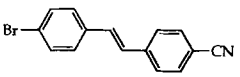	**6**	+	– BU; – PA
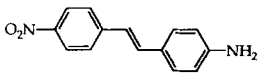	**7**	+	+ BU
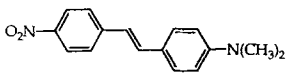	**8**	–	+ FR; + BU
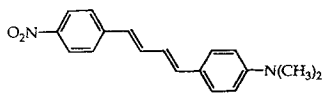	**9**	–	+ FR; + BU
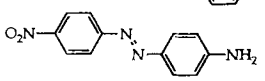	**10**	–	– FR; + BU
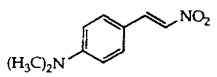	**11**	–	+ FR; + BU; + PA
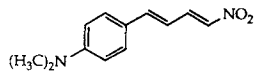	**12**	–	+ FR; + BU
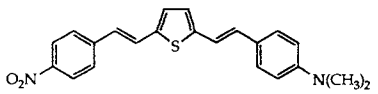	**13**	–	+ FR; + BU; + PA
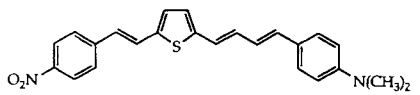	**14**	–	– FR; + BU; + PA
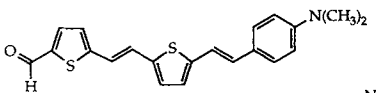	**15**	–	+ FR; + BU; + PA
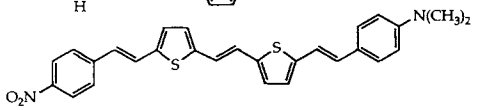	**16**	–	+ FR; + BU; + PA
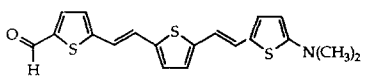	**17**	–	+ FR; + BU; + PA
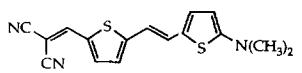	**18**	–	– FR; + BU; + PA
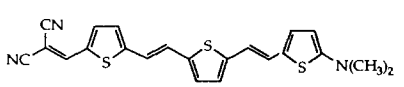	**19**	–	+ FR; + PA
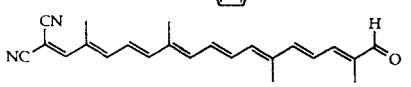	**20**	–	– FR; + BU; + PA

X-ray oscillation photographs of single crystals exhibited, apart from Bragg reflections stemming primarily from the PHTP host lattice, diffuse X-ray scattering phenomena that are caused by, among other things, a one-dimensional periodic arrangement of the guest molecules.[14] In the cases studied (**2**–**9**, **12**, **15**–**18**), the translational periods agree well with the calculated lengths of the corresponding molecules;[15] in some cases, the formation of hydrogen bonds is observed. The guest species that absorb visible light were all observed to exhibit a strong dichroism ($\alpha_{\parallel} \gg \alpha_{\perp}$), clearly indicating parallel charge-transfer axes.[16] A "closest packing" of guest molecules is important for two reasons: 1) the dilution of dipoles, caused by the host–guest lattice, is not further enhanced; 2) the observed intermolecular interactions along the D-π-A···D-π-A chains support the assumption that photoconduction might be possible upon a judicious choice of the D and A substituents. A new pathway for the formation of organic photorefractive crystals could be opened in this way.[1, 17]

The number of the obtained PHTP-guest systems exhibiting macroscopic polar properties was also determined. Frequency doubling experiments on polycrystalline samples[18] or small single crystals showed that 18 of the 20 systems studied exhibit a second-order NLO effect, while only four crystalline samples of the pure guest species were SHG active (SHG = *s*econd *h*armonic *g*eneration). A contribution to the SHG effect by crystallites of pure NLO species can be excluded for all samples obtained by solid-state reactions, as only crystal modifications that are SHG inactive were used. With respect to the high proportion of SHG-active PHTP-guest systems it remains to be examined how much the theoretically maximum NLO or electrooptic effect is reduced by orientational disorder or by domain formation (regions showing antiparallel orientations of the β_z axes). The EO characterizations of PHTP-**5** performed so far allow the exclusion of domains that are substantially larger than the wavelength of visible light. For the PHTP–guest complexes with **5**, **8**, **9**, **13**, **14**, as well as **16**–**20**, the 2ω response was sufficiently intense relative to that of pure 4′-dimethylamino-*N*-methyl-stilbenazolium-*p*-tosylate[1] to assume a primarily parallel arrangement of dipoles. In terms of potential crystallization mechanisms it is surprising that even solid-state reactions between PHTP and apolar crystalline samples of the guest species lead to polar PHTP–guest materials, as does the co-inclusion of 2-butanone.

With a representative sample of compounds we could show that racemic PHTP forms stable channel-inclusion lattices with many electronically interesting guest molecules. Through the supramolecular approach, the use of D-π-A guest molecules yields crystals exhibiting macroscopic polar properties in about 90% of

the cases studied. For now, the question why the formation of a polar arrangement for PHTP inclusion complexes is so strongly preferred over a pure NLO species remains unanswered.

Experimental Procedure

The guest species were purified by chromatography before cocrystallization and characterized with the usual analytical techniques. Of the large number of NLO compounds [1–4] only the 20 D-π-A systems described herein were available to us. The crystallizations by controlled isothermal evaporation of 2-butanone or paraldehyde were performed as described [14,19]. When solid starting materials were employed, the first step was grinding with a mortar and pestle, followed by isothermal annealing at 80–100 °C. Crystallization from the gas phase can be performed (e.g., for PHTP-**5**) according to reference [19] (evaporation from Knudsen cells) or in sealed ampules with $\Delta T < 1$ K, $T = 60$–120 °C, depending on the vapor pressure of the guest species.

The PHTP–guest systems were detected and characterized by gas chromatography and ^{1}H NMR spectroscopy in solution, as well as by single crystal X-ray structure analysis. The melting points of these systems were above that of pure PHTP (125.2 °C). Oscillation photographs show a system of diffuse layer lines perpendicular to the channel axis [14]. From this data, the translational periods of the guest molecules were calculated. In all studied cases this period corresponded well to the calculated length of the molecule (e.g., $\mathbf{15}_{obs}/\mathbf{15}_{calc} = 22.9(3)/22.8(5)$ Å, $\mathbf{16}_{obs}/\mathbf{16}_{calc} = 27.1(5)/28.8(7)$ Å, $\mathbf{18}_{obs}/\mathbf{18}_{calc} = 18.0(4)/19.2(6)$ Å).[15] The lattice constant c of the host lattice was also determined from oscillation photographs and was always found to be 4.75(5) Å. Precession photographs indicated a host unit cell with either orthorhombic C-centered (**5**, **8**, **15**) or monoclinic symmetry (**16**, **17**, **18**).

As summarized in Table 1, polycrystalline samples and small single crystals of the PHTP–guest complexes were examined for SHG at 1064 or 1300 nm (for **1**–**6** and **7**–**20**, respectively). To eliminate potential effects of trapped solvents, measurements involving guest species that do not show SHG effects as pure solids were performed on samples from solid-state reactions.

Received: November 6, 1995
Revised version: February 12, 1996 [Z 8527IE]
German version: *Angew. Chem.* **1996**, *108*, 1774–1776

Keywords: electrooptical properties · inclusion compounds

[1] "Organic Nonlinear Optical Materials", C. Bosshard, K. Sutter, P. Prêtre, J. Hulliger, M. Flörsheimer, P. Kaatz, P. Günter in *Advances in Nonlinear Optics, Vol. 1* (Eds.: A. F. J. Garito, F. Kajzar), Gordon and Breach, New York, **1995**.
[2] *Molecular Nonlinear Optics* (Ed.: J. Zyss), Academic Press, New York, **1994**.
[3] *Nonlinear Optical Properties of Organic Molecules and Crystals, Vol. 1, 2* (Eds.: D. S. Chemla, J. Zyss), Academic Press, New York, **1987**.
[4] "Materials for Nonlinear Optics", *ACS Symp. Ser.* **1991**, 455.
[5] N. J. Long, *Angew. Chem.* **1995**, *107*, 37–56, *Angew. Chem. Int. Ed. Engl.* **1995**, *34*, 6–20.
[6] M. Farina, *Inclusion Compd.* **1984**, 69–95; G. Allegra, M. Farina, A. Immirzi, A. Colombo, U. Rossi, R. Broggi, G. Natta, *J. Chem. Soc. B* **1967**, 1020–1028; M. Farina, G. di Silvestro, P. Sozzani, *Comp. Supramol. Chem., Vol. 6, Solid-State Supramolecular Chemistry: Crystal Engineering* (Eds.: D. D. MacNicol, F. Toda, R. Bishop), Pergamon, in press.
[7] V. Ramamurthy, D. F. Eaton, *Chem. Mater.* **1994**, *6*, 1128–1136.
[8] S. Tomaru, S. Zembutsu, M. Kawachi, M. Kobayashi, *J. Chem. Soc. Chem. Commun.* **1984**, 1207–1208.
[9] A. G. Anderson, D. F. Eaton, W. Tam, Y. Wan (E. I. Du Pont de Nemours), US-4818898, **1989** [*Chem. Abs.* **1991**, *115*, 243514t]
[10] E. Weber in *Top. Curr. Chem.* **1987**, *140*, 3–20; J. E. D. Davies, W. Kemula, H. M. Powell, N. O. Smith, *J. Inclusion Phenom. Mol. Recognit. Chem.* **1983**, *1*, 3–44.
[11] D. F. Eaton, A. G. Anderson, W. Tam, Y. Wang, *J. Am. Chem. Soc.* **1987**, *109*, 1886–1888; W. Tam, D. F. Eaton, J. Calabrese, I. Williams, Y. Wang, A. G. Anderson, *Chem. Mater.* **1989**, *1*, 128–140.
[12] S. D. Cox, T. E. Gier, G. D. Stucky, J. D. Bierlein, *J. Am. Chem. Soc.* **1988**, *110*, 2986–2987.
[13] I. Girnus, M.-M. Pohl, J. Richter-Mendau, M. Schneider, M. Noack, D. Venzke, J. Caro, *Adv. Mater.* **1995**, *7*, 711–714.
[14] J. Hulliger, O. König, R. Hoss, *Adv. Mater.* **1995**, *7*, 719–721.
[15] We calculated the lengths of the molecules using the program *Batchmin* from the program package *MakroModel 4.5*, Columbia University, Cleveland, OH.
[16] S. K. Lee, Q. Y. Shang, B. Hudson, *Mol. Cryst. Liq. Cryst.* **1992**, *211*, 147–156.
[17] K. Sutter, J. Hulliger, P. Günter, *Solid State Commun.* **1990**, *74*, 867–870; J. Hulliger, K. Sutter, Y. Schumacher, B. Březina, V. A. Ivanshin, *J. Cryst. Growth* **1993**, *128*, 886–890.
[18] S. K. Kurtz, T. T. Perry, *J. Appl. Phys.* **1968**, *39*, 3798–3813.
[19] J. Hulliger, *Angew. Chem.* **1994**, *106*, 151–171; *Angew. Chem. Int. Ed. Engl.* **1994**, *33*, 143–163.
[20] O. König, H. B. Burgi, T. Armbruster, J. Hulliger, *Z. Kristallogr. Suppl. 11* **1996**, 106.

Oscillating Crystallization of (+) and (−) Enantiomers during Resolution by Entrainment of 2-Azabicyclo[2.2.1]hept-5-en-3-one**

Gerard A. Potter, Chantal Garcia, Raymond McCague, Brian Adger, and André Collet*

The (−) enantiomer of the bicyclic lactam **1** is a key synthon for the preparation of enantiopure carbocyclic nucleosides[1, 2] used as chemotherapic agents for the treatment of viral infections (HIV, herpes) and as coronary vasodilatators[3] in certain cardiac diseases.[4, 5] At present the manufacture of this important compound is effected by biocatalytic resolution of the racemate with suitable microbial strains.[6] We recently discovered that (±)-**1** is a conglomerate (a feature that had not been reported before),[7] and this finding led us to focus on the possibility of resolving this compound by the preferential crystallization (or entrainment) method,[8–11] which is well suited to large scale applications. In this communication we report an amazing observation made during the development of a practical entrainment process for **1**; we found that the crystallization of supersaturated solutions of this lactam proceeds by a series of oscillations of their enantiomeric composition (the optical rotation value varies from (−) to (+) and back), until the final racemic composition corresponding to the solubility equilibrium is attained. This unprecedented physical phenomenon provides a new insight into some of the factors that determine the kinetics of crystallization of enantiomeric mixtures remote from their solubility equilibrium.

(+)-**1** (−)-**1**

We first examined the crystallization and solubility properties of lactam **1** in various solvents. This compound crystallizes well from diisopropyl ether, in which it is sparingly soluble at 20 °C (racemate: $S_R = 3.56$ wt %, enantiomer: $S_A = 1.1$ wt %).[12] In this apolar solvent, however, the solubility ratio $\alpha = S_R/S_A$ has an anomalously high value ($\alpha = 3.24$), indicating that each enantiomer of **1** enhances the solubility of its mirror image beyond what is usually observed. The same solubility properties were observed in other ethereal solvents such as *tert*-butyl methyl ether (TBME, $\alpha = 3.4$). In most conglomerates there is not normally such mutual solubility enhancement, and the racemate is usually about twice as soluble as the individual enantiomers (that is, α is close to 2).[13] The amide structure of **1** lends itself to the formation of strong intermolecular hydrogen bonds, and the enhancement of the racemate solubility is possibly due to the existence of preferential heterochiral H-bonding in solution. This is substantiated by the observation that addition of an alcoholic solvent to diisopropyl ether, which can disrupt the intermolecular H-bonding, increases the solubility of **1** and significantly decreases α. Since a high value of α is not favorable for the method of enantiomeric resolution by preferential crystallization,[14] we attempted carrying out the entrainment experiments in a 90:10 (w/w) mixture

[*] Prof. A. Collet, Dr. C. Garcia
École normale supérieure de Lyon
Stéréochimie et Interactions Moléculaires (UMR CNRS 117)
46, Allée d'Italie, 69364 Lyon cedex 07 (France)
Fax: Int. code +(33)72 72 84 83
e-mail: andre.collet@chimie.ens-lyon.fr
Dr. G. A. Potter, Dr R. McCague, Dr. B. Adger
Chiroscience, Cambridge (UK)

[**] This work was supported by sabbatical funding from Chiroscience (to G. A. P.)

of diisopropyl ether and 2-propanol at 20 °C, where S_R and $S_A = 12.71$ and 4.54 wt%, respectively, and α is reduced to 2.8. This value is still too high, but we could not improve on this. Figure 1a displays the ternary phase diagram of (+)- and (−)-**1** at 20 °C in this mixed solvent system, and Figure 1b) focuses on the region of this diagram located in the vicinity of the

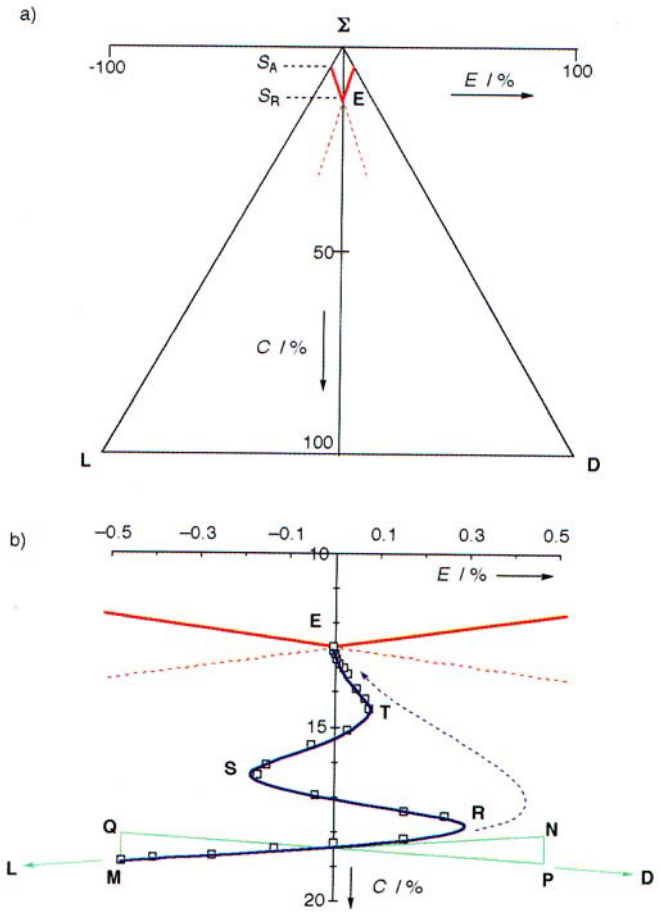

Fig. 1. a) Solubility isotherm at 20 °C of mixtures of (+)-**1** (**D**) and (−)-**1** (**L**) in solvent Σ (diisopropyl ether/2-propanol 90:10 w/w); b) enlargement of the region of diagram (a) situated below the eutectic **E**, showing the oscillating crystallization path (□ represent the experimental points); units for C and E in wt%.

eutectic **E**. In the area situated below the red dotted lines, which represent the extensions of the solubility isotherms beyond **E**, both enantiomers are supersaturated; this is the region suitable for the preferential crystallization method, and by way of example, the indicated paths **M** → **N** or **P** → **Q** represent the expected variation of the composition of a supersaturated solution during the crystallization of a pure enantiomer in a typical entrainment process. Note that segments **N** → **P** and **Q** → **M** correspond to the addition of racemate after each crystallization cycle, and that the extensions of **NM** and **QP** intersect the **L** and **D** apexes of the triangle of Figure 1a.

We then sought conditions that allow a supersaturated solution to follow path **M** → **N** after addition of seeds of (−) enantiomer. Typically, 500 g of a batch solution with composition **M** ($C_0 = 18.9$ wt% and $E_0 = -0.47$ wt%) were stirred at 360 rpm and seeded at 20 °C with 50 mg of finely ground (−)-**1**. The composition of the solution was derived from its rotation α_{436}^{30} (E) and index of refraction n_D^{30} (C), which were recorded every 2 minutes during the initial period (24 min), then every 10 minutes or more at the end. Plots of E vs. C and of α_{436}^{30} vs. the time t are shown in Figure 1b and 2, respectively.

During the first 10 minutes, the composition of the solution closely followed line **MN**, indicating that crystallization of pure (−)-**1** was taking place. Sign inversion from (−) to (+) occurred at the end of 8 minutes; what we then expected was that the solution would attain a maximum positive rotation, followed by a slow decrease eventually reaching zero at the eutectic point **E** (dotted curve in Figs. 1b and 2); this normal behavior

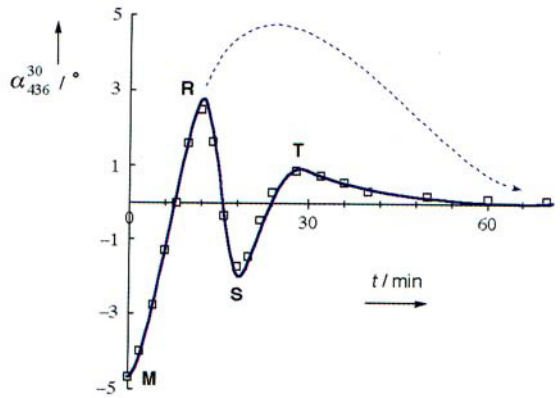

Fig. 2. Optical rotation of the solution vs. time during the oscillating crystallization (□ represent the experimental points).

corresponds to the spontaneous nucleation of the nonseeded enantiomer, which then starts to crystallize along with the seeded enantiomer until the thermodynamic equilibrium is attained. Instead of this, we observed after 12 min a sharp turn (**R**) followed by a straight segment **RS** parallel to **PQ** and corresponding to the crystallization of pure (+)-**1**. This was followed after 16 min by a second change of sign of the solution from (+) to (−), then by a second turn (**S**, 18 min) where (−)-**1** started to crystallize again; a third change of sign from (−) to (+) occurred after 24 min and a last turn at the end of 28 min (**T**). After this point the equilibrium state **E** was finally attained by the end of 1 h, and no further oscillation was observed. This phenomenon was observed consistently and proved to be perfectly reproducible.[15]

An explanation of this behavior can be provided on consideration of two factors. 1) As stated above, the α value is high; that is, one enantiomer aids the solubility of the other. Therefore, as one enantiomer crystallizes from a supersaturated solution, the other enantiomer becomes critically supersaturated, and has a much greater tendency to crystallize than in the racemic solution. This is not sufficient, however, to explain the oscillations. 2) It must be assumed that the conglomerate crystals are *twinned*, and that one enantiomer (+) can grow on the surface of the other (−) (and vice versa) in such a way that the apparent handedness of the seeds is periodically inverted during the crystallization process. This inversion occurs at **R**, **S**, and **T** on the crystallization path displayed Figures 1b and 2. The twinning hypothesis is substantiated by the fact that, although the compound is a conglomerate, individual crystals sorted from the racemate only show weak rotations, and a well formed (apparently) single crystal was found to be almost racemic. Examples of lamellar twinning of (+) and (−) enantiomers in conglomerates have previously been reported, and the case of [6]-helicene is well documented.[16] Along these lines, we explain the observed oscillations as follows. The (−) enantiomer crystallizes rapidly first, on the (−) seeds added. A point is reached (**R**)

 © VCH Verlagsgesellschaft mbH, D-69451 Weinheim, 1996 0570-0833/96/3515-1667 $ 15.00+.25/0

where the (−) enantiomer has crystallized to the extent that the (+) enantiomer left in solution is now in excess and becomes critically supersaturated. At this point the (+) crystals start to grow on the surface of the (−) crystals that have already formed, which stops the crystallization of the (−) enantiomer; a point is then reached (**S**) where the (+) enantiomer has crystallized to the extent that the (−) is now left in solution in excess and becomes critically supersaturated. The (−) enantiomer then starts to grow on the surface of the (+) crystals, and so on. The process repeats until the solubility equilibrium is attained (**E**). If this explanation is correct, then the crystals thus formed would consist of distinct alternating layers of (−)/(+)/(−)/(+) enantiomers, as has been observed in [6]-helicene.

In order to test the hypothesis that one enantiomer of the bicyclic lactam **1** can grow on the surface of the opposite enantiomer, an experiment was conducted in which a supersaturated solution of **1** containing a small excess of the (−) enantiomer was seeded with crystals of the *opposite* (+) enantiomer. Indeed, in this experiment carried out on a 500 g scale with an initial composition of $E_0 = -0.42$ wt% and $C_0 = 17.12$ wt% by seeding with 50 mg of (+) enantiomer and collecting the crystals thus formed just before the first oscillation, it was possible to obtain 4.0 g of the (−) enantiomer having 86% *ee*! Following on from this result, seeding with crystals of the racemate was examined. From a solution with the same starting composition as the previous experiment and seeded with 50 mg of racemic seed crystals, 3.9 g of the (−) enantiomer of 90% *ee* was obtained. For seeding with the opposite enantiomer and racemate to be successful, the initial enantiomeric excess (E_0) needed to be greater than about 0.35 wt% (ca. 2 % *ee*) at the initial concentration employed. Thus above a certain critical enantiomeric excess, which is dependent upon the degree of supersaturation, the enantiomer in excess crystallizes on the surface of the seed crystals, irrespective of which enantiomer it is, verifying that one enantiomer of **1** can grow on the surface of its opposite enantiomer.

The fact that oscillating crystallizations of this kind have not been observed earlier is not surprising. The conditions that must be fulfilled are in fact very difficult to meet: conglomerates represent only 5–10 % of crystalline racemates, the vast majority of these display normal solubility behavior (α close to 2), and lamellar twinning of enantiomers is not so common. Moreover, the region of the phase diagram where such oscillations can take place is very narrow (compare the scales of Figure 1a and b).

Although the crystallization of **1** was observed to proceed in this oscillating manner, successful resolution by a cyclic entrainment process was found to be possible by seeding with the desired enantiomer and collecting the crystals formed just before the onset of the first oscillation through careful monitoring of the crystallization process.

Experimental Procedure

Suitable operating conditions for entrainment were as follows: solvent 90:10 (w/w) mixture of diisopropyl ether and 2-propanol; $T = 20\,^{\circ}C$; 1 kg of batch solution having $C_0 = 16.6$ to 17.1 wt% and $E_0 = +$ or -0.28 wt%; stirring speed 500 rpm; seeding with 50 mg of enantiomer per cycle; crystallization duration from 30 to 60 min; yield *ca.* 6 g of enantiomer per cycle, with 85-90 % *ee*. Under these conditions, a series of ten successive cycles furnished 31.9 g of (−)-**1** and 31.1 g of (+)-**1** having 86 % *ee*, which after one recrystallization yielded 25.6 and 24.8 g, respectively, of pure lactam enantiomers.

Received: February 16, 1996 [Z 8827 IE]
German version: *Angew. Chem.* **1996**, *108*, 1780–1782

Keywords: crystallization · enantiomeric resolution · lactams · oscillating systems

[1] J. J. C. Taylor, A. G. Sutherland, C. Lee, R. Wilson, S. Thomas, S. M. Roberts, C. Evans, *J. Chem. Soc. Chem. Commun.* **1990**, 1120; C. Evans, S. M. Roberts, K. A. Skoberu, A. G. Sutherland, *J. Chem. Soc. Perkin Trans. 1* **1992**, 589.
[2] B. L. Bray, S. C. Dolar, B. Halter, J. W. Lackey, M. B. Schilling, D. J. Tapolczay, *Tetrahedron Lett.* **1995**, *36*, 4483; for alternative routes to carbocyclic nucleosides and leading references see B. M. Trost, D. Stenkamp, S. R. Pulley, *Chem. Eur. J.* **1995**, *1*, 568.
[3] J. W. Daly, D. Ukena, R. A. Olsson, *Can. Physiol. Pharmacol.* **1987**, *65*, 365.
[4] C. Evans, R. McCague, S. M. Roberts, A. G. Sutherland, *J. Chem. Soc. Perkin Trans. 1* **1991**, 656.
[5] V. E. Marquez, M.-I. Lim, *Med. Res. Rev.* **1986**, *6*, 1; J. W. Daly, D. Ukena, R. A. Olsson, *J. Physiol. Pharmacol.* **1987**, *65*, 365.
[6] S. J. C. Taylor, R. McCague, R. Wisdom, C. Lee, K. Dickson, G. Ruecroft, F. O'Brien, J. Littlechild, J. Bevan, S. M. Roberts, C. T. Evans, *Tetrahedron: Asymmetry* **1993**, *4*, 1117.
[7] (+)- or (−)-**1**: m.p. 95 °C, $\Delta H_A = 17.8$ kJ mol^{-1}; (±)-**1**: m.p. 56 °C, $\Delta H_R = 15.2$ kJ mol^{-1}; the calculated melting point for a conglomerate is 55.8 °C (see ref. [9]; the variation of ΔH with T is neglected in this calculation). The solid state IR spectra of the racemate and of the enantiomers are identical.
[8] A. Collet, M.-J. Brienne, J. Jacques, *Chem. Rev.* **1980**, *80*, 215.
[9] J. Jacques, A. Collet, S. H. Wilen, *Enantiomers, Racemates and Resolutions*, Wiley-Interscience, New York, **1981**; revised edition: Krieger, Malabar, FL, USA, **1994**.
[10] M.-J. Brienne, A. Collet, J. Jacques, *Synthesis* **1983**, 704.
[11] A. Collet in *Comprehensive Supramolecular Chemistry, Vol. 10* (Ed.: D. N. Reinhoudt), Pergamon, Oxford, **1996**, Chapter 5; see also: *Chirality and Industry* (Eds.: A. N. Collins, G. N. Sheldrake, J. Crosby), Wiley, Chichester, **1992**.
[12] The following units are used throughout this paper: in a quantity σ g of solvent, the solubility (S) or concentration C of a mixture of d g of (+) and l g of (−) enantiomers is defined as $(d+l)/(d+l+\sigma)$ in wt % and the excess of enantiomer E as $(d-l)/(d+l+\sigma)$ also in wt %. Note that C and E define the vertical and horizontal axes of the ternary phase diagram of Fig. 1, and that E/C corresponds to *ee*, the usual enantiomeric excess of the considered mixture.
[13] There are very few reported examples of conglomerates with α greater than 3: in water at 30 °C *N*-acetyl- and *N*-butyrylproline have $\alpha = 3.34$ and 3.24, respectively: C. Hongo, M. Shibazaki, S. Yamada, I. Chibata, *J. Agric. Food Chem.* **1976**, *24*, 903.
[14] See Ref. [9] pp. 233–235; a value of α greater than 2 reduces the size of the region of the phase diagram suitable for the entrainment (lower productivity), and has a detrimental effect on the stability of the supersaturation of the nonseeded enantiomer, which leads to spontaneous nucleation of the undesired enantiomer.
[15] The oscillation frequency was found to increase with the degree of supersaturation and the rate of stirring, but this dependence is complex, and was not investigated further in this work.
[16] B. S. Green, M. Knossow, *Science* **1981**, *214*, 795; see also R. J. Davey, S. N. Black, L. J. Williams, D. McEwan, E. Sadler, *J. Cryst. Growth* **1990**, *102*, 97.

Discovery of Chiral Catalysts through Ligand Diversity: Ti-Catalyzed Enantioselective Addition of TMSCN to *meso* Epoxides**

Bridget M. Cole, Ken D. Shimizu, Clinton A. Krueger, Joseph P. A. Harrity, Marc L. Snapper,* and Amir H. Hoveyda*

Herein we report a new method for the rapid development of catalysts used in enantioselective synthesis of chiral molecules. Our approach is general, does not require immunization pro-

[*] Prof. M. L. Snapper, Prof. A. H. Hoveyda, Dr. B. M. Cole, Dr. K. D. Shimizu, C. A. Krueger, Dr. J. P. A. Harrity
Department of Chemistry, Merkert Chemistry Center, Boston College
Chestnut Hill, MA 02167-3860 (USA)
Fax: Int. code + (617) 552-2705

[**] Financial support from Johnson and Johnson (Focused Giving Grant to A. H. H.), Pfizer (Young Faculty Award to A. H. H.), and the Massachusetts Department of Public Health (Breast Cancer Scholar Award to M. L. S.) is gratefully acknowledged. We thank Pfizer for additional funds for the purchase of a high-throughput GLC system. K. D. S. is an NIH postdoctoral fellow; A. H. H. is a Sloan Research Fellow and a Camille Dreyfus Teacher-Scholar. We are grateful to Professors S. L. Schreiber and J. Rebek, Jr., for critical readings of this manuscript and to Professor M. R. Ghadiri for invaluable technical advice.

cesses,[1] and leads to the discovery of low molecular weight ligands that effect formation of chiral molecules efficiently. This research was undertaken since we judged that, given the ability of enzymes to serve as asymmetric catalysts,[2] potent stereoselective reactions catalyzed by transition metal peptide complexes may be uncovered. As the search for an optimal ligand was inspired by combinatorial and related strategies, peptide-derived ligands represent an attractive option: they have modular structures within which asymmetry can be easily varied. Furthermore, amino acid building blocks are environmentally benign, readily available in optically pure form, and inexpensive.[3] We thus present the first enantioselective formation of β-cyanohydrins achieved by the asymmetric opening of *meso* epoxides.[4] Our studies demonstrate that diverse peptide-based structures can be rapidly synthesized and screened collectively for their ability to induce appreciable levels of enantiocontrol.

The Ti-catalyzed addition of trimethylsilylcyanide to epoxides is facilitated by the presence of an alkoxide Schiff base [Eq. (a)].[5] Reaction of **1** with 10 mol% $Ti(OiPr)_4$ provided

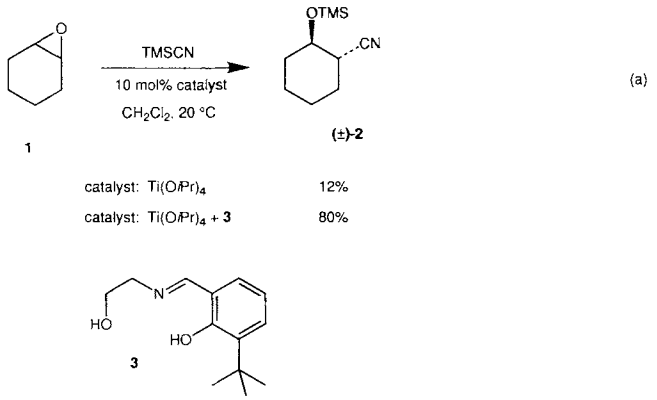

(a)

(±)-**2** in only 12% yield (18 h), whereas when **3** was also present (10 mol%), (±)-**2** was isolated in 80% yield. We surmised that if ligands such as **3** are effective in accelerating C–C bond formation, dipeptide Schiff bases with the general structure shown in Scheme 1 may also give rise to effective *chiral* catalysts. The availability of two amino acid residues presents opportunities for fine-tuning catalyst efficiency; the aromatic Schiff base allows for electronic adjustment of the ligand.[6] Similar ligand systems have been used by Inoue et al. for catalytic enantioselective cyanohydrin synthesis;[3] however, these studies followed

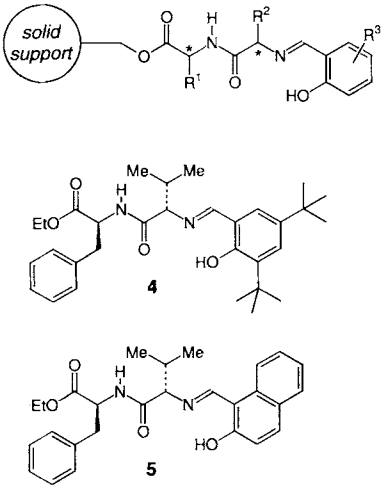

Scheme 1. General structure of support-bound dipeptide Schiff bases, and ligands **4** and **5**. R^1 and R^2 can contain stereogenic centers.

the classical approach to catalyst optimization: ligands were modified in a serial manner.

To establish the efficacy of dipeptide Schiff bases, the reaction illustrated in Equation (a) was performed in the presence of **4** (see Experimental Procedure): at 4 °C (9 h, CH_2Cl_2), **2** was isolated in 68% yield (6% *ee*); with **5** present (toluene, 4 °C), a 58% yield of **2** was achieved (40% *ee*). Reasonable levels of reaction acceleration can thus be expected from this class of chiral ligands. This transformation and the variety of related ligand systems render the aforementioned strategy for catalyst development attractive, because solid-support techniques can be used for the high-throughput search for an effective catalyst. It is notable that since reactions are accelerated by the dipeptide Schiff base,[7] adventitious side products present from ligand synthesis on solid support should not provide a serious hindrance to accurate analysis (impurities are less likely to serve as ligands).[8]

Dipeptide Schiff bases can be prepared rapidly and efficiently in a parallel manner by standard methods (Scheme 2).[9,10] Schiff base **8** is prepared by subjecting the polymer-bound **7** to the requisite aromatic aldehyde. Accordingly, more than twenty different ligands can be prepared in the course of a single day, a feat that would be difficult by traditional techniques.

Next, we established whether the levels of selectivity observed for the dipeptide Schiff base bound to the solid support correspond to those of reactions with the free ligand. With support-

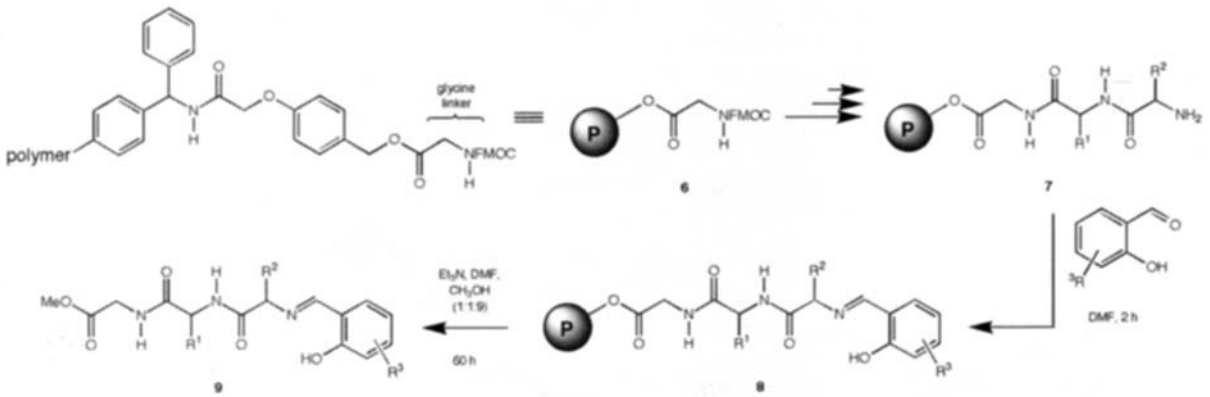

Scheme 2. Solid-phase synthesis of **9**. FMOC = 9-fluorenylmethyloxycarbonyl.

 © VCH Verlagsgesellschaft mbH, D-69451 Weinheim, 1996 0570-0833/96/3515-1669 $ 15.00+.25/0

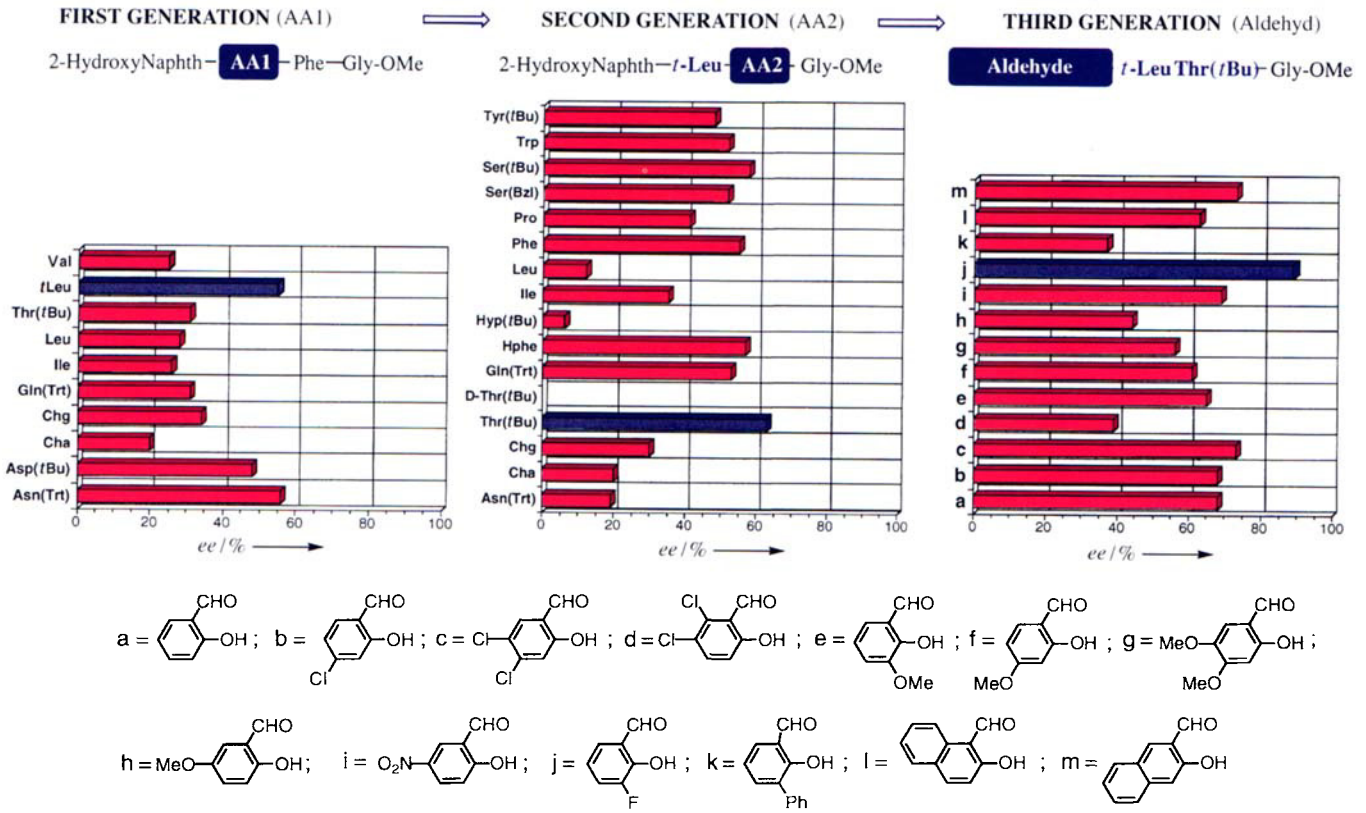

Fig. 1. Ligand optimization by variation of the ligand components AA1 (first generation), AA2 (second generation), and aldehyde (third generation). Asn(Trt) = *N*-β-trityl-L-asparagine; Asp(*t*Bu) = L-aspartic acid β-*tert*-butyl ester; Cha = L-cyclohexylalanine; Chg = L-cyclohexylglycine; D-Thr(*t*Bu) = *O*-*tert*-butyl-D-threonine; Gln(Trt) = *N*-γ-trityl-L-glutamine; Hphe = L-homophenylalanine; Hyp(*t*Bu) = *O*-*tert*-butyl-L-hydroxyproline; Ile = L-isoleucine; Leu = L-leucine; Phe = L-phenylalanine; Pro = L-proline; Ser(Bzl) = *O*-benzyl-L-serine; Ser(*t*Bu) = *O*-*tert*-butyl-L-serine; Thr(Bzl) = *O*-benzyl-L-threonine; Thr(TBS) = *O*-*tert*-butyldimethylsilyl-L-threonine; Thr(*t*Bu) = *O*-*tert*-butyl-L-threonine; Thr(Trt) = *O*-trityl-L-threonine; *t*-Leu = L-*tert*-leucine; Val = L-valine; trityl = triphenylmethyl.

bound **4**, reaction of **1** with TMSCN affords cyanohydrin **2** in 56% *ee* (vs 6% *ee* with the free ligand). When **5** is tethered to the solid support with the longer chain 6-amino caproic acid linker, (±)-**2** is obtained (vs 58% *ee* with a glycine linker). Thus, enantioselective processes are possible with immobilized ligands, but it appeared that, at least initially, a more reliable approach for discovery of catalysts in solution would require cleavage of the ligand from the polymer support, a process that delivers ligands in excellent yields as yellow crystalline solids.[7]

In a manner similar to "positional scanning",[8] each of the basic structural modules of the chiral ligand system was modified systematically (Fig. 1). Because in our preliminary studies **5** led to the highest enantioselectivities (40% *ee*), we decided to use it as our starting system. To determine the best candidate for the amino acid unit AA1, ten ligand systems were prepared on solid support (other two components were retained), cleaved, and screened in a parallel fashion as catalysts for the enantioselective formation of **2** (10 mol% ligand and $Ti(OiPr)_4$). *t*Leu emerged as a superior AA1 unit. With *t*Leu as AA1 and 2-hydroxy-1-naphthaldehyde (2-hydroxynaphth) as the Schiff base, the search for the most appropriate AA2 unit (second-generation ligands, sixteen different amino acids) led us to Thr(*t*Bu). It is noteworthy that the unnatural enantiomer D-Thr(*t*Bu) did not afford any of the desired product. With *t*Leu as AA1 and Thr(*t*Bu) as AA2, thirteen aldehydes with a range of steric and electronic properties were selected, synthesized, and screened; 3-fluorosalicaldehyde stood as the best choice (third-generation ligand). Hence, through rapid screenings of three ligand classes each consisting of ten to seventeen members, a ligand structure (AA1 = *t*Leu, AA2 = Thr(*t*Bu), aldehyde = 3-fluorosalicaldehyde) was found that effects enantioselective formation of **2** in 89% *ee*.

Dipeptide Schiff base **10** is therefore implicated to be an effective chiral ligand for the Ti-catalyzed addition. Indeed, conversion of **1** to **2** in the presence of **10** proceeds in 86% *ee* (Table 1,

Table 1. Ti-catalyzed enantioselective addition of TMSCN to *meso* epoxides [a].

Entry	Substrate	Product	Ligand	e.r. [b]	*ee* [%]	Yield [%]	Conv. [%]
1		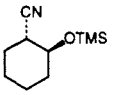	i	13.3:1	86	65	80
2			ii	5.6:1	70	62	–
	1	**2**					
3		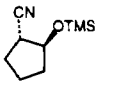	i	4.5:1	64	56	–
4			ii	7:1	75	57	72
	11	**12**					
5		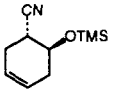	i	7:1	75	50	62
6			ii	2.7:1	46	48	
	13	**14**					

[a] Conditions: 20 mol% $Ti(OiPr)_4$, 20 mol% ligand, 4 °C, toluene, 6–12 h. [b] Enantiomeric ratio determined by GLC (BETA-DEX 120 column) by comparison with authentic material. [c] Yields after chromatography. [d] Determined by GLC analysis.

entry 1). However, **10** is not the most suitable ligand for the reaction of **11**. In the presence of **10**, addition product **12** is obtained in 64% *ee* (entry 3), whereas with **15** as the chiral ligand, **12** is obtained in a higher 75% *ee* (entry 4). In direct contrast, **15** is an inferior ligand for Ti-catalyzed TMSCN addition to **1**; **2** is formed in 70% *ee* (vs 86% *ee* with **10**). This

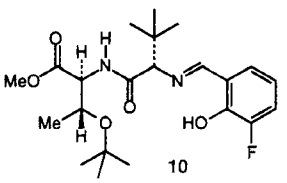

10

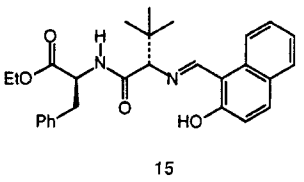

15

substrate specificity in asymmetric induction as a function of the ligand structure is a notable attribute of the present method (similar to what is found in enzyme-catalyzed reactions). Ligand optimization can be carried out for *each* particular class of substrates, since the best chiral ligand for six-membered epoxides may not be the most effective for reactions of five-membered ring substrates (compare entry 1 to 3 or entry 2 to 4). The outcome of the Ti-catalyzed asymmetric opening of **13** (entries 5 and 6) supports this contention.

The present report delineates several advances. 1) We put forth the first example of a catalytic and enantioselective method for the addition of TMSCN to *meso* epoxides. 2) We illustrate that peptide-based systems are amenable to high-throughput screening. The reaction outcomes observed in the initial screening correlate well with the subsequent solution chemistry. 3) We demonstrate a novel strategy for the development of new catalysts for asymmetric transformations; stepwise modification of the modular ligand structure leads to the identification of a system that affords high enantioselectivity. In the case of **1** → **2**, reaction enantioselectivity is improved from 40 to 86% *ee*.[9] The present strategy does not allow for an exhaustive examination of every ligand structure; our iterative approach, however, allows one to eliminate—quickly and logically—certain combinations. We have scanned much of the conformational space at each position of the modular ligand by varying various subunits in a random fashion and combining the best set of building blocks. The described strategy assumes that the influence of each ligand subunit is independent and additive; it is impossible to rule out cooperative effects without individually testing each combination. Nonetheless, additivity effects are apparent from the above data and our studies corroborate that if ligand **10** is optimized in the reverse fashion (i.e. aldehyde→AA2→AA1), the same ligand structure is identified. The dipeptide-based ligands discussed here, the attendant method for examination of their efficiency, and the catalytic enantioselective addition of TMSCN to *meso* epoxides should find extensive applications in the synthesis of chiral compounds.

Experimental Procedure

General procedure for the solid-phase synthesis of ligands: Solid-phase synthesis was carried out on the functionalized resin, FMOC-Gly-PAC (Millipore; 0.42 mmol g^{-1} loading). Reactions were performed in polypropylene Bio-Spin chromatography columns from Bio-Rad Laboratories, Inc. PAC-Gly-Fmoc resin (100 mg, 0.04 mmol) was placed in the polypropylene reaction vessel and washed with DMF (3 × 1.5 mL). The resin became swollen through by agitation in DMF (1.5 mL) for 2 h, washed with additional DMF (3 × 1.5 mL), and subsequently deprotected by washing with 20% piperidine/DMF (1.5 mL), agitation for 1.5 h in 20% piperidine/DMF (1.5 mL), and washing with DMF (10 × 1.5 mL). The FMOC-protected amino acid (0.17 mmol) was activated as a symmetrical anhydride by treatment with an excess of 1,3-diisopropylcarbodiimide (49 μL, 0.25 mmol) in DMF (1.5 mL, 20 min). The resulting solution was added to H_2N-Gly-PAC, mixed for 1 h, and then washed with DMF (10 × 1.5 mL). A sample of the resin was subjected to a ninhydrin test [10]. Samples testing positive were resubjected to the coupling conditions. FMOC-AA2-Gly-PAC was deprotected by washing with 20% piperidine/DMF (1 × 1.5 mL), mixing for 1.5 h in 20% piperidine/DMF (1.5 mL), and washing with DMF (10 × 1.5 mL). The second amino acid coupling and deprotection was performed similarly. Following coupling and deprotection, H_2N-AA1-AA2-Gly-PAC was treated with 4.0 equiv (0.17 mmol) of an *ortho*-hydroxy aldehyde (1.5 mL DMF, 2 h) and washed with DMF (10 × 1.5 mL). The ligand was cleaved from the resin by stirring with 2.0 mL of triethylamine/DMF/MeOH (1:1:9) for 60 h. The solution was filtered and the resin washed with distilled THF (3 × 2 mL). Solvent was removed in vacuo; the resulting yellow solid was taken up in CH_2Cl_2 (1.0 mL) and loaded onto a pipet packed with a cotton plug and silica gel. The ligand was eluted with EtOAc (ca. 10 mL); the product was dissolved in toluene (5 mL) and concentrated in vacuo to remove water and DMF as the azeotrope; the product was dried in vacuo to give a pale to a bright yellow solid (yields: 80–100%).

Testing of the ligands in the epoxide ring opening reaction: The ligand (0.02 mmol) prepared by solid-phase synthesis was taken up in $CHCl_3$ (1.0 mL). Toluene (2.0 mL) was added and the solution concentrated to a yellow solid in vacuo. The reaction vessel was evacuated and flushed with argon three times before $Ti(OiPr)_4$ (1 equiv of a 0.1 M solution in toluene; 200 μL, 0.02 mmol) was added; the reaction mixture and stirred for 1 h at 22 °C. Subsequently, cyclohexene oxide was added (1.0 M in toluene; 200 μL, 0.2 mmol), followed by TMSCN (1.0 M in toluene; 200 μL, 0.2 mmol). The reaction mixture was allowed to stir for 20 h (4 °C). Reactions were quenched by the addition of 1.0 mL of ether/hexanes (1:1) and forced through a silica gel plug with an additional 1.0 mL of ether/hexanes (1:1). Reaction selectivity was determined by GLC analysis (BETADEX-120 chiral column).

Received: May 22, 1996 [Z9146IE]
German version: *Angew. Chem.* **1996**, *108*, 1776–1779

Keywords: asymmetric catalysis · combinatorial chemistry · cyanohydrins · epoxides · peptides

[1] a) T. Li, K. D. Janda, J. A. Ashley, R. A. Lerner, *Science* **1994**, *264*, 1289–1293; b) P. G. Shultz, R. A. Lerner, *ibid.* **1995**, *269*, 1835–1842; c) M. M. Davis, *ibid.* **1996**, *271*, 1078–1079.

[2] C.-H. Wong, G. M. Whitesides, *Enzymes in Synthetic Organic Chemistry*, Pergamon, Oxford, New York, **1994**.

[3] Yet, with a few exceptions, dipeptide systems have not been used in this context. See: a) H. Nitta, D. Yu, M. Kudo, A. Mori, S. Inoue, *J. Am. Chem. Soc.* **1992**, *114*, 7969–7975, and references therein; b) M. Hayashi, Y. Miyamoto, T. Inoue, N. Oguni, *J. Org. Chem.* **1993**, *58*, 1515–1522.

[4] For a brief overview of related processes, see: I. Paterson, D. J. Berrisford, *Angew. Chem.* **1992**, *104*, 1204–1205; *Angew. Chem. Int. Ed. Engl.* **1992**, *31*, 1179–1180. Catalytic enantioselective opening of *meso* epoxides by $TMSN_3$ has been reported: a) W. A. Nugent, *J. Am. Chem. Soc.* **1992**, *114*, 2768–2769. b) L. E. Martinez, J. L. Leighton, E. N. Jacobsen, *ibid.* **1995**, *117*, 5897–5898.

[5] M. Hayashi, M. Tamura, N. Oguni, *Synlett.* **1992**, 663–664.

[6] For examples of electronic tuning of transition metal catalyzed reactions, see: a) E. N. Jacobsen, W. Zhang, M. L. Guler, *J. Am. Chem. Soc.* **1991**, *113*, 6703–6704; b) T. V. Rajanbabu, T. A. Ayers, A. L. Casalnuovo, *ibid.* **1994**, *116*, 4101–4102; c) A. Schnyder, L. Hintermann, A. Togni, *Angew. Chem.* **1995**, *107*, 628–630; *Angew. Chem. Int. Ed. Engl.* **1995**, *34*, 931–933, and references therein.

[7] For a recent review of ligand-accelerated catalysis, see: D. J. Berrisford, C. Bolm, K. B. Sharpless, *Angew. Chem.* **1995**, *107*, 1159–1170; *Angew. Chem. Int. Ed. Engl.* **1995**, *34*, 1059–1070.

[8] G. Liu, J. A. Ellman, *J. Org. Chem.* **1995**, *60*, 7712–7713.

[9] A. Tartar, J.-C. Gesquiere, *J. Org. Chem.* **1979**, *44*, 5000–5003.

[10] a) L. A. Carpino, G. Y. Han, *J. Org. Chem.* **1972**, *37*, 3404–3405; b) G. B. Fields, R. L. Nobel, *Int. J. Peptide Protein Res.* **1990**, *35*, 161–214.

[11] The notably higher levels of enantioselectivity obtained with support-bound peptides will be the subject of future investigations.

[12] The present approach is related to "positional scanning" of peptide libraries for the study of receptor interactions: C. T. Dooley, R. A. Houghten, *Life Sciences* **1993**, *52*, 1509–1517.

[13] We find that, unlike the relative levels of enantioselectivity, the relative reaction efficiencies observed in our screening process cannot be reliably extrapolated to larger scale reactions.

[14] E. Kaiser, R. L. Colescott, C. D. Bossinger, P. I. Cook, *Anal. Biochem.* **1970**, *34*, 595–598.

The Complete Structure of Maitotoxin, Part I: Configuration of the C1–C14 Side Chain**

Makoto Sasaki, Nobuaki Matsumori, Takahiro Maruyama, Taro Nonomura, Michio Murata, Kazuo Tachibana,* and Takeshi Yasumoto

Maitotoxin (MTX, **1**) was first discovered as one of the toxins responsible for ciguatera seafood poisoning and was afterward found to be produced by the dinoflagellate *Gambierdiscus toxicus*.[1] MTX is the largest non-biopolymer known to date (M_r = 3422),[2] thus attracting considerable attention from natural products and synthetic chemists. Additionally, MTX has remarkable biological activities; particularly, its lethality against mammalians is extremely potent (50 ng per kg, mouse, ip.) and exceeded by that of only a few proteinous toxins.[2b,3] Therefore, the elucidation of its structure has been regarded as one of the most exciting challenges in natural products chemistry. In this and the following communication[20] we wish to report the complete structural determination including the absolute configuration of **1**.

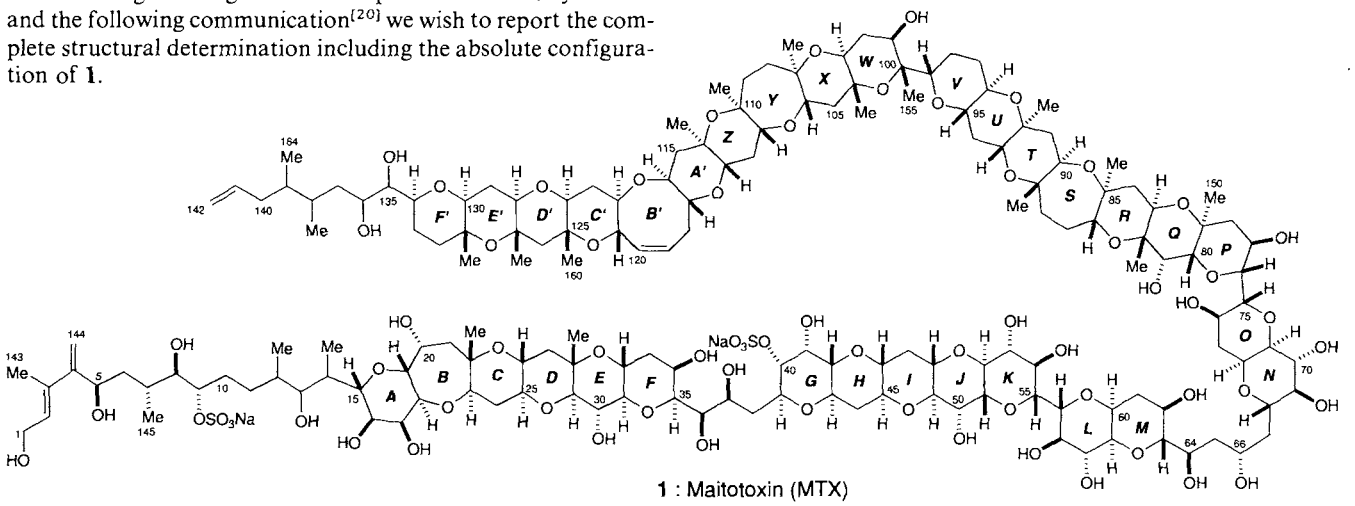

1 : Maitotoxin (MTX)

We have recently succeeded in determining the relative configuration along the polyether entity of MTX encompassing ether rings A through F'.[4] Yet the configuration of both side chains (C1–C14 and C135–C142) has remained unknown. Our strategy in previous work was based on the diastereospecific syntheses of fragment structures in combination with stereochemical analysis with use of NMR data ($^{2,3}J_{C,H}$ and $^{3}J_{H,H}$).[4] Upon determination of configuration by synthetic methods, all possible diastereomers are usually synthesized and their spectroscopic data compared with those of a derivative of the natural product. However, in the case of the C1–C14 side chain of MTX, which contains seven asymmetric carbons, the total number of the possible stereoisomers amounts to 128. In previous studies[4,5] we have demonstrated that the number of possible candidates requiring synthesis can be greatly reduced by careful examination of the NMR data of the natural product. Therefore, we first used this approach to select diastereomers of the C1–C14 side chain to be synthesized. For the C5–C9 part, the configuration was previously deduced as 5*R**, 7*R**, 8*R**, and 9*S** based on the long-range carbon–proton and proton–proton coupling constants ($^{2,3}J_{C,H}$ and $^{3}J_{H,H}$).[5] This method failed to be convincing for the C9–C12 portion mainly because of extreme overlap and broadening of the corresponding ^{1}H signals. Instead, conventional NOE analysis was informative (Fig. 1), since the C9–C12 portion appeared to take a relatively rigid conformation (1,2-disubstituted ethanes are known to be mostly in the *anti* orientation). NOEs between H-7 and H-10 (δ = 2.03) and the coupling constants $^{3}J_{H\text{-}9/H2\text{-}10}$ (7.9 and 3.2 Hz) showed that the chain C8-C9-C10-C11 takes an extended conformation, which allowed us to assign the signals for H_2-10 at δ = 1.81 and 2.03 to H_α-10 and H_β-10, respectively. NOEs arising from probable 1,3-*syn* interaction of H-9/H-11 (δ = 1.47) and H_β-10/H_3-146 indicated the extended conformation of C9-C10-C11-C12 with the following stereospecific assignments for H_2-11: H-11 (δ = 1.47) is a β-proton and H-11 (δ = 2.14) is an α-proton (Fig. 1). An intense cross peak due to C146/H_α-11 in phase-sensitive HMBC spectra (HMBC = heteronuclear multiple bond correlation)[6] suggested the dihedral angle C146-C12-C11-H_α-11 to be nearly 180°. Furthermore, the fact that $^{3}J_{H_\beta\text{-}11/H\text{-}12}$ is much larger than $^{3}J_{H_\alpha\text{-}11/H\text{-}12}$, as estimated from the intensity of the cross peaks in the DQF-COSY spectrum (double quantum filtered correlation spectrum), indicates that H_β-11 is *anti* to H-12. The relationship between C9 and C12 was therefore suggested to be 9*S**/12*R** through the double stereospecific assignments for H-9/H_2-10 and H_2-11/H-12.

Unlike the case for C9–C12, the relative configurations of C12, C13, and C14 were hardly assignable by NOE analysis

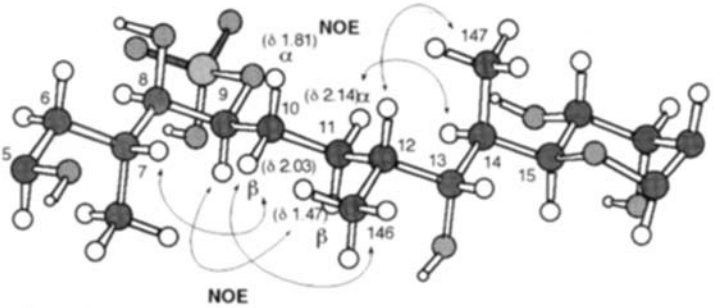

Fig. 1. Deduced conformation of the C1–C14 side chain of maitotoxin with the stereospecific assignments for H_2-10 and H_2-11. Double-headed arrows denote key NOEs necessary for deducing the conformation of the C8–C12 portion.

[*] Prof. Dr. K. Tachibana, Dr. M. Sasaki, N. Matsumori, T. Maruyama, T. Nonomura, Prof. Dr. M. Murata
Department of Chemistry, School of Science, The University of Tokyo
Hongo, Bunkyo-ku, Tokyo 113 (Japan)
Fax: Int. code + (3) 5800-6898
e-mail: ktachi@chem.s.u-tokyo.ac.jp
Prof. Dr. T. Yasumoto
Faculty of Agriculture, Tohoku University (Japan)

[**] This work was supported in part by a Grant-in-Aid from the Ministry of Education, Science and Culture, Japan.

because of the suggested presence of two alternating conformers.[7] Nevertheless, the relationship between C12 and C13 could be established based on the coupling constants $^{3}J_{H,H}$ and $^{2,3}J_{C,H}$, since unlike the NOEs these were obtained as the weighted average of those from both conformers. As shown in Figure 2, the small value of $^{3}J_{H\text{-}12/H\text{-}13}$ of 4.0 Hz revealed that the H-12/H-13 *gauche* conformer is dominant. The large $^{3}J_{C11/H\text{-}13}$ and small $^{2}J_{H\text{-}12/C13}$ values, which were determined by HETLOC spectra,[8] were indicative of the *anti* orientation of both C11/H-13 and H-12/13-OH, respectively (Fig. 2).[15a,9] The relationship

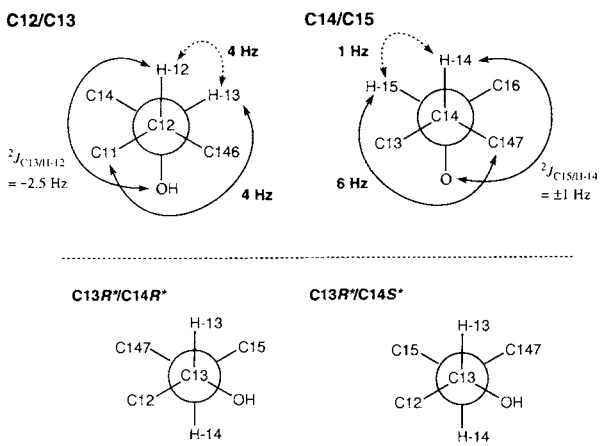

Fig. 2. Newman projections along the C12–C13 and C14–C15 bonds with vicinal H–H coupling constants ($^{3}J_{H,H}$, broken lines) and geminal/vicinal C–H coupling constants ($^{2,3}J_{C,H}$, solid lines), and Newman projections along the C13–C14 bonds of the two H-13 H-14-*anti* diastereomers. $^{2}J_{C,H}$ values are known to depend on the dihedral angle between a proton and an oxygen atom at the vicinal position and are thus utilized to deduce the rotational conformations between H-12/13-OH and H-14/15-O [9]. The value for $^{2}J_{C15,H\text{-}14}$ (±1 Hz) was obtained from phase-sensitive HMBC, in which the signs of coupling constants are not determined [6].

between C14 and C15 was unambiguously established by a similar method on the basis of coupling constants ($^{3}J_{H\text{-}14/H\text{-}15}$ = 1 Hz, $^{3}J_{C147/H\text{-}15}$ = 6 Hz, $^{2}J_{C15/H\text{-}14}$ = ±1 Hz). On the other hand, the relative configuration between C13 and C14 could not be assigned because of the dominant conformation with the *anti* H-13/H-14 orientation, in which the diastereomers are not distinguishable since in either case the implicated $^{3}J_{C,H\text{-}13}$ and $^{2,3}J_{C,H\text{-}14}$ couplings (due to H-13/C15, H-13/C147, H-14/C12, and H-14/13-OH) would have similar values for the *gauche* interactions (Fig. 2 bottom).

These data suggested the configuration of the side chain to be either **2A** or **2B**, in which the diastereomeric relationship is inverted at the C13–C14 bond. Thus, in order to assign this diastereomeric relationship, and also to confirm the relative configurations at C9, C12, and C13 as deduced from the NMR data, the diastereomeric fragments **2A** and **2B** were chosen to be

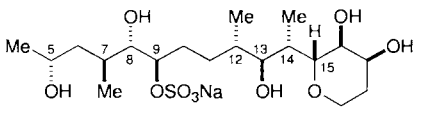

2A

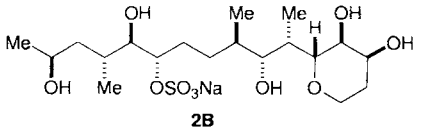

2B

synthesized for comparison of their NMR data with those of MTX.[4b] These fragments were designed also to incorporate the asymmetric centers whose configuration had already been determined (C5–C8 and C15–C17) so as to reproduce the ^{1}H and ^{13}C chemical shifts of the natural product.

The synthesis of aldehyde **7**, the left half of **2A**, started with methyl (*S*)-(+)-3-hydroxybutyrate ((*S*)-(+)-**3**) (Scheme 1),

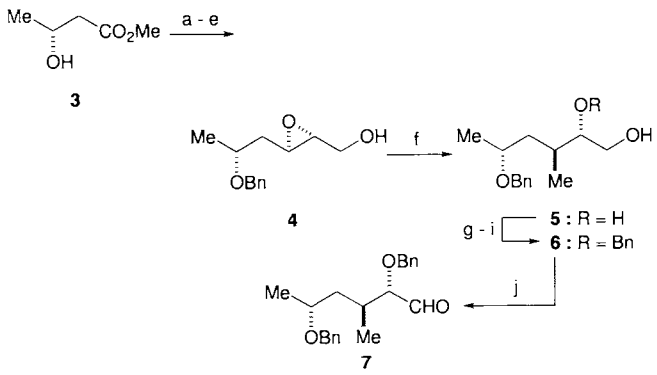

Scheme 1. Synthesis of aldehyde **7**. a) $BnOC(=NH)CCl_3$, TfOH (cat.), CH_2Cl_2/hexane (2/1), 0 °C, 84%; b) DIBAL-H, CH_2Cl_2, −78 °C; c) $Ph_3P{=}CHCO_2Me$, benzene, RT, 70% (two steps), d) DIBAL-H, CH_2Cl_2, −78 °C, 92%; e) *t*BuOOH, (−)-diethyl tartrate, $Ti(OiPr)_4$, CH_2Cl_2, 4 Å molecular sieves, −20 °C, 77%; f) $AlMe_3$, CH_2Cl_2/hexane (1/3), RT; g) MMTrCl, iPr_2NEt, CH_2Cl_2, RT, 62% (two steps); h) NaH, BnBr, DMF, RT; i) *p*TsOH (cat.), CH_2Cl_2/MeOH (1/1), RT, 72% (two steps); j) $(COCl)_2$, DMSO, Et_3N, CH_2Cl_2, −78 °C→RT. Bn = benzyl, TfOH = trifluoromethanesulfonic acid, DIBAL-H = diisobutylaluminum hydride, RT = room temperature, MMTr = *p*-methoxyphenyldiphenylmethyl, DMF = *N*,*N*-dimethylformamide, *p*TsOH = *p*-toluenesulfonic acid, DMSO = dimethylsulfoxide.

which was converted into epoxy alcohol **4** by the following sequence: 1) protection as its benzyl ether, 2) reduction with diisobutylaluminum hydride (DIBAL-H), 3) Wittig homologation, 4) reduction to the allylic alcohol, and 5) Sharpless asymmetric epoxidation.[10] The C7[11] methyl group was introduced by the regioselective opening of the epoxide ring with trimethylaluminum[12] to give *vic*-diol **5**. In this transformation the regioisomeric 1,3-diol was not produced. Routine protecting group manipulations allowed the conversion of **5** into primary alcohol **6**, which was oxidized under Swern conditions to give the desired aldehyde **7**. The enantiomer of **7** was synthesized from (*R*)-(−)-**3** analogously.

Elaboration of the vinyl iodide **15**, which corresponds to the right half of **2A**, started with optically active alcohol **8**[13] (Scheme 2). Swern oxidation of **8** followed by Wittig olefination and DIBAL-H reduction gave the allylic alcohol, which was subjected to Sharpless asymmetric epoxidation to furnish epoxy alcohol **9**. Treatment of **9** with trimethylaluminum[12] provided *vic*-diol **10** as a single regioisomer, which was then converted into allylic alcohol **11** by the three-step sequence of reactions comprising periodate oxidation, Horner–Emmons olefination, and DIBAL-H reduction. Sharpless asymmetric epoxidation of **11** and regioselective opening of the resulting epoxide **12** with lithium dimethylcuprate[14] gave 1,3-diol **13** (>90% regioselectivity), which was then transformed into the primary alcohol **14**. Swern oxidation of **14** and subsequent treatment of the resulting aldehyde with iodoform and $CrCl_2$[15] provided (*E*)-vinyl iodide **15**. Similarly, the diastereomeric iodide **18** was prepared from **11** via epoxy alcohol **16**, which was produced by use of the antipodal tartrate in the Sharpless epoxidation.

The crucial $NiCl_2/CrCl_2$-mediated coupling reaction[16] of **7** and **15** provided allylic alcohol **19** in 52% yield (based on **15**, Scheme 3) as a 1:1 mixture of diastereoisomers (500 MHz

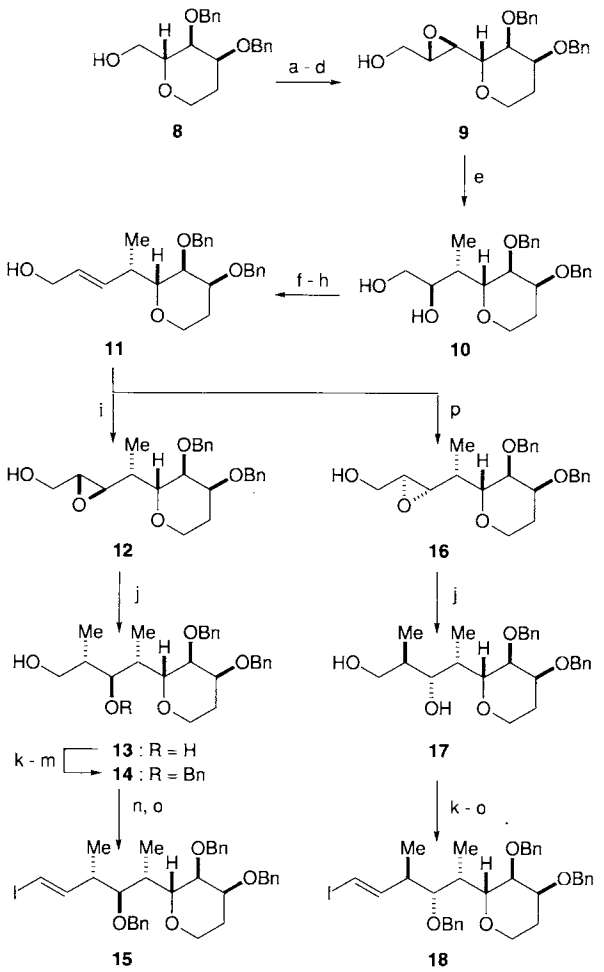

Scheme 2. Synthesis of diastereomeric vinyl iodides **15** and **18**. a) $(COCl)_2$, DMSO, Et_3N, CH_2Cl_2, $-78\,^{\circ}C \rightarrow RT$; b) $Ph_3P{=}CHCO_2Me$, benzene, RT, 73% (two steps); c) DIBAL-H, CH_2Cl_2, $-78\,^{\circ}C$, 88%; d) *t*BuOOH, (+)-diethyl tartrate, $Ti(O{i}Pr)_4$, CH_2Cl_2, 4 Å molecular sieves, $-20\,^{\circ}C$, 85%; e) $AlMe_3$, CH_2Cl_2/hexane (1/2), $0\,^{\circ}C$; f) $NaIO_4$, THF/H_2O (2/1), RT; g) $(iPrO)_2POCH_2CO_2Et$, *t*BuOK, THF, $-78\,^{\circ}C$, 68% (three steps); h) DIBAL-H, CH_2Cl_2, $-78\,^{\circ}C$, 96%; i) *t*BuOOH, (−)-diethyl tartrate, $Ti(O{i}Pr)_4$, CH_2Cl_2, 4 Å molecular sieves, $-20\,^{\circ}C$; j) Me_2CuLi, Et_2O, $-20\,^{\circ}C$, then $NaIO_4$, THF/H_2O (2/1), RT, 68% (three steps); k) TrCl, iPr_2NEt, DMAP (cat.), CH_2Cl_2, RT, 82%; l) NaH, BnBr, TBAI (cat.), DMF, RT; m) *p*TsOH (cat.), MeOH, RT, 82% (two steps); n) $(COCl)_2$, DMSO, Et_3N, CH_2Cl_2, $-78\,^{\circ}C$ to RT; o) CHI_3, $CrCl_2$, THF, $0\,^{\circ}C$, 77% (two steps); p) *t*BuOOH, (+)-diethyl tartrate, $Ti(O{i}Pr)_4$, CH_2Cl_2, 4 Å molecular sieves, $-20\,^{\circ}C$. Tr = triphenylmethyl, DMAP = 4-dimethylaminopyridine, TBAI = tetrabutylammonium iodide.

^{1}H NMR spectrum). Oxidation of **19** with pyridinium dichromate gave the α,β-unsaturated ketone, which was reduced with NaHTe[17] to afford ketone **20**. Chelation-controlled $Zn(BH_4)_2$ reduction of ketone **20** proceeded in a highly stereoselective manner[18] to yield the desired alcohol **21**. Finally, sulfation of **21** followed by ion exchange to give the sodium salt and hydrogenation of the benzyl ethers with $Pd(OH)_2$/C furnished the target compound **2A**. Diastereomer **2B** was synthesized analogously from the enantiomer of **7** and iodide **18**.

In the comparison of the ^{1}H and ^{13}C NMR data of **2A** and **2B** with those of MTX, the observed chemical shifts of **2A** clearly match those of MTX (Table 1) more closely. In particular, the δ_C values of C11, C13, and C147 in **2B** deviate from those of MTX by over 1 ppm, while the relevant values of **2A** (C9–C14, C146, and C147) match those of MTX within 0.5 ppm. Furthermore, $^3J_{H,H}$ data of the C7–C9 and C12–C15 portions of **2A** alone correspond well with the those of MTX (Table 2). These results unambiguously establish the configura-

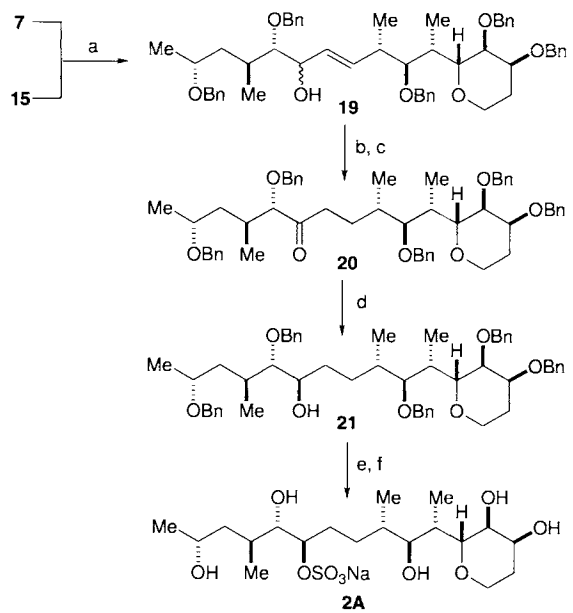

Scheme 3. Synthesis of compound **2A**. a) $CrCl_2$, $NiCl_2$ (cat.), DMSO, RT, 52%; b) PDC, 4 Å molecular sieves, CH_2Cl_2, RT, 91%; c) NaHTe, EtOH, RT, 79%; d) $Zn(BH_4)_2$, Et_2O, $-15\,^{\circ}C$, 94%; e) $SO_3{\cdot}NMe_3$, pyridine, RT, then ion exchange, quant.; f) H_2, $Pd(OH)_2$/C, MeOH, RT, quant. PDC = pyridinium dichromate.

Table 1. Selected ^{1}H and ^{13}C NMR chemical shifts of maitotoxin (MTX) and synthetic fragments **2A** and **2B** in [D_5]pyridine/[D_4]methanol (1/1).

Position	^{1}H NMR [a] MTX	2A	2B	Position	^{13}C NMR [b] MTX	2A	2B
7	2.35	2.14	2.14	7	33.1	33.0	33.1
8	3.93	3.93	3.94	8	77.7	77.7	77.7
9	4.73	4.71	4.71	9	81.5	82.0	81.8
10_α	1.81	1.77	1.80	10	28.6	28.3	28.0
10_β	2.03	1.97	2.02				
11_α	2.14	2.16	2.21	11	26.7	26.8	27.8
11_β	1.47	1.42	1.45				
12	1.66	1.63	1.68	12	37.0	37.1	37.1
13	3.50	3.43	3.51	13	78.8	78.8	80.5
14	2.30	2.29	2.28	14	35.8	35.4	35.5
15	4.29	4.20	3.88	15	74.8	75.7	79.9
145	1.04	0.97	0.97	145	17.4	17.5	17.6
146	0.98	0.94	0.85	146	18.0	17.8	17.1
147	0.93	0.92	1.03	147	11.0	11.0	8.0

[a] Relative to the signal of CHD_2OD ($\delta = 3.310$) [2b]. [b] Relative to the signal of $^{13}CD_3OD$ ($\delta = 48.94$) [2c]; assignment for C146 has been revised.

Table 2. Selected ^{1}H NMR coupling constants [Hz] for maitotoxin (MTX) and synthetic fragments **2A** and **2B** in [D_5]pyridine/[D_4]methanol (1/1).

	MTX	2A	2B
$^3J_{7,8}$	6.3	6.7	6.4
$^3J_{8,9}$	4.7	4.3	4.6
$^3J_{12,13}$	4.0	4.7	6.1
$^3J_{13,14}$	7.2	7.5	4.9
$^3J_{14,15}$	1.0	1.2	2.1

tional assignment of the C1–C15 acyclic chain of MTX as represented by structure **2A**: 5*R**, 7*R**, 8*R**, 9*S**, 12*R**, 13*R**, 14*R**, and 15*S**.[19]

Received: April 1, 1996 [Z89901E]
German version: *Angew. Chem.* **1996**, *108*, 1782–1785

Keywords: configuration determination · conformation · maitotoxin · natural products · NMR spectroscopy

[1] T. Yasumoto, R. Bagnis, J. P. Venoux, *Bull. Jpn. Soc. Sci. Fish.* **1976**, *42*, 359–365.

[2] a) M. Murata, H. Naoki, T. Iwashita, M. Sasaki, A. Yokoyama, T. Yasumoto, *J. Am. Chem. Soc.* **1993**, *115*, 2060–2062; b) M. Murata, H. Naoki, S. Matsunaga, M. Satake, T. Yasumoto, *ibid.* **1994**, *116*, 7098–7107; c) M. Satake, S. Ishida, T. Yasumoto, M. Murata, H. Utsumi, T. Hinomoto, *ibid.* **1995**, *117*, 7019–7020; d) A. Yokoyama, M. Murata, Y. Oshima, T. Iwashita, T. Yasumoto, *J. Biochem.* **1988**, *104*, 184–187.

[3] For a review, see F. Gusovsky, J. W. Daly, *Biochem. Pharmacol.* **1990**, *39*, 1633–1639.

[4] a) M. Sasaki, T. Nonomura, M. Murata, K. Tachibana, *Tetrahedron Lett.* **1994**, *35*, 5023–5026; b) M. Sasaki, T. Nonomura, M. Murata, K. Tachibana, *ibid.* **1995**, *36*, 9007–9010; c) M. Sasaki, N. Matsumori, M. Murata, K. Tachibana, T. Yasumoto, *ibid.* **1995**, *36*, 9011–9014.

[5] a) N. Matsumori, M. Murata, K. Tachibana, *Tetrahedron* **1995**, *51*, 12229–12238; b) N. Matsumori, T. Nonomura, M. Sasaki, M. Murata, K. Tachibana, M. Satake, T. Yasumoto, *Tetrahedron Lett.* **1996**, *37*, 1269–1272.

[6] For the phase-sensitive HMBC spectrum, ^{13}C-enriched MTX [2c] (ca. 4%, 9 mg) was used; the spectrum was recorded on a JEOL A-500 spectrometer (500 MHz). The pulse sequence proposed by D. G. Davis was used (*J. Am. Chem. Soc.* **1989**, *111*, 5466–5468). The acquisition data points were 2K (*F2*) vs. 512 (*F1*) and twofold zero-filling was carried out for each dimension to furnish the 2D spectrum with 4K (*F2*) and 1K (*F1*) data points. Digital resolution in the *F2* (^{1}H) dimension was 0.75 Hz.

[7] The major conformer is shown in Figure 1. In the minor conformer, C11 is thought to be *anti* to C14 along the C12–C13 bond, while C12 is *anti* to C147 along the C13–C14 bond.

[8] The HETLOC spectrum was measured with ^{13}C-enriched MTX (9 mg) on a JEOL A-500 spectrometer (500 MHz). The pulse sequence reported by U. Wollborn and D. Leibfritz (*J. Magn. Reson.* **1992**, *98*, 142–146) was used for the experiments. The data dimensions for acquisition and for 2D charts were the same as those for the HMBC spectrum [6].

[9] J. A. Schwarez, N. Cyr, A. S. Perlin, *Can. J. Chem.* **1975**, *53*, 1872–1875; for a review, see P. E. Hansen, *Prog. NMR Spectr.* **1981**, *14*, 175–296.

[10] a) T. Katsuki, K. B. Sharpless, *J. Am. Chem. Soc.* **1980**, *102*, 5974–5976; b) Y. Gao, R. M. Hanson, J. M. Klundder, S. Y. Ko, H. Masamune, K. B. Sharpless, *ibid.* **1987**, *109*, 5765–5780.

[11] The numbering of the compounds in this paper corresponds to that of maitotoxin.

[12] a) T. Suzuki, H. Saimoto, H. Tomioka, K. Oshima, H. Nozaki, *Tetrahedron Lett.* **1982**, *23*, 3597–3600; b) W. R. Roush, M. A. Adam, S. M. Peseckis, *ibid.* **1983**, *24*, 1377–1380.

[13] Compound **8** was prepared in ten steps from tri-*O*-acetyl-D-glucal: 1) H_2, Pd-C, EtOAc, RT; 2) NaOMe (cat.), MeOH, RT; 3) $PhCH(OMe)_2$, *p*TsOH (cat.), DMF, RT, 93% (three steps); 4) $(COCl)_2$, DMSO, Et_3N, CH_2Cl_2, −78 °C→RT; 5) L-Selectride, THF, −78 °C; 6) NaH, BnBr, DMF, RT, 74% (three steps); 7) *p*TsOH (cat.), MeOH, RT, 94%; 8) TrCl, Et_3N, DMAP (cat.), CH_2Cl_2, RT; 9) NaH, BnBr, DMF, RT; 10) *p*TsOH, MeOH, RT, quant. (three steps).

[14] M. R. Johnson, T. Nakata, Y. Kishi, *Tetrahedron Lett.* **1979**, 4343–4346.

[15] K. Takai, K. Nitta, K. Utimoto, *J. Am. Chem. Soc.* **1986**, *108*, 7408–7410.

[16] a) K. Takai, K. Kimura, T. Kuroda, T. Hiyama, H. Nozaki, *Tetrahedron Lett.* **1983**, *24*, 5281–5284; b) H. Jin, J. Uenishi, W. J. Christ, Y. Kishi, *J. Am. Chem. Soc.* **1986**, *108*, 5644–5646; c) K. Takai, K. Yagashira, T. Kuroda, K. Oshima, K. Uchimoto, H. Nozaki, *ibid.* **1986**, *108*, 6048–6050.

[17] a) M. Yamashita, Y. Kato, R. Suemitsu, *Chem. Lett.* **1980**, 847–848; b) D. H. R. Barton, W. McCombie, *J. Chem. Soc. Perkin Trans. 1* **1975**, 1574–1585.

[18] T. Nakata, T. Tanaka, T. Oishi, *Tetrahedron Lett.* **1983**, *24*, 2653–2656.

[19] The relative configuration was denoted in this way, although it is enantiomeric to **2A**, to be consistent with the absolute configuration in the following communication [20].

[20] T. Nonomura, M. Sasaki, N. Matsumori, M. Murata, K. Tachibana, T. Yasumoto, *Angew. Chem.* **1996**, *108*, 1786–1791; *Angew. Chem. Int. Ed. Engl.* **1996**, *35*, 1675–1678.

The Complete Structure of Maitotoxin, Part II: Configuration of the C135–C142 Side Chain and Absolute Configuration of the Entire Molecule**

Taro Nonomura, Makoto Sasaki, Nobuaki Matsumori, Michio Murata, Kazuo Tachibana,* and Takeshi Yasumoto

Maitotoxin (MTX, **1**; structural formula given in the preceding communication[1]) is one of the most intriguing natural products with extremely potent biological activity[1,2] and has thus attracted considerable attention. We have thus far succeeded in elucidating the relative configurations of most of the stereogenic carbon atoms in MTX; the assignment of those in the C1–C14 side chain is described in ref. [1]. In this communication we wish to report determination of the absolute configuration of MTX together with the relative configurations in the C135–C142 side chain, which results in completion of the full structural determination.

In a previous study we showed that MTX is cleaved by periodate oxidation into three pieces, the smallest of which is fragment C (3,4-dimethyl-6-hepten-1-ol) with a molecular mass of 142.[2,3] For determining the absolute configuration of this fragment, we decided to synthesize its four possible stereoisomers **2a–d** for comparison by chiral gas chromatography with fragment C obtained from the natural product. Preceding this, the relative configuration of the side chain attachment at C134 was determined with respect to the four stereogenic centers in the side chain (C135, C136, C138, and C139).

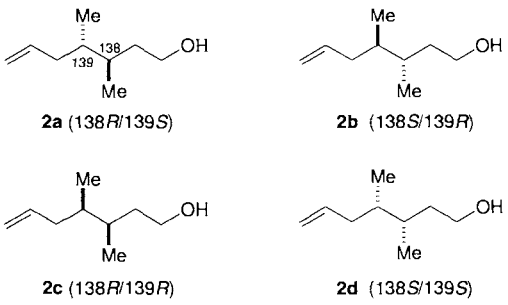

As described in the preceding communication,[1] the $^{2,3}J_{C,H}$ coupling constants provide essential information on the configuration of acyclic structures.[1,4] In the same manner the relationship between C136 and C138 could be unambiguously assigned (Fig. 1). A large value for $^3J_{H\text{-}136/H\text{-}137}$ (10 Hz) revealed the antiperiplanar relationship between H-136 and H-137 ($\delta = 1.76$), and a small value for $^2J_{C136/H-137}$ (−1 Hz) indicated 136-OH to take the *anti* position to H-137 ($\delta = 1.25$).[4,5]

[*] Prof. Dr. K. Tachibana, T. Nonomura, Dr. M. Sasaki, N. Matsumori, Prof. Dr. M. Murata
Department of Chemistry, School of Science, The University of Tokyo
Hongo, Bunkyo-ku, Tokyo 113 (Japan)
Fax: Int. code + (3) 5800-6898
e-mail: ktachi@chem.s.u-tokyo.ac.jp

Prof. Dr. T. Yasumoto
Faculty of Agriculture, Tohoku University (Japan)

[**] This work was supported in part by a Grant-in-Aid from the Ministry of Education, Science, and Culture of Japan, and by the Special Coordination Fund for Promoting Science and Technology from the Science and Technology Agency of Japan. We are grateful to Y. Kumaki and T. Hinomoto of JEOL for NMR measurements, and to Dr. M. Satake, Tohoku University, for preparation of ^{13}C-enriched maitotoxin.

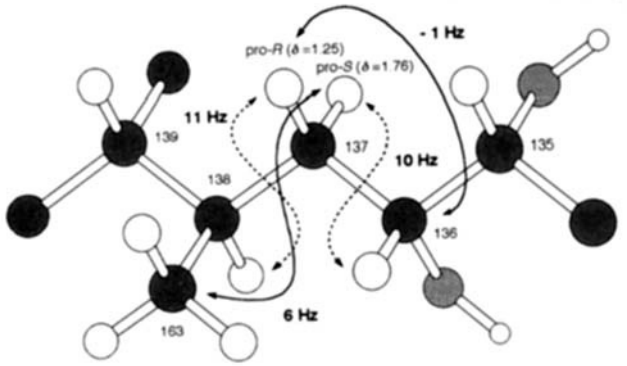

Fig. 1. The configuration and conformation of the C136–C139 portion of MTX deduced from the $^{2,3}J_{C,H}$ and $^{3}J_{H,H}$ couplings (marked with arrows).

These two relationships enabled us to determine the predominant rotational isomer with respect to the C136–C137 bond and thus to assign the prochiral protons on C137, namely, H-137$^{pro\text{-}R}$ at $\delta = 1.25$ and H-137$^{pro\text{-}S}$ at $\delta = 1.76$. We used this assignment and the analogous conformational analysis based on $^{3}J_{H\text{-}137^{pro\text{-}R}/H\text{-}138}$ and $^{3}J_{C163/H\text{-}137^{pro\text{-}S}}$ to identify the dominant rotamer around the C137–C138 bond and thus the relative configurations between C136 and C138 (Fig. 1).

The stereochemical relationships between C134, C135, and C136 were deduced in a similar manner from the results shown in Figure 2. However, NOEs together with the coupling constants $^{3}J_{H\text{-}134/H\text{-}135}$ and $^{3}J_{H\text{-}135/H\text{-}136}$, which deviate from typical values (2–3 Hz) for a *gauche* orientation, suggested that the C134–C136 portion assumes two conformations (Fig. 2), hence

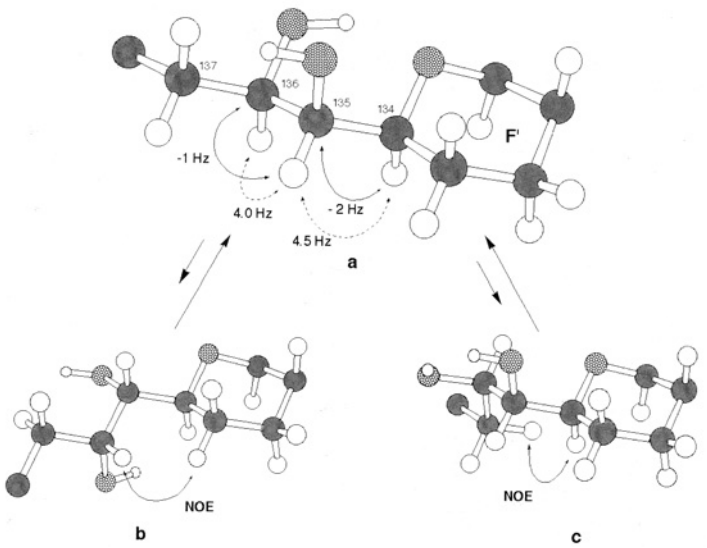

Fig. 2. Conformational changes in the C134–C137 side chain attached to the F' ring of MTX that were suggested by NOEs and $^{3}J_{H,H}$ coupling constants. a) The predominant conformer; b, c) two minor conformers with C–C *gauche* interactions at bonds C134–C135 and C135–C136, respectively.

obscuring unequivocal configurational assignment. To remove this ambiguity, we proceeded to synthesize a fragment representing this portion of MTX with the proposed configurations; the $^{2}J_{C,H}$ and $^{3}J_{H,H}$ values of this synthetic fragment would then be compared with those of MTX.

The synthesis of model compound **3** started with the optically active alcohol **4**[6] (Scheme 1), which was oxidized to the aldehyde and subjected to Wittig reaction to give the α,β-unsaturated ester **5**. Asymmetric dihydroxylation of **5** with AD-mix β, which contains 1,4-bis(10,11-dihydro-7-*O*-quinidine)phthalazine as the chiral ligand,[7,8] provided a 6:1 ratio of products in favor of the desired diastereomer **7**, although the intrinsic diastereofacial preferences of **5** and the ligand used were "mismatched". Improved and reversed selectivity was obtained in the same reaction with the use of AD-mix α, containing the pseudo-enantiomeric ligand; diol **6** was then the major product with a diastereoselectivity of >10:1, thereby indicating that the stereoselectivity was controlled by the chirality of the reagent rather than that of **5**. After protection of the mixture of diols as acetonides, pure diastereoisomer **8** was separated by silica gel chromatography. Diisobutylaluminum hydride (DIBAL-H) reduction of **8** followed by Wittig homologation gave the α,β-unsaturated ester **9**, which was converted into alcohol **10** in three steps. Removal of the hydroxyl group in **10** via the phenyl thionocarbonate ester[9] and acid hydrolysis of the acetonide furnished the target compound **3** (Table 1). As shown in Table 2,[10] the $^{2}J_{C,H}$ and $^{3}J_{H,H}$ values of **3** agreed very well with those of MTX, verifying not only the deduced configuration but the presence of two conformers for the C134–C136 portion (Fig. 2).

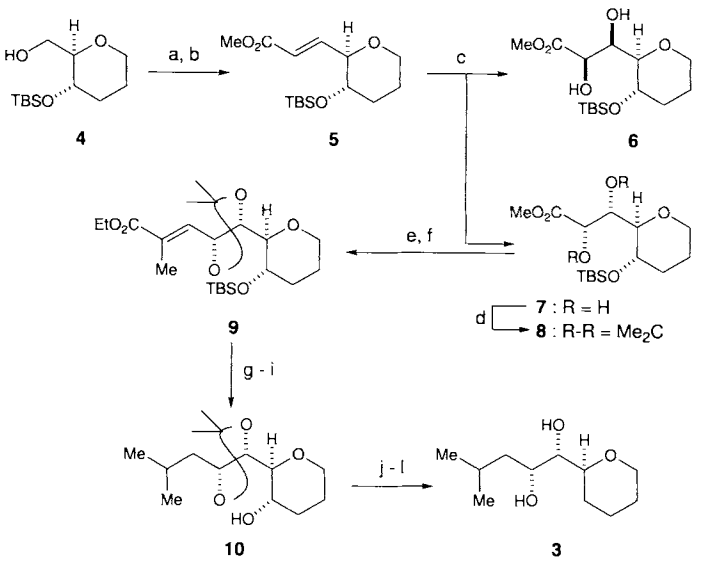

Scheme 1. Synthesis of model compound **3**. a) SO_3·pyridine, Et_3N, DMSO/CH_2Cl_2 (1/5), 0 °C; b) $Ph_3P{=}CHCO_2Me$, toluene, 80 °C, quant. (two steps); c) AD-mix β, OsO_4 (cat.), $MeSO_2NH_2$, *t*BuOH/H_2O (1/1), RT, 75% (**6**:**7** = 1:6); d) CSA (cat.), $Me_2C(OMe)_2$, CH_2Cl_2, RT, then separation, 46%; e) DIBAL-H, CH_2Cl_2, −78 °C; f) $Ph_3P{=}C(Me)CO_2Et$, toluene, 80 °C, quant. (two steps); g) $LiAlH_4$, THF, 0 °C; h) TBAF, THF; i) H_2, Pd/C, EtOAc/MeOH (1/1), RT, 86% (three steps); j) PhOC(S)Cl, DMAP, pyridine/CH_2Cl_2 (2/1), 50 °C; k) *n*Bu_3SnH, AIBN (cat.), toluene, 80 °C; l) CF_3CO_2H, MeOH, RT, 16% (three steps). DMSO = dimethylsulfoxide, RT = room temperature, CSA = camphorsulfonic acid, DIBAL-H = diisobutylaluminum hydride, TBAF = tetrabutylammonium fluoride, DMAP = 4-dimethylaminopyridine, AIBN = 2,2'-azobisisobutyronitrile.

At this point the only diastereomeric relationship not known in the whole molecule was that between C138 and C139 because the broadened signals of H-138 and H-139 (seven-spin systems) hampered the measurement of $^{3}J_{C,H}$ and $^{3}J_{H,H}$. Therefore, in order to determine this relative configuration and the absolute configuration, the four possible stereoisomers **2a–d** were synthesized.[10] Preparation of the the *anti* isomers **2a** (138*R*/139*S*) and **2b** (138*S*/139*R*) relied on the Sharpless epoxidation, and that of the *syn* isomers **2c** (138*R*/139*R*) and **2d** (138*S*/139*S*) on the enantioselective Diels–Alder reaction. Both asymmetric reactions provided the products with about 90% enantiomeric excess, thereby securing the validity of the absolute configurations of the four isomers.

 © VCH Verlagsgesellschaft mbH, D-69451 Weinheim, 1996 0570-0833/96/3515-1676 $ 15.00+.25/0

Table 1. Selected NMR data for compounds **2a**, **2c**, and **3** [a].

2a: ^{1}H NMR (500 MHz): δ = 5.67 (ddt, J = 17, 10, 7 Hz, 1H, H-141 [10]), 4.90 (br. d, J = 17 Hz, 1H, H-142), 4.88 (br. d, J = 10 Hz, 1H, H-142), 3.65 (ddd, J = 11, 8, 5.5 Hz, 1H, H-136), 3.55 (ddd, J = 11, 7.5, 7 Hz, 1H, H-136), 2.00 (m, 1H, H-140), 1.69 (m, 1H, H-140), 1.61 (m, 1H, H-137), 1.53 (m, 1H, H-138), 1.34 (m, 1H, H-139), 1.24 (m, 1H, H-137), 0.75 (d, J = 7 Hz, 3H, H-163), 0.71 (d, J = 7 Hz, 3H, H-164); ^{13}C NMR (125 MHz): δ = 139.1, 115.9, 61.2, 38.7, 38.6, 36.7, 34.5, 17.0, 16.4

2c: ^{1}H NNR (500 MHz): δ = 5.65 (ddt, J = 17, 10, 7 Hz, 1H, H-141 [10]), 4.90 (br. d, J = 17 Hz, 1H, H-142), 4.87 (br. d, J = 10 Hz, 1H, H-142), 3.63 (ddd, J = 10, 7.6, 5.8 Hz, 1H, H-136), 3.57 (dt, J = 10, 6.7 Hz, 1H, H-136), 1.94 (m, 1H, H-140), 1.75 (m, 1H, H-140), 1.62–1.52 (m, 2H, H-138, H-137), 1.42–1.28 (m, 2H, H-139, H-137), 0.68 (d, J = 6.7 Hz, 3H, H-163), 0.66 (d, J = 7 Hz, 3H, H-164); ^{13}C NMR (125 MHz): δ = 139.1, 115.8, 61.0, 40.4, 38.7, 37.8, 33.7, 14.7, 14.6

3: ^{1}H NMR (500 MHz): δ = 3.86 (m, 1H, H-130$_{eq}$ [10]), 3.81 (ddd, J = 9.2, 4.0, 3.7 Hz, 1H, H-136), 3.46 (ddd, J = 10.7, 5.2, 2.4 Hz, 1H, H-134), 3.28 (dd, J = 5.2, 3.7 Hz, 1H, H-135), 3.28 (m, 1H, H-130$_{ax}$), 1.83 (m, 1H, H-138), 1.68 (m, 1H, H-132), 1.59 (m, 1H, H-137), 1.56 (m, 1H, H-133), 1.48 (m, 1H, H-133), 1.46–1.26 (m, 4H, H-131, H-132, H-137, H-131), 0.83 (d, J = 6.7 Hz, 6H); ^{13}C NMR (125 MHz): δ = 80.3, 77.6, 70.2, 69.1, 43.7, 28.6, 26.9, 25.3, 24.12, 24.07, 22.4

[a] Recorded in [D_5]pyridine/[D_4]methanol (1/1).

Table 2. Comparison of the $^2J_{C,H}$ and $^3J_{H,H}$ values [Hz] of MTX and fragment **3**.

Position	MTX	**3**	Position	MTX	**3**
$^2J_{C134,H-135}$	−1	−1	$^3J_{H-134,H-135}$	5	5
$^2J_{C135,H-134}$	−2	−2	$^3J_{H-135,H-136}$	4	4
$^2J_{C135,H-136}$	0	0	$^3J_{H-136/H-137pro-R}$	3	4
$^2J_{C136,H-135}$	−1	−1	$^3J_{H-136,H-137pro-S}$	10	9

In the synthesis of **2a** (Scheme 2) starting with allylic alcohol **11**,[11] which was readily prepared from 3-butenol, Sharpless asymmetric epoxidation[12] afforded alcohol **12**. Treatment of **12** with trimethylaluminum[13] provided *vic*-diol **13** as a single regioisomer, which was then converted into epoxy alcohol **14** in four-step sequence comprising 1) periodate oxidation, 2) Wittig homologation, 3) DIBAL-H reduction, and 4) Sharpless asymmetric epoxidation. The epoxide ring opening of **14** with trimethylaluminum was expected to proceed regio- and stereoselectively to provide the *syn*-dimethylated isomer **16**. However, an approximately 7:3 mixture of *vic*-diols resulted; the unexpected *anti*-dimethylated isomer **15** predominated as indicated by the alternative synthesis of **16** described later. After purification of the mixture by column chromatography, the major isomer **15**[14] was converted into olefin **17** and thence to the (138*R*,139*S*) isomer **2a** (Table 1) by routine synthetic operations. The enantiomer of **2a** (**2b**) was prepared by the same route except the enantiomeric tartrate was used in the Sharpless epoxidation.

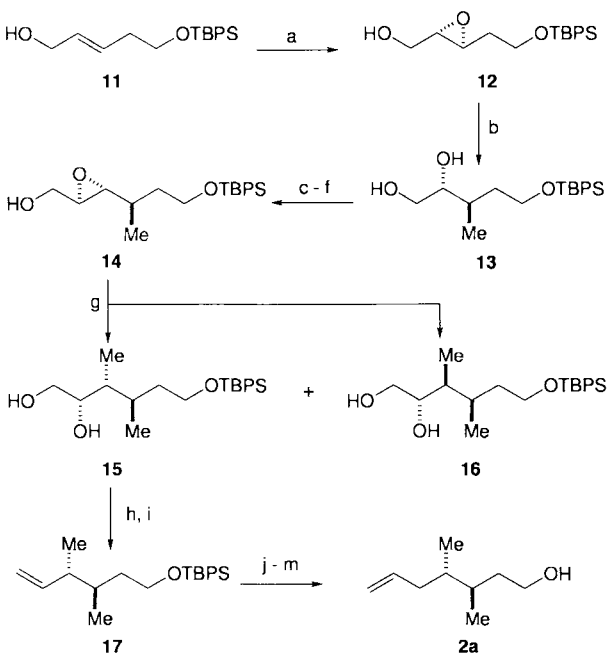

Scheme 2. Synthesis of the (138*R*,139*S*) isomer **2a**. a) *t*BuOOH, Ti(O*i*Pr)$_4$, (+)-diethyl tartrate, CH_2Cl_2, 4 Å molecular sieves, −20 °C, 62%; b) $AlMe_3$, hexane, 0 °C, 97%; c) $NaIO_4$, THF/H_2O (2/1), RT; d) $Ph_3P{=}CHCO_2Me$, benzene, 70 °C; e) DIBAL-H, CH_2Cl_2, −78 °C; f) *t*BuOOH, Ti(O*i*Pr)$_4$, (+)-diethyl tartrate, CH_2Cl_2, 4 Å molecular sieves, −20 °C, 78% (four steps); g) $AlMe_3$, hexane, 0 °C, 69% (**15**:**16** = 7:3); h) $NaIO_4$, THF/H_2O (1/1), RT; i) CH_2I_2, $TiCl_4$, Zn, THF, RT; j) 9-BBN, THF, RT, then 30% H_2O_2, 3 M NaOH, RT; k) SO_3·pyridine, Et_3N, DMSO/CH_2Cl_2 (1/5), 0 °C; l) $Ph_3P^+CH_3Br^-$, LiHMDS, THF, 0 °C, 17% (four steps); m) TBAF, THF, RT. 9-BBN = 9-borabicyclononane. LiHMDS = lithium bis(trimethylsilyl)amide.

To confirm the configurations assigned for **2a** and **2b** unambiguously, the (138*R*,139*R*) isomer **2c** was synthesized by the more established synthetic route (Scheme 3), instead of that originally intended from **16**. The synthesis began with the known optically active diol (−)-**18**, which was prepared by the Diels–Alder reaction of di-(+)-menthyl fumarate with 1,3-butadiene and subsequent lithium aluminum hydride reduction.[15,16] Iodination of **18** followed by catalytic osmylation gave *vic*-diol **19**, which was converted into diol **20** by a three-step sequence: 1) reductive deiodination, 2) oxidative cleavage of the *vic*-diol, and 3) sodium borohydride reduction. Monosilylation of **20**, oxidation to the aldehyde, Wittig methylenation, and desilylation furnished the desired (138*R*,139*R*) isomer **2c** (Table 1). The (138*S*,139*S*) isomer **2d** was synthesized analogously from the (+)-**18**.

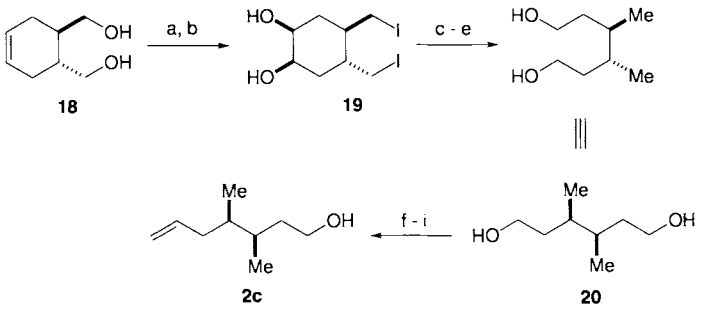

Scheme 3. Synthesis of the (138*R*,139*R*) isomer **2c**. a) I_2, Ph_3P, imidazole, benzene, RT, 58%; b) OsO_4 (cat.), NMO, THF/H_2O (2/1), RT, 99%; c) nBu_3SnH, AIBN, toluene, 80 °C, quant.; d) $NaIO_4$, THF/H_2O (2/1), RT; e) $NaBH_4$, MeOH, 0 °C, 83% (two steps); f) *t*BuPh$_2$SiCl, imidazole, DMF, RT, 43%; g) SO_3·pyridine, Et_3N, DMSO/CH_2Cl_2 (1/4), 0 °C; h) $Ph_3P^+CH_3Br^-$, NaHMDS, THF, 0 °C, 90% (two steps); i) TBAF, THF, RT. NMO = 4-methylmorpholine *N*-oxide, DMF = *N*,*N*-dimethylformamide, NaHMDS = sodium bis(trimethylsilyl)amide.

The stereoisomers were separated completely by chiral gas chromatography.[17] Fragment C was prepared from MTX (50 μg) by treatment with $NaIO_4$ and then with $NaBH_4$.[2] The product was extracted with hexane and analyzed by GC-MS under the same conditions.[17] The extract gave a single peak in the gas chromatogram at 13 min 52 s; the retention time and mass spectrum for that peak are identical with those of the (138*R*,139*S*) isomer **2a** (Fig. 3). Thus we successfully determined the absolute configuration of the C135–C142 side chain as 134*S*, 135*S*, 136*R*, 138*R*, and 139*S*, which leads to the complete structure of MTX **1**[18] (Scheme 4; please note that the absolute configuration of **1** is different from that drawn in our previous publications[2,3]).

Received: April 1, 1996 [Z8991IE]
German version: *Angew. Chem.* **1996**, *108*, 1786–1789

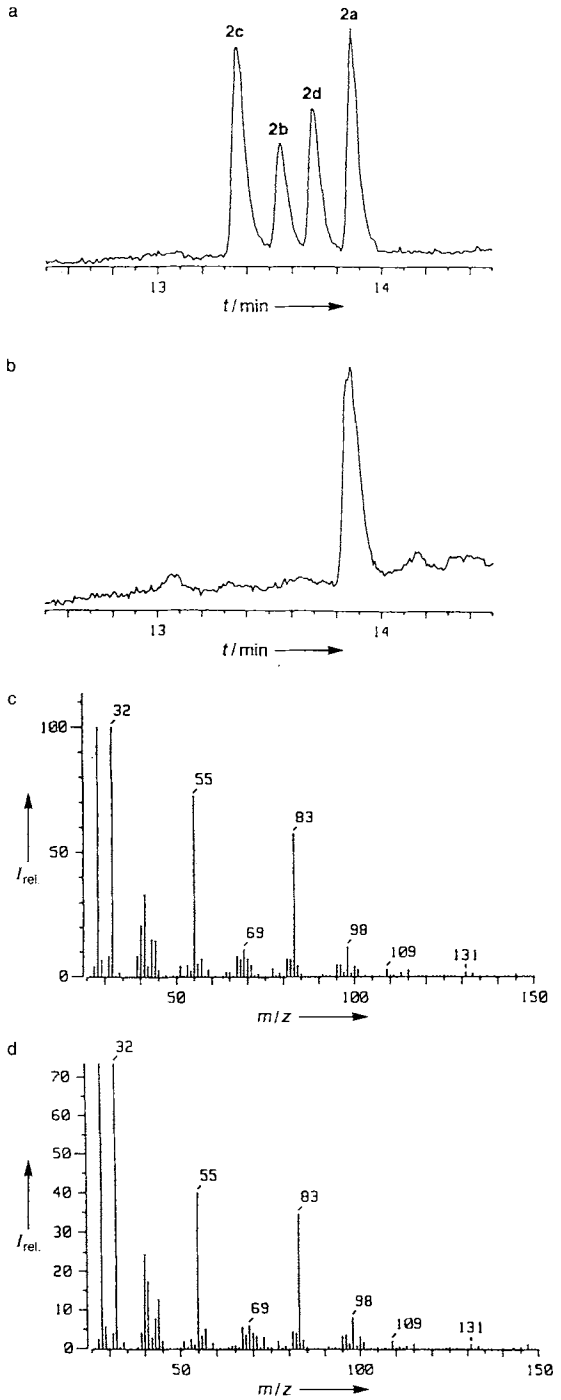

Fig. 3. Gas chromatograms (chiral column) [17] of **2a–d** (a) and of fragment C (b); mass spectra of **2a** (c) and fragment C (d).

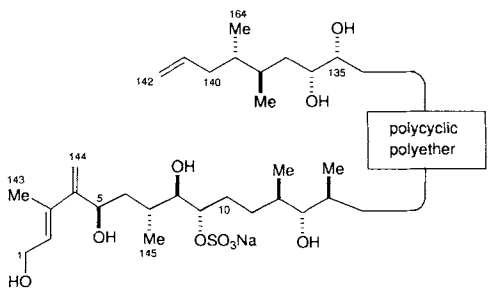

Scheme 4. The two side chains of MTX and the correct absolute configuration (the complete structure of the polycyclic polyether is given in the preceding communication [1]).

Keywords: asymmetric syntheses · maitotoxin · natural products · NMR spectroscopy · structure elucidation

[1] M. Sasaki, N. Matsumori, T. Maruyama, T. Nonomura, M. Murata, K. Tachibana, T. Yasumoto, *Angew. Chem.* **1996**, *108*, 1782–1785; *Angew. Chem. Int. Ed. Engl.* **1996**, *35*, 1672–1675.
[2] M. Murata, H. Naoki, S. Matsunaga, M. Satake, T. Yasumoto, *J. Am. Chem. Soc.* **1994**, *116*, 7098–7107.
[3] M. Sasaki, N. Matsumori, M. Murata, K. Tachibana, T. Yasumoto, *Tetrahedron Lett.* **1995**, *36*, 9011–9014.
[4] N. Matsumori, M. Murata, K. Tachibana, *Tetrahedron* **1995**, *51*, 12229–12238.
[5] Vicinal C–H coupling constants ($^3J_{C,H}$) are known to depend on the dihedral angle between the proton and an oxygen atom on the vicinal carbon; when the proton is antiperiplanar to the oxygen (as is the case for H-137^{pro-R} and 136-OH in Figure 1), $^3J_{C,H}$ is about -1 to -2 Hz; in the *gauche* orientation, the value is about -4 to -6 Hz; J. A. Schwarcz, N. Cyr, A. S. Perlin, *Can. J. Chem.* **1975**, *53*, 1872–1875; For a review, see P. E. Hansen, *Prog. NMR Spectr.* **1981**, *14*, 175–296.
[6] K. C. Nicolaou, C.-K. Hwang, B. E. Marron, S. A. DeFrees, E. A. Couladouros, Y. Abe, P. J. Carroll, J. P. Snyder, *J. Am. Chem. Soc.* **1990**, *112*, 3040–3054.
[7] K. B. Sharpless, W. Amberg, Y. L. Bennani, G. A. Crispino, J. Hartung, K. S. Jeong, H. L. Kwong, K. Morikawa, Z. M. Wang, D. Xu, X. L. Zhang, *J. Org. Chem.* **1992**, *57*, 2768–2771; for a review, see H. C. Kolb, M. S. Van Nieuwenhze, K. B. Sharpless, *Chem. Rev.* **1994**, *94*, 2483–2547.
[8] Since osmylation of **5** was very slow under the standard asymmetric dihydroxylation conditions (0.2–0.4 mol% of Os), the amount of Os was increased to ca. 4 mol% by the addition of OsO_4 and a dramatic increase of the reaction rate was realized.
[9] M. J. Robins, J. S. Wilson, F. Hansske, *J. Am. Chem. Soc.* **1983**, *105*, 4059–4065.
[10] The numbering of compounds **2** and **3** in this paper corresponds to that of maitotoxin.
[11] Compound **11** was prepared from 3-buten-1-ol by the following sequence of reactions: 1) *t*BuPh$_2$SiCl, imidazole, DMF, RT, quant.; 2) O_3, CH_2Cl_2, -78 °C, then Me_2S, -78 °C → RT; 3) $Ph_3P{=}CHCO_2Et$, benzene, 60 °C, 75 % (two steps); 4) DIBAL-H, CH_2Cl_2, -78 °C, 84 %.
[12] a) T. Katsuki, K. B. Sharpless, *J. Am. Chem. Soc.* **1980**, *102*, 5974–5976; b) Y. Gao, R. M. Hanson, J. M. Klunder, S. Y. Ko, H. Masamune, K. B. Sharpless, *ibid.* **1987**, *109*, 5765–5780.
[13] a) T. Suzuki, H. Saimoto, H. Tomioka, K. Oshima, H. Nozaki, *Tetrahedron Lett.* **1982**, *23*, 3597–3600; b) W. R. Roush, M. A. Adam, S. M. Peseckis, *ibid.* **1983**, *24*, 1377–1380.
[14] Compound **15** was still contaminated with roughly 10 % of the undesired diastereomer **16** after chromatographic separation, and this 9:1 mixture was used without further purification in the subsequent reactions.
[15] C. H. Heathcock, B. R. Davis, C. R. Hadley, *J. Med. Chem.* **1989**, *32*, 197–202.
[16] K. Furuta, K. Iwanaga, H. Yamamoto, *Tetrahedron Lett.* **1986**, *27*, 4507–4510.
[17] Chiral GC column: Chirasil-DEX CB, Chrompack, 0.25 mm × 25 m; gas chromatograph: HP5890, Hewlett Packard; mass spectrometer: JMS-SX 102, JEOL. The column temperature was kept at 90 °C for the first 10 min and then raised by 10 °C min^{-1} to 190 °C.
[18] The complete relative configuration of maitotoxin given here has also been determined independently by synthetic methods: Y. Kishi et al., personal communication.

Diastereoselective C–C Bond Formation with Nonracemic Planar-Chiral η^2-Manganese Complexes**

Dieter Schinzer* and Heiko Bärmann

We report here for the first time the enantioselective preparation of planar-chiral η^2-manganese complexes and their use in diastereoselective C–C bond forming reactions.[1] In the racemic series we have already described diastereoselective alkylations and aldol reactions with η^2-manganese complexes.[2, 3]

[*] Prof. Dr. D. Schinzer, Dipl.-Chem. H. Bärmann
Institut für Organische Chemie der Technischen Universität
Hagenring 30, D-38106 Braunschweig (Germany)
Fax: Int. code +(531)391-5386
e-mail: d.schinzer@tu-bs.de

[**] This work was supported by the Deutsche Forschungsgemeinschaft (DFG) and by the Fonds der Chemischen Industrie. We also thank Schering AG, Berlin, for generous gifts of chemicals.

We have now successfully prepared these complexes enantioselectively and also utilized the reactions in the nonracemic (enantiomerically enriched) series. Bromocyclopentenone (**1**) is easily reduced to the racemic cyclopentenol *rac*-**2**,[4, 5] which reacts with an immobilized lipase (Novozym 435, *candida antarctia*) to (*S*)-**2** in 45% yield (94% *ee*) and to the corresponding acetate (*R*)-**2'** in 46% yield (94% *ee*).[6, 7] Conversion of (*S*)-**2** with *tert*-butyllithium produces (*S*)-**3** in 69% yield ($[\alpha]_D^{20} = +29.3$ ($c = 1.1$ in $CHCl_3$)).[8] The (*S*)-cyclopentenol (*S*)-**3** was then treated with the $[Mn(MeCp)(CO)_2]\cdot THF$ complex (formed in situ photochemically) to form the chiral η^2-manganese complex (*S,S*)-**4** ($[\alpha]_D^{20} = +31.0$ ($c = 0.5$ in benzene) by *syn* addition in 25% yield (50% conversion).[2, 3, 9] The oxidation of this material with tetra-*n*-propylammonium perruthenate (TPAP) as catalyst and *N*-methylmorpholine-*N*-oxide (NMO) as oxidant[10] delivered the planar-chiral η^2-manganese complex (*S*)-**5** in 90% yield ($[\alpha]_D^{20} = +78.8$ ($c = 0.5$ in benzene)).[11, 12] This oxidation is remarkable because η^2-manganese fragments are particularly sensitive towards oxidation. With the majority of modern oxidation systems tested in the course of this work, the only product obtained was a manganese dioxide.

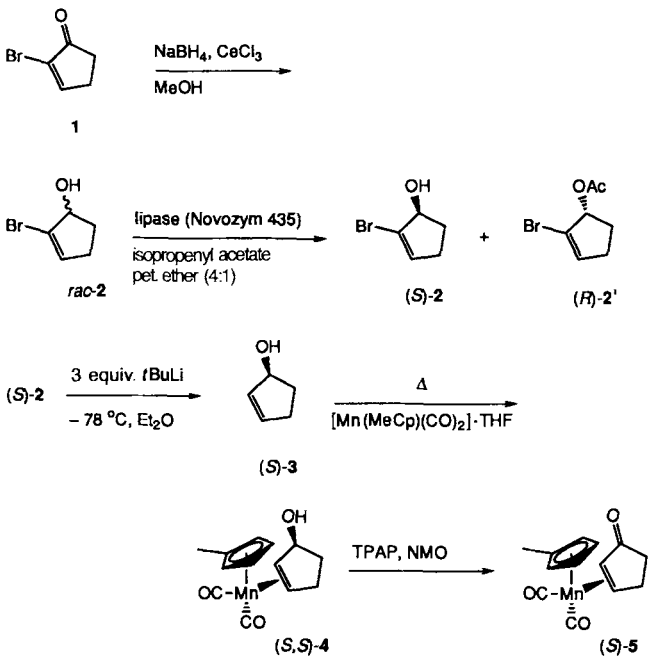

The complex (*S*)-**5** can be deprotonated in situ with lithium diisopropylamide (LDA) in THF at $-78\,^{\circ}C$, under conditions of kinetic control, to give the enolate (*S*)-**5a**, which can be transformed diastereoselectively with alkylating agents:[2, 13] the enolate reacts exclusively on the side away from the metal atom (the *exo* side) to give the manganese complex **6**.[13] In all the examples investigated, the 100 MHz ^{13}C NMR spectrum of **6** displayed signals arising from only one diastereomer. This stereochemical result could be unambiguously determined by a crystal structure analysis from the racemic series.[2] The manganese fragment was oxidatively cleaved by warming in acetonitrile in the presence of air. The product was the alkylated α-chiral cyclopentenone **7**, which is not easily accessible by other methods.[14] The *ee* values of **7** were determined by gas chromatography on the chiral stationary phase Lipodex E (Table 1). (*S*)-**7** (R = Ph) was the only example in which enantiomers did not separate; nevertheless, the *ee* value is expected to be at least as high as that for (*R*)-**7** (R = Me, allyl), since also in the 100 MHz ^{13}C NMR spectrum of (*S,S*)-**6** (R = Bn) only one diastereoisomer was detected.

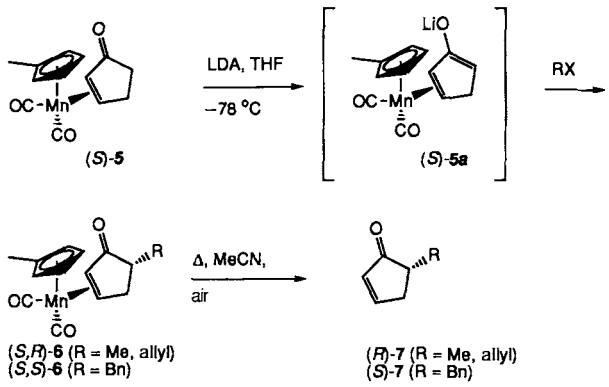

Kinetically controlled aldol reactions can be carried out analogously.[3, 13] Stereoselective aldol reactions are extremely important C–C bondforming reactions. The conversion of cyclic lithium enolates with good diastereoselectivity is particularly difficult.[15] For this reason, we investigated, for the first time, the asymmetric aldol reaction using planar, chiral η^2-manganese complexes. In this case, too, the desired *anti* aldol products **8** are obtained exclusively with a high degree of optical purity. Mild demetalation in acetonitrile in the presence of air affords the *anti* aldol product **9**. The *ee* value of (*S,R*)-**9** (R = Ph) could not be measured by gas chromatography (Lipodex E), even after derivatization to a camphanic acid ester,[16] which yielded elimination products. Nevertheless, one

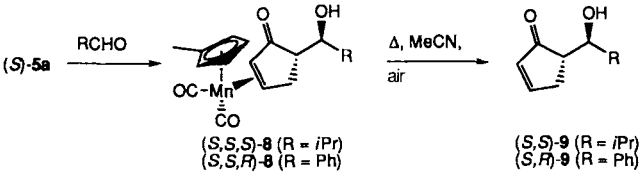

Table 1. Alkylations and aldol reaktions with the planar-chiral manganese complex (*S*)-**5** [a].

Manganese complex	$[\alpha]_D^{20}$ (*c* in benzene)	Yield [%]	Product	$[\alpha]_D^{20}$ (*c* in $CHCl_3$)	*ee* [%]	Yield [%]
(*S,R*)-**6** (R = Me)	−119.8 (1.0)	59	(*R*)-**7** (R = Me)	+41.5 (0.85)	85[b]	44
(*S,S*)-**6** (R = Bn)	−149.4 (0.5)	55	(*S*)-**7** (R = Bn)	+91.0 (0.8)	– [c]	63
(*S,R*)-**6** (R = allyl)	−103.3 (1.0)	41	(*R*)-**7** (R = allyl)	+67.5 (0.8)	85[b]	66
(*S,S,R*)-**8** (R = Ph)	−284.0 (0.5)	52	(*S,R*)-**9** (R = Ph)	−7.98 (1.05)	– [c]	75
(*S,S,S*)-**8** (R = *i*Pr)	−194.4 (1.0)	65	(*S,S*)-**9** (R = *i*Pr)	+7.35 (0.34)	88[b]	75

[a] 94% *ee*. [b] Determined by gas chromatography (baseline separation) with the chiral stationary phase Lipodex E (Macherey-Nagel, Düren). [c] The *ee* value could not be determined. The 100 MHz ^{13}C NMR spectra of (*S,S*)-**6** (R = Bn) and (*S,S,R*)-**8** (R = Ph), however, show signals from only one diastereomer.

can assume that the *ee* value is very high in this reaction, since the 100 MHz ^{13}C NMR spectrum of (*S,S,R*)-**8** (R = Ph) shows signals from only one diastereoisomer.

We can therefore access interesting synthetic building blocks in high optical yield using this new method of asymmetric C–C bond formation. In this way the principle of diastereoselective complexation of a temporarily chirally modified ligand[1] is used for enantioselective preparation of the chiral η^2-enone–manganese complex **5**, from which, after diastereoselective conversion and decomplexation, chiral, nonracemic, synthetically useful products can be obtained. Further investigations are currently underway, which focus predominantly on the use of functionalized alkylating reagents, as well as reactions at the carbonyl group of the planar-chiral enone–metal complex.

Experimental Procedure

(*R*)-**7** (R = allyl): *n*-Butyllithium (515 μL, 0.77 mmol, 1.5 M in hexane) was added dropwise to a solution of diisopropylamine (101 μL, 0.77 mmol) in THF (5 mL) at 0 °C. The resulting solution was stirred for 30 min at 0 °C. This LDA solution was then added dropwise over a period of 10 min to a solution of (*S*)-**5** (150 mg, 0.55 mmol) in THF (5 mL), precooled to −78 °C. After addition, the solution was stirred for 2 h at −78 °C. Finally allyl bromide (67 μL, 0.77 mmol) was added, and the solution allowed to warm to 0 °C over a period of about 12 h. The reaction mixture was concentrated on a rotary evaporator, and the components separated by flash chromatography with diethyl ether as eluent. Yield: 70 mg of (*S,R*)-**6**, yellow powder (41 %). $[\alpha]_D^{20} = -103$ (*c* = 1.0 in benzene); ^1H NMR (400 MHz, C_6D_6): δ = 5.65 (br., 1H), 4.93 (2H), 3.91 (1H), 3.73–3.67 (4H), 3.30 (1H), 2.66–2.52 (2H), 2.21 (1H), 1.98 (1H), 1.78 (1H), 1.24 (s, 3H); ^{13}C NMR (100 MHz, C_6D_6; * = quaternary C, + = CH_2, − = CH, CH_3): δ = 233.6 (*), 232.7 (+), 214.7 (*), 136.6 (−), 116.2 (+), 101.2 (*), 85.3 (−), 85.2 (−), 84.5 (−), 84.2 (−), 67.3 (−), 53.9 (−), 40.8 (−), 34.8 (+), 33.7 (+), 12.1 (−); IR (KBr): $\tilde{\nu}$ = 1965 (s), 1904 (s), 1699 (s), 1457 (w), 1175 (w), 917 (w), 601 (m), 573 (m) cm^{-1}; MS (CI, NH_3): *m/z* (%): 313 (9) [M^+ + H], 256 (4), 140 (44) [NH_4^+ + enone], 123 (100) [enone$^+$ + H].

(*S,R*)-**6** (R = allyl) (62 mg, 0.198 mmol) was dissolved in acetonitrile (5 mL), and the yellow solution heated under reflux for 1 h. It was then allowed to cool, and air was introduced into the flask through a needle for 20 min at room temperature. The brown precipitate that formed was separated by filtration, and the solvent removed on a rotary evaporator. After flash chromatography with pentane/diethyl ether (1/1) as eluent, 16 mg (*R*)-**7** (R = allyl) was obtained in the form of a colorless oil (66 % yield). $[\alpha]_D^{20} = +67.5$ (*c* = 0.8 in $CHCl_3$); 85 % *ee* (GC, Lipodex E); ^1H NMR (400 MHz, $CDCl_3$) : δ = 7.69 (dt, 1H, *J* = 2.6, 5.7 Hz), 6.18 (m, 1H), 5.75 (m, 1H), 5.06 (2H), 2.83 (dm, 1H, *J* = 19.3 Hz), 2.55 (m, 1H), 2.45–2.38 (2H), 2.19–2.11 (1H); ^{13}C NMR (100 MHz, $CDCl_3$): δ = 211.6 (*), 163 (−), 135.2 (−), 133.8 (−), 116.8 (+), 43.9 (−), 35.2 (+), 34.8 (+).

Received: February 26, 1996 [Z 8870 IE]
German version: *Angew. Chem.* **1996**, *108*, 1825–1827

Keywords: aldol reactions · alkylations · asymmetric syntheses · manganese compounds

[1] Examples of planar-chiral η^6-, η^4-, and η^3-complexes: H. G. Schmalz, B. Millies, J. W. Bats, G. Dürner, *Angew. Chem.* **1992**, *104*, 640; *Angew. Chem. Int. Ed. Engl.* **1992**, *31*, 631; H.-J. Knölker, H. Herrmann, *ibid.* **1996**, *108*, 363 and **1996**, *35*, 341; D. Enders, S. von Berg, B. Jandeleit, *Synlett* **1996**, 18.
[2] D. Schinzer, T. Blume, R. U. Rojas-Wahl, *Synlett*, **1994**, 297.
[3] D. Schinzer, T. Blume, M. Woltering, *Synlett* **1994**, 1045.
[4] C. J. Kowalski, A. E. Weber, A. W. Fields, *J. Org. Chem.* **1982**, *47*, 5089.
[5] F. E. Ziegler, A. Nangia, G. Schulte, *J. Am. Chem. Soc.* **1987**, *109*, 3987.
[6] C. R. Johnson, H. Sakaguchi, *Synlett* **1992**, 813.
[7] A. Wahhab, D. F. Tovares, A. Rauk, *Can. J. Chem.* **1990**, *68*, 1559.
[8] X. Zhou, P. J. De Clercq, *Tetrahedron: Asymmetry* **1995**, *6*, 1551.
[9] A. M. Rosan, *J. Chem. Soc. Chem. Commun.* **1981**, 311.
[10] W. G. Griffith, S. V. Ley, G. P. Withcombe, A. D. White, *J. Chem. Soc. Chem. Commun.* **1987**, 1625.
[11] The absolute configuration of (*S*)-**5** was determined by conversion of the aldol product (*S,S*)-**9** to the diastereomeric Mosher esters **a** und **b** and determination of the ^1H NMR shift differences in the spectra of these compounds (I. Ohtain, Kusumi, Y. Kashman, H. Kakisawa, *J. Am. Chem. Soc.* **1991**, *113*, 4092), since we could decide the absolute configuration of (*S,S*)-**9** based on that of (*S*)-**5**. Thus, (*S,S*)-**9** (R = *i*Pr) was treated with (*R*)-(−)-α-methoxy-α-trifluoromethylphenylacetyl chloride to give **a** and with (*S*)-(+)-α-methoxy-α-trifluoromethylphenyl acetyl chloride to give **b**. The ^1H NMR signals were assigned with the H-H COSY experiments. **a**: ^1H NMR (400 MHz, $CDCl_3$): δ = 7.57 (m, 2H; H15, H19), 7.43–7.36 (m, 4H; H3, H16–H18), 6.05 (dt, 1H, *J* = 2.1, 5.8 Hz; H2), 5.16 (dd, 1H, *J* = 8.3, 3.9 Hz; H6), 3.52 (d, 3H, *J* = 1.2 Hz; H13), 2.81–2.77 (m, 1H; H5), 2.74–2.66 (dm, 1H, *J* = 19.1 Hz; H4), 2.42–2.33 (m, 2H; H4′, H7), 0.95 (d, 3H, *J* = 6.8 Hz; H8/9), 0.88 (d, 3H, *J* = 6.8 Hz; H8/9); ^{13}C NMR (100 MHz, $CDCl_3$): δ = 207.3 (*; C1), 166.5 (*; C10), 162.6 (−; C3), 134.4 (−); C2), 131.7 (*; C11/14), 131.6 (*; C11/14), 129.6 (−), 128.4 (−), 127.6 (−) (C15–C19), 122 (*; C12), 81.6 (−; C6), 55.5 (−; C13), 45.3 (−; C5), 32.8 (+; C4), 29.6 (−; C7), 19.5 (−; C8/9), 18.8 (−; C8/9). **b**: ^1H NMR (400 MHz, $CDCl_3$): δ = 7.56 (m, 2H; H15, H19), 7.41–7.36 (m, 4H; H3, H16–H18), 6.12 (dt, 1H, *J* = 2.0, 5.9 Hz; H2), 5.18 (dd, 1H, *J* = 8.3, 3.7 Hz; H6), 3.49 (d, 3H, *J* = 1.0 Hz; H13), 2.84–2.76 (m, 2H; H4, H5), 2.53–2.47 (m, 1H; H4′), 2.41–2.32 (m, 1H; H7), 0.91 (d, 3H, *J* = 6.8 Hz; H8/9), 0.81 (d, 3H, *J* = 6.9 Hz; H8/9); ^{13}C NMR (100 MHz, $CDCl_3$): δ = 207.2 (*; C1), 166.4 (*; C10), 162.6 (−; C3), 134.4 (−; C2), 131.7 (*; C11/14), 131.6 (*; C11/14), 129.5 (−), 128.3 (−), 127.6 (−) (C15–C19), 122 (*; C12), 81.4 (−; C6), 55.3 (−; C13), 45.4 (−; C5), 32.8 (+; C4), 29.5 (−; C7), 19.4 (−; C8/9), 18.5 (−; C8/9); shift differences: $\delta_S - \delta_R = \delta$(**b**) − δ(**a**): 0.07 (H2), 0.1 (H4), 0.11 (H4′), 0.03 (H5), −0.04 (H8/9), −0.07 (H8/9).
[12] Nomenclature of the configuration of planar-chiral complexes: G. Paiaro, A. Panunzi, *J. Am. Chem. Soc.* **1964**, *86*, 5148; G. Helmchen in *Houben-Weyl, Vol. 21a* (Eds.: G. Helmchen, R. W. Hoffmann, J. Mulzer, E. Schaumann), Thieme, Stuttgart, **1995**, p. 33.
[13] All new compounds were fully characterized with standard methods.
[14] M. Göres, E. Winterfeldt, *J. Chem. Soc. Perkin 1* **1994**, 3525.
[15] J. S. Panek, O. A. Bula, *Tetrahedron Lett.* **1988**, *29*, 1661.
[16] Y. Hu, H. Ziffer, *J. Chromatogr.* **1989**, *482*, 227.

Absolute Configurations of the Inhalation Anesthetics Isoflurane and Desflurane

Volker Schurig,* Markus Juza, Bernard S. Green, Jörg Horakh, and Arndt Simon*

The chiral inhalation anesthetics isoflurane (2-chloro-2-(difluoromethoxy)-1,1,1-trifluoro-ethane, **1**) and desflurane (2-(difluoromethoxy)-1,1,1,2-tetrafluoroethane, **2**) are clinically administered as synthetic racemic mixtures, although the stereoselective interaction of pure isoflurane enantiomers with neuronal ion channels implies the role of proteins of the central nervous system for anesthetic action.[1, 2] In the patent literature, both the (*R*) and (*S*) enantiomers of **1** and **2** (*ee* ≥ 80 %) are astoundingly claimed to be associated with less adverse effects than the racemic mixtures.[3, 4] Both documents fail to identify the enantiomers by their sign of optical rotation.[3, 4] According to another patent, (+)-**2** possesses more favorable pharmacological properties than the (−)-enantiomer or the racemate.[5] The knowledge of the absolute configurations of the commercially important haloethers **1** and **2** is therefore of general interest.

[*] Prof. Dr. V. Schurig, Dipl.-Chem. M. Juza
Institut für Organische Chemie der Universität
Auf der Morgenstelle 18, D-72076 Tübingen (Germany)
Fax: Int. code + (7071) 296257
e-mail: volker.schurig@uni-tuebingen.de
Prof. Dr. A. Simon, Dr. J. Horakh
Max-Planck-Institut für Festkörperforschung
Heisenbergstrasse 1, D-70569 Stuttgart (Germany)
Telefax: Int. code + (711) 6891642
Prof. B. S. Green, PhD
Department of Pharmaceutical Chemistry
The Hebrew University of Jerusalem, Jerusalem (Israel)

[**] V.S. thanks the Deutsche Forschungsgemeinschaft and the Fonds der Chemischen Industrie for support of this work. V. S. and B. S. G. thank The Institute of Advanced Studies at the Hebrew University, Jerusalem, for providing research facilities. We thank Professor I. Agranat and Dipl-Chem. U. Biedermann, Jerusalem, for valuable discussions and Mr. G. J. Nicholson and Mr. E. Braun, Tübingen, for assistence in the maintainance of the preparative gas chromatograph (Model APG 402, Hupe).

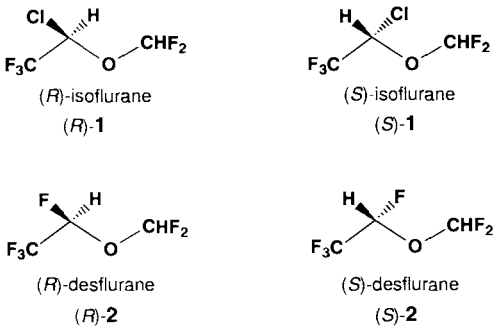

Polavarapu et al. determined the absolute configurations of **1** and **2** by vibrational circular dichroism (VCD) in the infrared region between 1400–700 cm^{-1}. Firstly, the conformations of the haloethers **1** and **2** were optimized by ab initio calculations, and afterwards the vibrational frequencies and circular dichroism intensities of the two lowest energy conformers were calculated. The theoretical spectra were then presented as the sum of the spectra of the conformers and compared with the experimental VCD spectra of the pure enantiomers of **1** and **2**. Polavarapu et al. assigned the (*S*)-configuration to dextrorotatory isoflurane, (+)-(*S*)-**1** (VCD),[6], and the (*R*)-configuration to dextrorotatory desflurane, (+)-(*R*)-**2** (VCD).[7] Although for **1** and **2** a conformer equilibrium of 80:20 and 85:15, respectively, had been calculated, a 50:50 conformer population was used for a better fit between the theoretical and experimental spectra.

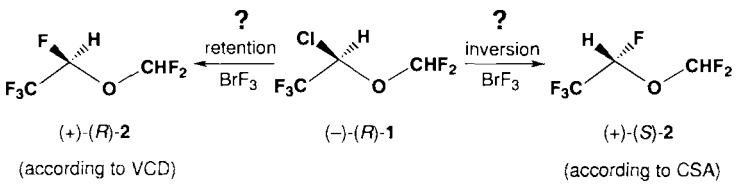

Moreover, the experimental spectra were not recorded in the gas phase but in solution (**1** in CS_2, **2** in $CDCl_3$). Isomer (+)-**2** was synthesized from (−)-**1** with the expected inversion of configuration (Walden inversion) on substituting chlorine with fluorine by using BrF_3 in the solvent Br_2.[5] In light of the absolute configuration assignment by VCD, this substitution was later reinterpreted as proceeding with retention of configuration.[8]

In this journal, the decarboxylation of (+)-(*R*)-1-methoxytetrafluoropropanoic acid [(+)-(*R*)-**3**] to (−)-(*S*)-1,2,2,2,-tetrafluoroethyl methyl ether [(−)-(*s*)-**4**] was proposed to proceed

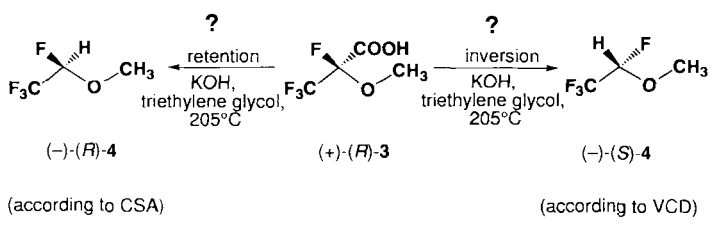

with complete inversion of configuration. The surprising stereochemical course of this reaction was based exclusively on the VCD assignment of the subsequent product desflurane as (−)-(*S*)-**2** (VCD).[9, 10]

Based on the absolute configuration assigned by VCD, the gas chromatographic elution order of the enantiomers of **1** (and two congeners) on several cyclodextrin derivatives was given as (*S*) before (*R*) while that of the enantiomers of **2** (and two congeners) was given as (*R*) before (*S*) (Table 6 in Ref. [11]). In addition, based on the absolute configuration assigned by VCD, the NMR-spectroscopic low-field shift of the proton signals of the enantiomers of **1** (and two congeners) in the presence of several cyclodextrin derivatives was greater for (*R*) than for (*S*), whereas that of the enantiomers of **2** (and two congeners) was reversed ((*S*)>(*R*), Table 6 in Ref. [11]).

The pure enantiomers of **1** and **2** can be isolated by preparative gas chromatography on two γ-cyclodextrin derivatives;[12, 13] the dextrorotatory enantiomers are always eluted first and the levorotatory enantiomers second.[12] From thermodynamic measurements it was concluded that the enantiomers of **1** and **2** with identical absolute configuration and differing only in the haloatom at the stereogenic center, possess the same sign of optical rotation and the same elution order in contrast to the chiroptical assignment (VCD).[12]

Determining the absolute configuration of **2** by anomalous dispersion of X-rays was considered impossible because the highly volatile ether was suspected to be noncrystallizable,[7] and indeed, it failed for the less volatile **1**.[2] In the present work the dextrorotatory (sodium D line) enantiomers of isoflurane, (+)-**1**, and desflurane, (+)-**2**, each obtained by preparative gas chromatography as the first fraction,[12] were investigated with X-ray crystallography. From both compounds single crystals could be grown, which were suitable for the crystal structure analysis (CSA) at −180 °C.

As seen in Figure 1 both dextrorotatory enantiomers possess the (*S*)-configuration.[16] Thus, the chiroptical assignment of dextrorotatory isoflurane as (+)-(*S*)-**1** (VCD) is confirmed,

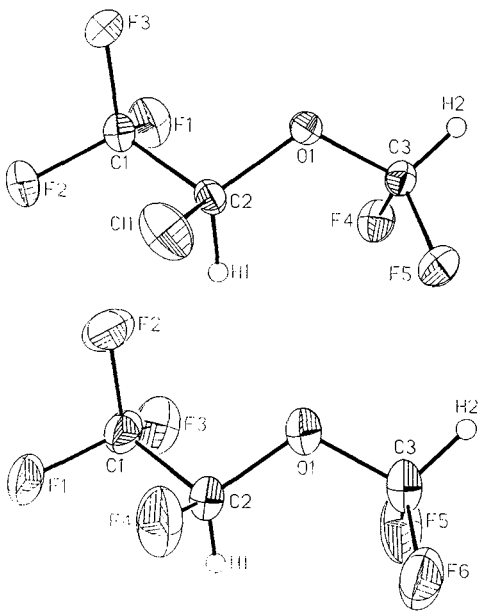

Fig. 1. Molecular structure of (+)-(*S*)-**1** (top) and (+)-(*S*)-**2** (bottom) at −180 °C; displacement ellipsoids for 50% probability; the size of the hydrogen atoms is arbitrary.

while the chiroptical assignment of dextrorotatory desflurane as (+)-(*R*)-**2** (VCD) must be revised as (+)-(*S*)-**2** (CSA). Due to the absence of heavy atoms and the low anomalous diffraction difference of the atoms hydrogen and fluorine at the stereogenic center, the determination of the absolute configuration for **2** is somewhat ambiguous. Yet, the Flack-parameter[17] of **2**[16] supports the (+)-(*S*) configuration. This result is in agreement with the following conclusions:

- Enantiomers of **1** and **2** with the same sign of optical rotation possess identical absolute configurations.
- Enantiomers of **1** and **2** with identical absolute configurations exhibit the same gas-chromatographic elution order (*S*) before (*R*) on γ-cyclodextrin derivatives (derived from D-glucose).[12]
- Enantiomers of **1** and **2** with identical absolute configurations exhibit the same NMR-spectroscopic, low-field shift of the proton resonances [(*R*)>(*S*)] on γ-cyclodextrin derivatives (derived from D-glucose).[18]
- Enantiomers of **1** and **2** are transformed into each other with inversion of configuration (Walden inversion) by halogen exchange (e.g., BrF_3 in the solvent Br_2).[5]
- (+)-(*R*)-1-Methoxytetrafluoropropanoic acid (**3**) is transformed into (−)-1,2,2,2,-tetrafluoroethyl methyl ether (**4**) with retention of configuration, and the ether possesses the (*R*) and not the (*S*) configuration.[9, 10]

The revised assignment of the absolute configuration of **2** (and of congeners[11]) has consequences for the CAS-numbering, patent literature, and the stereochemical course of reactions.[8–11]

Experimental Procedure

The sign of the optical rotation of **1** and **2** is based on the sodium D line at 20 °C (at other wavelengths no change of the sign of optical rotation was observed).

a) *Preparative enantiomer separations:* (+)-**1** (*ee*>99.9%) and (+)-**2** (*ee*=80.8%) were obtained by preparative gas chromatography on octakis (3-*O*-butanoyl-2,6-di-*O*-*n*-pentyl)-γ-cyclodextrin [15] dissolved in the polysiloxane SE-54 [12]. The enantiomers were checked before crystal sample preparation by analytical enantioselective gas chromatography for enantiomeric purity and elution order to preclude fortuitous errors.

b) *Crystal sample preparation:* An X-ray-capillary (0.2 mm diameter) was filled to a length of 1 cm by dipping its open end into the liquid. The sample was kept cold on a dry-ice block, and the capillary was sealed on both sides. Investigations with the modified Guinier technique [14] did not show any evidence of a phase transition, in the case of (+)-**2** between −185 °C and the melting point at −126 °C. (+)-**1** could not be investigated with the Guinier camera because of delayed crystallization accompanied by the destruction of the capillary.

c) *Crystal growth:* Single crystals of (+)-**1** and (+)-**2** were grown in situ on a Syntex $P2_1$ four-circle diffractometer. After cooling to a temperature below −110 °C (+)-**1** crystallized as a colorless powder. Annealing for several hours 1–2 °C below the melting point at −98 °C resulted in larger crystallites. While the temperature was carefully increased in steps of 0.1–0.2 °C, the extensive melting of a crystallite could be monitored by the decrease of a strong reflection to 1/20 of the original value of its intensity. After repeated cycles of partial melting and slow cooling, rotation and oscillation photographs showed the formation of a suitable single crystal, which could be cooled for X-ray analysis down to −180 °C without undergoing a phase transition. The growth of a single crystal of (+)-**2** was succesful by the method described above for (+)-**1** at a correspondingly lower temperature. The melting point of a (+)-**2** sample, considered to be enantiomerically pure, was −126 °C.

Received: March 1, 1996 [Z 8890 IE]
German version: *Angew. Chem.* **1996**, *108*, 1814–1816

Keywords: configuration determination · inhalation anesthetics

[1] a) N. P. Franks, W. R. Lieb, *Science* **1991**, *254*, 427–430; b) R. Matthews, *ibid.* **1992**, *255*, 156–157; c) N. P. Franks, R. Dickerson, W. R. Lieb, *Conf. Pap. Fluorine Med. 21st Century* (Manchester) **1994**, No. 16; d) N. P. Franks, W. R. Lieb, *Nature* **1994**, *367*, 607–614; e) E. J. Moody, B. D. Harris, P. Skolnick, *Trends Pharmacol. Sci.* **1994**, *15*, 387–391.

[2] C. G. Huang, L. A. Rozov, D. F. Halpern, G. G. Vernice, *J. Org. Chem.* **1993**, *58*, 7382–7387.

[3] J. W. Young, S. Brandt (Sepracor, Inc.), US-A 5114714, **1992** [*Chem. Abstr.* **1992**, *117*, 83458].

[4] J. W. Young, S. Brandt (Sepracor, Inc.), US-A 5114715, **1992** [*Chem. Abstr.* **1992**, *117*, 83459].

[5] L. A. Rozov, C. Huang, D. F. Halpern, G. G. Vernice (Anaquest, Inc.), US-A 5283372, **1994** [*Chem. Abstr.* **1994**, *120*, 322740].

[6] P. L. Polavarapu, A. L. Cholli, G. Vernice, *J. Am. Chem. Soc.* **1992**, *114*, 10953–10955.

[7] P. L. Polavarapu, A. L. Cholli, G. Vernice, *J. Phar. Sci.* **1993**, *82*, 791–793.

[8] a) "Organofluorine Compounds in Medical Chemistry and Biomedical Applications": D. F. Halpern, *Stud. Org. Chem. (Amsterdam)* **1993**, *48*, 125; b) *Conf. Pap. Fluorine Med. 21st Century* (Manchester) **1994**, No. 15.

[9] K. Ramig, L. Brockunier, P. W. Rafalko, L. A. Rozov, *Angew. Chem.* **1995**, *107*, 254–255; *Angew. Chem. Int. Ed. Engl.* **1995**, *34*, 222–223.

[10] L. A. Rozov, P. W. Rafalko, S. M. Evans, L. Brockunier, K. Ramig, *J. Org. Chem.* **1995**, *60*, 1319–1325. See also ref. [28] of this publication.

[11] K. Ramig, A. Krishnaswami, L. A. Rozov, *Tetrahedron* **1996**, *52*, 319–330. This work contains conclusions that we had already verified [12].

[12] V. Schurig, M. Juza, H. Grosenick, *Rec. Trav. Chim. Pays-Bas* **1995**, *114*, 211–219.

[13] D. U. Staerk, A. Shitangkoon, G. Vigh, *J. Chromatogr. A* **1994**, *663*, 79–85.

[14] A. Simon, *J. Appl. Crystallogr.* **1971**, *4*, 138–145.

[15] W. A. König, R. Krebber, P. Mischnick, *J. High Resolut. Chromatogr.* **1989**, *12*, 732–738.

[16] Data collection was performed for both compounds on a Syntex $P2_1$ diffractometer with graphite monochromator. a) Crystal data for (+)-**1**: space group: $P6_1$ (No. 169); a = 699.97(10), c = 2182.91(78) pm, $\rho_{ber.}$ = 1.985 g cm^{-3} at a recording temperature of −180 °C; Z = 6, $Ag_{K\alpha}$ irradiation, structure solution with direct methods [19], refinement with SHELXL-93 [20], $wR2$ = 0.159 and $R1$ = 0.049 for all 2732 data with 4 ≤ 2θ ≤ 54° and 100 refined parameters; Flack-parameter [17]: x = 0.04(10) for the conformation described above and 0.96(10) for the inverted configuration in the enantiomorphous space group $P6_5$. b) Crystal data for (+)-**2**: space group $P2_1$ (No. 4); a = 454.97(8), b = 793.68(18), c = 762.75(11) pm, β = 92.510(13)°, $\rho_{ber.}$ = 2.028 g cm^{-3} at the recording temperature at −180 °C; Z = 2, $Mo_{K\alpha}$ irradiation, structure solution with direct methods [19], refinement with SHELXL-93 [20], $wR2$ = 0.112 and $R1$ = 0.045 for all 2621 data with 4 ≤ 2θ ≤ 72° and 100 refined parameters; Flack-parameter [17]: x = −0.24(48) for the configuration described above and 1.24(48) for the inverted configuration. c) Crystallographic data (excluding structure factors) for the structure(s) reported in this paper have been deposited with the Cambridge Crystallographic Data Centre as supplementary publication no. CCDC-179-65. Copies of the data can be obtained free of charge on application to The Director, CCDC, 12 Union Road, Cambridge CB2 1EZ, UK (fax: int. code + (1223) 336-033; e-mail: teched@chemcrys.cam.ac.uk).

[17] x = 0 for the correct configuration, x = 0.5 for both configurations (racemic mixture), and x = 1 for the inverted configuration: G. Bernadelli, H. D. Flack, *Acta Crystallogr. Sect. A* **1985**, 500–511.

[18] Our investigations showed that both enantiomers (−)-**1** and (−)-**2**, eluted as the second peak in GC, exhibited a stonger down-field shift in the ^{1}H NMR spektrum in the presence of octakis(3-*O*-butanoyl-2,6-di-*O*-*n*-pentyl)-γ-cyclodextrin.

[19] G. M. Sheldrick, SHELXTL-PLUS, *Structure Determination Software*, Nicolet Instruments, Madison, WI (USA), **1990**.

[20] G. M. Sheldrick, SHELXL-93, Göttingen, **1993**.

Influence of Anchor Lipids on the Homogeneity and Mobility of Lipid Bilayers on Thin Polymer Films

Dierk Beyer, Gunther Elender, Wolfgang Knoll, Martin Kühner, Steffen Maus, Helmut Ringsdorf,* and Erich Sackmann

Supported phospholipid bilayers were first described by McConnell et al.[1] and are supposed to be ideal systems for investigations on incorporated membrane proteins and are expected to form the basis for future biosensors.[2] They allow application of a variety of methods for the investigation of biomembranes that are restricted to planar surfaces,[3] which are generally not applicable for known model membranes.

[*] Prof. Dr. H. Ringsdorf, Dipl.-Chem. D. Beyer
Institut für Organische Chemie der Universität
J.-J.-Becher Weg 18–22, D-55099 Mainz (Germany)
Fax: Int. code + (6131) 393145
Prof. Dr. W. Knoll, Dipl.-Chem. S. Maus
Max-Planck-Institut für Polymerforschung, Mainz (Germany)
Dipl.-Phys. G. Elender, Dipl.-Phys. M. Kühner, Prof. Dr. E. Sackmann
Institut für Biophysik der Technische Universität München (Germany)

A variety of techniques such as vesicle fusion, Langmuir–Blodgett transfer, and self-assembly can be applied on very different surfaces to establish planar model membranes.[4–9] Nevertheless, such systems are not ideally suited for investigations on membrane-spanning proteins,[1, 10, 11] because their mobility is limited due to friction with the substrate,[12, 13] which ultimately disturbs the conformation and therefore the function of the protein.[14]

Thus, an insulating barrier is required between the lipid bilayer and the substrate. This cushion layer may be achieved by using a water-swellable thin polymer layer (whose function is comparable to that of the cytoskeleton of the cell), which is covalently linked to the substrate, upon which the lipid bilayer is deposited.[15] A representation of a model biomembrane based on a polymer-supported lipid bilayer is presented in Figure 1.

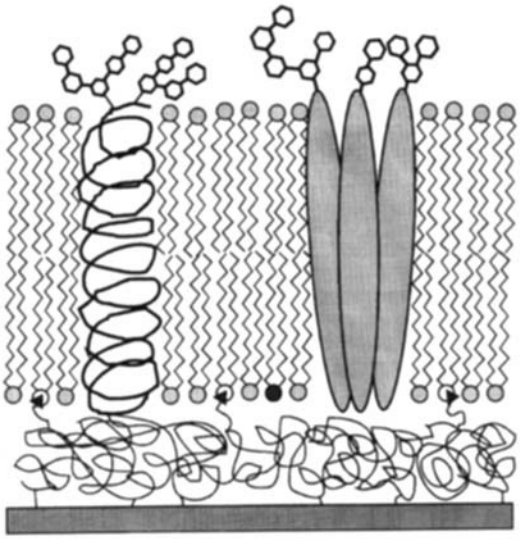

Fig. 1. Representation of a polymer-supported biomembrane (tethered supported bilayer) with membrane-spanning proteins.

The realization of such model systems still poses problems. It is still difficult to obtain homogeneous and fluid bilayers on polymer films that display long-term stability. In this communication we present an approach for covalently attaching homogeneous fluid lipid bilayers, which are stable for several days, on hydrophilic polymer films covalently attached to the substrate.

Glass slides were first functionalized with 4-aminobutyl(methoxy)dimethylsilane. Then, the alternating reactive copolymer **1** (Fig. 2), prepared from maleic acid anhydride and 1-methyl-vinylisocyanate, (poly[(1-methylvinylisocyanate)-*alt*-(maleic acid anhydride)]),[16] was chemisorbed from a solution in CH_2Cl_2/DMF.

The FTIR spectrum[17] of this reactive polymer layer is presented in Figure 2a. The bands of both the isocyanate (2272 cm^{-1}) and the anhydride (1858, 1791 cm^{-1}) remain clearly visible after reaction of the polymer on the substrate. Due to the excess of the reactive functionalities, the surface of this layer

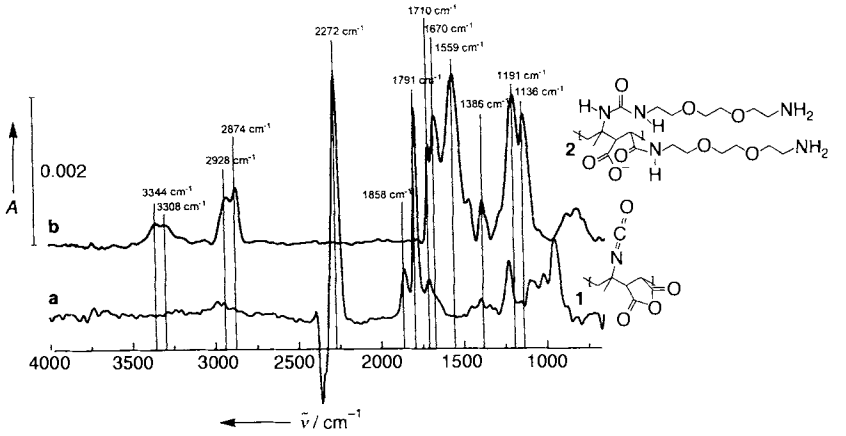

Fig. 2. FTIR spectra of the layer of reactive polymer **1** on an aminosilananized SiO_2 surface before (a) and after (b) reaction with the α,ω-diamine **3** to give **2**. A = absorbance [arbitrary units].

can be further derivatized. Reaction with an excess of α,ω-diamines such as **3** produces a polymer layer (**2**) containing

$H_2N(CH_2)_2O(CH_2)_2O(CH_2)_2NH_2$ **3**

containing hydrophilic amino groups (black triangles in Fig. 3). This layer remains stable even to extensive rinsing with CH_2Cl_2, methanol, and water. Figure 2b shows the FTIR spectrum of this amino group containing layer, which has a thickness of 81 ± 5 Å.[18, 19] The spectrum shows a strong C–O stretching vibration at 1136 cm^{-1}, as well as urea and amide bands at 1670, 1710, and 1559 cm^{-1}, which arise from the reaction of the reactive polymer layer with the α,ω-diamine. Furthermore, N–H stretching vibrations at 3344 and 3308 cm^{-1}, as well as a H–CHO alkyl stretching vibration at 2874 cm^{-1} is observed. The contact angles of layer of polymer **2** have the values $\theta_a = 15°$, $\theta_r = 10°$, whereas the contact angle of the original silanized glass slide has a value of $\theta_a = 63°$, $\theta_r = 45°$, indicating that the polymer surface formed is more hydrophilic than the hydrophobic precursor silane layer.[20]

The Langmuir–Blodgett technique was used to transfer the first lipid monolayer onto this polymer layer on the substrate. The second, outer lipid layer was deposited by dipping the substrate horizontally through a prespread monolayer of pure dimyristoylphosphatidylcholine (DMPC, **4**) on the film balance (the Langmuir–Schaefer technique). The preparation of this lipid layer system is shown schematically in Figure 3.

The composition of the lipid monolayer directly on the polymer substrate is a crucial parameter in our examination of the properties of the bilayer. In addition to the system in which pure DMPC forms the first lipid monolayer, systems with 20 mol% myristidic acid in DMPC, and 20 mol% *N*-succinimidomyristidic ester (**5**), a covalently linked anchor lipid reactive towards amino groups, in DMPC were prepared (Fig. 3). The additional incorporation of 0.8 mol% of the fluorescent lipid 7-nitrobenzo-2-oxa-1,3-diazol-dimyristoylphosphatidylethanolamine (NBD-DMPE, **6**) allowed investigation of the lipid bilayers by fluorescence microscopy.

To investigate the influence of these additional anchor lipids on the homogeneity and mobility of these "tethered, supported dilayers", three types of lipid bilayers with different compositions were prepared; their fluorescence images are displayed in Figure 4. As a reference a lipid bilayer made of pure DMPC with 0.8 mol% NBD-DMPE in the monolayer facing the substrate was prepared (Fig. 4 top). The fluorescence image record-

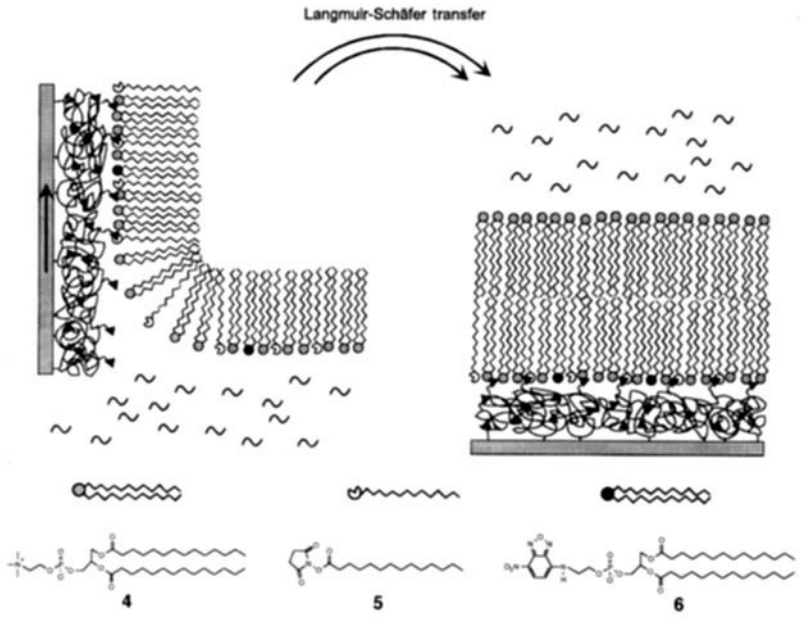

Fig. 3. Representation of the buildup of the bilayer by application of the Langmuir–Blodgett and the Langmuir–Schäfer techniques; NBD-DMPE (**6**, lipids with black headgroups), DMPC (**4**, lipids with shaded headgroups), anchor lipid (**5**, with white headgroups). Black triangles symbolize amino groups.

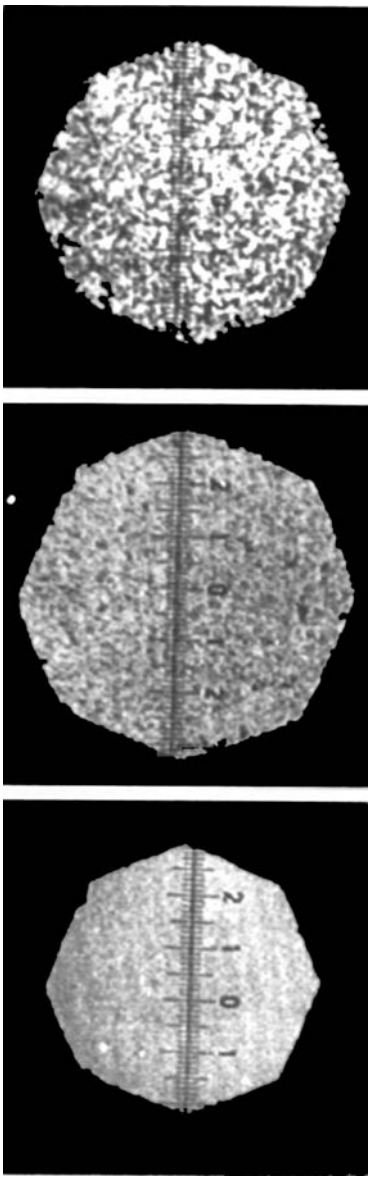

Fig. 4. Top: Fluorescence microscopy image of a lipid bilayer consisting of pure DMPC **4** without incorporation of anchor lipid into the monolayer facing the substrate. Middle: Fluorescence microscopy image of a lipid bilayer consisting of DMPC **4** with incorporation of 20 mol% myristidic acid into the monolayer facing the substrate. Bottom: Fluorescence microscopy image of a lipid bilayer consisting of DMPC **4** with incorporation of 20 mol% anchor lipid **5** into the monolayer facing the substrate. Distance between numbered lines: 13 μm, $T = 25\,^{\circ}C$.

ed directly after preparation shows a strongly inhomogeneous lipid bilayer on the polymer "cushion", as concluded from the very inhomogeneous and grainy texture. A fluorescence image of the same lipid bilayer after 24 h shows further enlargement of the inhomogeneous areas.

The incorporation of 20 mol% myristidic acid into the lipid monolayer facing the substrate leads to a bilayer displaying a more homogeneous fluorescence image (Fig. 4 middle). The homogeneity of this bilayer is significantly improved and holes appear much less frequently. This effect may be due to an ionic interaction between the myristidic acid and its anion and the partially protonated amino groups of the polymer substrate, leading to a loose attachment of the lipids on the polymer layer.

The incorporation of 20 mol% *N*-succinimidomyristidic ester (**5**) instead of the pure myristidic acid into the monolayer facing the substrate obviously leads to the covalent attachment of some of the lipids and results in a homogeneous fluorescence image (Fig. 4 bottom) without noticeable aggregation or phase separation of the lipids in the bilayer. The fluorescence image of this tethered, supported bilayer was checked over several days and did not exhibit any changes in the bilayer.

Measurements on the lateral diffusion of the fluorescence dye **6** in the monolayer of the lipid membrane facing the substrate were performed using the FRAP technique (FRAP = fluorescence recovery after photobleaching)[21] at a temperature of 25 °C. These measurements show the dependence of the diffusion constant of the dye-labeled lipid **6** upon incorporation of anchor lipid into the bilayer. A series of bilayers of different compositions was investigated. For a polymer-supported lipid bilayer of DMPC without incorporated anchor lipids or myristidic acid, a diffusion constant of $3.12 \pm 0.3\ \mu m^2 s^{-1}$ was established.[22] The value observed after incorporation of 20 mol% myristidic acid (ionic attachment) is significantly lower ($2.4 \pm 0.3\ \mu m^2 s^{-1}$). The diffusion constant of an analogously prepared lipid bilayer with the incorporation of 20 mol% anchor lipid **5** is considerably lower ($1.3 \pm 0.06\ \mu m^2 s^{-1}$) than that recorded for pure DMPC. A double layer of pure DMPC on a hydrophilic and not polymer-coated glass substrate shows a diffusion constant of roughly $4 \pm 0.3\ \mu m^2 s^{-1}$.[11, 21]

These differences in the diffusion constants are a further indication of the covalent attachment of some of the anchor lipids to the polymer film on the glass substrate. This covalent attachment forces the dye molecules to "diffuse around" the bound lipids and lowers the macroscopic diffusion constant as established by means of FRAP even further than would be achieved by the incorporation of just the myristidic acid, which is not able to form any covalent attachment with the polymer layer. The bilayer remains fluid but at the same time exhibits improved homogeneity.

The approach described here allows the preparation of homogeneous, lipid bilayers that are fluid and stable on solid substrates over several days as observed by fluorescence microscopy. Such anchored lipid bilayers (tethered supported bilayers) should, owing to the "decoupling" of the lipid bilayer from the substrate, be more suitable for the investigation of membrane proteins. Possible interactions with the substrate, which disturb the conformation and function of the protein,[14] should be reduced due to the water-swellable polymer film.

 © VCH Verlagsgesellschaft mbH, D-69451 Weinheim, 1996 0570-0833/96/3515-1684 $ 15.00+.25/0

Experimental Procedure

The reactive polymer **1** was prepared according to the procedure of Mormnn et al. [16].

Synthesis of anchor lipid **5**: Myristidic acid (5.6 g, 24.5 mmol) and *N*-hydroxysuccinimide (3.52 g, 30.7 mmol) were dissolved in a mixture of chloroform/acetone (180 mL, volume ratio 9:1) at room temperature, and a small amount of 4-dimethylaminopyridine (DMAP) was added as catalyst. Argon was bubbled through the solution, which was then cooled to 0 °C. A solution of dicyclohexylcarbodiimide (3.09 g, 15 mmol) in chloroform (10 mL) was added slowly to the reaction mixture. The resulting solution was stirred for an additional hour at 0 °C and then for 24 h at room temperature. The precipitate formed was then filtered off and and washed with chloroform. The filtrate was concentrated to dryness in vacuo and the residue recrystallized from petroleum ether. Afterwards the crude product was purified by flash chromatography on neutral Al_2O_3 with chloroform as eluent to provide 6.6 g (82%) of the lipid. M.p. 80.5 °C; ^{1}H NMR (200 MHz, $CDCl_3$, 20 °C): $\delta = 2.85$ (s, 4H; $OCCH_2CH_2CO$), 2.58 (t, 2H; OCH_2CH_2), 1.71 (m, 2H; $OCH_2CH_2CH_2$), 1.24 (m, 20H; $(CH_2)_{10}$), 0.85 (t, 3H; CH_3).

Adsorption and reaction of the polymer: The cleaned and silanized substrate was placed in a 2.2×10^{-3} M solution of the reactive polymer **1** dissolved in DMF/CH_2Cl_2 (1:9) for 12 h. Afterwards the slides were rinsed with DMF/CH_2Cl_2 (1:9) and then placed into a 0.5 M solution of α,ω-diamine **3** in CH_2Cl_2 for 12 h. Subsequently the slides were rinsed three times each with CH_2Cl_2, methanol, water, and again methanol. The slides were then dried in vacuum.

Transfer of the lipid bilayers: The bilayers were prepared using the Langmuir–Blodgett and the Langmuir–Schäfer techniques at 25 °C and at a lateral pressure of 30 mN m^{-1} on a film balance (constructed in our institute). In all cases a complete transfer was observed. The second lipid layer was prepared by pressing the substrate with the first monolayer horizontally through a monolayer of pure DMPC compressed at 30 m Nm^{-1} onto a hollow-dip microscope slide.

Received: November 21, 1995
Revised version: March 4, 1996 [Z 8575 IE]
German version: *Angew. Chem.* **1996**, *108*, 1791–1794

Keywords: biomembranes · fluorescence · lipid bilayers · polymer films

[1] L. K. Tamm, H. M. McConnel, *Biophys. J.* **1985**, *47*, 105.
[2] W. Müller, H. Ringsdorf, E. Rump, G. Wildburg, X. Zhang, L. Angermaier, W. Knoll, M. Liley, J. Spinke, *Science* **1992**, *262*, 1706–1708.
[3] A. Ulman, *An Introduction to Ultrathin Organic Films*, Academic Press, San Diego, **1991**
[4] E. Kalb, S. Frey, L. K. Tamm, *Biochim. Biophys. Acta.* **1992**, *1103*, 307.
[5] J. Spinke, J. Yang, H. Wolf, M. Liley, H. Ringsdorf, W. Knoll, *Biophys. J.* **1992**, *63*, 1667.
[6] H. T. Tien, Z. Salamon, *Bioelectrochem. Bioenerg.* **1989**, *22*, 211.
[7] C. Duschl, M. Liley, G. Corradin, H. Vogel, *Biophys. J.* **1994**, *67*, 1229.
[8] P. A. Ohlsson, P.-A. Gustafson, G. Puu, G. Olofsson, A. Sellström, in *Progress in Membrane Biotechnology* (Eds.: J. C. Gomez-Fernandez, D. Chapman, L. Packer), Birkhäuser Verlag, Basel, Switzerland, **1991**, p. 279.
[9] R. Naumann, A. Jonczyk, R. Kopp, J. van Esch, H. Ringsdorf, W. Knoll, P. Gräber, *Angew. Chem.* **1995**, *107*, 2168; *Angew. Chem. Int. Ed. Engl.* **1995**, *34*, 2056.
[10] H. M. McConnell, T. H. Watts, R. M. Weis, A. A. Brian, *Biochim. Biophys. Acta* **1986**, *864*, 95.
[11] L. K. Tamm, *Biochemistry*. **1988**, *27*, 1450.
[12] R. Merkel, E. Sackmann, E. Evans, *J. Phys. (Paris)* **1989**, *50*, 1535.
[13] M. Kühner, R. Tampé, E. Sackmann, *Biophys. J.* **1994**, *67*, 217.
[14] N. Thompson, C. Poglitsch, M. Timbs, M. Pisarchick, *Acc. Chem. Res.* **1993**, *26*, 567.
[15] E. Sackmann, *Science*, **1996**, *271*, 43; C. Erdelen, L. Häussling, R. Naumann, H. Ringsdorf, H. Wolf, J. Yang, M. Liley, J. Spinke, W. Knoll, *Langmuir* **1994**, *10*, 1246.
[16] W. Mormann, K. Schmalz, *Macromolecules* **1994**, *147*, 103.
[17] FTIR spectra were recorded at grazing incidence with an angle of incidence of 80° with a Nicolet 5DXC FTIR spectrometer. The reflecting layer was 80 nm of silver, and 14 nm of SiO_x was deposited for the silanization.
[18] G. Elender, E. Sackmann, *J. Phys. II* **1994**, *4*, 455.
[19] This layer thickness was determined using ellipsometry as described in ref. [18] using a refractive index of $n = 1.506$.
[20] Contact angle measurements were performed by the dynamic method with a Krüss G-1 contact angle microscope.
[21] O. Axelrod, D. E. Kappel, J. Schlessinger, E. Elson, W. W. Webb, *Biophys. J.* **1976**, *16*, 1055.
[22] Diffusion measurements using FRAP were performed with the setup described in refs. [12,13] at 25 °C. The values for the relative recovery were between 0.95 and 0.98. A more detailed description of the procedure can be found in ref. [21].

$La_9Br_5(CBC)_3$: A New Superconductor**

Hansjürgen Mattausch, Arndt Simon,* Claudia Felser, and Richard Dronskowski

Dedicated to Professor Hanskarl Müller-Buschbaum on the occasion of his 65th birthday

The superconducting carbide halides $M_2X_2C_2$ of the nonmagnetic rare earth metals (M) constitute model systems which illustrate the hypothesis[1, 2] that superconductivity originates from the tendency of a pairwise localization of conduction electrons.[3, 4] In these materials, an attractive interaction between the conduction electrons is attributed to the presence of pseudomolecular C_2-π^* levels at the Fermi edge E_F. Band structure calculations[4] for $Y_2Br_2C_2$ reveal a very flat band (localization) at E_F with a significant C_2-π^* contribution, which corresponds to a maximized density of states at E_F, as well as other bands with a large slope at the Fermi edge (delocalization). This characteristic feature in the band structure may serve as a "fingerprint" in the search of new superconductors.

In the course of new investigations on quaternary compounds with Ln, B, C, and X (X = Cl, Br, I),[5] $Ce_3Br_3(BC)$[6] and $Ce_9Br_5(CBC)_3$ were obtained for the first time. The phases form as air-sensitive, rod-shaped, metallic bronze crystals after heating the corresponding mixtures of $CeBr_3$, Ce, B, and C in sealed tantalum capsules for several days.[7] The structure of $Ce_9Br_5(CBC)_3$,[9] obtained from a single-crystal study, is given as a projection along [010] in Figure 1.[11] The B atoms are surrounded by a trigonal prism of Ce atoms, while the coordination of the C atoms almost resembles a quadratic pyramid. A single prism and two pyramids constitute the central building block (highlighted in ref. [5]) that contains the pseudomolecular C-B-C unit in its interior. Such blocks are connected parallel (100) to give corrugated sheets and these are bonded to each other by Br atoms.[12] The B–C distances (151 pm) are identical within 1σ (2 pm) in both crystallographically different C-B-C

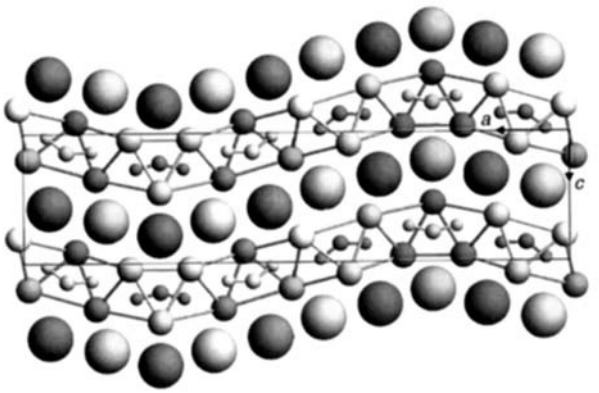

Fig. 1. Projection of the structure of $Ln_9Br_5(CBC)_3$ along [010]. Trigonal prismatic units around the B atoms, which are merged on both sides with tetragonal pyramids around the C atoms, are condensed into layers. Br atoms are found in the remaining void. Br, Ln, B, and C atoms are drawn as circles of decreasing sizes.

[*] Prof. Dr. A. Simon, Dr. C. Felser, Dr. H. Mattausch, Priv.-Doz. Dr. R. Dronskowski
Max-Planck-Institut für Festkörperforschung
Heisenbergstrasse 1, D-70569 Stuttgart (Germany)
Fax: Int. code +(711)689-1642
e-mail: hansm@vaxff2.mpi-stuttgart.mpg.de

[**] We thank C. Hochrathner for the structural drawings, R. Eger for his preparative help, R. Pöttgen for having collected the intensity data, and N. Weishaupt and E. Brücher for having measured both electrical conductivity and magnetic susceptibility.

groups. Furthermore, the C-B-C angles are 141(3)° for C3-B1-C3 and 151(3)° for C2-B2-C2. The compound is a metallic conductor, and its specific resistance[15] is almost temperature-independent above 50 K (about 120 mΩcm).

The chemical bonding in $Ce_9Br_5(CBC)_3$ can be considered as $(Ce^{3+})_9(Br^-)_5(CBC^{7-})_3 \cdot e^-$ according to the Zintl–Klemm concept, which indicates that the CBC^{7-} ions are formally isovalence electronic with molecular SO_2. Semiempirical band structure calculations and COOP (*c*rystal *o*rbital *o*verlap *p*opulation) analyses[13] show that the excess electrons occupy bands with Ce–Ce bonding character at the Fermi edge. There is a sharp maximum in the density of states at E_F, and the COOP analysis reveals, besides the already mentioned Ce–Ce bonds, strongly bonding Ce–B, weakly bonding Ce–Ce, and antibonding B–C interactions. Thus, the characteristic "fingerprint" known from the superconducting carbide halides is present. The experiments that were performed were successful in two respects. First, the isotypical compound containing the nonmagnetic La^{3+} ion could be synthesized. This compound showed the same band structure characteristics as the Ce compound, despite having different lattice constants and atomic energy levels. Second, $La_9Br_5(CBC)_3$ exhibits superconductivity at 6 K, as supported by the appearance of diamagnetic shielding (Fig. 2)[14] and vanishing electrical resistance[15] (Fig. 2, insert).

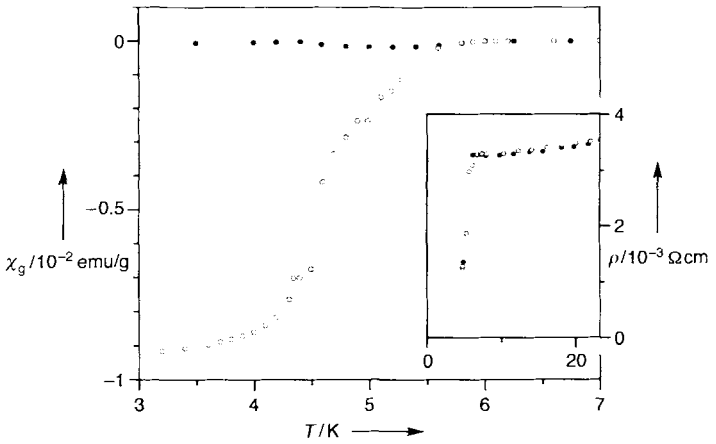

Fig. 2. Diamagnetic screening (open circles) and Meissner effect (filled circles) of $La_9Br_5(CBC)_3$ as a function of the temperature. The insert shows the electrical resistance as a function of the temperature (open circles: heating curve, filled circles: cooling curve).

The calculation of the electronic band structure[16] of $La_9Br_5(CBC)_3$ with density functional theory reveals a local maximum in the density of states at E_F. The k dependence of the bands (Fig. 3) shows that this maximum essentially arises from a flat band (van Hove singularity) with its center of gravity at the Fermi edge.

The bands' orbital character has been represented with the "fat band" technique, in which the width of the bands are drawn such as to reflect the weight of the contributing orbital. To do so, the internal coordinate system was set up such that the C-B-C unit points into the approximate x direction. The "fat band" representation confirms that the flat band at E_F arises from the covalent mixing of BC_2-centered MOs with approximate π^* symmetry and La-$d_{xz,yz}$ atomic levels. At the same time, there are bands of predominantly La-$d_{x^2-y^2}$ character at E_F, having a large absolute slope.[18] Despite the chemical and structural differences of the compounds $Y_2Br_2C_2$[4] and $La_9Br_5(CBC)_3$, their electronic structures strongly resemble each other with respect to the bands' characteristic course at E_F.

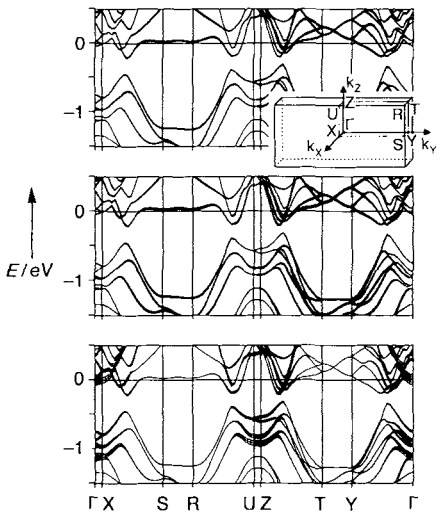

Fig. 3. Band structure of $La_9Br_5(CBC)_3$. The BC_2-centered levels of approximate π^* symmetry, the La-$d_{xz,yz}$ atomic levels, and the La-$d_{x^2-y^2}$ atomic levels (from top to bottom) are emphasized as "fat bands" [18]. The Fermi energy is the zero energy. The principal directions of the Brillouin zone are indicated.

A molecular orbital analysis of the the C-B-C units elucidates the chemical bonding of the pseudomolecular entity inside the crystal and indicates a specific electron–phonon interaction with the electrons at the Fermi edge. The result supports the formal charge assignment according to Zintl and Klemm. Within the one-electron picture, a doubly degenerate C–B antibonding π_u level is populated for a linear C-B-C unit of overall charge −7, in complete analogy to the carbide halides. The latter molecular orbital may mix with the σ_g-like LUMO through a bending vibration of symmetry π_u (Fig. 4). Such a coupling corresponds

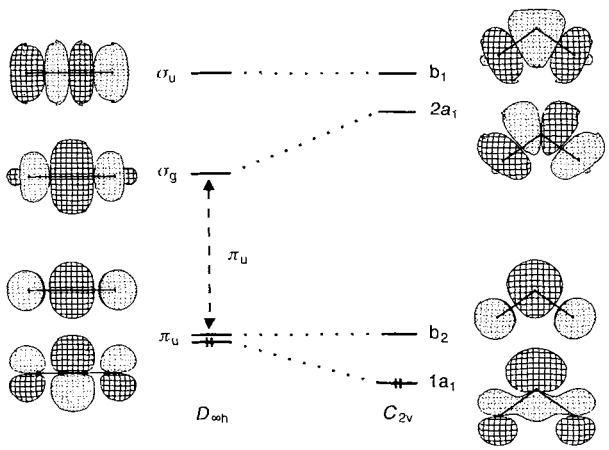

Fig. 4. Schematic Walsh diagram of a CBC^{7-} molecular anion. The molecular orbitals originate from a semiempirical (EH) calculation [23] that has been parameterized to numerical (HF) orbital energies and valence functions.

to a second order Jahn–Teller instability[19, 20] and allows the energetic stabilization/destabilization of the HOMO/LUMO under symmetry reduction from $D_{\infty h}$ to C_{2v}. This effect may be expected for all triatomic species with 18 valence electrons (O_3, SO_2, CF_2, CBC^{7-}). In the present case of CBC^{n-}, the group theory arguments are also corroborated by further ab initio calculations.[21] The influence of the matrix and the cation–anion backbonding (see above), however, is apparent from a comparison between the calculated C-B-C angle of 121° for the

isolated species and the widened angle (148°) that has been experimentally found.[22] The energy of the molecular $1a_1$ level (compared to E_F) is extremely sensitive to the size of the C-B-C angle, thus stressing the importance of the bending vibration for the appearance of superconductivity.

Superconducting boride carbides such as YB_2C_2 with $T_c = 3.6$ K[24] and $La_5B_2C_6$ with $T_c = 6.9$ K[25] have been known for a long time. Recently a lot of interest has focused on boride carbides with the composition $LnNi_2B_2C$ (T_c(max) = 16.6 K).[26–29] The bonding is complicated in all of these phases: YB_2C_2 contains B–C networks, in $La_5B_2C_6$ ($= La_5C_2(CBC)_2$) there are CBC and C_2 anions, and in $LnNi_2B_2C$ the bands carry contributions from all atoms at the Fermi edge. In comparison, the bonding conditions in the superconductor $La_9Br_5(CBC)_3$ are fairly clear. The "fingerprint" for superconductivity is similarly present for the compound $La_9Br_6(CBC)_3$,[5] which is structurally closely related. There are bands with large and negligible dispersions about 0.5 eV above and below E_F. Attempts to change E_F by substitution of La^{3+} are currently in progress.

Received: February 28, 1996 [Z8879IE]
German version: *Angew. Chem.* **1996**, *108*, 1805–1807

Keywords: carbide borides · halides · lanthanides · solid-state structures · superconductivity

[1] A. Simon, *Angew. Chem.* **1987**, *99*, 602; *Angew. Chem. Int. Ed. Engl.* **1987**, *26*, 579.
[2] A. Simon, *Chem. Uns. Zeit* **1988**, *22*, 1.
[3] A. Simon, H. Mattausch, R. Eger, R. K. Kremer, *Angew. Chem.* **1991**, *103*, 1209; *Angew. Chem. Int. Ed. Engl.* **1991**, *30*, 1188.
[4] A. Simon, A. Yoshiasa, M. Bäcker, R. W. Henn, C. Felser, R. K. Kremer, H. Mattausch, *Z. Anorg. Allg. Chem.* **1996**, *622*, 123.
[5] H. Mattausch, A. Simon, *Angew. Chem.* **1995**, *107*, 1764; *Angew. Chem. Int. Ed. Engl.* **1995**, *34*, 1633.
[6] H. Mattausch, A. Simon, *Jahresber. MPI-FKF, Stuttgart*, (**1996**). The lattice constants, atomic parameters, and details of the crystal structure analysis may be obtained from the Fachinformationszentrum Karlsruhe, D-76344 Eggenstein-Leopoldshafen, on quoting the depository number CSD-404168.
[7] The Ta ampoules were filled with starting material (ca. 2 g), welded under an argon pressure of 1 atm, sealed into quartz glass ampoules, heated at 1460 K ($Ce_9Br_5(CBC)_3$: 1 day; 30% yield), at 1700 K ($La_9I_5(CBC)_3$: 1 day; X-ray pure), at 1460 K ($La_9Br_5(CBC)_3$: 7 days; X-ray pure), and then quenched to room temperature. The quantitative synthesis of the samples (especially B:C = 1:2) proves the correct atomic assignment from the X-ray analysis [9]. For details on the synthesis and handling of the starting material, see ref. [8].
[8] H. Mattausch, H. Borrmann, R. Eger, R. K. Kremer, A. Simon, *Z. Anorg. Allg. Chem.* **1994**, *620*, 1889.
[9] Single-crystal intensity measurements on a four-circle diffractometer (CAD4, Enraf-Nonius) with $Ag_{K\alpha}$ radiation. Semiempirical absorption correction (ψ scan). Full-matrix least-squares refinement on F^2 [10]. $Ce_9Br_5(CBC)_3$: *Pmmn*; $a = 3293.5(3)$, $b = 380.4(1)$, $c = 781.6(1)$ pm. Ce1: 0.5094(1), 1/4, 0.1970(2); Ce2: 1/4, 1/4, 0.5475(3); Ce3: 0.5956(1), 1/4, 0.9135(2); Ce4: 0.3056(1), 1/4, 0.9530(2); Ce5: 0.6329(1), 1/4, 0.3502(2); Br1: 0.5481(1), 1/4, 0.5747(3); Br2: 0.3481(1), 1/4, 0.3258(3); Br3: 3/4, 1/4, 0.7875(5); C1: 0.6241(7), 3/4, 0.136(3); C2: 0.2937(8), 3/4, 0.728(3); C3: 0.4561(7), 1/4, 0.973(3); B1: 0.5794(9), 3/4, 0.139(4); B2: 1/4, 3/4, 0.776(5). $R1 = 0.069$; $wR2 = 0.135$ for 1463 independent reflections. $La_9Br_5(CBC)_3$: *Pmmn*; $a = 3319(2)$, $b = 385.3(1)$, $c = 790.6(3)$ pm. La1: 0.5093(1), 1/4, 0.1973(2); La2: 1/4, 1/4, 0.5464(3); La3: 0.5959(1), 1/4, 0.9113(2); La4: 0.3054(1), 1/4, 0.9543(2); La5: 0.6330(1), 1/4, 0.3503(2); Br1: 0.5481(1), 1/4, 0.5728(3); Br2: 0.3480(1), 1/4, 0.3276(3); Br3: 3/4, 1/4, 0.7858(5); C1: 0.6253(7), 3/4, 0.137(3); C2: 0.2940(7), 3/4, 0.726(3); C3: 0.4566(7), 1/4, 0.977(3); B1: 0.579(1), 3/4, 0.144(4); B2: 1/4, 3/4, 0.774(4). $R1 = 0.053$; $wR2 = 0.103$ for 1097 independent reflections. The correct assignment of B and C is clearly visible from the R values and the corresponding displacement parameters. Isotypic is $La_9I_5(CBC)_3$ with $a = 3385.7(4)$, $b = 394.81(4)$, $c = 821.8(1)$ pm. Further details of the crystal structures may be obtained from the Fachinformationszentrum Karlsruhe, D-76344 Eggenstein-Leopoldshafen (Germany), upon quoting the depository numbers: CSD-404170 ($La_9Br_5(CBC)_3$), CSD-404708 ($La_9I_5(CBC)_3$), and CSD-404169 ($Ce_9Br_5(CBC)_3$).
[10] G. M. Sheldrick, *SHELXTL-PLUS*, Göttingen, **1992** and *SHELXL-93*, Göttingen, **1993**.
[11] E. Dowty, *ATOMS for Windows*, Version 3.1, Shape Software, Kingsport, TN 37663, **1995**.
[12] The structure is closely related to the one of $La_9Br_6(CBC)_3$ [5]. The lowered Br content of $Ce_9Br_5(CBC)_3$ leads to a stronger corrugation of the sheets.
[13] QCPE program EHMACC by M.-H. Whangbo, M. Evain, T. Hughbanks, M. Kertesz, S. Wijeyesekera, C. Wilker, C. Zheng, and R. Hoffmann; Parametrization according to S. Alvarez.
[14] The magnetic susceptibilities were measured at 10 G with an MPMS Quantum Design SQUID magnetometer.
[15] L. J. van der Pauw, *Philips Res. Rep.* **1958**, *13*, 1.
[16] Program TB-LMTO-ASA 4.7 (tight binding-linear muffin tin orbital-atomic spheres approximation) [17] by G. Krier, O. Jepsen, A. Burkhardt, and O. K. Andersen.
[17] O. K. Andersen, *Phys. Rev. B* **1975**, *12*, 3060; O. K. Andersen, O. Jepsen, *Phys. Rev. Lett.* **1984**, *53*, 2571.
[18] The conventional orbital representation is obtained by exchanging the x and z directions.
[19] L. S. Bartell, *J. Chem. Educ.* **1968**, *45*, 754.
[20] R. G. Pearson, *J. Am. Chem. Soc.* **1969**, *91*, 4947.
[21] ADF 1.1.4, Department of Theoretical Chemistry, Vrije Universiteit, Amsterdam; E. J. Baerends, D. E. Ellis, P. Ros, *Chem. Phys.* **1973**, *2*, 41; G. te Velde, E. J. Baerends, *J. Comp. Phys.* **1992**, *99*, 84.
[22] We have performed quantum mechanical optimizations (triple-zeta basis sets including two polarization functions for all valence orbitals, local density functional) of the bridging angles of CBC^{n-} molecular ions, with a fixed C–B distance (151 pm). The calculations are model-like because of the Coulomb explosions that may be expected for such high charges. $D_{\infty h}$ symmetry is only found for CBC^{3-} and CBC^{5-}, whereas CBC^{7-} and CBC^{9-} adopt C_{2v} symmetry with angles of 121 and 110°. Test calculations on SO_2 show these calculations to be better than 2°, and they strongly favor the LDA with respect to gradient-corrected functionals.
[23] Program CACAO by C. Mealli, D. Proserpio, *J. Chem. Educ.* **1990**, *67*, 399.
[24] T. Sakai, G.-Y. Adachi, J. Shiokawa, *J. Less-Common. Met.* **1982**, *84*, 107.
[25] J. Bauer, O. Bars, *J. Less-Common. Met.* **1983**, *95*, 267.
[26] R. J. Cava, H. Tagaki, H. W. Zandbergen, J. J. Krajewski, W. F. Peck, T. Siegrist, B. Batlogg, R. B. van Dover, R. J. Felder, K. Mizuhashi, J. O. Lee, H. Eisaki, S. Uchida, *Nature* **1994**, *367*, 252.
[27] T. Siegrist, H. W. Zandbergen, R. J. Cava, J. J. Krajewski, W. F. Peck, *Nature* **1994**, *367*, 254.
[28] T. Siegrist, R. J. Cava, W. F. Peck, *J. Alloys Comp.* **1994**, *216*, 135.
[29] W. R. Pickett, D. J. Singh, *Phys. Rev. Lett.* **1994**, *27*, 3702.

Modeling of the Chemistry of the Active Site of Galactose Oxidase**

Jason A. Halfen, Victor G. Young, Jr., and William B. Tolman*

Arrays consisting of organic free radicals proximate to metal centers recently have been identified as important components of active sites in enzymes that catalyze multielectron redox reactions.[1] An intriguing example of a functionally significant metal-radical pair is found in galactose oxidase (GAO),[2] a fungal enzyme containing a monocopper active site that effects the two-electron oxidation of primary alcohols to aldehydes. Extensive biophysical studies[2a, 3] including X-ray structures[4] have resulted in the elucidation of the topology of the active site (Fig. 1, inset) and an electronic structural description of the functionally competent form. This form (structure **A**, Fig. 1) is postulated to contain a Cu^{II} ion tightly coupled to a radical localized on an equatorial, covalently S-cys-modified tyrosinato

[*] Prof. W. B. Tolman, J. A. Halfen, Dr. V. G. Young, Jr.
Department of Chemistry
University of Minnesota
207 Pleasant Street S. E., Minneapolis, MN 55455 (USA)
Fax: Int. code +(612)624-7029
e-mail: tolman@chemsun.chem.umn.edu

[**] This work was supported by grants from the National Institutes of Health (GM 47365), the National Science Foundation (National Young Investigator Award to W. B. T.), the Alfred P. Sloan and Camille and Henry Dreyfus Foundations (fellowships to W. B. T.), and the University of Minnesota (Dissertation Fellowship to J. A. H.). One of the diffractometers used was purchased in part from funds from the NSF (CHE-9413114).

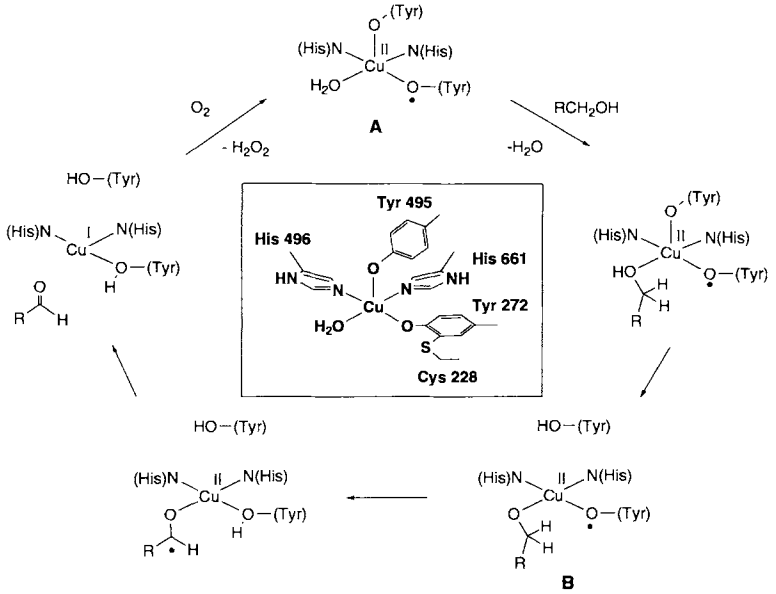

Fig. 1. Schematic drawings of the crystallographically characterized active site of galactose oxidase at pH 7.0 (inset, from Ref. [4]) and the proposed mechanism for alcohol oxidation by the enzyme (from Ref. [2]).

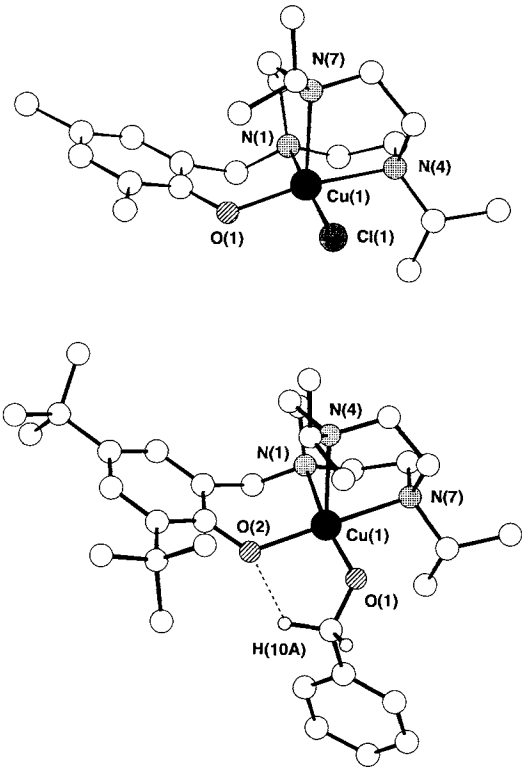

Fig. 2. X-ray crystal structures of **1** (top) and **4** (bottom). Selected bond lengths [Å] and angles [°] for **1**: Cu1–O1 1.916(5), Cu1–N1 2.069(5), Cu1–N4 2.148(6), Cu1–N7, 2.291(6), Cu1–Cl1, 2.286(2); Cl1-Cu1-O1 90.3(2), Cl1-Cu1-N1 171.4(2), Cl1-Cu1-N4 92.4(2), Cl1-Cu1-N7 102.7(2), O1-Cu1-N1 92.8(2), O1-Cu1-N4 167.4(2), O1-Cu1-N7 109.3(2), N1-Cu1-N4 83.0(2), N1-Cu1-N7 83.9(3), N4-Cu1-N7 82.2(2). Selected bond distances [Å] and angles [°] for **4**: Cu1–O1 1.893(1), Cu1–O2 1.931(1), Cu1–N1 2.082(2), Cu1–N4 2.397(2), Cu1–N7 2.140(2), N1-Cu1-N4 80.45(6), N1-Cu1-N7 82.89(6), N4-Cu1-N7 82.29(6), N1-Cu1-O1 169.80(6), N1-Cu1-O2 92.88(6), O1-Cu1-N7 88.23(6), O1-Cu1-O2 94.85(6), O1-Cu1-N4 103.39(6), N4-Cu1-O2 107.94(6), N7-Cu1-O2 168.21(6).

ligand and stabilized by π-stacking interactions with a nearby tryptophan residue (not shown). Poised to perform two-electron redox chemistry, the free- radical-coupled copper complex **A** has been proposed to yield intermediate adduct **B** upon deprotonation of the alcohol substrate by the axial tyrosinato ligand.[2a] The subsequent alcohol oxidation has been suggested to occur by initial hydrogen atom abstraction by the appended tyrosyl radical,[5] followed by electron transfer to copper to afford the aldehyde and the reduced Cu^{I} active site (Fig. 1).[6] Two-electron oxidation by O_2 completes the hypothetical catalytic cycle.

We wish to assess the viability of this interesting mechanism by examining appropriate synthetic model complexes. Previous modeling studies have demonstrated the feasibility of phenolato–Cu^{II} units found in the inactive form of GAO (one-electron reduced form of **A**)[7] and the functional competence of free-radical-coupled copper compounds to oxidize alcohols, albeit with an abiological radical cofactor (2,2,6,6-tetramethyl-1-piperidinyloxy, TEMPO).[8] Here we report the identification of synthetic analogs of **A** and a novel mixed alcoholato–phenolato complex of Cu^{II} that models reduced **B**. Moreover, we find that one-electron oxidation of **B** induces aldehyde production.

Reasoning that any attempt to generate a functional pair consisting of a phenoxyl radical and a Cu^{II} ion would be thwarted by inactivation reactions at the *ortho* and *para* positions of the arene ring, we prepared the protected monophenolato ligands $\mathbf{L^1}$ and $\mathbf{L^2}$. Deprotonation with NaH followed by treatment with the appropriate anhydrous Cu^{II} salt yielded the deep purple complexes [LCuX] (**1**: L = $\mathbf{L^1}$, X = Cl; **2**: L = $\mathbf{L^2}$, X = Cl; **3**: L = $\mathbf{L^2}$, X = O_3SCF_3), one of which (**1**) was structurally characterized by X-ray crystallography (Fig. 2, top).[9] The complex adopts a square-pyramidal geometry[10] with the chloro and phenolato ligands in *cis*-equatorial positions; spectroscopic comparisons implicate a similar arrangement in **2** and **3**.[11] The stabilizing effect of the the *tert*-butyl groups[12] is manifested in the unique electrochemical behavior of **2** and **3**, both of which exhibit reversible one-electron oxidation waves in their cyclic voltammograms (CVs) obtained with 0.25 M Bu_4NPF_6 in CH_2Cl_2 (**2**: $E_{1/2} = +0.59$ V, $\Delta E_p = 86$ mV; **3**: $E_{1/2} = +0.72$ V, $\Delta E_p = 96$ mV; both vs. SCE at 100 mV s^{-1}). One-electron oxidation of purple, EPR-active **3** could be accomplished at −40 °C electrochemically by controlled potential electrolysis at +1.0 V vs. SCE or chemically by treatment with equimolar $(NH_4)_2[Ce(NO_3)_6]$ in CH_3CN. Both procedures resulted in the production of a new green species. Consistent with the electrochemical reversibility evident in the CV of **3**, reaction of stoichiometric amounts of ferrocene [Cp_2Fe] with the green complex resulted in the quantitative regeneration of **3** and the production of $[Cp_2Fe]^+$. The green, oxidized species lacks an EPR signal and exhibits an optical absorption feature at 410 nm ($\varepsilon = 4000\ M^{-1}cm^{-1}$) similar to that observed in active GAO (445 nm, $\varepsilon = 5400\ M^{-1}cm^{-1}$)[13] and many 2,4,6-trisubstituted phenoxyl radicals.[14] These results support assignment of the green oxidized species ($\mathbf{3^{+\cdot}}$) as a magnetically coupled phenoxyl–Cu^{II} radical complex akin to GAO species **A**.

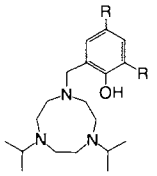

$\mathbf{L^1}$: R = CH_3
$\mathbf{L^2}$: R = $C(CH_3)_3$

In an approach toward modeling substrate interactions with the enzyme we treated **2** with $NaOCH_2Ph$ to yield [$L^2Cu(OCH_2Ph)$] (**4**) as green crystals suitable for X-ray crystallographic characterization (Fig. 2, bottom).[9, 11] The *cis*-equatorial arrangement of the alcoholato and phenolato ligands in the square-pyramidal[10] complex mimics the proposed disposi-

tion of these groups in GAO during enzyme turnover. Additional noteworthy features of **4** are the short Cu^{II}–alcoholato bond length [Cu1–O1 = 1.893(1) Å] and a 2.36 Å distance between a benzylic hydrogen (H10A) and the phenolate oxygen (O2) that implicates an O···H-C interaction of possible functional importance,[16] insofar as such an arrangement may be viewed as necessary for the hypothesized hydrogen atom abstraction that is the first step in alcohol oxidation. Indeed, the cyclic voltammogram of **4** exhibits an irreversible oxidation wave (E_{pa} = + 0.37 V vs. SCE in CH_3CN) and upon bulk electrolysis at + 0.5 V, 0.9 ± 0.1 e^- mol^{-1} was abstracted from the complex concomitant with bleaching of its EPR and UV/Vis features. ^1H NMR and GC/MS analysis of the resulting solution (after removal of copper-containing species) revealed the production of benzaldehyde (46% based on **4**) and small amounts of 1,4-diisopropyl-1,4,7-triazacyclononane[17] and 4,6-di-*tert*-butyl-2-formylphenol (Scheme 1).

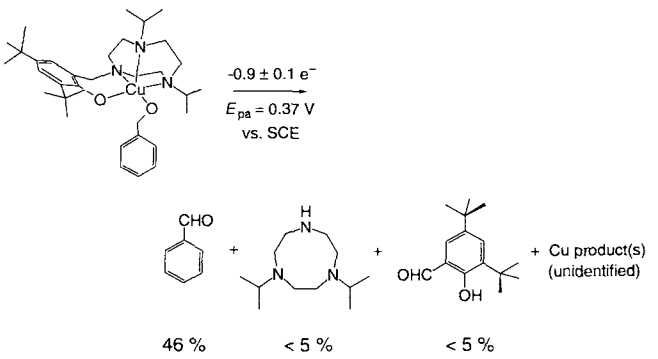

Scheme 1. SCE = saturated calomel electrode.

The overall reaction whereby one-electron oxidation of **4** yields benzaldehyde and, presumably, Cu^I coproduct(s) parallels that promoted by GAO. By analogy to the electrochemical behavior exhibited by **2** and **3**, we suggest that electrolysis of **4** generates $\mathbf{4}^{+\bullet}$, a reactive Cu^{II} complex with coupling between the free radical and the copper center that binds the substrate, analogous to enzyme intermediate **B**. Hydrogen atom abstraction (cf. H10A) by the phenoxyl oxygen (O2) would initiate benzaldehyde generation, while abstraction from the activated benzylic position of the phenoxyl group would afford the byproducts.[14] Inter- or intramolecular paths are possible, although we view internal delivery of a hydrogen atom from the benzyl alcoholate to the phenoxyl oxygen as a particularly attractive alcohol oxidation route in view of the O···H–C interaction identified by crystallography for **4**.

In sum, we have obtained chemical precedents for key intermediates hypothesized in alcohol oxidation catalyzed by the unique active site of GAO comprising a monocopper center coupled to a free radical. Important findings include the identification of species derived from one-electron oxidation of phenolato–Cu^{II} compounds that model the active form of the enzyme (**A**), structural characterization of a mixed phenolato–alcoholato complex that models the reduced enzyme–substrate adduct (reduced **B**), and aldehyde evolution from the phenolato–alcoholato compound upon its one-electron oxidation, a reaction that mimics GAO function.

Experimental Procedure

All compounds yielded satisfactory mass spectra and C,H,N analyses. The copper complexes were prepared under an inert atmosphere.

L^1: A solution of the Mannich base of 1,4-diisopropyl-1,4,7-triazacyclononane (4.95 mmol) [17] and 2,4-dimethylphenol (5.16 mmol) were heated at reflux in methanol for 12 h according to ref. [18]. Addition of water to the reaction mixture caused the deposition of a colorless oily mass, which crystallized on standing. Yield: 1.22 g (71%). ^1H NMR (500 MHz, $CDCl_3$): δ = 6.81 (s, 1H), 6.60 (s, 1H), 3.73 (s, 2H), 3.02–2.96 (*m*, 4H), 2.88 (sept, J = 6.5 Hz, 2H), 2.67 (t, J = 5.0 Hz, 4H), 2.43 (s, 4H), 2.19 (s, 3H), 2.17 (s, 3H), 0.95 (d, J = 6.5 Hz, 12H); $^{13}C\{^1H\}$ NMR (125 MHz, $CDCl_3$): δ = 154.2, 130.0, 126.8, 126.4, 124.5, 121.9, 60.8, 54.8, 53.6, 53.4, 52.9, 20.4, 18.3, 15.6. An analogous procedure was used to prepare **L^2** from 2,4-di-*tert*-butylphenol in 90% yield. Data for **L^2**: ^1H NMR (300 MHz, $CDCl_3$): δ = 7.17 (d, J = 2.4 Hz, 1H), 6.81 (d, J = 2.4 Hz, 1H), 3.76 (s, 2H), 3.04–2.85 (overlapping multiplet and septet, 6H), 2.68 (t, J = 4.8 Hz, 4H), 2.46 (s, 4H), 1.42 (s, 9H), 1.28 (s, 9H), 0.97 (d, J = 6.6 Hz, 12H); $^{13}C\{^1H\}$ NMR (75 MHz, $CDCl_3$): δ = 155.0, 139.6, 135.3, 123.2, 122.4, 122.1, 61.5, 54.6, 54.1, 53.7, 53.1, 34.8, 34.1, 31.7, 29.6, 18.4.

1–**3**: The sodium salt of **L^1** (prepared by the reaction of **L^1** (0.21 g, 0.60 mmol) with NaH in THF) and anhydrous $CuCl_2$ (0.081 g, 0.60 mmol) were stirred in THF (5 mL) for 2 h. The mixture was then filtered through a pad of celite, and the filtrate evaporated under reduced pressure. Recrystallization of the residue from CH_2Cl_2/pentane yielded **1** as purple crystals suitable for a single-crystal X-ray analysis, 0.189 g (70%). An analogous method was used to prepare **2** from **L^2** and $CuCl_2$ in 86% yield; complex **3** was prepared similarly using **L^2** and $Cu(O_3SCF_3)_2$ in 85% yield.

4: A solution of **2** (0.163 g, 0.31 mmol) and $NaOCH_2Ph$ (0.062 g, 0.48 mmol) were stirred in THF (5 mL) for 1 h. Pentane (10 mL) was then added, and the green mixture filtered through a pad of celite. Concentration of the filtrate and storage at −20 °C for several days caused the deposition of small green crystals of the product, 0.050 g (27%). Recrystallization from toluene/pentane at −20 °C yielded crystals of **4**·0.5 toluene suitable for a single-crystal X-ray analysis.

Received: January 11, 1996
Revised version: March 18, 1996 [Z87161E]
German version: *Angew. Chem.* **1996**, *108*, 1832–1835

Keywords: copper compounds · galactose oxidase · oxidations · radicals

[1] a) J. A. Stubbe, *Annu. Rev. Biochem.* **1989**, *58*, 257–285; b) J. Z. Pedersen, A. Finazzi-Agro, *FEBS Lett.*, **1993**, *325*, 53–58.

[2] a) J. W. Whittaker in *Metalloenzymes Involving Amino Acid Residue and Related Radicals, Vol. 30* (Eds.: H. Sigel, A. Sigel), Marcel Dekker, New York, **1994**, pp. 315–360; b) P. F. Knowles, N. Ito in *Perspectives in Bio-inorganic Chemistry, Vol. 2*, Jai Press LTD, London, **1994**, pp. 207–244.

[3] a) A. J. Baron, C. Stevens, C. Wilmot, K. D. Seneviratne, V. Blakeley, D. M. Dooley, S. E. V. Phillips, P. F. Knowles, M. J. McPherson, *J. Biol. Chem.* **1994**, *269*, 25095–25105; b) P. F. Knowles, R. D. Brown III, S. H. Koenig, S. Wang, R. A. Scott, M. A. McGuirl, D. E. Brown, D. M. Dooley, *Inorg. Chem.* **1995**, *34*, 3895–3902.

[4] a) N. Ito, S. E. V. Phillips, C. Stevens, Z. B. Ogel, M. J. McPherson, J. N. Kee'n, K. D. S. Yadav, P. F. Knowles, *Nature* **1991**, *350*, 87–90; b) N. Ito, S. E. V. Phillips, C. Stevens, Z. B. Ogel, M. J. McPherson, J. N. Keen, K. D. S. Yadav, P. R. Knowles, *Faraday Discuss.* **1992**, *93*, 75–84; c) N. Ito, S. E. V. Phillips, K. D. S. Yadav, P. F. Knowles, *J. Mol. Biol.* **1994**, *238*, 794–814.

[5] An alternative route involving deprotonation by the stacked tryptophan residue also has been suggested [4b].

[6] a) B. P. Branchaud, M. P. Montague-Smith, D. J. Kosman, F. R. McLaren, *J. Am. Chem. Soc.* **1993**, *115*, 798–800; b) K. Clark, J. E. Penner-Hahn, M. M. Whittaker, J. W. Whittaker, *ibid.* **1990**, *112*, 6433–6434; c) R. M. Wachter, B. P. Branchaud, *J. Am. Chem. Soc.* **1996**, *118*, 2782–2789.

[7] a) U. Rajendran, R. Viswanathan, M. Palaniandavar, M. Lakshminarayanan, *J. Chem. Soc. Dalton Trans.* **1992**, 3563–3564; b) R. Uma, R. Viswanathan, M. Palaniandavar, M. Lakshminarayanan, *J. Chem. Soc. Dalton Trans.* **1994**, 1219–1226; c) H. Adams, N. A. Bailey, D. E. Fenton, Q. He, *Inorg. Chim. Acta* **1994**, *215*, 1–3; d) H. Adams, N. A. Bailey, C. O. R. de Barbarin, D. E. Fenton, Q.-Y. He, *J. Chem. Soc. Dalton Trans.* **1995**, 2323–2331; e) M. Whittaker, Y. Chuang, J. Whittaker, *J. Am. Chem. Soc.* **1993**, *115*, 10029–10035; f) N. Kitajima, K. Whang, Y. Moro-oka, A. Uchida, Y. Sasada, *J. Chem. Soc. Chem. Commun.* **1986**, 1504–1505; g) M. M. Whittaker, W. R. Duncan, J. W. Whittaker, *Inorg. Chem.* **1996**, *35*, 382–386.

[8] J. Laugier, J.-M. Latour, A. Caneschi, P. Rey, *Inorg. Chem.* **1991**, *30*, 4474–4477.

[9] X-ray crystal structure analysis of **1**: purple block crystal (0.50 × 0.50 × 0.20 mm): $C_{21}H_{36}ClCuN_3O$, M_r = 445.53, monoclinic, space group $P2_1/c$, a = 15.18(4) Å, b = 7.538(1) Å, c = 20.58(5) Å, β = 109.1(1)°, V = 2225(8) Å^3, Z = 4 at 298(2) K; ρ_{calcd} 1.330 g cm^{-3}; $2\theta_{max}$ = 50.00°; μ_{Mo} = 11.19 cm^{-1}. The structure was solved by direct methods; hydrogen atoms were placed at calculated positions but were not refined. A semiempirical absorption correction (DIFABS) was applied. The final cycle of full-matrix least-squares refinement (on F), based on 4319 reflections [$I > 2\sigma(I)$] and 245 variable parameters, converged at R = 0.071 and wR = 0.096 (max/min residual electron density 0.72

$-1.03\ e^{-}\ Å^{-3}$). Data were collected on an Enraf–Nonius CAD-4 diffractometer, and calculations were performed with the TEXSAN software package. X-ray crystal structure analysis of **4**·0.5toluene: green block crystal ($0.50 \times 0.50 \times 0.25$ mm); $C_{37.50}H_{59}CuN_3O_2$, $M = 647.42$, monoclinic, space group $P2_1/n$, $a = 17.5316(4)$ Å, $b = 9.3694(3)$ Å, $c = 22.1187(5)$ Å, $\beta = 91.444(1)°$, $V = 3632.1(2)$ Å^3, $Z = 4$ at 173(2) K; $\rho_{calcd} = 1.184\ g\,cm^{-3}$; $2\theta_{max} = 50.18°$; $\mu_{Mo} = 6.36\ cm^{-1}$. The structure was solved by direct methods; non-hydrogen atoms were refined anisotropically, and hydrogen atoms were placed at calculated positions and refined as riding atoms with individual isotropic displacement parameters. A semiempirical absorption correction was applied. A disordered toluene molecule was located on an inversion center; the occupancies of its atoms were fixed at 0.5 to account for the disorder. The final cycle of full-matrix least-squares refinement (on F^2), based on 6402 reflections [$I > 2\sigma(I)$] and 495 variable parameters, converged at $R1 = 0.0359$ and $wR2 = 0.0865$ (max/min residual electron density 0.264/ $-0.369\ e\ Å^{-3}$). Data were collected on a Siemens SMART system and calculations were performed using the SHELXTL V5.0 suite of programs. Crystallographic data (excluding structure factors) for the structures reported in this paper have been deposited with the Cambridge Crystallographic Data Centre as supplementary publications no. CCDC-179-44. Copies of the data can be obtained free of charge on application to The Director, CCDC, 12 Union Road, Cambridge CB2 1EZ UK (Telefax: Int. code +(1223) 336-033; e-mail: teched(@) chemcrys.cam.ac.uk).

[10] For **1** and **4**, $\tau = 0.07$ and $\tau = 0.03$, respectively, where values of 0 or 1, respectively, refer to ideal square-pyramidal or trigonal-bipyramidal geometries as described in A. W. Addison, T. N. Rao, J. Reedijk, J. van Rijn, G. C. Verschoor, *J. Chem. Soc. Dalton Trans.* **1984**, 1349–1356.

[11] **1**: EPR (1:1 CH_2Cl_2:toluene, 77 K, 9.46 GHz): $g_\parallel = 2.25$, $A_\parallel = 152$ G, $g_\perp = 2.03$; UV/Vis (CH_2Cl_2): λ_{max} (ε) = 340 (3.1×10^3), 520 (1.5×10^3), 710 nm (sh, 440). **2**: EPR (1:1 CH_2Cl_2:toluene, 77 K, 9.46 GHz): $g_\parallel = 2.26$, $A_\parallel = 153$ G, $g_\perp = 2.04$; UV/Vis (CH_2Cl_2): λ_{max} (ε) = 350 (3.0×10^3), 526 (1.2×10^3), 720 nm (sh, 400). **3**: EPR (1:1 CH_2Cl_2:toluene, 77 K, 9.46 GHz): $g_\parallel = 2.25$, $A_\parallel = 152$ G, $g_\perp = 2.03$; UV/Vis (CH_2Cl_2): λ_{max} (ε) 328 (3.3×10^3), 532 (1.1×10^3), 696 nm (sh, 450). **4**: EPR (1:1 THF:toluene, 77 K, 9.46 GHz): $g_z = 2.26$, $A_z = 153$ G, $g_y = 2.03$, $g_x = 2.02$; UV/Vis (THF): λ_{max} (ε) = 436 (700), 760 nm (130).

[12] Oxidation of **1** was irreversible ($E_{pa} = +0.71$ V vs. SCE at 100 mVs^{-1} with 0.2 M Bu_4NPF_6 in CH_2Cl_2).

[13] M. M. Whittaker, J. W. Whittaker, *J. Biol. Chem.* **1988**, *263*, 6074–6080.

[14] E. R. Altwicker, *Chem. Rev.* **1967**, *67*, 475–531.

[15] Report describing species in which phenoxyl radicals are coordinated to iron: J. Hockertz, S. Steenken, K. Wieghardt, P. Hildebrandt, *J. Am. Chem. Soc.* **1993**, *115*, 11222–11230.

[16] T. Steiner, W. Saenger, *J. Am. Chem. Soc.* **1993**, *115*, 4540–4547, and references cited therein.

[17] R. P. Houser, J. A. Halfen, V. G. Young, Jr., N. J. Blackburn, W. B. Tolman, *J. Am. Chem. Soc.* **1995**, *117*, 10745–10746.

[18] D. A. Moore, P. E. Fanwick, M. J. Welch, *Inorg. Chem.* **1989**, *28*, 1504–1506.

A Cubic (3,4)-Connected Net with Large Cavities in Solvated $[Cu_3(tpt)_4](ClO_4)_3$ (tpt = 2,4,6-Tri(4-pyridyl)-1,3,5-triazine)**

Brendan F. Abrahams, Stuart R. Batten, Hasan Hamit, Bernard F. Hoskins, and Richard Robson*

Early studies suggest that the simple trigonal building block 2,4,6-tri(4-pyridyl)-1,3,5-triazine (tpt) may provide coordination polymers with diverse structures; examples known to date reveal high symmetry, unusual topology and, as a result of the large size and rigidity of the ligand, large intraframework spaces. The mercury(II) complex $[Hg(tpt)_2](ClO_4)_2 \cdot 6C_2H_2Cl_4$ has a highly symmetrical cubic structure involving a new type of (6,3)-connected net with spacious interconnected cavities that enclose large amounts of unusually well-ordered solvent and anions.[1] The cyanozinc derivative $[Zn_3(tpt)_2(CN)_3(NO_3)_3]$· solvate, which is also cubic, consists of two infinite networks of a previously unknown topology which interpenetrate so as to produce extraordinarily large but completely sealed-off chambers capable of enclosing of the order of twenty molecules of solvent (e.g. ca. $18CHCl_3 + 4CH_3OH$ per chamber or $9C_2H_2Cl_4 + 9CH_3OH$ per chamber)—essentially minute droplets of liquid imprisoned in microscopic cells.[2] A zinc hexafluorosilicate derivative (also cubic) consists of multiply interpenetrating enantiomorphic (10,3)a nets.[3] Recently a different type of (10,3) net, namely Wells's (10,3)b net, was reported by Moore et. al. in a coordination polymer of Ag^+ ions with the related trigonal building block 1,3,5-tris(4-ethynylbenzonitrile)benzene.[4] We report here yet another highly symmetrical coordination polymer of tpt that consists of two independent and interpenetrating cubic nets, producing large, solvent-filled cavities.

Diffusion of a solution of $[Cu(CH_3CN)_4]ClO_4$ in acetonitrile into a solution of tpt in chloroform/1,1,2,2-tetrachloroethane gave very dark red, almost black crystals of solvated $[Cu_3(tpt)_4](ClO_4)_3$ whose structure was determined from single-crystal X-ray diffraction data collected at 110 K. All tpt units are equivalent and are attached to three copper centers at the corners of an equilateral triangle (edge length 12.898(3) Å). All copper centers are equivalent and are coordinated by four tpt-derived pyridine donors in a distorted tetrahedral arrangement (N-Cu-N, 111.0(3) and 106.4(5)°). This results in an infinite (3,4)-connected three-dimensional network with $(6^3)_4(6^28^4)_3$ topology.[5] A repeated structural motif immediately apparent in the network comprises six copper centers at the corners of a regular octahedron, with tpt units occupying alternate triangular faces of the octahedron. These octahedral chambers are large: the diametrically opposed copper atoms are separated by 18.241(4) Å (a unit cell length). Each copper atom is shared by two such units as shown in Figure 1. The tpt units are significantly bowed away from the center of the chamber, one consequence of which is to allow the coordination geometry of the copper atom to approach more closely the tetrahedral ideal. These chambers can be imagined to be derived from the adamantanoid cages of a diamond net by replacing the four 3-connecting centers of the adamantane unit by four trigonal nodes.

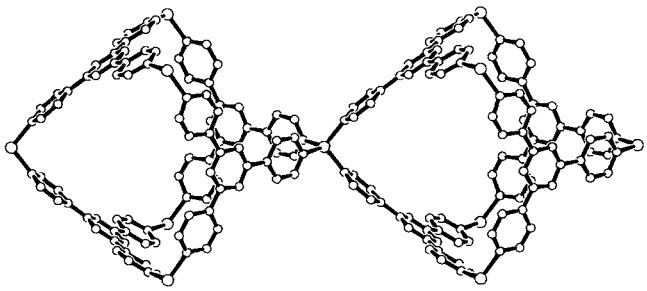

Fig. 1. Two adjacent chambers in the structure of $[Cu_3(tpt)_4](ClO_4)_3$·solvate. Each chamber comprises six Cu^{I} centers (the larger circles) at the corners of a regular octahedron and tpt units occupy alternate triangular faces. Smaller circles represent C and N. Cu–N,2.014(9) Å.

Every chamber is connected by its six copper vertices to six others whose centers are arranged octahedrally around the first. An infinite cubic collection of chambers is thereby produced as shown schematically in Figure 2. At the center of each collection

[*] Dr. R. Robson, Dr. B. F. Abrahams, S. R. Batten, H. Hamit, Dr. B. F. Hoskins
School of Chemistry, University of Melbourne
Parkville, Victoria 3052 (Australia)
Fax: Int. code +(3)347-5180
e-mail: richard_robson(@) muwayf.unimelb.edu.au

[**] This work was supported by the Australian Research Council. We thank Dr. K. Nugent of the School of Physics, University of Melbourne for measuring the UV/Vis spectrum.

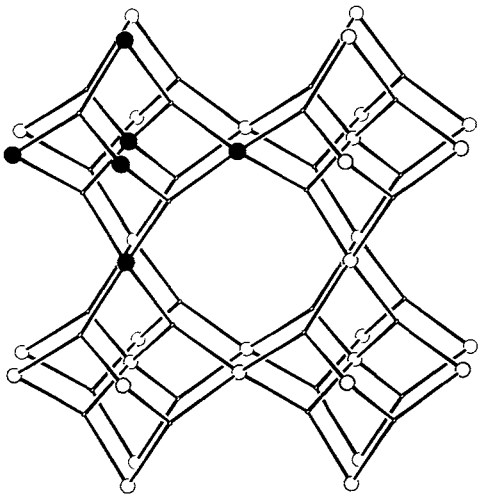

Fig. 2. A cubic tpt Cu framework. Tpt units are represented schematically by three spokes radiating from a point and Cu centers by circles. One octahedral group of Cu centers is highlighted by black circles.

of eight chambers of the type seen in Figure 2 is a cavity which is of the appropriate size, shape, and chemical character to accommodate very neatly a chamber belonging to a second completely independent but identical infinite network. A schematic representation of the two independent interpenetrating networks is shown in Figure 3. Neither framework intrudes inside

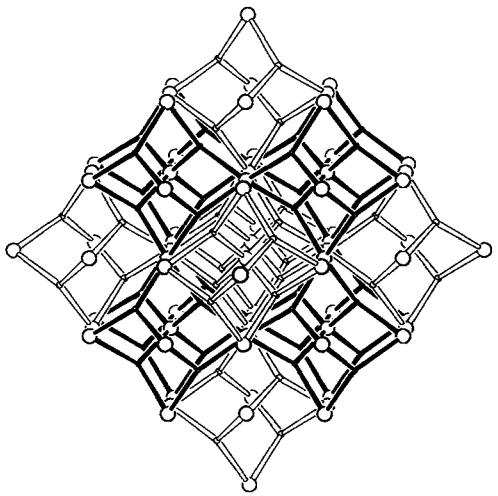

Fig. 3. Schematic representation of two interpenetrating, identical frameworks. Eight chambers of one framework ("black" connections) are disposed at the corners of a cube in the central cavity of which is a chamber of the second framework ("white"), which, in turn, is connected octahedrally to six other "white" chambers.

the octahedral chambers of the other, so the composite structure remains very spacious. Each octahedral chamber in essence has only four of its eight triangular "windows" blocked off by tpt units, the other four remaining "open". The two independent networks are so arranged that the occupied faces of one chamber butt against the occupied faces of a neighboring chamber belonging to the other framework to give discrete, centrosymmetrically related tpt pairs. Likewise the four "open windows" of a given chamber immediately face the "open windows" of four neighboring chambers belonging to the other framework. In contrast to $[Zn_3(tpt)_2](CN)_3(NO_3)_3 \cdot$solvate in which the large chambers are completely sealed off from each other by an impenetrable shell of tpt pairs,[2] $[Cu_3(tpt)_4](ClO_4)_3 \cdot$solvate allows ready access from any chamber to four of its neighbors. The bowing of the tpt ligands away from the interior of the cavity, mentioned earlier, means that within a discrete tpt pair the triazine rings are much closer together (3.29(2) Å) than the two associated Cu_3 triangles (5.27 Å).

The extremely dark red color of the crystals is unusual for Cu^I complexes (λ_{max} 420–550 nm, very broad). In those cases where visible absorption has previously been observed in Cu^I complexes this has been ascribed to metal-to-ligand charge-transfer transitions.[6]

A dark red, almost black, crystalline solid with essentially the same cubic unit cell dimensions (18.236(5) Å) as those of the perchlorate is obtained by using $CuBF_4$ in place of $CuClO_4$ following an otherwise identical procedure. The IR spectrum (KBr disc) of the tetrafluoroborate shows an anion-derived band at 1060 cm^{-1}, that of the perchlorate at 1100 and 625 cm^{-1}.

We are presently investigating whether selective incorporation of various species into the large chambers of $[Cu_3(tpt)_4](ClO_4)_3$ can be achieved.

Experimental Procedure

A buffer zone of chloroform (10 mL) was carefully layered on top of a solution of tpt (25 mg) in 1,1,2,2-tetrachloroethane (10 mL) and then a solution of $[Cu(CH_3CN)_4]ClO_4$ (45 mg) in acetonitrile (5 mL) was carefully layered on top of that. Very dark red, almost black crystals of solvated $[Cu_3(tpt)_4](ClO_4)_3$ grew on the vessel walls just below the buffer region over a period of several days. The crystals, which were sensitive to solvent loss upon exposure to the atmosphere, were transferred directly from solution to oil and cooled to 110 K on an Enraf-Nonius CAD-4MachS diffractometer for crystallographic analysis. The product obtained in this way was accompanied by a small amount of orange material and was therefore unsuitable for elemental analysis. Formation of the orange solid could be eliminated by replacing a large fraction of the acetonitrile in which the $[Cu(CH_3CN)_4]ClO_4$ was dissolved by methanol and by reducing the proportion of copper. The sample for analysis was obtained exactly as above except that the top layer consisted of $[Cu(CH_3CN)_4]ClO_4$ (22 mg) in acetonitrile:methanol (1:9, 10 mL). Even after it had been dried to constant weight at 160 C under vacuum and thereby losing 30.7% by weight, the sample still clearly retained considerable solvent. Elemental analysis calcd. for $[Cu_3(tpt)_4](ClO_4)_3 \cdot 1.5CH_3OH \cdot 1.17C_2H_2Cl_4$ ($C_{75.84}H_{56.34}Cl_{5.68}Cu_3N_{24}O_{13.5}$): C 45.9, H 2.9, Cu 9.6, Cl 13.7, N 17.0; found: C 45.4, H 2.6, Cu 9.6, Cl 13.2, N 17.1; IR (Kbr): $\tilde{\nu}$ = 1100, 625 (ClO), 1580 (CN) cm^{-1}. Crystal dimensions: 0.4 × 0.4 × 0.4 mm; cubic, space group $Pn\bar{3}m$ (no. 224), a = 18.241(4) Å, V = 6069(2) Å^3, Z = 2, ρ_{calcd} = 1.572 gcm^{-3}, $2\theta_{max}$ = 150°, $Cu_{K\alpha}$ radiation, λ = 1.5418 Å, ω:2θ scan, 1457 reflections collected, 1194 independent reflections, all reflections included in the refinement. Corrections applied for Lorentz and polarization effects. Absorption corrections were numerically evaluated by Gaussian integration (SHELX-76 [7]), μ = 75.18 cm^{-1}, min./max. transmission 0.2205/0.1069. The structure was solved by using direct methods (SHELXS-86 [8]) and refined by using a full-matrix least squares refinement based on F^2 (SHELXL-93 [9]), 62 parameters. The four unique pyridyl hydrogen atoms were located in difference electron density maps and were assigned to calculated positions. $R1$ [$I > 2\sigma(I)$] = 0.1473, $wR2$ [$I > 2\sigma(I)$] = 0.3938 [10]. Residual electron density = 0.634 e Å^{-3}. Crystallographic data (excluding structure factors) for the structure(s) reported in this paper have been deposited with the Cambridge Crystallographic Data Centre as supplementary publication no. CCDC-179-38. Copies of the data can be obtained free of charge on application to The Director, CCDC, 12 Union Road, Cambridge CB2 1EZ, UK (fax: Int. code +(1223) 336-033; e-mail: teched@chemcrys.cam.ac.uk).

Received: January 8, 1996
Revised version: March 26, 1996 [Z8704IE]
German version: *Angew. Chem.* **1996**, *108*, 1794–1796

Keywords: complexes with nitrogen ligands · coordination polymers · copper compounds · triazines

[1] S. R. Batten, B. F. Hoskins, R. Robson, *Angew. Chem.* **1995**, *107*, 884; *Angew. Chem. Int. Ed. Engl.* **1995**, *34*, 820.
[2] S. R. Batten, B. F. Hoskins, R. Robson, *J. Am. Chem. Soc.* **1995**, *117*, 5385.
[3] B. F. Abrahams, S. R. Batten, H. Hamit, B. F. Hoskins, R. Robson, *Chem. Commun.* **1996**, in press.
[4] G. B. Gardner, D. Venkataraman, J. S. Moore, S. Lee, *Nature*, **1995**, *374*, 792.

[5] A. F. Wells, *Acta Crystallogr. Sect. A*, **1986**, *42*, 133. We are indebted to one of the referees who drew our attention to this reference.
[6] M. Melnik, L. Macaskova, C. E. Holloway, *Coord. Chem. Rev.* **1993**, *126*, 92.
[7] G. M. Sheldrick, *SHELX-76, Program for Crystal Structure Determination*, University of Cambridge, Cambridge, UK, **1976**.
[8] G. M. Sheldrick, *SHELXS-86, Program for Crystal Structure Solution*, Universitat Gottingen, **1986**.
[9] G. M. Sheldrick, *SHELXL-93, Program for Crystal Structure Refinement*, Universitat Gottingen, **1993**.
[10] The problem of relatively high R values is far from unusual in materials of this type in which highly disordered solvent constitutes a very significant fraction of the volume of the crystal. There are numbers of examples of crystal structure analyses in the literature where similar problems have been encountered and where refinements have converged with comparably high R values.

Total Synthesis of (+)-Camptothecin**

Marco A. Ciufolini* and Frank Roschangar

Camptothecin (CPT, **1**)[1] and related compounds (e.g. **2** and **3**)[2] have lately reestablished themselves as important antitumor agents.[3] Consensus has developed regarding their biomolecular target and mode of action,[4] and new biological properties of **1** have recently been discovered.[5] A good synthesis of CPT appears to be necessary in light of its biomedical significance and of its natural scarcity. As a consequence, synthetic activity in this area has experienced a major revival, and elegant new solutions have emerged.[6]

Our own interest in developing a practical synthesis of CPT and analogues led us to envision retrosynthetic dissection of the N4–C5 bond as the last stage of ring C construction. A concise synthesis might result by the merger of quinoline **4**, scalemic aldehyde **5**, and cyanoacetamide (**6**), through the agency of our recently described pyridone chemistry (Scheme 1).[7] Minor

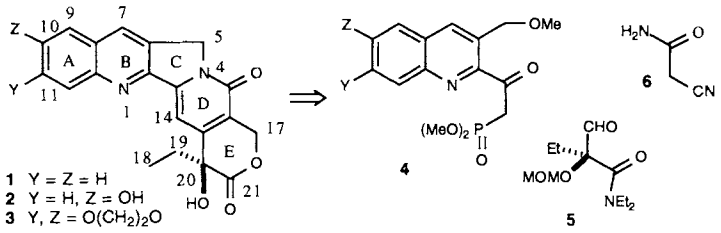

Scheme 1. Retrosynthetic analysis of 1 and analogues. MOM = methoxymethyl.

modifications of the same general approach could also result in diverse analogues of **1**. The above mode of ring C formation is indeed facile. The strategy described here utilizes an enzymatic desymmetrization of a malonate, instead of chiral auxiliaries,[6e] Sharpless dihydroxylation,[6f-h] or resolution,[1] as a means to control absolute stereochemistry at C20.

[*] Prof. Dr. M. A. Ciufolini, F. Roschangar
Department of Chemistry, Rice University
P. O. Box 1892
Houston, TX 77251 (USA)
Fax: Int. code +(713)285-5155
e-mail: ciufi@ ruf.rice.edu

[**] We thank the National Institutes of Health (CA-55268), the National Science Foundation (CHE 95-26183), the Robert A. Welch Foundation (C-1007), and the Alfred P. Sloan Foundation, for support of our research, and Dr. Monroe E. Wall, Research Triangle Institute, North Carolina, for a gift of authentic camptothecin.

Condensation of phosphonate **4**, Y = Z = H, with aldehyde **5** (vide infra) afforded enone **7**, $[\alpha]_D^{25} = -56.1$ ($c = 4.720$ in $CHCl_3$), in 80% yield (Scheme 2). For reasons that are not yet

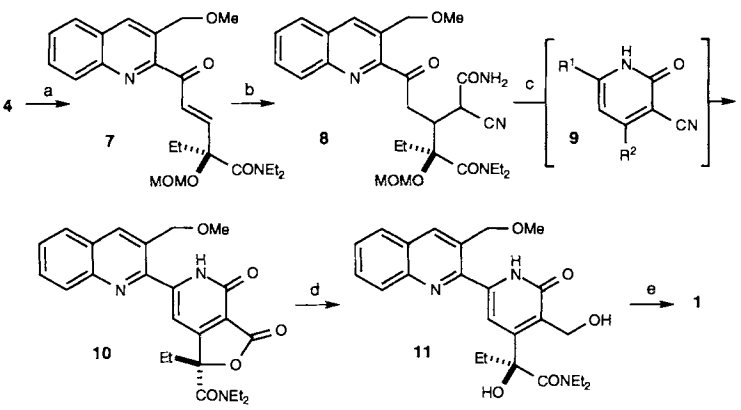

Scheme 2. a) *t*BuOK, 1,2-dimethoxyethane (DME), 5, 50 C, 12 h, 80%; b) **6**, *t*BuOK, DMSO, 25 C; c) 0.2 equiv of 5% SeO_2 on silica gel, *t*BuOOH, AcOH, 110 C, then 10% aq H_2SO_4 (see text), 68% combined yield for steps b and c; d) $NaBH_4$ (10 equiv) $CeCl_3$ (2.5 equiv), EtOH, 0 C for 20 min, then 45 C for 30 min; e) 60% H_2SO_4 in EtOH, 115 C, 94% combined yield for steps d,e.

fully understood, **7** was a poor substrate for our pyridone-forming reaction.[7] However, **7** combined with the potassium enolate of **6**[8] in DMSO to afford Michael adduct **8** in quantitative yield.[9] Subsequent oxidation with *t*BuOOH in AcOH in the presence of 20 mol% SeO_2 adsorbed on silica gel[10] gave pyridone **9**, $[\alpha]_D^{25} = -71.0$ ($c = 6.650$ in $CHCl_3$), in 74% yield. Exposure of **9** to acidic conditions induced conversion into the more synthetically useful lactone **10**, $[\alpha]_D^{25} = -38.8$ ($c = 1.025$ in $CHCl_3$). More conveniently, **10** was obtained directly from **8** simply by allowing the oxidation to reach completion (1 h), adding 10% vol/vol of 10% aqueous H_2SO_4 to the mixture, and heating at reflux for one more hour. The overall yield of **10** from **7** was thus 68%.

Lactones of the type **10** had been previously regarded as poor synthetic intermediates for **1**, because their reduction to diols like **11** is highly troublesome.[11] We confirmed these difficulties, but after much research we found that a modification of the Luche[12] protocol accomplished reduction of **10** to **11**, $[\alpha]_D^{25} = +72.1$ ($c = 1.200$ in $CHCl_3$), in over 95% yield. When crude **11** was heated at 115 °C for 5 h in 60% ethanolic H_2SO_4, fully synthetic, pure (20*S*)-(+)-camptothecin (**1**), identical in all respects including optical rotation, $[\alpha]_D^{25} = +34.8$ ($c = 0.400$ in 8:2 $CHCl_3$/CH_3OH; lit. $+35.0$[11]), to authentic samples from two different sources,[13] emerged in 94% overall yield from **10** after flash chromatography.[14] The merger of fragments **4**, **5**, and **6** to give CPT thus occurs in five steps and in 51% overall yield.

Compound **4** was obtained as follows. Readily available quinoline **12**[15] underwent smooth carbomethoxylation to **13** under catalysis by 5 mol% $[Pd(OAc)_2(dppp)_2]$ (dppp = 1,3-bis-(diphenylphosphino)propane) (Scheme 3). While aryl chlorides

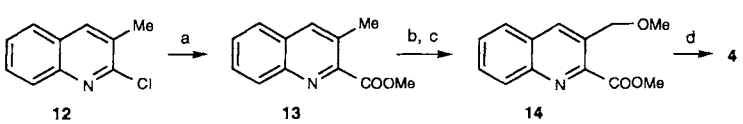

Scheme 3. a) 5 mol% $[Pd(dppp)_2Cl_2]$, NaOAc, MeOH, DMF, 105 atm (1500 psi) CO, 140 C, 98%; b) *N*-bromosuccinimide (NBS), CCl_4, $(BzO)_2$, hv; c) MeOH, 5% H_2SO_4, reflux, 55% combined yield for steps b and c; d) $(MeO)_2P(O)CH_2Li$ (2 equiv), THF, −78 C, 100%.

are generally unreactive in carbonylation reactions and normally require complex catalysts,[16] the great reactivity of 2-haloquinolines seems to overcome these problems. Radical bromination and methanolysis[17] advanced **13** to **14**, which delivered phosphonate **4** upon Corey–Kwiatkowski reaction.[18]

Compound **5** was prepared by the following sequence. Dimethyl 2-ethylmalonate adsorbed on silica gel was cleanly hydroxylated by ozone[19] at room temperature to give **15** (Scheme 4). Methoxymethyl (MOM) protection of the hydroxyl

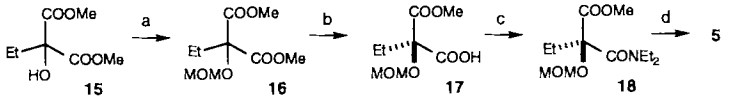

Scheme 4. a) MOMCl, diisopropylethylamine, CH_2Cl_2, 25 °C, 100%; b) PLE, 25% aq DMSO, pH 6.8–7.4, 35 °C, 90%, >98% *ee* (see text); c) *N*-methyl-2-chloropyridinium iodide, Et_2NH, Et_3N, CH_2Cl_2, 25 °C, 90%; d) DIBAL, THF, −78 °C, 100%.

group[20] and enantioselective hydrolysis with pig liver esterase (PLE)[21] furnished **17**, $[\alpha]_D^{25} = +10.0$ ($c = 6.150$ in $CHCl_3$), in 90% overall yield and in >98% *ee*.[22] This carboxylic acid was converted to diethylamide **18**, $[\alpha]_D^{25} = -67.4$ ($c = 6.850$ in $CHCl_3$), under Mukaiyama conditions.[23] Subsequent exposure to diisobutylaluminum hydride (DIBAL) resulted in chemoselective and quantitative reduction of the ester to aldehyde **5**, $[\alpha]_D^{25} = -40.8$ ($c = 10.25$ in $CHCl_3$), which was spectroscopically and microanalytically pure in "crude" form and was therefore not further purified.[24]

In summary, CPT may now be obtained in ten linear steps in 30% overall yield starting from dimethyl ethylmalonate. As shown in Scheme 5, the present synthesis is twice as efficient as

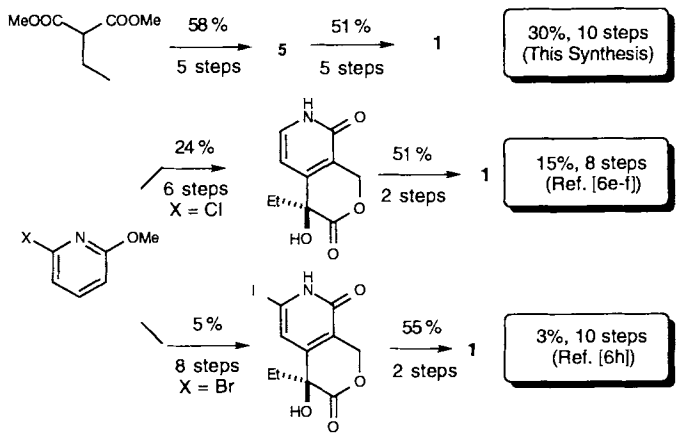

Scheme 5. Comparison of published syntheses of (+)-camptothecin (**1**).

the best enantioselective alternative currently available (eight steps, 15% overall yield),[6e, f] and ten times higher yielding than the next best enantioselective protocol (ten steps, 3% overall yield).[6h] We are hopeful that our synthesis will facilitate the creation of novel CPT analogues for bioassay and for the eventual development of better anticancer resources.

Received: November 16, 1995
Revised version: March 13, 1996 [Z 5591E]
German version: *Angew. Chem.* **1996**, *108*, 1789–1791

Keywords: alkaloids · asymmetric syntheses · camptothecin · natural products

[1] Leading references and reviews: a) M. E. Wall, M. Wani in *The Chemistry of Heterocyclic Compounds: Monoterpenoid Indole Alkaloids, Vol. 25* (Ed.: J. E. Saxton), Wiley, Chichester, UK, **1994**, p. 689; b) M. E. Wall, M. Wani, A. W. Nicholas, G. Manikuma, C. Tele, L. Moore, A. Truesdale, P. Leitner, J. M. Besterman, *J. Med. Chem.* **1993**, *36*, 2689; c) M. Suffness, G. A. Cordell in *The Alkaloids, Vol. 25* (Ed.: A. Brossi), Academic Press, Orlando, FL, **1985**, Chapter 1, see especially p. 75ff.

[2] Cf. ref. [1] as well as: a) M. J. Luzzio, J. M. Besterman, D. L. Emerson, M. G. Evans, K. Lackey, P. L. Leitner, G. McIntyre, B. Morton, P. L. Myers, M. Peel, J. M. Sisco, D. D. Sternbach, W. Q. Tong, A. Truesdale, D. E. Uehling, A. Vuong, J. Yates, *J. Med. Chem.* **1995**, *38*, 395; b) D. E. Uehling, S. S. Nanthakumar, D. Croom, D. L. Emerson, P. L. Leitner, M. J. Luzzio, G. McIntyre, B. Morton, S. Profeta, J. M. Sisco, D. D. Sternbach, W. Q. Tong, A. Vuong, J. Yates, J. M. Besterman, *ibid.* **1995**, *38*, 1106.

[3] a) D. P. Curran, *J. Chin. Chem. Soc. (Peking)* **1993**, *40*, 1; b) M. Potmesil, *Cancer Res.* **1994**, *54*, 1431.

[4] The activity of **1** is believed to result from inhibition of topoisomerase I. See e.g. a) W. D. Kingsbury, J. C. Boehm, D. R. Jackas, K. G. Holden, S. M. Hecht, G. Gallagher, M. J. Caranfa, F. L. McCabe, L. F. Faucette, R. K. Johnson, R. P. Hertzberg, *J. Med. Chem.* **1991**, *34*, 98; b) E. Kjeldsen, J. Q. Svejstrup, I. I. Gromova, J. Alsner, O. Westergaard, *J. Mol. Biol.* **1992**, *228*, 1025; c) F. Jakob, J. Seufert, C. Sarrazin, D. Schneider, J. Kohrle, H. P. Tony, *Bioch. Biophys. Res. Commun.* **1994**, *199*, 531; d) I. Husain, J. L. Mohler, H. F. Seigler, J. M. Besterman, *Cancer Res.* **1994**, *54*, 539, and references therein.

[5] Antiretroviral activity: a) E. Priel, S. D. Showalter, D. G. Blair, *AIDS Res. Hum. Retroviruses* **1991**, *7*, 65; b) I. Pendrak, R. Whittrock, W. D. Kingsbury, *J. Org. Chem.* **1995**, *60*, 2912. Modulation of protein synthesis: c) J. L. Janavs, J. C. Florez, M. E. Pierce, J. S. Takahashi, *J. Neurosci.* **1995**, *15* (1), 298.

[6] Thorough reviews of earlier synthetic activity are listed in ref. [1]. Recent syntheses of (±)-**1**: a) D. P. Curran, H. Liu, *J. Am. Chem. Soc.* **1992**, *114*, 5863; b) S. Wang, C. A. Coburn, W. G. Bornmann, S. J. Danishefsky, *J. Org. Chem.* **1993**, *58*, 611; c) A. V. Rama Rao, J. S. Yadav, M. Valluri, *Tetrahedron Lett.* **1994**, *35*, 3613; d) D. L. Comins, H. Hong, J. K. Saha, J. H. Gao, *J. Org. Chem.* **1994**, *59*, 5120. Recent syntheses or formal syntheses of (+)-**1**: e) D. L. Comins, M. F. Baevsky, H. Hong, *J. Am. Chem. Soc.* **1992**, *114*, 10971; f) F. G. Fang, S. P. Xie, M. W. Lowery, *J. Org. Chem.* **1994**, *59*, 6142; g) S. S. Jew, K. D. Oh, H. J. Kim, J. M. Kim, J. M. Hah, Y. S. Cho, *Tetrahedron Asymmetry* **1995**, *6*, 1245; h) D. P. Curran, S. B. Ko, H. Josien, *Angew. Chem.* **1995**, *107*, 2948; *Angew. Chem., Int. Ed. Engl.* **1995**, *34*, 2683.

[7] R. Jain, F. Roschangar, M. A. Ciufolini, *Tetrahedron Lett.* **1995**, *36*, 3307.

[8] From equimolar amounts of **6** and *t*BuOK.

[9] The Michael product was obtained as a mixture of diastereomers of the ring and chain tautomers.

[10] Use of adsorbed SeO_2: a) T. Ohtsuka, H. Shirahama, T. Matsumoto, *Chem. Lett.* **1981**, 1703. Similar oxidations with stoichiometric or even excess SeO_2 have been described, inter alia, by b) H. H. Otto, O. Rinus, *Arch. Pharm.* **1979**, *312*, 548; c) Wojcik, M., *Dissertation*, Harvard University, **1970**.

[11] A. G. Schultz, *Chem. Rev.* **1973**, *73*, 385.

[12] J. L. Luche, L. Rodriguez-Hahn, P. Crabbé, *J. Chem. Soc. Chem. Commun.* **1978**, 601. Reducing agents explored included $LiAlH_4$ (destruction of the substrate), DIBAL or $LiBH_4$ in THF and ethanolic $NaBH_4$ (competing quinoline reduction), $NaBH_4$ suspended in refluxing THF (45% yield of **11** plus overreduced products), KBH_4 with or without [18]crown-6 and $Zn(BH_4)_2$, both with or without added EtOH (no reaction), and $LiEt_3BH$ (demethoxylation probably through single electron transfer).

[13] Samples of natural **1** were purchased from Aldrich and received as a gift through the courtesy of Dr. Monroe E. Wall, Research Triangle Institute, NC (USA).

[14] Formation of the ring E lactone is rapid; the resulting intermediate cyclizes more slowly to **1**.

[15] One step from propionanilide by the Meth-Cohn quinoline synthesis: O. Meth-Cohn, B. Narine, B. Tarnowski, *J. Chem. Soc. Perkin Trans. 1* **1981**, 1537.

[16] Y. Ben-David, M. Portnoy, D. Milstein, *J. Am. Chem. Soc.* **1989**, *111*, 8742.

[17] Methanolysis was best carried out under acidic conditions.

[18] E. J. Corey, G. T. Kwiatkowski, *J. Am. Chem. Soc.* **1966**, *88*, 5654.

[19] Cf. Z. Cohen, H. Varkony, E. Keinan, Y. Mazur in *Org. Synth. Coll. Vol. VI*, **1988**, 43. Apparently, no examples of hydroxylation of malonates with ozone have been recorded in the literature.

[20] A MOM group promotes high enantioselectivity and fast rate of hydrolysis, in agreement with the report of M. Luyten, S. Müller, B. Herzog, R. Keese, *Helv. Chim. Acta* **1987**, *70*, 1250.

[21] Cf. a) R. Azerad, *Bull. Soc. Chim. Fr.* **1995**, *132*, 17; b) E. Santaniello, P. Ferraboschi, P. Grisenti, A. Manzocchi, *Chem. Rev.* **1992**, *92*, 1071; c) M. Ohno, M. Otsuka, *Org. React.* **1989**, *37*, 1. Maximum enantioselectivity is obtained when the reaction is conducted in 25% aqueous DMSO at 35 C; d) M. A. C. Andrade, F. A. C. Andrade, R. S. Phillips, *Bioorg. Med. Chem. Lett.* **1991**, *1*, 373.

[22] Determined by comparison of the ^{1}H NMR spectra of the amides obtained from racemic and scalemic **17** and (*S*)-(−)-α-methylbenzylamine. Amide formation was best carried out with the Mukaiyama reagent [23].

[23] T. Mukaiyama, M. Usui, E. Shimada, K. Saigo, *Chem. Lett.* **1975**, 1045. The DCC procedure gave poor results.

[24] *ent*-**5** is readily available from **17** by reaction with excess Et_2NLi (methyl ester/diethylamide exchange) and esterification (CH_2N_2, 63% over the two steps), followed by DIBAL reduction (100%). Biologically inactive *ent*-**1** was obtained from *ent*-**5** as described above, confirming the absolute configuration of **5**.

Ancillary Ligand Dependent Shifts in Charge Distribution for Cobalt–Quinone Complexes**

Ok-Sang Jung,* Du Hwan Jo, Young-A Lee, Youn Soo Sohn, and Cortlandt G. Pierpont*

Transition metal complexes containing chelated *o*-quinone ligands have metal- and quinone-localized electronic levels that are unusually close in energy.[1] As a consequence, intramolecular charge transfer between metal and ligand occurs at low energy, and, in some cases, under conditions of thermal equilibrium.[2, 3] Structural changes that accompany shifts in metal oxidation and spin states have been applied to materials that exhibit photomechanical properties and optical switching effects.[4, 5] The most extensively studied equilibria of this type occur for complexes of cobalt with general formula [Co(N–N)(dbq)$_2$], where dbq is the semiquinonate (dbsq) or catecholate (dbcat) form of either 3,5- or 3,6-di-*tert*-butyl-1,2-benzoquinone and N–N is a bidentate nitrogen-donor ancillary ligand.[2] Temperature-dependent equilibria [Eq. (a)] may be

$$[Co^{III}(N-N)(dbsq)(dbcat)] \rightleftharpoons [Co^{II}(N-N)(dbsq)_2] \quad (a)$$

observed in the solid state as well as in solution by monitoring changes in the optical spectrum or in the magnetism for the shift from the low-spin Co^{III} ion to the high-spin Co^{II} ion.[6] The Co^{III}/Co^{II} transition temperature (T_c) is dependent upon the nature of the nitrogen coligand.[7] By defining the transition temperature as the point where concentrations of redox isomers are equal, T_c is equal to the ratio of enthalpic and entropic changes associated with the equilibrium.[6] The enthalpy change is primarily associated with changes in bond energy that occur with the shift in metal charge and spin state. Low-frequency vibrational shifts that accompany the transition to the high-spin Co^{II} ion provide the greatest contribution to ΔS, and both effects are associated with the change in population of the metal d_σ (e_g) orbitals. Donor effects of the coligands are clearly important in defining T_c through both enthalpic and entropic contributions, and the properties of ancillary ligands may be used to tune transition temperature with great sensitivity.[8] Herein we describe an unexpectedly large change in T_c associated with a minor change in coligand structure.

In an earlier study we described the properties of [Co^{III}(tmeda)(3,6-dbsq)(3,6-dbcat)] (tmeda = *N*,*N*,*N*′,*N*′-tetramethylethylenediamine).[2] The hard-donor coligand used in this case provides stabilization for the Co^{III} isomer and is responsible for the relatively high transition temperature of 310 K in solution (toluene). The T_c value for this complex is 35 K higher than that of the related bipyridine complex, even though the Co–N bond lengths are 0.1 Å longer with tmeda. Temperature-dependent changes in magnetic moment that accompany shifts in equilibrium are shown in Figure 1 for complexes prepared with *N*,*N*,*N*′,*N*′-tetramethylmethylenediamine (tmmda),

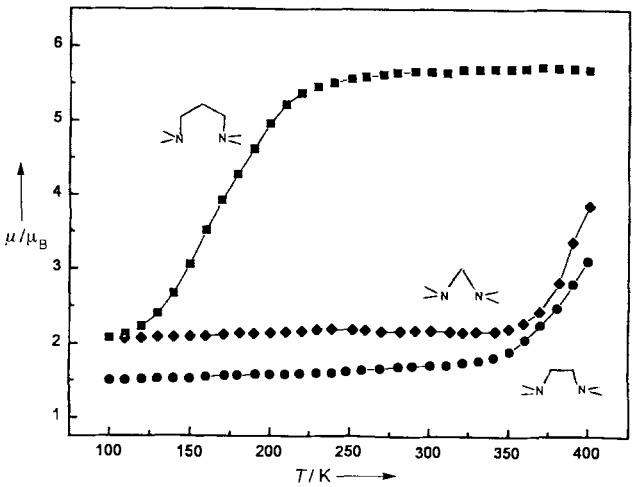

Fig. 1. Temperature dependence of the magnetic moments of complexes of the type [$Co\{Me_2N(CH_2)_nNMe_2\}(3,6\text{-dbq})_2$], $n = 1-3$.

tmeda, and *N*,*N*,*N*′,*N*′-tetramethylpropylenediamine (tmpda). The Co^{III} redox isomer has a single unpaired electron localized on the sq ligand. Metal–radical magnetic exchange that occurs for the Co^{II} isomer is responsible for values in magnetic moment that generally range between 4.5 and 5.5 μ_B. The solid-state T_c for [Co(tmeda)(3,6-dbsq)(3,6-dbcat)] lies above 400 K, and magnetic measurements made on [Co(tmmda)(3,6-dbsq)(3,6-dbcat)] indicate that it behaves similarly. In marked contrast, the related complex prepared with a propylene bridge between nitrogen donors has a solid-state T_c of 178 K, more than 200 K below the value for the corresponding complex with tmeda ligands. Solid-state equilibria have been monitored spectroscopically by observing intensity changes for a low-energy charge transfer transition that occurs characteristically for the Co^{III} redox isomers.[2] This band appears at 2500 nm for [Co(tmpda)(3,6-dbsq)(3,6-dbcat)], and temperature-dependent changes in intensity are shown in Figure 2. Structural features of [Co^{II}(tmpda)(3,6-dbsq)$_2$] in the solid state are shown in Figure 3.[9] In contrast to the features of [Co^{III}(tmeda)(3,6-dbsq)(3,6-dbcat)], Co–N and Co–O bond lengths are typical of high-spin Co^{II} ions, and dimensions of the quinone ligands are those of a semiquinone. The tmpda ligand is disordered in the structure by rotation about the Co–N2 bond. Crystallographic data collected at room temperature failed to provide clear resolution of the disordered carbon atoms, but data collected at

[*] Prof. O.-S. Jung, Dr. D. H. Jo, Prof. Y.-A. Lee, Dr. Y. S. Sohn
Inorganic Chemistry Laboratory
Korea Institute of Science and Technology
Cheongryang, Seoul 136-791 (Korea)
Prof. C. G. Pierpont
Department of Chemistry and Biochemistry
University of Colorado, Boulder, CO 80309 (USA)
Fax: Int. code +(303)492-5894

[**] Support for research carried out at KIST was provided as part of the E-project under grant 2N13694. Research at the University of Colorado was supported by the National Science Foundation through grant CHE 9023636.

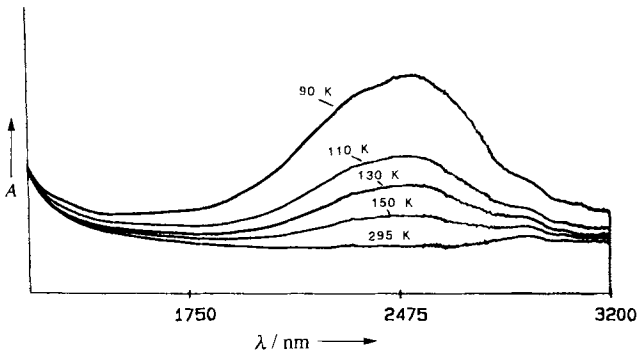

Fig. 2. Changes in the intensity of the transition at 2500 nm in [Co^{III}(tmpda)(3,6-dbsq)(3,6-dbcat)] with the equilibrium shift to [Co^{II}(tmpda)(3,6-dbsq)$_2$] at higher temperature in the solid state. Spectra were recorded on a sample prepared as a KBr disk. A = absorption.

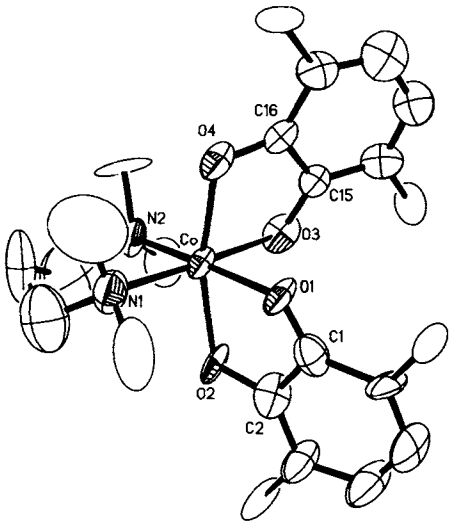

Fig. 3. View of the structure of [Co^{II}(tmpda)(3,6-dbsq)]. Carbon atoms bonded to N2 are shown in one of two disordered locations. Selected average bond lengths [Å]: Co–O 2.019(6), Co–N 2.181(10), C–O (quinone ligands) 1.29(1).

150 K gave locations for two sets of carbon atoms bonded to N2. Furthermore, data collected at 110 K has given clear resolution of the disorder and provided structural evidence for the transition to the Co^{III} isomer at low temperature.[10] The results of these structural studies will be described in a separate publication, but they show no evidence for an axially elongated low-spin Co^{II} intermediate that might appear with the high-spin Co^{II}/low-spin Co^{III} transition.

Energy changes that influence the equilibrium shown in Equation (a) provide fundamental insights on intramolecular metal–ligand electron transfer, information that is difficult to obtain directly for systems studied under conditions that are often dominated by solvation effects.[11, 12] Solid-state equilibria are of particular interest since the molecular environment can be precisely defined. Structural characterization on both [Co^{II}(tmpda)(3,6-dbsq)$_2$] and [Co^{III}(tmeda)(3,6-dbsq)(3,6-dbcat)] has shown that there are no close intermolecular contacts in the solid state. Temperature-dependent changes in both magnetism and the intensity of the band at 2500 nm in the spectrum have been used to calculate relative concentrations of Co^{II} and Co^{III} isomers present in the solid state, and from this data thermodynamic parameters have been obtained for the equilibrium.[6] The enthalpy change has been determined to be 14.2 kJ mol^{-1}, and the entropy change is 80 J mol^{-1} K^{-1}. The value for ΔS is large, but in agreement with values obtained for metal redox processes that place charge in M–L antibonding d_σ orbitals.[11] A value of 98 J mol^{-1} K^{-1} was obtained from a similar analysis on [Co(bpy)(3,5-dbq)$_2$] (bpy = 2,2′-bipyridine) in the solid state. The enthalpy change for [Co(tmpda)(3,6-dbq)$_2$] is roughly half the value of 32 kJ mol^{-1} obtained for the bipyridine complex, but within the range of values associated with Co^{II}/Co^{III} electron transfer reactions.[12] A detailed thermodynamic analysis has not been carried out for [Co(tmeda)(3,6-dbsq)(3,6-dbcat)] due to its high T_c, but the difference between complexes containing tmeda and tmpda ancillary ligands seems clearly related to the difference in chelate ring size. The six-membered chelate ring of tmpda permits greater vibrational flexibility and a N-Co-N bond angle that is more conducive to high-spin Co^{III} ions.

Experimental Procedure

[Co{$Me_2N(CH_2)_nNMe_2$}(3,6-dbq)$_2$], n = 1–3: Synthetic procedures used to prepare complexes with tmmda (n = 1) and tmpda (n = 3) coligands were similar to the synthesis of the related tmeda (n = 2) complex described previously [2].

Received: January 15, 1996 [Z 8719 IE]
German version: *Angew. Chem.* **1996**, *108*, 1796–1797

Keywords: cobalt compounds · complexes with quinone ligands · electron transfer · isomerism · redox systems

[1] C. G. Pierpont, C. W. Lange, *Prog. Inorg. Chem.* **1993**, *41*, 381.
[2] O.-S. Jung, C. G. Pierpont, *Inorg. Chem.* **1994**, *33*, 2227.
[3] A. S. Attia, C. G. Pierpont, *Inorg. Chem.* **1995**, *34*, 1172.
[4] O.-S. Jung, C. G. Pierpont, *J. Am. Chem. Soc.* **1994**, *116*, 2229.
[5] O.-S. Jung, D. H. Jo, Y.-A Lee, B. J. Conklin, C. G. Pierpont, *Angew. Chem.* submitted.
[6] C. G. Pierpont, O.-S. Jung, *Inorg. Chem.* **1995**, *34*, 4281.
[7] Transition temperature (T_c) for the equilibrium described in Equation (a) is defined as the temperature at which concentrations of the Co^{III} and Co^{II} redox isomers are equal.
[8] O.-S. Jung, C. G. Pierpont, *J. Am. Chem. Soc.* **1994**, *116*, 1127.
[9] Dark blue-green prismatic crystals of [Co(tmpda)(3,6-dbsq)$_2$] were obtained by slow evaporation of a saturated solution in toluene. Monoclinic crystal system, space group $P2_1/c$, a = 16.987(2), b = 11.771(2), c = 19.723(3) Å, β = 111.82(1)°, V = 3661.1(9) Å^3, Z = 4, T = 24 °C. At T = −125 °C: a = 16.804(2), b = 11.691(2), c = 19.415(3) Å, β = 111.52(1)°, V = 3548.3(9) Å^3. Data were collected on a Siemens P3F diffractometer at both temperatures. Calculations were carried out by using the SHELXTL library of crystallographic programs. The structure was solved by using a sharpened Patterson map. Refinement with data collected at 24 °C converged with R = 0.080 and Rw = 0.100 for 2242 observed ($I > 2\sigma(I)$) reflections. Data collected at −125 °C converged with R = 0.074 and Rw = 0.105 for 2753 observed reflections. Crystallographic data (excluding structure factors) for the structure(s) reported in this paper have been deposited with the Cambridge Crystallographic Data Centre as supplementary publication no. CCDC-179-40. Copies of the data can be obtained free of charge on application to The Director, CCDC, 12 Union Road, Cambridge CB2 1EZ, UK (fax: Int. code +(1223) 336-033; e-mail: teched@chemcrys.cam.ac.uk).
[10] O.-S. Jung, D. H. Jo, Y.-A Lee, C. G. Pierpont, *Inorg. Chem.* submitted.
[11] a) D. E. Richardson, P. Sharpe, *Inorg. Chem.* **1991**, *30*, 1412; b) *ibid.* **1993**, *32*, 1809.
[12] a) P. W. Crawford, F. A. Schultz, *Inorg. Chem.* **1994**, *33*, 4344; b) Y.-D. Gao, K. B. Lipkowitz, F. A. Schultz, *J. Am. Chem. Soc.* **1995**, *117*, 11932.

 © VCH Verlagsgesellschaft mbH, D-69451 Weinheim, 1996 0570-0833/96/3515-1695 $ 15.00+.25/0

Diisocyanate**

Günther Maier,* Matthias Naumann,
Hans Peter Reisenauer, and Jürgen Eckwert

After the first synthesis of cyanogen (**1**) by Gay-Lussac in 1815[1] 173 years passed until Bickelhaupt and van der Does[2] described the formation of a second C_2N_2 isomer (**2**).[3] It took only four more years until diisocyanogen (**3**) was detected by matrix spectroscopy.[4]

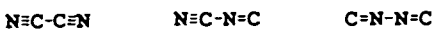

In analogy to the CN radical the ambivalent fragments CNO and NCO can formally be combined to give structurally different isomers of the formula $C_2N_2O_2$. Three of a total of ten typical atomic arrangements are compounds **4**–**6**. The first species of this kind, cyanogendi-*N*-oxide (**4**), was obtained by Grundmann in 1963.[5] Here we report on the identification of the structural isomer diisocyanate (**6**).

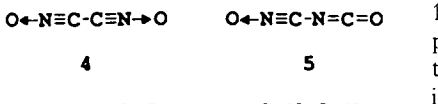

Our aim was not only to prove the existence of **6**. In addition, we assumed that upon matrix-photolysis of **6** in argon at 10 K two CO molecules would be formed in the same rare gas matrix cage without interfering by-products. A singlet/triplet-photoexcitation of one of the ^{1}CO molecules followed by a [^{1}CO + ^{3}CO]addition might provide an access to the still unknown carbon monoxide dimer C_2O_2 (triplet ground state[6]).

Matrix-irradiation[7] of **4** does not lead to the desired diisocyanate **6** but yields—presumably via the primary, singly rearranged product **5**—nitrosyl cyanide **7**. Therefore, we had to find another route to **6**. A promising precursor for **6** is oxalic acid diazide (**9**). We first tried to obtain matrix-isolated diazide **9** by passing oxalic azid dibromide over solid sodium azide.[8] This reaction turned out to be poorly reproducible. Hence, we synthesized **9** in a reaction of oxalic azid dichloride (**8**) with tri-*n*-butyltin azide.[9] However, in this case the formation of two by-products, azidoformyl isocyanate (**10**) and the fairly explosive carbonyl diazide, is disadvantageous. In the meantime we learned that it is more convenient and safer to synthesize **9**, in a modified procedure of Roesky and Glemser,[10] by the reaction of oxalic acid dihydrazide (**11**) with nitrous acid. Utilizing this approach we isolated pure, crystalline oxalyl diazide and deposited it on a matrix window. In solution (CH_2Cl_2) at room temperature **9** loses one molecule of nitrogen, and **10** is formed. Removal of the solvent yields **10** as a colorless, pure liquid that can be safely handled, easily evaporated, and condensed on a spectroscopic window.

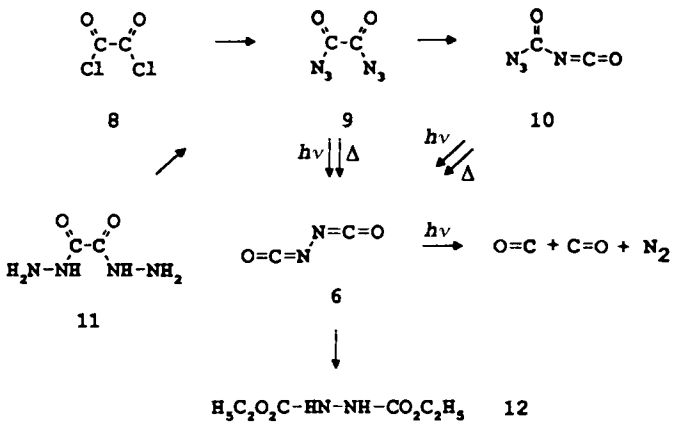

Irradiation of **9** and **10** in argon at 10 K with light of the wavelength 254 nm furnishes **6**. Compound **6** is also formed upon high-vacuum flash pyrolysis of **9** and **10** (quartz tube filled with quartz wool, 900 °C).

The proof of the identity of **6** is based on the following findings: Independently of the applied method of generation the IR spectrum exhibits a very intense absorption at 2201 cm^{-1}, two much weaker bands at 661 and 534 cm^{-1}, and six additional, very weak bands above 2000 cm^{-1}. All absorptions diminish simultaneously upon irradiation with 254 or 193 nm light, and CO is produced. A comparison with the spectrum of **6** calculated by ab initio methods unequivocally shows that all bands belong to diisocyanate (Fig. 1, Table 1).

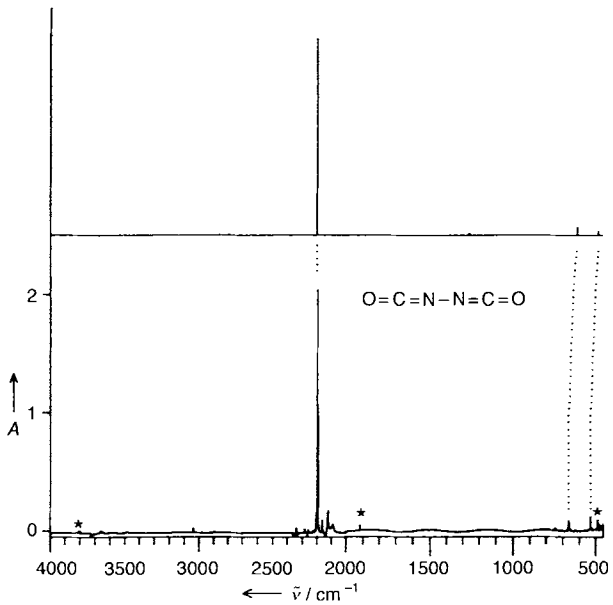

Fig. 1. IR spectrum of **6**. Top: Spectrum calculated by ab initio methods (BLYP/6-311G*). Bottom: Experimentally observed spectrum (Ar matrix, 15 K, from flash pyrolysis of **10**). The experimental spectrum is a difference spectrum of the photofragmentation of **6** into CO and N_2. *: NCO radical. A = absorbance.

The geometry optimization of **6** at the BLYP/6-311G* level[11] results in a minimum for the *s-trans*-conformation (d(C–O) = 1.178, d(C–N) = 1.233, d(N–N) = 1.387 Å, ∢(O-C-N) = 168.8°, ∢(C-N-N) = 125.9°) with C_{2h} symmetry (only real frequencies). In contrast, the C_{2v}-symmetrical molecule with *s-cis*-conformation is calculated to be a transition state (one imaginary frequency). Due to the high symmetry only six of the twelve fundamental vibrations belong to the IR-active species a_u and b_u, and only four should be found in the investigated spectral range (5000–400 cm^{-1}). The three most intense ones are readily assigned to the measured bands at 2201 (NCO

[*] Prof. Dr. G. Maier, Dipl.-Chem. M. Naumann, Dr. H. P. Reisenauer, Dr. J. Eckwert
Institut für Organische Chemie der Universität
Heinrich-Buff-Ring 58, D-35392 Giessen (Germany)
Fax: Int. code +(641)702-5712

[**] In this communication in analogy to the trivial names used for compounds **1**–**3** (cyanogen, isocyanogen, and diisocyanogen) [4], the title compound is referred to as diisocyanate instead of isocyanato isocyanate.

Table 1. Calculated (BLYP/6-311G*) and experimentally observed vibrational spectral data of **6** (Ar matrix, 15 K, from pyrolysis of **10**; relative intensities in parentheses).

		Type	$\tilde{\nu}_{calcd}$ [cm^{-1}]	$\tilde{\nu}_{exp.}$ [cm^{-1}]
ν_1	a_g	NCO str	2265 (i.a.)	(ca. 2235) [b]
			^{13}C: 2248	2225.7
ν_9	b_u	NCO str	2209 (100.0) [a]	2200.6 (100.0)
			^{13}C: 2165	2164.9
			^{18}O: 2198	2184.4
ν_2	a_g	NCO str	1451 (i.a.)	(ca. 1460) [b]
ν_{10}	b_u	NCO str	1269 (0.5)	
ν_3	a_g	NN str	786 (i.a.)	(ca. 840) [b]
ν_{11}	b_u	ip bend [c]	625 (3.8)	661.0 (4.2)
ν_4	a_g	ip bend	595 (i.a.)	
ν_8	b_g	oop bend [d]	506 (i.a.)	
ν_6	a_u	oop bend	494 (1.7)	533.5 (1.7)
ν_5	a_g	ip bend	271 (i.a.)	
ν_{12}	b_u	ip bend	133 (0.5)	
ν_7	a_u	oop bend	72 (0.0)	

Combination bands (plausible assignment): 3660.9 ($\nu_2 + \nu_9$), 3488.7 ($\nu_1 + \nu_{10}$), 3040.6 ($\nu_3 + \nu_6$), 2895.6 ($\nu_1 + \nu_{11}$), 2124.3 ($\nu_2 + \nu_{11}$), 2089.0 ($\nu_3 + \nu_{10}$)

[a] Absolute intensity: 1731 km mol^{-1}. [b] Calculated from combination bands. [c] ip = in-plane. [d] oop = out-of-plane.

stretching vibration, ν_9, b_u), 661 (in-plane bending, ν_{11}, b_u), and 534 cm^{-1} (out-of-plane bending, ν_6, a_u). The missing fourth fundamental absorption (NCO stretching vibration, ν_{10}, b_u) is very weak in accordance with the calculation. Besides these fundamental vibrations six other weak bands of **6** were identified, which can, aided by the calculation, be interpreted as combination bands of IR-inactive and IR-active transitions (Table 1). The band ν_9 possesses an intensity high enough to enable the detection of the corresponding absorptions of the ^{13}C and ^{18}O isotopomers in natural abundance. The measured intensity of the ^{13}C band (2.2%) confirms that the molecule contains two symmetry-equivalent carbon atoms. Due to the breakdown of symmetry in the ^{13}C/^{12}C isotopomer the ν_1 band, which is inactive in the parent **6**, can be detected.

The photolability of **6** towards light with short (λ = 254 or 193 nm), but not towards longer wavelengths (λ > 310 nm) demands an absorption in the UV range. Indeed, an electronic transition with a λ_{max} = 220 nm can be registered in the UV spectrum. This band position shows that the bathochromic shift from an isolated monoisocyanate (HCNO: λ_{max} = 167 nm[12]) to the conjugated diisocyanate (**6**) is of the same order of magnitude as in the pair ethene (λ_{max} = 165 nm)/butadiene (λ_{max} = 217 nm).

The correctness of the identification of **6** is further supported by its reaction with ethanol: We cocondensed **6** and ethanol on a cold finger at 77 K and obtained after thawing exclusively diethyl 1,2-hydrazinedicarboxylate (**12**).

How stable is **6**? As mentioned above, **6** survives the conditions of flash pyrolysis. In this case cleavage into NCO radicals[13] was observed only to a small extent. If the thermal products of the precursor **10** are condensed without argon on a spectroscopic window at 80 K, the IR spectra reveal that **6** is viable under these conditions. Subsequent annealing results in the onset of a reaction at about 130 K. At 190 K all IR bands of **6** have vanished. While **6** does not exist in pure form at room temperature its lifetime in diluted form in the gas phase is much higher. We mixed **10** and argon (1:1000) and irradiated this sample at room temperature in an IR gas cell with 254 nm light. Spectra measured immediately thereafter exhibited the strongest absorption of **6** as a weak band with clearly visible P- and R-branches (centered at 2208 cm^{-1}). The intensity of this band decreased with a half-life of about 10 minutes.

With respect to the aforementioned C_2O_2 problem we would like to add that so far a photoinduced dimerization of the two CO molecules trapped in the same matrix cage could not be achieved.

Received: February 26, 1996 [Z 8860 IE]
German version: *Angew. Chem.* **1996**, *108*, 1800–1801

Keywords: ab initio calculations · density functional theory · IR spectroscopy · isocyanates · matrix isolation

[1] L. J. Gay-Lussac, *Ann. Chim. (Paris)* **1815**, *95*, 175.
[2] T. van der Does, F. Bickelhaupt, *Angew. Chem.* **1988**, *100*, 998–1000; *Angew. Chem. Int. Ed. Engl.* **1988**, *27*, 936–938.
[3] Structural proofs: a) Microwave spectroscopy: F. Stroh, M. Winnewisser, *Chem. Phys. Lett.* **1989**, *155*, 21–26; b) matrix IR spectroscopy: F. Stroh, M. Winnewisser, B. P. Winnewisser, H. P. Reisenauer, G. Maier, S. J. Goede, F. Bickelhaupt, *ibid.* **1989**, *160*, 105–112.
[4] G. Maier, H. P. Reisenauer, J. Eckwert, C. Sierakowski, T. Stumpf, *Angew. Chem.* **1992**, *104*, 1287–1289; *Angew. Chem. Int. Ed. Engl.* **1992**, *31*, 1218–1220.
[5] a) C. Grundmann, *Angew. Chem.* **1963**, *75*, 450; *Angew. Chem. Int. Ed. Engl.* **1963**, *2*, 260; b) C. Grundmann, V. Mini, J. M. Dean, H.-D. Frommeld, *Justus Liebigs Ann. Chem.* **1965**, *687*, 191–214.
[6] G. Maier, H. P. Reisenauer, B. Röther, J. Eckwert, *Liebigs Ann.* **1996**, 303–306, and references therein.
[7] G. Maier, J. H. Teles, *Angew. Chem.* **1987**, *99*, 152–153; *Angew. Chem. Int. Ed. Engl.* **1987**, *26*, 155–156.
[8] J. Eckwert, Diplomarbeit, Universität Giessen, **1990**.
[9] H. R. Kricheldorf, E. Leppert, *Synthesis*, **1976**, 229–230.
[10] H. Roesky, O. Glemser, *Chem. Ber.* **1964**, *97*, 1710–1712.
[11] Gaussian 94, Revision B.1, M. J. Frisch, G. W. Trucks, H. B. Schlegel, P. M. W. Gill, B. G. Johnson, M. A. Robb, J. R. Cheeseman, T. Keith, G. A. Petersson, J. A. Montgomery, K. Raghavachari, M. A. Al-aham, V. G. Zakrzewski, J. V. Ortiz, J. B. Foresman, J. Cioslowski, B. B. Stefanov, A. Nanayakkara, M. Challacombe, C. Y. Peng, P. Y. Ayala, W. Chen, M. W. Wong, J. L. Andres, E. S. Replogle, R. Gomperts, R. L. Martin, D. J. Fox, J. S. Binkley, D. J. Defrees, J. Baker, J. P. Stewart, M. Head-Gordon, C. Gonzalez, J. A. Pople, Gaussian, Inc., Pittsburgh PA, **1995**.
[12] H. Okabe, *J. Chem. Phys.* **1970**, *53*, 3507–3515.
[13] D. E. Milligan, M. E. Jacox, *J. Chem. Phys.* **1967**, *47*, 5157–5168.

Prenylation of Benzoic Acid Derivatives Catalyzed by a Transferase from *Escherichia coli* Overproduction: Method Development and Substrate Specificity**

Ludger Wessjohann* and Bernd Sontag

Enzyme-catalyzed reactions offer possibilities that extend beyond their obvious advantages of chemo-, regio-, and stereoselectivity, such as especially mild conditions, use in water and reproducibility on a microscale basis.[1–4] This is especially important for those reactions for which classical methods are not available. Due to their easy accessibility, hydrolases (peptidases, lipases, and esterases) now belong to the standard repertoire for organic synthesis,[1b,d] whereas enzyme-catalyzed C–C bond formations[1c,2] have not yet found widespread application. To

[*] Dr. L. A. Wessjohann, B. Sontag
Institut für Organische Chemie der Universität
Karlstrasse 23, D-80333 München (Germany)
Fax: Int. code +(89) 5902-483
e-mail: law@org.chemie.uni-muenchen.de

[**] This work was supported by the Fonds der Chemischen Industrie. We thank the Bayer AG and the BASF AG for the donation of chemicals and equipment. We also thank Prof. Dr. L. Heide for providing us with the bacteria strains, Dr. K. Severin, Dr. M. Melzer, and Dr. T. Kutchan for their assistance in molecular biological and microbiological discussions, as well as Prof. Dr. W. Steglich, Prof. Dr. M. Zenk, and Dr. G. Greull for the use of their instruments and facilities.

date, only the oxynitrilase-catalyzed cyanohydrin reaction has been able to become established.[3] For more complex C–C bond formations, the aldolases have been the main focus of investigations.[1c, 2, 4]

The use of prenyltransferases in chemistry has so far been described only to a minor extent.[5] This may be because they are predominantly membrane-dependent[6–8] and therefore generally less accessible, less stable, and more difficult to characterize than globular enzymes. An important group of these enzymes catalyze the prenylation in the *ortho* position of phenols such as 4-hydroxybenzoic acid (PHB), which is a key step in the synthesis of biologically active compounds such as ubiquinone[9] and vitamin E[10] as well as many secondary metabolism products, including the Japanese drug and dye compound shikonin,[8, 11, 12] the anti-HIV-active conocurvone,[13] boviquinones,[14, 15] tridentoquinone[15–17] and others.[18, 19]

Herein we describe the regioselective prenylation of benzoic acid derivatives with a very stable and easily accessible transferase, which was first discovered in 1972 by Young et al.[20] in cell-free extracts of *Escherichia coli* and which in vivo probably catalyzes the reaction (with $n = 8$) shown in Scheme 1,[21] a

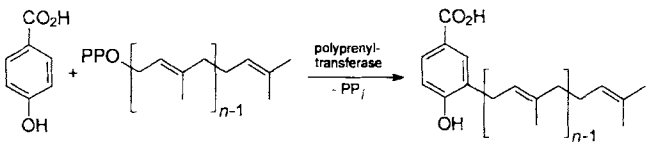

1 2 3

Scheme 1. Prenylation of 4-hydroxybenzoic acid (OPP = pyrophosphate, n = 1–12).

partial step in the ubiquinone biosynthesis.[6, 22] This enzyme is a polyprenyldiphosphate:4-hydroxybenzoate polyprenyl-transferase. Recently, Heide et al.[23, 24] were able to clone the corresponding gene (*ubiA*) to obtain recombinant overproducing strains, which they kindly made available to us.

The harvest of the enzyme fraction is readily accomplished in two days. A 500 mL batch yields enough material for approximately 200 prenylation experiments. The bacteria are initially grown from a main culture (glycerine culture) on an agar plate, then inoculated to a standard liquid medium (LB), where they are incubated at 37 °C to an optical density of approximately 1. The isolation of the enzyme proceeds by centrifugation and separation of the bacteria, the cell walls are destroyed with ultrasound, and the enzyme fraction is separated by centrifugation. To raise the specific activity to approximately 3 nkat mg^{-1} and to obtain better reproducibility from different batches, the membrane fractions are enriched by ultracentrifugation.[11, 24] This step, which brings about a loss of up to three quarters of the total activity of approximately 12 nkat, can be omitted for applications. The obtained membrane fraction is combined with 10 mL of a buffer solution (50 mM tris(hydroxymethyl)-aminomethane hydrochloride (TRIS·HCl; pH = 7.50), 2 mM 1,4-dithiothreitol), suspended, and immediately frozen at −25 °C. It is stable for many months without significant activity loss. After more than one year, the activity of the frozen suspension in the standard assay (see Experimental) was only approximately 20% lower than that of a fresh suspension and therefore still within the normal range of activity deviations for enzyme preparations.

The reaction of geranyl pyrophosphate (GPP) with *p*-hydroxybenzoic acid (PHB) to 3-geranyl-4-hydroxybenzoic acid (GBA) proved to be a good reference system (Scheme 1, $n = 2$). A calibration curve determined with classically synthesized GBA was used for the quantitative analysis by reversed-phase HPLC (4-ethylbenzoic acid as internal standard). For the standard assay (see Experimental) the reaction was stopped after one hour. The chemical yield for the PHB/GPP-reaction at this time was 62%; after three hours, synthetically useful yields of approximately 80% were obtained. The reproducibility of the reaction with enzyme preparations from the same batch is ±5%, excellent for these microreactions, and the deviations within one experimental series is only ±1%. Scale-up by a factor of 30 was easily accomplished and suggests no complications for larger batches.

The successful variation of the polyprenyl substituent (both GPP and geranylgeranyl pyrophosphate[27] were used) is not surprising based on the variation in the chain length in ubiquinones from *E. coli* and the resulting successful transformation of long-chain prenyl pyrophosphates.[11, 20, 24, 28] It is remarkable that the shorter GPP reacted with the highest rate, whereas, for the optimal compatibility with the chain length of the ubiquinones in *E. coli*, long-chain prenyl diphosphates such as octaprenyl[20, 29] were expected to be the best substrates. As expected, geranyl monophosphate was not converted.

The enzyme accepts a variety of 4-hydroxybenzoic acid derivates and related compounds as the substrate, of which a few are shown in Scheme 2. A systematic variation of the sub-

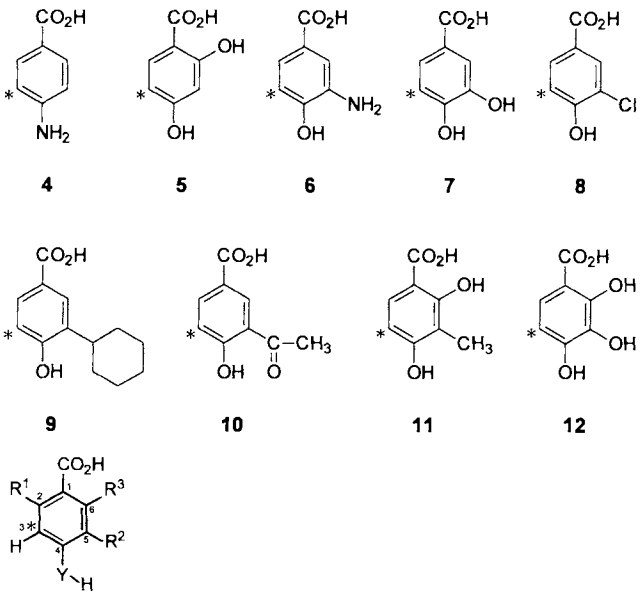

4 5 6 7 8

9 10 11 12

Scheme 2. Some of the successfully converted benzoic acid derivatives and a preliminary substrate model. (The prenylated position is marked with a star.) R^1 = H (other substituents are probably not allowed); R^2 = H, OH, NH_2, OCH_3, Cl, $COCH_3$, CH_3, cyclohexyl, etc., not polyprenyl or very strongly electron-withdrawing substituents like NO_2; R^3 = H, OH and others; Y = O, NH (other substituents likely to be possible).

stituents on the aromatic ring resulted in the following preliminary picture for the prenylation of the *meta*-position (C-3): 1) The acidic group is invariant: only benzoic acid derivatives are substrates. 2) The *para*-hydroxy functional group can be replaced, for example, by an amino group (**4**). Derivatives in which the hydrogen atom has been replaced, for example, by methylation to 4-methoxy- or 4-*N*,*N*-dimethylaminobenzoic acids, do not react. 3) As expected, the reaction does not take place if both *meta*-positions are blocked. However, these substances are not inhibitors either. 4) Substituents in the 5- and/or

6-position (R^2 and R^3, respectively) appear to be tolerated (**5**–**12**). Thus it is possible to carry out the one-step synthesis of 4,5-dihydroxy- and 4-hydroxy-5-methoxy-3-polyprenylbenzoic acid isolated from *Saccharomyces cerevisiae*.[18] Only very strongly electron-withdrawing substituents, such as the nitro group, lead to activity loss, whereas 5-chloro and 5-acetyl derivatives (**8** and **10**, respectively) can still be transformed at an acceptable rate. Donor-substituted substrates, such as the bulky 5-cyclohexyl-4-hydroxybenzoic acid **9**, react without any reactivity loss. 5) An additional hydroxy group in 2-position (R^1) is not acceptable.

Based on these results we have developed a model for the requirements of the enzyme with respect to the aromatic component, which has proven reliable for all of the tested compounds. The following is crucial for a successful experiment: Only those benzoic acid derivatives are transformed that bear an electron donor and a hydrogen-bond donor in *para*-position and are not substituted in the *meta*-position to be alkylated or in the adjacent *ortho*-position.

In contrast, the classical Friedel–Crafts alkylation of 4-hydroxybenzoic acid with prenyl compounds does not work. Even the reaction of methyl ester with phytol yields the 3-phytyl derivative in only 9% yield, and the important polyunsaturated all-*trans*-prenyl electrophiles did not yield the desired products at all. Not only the poor regioselectivity, but also the isomerization, overalkylation, and *O*-alkylation products were detected in these reactions.[17, 30] Such products are not formed when using the enzyme catalyst.

The investigations discussed herein for the overproduction of polyprenyl diphosphate:4-hydroxybenzoate-polyprenyltransferase from *E.-coli* demonstrate for the first time the potential of this almost unused class of C–C bond forming enzyme for the directed catalysis of a Friedel–Crafts type alkylation in water, the *meta*-prenylation of benzoic acid derivatives.

Experimental Procedure

The polyprenyl pyrophosphates were obtained from the respective polyprenyl alcohols or halides [31] according to the method of Poulter et al. [32]. Geranyl phosphate can be synthesized according to the procedure for pyrophosphates.

Enzyme assay: 100 nmol of the benzoic acid derivative (reference: PHB), 100 nmol polyprenyl pyrophosphate (reference: GPP), 50 μmol $MgCl_2$ (Mg^{2+} as the cofactor) in 50 μL of TRIS buffer (50 mM TRIS·HCl; pH = 7.5) and 50 μL of the enzyme suspension (approx. 25 pcat) were incubated for 60 min at 37 °C. The reaction was stopped by adding 2 μL of formic acid, and the reaction mixture was extracted with 500 μL of 4-ethylbenzoic acid (PEB) solution (100 μM in ethyl acetate; internal standard). After phase separation (centrifuge if necessary), a 450 μL sample of the organic phase was drawn, and the solvent removed in vacuo. The residue was dissolved in 60 μL of methanol and analyzed by HPLC (20 μL of the solution, column 250 × 4 mm, RP-18 (7 μm), 100 bar, detection at 240 nm (λ_{max} PEB) or 254 nm). The retention time of the geranylated compounds was 2.5 to 4 times that of the respective arene (eluent: methanol/water/formic acid 750/245/5, isocratic), that of geranylgeranylated compounds 6 to 7 times (eluent A (2 min), followed by gradient elution (13 min) to eluent B: methanol/isopropanol/formic acid 800/195/5). PEB elutes between the reactant and the product. The UV spectra of the prenylated benzoic acids show a bathochromic shift of 5–10 nm for the K band ($\pi \rightarrow \pi^*$) of the arene.

Received: February 15, 1996 [Z8826]
German version: *Angew. Chem.* **1996**, *108*, 1821–1823

Keywords: alkylations · enzyme catalysis · prenylations

[1] a) *Enzyme Catalysis in Organic Synthesis – A Comprehensive Handbook, Vol. 1* (Eds.: K. Drauz, H. Waldmann), VCH, Weinheim, **1995**; b) Ref. [1a], pp. 165–504; c) *Enzyme Catalysis in Organic Synthesis – A Comprehensive Handbook, Vol. 2* (Eds.: K. Drauz, H. Waldmann), VCH, Weinheim, **1995**, pp. 547–593; d) C.-H. Wong, G. M. Whitesides, *Enzymes in Synthetic Organic Chemistry*, Pergamon, Oxford, **1994**; e) *Enzyme Chemistry – Impact and Applications*, 2nd ed. (Ed.: C. J. Suckling), Chapman and Hall, London, **1990**.

[2] H. Waldmann, *Nachr. Chem. Tech. Lab.* **1991**, *39*, 1408–1414.

[3] F. Effenberger, *Angew. Chem.* **1994**, *106*, 1609–1619; *Angew. Chem. Int. Ed. Engl.* **1994**, *33*, 1555–1565.

[4] W.-D. Fessner, G. Sinerius, *Angew. Chem.* **1994**, *106*, 217–220; *Angew. Chem. Int. Ed. Engl.* **1994**, *33*, 209–212.

[5] The enzymatic synthesis of 4-methyldihomofarnesol is the only similar synthesis: T. Koyama, K. Ogura, F. C. Baker, G. C. Jamieson, D. A. Schooley, *J. Am. Chem. Soc.* **1987**, *109*, 2853–2854; Ref. [1c,d].

[6] K. Momose, H. Rudney, *J. Biol. Chem.* **1972**, *247*, 3930–3940.

[7] G. Wu, H. D. Williams, F. Gibson, R. K. Poole, *J. Gen. Microbiol.* **1993**, *139*, 1795–1805.

[8] Y. Yamaga, K. Nakanishi, H. Fukui, M. Tabata, *Phytochemistry* **1993**, *32*, 633–636.

[9] R. E. Olson, H. Rudney, *Vitam. Horm. (NY)* **1983**, *40*, 1–43.

[10] R. E. Beyer, K. Nordenbrand, L. Ernster, *Chem. Scr.* **1987**, *27*, 145–153; G. W. Burton, K. U. Ingold, *Acc. Chem. Res.* **1986**, *19*, 194–201; S. Kasparek in *Vitamin E: A Comprehensive Treatise, Vol. 1* (Ed.: L. J. Machlin), Marcel Dekker, New York, **1980**, pp. 7–65.

[11] M. Melzer, Dissertation, Universität Tübingen, **1995**.

[12] M. Hayashi, *Nippon Yakurigaku Zasshi* **1977**, *73*, 193–203 [*Chem. Abstr.* **1978**, *88*, 44863e]; L. Heide, M. Tabata, *Phytochemistry* **1987**, *26*, 1645–1650, 1651–1655.

[13] H. Laatsch, *Angew. Chem.* **1994**, *104*, 438–440, 1865; *Angew. Chem. Int. Ed. Engl.* **1994**, *33*, 422–424, 1668.

[14] E. Jägers, W. Steglich, *Angew. Chem.* **1981**, *93*, 1105; *Angew. Chem. Int. Ed. Engl.* **1981**, *20*, 1016; W. Steglich, F. Esser, I. Pils, *Z. Naturforsch. B* **1971**, *26*, 336–338; D. Brewer, W. C. Jen, G. A. Jones, A. Tayler, *Can. J. Microbiol.* **1984**, *30*, 1068–1072; P. C. Beaumont, R. L. Edwards, *J. Chem. Soc. C* **1971**, 2582–2585; K. Minami, K. Asawa, M. Sawada, *Tetrahedron Lett.* **1968**, 5067–5070.

[15] J. Miersch, *Biochem. Physiol. Pflanz.* **1986**, *181*, 405–410.

[16] H. Besl, H.-J. Hecht, P. Luger, V. Pasupathy, W. Steglich, *Chem. Ber.* **1975**, *108*, 3675–3691; H. Schwarz, V. Pasupathy, W. Steglich, *Org. Mass Spectrom.* **1976**, *11*, 472–478; R. F. C. Brown, A. J. Robinson, *Aust. J. Chem.* **1995**, *48*, 515–529.

[17] J. Beyer, Dissertation, Ludwig-Maximilians-Universität München, **1995**; W. Steglich, J. Beyer, München, unpublished results.

[18] R. R. Goewert, J. Sippel, M. F. Grimm, R. E. Olson, *Biochemistry* **1981**, *20*, 5611–5616; R. R. Goewert, J. Sippel, R. E. Olson, *ibid.* **1981**, *20*, 4217–4223.

[19] a) G. Cimino, S. De Stefano, L. Minale, *Experientia* **1972**, *28*, 1401–1402; b) W. Kramp, F. Bohlmann, *Liebigs Ann. Chem.* **1986**, 226–233.

[20] I. G. Young, R. A. Leppik, J. A. Hamilton, F. Gibson, *J. Bacteriol.* **1972**, *110*, 18–25 [*Chem. Abstr.* **1972**, *76*, 138015j].

[21] I. G. Young, P. Stroobant, C. G. Macdonald, F. Gibson, *J. Bacteriol.* **1973**, *114*, 42–52 [*Chem. Abstr.* **1973**, *79*, 2615j].

[22] G. D. Daves, Jr., R. F. Muraca, J. S. Whittick, P. Friis, K. Folkers, *Biochemistry* **1967**, *6*, 2861–2866.

[23] L. Heide, M. Melzer, M. Siebert, A. Bechthold, J. Schröder, K. Severin, *J. Bacteriol.* **1993**, *175*, 5728–5729; M. Melzer, M. Siebert, A. Bechthold, L. Heide, *Planta Med.* **1992**, *58*, A596.

[24] M. Melzer, L. Heide, *Biochim. Biophys. Acta* **1994**, *1212*, 93–102.

[25] Overproducing mutants were obtained by insertion in a multicopy plasmid, which contained an ampicillin resistance gene for selectivity purposes, and transfer to the wild type K-12 or in a *ubiA*-deficient *E.-coli* strain AN385. For the investigations, *E. coli* K-12:pALMU3 was used, the membrane fraction of which exhibits an approximate 600-fold activity. For recent clonings, see P. E. Lilley, N. P. J. Stamford, S. G. Vasudevan, N. E. Dixon, *Gene* **1993**, *129*, 9–16; K. Suzuki, U. Minoru, M. Yuasa, T. Nakagawa, M. Kawamukai, H. Matsuda, *Biosci. Biotech. Biochem.* **1994**, *58*, 1814–1819; G. Wu, H. D. Williams, F. Gibson, R. K. Poole, *J. Gen. Microbiol.* **1993**, *139*, 1795–1805.

[26] The half-life of the enzyme in the reaction medium at 37 °C in air is approximately 1.5 h.

[27] The product 3-geranylgeranyl-4-hydroxybenzoic acid, obtained with PHB, was also isolated from the marine sponge *Ircinia muscarum* [19a].

[28] Z. El Hachimi, O. Samuel, R. Azerad, *Biochimie* **1974**, *56*, 1239–1247 [*Chem. Abstr.* **1975**, *82*, 121392f].

[29] M. Siebert, A. Bechthold, M. Melzer, U. May, U. Berger, G. Schröder, J. Schröder, K. Severin, L. Heide, *FEBS Lett.* **1992**, *307*, 347–350.

[30] S. Lang-Fugmann, Dissertation, Universität Bonn, **1987**.

[31] S. Klinge, M. Demuth, *Synlett* **1993**, 783–784; E. J. Corey, W.-C. Shieh, *Tetrahedron Lett.* **1992**, *33*, 6435–6438; A. Yanagisawa, H. Hibino, S. Habaue, Y. Hisada, H. Yamamoto, *J. Org. Chem.* **1992**, *57*, 6386–6387; J. D. Faulkner, *Synthesis* **1971**, 175–189.

[32] V. J. Davisson, A. B. Woodside, C. D. Poulter in *Steroids and Isoprenoids, Part A, Vol. 110* (Eds.: J. H. Law, H. C. Rilling), Academic Press, Orlando, **1985**, pp. 130–144.

 © VCH Verlagsgesellschaft mbH, D-69451 Weinheim, 1996 0570-0833/96/3515-1699 $ 15.00+.25/0

New Cobalt- and Iron-Catalyzed Reactions of Organozinc compounds**

C. Kishan Reddy and Paul Knochel*

σ-Alkyl transition metal complexes are important intermediates in many transition-metal-mediated organic reactions.[1] Most of these compounds are highly unstable and undergo decomposition even at low temperature.[1, 2] It was thought that the stability of these organometallic reagents could be increased by an appropriate choice of the ligands, by using alkyl groups that do not contain β-hydrogen atoms, or by steric protection.[3] Recently we have found that the organometallic reagent used for the preparation of these transition metal alkyl species is also important for their stability. Whereas the treatment of $Co^{II}Br_2$ with highly reactive organolithium or Grignard reagents leads to decomposition even at very low temperature,[2, 4, 5] the same reaction performed with organozinc halide (RZnX) or diorganozinc (R_2Zn) reagents in THF:NMP mixtures (NMP = 1-methyl-2-pyrrolidinone) leads to deep blue solutions of RCoBr·RZnX, which are relatively stable at 0 °C.[6] Bubbling CO through these reaction mixtures (0 °C to 25 °C, 3 h) provides symmetrical ketones like **1** in excellent yield [Eq. (a)].[7] In this

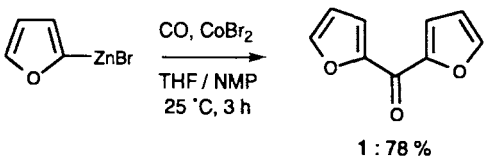

(a)

work, we report several new cobalt(II)- and iron(III)-catalyzed reactions of organozinc reagents. The direct acylation of diorganozinc compounds is a low-yield reaction for which palladium-[8] and copper-catalyzed[9] reactions have been developed. The disadvantages of these methods are a lack of generality for the palladium catalysis[10] and the need for a stoichiometric amount of copper salts (CuCN·2 LiCl) for the copper-catalyzed acylations.[9-11]

We have found that $Co^{II}Br_2$ is a very efficient catalyst for the acylation of diorganozinc compounds in NMP/THF mixtures. The reaction of various functionalized diorganozinc compounds with acid chlorides in the presence of $CoBr_2$ (10 mol%) in THF:NMP (1:1) at −10 °C affords polyfunctional ketones **2**–**7** in 78–84% yield [Eq. (b) and Scheme 1]. The reactions are

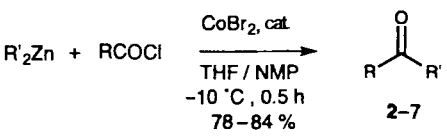

(b)

complete in less than 0.5 h and proceed well with aliphatic and aromatic acid chlorides, oxalyl chloride, or even trifluoroacetic anhydride.

[*] Prof. Dr. P. Knochel, Dr. C. K. Reddy
Fachbereich Chemie der Universität
Hans-Meerwein-Strasse, D - 35032 Marburg (Germany)
Fax: Int. code +(6421)282189
e-mail: knochel@ps1515.uni-marburg.de

[**] We thank the DFG (SFB 260) for generous financial support. C. K. R. thanks the Alexander-von-Humboldt-Stiftung for a fellowship. We thank BASF AG, Witco AG, Bayer AG, Schering AG, Callery, Sipsy, and Chemetall GmbH for the generous gift of chemicals.

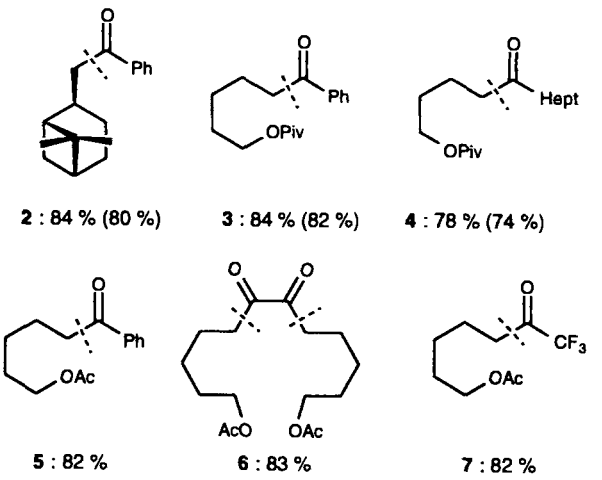

Scheme 1. Products from cobalt(II)- or iron(II)-catalyzed acylations.

Interestingly, catalysis with $FeCl_3$ (10 mol%) can also be performed (−10 °C, 1 h). Compared to the Co^{II} catalysis, slightly lower yields (yields in parenthesis in Scheme 1) and longer reaction times are required. In the course of this work, it was found that allylations of organozinc reagents (R_2Zn or RZnX) are very efficiently catalyzed by $CoBr_2$ in THF and lead with greater than 98% selectivity to the S_N2-substitution products[12] with complete retention of the stereochemistry of the double bond [>99%, Eq. (c)]. Thus, the reaction of dipentylzinc ($Pent_2Zn$)

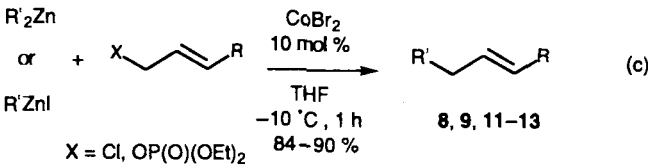

(c)

with geranyl chloride gives the (*E*)-diene **8** (>98% *E*; 90% yield), whereas its reaction with neryl chloride provides the isomeric (*Z*)-diene **9** (98% *Z*; 89% yield). Interestingly, the reaction of geranyl chloride with $Pent_2Zn$ in the presence of the soluble copper salt CuCN·2 LiCl (10 mol%, 0 °C, 1 h) furnishes selectively the S_N2'-substitution product **10** (90% yield, >98% S_N2'; Scheme 2).

Alkylzinc halides[9, 13] undergo the allylation reaction, giving similar yields as dialkylzinc compounds but requiring longer

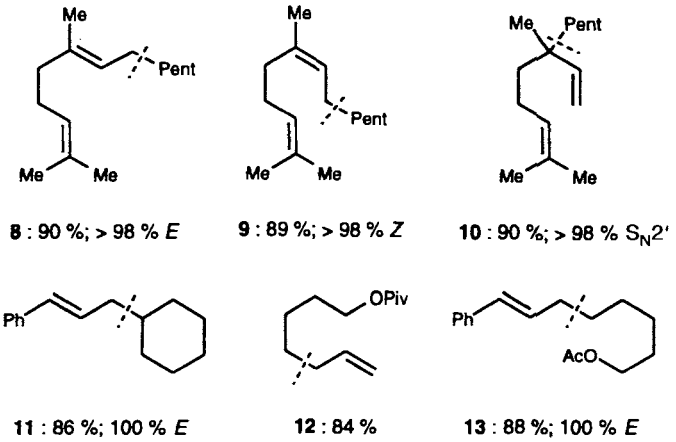

Scheme 2. Products from cobalt(II)- or copper(II)-catalyzed allylations.

reaction times (about 5 h at $-10\,^{\circ}C$). Contrary to the Co^{II}-catalyzed acylation, both functionalized R′ groups from the dialkylzinc compounds ZnR'_2 are transferred in these allylation reactions (see products **11**–**13** of Scheme 2). In addition, allylic phosphates as well as allylic chlorides react, and with the same high stereoselectivity. Thus the reaction of $Pent_2Zn$ with diethyl cinnamylphosphate (THF, $-10\,^{\circ}C$, 0.5 h) furnishes the S_N2 allylated product (*E*)-1-phenyloctene (88% yield, 100% *E*, 100% S_N2 substitution). Organozinc reagents also undergo coupling reactions with benzylic bromides. In the reaction of benzyl bromide with 4-acetoxybutylzinc iodide in the presence of $CoBr_2$ (10 mol%) in THF:NMP (1:1) at $-10\,^{\circ}C$ for 5 h, 5-phenylpentyl acetate is isolated in 60% yield.

In conclusion, we have described a new and efficient cobalt(II)- and iron(III)-catalyzed acylation, which provides a general synthesis of polyfunctional ketones. Remarkably the cobalt(II)-catalyzed allylation provides exclusively S_N2 products with complete retention of the double bond geometry. Further studies involving cobalt(II)- and iron(III)-catalyzed reactions of organozinc compounds are underway.

Experimental Procedure

Typical syntheses are as follows:

Bis(4-pivaloxybutyl)zinc: A 50 mL, three-necked flask was charged with 4-iodobutyl pivalate (8.52 g, 30 mmol), CuI (60 mg, 0.3 mol%), and Et_2Zn (4.5 mL, 40 mmol, 1.3 equiv). The reaction mixture was stirred at 55 °C for 14 h. The volatiles were removed under vacuum (55 °C, 0.1 mm Hg, 2 h). After addition of decane (10 mL), all traces of Et_2Zn were removed under high vacuum (1 h). This last operation was performed twice. The resulting zinc reagent was diluted in ether (10 mL) and was ready to use.

5-Oxododecyl pivalate (**4**): A 50 mL three-necked flask was charged with $CoBr_2$ (218 mg, 1 mmol) in NMP (4 mL) and ether (2 mL). The reaction mixture was cooled to −10 °C and *n*-octanoyl chloride (1.62 g, 10 mmol) was added followed by bis(4-pivaloxy-butyl)zinc (4 mL of the solution prepared as described above, 10 mmol). The resulting deep blue solution was stirred for 0.5 h at −10 °C and worked up as usual. After evaporation of the solvents, the crude residue was purified by flash chromatography (hexane:ether = 95:5), providing **4** (2.2 g, 78% yield) as a colorless oil.

6-Heptenyl pivalate (**12**): A 50 mL three-necked flask was charged with $CoBr_2$ (218 mg, 1 mmol) in THF (5 mL). The reaction mixture was cooled to −10 °C, and allyl bromide (2.42 g, 20 mmol) followed by bis(4-pivaloxybutyl)zinc (4 mL, 10 mmol) was added. The resulting solution was stirred for 5 h at this temperature and worked up as usual to afford, after flash chromatography, 3.32 g of the ester **12** (16.8 mmol, 84% yield).

Received: February 13, 1996 [Z88171E]
German version: *Angew. Chem.* **1996**, *108*, 1812–1813

Keywords: acylations · allylations · catalysis · cobalt compounds · zinc compounds

[1] a) L. S. Hegedus, *Transition Metals in the Synthesis of Complex Organic Molecules*, University Science Science, Mill Valley, CA, **1994**; b) A. J. Pearson, *Metallo-organic Chemistry*, Wiley, New York, **1985**; c) A. Yamamoto, *Organotransition Metal Chemistry*, Wiley, New York, **1986**.

[2] B. J. Wakefield, *The Chemistry of Organolithium Compounds*, Pergamon, **1976**, pp. 290.

[3] a) R. R. Schrock, G. W. Parshall, *Chem. Rev.* **1976**, *76*, 243–268; some alkylchromium(III) compounds are quite stable, but display a low reactivity toward most organic electrophiles; b) T. Kauffmann, A. Hamsen, C. Beirich, *Angew. Chem.* **1982**, *94*, 145–146; *Angew. Chem. Int. Ed. Engl.* **1982**, *21*, 144–145; c) T. Kauffmann, R. Abeln, D. Wingbermühle, *ibid.* **1984**, *96*, 724–725 and **1984**, *23*, 724–725.

[4] Recent review on organocobaltate reagents for organic synthesis: T. Kauffmann, *Angew. Chem.* **1996**, *108*, 401–418; *Angew. Chem. Int. Ed. Engl.* **1996**, *35*, 386–403.

[5] a) K. Jacob, E. Pietzner, S. Vastag, K.-H. Thiele, *Z. Anorg. Chem.* **1977**, *432*, 187–192; b) W. B. Smith, *J. Org. Chem.* **1958**, *23*, 509–512; c) *ibid.* **1961**, *26*, 4206–4209.

[6] RCoBr·RZnX merely reflects the stoichiometry used. A structure determination is underway. Equimolar solutions of dipentylzinc and $CoBr_2$ or $FeCl_3$ in Et_2O:NMP (1:1) decompose slowly at −10 °C. The half-lives are 40 min and 2.5 h, respectively.

[7] A. Devasagayaraj, P. Knochel, *Tetrahedron Lett.* **1995**, *36*, 8411–8114.

[8] a) E. Negishi, V. Bagheri, S. Chatterjee, F.-T. Luo, *Tetrahedron Lett.* **1983**, *24*, 5181–5184; b) R. A. Grey, *J. Org. Chem.* **1984**, *49*, 2288–2289; c) R. F. W. Jackson, N. Wishart, A. Wood, K. James, M. J. Wythes, *ibid.* **1992**, *57*, 3397–3404; d) J. L. Fraser, R. F. W. Jackson, B. Porter, *Synlett* **1995**, 819–820.

[9] P. Knochel, M. C. P. Yeh, S. C. Berk, J. Talbert, *J. Org. Chem.* **1988**, *53*, 2392–2394.

[10] P. Knochel, R. Singer, *Chem. Rev.* **1993**, *93*, 2117–3404.

[11] Manganese(II)-mediated acylations with organolithium compounds and magnesium reagents proceed very efficiently: a) G. Cahiez, B. Laboue, *Tetrahedron Lett.* **1992**, *33*, 4439–4442; b) G. Cahiez, P.-Y. Chavant, E. Métais, *ibid.* **1992**, *33*, 5245–5248; c) G. Cahiez, S. Marquais, *Pure Appl. Chem.* **1996**, *68*, 53–60.

[12] Nickel-catalyzed allylations of organozinc compounds also furnish S_N2-substitution products: a) Y. Yamamoto, S. Yamamoto, H. Yatagai, K. Maruyama, *J. Am. Chem. Soc.* **1980**, *102*, 2318–2325; b) K. Sekiya, E. Nakamura, *Tetrahedron Lett.* **1988**, *29*, 5155–5156.

[13] a) E. Nakamura, K. Sekiya, M. Arai, S. Aoki, *J. Am. Chem. Soc.* **1989**, *111*, 3091–3093; b) M. Arai, E. Nakamura, *J. Org. Chem.* **1991**, *56*, 5489–5491; c) M. Arai, T. Kawasuji, E. Nakamura, *ibid.* **1993**, *58*, 5121–5129.

Hexakis(but-3-ynyl)benzene**

Hans-W. Marx, Françoise Moulines, Trixie Wagner, and Didier Astruc*

Interest in polyalkyne compounds has increased over the last few years[1–5] due to their use as building blocks for the construction of extended molecular frameworks needed in supramolecular assemblies[1a] and molecular electronic devices.[2] For instance, Diederich et al. have synthesized various polyalkynes with exotic shapes,[3] and Bunz et al. have devised a strategy to couple alkyne-derived transition metal complexes to form linear arrays and grids.[4] Vollhardt et al. have reported on two appealing compounds in the hexaalkynylbenzene family, hexaethynyl-[5a] and hexabutadiynylbenzene.[5b] However, little is known concerning hexaalkynylbenzenes in which methylene units separate the benzene ring and the alkyne functions.[6]

The $FeCp^+$-induced formation of multiple C–C bonds in Equation (a) proceeds readily with alkyl, allyl, and benzyl

$$[FeCp(C_6Me_6)]^+PF_6^- \xrightarrow[\text{base}]{RX} [FeCpC_6(CH_2R)_6]^-PF_6^- \qquad \text{(a)}$$

halides;[7] however, this reaction does not allow the direct introduction of alkynes. Indeed, triple bonds are not compatible with the required base. For instance, the reactions of propargyl bromide with KOH in DME or KO*t*Bu in THF with complexes of the series $[FeCp(C_6H_{6-n}Me_n)]^+PF_6^-$ give polymers. Since the $FeCp^+$-induced hexaallylation of C_6Me_6 proceeds readily,[8] we attempted to use this indirect route to synthesize hexakis(but-3-ynyl)benzene. We now report on the synthesis, structure, and reactions of this compound.

The reaction of excess allyl bromide and KO*t*Bu in THF with $[FeCp(C_6Me_6)]^+PF_6^-$ (**1**) gave the hexaallylated complex $[FeCp\{C_6(CH_2CH_2CH{=}CH_2)_6\}]^+PF_6^-$ (**2**) [Eq. (a), R = $CH_2CH{=}CH_2$; Scheme 1). Although **2** can be transformed into

[*] Prof. D. Astruc, Dr. H.-W. Marx, Dr. F. Moulines
Laboratoire de Chimie Organique et Organométallique
URA CNRS No. 35, Université Bordeaux I
351, Cours de la Libération, F-33405 Talence Cédex (France)
Fax: Int. code +(56)846646
e-mail: astruc@cribx1.u-bordeaux.fr
Dr. T. Wagner
Institut für Anorganische Chemie der Technischen Hochschule
Professor-Pirlet-Strasse 1, D-52074 Aachen (Germany)

[**] Financial support from the Institut Universitaire de France, the Région Aquitaine, the CNRS, the Université Bordeaux I, and the DAAD (NATO grant to H.-W. M.) is gratefully acknowledged. We thank Dr S. Moss for the force-field calculations.

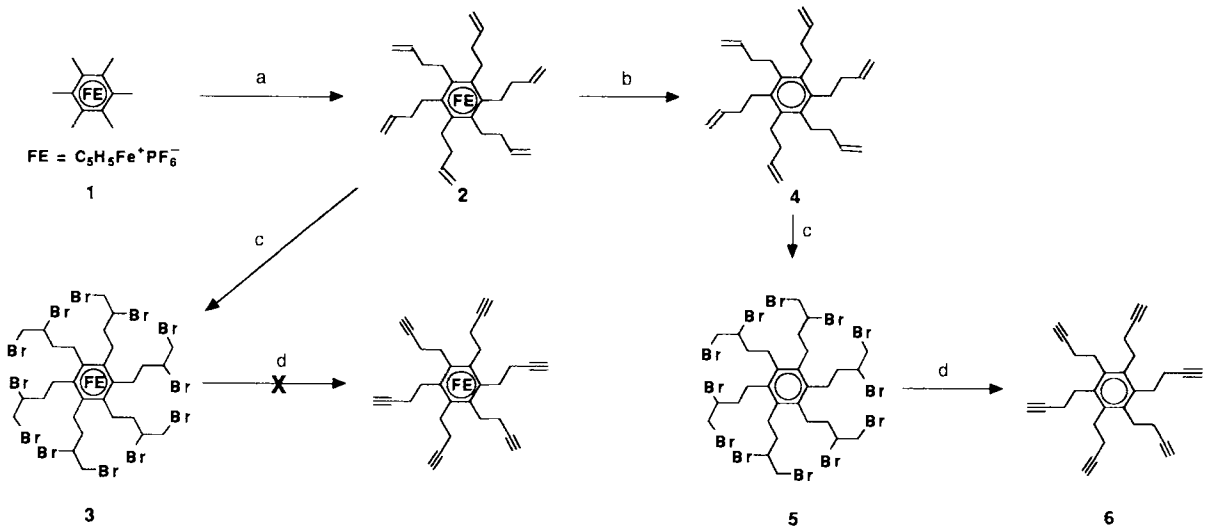

Scheme 1. Synthesis of **6**: a) CH_2=CHBr, KOH, 40 °C; b) $h\nu_{(vis)}$, CH_3CN, PPh_3, room temperature; c) Br_2 in CH_2Cl_2, room temperature; d) $NaNH_2$ in NH_3, −33 °C.

its dodecabromo derivative **3**,[8] we found that the dehydrohalogenation of the latter using $NaNH_2$ in liquid NH_3 gave a product whose ^1H and ^{13}C NMR spectra show the presence of double bonds and of several kinds of triple bonds, presumably resulting from isomerization under the reaction conditions.[9a] The analogous dehydrohalogenation of the metal-free analogue **5** was successful. Photochemical decomplexation of **2** using visible light in CH_2Cl_2 or CH_3CN quantitatively gave **4**.[8] Reaction of Br_2 with **4** in CH_2Cl_2 provided the new insoluble dodecabromo derivative **5** (negative-ion FAB mass spectrum: $[M+Br^-]$), which is also characterized by its correct elemental analysis. Dehydrohalogenation of **5** proceeded by reaction with $NaNH_2$ in liquid NH_3[9] and gave hexakis(but-3-ynyl)benzene (**6**) in 74–81% yield as a white powder (Scheme 1); this synthesis was reproduced many times.

In the pure state, **6** is air-stable at ambient temperature for weeks and thermally stable. The ^1H NMR spectrum of **6** does not change upon heating in [D_8]toluene at 100–110 °C for 18 h. The slow evaporation of a saturated THF solution of **6** provides large transparent crystals. The X-ray structure determination reveals crystallographic $\bar{1}$ symmetry for **6**.[10] The C≡CCH$_2$ units are almost linear, with angles between 176.2(1) and 177.9(1)°. The branches are alternating above and below the plane of the aromatic ring (Fig. 1). Two of the three symmetrically independent substituents have a stretched conformation (*trans* with regard to the CH_2–CH_2 bond, with torsion angles of 168.3(1) and 163.6(1)°); the third substituent has a folded conformation (*gauche* arrangement, with a torsion angle of 57.1(2)°). The C-C-C angles of the latter are larger than those of the two other branches. All equivalent C–C bonds have almost identical lengths within the limits of their estimated standard deviations.

Force-field calculations on **6** show the all-*trans* (D_{3d}) conformation to be the most stable and 11.3 kJ mol^{-1} lower in energy than the C_i arrangement found in the crystal structure (Fig. 1; four *trans* and two *gauche* conformations, Table 1). A decrease in molecular symmetry due to crystal forces is a common phenomenon. Since small energy differences like that calculated here can readily be compensated by lattice energy differences between conformers, the order of stability in the solid state may be reversed.[11]

Reactions of **6** are illustrated in Scheme 2. Addition of BuLi in hexane to **6** in THF immediately provided a white precipitate, which is only poorly soluble in *N,N,N',N'*-tetramethylethylenediamine (TMEDA). Further reactions show that this compound is the hexalithiated derivative **7**. Various electrophiles (MeI, $SiMe_3Cl$, CO_2) were added to a suspension of **7** to furnish the hexasubstituted derivatives **8**–**10** (Scheme 2, Table 2). Hexakis(pent-3-ynyl)benzene (**8**) was obtained in crystalline form in 90% yield by slow evaporation of an etheral solution of the reaction mixture. The trimethylsilyl derivative **9** was obtained as

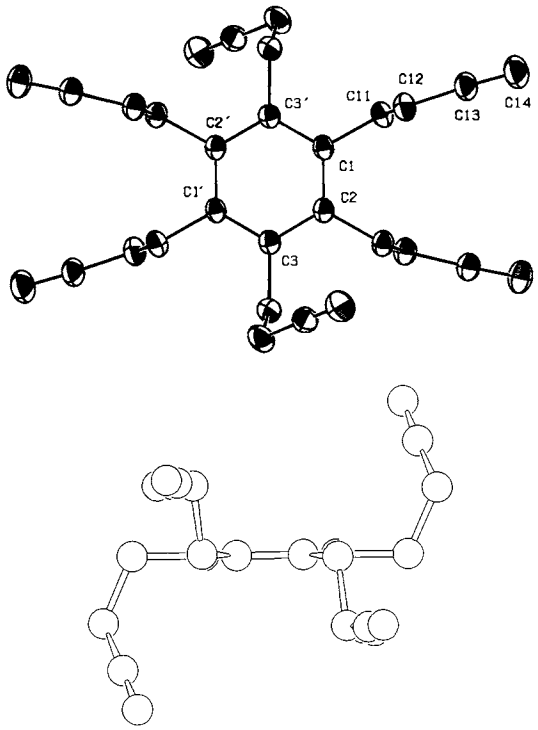

Fig. 1. X-ray crystal structure of **6**. Top: View onto the plane of the benzene ring (ORTEP plot, the ellipsoids are scaled to 30% probability). Bottom: Side view (SCHAKAL plot). Primed atoms are related to the unprimed by the symmetry operation $-x, -y, -z$. Selected distances [Å] and angles [°]: C1–C2 1.408(1), C2–C3 1.404(1), C1–C3 1.405(1), C1–C11 1.515(1), C2–C21 1.518(1), C3–C31 1.518(1), C11–C12 1.541(2), C21–C22 1.541(1), C31–C32 1.545(2), C12–C13 1.461(1), C22–C23 1.464(1), C32–C33 1.452(2), C13–C14 1.179(2), C23–C24 1.189(2), C33–C34 1.182(2); C1-C11-C12 111.71(8), C2-C21-C22 111.41(8), C3-C31-C32 113.9(1), C11-C12-C13 111.3(1), C21-C22-C23 112.67(9), C31-C32-C33 115.0(1), C12-C13-C14 176.2(1), C22-C23-C24 177.2(1), C32-C33-C34 177.9(1).

Table 1. Conformations of **6** obtained by force-field calculations.

Conformation	Symmetry	E [kJ mol^{-1}]	Torsion angle [ ]
all-*trans*	D_{3d}	0.0	-
4 × *trans*, 2 × *gauche*	C_i	−11.3	55.7
all-*gauche*	C_{3i}	−23.7	57.2
all-*gauche*	D_3	−27.4	

a white powder in 97% yield. The carboxylic acid **10** was isolated after hydrolysis and acidic workup. Reaction of **6** with Lappert's reagent Me_2NSnMe_3[12] afforded the hexastannyl derivative **11** as a white powder in 95% yield after standard purification.

The six triple bonds of **6** were π-complexed by $[Co_2(CO)_6]$[1b,c] by reaction with $[Co_2(CO)_8]$ in pentane. The

Table 2. Selected spectroscopic and physical data for compounds **6**, **8**–**13**.

6: ^{1}H NMR (250 MHz, $CDCl_3$): δ = 2.90 (t, J = 8 Hz, 12H, CH_2C_{Ar}), 2.33 (td, J = 8, 2 Hz, 12H, CH_2CC), 2.05 (t, J = 2 Hz, 6H, CCH); ^{13}C NMR (62.9 MHz, $CDCl_3$): δ = 136.2 (C_{Ar}, s), 83.5 (*C*CH, dm, ^2J(C,H) = 50 Hz), 69.4 (C*C*H, dt, ^1J(C,H) = 248 Hz, ^3J(C,H) = 4 Hz), 28.9 (CH_2C_{Ar}, t, ^1J(C,H) = 129 Hz), 20.4 (CH_2CC, t, ^1J(C,H) = 132 Hz)

8: ^{1}H NMR (250 MHz, $CDCl_3$): δ = 2.81 (pseudo-t, J = 8 Hz, 12H, CH_2C_{Ar}), 2.24 (br., 12H, CH_2CC), 1.81 (s, 18H, CH_3); ^{13}C NMR (62.9 MHz, $CDCl_3$): δ = 136.2 (C_{Ar}), 78.7 (*C*CMe), 76.4 (C*C*Me), 29.4 (CH_2C_{Ar}), 20.8 (CH_2CC), 3.7 (Me); Anal. calcd. for $C_{36}H_{42}$: 91.08 C, 8.92 H; found: 91.24 C, 8.90 H; m.p. 172 °C

9: ^{1}H NMR (250 MHz, $CDCl_3$): δ = 2.86 (pseudo-t, J = 8.1 Hz, 12H, CH_2C_{Ar}), 2.34 (pseudo-t, J = 8.1 Hz, 12H, CH_2CC), 1.50 (s, 2H, H_2O), 0.17 (s, 54H, $SiMe_3$); ^{13}C NMR (62.9 MHz, $CDCl_3$): δ = 136.3 (C_{Ar}), 106.4 (*C*CSi), 85.4 (C*C*Si), 29.1 (CH_2C_{Ar}), 21.8 (CH_2CC), 0.2 ($SiMe_3$); Anal. calcd. for $C_{48}H_{80}SiO$: 68.50 C, 9.58 H; found: 68.93 C, 9.58 H; m.p. 191–192 °C

10: ^{1}H NMR (250 MHz, [D$_6$]acetone): δ = 7.8 (br., 6H, CO_2H), 3.11 (pseudo-t, J = 7.5 Hz, 12H, CH_2C_{Ar}), 2.63 (pseudo-t, J = 7.5 Hz, 12H, CH_2CC); ^{13}C NMR (62.9 MHz, [D$_6$]acetone): δ = 154.6 (CO_2H), 137.0 (C_{Ar}), 88.6 (*C*CCO$_2$H), 75.0 (C*C*CO$_2$H), 28.3 (CH_2C_{Ar}), 20.5 (CH_2CC); IR (film): $\tilde{\nu}$ = 2230 (C≡C), 1680 (CO) cm^{-1}

11: ^{1}H NMR (250 MHz, $CDCl_3$): δ = 2.87 (pseudo-t, J = 7.3 Hz, 12H, CH_2C_{Ar}), 2.35 (br., 12H, CH_2CC), 0.29 (s, 54H, Sn Me_3, ^{119}Sn satellites: J(Sn,H) = 59.0 Hz); ^{13}C NMR (62.9 MHz, $CDCl_3$): δ = 136.3 (C_{Ar}), 110.0 (*C*CSn), 83.2 (C*C*-Sn), 29.5 (CH_2C_{Ar}), 22.1 (CH_2CC), −7.7 ($SnMe_3$, Sn satellites of various isotopes); IR (film): $\tilde{\nu}$ = 214 (C≡C) cm^{-1}

12: ^{1}H NMR (250 MHz, $CDCl_3$): δ = 6.19 (s, 6H, CCH), 3.07 and 2.98 (br., 12H each, CH_2CH_2); IR (film): $\tilde{\nu}$ = 2090, 2055, 2022 cm^{-1}; Anal. calcd. for $C_{66}H_{30}Co_{12}O_{36}$: 37.64 C, 1.44 H, 33.58 Co; found: 37.64 C, 1.68 H, 33.04 Co

13: ^{1}H NMR (250 MHz, $CDCl_3$): δ = 3.22 and 3.10 (br., 12H each, CH_2CH_2), 0.26 (s, 54H, $SiMe_3$); ^{13}C NMR (62.9 MHz, $CDCl_3$): δ = 200.4 (CO), 137.4 (C_{Ar}), 110.3 and 80.4 (CC), 37.2 and 31.4 (CH_2CH_2), 0.5 ($SiMe_3$); IR (film): $\tilde{\nu}$ = 2085, 2070, 2045, 2020 cm^{-1}

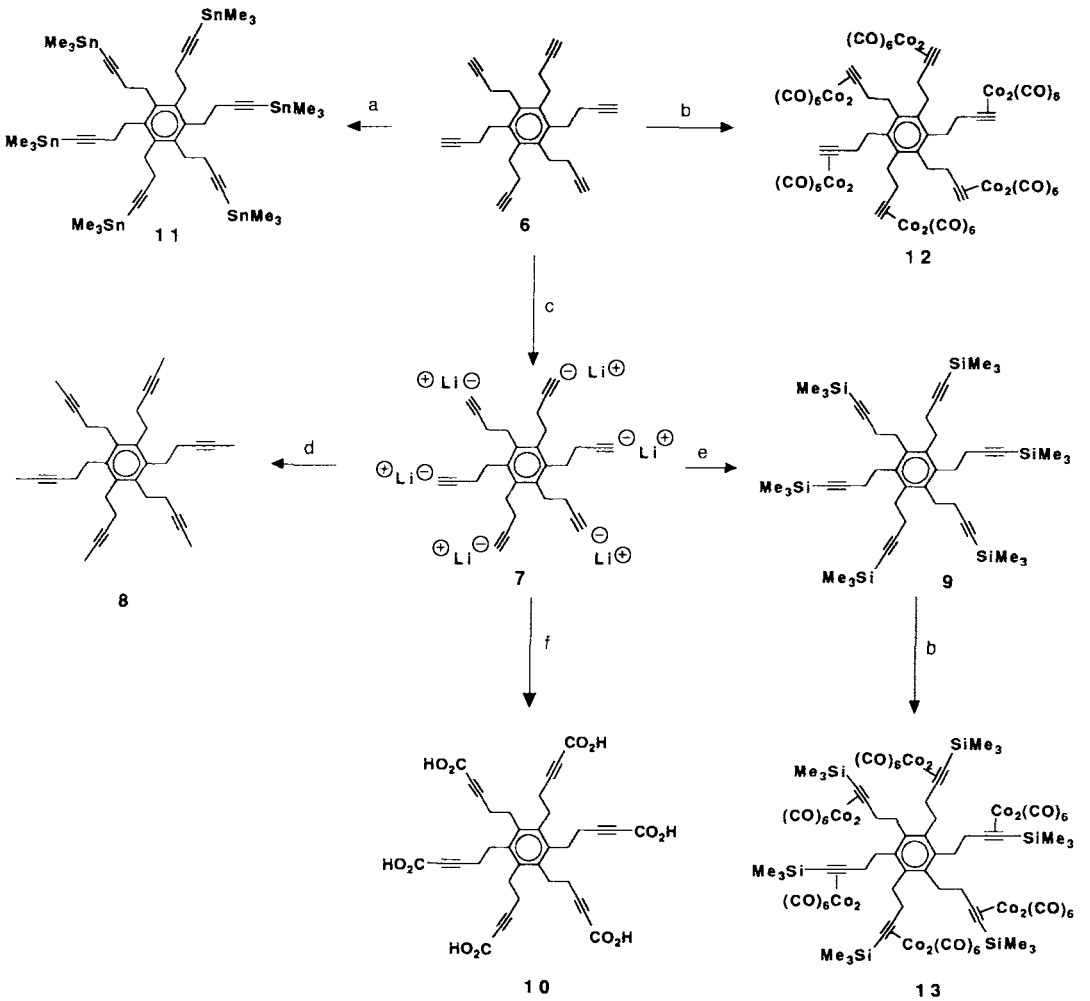

Scheme 2. Reactions of **6**: a) Me_2NSnMe_3; b) $[Co_2(CO)_8]$, pentane, room temperature; c) *n*BuLi, THF, room temperature; d) MeI, THF, room temperature; e) Me_3SiCl, THF, room temperature; f) CO_2, THF then aq. HCl, room temperature.

reaction was accompanied by violent evolution of CO and after a few minutes the red compound **12** formed. This compound is almost insoluble in standard solvents but gave satisfactory elemental analysis and a clean ^{1}H NMR spectrum (after 2000 scans (!), 250 MHz, $CDCl_3$). In contrast, analogue **13**, which has six $SiMe_3$ groups, is readily soluble in various solvents and was easily characterized by ^{1}H and ^{13}C NMR spectroscopy (Scheme 2, Table 2).

In conclusion, hexakis(butynyl)benzene (**6**), now easily and reproducibly accessible, is a very stable compound which shows a well-defined conformation in the solid state and a rich synthetic chemistry. Various hexaalkynylbenzenes, including functionalized derivatives and potentially useful synthetic intermediates, can be obtained from hexamethylbenzene in high yield.

Experimental Procedure

5: To a cold solution (−80 °C) of hexakis(butenyl)benzene (1.00 g, 2.48 mmol) in 50 mL of CH_2Cl_2 was added dropwise Br_2 (0.8 mL, 2.5 g, 15.6 mmol). The solution was stirred for 30 min at room temperature before the product was filtered off, washed with pentane (3 × 10 mL), and dried in vacuo. This gave 3.04–3.21 g (90–95%) of **5** as a white powder.

6: At −70 °C, 100 mL of NH_3 was condensed into a large Schlenk tube. After addition of a small amount of $Fe(NO_3)_3 \cdot 9H_2O$, Na (6.10 g, 265 mmol) was added in small portions. When H_2 evolution had ceased (the slurry was now gray), 3.00 g of **5** was added. The temperature was first raised to −60 °C (16 h), then to −35 °C (5 h). The mixture was hydrolyzed by addition of NH_4Cl (14.40 g, 269 mmol) and NH_3 was evaporated under reduced pressure. After addition of aq. HCl (pH < 4), the product was extracted with CH_2Cl_2. The organic layers were washed with water, dried over Na_2SO_4, filtered, and concentrated to dryness. Flash chromatography (Al_2O_3, 8 × 2 cm, Et_2O) yielded 640–700 mg (74–81%) of **6** as a white powder.

7: A solution of BuLi in hexane (0.92 mL, 1.6 M, 1.47 mmol) was slowly added to a cold (−70 °C) solution of **6** (95.3 mg, 0.244 mmol) in 20 mL of THF. After 15 min lithiation was complete and a white precipitate had formed. This suspension was used in subsequent reactions.

9: A twofold excess of Me_3SiCl was added to the suspension of **7** prepared as described above. The precipitate dissolved immediately. The solvent was evaporated and the product was dissolved in Et_2O. The organic phase was washed twice with water, dried over Na_2SO_4, and filtered. After evaporation of the solvent, the product was purified by flash chromatography (Al_2O_3, 5 × 2 cm, Et_2O). The white powder (97%) contained 1 equiv of water and was very soluble in Et_2O, THF, and CH_2Cl_2, but only sparingly soluble in pentane.

10: A stream of dry CO_2 was bubbled through a suspension of **7** first at −70 °C, later at room temperature. After evaporation of the solvent, water was added, the suspension was filtered, and the solution was acidified with aq. HCl. The solid that had formed was filtered, dissolved in Et_2O, and precipitated with pentane. The product (70%) was filtered and dried. It was soluble in Et_2O, acetone, and aq. NaOH, but only sparingly soluble in pentane and CH_2Cl_2.

Received: February 26, 1996 [Z8869IE]
German version: *Angew. Chem.* **1996**, *108*, 1842–1845

Keywords: alkynes · arenes · hexaalkynylbenzenes · sandwich complexes

[1] a) S. Claude, J.-M. Lehn, M.-J. Perez de Vega, J.-P. Vigneron, *New J. Chem.* **1992**, *16*, 21–28; b) R. J. Lagow, J. J. Kampa, H. C. Wei, S. L. Battle, J. W. Genge, D. A. Laude, C. J. Harper, R. Bau, R. C. Stevens, J. F. Haw, E. Munson, *Science* **1995**, *267*, 362–367; c) U. Bunz, K. P. C. Vollhardt, J. S. Ho, *Angew. Chem.* **1992**, *104*, 1645–1648, *Angew. Chem. Int. Ed. Engl.* **1992**, *31*, 1648–1651; d) U. H. F. Bunz *ibid.* **1994**, *106*, 1127–1131 and **1994**, *33*, 1073–1076; e) R. Gleiter, D. Kratz, *ibid.* **1993**, *32*, 884–887 and **1993**, *32*, 842–845; f) The alkyne function has been astutely used by Newkome et al. to build globular arborols and micellanes: G. R. Newkome, C. N. Moorefield, G. R. Baker, A. L. Johnson, R. K. Behera, *ibid.* **1991**, *103*, 1205–1207 and **1991**, *30*, 1176–1180; g) H. Hopf, G. Maas, *ibid.* **1992**, *104*, 953–977 and **1992**, *31*, 931–954; h) D. Seyferth, T. Kugita, A. L. Rheingold, G. P. A. Yap, *Organometallics* **1995**, *14*, 5362–5366; i) H. Lang, *Angew. Chem.* **1994**, *106*, 569–572, *Angew. Chem. Int. Ed. Engl.* **1994**, *33*, 547–550; j) M. Brady, W. Weng, J. A. Gladysz, *J. Chem. Soc. Chem. Commun.* **1994**, 2655–2656.

[2] For a recent review on molecular electronics in transition metal chemistry, see D. Astruc, *Electron Transfer and Radical Processes in Transition-Metal Chemistry*, VCH, New York, **1995**, Chapter 4.

[3] a) L. Isaacs, P. Seiler, F. Diederich, *Angew. Chem.* **1995**, *107*, 1636–1639, *Angew. Chem. Int. Ed. Engl.* **1995**, *34*, 1466–1469; b) S. Anderson, U. Neidlein, V. Gramlich, F. Diederich, *ibid.* **1995**, *107*, 1722–1725 and **1995**, *34*, 1596–1599; c) A. M. Boldi, F. Diederich, *ibid.* **1994**, *106*, 482–485 and **1994**, *33*, 468–471; d) J. Anthony, C. Boudon, F. Diederich, J.-P. Gisselbrecht, V. Gramlich, M. Gross, M. Hobi, P. Seiler, *ibid.* **1994**, *106*, 794–798 and **1994**, *33*, 763–766.

[4] a) M. Altmann, U. H. F. Bunz, *Angew. Chem.* **1995**, *107*, 603–605, *Angew. Chem. Int. Ed. Engl.* **1995**, *34*, 569–571; b) U. H. F. Bunz, V. Enkelmann, F. Beer, *Organometallics* **1995**, *14*, 2490–2495; c) U. H. F. Bunz, V. Enkelmann, *ibid.* **1994**, *13*, 3823–3833; d) J. E. C. Wiegelmann, U. H. F. Bunz, P. Schiel, *ibid.* **1994**, *13*, 4649–4651.

[5] a) R. Diercks, J. C. Armstrong, R. Boese, K. P. C. Vollhardt, *Angew. Chem.* **1986**, *98*, 270–271, *Angew. Chem. Int. Ed. Engl.* **1986**, *25*, 268–269; b) R. Boese, J. R. Green, J. Mittendorf, D. L. Mohler, K. P. C. Vollhardt, *ibid.* **1992**, *104*, 1643–1645 and **1992**, *31*, 1643–1645.

[6] Hexakis(pent-4-ynyl)benzene has been synthesized in 5% yield by trimerization of 1,8-dichlorooct-4-yne followed by coupling with ethynyl sodium: A. J. Hubert, *J. Chem. Soc. C* **1967**, 13–14.

[7] a) D. Astruc, *Acc. Chem. Res.* **1986**, *19*, 377–383; b) D. Astruc, *Top. Curr. Chem.* **1991**, *160*, 47–95.

[8] F. Moulines, D. Astruc, *Angew. Chem.* **1988**, *100*, 1394–1396, *Angew. Chem. Int. Ed. Engl.* **1988**, *27*, 1347–1349.

[9] a) "Preparative Acetylenic Chemistry": L. Brandsma, *Stud. Org. Chem. (Amsterdam)* **1988**, *34*, Chapters 9 and 11; b) V. Jäger, H. G. Viehe in *Houben-Weyl Methoden der Organischen Chemie, Vol. 5, Part 2a*, 4th ed. (Ed.: E. Müller), Thieme, Stuttgart, **1977**, pp. 677–912.

[10] Crystal structure determination of **6** ($C_{30}H_{30}$): Enraf-Nonius CAD4 diffractometer, $Cu_{K\alpha}$ radiation ($\lambda = 1.5418$ Å), $T = -45$ °C, crystal size $0.30 \times 0.40 \times 0.60$ mm^3; $M_r = 390.57$; $a = 8.141(4)$, $b = 11.512(3)$, $c = 12.812(4)$ Å, $\alpha = 96.04(3)$°, $V = 1194(1)$ Å^3, monoclinic, space group $P2_1/n$ (no. 14), $Z = 2$, $\rho_{calcd} = 1.088$ g cm^{-3}, $\mu = 4.27$ cm^{-1}, $F_{000} = 420.0$; 2419 reflections were measured in the range $5 \le \theta \le 70$° (ω-scan), 2034 of which with $I > 3\sigma(I)$; 2011 independent reflections with $I > 1\sigma(I)$ were used for 197 parameters; solution and refinement of the structure with SDP [13]; $R(F) = 0.054$, $R_w(F) = 0.081$, GOF = 2.655, residual electron density 0.15 e Å^3. Non-hydrogen atoms were refined anisotropically, hydrogen atoms istropically. No correction for ahsorption; secondary extinction coefficient 1.06×10^{-5} [14]. A weighting scheme $1/\sigma^2(F_o)$ was applied to all reflections. Crystallographic data (excluding structure factors) for the structure reported in this paper have been deposited with the Cambridge Crystallographic Data Centre as supplementary publication no. CCDC-179-39. Copies of the data can be obtained free of charge on application to The Director, CCDC, 12 Union Road, Cambridge CB2 1EZ, UK (fax: Int. code +(1223)336-033; e-mail: teched@chemcrys.cam.ac.uk).

[11] a) J. Bernstein, *Accurate Molecular Structures. Their Determination and Importance* (Eds.: A. Domenicano, I. Hargittai), Oxford University Press, Oxford, **1992**; b) A. I. Kitaigorodskii, *Molecular Crystals and Molecules*, Academic Press, New York, **1973**.

[12] K. Jones, M. F. Lappert, *J. Chem. Soc.* **1965**, 1944–1951.

[13] *SDP, Version 5.0B*: A. Frenz, Enraf-Nonius, Delft, The Netherlands, **1988**.

[14] W. H. Zachariasen, *Acta Crystallogr.* **1963**, *16*, 1139–1144.

The Novel Encapsulation of Transition Metals in a Bioctahedral Rare Earth Metal Cluster: $Cs_2La_{10}I_{17}Co_2$

Michael Lulei, Paul A. Maggard, and John D. Corbett*

Dedicated to Professor Hans Georg von Schnering on the occasion of his 65th birthday

The rare earth metal halides form a remarkable variety of highly reduced phases that contain metal clusters.[1, 2] The great majority of these clusters are derived from octahedral units M_6 that are centered by an interstitial atom and are bridged over

[*] Prof. J. D. Corbett, Dr. M. Lulei, P. A. Maggard
Department of Chemistry
Iowa State University, Ames, IA 50011 (USA)
Fax: Int. code +(515) 294-5718

[**] This research was supported by the National Science Foundation—Solid State Chemistry—under DMR-9207361 and DMR-9510278, and was carried out in the facilities of Ames Laboratory, U. S. Department of Energy. M. L. thanks the Alexander von Humboldt Foundation for a Feodor Lynen Fellowship.

each edge by a halide atom to form $M_6X_{12}Z$ units. Possible interstitial atoms are transition metals (i.e. elements from Groups 7–9), main group elements from the second period such as C and N, and even small diatomic C_2 units. The encapsulated elements provide not only central bonding to the cluster but also valence electrons that aid in fulfilling certain minimal electron counts necessary for cluster bonding of the electron-poor rare earth metals.

Our research in recent years has focused on the condensation of clusters into oligomers and chains, as well as on the different patterns of connectivity displayed by the halide atoms that link the clusters into diverse frameworks. Compounds in which R_6Z clusters occur isolated from each other in the structure or are condensed into infinite chains are well investigated and common. However, so far only a very limited group are known with bioctahedral clusters, such as $Gd_{10}Cl_{17}C_4$, or more recently, $CsEr_{10}I_{18}C_4$, in which two M_6 octahedra share a common edge and are each centered by a C_2 group.[3–5] In addition, there are oligomers derived from the spherical condensation of four R_6Z octahedra as in the structures of $Y_{16}I_{20}Ru_4$, $Y_{16}Br_{24}Ir_4$, and $Gd_{20}I_{28}Mn_4$.[6–8] We have also found that the introduction of alkali metal atoms into these systems leads to new quaternary compounds with different compositions and cluster arrangements, as observed in $Cs_4Pr_6I_{13}Os$ and $KPr_6I_{10}Os$ for example.[9, 10] In addition, there is a bioctahedral cluster $La_{10}I_{15}Os_2$ under further study which is apparently formed only in the presence of KI flux.[11]

We report here a novel feature in the chemistry of transition metal stabilized cluster compounds—a bioctahedral cluster unit centered by Co. The new compound with the formula $Cs_2La_{10}I_{17}Co_2$ crystallizes as irregular-shaped, black, air- and moisture-sensitive crystals.[12] As shown in Figure 1,[16] the

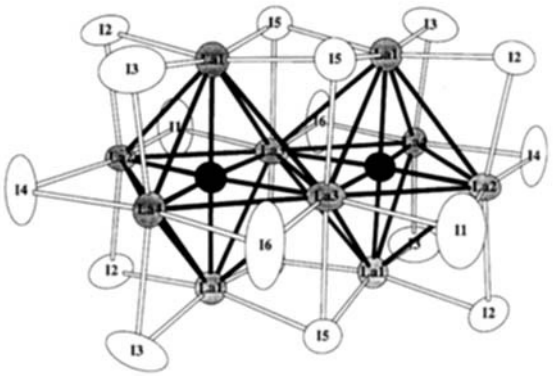

Fig. 1. Structure of the $La_{10}Co_2I_{17}^{2-}$ cluster unit (C_{2h} symmetry, ellipsoids at 99% probability with Co atoms as black circles). Selected interatomic distances [Å]: Co–Co 4.416, La1–Co 2.885, La2–Co 2.779, La3–Co 2.794/3.000, La4–Co 2.659, La1–La2 4.019, La1–La3 4.024/4.148, La1–La4 3.914, La2–La3 4.011, La2–La4 3.951, La3–La3 3.757, La3–La4 4.144.

most remarkable structural feature is a cluster of ten La atoms in the form of two edge-sharing octahedra, each centered by a Co atom. The cluster is centrosymmetric with an inversion center at the midpoint of the La3–La3 axis (site symmetry $2/m$), which is considerably shorter than the other metal–metal separations (by about 0.2 Å).

All 22 outer La–La edges of this bioctahedral cluster are bridged by one of six crystallographically distinct iodine atoms (Fig. 1), which also serve to connect the metal clusters into a three-dimensional network (Figs. 2 and 3). I1 and I4 bridge the La2–La3 and La2–La4 edges, respectively, and connect the clusters as I^{i-a}[1] into layers about (0, 0, 0) and (0, 1/2, 0) along

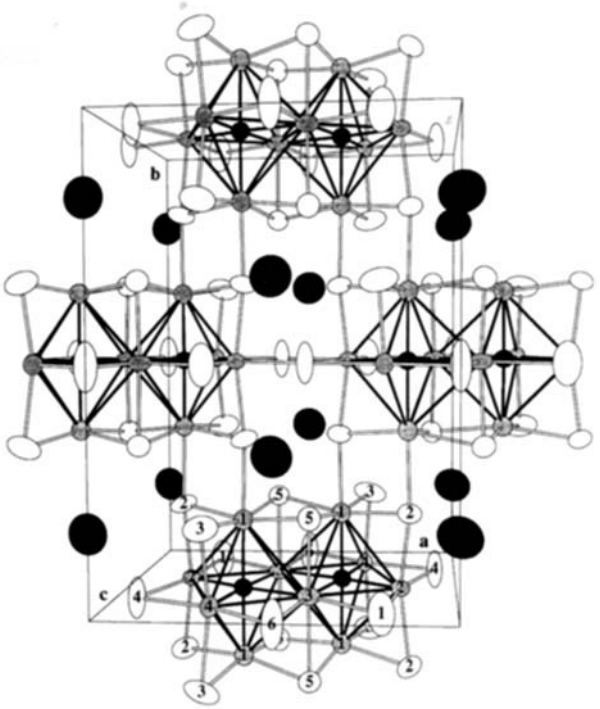

Fig. 2. Structure of $Cs_2La_{10}I_{17}Co_2$. The view of the unit cell along [001] showing the arrangement of the clusters, the iodine connectivity, and the Cs atoms (Cs: large black circles, La: gray, I: white, Co: small black circles, ellipsoids at 99% probability).

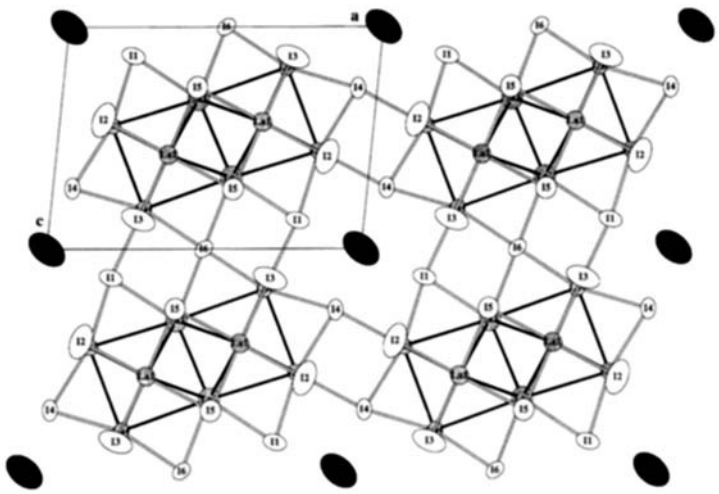

Fig. 3. Structure of $Cs_2La_{10}I_{17}Co_2$. Projection of one layer at (0, 0, 0) on (101) to show the iodine connectivity (atoms are marked as in Fig. 2).

[010] in the unit cell (Fig. 2). The I6 atoms bridge La3–La4 edges in two adjoining clusters within one layer and have, therefore, the functionality I^{i-i}. I2 atoms cover the La1–La2 edges and link the clusters as I^{i-a} along [010]. The La1–La4 edges are capped by I3 atoms (I^i) that form no bonds to neighboring clusters. Finally, two I5 atoms each bridge pairs of La1–La3 edges as I^i in the saddles of the bioctahedral cluster, and hence are each coordinated to three La atoms. All I atoms with the functionality I^{i-a} are naturally complemented by an equal number of I atoms that link the clusters as I^{a-i}. Therefore, the interconnection pattern of the structure can be formulated as $Cs_2(La_{10}Co_2)I^i_8I^{i-i}_{2/2}I^{i-a}_{8/2}I^{a-i}_{8/2}$.

The Cs atoms are located in iodine-lined, slightly distorted and somewhat oversized cuboctahedral cavities within the framework of clusters and halide atoms (Fig. 4). The inter-

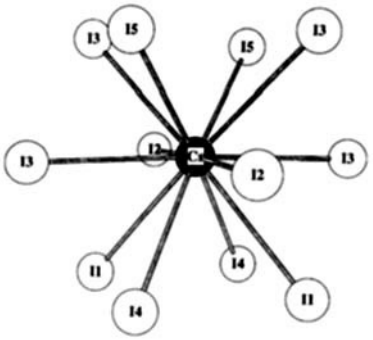

Fig. 4. Coordination polyhedron of the Cs atoms in $Cs_2La_{10}I_{17}Co_2$.

atomic distances range from 4.144 Å for Cs–I5 to 4.514 Å for the Cs–I1 separations. The electron count for $Cs_2La_{10}I_{17}Co_2$ reveals that there are 33 electrons per cluster available for metal–metal bonding. Interestingly, since there are two interstitial atoms per cluster, and an odd number of iodine atoms, it is impossible to reach an even number of cluster electrons by a complete exchange to other interstitial elements. $Cs_2La_{10}I_{17}Fe_2$ would have 31 and the Ni analogue 35 electrons available for metal–metal bonding.

The structure described here is related to those that contain the $Gd_{10}(C_2)_2$ biclusters. In all of these compounds, the halides and the interstitial species, and in case of $Cs_2La_{10}I_{17}Co_2$ also the Cs atoms, approximate a cubic close packing with the rare earth metals in the octahedral holes. Indeed, the interconnection pattern among the halide atoms for $Cs_2La_{10}I_{17}Co_2$ and $Gd_{10}Cl_{17}C_4$ is the same, although the arrangement of the bioctahedral units to each other is altered in order to accommodate the large Cs atoms. This is also reflected by the higher symmetry of the present compound.

Following up on the discovery of this new quaternary example of bioctahedral rare earth metal clusters stabilized by Co, we are exploring the range of this chemistry and also the properties of these phases. The structure pertains to other rare earth metals and interstitials such as Os as well, and preliminary magnetic data and MO calculations are consistent with the expectations (above). These aspects will be reported in a subsequent full paper.

Experimental Procedure

The synthetic and sublimation techniques for LaI_3 and the reaction procedures utilizing welded Nb tubing have been described before [17,18]. CsI (Alfa, 99.9%) was dried by slow heating under dynamic high vacuum and then sublimed. La metal (Ames Laboratory) and Co powder (Alfa, 99.95%) were used as received and were handled in a glovebox. Initially mixtures with an overall stoichiometry $Cs_2La_6I_9Co$ were heated at 800 °C for 27 days, slowly cooled at 5 °C h^{-1} to 300 °C, and then the furnace was turned off. According to Guinier powder pattern, the products were 80% $Cs_2La_{10}I_{17}Co_2$, 10% CsI and 10% LaOI (from traces of water, as usual [1]). Subsequent reactions of starting materials with the refined stoichiometry gave the compound in high yields (90%, in addition to about 10% LaOI) under the same reaction conditions.

Received: February 22, 1996 [Z8847IE]
German version: *Angew. Chem.* **1996**, *108*, 1798–1799

Keywords: clusters · rare earth metal compounds · solid-state structures

[1] J. D. Corbett in *Modern Perspectives in Inorganic Crystal Chemistry* (Ed.: E. Parthé), Kluwer, Dordrecht, The Netherlands, **1992**, p. 27; J. D. Corbett, *J. Alloys Compd.* **1995**, *229*, 10.
[2] A. Simon, H. Mattausch, G. J. Miller, W. Bauhofer, R. K. Kremer in *Handbook on the Physics and Chemistry of Rare Earths, Vol. 15* (Eds.: K. A. Gschneidner Jr., L. Eyring), Elsevier, Amsterdam, **1991**, p. 191.
[3] A. Simon, *Angew. Chem.* **1981**, *93*, 23; *Angew. Chem. Int. Ed. Engl.* **1981**, *20*, 1.
[4] E. Warkentin, R. Masse, A. Simon, *Z. Anorg. Allg. Chem.* **1982**, *491*, 323.
[5] S. Uhrlandt, H. M. Artelt, G. Meyer, *Z. Anorg. Allg. Chem.* **1994**, *620*, 1532.
[6] M. W. Payne, M. Ebihara, J. D. Corbett, *Angew. Chem.* **1991**, *103*, 842; *Angew. Chem. Int. Ed. Engl.* **1991**, *30*, 856.
[7] S. J. Steinwand, PhD thesis, Iowa State University, Ames, **1994**.
[8] M. Ebihara, J. D. Martin, J. D. Corbett, *Inorg. Chem.* **1994**, *33*, 2079.
[9] M. Lulei, J. D. Corbett, *Inorg. Chem.* **1996**, *35*, 4084.
[10] M. Lulei, J. D. Corbett, *Z. Anorg. Allg. Chem.*, in press.
[11] J. D. Martin, J. D. Corbett, unpublished results.
[12] Crystal structure analysis of $Cs_2La_{10}I_{17}Co_2$: Lattice constants for the monoclinic cell (space group $C2/m$), $a = 13.865(5)$, $b = 18.986(5)$, $c = 9.887(3)$ Å, $\beta = 96.00(3)°$ were refined from Guinier powder pattern data ($\lambda = 1.540562$ Å), $V = 2588(1)$ Å^3, $Z = 2$, $\rho = 5.042$ g cm^{-3}. 2823 data (h, k, $\pm l$; $2 < 50°$) were collected with the aid of a CAD4 diffractometer (23 °C, $Mo_{K\alpha}$ radiation, $\mu = 201.3$ cm^{-1}, crystal dimensions $0.2 \times 0.1 \times 0.1$ mm, min./max. transmission: 0.798/1.276). The structure was solved by direct methods (SHELXS) [13]. Programs utilized were those in the instrument package TEXSAN [14]. The residuals for the anisotropic refinement were $R(F) = 0.037$, $R_w = 0.045$ with 1827 independent reflections and 83 variables ($I_0 > 3\sigma(I_0)$), and empirical absorption correction at the isotropic level by four Ψ scans followed by DIFABS, as recommended [15]. Further details of the crystal structure investigation may be obtained from J. D. C. or the Fachinformationszentrum Karlsruhe, D-76344, Eggenstein-Leopoldshafen (Germany), on quoting the depository number CSD-405076.
[13] G. M. Sheldrick, SHELXS-86, Universität Göttingen, **1986**.
[14] TEXSAN, version 6.0, Molecular Structure Corp., The Woodlands, TX, **1990**.
[15] N. Walker, D. Stuart, *Acta Crystallogr. Sect. A*, **1983**, *39*, 159.
[16] All drawings were produced with ATOMS, Shape Software, Kingsport, TN.
[17] J. D. Corbett, *Inorg. Synth.* **1983**, *22*, 15, 31.
[18] T. Hughbanks, J. D. Corbett, *Inorg. Chem.* **1989**, 28, 631.

Like on Heterogeneous Hydrodesulfurization (HDS) Catalysts, the Homogeneous HDS of Benzo[*b*]thiophene Is Achieved by the Concomitant Action of a Metal Promoter (Rh) and an Active HDS Component (W)**

Claudio Bianchini,* M. Victoria Jiménez, Carlo Mealli, Andrea Meli, Simonetta Moneti, Véronique Patinec, and Francesco Vizza

The commercial hydrodesulfurization (HDS) catalysts generally comprise metal sulfides supported on γ-alumina. Molybdenum or tungsten are essential components but the catalytic activity increases remarkably by addition of other transition metals (Ni, Co, Ru, Ir, Rh, Pt, Pd, Os, Re) as promoters.[1, 2] The role played by these promoters is still a matter of debate. According to a recent mechanistic interpretation, the active centers for thiophene activation are the promoter atoms located at the edge plane of a MoS_2 (or WS_2) single slab, whereas H_2 activation occurs on MoS_2 (or WS_2).[2] Modeling studies for the homogeneous reaction support this hypothesis since the large majority of the known C–S bond scissions of thiophenes are brought about by promoter metal complexes.[3] On the other hand, the activation of the thiophene molecules by promoter metal complexes is never followed by the desulfurization of the substrate unless polymetallic metal systems[4] or external sources of "activated" hydrogen atoms are employed.[5] We report herein that benzo[*b*]thiophene, in which a metal promoter (Rh) is inserted into a C–S bond, is desulfurized by H_2 only with the mandatory cooperation of a W center bound to the sulfur atom. For the first time, the heterobimetallic intermediate species that is formed prior to the desulfurization step has been intercepted and characterized.

[*] Dr. C. Bianchini, Dr. M. V. Jiménez, Dr. C. Mealli, Dr. A. Meli, Dr. S. Moneti, Dr. V. Patinec, Dr. F. Vizza
Istituto per lo Studio della Stereochimica ed Energetica dei Composti di Coordinazione, C. N. R.
Via J. Nardi 39, I-50132 Firenze (Italy)
Fax: Int. code + (55)2478366
e-mail: bianchin@cacao.issecc.fi.cnr.it

[**] We thank Progetto Strategico "Tecnologie Chimiche Innovative", CNR, Rome (Italy), and EC (contract no. CHRX-CT930147) for financial support and Mr. Dante Masi for technical assistance.

The 2-vinylthiophenolate complex [(triphos)Rh{η^3-S(C_6H_4)CH=CH_2}] (**1**), obtained by reaction of the 16-electron fragment [(triphos)RhH] (triphos = $MeC(CH_2PPh_2)_3$) with benzo[*b*]thiophene,[3h] is an efficient catalyst for the hydrogenolysis of benzo[*b*]thiophene to 2-ethylthiophenol.[6] High-pressure NMR spectroscopy (HPNMR) has shown that, under catalytic conditions, an active species is the dihydride **2**.[6] In the absence of BT, **1** in THF reacts with H_2 (30 atm, >120 °C) to give free 2-ethylthiophenol and various Rh compounds via the intermediacy of the dihydride **2** which is formed at lower temperature (20–120 °C) (Scheme 1).

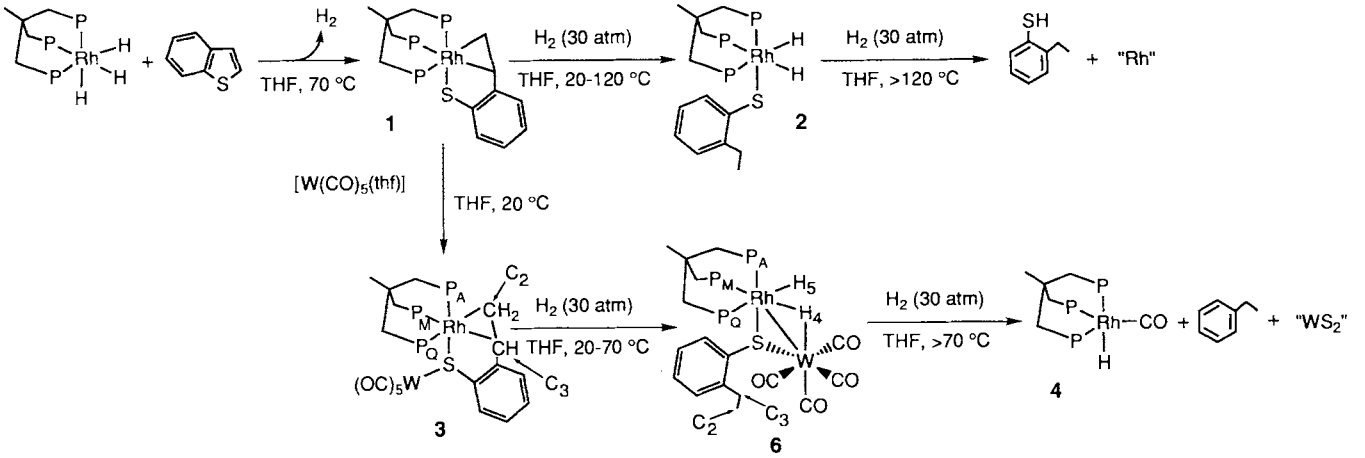

Scheme 1. Synthesis of **1**–**4** and **6**.

A quite different reaction with H_2 (30 atm) is observed when **1** is previously treated with [$W(CO)_5$(thf)] to give the adduct **3**, which is isolated as orange-yellow crystals. In this case, in fact, the hydrodesulfurization of the thiolate ligand (THF, 30 atm H_2, >70 °C) occurs with formation of ethylbenzene (GC-MS), **4**,[7] and an insoluble black material that contains W and S in an approximate ratio of 1 to 2 (atomic absorption analysis). Analysis of the crude product shows that traces of $W(CO)_6$ (GC-MS) and of **5**[6] (NMR) are also formed.

[(triphos)Rh(CO){*o*-S(C_6H_4)C_2H_5}] **5**

Monitoring the reaction between **3** and H_2 by variable-temperature HPNMR shows that the degradation of **3** to **4** is traversed by an intermediate species **6**, which incorporates all the rhodium at temperatures below 70 °C. This species has been isolated as brick red crystals by reaction of **3** in THF with H_2 (30 atm) at a constant temperature of 70 °C for 3 h. The molecular structure of **6** has been elucidated in both solution and the solid state by multinuclear NMR spectroscopy and an X-ray structure analysis,[8] respectively. A Zortep drawing of this binuclear complex **6** is shown in Figure 1.

The X-ray structure analysis, carried out on crystals of **6**·CH_2Cl_2, confirms the NMR spectroscopic results: a hydride anion bridges the Rh and W metal centers (^{1}H NMR, CD_2Cl_2, 20 °C: $\delta(H_b) = -9.88$, $J(H,Rh) = 19.0$, $J(H,P)_{trans} = 100.6$, ^{183}W satellites with $J(H,W) = 34.2$ Hz). Unfortunately, the second hydrido ligand could not be located and its position is only indirectly placed (^{1}H NMR, CD_2Cl_2, 20 °C: $\delta(H_t) = -10.07$, $J(H,Rh) = 6.8$, $J(H,P)_{trans} = 181.5$, $J(H,H) = 5.4$ Hz; IR (CH_2Cl_2): $\tilde{\nu} = 1996$ cm^{-1} (νRh–H)). In fact, there is a vacant octahedral site at the Rh center, and the opposite P_1 atom is the most *trans*-influenced (d_{Rh-P1} 2.414(4), $\bar{d}_{Rh-P2,3}$ 2.293(4) Å).

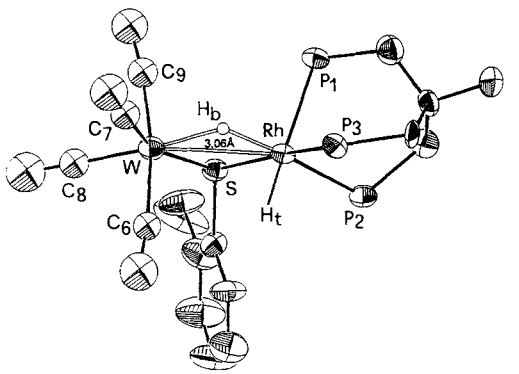

Fig. 1. Zortep drawing of the structure of **6**. Phenyl rings of the triphos ligand are omitted for clarity. The atom H_t could not be located by normal X-ray procedures and it is shown at the vacant octahedral site about the rhodium atom. The positioning is supported by the Rh–P_1 bond, which is significantly longer than the other two Rh–P bonds [2.414(4) vs. av 2.293(4) Å]. Selected bond lengths [Å] and angles [°]: W–S 2.493(4), Rh–S 2.407(4), W–C 1.93(3) (av), W–H_b 1.75(16), Rh–H_b 1.57(16); P-Rh-P 90.0(6) (av), C_6-W-C_9 170.8(7), C_7-W-C_8 91.4(7), W-S-Rh 77.1(1), S-Rh-P_3 169.9(1), S-W-C_7 159.8(5), P_2-Rh-H_b 170(5), C_8-W-H_t 172(5), W-H_b-Rh 134(3).

The overall structure can be described as follows: By initially neglecting the H_b ligand, the two formal d^6 metal centers (W^0 and Rh^{III}) appear as the central atoms of two square pyramids sharing a basal site (namely, the bridging S donor of the thiophenolate ligand). Although the H_b ligand seems to be in the proper position to complete the octahedra of both metal centers, its two electrons cannot saturate the metals (in terms of the effective atomic number (EAN) rule, the total electron count of 34 implies a M–M bond). Essentially, the situation closely resembles that of the $[M(CO)_5(\mu\text{-H})]^-$ ions (M = Cr, W),[14] which contain two isoelectronic terminal ML_5 fragments and a bent M-H_b-M bridge. The latter, also described as a three-center–two-electron bond, involves the formally empty σ-hybrid orbitals of the two ML_5 fragments and the filled H_{1s} orbital. The W–Rh distance of 3.06 Å and the W-H_b-Rh angle of 134° are consistent with the corresponding parameters of the quoted compounds.

To confirm the intermediacy of **6** in the desulfurization step, an isolated sample of this compound in THF was treated with H_2 (30 atm) at a constant temperature of 120 °C. This led to the (carbonyl)hydride **4**, ethylbenzene, and the black material

"WS_2". Also, the thermal decomposition of **6** at 120 °C under nitrogen (NMR experiment in [D$_8$]THF) gave **4** (together with some **5** and decomposition products), thus indicating that the desulfurization step involves an intramolecular hydrogen atom migration.

The overall structural motif of **6** has no experimental precedent in modeling studies on homogeneous systems, but heterobimetallic moieties with a similar structure have been suggested to form on the surface of heterogeneous HDS catalysts.[4a]

Experimental Procedure

3: A sample of $W(CO)_6$ (0.12 g, 0.33 mmol), dissolved in THF (30 mL), was placed in a quartz reactor and converted to [$W(CO)_5$(thf)] by photolysis at −10–10 °C under a flow of nitrogen. After 4 h, this solution was transferred by cannula to a flask containing **1** [3h] (0.28 g, 0.33 mmol) in THF (20 mL) and the resulting mixture stirred for 1 h at room temperature. The volume of the solvent was reduced to about 15 mL and ethanol (40 mL) added. Orange-yellow microcrystals of **3** were obtained in 85% yield after filtering and drying. $^{31}P\{^1H\}$ NMR (81.01 MHz, CD_2Cl_2, 20 °C): AMQX spin system, δ = 30.9 (ddd, $J(P_A,P_M)$ = 36.0, $J(P_A,P_Q)$ = 32.0, $J(P_A,Rh)$ = 115.8 Hz; P_A), −7.1 (ddd, $J(P_M,P_Q)$ = 42.6, $J(P_M,Rh)$ = 112.4 Hz; P_M), −10.0 (ddd, $J(P_Q,Rh)$ = 104.6 Hz; P_Q); ^1H NMR (200.13 MHz, CD_2Cl_2, 20 °C): δ = 3.84 (m, $J(H_2,H_3)$ = 9.5 Hz, $J(H_2,H_2)$ = 1.7, $J(H_2,Rh)$ = 1.8 Hz; H_2), 2.86 (m, $J(H_3,H_2)$ = 8.3, $J(H_3,Rh)$ = 0.9 Hz; H_3), 2.70 (m, $J(H_2,Rh)$ = 1.5 Hz; H_2). The J(H,H) and J(H,Rh) values were determined on the basis of $^1H\{^{31}P\}$ NMR experiments. $^{13}C\{^1H\}$ NMR (50.32 MHz, CD_2Cl_2, 20 °C): δ = 42.5 (dm, J(C,P) 35.9; C_2), 65.5 (dm, J(C,P) 28.7; C_3), 200.1 (s, ^{183}W satellites with J(C,W) = 128.7 Hz; CO_{eq}), 202.6 (s, CO_{ax}). Remaining ^{13}C resonances were obscured by those of triphos carbon atoms. IR (Nujol): $\tilde{\nu}$ = 2060 (m), 1966 (m), 1917 (vs), 1872 (s) cm^{-1} (CO). $C_{54}H_{46}O_5P_3RhSW$ (1186.7): calcd: C 54.65, H 3.91, Rh 8.67; found: C 54.55, H 3.81, Rh 8.49.

6: A solution of **3** (0.24 g, 0.2 mmol) in THF (50 mL) was treated with H_2 (30 atm) at 70 °C for 3 h in a Parr reactor. After the bomb was depressurized and vented under a nitrogen stream, the contents were transferred into a Schlenk-type flask. The solution was concentrated to about 20 mL under vacuum. Portionwise addition of *n*-heptane (10 mL) led to the precipitation of brick red crystals of **6** in 75% yield. $^{31}P\{^1H\}$ NMR (81.01 MHz, CD_2Cl_2, 20 °C): AMQX spin system, δ = 23.1 (ddd, $J(P_A,P_M)$ = 34.1, $J(P_A,P_Q)$ = 26.9, $J(P_A,Rh)$ = 109.7 Hz; P_A), 13.6 (ddd, $J(P_M,P_Q)$ = 21.7, $J(P_M,Rh)$ = 105.5 Hz; P_M), −9.2 (ddd, $J(P_Q,Rh)$ = 74.5 Hz; P_Q); ^1H NMR (200.13 MHz, CD_2Cl_2, 20 °C): δ = 2.63 (dq, $J(H_3,H_3)$ = 14.0, $J(H_3,H_2)$ = 7.4 Hz; H_3), 2.18 (dq, $J(H_3,H_2)$ = 7.4 Hz; H_3), 1.10 (t; H_2), −9.88 (dm, $J(H_4,Rh)$ = 19.0 Hz, $J(H_4,H_5)$ = 5.4 Hz, $J(H_4,P_M)$ = 100.6 Hz, ^{183}W satellites with $J(H_4,W)$ = 34.2 Hz; H_4), −10.07 (dm, $J(H_5,Rh)$ = 6.8 Hz, $J(H_5,P_Q)$ = 181.5 Hz; H_5). The J(H,H), J(H,Rh) and J(H,W) values were determined on the basis of $^1H\{^{31}P\}$ NMR experiments. $^{13}C\{^1H\}$ NMR (50.32 MHz, CD_2Cl_2, 20 °C): δ = 213.9 (s; CO), 210.6 (d, J(C,P) = 5.3 Hz; CO), 205.5 (d, J(C,P) = 3.8 Hz; CO), 205.2 (d, J(C,P) = 6.0 Hz; CO), 29.1 (s; C_2), 14.9 (s; C_3). IR (Nujol): $\tilde{\nu}$ = 1995 (s) (Rh–H), 2057 (w), 1868 (s), 1852 (s), 1811 (s) cm^{-1} (CO); (CH_2Cl_2 solution): ν = 1996 (s) (Rh–H), 2058 (w), 1872 (vs), 1860 (sh), 1822 (s) cm^{-1} (CO). $C_{53}H_{50}O_4P_3RhSW$ (1162.7): calcd: C 54.75, H 4.33, Rh 8.85; found: C 54.68, H 4.25, Rh 8.69. Crystals of **6**·CH_2Cl_2 suitable for an X-ray structure analysis were obtained by slow crystallization of **6** from CH_2Cl_2/ethanol under nitrogen at room temperature. $C_{54}H_{52}Cl_2O_4P_3RhSW$ (1246.1): calcd: C 51.99, H 4.20, Rh 8.25; found: C 51.21, H 4.22, Rh 8.12.

Received: March 20, 1996 [Z 8953 IE]
German version: *Angew. Chem.* **1996**, *108*, 1845–1847

Keywords: catalysis · desulfurization · NMR spectroscopy · rhodium compounds · tungsten compounds

[1] a) M. J. Girgis, B. C. Gates, *Ind. Eng. Chem. Res.* **1991**, *30*, 2021; b) B. C. Wiegand, C. M. Friend, *Chem. Rev.* **1992**, *92*, 491.
[2] A. N. Startsev, *Catal. Rev.-Sci. Eng.* **1995**, *37*, 353.
[3] a) T. B. Rauchfuss, *Prog. Inorg. Chem.* **1991**, *39*, 259; b) J. G. Reynolds, *Chem. Ind.* **1991**, 570; c) R. A. Sánchez-Delgado, *J. Mol. Catal.* **1994**, *86*, 287; d) R. J. Angelici, *Bull. Soc. Chim. Belg.* **1995**, *104*, 265; e) C. Bianchini, A. Meli, *J. Chem. Soc., Dalton Trans.* **1996**, 801; f) C. Bianchini, A. Meli, M. Peruzzini, F. Vizza, S. Moneti, V. Herrera, R. A. Sánchez-Delgado, *J. Am. Chem. Soc.* **1994**, *116*, 4370; g) C. Bianchini, M. V. Jiménez, A. Meli, S. Moneti, F. Vizza, V. Herrera, R. A. Sánchez-Delgado, *Organometallics* **1995**, *14*, 2342; h) C. Bianchini, P. Frediani, V. Herrera, M. V. Jiménez, A. Meli, L. Rincón, R. A. Sánchez-Delgado, F. Vizza, *J. Am. Chem. Soc.* **1995**, *117*, 4333.
[4] a) J. Chen, L. M. Daniels, R. J. Angelici, *J. Am. Chem. Soc.* **1991**, *113*, 2544; b) S. Luo, A. E. Ogilvy, T. B. Rauchfuss, A. L. Rheingold, S. R. Wilson, *Organometallics* **1991**, *10*, 1002; c) W. D. Jones, R. M. Chin, *J. Am. Chem. Soc.* **1994**, *116*, 198; d) U. Riaz, O. J. Curnow, M. D. Curtis, *ibid.* **1995**, *117*, 6366.
[5] a) C. Bianchini, A. Meli, M. Peruzzini, F. Vizza, P. Frediani, V. Herrera, R. A. Sánchez-Delgado, *J. Am. Chem. Soc.* **1993**, *115*, 2731; b) J. J. Garcia, B. E. Mann, H. Adams, N. A. Bailey, P. M. Maitlis, *ibid.* **1995**, *117*, 2179.
[6] C. Bianchini, V. Herrera, M. V. Jiménez, A. Meli, R. A. Sánchez-Delgado, F. Vizza, *J. Am. Chem. Soc.* **1995**, *117*, 8567.
[7] J. Ott, L. M. Venanzi, C. A. Ghilardi, S. Midollini, A. Orlandini, *J. Organomet. Chem.* **1985**, *291*, 89.
[8] Crystal structure data for $C_{53}H_{50}O_4P_3RhSW\cdot CH_2Cl_2$: monoclinic, space group $P2_1/n$, ρ_{calcd} = 1.607 g cm^{-3}, Z = 4, a = 15.626(5), b = 19.129(5), c = 17.270(5) Å, β = 92.33(1)°, V = 5158(3) Å^3, number of unique data = 6486, $R1$ [$I > 2\sigma(I)$] = 0.081. Data were collected on a Philips PW1100 FEBO diffractometer at 293(2) K using $Cu_{K\alpha}$ (λ = 1.5418 Å) radiation. A set of 25 carefully centered reflections having $10 < \theta < 16.5$ were used to determine the cell constants. Three standard reflections were measured every 2 h for the orientation and the intensity control. During data collection no decay for the specimen was noticed. Intensity data were corrected for Lorentz-polarization effects. Atomic scattering factors were those reported by Cromer and Waber [9] with anomalous dispersion correction taken from reference [10]. An empirical absorption correction was applied by Ψ scan with transmission factors in the range 1.001–1.46 [11]. The computational work was carried out with the program SHELXL93 [12]. The structure was solved by direct methods using the SIR92 programm [13] and all of the non-hydrogen atoms were found through a series of F_o Fourier maps. A CH_2Cl_2 solvent molecule was also introduced although affected by some disorder. Nonmetal-bound hydrogen atoms were introduced at calculated positions at the late stage of refinement. The latter was done by full-matrix least square calculations, initially with isotropic thermal parameters. In the last least square cycles anisotropic thermal parameters were used for Rh, W, S, and P, and also for the C atoms except for those of the P phenyl substituents and of the CO molecules. In the last stage of refinement a peak of 0.9 e Å^{-3} was detected in the ΔF map corresponding to the expected bridging hydrido ligand, and it was succesfully refined. No evidence was found for the terminal H ligand. In the final ΔF maps significant peaks were found close to the heavy metal (largest value ca. 1.2 e Å^{-3}), and were considered as ripples of no chemical relevance. Crystallographic data (excluding structure factors) for the structure(s) reported in this paper have been deposited with the Cambridge Crystallographic Data Centre as supplementary publication no. CCDC-179-71. Copies of the data can be obtained free of charge on application to The Director, CCDC, 12 Union Road, Cambridge CB2 1EZ, UK (fax: Int. code + (1223) 336-033; e-mail: teched@chemcrys.cam.ac.uk).
[9] D. T. Cromer, J. T. Waber, *Acta Crystallogr.* **1965**, *18*, 104.
[10] *International Tables of Crystallography, Vol. 4*, Kynoch, Birmingham, England, **1974**.
[11] N. Walker, D. Stuart, *Acta Crystallogr. Sect. A* **1983**, *39*, 158.
[12] G. M. Sheldrick, *SHELXL93. Program for structure refinement*, Universität Göttingen, Germany, **1994**.
[13] A. Altomare, G. Cascarano, C. Giacovazzo, A. Guagliardi, M. C. Burla, G. Polidori, M. Camalli, *J. Appl. Crystallogr.* **1994**, *27*, 435.
[14] a) J. L. Petersen, R. K. Brown, J. M. Williams, *Inorg. Chem.* **1981**, *20*, 158; b) J. Roziere, J. M. Williams, R. P. Stewart, Jr., J. L. Petersen, L. F. Dahl, *J. Am. Chem. Soc.* **1977**, *99*, 4497.

Two-Phase Catalysis: A Strategy for Avoiding Consecutive Reactions as Exemplified in the Telomerization of Butadiene and Ammonia**

Thomas Prinz, Wilhelm Keim, and Birgit Driessen-Hölscher*

Liquid/liquid two-phase processes nowadays play a major role in homogeneous catalysis,[1–4] and are increasingly used in industrial applications.[5–7] Several homogeneously catalyzed telomerizations, that is the dimerization of a diene coupled with the addition of a nucleophile, have been carried out in two-phase systems.[8–12] One example that has already achieved

[*] Dr. B. Driessen-Hölscher, Dipl.-Chem. T. Prinz, Prof. Dr. W. Keim
Institut für Technische Chemie und Petrolchemie der Technischen Hochschule Templergraben 55, D-52056 Aachen (Germany)
Fax: Int. code +(241)8888-177
e-mail: driessen-hoelscher@itc.itc.rwth-aachen.de

[**] We thank the Bayer AG (Leverkusen) for financial support. B. D.-H. thanks the Land Nordrhein-Westfalen for a stipendium (Hochschulsonderprogramm II).

industrial significance is the synthesis of 1,7-octadienol from butadiene and water.[7] In contrast, the catalytic telomerization of butadiene and ammonia has so far only been carried out in one-phase systems,[13-15] leading to the products shown in Scheme 1.

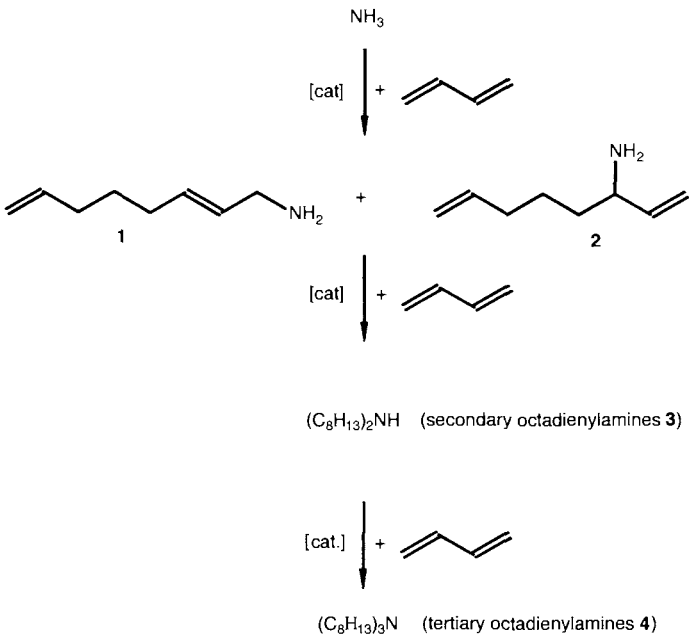

Scheme 1. Telomerization of butadiene and ammonia.

Since the primary and secondary octadienylamines **1**/**2** and **3**, respectively, are more nucleophilic than ammonia and therefore react further, it is not possible to synthesize them in good yields and selectivities by the above-mentioned telomerization. Even at low conversions, the primary octadienylamines **1** and **2** are only obtained with poor selectivities (Table 1, entry 1). If it were possible to control this telomerization to selectively yield only the primary products **1** and **2**, a potential route for the synthesis of primary octadienylamines would be available. Hydrogenation of **1** yields the industrially important *n*-octylamine, which is used for the production of water softeners, corrosion inhibitors, and flotation agents.

We report herein that **1** and **2** can be synthesized selectively by the catalytic two-phase telomerization of butadiene and ammonia, providing that the two amines are extracted from the aqueous catalyst phase immediately after their synthesis by using a solvent with appropriate polarity. In this way, the consecutive reactions to higher amines in the aqueous phase are avoided. The catalyst system employed consists of palladium acetate/tppts (tppts = trisodium salt of 3,3′,3″-phosphanetriylbenzenesulfonic acid) dissolved in water. The second phase is an organic solvent such as toluene to which butadiene and ammonia is added. The results of the known one-phase telomerizations are listed in Table 1 together with the results of our two-phase experiments.

When the telomerization is carried out in *tert*-butyl alcohol as a single-phase process (reaction time 1 h), tertiary amines **4** are obtained as the major product with 61% selectivity in a total yield of 21% (Table 1, entry 1). In contrast, the two-phase process under otherwise identical conditions leads preferentially to the primary amines **1** and **2** (Table 1, entry 2). The high selectivity of 25.8% with which the secondary amines **3** are formed can be attributed to the high reaction temperature of 100 °C and to the small amount of ammonia present. When the two-phase telomerization is carried out at 60 °C with a large excess of ammonia and under otherwise identical conditions, the secondary amines **3** are obtained with a selectivity of only 1%. Typical results of two-phase telomerizations with various solvents are listed in Table 2. Without the organic phase—using only water as solvent—under otherwise identical conditions, the preferred products are the primary (**1**, **2**) and secondary amines **3** (Table 2, entry 1). The solubility of butadiene in the aqueous catalyst phase is sufficient to allow medium conversions. However, the octadienylamines **1** and **2** are slightly soluble in the aqueous phase and thus the consecutive reaction to the secondary amines **3** takes place to a considerable extent. Similar results are achieved when ethyl acetate is used as the organic phase (Table 2, entry 4), since it mixes better with water than the other solvents and thus compounds **1** and **2** cannot be extracted. Toluene serves as a suitable solvent for extraction; the primary amines are formed with a selectivity of 88%.

Table 1. Comparison of one-phase versus two-phase catalytic process in the telomerization of butadiene and ammonia [a].

Entry	Process	Selectivity [%]			Ratio	Total yield
		1+**2**	**3**	**4**	(**1**+**2**):**3**:**4**	[%] [b]
1	one-phase	2	4	61	1:2:31	21
2	two-phase	31.5	25.5	1.5	21:17:1	24

[a] Reaction conditions: Single-phase: $T = 100$ C, $t = 1$ h, butadiene:ammonia = 10:1, Pd : butadiene = 1:1000, 20 mL *tert*-butyl alcohol, Pd:PPh_3 = 1:3.4; two-phase: $T = 100$ C, $t = 1$ h, butadiene:ammonia = 10:1, Pd:butadiene = 1:1000, H_2O:CH_2Cl_2 = 2:1, Pd:tppts = 1:4. [b] Total yield based on ammonia.

Table 2. Influence of the organic solvent on the catalytic two-phase telomerization of butadiene and ammonia [a].

Entry	Second phase	Selectivity [%]			Total yield
		1+**2**	**3**	**4**	[%] [b]
1	–	60.5	30	·	41
2	toluene	88	6	·	55
3	pentane	79	16	·	61
4	ethyl acetate	53	18	·	40

[a] Reaction conditions: $Pd(OAc)_2$ (0.15 mmol), tppts (0.6 mmol), H_2O (20 mL), organic solvent (12.5 mL), ammonia (300 mmol), butadiene (75 mmol), $T = 80$ C, $t = 1.5$ h. [b] Total yield based on butadiene.

The total yields show that the second phase has a significant influence on the mass transfer of reactants and products between the aqueous and the organic phase. It is known that reaction rates of two-phase reactions are limited by mass transfer.[16]

In a pilot plant for batchwise operation, comprising a 900 mL reactor and a coupled separator, the catalyst phase could be recycled ten times without loss of selectivity and with only small loss of activity. Our results show that two-phase catalysis is a suitable method for avoiding consecutive reactions of primary products that are sparingly soluble in water. Further applications are conceivable such as in the hydroformylation of alkynes.

Experimental Procedure

In a typical experiment palladium(II) acetate (0.15 mmol) and tppts (0.6 mmol) (synthesized according to the procedure given by Gärtner et al. [17]) were dissolved in water (5 mL) and placed under argon into an autoclave (75 mL). Aqueous ammonia solution (300 mmol, 20 mL of a 27.13 M solution) and organic solvent (12.5 mL; mostly toluene) were added, followed by condensation of butadiene (4.1 g, 75 mmol, 5.8 mL). The autoclave was heated in an oil bath (80 C) and the mixture

stirred. After the reaction, the autoclave was cooled, degassed, and the phases were separated in a separating funnel. The aqueous phase was extracted with an organic solvent (10 mL). *n*-Hexanol was added as internal standard to the combined organic phases for analysis. A sample was dried over molecular sieves and analyzed by quantitative gas chromatography (Pona, 50 m, 1.5 bar Helium). Amines were not observed either in the aqueous phase or in the gas phase. The experimental results are given in Tables 1 and 2.

Received: February 19, 1996 [Z88301E]
German version: *Angew. Chem.* **1996**, *108*, 1835–1836

Keywords: amines · homogeneous catalysis · palladium compounds · telomerization · two-phase catalysis

[1] A. Behr, W. Keim, *Erdoel Erdgas Kohle* **1987**, *3*, 126.
[2] W. A. Herrmann, C. W. Kohlpaintner, *Angew. Chem.* **1993**, *105*, 1588; *Angew. Chem. Int. Ed. Engl.* **1993**, *32*, 1524.
[3] P. Kalck, F. Monteil, *Adv. Organomet. Chem.* **1992**, *34*, 219.
[4] T. Horvath, F. Joo, *Aqueous Organometallic Chemistry and Catalysis*, Kluwer, Dordrecht, **1995**.
[5] B. Cornils, E. Wiebus, *CHEMTECH* **1995**, *25*, 33.
[6] W. Keim, *Chem. Ing. Tech.* **1984**, *56*, 850.
[7] Y. Noriaki, T. Masuliko (Kuraray), US-A 4356333, **1982**.
[8] A. Durocher, W. Keim, *Erdoel, Kohle* **1976**, *29*, 31.
[9] E. Kuntz (Rhone-Poulenc), DE-B 2733516, **1978**.
[10] G. Pfeiffer, S. Chan, A. Bendayan, B. Waegell, J.-P. Zahra, *J. Mol. Catal.* **1990**, *59*, 1.
[11] J. Pennequin, A. Mortreux, F. Petit, J. Mentech, B. Thiriet, FR 2 693 188, **1994**.
[12] E. Monflier, P. Bourdauducq, J.-L. Couturier, J. Kervennal, A. Mortreux, *J. Mol. Catal.* **1995**, *97*, 29.
[13] a) T. Mitsuyasu, M. Hara, J. Tsuji, *J. Chem. Soc. Chem. Commun.* **1971**, 345; b) J. Tsuji, M. Takahashi, *J. Mol. Catal.* **1981**, *10*, 107.
[14] R. N. Fakhretdinov, G. A. Tolstikov, U. M. Dzhemilev, *Neftekhimiya (Engl. Trans.)* **1979**, *19*, 468.
[15] C. F. Hobbs, D. E. McMackins (Monsanto), US-A 4100194, **1978** and US-A 4130590, **1978**.
[16] S. S. Divekar, B. M. Bhanage, R. M. Deshpande, R. V. Gholap, R. V. Chaudhari, *J. Mol. Catal.* **1994**, *91*, L1.
[17] R. Gärtner, B. Cornils, H. Springer, P. Lappe (Ruhrchemie), DE-B 3235030, **1982** [*Chem. Abstr.* **1984**, *101*, P55331t].

$[Mn(CO)_5]^-$, the First Square-Pyramidal Pentacarbonyl Complex in the Complex Salt $[Ph_4P][Mn(CO)_5]$, and $[Mn_3Se_2(CO)_9]^{2-}$, the First Mixed Carbonyl-Selenido Complex of Manganese**

Renate Seidel, Birgit Schnautz, and Gerald Henkel*

Dedicated to Professor Hans Georg von Schnering on the occasion of his 65th birthday

Whereas the chemistry of sulfur-containing transition metal complexes is well-developed,[1] comparatively few of the corresponding selenido and tellurido compounds are known.[2] In an approach to synthesize chalcogenido complexes with unprecedented chemical properties, we recently characterized the compounds $[Co_{11}Te_7(CO)_{10}]^{2-}$ and $[Co_4Te_2(CO)_{11}]$ obtained by oxidation of $[Co_2(CO)_8]$ with Na_2Te_2.[3] Herein we report on an unexpected disproportionation of $[Mn_2(CO)_{10}]$ that occurs when it is treated with Na_2Se in solvents like methanol or THF. Besides the mononuclear complex $[Mn(CO)_5]^-$ **2**, the trinuclear complex $[Mn_3Se_2(CO)_9]^{2-}$ **4** is formed, which is the first manganese complex with a mixed carbonyl-selenido ligand sphere. Anions **2** and **4** were isolated as tetraphenylphosphonium salts **1** and **3**, respectively, and were fully characterized by X-ray structure determinations at $-120\,^{\circ}C$.[4]

$[Ph_4P][Mn(CO)_5]$ **1** $\qquad$ $[Mn(CO)_5]^-$ **2**

$[Ph_4P]_2[Mn_3Se_2(CO)_9]\cdot THF$ **3** $\qquad$ $[Mn_3Se_2(CO)_9]^{2-}$ **4**

Very recently the mixed-metal complex $[MnFe_2Se_2(CO)_9]^-$ related to **4** was synthesized and described as isostructural with $[Fe_3Se_2(CO)_9]$.[5] The X-ray structure determination was based on a disordered model in which two of the three metal positions are statistically occupied by Mn and Fe. Because of the unexpected coordination properties of **4** (see below), the related complex $[Fe_3Se_2(CO)_9]$ **5** as well as its sulfur-containing analogue $[Fe_3S_2(CO)_9]$ **6** were prepared for comparison purposes. The structures of **5** and **6**, which were described by Dahl et al.[6] and by Bard et al.,[7] respectively, were redetermined by using high-quality low-temperature X-ray data.[4] The resulting structural parameters were used as reference material.

$[Fe_3Se_2(CO)_9]$ **5** $\qquad$ $[Fe_3S_2(CO)_9]$ **6**

Crystals of **1** are composed of discrete mononuclear anions **2** and tetraphenylphosphonium cations. The most important feature of this compound is that **2** does not possess the expected trigonal-bipyramidal structure observed in crystals of $[Ni(phen)_3][Mn(CO)_5]_2$[8] (phen = 1,10-phenanthroline) and $[Mn(thf)_6][Mn(CO)_5]_2$,[9] which is also characteristic for the isoelectronic molecule $[Fe(CO)_5]$.[10] To our surprise, the coordination polyhedron of **2** is a regular square pyramid of nearly perfect symmetry (point group C_{4v}, Fig. 1), and as such possesses a spatial distribution of the CO ligands similar to that of the protonated compound $[HMn(CO)_5]$.[11] These structural similarities might be indicative of a stereochemically active lone pair of electrons in **2**. Contrary to this hypothesis, however, the C_{ax}-Mn-C_{eq} valence an-gle (102.6(1)°) is about 5° larger than the corresponding angle in $[HMn(CO)_5]$. In the crystalline state, **2** sits on a fourfold rotation axis of the space group.

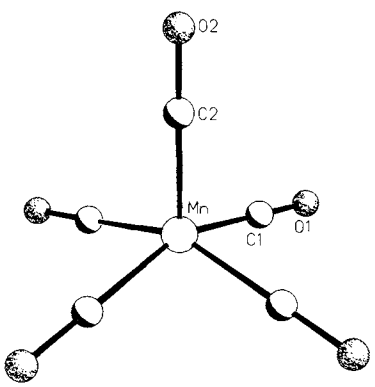

Fig. 1. Structure of **2** in crystals of **1**. Selected distances [Å] and angles [°]: Mn–C1 1.809(2) (4×), Mn–C2 1.794(3), C1–O1 1.159(2), C2–O2 1.155(4); C1-Mn-C2 102.6(1) (4×), C1-Mn-C1 154.7(1) (2×) and 87.3(1) (4×), Mn-C1-O1 179.5(2), Mn-C2-O2 180.

According to the results of the X-ray structure analysis, in addition to trinuclear mixed-valence complex anions **4** and tetraphenylphosphonium ions, crystals of **3** contain stabilizing THF molecules (ratio 1:2:1). The description of **4** as a complex anion with an odd number of valence electrons was further supported by magnetic measurements. These revealed that **4** has the expected paramagnetic properties ($\mu_{eff} = 1.8\ \mu_B$ for $[Ph_4P]_2[Mn_3Se_2(CO)_9]$ at 100 K). Paramagnetic behavior is also manifested by broadening of the resonance signals of the phenyl protons in the ^1H NMR spectrum compared to those in the diamagnetic reference compound $[Ph_4P]_2[Mn_3Se_2(SeMe)(CO)_9]$.[12]

[*] Prof. Dr. G. Henkel, Dipl.-Chem. R. Seidel, Dipl.-Chem. B. Schnautz
Fachgebiet Anorganische Chemie der Universität
Lotharstrasse 1, D-47048 Duisburg (Germany)
Fax: Int. code +(203)379-2110
e-mail: biohenkel@uni-duisburg.de

[**] This work was supported by the Deutsche Forschungsgemeinschaft, the Bundesministerium für Bildung, Wissenschaft, Forschung und Technologie (BMBF), and the Fonds der chemischen Industrie. We thank Dr. E. Bill (Mülheim an der Ruhr) for carrying out the magnetic measurements.

With a total of 49 valence electrons and two Mn–Mn bonds, **4** falls short of the value required by the 18 electron rule (PSEP theory[13]) by one. The heavy atom frame is a slightly distorted square pyramid in which alternating Mn and Se atoms occupy the base, and a third Mn atom defines the top (Fig. 2).

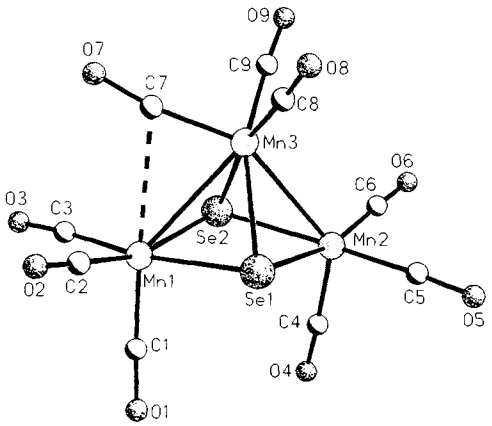

Fig. 2. Structure of **4** in crystals of **3**. Selected distances [Å] and angles [°]: Mn1···Mn2 3.647(2), Se1···Se2 3.171(2), Mn1···Mn3 2.803(3), Mn2–Mn3 2.724(2), Mn1–Se1 2.407(2), Mn1–Se2 2.402(2), Mn1–C1 1.769(9), Mn1–C2 1.805(8), Mn1–C3 1.804(6), Mn1–C7 2.726(7), Mn2–Se1 2.458(2), Mn2–Se2 2.439(2), Mn2–C4 1.768(8), Mn2–C5 1.793(6), Mn2–C6 1.793(8), Mn3–Se1 2.446(2), Mn3–Se2 2.444(2), Mn3–C7 1.794(7), Mn3–C8 1.775(7), Mn3–C9 1.783(8); Mn3-C7-O7 171.0(8).

While the heavy atom frame of **5** (50 electrons) is of comparable geometry, both compounds differ with respect to the arrangement of the carbonyl ligands around the metal atom on top of the M_3Se_2 pyramid. Evidently, an asymmetric carbonyl bridge (C7) between Mn3 and Mn1 is induced by an electronic nonequivalence of Mn1 and Mn2 in **4**, which is not observed in the structure of **5**. This nonequivalence is particularly apparent from a comparison of the Mn–Se bond lengths (Mn1–Se1 2.407(2), Mn1–Se2 2.402(2) Å; Mn2–Se1 2.458(2), Mn2–Se2 2.439(2) Å). The observed differences can be attributed to different oxidation states of the manganese atoms; the mean value is calculated to be +0.67. Based on the observed bond lengths and coordination numbers, a formal oxidation state of +1 can be assigned to the atoms Mn1 and Mn3, wheras a value of 0 seems to be appropriate for Mn2. The point symmetry of **4** is C_s; the Mn atoms define the mirror plane. All three of the Mn atoms are surrounded by three carbonyl and two selenido ligands in a square-pyramidal fashion, if the weak interaction of the asymmetric CO bridge (Mn1–C7: 2.726(7) Å) is neglected. On the other hand, if this bridge is considered to be a bond, Mn1 has a distorted octahedral ligand sphere. In contrast to Mn3 in **4**, the coordination of Fe3 in **5** is trigonal-bipyramidal (Fig. 3).

The arrangement of the carbonyl groups around Fe3 leads to identical ligand environments for both Fe1 and Fe2. Both metal atoms are chemically equivalent with similar Fe–Se bond lengths (Fe1–Se1 2.351(1), Fe1–Se2 2.359(1) Å; Fe2–Se1 2.354(1), Fe2–Se2 2.358(1) Å). The point symmetry of **5** is C_s; the mirror plane is now defined by the two Se atoms and the Fe3 center. In the mixed-valence compound **5** the formal oxidation state of Fe3 is +2, whereas Fe1 and Fe2 are monovalent.

These results support the assumption that in complexes of formula $[M_3X_2(CO)_9]^z$ (X = S, Se, Te; $z = -2, -1, 0, +1$) an asymmetric carbonyl bridge is established if the two metal atoms in the base of the M_3X_2 pyramid are electronically nonequivalent. As a consequence, the metal atom in the higher

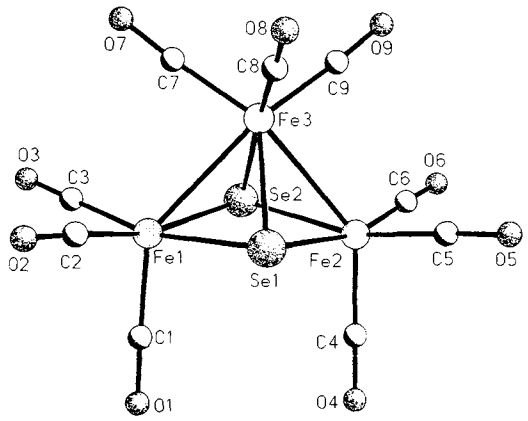

Fig. 3. Structure of **5** in the crystal. Selected distances [Å]: Fe1···Fe2 3.520(1), Se1···Se2 3.105(1), Fe1–Fe3 2.657(1), Fe2–Fe3 2.645(1), Fe1–Se1 2.351(1), Fe1–Se2 2.359(1), Fe1–C1 1.790(5), Fe1–C2 1.822(5), Fe1–C3 1.821(6), Fe2–Se1 2.354(1), Fe2–Se2 2.358(1), Fe2–C4 1.780(5), Fe2–C5 1.801(7), Fe2–C6 1.798(5), Fe3–Se1 2.354(1), Fe3–Se2 2.375(1), Fe3–C7 1.790(6), Fe3–C8 1.801(6), Fe3–C9 1.798(5).

oxidation state is stabilized probably by a $(p_\pi)_{CO}$-d_M interaction. The change from the nonbridged (**5**, Fig. 3) to the bridged state (**4**, Fig. 2) is accompanied by a rotation of the apical $M(CO)_3$ fragment by 30° around its local symmetry axis followed by a bend of this axis by about 15° in the direction of M1. At the same time, the coordination polyhedron changes from the trigonal bipyramid to the square pyramid.

Based on these results, we can now solve the problem of the Fe/Mn distribution in the complex ion $[MnFe_2Se_2(CO)_9]^-$ (see above). According to the literature, this compound is isostructural with **5**.[5] In fact, however, the complex possesses the characteristic asymmetric carbonyl bridge identified in **4** for the first time and therefore is rather built-up like **4** and not like **5**. Taking the individual metal–selenium distances into account, our analysis indicates that the metal positions in the base of the M_3Se_2 pyramid are filled most probably in an ordered fashion with manganese (position M1) and iron (position M2), contrary to the previously proposed statistical arrangement. The metal atom in the higher formal oxidation state (here Mn) is stabilized by the asymmetic carbonyl bridge in accordance with our hypothesis.

Though asymmetric carbonyl bridges are widespread in chemistry,[14] only very few other examples of the type identified in **4** with an unexpected long secondary Mn···C bond exist. A prominent example for an asymmetric bond of this type, the realization of which has only now become apparent, is found in the $[Fe_3S_2(CO)_9]$ component of the 1:1 adduct of the formula $[Fe_3S_2(CO)_9][Fe_2(S_2)(CO)_6]$, which is also known as the "King complex".[15] To our surprise, this component exhibits the same long M···C contact that is typical for **4**, although both Fe atoms in the base of the Fe_3S_2 pyramid should be chemically equivalent. The unusual orientation of the apical $Fe(CO)_3$ fragment in comparison with the expected geometry observed in **5** is described by Dahl et al. as an alternative conformation.[15] Based upon our knowledge derived from the structures of **4** and **5**, however, the existence of an asymmetric carbonyl bridge in the $[Fe_3S_2(CO)_9]$ adduct component has to be proposed. To test whether this is an exception of our hypothesis, the compound $[Fe_3S_2(CO)_9]$ **6** was crystallized and investigated at low temperatures. According to the results of an X-ray structure investigation,[4] crystals of **6** are isotypic with crystals of **5** even at −120 °C. In the structure at low temperatures no carbonyl bridges are observed. The reason for the unexpected behavior of

the $[Fe_3S_2(CO)_9]$ component within crystals of the 1:1 adduct, however, is evident on careful analysis of the packing. In fact, both components form charge transfer adducts in which trinuclear $[Fe_3S_2(CO)_9]$ and binuclear $[Fe_2(S_2)(CO)_6]$ molecules are associated alternately by intermolecular S···S bridges (3.157 Å) to form one-dimensional endless strands (Fig. 4).

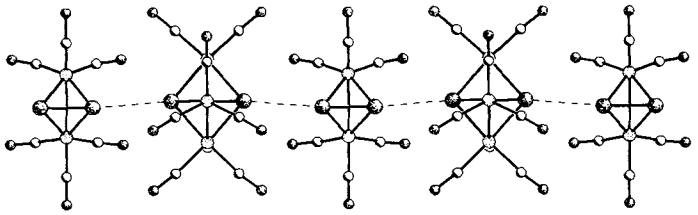

Fig. 4. Section of the alternating chain in crystals of $[Fe_3S_2(CO)_9][Fe_2(S_2)(CO)_6]$ (S···S = 3.157 Å).

Within these charge transfer adducts, electron density is transferred from the trinuclear component to the disulfide group of the binuclear complex. The resulting electron deficit in $[Fe_3S_2(CO)_9]$ is most probably stabilized by the asymmetric carbonyl bridge. This may also explain why the Mössbauer spectrum of $[Fe_3S_2(CO)_9][Fe_2(S_2)(CO)_6]$ differs significantly from that of the single complexes **5** and **6**.[16] Thorough characterization of these and related charge transfer complexes is currently in progress.

Experimental Procedure

All experiments were performed under oxygen-free nitrogen.

1 and **3**: $[Mn_2(CO)_{10}]$ (0.044 g, 0.11 mmol), Na_2Se (0.024 g, 0.19 mmol), $[Ph_4P]Cl$ (0.083 g, 0.22 mmol), and THF (1 mL) were placed in a pyrex-glass ampoule (20 cm in length, 1 cm in diameter). The ampoule was then cooled with liquid nitrogen and sealed up under vacuum (10^{-3} mbar) followed by subsequent heating of the reaction mixture for 72 h at 80 °C in an oven. After cooling the mixture to 5° C, yellow platelike crystals of **1** appeared together with dark red blocks of **3**. IR(KBr): $\tilde{\nu}$ = 1944, 1845 cm^{-1} (C=O) (**1**); $\tilde{\nu}$ = 1979, 1943, 1890, 1859 cm^{-1} (C=O) (**3**).

5 and **6** were prepared as described in the literature [17]. Crystals of **5** and **6** of better quality that were used for the X-ray structure determinations were isolated as by-products from reactions of $[Fe(CO)_5]$ with Na_2S_2 and NiI_2, and of $[Ph_4P]_2[Fe_6Se_6(CO)_{12}]$ [18] with I_2, respectively.

Received: January 8, 1996 [Z8701IE]
German version: *Angew. Chem.* **1996**, *108*, 1836–1839

Keywords: charge transfer complexes · iron compounds · manganese compounds · structure elucidation

[1] a) B. Krebs, G. Henkel, *Angew. Chem.* **1991**, *103*, 785; *Angew. Chem. Int. Ed. Engl.* **1991**, *30*, 769, and references therein; b) I. G. Dance, K. Fisher, *Prog. Inorg. Chem.* **1994**, *41*, 637.

[2] a) L. C. Roof, J. W. Kolis, *Chem. Rev.* **1993**, *93*, 1037; b) D. Fenske, J. Ohmer, J. Hachgenei, K. Merzweiler, *Angew. Chem.* **1988**, *100*, 1300; *Angew. Chem. Int. Ed. Engl.* **1988**, *27*, 1277; c) M. A. Ansari, J. A. Ibers, *Coord. Chem. Rev.* **1990**, *100*, 223; d) S.-P. Huang, M. G. Kanatzidis, *ibid.* **1994**, *130*, 509; e) J. W. Kolis, *ibid.* **1990**, *105*, 195.

[3] R. Seidel, R. Kliss, S. Weissgräber, G. Henkel, *J. Chem. Soc. Chem. Commun.* **1994**, 2791.

[4] Crystal data: Siemens P4RA four-circle diffractometer, $Mo_{K\alpha}$ radiation (λ = 0.71073 Å), graphite monochromator, rotating anode generator, scintillation counter, 150 K, empirical absorption corrections, SHELXTL-PLUS programs, direct methods, least-squares refinements, one scaling factor, one isotropic extinction parameter. **1**: $C_{20}H_{20}O_5PMn$, M_r = 534.36, tetragonal, space group $P4/n$, a = 13.166(4), c = 7.276(3) Å, V = 1261.25 Å^3, Z = 2, ρ_{calcd} = 1.407 g cm^{-3}, $\mu(Mo_{K\alpha})$ = 0.62 mm^{-1}, transmission range 0.984–0.801, crystal dimensions ca. 0.49 × 0.42 × 0.18 mm, ω scan, $2\theta_{max}$ = 54°, 2875 reflections, $R(R_w)$ = 0.0295 (0.0380) for 1221 observed reflections ($I > 2\sigma(I)$), 86 variables, non-hydrogen atoms anisotropic, H atoms at idealized positions. **3**: $C_{61}H_{48}O_{10}P_2Se_2Mn_3$, M_r = 1325.67, monoclinic, space group $P2_1/c$, a = 11.574(8), b = 46.18(2), c = 11.656(7) Å, β = 112.37(4)°, V = 5761.52 Å^3, Z = 4, ρ_{calcd} = 1.528 g cm^{-3}, $\mu(Mo_{K\alpha})$ = 2.02 mm^{-1}, transmission range 0.541–0.304, crystal dimensions ca. 0.38 × 0.22 × 0.17 mm, ω scan, $2\theta_{max}$ = 54°, 12101 unique reflections, $R(R_w)$ = 0.0649 (0.0549) for 7578 observed reflections ($I > 2\sigma(I)$), 694 variables, all heavy atoms with the exception of the disordered THF molecule anisotropic, H atoms at idealized positions. **5**: $C_9O_9Se_2Fe_3$, M_r = 577.56, triclinic, space group $P\bar{1}$, a = 6.748(1), b = 9.163(1), c = 13.044(1) Å, α = 93.97(1), β = 94.54(1), γ = 110.75(1)°, V = 747.75 Å^3, Z = 2, ρ_{calcd} = 2.565 g cm^{-3}, $\mu(Mo_{K\alpha})$ = 7.78 mm^{-1}, transmission range 0.977–0.323, crystal dimensions ca. 0.55 × 0.23 × 0.21 mm, ω scan, $2\theta_{max}$ = 54°, 3266 unique reflections, $R(R_w)$ = 0.0360 (0.0359) for 2761 observed reflections ($I > 2\sigma(I)$), 209 variables, all atoms anisotropic. **6**: $C_9O_9S_2Fe_3$, M_r = 483.76, triclinic, space group $P\bar{1}$, a = 6.682(2), b = 9.047(2), c = 12.998(3) Å, α = 93.96(2), β = 94.42(2), γ = 111.03(2)°, V = 727.56 Å^3, Z = 2, ρ_{calcd} = 2.208 g cm^{-3}, $\mu(Mo_{K\alpha})$ = 3.28 mm^{-1}, transmission range 0.470–0.284, crystal dimensions ca. 0.74 × 0.28 × 0.28 mm, ω scan, $2\theta_{max}$ = 54°, 3192 unique reflections, $R(R_w)$ = 0.0231 (0.0292) for 2937 observed reflections ($I > 2\sigma(I)$), 209 variables, all atoms anisotropic. Further details of the crystal structure investigation may be obtained from the Fachinformationszentrum Karlsruhe, D-76344 Eggenstein-Leopoldshafen, on quoting the depository number CSD-59402.

[5] M. Shieh, T.-F. Tang, S.-M. Peng, G.-H. Lee, *Inorg. Chem.* **1995**, *34*, 2797.

[6] L. F. Dahl, P. W. Sutton, *Inorg. Chem.* **1963**, *2*, 1067.

[7] A. J. Bard, A. H. Cowley, J. K. Leland, G. J. N. Thomas, N. C. Norman, P. Jutzi, C. P. Morley, E. Schlüter, *J. Chem. Soc., Dalton Trans.* **1985**, 1303.

[8] B. A. Frenz, J. A. Ibers, *Inorg. Chem.* **1972**, *11*, 1109.

[9] G. Kong, G. N. Harakas, B. R. Whittlesey, *J. Am. Chem. Soc.* **1995**, *117*, 3502.

[10] B. Beagley, D. W. J. Cruickshank, P. M. Pinder, A. B. Robiette, G. M. Sheldrick, *Acta Crystallogr. Sect. B* **1969**, *25*, 737.

[11] a) S. J. La Placa, W. C. Hamilton, J. A. Ibers, A. Davison, *Inorg. Chem.* **1969**, *8*, 1928; b) S. J. La Placa, W. C. Hamilton, J. A. Ibers, *ibid.* **1964**, *3*, 1491.

[12] R. Seidel, G. Henkel, unpublished results.

[13] D. M. P. Mingos, R. L. Johnston, *Struct. Bond.* **1987**, *68*, 29.

[14] See for example R. H. Crabtree, M. Lavin, *Inorg. Chem.* **1986**, *25*, 805.

[15] C. H. Wei, L. F. Dahl, *Inorg. Chem* **1965**, *4*, 493.

[16] J. R. Dilworth, S. Morton, M. O'Connor, J. Silver, *Inorg. Chim. Acta.* **1987**, *127*, 91.

[17] W. Hieber, J. Gruber, *Z. Anorg. Allg. Chem.* **1958**, *296*, 91.

[18] R. Seidel, G. Henkel, unpublished results.

A Designed Non-Peptidic Receptor that Mimics the Phosphocholine Binding Site of the McPC603 Antibody**

J. Oriol Magrans, Angel R. Ortiz, M. Antònia Molins, Paul H. P. Lebouille, Jorge Sánchez-Quesada, Pilar Prados, Miquel Pons, Federico Gago, and Javier de Mendoza*

Biotechnological applications of catalytic antibodies[1] meet with considerable problems such as high cost and lability at high temperatures and in nonaqueous solvents. Potentially, most of these problems could be obviated by using synthetic molecules with similar binding properties and predicted biological activities, whose design could be guided by the binding strategy found in crystal structures of antibody–antigen complexes. We describe herein a non-peptidic abiotic receptor **1**, which binds dioctanoyl-L-α-phosphatidylcholine (DOPC) by making use of

[*] Prof. Dr. J. de Mendoza, J. O. Magrans, J. Sánchez-Quesada, Prof. Dr. P. Prados
Departamento de Química Orgánica
Universidad Autónoma de Madrid
Cantoblanco, E-28049 Madrid (Spain)
Fax: Int. +code (1)397-3966

Dr. A. R. Ortiz, P. H. P. Lebouille, Prof. Dr. F. Gago
Departamento de Fisiología y Farmacología
Universidad de Alcalá de Henares
E-28871 Alcalá de Henares (Spain)

Dr. M. A. Molins, Prof. Dr. M. Pons
Departament de Química Orgànica, Facultat de Química
Universitat de Barcelona, E-08028 Barcelona (Spain)

[**] This work was supported by Dirección General de Investigación Científica y Técnica (DGICYT PB93 0283).

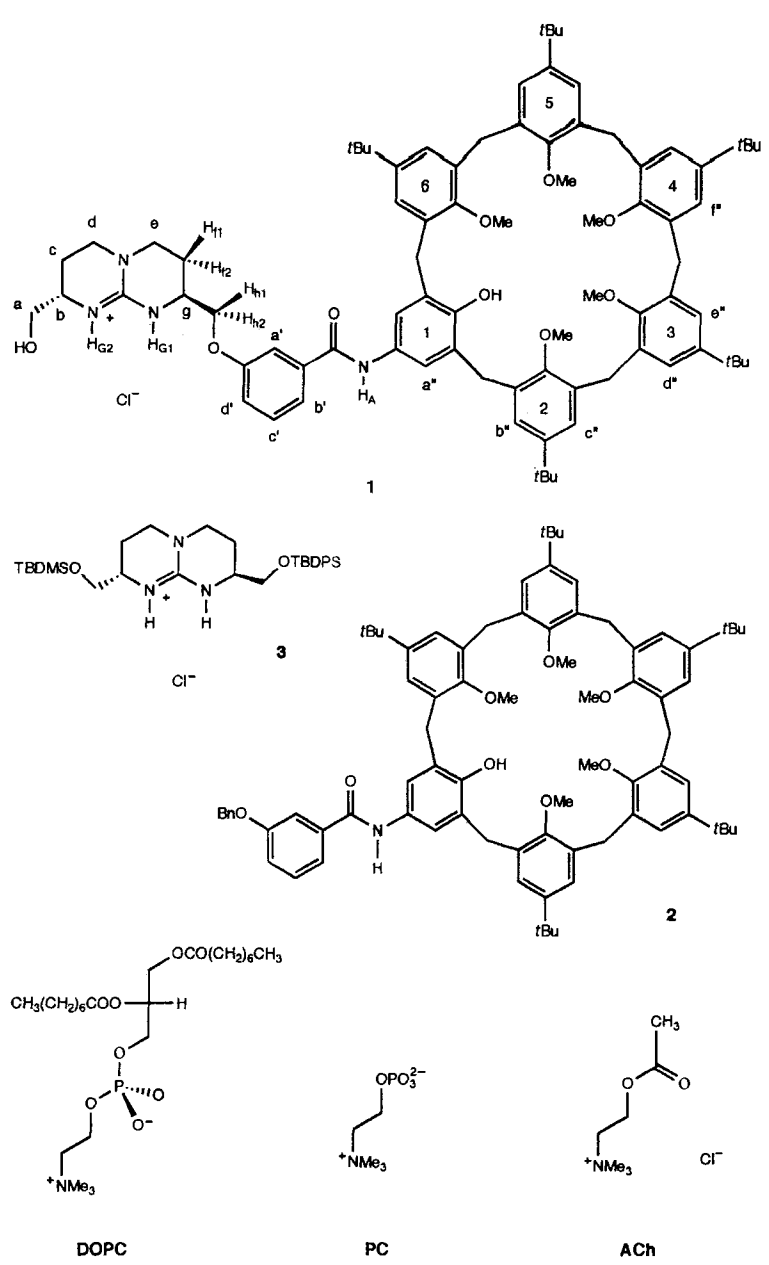

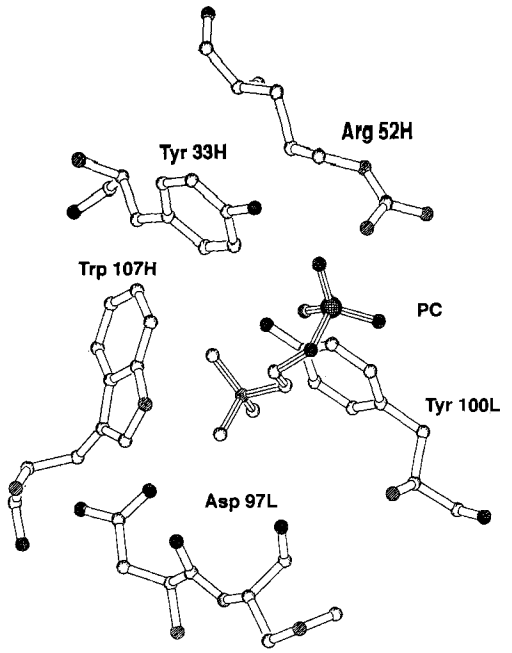

Fig. 1. Phosphocholine binding site of McPC603 [2].

the key interactions found in the crystal structure of the Fab domain of the McPC603 antibody complexed with phosphorylcholine (PC).[2, 3] In the McPC603–PC complex (Fig. 1) the PC phosphate group interacts with the positively charged Arg 52H residue, and its quaternary ammonium head establishes both ion–ion (Asp 97L) and cation–π interactions (Trp 107H, Tyr 33H, and Tyr 100L). Both types of interactions have been considered crucial determinants of binding specificity.[4]

Thus, receptor **1** was designed to provide chemical complementarity to both the phosphate and trimethylammonium groups of DOPC. It contains a bicyclic guanidinium moiety for the selective complexation of phosphate monoanion and a calix[6]arene subunit for the complexation of the quaternary ammonium salt through cation–π interactions. The two subunits are linked through a short spacer containing an amide bond.

The synthesis of **1** was achieved in five steps from readily available mononitrocalix[6]arene **4**[5] and the bicyclic guanidinium compound **5** (TBDPS = *tert*-butyldiphenylsilyl)[6] with an overall yield of 30% (Scheme 1). Compound **1** was fully characterized by mass spectrometry, NMR spectroscopy (500 MHz), and microanalysis. Its NMR spectrum is consistent with the presence of an average symmetry plane bisecting the calix[6]arene macrocycle. Complete assignment of the spectrum was straightforward using a combination of COSY and ROESY experiments. ROE cross-peaks between aromatic protons on neighboring phenolic rings indicate that the *cone* conformation required for encapsulation of trimethylammonium is predominant, although the fact that methylene groups appear as singlets suggests that rapid inversion of the cone takes place at room temperature.

Addition of one equivalent of DOPC to a CD_2Cl_2 or a $CDCl_3$ solution of **1** resulted in a single set of NMR resonances substantially different from those of the component molecules. Complete assignment was also carried out by a combination of COSY and ROESY spectra. In $CDCl_3$, the important downfield shifts of $\Delta\delta = 1.76$ for the amide proton (H_A) in the side chain and of $\Delta\delta = 0.81$ for the guanidine NH proton closer to the calixarene ring (H_{G1}) were observed, indicating strong hydrogen bonds. The signal of the other guanidinium NH proton (H_{G2}) was shifted upfield by $\Delta\delta = 0.51$ in the complex.[7] Similar changes were observed in the spectra recorded in CD_2Cl_2 (Fig. 2).

The signals of the methyl and methylene protons bound to the quaternary nitrogen of the choline group were strongly shifted upfield by $\Delta\delta = 0.51$ and 0.35, respectively. This can be interpreted as being caused by the inclusion of the choline group inside the cavity formed by the aromatic groups of the calixarene. Inclusion was confirmed by the observation of a rotating-frame NOE beween the methyl group of choline and the aromatic protons ($H_{a''}$) in ring 1 in CD_2Cl_2.

A *cone* conformation of the calix[6]arene in the complex is indicated by ROE cross-peaks between aromatic protons in neighboring rings and by the chemical shifts of calixarene methylene carbons.[8] Cone inversion in the complex is slower than in the free calixarene, allowing the observation of an AB

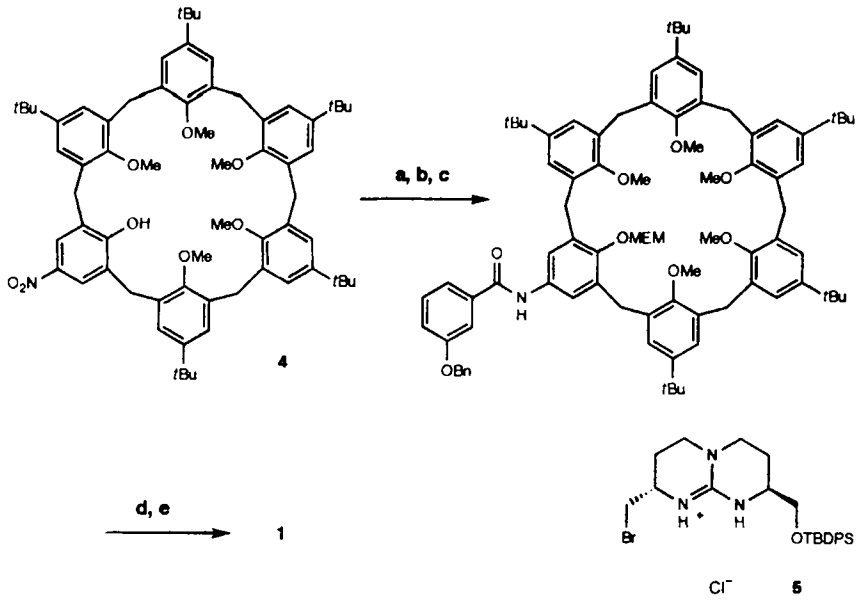

Scheme 1. Synthesis of receptor **1**. a) K_2CO_3 (1.1 equiv), CH_3CN, room temperature, 1 h, then methoxyethoxymethyl chloride (1.5 equiv), room temperature, 24 h (yield 85%); b) H_2PtO_2 (1 equiv), THF, room temperature, 48 h (yield 100%); c) Et_3N (cat.), 3-benzyloxybenzoyl chloride (1.1 equiv), THF, reflux, 16 h (yield 88%); d) H_2, 10% Pd–C, THF, room temperature, 24 h (yield 85%); e) K_2CO_3 (1 equiv), CH_3CN, reflux, 1 h, then **5** (1.3 equiv, 20 h, 0.3 equiv, 24 h, 0.1 equiv, 24 h), 55 °C, then aq. HCl, room temperature, 16 h (yield 48%).

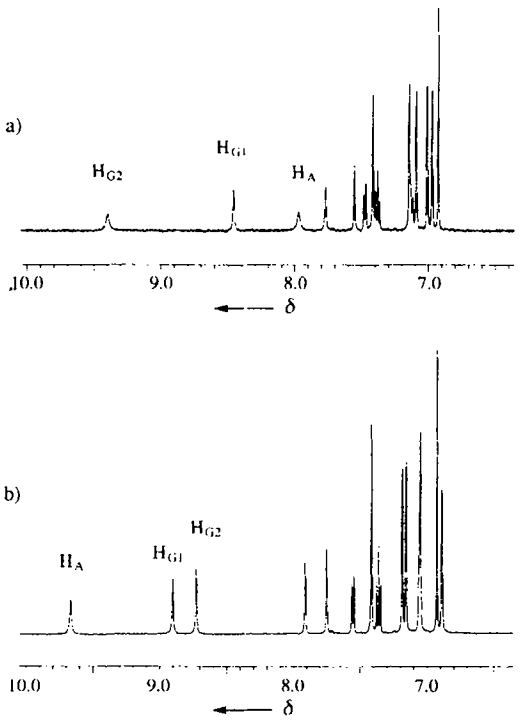

Fig. 2. Changes in the ^1H NMR signals of the aromatic protons of **1** (in CD_2Cl_2) upon complexation of DOPC. a) Pure **1**. b) DOPC–**1** complex (1:1).

system for the methylene group between rings 2 and 3. However, the fact that the remaining methylenes give rise to singlets and that weak ROEs are observed between methoxy protons in ring 4 and one of the aromatic protons in rings 3 and 5 suggests that some flexibility persists.

The linker region also appears to be more structured in the complex. In particular, proton H_a shows intense ROEs to the amide proton H_A and to the methylene group (H_{h1} and H_{h2}) directly attached to the bicyclic guanidine. This indicates that the side chain is folded such that both the guanidinium and amide protons participate simultaneously in hydrogen bonding to the guest phosphate group.

Extensive molecular modeling studies were performed for the DOPC–**1** complex. In keeping with the results of the NMR experiments, the calix[6]arene moiety was initially set in an all-*syn cone* conformation, with the trimethylammonium group of DOPC docked into its cavity. Then, 500 ps restrained molecular dynamics (MD) simulations in vacuo were employed to search for low-energy conformations compatible with the NOE results. The conformation optimized in vacuo was then subjected to an unrestrained 500 ps MD simulation at 298 K in chloroform[9] (Fig. 3). In full agreement with the NMR data, the calix[6]arene moiety displays a *cone* conformation in the calculated structure; the choline head remains inside the cavity, while the phosphate group interacts through strong hydrogen bonds with proximal guanidinium (H_{G1}) and amide (H_A) protons. Structures computed for the DOPC–**1** complex

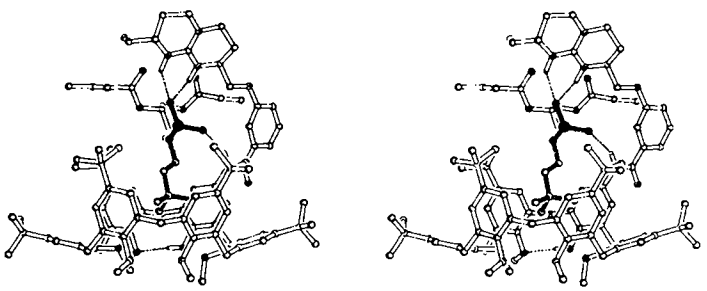

Fig. 3. Stereoview of the energy-minimized averaged structure of the DOPC–**1** complex in chloroform. For clarity the octanoyl residues have been truncated to butyroyl. Hydrogen bonds involving protons that are deshielded in the ^1H NMR spectrum are shown as dotted lines.

in chloroform are fully compatible with the relative intensities of the observed NOEs.

The structure of DOPC–**1** complex has a close resemblance to the antigen binding site in the McPC603–PC complex. In both cases the phosphocholine head adopts a linear conformation, is oriented in a similar way within the binding site, and gives rise to similar interactions: 1) the phosphate group interacts strongly with one of the nitrogens of a cationic guanidinium group (Arg52H in McPC603, the bicyclic guanidinium subunit in **1**); 2) a similarly oriented hydrogen bond is established between one of the phosphate oxygens and either the hydroxyl group of Tyr33H or the amide nitrogen of the receptor's side chain; 3) the aromatic rings are oriented toward the methyl groups on the choline head in such a way that each of the N–C vectors is perpendicular to the plane of the opposing ring; and 4) the floor of the binding site is made up of electron-rich groups, the side chain of Asp97L in the antibody, and methoxy groups and the additional hydroxyl group in the synthetic receptor.

A high binding constant K_{ass} (298 K) = 73000 ± 5000 M^{-1} ($\Delta G^\circ = -6.7$ kcal mol^{-1}) was obtained for the DOPC–**1** complex in chloroform,[10] which is very similar to that observed for the complex of McPC603 with PC in water ($\Delta G^\circ =$

-6.6 kcal mol^{-1}).[3] Since the NMR spectra of model compounds **2** and **3** did not show significant shifts upon addition of DOPC, binding was not measurable by NMR in these cases. Complexation of single quaternary ammonium salts such as acetyl choline (ACh) resulted in $K_{ass} = 730 \pm 30$ M^{-1} and 138 ± 27 M^{-1} for **1** and **2**, respectively. Weaker complexes were also formed between simple phosphodiester salts and guanidinium models. For example, triethylammonium dihexadecylphosphate is bound by guanidinium **3** with a K_{ass} of roughly 7000 M^{-1}. Thus, *both* guanidinium and calixarene subunits of **1** participate in binding DOPC, in agreement with structural data provided by the NMR studies. The fact that the experimental binding constant is still below the one estimated from model compounds of each isolated binding subunit suggests that there is still room for improvement in the design of the spacer unit. Finally, thermodynamic data were determined from titrations of **1** in tetrachloroethane with DOPC in the 330–350 K range (van't Hoff plot): ΔG° (298 K) $= -6.4$ kcal mol^{-1}, $\Delta H^{\circ} = -10$ kcal mol^{-1}, and $\Delta S^{\circ} = -12$ cal K^{-1} mol^{-1}. Thus, binding is mostly enthalpically driven.

Energy calculations were carried out both on a representative DOPC–**1** complex and on the crystal structure of the variable portion of the PC–McPC603 complex (Table 1). The binding free energy was factorized as a sum of electrostatic and non-electrostatic contributions.[11] Binding appears to be driven by different contributions in each case: binding of DOPC to **1** in chloroform is enthalpically driven, in agreement with the ΔH° and ΔS values, as a result of the favorable electrostatic contribution to the binding free energy; however, in the binding of PC to McPC603 in water the driving force appears to be the hydrophobic effect, as desolvation of the charged ligand in water greatly reduces the net electrostatic contribution to the binding free energy. This finding highlights the importance of evaluating accurately the energy penalty associated with removing the interacting moieties from water when dealing with molecular associations in aqueous media.[12] The fact that the electrostatic contribution for DOPC–**1** in chloroform and the hydrophobic contribution for PC–McPC603 in water appear to be of the same magnitude is fortuitous. On the other hand, the analysis of the contributions to the binding free energy suggests that it should be possible for a water-soluble derivative of **1** to attain substantially high affinities for biological applications in water, as the hydrophobic and electrostatic contributions to the binding free energy are expected to be similar to those of McPC603. In addition, our calculations suggest that the entropic penalties arising from the fixation of torsional degrees of freedom are also similar in both cases.

Table 1. Binding free energy [kcal mol^{-1}] and its different contributions for PC–McPC603 and DOPC–**1** complexes.

	ΔG_{exp} [a]	ΔG_{tot} [b]	ΔG_{ele} [c]	ΔG_{hyd} [d]	ΔG_{conf} [e]	ΔG_{T+R} [f]
PC–McPC603	-6.6	-5.4	-2.4	-23.0	11.0	9.0
DOPC–**1**	-6.7	-5.6	-25.4	0.0	9.8	10.0

[a] Experimental values at 298 K taken from ref. [3] for PC–McPC603 and from the K_{ass} for DOPC–**1** determined by UV titrations. [b] $\Delta G_{tot} = \Delta G_{ele} + \Delta G_{hyd} + \Delta G_{conf} + \Delta G_{T+R}$; tot = total, ele = electrostatic, hyd = hydrophobic, conf = conformational, T + R = translation and rotation; according to ref. [11]. The bound conformations were the energy-refined crystal structure of PC–McPC603 and a representative average structure [9] of DOPC–**1**. A rigid model for noncovalent complex formation was assumed. [c] The electrostatic contribution to the binding free energy was calculated by solving the Poisson–Boltzmann equation with the program DelPhi [13]. [d] The hydrophobic contribution to the free energy of complex formation was obtained from the solvent-accessible surface [14] of PC and McPC603 buried upon complex formation (400 Å^2) multiplied by a factor of -57.42 cal mol^{-1} Å^{-2} [11]. It is assumed that there is no hydrophobic effect in chloroform. [e] Entropic cost of fixing torsional degrees of freedom in the binding process. A total of eight torsional angles were fixed in DOPC–**1**, each contributing 1.22 kcal mol^{-1} [11]. For PC–McPC603 the lower limit estimated by Novotny et al. [4a, b] was used, which corresponds to nine fixed torsional angles. [f] Entropy less on translation and rotation. For PC, the value of ref. [4a, b] was used. For DOPC, an extra 1 kcal mol^{-1} was added due to the increase in molecular weight [11].

In summary, we have shown that a synthetic non-peptidic receptor displaying the binding properties of a whole antibody can be designed by mimicking the key interactions found in the crystal structure of an hapten–antibody complex. Incorporation of suitable reactive functional groups into the recognition binding site should open a new avenue for research into antibody or enzyme mimics.

Received: January 19, 1996
Revised version: April 10, 1996 [Z 8767 IE]
German version: *Angew. Chem.* **1996**, *108*, 1816–1819

Keywords: calixarenes · molecular dynamics simulations · molecular recognition · phospholipids

[1] a) P. G. Schultz, R. A. Lerner, *Acc. Chem. Res.* **1993**, *26*, 391; b) J. D. Stewart, L. J. Liotta, S. J. Benkovic, *ibid.* **1993**, *26*, 396; c) D. Hilvert, *ibid.* **1993**, *26*, 552; M. R. Haynes, E. A. Stura, D. Hilvert, I. A. Wilson, *Science* **1994**, *263*, 646; d) P. G. Schultz, R. A. Lerner, *ibid.* **1995**, *269*, 1835.

[2] For X-ray structures, see a) D. M. Segal, E. A. Padlan, G. H. Cohen, S. Rudikoff, M. Potter, D. R. Davies, *Proc. Natl. Acad. Sci. USA* **1974**, *71*, 4298; b) Y. Satow, G. H. Cohen, E. A. Padlan, D. R. Davies, *J. Mol. Biol.* **1986**, *190*, 593.

[3] For accurate binding studies, see a) S. Rudikoff, M. Potter, D. M. Segal, E. A. Padlan, D. R. Davies, *Proc. Natl. Acad. Sci. USA* **1972**, *66*, 3689; b) A. Skerra, A. Plückthun, *Science* **1988**, *240*, 1038; c) R. Glockshuber, J. Stadlmüller, A. Plückthun, *Biochemistry* **1991**, *30*, 3049.

[4] a) J. Novotny, R. E. Bruccoleri, F. A. Saul, *Biochemistry* **1989**, *28*, 4735; b) F. S. Lee, Z.-T. Chu, M. B. Bolger, A. Warshel, *Prot. Eng.* **1992**, *5*, 215. For cation–π interactions with synthetic models containing aromatic units, see c) D. A. Dougherty, *Science* **1996**, *271*, 163, and references therein; d) K. Araki, H. Shimizu, S. Shinkai, *Chem. Lett.* **1993**, 205; M. Inouye, K. Hashimoto, K. Isagawa, *J. Am. Chem. Soc.* **1994**, *116*, 5517; e) J.-M. Lehn, R. Meric, J.-P. Vigneron, M. Cesario, J. Guilhem, C. Pascard, Z. Asfari, J. Vicens, *Supramol. Chem.* **1995**, *5*, 97; f) A. Casnati, P. Jacopozzi, A. Pochini, F. Ugozzoli, R. Cacciapaglia, L. Mandolini, R. Ungaro, *Tetrahedron* **1995**, *51*, 591.

[5] J. de Mendoza, M. Carramolino, F. Cuevas, P. M. Nieto, P. Prados, D. N. Reinhoudt, W. Verboom, R. Ungaro, A. Casnati, *Synthesis* **1994**, 47.

[6] W. Peschke, P. Schiessl, F. P. Schmidtchen, P. Bissinger, A. Schier, *J. Org. Chem.* **1995**, *60*, 1039.

[7] The opposite effect of complexation on the chemical shifts of the two NH protons is consistent with the idea that hydrogen bonding to phosphate is actually taking place only through the proximal NH proton. Significant downfield shifts have been observed in model guanidinium ions by changing the counterion from chloride to carboxylate or phosphate: a) A. Echavarren, A. Galán, J.-M. Lehn, J. de Mendoza, *J. Am. Chem. Soc.* **1989**, *111*, 4994; b) A. Galán, E. Pueyo, A. Salmerón, J. de Mendoza, *Tetrahedron Lett.* **1991**, *32*, 1830.

[8] C. Jaime, J. de Mendoza, P. Prados, P. M. Nieto, C. Sánchez, *J. Org. Chem.* **1991**, *56*, 3372.

[9] MD simulations were carried out using the AMBER 4.0 suite of programs (University of California at San Francisco, **1991**). OPLS parameters were used for chloroform. All distances obtained from the NOE studies were maintained within the expected values during the MD trajectories. The energy-minimized average structure was in agreement with the NOE distances and was chosen to represent the solution structure of DOPC–**1** in the analysis of the contributions to the binding free energy. Full details will be reported elsewhere.

[10] In the direct NMR titration of **1** with DOPC in $CDCl_3$ complete saturation was reached at a ratio of 1:1, indicating $K_{ass} > 50000$ M^{-1}. Thus, binding was measured by UV spectroscopy in $CHCl_3$ by competition with Methyl Orange tetraethylammonium salt ($K_{ass} = 21500 \pm 1000$ M^{-1}). Examination of CPK models suggested that the dye sulfonate group could bind to the guanidinium group of **1** and that the rest of the molecule could easily be encapsulated by the calixarene cavity.

[11] D. H. Williams, M. S. Searle, J. P. Mackay, U. Gerhard, R. A. Maplestone, *Proc. Natl. Acad. Sci. USA* **1993**, *90*, 1172.

[12] a) K. A. Sharp, B. Honig, *Ann. Rev. Biophys. Biophys. Chem.* **1990**, *19*, 301; b) J. Novotny, K. A. Sharp, *Prog. Biophys. Mol. Biol.* **1992**, *58*, 203; c) B. Honig, A. Nicholls, *Science* **1995**, *68*, 1144.

[13] A. Nicholls, B. Honig, *J. Comput. Chem.* **1991**, *12*, 435.

[14] B. Lee, F. M. Richards, *J. Mol. Biol.* **1971**, *55*, 379.

Selection of Different Reactive Sites by Enantiomers in Electron-Transfer Reactions Involving Metalloproteins**

Klaus Bernauer* and Luca Verardo

The identification of the exact site of attack in electron-transfer reactions involving metalloproteins has been the object of many studies.[1-3] In the case of plastocyanin ($PcCu^{II}$) two sites have been identified, the "adjacent site" near the copper center and the "remote site" located near a negative patch of the protein, some 16 Å away from the copper center. Negatively charged or neutral metal complexes are thought to react exclusively at the hydrophobic adjacent site, whereas positively charged reagents can react at both the adjacent and/or the remote site.[3] In the latter case the neighboring Tyr83 probably intervenes in the electron transfer pathway. In order to obtain more detailed information on the location of the attack of electron-transfer reagents, we used optically active metal complexes, our aim being the detection of chiral recognition by means of kinetic stereoselectivity.[4-7]

A useful technique to identify electron-transfer sites in inner-sphere reactions is the use of reagents like Cr^{2+}, which form inert reaction products and therefore remain attached to the bridging atom of the electron-transfer precursor complex.[8] This technique has also been applied to metalloproteins, but identification of the exact structure of the reaction products proved to be difficult.[9,10] In the present communication we report the first use of circular dichroism (CD) for the identification of specific sites in the reaction of plastocyanin with optically active Co^{2+} complexes.

In a previous communication we have shown that the electron-transfer reaction between spinach plastocyanin and the optically active Fe^{2+} complexes with **1** and **2** as ligands takes place

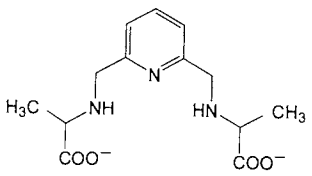

1

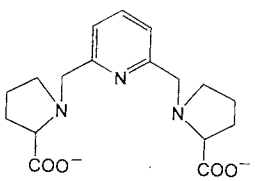

2

at the hydrophobic adjacent site of this blue copper protein and that significant chiral recognition occurs in the formation of the transition state.[4] From these results the question arose whether the imidazole unit of His87 was involved in the electron transfer. Therefore, plastocyanin was treated with the Co^{2+} complexes of both the (*S*,*S*) and (*R*,*R*) enantiomers of **1** and **2** in phosphate buffer at pH 7 and 20 °C. Under these conditions electron transfer, monitored by the variation of the UV/Vis and CD spectra, is quantitative and occurs at similar rates with all the Co^{II} complexes used. As the reduced protein has no CD activity in the visible range, the CD spectrum of the Co^{III} species formed during the reaction can be obtained by accounting for the remaining Co^{2+} complex in the final spectrum, which was initially present in excess. If the reaction occurs by a His87-bridged transition state, the imidazole moiety would be coordinated to the produced inert Co^{III} complex, which remains attached to the protein. In the case of an outer-sphere reaction, on the other hand, the Co^{III} aqua complex would be formed, and no metal would be bound to the protein. The amount of the fixed Co^{III} is then obtained by comparison of the final CD spectrum with the spectrum of the corresponding Co^{III} complexes containing H_2O or imidazole (or histidine) at the sixth coordination site. The results shown in Figure 1 indicate that *Λ*-[Co((*S*,*S*)-**1**)]

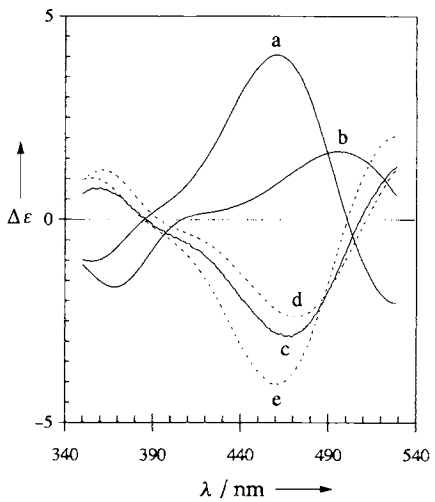

Fig. 1. Circular dichroism spectra of the species involved in the reaction at pH 7 (other reaction conditions as indicated in Table 1) of plastocyanin with complexes of Co^{2+} with both enantiomers of **1** and **2**. The solid lines are the residual spectra of the reaction product of PcCu(II) with *Λ*-[Co((*S*,*S*)-**1**)] (a, identical to the spectrum of *Λ*-[Co((*S*,*S*)-**1**)(imidazole)]$^+$), *Λ*-[Co((*S*,*S*)-**2**)] (b, identical to the spectrum of *Λ*-[Co((*S*,*S*)-**2**)H_2O]$^+$), and *Δ*-[Co((*R*,*R*)-**1**)] (c); the dashed lines are the reference spectra of *Δ*-[Co((*R*,*R*)-**1**)H_2O]$^+$ (d) and *Δ*-[Co((*R*,*R*)-**1**)(imidazole)]$^+$ (e). (The residual spectrum for *Δ*-[Co((*R*,*R*)-**2**)] was omitted for clarity.)

is quantitatively fixed, whereas only the aqua complexes are obtained with both enantiomers of [Co(**2**)]. In the case of *Δ*-[Co((*R*,*R*)-**1**)] an intermediate situation is observed: the final spectrum corresponds to a mixture of the imidazole and the aqua complexes.

When the final solution of the reaction with *Λ*-[Co((*S*,*S*)-**1**)] as the reducing agent is dialyzed, the Co^{III} complex formed is completely retained with the protein. Furthermore, reoxidation by $[Fe(CN)_6]^{3-}$ does not restore the initial CD spectrum of the protein in this case. With the two enantiomers of [Co(**2**)], on the other hand, all the Co^{III} complex is eliminated by dialysis and the initial CD spectrum of the protein is obtained on reoxidation. Again the reaction product obtained with *Δ*-[Co((*R*,*R*)-**1**)] shows intermediate behavior. Only part of the Co^{III} formed is removed by dialysis, and the CD spectrum of the Co^{III} complex retained with the protein is identical to that of the imidazole complex, but the intensity is lower than that expected for the total amount of Co^{III} formed.

The question arises whether the Co^{III} center was attached to the protein in a reaction subsequent to the electron transfer. However, when the protein is reduced in the presence of *Λ*-[Co((*S*,*S*)-**1**)H_2O]$^+$ by ascorbic acid, which does not react with the Co^{III} complex in the time scale of interest, no Co^{III} is bound to the protein. Finally, the reagents leading to the Co^{III} aqua complex do not attack at the remote, negatively charged area of the protein, as the reaction rate with all the reagents used is

[*] Prof. K. Bernauer, Dipl.-Chem. L. Verardo
Institut de chimie
Université de Neuchâtel
51, Av. de Bellevaux, CH-2000 Neuchâtel (Switzerland)
Fax: Int. code +(38)232511

[**] This work was supported by the Swiss National Science Foundation (Grant Nos. 20-37'224.93 and 20-41'206.94). The authors thank Professor P. Schürmann for providing samples of plastocyanin and for many useful discussions.

completely unaffected by the presence of highly charged cations like $[Co(NH_3)_6]^{3+}$.

An additional question concerns the exact structure of the transition state involving the bridging imidazole unit of His87. Measurements of the amount of covalently bound Co^{III} at different pH (Table 1) suggest that deprotonation occurs in the transition state and that the metal centers are linked together by the negatively charged imidazole moiety (Scheme 1). This is

Table 1. Relative amount [%] of Co^{III} complexes bound to plastocyanin after electron transfer [a].

pH	Λ-[Co((*S*,*S*)-**1**)]	Δ-[Co((*R*,*R*)-**1**)]	Λ-[Co((*R*,*R*)-**2**)]	Δ-[Co((*S*,*S*)-**2**)]
5.5	80	13	–	–
6.0	>95	21	–	–
7.0	ca. 100	40	0	0
8.0	ca. 100	50	–	–

[a] Determined from CD spectra; error limit ±5%; reaction conditions: $[PcCu^{II}] \approx 10^{-4}$ M, $[Co^{2+}]_{tot} = [ligand]_{tot} = 10^{-3}$ M, [buffer] = 0.1 M (phosphate), $T = 20$ °C.

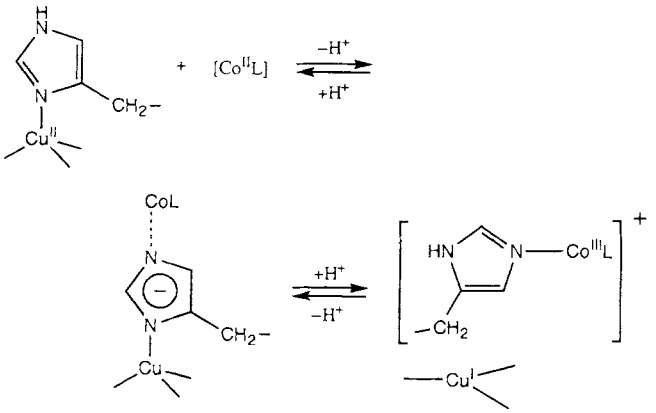

Scheme 1. Electron transfer reaction between Λ-[Co((*S*,*S*)-**1**)] and $PcCu^{II}$ at His87 (site a) and the possible structure of the transition state.

analogous to what is known for the binding between Cu^{2+} and Zn^{2+} in superoxide dismutase[11] or in corresponding model systems.[12] Even at pH 5.5, 80% of the Co^{III} species still remains attached to the protein in the reaction with the Λ-[Co((*S*,*S*)-**1**)], whereas the reaction with its enantiomer Δ-[Co((*R*,*R*)-**1**)] under the same conditions affords more than 85% of the aqua complex.

From these results some important conclusions can be drawn. Electron transfer at the hydrophobic area of plastocyanin must occur by at least two different pathways, one of them involving the imidazole unit of His87 as a bridging group (site a). Important information about the pathway used in the outer-sphere mechanism (site b) leading to the aqua complexes is obtained from genetically mutated plastocyanin. Site-directed mutations at Leu12 suggest that the reaction with [Co(**2**)] takes place at a position distant from this amino acid.[13]

However, the most important feature in the present case is that the choice of the different pathways can not only be controlled by the structure of different ligands, but also by their chirality. From the data for Δ-[Co((*R*,*R*)-**1**)] and Λ-[Co((*S*,*S*)-**1**)] at pH 5.5 and 20 °C (Table 1), it is concluded that under these conditions the free activation energy for reaction at site (a) is lower by about 3.4 kJ mol^{-1} for Λ-[Co((*S*,*S*)-**1**)], and for the reaction at site (b) by about 4.6 kJ mol^{-1} for Δ isomer than for the other enantiomer investigated in each case. Interestingly, the measured global free activation energy of the reaction at pH 7 and 19 °C is exactly the same for the two enantiomers (crossing point of the Eyring plots; $\Delta G^{\neq} = 72.2$ kJ mol^{-1}).[14] This clearly shows that site (b) is not simply a bypass for the case when site (a) becomes unfavorable, but that each site definitely favors one of the two enantiomers over the other. Apparently, the enantiomers of a chiral reagent can react with high preference at completely different positions on the protein surface.

Received: February 19, 1996 [Z8834IE]
German version: *Angew. Chem.* **1996**, *108*, 1823–1825

Keywords: circular dichroism · electron transfer · molecular recognition · plastocyanin

[1] D. N. Beratan, J. N. Onuchic, H. B. Gray, *Met. Ions Biol. Syst.* **1991**, *27*, 97–127.
[2] A. G. Lappin, *Redox Mechanisms in Inorganic Chemistry*, Ellis Horwood, **1994**, S. 195–215.
[3] A. G. Sykes, *Struct. Bonding (Berlin)* **1991**, *75*, 175–225.
[4] K. Bernauer, J.-J. Sauvain, *J. Chem. Soc. Chem. Commun.* **1988**, 353–354.
[5] K. Bernauer, M. Monzione, P. Schürmann, V. Viette, *Helv. Chim. Acta* **1990**, *73*, 346–352.
[6] K. Bernauer, *Met. Ions Biol. Syst.* **1991**, *27*, 265–289.
[7] K. Bernauer, P. Jauslin, *Chimia* **1993**, 218–219.
[8] H. Taube, H. Myers, R. R. Rich, *J. Am. Chem. Soc.* **1953**, 75, 4118–4119.
[9] O. Farver, I. Pecht, *Coord. Chem. Rev.* **1989**, *94*, 17–45.
[10] O. Farver, I. Pecht, *Proc. Natl. Acad. Sci. USA* **1981**, *78*, 4190–4193.
[11] H. A. Azab, L. Banchi, M. Bosari, C. Luchinat, M. Sola, M. S. Viezzoli, *Inorg. Chem.* **1992**, *31*, 4649–4655.
[12] J.-P. Pierre, P. Chautemps, S. Refaif, C. Beguin, A. El Marzouki, G. Serratrice, E. Saint-Aman, P. Rey, *J. Am. Chem. Soc.* **1995**, *117*, 1965–1973.
[13] C. Nusbaumer, P. Schürmann, K. Bernauer, unpublished results.
[14] K. Bernauer, L. Verardo, *Inorg. Chem.*, submitted.

A Mobility Filter for the Detection and Identification of Charged Species in Complex Liquid Mixtures by ENMR Phase Difference Spectroscopy**

Stefan R. Heil and Manfred Holz*

NMR experiments in the presence of an electric direct current in the sample under observation (DCNMR) can provide interesting information about charged particles in liquid solutions.[1–4] We and later also other groups have shown that by so-called electrophoretic NMR (ENMR)[5] the migration of simple ions, charged molecules, and charged molecular aggregates can be observed and their mobilities can be measured by applying pulsed field gradient spin-echo (PGSE) techniques in one-dimensional (1D)[2, 3, 7] and two-dimensional (2D) ENMR experiments.[5, 6, 8] In particular 2D ENMR spectroscopy proved to be the method of choice for the investigation of complex systems with charged molecular aggregates, since the charged species can be distinguished from the neutral species due to the fact that their NMR lines appear in a second "mobility dimension".

[*] Dr. M. Holz, Dipl.-Phys. S. R. Heil
Institut für Physikalische Chemie und Elektrochemie der Universität
Kaiserstrasse 12, D-76128 Karlsruhe (Germany)
Fax: Int. code +(721)608-3310
e-mail: cd59@rz.uni-karlsruhe.de

[**] This research was supported financially by the Deutsche Forschungsgemeinschaft.

However, 2D ENMR experiments are restricted to nuclides with a high gyromagnetic ratio γ, for example ^{1}H and ^{19}F, and to systems amenable to relatively high electric fields, which results in comparatively high migration velocities v of the charged species. Consequently, 2D ENMR experiments have been performed previously only with the nucleus ^{1}H.[4, 5] 2D ENMR spectroscopy is hardly feasible for other important nuclides such as ^{13}C, ^{29}Si, and ^{31}P. Furthermore, if in a system of interest the ionic concentration is relatively high and exceeds say 0.5 M, the applied electric fields must be reduced to avoid resistive heating of the sample.[4, 5] Both low electric fields and low mobilities, for example of large molecular aggregates, result in low migration velocities during the experiment, which again restrict the applicability of 2D ENMR spectroscopy. Finally, in principle 2D NMR experiments are more time-consuming than 1D NMR experiments and therefore it is generally worthwhile to search for alternative quick 1D NMR experiments.

We report here on a simple 1D ENMR experiment in which a "mobility filter" is generated such that in a complex NMR spectrum of a multicomponent liquid mixture the resonance lines of electrically charged species can be filtered. In this way the electric charge is introduced as a spectral parameter in the 1D NMR experiment. Such an experiment would not only detect charged particles containing the nucleus under observation, but it should simultaneously allow the identification of these particles by their NMR lines. By repeating measurements with varying experimental parameters the mobilities of the detected species can also be measured. In addition, we demonstrate the practicability of ^{13}C ENMR, which results in an extension of possible applications of this special field of NMR spectroscopy. For this reason we have chosen an aqueous solution of three ^{13}C-containing solutes, namely acetonitrile and ethanol as uncharged components, and the formate ion as a charged solute.

We performed the ^{13}C NMR experiments at 25 °C using a Bruker AM 300 spectrometer operating at 75.45 MHz. The gradient unit, the constant current power supply for the electrophoretic cell, and the ENMR probehead are described elsewhere.[7] In the sample cell we used platinated Pt electrodes and applied electric fields of typically $0.5-4\,V\,cm^{-1}$, resulting in pulsed electric currents of 12.5–100 mA in the sample. The simplest PGSE pulse sequence for ENMR experiments is given in Figure 1. The actual values for the gradient pulse sequence were $\delta = 1.5$ ms, $\Delta = 150$ ms, and the gradient strength G could be varied between 0 and approximately $0.5\,T\,m^{-1}$. The composition of the liquid mixture given by the mole fractions x of the four components was: $x(H_2O) = 0.81$, $x(CH_3CN) = 0.06$, $x(CH_3CH_2OH) = 0.05$, and $x(HCOONa) = 0.08$. The measurements were performed in a solution not stabilized by a gelling agent.

The basic idea of our mobility filter is described by the following. In an ENMR experiment only charged particles move with constant drift velocity in an electric field. In a PGSE experiment this drift velocity v results in a phase shift $\Delta\varphi = \gamma G v \delta \Delta$ of the NMR signal at $t = 2\tau$,[4, 5] the time at which the echo maximum appears and when the signal acquisition is started. The quantities G, Δ, δ, and 2τ are shown in Figure 1. (Here the reasons for the previously mentioned restrictions of 2D ENMR spectroscopy are evident. In such an experiment phase shifts $\Delta\varphi$ of at least 360° must be achieved.[4, 5] Since the applicable G, Δ, and δ values are limited owing to the spin-echo signal intensity, successful 2D ENMR experiments require high γ and v values.)

Thus, if we record first an NMR spectrum by using the PGSE sequence in Figure 1, in the absence of an electric field and thus in the absence of an electric current I, and if we then record a second ENMR spectrum in the presence of I and subtract the first spectrum from the second, the resulting difference spectrum should no longer contain NMR signals from uncharged species, since their signals are theoretically equal in both experiments, whereas the signals of charged particles experience a characteristic phase shift $\Delta\varphi$.

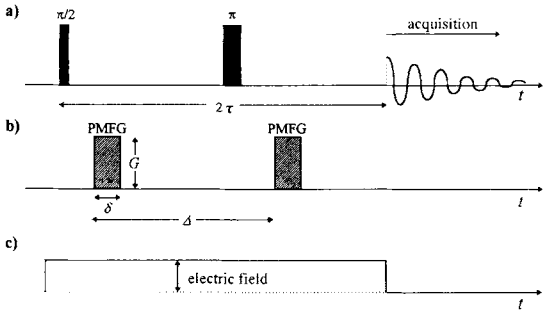

Fig. 1. Pulse sequence for a PGSE experiment in electrophoretic NMR spectroscopy. a) High-frequency pulses; b) magnetic field gradient pulses; c) electric field pulse applied in the sample cell. Signal acquisition starts at 2τ.

Therefore, we applied the following procedure and illustrate it with the results of our ^{13}C ENMR experiment (Fig. 2; the spectra a) and b) show the undecoupled ^{13}C NMR signals of the three aforementioned solutes in the range of higher chemical shifts).

1) Signal acquisition (as in Fig. 1) of the mixture without applied electric field ($I = 0$). If in the very first step (0) an original spectrum is also recorded without gradient pulses, steps 0) and 1) correspond to a normal PGSE experiment for the measurement of self-diffusion coefficients of the different components.[9]

2) Signal acquisition (as in Fig. 1), now with an applied electric field ($I \neq 0$).

3) Fourier transformation and phasing of both spectra. For the phasing procedure a known line of a neutral component in the spectrum from 1) must be used, and finally the spectrum from 2) is phased with identical phasing parameters (Fig. 2a, b). For NMR lines of charged species a phase shift in the spectrum from 2) is evident relative to the spectrum from 1). We emphasize that, as in our case, small phase shifts $\Delta\varphi$ of, for example, 5 to 20° are difficult to observe by simple inspection of the actual spectra.

4) Both spectra are normalized to the same intensity, again using the known line of an uncharged component. We point out that we apply "phase difference spectroscopy" here and thus the absolute intensities play a minor role. (To our knowledge this is the first NMR phase difference spectroscopy experiment, since in common NMR difference spectroscopy line intensity differences are of interest.[10])

5) Spectrum subtraction delivers the difference spectrum (see Fig. 2c). The NMR lines of the neutral species have disappeared and we obtain only non-zero intensities at the position of lines arising from charged species.

6) For a clearer presentation the difference spectrum can be optimized by further data processing, for example further phasing (Fig. 2d).

Inspection of our results given in Figure 2 clearly indicates that the proposed mobility filter works excellently, since in the phase difference spectra c) and d), as expected, only the ^{13}C signal of the formate anion is seen. In spectrum b) the signal-to-noise ratio (S/N) is smaller than that in a) since we had used a smaller number of signal accumulations with $I \neq 0$, with the intention of keeping electrode processes and heating of the sample to a minimum. Convective motion may further reduce

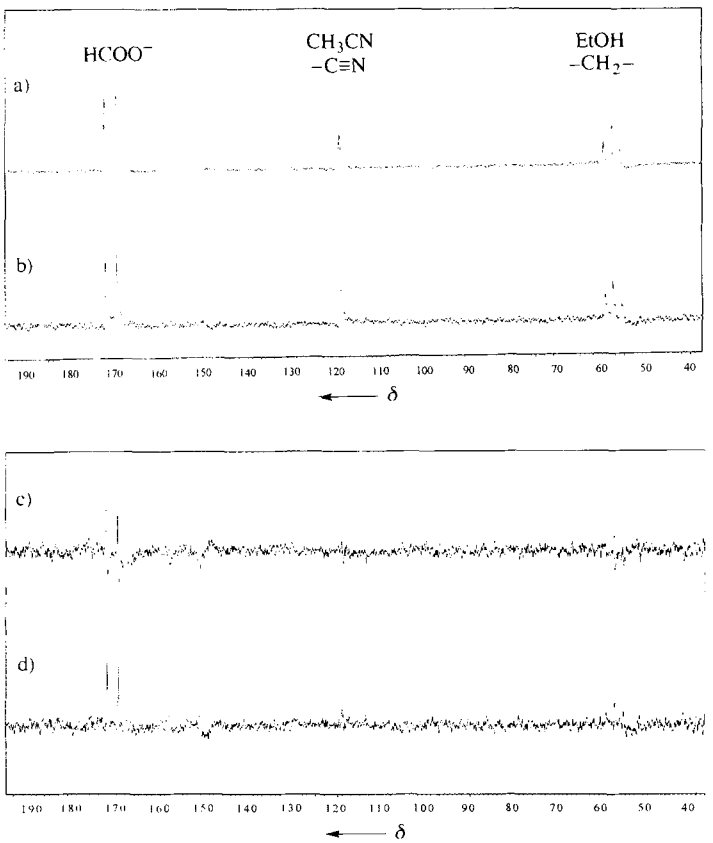

Fig. 2. The high-frequency part of the ^{13}C NMR spectrum of the mixture of water, ethanol, acetonitrile, and sodium formate obtained with the pulse sequence given in Figure 1. a) Electric field off, $I = 0$; b) electric field on, $I \neq 0$; c) phase difference spectrum of a) and b); d) rephased difference spectrum, the "mobility-filtered" spectrum.

the S:N ratio.[11] At the position of the $-^{13}CH_2-$ signal of EtOH and the $-^{13}C\equiv N$ signal of CH_3CN in the difference spectra c) and d) very weak residual signals on the order of the noise intensity can be seen; however, we can state that this small artifact does not affect the effectiveness of the ENMR mobility filter. Of course, in the phase difference spectrum the information about the concentration ratios of the different species in terms of the peak intensities is lost; however, if the lines of the different species are resolved, these ratios can be determined easily from the original spectrum recorded in step 0), by using the assignment gained from the final difference spectrum.

We should add some further general remarks with respect to the phase difference spectroscopy. For this reason we show in Figure 3 a typical NMR line (a) and the phase-shifted line, with varying $\Delta\varphi$ between 0 and 360° (b). The corresponding line shapes in the difference spectrum are also given (c), showing the behavior of the line of interest in the difference spectrum as a function of the shift angle. We recognize two important facts with implications for the application of phase difference spectroscopy. First, the line intensity in the difference spectrum increases with increasing $\Delta\varphi$ between 0 and 180°, reaches twice the intensity of the orignal line at $\Delta\varphi = 180°$, and then decreases at higher angles. Thus, the method has its highest sensitivity when phase shifts of about 180° are produced. Although the typical application of our mobility filter is intended for systems with small shift angles, the experimental aim remains to achieve comparatively high $\Delta\varphi$ values by an appropriate choice of G, Δ, and δ, and the highest applicable electric field (which means the

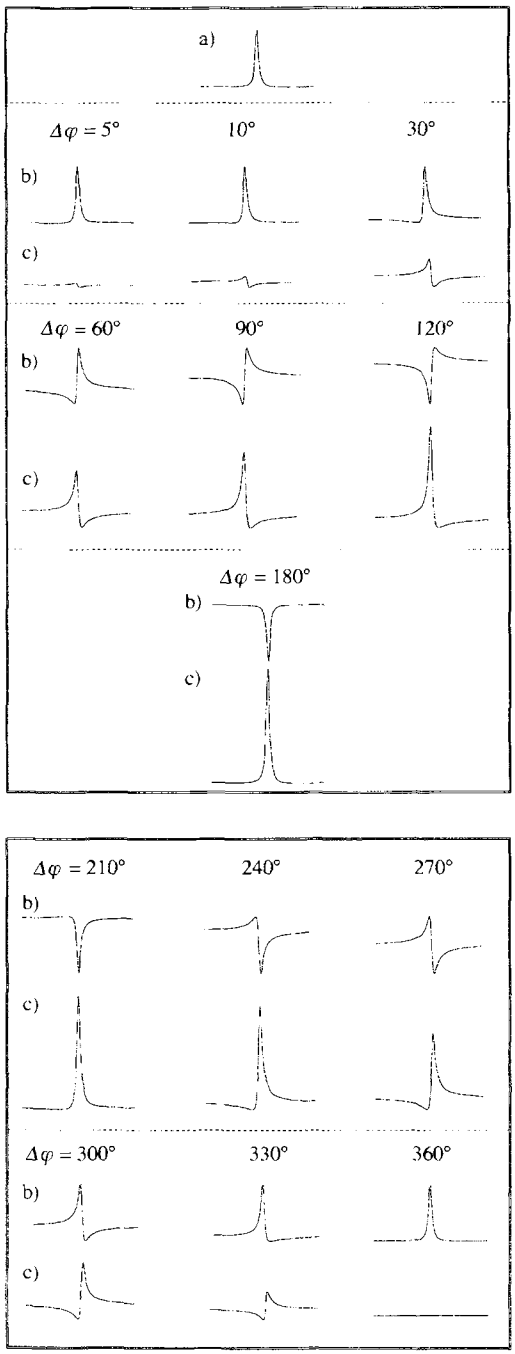

Fig. 3. Signal shapes in NMR phase difference spectroscopy. a) Original typical NMR line; b) the same line as in a) but phase-shifted by $\Delta\varphi$ due to migration of the nucleus-bearing particle in a magnetic field gradient; c) line of interest in the difference spectrum.

highest possible v). Second, we can see from Figure 3 that in those cases in which high phase shifts in the range of 360° can occur, for example with nuclides with high γ values, a problem arises if the phase shift is exactly 360° or generally $n \times 360°$. For this case the intensity is zero in the difference spectrum, and we would not be able to differentiate between neutral and charged species. However, this problem can be easily overcome by performing a second experiment in which one of the parameters—G, Δ, δ, or v—is varied, leading then to a phase shift $\Delta\varphi$ not equal to 360°. But it should be emphasized that in cases with high shift angles the method of choice should be 2D ENMR spectroscopy.

To return to our experiment, it is clear that only charged particles containing carbon are detected in our ^{13}C ENMR experiment. Thus, in the present case the $^{23}Na^+$ ion could not be detected. However, we point out that the sign of the charge of the detected particle is available from the sign of the phase shift generated in the ENMR experiment.[4, 5] In conclusion we can state that the mobility filter described here should provide a good tool for the detection and identification of carbon-containing ions or charged molecules in complex mixtures, in particular if the charged species do not contain hydrogen or only hydrogen atoms that can undergo chemical exchange. In analogy, the same should be valid for charged systems containing ^{29}Si or ^{31}P nuclei. If, as in most organic ions or charged molecular aggregates, suitable hydrogen atoms are present, but the above-mentioned conditions prevent the application of 2D ENMR techniques, an analogous ^1H ENMR mobility filter might even be much better suited than heteronuclear ENMR experiments, due to the sensitivity of ^1H NMR spectroscopy. An interesting additional aspect of the mobility filter is also its possible use for signal assignment. For example, if the charged particles in a mixture are known, a mobility filter with a slightly modified phasing procedure, in which only the lines of charged particles disappear in the difference spectrum, can be used to simplify a complex spectrum and facilitate the assignment of lines of unknown uncharged species.

In these studies we could also demonstrate the feasibility of ^{13}C ENMR spectroscopy, and we will briefly mention the advantages and disadvantages of ^{13}C ENMR. As can be seen in Figure 2 the main advantage is the large chemical shift range in ^{13}C NMR spectroscopy, which results in a well-resolved spectrum even though no sample spinning techniques are applied currently in ENMR studies. (Of course switchable sample spinning[12] during the signal acquisition could in principle be possible, but so far this has not been applied in ENMR.) A further advantage of ^{13}C ENMR spectroscopy lies in the typically long T_2 relaxation times, allowing the application of long Δ values, which are favorable in ENMR experiments.[4, 5] The disadvantage of ^{13}C NMR is its low sensitivity; relatively high signal accumulation numbers are required, which in certain ENMR experiments can lead to problems with electrode processes such as changing concentrations of charged particles during the experiment.

Finally, it should be emphasized that in addition to qualitative results like those described here obtained with the mobility filter, quantitative information can also be derived from the ENMR experiment if required. As already mentioned, information about the single components can be obtained by repeating the experiment, for example, with different G values, which delivers as a byproduct the translational diffusion coefficients D.[9] Moreover, analysis of the phase shift $\Delta\varphi$ as a function of the applied electric current I yields the electrophoretic mobility u.[4, 5] For example, in our experiment we obtain the following results for the previously mentioned mixture at 25 °C: $D(CH_3CN) = 1.4 \times 10^{-9}\ m^2 s^{-1}$, $D(EtOH) = 1.1 \times 10^{-9}\ m^2 s^{-1}$, and $D(HCOO^-) = 1.3 \times 10^{-9}\ m^2 s^{-1}$. The mobility of the formate ion is found to be $u^- = 6.3 \times 10^{-8}\ m^2 s^{-1} V^{-1}$. The data, derived here only for demonstration purposes from experiments with five different G and I values, have a relatively high experimental error of 15%. Unfortunately, our quantitative results cannot be compared with literature data, because this particular mixture has not been investigated previously. However, we want to point out that the diffusion coefficient and in particular the mobility of the formate ion in this multicomponent mixture are unexpectedly high compared with the values in pure water ($u^- = 4.2 \times 10^{-8}\ m^2 s^{-1} V^{-1}$). We ascribe this increased translational mobility of the ion to the influence of the component acetonitrile, since the u and D values in the acetonitrile-free mixture were, as expected, close to those in pure water.

Received: February 28, 1996 [Z8876IE]
German version: *Angew. Chem.* **1996**, *108*, 1801–1804

Keywords: electrolytes · electrophoretic NMR spectroscopy · liquid mixtures · NMR spectroscopy

[1] M. Holz, C. Müller, *J. Magn. Reson.* **1980**, *40*, 595–599.
[2] M. Holz, C. Müller, *Ber. Bunsenges. Phys. Chem.* **1982**, *86*, 141–147.
[3] M. Holz, *Prog. NMR Spectrosc.* **1986**, *18*, 327–403.
[4] M. Holz, *Chem. Soc. Rev.* **1994**, *23*, 165–174.
[5] C. S. Johnson, Jr., Q. He, *Adv. Magn. Reson.* **1989**, *13*, 131–159.
[6] C. S. Johnson, Jr. in *Nuclear Magnetic Resonance Probes of Molecular Dynamics* (Ed.: R. Tycko), Kluwer, Dordrecht, **1994**, pp. 455–488.
[7] M. Holz, D. Seiferling, X. Mao, *J. Magn. Reson. A* **1993**, *105*, 90–94.
[8] C. S. Johnson, Jr., K. F. Morris, *J. Magn. Reson. A* **1993**, *101*, 67–73.
[9] P. Stilbs, *Prog. NMR Spectrosc.* **1987**, *19*, 1–45.
[10] See for example J. K. M. Sanders, B. K. Hunter, *Modern NMR Spectroscopy*, Oxford University Press, Oxford, **1988**.
[11] F. M. Coveney, J. H. Strange, E. G. Smith, *Mol. Phys.* **1992**, *75*, 127–137.
[12] D. Wu, W. S. Woodward, C. S. Johnson, Jr., *J. Magn. Reson. A* **1993**, *104*, 231–233.

Enzymatic Synthesis of a Characteristic Phosphorylated and Glycosylated Peptide Fragment of the Large Subunit of Mammalian RNA Polymerase II**

Torsten Pohl and Herbert Waldmann*

The transduction of signals from the extracellular space across the plasma membrane into the interior of the cell and ultimately to the cell nucleus in general is achieved by employing covalently modified proteins.[1] Among the different types of covalent protein modification, in particular, the dynamic phosphorylation and dephosphorylation of hydroxyamino acids[2] but also the β-O-glycosidic attachment of single N-acetylglucosamine (O-GlcNAc) residues to serine and threonine units of intracellular proteins[3] mediate the intracellular response to a wide variety of extracellular stimuli. An illustrative example is provided by mammalian RNA polymerase II[4] **1** (Scheme 1). In its cytosolic form the C-terminal domain of its large subunit is heavily glycosylated, probably to facilitate the transport of the enzyme into the cell nucleus. During the intranuclear transition of RNA polymerase II from an initiating to an elongating transcription complex the GlcNAc glycosides are removed and the protein is rapidly and repeatedly phosphorylated. Thus, O-GlcNAc may mask or tag phosphorylation sites, and the covalent modifications with both O-GlcNAc and phosphate fulfil a decisive role in the expression of genes that are transcribed under control of RNA polymerase II.

To study the biological phenomena associated with such covalently modified protein conjugates appropriate tools are needed. The use of characteristic partial structures of the parent proteins that embody both types of modifications as well as

[*] Prof. Dr. H. Waldmann, Dr. T. Pohl
Institut für Organische Chemie der Universität
Richard-Willstätter-Allee 2, D-76128 Karlsruhe (Germany)
Fax: Int. code + (721)608-4825
e-mail: waldmann@ochhades.chemie.uni-karlsruhe.de

[**] This work was supported by the Deutsche Forschungsgemeinschaft and the Fonds der Chemischen Industrie.

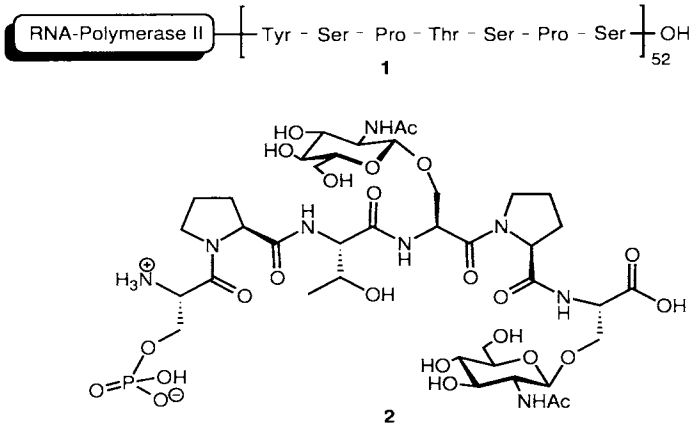

Scheme 1. Repeat sequence **1** of the large subunit of mammalian RNA polymerase II and the structure of the phosphorylated and glycosylated hexapeptide target **2**.

underivatized hydroxyamino acids may open up new opportunities for bioorganic investigations, for example for the generation of monoclonal antibodies (O-GlcNAc-modified peptides are highly antigenic[3]), or for inhibition and microinjection studies. However, the synthesis of phospho-[5] or glycopeptides[6] alone is severely complicated by their pronounced acid and base sensitivity as well as their multifunctionality which make the application of a variety of protecting groups necessary that can be removed selectively under very mild, preferably neutral conditions. In the construction of peptides that embody both modifications these difficulties are potentiated and, consequently to date the synthesis of phosphoglycopeptides has not been described.

We now report that such multifunctional and sensitive peptide conjugates can advantageously be built up under very mild conditions (pH 7.5, 25 °C) by employing enzymatic protecting group techniques.[7] The hexapeptide **2**, which carries one phosphorylated, two glycosylated, and one unmodified hydroxyamino acid, was chosen as biologically relevant target.[8] Compound **2** represents a characteristic partial structure of the repeat sequence of the large subunit of mammalian RNA polymerase II which becomes glycosylated or phosphorylated while the enzyme carries out its biological functions (vide supra).

For the choice of appropriate enzyme-labile blocking functions we have drawn from our previous experience in the biocatalyzed synthesis of multifunctional and sensitive peptide conjugates.[9] As enzymatically removable N-terminal blocking group the *p*-phenylacetoxybenzyloxycarbonyl (PhAcOZ) group was developed, that is a urethane which embodies a functional group (here: a phenylacetate) that is recognized by the biocatalyst (here: penicillin G acylase) and that is bound by an enzyme-labile linkage (here: an ester) to a functional group that undergoes a spontaneous fragmentation upon cleavage of the enzyme-sensitive bond (here: a *p*-hydroxybenzyl urethane) resulting in the liberation of a carbamic acid derivative, which decarboxylates to give the desired peptide or peptide conjugate (Scheme 2).

In an orienting experiment the PhAcOZ-protected peptide **3**[10] was treated with penicillin G acylase, that is an enzyme which specifically recognizes and saponifies phenylacetic acid esters and amides under very mild conditions[11] (Scheme 2). In the course of the ensuing enzymatic reaction the phenylacetate **3** was smoothly hydrolyzed to give the phenolate **4**, which spontaneously fragmented and liberated the peptide **5** in high yield. In this process no undesired side reaction was observed. On the one hand, the quinone methide **6**, which was formed from the phenolate, was trapped by water or—more efficiently—by an

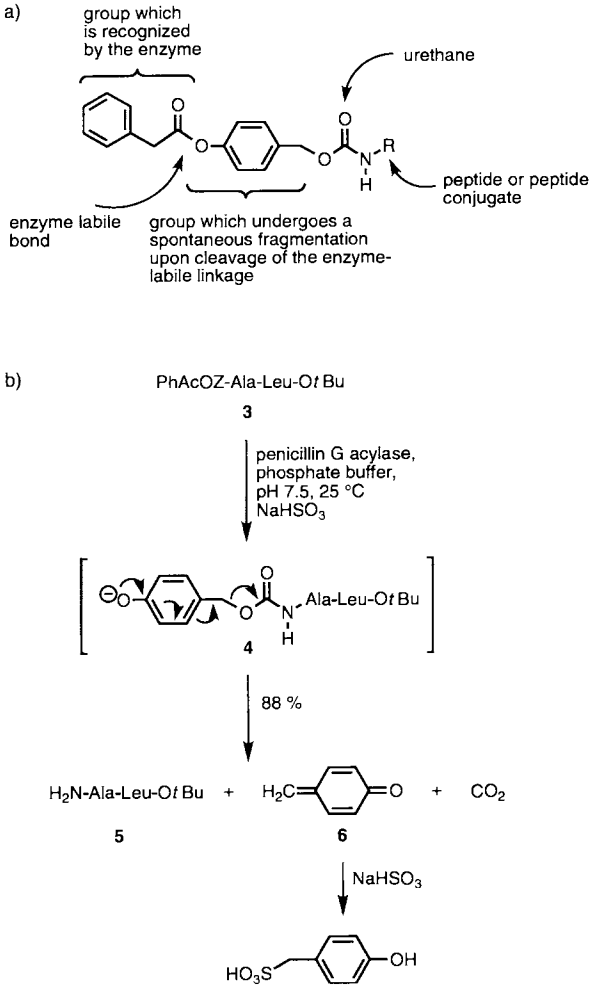

Scheme 2. Enzymatic cleavage of the PhAcOZ group with penicillin G acylase. a) Concept for the cleavage; b) cleavage of the PhAcOZ protecting group of **3** leading to the formation of **5**.

added nucleophile like $NaHSO_3$, so that an attack of **6** on the liberated amine **5** was completely avoided. On the other hand, the substrate specificity of penicillin acylase guarantees that exclusively the phenylacetic acid ester is cleaved and that the C-terminal ester group and the peptide bonds are left intact.

To build up the complex phosphoglycohexapeptide **2** by means of this advantageous enzymatic method, the PhAcOZ-protected serine glycoside **8** was synthesized from the oxazoline **7**[12] and PhAcOZ-Ser and then condensed with proline allyl ester **9** to give the completely protected glycodipeptide **10** in high yield (Scheme 3). From **10** the C-terminal ester was selectively removed by Pd^0-mediated allyl transfer to morpholine to give **12**.[13] In addition, **8** was masked as *tert*-butyl ester **11**, which could be deprotected under very mild conditions at the N-terminus by penicillin G acylase catalyzed cleavage of the PhAcOZ-urethane to give **13**. The selectively unmasked glycosylated fragments **12** and **13** were then coupled to give a high yield of the diglycotripeptide **14**, whose N-terminal blocking group was removed by penicillin G acylase induced fragmentation of the PhAcOZ-urethane under virtually neutral conditions. This gave the selectively deprotected diglycotripeptide **15** whose amino acid chain was readily elongated by condensation with the PhAcOZ-masked dipeptide carboxylic acid **16**.[14] Furthermore, from the resulting complex and sensitive diglycopentapeptide **17** the PhAcOZ group was cleaved with penicillin G acylase to

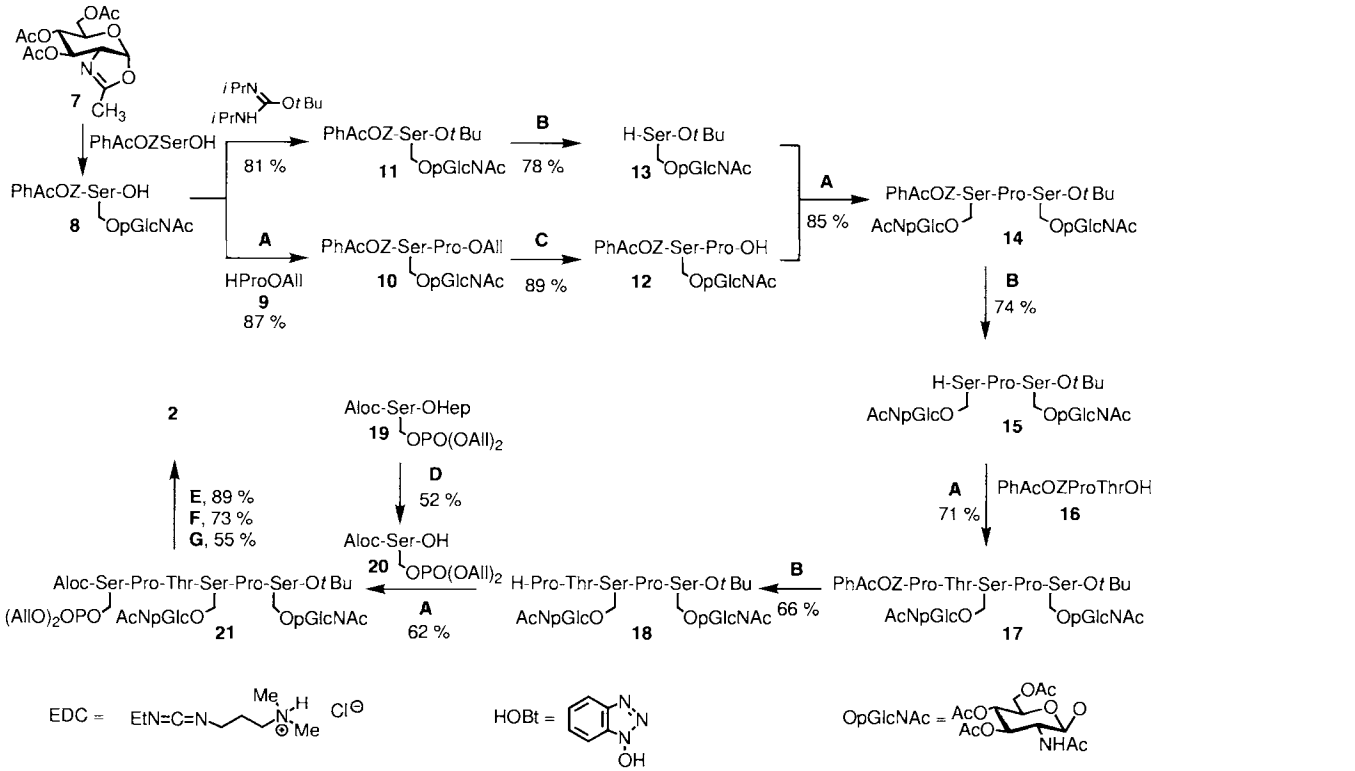

Scheme 3. Enzymatic synthesis of the phosphoglycohexapeptide **2**. A) EDC, HOBt (2 equiv:2 equiv); B) penicillin G acylase, 0.07 M phosphate buffer, 30 vol% methanol, $NaHSO_3$ (500 equiv), pH 7.5, 25 °C; C) $[Pd(Ph_3P)_4]$, morpholine (1.1 equiv); D) lipase from *Aspergillus niger*; 0.2 M phosphate buffer (pH 7, 37 °C); E) $[Pd(Ph_3P)_4]$, formic acid:*n*-butylamine (10 equiv: 6 equiv), room temperature; F) trifluoroacetic acid (TFA), room temperature; G) hydrazine hydrate (3000 equiv), methanol, room temperature.

deliver a satisfactory yield of the selectively unmasked intermediate **18**, which embodies two glycosylated and one unfunctionalized hydroxyamino acid. To guarantee that the PhAcOZ-protected substrates are soluble under the reaction conditions and thereby accessible to the biocatalyst, the enzymatic transformations are most advantageously carried out in the presence of 30 vol% of methanol as cosolvent.

For the subsequent introduction of a phosphorylated, that is differently modified serine residue, the phosphoserine **20** was required. Compound **20** was synthesized by selective saponification of the heptyl ester present in the fully masked phosphoserine derivative **19** with lipase from *Aspergillus niger*[15] under very mild conditions. Finally, **18** and **20** were condensed to give the desired complex multifunctional phosphoglycohexapeptide **21**.[16]

Finally, all allylic protecting groups were removed simultaneously by treatment with formic acid/*n*-butylamine at room temperature in the presence of $[Pd(Ph_3P)_4]$.[17] Subsequently, the *tert*-butyl ester was cleaved with trifluoroacetic acid, and the selective unmasking of the hydroxy groups of the carbohydrates was achieved by employing hydrazine hydrate in methanol.[18]

In all enzymatic and nonenzymatic transformations described above, no undesired side reactions were observed. Thus, the peptide bonds and the O-acetates in the carbohydrates as well as the phosphate remained intact. In addition, an anomerization or cleavage of the glycosidic bonds which may occur under acidic conditions[19] as well as a β-elimination of the phosphate or the carbohydrates which has to be feared under basic conditions[18, 20] could not be detected.

In conclusion, we have developed an enzymatic strategy for the synthesis of differently functionalized complex peptide conjugates and demonstrated its usefulness in the first construction of a phosphoglycohexapeptide that represents a characteristic partial structure of the C-terminal repeating domain of the large subunit of mammalian RNA polymerase II. By using this technique further O-phosphorylated and O-glycosylated peptide conjugates are potentially accessible, which may open up new avenues of research in bioorganic chemistry and biology.

Received: March 21, 1996 [Z 8954 IE]
German version: *Angew. Chem.* **1996**, *108*, 1829–1832

Keywords: enzymes · glycopeptides · peptides · protecting groups

[1] a) T. Hunter, M. Karin, *Cell* **1992**, *70*, 375; b) A. Levitzki, *Eur. J. Biochem.* **1994**, *226*, 1; c) P. J. Casey, *Science* **1995**, *268*, 221; d) S. E. Egan, R. A. Weinberg, *Nature* **1993**, *365*, 781; e) M. S. Boguski, F. McCormick, *Nature* **1993**, *366*, 643.

[2] Review: A. J. Bridges, *Chemtracts Org. Chem.* **1995**, *8*, 73.

[3] G. W. Hart, W. G. Kelly, M. A. Blomberg, E. P. Roquemore, L.-Y. D. Dong, L. Kreppel, T.-Y. Chou, D. Snow, K. Greis, *Glyco- and Cellbiology*, Springer, Heidelberg, **1994**, and references therein.

[4] W. G. Kelly, M. E. Dahmus, G. W. Hart, *J. Biol. Chem.* **1993**, *268*, 10416.

[5] J. W. Perich in *Peptides and Protein Phosphorylation* (Ed. B. E. Kemp), CRC Press, **1990**, p. 289.

[6] Review: H. Kunz, *Angew. Chem.* **1987**, *99*, 297; *Angew. Chem. Int. Ed. Engl.* **1987**, *26*, 294.

[7] Review: H. Waldmann, D. Sebastian, *Chem. Rev.* **1994**, *94*, 911.

[8] For a synthesis of a glycosylated analog to **2** see E. Meinjohanns, A. Vargas-Berenguel, M. Meldal, H. Paulsen, K. Bock, *J. Chem. Soc. Perkin Trans. 1*, **1995**, 2165.

[9] a) H. Waldmann, E. Nägele, *Angew. Chem.* **1995**, *107*, 2425; *Angew. Chem. Int. Ed. Engl.* **1995**, *34*, 2259; b) H. Waldmann, M. Schelhaas, *ibid.* **1996**, *108*, 82 and **1996**, *35*, 106; c) H. Waldmann, E. Nägele, M. Schelhaas, *Bioorg. Med. Chem.* **1996**, in press.

[10] Compound **3** was obtained from *p*-PhAcOZ-Ala-OH and H-Leu-O*t*Bu by coupling with *N*-ethoxycarbonyl-2-ethoxy-1,2-dihydro-quinoline without any detectable racemization (HPLC, NMR) in 94% yield. PhAcOZ-protected amino acids are readily available from *p*-phenylacetoxybenzyl chloroformate and *N,O*-bis(trimethylsilyl) amino acids. D. R. Bolin, I. I. Sytwu, F. Humiec, J. Meienhofer, *Int. J. Peptide Protein Res.* **1989**, *33*, 353, and references therein.

[11] T. Pohl, H. Waldmann, *Tetrahedron Lett.* **1995**, *36*, 2963, and references therein.
[12] G. Arsequell, L. Krippner, R. A. Dwek, S. Y. C. Wong, *J. Chem. Soc. Chem. Commun.* **1994**, 2383.
[13] S. Friedrich-Bochnitschek, H. Waldmann, H. Kunz, *J. Org. Chem.* **1989**, *54*, 751.
[14] Compound **16** was synthesized from PhAcOZ-Pro-Thr-OAll by selective cleavage of the allyl ester with $[Pd(Ph_3P)_4]$ / morpholine in 93% yield.
[15] D. Sebastian, H. Waldmann, unpublished results. For the removal of heptyl esters from *O*-glycopeptides with a different lipase see: P. Braun, H. Waldmann, H. Kunz, *Bioorg. Med. Chem.* **1993**, *1*, 197.
[16] **21**: colorless amorphous solid; R_f: 0.37 (chloroform/methanol 6:1 (v/v)); $[\alpha]_D^{22} = -65.4$ ($c = 1$ in MeOH); ^{1}H NMR (400 MHz, CD_3OD, 25 °C, TMS), characteristic signals: $\delta = 6.06-5.88$ (m, 3H, $CH=CH_2$), 5.43–5.08 (m, 8H, 3-H, 3'-H, $CH=CH_2$), 5.01 (dd, $J(3,4) = J(4,5) = J(3',4') = J(4',5') = 9$ Hz, 2H, 4-H, 4'-H), 4.78 (d, $J(1,2) = 8.5$ Hz, 1H, 1-H), 4.73 (d, $J(1',2') = 8.5$ Hz, 1H, 1'-H), 4.71 (t, $J = 6$ Hz, 1H, α-CH Ser), 2.40–2.19 (m, 2H, β-CH_{2a} Pro, β'-CH_{2a} Pro), 2.16–1.85 (m, 30H, β-CH_{2b} Pro, β'-CH_{2b} Pro, γ-CH_2 Pro, γ'-CH_2 Pro, $COCH_3$), 1.46 (s, 9H, $C(CH_3)_3$), 1.19, 1.14 (d, $J = 6$ Hz, 3H, γ-CH_3 Thr, two rotamers); FAB-MS (glycerol): m/z: 1533.602 [$M^+ + H$].
[17] Y. Hayakawa, H. Kato, M. Uchiyama, H. Kajino, R. Noyori, *J. Org. Chem.* **1986**, *51*, 2402.
[18] P. Schultheiss-Reimann, H. Kunz, *Angew. Chem.* **1983**, *95*, 64; *Angew. Chem. Int. Ed. Engl.* **1983**, *22*, 62.
[19] H. Kunz, *Pure Appl. Chem.* **1993**, *65*, 1223.
[20] a) G. Shapiro, D. Büchler, C. Dalvit, M. Fernandez, B. Gomez-Lor, E. Pombo-Villar, U. Stauss, R. Swoboda, *Bioorg. Med. Chem. Lett.* **1996**, *4*, 409; b) J. R. Vercellotti, R. Fernandez, C. J. Chang, *Carbohydr. Res.* **1974**, *5*, 97.

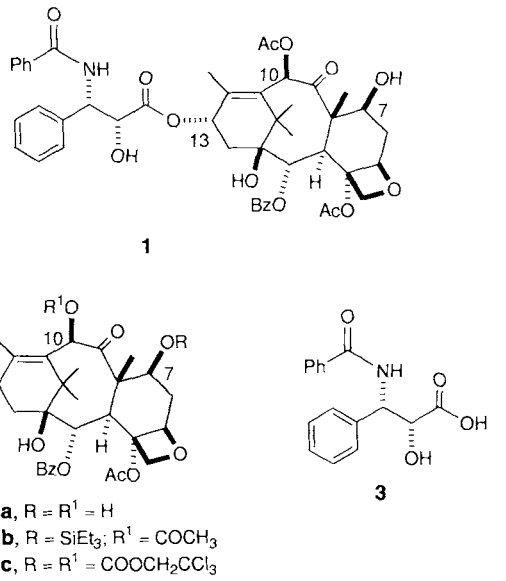

Scheme 1. Paclitaxel (**1**), free (**2a**) and protected 10-deacetylbaccatin III (**2b,c**), and *N*-benzoyl-(2*R*,3*S*)-3-phenyl isoserine (**3**).

Semisynthesis of Taxol: A Highly Enantio- and Diastereoselective Synthesis of the Side Chain and a New Method for Ester Formation at C13 Using Thioesters**

Cesare Gennari,* Anna Vulpetti, Monica Donghi, Nicola Mongelli, and Ermes Vanotti

Paclitaxel (Taxol, **1**), isolated from the bark of the Pacific yew *Taxus brevifolia*, is considered the most promising cancer chemotherapeutic agent and has recently been approved for treatment of metastatic ovarian and breast cancer.[1] It is also undergoing clinical trials in non-small cell lung cancer, head and neck cancer, glioblastoma, and esophageal cancer. The scarcity of **1** and its highly challenging structure have stimulated interest in its synthesis. Central to all synthetic strategies is the attachment of the C13 side chain to the baccatin III nucleus, since the presence of this side chain has proven to be essential for the biological activity of **1**.[1] Owing to the chemical complexity of Paclitaxel (**1**), its commercial production by total synthesis is not likely to be economical. However, the naturally derived 10-deacetylbaccatin III (**2a**, Scheme 1) is readily available in relatively high yield from the needles of the European yew *T. baccata*. Preparation of quantities of Paclitaxel economically by semisynthesis by condensing suitably protected 10-deacetylbaccatin III (**2b,c**) with suitably protected *N*-benzoyl-(2*R*,3*S*)-3-phenylisoserine (**3**) provides an alternative source of this important natural product and access to semisynthetic analogs. Therefore, the development of short and practical synthetic routes to phenylisoserine derivatives, as well as procedures for attaching the C13 side chain to the baccatin III nucleus, which are adaptable for industrial-scale production, have become very important.

The numerous papers devoted to the preparation of enantiomerically enriched **3** include research on semisynthesis drawing from the chiral pool, enzymatic and/or microbial processes, diastereoselective reactions with covalently bound chiral auxiliaries or with chiral substrates, asymmetric catalysis, and chemical resolution of racemic carboxylic acids.[1] In contrast, only a few reactions have been developed to attach the side chain to the free OH group at C13 of baccatin derivatives. This esterification reaction appears to be hampered by the steric congestion around the C13 OH group. Essentially only two general methods have been developed to solve this problem: the first one relies on the dicyclohexylcarbodiimide protocol by Rhône-Poulenc/Gif/Grenoble,[2, 3] and the second one on the β-lactam protocol by Holton et al. and Ojima et al.[4]

We have developed a very simple, new, straightforward approach to the Paclitaxel side chain using the imine addition reaction of thioester-derived boron enolates bearing chiral ligands.[5–7] The side chain is assembled in one step with the correct relative (*syn*) and absolute stereochemistry (2*R*,3*S*). The easily accessible *tert*-butyl (benzoyloxy)thioacetate (**4**)[8] was enolized with triethylamine and the chiral boron reagent **5** derived from (+)-menthone,[6] and then treated with *N*-(trimethylsilyl)benzaldimine (**6**)[9] (Scheme 2). After quenching and extraction, the crude product was transformed into the amine hydrochloride. Salt formation freed the reaction product from the boron ate complex and all of the by-products could be removed simply by washing the resulting white solid with ether. Treatment with buffered MeOH/H_2O at pH 8.0 caused clean intramolecular COPh migration from oxygen to nitrogen[10] to give the desired compound **7**, which was isolated in practically pure form by simple solvent extraction. The overall yield is around 60% (starting from **4**), and the stereochemical control is high (*syn*:*anti* ≥ 96:4; *ee* ≥ 96%).[11] Treatment of **7** with 2-methoxypropene and pyridinium toluene-4-sulfonate (PPTS)

[*] Prof. Dr. C. Gennari, Dr. A. Vulpetti,[+] M. Donghi
Dipartimento di Chimica Organica e Industriale, Università di Milano
Centro CNR per lo Studio delle Sostanze Organiche Naturali
via G. Venezian 21, I-20133 Milano (Italy)
Fax: Int. code +(2)236-4369
e-mail: cesare@iumchx.chimorg.unimi.it
Dr. N. Mongelli, Dr. E. Vanotti
Pharmacia & Upjohn, Milano (Italy)
[+] New address: Pharmacia & Upjohn, Milano (Italy)

[**] This work was supported financially by Pharmacia & Upjohn (postdoctoral fellowship to A. V. and postgraduate gellowship to M. D.).

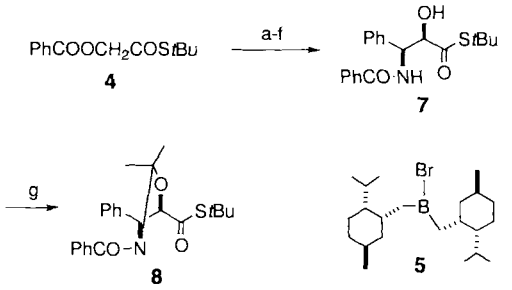

Scheme 2. a) **5** [6], Et_3N, CH_2Cl_2, Et_2O, $-25\,^{\circ}C$, 7 h; b) $PhCH{=}NSiMe_3$ (**6**), $-78\,^{\circ}C \rightarrow -5\,^{\circ}C$; c) quenching with phosphate buffer (pH 6), extraction with CH_2Cl_2, concentration to dryness; d) MeOH/1 N aqueous HCl (1/1), room temperature; concentration to dryness; e) solid washed with Et_2O; f) aqueous phosphate buffer (pH 8), MeOH, room temperature; extraction with CH_2Cl_2 (60% yield over steps a–f); g) $CH_2{=}C(OMe)Me$, PPTS, toluene, 80 °C, ≥90%.

in toluene smoothly furnished oxazolidine **8** (≥90%), and the small amount of the unwanted *anti* diastereomer was removed in this step by chromatography (the *anti* compound does not cyclize under these conditions). The absolute configuration was checked by chemical correlation to known intermediates,[12] and the enantiomeric excess was determined by ^1H NMR analysis of the Mosher ester derivative of **7**.[13]

Following a different approach, the easily accessible phenyl (*tert*-butyldimethylsilyloxy)thioacetate (**9**)[14] was enolized with triethylamine and *ent*-**5**, the chiral boron reagent derived from (−)-menthone,[6] and then treated with *N*-(trimethylsilyl)benzaldimine (**6**)[9] (Scheme 3). After quenching and extraction, the

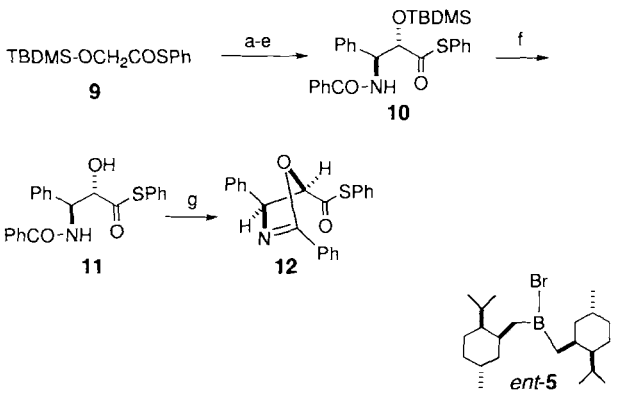

Scheme 3. a) *ent*-**5** [6], Et_3N, CH_2Cl_2, Et_2O, 0 °C → room temperature, 5 h; b) $PhCH{=}NSiMe_3$ (**6**), $-78\,^{\circ}C \rightarrow -5\,^{\circ}C$; c) quenching with phosphate buffer (pH 7), extraction with CH_2Cl_2, concentration to dryness; d) 0.25 N HCl in MeOH/H_2O (1/1), room temperature; concentration to dryness; e) PhCOCl, Et_3N, CH_2Cl_2, 4-dimethylaminopyridine, 0 °C; workup and chromatography (71% yield over steps a–e); f) HF, CH_3CN, H_2O, 100%; g) $SOCl_2$, $CHCl_3$, 45 °C; 1,2-dichloroethane, 100 °C, 65%.

crude product was transformed into the amine hydrochloride to free the reaction product from the boron ate complex. The white solid salt was then treated with PhCOCl, Et_3N, and a catalytic amount of 4-dimethylaminopyridine, and the resulting crude product was purified by filtration through silica gel to give the *anti* compound **10** and traces of the *syn* diastereomer.[11] The overall yield was 71% (starting from **9**), the *anti*:*syn* ratio is 97:3, and the major *anti* compound (**10**) is ≥95% enantiomerically pure (average over several experiments). The *anti* compound **10** (and traces of the *syn* isomer) was then treated with aqueous HF in acetonitrile, and the resulting crude compound **11** (100%; *anti*:*syn* 97:3, average over several experiments)[11] was cyclized by treatment with thionyl chloride in refluxing 1,2-dichloroethane. Oxazoline formation occurred uneventfully with complete inversion of stereochemistry at the C2 stereocenter[10a, 15] to give **12** (65% yield, average over several experiments), and traces of the unwanted *syn* diastereomer were removed in this step by chromatography (the *syn* compound does not cyclize under these conditions). The absolute configuration was checked by chemical correlation with known intermediates,[16] and the enantiomeric excess was determined by ^1H NMR analysis of the Mosher ester derivative of **11**. The synthesis of **12** has an overall yield of 46% (starting from **9**) and requires only two chromatographic purifications.

Thioesters **8** and **12** were attached directly to the baccatin nucleus. By treatment of a mixture of **2b**[2a] or **2c**[17] and **8** or **12** with $LiN(SiMe_3)_2$, the 13-O-acylated compounds **13** and **14** were obtained with high conversion and yield (74–75% for **13** and 89–90% for **14**, Scheme 4).[5] The use of lithium amides for

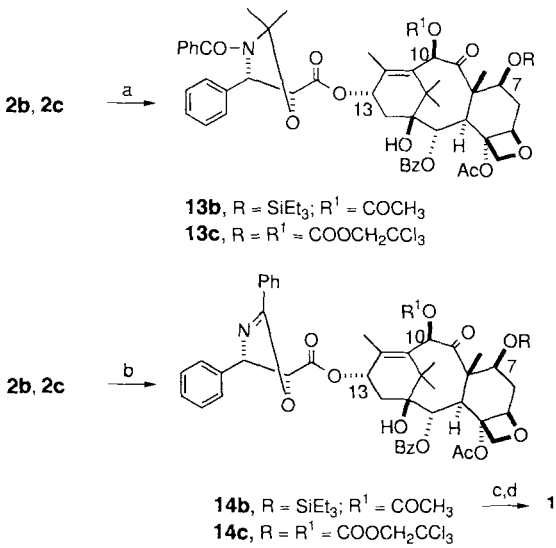

Scheme 4. a) **8** (3.5 equiv), $LiSi(Me)_{32}$ (2.0 equiv), THF, 24 h at 0 °C, 74–75%; b) **12** (3.5 equiv), $LiSi(Me)_{32}$ (4.5 equiv), THF, 15 min at 0 °C, 89–90%; c) 0.04 N HCl in MeOH/H_2O (1.5/1), 60–80 °C; d) $NaHCO_3$, H_2O, pH 7.5, 16 h, room temperature, (80% yield over steps c and d).

metalation of the C13 OH group of protected baccatin III is well precedented.[4a–c] The most surprising, yet gratifying aspect of this new coupling reaction is the high reactivity of the thioester derivatives, given the scarcity of methods for this important transformation and its difficulty. Thioesters have attracted the interest of organic chemists since the discovery that they are used by Nature in enzymatic acylation processes.[18] The resonance overlap of the lone-pair electrons with the carbonyl group is much weaker for the sulfur atom than for the oxygen atom, thus a thioester carbonyl group is much less stabilized by resonance than the carbonyl group of an ester, and is therefore much more reactive.[18] In addition, thioesters **8** and **12** are particularly electrophilic due to presence of electron-withdrawing substituents in both the α and β position.

Compounds **13**[2b–d] and **14**[3] have been deprotected to give Paclitaxel (**1**) in high yields. In our preferred route **14b** is hydrolyzed to give **1** in 80% yield. This represents the third original approach (after the two described in the introduction)[2–4] for the attachment of the Paclitaxel side chain.

From a mechanistic standpoint, the stereochemical divergence of the reactions of aldehydes[6c] and imines was reason-

ably expected based on the different coordination of aldehydes and *trans* imines to the boron atom in chairlike transition state structures (cf. the two chair transition state structures in Scheme 5). However, the stereodivergence caused by the type of thioester (COSPh vs. COS*t*Bu) in the addition to imines is quite surprising. The stereochemical outcome can be rationalized by using corresponding chair and boat transition structures (Scheme 5).[19] However, there is no obvious explanation why this strong stereocontrol is operating as a function of R^2. Experiments not reported here show that the role of the oxygen protecting group R^1 is relatively minor.

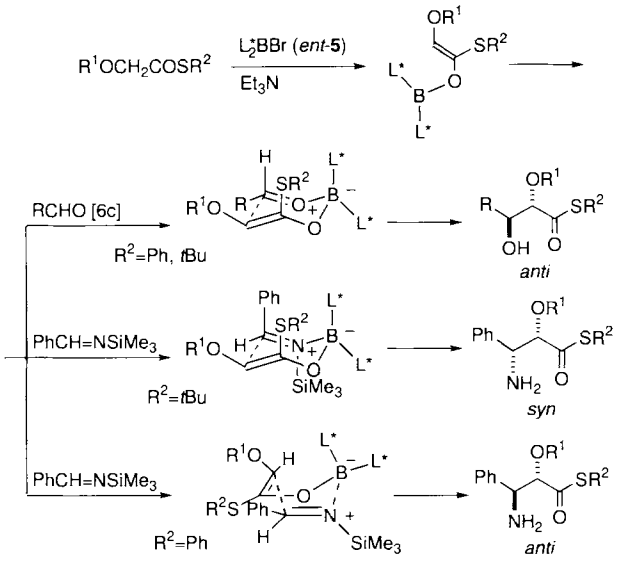

Scheme 5. Transition state models for the boron aldol addition to imines. Products with *anti* configuration arise from attack on the *Re* face of the aldehyde or imine, products with *syn* configuration from attack on the *Si* face.

Received: February 28, 1996 [Z8880IE]
German version: *Angew. Chem.* **1996**, *108*, 1809–1812

Keywords: asymmetric syntheses · enolates · imines · taxol · thioesters

[1] Taxol is the registered trademark of Bristol-Myers Squibb Company for Paclitaxel. For a review, see: K. C. Nicolaou, W.-M. Dai, R. K. Guy, *Angew. Chem.* **1994**, *106*, 38–67; *Angew. Chem. Int. Ed. Engl.* **1994**, *33*, 15–44.

[2] a) J.-N. Denis, A. E. Greene, D. Guenard, F. Gueritte-Voegelein, L. Mangatal, P. Potier, *J. Am. Chem. Soc.* **1988**, *110*, 5917–5919; b) A. Commercon, D. Bezard, F. Bernard, J. D. Bouzard, *Tetrahedron Lett.* **1992**, *33*, 5185–5188; c) J. N. Denis, A. M. Kanazawa, A. E. Greene, *ibid.* **1994**, *35*, 105–108; (Rhône-Poulenc Rorer S.A.), WO 94/10169, **1994**, FR-A 92/13000, **1992**; d) A. M. Kanazawa, J. N. Denis, A. E. Greene, *J. Chem. Soc. Chem. Commun.* **1994**, 2591–2592.

[3] D. G. I. Kingston, A. G. Chaudhary, A. A. L. Gunatilaka, M. L. Middleton, *Tetrahedron Lett.* **1994**, *35*, 4483–4484.

[4] a) R. A. Holton, EP-A 400971, **1990** [*Chem. Abstr.* **1991**, *114*, 164568q]; US 5015744, **1991**; US 5136060, **1992**; US 5175315, **1992**; WO 93/06079, **1993**; US 5229526, **1993**; b) I. Ojima, I. Habus, M. Zhao, M. Zucco, Y. H. Park, C. M. Sun, T. Brigaud, *Tetrahedron* **1992**, *48*, 6985–7012; c) I. Ojima, C. M. Sun, M. Zucco, Y. H. Park, O. Duclos, S. Kuduk, *Tetrahedron Lett.* **1993**, *34*, 4149–4152; d) I. Ojima, WO 94/18164, **1994**; US Serial N. 93/11922, **1993**; e) R. A. Holton, K. Rengan, H. Nadizadeh, US 5283253, **1994**.

[5] C. Gennari, N. Mongelli, E. Vanotti, A. Vulpetti (Pharmacia), GB-A 9512471.5, **1995**.

[6] a) C. Gennari, C. T. Hewkin, F. Molinari, A. Bernardi, A. Comotti, J. M. Goodman, I. Paterson, *J. Org. Chem.* **1992**, *57*, 5173–5177; b) C. Gennari, D. Moresca, S. Vieth, A. Vulpetti, *Angew. Chem.* **1993**, *105*, 1717–1719; *Angew. Chem. Int. Ed. Engl.* **1993**, *32*, 1618–1621; c) C. Gennari, A. Vulpetti, D. Moresca, *Tetrahedron Lett.* **1994**, *35*, 4857–4860; d) A. Bernardi, C. Gennari, J. M. Goodman, I. Paterson, *Tetrahedron: Asymmetry* **1995**, *6*, 2613–2636; e) C. Gennari, G. Pain, D. Moresca *J. Org. Chem.* **1995**, *60*, 6248–6249.

[7] For related chemistry involving silyl ketene acetal additions to chiral imines mediated by a chiral boron Lewis acid, see: a) K. Hattori, M. Miyata, H. Yamamoto, *J. Am. Chem. Soc.* **1993**, *115*, 1151–1152; b) K. Hattori, H. Yamamoto, *Tetrahedron* **1994**, *50*, 2785–2792.

[8] Prepared from methyl glycolate in two steps: a) *t*BuSH, $AlMe_3$, hexanes, CH_2Cl_2, 0 °C, 53%; b) PhCOCl, Et_3N, 4-(dimethylamino)pyridine, CH_2Cl_2, 0 °C, 89%.

[9] D. J. Hart, K. Kanai, D. G. Thomas, T. K. Yang, *J. Org. Chem.* **1983**, *48*, 289–294.

[10] a) M. E. Bunnage, S. G. Davies, C. J. Goodwin, *J. Chem. Soc. Perkin Trans. 1* **1993**, 1375–1376; b) *ibid.* **1994**, 2385–2391; c) J.-N. Denis, A. E. Greene, A. A. Serra, M.-J. Luche, *J. Org. Chem.* **1986**, *51*, 46–50.

[11] The *syn*:*anti* mixture was used in the next synthetic step. The *syn* and *anti* compounds were separated and isolated only for analytical purposes.

[12] Compound **7** was transformed into the known (−)-methyl (2*R*,3*S*)-3-benzoylamino-2-hydroxy-3-phenylpropionate by the following steps: a) 30% H_2O_2 (4 equiv), LiOH aq. (8 equiv), THF, 0 °C, 15 h; Na_2SO_3; b) CH_2N_2, Et_2O, MeOH. For optical rotation values, see: a) M. C. Wani, H. L. Taylor, M. E. Wall, P. Coggon, A. T. McPhail, *J. Am. Chem. Soc.* **1971**, *93*, 2325–2326; b) J.-N. Denis, A. Correa, A. E. Greene, *J. Org. Chem.* **1990**, *55*, 1957–1959; c) refs. [10b, c].

[13] Determination of the absolute configuration by means of the Mosher method (a) I. Ohtani, T. Kusumi, Y. Kashman, H. Kakisawa, *J. Am. Chem. Soc.* **1991**, *113*, 4092–4096; b) S. Izumi, H. Moriyoshi, T. Hirata, *Bull. Chem. Soc. Jpn.* **1994**, *67*, 2600–2602) was in accord with the determination by chemical correlation.

[14] Prepared from methyl glycolate in two steps: a) TBDMSCl, imidazole, DMF, 0 °C to room temperature, 100%; b) PhSH, $AlMe_3$, hexanes, CH_2Cl_2, 0 °C to room temperature, 79%.

[15] D.-M. Gou, Y.-C. Liu, C.-S. Chen, *J. Org. Chem.* **1993**, *58*, 1287–1289.

[16] Compound **11** was transformed into the known (+)-methyl (2*S*,3*S*)-3-benzoylamino-2-hydroxy-3-phenylpropionate by the following steps: a) 30% H_2O_2 (4 equiv), LiOH aq. (2 equiv), THF, 0 °C, 15 h; Na_2SO_3; b) CH_2N_2, Et_2O, MeOH. For optical rotation values, see: a) F. A. Davis, R. T. Reddy, R. E. Reddy, *J. Org. Chem.* **1992**, *57*, 6387–6389; b) ref. [10b].

[17] F. Guéritte-Voegelein, V. Sénilh, B. David, D. Guénard, P. Potier, *Tetrahedron* **1986**, *42*, 4451–4460.

[18] T. C. Bruice, S. J. Benkovic, *Bioorganic Mechanisms*, W. A. Benjamin Inc., New York, **1966**, Vol. 1, Chapter 3.

[19] Recent ab initio MO calculations (3-21G basis set) featuring the addition of the BH_2 enol borinate derived from acetaldehyde to formaldehyde-imine have shown that two competing cyclic transition structures are important: the chair and the boat (A. Bernardi, C. Gennari, L. Raimondi, M. Villa (University of Milano), unpublished results).

Asymmetric Epoxidation of Enones With Oxygen in the Presence of Diethylzinc and (*R*,*R*)-*N*-Methylpseudoephedrine**

Dieter Enders,* Jiqun Zhu, and Gerhard Raabe

The asymmetric epoxidation of C–C double bonds plays an important role in the synthesis of optically active organic compounds. In 1980 Sharpless et al. reported the titanium-mediated enantioselective epoxidation of allylic alkohols with *t*BuOOH,[1] which was later achieved catalytically by addition of molecular sieves.[2] Based on cationic salen–manganese complexes Jacobsen et al.[3] and Katsuki et al.[4] developed an efficient method for the enantioselective epoxidation of unfunctionalized olefins.

[*] Prof. Dr. D. Enders, Dr. J. Zhu, Dr. G. Raabe
Institut für Organische Chemie der Technischen Hochschule
Professor-Pirlet-Strasse 1, D-52074 Aachen (Germany)
Fax: Int. code +(241)8888 127
e-mail: enders@rwth-aachen.de

[**] This work was supported by the Fonds der Chemischen Industrie, the Deutsche Forschungsgemeinschaft (Leibniz Prize), and the European Union (HCM network: Metal Mediated and Catalysed Organic Synthesis). We are obliged to the companies Degussa AG, BASF AG, Bayer AG, Hoechst AG, and Knoll AG for donations of chemicals.

The asymmetric epoxidation of chalcone in high optical yields was achieved by Juliá et al. with H_2O_2/NaOH in a three-phase system over chiral polypeptides.[5] However, the success of this method is as yet usually limited to chalcones.[6] Other methods for the enantioselective epoxidation of α,β-unsaturated ketones, for example by use of benzylquininium chloride,[7] bovine serum albumin,[8] cyclodextrins,[9] or chiral platinum complexes,[10] generally gave only low to moderate enantiomeric excesses.

We now report a new method for the enantioselective epoxidation of α,β-unsaturated ketones **1** with O_2 in the presence of Et_2Zn[11] and (*R,R*)-*N*-methylpseudoephedrine to afford the chiral α,β-epoxyketones (*R,S*)-**2** (Scheme 1). The epoxidation proceeds with excellent yields (94–99%), virtually complete diastereoselectivities (*de* > 99%), and except for one case, with high enantiomeric excesses (*ee* = 61, 82–92%) (Table 1). The

Table 1. α,β-Epoxyketones **2** prepared by diastereo- and enantioselective epoxidation of α,β-unsaturated ketones **1**.

2	R^1	R^2	*t* [h]	Yield [%]	*de* [%]	*ee*[a] [%]	$[\alpha]_D^{26}$ (c, CH_2Cl_2)	Conf.[b] (α,β)
a	Ph	Me	3	96	>99	85	+0.4 (1.2)	(*R,S*)
b	Ph	Et	3	99	>99	91	+13.8 (1.4)	(*R,S*)
c	Ph	*n*Pr	3	99	>99	87	+0.9 (1.1)	(*R,S*)
d	Ph	*i*Pr	3	97	>99	92	+32.0 (1.3)	(*R,S*)
e	Ph	Ph	16	94	>99	61	−130 (1.1)	(*R,S*)[c]
f	*t*Bu	$PhCH_2CH_2$	41	99	>99	90	−50.1 (1.2)	(*R,S*)
g	2,4,6-$Me_3C_6H_2$	Et	89	94	>99	82	+20.9 (1.1)	(*R,S*)

[a] Determined by NMR-shift experiments with [Eu(tfc)$_3$] (tfc = 3-(trifluoromethylhydroxymethylene)-*d*-camphorate). [b] Derived from **2e** based on the assumption of a uniform reaction mechanism. [c] Determined by comparison of the optical rotation with literature data [13].

chiral alcohol (*R,R*)-*N*-methylpseudoephedrine employed is readily accessible from cheap (*R,R*)-pseudoephedrine by methylation[12] and can be virtually quantitatively recovered after the reaction by a simple chromatographic elution (Scheme 1).

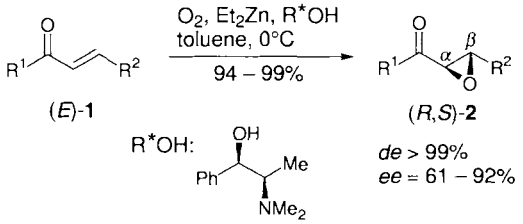

Scheme 1. Asymmetric epoxidation of enones with O_2 in the presence of Et_2Zn and *N*-methylpseudoephedrine.

The epoxidation, which is carried out as a "one-pot" reaction probably proceeds as follows:[14] Firstly, ethyl zinc alkoxide **3** is formed from diethylzinc and the chiral alcohol.[15] The expected evolution of a gas (ethane) was observed. The substitution of the second ethyl group by an alkoxy ligand is very slow. Therefore, insertion of O_2 into the Zn–C bond between the remaining ethyl ligand and the zinc atom is preferred.[16] In the course of this process the chirally modified alkoxy(ethylperoxy)zinc **4** is formed. The measurement of the absorption of oxygen by a solution of **3** in toluene at room temperature gave a value of 25.8 mL (1.06 mmol). According to the Van der Waals equation absorption of 26.9 mL O_2 was expected for 1.1 mmol **3**. After removal of the solvent in vacuo, **4** remained as a colorless powder. Upon addition of **4** to an aqueous Fe^{II} solution, oxidation to Fe^{III} occurs, which can be proved by the characteristic color change upon treatment with $K_4[Fe(CN)_6]$ and KSCN.[17] It is likely that **4** is the species that actually epoxidizes the α,β-unsaturated ketones asymmetrically. In the epoxidation process the oxygen of the carbonyl function first coordinates the zinc atom in **4**, with concomitant attack of the ethylperoxy anion in β-position to form the intermediate **5**. This reaction constitutes a Michael-type addition. The subsequent cyclization gives the epoxyketone **2** and **6**.[18] In this way, *trans*-epoxides are exclusively formed from (*E*)-α,β-unsaturated ketones (*de* > 99%).[19] Since the reaction rate strongly decreases upon introduction of voluminous groups adjacent to the carbonyl function (see **2f**, **2g**), the formation of **5** is probably the rate-determining step. Upon hydrolysis of **6** the chiral amino alcohol is formed, which can be virtually quantitatively recovered with unchanged enantiomeric purity (Scheme 2).

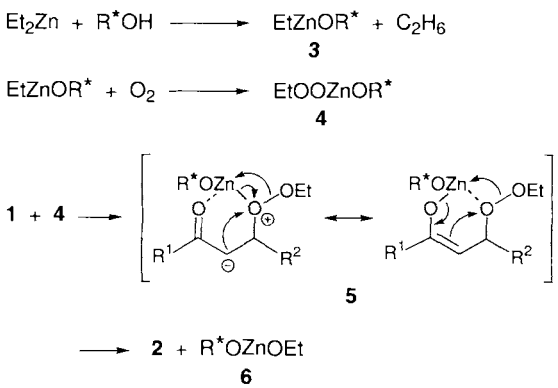

Scheme 2. Proposed reaction mechanism for the asymmetric epoxidation of enones.

The substituents R^2 in β-position have only a slight influence on the enantioselectivity. Only the phenyl group leads to a significant decrease in the enantiomeric excess (see **2e**). In the scope of this work 35 chiral alcohols such as (*S*)-1-phenylethanol, (*R,R*)-*N*-ethylpseudoephedrine, (−)-menthol, (−)-8-phenylmenthol, (*S*)-2,2-dimethyl-1,3-dioxolan-4-methanol, as well as nine solvents were tested in the asymmetric epoxidation of enones. (*R,R*)-*N*-Methylpseudoephedrine and toluene proved to be best suited. The stereochemical result (that is, the *trans*-(*R,S*) configuration of the epoxyketones **2**) can be explained by means of the transition states **A** or **B** with *R* or *S* configuration at the zinc atom, respectively, which are depicted in Figure 1. In this picture the chiral alkoxy(ethylperoxy)zinc **4** attacks the *si* face of the s-*cis* conformation of the (*E*) enones in the fashion of an oxa-Michael addition. Transition state **A** shows particularly well that the steric hindrance between R^1 and

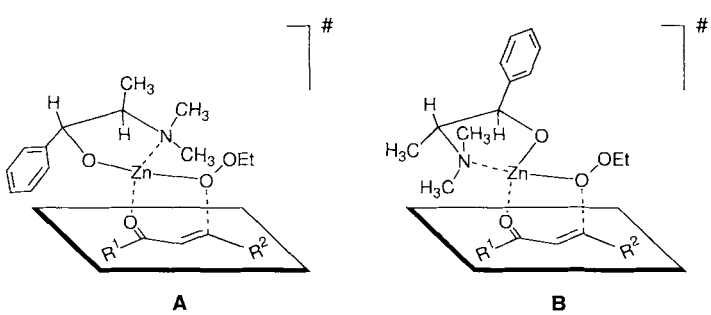

Fig. 1. Postulated transition states for the asymmetric epoxidation.

the phenyl group as well as the interaction between R^2 and the dimethylamino group, which are caused by a rotation of the enone plane by 180°, significantly impedes the attack at the *re* face of the enone.

The zinc bis-alkoxide **7** was obtained by the reaction of two equivalents of (*R*,*R*)-*N*-methylpseudoephedrine with diethylzinc in pentane (Scheme 3). However, **7** does not react with the enones **1** under standard conditions. As can be seen from Figure 2, the zinc bis-alkoxide **7** exists as a dimer in the solid

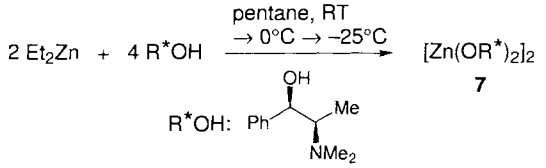

Scheme 3. Preparation of the chiral zinc bis-alkoxide **7**. RT = room temperature.

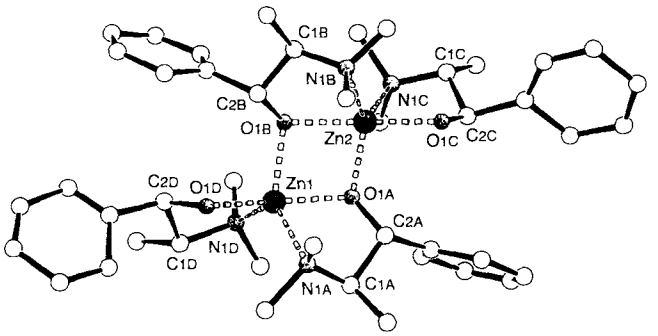

Fig. 2. Structure of the enantiomerically pure zinc bis-alkoxide **7** in the solid state (SCHAKAL plot).

state[20] in which the zinc atoms are surrounded by three oxygen and two nitrogen atoms each to form a distorted trigonal bipyramid (coordination number 5).[21] The structure is C_2-symmetrical and is, to the best of our knowledge, the first crystal structure of a chiral zinc bis-aminoalkoxide.

This new method for the zinc-mediated asymmetric epoxidation of α,β-unsaturated ketones opens an efficient diastereo- and enantioselective access to *trans*-configured α,β-epoxyketones. The use of the cheap chemicals O_2 and Et_2Zn as well as the possibility of recovering the employed chiral additive quantitatively makes this method interesting also in terms of industrial applications. Further work on the optimization of the method and extension to other electron-deficient alkenes is underway.[22]

Experimental Procedure

Asymmetric epoxidation of α,β-unsaturated ketones **1**: A solution of diethylzinc in toluene (1.0 mL, 1.1 M) was added to a stirred solution of (1*R*,2*R*)-*N*-methylpseudoephedrine ([23], 2.4 mmol) in dried toluene (10 mL) in a 50 mL Schlenk flask under an argon atmosphere at 0 °C. After 80 min a slight O_2 pressure was applied from a balloon filled with O_2 so that the argon inside the flask was not removed. After stirring for 2.5 h the reaction mixture was cooled to −78 °C and α,β-unsaturated ketone **1** (1 mmol in 2 mL dried toluene) was added. The reaction mixture was stirred for 30 min at this temperature and then rapidly warmed up to 0 °C (ice/water bath) under constant stirring [24]. At the end of the reaction (TLC control), aqueous phosphate buffer solution (8 mL, pH 7) was added. After the separation of the layers and extraction of the aqueous layer with dichloromethane, the combined organic layers were dried over Na_2SO_4 and concentrated. After purification by flash chromatography (ether/petroleum ether 1/24 to 1/4) the α,β-epoxyketones **2** were obtained [25]. (*R*,*R*)-*N*-Methylpseudoephedrine could be recovered virtually quantitatively with an unchanged enantiomeric purity from the same chromatographic column with a polar eluent (methanol/ether 1/9, mixed with 1 vol% isopropylamine).

Received: March 18, 1996 [Z 89341E]
German version: *Angew. Chem.* **1996**, *108*, 1827–1829

Keywords: asymmetric epoxidation · chiral auxiliaries · enones · epoxyketones · zinc compounds

[1] K. Katsuki, K. B. Sharpless, *J. Am. Chem. Soc.* **1980**, *102*, 5974–5976.
[2] a) R. M. Hanson, K. B. Sharpless, *J. Org. Chem.* **1986**, *51*, 1922–1925; reviews: b) R. A. Johnson, K. B. Sharpless in *Catalytic Asymmetric Synthesis* (Ed.: I. Ojima), VCH, New York, **1993**, p. 103; c) A. C. Oehlschlager in *Houben-Weyl, Methods of Organic Chemistry, Bd. E21e* (Eds.: G. Helmchen, R. W. Hoffmann, J. Mulzer, E. Schaumann), Thieme, Stuttgart, **1995**, p. 4675.
[3] a) W. Zhang, J. L. Loebach, S. R. Wilson, E. N. Jacobsen, *J. Am. Chem. Soc.* **1990**, *112*, 2801–2803; b) B. D. Brandes, E. N. Jacobsen, *Tetrahedron Lett.* **1995**, *36*, 5123–5126; c) reviews: E. N. Jacobsen in *Catalytic Asymmetric Synthesis*, (Ed.: I. Ojima), VCH, New York, **1993**, p. 159.
[4] a) R. Irie, K. Noda, Y. Ito, N. Matsumoto, T. Katsuki, *Tetrahedron Lett.* **1990**, *31*, 7345–7348; b) T. Fukuda, R. Irie, T. Katsuki, *Synlett* **1995**, 197–198; c) reviews: T. Katsuki, *Coord. Chem. Rev.* **1995**, *140*, 189–214.
[5] S. Juliá, J. Masana, J. C. Vega, *Angew. Chem.* **1980**, *92*, 968–969; *Angew. Chem. Int. Ed. Engl.* **1980**, *19*, 929–931.
[6] a) S. Juliá, J. Guixer, J. Masana, J. Rocas, S. Colonna, R. Annunziata, H. Molinari, *J. Chem. Soc. Perkin Trans. 1* **1982**, 1317–1324; b) S. Banfi, S. Colonna, H. Molinari, S. Juliá, J. Guixer, *Tetrahedron* **1984**, *40*, 5207–5211; c) B. C. B. Bezuidenhoudt, A. Swanepoel, J. A. N. Augustyn, D. Ferreira, *Tetrahedron Lett.* **1987**, *28*, 4857–4860; d) S. Itsuno, M. Sakakura, K. Ito, *J. Org. Chem.* **1990**, *55*, 6047–6049; e) P. W. Baures, D. S. Eggleston, J. R. Flisak, K. Gombatz, I. Lantos, W. Mendelson, J. J. Remich, *Tetrahedron Lett.* **1990**, *31*, 6501–6504; f) C. Bolm, *Angew. Chem.* **1991**, *103*, 414–415; *Angew. Chem. Int. Ed. Engl.* **1991**, *30*, 403–404; g) J. R. Flisak, K. J. Gombatz, M. M. Holmes, A. A. Jarmas, I. Lantos, W. L. Mendelson, V. J. Novack, J. J. Remich, L. Snyder, *J. Org. Chem.* **1993**, *58*, 6247–6254; h) M. E. Lasterra Sanchez, S. M. Roberts, *J. Chem. Soc. Perkin Trans. 1* **1995**, 1467–1468; i) M. E. Lasterra Sanchez, U. Felfer, P. Mayon, S. M. Roberts, S. R. Thornton, C. J. Todd, *ibid.* **1996**, 343–348.
[7] Benzylquininium chloride: a) R. Helder, J. C. Hummelen, R. W. P. M. Laane, J. S. Wiering, H. Wynberg, *Tetrahedron Lett.* **1976**, 1831–1834; b) J. C. Hummelen, H. Wynberg, *ibid.* **1978**, 1089–1092; c) H. Wynberg, B. Marsman, *J. Org. Chem.* **1980**, *45*, 158–161; d) H. Pluim, H. Wynberg, *ibid.* **1980**, *45*, 2498–2502; e) Y. Harigaya, H. Yamaguchi, M. Onda, *Heterocycles* **1981**, *15*, 183–185.
[8] Bovine serum albumin: a) S. Colonna, A. Manfredi, *Tetrahedron Lett.* **1986**, *27*, 387–390; b) S. Colonna, A. Manfredi, A. M. Spadoni, *ibid.* **1987**, *28*, 1577–1580; c) S. Colonna, N. Gaggero, A. Manfredi, A. M. Spadoni, L. Casella, G. Carrea, P. Pasta, *Tetrahedron* **1988**, *44*, 5169–5178.
[9] Cyclodextrins: a) S. Banfi, S. Colonna, S. Julia, *Synth. Commun.* **1983**, *13*, 1049–1052; b) S. Colonna, S. Banfi, A. Pagagni, *Gazz. Chim. Ital.* **1985**, *115*, 81–83; c) Y. Hu, A. Harada, S. Takahashi, *Synth. Commun.* **1988**, *18*, 1607–1610; d) S. Colonna, A. Manfredi, R. Annunziata, N. Gaggero, *J. Org. Chem.* **1990**, *55*, 5862–5866.
[10] Chiral platinum complexes: C. Baccin, A. Gusso, F. Pinna, G. Strukul, *Organometallics* **1995**, *14*, 1161–1167.
[11] Diastereoselective epoxidation of enones with the system O_2/R_2Zn have already been reported: K. Yamamoto, N. Yamamoto, *Chem. Lett.* **1989**, 1149–1152. The authors postulated ROOZnR as the oxidizing species. However, our asymmetric variant supports the reaction mechanism depicted in Scheme 2 via **4**. Cyclohexenone is not epoxidized under our conditions.
[12] Prepared according to a) S. Smith, *J. Chem. Soc.* **1927**, 2056–2059 (65% yield, m.p. 29 °C, b.p. 91–92 °C (8 mbar), $[\alpha]_D^{22} = -48.6$ ($c = 5.1$ in MeOH)), in agreement with literature data: b) W. N. Nagai, S. Kanao, *Justus Liebigs Ann. Chem.* **1929**, *470*, 157–182; c) T. Kanzawa, *Bull. Chem. Soc. Jpn.* **1956**, *29*, 398–403; d) K. Yamamoto, K. Tsuruoka, J. Tsuji, *Chem. Lett.* **1977**, 1115–1116; e) H.-J. Schneider, M. Lonsdorfer, *Org. Magn. Reson.* **1981**, *16(2)*, 133–137.
[13] B. Marsman, H. Wynberg, *J. Org. Chem.* **1979**, *44*, 2312–2314.
[14] The zinc complexes depicted in the formulas are presented as monomers for the sake of simplicity. They do not account for the fact that these species could possibly exist as dimers.
[15] Alkyl zinc alkoxides were successfully employed in the enantioselective addition of dialkylzinc to aldehydes. Reviews: a) R. Noyori, M. Kitamura, *Angew. Chem.* **1991**, *103*, 34–55; *Angew. Chem. Int. Ed. Engl.* **1991**, *30*, 49–69; b) K. Soai, S. Niwa, *Chem. Rev.* **1992**, *92*, 833–856.
[16] G. Sosnovsky, J. H. Brown, *Chem. Rev.* **1966**, *66*, 529–566.
[17] G. Jander, E. Blasius, *Lehrbuch der analytischen und präparativen anorganischen Chemie*, 14th ed., Hirzel, Stuttgart, **1995**, p. 422.
[18] An analogous mechanism was postulated for the epoxidation of enones with H_2O_2 in alkaline medium: H. O. House, R. S. Ro, *J. Am. Chem. Soc.* **1958**, *80*, 2428–2433.
[19] The coupling constants of the vicinal protons in *trans* positions at the oxirane ring of the epoxyketones **2** are 1.68–2.02 Hz (^{1}H NMR spectrum). They are in accord with the literature data for *trans* epoxides: C. A. Reilly, J. D. Swalen, *J. Chem. Phys.* **1960**, *32*, 1378–1384; b) K. L. Williamson, C. A. Lanford, C. R. Nicholson, *J. Am. Chem. Soc.* **1964**, *86*, 762–765.

 © VCH Verlagsgesellschaft mbH, D-69451 Weinheim, 1996 0570-0833/96/3515-1727 $ 15.00+.25/0

[20] X-ray crystal analysis of **7**: monoclinic, space group $P2_1(4)$, $a = 13.988(2)$, $b = 18.846(17)$, $c = 14.141(9)$ pm, $\beta = 106.09(2)^\circ$; 25 reflections, $12.23^\circ < \theta < 16.98^\circ$; $Z = 2$, $V = 3581.8$ Å^3, $M_r = 1202.29$, $\rho_{calcd} = 1.115$ g cm^{-3}. The crystal was measured directly without capillary in a stream of cold nitrogen ($T = 190$ K), $F(000) = 1288$, $Mo_{K\alpha}$ radiation ($\lambda = 0.71069$ Å), $\sin\theta/\lambda_{max} = 0.651$, $\mu = 7.32$ cm^{-1} (no absorption correction), $R_{int} = 0.102(30)$, 4963 observed reflections ($I > 2\sigma(I)$) in the range $-18 < h < 17$, $0 < k < 24$, $0 < l < 18$. The structure was solved by the heavy atom method (SHELXS86 [26]), refinement with XTAL3.2 [27]. 4963 reflections in final least-squares full-matrix refinement of 410 parameters. $R = 0.103$, $R_w = 0.077$ ($w = 1/\sigma^2$). $S = 2.717$, residual electron density 1.6 e Å^3. Compound **7** crystallizes with two free molecules of the ligand (disordered) per molecular unit. The poor quality of the crystals allowed only the anisotropic refinement of the Zn atoms and of their immediate environment (O1A–D, N1A–D, C1A–D, C2A–D). All other atomic parameters were refined isotropically. The positions of the hydrogen atoms were calculated. All attempts to prepare crystals of superior quality were unsuccessful. The crystallographic data (without structure factors) of the structure described in this publication were deposited as "supplementary publication no. CCDC-179-57" at the Cambridge Crystallographic Data Centre. Copies of the data can be ordered free of charge from the following address: The Director, CCDC, 12 Union Road, GB-Cambridge CB2 1EZ (fax: Int. code + (1223) 336-033; e-mail: teched(*a*) chemcry.cam.ac.uk)

[21] A related achiral zinc bis-alkoxide structure with C_i symmetry is known: P. L. Orioli, M. Di Vaira, L. Sacconi, *Inorg. Chem.* **1966**, *5*, 400–405.

[22] We have already succeeded in epoxidizing a nitro alkene diastereo- and enantioselectively by the same method: J. Zhu, Dissertation, Technische Hochschule Aachen, **1996**.

[23] The epoxidation carried out with half the amount of (1*R*,2*R*)-*N*-methylpseudoephedrine gave comparable yields at longer the reaction times. However, the enantiomeric excesses fell by several percent in most cases (example **4b**: 17 h, 94% yield, 87% *ee*).

[24] Since extensive exposure to O_2 can have an adverse influence on the reaction, it is recommended to replace the oxygen balloon with an argon balloon after 3.5 h.

[25] In addition, **2g** was prepared by preparative HPLC. All new compounds gave consistent spectroscopic data (IR, NMR, MS) and correct elemental analysis or high-resolution mass spectra.

[26] G. M. Sheldrick in *Crystallographic Computing C* (Eds.: G. M. Sheldrick, C. Krüger, R. Goddard), University Press, **1985**, p. 175.

[27] S. R. Hall, H. D. Flack, J. M. Stewart, *XTAL3.2 Reference Manual*, Universities of West Australia, Geneva, and Maryland, Lamb, Perth **1992**.

cis-Sodium Hyponitrite—A New Preparative Route and a Crystal Structure Analysis**

Claus Feldmann and Martin Jansen*

Dedicated to Professor Hans Georg von Schnering on the occasion of his 65th birthday

The family of triatomic molecular 16-electron species has attained an impressive size. Previous studies on these molecules or molecular ions have concentrated on their preparation and structural and spectroscopic characterization.[1] Their electronic structures correspond to a large extent and should, as a result, lead to similar chemical behavior—an aspect that has previously been given scant regard with respect to their use in synthesis. The central atom, being generally positively polarized, should function as a Lewis acid center. This behavior is well-known for CO_2, but otherwise only described for CS_2.[2] Novel interesting tetraatomic complex anions should be accessible by the addition of oxide, nitride, or sulfide ions, for example. To test this idea we studied the effect of laughing gas (N_2O) on Na_2O, which—if the reaction proceeds analogous to that of CO_2—should lead to the formation of sodium nitridonitrate.

At a temperature between 300 and 400 °C, Na_2O does indeed take up an equimolar amount of N_2O. According to the X-ray powder diagrams the reaction goes to completion (no Na_2O reflections were detected), and the elemental analysis confirms the expected composition $Na_2N_2O_2$.[3] The colorless, extremely moisture-sensitive product is obtained as microcrystals. It is thermally stable up to 325 °C; above this temperature quantitative disproportionation occurs with N_2 cleavage and formation of "sodium orthonitrite" [Eq. (a)].[4]

$$3\,Na_2N_2O_2 \longrightarrow 2\,Na_3O(NO_2) + 2\,N_2 \qquad (a)$$

Neither by annealing (due to the low decomposition temperature) nor by recrystallization (due to the insolubility in aprotic solvents and the decomposition in protic solvents) was it possible to obtain single crystals of $Na_2N_2O_2$. The proof of its constitution was therefore undertaken by a crystal structure determination from X-ray powder data without using any a priori knowledge[5] and confirmed spectroscopically (^{15}N MAS-NMR, vibrational spectroscopy).

According to the results of the X-ray structure analysis (Fig. 1),[6] the product of the reaction of N_2O with Na_2O is

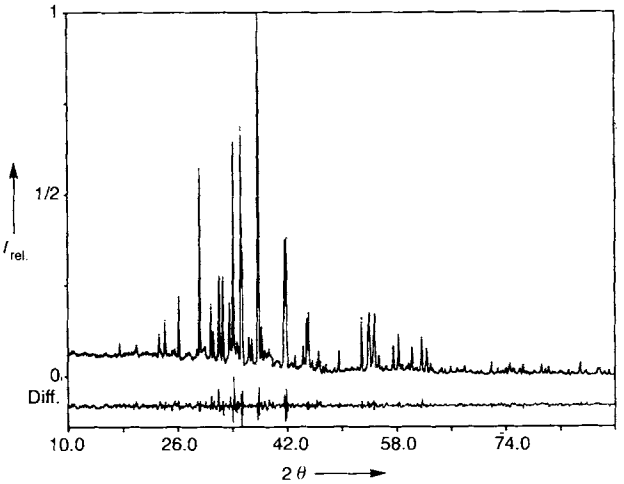

Fig. 1. Profile fitting for *cis*-$Na_2N_2O_2$. Top: measured intensities; bottom: difference.

unexpectedly *cis*-$Na_2N_2O_2$, the constitution of which was thus unequivocally confirmed for the first time. The bond lengths of the *cis*-hyponitrite ion of 1.20(3) (N1–N2), 1.40(3) (N1–O1), and 1.39(3) Å (N2–O2) correspond approximately to those of a N–N double bond (1.15 Å) and two N–O single bonds (1.40 Å).[7] The bond angles of 119.8(4) (O1–N1–N2) and 119.2(4)° (O2–N2–N1) agree with those expected for a pseudo trigonal-planar arrangement.[8] With a dihedral angle (O1–N1–N2–O2) of 0.6(3)°, *cis*-$N_2O_2^{2-}$ is, within the limits of error, planar. The anion has C_1 site symmetry; the measured deviations from the highest possible symmetry (point group C_{2v}) lie within the standard deviations, however.

The ^{15}N MAS-NMR spectrum of *cis*-$Na_2{}^{15}N_2O_2$ (99 % ^{15}N) has, in addition to the rotational side bands, just one isotropic signal ($\delta = 364(1)$). At a line width of $\Delta\delta = 2.0(5)$, the nitrogen atoms can be considered as chemically equivalent, which would agree with the point groups C_{2v} or C_2 for *cis*-$N_2O_2^{2-}$. The vibrational spectra show a clear splitting of all significant peaks, which in accordance with a point or factor group analysis is to be expected (Table 1). Interestingly in this case, the vibrational

[*] Prof. Dr. M. Jansen
Institut für Anorganische Chemie der Universität
Gerhard-Domagk-Strasse 1, D-53121 Bonn (Germany)
Fax: Int. code + (228) 735660
Dr. C. Feldmann
Max-Planck-Institut für Festkörperforschung, Stuttgart (Germany)

[**] This work was supported by the Deutsche Forschungsgemeinschaft and the Fonds der Chemischen Industrie.

Table 1. Factor group analysis and measured internal vibrations of *cis*-$Na_2N_2O_2$ [a].

Type of band	Point group of the free anion C_{2v}	Site symmetry in the solid C_1	Factor group C_{2h}	$\tilde{\nu}$ [cm^{-1}]
ν(N-N)	A_1	A	$A_g + B_g$ (2 Ra)	Ra: 1325
			$A_u + B_u$ (2 IR)	IR: 1320, 1329
ν(N-O)	A_2	A	$A_g + B_g$ (2 Ra)	Ra: 1062, 1074
			$A_u + B_u$ (2 IR)	IR: 1065, 1097
ν(N-O)	B_1	A	$A_g + B_g$ (2 Ra)	Ra: 863, 874
			$A_u + B_u$ (2 IR)	IR: 860, 885

[a] The bending vibrations were not detectable because the intensities were too small.

spectroscopy reacts considerably more sensitively to crystal field effects than the MAS nuclear magnetic resonance spectroscopy, which is usually known for its extreme sensitivity.[9]

The *cis*-$N_2O_2^{2-}$ ions are arranged around the Na cations in such a way that each takes on a pseudo octahedral coordination sphere (Fig. 2; if *cis*-$N_2O_2^{2-}$ is coordinated to two adjacent atoms, these are counted as one ligand). A stacking of the *cis*-$N_2O_2^{2-}$ ions along the direction [001] can be considered as the spatial packing principle, whereby the plane of the molecular anions is tilted relative to the *a,b* plane by about 25° (Fig. 3). The cations form linear strings along [001] in the channels remaining between the anions. Astonishingly enough, the packing of *cis*-$Na_2N_2O_2$ has a great deal in common with that of the alkali metal carbonates, in spite of the different symmetries of the anions. If the cations and two of the oxygen atoms are left in almost the same positions as in β-Na_2CO_3 (space group $C2/m$),[10] the crystal structure of *cis*-$Na_2N_2O_2$ is attained by turning the remaining C–O group by 90° and exchanging it for N–N (Fig. 3).

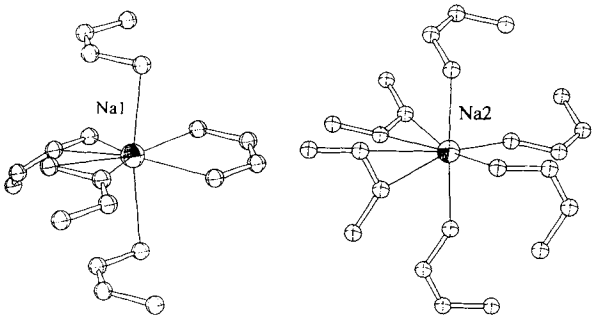

Fig. 2. Coordination spheres around Na (atomic distances: Na–O 2.30 to 2.81 Å, Na–N 2.47 to 3.03 Å).

The hyponitrite class of substances as a whole now appears in a clearer light. Among the three reasonable constitutional isomers for $N_2O_2^{2-}$ (namely, *cis*-hyponitrite, *trans*-hyponitrite, and nitridonitrate), *cis*-$N_2O_2^{2-}$ had only been confirmed structurally as a complex ligand;[11] moreover, the structural suggestions for *cis*- and *trans*-hyponitrite were based on vibrational spectroscopy only (Table 2).[12] Thus, *cis*-$Na_2N_2O_2$ provides the first crystal structure analysis of a simple salt of hyponitrous acid. At the same time, the product of the reduction of NO with Na in liquid ammonia, originally described as sodium nitrosyl, can be recategorized.[13] Based on vibrational spectra of this compound, Goubeau and Laitenberger were able to show that $N_2O_2^{2-}$ ions were present and not NO^- ions. The decision between nitridonitrate and *cis*-hyponitrite fell on the latter.[14] Similarly situated cases such as N_2F_2 and S_2F_2 have shown, however, how difficult a differentiation between these two possible isomers can be, when based solely on vibrational spectra.[15]

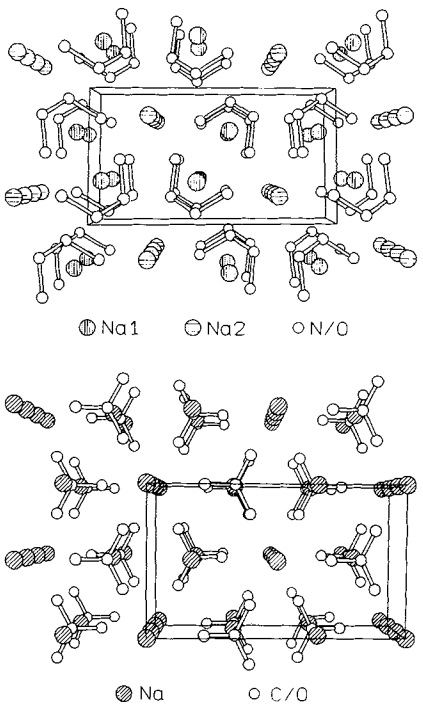

Fig. 3. Packing of the crystal building blocks of *cis*-$Na_2N_2O_2$ (top) and β-Na_2CO_3 (bottom) in the [001] direction (unit cells indicated).

Table 2. Physical and chemical properties of sodium hyponitrite.

	trans-$Na_2N_2O_2$ [12]	*cis*-$Na_2N_2O_2$	*cis*-$Na_2N_2O_2$ ("NaNO") [14]
preparation	$NaNO_2$ + Na(Hg) 0 °C, H_2O	$N_2O + Na_2O$ 360 °C, 2 h	NO + Na −50 °C, fl. NH_3
thermal decomposition	$Na_3O(NO_2) + N_2$ 260 °C	$Na_3O(NO_2) + N_2$ 325 °C	$N_2O + Na_2O$ 100 °C
crystal system	tetragonal	monoclinic	(amorphous)
point group of the anion	C_{2h}	C_{2v}	C_{2v}

A comparison between the *cis*-$Na_2N_2O_2$ prepared by Goubeau and Laitenberger and that described here shows significant differences in the chemical properties and the vibrational spectra (Table 2, Fig. 4). The fundamentally different temperatures of decomposition and the clearly divergent vibrational spectra irritated us at first, and we assumed that they represented different species. However, the differences are apparently due to the absence of structural order already on a local scale on the one hand and the presence of well-formed long-range crystalline order in the *cis*-$Na_2N_2O_2$ prepared by the solid-state reaction on the other. This is the only convincing explanation for the observation that a local probe such as vibrational spectroscopy in the case of amorphous *cis*-$Na_2N_2O_2$ shows no splitting due to reduced site symmetry. This is an impressive example for different chemical and physical behaviors of solids having the same composition, but different conditioning.

Experimental Procedure

cis-$Na_2N_2O_2$ was prepared by the gas–solid reaction of Na_2O (0.3 g, 4.8 mmol) and excess N_2O (0.77×10^5 Pa at the start of the reaction) in a sealed Duran glass cylinder (l = 425 mm, diameter 45 mm). The cylinder was heated to 360 °C for two hours in a tube furnace. The course of the reaction (complete conversion, start of

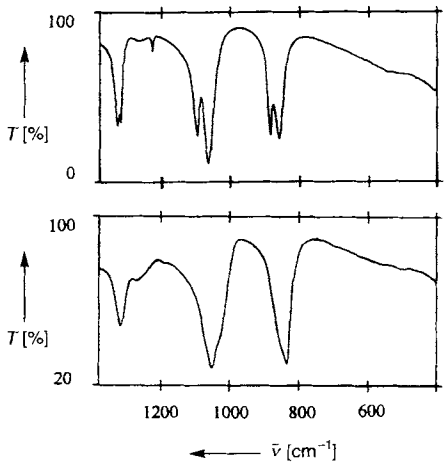

Fig. 4. IR spectra of *cis*-$Na_2N_2O_2$. Top (this paper): $\tilde{\nu}$ = 860/885, 1065/1097, 1320/1329 cm^{-1}; bottom (according to Ref [14]): $\tilde{\nu}$ = 839, 1053, 1316 cm^{-1}.

decomposition) is extremely sensitive to the temperature and duration of reaction, and to the N_2O pressure. The conditions mentioned are the result of careful optimization. The preparation of $Na_2{}^{15}N_2O_2$ was carried out analogously with Na_2O and $^{15}N_2O$ (99 % ^{15}N, Chemotrade, Düsseldorf).

Received: March 19, 1996
Revised version: May 6, 1996 [Z8948IE]
German version: *Angew. Chem.* **1996**, *108*, 1807–1809

Keywords: sodium compounds · nitrogen compounds · structure elucidation

[1] T. M. Klapötke, *Angew. Chem.* **1994**, *106*, 1651; *Angew. Chem. Int. Ed. Engl.* **1994**, *33*, 1575; H. G. von Schnering, M. Somer, M. Hartweg, K. Peters, *ibid.* **1990**, *102*, 63 and **1990**, *29*, 65; P. Pyykkö, Y. Zhao, *J. Phys. Chem.* **1990**, *94*, 7753.

[2] A. F. Hollemann, E. Wiberg, *Lehrbuch der Anorganischen Chemie*, 101. Aufl., de Gruyter, Berlin, **1995**, pp. 859 and 871; U. Henseler, M. Jansen, *Z. Anorg. Allg. Chem.* **1993**, *619*, 1203.

[3] Quantitative analysis of *cis*-$Na_2N_2O_2$: Na 43.4 (calcd 43.4), N 24.9 (calcd 26.4), O 28.9 (calcd 30.2) wt %. Sodium was determined by flame photometry, oxygen acidimetrically after hydrolysis, N gravimetrically after the thermal decomposition of *cis*-$Na_2N_2O_2$ to $Na_3O(NO_2)$.

[4] M. Jansen, *Angew. Chem.* **1976**, *88*, 410; *Angew. Chem. Int. Ed. Engl.* **1976**, *15*, 376; *Z. Anorg. Allg. Chem.* **1977**, *435*, 13.

[5] L. G. Akselrud, J. N. Grin, P. Y. Zavalii, V. K. Pecharskii, V. S. Fundamenskii, *CSD – Universal Program Package for Single Crystal and/or Powder Structure Data Treatment*, 12. European Crystallographic Meeting, Collected Abstracts, Moskow, **1989**, *3*, 155.

[6] X-ray structure analysis of *cis*-$Na_2N_2O_2$: space group $P2_1/c$, a = 5.11(1), b = 9.21(2), c = 6.16(1) Å, β = 97.9(1)°, V = 286(2) Å^3, Z = 4, $F(000)$ = 208, ρ_{calcd} = 2.45(1) gcm^{-3}. X-ray diffraction studies on powders were performed on a Stoe-Stadi-P diffractometer: $Cu_{K\alpha1}$ radiation, Ge monochromator, small PSD, 2θ = 5–100°. The crystal structure was solved using the CSD program package [5] with direct methods and refined with the Rietveld method: 270 observed reflections, 57 free parameters, Na, N, O to 4e, $R_{intensity}$ = 0.07, $R_{profile}$ = 0.13. Further details of the crystal structure investigation may be obtained from the Fachinformationszentrum Karlsruhe, D-76344 Eggenstein-Leopoldshafen (Germany) on quoting the depository number CSD-405055.

[7] J. E. Huheey, E. A. Keiter, R. C. Keiter, *Anorganische Chemie*, 2nd ed., de Gruyter, Berlin, **1995**, p. 1165.

[8] R. J. Gillespie, E. A. Robinson, *Angew. Chem.* **1996**, *108*, 539; *Angew. Chem. Int. Ed. Engl.* **1996**, *35*, 477.

[9] U. Fleischer, F. Frick, A. R. Grimmer, W. Hoffbauer, M. Jansen, W. Kutzelnigg, *Z. Anorg. Allg. Chem.* **1995**, *621*, 2012.

[10] C. J. de Pater, *Physica B* **1979**, *96*, 89.

[11] B. F. Hoskins, F. D. Whillans, *J. Chem. Soc. Chem. Commun.* **1969**, 69; S. Bhaduri, B. F. G. Johnson, A. Pickard, P. R. Raithby, G. M. Sheldrick, C. I. Zuccaro, *ibid.* **1977**, 354.

[12] C. C. Addison, G. A. Gamelen, R. Thompson, *J. Chem. Soc.* **1952**, 338; M. N. Hughes, *Quart. Rev.* **1968**, *22*, 1.

[13] E. Zintl, A. Harder, *Ber. Dtsch. Chem. Ges.* **1933**, *66*, 760.

[14] J. Goubeau, K. Laitenberger, *Z. Anorg. Allg. Chem.* **1963**, *320*, 78.

[15] R. H. Sanborn, *J. Chem. Phys.* **1960**, *33*, 1855; F. Seel, R. Budenz, *Chem. Ber.* **1965**, *98*, 251.

Transition-Metal-Mediated Radical Reactions as an Easy Route to 2-C-Analogues of Carbohydrates**

Torsten Linker,* Klaus Hartmann, Thomas Sommermann, Dieter Scheutzow, and Elfriede Ruckdeschel

Dedicated to Professor Siegfried Hünig on the occasion of his 75th birthday

C-Disaccharides represent an interesting class of compounds in which the glycosidic oxygen atom is replaced by a methylene group.[1] During the last few years the conformational properties of such carbohydrate analogues were investigated intensively.[2] Besides ionic[1a–d, 2] and enzymatic[1e] approaches, radical reactions[3] are especially attractive for the synthesis of *C*-disaccharides. Conveniently, C-analogues of monosaccharides serve as precursors for the different synthetic routes. Carbon substituents can be easily introduced at the anomeric center (synthesis of *C*-glycosides),[4] whereas C-functionalizations at other positions require many steps[2, 5] or the use of toxic tin and mercury compounds.[6] Herein we present a practical protocol, notable for the easy availability of the starting materials, for the synthesis of 2-C-analogues of D-glucose.

Glycals can be prepared on a multigram scale and allow various functionalizations. Epoxidations, cycloadditions, and the introduction of heteroatoms in the 2-position represent the most important transformations.[7] However, the synthetic potential of glycals was not used for intermolecular additions of carbon-centered radicals up to now. In the course of our investigations on manganese(III)-mediated radical reactions,[8] we became interested in the addition of dimethyl malonate (**2**) to tri-*O*-acetyl-D-glucal (**1**, Scheme 1).

Indeed, the C–C bond-formation products **3** and **4** are obtained highly regioselectively in 66% yield. The unsaturated carbohydrates **5** are formed as by-products due to acid-catalyzed Ferrier rearrangement,[9] but are easily separated by column chromatography. The configuration of the C-analogues **3** and **4**, which are obtained as a mixture of diastereomers, was

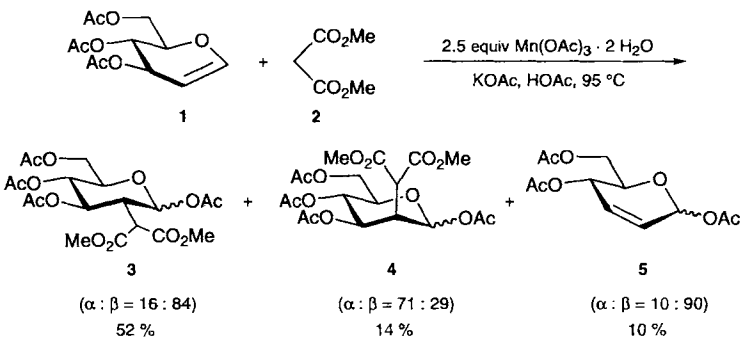

Scheme 1. Manganese(III)-mediated radical addition of dimethyl malonate (**2**) to tri-*O*-acetyl-D-glucal (**1**).

[*] Dr. T. Linker, K. Hartmann, T. Sommermann
Institut für Organische Chemie der Universität
Am Hubland, D-97074 Würzburg (Germany)
Fax: Int. code +(931)888-4606
e-mail: linker@chemie.uni-wuerzburg.de
Dr. D. Scheutzow, E. Ruckdeschel
NMR-Abteilung, Institut für Organische Chemie der Universität Würzburg

[**] Transition-Metal-Mediated Radical Reactions, Part 3. This work was generously supported by the Deutsche Forschungsgemeinschaft (Li 556/3-1, SFB 347 "Selektive Reaktionen Metall-aktivierter Moleküle") and the Volkswagen-Stiftung. We thank Prof. W. Adam for his constant support. Part 2: [8b].

determined by a complete assignment of all ring protons by means of 600 MHz 1D TOCSY NMR spectroscopy.[10] The product ratios and regioselectivities can be rationalized by the mechanism outlined in Scheme 2. In the first step, the malonyl

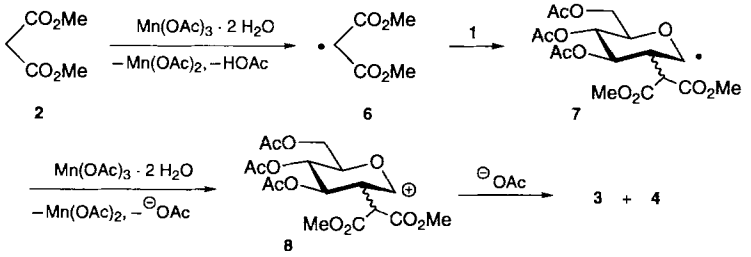

Scheme 2. Mechanism of the manganese(III)-mediated radical addition of dimethyl malonate (**2**) to tri-*O*-acetyl-D-glucal (**1**).

radicals **6** are generated from dimethyl malonate (**2**) and manganese(III) acetate dihydrate by an inner-sphere electron transfer;[11] these radicals react with tri-*O*-acetyl-D-glucal (**1**) to form the adduct radicals **7**. Oxidation by a second equivalent of manganese(III) affords the cations **8**, which are trapped by the solvent acetic acid to yield the products **3** and **4**. Due to the electrophilic nature of malonyl radicals,[12] the addition is highly regioselective at the 2-position in an orbital-controlled reaction. The preferred formation of *gluco*-configurated products can be rationalized by a *trans* attack at the 3-*O*-acetyl group, which is in accordance with cycloadditions to glucals.[7c-e] Presumably, the same steric effects operate at the anomeric center, where the malonyl substituent controls the reaction. Thus, the *β-gluco* and *α-manno* isomers are obtained predominantly.

In order to suppress the undesired formation of the rearrangement products **5**, we subsequently became interested in additions mediated by ceric(IV) ammonium nitrate (CAN), since the milder reaction conditions are advantageous.[13] For both manganese(III) and cerium(IV) several precedents exist for the generation of electrophilic carbon-centered radicals.[11] However, the application of such radicals in carbohydrate chemistry was hitherto unknown. Indeed, a smooth addition of dimethyl malonate (**2**) to tri-*O*-acetyl-D-glucal (**1**) takes place even at 0 °C, and the formation of the rearrangement products **5** was suppressed completely (Scheme 3). Furthermore, because of the lower reaction temperature higher stereoselectivities are obtained with cerium(IV) than with manganese(III). The methyl glycosides **9** and **11** are formed by trapping of the cationic intermediates **8** (Scheme 2) with solvent, whereas the nitrate **10** results from a ligand transfer reaction with CAN. This ligand transfer offers an explanation for the exclusive formation of the α-anomer **10**,

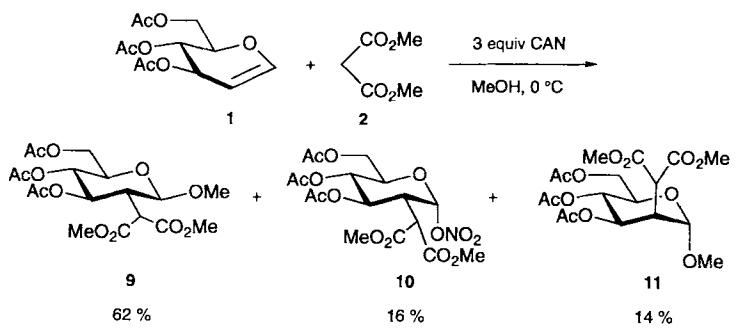

Scheme 3. Cerium(IV)-mediated radical addition of dimethyl malonate (**2**) to tri-*O*-acetyl-D-glucal (**1**).

since a coordination of the adduct radical to the transition metal is proposed in literature.[14] Thus, the nitrate group should be stereoselectively transferred *cis* to the 2-position, which is indeed the case. Another advantage of the cerium(IV)-mediated reactions is reflected in the easy separation of the *gluco*-configurated main products by column chromatography, which are then isolated in analytically pure form.

In summary, the transition-metal-mediated radical reactions presented herein provide an easy route to 2-C-analogues of D-glucose. Since a broad variety of CH-acidic precursors are available and malonates can be added to glycosyl halides after deprotonation, this methodology should open up interesting prospects for the synthesis of *C*-disaccharides.

Experimental Procedure

A solution of tri-*O*-acetyl-D-glucal (**1**, 1.36 g, 5.0 mmol) and dimethyl malonate (**2**, 6.61 g, 50 mmol) in methanol (10 mL) was cooled to 0 °C under an argon atmosphere. At this temperature a solution of ceric(IV) ammonium nitrate (8.22 g, 15 mmol) in methanol (30 mL) was added dropwise over a period of 4 h. After stirring for 30 min at 0 °C an ice-cold, dilute sodium thiosulfate solution (200 mL) was added, and the mixture was extracted with dichloromethane (4 × 80 mL). The combined organic extracts were dried (sodium sulfate) and concentrated, and the excess of dimethyl malonate was removed at 0.01 mbar. Column chromatography on silica gel (hexane/ethyl acetate 7/3 → 5/5) afforded 370 mg (16%) of **10**, 1.35 g (62%) of **9**, and 350 mg (16%) of **11** containing a small amount of **9**.

9: ^{1}H NMR (600 MHz, $CDCl_3$): δ = 1.98, 1.99, 2.06 (3s, 3H, OAc), 2.57 (ddd, J = 11.6, 8.6, 3.6 Hz, 1H, 2-H), 3.45 (s, 3H, OMe), 3.57 (d, J = 3.6 Hz, 1H, 7-H), 3.69 (ddd, J = 10.0, 4.6, 2.4 Hz, 1H, 5-H), 3.70, 3.73 (2s, 3H, CO_2Me), 4.10 (dd, J = 12.2, 2.4 Hz, 1H, 6-H), 4.28 (dd, J = 12.2, 4.6 Hz, 1H, 6'-H), 4.95 (d, J = 8.6 Hz, 1H, 1-H), 4.98 (dd, J = 10.0, 9.0 Hz, 1H, 4-H), 5.27 (dd, J = 11.6, 9.0 Hz, 1H, 3-H). ^{13}C NMR (151 MHz, $CDCl_3$): δ = 20.5, 20.6, 20.7 (3q, OAc), 46.3, 48.0 (2d, C-2, C-7), 52.4, 52.5 (2q, CO_2Me), 57.5 (q, OMe), 62.2 (t, C-6), 69.8, 71.3, 71.6 (3d, C-3, C-4, C-5), 101.6 (d, C-1), 168.2, 168.5, 169.7, 170.0, 170.7 (5s, OAc, CO_2Me). M.p. 101 °C, $[\alpha]_D^{20}$ = −6.9 (c = 1.08, $CHCl_3$). Anal. Calcd. for $C_{18}H_{26}O_{12}$: C 49.77, H 6.03; Found: C 49.51, H 5.92.

10: ^{1}H NMR (600 MHz, $CDCl_3$): δ = 2.01, 2.03, 2.10 (3s, 3H, OAc), 3.09 (ddd, J = 12.0, 6.1, 3.7 Hz, 1H, 2-H), 3.58 (d, J = 6.1 Hz, 1H, 7-H), 3.76, 3.78 (2s, 3H, CO_2Me), 4.08 (dd, J = 12.6, 2.2 Hz, 1H, 6-H), 4.17 (ddd, J = 10.3, 4.0, 2.2 Hz, 1H, 5-H), 4.33 (dd, J = 12.6, 4.0 Hz, 1H, 6'-H), 5.07 (dd, J = 10.3, 9.3 Hz, 1H, 4-H), 5.45 (dd, J = 12.0, 9.3 Hz, 1H, 3-H), 6.70 (d, J = 3.7 Hz, 1H, 1-H). ^{13}C NMR (151 MHz, $CDCl_3$): δ = 20.4, 20.5, 20.6 (3q, OAc), 42.1, 49.1 (2d, C-2, C-7), 53.0, 53.2 (2q, CO_2Me), 61.3 (t, C-6), 68.9, 69.4, 70.3 (3d, C-3, C-4, C-5), 97.3 (d, C-1), 167.2, 167.4, 169.5, 169.7, 170.5 (5s, OAc, CO_2Me). Syrup, $[\alpha]_D^{20}$ = +138.7 (c = 0.86, $CHCl_3$). Anal. Calcd. for $C_{17}H_{23}NO_{14}$: C 43.88, H 4.98, N 3.01; Found: C 44.12, H 5.14, N 2.79.

Received: April 1, 1996 [Z 8989 IE]
German version: *Angew. Chem.* **1996**, *108*, 1819–1821

Keywords: carbohydrates · cerium compounds · manganese compounds · radical reactions

[1] a) D. Rouzaud, P. Sinaÿ, *J. Chem. Soc. Chem. Commun.* **1983**, 1353–1354; b) S. Hanessian, M. Martin, R. C. Desai, *ibid.* **1986**, 926–927; c) H. Dietrich, R. R. Schmidt, *Liebigs Ann. Chem.* **1994**, 975–981; d) R. W. Armstrong, D. P. Sutherlin, *Tetrahedron Lett.* **1994**, *35*, 7743–7746; e) O. Eyrisch, W.-D. Fessner, *Angew. Chem.* **1995**, *107*, 1738–1740; *Angew. Chem. Int. Ed. Engl.* **1995**, *34*, 1639–1641.

[2] a) Y. Wang, S. A. Babirad, Y. Kishi, *J. Org. Chem.* **1992**, *57*, 468–481; b) Y. Wang, P. G. Goekjian, D. M. Ryckman, W. H. Miller, S. A. Babirad, Y. Kishi, *ibid.* **1992**, *57*, 482–489; c) J.-F. Espinosa, H. Dietrich, M. Martín-Lomas, R. R. Schmidt, J. Jiménez-Barbero, *Tetrahedron Lett.* **1996**, *37*, 1467–1470.

[3] a) B. Giese, T. Witzel, *Angew. Chem.* **1986**, *98*, 459–460; *Angew. Chem. Int. Ed. Engl.* **1986**, *25*, 450–451; b) B. Giese, M. Hoch, C. Lamberth, R. R. Schmidt, *Tetrahedron Lett.* **1988**, *29*, 1375–1378; c) A. Chénedé, E. Perrin, E. D. Rekai, P. Sinaÿ, *Synlett* **1994**, 420–422; d) R. Ferritto, P. Vogel, *Tetrahedron Lett.* **1995**, *36*, 3517–3518.

[4] Reviews: a) S. Hanessian, A. G. Pernet, *Adv. Carbohydr. Chem. Biochem.* **1976**, *33*, 111–188; b) M. H. D. Postema, *Tetrahedron* **1992**, *48*, 8545–8599.

[5] a) R. H. Hall, K. Bischofberger, A. J. Brink, O. G. de Villiers, A. Jordaan, *J. Chem. Soc. Perkin Trans. 1* **1979**, 781–786; b) B. Fraser-Reid, L. Magdzinski, B. F. Molino, D. R. Mootoo, *J. Org. Chem.* **1987**, *52*, 4495–4504.

[6] a) B. Giese, J. A. González-Gomez, T. Witzel, *Angew. Chem.* **1984**, *96*, 51–52; *Angew. Chem. Int. Ed. Engl.* **1984**, *23*, 69–70; b) B. Giese, K. Gröninger, *Tetrahedron Lett.* **1984**, *25*, 2743–2764; c) M. E. Jung, S. W. T. Choe, *ibid.* **1993**, *34*, 6247–6250.

[7] Selected examples of additions to glycals: a) J. Thiem, H. Karl, J. Schwentner, *Synthesis* **1978**, 696–698; b) R. U. Lemieux, R. M. Ratcliffe, *Can. J. Chem.* **1979**, *57*, 1244–1251; c) M. Chmielewski, Z. Kaluza, C. Belzecki, P. Salanski, J. Jurczak, *Tetrahedron Lett.* **1984**, *25*, 4797–4800; d) R. L. Halcomb, S. J. Danishefsky, *J. Am. Chem. Soc.* **1989**, *111*, 6661–6666; e) C. M. Timmers, M. A. Leeuwenburgh, J. C. Verheijen, G. A. van der Marel, J. H. van Boom, *Tetrahedron Asym.* **1996**, *7*, 49–52.

[8] a) U. Linker, B. Kersten, T. Linker, *Tetrahedron* **1995**, *51*, 9917–9926; b) T. Linker, B. Kersten, U. Linker, K. Peters, E.-M. Peters, H.-G. von Schnering, *Synlett* **1996**, 468–470.

[9] a) R. J. Ferrier, N. Prasad, *J. Chem. Soc. C* **1969**, 581–586; b) R. D. Dawe, B. Fraser-Reid, *J. Chem. Soc. Chem. Commun.* **1981**, 1180–1181; c) K. Inaba, S. Matsumura, S. Yoshikawa, *Chem. Lett.* **1991**, 485–488.

[10] a) H. Kessler, H. Oschkinat, C. Griesinger, W. Bermel, *J. Magn. Reson.* **1986**, *70*, 106–133; b) H. Günther, NMR-Spektroskopie, 3rd ed., Thieme, Stuttgart, **1993**, p. 375.

[11] Reviews of transition-metal-mediated radical reactions: a) J. Iqbal, B. Bhatia, N. K. Nayyar, *Chem. Rev.* **1994**, *94*, 519–564; b) P. I. Dalko, *Tetrahedron* **1995**, *51*, 7579–7653; c) B. B. Snider, *Chem. Rev.* **1996**, *96*, 339–363.

[12] a) B. Giese, *Angew. Chem.* **1983**, *95*, 771–782; *Angew. Chem. Int. Ed. Engl.* **1983**, *22*, 753–764; b) B. Giese, *ibid.* **1985**, 97, 555–567 and **1985**, *24*, 553–565.

[13] a) A. Citterio, L. Pesce, R. Sebastiano, R. Santi, *Synthesis* **1990**, 142–144; b) E. Baciocchi, R. Ruzziconi, *J. Org. Chem.* **1991**, *56*, 4772–4778; c) V. Nair, J. Mathew, *J. Chem. Soc. Perkin Trans. 1* **1995**, 1881–1882.

[14] a) B. B. Snider, J. J. Patricia, S. A. Kates, *J. Org. Chem.* **1988**, *53*, 2137–2143; b) K. Narasaka, K. Iwakura, T. Okauchi, *Chem. Lett.* **1991**, 423–426; c) R. Warsinsky, E. Steckhan, *J. Chem. Soc. Perkin Trans. 1* **1994**, 2027–2037.

Isolation and Characterization of C_{80}**

Frank H. Hennrich, Rudi H. Michel, Achim Fischer, Sabine Richard-Schneider, Stefan Gilb, Manfred M. Kappes,* Dirk Fuchs, Martin Bürk, Kaoru Kobayashi, and Shigeru Nagase

It is well established that fullerenes comprise carbon cage structures consisting of pentagon and hexagon rings.[1] Of the many air-stable fullerene cages (C_{2n}, $n \geq 30$) so far extracted from fullerene soot generated by the Krätschmer–Huffman (K–H) method, all have nonadjacent or "isolated" pentagon rings (isolated pentagon rule, IPR).[2] This has been rationalized on energetic grounds. The smallest fullerene cage that allows such pentagon isolation is C_{60}. Only one form that obeys the IP rule exists for this well-known vertex count (I_h-C_{60}).[3] Beyond C_{60}, the next vertex count that supports an IPR structure is C_{70}. Here again only one IPR isomer is possible (and formed) and has D_{5h} symmetry.[4] After C_{70}, in principle, all C_{2n} cages can have IPR isomers. Furthermore, beyond C_{74} all vertex counts support more than one IPR isomer. Indeed, several IPR isomers of one carbon atom count are often formed in extractable amounts upon fullerene soot generation by graphite arc discharge[5,6] (and by other methods[7]). For example, three of the five theoretically possible C_{78} IPR isomers have been experimentally detected.[8] Furthermore, two of the 24 theoretically possible isomers of C_{84} occur predominantly.[6,9] Study of the symmetries and relative amounts of IPR isomers found for given experimental conditions is of interest towards understanding how the kinetics and energetics of growth and unimolecular dissociation determine fullerene yield in the K–H arc discharge "synthesis". In this work, which has in the meantime led to the isolation and characterization of many IPR C_{2n} fullerenes between C_{76} and C_{96},[10] there have been three notable exceptions. C_{72} (one IPR isomer), C_{74} (one IPR isomer), and C_{80} (seven IPR isomers) have not as yet proven isolable.[11] This has been attributed to their comparatively low abundance in or even outright absence from soot extracts. Herein we report the isolation and characterization of one of these "missing" fullerenes, namely C_{80}.

Apart from inherent questions concerning isomer distribution and relative stability of empty cages, C_{80} is presently also of interest with respect to the mechanism of formation of endohedrally metal doped cages in modified K–H composite arcs. Here it has been found that for several lanthanide metals,[12] the most abundant metallofullerenes after extraction comprise $M@C_{82}$[13] and—remarkably—$M_2@C_{80}$.[14] In both cases the appropriate cage structure still remains to be determined experimentally. Recent ab initio calculations for $La_2@C_{80}$ (which to a first approximation can be described as $(La^{3+})_2@C_{80}^{6-}$) predict an I_h cage derived ground state isomer in contrast to calculations for empty C_{80} which predict a D_2 isomer at the same level of theory (see below).[15]

Fullerene soot formation and extraction was carried out as previously described.[16] The soot extract was fractionated by preparative-scale HPLC in three steps. The optimized protocol consisted of two initial passes using a 250 × 20 mm Cosmosil PYE column (Nacalai Tesque, Kyoto, Japan, toluene eluent), followed by a third pass using a 250 × 21.1 mm Buckyclutcher-1-Prep-Trident-Tri-DNP column (Regis Technologies, Illinois, USA, toluene eluent).[17] The purity of the isolated C_{80} sample (>98%; >1 mg of material) was determined by analytical HPLC and laser desorption time-of-flight mass spectrometry (LD-TOF, N_2-laser). Figure 1 shows the corresponding LD-TOF mass spectrum and the UV/Vis absorption spectrum for the yellow solution of C_{80} in CH_2Cl_2 (main peaks at $\lambda(\varepsilon[\mathrm{L\,mol^{-1}\,cm^{-1}}]) = 860$ (1400), 775 (1400), 714 (1400), 596 (1700), 466 (2100), 420 (2400), 343 (3300) and 276 nm (4200)).

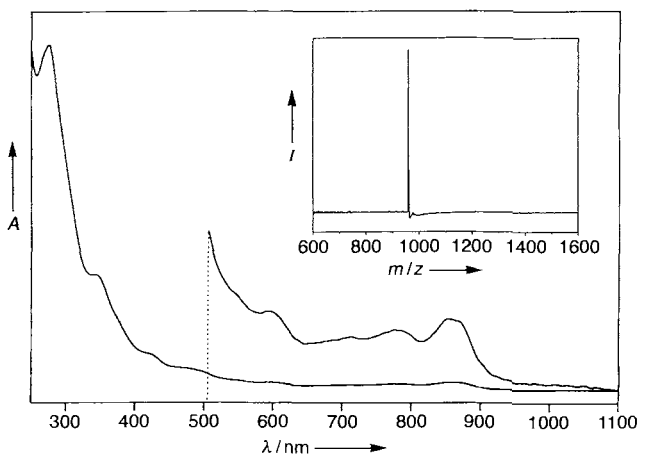

Fig. 1. UV/Vis spectrum of D_2-C_{80} in CH_2Cl_2 (the spectrum enhanced by a factor of 10 is shown in the range from 1100 to about 500 nm). A = absorption. The insert shows the laser-desorption time-of-flight mass spectrum (337 nm) obtained for the purified sample.

[*] Prof. M. Kappes, F. H. Hennrich, R. H. Michel, A. Fischer, S. Richard-Schneider, S. Gilb
Institut für Physikalische Chemie II der Universität
Kaiserstrasse 12, D-76128 Karlsruhe (Germany)
Fax: Int. code + (721)608 3310
e-mail: manfred.kappes@chemie.uni-karlsruhe.de
Dr. D. Fuchs, M. Bürk
Institut für Nukleare Festkörperphysik
Forschungszentrum Karlsruhe, D-76021 Karlsruhe (Germany)
Dr. K. Kobayashi, Prof. S. Nagase
Department of Chemistry, Faculty of Science
Tokyo Metropolitan University
Hachioji, Tokyo 192-03 (Japan)

[**] This work was supported by the Bundesministerium für Bildung und Forschung. We thank Prof. H.-J. Knölker (Institut für Organische Chemie, Karlsruhe) for facilitating the NMR measurement and Dr. Röttele for performing it.

Note that the absorption of C_{80} in CH_2Cl_2 (and toluene) solution between 325–335 nm is significantly smaller than that for other previously characterized higher fullerenes.[9,18] In contrast, the solubility of C_{80} in toluene (and CS_2) at room temperature was found to be roughly equivalent to that of C_{78} and C_{82}.

A ^{13}C NMR spectrum of the material dissolved in CS_2 (500 MHz Bruker pulsed FT NMR spectrometer, CCl_3D as internal lock) was obtained after accumulating 60000 scans (measurement time 3.5 days). In the region from $\delta = 129.3$ to 152.9 and at lower resolution the spectrum shows 18 lines with relative intensities between 2.77 and 4.10 and one stronger line of relative intensity 6.00, which at higher resolution splits into two resonances of roughly equal intensity. Considering the signal-to-noise ratio, the measurement is consistent with the presence of 20 groups of four symmetry equivalent carbon atoms (20×4). The experimentally determined chemical shifts and intensities are summarized in Table 1.

Table 1. C_{80} ^{13}C NMR line positions (experimental).

No.	δ [a]	$I_{rel.}$	No.	δ [a]	$I_{rel.}$
1	152.9	3.57	11	138.1	2.77
2	152.6	2.92	12	137.1	3.39
3	151.4	3.21	13	136.9	4.06
4	146.1	3.61	14	136.1	3.98
5	144.4	6.00[b]	15	135.3	3.33
6	143.8	4.10	16	134.2	2.88
7	142.8	3.93	17	133.0	3.54
8	142.6	4.00	18	131.1	3.31
9	138.9	3.22	19	129.3	3.63
10	138.7	3.32			

[a] Measurements in CS_2 solution at a signal-to-noise ratio of maximally 6. [b] At high resolution this line splits into two signals of roughly equal intensity at $\delta = 144.43$ and 144.45.

C_{80} has been the subject of numerous calculations at various levels.[15,19–22,28] There are seven possible IPR isomers of C_{80} at the level of ring combinatorics, which assumes identical pentagons and hexagons throughout.[1] Their symmetries are: I_h, D_{5d}, D_{5h}, D_3, D_2, C_{2v}, and C_{2v} (interestingly C_{80} is the first fullerene beyond C_{60} to allow an IPR isomer with I_h symmetry—albeit open shell). Several calculations that start from these structures and that allow some level of symmetry relaxation to take into account partially filled electronic levels have been performed.[19–21,28] Of these the most extensive so far predicts a (vibrationless) energy ordering at the HF/AM1 level (energy optimization in AM1 followed by single point HF/3-21G calculations): $D_5(D_{5d}) < D_2$ [+2.3] $< C_{2v}$ [+23.6] $< C_3(D_3)$ [+36] $< C_s(C_{2v})$ [+38.5] $< C_s(D_{5h})$ [+49.9] $< D_2(I_h)$ [+102], where the relaxed symmetry indicated (corresponding to optimized structures only slightly distorted away from the higher symmetry topological cage) derives from that in parentheses, and energies are listed in square brackets [kcal mol^{-1}] relative to the most stable $D_5(D_{5d})$ isomer.[15] Within the limits of error this cage is essentially isoenergetic with the D_2 isomer. In fact at the level of B3P density functional theory, the same study reveals a reversed ordering between these two structures with an even smaller energy difference. Note that in these calculations the optimal I_h derived cage is also found to have D_2 symmetry [$D_2(I_h)$]. The number of symmetry distinguishable carbon atoms corresponding to the seven relaxed structures derived from reference [15] and listed above are: 8 (8×10), 20 (20×4), 23 (6×2; 17×4), 28 (2×1; 26×3), 41 (39×2; 2×1), 44 (8×1; 36×2), and 20 (20×4). In principle, both D_2 structures would be consistent with the 20 distinguishable carbon atoms observed in the ^{13}C NMR spectrum. Furthermore, simple algebra shows that it is not possible to obtain these 20 lines by judicious combination of two or more of the other possible isomers. We therefore conclude on the basis of the calculations in reference [15] that the sample comprises D_2 or $D_2(I_h)$-C_{80}. Given the signal-to-noise ratio and the smaller number of NMR lines expected for the more symmetrical $D_5(D_{5d})$ isomer, we can further state that our isolated sample must contain $< 10\%$ $D_5(D_{5d})$-C_{80}.

While already unlikely on energetic grounds, we can rule out the presence of $D_2(I_h)$-C_{80} on the basis of NMR chemical shift calculations. For this purpose both D_2 isomers were examined with the HF-GIAO chemical shift subroutine implemented in Gaussian 94 using a 6-31G basis set and the HF/3-21G optimized structures of reference [15].[23,24] While not quantitatively predictive, the same procedure has previously been used with some success to calculate NMR chemical shift ranges for a number of higher fullerenes.[25] The ranges predicted here for both D_2 and $D_2(I_h)$ isomers were $\Delta\delta = 21.1$ and 38.9, respectively. Clearly the prediction for the D_2 isomer is in much better agreement with the measured value. Note that the correlation between local cage "surface" curvature (as quantified by π orbital axis vector (POAV) angle[26]) and chemical shift inferred in analogous work on C_{84} isomers[27] fails here—the $D_2(I_h)$ isomer, while predicted to have the larger shift range, is only slightly distorted away from I_h symmetry and therefore more spherical than the D_2 form. This is likely a function of the significantly less homogeneous charge density distribution about the atoms of the $D_2(I_h)$-C_{80} isomer.

In conclusion C_{80} can be isolated from K–H fullerene soot. Only one isomer is observed. This isomer has D_2 symmetry and as such is a chiral molecule. Its topology corresponds to one of the two essentially equienergetic IPR isomeric forms predicted to be the most stable on the basis of (vibrationless) ab initio calculations (Fig. 2).[15] We cannot completely rule out that the other stable $D_5(D_{5d})$-C_{80} form is also present in the soot extract (perhaps coeluting together with and therefore not separable from other much more abundant higher fullerenes). Note, however, that $D_5(D_{5d})$-C_{80} is expected to be more reactive (and perhaps less air-stable) than D_2-C_{80} on the basis of the HOMO–LUMO gap.[15] Furthermore, AM1 calculations performed to calculate hypothetical (isomerization) equilibrium constants K for C_{80} isomers at finite temperatures predict the D_2:$D_5(D_{5d})$ abundance ratio to increase with temperature on entropic grounds ($K > 1$ for $T > 1485$ K—much below arc temperature).[20]

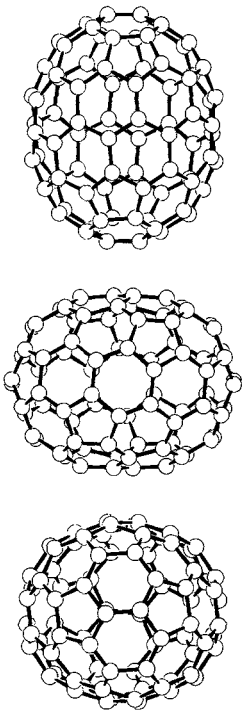

Fig. 2. Inertial axis projections of the D_2-C_{80} molecular structure (as derived from ab initio calculations in ref. [15]; only one enatiomer is shown; relative moments of inertia top:middle:bottom 1:0.95:0.80).

C_{80} appears in positive ion LD-TOF mass spectra of soot extracts with an intensity of less than the 20% of that of the most abundant high fullerene C_{84}.[11] In retrospect it may be that C_{80} has eluded isola-

tion due to an unfortunate combination of relatively low abundance in soot extract (it is the least abundant fullerene ion between C_{76}^+ and $>C_{96}^+$) and small near UV extinction coefficient (typical HPLC separation protocols use absorption detectors set to 330 nm). While a quantitative analysis of raw soot composition is not available, the solubility of C_{80} in solvents used for extraction is not dramatically less than that of other previously isolated cages. This suggests that the apparent low abundance of C_{80} in soot extracts may correlate with a low abundance in the raw material.

While a pronounced lability of C_{80} towards dissociation cannot be postulated on the basis of comparative electronic structure calculations published so far,[28] fragment mass spectra obtained for surface-collisionally activated C_{94}^+ ions, which dissociate by sequential C_2 loss, show an abundance discontinuity at C_{78}^+/C_{80}^+[29] (similar "ledges" occur also at C_{50}^+/C_{52}^+, C_{60}^+/C_{62}^+, and C_{70}^+/C_{72}^+). Such discontinuities have been observed in a variety of carbon cluster ion beam experiments sensitive to metastable decay rates which in turn reflect relative dissociation energies (evaporative ensembles[30]).[31] They generally occur at cluster sizes for which the higher mass is relatively labile and/or the fragment particularly stable. Conceivably then, the reaction

$$C_{80}^{+\bullet} \longrightarrow C_{78}^{+} + C_2 \qquad \text{(a)}$$

may be less endothermic than the corresponding dissociation of $C_{82}^{+\bullet}$ or $C_{78}^{+\bullet}$. There are indications that fullerene formation by graphite/helium arc proceeds at least in part by way of cations—such that these reactions may in fact occur within and at the boundary of the discharge.[32] Might the low abundance of C_{80} (as well as C_{74} and C_{72}?) reflect rate differences in a last evaporative step—before helium collisions freeze out the isomer distribution? Alternative (and perhaps complementary) explanations in terms of cage electron affinity/soot extraction kinetics need to be quantitatively explored.[33]

Received: April 9, 1996 [Z9006IE]
German version: *Angew. Chem.* **1996**, *108*, 1839 -1841

Keywords: ab initio calculations · fullerenes · NMR spectroscopy

[1] P. W. Fowler, D. E. Manolopoulos, *An Atlas of Fullerenes*, Oxford University Press, Oxford, **1995**.
[2] W. Krätschmer, L. D. Lamb, K. Fostiropoulos, D. R. Huffman, *Nature* **1990**, *347*, 354.
[3] H.-B. Bürgi, E. Blanc, D. Schwarzenbach, S. Liu, Y. Lu, M. M. Kappes, J. A. Ibers, *Angew. Chem.* **1992**, *104*, 667; *Angew. Chem. Int. Ed. Engl.* **1992**, *31*, 640.
[4] G. Roth, P. Adelmann, *J. Phys. I (France)* **1992**, *2*, 1541.
[5] R. Ettl, J. Chao, F. Diederich, R. Whetten, *Nature* **1991**, *353*, 149.
[6] K. Kikuchi, N. Nakahara, T. Wakabayashi, S. Suzuki, H. Shiromaru, Y. Miyake, K. Saito, I. Ikemoto, M. Kainosho, Y. Achiba, *Nature* **1992**, *357*, 142.
[7] See for example: A. Fonseca, H. Richter, R. Doome, J. Nagy, J. Gilles, P. Thiry, A. Lucas in *Proceedings of the International Winterschool on Electronic Properties of Novel Materials 1995* (Eds.: K. Kuzmany, J. Fink, M. Mehring, S. Roth), World Scientific, Singapore, **1995**, p. 17.
[8] T. Wakabayashi, K. Kikuchi, S. Suzuki, H. Shiromaru, Y. Achiba, *J. Phys. Chem.* **1994**, *98*, 3090.
[9] F. Diederich, R. Whetten, *Acc. Chem. Res.* **1992**, *25*, 119; R. Taylor, G. Langley, A. Avent, T. Dennis, H. Kroto, D. Walton, *J. Chem. Soc. Perkin Trans. 2* **1993**, 1029.
[10] Y. Achiba, K. Kikuchi, Y. Aihara, T. Wakabayashi, Y. Miyake, M. Kainosho in *Proceedings of the Nato Advanced Workshop on the Chemical Physics of Fullerenes* (Ed.: W. Andreoni), Kluwer, Dordrecht, **1996**.
[11] T. Kimura, T. Sugai, H. Shinohara, T. Goto, K. Tohji, J. Matsuoka, *Chem. Phys. Lett.* **1995**, *246*, 571.
[12] R. Michel, D. Fuchs, R. Beck, M. M. Kappes in *Proceedings of the International Winterschool on Electronic Properties of Novel Materials 1995* (Eds.: K. Kuzmany, J. Fink, M. Mehring, S. Roth), World Scientific, Singapore, **1995**, p. 89.
[13] M. Alvarez, E. Gillan, K. Holczer, R. Kaner, K. Min, R. Whetten, *J. Phys. Chem.* **1991**, *95*, 10561; D. Bethune, R. Johnson, J. Salem, M. de Vries, C. Yannoni, *Nature* **1993**, *366*, 123.
[14] T. Suzuki, Y. Maruyama, T. Kato, K. Kikuchi, Y. Nakao, Y. Achiba, K. Kobayashi, S. Nagase, *Angew. Chem.* **1995**, *107*, 1229; *Angew. Chem. Int. Ed. Engl.* **1995**, *34*, 1094.
[15] K. Kobayashi, S. Nagase, T. Akasaka, *Chem. Phys. Lett.* **1995**, *245*, 230.
[16] D. Fuchs, H. Rietschel, R. Michel, M. Benz, A. Fischer, M. M. Kappes in ref. [12], p. 105; see also: D. Fuchs, Dissertation, Universität Karlsruhe, **1996**.
[17] R. Michel, Dissertation, Universität Karlsruhe, **1996**.
[18] H. Ajie, M. Alvarez, S. Anz, R. Beck, F. Diederich, K. Fostiropoulos, D. R. Huffman, W. Krätschmer, Y. Rubin, K. Schriver, D. Sensharma, R. Whetten, *J. Phys. Chem.* **1990**, *94*, 8630.
[19] K. Nakao, N. Kurita, M. Fujita, *Phys. Rev. B* **1994**, *49*, 11415.
[20] M. Sun, Z. Slanina, S. Lu, F. Uhlik, L. Adamowicz, *Chem. Phys. Lett.* **1995**, *246*, 66.
[21] G. Scuseria in *Buckminsterfullerenes* (Eds.: W. Billups, M. Ciufolini), VCH, Weinheim, **1993**, p. 103.
[22] P. W. Fowler, F. Zerbetto, *Chem. Phys. Lett.* **1995**, *243*, 36.
[23] K. Wolinski, J. Hinton, P. Pulay, *J. Am. Chem. Soc.* **1990**, *112*, 8251.
[24] M. J. Frisch, G. W. Trucks, H. B. Schlegel, P. M. W. Gill, B. G. Johnson, M. A. Robb, J. Cheeseman, T. Keith, G. Petersson, J. Montgomery, K. Raghavachari, M. Al-Laham, V. Zakrzewski, J. Ortiz, J. B. Foresman, J. Cioslowski, B. Stefanov, A. Nanayakkara, M. Cahallacombe, C. Peng, P. Ayala, W. Chen, M. W. Wong, J. L. Andres, E. S. Replogle, R. Gomperts, R. L. Martin, D. J. Fox, J. S. Binkley, D. J. Defrees, J. Baker, J. J. P. Stewart, M. Head-Gordon, C. Gonzalez, J. A. Pople, Gaussian Inc., Pittsburgh, **1995**.
[25] C_{76} (D_2), C_{78} (C_{2v}) and C_{84} (D_{2d}) chemical shift ranges were calculated at the same level of theory as used here for C_{80}. Theoretical and corresponding experimental values were $\Delta\delta$ = 20.4/20.5, 18.1/14.8, and 9.7/9.6, respectively.
[26] R. Haddon, L. Scott, *Pure Appl. Chem.* **1986**, *58*, 137.
[27] U. Schneider, S. Richard, M. M. Kappes, R. Ahlrichs, *Chem. Phys. Lett.* **1993**, *210*, 165; D. Bakowies, M. Kolb, W. Thiel, S. Richard, R. Ahlrichs, M. M. Kappes, *Chem. Phys. Lett.* **1992**, *200*, 411.
[28] See for example: B. Zhang, C. Wang, K. Ho, C. Xu, C. Chan, *J. Chem. Phys.* **1993**, *98*, 3095.
[29] R. Beck, J. Rockenberger, C. Warth, P. Weis, M. M. Kappes, *J. Chem. Phys.* **1996**, *104*, 3629.
[30] See for example: E. Rohlfing, D. Cox , A. Kaldor, *J. Chem. Phys.* **1984**, *81*, 3322; P. Radi, T. Brunn, P. Kemper, M. Molchan, M. Bowers, *ibid.* **1988**, *88*, 2809; P. Radi, M. Rincon, M. Hsu, J. Brodbelt-Lustig, P. Kemper, M. Bowers, *J. Phys. Chem.* **1989**, *93*, 6187.
[31] See for example: R. Wörgötter, B. Dünser, P. Scheier, T. Märk, *J. Chem. Phys.* **1996**, *104*, 1225.
[32] See for example: R. Bunshah, S. Jou, S. Prakash, H. Doerr, L. Isaacs, A. Wehosig, C. Yeretzian, H. Cynn, F. Diederich, *J. Phys. Chem.* **1992**, *96*, 6866.
[33] See for example: O. Boltalina, E. Dashkova, L. Sidorov in *Proceedings of the International Winterschool on the Properties of Novel Materials 1996* (Eds.: H. Kuzmany, S. Roth, J. Fink, M. Mehring), unpublished results.

 © VCH Verlagsgesellschaft mbH, D-69451 Weinheim, 1996 0570-0833/96/3515-1734 $ 15.00+.25/0

A "Heck" of a Lot of Chemistry

Palladium Reagents and Catalysts. Innovations in Organic Synthesis. By *J. Tsuji*. Wiley, Chichester, 1995. 560 pp., hardcover £125.00.–ISBN 0-471-95483-7

Palladium is justifiably regarded as the transition metal with the greatest variety of potential applications in organic synthesis. Many different reactions are catalyzed or initiated by palladium complexes, and the leading chemistry journals contain articles reporting synthetic uses of palladium in almost every issue. Because of the continuing flood of new publications in this area, much time and effort is absorbed in keeping up with the latest developments. Thus there was certainly a need for an up-to-date monograph on palladium reagents in organic synthesis.

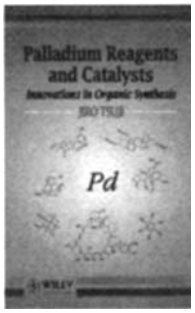

The book by J. Tsuji fulfills this need in exemplary style. Over 2500 literature references, extending up to the beginning of 1994, are treated under the relevant topic areas with succinct commentaries, in a way that ensures lucidity and ease of use despite the vast amount of information. The schemes showing the important reactions and mechanisms are clear and of a high quality.

The subject index lists reagents, substrates, target molecules, and some named reactions. Reactions of a particular type can be found by using the contents list in conjunction with following the systematic arrangement of the subject matter. This system is based on the mechanisms that the reactions are assumed to involve according to current knowledge. It is a pragmatic and effective approach, although one may occasionally question the assumptions, as there still remains much to be learned about the mechanisms of palladium-catalyzed reactions.

The contents are arranged in five chapters of widely differing lengths. Chapter 1 (12 pp.) summarizes the fundamentals and main features of palladium chemistry, including the structures and properties of some important (mostly commercially available) palladium complexes and information about commonly used ligands. Some basic reactions of palladium complexes are described, and the chapter ends with a comprehensive list of references for further reading. Chapter 2 consists of only six pages, giving additional basic information about stoichiometric and catalytic reactions of palladium.

Chapter 3 is much longer (106 pp.), and covers oxidative reactions using palladium(II) compounds. After a short introduction (Section 1), the Wacker process and related reactions are described in Section 2. The following sections are devoted to stoichiometric reactions of π-allyl complexes and to transformations of various compounds (dienes, allenes, alkynes, arenes, and many more) that are induced or catalyzed by palladium(II) compounds.

Chapter 4 is by far the longest (over 400 pp.) and deals with catalytic reactions of palladium(0) and palladium(II). The two main topics are the reactions of organic halides and pseudohalides catalyzed by palladium(0), including examples such as the Heck reaction and the Suzuki coupling (Section 1), and the reactions of allyl compounds, again catalyzed by palladium(0) (Section 2). As an example to illustrate the systematic arrangement of the subject matter adopted throughout the book, let us assume that we wish to find the Stille reaction in Chapter 4. This reaction uses organic halides or pseudohalides as substrates, so we go first to Section 1.1. An organometallic compound is used as the coreactant, which takes us to Section 1.1.4. More specifically this is an organotin compound, so finally we arrive at Section 1.1.4.5. The Stille reaction could actually be found more easily from the contents list, but the same would not be true of the related coupling reactions using organocopper or organozinc compounds, as these are not named reactions–for these one must rely on the system described above.

Chapter 5 (22 pp.) covers other reactions that could not appropriately be included in the preceding chapters, such as the palladium-catalyzed Cope rearrangement and the decarbonylation of aldehydes.

In his preface the author writes that it is better to finish an imperfect book than never to finish a perfect one. In any event this is a very good and useful book which provides a detailed survey of palladium chemistry. There is scarcely a single important publication that is not cited. It should be followed in due course by an updated second edition.

Gerald Dyker
FB6, Organische
und Metallorganische Chemie
der Universität-Gesamthochschule
Duisburg
Duisburg (Germany)

Metals and Ligand Reactivity. By *E. C. Constable*. VCH Verlagsgesellschaft, Weinheim, 1996. 308 pp., hardcover DM 128.00/paperback DM 68.00.—ISBN 3-527-29278-0/3-527-29277-2

What common ground is there between coordination chemistry, a traditional area of inorganic chemistry, and organic chemistry? That is the question addressed by Edwin C. Constable in the new and completely revised edition of the above book; the reader seeking an answer will find it here. The author discusses a large number of examples which show that "inorganic" coordination compounds can certainly undergo "organic" reactions, and that complexation with metal ions alters the reactivity of "organic" molecules. The discussion spans the range from special types of syntheses and aspects of (metallo)supramolecular chemistry—a modern

This section contains book reviews and a list of new books received by the editor. Book reviews are written by invitation from the editor. Suggestions for books to be reviewed and for book reviewers are welcome. Publishers should send brochures or (better) books to the editorial office: Redaktion Angewandte Chemie, Postfach 101161, D-69451 Weinheim, Germany. The editor reserves the right of selecting which books will be reviewed. Uninvited books not chosen for review will not be returned.

symbiosis of organic and inorganic chemistry—to bioinorganic chemistry.

The first chapter gives a concise but clear and understandable introduction to the basic principles of coordination chemistry, from crystal field theory via MO theory to the thermodynamic and kinetic aspects of coordination compounds. In the second chapter the author begins by discussing the effects of ligands on metal centers, then considers the situation from the opposite standpoint by focusing attention on the effects of coordinated metals on the properties of the ligands, taking into account electronic effects as well as steric and conformational effects. Unfortunately the book is so constructed that these first two chapters have had to be kept rather brief, and consequently they give only a sketchy outline and cannot equip the reader with a detailed understanding.

The chemistry of carbonyl compounds and their derivatives has an important role in organic chemistry, and accordingly it is a central theme of Chapters 3 and 4 (which cover reactions with nucleophiles) and Chapter 5 (reactions with electrophiles). The various types of reactions that can occur are described and illustrated by many examples.

Chapter 6 is concerned with the template effect and the synthesis of macrocyclic ligands. In Chapter 7 the results from the previous chapter are extended to three-dimensional space, which leads to the introduction and detailed discussion of concepts such as supramolecular chemistry, molecular topology, molecular recognition, and self-assembly.

Chapter 8 deals with the chemistry of arenes. The author shows that the typical reactions of aromatic compounds [such as $S_E(Ar)$ and $S_N(Ar)$ reactions] can certainly also occur in the ligand sphere of metal complexes. Chapter 9 is concerned with oxidation and reduction reactions, then the tenth and final chapter emphasizes the importance of the reactive properties of coordination compounds in biological processes, illustrated by a few well-chosen examples. In this chapter the author bridges the gap between coordination chemistry and the area generally called bioinorganic chemistry. Examples drawn from metallo-enzyme chemistry and protein chemistry serve as a brief introduction to this interdisciplinary field between inorganic chemistry and biochemistry.

Regrettably, catalytic reactions of coordination compounds are not included, despite this being a potentially fruitful area for applying the principles of coordination chemistry to organic synthesis. A nice example of this would be the Sharpless epoxidation, illustrating the high catalytic efficiency and degree of stereochemical control that can be achieved using metal complexes.

The book has not been written for the reader whose main interest is in preparing organometallic compounds (e.g. carbene complexes) and in organometallic syntheses. The author has deliberately limited the scope to classical "Alfred Werner" complexes. Thus, the book contains an excellent collection of examples illustrating the "organic chemistry" of coordination compounds, and it is suitable both for students majoring in chemistry and for more advanced readers.

The author's clear and systematic presentation aids the reader's understanding, while the excellent figures and schematic diagrams illustrating chemical principles explain the important relationships very effectively. However, a few small errors in the formulas have slipped through; for example in Figure 2-31 the charges are incorrect, in Figure 3-14 an NH group is missing from the formula of the likely intermediate, and the ligand 7.57 shown on page 220 has two extra methylene groups which should not be present. References to material for further reading enable the reader to follow up selected topics in greater depth. These references concentrate on secondary rather than primary literature, so as to give as broad a range of information sources as possible. The author's comments on the publications cited are an additional aid to selection.

Compared with the first edition (published in 1990 by Ellis Horwood) the most important difference is in the more detailed treatment of supramolecular chemistry. Also the examples discussed and the clear definitions of relevant basic terms are undoubtedly an improvement on the earlier version. I unhesitatingly recommend everyone with an interest in the subject to buy this book.

Markus Albrecht
Institut für Organische Chemie
der Universität Karlsruhe (Germany)

Encyclopedia of Reagents for Organic Synthesis. Vols. 1–8. Supervising editor: *L. A. Paquette*. Wiley, Chichester, 1995. 6223 pp., hardcover £ 1750.00.—ISBN 0-471-93623-5

"Paquette": a reference source on reagents. There can scarcely be a student who, when reading the current literature, does not frequently encounter reagents about which he or she knows little or nothing, often in the form of strange abbreviations above reaction arrows (such as DMTSF, MoOPH, PMDTA, or TMANO), and without even a reference to the original publications. Is it not also true that even experienced synthetic chemists need quick access to information about this or that reagent in their everyday work, especially when they must decide which one to try next for performing a desired transformation? The choice of reagents nowadays available for organic syntheses is enormous. The development of new synthetic methods and the discovery of new applications for familiar reagents has progressed steadily for many decades. In some cases reagents described in the literature have been shown to be dangerous, or their synthetic applications have not developed further and they have disappeared into the back of the filing cabinet. It is becoming increasingly difficult to find one's way through this jungle of information on potential applications, knowledge, and experience.

It is not surprising, therefore, that there is a great demand for easily accessible, concise, and above all reliable sources of information about synthetic reagents. One can well understand the success of "Fieser and Fieser" (*Reagents for Organic Synthesis*), which has served its readers for nearly thirty years, but is now showing its age and becomes more expensive and less convenient with each supplementary volume.

However, thanks to this work edited by L. A. Paquette and a team of well-known American synthetic chemists (S. D. Burke, R. M. Coates, R. L. Danheiser, S. E. Denmark, F. J. Hart, L. S. Liebeskind, D. C. Liotta, A. J. Pearson, H. J. Reich, J. H. Rigby, and W. R. Roush), life is now becoming a little easier. The eight volumes in their brick-red colored bindings contain about 6000 approximately A4-sized pages printed in two-column format, covering over 3500 reagents in alphabetical order (named according to IUPAC rules, from acetaldehyde to zirconium tetraisopropoxide). A comprehensive index is provided at the end of the last volume.

This "Paquette" makes a favorable impression from the start, with its handsome appearance, the very clear typeface with tastefully inserted structural formulas, and a good quality paper which is not too thin and will withstand photocopying. More important, however, is the outstandingly high quality of its contents. All the contributions on individual reagents have been written by carefully chosen experts, often by those whose names one automatically associates with those reagents, and the effort devoted to bring-

 © VCH Verlagsgesellschaft mbH, D-69451 Weinheim, 1996 0570-0833/96/3515-1736 $ 15.00+.25/0

ing together the best expert knowledge has paid off handsomely. Altogether more than a thousand scientists from 40 countries were involved, and the editors must be admired and congratulated on the excellent coordination that they have achieved.

Each reagent is treated in a clear and unambiguous style, beginning with the structural formula, the CA Registry number(s), the molecular formula, the molecular mass, and the function of the reagent (in abbreviated form). These details are followed by the main features of its physical properties, solubility, the form in which it occurs and is commercially available, its preparation, purification, and analysis for purity, then information about its handling, storage, possible hazards, and necessary precautions. There is then a brief and succinct description of the reagent's uses, always with references to the original publications. The descriptions are mainly along phenomenological lines; thus, with few exceptions the reaction mechanisms are not discussed.

The lengths of the articles on individual reagents vary from half a page to ten pages; for a few reagents the number of literature references is well over 100. To save space journals are abbreviated according to initial letter codes [e.g., *Angew. Chem. Int. Ed. Engl.* becomes *AG(E)*]; however, these are always easily decoded by referring to a list inside the back cover. Another very useful feature is the general glossary of abbreviations provided on the front inside cover of each volume, which allows one to quickly find the meaning of reagent abbreviations such as those mentioned earlier—for example, DMTSF is dimethyl(methylthio)sulfonium tetrafluoroborate). Both these lists of abbreviations are mentioned at the foot of every other page, alternating with the thoughtful warning "Avoid skin contact with all reagents".

The clear structure and systematic layout of "Paquette" deserve praise, and in this connection one must also mention the index of more than 600 pages, which consists of four parts. If one were looking for a particular reagent (e.g., "Eschenmoser's salt") but did not know its IUPAC name [which in this example would be dimethyl(methylene)ammonium iodide], it could be found easily by searching in one of the other three separate indexes via the molecular formula (under "C_3H_8IN") or the structural class ("Nitrogen reagents: Iminium salts") or the mode of action ("Alkylating reagents: Electrophilic"). Alternatively, however, one could find it in the general subject index (which is itself enormously long) by searching under either the trivial name or the systematic name. This reagent also appears elsewhere in the general index, for example under "Mannich reaction" and under "Amines, tertiary, synthesis". Having then found the actual article, one discovers that the information is not confined to the iodide but also covers other salts such as the chloride (although this is not listed anywhere in the index!). This illustrates another characteristic of "Paquette", namely that although most of the articles belong nominally to a single reagent they often contain information on other closely related reagents. Thus, for example, one finds information on trimethylsilylacetic acid methyl ester in the article on the corresponding *ethyl* ester, and lithium-trimethoxyaluminum hydride is mentioned in the article on lithium-tri-*t-butoxy*-aluminum-hydride.

It is obvious that with these different indexes one has at one's disposal a variety of "navigational instruments". Thus every serious user of the work will quickly learn to find his or her way around within it and obtain answers to different types of questions. In this respect the notes on related reagents included at the ends of many of the articles are very useful, as they allow one to quickly find information about alternatives.

However, care is also needed! For example, a reader wanting information about the asymmetric reduction of ketones will quickly discover that the general subject index cannot always be relied on, despite its comprehensiveness. Thus the CBS reduction method (arguably the most important for enantioselective reductions) can only be found indirectly in this index, by looking up keywords such as "Oxazaborolidines" or "α,α-Diphenyl-2-pyrrolidinemethanol". Evidently, therefore, the user with some previous knowledge would fare better; in fact he or she could also find the CBS reagents by looking in the *Reagent Structural Class Index* under "Boron reagents: Boranes". However, in a case like this it would seem even better to use the *Reagent Function Index*; here, under "Reducing reagents: Chiral", we find a list of 15 reagents, including the one we are looking for under the name "Tetrahydro-1-methyl-3,3-diphenyl-1H,3H-pyrrolo[1,2-c]-[1,3,2]oxazaborole". When we look up the information on this reagent we find an excellent review of the method in question, in an article whose content overlaps considerably with that on "α,α-Diphenyl-2-pyrrolidinemethanol".

It is obvious that a work of this kind cannot be completely encyclopedic in the strict sense of the word. However, the editors have presented an excellent and well-balanced selection which includes most of the important reagents. Transition metal reagents and catalysts are particularly well covered. On the other hand there is far too little on enzymes. The two short articles on bakers' yeast and esterases are all that I could find in this area, and it is unfortunate that other "bioreagents" such as aldolases, alcohol dehydrogenases, lipases, and glycosyl transferases are completely absent. Also, in this era of combinatorial chemistry it would have been desirable to include some articles on support materials for solid phase synthesis, such as Merrifield resins or modified silica gels. Another shortcoming, which "Paquette" has in common with many other large works of reference, is the wide variation in the up-to-dateness of the contributions. A glance at the lists of references shows that in many of the articles the literature coverage extends only to 1992 or 1993. This seems all the more surprising when, on leafing through the volumes, one suddenly (although rarely) comes across references from 1994 or even 1995 (!).

However, on the whole this is an excellent work which fully meets its objectives and comes up to one's highest expectations. It will be of enormous value to both students and practicing chemists. The publication of this new reference source is evidence that even in the age of computerized information media the conventional form of the encyclopedia is still a worthwhile endeavor (although that is not to say that a CD-ROM version would not find a ready market, especially since it would be easier to update).

This "Paquette" should find an honored place in every laboratory engaged in synthesis and in every chemistry library. Chemists working on organic synthesis will gain a competitive advantage by keeping it within easy reach. I fully share the view expressed by L. A. Paquette in his preface that we can "...expect the *Encyclopedia of Reagents for Organic Synthesis* to play a vital role in stimulating creative research in organic chemistry in the years immediately ahead".

Hans-Günther Schmalz
Institut für Organische Chemie
der Technischen Universität Berlin
Berlin (Germany)

 © *VCH Verlagsgesellschaft mbH, D-69451 Weinheim, 1996* *0570-0833/96/3515-1737 $ 15.00+.25/0*

Encyclopedia of Inorganic Chemistry. Edited by *R. B. King*. Wiley, Chichester/New York, 1994. Eight volumes. CLXXVI, 4819 pp., hardcover $ 2500.00.—ISBN 0-471-93620-0

During the first four decades of this century inorganic chemistry languished in the doldrums until World War II ushered in the resurgence in the field that the late Sir Ronald S. Nyholm called the "renaissance in inorganic chemistry". Inorganic chemistry encompasses an amazing variety of structurally diverse substances—molecular, ionic, coordination, and organometallic compounds of the roughly one hundred elements now known (with the exception of those compounds of carbon that are the province of organic chemistry) as well as materials such as metallobiomolecules, semiconductors, ceramics, and minerals.

Yet, despite the increased activity in the field during the past half-century, inorganic chemistry has lacked a modern comprehensive encyclopedia, although multivolume treatises on the elements and their compounds such as *Gmelins Handbuch der anorganischen Chemie*, J. N. Friend's *Textbook of Inorganic Chemistry*, J. W. Mellor's *Comprehensive Treatise on Inorganic and Theoretical Chemistry*, P. Pascal's *Nouveau Traité de chimie minérale*, and N. V. Sidgwick's *The Chemical Elements and Their Compounds* have long been available. More recently, modern comprehensive monographs on specialized aspects of inorganic chemistry have appeared, such as Sir Geoffrey Wilkinson, Robert D. Gillard, and Jon A. McCleverty's 7-volume *Comprehensive Coordination Chemistry* (Pergamon, 1987), G. Wilkinson, F. Gordon A. Stone, and Edward W. Abel's 9-volume *Comprehensive Organometallic Chemistry* (Pergamon, 1982), and E. W. Abel, F. G. A. Stone, and G. Wilkinson's 14-volume *Comprehensive Organometallic Chemistry II* (Pergamon, 1995). Perhaps the multivolume set that came closest to the volume under review here is M. Cannon Sneed, J. Lewis Maynard, and Robert C. Brasted's projected 11-volume *Comprehensive Inorganic Chemistry* (only 8 volumes of which were published; 1979 pp., Van Nostrand, 1953–1961), but it was more of a textbook by a limited number of authors (15) than a true encyclopedia. Thus the *Encyclopedia of Inorganic Chemistry* (*EIC*) reviewed here fills a real gap in the literature.

Editor-in-Chief R. Bruce King of the University of Georgia, together with an Editorial Board of five prominent American chemists and an International Advisory Board of 11 chemists from nine countries, including 1987 Nobel laureate Jean-Marie Lehn, has assembled an outstanding group of 304 contributors from 21 countries to produce what should be a definitive reference source for some time to come. The authors, whose names and addresses are listed in Vol. 8, are all prominent authorities who were selected for their expertise in the subjects of their articles, e.g., Robert J. Brotherton (Boron: Inorganic Chemistry), Harold W. Kroto (Carbon: Fullerenes), Stephen J. Lippard (Platinum-Based Anticancer Drugs), Gabor A. Somorjai (Heterogeneous Catalysis by Metals), and Robert C. West (Polysiloxanes and Polysilanes).

For ready reference the *EIC* is arranged alphabetically from Ab Initio Calculations to Zwitterion, with 260 signed main articles (with their contents clearly listed at the beginnings and with numbered sections, subsections, and sub-subsections) dealing with individual topics in a self-contained manner but with frequent references to other articles; 864 short entries defining or explaining important concepts or providing valuable data; and more than 340 cross-reference entries to help locate specific topics. In any article cross-references to definition entries are indicated by italics, while cross-references to other main articles are indicated by bold italics. Abbreviations and terms specific to a given article are defined in the Abbreviations and Glossary sections at the beginning of the article. A list of related main articles is given at the end of each article, followed by extensive, up-to-date literature references, some as recent as 1993 and many to review articles and seminal papers to guide the reader to sources of more detailed information. (For all articles the number of the page on which the references begin is given as a footnote on each right-hand page). A particular subject can be located either directly, by consulting the appropriate alphabetical place, or from the detailed (295 pp.) index in Vol. 8.

The Periodic Table, with the group numbers 1 to 18 as recommended by the International Union of Pure and Applied Chemistry (IUPAC) rather than the older Mendeleev numbers I–VIII and with the symbols for elements 104–109 as endorsed by the Nomenclature Committee of the American Chemical Society (rather than the controversial ones proposed by IUPAC after the *EIC*'s publication) appears on the inside front cover, while four columns of general abbreviations appear on the back endpapers. Each volume contains: Preface; Foreword, which lists the main articles under the six areas of inorganic chemistry assigned to the editors—main group elements, transition metals, organometallics, bioinorganic chemistry, solid state, and physical and theoretical methods (4 pp.); and Table of Contents, which lists alphabetically, with page numbers, all the main and definition articles in the entire *EIC* (10 pp.). Most of the articles are written at an appropriate level for a research student seeking an entry to the literature of an area. The index does not direct readers to authors of references cited in the main articles; an author index of this sort would have been quite useful.

The listing of the articles under the six areas covers the field of inorganic chemistry quite well. This umbrella covers many new areas although it is not, nor could it be, completely exhaustive.

The sections that include main group element chemistry will be particularly useful, since this area has not been reviewed in such detail for many years. It is gratifying to see the excellent treatment of the inorganic chemistry of the noble gases (Boris Žemva) and the discussion of hypervalent compounds (Michael Lattman). The coverage here is reasonably complete and greatly adds to the more classical and narrower focus found in other treatises such as *Comprehensive Coordination Chemistry* and *Comprehensive Inorganic Chemistry*. Of course, the organizational method by bond type generally conceals many of the periodic relationships that already exist and continue to be revealed in this chemistry. Nonetheless, the knowledgeable reader will be able to extract relationships as desired.

The transition metal articles give excellent coverage of inorganic and coordination chemistry of the actinide elements (Grigorii L. Soloveichik), an ambitious undertaking in view of the specialized nature of these elements. The table summarizing "Discovery of the Actinides" is remarkably accurate except for inclusion of a curious reaction to represent the synthesis of plutonium. The table "Main Properties of the Actinides" is generally well done but includes unexpected mistakes (such as in the electronic configuration of Cm^{3+} ions).

Unfortunately, the chemistry of the transactinide elements, rutherfordium (Rf) and hahnium (Ha), is ignored; this is a very interesting area of recent research. Also, a more extensive discussion of the Periodic Table would have been appreciated in view of recent developments at the heavy end.

The sections on organometallics and bioinorganic chemistry cover these areas very well.

Although there are concise and accurate discussions of nuclear matters, a brief discussion of nuclear chemistry might have been appropriate. The use of inorganic chemistry in nuclear studies has a long history and is of continuing importance.

In keeping with the traditional interests of inorganic chemists, most of the theoretical content of the *EIC* concerns bonding models. Three articles on the electronic structures of main-group compounds (Jeremy K. Burdett), organometallics (Thomas A. Albright), and solids (Enric Canadell) all emphasize qualitative, one-electron aspects of bonding. Readers will find much in the first two articles that these authors have previously discussed in books. Canadell expends some effort in weaving the terminology of solid state physics with bonding concepts familiar to many inorganic chemists. Paul T. Czech gives a fairly standard account of qualitative molecular orbital theory in general. The discussion of bonding in clusters given by David J. Wales leans on electron counting and topological schemes, having much in common with his recent book with D. Michael P. Mingos.

It is fair to say that quantitative computational approaches have not yet had as much impact on inorganic chemistry as on organic chemistry, and this is reflected in the coverage in the *EIC*. It is probably also inherently difficult to give an effective treatment of quantitative theoretical approaches in an encyclopedia format aimed at non-theoreticians. Brief accounts tend to be useless; if the reader does not know what the Fock equations are or has not been introduced to density functional theory, the *EIC* is not a realistic place to start. Still, given the pace of change in computing and computational methodology, we suspect that the relatively low profile of quantitative theory in the *EIC* may soon be inappropriate.

Solid state chemistry is much more prominently represented in the *EIC* than in even the most recent textbooks of inorganic chemistry, where the discipline is still given a rather peripheral role. Textbook authors would do well to bear this in mind. Many of the articles are quite good; some are truly outstanding. Klaus Yvon gives a comprehensive and nicely illustrated treatment of solid state hydrides, Hans Georg von Schnering and Wolfgang Hönle present a valuable and authoritative article on phosphides, and William H. McCarroll gives a concise and elegant introduction to solid state oxides. Douglas A. Keszler's article on borates is a fine blend of basic preparative and structural chemistry combined with a useful discussion of physical properties. Indeed, there are several other good articles concerning boron chemistry. The article by Jeremy K. Burdett and John R. Rodgers on structure–property maps is a welcome contribution; such maps seem destined to influence workers who wish to find empirical guides for preparing materials with particular properties in mind. Some connections to topical materials preparation can be found in articles on thin-film synthesis (Chunming Niu and Charles M. Lieber) and organometallic precursors to metallic materials (Herbert D. Kaesz, Alfred Zinn, and Lutz Brandt). Readers will also find good introductory articles on sol–gel synthesis (Jacques Livage) and intercalation chemistry (Allan J. Jacobson). Solid state chemistry tends to have a strong structural emphasis, but many of the articles in the *EIC* will be useful because they also contain good discussions of synthesis and/or properties of compounds.

The encyclopedia is extensively illustrated with photographs, concise tables, line drawings, diagrams, figures, equations, reaction schemes, and computer-drawn structural formulas. Many subjects or terms are defined in only one or two sentences; others are reviewed and referenced in great detail over several pages. This contrast in coverage is to be expected from a comprehensive reference that is less than 5000 pages long. The emphasis on recent developments such as fullerenes, superconductivity, bioinorganic catalysts, and the biology of nitric oxide ensures that the *EIC* will remain topical for many years.

Considering its broad scope and multiple authorships, the *EIC* is exceptionally accurate; the few errors are decidedly minor, such as misspellings (Herault for Héroult, p. 1357), lack of diacritical marks (Delepine for Delépine, p. 985), and the listing of Vaska's complex twice in the Contents (p. XXII). This excellent, up-to-date, comprehensive, easy-to-use, and modestly priced reference work provides more information than is available in single-volume works, without being so large as to be beyond the reach of all but a few well-endowed academic and industrial libraries or affluent individuals. It should be of interest and use not only to inorganic chemists but also to organic, physical, and analytical chemists, biochemists, chemical engineers, materials, earth, and environmental scientists, physicists, biologists, and anyone seeking information on and ideas for new research in one of the most active fields of chemistry today.

George B. Kauffman
California State University
Fresno, CA (USA)

Timothy R. Hughbanks
Texas A & M University
College Station, TX (USA)

Glenn T. Seaborg
Lawrence Berkeley Laboratory
Berkeley, CA (USA)

Harry B. Gray
California Institute of Technology
Pasadena, CA (USA)

Robert T. Paine, Jr.
University of New Mexico
Albuquerque, NM (USA)

 © *VCH Verlagsgesellschaft mbH, D-69451 Weinheim, 1996* *0570-0833/96/3515-1739 $ 15.00+.25/0*

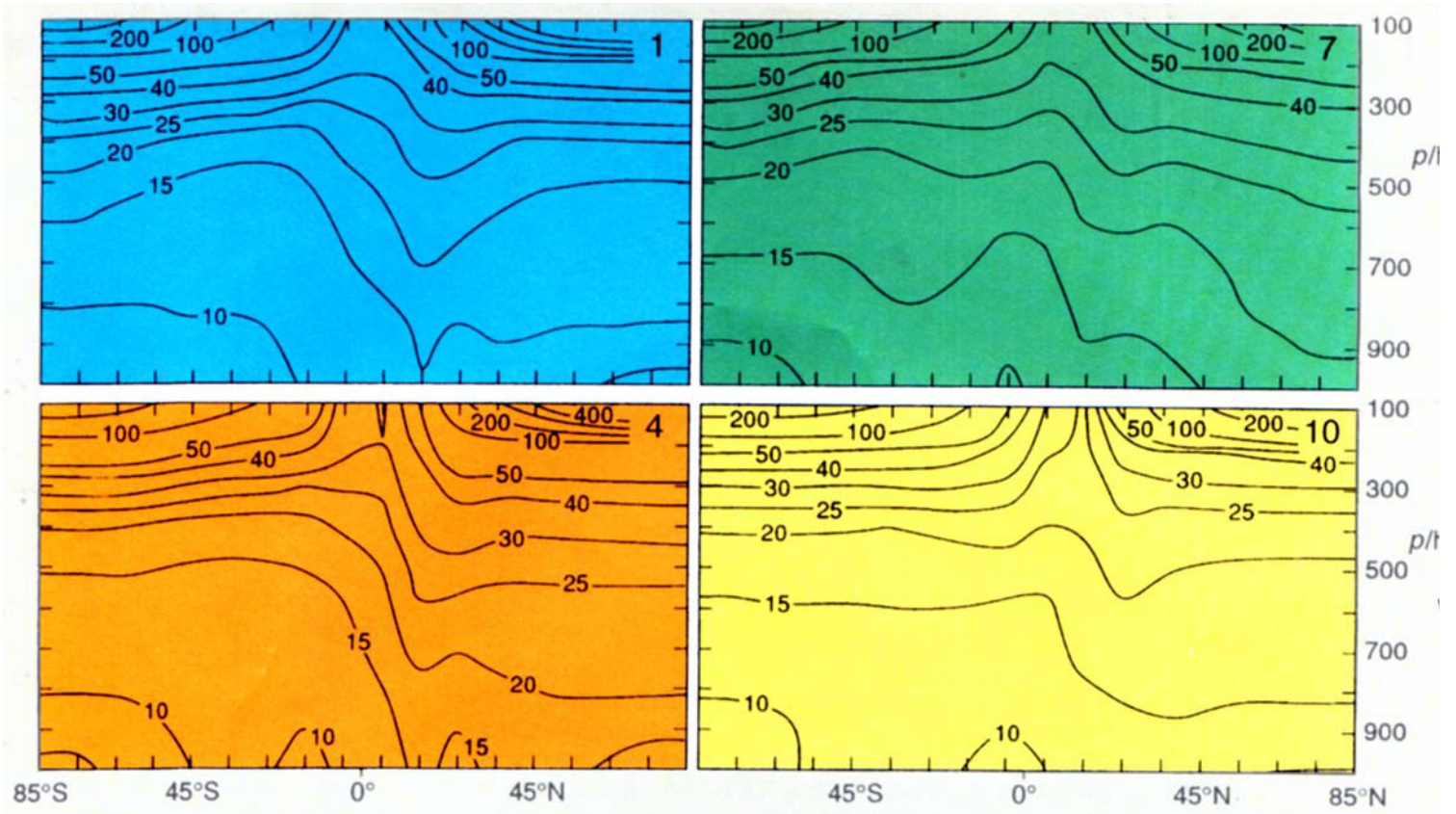

The calculated zonal monthly average concentrations of O_3 in the troposphere have changed substantially from the preindustrial period (top) to 1985 (bottom). Particularly in the northern hemisphere the O_3 concentration has increased substantially as a result of increased emissions of NO, CH_4 and CO.

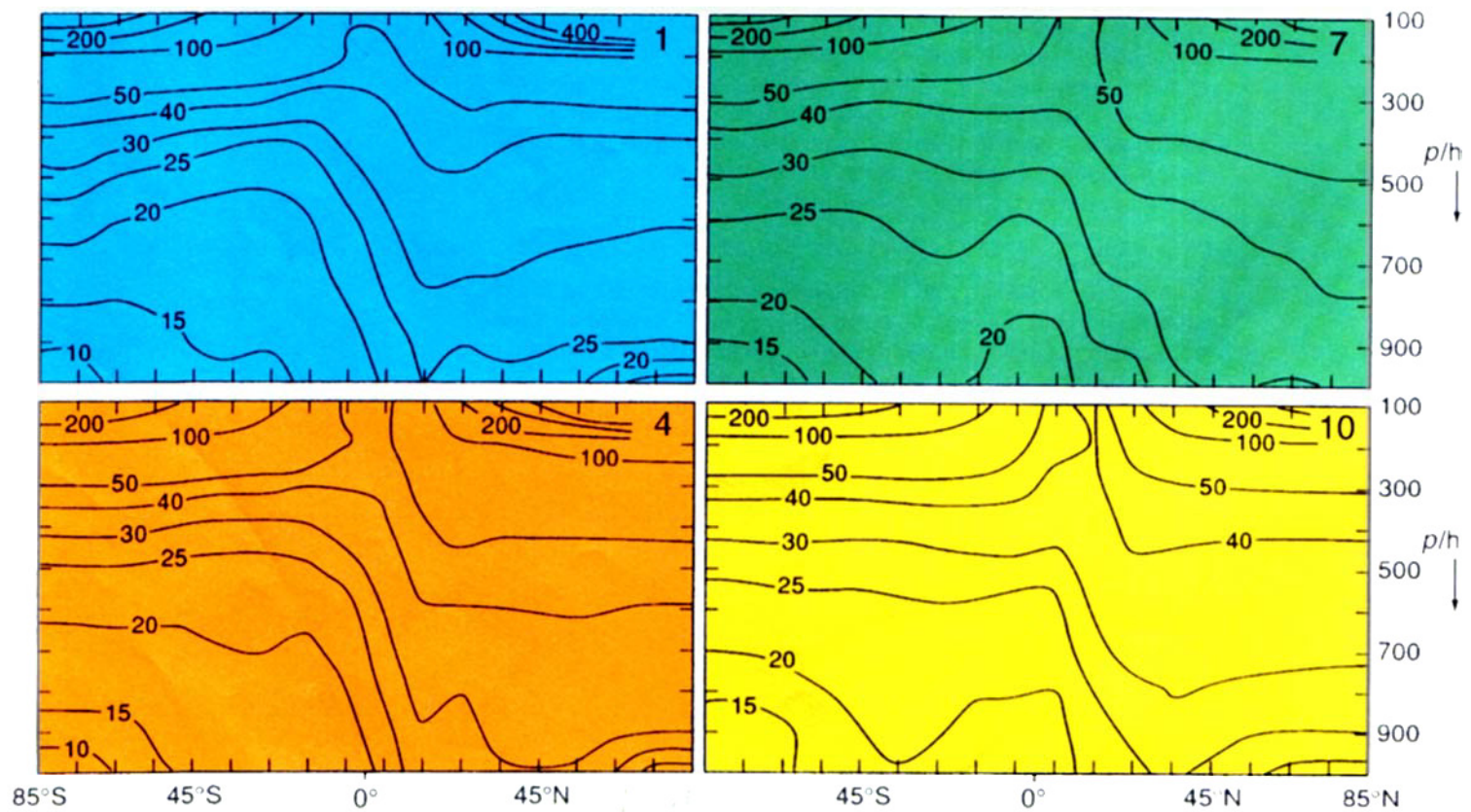

My Life with O_3, NO_x, and Other YZO_x Compounds (Nobel Lecture)**

Paul J. Crutzen*

To the generation of Jamie Paul and our future grandchildren, who will know so much more and who will celebrate the disappearance of the ozone hole. I hope you will not be disappointed with us.

The Background of an Ozone Researcher

I was born in Amsterdam on December 3, 1933, the son of Anna Gurk and Jozef Crutzen. I have one sister, who still lives there with her family. My mother's parents moved to the industrial Ruhr region in Germany from East Prussia towards the end of the last century. They were of mixed German and Polish origin. In 1929 at the age of 17, my mother moved to Amsterdam to work as a housekeeper. There she met my father. He came from Vaals, a little town in the southeastern corner of the Netherlands, bordering Belgium and Germany and very close to the historical German city of Aachen. He died in 1977. He had relatives in the Netherlands, Germany, and Belgium. Thus, from both parents I inherited a cosmopolitan view of the world. My mother, now 84 years old, still lives in Amsterdam, mentally very alert, but since a few months ago, wheelchair-bound. Despite having worked in several countries outside the Netherlands since 1958, I have remained a Dutch citizen.

Paul Crutzen

In May 1940 the Netherlands were overrun by the German army. In September of the same year I entered elementary school, "de grote school" (the big school), as it was popularly called. My six years of elementary school largely overlapped with the Second World War. Our school class had to move several times to different premises in Amsterdam after the German army had confiscated our original school building. The last months of the war, between the fall of 1944 and Liberation Day on May 5, 1945, were particularly horrible. During the cold "hongerwinter" (winter of famine) of 1944–1945 there was a severe lack of food and heating fuels. Also water for drinking, cooking, and washing was available only in limited quantities for a few hours per day, which caused poor hygienic conditions. Many died of hunger and disease, including several of my schoolmates. Some relief came at the beginning of 1945 when the Swedish Red Cross dropped food supplies by parachute from airplanes. To welcome them we waved our red, white, and blue Dutch flags in the streets. I had, of course, not the slightest idea how important Sweden would become later in my life. We only had a few hours of school each week, but because of special help from one of the teachers, I was allowed, together with two other schoolmates, to continue to the next and final class of elementary school; unfortunately all the others lost a year. More or less normal school education only became possible again with the start of the new school year in the fall of 1945.

In 1946 after a successful entrance exam, I entered the "Hogere Burgerschool" (HBS), Higher Citizen School, a five-year long middle school which prepared scholars for University entrance. I finished this school in June 1951, with natural sciences as my focal subjects. However, we all also had to become proficient in 3 foreign languages: French, English, and German. I was given considerable help in learing languages from my parents: German from my mother, French from my father. During those years, chemistry definitely was not one of my favorite subjects. They were mathematics and physics, but I also did very well in the three foreign languages. During my school years I spent considerable time at sport: football, cycling, and my greatest passion, long distance skating on the Dutch canals and lakes. I also played chess, which in the Netherlands is ranked as a "denksport" (thought sport). I read widely about travels in distant lands, about astronomy, as well as about bridges and tunnels. Unfortunately, because of a heavy fever, my grades in the final exam of the HBS were not good enough to qualify for a university study stipend, which was very hard to obtain at that time, only six years after the end of the Second World War and a few years after the end of colonial war in Indonesia, which had been a large drain on Dutch resources. As I did not want to be a further financial burden on any parents for another four years or more (my father, a waiter, was often unemployed; my mother worked in the kitchen of a hospital), I chose to attend the Middelbare Technische School (MTS), middle technical school, now called the Higher Technical School (HTS), to train as a civil

[*] Prof. Dr. P. J. Crutzen
Max-Planck-Institut für Chemie
Abteilung Chemie der Atmosphäre
Postfach 3060, D-55020 Mainz (Germany)
Fax: Int. code +(6131) 305-511

[**] Copyright © The Nobel Foundation 1996. We thank the Nobel Foundation, Stockholm, for permission to print this lecture.

engineer. Although the MTS took three years, the second year was a practical year during which I earned a modest salary, enough to live on for about two years.

From the summer of 1954 until February 1958, with a 21-month interruption for compulsory military service, I worked at the Bridge Construction Bureau of the City of Amsterdam. In the meanwhile, on a vacation trip in Switzerland I met a sweet girl, Terttu Soininen, a student of Finnish history and literature at the University of Helsinki. A few years later I was able to entice her to marry me. What a great choice I made! She has been the center of a happy family; without her support, I would never have been able to devote so much of my time to studies and science. After our marriage in February 1958, we settled in Gävle, a little town about 200 km north of Stockholm, where I had found a job in a building construction bureau. In December of that same year our daughter Ilona was born. In March 1964, she gained a little sister, Sylvia. Ilona is a registered nurse, now living in Boulder, Colorado. Her son Jamie Paul is 12 years old. Sylvia is a marketing assistant in München, Germany. All were present in Stockholm, Upsala, and Gävle during the Nobel week. We had a happy and unforgettable time.

All this time I had longed for an academic career. One day at the beginning of 1958, I saw an advertisement in a Swedish newspaper by the Department of Meteorology of Stockholm Högskola (from 1961, Stockholm University) announcing an opening for a computer programmer. Although I had not the slightest experience in such work, I applied for the job and had the great luck to be chosen from among many candidates. On July 1, 1959, we moved to Stockholm and I started with my second profession. At that time the Meteorology Institute of Stockholm University (MISU) and the associated International Meteorological Institute (IMI) were at the forefront of meteorological research, and many top researchers worked in Stockholm for extended periods. Only about a year earlier the founder of the institutes, Prof. Gustav Rossby, one of the greatest meteorologists ever, had died suddenly and was succeeded by Dr. Bert Bolin, another famous meteorologist, now "retired" as director of the Intergovernmental Panel on Climate Change (IPCC). At that time Stockholm University housed the fastest computers in the world (BESK and its successor FACIT).

With the exception of participation in a field campaign in northern Sweden, led by Dr. Georg Witt to measure the properties of noctilucent clouds that appear during summer at about 85 km altitude in the coldest parts of atmosphere, and some programming work related to this, I was mainly involved in various meteorological projects until about 1966, especially helping to build and run some of the first numerical (barotropic) weather prediction models. I also programmed a model of a tropical cyclone for a good friend, Hilding Sundquist, now a professor at MISU. At that time programming was a special art. Advanced general computer languages, such as Algol or Fortran, had not been developed, so all programmes had to be written in specific machine code. One also had to make sure that all operations yielded numbers in the range $-1 \leq x < 1$, which meant that one had to scale all equations to stay within these limits; otherwise the computations would yield wrong results.

The great advantage of being at a university department was that I got the opportunity to follow some of the lecture courses that were offered. By 1963 I could thus fulfill the requirement for the "filosofie kandidat" (corresponding to a Master of Science) degree, combining the subjects mathematics, mathematical statistics, and meteorology. Unfortunately I could include neither physics nor chemistry in my formal education, because this would have required my participation in time consuming laboratory courses. In this way I became a pure theoretician. I have, however, always felt close to experimental work, which I have strongly supported during my later years as director of research at the National Center of Atmospheric Research (NCAR) in Boulder, Colorado (1977–1980), and at the Max-Planck-Institute for Chemistry in Mainz, Germany (since 1980).

Being employed at the meteorological research institute, I quite naturally chose a meteorological topic for my filosofie licentiat thesis (comparable to a Ph.D. thesis). Originally, work on the further development of a numerical model of a tropical cyclone had been proposed to me. However, around 1965 I was given the task of helping a scientist from the United States to develop a numerical model of the oxygen allotrope distribution in the stratosphere, mesosphere, and lower thermosphere. This project got me highly interested in the photochemistry of atmospheric ozone, and I started an intensive study of the scientific literature. This gave me an understanding of the status of scientific knowledge on stratospheric chemistry by the latter half of the 1960s, thus setting the "initial conditions" for my scientific career. Instead of the initially proposed research project, I preferred research on stratospheric chemistry, which was generously accepted. At that time the main topics of research at the MISU were dynamics, cloud physics, the carbon cycle, studies of the chemical composition of rainwater, and especially the "acid rain" problem which was largely "discovered" at MISU through the work of Svante Odén and Erik Eriksson. Several researchers at MISU, among them Prof. Bolin and my good friend and fellow student Henning Rodhe, now Professor in Chemical Meteorology at MISU, became heavily involved in the issue, which drew considerable political interest at the first United Nation Conference on the Environment in Stockholm in 1972.[1] However, I wanted to do pure science related to natural processes and therefore I picked stratospheric ozone as my subject, without the slightest anticipation of what lay ahead. In this choice of research topic I was left totally free. I can not overstate how I value the generosity and confidence that were conveyed to me by my supervisors Prof. Georg Witt, an expert on the aeronomy of the upper atmosphere, and the head of MISU Prof. Bert Bolin. They were always extremely helpful and showed great interest in the progress of my research.

Stratospheric Ozone Chemistry

As early as 1930 the famous British scientist Sydney Chapman[2] had proposed that the formation of "odd oxygen" O_x (= O, O_3) is due to photolysis of O_2 by solar radiation at wavelengths shorter than 240 nm [Eq. (1)].

$$O_2 + h\nu \longrightarrow 2O \quad (\lambda \leq 240\ \text{nm}) \tag{1}$$

Fast reactions (2), where M is a mediator, and (3) next lead to the rapid establishment of a steady state for the concentrations of O and O_3 without affecting the concentration of odd

oxygen. Destruction of odd oxygen, counteracting its production by reaction (1), occurs by reaction (4).

$$O + O_2 + M \longrightarrow O_3 + M \quad (2)$$

$$O_3 + h\nu \longrightarrow O + O_2 \quad (\lambda \leq 1180\ nm) \quad (3)$$

$$O + O_3 \longrightarrow 2O_2 \quad (4)$$

Until about the middle of the 1960s it was generally believed that reactions (1)–(4) sufficed to explain the ozone concentration distribution in the stratosphere. However, by the mid 1960s, especially following a study by Benson and Axworthy,[3] it became clear that reaction (4) is much too slow to balance the production of odd oxygen by reaction (1) (Fig. 1). In 1950

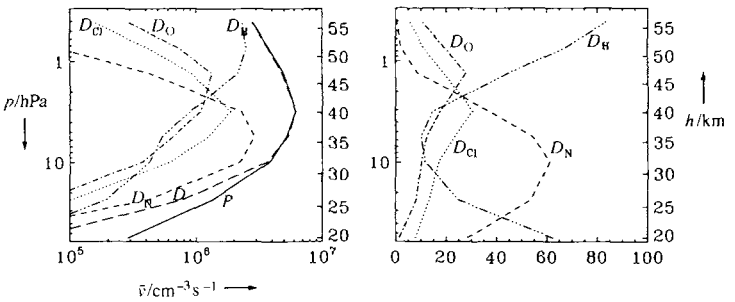

Fig. 1. Dependence of the influence of ozone production and destruction reactions on altitude: D_O = Chapman reaction (4), D_N = NO_x catalysis [Eqs. (11) + (12)], D_H = HO_x catalysis by H, OH, and HO_2, and D_{Cl} = ClO_x catalysis [120]. The calculations neglect the heterogeneous activation by halogen compounds, which becomes very important below 25 km under cold conditions. v = average reaction rate. % k_{tot} = contribution to the total O_3 loss rate. P = production of odd oxygen by reaction (1); D = total ozone destruction.

David Bates and Marcel Nicolet,[4] together with Sydney Chapman, the great pioneers of upper atmospheric photochemistry research, proposed that catalytic reactions involving OH and HO_2 radicals could counterbalance the production of odd oxygen in the mesosphere and thermosphere. Building on their work and on laboratory studies conducted by one of the 1967 Nobel Prize Laureates in Chemistry, Prof. R. Norrish of Cambridge University and his co-workers,[5, 6] the ozone destruction reaction pair (5) and (6) involving OH and HO_2 radicals as catalysts were postulated by Hampson[7] and incorporated into an atmospheric chemical model by Hunt.[8]

$$OH + O_3 \longrightarrow HO_2 + O_2 \quad (5)$$

$$HO_2 + O_3 \longrightarrow OH + 2O_2 \quad (6)$$

$$2O_3 \longrightarrow 3O_2 \quad (5) + (6)$$

The proposed primary source for the OH radicals was photolysis of O_3 by solar ultraviolet radiation of wavelengths shorter than about 320 nm [Eq. (7)], which leads to electronically excited $O(^1D)$ atoms, a small fraction of which reacts with water vapor [Eq. (8)]. Most $O(^1D)$ reacts with O_2 and N_2 to reproduce

$$O_3 + h\nu \longrightarrow O(^1D) + O_2 \quad (\lambda \leq 320\ nm) \quad (7)$$

$$O(^1D) + H_2O \longrightarrow 2OH \quad (8)$$

O_3 rapidly [Eqs. (9) and (2)], producing a null cycle with no effect on the concentrations of ozone or odd oxygen.

$$O(^1D) + M \longrightarrow O + M \quad (9)$$

In the absence of laboratory measurements for the rate constants of reactions (5) and (6), and in order for these reactions to counterbalance the production of odd oxygen by reaction (1), Hunt adopted the rate constants $k_5 = 5 \times 10^{-13}$ cm^{3}molec^{-1}s^{-1} and $k_6 = 10^{-14}$ cm^{3}molec^{-1}s^{-1}, respectively.

In my filosofie licentiat thesis of 1968 I analyzed the proposal by Hampson and Hunt and concluded that the rate constants for reactions (5) and (6) that they had chosen could not explain the vertical distribution of ozone in the photochemically dominated stratosphere above 25 km. Furthermore, I pointed out[9] that the above choice of rate constants would also lead to unrealistically rapid loss of ozone (on a timescale of only a few days) in the troposphere. Anticipating a possible role of OH in tropospheric chemistry, I also briefly mentioned the potential importance of a reaction between OH with CH_4. We now know that reactions (5) and (6) proceed about 25 and 10 times slower, respectively, that postulated by Hunt and Hampson and that the CH_4 oxidation cycle plays a very large role in tropospheric chemistry, a topic to which I will return.

With respect to stratospheric ozone chemistry, I discarded the theory of Hampson and Hunt and concluded "...at least part of the solution of the problem of the ozone distribution might be the introduction of photochemical processes other than those treated here. The influence of nitrogen compounds on the photochemistry of the ozone layer should be investigated."

Unfortunately no measurements of stratospheric NO_x (NO and NO_2) were available to confirm my thoughts about their potential role in stratospheric chemistry. By the summer of 1969 I had joined the Department of Atmospheric Physics at the Clarendon Laboratory of Oxford University as a postdoctoral fellow of the European Space Research Organization and stayed there for a two year period. The head of the research group, Dr. (now Sir) John Houghton, hearing of my idea on the potential role of NO_x, handed me a solar spectrum, taken on board a balloon by Dr. David Murcray and co-workers of the University of Denver, and indicated to me that it might reveal the presence of HNO_3.[10] After some analysis I could derive the approximate amounts of stratospheric HNO_3, including a rough idea of its vertical distributions. I did not get the opportunity to write up the result, because at about the same time, Rhine et al.[11] published a paper, showing a vertical HNO_3 column density of 2.8×10^{-4} atm cm ($\approx 7.6 \times 10^{15}$ molecules per cm^2) above 18.8 km. With this information I knew that NO_x should also be present in the stratosphere as a result of the reactions (10a) and (10b).

$$OH + NO_2(+M) \longrightarrow HNO_3(+M) \quad (10a)$$

$$HNO_3 + h\nu \longrightarrow OH + NO_2 \quad (\lambda \leq 320\ nm) \quad (10b)$$

This gave me enough confidence to submit my paper[12] on catalytic ozone destruction by NO and NO_2, based on the simple catalytic set of reactions [Eqs. (11) + (12)].

$$NO + O_3 \longrightarrow NO_2 + O_2 \quad (11)$$

$$NO_2 + O \longrightarrow NO + O_2 \quad (12)$$

$$O + O_3 \longrightarrow 2O_2 \quad (11) + (12)$$

The net result of reactions (11) and (12) is equivalent to the direct reaction (4). However, the rate of the net reaction can be greatly enhanced by relatively small quantities of NO_x on the order of a few nanomole per mole. I also included a calculation of the vertical distribution of stratospheric HNO_3. As the source of stratospheric NO_x, I initially accepted the proposal by Bates and Hays[13] that about 20% of the photolysis of N_2O would yield N and NO. Subsequent work showed that this reaction does not take place. However, it was soon shown that NO could also be formed to a lesser extent, but still in significant quantities, by the oxidation of nitrous oxide (N_2O) by $O(^1D)$.[14–16] It was further shown by Davis et al.[17] that reac-

$$N_2O + O(^1D) \longrightarrow 2NO \quad (13)$$

tion (12) proceeds about 3.5 times faster than I had originally assumed based on earlier laboratory work. A few years later it was also shown that earlier estimates of O_3 production by reactions (1) and (2) had been too large due to overestimations of both the absorption cross-sections of molecular oxygen[18] and solar intensities in the ozone-producing 200–240 nm wavelength region.[19, 20] As a result of these developments it became clear that enough NO is produced in reaction (13) to make reactions (11) and (12) the most important ozone loss reactions in the stratosphere in the altitude region between about 25 and 45 km (see Fig. 1).

N_2O is a natural product of microbiological processes in soils and waters. A number of anthropogenic activities, such as the application of nitrogen fertilizers in agriculture, also lead to significant N_2O emissions. The rate of increase in atmospheric N_2O concentrations for the past decades has been about 0.3% per year.[21] That, however, was not known in 1971. The discovery of the indirect role of a primarily biospheric product on the chemistry of the ozone layer has greatly stimulated interest in bringing biologists and atmospheric scientists together.

Man's Impact on Stratospheric Ozone

In the fall of 1970, still in Oxford, I obtained a preprint of a study sponsored by the Massachusetts Institute of Technology (MIT), the Study on Critical Environmental Problems (SCEP), which was held in July of that year.[22] This report also considered the potential impact of the introduction of large stratospheric fleets of supersonic aircraft (US: Boeing, Britain France: Concorde, Soviet Union: Tupolev; in the following, supersonic stratospheric transport is abbreviated SST) and gave me the first quantitative information on the stratospheric inputs of NO_x that would result from these operations. By comparing these with the production of NO_x by reaction (13), I realized immediately that we could be faced with a severe global environmental problem. Although the paper in which I proposed the important catalytic role of NO_x on ozone destruction had already been published in April 1970, the participants in the study conference had clearly not taken any note of it, since they concluded "The direct role of CO, CO_2, NO, NO_2, SO_2, and hydrocarbons in altering the heat budget is small. It is also unlikely that their involvement in ozone photochemistry is as significant as water vapour." I was quite upset by the statement. Somewhere in the margin of this text I wrote "Idiots".

After it became quite clear to me that I had stumbled on a hot topic, I decided to extend my 1970 study by treating in much more detail the chemistry of the oxides of nitrogen (NO, NO_2, NO_3, N_2O_4, N_2O_5), hydrogen (OH, HO_2), and HNO_3, partially building on a literature review by Nicolet.[23] I soon got into big difficulties. In the first place, adopting Nicolet's reaction scheme I calculated high concentrations of N_2O_4, a problem that I could soon resolve when I realized that this compound is thermally unstable, a fact not considered by Nicolet. An even greater headache was caused by reactions (14) and (15)

$$N_2O_5 + H_2O \longrightarrow 2HNO_3 \quad (14)$$

$$O + HNO_3 \longrightarrow OH + NO_3 \quad (15)$$

for which the only laboratory studies available at that time had yielded rather high rate coefficients: $k_{14} = 1.7 \times 10^{-18}$ and $k_{15} = 1.7 \times 10^{-11} - 17 \times 10^{-11}$ cm^3 molec^{-1} s^{-1} at room temperatures. A combination of reactions (14) and (15) with these rate constants would provide a very large source of OH radicals, about a thousand times larger than supplied by reaction (8), and would lead to prohibitively rapid catalytic ozone loss. This was a terribly nervous period for me. At that time no critical reviews and recommendations of rate coefficients were available. With no formal background in chemistry, I basically had to compile and comprehend much of the needed chemistry by myself from the available publications, although I profited greatly from discussions with colleagues at the University of Oxford, especially Dr. Richard Wayne of the Physical Chemistry Laboratory, a former student of Prof. R. Norrish in Cambridge. I discussed all these difficulties and produced extensive model calculations on the vertical distributions of trace gases in the $O_x/NO_x/HO_x/HNO_x$ system in a paper which was submitted by the end of 1970 to the Journal of Geophysical Research (received there on January 13, 1971) and which, after revision, was finally published in the October 20 issue of 1971.[15] The publication of this paper was much delayed because of an extended mail strike in Britain. Because of the major problems I had encountered, I did not make any calculations of ozone depletions, but instead drew attention to the potential seriousness of the problem by stating:

> "An artificial increase of the mixing ratio of the oxides of nitrogen in the stratosphere by about 1×10^{-8} may lead to observable changes in the atmospheric ozone level... It is estimated that global nitrogen oxide mixing ratios may increase by almost 10^{-8} from a fleet of 500 SSTs in the stratosphere. Larger increases, up to 7×10^{-8}, are possible in regions of high traffic densities... Clearly, serious decreases in the total atmospheric ozone level and changes in the vertical distributions of ozone, at least in certain regions, can result from such an activity...".

The Supersonic Transport Controversy in the USA

Unknown to me, a debate on the potential environmental impact of supersonic stratospheric transport had erupted in the USA. Initially the concern was mainly enhanced catalytic ozone destruction by OH and HO_2 radicals resulting from the release of H_2O in the engine exhausts.[24] By mid-March 1971, a workshop was organized in Boulder, Colorado, by an advisory board of the Department of Commerce, to which Prof. Harold Johnston of the University of California, Berkeley, was invited. As an expert in laboratory kinetics and reaction mechanisms of NO_x compounds,[25-27] he immediately realized that the role of NO_x in reducing stratospheric ozone had been grossly underestimated. Very quickly (submission 14 April, revision 14 June) on August 6, 1971, his paper appeared in Science[27] with the title "Reduction of Stratospheric Ozone by Nitrogen Oxide Catalysts from Supersonic Transport Exhaust". In the abstract of this paper Johnston stated "...oxides of nitrogen from SST exhaust pose a much greater threat to the ozone layer than does the increase in water. The projected increase in stratospheric oxides of nitrogen could reduce the ozone shield by about a factor of 2, thus permitting the harsh radiation below 300 nanometers to permeate the lower atmosphere." During the summer of 1971 I received a preprint of Johnston's study via a representative of British Aerospace, one of the Concorde manufacturers. This was the first time I had heard of Harold Johnston, for whom I quickly developed a great respect both as a scientist and a human being. Although I had expressed myself rather modestly about the potential impact of stratospheric NO_x emissions from SSTs, for the reasons given above, I fully agreed with Prof. Johnston on the potential severe consequences for stratospheric ozone, and I was really happy to have support for my own ideas from such an eminent scientist. For a thorough resumé of the controversies between scientists and industry, and between meteorologists and chemists (recurring themes also in later years) I refer to Johnston's article "Atmospheric Ozone".[28] It should also be mentioned here that Prof. Johnston's publications in the early 1970s removed several of the major reaction kinetic problems that I had encountered in my 1971 study.[15] It was shown, for instance, that neither reaction (14) nor (15) occur to a significant degree in the gas phase, and that the earlier laboratory studies had been significantly influenced by reactions on the walls of the reaction vessels,[29] advice that was earlier also given to me in a private communication from Prof. Sydney Benson of the University of Southern California.

In July 1971, I returned to the University of Stockholm and devoted myself mainly to studies concerning the impact of NO_x releases from SSTs on stratospheric ozone. In May 1973, I submitted my inaugural dissertation "On the Photochemistry of Ozone in the Stratosphere and Troposphere and Pollution of the Stratosphere by High-Flying Aircraft" to the Faculty of Natural Sciences and was awarded the degree of Doctor of Philosophy with the highest possible distinction, the third time this had ever happened during the history of Stockholm University (and earlier Stockholm "Högskola"). This was one of the last occasions in which the classical and rather solemn "Filosofie Doktor", similar to the Habilitation in Germany and France, was awarded. I had to dress up as for the Nobel Ceremonies. First and second "opponents" were Dr. John Houghton and Dr. Richard Wayne of the University of Oxford, who wore their college gowns for the occasion. Dr. Wayne also served as a most capable, nonobligatory third opponent, whose task it was to make fun of the candidate. Unfortunately, the classical doctoral degree has been abolished (I was one of the last ones to go through the procedure). The modern Swedish Filosofie Doktor degree corresponds more closely to the former Filosofie Licentiat degree.

In large part as a result of the proposal by Johnston[27] that NO_x emissions from SSTs could severely harm the ozone layer, major research programs were started: the Climate Impact Assessment Program (CIAP), organized by the US Department of Transportation,[30] and the COVOS/COMESA[31,32] program, jointly sponsored by France and Great Britain (the producers of the Concorde Aircraft). The aim of these programs was to study the chemical and meteorological processes that determine the abundance and distribution of ozone in the stratosphere, about which so little was known then that the stratosphere was sometimes dubbed the "ignorosphere". The outcome of the CIAP study was summarized in a publication by the US National Academy of Sciences in 1975.[33] "We recommend that national and international regulatory authorities be alerted to the existence of potentially serious problems arising from growth of future fleets of stratospheric airlines, both subsonic and supersonic. The most clearly established problem is a potential reduction of ozone in the stratosphere, leading to an increase in biologically harmful ultraviolet light at ground level."

The proposed large fleets of SSTs never materialized, largely for economic reasons; only a few Concordes are currently in operation. The CIAP and COVOS/COMESA research program, however, greatly enhanced knowledge about stratospheric chemistry. They confirmed the catalytic role of NO_x in stratospheric ozone chemistry. A convincing example of this was provided by a major solar proton event which occurred in August 1972 and during which, within a few hours, large quantities of NO, comparable to the normal NO_x content were produced at high geomagnetic latitudes ($> 65°$), as shown in Figure 2.

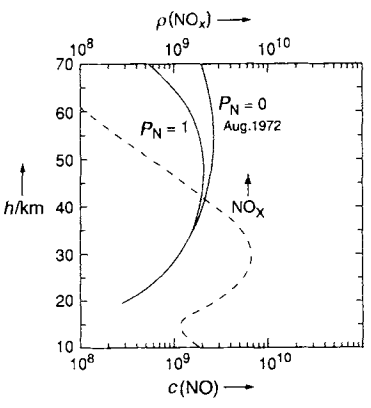

Fig. 2. Production of NO (c in molecules per cm^3; solid line) at high geomagnetic latitudes during the solar proton event of 1972 for two assumptions about the electronic states of the N atoms formed ($P_N = 0$, or 1). Also shown are the average NO_x concentration for these locations (broken line).

With such a large input of NO, a clear depletion of stratospheric ozone was expected,[34] a hypothesis which was confirmed by analysis of satellite observations.[35] Figure 3 shows results of the calculated and observed ozone depletions, the former obtained with a model that also considered chlorine chemistry.[36]

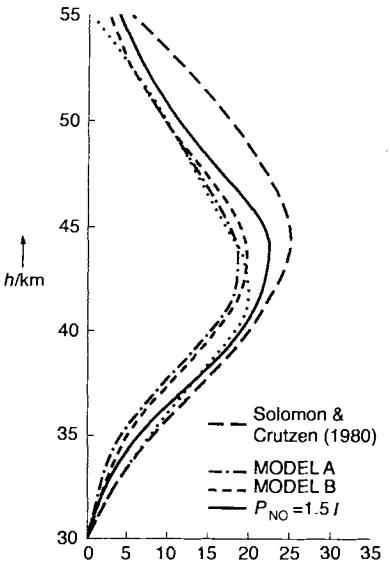

Fig. 3. Observed (····) and calculated percentage depletion of ozone resulting from the 1972 solar proton event. The various calculated curves correspond to assumed values of parameters that were not well known. P = production of NO, I = ionization rate.

Although I had started my scientific career with the ambition to do basic research related to natural processes, the experiences of the early 1970s had made it utterly clear to me that human activities had grown so much that they could compete and interfere with natural processes. Since then this has been an important factor in my research efforts. Already by the end of 1971 I wrote in an article published in the "The Future of Science Year Book" of the USSR in 1972:

> "...the upper atmosphere is an important part of our environment. Let us finish by expressing a sincere hope that in the future environmental dangers of new technological development will be recognizable at an early stage. The proposed supersonic air transport is an example of a potential threat to the environment by future human activities. Other serious problems will certainly arise in the increasingly complicated world of tomorrow."

Tropospheric Ozone

My first thoughts on tropospheric photochemistry go back to about 1968, as discussed briefly above.[9] However, in the following three years, my research was largely devoted to stratospheric ozone chemistry. Then in 1971 a very important paper with the title "Normal Atmosphere: Large Radical and Formaldehyde Concentrations Predicted" was published by Hiram Levy III, then of the Smithsonian Astrophysical Observatory in Cambridge, Massachusetts.[37] Levy proposed that OH radicals could also be produced in the troposphere by the action of solar ultraviolet radiation on ozone [Eqs. (7) and (8)], and that they are responsible for the oxidation of CH_4 and CO, an idea that was also quickly adopted by Jack McConnell, Michael McElroy, and Steve Wofsy[38] of Harvard University. The recognition of the important role of OH was a major step forward in our understanding of atmospheric chemistry. Despite very low atmospheric concentrations, currently estimated at 10^6 molecules per cm^3, corresponding to a mean tropospheric volume mixing ratio of 4×10^{-14},[39] it is this ultraminor constituent—and not the 10^{13} times more abundant O_2—that is responsible for the oxidation of almost all compounds emitted into the atmosphere by natural processes and anthropogenic activities. The lifetimes of most atmospheric gases are, therefore, largely determined by the concentrations of OH and the corresponding reaction coefficients[40] (Scheme 1). Those gases that do not react with OH have very long atmospheric residence times and are largely destroyed in the stratosphere. Examples of the latter class of compounds are N_2O and several fully halogenated, industrial organic compounds, such as $CFCl_3$, CF_2Cl_2, and CCl_4. These play a major role in stratospheric ozone chemistry, an issue to which we will return.

Primary Production of OH Radicals

$O_3 + h\nu\ (\leq 320\ nm) \longrightarrow O(^1D) + O_2$

$O(^1D) + H_2O \longrightarrow 2OH$

Global 24-Hour Average:

$c(OH) \approx 10^6$ molecules per cm^3

molar mixing ratio in troposphere $\approx 4\times10^{-14}$

Reaction with OH Determines the Lifetime of Most Gases in the Atmosphere:

CH_4:	8 years	$(CH_3)_2S$:	2–3 days
C_2H_6:	2 months	CH_3Cl:	≈ 1 year
C_3H_8:	10 days	CH_3CCl_3:	≈ 5 years
C_5H_8:	hours	NO_2:	≈ 1 day

$CFCl_3$, CF_2Cl_2, and N_2O do not react with OH. They are broken down in the stratosphere and have a large influence on ozone chemistry.

Scheme 1. The importance of OH radicals in atmospheric chemistry.

Following Levy's paper my attention turned strongly to tropospheric chemistry. Starting with a presentation at the 1972 International Ozone Symposium in Davos, Switzerland, I proposed that in situ chemical processes could produce or destroy ozone in quantities larger than the estimated downward flux of ozone from the stratosphere to the troposphere.[41,42] Destruction of ozone occurs by reactions (5) + (6) and (7) + (8). Ozone production takes place in environments containing sufficient NO_x by reactions (16), (17), and (2), where R = H, CH_3, or other organoperoxy radicals.

$$RO_2 + NO \longrightarrow RO + NO_2 \quad (16)$$

$$NO_2 + h\nu \longrightarrow NO + O \quad (\lambda \leq 405\ nm) \quad (17)$$

$$O + O_2 + M \longrightarrow O_3 + M \quad (2)$$

$$RO_2 + O_2 \longrightarrow RO + O_3 \quad (16) + (17) + (2)$$

The catalytic role of NO in atmospheric chemistry is, therefore, twofold. At altitudes above about 25 km, where O atom concentrations are high, ozone destruction by reactions (11) + (12) dominates over ozone production by reactions (16) + (17) + (2). The latter chain of reactions is at the base of all photochemical ozone formation in the troposphere, including that taking place during photochemical smog episodes, originally discovered in southern California, as discussed by Johnston.[28] Such reactions can, however, also take place in

background air with ubiquitous CO and CH_4 serving as fuels: in the case of CO oxidation the course is (18)→(19)→(16')→(17)→(2).

$$CO + OH \rightarrow CO_2 + H \quad (18)$$

$$H + O_2 + M \rightarrow HO_2 + M \quad (19)$$

$$HO_2 + NO \rightarrow OH + NO_2 \quad (16')$$

$$NO_2 + h\nu \rightarrow NO + O \quad (17)$$

$$O + O_2 + M \rightarrow O_3 + M \quad (2)$$

$$CO + 2O_2 \rightarrow CO_2 + O_3 \quad (18) + (19) + (16') + (17) + (2)$$

This reaction chain requires the presence of sufficient concentrations of NO. At low NO volume mixing ratios, below about 10 pmol mol^{-1}, oxidation of CO may lead to ozone destruction, since the HO_2 radical then reacts mostly with O_3 [see Eq. (6)]. The result of the participating reactions [(18) + (19) + (6)] is: $CO + O_3 \rightarrow CO_2 + O_2$. In a similar way, the oxidation of CH_4 in the presence of sufficient NO_x will lead to tropospheric ozone production.

Besides reacting with NO or O_3, HO_2 can also react with itself [Eq. (20)] to produce H_2O_2 which serves as a strong oxidizer of S^{IV} compounds in cloud and rain water.

$$HO_2 + HO_2 \rightarrow H_2O_2 + O_2 \quad (20)$$

My talk at the International Ozone Symposium was not well received by some members of the scientific establishment of the time. However, in the following years the idea gradually received increased support. In particular, Bill Chameides and Jim Walker,[43] then of Yale University, took it up and went as far as proposing that even the diurnal variation of lower tropospheric ozone could be explained largely by in situ photochemical processes. Although I did not agree with their hypothesis (CH_4 and CO oxidation rates are just not rapid enough), it was good to note that my idea had been taken seriously. (I should also immediately add that especially Bill Chameides in subsequent years add much to our knowledge of tropospheric ozone.) A couple of years later, together with two of my finest students, Jack Fishman and Susan Solomon, we presented observational evidence for a strong in situ tropospheric ozone chemistry.[44, 45] Laboratory measurements by Howard and Evenson[46] next showed that reaction (16) proceeded about 40 times faster than determined earlier, strongly promoting ozone production and increased OH concentrations with major consequences for tropospheric and stratospheric chemistry.[47] A consequence of the faster rate of this reaction is a reduction in the estimated ozone depletions by stratospheric aircraft as the ozone production reactions (16) + (17) + (2) are favored over the destruction reaction (6). Furthermore, a faster reaction (16) leads to enhanced OH concentrations and thus a faster conversion of reactive NO_x to far less reactive HNO_3. Table 1 summarizes a recent ozone budget calculated with a three-dimensional chemical transport model of the troposphere. The results clearly show the dominance of in situ tropospheric ozone production and destruction. With the same model, estimates were also made of the present and pre-industrial ozone concentration distributions (Fig. 4). The calculations indicate a clear increase in tropospheric ozone concentrations over the past centuries.[48] In Figure 5 we also show the meridional cross sections of zonal average ozone, as compiled by Jack Fishman (unpublished data).

Table 1. Tropospheric ozone budgets, globally and for the northern (NH) and southern hemisphere (SH) in 10^{13} mol per year. Only CH_4 and CO oxidation cycles were considered. Calculations were made with the latest version of the global, three-dimensional MOGUNTIA model [48].

	Global	NH	SH
Sources			
$HO_2 + NO$	6.5	4.1	2.4
$CH_3O_2 + NO$	1.7	1.0	0.7
Transport from the stratosphere	1.0	0.7	0.3
Sinks			
$O(^1D) + H_2O$	3.8	2.2	1.6
$HO_2 + O_3$ and $OH + O_3$	2.8	1.8	1.0
Deposition on the surface	2.7	1.8	0.9
Net chemical source [a]	1.6	1.1	0.5

[a] Difference between the two chemical sources and the two chemical sinks.

With the same model we have also calculated the OH concentration distributions for pre-industrial and present conditions. Since pre-industrial times, the CH_4 volume mixing ratio in the atmosphere has increased[49] from about 0.7 to 1.7 ppmv (v indicates a volume/volume comparison). Because reaction with CH_4 is one of the main sinks for OH, an increase in CH_4 should have led to a decrease in OH concentrations. On the other hand, increased ozone concentrations, which enhance OH production by reactions (7) + (8), and the reactions (6) and (16'), both stimulated by strongly enhanced anthropogenic NO production, should exert the opposite effect. Figure 6 shows the zonally averaged, meridional distributions of the diurnally averaged OH concentrations, both for the pre-industrial and industrial periods. They indicate:

a) strong maxima of OH concentrations in the tropics, largely due to high intensities of ultraviolet radiation as a consequence of a minimum in the vertical ozone column. Consequently the atmospheric oxidation efficiency is strongly determined by tropical processes. For instance, most CH_4 and CO is removed from the atmosphere by reaction with OH in the tropics.

b) the possibility of a significant decline in OH concentrations from pre-industrial to industrial conditions.

The results presented in Figure 6, bottom, are of great importance, as they allow estimations of the sink of atmospheric CH_4 by reaction with OH. Prior to the discovery of the fundamental role of the OH radical,[37] estimates of the sources and sinks of trace gases were largely based on guess work without a sound scientific basis. As shown in Scheme 2, this recognition has led to very large changes in the budget estimates of CH_4 and CO. "Authoritative" estimates of the CH_4 budget of 1968 (no reference will be given) gave much higher values for CH_4 releases from natural wetlands. With such a dominance of natural sources, it would have been impossible to explain the annual increase in atmospheric CH_4 concentrations by almost 1% per year. Early estimates of CO sources, on the other hand, were much too low.

The dominance of OH concentrations and the high photochemical activity in the tropics clearly points at the great impor-

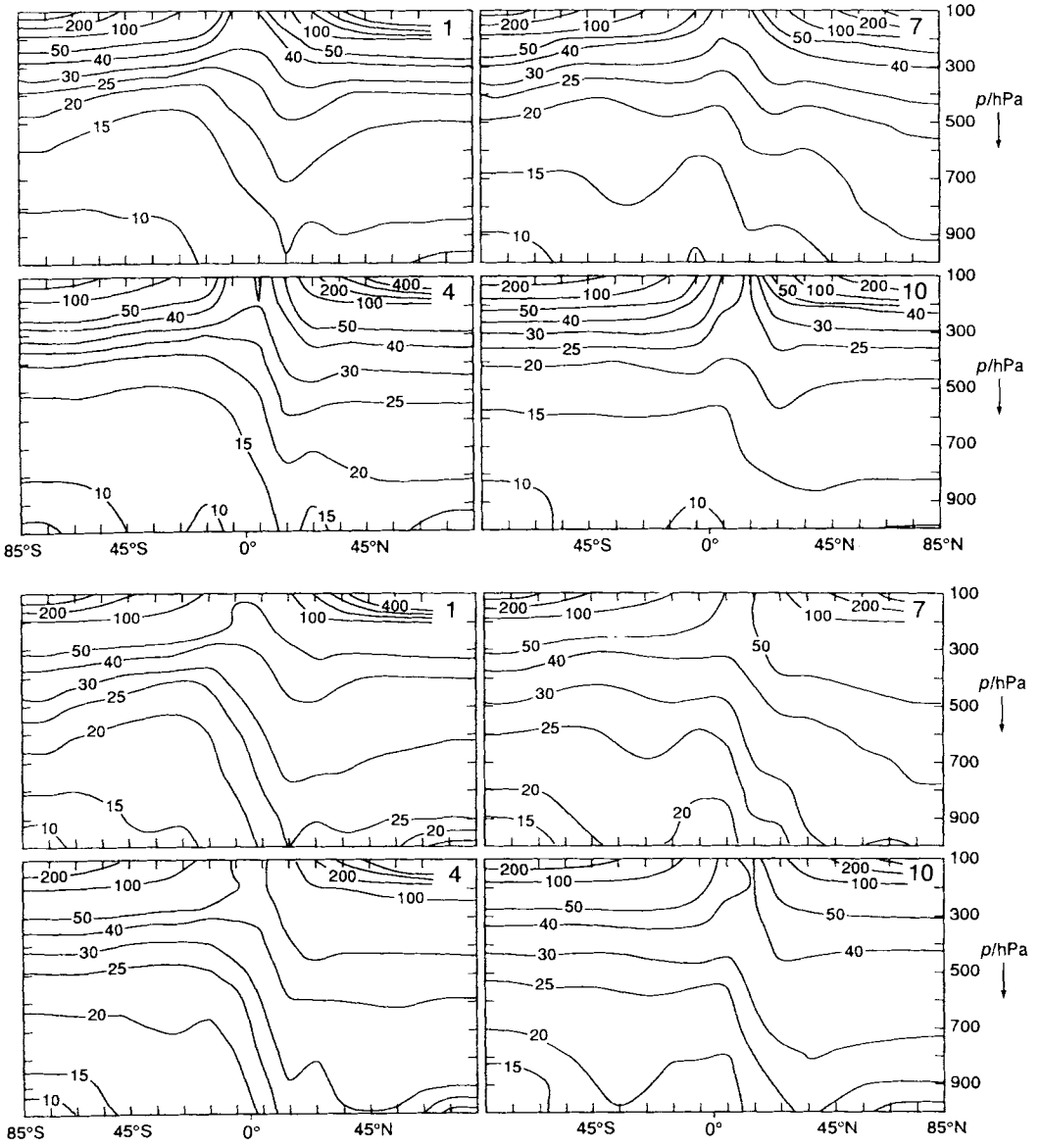

Fig. 4. Calculated zonal average ozone volume mixing ratios in units of nmol per mol for the months January (1 in upper right corner), April (4), July (7), and October (10) in the pre-industrial era (top) and in 1985 (bottom).

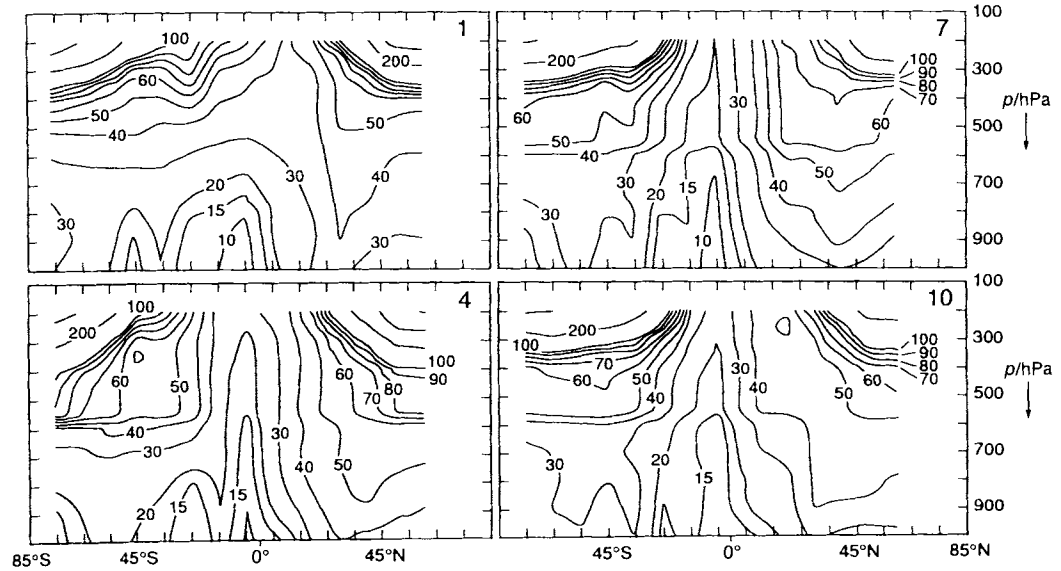

Fig. 5. Compilation of observed meridional ozone distributions (in nmol per molecule) prior to 1989, compiled by Jack Fishman of NASA Langley Research Center, for the months January (1), April (4), July (7), and October (10). It should be mentioned that the data base is very limited and has not improved much for the tropics and subtropics.

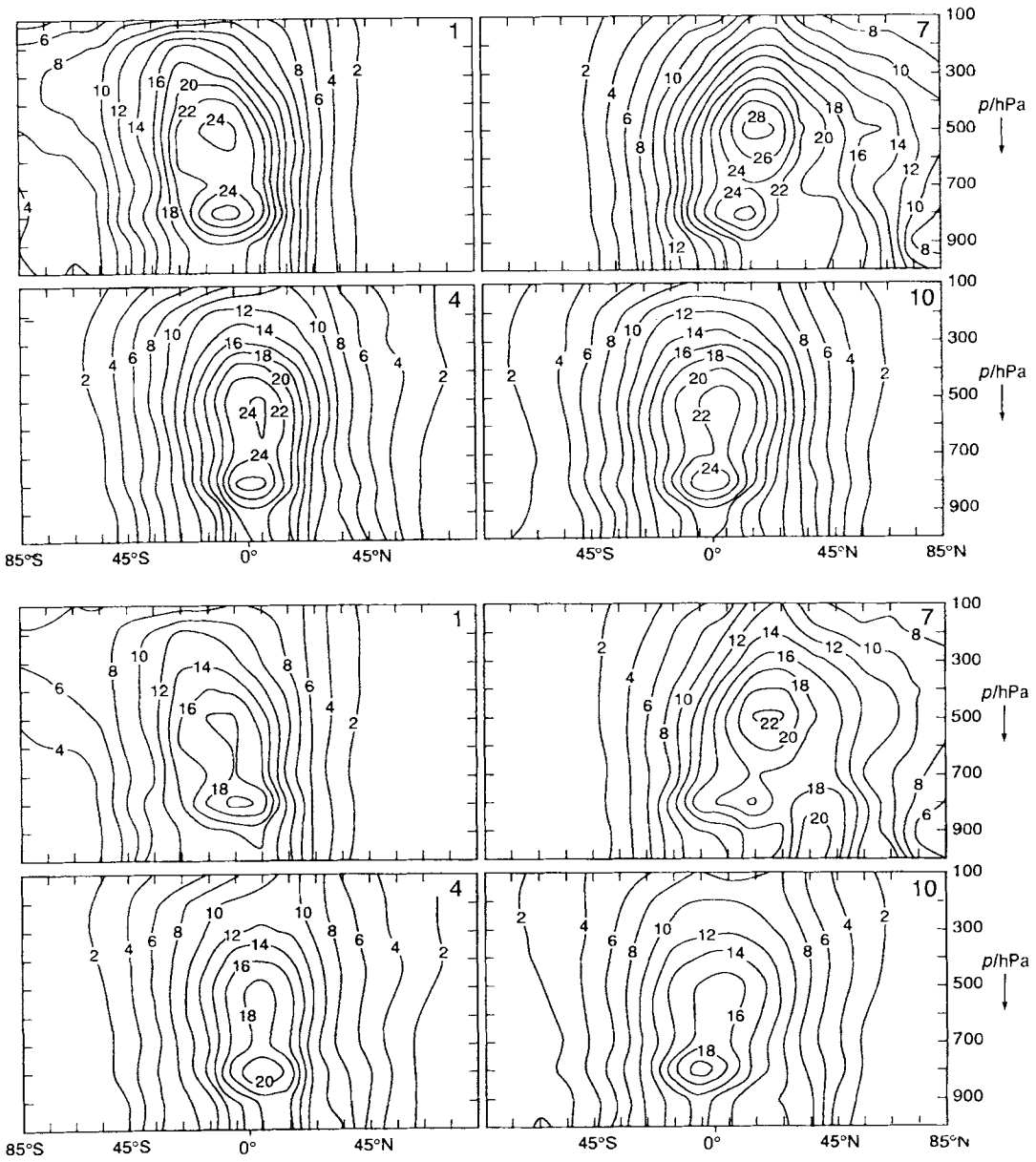

Fig. 6. Calculated zonal and 24-hour average OH concentrations in units of 10^5 molecules per cm^3 for January (1), April (4), July (7), and October (10) in the pre-industrial period (top) and 1985 (bottom).

	1968	1995		1968	1995
CH_4:			NO_x:		
natural wetlands	1180	275	biological sources	150	10
anthropogenic sources	270	265	pollutants	15	24
	1450	540	lightning		2–10
				165	36–44
CO:			N_2O:		
natural sources	75	860	biological sources	340	15
anthropogenic sources	274	1640	anthropogenic sources		3.5
	350	2500		340	18.5
S:					
pollutants	76	78			
oceanic emissions	30 (H_2S)	25 (Me_2S)			
land emissions	70 (H_2S)	few (various compounds)			
	176	105			

Scheme 2. Estimated budgets of important atmospheric trace gases made in 1968 and 1995. The amounts are given in 10^{12} g per year (for the S- and N-containing compounds, with respect to S or N).

tance of the tropics and subtropics in atmospheric chemistry. Despite this fact, research on low latitude chemistry is much neglected, with the consequence that we do not even have satisfactory statistics on the ozone distribution in this part of the world. Tropical chemistry is a topic that has played and will continue to play a large role in my research. Contrary to what was commonly believed prior to the early 1980s, the chemical composition of the tropical and subtropical atmosphere is substantially affected by human activities, in particular biomass burning, which takes place during the dry season. The high temporal and spatial variability of ozone in the tropics is shown in Figure 7. Highest ozone concentrations are observed over the polluted regions of the continents during the dry season, lowest values in the clean air over the Pacific. I will return to the topic of tropical tropospheric ozone, but will first review the stormy developments in stratospheric ozone depletion by halogen compounds that started in 1974.

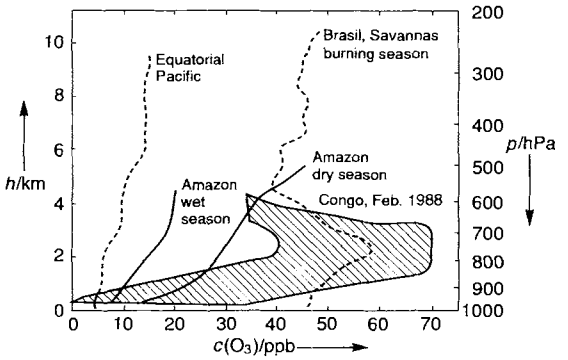

Fig. 7. Variability of ozone profiles in the tropics, displaying the contrast between the dry and the wet season, and between continents and marine sites.

Pollution of the Stratosphere by ClO_x Compounds

Towards the end of the CIAP programme some researchers had turned their interest to the potential input of reactive chlorine radicals on stratospheric ozone. In the most thorough of these studies, Stolarski and Cicerone[50] calculated significant ozone depletions if inorganic chlorine were present in the stratosphere at a volume mixing ratio of 1 nmol per mole of air. Odd oxygen destruction would take place by the catalytic reaction cycle (21) + (22). This reaction sequence is very similar to the

$$Cl + O_3 \longrightarrow ClO + O_2 \quad (21)$$

$$O + ClO \longrightarrow Cl + O_2 \quad (22)$$

$$O + O_3 \longrightarrow 2O_2 \quad (21) + (22)$$

catalytic NO_x cycle (11) + (12) introduced before. The study by Stolarski and Cicerone, first presented at a conference in Kyoto, Japan, in the fall of 1973, mainly considered volcanic injections as a potential source of ClX compounds (their initial interest in chlorine chemistry was, however, concerned with the impact of the exhaust of solid rocket fuels of the space shuttle). Two other conference papers[51, 52] also dealt with ClO_x chemistry. All three papers struggled, however, with the problem of a missing chlorine source in the stratosphere (research over the past 20 years has shown that the volcanic source is rather insignificant).

In the fall of 1973 and early 1974 I spent some time looking for potential anthropogenic sources of chlorine in the stratosphere. Initially my main interest was with DDT and other pesticides. Then by the beginning of 1974 I read a paper by James Lovelock and co-workers,[53] who reported atmospheric measurements of $CFCl_3$ (50 picomol mol^{-1}) and CCl_4 (71 pmol mol^{-1}) over the Atlantic. (Such measurements had been made possible by Lovelock's invention of the electron capture detector for gas chromatographic analysis, a major advance in the environmental sciences.) Lovelock's paper gave me the first estimates of the industrial production rates of CF_2Cl_2 and $CFCl_3$. It also stated that these compounds "are unusually stable chemically and only slightly soluble in water and might therefore persist and accumulate in the atmosphere... The presence of these compounds constitutes no conceivable hazard." This statement had just aroused my curiosity about the fate of these compounds in the atmosphere when a preprint of a paper by M. J. Molina and F. S. Rowland with the title "Stratospheric Sink for Chlorofluoromethanes—Chlorine Atom Catalyzed Destruction of Ozone" was sent to me by the authors. I knew immediately that this was a very important paper and decided to mention it briefly during a presentation on stratospheric ozone to which I had been invited by the Royal Swedish Academy of Sciences in Stockholm. What I did not know was that the press was likewise invited to the lecture. To my great surprise, within a few days, an article appeared in the Swedish newspaper *Svenska Dagbladet*, which drew attention to the topic. This article quickly attracted wide international attention, and soon I was visited by representatives of the German chemical company Hoechst and also by Professor Rowland, who at that time was spending a sabbatical at the Atomic Energy Agency in Vienna. This was the first time I had ever heard of Molina or Rowland, which is not surprising as they had not been active in studies on the chemistry of the atmosphere. Needless to say, I remained highly interested in the topic, and by September 1974, about 2 months after the publication of Molina and Rowland's paper,[54] I presented a model analysis of the potential ozone depletion resulting from continued use of chlorofluoro carbons (CFCs),[55] which indicated the possibility of up to about 40% ozone depletion near 40 km altitude as a result of continued use of these compounds at 1974 rates. Almost simultaneously, Cicerone et al.[56] published a paper in which they predicted that by 1985–1990, continued use of CFCs at early 1970 levels could lead to ClO_x-catalyzed ozone destruction of a similar magnitude to the natural sinks of ozone. Following Molina and Rowland's proposal, research on stratospheric chemistry further intensified, now with the emphasis on chlorine compounds.

By the summer of 1974, together with my family, I moved to Boulder, Colorado, where I assumed two halftime positions, one as a consultant at the Aeronomy Laboratory of the National Oceanic and Atmospheric Administration (NOAA) and the other at the Upper Atmosphere Project of the National Center for Atmospheric Research (NCAR). The NOAA group, which under the able direction of Dr. Eldon Ferguson had become the world leading group in the area of laboratory studies of ion–molecule reactions, had just decided to direct their considerable experimental skills to studies of stratospheric chemistry. My task was to guide them in that direction. I still feel proud to have been part of a most remarkable transformation. Together with Eldon Ferguson, scientists like Dan Albritton, Art Schmeltekopf, Fred Fehsenfeld, Paul Goldan, Carl Howard, George Reid, John Noxon, and Dieter Kley rapidly made major contributions to stratospheric research, including such activities as air sampling with balloon-borne evacuated cans, so-called "salad bowls" for later gas chromatographic analysis, optical measurements of the vertical abundances and distributions of NO_2 and NO_3 (later expanded by Susan Solomon to BrO and OClO), the design and operation of an instrument to measure extremely low water vapor mixing ratios, and laboratory simulations of important, but previously poorly known rate coefficients of important reactions. In later years the NOAA group also devoted itself to studies of tropospheric chemistry, reaching a prominent position in this research area as well. At NCAR the emphasis was more on infrared spectrographic measurements by John Gille and Bill Mankin, work that also developed into satellite-borne experiments. Another prominent activity was the

analysis of the vertical distributions of less reactive gases, such as CH_4, H_2O, N_2O, and the CFCs, employing the cryogenic sampling technique which had been pioneered by Ed Martell and Dieter Ehhalt.

In 1977 I took up the directorship of the Air Quality Division of NCAR, my first partially administrative position. I continued, however, my scientific work, something which many thought would be impossible. Fortunately, in Nelder Medrud I had a highly competent administrative officer. In my position as director I promoted work on both stratospheric and tropospheric chemistry. My own research was mostly devoted to the development of photochemical models, conducted mostly with my students Jack Fishman, Susan Solomon, and Bob Chatfield. Together with Pat Zimmerman we started studies on atmosphere–biosphere interactions, especially the release of hydrocarbons from vegetation and pollutant emissions due to biomass burning in the tropics. I also tried to strengthen interactions between atmospheric chemists and meteorologists to improve the interpretation of the chemical measurements obtained during various field campaigns. To get this interdisciplinary research going was a challenge in those days.

During this period, as part of various activities in the United States and internationally, much of my research remained centered on the issue of anthropogenic, chlorine-catalyzed ozone destruction. However, because I am sure that this topic will be covered extensively by my two fellow recipients of this year's Nobel Prize, I would like to make a jump to the year 1985, when Joe Farman and his colleagues[57] of the British Antarctic Survey published their remarkable set of October total ozone column measurements from the Halley Bay station, showing a rapid depletion on the average by more than 3% per year, starting from the latter half of the 1970s. Although their explanation (ClO_x/NO_x interactions) was wrong, Farman et al.[57] correctly suspected a connection with the continued increase in stratospheric chlorine (nowadays more than five times higher than natural levels). Their display of the downward trend of ozone, matching the upward trend of the chlorofluorocarbons (with the appropriate scaling) was indeed highly suggestive.

The discovery of the ozone hole came during a period in which I was heavily involved in various international studies on the potential environmental impacts of a major nuclear war between the NATO and Warsaw Pact nations, an issue to which I will briefly return in one of the following sections. Because so many researchers became quickly involved in the "ozone hole" research, initially I stayed out of it. Then, in early 1986 I attended a scientific workshop in Boulder, Colorado, which brought me up-to-date with the various theories that had been proposed to explain the ozone hole phenomenon. Although it turned out that some of the hypotheses had elements of the truth, in particular the idea put forward by Solomon et al.[58] of chlorine activation on the surface of stratospheric ice particles, by reaction (23) followed by rapid photolysis of Cl_2 and production of highly reactive Cl atoms [Eq. (24)], I felt dissatisfied with the treatment of the chemistry in the heterogeneous phase. On my flight back to Germany (I hardly sleep on trans-Atlantic flights), I had good time to think it over and suddenly realized that if HNO_3 and NO_x were removed from the gas phase into the particulate phase, then an important defense against the attack of ClO_x on O_3 would be removed. The thought goes as follows: Under normal stratospheric conditions, there are strong interactions between the NO_x and ClO_x radicals, which lead to protection of ozone from otherwise much more severe destruction. Important examples of these are reaction (25) and the pair of reactions (26) + (27), producing HCl and $ClONO_2$,

$$HCl + ClONO_2 \longrightarrow Cl_2 + HNO_3 \quad (23)$$

$$Cl_2 + h\nu \longrightarrow 2Cl \quad (24)$$

$$ClO + NO_2 + M \longrightarrow ClONO_2 + M \quad (25)$$

$$ClO + NO \longrightarrow Cl + NO_2 \quad (26)$$

$$Cl + CH_4 \longrightarrow HCl + CH_3 \quad (27)$$

which do not react with odd oxygen. Because of these reactions, under normal stratospheric conditions most of the inorganic chlorine is present as HCl and $ClONO_2$. Like two Mafia families, the ClO_x and NO_x thus fight each other, to the advantage of ozone. As shown in Figure 8, there are plenty of complex interactions between the OX, HX, NX, and ClX families (for definitions see the legend of Fig. 8). Now, if the NX compounds were removed from the gas phase, reactions (25)–(27) would not occur and most inorganic chlorine may become available in the activated forms. During my return trip to Germany I started to think about this possibility. First, all NO_x compounds are converted to HNO_3 either by reaction (10a) or, especially during the long polar nights, by the night-time reactions (11), (14′), and (28)–(30).

$$NO + O_3 \longrightarrow NO_2 + O_2 \quad (11)$$

$$NO_2 + O_3 \longrightarrow NO_3 + O_2 \quad (28)$$

$$NO_3 + NO_2(+M) \longrightarrow N_2O_5(+M) \quad (29)$$

$$N_2O_5 + H_2O(\text{surface}) \longrightarrow 2HNO_3\,(\text{gas}) \quad (14')$$

$$HNO_3(\text{gas}) \longrightarrow HNO_3(\text{particles}) \quad (30)$$

As noted before, reaction (14) does not occur in the gas phase, but it readily occurs on wetted particulate surfaces. These are always present in the lower stratosphere in the form of sulfate particles, a fact which was first discovered by Christian Junge, a pioneer in atmospheric chemistry and my predecessor as director at the Max-Planck-Institute of Chemistry in Mainz.[59] The sulfate particles are formed by nucleation of gas phase H_2SO_4, which is formed from SO_2, following attack by OH[60, 61] [Eqs. (31)–(33)].

$$SO_2 + OH + M \longrightarrow HSO_3 + M \quad (31)$$

$$HSO_3 + O_2 \longrightarrow SO_3 + HO_2 \quad (32)$$

$$SO_3 + H_2O \longrightarrow H_2SO_4 \quad (33)$$

The sources of stratospheric SO_2 are either direct injections by volcanic explosions[59] or oxidation of OCS, produced at the earth's surface,[62] by reactions (34)–(36).

$$OCS + h\nu \longrightarrow S + CO \quad (34)$$

$$S + O_2 \longrightarrow SO + O \quad (35)$$

$$SO + O_2 \longrightarrow SO_2 + O \quad (36)$$

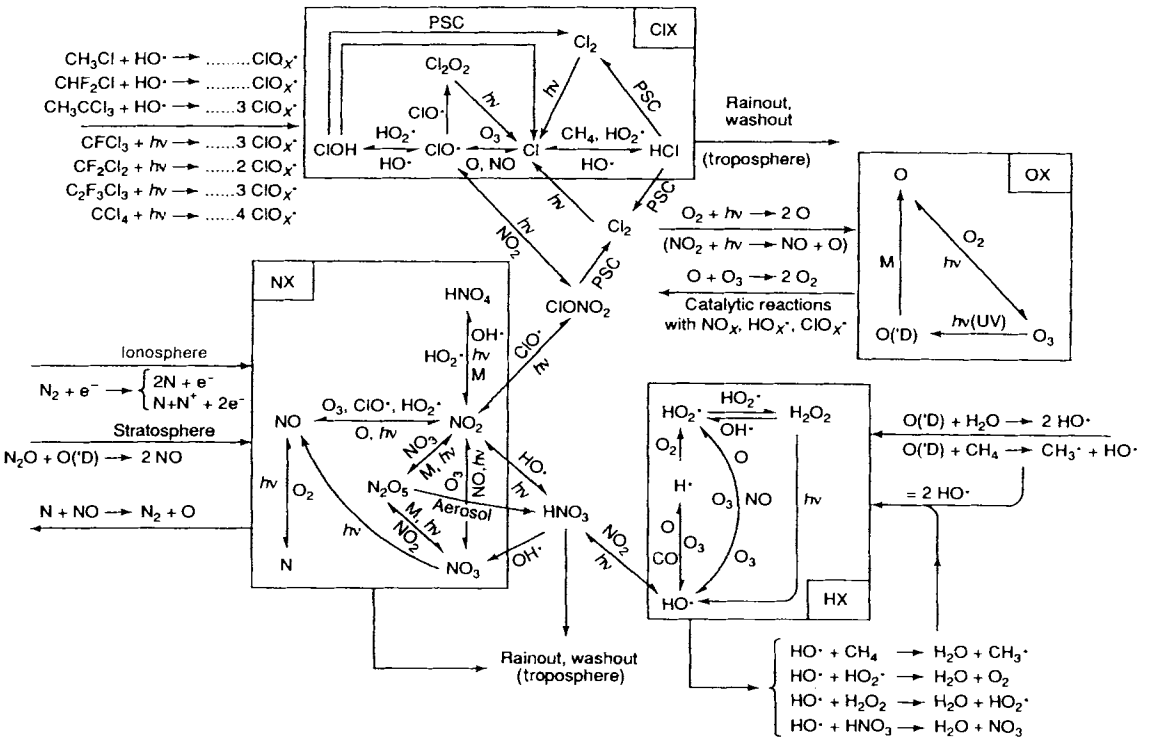

Fig. 8. Schematic presentation of the chemical interactions in the stratosphere. At the start of my scientific career only the OX reactions and some of the HX reactions had been taken into account. Note that OX stands for the odd oxygen compounds, HX for H, OH, HO_2, and H_2O_2; NX for N, NO, NO_2, NO_3, N_2O_5, HNO_3, and HNO_4; and ClX for all inorganic chlorine compounds, Cl, ClO, Cl_2O_2, $ClONO_2$, HCl, OClO, and Cl_2. Not included are the bromine compounds, which likewise play a significant role in stratospheric ozone depletion. PSC = polar stratospheric clouds.

The possibility of HNO_3 formation by heterogeneous reactions on sulfate particles had already been considered in a 1975 paper that I had co-authored with Richard Cadle and Dieter Ehhalt.[63] Based on laboratory experiments, this reaction was for a long while thought to be unimportant, until it was discovered that the original laboratory measurements were grossly incorrect and that reaction (14) readily occurs on H_2O-containing surfaces.[64–66] Earlier tropospheric measurements had, however, already indicated this.[67] The introduction of reaction (14) leads to a significant conversion of reactive NO_x to much less reactive HNO_3, thus diminishing the role of NO_x in ozone chemistry, especially in the lower stratosphere. By including reaction (14), better agreement was obtained between theory and observations.[68] The experience with reaction (14) emphasizes again the importance of high-quality measurements. It is clearly better to have no measurements at all than bad measurements.

As soon as I returned to Mainz, I contacted Dr. Frank Arnold of the Max-Planck-Institute for Nuclear Physics in Heidelberg to explain my idea about NO_x removal from the gas phase to him. After about a week he had shown that under stratospheric conditions, solid nitric acid trihydrate (NAT) particles could be formed at temperatures below about 200 K, that is, a temperature about 10 K higher than that needed for water ice particle formation. The paper about our findings was published in Nature at the end of 1986.[69] Independently, the idea had also been developed by Brian Toon, Rich Turco, and co-workers.[70] Subsequent laboratory investigations, notably by David Hanson and Konrad Mauersberger,[71] then of the University of Minnesota, provided accurate information on the thermodynamic properties of NAT. Next it was also shown that the NAT particles could provide efficient surfaces to catalyze the production of ClO_x by reactions (23) and (24).[72, 73] Finally, Molina and Molina[74] proposed a powerful catalytic reaction cycle involving ClO-dimer formation [Eqs. (21), (37), and (38)], which

$$Cl + O_3 \longrightarrow ClO + O_2 \quad (2\times) \tag{21}$$

$$ClO + ClO + M \longrightarrow Cl_2O_2 + M \tag{37}$$

$$Cl_2O_2 + h\nu \longrightarrow Cl + ClO_2 \rightarrow 2Cl + O_2 \tag{38}$$

$$2O_3 \longrightarrow 3O_2 \qquad (21) + (37) + (38)$$

could complete the chain of events causing rapid ozone depletion under cold, sunlit stratospheric conditions. Note that reaction (37) implies an ozone depletion response that is proportional to the square of the ClO concentration. Furthermore, as chlorine activation by reaction (23) is also nonlinearly dependent on the stratospheric chlorine content, a powerful, nonlinear, positive feedback system is created, which is responsible for the accelerating loss of ozone under "ozone hole" conditions. The "ozone hole" is a drastic example of a man-made chemical instability, which developed at a location most remote from the industrial releases of the chemicals responsible for the effect.

The general validity of the chain of events leading to chlorine activation has been confirmed by both ground-based[75, 76] and airborne, in situ[77] radical observations. Especially the latter, performed by James Anderson and his students of Harvard University, have been very illuminating, showing large enhancements in ClO concentrations in the cold, polar region of the

lower stratosphere, coincident with a rapid decline in ozone concentrations. Together with other observations this confirms the correctness of the ozone depletion theory as outlined above. In the meanwhile the seriousness of this global problem has been recognized by all nations of the world, and international agreements have been signed to halt the production of CFCs and halons from this year on. Although the cause–effect relationship is very clear, for the layperson as well, it is depressing to see that it is, nevertheless, not accepted by a small group of very vocal critics without any record of achievements in this area of research. Some of these have recently even succeeded in becoming members of the U.S. Congress.

And Things Could Have Been Much Worse

Gradually, over a period of a century or so, stratospheric ozone should recover. However, it was a close call. Had Joe Farman and his colleagues from the British Antarctic Survey not persevered in making their measurements in the harsh Antarctic environment for all those years since the International Geophysical Year 1958/1959, the discovery of the ozone hole may have been substantially delayed, and there may have been far less urgency to reach international agreement on the phasing out of CFC production. There might thus have been a substantial risk that an ozone hole could also have developed in the higher latitudes of the northern hemisphere.

Furthermore, while the establishment of an instability in the O_x/ClO_x system requires chlorine activation by heterogeneous reactions on solid or supercooled liquid particles, this is not required for inorganic bromine, which is normally largely present in its activated forms due to gas-phase photochemical reactions. This makes bromine almost a hundred times more dangerous for ozone than chlorine on an atom to atom basis.[52, 78] This brings up the nightmarish thought that if the chemical industry had developed organobromine compounds instead of the CFCs –or alternatively, if chlorine chemistry had behaved more like that of bromine–—then without any preparedness, we would have been faced with a catastrophic ozone hole everywhere and at all seasons during the 1970s, probably before the atmospheric chemists had developed the necessary knowledge to identify the problem and the appropriate techniques for the necessary critical measurements. Noting that nobody had worried about the atmospheric consequences of the release of Cl or Br before 1974, I can only conclude that we have been extremely lucky, which shows that we should always be on our guard for the potential consequences of the release of new products into the environment. Continued surveillance of the composition of the stratosphere, therefore, remains a matter of high priority for many years ahead.

In the meanwhile, we know that freezing of $H_2SO_4/HNO_3/H_2O$ mixtures to give NAT particle formation does not always occur and that supercooled liquid droplets can exist in the stratosphere substantially below nucleation temperatures, down to the ice freezing temperatures.[79] This can have great significance for chlorine activation.[80, 81] This issue, and its implications for heterogeneous processes, have been under intensive investigation at a number of laboratories, especially in the United States, notably by the groups headed by A. R. Ravishankara at the Aeronomy Laboratory of NOAA, Margaret Tolbert at the University of Colorado, Mario Molina at MIT, Doug Worsnop and Chuck Kolb at Aerodyne, Boston, and Dave Golden at Stanford Research Institute in Palo Alto. I am very happy that a team of young colleagues at the Max-Planck-Institute for Chemistry under the leadership of Dr. Thomas Peter is likewise very successfully involved in experimental and theoretical studies of the physical and chemical properties of stratospheric particles at low temperatures. A highly exciting new finding from this work was that freezing of supercooled ternary $H_2SO_4/HNO_3/H_2O$ mixtures may actually start in the small aerosol size range when air parcels go through orographically induced cooling events. Under these conditions the smaller particles, originally mostly consisting of a mixture of H_2SO_4 and H_2O, will most rapidly be diluted with HNO_3 and H_2O and attain a chemical composition resembling that of a NAT aerosol, which, according to laboratory investigations, can readily freeze.[82, 83]

Biomass Burning in the Tropics

By the end of the 1970s considerable attention was given to the possibility of a large net source of atmospheric CO_2 due to tropical deforestation.[84] Biomass burning is, however, not only a source of CO_2, but also of a great number of photochemically and radiatively active trace gases, such as NO_x, CO, CH_4, reactive hydrocarbons, H_2, N_2O, OCS, and CH_3Cl. Furthermore, biomass burning in the tropics is not restricted to forest conversion, but is also a common activity related to agriculture, involving the burning of savanna grasses, wood, and agricultural wastes. In the summer of 1978, on our way back to Boulder from measurements of the emissions of OCS and N_2O from feedlots in Northeastern Colorado, we saw a big forest fire high up in the Rocky Mountain National Forest, which provided us with the opportunity to collect air samples from a major forest fire plume. After chemical analysis in the NCAR Laboratories by Leroy Heidt, Walt Pollock, and Rich Lueb the emission ratios of the above gases relative to CO_2 could be established. Multiplying these ratios with estimates of the global extent of CO_2 production by biomass burning, estimated to be of the order of $2 \times 10^{15} - 4 \times 10^{15}$ g C per year,[85] we next derived the first estimates of the global emissions of H_2, CH_4, CO, N_2O, NO_x, COS, and CH_3Cl, and could show that the emissions of these gases could constitute a significant fraction of their total global emissions. These first measurements stimulated considerable international research efforts. Except for N_2O (for which our first measurements have since proved incorrect) our original findings were largely confirmed, although large uncertainties in the quantification of the various human activities contributing to biomass burning and individual trace gas releases remain.[86] Because biomass burning releases substantial quantities of reactive trace gases, such as hydrocarbons, CO, and NO_x, in photochemically very active environments, large quantities of ozone were expected to be formed in the tropics and subtropics during the dry season. Several measurement campaigns in South America and Africa, starting in 1979 and 1980 with NCAR's Quemadas expedition in Brazil, have confirmed this expectation.[87–92] The effects of biomass burning are especially

noticeable in the industrially lightly polluted southern hemisphere, as is clearly shown from satellite observations of the tropospheric column amounts of CO and O_3 in Figures 9 and 10.[93, 94]

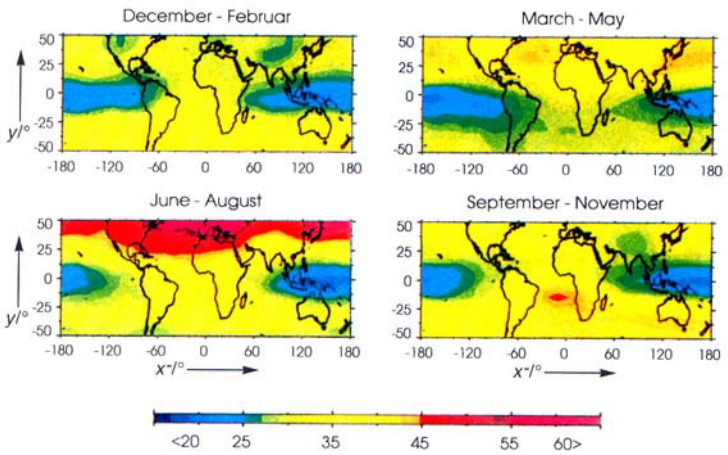

Fig. 9. Observed distributions of vertical column ozone in the troposphere for four seasonal periods in 1994 (from [91, 93]). The color scale is in Dobson units. x = geographic longitude, y = geographic latitude.

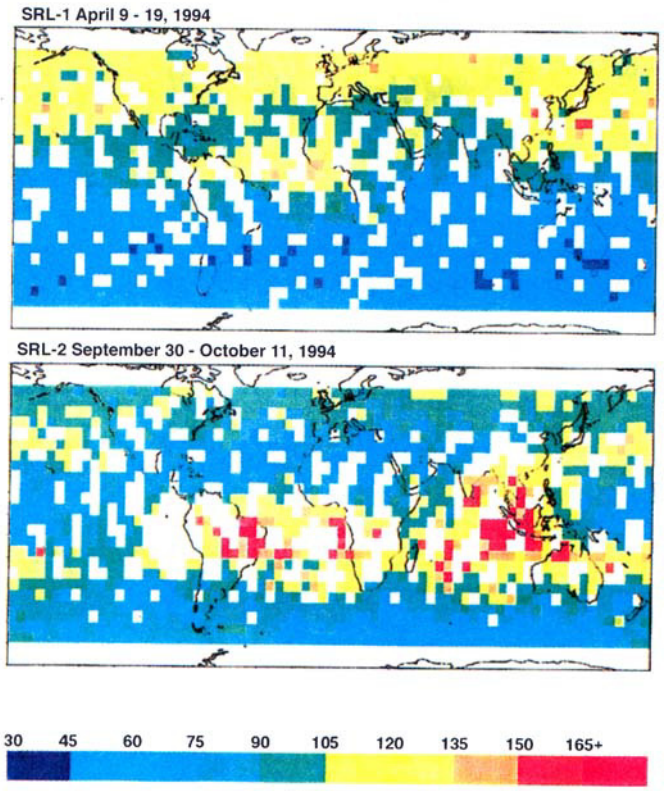

Fig. 10. Observed distribution of vertical column CO in the troposphere, measured on the space shuttle during April and October, 1994 (by courtesy of Dr. Vicki Connors, Dr. Hank Reichle, and the MAPS team [94]). The color scale represents the volume mixing ratios in ppb (1 ppb = 1 nmol per mol).

"Nuclear Winter"

My research interests both into the effects of NO_x on stratospheric ozone and in biomass burning explain my involvement in the "nuclear winter" studies. When in 1981 I was asked by the editor of *Ambio* to contribute to a special issue on the environmental consequences of a major nuclear war, an issue co-edited by Dr. Joseph Rotblat, this year's Nobel Peace Prize awardee, the initial thought was that I would make an update on predictions of the destruction of ozone by the NO_x that would be produced and carried up by the fireballs into the stratosphere.[95, 96] Prof. John Birks of the University of Colorado, Boulder, one of the coauthors of the Johnston study on this topic,[96] who spent a sabbatical in my research division in Mainz, joined me in this study. Although the ozone depletion effects were significant, it was also clear to us that these effects could not compete with the direct impacts of the nuclear explosions. However, we then came to think about the potential climatic effects of the large amounts of sooty smoke from fires in the forests and in urban and industrial centers and oil storage facilities, which would reach the middle and higher troposphere. Our conclusion was that the absorption of sunlight by the black smoke could lead to darkness and strong cooling at the earth's surface, and a heating of the atmosphere at higher elevations, thus creating atypical meteorological and climatic conditions that would jeopardize agricultural production for a large part of the human population.[97] This idea was picked up by others, especially the so-called TTAPS (Turco, Toon, Ackerman, Pollack, Sagan) group,[98] who even predicted that subfreezing temperatures could be possible over much of the earth. This was supported by detailed climate modeling.[99] A major international study of the issue, which was conducted by a group of scientists working under the auspices of SCOPE (Scientific Committee on Problems of the Environment) of the ICSU (International Council of Scientific Unions), also supported the initial hypothesis, and concluded that far more people could die because of the climatic and environmental consequences of a nuclear war than directly because of the explosions.[100, 101]

Although I do not count the nuclear winter idea among my greatest scientific achievements (in fact, the hypothesis can not be tested without performing the "experiment"), I am convinced that, from a political point of view, it is by far the most important, because it magnifies and highlights the dangers of a nuclear war and convinces me that in the long run mankind can only escape such horrific consequences if nuclear weapons are totally abolished by international agreement. I thus wholeheartedly agree in this respect with Joseph Rotblat and the Pugwash organization, this year's recipients of the Nobel Prize for Peace.

Current Research Interests

Realizing the great importance of heterogeneous reactions in stratospheric chemistry, together with my Dutch students Jos Lelieveld (now professor at the University of Utrecht) and Frank Dentener, I have been involved in studies on the effects of reactions taking place in cloud droplets and tropospheric aerosol particles. In general, such reactions result in removal of NO_x and lower concentrations of O_3 and OH.[102, 103] Furthermore, even at high enough NO_x concentrations to allow ozone formation by reactions (16') + (17) + (2), such reactions would be much limited within clouds, because the NO_x molecules, which are only slightly water soluble, stay in the gas phase, while

the HO_2 radicals readily dissolve in the cloud droplets [Eq. (39)], where they can destroy ozone by reaction (40).

$$HO_2(gas) \longrightarrow HO_2(aq) \rightleftarrows H^+ + O_2^- \quad (39)$$

$$O_2^- + O_3 + H^+ \longrightarrow OH + 2O_2 \quad (40)$$

The role of rapid transport of reactive compounds from the planetary boundary layer into the upper troposphere is another topic with which I have been involved with some of my students over the past decade. This may have important effects on the chemistry of the upper troposphere.[104, 105] My great interest in the role of clouds in atmospheric chemistry has brought me in close contact with a major research group at the University of California, San Diego, headed by my good friend Prof. V. Ramanathan.

A new project in which I am currently much interested is the possibility of Cl and especially Br activation in the marine boundary layer. It is already known that Br activation can explain the near-zero O_3 concentrations, which are often found in the high-latitude, marine boundary layer during springtime.[106] In our most recent papers we discuss the possibility that Br activation may also occur in other marine regions and seasons.[107, 108]

The ideas outlined above will be tested by field programs and, if confirmed, introduced in advanced photochemical-transport models. The field programs will be mostly carried out by members of my research division at the Max-Planck-Institute for Chemistry, often in collaboration with other experimental groups. The modeling work is conducted within a consortium of researchers from Sweden, The Netherlands, France, Italy, and Germany. This effort is funded by the European Union and coordinated by Professors Lennart Bengtsson from Hamburg, Henning Rodhe from Stockholm, and Jos Lelieveld from Utrecht.

A Look Ahead

Despite the fundamental progress that has been made over the past decades, much research will be needed to fill major gaps in our knowledge of atmospheric chemistry. In closing I will try to indicate some of those research areas that I consider to be of greatest interest.[109]

Observations of the Tropospheric Ozone

Despite the great importance of tropospheric ozone in atmospheric chemistry, there are still major uncertainties concerning its budget and global concentration distribution. Everywhere, but especially in the tropics and the subtropics, there is a severe lack of data on tropospheric ozone concentrations. Considering the enormous role of tropical ozone in the oxidation efficiency of the atmosphere, the already recognized large anthropogenic impact on ozone through biomass burning, and the expected major agricultural and industrial expansion of human activities in this part of the world, this knowledge gap is very serious. At this stage it is not possible to test photochemical transport models owing to the severe scarcity of ozone observations, especially in the tropics and subtropics. Of critical importance in the effort to obtain data from the tropics and subtropics will be the *training and long-term active participation of scientists from the developing countries.* Besides the ozone measurements at a number of stations and during intensive measurement campaigns, it will be important to also obtain data on reactive hydrocarbons, CO, NO_x, NX, and on chemical constituents in precipitation. Unfortunately, it has been frustrating to note how little response there has been from potential funding agencies to support efforts in this direction.

Long-Term Observations of Properties of the Atmosphere

Two major findings have demonstrated the extreme value of long-term observations of important chemical properties of the atmosphere. One example was the discovery of the rapid depletion of stratospheric ozone over Antarctica during the spring months, as discussed before. Another is the recent, unexpected major, temporary break in the trends of CH_4 and CO. Most surprising were the changes in CO, for which Khalil and Rasmussen[110] derived a downward trend in surface concentrations by $(1.4 \pm 0.9)\%$ per year in the northern hemisphere and by as much as $(5.2 \pm 0.7)\%$ per year in the southern hemisphere between 1987 and 1992. Even larger downward trends, $(6.1 \pm 1)\%$ per year in the northern hemisphere and $(7 \pm 0.6)\%$ per year in the southern hemisphere, were reported for the period between June 1990 and June 1993 by Novelli et al.[111] Although these trends have again reversed (P. Novelli, private communication) into the previous upward trend of $+0.7\%$ per year for CO and almost 1% per year for CH_4,[112, 113] the temporary break is remarkable. The reasons for this surprising behavior are not known. They may consist of a combination of: 1) variable annual emissions from biomass burning, 2) higher concentrations of OH radicals, maybe due to loss of stratospheric ozone, triggered by an increase in reactive aerosol surfaces in the stratosphere following the Pinatubo volcanic eruption in June 1991, 3) a dynamically forced global redistribution of CO, introducing a bias due to the location of the limited number of measuring sites, 4) reduced CO formation from the oxidation of natural hydrocarbons emitted by tropical forests due to globally altered precipitation and temperature patterns, or, most likely, a combination of these and other, yet unknown factors. At this stage we can only conclude that the causes for the surprisingly rapid changes in CO trends are not known, mainly because of incomplete global coverage of the CO measurement network. The same applies for CH_4.

Intensive Measurement Campaigns

Comprehensive field programmes that have been conducted in the past with detailed observations of all factors that influence the photochemistry of the troposphere will also be much needed in the future, especially in various regions of the marine and continental tropics and subtropics, to find out whether we understand the major processes that determine the chemistry of ozone and related photochemically active compounds. Applica-

tions of comprehensive chemical and transport models should be an important part of these activities. Topics in which greatly improved knowledge is necessary are especially the improved quantification of the stratospheric influx of ozone; distributions, sources, and sinks of CH_4, reactive hydrocarbons, CO, NO_x, and NX; and the quantification of natural NO emissions from lightning and soils.

Cloud Transport

The role of clouds as transporters of chemical constituents such as CO, NO_x, reactive hydrocarbons, and their oxidation products from the boundary layer to the middle and upper troposphere (and possibly into the lower stratosphere) should be better understood and quantified, so that they can be parameterized for inclusion in large scale photochemical models of the atmosphere. Similarly the production of NO by lightning and its vertical redistribution by convective storms should also be much better quantified, both for marine and continental conditions. Current uncertainties of NO production by lightning are at least a factor of 4.

Chemical Interactions with Hydrometeors

The interactions of chemical constituents emanating from the boundary layer with liquid and solid hydrometeors in the clouds will be of special importance. There is, for instance, the question of why strong ozone formation has not been noticed around the most convective regions in the continental tropics, in which large amounts of forest-derived reactive hydrocarbons such as isoprene (C_5H_8) and their oxidation products are rapidly lifted to the middle and upper troposphere and mixed with lightning-produced NO to provide favorable conditions for photochemical ozone formation. Could it be that the expected ozone formation is prevented by chemical interactions of the hydrocarbon reaction products and NO_x with the hydrometeors? Could significant ozone destruction take place in cloud water or on the surface of ice particles that may be partially covered by water?[114, 115] Such questions regarding potential loss of ozone by reactions with hydrometeors may be especially relevant in connection with observations of record low O_3 volume mixing ratios often of less than 10 nmol per mol over much of the entire tropospheric column in March 1993 in an extended, heavily convective region between Fiji and Christmas Island over the Pacific Ocean.[116] Although such low ozone volume mixing ratios had been noted on several occasions in the tropical marine boundary layer and can be explained by the ozone-destroying reactions (5)–(8) in the lower troposphere, it should be ascertained whether these reactions alone suffice to explain the extremely low ozone concentrations in such a large volume of air.

Photolysis Rates in Cloudy Atmospheres

Regarding the photochemistry taking place in cloudy atmospheric conditions, recent observations of unexpectedly high absorption of solar radiation in cloudy atmospheres[117] point to the possibility that multiple scattering in broken cloud systems may lead to strongly enhanced photolysis rates and photochemical activity, leading, for example, to much higher O_3 destruction and OH production rates by reactions (7) and (8), or ozone production by reactions (16) + (17) + (2), than thought so far. The influence of clouds on the photochemically active UV radiation field is a potentially very important research topic, which should be pursued by measurements and the development of appropriate radiative transfer models.

Biogenic Sources of Hydrocarbons, CO, and NO

The continental biosphere is a large source of hydrocarbons. Quantification of these sources in terms of geophysical (e.g., temperature, humidity, light levels) and biogeochemical (soil physical and chemical properties, land use) parameters are urgently needed for inclusion in atmospheric models. The hydrocarbon oxidation mechanisms in the atmosphere should also be better understood, so that formation of ozone, carbon monoxide, partially oxidized gaseous hydrocarbons, and organic aerosol can be better quantified. The formation of organic aerosol from hydrocarbon precursors and their capability to serve as cloud condensation nuclei are related, potentially important, subjects that have not been studied in any depth so far.

Potential Role of Halogen Radicals in Ozone Destruction

There are strong indications that tropospheric ozone can be destroyed by reactions in addition to those discussed so far. Observations of surface ozone levels during polar sunrise in the Arctic have frequently shown the occurrence of immeasurably low ozone concentrations, coinciding with high "filterable Br".[106] Further measurements[118] identified BrO as one of the active Br compounds, which, as is well known from stratospheric measurements, may rapidly attack ozone by a series of catalytic reactions, such as the following:

$$2 \times (Br + O_3 \rightarrow BrO + O_2) + (BrO + BrO \rightarrow 2\,Br + O_2) = (2\,O_3 \rightarrow 3\,O_2)$$

or

$$(Br + O_3 \rightarrow BrO + O_2) + (BrO + HO_2 \rightarrow HOBr + O_2) +$$
$$(HOBr + h\nu \rightarrow OH + Br) + (OH + CO + O_2 \rightarrow HO_2 + CO_2)$$
$$= (CO + O_3 \rightarrow CO_2 + O_2).$$

It should be explored whether halogen activation reactions may also occur under different circumstances than indicated above.[105–107]

Heterogeneous Reactions on Aerosol Particles

The issue of interactions between gases and atmospheric aerosol is largely unexplored and very little considered in tropospheric chemistry models. Examples are interactions of dimethylsulfide-derived sulfur compounds with sea salt in the marine boundary layer and reactions of SO_2, H_2SO_4, NO_x, N_2O_5, and HNO_3 on soil dust particles, which remove these

compounds from the gas phase. In the case of industrial SO_2, the neglect of such heterogeneous reactions may well have led to overestimations of the climatic cooling effects of anthropogenic aerosol, as any incorporation of sulfur in soil dust or sea salt will prevent the nucleation of new sunlight backscattering sulfate particles.

Ozone/Climate Feedbacks in the Stratosphere

Ozone is a significant greenhouse gas with an infrared absorption band in the atmospheric window region, centered at 9.6 μm. Although the amount of ozone in the troposphere is only about 10% of that of the stratosphere, the effective long-wave optical depth of tropospheric ozone is larger. Of greatest importance would be any changes that might take place in the ozone concentrations in the tropopause regions as a result of human activities, such as those caused by H_2O, NO, SO_2, and particulate emissions from expanding fleets of civil aircraft flying in the stratosphere and upper troposphere. On one hand this may lead to increasing temperatures in the lower stratosphere. However, increased HNO_3 and H_2O concentrations in the lower stratosphere may increase the likelihood of polar stratospheric particle formation and ozone destruction. Such a course of events is also promoted by cooling of the stratosphere through increasing concentrations of CO_2. This cooling effect also increases with height in the stratosphere and mesosphere. The implications of this for the future dynamics of the stratosphere, mesosphere, and lower thermosphere is likewise a topic deserving considerable attention. Changes in chemical and radiative conditions in the lower stratosphere may, therefore, create feedbacks that we need to understand well. They include understanding their potential impact on tropopause heights and temperatures, stratospheric water vapor, lower stratospheric cloud characteristics, and the tropospheric hydrological cycle. Recent observations of increasing trends of water vapor concentrations in the lower stratosphere over Boulder emphasize this point.[119] All these factors should be taken into account before decisions are taken on vast expansions of aircraft operations in the stratosphere.

In my acknowledgements, I firstly have to thank my parents, my wife, and my family for their love and support, and for creating the personal environment without which nothing will go.

I thank my secretaries Anja Wienhold and Bettina Krüger for their joyful attitude and hard work in sometimes chaotic times, especially in connection with the "Nobel hustle and bustle". Many thanks to Geoff Harris, Mark Lawrence, and Jens-Uwe Grooss for a final reading of the manuscript.

I thank my current and former students, post-docs, and coworkers at the Max-Planck-Institute for Chemistry for their enthusiastic research efforts. Several of them are now professors at universities or directors of major research activities. With most of them I keep a close contact, and we are friends for life.

I also thank the Max-Planck-Society and the various organizations with which I am or have been associated during my scientific career. All of them have been very important in trusting me with long-term funding and in giving me excellent opportunities to do research without major interferences. I am particularly happy to be a member of the NSF Center on the role of Clouds in Atmospheric Chemistry and Climate at the Scripps Institution of Oceanography (SIO) of the University of California, San Diego, where I am learning a lot about clouds, one of the most important elements in the climate system. I thank my good friend Prof. V. Ramanathan and SIO for this great opportunity to rejuvenate myself during a few months of the year.

I thank my director colleagues and the personnel of the Max-Planck-Institute for Chemistry, the University of Mainz, the City of Mainz, and the "Sonderforschungsbereich" for a wonderful welcome and party after my return to Mainz as a fresh Nobel Laureate following a brief vacation in Spain. I will also never forget my "homecoming" at MISU, Stockholm, and the welcome (with illegal fireworks) by my Dutch students and "grandstudents" in Wageningen, The Netherlands.

Finally, I have to thank the many colleagues, all around the world, who have congratulated me on the Nobel Prize award. Many of them have themselves contributed greatly to the remarkable progress in our research field over the past quarter of a century; only a few of these I could recognize in this Novel Lecture. As most of them have written, this is an award to the entire atmospheric chemistry and environmental field. I totally agree and thank you all.

And last but not least, a great Thank You to the Nobel Committee of the Royal Swedish Academy of Sciences. Your decision is an enormous boost for environmental research.

Received: February 29, 1996 [A 149 IE]
German version: *Angew. Chem.* **1996**, *108*, 1878–1898

Keywords: atmospheric chemistry · Nobel lecture · ozone

[1] Sweden's Case Study for the United Nations Conference on the Human Environment 1972: *Air Pollution Across National Boundaries. The Impact on the Environment of Sulfur in Air and Precipitation*, Stockholm, **1972**.
[2] "A theory of upper atmospheric ozone": S. Chapman, *Mem. R. Soc.* **1930**, *3*, 103–125.
[3] "Reconsiderations of the rate constants from the thermal decomposition of ozone": S. W. Benson, A. E. Axworthy, *J. Chem. Phys.* **1965**, *42*, 2614.
[4] "The photochemistry of atmospheric water vapour": D. R. Bates, M. Nicolet, *J. Geophys. Res.* **1950**, *55*, 301.
[5] "Studies of the reaction of excited oxygen atoms and molecules produced in the flash photolysis of ozone": W. D. McGrath, R. G. W. Norrish, *Proc. R. Soc. London A* **1960**, *254*, 317.
[6] "The photolysis of ozone by ultraviolet radiation. The photolysis of ozone mixed with certain hydrogen-containing substances": R. G. W. Norrish, R. P. Wayne, *Proc. R. Soc. London A* **1965**, *288*, 361.
[7] "Chemiluminescent emission observed in the stratosphere and mesosphere": J. Hampson, *Les problèmes météorologiques de la stratosphère et de la mésosphère*, Presses universitaires de France, Paris, **1965**, p. 393.
[8] "Photochemistry of ozone in a moist atmosphere": B. G. Hunt, *J. Geophys. Res.* **1966**, *71*, 1385.
[9] "Determination of parameters appearing in the "dry" and "wet" photochemical theories for ozone in the stratosphere": P. J. Crutzen, *Tellus* **1969**, *21*, 368–388.
[10] "Nitric acid and nitric oxide in the lower stratosphere": D. G. Murcray, T. G. Kyle, F. H. Murcray, W. J. Williams, *Nature* **1968**, *218*, 78.
[11] "Nitric acid vapor above 19 km in the Earth's atmosphere": P. E. Rhine, L. D. Tubbs, D. Williams, *Appl. Opt.* **1969**, *8*, 1501.
[12] "The influence of nitrogen oxides on the atmospheric ozone content": P. J. Crutzen, *Q. J. R. Meteorol. Soc.* **1970**, *96*, 320–325.
[13] "Atmospheric nitrous oxide": D. R. Bates, P. B. Hays, *Planet. Space Sci.* **1967**, *15*, 189.
[14] "Reaction of $O(^1D)$ with N_2O": R. I. Greenberg, J. Heicklen, *Int. J. Chem. Kinet.* **1970**, *2*, 185.
[15] "Ozone production rates in an oxygen–hydrogen–nitrogen oxide atmosphere": P. J. Crutzen, *J. Geophys. Res.* **1971**, *76*, 7311.
[16] "Nitrous oxide. A natural source of stratospheric NO": M. B. McElroy, J. C. McConnell, *J. Atmos. Sci.* **1971**, *28*, 1085.
[17] "Recent kinetic measurements on the reactions of $O(^3P)$, H and HO_2": D. D. Davis et al., **1973**, DOT-TSC-OST-73-4, p. 126.
[18] "Improved absorption cross-sections of oxygen in the wavelength region 205–240 nm of the Herzberg Continuum": K. Yoshino et al., *Planet. Space Sci.* **1988**, *36*, 1469.

[19] "Solar irradiance in the stratosphere: Implications for the Herzberg Continuum Absorption of O_2": J. E. Frederick, J. E. Mentall, *Geophys. Res. Lett.* **1982**, *9*, 461.

[20] "The solar spectral irridiance and its action in the atmospheric photodissociation processes": M. Nicolet, *Planet. Space Sci.* **1981**, *29*, 951.

[21] "The temporal and spatial distribution of tropospheric nitrous oxide": R. F. Weiss, *J. Geophys. Res.* **1981**, *86*, 7185.

[22] SCEP (Study on Critical Environmental Problems): *Man's Impact on the Global Environment. Assessment and Recommendations for Action*, The MIT Press, Cambridge, **1970**.

[23] "Nitrogen oxides in the chemosphere": M. Nicolet, *J. Geophys. Res.* **1965**, *70*, 679.

[24] "Stratospheric ozone with added water vapour: influence of high altitude aircraft": H. S. Harrison, *Science* **1970**, *170*, 734.

[25] "Kinetics of the fast gas phase reaction between ozone and nitric oxide": H. S. Johnston, H. J. Crosby, *J. Chem. Phys.* **1954**, *22*, 689.

[26] "Working Papers for a Survey of Rate Data for Chemical Reactions in the Stratosphere": H. S. Johnston, D. Garvin, *NBS Rep.* **1972**, *10931*.

[27] "Reduction of stratospheric ozone by nitrogen oxide catalysts from supersonic transport exhaust": H. S. Johnston, *J. Geophys. Res.* **1971**, *173*, 517.

[28] "Atmospheric Ozone": H. S. Johnston, *Annu. Rev. Phys. Chem.* **1992**, *43*, 1.

[29] "Photochemistry of NO_x and HNO_x compounds": H. S. Johnston, R. A. Graham, *Can. J. Chem.* **1974**, *52*, 1415.

[30] CIAP (Climate Impact Assessment Program): *Report of Findings: The Effects of Stratospheric Pollution by Aircraft*, US Department of Transportation, Washington, DC, **1974**, DOT-TSC-75-50.

[31] COMESA (The Report of the Committee on Meteorological Effects of Stratospheric Aircraft), UK Meteorological Office, Bracknell, England, **1975**.

[32] COVOS (Comité d'Etudes sur les Conséquences des Vols Stratosphériques), Société Météorologique de France, Boulogne, France, **1976**.

[33] *Environmental Impact of Stratospheric Flight* (Ed.: National Academy of Sciences), Washington, DC, **1975**.

[34] "Solar proton events: Stratospheric sources of nitric oxide": P. J. Crutzen, I. S. A. Isaksen, G. C. Reid, *Science* **1975**, *189*, 457.

[35] "Solar proton event: Influence on stratospheric ozone": D. F. Heath, A. J. Krueger, P. J. Crutzen, *Science* **1977**, *197*, 886.

[36] "Analysis of the August 1972 solar proton event, including chlorine chemistry": S. Solomon, P. J. Crutzen, *J. Geophys. Res.* **1981**, *86*, 1140.

[37] "Normal atmosphere: Large radical and formaldehyde concentrations predicted": H. Levy, *Science* **1971**, *173*, 141.

[38] "Natural sources of atmospheric CO": J. C. McConnell, M. B. McElroy, S. C. Wofsy, *Nature* **1971**, *233*, 187.

[39] "Atmospheric trends and lifetime of trichloroethane and global average hydroxyl radical concentrations based on 1978–1994 ALE/GAGE measurements": R. G. Prinn, R. F. Weiss, B. R. Miller, J. Huang, F. N. Alyea, D. H. Cunnold, P. J. Fraser, D. E. Hartley, P. G. Simmonds, *Science* **1995**, *269*, 187.

[40] "Photochemistry of the lower troposphere": H. Levy III, *Planet. Space Sci.* **1972**, *20*, 919.

[41] "A discussion of the chemistry of some minor constituents in the stratosphere and troposphere": P. J. Crutzen, *Pure Appl. Geophys.* **1973**, *106–108*, 1385.

[42] "Photochemical reactions initiated by an influencing ozone in unpolluted tropospheric air": P. J. Crutzen, *Tellus* **1974**, *26*, 47.

[43] "A photochemical theory of tropospheric ozone": W. L. Chameides, J. C. G. Walker, *J. Geophys. Res.* **1973**, *78*, 8751.

[44] "The origin of ozone in the troposphere": J. Fishman, P. J. Crutzen, *Nature* **1978**, *274*, 855.

[45] "Observational and theoretical evidence in support of a significant in-situ photochemical source of tropospheric ozone": J. Fishman, S. Solomon, P. J. Crutzen, *Tellus* **1979**, *31*, 432.

[46] "Kinetics of the reaction of HO_2 radicals with NO": C. J. Howard, K. M. Evenson, *Geophys. Res. Lett.* **1977**, *4*, 437.

[47] "The effect of the HO_2 + NO reaction rate constant on one-dimensional model calculations of stratospheric ozone depletions": P. J. Crutzen, C. J. Howard, *Pure Appl. Geophys.* **1978**, *116*, 497.

[48] "The changing photochemistry of the troposphere": P. J. Crutzen, P. H. Zimmermann, *Tellus* **1991**, *43 A/B*, 136.

[49] Intergovernmental Panel on Climate Change, *Climate Change: The IPCC Scientific Assessment* (Ed.: J. T. Houghton et al.), Cambridge University Press, **1990**, p. 365.

[50] "Stratospheric chlorine: A possible sink for ozone": R. S. Stolarski, R. J. Cicerone, *Can. J. Chem.* **1974**, *52*, 1610.

[51] "HO_x, NO_x and ClO_x: Their role in atmospheric photochemistry": S. C. Wofsy, M. B. McElroy, *Can. J. Chem.* **1974**, *52*, 1582.

[52] "A review of upper atmospheric photochemistry": P. J. Crutzen, *Can. J. Chem.* **1974**, *52*, 1569.

[53] "Halogenated hydrocarbons in and over the Atlantic": J. E. Lovelock, R. J. Maggs, R. J. Wade, *Nature* **1973**, *241*, 194.

[54] "Stratospheric sink of chlorofluoromethanes: Chlorine atom-catalyzed destruction of ozone": M. J. Molina, F. S. Rowland, *Nature* **1974**, *249*, 810.

[55] "Estimates of possible future ozone reductions from continued use of fluorochloromethanes (CF_2Cl_2, $CFCl_3$)": P. J. Crutzen, *Geophys. Res. Lett.* **1974**, *1*, 205.

[56] "Stratospheric ozone destruction by man-made chlorofluoromethanes": R. J. Cicerone, R. S. Stolarski, S. Walters, *Science* **1974**, *185*, 1165.

[57] "Large losses of total ozone in Antarctica reveal seasonal ClO_x/NO_x interaction": J. C. Farman, B. G. Gardiner, J. D. Shanklin, *Nature* **1985**, *315*, 201.

[58] "On the depletion of Antarctic ozone": S. Solomon, R. R. Garcia, F. S. Rowland, D. J. Wuebbles, *Nature* **1986**, *321*, 755.

[59] "Stratospheric aerosols": C. E. Junge, C. W. Chagnon, J. E. Manson, *J. Meteorol.* **1961**, *18*, 81.

[60] "SO oxidation via the hydroxyl radical: atmospheric fate of the HSO_x radicals": D. D. Davis, A. R. Ravishankara, S. Fischer, *Geophys. Res. Lett.* **1979**, *6*, 113.

[61] "The mechanism of the $HO-SO_2$ reaction": W. R. Stockwell, J. G. Calvert, *Atmos. Environ.* **1983**, *17*, 2231.

[62] "The possible importance of CSO for the sulfate layer of the stratosphere": P. J. Crutzen, *Geophys. Res. Lett.* **1976**, *3*, 73.

[63] "Heterogeneous chemical reactions in the stratosphere": R. D. Cadle, P. J. Crutzen, D. H. Ehhalt, *J. Geophys. Res.* **1975**, *80*, 3381.

[64] "Reaction probabilities of N_2O_5 on aqueous aerosols": M. Mozurkewich, J. G. Calvert, *J. Geophys. Res.* **1988**, *93*, 15889.

[65] "The reaction probabilities of $ClONO_2$ and N_2O_5 on 40 to 75 percent sulfuric acid solutions": D. R. Hanson, A. R. Ravishankara, *J. Geophys. Res.* **1991**, *96*, 17307.

[66] "Temperature dependence of the uptake coefficients of HNO_3, HCl, and N_2O_5 by water droplets": J. M. Van Doren, L. R. Watson, P. Davidovits, D. R. Worsnop, M. S. Zahniser, C. E. Kolb, *J. Phys. Chem.* **1990**, *94*, 3265.

[67] "Detection of NO_3 in the polluted troposphere by differential optical absorption": U. Platt, D. Perner, A. M. Winer, G. W. Harris, J. N. Pitts, Jr., *Geophys. Res. Lett.* **1980**, *7*, 89.

[68] "Stratospheric O_3 and NO_2 observations at the southern polar circle in summer and fall 1988": J. F. Pommereau, F. Goutail, *Geophys. Res. Lett.* **1988**, *15*, 895.

[69] "Nitric acid cloud formation in the cold Antarctic stratosphere: a major cause for the springtime 'ozone hole'": P. J. Crutzen, F. Arnold, *Nature* **1986**, *324*, 651.

[70] "Condensation of HNO_3 and HCl in the winter polar stratosphere": O. B. Toon, P. Hamill, R. P. Turco, J. Pinto, *Geophys. Res. Lett.* **1986**, *13*, 1284.

[71] "Vapor pressures of HNO_3/H_2O solutions at low temperatures": D. R. Hanson, K. Mauersberger, *J. Phys. Chem.* **1988**, *92*, 6167.

[72] "Antarctic stratospheric chemistry of chlorine nitrate, hydrogen chloride and ice": M. J. Molina, T. L. Tso, L. T. Molina, F. C.-Y. Wang, *Science* **1987**, *238*, 1253.

[73] "Reaction of chlorine nitrate with hydrogen chloride and water at Antarctic stratospheric temperatures": M. A. Tolbert, M. J. Rossi, R. Malhotra, D. M. Golden, *Science* **1987**, *238*, 1258.

[74] "Production of Cl_2O_2 from the self-reaction of the ClO radical": L. T. Molina, M. J. Molina, *J. Phys. Chem.* **1987**, *91*, 433.

[75] "High concentration of chlorine monoxide at low altitudes in the Antarctic spring stratosphere, I. Diurnal variation": R. L. de Zafra, M. Jaramillo, A. Parrish, P. M. Solomon, B. Connor, J. Barrett, *Nature* **1987**, *328*, 408.

[76] "Visible spectroscopy at McMurdo Station, Antarctica: Observations of OClO": S. Solomon, G. H. Mount, R. W. Sanders, A. L. Schmeltekopf, *J. Geophys. Res.* **1987**, *92*, 8329.

[77] "Ozone destruction by chlorine radicals within the Antarctic vortex: The spatial and temporal evolution of $ClO-O_3$ anticorrelation based on in situ ER-2 data": J. G. Anderson, W. H. Brune, M. H. Proffitt, *J. Geophys. Res.* **1989**, *94*, 11465.

[78] "The chemistry of atmospheric bromine": S. C. Wofsy, M. B. McElroy, Y. L. Yung, *Geophys. Res. Lett.* **1975**, *2*, 215.

[79] "Particle size distribution in Arctic polar stratospheric clouds, growth and freezing of sulfuric acid droplets, and implications for cloud formation": J. E. Dye, D. Baumgardner, B. W. Gandrud, S. R. Kawa, K. K. Kelly, M. Loewenstein, G. V. Ferry, K. R. Chan, B. L. Gary, *J. Geophys. Res.* **1992**, *97*, 8015.

[80] "Activation of stratospheric chlorine by reactions in liquid sulphuric acid": R. A. Cox, A. R. MacKenzie, R. Müller, T. Peter, P. J. Crutzen, *Geophys. Res. Lett.* **1994**, *21*, 1439.

[81] "Heterogeneous reactions in sulfuric acid aerosol: A framework for model calculations": D. R. Hanson, A. R. Ravishankara, S. Solomon, *J. Geophys. Res.* **1994**, *99*, 3615.

[82] "Size-dependent stratospheric droplet composition in lee wave temperature fluctuations and their potential role in PSC freezing": S. K. Meilinger, T. Koop, B. P. Luo, T. Huthwelker, K. S. Carslaw, P. J. Crutzen, T. Peter, *Geophys. Res. Lett.* **1995**, *22*, 3031.

[83] "Freezing of $HNO_3/H_2SO_4/H_2O$ solutions at stratospheric temperatures: Nucleation statistics and Experiments": T. Koop, B. P. Luo, U. M. Biermann, P. J. Crutzen, T. Peter, noch unveröffentlicht.

[84] "The biota and the world carbon budget": G. M. Woodwell, R. H. Whittaker, W. A. Reiners, G. E. Likens, C. C. Delwiche, D. B. Botkin, *Science* **1978**, *199*, 141.

[85] "Estimates of gross and net fluxes of carbon between the biosphere and the atmosphere from biomass burning": W. Seiler, P. J. Crutzen, *Clim. Change* **1980**, *2*, 207.
[86] "Biomass burning in the Tropics: Impact on atmospheric chemistry and biogeochemical cycles": P. J. Crutzen, M. O. Andreae, *Science* **1990**, *250*, 1669.
[87] "Tropospheric chemical composition measurements in Brazil during the dry season": P. J. Crutzen, A. C. Delany, J. Greenberg, P. Haagenson, L. Heidt, R. Lueb, W. Pollock, W. Seiler, A. Wartburg, P. Zimmerman, *J. Atmos. Chem.* **1985**, *2*, 233.
[88] Amazon Boundary Layer Experiment (ABLE 2A): Dry season 1985, Collection of 24 papers (*J. Geophys. Res.* **1988**, *93 (D2)*, 1349–1624).
[89] "Biomass burning emissions and associated haze layers over Amazonia": M. O. Andreae et al., *J. Geophys. Res.* **1988**, *93*, 1509.
[90] "Ozone and Aitken nuclei over equatorial Africa: Airborne observations during DECAFE 88": M. O. Andreae et al., *J. Geophys. Res.* **1992**, *97*, 6137.
[91] "Identification of widespread pollution in the southern hemisphere deduced from satellite analyses": J. Fishman, K. Fakhruzzaman, B. Cros, D. Nyanga, *Science* **1991**, *252*, 1693.
[92] FOS/DECAFE 91 Experiment, Collection of 13 papers (*J. Atmos. Chem.* **1995**, *22*, 1–239).
[93] "Probing planetary pollution from space": J. Fishman, *Environ. Sci. Technol.* **1991**, *25*, 612.
[94] "Global distribution of biomass burning and carbon monoxide in the middle troposphere during early April and October 1994": V. Connors, M. Flood, T. Jones, B. Gormsen, S. Nolt, H. Reichle in *Biomass Burning and Global Change* (Ed.: J. Levine), MIT Press, **1996**, in press.
[95] "Stratospheric NO production from past nuclear explosions": H. M. Foley, M. A. Ruderman, *J. Geophys. Res.* **1973**, *78*, 4441.
[96] "Effects of nuclear explosions on stratospheric nitric oxide and ozone": H. S. Johnston, G. Whitten, J. W. Birks, *J. Geophys. Res.* **1973**, *78*, 6107.
[97] "The atmosphere after a nuclear war: Twilight at noon": P. J. Crutzen, J. Birks, *Ambio* **1982**, *12*, 114.
[98] "Nuclear winter: Global consequences of multiple nuclear explosion": R. P. Turco, O. B. Toon, R. P. Ackerman, H. B. Pollack, C. Sagan, *Science* **1983**, *222*, 1283.
[99] "Global climatic consequences of nuclear war: Simulations with three-dimensional models": S. L. Thompson, V. Alexandrov, G. L. Stenchikov, S. H. Schneider, C. Covey, R. M. Chervin, *Ambio* **1984**, *13*, 236.
[100] A. B. Pittock, T. P. Ackerman, P. J. Crutzen, M. C. MacCracken, C. S. Shapiro, R. P. Turco, *Environmental Consequences of Nuclear War, Volume I: Physical and Atmospheric Effects, SCOPE 28*, Wiley, New York, **1986**.
[101] M. A. Harwell, T. C. Hutchinson, *Environmental Consequences of Nuclear War, Volume II: Ecological and Agricultural Effects, SCOPE 28*, Wiley, New York, **1985**.
[102] "Influences of cloud photochemical processes on tropospheric ozone": J. Lelieveld, P. J. Crutzen, *Nature* **1990**, *343*, 227.
[103] "Reaction of N_2O_5 on tropospheric aerosols: Impact on the global distributions of NO_x, O_3, and OH": F. J. Dentener, P. J. Crutzen, *J. Geophys. Res.* **1993**, *98 (D14)*, 7149.
[104] "Sulfur dioxide in remote oceanic air: Cloud transport of reactive precursors": R. Chatfield, P. J. Crutzen: *J. Geophys. Res.* **1984**, *89 (D5)*, 711.
[105] "Role of deep convection in the ozone budget of the troposphere": J. Lelieveld, P. J. Crutzen, *Science* **1994**, *264*, 1759.
[106] "Ozone destruction and photochemical reactions at polar sunrise in the lower Arctic atmosphere": L. A. Barrie, J. W. Bottenheim, R. C. Schnell, P. J. Crutzen, R. A. Rasmussen, *Nature* **1988**, *334*, 138.
[107] "Model study indicating halogen activation and ozone destruction in polluted air masses transported to the sea": R. Sander, P. J. Crutzen, *J. Geophys. Res.* **1996**, *101*, 9121.
[108] "A new mechanism for bromine and chlorine release from sea salt aerosol in the unpolluted marine boundary layer": R. Vogt, P. J. Crutzen, R. Sander, *Nature*, in press.
[109] "Overview of tropospheric chemistry: Developments during the past quarter century and a look ahead": P. J. Crutzen, *Faraday Discuss.* **1995**, *100*, 1.
[110] "Global decrease of atmospheric carbon monoxide": M. A. K. Khalil, R. A. Rasmussen, *Nature* **1993**, *370*, 639.
[111] "Recent changes in atmospheric carbon monoxide": P. C. Novelli, K. A. Masario, P. P. Tans, P. M. Lang, *Science* **1994**, *263*, 1587.
[112] "Secular increases in the total vertical abundances of carbon monoxide above central Europe since 1950": R. Zander, P. Demoulin, D. H. Ehhalt, U. Schmidt, C. P. Rinsland, *J. Geophys. Res.* **1989**, *94*, 11021.
[113] "Secular increases of the vertical abundance of methane derived from IR solar spectra recorded at the Jungfraujoch station": R. Zander, P. Demoulin, D. H. Ehhalt, U. Schmidt, *J. Geophys. Res.* **1989**, *94*, 11029.
[114] "Global tropospheric chemistry": P. J. Crutzen in *Low-Temperature Chemistry of the Atmosphere* (Ed.: G. K. Moortgat et al.), Springer, Berlin, **1994**, p. 467–498.
[115] "Ozone in the Troposphere": P. J. Crutzen in *Composition, Chemistry and Climate of the Atmosphere* (Ed.: H. B. Singh), Von Nostrand Reinhold, New York, **1995**, p. 349–393.
[116] "Extremely low upper tropospheric ozone observations in the convective regions of the Pacific": D. Kley, H. G. J. Smit, H. Vömel, S. Oltmans, H. Grassl, V. Ramanathan, P. J. Crutzen, *Science*, submitted.
[117] "Warm pool heat budget and shortwave cloud forcing: a missing physics?": V. Ramanathan, B. Subasilar, G. J. Zhang, W. Conant, R. D. Cess, J. T. Kiehl, H. Grassl, L. Shi, *Science* **1995**, *267*, 499.
[118] "Spectroscopic measurement of bromine oxide and ozone in the high Arctic during Polar Sunrise Experiment 1992": M. Hausmann, U. Platt, *J. Geophys. Res.* **1994**, *99*, 25399.
[119] "Increase in lower-stratospheric water vapour at a mid-latitude northern hemisphere site from 1981 to 1994": S. J. Oltmans, D. J. Hofmann, *Nature* **1995**, *374*, 146.
[120] "A reevaluation of the ozone budget with HALOE UARS data: No evidence for the ozone deficit": P. J. Crutzen, J. U. Grooß, C. Brühl, R. Müller, J. M. Russell III, *Science* **1995**, *268*, 705.

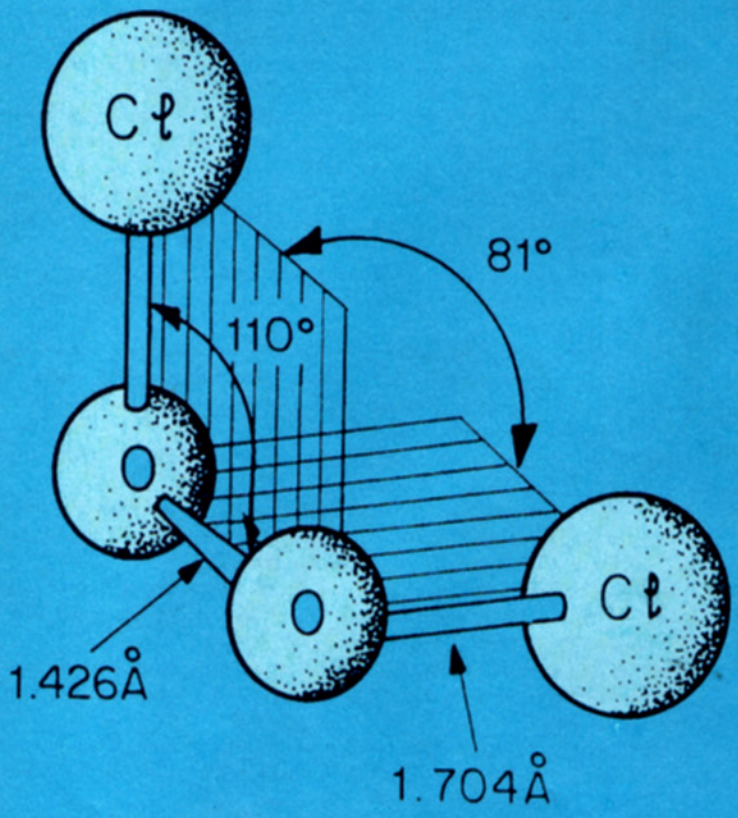

Schematic representation of the chlorine chemistry in the polar stratosphere and the theoretically and experimentally determined structure of the important molecule, chlorine peroxide.

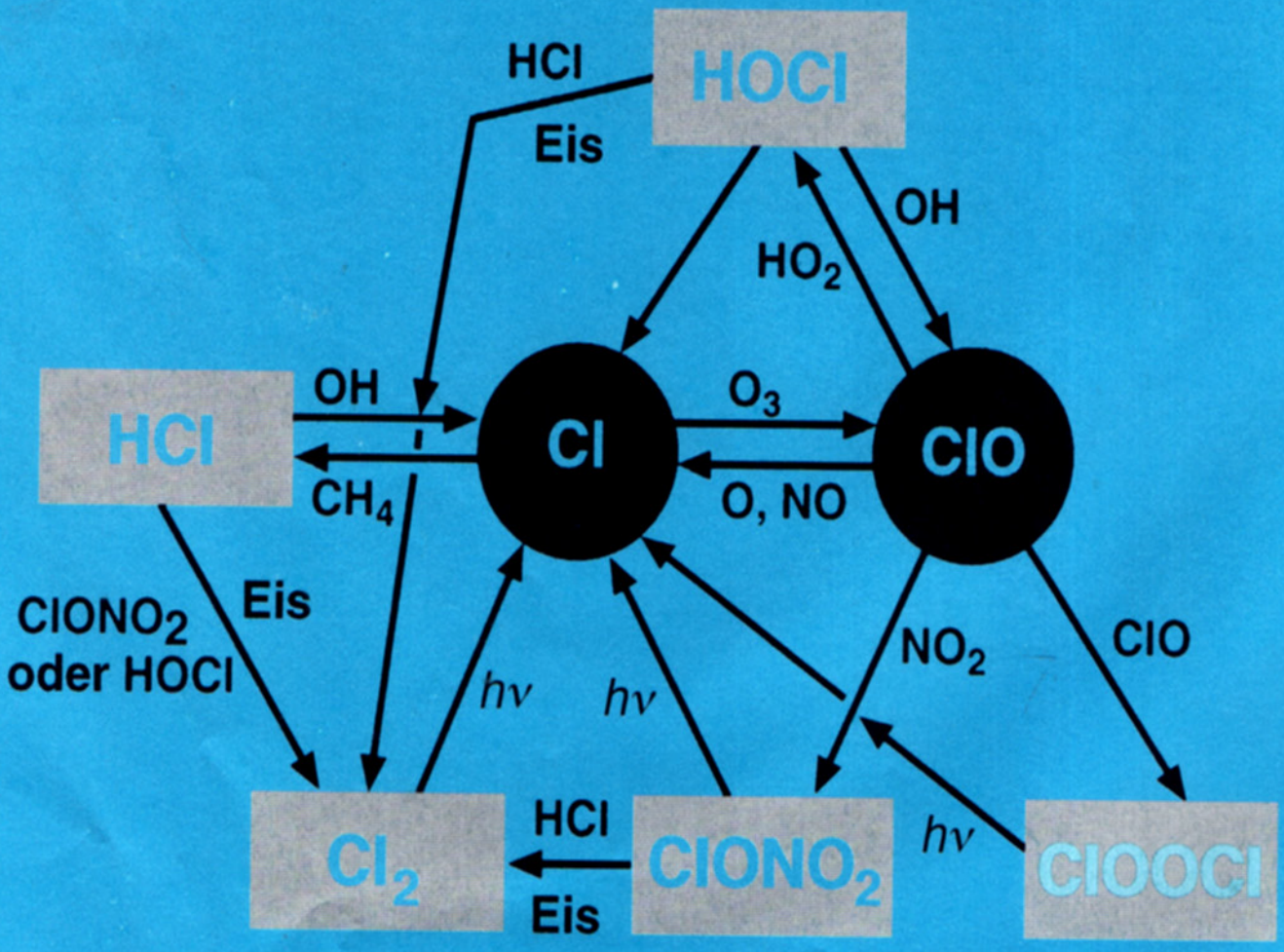

Polar Ozone Depletion (Nobel Lecture)**

Mario J. Molina*

On the rigor of Science

...In that Empire, the Art of Cartography achieved such Perfection that the map of a single Province occupied an entire City, and the map of the Empire an entire Province. With time, those unwieldy maps did not satisfy and the Cartographers raised a Map of the Empire, with the size of the Empire and which coincided with it on every point...

Jorge Luis Borges, *El Hacedor*

Introduction

The ozone layer acts as an atmospheric shield that protects life on earth against harmful ultraviolet radiation from the sun. This shield is fragile: in the past two decades it has become very clear that it can be affected by human activities.

Roughly 90% of the earth's ozone resides in the stratosphere, which is the atmospheric layer characterized by an inverted—that is, increasing—temperature profile that rises typically from about 210 K at its base at 10–15 km altitude, to roughly 275 K at 50 km altitude. The maximum concentration of ozone is several parts per million; it is continuously being produced in the upper stratosphere by the action of solar radiation on molecular oxygen, and continuously being destroyed by chemical processes involving free radicals. Work by Paul Crutzen in the early 1970s[1] established that nitrogen oxides of natural origin, present at parts per billion levels in the stratosphere, are responsible for most of this chemical destruction, which occurs by means of catalytic cycles. Harold Johnston pointed out in 1972[2] that the large fleets of supersonic aircraft, which were being considered at that time, could have seriously affected the ozone layer through their emissions of nitrogen oxides.

In early 1974 F. Sherwood (Sherry) Rowland and I proposed that chlorofluorocarbons (CFCs) would decompose in the stratosphere, releasing chlorine atoms that would catalytically destroy ozone.[3] The CFCs are industrial compounds that have been used as refrigerants, solvents, propellants for spray cans, blowing agents for the manufacture of plastic foams, etc. The two important properties make these compounds very useful: 1) they can be readily transformed from a liquid into a vapor under mild temperature and pressure conditions, as can be seen in Table 1, which displays vapor pressures and boiling points for some of the most common CFCs; and 2) they are chemically very inert and hence nontoxic, nonflammable, and do not decompose inside a spray can or a refrigerator.

Table 1. Physical properties of some common CFCs.

Compound	Formula	Vapor pressure [atm] 260 K	300 K	Boiling point [°C]
CFC-11	$CFCl_3$	0.22	1.12	23.8
CFC-12	CF_2Cl_2	1.93	6.75	−29.8
CFC-113	$CFCl_2CClF_2$	0.08	0.47	47.7

Measurements reported by James Lovelock and co-workers[4] had indicated that the CFCs were accumulating throughout the earth's atmosphere. In our 1974 paper we suggested that the CFCs will not be destroyed by the common cleansing mechanisms that remove most pollutants from the atmosphere, such as rain, or oxidation by hydroxyl radicals. Instead, the CFCs will be decomposed by short wavelength solar ultraviolet radiation, but only after drifting to the upper stratosphere—above much of the ozone layer—where they will first encounter such radiation. Upon absorption of solar radiation the CFC molecules will rapidly release their chlorine atoms, which will then participate in the catalytic reactions (1)–(3).[3, 5]

$$Cl + O_3 \longrightarrow ClO + O_2 \quad (1)$$

$$ClO + O \longrightarrow Cl + O_2 \quad (2)$$

$$O + O_3 \longrightarrow 2O_2 \quad (1) + (2) = (3)$$

These free radical chain reactions are terminated by reactions forming temporary reservoirs, the three most important ones being hydrogen chloride, chlorine nitrate, and hypochlorous acid [Eqs. (4)–(6)]. The free radicals are regenerated by reactions such as (7)–(9).

$$Cl + CH_4 \longrightarrow HCl + CH_3 \quad (4)$$

$$ClO + NO_2 + M \longrightarrow ClONO_2 + M \quad (5)$$

$$ClO + HO_2 \longrightarrow HOCl + O_2 \quad (6)$$

$$HCl + OH \longrightarrow Cl + H_2O \quad (7)$$

$$ClONO_2 + h\nu \longrightarrow Cl + NO_3 \quad (8)$$

$$HOCl + h\nu \longrightarrow Cl + OH \quad (9)$$

[*] Prof. Dr. M. J. Molina
Department of Earth, Atmospheric, and Planetary Sciences
and
Department of Chemistry
Massachusetts Institute of Technology
Cambridge, MA 02139 (USA)
Fax: Int. code +(617) 258-6525
e-mail: mmolina@mit.edu

[**] Copyright© The Nobel Foundation 1996. We thank the Nobel Foundation, Stockholm, for permission to print this lecture.

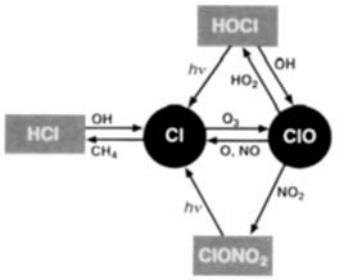

Fig. 1. Schematic representation of chlorine chemistry in the stratosphere at mid and low latitudes.

There are other reactions that affect the chlorine balance in the stratosphere; a schematic representation of the most important ones is shown in Figure 1. The net effect of this chemistry is that the inorganic chlorine produced by the decomposition of the CFCs exists in free radical form—that is, as "active chlorine"—only a few percent of the time. We have published more detailed reviews of stratospheric halogen chemistry; see, for example, Shen et al.[6] and Abbatt and Molina.[7]

In the decade following the publication of our Nature paper, field observations corroborated many of the predictions based on model calculations and on laboratory measurements of reaction rates. However, the effects on ozone were unclear, because the natural ozone levels have relatively large fluctuations.

Ozone Loss in the Polar Atmosphere

The rapid seasonal decline of stratospheric ozone over the South Pole—the so-called Antarctic ozone hole—is a startling phenomenon: a large fraction of the total column ozone (more than a third) disappears in the spring months over an area coinciding largely with the Antarctic continent (Fig. 2). In recent years it has become more severe: in October 1992 and 1993 more than 99% of the ozone disappeared at altitudes between about 14 and 19 km,[8] where concentrations of this species are usually largest; and in 1995, in mid-September, the ozone hole was the largest ever recorded that early in the austral spring.

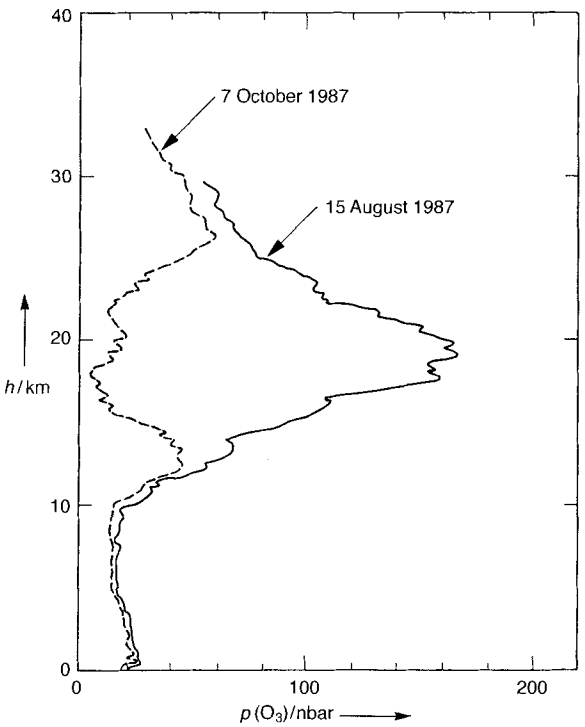

Fig. 2. Balloon measurements of ozone profiles over Halley Bay, Antarctica [30]. $p(O_3)$ = partial pressure of ozone.

Significant ozone depletion over Antarctica started in the early 1980s, but it was not until 1985 that Farman et al.[9] announced their discovery of the ozone hole, suggesting furthermore a possible link with the growth of active chlorine in the stratosphere released by the decomposition of CFCs. Satellite data subsequently confirmed their findings. This discovery was surprising, not only because of the magnitude of the depletion, but also because of its location. We had originally predicted that chlorine-initiated ozone loss would occur in regions of efficient ozone production, that is, predominantly in the upper stratosphere at middle and low latitudes; it is only there that the concentration of free oxygen atoms is large enough for catalytic reactions such as (1) and (2) to occur efficiently. Furthermore, the expectation was that at high latitudes active chlorine would be relatively less abundant, because the reservoir species would be more stable: reactions such as (7) and (8) slow down as a consequence of the decrease in temperature as well as the decrease in solar radiation at the higher zenith angles, that is, the lower sun elevation.

The initial question was, thus, whether the observed polar ozone loss was of human origin, or else merely a periodic natural phenomenon, only never before noticed. A prominent early theory put forth to explain this phenomenon had as a principal cause atmospheric dynamics driven by extreme cold temperatures: the hypothesis was that upon first sunrise in the spring, warming of the Antarctic stratosphere would lead to a net upward lifting of ozone-poor air from the troposphere or lower stratosphere. If so, no ozone destruction would be taking place; it would merely be redistributed periodically. Another theory suggested that the 11-year solar cycle was responsible for the effect: chemical destruction of ozone involving catalytic NO_x cycles would occur, with participation of catalysts generated in the upper stratosphere by high energy particles or by ultraviolet radiation following enhanced solar activity. A third theory suggested that chlorine and bromine free radicals were the catalysts for the chemical destruction of ozone, the source of these radicals being compounds of industrial origin—CFCs and halons (these are compounds containing bromine, which are used as fire extinguishers). This third theory is discussed next in more detail. It is based on our original hypothesis of ozone depletion by CFCs, but it is modified and extended to take into account the peculiar conditions prevailing over Antarctica Figure 3

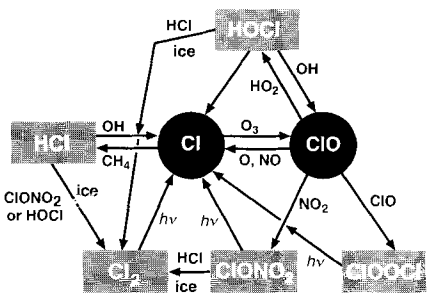

Fig. 3. Schematic representation of chlorine chemistry in the polar stratosphere.

displays schematically the most important reactions of the modified theory (compare to Fig. 1, the original chemistry).

Gas-Phase Chemistry of the Polar Stratosphere

The large solar zenith angle characteristic of the polar stratosphere results in little, if any photodissociation of oxygen, and hence in practically no new ozone production. Similarly, ozone itself photolyzes only rather slowly in those regions, so that the concentration of free oxygen atoms remains very small, particularly in the lower stratosphere where the ozone loss is largest. Consequently, catalytic cycles that require the presence of atomic oxygen are ineffective for ozone destruction, as mentioned above. Several cycles not involving oxygen atoms were proposed after the discovery of the ozone hole, such as the one depicted in Scheme 1, based on the coupling of HO_x and ClO_x radicals.[10]

$$\begin{aligned} &OH + O_3 \longrightarrow HO_2 + O_2 \\ &Cl + O_3 \longrightarrow ClO + O_2 \qquad (1) \\ &ClO + HO_2 \longrightarrow HOCl + O_2 \\ &HOCl + h\nu \longrightarrow OH + Cl \\ &\text{Net: } 2O_3 + h\nu \longrightarrow 3O_2 \end{aligned}$$

Scheme 1. A possible reaction sequence for ozone depletion without the participation of oxygen atoms.

Measurements of the abundance of HOCl in the Antarctic stratosphere indicate, however, that this cycle does not make a major contribution to ozone depletion. McElroy et al.[11] proposed another cycle involving bromine (Scheme 2).

$$\begin{aligned} &Cl + O_3 \longrightarrow ClO + O_2 \qquad (1) \\ &Br + O_3 \longrightarrow BrO + O_2 \\ &ClO + BrO \longrightarrow Cl + Br + O_2 \\ &2O_3 \longrightarrow 3O_2 \end{aligned}$$

Scheme 2. Another possible reaction sequence, which involves bromine, for ozone depletion without participation of oxygen atoms.

The reaction between ClO and BrO regenerates the free atoms in this cycle, but the reaction has actually three channels (Scheme 3). Laboratory investigations have shown that the first and third channels are approximately equally fast, whereas production of BrCl is relatively slow.

$$\begin{aligned} &ClO + BrO \longrightarrow Cl + Br + O_2 \\ &ClO + BrO \longrightarrow BrCl + O_2 \\ &ClO + BrO \longrightarrow Br + OClO \end{aligned}$$

Scheme 3. The three possible reactions between ClO and BrO.

In 1987 we proposed a mechanism involving the self-reaction of ClO to form chlorine peroxide,[12] a compound not previously characterized (Scheme 4, top). The reaction of ClO with itself has three bimolecular channels, as is the case for the ClO + BrO reaction (Scheme 4, bottom). These bimolecular reactions are

$$\begin{aligned} &ClO + ClO + M \longrightarrow Cl_2O_2 + M \\ &Cl_2O_2 + h\nu \longrightarrow 2Cl + O_2 \\ &2Cl + 2O_3 \longrightarrow 2ClO + 2O_2 \qquad 2\times(1) \\ &\text{Net: } 2O_3 + h\nu \longrightarrow 3O_2 \\ &ClO + ClO \longrightarrow Cl_2 + O_2 \\ &ClO + ClO \longrightarrow Cl + ClOO \\ &ClO + ClO \longrightarrow Cl + OClO \end{aligned}$$

Scheme 4. Postulated ozone depletion by participation of Cl_2O_2 (top) and the three possible reactions between two ClO molecules (bottom).

too slow to be of importance in the atmosphere. However, the termolecular reaction that leads to the formation of chlorine peroxide can occur efficiently in the lower stratosphere at high latitudes, as it is facilitated by the lower temperatures and higher pressures prevailing in those regions.

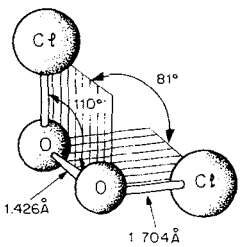

Fig. 4. Structure of chlorine peroxide [14].

The structure of the product formed in the termolecular ClO self-reaction has been shown by both theory[13] and experiment[14] to be indeed ClOOCl, rather than ClOClO (Fig. 4). Furthermore, photodissociation of ClOOCl yields predominantly Cl atoms, rather than ClO radicals, as we and others have shown in laboratory experiments.[15, 16] Formation of ClOO is also possible; however, even under polar stratospheric conditions ClOO rapidly decomposes to yield free chlorine atoms, since the Cl–OO bond strength is only about 5 kcal mol^{-1}.

Polar Stratospheric Clouds

In contrast to the troposphere, the stratosphere is extremely dry and practically cloudless. The concentration of water vapor is measured in parts per million, and is, in fact, comparable to that of ozone. Normally, there is a thin layer of aerosol throughout the lower stratosphere—a haze—first described in 1961 by Junge and co-workers.[17] The aerosol's droplets are mostly liquid and consist of supercooled aqueous sulfuric acid solutions (about 75% H_2SO_4 by weight at mid and low latitudes, with a radius of roughly 0.1 μm). The "background" number density falls typically in the 1–10 cm^{-3} range, but it may increase by between one and two orders of magnitude following the injection of SO_2 directly into the stratosphere by major volcanic eruptions, such as El Chichon in 1982 and Mount Pinatubo in 1991. The SO_2 is oxidized in the stratosphere to form H_2SO_4 on a time scale of months, and the excess particles decay over a period of a few years. SO_2 emitted at the earth's surface by processes such as the combustion of coal is mostly oxidized and removed from the atmosphere (as acid rain) before reaching the stratosphere. The background aerosols arise mainly from OCS, which is also emitted at the earth's surface but is sufficiently

stable to reach the stratosphere, where it photooxidizes to yield SO_2 and subsequently H_2SO_4.

Polar stratospheric clouds (PSCs) form seasonally over the polar regions. Satellite-based instruments have been monitoring these clouds long before the discovery of the ozone hole by observing the attenuation of sunlight, which is scattered at wavelengths characteristic of the size of the cloud particles. In the winter and spring months, sharp increases in the attenuation resulting from the presence of PSCs are evident, followed by a decrease in the summer after the cloud particles evaporate or sediment out.

The PSC particles form by condensation of vapors on the pre-existing sulfuric acid aerosols. Observations have also indicated the existence of different types of clouds, the two most common ones being often referred to as Type I and Type II PSCs. The latter are present only when the temperatures fall below the frost point of water, which is typically about 185–187 K; the particles are roughly 10 μm in diameter and are composed principally of water-ice crystals. The Type II clouds are more prevalent over Antarctica, because of its lower temperatures compared to the Arctic. Type I PSCs are observed more frequently, forming at temperatures above the frost point of water but below 190–195 K, with particle diameters of roughly one micrometer. Thermodynamic considerations coupled with laboratory experiments indicate that Type I PSC particles consist most likely of nitric acid trihydrate (NAT), which is the most stable condensed phase under the conditions leading to the formation of these clouds. However, more recent laboratory experiments indicate that the aerosol particles are not likely to freeze at temperatures above the water frost point.[18] Furthermore, investigations performed in the field[19] and in the laboratory[20, 21] indicate that the liquid sulfuric acid droplets should absorb significant amounts of nitric acid and water vapor under polar stratospheric conditions, and a very rapid change in composition (and hence size) should occur over a narrow temperature range,[22, 23] thus explaining the formation of Type I clouds below a certain temperature threshold. Hence, it appears that Type I PSCs are sometimes liquid—particularly over the Arctic—and sometimes solid.

Chemistry on Cloud Particles

Laboratory experiments, field observations, and atmospheric modeling calculations have now established that chemical reactions occurring on PSC particles play a central role in polar ozone depletion. These reactions have two separate effects, referred to as chlorine activation and nitrogen deactivation: first, chlorine is transferred from the relatively inert reservoir compounds HCl and $ClONO_2$ into forms that can be readily photolyzed (mostly Cl_2); and second, nitrogen oxides are removed from the gas phase, through incorporation of nitric acid into the PSCs, thus preventing the formation of $ClONO_2$, a species that interferes with the catalytic chlorine cycles that destroy ozone. In fact, some PSC particles grow large enough to precipitate, permanently removing nitric acid from the stratosphere; this process is labeled denitrification.

Of the key chlorine activation reactions [Eqs. (10)–(12)], the most important is (10). Our early laboratory experiments indi-

$$ClONO_2 + HCl \longrightarrow Cl_2 + HNO_3 \quad (10)$$

$$ClONO_2 + H_2O \longrightarrow HOCl + HNO_3 \quad (11)$$

$$HOCl + HCl \longrightarrow Cl_2 + H_2O \quad (12)$$

cated that this reaction does not occur in the gas phase at significant rates.[24] However, we noticed in those experiments that this and other reactions involving chlorine nitrate are very sensitive to surface effects; similar observations had been reported by Sherry Rowland's group. In 1986 Solomon et al.[10] suggested that reactions (10) and (11) would be promoted by PSCs, setting the stage for efficient ozone depletion over Antarctica. In 1987 we carried out a series of laboratory measurements showing that reaction (10) is indeed remarkably efficient, requiring only a few collisions of the reactant $ClONO_2$ with ice exposed to HCl vapor.[25] This peculiar chemical reactivity of ice was surprising; in contrast to liquid water—and the well-established chemistry of aqueous ions—reactions promoted by ice at temperatures down to 180 K were unprecedented. Our results were subsequently corroborated by several other groups (for a review, see Kolb et al.[26]).

Mechanism for Chlorine Activation Reactions

The net effect of reactions (11) and (12) occurring sequentially is reaction (10), which suggests that the mechanism for this last reaction involves the two steps (11) and (12). Also, while the high efficiency of reaction (11) on ice is understandable—the reactant H_2O is already in condensed phase—both reactants for reaction (10) are originally in the gas phase; hence, it proceeds most likely through sequential, rather than simultaneous collisions of the reactants with the surface. This implies that at least one of the reactants, most likely HCl, has a high affinity for the condensed phase. Previous measurements had shown, though, that HCl is only sparingly soluble in ice; more recent investigations have indicated, however, that monolayer amounts of HCl are taken up by the ice surface under temperature and HCl partial pressure conditions similar to those prevailing in the polar stratosphere.[26, 27]

Physical adsorption of HCl is expected to incorporate only negligible amounts of HCl on the ice surface,[28] even allowing for a very strong hydrogen bond. These expectations led early on to the suggestion that reaction (10) should not occur on ice under stratospheric conditions of temperature and HCl partial pressure, and the results of laboratory measurements were considered to be artifacts resulting from grain boundary effects.

The high affinity of HCl for the ice surface can be explained, however, by assuming that the HCl solvates, forming hydrochloric acid, as is the case with liquid water. This process is exothermic by about 18 kcal mol^{-1}; in contrast, a hydrogen bond of HCl with ice is estimated to be only 5 kcal mol^{-1}. Solvation can occur because the surface layers of ice are disordered and the water molecules there have much larger mobility than in the bulk crystal. This behavior leads to the formation of a quasi-liquid layer on the ice surface, which can be experimentally observed at temperatures down to about 240 K. The presence of HCl strongly depresses the freezing point (a 9-molal HCl solu-

tion freezes at about 190 K), with the result that formation of a quasi-liquid HCl solution layer appears plausible under polar stratospheric conditions.[28] Furthermore, the large reaction probabilities for reactions (10) and (12) can be understood with the quasi-liquid layer model: the mechanism for these reactions most likely involves aqueous-like ions. In contrast, adsorbed molecular HCl is expected to behave rather similarly to gaseous HCl, and hence should react only very slowly with $ClONO_2$, as noted above.

Laboratory measurements of the uptake of HCl by NAT have also been conducted. For NAT, however, an additional parameter that needs to be taken into account is its H_2O vapor pressure: at any given temperature it can have a range of values, whereas for water-ice it has, of course, only one value. Observations show that when the H_2O vapor pressure of NAT approaches that of ice its surface takes up as much HCl as ice, whereas the amount decreases by more than two orders of magnitude as the H_2O vapor pressure drops. The reaction probabilities for reactions (10) and (12) behave accordingly: they have large values when the H_2O vapor pressure of NAT is within a factor of about 3 of that of ice.[26, 29] It appears that the uptake as well as the reaction probabilities are controlled by the availability of water at the surface.

The chlorine activation reactions (10–12) occur rather slowly on sulfuric acid aerosols at mid latitudes, because HCl is only very sparingly soluble in relatively concentrated H_2SO_4 solutions, and because the water in those solutions is not available for reaction with $ClONO_2$. However, as the temperature drops towards high latitudes and the sulfuric acid solution becomes more dilute, the HCl becomes more soluble, and the efficiency of these reactions increases dramatically over a relatively narrow temperature range: under conditions of thermodynamic stability for Type I PSCs, chlorine activation occurs rapidly on both liquid and solid particles.[20]

Measurements of Key Species over Antarctica

Beginning in 1986, a series of field experiments were designed to test the various hypotheses that had been put forth to explain the Antarctic ozone hole. For example, observations of upward flow in the polar stratosphere would have verified the "dynamics only" theory. The solar cycle theory would have been supported by observations of high NO_x levels in regions where ozone was being depleted; furthermore, according to this theory in years of low solar activity the polar stratosphere would recover to normal pre-ozone hole conditions. In contrast, expectations from the halogen theory were low levels of nitrogen oxides, and high levels of active chlorine.

The first observational campaign designed to test these theories, the National Ozone Experiment (NOZE), was mounted in the winter of 1986. The NOZE scientists, based at McMurdo, Antarctica, and led by Susan Solomon, performed remote sensing measurements of key stratospheric species such as NO_2, O_3, and chlorine free radicals. Their findings provided the first evidence that the chemistry of the Antarctic stratosphere was highly perturbed, and the halogen chemistry mechanism appeared most likely. A second NOZE campaign, as well as the Airborne Antarctic Ozone Experiment (AAOE) were conducted in 1987. This expedition was based at Punta Arenas, Chile: the results from flights conducted over a six week period largely confirmed and extended the results from the NOZE experiment. The observations provided very clear evidence of a strong downward flow within the Antarctic polar vortex, which is the region of the stratosphere where the ozone hole develops: contrary to predictions based on the dynamics only theory, the levels of tracers such as the CFCs, CH_4, and N_2O were typical of air coming from higher altitudes—"aged" air which had been exposed to short-wavelength ultraviolet radiation. Furthermore, the concentration of NO_x was remarkably low, in contrast with expectations from the solar cycle theory.

The chemical CFC–halogen hypothesis received strong support from the results of the field experiments. The measurements conducted by James Anderson and co-workers[31] showed that the ClO concentrations in the polar vortex were greatly enhanced (Fig. 5), revealing that more than half of the

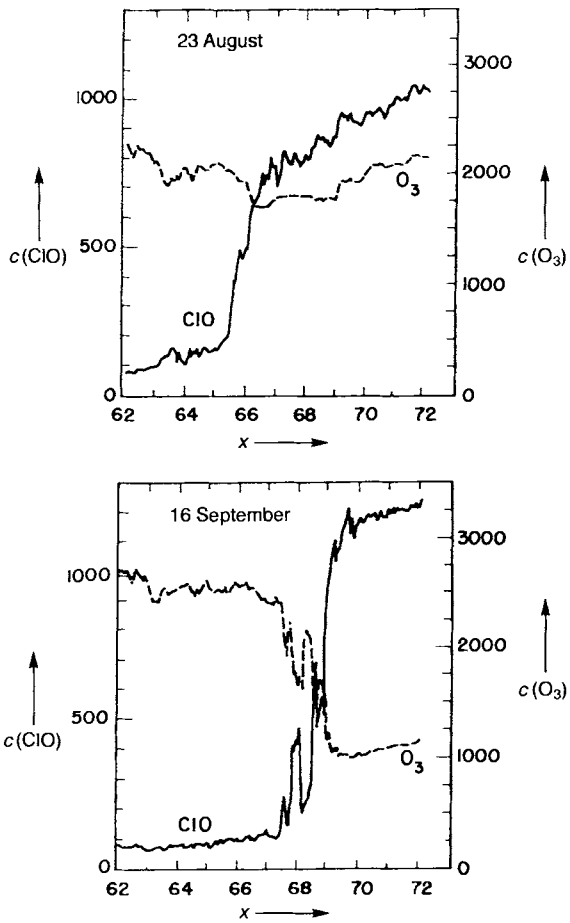

Fig. 5. Mixing ratios c (in ppb) of ClO and ozone measured in 1987 during the AAOE expedition; adapted from Ref. [31]. x = latitude (degrees south).

chlorine was present there as a free radical—chlorine that had been released in the stratosphere at lower latitudes by the decomposition of the CFCs. These measurements, coupled with the observations of the rate of disappearance of ozone, indicated that the chlorine peroxide cycle that we had suggested (Scheme 4, top) was responsible for more than two-thirds of the ozone loss. Most of the rest of the loss resulted from bromine chemistry.

The unique instruments required for all these experiments, as well as the halogen hypothesis itself, were developed in a relatively short time. The community was well prepared for these new developments, since it had vigorously continued for over a decade the pursuit of scientific research on the stratospheric ozone issue.

Conclusions

Much remains to be learned about stratospheric chemistry—and, in more general terms, about the physics and chemistry of the global atmosphere. On the other hand, the cause–effect relationship between human-produced chemicals and ozone depletion is rather well established now: the signals connected with the Antarctic ozone hole are very large indeed. The stratospheric ozone issue has shown us that mankind is quite capable of significantly affecting the atmosphere on a global scale: the most striking effects of CFCs, which are emitted mostly in the north, are seen as far away as possible from the sources, namely over the South Pole. This global problem has also shown us that different sectors of society can work together—the scientific community, industry, environmental organizations, government representatives, and policy makers—to reach international agreements: the Montreal Protocol on Substances that Deplete the Ozone Layer has established a very important precedent for the solution of global environmental problems.

Biographical Notes

Finally, a short resumé of my life. I was born in Mexico City on March 19, 1943, the son of Roberto Molina Pasquel and Leonor Henriquez de Molina. My father was a lawyer in private practice, but he also taught at the National University of Mexico (Universidad Nacional Autonoma de Mexico (UNAM)). In his later years, after I had left Mexico, he served as Mexican Ambassador to Ethiopia, Australia, and the Philippines. I was already fascinated by science before entering high school. Aware of my interest in chemistry, my parents kept with the family tradition of sending children abroad for a couple of years and sent me to a boarding school in Switzerland when I was 11 years old, on the assumption that German was an important language for a prospective chemist to learn. After finishing my undergraduate studies in Mexico with the aim of becoming a research chemist, I spent nearly two years doing research in kinetics of polymerizations at the University of Freiburg, Germany. Subsequently, I returned to Mexico as an Assistant Professor at the UNAM and set up the first graduate program in chemical engineering. Finally, to broaden my background and to explore other research areas, I began my graduate studies in physical chemistry in 1968 at the University of California at Berkeley in the research group of Professor George C. Pimentel. There I met Luisa Tan, a fellow graduate student in Pimentel's group, who later became my wife and close scientific collaborator. We have one son.

M. J. Molina

After completing my Ph.D. degree on the investigation of the distribution of internal energy in the products of chemical and photochemical reactions in 1972, I joined the group of Professor F. Sherwood (Sherry) Rowland as a postdoctoral fellow in 1973 and chose to study the environmental fate of CFCs.

In 1975 I was appointed as a member of the faculty at the University of California, Irvine and set up an independent program to investigate chemical and spectroscopic properties of compounds of atmospheric importance, focusing on those that are unstable and difficult to handle in the laboratory, such as HClO, ClONO, $ClONO_2$, and $HOONO_2$.

Although my seven years at Irvine were very productive, I missed not doing experiments myself because of the many responsibilities associated with a faculty position. I decided to move to a nonacademic position and joined the Molecular Physics and Chemistry Section at the Jet Propulsion Laboratory in 1982. Around 1985 after becoming aware of the discovery by Joseph Farman and his co-workers of the seasonal depletion of ozone over Antarctica, my research group at JPL investigated the peculiar chemistry promoted by polar stratospheric clouds. In 1989 I returned to academic life at the Massachusetts Institute of Technology, where I have continued with research on global atmospheric chemistry issues. Although I no longer spend much time in the laboratory, I very much enjoy working with my graduate and postdoctoral students, who provide me with invaluable intellectual stimulus. I have also benefited from teaching; as I try to explain my views to students with critical and open minds, I find myself continually challenged to go back and rethink ideas. I now see teaching and research as complementary, mutually reinforcing activities.

One of the very rewarding aspects of my work has been the interaction with a superb group of colleagues and friends in the atmospheric sciences community. I truly value these friendships, many of which go back 20 years or more, and which I expect to continue for many more years to come. I feel that this Nobel Prize represents a recognition for the excellent work that has been done by my colleagues and friends in the atmospheric chemistry community on the stratospheric ozone depletion issue. Many colleagues and collaborators have contributed to the work described above; while only some of them have been mentioned here, I would like to express my appreciation to all of them. I am grateful to my past and present students and associates for their dedication in carrying out research in my laboratory. I am especially indebted to my wife, Luisa, who has been my closest collaborator for many years. I also want to acknowledge the sponsors of our research, which have included the National Aeronautics and Space Administration and the National Science Foundation.

Received: March 4, 1996 [A 155 IE]
German version: *Angew. Chem.* **1996**, *108*, 1900

[1] "The Influence of Nitrogen Oxides on Atmosphere Ozone Content": P. J. Crutzen, *Q. J. R. Meteorol. Soc.* **1970**, *96*, 320–325.
[2] "Reduction of Stratospheric Ozone by Nitrogen Oxide Catalysts from Supersonic Transport Exhaust": H. S. Johnston, *Science* **1971**, *173*, 517–522.
[3] "Stratospheric Sink for Chlorofluoromethanes: Chlorine Catalysed Destruction of Ozone": M. J. Molina, F. S. Rowland, *Nature* **1974**, *249*, 810–814.

[4] "Halogenated Hydrocarbons in and over the Atlantic": J. E. Lovelock, R. J. Maggs, R. J. Wade, *Nature* **1973**, *241*, 194–196.
[5] "Stratospheric Chlorine: A Possible Sink for Ozone": R. S. Stolarski, R. Cicerone, *Can. J. Chem.* **1974**, *52*, 1610–1615.
[6] "Stratospheric Pollution and Ozone Depletion": T.-L. Shen, P. J. Wooldridge, M. J. Molina in *Composition, Chemistry, and Climate of the Atmosphere* (Ed.: H. B. Singh). Van Nostrand Reinhold, New York, **1995**.
[7] "Status of Stratospheric Ozone Depletion": J. P. D. Abbatt, M. J. Molina, *Annu. Rev. Energy Environ.* **1993**, *18*, 1–29.
[8] "Scientific Assessment of Ozone Depletion 1994": World Meteorological Organization, *WMO Global Ozone Research and Monitoring Project, Report No. 37*, **1995**.
[9] "Large Losses of Total Ozone in Antarctica Reveal Seasonal ClO_x/NO_x Interactions": J. C. Farman, B. G. Gardiner, J. D. Shanklin, *Nature* **1985**, *315*, 207–210.
[10] "On the Depletion of Antarctic Ozone": S. Solomon, R. R. Garcia, F. S. Rowland, D. J. Wuebbles, *Nature* **1986**, *321*, 755–758.
[11] "Reduction of Antarctic Ozone due to Synergistic Interactions of Chlorine and Bromine": M. B. McElroy, R. J. Salawitch, S. C. Wofsy, J. A. Logan, *Nature* **1986**, *321*, 759–762.
[12] "Production of the Cl_2O_2 from the Self-Reaction of the ClO Radical": L. T. Molina, M. J. Molina, *J. Phys. Chem.* **1987**, *91*, 433–436.
[13] "Structures, Relative Stabilities, and Vibrational Spectra of Isomers of Cl_2O_2: The Role of Chlorine Oxide Dimer in Antarctic Ozone Depleting Mechanism": M. P. McGrath, K. C. Clemitshaw, F. S. Rowland, W. G. Hehre, *J. Phys. Chem.* **1990**, *94*, 6126–6132.
[14] "The Rotational Spectrum and Structure of Chlorine Peroxide": M. Birk, R. R. Friedl, E. A. Cohen, H. M. Pickett, S. P. Sander, *J. Chem. Phys.* **1989**, *91*, 6588–6597.
[15] "Quantum Yield of Chlorine-Atom Formation in the Photodissociation of Chlorine Peroxide (ClOOCl) at 308 nm": M. J. Molina, A. J. Colussi, L. T. Molina, R. N. Schindler, T.-L. Tso, *Chem. Phys. Lett.* **1990**, *173*, 310–315.
[16] "The Stability and Photochemistry of Dimers of the ClO Radical and Implications for Antarctic Ozone Depletion": R. A. Cox, G. D. Hayman, *Nature* **1988**, *332*, 796–800.
[17] "Stratospheric Aerosols": C. E. Junge, C. W. Chagnon, J. E. Manson, *J. Meteorol.* **1961**, *18*, 81–108.
[18] "Do Stratospheric Aerosol Droplets Freeze Above the Ice Frost Point?": T. Koop, U. M. Biermann, W. Raber, B. Luo, P. J. Crutzen, T. Peter, *Geophys. Res. Lett.* **1995**, *22*, 917–920.
[19] "Stratospheric Aerosol Increases and Ozone Destruction: Implications from Mass Spectrometer Measurements": F. Arnold, *Ber. Bunsenges. Phys. Chem.* **1992**, *96*, 339–350.
[20] "Vapor Pressure Measurements for the $H_2SO_4/HNO_3/H_2O$ and $H_2SO_4/HCl/H_2O$ Liquid Systems, Incorporation of Stratospheric Acids into Background Sulfate Aerosols": R. Zhang, P. J. Wooldridge, M. J. Molina, *J. Phys. Chem.* **1993**, *97*, 8541–8548.
[21] "Physical Chemistry of the $H_2SO_4/HNO_3/H_2O$ System: Implications for Polar Stratospheric Clouds": M. J. Molina, R. Zhang, P. J. Wooldridge, J. R. McMahon, J. E. Kim, H. Y. Chang, K. D. Beyer, *Science* **1993**, *261*, 1418–1423.
[22] "Composition and Freezing of Aqueous H_2SO_4/HNO_3 Solutions under Polar Stratospheric Conditions": K. D. Beyer, S. W. Seago, H. Y. Chang, M. J. Molina, *Geophys. Res. Lett.* **1994**, *21*, 871–874.
[23] "Stratospheric Aerosol Growth and HNO_3 Gas Phase Depletion from Coupled HNO_3 and Water Uptake by Liquid Particles": K. S. Carslaw, B. P. Luo, S. L. Clegg, T. Peter, P. Brimblecombe, P. J. Crutzen, *Geophys. Res. Lett.* **1994**, *21*, 2479–2482.
[24] "An Upper Limit to the Rate of the HCl + $ClONO_2$ Reaction": L. T. Molina, M. J. Molina, R. A. Stachnick, R. D. Tom, *J. Phys. Chem.* **1985**, *89*, 3779–3781.
[25] "Antarctic Stratospheric Chemistry of Chlorine Nitrate, Hydrogen Chloride and Ice: Release of Active Chlorine": M. J. Molina, T.-L. Tso, L. T. Molina, F. C.-Y. Wang, *Science* **1987**, *238*, 1253–1257.
[26] "Laboratory Studies of Atmospheric Heterogeneous Chemistry": C. E. Kolb, D. R. Worsnop, M. S. Zahniser, P. Davidovits, C. F. Keyser, M.-T. Leu, M. J. Molina, D. R. Hanson, A. R. Ravishankara, L. R. Williams, M. A. Tolbert in *Advances in Physical Chemistry Series* (Current Problems and Progress in Atmospheric Chemistry) (Ed.: J. R. Barker), World Scientific Publishing, **1995**.
[27] "Interaction of HCl Vapor with Water-Ice: Implications for the Stratosphere": J. P. D. Abbatt, K. D. Beyer, A. F. Fucaloro, J. R. McMahon, P. J. Wooldridge, R. Zhang, M. J. Molina, *J. Geophys. Res.* **1992**, *97*, 15819–15826.
[28] "The Probable Role of Stratospheric 'Ice' Clouds: Heterogeneous Chemistry of the Ozone Hole": M. J. Molina in *Chemistry of the Atmosphere: The Impact of Global Change* (Ed.: J. G. Calvert), Blackwell, Oxford, **1994**.
[29] "Heterogeneous Interactions of $ClONO_2$ and HCl on Nitric Acid Trihydrate at 202 K": J. P. D. Abbatt, M. J. Molina, *J. Phys. Chem.* **1992**, *96*, 7674–7679.
[30] "What Hope for the Ozone Layer Now?" J. C. Farman, *New Scientist* **1987**, *116* (1586), 50–54.
[31] "Ozone Destruction by Chlorine Radicals within the Antarctic Vortex: The Spatial and Temporal Evolution of $ClO-O_3$ Anticorrelation Based on In Situ ER-2 Data": J. G. Anderson, W. H. Brune, M. H. Proffitt, *J. Geophys. Res.* **1989**, *94*, 11465–11479.

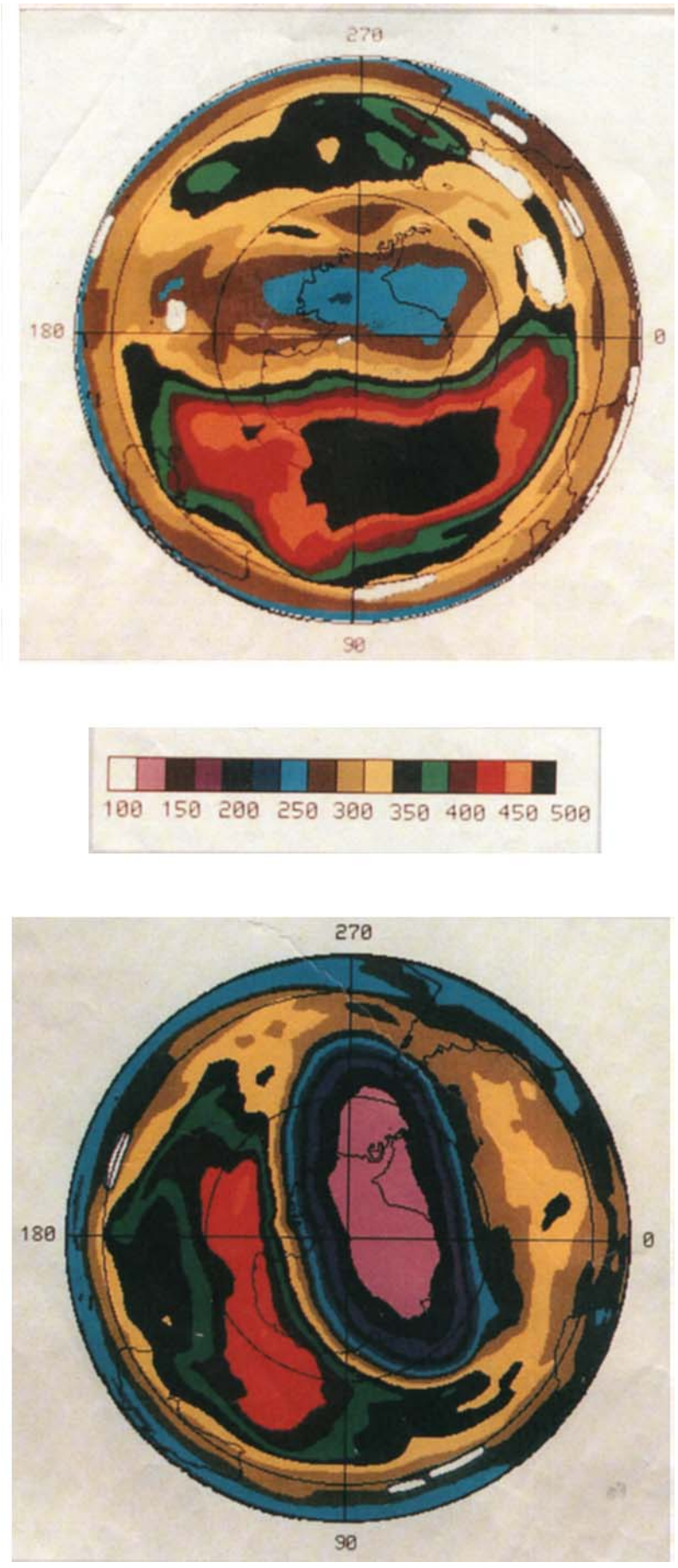

These images from the NASA TOMS (Total Ozone Mapping Spectrometer) satellite of October 3, 1979 (top) and October 4, 1992 (bottom) clearly show how the total ozone concentration has changed in spring over the southern hemisphere. The color key (in Dobson Units) interprets the measurements. The data return from October 3, 1979, was flawed, and missing data are shown as irregular white spaces.

Stratospheric Ozone Depletion by Chlorofluorocarbons (Nobel Lecture)**

F. Sherwood Rowland*

Introduction

There is a well-known mathematical exercise called the Konigsberg Bridge Problem in which the solution involves crossing each of the city's bridges once and only once. When my wife and I first visited Stockholm together in April 1974, we had the distinct impression that our host, Paul Crutzen, was trying to illustrate the corresponding solution for Stockholm by leading us across every single bridge, on foot. We were in Stockholm, because I had sent Paul a preprint of our first scientific paper on the chlorofluorocarbon/stratospheric ozone problem,[1] and he had invited me to present a lecture about this work to the Department of Meteorology of Stockholm University.

The starting point for that work was the discovery by Jim Lovelock that CCl_3F, a substance for which no natural sources have been found, was present in the earth's atmosphere in quantities roughly comparable to the total amount manufactured up to that date. Lovelock had earlier invented an extremely sensitive detection system employing electron capture (EC) by trace impurities, and attached it to the column of effluent gases from a gas chromatograph (GC), a device which separates a mixture of gases into its individual components. With this EC-GC apparatus, Lovelock initially established that CCl_3F was always detectable in the atmosphere near his home in western Ireland, and then that it was also present in all of the air samples tested on the voyage of the R.V. Shackleton from England to Antarctica (Fig. 1).[2] The EC-GC instrument is especially sensitive for CCl_3F, as well as for many other similar molecules in this class of chlorofluorocarbons (CFCs).

The appearance in the atmosphere of a new, man-made molecule provided a scientific chemical challenge: Was enough known about the physicochemical behavior under atmospheric conditions of molecules such as CCl_3F to allow prediction of its fate, once released into the environment? In 1973 I included in my yearly proposal to the U.S. Atomic Energy Commission (AEC), which had sponsored my research involving radioactive tracer species since 1956, a predictive study of the atmospheric chemistry of CCl_3F, in addition to the continuation of other

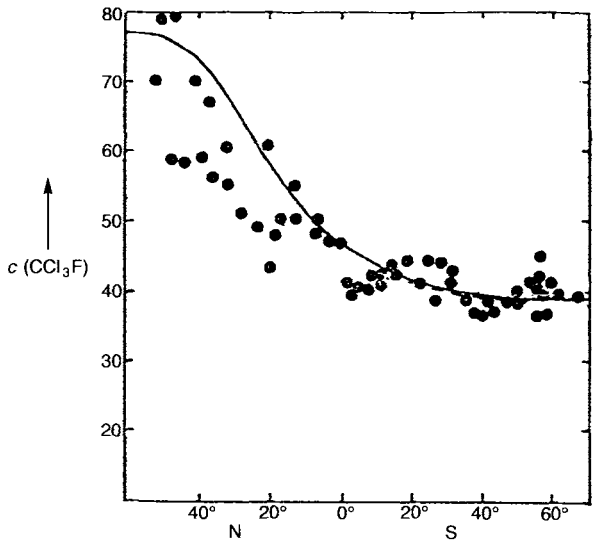

Fig. 1. Mixing ratios of CCl_3F (c in ppbv ($1:10^9$ by volume) measured by James Lovelock [2] on board the R. V. Shackleton in 1971. The x axis represents latitude from 40°N to 60°S.

studies already in progress. The A.E.C. agreed to permit this new venture, subject only to the requirement that I shift some of the funding already scheduled for the studies on radioactivity.

When Mario Molina joined my research group as a postdoctoral research associate later in 1973, he elected the chlorofluorocarbon problem from several offered to him, and we began the scientific search for the ultimate fate of such molecules. At the time, neither of us had any significant experience in treating chemical problems of the atmosphere, and each of us was now operating well away from our previous areas of expertise.

The search for any removal process that might affect CCl_3F began with the reactions that normally affect molecules released to the atmosphere at the surface of the earth. Several well-established tropospheric sinks – chemical or physical removal processes in the lower atmosphere – exist for most molecules released at ground level:

1) Colored species such as the green molecular chlorine (Cl_2) absorb visible solar radiation and break apart, or photodissociate, into individual atoms.

2) Highly polar molecules, such as hydrogen chloride (HCl) dissolve in raindrops to form hydrochloric acid, and are removed when the drops actually fall.

[*] Prof. F. S. Rowland
Department of Chemistry, University of California
Irvine, CA 92697-2025 (USA)
Fax: Int. code +(714)824-2905
e-mail: rowland@uci.edu

[**] Copyright © The Nobel Foundation 1996. We thank the Nobel Foundation, Stockholm, for permission to print this lecture.

3) Almost all compounds containing carbon-hydrogen bonds, for example CH_3Cl, are oxidized in our oxygen-rich atmosphere, often by the hydroxyl radical [Eq. (1)].

$$CH_3Cl + HO \longrightarrow H_2O + CH_2Cl \quad (1)$$

However, CCl_3F and the other chlorofluorocarbons such as CCl_2F_2 and CCl_2FCClF_2[*] are transparent to visible solar radiation and those wavelengths of ultraviolet (UV) radiation that penetrate to the lower atmosphere, are basically insoluble in water, and do not react with HO, O_2, O_3, or other oxidizing agents in the lower atmosphere. When all of these usual decomposition routes are closed, what happens to such survivor molecules?

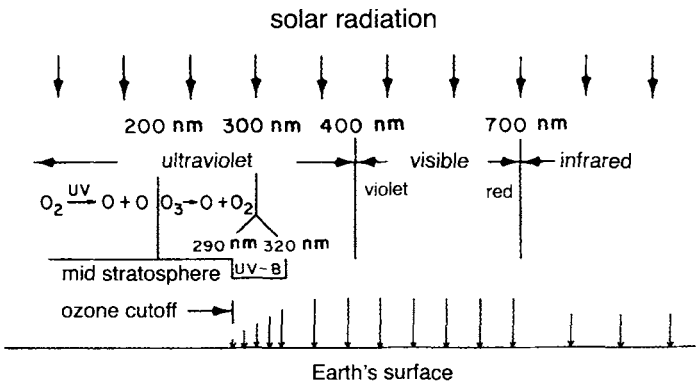

Fig. 2. The solar spectrum, illutrating the absorption of ultraviolet radiation by O_2 and O_3, and the location of the UV-B range between 290 and 320 nm. UV radiation at wavelengths shorter than 290 nm, "the ozone cutoff", does not reach the earth's surface.

Stratospheric Chemical Processes

The radiation from the sun has wavelengths visible to humans from violet (400 nm) to red (700 nm), plus invisible infrared (> 700 nm) and ultraviolet (< 400 nm) wavelengths. The energy of the radiation increases as the wavelengths shorten, and the absorption of highly energetic UV radiation usually causes the decomposition of simple atmospheric molecules.

All multiatom compounds are capable of absorbing UV radiation if the wavelength is short enough, and almost all will decompose after absorbing the radiation. At the top of the atmosphere, the process is so rapid that a CFC molecule would last at most a few weeks if directly released there. However, CFC molecules in the lower atmosphere are protected against this very energetic UV radiation by O_2 and O_3 molecules at higher altitudes. In the upper atmosphere, the UV wavelengths shorter than 242 nm can be absorbed by O_2 (Fig. 2), splitting it into two oxygen atoms [Eq. (2)]. Each of these O atom products normally adds to another O_2 molecule [Eq. (3)] to form ozone (O_3). Collision with some third molecule M is needed to stabilize the O_3 product. These ozone molecules in turn can absorb UV radiation [Eq. (4)] and split off an O atom. Such absorption is especially strong for wavelengths shorter than 290 nm. Again, these O atoms usually reform ozone by reacting with O_2.

$$O_2 + \text{UV light} \longrightarrow O + O \quad (2)$$

$$O + O_2 + M \longrightarrow O_3 + M \quad (3)$$

$$O_3 + \text{UV light} \longrightarrow O + O_2 \quad (4)$$

Ozone is actually quite chemically reactive and sometimes intercepts the O atoms [Eq. (5)]. This set of four reactions involving

$$O + O_3 \longrightarrow O_2 + O_2 \quad (5)$$

O, O_2, and O_3 was already recognized by Chapman in 1930.[3] Through these processes, and others such as the free radical reactions of NO_x and ClO_x described below, a balance of ozone is maintained in the atmosphere by which about 3 parts in 10^7 of the entire atmosphere are present as O_3, versus almost 21% as O_2. About 90% of these ozone molecules are present at altitudes between 10 and 50 km, that is, in the stratosphere, where the mixing ratio of O_3 can rise as high as 1 part in 10^5.

The solar UV energy absorbed in reaction (4) is converted into heat by processes such as energy transfer to M in Equa-

[*]The CFCs are often technically identified by a numerical formula that gives the number of F atoms in the units digit, the number of H atoms plus 1 in the tens digit, and the number of C atoms minus 1 in the hundreds digit: CCl_2FCClF_2 → CFC-113; CCl_3F → CFC-11, dropping the 0 from 011; and CCl_2F_2 → CFC-12. During the past decade, the hydrogen-containing species have been distinguished from the fully-halogenated CFCs by subdivision into the two new categories of HCFCs (e.g., $CHClF_2$ → HCFC-22) and HFCs (e.g., CH_2FCF_3 → HFC-134A; the A distinguishes this molecule from its isomer CHF_2CHF_2).

F. Sherwood Rowland was born on June 28, 1927, in Delaware, Ohio. At not quite sixteen he completed his High School education and then spent two years on an accelerated university course until he was old enough to enlist in the Navy in 1945. After the war he decided to extend the time he still needed to graduate by a year to broaden his studies. In 1948 he enrolled for graduate work in the Department of Chemistry at the University of Chicago. His supervisor was Willard F. Libby, who won the Nobel Prize in 1960 for his work on the ^{14}C dating technique. In his doctoral thesis he worked on the chemical state of radioactive bromine atoms generated in a cyclotron. After attaining his doctorate in 1952 he moved to Princeton University with his wife Joan Lundberg. They have two children. The particularly good facilities for radiochemistry attracted him to the University of Kansas in 1956. From 1964 to 1970 he was the first Chairman of the Chemistry Department at the Irvine campus of the University of California. Since the early 1970s he has devoted his time increasingly to a new research field, atmospheric chemistry, and in particular to the chemistry of chlorofluorocarbons.

tion (3), providing a heat source in the 30–50 km altitude range. This heat source creates the stratosphere, the region between 15 and 50 km in which the temperature increases with altitude. The ozone layer thus performs two important physical processes: it removes short wavelength UV radiation and changes this energy into heat, both creating and maintaining the stratosphere.

Because both O_2 and O_3 can absorb short wavelength UV radiation, no solar radiation with wavelengths shorter than 290 nm penetrates below the stratosphere. The CCl_3F molecule was known from laboratory studies to be able to absorb UV radiation at wavelengths shorter than 220 nm, but to encounter such solar radiation in the atmosphere the molecule must first drift randomly through the atmosphere to altitudes higher than most of the O_2 and O_3 molecules – roughly to 25 or 30 km. More than 98% of the atmosphere and 80% of the ozone lies below 30 km altitude. In this rarefied air, the CFC molecules are exposed to very short wavelength UV radiation and decompose with the release of Cl atoms [Eqs. (6) and (7)]. Because at any

$$CCl_3F + \text{UV light} \longrightarrow Cl + CCl_2F \quad (6)$$

$$CCl_2F_2 + \text{UV light} \longrightarrow Cl + CClF_2 \quad (7)$$

given time, only a very small fraction of CFC molecules are found at altitudes of 30 km or higher, the average molecule survives for many decades before it is decomposed by solar UV radiation.

In 1974 we calculated the vertical profile to be expected for CCl_3F in the stratosphere, using several different sets of eddy diffusion coefficients, the parameter used to simulate vertical motions in these calculations.[4] The resulting vertical profiles for CCl_3F are all quite similar (Fig. 3), because the decomposition rate for this molecule escalates rapidly with increasing altitude in the 20–30 km range. With each of these parameters, the estimated average lifetime in the atmosphere for CCl_3F was in the range from 40 to 55 years, and others extended the lifetime to 75 years. The range of lifetimes calculated for CCl_2F_2 was 75 to 150 years.[1,4]

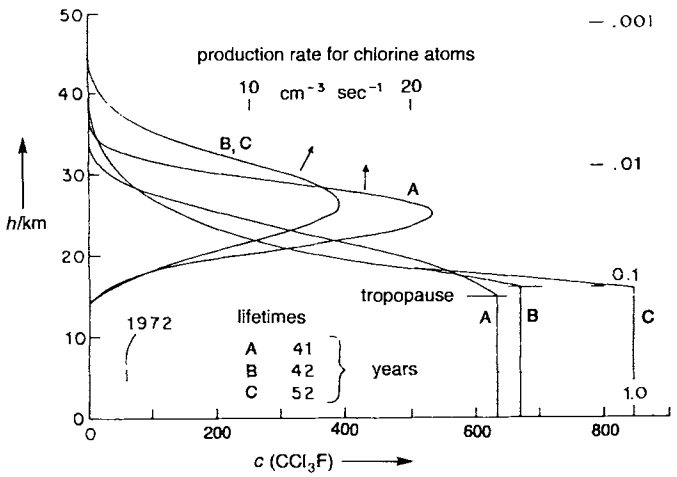

Fig. 3. Vertical profiles of the CCl_3F content c in pptv ($1:10^{12}$ by volume) at steady state, as calculated for three different diffusion models (A, B, C) and the 1972 emission rate [4]. Photolytic destruction of CCl_3F occurs most efficiently at an altitude of 28 kilometers. On the right the pressure is given in atmospheres.

The answer to our original scientific question is that the eventual fate of the CFC molecules is photodissociation in the mid-stratosphere with the release of atomic chlorine, but on a time scale of many decades. What is the fate of these chlorine atoms at an altitude of 30 km?

Chlorine Chemistry in the Stratosphere

The major chemical components of the mid-stratosphere are well known, and their reaction rate constants with atomic Cl have been measured in the laboratory. By combining these data, the conclusion is readily reached that almost all chlorine atoms react with ozone by Equation (8), forming another reactive molecule, ClO. This probability is about 1000 times more likely than reaction with methane according to Eq. (9). The questions of

$$Cl + O_3 \longrightarrow ClO + O_2 \quad (8)$$

$$Cl + CH_4 \longrightarrow HCl + CH_3 \quad (9)$$

the ultimate sinks, first for CCl_3F and then for Cl, have thus been answered, and the question now moves to a third molecule, the ClO product from reaction (8): What happens to ClO at 30 km?

Two important answers appear: reaction with O atoms [Eq. (10)] or with NO [Eq. (11)]. The combination of reactions

$$ClO + O \longrightarrow Cl + O_2 \quad (10)$$

$$ClO + NO \longrightarrow Cl + NO_2 \quad (11)$$

(8) and (10) corresponds to reaction (5) and constitutes a free radical catalytic chain reaction in which the Cl atom alternates between the chemical species Cl and ClO. The first step removes one O_3 molecule, while the second intercepts an O atom which could have become an O_3 by reaction (3), but is instead also converted into O_2. The Cl atom, however, is only a catalyst, and remains to initiate the process once more.

This Cl/ClO cycle can be repeated hundreds or thousands of times, converting back into molecular O_2 one ozone molecule and one oxygen atom. When this catalytic efficiency of about 100000 ozone molecules removed per chlorine atom is coupled with the yearly release to the atmosphere of about one million tons of CFCs, the original question chiefly of scientific interest has now been converted into a very significant global environmental problem – the depletion of stratospheric ozone by chlorine contained in the chlorofluorocarbons.

The ClO_x chain of reactions (8) and (10) was discovered earlier in 1973 by Stolarski and Cicerone, who were interested in the possible natural release of HCl to the atmosphere from volcanoes or from man-made sources in the exhaust of the rockets scheduled for propulsion of the space shuttle.[5] The ClO_x chain has a close analogy with the NO_x free radical catalytic chain of reactions (12) and (13), which also combine to convert

$$NO + O_3 \longrightarrow NO_2 + O_2 \quad (12)$$

$$NO_2 + O \longrightarrow NO + O_2 \quad (13)$$

O and O_3 into two molecules of O_2. This chain can be initiated in the stratosphere by the decomposition of the long-lived mol-

ecule nitrous oxide, N_2O.[6] Alternatively, the NO_x chain can also be triggered by the direct release of NO and NO_2 in the exhaust of high-flying aircraft.[7, 8] The potential effects on stratospheric ozone of NO_x from supersonic transport aircraft such as the Concorde and the proposed Boeing aircraft were discussed in detail during the period 1971 to 1974 under the Climatic Impact Assessment Program.[9, 10]

Reactions such as (9), (11), and (14) show that the distribution of chlorine is closely intertwined with the concentrations of

$$HO + HCl \longrightarrow Cl + H_2O \qquad (14)$$

other stratospheric species, including the nitrogen oxides, methane, and oxides of hydrogen. The most significant homogeneous gas phase interconnections among the active chain species (Cl, ClO) and the reservoir molecules (HCl, HOCl, $ClONO_2$) in the stratosphere above the tropics and the temperate zones are shown in Figure 4. Because of the large-scale mixing processes

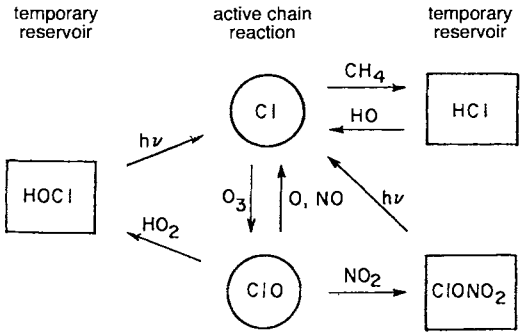

Fig. 4. The most important chemical transformations among inorganic chlorine species in the stratosphere except during the polar winter. Ozone depletion occurs only while chlorine is in the forms of Cl and ClO.

that dominate throughout the troposphere and stratosphere, the total mixing ratio of Cl from any species released at the earth's surface is essentially constant with altitude. However, the fraction in each of the various chlorine-containing chemical forms varies significantly with altitude (Fig. 5).

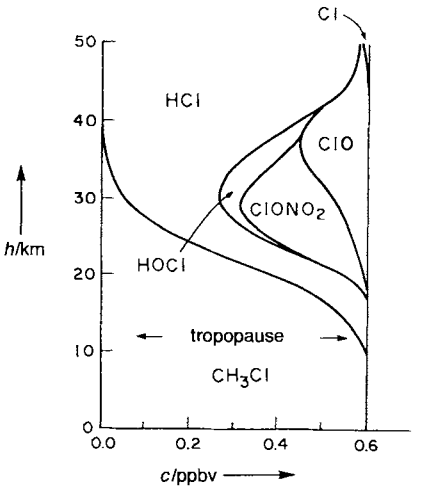

Fig. 5. Schematic illustration of the distribution of chlorine among various chemical forms after release to the atmosphere in the form of methyl chloride. At steady state, the sum of the mixing ratios c at all altitudes is constant and equal to the tropospheric mixing ratios of CH_3Cl.

Our original calculations about the behavior of CFCs in the stratosphere were actually predictions of the vertical distribution, because no measurements were then available for any chlorinated species in the stratosphere, and certainly not for CFCs. During 1975 two different research groups sent evacuated containers equipped with pressure-sensitive values up on high-altitude balloons, and recovered air samples from the stratosphere. The measured mixing ratios for CCl_3F (Fig. 6) were in excellent agreement with the vertical profiles calculated by us in the previous year. This fit between theory and experiment demonstrates both that CFCs reach the stratosphere and that they are decomposed there by solar ultraviolet radiation at the altitudes predicted earlier.[11, 12]

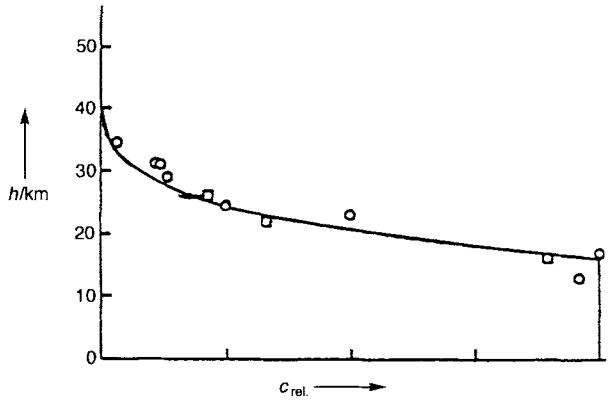

Fig. 6. Relative mixing ratios c_{rel} for CCl_3F, observed in 1975 by research groups from NCAR (○) [12] and NOAA (□) [11] normalized to tropospheric value as 1.0. The solid line was calculated with diffusion coefficient C in Fig. 3 [4].

Growth of Tropospheric CFC Concentrations

When the rate of upward transport of the CFCs into the stratosphere proved to be the same as for all other molecules, attention returned to the possibility of tropospheric sinks. The rapid tropospheric removal processes (photolysis, rainout, oxidation) were readily eliminated. Nevertheless, the calculated 50 to 100 year lifetimes for the various CFCs left room for concern about the possibility of an accumulation of minor sinks, or even of an undiscovered tropospheric sink. While atmospheric and laboratory tests can be conducted appropriate to each proposed individual sink, an even more comprehensive approach is the measurement of the sum for all tropospheric removal processes, including those not yet specifically identified. This can be accomplished by measurement of the actual lifetime of the CFCs in the atmosphere itself, and requires accurate knowledge both of the amounts of a particular CFC released to the atmosphere and of the amount still there.

An electron capture gas chromatographic trace, taken by the same technique originally developed by Lovelock, is shown in Figure 7 for an air sample collected in Tokyo in 1989.

Tokyo is not unusual. Similar high concentrations are found in all major cities, because most of the technological uses of CFCs take place in urban areas. While this is an accurate assessment of the halocarbon impurities found in Tokyo air on that date, it is not very useful for a global assessment of total CFC

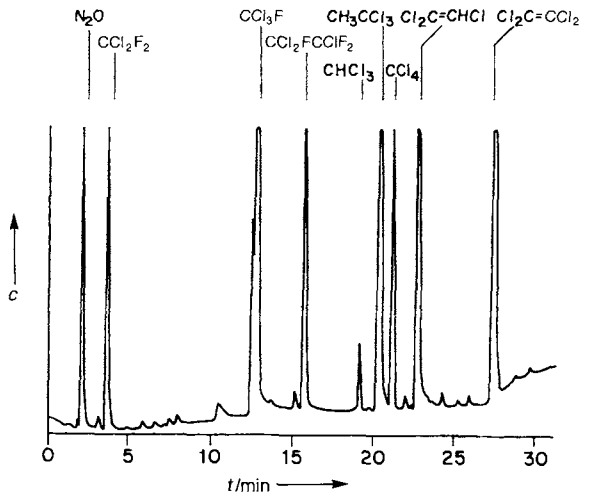

Fig. 7. Analysis by EC-GC of a Tokyo air sample collected on May 20, 1989. Four of the peaks rise above the printed scale values. The detector has a different response for each compound, requiring calibration for each. c = concentration.

concentrations because the measurement is not representative of the whole atmosphere.

The air volume associated with cities, and the amounts of CFCs in that air, represent minuscule fractions of the total atmosphere and of its total CFC content. Instead, what is required are measurements at enough representative remote locations to permit a global assay. A comparable EC-GC display from an air sample collected a few miles from Barrow, Alaska, (71°N Latitude) in 1989 is shown in Figure 8. Although the

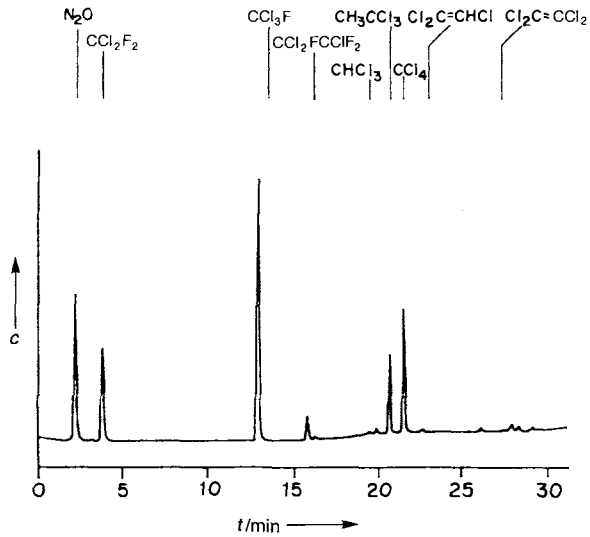

Fig. 8. Analysis by EC-GC of an air sample collected in Barrow, Alaska, on September 15, 1989. The detector has a different response for each compound, requiring calibration for each. c = concentration.

amounts are certainly smaller, the three major CFC molecules are all clearly present near Barrow. Many of the other molecules found in Tokyo (Fig. 7) have atmospheric lifetimes of one year or less, and are detected only in very low concentration or not at all in northern Alaska.

The west-east global mixing processes across longitudinal lines are sufficiently rapid that good estimates can be obtained for molecules as long-lived as the CFCs from a set of air samples collected within a short time period from remote locations across most of the north-south latitudinal spread. The CCl_3F concentration found at such a set of remote locations are illustrated in Fig. 9 for the summer of 1979 (top) and for December

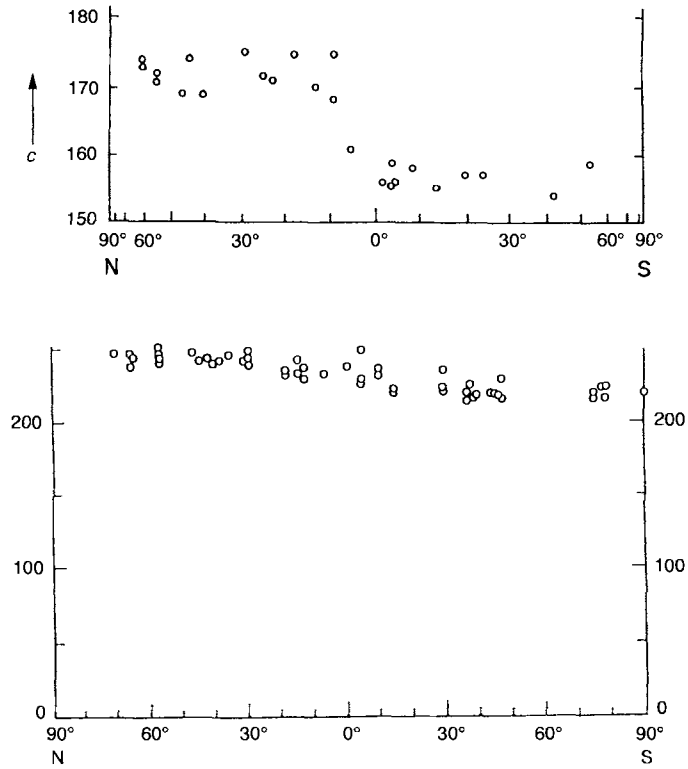

Fig. 9. Mixing ratios c of CCl_3F in pptv for different latitudes, as measured at remote sites in summer 1979 (top) and December 1987 (bottom).

1987 (bottom). Both of these figures illustrate that north-south mixing is quite rapid in the atmosphere, for the gradient from north-to-south is only about 10%, despite the release of about 95% of CCl_3F in the northern hemisphere, mostly between 30°N and 60°N latitudes. The average time for a molecule to mix from the northern to southern hemisphere, or vice versa, has been calculated from the release patterns in comparison with these measured concentrations and is approximately 15 months. The average CFC molecule therefore mixes back and forth between the northern and southern hemispheres 20 to 40 times or more before its ultimate decomposition in the stratosphere. Only the continued injection of CCl_3F into the northern hemisphere maintained the observed north-south concentration gradient from 1971 into the late 1980s.

Comparison of the data in Figure 9 with the Lovelock data demonstrates that the northern hemisphere concentration of CCl_3F increased from about 70 pptv (that is, $1:10^{-12}$) in 1971 to 170 pptv in 1979 and 250 pptv in 1987. This steady increase in concentration with time is precisely what is expected for a molecule with an atmospheric lifetime in the 50 to 100 year range. In 1995 the best estimate for these CFC lifetimes made from a comparison of total atmospheric burden versus total

release is 50 years for CCl_3F and 102 years for CCl_2F_2.[13] Both estimates are well within the ranges of lifetimes calculated 20 years earlier.[1,4] This close agreement between measured lifetimes and those calculated on the assumption that no important tropospheric loss processes exist is a clear indication that this assumption is correct. The ultimate fate for the CFC compounds lies in their photodissociation by solar ultraviolet radiation in the mid-stratosphere.

A typical measurement with the current version of our analytical system for chlorocarbon molecules is shown in Figure 10 for an air sample collected through an external air intake on a C-130 Hercules aircraft 850 miles south of New Zealand on November 15, 1995. Even in this remote location, sixteen different low molecular weight compounds containing Cl or Br atoms were readily detected, together with others such as O=C=S and N_2O (not shown), the molecule whose atmospheric chemistry was considered by Crutzen 25 years ago.[6]

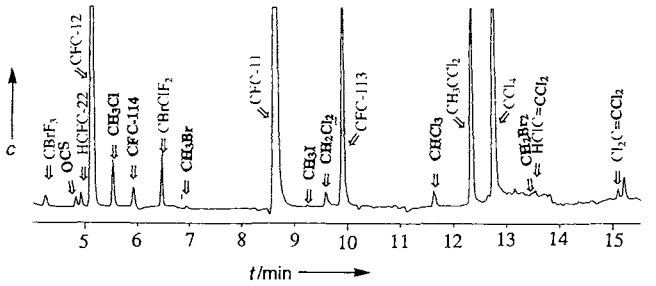

Fig. 10. EC-GC analysis of an air sample collected with an aircraft south of New Zealand on November 15, 1995, at Oh 45 GMT and 800 m altitude. c = concentration.

Springtime Loss of Ozone in the Antarctic

The greatest surprise in the CFC-ozone story was revealed in the spring of 1985 with the discovery by Joe Farman and his colleagues from the British Antarctic Survey of massive springtime losses of ozone over their station at Halley Bay, Antarctica (75.5°S Latitude.[14] This station was established in preparation for the International Geophysical Year of 1957–1958 and was equipped with a Dobson ultraviolet spectrometer for the measurement of total ozone. The principle of this instrument, designed by Dobson in the 1920s, relies on the measurement at the surface of the earth of the ratio of received solar radiation for two UV wavelengths. One of these is moderately absorbed by ozone, and one is almost unaffected, as illustrated in Figure 11. A typical wavelength pair is the C pair that uses 311.45 nm for the former, and 332.4 nm for the latter.

While the absorbing characteristics of most molecules vary continuously with wavelength, the ultraviolet region is often divided for convenience in description into three arbitrary wavelength regions: UV-A, 400 nm to 320 nm (most reaches the earth's surface); UV-B, 320 nm to 290 nm (some reaches the surface); UV-C, shorter than 290 nm (none reaches the surface). The wavelength pairs used with a Dobson spectrometer usually compare one UV-B wavelength against one from the UV-A range. Most concerns about UV effects on biology are directed toward the UV-B range because UV-C radiation does not get

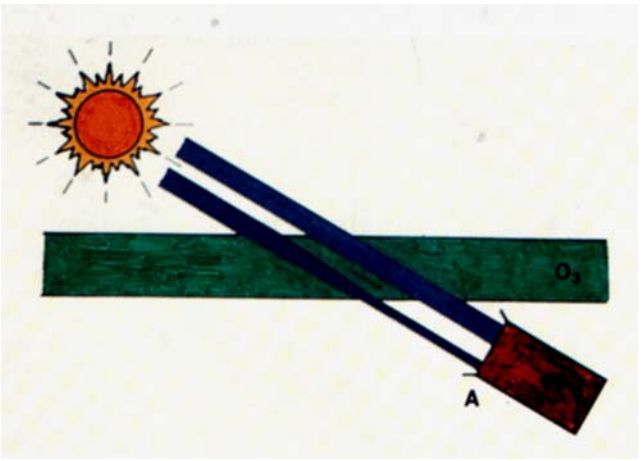

Fig. 11. Standard technique for measurement of ozone with a Dobson ultraviolet spectrometer. The ratio of the intensities at two UV wavelengths is dependent upon the ozone content of the atmosphere and the solar zenith angle.

down to the levels where biological species flourish, and UV-A radiation at the surface is so intense that species without some mechanism for dealing with UV-A would long since have become extinct.

In the northern hemisphere, the highest total ozone concentrations are observed in the polar regions around the spring equinox (March/April), as shown in Figure 12. (The technical

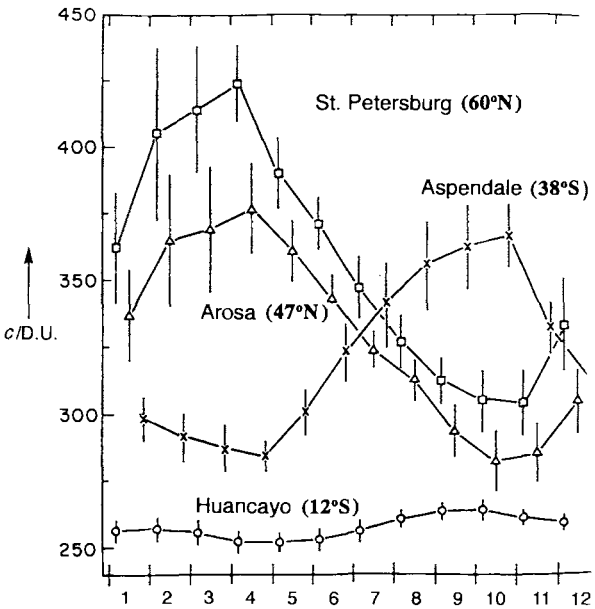

Fig. 12. Seasonal variation of ozone concentrations as measured with a Dobson spectrometer for two stations in the northern hemisphere (St. Petersburg, Russia; Arosa, Switzerland), one station in the tropics (Huancayo, Peru), and one station in the southern hemisphere (Aspendale, Australia). The vertical bars indicate the natural variability of ozone measurements for that location and that calendar month (1 = January, ...12 = December) averaged over 25 years.

unit used to measure total ozone is the milliatmosphere centimeter, but this has been almost universally superseded by its other name, the Dobson Unit (D.U.). The Dobson unit represents approximately 1 part in 10^9 of the atmospheric molecules by volume, and the average global concentration is about 300 D.U.). The spring maximum values are higher at the higher

latitudes, as at St. Petersburg, Russia, versus Arosa, Switzerland, while the highest of all are found in the north polar region. On the other hand, tropical locations have the lowest year-round levels of ozone, with little seasonal variation, as illustrated for Huancayo, Peru.

With no significant prior information about Antarctic meteorology, in 1956 Dobson anticipated finding a spring equinoctial maximum over Halley Bay similar to that previously observed at Spitzbergen, Norway. However, instead of increasing steadily through the autumn and winter, as observed in the north, the southern polar ozone values remained essentially constant through the autumn and winter darkness, and into mid-spring. They then increased sharply to a peak in mid-November, as illustrated in Figure 13 for the summers of 1956–1957, 1957–1958 and 1958–1959.[15] Dobson recognized that this represented the discovery of a very strong Antarctic polar vortex, which until its breakdown in mid-spring prevented the arrival over the polar regions of ozone-richer stratospheric air from the temperate zone.

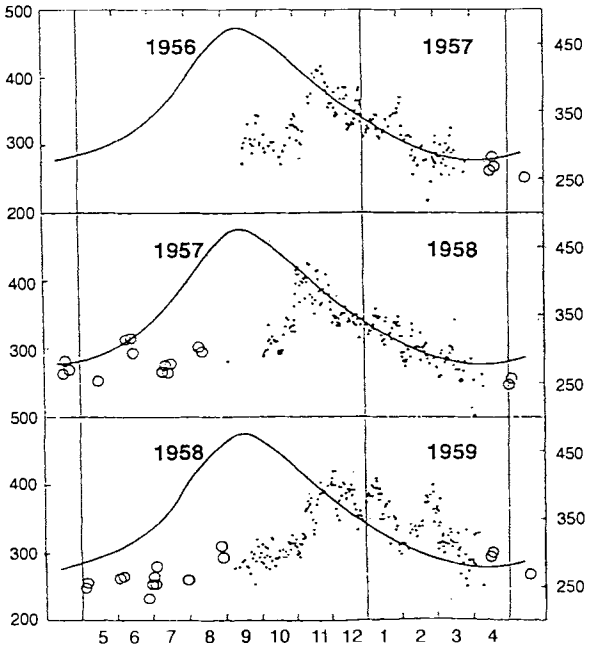

Fig. 13. Daily ozone measurements at Halley Bay, Antarctica, from 1956 to 1959, and, for comparison, the pattern previously observed (solid line) in the north polar region at Spitzbergen, Norway [15]. Dots indicate data using the sun as the UV source, and the less accurate circles those with the moon as the source. Vertical scale: ozone in Dobson units; horizontal axis: months (5 = May, ...4 = April).

This pattern of level ozone values into mid-spring was observed throughout the 1960s and early 1970s. However, in the late 1970s, the average October ozone values over Halley Bay began to decrease, dropping below 200 D.U. in 1984 versus the 300–320 D.U. values of the 1960s (Fig. 14). These data were reported in May 1985, together with the hypothesis that the ozone decrease was correlated with the increasing CFC concentrations in the atmosphere.[14] This loss of ozone begins soon after the end of the polar winter darkness, and proceeds very rapidly for the next six or seven weeks into mid-October.

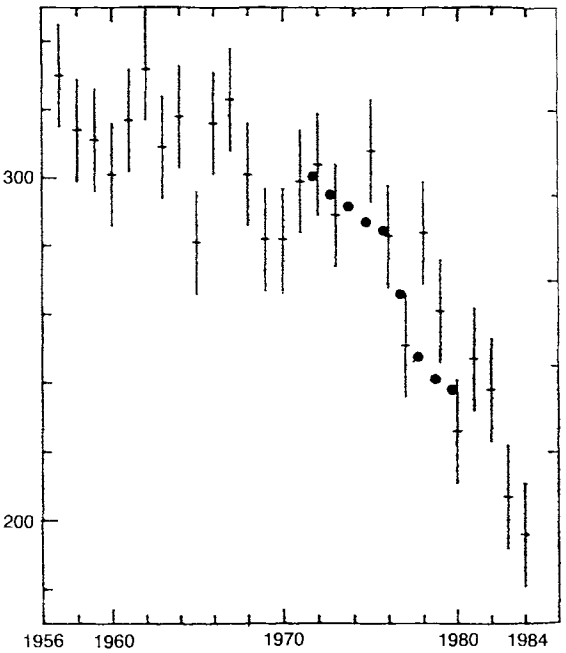

Fig. 14. Average ozone concentrations in Dobson units for October, for the years 1957–1984, at Halley Bay, Antarctica. The black dots indicate on a relative scale the concentrations of CCl_3F versus time, plotted downward from zero at the top.

These substantially smaller ozone values over Halley Bay in October in the 1980s were quickly shown to be characteristic of the entire south polar region by the measurements of the TOMS (Total Ozone Mapping Spectrometer) on the Nimbus-7 satellite.[16] This instrument also measures ozone from the ratio of two UV wavelengths, utilizing solar UV back-scattered from the troposphere through the stratosphere. More than 100000 daily ozone measurements with TOMS over the entire Southern hemisphere are expressed in Figure 15 through a color code for one early October day each in 1979, 1983, 1987, and 1992. In these TOMS displays, the lowest October ozone values fell rapidly from 250 to 175 D.U. and then 125 D.U. between 1979 and 1987. The ozone loss is not confined to the central area: as shown in Figure 15, by 1983 substantial reductions occurred in the areas originally covered by 450–500 D.U. in 1979. A totally different kind of ozone measurement, utilizing its chemical capability for oxidizing the iodide ion to elemental iodine, was used on balloon sondes and demonstrated that most of this ozone loss occurred in the lower stratosphere (Fig. 16). Again, the loss of ozone was observed to be very rapid between late August and October.

Chemistry of the Polar Stratosphere

Numerous theories were suggested for this new observation of ozone loss, and can generally be classified into three groups: a) natural change in the dynamics of the Antarctic stratosphere; b) change in the natural chemistry, e.g. NO_x, of the stratosphere; or c) chemical changes induced by mankind, especially through the introduction of artificial chlorine-containing compounds such as the CFCs. A decrease in the springtime stratospheric temperatures was observed to accompany the observa-

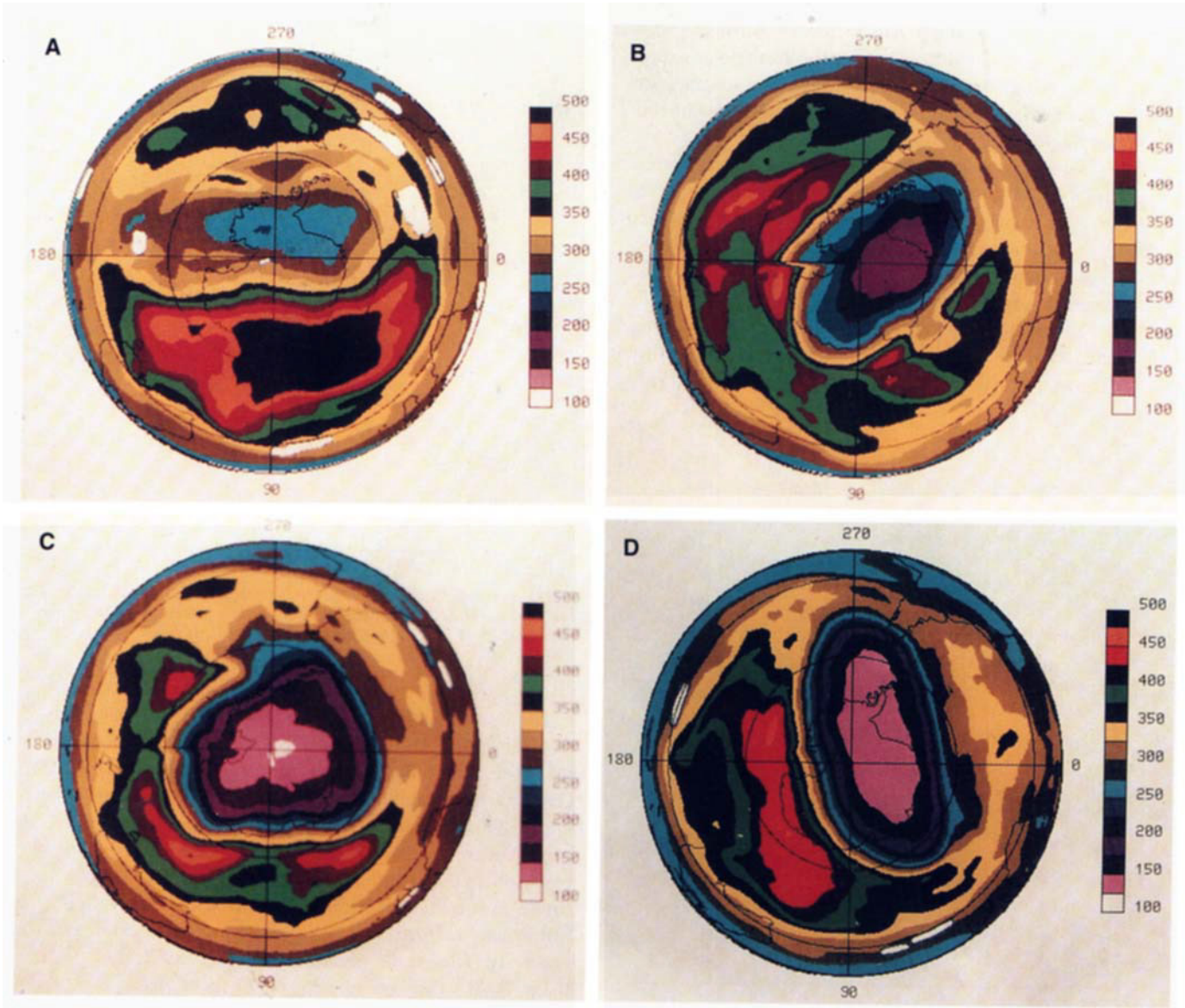

Fig. 15. Total ozone concentrations for the southern hemisphere measured with the TOMS on the Nimbus 7 satellite: A: October 3, 1979; B: October 5, 1983; C: October 5, 1987; D: October 4, 1992. The color code for the measured numerical values in Dobson Units is given to the right. (Missing data is also shown in white.)

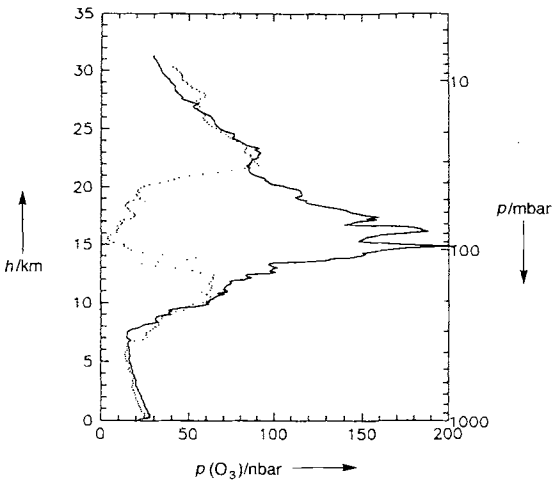

Fig. 16. Dependence of the partial pressures of ozone $p(O_3)$ on altitude, as measured by balloon sondes from McMurdo, Antarctica. Solid line: August 23, 1989, in late winter at the end of the polar night. Dotted line: October 20, 1989, after two months of sunlight. p = approximate total pressure.

tions of lessened quantities of ozone, and was briefly considered as a possible cause for its destruction.[17] However, the lowered temperatures were soon established to be occurring after the ozone loss, and to be the consequence of reduced UV absorption by reduced amounts of ozone, not a cause of the ozone loss. The observed temperature decreases are, in fact, a slower warm-up from the wintertime temperature minimum.

Three polar expeditions in 1986 and 1987 provided the scientific basis for the conclusion that the ozone losses over Antarctica were indeed the consequence of chemical reactions driven by the much higher stratospheric chlorine concentrations of the mid-1980s than those of 1950–1970. Two of these were ground-based expeditions to McMurdo, Antarctica, led by Susan Solomon. Two maxima were detected in 1986 in the vertical profile of the important free radical, ClO, by ground-based millimeter wave spectroscopy.[18] The larger maximum in ClO concentrations, reaching ppbv concentrations ($1:10^9$ by volume), was found in the lower stratosphere coincident with the altitudes of major ozone loss. These results were then followed in 1987 by

in situ measurements of ClO and O_3 within the polar vortex by instruments on the high-flying ER-2 aircraft.[19] These experiments were carried out from a base in Punta Arenas, Chile (53°S latitude), from aircraft which entered the polar vortex over the Antarctic peninsula. The data of Jim Anderson clearly showed levels of 10^{-9} parts by volume of ClO over Antarctica (Fig. 17)

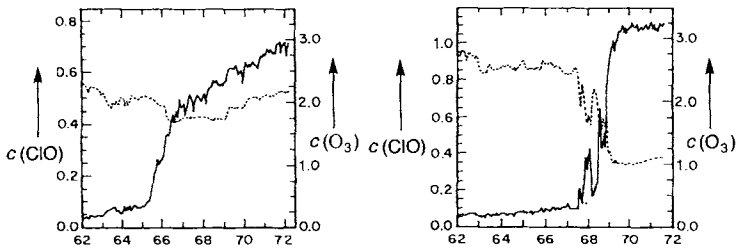

Fig. 17. Chlorine oxide (solid line; scale: parts per 10^9 by volume) and ozone (dotted line; scale: parts per 10^6 by volume) measurements taken on flights with the ER-2 aircraft from Punta Arenas, Chile, over Antarctica [19]. Left: August 23, 1987; Right: September 16, 1987. The x axis represents the latitude in °S.

on the first successful flight on August 23. However, the simultaneous ER-2 data for ozone showed little or no change in concentration inside or outside the polar vortex. At this late-winter date, sunlight had only been available in the Antarctic stratosphere for a few days. In contrast, 24 days later on September 16, the ClO levels over Antarctica were again in the same range, but this time approximately two-thirds of the ozone within the polar vortex had already disappeared. The edge of the Antarctic polar vortex was particularly ragged on September 16, and the high values of ClO and low values of O_3 tracked each other in perfect anti-coordination (Fig. 17, right).

The chlorine chemistry of the lower Antarctic stratosphere has some substantial differences from that of the upper stratosphere in the temperate and tropical zones. Because the concentration of O atoms is very low in the polar lower stratosphere, reaction (10) is quite slow and the ClO_x chain of (8) + (10) is no longer effective. At these altitudes, the winter temperatures drop to the −80 °C range, low enough for the formation there of polar stratospheric clouds (PSCs), which can contain both HNO_3 and H_2O.[20–22] Such low temperatures, and the accompanying clouds, are not generally found in the stratosphere of the temperate zone. However, the same air remains trapped in the strong Antarctic polar vortex throughout the total winter darkness, and the temperatures drop low enough for cloud formation.

These polar clouds furnish active surfaces on which chemical reactions can occur, including reactions such as (15) and (16)

$$HCl + ClONO_2 \xrightarrow{PSC} Cl_2 + HNO_3 \quad (15)$$

$$H_2O + ClONO_2 \xrightarrow{PSC} HOCl + HNO_3 \quad (16)$$

involving reservoir molecules HCl and $ClONO_2$.[23–26] surface back into the gas phase, where they are photolyzed when the sun returns from its months-long absence. The HNO_3 from such reactions remains in these clouds, a process which denitrifies the air mass. When cold enough, sufficient water molecules can also add to the PSC particles to make them fall by gravitation, which dehydrates the air mass as well.

An important aspect of the denitrification process is the very low residual concentration of NO and NO_2; the absence of the latter severely curtails the formation reaction for chlorine nitrate by Equation (17). Without this removal process for ClO

$$ClO + NO_2 + M \longrightarrow ClONO_2 + M \quad (17)$$

radicals, the ClO concentrations rise to mixing ratios in the ppbv range and begin to react in significant numbers with other ClO radicals to form Cl_2O_2 by Equation (18).[27] The chlorine oxide dimer, ClOOCl, can then be destroyed by sunlight [Eq. (19)], releasing one Cl atom each in reactions (19) and (20). The sum of reactions 2 × (8) + (18) + (19) + (20) gives (21) by

$$ClO + ClO + M \longrightarrow ClOOCl + M \quad (18)$$

$$ClOOCl + light \longrightarrow Cl + ClOO \quad (19)$$

$$ClOO + M \longrightarrow Cl + O_2 + M \quad (20)$$

$$O_3 + O_3 \longrightarrow O_2 + O_2 + O_2 \quad (21)$$

which two O_3 molecules are transformed into three O_2 molecules. This alternate polar ClO_x chain reaction converts ozone into molecular O_2 without the need for the O atom step of reaction (10). Other reactions involving Br atoms from halon molecules such as $CBrF_3$ and $CBrClF_2$ or methyl bromide are exceedingly efficient in removing ozone as well.

Ozone Losses in the Northern Temperate Zone

In 1985 the several existing statistical evaluations of the combined data from the Dobson stations in the northern hemisphere appeared to indicate that no significant loss in total ozone had occurred there.[28] The longest series of these ozone measurements without any significant breaks has been carried out since August 1931 in the Swiss alpine community of Arosa. In 1986 Neil Harris and I began a reexamination of the Arosa data series, treating it not as a single comprehensive set, but as a collection of twelve separate data sets, one for each calendar month. Interannual ozone comparisons (see Fig. 2) show substantial seasonal differences in the variability of the monthly averages. While each year individually shows the normal north temperate zone pattern of maximum ozone values around the spring equinox, and a minimum at the beginning of autumn, the year-to-year variability in average ozone concentration for each month is much greater for the January-to-April period than it is for July-to-October. When this 56-year data series from Arosa was broken into two periods – the 39 year period 1931–1969, and the 17-year period 1970–1986 – the interesting result emerged that significantly less ozone was measured for several of the autumn-winter months after 1970 than in the previous four decades.[29] Figure 18 shows this Arosa wintertime ozone loss after the inclusion of data from 1987/88.

We then extended this inquiry to two U.S. ozone stations, Caribou (Maine) and Bismarck (North Dakota), and found that these two also exhibited wintertime losses when the data for 1965–1975 were compared with 1976–1986.[29] This comparison of consecutive 11-year periods corresponding to the well-

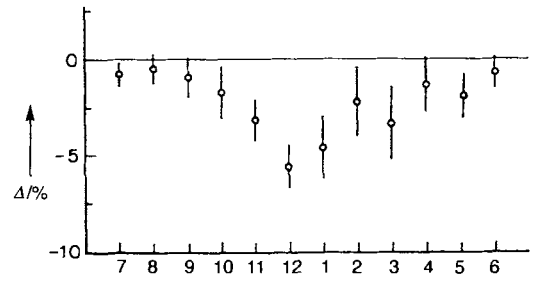

Fig. 18. Changes Δ in monthly average total ozone concentrations measured with a Dobson spectrometer at Arosa for the period 1970–1988 relative to 1931–1969 (updated from [29]). Negative values represent smaller average concentrations after 1970. The x axis represents the months from July (7) to June (6).

known 11-year solar cycle minimizes any influence of variations in UV emission on the evaluation of the long-term trends. Subsequently, the WMO/NASA Ozone Trends Panel confirmed (Fig. 19) that all 18 of the ozone stations between 35°N and

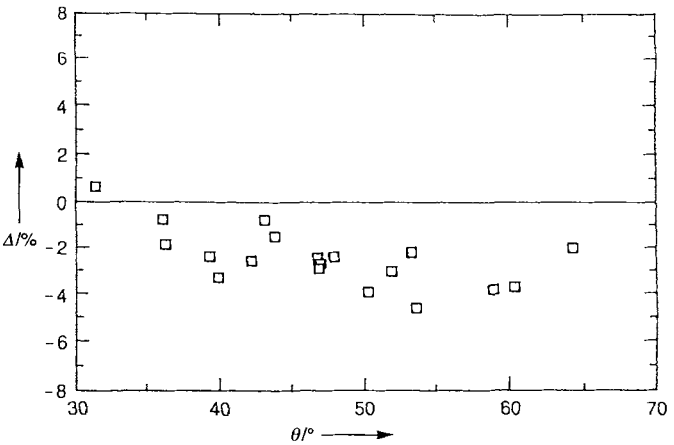

Fig. 19. Changes Δ in average total ozone concentrations in the "winter" season (December to March) for 1976–1986 relative to values for 1965–1975 for all Dobson stations north of 30° North latitude that have a complete 22 year record (two complete solar cycles) [30]. Negative values represent smaller average concentrations after 1975.

60°N latitudes with at least 22 years of data (that is, also covering two complete 11-year solar cycles) had less wintertime ozone in 1976–1986 than in the earlier period.[30] An earlier National Academy of Sciences/National Research Council report had concluded that loss of ozone had already occurred at the altitudes between 35 and 40 km for which the ClO_x chain reaction of (8) + (10) was predicted to be most effective.[31] However, the Ozone Trends Panel report was the first assessment document to assert that significant ozone loss had already been observed over the highly populated areas of North America, Europe, the Soviet Union, and Japan. The combination of very large springtime losses of ozone over Antarctica directly attributable to man-made chlorine compounds introduced into the stratosphere, and measurable ozone losses in the north temperate zone, brought a rapid change in the attitudes of CFC producers and many of the users, and a complete phaseout of CFC production and uses became a widely accepted goal.

The Montreal Protocol for Regulation of CFCs

Regulations for the control of CFC emissions had first been introduced during the late 1970s for the use of CFC-11 and CFC-12 as propellant gases for aerosol sprays, but only in the United States, Canada, Sweden, and Norway. In 1985 a United Nations meeting in Vienna, Austria, had agreed to a convention on the protection of the stratospheric ozone layer. Then, in September 1987 a further agreement, known as the Montreal Protocol, called for actual limitations on the emissions of CFCs, and a 50% cutback in CFC production was scheduled by the end of the century.[32] The terms of the Montreal Protocol called for periodic revisits to the controls, and a meeting in London in 1990 changed the restricted production into an outright phaseout of CFCs by the year 2000. A further meeting in Copenhagen in 1992 accelerated the phaseout to January 1, 1996, for the major industrial countries and included compounds such as 1,1,1-trichloroethane (CH_3CCl_3), carbon tetrachloride (CCl_4), and the bromine-containing halons H-1301($CBrF_3$), H-1211 ($CBrClF_2$), and H-2402 ($CBrF_2CBrF_2$).

Changes in Ultraviolet Flux at the Earth's Surface

Most of the measurements of total ozone, including the Dobson and TOMS data, actually depend upon the ratio of two wavelengths of solar ultraviolet radiation, as described earlier. A change in the amount of ozone along the path of the UV radiation is inferred from a change in the intensity of the wavelengths of the detected radiation. In these cases, the existence of a correlation between ozone and UV-B radiation under clear-sky conditions is a tautology. Less reported ozone means either more UV-B or less UV-A or both, and no mechanisms for significant changes in UV-A radiation intensity have been put forward. However, because actual well-calibrated, precise absolute measurements of ultraviolet radiation over many decades do not exist, no long-term comparison of trends in ozone concentrations and the intensity of UV-B radiation has been possible.

In the past decade, instruments capable of such ultraviolet measurements have been deployed in various locations, especially in the south polar region, including three Antarctic stations – South Pole, McMurdo (78°S), and Palmer (64°S), as well as Ushuaia, Argentina (55°S). Because the Antarctic polar vortex, and its region of low ozone concentrations during recent Octobers, can be very elongated (see Fig. 15 for October 4, 1992), the possibility now exists for much higher UV-B exposures in the southern high latitudes than in previous times.

Comparison of the measured UV-B intensities for the same solar zenith angle in spring (that is, when ozone is depleted) and autumn (relatively normal ozone) allow an experimental confirmation of the anticipated anticorrelation between UV-B and total ozone. The measured correlation in Figure 20 for the South pole in 1991/1992 shows a 150% increase in UV-B for a 50% decrease in ozone content.[33] Furthermore, on October 26, 1993, when a particularly low ozone value existed over Palmer in the Antarctic peninsula, the UV-B intensity exceeded by 25% the highest intensity recorded in San Diego, California, for any day of 1993 (the most intense there was June 21, 1993, Fig. 21).[34] A remarkable further observation was also record-

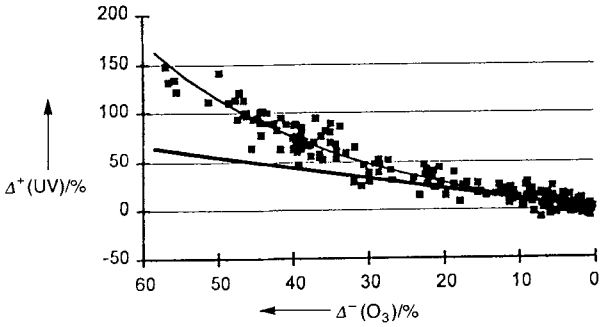

Fig. 20. Percentage increases Δ^+ (UV) in UV-B radiation (erythemally weighted) plotted against percentage decreases in total ozone at the South Pole, 1991/1992 [33]. RAF = 1.1 (RAF = radiation amplification factor).

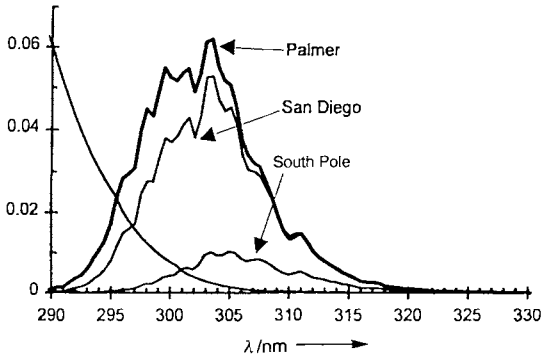

Fig. 21. Maximum UV-B spectral intensities measured at three stations during 1992/1993, weighted by the experimental absorption spectrum of DNA (shown as falling curve at the left of the figure) [34]. At San Diego the maximum intensity occurred on June 21, 1993 (10° solar zenith angle), at Palmer in the Antarctic peninsula (64°S) on October 26, 1993 (52° solar zenith angle), and at the South Pole on November 29, 1992 (68° solar zenith angle). The relative integrated intensities are 0.11 at the South Pole, 0.59 at San Diego, and 0.74 at Palmer.

ed: the most intense weekly UV-B exposure in any single week at any of these stations was recorded at the South Pole. There, even though the sun is low on the horizon, the very low concentrations of ozone in the late Antarctic spring, the general absence of clouds, and the 24 hours per day of continuous sunlight combined to permit a higher weekly dose of UV-B than in any week in San Diego, California.[34] The often-heard statement that UV-B intensities in the Antarctic can never be very large is no longer true. The question of possible biological damage associated with UV-B radiation then requires a separate assessment for each biological species of whether such damage is the result of cumulative UV-B exposure over an entire season or of a single, extremely intense exposure; both circumstances exist elsewhere.

Changing O_3 and CFC Concentrations in the 1990s

Ozone concentrations have continued to fall during the early 1990s. The measured value at the South Pole was only 91 D.U. on October 12, 1993, and the vertical profile data from the corresponding balloon sonde indicated that all ozone had been removed from a 5-kilometer altitude band between 14 and 19 kilometers. The TOMS satellite registered many new daily record low global ozone values in early 1992, and then for nearly 13 months from mid-April 1992, a new daily low global ozone

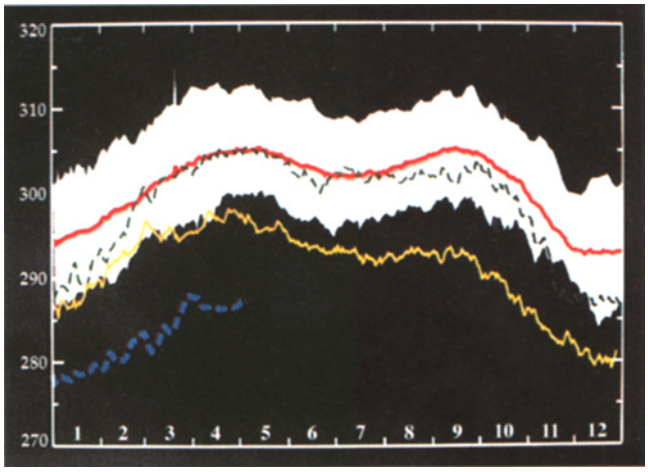

Fig. 22. Global ozone values in Dobson Units as measured with the TOMS on the Nimbus 7 Satellite. The range of values recorded on each day from 1979 to 1990 is outlined in white and the average for these years in red. The values for 1991, 1992, and 1993 are shown in green, yellow, and blue, respectively. The spectrometer failed on May 7. 1 = 1–31 January, etc.

value was measured (Fig. 22). This measurement series ended when the spectrometer finally failed on May 7, 1993. The ozone data interpretations were complicated by the eruption of Mount Pinatubo in the Philippines in June 1991. This volcano, while not providing any significant amount of hydrogen chloride to the stratosphere, did introduce particulate surfaces on which reactions similar to those taking place on the PSCs could occur. The Dobson stations in the northern hemisphere continued to report declining ozone concentrations, with the losses now spreading into the summer. By 1995 the total ozone losses for the north temperate zone approached 10% during winter and spring and 5% in the summer and autumn.[13]

In contrast, the measured tropospheric concentrations of the various halocarbon gases deviated in the 1990s from their earlier pattern of steady increases in response to the restrictions of the Montreal Protocol. The concentrations of the three major CFCs, which had risen almost linearly during the 1980s, markedly slowed their pace of increase. By 1995, the concentrations of CCl_3F measured regularly at seven different stations varying in latitude from the polar Arctic to the South Pole had essentially leveled off (Fig. 23). The CCl_2F_2 and CCl_2FCClF_2

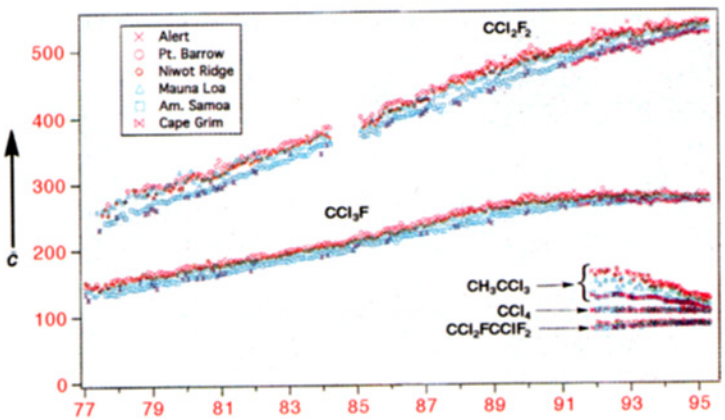

Fig. 23. Measured mixing ratios in pptv for the period 1977–1995 for CCl_3F, CCl_2F_2, CCl_2FCClF_2, CH_3CCl_3, and CCl_4, determined at seven sites. ▽ = South Pole.

concentrations were still rising, but at no more than half the rate of the 1980s. The sharpest changes were observed with the organic solvent 1,1,1-trichloroethane for which controls were added in revisions of the original Montreal Protocol. This substance has three hydrogen atoms that are susceptible to attack by HO radicals in the troposphere, in analogy with reaction (1), and therefore has an average lifetime of only about 5 years. With its rapidly diminishing emission rate under the limitations of the Protocol, the tropospheric concentrations of CH_3CCl_3 reached a maximum in 1992 and have declined significantly since (Fig. 23).

The situation at the end of 1995 is therefore a mixed one. The three most important CFC molecules have atmospheric lifetimes measured from many decades to a century or more, with the consequence that there will be significant quantities of them present in the atmosphere throughout the 21st century. The major springtime losses in the Antarctic will probably continue at least until mid-century. However, because the primary cause of these ozone losses are the man-made chlorine and bromine compounds limited by the Montreal Protocol, the amount of organochlorine in the troposphere will peak soon, if it hasn't already. When the weighted effects of bromine compounds are added in, the peak in tropospheric halocarbons will occur within this decade. Because of the delay time in rising upward, the stratospheric peak will follow within a few years. For the next few decades, the atmosphere will be loaded with chlorine and bromine compounds, so that a really large volcanic explosion with major increases in the particulate surface area of the stratosphere might cause transitory large ozone decreases. Another area for concern is the changing temperature structure of the stratosphere because of the steady increases in the greenhouse gases, especially carbon dioxide. The effect of more carbon dioxide is to decrease temperatures in the lower stratosphere, and this could lead to more extensive cloud formation, and more particulate surface area as well. However, with the limitations just expressed, the threat of extensive further stratospheric ozone depletion during the 21st century appears to be under control.

Received: March 4, 1996 [A 156IE]
German version: *Angew. Chem.* **1996**, *108*, 1908–1921

Keywords: atmospheric chemistry · Nobel lecture · ozone

[1] "Stratospheric sink for chlorofluoromethanes: Chlorine atom-catalysed destruction of ozone": M. J. Molina, F. S. Rowland, *Nature* **1974**, *249*, 810–812.
[2] "Halogenated hydrocarbons in and over the Atlantic": J. E. Lovelock, R. J. Maggs, R. J. Wade, *Nature* **1973**, *241*, 194–196.
[3] "A theory of upper atmospheric ozone": S. Chapman, *Mem. Meteorol. Soc.* **1930**, *3*, 103–125.
[4] "Chlorofluoromethanes in the environment": F. S. Rowland, M. J. Molina, *Rev. Geophys. Space Phys.* **1975**, *13*, 1–35.
[5] "Stratospheric chlorine: a possible sink for ozone": R. S. Stolarski, R. J. Cicerone, *Can. J. Chem.* **1974**, *52*, 1610–1615.
[6] "The influence of nitrogen oxides on the atmospheric ozone content": P. J. Crutzen, *R. Meteorol. Soc. Quart. J.* **1970**, *96*, 320–325.
[7] "Reduction of stratospheric ozone by nitrogen oxide catalysts from supersonic transport exhaust": H. S. Johnston, *Science* **1971**, *173*, 517–522.
[8] "Ozone production rates in an oxygen–hydrogen–nitrogen oxide atmosphere": P. J. Crutzen, *J. Geophys. Res.* **1971**, *76*, 7311–7327.
[9] "Environmental Impact of Stratospheric Flight, Biological and Climatic Effects of Aircraft Emissions in the Stratosphere": Climatic Impact Committee, National Academy of Sciences, Washington, DC, **1975**.
[10] "The Natural Stratosphere of 1974": *CIAP Monograph 1* (Ed.: A. J. Grobecker), Final Report, US Dept. of Transportation, DOT-TST-75-51, Washington, DC, **1975**.
[11] "Measurements of stratospheric $CFCl_3$, CF_2Cl_2 and N_2O": A. L. Schmeltekopf, P. D. Goldan, W. R. Henderson, W. J. Harrop, T. L. Thompson, F. C. Fehsenfeld, H. I. Schiff, P. J. Crutzen, I. S. A. Isaksen, E. E. Ferguson, *Geophys. Res. Lett.* **1975**, *2*, 393–396.
[12] "Stratospheric profiles of CCl_3F and CCl_2F_2": L. E. Heidt, R. Lueb, W. Pollock, D. H. Ehhalt, *Geophys. Res. Lett.* **1975**, *2*, 445–447.
[13] World Meteorological Organization, Global Ozone Research and Monitoring Project, Report No. 37, Scientific Assessment of Ozone Depletion: 1994, WMO/NASA, **1995**.
[14] "Large losses of ozone in Antarctica reveal seasonal ClO_x/NO_x interaction": J. C. Farman, B. G. Gardiner, J. D. Shanklin, *Nature* **1985**, *315*, 207–210.
[15] "Forty years' research on atmospheric ozone at Oxford: A history": G. M. B. Dobson, *Appl. Opt.* **1968**, *7*, 401.
[16] "Nimbus 7 SBUV/TOMS measurements of the springtime Antarctic ozone decrease": R. S. Stolarski, A. J. Krueger, M. R. Schoeberl, R. D. McPeters, P. A. Newman, J. C. Alpert, *Nature* **1986**, *322*, 808–811.
[17] "Total ozone variations at Syowa, Antarctica": a) S. Chubachi, R. Kajawara, *Geophys. Res. Lett.* **1986**, *13*, 1197–1198; b) "Antarctic ozone change correlated to the stratospheric temperature field": Y. Sekiguchi, *ibid.* **1986**, *13*, 1202–1205; c) "October Antarctic temperature and total ozone trends from 1979–1985": P. Newman, M. Schoeberl, *ibid.* **1986**, *13*, 1206–1209; d) "The close relationship between Antarctic total ozone depletion and cooling of the Antarctic lower stratosphere": J. K. Angell, *ibid.* **1986**, *13*, 1240–1243.
[18] "High concentrations of chlorine monoxide at low altitudes in the Antarctic spring stratosphere, I, Diurnal variation": R. L. deZafra, M. Jaramillo, A. Parrish, P. M. Solomon, B. Connor, J. Barrett, *Nature* **1987**, *328*, 408–411.
[19] "Ozone destruction by chlorine radicals within the Antarctic vortex: the spatial and temporal evolution of $ClO-O_3$ anticorrelation based on in situ ER-2 data": J. G. Anderson, W. H. Brune, M. H. Proffitt, *J. Geophys. Res.* **1989**, *94*, 11465–11479.
[20] "Polar stratospheric cloud sightings by SAM II": M. P. McCormick, H. M. Steele, P. Hamill, W. P. Chu, T. J. Swissler, *J. Atmos. Sci.* **1982**, *3*, 1387–1397.
[21] "Nitric acid cloud formation in the cold Antarctic stratosphere: A major cause for the springtime ozone hole": P. J. Crutzen, F. Arnold, *Nature* **1986**, *324*, 651–655.
[22] "Condensation of HNO_3 and HCl in the winter polar stratosphere": O. B. Toon, P. Hamill, R. P. Turco, J. Pinto, *Geophys. Res. Lett.* **1986**, *13*, 1284–1287.
[23] a) H. Sato, F. S. Rowland, paper at the International Meeting on Current Issues in our Understanding of the Stratosphere and the Future of the Ozone Layer, Feldafing, Germany, **1984**; b) "The hydrolysis of chlorine nitrate and its possible atmospheric significance": F. S. Rowland, H. Sato, H. Khwaja, S. M. Elliott, *J. Phys. Chem.* **1986**, *90*, 1085–1088.
[24] "On the depletion of Antarctic ozone": S. Solomon, R. R. Garcia, F. S. Rowland, D. J. Wuebbles, *Nature* **1986**, *321*, 755–758.
[25] "Antarctic stratospheric chemistry of chlorine nitrate, hydrogen chloride and ice. Release of active chlorine": M. J. Molina, T.-L. Tso, L. T. Molina, F. C.-Y. Wang, *Science* **1987**, *238*, 1253–1257.
[26] "Reaction of chlorine nitrate with hydrogen chloride and water at Antarctic stratospheric temperatures": M. A. Tolbert, M. J. Rossi, R. Malhotra, D. M. Golden, *Science* **1987**, *238*, 1258–1260.
[27] "Production of Cl_2O_2 from the self-reaction of the ClO radical": L. T. Molina, M. J. Molina, *J. Phys. Chem.* **1987**, *91*, 433–436.
[28] "Atmospheric Ozone 1985", WMO Report No. 16, 3 Volumes, **1986**.
[29] "Trends in total ozone at Arosa": N. R. P. Harris, F. S. Rowland, *EOS* **1986**, *67*, 875.
[30] a) "Trends in Total Column Ozone Measurements": Chapter 4, in Report of the International Ozone Trends Panel, WMO Report No. 18, Volume 1, **1990**; b) "Statistical Error Analyses of Ozone Trends—Winter Depletion in the Northern Hemisphere": F. S. Rowland, N. R. P. Harris, R. D. Bojkov, P. Bloomfield in *Ozone in the Atmosphere* (Eds.: R. D. Bojkov, P. Fabian), Deepak Publishing, Hampton, **1989**, pp 71–75.
[31] Committee on the Chemistry and Physics of Ozone Depletion, National Research Council, *Causes and Effects of Stratospheric Ozone Reduction: An Update*, National Academy Press, Washington, DC, **1982**.
[32] R. E. Benedick, *Ozone Diplomacy*, Harvard University Press, Cambridge, MA, **1991**.
[33] "Radiation amplification factors: improved formula accounts for large increases in ultraviolet radiation associated with Antarctic ozone depletion": C. R. Booth, S. Madronich, *Antarct. Res. Ser.* **1994**, *62*, 39–42.
[34] C. R. Booth, T. B. Lucas, T. Mestechkina, J. Tusson, *Antarct. J. US* **1994**, *39*, 256–259.

ANGEWANDTE
CHEMIE
International Edition in English

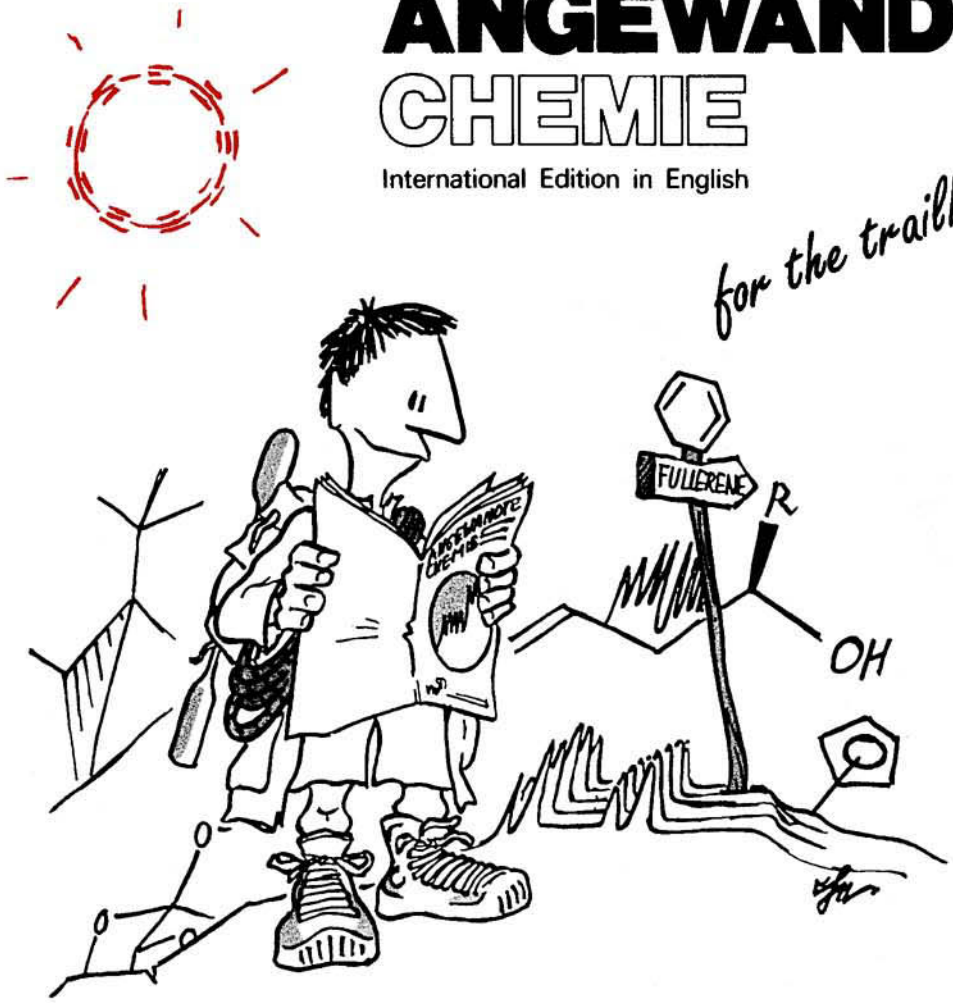

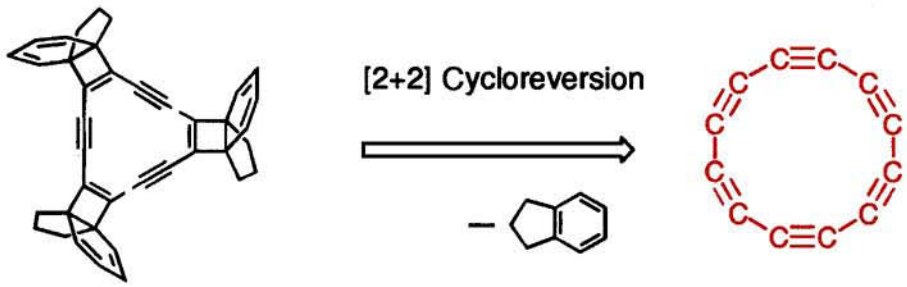

The synthesis of the smallest *cyclo*-carbon C_{12} was achieved by Y. Tobe et al. by the route sketched above (see p. 1800 ff).

 © *VCH Verlagsgesellschaft mbH, D-69451 Weinheim, 1996* *0570-0833/96/3516-1799 $ 15.00+.25/0*

Generation of Cyclocarbons with 4*n* Carbon Atoms (C_{12}, C_{16}, and C_{20}) by [2+2] Cycloreversion of Propellane-Annelated Dehydroannulenes**

Yoshito Tobe,* Hideki Matsumoto, Koichiro Naemura, Yohji Achiba,* and Tomonari Wakabayashi

Dedicated to Professor Philip E. Eaton on the occasion of his 60th birthday

Recent studies on the spectroscopic, chemical, and physical behavior of carbon clusters revealed that small clusters of C_{10}–C_{20} possess monocyclic form.[1] All-carbon molecules of this type, called cyclo[*n*]carbons,[2] are of particular interest because they play an important role in the formation of fullerenes[3] and because for some of them more than one structure has been predicted by calculations.[4] We and Diederich et al. have synthesized a number of precursors of cyclo[*n*]carbons with well-defined cyclic structures and readily removable groups, which eventually generated *cyclo*-C_{18} (and *cyclo*-C_{24} and *cyclo*-C_{30} as well) by laser desorption induced [4+2] cycloreversion (retro-Diels–Alder reaction),[5a,d] decarbonylation,[5b–d] or [2+2] cycloreversion.[6] The advantage of the [4.3.2]propellane-type precursors lies in their thermal stability and facility to undergo cycloreversion on both laser desorption and ultraviolet irradiation.[6] However, these methods have been only applied so far to generate cyclocarbons with 6*n* carbon atoms (n = 3–5), and no precursors to cyclocarbons of other ring sizes were known despite the importance of these carbon clusters.[7,8] Moreover, cyclocarbons having 4*n* carbon atoms should give dianions by two-electron reduction[9] and form transition metal complexes (in the case of *cyclo*-C_{12}),[10] in view of the chemistry of the dehydroannulenes with 4*n* π-electron systems. In this connection, we report herein the synthesis of hexadehydro[12]annulene **1**, octadehydro[16]annulene **2**, and decadehydro[20]annulene **3** with annelated [4.3.2]propellatriene units and their laser desorption induced fragmentation generating *cyclo*-C_{12}, *cyclo*-C_{16}, and *cyclo*-C_{20}, respectively, by extrusion of indan.

Palladium(0)-catalyzed coupling[11] of dichloro[4.3.2]propellatriene **4**[12] with 2-methyl-3-butyn-2-ol gave mainly the monosubstitution product **5** (70%). Attempted cyclization of **6**, prepared by deprotection of **5**, by Pd^0-catalyzed coupling under a variety of conditions resulted in the formation of dimer **7** (mixture of diastereomers); none of the desired cyclization products were detected. In contrast, when **5** was subjected to phase-transfer conditions for deprotection and subsequent coupling,[15] the dehydroannulenes **1**, **2**, and **3** were obtained in 0.9, 11, and 0.9%, respectively (Scheme 1). Although the dehydroannulenes **1**–**3** are inseparable mixtures of diastereomers (two isomers of **1**, four each of **2** and **3**), only those with the highest symmetry are drawn in Scheme 1 for clarity. The fact that the tetramer **2** is obtained in higher yield than the trimer **1** is explained by the smaller geometrical deformation in the cyclobutene-annelated [16]dehydroannulene ring.[16] The trimer **1** was also prepared in a stepwise manner by three successive Pd^0-catalyzed coupling reactions (Scheme 2). The reaction of diethynylpropellane **8**[17] with an excess of **4** yielded the 1:2 coupling product **9** (50%); **9** was coupled with 2-methyl-3-butyn-2-ol to give monosubstituted **10** (54%); and finally in-

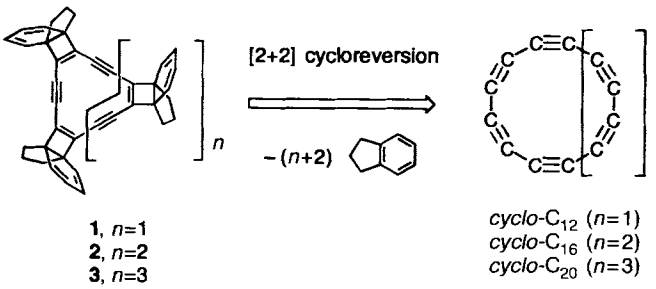

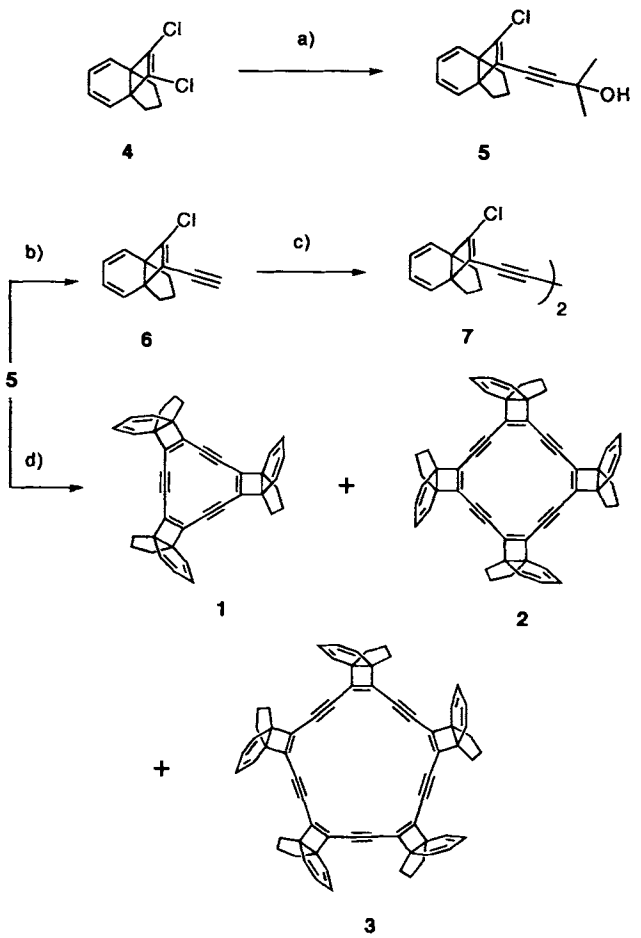

Scheme 1. a) 2-Methyl-3-butyn-2-ol, $[Pd(PPh_3)_4]$, CuI, $BuNH_2$, THF, room temperature (rt); b) NaOH, MeOH, toluene, 110°C; c) $[Pd(PPh_3)_4]$, CuI, $BuNH_2$, THF, rt; d) $[Pd(PPh_3)_4]$, CuI, aq NaOH, benzyltriethylammonium chloride, benzene, 80°C. Compounds **1**–**3** and **7** are inseparable mixtures of diastereomers.

[*] Prof. Dr. Y. Tobe, H. Matsumoto, Prof. Dr. K. Naemura
Department of Chemistry, Faculty of Engineering Science
Osaka University, Toyonaka, Osaka 560 (Japan)
Fax: Int. code + (6)850-6229
e-mail: tobe@chem.es.osaka-u.ac.jp
Prof. Dr. Y. Achiba, Dr. T. Wakabayashi[+]
Department of Chemistry, Faculty of Science
Tokyo Metropolitan University
Hachioji, Tokyo 192-03 (Japan)
Fax: Int. code + (426)77-2525
[+] Present Address:
Department of Chemistry, Faculty of Science
Kyoto University, Sakyo-ku, Kyoto 606-01 (Japan)

[**] This work was supported by Grants-in-Aid for Scientific Research on Priority Areas from the Ministry of Education, Science, Sports and Culture of Japan. Y. T. is grateful to Shin-Etsu Chemicals Co. for a generous gift of organosilicon reagents.

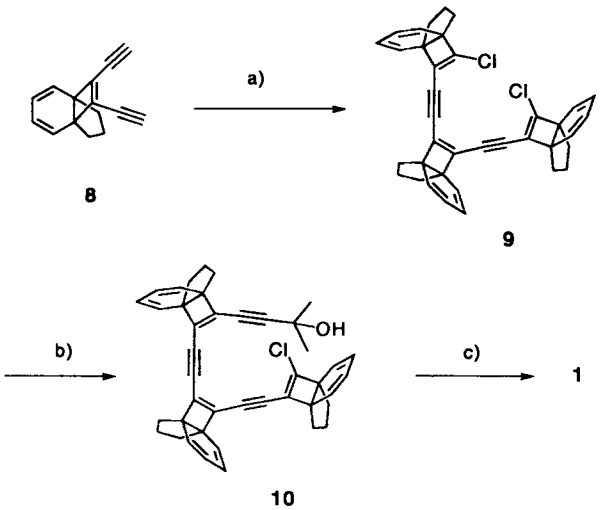

Scheme 2. a) **4** (15 equiv), $[Pd(PPh_3)_4]$, CuI, $BuNH_2$, THF, rt; b) 2-methyl-3-butyn-2-ol, $[PdCl_2(PhCN)_2]$, CuI, piperidine, THF, rt; c) $[Pd(PPh_3)_4]$, CuI, aq NaOH, benzyltriethylammonium chloride, benzene, 80 °C. Compounds **9** and **10** are inseparable mixtures of diastereomers.

tramolecular cyclization of **10** under the phase-transfer conditions provided **1**(14%).

The parent hexadehydro[12]annulene[18] and its benzo[15b, 19] and tris(bicyclo[2.2.2]octeno)[20] derivatives are known and their chemistry has been well studied.[9, 10] However, the properties of **1** might be considerably different, as the triple bonds must be substantially deformed from linearity because of the cyclobutene fusion; the AM1-calculated bond angle of the triple bond is 170.2°. The tetrabenzo[19b, 21] and tetrakis(bicyclo-[2.2.2]octeno)[20] derivatives of octadehydro[16]annulene are known, and both have a nonplanar puckered conformation. We deduce, on the other hand, that dehydroannulene **2** adopts a planar conformation on the basis of the paratropic shift[22] of the signals of the vinyl protons in the ^1H NMR spectrum and long-wavelength absorption maxima in the electronic spectrum (Fig. 1). The dodecadehydro[20]annulene system was previously unknown; the conformation of the pentamer **3** should be nonplanar in view of the small paratropic NMR shift[22] and the absence of long-wavelength absorption maxima.

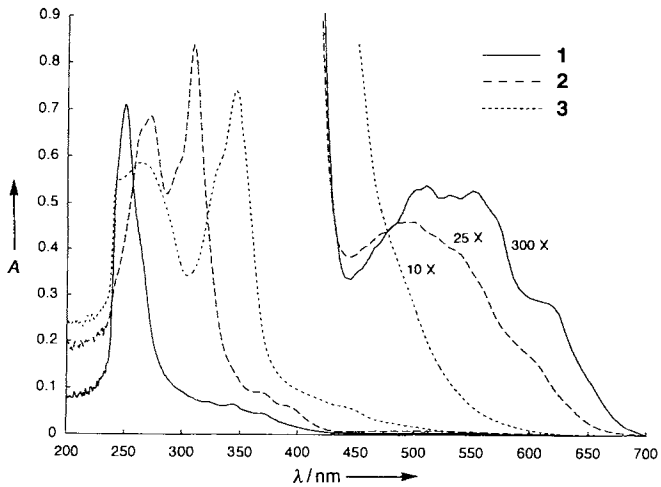

Fig. 1. UV/Vis spectra of **1** (1.04×10^{-6} mol dm^{-3}), **2** (3.43×10^{-6} mol dm^{-3}), and **3** (2.17×10^{-6} mol dm^{-3}) in chloroform. A = absorbance.

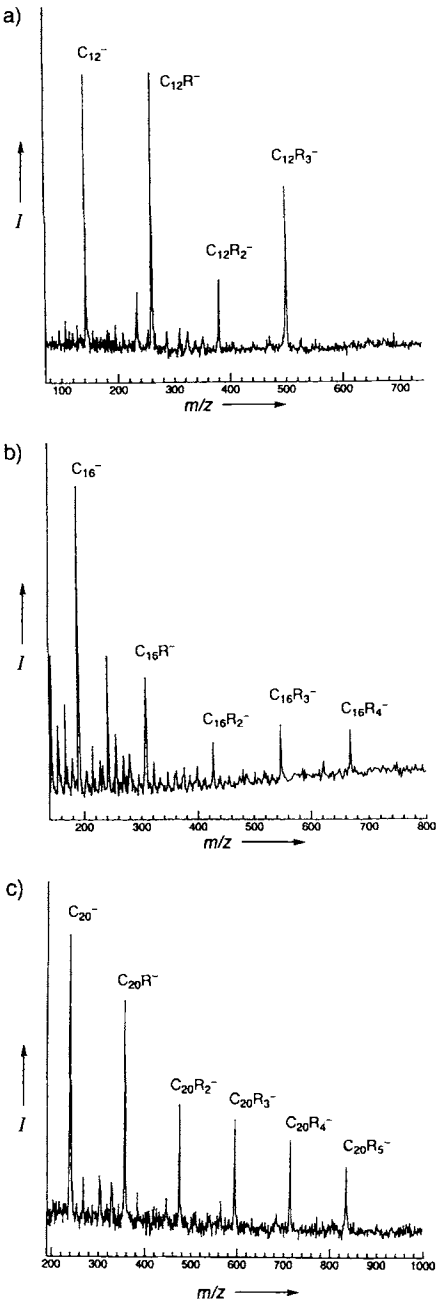

Fig. 2. Laser-desorption time of flight mass spectra of a) **1**, b) **2**, and c) **3** (R = indan). The compounds were dissolved in liquid paraffin as a matrix. For simultaneous desorption and ionization, the fourth harmonic of a Nd:YAG laser (266 nm, typically 0.6 mJ per pulse) was focused on an area of 3 mm^2. The vacuum chamber was maintained at 1×10^{-6} Torr during the operation.

In the positive-ion laser desorption time-of-flight (LD-TOF) mass spectra of **1**–**3**, like that of the related *cyclo*-C_{18} precursor, only the peak due to the indan fragment is observed. However, in the negative-ion mass spectra of **1**–**3** (Fig. 2) the peaks due to the parent ions ($C_{12}R_3^-$, ($C_{16}R_4^-$, ($C_{20}R_5^-$ (R = indan)) and the ions resulting from the successive loss of one, two, and three indan fragments were observed.[23] Thus for the first time cyclo[*n*]carbons with 4*n* carbon atoms have been obtained efficiently from organic precursors with well-defined structures.[7]

Received: February 27, 1996 [Z8873IE]
German version: *Angew. Chem.* **1996**, *108*, 1923–1926

Table 1. Physical and spectroscopic properties of compounds **1**–**3**, **9**, and **10**.

1 (mixture of diastereomers): dark purple solid; m.p. 117 °C (decomp); ^{1}H NMR ($CDCl_3$, 500 MHz): δ = 5.77–5.83 (m, 6H), 5.28–5.35 (m, 6H), 1.96–2.06 (m, 3H), 1.50–1.63 (m, 9H), 0.80–0.88 (m, 6H); ^{13}C NMR ($CDCl_3$, 125 MHz): δ = 139.91 (s), 139.89 (s), 139.78* (s), 139.76 (s), 126.26 (d), 126.19 (d), 126.17 (d), 126.15* (d), 122.00 (d), 121.98* (d), 121.97(d), 121.94 (d), 93.47 (s), 93.35* (s), 93.33 (s), 93.30 (s), 54.47 (s), 54.46* (s), 54.45 (s), 54.41 (s), 32.14 (t), 32.11* (t), 32.08 (t), 32.06 (t), 18.86 (t), 18.81 (t), 18.77* (t). The signals marked by asterisk are due to the C_{3v} isomer, because the intensities of these signals are slightly larger than those expected from the statistical distribution (1:3) of C_{3v} and C_s isomers. UV/Vis ($CHCl_3$): λ_{max} (log ε) = 250 (4.83), 509 (2.24), 550 (2.23), 614 (sh, 1.96) nm; FAB MS: *m/z* (%): 498 (100) [M^+], 261 (30) [$M^+ - 2(C_9H_{10}) - H$]

2 (mixture of diastereomers): dark purple solid; m.p. 218–221 °C (decomp); ^{1}H NMR ($CDCl_3$, 500 MHz): δ = 5.76–5.81 (m, 8H), 5.37–5.44 (m, 8H), 1.68–1.74 (m, 4H), 1.54–1.66 (m, 12H), 0.92–1.01 (m, 8H); ^{13}C NMR ($CDCl_3$, 125 MHz): δ = 135.65 (s), 135.62 (s), 135.58 (s), 135.54 (s), 135.53 (s), 135.52 (s), 135.51 (s), 135.49* (s), 127.26 (d), 127.25 (d), 127.21 (d), 127.14 (d), 127.01* (d), 121.91 (d), 121.90* (d), 121.87 (d), 121.86 (d), 121.85 (d), 121.81 (d), 89.98 (s), 89.95 (s), 89.93 (s), 89.92 (s), 89.91 (s), 89.91 *(s), 89.90 (s), 89.88 (s), 54.93 (s), 54.90 (s), 54.88 (s), 54.87* (s), 32.49 (t), 32.47 (t), 32.45 (t), 18.73 (t), 18.69, (t), 18.66 (t), 18.65 (t). The signals marked by asterisk are due to the statistically least feasible C_{2v} isomer, because these signals have apparently low intensities. UV/Vis ($CHCl_3$): λ_{max} (log ε) = 272 (4.30), 309 (4.39), 502 (2.72) nm; FAB MS: *m/z* (%): 664 (100) [M^+], 309 (53) [$M^+ - 3(C_9H_{10}) - H$]

3 (mixture of diastereomers): orange solid; m.p. 108 °C (decomp); ^{1}H NMR ($CDCl_3$, 500 MHz): δ = 5.82–5.88 (m, 10H), 5.68–5.65 (m, 10H), 1.84–1.87 (m, 10H), 1.59–1.61 (m, 10H), 1.14–1.22 (m, 10H); ^{13}C NMR ($CDCl_3$, 125 MHz): δ = 132.99(s), 132.97 (s), 132.95 (s), 132.92 (s), 132.86 (s), 132.82 (s), 132.80 (s), 132.78 (s), 128.35 (d), 128.33 (d), 128.29 (d), 128.25 (d), 128.21 (d), 128.20 (d), 128.18 (d), 128.16 (d), 128.11 (d), 121.96 (d), 121.94 (d), 121.91 (d), 121.89 (d), 121.85 (d), 88.80 (s), 88.79 (s), 88.77 (s), 88.75 (s), 88.74 (s), 88.73 (s), 56.08 (s), 56.07 (s), 56.06 (s), 56.05 (s), 56.04 (s), 56.03 (s), 56.02 (s), 32.94 (t), 18.74 (t), 18.71 (t), 18.67 (t); UV/Vis ($CHCl_3$): λ_{max} (log ε) = 263 (4.43), 345 (4.53) nm; FAB MS: *m/z* (%): 830 (37) [M^+], 357 (100) [$M^+ - 4(C_9H_{10}) - H$], 240 (65) [C_{20}^+, $M^+ - 5(C_9H_{10})$]

9 (mixture of diastereomers): colorless solid; m.p. 68–70 °C; ^{1}H NMR ($CDCl_3$, 270 MHz): δ = 5.77–5.95 (m, 12H), 1.96–2.03 (m, 6H), 1.16–1.67 (m, 12H); ^{13}C NMR ($CDCl_3$, 67.5 MHz): δ = 133.03 (s), 133.01 (s), 132.98 (s), 131.91 (s), 131.90 (s), 131.83 (s), 128.83 (d), 128.44 (d), 127.33 (d), 127.31 (d), 125.67 (s), 122.61 (d), 121.85 (d), 121.58 (d), 86.57 (s), 84.94 (s), 59.64 (s), 56.33 (s), 56.31 (s), 56.16 (s), 33.00 (t), 32.28 (t), 31.83 (t), 18.78 (t), 18.50 (t), 18.48 (t)

10 (mixture of diastereomers): colorless solid; m.p. 97–100 °C; ^{1}H NMR ($CDCl_3$, 270 MHz): δ = 5.76–5.95 (m, 12H), 2.12 (s, 1H), 1.91–1.99 (m, 6H), 1.64–1.16 (m including singlet at 1.55, 10H); ^{13}C NMR ($CDCl_3$, 67.5 MHz): δ = 133.12 (s), 133.09 (s), 133.07 (s), 133.03 (s), 132.98 (s), 132.97 (s), 132.62 (s), 132.60 (s), 132.57 (s), 131.87 (s), 131.85 (s), 131.81 (s), 128.73 (d), 128.71 (d), 128.67 (d), 128.63 (d), 128.57 (d), 128.47 (d), 128.45 (d), 127.29 (d), 125.66 (s), 122.64 (d), 122.59 (d), 121.83 (d), 121.81 (d), 121.68 (d), 121.64 (d), 121.61 (d), 100.31 (s), 87.63 (s), 87.61 (s), 87.60 (s), 87.58 (s), 86.92 (s), 86.09 (s), 86.64 (s), 86.63 (s), 84.87 (s), 84.84 (s), 74.62 (s), 65.65 (s), 59.61 (s), 59.38 (s), 56.31 (s), 56.30 (s), 56.16 (s), 56.14 (s), 56.09 (s), 33.00 (t), 32.87 (t), 32.76 (t), 32.28 (t), 31.80 (t), 31.39 (q), 31.36 (q), 18.73 (t), 18.47 (t)

Keywords: carbon clusters · cyclo[*n*]carbons · cycloreversion · dehydroannulenes

[1] a) S. Yang, K. J. Taylor, M. J. Craycraft, J. Conceicao, C. L. Pettiette, O. Cheshnovsky, R. E. Smalley, *Chem. Phys. Lett.* **1988**, *144*, 431–436; b) D. C. Parent, S. W. McElvany, *J. Am. Chem. Soc.* **1989**, *111*, 2393–2401; c) G. von Helden, M.-T. Hsu, P. R. Kemper, M. T. Bowers, *J. Chem. Phys.* **1991**, *95*, 3835–3837; d) review: W. Weltner, Jr., R. J. van Zee, *Chem. Rev.* **1989**, *89*, 1713–1747.

[2] Reviews: a) F. Diederich, Y. Rubin, *Angew. Chem.* **1992**, *104*, 1123–1146; *Angew. Chem. Int. Ed. Engl.* **1992**, *31*, 1101–1123; b) F. Diederich, *Nature* **1994**, *369*, 199–207; c) F. Diederich in *Modern Acetylene Chemistry* (Eds.: P. J. Stang, F. Diederich), VCH, Weinheim, **1995**, p. 443.

[3] a) G. von Helden, N. G. Gotts, M. T. Bowers, *Nature* **1993**, *363*, 60–63; b) *J. Am. Chem. Soc.* **1993**, *115*, 4363–4364; c) J. M. Hunter, J. L. Fye, M. F. Jarrold, *J. Chem. Phys.* **1993**, *99*, 1785–1795; d) J. M. Hunter, J. L. Fye, E. J. Roskamp, M. F. Jarrold, *ibid.* **1994**, *98*, 1810–1818.

[4] Review: D. Plattner, Y. Li, K. N. Houk in *Modern Acetylene Chemistry* (Eds.: P. J. Stang, F. Diederich), VCH, Weinheim, **1995**, p. 1.

[5] a) F. Diederich, Y. Rubin, C. B. Knobler, R. L. Whetten, K. E. Schriver, K. N. Houk, Y. Li, *Science* **1989**, *245*, 1088–1090; b) Y. Rubin, M. Kahr, C. B. Knobler, F. Diederich, C. L. Wilkins, *J. Am. Chem. Soc.* **1991**, *113*, 495–500; c) S. W. McElvany, M. M. Ross, N. S. Goroff, F. Diederich, *Science* **1993**, *259*, 1594–1596; d) F. Diederich, Y. Rubin, O. L. Chapman, N. S. Goroff, *Helv. Chim. Acta* **1994**, *77*, 1441–1457.

[6] Y. Tobe, T. Fujii, H. Matsumoto, K. Naemura, Y. Achiba, T. Wakabayashi, *J. Am. Chem. Soc.* **1996**, *118*, 2758–2759.

[7] Cyclo[*n*]carbons can be produced by electron impact induced fragmentation of perchlorinated aromatic compounds; however, many side reactions due to fragmentation under standard conditions in a mass spectrometer are also possible: J. Sun, H.-F. Grützmacher, C. Lifshitz, *J. Am. Chem. Soc.* **1993**, *115*, 8382–8388, and references therein.

[8] Recently, Diederich et al. described fullerene-substituted pericyclene derivatives that produced *cyclo*-C_{15} and *cyclo*-C_{20} by cheletropic fragmentation: L. Issacs, P. Seiler, F. Diederich, *Angew. Chem.* **1995**, *107*, 1636–1639; *Angew. Chem. Int. Ed. Engl.* **1995**, *34*, 1466–1469.

[9] For the reduction of hexadehydro[12]annulene, see: P. Garratt, N. E. Rowland, F. Sondheimer, *Tetrahedron* **1971**, *27*, 3157–3162.

[10] For transition metal complexes of tribenzohexadehydro[12]annulene, see: J. D. Ferrara, A. A. Tanaka, C. Fierro, C. A. Tessier-Youngs, W. J. Youngs, *Organometallics*, **1989**, *8*, 2089–2098, and references therein.

[11] For a review, see: K. Sonogashira in *Comprehensive Organic Synthesis, Vol. 3* (Eds.: B. M. Trost, I. Fleming), Pergamon, Oxford, **1991**, p. 521.

[12] Dichloropropellatriene **4** was prepared by the following sequence of reactions: 1) photocycloaddition of trichloroethylene with bicyclo[4.3.0]non-1(6)-en-2-one, 2) elimination of hydrogen chloride with *t*BuOK (75% for two steps), 3) bromination with 5,5-dibromo-2,2-dimethyl-1,3-dioxane-4,6-dione (dibromomeldrum's acid), 4) elimination of hydrogen bromide with $LiBr/Li_2CO_3$ in DMF (70% for two steps), 5) 1,2-reduction with $NaBH_4$/ $CeCl_3$ [13] 6) 1,4-elimination with 3,5-dinitrophenylsulfenyl chloride [14] (79% for two steps).

[13] A. L. Gemal, J. L. Luche, *J. Am. Chem. Soc.* **1981**, *103*, 5454–5459.

[14] H. J. Heich, S. Wollowitz, *J. Am. Chem. Soc.* **1982**, *104*, 7051–7059.

[15] a) R. Rossi, A. Carpita, M. G. Quirici, M. L. Gaudenzi, *Tetrahedron* **1982**, *38*, 631–637; b) C. Huynh, G. Linstrumelle, *Tetrahedron* **1988**, *44*, 6337–6344.

[16] For a related discussion on the cyclobutene-annelated [18]- and [24]dehydroannulenes, see: Y. Li, Y. Rubin, F. Diederich, K. N. Houk, *J. Am. Chem. Soc.* **1990**, *112*, 1618–1623.

[17] Y. Tobe, T. Fujii, K. Naemura, *J. Org. Chem.* **1994**, *59*, 1236–1237. Alternatively, diethynylpropellane **8** was prepared by Pd^0-catalyzed coupling of dichloride **4** with triisopropylsilylacetylene followed by deprotection (quantitative yield).

[18] a) K. G. Untch, D. C. Wysocki, *J. Am. Chem. Soc.* **1966**, *88*, 2608–2610; b) F. Sondheimer, R. Wolovsky, P. J. Garratt, I. C. Calder, *ibid.* **1966**, *88*, 2610.

[19] a) H. A. Staab, F. Graf, *Tetrahedron Lett.* **1966**, 751–757; b) I. D. Campbell, G. Eglinton, W. Henderson, R. A. Raphael, *J. Chem. Soc. Chem. Commun.* **1966**, 87–89; c) H. A. Staab, F. Graf, *Helv. Chim. Acta* **1970**, *103*, 1107–1118; d) J. W. Barton, M. K. Shepherd, *Tetrahedron Lett.* **1984**, *25*, 4967–4970.

[20] Recently, bicyclo[2.2.2]octene-annelated dehydro[12]- and -[16]annulenes were synthesized by Komatsu et al. We are grateful to Professor Komatsu for providing us with the unpublished data.

[21] J. D. Bradshaw, D. Solooki, C. A. Tessier, W. J. Youngs, *J. Am. Chem. Soc.* **1994**, *116*, 3177–3179.

[22] While the ^{1}H NMR signals of both of the vinyl protons of **8** appear at δ = 5.8–5.9 [17], those of **1**–**3** were observed at δ = 5.8 and 5.3, 5.8 and 5.4, and 5.85 and 5.65, respectively (Table 1). The signals at higher field are assigned to the protons located closer to the annulene rings, which are shifted upfield due to the paratropicity of the $4n\pi$ ring systems.

[23] In the positive-ion FAB mass spectra of **1**–**3**, peaks due to the loss of the indan fragments were also observed; however, the cyclocarbon cation (C_{20}^+) was observed only in the case of **3** (Table 1).

 © VCH Verlagsgesellschaft mbH, D-69451 Weinheim, 1996 0570-0833/96/3516-1802 $ 15.00+.25/0

1,2-Distanna[2]- and 1,2,3-Tristanna[3]-ferrocenophanes**

Max Herberhold,* Udo Steffl, Wolfgang Milius, and Bernd Wrackmeyer

Dedicated to Professor Hans Georg von Schnering on the occasion of his 65th birthday

[*n*]Ferrocenophanes,[1] in which the two cyclopentadienyl ligands are connected by an intramolecular bridge of $n = 1$, 2, or 3 links, have attracted interest as monomer precursors for the ring-opening polymerization (ROP) to metal-containing polymers.[2, 3] In addition, they can serve as models for the study of molecular dynamics[1a, 4] and for the study of the reactivity of element–element bonds in the bridge[4–8] as a function of the more or less strained bonding situation.

Although 1,1′-disubstituted ferrocene derivatives such as $[Fe(C_5H_4SnMe_3)_2]$[9, 10] and $[Fe(C_5H_4SnMe_2Cl)_2]$ (**1**) (Scheme 1)[10] have been described, their chemistry has not been explored in a systematic manner, and [*n*]ferrocenophanes containing tin directly attached to the two cyclopentadienyl ligands were unknown until very recently: I. Manners and coworkers[20] have succeeded in characterizing the first 1-stanna[1]ferrocenophane $[Fe(C_5H_4)_2(SntBu_2)]$; earlier attempts to synthesize 1-stanna[1]ferrocenophanes had produced only the dinuclear distanna[1.1]ferrocenophanes $[Fe(C_5H_4SnR_2C_5H_4)_2Fe]$ (R = Et[11], *n*Bu[11, 12]) in very low yield in addition to polymeric products. In contrast, sila[*n*]ferrocenophanes such as $[Fe(C_5H_4)_2(SiR_2)_n]$ (R = Me: $n = 1$,[7, 13] 2,[6–8, 14] 3;[8, 14] R = Ph: $n = 1$,[13, 15] R = Cl: $n = 1$[13]) and germa[*n*]ferrocenophanes such as $[Fe(C_5H_4)_2GePh_2]$[16] and $[Fe(C_5H_4GeMe_2)_2]$[14] are well known. We have found a convenient access to 1,1′-bis(chlorodimethylstannyl)ferrocene (**1**),[10] which can be readily converted to the new hydride **2** (Scheme 1).

Both **1** and **2** are useful starting materials for the synthesis of stanna[*n*]ferrocenophanes. Treatment of **1** with bis(trimethylsilyl)mercury affords **3** in moderate yield, whereas the reaction of **2** with bis(diethylamino)dimethyltin liberates two equivalents of diethylamine to give **4** in high yield. However, if other diethylaminotin compounds such as $Et_2Sn(NEt_2)_2$, $nBu_2Sn(NEt_2)_2$, and $Sn(NEt_2)_4$ were treated with **2** under the same conditions, only the distannane **3** was obtained (Scheme 1). The molecular structure[17] of the 1,2-distanna[2]ferrocenophane **3** (Fig. 1) reveals some slight but typical deformations (Fig. 2).

The cyclopentadienyl rings are almost parallel (with a tilt angle α of 0.7° towards the bridge) and adopt a nearly eclipsed conformation (with a twist angle τ of 2.9°). The distance between the cylopentadienyl rings (331.2 pm) is similar to that in ferrocene (332 pm).[18] Both the C(1)–Sn(1) and the C(6)–

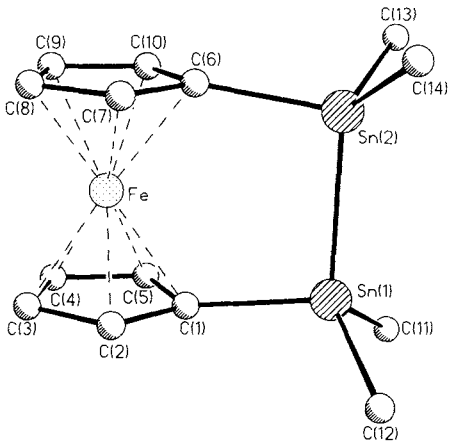

Fig. 1. Structure of **3** in the crystal. Selected bond lengths [pm] and angles [°]: Sn(1)–Sn(2) 276.2(1), Sn(1)–C(1) 214.8(5), Sn(1)–C(11) 213.5(6), Sn(1)–C(12) 213.9(6), Sn(2)–C(6) 213.3(6), Sn(2)–C(13) 213.0(7), Sn(2)–C(14) 213.5(8); Sn(2)-Sn(1)-C(1) 97.5(1), Sn(2)-Sn(1)-C(11) 114.7(2), Sn(2)-Sn(1)-C(12) 117.1(2), C(1)-Sn(1)-C(11) 108.5(3), C(1)-Sn(1)-C(12) 109.5(3), C(11)-Sn(1)-C(12) 108.7(2); Sn(1)-Sn(2)-C(6) 97.7(1), Sn(1)-Sn(2)-C(13) 115.8(2), Sn(1)-Sn(2)-C(14) 115.9(2), C(6)-Sn(2)-C(13) 107.2(3), C(6)-Sn(2)-C(14) 110.4(3), C(13)-Sn(2)-C(14) 108.9(3).

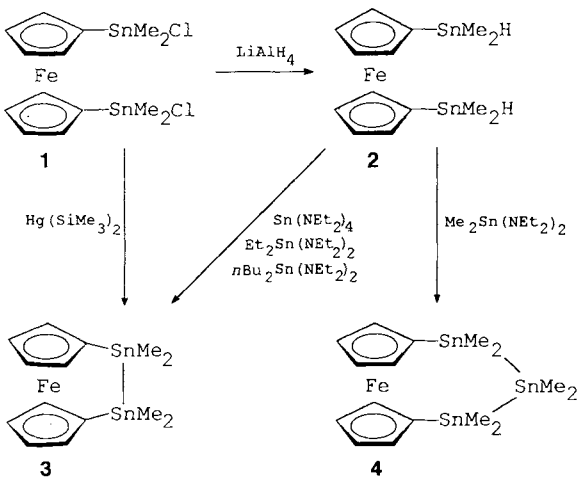

Scheme 1. Synthetic routes to **2**–**4**.

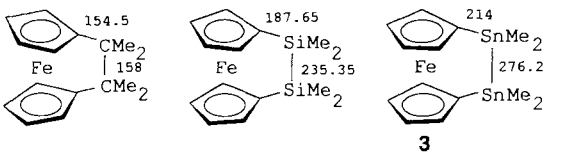

Angle	$[Fe(C_5H_4)_2[CMe_2]_2]$ [19]	$[Fe(C_5H_4)_2[SiMe_2]_2]$ [7]	$[Fe(C_5H_4)_2[SnMe_2]_2]$ **3**
α	23.2°	4.19°	0.7°
β	10; 12°	10.8°	10.3; 10.6°
δ	156.8°	176.48°	179.4°
τ	9–10°	6.0°	2.9°
ε	26; 28°	7.85; 8.35°	5.2; 5.5°

Fig. 2. Comparison of the structures of the homologous [2]ferrocenophanes. The twist angle τ and the torsion angle ε are defined in the text.

[*] Prof. Dr. M. Herberhold, Dipl.-Chem. U. Steffl, Dr. W. Milius, Prof. Dr. B. Wrackmeyer
Laboratorium für Anorganische Chemie der Universität
Postfach 101251, D-95440 Bayreuth (Germany)
Fax: Int. code +(921)552157
e-mail: max.herberhold@uni-bayreuth.de.

[**] This work was supported by the Deutsche Forschungsgemeinschaft and the Fonds der Chemischen Industrie.

Sn(2) distances (av 214 pm) and the Me-Sn-Me angles (av 108.8°) are in the expected ranges; the corresponding values in $[Fe(C_5H_4Sn(nBu)_2C_5H_4)_2Fe]$[12] are 212.5(3) and 214.6(3) pm, and 110.1(2)°, respectively. The two $SnMe_2$ units are displaced from the eclipsed arrangement by a torsion angle ε of about 5.3°.

The NMR data of the new stanna[*n*]ferrocenophanes **3** and **4** are consistent with the proposed structures. Of particular interest are the ^{119}Sn NMR spectra, which show typical ^{117}Sn satellite signals of $^1J(^{119}Sn,^{117}Sn) = 5274.0$ Hz (**3**) and 3223.9 Hz (**4**) as well as $^2J(^{119}Sn,^{117}Sn) = 537.2$ Hz (**4**). The bridge consisting of three $SnMe_2$ units in **4** appears to be highly flexible, since no changes were observed in the $^1H(C_5H_4)$ and $^1H(SnMe_2)$ resonance signals, recorded in $[D_8]$toluene between 25 °C and −90 °C.

Evidently, the strain in the [2]ferrocenophanes (Fig. 2) decreases as the E–E bond lengths increase in the order E = $CMe_2 < SiMe_2 < SnMe_2$. Taking into account the well known reactivity of Sn–Sn bonds in distannanes and polystannanes, the new ferrocenophanes **3** and **4** must be considered as model compounds for studying exchange and insertion[21] reactions, opening the way to a rich chemistry of stanna[*n*]ferrocenophanes in general.

Experimental Procedure

All coupling constants to ^{119}Sn are determined from the satellite signals. The ^1H, ^{13}C, and ^{119}Sn NMR spectra were measured at 250, 62.9, and, 93.3 MHz, respectively.

1: A mixture of 1,1′-bis(trimethylstannyl)ferrocene (1.41 g, 2.8 mmol) and dimethyltin dichloride (1.3 g, 5.9 mmol) was heated at 130 °C for 3 h. Trimethyltin chloride was removed from the equilibrium by sublimation onto a cooling finger (15 °C). Traces of further trimethyltin chloride or dimethyltin dichloride were removed in vacuo, and 1.39 g (90%) of **1** was left as a dark-orange oil. Recrystallization from hexane gave an orange solid (m.p. 85 °C). EI MS: *m/z* (%) = 554 (100) $[M^+]$. ^1H NMR (C_6D_6, $J(^{119}Sn,^1H)$): $\delta = 0.55$ (s, 12H, Me_2Sn, $J = 60.9$ Hz); 4.08 (m, 4H, 2,5-H, $J = 9.6$ Hz), 4.25 (m, 4H, 3,4-H); ^{13}C NMR (C_6D_6, $J(^{119}Sn,^{13}C)$): $\delta = -1.1$ (Me_2Sn, $J = 415.6$), 70.7 (C-1, $J = 590.0$ Hz), 74.5 (C-2,5, $J = 66.9$), 72.0 (C-3,4, $J = 51.2$ Hz); ^{119}Sn NMR (C_6D_6): $\delta = 125.5$.

2: A solution of **1** (0.73 g, 1.3 mmol) in ether (20 mL) was slowly added to a cooled (0 °C) suspension of $LiAlH_4$ (0.05 g, 1.3 mmol) in ether, and the mixture was stirred for 3 h at room temperature. Insoluble material was filtered off, and the solvent was removed in vacuo, leaving 0.61 g (96%) of **2** as an orange oil. EI MS: *m/z* (%) = 486 (100) $[M^+]$. ^1H NMR (C_6D_6, $J(^{119}Sn,^1H)$): $\delta = 0.26$ (d, 12H, Me_2Sn, $J = 57.9$ Hz, $^3J(^1H,^1H) = 2.2$ Hz), 3.99 (m, 4H, 2,5-H, $J = 9.4$ Hz), 4.23 (m, 4H, 3,4-H), 5.45 (sept, 2H, HSn, $J = 1824.0$); ^{13}C NMR (C_6D_6, $J(^{119}Sn,^{13}C)$): $\delta = -7.5$ (Me_2Sn, $J = 371.8$ Hz), 65.8 (C-1, $J = 515.4$ Hz), 75.0 (C-2,5, $J = 53.8$ Hz), 71.4 (C-3,4, $J = 42.4$ Hz). ^{119}Sn NMR (C_6D_6): $\delta = -102.4$.

3: From **1** and $Hg(SiMe_3)_2$: To a solution of **1** (0.58 g, 1 mmol) in toluene (20 mL), bis(trimethylsilyl)mercury (0.47 g, 1.3 mmol) was added in one portion. The mixture was stirred at room temperature for 5 h. The toluene was then removed in vacuo and the residue was dissolved in pentane. After filtration and evaporation of most of the pentane, chromatography on silica with hexane/dichloromethane (3:2) gave 0.14 g (29%) of **3** as a yellow, crystalline solid (m.p. 105 °C).

3: From **2** and $R_2Sn(NEt_2)_2$ (R = Et, Bu) or $Sn(NEt_2)_4$: The stoichiometric amount of the diethylaminotin compound was added to a solution of **2** (0.2 g, 0.41 mmol) in ether (20 mL) at 0 °C, and the mixture was heated to reflux for 2 h. After all volatile material had been removed in vacuo the residue was purified by chromatography on silica (vide supra) to give **3** in yields up to 52%. EI MS: *m/z* (%) = 484 (100) $[M^+]$. ^1H NMR (C_6D_6, $J(^{119}Sn,^1H)$): $\delta = 0.40$ (s, 12H, Me_2Sn; $J_1 = 50.2$, $J_2 = 15.4$ Hz), 4.34 (m, 4H, 2,5-H, $J = 9.8$ Hz), 4.22 (m, 4H, 3,4-H); ^{13}C NMR (C_6D_6, $J(^{119}Sn,^{13}C)$): $\delta = -8.2$ Me_2Sn $J_1 = 227.0$, $J_2 = 74.2$ Hz), 77.8 (C-1, $J_1 = 338.9$, $J_2 = 49.9$ Hz), 74.8 (C-2,5, $J = 44.6$ Hz), 69.5 (C-3,4, $J_1 = 32.7$, $J_2 = 4.4$ Hz); ^{119}Sn NMR (C_6D_6, $J(^{119}Sn,^{117}Sn)$): $\delta = -43.4$ ($J = 5274.0$ Hz).

4: A solution of **2** (0.2 g, 0.41 mmol) in ether (20 mL) was cooled to 0 °C, and bis(diethylamino)dimethyltin (0.1 g, 0.41 mmol) was slowly added through a syringe. The mixture was heated to reflux for 3 h, then all volatile material was removed in vacuo. After chromatography on silica with hexane, 0.11 g (43%) of **4** were obtained as a yellow, crystalline solid (m.p. 117 °C). EI MS: *m/z* (%) = 630 (43) $[M^+]$; 467 (100) $[M^+ - SnMe_3]^+$; ^1H NMR (C_6D_6, $J(^{119}Sn,^1H)$): $\delta = 0.53$ (s, 12H, Me_2Sn, $J_1 = 44.6$, $J_2 = 22.6$ Hz), 0.45 (s, 6H, $SnSnMe_2Sn$, $J_1 = 48.7$, $J_2 = 13.8$, $J_3 = 5.0$ Hz), 3.99 (m, 4H, 2,5-H, $J = 10.4$ Hz), 4.26 (m, 4H, 3,4-H); ^{13}C NMR (C_6D_6, $J(^{119}Sn,^{13}C)$): $\delta = -9.0$ ($C_5H_4SnMe_2$, $J_1 = 244.7$, $J_2 = 42.7$, $J_3 = 17.7$ Hz), −13.5 ($SnSnMe_2Sn$, $J_1 = 185.0$, $J_2 = 30.5$ Hz) 72.2 (C-1, $J_1 = 362.9$, $J_2 = 54.1$, $J_3 = 8.3$ Hz), 78.9 (C-2,5, $J_1 = 46.5$, $J_2 = 10.5$ Hz), 74.3 (C-3,4, $J_1 = 35.0$, $J_2 = 5.0$ Hz). ^{119}Sn NMR (C_6D_6, $J(^{119}Sn,^{117}Sn)$): $\delta = -102.5$ ($C_5H_4SnMe_2$, $J_1 = 3223.9$, $J_2 = 537.2$ Hz), −249.3 ($SnSnMe_2Sn$, $J = 3225.7$ Hz).

Received: February 26, 1996 [Z8868IE]
German version: *Angew. Chem.* **1996**, *108*, 1927–1928

Keywords: iron compounds · metallocenophanes · sandwich complexes · stannylations · tin compounds

[1] a) M. Herberhold, *"Ferrocene Compounds containing Heteroelements"* in *Ferrocenes, Homogeneous Catalysis, Organic Synthesis, Materials Science* (Eds.: A. Togni, T. Hayashi), VCH Weinheim, **1995**, pp. 219–278; b) M. Herberhold, *Angew. Chem.* **1995**, *107*, 1985–1987; *Angew. Chem. Int. Ed. Engl.* **1995**, *34*, 1837–1840.

[2] a) I. Manners, *Adv. Organomet. Chem.* **1995**, *37*, 131–168; b) *Phosphorus, Sulfur, Silicon* **1994**, *93/94*, 143–151.

[3] a) P. F. Brandt, T. B. Rauchfuss, *J. Am. Chem. Soc.* **1992**, *114*, 1926–1927; b) C. P. Galloway, T. B. Rauchfuss, *Angew. Chem.* **1993**, *105*, 1407–1409; *Angew. Chem. Int. Ed. Engl.* **1993**, *32*, 1319–1321; c) *Phosphorus, Sulfur, Silicon* **1994**, *93/94*, 117–128.

[4] a) E. W. Abel, K. G. Orrell, A. G. Osborne, V. Sik, W. Guoxiong, *J. Organomet. Chem.* **1991**, *411*, 239–249; b) M. Herberhold, U. Dörfler, W. Milius, B. Wrackmeyer, *ibid.* **1995**, *492*, 59–63; c) A. Davison, J. C. Smart, *ibid.* **1979**, *174*, 321–334.

[5] a) M. Kumada, T. Kondo, K. Mimura, K. Yamamoto, M. Ishikawa, *J. Organomet. Chem.* **1972**, *43*, 307–314; b) M. Kumada, T. Kondo, K. Mimura, K. Yamamoto, *ibid.* **1972**, *43*, 315–321.

[6] W. Finckh, B.-Z. Tang, A. Lough, I. Manners, *Organometallics* **1992**, *11*, 2904–2911.

[7] W. Finckh, B.-Z. Tang, D. A. Foucher, D. B. Zamble, R. Ziembinski, A. Lough, I. Manners, *Orgunometallics* **1993**, *12*, 823–829.

[8] V. V. Dement'ev, F. Cervantes-Lee, L. Parkányi, H. Sharma, K. H. Pannell, M. T. Nguyen, A. Diaz, *Organometallics* **1993**, *12*, 1983–1987.

[9] F. H. Köhler, W. A. Geike, N. Hertkorn, *J. Organomet. Chem.* **1987**, *334*, 359–367.

[10] Z. Kabouche, Nguyen Huu Dinh, *J. Organomet. Chem.* **1989**, *375*, 191–195.

[11] D. Seyferth, H. P. Withers, Jr., *Organometallics* **1982**, *1*, 1275–1282.

[12] A. Clearfield, C. J. Simmons, H. P. Withers, Jr., D. Seyferth, *Inorg. Chim. Acta* **1983**, *75*, 139–144.

[13] A. R. Fischer, J. B. Kinney, R. H. Staley, M. S. Wrighton, *J. Am. Chem. Soc.* **1979**, *101*, 6501–6506.

[14] M. Kumada, T. Kondo, K. Mimura, M. Ishikawa, K. Yamamoto, S. Ikeda, M. Kondo, *J. Organomet. Chem.* **1972**, *43*, 293–305.

[15] H. Stoeckli-Evans, A. G. Osborne, R. H. Whiteley, *Helv. Chim. Acta* **1976**, *59*, 91–101.

[16] a) A. G. Osborne, R. H. Whiteley, R. E. Meads, *J. Organomet. Chem.* **1980**, *193*, 345–357; b) H. Stoeckli-Evans, A. G. Osborne, R. H. Whiteley, *ibid.* **1980**, *194*, 91–101.

[17] X-Ray structure analysis of compound **3**: $C_{14}H_{20}FeSn_2$, orange platelet with dimensions $0.42 \times 0.35 \times 0.10$ mm^3; **3** crystallizes in the monoclinic space group $P2_1/c$ with the lattice parameters $a = 1309.0(2)$, $b = 657.5(2)$, $c = 1887.4(2)$ pm, $\beta = 100.76(2)°$, $Z = 4$ and $\mu(Mo_{K\alpha}) = 3.981$ mm^{-1}. On a Siemens P4 diffractometer with $Mo_{K\alpha}$-radiation ($\lambda = 71.073$ pm, graphite monochromator) 4832 reflections were collected in the range $3° \le 2\theta \le 55°$ ($T = 296$K). Solution and refinement (Program SHELXTL PLUS) was done with 3547 independent and observed ($F_0 \ge 0\sigma(F_0)$, no reflections omitted) reflections; the data were corrected empirically for absorption effects by using Ψ scans of ten selected reflections (min./max. transmission factors: 0.3847/0.8034). All non-hydrogen atoms were refined anisotropically, the hydrogen atoms are in calculated positions. The refinement of 155 parameters converged at *R*/*wR*-values of 0.0403/0.0360 with $w^{-1} = \sigma^2(F_0)$; the max./min. residual electron density was 1.09/−0.60 e Å^{-3}. Crystallographic data (excluding structure factors) for the structure(s) reported in this paper have been deposited with the Cambridge Crystallographic Data Centre as supplementary publication no. CCDC-179-54. Copies of the data can be obtained free of charge on application to The Director, CCDC, 12 Union Road, Cambridge CB2 1EZ, UK (fax: Int. code +(1223) 336-033; e-mail: teched(@chemcrys.cam.ac.uk).

[18] a) J. D. Dunitz, L. E. Orgel, A. Rich, *Acta Crystallogr.* **1956**, *9*, 373–375; P. Seiler, J. D. Dunitz, *Acta Crystallogr. Sect. B* **1979**, *35*, 1068–1074; b) F. Takusagawa, T. F. Koetzle, *ibid.* **1979**, *35*, 1074–1081.

[19] M. Burke Laing, K. N. Trueblood, *Acta Crystallogr.* **1965**, *19*, 373–381.

[20] R. Rulkens, A. J. Lough, I. Manners, *Angew. Chem.* **1996**, *108*, 1929; *Angew. Chem. Int. Ed. Engl.* **1996**, *35*, 1805.

[21] Preliminary results have shown that oxygen, sulfur, and selenium insert into the Sn–Sn bond of **3** to give the 1,3-distanna-2-chalcogena[3]ferrocenophanes.

Synthesis and Ring-Opening Polymerization of a Tin-Bridged [1]Ferrocenophane**

Ron Rulkens, Alan J. Lough, and Ian Manners*

[1]Ferrocenophanes **1** possess a single-atom bridge ER_x linking the two cyclopentadienyl ligands. The idea that species such as **1** (E = Si) might exist was (understandably) dismissed by Rosenberg and Neuse in 1970 who stated that such structures would be "impossibly strained."[1] Since the synthesis of the first [1]ferrocenophane **1**, $ER_x = SiPh_2$, in 1975 by the reaction of dilithioferrocene·tmeda (tmeda = tetramethylethylenediamine) with Ph_2SiCl_2,[2] a range of analogous species with Group 14 (Si, Ge),[3,4] Group 15 (P, As),[4-6] Group 16 (S),[7] and Group 4 (Ti, Zr, Hf)[8,9] bridging elements have subsequently been prepared. These molecules possess interesting strained structures with tilt angles between the planes of the cyclopentadienyl ligands between 6° (for **1** (E = Zr)) and 31° (for **1** (ER_x = S)). Recently [1]ferrocenophanes have attracted attention as precursors to novel high molecular weight poly(metallocene)s **2** by ring-opening polymerization (ROP).[10-15]

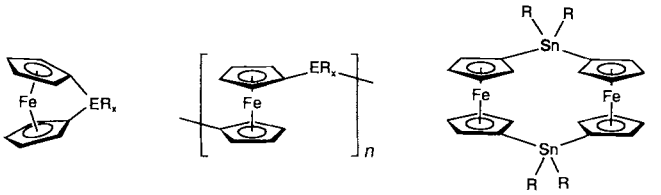

1 **2** **3**

As the properties of the resulting organometallic materials **2** are modified significantly by the nature of the spacer ER_x, the extension of the range of [1]ferrocenophanes by the incorporation of other bridging elements is of considerable interest.[14,16,17] Despite their large covalent radii, the introduction of heavier elements (fifth period and higher) would be expected to be synthetically challenging because of the weakness of the bonds between the *ipso*-carbon atoms and the bridging element. Herein we report on the first [1]ferrocenophane to be bridged by the heavy main group element tin.[18]

Although [1]ferrocenophanes containing silicon and germanium as bridging elements are now well known,[3,4] previous attempts to synthesize stanna[1]ferrocenophanes by the reaction of dilithioferrocene·tmeda with R_2SnCl_2 (R = Me, Et, *n*Bu, or Ph) were unsuccessful and resulted only in low molecular weight oligomers **2** ($ER_x = SnR_2$) ($M_n < 4600$) and cyclic dimers **3**.[4,5,19] The absence of a stanna[1]ferrocenophane in the product mixture was attributed to the high reactivity of the Sn–Cl bonds, which might favor intermolecular condensation reactions over intramolecular cyclizations.[19]

We initially attempted to isolate a tin-bridged [1]ferrocenophane by the reaction of dilithioferrocene·2/3tmeda with nBu_2SnCl_2 in Et_2O at low temperature.[20] Although a color change from amber to orange was detected below −40 °C, warming the reaction mixture led to amber oligomeric products similar to those previously reported.[19] Since the presence of bulkier substituents at the tin atom should stabilize a stanna[1]ferrocenophane, we studied the reaction of dilithioferrocene·2/3tmeda with tBu_2SnCl_2 in diethyl ether. At −35 °C the reaction showed a subtle color change from amber to orange. When it reached −30 °C the reaction mixture was rapidly warmed to 20 °C and filtered to remove LiCl. The filtrate was collected at −78 °C and the stanna[1]ferrocenophane **4** was isolated as orange needles in 65% yield.

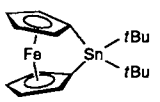

4

The structure of **4** was confirmed by ^1H, ^{13}C, and ^{119}Sn NMR, UV/Vis spectroscopy, and by mass spectrometry. NMR and UV/Vis spectroscopic results indicated a less strained structure for **4** compared to that of the Si and Ge analogues **1**, $ER_2 = SiMe_2$ and $GeMe_2$, respectively (see Table 1).[21] For example, the ^1H NMR spectrum of **4** (in $CDCl_3$) shows of a pair of less widely separated pseudo triplets (δ = 4.22 and 4.44) assigned to the α and β protons of the cyclopentadienyl ligands. Thus the splitting between the pseudo triplets, $\Delta\delta$, is 0.22, 0.26, and 0.40 for **4**, **1**, $ER_x = GeMe_2$, and **1**, $ER_x = SiMe_2$, respectively. In the ^{13}C NMR spectrum (in $CDCl_3$) the resonance of the *ipso*-carbon atoms of the cyclopentadienyl ligands of **4** at δ = 34.9 lies at slightly higher field than those of **1** (E = Si, Ge); but these C atoms are still extremely shielded compared to those of unstrained ferrocene derivatives.

Table 1. Comparison of data indicating ring strain in Group 14 bridged [1]ferrocenophanes.

	α [°]	β [a] [°]	λ_{max} [b] [nm]	ε [M^{-1} cm^{-1}]	$\delta_{(ipso\text{-}C)}$ [c]	$\Delta\delta$(H-Cp) [d]
1 ($ER_2 = SiMe_2$)	20.8(5)	37.0(6)	481	341	33.1	0.40
1 ($ER_2 = GeMe_2$)	19.0(9)	36.8(5)	420/486	75/283	30.0	0.26
4	14.1(2)	36.2(2)	418/485	75/158	34.9	0.22
Fe(η-$C_5H_4SiMe_3$)$_2$	0	0	448	130	72.0	0.22

[a] Average values. [b] 1.1×10^{-3} M in THF. [c] ^{13}C NMR spectra in $CDCl_3$. [d] ^1H NMR spectra in $CDCl_3$.

Crystals of the tin-bridged [1]ferrocenophane **4** suitable for a single-crystal X-ray diffraction study were obtained by recrystallization from Et_2O/THF (10:1) at low temperature (< −20 °C). The molecular structure of **4** is shown in Figure 1.[22] The most important structural features indicating ring strain are

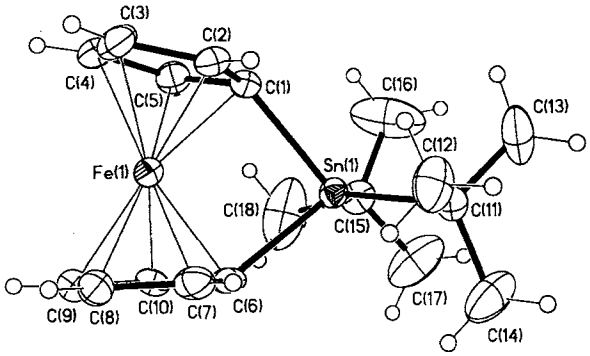

Fig. 1. Crystal structure of **4**. Selected bond lengths [Å] and angles [°]: Sn–C(1) 2.174(4), Sn–C(6) 2.171(5), Sn–C(11) 2.180(5), Sn–C(15) 2.190(6), Sn–Fe 2.9761(8), Fe–C(1) 2.036(5), Fe–C(2) 2.026(5), Fe–C(3) 2.059(5), Fe–C(4) 2.062(5), Fe–C(5) 2.027(5), Fe–C(6) 2.041(5), Fe–C(7) 2.027(5), Fe–C(8) 2.068(5), Fe–C(9) 2.063(6), Fe–C(10) 2.036(6); C(1)-Sn-C(6) 86.5(2), C(11)-Sn-C(15) 115.1(2).

[*] Prof. I. Manners, R. Rulkens, A. J. Lough
Department of Chemistry, University of Toronto
80 St. George Street
Toronto, ON, M5S 3H6 (Canada)
Fax: Int. code +(416) 978-6157
e-mail: imanners@alchemy.chem.utoronto.ca

[**] We thank the donors of the Petroleum Research Fund, administered by the American Chemical Society, for financial support of this work. We also wish to acknowledge an Ontario Graduate Student Fellowship for R. R., and I. M. is grateful to the Alfred P. Sloan Foundation for a Research Fellowship (1994–1998).

the tilt angle α between the planes of the cyclopentadienyl rings (14.1(2)°) and the angles β between the cyclopentadienyl ring planes and the exocyclic C–Sn bonds (36.2(2)° and 36.1(2)°). The tilt angle α for **4** is the smallest yet reported for a [1]ferrocenophane with a main group element in the bridge and is significantly less than that for silicon- and germanium-bridged analogues (Table 1). The tilting of the cyclopentadienyl ligands is accompanied by a RC1-Fe-RC2 (RC = ring centroid) angle of 168.6(2)° (180° in ferrocene) and a 0.164(6) Å displacement of the iron atom from the line joining the two ring centroids. The tilted cyclopentadienyl ligands maintain an eclipsed conformation. The angle between the *ipso* carbon atoms of the cyclopentadienyl ligands and the tin atom (C1-Sn-C6) is 86.5(2)°; this is smaller than the analogous angles for **1**, $ER_2 = SiMe_2$, and $ER_2 = GeMe_2$, (95.7(4)° and 91.7(3)°, respectively). The average Sn–C bond lengths ($Sn-C_{Cp} = 2.173(4)$, $Sn-C_{tBu} = 2.185(5)$ Å) are typical for Sn–C single bonds. The Sn–Fe distance in **4** is 2.9761(8) Å, which is only 14–17% longer than Fe–Sn bond lengths found in the species $[CpL_2FeSnR_3]$ (2.537–2.605 Å).[23] This indicates that probably there is significant overlap of the orbitals of iron and tin to give a weak bond.[11, 24]

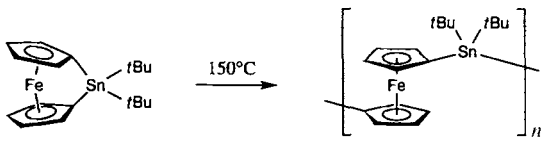

4 **5**

When **4** was heated at 150 °C the amber poly(ferrocenylstannane) **5** was formed,[25] which is soluble in fairly polar and aromatic organic solvents (e.g. THF, CH_2Cl_2, toluene). Analysis by gel permeation chromatography (GPC) in THF versus polystyrene standards showed that the material was of high molecular weight ($M_w = 133000$, $M_n = 83000$, polydispersity index $M_w/M_n = 1.6$). Despite its strained structure, **4** is air-stable over several days in the solid state. However, in solution in $CHCl_3$ ROP occurs at room temperature to form a low molecular weight poly(ferrocenylstannane) **5** ($M_w = 10000$, $M_n = 4700$, polydispersity index $M_w/M_n = 2.2$) and as a side product the cyclic dimer **3** (R = *t*Bu). However, when **4** was dissolved in toluene, high molecular weight **5** ($M_w = 900000$, $M_n = 560000$, $M_w/M_n = 1.6$) and a small amount of the dimer **3** were formed within 3 h.

The tin-bridged species **4** represents the least ring-tilted [*n*]metallocenophane to undergo ROP to date. We have previously prepared [2]metallocenophanes with tilt angles up to 13° that were found to be resistent to ROP.[26, 27] In order to compare the strain energy of **4** to that of other polymerizable [1]ferrocenophanes the thermal ROP was studied by differential scanning calorimetry (DSC) (see Fig. 2). We found that when heated above 100 °C, the sample showed a ROP exotherm but no melt transition. By integration of the ROP exotherm we found that **4** has a strain energy of $36(\pm 9)$ kJ mol^{-1}. This is approximately half the enthalpy of polymerization found by DSC analysis of the ROP of silicon-bridged [1]ferrocenophanes (70–80 kJ mol^{-1}).[10, 28] Analysis of **5** by cyclic voltammetry showed the presence of two reversible oxidation waves (separation $\Delta E = 0.24$ V)[29] consistent with the presence of significant bridge-mediated interactions between the iron atoms.[10, 14, 16, 30–32] Thermogravimetric analysis (TGA) under nitrogen (heating rate of 10 K min^{-1}) revealed that polymer **5** is stable to weight loss below about 230 °C. The ceramic yield at 900 °C was 44%.

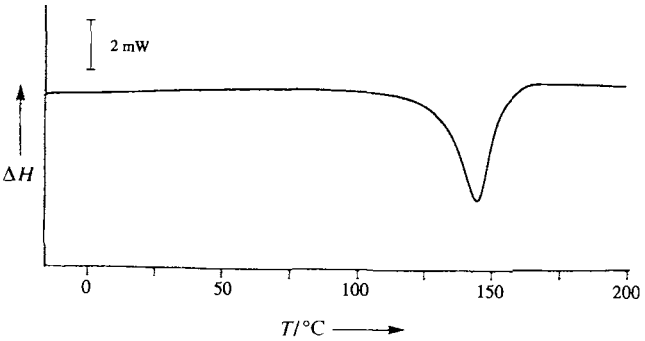

Fig. 2. DSC of the polymerization of **4** (5.8 mg, heating rate: 10 K min^{-1}).

Further studies of **4** and the polymer **5** will allow detailed comparisons with the analogous Si and Ge monomers and high polymers. In addition, the ROP of **4** in solution at room temperature provokes intriguing mechanistic questions. Relevant investigations are now in progress.

Experimental Procedure

4: A solution of tBu_2SnCl_2 (2.32 g, 7.64 mmol) in diethyl ether (20 mL) was added dropwise to a suspension of dilithioferrocene·2/3 tmeda (2.00 g, 7.27 mmol) in diethyl ether (100 mL) that was cooled to −78 °C. The reaction mixture was allowed slowly to warm to −30 °C over 4 h after which it was rapidly warmed to 20 °C and vacuum filtered through a fritted glass disk. The orange filtrate was collected at −78 °C which resulted in the precipitation of the orange product. After the mixture had been cooled for 30 minutes at −78 °C, the solvent was decanted off and the product was dried under vacuum. This gave 1.98 g (65%) of analytically pure orange crystalline needles of **4**. ^{1}H NMR (300 MHz, $CDCl_3$, −20 °C; ps. t: pseudo triplet): $\delta = 4.44$ (ps. t, $J = 2$ Hz, 4H, cyclopentadienyl), 4.22 (ps. t, $J = 2$ Hz, 4H, cyclopentadienyl), 1.48 *t*Bu (s/d, $J(H,^{117/119}Sn) = 75$ Hz, 18H); ^{13}C NMR (75.5 MHz, $CDCl_3$, −20 °C): $\delta = 77.9$ ($J(C,^{117/119}Sn) = 28$ Hz, cyclopentadienyl), 75.7 ($J(C,^{117/119}Sn) = 26$ Hz, cyclopentadienyl), 34.9 (*ipso*-cyclopentadienyl), 32.8 (*ipso*-*t*Bu), 31.8 (*t*Bu); ^{119}Sn NMR (111.8 MHz, $CDCl_3$, −20 °C): $\delta = -23.7$; UV/Vis. (THF): 340 nm (sh.), 418 nm ($\varepsilon = 75\,M^{-1}cm^{-1}$), 485 nm ($\varepsilon = 158\,M^{-1}cm^{-1}$); MS: *m/z* (%): 418 (62) [M^+], 362 (28) [$M^+ - t$Bu], 304 (100) [$M^+ - 2t$Bu], 248 (46) [$Sn(\eta\text{-}C_5H_5)_2^+$], 186 [$Fe(\eta\text{-}C_5H_5)_2^+$]; anal calcd. for $C_{18}H_{26}FeSn$: C 51.85, H 6.29; found: C 51.51, H 6.29; DSC: polymerization exotherm 145 °C (peak), 130 °C (onset), $\Delta H = -36(\pm 9)$ kJ mol^{-1}.

ROP of **4**: The poly(ferrocenylstannane) **5** was obtained from **4** in two ways: 1) Thermal ROP: Solid-state polymerization was carried out by heating crystalline **4** in a sealed evacuated Pyrex tube at 150 °C for 30 min. This resulted in the formation of monomodel high molecular weight poly(ferrocenylstannane) **4** in a quantitative yield. 2) ROP in solution: After the dissolution of **4** (50 mg, 0.10 mmol) in $CHCl_3$ (0.5 mL) at 20 °C, it underwent complete conversion over 3 h to the cyclic dimer **3** (R = *t*Bu) (30%) and to polymeric material **5** (70%), which was isolated by precipitation into hexanes and was shown to have a monomodel low molecular weight. The remaining solution contained the cyclic dimer **3** (R = *t*Bu), which was isolated by recrystallization from pentanes. In toluene, high molecular weight polymer **5** and only a small amount of dimer **3** were formed.

3 (R = *t*Bu): ^{1}H NMR (200 MHz, $CDCl_3$, 20 °C): $\delta = 4.41$ (ps. t, $J = 2$ Hz, 8H, cyclopentadienyl), 4.18 (ps. t, $J = 2$ Hz, 8H, cyclopentadienyl), 1.18 *t*Bu (s/d, J (H, $^{117/119}$Sn) = 64 Hz, 36H); ^{13}C NMR (50.3 MHz, $CDCl_3$, 20 °C): $\delta = 75.2$ (J ($C,^{117/119}Sn$) = 40 Hz, cyclopentadienyl), 70.2 ($J(C,^{117/119}Sn) = 34$ Hz, cyclopentadienyl), 69.2 (*ipso*-cyclopentadienyl), 31.3 (*t*Bu), 28.1 (*ipso*-*t*Bu); MS: *m/z* (%): 834 (2) [M^+], 777 (73) [$M^+ - t$Bu], 663 (67) [$M^+ - 3t$Bu], 606 (57) [$M^+ - 4t$Bu], 368 (100) [$M^+ - 2Sn(t\text{Bu})_2$], 304 (58) [$[Fe(\eta\text{-}C_5H_5)_2Sn^+$].

5: ^{1}H NMR (300 MHz, $CDCl_3$, 20 °C): $\delta = 4.24$ (s,br., 4H, cyclopentadienyl), 3.97 (s,br., 4H, cyclopentadienyl), 1.34 *t*Bu (s/d, J (H, $^{117/119}$Sn) = 65 Hz, 18H); ^{13}C NMR (75.5 MHz, $CDCl_3$, 20 °C): $\delta = 74.5$ ($J(C,^{117/119}Sn) = 24$ Hz, cyclopentadienyl), 71.1 (J ($C,^{117/119}Sn$) = 32 Hz, cyclopentadienyl), 70.6 (*ipso*-cyclopentadienyl), 31.8 (*t*Bu), 29.0 (*ipso*-*t*Bu); ^{119}Sn NMR (111.8 MHz, $CDCl_3$, 20 °C): $\delta = -45.2$; UV/Vis. (THF): 340 nm (sh.), 452 nm ($\varepsilon = 152\,M^{-1}cm^{-1}$); anal calcd. for $C_{18}H_{26}FeSn$: C 51.85, H 6.29; found: C 51.86, H 6.37; DSC: T_g 120 °C ($\Delta C_p = 28(5)$ J mol^{-1}), T_{decomp} 205 °C; GPC (THF, vs. polystyrene): thermal polymerization $M_n = 83000$ (PDI = 1.6); polymerization in solution (20 °C): $CHCl_3$, $M_n = 4700$ (PDI = 2.2); toluene, $M_n = 560000$ (PDI = 1.6).

Received: February 27, 1996 [Z8875IE]
German version: *Angew. Chem.* **1996**, *108*, 1929–1931

Keywords: iron compounds · metallocenophanes · poly(metallocene)s · ring-opening polymerization · sandwich complexes

[1] E. W. Neuse, H. Rosenberg, *J. Macromol. Sci.* **1970**, *C4(1)*, 110.
[2] A. G. Osborne, R. H. Whiteley, *J. Organomet. Chem.* **1975**, *101*, C27.
[3] H. Stoeckli-Evans, A. G. Osborne, R. H. Whiteley, *J. Organomet. Chem.* **1980**, *194*, 91.
[4] A. G. Osborne, R. H. Whiteley, R. E. Meads, *J. Organomet. Chem.* **1980**, *193*, 345.
[5] D. Seyferth, H. P. Withers, *Organometallics* **1982**, *1*, 1275.
[6] I. R. Butler, W. R. Cullen, F. W. B. Einstein, S. J. Rettig, A. J. Willis, *Organometallics* **1983**, *2*, 128.
[7] J. K. Pudelski, D. G. Gates, R. Rulkens, I. Manners, *Angew. Chem.* **1995**, *107*, 1633; *Angew. Chem. Int. Ed. Engl.* **1995**, *34*, 1506.
[8] R. Broussier, A. Da Rold, B. Gautheron, Y. Dromzee, Y. Jeannin, *Inorg. Chem.* **1990**, *29*, 1817.
[9] R. Broussier, A. Da Rold, B. Gautheron, *J. Organomet. Chem.* **1992**, *427*, 231.
[10] D. A. Foucher, B. Z. Tang, I. Manners, *J. Am. Chem. Soc.* **1992**, *114*, 6246.
[11] D. A. Foucher, M. Edwards, R. A. Burrow, A. J. Lough, I. Manners, *Organometallics* **1994**, *13*, 4959.
[12] C. H. Honeyman, D. A. Foucher, F. Y. Dahmen, R. Rulkens, A. J. Lough, I. Manners, *Organometallics* **1995**, *14*, 5503.
[13] Y. Ni, R. Rulkens, I. Manners, *J. Am. Chem. Soc.* **1996**, *118*, 4102.
[14] I. Manners, *Adv. Organomet. Chem.* **1995**, *37*, 131, and references therein.
[15] For recent work on organometallic polymers see, for example, a) O. Nuyken, T. Pöhlmann, M. Herberhold *Macromol. Rep.* **1992**, A29(3), 211; b) C. P. Galloway, T. B. Rauchfuss *Angew. Chem* **1993**, *105*, 1407; *Angew Chem. Int. Ed. Engl.* **1993**, *32*, 1319; c) H. Chen, R. D. Archer, *Macromolecules* **1995**, *28*, 1609; d) H. M. Nugent, M. Rosenblum, P. Klemarczyk, *J. Am. Chem. Soc.* **1993**, *115*, 3848; e) R. Bayer, T. Pöhlmann, O. Nuyken, *Makromol. Chem. Rapid. Commun.* **1993**, *14*, 359; f) M. Altmann, U. H. F. Bunz, *Angew. Chem* **1993**, *107*, 603; *Angew. Chem. Int. Ed. Engl.* **1995**, *34*, 569; g) H. B. Fyfe, M. Mlekuz, D. Zargarian, N. J. Taylor, T. B. Marder, *J. Chem. Soc. Chem. Commun.* **1991**, 188; h) M. S. Khan, A. K. Kakkar, S. L. Ingham, P. R. Raithby, J. Lewis, B. Spencer, F. Wittman, R. H. Friend, *J. Organomet. Chem.* **1994**, *472*, 247; i) M. C. Carmen, M. Morán, J. Losada, I. Cuadrado, *Inorg. Chem.* **1995**, *34*, 1668.
[16] D. A. Foucher, C. H. Honeyman, J. M. Nelson, B. Z. Tang, I. Manners, *Angew. Chem.* **1993** *105*, 1843; *Angew. Chem. Int. Ed. Engl.* **1993**, *32*, 1709.
[17] a) T.-Y. Dong, M.-Y. Hwang, Y.-S. Wen, W.-S. Hwang, *J. Organomet. Chem.* **1990**, *391*, 377; b) V. V Dement'ev, F. Cervantes-Lee, L. Parkanyi, H. Sharma, K. H. Pannell, M. T. Nguyen, A. Diaz, *Organometallics* **1993**, *12*, 1983.
[18] The first 1,2-distanna[2]- and 1,2,3-tristanna[3]ferrocenophanes have now been made by Herberhold and co-workers. See M. Herberhold, U. Steffl, W. Milius, B. Wrackmeyer, *Angew. Chem.* **1996**, *108*, 1927; *Angew. Chem. Int. Ed. Engl.* **1996**, *35*, 1803.
[19] A. Clearfield, C. J. Simmons, H. P. Withers, D. Seyferth, *Inorg. Chim. Acta* **1983**, *75*, 139.
[20] D. A. Foucher, Ph.D. Thesis, University of Toronto, **1993**.
[21] This is also expected based on the large covalent radius of tin (140 pm) compared to those of germanium (122 pm) and silicon (118 pm).
[22] Crystal data for $C_{18}H_{26}FeSn$ **3**: tetragonal $P\bar{4}2_1c$, $a = b = 19.667(2)$, $c = 9.0997(8)$ Å, $V = 3519.7(2)$ Å^3, $Z = 8$, $\mu = 2.233$ mm^{-1}, $Mo_{K\alpha}$ ($\lambda = 0.71073$ Å), $\rho_{calcd} = 1.574$ Mgm^{-3}, 173(2) K, Siemens P4 diffractometer with graphite monochromator, orange crystal ($0.08 \times 0.08 \times 0.50$ mm). Absorption correction by integration (0.7876, 0.8422). Of 4225 reflections collected ($2.93 \le 2\theta \le 27.00^\circ$) 2158 were independent $R_{int} = 0.0360$, and 1758 were observed with $F_o \ge 4\sigma(F_o)$. Solution by direct methods and refinement on F^2 using SHELXTL-PC V5.03 (Sheldrick, G. M., Siemens Analytical X-ray Instruments Inc., Madison, WI, USA, **1994**), non-hydrogen atoms were refined with anisotropic thermal parameters, hydrogen atoms were refined with isotropic thermal parameters, $R1 = 0.0267$, $wR2 = 0.0473$ ($R1 = \Sigma(F_o - F_c)/\Sigma F_o$ observed data, $wR2 = \{\Sigma[w(F_o^2 - F_c^2)^2]/\Sigma[w(F_o^2)^2]\}^{1/2}$ for all data), GOF = 0.864, $N_o/N_v = 11.24$ and $\Delta\rho_{max} = 0.274$ and $\Delta\rho_{min} = -0.321$ e Å^{-3}. Further details of the crystal structure investigation may be obtained from the Fachinformarmationszentrum Karlsruhe, D-76344 Eggenstein-Leopoldshafen (Germany), on quoting the depository number CSD-405528.
[23] a) R. F. Bryan, *J. Chem. Soc. (A)* **1967**, 192; b) F. W. B. Einstein, R. Restivo, *Inorg. Chim. Acta* **1971**, *5*, 501; c) M. Veith, L. Stahl, V. Huch, *Organometallics* **1993**, *12*, 1914.
[24] J. Silver, *J. Chem. Soc., Dalton Trans.* **1990**, 3513.
[25] High molecular weight polymers with tin-based polymers are very rare. For the recent synthesis of poly(stannane)s $[SnR_2]_n$ see: a) T. Imori, T. D. Tilley, *J. Chem. Soc. Chem. Commun.* **1993**, 1607; b) T. Imori, V. Lu, H. Cai, T. D. Tilley, *J. Am. Chem. Soc.* **1995**, *117*, 9931; c) N. Devylder, M. Hill, K. C. Molloy, G. J. Price, *J. Chem. Soc. Chem. Commun.* **1996**, 711.
[26] J. M. Nelson, A. J. Lough, I. Manners, *Organometallics* **1994**, *13*, 3703.
[27] Hydrocarbon-bridged [2]metallocenophanes with ring-tilts of 21–29° have been found to undergo thermal ROP, see: a) J. M. Nelson, H. Rengel, I. Manners, *J. Am. Chem. Soc.* **1993**, *115*, 7035; b) J. M. Nelson, A. J. Lough, I. Manners, *Angew. Chem.* **1994**, *106*, 1019; *Angew. Chem. Int. Ed. Engl.* **1994**, *33*, 989.
[28] J. K. Pudelski, D. A. Foucher, C. H. Honeyman, P. M. Macdonald, I. Manners, S. Barlow, D. O'Hare, *Macromolecules* **1996**, *29*, 1894.
[29] Cyclic voltammetry was performed on a CH_2Cl_2 solution which was 1.0 g L^{-1} in poly(ferrocenylstannane) **5** and 0.1 M in $[Bu_4N][PF_6]$ at 20 °C. Two $E_{1/2}$ values of 0.04 and 0.28 V vs. the ferrocene/ferrocenium ion couple were observed. The [1]stannaferrocenophane **4** undergoes reversible one-electron oxidation ($E_{1/2} = 0.00$ V vs. ferrocene/ferrocenium) as found previously for silicon-bridged [1]ferrocenophanes. See: J. K. Pudelski, D. A. Foucher, C. H. Honeyman, A. J. Lough, I. Manners, S. Barlow, D. O'Hare, *Organometallics* **1995**, *14*, 2470.
[30] P. F. Brandt, T. B. Rauchfuss, *J. Am. Chem. Soc.* **1992**, *114*, 1926.
[31] a) I. Manners, *J. Inorg. Organomet. Polym.* **1993**, *3*, 185; b) R. Rulkens, A. J. Lough, I. Manners, *J. Am. Chem. Soc* **1994**, *116*, 797.
[32] M. T. Nguyen, A. F. Diaz, V. V. Dement'ev, K. H. Pannell, *Chem. Mater.* **1993**, *5*, 1389.

Azido and 2,2′-Bipyrimidine Ligands as Useful Tools in Designing Two- and Three-Dimensional Manganese(II) Networks

Giovanni De Munno,* Miguel Julve,* Guillaume Viau, Francesc Lloret, Juan Faus, and Davide Viterbo

Magneto-structural studies on azido-bridged dinuclear copper(II) complexes[1] have shown that the end-to-end and end-on azido bridging ligands are able to mediate large antiferromagnetic[1b–e] and ferromagnetic[1b,f,g] interactions, respectively. The concept of accidental orthogonality[1b] and the theory of spin polarization[2] have been applied by Kahn et al. to account for these magnetic interactions. Calculations have revealed that the interaction between the in-plane π_g HOMOs of the azido ligand and the d_{xy} metal orbitals containing the unpaired electron favors either the singlet (end-to-end azido bridge) or the triplet (end-on azido bridge) as ground state. The extension of these magneto-structural studies to other complexes with transition metal ions such as nickel(II) cation afforded azido-bridged dinuclear,[3] square[4] and cubane[5] tetranuclear, and one-[6] and two-dimensional[7] compounds.

Extensive magneto-structural work has been carried out also with metal complexes that contain 2,2′-bipyrimidine (bpym) ligands, taking advantage of the chelating and bis(chelating) coordination modes of this bis(α-diimine) type ligand. The most striking features of this class of compounds are the easy access to dinuclear complexes,[8] the possibility of tailoring the number of metal atoms in the molecule from the mononuclear species to *n*-dimensional (*n*D) networks ($n = 1-3$),[9] the preparation of novel dicubane type complexes,[10] the rational design of chain-like multinuclear complexes with a regular alternation of ferro- and antiferromagnetic interactions[11] or with two antiferro-

[*] Prof. G. De Munno
Dipartimento di Chimica, Università della Calabria
I-87030 Arcavacata di Rende, Cosenza (Italy)
Fax: Int. code +(984)49-2044
Prof. M. Julve, Dr. G. Viau, Dr. F. Lloret, Prof. J. Faus
Departament de Química Inorgànica, Facultat de Química
Dr. Moliner 50, E-46100 Burjassot, València (Spain)
Fax: Int. code +(6)3864322
e-mail: miguel.julve@uv.es
Prof. D. Viterbo
Dipartimento di Chimica IFM, Università di Torino
Via P. Giuria 7, 10125 Torino (Italy)

[**] This work was supported by the Spanish DGICYT (Project PB94-1002), the Italian Ministero dell'Università e della Ricerca Scientifica e Tecnologica, and the Human Capital and Mobility Program (Network on Magnetic Molecular Materials from the EU) through Grant ERBCHRX-CT920080. G. V. thanks the Spanish Ministery of Education and Science for a postdoctoral fellowship.

magnetic[12] interactions, and finally, the preparation of new honeycomb layered materials, which exhibit alternating antiferromagnetic interactions within the hexagonal layer.[8c, 13]

In view of the remarkable ability of the end-on azido and bis(chelating) bpym bridging units to mediate relatively strong ferro- and antiferromagnetic interactions, respectively, we tried to prepare honeycomb layered materials with these two types of bridges and first row transition metal ions. Preliminary attempts resulted in the isolation and structural characterization of the sheetlike polymer **1** and the three-dimensional polymeric compound **2**, which both have the same composition.

$[Mn_2(bpym)(N_3)_4]$ **1**, **2**

The crystal structure of **1** reveals parallel sheets of manganese atoms linked by two end-on azido and one bis(chelating) bpym ligands (Fig. 1). Each sheet comprises double azido-bridged manganese(II) chains that are connected by bridging bpym ligands, leading to the formation of a honeycomb network. Each manganese atom is in an highly distorted octahedral MnN_6 environment. If we assume that the equatorial plane is defined by the two bpym nitrogen atoms and the nitrogen atoms N(2) and N(2c) of the azido ligands, the two bonds between the axial azido ligand and the metal are longer than those between the equatorial azido ligands and the metal, and are all significantly shorter than that between the metal and the bpym ligand. The intraring metal–metal separations are Mn(1)···Mn(1a) 6.142(1), Mn(1)···Mn(1b) 3.428(1), Mn(1)···Mn(1d) 6.234(1), Mn(1)···Mn(1e) 8.751(1), Mn(1)···Mn(1f) 8.186(1), and Mn(1b)···Mn(1f) 8.996(1) Å [(a) = x, $1-y$, z; (d) $1+x$, y, z; (e) $1+x$, $1-y$, z; (f) $1.5-x$, $y-0.5$, $-z$]. The distances between Mn centers separated by bpym and azido ligands compare well with corresponding values reported for bpym[8c] or double end-on azido-bridged[14] manganese(II) dimers. Compound **1** is very similar to the parent complex of formula **3**,[8e]

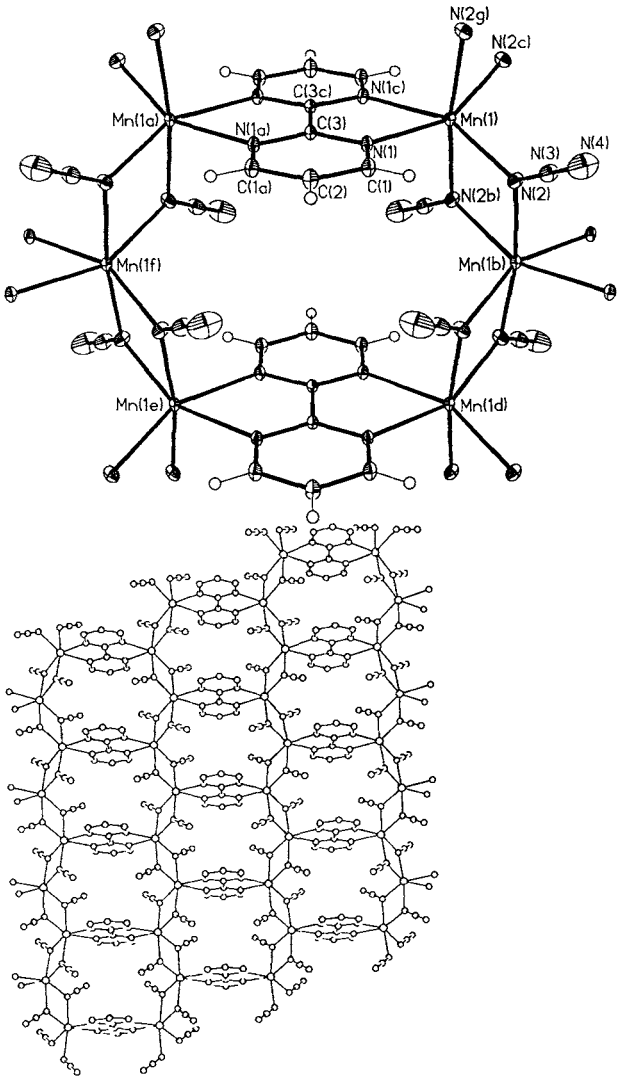

Fig. 1. Crystal structure of **1** (ellipsoids at the 30% probability level). Top: Hexanuclear repeating unit. Bottom: View of a sheet of **1** perpendicular to the xy plane (hydrogen atoms have been omitted for clarity). Selected distances [Å] and angles [°] with standard deviations in parentheses: Mn(1)–N(1) 2.315(1), Mn(1)–N(2) 2.178(1), Mn(1)–N(2b) 2.234(1); N(1)-Mn(1)-N(2) 92.8(1), N(1)-Mn(1)-N(1c) 71.3(1), N(2)-Mn(1)-N(1c) 154.8(1), N(1)-Mn(1)-N(2b) 100.7(1), N(2)-Mn(1)-N(2b) 78.0(1), N(2)-Mn(1)-N(2c) 108.2(1), N(1)-Mn(1)-N(2g) 85.7(1), N(2)-Mn(1)-N(2g) 97.4(1), N(2b)-Mn(1)-N(2g) 172.3(1), Mn(1)-N(2)-Mn(1b) 102.0(1), N(2)-N(3)-N(4) 178.5(2) (symmetry code: (b) $1.5-x$, $1.5-y$, $-z$; (c) $1-x$, y, $-z$; (g) $x-0.5$, $1.5-y$, z).

$[Mn_2(bpym)(ox)_2]\cdot 6H_2O$ **3**

in which the double azido bridge is replaced by the bis(chelating) oxalato ligand. Since the Mn···Mn distances are shortened for the complex with azido ligands in comparison to that with oxalato ligands, the size of the cavity in the hexameric ring of **1** is reduced to such an extent that the inclusion of solvent molecules is precluded. The bpym ligand is planar and its bond lengths and angles are consistent with known values. The distance between the two bpym units within the hexameric ring is 5.876(2) Å.

The crystal structure of **2** consists of chains of manganese atoms; the Mn centers are alternatively bridged by bpym and two end-on azido ligands (Fig. 2). The chains are connected by end-to-end azido ligands in vicinal positions, which ensures linkages along two different directions. Each metal atom is in a highly distorted octahedral MnN_6 environment. If we assume that two bpym-nitrogen atoms occupy two equatorial positions of the octahedron around Mn^{II} (Fig. 2), the other two equatorial positions are occupied by N(6) of the end-on azido ligand and by N(3) of the end-to-end azido ligand, while the axial positions are occupied by N(5c) and N(6b). The axial positions of each Mn^{II} center are connected with the equatorial ones of the adjacent Mn^{II} center (and vice versa) by end-on and end-to-end azido ligands. Although bpym is coordinated to the metal ion in an asymmetrical bis(chelating) fashion, the average Mn–N(bpym) bond length in **2** and the distance between the metal centers separated by the bpym bridge [Mn(1)···Mn(1a) = 6.177(1) Å] are close to that in **1**. The Mn(1)–N(3) bond length is significantly shorter than the other equatorial distances. The bpym ligand is planar and the Mn(1) atom lies 0.036(1) Å out of this plane. The distance between the metal centers separated by end-on azido ligands is somewhat longer that those in **1** and in similar complexes.[14] The structure of **2** is very similar to that of $[Cu_2(bpym)(NCO)_4]$,[9b] because the metal atoms in both compounds are bridged by bpym and end-on and end-to-end pseudohalide ligands. The only remarkable difference concerns the connections of adjacent chains: in the copper complex they are connected in such a way to form a two-dimensional polymer, whereas in **2** a three-dimensional network occurs.

The $\chi_m T$ values (χ_m is the magnetic susceptibility per two Mn^{II} ions) for **1** and **2** at room temperature are similar to one another and lie in the range expected for two $S = 5/2$ ground states. However, the temperature dependence of the $\chi_m T$ values for these compounds is very different: the $\chi_m T$ value for **1** continuously increases as the sample is cooled and reaches a maximum at 25 K (χ_m shows a maximum at 14 K) then decreases very

 © VCH Verlagsgesellschaft mbH, D-69451 Weinheim, 1996 0570-0833/96/3516-1808 $ 15.00+.25/0

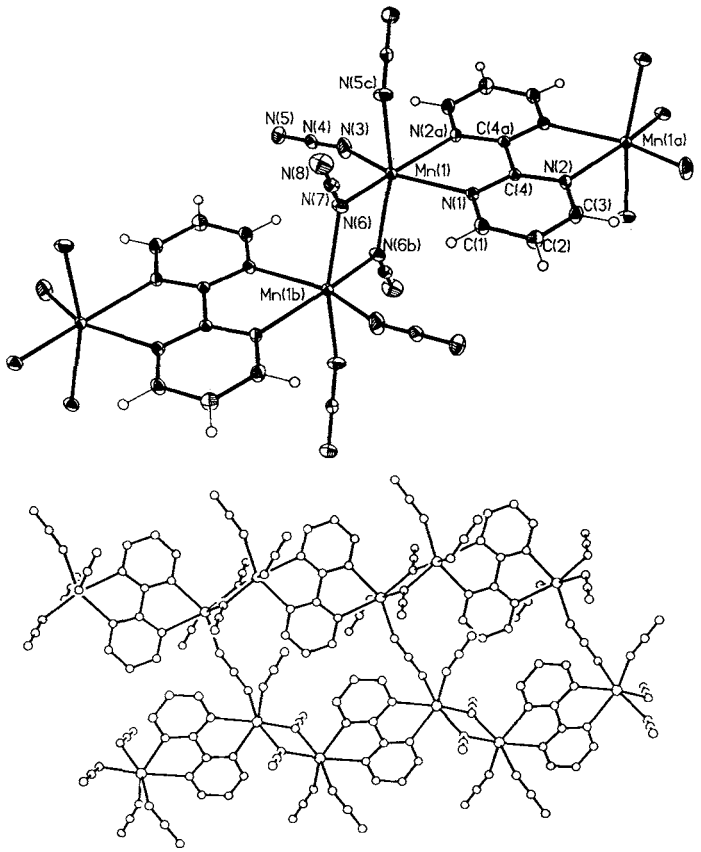

Fig. 2. Crystal structure of **2** (ellipsoids at the 30% probability level). Top: Tetranuclear fragment. Bottom: Best view of two chains in the layer (hydrogen atoms have been omitted for clarity). Selected distances [Å] and angles [°] with standard deviations in parentheses: Mn(1)-N(1) 2.294(2), Mn(1)-N(3) 2.177(2), Mn(1)-N(6) 2.230(2), Mn(1)-N(2a) 2.356(1), Mn(1)-N(5c) 2.217(2), Mn(1)-N(6b) 2.215(2); N(1)-Mn(1)-N(3) 151.8(1), N(1)-Mn(1)-N(6) 97.1(1), N(3)-Mn(1)-N(6) 110.8(1), N(1)-Mn(1)-N(2a) 70.4(1), N(3)-Mn(1)-N(2a) 82.8(1), N(6)-Mn(1)-N(2a) 164.2(1), N(1)-Mn(1)-N(5c) 96.0(1), N(3)-Mn(1)-N(5c) 90.3(1), N(6)-Mn(1)-N(5c) 86.5(1), N(2a)-Mn(1)-N(5c) 85.4(1), N(1)-Mn(1)-N(6b) 91.1(1), N(3)-Mn(1)-N(6b) 91.6(1), N(6)-Mn(1)-N(6b) 75.5(1), N(2a)-Mn(1)-N(6b) 113.2(1), N(5a)-Mn(1)-N(6b) 161.4(1), Mn(1)-N(6)-Mn(1b) 104.5(1), Mn(1)-N(3)-N(4) 161.3(2), N(3)-N(4)-N(5) 178.4(3), Mn(1)-N(5c)-N(4c) 126.6(2), N(6)-N(7)-N(8) 179.2(2) (symmetry code: (a) $1-x, -y, 1-z$; (b) $-x, -y, -z$; (c) $x, 0.5-y, 0.5+z$).

quickly at lower temperatures; the $\chi_m T$ value for **2** continuously decreases as the sample is cooled, and a susceptibility maximum occurs at 35 K. These results correspond to overall ferromagnetic (**1**) and antiferromagnetic behavior (**2**) and can be easily understood by considering the structures. In the case of **1**, the ferromagnetic interaction between the metal ions through the end-on azido bridge is larger (J ca. $+2\ cm^{-1}$)[14] than the antiferromagnetic interaction through the bpym ligand (J ca. $-1\ cm^{-1}$).[8c] This is the first example of a honeycomb layered material with alternating ferro- and antiferromagnetic interactions within the layers. In the case of **2**, the single end-to-end azido ligand and the bridging bpym ligand would provide the pathways for the antiferromagnetic coupling, whereas the double end-on azido ligand mediates the ferromagnetic coupling. The antiferromagnetic interaction through the end-to-end azido ligand should be larger[1d] than the ferromagnetic one and the overall antiferromagnetic coupling results. Additional new compounds and calculations are needed in order to extend these investigations to other spin systems and to get suitable theoretical models to analyze the magnetic properties of these exotic new systems. This kind of compound containing ferro- and antiferromagnetic interactions is very interesting with regard to understanding and designing metamagnetic compounds. Indeed, **1** shows metamagnetic behavior with a critical magnetic field about 2 T.

Experimental Procedure

Synthesis of **1** and **2**: Orange hexagonal needles of **1** (main product) and yellow prisms of **2** were grown by slow evaporation of aqueous solutions (60 mL) containing $Mn(NO_3)_2 \cdot 4H_2O$ (1 mmol), 2,2'bipyrimidine (1 mmol), and sodium azide (2 mmol). The crystals of **2** were separated by hand and dried on filter paper. Crystals of **1** were filtered off, washed with water and dried in air. The crystals obtained in this way were suitable for X-ray diffraction. The main difference in the IR spectra of **1** and **2** is the occurrence of three peaks (**2**) instead of two (**1**) in the region 2120–2040 cm^{-1} (ν_{as} (N_3^-)).

Crystal structure analyses of **1** and **2**: Siemens R3m/V automatic diffractometer, $Mo_{K\alpha}$, $\lambda = 0.71073$ Å, graphite monochromator, 295 K. Data collection, solution, and refinement: ω-2θ scan, standard Patterson methods with subsequent Fourier recycling. SHELXTL-PLUS [15]. **1**: $C_8H_4Mn_2N_{16}$, monoclinic, space group $C2/m$, $a = 6.234(2)$, $b = 15.138(3)$, $c = 8.934(2)$ Å, $\beta = 95.60°$, $V = 839.1(4)$ Å^3, $Z = 2$, $\rho_{calcd} = 1.726\ g\,cm^{-3}$, $3 < 2\theta < 85°$, crystal size $0.12 \times 0.26 \times 0.44$ mm. 3100 unique reflections, and 2259 assumed as observed with $I > 3\sigma(I)$. Refinement of 65 variables with anisotropic thermal parameters for all non-hydrogen atoms gave $R = 0.034$, $R_w = 0.038$ and $S = 1.10$ [16]. **2**: $C_8H_4Mn_2N_{16}$, monoclinic, space group $P2_1/c$, $a = 7.695(2)$, $b = 13.114(3)$, $c = 7.813(2)$ Å, $\beta = 111.67°$, $V = 732.7(3)$ Å^3, $Z = 2$, $\rho_{calcd} = 1.977\ g\,cm^{-3}$, $3 < 2\theta < 54°$, crystal size $0.14 \times 0.15 \times 0.18$ mm. 1606 unique reflections, and 1346 assumed as observed with $I > 3\sigma(I)$. Refinement of 127 variables with anisotropic thermal parameters for all non-hydrogen atoms gave $R = 0.022$, $R_w = 0.025$ and $S = 1.19$. Crystallographic data (excluding structure factors) for the structure(s) reported in this paper have been deposited with the Cambridge Crystallographic Data Centre as supplementary publication no. CCDC-179-56. Copies of the data can be obtained free of charge on application to The Director, CCDC, 12 Union Road, Cambridge CB2 1EZ, UK (fax: Int. code +(1223) 336-033; e-mail: teched@chemcrys.cam.ac.uk).

Received: March 5, 1996 [Z8907IE]
German version: *Angew. Chem.* **1996**, *108*, 1931–1934

Keywords: azides · complexes with nitrogen ligands · layer compounds · magnetic properties · manganese compounds

[1] a) O. Kahn, *Comments Inorg. Chem.* **1984**, *3*, 105; b) J. Commarmond, P. Plumeré, J. M. Lehn, Y. Agnus, R. Louis, R. Weiss, O. Kahn, I. Morgenstern-Badarau, *J. Am. Chem. Soc.* **1982**, *104*, 6330; c) Y. Agnus, R. Louis, J. P. Gisselbrecht, R. Weiss, *ibid.* **1984**, *106*, 93; d) I. Bkouche-Waksman, M. L. Boillot, O. Kahn, S. Sikorav, *Inorg. Chem.* **1984**, *23*, 4454; e) P. Chaudhuri, K. Oder, K. Wieghardt, B. Nuber, J. Weiss, *ibid.* **1986**, *25*, 2818; f) O. Kahn, S. Sikorav, J. Gouteron, S. Jeannin, Y. Jeannin, *ibid.* **1983**, *22*, 2877; g) S. Sikorav, I. Bkouche-Waksman, O. Kahn, *ibid.* **1984**, *23*, 490.

[2] M. F. Charlot, O. Kahn, M. Chaillet, C. Larrieu, *J. Am. Chem. Soc.* **1986**, *108*, 2574.

[3] a) C. G. Pierpont, D. N. Hendrickson, D. M. Duggan, F. Wagner, E. K. Barefield, *Inorg. Chem.* **1975**, *14*, 604; b) P. Chaudhuri, M. Guttmann, D. Ventur, K. Wieghardt, B. Nuber, J. Weiss, *J. Chem. Soc. Chem. Commun.* **1985**, 1618; c) R. Cortés, J. I. Ruiz de Larramendi, L. Lezama, T. Rojo, K. Urtiaga, M. I. Arriortua, *J. Chem. Soc. Dalton Trans.* **1992**, 2723; d) J. Ribas, M. Monfort, C. Diaz, C. Bastos, X. Solans, *Inorg. Chem.* **1993**, *32*, 3557, and references therein.

[4] J. Ribas, M. Monfort, R. Costa, X. Solans, *Inorg. Chem.* **1993**, *32*, 695.

[5] M. A. Halcrow, J. C. Huffman, G. Christou, *Angew. Chem.* **1995**, *107*, 971; *Angew. Chem. Int. Ed. Engl.* **1995**, *34*, 889.

[6] a) A. Escuer, R. Vicente, J. Ribas, M. Salah el Fallah, X. Solans, M. Font-Badia, *Inorg. Chem.* **1994**, *33*, 1842; b) R. Cortés, K. Urtiaga, L. Lezama, J. L. Pizarro, A. Goñi, M. I. Arriortua, T. Rojo, *ibid.* **1994**, *33*, 4009; c) J. Ribas, M. Monfort, B. K. Ghosh, X. Solans, *Angew. Chem.* **1994**, *106*, 2177; *Angew. Chem. Int. Ed. Engl.* **1994**, *33*, 2087; d) J. Ribas, M. Monfort, B. K. Ghosh, X. Solans, M. Font-Badia, *J. Chem. Soc. Chem. Commun.* **1995**, 2375.

[7] M. Monfort, J. Ribas, X. Solans, *J. Chem. Soc. Chem. Commun.* **1993**, 350.

[8] a) G. Brewer, E. Sinn, *Inorg. Chem.* **1985**, *24*, 4580; b) G. De Munno, M. Julve, F. Lloret, J. Faus, A. Caneschi, *J. Chem. Soc. Dalton Trans.* **1994**, 1175; c) G. De Munno, R. Ruiz, F. Lloret, J. Faus, R. Sessoli, M. Julve, *Inorg. Chem.* **1995**, *34*, 408; d) G. De Munno, M. Julve, F. Lloret, J. Cano, A. Caneschi, *ibid.* **1995**, *34*, 2048; e) I. Castro, J. Sletten, L. K. Glærum, J. Cano, F. Lloret, J. Faus, M. Julve, *J. Chem. Soc., Dalton Trans.* **1995**, 3207.

[9] a) M. Julve, G. De Munno, G. Bruno, M. Verdaguer, *Inorg. Chem.* **1988**, *27*, 3160; b) M. Julve, M. Verdaguer, G. De Munno, J. A. Real, G. Bruno, *ibid.* **1993**, *32*, 795; c) G. De Munno, M. Julve, M. Verdaguer, G. Bruno, *ibid.* **1993**, *32*, 2215.

[10] J. A. Real, G. De Munno, R. Chiappetta, M. Julve, F. Lloret, Y. Journaux, J. C. Colin, G. Blondin, *Angew. Chem.* **1994**, *106*, 1223; *Angew. Chem. Int. Ed. Engl.* **1994**, 33, 1184.

[11] G. De Munno, M. Julve, F. Lloret, J. Faus, M. Verdaguer, A. Caneschi, *Inorg. Chem.* **1995**, *34*, 157.
[12] S. Decurtins, A. W. Schmalle, P. Schnewly, L. M. Zheng, J. Ensling, A. Hauser, *Inorg. Chem.* **1995**, *34*, 5501.
[13] a) G. De Munno, M. Julve, F. Nicoló, F. Lloret, J. Faus, R. Ruiz, E. Sinn, *Angew. Chem.* **1993**, *105*, 588; *Angew. Chem. Int. Ed. Engl.* **1993**, *34*, 613.
[14] R. Cortés, J. L. Pizarro, L. Lezama, M. I. Arriortua, T. Rojo, *Inorg. Chem.* **1994**, *33*, 2697.
[15] SHELXTL PLUS, Version 4.21/V, Siemens Analytical X-Ray Instruments Inc., Madison, WI, 1990.
[16] Almost simultaneously to our paper, another paper containing the same crystal structure for complex **1** was submitted by another research group (see next communication): R. Cortés, L. Lezama, J. L. Pizarro, M. I. Arriortua, T. Rojo, *Angew. Chem.* **1996**, *108*, 1934; *Angew. Chem. Int Ed. Engl.* **1996**, *35*, 1810.

Alternating Ferro- and Antiferromagnetic Interactions in Honeycomb-Like Layers of an Azidomanganese(II) Compound**

Roberto Cortés,* Luis Lezama, J. Luis Pizarro, M. Isabel Arriortua, and Teófilo Rojo*

Alternating ferro-and antiferromagnetic interactions is a rather rare phenomenon in molecular-based magnetic materials. Very few examples are known in one-dimensional (1D) copper(II) compounds[1] and recently this has also been observed in one manganese(II) chain.[2] Interchain interactions in 1D systems are very weak compared with intrachain interactions and, therefore, there is no magnetic ordering except at absolute zero. Thus, in order to obtain high magnetic ordering it appears necessary to increase the dimensionality. To our knowledge, two- (2D) or three-dimensional (3D) systems showing this kind of magnetic alternation have not yet been reported.

Extended lattices of antiferromagnetic or ferrimagnetic systems have been obtained by using adequate superexchange bridging groups such as oxalates or cyanides.[3] Thus, the azido ligand should be a suitable candidate for the design of new magnetic systems because the azido ion has shown great versatility in its coordination modes in different transition metal complexes. Thus, double- or triple-bridged dinuclear complexes,[4–6] square-planar[7] and cubane tetranuclear complexes,[8] and polymeric 1D,[2, 5, 9] 2D,[10] and 3D complexes[11] have been characterized.

The wide variety of molecular architectures obtained has given rise to a broad range of magnetic couplings. In fact, the azido ligand can mediate antiferromagnetic interactions when it bridges end-to-end (EE)[9] or is coordinated through end-on (EO) bridges with angles greater than 108°.[12] In contrast, ferromagnetic coupling is observed through EO bridges with angles less than 108°.[2, 6, 13] Alternating ferro- and antiferromagnetic interactions in a 1D compound containing both types of bridging[2] have also been described.

[*] Dr. R. Cortés
Departamento de Química Inorgánica, Facultad de Farmacia
Aptdo. 450, E-01080 Vitoria-Gasteiz (Spain)
Prof. T. Rojo, Dr. L. Lezama
Departamento de Química Inorgánica, Facultad de Ciencias
Universidad del País Vasco
Aptdo. 644, E-48080 Bilbao (Spain)
Fax: Int. code +(4)4648500
e-mail: qiproapt@lg.ehu.es
Prof. M. I. Arriortua, Dr. J. L. Pizarro
Departamento de Mineralogía y Petrología Universidad del País Vasco
Aptdo. 644, E-48080 Bilbao (Spain)

[**] We thank the University of the Basque Country (UPV EB234/95) for financial support.

In the case of bis(bidentate) ligands such as 2,2′-bipyrimidine (bpym), high-dimensional polynuclear species have been found.[14] This ligand, in its bis(chelating) coordination mode, has a remarkable ability to mediate strong antiferromagnetic exchange interactions between metal ions.[14] Thus, a suitable combination of bpym and the azido ligand (in EO coordination) could therefore lead to the preparation of the desired high-dimensional species with alternating ferro- and antiferromagnetic interactions. Herein we report the results on an unusual polymeric layered system of the formula $[Mn_2(bpym)(N_3)_4]$ **1**, whose molecular structure can be considered as a honeycomb-like layer.

The X-ray crystal structure analysis of the Mn complex **1** (Fig. 1)[15] shows chains of manganese(II) ions connected by

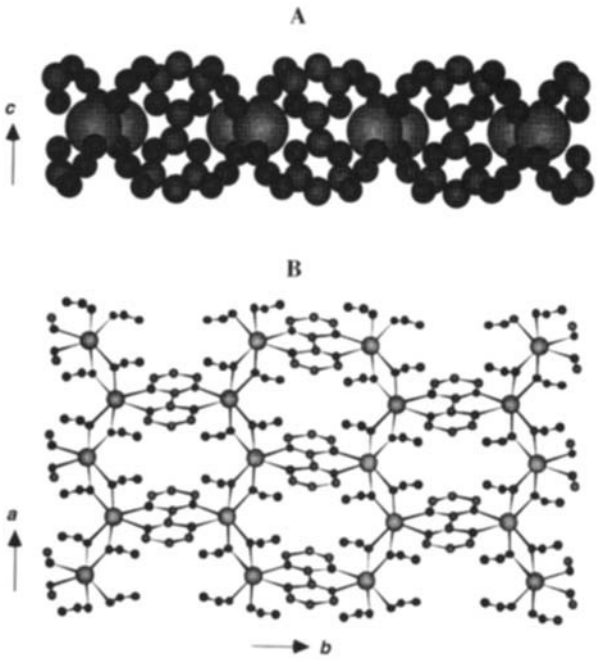

Fig. 1. Crystal structure of **1**. A) Space-filling view of one layer. B) View along the *c* axis of a layer showing the Mn_6^{II} hexagons. The H atoms have been omitted for clarity.

double EO azido bridges. These chains are alternately bridged by bis(bidentate) bpym ligands. The whole structure can be described as parallel honeycomb-like sheets, each consisting of an infinite hexagonal array of manganese(II) ions bridged by bis(chelating) bpym ligands and by double end-on azido bridges. The nearly planar hexagonal units are compressed, with two long and four short edges (Fig. 2). The 2D polymer extends in the *xy* plane by repetition of edge-sharing hexagons. The layers of the polymer are held together by hydrogen bonding between the bpym ligands and the terminal nitrogen atoms of the azido ligands; the interplane separation is 8.88 Å. Each Mn^{II} ion resides in a distorted octahedral environment formed by six nitrogen atoms, four from the azido ligands and two from the bpym ligand. The Mn–N distances range from 2.08 to 2.33 Å. The Mn–N(bpym) distances are slightly larger than those in the dinuclear complex $[Mn_2(bpym)(H_2O)_6(SO_4)_2]$ **2**[14] and as a consequence the value of the bite angle N2-Mn-N1 decreases from 71.5° in the dimer to 70.9(3)° in **1**. Regarding the azido bridges, only the Mn–$N3^I$ distance [2.33(2) Å] can be considered larger than that usually obtained from the azidomanganese compounds. The two EO azido bridges form different angles with the metal centers (98.5(3)° and 107.2(4)°). The distance

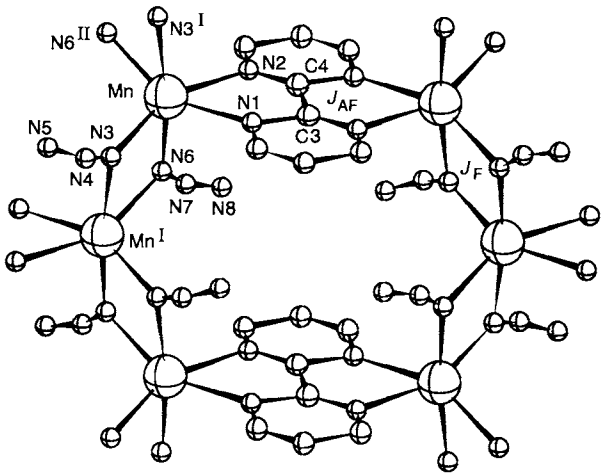

Fig. 2. Compressed hexagonal unit showing selected atom numbering and the exchange coupling constants. Selected distances [Å] and bond angles [°] (standard deviations in parentheses): Mn–N1 2.33(1), Mn–N2 2.289(8), Mn–N3 2.191(9), Mn–N3^{I} 2.33(2), Mn–N6 2.17(1), Mn–N6^{II} 2.08(1); Mn-N3-Mn^{II} 98.5(3), Mn-N6-Mn^{I} 107.2(4), Mn-N1-C4 121.9(4), Mn-N2-C4 114.6(7); symmetry code: I $x-1/2,1/2-y,z$; II $1/2+x,1/2-y,z$.

between the Mn centers separated by the double azido bridge is 3.425(4) Å, that between the Mn centers separated by the bpym ligand 6.127(2) Å.

The variation of the molar magnetic susceptibility χm as a function of the temperature in the temperature range 4–300 K is shown in Figure 3a. When the sample is cooled χ_m gradually increases and reaches a sharp maximum near 12 K after which it rapidly decreases. The value of $\chi_m T$ at room temperature is 9.9 $cm^3 mol^{-1}$ K, which is slightly higher than that calculated for two noninteracting manganese(II) ions (8.76 $cm^3 mol^{-1}$ K). The product $\chi_m T$ continuously increases from room temperature to 22 K and then decreases down to 4 K (see Fig. 3b). This behavior is characteristic of dominant ferromagnetic interactions in the high-temperature range, followed by antiferromagnetic interactions at lower temperatures. The maximum observed is indicative of the existence of two-dimensional antiferromagnetic ordering at temperatures lower than 20 K.

The presence of bridging bpym and EO azido ligands in **1** allows the existence of antiferromagnetic and ferromagnetic interactions through the bpym and EO azido bridges, respectively. This can be explained by the results obtained from other compounds with these kinds of bridges. Thus, the Mn-bpym-Mn fragment is similar to that in the dinuclear compound **2**,[14] which reveals antiferromagnetic interactions with a J value of -1.1 cm^{-1}. On the other hand, ferromagnetic coupling has been observed in the dinuclear compound $[Mn(terpy)(N_3)_2]\cdot H_2O$[13] (terpy = 2,2′-6′,2″-terpyridine) and in the 1D compound $[Mn(bpy)(N_3)_2]$[2] (bpy = 2,2′-bipyridine), which both have EO azido bridges ($J = 1.5$ and 2.5 cm^{-1}, respectively). These data strongly suggest the existence of alternating ferromagnetic and antiferromagnetic interactions in **1**, which to our knowledge, is the first example of a 2D sheetlike molecular compound in which the magnetic interactions alternate in sign. Since no theoretical studies have been carried out on this sort of magnetic behavior in which the magnetic interactions alternate in sign, a detailed analysis of the behavior of **1** is not possible. Two simple models have been employed to evaluate the magnitude of the exchange couplings; however, one should be mindful of their limitations. The first model was based on a Heisenberg type chain in which interchain interactions (J') were treated with

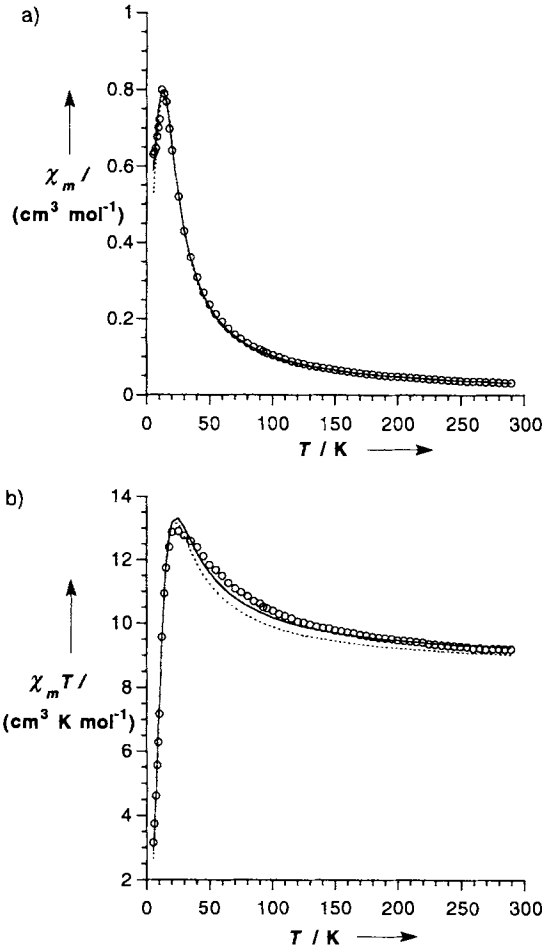

Fig. 3. Temperature dependence of the molar susceptibility χ_m (a), and of the product $\chi_m T$ (b) of **1**. o: experimental values; —: fit for interacting Heisenberg type chain model; - - -: fit for ferromagnetically coupled antiferromagnetic dimer model.

the molecular field approximation.[17] In the second model, antiferromagnetic dimers ferromagnetically coupled to each other were considered.[18] The results for these theoretical models are shown in Figure 3. The best fit for both χ_m and $\chi_m T$ with the first model leads to the parameters $J = -1.06$ cm^{-1} and $zJ' = 1.99$ cm^{-1} and with the second model to $J = -1.18$ cm^{-1} and $zJ' = 1.53$ cm^{-1}. On the basis of these models, and taking their limitations into consideration, the ferromagnetic interactions are predominant in the compound **1** and the magnitude of the exchange parameters obtained are in good agreement with those observed in the literature for both types of bridging.[13, 14]

The connection of 1D compounds through bis(chelating) ligands such as 2,2′-bipyrimidine has been shown to be a good strategy for obtaining 2D systems. The resulting compound **1** shows a honeycomb-like layer structure, which is formed by Mn_6 hexagons and is rather unusual. The bridging ligands between Mn^{II} ions are capable of mediating antiferromagnetic (bpym) and ferromagnetic (EO azide) exchange interactions. This has led to a 2D sheetlike structure with magnetic interactions that alternate in sign. As far as we are aware, this kind of alternating system is unique.

Experimental Procedure

Compound **1** was synthesized by slow addition of bpym (0.158 g, 1 mmol) in methanol (15 mL) to a solution prepared by mixing $Mn(NO_3)_2\cdot 4H_2O$ (0.251 g, 1 mmol) and NaN_3 (0.130 g, 2 mmol) in water/methanol (20 mL). The reaction mixture was stirred continuously at 45 °C. Orange-yellow long prismatic crystals

were obtained from the resulting solution after it had been left to stand at room temperature for two weeks. Elemental analysis: Calc. (found): Mn 25.2 (25.4), N 51.4 (51.3), C 22.0 (22.1), H 1.4 (1.4)%.

Received: March 15, 1996 [Z89291E]
German version: *Angew. Chem.* **1996**, *108*, 1934–1936

Keywords: azides · complexes with nitrogen ligands · layer compounds · magnetic properties · manganese compounds

[1] H. J. M. de Groot, L. J. de Jongh, R. D. Willet, J. Reedijk, *J. Appl. Phys.* **1982**, *53*, 8038; C. Benelli, D. Gatteschi, D. W. Carnegie, R. L. Carlin, *J. Am. Chem. Soc.* **1985**, *107*, 2560; I. Vasilevesky, N. R. Rose, R. Stenkamp, R. D. Willet, *Inorg. Chem.* **1991**, *30*, 4082; G. de Munno, M. Julve, F. LLoret, J. Faus, M. Verdaguer, A. Caneschi, *Angew. Chem.* **1993**, *105*, 1122; *Angew. Chem. Int. Ed. Engl.* **1993**, *32*, 1046.

[2] R. Cortés, L. Lezama, J. L. Pizarro, M. I. Arriortua, X. Solans, T. Rojo, *Angew. Chem.* **1994**, *106*, 2520; *Angew. Chem. Int. Ed. Engl.* **1994**, *33*, 2488.

[3] J. S. Miller, A. J. Epstein, *Angew. Chem.* **1994**, *106*, 399; *Angew. Chem. Int. Ed. Engl.* **1994**, *33*, 385; W. R. Entley, G. S. Girolami, *Inorg. Chem.* **1994**, *33*, 5165.

[4] D. M. Duggan, D. N. Hendrickson, *Inorg. Chem.* **1973**, *12*, 2422; J. Commarmond, P. Plumeré, J. M. Lehn, Y. Agnus, R. Louis, R. Weiss, O. Kahn, I. Morgenstern-Badarau, *J. Am. Chem. Soc.* **1982**, *104*, 6330; P. Chaudhuri, M. Guttmann, D. Ventur, K. Wieghardt, B. Nuber, J. Weiss, *J. Chem. Soc. Chem. Commun.* **1985**, 1618; T. Rojo, L. Lezama, R. Cortés, J. L. Mesa, M. I. Arriortua, G. Villeneuve, *J. Magn. Magn. Mat.* **1990**, *83*, 519; R. Cortés, J. I. R. de Larramendi, L. Lezama, T. Rojo, M. K. Urtiaga, M. I. Arriortua, *J. Chem. Soc. Dalton Trans.* **1992**, 2723; R. Cortés, M. K. Urtiaga, L. Lezama, J. I. R. de Larramendi, M. I. Arriortua, T. Rojo, *ibid.*, **1993**, 3685, and references therein.

[5] R. Vicente, A. Escuer, J. Ribas, M. S. El Fallah, X. Solans, M. Font-Bardia, *Inorg. Chem.* **1993**, *32*, 1920; J. Ribas, M. Monfort, C. Diaz, C. Bastos, X. Solans, *ibid.* **1994**, *33*, 484.

[6] J. Ribas, M. Monfort, C. Diaz, C. Bastos, X. Solans, *Inorg. Chem.* **1993**, *32*, 3557.

[7] J. Ribas, M. Monfort, R. Costa, X. Solans, *Inorg. Chem.* **1993**, *32*, 695.

[8] M. A. Halcrow, J. C. Huffman, G. Christou, *Angew. Chem.* **1995**, *107*, 971; *Angew. Chem. Int. Ed. Engl.* **1995**, *34*, 889.

[9] C. G. Pierpont, D. N. Hendrickson, D. M. Duggan, F. Wagner, E. K. Barefield, *Inorg. Chem.* **1975**, *14*, 604; A. Escuer, R. Vicente, J. Ribas, M. S. El Fallah, X. Solans, M. Font-Bardia, *ibid.* **1993**, *32*, 3727; R. Cortés, M. K. Urtiaga, L. Lezama, J. L. Pizarro, A. Goñi, M. I. Arriortua, T. Rojo, *ibid.* **1994**, *33*, 4009.

[10] J. Ribas, M. Monfort, X. Solans, M. Drillon, *Inorg. Chem.* **1994**, *33*, 742; M. A. S. Goher, F. A. Mautner, *Croat. Chem. Acta* **1990**, *63*, 559.

[11] F. A. Mautner, R. Cortés, L. Lezama, T. Rojo, *Angew. Chem.* **1996**, *108*, 96; *Angew. Chem. Int. Ed. Engl.* **1996**, *35*, 78.

[12] L. K. Thompson, S. S. Tandon, M. E. Manuel, *Inorg. Chem.* **1995**, *34*, 2356.

[13] R. Cortés, J. L. Pizarro, L. Lezama, M. I. Arriortua, T. Rojo, *Inorg. Chem.* **1994**, *33*, 2697.

[14] G. de Munno, M. Julve, F. Nicolo, F. Lloret, J. Faus, R. Ruiz, E. Sinn, *Angew. Chem.* **1993**, *105*, 588; *Angew. Chem. Int. Ed. Engl.* **1993**, *32*, 613; G. de Munno, R. Ruiz, F. Lloret, J. Faus, R. Sessoli, M. Julve, *Inorg. Chem.* **1995**, *34*, 408.

[15] X-ray structure analysis: Enraf-Nonius CAD-4 diffractometer. Unit cell parameters were determined from automatic centering of 25 reflections ($12 < 2\theta < 30°$) and refined by least-squares method. Intensities were collected with graphite monochromatized $Mo_{K\alpha}$ (0.71069 Å) radiation using the ω scan technique. Lorentz polarization and extinction corrections were made. The structure was solved by direct methods and successive Fourier difference syntheses, using the SHELXL-93 computing program. $C_8H_6N_{16}Mn_2$ ($M = 436$), monoclinic system, space group $P2_1/a$, $a = 6.229(1)$, $b = 15.104(1)$, $c = 8.923(1)$ Å, $\beta = 95.72(2)°$, $V = 835.3(2)$Å^3, $Z = 4$, $\rho_{calcd} = 1.734\ g\,cm^{-3}$, $\mu = 15.4\ cm^{-1}$, $F(000) = 432$. The refinements by full matrix least-squares gave final $R1(F_o) = 0.028$, $wR2(F_o^2) = 0.1356$ and $S = 0.78$ [16] from 2432 reflections with intensity $I \geq 2\sigma(I)$ for 137 variables. All non-hydrogen atoms were refined anisotropically. The extreme nitrogen atom (N8) of one of the azido bridges is disordered. A strong pseudo-C symmetry is observed in the compound. Crystallographic data (excluding structure factors) for the structure(s) reported in this paper have been deposited with the Cambridge Crystallographic Data Centre as supplementary publication no. CCDC-179-81. Copies of the data can be obtained free of charge on application to The Director, CCDC, 12 Union Road, Cambridge CB2 1EZ, UK (fax: Int. code +(1223) 336-033; e-mail: teched(*a*) chemcrys.cam.ac.uk).

[16] Almost simultaneously to our paper, another paper containing the same crystal structure was submitted by another research group (see preceeding communication). G. De Munno, M. Julve, G. Viau, F. Llore, J. Faus, D. Viterbo, *Angew. Chem.* **1996**, *108*, 1931; *Angew. Chem. Int Ed. Engl.* **1996**, *35*, 1807.

[17] M. E. Fisher, *Am. J. Phys.* **1964**, *32*, 343.

[18] J. H. Van Vleck, *Electrical and Magnetic Susceptibilities*, Oxford University Press, **1965**.

Chemoenzymatic Synthesis of Sialyl Lewis^x Glycopeptides**

Gabi Baisch and Reinhold Öhrlein*

Invasive leukocytes play a decisive role in acute and chronic inflammation.[1] They reach the site of inflammation through a multistep process initiated by "leukocyte rolling".[2, 3] This "rolling" is caused by the interaction of carbohydrate ligands on the surface of leukocytes and receptors, the E- and P-selectins, which are found on the surface of activated endothelial cells.[4] A disruption of this early interaction is considered to be a promising therapeutic approach.[5] The tetrasaccharide sialyl Lewis^x (SLe^x) and various derivatives have been identified as ligands for selectins.[6] Because monovalent SLe^x shows only

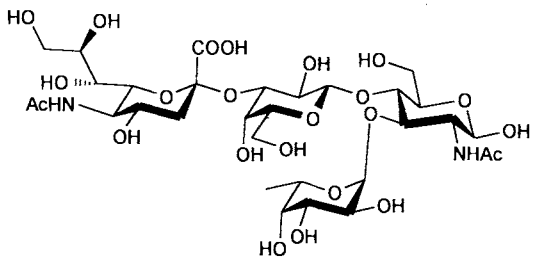

siaα(2-3)galβ(1-4)(fucα(1-3))glcNAc = SLe^x

relatively weak binding to E-selectin ($IC_{50} = 0.75$ mM),[7] it is assumed that the E-selectin–SLe^x interaction is enhanced in vivo through "clustering" (multivalency) by either E-selectin or SLe^x[8] or both. In some early investigations up to 18 preassembled SLe^x moieties were attached with a spacer to bovine serum albumin in order to evaluate this hypothesis.[9] The positive results of assays obtained with these artificial glycoproteins stimulated the search for methods to synthesize well-defined oligovalent SLe^x conjugates. Thus three chemically synthesized SLe^x moieties were linked to nitromethane tricarbonic acids[10] and to cyclopeptide templates.[11] More rigid, divalent SLe^x conjugates were obtained chemoenzymatically with trisaccharide templates.[12]

Up to now there have been no systematic studies concerning the number of SLe^x units necessary and their three-dimensional arrangements. The following strategy for the synthesis of oligovalent SLe^x conjugates enables rapid screening of these parameters. We selected oligopeptide chains as the framework on which to attach the carbohydrate moieties. A proper choice of the monomeric building blocks renders the backbone more rigid or more flexible, thus markedly influencing the presentation of the SLe^x moieties. Additionally, the peptide linker can be optimized by the well-established peptide chemistry.[13, 14]

Complex glycopeptide clusters containing natural hexoses are most efficiently prepared by enzyme-mediated synthesis. With the help of glycosyl transferases, glycosylations can be performed with predictable, excellent stereo- and regioselectivity,[15] thereby circumventing the highly demanding chemical synthesis of the SLe^x tetrasaccharide.[16] The inefficient and cumbersome protecting group manipulations inevitable in the

[*] Dr. R. Öhrlein, G. Baisch
Central Research Laboratories
Schwarzwaldallee 211, CH-4002 Basel (Switzerland)
Telefax: Int. code +(61)697-8975

[**] The authors thank Dr. A. Katopodis and Dr. M. Streiff for the biotechnological preparation of α(2-3)sialyl transferase and fucosyl transferase VI.

chemical glycopeptide synthesis are avoided.[17] The enzymes function in aqueous buffer systems without poisonous metal salt promotors.

The scope of the enzymatic methodology is presently limited by the availability of transferases[18] and the necessary activated donor sugars. These have to be synthesized,[19] although they are commercially available on a small scale. Alternatively some donor sugars may be produced in situ.[20]

Our synthesis started with the *N*-acetyl glucosamine building blocks **2** and **3** (Scheme 1). Deprotection of the amino group of the glycoside **1**[21] with morpholine[22] provided the amine **2**, which was subsequently N-acetylated, treated with trifluoroacetic acid to remove the *tert*-butyl ester, and finally deacetylated to yield the building block **3**.

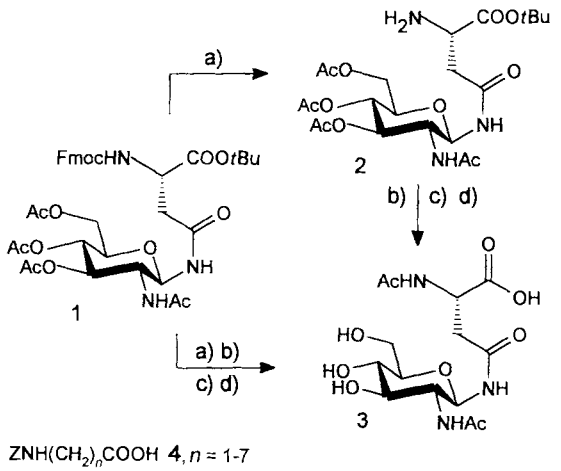

Scheme 1. a) Morpholine, 77%; b) CH_2Cl_2, Ac_2O, py, 96%; c) CF_3COOH, 94%; d) MeOH, MeONa, 76%; Fmoc = 9-fluorenylmethyloxycarbonyl, Z = benzyloxycarbonyl.

Amino acids **4** of various lengths—flexible spacers—were synthesized according to the Schotten–Baumann procedure from the corresponding free amino acids and benzyloxycarbonyl chloride in quantitative yields.[13] The building blocks **2** and **4** were linked in the presence EDCI[23] and subsequently deacetylated and hydrogenated (Scheme 2). The resulting compounds **5** were connected with building block **3**. DCC/HOBt or BBC proved to be reliable condensing reagents in this case.[24] The trimeric structures **7**[25] were finally reached after deblocking of **6** and subsequent condensation of the resulting acid with **5**. The versatility of this strategy can be exploited through repetition of steps (d) and (e) of Scheme 2 to generate defined "tetravalent" compounds and structures of even higher "valency".

Compounds **6** and **7** were treated with uridine 5′-diphosphogalactose (UDP-gal)[26] and commercially available galactosyl transferase (EC 2.4.1.22)[27] in a sodium cacodylate buffer (pH 7.5) in the presence of calf intestine alkaline phosphatase (CIAP, EC 3.1.3.1) (Scheme 3).[28] The latter enzyme destroys the inhibiting uridine 5′-diphosphate,[29] which is concomittantly formed as a by-product. The completion of the enzymatic reaction can be checked by thin-layer chromatography or preferably by MALDI-TOF (matrix-assisted laser desorption ionization time-of-flight) mass spectrometry of a small sample of the incubation mixture (see Fig. 1).

The galactosylated intermediates were filtered through Sephadex (G-25 superfine (Pharmacia)) and characterized by ^1H and ^{13}C NMR spectroscopy. Subsequently sialic acid was introduced by incubation with cytidine 5′-monophospho-sialic acid (CMP-sia)[30] and α(2-3)sialyl transferase (EC 2.4.99.6)[31] at

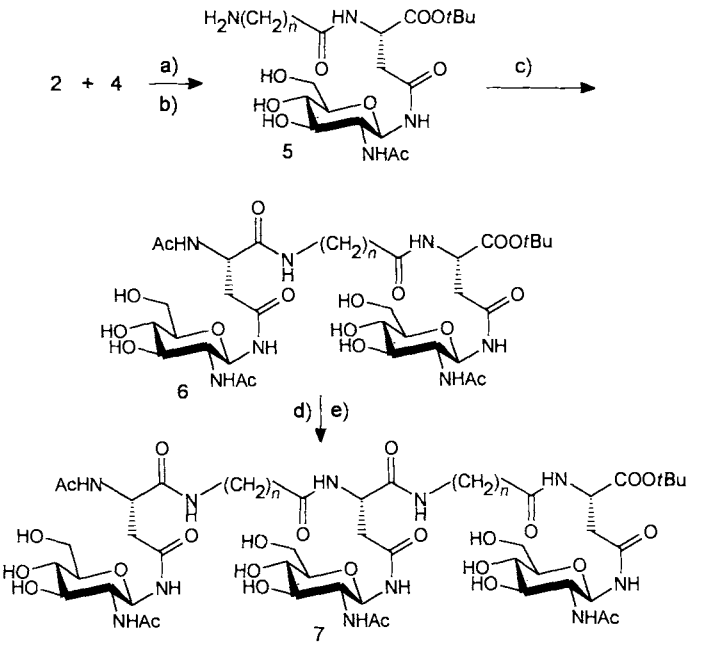

Scheme 2. a) THF, EDCI, 62–94%; b) 1% NaOMe in methanol then MeOH, H_2/Pd/C, 93–97%; c) DMF, **3** + DCC/HOBt or **3** + BBC, (56% (n = 1), 47% (2), 54% (3), 80% (4), 67% (5), 84% (6), 97% (7)); d) valid for n = 4–7: CF_3COOH, 0 °C, (43% (n = 4), 82% (5), 53% (6), 55% (7)); e) DMF, **5** + DCC/HOBt or **5** + BBC, 43–53%; EDCI = 1-ethyl-3-[3-(dimethylamino)propyl]carbodiimide hydrochloride, DCC = dicyclohexylcarbodiimide, HOBt = hydroxybenzotriazole, BBC = benzotriazolyloxybis(pyrrolidino)carbonium hexafluorophosphate.

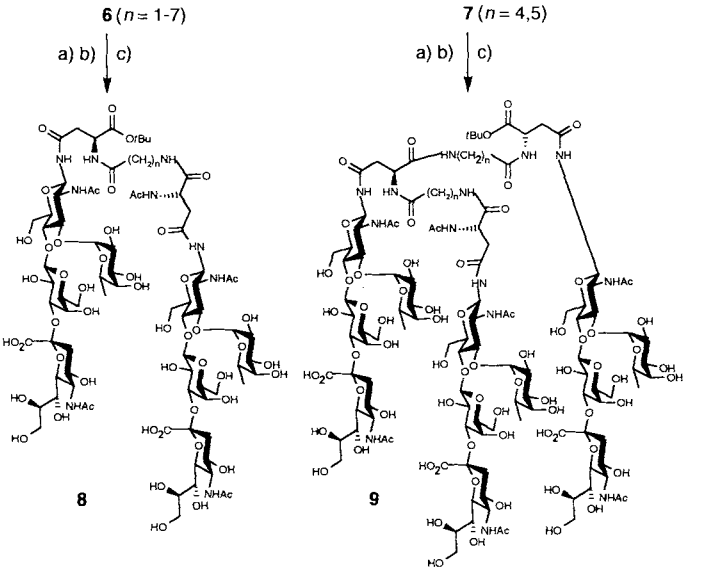

Scheme 3. a) 2.2 and 3.3 equiv UDP-gal, gal-t for **8** (75%, 85%, 92%, 70%, 81%, 96%, 64%) and **9**, respectively (88%, 75%); b) 2.2 and 3.3 equiv CMP-sia, α(2-3)sia-t for **8** (73%, 97%, 73%, 99%, 64%, 77%, 77%) and **9**, respectively (85%, 99%); c) 2.2 and 3.3 equiv. GDP-fuc,fuc-t VI for **8** (99%, 85%, 95%, 77%, 73%, 74%, 67%) and **9**, respectively (68%, 67%).

pH 6.5 in the presence CIAP.[29] Filtration of the reaction mixture through Sephadex provided the sialylated saccharides, which were characterized by ^1H NMR spectroscopy and MALDI-TOF mass spectometry. Finally fucose was introduced with guanosine 5′-diphospho-fucose (GDP-fuc)[32] as the fucose donor and fucosyl transferase VI[33] in a cacodylate buffer at pH 6.5, again in the presence of CIAP. Thus the desired compounds **8** and **9** could be obtained in 6–20 mg amounts, which was sufficient for the ensuing biological assays.[34]

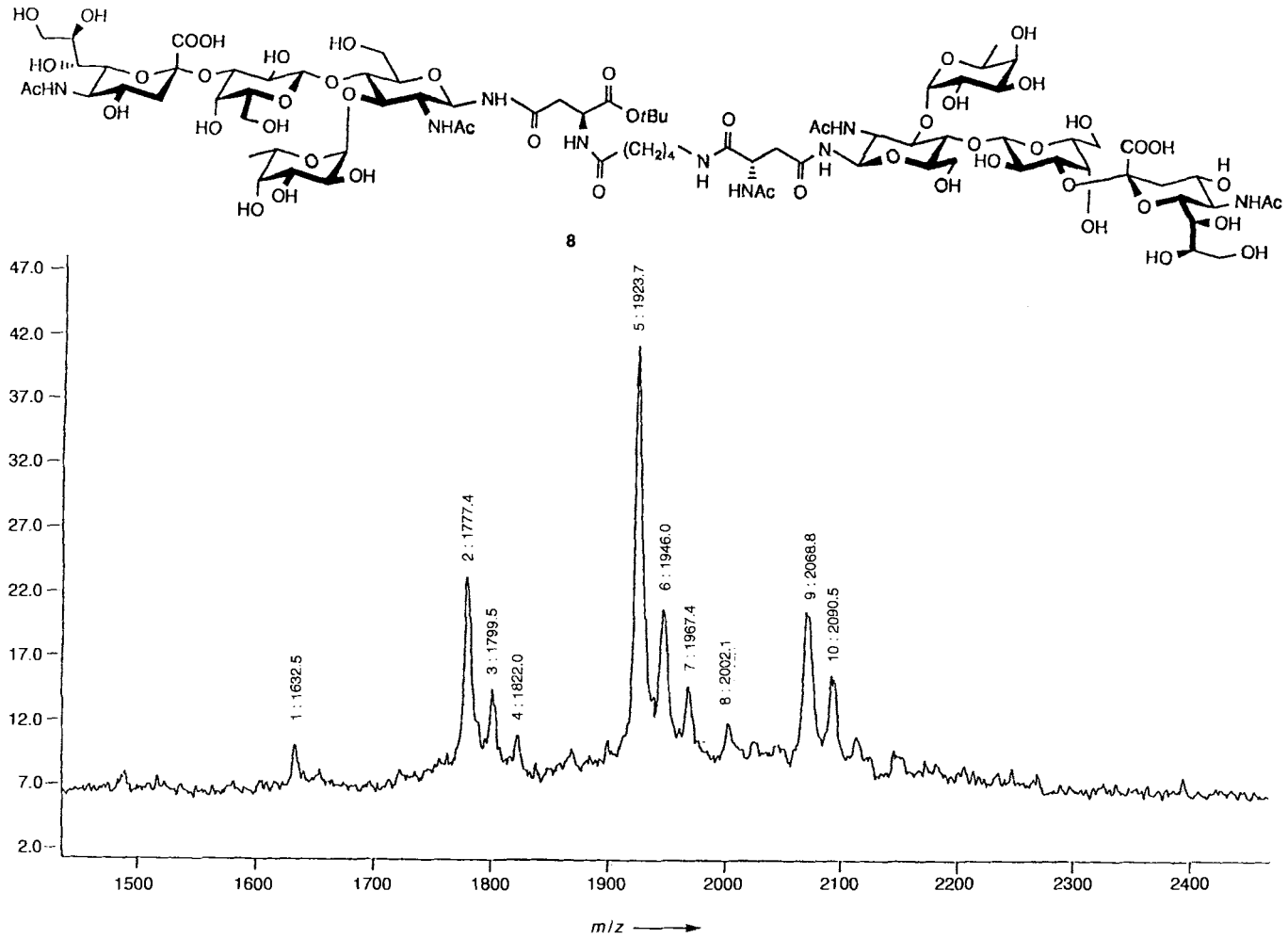

Fig. 1. MALDI-TOF mass spectrum of the reaction mixture from the fucosylation of **6** ($n = 4$); matrix: 0.1 M 2,4,6-trihydroxyacetophenone in ethanol.

All IC_{50} values have been normalized to one SLe^x unit. Although the divalent compounds **8** show varying binding affinities, their overall affinity to E-selectin is not significantly enhanced over that of the monovalent SLe^x, which was attached β-glycosidically to the aglycon (N-acetylated, O-*tert*-butyl protected aspartic acid). In contrast, the affinity of the trimeric compound **9** ($n = 4$) to E-selectin is four times higher than that of the monomer and almost nine times higher than that of the corresponding dimer **8** (Table 1).

For monitoring the progress of the formation of these complex glycopeptides MALDI-TOF mass spectrometry proved to be an indispensable analytical tool.[35] Figure 1 shows a spectrum of a small sample drawn from the incubation mixture from the fucosylation of compound **6** ($n = 4$). All final compounds were additionally characterized by ^1H NMR spectroscopy.[36] In Figure 1 peaks 2–4 arise from nonfucosylated starting material ($M = 1756.7$) with Na^+, $2\,Na^+$, and $3\,Na^+$ ions. Peaks 5–7 correspond to monofucosylated intermediates ($M = 1902.8$) associated similarly with Na^+ ions. Peaks 9–10 arise from the desired difucosylated final compound ($M = 2047.0$), again associated with Na^+ and $2\,Na^+$ ions. The incubation was terminated when no peaks corresponding to either the starting material or intermediates were detected. The final fucosylated glycopeptides were purified by filtration through Sephadex. MALDI-TOF mass spectrometry can also be used to check the purity of the end products.

Table 1. IC_{50} values of the octa- (**8**) and dodecasaccharides (**9**) [34].

Compound	IC_{50} [mM]
SLe^x aglycon	0.60
8 ($n = 1$)	0.46
8 ($n = 2$)	–
8 ($n = 3$)	0.64
8 ($n = 4$)	1.20
8 ($n = 5$)	0.47
8 ($n = 6$)	0.80
8 ($n = 7$)	0.48
9 ($n = 4$)	0.14
9 ($n = 5$)	0.39

Our method, which relies on a set of accessible transferases and activated donor sugars, allows the rapid assembly of oligovalent SLe^x conjugates. The rigidity of the peptide backbone (→ presentation of the SLe^x moieties) and the individual distances of the SLe^x moieties are controlled by the proper choice of amino acid monomers. SLe^x analogues of higher "valency" can be formed sequentially by known peptide chemistry.

The enzymatic methodology is not limited to the formation of the natural SLe^x structure.[37] It has been shown recently that nonnatural substrates (donors and acceptors) are recognized by glycosyl transferases, and glycosides are produced with high regio- and stereoselectivity.[38] The breadth of substrates amenable to glycosyl transferase catalysis is not yet fully investigated. Even pseudo-sugars can be synthesized efficiently with

 © VCH Verlagsgesellschaft mbH, D-69451 Weinheim, 1996 0570-0833/96/3516-1814 $ 15.00+.25/0

the help of glycosyl transferases in a stereospecific manner without protecting group manipulations.[38, 39] Thus SLe^x mimetics,[37] some of them showing surprisingly high affinities to E-selectin,[40] may be accessible easily.

Received: December 7, 1995
Revised version: March 4, 1996 [Z 8621 IE]
German version: *Angew. Chem.* **1996**, *108*, 1949–1952

Keywords: glycopeptides · glycosyl transferases · mass spectrometry · sialyl Lewis^x

[1] J. B. Lowe in *Molecular Glycobiology* (Eds.: M. Fukuda, O. Hindsgaul), IRL-Press, **1994**, p. 163, and references therein.
[2] M. B. Lawrence, T. A. Springer, *Cell* **1991**, *65*, 859.
[3] K. Ley, P. Gaethgens, C. Fennie, M. S. Singer, L. A. Lasky, S. D. Rosen, *Blood* **1991**, *77*, 2553.
[4] L. A. Lasky, *Ann. Rev. Biochem.* **1995**, *64*, 113.
[5] C. R. Bertozzi, *Chem. Biol.* **1995**, *2*, 703.
[6] M. Edwards, *Curr. Opin. Therap. Pat.* **1991**, 1617.
[7] R. M. Nelson, S. Dolich, A. Aruffo, O. Cecconi, M. P. Bevilaqua, *J. Clin. Invest.* **1993**, *91*, 1157.
[8] T. Feizi, *Curr. Opin. Struct. Biol.* **1993**, *3*, 701.
[9] J. K. Welply, S. Z. Abbas, P. Scudder, J. L. Keene, K. Broschat, S. Casnocha, C. Gorka, C. Steiniger, S. C. Howard, J. J. Schmuke, M. Graneto, J. M. Rotseart, J. D. Manger, G. S. Jacob, *Glycobiology* **1994**, *4*, 259.
[10] G. Kretzschmar, U. Sprengard, H. Kunz, E. Bartnik, W. Schmidt, A. Töpfer, B. Hörsch, M. Krause, D. Seiffge, *Tetrahedron* **1995**, *51*, 13015.
[11] After submission of this paper the synthesis of a trivalent SLe^x conjugate on a cyclopeptide template was published: U. Sprengard, M. Schudok, W. Schmidt, G. Kretzschmar, H. Kunz, *Angew. Chem.* **1996**, *108*, 359; *Angew. Chem. Int. Ed. Engl.* **1996**, *35*, 321.
[12] S. A. DeFrees, W. Kosch, W. Way, J. C. Paulson, S. Sabesan, R. R. Halcomb, D.-H. Huang, Y. Ichikawa, C.-H. Wong, *J. Am. Chem. Soc.* **1995**, *117*, 66.
[13] H. Benz, *Synthesis* **1994**, 337.
[14] C. Unverzagt, S. Kelm, J. C. Paulson, *Carbohydr. Res.* **1994**, *251*, 285.
[15] C.-H. Wong, R. R. Halcomb, Y. Ichikawa, T. Kajimoto, *Angew. Chem.* **1995**, *107*, 569; *Angew. Chem. Int. Ed. Engl.* **1995**, *34*, 521.
[16] O. Hindsgaul, *Sem. Cell Biol.* **1991**, *2*, 319.
[17] K. von dem Bruch, H. Kunz, *Angew. Chem.* **1994**, *106*, 87; *Angew. Chem. Int. Ed.* **1994**, *33*, 101.
[18] The cDNA sequences of a large number of transferases are deposited and cell clones that express the desired transferase can often be obtained; see M. C. Field, L. J. Wainwright, *Glycobiology* **1995**, *5*, 463.
[19] J. E. Heidlas, K. J. Williams, G. M. Whitesides, *Acc. Chem. Res.* **1992**, *25*, 307.
[20] Y. Ichikawa, J. L. Liu, G.-J. Shen, C.-H. Wong, *J. Am. Chem. Soc.* **1991**, *113*, 6300.
[21] T. Inazu, K. Kobayashi, *Synlett* **1993**, 869.
[22] P. Schultheiss-Reimann, H. Kunz, *Angew. Chem.* **1983**, *95*, 64; *Angew. Chem. Ed. Int. Engl.* **1983**, *22*, 62; *Angew. Chem. Suppl.* **1983**, 39.
[23] D. Seghal, I. K. Vijay, *Anal. Biochem.* **1994**, *218*, 87.
[24] S. Chen, J. Xu, *Tetrahedron Lett.* **1992**, *33*, 647.
[25] Compounds **1**–**5** were obtained easily in pure form (^{1}H NMR spectroscopy) in gram amounts by silica gel chromatography. Compounds **6** and **7** were obtained in pure form in 100–250 mg amounts by chromatography over RP-18-gel.
[26] J. E. Heidlas, W. J. Lees, G. M. Whitesides, *J. Org. Chem.* **1992**, *57*, 152; commercially available from Sigma (U-4500).
[27] Sigma G-5507.
[28] Boehringer No. 108146.
[29] M. M. Palcic, *Methods Enzymol.* **1994**, *230*, 300.
[30] M. Kittelmann, T. Klein, U. Kragl, C. Wandrey, O. Ghisalba, *Appl. Microbiol. Biotechnol.* **1995**, *44*, 59.
[31] S. Gosselin, M. Alhussaini, M. Streiff, K. Takabayashi, M. M. Palcic, *Anal. Biochem.* **1994**, *220*, 92.
[32] U. B. Gokhale, O. Hindsgaul, M. M. Palcic, *Can. J. Chem.* **1990**, *68*, 1063; gram amounts of this donor and different derivatives thereof are easily prepared chemoenzymatically: R. Öhrlein, G. Baisch, unpublished.
[33] Soluble fucosyl transferase VI was obtained from the supernatant of a highly productive, transfected CHO cell line; A. Katopodis, B. Bowen, unpublished.
[34] The inhibition constants (IC_{50}) were obtained from a static assay with recombinant human E-selectin. The assays were performed by Dr. J. Magnani (GlycoTech Corp., 14915 Broschart Road, Rockville, MD 20850, USA).
[35] This very sensitive and mild method was originally developed to analyze oligonucleotides (U. Pieles, W. Zürcher, M. Schär, H. E. Moser, *Nucleic Acids Res.* **1993**, *21*, 3191). We could apply this method to analyze complex glycopeptides in a reliable manner.
[36] Selected ^{1}H NMR data (D_2O, 500 MHz): **8** ($n = 4$): $\delta = 1.27$ (d, $J = 7.0$ Hz, 6H, 6-H(fuc)), 1.54 and 1.68 (each m and 2H, $O_2CCH_2CH_2CH_2CH_2N$), 1.76 (t, $J = 11$ Hz, 2H, 3-H_{ax}(sia)), 1.94 and 1.96 (each s and 3H, NH*Ac*), 2.00 (s, 9H, NH*Ac*), 2.25 (m, 2H, $O_2CCH_2CH_2CH_2CH_2N$), 2.75 (m, 6H, 3-H_{eq}(sia) and β-H(asn)), 3.15 (m, 2H, $O_2CCH_2CH_2CH_2CH_2N$), 4.49 (d, $J = 7.5$ Hz, 1H, 1-H(gal)), 4.51 (d, $J = 7.5$ Hz, 1H, 1-H(gal)), 4.60 (m, 2H, α-H(asn)), 5.14 (m, 4H, 1-H(fuc) and 1-H″(glcNAc)). **9** ($n = 4$): $\delta = 1.31$ (d, $J = 7.0$ Hz, 9H, 6-H(fuc)), 1.68 (m, 8H, $O_2CCH_2CH_2CH_2CH_2N$), 1.94 (t, $J = 11$ Hz, 3H, 3-H_{ax}(sia)), 2.15 (s, 9H, NH*Ac*), 2.20 (s, 12H, NH*Ac*), 2.46 (m, 4H, $O_2CCH_2CH_2CH_2CH_2N$), 2.92 (m, 9H, 3-H_{eq}(sia) and β-H(asn)), 3.48 (m, 4H, $O_2CCH_2CH_2CH_2CH_2N$), 4.71 (d, $J = 7.5$ Hz, 3H, 1-H(gal)), 4.79 (m, 3H, α-H(asn)), 5.25 (m, 6H, 1-H(fuc) and 1-H(glcNAc)).
[37] Recently we could show that all three glycosyl transferases used in this study readily accepted a number of nonnatural substrates in vitro: G. Baisch, R. Öhrlein, B. Ernst, *Biorg. Med. Chem. Lett.* **1996**, *6*, 749; G. Baisch, R. Öhrlein, B. Ernst, M. Streiff, *ibid.*, *6*, 755; G. Baisch, R. Öhrlein, B. Ernst, A. Katopodis *ibid.*, *6*, 759.
[38] For a recent review, see: M. M. Palcic, O. Hindsgaul, *Trends Glycosci. Glycotechnol.* **1996**, *8*, 37.
[39] L. Yu, R. Cabrera, J. Ramirez, V. A. Malinoskii, K. Brew, P. G. Wang, *Tetrahedron Lett.* **1995**, *36*, 2897; C.-H. Wong, Y. Ichikawa, T. Krach, C. Gautheron-LeNarvor, D. P. Dumas, G. C. Look, *J. Am. Chem. Soc.* **1991**, *113*, 8137; R. Öhrlein, unpublished.
[40] N. M. Allanson, A. H. Davidson, C. D. Floyd, F. M. Martin, *Tetrahedron Asymmetry* **1994**, *5*, 2061; A. Töpfer, G. Kretzschmar, E. Bartnik, *Tetrahedron Lett.* **1995**, *36*, 9161.

Molecular Recognition Analyzed by EPR, ENDOR, and NMR Spectroscopy**

Martin Jäger and Hartmut B. Stegmann*

The formation of complexes between model receptors and substrates is known as molecular recognition.[1] Since natural phenomena like transport, catalysis, and regulation are based on it, extraordinary interest in intermolecular interactions has been aroused. The formation equilibrium and the conformation of all the components of these lock-and-key interdependencies are dynamic systems.

We therefore decided to study these kinds of systems with nuclear magnetic resonance spectroscopy (^{1}H NMR; 250 MHz) in parallel with electron paramagnetic (EPR; 10 GHz) and electron nuclear double resonance (ENDOR) spectroscopy. The difference in time resolution of the methods provides complementary information. The receptor **A** (Scheme 1) proved to be suitable for this investigation because of its converging functional groups, providing a cylinder-lock-like cavity with specific affinity to purine and benzimidazole moieties.[2] To introduce a part of the molecule that can be converted into a paramagnetic state, we modified these heterocycles with suitable phenol-type substituents in sites where they do not hinder the intermolecular interactions. Hence the resulting compounds **1**, **2**, **3** could still be recognized as substrates. One-electron oxidation of the phenols **1**–**3** leads to the paramagnetic complexes **A1***–**A3***.

The spectra of both the diamagnetic and paramagnetic associates depend on concentration and temperature. Since the number of NMR signals remains constant, the chemical shifts repre-

[*] Prof. Dr. H. B. Stegmann, Dipl.-Chem. M. Jäger
Institut für Organische Chemie der Universität
Auf der Morgenstelle 18, D-72076 Tübingen (Germany)
Fax: Int. code +(7071)29-5246
e-mail: stegmann@uni-tuebingen.de

[**] This work was supported by the Fonds der Chemischen Industrie and the Deutsche Forschungsgemeinschaft within the Graduiertenkolleg "Analytische Chemie" (scholarship for M. J.). We thank Dr. H.-J. Egelhaaf and Dipl.-Chem. B. Lehr for carrying out the optical investigations.

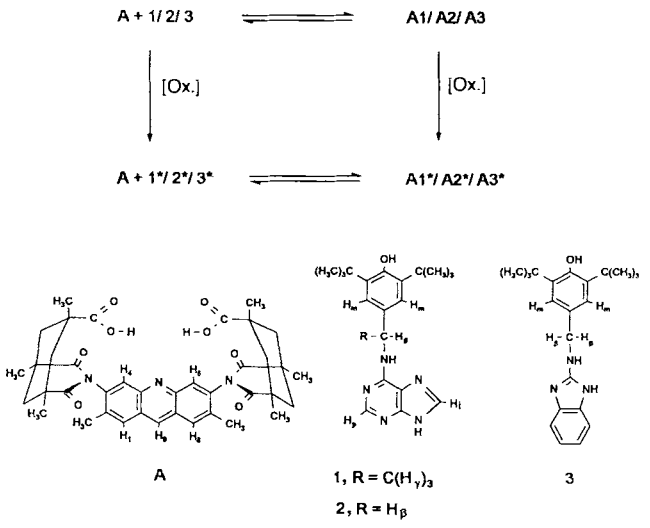

Scheme 1. Interdependence between receptor (**A**) and substrate (**1/1***, **2/2***, **3/3***) and pathways of oxidative radical generation. The nomenclature of the probes is given under the structural formulas.

sent averaged values. On the other hand, characteristic[3, 4] shifts of the signals are observed, which are most distinct for the aromatic protons. Examples of this behavior are demonstrated by the temperature-dependence of the $\Delta\delta$ values in Figures 1 and 2. The difference in the chemical shifts of complexed and free species, $\Delta\delta = \delta_{compl} - \delta_{free}$, eliminates the temperature dependence of the free species, thus takes into account only properties arising from complexation, and therefore indicates the existence of intermolecular interactions. In detail, these shift differences are influenced by association–dissociation equilibria, the complex conformation, and an additional protonation equilibrium, as will be discussed subsequently.

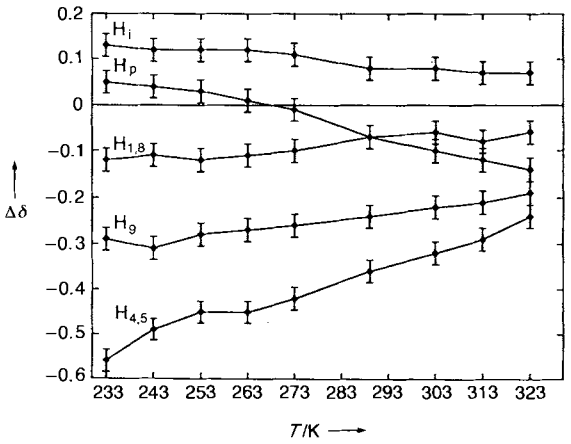

Fig. 1. Chemical shift difference $\Delta\delta$ of H_9, $H_{1,8}$ $H_{4,5}$, H_p, and H_i as a function of the temperature for the equilibrium **A** + **1** ⇌ **A1** in $CDCl_3$.

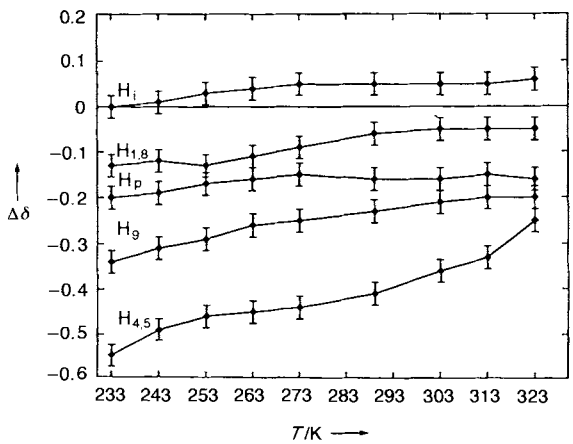

Fig. 2. Chemical shift difference $\Delta\delta$ of H_9, $H_{1,8}$ $H_{4,5}$, H_p, H_i as a function of the temperature for the equilibrium **A** + **2** ⇌ **A2** in $CDCl_3$.

Essentially, the temperature-dependent $|\Delta\delta|$ values converge to zero as shown in Figures 1 and 2. In the same way, if the concentration ratio of the components is systematically varied at constant temperature, the measured chemical shifts approach those of the free species ($lim_{c(comp)\to 0}\Delta\delta_{free} = 0$, $lim_{c(free)\to 0}\Delta\delta_{comp} = 0$) is observed. These results confirm the existence of an equilibrium that is rapid on the NMR time frame.

When complexed, the protons H_9, $H_{4,5}$, and $H_{1,8}$ of the acridine base of **A** are shielded by the purine and benzimidazole moieties and therefore resonate at higher field. In addition, the intramolecular proton transfer equilibrium[5] must be taken into account, as explained below. In the case of the purine derivatives **1** and **2**, the electron density in the imidazole ring is diminished by the "grasp of the carboxyl pincers", causing a downfield shift of the H_i signals. The quantitative investigation of the substrate's concentration dependence (NMR titration) allows an estimation of the association constants. For this purpose, we took the chemical shifts obtained at the experimentally highest receptor–substrate ratio as the chemically induced shifts (CIS)[6] for completely bound substrate at room temperature, because a numerical approximation (curve fitting by means of the nonlinear, least-squares method with a Marquardt algorithm) indicates that they are limiting values. An analysis of the measured data by a Hill plot[7, 8] not only yielded a Hill coefficient of $n_H = 1$ and confirmed the anticipated receptor–substrate complex formation ratio of 1:1, but also enabled the determination of the following association constants: $K_A = 1 \times 10^3\,M^{-1}$ for **A1** and $K_A = 3 \times 10^3\,M^{-1}$ for **A2**. A comparison of these data with those of the unsubstituted heterocyclic bases[3] indicates that the benzyl substituent hardly influences the molecular recognition.

UV, VIS, and fluorescence measurements verify the existence of the equilibrium between the protonated and deprotonated acridine moiety. The fluorescence excitation spectrum of the protonated form of **A** presents a clear bathochromic shift of the transition $S_0 \to S_1$ (band at 410–430 nm) relative to that of the deprotonated form (band maximum at 390 nm). The emission spectrum (excitation at 360 nm) is a composite spectrum superimposing both forms; a series of concentration measurements that determine the proportions of the two forms show that the autoprotolysis of the receptor is suppressed by addition of **1**, **2**, or **3**.

In contrast to the ^1H NMR spectra, EPR and ENDOR spectra are to be interpreted in terms of superposition signals from separate "key" compounds and lock-and-key complex because of the faster time scale of the latter methods. For example, Figure 3 illustrates that in the ENDOR spectra of **1*** new lines appear after addition of **A**, but the number is again reduced to the original seven absorptions with further increase of the receptor concentration, though their frequencies are different.

We attribute the spectrum in Figure 3c to the complex **A1***. Consequently, Figure 3b has to be a superposition of **1*** and **A1***. At $T = 243$ K, the phenoxyl radical **1*** is characterized by the parameters given in Table 1. The addition of the receptor **A** results in a decrease of the β-proton coupling and an increase of a_{H_γ}. The assignment of the coupling constants could be additionally verified by general triple experiments. At $T = 203$ K, new signals are observed in the frequency area of the β-proton

 © VCH Verlagsgesellschaft mbH, D-69451 Weinheim, 1996 0570-0833/96/3516-1816 $ 15.00+.25/0

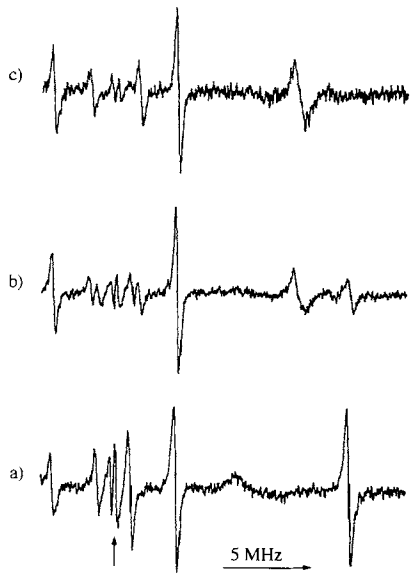

Fig. 3. ENDOR spectra in CH_2Cl_2 at $T = 243$ K of **1*** (a) and mixtures with the concentration ratios **1***:**A** = 1:1 (b), and **1***:**A** = 1:2 (c). Arrow: Larmor frequency of the free proton at $\nu = 14.32$ MHz.

Table 1. EPR and ENDOR data of **1***, **A1***, **2***, **A2***, and **3***, recorded in CH_2Cl_2.

1* (T = 243 K)	**A1*** (T = 243 K)	**2*** (T = 298 K)	**A2*** (T = 252 K)	**3*** (T = 298 K)
$a_{H\beta} = 6.95$ G	$a_{H\beta} = 5.37$ G	$a_{H\beta}^{(2)} = 9.18$ G	$a_{H\beta} = 10.90$ G $a_{H\beta'} = 8.32$ G	$a_{H\beta}^{(2)} = 11.80$ G
$a_N = 1.81$ G		$a_N = 2.15$ G	$a_N = 2.04$ G	$a_N = 1.25$ G
$a_{Hm}^{(2)} = 1.81$ G	$a_{Hm}^{(2)} = 1.81$ G	$a_{Hm}^{(2)} = 1.88$ G	$a_{Hm}^{(2)} = 1.88$ G	$a_{Hm}^{(2)} = 1.84$ G
$a_{H_p}^{(3)} = 0.49$	$a_{H_p}^{(3)} = 0.71$ G			
$g = 2.00456$		$g = 2.00455$		$g = 2.00458$

coupling of the complex **A1***. We therefore trace them back to different conformations of the key in the lock according to refs. [3, 4].

Similarly, Figure 4b can be explained as a superimposed spectrum of free and complexed **3***. The signal of the phenoxyl radical **3*** is interpreted with the data in Table 1. The hyperfine structure (hfs) changes on addition of **A** (Fig. 4b). Obviously, a

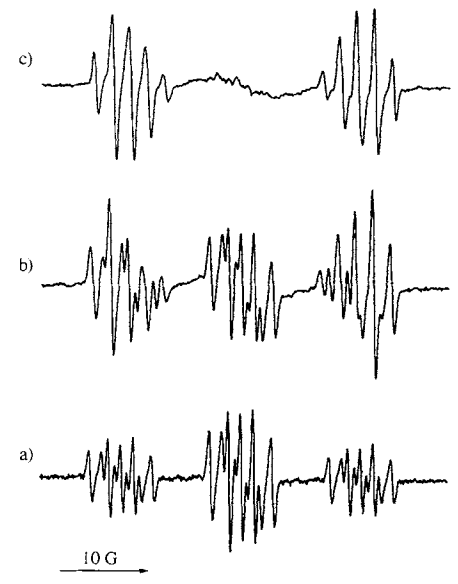

Fig. 4. EPR spectra in CH_2Cl_2 at $T = 293$ K: (a) **3***, (b) **3*** + **A**, (c) difference spectrum b − a.

superposition of the signals of at least two species takes place. In fact, the subtraction of the spectrum of free **3*** leads to the hyperfine structure shown in Figure 4c.

The spectrum can only be understood if complexation influences the intramolecular flexibility of **3***. While in the case of uncomplexed **3*** those processes causing the two β-protons to be equivalent are fast enough to generate a triplet structure, the signals coalesce at the same temperature on interaction with the receptor **A**. The influence of the temperature variation on the molecular dynamics of the substrate at a constant concentration ratio is illustrated for system **A2*** in Figure 5. Whereas the sig-

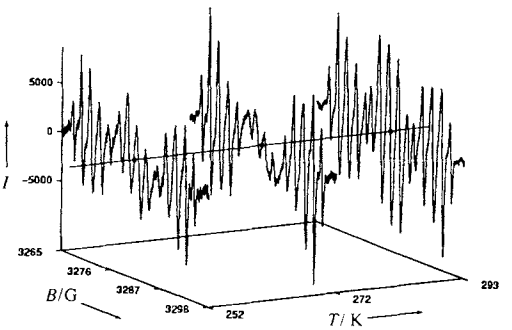

Fig. 5. EPR spectra of **2*** + **A** at different temperatures. I = intensity (arbitrary units).

nal of free **2*** is characterized by a triplet structure with an intensity ratio of 1:2:1 ($a_{H\beta}^{(2)} = 9.18$ G; other hf parameters are shown in Table 1) resulting from an equivalence of the β-protons at $T = 293$ K, the addition of the receptor hinders the flexibility of **2*** even at room temperature; consequently, the three signal groups due to the β-proton coupling have nearly equal intensity. With decreasing temperature, the central hfs components become broader in order to regain intensity after coalescence. The hyperfine coupling constants $a_{H\beta} = 10.90$ G and $a_{H\beta'} = 8.32$ G (all other data given in Table 1) can be deduced from Figure 5 as characteristic for the complex **A2***. Thus, this hfs now provides a quartet pattern. The β-proton coupling ($a_{H\beta}^{(2)} = 9.18$ G) observed for free **2*** is not yet the average of both β-couplings of **A2***. In the absence of **A**, no comparable temperature dependence for **2*** can be found. Thus, the magnetic inequivalence of the β-protons of **2*** at $T < 272$ K is a consequence of the lock-and-key interaction.

The quantitative evaluation of the molecular dynamics of **A2*** according to Arrhenius for a two-jump model yields an activation energy of 8.2 kcal mol^{-1} and $k_{293} = 47$ MHz for the experimentally accessible temperature range between 252 and 333 K.

A two-jump mechanism as interpretation of such a temperature dependence for analogous systems with a tertiary nitrogen atom (Fig. 6) is attributed to hindrance of rotation around the C–C_{aroxyl} bond or to inversion of the nitrogen atom,[9, 10] whereas in this case the magnitude of the activation energy found favors the inhibition of rotation as an explanation. Aroxyls

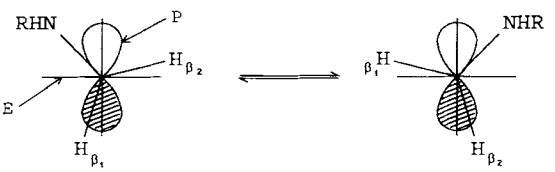

Fig. 6. Illustration of the two-jump mechanism. R = purinyl, E = plane of the arene ring of the phenoxyl radical, P = p orbital perpendicular to E.

 © VCH Verlagsgesellschaft mbH, D-69451 Weinheim, 1996 0570-0833/96/3516-1817 $ 15.00+.25/0

substituted with a secondary amino group at the methylene carbon do not show any inequivalence of the β-protons over the whole temperature range. Thus, only the key-in-the-lock possesses the sufficiently large activation energy necessary for the observation of coalescence under the existing conditions.

Experimental Procedure

The receptor **A** is well known [5]. Phenol **1** was synthesized by addition of adenine to 3,5-di-*tert*-butylquinonemethide [11]. Phenols **2** and **3** were obtained by condensation of 4-bromomethyl-2,6-di-*tert*-butylphenol with adenine and with 2-aminobenzimidazole [10], respectively. All compounds were characterized by current methods. The ^{1}H NMR spectra were obtained on a Bruker AC 250 (250 MHz) spectrometer in CDCl3.

The radicals **1***, **2***, and **3*** were generated in CH_2Cl_2 by oxidation of the corresponding phenols with PbO_2; **A** can be added before or after radical generation. Deoxygenation was done by bubbling argon through the samples. The spectra were recorded with a Bruker ESP 300E spectrometer equipped with an ENDOR unit (Bruker ER 810). Typical instrumental parameters for ENDOR investigations: MW power 30 mW; RF power 7 dB, 500 W; modulation 70 kHz.

Received: December 11, 1995
Revised version: February 19, 1996 [Z 8631 IE]
German version: *Angew. Chem.* **1996**, *108*, 1943–1946

Keywords: ENDOR spectroscopy · molecular dynamics · molecular recognition

[1] Recent comprehensive review: J.-M. Lehn *Supramolecular Chemistry*, VCH, Weinheim, **1995**.
[2] J. Rebek, Jr., *Angew. Chem.* **1990**, *102*, 261; *Angew. Chem. Int. Ed. Engl.* **1990**, *29*, 245.
[3] J. Rebek, Jr., B. Askew, M. Killoran, D. Nemeth, F.-T. Lin, *J. Am. Chem. Soc.* **1987**, *109*, 2426.
[4] J. Rebek, Jr., D. Nemeth, *J. Am. Chem. Soc.* **1986**, *108*, 5637.
[5] J. Rebek, Jr., L. Marshall, R. Wolak, K. Parris, M. Killoran, B. Askew, D. Nemeth, N. Islam, *J. Am. Chem. Soc.* **1985**, *107*, 7476.
[6] H.-J. Schneider, R. Kramer, S. Simova, U. Schneider, *J. Am. Chem. Soc.* **1988**, *110*, 6442.
[7] A. V. Hill, *J. Physiol.* **1910**, *40*, iv.
[8] A. Cornish-Bowden, D. E. Koshland, Jr., *J. Mol. Biol.* **1975**, *95*, 201.
[9] V. Fischer, W. Bühler, K. Scheffler, *Z. Naturforsch. Part A* **1983**, *38*, 570.
[10] V. Fischer, *Dissertation*, Universität Tübingen **1981**.
[11] U. Höfler, *Dissertation*, Universität Tübingen **1994**.

Bis(bipyridine) Ligands in Manganese Carboxylate Cluster Chemistry: Self-Assembly of a Cluster Complex with Two Butterfly-Like $[Mn_4(\mu_3\text{-}O)_2]^{8+}$ Cores**

Vincent A. Grillo, Michael J. Knapp, John C. Bollinger, David N. Hendrickson,* and George Christou*

Polypyridyl, oligo-2,2′-bipyridine, and related ligands L have received considerable attention over the last several years.[1–11] The use of such ligands as "programmed" components in self-assembly reactions with metal ions has been a central theme in supramolecular chemistry, and has led to the formation of a variety of metal/ligand supramolecular ensembles. The latter have fascinating structures such as double or triple helices, and "capped", "cylindrical" and "circular" architectures. The resulting redox and photophysical properties have also been of interest. In all the work to date the ligands L have been bound to mononuclear centers and they have also been the only (or in some cases, the majority) ligands to the metals.

Metal cluster chemistry is another area in which self-assembly of multiple components occurs to produce a "supermolecular" product. We have been interested in carboxylatomanganese clusters for a number of reasons, including the fact that they exhibit highly unusual magnetic properties and, in some cases, are single-molecule magnets.[12, 13]

We report herein the amalgamation of the above two areas, namely the use of bis-2,2′-bipyridine ligands L in carboxylatomanganese cluster formation, in order to explore the influence of the ligand "programming" on both the cluster formed and the nature of the multicomponent assembly; the overall objective is the development of supramolecular chemistry involving metal clusters as components of the supramolecular ensemble.

The two ligands employed were L1[14] and L2.[15] Treatment of $[Mn_3O(O_2CMe)_6(py)_3](ClO_4)$[16] (py = pyridine) with L1 in a 1:1.5 molar ratio in MeCN led to a dark brown solution and subsequent isolation of the tetranuclear complex **1** as a perchlorate salt. Similarly, treatment of $[Mn_3O(O_2CEt)_6(py)_3](ClO_4)$[17] with L2 in a 1:1.5 molar ratio in CH_2Cl_2 led to subsequent isolation of the octanuclear complex **2** as a perchlo-

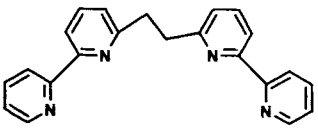

L1

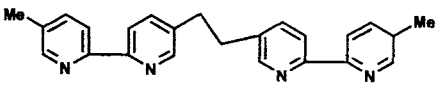

L2

$[Mn_4O_2(O_2CMe)_4(L1)_2](ClO_4)_2$ **1**-$(ClO_4)_2$

$[Mn_8O_4(O_2CEt)_{14}(L2)_2](ClO_4)_2$ **2**-$(ClO_4)_2$

rate salt. The structure of the cation **1** (Fig. 1)[18] consists of two $[Mn_2O(O_2CMe)_2(L1)]^+$ fragments held together by interfragment linkages Mn1–O3′ and Mn1′–O3. The cation is centrosymmetric and mixed-valent (two Mn^{II}, two Mn^{III}) and, on the basis of the structural parameters, the Mn^{II} and Mn^{III} centers are five-coordinate (Mn2) and six-coordinate (Mn1), respectively. Each resulting $Mn^{II}Mn^{III}$ pair is quadruply bridged by O3, two *syn,syn*-$MeCO_2^-$ groups, and the L1 ligand, which is attached to both metals. There are three types of Mn···Mn distances, $Mn^{III}\cdots Mn^{III}$ (2.784(4) Å), intrafragment $Mn^{II}\cdots Mn^{III}$ (3.208(4) Å), and interfragment $Mn^{II}\cdots Mn^{III}$ (3.632(4) Å). The central $[Mn_2O_2]$ unit is asymmetrical; the interfragment Mn^{III}–O bonds (1.8787(6) Å) are noticeably longer than the intrafragment Mn^{III}–O bonds (1.8391(6) Å). Interestingly, all bipyridine (bpy) rings are essentially parallel, providing additional interfragment interactions by π stacking. Complex **1** is a new addition to the family of Mn_4 clusters with a "dimer-of-dimers" structure.[19]

[*] Prof. Dr. D. N. Hendrickson, M. J. Knapp
Department of Chemistry, University of California at San Diego
La Jolla, CA 92093-0358 (USA)
Fax: Int. code +(619) 534-5383
e-mail: dhendrickson@ucsd.edu
Prof. Dr. G. Christou, Dr. V. A. Grillo, Dr. J. C. Bollinger
Department of Chemistry and the Molecular Structure Center
Indiana University, Bloomington, IN 47405-4001 (USA)
Fax: Int. +(812) 855-2399
e-mail: christou@indiana.edu

[**] This work was supported by the U. S. National Science Foundation (Grants CHE 9115286 and CHE 9311904) and National Institutes of Health (Grant GM 39083).

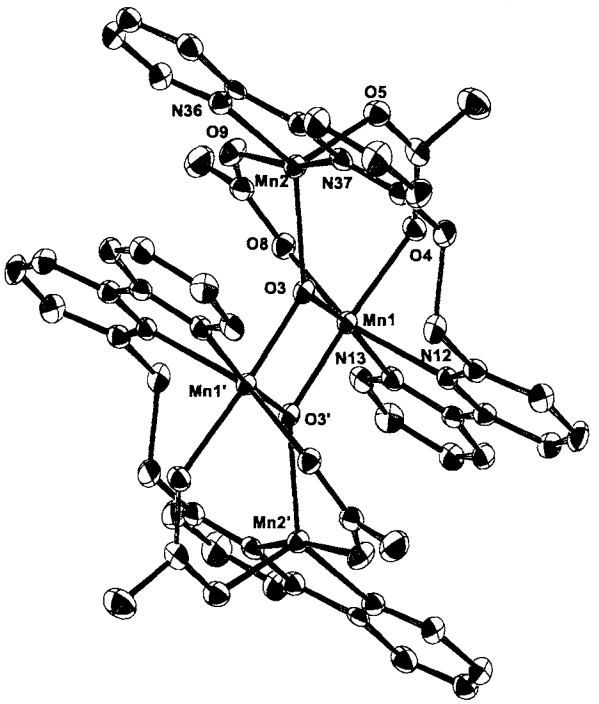

Fig. 1. ORTEP representation of the cation **1**. Selected distances [Å] and angles [°]: Mn1···Mn1' 2.784(4), Mn1···Mn2 3.208(4), Mn1···Mn2' 3.632(4), Mn1–O3 1.839(1), Mn1–O3' 1.879(1), Mn2–O3 2.030(1), O3-Mn1-O3' 83.01(3), Mn1-O3-Mn1' 96.99(3), Mn1-O3'-Mn2' 136.60(3), Mn1-O3-Mn2 111.93(3).

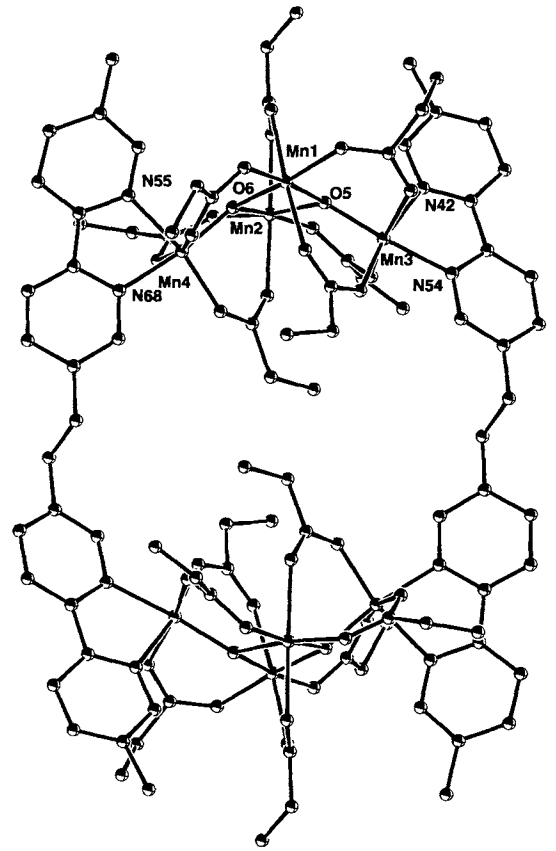

Fig. 2. ORTEP representation of the cation **2**. Selected distances [Å] and angles [°]: Mn1···Mn2 2.843(4), Mn1–O5 1.889(13), Mn1–O6 1.890(12), Mn2–O6 1.893(13), Mn2–O5 1.899(13), Mn3–O5 1.831(13), Mn4–O6 1.845(13), O5-Mn1-O6 81.6(6), O5-Mn2-O6 81.2(6).

The structure of the centrosymmetric cation **2** (Fig. 2)[18] likewise consists of two fragments, but interfragment linkages are now provided by the two L2 ligands. The fragments have $[Mn_4(\mu_3\text{-}O)_2]^{8+}$ (i.e. four Mn^{III}) butterfly-like cores, arranged face-to-face. If the $\text{-}CH_2\text{-}CH_2\text{-}$ linker groups of the L2 ligands were removed, two previously reported $[Mn_4O_2(O_2CEt)_7(bpy)_2]^+$ units result; this shows that **2** can be viewed as a dimer of clusters with butterfly-like cores in which the fragments are only slightly distorted compared with discrete $[Mn_4O_2(O_2CR)_7(bpy)_2]^+$ species.[17] Inspection of a space-filling model shows no cavity in the center of the cluster.

Variable-temperature magnetic susceptibility data were collected on complexes **1** and **2** (SQUID magnetometer, 10.0 kG field) to investigate the degree of interfragment interaction. Complex **1** exhibits an effective magnetic moment (μ_{eff}) per molecule that smoothly decreases from 8.05 μ_B at 320 K to 1.05 μ_B at 2.0 K (Fig. 3). The data were fit to a model in which the exchange interaction between the interfragment $Mn^{II}\cdots Mn^{III}$ pairs was considered to be negligible because of the relatively long separation. The fit (Fig. 3) employed $-2J\hat{S}_i\cdot\hat{S}_j$ terms for exchange interactions and gives $J(Mn^{III}\cdots Mn^{III}) = -3.2\ cm^{-1}$, J(intrafragment $Mn^{II}\cdots Mn^{III}$) $= -2.3\ cm^{-1}$, $g = 1.86$ and a small contamination (4%) by paramagnetic Mn^{II} ions. The value of $J(Mn^{III}\cdots Mn^{III})$ shows that interfragment interactions exist in **1**. The variable-field and variable-temperature data indicate that **1** has an $S = 0$ ground state.

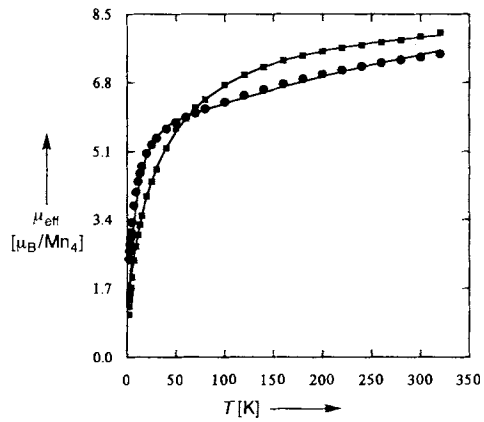

Fig. 3. Plot of the effective magnetic moment, μ_{eff}/Mn_4, vs. temperature for $[Mn_4O_2(OAc)_4(L1)_2](ClO_4)_2$ (**1**, ■) and $[Mn_8O_4(O_2CEt)_{14}(L2)_2](ClO_4)_2$ (**2**, ●) in an applied magnetic field of 10.00 kG. The solid line represents the best fit to the theoretical equation. See text for fitting parameters.

The data for **2** indicate there is negligible exchange interaction between the two butterfly-like $Mn^{III}_4O_2$ fragments. In Figure 3, μ_{eff} per butterfly unit is plotted as a function of temperature. The decrease from 7.51 μ_B (per Mn_4O_2 fragment) at 320 K to 5.82 μ_B at 50.0 K, followed by a rapid decrease to 2.42 μ_B at 2.0 K, parallels what has been seen[17, 20] for other butterfly-like $Mn^{III}_4O_2$ complexes. In fact, the data could be fit assuming the two butterfly-like fragments do not interact to give $J_{wb} = -10.5\ cm^{-1}$, $J_{bb} = -27.4\ cm^{-1}$, and $g = 2.00$, where J_{wb} characterizes the wing-tip-body $Mn^{III}\cdots Mn^{III}$ interaction and J_{bb} the body–body interaction. The rapid decrease in μ_{eff} at low temperatures was accommodated by assuming the $S = 3$ ground state in each butterfly-like core has an axial zero-field splitting with $|D| = 3.0\ cm^{-1}$.

L1 and L2 possess two important properties: 1) the 2,2′-bpy character of each half of the ligands and 2) their overall "linked-

 © VCH Verlagsgesellschaft mbH, D-69451 Weinheim, 1996 0570-0833/96/3516-1819 $ 15.00+.25/0

bpy" nature. Given that bpy itself will react with $[Mn_3O(O_2CR)_6(py)_3](ClO_4)$ to afford butterfly-like clusters of the type $[Mn_4O_2(O_2CR)_7(bpy)_2](ClO_4)$,[17] it can be seen that in L2 the 5,5″ linkage results in the above-mentioned properties being independent: property 1) triggers self-assembly of a butterfly-like $[Mn_4O_2]^{8+}$ cluster (as does free bpy), and property 2) yields a resulting "dimer-of-clusters" supramolecular assembly. In contrast, properties 1) and 2) are coupled (not independent) in L1, and the 6,6″ linkage therefore yields the new cluster type in complex **1**.

It is clear that there is great potential for suitably "programmed" polypyridyl and related ligands in this area of supramolecular chemistry involving metal clusters, complementing the current use of mononuclear metal centers. Such an approach might be one potential means of amalgamating, for example, the often unusual magnetic properties of metal clusters and the multidimensional controlled ordering of supramolecular chemistry.

Experimental Procedure

$[Mn_4O_2(O_2CMe)_4(L1)_2](ClO_4)_2$ (**1**). Solid L1 (0.30 g, 0.90 mmol) was added to a stirred red-brown solution of $[Mn_3O(O_2CMe)_6(py)_3](ClO_4)$ (0.52 g, 0.60 mmol) in MeCN (60 mL), which caused a rapid color change to dark red-brown. The solution was stirred for 12 h, filtered, and the filtrate layered with an equal volume of THF. After several days, dark red-brown block-shaped crystals of **1**·2THF had formed; this formulation was indicated crystallographically, but dried solid analyzed as **1**·THF·$2H_2O$. Yield 46%. Anal. calcd (found) for $C_{56}H_{60}N_8O_{21}Cl_2Mn_4$: C 45.70 (45.87), H 4.11 (3.96), N 7.61 (7.67), Mn 14.93 (14.99)%.

$[Mn_8O_4(O_2CEt)_{14}(L2)_2](ClO_4)_2$ (**2**). Solid L2 (0.10 g, 0.30 mmol) was added to a stirred red-brown solution of $[Mn_3O(O_2CEt)_6(py)_3](ClO_4)$ (0.19 g, 0.20 mmol) in CH_2Cl_2 (50 mL). The solution was stirred for 2 h, filtered, and the filtrate layered with an equal volume of hexanes. After several days, dark red crystals of $2\cdot4CH_2Cl_2\cdot xC_6H_{14}$ were collected; this formulation was indicated crystallographically, but dried solid analyzed as solvent free. Yield 65%. Anal. calcd (found) for $C_{90}H_{114}N_8O_{40}Cl_2Mn_8$: C 43.97 (44.04), H 4.67 (4.53), N 4.56 (4.66), Mn 17.88 (17.92)%.

Received: December 13, 1995 [Z 8643 IE]
German version: *Angew. Chem.* **1996**, *108*, 1962–1964

Keywords: · clusters · complexes with carboxylato ligands · magnetic properties · manganese compounds

[1] J.-M. Lehn, *Supramolecular Chemistry*, VCH, Weinheim, **1995**.
[2] a) R. Krämer, J.-M. Lehn, A. DeCian, J. Fischer, *Angew. Chem.* **1993**, *105*, 764; *Angew. Chem. Int. Ed. Engl.* **1993**, *32*, 703; b) E. Leize, A. Van Dorsselaer, R. Krämer, J.-M. Lehn, *J. Chem. Soc. Chem. Commun.* **1993**, 990.
[3] C. Piguet, G. Bernardinelli, B. Bocquet, A. Quattropani, A. F. Williams, *J. Am. Chem. Soc.* **1992**, *114*, 7440.
[4] W. Zarges, J. Hall, J.-M. Lehn, C. Bolm, *Helv. Chim. Acta* **1991**, *74*, 1843.
[5] T.-M. Garrett, U. Koert, J.-M. Lehn, A. Rigault, D. Meyer, J. Fischer, *J. Chem. Soc. Chem. Commun.* **1990**, 557.
[6] J.-M. Lehn, J.-P. Sauvage, J. Simon, R. Ziessel, C. Piccini-Leopardi, G. Germain, J.-P. Declercq, M. Van Meerssche, *Nouv. J. Chim.* **1983**, *7*, 413.
[7] J.-M. Lehn, A. Rigault, J. Siegel, J. Harrowfield, B. Chevrier, D. Moras, *Proc. Natl. Acad. Sci. USA* **1987**, *84*, 2565.
[8] a) P. Baxter, J.-M. Lehn, A. DeCian, J. Fischer, *Angew. Chem.* **1993**, *105*, 92; *Angew. Chem. Int. Ed. Engl.* **1993**, *32*, 69; b) P. Baxter, J.-M. Lehn, J. Fischer, M.-T. Youinou, *ibid.* **1994**, *106*, 2432 and **1994**, *33*, 2284.
[9] a) M.-T. Youinou, R. Ziessel, J.-M. Lehn, *Inorg. Chem.* **1991**, *30*, 2144; b) M.-T. Youinou, N. Rahmouni, J. Fischer, J. A. Osborn, *Angew. Chem.* **1992**, *104*, 771; *Angew. Chem. Int. Ed. Engl.* **1992**, *31*, 733.
[10] K. T. Potts, K. A. Gheysen Raiford, M. Keshavarz-K, *J. Am. Chem. Soc.* **1993**, *115*, 2793.
[11] a) E. C. Constable, R. Chotalia, D. A. Tocher, *J. Chem. Soc. Chem. Commun.* **1992**, 771; b) E. C. Constable, *Tetrahedron* **1992**, *48*, 10013; *Prog. Inorg. Chem.* **1994**, *42*, 67; c) E. C. Constable, M. D. Ward, D. A. Tocher, *J. Am. Chem. Soc.* **1990**, *112*, 1256, *J. Chem. Soc. Dalton Trans.* **1991**, 1675; d) E. C. Constable, R. Chotalia, *J. Chem. Soc. Chem. Commun.* **1992**, 64.
[12] H. J. Eppley, H.-L. Tsai, N. de Vries, K. Folting, G. Christou, D. N. Hendrickson, *J. Am. Chem. Soc.* **1995**, *117*, 301, and references therein.
[13] a) M. W. Wemple, D. M. Adams, K. S. Hagen, K. Folting, D. N. Hendrickson, G. Christou, *J. Chem. Soc. Chem. Commun.* **1995**, 1591; b) H.-L. Tsai, S. Wang, K. Folting, W. E. Streib, D. N. Hendrickson, G. Christou, *J. Am. Chem. Soc.* **1995**, *117*, 2503.
[14] T. Garber, S. Van Wallendael, D. P. Rillema, M. Kirk, W. E. Hatfield, J. H. Welch, P. Singh, *Inorg. Chem.* **1990**, *29*, 2863.
[15] J.-M. Lehn, R. Ziessel, *Helv. Chim. Acta* **1988**, *71*, 1511.
[16] J. B. Vincent, H.-R. Chang, K. Folting, J. C. Huffman, G. Christou, D. N. Hendrickson, *J. Am. Chem. Soc.* **1987**, *109*, 5703.
[17] J. B. Vincent, C. Christmas, H.-R. Chang, Q. Li, P. D. W. Boyd, J. C. Huffman, D. N. Hendrickson, G. Christou, *J. Am. Chem. Soc.* **1989**, *111*, 2086.
[18] Crystal data for **1**·2THF: $C_{52}H_{48}N_8O_{18}Cl_2Mn_4\cdot2C_4H_8O$, triclinic, $P\bar{1}$, $T = -169\,^{\circ}C$, $a = 12.017(2)$, $b = 12.197(2)$, $c = 12.343(2)$ Å, $\alpha = 73.29(1)$, $\beta = 78.02(1)$, $\gamma = 68.36(1)^{\circ}$, $V = 1600.1$ Å^3, $Z = 1$, $6^{\circ} \le 2\theta \le 45^{\circ}$. 4176 unique reflections, 3757 unique reflections with $F > 2.33\sigma(F)$; $R(F) = 0.0448$, $R_w(F) = 0.0419$. Crystal data for $2\cdot4CH_2Cl_2\cdot xC_6H_{14}$: $C_{90}H_{114}N_8O_{40}Cl_2Mn_8\cdot4CH_2Cl_2\cdot xC_6H_{14}$, monoclinic, $C2/c$, $T = -164\,^{\circ}C$, $a = 22.189(4)$, $b = 32.402(6)$, $c = 22.521(4)$ Å, $\beta = 115.60(1)^{\circ}$, $V = 14602$ Å^3, $Z = 4$, $6^{\circ} \le 2\theta \le 45^{\circ}$. 9508 unique reflections, 5341 unique reflections with $F > 4\sigma(F)$; $R(F) = 0.0914$, $R_w(F^2$; all data$) = 0.1777$. Crystallographic data (excluding structure factors) for the structure(s) reported in this paper have been deposited with the Cambridge Crystallographic Data Centre as supplementary publication no. CCDC-179-52. Copies of the data can be obtained free of charge on application to The Director, CCDC, 12 Union Road, Cambridge CB2 1EZ, UK (fax: Int. code +(1223) 336-033; e-mail: teched@chemcrys.cam.ac.uk).
[19] a) M. K. Chan, W. H. Armstrong, *J. Am. Chem. Soc.* **1991**, *113*, 5055; b) M. L. Kirk, M. K. Chan, W. H. Armstrong, E. I. Solomon, *ibid.* **1992**, *114*, 10432; c) H. Sakiyama, K. Tokuyama, Y. Matsumura, H. Okawa, *J. Chem. Soc. Dalton Trans.* **1993**, 2329; d) H. Kawasaki, M. Kusunoki, Y. Jayashi, M. Suzuki, K. Munezawa, M. Suenaga, H. Senda, A. Uehara, *Bull. Chem. Soc. Jpn.* **1994**, *67*, 1310; e) C. Philouze, G. Blondin, J.-J. Girerd, J. Guilhem, C. Pascard, D. Lexa, *J. Am. Chem. Soc.* **1994**, *116*, 8557; f) G. Haselhorst, K. Wieghardt, *J. Inorg. Biochem.* **1995**, *59*, 624.
[20] E. Libby, K. Folting, C. J. Huffman, J. C. Huffman, G. Christou, *Inorg. Chem.* **1993**, *32*, 2549.

Carbaporphyrins**

Kurt Berlin*

In recent years numerous structural variants of porphyrins have been synthesized[1, 2b] which are not only interesting as 18π arenes, but also because of their diverse applications in medicine,[2] and as catalysts and chromophores.[1, 2b] In most of these porphyrinoids, including porphyrin isomers,[3–5] porphyrin analogs, and expanded porphyrins,[1b, 2b, 4] either a pyrrole ring has been formally replaced by a unit containing a nitrogen or a different heteroatom, or the arrangement of pyrroles and CH groups has been changed. But few porphyrinoids with less than four heteroatoms in the inner cycle have been reported that can bridge the gap to the formally related C-annulenes, which are prepared by completely different synthetic strategies and display strongly contrasting spectroscopic and physical properties.[6]

Novel porphyrin isomers, in particular one with an inverted pyrrole ring and an inner CH unit,[5] were inspiration to proceed further and replace one pyrrole ring of porphine by a five-membered unsaturated all-carbon ring. In these compounds only one nitrogen atom of the porphyrin system is replaced by carbon; thus they are referred to as carbaporphyrins.

Since the replacement of one pyrrole ring of the porphyrin core by 6π arenes was successful,[7] the reaction of a tripyrrane like **2b** (see Scheme 1) with a cyclopentadiene-1,3-dialdehyde appeared to be promising. Unfortunately the latter compound is not known, and it would probably be unstable under the

[*] Dr. K. Berlin
Tufts University, Department of Chemistry
62 Talbot Avenue, Medford, MA 02155 (USA)
Telefax: Int. code +(617)627-3443
e-mail: kberlin@emerald.tufts.edu

[**] I thank Prof. Dr. E. Breitmaier, Institut für Organische Chemie und Biochemie, Bonn, Germany, for suggesting and supporting this project.

acidic conditions required for cyclization. An alternative approach based on the condensation of 6-(2-pyrryl)fulvenes with dipyrrylmethanedialdehydes to yield carbaporphyrins[8] was thwarted by the instability of the fulvene starting material. An additional electron-withdrawing group attached to an unsaturated five-membered ring dialdehyde should increase the stability of the cyclopentadiene unit and provide a welcome function in the carbaporphyrins for further reactions.

As far back as 1963 Hafner et al. described Vilsmeier formylations of cyclopentadiene[9] that furnished mixtures of isomers in the form of immonium salts. These can be converted into aldehydes by basic hydrolysis. The hydroxyfulvenedialdehyde **1a**, which is stabilized by an intramolecular hydrogen bond,[10] was always isolated regardless of the original substitution pattern. This compound can also be regarded formally as the enol form of cyclopentadienetrialdehyde. The mesomeric stabilization of compounds **1a** and **1b** (Scheme 1) is probably responsible for their sufficient stability even under acidic reaction conditions.

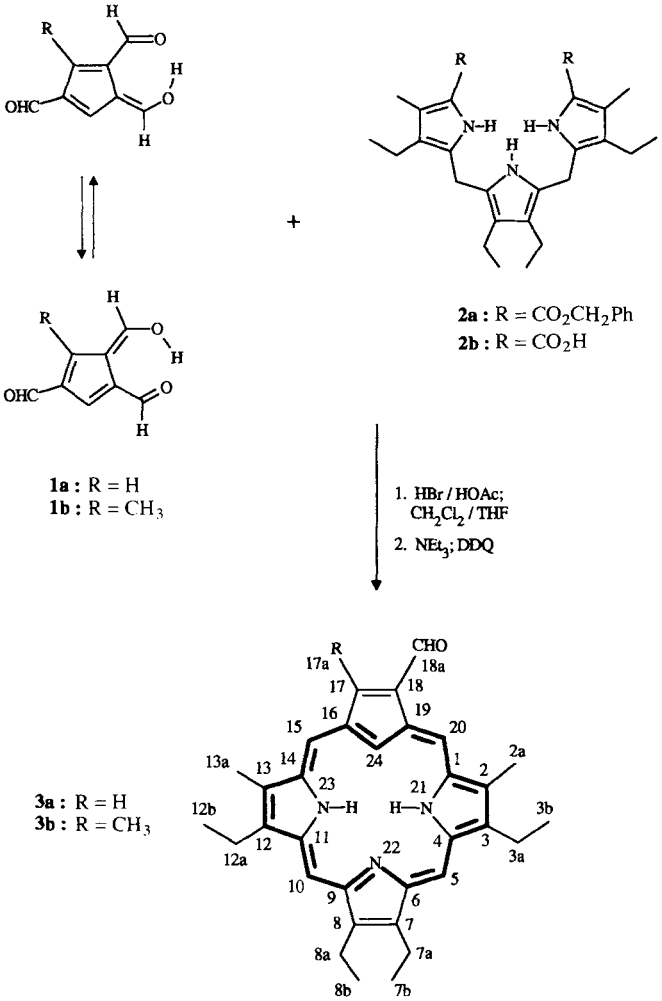

Scheme 1.

The hydroxyfulvenedialdehyde **1a** and compound **1b**, which was prepared analogously from methylcyclopentadiene, reacted as expected with the in situ decarboxylated tripyrranedicarboxylic acid **2b**[11] in dichlormethane/THF with HBr/glacial acetic acid as the catalyst. Oxidation of the products with 2,3-dichloro-5,6-dicyano-1,4-benzoquinone (DDQ) yielded the carbaporphyrins **3a** and **3b**, respectively (Scheme 1), which were obtained from yellow-brown fractions by column chromatography on silica gel. The products were identified unambiguously by two-dimensional NMR spectroscopy (HMQC, HMBC) and high-resolution mass spectrometry.[12]

Table 1. Selected physical and spectroscopic data of **1a**, **1b**, **3a**, and **3b**.

1a: ^{13}C NMR (100 MHz, acetone): δ = 127.8 (C-1/C-2), 138.3 (C-4), 142.3 (C-3/C-5), 182.5(C-2a/C-6), 186.9 (C-4a).

1b: M.p. 131–132 °C; ^{1}H NMR (200 MHz, $CDCl_3$): δ = 2.72 (s, 3H, 3a-H), 7.79 (s, 1H, 5-H), 8.77, 8.92 (2d, J = 8.7 Hz, 2H, 2a-H/6-H), 9.99 (s, 1H, 4a-H), 16.87 (t, J = 8.7 Hz, 1H, O-H); ^{13}C NMR (100 MHz, acetone): δ = 12.3 (C-3a), 125.9 (C-2), 127.1 (C-1), 135.8 (C-4), 141.8 (C-5), 144.7 (C-3), 179.6, 181.1 (C-2a/C-6), 187.4 (C-4a).

3a: M.p. > 250 °C; ^{1}H NMR (500 MHz, $CDCl_3$): δ = −7.23 (s, 1H, 24-H), −4.21 (br. s, 2H, NH), 1.76 (4t, 12H, 3b/7b/8b/12b-H), 3.31 (s, 3H, 13a-H), 3.50 (s, 3H, 2a-H), 3.75 (2q, 4H, 7a/8a-H), 3.82 (q, 2H, 12a-H), 3.88 (q, 2H, 3a-H), 8.39 (s, 1H, 17-H), 9.11 (s, 1H, 15-H), 9.18, 9.26 (2s, 2H, 5-H/10-H), 10.43 (s, 1H, 20-H), 10.59 (s, 1H, 18a-H); ^{13}C NMR (125 MHz, $CDCl_3$): δ = 11.4 (C-13a), 11.7 (C-2a), 17.5, 17.6 (C-3b/C-12b), 18.7 (C-7b/C-8b), 19.6 (C-12a), 19.7 (C-3a), 20.1 (C-7a/C-8a), 94.1, 94.8 (C-5, C-10), 103.9 (C-24), 106.4 (C-15), 108.1 (C-20), 132.1 (C-16), 132.4 (C-19), 134.7, 134.8 (C-13/C-14), 135.3 (C-2), 135.6 (C-1), 136.4 (C-18), 137.4 (C-3/C-12), 138.1, 138.5 (C-4/C-11), 143.3 (C-17), 145.0, 145.3 (C-7/C-8), 155.0, 155.4 (C-6/C-9), 188.8 (C-18a); HRMS: m/z = 477.2777 (calcd 477.2780 for $C_{32}H_{35}N_3O$); UV/Vis (CH_2Cl_2): λ_{max} [nm] (lg ε) = 316 (4.12), 366 (4.36), 433 (4.59), 524 (3.77), 564 (3.81), 618 (3.23), 636 (3.25), 704 nm (3.15).

3b: M.p. > 250 °C; ^{1}H NMR (500 MHz, $CDCl_3$): δ = −6.82 (s, 1H, 24-H), −3.71 (br. s, 2H, NH), 1.80 (2t, 6H, 3b/12b-H), 1.83 (2t, 6H, 7b/8b-H), 3.47 (s, 3H, 13a-H), 3.50 (s, 3H, 17a-H), 3.57 (s, 3H, 2a-H), 3.87 (2q, 4H, 7a/8a-H), 3.94 (2q, 4H, 3a/12a-H), 9.50 (s, 1H, 10-H), 9.57 (2s, 2H, 5/15-H), 10.71 (s, 1H, 20-H), 10.96 (s, 1H, 18a-H); ^{13}C NMR (125 MHz, $CDCl_3$): δ = 11.6 (C-13a), 11.8 (C-2a), 12.3 (C-17a), 17.6 (C-3b/C-12b), 18.7, 18.8 (C-7b/C-8b), 19.7, 19.8 (C-3a/C-12a), 20.2 (C-7a/C-8a), 94.3 (C-10), 95.5 (C-5), 102.2 (C-15), 103.7 (C-24), 108.0 (C-20), 131.5 (C-18), 133.7 (C-16), 133.8 (C-19), 134.7 (C-13), 135.1 (C-14), 135.4 (C-1), 135.5 (C-2), 137.6 (C-3), 137.7 (C-4), 137.8 (C-12), 138.6 (C-11), 145.1 (C-8), 145.5 (C-7), 153.1 (C-17), 154.8, 155.5 (C-6/C-9), 188.2 (C-18a); HRMS: m/z = 491.2936 (calcd 491.2937 for $C_{33}H_{37}N_3O$); UV/Vis (CH_2Cl_2): λ_{max} [nm] (lg ε) = 320 (4.22), 371 (4.39), 434 (4.53), 523 (3.91), 564 (3.87), 638 (3.54), 703 nm (3.39).

In the ^{1}H NMR spectrum of **3a** (Fig. 1) the signal of the inner NH protons appears at δ_H = −4.21, whereas the sharp signal

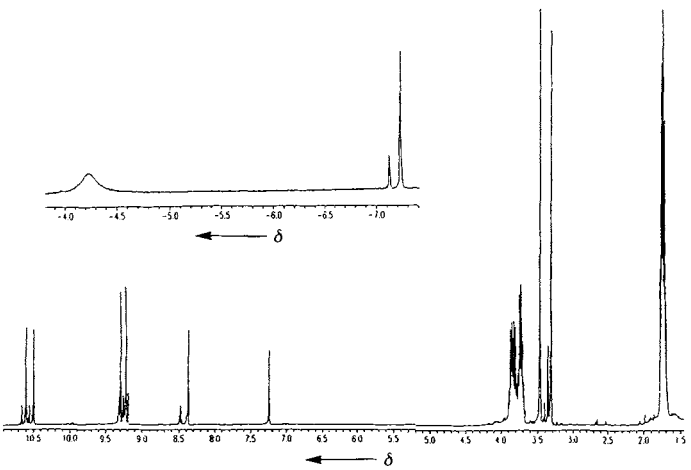

Fig. 1. ^{1}H NMR spectrum ($CDCl_3$) of **3a**.

corresponding to the inner CH group is observed at δ_H = −7.23. Thus the carbaporphyrins exhibit a ring current comparable to that of porphyrins, and there is no doubt that these compounds are 18π arenes. This is also confirmed by the low-field shifts of the signals corresponding to the *meso* protons (between δ_H = 9.1 and 10.7) and by those of the alkyl substituents. The chemical shifts of δ_H = −7.23 and −6.81 for the inner CH group are equivalent to values given by Lash et al. for

 © VCH Verlagsgesellschaft mbH, D-69451 Weinheim, 1996 0570-0833/96/3516-1821 $ 15.00+.25/0

the oxibenziporphyrin[13] and also to those of comparable benzo-condensed carbaporphyrins.[14]

The UV/Vis spectra (Fig. 2) include a characteristic Soret absorption[15] at 433 nm and also resemble the spectra of alkylporphyrins in the visible range. In distinct contrast to porphyrins, the carbaporphyrins do not display a red fluorescence at 366 nm, so that the yellow-brown target compounds look quite unspectacular on the TLC plate.

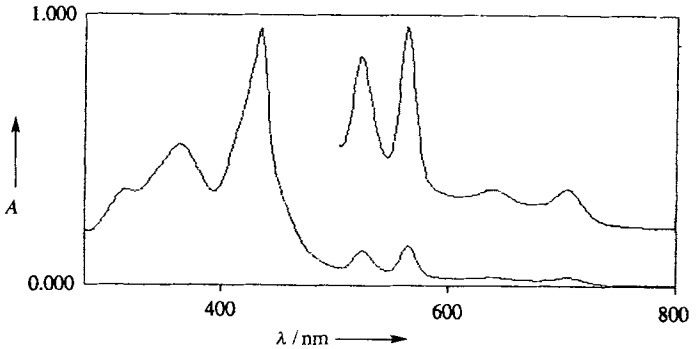

Fig. 2. UV/Vis spectrum of **3a**. A = absorption (arbitrary units).

While the carbaporphyrins appear uniform in the ^{13}C NMR spectra, in the 500 MHz ^1H NMR spectra each signal is accompanied by two weaker ones with identical multiplicity (ca. 13% und 1%). Since they correlate to the same carbon signals in the two-dimensional spectra (HMBC, HMQC), they provide the identical structure information. This confirms that the material is pure with respect to its constitution. Apparently either the three possible tautomers of the carbaporphyrin can be observed on the NMR time scale, or different stable conformations coexist due to steric strain resulting from the three inner protons. It has not yet been possible to achieve coalescence in high-temperature NMR experiments (deuteronaphthalene). In ^{15}N NMR experiments (50 MHz, $CDCl_3$, sample enriched with 5% ^{15}N) the chemical shifts of $\delta_N = 130.4$ and 130.9 (**3a**, NH_3 as a standard) for N-21 and N-23 indicate that the N–H units are located at least predominantly at these positions.[16]

Efforts to synthesize metal complexes (Zn^{2+}, Ni^{2+}) of the carbaporphyrins have not yet been successful. This can probably be attributed to the even lower CH acidity of the carbaporphyrins compared to that of the porphyrin isomers with an inverted pyrrole ring and an inner CH unit; chelates of the latter compounds having a carbon–metal bond are known.[5]

The carbaporphyrins are quite similar to porphyrins with regard to other chemical and spectroscopic properties. Hence carbaporphyrins could be suitable for special applications that require the spectroscopic properties of porphyrins but not their complexation behavior with certain metal ions.

The further development of the synthetic strategy introduced here for the preparation of carbaporphyrins to eventually prepare a tetracarbaporphyrin remains a great challenge and would link annulene and porphyrin chemistry. A dicarbaporphyrin would contain two inner CH units and a total of four inner protons. This would result not only in total cancellation of the tautomerism characteristic of porphyrins, but also in an increase of steric strain which should influence the aromaticity of the molecule. The effects of the inner methylene groups in a tetracarbaporphyrin are the subject of speculation.

Experimental Procedure

The hydroxyfulvenedialdehydes **1a** and **1b** were prepared according to the procedure published by Hafner et al. [9].

3a and **3b**: To a solution of **2a** (635 mg, 1 mmol) in anhydrous THF (80 mL) were added triethylamine (0.1 mL) and palladium on charcoal (200 mg, 10 % Pd, oxidic form, Merck). The mixture was hydrogenated for 3 h at atmospheric pressure. The catalyst was filtered off, and the filtrate was added to a solution of **1a** (150 mg, 1 mmol) or **1b** (164 mg, 1 mmol) in dichloromethane (750 mL). The orange-red solution was degassed with argon and charged with hydrogen bromide in glacial acetic acid (33 %, 1.5 mL) and glacial acetic acid (0.3 mL). The reaction mixture was stirred for 3 h with exclusion of light and neutralized with triethylamine (2.5 mL). DDQ (250 mg) was added and the mixture was stirred an additional 12 h. The solvent was evaporated and the residue purified by column chromatograpy on silica gel (eluent cyclohexane:ethyl acetate 3:1). Yield of **3a**: 37 mg (77.6 μmol, 7.8 %); yield of **3b**: 32 mg (65.2 μmol, 6.5 %) of **3b**. Both are dark green-brown microcrystalline compounds.

Received: December 27, 1995 [Z 8685 IE]
German version: *Angew. Chem.* **1996**, *108*, 1955–1957

Keywords: annulenes · fulvenes · porphyrinoids

[1] a) J. L. Sessler, S. J. Weghorn, Y. Hiseada, V. Lynch, *Chem. Eur. J.* **1995**, *1*, 56; b) J. L. Sessler, A. K. Burrell, *Top. Curr. Chem.* **1991**, *161*, 177, and references therein; c) T. Wessel, B. Franck, M. Möller, U. Rodewald, M. Läge, *Angew. Chem.* **1993**, *105*, 1201; *Angew. Chem. Int. Ed. Engl.* **1993**, *32*, 1148; d) J. L. Sessler, S. J. Weghorn, T. Morishima, M. Rosingana, V. Lynch, V. Lee, *J. Am. Chem. Soc.* **1992**, *114*, 8306; e) J. L. Sessler, T. D. Mody, D. A. Ford, V. Lynch, *Angew. Chem.* **1992**, *104*, 461; *Angew. Chem. Int. Ed. Engl.* **1992**, *31*, 452; f) M. Pohl, H. Schmickler, J. Lex, E. Vogel, *ibid.* **1991**, *103*, 1737 and **1991**, *30*, 1693; g) H. König, C. Eickmeier, M. Möller, U. Rodewald, B. Franck, *ibid.* **1990**, *102*, 1437 and **1990**, *29*, 1393; h) S. Beckmann, T. Wessel, B. Franck, W. Hönle, H. Borrmann, H. G. von Schnering, *ibid.* **1990**, *102*, 1439 and **1990**, *29*, 1395; i) M. Bröring, J. Jendrny, L. Zander, H. Schmickler, J. Lex, Y.-D. Wu, M. Nendel, J. Chen, D. A. Plattner, K. N. Houk, E. Vogel, *ibid.* **1995**, *107*, 2709 and **1995**, *34*, 2515.

[2] a) R. Bonnett, *Chem. Soc. Rev.* **1995**, 19, and references therein; b) B. Franck, A. Nonn, *Angew. Chem.* **1995**, *107*, 1941; *Angew. Chem. Int. Ed. Engl.* **1995**, *34*, 1795; c) R. K. Pandey, F.-Y. Shiau, T. J. Dougherty, K. M. Smith, *Tetrahedron* **1991**, *47*, 9571.

[3] J. L. Sessler, *Angew. Chem.* **1994**, *106*, 1410; *Angew. Chem. Int. Ed. Engl.* **1994**, *33*, 1348, and references therein; E. Vogel, M. Köcher, H. Schmickler, J. Lex, *ibid.* **1986**, *98*, 262 and **1986**, *25*, 257; J. L. Sessler, E. A. Brucker, S. J. Weghorn, M. Kisters, M. Schäfer, J. Lex, E. Vogel, *ibid.* **1994**, *106*, 2402 and **1994**, *33*, 2308.

[4] E. Vogel, M. Bröring, J. Fink, D. Rosen, H. Schmickler, J. Lex, K. W. K. Chan, Y.-D. Wu, M. Nendel, D. A. Plattner, K. N. Houk, *Angew. Chem.* **1995**, *107*, 2705; *Angew. Chem. Int. Ed. Engl.* **1995**, *34*, 2511.

[5] a) P. J. Chmielewski, L. Latos-Grazynski, K. Rachlewicz, T. Glowiak, *Angew. Chem.* **1994**, *106*, 805; *Angew. Chem. Int. Ed. Engl.* **1994**, *33*, 779; P. J. Chmielewski, L. Latos-Grazynski, *J. Chem. Soc. Perkin Trans. 2* **1995**, 503; b) H. Furuta, T. Asano, T. Ogawa, *J. Am. Chem. Soc.* **1994**, *116*, 767.

[6] E. Vogel, *Pure Appl. Chem.* **1993**, *65*, 143.

[7] K. Berlin, E. Breitmaier, *Angew. Chem.* **1994**, *106*, 229; *Angew. Chem. Int. Ed. Engl.* **1994**, *33*, 219; b) K. Berlin, E. Breitmaier, *ibid.* **1994**, *106*, 1356 and **1994**, *33*, 1246.

[8] K. Berlin, Dissertation, Universität Bonn, **1994**.

[9] K. Hafner, K. H. Vöpel, G. Ploss, C. König, *Liebigs Ann. Chem.* **1963**, *661*, 52.

[10] K. Hafner, H. E. A. Kramer, H. Musso, G. Ploss, G. Schulz, *Chem. Ber.* **1964**, *97*, 2066.

[11] J. L. Sessler, M. R. Johnson, V. Lynch, *J. Org. Chem.* **1987**, *52*, 4394.

[12] I thank M. Gondorf, R. Hartmann, T. Schönemeier, and C. Steinbeck for carrying out NMR experiments, and G. Eckhardt and his co-workers for recording the mass spectra.

[13] T. D. Lash, *Angew. Chem.* **1995**, *107*, 2703; *Angew. Chem. Int. Ed. Engl.* **1995**, *34*, 2533.

[14] K. Berlin, C. Steinbeck, E. Breitmaier, *Synthesis* **1996**, *336*.

[15] J. L. Soret, *C. R. Hebd. Seances Acad. Sci* **1883**, *97*, 1207.

[16] ^{15}N NMR chemical shifts of porphyrins: H. J. C. Yeh, M. Sato, I. Morishima, *J. Magn. Res.* **1977**, *26*, 365; C. S. Irving, A. Lapidot, *J. Chem. Soc. Chem. Commun.* **1977**, 184.

 © VCH Verlagsgesellschaft mbH, D-69451 Weinheim, 1996 0570-0833/96/3516-1822 $ 15.00+.25/0

Rhodium(I)-Catalyzed Cycloaromatization of Acyclic 3-Ene-1,5-diynes**

Kouichi Ohe,* Masa-aki Kojima, Koji Yonehara, and Sakae Uemura*

Calicheamicins, esperamicin, dynemicin A, and the neocarzinostatin chromophore belong to a rapidly growing class of anticancer antibiotics from bacterial sources. Their characteristic enediyne subunit, which acts as a "warhead" and induces DNA cleavage, is proposed to be the source of their remarkable antitumor activity.[1] The fascinating mode of the action can be attributed to two types of cycloaromatization, both of which proceed via diradical intermediates (Scheme 1). One is the generation of 1,4-didehydrobenzene from (*Z*)-3-hexene-1,5-diyne (**1**) (Bergman reaction);[2] the other is the cycloaromatization of (*Z*)-1,2,4-heptatrien-6-yne (**2**) producing α,3-didehydrotoluene (Myers reaction).[3] Acyclic enediynes like **1** cyclize only at high temperatures (≈200 °C) and are otherwise quite stable. In contrast, acyclic allene-enynes like **2** undergo facile cycloaromatization at much lower temperatures (≈40 °C).[3a, c] Similar reactions of (*Z*)-1-oxa-2,4-heptatrien-6-yne as an isostructure of **2** have been reported by Moore et al.[4] and by Saito et al.[5] We envisaged a catalytic cycloaromatization of the acyclic enediyne via an intermediary vinylidene–metal complex **3** (Scheme 2).[6]

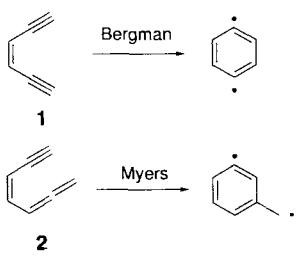

Scheme 1. Bergman and Myers cycloaromatizations.

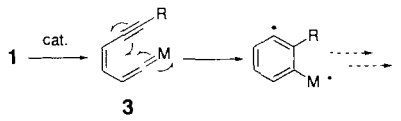

Scheme 2. Catalytic cycloaromatization of **1**. cat. = transition metal catalyst.

In the course of our study Finn and Wang have reported the cycloaromatization of the isolated vinylidene–ruthenium complex based on the same concept.[7] Here we describe the first rhodium-catalyzed cycloaromatization of an acyclic enediyne.

We examined the reaction of (*Z*)-3-dodecene-1,5-diyne (**1a**) with a coordinatively unsaturated rhodium(I) complex suitable for generating a vinylidene complex.[8] The treatment of **1a** with 10 mol% $[RhCl(iPr_3P)_2]$[9] in the presence of ten equivalents of 1,4-cyclohexadiene as a hydrogen donor in cyclohexane at 80 °C afforded an unexpected product, 1-phenylhex-2-ene (**4a**) (*E*/*Z* = 80/20) in 20% yield (Scheme 3). When 5 mol% $[CpRuCl(PPh_3)_2]$ and NH_4PF_6[10] were used, no reaction took place and **1a** was recovered intact. Even in the absence of 1,4-cyclohexadiene the rhodium(I) complex catalyzed the reaction of **1a** to give **4a** in 22% yield with the same ratio of isomers. Apparently two hydrogens on the alkyl group of **1a** migrate to the phenyl ring. Although the reaction of **1a** was complete, **4a**

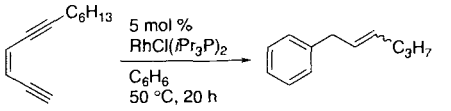

Scheme 3. Synthesis of **4a**. In the presence of Et_3N **4a** was obtained in 58% yield (*E*/*Z* = 86/14).

was obtained in low yield because of undesired polymerization. Extensive efforts to improve the yield were made and the addition of triethylamine was found to be effective. Thus, the reaction of **1a** with 5 mol% $[RhCl(iPr_3P)_2]$ and Et_3N in benzene at 50 °C under argon was complete within 20 h and gave **4a** in 58% yield (*E*/*Z* = 86/14) (see Experimental Procedure).

The results of the cycloaromatization of a variety of enediynes under the optimum conditions are listed in Table 1. In all cases

Table 1. Rhodium(I)-catalyzed cycloaromatization of enediynes [a].

Enediyne	Product	Yield [%] (*E*/*Z*)
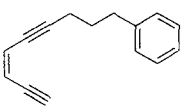 **1b**	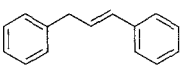 **4b**	68 (100/0)
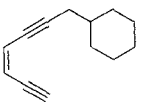 **1c**	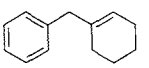 **4c**	64
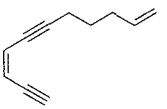 **1d**	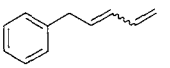 **4d**	10 (88/12)
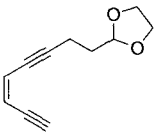 **1e**	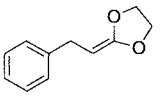 **4e**	52 [b]
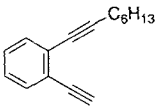 **1g**	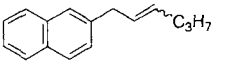 **4g**	46 (86/14)

[a] Reaction conditions: 5 mol% $[RhCl(iPr_3)_2]$ and Et_3N (70 μL) in C_6H_6 (4 mL) at 50 °C for 20 h. [b] Yield as the hydrolyzed product $PhCH_2CH_2CO_2CH_2CH_2OH$ after purification of **4e** by column chromatography on silica gel.

the products obtained have a β,γ double bond in the side chain attached to the benzene ring formed. The cyclizations of **1b** and **1c** led to (*E*)-1,3-diphenylpropene (**4b**) and **4c** in yields of 68 and 64%, respectively. Enediyne **1d** bearing an isolated double bond gave diene **4d** in low yield (10%), although **1d** was completely consumed. The formation of 2-alkylidene-1,3-dioxolane **4e** from **1e** demonstrated the tolerance of oxygen functionality, but cycloaromatization of **1f** bearing a cyano group did not proceed

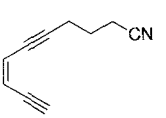

[*] Dr. K. Ohe, Prof. Dr. S. Uemura, M. Kojima, K. Yonehara
Department of Energy and Hydrocarbon Chemistry
Graduate School of Engineering, Kyoto University
Sakyo-ku, Kyoto 606-01 (Japan)
Telefax: Int. code +(75)753-5697

[**] This work was supported by a Grant-in-Aid for Scientific Research from the Ministry of Education, Science and Culture, Japan.

probably due to the strong coordination of the cyano group to rhodium. Similarly, 1-(1-octynyl)-2-ethynylbenzene (**1g**) underwent cyclization to give 2-(2-hexenyl)naphthalene (**4g**) (E/Z = 86/14) in 46% yield.

A plausible catalytic cycle for this reaction is shown in Scheme 4. Triethylamine seems to facilitate the rapid formation

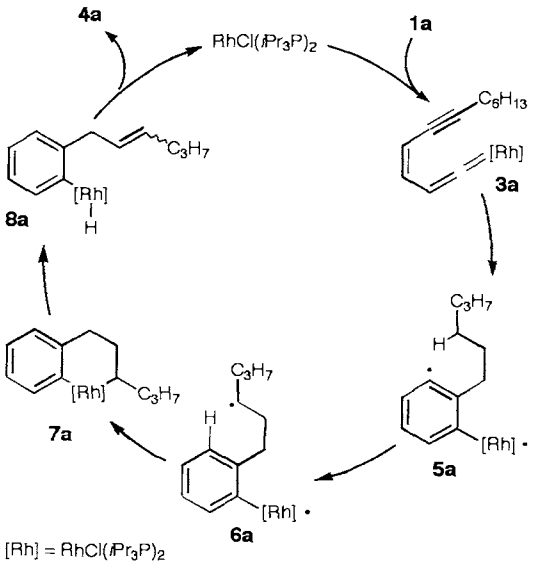

Scheme 4. Postulated mechanism for the catalytic cycloaromatization of **1a** to give **4a**.

of a vinylidene–rhodium complex [RCH=C=Rh] from an alkynyl(hydrido)–rhodium complex [RC≡CRhH].[11] Thus, this reaction might proceed via the vinylidene–rhodium complex **3a**, which, in analogy to the Myers reaction, cyclizes to afford the 1,4-diradical **5a**. The intramolecular 1,5-hydrogen shift from the hexyl chain to the benzenoid radical takes place to give the intermediate **6a**.[12] Two pathways from **6a** to **8a** might be accessible. The two radical centers in **6a** could couple to form **7a**; subsequent *syn* elimination of the β-hydride ($\rightarrow$ **8a**) followed by reductive elimination would then give **4a**. Alternatively, a second 1,5-hydrogen shift in **6a** from the alkyl chain to the rhodium radical could occur directly to give **8a**, which would lead to **4a**. It is not clear at present by which mechanism the reaction proceeds.

The formation of **3a** was supported by the fact that the reaction of 1-deuterio-3-dodecene-1,5-diyne (**1aD**) (97% deuterium incorporation) afforded 1-(3-deuteriophenyl)hex-2-ene (**4aD**)[15] in 58% yield (52% deuterium incorporation) (Scheme 5).[16] In another experiment diradical **5a** was intercepted intermolecularly with hydrogens from 1,4-cyclohexadiene. In the presence of 25 equiv 1,4-cyclohexadiene, the reaction of **1a** gave 1-hexylbenzene (6%) and **4a** (5%) in addition to recovered **1a** (23%).[17] Interestingly, the reaction of **1a** with two equivalents of ethyl acrylate afforded the (*E*) olefin **9** stereospecifically in 5% yield

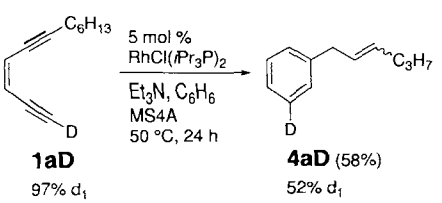

Scheme 5. Conversion of **1aD** into **4aD**. MS4A = molecular sieves 4 Å.

together with **4a** in 38% yield (Scheme 6). The formation of **9** is explained by the addition of the benzenoid radical **5a** to ethyl acrylate producing the 1,6-diradical **10**; abstraction of two vicinal hydrogens of the hexyl group then yields **9**. The intermediacy of the metallacycle **7a** was supported by the reaction of **1h** with a stoichiometric amount of [RhCl(iPr$_3$P)$_2$] (Scheme 7). Fluorene (**12**) formed as a result of reductive elimination from metallacycle **11**, which is analogous to **7a**.

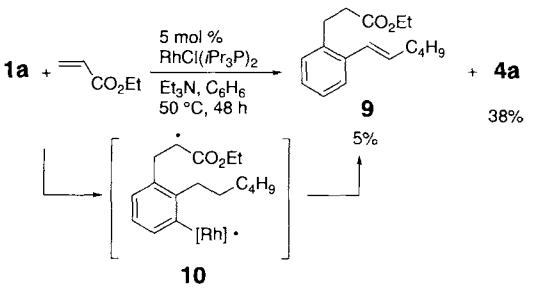

Scheme 6. Cyclization of **1a** in the presence of ethyl acrylate. Only the (*E*) isomer of **9** was obtained.

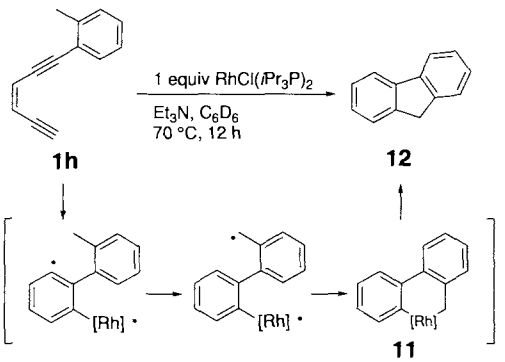

Scheme 7. Cyclization of **1h** leading to fluorene (**12**) (in quantitative yield).

We have demonstrated the first catalytic cycloaromatization of an enediyne via a vinylidene–rhodium intermediate. It should be noted that the transition metal can act as a trigger for the cycloaromatization of the acyclic enediyne. Applications of this reaction will be reported in due course.

Experimental Procedure

To a solution containing [RhCl(iPr$_3$P)$_2$] prepared in situ from [{RhCl(C$_8$H$_{14}$)$_2$}$_2$] (0.007 g, 0.01 mmol) and iPr$_3$P (10 μL, 0.05 mmol) in benzene (1 mL) were added Et$_3$N (70 μL, 0.5 mmol) and a solution of (*Z*)-3-dodecene-1,5-diyne (**1a**) (0.064 g, 0.4 mmol) in benzene (3 mL). The reaction mixture was stirred under argon at 50 °C for 20 h. Filtration through Florisil and further purification by column chromatography on SiO_2 eluting with hexane afforded 0.037 g (0.23 mmol, 58%) of 1-phenylhex-2-ene (**4a**) (E/Z = 86/14) as a colorless liquid. ^{1}H NMR (270 MHz, $CDCl_3$, 25 °C, TMS): *E* isomer: δ = 0.90 (t, J = 7.3 Hz, 3H), 1.38 (tq, J = 7.3, 7.3 Hz, 2H), 1.97–2.04 (m, 2H), 3.33 (d, J = 5.1 Hz, 2H), 5.50 (dt, J = 15.1, 5.1 Hz, 1H), 5.58 (dt, J = 15.1, 6.2 Hz, 1H), 7.17–7.20 (m, 3H, *o*- and *p*-Ar), 7.25–7.31 (m, 2H, *m*-Ar); *Z* isomer: δ = 0.96 (t, J = 7.3 Hz, 3H), 1.3–1.5 (m, 2H), 2.1–2.2 (m, 2H), 3.40 (d, J = 5.9 Hz, 2H), 5.5–5.6 (m, 2H), 7.1–7.25 (m, 3H), 7.25–7.30 (m, 2H); ^{13}C NMR (67.5 MHz, $CDCl_3$, 25 °C, TMS): *E* isomer: δ = 14.1, 22.9, 35.0, 39.4, 126.1, 128.6, 128.8, 129.2, 132.2, 141.6; *Z* isomer: δ = 14.2, 23.2, 33.8, 36.5, 126.0, 128.5, 128.7, 131.4, 133.0, 142.6. Anal. calcd for $C_{12}H_{16}$: C 89.94; H 10.06; found: C 89.65, H 10.26.

Received: December 28, 1995
Revised version: February 23, 1996 [Z8688IE]
German version: *Angew. Chem.* **1996**, *106*, 1959–1962

Keywords: catalysis · cycloaromatizations · enediynes · rhodium compounds

[1] For reviews, see: a) K. C. Nicolaou, W.-M. Dai, *Angew. Chem.* **1991**, *103*, 1453; *Angew. Chem. Int. Ed. Engl.* **1991**, *30*, 1387; b) K. C. Nicolaou, A. L. Smith, E. W. Yue, *Proc. Natl. Acad. Sci. USA* **1993**, *90*, 5881; c) R. Gleiter, D. Kratz, *Angew. Chem.* **1993**, *105*, 884; *Angew. Chem. Int. Ed. Engl.* **1993**, *32*, 842; d) M. E. Maier, *Synlett* **1995**, 1; e) J. W. Grissom, G. U. Gunawardena, D. Klingberg, D. Huang, *Tetrahedron* **1996**, *52*, 6453.

[2] a) R. R. Jones, R. G. Bergman, *J. Am. Chem. Soc.* **1972**, *94*, 660; b) R. G. Bergman, *Acc. Chem. Res.* **1973**, *6*, 5; c) T. P. Lockhart, P. B. Comita, R. G. Bergman, *J. Am. Chem. Soc.* **1981**, *103*, 4082; d) T. P. Lockhart, R. G. Bergman, *ibid.* **1981**, *103*, 4091.

[3] a) A. G. Myers, E. Y. Kuo, N. S. Finney, *J. Am. Chem. Soc.* **1989**, *111*, 8057; b) R. Nagata, H. Yamanaka, E. Okazaki, I. Saito, *Tetrahedron Lett.* **1989**, *30*, 4995; c) A. G. Myers, P. S. Dragovich, E. Y. Kuo, *J. Am. Chem. Soc.* **1992**, *114*, 9369; d) J. W. Grissom, D. Huang, *Angew. Chem.* **1995**, *107*, 2196; *Angew. Chem. Int. Ed. Engl.* **1995**, *34*, 2037, and references therein.

[4] a) L. D. Foland, J. O. Karlsson, S. T. Perri, R. Schwabe, S. L. Xu, S. Patil, H. W. Moore, *J. Am. Chem. Soc.* **1989**, *111*, 975; b) R. W. Sullivan, V. M. Coghlan, S. A. Munk, M. W. Reed, H. W. Moore, *J. Org. Chem.* **1994**, *59*, 2276.

[5] a) K. Nakatani, S. Isoe, S. Maekawa, I. Saito, *Tetrahedron Lett.* **1994**, *35*, 605; b) K. Nakatani, S. Maekawa, K. Tanabe, I. Saito, *J. Am. Chem. Soc.* **1995**, *117*, 10635.

[6] This work was reported in part at the 69th Annual Meeting of the Chemical Society of Japan, Kyoto (Japan), March 27, 1995; Abstract Vol. II, p. 1131.

[7] Y. Wang, M. G. Finn, *J. Am. Chem. Soc.* **1995**, *117*, 8045.

[8] a) F. J. G. Alonso, A. Höhn, J. Wolf, H. Otto, H. Werner, *Angew. Chem.* **1985**, *97*, 401; *Angew. Chem. Int. Ed. Engl.* **1985**, *24*, 406; b) R. Wiedemann, J. Wolf, H. Werner, *Angew. Chem.* **1995**, *107*, 1359; *Angew. Chem. Int. Ed. Engl.* **1995**, *34*, 1244.

[9] This rhodium complex is known to be dimeric; see for example: a) H. Werner, J. Wolf, A. Höhn, *J. Organomet. Chem.* **1985**, *287*, 395; b) P. Binger, J. Haas, G. Glaser, R. Goddard, C. Krüger, *Chem. Ber.* **1994**, *127*, 1927.

[10] M. I. Bruce, *Chem. Rev.* **1991**, *91*, 197.

[11] It is known that the addition of pyridine shifts the equilibrium between an alkyne complex [(RC≡CH)Rh] and an alkynyl(hydrido) complex [RC≡CRhH], which is converted to a vinylidene complex: J. Wolf, H. Werner, O. Serhadli, M. L. Ziegler, *Angew. Chem.* **1983**, *95*, 428; *Angew. Chem. Int. Ed. Engl.* **1983**, *22*, 414. However, pyridine deterred the present reaction. *N,N*-Diisopropylethylamine and tetramethylethylenediamine were moderately effective and after two days gave **4a** in 42 and 23% yield, respectively.

[12] The heat of the formation of diradical **6a** is estimated to be about 16 kcal mol^{-1} less than that of **5a** [13]. This value corresponds to the difference in the strength of the secondary alkyl (95 kcal mol^{-1}) and aryl C–H (110 kcal mol^{-1}) bonds. It is less likely that the rhodium center abstracts hydrogen before the benzenoid radical does, because the bond dissociation energy of a secondary C–H bond is greater than that of a Rh–H bond (ca. 54–64 kcal mol^{-1}) [14].

[13] N. S. Issacs, *Physical Organic Chemistry*, Wiley, New York, **1987**, p. 24.

[14] S. J. A. Martinho, J. L. Beauchamp, *Chem. Rev.* **1990**, *90*, 629.

[15] The incorporation of deuterium at the *meta* position was confirmed by comparison of the intensity of ^{1}H NMR signals of the *meta* protons (δ = 7.23–7.32) with those of the *ortho* and *para* protons (δ = 7.12–7.22) in CD_2Cl_2. The ratio of the integrations of the signals in these two regions is 1.48:3.0, which means that one of the *meta* positions had 52% deuterium incorporation. No incorporation of deuterium in the side chain was apparent. The observation of two isotope peaks for [M^+] at m/z = 160 (22.8%) and 161 (24.0%) in the EI mass spectrum (70 eV) of **4aD** also supports the assignment of the product (51.3% deuterium incorporation).

[16] In the absence of molecular sieves 4 Å no incorporation of deuterium into **4a** was observed and recovered **1aD** had a reduced deuterium content. This is probably due to rapid D/H exchange during the isomerization between the alkynyl(hydrido) complex and the vinylidene complex owing to trace amounts of H_2O.

[17] The reaction of **1a** (0.4 mmol) was carried out with 1,4-cyclohexadiene (10 mmol) in benzene (3 mL) in the presence of 5 mol% Rh catalyst and Et_3N (0.5 mmol) at 50 °C for 30 h. The use of greater excesses of 1,4-cyclohexadiene deterred the cyclization.

Ferric Wheels and Cages: Decanuclear Iron Complexes with Carboxylato and Pyridonato Ligands

Cristiano Benelli, Simon Parsons, Gregory A. Solan, and Richard E. P. Winpenny*

The study of polymetallic complexes has recently begun to lead to not only fascinating structures but also interesting properties. In particular the magnetic relaxation and hysteresis effects first shown for a dodecanuclear manganese cluster[1] and recently found in deca-[2] and tetranuclear[3] manganese species are novel and have implications for fundamental science and potential future applications. To understand and exploit these phenomena more examples are required, and therefore the greatest need in this area remains the design of reliable synthetic routes to produce nanoscale clusters with the potential for high-spin ground states.

We have developed the reaction of metal carboxylates with pyridone ligands leading to incomplete replacement of the carboxylates and large polynuclear arrays of copper[4] and nickel.[5, 6] We hoped that this strategy would prove general for the 3d metals, but on examination of the reactivity of $[Fe_3O(O_2CMe)_6(H_2O)_3]Cl$ with pyridones we isolated solids, which on dissolution in MeOH led to the isolation of a yellow powder that analyzed as $[Fe(OMe)_2(O_2CMe)]$. This could be recrystallized from MeOH/THF in low yield, and X-ray structure determination[7] revealed the compound to be complex **1**, which is very similar to the "ferric wheel" **2** reported by Lippard

$[\{Fe(OMe)_2(O_2CMe)\}_{10}]$ **1** $[\{Fe(OMe)_2(O_2CCH_2Cl)\}_{10}]$ **2**

and co-workers.[8] A centrosymmetric cyclic decanuclear array of iron atoms is held together by twenty μ_2-OMe ligands and ten 1,3-bridging acetato ligands (Fig. 1).

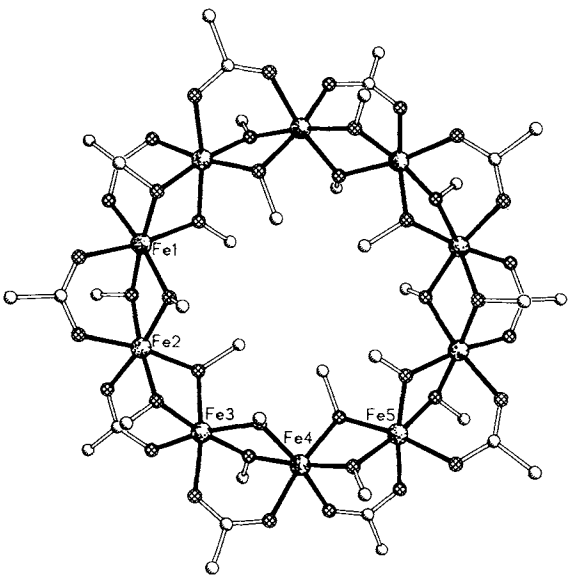

Fig. 1. The structure of the cyclic Fe_{10} complex **1** in the crystal.

[*] Dr. R. E. P. Winpenny, Dr. S. Parsons, Dr. G. A. Solan
Department of Chemistry, The University of Edinburgh
West Mains Road, Edinburgh, EH9 3JJ (UK)
Fax: Int. code +(131)667-4743
Prof. C. Benelli
Dipartimento di Chimica, Universita degli Studi di Firenze (Italy)

[**] This work was supported by the Engineering and Physical Sciences Research Council and the Leverhulme Trust.

Yellow powders with identical elemental composition can be produced from many reactions involving iron(III) and acetate in methanol, for example by mixing ferric chloride with sodium acetate in this solvent, or by refluxing a solution of $[Fe_3O(O_2CMe)_6(H_2O)_3]Cl$ in methanol. Whether the unrecrystallized powder contains exclusively cyclic oligomers is unclear; unfortunately powder diffraction studies failed as the powder is amorphous. We suspect that a polymeric material may be present and that cyclization occurs during crystallization; however, mass spectrometric studies of the powder show an intense high-mass peak at m/z 1710 corresponding to $[\mathbf{1} - O_2CMe]^+$. Only one significant peak is observed at a mass above that of **1**, at m/z 1831, which arises from $[\mathbf{1} + O_2CMe]^+$. This cut-off in the mass spectrum may be coincidental.

The magnetic behavior of the yellow powder is similar to that reported for **2**[8] down to about 50 K, but below this temperature the magnetic susceptibility increases dramatically. Such behavior is not compatible with the existence of rings with an even number of ions having a magnetic moment if only one type of magnetic interaction is present, as would be expected from the molecular structure of **1**. Probably the powder contains some oligomeric impurities that prevent detailed analysis of the low-temperature data at this time. Similar yellow powders result from reactions of other iron carboxylates in MeOH; however, their exact nature is currently unclear.

To synthesize acyclic polynuclear iron complexes we have utilized other precursors and other solvents. The salt $[NEt_4]_2[Fe_2OCl_6]$[9] has proved ideal for such studies.[10, 11] Dissolution of this salt with two molar equivalents of sodium benzoate in acetonitrile, followed by addition of three equivalents of sodium 6-chloro-2-pyridonate, Na(chp), gives a red solution, which we believe contains a dinuclear species of approximate formula $[Fe_2O(O_2CPh)_2(chp)_2(CH_3CN)_4]$.[12] Filtration of the solution followed by mixing with acetone gives, after one week, orange-brown crystals suitable for diffraction studies.[7] The structure in the crystal (Fig. 2) corresponds to a decanuclear iron complex capped by two sodium atoms with the stoichiometric formula **3**.

$[Fe_{10}Na_2(\mu_4\text{-}O)_2(\mu_3\text{-}O)_4(\mu_3\text{-}OH)_4(O_2CPh)_{10}(chp)_6(H_2O)_2(Me_2CO)_2]$ **3**

The metal atoms in **3** are held together by a combination of μ_4-oxo groups each bridging three Fe atoms and one Na atom, μ_3-oxo and μ_3-hydroxo units bridging exclusively Fe centers,

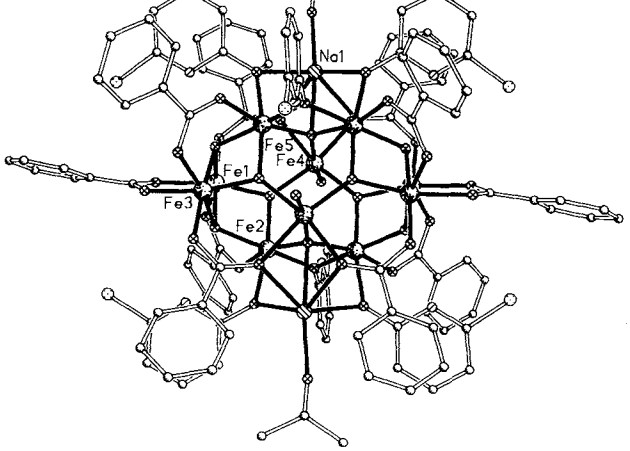

Fig. 2. The structure of the $Fe_{10}Na_2$ cage complex **3** in the crystal.

1,1′,3-bridging and 1,3-bridging benzoates, and chp ligands bridging in a μ_2-fashion through the exocyclic O atom. Terminally bound water molecules are attached to Fe4 and Fe4a, and acetone molecules are bound to the Na atoms. The iron–oxo core can be considered to contain two distorted Fe_6O_6 hexagonal prisms sharing one "square" face containing Fe4, O4, Fe4a, and O4a (Fig. 3). Similar hexagonal prisms are found as segments of other iron–oxo complexes such as $[Fe_{11}(O)_6(OH)_6(O_2CPh)_{15}]$[13] and $[Fe_{16}CoO_{10}(OH)_{10}(O_2CPh)_{20}]$;[14] however, in these complexes the hexagonal prisms do not share faces. Both of these complexes were also synthesized in CH_3CN, starting with $[NEt_4]_2[Fe_2OCl_6]$ and iron benzoate, respectively,[13, 14] possibly indicating an important role for this solvent in the formation of such cage structures. We have not yet been able to produce **3** from the reaction of preformed iron benzoate, for example $[Fe_3O(O_2CPh)_6(H_2O)_3]Cl$ with pyridonate precursors.

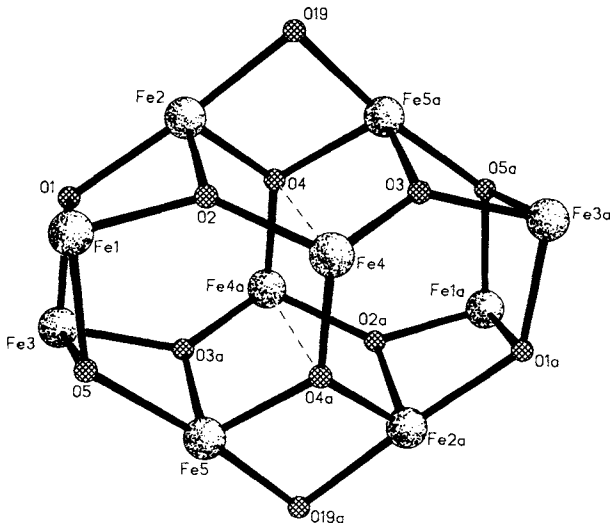

Fig. 3. The central $Fe_{10}O_{12}$ core of **3** showing the atom numbering scheme. Only μ_4-oxo, μ_3-oxo, and μ_3-hydroxo groups are shown. Selected bond angles [°]: Fe2-O1-Fe3 128.7, Fe2-O1-Fe1 91.4, Fe2-O1-Fe1 97.4, Fe1-O2-Fe4 130.2, Fe1-O2-Fe2 100.8, Fe2-O2-Fe4 127.0, Fe-4-O3-Fe3a 130.2, Fe4-O3-Fe5a 126.9, Fe3a-O3-Fe5a 100.6, Fe4a-O4-Fe5a 126.8, Fe4a-O4-Fe2 129.0, Fe2-O4-Fe5a 100.6 (average esd 0.3).

Cluster **3** contains three chemically distinct octahedral iron centers, all of which are bound exclusively to oxygen donors. The first group comprises Fe4 and Fe4a, and they are bonded to oxygen atoms from two benzoato ligands, two μ_3-oxo groups, one μ_4-oxo group, and one terminal aqua ligand. The second group consists of Fe1, Fe1a, Fe3, and Fe3a, each of which is bonded to three benzoato ligands and one μ_3-oxo and two μ_3-OH units. The remaining iron atoms, Fe2, Fe2a, Fe5, and Fe5a, are bonded to one benzoate oxygen, two μ_2-oxygens from chp, and one of each of μ_3-oxo, μ_4-oxo, and μ_3-OH units. The sodium sites are six-coordinate with O-donors derived from one μ_4-oxo, two μ_2-chp ligands, two benzoate groups, and a terminal acetone ligand.

The assignment of groups as oxo or hydroxo was made on the basis of bond length considerations. Fe–O(hydroxo) bonds are known to be significantly longer than Fe–O(oxo) bonds, and in **3** we find that Fe–O distances to such groups fall into two distinct regions. Fe–O(oxo) bonds vary from 1.900 to 1.951 Å, while Fe–O(hydroxo) bonds span the range 2.017 to 2.135 Å (average estimated standard deviation 0.005 Å). The shortest Fe···Fe contact found in **3** is 2.974(2) Å between Fe3 and Fe5. Further evidence of the identity of the O atoms comes from their

 © VCH Verlagsgesellschaft mbH, D-69451 Weinheim, 1996 0570-0833/96/3516-1826 $ 15.00+.25/0

coordination geometry; the μ_3-oxo groups are planar while the μ_3-hydroxides are not. The μ_4-oxo groups have a trigonal-pyramidal geometry and are planar with respect to the three nearest Fe atoms; a Na atom occupies an apical position.

The temperature dependence of the magnetic susceptibility χ_m of **3** was measured between 260 and 2.5 K. The values of χ_m were calculated on the basis of the elemental analysis of the crystals used (C,H, N, Fe), which indicate that the sample has desolvated; hence the molecular weight is about 2900 u rather than 3347 u as indicated in the crystal structure. The observed high-temperature value of the product $\chi_m T$ of approximately 35 emu K mol^{-1} is lower than that calculated for ten non-interacting $S = 5/2$ centers with a g-value of 2 (calcd 43.75 emu K mol^{-1}) (Fig. 4 top). However, the value of $\chi_m T$ increases steadily down to 40 K, where a plateau is reached at a $\chi_m T$ value of roughly 64 emu K mol^{-1}. Such a value is close to that expected for an $S = 11$ spin state (calcd $\chi_m T =$ 66 emu K mol^{-1}). Below 20 K a slight fall in $\chi_m T$ is observed, possibly due to zero-field splitting within the spin ground state or due to intermolecular coupling. This decrease is largely independent of the magnitude of the external magnetic field. In an attempt to clarify the nature of the spin ground state the magnetization of **3** was measured at 2.26 K in an external magnetic field from 0.5 to 7 T. The magnetization shows an increase with the field up to 21.85 μ_B per molecule (Fig. 4 bottom). For a ground state with $S = 11$ a value of 22 μ_B is expected.

A high-spin ground state for **3** could be predicted based on known magneto-structural correlations. Previous work[15] demonstrates that antiferromagnetic exchange between Fe^{III} centers is stronger when mediated by oxo rather than hydroxo groups. This allows us to assume that antiferromagnetic exchange through O2, O3, and O4, and their symmetry equivalents will be dominant, and exchange through O1 and O5 will be of secondary importance (Fig. 3). Secondly, we can assume that

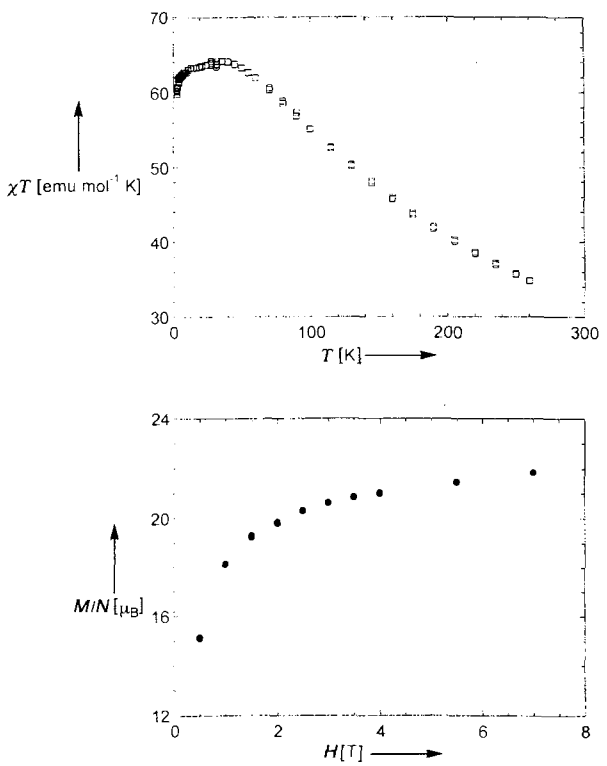

Fig. 4. Top: The temperature dependence of $\chi_m T$ for **3**. Bottom: Magnetization M of **3** at 2.26 K against magnetic field strength. M/N = reduced magnetic moment.

the magnitude of the exchange interaction will be related to the Fe-O-Fe angles at these bridging oxo units; the more obtuse the angle the larger the antiferromagnetic exchange.[16] All the most obtuse angles at oxo groups involve either Fe4 or Fe4a. For example, at O4a the two angles involving Fe4 are roughly 130°; the Fe2a-O4a-Fe5 angle is 100.6(3)°. Therefore we assume the strongest antiferromagnetic exchange interactions within this Fe_3 triangle are between Fe4 $\cdots$ Fe2a and Fe4 $\cdots$ Fe5. Similar considerations lead to all the largest antiferromagnetic exchange interactions coupling Fe4 and Fe4a antiparallel with the other eight spin centers in the molecule.

Although the magnetic susceptibility and magnetization experiments are in good agreement with an $S = 11$ ground state, on the basis of these results we cannot rule out the possibility of a ground state with a higher spin value. The magnetization curve did not reach a saturation plateau and, in any case, in the presence of significant zero-field splitting of ground states with a high spin value the magnetic susceptibility might not attain the expected upper limit. The spin value of the ground state is far from that expected in the presence of simple antiferromagnetic exchange (which would give $S = 15$ and $S = 10$ for a total of six and four $S = 5/2$ centers, respectively). Therefore we believe that some level of spin frustration must exist to explain these preliminary results. Confirmation of the exact spin ground state will require further experiments which we are presently undertaking.

Experimental Procedure

1·2THF: A solution of $[Fe_3O(O_2CMe)_6(H_2O)_3Cl]\cdot 5H_2O$ [17] (0.63 g, 0.9 mmol) in MeOH (30 mL) was stirred at reflux for 3 h to give a yellow precipitate (0.276 g). Yield: 18%. The yellow solid was extracted with a Soxhlet apparatus (40 mL MeOH, 10 mL THF) for 12 h, and the resulting solution was allowed to stand for several weeks to give pale yellow crystals of **1**·2THF. Both the yellow precipitate and crystals analyze satisfactorily for $[\{Fe(OMe)_2(O_2CMe)\}_{10}]$. FAB-MS: m/z: 1832 $[Fe_{10}(OMe)_{20}(O_2CMe)_{11}]^+$, 1739 $[Fe_{10}(OMe)_{19}(O_2CMe)_{10}]^+$, 1711 $[Fe_{10}(OMe)_{20}(O_2CMe)_9]^+$, 1386 $[Fe_9(OMe)_{19}(O_2CMe)_5]^+$, 1357 $[Fe_9(OMe)_{18}(O_2CMe)_5]^+$, 1208 $[Fe_9(OMe)_{19}(O_2CMe)_2]^+$, 1180 $[Fe_9(OMe)_{18}(O_2CMe)_2]^+$, 1031 $[Fe_6(OMe)_{13}(O_2CMe)_5]^+$, 1003 $[Fe_6(OMe)_{12}(O_2CMe)_5]^+$, 854 $[Fe_6(OMe)_{11}(O_2CMe)_3]^+$, 826 $[Fe_5(OMe)_{10}(O_2CMe)_4]^+$, 675 $[Fe_5(OMe)_{11}]^+$.

3·8MeCN·2Me_2CO: A solution of $[NEt_4]_2[Fe_2OCl_6]$ (0.25 g, 0.4 mmol) and $Na(O_2CPh)$ (0.12 g, 0.8 mmol) in MeCN (30 mL) was stirred for 15 min before Na(chp) (0.19 g, 1.2 mmol, 3 equiv) was added. The resultant red solution was stirred for 2 h then filtered and acetone (4 mL) was added. After one week at 253 K orange-brown rhombic prisms of **3**·8MeCN·2Me_2CO had formed. Yield: 15%. The sample analyzed well for $[Fe_{10}Na_2(\mu_4\text{-}O)_2(\mu_3\text{-}O)_4(\mu_3\text{-}OH)_4(O_2CPh)_{10}(chp)_6(H_2O)_2(Me_2CO)_2]\cdot$MeCN. No significant peaks were observed in the FAB mass spectrum.

Received: January 15, 1996 [Z 8726 IE]
German version: *Angew. Chem.* **1996**, *108*, 1967–1970

Keywords: complexes with oxygen ligands · iron compounds · magnetic properties

[1] a) R. Sessoli, D. Gatteschi, A. Caneschi, M. A. Novak, *Nature* **1993**, *365*, 141; b) H. J. Eppley, H.-L. Tsai, N. de Vries, K. Folting, G. Christou, D. N. Hendrickson, *J. Am. Chem. Soc.* **1995**, *117*, 301.
[2] D. P. Goldberg, A. Caneschi, S. J. Lippard, *J. Am. Chem. Soc.* **1993**, *115*, 9299.
[3] M. W. Wemple, D. Adams, K. S. Hagen, K. Folting, D. N. Hendrickson, G. Christou, *J. Chem. Soc. Chem. Commun.* **1995**, 1591.
[4] A. J. Blake, C. M. Grant, C. I. Gregory, S. Parsons, J. M. Rawson, D. Reed, R. E. P. Winpenny, *J. Chem. Soc. Dalton Trans.* **1995**, 195.
[5] A. J. Blake, C. M. Grant, S. Parsons, J. M. Rawson, R. E. P. Winpenny, *J. Chem. Soc. Chem. Commun.* **1994**, 2363.
[6] A. J. Blake, E. K. Brechin, A. Codron, R. O. Gould, C. M. Grant, J. M. Rawson, R. E. P. Winpenny, *J. Chem. Soc. Chem. Commun.* **1995**, 1983.
[7] Crystal data for **1**·2THF ($C_{48}H_{106}Fe_{10}O_{42}$): monoclinic, $P2_1/n$, $a = 9.027(3)$, $b = 22.101(8)$, $c = 20.159(12)$ Å, $\beta = 102.54(3)°$, $V = 3926$ Å^3, $M = 1914$, $Z = 2$ (the molecule lies on an inversion center), $\rho_{calcd} = 1.619$ g cm^{-3}, $T = 150.0(2)$ K, crystal size $0.35 \times 0.15 \times 0.05$ mm, $\mu(Mo_{K\alpha}) = 1.879$ mm^{-1}. Crystal data for **3**·8MeCN·2Me_2CO ($C_{128}H_{124}Cl_6Fe_{10}N_{14}Na_2O_{42}$): triclinic, $P\bar{1}$, $a = 16.195(12)$, $b = 17.604(14)$, $c = 17.593(14)$ Å, $\alpha = 61.48(5)$, $\beta = 63.18(5)$, $\gamma = 62.72(5)°$, $V = 3740$ Å^3, $M = 3347$, $Z = 1$ (the molecule lies on an inver-

 © VCH Verlagsgesellschaft mbH, D-69451 Weinheim, 1996 0570-0833/96/3516-1827 $ 15.00+.25/0

sion center), $\rho_{calcd} = 1.487\ g\,cm^{-3}$, $T = 150.0(2)$ K, crystal size $0.78 \times 0.58 \times 0.35$ mm, $\mu(Mo_{K\alpha}) = 1.134\ mm^{-1}$. Data were collected with a Stoe-Stadi-4 diffractometer, graphite monochromator, $Mo_{K\alpha}$, $\omega - 2\theta$ scans with on-line profile-fitting (W. Clegg, *Acta Crystallogr. Sect. A* **1981**, *37*, 22). An absorption correction was applied using Ψ-scan data for **3** (min./max. transmission 0.392, 0.560). For both **1** and **3** the crystals were cooled using an Oxford Cryosystems low-temperature device (J. Cosier, A. M. Glazer, *J. Appl. Crystallogr.* **1986**, *19*, 105). Both structures were solved by direct methods and completed by iterative cycles of difference Fourier syntheses and full-matrix least-squares refinement against F^2 (G. M. Sheldrick, SHELXL-93, University of Göttingen, **1993**). Hydrogen atoms were included in both structures in calculated positions, riding on parent C atoms, with $U(H) = 1.2\ U_{eq}(C)$ for chp H atoms and $U(H) = 1.5\ U_{eq}(C)$ for methyl H atoms. For **1** four bridging MeO groups are disordered, and one molecule of THF solvate is also disordered over two positions and was refined with similarity restraints. All iron and fully weighted oxygen atoms (with the exception of O10 which is part of the THF solvate) were refined with anisotropic displacement parameters to give, using 349 parameters, $wR2 = 0.2357$ for 3651 unique data ($2\theta \leq 40^\circ$) [$R1 = 0.0941$ for 1820 observed reflections, $F_o > 4\sigma(F)$]. The largest residual difference peak and hole were 0.977 and $-0.749\ e\,Å^{-3}$, respectively. For **3** all non-hydrogen atoms were refined anisotropically, except atoms in several disordered solvent molecules, which were refined isotropically, to give, using 864 parameters, $wR2 = 0.2236$ for 13157 unique data ($2\theta \leq 50^\circ$) [$R1 = 0.0798$ for 7629 observed reflections, $F_o > 4\sigma(F)$]. The largest residual difference peak and hole were 1.472 and $-1.349\ e\,Å^{-3}$, Crystallographic data (excluding structure factors) for the structures reported in this paper have been deposited with the Cambridge Crystallographic Data Centre as supplementary publication no. CCDC-179-75. Copies of the data can be obtained free of charge on application to The Director, CCDC, 12 Union Road, Cambridge CB21EZ, UK (fax: Int. code +(1223)336-033; e-mail: teched@chemcrys.cam.ac.uk).

[8] K. L. Taft, C. D. Delfs, G. C. Papefthymiou, S. Foner, D. Gatteschi, S. Lippard, *J. Am. Chem. Soc.* **1994**, *116*, 823.

[9] W. Armstrong, S. J. Lippard, *Inorg. Chem.* **1985**, *24*, 981.

[10] S. Parsons, G. A. Solan, R. E. P. Winpenny, *J. Chem. Soc. Chem. Commun.* **1995**, 1987.

[11] A. J. Blake, S. Parsons, G. A. Solan, R. E. P. Winpenny, *J. Chem. Soc. Dalton Trans.* **1996**, 321.

[12] The related dinuclear complex $[Fe_2O(O_2CPh)_2(chp)_2(phen)_2]$, which we have structurally characterized, can be isolated by addition of 1,10-phenanthroline (phen). S. Parsons, G. A. Solan, R. E. P. Winpenny, unpublished results.

[13] K. L. Taft, G. C. Papaefthymiou, S. J. Lippard, *Science* **1993**, *259*, 1302.

[14] W. Micklitz, S. J. Lippard, *J. Am. Chem. Soc.* **1989**, *111*, 6856.

[15] A. K. Powell, S. L. Heath, D. Gatteschi, L. Pardi, R. Sessoli, G. Spina, F. Del Giallo, F. Pieralli, *J. Am. Chem. Soc.* **1995**, *117*, 2491.

[16] D. M. Kurtz, Jr., *Chem. Rev.* **1990**, *90*, 589.

[17] A. Earnshaw, B. N. Figgis, J. Lewis, *J. Chem. Soc. A.* **1966**, 1656.

Structural Reorganization of the Doubly Protonated [222]Cryptand through Cation–π and Charge–Charge Interactions: Synthesis and Structure of Its $[CoCl_4]\cdot 0.5\,C_6H_5CH_3$ Salt

Leonard R. MacGillivray and Jerry L. Atwood*

For molecular recognition processes, understanding the influence of noncovalent interactions on the conformation and corresponding ionophoric properties of macro(poly)cyclic receptors (e.g. crown ethers, cryptands)[1, 2] in solution,[3a, b] the gas phase,[3c] and the solid state[3d] is an area of much current interest. In this context, the cation–π interaction[4] is a stabilizing interaction for the binding of positively charged guests (e.g. ammonium cations) by a number of preorganized electron-rich synthetic hosts (e.g. cyclophanes)[5] and hydrophobic binding sites in proteins (e.g. acetylcholine esterase).[4a, 6] Indeed, both experimental and theoretical studies have determined the interaction energies between $N(CH_3)_4^+$ and NH_4^+ cations and the quadrupole moment of benzene to be 9 and 19 kcal mol^{-1}, respectively,[7] and close contacts between cationic amines and aromatic residues in a limited number of protein structures have been noted.[6, 8]

Extensive work has demonstrated the formation of two-phase liquid clathrate systems[9] resulting from the interaction of a wide range of salts with aromatic solvents.[10] Recently we reported the self-assembly of proton cryptate complexes of the macrobicyclic ionophore [222]cryptand (**1**) with inorganic anions isolated from such liquid clathrate media.[10a, b] In particular, we illustrated the ability of two trifurcated intraionic N^+-H···O hydrogen bonds to reorganize the flexible ligand to a chiral, *in–in* conformation with approximate D_3 symmetry in the solid state.[10b] Furthermore, we also studied its mechanism of protonation and revealed the ability of the oxonium ion (H_3O^+) to interact with the $[\mathbf{1}\text{-}2H]^{2+}$ ion through two strong interionic O^+-H···O hydrogen bonds.[10a]

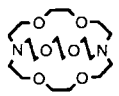

1

As part of our ongoing studies of liquid clathrate systems we now report the synthesis and X-ray crystal structure of complex **2**, which provides structural insight into the nature of the

$[\mathbf{1}\text{-}2H][CoCl_4]\cdot 0.5\,C_6H_5CH_3$ **2**

ammonium–π interaction. The complex includes a $[\mathbf{1}\text{-}2H]^{2+}$ ion that engages in both a cation–π interaction with a single molecule of toluene and charge–charge interaction with the $[CoCl_4]^{2-}$ ion. Moreover, as a consequence of these interactions, the ligand has undergone a structural reorganization from approximate D_3 symmetry to an elongated *in–in* conformation. To our knowledge, this represents the first case in which an ammonium–π interaction contributes to the structural stability of an ionophore in the solid state.

Addition of anhydrous HCl(g) to a toluene solution of the [2.2.2]cryptand **1** in the presence of an equimolar amount $CoCl_2\cdot 6H_2O$ and a further 2–3 equivalents of H_2O immediately yielded a two-phase liquid clathrate solution. Light blue crystals of **2** suitable for X-ray analysis were obtained from the lower layer by allowing the reaction mixture to stand at room temperature for approximately four weeks. The formula of **2** was confirmed by single-crystal X-ray diffraction,[11] ^{1}H NMR spectroscopy,[12] and analytical data.[13]

An ORTEP perspective of the $[\mathbf{1}\text{-}2H]^{2+}$ ion is shown in Figure 1. As in $[H_3O]_2[\mathbf{1}\text{-}2H][4Cl]\cdot 4H_2O$ (**3**), *endo* protonation of the macrobicycle leads to the formation of two intraionic trifurcated[14] N^+-H···O hydrogen bonds, and hence, an *in–in* conformation is adopted by the cryptate. As a result, all six oxygen atoms are directed inward toward the cavity, as illustrated by NCCO torsion angles, which range from 51(1)° to 53(1)° for N1–CCO and −49(1)° to −53(1)° for N2–CCO. However, unlike the cryptates in **3**, each of which lie on a crystallographic twofold axis,[10b] all atoms of the $[\mathbf{1}\text{-}2H]^{2+}$ ion in **2** are contained within the asymmetric unit. Moreover, the intraionic N^+-H···O interactions in **2** are distinct as revealed by their average N^+···O(cryptate) separations of 2.73(2) and 2.85(2) Å to N1 and N2, respectively. Similarly, the average distances for the edges of the two triangular faces formed by atoms O1,O3,O5 [3.65(2) Å] and O2,O4,O6 [3.89(2) Å] are also different. The

[*] Prof. J. L. Atwood, L. R. MacGillivray
Department of Chemistry
University of Missouri-Columbia
Columbia, MO 65211 (USA)
Fax: Int. code +(573)884-9606
e-mail: chemja@mizzou1.missouri.edu

[**] We are grateful for funding from the National Science Foundation, the Natural Sciences and Engineering Research Council of Canada (NSERC) (research fellowship for L. R. M.), and the International Centre for Diffraction Data (research scholarship for L. R. M.).

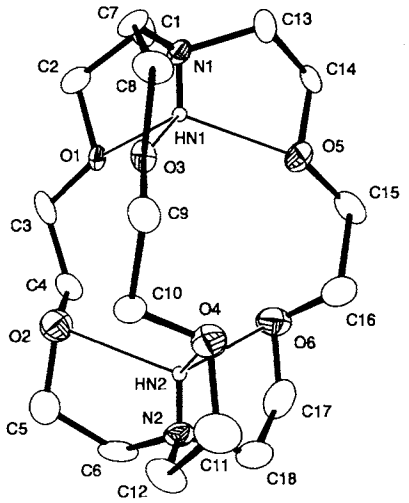

Fig. 1. X-ray crystal structure of the $[1\text{-}2H]^{2+}$ ion. Selected interatomic distances (Å): N1···N2 6.36(2), N1–HN1 1.03, N1···O1 2.75(2), N1···O3 2.71(2), N1···O5 2.74(2), O1···HN1 2.21, O3···HN1 2.25, O5···HN1 2.22, N2–HN2 1.02, N2···O2 2.85(2), N2···O4 2.83, N2···O6 2.87(2), O2···HN2 2.38, O4···HN2 2.31, O6···HN2 2.41.

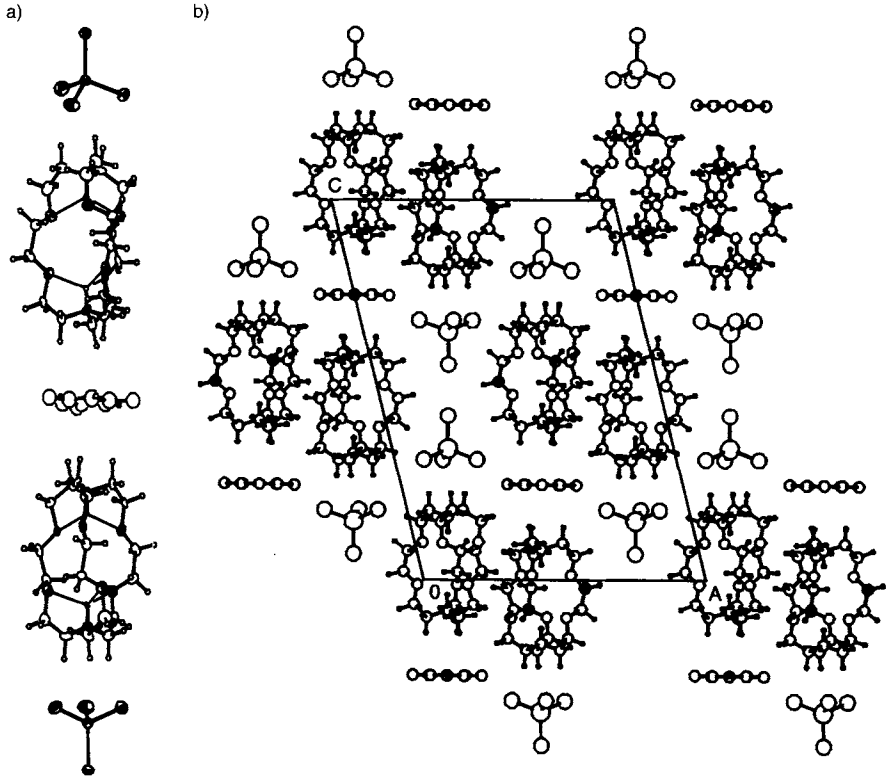

Fig. 2. a) View of the five component supramolecular complex; b) the 2D assembly along the crystallographic *b* axis.

corresponding $N^+\cdots O$ and $O\cdots O$ separations in **3** are 2.77(2) and 3.74(1) Å, respectively.[10b] Furthermore, the nonbonding $N\cdots N$ separation (6.36 Å), which is shorter than that of the empty cryptand (6.87 Å),[15] is substantially longer than in **3** (5.71 Å).[10b, 16]

The surprising geometry of the cavity of the cryptate may be attributed to the contributions of attractive ammonium-π and charge–charge interactions, which induce a structural reorganization upon the flexible macrobicycle causing the ligand to elongate along its $N\cdots N$ axis. Indeed, solution and structural data have suggested the coexistence of both interactions in a number of synthetic and biological receptors.[4] As shown in Figure 2a, the toluene molecule in **2** is sandwiched between two equivalent ends of two symmetry related $[1\text{-}2H]^{2+}$ ions in a position [distance between N1 and the ring centroid: 4.34(1) Å] that facilitates edge-type $C-H^{\delta+}\cdots\pi$ interactions[17] between three α-hydrogen atoms of each dication, each from a different methylene group, and the π face of the aromatic.[18] Similar $C-H^{\delta+}\cdots$ π(arene) interactions have been recently reported in a solid isolated from a liquid clathrate whose composition is water-dependent.[19] The $H\cdots C$(arene) separations in **2**, which range from 2.89(3) to 3.00(3) Å, fall at the upper limit of those calculated in a number of $N(CH_3)_4^+$·n-donor systems[7a] and are consistent with the observation that the interaction energy of such complexes decreases upon increasing the size of the quaternary ion which, in turn, decreases the charge on each proton.[7a] In a similar manner, the $[CoCl_4]^{2-}$ ion, located near N2 [$N2\cdots Co$ 4.54(1) Å], interacts with each cryptate through three $C-H^{\delta+}\cdots Cl$ interactions (2.924(6)–3.029(6) Å) resulting in the formation of a linear five component supramolecular complex.

A view along the crystallographic *b* axis depicting the assembly of **2** is shown in Figure 2(b). Internal protonation results in a deficiency of strong hydrogen-bond donors between constituent ions and molecules; consequently an excess of available hydrogen-bond acceptors are present in **2**.[20] As a result, the assembly process is controlled by weaker electrostatic interactions, which result in the formation of a 2D, layered architecture within the *ac* plane.[21] Interestingly, each layer exhibits pairs of $[1\text{-}2H]^{2+}$ ions surrounded by electron-rich moieties, which lends a measure of support for the proposed model of a liquid clathrate in which cation–cation repulsions are reduced by insulating assemblies of anions and aromatic molecules.[22]

That attractive cation–π and charge–charge interactions may induce a structural reorganization in the flexible $[1\text{-}2H]^{2+}$ ion in a solid isolated from a liquid clathrate medium has been demonstrated. Moreover, such observations provide insight into the ability of noncovalent interactions to impart conformational stability to macro(poly)cyclic hosts. This stability is thought to play an important role in determining their ionophoric properties.

Received: March 13, 1996 [Z89231E]
German version: *Angew. Chem.* **1996**, *108*, 1937–1939

Keywords: clathrates · cryptands · noncovalent interactions

[1] G. Gokel in *Crown Ethers & Cryptands* (Ed. J. F. Stoddart), Black Bear Press, Cambridge, **1991**.
[2] M. Dobler, *Ionophores and Their Structures*, Wiley, New York, **1981**.
[3] Lead references: a) R. M. Izatt, K. Pawlak, J. S. Bradshaw, R. L. Bruening, *Chem. Rev.* **1991**, *91*, 1721; b) L. Troxler, G. J. Wipff, *J. Am. Chem. Soc.* **1994**, *116*, 1468; c) S. Lee, T. Wyttenbach, G. Von Helden, M. T. Bowers, *ibid.* **1995**, *117*, 10159; d) G. Papoyan, K. Gu, J. Wiorkiewicz-Kuczera, K. Kuczera, K. Bowman-James, *ibid.* **1996**, *118*, 1354.
[4] a) D. A. Dougherty, *Science* **1996**, *271*, 163; b) R. A. Kumpf, D. A. Dougherty, *ibid.* **1993**, *261*, 1708; c) J. W. Caldwell, P. A. Kollman, *J. Am. Chem. Soc.* **1995**, *117*, 4177.
[5] a) J. Gross, G. Harder, F. Vögtle, H. Stephan, K. Gloe, *Angew. Chem.* **1995**, *107*, 523; *Angew. Chem. Int. Ed. Engl.* **1995**, *34*, 481; b) P. C. Kearney, L. S. Mizoue, R. A. Kumpf, J. E. Forman, A. McCurdy, D. A. Dougherty, *J. Am. Chem. Soc.* **1993**, *115*, 9907; c) M. A. Petti, T. J. Shepodd, R. E. Barrans, Jr., D. A. Dougherty, *ibid.* **1988**, *110*, 6825.
[6] D. A. Dougherty, D. A. Stauffer, *Science* **1990**, *250*, 1558.
[7] a) M. Meot-Ner (Mautner), C. A. Deakyne, *J. Am. Chem. Soc.* **1985**, *107*, 469; b) C. A. Deakyne, M. Meot-Ner (Mautner), *ibid.* **1985**, *107*, 474.

[8] J. Novotny, R. E. Bruccoleri, F. A. Saul, *Biochemistry* **1989**, *28*, 4735.
[9] J. L. Atwood in *Separation Technology* (Eds.: N. N. Li, H. Strathmann), United Engineering Trustees, New York, **1988**, pp. 46–56.
[10] a) L. R. MacGillivray, J. L. Atwood, *J. Chem. Soc. Chem. Commun.* **1996**, 735; b) *J. Org. Chem.* **1995**, *60*, 4972; c) P. C. Junk, J. L. Atwood, *J. Chem. Soc. Chem. Commun.* **1995**, 1552; d) P. C. Junk, L. R. MacGillivray, M. T. May, K. D. Robinson, J. L. Atwood, *Inorg. Chem.* **1995**, *34*, 5395; e) J. L. Atwood, S. G. Bott, A. W. Coleman, K. D. Robinson, S. B. Whetstone, C. M. Means, *J. Am. Chem. Soc.* **1987**, *109*, 8100.
[11] Crystal data for $[1\text{-}2H][CoCl_4]\cdot 0.5C_6H_5CH_3$: crystal size: $0.10\times0.20\times0.20$ mm, monoclinic, space group $C2/c$, $a=19.478(7)$, $b=11.245(1)$, $c=26.43(1)$ Å, $\beta=104.24(2)$, $V=5611(3)$ Å^3, $\rho_{calcd}=1.48$ g cm^{-3}, $2\theta_{max}=46°$; $\mu=0.52$ mm^{-1}, $Mo_{K\alpha}$ radiation ($\lambda=0.71069$ Å) for $Z=8$. Intensity data were collected using the $\omega-2\theta$ scan mode on an Enraf Nonius CAD-4 diffractometer and were corrected for Lorentz, polarization, and absorption effects, but not for extinction. The structure was solved with direct methods. Least-squares refinement based on 1301 reflections with $I_{net}>2.0\sigma(I_{net})$ (out of 4043 unique reflections), and 298 parameters on convergence gave final values of $R=0.081$ and $R_w=0.065$. Methylene and aromatic hydrogen atoms were placed in calculated positions (d(C,H) = 1.08 and 1.00 Å, respectively) with their positional and thermal parameters fixed, temperature factors being based upon the carbon atoms to which they are bonded. Quaternary ammonium hydrogen atoms were located by inspection of a difference Fourier map, and their positional and thermal were fixed, temperature factors being based upon the atoms to which they are bonded. The toluene molecule was observed to lie on a crystallographic twofold axis and exhibit threefold disorder with the carbon atoms of the methyl group displaying site occupancies of 0.4 (CS5) and 0.3 (CS5B). Crystallographic calculations were conducted with the NRCVAX program package (E. J. Gabe, Y. Le Page, J.-P. Charland, F. L. Lee, P. S. White, *J. Appl. Cryst.* **1989**, *22*, 384) on a pentium-based IBM compatible computer. Crystallographic data (excluding structure factors) for the structure reported in this paper have been desposited with the Cambridge Crystallographic Data Centre as supplementary publication no. CCDC-179-83. Copies of the data can be obtained free of charge on application to The Director, CCDC, 12 Union Road, Cambridge CB2 1EZ, UK (fax: Int. +(1223)336-033; e-mail: teched@chemcrys.cam.ac.uk).
[12] The ^{1}H NMR spectrum exhibits resonances typical of the $[1\text{-}2H]^{2+}$ ion (see ref. [10b]) and toluene.
[13] Satisfactory elemental analysis was obtained for **2** as formulated.
[14] C. B. Aakeröy, K. R. Seddon, *Chem Soc. Rev.* **1993**, 397.
[15] B. Metz, D. Moras, R. Weiss, *J. Chem Soc. Perkin Trans. 2* **1976**, 423.
[16] The N···N separation in **2** is also comparable to that in $[H_3O][1\text{-}2H][(CoCl_3)_2(\mu\text{-}Cl)]$ (6.44 Å)[10a] in which two strong *inter*ionic O^+-H···O hydrogen bonds cause reorganization of the cryptate and result in the formation of two bifurcated *intra*ionic hydrogen bonds within the cavity.
[17] M. A. Viswamitra, R. Radhakrishnan, J. Bandekar, G. R. Desiraju, *J. Am. Chem. Soc.* **1993**, *115*, 4868.
[18] Ab initio calculations involving the $N(CH_3)_4^+$ ion confirm the electrostatic nature of such interactions and demonstrate that a conformation in which three hydrogen atoms are attached to three different alkyl groups is preferred [7].
[19] R. Hunter, R. H. Haueisen, A. Irving, *Angew. Chem.* **1994**, *106*, 588; *Angew. Chem. Int. Ed. Engl.* **1994**, *33*, 566.
[20] L. R. Hanton, C. A. Hunter, D. H. Purvis, *J. Chem. Soc. Chem. Commun.* **1992**, 1134.
[21] We also note the following data: a) an interionic Cl···Cl separation of 3.465(8) Å and a Co-Cl-Cl angle of 179.6(2)° between Cl4 and Cl4a (a: $1.5-x$, $0.5-y$, $-z$), which is indicative of a Cl···Cl interaction [see V. R. Pedireddi, D. S. Reddy, B. S. Goud, D. C. Craig, A. D. Rae, G. R. Desiraju, *J. Chem. Soc. Perkin Trans. 2* **1994**, 2354]; and b) close approach between the methyl group of the disordered toluene molecule and the $[CoCl_4]^{2-}$ ion ($C_{Me}\cdots Cl<3.60$ Å), which suggests the presence of a stabilizing interaction between the hydrogen atoms of the substituent and the anion.
[22] J. L. Atwood, *J. Inclusion Phenom.* **1985**, *3*, 13.
[23] Note added in proof (August 1, 1996): Using data collected on the Siemens SMART system we have recently discovered that **2** may also be solved in the trigonal space group $R\bar{3}c$ with $a=11.2733(5)$, $c=77.002(5)$ Å. The dication and anion lie on a crystallographic threefold axis and the toluene molecule exhibits threefold disorder across a crystallographic *32* site. Interpretation of the assembly process, however, remains the same.

Enantioselective Synthesis of Copper(I) Bipyridine Based Helicates by Chiral Templating of Secondary Structure: Transmission of Stereochemistry on the Nanometer Scale**

Craig R. Woods, Maurizio Benaglia, Franco Cozzi, and Jay S. Siegel*

Achiral oligobipyridines spontaneously wrap around copper(I) ions to create the beautiful secondary structure of a double helix in racemic modification (Fig. 1).[1, 2] In cases where

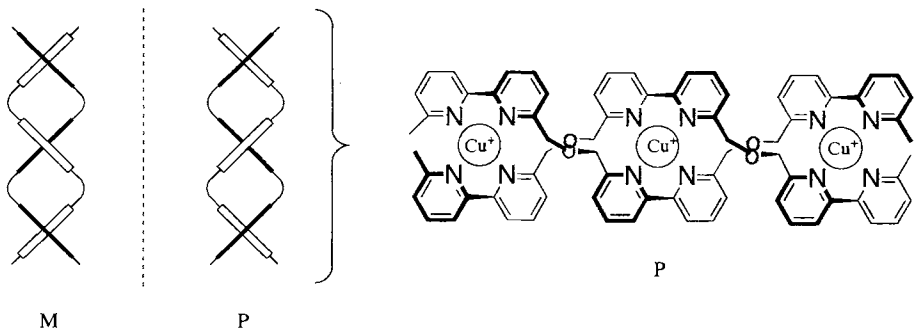

Fig. 1. Enantiomers of helicates.

the bipyridine strands possess a directionality,[3] the pair of enantiomers further speciates into isomers of the head-to-head and head-to-tail variety.[4] Stereoselective control of this secondary structure is an integral component in the synthesis of enantiopure topologically complex supramolecular structures.[5] A classical strategy to such stereocontrol involves altering the parent structure by incorporation of a stereochemical director.[6] Lehn et al. demonstrated this approach by placing chiral linkers between bipyridines which when bound with copper, preferentially formed helicates of one handedness.[7] Less invasive control of stereochemistry can result from an auxiliary template that predetermines stereochemistry and then is removed.[8] Such a scheme opens the possibility of preparing and analyzing specific stereoisomers of the parent helicate in a nonequilibrium mixture. This idea led us to investigate the synthesis and metal complexing behavior of a series of oligobipyridines hybridized to chiral organic templates.

A chiral template provides the necessary symmetry condition for distinguishing right- from left-handed helicates, and the conformational energetics of the chosen template sets the pitch and direction of the helix by restricting the conformational freedom of the bipyridine strands as the metal binds to the ligand. Given sufficient binding strength and helical stability of the helicates, the template can be removed without racemizing the system and the enantiomerically enriched helicate may be used or investigated further. These structural and energetic factors play an important role in determining which template will be an effec-

[*] Prof. J. S. Siegel, C. R. Woods, Dr. M. Benaglia
Department of Chemistry, University of California at San Diego
La Jolla, CA 92093-0358 (USA)
Fax: Int. code +(619)534-5383
e-mail: jss@chem.ucsd.edu
Prof. F. Cozzi
Dipartimento di Chimica Organica e Industriale
Università di Milano (Italy)

[**] This work was supported by the National Science Foundation (CHE-9307582), MURST-Roma, the NATO Collaborative Research Grants Programme, and the CNR-NATO Postdoctoral Fellowship Program (M. B.).

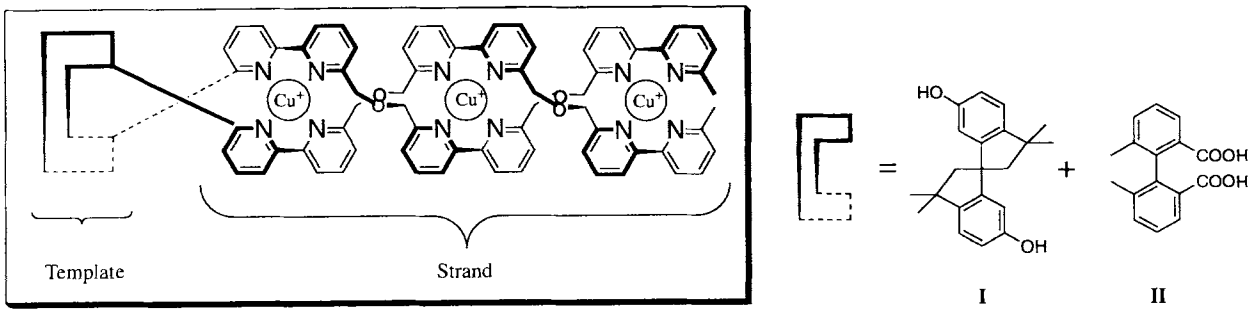

Fig. 2. Representation of the template strategy. The systems discussed were realized with spirobisindane **I** and dimethylbiphenic acid **II**.

tive auxiliary. For the copper(I) bipyridine based helicates spirobisindanol **I** and dimethylbiphenic acid **II** presented the necessary match of symmetry, dimensions, and accessibility (Fig. 2). Hybrids of **I** or **II** with oligobipyridine strands thus became our specific synthetic targets. All of these targets contain numerous carbon–oxygen bonds, suitable sites for retrosynthetic disconnection. The pattern of these disconnections can follow various schemes: 1) strand synthesis, followed by hybridization to the template; 2) template modification by linear addition of bipyridine units; 3) convergent combination of an extended template with oligobipyridines. Methods 1 and 3 proved most expedient.

Synthesis of the bipyridine strands **1**-OH–**3**-OH, proceeds, after initial photobromination, by an iterative series of hydrolysis and Williamson etherification steps (Scheme 1). Initially, 6,6′-dimethyl bipyridine (**1**)[9] is brominated to yield the 6-bromomethyl-6′-methyl (**1**-Br) and 6,6′-bis(bromomethyl) (**1**-Br_2) derivatives. Hydrolysis of **1**-Br is effected with potassium carbonate in aqueous dioxane to form the alcohol **1**-OH, the alkoxide of which reacts with **1**-Br_2 to yield the bisbipyridine **2**-Br.[10] The strand is extended by repeating these steps to produce **2**-OH, **3**-Br, and **3**-OH, sequentially. Enantiomerically resolved **I**[11] and **II**[12] were obtained by literature methods. The bipyridine strands are attached to the template at the bromide or alcohol stages depending on the template. The alkoxide of **I** is formed with sodium hydride and reacts with bromomethylbipyridines **1**-Br, **2**-Br, and **3**-Br to form the template/strand hybrids **I-1**, **I-2**, and **I-3**, respectively. The action of oxalyl chloride converts **II** to its acid chloride, and subsequent reaction with the hydroxymethylbipyridines **1**-OH, **2**-OH, and **3**-OH yields the strand/template hybrids **II-1**, **II-2**, and **II-3**, respectively. Additionally, a convergent approach may be taken, in which **I** is combined with **1**-Br_2 to yield **I-1**-Br, which can be subsequently allowed to react with the alkoxide of **2**-OH to give **I-3**. Metal complexation is accomplished by adding copper(I) triflate or trifluoroacetate to a stirred solution of ligand in acetonitrile.[13]

The ^1H and ^{13}C NMR spectra of the strand/template hybrids clearly display discrete regions for each of the respective proton and carbon types. Upon metal complexation specific signal regions of the ^1H NMR spectra undergo significant and telling changes, which make these signals key reporters of helicate formation (Fig. 3). In particular, the methylene region in the spectra of the free ligands appears primarily as a set of singlets ($\delta \approx 5.0-5.2$), due to accidental isochrony of the diastereotopic protons. Only the methylene closest to the template in the **I** series displays a four-line AB pattern. Upon helicate formation all of the methylene signals shift upfield ($\Delta\delta \approx 1$) and the diastereotopism amplifies such that full four-line AB patterns are seen throughout. The proximity of the methylene groups to the shielding cone of the heterocycles is the likely cause of the

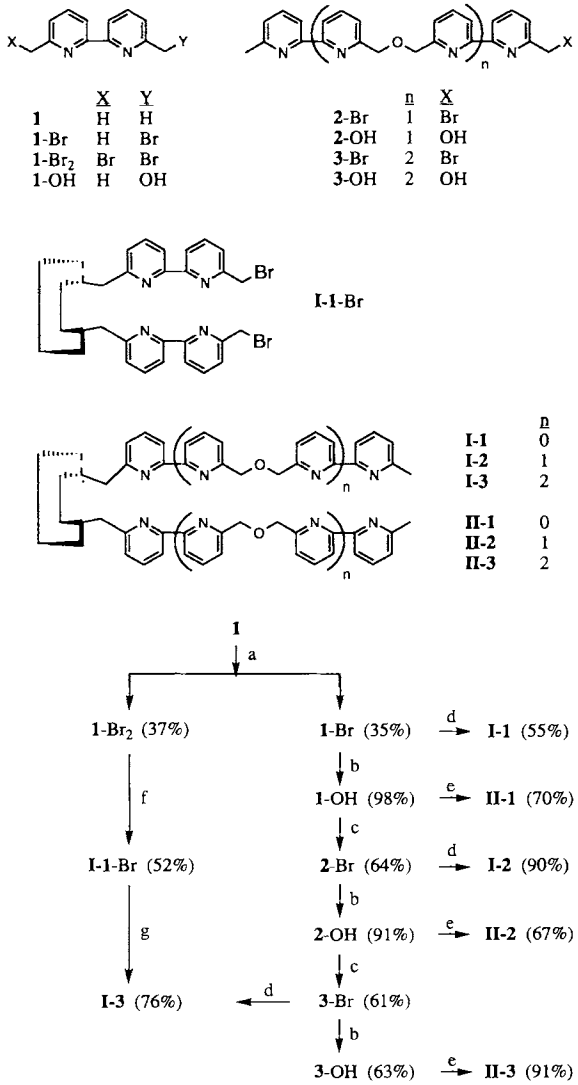

Scheme 1. a) *N*-bromosuccinimide (NBS), CCl_4, benzoyl peroxide; b) K_2CO_3, aqueous dioxane; c) NaH, THF, **1**-Br_2 (1 equiv); d) **I** (0.5 equiv), NaH (1 equiv), THF; e) **II**-acid chloride (0.5 equiv), $CHCl_3$; f) **I** (0.25 equiv), NaH (0.5 equiv), THF; g) **2**-OH, NaH (1 equiv), THF.

upfield shift and the greater manifestation of diastereotopism. The signal for the proton *ortho* to the oxygen in **I** ($\delta = 6.5$) also experiences a strong upfield shift ($\Delta\delta \approx 1.5$) upon complexation. Together these spectral changes indicate helix formation with close participation from the template. Thus, the single stereoelement of the template controls the stereochemistry of the complex throughout a span of 20 Å.

 © VCH Verlagsgesellschaft mbH, D-69451 Weinheim, 1996 0570-0833/96/3516-1831 $ 15.00+.25/0

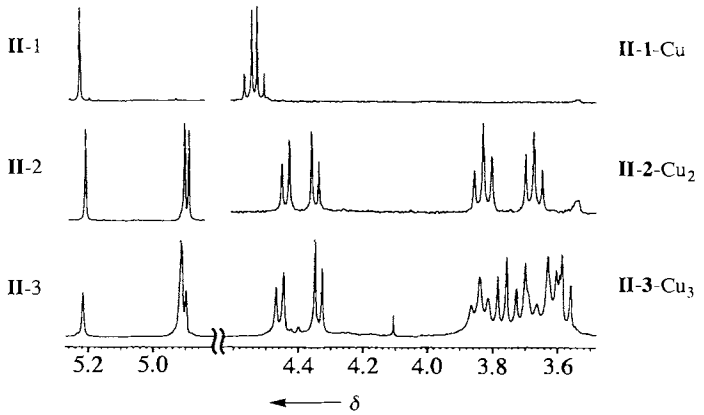

Fig. 3. ^{1}H NMR spectra showing signals of the linking methylene regions of the **II** series of ligands before (left) and after (right) complexation.

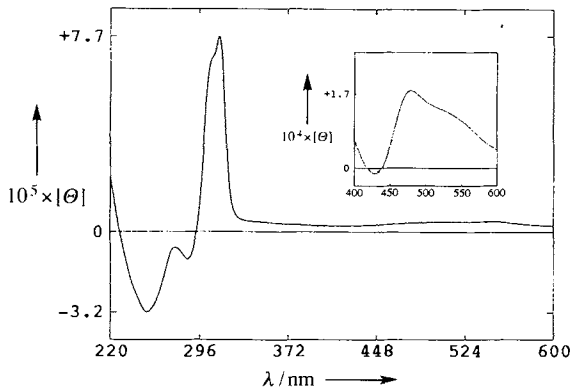

Fig. 4. CD spectra of **II**-3-Cu_3 (CH_3CN). Inset: Cotton effect in the visible region. θ = molecular ellipticity [° $cm^2 dmol^{-1}$].

Although the copper(I) complexes of **I** and **II** have complex spectra, the collection of signals can be accounted for by only one species in each case:[13] a single enantiomer of the head-to-head isomer. Previous work on helix reversion excludes the possibility that this set of signals is due to diastereomeric equilibration on the NMR time scale.[1] Chiroptical measurements also support a highly diastereoselective complexation (Table 1). The

Table 1. Spectral characteristics of ligands and helicates [a].

Cmpd.	λ_{max} (ε)	$[\alpha]_D$ (conc./solv.)
I-1	233 (17000), 285 (20000)	45.9 (0.082/$CHCl_3$)
I-2	235 (44000), 289 (62000)	72.1 (0.20/$CHCl_3$)
I-3	236 (86000), 289 (130000)	108.2 (0.17/$CHCl_3$)
II-1	242 (27000), 290 (37000)	−27.1 (1.2/$CHCl_3$)
II-2	242 (99000), 291 (110000)	−18.1 (0.80/$CHCl_3$)
II-3	242 (190000), 290 (270000)	−7.3 (0.26/$CHCl_3$)
I-1-Cu	265 (23000), 299 (27000), 452 (5000)	419 (0.14/CH_3CN)
I-2-Cu_2	265 (31000), 301 (39000), 450 (7500)	778 (0.13/CH_3CN)
I-3-Cu_3	266 (42000), 303 (52000), 450 (9100)	
II-1-Cu	242 (31800), 300 (31900), 450 (5100)	317 (0.08/CH_3CN)
II-2-Cu_2	242 (45000), 266 (44000), 302 (57000), 450 (9400)	472 (0.10/CH_3CN)
II-3-Cu_3	246 (47000), 268 (51300), 302 (63000), 450 (11000)	501 (0.04/CH_3CN)

[a] All measurements were taken at 25 °C. λ_{max} in nm, concentrations in grams per 100 mL.

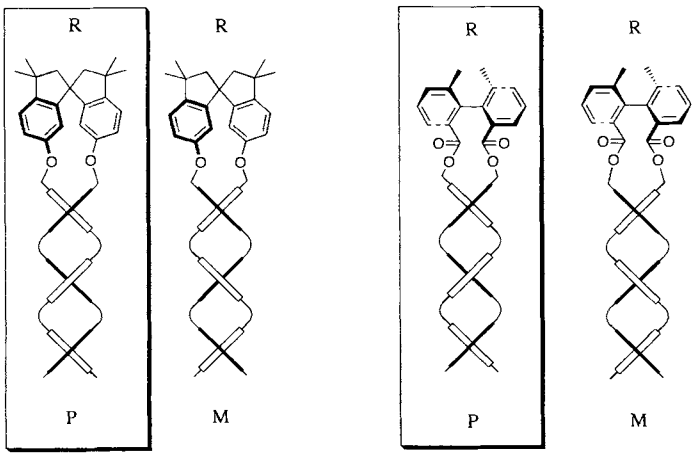

Fig. 5. The possible stereoisomers of the complexes of **I** (left) and **II** (right); the species formed are boxed.

template and the free ligand/template hybrids show $[\alpha]_D$ values that are small in absolute value (<100°); the metal complexes display much greater $[\alpha]_D$ values (ca. +500°). Circular dichroism (CD) spectra (Fig. 4) confirm the helicity of **II**-3-Cu_3.[14]

The absolute configurations of the helicates were deduced by comparison of their CD spectra and $[\alpha]_D$ values with those of Lehn's compound.[7a] The CD spectra show an identical Cotton effect and $[\alpha]_D$ values of the same sign and magnitude.[15, 16] The absolute configurations of the templates have been correlated to the optical rotation in the literature. Thus, for **I**-3-Cu_3 and **II**-3-Cu_3 the absolute configurations must be R-P and R-P, respectively (Fig. 5).

The present results bode well for the general isolation of enantiomerically pure head-to-head double helicates. The stereochemical integrity observed in these compounds demonstrates the ability to transmit stereochemical information over nanometer distances. These complexes will allow direct studies on the mechanism of helicate ligand exchange and recognition processes.[17] Having a general route to the enantiopure helicates with sites for modification opens new avenues for selective bioconjugates involving helicates.[18] From an organic perspective these helicates may provide the foundation for the development of new enantioselective reagents.[19]

January 29, 1996 [Z8766IE]
German version: *Angew. Chem.* **1996**, *108*, 1977–1980

Keywords: chirality · copper compounds · helices · self-assembly

[1] a) J.-M. Lehn, A. Rigault, J. Siegel, J. Harrowfield, B. Chevrier, D. Moras, *Proc. Natl. Acad. Sci. USA* **1987**, *84*, 2565; b) J.-M. Lehn, *Supramolecular Chemistry, Concepts and Perspectives*, VCH, Weinheim, **1995**, Chapter 9; c) C. O. Dietrich-Buchecker, J.-P. Sauvage, A. de Cian, J. Fischer, *J. Chem. Soc. Chem. Commun.* **1994**, *19*, 2231.

[2] The principle of helical metal · ligand association manifests itself in a wide area of chemistry. For a selection of representative examples, see: J.-C. Chambron, C. O. Dieterich-Buchecker, V. Heitz, J.-F. Nierengarten, J.-P. Sauvage, C. Pascard, J. Guilhem, *Pure Appl. Chem.* **1995**, *67*, 233; b) E. C. Constable, *Tetrahedron* **1992**, *48*, 10013; c) C. Piguet, G. Bernardinelli, A. F. Williams, B. Bocquet, *Angew. Chem.* **1995**, *107*, 618; *Angew. Chem. Int. Ed. Engl.* **1995**, *34*, 582; d) C. Piguet, G. Hopfgartner, A. F. Williams, J.-C. G. Bünzli, *J. Chem. Soc. Chem. Commun.* **1995**, *4*, 491; e) T. W. Bell, A. M. Heiss, H. Jousselin, R. T. Ludwig in *Supramolecular Stereochemistry*, (Ed.: J. S. Siegel), Kluwer, Dordrecht, **1995**, pp. 161–168; f) K. T. Potts, K. A. Gheysen Raiford, M. Keshavarz-K, *J. Am. Chem. Soc.* **1993**, *115*, 2793; g) J. Sánchez-Quesada, C. Seel, P. Prados, J. de Mendoza, *J. Am. Chem. Soc.* **1996**, *118*, 277; h) For an example of a triple helix that spontaneously resolves, see: R. Kramer, J.-M. Lehn, A. de Cian, J. Fischer, *Angew. Chem.* **1993**, *105*, 764; *Angew. Chem. Int. Ed. Engl.* **1993**, *32*, 703.

[3] We assume a symmetry argument for strand directionality analogous to that defined by Mislow for cycles, in other words, absence of C_2 or σ symmetry perpendicular to the strand. See: K. Mislow, *Chimia* **1986**, *40*, 395.

[4] a) E. C. Constable, F. R. Heirtzler, M. Neuburger, M. Zehnder, *Supramol. Chem.* **1995**, *5*, 197; b) C. Piguet, G. Hopfgartner, B. Bocquet, O. Schaad, A. F. Williams, *J. Am. Chem. Soc.* **1994**, *116*, 9092.
[5] See for example: a) K. Judice, S. J. Keipert, D. J. Cram, *J. Chem. Soc. Chem. Commun.* **1993**, 1323; b) K. Deshayes, R. D. Broene, I. Chao, C. B. Knobler, F. Diederich, *J. Org. Chem.* **1991**, *56*, 6787; c) P. Hayoz, A. von Zelewsky, H. Stoeckli-Evans, *J. Am. Chem. Soc.* **1993**, *115*, 5111; d) V. Prelog, *Pure Appl. Chem.* **1978**, *50*, 893.
[6] a) J. P. Schneider, J. W. Kelly, *J. Am. Chem. Soc.* **1995**, *117*, 2533; b) D. S. Kemp, T. J. Allen, S. L. Oslick, *ibid.* **1995**, *117*, 6641; d) G. Tuchscherer, M. Mutter, *J. Biotech.* **1995**, *41*, 197; e) P. Wittung, M. Eriksson, R. Lyng, P. E. Nielson, B. Nordén, *J. Am. Chem. Soc.* **1995**, *117*, 10167; f) M. M. Green, N. C. Peterson, T. Sato, A. Teramoto, R. Cook, S. Lifson, *Science*, **1995**, *268*, 1860.
[7] a) W. Zarges, J. Hall, J.-M. Lehn, C. Bolm, *Helv. Chim. Acta* **1991**, *74*, 1843; b) for the use of chiral amino acids to control the helicity of ferric ion binders, see: J. Libman, Y. Tor, A. Shanzer, *J. Am. Chem. Soc.* **1987**, *109*, 5880; A. Shanzer, J. Libman, S. Lifson, *Pure Appl. Chem.*, **1992**, 64, 1421.
[8] For a didactic discussion of chiral auxiliaries, see: E. L. Eliel, S. H. Wilen, L. N. Mander, *Stereochemistry of Organic Compounds*, Wiley, New York, **1994**, pp. 868–870.
[9] T. Rode, E. Breitmaier, *Synthesis* **1987**, 574.
[10] M. M. Harding, U. Koert, J.-M. Lehn, A. Marquis-Rigault, C. Piguet, J. Siegel, *Helv. Chim. Acta* **1991**, *74*, 594.
[11] R. J. Kazlauskas, *J. Am. Chem. Soc.* **1989**, *111*, 4953.
[12] M. Siegel, K. Mislow, *J. Am. Chem. Soc.* **1958**, *80*, 473.
[13] All new compounds were fully characterized by mass spectrometry, ^{1}H NMR, ^{13}C NMR, and UV spectroscopy, and by determination of $[z]_D$ values.
[14] CD data from Figure 5. Wavelengths [nm], followed by molecular ellipticity [$cm^2 dmol^{-1}$]: 251.5 (-3.16×10^{-5}), 313.5 (7.69×10^{5}), 428.3 (-1.26×10^{-3}), 479.3 (1.73×10^{4}).
[15] The small magnitude of the template rotation and van't Hoff's additivity principle for optical activity allows the sign of the larger rotation of the complex to be correlated directly.
[16] J. H. van't Hoff, *Arrangement of Atoms in Space*, 2nd ed. in English, Longmans, London, **1898**, Chapter 7, pp. 160–169.
[17] D. A. Buckingham, A. M. Sargeson, *Top. in Stereochem.* **1971**, *6*, 219–279.
[18] a) B. Schoentjes, J.-M. Lehn, *Helv. Chim. Acta* **1995**, *78*, 1; b) U. Koert, M. M. Harding, J.-M. Lehn, *Nature* **1990**, *346*, 339; c) D. S. Sigman, A. Mazumder, D. M. Perrin, *Chem. Rev.* **1993**, *93*, 2295; d) J. K. Barton, *Science* **1986**, *233*, 727.
[19] a) A. M. Gilbert, T. J. Katz, W. E. Geiger, M. P. Robben, A. L. Rheingold, *J. Am. Chem. Soc.* **1993**, *115*, 3199; b) A. Pfaltz, *Acc. Chem. Res.* **1993**, *26*, 339; c) *Catalytic Asymmetric Synthesis*, (Ed.: I. Ojima), **1993**, VCH, Weinheim; d) K. Maruoka, N. Murase, H. Yamamoto, *J. Org. Chem.* **1993**, *58*, 2938.

Metalloporphyrins as Ligands: Synthesis and Characterization of $[(\eta^6\text{-cymene})\text{-Ru}\{\eta^5\text{-Ni(OEP)}\}]^{2+}$**

Karen Koczaja Dailey, Glenn P. A. Yap, Arnold L. Rheingold, and Thomas B. Rauchfuss*

Interactions between transition metals and heterocycles are relevant to many areas of science and technology. This topic has elicited recent interest in the context of hydrotreating catalysis, the industrial process by which heteroatom-containing contaminants are removed from fossil fuels.[1] Studies to date have focused on two aspects of hydrotreating, hydrodesulfurization (HDS) and hydrodenitrification (HDN), which can be modeled through the study of thiophene–metal[2] and pyridine–metal interactions,[3] respectively.

Hydrotreating also encompasses hydrodemetalation (HDM), which primarily involves the removal of nickel and vanadium from crude oil stocks.[4] These metals are typically found in fossil fuels as metalloporphyrins.[5] Such species arise from the dehydrogenation and transmetalation of chlorophyll and related pigments present in fossil plants. Because HDS and HDN catalysts are poisoned by these metals, HDM reactors typically precede other petroleum processing steps. We have prepared what appear to be the first π–metal complexes of metalloporphyrins as models for the initial stages of HDM catalysis. Since metalloporphyrins are of widespread interest in catalysis,[6] energy conversion,[7] and supramolecular chemistry in general,[8] the new coordination mode may be more broadly applicable, especially as we show that the π complexation strongly affects the structural and spectroscopic properties of the porphyrin.

We have previously demonstrated that the reagent [(cymene)Ru(OTf)$_2$] **1** (cymene = *p*-isopropyltoluene; OTf = $CF_3SO_3^-$) is a potent arenophile, which rapidly forms π complexes with a variety of arenes and heterocycles.[9] We have now found that **1** reacts with octaethylporphyrinatonickel, [Ni(OEP)] **2**, to give the adduct $[(\eta^6\text{-cymene})\text{Ru}\{\eta^5\text{-Ni(OEP)}\}](\text{OTf})_2$ **3** [Eq. (a)].

$$[(R)M(OTf)_2] + [Ni(OEP)] \longrightarrow [(R)M\{\eta^5\text{-Ni(OEP)}\}](OTf)_2 \quad (a)$$

$(R)M^{n+}$ = (cymene)Ru^{2+}, (cymene)Os^{2+}, $(C_5Me_5)Ir^{2+}$

The reaction occurs readily at room temperature and is signaled by a conversion of the magenta color characteristic of the nickel porphyrin to deep green. Addition of hexanes to these solutions precipitates **3**, leaving unconverted **2** in solution. The new compound is air-stable and soluble in a variety of polar organic solvents. Coordinating solvents, such as MeCN, reverse the complexation to give free **2**.

The ^{1}H NMR spectrum of **3** illustrates that the complex lacks the D_{4h} symmetry of **2**. Two methyne singlets are observed at $\delta = 8.13$ and 8.72. These signals are shifted upfield relative to the methyne signal found in **2** at $\delta = 9.7$, indicating the reduced ring current of the metalloporphyrin upon complexation. Homonuclear decoupling experiments show that the methylene hydrogen atoms are diastereotopic, for example the overlapping doublet of quartets at $\delta = 3.83$ is coupled to the overlapping doublet of quartets at $\delta = 3.03$, consistent with C_s symmetry of the π complex. Typical for other π-arene complexes, it is assumed that the $\{\eta^5\text{-Ni(OEP)}\}$, as well as the η^6-cymene ligand, rotates freely about the metal–ring centroid axis. The ^{13}C NMR data are consistent with the ^{1}H NMR spectroscopic results. The lower symmetry of the complex may also be responsible for the broadening of the Soret band, which has shifted from 392 nm to 406 nm, and appearance of a band at 672 nm, which is similar to those exhibited by metallochlorins (Fig. 1).[10]

While **3** did not afford crystals, X-ray quality crystals of the tetrafluoroborate salt, $[(\eta^6\text{-cymene})\text{Ru}\{\eta^5\text{-Ni(OEP)}\}](BF_4)_2$, were obtained, although due to disorder in the anion and solvent, the structure is of limited quality. The crystallographic results confirm that **2** is indeed serving as a π ligand for the Ru dication (Fig. 2).[11] The pyrrolide and π arene deviate from parallel by only 4.13°. The Ni(OEP) ligand is strongly distorted, being folded along the C28-Ni-C46 axis. The planes defined by the pyrrolides containing N1, N3, and N4 are twisted 10°, 28°, and 27°, respectively, from the least-squares plane calculated

[*] Prof. T. B. Rauchfuss, K. K. Dailey
School of Chemical Sciences
University of Illinois, Urbana, IL 61801 (USA)
Fax: Int. code +(217)333-2685
e-mail: rauchfuz@ux1.cso.uiuc.edu
Dr. G. P. A. Yap, Prof. A. L. Rheingold
Department of Chemistry & Biochemistry
University of Delaware, Newark, DE 19716 (USA)

[**] This research was funded by the U. S. Department of Energy through contract DOE DEFGO2-90ER14146. The Fluorescence Dynamics Laboratory at the University of Illinois, Urbana-Champaign, is supported by the Division of Research Resources of the National Institutes of Health through grant PHS-P41-RRO3155. OEP = octaethylporphyrin.

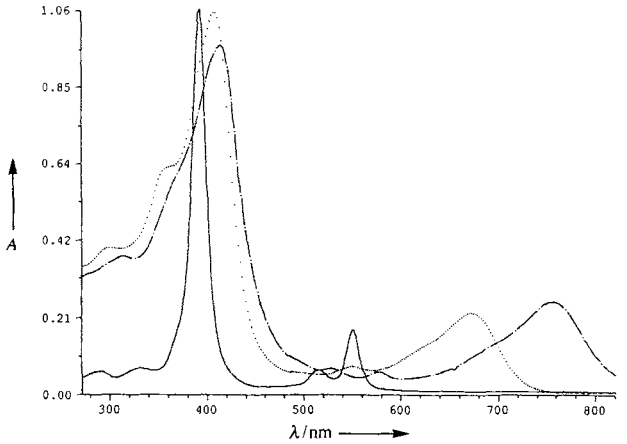

Fig. 1. Absorption spectra of [Ni(OEP)] (—), $[(\eta^6\text{-cymene})Ru\{\mu^5\text{-}Ni(OEP)\}](BF_4)_2$ (····), and $[(\eta^6\text{-cymene})Ru\{\eta^5\text{-}Zn(OEP)\}](OTf)_2$ (–·–·–) in CH_2Cl_2. A = absorption.

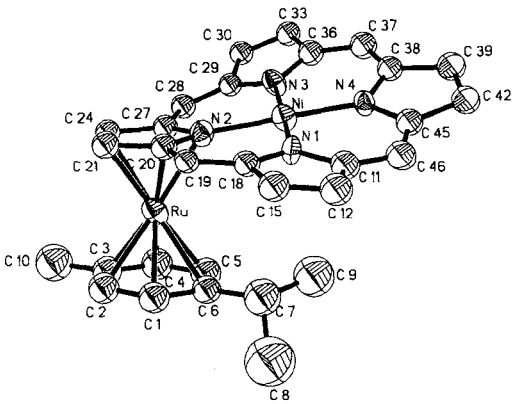

Fig. 2. Structure of the dication in $[(\eta^6\text{-cymene})Ru\{\eta^5\text{-}Ni(OEP)\}](BF_4)_2$ with thermal ellipsoids drawn at the 50% probability level. (Ethyl groups omitted for clarity.) Selected bond lengths [Å]: Ru–N2 2.230, Ru–C20 2.169, Ru–C21 2.216, Ru–C24 2.237, Ru–C27 2.181, Ni–N1 1.922, Ni–N2 1.963, Ni–N3 1.945, Ni–N4 1.924.

for the π-complexed pyrrolide. The competition between Ni and Ru for electron density at N2 is also manifested in the structural data. The Ru–N2 distance is 0.081 Å longer than that in $[(\eta^6\text{-cymene})Ru(\eta^5\text{-}C_4Me_4N)](OTf)_2$ (2.149 Å).[12] The Ni–N2 distance (1.963 Å) in **1** is only slightly longer than that found in the three known crystalline forms of **2**,[13–15] while the remaining three Ni–N bond lengths of the complex are either comparable or slightly shorter. It has been postulated[16] that 1.96 Å is the shortest metal–N bond length necessary to retain a planar macrocycle.[13] Thus, the somewhat shorter Ni–N1, Ni–N3, and Ni–N4 bond lengths are in accord with the severe nonplanarity of the Ni(OEP) ligand in **3**.

The new type of sandwich complex enjoys some the generality. ^{1}H NMR experiments confirm that both $[(C_5Me_5)Ir(OTf)_2]$ and $[(cymene)Os(OTf)_2]$ react with **2** in a manner analogous to **1**. The iridium adduct is deep blue, while the (cymene)Os derivative is green. We investigated the possibility that more than one metal could be attached to the porphyrin ring by treating **2** with an excess of **1**, but only the 1:1 adduct was isolated. We conclude that the first metalation diminishes the basicity of the entire porphyrin.

Interestingly, H_2(OEP) itself does not form a complex with **1**. Stable π complexes derived from pyrroles typically feature the deprotonated heterocycle.[17] We reason that the greater coordinating power of **2** relative to H_2(OEP) reflects the electron-releasing tendency of the electropositive Ni center. Consistent with this view, [Zn(OEP)] forms a very stable adduct with $Ru(cymene)^{2+}$ ions but [VO(OEP)] does not appear to bind at all. Spectroscopic and microanalytical data for $[(cymene)Ru\{Zn(OEP)\}](OTf)_2$ (**4**) suggest that this olive green species adopts a structure similar to that of the cation of **3** [Eq. (b)]. In

$$[(R)Ru(OTf)_2] + [Zn(OEP)] \longrightarrow [(R)M\{\eta^5\text{-}Zn(OEP)\}](OTf)_2 \quad (b)$$
$$(R)M^{n+} = (cymene)Ru^{2+},\ (C_5Me_5)Ir^{2+}$$

contrast to Zn(OEP),[18] whose photophysical properties have been widely studied, neither $[(cymene)Ru\{Zn(OEP)\}]^{2+}$ nor $[(C_5Me_5)Ir\{Zn(OEP)\}]^{2+}$ fluoresces.

The results define a new mode for metal–porphyrin interactions potentially relevant to catalyst–metalloporphyrin interactions in the hydrodemetalation process. The π-complexation strongly perturbs the electronic and structural properties of this important family of heterocycles. This new coordination mode presents new opportunities for the design of metal–metalloporphyrin superstructures.

Experimental Procedure

All preparative operations were conducted under purified nitrogen unless otherwise stated.

$[(cymene)Ru\{Ni(OEP)\}](BF_4)_2$: In a 100 mL Schlenk flask $[(cymene)RuCl_2]_2$ (0.078 g, 0.127 mmol) and $AgBF_4$ (0.098 g, 0.507 mmol) were combined and CH_2Cl_2 (10 mL) was added. After the mixture had been stirred for 2 h at room temperature, the orange solution was filtered to remove AgCl. The solution of $[(cymene)Ru(BF_4)_2]$ was treated with **2** (0.158 g, 0.267 mmol). After about 16 h, the dark purple solution was reduced in volume to about 10 mL and diluted with hexane. The green solid precipitate was washed with hexane until the filtrate was colorless. The green powder was collected and dried under vacuum. Yield: 0.150 g (60%). Single crystals were obtained from a THF/hexane solvent system. ($[(\eta^6\text{-cymene})Ru\{\eta^5\text{-}Ni(OEP)\}][OTf]_2$ was prepared analously using AgOTf, but no crystals were isolated.) Anal. calcd for $C_{46}H_{58}N_4B_2F_8NiRu \cdot 0.6$ THF (found): C 55.70 (54.60), H 6.07 (6.18), N 5.37 (4.48). ^{1}H NMR (CD_2Cl_2): $\delta = 0.54$ (d, 6H), 1.39 (t, 6H), 1.52 (m, 18H), 1.60 (m, 1H), 2.00 (s, 3H), 3.03 (m, 2H), 3.25 (m, 10H), 3.57 (m, 2H), 3.83 (m, 2H), 5.52 (d, 2H), 6.10 (d, 2H), 8.13 (s, 2H), 8.72 (s, 2H). $^{13}C\{^1H\}$ NMR (CD_2Cl_2): δ = 16.0, 16.3, 16.7, 17.1, 17.8, 18.6, 18.7, 19.0, 19.2, 21.8, 31.0, 86.0, 89.8, 97.3, 102.9, 103.0, 106.2, 106.7, 112.5, 145.9, 148.5, 148.8, 151.1, 154.6, 159.2. FAB-MS: m/z: 826.3 ($[(cymene)Ru\{Ni(OEP)\}]^{2+}$). UV/Vis ($CH_2Cl_2$): λ [nm] (ε[$M^{-1}cm^{-1}$]) 300 (20500), 360 (32400), 406 (55000), 490 (2800), 550 (3700), 624 (6700), 672 (11600).

$[Cp^*Ir\{Ni(OEP)\}](OTf)_2$: The synthesis was carried out as for $[(cymene)Ru\{Ni(OEP)\}](BF_4)_2$ by using $[Cp^*IrCl_2]_2$ (0.038 g, 0.048 mmol), AgOTf (0.051 g, 0.198 mmol), and [Ni(OEP)] (0.060 g, 0.101 mmol). A blue powder was isolated. Yield: 0.070 g (60%). ^{1}H NMR (CD_2Cl_2): δ = 1.26 (s, 5H), 1.58 (m, 24H), 3.16 (m, 2H), 3.37 (m, 10H), 3.60 (m, 2H), 3.84 (m, 2H), 8.36 (s, 2H), 8.64 (s, 2H). $^{13}C\{^1H\}$ NMR (CD_2Cl_2): δ = 8.4, 15.9, 16.7, 16.9, 17.1, 17.5, 19.1, 19.2, 19.4, 96.7, 96.9, 100.4, 106.0, 108.6, 147.4, 149.7, 150.0, 152.0, 155.7, 159.3. FAB-MS: m/z: 918.4 ($[Cp^*Ir\{Ni(OEP)\}]^{2+}$). UV/Vis (CD_2Cl_2): λ [nm] (ε [$M^{-1}cm^{-1}$]) 312 (16000), 394 (39000), 410 (49000), 550 (6000), 582 (7000), 636 (10000).

4: A solution of **1**, generated from $[(cymene)RuCl_2]_2$ (0.026 g, 0.042 mmol) and AgOTf (0.044 g, 0.170 mmol) in CH_2Cl_2 (10 mL) was treated with [Zn(OEP)] (0.075 g, 0.125 mmol). The slurry was refluxed at 65 °C for about 16 h. After the mixture had been cooled to room temperature, the dark purple solution was filtered (in air) to remove the unconverted, solid [Zn(OEP)]. The remaining [Zn(OEP)] was removed by first precipitating the complex with diethyl ether and washing with this solvent until the filtrate was colorless. The complex was recrystallized from a CH_2Cl_2/hexane solvent system to give olive green microcrystals. Yield: 0.065 g (67%). Anal. calcd for $C_{48}H_{58}N_4F_6O_6RuS_2Zn$ (found): C 50.95 (50.83), H 5.17 (5.50), N 4.95 (4.39). ^{1}H NMR (CD_2Cl_2): δ = 0.92 (d, 6H), 1.29 (m, 6H), 1.54 (m, 18H), 2.09 (s, 3H), 2.43 (m, 1H), 3.30 (m, 14H), 3.44 (m, 2H), 5.7 (dd, 4H), 7.89 (s, 1H), 8.05 (s, 1H). $^{13}C\{^1H\}$ NMR (CD_2Cl_2): δ = 15.89, 16.51, 16.90, 17.34, 18.67, 18.70, 18.91, 18.92, 19.02, 22.18, 31.40, 86.10, 88.37, 96.63, 102.07, 102.56, 104.98, 108.78, 111.96, 145.81, 147.11, 147.34, 155.78, 163.80, 167.24. FAB-MS: m/z: 832.3 ($[(cymene)Ru\{Zn(OEP)\}]^{2+}$). UV/Vis ($CH_2Cl_2$): λ [nm] (ε [$M^{-1}cm^{-1}$]) 274 (22000), 312 (25000), 370 (41000), 412 (65000), 528 (4000), 576 (3500), 692 (8500), 754 (17000).

$[Cp^*Ir\{Zn(OEP)\}](OTf)_2$: $[Cp^*Ir(OTf)_2]$ was generated from $[Cp^*IrCl_2]_2$ (0.033 g, 0.042 mmol) and AgOTf (0.043 g, 0.166 mmol) in CH_2Cl_2 (10 mL). To this solution, [Zn(OEP)] (0.075 g, 0.125 mmol) was added as a solid. The reaction mixture was heated to reflux for about 16 hours. After cooling to room temperature, the reaction mixture was filtered (in air) to remove the unconverted [Zn(OEP)]. The crude

 © VCH Verlagsgesellschaft mbH, D-69451 Weinheim, 1996 0570-0833/96/3516-1834 $ 15.00+.25/0

product was repeatedly precipitated from a thf/hexane solvent system until the washings were colorless. A green powder was recovered. Yield: 0.065 g (64%). Anal. calcd for $C_{48}H_{59}N_4F_6IrO_6S_2Zn$ (found): C 47.11 (47.20), H 4.86 (4.97), N 4.58 (4.50). ^{1}H NMR (CD_2Cl_2): $\delta = 0.88$ (s, 15H), 1.60 (m, 18H), 1.70 (t, 6H), 3.19 (m, 2H), 3.38 (m, 12H), 3.49 (m, 2H), 8.14 (s, 2H), 8.27 (s, 2H). ^{13}C{^{1}H} NMR (CD_2Cl_2): $\delta = 8.04$, 15.90, 16.83, 17.05, 17.43, 17.85, 19.03, 19.05, 19.14, 94.53, 95.94, 98.87, 107.09, 108.94, 145.83, 147.32, 148.14, 155.65, 163.59, 166.68. FAB-MS: m/z: 924.2 ([Cp*Ir{Zn(OEP)}]$^{2+}$). UV/Vis (CH_2Cl_2): λ [nm] (ε [$M^{-1}cm^{-1}$]) 334 (29000), 404 (51000), 420 (71000), 526 (4400), 572 (5000), 712 (19000).

Received: February 27, 1996 [Z 8871 IE]
German version: *Angew. Chem.* **1996**, *108*, 1985–1987

Keywords: metalloporphyrins · nickel compounds · ruthenium compounds · sandwich complexes

[1] B. C. Gates, *Catalytic Chemistry*, Wiley, New York, **1992**; J. G. Reynolds, *Chem. Ind. (London)* **1991**, p. 570.
[2] R. J. Angelici in *Encyclopedia of Inorganic Chemistry, Vol. 3* (Ed.: R. B. King), Wiley, New York, **1994**, p. 1433; T. B. Rauchfuss, *Prog. Inorg. Chem.* **1991**, *31*, 259.
[3] S. D. Gray, K. J. Weller, M. A. Bruck, P. M. Briggs, D. E. Wigley, *J. Am. Chem. Soc.* **1995**, *117*, 10678.
[4] R. A. Ware, J. Wei, *J. Catal.* **1985**, *93*, 100; C. Hung, R. L. Howell, D. R. Johnson, *Chem. Eng. Prog.* **1986**, 57.
[5] E. W. Baker, S. E. Palmer in *The Porphyrins, Vol. 1* (Ed.: D. Dolphin), Academic Press, New York, **1978**, p. 485; *Metal Complexes in Fossil Fuels: Geochemistry, Characterization and Processing* (Eds.: R. H. Filby, J. F. Branthaver), American Chemical Society, Washington DC, **1987**.
[6] J. E. Lyons, P. E. Ellis, H. K. Myers, *J. Catal.* **1995**, *155*, 59; F. Minisci, F. Fontana, S. Araneo, F. Recupero, S. Banfi, S. Quici, *J. Am. Chem. Soc.* **1995**, *117*, 226; J. T. Groves, S. B. Ungashe, *ibid.* **1990**, *112*, 7796.
[7] M. R. Wasielewski, *Chem. Rev.* **1992**, *92*, 435.
[8] J.-M. Lehn, *Supramolecular Chemistry: Concepts and Perspectives*, VCH, Weinheim, **1995**.
[9] E. A. Ganja, T. B. Rauchfuss, *Organometallics* **1991**, *10*, 270.
[10] M. Gouterman in *The Porphyrins, Vol. 3* (Ed.: D. Dolphin), Academic Press, New York, **1978**, p. 1.
[11] Crystal data of $[(\eta^6\text{-cymene})Ru\{\eta^5\text{-Ni(OEP)}\}](BF_4)_2 \cdot 0.5THF$: $C_{48}H_{62}B_2F_8N_4NiO_{0.5}Ru$ crystals were grown from a THF/hexane solution, $M_r = 1036.42$, monoclinic, space group $P2_1/n$, $a = 13.413(3)$, $b = 17.017(3)$, $c = 22.516(5)$ Å, $\beta = 101.93(3)°$; $V = 5028(2)$; $Z = 4$; $\rho_{calcd} = 1.369$ Mgm^{-3}, $F(000) = 2144$, $\lambda = 0.71073$ Å, $T = 247(2)$ K, $\mu(Mo_{K\alpha}) = 0.741$ mm^{-1}, reflections were collected on a $0.2 \times 0.1 \times 0.1$ mm^3 crystal using a Siemens diffractometer, of a total of 6415 reflections, 5392 were independent, largest peak and hole: 0.806 and -0.549 e^{-3}, $R1(I > 2\sigma(I)) = 0.721$ and $wR2 = 0.1703$ (final data) with $R1 = \Sigma||F_o| - |F_c||/\Sigma|F_o|$ and $wR2 = (\Sigma w(F_o^2 - F_o^2)^2/\Sigma w(F_o^2)^2)^{0.5}$. The structure was solved with direct methods (SHLETXL version 5.03) and refined by full-matrix least squares based on F^2. A riding model was applied to refine the hydrogen atom positions. The uncoordinated disordered thf molecules were refined at half occupancy. Crystallographic data (excluding structure factors) for the structure(s) reported in this paper have been deposited with the Cambridge Crystallographic Data Centre as supplementary publication no. CCDC-179-53. Copies of the data can be obtained free of charge on application to The Director, CCDC, 12 Union Road, Cambridge CB2 1EZ, UK (fax: Int. code +(1223) 336-033; e-mail: teched@chemcrys.cam.ac.uk).
[12] F. Kvietok, V. Allured, M. Rakowski DuBois, *Organometallics* **1994**, *13*, 60.
[13] E. F. Meyer, *Acta Crystallogr. Sect. B.* **1972**, *28*, 2162.
[14] D. L. Cullen, E. F. Meyer, *J. Am. Chem. Soc.* **1974**, *96*, 2095.
[15] T. D. Brennan; W. R. Scheidt, J. A. Shelnutt, *J. Am. Chem. Soc.* **1988**, *110*, 3919.
[16] J. L. Hoard, *Ann. N. Y. Acad. Sci.* **1973**, *206*, 18.
[17] W. J. Kelly, W. E. Parthun, *Organometallics* **1992**, *11*, 4348; N. Kuhn, M. Kockerling, S. Stubenrauch, D. Blaser, R. Boese, *J. Chem. Soc. Chem. Commun.* **1991**, 1368; K. J. Chase; R. F. Bryan, M. K. Woode, R. N. Grimes, *Organometallics* **1991**, *10*, 2631; N. Kuhn, A. Kuhn, E. M. Lampe, *Chem. Ber.* **1991**, *124*, 997; J. Zakrzewski, *Organomet. Chem.* **1987**, *326*, C17.
[18] N. Barboy, J. Feitelson, *J. Chem. Phys.* **1984**, *88*, 1065.

DNA Cleavage by a Nine-Membered Masked Enediyne, an Analogue of the Kedarcidin and C-1027 Chromophores**

Takashi Takahashi,* Hiroshi Tanaka, Haruo Yamada, Takuyuki Matsumoto, and Yukio Sugiura

Kedarcidin (KD)[1] and C-1027[2] belong to a new class of chromoprotein antitumor antibiotics consisting of a 1:1 complex of apoproteins and cytotoxic nonprotein chromophores. Their chromophores, KD-chr (**1**) and C-1027-chr (**2**), possess a

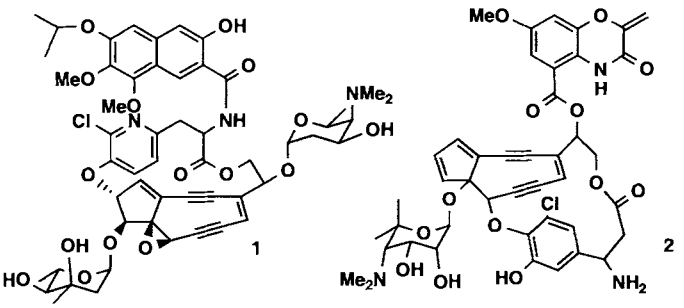

common nine-membered enediyne core structure. Their biological activities are associated with their ability to cause strong DNA cleavage. The proposed mechanism of the DNA cleavage is that biradical species generated from the highly strained nine-membered enediyne chromophores abstract hydrogens from deoxyribose.[1d,2d] Unlike other enediynes, C-1027 shows predominant DNA-cleaving activity even in the absence of thiols or reducing agents, a valuable implication for its application as a potent cancer chemotherapeutic agent.[3]

The design and synthesis of DNA-cleaving molecules has been a subject of recent synthetic and biochemical investigations.[4,5] We have already reported an approach to the enediyne **4a** (Scheme 1) as a nine-membered esperamicin–calicheamicin

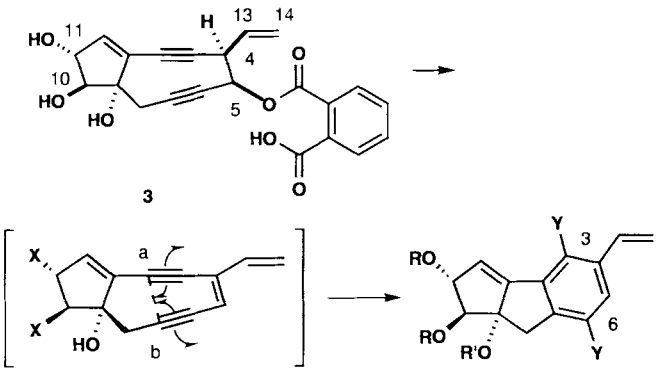

4a: X=H
4b: X=OH

5a: R=R'=H, Y= •
5b: R=R'=OAc, Y=H
5c: R=TBS, R'=TMS, Y=D

Scheme 1. Mechanism of enediyne and biradical generation from **3**.

[*] Prof. Dr. T. Takahashi, H. Tanaka, Dr. H. Yamada
Tokyo Institute of Technology, Merguo
Tokyo 152 (Japan)
Fax: Int. code +(3)5734-2884
T. Matsumoto, Prof. Dr. Y. Sugiura
Institute for Chemical Research, Kyoto University Uji
Kyoto 611 (Japan)

[**] This research was supported by a Grant-in-Aid for Scientific Research on Priority Area No. 06240104 from the Ministry of Education, Science and Culture, Japan.

analogue.[6] However, **4a** did not cause any DNA cleavage, probably because it is not soluble in water and not stable enough to be handled at ambient temperature. In this communication we report the design, synthesis, and DNA-cleaving activity of the new nine-membered pro-enediyne **3**, which is sufficiently stable at ambient temperature to allow its isolation and handling and which shows a strong DNA-cleaving activity without addition of thiols.

Compound **3** was designed as a potential precursor for the KD-chr analogue **4b** based on the following considerations. The 1,5-diyne system in **3** should be stable enough to allow isolation and handling at ambient temperature, and the phthalic acid moiety should improve the solubility of **3** in water. Removal[7] of the phthalic acid in **3** in weakly basic buffer solution should lead to the highly reactive nine-membered enediyne **4b**, which based on MM2 calculations (distance between a and b in **4b** is 2.82 Å) should undergo spontaneous Bergman cyclization at room temperature to give the benzenoid biradical **5a**.[8] Thus, like C-1027-chr, the pro-enediyne molecule **3** should cleave DNA without added thiols or reductants. The *trans*-dihydroxy groups at C(10) and C(11) in **3** should also increase its solubility in water and could be used to attach a DNA sequence recognition element in DNA binding studies. In addition, at a later stage of this program the vinyl group at C(4) in **3** could be used to introduce dihydroxy groups at C(13) and C(14), which could be elaborated in analogy to **1** and/or **2**.

The nine-membered diyne **3** was synthesized from the (±)-epoxyketone **6** by using a modification of the general methodology developed previously in our laboratory (Scheme 2).[6,9] Addition of magnesium trimethylsilylacetylide to ketone **6** (80%), followed by treatment of the resultant alcohol with $(CF_3SO_2)_2O$ (Tf_2O) and lutidine gave the enoxide **7** in 70% yield.[10] Palladium-catalyzed ([Pd(OAc)$_2$]/PPh$_3$ in THF) opening of the epoxide ring[11] of **7** in the presence of benzoic acid gave a 4:1 mixture of the 1,4-adduct and 1,2-adduct in 94% combined yield. HPLC and NMR analysis of the products indicate that the major 1,4-adduct is exclusively the α-benzoate but the minor 1,2-adduct is a 2:1 mixture of the α- and β-benzoates. The mixture of isomers was not separated but converted directly to the enone. Protection of the alcohol resulting from the epoxide opening by treatment with *tert*-butyldimethylsilyl chloride (TBSCl)/imidazole, removal of benzoate group in **8a** (MeLi/Et_2O; 83% over two steps), and oxidation of the resultant alcohol with pyridinium chlorochromate (PCC) in CH_2Cl_2 (yield 80%) afforded enone **8b**. 1,2-Addition of propargylmagnesium bromide to **8b** in the presence of $ZnCl_2$ in Et_2O at −78 °C, followed by protection of the alcohol with TMSOTf gave a separable 5:1 mixture of α-trimethylsilyl ether **9** and its β-isomer in 85% yield. Metalation of the alkyne (EtMgBr/THF, at 0 °C), followed by addition of paraformaldehyde gave the alcohol, which was converted to diol **10** by removal of the trimethylsilyl group (K_2CO_3, MeOH) in 97% overall yield. Compound **10** was coupled to (*Z*)-3-iodo-2-propenyl *tert*-butyldimethylsilyl ether with [Pd(OAc)$_2$] and CuI as catalysts[12] (97%). Subsequent bromination of the propargyl alcohol (CBr_4, PPh_3, lutidine/CH_3CN) and selective removal of the primary TBS group (HF_{aq}/CH_3CN, at −20 °C) gave bromide **11** in 57% yield. The cyclization of **11** under high-dilution conditions (10^{-2} M/THF, NaH, room temperature) and protection of the tertiary alcohol (TMSOTf, Et_3N, CH_2Cl_2) gave the cyclic ether **12** in 77% yield. The [2,3]Wittig rearrangement[13] of **12** under our previously described conditions[6,9] (*t*BuLi/THF, at −110 °C) was complete within 10 min. The rearrangement product **13** was obtained in 65% yield with high *cis* selectivity (90%) at the newly formed stereocenters.[14] Alcohol **13** was treated with phthalic anhydride, pyridine, and 4-(dimethylamino)pyridine (DMAP) at room temperature to afford the half ester, which was not isolated but desilylated directly under mild acidic conditions (40% HF_{aq}:CH_3CN = 5:95) at room temperature for 4 h to give the half ester **3**[16] in 47% overall yield after purification by column chromatography.

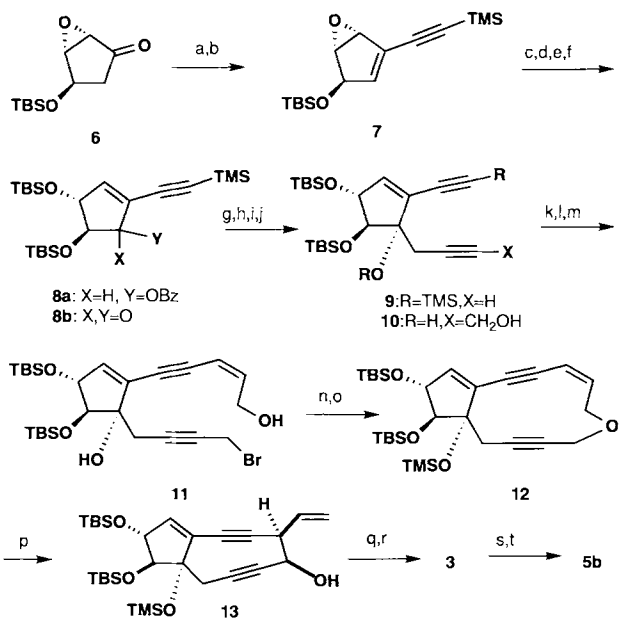

Scheme 2. Synthesis of **3** and **5b**. a) Trimethysilylacetylene, EtMgBr; b) Tf_2O, lutidine; c) [Pd(OAc)$_2$], PPh_3, BzOH; d) TBSCl, imidazole; e) MeLi; f) PCC; g) propargylmagnesium bromide, $ZnCl_2$; h) TMSOTf, NEt_3; i) EtMgBr, $(CH_2O)_n$; j) K_2CO_3; k) (*Z*)-3-iodo-2-propenyl *tert*-butyldimethylsilyl ether, [Pd(OAc)$_2$], PPh_3, CuI, *t*BuNH$_2$; l) CBr_4, PPh_3, lutidine; m) HF_{aq}, CH_3CN; n) NaH, THF; o) TMSOTf, NEt_3; p) *t*BuLi, THF, −110 °C; q) phthalic anhydride, pyridine, DMAP; r) HF_{aq}, CH_3CN, room temperature; s) DBU, THF, cyclohexadiene; t) Ac_2O, pyridine, DMAP.

As expected, the masked enediyne **3** was readily soluble in 10% MeOH aqueous solution and stable for more than 24 h at room temperature under neutral conditions and for more than one month at −20 °C. But under basic conditions (1,8-diazabicyclo[5.4.0]undec-7-ene (DBU), THF, cyclohexadiene), β-elimination of the phthalate in **3**, followed by cycloaromatization of **4b** proceeded to give the aromatized product (see Scheme 1), which was converted to **5b**[17] in 25% overall yield for structure determination. When the phthalate derivative of **13** was treated with DBU in [D$_8$]THF, deuterium was incorporated at C(3) and C(6) of **5c** to the extent of 67% and 53%, respectively. The hypothesis that the biradical is generated from **3** is supported by deuterium incorporation at these positions.

The DNA-cleaving activity of the masked enediyne **3** was then examined. Supercoiled pBR322 DNA was incubated with **3** at various concentrations in 20 mM Tris-HCl buffer (pH 7.5) at 37 °C for 5 h in the absence of thiol (Fig. 1, lanes 6–8; Table 1). Lane 6 (0.1 mM **3**) indicated single strand DNA cleavage with the formation of Form II DNA. Form III DNA, the result of double strand cleavage, was observed with 1.0 mM **3** (lane 8).

Fig. 1. The concentration- and temperature-dependence of the DNA-cleaving activity of **3**; bands obtained on agarose gel by electrophoretic analysis after DNA strand scission.

Table 1. Percentages of Form I, Form II, and Form III DNA after treatment of pBR322 DNA with **3** under various conditions.

Lane	T [°C]	c(**3**) [mM]	Form I	Form II	Form III
1	[a]		85.9	14.1	0.0
2	4	1.0	16.4	74.7	8.9
3	20	1.0	13.6	77.7	8.7
4	37	1.0	7.9	63.3	28.7
5	50	1.0		fragmentation	
6	37	0.1	33.9	63.3	2.8
7	37	0.5	11.6	75.2	13.2
8	37	1.0	8.0	57.9	34.1
9	37	1.0(+DTT)	25.6	72.2	2.2

[a] Intact DNA.

This is in contrast to other DNA-cleaving molecules that alkylate DNA. In the presence of dithiothreitol (lane 9) the DNA-cleaving activity of **3** was not accelerated, indicating that the masked enediyne **3** is activated even in the absence of thiol. Next, the temperature-dependent DNA-cleaving activity was examined by incubation with 1 mM **3** for 5 h (lanes 2–5). As shown in lane 2, appreciable activity is apparent even at 4 °C. A kinetic study with 1.0 mM **3** showed that single strand DNA cleavage proceeded within 5 min on incubation at 37 °C (Table 2). These results suggest that **3** cleaves DNA through a biradical intermediate, which is generated by Bergman cycloaromatization of the highly strained nine-membered enediyne skeleton.

Table 2. Kinetic study of DNA cleavage by **3** (1 mM).

Incubation time [min]	Form I [%]	Form II [%]	Form III [%]
0	94.9	5.1	0
5	21.9	67.2	10.9
10	23.5	66.7	9.8
30	19.3	75.6	5.1
60	12.5	81.6	5.9

In summary, we have succeeded in the design and synthesis of a nine-membered KD analogue with DNA-cleaving activity in the absence of thiols. The biological properties of the designed analogue may underscore it as a potential lead for the further development of DNA-cleaving molecules. Introduction of DNA recognition sites at C(10) and/or C(11) is under investigation in our laboratory.

Received: February 8, 1996 [Z 8795 IE]
German version: *Angew. Chem.* **1996**, *108*, 1946–1949

Keywords: DNA cleavage · enediynes · natural products

[1] a) K. S. Lam, G. A. Hesler, D. R. Gustavson, A. R. Crosswell, J. M. Veitch, S. Forenza, K. Tomita, *J. Antibiot.* **1991**, *44*, 472–478; b) S. J. Hofstead, J. A. Matson, A. R. Malacko, H. Marquardt, *ibid.* **1992**, *45*, 1250–1254; c) J. E. Leet, D. R. Schroeder, S. J. Hofstead, J. Golik, K. L. Colson, S. Huang, S. E. Klohr, T. W. Doyle, J. A. Matson, *J. Am. Chem. Soc.* **1992**, *114*, 7946–7948; d) J. E. Leet, D. R. Schroeder, D. R. Langley, K. L. Colson, S. Huang, S. E. Klohr, M. S. Lee, J. Golik, S. J. Hofstead, T. W. Doyle, J. A. Matson, *ibid.* **1993**, *115*, 8432–8443; e) N. Zein, K. L. Colson, J. E. Leet, D. R. Schroeder, W. Solomon, T. W. Doyle, A. M. Casazza, *Proc. Natl. Acad. Sci. USA* **1993**, *90*, 2822–2826.

[2] a) J. Hu, Y.-C. Xue, M.-Y. Xie, R. Zhang, T. Otani, Y. Minami, Y. Yamada, T. Marunaka, *J. Antibiot.* **1988**, *41*, 1575–1579; b) T. Otani, Y. Minami, Y. Yamada, T. Marunaka, R. Zhang, M.-Y. Xie, *ibid.* **1988**, *41*, 1580–1585; c) Y. Minami, K. Yoshida, R. Azuma, M. Saeki, T. Otani, *Tetrahedron Lett.* **1993**, *34*, 2633–2636; d) K. Yoshida, Y. Minami, R. Azuma, M. Saeki, T. Otani, *ibid.* **1993**, *34*, 2637–2640.

[3] a) Y. Suigimoto, T. Otani, S. Oie, *J. Antibiot.* **1990**, *43*, 417–421; b) Y. Sugiura, T. Matsumoto, *Biochemistry* **1993**, *32*, 5548–5553; c) Y.-J. Xu, Y.-S. Zhen, I. H. Goldberg, *ibid.* **1994**, *33*, 5947–5954; d) T. Matsumoto, Y. Sugiura, *Biochem. Biophys. Res. Commun.* **1994**, *205*, 1533–1538; e) R. J. Cobuzzi Jr., S. K. Kotsopoulos, T. Otani, T. A. Beerman, *Biochemistry* **1995**, *34*, 583–592; f) M. M. McHugh, J. M. Woynarowski, L. S. Gawron, T. Otani, T. A. Beerman, *ibid.* **1995**, *34*, 1805–1814; g) Y.-J. Xu, Z. Xi, Y.-S. Zhen, I. H. Goldberg, *ibid.* **1995**, *34*, 12451–12460.

[4] a) K. C. Nicolaou, Y. Ogawa, G. Zuccarello, H. Kataoka, *J. Am. Chem. Soc.* **1988**, *110*, 7247–7248; b) K. C. Nicolaou, W.-M. Dai, S.-C. Tsay, Y. A. Estevez, W. Wrasidlo, *Science* **1992**, *256*, 1172–1178; Reviews: c) K. C. Nicolaou, A. L. Smith, E. W. Yue, *Proc. Natl. Acad. Sci. USA* **1993**, *90*, 5881–5888; d) M. E. Maier, *Synlett* **1995**, 16–24; e) K. C. Nicolaou, W.-M. Dai, *Angew. Chem.* **1991**, *103*, 1453–1481; *Angew. Chem. Int. Ed. Engl.* **1991**, *30*, 1387–1416; f) K. C. Nicolaou, A. L. Smith, *Acc. Chem. Res.* **1992**, *25*, 497–503.

[5] a) P. A. Wender, M. Harmata, D. Jeffrey, C. Mukai, J. Suffert, *Tetrahedron Lett.* **1988**, *29*, 909–912; b) P. A. Wender, J. A. McKinney, C. Mukai, *J. Am. Chem. Soc.* **1990**, *112*, 5369–5370; c) P. Magnus, T. Pitterna, *J. Chem. Soc. Chem. Commun.* **1991**, 541–543; d) P. Magnus, M. Davies, *ibid.* **1991**, 1522–1524; e) A. G. Myers, P. M. Harrington, E. Y. Kuo, *J. Am. Chem. Soc.* **1991**, *113*, 694–695; f) A. G. Myers, P. M. Harrington, B.-M. Kwon, *ibid.* **1992**, *114*, 1086–1087; g) K. R. Buszek, Y. Jeong, *Syn. Commun.* **1994**, *24*, 2461–2470; h) K. Iida, M. Hirama, *J. Am. Chem. Soc.* **1994**, *116*, 10310–10311; i) *ibid.* **1995**, *117*, 8875–8876.

[6] T. Doi, T. Takahashi, *J. Org. Chem.* **1991**, *56*, 3465–3467.

[7] a) M. E. Maier, T. Brandstetter, *Tetrahedron Lett.* **1991**, *32*, 3679–3682; b) A. G. Myers, P. S. Dragovich, *J. Am. Chem. Soc.* **1992**, *114*, 5859–5860; c) H. Audrain, T. Skrydstrup, G. Ulibarri, D. S. Grierson, *Synlett* **1993**, 20–22; d) H. Audrain, T. Skrydstrup, G. Ulibarri, C. Riche, A. Chiaroni, D. S. Grierson, *Tetrahedron* **1994**, *50*, 1469–1502; e) J. M. Nuss, M. M. Murphy, *Tetrahedron Lett.* **1994**, *35*, 37–40.

[8] K. C. Nicolaou, G. Zuccarello, Y. Ogawa, E. J. Schweiger, T. Kumazawa, *J. Am. Chem. Soc.* **1988**, *110*, 4866–4868.

[9] T. Takahashi, H. Tanaka, Y. Hirai, T. Doi, H. Yamada, T. Shiraki, Y. Sugiura, *Angew. Chem.* **1993**, *105*, 1719–1722; *Angew. Chem. Int. Ed. Engl.* **1993**, *32*, 1657–1659.

[10] Addition of (*Z*)-1-(tetrahydro-2*H*-pyran-2-yloxy)pent-2-en-4-yne to enone **6** and dehydration of the resultant tertiary alcohol with $(CF_3SO_2)_2O$ and lutidine gave the *E*-configurated cyclopentenylpentenyne, which complicated the cyclization analogous to **11** → **12**.

[11] a) T. Takahashi, H. Kataoka, J. Tsuji, *J. Am. Chem. Soc.* **1983**, *105*, 147–149; b) D. R. Deardorff, D. C. Myles, K. D. MacFerrin, *Tetrahedron Lett.* **1985**, *26*, 5615–5618.

[12] a) R. D. Stephens, C. E. Castro, *J. Org. Chem.* **1963**, *28*, 3313–3315; b) K. Sonogashira, Y. Tohada, N. Hagihara, *Tetrahedron Lett.* **1975**, 4467–4470; c) V. Ratovelomanana, G. Linstrumellle, *Tetrahedron Lett.* **1981**, *22*, 315–318.

[13] Transannular [2,3] Wittig rearrangement: a) T. Takahashi, H. Nemoto, Y. Kanda, J. Tsuji, Y. Fujise, *J. Org. Chem.* **1986**, *51*, 4315–4316; b) J. A. Marshall, T. M. Jensojn, B. S. DeHoff, *ibid.* **1986**, *51*, 4316–4319; c) reviews on the acyclic [2,3] Wittig rearrangement: T. Nakai, K. Mikami, *Chem. Rev.* **1986**, *86*, 885–902.

[14] The *cis* relationship between C(4) vinyl and C(5) hydroxyl groups was established by NOE experiments. The relative configuration between the C(5) and C(11) hydroxyl groups was determined based on modified MTPA method [15]. For further details of the structural determination of **13**, see: T. Takahashi, H. Tanaka, Y. Sakamoto, H. Yamada, *Heterocycles* **1996**, *43*, 945–948.

[15] I. Ohtani, T. Kusumi, Y. Kashman, H. Kakisawa, *J. Am. Chem. Soc.* **1991**, *113*, 4092–4096.

[16] **3**: ^{1}H NMR (270 MHz, [D$_6$]DMSO): δ = 7.6–7.8 (m, 4H), 5.84 (ddd, 1H, J = 6.9, 9.9, 17.2 Hz), 5.76 (d, 1H, J = 2.0 Hz), 5.47 (dd, 1H, J = 2.6, 6.6 Hz), 5.45 (br., 1H, J = 17.2 Hz), 5.20 (br., 1H, J = 9.9 Hz), 4.14–4.24 (m, 1H), 3.98 (br., 1H, J = 6.6, 6.9 Hz), 3.75–3.84 (m, 1H), 2.41 (d, 1H, J = 17.5 Hz), 2.34 (dd, 1H, J = 2.6, 17.5 Hz); ^{13}C NMR (67.8 MHz, [D$_6$]DMSO): δ = 170.2, 167.7, 133.9, 132.3, 132.0, 131.3, 131.3, 129.5, 128.8, 128.3, 118.7, 97.6, 94.3, 91.1, 87.4, 84.8, 81.2, 76.9, 69.0, 43.1, 26.6; IR (KBr): 3402, 2212, 1719, 1259, 1118, 1069, 1038, 789, 744, 712 cm^{-1}; MS (FAB): *m/z*: 417 [M^+ + Na], 433 [M^+ + K], 471 [M^+ − H + 2K].

[17] **5b**: ^{1}H NMR (270 MHz, CD_2Cl_2): δ = 7.59 (d, 1H, J = 1.7 Hz), 7.39 (dd, 1H, J = 1.7, 7.9 Hz), 7.26 (d, 1H, J = 7.9 Hz), 6.74 (dd, 1H, J = 10.9, 17.5 Hz), 6.23 (d, 1H, J = 3.3 Hz), 5.78 (d, 1H, J = 17.5 Hz), 5.52 (d, 1H, J = 3.3 Hz), 5.44 (s, 1H), 5.28 (d, 1H, J = 10.9 Hz), 3.36 (d, 1H, J = 18.1 Hz), 3.24 (d, 1H, J = 18.1 Hz), 2.08(s, 3H), 2.07 (s, 3H), 1.99 (s, 3H); ^{13}C NMR (67.8 MHz, CD_2Cl_2): δ = 171.0, 170.2, 169.3, 156.1, 148.1, 137.6, 136.6, 133.8, 128.6, 126.6, 121.1, 120.8, 114.4, 97.2, 85.7, 76.7, 35.3, 22.1, 21.2, 21.2; IR (Film): 2926, 2250, 1735, 1429, 1368, 1226, 1025, 929, 827, 732, 608 cm^{-1}; MS (FAB): *m/z*: 379 [M^+ + Na].

 © VCH Verlagsgesellschaft mbH, D-69451 Weinheim, 1996 0570-0833/96/3516-1837 $ 15.00+.25/0

Self-Assembly of a Circular Double Helicate**

Bernold Hasenknopf, Jean-Marie Lehn,* Boris O. Kneisel, Gerhard Baum, and Dieter Fenske

Dedicated to Professor Guy Ourisson on the occasion of his 70th birthday

Helicates, metal complexes that form double[1-4] or triple helices[5-7] in solution and/or in the solid state, are generated by self-assembly of two or three ligand strands around suitable metal ions. Whereas the double helix of DNA results from the assembly of two complementary chains of nucleotides through hydrogen bonding, helicates form spontaneously from linear ligands composed of a series of discrete binding subunits through metal ion coordination. The process may be considered as resulting from the operation of a programmed system, in which the steric and interactional information stored in the ligands is read out by the metal ions following the algorithm defined by their coordination geometry.[3] Thus homostranded double[1,3,4] and triple[5,7] helicates have been obtained from chains of 2,2′-bipyridine (bpy) or 2,2′:6′,2″-terpyridine (terpy) groups connected by short covalent bridges, and metal ions having tetrahedral or octahedral coordination geometry. Recently, a heteroduplex helicate based on a tris-bpy strand, a tris-terpy strand, and pentacoordinated Cu^{II} ions has been described.[8]

The DNA double helix is usually acyclic but can also be closed into a cyclic structure, a circular DNA, as found in some viruses. By analogy, it would be of great interest to devise means of generating closed, circular helicates. We describe herein the self-assembly of such a supramolecular architecture. The tris-bpy ligand **L** and iron(II) chloride have been found to form spontaneously and quantitatively a circular double helicate, **cH** (Fig. 1), in other words, a double helicate closed into a ring, as indicated by ^{1}H NMR spectroscopy and mass spectrometry as well as by X-ray crystal structure determination.

The reaction of ligand **L**[5] with an equimolar amount of $FeCl_2$ in ethylene glycol at 170 °C gave a clear red solution, as expected for an iron–bpy complex. Addition of NH_4PF_6 precipitated a red solid, which was separated and analyzed. Its electronic absorption spectrum shows a band at 523 nm in the visible range, which corresponds to the metal–ligand charge transfer (MLCT) band of an "$Fe(bpy)_3$" unit.[9] This agrees with the complexation of three bpy units by each iron(II) ion. In view of the structure of ligand **L**, these three bpy units cannot belong to the same ligand strand. An inspection of molecular models shows that the central and a terminal bpy of one ligand strand cannot be arranged around the same Fe^{II} ion; also the complexation of the two terminal bpys of one ligand by one Fe^{II} ion results in deformation of the central bpy. Therefore, every Fe^{II} ion should complex one bpy from each of three different ligands **L**.

The ^{1}H NMR spectrum of the complex displays a singlet for the methyl groups, pointing to a similar environment for all the ligands in the Fe^{II} complex. The signals of CH_2 groups of the bridges between the bpy units appear as a singlet in the free ligand and as a multiplet in the complex. This splitting agrees with the formation of a helicoidal structure, in which these protons form an AA′BB′ system. The aromatic part of the spectrum shows three singlets and six doublets for the complex, each of which corresponds to two protons. Hence, the complex has a twofold symmetry axis through the C2–C2′ bond of the central bpy. The signals of the protons α to the nitrogens of both the central and the lateral bpys are shifted upfield relative to the signals of the free ligand. This indicates that all the bpy groups of the ligand are coordinated, since octahedral coordination of three bpy units on one metal ion brings these protons in proximity to the aromatic system of another bpy on the same metal center, resulting in the observed upfield shift.

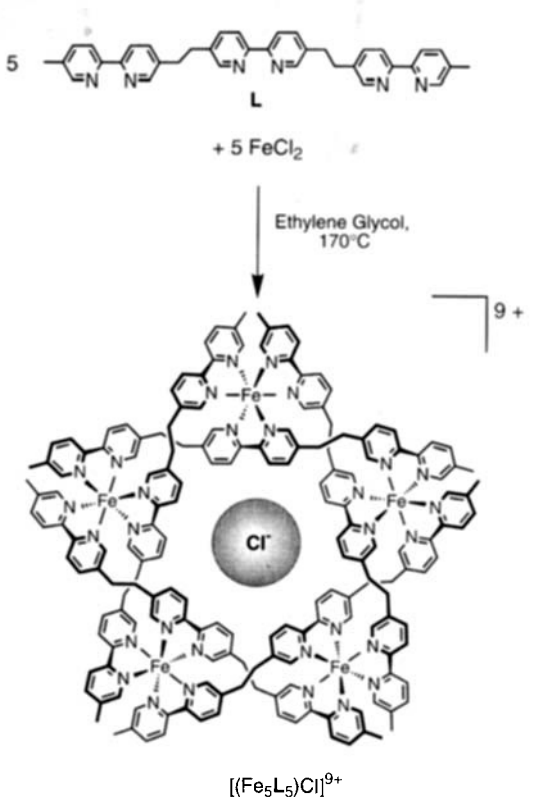

Fig. 1. Self-assembly of the circular helicate $[(Fe_5\mathbf{L}_5)Cl]^{9+}$ from five tris-bpy ligand strands **L** and five equivalents of $FeCl_2$.

All signals have been assigned unequivocally by a series of decoupling and NOE measurements. The NOE measurements allowed a further look into the structure of the complex. One observes interactions between all the protons α to the nitrogens, which must therefore be close in space. This is only possible if central and terminal bpys are coordinated to the same Fe^{II} ion. In view of the limited flexibility of ligand **L** it implies that the central bpy of one strand and the terminal bpys of two other strands are brought into proximity. To assure that all the coordination sites are occupied and open ends are avoided, the whole complex must be closed into a ring.

The electrospray mass spectrum (ESI-MS) indicates a complex with the composition $[(Fe_5\mathbf{L}_5)Cl](PF_6)_9$. The signals of cations arising from an initial complex $[(Fe_5\mathbf{L}_5)Cl](PF_6)_7^{2+}$ through the successive loss of PF_6 anions down to $[(Fe_5\mathbf{L}_5)Cl](PF_6)_2^{7+}$ are observed. The chloride ion must be bound strongly to the complex, since it is found in all fragments.

Single crystals were obtained from nitromethane/benzene and analyzed by X-ray diffraction.[10] The structure determination

[*] Prof. Dr. J.-M. Lehn, B. Hasenknopf
Laboratoire de Chimie Supramoléculaire
Institut Le Bel, Université Louis Pasteur
CNRS URA 422
4, rue Blaise Pascal, F-67000 Strasbourg (France)
Fax: Int. code +8841 1020
B. O. Kneisel, G. Baum, Prof. Dr. D. Fenske
Institut für Anorganische Chemie der Universität Karlsruhe (Germany)

[**] We thank Prof. Dr. A. Van Dorsselaer and A. Dupont-Gervais for determining the electrospray mass spectra and P. Maltèse for the NOESY NMR spectra.

 © VCH Verlagsgesellschaft mbH, D-69451 Weinheim, 1996 0570-0833/96/3516-1838 $ 15.00+.25/0

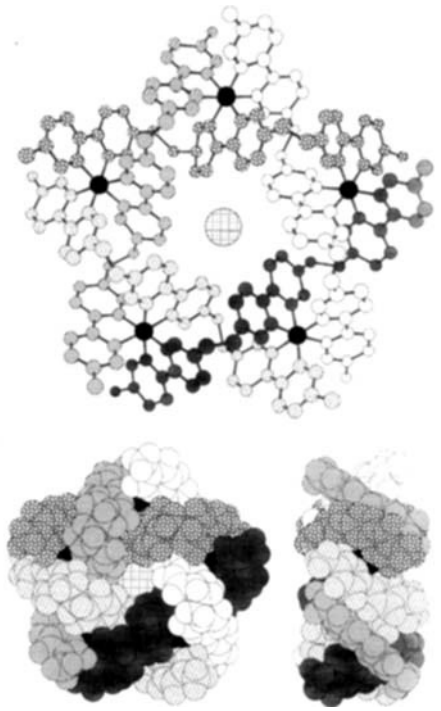

Fig. 2. Top: ball-and-stick representation of the crystal structure of the circular helicate $[(Fe_5L_5)Cl]^{9+}$ in the PF_6 salt. Bottom: CPK representations; left: top view; right: side view. The five ligand strands **L** are shown in different patterns, the Fe^{II} centers are black.

confirms the other results (Fig. 2). The complex consists of five Fe^{II} ions, five ligands **L**, and a chloride ion: $[(Fe_5L_5)Cl]^{9+}$. Each Fe^{II} ion has a distorted octahedral coordination sphere occupied by three bpy groups,[14] two terminal and one central, belonging to three different ligand strands. The metal ions lie almost in one plane and form the corners of a pentagon with an edge length of 8.4 Å (Fe–Fe distance). Neighboring Fe^{II} ions are connected by two strands **L**, which cross each other, resulting in a rotatory sense of the structure. The ligands wrap helically around the connecting line between the Fe^{II} ions. A full turn is completed between three successive metal centers. The rotatory sense between the metals in the complex is the same throughout the structure.

The $[Fe_5L_5]^{10+}$ cation can be described as a *circular double helix* resulting in a torus, with an outer diameter between two opposite carbon atoms of about 22 Å. The inner cavity has a radius of 1.75 Å and contains a chloride ion (ionic radius 1.8 Å). This tight inclusion into a cavity bearing ten positive charges agrees with the strong binding of the chloride ion indicated by the stability of the complex in ESI-MS with respect to the loss of Cl^- and by the fact that no exchange takes place in the presence of a large excess of another anion such as PF_6^- or $CF_3SO_3^-$. The torus $[Fe_5L_5]^{10+}$ is thus a specific receptor for chloride.

The salt of the chiral cation is obtained as a racemic mixture. The unit cell contains two tori of opposite rotatory sense. First attempts at chromatographic separation (Sephadex-SP C-25, 40–120 μm, eluting with an aqueous solution of sodium (+)-tartratoantimonate[15]) yielded two optically active fractions. Their circular dichroism spectra display an opposite Cotton effect at the same wavelength maxima. Full resolution of the two enantiomers was not achieved at this stage.

A number of multinuclear complexes present a circular arrangement of metal centers[16] and may include small atoms or molecules.[17] In these structures the ligands bridge two adjacent metal centers. The supramolecular architecture of $[(Fe_5L_5)Cl]^{9+}$ exhibits unique features: each ligand strand bridges three metal centers and together they form a double helix, which is closed into a torus, representing therefore a circular helicate of fivefold symmetry [5]**cH**, the helicate analog of circular DNA.

The complexation of ligand **L** with Ni^{II} resulted in an architecture also containing octahedrally coordinated metal centers.[5] However, in this case a triple helix formed, in which three ligand strands **L** are wrapped around three Ni^{II} ions. This triple helicate composition $[Ni_3L_3]^{6+}$ was obtained with both $Ni(ClO_4)_2$ and $NiCl_2$ under exactly the same conditions as those leading to the formation of the torus using $FeCl_2$. Thus, different supramolecular architectures are generated with two metal ions which both display octahedral coordination geometry. Preliminary results indicate that the two architectures can be obtained from both metal ions under suitable reaction conditions; the triple helicate is formed first and then converted into the cyclic structure.

Furthermore, the reaction of the ligand **L** with different iron salts yields different complexes. Preliminary results show that $Fe(BF_4)_2$ gives a hexameric $[Fe_6L_6]^{12+}$ complex which could also have a circular structure. The self-assembly is therefore not only determined by the ligand and the coordination geometry of the metal ion, but also by the nature of the counteranion, thus opening the way to a range of novel architectures.

The torus also lends itself to further elaboration. For instance, the covalent connection of the two terminal bpy units of two different strands at each Fe^{II} ion would yield a molecule with the topology of a fivefold knot.[18] The addition of the circular [5]**cH** structure to the linear double[1–4] and triple[5–7] helicates described previously, represents a novel step and warrants further exploration of the developing "helicate world".

The present results are also of much significance from another point of view related to an area of great current activity—combinatorial chemistry. The generation of a defined assembly that depends on the nature of a bound substrate (for example the chloride ion in $[(Fe_5L_5)Cl]^{9+}$) may be considered either as the result of templating by the substrate, or conversely, and much more interestingly, as the result of the spontaneous assembly of a suitable number of components to form a species capable of strongly binding a given substrate. In other words, the latter represents a combinatorial generation of a receptor by self-assembly of a set of components (identical or different) into the entity that most strongly binds the substrate. Thus, the pentameric cyclic structure $[(Fe_5L_5)Cl]^{9+}$ is selected[19] among all possible oligomers when chloride ions are present; other entities may be formed with other anions.

In general terms, such multicomponent self-assembly of a receptor amounts to the generation/selection from a *virtual combinatorial library* (VCL, a library made up of all possible combinations in number and nature of the available components) of that supramolecular entity, among all those possible, that best binds a given substrate, by recruiting the best suited components from the set of those available. Further exploration of this VCL concept is being actively pursued.[21]

Experimental Procedure

The tris-bpy ligand **L** (67 mg, 0.12 mmol) and iron(II) chloride ($FeCl_2 \cdot 4H_2O$, 24 mg, 0.12 mmol) were mixed in ethylene glycol (10 mL) under argon. The red suspension was heated to 170–180 °C overnight. A dark red solution formed. After the reaction mixture had cooled down to room temperature, an aqueous solution of NH_4PF_6 (ca. 1 g in 40 mL) was added. A red gellike solid formed, which was isolated by centrifugation, washed with methanol/ether 1/1, and dried in a desiccator to provide 104 mg of a red powder. Thin-layer chromatography: Al_2O_3, $CH_3CN:H_2O$ (5% NH_4PF_6), $R_f = 0.8$; SiO_2, $CH_3CN:H_2O:KNO_3$ aq. sat. 5:4:1, $R_f = 0.3$;

^{1}H NMR (400 MHz, CD_3CN, 25 °C, TMS): δ = 2.21 (s, 6H; CH_3), 2.6–3.0 (m, 8H; CH_2), 6.47 (s, 2H; 6_A), 6.57 (s, 2H; 6_B), 7.23 (s, 2H; $6'_A$), 7.52 (br. d, 4H; $4_A + 4_B$), 8.08 (d, 7.2 Hz, 2H; $4'_A$), 8.25 (d, 8.3 Hz, 2H; 3_A), 8.47 (d, 8.3 Hz, 2H; $3'_A$), 10.02 (d, 8.3 Hz, 2H; 3_B); A = terminal bpy, B = central bpy; ESI-MS: m/z 2034.24 $[(Fe_5L_5Cl)(PF_6)_7]^{2+}$, 1308.73 $[(Fe_5L_5Cl)(PF_6)_6]^{3+}$, 945.15 $[(Fe_5L_5Cl)(PF_6)_5]^{4+}$, 726.98 $[(Fe_5L_5Cl)(PF_6)_4]^{5+}$, 581.54 $[(Fe_5L_5Cl)(PF_6)_3]^{6+}$, 477.52 $[(Fe_5L_5Cl)(PF_6)_2]^{7+}$; IR (KBr): ν = 3406 (br), 3032 (m), 1602 (m), 1477 (s), 1401 (m), 1247 (m), 1041 (m), 840 (vs), 732 (m), 558 (s) cm^{-1}; UV/Vis (CH_3CN): λ_{max} (ε_{max}): 523 (3.80×10^4), 313 (2.37×10^5), 269 (1.36×10^4), 257 nm (1.38×10^4 $dm^3 mol^{-1} cm^{-1}$); correct C, H, N analysis.

Received: March 1, 1996 [Z8887IE]
German version: *Angew. Chem.* **1996**, *108*, 1987–1990

Keywords: helicates · iron compounds · supramolecular chemistry

[1] J.-M. Lehn, A. Rigault, J. Siegel, J. Harrowfield, B. Chevrier, D. Moras, *Proc. Natl. Acad. Sci. USA* **1987**, *84*, 2565.
[2] E. C. Constable, *Prog. Inorg. Chem.* **1994**, *42*, 67; K. T. Potts, M. Keshavarz-K, F. S. Tham, H. D. Abruna, C. R. Arana, *Inorg. Chem.* **1993**, *32*, 4422, 4436; J.-M. Lehn, A. Rigault, *Angew. Chem.* **1988**, *100*, 1121; *Angew. Chem. Int. Ed. Engl.* **1988**, *27*, 1095.
[3] J.-M. Lehn, *Supramolecular Chemistry—Concepts and Perspectives*, VCH, Weinheim, **1995**.
[4] J. D. Crane, J.-P. Sauvage, *New J. Chem.* **1992**, *16*, 649.
[5] R. Krämer, J.-M. Lehn, A. De Cian, J. Fischer, *Angew. Chem.* **1993**, *105*, 764; *Angew. Chem. Int. Ed. Engl.* **1993**, *32*, 703.
[6] L. J. Charbonnière, G. Bernardinelli, C. Piguet, A. M. Sargeson, A. F. Williams, *J. Chem. Soc. Chem. Commun.* **1994**, 1419; K. T. Potts, C. P. Horwitz, A. Fessak, M. Keshavarz-K, K. E. Nash, P. J. Toscano, *J. Am. Chem. Soc.* **1993**, *115*, 10444; C. Piguet, J.-C. G. Bünzli, G. Bernardinelli, C. G. Bochet, P. Froidevaux, *J. Chem. Soc. Dalton Trans.* **1995**, 83; E. J. Enemark, T. D. P. Stack, *Angew. Chem.* **1995**, *107*, 1082; *Angew. Chem. Int. Ed. Engl.* **1995**, *34*, 996.
[7] D. Zurita, P. Baret, J.-L. Pierre, *New J. Chem.* **1994**, *18*, 1143.
[8] B. Hasenknopf, J.-M. Lehn, G. Baum, D. Fenske, *Proc. Natl. Acad. Sci. USA* **1996**, *93*, 1397.
[9] F. W. Cagle, G. F. Smith, *J. Am. Chem. Soc.* **1947**, *69*, 1860.
[10] Crystal data for $[\{Fe_5L_5)Cl\}_2](PF_6)_{17.5}Cl_{0.5} \cdot 11\,H_3CNO_2 \cdot 40.5\,H_2O$: diffractometer and data collection: STOE IPDS (−80 °C), graphite-monochromated $Mo_{K\alpha}$ radiation (λ = 0.71073 Å), monoclinic, space group $P2/n$, a = 38.918(8), b = 27.036(5), c = 52.492(11) Å, β = 97.42(3)°, V = 54769(19) Å^3, Z = 2, μ = 0.417 mm^{-1}, $F(000)$ = 20212, ρ_{calc} = 1.208 $Mg\,m^{-3}$, M_r = 19914.16, $2\theta_{max}$ = 45°. Structure solution and refinement: Primary structure solution by direct methods (SHELXS-92) [11a]. Anisotropic refinement for all non-hydrogen atoms (SHELXL-93) [11b], as indicated by R_{free} tests [12]. A riding model starting from calculated positions was employed for the hydrogen atoms; no hydrogen positions were calculated for nitromethane and water molecules. 162803 measured reflections, 69755 independent [R(int) = 0.0874], of which 42481 within a resolution shell of $8.00 \geq d \geq 1.06$ Å were employed in the refinement of 6004 parameters using 126032 restraints, as described in the following. 1) Ligands L: planarity for the aromatic systems and for the coordination spheres around each 1- and 4-position of the pyridyl rings; combined 1,2/1,3 distance restraints for chemically equivalent distances within the bpy units allowing free rotation between the aromatic systems; rigid-bond and similarity restraints for the anisotropic displacement parameters. 2) PF_6 Anions: combined 1,2/1,3 distance restraints for chemically equivalent distances, additional fitting of P···F and F···F distances to target values of 1.60 and 2.24 Å, respectively (e.s.d. 0.03 Å). Rigid-bond and similarity restraints for the anisotropic displacement parameters. Constraints were employed for the anisotropic displacement parameters of opposite fluorine positions. Most of the anions show up to threefold positional disorder, which could not always be resolved and modeled completely. 3) "Free" chlorine anions: the anisotropic displacement parameters were restrained to be approximately isotropic (e.s.d. 0.10 Å). Two positions were treated as being one-fourth occupied. "Anti-bumping" restraints were applied to prevent close contacts between isolated ions and other molecules. 4) Nitromethane: planarity for the coordination spheres around the nitrogen atoms; combined 1,2/1,3 distance restraints for chemically equivalent distances; additionally fitting of N–C, N–O, and O···O distances to target values of 1.55, 1.20, and 2.16 Å, respectively (e.s.d. 0.03 Å). Rigid-bond, similarity, and isotropic restraints for the anisotropic displacement parameters. Some of the solvent molecules show twofold positional disorder, which could be resolved. 5) Water: the anisotropic displacement parameters were restrained to be approximately isotropic (e.s.d. 0.10 Å). Some water positions were treated as half occupied, most water sites were given full occupancies. "Anti-bumping" restraints were applied to prevent close contacts between isolated molecules, and "Babinet's principle" was employed to model diffuse water [13]. The structure was refined against F^2 (full matrix least squares) with the weighting scheme $w^{-1} = \sigma^2(F_o^2) + (0.3526\,P)^2 + 207.5267\,P$, with $P = (F_o^2 + 2F_c^2)/3$, $R1$ = 0.1552 ($F > 4\sigma F$) [$R1$ = 0.2298 (all data)] and $wR2$ = 0.5332 (all data), GooF on F^2 = S = 1.058, max./min. residual density: +1.132/−0.981 e Å^{-3}. ($R1 = \Sigma||F_o| - |F_c||/\Sigma|F_o|$, $wR2 = [\Sigma w(F_o^2 - F_c^2)^2/\Sigma wF_o^4]^{1/2}$, GooF = $S = \{\Sigma[w(F_o^2 - F_c^2)^2]/(n-p)\}^{1/2}$, where n = number of reflections and p = number of parameters). Crystallographic data (excluding structure factors) for the structure reported in this paper have been deposited with the Cambridge Crystallographic Data Centre as supplementary publication no. CCDC-179-46. Copies of the data can be obtained free of charge on application to The Director, CCDC, 12 Union Road, Cambridge CB21EZ, UK (fax: Int. code +(1223)336-033; e-mail: teched@chemcrys.cam.ac.uk).
[11] a) G. M. Sheldrick, *Acta Crystallogr. Sect. A* **1990**, *46*, 467; b) G. M. Sheldrick, SHELXL-93, program for crystal structure refinement, University of Göttingen, **1993**.
[12] A. T. Brünger, *Nature* **1992**, *355*, 472.
[13] R. Langridge, D. A. Marvin, W. E. Seeds, H. R. Wilson, C. P. Hooper, M. H. F. Wilkins, L. D. Hamilton, *J. Mol. Biol.* **1960**, *2*, 38; H. Driessen, M. I. J. Haneef, G. W. Harris, B. Howlin, G. Khan, D. C. Mos, *J. Appl. Crystallogr.* **1989**, *22*, 510.
[14] The coordination geometry is similar to that found in $[Fe(bpy)_3]^{2+}$ itself (N-Fe-N angles of about 80°, N–Fe distances of about 1.96 Å), see for instance: M. E. García Posse, M. A. Juri, P. J. Aymonino, O. E. Piro, H. A. Negri, E. E. Castellano, *Inorg. Chem.* **1984**, *23*, 948.
[15] Y. Yoshikawa, K. Yamasaki, *Coord. Chem. Rev.* **1979**, *28*, 205.
[16] See for instance: S. Gambarotta, C. Floriani, A. Chiesi-Villa, C. Guastini, *J. Chem. Soc. Chem. Commun.* **1983**, 1304; O. Poncelet, L. G. Hubert-Pfalzgraf, J.-C. Daran, R. Astier, *J. Chem. Soc. Chem. Commun.* **1989**, 1846; K. L. Taft, C. D. Delfs, G. C. Papaefthymiou, S. Foner, D. Gatteschi, S. J. Lippard, *J. Am. Chem. Soc.* **1994**, *116*, 823; P. J. Stang, D. H. Cao, S. Saito, A. M. Arif, *J. Am. Chem. Soc.* **1995**, *117*, 6273.
[17] M. S. Lah, V. L. Pecoraro, *Comments Inorg. Chem.* **1990**, *11*, 59; H. Barrow, D. A. Brown, N. W. Alcock, H. J. Clase, M. G. H. Wallbridge, *J. Chem. Soc. Chem. Commun.* **1995**, 1231; R. N. Grimes, *Angew. Chem.* **1993**, *105*, 1350; *Angew. Chem. Int. Ed. Engl.* **1993**, *32*, 1289. A. Caneschi, A. Cornia, S. J. Lippard, *ibid.* **1995**, *107*, 511 and **1995**, *34*, 467.
[18] N. van Gulick, *New J. Chem.* **1993**, *17*, 619.
[19] This selection bears some relationship to the self-recognition processes described earlier where specific ligands are preferentially incorporated into a given inorganic superstructure [20].
[20] J.-M. Lehn, R. Krämer, A. Marquis-Rigault, *Proc. Natl. Acad. Sci. USA* **1993**, *90*, 5394.
[21] D. P. Funeriu, B. Hasenknopf, Y. Huc, J.-M. Lehn, unpublished results.

Planar Bischlorophyll Derivatives with a Completely Conjugated π-System: Model Compounds for the Special Pair in Photosynthesis**

Laurent Jaquinod, Mathias O. Senge, Ravindra K. Pandey, Timothy P. Forsyth, and Kevin M. Smith*

Chlorophylls play a central role in photosynthesis as both antenna arrays and reaction centers. One of the most intriguing problems associated with mimicking their biological function in model systems has been the synthesis of suitable model compounds for the delocalized state of the "special pair" chlorophylls in the reaction center.[1] Numerous attempts have been made to develop model compounds for reaction center chloro-

[*] Prof. Dr. K. M. Smith, Dr. L. Jaquinod, T. P. Forsyth
Department of Chemistry, University of California
Davis, CA 95616 (USA)
Fax: Int. code +(916)752-8995
e-mail: smith@chem.ucdavis.edu
Dr. M. O. Senge
Institut für Organische Chemie (WE02) der Freien Universität Berlin
Takustrasse 3, D-14195 Berlin (Germany)
Dr. R. K. Pandey
Department of Radiation Biology
Roswell Park Cancer Institute
Buffalo, NY 14263 (USA)

[**] This work was supported by grant CHE-93-05577 from the National Science Foundation, grants from the Deutsche Forschungsgemeinschaft and the Fonds der Chemischen Industrie, and a grant from Oncologic Foundation of Buffalo.

phylls in general.[2] Supramolecular approaches towards the reaction center have yielded promising results,[3a] but only few attempts have been made to address models of the special pair.[2, 3b] Criteria for a good model of the special pair excited state include two chlorin macrocycles in close proximity, a substituent pattern as close as possible to that in natural chlorophylls, and interaction between the π-electron systems of the pair. Even though the special pair itself consists of partly cofacial bacteriochlorophylls overlapping in the ring A area, any kind of electronic coupling between the two components of a pair should produce models worthy of investigation. Along these lines, much recent work has been devoted to the preparation of bismacrocycles in which the two chromophores are coplanar,[4] thereby allowing electronic coupling between the two macrocycles. To date, these systems have consisted of porphyrin subunits. We felt that a more meaningful model for the special pair would consist of a bischlorin in which the two chlorin subunits are coplanar and thus strongly coupled electronically.

We report here the synthesis, spectroscopic properties, and structural analysis of a novel planar bisphaeophorbide system in which the two macrocycles are connected directly by a C=C bridge. The titanium-mediated, reductive coupling of ketones (McMurry reaction)[5] was the key reaction in our approach, and the substrates were derived, initially, from methyl mesopyrophaeophorbide *a* **1**, which possesses a reactive 13^1-carbonyl function, still contains the major structural features of native chlorophyll, and is easily prepared from chlorophyll *a*.[6] McMurry coupling of nickel(II) complex **2** at $-10\,^{\circ}C$ in dimethoxyethane (DME) produced the green nickel(II) bischlorin **3** in 44% yield (61% based on recovered starting material). The ^1H NMR spectrum of **3** indicated a single diastereomer with C_2 symmetry. When the coupling reaction of **2** was performed at $-30\,^{\circ}C$, the formation of the pinacol intermediate could be monitored by disappearance of the Q-band at 638 nm and appearance of another at 620 nm. Chromatography on alumina (Brockmann activity III) or dissolution in dimethyl sulfoxide (DMSO) caused reversion of the pinacol to starting material.[7]

Since attempts to demetalate **3** with concentrated H_2SO_4 led to decomposition, the metal-free bisphaeophorbide **4** was prepared by coupling the zinc(II) monomer **5** in the presence of 3.5 equivalents of pyridine. The zinc(II) ion was removed readily upon treatment with trifluoroacetic acid (TFA) in CH_2Cl_2. After chromatographic purification the free-base bisphaeophorbide **4** was obtained in 46% yield. Hydrogenation (10% Pd/C) of **4** gave quantitatively **6**, and the main Q-band shifted from 752 to 740 nm. Reaction of **6** with $Zn(OAc)_2$ gave the bischlorin **7**.

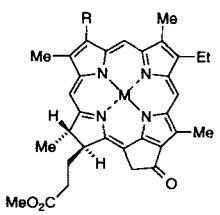

1 M = 2H; R = Et
2 M = Ni; R = Et
5 M = Zn; R = CH=CH$_2$

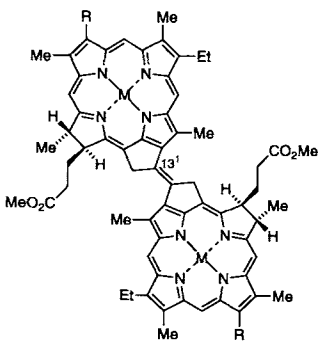

3 M = Ni; R = Et
4 M = 2H; R = CH=CH$_2$
6 M = 2H; R = Et
7 M = Zn; R = Et

To extend this methodology we examined other chlorin substrates containing ketone groups. When a McMurry coupling of the nickel(II) complex **8**[8] was attempted, the expected bischlorin was not produced. Instead chlorin **9** was obtained in quantitative yield. In the case of the zinc(II) analogue **10**, a similar reduction (in presence of pyridine) could be effected, giving compound **11** in 60% yield. This direct reduction of ketochlorins is unusual, as they have been shown to be unreactive to most reducing agents[8] except for alkyllithiums, though a two-step reduction has been reported.[9] McMurry coupling between acetone and **2** (acetone/**2** = 10/1) gave the isopropylidene adduct in moderate yield; the Q-band of this compound is only slightly blue-shifted ($\Delta\lambda = 14$ nm) compared to that of the starting material.

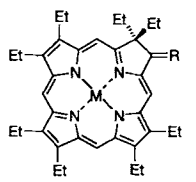

8 M = Ni; R = O
9 M = Ni; R = 2H
10 M = Zn; R = O
11 M = Zn; R = 2H

The most notable feature of the bischlorins is the large bathochromic shifts of the main Q-band relative to the those of the monomeric chlorins (Fig. 1). For instance **3** shows a 92 nm

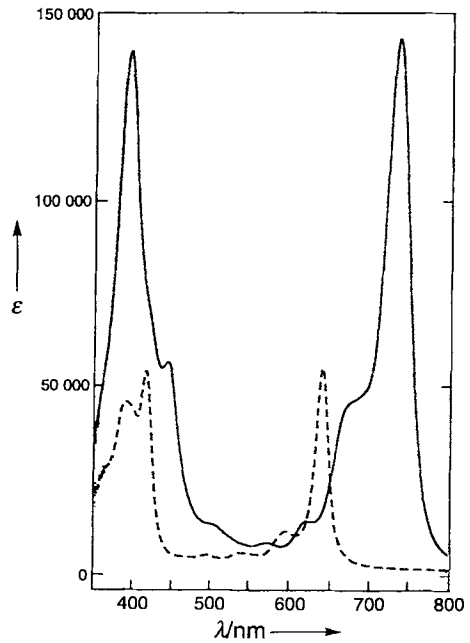

Fig. 1. UV/Vis spectra of **3** (—) and **2** (– – –) in CH_2Cl_2.

red-shift of the highest wavelength absorbance relative to the that of the monomeric nickel(II) compound. The bathochromic shift and the hyperchromic effect displayed by **3** support the hypothesis of "electronic delocalization" within the two phaeophorbide subunits. The Q-bands are sensitive to concentration changes, undergoing a slight blue shift with increased concentration. In the ^1H NMR spectrum of **6** the additional upfield shift for the NH protons ($\delta = -0.95$ and -2.81 versus 0.60, -1.60 for **1**) and the extra downfield chemical shifts of the *meso* protons further support the existence of electronic delocalization.

The molecular structure was established by X-ray crystallography (Fig. 2).[10a] The double bond character of the connecting bridge in **6** is clearly shown by the $C(13^1)-C(13^1)'$ bond length of 1.34(2) Å. With the exception of the reduced pyrrole rings the

 © VCH Verlagsgesellschaft mbH, D-69451 Weinheim, 1996 0570-0833/96/3516-1841 $ 15.00+.25/0

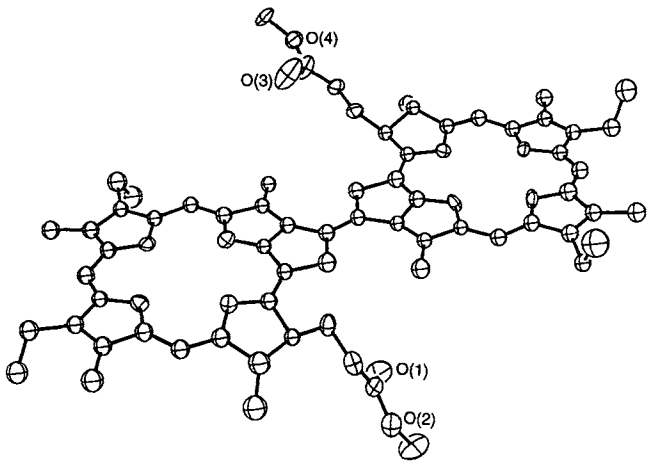

Fig. 2. Molecular structure of **6** in the crystal. Ellipsoids are drawn for 50% occupancy. Hydrogen atoms have been omitted for clarity.

molecule is essentially planar. Deviations from planarity of the macrocycle atoms from their least-squares plane are 0.125 and 0.09 Å for the two phytochlorin units. Delocalization of the electrons in the bischlorin system is also emphasized by the planar arrangement of both phytochlorin systems; the two N_4 planes form an angle of only 2.2°. For steric reasons the two reduced pyrrole rings occupy opposite sides of the plane formed by the ethene bridge and the two propionic ester side chains point to opposite sides of the bischlorin.

The fusion of two chlorophyll derivatives through a direct ethene linkage gives rise to some interesting chemical properties. Both the nickel(II) and zinc(II) bischlorins **3** and **4**, respectively, decompose slowly in solution, whereas the metal-free dimer **6** is quite stable for long periods in solution. But after several months in a chloroform/methanol solution in the presence of air, compound **6** is converted into another compound (Q-band at 726 nm). X-ray crystallography showed the new compound to be the 13^2,$(13^2)'$-dimethoxy derivative **12** (Fig. 3).[10b] Formation of **12** can be explained by an oxygen-promoted double allylic oxidation of **6**, suggesting a lower oxidation potential for **6** than in methyl mesopyrophaeophorbide *a*. The molecular structure of **12** is similar to that of **6**, with an [1.378(12) Å]. One interesting feature is the uniquely *syn* orientation of the methoxy groups at $C13^2$ on one face of the molecule and the C17-propionic ester groups on the other face.

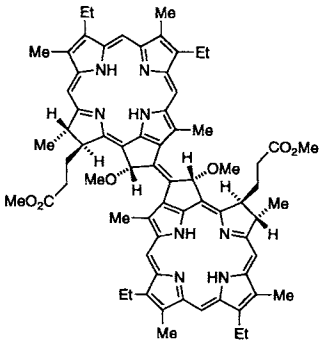

12

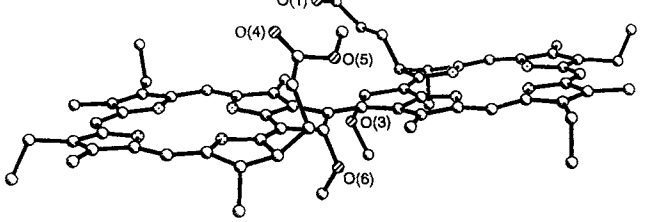

Fig. 3. Molecular structure of **12** in the crystal. Ellipsoids are drawn for 50% occupancy. Hydrogen atoms have been omitted for clarity.

Experimental Procedure

Bischlorin **4:** $TiCl_3(DME)_{1.5}$ (1.20 g, 4.12 mmol) and Zn/Cu couple (1.10 g, 15.6 mmol) were added to a dry flask in a dry box. Anhydrous THF (40 mL) was added to the reaction flask, and the resulting mixture was heated at reflux for 3 h under an inert atmosphere. The mixture was then cooled to room temperature; pyridine (0.12 mL, 1.5 mmol, 3.65 equiv) and zinc(II) methyl pyrophaeophorbide *a* **5** (250 mg, 0.41 mmol) were added. The resulting mixture was stirred for 2 h at room temperature and then filtered through a short plug of Grade III alumina, eluting with CH_2Cl_2/THF (10/1). The solvents were evaporated and the residue was redissolved in CH_2Cl_2 (20 mL). TFA (5 mL) was added and the mixture was stirred at room temperature for 0.5 h. The organic phase was washed with water, saturated aqueous sodium carbonate, and again with water, and was concentrated to dryness. The final residue was chromatographed on Grade III alumina, eluting with CH_2Cl_2/cyclohexane (2/1). The main brown fraction was collected and recrystallized from CH_2Cl_2/toluene to give 100 mg (46%) of **4**. M.p. > 330 °C; UV/Vis (CH_2Cl_2): λ_{max} (ε) = 404 (208 500), 486 (87 800), 526 (49 800), 564 (31 600), 600 (19 900), 674 (18 700), 692 (44 500), 752 nm (253 000); ^{1}H NMR (300 MHz, $CDCl_3$): δ = 9.73, 9.68, 8.95 (s, 2H each, *meso* H), 7.91 (dd, 2H, 3^1-CH, J = 18, 12 Hz), 6.02 (m, 4H, 3^2-CH *trans* to 3^1-CH + 2H 13^2-CH_2), 5.83 (d, 2H, 3^2-CH *cis* to 3^1-CH, J = 12 Hz), 5.56 (d, 2H, 13^2-CH_2, J = 18 Hz), 4.78 (m, 4H, 17-CH + 18-CH), 3.91 (q, 4H, CH_2CH_3, J = 7.5 Hz), 4.08, 3.65, 3.42, 3.39 (each s, 6H each), 2.95–2.20 (m, 8H), 2.16 (d, 6H, 18-CH_3, J = 6.9 Hz), 1.83 (t, 6H, CH_3 of Et, J = 7.5 Hz), −1.04 (s, 2H, NH), −2.73 (s, 2H, NH). The compound gave the expected mass spectrum and elemental analysis.

Received: February 9, 1996 [Z 8804 IE]
German version: *Angew. Chem.* **1996**, *108*, 1982–1984

Keywords: bischlorins · McMurry reactions · porphyrinoids

[1] *The Photosynthetic Reaction Center* (Eds.: J. R. Norris, J. Deisenhofer), Academic, San Diego, **1993**.
[2] M. R. Wasielewski, *Chem. Rev.* **1992**, *92*, 435–461.
[3] a) A. M. Brun, A. Harriman, V. Heitz, J.-P. Sauvage, *J. Am. Chem. Soc.* **1991**, *113*, 8657–8663; J.-C. Chambron, A. Harriman, V. Heitz, J.-P. Sauvage, *ibid.* **1993**, *114*, 7419–7425; b) H. Kurreck, M. Huber, *Angew. Chem.* **1995**, *34*, 929–947; *Angew. Chem. Int. Ed. Engl.* **1995**, *104*, 849–866.
[4] a) V. S.-Y. Lin, S. G. DiMagno, M. J. Thieren, *Science* **1994**, *264*, 1105–1111; b) T. X. Lü, J. R. Reimus, M. J. Crossley, N. S. Hush, *J. Phys. Chem.* **1994**, *98*, 11878–11884; c) M. J. Crossley, L. J. Govenlock, J. K. Prashar, *J. Chem. Soc. Chem. Commun.* **1995**, 2379–2380.
[5] M. G. H. Vicente, K. M. Smith, *Synlett* **1990**, 579; *J. Org. Chem.* **1991**, *56*, 4407–4418; M. O. Senge, K. R. Gerzevske, M. G. H. Vicente, T. P. Forsyth, K. M. Smith, *Angew. Chem.* **1993**, *105*, 745–747; *Angew. Chem. Int. Ed. Engl.* **1993**, *32*, 750–754; L. Jaquinod, D. J. Nurco, C. J. Medforth, R. K. Pandey, T. P. Forsyth, M. M. Olmstead, K. M. Smith, *ibid.* **1996**, *105*, 1085–1087 and **1996**, *35*, 1013–1016.
[6] K. M. Smith, D. A. Goff, D. J. Simpson, *J. Am. Chem. Soc.* **1985**, *107*, 4946–4954.
[7] J. E. McMurry, W. Choy, *J. Org. Chem.* **1978**, *43*, 1800–1803, and references therein.
[8] A. M. Stolzenberg, P. A. Glazer, B. M. Foxman, *Inorg. Chem.* **1986**, *25*, 983–991.
[9] a) K. R. Adams, M. C. Berenbaum, R. Bonnett, A. N. Nizhnik, A. Salgado, M. A. Vallés, *J. Chem. Soc. Perkin Trans. 1* **1992**, 1465–1470; b) C. K. Chang, *Biochemistry* **1980**, *19*, 1971–1976.
[10] a) **6**: $C_{68}H_{76}N_8O_4$, M_r = 1069.76, green parallelepiped from CH_2Cl_2/CH_3OH, crystal size 0.9 × 0.1 × 0.1 mm, monoclinic, space group $P2_1$, a = 12.495(7), b = 7.436(2), c = 31.062(8) Å, β = 100.94(2)°, V = 2834(2) Å^3, Z = 2, ρ_{calcd} = 1.253 Mg m^{-3}, Siemens P4/RA diffractometer, θ_{max} = 52.52°, $Cu_{K\alpha}$ radiation (λ = 1.54178 Å), T = 128 K, $2\theta - \theta$ scans, structure solution with direct methods, refinement on F^2, 3541 independent reflections, 1973 with $I > 2\sigma(I)$, 424 parameters, observed data: $R1$ = 0.087, $wR2$ = 0.184; all data: $R1$ = 0.171, $wR2$ = 0.244. b) **12**: $C_{70}H_{80}N_8O_4 \cdot CH_2Cl_2$, M_r = 1214.3, blue parallelepiped from CH_2Cl_2/CH_3OH, crystal size 0.3 × 0.1 × 0.03 mm, monoclinic, space group $P2_1$, a = 11.269(4), b = 18.475(7), c = 15.466(7) Å, β = 95.46(2)°, V = 3205(2) Å^3, Z = 2, ρ_{calcd} = 1.258 Mg m^{-3}, Siemens P4/RA diffractometer, θ_{max} = 57°, $Cu_{K\alpha}$ radiation (λ = 1.54178 Å), T = 128 K, $2\theta - \theta$ scans, structure solution with direct methods, refinement on $|F|$, 4393 independent reflections, 3528 with $I > 2\sigma(I)$, 784 parameters, observed data: R = 0.073, wR = 0.085. Crystallographic data (excluding structure factors) for the structures reported in this paper have been deposited with the Cambridge Crystallographic Data Centre as supplementary publication no. CCDC-179-78. Copies of the data can be obtained free of charge on application to The Director, CCDC, 12 Union Road, Cambridge CB2 1EZ, UK (fax: Int. + (1223) 336-033; e-mail: teched@chemcrys.cam.ac.uk).

An Unprecedented Biradical Cyclization as an Alternative Pathway to the Myers–Saito Cycloaromatization in the Thermal Reactions of Enyne Allenes**

Michael Schmittel,* Marc Strittmatter, and Susanne Kiau

Dedicated to Professor Horst Prinzbach on the occasion of his 65th birthday

During the last few years interest in the thermal biradical cyclizations[1] of enediynes, enyne cumulenes, and enyne allenes has increased dramatically. This trend is due to the fascinating mechanisms of these systems operative in natural antitumor antibiotics[2] as well as their potential in the synthesis of carbocyclic systems.[3] Consequently, numerous derivatives of enyne allenes with various substituents and substitution patterns, which on heating generally furnish the expected Myers–Saito cyclization products,[1b,d] have already been studied.[4] However, we found quite unexpectedly that the simple attachment of an aryl group to the alkyne terminus of the enyne allenes redirects the reaction course to a novel C^2-C^6 cyclization, giving rise to formal ene[5] and Diels–Alder products (Scheme 1).[6]

To account for this surprising C^2-C^6 cyclization of **1a,c,d** we have postulated[5,6] the biradical intermediate $\mathbf{B}^{2,6}$ (Scheme 2), although in principle, **2a**, **4** (R = CH_3), and **5** may also arise from a concerted reaction. However, since aryl groups are known to stabilize vinyl radicals,[7] it was suggested that this stabilizing effect would favor formation of biradical $\mathbf{B}^{2,6}$ over biradical $\mathbf{B}^{1,6}$, which is a key intermediate in the Myers–Saito cyclization.[8]

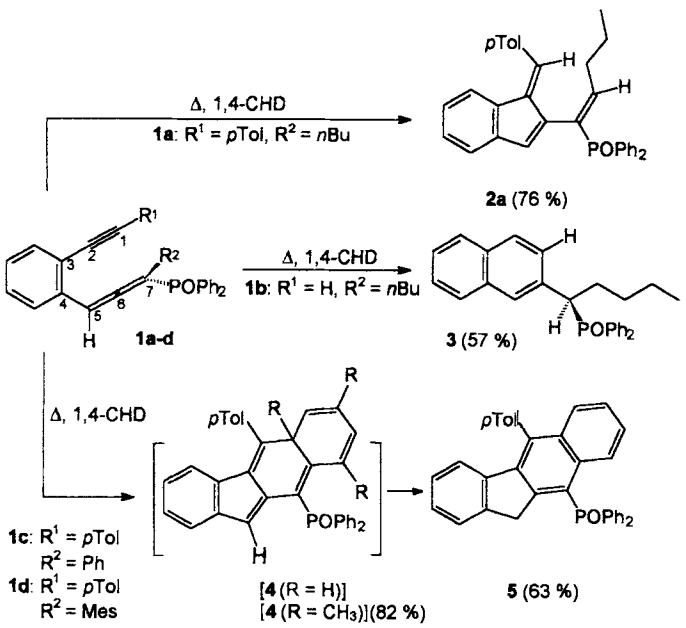

Scheme 1. The switch from the Myers–Saito to a novel C^2-C^6 cyclization in the thermal reaction of enyne allenes (1,4-CHD = 1,4-cyclohexadiene; Mes = 2,4,6-trimethylphenyl).

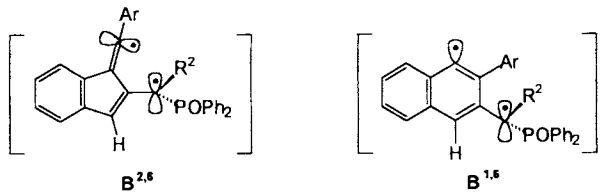

Scheme 2. Biradicals $\mathbf{B}^{2,6}$ resulting from C^2-C^6 cyclization and $\mathbf{B}^{1,6}$ from the Myers–Saito cycloaromatization of aryl-substituted enyne allenes.

The biradical intermediate $\mathbf{B}^{2,6}$ could easily lead to ene- and Diels–Alder-type products depending on the nature of group R^2 (Scheme 3), and a plethora of other useful reactions should be possible as well. Consequently, we have conducted a series of experiments to elucidate the mechanism of the novel C^2-C^6 cyclization and herein present evidence for a benzofulvene biradical $\mathbf{B}^{2,6}$ intermediate in the cyclizations examined.

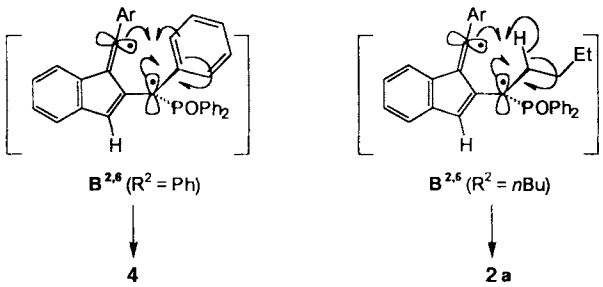

Scheme 3. Two follow up reactions of the postulated biradical intermediate $\mathbf{B}^{2,6}$ generated from aryl-substituted enyne allenes.

The first evidence for a stepwise mechanism was provided by the activation barriers for the reactions presented in Scheme 1. The activation data for the formal ene and Diels–Alder reaction (Table 1) proved to be remarkably similar. In addition, the almost identical activation barriers for the formal Diels–Alder reactions of the aryl-substituted enyne allenes **1c** and **1d** are definitely not reconcilable with a concerted reaction. In such a case, the activation energy of **1d** would be expected to be much higher than that of **1c**, since the bulky mesityl group should slow down the pericyclic reaction. Indeed, we are not aware of any examples of an analogous cycloaddition across a mesitylene ring.[9] Even under much more extreme conditions than those applied for the phenyl analogues, cycloaddition does not occur.[10] Another mechanistically significant result is that the rates of the transformations **1a** → **2a** and **1c** → **5** were not affected by the change from an unpolar solvent (mesitylene or benzene) to DMSO. This finding precludes a zwitterion as an alternative intermediate.

Unfortunately, all attempts to trap the postulated biradical $\mathbf{B}^{2,6}$ by an intermolecular reaction (O_2, PhSH, $(Me_3Si)_3SiH$, 1,4-cyclohexadiene 2,2,6,6-tetramethylpiperidine *N*-oxide) failed so far. Thus, in order to obtain information about the lifetime of the presumably short-lived biradical, experiments based on the cyclopropylmethyl radical clock were devised, using the cyclopropyl-substituted enyne allene **1e** (Scheme 4).[11,12] The ring opening of the *trans*-(2-phenylcyclopropyl)benzyl radical is known to be extremely rapid (*k* (80 °C) =

[*] Prof. Dr. M. Schmittel, Dipl.-Chem. M. Strittmatter, Dipl.-Chem. S. Kiau
Institut für Organische Chemie der Universität
Am Hubland, D-97074 Würzburg (Germany)
Fax: Int. code +(931)888-4606
e-mail: mjls@chemie.uni-wuerzburg.de

[**] Thermal and Electron Transfer Induced Reactions of Enediynes and Enyne Allenes, Part 4. Financial support from the Volkswagen-Stiftung and the Fonds der Chemischen Industrie is gratefully acknowledged. We thank Prof. Dr. C. Rüchardt and E. Hickl (Freiburg) for their kind help with the DSC experiments. Part 3: [6].

Table 1. Activation parameters for the thermal reaction of **1** determined by DSC [11] and ^{1}H NMR experiments (in the presence of 2000 mol% 1,4-cyclohexadiene).

Reaction	$\Delta G^{\neq}$ [kcal mol^{-1}] at 80 °C [a]	k [s^{-1}] at 73 °C [b]	$\Delta H^{\neq}$ [a] [kcal mol^{-1}]	$\Delta S^{\neq}$ [a] [cal K^{-1} mol^{-1}]
1a → **2a**	+26.4 (mesitylene) [c]	–	+ 23.9 [c]	– 9.8 [c]
	+ 26.7 (DMSO)	–	+ 24.9	– 5.3
1c → **5**	+ 25.9 (mesitylene)	4.9×10^{-4} (C_6D_6)	–	–
		3.4×10^{-4} ([D$_6$]DMSO)	–	–
1d → **4** (R = CH$_3$)	+ 26.3 (mesitylene)	3.7×10^{-4} (C_6D_6)	–	–

[a] Based on kinetic data determined by DSC. [b] Based on kinetica data determined by ^{1}H NMR spectroscopy. [c] From ref. [5].

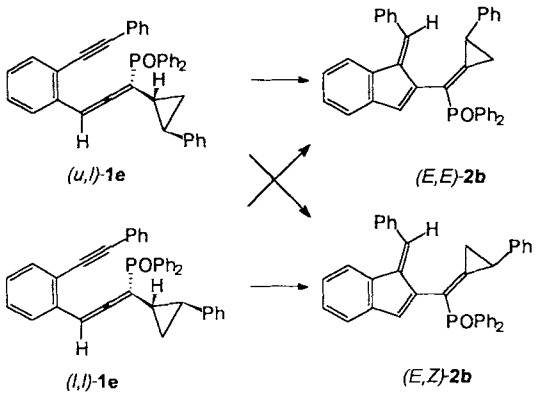

Scheme 4. Thermal reactions of enyne allenes **1e**.

1.1×10^9 s^{-1}).[13] When **1e** (1:1 mixture of the two *trans* diastereomers) was heated gently to 80 °C, benzofulvenes **2b** formed in 52% yield, also as a mixture of two diastereomers ((*E,Z*)-**2b**:(*E,E*)-**2b** = 1.0:0.6). The structures of the products were determined unambiguously by ^{1}H, ^{13}C, ^{31}P NMR and 2D NMR experiments (Table 2).[12]

Table 2. NMR and IR spectroscopic data for **1e** and **2b** [a].

(*u,l*)-**1e**: ^{1}H NMR (250 MHz, $CDCl_3$): δ = 1.23 (td, J_1 = 7.0 Hz, J_2 = 1.6 Hz, 2H, CH_2), 1.83 (m, 1H, C*H), 2.09 (dd, J_1 = 7.0 Hz, J_2 = 1.6 Hz, 1H, C*HPh), 6.80 (dd, J_1 = 10.7 Hz, J_2 = 1.3 Hz, 1H, =C=CH), 6.88 (d, J_1 = 7.0 Hz, J_2 = 1.6 Hz, 2H, arom. H), 7.01–7.20 (m, 7H), 7.24–7.50 (m, 11H), 7.66 (dd, J_1 = 12.3 Hz, J_2 = 1.3 Hz, 1H, *o*-H(OPPh$_2$)), 7.69 (dd, J_1 = 12.3 Hz, J_2 = 1.6 Hz, 2H, *o*-H(OPPh$_2$)), 7.73 (dd, J_1 = 12.3 Hz, J_2 = 1.3 Hz, 1H, *o*-H(OPPh$_2$)); IR (neat): $\tilde{\nu}$ [cm^{-1}] = 2222 (s, C≡C), 1931 (s, C=C=C)

(*l,l*)-**1e**: ^{1}H NMR (250 MHz, $CDCl_3$): δ = 1.23 (td, J_1 = 7.0 Hz, J_2 = 1.6 Hz, 2H, CH_2), 1.80 (m, 1H, C*H), 2.03 (m, J_1 = 7.0 Hz, J_2 = 1.6 Hz, 1H, C*HPh), 6.80 (dd, J_1 = 10.7 Hz, J_2 = 1.3 Hz, 1H, =C=CH), 6.82 (dd, J_1 = 7.0 Hz, J_2 = 1.6 Hz, 2H, arom. H), 7.01–7.40 (m, 18H), 7.63 (dd, J_1 = 11.9 Hz, J_2 = 1.6 Hz, 1H, *o*-H(OPPh$_2$)), 7.67 (dd, J_1 = 11.9 Hz, J_2 = 1.3 Hz, 1H, *o*-H(OPPh$_2$)), 7.73 (dd, J_1 = 11.9 Hz, J_2 = 1.6 Hz, 1H, *o*-H(OPPh$_2$)), 7.77 (dd, J_1 = 11.9 Hz, J_2 = 1.3 Hz, 1H, *o*-H(OPPh$_2$)); IR (neat): $\tilde{\nu}$ [cm^{-1}] = 2222 (s, C≡C), 1931 (s, C=C=C)

(*E,E*)-**2b**: ^{1}H NMR (250 MHz, $CDCl_3$): δ = 1.13 (ddd, J_1 = 11.1 Hz, J_2 = 6.6 Hz, J(^{1}H,^{31}P) = 2.8 Hz, 1H, CH_2), 1.57 (ddd, J_1 = 11.1 Hz, J_2 = 10.4 Hz, J(^{1}H,^{31}P) = 2.9 Hz, 1H, CH_2), 2.70 (ddd, J_1 = 10.4 Hz, J_2 = 6.6 Hz, J(^{1}H,^{31}P) = 3.4 Hz, 1H, C*HPh), 6.78 (m, 3H), 7.02 (dd, J_1 = 7.0 Hz, J_2 = 1.6 Hz, 2H), 7.05–7.45 (m, 17H), 7.67 (dd, J_1 = 12.3 Hz, J_2 = 1.3 Hz, 1H, *o*-H(OPPh$_2$)), 7.69 (ddd, J_1 = 12.3 Hz, J_2 = 1.6 Hz, J_3 = 1.3 Hz, 2H, *o*-H(OPPh$_2$)), 7.72 (dd, J_1 = 12.3 Hz, J_2 = 1.3 Hz, 1H, *o*-H(OPPh$_2$)); ^{13}C NMR (63 MHz, $CDCl_3$): δ = 16.1 (d, J(^{13}C,^{31}P) = 3.1 Hz, CH_2), 21.4 (d, J(^{13}C,^{31}P) = 13.3 Hz, C*HPh)

(*E,Z*)-**2b**: ^{1}H NMR (250 MHz, $CDCl_3$): δ = 1.34 (ddd, J_1 = 10.4 Hz, J_2 = 6.4 Hz, J(^{1}H,^{31}P) = 4.0 Hz, 1H, CH_2), 1.78 (ddd, J_1 = 10.5 Hz, J_2 = 10.4 Hz, J(^{1}H,^{31}P) = 3.5 Hz, 1H, CH_2), 2.75 (ddd, J_1 = 10.5 Hz, J_2 = 6.4 Hz, J(^{1}H,^{31}P) = 2.4 Hz, 1H, C*HPh), 6.67 (m, 2H), 6.83 (m, 2H), 6.96 (d, 1H, J(^{1}H,^{31}P) = 2.4 Hz), 7.10–7.47 (m, 17H), 7.66 (dd, J_1 = 12.3 Hz, J_2 = 1.3 Hz, 1H, *o*-H(OPPh$_2$)), 7.69 (dd, J_1 = 12.3 Hz, J_2 = 1.6 Hz, 2H, *o*-H(OPPh$_2$)), 7.73 (dd, J_1 = 12.3 Hz, J_2 = 1.3 Hz, 1H, *o*-H(OPPh$_2$)); ^{13}C NMR (63 MHz, $CDCl_3$): δ = 15.8 (d, J(^{13}C,^{31}P) = 13.8 Hz, CH_2), 24.1 (d, J(^{13}C,^{31}P) = 4.7 Hz, C*HPh)

[a] Chiral centers are denoted as C*.

At this point the failure to observe ring-opened products rather seemed to testify against a biradical intermediate. However, we were finally able to separate the two diastereomeric *trans* enyne allenes **1e** ((*u,l*) and (*l,l*))[14] by HPLC. The thermal cyclization of (*u,l*)-**1e** furnished a mixture of (*E,E*)-**2b** and (*E,Z*)-**2b** (33:21, overall yield 54%), while that of (*l,l*)-**1e** provided a mixture of (*E,Z*)-**2b** and (*E,E*)-**2b** (53:7, overall yield 60%) (Scheme 5). Control experiments confirmed that neither

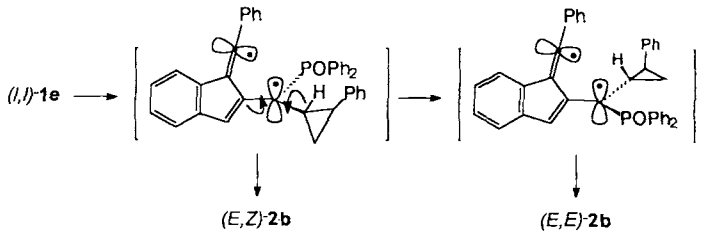

Scheme 5. Proposed mechanism for the thermal cyclization of (*l,l*)-**1e**: Coupled bond rotation in the biradical intermediate.

the enyne allenes (*u,l*)- and (*l,l*)-**1e** nor the products (*E,E*)-**2b** and (*E,Z*)-**2b** interconvert. As a consequence, this ene reaction is not stereospecific, which indicates that a stepwise mechanism proceeding via a reactive intermediate such as biradical **B**[2,6] may be in operation.

Two plausible pathways for the conversion of biradical **B**[2,6] into a mixture of (*E,E*)-**2b** and (*E,Z*)-**2b** are open for discussion: a coupled rotation about the bonds linking the radical center to the cyclopropyl group and to the benzofulvene moiety, and reversible opening of the cyclopropyl ring. PM3 calculations[15] indicate that the activation barrier for the coupled bond rotations should be on the order of 6 kcal mol^{-1}, which is similar to the barrier for cyclopropyl ring opening (E_a = 6.15 kcal mol^{-1}).[13] The rate constant for hydrogen transfer in **B**[2,6] has to be much faster than 10^6 s^{-1} (80 °C), a value found for intramolecular hydrogen transfer from an alkyl group to a vinyl radical via a six-membered ring transition state.[16] At present, however, further investigations are required to obtain a more precise value.

With the assumption of a biradical intermediate all of the experimental results can be readily rationalized: a) The switch from the Myers–Saito cyclization to a novel C^2–C^6 cyclization that occurs when hydrogen or alkyl substituents[3a,b] at the alkyne terminus are replaced by an aryl group results from the stabilization of biradical **B**[2,6] through an adjacent aryl group. b) A biradical intermediate convincingly explains how formally different reactions like the ene reaction and the Diels–Alder cycloaddition can have almost identical activation barriers. c) The almost identical activation barriers for the cycloadditions of **1c** and **1d**, which does not support a concerted reaction pathway due to the different steric demands of the aryl substituents,

is readily explained by a two-step process with formation of $\mathbf{B}^{2,6}$ as the rate-determining step. d) The existence of an intermediate is the only rationalization for the nonstereospecific hydrogen transfer in the reaction of **1e**. e) The lack of solvent effects on the rates of the formal ene and Diels–Alder reactions supports the proposed biradical and excludes a zwitterionic intermediate.

In summary, a novel thermal C^2-C^6 cyclization of substituted enyne allenes has been established for substrates in which an aryl group is affixed to the alkyne terminus. Apparently, aryl substitution raises the barrier for the Myers cycloaromatization and lowers the barrier for the biradical C^2-C^6 cyclization, rendering the latter one the exclusive pathway.[17] Further mechanistic work on this intriguing reaction and its synthetic applications is currently in progess in our group.

Received: February 19, 1996 [Z 88361E]
German version: *Angew. Chem.* **1996**, *108*, 1952–1954

Keywords: enyne allenes · cycloaromatizations · diradicals · reaction mechanisms

[1] a) R. G. Bergman, R. R. Jones, *J. Am. Chem. Soc.* **1972**, *94*, 660–661; b) A. G. Myers, *Tetrahedron Lett.* **1987**, *28*, 4493–4496; c) A. G. Myers, E. Y. Kuo, N. S. Finney, *J. Am. Chem. Soc.* **1989**, *111*, 8057–8059; d) R. Nagata, H. Yamanaka, E. Okazaki, I. Saito, *Tetrahedron Lett.* **1989**, *30*, 4995–4998; e) R. Nagata, H. Yamanaka, E. Murahashi, I. Saito, *ibid.* **1990**, *31*, 2907–2910.

[2] a) M. E. Maier, *Synlett* **1995**, 13–26; b) K. C. Nicolaou, P. Maligres, J. Shin, E. de Leon, D. Rideout, *J. Am. Chem. Soc.* **1990**, *112*, 7825–7826; c) K. C. Nicolaou, G. Skokotas, P. Maligres, G. Zuccarello, E. J. Schweiger, K. Toshima, S. Wendeborn, *Angew. Chem.* **1989**, *101*, 1255–1257; *Angew. Chem. Int. Ed. Engl.* **1989**, *28*, 1272–1275; d) K. C. Nicolaou, W. M. Dai, *ibid.* **1991**, *103*, 1453–1481 and **1991**, *30*, 1387–1416.

[3] a) Y. W. Andemichael, Y. G. Gu, K. K. Wang, *J. Org. Chem.* **1992**, *57*, 794–796; b) J. W. Grissom, B. J. Slattery, *Tetrahedron Lett.* **1994**, *35*, 5137–5410; c) J. W. Grissom, D. Huang, *J. Org. Chem.* **1994**, *59*, 5114–5116; d) *Angew. Chem.* **1995**, *107*, 2196–2198; *Angew. Chem. Int. Ed. Engl.* **1995**, *34*, 2037–2039.

[4] Even enyne ketenes undergo a reaction analogous to the Myers–Saito cyclization: a) K. Nakatani, S. Isoe, S. Maekawa, I. Saito, *Tetrahedron Lett.* **1994**, *35*, 605–608; b) H. Xia, H. W. Moore, *J. Org. Chem.* **1992**, *57*, 3765–3766; c) A. Padwa, D. J. Austin, U. Chiacchio, J. M. Kassir, A. Rescifina, S. L. Xu, *Tetrahedron Lett.* **1991**, *32*, 5923–5926.

[5] M. Schmittel, M. Strittmatter, S. Kiau, *Tetrahedron Lett.* **1995**, *36*, 4975–4979.

[6] M. Schmittel, M. Strittmatter, K. Vollmann, S. Kiau, *Tetrahedron Lett.* **1996**, *37*, 999–1002.

[7] J. E. Bennett, J. A. Howard, *Chem. Phys. Lett.* **1971**, *9*, 460–462.

[8] The C^1-C^6 and C^2-C^6 distances determined by AM1 calculations (cf. M. J. S. Dewar, E. G. Zoebisch, E. F. Healy, J. J. P. Stewart, *J. Am. Chem. Soc.* **1985**, *107*, 3902–3909) for **1a** in the s-*cis* conformation are 3.47 and 2.98 Å, respectively.

[9] W. Carruthers, *Cycloaddition Reactions in Organic Synthesis*, Pergamon, Oxford **1990**.

[10] a) R. Brückner, R. Huisgen, J. Schmid, *Tetrahedron Lett.* **1990**, *31*, 7129–7132; b) J. Sauer, R. Sustmann, *Angew. Chem.* **1980**, *92*, 773–801; *Angew. Chem. Int. Ed. Engl.* **1980**, *19*, 779–807.

[11] a) M. Schmittel, C. Rüchardt, *J. Am. Chem. Soc.* **1987**, *109*, 2750–2759; b) M. A. Flamm-ter Meer, H.-D. Beckhaus, K. Peters, H.-G. von Schnering, C. Rüchardt, *Chem. Ber.* **1985**, *118*, 4665–4673.

[12] All enyne allenes described in this paper were prepared from the corresponding propargyl alcohols by rearrangement in the presence of chlorodiphenylphosphane. All starting materials and products were isolated as pure compounds and fully characterized by ^1H, ^{13}C, and ^{31}P NMR spectroscopy, mass spectrometry, and IR spectroscopy (see Table 2).

[13] R. Hollis, L. Hughes, V. W. Bowry, K. U. Ingold, *J. Org. Chem.* **1992**, *57*, 4284–4287.

[14] The relative configuration is determined by the three contiguous stereogenic units: the stereogenic axis of the allene and the stereogenic centers in the cyclopropyl ring, C*H and C*HPh.

[15] a) J. J. P. Stewart, *J. Comput. Chem.* **1989**, *10*, 209–221; b) *J. Comput. Aided Mol. Design* **1990**, *4*, 1–105.

[16] D. P. Curran, W. Shen, *J. Am. Chem. Soc.* **1993**, *115*, 6051–6059.

[17] a) Since our first report on a C^2-C^6 cyclization two other papers have been published [17b,c] that report on a similar reaction leading to benzofulvene derivatives. However, in these cases owing to the substitution patterns a zwitterionic intermediate seems to be more plausible than a biradical. b) T. Gillmann, T. Hülsen, W. Massa, S. Wocadlo, *Synlett* **1995**, 1257–1259; c) J. G. Garcia, B. Ramos, L. M. Pratt, A. Rodriguez, *Tetrahedron Lett.* **1995**, *36*, 7391–7394.

Photoinduced Ring-Opening Metathesis Polymerization (PROMP) with Photochemically Generated Schrock-Type Catalysts

Paul A. van der Schaaf,* Andreas Hafner, and Andreas Mühlebach

Ring-opening metathesis polymerization (ROMP) is a versatile tool for the preparation of a wide variety of polymers.[1] Since the postulated mechanism by Herisson and Chauvin in 1970[2] that metal alkylidenes[3] are the active species in this type of reaction and the discovery by Schrock et al. in 1974 that these are generated by an α-H abstraction reaction between two alkyl substituents,[4] a tremendous amount of effort has been directed, successfully, to the design of well-defined one-component ROMP initiators. To date, a broad range of initiators is known with a versatile range of applications. The best studied initiators are those based on early transition metals, in particular molybdenum and tungsten complexes developed by Schrock et al.[5] These compounds are excellent initiators for a wide variety of monomers, but their main disadvantage is their lack of latency (thermal stability) in the presence of pure monomers. Although there are indications that alkyl complexes of early transition metals can be light-sensitive and even that irradiation can accelerate α-H abstraction reactions,[6] no examples are known, besides our own work on Ru^{II} complexes, using the principle of photoinduced ring-opening metathesis polymerization (PROMP) with well-defined, one-component metal complexes.[7, 8] This is even more surprising when one considers that photoprocesses are known for almost all other polymerization reactions and employed in numerous commercial applications.[9] We report here the first results in the field of photoinduced ROMP (PROMP) reactions using simple alkyl tungsten complexes *and* light for the in situ generation of active ROMP initiators.[10]

Complexes **1** and **2** are easily prepared by standard transmetalation procedures (Scheme 1). Both **1** and **2** are mois-

$[W(=NPh)(CH_2SiMe_3)_2\{OCMe(CF_3)_2\}_2]$ **1**

$[W(=NPh)(CH_2SiMe_3)_3Cl]$ **2**

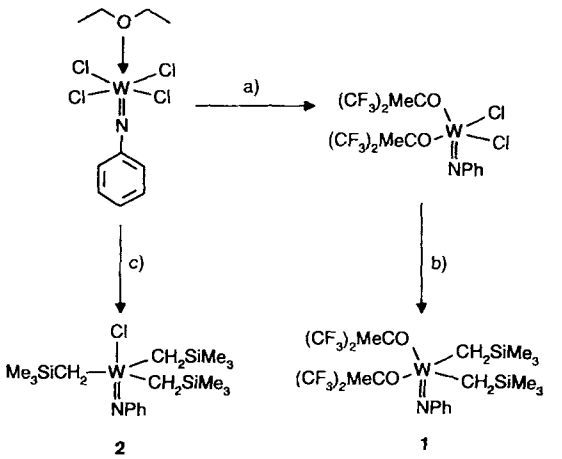

Scheme 1. Synthesis of the complexes **1** and **2**: a) 2 equiv $LiOCMe(CF_3)_2$ in Et_2O at 0 °C, b) NEt_4Cl and $Zn(CH_2SiMe_3)_2$ in CH_2Cl_2 at 0 °C, c) NEt_4Cl and 1.5 equiv $Zn(CH_2SiMe_3)_2$ in CH_2Cl_2 at 0 °C.

[*] Dr. P. A. van der Schaaf, Dr. A. Hafner, Dr. A. Mühlebach
Ciba-Geigy Ltd.
Corporate Research Units, Materials Reasearch
CH-1723 Marly (Switzerland)
Fax: Int. code +(37)856219

ture-sensitive compounds; **1**, as a crystalline material, can be handled in air for short periods. Both complexes are thermally very stable. Solutions in [D_8]toluene can be heated at 80 °C for at least one day without decomposition products apparent by ^{1}H NMR spectroscopy. The ^{1}H NMR data (see Experimental Procedure) suggest that in both complexes the alkyl groups are *cis* positioned. For direct proof of the stereochemistry an X-ray structural determination of **1** was carried out (Fig. 1).[11]

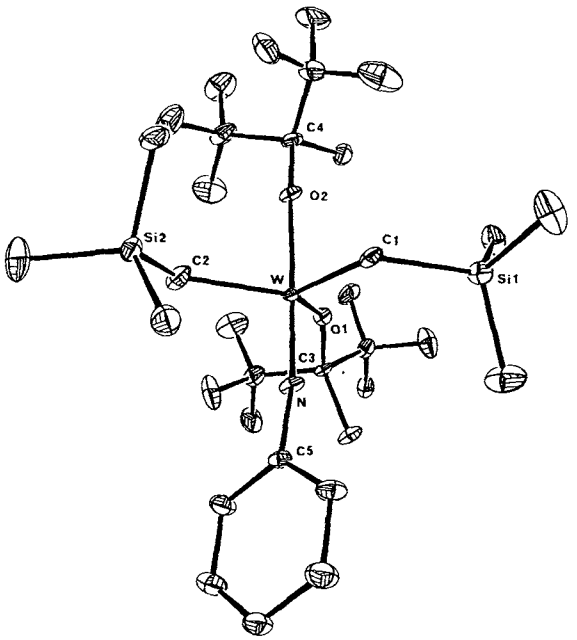

Fig. 1. Molecular structure of **1** (hydrogen atoms are ommited for clarity). Selected bond lengths [Å] and angles [°]: W–C1 2.11(1), W–C2 2.09(1), W–O1 1.919(7), W–O2 1.982(6), W–N 1.753(7); W-C1-Si1 121.7(7), W-C2-Si2 117.2(5), W-O1-C3 137.3(6), W-O2-C4 161.5(7), W-N-C5 171.2(7).

The crystal structure of **1** shows clearly that the two trimethylsilylmethyl groups have a *cis* relationship, as desired for an α-H abstraction reaction. To prove that Schrock-type initiators are formed during irradiation, solutions of **1** and **2** in C_6D_6 were irradiated with UV light and ^{1}H NMR spectra were recorded (Scheme 2). Unfortunately, only decomposition products were observed. However, the in situ formation of an alkylidene metal complex could be proven indirectly by trapping reactions with an aldehyde.[12]

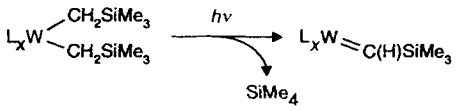

Scheme 2. Schemetic representation of a photoinduced α-H abstraction reaction.

Useful photoinitiators must fulfill several requirements. Firstly, they should, of course, be photoactive, and secondly, they should be latent, that is thermally stable, in the presence of the monomer and initiate the polymerization reaction only when activated with light.

UV irradiation of **1** and **2** in the presence of norbornene or dicyclopentadiene (DCPD) yielded the ring-opening metathesis polymers quantitatively.[13] The photoactivity was demonstrated as well by photo-DSC (DSC = differential scanning calorimetry) experiments and viscosity measurements during UV irradiation of solutions of **1** or **2** in DCPD. The results of the photo-DSC experiments for solutions of 1% of **1** and **2** in DCPD are given in Figure 2. As soon as the light beam is switch on the polymerization is initiated. Whereas the polymerization reaction with **2** is complete after 30 seconds of irradiation, the polymerization reaction with **1** continues when the light is switched off after 3 minutes of irradiation.

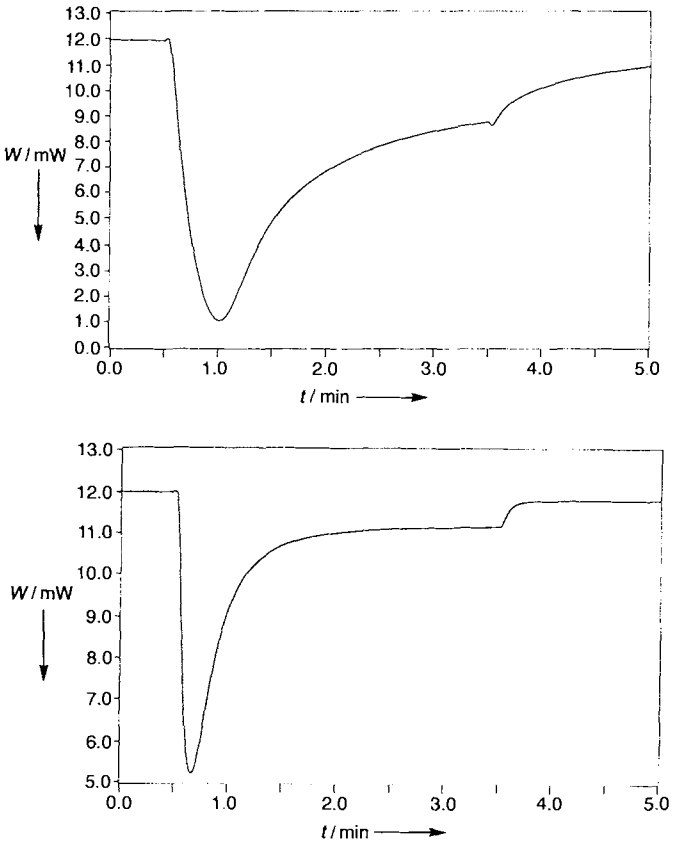

Fig. 2. Results of photo-DSC experiments of **1** (top) and **2** (bottom) in DCPD. *W* = heat flow.

The latency of complexes **1** and **2** in DCPD was tested by using a viscosity apparatus. During these experiments the samples could be either heated or irradiated with a UV lamp. The viscosity of the samples (1% initiator in DCPD containing 5% octane) was determined every minute. The results of the experiments for **1** and **2** are given in Figure 3. Complex **1** slowly polymerizes DCPD at 60 °C in the dark (Fig. 3 top). After 2 h the DCPD starts to gel and after 3 h it is fully polymerized. When the same solution at room temperature is irradiated with a UV lamp, polymerization starts directly and within 15 min the reaction is complete. Surprisingly, complex **2** in DCPD is even more latent (Fig. 3 bottom). Again, irradiation leads to a fast DCPD polymerization. However, when the solution is heated to 80 °C in the absence of light, no polymerization takes place. Moreover, this solution can be stored for days at room temperature without an increase of viscosity, and, even more importantly, without loss of photoactivity.

To our knowledge, these are the first examples of photo-induced ROMP reactions with well-defined early transition metal complexes. With these experiments we showed that simple alkyl tungsten complexes can act as one-component photo-ROMP initiators, and that their photoactivity as well as latency is very

 © VCH Verlagsgesellschaft mbH, D-69451 Weinheim, 1996 0570-0833/96/3516-1846 $ 15.00+.25/0

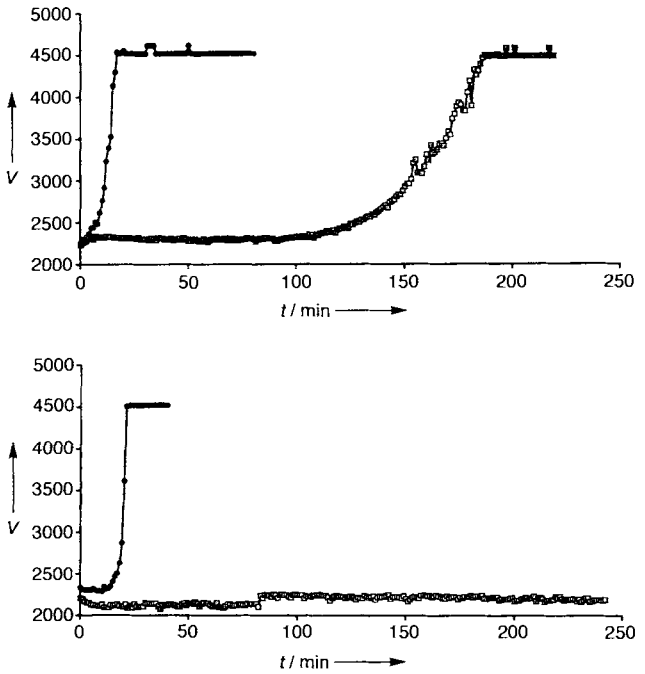

Fig. 3. Plots of real-time viscosimetric measurements of **1** (top) and **2** (bottom) in DCPD, showing the latency of the initiators in the dark. V = viscosity (arbitrary units). Top: ▣: 60 °C, in the dark; ●: 30 °C, UV irradiation. Bottom: ▣: 80 °C, in the dark; ●: 30 °C, UV irradiation.

high. In further studies on these and related complexes we are examining their reactivity with other cyclic olefins as well as the kinetics and quantum yields of these reactions. Applications of this new photopolymerization principle are also being studied.

Experimental Procedure

1: A green solution of $[W(=NPh)Cl_4 \cdot OEt_2]$ (11.58 g, 23.59 mmol) in Et_2O (50 mL) at −78 °C was treated with a solution of $[LiOCMe(CF_3)_2]$ (8.87 g, 47.18 mmol) in Et_2O (50 mL). The brownish reaction mixture was warmed to room temperature, stirred for 30 min, and centrifuged. The orange solution was decanted from a white precipitate (LiCl). Volatiles were removed in vacuo leaving a red solid. The crude product was extracted with hexane (2 × 80 mL). The hexane fractions were combined and dried in vacuo leaving $[W(=NPh)\{OCMe(CF_3)_2\}_2Cl_2]$ as a red powder; yield 16.54 g (90%). To a solution of $[W(=NPh)\{OCMe(CF_3)_2\}_2Cl_2]$ (16.54 g, 21.15 mmol) in CH_2Cl_2 (50 mL) was added NEt_4Cl (4.00 g, 24.14 mmol) as a solid. After 10 min the resulting dark red suspension was cooled to 0 °C and a solution of $Zn(CH_2SiMe_3)_2$ (5.08 g, 21.24 mmol) in CH_2Cl_2 (20 mL) was added within 5 min. Upon addition the color of the reaction mixture turned yellow/orange and a precipitate formed. The reaction mixture was then warmed to room temperature and stirred for an additional hour. Volatiles were evaporated in vacuo leaving a light-yellow solid, which was extracted with hexane (80 and 50 mL). The combined hexane fractions were concentrated to ca. 70 mL and stored at −30 °C. The pure product was obtained, in two crops, as yellow crystalline needles; yield 12.57 g (73.2%). C, H, N analysis: found C 32.61, H 3.89, N 1.79%; calcd C 32.56, H 4.10, N 1.73%; ^{1}H NMR (300 MHz, C_6D_6): δ = 7.22 (d, 2H, *o*-H, NPh), 7.10 (t, 2H, *m*-H, NPh), 6.76 (t, 1H, *p*-H NPh), 2.57 (d, 2H, $^2J(H_a,H_a)$ = 7.5 Hz, $^2J(W,H)$ = 5.1 Hz, CH_aH_aSi), 2.28 (d, 2H, $^2J(H_a,H_a)$ = 7.5 Hz, $^2J(W,H)$ = 5.0 Hz, CH_aH_aSi), 1.87 and 1.37 (2s, 6H, 2 × OCMe), 0.09 (s, 18, $SiMe_3$).

2: A green solution of $[W(=NPh)Cl_4 \cdot OEt_2]$ (8.98 g, 18.29 mmol) in CH_2Cl_2 (60 mL) was treated with powdered NEt_4Cl (3.20 g, 19.31 mmol) and stirred for 30 min. The resulting green suspension was cooled to 0 °C, and a solution of $[Zn(CH_2SiMe_3)_2]$ (6.58 g, 27.44 mmol) in CH_2Cl_2 (25 mL) was added dropwise within 15 min. Upon addition the color of the reaction mixture changed immediately to light brown. The reaction mixture was then stirred for an additional hour. The volatiles were removed in vacuo leaving a sticky light-brown solid. The crude product was extracted with pentane (2 × 60 mL). The combined pentane fractions were concentrated to ca. 50 mL and stored at −30 °C. The pure product was obtained as off-white crystals in 85% yield. C,H,N analysis: found C 37.91, H 6.80, N 2.40%; calcd C 37.79, H 6.70, N 2.45%; ^{1}H NMR (250 MHz, C_6D_6): δ = 7.43 (d, 2H, *o*-H, NPh), 7.09 (t, 2H, *m*-H, NPh), 6.89 (t, 1H, *p*-H, NPh), 2.17 (s, 6H, $^2J(W,H)$ = 4.3 Hz, CH_2Si), 0.20 (s, 27H, $SiMe_3$).

Photo-DSC experiments were carried out at room temperature using a Perkin-Elmer DSC-7 equipped with a Perkin-Elmer DPA-7 light unit. The light source was a 200 W Hg/Xe lamp with 2.5 mW cm^{-2} power. Samples of 1% **1** or **2** in DCPD containing 5% octane were transferred in a sapphire cell under a flow of argon.

Viscosity measurements were performed with a real-time viscosity apparatus of our own construction. Samples of 1% **1** or **2** in DCPD containing 5% octane were heated or irradiated in a pyrex or quartz test tube under a flow of argon while the viscosity was measured every minute. Irradiation was carried out using a 200 W Hg lamp.

Received: February 19, 1996
Revised: May 9, 1996 [Z8840IE]
German version: *Angew. Chem.* **1996**, *108*, 1974–1977

Keywords: catalysis · metathesis · photochemistry · polymerizations · tungsten compounds

[1] a) R. H. Grubbs in *Comprehensive Organometallic Chemistry, Vol. 8* (Eds.: E. W. Abel, F. G. A. Stone, G. Wilkinson), Pergamon, New York, **1982**. b) K. J. Ivin, *Olefin Metathesis*, Academic, London, **1983**. c) R. R. Schrock, *Acc. Chem. Res.* **1990**, *23*, 158.

[2] J. L. Herisson, Y. Chauvin, *Makromol. Chem.* **1970**, *141*, 161.

[3] The term "alkylidene complex" is commonly used for a complex distinguished by a double bond between a high-valent metal and carbon; according to IUPAC nomeclature these complexes are "metallaolefins".

[4] R. R. Schrock, *J. Am. Chem. Soc.* **1974**, *96*, 6796.

[5] J. Feldman, R. R. Schrock, *Prog. Inorg. Chem.* **1991**, *39*, 1.

[6] a) C. D. Wood, S. J. McLain, R. R. Schrock, *J. Am. Chem. Soc.* **1979**, *101*, 3210. b) L. R. Chamberlain, A. P. Rothwell, I. P. Rothwell, *ibid.* **1984**, *106*, 1847. c) M. D. Fryzuk, P. A. MacNeil, S. R. Rettig, *ibid.* **1985**, *107*, 6708. d) M. D. Fryzuk, X. Gao, K. Joshi, P. A. MacNeil, R. L. Massey, *ibid.* **1993**, *115*, 10581. e) J. Kress, M. Wesolek, J.-P. Le Ny, J. Osborn, *J. Chem. Soc. Chem. Commun.* **1981**, 1039. f) D. B. Pourreau, G. L. Geoffroy, *Adv. Organomet. Chem.* **1985**, *24*, 249. g) L. R. Chamberlain, I. P. Rothwell, *J. Chem. Soc. Dalton Trans.* **1987**, 155; *ibid.* **1987**, 163.

[7] A few examples of polymerization reactions are described in which solutions of $[Mo(CO)_6]$ or $[W(CO)_6]$ salts in CCl_4 are irradiated to initiate polymerization reactions: a) B. Gita, G. Sundararajan, *Tetrahedron Lett.* **1993**, *34*, 6123. b) K. Tamura, T. Masuda, T. Higashimura, *Polym. Bull.* **1994**, *32*, 289.

[8] Our initial work in the field of photo-ROMP was based on the photosolvation of bis(arene)Ru^{II} salts to form the active $[Ru(H_2O)_6]^{2+}$ catalyst: T. Karlen, A. Ludi, A. Mühlebach, P. Bernard, C. Pharisa, *J. Polym. Sci. Part A: Polym. Chem.* **1995**, *33*, 1665; A. Mühlebach, P. Bernard, A. Hafner, T. Karlen, A. Ludi, WO-P 95 07,310 [*Chem. Abstr.* **1993**, *123*, 287151].

[9] N. Bühler, D. Belluš, *Pure Appl. Chem.* **1995**, *67*, 25.

[10] A. Hafner, P. A. Van der Schaaf, A. Mühlebach, WO-P 95 14,051 [*Chem. Abstr.* **1993**, *123*, 314873].

[11] Crystals were grown by cooling a saturated hexane solution to −30 °C; crystal size 0.7 × 0.4 × 0.2 mm; monoclinic, space group $P2_1/c$; Z = 4; a = 9.913(3), b = 16.956(5), c = 18.755(6) Å, β = 102.34(2)°; V = 3082.9 Å^3, ρ_{calcd} = 1.748 g cm^{-3}; 2θ = 6–130° ($Cu_{K\alpha}$, λ = 1.5418 Å, graphite monochromator, 2θ–θ scan, T = 188 K); 5768 reflections measured, 4885 observed [$F > 3\sigma(F)$]. Crystallographic data (excluding structure factors) for the structure reported in this paper have been deposited with the Cambridge Crystallographic Data Centre as supplementary publication no. CCDC-179-82. Copies of the data can be obtained free of charge on application to The Director, CCDC, 12 Union Road, Cambridge CB2 1EZ UK (fax: Int. code +(1223) 336-033; e-mail: teched@chemcrys.cam.ac.uk).

[12] An example: irradiation of **1** in the presence of 3,4-dimethoxybenzaldehyde yielded trimethyl[2-(3,4-dimethoxyphenyl)ethenyl]silane (the product of a Wittig-like reaction) in 84% yield with an *E*/*Z* ratio of 1. A complete study on this subject will be published.

[13] Reaction with 100 equivalents of norbornene with **1** and **2** yielded ring-opened polynorbornene quantitatively with 85 and 50% *cis*-configurated double bonds, respectively. Polymerization of a 1% solution of **1** in neat DCPD gave a material with properties typical of metathesis-polymerized DCPD. T_g: 130 °C (after postcure at 120 °C for 30 min), E-modulus: 1920 MPa, crosslink density (from swelling in toluene): ca. 0.4%, weight loss (TGA, 10 °C min^{-1}, 20–300 °C): 3.0%).

 © VCH Verlagsgesellschaft mbH, D-69451 Weinheim, 1996 0570-0833/96/3516-1847 $ 15.00+.25/0

Asymmetric Synthesis of Alkyl Aziridine-2-Carboxylates from Chiral 3′-Benzyloxyaminoimides**

Giuliana Cardillo,* Sonia Casolari, Luca Gentilucci, and Claudia Tomasini

The use of aziridinecarboxylates as intermediates in the synthesis of optically active compounds is a subject of current interest.[1] The ring-opening of aziridines, a consequence of ring strain, is the most important feature of their chemistry and serves as the basis of the synthesis of substituted α- and β-amino acids,[2] which is a topic of interest in our laboratory.[3]

Enantiomerically pure aziridines are available not only by separation of racemic mixtures, successfully performed by enzymatic resolution,[4] but can also be prepared starting from β-hydroxy α-amino acids such as serine or threonine.[4a, 5] Recently Zwanenburg and co-workers reported an interesting synthesis of aziridine-2-carboxylates from the corresponding chiral oxiranes.[6] Furthermore, convenient methods have been reported for the synthesis of this class of compounds from α,β-unsaturated chiral imides relying on the reaction of 2,3-dihalocarboxylic acid derivatives with primary amines or ammonia.[7]

Interestingly, racemic keto aziridines can be prepared from α,β-unsaturated ketones by a two-step procedure: 1,4-addition of *O*-methylhydroxylamine to an unsaturated ketone followed by treatment with two equivalents of sodium methylate in methanol.[8] Under these conditions the *trans* aziridines are formed in excellent yields. Although the mechanism of this reaction is unknown, it is reasonable to assume that the aziridine is formed by cyclization of an intermediate enolate.

We recently reported a new synthesis of β-amino acids[3a] starting from the chiral[9] alkenoylimidazolidin-2-ones **1**, which

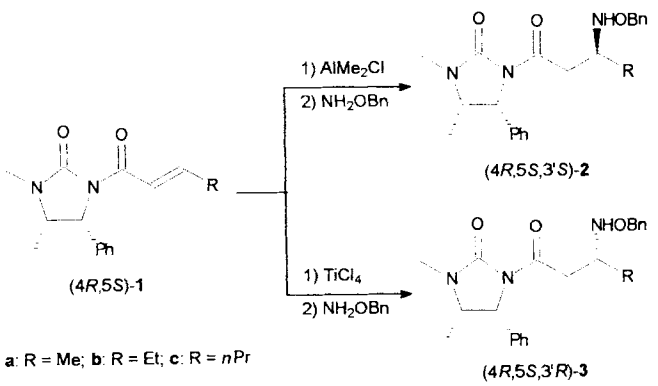

undergo selective 1,4-addition of *O*-benzylhydroxylamine promoted by Lewis acids. The predominant (*S*) or (*R*) configuration of the newly introduced stereogenic center depends on the Lewis acid selected as activating agent. Thus, nucleophilic attack on the aluminum-chelated alkenoylimide derivatives results in the formation of (4*R*,5*S*,3′*S*)-**2** as the major product, whereas the titanium-promoted addition of *O*-benzylhydroxylamine affords (4*R*,5*S*,3′*R*)-**3** as the major product. Each compound was obtained in pure form after flash chromatography.

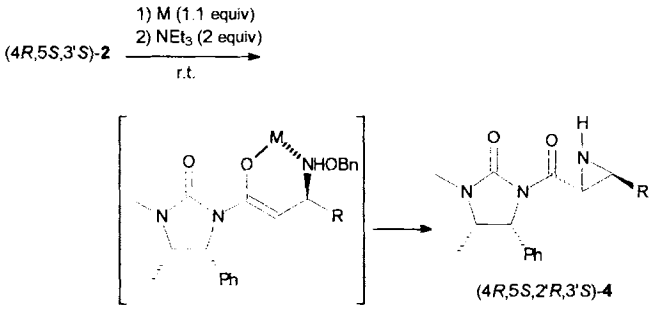

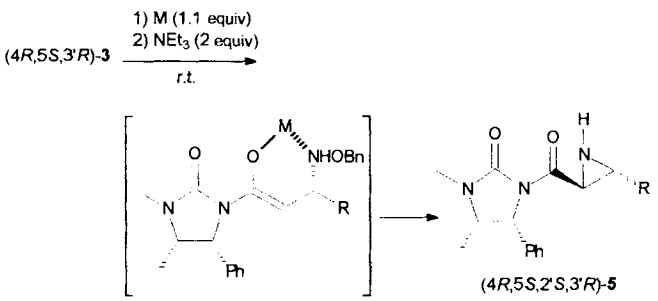

a: R = Me, **b**: R = Et, **c**: R = *n*Pr M = $TiCl_4$, $AlMe_2Cl$

In analogy with the preparation of ketoaziridines, we thought that if an enolate could be prepared from **2** or **3**, the subsequent cyclization would yield the corresponding aziridine. All attempts to prepare the enolate with sodium methylate failed, and a complex mixture of products was obtained without any traces of aziridine derivatives. In contrast, the excellent procedure of Evans et al.[10] for the formation of titanium enolates from the corresponding carbonyl precursors with titanium tetrachloride and a tertiary amine gave satisfactory results. After addition of a titanium complex of **2** or **3** to a solution of triethylamine in CH_2Cl_2 under argon at room temperature, the reaction mixture turned red,[10] thus implying the formation of the desired enolate. The solution was stirred for 30 min at room temperature and the aziridine was isolated after aqueous workup (Table 1). The order of reagent addition has a critical effect on the yield and formation of by-products. Furthermore, the yields are not always reproducible.

Repeating this protocol with $AlMe_2Cl$ as Lewis acid gave better results (Table 1).[11] A clean reaction took place affording a pale yellow solution, and **2** and **3** were converted smoothly to aziridines **4**[7b] and **5**,[12, 13] respectively, in 30 min. The ^1H and

Table 1. Synthesis of chiral *trans*-aziridine-2-imides **4** and **5** by $AlMe_2Cl$- or $TiCl_4$-promoted cyclizations of **2** and **3**, respectively [a].

Entry	Reagent	Lewis acid [b]	Solvent	Yield [%][c]
1	**2a**	$TiCl_4$	THF	74
2	**3a**	$TiCl_4$	THF	70
3	**2a**	$TiCl_4$	CH_2Cl_2	97
4	**3a**	$TiCl_4$	CH_2Cl_2	96
5	**2a**	$AlMe_2Cl$	CH_2Cl_2	80
6	**3a**	$AlMe_2Cl$	CH_2Cl_2	77
7	**2b**	$AlMe_2Cl$	CH_2Cl_2	67
8	**3b**	$AlMe_2Cl$	CH_2Cl_2	71
9	**2c**	$AlMe_2Cl$	CH_2Cl_2	70
10	**3c**	$AlMe_2Cl$	CH_2Cl_2	70

[a] In all cases examined the diastereomeric excess of the product was >99% (determined by NMR, GC, and HPLC analysis of the crude product). [b] 1.1 Equiv. [c] Yields after purification by flash chromatography on silica gel.

[*] Prof. G. Cardillo, Dr. S. Casolari, Dr. L. Gentilucci, Dr. C. Tomasini
Dipartimento di Chimica "G. Ciamician" and CSFM
Via Selmi 2, I-40128 Bologna (Italy)
Fax: Int. code +(51)259456

[**] We thank MURST and the CNR for financial support.

^{13}C NMR and HPLC analysis of the crude reaction mixture indicate that the *trans* aziridine, established on the basis of the ^1H NMR coupling constants ($J_{2',3'} = 2.2-2.5$ Hz), is formed exclusively.

The reaction provides better results in CH_2Cl_2 than in ethereal solvents, although the reaction proceeds also in THF in good yield and selectivity. Good to excellent yields of pure aziridines **4** and **5** are obtained after flash chromatography. In the examples given, the stereochemical outcome was uniformly excellent (>99% *de*). Since the configuration at C3′ is known, the configuration of the newly created stereogenic center at C2′ was unequivocally established based on the *trans* relationship of the hydrogens at C2′ and C3′.

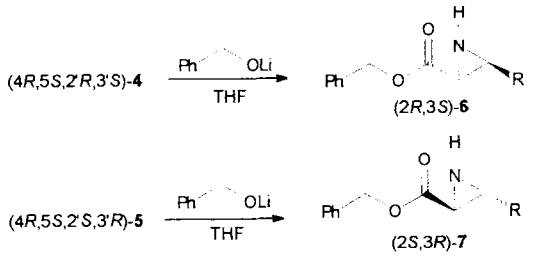

A major advantage of this methodology is the efficient and easy removal and recovery of the chiral auxiliary. Reaction of both **4** and **5** in THF with two equivalents of $PhCH_2OLi$[14] (prepared from benzyl alcohol and *n*BuLi) at 0 °C afforded the corresponding esters (2*R*,3*S*)-**6** and (2*S*,3*R*)-**7**, respectively, in good yield[15] after workup with a saturated solution of NH_4Cl (Table 2). Furthermore a small amount of the corresponding aziridine-2-carboxylic acid was recovered from the aqueous layer.[16]

Table 2. Synthesis of enantiomerically pure benzyl *trans*-aziridine-2-carboxylates (2*R*,3S)-**6** and (2*S*,3*R*)-**7**.

Entry	Reagent	Conv [%][a]	Yield [%][b]
1	**4a**	98	75
2	**5a**	96	73
3	**4b**	93	70
4	**4c**	85	75
5	**5c**	87	65

[a] Based on the recovered chiral auxiliary. [b] Yields of **6** and **7** after purification by flash chromatography; the remainder is the corresponding carboxylic acid. No traces of the *cis* epimers were detected by ^1H, ^{13}C NMR and HPLC analysis.

In conclusion, we have developed a practical, straightforward method for the synthesis of (*R*,*S*)- and (*S*,*R*)-aziridine-2-carboxylates, starting from enantiomerically pure (*S*)- and (*R*)-3′-benzyloxyaminoimide derivatives via titanium or aluminium enolate intermediates. The nondestructive removal of the chiral auxiliary was easily performed by treatment with lithium benzyloxide. Studies are in progress in our group to rationalize the high diastereoselectivity observed.

Received: March 5, 1996 [Z8898IE]
German version: *Angew. Chem.* **1996**, *108*, 1939–1941

Keywords: aziridines · chiral auxiliaries · cyclizations · enolates

[1] P. E. Fanta in *Heterocyclic Compounds with Three- and Four-membered Rings*, Part 1 (Ed.: A. Weissberger), Wiley Interscience, New York, **1964**, p. 524. For a recent review see: D. Tanner, *Angew. Chem.* **1994**, *106*, 625; *Angew. Chem. Int. Ed.* **1994**, *33*, 599.

[2] a) J. Legters, J. G. H. Willems, L. Thijs, B. Zwanenburg, *Recl. Trav. Chim. Pays-Bas* **1992**, *111*, 59; b) P. Dauban, L. Dubois, M. E. Tran Huu Dau, R. H. Dodd, *J. Org. Chem.* **1995**, *60*, 2035; c) K. Nakajima, T. Tanaka, K. Morita, K. Okawa, *Bull. Chem. Soc. Jpn.* **1980**, *53*, 283; d) K. Nakajima, M. Neya, S. Yamada, K. Okawa, *ibid.* **1982**, *55*, 3049; e) J. Bodenan, J. Chanet-Ray, R. Vassiere, *Synthesis* **1992**, 288; f) Z. Bernstein, D. Ben-Ishai, *Tetrahedron*, **1977**, *33*, 881; g) J. Legters, L. Thijs, B. Zwanenburg, *Recl. Trav. Chim. Pays-Bas* **1992**, *111*, 16; h) O. Ploux, M. Caruso, G. Chassaing, A. Marquet, *J. Org. Chem.* **1988**, *53*, 3154; i) K. Nakajima, H. Oda, K. Okawa, *Bull. Chem. Soc. Jpn.* **1983**, *56*, 520; l) K. Sato, A. P. Kozikowski, *Tetrahedron Lett.* **1989**, *30*, 4073; m) I. Shima, N. Shimazaki, K. Imai, K. Hemmi, M. Hashimoto, *Chem. Pharm. Bull.* **1990**, *38*, 564; n) E. P. Styngach, K. I. Kuchkova, T. M. Efremova, A. A. Semenov, *Chem. Heterocycl. Comp.* **1973**, 1378; o) J. E. Baldwin, R. M. Adlington, N. G. Robinson, *J. Chem. Soc. Chem. Comm.* **1987**, 153; p) J. E. Baldwin, R. M. Adlington, I. A. O'Neil, C. Schofield, A. C. Spivey, J. B. Sweeney, *ibid.* **1989**, 1852; q) Z. Bouyad, J. Chanet-Ray, S. Ducher, R. Vessiere, *J. Heterocycl. Chem.* **1991**, 1757.

[3] a) R. Amoroso, G. Cardillo, P. Sabatino, C. Tomasini, A. Trerè, *J. Org. Chem.* **1993**, *58*, 5615, and references therein; b) G. Cardillo, A. De Simone, L. Gentilucci, P. Sabatino, C. Tomasini, *Tetrahedron Lett.* **1994**, *35*, 5051; c) I. Braschi, G. Cardillo, C. Tomasini, R. Venezia, *J. Org. Chem.* **1994**, *59*, 7292, and references therein.

[4] a) O. Ploux, M. Caruso, G. Chassaing, A. Marquet, *J. Org. Chem.* **1988**, *53*, 3154; b) R. Haner, B. Olano, D. Seebach, *Helv. Chim. Acta* **1987**, *70*, 1676; c) G. V. Shustov, O. N. Krutius, V. N. Voznesensky, I. I. Chervin, A. V. Eremeer, R. G. Kostyanovsky, F. D. Polyak, *Tetrahedron*, **1990**, *46*, 6741.

[5] a) K. Nakajima, F. Takai, T. Tanaka, K. Okawa, *Bull. Chem. Soc. Jpn.* **1978**, *51*, 1577; b) E. Kuyl-Yeheskiely, M. Lodder, G. A. van der Marel, J. H. van Boom, *Tetrahedron Lett.* **1992**, *33*, 3013; c) T. Wakamiya, K. Shimbo, T. Shiba, K. Nakajima, M. Neya, K. Okawa, *Bull. Chem. Soc. Jpn.* **1982**, *55*, 3878; d) K. J. Shaw, J. R. Luly, H. Rapoport, *J. Org. Chem.* **1985**, *50*, 4515.

[6] J. Legters, L. Thijs, B. Zwanenburg, *Recl. Trav. Chim. Pays-Bas* **1992**, *111*, 1.

[7] a) P. Garner, O. Dogan, S. Pillai, *Tetrahedron Lett.* **1994**, *35*, 1653; b) G. Cardillo, L. Gentilucci, C. Tomasini, M. P. Visa Castejon-Bordas, *Tetrahedron: Asymmetry* **1996**, *7*, 755.

[8] a) A. H. Blatt, *J. Am. Chem. Soc.* **1939**, *61*, 3494; b) N. H. Cromwell, N. G. Barker, R. A. Wankel, P. J. Vanderhorst, F. W. Olson, J. H. Anglin, *ibid.* **1951**, *73*, 1044; c) L. D. Nagel, P. B. Woller, N. H. Cromwell, *J. Org. Chem.* **1971**, *36*, 3911.

[9] H. Roder, G. Helmchen, E. M. Peters, K. Peters, H. G. von Schnering, *Angew. Chem.* **1984**, *96*, 895; *Angew. Chem. Int. Ed. Engl.* **1984**, *23*, 898.

[10] D. A. Evans, F. Urpi, T. C. Somers, J. S. Clark, M. T. Bilodeau, *J. Am. Chem. Soc.* **1990**, *112*, 8215.

[11] R. Annunziata, M. Benaglia, M. Cinquini, F. Cozzi, *Tetrahedron* **1995**, *32*, 8941.

[12] **5a**: IR (nujol): $\tilde{\nu}$ = 3260, 1700, 1640, 1410, 1360, 1220, 1060, 930, 860, 790, 690 cm^{-1}; ^1H NMR ($CDCl_3$): δ = 0.82 (d, 3H, J = 6.6 Hz, $CH_3CHCHPh$), 1.30 (d, 3H, J = 5.2 Hz, CH_3), 1.80 (br. s, 1H, NH), 2.05 (dq, 1H, J = 5.2, 2.2 Hz, $HNCHCH_3$), 2.87 (s, 3H, NCH_3), 3.71 (d, 1H, J = 2.2 Hz, $OCCHNH$), 4.00 (dq, 1H, J = 8.4, 6.6 Hz, $CH_3CHCHPh$), 5.25 (d, 1H, J = 8.4 Hz, $CH_3CHCHPh$), 7.09–7.40 (m, 5H, Ph); ^{13}C NMR ($CDCl_3$): δ = 15.3, 18.6, 28.5, 36.2, 37.5, 54.9, 60.4, 127.2, 128.7, 129.2, 136.7, 156.2, 171.6; MS: *m/z*: 273 (M^+, 19), 231 (10), 217 (7), 191 (100), 175 (14), 160 (3), 148 (8), 132 (25), 113 (21), 91 (14), 77 (15), 56 (22); $[\alpha]_D$ = −63 (c = 1 in $CHCl_3$); m.p. 174–176 °C.

[13] **5b**: $[\alpha]_D$ = −75 (c = 1.2 in $CHCl_3$); m.p. 140–145 °C. **5c**: $[\alpha]_D$ = −54 (c = 1.4 in $CHCl_3$); m.p. 112–116 °C.

[14] D. A. Evans, M. D. Ennis, D. J. Mathre, *J. Am. Chem. Soc.* **1982**, *104*, 1737.

[15] **7a:** IR (neat): ν = 3280, 3040, 2960, 1730, 1500, 1450, 1410, 1200, 1080, 820, 705 cm^{-1}; ^1H NMR ($CDCl_3$): δ = 1.24 (d, 3H, J = 5.2 Hz, CH_3), 1.54 (s, 1H, NH), 2.28–2.37 (m, 2H, $CHCH$), 5.16 (d, 1H, J = 12.1 Hz, $OCHPh$), 5.21 (d, 1H, J = 12.1 Hz, $OCHPh$), 7.30–7.50 (m, 5H, Ph); ^{13}C NMR ($CDCl_3$): δ = 18.0, 34.9, 36.1, 67.2, 128.3, 128.5, 128.6, 135.3, 172.5; MS: *m/z*: 176 (2), 147 (3), 131 (3), 117 (2), 100 (60), 91 (100), 77 (6), 65 (20); $[\alpha]_D$ = +47.2 (c = 1.2 in $CHCl_3$).

[16] No traces of benzyl *cis*-aziridine-2-carboxylates or *cis*-aziridine-2-carboxylic acids were detected.

 © VCH Verlagsgesellschaft mbH, D-69451 Weinheim, 1996 0570-0833/96/3516-1849 $ 15.00+.25/0

Synthesis of New Hybrid Materials by Intercalation of a Bifunctional Aminophosphane and Its Tungsten Pentacarbonyl Complex in α-Zirconium Phosphate**

Jonathon S. Bone, David G. Evans,* J. John Perriam, and Robert C. T. Slade

In recent years a variety of catalytically active materials has been produced by anchoring transition metal complexes on the surface of insoluble supports such as organic polymers[1] or metal oxides[2] in order to exploit in tandem the well-known advantages of heterogenous and homogeneous systems. If the metal complex can be incorporated in the interlamellar region of a layered solid, the catalytic selectivity is potentially enhanced since the effect of the layers may limit absorption and reaction of substrates based on their size, shape, or polarity. The synthesis of such hybrid materials containing rhodium complexes intercalated in smectite clays has been reported.[3-5] α-Zirconium phosphate $Zr(HPO_4)_2 \cdot H_2O$ (**1**) represents an alternative layered solid, which has a number of advantages as a host lattice arising from the ease of synthesis of high purity material, its high exchange capacity, and chemical and thermal robustness.[6] Crystallographic studies[7] show that each layer consists of almost coplanar zirconium atoms bridged by tetrahedral O_3POH groups alternatively located above and below the plane. The acidic protons of the hydrogen phosphate groups may be readily substituted by other cations, which leads to an expansion of the interlayer distance. A wide variety of transition metal ions[8] and preformed transition metal coordination complexes[9] such as $[Cr(NH_3)_6]^{3+}$ and $[Co(en)_3]^{3+}$ (en = 1,2-diaminoethane) have been intercalated into the α-zirconium phosphate host lattice. An alternative procedure that has been effectively employed[10] is to pre-intercalate a ligand such as 2,2′-bipyridyl or 1,10-phenanthroline and form an intercalated metal complex in situ by subsequent reaction of this material with metal ions such as Rh^{3+}. A third route to intercalation compounds of α-zirconium phosphate involves its reaction with Brønsted bases such as amines, which leads to formation of products containing intercalated alkylammonium ions. If the amino group is incorporated in a suitable bifunctional cyclopentadienyl ligand, its reaction with interlayer acidic protons facilitates the intercalation of organometallic complexes such as $[(\eta^5\text{-}C_5H_5)Fe(\eta^5\text{-}C_5H_4CH_2CH_2NH_2)]$[11] and $[\{(OC)_3Mn(\eta^5\text{-}C_5H_3(CH_3)CH_2)\}_2NH]$[12] in the α-zirconium phosphate host **1**.

Transition metal phosphane complexes are active as both homogeneous and supported catalysts in a variety of important reactions. Herein we report on the synthesis of the first hybrid material containing such a complex incorporated in an α-zirconium phosphate host lattice. Our strategy has been to employ a bifunctional aminophosphane ligand in which the basic nitrogen center facilitates intercalation by reaction with the acidic protons of **1**. With careful choice of experimental conditions, the use of such hybrid ligands allows the incorporation of otherwise hydrophobic metal complexes in the hydrophilic interlayer region. Reaction (methanol solution, 65 °C, 48 h) of mechanically ground (micronized) **1**, prepared by a sol–gel route,[13] with the bifunctional ligand *N*,*N*-dimethylaminoethyldiphenylphosphane[14] afforded a material (**2**), which according to microanalysis and thermogravimetry has the empirical formula $[Zr(HPO_4)_2(Ph_2PCH_2CH_2NMe_2)_{0.46} \cdot 1.1\,H_2O]$ (Scheme 1, Table 1). The powder X-ray diffraction pattern ($\lambda = 1.54178$ Å) of **2** was consistent with the presence of a single crystalline phase and showed (002) and higher order reflections, indicating an expanded interlayer spacing (d_{002}) of 16.7 Å in comparison with the corresponding value of 7.6 Å in **1** (Fig. 1).[6] The increased $H_2O:Zr(HPO_4)_2$ ratio in **2** can be ascribed to the increased

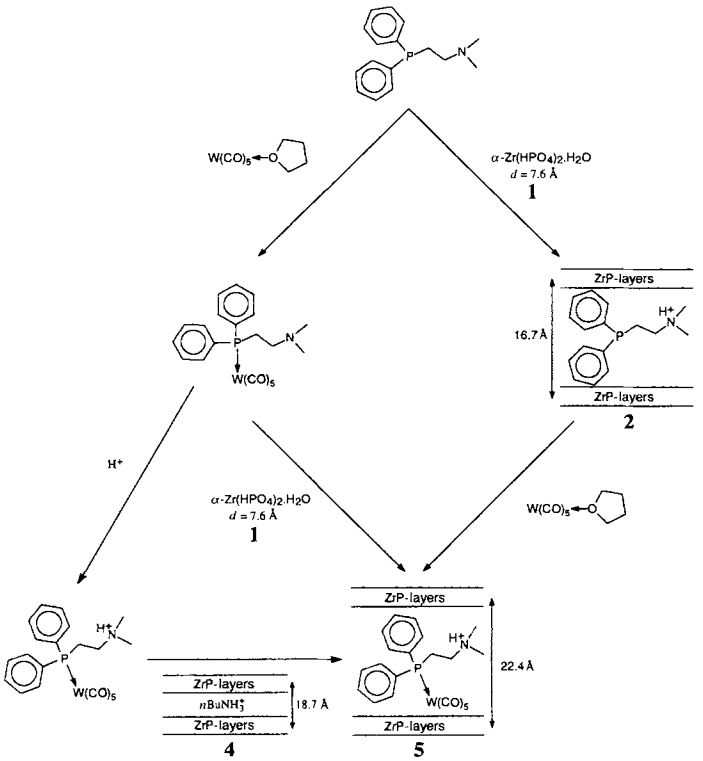

Scheme 1. Methods of intercalation of tungsten complexes with the ligand $Ph_2PCH_2CH_2NMe_2$.

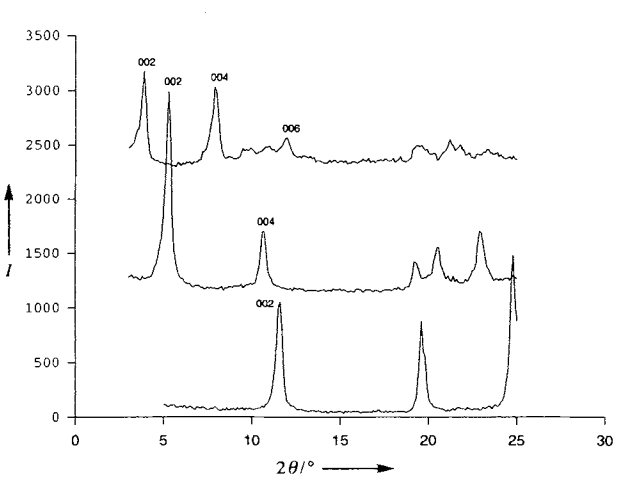

Fig. 1. X-ray powder diffraction patterns ($\lambda = 1.54178$ Å) of **1** (bottom), **2** (middle), and **5** (top). The variation in the position of the low angle reflection (indexed as d_{002}) is consistent with the expansion in interlayer spacing in **1**–**5**.

[*] Dr. D. G. Evans, J. S. Bone, J. J. Perriam, Dr. R. C. T. Slade
Department of Chemistry, University of Exeter
Stocker Road, Exeter EX4 4QD (UK)
Fax: Int code +(1392)263434
e-mail: DGEvans@exeter.ac.uk

[**] We thank EPSRC (UK) for a studentship (to J. J. P.) and access to MAS NMR facilities at the National Solid State NMR Service at Durham. Aspects of this work were funded by the European Commission under Brite-Euram II (Contract Number BRE2-CT93-0450). We thank Dr. K. E. Young for helpful discussions.

Table 1. Interlayer spacing d [Å], ^{31}P NMR chemical shifts δ, and compositions [%] of **1**–**5**.

Compound	Formula	d_{002}	δ [a] Host lattice [b]	Interlayer species	Composition [e, f] C	H	N	H_2O
1	α-$Zr(HPO_4)_2 \cdot H_2O$	7.6	−18.8	--	-	-	--	6.18 (6.35)
2	α-$Zr(HPO_4)_2(Ph_2PCH_2CH_2NMe_2)_{0.46} \cdot 1.1\ H_2O$	16.7	−11.2, −19.2, −20.0, −20.7	−26.5 [b] −19.1 [c]	21.10 (20.98)	3.25 (3.20)	1.57 (1.53)	4.64 (4.70)
3	α-$Zr(HPO_4)_2(Ph_2P(=O)CH_2CH_2NMe_2)_{0.43} \cdot 1.5\ H_2O$	16.4	−12.2, −20.6	31.8 [b] 31.7 [c]	19.14 (19.16)	3.03 (3.19)	1.48 (1.40)	6.39 (6.33)
4	α-$Zr(HPO_4)_2(n\text{BuNH}_2)_2 \cdot 0.7\ H_2O$	18.7	−14.8, −18.9	-	21.44 (21.41)	5.68 (5.70)	6.30 (6.24)	2.68 (2.70)
5	α-$Zr(HPO_4)_2 \cdot [(OC)_5W\{Ph_2PCH_2CH_2NMe_2\}]_{0.51} \cdot 1.5\ H_2O$	22.4	−19.4, −20.2, −20.9	8.2, 6.3 [b] 5.5 [d]	21.20 (21.22)	2.43 (2.50)	1.21 (1.18)	4.43 (4.45)

[a] Reference = 85% H_3PO_4. [b] Solid-state MAS NMR. [c] In $CDCl_3$ solution. [d] In CD_2Cl_2 solution. [e] C,H,N by microanalysis (calculated values are in parentheses). [f] Weight loss below 150 °C (by thermogravimetry) is assumed to arise from desorption of interlayer water.

gallery height, which makes the material more zeolitic in character, thus facilitating uptake of additional water. The ^{31}P MAS NMR spectrum of **2** (Table 1) showed a resonance with a chemical shift close to that observed for the free phosphane in solution[14] and a complex set of resonances indicating[15, 16] that the material contains both hydrogen phosphate ($\delta = -19.2$, -20.0, and -20.7) and phosphate ($\delta = -11.2$) groups. This suggests that it can be correctly formulated as $[Zr(HPO_4)_{1.54}(PO_4)_{0.46}(Ph_2PCH_2CH_2NHMe_2)_{0.46} \cdot 1.1\ H_2O]$. In order to confirm that oxidation of the phosphane had not taken place during the intercalation, reaction of an authentic sample[14] of *N*,*N*-dimethylaminoethyldiphenylphosphane oxide with micronized **1** was carried out under the same conditions as those for the phosphane itself. The product **3** had the empirical formula $[Zr(HPO_4)_2(Ph_2P(=O)CH_2CH_2NMe_2)_{0.43} \cdot 1.5\ H_2O]$ and an expanded interlayer spacing (Table 1). The ^{31}P MAS NMR spectrum of **3** (Table 1) showed resonances consistent with the presence of both hydrogen phosphate and phosphate groups, and in addition a broad resonance with a chemical shift very close to that of the free phosphane oxide in solution, suggesting that **3** can be correctly formulated as $[Zr(HPO_4)_{1.57}(PO_4)_{0.43}(Ph_2P(=O)CH_2CH_2NHMe_2)_{0.43} \cdot 1.5\ H_2O]$. No resonance in the phosphane oxide region of the spectrum is observed in the case of **2**, confirming its formulation as the phosphane intercalate.

The ability of **2** to incorporate metal fragments was investigated by studying its reaction with the labile complex $[W(CO)_5(thf)]$. Such compounds are known[17] to react readily with phosphane ligands in solution to afford complexes of the type $[W(CO)_5(PR_3)]$ that have a characteristic IR spectrum, which is therefore useful for diagnostic purposes. Reaction (THF/methanol, 60 °C, 48 h) of **2** with $[W(CO)_5(thf)]$ led to uptake of the carbonyl moiety by the intercalated phosphane ligand, as shown by the characteristic IR spectrum[12] ($\tilde{\nu}_{CO}$/cm^{-1} 2072 m, 1981 sh, 1936 vs) of the solid and the further expansion of the interlayer spacing to 22.6 Å. A similar material was prepared by direct reaction (THF/methanol, 60 °C, 108 h) of **1** with a solution of the $[(OC)_5W(Ph_2PCH_2CH_2NMe_2)]$ complex[14] (see Scheme 1). The resulting products from these reactions, however, were contaminated with poorly crystalline **1**, and a single phase could not be obtained. The following alternative synthetic strategy did, however, afford single-phase materials.

Reaction of **1** with butylamine vapor is known[18] to afford $[Zr(HPO_4)_2(n\text{BuNH}_2)_2 \cdot 0.7\ H_2O]$ (**4**), which has a greatly expanded interlayer spacing (see Table 1). The interlayer butylammonium cations may be readily replaced by a variety of other cations.[8, 9] Reaction of an ethereal solution of $[(OC)_5W(Ph_2PCH_2CH_2NMe_2)]$ with $HBF_4 \cdot Et_2O$ afforded the isolable salt $[(OC)_5W(Ph_2PCH_2CH_2NHMe_2)](BF_4)$. Reaction of a solution of this salt in methanol with **4** afforded a material (**5**) with the empirical formula $[Zr(HPO_4)_2\{(OC)_5W(Ph_2PCH_2CH_2NMe_2)\}_{0.51} \cdot 1.5\ H_2O]$ (Scheme 1, Table 1). The powder X-ray diffraction pattern contained (002) and higher order reflections, indicating an interlayer spacing of 22.4 Å. The ^{31}P MAS NMR spectrum of **5** (Table 1) showed a complex set of resonances consistent with the presence of both hydrogen phosphate and phosphate groups, and, in addition, two very broad resonances at a chemical shift very close to that of the free tungsten phosphane complex in solution (Table 1), indicating that **5** can be correctly formulated as $[Zr(HPO_4)_{1.49}(PO_4)_{0.51}\{(OC)_5W(Ph_2PCH_2CH_2NHMe_2)\}_{0.51} \cdot 1.5\ H_2O]$. The presence of two resonance signals may indicate that the intercalated phosphane occupies at least two distinct sites in a disordered interlayer region.

It is noteworthy that in the above reaction, two moles of butylamine are quantitatively replaced by 0.51 moles of the aminophosphane complex. In the starting material, $[Zr(PO_4)_2(n\text{BuNH}_3)_2 \cdot 0.7\ H_2O]$, the protonated amine ligands form a bilayer[16, 18] with their alkyl chains making an angle of 55° to the phosphate layers. Although it is to be expected that there will be strong forces between the anionic layers and the cationic guest species, a recent study[19] of quarternary ammonium ion intercalates derived from the closely related host lattice $[\gamma\text{-}Ti(HPO_4)_2 \cdot 2\ H_2O]$ has indicated that the van der Waals forces between the alkyl chains of the guest species make a significant contribution to the overall stability of the material. Replacement of a small amount of butylammonium cation by the intercalating protonated complex will presumably disrupt the bilayer, thus facilitating the expulsion of further butylamine with concomitant reprotonation of the host lattice O_3PO^- groups. A similar high selectivity for cationic transition metal complexes over butylamine has been observed previously.[9] For example, two moles of butylamine were shown to be quantitatively replaced by 0.28 moles of $[Cr(NH_3)_6]^{3+}$ ions or 0.24 moles of $[Co(en)_3]^{3+}$ ions, respectively.

In conclusion, an appropriately functionalized phosphane ligand and its tungsten pentacarbonyl complex may be incorporated into the α-zirconium phosphate host structure. Further studies on other complexes of $Ph_2PCH_2CH_2NMe_2$ and related ligands are in progress.

Experimental Procedure

2: A solution of *N*,*N*-dimethylaminoethyldiphenylphosphane (1.00 g, 3.88 mmol) in dry, degassed methanol (30 mL) was added to a slurry of α-zirconium phosphate (0.50 g, 1.66 mmol) in dry, degassed methanol (20 mL) and the reaction stirred at

65 °C for 48 h. The slurry was cooled and the solid isolated by centrifugation, washed with dried methanol and dried under reduced pressure.

3: The preparation was carried out in the same manner as for **2** starting from *N,N*-dimethylaminoethyldiphenylphosphane oxide.

5: A solution of $[(OC)_5W(Ph_2PCH_2CH_2NHMe_2)](BF_4)$ (0.75 g, 1.07 mmol) [prepared by reaction of $[(OC)_5W(Ph_2PCH_2CH_2NMe_2)]$ (0.80 g, 1.38 mmol) in dry degassed diethyl ether (50 mL) with an 85% solution of $HBF_4 \cdot Et_2O$ in diethyl ether (0.36 g, 1.89 mmol)] in dry, degassed methanol (20 mL) was added to a slurry of **4** (0.10 g, 0.22 mmol) in dry, degassed methanol (20 mL) and the reaction stirred at 60 °C for 48 h. The slurry was cooled and the solid isolated by centrifugation, washed with dried methanol and dried under reduced pressure.

Received: January 19, 1996 [Z 8737 IE]
German version: *Angew. Chem.* **1996**, *108*, 1972–1974

Keywords: complexes with phosphorus ligands · intercalation compounds · tungsten compounds · zeolites · zirconium compounds

[1] B. Heinrich, Y. Chen, J. Hjortkjoer, *J. Mol. Catal.* **1993**, *80*, 365.
[2] M. Lenarda, R. Ganzerla, L. Storaro, R. Zanoni, *J. Mol. Catal.* **1993**, *78*, 339.
[3] T. J. Pinnavaia, R. Raythatha, J. G.-S. Lee, L. J. Halloran, J. F. Hoffman, *J. Am. Chem. Soc.* **1979**, *101*, 6891.
[4] F. Farzaneh, T. J. Pinnavaia, *Inorg. Chem.* **1983**, *22*, 2216.
[5] V. L. K. Valli, H. Alper, *Chem. Mater.* **1995**, *7*, 359.
[6] Y. Ding, D. J. Jones, P. Maireles-Torres, J. Rozière, *Chem. Mater.* **1995**, *7*, 562.
[7] J. M. Troup, A. Clearfield, *Inorg. Chem.* **1977**, *16*, 3311.
[8] G. L. Rosenthal, J. Caruso, *Inorg. Chem.* **1992**, *31*, 144.
[9] G. L. Rosenthal, J. Caruso, *J. Solid State. Chem.* **1991**, *93*, 128.
[10] C. Ferragina, A. La Ginestra, M. A. Massucci, G. Mattogno, P. Patrono, P. Giannoccaro, P. Cafarelli, M. Arfelli, *J. Mater. Chem.* **1995**, *5*, 461, and references therein.
[11] S. J. Mason, L. M. Bull, C. P. Grey, S. J. Heyes, D. O'Hare, *J. Mater. Chem.* **1992**, *2*, 1189.
[12] C. F. Lee, M. E. Thompson, *Inorg. Chem.* **1991**, *30*, 4.
[13] H. Benhamza, P. Barboux, A. Bouhaouss, F. Josien, J. Livage, *J. Mater. Chem.* **1991**, *1*, 681.
[14] R. T. Smith, M. C. Baird, *Inorg. Chim. Acta*, **1982**, *62*, 135.
[15] D. J. MacLachlan, K. R. Morgan, *J. Phys. Chem.* **1990**, *94*, 7656.
[16] D. J. MacLachlan, K. R. Morgan, *J. Phys. Chem.* **1992**, *96*, 3458.
[17] D. J. Darensbourg, C. J. Bischoff, *Inorg. Chem.* **1993**, *32*, 47.
[18] A. Clearfield, R. M. Tindwa, *J. Inorg. Nucl. Chem.* **1979**, *41*, 871.
[19] M. Danjo, Y. Baba, M. Tsuhako, S. Yamaguchi, M. Hayama, H. Nariai, I. Motooka, *Bull. Chem. Soc. Jpn.* **1995**, *68*, 1607.

Nonlinear Temperature Behavior of Product Ratios in Selection Processes**

Detlef Heller,* Helmut Buschmann, and Hans-Dieter Scharf

Dedicated to Professor Ivar Ugi on the occasion of his 65th birthday

For selective reactions it has long been known that a logarithmic plot of the product ratio as a function of reciprocal temperature does not always display linear behavior.[1–3] That the selectivity of a reaction need not fall regularly with decrease in temperature is of considerable practical significance in efforts to attain higher selectivity. In addition, interpretation of the temperature dependence can provide information on the mechanism of a reaction.[3] The temperature dependence has been examined in detail in the case of the Paternò–Büchi reaction, which led to the empirically derived isoinversion principle.[4] Accordingly, at the inversion point of two roughly linear regions, obtained by plotting the logarithm of the product ratios $[\ln(R/S)]$ versus $1/T$, there is a change in dominance between differences in activation enthalpy ($\Delta\Delta H^{\neq}$) and activation entropy ($\Delta\Delta S^{\neq}$) for various selection levels. The difference in the values of $\Delta\Delta H^{\neq}$ and $\Delta\Delta S^{\neq}$ before and after the point of inversion—in this case the inversion temperature T_{inv}—leads to the isoinversion temperature T_i [Eq. (a)], which describes the selectivity of a reaction as a characteristic quantity. This is the so-called *isoinversion principle*.

$$\partial\Delta\Delta H^{\neq} = T_i \cdot \partial\Delta\Delta S^{\neq} \qquad \text{(a)}$$

As an "abrupt" change of dominance between $\Delta\Delta H^{\neq}$ and $\Delta\Delta S^{\neq}$ is rather unlikely, according to Ridd,[5] he interpreted the experimentally determined nonlinear temperature dependence of the logarithmic product ratios as a shift in the rate-determining step of the reaction with change in temperature. This alternative interpretation is based on a simulation with empirical energy levels. The shift in the rate-determining step has also been invoked by Sharpless for the asymmetric olefin dihydroxylation with OsO_4 (in the presence of chiral bases).[3]

Common to the two apparently contradictory viewpoints is the consideration of the temperature dependence of the ratio of the overall rate constants in terms of Eyring theory.[6] The subsequent difference in free activation enthalpy $\Delta\Delta G^{\neq}$ resulting from processes leading to selection is also the basis of the stereochemical structure model of Ugi and Ruch.[7]

The aim of the present work was to extend the previous examples and interpretations of the nonlinear temperature dependence in selection processes, and to trace this exclusively back to the nonlinear change in the concentration ratio of the intermediate with the variation in temperature. This should be demonstrated with one of the best understood selection processes, catalytic asymmetric hydrogenation. According to Halpern[8] and Brown,[9] asymmetric catalytic hydrogenation with five-membered Rh chelate complexes proceeds as shown in Scheme 1. All subsequent considerations are based exclusively on two diastereomeric intermediates, which are prepared with chiral C_2-symmetric ligands, for example, Kagan's DIOP ligand (Fig. 1).[10]

As shown in Scheme 1, the diastereomeric substrate complexes E_{ma} and E_{mi} are formed in the first selection level in a preequilibrium. In a series of elementary steps—oxidative addition of hydrogen, insertion, reductive elimination—these react at different rates in the second selection level to give the enantiomers. Under normal conditions the rate of the oxidative addition is recognized to be rate-determining.

The ratio of enantiomers is described by Equation (b). Whereas a plot of $\ln(R/S)$ against $1/T$ gives, in principle, a

$$\frac{R}{S} = \frac{k_{2mi}}{k_{2ma}} \cdot \frac{E_{mi}}{E_{ma}} = \frac{k_{2mi} \cdot \dfrac{k_{1mi}}{k_{-1mi} + k_{2mi}}}{k_{2ma} \cdot \dfrac{k_{1ma}}{k_{-1ma} + k_{2ma}}} \qquad \text{(b)}$$

straight line for established preequilibria ($k_{2ma} \ll k_{1ma}$ or k_{-1ma}; $k_{2mi} \ll k_{1mi}$ or k_{-1mi}), for a nonestablished preequilibrium this

[*] Dr. D. Heller
Max-Planck-Gesellschaft
Arbeitsgruppe "Asymmetrische Katalyse" an der Universität
Buchbinderstrasse 5/6, D-18055 Rostock (Germany)
Fax: Int. code +(381)4669324
e-mail: dhelle@chemie1.uni-rostock.de
Dr. H. Buschmann
Grünenthal GmbH Aachen, Forschungszentrum
Zieglerstrasse 6, D-52078 Aachen (Germany)
Prof. Dr. H.-D. Scharf
Institut für Organische Chemie der Technischen Hochschule
Professor-Pirlet-Strasse 1, D-52056 Aachen (Germany)

[**] The authors thank Prof. D. Haberland for stimulating discussions and Prof. J. Ridd, London, for communicating his results. This work was supported by Prof. R. Selke, the Max-Planck-Gesellschaft, and the Fonds der Chemischen Industrie.

 © VCH Verlagsgesellschaft mbH, D-69451 Weinheim, 1996 0570-0833/96/3516-1852 $ 15.00+.25/0

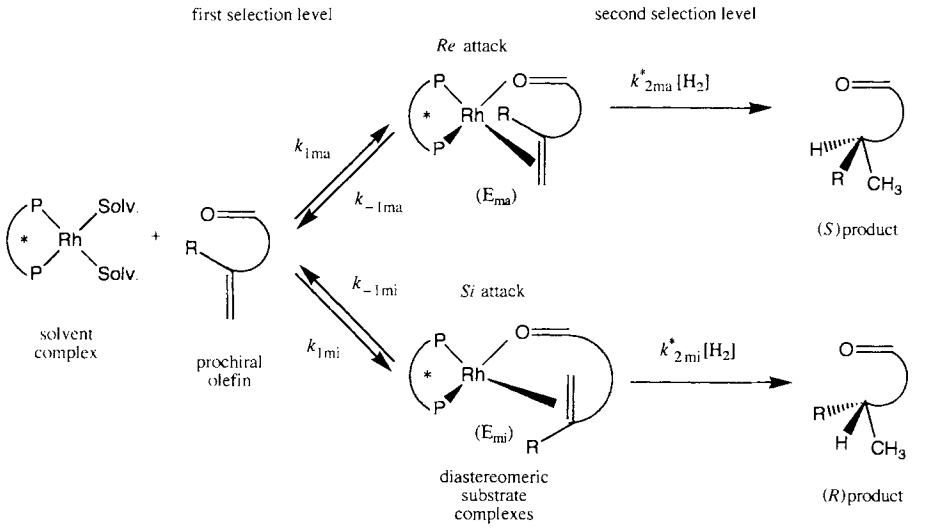

Scheme 1. Example of an asymmetric hydrogenation catalyzed by a rhodium complex. The (*R*) amino acid is formed in excess. (E_{ma} and E_{mi} are the major and minor substrate complexes, respectively; k_i: rate constants; $k^*_{2ma}[H_2] = k_{2ma}$; $k^*_{2mi}[H_2] = k_{2mi}$).

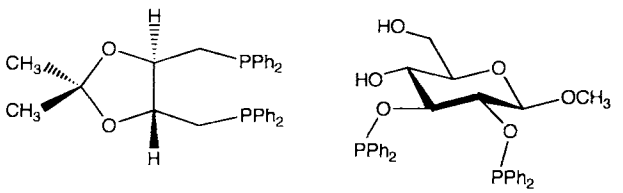

(*R*,*R*)-DIOP **1a** Phenyl-β-glup-OH **1b**

Fig. 1. Chiral ligands for asymmetric hydrogenation. DIOP = 4,5-bis(diphenylphosphinomethyl)-2,2-dimethyl-1,3-dioxolane.

can no longer be the case because of the additive coupling of the rate constants. As the ratio of the rate constants k_{2mi}/k_{2ma} leads in principle to a linear temperature dependence, the experimentally observed nonlinearity must depend on a change in the concentration ratio of the diastereomeric substrate complexes with temperature. This will be explained with an example.

Table 1. Values for $\Delta H^{\ddagger}$ [kcal mol^{-1}] and $\Delta S^{\ddagger}$ [cal mol^{-1} K^{-1}] for the calculation of the rate constants according to Equation (b).

	k_{1mi}	k_{1ma}	k_{-1mi}	k_{-1ma}	k_{2mi}	k_{2ma}
$\Delta H^{\ddagger}$	6.9	4.9	13.0	13.3	8.5	13.5
$\Delta S^{\ddagger}$	−17.0	−24.6	−12.9	−17.9	−27.0	−24.0

Table 1 contains $\Delta H^{\ddagger}$ and $\Delta S^{\ddagger}$ values for the determination of rate constants according to Equation (b). The rate constants for the preequilibrium are those found for asymmetric hydrogenation.[8] Because the thermodynamically less stable minor substrate complex reacts at a higher rate to give the enantiomer found in excess, as shown by Halpern in terms of the major/minor concept,[8] only the values for calculation of the rate constants of the oxidative addition, k_{2mi} and k_{2ma}, have been simulated. The temperature dependence of the product ratio (R/S) is shown in Figure 2. In the temperature range from roughly −25 °C to about +130 °C a characteristic maximum can be seen.

The upper part of Figure 3 shows the expected linearity in the temperature dependence of the ratio of the rate constants for the oxidative addition as one of the factors on the left-hand side of Equation (b). The temperature dependence of the ratio of the diastereomeric substrate complexes is shown in the lower part of Figure 3. Whereas the curve is still linear at higher temperatures as expected, at lower temperatures the curve deviates increasingly from linearity. Although all rate constants become smaller with decreasing temperature, the displacement of establishment of the preequilibrium becomes more pronounced with decreasing temperature.

Summation of the individual factors from Equation (b) for the temperature dependence shown in Figure 3 gives the temperature dependence of the enantiomer ratio for the overall reaction, as shown in Figure 2. When Figure 3 is considered from this aspect, it is apparent that at higher temperatures the oxidative addition (second selection level) is the major contribution to the enantiomer ratio. In contrast, at very low temperatures the selectivity results predominantly from the ratio of the diastereomeric substrate complexes (first selection level). This increasing dominance of the first selection level is caused exclusively by the increasing deviation, with decreasing temperature, from linearity of the temperature dependence of the ratio of the diastereomer concentrations (E_{mi}/E_{ma}), which is the real cause for the nonlinear temperature dependence of the enantiomer ratio. Thus, both

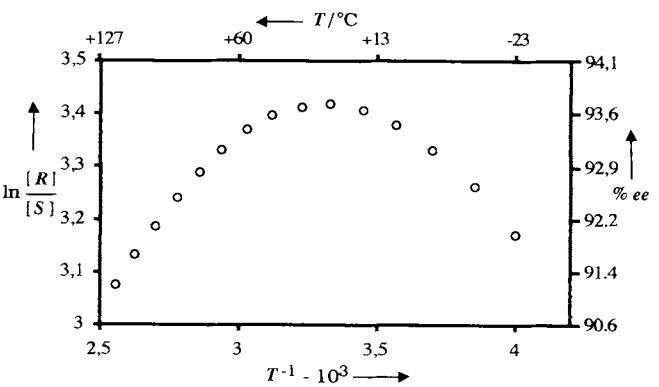

Fig. 2. Temperature dependence of the enantiomer ratio (calculated with the constants from Table 1).

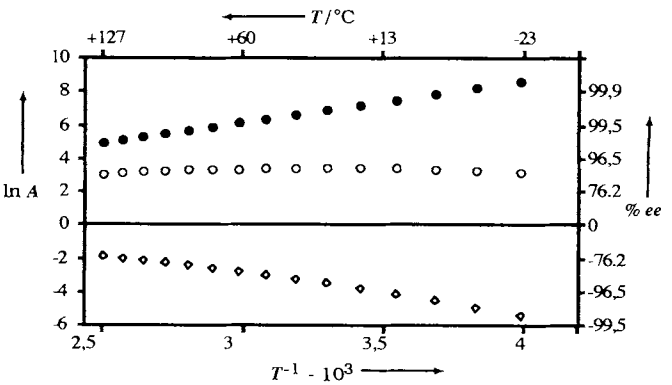

Fig. 3. Temperature dependence of the individual factors from Equation (b) [•: $A = (k_{2mi}/k_{2ma})$; ○: $A = (R/S)$; ◇: $A = (E_{mi}/E_{ma})$].

sides of the maximum can, in principle, be explained as resulting from the dominance of different selection levels in different temperature ranges. This is an essentially empirical statement of the inversion principle.[4]

We will now discuss the nonlinear temperature dependence of the concentration ratio of the intermediates as the cause for the nonlinear behavior of the product ratio in a selection process. In principle, for the asymmetric hydrogenation with C_2-symmetric ligands as an example of a selection process, this behavior can be traced back to two possible causes:[17] 1) displaced (intermolecular) preequilibria and 2) intramolecular equilibria.

The displacement in the establishment of a preequilibrium, the position of which is temperature dependent, means that the stationary concentration of the affected substrate complex will become smaller. Coupling of the diastereomeric substrate complexes through their the common substrate leads to a change in the ratio of the intermediates (see also ref. [12]). The increasing displacement in reaching the preequilibrium through increasingly faster subsequent reactions of the intermediate ultimately results in other steps becoming rate-determining; this corresponds to the "transition region" described by Ridd.[5] The nonlinear temperature dependence of the logarithmic product ratio in this transition region is based on a change in the rate-determining step. In our opinion this is caused by the nonlinear shift of the concentration ratio of the intermediate as a function of temperature.

A second possible cause is the intramolecular exchange between diastereomeric substrate complexes, as described for five-membered chelate rings[13, 14] and recently quantified for seven-membered chelate rings.[15] In principle, even when all equilibria are established, this leads to a nonlinear temperature dependence of the ratio of the diastereomeric substrate complexes (for a derivation, see ref. [16]). This is particularly valid when the intramolecular exchange processes are more dominant than the intermolecular equilibria.

Thus, we have shown that the arguments in the discussion[4, 5] on the interpretation of the nonlinear temperature dependence of logarithmic product ratios are not contradictory. Both interpretations are possible within defined limits. The cause for the experimentally observed dependence can be reduced to the concentration ratio of two intermediates that changes with temperature in nonlinear fashion; further reaction of these two intermediates then leads to selective product formation. The causes of the nonlinear changes in the ratio of intermediates are then displaced intermolecular preequilibria and intramolecular exchange processes of substrate complexes that appear as intermediates.

Received: January 8, 1996
Revised version: March 26, 1996 [Z 8706 IE]
German version: *Angew. Chem.* **1996**, *108*, 1964–1967

Keywords: asymmetric hydrogenations · isoinversion principle · selection processes

[1] H. Pracejus, *Liebigs Ann. Chem.* **1960**, *634*, 9–22.
[2] E. Anders, E. Ruch, I. Ugi, *Angew. Chem.* **1973**, *85*, 16–20; *Angew. Chem. Int. Ed. Engl.* **1973**, *12*, 25–29.
[3] T. Göbel, K. B. Sharpless, *Angew. Chem.* **1993**, *105*, 1417–1418; *Angew. Chem. Int. Ed. Engl.* **1993**, *32*, 1329–1330.
[4] H. Buschmann, H.-D. Scharf, N. Hoffmann, P. Esser, *Angew. Chem.* **1991**, *103*, 480–518; *Angew. Chem. Int. Ed. Engl.* **1991**, *30*, 477–515.
[5] K. J. Hale, J. H. Ridd, *J. Chem. Soc. Perkin 2* **1995**, 1601–1605.
[6] S. Glasstone, K. J. Laidler, H. Eyring, *The Theory of Rate Processes*, McGraw-Hill, New York, **1941**.
[7] I. Ugi, *Z. Naturforsch. B* **1965**, *20*, 405–409.
[8] C. R. Landis, J. Halpern, *J. Am. Chem. Soc.* **1987**, *109*, 1746–1754.
[9] J. M. Brown, P. A. Chaloner in *Homogeneous Catalysis with Metal-Phosphine Complexes* (Ed.: L. H. Pignolet), Plenum, New York, **1983**, pp. 137–165.
[10] H. B. Kagan, T. P. Dang, *J. Am. Chem. Soc.* **1972**, *94*, 6429–6433.
[11] R. Selke, *J. Organomet. Chem.* **1989**, *370*, 241–248.
[12] D. Heller, S. Borns, W. Baumann, R. Selke, *Chem. Ber.* **1996**, *129*, 85–89.
[13] H. Bircher, B. R. Bender, W. von Philipsborn, *Magn. Reson. Chem.* **1993**, *31*, 293–298.
[14] J. A. Ramsden, T. D. W. Claridge, J. M. Brown, *J. Chem. Soc. Chem. Commun.* **1995**, 2469–2471.
[15] R. Kadyrov, T. Freier, D. Heller, M. Michalik, R. Selke, *J. Chem. Soc. Chem. Commun.* **1995**, 1745–1746.
[16] D. Heller, R. Thede, D. Haberland, unpublished results.
[17] By the use of C_1-symmetrical ligands (an example is shown in Fig. 1 (**1b**) [11]) formation of individual enantiomers can be the result of two independent processes, because four substrate complexes are possible in principle. This means that the logarithmic product ratio changes with temperature in principle in nonlinear fashion.

Synthesis of New Dialkylmagnesium Compounds by Living Transfer Ethylene Oligo- and Polymerization with Lanthanocene Catalysts

Jean-François Pelletier, André Mortreux,* Xavier Olonde, and Karel Bujadoux

Dedicated to the memory of Professor Francis Petit

Considerable interest has been devoted to oligomerization and polymerization of ethylene on transition metal catalysts. The aim of these reactions is to produce higher olefins (Alfen, Alphabutol, SHOP processes) or polymers of higher molecular weight (Ziegler–Natta catalysis). Such reactions and those with the relatively recently discovered metallocene-based catalysts produce linear, vinyl-terminated chains, which can be transformed by the use of stoichiometric amounts of zirconocene compounds into functionalized compounds.[1] This kind of functionalized oligomers, however, can be obtained by anionic polymerization of ethylene with *n*-butyllithium followed by electrophilic substitution of the resulting living oligomer.[2] In contrast, organomagnesium compounds have been synthesized from olefins by using zirconocene-based catalysts and dialkylmagnesium compounds or Grignard reagents as coreactants,[3] and zirconium tetrachloride has been used as catalyst for the synthesis of dialkylmagnesium compounds from MgH_2 and α-olefins, a process, which could be followed by ethylene addition, but only under severe conditions.[4]

We report herein that the ethylene insertion into a Mg–C bond can be catalyzed under very mild conditions by an alkyl chain transfer through chain growth polymerization on a lanthanocene-based catalyst.[5] This new reaction is a useful method for the synthesis of compounds of the type P-Mg-P′ (P = alkyl chain), in which, depending on the reaction parameters, P or P′ can contain between four and 200 C atoms, and a narrow distribution of products is obtained [Eq. (a)].

$$BuMgEt + (n+m)CH_2{=}CH_2 \xrightarrow[80\,^{\circ}C,\ 1\ atm]{[Cp^{*}_{2}SmCl_2Li(OEt_2)_2]} P\text{-}Mg\text{-}P' \qquad (a)$$

$P = Bu\{CH_2\text{-}CH_2\}_n$; $P' = Et\{CH_2\text{-}CH_2\}_m$.

[*] Prof. Dr. A. Mortreux, Dr. J.-F. Pelletier
Laboratoire de Catalyse Hétérogène et Homogène
Ecole Nationale Supérieure de Chimie de Lille
URA CNRS 402, BP 108
F-59652 Villeneuve d'Ascq (France)
Fax: Int. code +2043-6585
Dr. X. Olonde, Dr. K. Bujadoux
ECP Enichem Polymères France, Centre de recherches, BP 2 F-62670 Mazingarbe (France)

Typical experiments were conducted at 80 °C in hydrocarbon solvents. Upon introduction of a premixed mixture of the catalyst $[Cp^*_2SmCl_2Li(OEt_2)_2]$[6] (0.1 mmol, $Cp^* = C_5Me_5$) and butylethylmagnesium (20 mmol) into the hydrocarbon solvent (500 mL), the consumption of the ethylene begins immediately and remains constant until the growing alkyl chains of the dialkylmagnesium compound reach such a length that the products precipitate from the solution. The reaction of these new P-Mg-P′ compounds, which were initially obtained from ethylene (0.31 g) and a catalytic solution with a butylethylmagnesium/samarium ratio of 1:100 during 60 s, with CO_2 affords linear carboxylic acids with an odd number of carbon atoms in the chain (between five and 13 C atoms) upon further hydrolysis (FAB^+ MS analysis, $m/z = 101$ to 213).

Table 1 summarises our results obtained by using different Mg/Sm ratios. The lengths of the alkyl chains in the dialkylmagnesium units P-Mg-P′, which are given by the number average molecular weight ($\bar{M}_n$), depend on the Mg/Sm ratio and on the polymerization time. As long as P-Mg-P′ remains in solution (entries 1 to 7), the polydispersity index (PDI) is close to 1. This indicates that a reversible and very efficient transfer reaction occurs, leading to a pseudo-living polymerization process. The number of growing chains (yield/$\bar{M}_n$) is close to the number of Mg–C bonds available. Such transfers between catalyst (Zr or Ti) and trialkylaluminum occur in Ziegler–Natta polymerization, but are effective only at low temperature.[7] The key point in our process is that these transfer reactions are fast and reversible at 80 °C. This is the first example in which a polymerization with transfer reactions between two different metals can be considered as living.

Table 1. Ethylene polymerization with $BuMgEt/[Cp^*_2SmCl_2Li(OEt_2)_2]$ catalysts [a].

Entry	Mg/Sm	Polymerization time [min]	Ethylene consumption [g]	$\bar{M}_n$ [b]	PDI [c]	$N_{exp.}/N_{th.}$ [d]
1	10	5	4.7	1870	1.2	1.25
2	20	5	3.3	690	1.3	1.17
3	50	5	2.9	400	1.3	0.72
4	1000	1480	93.0	460	1.1	1.01
5	50	8.3	5.5	580	1.2	0.95
6	50	20.3	11.0	900	1.2	1.20
7	50	31	15.4	1300	1.3	1.20
8	50	41	30.0	1530	4.0	2.00
9 [e]	20	2.5	2.2	1070	1.3	1.05
10 [f]	50	108	42.2	3070	1.5	1.37
11 [g]	50	220	180.0	2110	2	8.50

[a] Solvent: 500 mL, catalyst: $[Cp^*_2SmCl_2Li(OEt_2)_2]$, (0.1 mmol) 80 °C. [b] Determined by GPC analysis. [c] PDI: polydispersity index = $\bar{M}_w/\bar{M}_n$ of the resulting polymer after hydrolysis. [d] N_{exp}: Experimental chain number [yield (in g)/$\bar{M}_n$]; N_{th}: Theoretical chain number, considering a living polymerization on both Mg (two chains per Mg atom) and Sm. [e] Catalyst: 0.05 mmol. [f] Solvent: xylene. [g] Reaction temperature = 100 °C.

According to our previous observations on the effect of an excess of dialkylmagnesium compound on the ethylene polymerization kinetic profiles,[8] it may be assumed that the polymerization occurs by the formation of a double R-bridged complex (in equilibrium with the free lanthanocene species, which is responsible for the chain growth catalysis, and MgR_2, Scheme 1, left), by which the interchange of the alkyl groups could take place (Scheme 1).

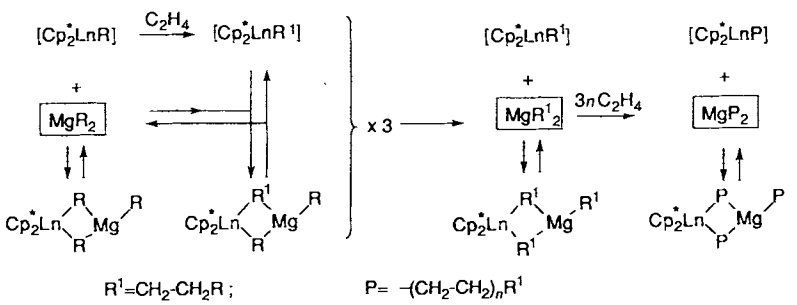

Scheme 1. Proposed reaction mechanism for the synthesis of MgP_2.

If the reaction is allowed to continue after the P-Mg-P′ precipitation, this chain transfer to magnesium is no longer possible, and classical polymerization occurs on the lanthanocene complex with β-H elimination reactions, leading to an increase of the PDI (entry 8).

The $\bar{M}_n$ numbers of each alkyl chain bound to Mg are governed by the solubility of the P-Mg-P′ compound in the reaction medium. A considerable increase in the lengths of the chains could be achieved (entries 10 and 11) by varying the solvent and temperature. However, increasing the temperature to 100 °C gave mainly α-olefins as by-products due to competitive β-H elimination reactions.

In order to check the molecular distribution of the first phase of the polymerization reaction, we performed an experiment with di-*n*-hexylmagnesium. This symmetrical dialkylmagnesium compound was chosen to avoid the possible difference in reactivity that could occur from the BuMg and EtMg moieties in BuMgEt during the initiation step. The distribution of the oligomers obtained by hydrolysis of the reaction products after 9 min (Mg/Sm = 134) is given in Figure 1. As expected, the products are exclusively alkanes with a very low polydispersity ($\bar{M}_w/\bar{M}_n = 1.11$). A Poisson distribution was calculated and is likewise shown. The good agreement between the experimental data and this curve indicates that most of the Mg–C bonds have been exchanged and that the oligomeric distribution can be considered as monodisperse.[9]

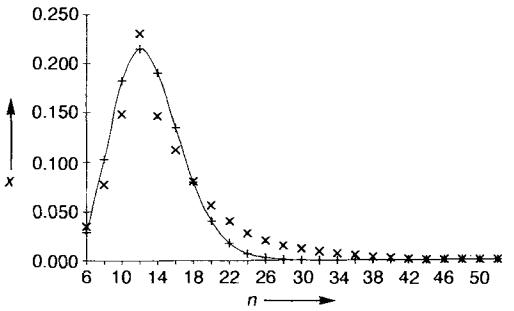

Fig. 1. Comparison of the experimental (×) and calculated (+) distribution of oligomers in the polymerization with di-*n*-hexylmagnesium. The solid line indicates the Poisson distribution. The experimental data were obtained by GC analysis of the products obtained after 9 min from the oligomerization of ethylene (115 mmol) with the catalyst (0.1 mmol) and di-*n*-hexylmagnesium (13.4 mmol) at 80 °C. n = number of C atoms, x = molar fraction. λ = ethylene/Mg–C = 3.54, where λ = average number of ethylene insertions in $Mg(n\text{-hexyl})_2$.

One of the most interesting of the numerous potential applications of these new P-Mg-P′ compounds (Scheme 2) is their use as macroinitiator in diblock copolymerization reactions with some polar monomers.

 © VCH Verlagsgesellschaft mbH, D-69451 Weinheim, 1996 0570-0833/96/3516-1855 $ 15.00+.25/0

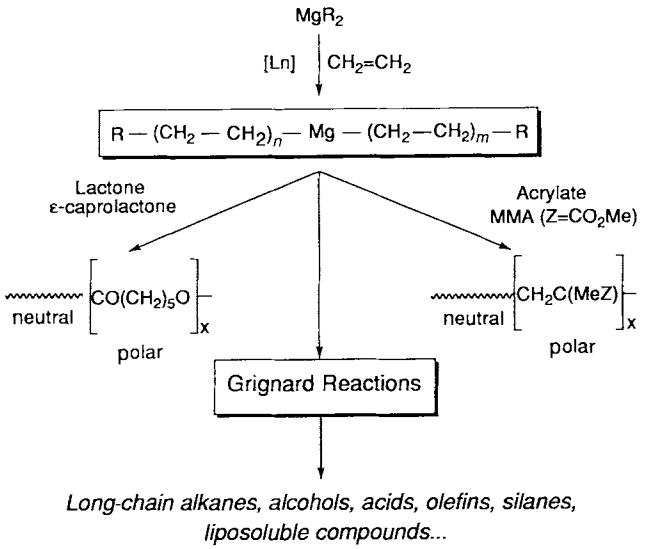

Scheme 2. Synthesis and applications of higher dialkylmagnesium compounds.

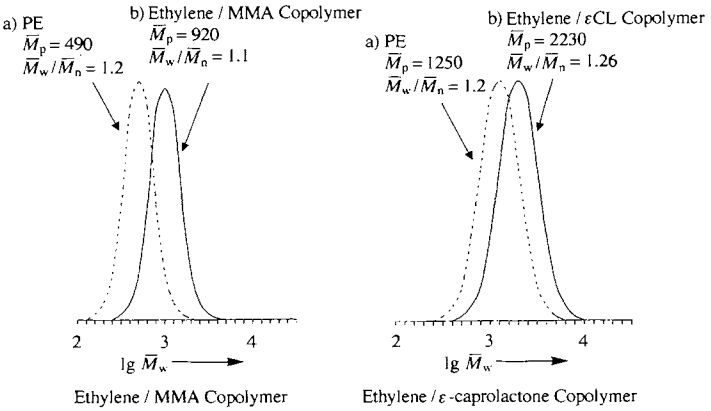

Fig. 2. GPC profiles of diblock ethylene/methylmethacrylate (MMA) and ethylene/ε-caprolactone (CL) copolymers (insoluble fractions after acetone extraction). PE = polyethylene. M_p = peak mass.

Figure 2 shows the gel permeation chromatography (GPC) profiles of polymer samples obtained a) by hydrolysis of P-Mg-P′ compounds, b) by further in situ reaction with ε-caprolactone at 80 °C, and c) by the same consecutive procedure after decreasing the temperature and addition of methyl methacrylate at −78 °C.

As expected, the first ethylene polymerization step occurs in an almost "living" fashion to produce the dialkylmagnesium compound P-Mg-P′. Subsequent addition of the lactone or the acrylate leads to diblock copolymers whose polydispersity index indicates that again, the copolymerization can be considered as living.

We have developed an efficient synthesis of dialkylmagnesium compounds that were hitherto only accessible under severe conditions,[4] and have shown that a living ethylene growth chain transfer reaction between dialkylmagnesium derivatives and lanthanocene complexes is possible. Because of the high reactivity of the Mg–C bond, such dialkylmagnesium compounds with a narrow distribution of molecular weights may eventually be used to introduce lipophilic chains of well-defined lengths in a series of compounds.

Received: February 1, 1996 [Z 8778 IE]
German version: *Angew. Chem.* **1996**, *108*, 1980–1982

Keywords: Grignard reactions · lanthanides · magnesium compounds · polymerizations

[1] J. Schwartz, J. A. Labinger, *Angew. Chem.* **1976**, *88*, 402; *Angew Chem. Int. Ed. Engl.* **1976**, *15*, 333.
[2] D. E. Bergbreiter, J. R. Blanton, R. Chandran, M. D. Hein, K. J. Huang, D. R. Treadwell, S. A. Walker, *J. Polym. Sci. Part A: Polym. Chem.*, **1989**, *27*, 4205.
[3] a) U. M. Dzhemilev, O. S. Vostrikova, R. M. Sultanov, *Izv. Akad. Nauk. SSSR Ser. Khim.* **1983**, *32*, 218; b) U. M. Dzhemilev, R. M. Sultanov, R. G. Gaimaldinov, *Russian Chem. Bull.* **1993**, *42*, 149, and references therein; c) C. J. Rousset, E. Negishi, N. Suzuki, T. Takahashi, *Tetrahedron Lett.* **1992**, *33*, 1965. d) A. H. Hoveyda, J. P. Morken, A. F. Houri, Z. Xu, *J. Am. Chem. Soc.* **1992**, *114*, 6692. See also K. S. Knight, D. Wang, R. W. Waymouth, J. Ziller, *ibid.* **1994**, *116*, 1845 for the zirconocene-catalyzed cyclomagnesation of dienes.
[4] B. Bogdanovic, P. Bons, S. Konstantinovic, M. Schwickardi, U. Westeppe *Chem. Ber.* **1993**, *126*, 1371.
[5] *Fr Demande by* ECP Enichem Polymères France and Université des Sciences et Technologies de Lille, FR-A 04203 **1995**.
[6] T. Don Tilley, R. A. Andersen, *Inorg. Chem.* **1981**, *20*, 3267.
[7] L. Resconi, F. Piemontesi, G. Franciscono, G. Abis, T. Fiorani, *J. Am. Chem. Soc.* **1992**, *114*, 1025.
[8] X. Olonde, A. Mortreux, F. Petit, K. Bujadoux, *J. Mol. Cat.* **1993**, *82*, 75.
[9] J. B. Burger, M. E. Thompson, W. D. Cotter, J. E. Bercaw, *J. Am. Chem. Soc.* **1990**, *112*, 1566.

The First Silylpalladium(IV) Complex

Shigeru Shimada, Masato Tanaka,* and Motoo Shiro

Owing to the intense interest in the silicon-based materials, the chemistry of (silyl)metals is a vigorously growing research field. In particular, an understanding of the reactivities of palladium complexes is highly desired, since palladium complexes are versatile catalysts in a number of transformations of hydrosilanes and disilanes.[1] In these reactions, silylpalladium(IV) species are occasionally suggested to be key intermediates, based on the relevant chemistry of silylplatinum(IV)[2, 3] and organopalladium(IV)[4] complexes. However, no unequivocal evidence that substantiates silylpalladium(IV) species has been reported to date. Accordingly, discussions about their intermediacy have usually been speculative, and elementary steps that may involve silylpalladium(IV) species have been often described simply as "metathesis".[5, 6] Our recent paper reporting isolation of a tetrakis(silyl)platinum(IV) complex (**1**)[3] appears to imply that the chelation, rigid conformation, and small steric size of the 1,2-phenylenedisilyl ligand might be ideal for the stabilization of possible palladium(IV) complexes. Here we disclose the very first isolation and characterization of a silylpalladium(IV) complex.

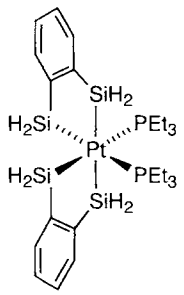

1

After the survey of several palladium complexes,[7] we found that the reaction of [Me_2Pd(dmpe)] (**2**, dmpe = 1,2-bis(dimethylphosphanyl)-ethane)[8] with 3 equivalents of 1,2-disilylbenzene (**3**)[3, 9] in toluene

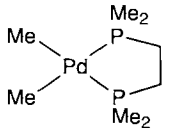

2

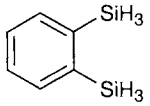

3

[*] Prof. Dr. M. Tanaka, Dr. S. Shimada
National Institute of Materials and Chemical Research
1-1 Higashi, Tsukuba, Ibaraki 305 (Japan)
Fax: Int. code +(298) 54-4709
e-mail: mtanaka@ccmail.nimc.go.jp
Dr. M. Shiro
Rigaku Corporation (Japan)

 © VCH Verlagsgesellschaft mbH, D-69451 Weinheim, 1996 0570-0833/96/3516-1856 $ 15.00+.25/0

proceeded slowly even at room temperature, and after heating at 50 °C a new complex was isolated as a microcrystalline white solid in 67% yield, which was not a usual bis(silyl)palladium(II) complex like **4** but the tetrakis(silyl)palladium(IV) complex **5**.[10]

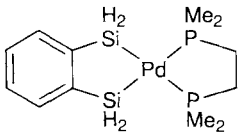

4

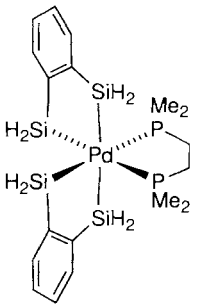

5

Several silanes were also formed by methyl-hydrogen exchange processes (according to ^{1}H NMR and GC-MS studies, mainly monomethylsilane **6** (about 30 mol%, based on the consumed **2**), together with dimethyl and trimethyl derivatives of **3**). The ^{29}Si{^{1}H} NMR spectrum (DEPT 45 and 135) of **5** clearly displayed two signals for SiH_2; one SiH_2 group is *cis* to two phosphane ligands (t, ^2J(P,Si) = 17 Hz) and the other *cis* to one and *trans* to another phosphane ligand (dd, $^2J(P_{cis},Si) = 17$ Hz, $^2J(P_{trans},Si) = 162$ Hz). The ^{1}H and ^{13}C NMR spectra similarly displayed two PCH_3 signals. Finally, the structure of **5** was unambiguously confirmed by X-ray diffraction analysis (Fig. 1).[11] Complex **5** is C_2 symmetric, and the Si3–Pd bond is longer than the Si2–Pd bond as a result of the stronger *trans* influence of silicon than that of phosphorus.

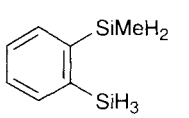

6

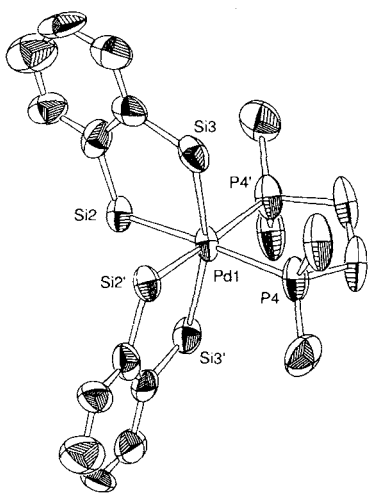

Fig. 1. Molecular structure of **5**. Selected bond lengths [Å] and angles [°]: Pd1–P4 2.337(2), Pd1–Si2 2.345(2), Pd1–Si3 2.394(4); P4-Pd1-P4' 86.1(2), P4-Pd1-Si2 175.5(1), P4-Pd1-Si2' 93.3(1), P4-Pd1-Si3 99.6(1), P4-Pd1-Si3' 93.8(1), Si2-Pd1-Si2' 87.7(2), Si2-Pd1-Si3 84.9(1), Si2-Pd1-Si3' 81.9(1), Si3-Pd1-Si3' 161.6(1).

In order to elucidate the mechanism of the reaction, an attempt was made to isolate a possible intermediate (**4**) by treating **2** with 1.1 equivalents of **3**, but the main product that formed was **5**.[12] However, an analogous complex (**7**) was obtained as a dimer[13] by the phosphane exchange reaction of [1,2-$C_6H_4(SiH_2)_2$Pd(PMePh$_2$)$_2$][7] with dmpe. As expected, **7** reacted smoothly with **3** (3 equivalents) at 50 °C to give **5** nearly quantitatively. Based on the above results, we tentatively propose the following mechanism. The formation of **6** and the thermal stability of complex **2**[14] suggest that the initial step is the oxidative addition of one of the Si–H bonds of **3** to **2** to give the silylpalladium(IV) intermediate **8**, which then reductively

[{1,2-$C_6H_4(SiH_2)_2$Pd(dmpe)}$_2$(μ-dmpe)] **7**

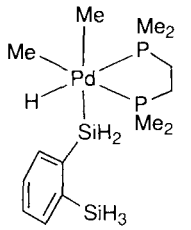

8

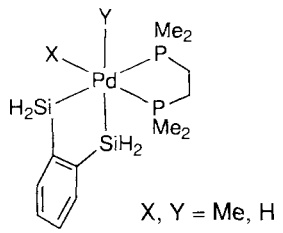

9

eliminates methane, ethane, or **6**. In the former two cases, further intramolecular oxidative addition of the other Si–H bond gives complex **9**, which then produces **4** by reductive elimination of hydrogen or methane. The next step is presumably the oxidative addition of the Si–H bond of another molecule of **3** to **4** as in the corresponding platinum case,[3] although no evidence was obtained at present.

The results disclosed here emphasize the significance of the intermediacy of silylpalladium(IV) species in the palladium-promoted reactions of hydrosilanes and disilanes. Tetrakis(silyl)-palladium(IV) intermediates, in particular, should be more seriously considered in the metathesis reactions of disilanes catalyzed by palladium complexes.[5a, 5e, 10f, 10g, 15]

Detailed mechanistic aspects as well as the reactivities of complex **5** are now under investigation in our laboratory.

Experimental Procedure

5: To a toluene solution (2 mL) of **2** (177 mg, 0.618 mmol) was added **3** (256 mg, 1.85 mmol), and the resulting mixture was stirred first at room temperature for 78 h and then at 50 °C for 58 h. A large amount of a white precipitate was observed even after the room temperature reaction. After addition of pentane (3 mL), the supernatant was filtered off, and the remaining solid was washed with toluene/pentane (2:1, 2 × 3 mL). After drying under vacuum, **5** was obtained as a microcrystalline white solid, 220 mg (67% yield). The combined mixture of the filtrate and the washings was kept at room temperature to give additional **5** as a hexagonal single crystal suitable for X-ray structure analysis. M.p. 195–220 °C (decomp. under vacuum); ^{1}H NMR (300 MHz, C_6D_6): δ = 0.78 (d, 6H, J = 9 Hz, PCH_3), 0.9–1.2 (m, 4H, PCH_2CH_2P), 1.02 (d, 6H, J = 9 Hz, PCH_3), 4.7–4.8 (m, 2H, SiH_2), 4.83–4.95 (m, 4H, SiH_2), 4.98–5.17 (m, 2H, SiH_2), 7.11–7.21 (m, 4H), 7.75 (d, 2H, J = 7 Hz), 8.04 (d, 2H, J = 7 Hz); ^{13}C{^{1}H} NMR (75.5 MHz, C_6D_6): δ = 11.45 (m, PCH_3), 12.65 (m, PCH_3), 28.69 (t, ^1J(P,C) = 23 Hz, PCH_2CH_2P), 127.5 (2C), 134.22 (t, ^4J(P,C) = 2.5 Hz), 134.89 (s), 147.29 (t, ^3J(P,C) = 3.0 Hz), 150.69 (t, ^3J(P,C) = 2.3 Hz); ^{31}P{^{1}H} NMR (121.5 MHz, C_6D_6): δ = 15.87 (s); ^{29}Si{^{1}H} NMR (59.6 MHz, C_6D_6): δ = −8.31 (t, ^2J(P,Si) = 17 Hz), −6.58 (dd, $^2J(P_{cis},Si) = 17$, $^2J(P_{trans},Si) = 162$ Hz); IR (KBr): $\tilde{\nu}$ = 2070, 2032 cm^{-1} (SiH); C,H analysis: calcd for $C_{18}H_{32}P_2PdSi_4$: C 40.86, H 6.10; found: C 41.21, H 6.01.

Received: February 5, 1996 [Z8785IE]
German version: *Angew. Chem.* **1996**, *108*, 1970–1972

Keywords: catalysis · palladium compounds · silicon compounds

[1] Recent reviews: H. Yamashita, M. Tanaka, *Bull. Chem. Soc. Jpn.* **1995**, *68*, 403–419; K. A. Horn, *Chem. Rev.* **1995**, *95*, 1317–1350; H. K. Sharma, K. H. Pannell, *ibid.* **1995**, *95*, 1351–1374; P. Braunstein, M. Knorr, *J. Organomet. Chem.* **1995**, *500*, 21–38.

[2] a) J. E. Bentham, S. Cradock, E. A. V. Ebsworth, *J. Chem. Soc. A* **1971**, 587–593; b) D. W. W. Anderson, E. A. V. Ebsworth, D. W. H. Rankin, *J. Chem. Soc. Dalton Trans.* **1973**, 2370–2373; c) D. W. W. Anderson, E. A. V. Ebsworth, J. K. Macdougall, D. W. H. Rankin, *J. Inorg. Nucl. Chem.* **1973**, *35*, 2259–2263; d) E. A. V. Ebsworth, V. M. Marganian, F. J. S. Reed, *J. Chem. Soc. Dalton Trans.* **1978**, 1167–1170; e) S. L. Grundy, R. D. Holmes-Smith, S. R.

Stobart, M. A. Williams, *Inorg. Chem.* **1991**, *30*, 3333–3337; f) R. H. Heyn, T. D. Tilley, *J. Am. Chem. Soc.* **1992**, *114*, 1917–1919; g) M. J. Michalczyk, C. A. Recatto, J. C. Calabrese, M. J. Fink, *ibid.* **1992**, *114*, 7955–7957; h) C. J. Levy, R. J. Puddephatt, J. J. Vittal, *Organometallics* **1994**, *13*, 1559–1560.

[3] S. Shimada, M. Tanaka, K. Honda, *J. Am. Chem. Soc.* **1995**, *117*, 8289-8290.

[4] Isolated examples: a) A. J. Canty, *Acc. Chem. Res.* **1992**, *25*, 83–90, and references therein; b) A. N. Vedernikov, A. I. Kuramshin, B. N. Solomonov, *J. Chem. Soc. Chem. Commun.* **1994**, 121–122; c) R. van Asselt, E. Rijnberg, C. J. Elsevier, *Organometallics* **1994**, *13*, 706–720; d) B. A. Markies, A. J. Canty, J. Boersma, G. van Koten, *ibid.* **1994**, *13*, 2053–2058; e) A. J. Canty, R. T. Honeyman, A. S. Roberts, P. R. Traill, R. Colton, B. W. Skelton, A. H. White *J. Organomet. Chem.* **1994**, *471*, C8–C10; f) W. Kläui, M. Glaum, T. Wagner, M. A. Bennett, *ibid.* **1994**, *472*, 355–358; g) A. J. Canty, H. Jin, A. S. Roberts, B. W. Skelton, P. R. Traill, A. H. White, *Organometallics* **1995**, *14*, 199–206.

[5] a) H. Sakurai, Y. Kamiyama, Y. Nakadaira, *J. Organomet. Chem.* **1977**, *131*, 147–152; b) H. Urata, H. Suzuki, Y. Moro-oka, T. Ikawa, *ibid.* **1982**, *234*, 367–373; c) H. Matsumoto, M. Kasahara, I. Matsubara, M. Takahashi, T. Arai, M. Hasegawa, T. Nakano, Y. Nagai, *ibid.* **1983**, *250*, 99–107; d) S. Cros, B. Bennetau, J. Dunoguès, P. Babin, *ibid.* **1994**, *468*, 69–74; e) T. Kusukawa, Y. Kabe, B. Nestler, W. Ando, *Organometallics* **1995**, *14*, 2556–2564; f) Y. Obora, Y. Tsuji, T. Kawamura, *J. Am. Chem. Soc.* **1995**, *117*, 9814–9821.

[6] Silylpalladium(IV) intermediates have been proposed without any direct evidence: a) C. Eaborn, R. W. Griffiths, A. Pidcock, *J. Organomet. Chem.* **1982**, *225*, 331–341; b) D. Seyferth, E. W. Goldman, J. Escudie, *ibid.* **1984**, *271*, 337–352; c) J. D. Rich, T. E. Krafft, *Organometallics* **1990**, *9*, 2040–2045.

[7] The formation of bis(silyl)palladium(II) complexes was observed in the reactions of **3** with several palladium complexes ($[Pd(PPh_3)_4]$, $[Pd(dba)_2]/2PEt_3$ (dba = dibenzylideneacetone), $[Me_2Pd(PPh_2Me)_2]$), while decomposition to black precipitates occurred in the case of $[Me_2Pd(tmeda)]$ (tmeda = *N,N,N',N'*-tetramethylethylenediamine) and $[Me_2Pd(bpy)]$ (bpy = 2,2'-bipyridyl). The detailed results will be reported separately.

[8] W. de Graaf, J. Boersma, W. J. J. Smeets, A. L. Spek, G. van Koten, *Organometallics* **1989**, *8*, 2907–2917.

[9] R. Schröck, A. Sladek, H. Schmidbaur, *Z. Naturforsch. B* **1994**, *49*, 1036–1040.

[10] Examples of bis(silyl)palladium(II) complexes: a) M. D. Curtis, J. Greene, *J. Am. Chem. Soc.* **1978**, *100*, 6362–6367; b) U. Schubert, C. Müller, *J. Organomet. Chem.* **1989**, *373*, 165–172; c) Y. Pan, J. T. Mague, M. J. Fink, *Organometallics* **1992**, *11*, 3495–3497; d) M. Murakami, T. Yoshida, Y. Ito, *ibid.* **1994**, *13*, 2900–2902; e) F. Ozawa, M. Sugawara, T. Hayashi, *ibid.* **1994**, *13*, 3237–3243; f) M. Suginome, H. Oike, Y. Ito, *ibid.* **1994**, *13*, 4148–4150; g) M. Suginome, H. Oike, Y. Ito, *J. Am. Chem. Soc.* **1995**, *117*, 1665–1666; see also refs. [6a, 6b].

[11] Crystal data for **5**: $0.30 \times 0.20 \times 0.20$ mm^3, hexagonal, space group $P6_122$ (No.178), $a = 8.583(1)$, $c = 60.373(3)$ Å, $V = 3851(1)$ Å^3, $Z = 6$, $\rho_{calcd} = 1.37$ g cm^{-3}, $\mu(Cu_{K\alpha}) = 87.9$ cm^{-1}, $T = -70$ °C; Rigaku AFC5R diffractometer, ω scans; 1351 measured reflections, of which 862 with $I > 3.0\sigma(I)$ were used in the refinement. The structure was solved by direct methods (SAPI91) and refined by full-matrix least-squares techniques against $|F|^2$ with teXsan crystallographic software package of Molecular Structure Corporation. The non-hydrogen atoms were refined anisotropically. Hydrogen atoms were included but not refined; $R = 0.035$, $Rw = 0.049$, residual electron density $+0.34/-0.40$ e Å^{-3}. Crystallographic data (excluding structure factors) for the structure reported in this paper have been deposited with the Cambridge Crystallographic Data Centre as supplementary publication no. CCDC-179-55. Copies of the data can be obtained free of charge on application to The Director, CCDC, 12 Union Road, Cambridge CB21EZ, UK (fax: Int. code +(1223) 336-033; e-mail: teched@chemcrys.cam.ac.uk).

[12] The reaction of **2** and **3** in C_6D_6 at 50 °C monitored over 5 days by NMR spectroscopy showed that another complex (^{31}P NMR: $\delta = 16.26$) was generated in the transformation as a transient intermediate. This signal appeared before the emergence of the signal assignable to **5** ($\delta = 15.87$). The amount of the transient species reached its maximum (about 15% by ^{31}P NMR integration) after 10 hours and then gradually decreased. Further characterization or isolation of the transient species was not feasible.

[13] Broad NMR signals appear to indicate that **7** is in equilibrium with monomer **4** in solution. **7**: M.p. 133–137 °C (decomp, under vacuum); ^{1}H NMR (300 MHz, [D$_8$]THF): $\delta = 1.25$–1.37 (br. m, 36H), 1.64 (br. d, 12H, $J = 14$ Hz), 4.94 (s, 8H, $^1J(Si,H) = 160$ Hz, SiH_2), 7.05 (dd, 4H, $J = 3$, 5 Hz), 7.54 (dd, 4H, $J = 3$, 5 Hz); ^{13}C{^{1}H} NMR (75.5 MHz, [D$_8$]THF): $\delta = 14.28$ (br., PCH_3), 29.65 (br. t, $J = 19$ Hz, PCH_2CH_2P), 126.84 (s), 134.37 (s), 152.42 (s); ^{31}P{^{1}H} NMR (121.5 MHz, [D$_8$]THF): $\delta = 2.68$ (br.); ^{29}Si{^{1}H} NMR (59.6 MHz, [D$_8$]THF): $\delta = -18.5$ (br); IR (KBr): $\tilde{\nu} = 2006$ cm^{-1} (SiH); C,H analysis: calcd for $C_{30}H_{64}P_6Pd_2Si_4$: C 38.50, H 6.89; found: C 38.72, H 6.78. The dimeric structure was confirmed by X-ray analysis. The detailed results will be reported separately.

[14] Note that complex **2** is thermally stable at room temperature and slowly decomposes at 90 °C to form methane and ethane; see ref. [8]. Accordingly, generation of palladium(0) species prior to the oxidative addition of **3** is unlikely.

[15] K. Tamao, T. Hayashi, M. Kumada, *J. Organomet. Chem.* **1976**, *114*, C19–C21; Y. Tanaka, Y. Uchimaru, M. Tanaka, *Chem. Lett.* **1995**, 164.

Metallomesogens with Branched, Dendrimeric Amino Ligands**

Uwe Stebani, Günter Lattermann,* Michael Wittenberg, and Joachim Heinz Wendorff

In the search for compounds with novel electric or magnetic behavior, the desire to combine the properties of liquid crystals (LC) with those of metal complexes has led to the synthesis of a large number of metallomesogens, mostly with square-planar or linear coordination geometry.[1] However, high-spin transition metal complexes often unavoidably have different geometries whose higher degree of isometry has been regarded for a long time as unsuitable for mesomorphic behavior.[2] Only recently have, for example, liquid-crystalline nickel(II) complexes with paramagnetic properties based on octahedral[3] and tetrahedral coordination[4] been described. The previously known LC complexes with trigonal-bipyramidal configuration have a distorted shape, as in the case of the dimeric zinc alkoxydithiobenzoates[5] and the iron complexes, which have coordination geometries lying between square-pyramidal and trigonal-bipyramidal.[4b, 6]

The branched amine ligands $\mathbf{L^1}$ and $\mathbf{L^2}$, which are ethyleneimine dendrimers of the first and second generation and are derivatives of tris(2-aminoethyl)amine (tren), allow access to a novel class of liquid-crystalline transition metal complexes with trigonal-bipyramidal or octahedral coordination geometry. The use of dendrimeric ligands in metallomesogens has not been reported before.

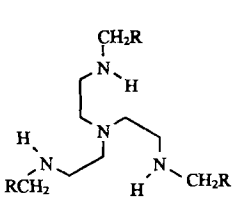

$\mathbf{L^1}$

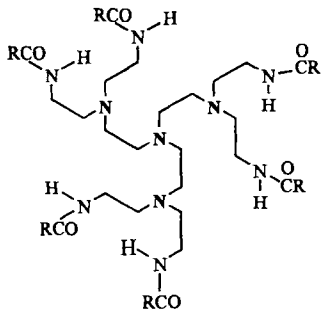

$\mathbf{L^2}$

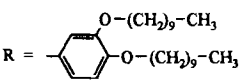

The transition temperatures (determined by polarization microscopy and differential calorimetry) of the metal complexes $\mathbf{K^1}$–$\mathbf{K^8}$ are listed in Table 1. Up to $\mathbf{K^3}$ ($\mathbf{L^1} \cdot Ni(NO_3)_2$), all complexes show mesomorphic behavior with relatively low glass transition temperatures. With $\mathbf{K^1}$, $\mathbf{K^4}$, and $\mathbf{K^7}$ there is no crystalline phase, for the other compounds a crystalline phase appears only before the first heating. No double refraction is ob-

[*] Dr. G. Lattermann, Dr. U. Stebani
Makromolekulare Chemie I der Universität
D-95440 Bayreuth (Germany)
Fax: Int. code +(921) 55-3206
e-mail: guenter.lattermann@uni-bayreuth.de
Dipl.-Chem. M. Wittenberg, Prof. Dr. J. H. Wendorff
Fachbereich Physikalische Chemie und wissenschaftliches Zentrum für Materialwissenschaften
der Universität Marburg
D-35032 Marburg (Germany)

[**] U. S. and G. L. acknowledge support from the Deutsche Forschungsgemeinschaft (La 662/1-2).

Table 1. Transition temperatures [°C] of complexes $\mathbf{K^1}$–$\mathbf{K^8}$ (in parentheses: ΔH [kJ mol^{-1}]).

Complex	T_g	ΔC_p	K		M		I
$\mathbf{K^1}$, $\mathbf{L^1}\cdot CoCl_2$	56	0.37	–		•	85.5 (0.4)	•
$\mathbf{K^2}$, $\mathbf{L^1}\cdot NiCl_2$	40	0.61	•	47.0 (3.4)[a]	•	64.5 (1.7)	•
$\mathbf{K^3}$, $\mathbf{L^1}\cdot Ni(NO_3)_2$	36	0.64	•	46.5 (11.1)[a]	–		•
$\mathbf{K^4}$, $\mathbf{L^1}\cdot CuCl_2$	41	0.57	–		•	75.0 (0.8)	•
$\mathbf{K^5}$, $\mathbf{L^1}\cdot Cu(SCN)_2$	41	0.39	•	48.5 (4.6)[a]	•	75.0 (1.1)	•
$\mathbf{K^6}$, $\mathbf{L^1}\cdot Cu(NO_3)_2$	36	0.88	•	47.5 (12.4)[a]	•	79.0 (1.4)	•
$\mathbf{K^7}$, $\mathbf{L^1}\cdot ZnCl_2$	60	0.41	–		•	126.0 (1.3)	•
$\mathbf{K^8}$, $\mathbf{L^2}\cdot CuCl_2$	49	0.64	–		•	140.0 (2.8)	•

[a] Only on first heating; T_g: glass transition temperature [°C]; ΔC_p [kJ mol^{-1} K^{-1}]; K: crystalline phase, M: mesophase, I: isotropic phase.

Table 2. X-ray reflections and lattice constants in the mesophase of complexes of $\mathbf{L^1}$ and $\mathbf{L^2}$ and of the ligand $\mathbf{L^2}$.

Complex	d_{10}	d_{11}	d_{20}	d_{30}	a_{hex}
$\mathbf{K^1}$, $\mathbf{L^1}\cdot CoCl_2$	28.67	–	–	–	–
$\mathbf{K^2}$, $\mathbf{L^1}\cdot NiCl_2$	30.13	–	–	–	–
$\mathbf{K^4}$, $\mathbf{L^1}\cdot CuCl_2$	30.48	–	15.37	–	–
$\mathbf{K^5}$, $\mathbf{L^1}\cdot Cu(SCN)_2$	32.63	–	16.34	–	–
$\mathbf{K^7}$, $\mathbf{L^1}\cdot ZnCl_2$	30.78	17.49	15.07	10.16	35.2
$\mathbf{L^2}$	31.09	18.64	15.93	–	36.4
$\mathbf{K^8}$, $\mathbf{L^2}\cdot CuCl_2$	31.98	18.99	16.09	10.57	36.9

served with the polarization microscope, but $\mathbf{K^7}$ has a fine, needlelike texture.

For the complexes $\mathbf{L^1}\cdot CoCl_2$ ($\mathbf{K^1}$) and $\mathbf{L^1}\cdot NiCl_2$ ($\mathbf{K^2}$), X-ray diffraction of the mesophase (Table 2) gave only a first order reflection apart from a halo at 4.4 Å. For $\mathbf{L^1}\cdot CuCl_2$ ($\mathbf{K^4}$) and $\mathbf{L^1}\cdot Cu(SCN)_2$ ($\mathbf{K^5}$), a second order reflection was observed as well, which is attributed to a lamellar phase. For $\mathbf{L^1}\cdot ZnCl_2$ ($\mathbf{K^7}$), the mixed d_{11} reflection is indicative of a hexagonal-columnar phase (Col_h).

The tren skeleton is in principle able to accomodate two coordination geometries: a) trigonal-bipyramidal (**1**) with fivefold coordination ("azatran geometry" with elements of Groups 1, 2, and 12–15[7] and with transition metals of Groups 3–11[8], resulting in ionic complexes), and b) octahedral geometry (**2**) in the case of neutral complexes of transition metals. The azatran geometry **1** is preferred with most divalent metal centers.[9] Only in the case of the Ni^{II} complex with unsubstituted tren ligands does the octahedral geometry **2** also occur;[8d] with hexamethyl-substituted tren, the trigonal-bipyramidal structure is again favored.[10]

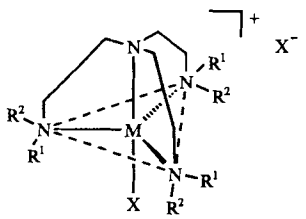

1

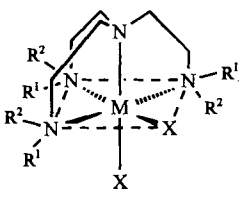

2

As the $\mathbf{L^1}$ complexes do not form stable crystalline phases, it was not possible to carry out X-ray structural analysis. However, the complex geometry can be established by comparison with known non-liquid-crystalline analogs. The trigonal-bipyramidal[11] complex formed from the unsubstituted tren ligands and $Cu(SCN)_2$ shows a special feature in the IR spectrum—two sets of two absorption bands corresponding to an isothiocyanato ligand and an ionic thiocyanate group.[12] Comparison of the IR data for this complex with those for $\mathbf{L^1}\cdot Cu(SCN)_2$ ($\mathbf{K^5}$) shows that the absorption bands of the coordinated isothiocyanate group and the thiocyanate anion correspond (Table 3). The trigonal-bipyramidal azatran structure may therefore also be assigned to $\mathbf{K^5}$ (Scheme 1).

Table 3. IR and UV absorption bands of the complexes $\mathbf{K^1}$–$\mathbf{K^6}$ and $\mathbf{K^8}$.

Complex	ν(C–N) st [cm^{-1}]	ν(C–S) st [cm^{-1}]	λ [nm]	ε_{mol} [L mol^{-1}]
$\mathbf{K^1}$, [$\mathbf{L^1}\cdot$CoCl]Cl			696, 668, 628	188, 180, 178
			616, 492, 468	–, 111, –
$\mathbf{K^2}$, [$\mathbf{L^1}\cdot NiCl_2$]			960, 624, 396	19, 20, 44
$\mathbf{K^3}$, [$\mathbf{L^1}\cdot Ni(NO_3)_2$]			908, 568, 372	26, 22, –
$\mathbf{K^4}$, [$\mathbf{L^1}\cdot$CuCl]Cl			924, 752	381, 289
[tren·Cu(NCS)](SCN)	2094[a], 2060[b]	818[a], 745[b]		
$\mathbf{K^5}$, [$\mathbf{L^1}\cdot$Cu(NCS)](SCN)	2087[a], 2059[b]	813[a], 748[b]	816, 672, 372	285, 258, 1167
$\mathbf{K^6}$, [$\mathbf{L^1}\cdot Cu(NO_3)$]($NO_3$)			844, 676	296, –
$\mathbf{K^8}$, [$\mathbf{L^2}\cdot$CuCl]Cl			926, 752	578, 761

[a] Stretching vibrations of the ligand NCS. [b] Stretching vibrations of the anion SCN^-.

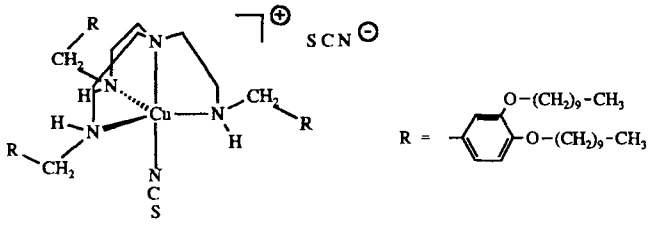

Scheme 1. Structure of [$\mathbf{L^1}\cdot$Cu(NCS)](SCN).

With the other complexes, the geometry cannot be deduced from the IR data. However, important information is available from the UV/Vis spectra (Table 3).[13] The measured wavelengths and molar extinction coefficients of the Co^{II} complex $\mathbf{K^1}$ (Fig. 1) would not expected from octahedral geometry,[13] but correspond to trigonal-bipyramidal coordination.[10] The two or three very intense bands of the Cu^{II} complexes $\mathbf{K^4}$–$\mathbf{K^6}$ cannot be due to an octahedral structure (only one band of low intensity),[13] but confirm the trigonal-bipyramidal coordination that was established by IR spectroscopy for $\mathbf{K^5}$, which can therefore also be assumed for $\mathbf{K^4}$ and $\mathbf{K^6}$. The absorption bands of the Ni^{II} complexes are of only low intensity. Their number, position, and extinction coefficients agree very well with typical values for

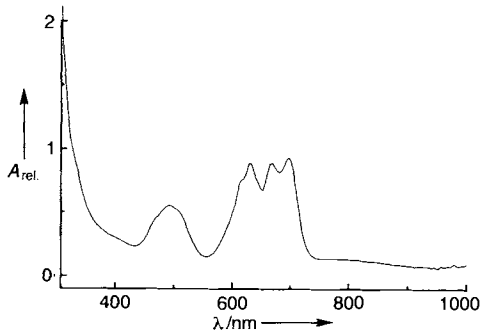

Fig. 1. UV/Vis spectrum of [$\mathbf{L^1}\cdot$CoCl]Cl ($\mathbf{K^1}$) (hexane, $c = 5\times10^{-3}$ mol L^{-1}).

octahedral nickel complexes.[13] No information on the coordination geometry of the complex $L^1 \cdot ZnCl_2$ (K^7) can be derived from the spectroscopic data.

Owing to the very low coordination tendency of the peripheral amide groups, the situation for L^2 is similar to that for L^1. The copper(II) dichloride complex $[L^2 \cdot CuCl]Cl$ (K^8) does not show any crystalline phase; the enantiotropic mesophase is frozen in the glassy state above room temperature (Table 1), and the texture is broken spherolitic (Fig. 2). X-ray diffraction experiments show the presence of a hexagonal-columnar mesophase (Col_h) with $a_{hex} = 36.9$ Å (Table 2, Fig. 3). The lattice constant is only 0.4 Å greater than that of the free ligand, which indicates that complexation has only a negligible influence on the space filling of the molecule. The UV/Vis spectrum of K^8 is almost identical to that of K^4 (Table 3), so that trigonal-bipyramidal coordination may also be assumed for K^8.

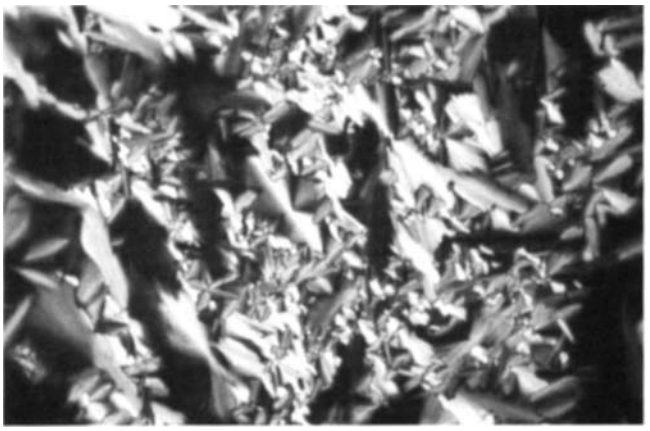

Fig. 2. Texture of the complex $[L^2 \cdot CuCl]Cl$ (K^8) ($T = 132$ C, 120-fold magnification, crossed polarizers).

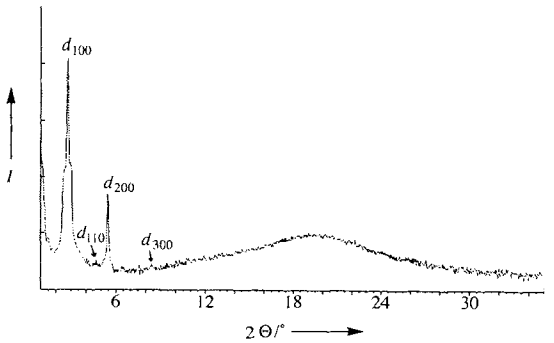

Fig. 3. X-ray diffraction diagram of the complex $[L^2 \cdot CuCl]Cl$ (K^8).

The complexes described here are the first examples of metallomesogens with branched, dendrimeric oligoalkyleneamino ligands. These mesogens are not based on the classical rod or disklike shape. They show a trigonal-bipyramidal coordination geometry; only the nickel complexes studied are octahedral. The transition temperatures of all the complexes—in the absence of a crystalline phase—are relatively low for metallomesogens. The hexagonal-columnar phase appears to be formed when either the larger ligand L^2 or the Zn^{II} ion are present. Initial measurements have shown that the nickel complexes described here are also paramagnetic.

Experimental Procedure

L^1: Tris(2-aminoethyl)amine was allowed to react with 3,4-bis(decyloxy)benzoyl chloride [14], and the product was reduced to the amine [3] (54% yield); IR (KBr): $\tilde{\nu} = 3302\ cm^{-1}$, 2925, 2855, 1606, 1589, 1512, 1467, 1380, 1264, 1231, 1134, 1044, 801, 722; ^1H NMR (250 MHz, $CDCl_3$): $\delta = 6.85$ (s, 1H, arom.), 6.65–6.80 (m, 2H, arom.), 3.95 (m, 4H, OCH_2), 3.65 (s, 2H, $ArCH_2$), 2.60 (m, 4H, CH_2N), 1.75 (m, 4H, OCH_2CH_2), 1.10–1.60 (m, 28H, alkoxy-CH_2), 0.85 (t, 6H, CH_3); EI-MS (70 eV): *m/z* (%): 1352 (11) [M^+], 460 (100); Elemental analysis (%): calcd for $C_{87}H_{150}N_4O_6$ (1354.15 $g\,mol^{-1}$): C 77.17, H 11.61, N 4.14, O 7.09; found: C 77.17, H 11.55, N 4.08.

L^2: This ligand was prepared as described elsewhere [15].

K^1–K^8: To L^1 or L^2 in EtOH at 60 C was added dropwise an equimolar amount of the metal salt dissolved in EtOH. The mixture was stirred for 3 h at 60 C, stored in a refrigerator for 12 h, and then filtered. The residue was recrystallized from EtOH, and the solid dissolved in benzene and freeze-dried. K^5 was synthesized by adding NaSCN in acetone to an equimolar amount of K^4 in acetone at 50 C. After 30 min, this was filtered hot, worked up as described, and recrystallized from benzene (85–92% yield).

Complexes with L^1 (for example: $L^1 \cdot ZnCl_2$): IR (KBr): $\tilde{\nu} = 3193\ cm^{-1}$, 2925, 2855, 1606, 1589, 1515, 1467, 1380, 1265, 1141, 1044, 812, 722; ^1H NMR (250 MHz, $CDCl_3$): $\delta = 7.05$ (br., 1H, arom.), 6.95 (br., 1H, arom.), 6.75 (d, 1H, arom.), 3.8–4.1 (m, 6H, OCH_2, $ArCH_2N$), 2.5–2.8 (br., 4H, NCH_2CH_2N), 1.6–1.9 (m, 4H, OCH_2CH_2), 1.1–1.5 (m, 28H, alkoxy-CH_2), 0.9 (t, 3H, CH_3); Elemental analysis (%): $[L^1 \cdot CoCl]Cl$ (K^1): calcd for $C_{87}H_{156}Cl_2CoN_4O_6$ (1483.99 $g\,mol^{-1}$): C 70.42, H 10.60, N 3.78, Cl 4.78, Co 3.97, O 6.47; found: C 70.25, H 10.60, N 3.94; $[L^1 \cdot NiCl_2]$ (K^2): calcd for $C_{87}H_{156}Cl_2NiN_4O_6$ (1483.75 $g\,mol^{-1}$): C 70.43, H 10.60, N 3.78, Cl 4.78, Ni 3.96, O 6.47; found: C 70.17, H 10.87, N 3.80; $[L^1 \cdot Ni(NO_3)_2]$ (K^3): calcd for $C_{87}H_{156}NiN_6O_{12}$ (1536.85 $g\,mol^{-1}$): C 67.99, H 10.23, N 5.47, Ni 3.82, O 12.49; found: C 68.05, H 10.11, N 5.37; $[L^1 \cdot CuCl]Cl$, (K^4): calcd for $C_{87}H_{156}Cl_2CuN_4O_6$ (1488.60 $g\,mol^{-1}$): C 70.20, H 10.56, N 3.76, Cl 4.76, Cu 4.27, O 6.45; found: C 69.69, H 10.95, N 4.28; $[L^1 \cdot Cu(NCS)](SCN)$ (K^5): calcd for $C_{89}H_{156}CuN_6O_6S_2$ (1533.93 $g\,mol^{-1}$): C 69.68, H 10.25, N 5.48, Cu 4.14, S 4.18, O 6.47; found: C 68.80, H 10.35, N 6.55, Cu 4.30, S 4.10; $[L^1 \cdot Cu(NO_3)](NO_3)$ (K^6): calcd for $C_{87}H_{156}CuN_6O_{12}$ (1541.70 $g\,mol^{-1}$): C 67.78, H 10.20, N 5.45, Cu 4.25, O 12.45; found: C 67.64, H 10.05, N 5.45; $L^1 \cdot ZnCl_2$ (K^7): calcd for $C_{87}H_{156}Cl_2ZnN_4O_6$ (1490.45 $g\,mol^{-1}$): C 70.11, H 10.55, N 3.76, Cl 4.76, Zn 4.39, O 6.44; found: C 68.95, H 10.38, N 4.07.

Complex with L^2: $[L^2 \cdot CuCl]Cl$ (K^8): IR (KBr): $\tilde{\nu} = 3304\ cm^{-1}$, 2924, 2855, 1635, 1602, 1581, 1508, 1468, 1392, 1270, 1131, 1040, 761, 722; Elemental analysis (%): calcd for $C_{180}H_{312}Cl_2CuN_{10}O_{18}$ (3038.81 $g\,mol^{-1}$): C 71.15, H 10.35, N 4.61, Cl 2.33, Cu 2.17, O 9.48; gef.: C 70.42, H 10.47, N 4.35, Cl 2.32, Cu 2.34.

Received: March 13, 1996 [Z8922IE]
German version: *Angew. Chem.* **1996**, *108*, 1941–1943

Keywords: complexes with nitrogen ligands · coordination · dendrimers · mesophases · metallomesogens

[1] a) A.-M. Giroud-Godquin, P. M. Maitlis, *Angew. Chem.* **1991**, *103*, 370; *Angew. Chem. Int. Ed. Engl.* **1991**, *30*, 375; b) P. Espinet, M. A. Esteruelas, L. A. Oro, J. L. Serrano, E. Sola, *Coord. Chem. Rev.* **1992**, *117*, 215; D. W. Bruce in *Inorganic Materials* (Eds.: D. W. Bruce, D. O'Haare), Wiley, New York, **1992**, p. 405; d) S. A. Hudson, P. M. Maitlis, *Chem. Rev.* **1993**, *93*, 861; e) L. Oriol, J. L. Serrano, *Adv. Mater.* **1995**, *7*, 348; f) J. L. Serrano, *Metallomesogens*, VCH, Weinheim, **1995**.

[2] A.-M. Giroud-Godquin, A. Rassat, *C. R. Acad. Sci. Ser. 2* **1982**, *294*, 241.

[3] G. Lattermann, S. Schmidt, R. Kleppinger, J. H. Wendorff, *Adv. Mater.* **1992**, *4*, 30.

[4] a) Yu. G. Galyametdinov, I. G. Bikchantaev, I. V. Ovchinnikov, *Zh. Obshch. Khim.* **1988**, *58*, 1326; b) Yu. G. Galyametdinov, O. N. Kadkin, A. V. Prosvirin, *Izv. Akad. Nauk. Ser. Khim.* **1994**, 941; *Russ. Chem. Bull.* **1994**, *43*, 887; c) K. Griesar, Y. Galyametdinov, M. Athanassopoulou, I. Ovchinnikov, W. Haase, *Adv. Mater.* **1994**, *6*, 381; d) W. Pyzuk, Yu. Galyametdinov, *Liq. Crystals* **1993**, *15*, 265.

[5] a) H. Adams, N. A. Bailey, D. W. Bruce, R. Dhillon, D. A. Dunmur, S. E. Hunt, E. Lalinde, A. A. Maggs, R. Orr, P. Styring, M. S. Wragg, P. Maitlis, *Polyhedron*, **1988**, *7*, 1861; b) D. Guillon, D. W. Bruce, P. Maldivi, M. Ibn-Elhaj, R. Dhillon, *Chem. Mater.* **1994**, *6*, 182.

[6] a) Y. G. Galyametdinov, G. I. Ivanova, I. V. Ovchinnikov, *Izv. Akad. Nauk. SSSR Ser. Khim.* **1989**, 1931; b) Y. Galyametdinov, G. Ivanova, K. Griesar, A. Prosvirin, I. Ovchinnikov, W. Haase, *Adv. Mater.* **1992**, *4*, 739; c) W. Haase, K. Griesar, M. F. Iskander, Y. Galyametdinov, *Mol. Cryst. Liq. Cryst. Sect. C.* **1993**, *3*, 115; d) M. Marcos, J. L. Serrano, P. J. Alonso, J. I. Martinez, *Adv. Mater.* **1995**, *7*, 173.

[7] J. G. Verkade, *Coord. Chem. Rev.* **1994**, *137*, 233.

[8] a) S. G. Zipp, A. P. Zipp, S. K. Madan, *Coord. Chem. Rev.* **1974**, *14*, 29, and references therein; b) P. Paoletti, L. Fabrizzi, *ibid.* **1975**, *15*, 435, and references therein; c) M. J. Gaudin, C. R. Clark, D. A. Buckingham, *Inorg. Chem.* **1986**, *25*, 2569, and references therein; d) G. J. Colpas, M. Kumar, R. O. Day, M. J. Maroney, *ibid.* **1990**, *29*, 4779.
[9] D. A. Buckingham, J. D. Edwards, G. M. McLaughlin, *Inorg. Chem.* **1982**, *21*, 2770.
[10] M. Ciampolini, N. Nardi, *Inorg. Chem.* **1966**, *5*, 41.
[11] P. C. Jain, E. C. Lingafelter, *J. Am. Chem. Soc.* **1967**, *89*, 724.
[12] K. N. Raymond, F. Basolo, *Inorg. Chem.* **1966**, *5*, 1632.
[13] M. Gerloch, E. C. Constable, *Transition Metal Chemistry*, VCH, Weinheim **1994**, p. 61 ff.
[14] U. Stebani, G. Lattermann, R. Festag, M. Wittenberg, J. H. Wendorff, *Adv. Mater.* **1994**, *6*, 572, 790.
[15] U. Stebani, G. Lattermann, *Adv. Mater.* **1995**, *7*, 578.

An Intermolecularly Donor-Stabilized Silanediyl(silyl)nickel Complex: Combined Si–Si Bond Cleavage and Methyl Migration between Silicon Centers**

Sylvain Nlate, Eberhardt Herdtweck, and Roland A. Fischer*

Dedicated to Professor Hans Georg von Schnering on the occasion of his 65th birthday

Cyclopentadienyl derivatives with Lewis bases in the side groups that are capable of binding to hard and soft centers in a hemilabile manner promise a rich coordination chemistry and unusual reactions at the metal center. Prominent ligands include [2-(*N*,*N*-dimethylamino)ethyl]cyclopentadienyl and its tetramethyl-substituted derivative (Cp^N and Cp^{*N}, respectively), and intermolecular adducts of these to various metal centers are known.[1] However, convincing examples in which reactions are specifically controlled by the binding properties of this ligand have not been reported.

The nickel dimer $[Cp^N_2(CO)_2Ni_2]$ can be synthesized quantitatively by the "classical" reaction of $[Cp^N_2Ni]$ and tetracarbonylnickel (the corresponding Cp* compound has been described previously[1b]). Oxidative cleavage of the nickel dimer with iodine, followed by decarbonylation gave the key compound **1** (Scheme 1). The quality of the crystallographic data[3a] (Fig. 1) of **1** is affected by dynamic disorder of the aminoethyl substituent (large anisotropic thermal parameters at C6 and C7). To the best of our knowledge there is only one further structurally characterized example of a nickel complex with intramolecular coordination of the substituent at Cp: $[\eta^5{:}\eta^2$-2,3,4,5-tetramethyl-1-(4-pentenyl)cyclopentadienyl](bromo)-nickel(II).[4]

Reaction of **1** with $[(thf)_3Li\{Si[Si(CH_3)_3]_3\}]$ selectively yields bright yellow, air-sensitive crystals of **2** in 80–90% yield (Fig. 2).[3b] This is the first structurally characterized example of a silanediyl(silyl) metal complex. The occurrence of both π(M=Si) and σ(M–Si) bonds in one molecule permits a direct comparison these two types of bonding. Complex **1** is related to some bissilanediyl complexes, for example $[(\eta^5\text{-}C_5Me_5)Ru(PPh_3)\{\eta^2\text{-}[(\mu\text{-}CH_3O)(SiMe_2)_2]\}]$,[5] which are also stabilized by intramolecular base coordination, but contain identical Si complex fragments. The only other known silanediylnickel complex is [bis(1,3-di-*tert*-butyl-2,3-dihydro-1*H*-1,3,2-diazasilol-2-ylidene)](dicarbonyl)nickel, which was described as a "donor-free" system. However, in this compound silicon is bound to two nitrogen atoms, and π(Si–N) interactions cannot be neglected.[6] Even when the reduced coordination number of three is taken into consideration, the Ni–Si4 bond length in **2** (213.7(1) pm; Fig. 2) is significantly shorter than the corresponding bonds in the above-mentioned $NiSi_2$ complex (220.7(2) pm and 221.6(2) pm).[6] According to T. D. Tilley et al.

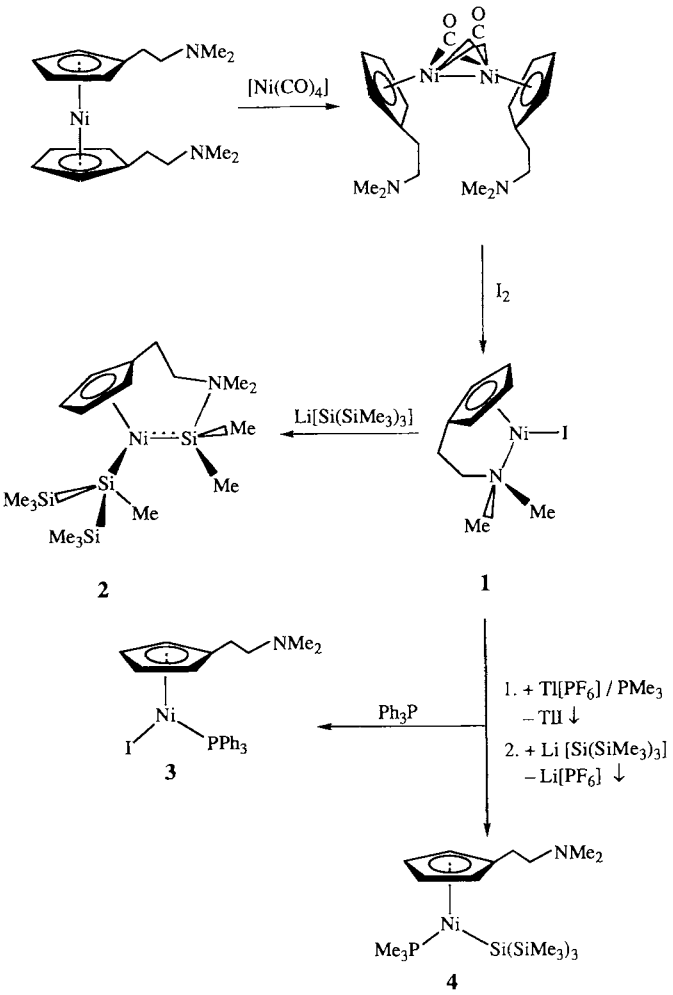

Scheme 1. Syntheses of the compounds discussed in this work.

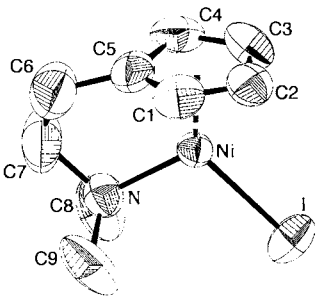

Fig. 1. Crystal structure of **1** (ORTEP, thermal ellipsoids at 50% probability level). Selected bond lengths [pm] and angles [°]: Ni–I 250.0(1), Ni–N 196.0(5), Ni–C1 212.8(6), Ni–C2 213.0(5), Ni–C3 214.2(7), Ni–C4 211.9(7), Ni–C5 199.7(7), N–C7 152(1), N–C8 146.6(8), N–C9 147.0(8), C5–C6 149(1), C6–C7 138(1); I-Ni-N 103.3(2), C1-C5-C6 125.8(7), C4-C5-C6 125.6(7), C5-C6-C7 112.1(8), N-C7-C6 116.2(8).

[*] Prof. Dr. R. A. Fischer
Anorganisch-chemisches Institut der Universität
Im Neuenheimer Feld 270, D-69120 Heidelberg (Germany)
Fax: Int. code +(6221)546617
e-mail: fischer@akcomba.aci.uni-heidelberg.de
Dr. S. Nlate, Dr. E. Herdtweck
Anorganisch-chemisches Institut der Technische Universität München
Lichtenbergstrasse 4, D-85747 Garching (Germany)

[**] The authors thank the Alexander-von-Humboldt-Stiftung (grant to S. N) and the Fonds der Chemischen Industrie for financial support.

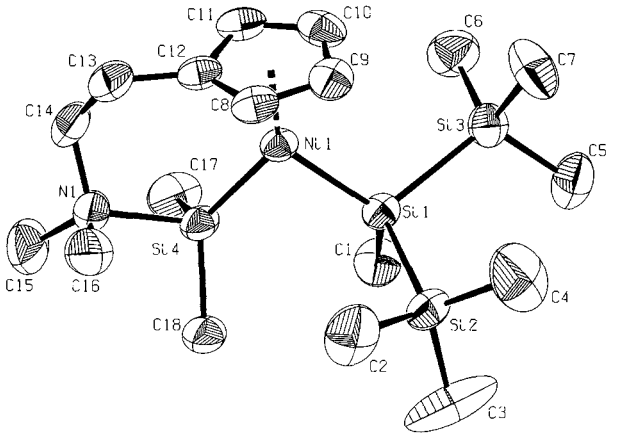

Fig. 2. Crystal structure of **2** (ORTEP, thermal ellipsoids at 50% probability level). Selected bond lengths [pm] and angles [°]: Ni–Si4 213.7(1), Ni–Si1 224.0(1), Ni–C8 211.8(3), Ni–C9 211.6(3), Ni–C10 214.1(3), Ni–C11 214.9(3), Ni–C12 209.3(3), Si1–C1 192.9(3), Si4–C18 188.7(4), Si4–C17 189.2(4), Si4–N1 200.2(3), N1–C14 151.2(4), C12–C13 149.6(5), C13–C14 152.1(5); Si4-Ni1-Si1 88.56(3), C18-Si4-C17 96.7(1), C18-Si4-N1 96.8(1), N1-Si4-Ni1 107.69(8).

donor stabilization or heteroatom substitution lead to elongated M–Si bonds.[7] Thus, the Ni–Si bond in a donor-free silanediylnickel complex should be shorter than 214 pm. In contrast, the Ni–Si1 bond, which is 10 pm longer, clearly lies in the range of Ni–Si single bonds.[8] Proton-decoupled ^{29}Si NMR spectroscopy shows three types of silicon atoms. The occurrence of a downfield signal for Si1 at $\delta = 107.8$ is consistent with the discussed binding mode.[9] The Si4–N donor–acceptor bond length (200.2(3) pm) is in the range of Si–N bond lengths determined for the related complexes $[(CO)_5Cr{=}Si(Ph)(Ar^N)]$ (204.6(2) pm, Ar^N = 2-(dimethylaminomethyl)phenyl[9b]) and $[\{(\eta^5\text{-}(C_5H_5)(CO)_2Fe{=}Si(CH_3)Ar^N\}^+]$ (194.9(3) pm[10]). The Ni atom in **2** is coordinated to the center of the Cp ligand, whereas in **1** a strongly decentralized binding mode exists. The formation of the bright yellow complex **2** evidently occurs via the primary intermediate **A** (Scheme 2); the aminoethyl substituent is replaced by the incoming nucleophile $\{Si[Si(CH_3)_3]_3\}^-$, a course analogous to that for the reaction of **1** with a phosphane ligand, which is isolobal to the silyl group (Scheme 1, **1** → **3**). The reaction is accompanied by a change of color from greenish black (**1**) to a dark red-purple (**A**). There are examples for the activation of Si–Si bonds at transition metal centers, for example with oligosilanyl systems $[L_nM{-}SiR_2{-}(SiR_2)_n{-}SiR_3]$,[11] and for [1,3] migration of a methyl group between silicon centers in bissilanyl complexes.[12] Intermediates analogous to **2** were claimed, but never isolated. Formation of **2** can be rationalized as follows (Scheme 2): In a first step, complex **B** is formed from intermediate **A** after elimination of LiI and [1,2] migration of a $(CH_3)_3Si$ group. Owing to steric hindrance the bis(trimethylsilyl)-substituted silanediyl center in **B** is apparently not sufficiently stabilized by the aminoethyl group. Then the [1,3] sigmatropic methyl shift from the $(CH_3)_3Si$ unit to Si1 stabilizes the system thermodynamically (**B** → **2**), and the resulting dimethylsilanediyl unit Si4 is trapped by intramolecular adduct formation. We assume that these reaction steps are assisted kinetically by the amino group, giving rise to weak hypervalent interactions with the reactive Si centers. Pentacoordinate intermediates were discussed for Si–Si and Si–C bond cleavage.[13]

The coordinative flexibility of the aminoethyl group thus causes a special reactivity of complex **1**. However, this can be strongly affected. Reaction of complex **1** with $[(thf)_3Li\{Si(CH_3)_3]_3\}]$ in the presence of PMe_3 only yields a stable, "trivial" substitution product **4** (see Scheme 1). In summary, only in the *absence* of strong π acceptors (CO) and soft Lewis bases (PR_3) as competing ligands, do aminoalkyl side chains of Cp ligands participate in the coordination to electron-rich transition metal centers. The aminoalkyl function on the Cp system can then be used to stabilize unusual silanediyl(silyl) complexes such as **2**.

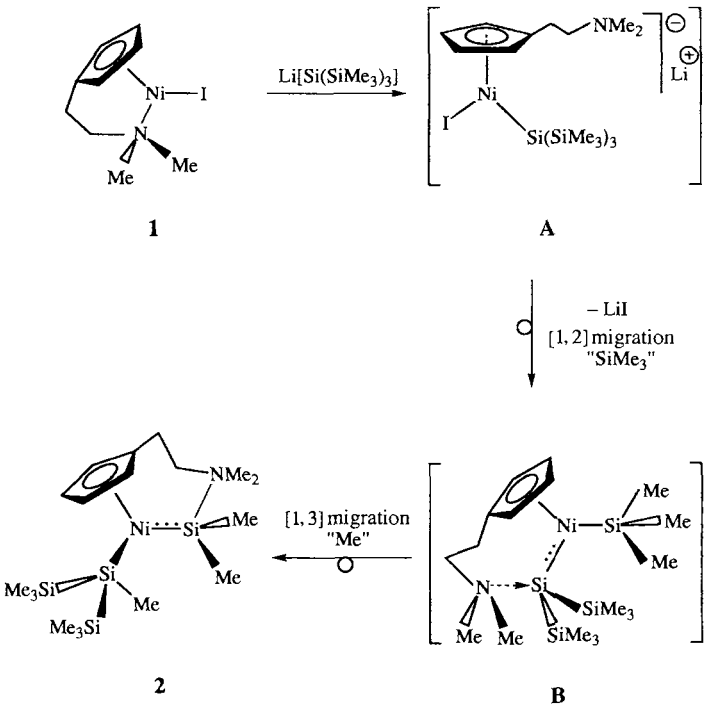

Scheme 2. Hypothetical mechanism of the formation of **2**.

Experimental Procedure

1: I_2 (1.02 g, 4 mmol) in THF (20 mL) was added to a stirred solution of $[Cp^N_2(CO)_2Ni_2]$ (1.8 g, 4 mmol) in THF (20 mL) at −78 °C over 30 min. The mixture was allowed to warm to 25 °C and stirred for 2 h. The solvent was evaporated in vacuo, the residue was washed with *n*-pentane (15 mL), and the product was extracted with toluene. Crystallization from toluene at −30 °C gave **1** (2.2 g, 85% based on Ni). Correct elemental analysis.

2: **1** (0.32 g, 1 mmol) was added to a solution of $(thf)_3Li\{Si[Si(CH_3)_3]_3\}$ (0.47 g, 1 mmol) in THF (20 mL) at −78 °C). The mixture was allowed to warm to 25 °C and stirred for 12 h. The solvent was evaporated in vacuo and the residue was extracted into *n*-pentane (20 mL). Crystallization from *n*-pentane at −30 °C gave **2** (0.38 g, 85%). Correct elemental analysis.

Received: March 14, 1996 [Z 8926 IE]
German version: *Angew. Chem.* **1996**, *108*, 1957–1959

Keywords: coordination · cyclopentadienyl complexes · nickel compounds

[1] a) P. Jutzi, U. Siemeling, *J. Organomet. Chem.* **1995**, *500*, 175–185; and references therein; b) P. Jutzi, T. Redeker, B. Neumann, H.-G. Sammler, *ibid.* **1995**, *498*, 127–134.

[2] E. O. Fischer, C. Palm, *Chem. Ber.* **1958**, *91*, 1725–1731.

[3] X-ray crystal structure analyses a) **1**: $C_9H_{14}INNi$, M = 321.82; black crystals (0.23 × 0.15 × 0.15 mm^3); orthorhombic, *Pbca* (no. 61), a = 900.0(1), b = 1320.6(1), c = 1891.3(1) pm, V = 2247.9(3) × 10^6 pm^3, Z = 8, ρ_{calc} = 1.902 g cm^{-3}; F_{000} = 1248; μ = 44.2 cm^{-1}; IPDS (STOE & CIE.), $Mo_{K\alpha}$ radiation, λ = 71.073 pm; oscillation; 2 min per image [14]. The calculations [15] converged at $R1$ = 0.057, $wR2$ = 0.112 and GOF = 0.953 for all 1864 reflections ($I > 2.0\sigma(I)$) and 109 parameters. b) **2**: $C_{18}H_4{}_1NNiSi_4$, M = 442.57; light yellow prisms (0.51 × 0.25 × 0.15 mm^3); triclinic, $P\bar{1}$ (no. 2), a = 888.0(1), b = 1717.1(2), c = 1763.8(2) pm, α = 76.46(1), β = 83.09(1), γ = 76.83(1)°, V = 2539.5(5) × 10^6 pm^3, Z = 4, ρ_{calc} = 1.158 g cm^{-3}; F_{000} = 960; μ =

9.5 cm^{-1}; IPDS (STOE & CIE.), $Mo_{K\alpha}$ radiation, $\lambda = 71.073$ pm; rotation; 6 min per image [14]. The calculations [15] converged at $R1 = 0.037$, $wR2 = 0.093$ and $GOF = 1.041$ for all 7461 reflections ($I > 2.0\sigma(I)$) and 452 parameters. The unit cell contains two independent molecules **2a** and **2b** with negligible differences in their geometry. Only molecule **2b** exhibits a slight disorder of the dimethylamino group. The data given in the text refer to molecule **2a**. Further details of the crystal structure investigations may be obtained from the Fachinformationszentrum Karlsruhe, D-76344 Eggenstein-Leopoldshafen (Germany), on quoting the depository number CSD-405435 for **1** and CSD-405436 for **2**.

[4] H. Lehmkuhl, J. J. Naser, G. G. Mehler, T. T. Keil, F. Danowski, R. Benn, R. Mynott, G. Schroth, B. Gabor, C. Krüger, P. Betz, *Chem. Ber.* **1991**, *124*, 441–452.

[5] H. Tobita, H. Wada, K. Ueno, O. Ogino, *Organometallics* **1994**, *13*, 2545–2547.

[6] M. Denk, R. K. Hayashi, R. West, *J. Chem. Soc. Chem. Commun.* **1994**, 33–34.

[7] S. K. Grumbine, T. D. Tilley, *J. Am. Chem. Soc.* **1994**, *116*, 5495–5496.

[8] T. R. Bierschenk, M. A. Guerra, T. J. Juhlke, S. B. Larson, R. J. Lagow, *J. Am. Chem. Soc.* **1987**, *109*, 4855–4860.

[9] a) C. Leis, D. L. Wilkinson, H. Handwerker, C. Zybill, *Organometallics* **1992**, *11*, 514–529; b) R. Probst, C. Leis, S. Gamper, E. Herdtweck, C. Zybill, N. Auner, *Angew. Chem.* **1991**, *103*, 1155–1157; *Angew. Chem. Int. Ed. Engl.* **1991**, *30*, 1132–1134.

[10] H. Kobayashi, K. Ueno, H. Ogino, *Organometallics* **1995**, *14*, 5490–5492.

[11] H. K. Sharma, K. H. Pannell, *Chem. Rev.* **1995**, *95*, 1351–1374.

[12] D. C. Pestana, T. S. Koloski, D. H. Berry, *Organometallics* **1994**, *13*, 4173–4175.

[13] C. Chuit, R. J. P. Corriu, C. Reye, J. C. Young, *Chem. Rev.* **1993**, *93*, 1371–1448.

[14] a) W. Schütt, E. Herdtweck, F. Hahn, F. R. Kreissl, *J. Organomet. Chem.* **1993**, *443*, C33-C36; and references therein; b) G. Artus, W. Scherer, E. Herdtweck, STRUX-V, Technische Universität München, Germany, **1994**.

[15] a) A. Altomare, G. Cascarano, C. Giacovazzo, A. Guagliardi, M. C. Burla, G. Polidori, M. Camalli, SIR-92, University Bari, Italy, **1992**; b) G. M. Sheldrick, SHELXL-93, Universität Göttingen, Germany, **1993**.

Synthesis and Asymmetric [3+2] Cycloaddition Reactions of Chiral Cyclic Nitrone: A Novel System Providing Maximal Facial Bias for both Nitrone and Dipolarophile**

Teruhiko Ishikawa, Yoshiaki Tajima, Miyuki Fukui, and Seiki Saito*

Asymmetric synthesis through [3 + 2] cycloadditions of chiral nitrones to dipolarophiles provides three contiguous stereogenic centers, the first and third of which are bound to oxygen and nitrogen atoms.[1] In spite of its important role in organic synthesis, a methodology for discriminating the diastereofaces of the nitrone and the enantiofaces of the dipolarophiles at the same time has been lacking.[2]

A cyclic nitrone such as **1** could realize such a high level of stereocontrol (Scheme 1). The role of the three substituents Z^1, Z^2, and Z^3 of **1** seems to be significant. Because Z^1 and Z^3 are located on the same side of the ring (concave space), only the approach to the convex side of dipolarophile (**2**) would be possible. If this is the case, Z^2 would force the smallest substituent

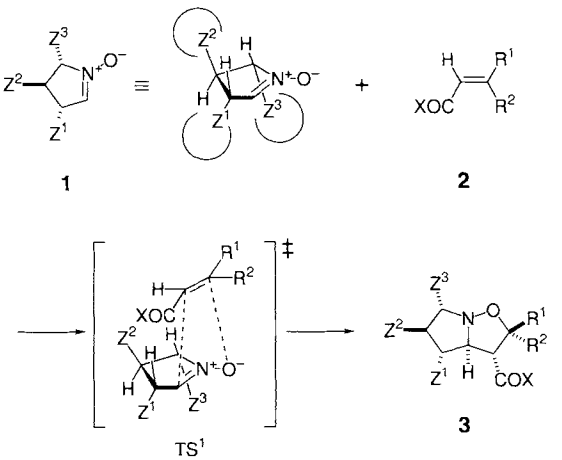

Scheme 1. Nitrone-dipolarophile arrangement in the transition state TS of the reaction of **1** with **2** to form **3**.

of **2** (H atom) to occupy the most demanding space in the transition state (TS^1). We have synthesized **1** by an intramolecular Michael addition of oxime enoates. Furthermore, the reactions of **1** with α,β-unsaturated carbonyl compounds (**2**) have resulted in almost perfect discrimination of the π faces of both **1** and **2**, exclusively affording cycloadducts such as **3**, bearing multiple stereogenic centers.

The cyclic nitrone **1b** that satisfies above-mentioned stereochemical features has been prepared on treatment of a formyl enoate derived from **4b**[3] with hydroxylamine hydrochloride and triethylamine (>99% *de*, Scheme 2). The reaction apparently involves the corresponding oxime enoate as an intermediate. The transition state of the reaction can be depicted as TS^2: TS^3 leading to **1b'** can be ruled out in this case.[4] In contrast, the corresponding formyl enoate derived from **4a** and lacking an α-methyl substituent gave a mixture of **1a** and **1a'** through TS^2 and TS^3, respectively (50% *de*). The structure of **1b** was con-

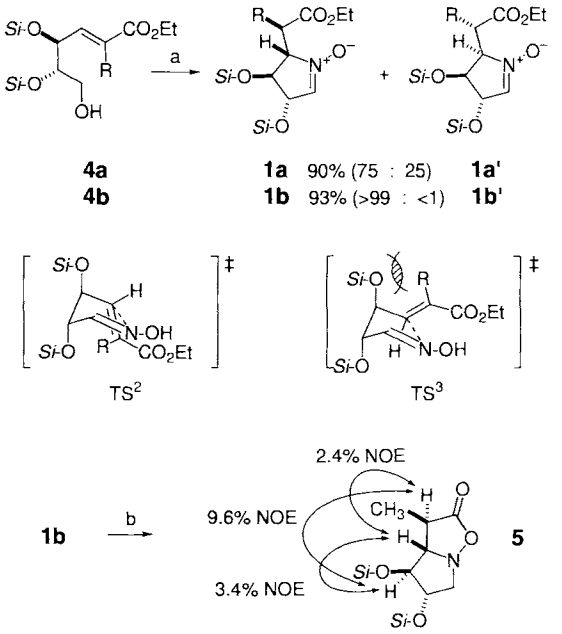

Scheme 2. Synthesis and characterization of the cyclic nitrone **1**. a) 1. Swern oxidation, 2. $NH_2OH \cdot HCl/Et_3N/CH_2Cl_2$ at room temperature; b) H_2/Pd-C. *Si* = TBDMS (*tert*-butyldimethylsilyl).

[*] Prof. Dr. S. Saito, Dr. T. Ishikawa, T. Tajima, M. Fukui
Department of Bioengineering Science, Faculty of Engineering
Okayama University
3-1-1, Tsushimanaka, Okayama 700 (Japan)
Fax: Int. code +(86)251-8209
e-mail: seisaito@cc.okayama-u.ac.jp

[**] This work was supported by a Grant-in-Aid for Scientific Research on Priority Areas (No. 07214221) from the Ministry of Education, Science, Sports, and Culture, Japan. We are grateful to "SC-NMR Laboratory of Okayama University" for high-field NMR experiments.

firmed on the basis of spectroscopic analyses, in particular by NOE measurements and mass spectrometry performed on derivative **5**.[5]

The cycloadditions of **1b** to the α,β-unsaturated carbonyl compounds **2a–f** gave the corresponding cycloadducts (**3a–f**, Table 1) in very high diastereomeric excess (>99% *de*).[6] For instance, the diastereofaces of **1b** have been perfectly distinguished by both maleate (**2b**) and maleimide (**2d**) or fumarate

Table 3. Results of the cycloaddition of **1b** to **2** (in C_6H_6 at 70 °C).

Dipolarophile	Equiv. **2**	Time [h]	Cycloadduct [a]	Yield [%]
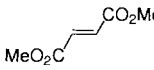 **2a**	3	12	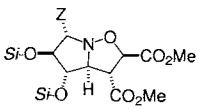 **3a**	82
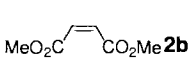 **2b**	3	24	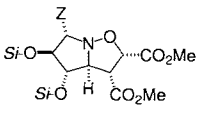 **3b**	85
2c	3	12	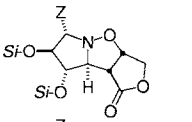 **3c**	84
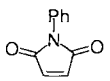 **2d**	3	4	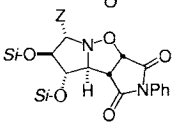 **3d**	89
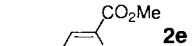 **2e**	4	12	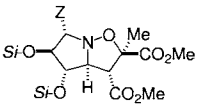 **3e**	62
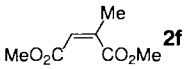 **2f**	4	18	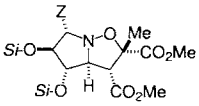 **3f**	60

[a] For chromatographically pure product, the absolute configuration was determined by NOE experiments.

(**2a**), which approach the reaction centers from the convex space exclusively in an *exo* manner and/or enantioselectively (>99% *ee*). The most striking observation is the almost perfect discrimination of enantiofaces of (*E*) and (*Z*) isomeric pairs such as **2e** and **2f**: these dipolarophiles exclusively afforded cycloadducts **3e** and **3f**, respectively. Thus, **1b** is the first chiral, cyclic nitrone capable of achieving an equally high level of face differentiation for the geometric isomers of 1,2-disubstituted and 1,1,2-trisubstituted olefins. The underlying concept for this class of facial bias has significant implications on the design of chiral reagents, catalysts, or ligands.

Experimental Procedure

1b: To a solution of $(COCl)_2$ (0.31 mL, 3.54 mmol, 3 equiv) in CH_2Cl_2 (6 mL) at −70 °C was added a solution of DMSO (0.5 mL, 7.1 mmol) in CH_2Cl_2 (6 mL), and the mixture was stirred for 5 min. To this mixture was added a solution of **4b** (0.511 g, 1.18 mmol) in CH_2Cl_2 (6 mL), the solution stirred for a further 15 min, and Et_3N (1.5 mL, 10.2 mmol, 9 equiv) was added. The mixture was allowed to warm up to 25 °C, quenched with water, and extracted with several portions of hexane/EtOAc (1/1). The combined organic extracts were dried (Na_2SO_4) and concentrated on a rotary evaporator to give the crude aldehyde, which, without purification, was dissolved in CH_2Cl_2 (6 mL). To this solution was added hydroxylamine hydrochloride (0.41 g, 5.90 mmol, 5 equiv) and Et_3N (0.82 mL, 5.90 mmol, 5 equiv) at about 25 °C. The mixture was stirred for 4 h, then poured into water, and extracted with several portions of hexane/EtOAc (1/1). The combined organic extracts were dried (Na_2SO_4) and concentrated on a rotary evaporator to give a crude residue, which was subjected to column chromatography (SiO_2) to give nitrone **1b** as a colorless oil (489 mg, 93%). $[\alpha]_D^{27} = +61.9$ ($c = 5.10$ in chloroform); IR (film): $\tilde{\nu}$ = 1740, 1580, 1460, 1260 cm^{-1}; ^1H NMR (500 MHz, $CDCl_3$, 23 °C): δ = 0.069, 0.087, 0.10, 0.17 (each s, each 3H), 0.86, 0.88 (each s, each 9H), 1.11 (d, 3H, J = 7.1 Hz), 1.28 (t, 3H, J = 7.2 Hz), 3.40 (dq, 1H, J = 7.2, 11.8 Hz), 4.13 (br.s, 1H), 4.17 (m, 1H), 4.12 and 4.22 (2 dq, 2H, J = 7.0, 10.8 Hz), 4.54 (d, 1H, J = 2.0 Hz), 6.83 (br. s, 1H); $^{13}C\{^1H\}$ NMR (125 MHz, $CDCl_3$, 23 °C): δ = −5.0, −4.8, −4.7, −4.3, 11.2, 14.1, 17.7, 17.8, 25.5, 25.6, 38.2, 61.0, 76.6, 79.3, 82.5, 133.8, 173.2; C,H analysis calcd for $C_{21}H_{43}O_5NSi_2$: H 9.73, C 56.60; found: H 9.85, C 56.45.

3a: A solution of **1b** (1 mmol) and dimethyl fumarate (3 equiv) in benzene (1 mL) was heated at 70 °C. The reaction was continued until **1b** was consumed (monitored by TLC). Then the mixture was concentrated on a rotary evaporator, and the residue was purified by column chromatography (SiO_2) to give **3a**. $[\alpha]_D^{21} = -2.71$ (c = 1.18 in chloroform); IR (film): $\tilde{\nu}$ = 1740, 1260, 1100 cm^{-1}; ^1H NMR (500 MHz, $CDCl_3$, 23 °C): δ = 0.055, 0.069, 0.078, 0.107 (each s, each 3H), 0.87 (s, 2 × 9H), 1.20 (d, 3H, J = 7.0 Hz), 1.26 (t, 3H, J = 7.1 Hz), 2.79 (dq, 1H, J = 7.0, 7.2 Hz), 3.61 (dd, 1H, J = 1.9, 7.2 Hz), 3.73 (m, 1H), 3.75 (s, 3H), 3.77 (s, 3H), 4.03 (t, 1H, J = 8.3 Hz), 4.04 (br. s, 1H), 4.12 and 4.17 (2 dq, 2H, J = 7.2, 7.6 Hz), 4.24 (s, 1H), 4.48 (d, 1H, J = 8.3 Hz); $^{13}C\{^1H\}$ NMR (50 MHz, $CDCl_3$, 23 °C): δ = −5.04, −4.96, −4.77, −4.66, 13.7, 14.2, 17.7, 17.8, 25.5, 25.6, 42.1, 52.5, 54.0, 60.3, 76.6, 77.0, 77.6, 79.6, 80.3, 81.0, 170.5, 170.6, 174.4; C,H analysis calcd for $C_{27}H_{51}O_9NSi_2$: H 8.72, C 54.98; found: H 8.77, C 54.88.

Received: March 13, 1996 [Z 8921 IE]
German version: *Angew. Chem.* **1996**, *108*, 1990–1991

Keywords: cycloadditions · nitrones · stereodifferentiation

[1] For chiral nitrones, see a) W. R. Raush, A. E. Watts, *J. Am. Chem. Soc.* **1984**, *106*, 721–723; b) P. DeShong, C. M. Dicken, J. M. Leginus, R. R. Whittle, *ibid.* **1984**, *106*, 5598–5602; c) T. Kametani, S.-D. Chu, T. Honda, *J. Chem. Soc. Perkin Trans. 1*, **1988**, 1593–1597; d) M. Ihara, M. Takahashi, K. Fukumoto, T. Kametani, *J. Chem. Soc. Chem. Commun.* **1988**, 9–10; e) D. Keirs, D. Moffat, K. Overton, *ibid.* **1988**, 654–655; f) S. Saito, T. Ishikawa, N. Kishimoto, T. Kohara, T. Moriwake, *Synlett* **1994**, 282–284; g) S. Saito, T. Ishikawa, T. Moriwake, *J. Org. Chem.* **1994**, *59*, 4375–4377; h) A. Brandi, S. Cicchi, A. Goti, M. Koprowski, K. M. Pietrusiewicz, *ibid.* **1994**, *59*, 1315–1318; i) F. M. Cordero, S. Cicchi, A. Goti, A. Brandi, *Tetrahedron Lett.* **1994**, *35*, 949–952.

[2] An intramolecular [3+2] cycloaddition reaction of a chiral nitrone unit with a prochiral dipolarophile unit in the same molecule has sometimes resulted in almost perfect discrimination of the diastereofaces of the nitrone unit and the enantiofaces of the dipolarophile unit: see ref. [1d].

[3] Compound **4b** was prepared in six steps starting from (2*S*,3*S*)-2,3-*O*-isopropylidene-L-threitol by the sequence of reactions 1) mono-O-*p*-methoxybenzylation, 2) oxidation, 3) Horner–Emmons condensation, 4) cleavage of an acetonide protecting group, 5) TBDMS-protection of a diol group, and 6) cleavage of a *p*-methoxybenzyl protecting group.

[4] For these transition states in which the TBDMSO groups arrange *anti* to each other, see ref. [1f,g] and S. Saito, Y. Hirohara, O. Narahara, T. Moriwake, *J. Am. Chem. Soc.* **1989**, *111*, 4533–4535; S. Saito, O. Narahara, T. Ishikawa, M. Asahara, T. Moriwake, *J. Org. Chem.* **1993**, *58*, 6292–6302 and references therein.

[5] Reduction of **1b** with Pd–charcoal took place at the C=N$^+$ bond to result in subsequent cyclization leading to **5**: the N–O bond was kept intact under the given reaction conditions, as clearly indicated by mass spectrometric analysis of **5**.

[6] Spectroscopic [NMR (^1H, ^{13}C, ^1H-COSY, ^1H-^{13}C-HETCOR, and NOE in some cases), IR, and HRMS] and analytical data for all new compounds were satisfactory.

 © VCH Verlagsgesellschaft mbH, D-69451 Weinheim, 1996 0570-0833/96/3516-1864 $ 15.00+.25/0

Black Gold

Hydrocarbon Chemistry. By *G. A. Olah* and *Á. Molnár*, Wiley-Interscience, New York, 1995. 632 pp., hardcover DM 134.90.-ISBN 0-471-11359-X

As a consequence of the increasing consumption of fossil raw materials and fuels – natural gas, oil, and coal – these important sources of hydrocarbons are being rapidly depleted. In the future, therefore, it may become necessary to produce hydrocarbon derivatives using building blocks from less natural sources. This viewpoint is one of the somewhat unconventional thoughts with which George A. Olah and Árpad Molnár introduce their new book *Hydrocarbon Chemistry*.

The book is divided into twelve chapters. After a general introduction describing the origins and uses of hydrocarbons (Chs. 1 and 2) and a short survey of classical synthetic methods based on C_1 sources (Ch. 3), the remaining chapters deal with specific types of reactions: isomerization, alkylation, addition, carbonylation, oxidation and oxygenation, heterosubstitution, reduction and hydrogenation, metathesis, and oligomerization and polymerization. Each of these chapters contains a survey of modern synthetic methods used in the large-scale production of various relevant hydrocarbon derivatives, and explains the most important reaction mechanisms.

Chapter 1 (27 pp., 80 literature references) deals concisely with general aspects, such as the relationship between energy demand and hydrocarbon demand, natural sources of hydrocarbons and extraction processes, the most important available synthetic routes to hydrocarbons, and their uses. Chapter 2 (35 pp., 251 references) describes the most important processes of the petrochemical industry, including cracking, reforming, and dehydrogenation, with their different thermal and catalytic variants, and the technological uses of the most important petrochemical products. Chapter 3 (37 pp., 307 references) describes methods for synthesizing hydrocarbons from C_1 building blocks such as CO_2, CO (Fischer–Tropsch processes), and methanol. Isomerization reactions of alkanes, arylalkanes, and alkenes are then discussed in Chapter 4 (41 pp., 288 references), which also covers some important technological uses such as the manufacture of detergents and polyesters. In Chapter 5 (54 pp., 341 references) the authors deal with methods for the alkylation of hydrocarbons, such as reacting with alkenes, or by the use of various catalysts and reagents such as metal halides (in Friedel–Crafts reactions), Brønsted acids, superacids, or zeolites. These processes are of great technological importance in the manufacture of isoalkanes and alkenes, antiknock fuels, ethylbenzene, cumene, and other alkyl-benzenes. Chapter 6 (68 pp., 558 references) is devoted to additions of electrophilic reagents to alkenes, dienes, and alkynes, with special emphasis on industrial applications. Chapter 7 (22 pp., 205 references) is concerned with carbonylation reactions using CO. These include hydroformylation, oxo reactions, and carboxylation of hydrocarbons using transition metal catalysts; industrial applications are also described. The chapter on oxidation and oxygenation is the longest (Ch. 8, 122 pp., 1041 references). It begins by describing methods for oxidizing saturated hydrocarbons. In addition to the classical methods using free radical initiation these include the use of oxidizing agents such as *m*-chloroperbenzoic acid, dimethyldioxirane, methyl(trifluoromethyl)dioxirane, or hydrogen peroxide in a superacidic medium. Linear alkanes can be converted into primary and secondary alcohols and ketones with regio- and stereoselectivity by using ozone in a superacidic medium or by a dry ozonation reaction using ozone on silica gel. Newer methods are also mentioned, including oxidation by metalloporphyrins and the use of metals as homogeneous oxidation catalysts. The chapter contains detailed explanations of industrial epoxidation processes and the use of oxygen for oxidizing a wide variety of compounds. Chapter 9 (31 pp., 248 references) contains a succinct treatment of heterosubstitution reactions of hydrocarbons. As well as electrophilic halogenation, nitration, and sulfonation reactions of alkanes and arenes the authors discuss free radical and metal-catalyzed reactions for achieving heterofunctionalization. Hydrogenation and reduction reactions and their practical applications are treated in Chapter 10 (56 pp., 345 references). After reviewing heterogeneously and homogeneously catalyzed hydrogenation reactions, the authors go on to discuss chemical and electrochemical reductions, ionic hydrogenations, e.g. using trifluoroacetic acid with trialkyl-silanes, and ionic and metal-catalyzed hydrogenolysis reactions (hydrogenation involving breaking of C–C s-bonds). The chapter ends by describing a number of technological applications, such as the hydro-refining of petroleum fractions and other industrially important hydrogenation processes. Chapter 11 (20 pp., 157 references) is devoted to metathesis reactions and their practical applications. Lastly, in Chapter 12 (70 pp., 500 references), the authors describe the most important methods for oligomerization and polymerization of hydrocarbons. They explain the main reaction mechanisms and discuss stereo- and regioselectivity in relation to industrially important reactions such as Ziegler–Natta polymerization; the effects of varying the catalyst and the reaction conditions are also discussed.

Considering the book as a whole, one particularly impressive feature is the provision of a comprehensive collection of references at the end of each chapter. Thus the interested reader has easy access not only to the earlier original papers extending back up to ten years or so, but also to quite recent publications that have appeared during the last two years. On the other hand, the mediocre quality of the presentation of chemical equations and formulas is disturbing, and is unnecessary with modern technology. Bonds are

This section contains book reviews and a list of new books received by the editor. Book reviews are written by invitation from the editor. Suggestions for books to be reviewed and for book reviewers are welcome. Publishers should send brochures or (better) books to the editorial office: Redaktion Angewandte Chemie, Postfach 101161, D-69451 Weinheim, Germany. The editor reserves the right of selecting which books will be reviewed. Uninvited books not chosen for review will not be returned.

shown extending into the chemical symbols, making the latter difficult to read. Broken-line bonds are sometimes missing or are printed in varying styles, double bonds in arenes are shown crookedly, ring structures are also crooked in some cases and the rings are often incomplete. The symbols in equations are not all of uniform size. In the main text superscripts and subscripts are a little too small, and the latter are printed too low down. Otherwise, however, the text is very clearly set out and easy to read.

The book provides a detailed and informative survey of synthetic methods for hydrocarbons and their derivatives, including industrial processes. This very useful compilation contains a wealth of literature references. Its special appeal lies in the excellent organization of the subject matter. The most important chemical reactions of hydrocarbons, the mechanisms involved, and the applications of these reactions in industrial processes are linked together and described in a concise and readable form. The book will be useful to all readers with an interest in the reactions of hydrocarbons as applied in industrial processes. It will also serve as an excellent foundation for newcomers to the petrochemical field and the chemistry of hydrocarbons, and for those switching interests in these areas, especially as the industrial processes described are identified by name. Industrial chemists, research chemists, and advanced students will also find useful material in this concise and up-to-date survey of all aspects of hydrocarbon chemistry.

Hans-Ullrich Siehl,
Alexander Christian Backes
Abteilung für Organische Chemie I
der Universität Ulm (Germany)

Organic Synthesis Highlights II. Edited by *H. Waldmann*. VCH Verlagsgesellschaft, Weinheim, 1995. 407 pp., hardcover DM 148.00.—ISBN 3-527-29200-4

Organic synthesis is nowadays more than ever before a meeting point of organic chemistry, biochemistry, biology, medicine, physics, and the material sciences. Books concerned with recent developments in this area are therefore of considerable interest to many readers other than synthetic chemists. *Organic Synthesis Highlights II* is a successor to the book *Organic Synthesis Highlights* (J. Mulzer et al.) published in 1990, also by VCH. It contains 40 contributions based on a series of review articles published in the journal *Nachr. Chem. Tech. Lab.* during the period 1989–1993, under the general title "Synthese im Blickpunkt".

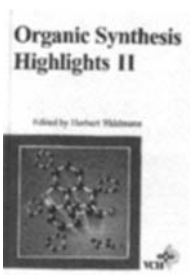

Eleven of the articles are by D. Schinzer and twelve are by H. Waldmann, who has also edited this volume. A further six articles are by M. Maier, and K. H. Dötz appears as coauthor in another five. The authors of the remaining contributions are six industrial chemists: R. Bohlmann, T. Brumby, H.-P. Fischer, P. Hammann, R. Henning, and G. Sedelmeier. The book is divided into two parts, the first dealing with new methods and reagents for organic synthesis and the second with their applications in total syntheses of natural products and analogs thereof.

Part 1 is concerned with six topical themes of organic synthesis. The first of these is asymmetric synthesis, to which six chapters are devoted; the subjects range from the Sharpless epoxidation and enantioselective *cis*-dihydroxylation, through asymmetric aza-Diels–Alder reactions, to the use of amines with C_2 symmetry as chiral auxiliaries. The second topic is organometallic chemistry, which is treated at considerable length in seven chapters, reflecting the growing importance of organometallic reactions in synthesis. The wide variety of topics covered includes rhodium-catalyzed carbenoid cyclizations, nickel-activated C_1 building blocks, C–C bond-forming reactions using metallocenes of sub-group 4 metals, and aluminum enolates. The third group of articles is concerned with modern aspects of organosilicon chemistry. In the three chapters in this group the authors report on selective transformations using pentacoordinated silicon compounds, oxidative cleavage of silicon-carbon bonds, and the temporary attachment of silicon-containing groups. The next group of articles has the general heading "Enzymes in Organic Synthesis"; here H. Waldmann reports on applications of enzymatic catalysis in the formation of C-C bonds and in syntheses of *O*-glycosides. The subject of the penultimate section of Part 1 is an "evergreen": the synthesis of heterocycles by cyclization reactions. In four chapters D. Schinzer deals very thoroughly with electrophilic cyclizations of iminium, oxonium, and sulfonium systems, and with the use of polycyclization reactions in the synthesis of alkaloids. Part 1 ends with five articles on "General Methods and Reagents for Organic Synthesis". The methods discussed here are domino reactions and group-selective reactions, and the reagents described are hypervalent iodine species, furan as a synthetic building block, and fluorine.

The articles in Part 2 describe total syntheses of natural products and active agents. The discussions illustrate the impressive capabilities of the techniques now available for organic synthesis, and also emphasize the need to continually develop new methods and reagents. The first of the two sections contains most of the contributions from authors in industry, and is concerned with syntheses of several important classes of natural products and active compounds, including hydroxyethylene-isosteric dipeptides, natural products for plant protection, penems, *O*-glycosides, carbacyclins, mitomycins, ergot and piperidine alkaloids, and taxanes. The concluding part of the book—which I might also describe as its crowning achievement—is an account of the total syntheses of several complex natural products. Here the authors have chosen some very interesting target molecules: CC-1065, morphine, calicheamicin γ_1^I, and rapamycin.

This list of topics is by no means complete, but is sufficient to show that the book covers a wealth of modern developments in organic synthesis. Although the articles treat such a wide variety of topics, the quality is consistently high throughout. All the authors have succeeded in presenting the essentials of their subjects concisely and clearly. The reader needing further details will benefit from the extensive lists of literature references.

Organic Synthesis Highlights II will obviously be of great value for post-graduate students and for everyone interested in modern synthetic methods. It is also eminently suitable as a source for preparing seminars and colloquia for advanced undergraduate students. From the standpoint of students especially, it would of course be helpful if this excellent book could also be published in a cheaper paperback edition.

Uwe Beifuss
Institut für Organische Chemie
der Universität Göttingen (Germany)

Theoretical and Physical Principles of Organic Reactivity. By *A. Pross*. Wiley, Chichester, 1995. 294 pp., hardcover £ 42.50.—ISBN 0-471-55599-1

Why do reactions have energy barriers? That is the fundamental question addressed in this monograph by A. Pross,

 © VCH Verlagsgesellschaft mbH, D-69451 Weinheim, 1996 0570-0833/96/3516-1866 $ 15.00+.25/0

one of the pioneers in the development and application of the theory of crossing potential curves, usually called the valence bond configurational mixing (VBCM) theory or the curve-crossing model. The book contains ten chapters which are grouped under three main sections: "Theoretical Principles", "Principles of Physical Organic Chemistry", and "Reaction Types". The first section introduces some basic concepts of molecular quantum mechanics. Here the author avoids using mathematical formalism as far as possible. The comparison between the molecular orbital and valence bond theories is well presented and instructive. The fourth chapter starts from simple potential energy curves and develops the theory to discuss reaction profiles using the VBCM method. The three most important "ingredients" of the VBCM theory are explained here, namely the initial excitation energy G, the fraction factor f, and the resonance energy B. Chapter 5 continues this theme with scarcely a perceptible break, explaining a number of well-established reactivity concepts such as the Hammond postulate, the Bell–Evans–Polanyi principle, and the Marcus theory. Both these chapters make easy reading as the arguments follow a clear sequence. However, they could have been improved by including a little more detail, especially in the treatment of the Marcus theory. Chapter 6 discusses empirical structure–reactivity relationships that are not based on a theoretical model, such as the Hammett and Brønsted relationships. In Chapter 7 the author provides the reader with all the theoretical tools needed to apply the VBCM theory qualitatively: the excitation energies, electron affinities, and ionization potentials. Chapter 8 then deals with solvent effects on reaction rates, describing various classical procedures for quantifying such effects, and finally considering solvent effects in terms of the VBCM theory.

The third section of the book is entirely devoted to applications of the VBCM theory to various types of reactions. In accordance with the historical development of the theory it is natural that the greatest emphasis is given to nucleophilic substitution reactions and to general considerations regarding the reactivity of nucleophiles. The last chapter describes recent work by the author on the reactivity of free radicals and carbenes and the application of the VBCM model to pericyclic reactions.

The author writes in an excellent and didactically clear style, both in explaining fundamental concepts and in discussing the many well-chosen examples; thus the central features of the VBCM theory come out especially clearly. Pross confines the discussion to considerations of energy level diagrams and variations in the initial excitation energy, and thus all aspects are treated qualitatively and in a comparative way. This makes the book especially suitable for the readership intended by the author, defined as "advanced undergraduate and graduate students as well as researchers in organic chemistry". The quantitative application of the VBCM theory has already been treated in a monograph by S. Shaik et al. published in 1992 and reviewed in this journal (*Angew. Chem.* **1993**, *105*, 1277; *Angew. Chem. Int. Ed. Engl.* **1993**, *32*, 1106). Perhaps the only complaint about this excellent introduction is that nearly all the publications on the VBCM theory cited here originate either from the author himself or from S. Shaik. Proposed extensions to the VBCM theory, such as those discussed in the literature by V. Parker, are not mentioned. Also the chosen examples are rather one-sided, in that they illustrate the scope but not the limitations of the VBCM theory. These become especially evident in reactions with very low energy barriers, such as those between nucleophiles and radical cations, and generally in bimolecular reactions where intermolecular attractive forces come into play.

Hendrik Zipse
Institut für Organische Chemie
der Technischen Universität Berlin
Berlin (Germany)

Organomagnesium Methods in Organic Synthesis. (Series: Best Synthetic Methods.) By *B. J. Wakefield.* Academic Press, London, 1995. 249 pp., hardcover £ 50.00.—ISBN 0-12-730945-4

Like the other volumes of this series, the book reviewed here is designed to inform synthetic organic chemists about the capabilities, advantages, and limitations of a particular class of synthetic methods from a practical standpoint. The approach is based not only on describing many examples from the literature but also on giving detailed laboratory procedures for carrying out the preparations. From this the reader can quickly gain a comprehensive picture of the reaction conditions, the techniques used, and the work-up procedures.

The first of the 16 chapters in this volume deals with general aspects, beginning with a fairly brief account of the structures and reactive properties of organomagnesium compounds, then discussing in more detail the methods for handling and using them. The author discusses the different solvents used and describes the techniques for working in an inert environment and performing titrations. This is followed by a chapter of more than fifty pages on the preparation of organomagnesium compounds, including detailed descriptions of 25 laboratory procedures. As well as methods based on activation of magnesium metal, this includes routes that start from other organomagnesium or organolithium compounds, and ligand exchange reactions. The chapters that follow describe applications of organomagnesium compounds in synthesis. The list includes addition reactions of alkenes, alkynes, carbon–nitrogen multiple bonds, carbonyl compounds, and thiocarbonyl compounds, followed by substitutions at carbon atoms, reactions yielding carbenes and arynes, reactions with acidic compounds, methods for forming carbon–nitrogen, carbon–oxygen, carbon–sulfur, carbon–selenium, carbon–tellurium, and carbon–halogen bonds, and methods for synthesizing organoboron, organophosphorus, organosilicon, and various organometallic compounds.

Reaction mechanisms are also explained in some cases, but the emphasis remains firmly on practical synthetic applications. The great value of the book lies in its presentation of the broad scope of applications of organomagnesium compounds, in the wealth of examples that are described, and in the detailed descriptions of experimental procedures. The examples from the literature are closely integrated with the selected laboratory recipes. In addition there are tables referring the reader to other published examples. Unfortunately the laboratory procedures are not easily distinguished at a glance from the main text, which would have made for easier reading. However, a very positive aspect of these descriptions is the attention to the detailed needs of the user, including not only valuable advice about special points concerning the reactions, but also about possible difficulties, such as side-reactions that may occur, or the extent to which the reaction is or is not compatible with the presence of certain functional groups. The coverage of the literature is very thorough, including some references as recent as 1994. The inclusion of the laboratory recipes in the list of contents is a useful aid, but it would also have been helpful to provide in addition a "graphic abstract" for quick access to the information.

To summarize, this should not be regarded as a textbook (nor is it intended to

 © VCH Verlagsgesellschaft mbH, D-69451 Weinheim, 1996 0570-0833/96/3516-1867 $ 15.00+.25/0

be), but it can be thoroughly recommended as a very useful reference source for libraries and for all chemists wishing to use organomagnesium compounds in synthetic work.

Sabine Laschat
Organisch-chemisches Institut
der Universität Münster (Germany)

Multidimensional NMR in Liquids. Basic Principles and Experimental Methods. By *F. J. M. van der Ven.* VCH Verlagsgesellschaft, Weinheim/ VCH Publishers, New York, 1995. 400 pp., hardcover DM 85.00.— ISBN 1-56081-665-1

This book is an up-to-date introduction to multidimensional NMR spectroscopy as applied to biomolecules. It has been written for chemists, biochemists, and biologists interested in problems of molecular structure, who wish to gain a deeper understanding of NMR spectroscopy and have the necessary background in physical chemistry. The mathematical and physical fundamentals of NMR spectroscopy are presented in an exemplary way, without assuming a great deal of previous knowledge. The theoretical tools introduced are later used repeatedly and consistently in the applications part of the book to describe pulsed NMR experiments, thus enabling the reader to relate them directly to practical situations. A particular peptide (His-Val-Tyr) and a protein (the Pf3-DNA binding protein) appear frequently thoughout the book as standard example molecules to illustrate and explain the various NMR experiments used in determining the structures of biomolecules.

The first of the six chapters begins by explaining the vector formalism used for NMR spectroscopy, and basic concepts such as radiofrequency pulses, the rotating frame, off-resonance effects, the free precession of a spin, and Bloch-Siegert effects. This is followed by a more technically-orientated description of the main components of an NMR spectrometer and of data processing methods. At the end of this chapter the author introduces the density matrix, and discusses the relationship between the quantum-mechanical description of a spin in Liouville space and the vector formalism.

Chapter 2 is concerned with the fundamental properties of multi-spin systems, introducing the scalar coupling and the chemical shift as the dominant parameters. The role of these parameters in the development of a spin system as a function of time is described using the product operator formalism, according to the theory formulated by the author simultaneously with the work of Sørensen, Bodenhausen, and Ernst. The product operator formalism using cartesian basis operators plays a central role in the description of NMR experiments throughout the book. The phenomenological description of relaxation in the product operator formalism is briefly discussed. The chapter ends by introducing and explaining the most important terms in the spin Hamiltonian operator (the chemical shift, the spin-spin coupling, and the interaction with the r.f. field).

Chapter 3 shows how a one-dimensional NMR experiment can be described as an assembly of modules in which the basic building blocks are a 90^0 pulse and a 180^0 pulse. These can produce many different effects, such as refocussing of the precessing spins, modulation of the J-coupling, the appearance of a spin-echo, etc. This chapter also describes experiments for measuring the longitudinal and transverse relaxation times and for calibrating pulses, and various types of experiments using heteronuclear detection, such as the well-known INEPT and DEPT procedures. Lastly some more complicated building blocks are described, such as "composite" pulses and decoupling sequences. Because ever more new and improved pulse sequences are continually being introduced, the author is here less concerned with evaluating the existing sequences than with showing the reader what factors should be considered in assessing the usefulness of any newly developed pulse or decoupling sequence.

Chapter 4 is concerned with two-dimensional NMR spectroscopy. The first 60 pages of the chapter are devoted to the COSY experiment, which was the earliest type of 2D experiment and is the simplest. The underlying philosophy here may have been that once one has understood the COSY experiment one has the key to the whole of 2D NMR spectroscopy. This method serves as an example for explaining various tools of 2D NMR spectroscopy, including phase cycles, field gradients, the BIRD pulse sequence, sign differentiation in indirect dimensions (TPPI, states, states-TPPI, etc.), multiquantum filters, and small flip-angle pulses. The other basic mixing schemes for magnetization transfer are then described: Hartmann-Hahn mixing, NOESY via the nuclear Overhauser effect, then ROESY and TOCSY. This is followed by a discussion of heteronuclear correlation experiments with proton detection (HSQC, HMQC, HMBC). Correlation experiments with heteronuclear detection are now scarcely used at all for applications to biomolecules, and are therefore not discussed further. The chapter ends with a detailed discussion of "coherence order pathways", which form the basis for the design of phase cycles and pulsed gradient sequences for suppressing unwanted signals.

Chapter 5 moves on to n-dimensional NMR spectroscopy. Many different experiments of this kind have been developed during the last six years. The author describes the most useful of these, using the product operator formalism. These are arranged in order of the complexity of the pulse sequences rather than according to the spectral or chemical information that they yield. A number of important experiments are described, including 3D and 4D versions of NOESY-HMQC, HCCH-TOCSY, HNCO, HN(CO)CA, and CBCA(CO)NH. Those treated here are only a selection of the many different methods that can be applied to tasks such as determining the structure of a protein. However, the author clearly explains the principles on which the sequences are based, so as to enable the reader to understand the original publications and to evaluate new sequences. The spectral information yielded by these methods plays only a secondary role in the discussions.

The final chapter is devoted to relaxation. This is undoubtedly the most difficult topic to treat. The author first sets out the fundamental principles of relaxation using the example of stochastic fields, leading to simple derivations of the most important mathematical expressions for dipolar relaxation (NOE, ROE, T_1, and T_2). He then goes on to derive a formalism for relaxation in terms of the density matrix. After a brief résumé of the Wangsness-Bloch-Redfield relaxation theory he then calculates the double commutators needed to describe the most important magnetic interactions, namely the dipolar relaxation and the chemical shift anisotropy, and the cross-correlation between these interactions. In contrast to the previous chapters, this chapter on relaxation devotes relatively little attention to relating the results to spectroscopic practice. However, the bibliography for this chapter includes references to review articles and other publications describing relevant experiments and the types of information that they can give about the dynamic structures of biomolecules.

The book can be thoroughly recommended for everyone who wishes to gain a deeper understanding of the applications of NMR spectroscopy to biomolecules in solution. It is unrivalled in its up-to-date

 © VCH Verlagsgesellschaft mbH, D-69451 Weinheim, 1996 0570-0833/96/3516-1868 $ 15.00+.25/0

coverage, in the thoroughness of the theoretical treatment, and in the skill of presentation.

Frank van der Ven died in March this year. His death is a painful loss for the many people who knew Frank. His scientific ability and, not least, his skill in teaching others in the field of NMR spectroscopy were outstanding. This book is an eloquent testimony to the deep understanding, sharp reasoning, and care that characterized his research.

Christian Griesinger
Institut für Organische Chemie
der Universität Frankfurt (Germany)

Chemistry of Waste Minimization. Edited by *J. H. Clark*. Blackie, Glasgow, 1995. 554 pp., hardcover £ 89.00.—ISBN 0-7514-0200-6

Attitudes towards caring for the environment are currently undergoing a shift in many sections of society, away from correcting damage towards preventing it in advance. In order to move towards a sustainable pattern of development that safeguards the future environment, the habits of both producers and consumers must change, and this will require some fundamental changes of attitude and also cause some others. For the chemical industry the future will demand a changeover to an ecologically orientated chemistry. The book *Chemistry of Waste Minimization* is an important contribution on this topic, in which J. H. Clark of the University of York has brought together 22 authors from universities and the chemical industry in Great Britain to cover this complex subject in 16 chapters of widely differing content.

In the introductory chapter T. Lester develops some general principles for the book as a whole, and defines the subject as follows: "Waste minimization involves any technique, process or activity which either avoids, eliminates or reduces a waste at its source, usually within the confines of the production unit, or allows reuse or recycling of the waste for benign purposes."

In the second chapter W. Braithwaite examines the industrial aspects of waste minimization, emphasizing that wherever possible this should be achieved in the production process itself, i.e. at the source. Of course the generation of waste products can never be completely eliminated, but wherever possible they should be recycled. Disposal of wastes into the environment should only be considered in cases where they can be treated in such a way that they have no harmful effects on ecosystems. The waste disposal costs must always be taken into account in the economics of the process. A process that at first sight seems expensive may then be found to be actually cheaper than one that generates a lot of waste which is costly to dispose of. Here it is important that chemists and chemical engineers should work closely together.

In Chapter 3, by P. J. Kinley, the environmental legislation in Great Britain, Europe, and the USA is described, and its effects on the chemical industry are discussed.

After these introductory chapters which are of a fairly general nature, we move on to chemistry. What contributions can chemistry offer in this area? There are undoubtedly many, and the selection presented in Chapters 4–16 often strikes one as rather arbitrary.

Catalysts which allow one to carry out a chemical reaction more selectively can make an important contribution. Chapter 4, by K. Smith, C. V. Fry, and M. Tzimas, deals with clays, zeolites, and other types of catalyst supports, and with the reagents used in this form and their applications to various reactions. As one expects, the examples are chosen on the basis that they are more environmentally friendly than conventional processes. However, no quantitative comparisons are made, nor are there any examples of processes that are already being operated commercially.

Chapter 5 (S. J. Tavener and J. H. Clark) describes the principles and applications of phase transfer catalysis. The authors state that "Phase transfer catalysis clearly has an important role to play in a cleaner future", but regrettably they do not support this by citing quantitative studies or giving an example.

Chapter 6, by D. C. Sherrington, contains a detailed description of the design and application of polymer supports for solid state syntheses. In Chapter 7, B. M. Adger reviews methods for synthesizing chiral compounds and describes several interesting examples of industrial applications. G. Webb and J. M. Winfield then examine in Chapter 8 the alternatives to chlorofluorocarbons and halogenated fire retardants.

Chapter 9 (W. R. Sanderson) is an excellent survey of the use of hydrogen peroxide as an environmentally friendly oxidizing agent for treating chemical wastes and as a reagent in syntheses, including many examples of industrial applications. Chapter 10, by T. J. Mason and S. S. Phull, is concerned with sonochemistry, including sonoelectrochemistry, and the use of these methods in synthesis and in waste water treatment. Chapter 11 (K. Scott) describes the many different applications of electrochemistry in treating chemical wastes; these include the recovery of metals from aqueous effluents, the treatment of effluents containing harmful substances such as cyanides, phenols, or organochloro compounds, and the removal of SO_2, H_2S, NO_x, or Cl_2 from gas emissions. However, electrochemical syntheses are only treated briefly. In Chapter 12, J. H. Atherton and I. K. Jones discuss the problem of choosing the best solvent for a reaction.

Chapter 13, by M. J. Ramsden, discusses the problem of polymer recycling, then in Chapter 14 P. H. Walton deals with the important question of the precipitation of metals from aqueous wastes (already partly covered in Chapter 11), and here includes also biological methods. The topical theme of the decomposition of waste substances in supercritical water is discussed by A. A. Clifford in Chapter 15. In the last chapter A. J. Butterworth, S. J. Tavener, and S. J. Barlow describe some further examples of the use of catalysts in the synthesis of fine chemicals. Enzymes are treated briefly, but more space is again devoted to zeolites and montmorillonite catalysts.

The appearance of this multiauthor work is to be welcomed. It should be available in every library and industrial chemical plant. Practitioners of applied chemistry will find in it many useful ideas for applying to their own operations, and it will help synthetic chemists involved in basic research to devise new synthetic routes that are more environmentally acceptable.

Jürgen Metzger
Fachbereich Chemie, Organische Chemie
der Universität Oldenburg (Germany)

Fifty Years of Free Radicals. (Series: Profiles, Pathways, and Dreams. Series editor: *J. I. Seeman.*) By *C. Walling*. American Chemical Society, Washington, DC, 1995. XXVI, 141 pp., hardcover $ 24.95.—ISBN 0-8412-1830-7

"Cheves Walling is one of the founding fathers of radical chemistry. He helped set the parameters twenty years before the explosive growth of the field. His work pervaded the thinking in radical chemistry... Radicals are not in general very selective, they are unusually reactive; but they are quite valuable in the craft that is synthesis. It just took many years for synthetic

 © VCH Verlagsgesellschaft mbH, D-69451 Weinheim, 1996 0570-0833/96/3516-1869 $ 15.00+.25/0

chemistry to catch up with Walling's contributions."

This statement by Albert Padwa, a professor at Emory University and a former student of Walling's at Columbia University, is not just a tribute to his mentor but a reflection of the fact that the current trend toward using free radicals in synthetic organic chemistry is based on Walling's pioneering contributions. In this 17th and latest volume, one of the shortest, in Jeff Seeman's projected 22-volume series of autobiographies of 20th-century organic chemists, Walling, a whimsical but classical gentleman-scholar with a quirky sense of humor, who often wears outrageously garish neckties and loud Hawaiian shirts to faculty and other professional meetings, modestly describes his life and career, with extensive discussions of the work of his students and of other chemists as well as his own. Thus most of the 52 informal photographs that grace this slim volume are of students and colleagues, with or without Walling, at the various meetings or places that he visited during his extensive travels.

Cheves Thomson Walling was born in Evanston, Illinois on February 28, 1916. His unusual first name derives from his great-great-grandfather, Langdon Cheves, who had been speaker of the U.S. House of Representatives and president of the Bank of the United States during the early 19th century. His parents were relative liberals in a conservative community who impressed upon him that success carried with it an obligation to public service and to those who were less fortunate, a trait that he exhibited throughout his life. Although there were no scientists in his direct family, as a youth he became interested in the physical world around him. His interest in chemistry dated from his encounter with a friend's chemistry set during the summer of 1925, and chemistry was the first branch of science that he encountered that he could actually do something about rather than merely read about. He did not take chemistry in high school and was largely self-taught in science.

In 1933 Walling enrolled in Harvard University, where, as an undergraduate, he worked with Charles H. ("Hap") Fisher, which led to his first two publications—on side-chain reactions of benzene derivatives. After his graduation in 1937, he enrolled in the University of Chicago, where he could work on free radicals with Morris Kharasch and continue his education nearer to home. That year three seminal publications on free radical intermediates that influenced his career appeared—Donald H. Hey and William A. Waters' review of free radical intermediates in solution (*Chem. Rev.* **1937**, *21*, 169); Kharasch's formulation of a bromine atom chain mechanism (*J. Org. Chem.* **1937**, *2*, 288); and Paul J. Flory's analysis of vinyl polymerization as a radical chain reaction (*J. Am. Chem. Soc.* **1937**, *59*, 241). Walling was so impressed with the first article that a half-century later he paid tribute to it in his own article, "Fifty Years of Free Radical Chemistry" (*Chem. Br.* **1987**, *23*, 767), from which the title of the book under review here was undoubtedly derived.

On receiving his Ph.D. degree in 1939, Walling accepted a position at E. I. du Pont de Nemours' Deepwater, New Jersey laboratory, where he worked on azo dyes and other substances. In 1940 he married Jane Wilson, a Vassar graduate whom he had met in Winnetka, Illinois. The couple had four daughters and a son. Frustrated by the largely empirical "Edisonian research" at Du Pont, in 1943 Walling moved to the U.S. Rubber Company in Passaic, New Jersey, where he worked on various aspects of polymer chemistry, which had become vitally important to the war effort, such as structure and reactivity in radical chemistry, emulsion polymerization, free radical additions, polyethylene, and autoxidation. In 1949 he became head of organic research at Lever Brothers Company in Cambridge, Massachusetts, where he was concerned with synthetic detergents and the development of new products and processes.

In 1952 Walling realized his longtime goal of returning to basic research when Louis P. Hammett, who, along with Frank Mayo, Paul Bartlett, and Frank Westheimer, was his scientific hero and role model, invited him to join the faculty of Columbia University. Here, during the 1950s and 1960s, his time in industry helped him to connect fundamental science with commercial practicality and to produce his most significant work—on high-pressure reactions; free radicals in solution (his book with this title appeared in 1957); hypochlorite chemistry and halogen carriers; alkoxy, thiyl, and phosphoranyl radicals; radical cyclizations; and peroxide chemistry. He was also a member of the American Chemical Society's Committee on Professional Training (1962–1975), serving as chairman from 1964 to 1972.

In 1969, disillusioned by the student revolts of the 1960s and because, in his words, "I had always liked the West. I'd gotten restless and felt the need for a change", Walling became Distinguished Professor of Chemistry at the University of Utah at Salt Lake City, where, in addition to continuing his peroxide and hypochlorite studies, he worked on hydroxyl radicals, radical cations, and chemically induced dynamic nuclear polarizations (CIDNP). In predicting the future of his field, he states, "The real frontier... is the understanding of the place of radicals as transient intermediates in living processes."

Walling taught undergraduate organic chemistry and graduate courses in physical organic chemistry and in kinetics as well as an experimental course on science, technology, and society. He also served as editor of the prestigious *Journal of the American Chemical Society* (1975–1981). In 1991 he retired and with his wife moved to their summer home in Jaffrey, New Hampshire.

In his last chapter Walling devotes a 7-page section to a unique insider's view of the cold fusion controversy, the bizarre and frustrating project on which he spent his last two years at Utah. He became involved by offering to assist Stanley Pons, then chairman of the Chemistry Department, and Martin Fleischmann. A compassionate man, Walling felt strongly that the two collaborators, both scientists whom he knew and respected, should be considered innocent before being judged guilty. When they and the university were overwhelmed by inquiries and visitors, many of these were referred to Walling, and he was drawn into the project, serving as consultant and advisor to the National Cold Fusion Institute (NCFI) until it closed and he retired in June 1991. He relates that "Fleischmann and Pons became increasingly secretive and began to consider critics as enemies." When the two learned that he was collecting data on his own, they were furious, demanded that the work stop, and regarded him as an enemy. In Walling's view, "the anomalous heat evolution... seems to be a real phenomenon, although its occurrence is still quite unpredictable", but he concludes, "Currently the field is in such bad repute in the United States that only a rash young investigator or student would touch it, and almost no money is available. I'd like to know the answer even if it does turn out to be trivial."

Although Walling was always available to students, he states, "I was not a demanding research supervisor. Students worked on their own. I was a better supervisor for people who themselves were quite good. Almost all of my students got their degrees." According to Utah colleague Peter Stang, "Walling's high standard of excellence and gentlemanly demeanor served as the role model for

 © VCH Verlagsgesellschaft mbH, D-69451 Weinheim, 1996 0570-0833/96/3516-1870 $ 15.00+.25/0

young faculty as well as students". Walling admits, "I wasn't as much interested in contact with students as I was in understanding physical phenomena and explaining them to other people". He won the 1970 James Flack Norris Award in Physical Organic Chemistry.

Like many of the other authors in Seeman's series, Walling summarizes his career in a few words: "To someone of my temperament, being able to pursue my curiosity through research and reading with freedom and adequate support and to receive some recognition for my work have been all I could ask for. I can't think of anything I'd rather have done... I'm also conscious of the part that chance (or luck) has played in my career."

This entertaining, informative, and attractively priced volume will be of interest to both present and future generations of students and instructors of chemistry and history of chemistry courses as well as to practicing chemists interested in the humanistic aspects of their science.

George B. Kauffman
California State University, Fresno
Fresno, CA (USA)

Symmetry and Structure. Readable Group Theory for Chemists. 2nd edition. By *S. F. A. Kettle*. Wiley, Chichester, 1995. 416 pp., paperback £ 18.99.–ISBN 0-471-95476-4

This book is intended mainly for chemistry students. The title is rather misleading, as the book is not basically about the symmetry of crystal structures. Instead it is an introductory text concerned with the relationship between the geometrical and electronic structures of molecules and their symmetry. Using the chemical bond as an example, the reader is introduced to group theory in a way that is both unconventional and easy to understand. The book consists of 13 chapters and six appendices. The changes that have been made in this second edition are mainly small, but two additional chapters have been included, on space groups and on spectroscopic studies of crystals.

Chapter 1 (9 pp.) describes different models for the bonding in the ammonia molecule. Chapter 2 (25 pp.) contains a lucid elementary introduction to point groups, group tables, character tables, and irreducible representations, using the water molecule as an example. Chapter 3 (28 pp.) then deals with the orthonormality properties of irreducible representations, the separation of reducible representations into their irreducible components, transformation properties of atomic orbitals, symmetry-adjusted combinations of orbitals, interactions between bonds, and orbital energy levels; the examples used for illustration are the electronic structure of water and the point group C_{2v}. Chapter 4 (34 pp.) introduces the point group D_{2h} as the direct product of its normal subgroups C_2 and C_i, then discusses the symmetry of the atomic orbitals in C_2H_6 and B_2H_6, the bonding in these molecules, and the method of projection operators. In Chapter 5 (26 pp.) the author takes the symmetry group C_{4v} of BrF_5 as an example of a fairly complex group, and shows how the orthonormality relationships provide a way of systematically deriving a complete character table. Chapter 6 (12 pp.) discusses again symmetry and bonding in the ammonia molecule. Chapter 7 (42 pp.) is concerned with the symmetry of cubic molecules (example: SF_6) and with octahedral transition metal complexes, and introduces the point groups O, O_h, and T_d together with their character tables. Chapter 8 (11 pp.) is of a more general nature, dealing with the relationships between groups and their subgroups and between the irreducible representations of a given group and those of its subgroups. Chapter 9 (14 pp.) explains how the symmetry of a molecule is related to its vibrational spectrum and introduces the normal modes of vibration. Chapter 10 (22 pp.) deals with the important topics of the direct products of irreducible representations, products of wave-functions, the symmetry of different electronic configurations, and spectroscopic selection rules. In Chapter 11 (18 pp.) the author introduces complex characters, illustrated by the relatively simple example of the π-orbitals of cyclobutadiene with C_4 symmetry, and discusses the occurrence of optical activity. Next, in Chapter 12 (46 pp.), we move from point groups to space groups. The chapter deals in turn with the crystal systems, the Bravais lattices, the crystallographic point groups, symmorphic and asymmorphic space groups, Hermann-Mauguin symbols, and unit cells. The final chapter (15 pp.) is devoted to spectroscopic investigations of crystals. The author shows that because most of the phenomena on which spectroscopic measurements depend are translationally invariant, one can in general limit the discussion to the factor groups of the space groups with respect to their translation subgroups, i.e. to point groups.

Appendices 1 and 2, covering 42 pages, give a brief mathematical introduction to group theory and to the matrix representations of groups. Appendix 3 contains the character tables of the "most important" point groups, namely I_h and I, O_h, O, T_d, T_h and T, D_{nh}, D_{nd}, D_n, C_{nv} and C_n (all with $2 \leq n \leq 6$), C_{2h}, C_{3h}, C_i, S_4, C_s and C_1. Appendix 4 (15 pp.) contains a derivation of the group orbitals with π-symmetry for fluorine in SF_6. Appendix 5 (5 pp.) treats the point groups $C_{\infty v}$ and $C_{\infty h}$. Appendix 6 consists of two tables listing the Schoenflies and Hermann-Mauguin symbols for point groups alongside each other.

With its lucid and unconventional mode of presentation the book makes good reading and is on the whole easily understandable. The number of printing errors is not excessive. Unfortunately, however, these comments do not apply to the last two chapters which have been added for this second edition, and they are especially untrue in the case of Appendix 6, where there is a much higher incidence of errors and the presentation is far from clear. Many of the Hermann-Mauguin symbols are garbled in such a way that it is difficult to identify the groups. These chapters cannot be recommended to anyone as an introduction to space groups. They should be either left out completely or thoroughly rewritten at the earliest opportunity.

Elke Koch
Institut für Mineralogie, Petrologie
und Kristallographie
der Universität Marburg (Germany)

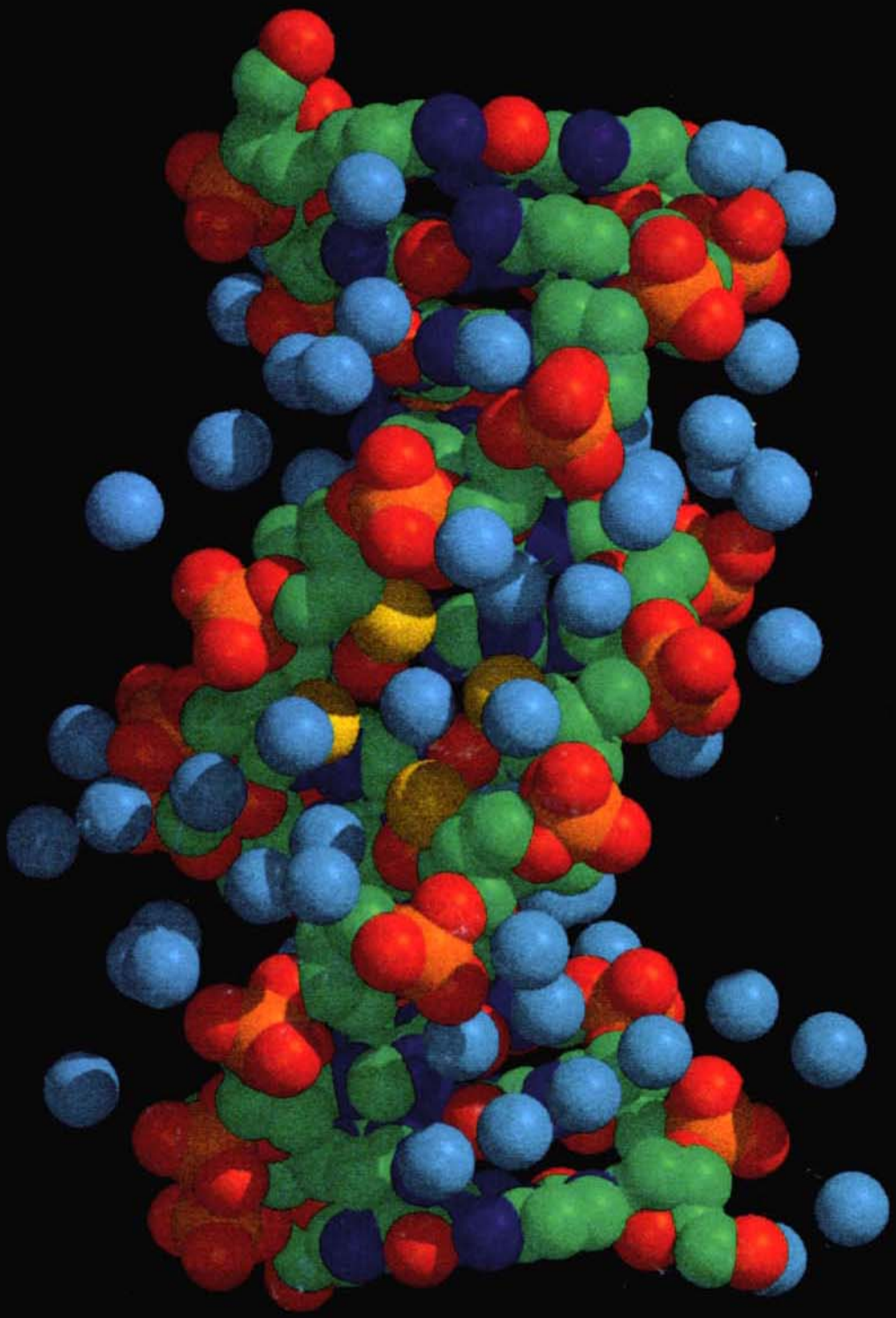

Hydration of the B-DNA duplex [d(CGCGAAT^{Me}T^{Me}CGCG)]$_2$ (T^{Me} = carbocyclic 6´-α-methylthymidine). Water molecules are shown as light blue spheres; the carbon atoms of the α-CH_3 substituents in the modified thymidine residues are represented by yellow spheres.

Structural Aspects of Nucleic Acid Analogs and Antisense Oligonucleotides

Martin Egli*

Hybridization of complementary oligonucleotides is essential to highly valuable research tools in many fields including genetics, molecular biology, and cell biology. For example, an antisense molecule for a particular segment of sense messenger RNA allows gene expression to be selectively turned off, and the polymerase chain reaction requires complementary primers in order to proceed. It is hoped that the antisense approach may lead to therapeutics for treatment of various diseases including cancer. Areas of active research in the antisense field focus on the mechanisms of cellular uptake of antisense molecules and their delivery to specific cell sites, an improved understanding of how these molecules inhibit the production of proteins, as well as the optimization of the chemical stability of antisense molecules and the thermodynamic stability of the duplexes they form with the mRNA targets. The last two issues in particular have prompted chemists to launch an extensive search for oligonucleotide analogs with improved binding properties for hybridization with RNA and higher resistance toward nuclease degradation. During the last years this research has resulted in a flurry of new chemical analogs of DNA and RNA with modifications in the sugar–phosphate backbone as well as in the nucleobase sites. However, to date little effort has been directed toward uncovering the exact origins of the gain or loss in stability when nucleic acid analogs bind to RNA. Although large amounts of thermodynamic data have been collected, the structural perturbations induced by the modifications in hybrid duplexes are only poorly understood. For many modified oligonucleotides the compatibility of protection, coupling, and deprotection chemistry with standard DNA and RNA synthesis protocols makes it now possible to generate modified nucleic acid fragments or mixed oligonucleotides containing modifications at selected sites in quantities suitable for three-dimensional structure investigations. Such studies should reveal the structural origins of the observed changes in affinity and specificity of binding for particular modifications and may guide the development of second- and third-generation antisense molecules. In addition, the availability of a previously unimaginable variety of modified building blocks and the investigation of their structures provides the basis for a deeper understanding of the native DNA and RNA structures. This contribution will summarize the results of X-ray crystallographic structure determinations of modified nucleic acid fragments conducted in our laboratory during the last three years and the insights gained from them.

Keywords: crystal structure analysis · DNA · hydrogen bonding · RNA

1. Introduction

The precisely ordered strings formed by the four nucleotide bases adenine (A), thymine (T), guanine (G), and cytosine (C), and the formation of complementary, hydrogen-bonded A–T and G–C base pairs provide the foundation for gene structure and expression. In chromosomes the DNA usually exists in the form of an antiparallel double helix composed of the sense strand and the antisense strand. Pairing specificity is the underlying principle of all biological information transfer—replication, recombination, transcription, and translation. In bacteria and viruses hybridization between sense RNA and antisense RNA is a common mechanism for regulation as well as inhibition of gene activity. Both replication and transcription were shown to be controlled by such mechanisms in prokaryotes.[1–4] In order to control replication of the *E. coli* plasmid ColE1, a sense–antisense RNA complex is formed between two complementary loop structures.[5, 6] These initial observations of a natural mechanism to suppress genetic information via nucleic acids were followed by a decade of intense exploration of the possibilities and limits of the antisense approach.

Antisense RNA need not necessarily be administered through expression vectors, but can be injected into cells in the form of short synthetic oligonucleotides. In addition, it was first shown by Zamecnik and coworkers that DNA can also be utilized to effectively inhibit protein expression.[7, 8] Messenger RNA in the unprocessed and processed state is not the only possible target; interference with the protein expression pathway can in

[*] Prof. M. Egli
Department of Molecular Pharmacology and Biological Chemistry
Northwestern University Medical School
303 East Chicago Avenue
Chicago, IL 60611-3008 (USA)
Fax: Int. code +(312)503-0796
e-mail: m-egli@nwu.edu

 © VCH Verlagsgesellschaft mbH, D-69451 Weinheim, 1996 0570-0833/96/3517-1895 $ 15.00+.25/0

principle also occur at the gene level. However, this approach is thus far restricted largely to homopurine target sites that allow triplex formation with the antigene strand.[9-11] More effective control of gene expression may be exhibited by antisense RNAs with functional properties, for example *trans*-acting hammerhead ribozymes that can cleave a target message after the sequence UH (H = A, C, or U) and will thus not only inhibit but actively degrade the sequence.[12, 13]

The experience gathered in various areas of the antisense field during the last years has indicated several critical points that must be addressed should the antisense technology become applicable in the treatment of human diseases. These obstacles for antisense drug development will only be briefly addressed here; most aspects have been exhaustively treated in a series of excellent recent reviews and books.[14-33] Potential pitfalls to successful application of antisense therapeutics are the often low cellular uptake and the insufficient chemical stability of natural and chemically modified oligonucleotides against degradation by various nucleases. Once resistant against nucleases and efficiently delivered, a modified oligonucleotide may not sufficiently discriminate between a chosen target and other sites. Further complications can arise from the fact that most of the modified DNAs and RNAs do not induce RNase H-mediated cleavage of mRNA,[34] that folding of cellular RNAs into secondary and tertiary structures may render the selected target sites inaccessible, and that the antisense strand and target may not be found in the same location within the cell.

It is anticipated that appropriate chemical modification of oligonucleotides may help overcome some of these problems. In particular, modifications may lead to improved hybridization properties, nuclease resistance, and cell permeation. The structural framework of DNA and RNA allows a multitude of chemical modifications on the phosphate backbone and on the sugar and base moieties. First-generation analogs based on these three constituents include the phosphorothioates,[35, 36] the methylphosphonates,[37, 38] and a range of O2′-modified oligonucleotides.[39-42] The current variety of analogs is overwhelming, and the interested reader is referred to other sources such as the previously mentioned reviews.[14-33]

Among the newer generation of backbone modifications are 3′-allylethers and 3′-allylsulfides,[43] amides,[44] amines,[45] carbon chains,[46] formacetals and thioformacetals,[47, 48] guanidinium linkages,[49] 5′-methyl DNA and RNA,[50] phosphoramidates,[51] phosphorodithioates,[52] sulfides,[53] sulfonamides,[54] and sulfones.[55] The analogs with modifications on the sugar portion comprise carbocyclic compounds,[56, 57] L-2′-deoxyriboses,[58] and hexoses.[59-61] Oligonucleotides in which the pyrimidine rings have propyne substituents at C5 display promising features for antisense applications,[62] and the peptide nucleic acids (PNAs) introduced in 1994 are the analogs with the highest divergence from the native nucleic acids.[63]

The abundant number of modifications is in stark contrast to the handful of detailed structural studies of analogs using either solution NMR or modeling methods. Among those analyzed are amide-linked DNA,[64, 65] formacetal DNA,[66, 67] thioformacetal DNA,[68] urea-linked DNA,[69] phosphorodithioate DNA,[70] 2′-*O*-methyl RNA,[71] 2′-5′-linked RNA,[72] a PNA–RNA duplex,[73] and a PNA–DNA duplex.[74] In addition, structural investigations conducted with PNAs include the crystal structure of a triple-stranded nucleic acid complex, consisting of a homopurine DNA nonamer and two homopyrimidine PNA nonamers, in which the latter strands are linked through six amino acids.[75] Much more structural work will be necessary to interpret the thermodynamic stability data of oligonucleotide modifications, and to begin to understand the complex interplay between enthalpic and entropic effects, including factors such as conformational preorganization, hydration, salt concentration, and cooperativity.[76, 77]

Beyond the search for therapeutically feasible antisense compounds, recent progress in the chemical alteration of DNA and RNA provides numerous opportunities to probe nucleic acid structure[78, 79] as well as interactions between proteins and nucleic acids.[80]

2. The Structures of DNA and RNA

RNA differs from DNA by the additional hydroxyl group at the 2′-position in the ribose. This seemingly subtle difference has important consequences for the chemical and structural properties of RNA and its biological role. DNA is normally a double-stranded molecule, while RNA is single-stranded and can adopt complex folding motifs with a range of structural elements such as double-helical stems, bulges (with unpaired bases), hairpin loops, and pseudoknots.[81] DNA has been observed in two general classes of right-handed duplexes with antiparallel orientation of strands, the A- and the B-form (Fig. 1). One should keep in mind, however, that nucleic acid structure is polymor-

M. Egli was born in 1961 in Schaffhausen, Switzerland. He studied chemistry at the ETH-Zürich, obtaining his diploma in 1984 and his PhD in 1988 under Professors V. Prelog, J. D. Dunitz, and M. Dobler for the structural investigation of the enantioselectivity of simple receptors such as tartrates toward biologically interesting substrates including α-amino alcohol salts. He then joined Professor A. Rich's research group at MIT in Cambridge, MA (USA), where he studied the structure of nucleic acids, their complexes with drugs, and the properties of chimeric RNA–DNA molecules by using X-ray crystallographic methods. In 1992 he moved to the Organic Chemistry Laboratory at the ETH to pursue independent research on the structures of chemically modified DNA and RNA. This account summarizes research conducted by the author while at the ETH. In the fall of 1995 Egli joined the faculty of the Northwestern University Medical School in Chicago, IL (USA), as an assistant professor.

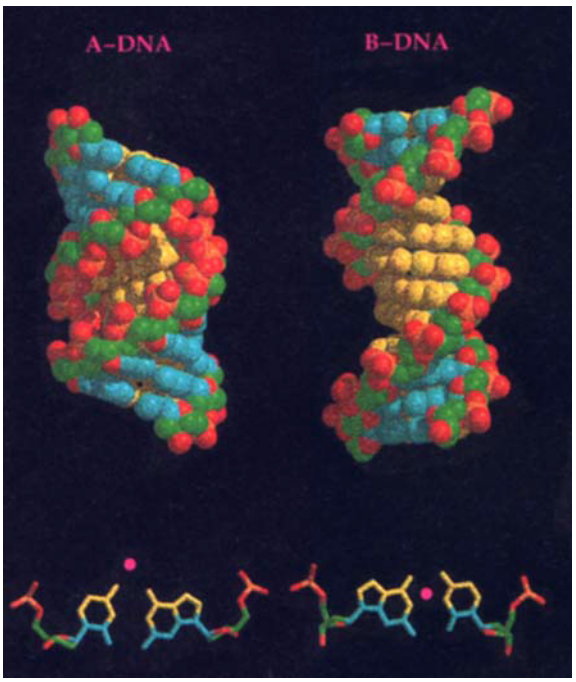

Fig. 1. Top: van der Waals models of the two basic right-handed double-helical conformations of DNA (RNA adopts an A-type duplex). The edges of the base pairs in the major groove are yellow and those in the minor groove are cyan. Bottom: Relative orientations of base pair and helix axis (pink) for A-DNA -RNA (left) and B-DNA (right) in axial projections.

phic; other stable conformations, although not necessarily double-stranded, exist.[82] In this discussion we will analyze DNA and RNA analogs in their right-handed duplex states.

Double-stranded RNA adopts an A-type conformation exclusively and is relatively inflexible. On the other hand, double-stranded DNA displays considerable conformational polymorphism and can exist in a range of conformations featuring both A- and B-like characteristics. These are influenced by the base sequence,[83] hydration state,[84, 85] the lattice contacts in a particular crystal form,[86-89] and the binding motif and interface in protein-DNA complexes,[90] among others. The crystal structure determinations of more than one hundred DNA fragments[91-94] and some four dozen protein-DNA complexes[95-98] have yielded a detailed picture of the DNA double helix. The impact of X-ray crystallography on our understanding of DNA structure and its biological role has thus far not been matched for RNA—apart from the early success with the elucidation of the tRNA structure—because of difficulties in generating highly pure RNA samples.

A- and B-type duplexes are characterized by very different topologies (Fig. 1). The major groove of the A-duplex is narrow and deep, and the minor groove is wide and shallow. The major groove of the B-duplex is wide but not as deep as that of the A-form, and the minor groove is narrower than that in the A-form but of similar depth. The A-duplex has a larger diameter and the helical axis is located in the major groove, whereas it runs through the centers of base pairs in the B-duplex. Several other features distinguish the two duplexes. The base pairs are inclined relative to the helix axis in the A-type duplex, but are more or less normal to the axis in the B-type. Phosphate groups are more closely spaced within strands in the former duplex (5.9 Å on average, B-DNA 7 Å, Fig. 2). These differences in geometry are a direct consequence of the conformational flexibility of the sugar moiety. In the A-DNA form the sugars adopt a so-called C3′-*endo* pucker, and in the B-DNA form the sugar conformation is of the C2′-*endo* type. Sugar conformations that fall into direct neighbor ranges of these two in the furanose pseudo-rotation phase cycle are also observed, but do not drastically change the overall conformations.

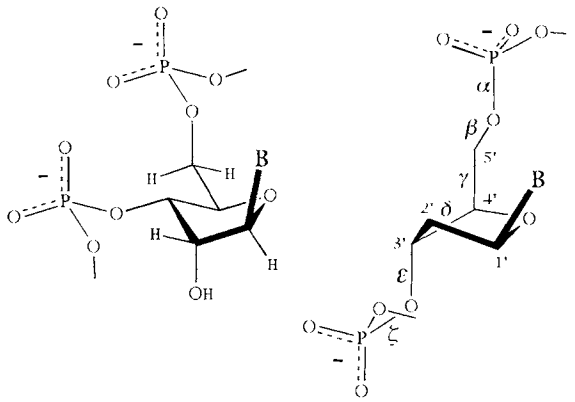

Fig. 2. Schematic diamond-lattice representations of the sugar-phosphate backbone conformations in A- and B-type duplexes. In A-DNA -RNA the six torsion angles α, β, γ, δ, ε, and ζ adopt the conformations sc^-, ap, sc^+, sc^+, ap, sc^-, respectively; in B-DNA, the conformations are sc^-, ap, sc^+, ap, ap, and sc^+. B = nucleobase.

The geometry of the sugar-phosphate backbone of oligonucleotides can be described by six torsion angles, α, β, γ, δ, ε, and ζ; the δ angle describes the torsion angle around the ribose C4′-C3′ bond (Fig. 2). In A-type duplexes δ has a sc^+ conformation, and in B-type duplexes, its conformation is *ap*. All other torsion angles fall into the same ranges in both duplexes. Readers who are not familiar with nucleic acid structure are referred to the excellent review article by Kennard and Hunter[91] for nomenclature and definitions, as well as to Saenger's book on the principles of nucleic acid structure.[99]

3. Crystallization of Oligonucleotide Analogs

3.1. Choosing the Template Sequence and the Sites for Incorporating Modified Nucleotides

A crucial step toward the exploration of chemically modified nucleic acids by X-ray crystallography is the availability of template sequences known to produce crystals that diffract reasonably well (typically to better than 2.5 Å resolution), and the determination of the number and the locations of incorporation sites with a particular nucleotide analog that will preserve crystallization. We have established such sequences and incorporation sites for both modified DNA and RNA oligonucleotides. Scheme 1 illustrates the trial-and-error approach that was used for growing high-resolution crystals of a B-DNA template containing carbocyclic residues. With this d(CGCGAATTCGCG)

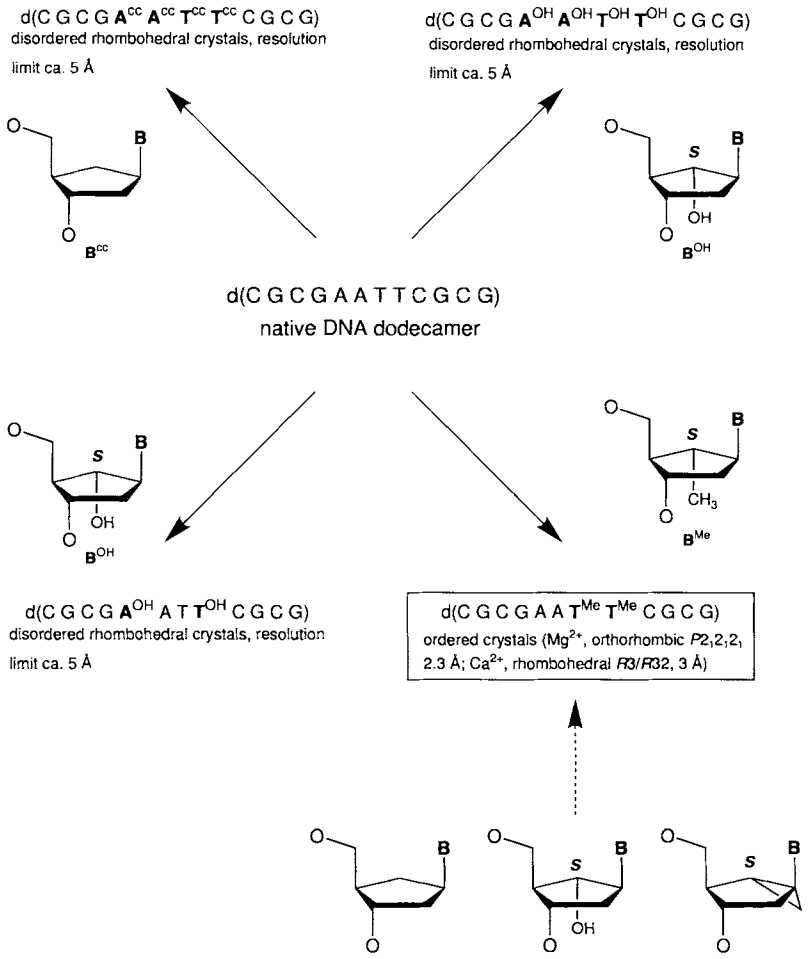

Scheme 1. Selection of incorporation sites for carbocyclic nucleotides in a B-DNA dodecamer [107] that will still yield well-diffracting crystals. Placing carbocyclic 6'-α-methylthymidines (T^{Me}) at positions 7 and 8 produced two crystal forms; the orthorhombic crystals are isomorphous with those of the native DNA oligonucleotide. Various carbocyclic analogs can now be incorporated at these sites (see bottom of scheme) with the goal of producing crystals of good diffraction quality and then comparing the structural changes.

or so-called Dickerson–Drew dodecamer, optimal crystallization results were obtained with carbocyclic analogs incorporated at locations T(7) and T(8). The dodecamer was originally selected because of its demonstrated mutation tolerance and lattice conservation in over 35 cases (NDB, Nucleic Acid Crystal Structure Data Base,[100] search December 1994).

It is now widely believed that the targeting of a particular stretch of messenger RNA with RNA analogs may hold certain advantages over the targeting with DNA analogs in terms of stability and selectivity. RNA·RNA duplexes are considerably more stable than the corresponding RNA·DNA hybrids.[101] This suggests that it is important to study RNA modifications within the context of an RNA or A-form double helix. We have relied on two template sequences for the incorporation of RNA analogs: the RNA octamer r(CCCCGGGG)[102,103] and the A-type DNA with sequence d(GCGTATACGC).[104–106]

3.2. Crystal Growth

A comparison of the conditions used to grow crystals of oligonucleotides discloses an amazing similarity between many of them. In probably more than 90% of the cases, the mother liquor components include sodium cacodylate buffer, magnesium chloride, spermine tetrahydrochloride, and 2-methyl-2,4-pentanediol (MPD) as the precipitant. At the onset of crystallization experiments with analogs, it is therefore reasonable to include these components. Obviously, such established techniques[108,109] do not always produce crystals. The conditions for growing protein crystals are considerably more diverse than those for nucleic acids. A common approach is the use of sparse matrix screens[110] that allow efficient sampling of a variety of buffers, cations, and precipitants. These screens are commercially available,[111] and modified versions have recently been applied successfully in the crystallization of medium- and large-sized RNAs .[112,113]

We have used commercial screen kits to crystallize double-helical RNA fragments. Two crystal forms of the octamer r(C_4G_4) could be grown from buffers with pH values between 4.5 and 8.5 and various precipitants, including high concentrations of ammonium sulfate, low molecular weight polyethylene glycols (PEGs), MPD, and others.[102] Successful use of smaller PEGs in the crystallization of RNA oligonucleotides has also been reported by other researchers.[114] The rhombohedral crystal form of the r(C_4G_4) octamer diffracts X-rays to exceptionally high resolution (better than 1.5 Å) and can also be grown from solutions containing 100–250 mM concentrations of various divalent metal cations (Mg^{2+}, Ca^{2+}, Zn^{2+}, etc.). Collection of high-resolution data with these crystals should enable investigation of the RNA binding modes of these ions. The particular arrangement of $[r(C_4G_4)]_2$ duplexes in the rhombohedral lattice displays no close packing contacts for many nucleotides. This renders the r(C_4G_4) sequence an ideal crystallization template for modified RNAs with alterations at a number of sites. Attempts at crystallizing such modified RNAs are under way. This example demonstrates that one should not rely only on classic crystallization ingredients but explore alternatives as well. Modifications alter the physical properties of nucleic acids, and to obtain diffraction-quality crystals of analogs, one will often have to adapt the typical DNA crystallization conditions or even choose an innovative approach.

3.3. Hydration

A deeper understanding of how antisense modifications affect the structure and stability of nucleic acid fragments requires the assessment of modification-induced hydration changes, both at the global and the local level. Besides determining the atomic coordinates, X-ray crystallography permits the visualization of the first hydration shell as well as the thermal motion of molecular fragments and water molecules. Provided atomic-resolu-

tion diffraction data is available, molecular hydration in crystals can be assessed in great detail.[103, 115] Comparison of the hydration of the same oligonucleotide fragment in distinct crystallographic environments can reveal preserved hydration patterns, and crystallization of modified fragments in the lattice of the native molecule can indicate the differences in hydration brought about by the chemical modification.

The so-called "spine of hydration" of B-DNA dodecamers is a conserved hydration pattern that involves backbone and base atoms in the minor groove.[116, 117] Crystallization of such dodecamers with substantial incorporation of nucleotide analogs that affect the topology of the minor groove (Scheme 1, Table 1) should expose alterations in the global hydration, that is, displacements and replacements of water molecules in the spine, caused by the modifications. Similarly, crystallization of oligonucleotides with built-in single modifications allows the consequences for the local hydration to be assessed. Thus, incorporation of a 2′-*O*-methyladenosine into a DNA template provided some clues on the hydration of 2′-O-methylated riboses and its contribution to the exceptional stability of RNAs methylated at the 2′-oxygen.[106]

3.4. The Modifications

Chemical modifications of DNA and RNA affect different areas in the double helix, and Table 1 summarizes the groove locations of selected sugar and base modifications. The nucleic acid modifications thus far analyzed in our laboratory with X-ray crystallography comprise bicyclo-DNA, sulfone-RNA, carbocyclic DNA, and 2′-O-methylated RNA. The chemical alterations associated with each analog are depicted in Figure 3. Three of the modifications concern the ribose moiety, but in sulfone-RNA, the neutral dimethylene sulfone linker replaces the negatively charged phosphate group. The following sections summarize the structural findings based on single-crystal X-ray analyses for each of these nucleic acid analogs.

Table 1. Location of modifications at selected sugar and base sites in the duplex (see Figs. 1 and 2).

Modification site	Location
C2′ (sugar)	minor groove
O4′ (sugar)	minor groove
C5′ (sugar) [50]	minor groove (substituent replacing H^{Re})
C5 (base)	major groove

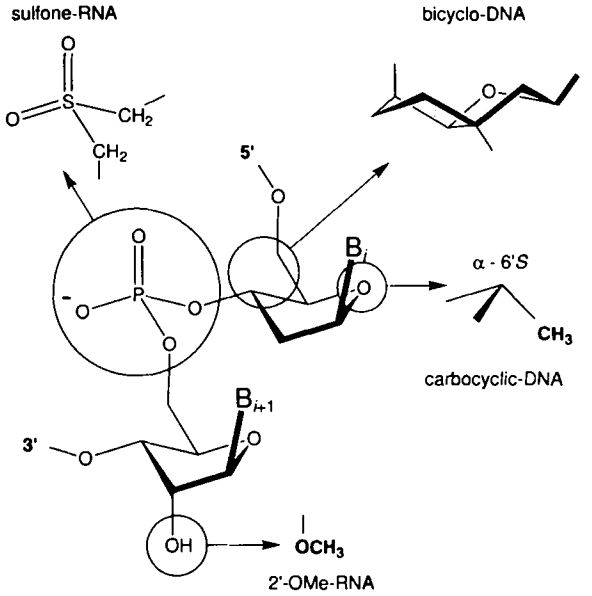

Fig. 3. Four types of DNA and RNA analogs.

4. Bicyclo-DNA

Preorganization and appropriate rigidity of the single strand are critical for the formation of stable duplexes. This was demonstrated by the drastically reduced T_m values of duplexes resulting from incorporation of open-chain glycerol building blocks into oligonucleotides,[118] as well as by the partly entropically stabilized duplexes formed by hexose-DNA.[119] Entropic stabilization of hybridization was tested in several cases. Constrained bicyclic sugar modifications include a neutral riboacetal internucleosidic linkage,[120] bicyclo-carbocyclic analogs,[121, 122] and a DNA analog with an ethylene bridge between C3′ and C5′, the so-called bicyclo-DNA (bcDNA, Fig. 3).[123] Although reduction of the entropy term upon duplex formation was achieved with the latter analogs, the affinity of the oligonucleotides containing bicyclic nucleotides for DNA and RNA was generally lower than that of the native molecules. This indicated that rigidity of the single strand alone is not sufficient for stable duplex formation, but that, in addition, the conformation adopted by the constrained nucleotide must be compatible with that of the target strand in the duplex.

The crystal structure of a bicyclic analog of the deoxycytidylyl-(3′-5′)-deoxycytidine dimer containing intranucleosidyl ethylene bridges between C3′ and C5′ (Fig. 3) was determined by X-ray diffraction at atomic resolution.[124, 125] In the crystal two bcd(CC) strands form a parallel-stranded duplex paired through hemiprotonated C–C^+ base pairs (Fig. 4). The conformations of the two single strands in the duplex deviate only minimally and, therefore, we will focus only on the conformation of the bcd(C1pC2) dimer in our discussion.

The distance between the stacked rings is 3.4 Å, and the right-handed helical twist is 34°. The paired bases display slight propeller twisting (Fig. 4, top). This arrangement leads to extensive overlap between cytosine rings within one strand, and the relative intrastrand positionings of the base carbonyl groups are likely to provide additional stability through dipole–dipole interactions (Fig. 4, bottom). The bicyclic sugars in the dimer adopt different conformations. The pucker of the C(1) deoxyribose moiety is of the C1′-*exo* type, and that of residue C(2) is of the C2′-*endo* type.

The conformations of the two cytidines also differ in their glycosidic torsion angles. Both fall into the *anti* range, but differ by about 40° (Fig. 5). Due to the conformational heterogeneity of residues in the duplex, it is impossible to build an extended parallel-stranded poly(bcdC)–poly(bcdC) duplex with continuous backbones and a single base pair as the repetitive unit.

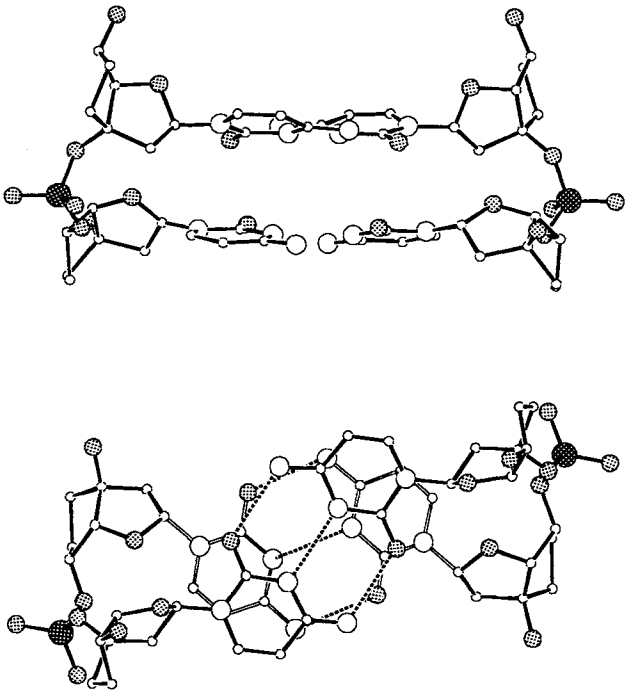

Fig. 4. The parallel-stranded [bcd(CC)]$_2$ duplex viewed along the planes of the base pairs (top), and in the direction of the helix axis (bottom). Here and in the following figures phosphorus atoms are dark gray, oxygen atoms are light gray, and hydrogen bonds are denoted by dashed lines.

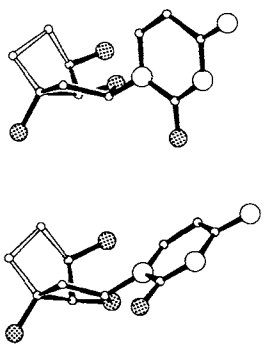

Fig. 5. Conformations of the nucleosides in bcd(CC). The deoxyribose puckers for residues C(1) and C(2) are C1′-*exo* (top) and C2′-*endo* (bottom), respectively. The ethylene bridge linking C3′ and C5′ in bcDNA is highlighted with white bonds.

In the bcDNA dimer the significant deviation from standard B-DNA geometry results in differences in the backbone torsion angles β and γ. These adopt sc^+ and *ap* conformations, respectively, in the bicyclic sugar–phosphate backbone, but are *ap* and sc^+ in B-DNA and A-RNA (where γ in an extended backbone variant can also be *ap*). The opening up of the torsion angle γ is a direct consequence of the modification in the sugar framework of bcDNA.

Cytidine-rich DNA can adopt a four-stranded arrangement composed of two interdigitated duplexes that are paired through hemiprotonated C–C$^+$ base pairs.[126] In this intercalated motif (i-motif) adjacent base pairs are about 6.2 Å apart, allowing for intercalation of base pairs from the second parallel-stranded interpenetrating duplex (Fig. 6). In this arrangement only exocyclic functions overlap, whereas the π-electron systems of the cytosine rings are not directly involved in stacking. Thus, the dipole–dipole interactions between adjacent C2=O2 carbonyl bonds and between adjacent C4–N4 bonds as well as C–H$\cdots$O4′ hydrogen bonds between more closely spaced pairs of sugar–phosphate backbones in intercalated duplexes (Fig. 6) appear to be the main stabilizing factors.[127] In the i-motif neighboring carbonyl bonds are oriented in an antiparallel fashion, while they are parallel in the [bcd(CC)]$_2$ duplex (see Figs. 4 and 6).

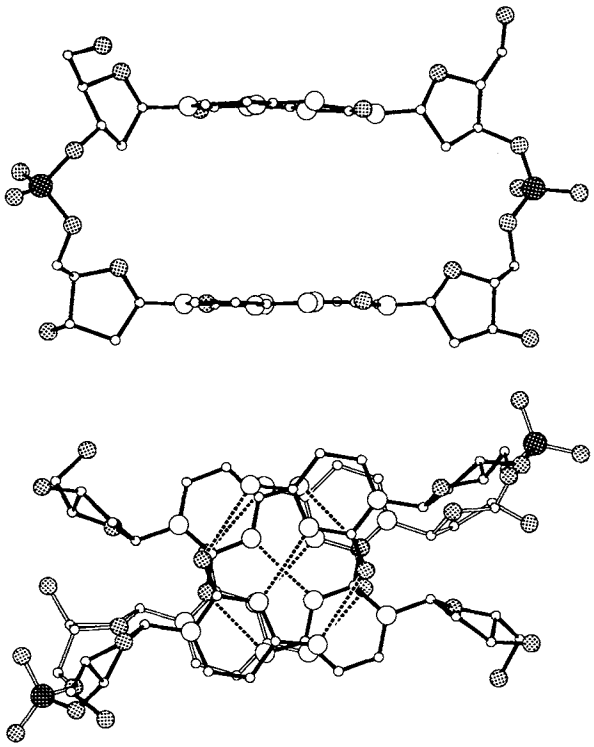

Fig. 6. The C(2)pC(3)·C(6)pC(7) base-pair step in one of the two parallel-stranded intercalated [d(CCCC)]$_2$ duplexes viewed along the planes of the base pairs (top) and in the direction of the helix axis (bottom). In the axial projection the intercalating C–C$^+$ base pair has been included and the C3–C7 base pair is highlighted with white bonds.

About half the deoxyriboses in the i-motif adopt A-type sugar puckers. The increase in the distances between adjacent base pairs in an axial direction is characterized by local changes in the backbone torsion angles. Thus, numerous α,γ pairs are found in the *ap*,*ap* range, a pattern commonly observed in the backbone region around the intercalation sites in DNA–drug complexes.[94]

The geometry of the sugar–phosphate backbone in bcDNA is different from that in B-DNA and in the i-motif. Although the ethylene bridge renders the sugar portion more rigid, the constraints introduced cause a significant deviation in strand conformation from that of a typical B-duplex and abate the entropic stability gains. To date, no diffraction-quality crystals of the native d(CC) dimer have been obtained. This may indicate that stable formation of the intercalated four-stranded motif requires a cytidine section of a minimum length. Perhaps the parallel-stranded zwitterionic bcDNA double helix constitutes an independent pairing structure that does not exist for cytidine-rich oligodeoxynucleotides.

5. Sulfone-RNA

The effect of removing the negative charge carried by phosphodiester backbones in DNA and RNA on the structure of the double helix has been relatively little studied. In duplex DNA the arrangement of negatively charged phosphates along the backbones creates a symmetric charge distribution. Disturbing this balance through neutralization of the negative charges on one face of the DNA bends the DNA toward that face.[78, 128]

With B-form DNA one can expect the degree of deformation to be more severe when the neutralization of charges concerns phosphates arranged on opposite sides of the narrow minor groove than when they flank the wide major groove.

The prospect of improved cell delivery with species that are more lipophilic than DNA and RNA has provided motivation for developing several nonionic nucleic acid analogs. Moreover, the lack of charge repulsion between phosphates in duplexes comprising an uncharged species and RNA may lead to enhanced binding stability of analogs compared with that of DNA and RNA. The methylphosphonates constitute the first uncharged nucleic acid analog. However, replacing one of the nonbridging phosphate oxygens by a methyl group leads to diastereoisomers. The dimethylene sulfone linker was conceived as a roughly isosteric, neutral, and achiral replacement for the phosphate group in DNA (Fig. 3).[55, 129] Synthetic protocols have recently been developed for the synthesis of dimethylene sulfone linked RNA.[130] The consequences of charge removal on the geometry of the RNA double helix were analyzed in the crystal structure of the dimethylene sulfone linked ribodinucleotide analog r(G-SO_2-C).[131] This crystal structure revealed that the neutral RNA analog adopts a relatively regular portion of a right-handed Watson–Crick-type double helix (Fig. 7). Overall,

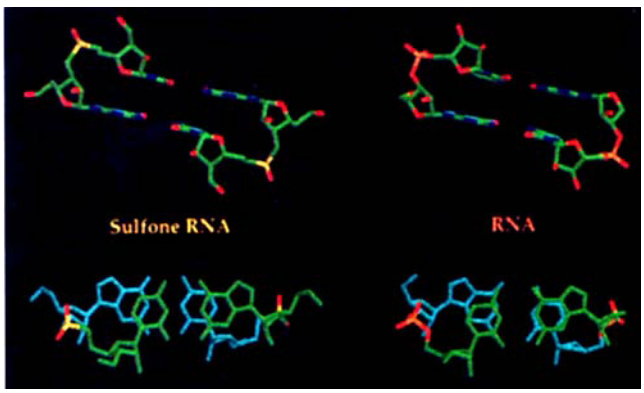

Fig. 7. The double helices formed by the nonionic dimethylene sulfone RNA analog r(G-SO_2-C) and the natural RNA dimer r(GpC) [132,133]. The images in the top half of the figure are projections into the minor groove, approximately along the crystallographic twofold rotation axes, and those in the bottom half are projections along the normal to the plane of the top base pair (green bonds). Sulfur atoms are yellow and phosphorus atoms are orange.

this duplex is quite similar to the one formed by the natural r(GpC) RNA dimer. Although the dimethylene sulfone RNA duplex appears wider at first glance, the actual S···S and P···P distances differ only by 0.3 Å. However, the backbones in the dimethylene sulfone duplex are more inclined relative to the base pair planes than those in $[r(GpC)]_2$. This is accompanied by a pronounced sliding of base pairs relative to one another in $[r(G\text{-}SO_2\text{-}C)]_2$, as well as a concomitant loss of overlap between the aromatic rings of stacked bases and a slightly decreased stacking distance in the sulfone duplex (3.4 Å vs. 3.68 Å in the phosphate duplex, Fig. 7). In addition to these changes, the helical twist in $[r(G\text{-}SO_2\text{-}C)]_2$ is about 14° less than that in $[r(GpC)]_2$, discernable by the angle between the glycosidic bonds of the guanosine and cytidine residues for both dimers (Fig. 7, bottom left and right).

Careful consideration of the possible causes of the structural perturbations in the sulfone-RNA duplex points largely to one of the methylene groups replacing the bridging phosphate ester oxygens, rather than the lack of charge. Notably, all the sugar–sulfone backbone torsion angles lie in the conformational ranges associated with an A-type duplex.[131] Both riboses adopt fairly standard C3′-*endo*-type puckers and the glycosidic bonds are in the *anti* conformation. The lack of *gauche* interactions, which are in natural nucleosides between O3′ and O4′, for 3′-CH_2-substituted (termed C3″ for sulfones) ribonucleosides would stabilize such a sugar pucker. However, the accommodation of the methylene group replacing O5′ (termed C6′ for sulfones) requires an adjustment of the nucleotide conformation (Fig. 8). Thus, the H^{Re} hydrogen of C6′ occupies roughly the position taken by O5′ in the standard phosphate backbone of A-form duplexes. This is achieved by slight changes in the sugar conformation, and in particular, by pushing the δ angle out toward 90° for a more equatorial arrangement of the C4′–C5′ and C1′–N1 bonds relative to the ribose ring. In addition, as a result of the more distinct antiperiplanar conformation of the glycosidic bond, the interaction between the H^{Re} hydrogen of C6′ and the hydrogen of C6 is minimized.

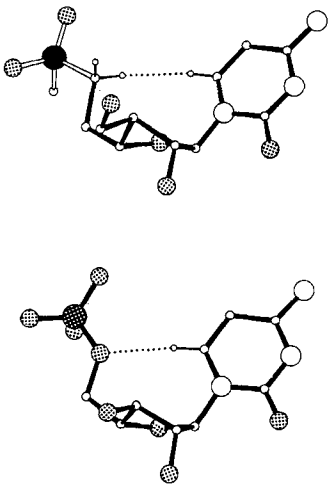

Fig. 8. The conformations of cytidine in the dimethylene sulfone RNA duplex $[r(G\text{-}SO_2\text{-}C)]_2$ (top) and in the natural $[r(GpC)]_2$ duplex (bottom). The dotted lines indicate the distances between H6 and $H6'^{Re}$ in the dimethylene sulfone duplex (2.21 Å) as well as between H6 and O5′ in the natural duplex (2.34 Å). Note the slight difference in ribose puckers in the two nucleotides. The sulfur atom is black, S=O and S–CH_2 bonds are highlighted, and the phosphorus is dark gray.

These changes in the relative positions of sugar and base together with the difference in the P–O and S–C bond lengths (the latter is approximately 0.2 Å longer) are largely responsible for the altered slide in $[r(G\text{-}SO_2\text{-}C)]_2$. Because the C6′–S bond is roughly parallel to the Watson–Crick hydrogen bonds (Fig. 7), the C6′ carbon contributes more substantially to the pronounced slide than the C3″ carbon. The lower twist in the dimethylene sulfone duplex is most likely the consequence of the difference between the S-C6′-C5′ (111°) and the P-O5′-C5′ (120°) bond angles (Fig. 7, bottom). The tighter elbow in $[r(G\text{-}SO_2\text{-}C)]_2$ rotates the green C(2)–G(3) base pair back over the blue G(1)–C(4) base pair.

The almost identical conformations of nucleosides in the dimethylene sulfone dimer allow the construction of an extended oligonucleotide duplex based on the helical twist and rise in $[r(G\text{-}SO_2\text{-}C)]_2$. A comparison between such a duplex and a standard A-RNA duplex is depicted in Figure 9. The sulfone-RNA duplex has about 17 repeats per full turn compared with the 11 repeats in standard A-RNA, and its diameter is 50% larger than that of RNA. This generates a hollow cylinder around the helix axis on the inside. The deep major groove

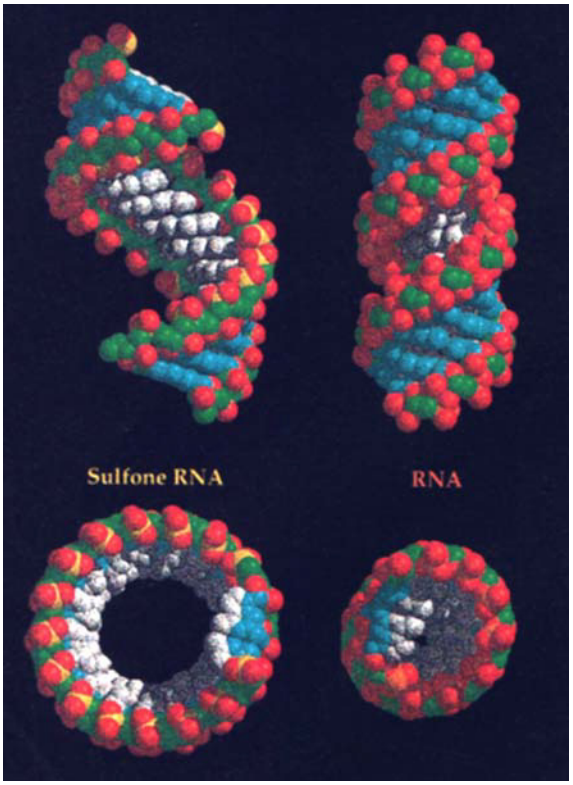

Fig. 9. Projections along the normal to the helix axis (top) and along the helix axis (bottom) of a full turn of a sulfone-RNA double helix (construction of the 17mer is based on the conformation of the $[r(G\text{-}SO_2\text{-}C)]_2$ dimer duplex) and a standard A-RNA of equal length. The edges of base pairs along the major groove are white and those along the minor groove are cyan. Sulfur atoms are yellow and phosphorus atoms are orange.

of A-RNA is opened up greatly in the sulfone duplex, and the distance separating sulfurs of opposite strands across that groove is extended to about 15 Å, or roughly three times the distance between phosphates in standard RNA. The changes in the minor groove are much less severe by comparison.

The reader should note that the rather drastic topological differences between sulfone-RNA and RNA as assessed by the structure determination of the $[r(G\text{-}SO_2\text{-}C)]_2$ duplex may represent a "worst case" scenario. The incorporation of a short stretch of sulfone-RNA into a native or otherwise modified RNA oligonucleotide may have less severe conformational consequences. Likewise, the larger slide and the smaller twist between base pairs in sulfone-RNA could lead to improved stacking beween interstrand purines in 5′-pyrimidine–purine-3′ steps and therefore higher stability. The synthesis of chimeric DNA/sulfone-DNA and RNA/sulfone-RNA oligonucleotides is under way, and it will be interesting to analyze their structures and to assess the consequences of incorporating dimethylene sulfone linked dimers into standard oligonucleotides on thermodynamic stability.

The conformational consequences of the replacement of O5′ by a methylene group have been studied with the r(UpcA) 5′-deoxy-5′-phosphonomethylene dimer,[134] and with r(A-$(pcA)_8$-pcA) 5′-deoxy-5′-phosphonomethylene-adenosine decamers.[135] For the former, circular dichroism experiments indicated that the incorporated methylene group destroyed the stacking in the dimer. However, the stability of triplexes formed by the above 5′-modified homo(A) decamer with two $r(U)_{10}$ strands was similar to that exhibited by the natural RNA oligonucleotides. The contradictory findings may be related to the different lengths and sequences of the molecules investigated. The conformational consequences of replacing O5′ by a methylene group are most likely different for purine and pyrimidine nucleosides. Thus, the methylene group may be more easily accommodated opposite H8 of adenosine than in the vicinity of H6 in cytidine as in $[r(G\text{-}SO_2\text{-}C)]_2$ (Fig. 8). Since the S–C and P–C bond lengths differ only minimally, it is unlikely that phosphonomethylene and dimethylene sulfone linkers lead to much different stacking. Further, an assumed slight loss of intrastrand stacking as observed in $[r(G\text{-}SO_2\text{-}C)]_2$ could affect the stability of double or triple helical arrangements of homopurine strands less severely (cf. the stability of the above-mentioned oligo-5′-deoxy-5′-phosphonomethylene-adenosine) than that of double and triple helices composed of mixed purine–pyrimidine sequences. Recently the synthesis and incorporation in oligonucleotides of a thymidine dimer containing an internucleoside phosphinato linkage (O5′ as well as O3′ replaced by methylene groups) have been reported.[136] It is noteworthy that the hybridization of a DNA with ten consecutive phosphinate nucleotides and its RNA complement resulted in a reduction in the melting temperature of slightly less than 2 °C per modification relative to that of the native hybrid. It remains to be seen how additional replacement of the negatively charged PO_2^- portion by SO_2, as in dimethylene sulfone RNA, will affect the RNA affinity.

The crystal structure of the dimethylene sulfone linked $r(A\text{-}SO_2U)$ dimer in a single-stranded state and a comparison of its conformation to that of the $r(G\text{-}SO_2\text{-}C)$ strand in the duplex state have shed some light on the conformational rearrangements required—in this particular case—for the transformation of a single strand into a duplex.[137] The single-stranded dimer shows an extended conformation, in which all torsion angles in the sugar–sulfone backbone (except δ) adopt an *ap* conformation. Interestingly, the riboses in the $r(ASO_2U)$ dimer have C2′-*exo* puckers (Fig. 10). The *ap* conformation of γ rotates one of the C5′ hydrogens much more toward the β-face of the ribose ring. A standard C3′-*endo* conformation of the ribose as seen in the duplex would cause an unfavorable steric interaction between this C5′ hydrogen and H3′. This is avoided by folding down the C4′-C3′-C2′ elbow in the ribose (Fig. 10). Flipping α

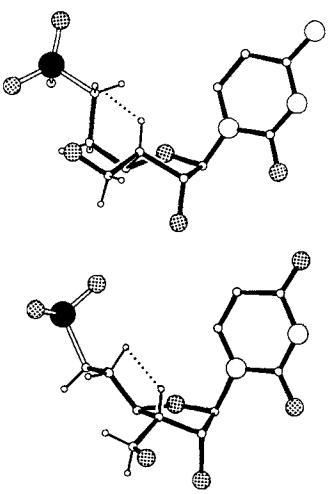

Fig. 10. C3′-*endo* pucker of cytidine in $[r(G\text{-}SO_2\text{-}C)]_2$ (top) and C2′-*exo* pucker of uridine in the $r(A\text{-}SO_2\text{-}U)$ single strand (bottom). The dotted lines mark the distances between H^{Si} of C6′ and H3′ in cytidine (2.16 Å) and between one of the C5′ hydrogens and H3′ in uridine (2.35 Å). Note the different conformations of torsion angle γ in the two nucleotides. Adoption of a C3′-*endo* pucker in uridine would generate an unfavorable interaction between H^{Re} and C5′. The sulfur atom is black.

and γ into a sc^+ conformation could allow the ribose to assume a C3′-*endo* pucker, and additional rotation around ζ would then convert the extended single-stranded conformation in r(A-SO_2-U) to a stacked arrangement similar to the one in the [r(G-SO_2-C)]$_2$ A-type duplex.

6. 6′-α-Substituted Carbocyclic DNA

In carbocyclic analogs the 4′-oxygen of the natural furanosyl nucleoside is replaced by a substituted methylene group (Fig. 3, Scheme 1). Removal of the electron-withdrawing 4′-oxygen in the furanosyl moiety has a significant effect on the basicity of the pyrimidine heterocycle. The carbocyclic analog of 5-methyl-2′-deoxycytidine has a higher pK_a than the parent compound and was shown to increase the stability of Pu·Py–Py type triple helices (requiring protonation of cytidine in the third strand).[156] In addition, the higher stability conferred by carbocyclic residues in the pyrimidine strand may be related to the absence of repulsive interactions between phosphates of the purine strand and the 4′-oxygens of the third strand bound in the major groove.[25] Carbocyclic analogs exhibit greater resistance to enzymatic cleavage of the glycosidic linkage and therefore may be useful in therapeutic applications.[138]

Although oligonucleotides containing carbocyclic building blocks showed favorable RNA-binding properties, it is believed that their stability against nuclease degradation does not suffice for biological applications.[25] Oligonucleotides containing carbocyclic analogs with α-substituents on the CH_2 group (termed C6′, Fig. 3) were found to be more resistant to degradation.[57] However, those analogs with the most significant decrease in DNA/RNA duplex stability are the very ones that show the highest degree of nuclease resistance. The experiences gathered thus far on the stability of DNA homo- and DNA/RNA heteroduplexes containing carbocyclic oligonucleotides are consistent with no particular conformational preference of the cyclopentane ring. Rather, the lack of stereoelectronic effects influencing the conformation in the furanosyl moiety render the five-membered ring much more flexible, and may allow carbocyclic nucleotides to adapt to a variety of induced duplex geometries.

In order to assess the conformational features of carbocyclic nucleotides, we incorporated three types of carbocyclic analogs, both with and without 6′-α-substituents, into a Dickerson–Drew d(CGCGAATTCGCG) template sequence (Scheme 1). Crystals could be grown of all four modified strands synthesized thus far. However, in all but one case, the crystals diffracted to relatively low resolution. To our knowledge, the rhombohedral space group of the carbocyclic dodecamer crystals has never been observed with any of the numerous variants of the dodecamer sequence crystallized during the last 15 years. More than 30 d(CGCxyyyyzGCG)-type (x = G, A, T; y = A, T; z = C, A, T) dodecamers with either sequence alterations, chemical modifications, or minor groove binding drugs complexed to them all crystallized in the orthorhombic $P2_12_12_1$ space group of the native dodecamer.[107] It is noteworthy that an apparently subtle chemical modification like the replacement of O4′ by CH_2 in a few nucleotides causes the dodecamer to pack in a different fashion, perhaps resulting in an altered conformation of the DNA.

The crystal structure of d(CGCGAAT^{Me}T^{Me}CGCG) (T^{Me} = 6′-α-methylthymidine) has been determined at 2.5 Å resolution.[139] The structure is isomorphous to that of the unmodified dodecamer, and the four modified nucleotides per duplex adopt conformations compatible with a B-DNA. Of the twenty sugar units (omitting terminal residues) in the native structure, ten have C1′-*exo*, seven have C2′-*endo*, and two have O4′-*endo* conformations, and one assumes an O4′-*exo* pucker.[140, 141] In the native structure, residues T(7) and T(8) adopt O4′-*endo* and C1′-*exo* puckers, respectively, while they display C2′-*endo* and C1′-*exo* conformations, respectively, in the modified dodecamer (Fig. 11). In the second strand, residues T(19) and T(20) in the native dodecamer both adopt C1′-*exo* puckers, while T^{Me}(19) and T^{Me}(20) in the modified duplex have C2′-*endo* and C1′-*exo* puckers, respectively. Thus, the carbocyclic residues cause only very minor deviations from the standard geometry of the deoxyoligonucleotide duplex, and the cyclopentane rings adjust smoothly to the geometrical constraints posed by the furanosyl–phosphate backbone. This may indicate that the cyclopentane ring of unsubstituted and 6′-α-substituted carbocyclic nucleotides is "conformationally promiscuous", and can comply with a range of geometries dictated by either RNA or DNA backbones.

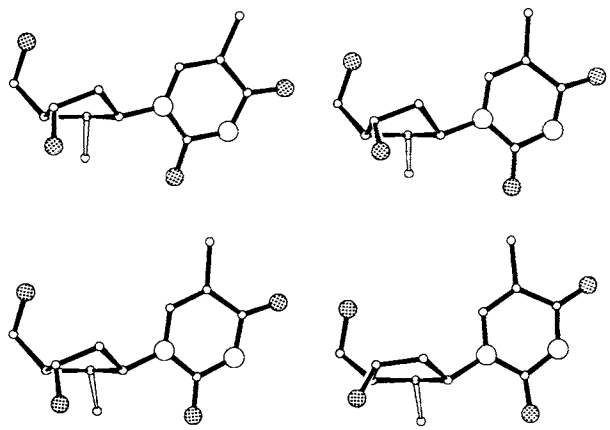

Fig. 11. Conformations of the four carbocyclic 6′-α-methylthymidines in [d(CGCGAAT^{Me}T^{Me}CGCG)]$_2$: T(8) (C2′-*endo*, top left), T(9) (C1′-*exo*, top right), T(19) (C2′-*endo*, bottom left), and T(20) (C1′-*exo*, bottom right). The C6′–C7′ bonds are highlighted.

In the central portion of the minor groove in [d(CGCGAATTCGCG)]$_2$, seven water molecules in the first hydration shell were found to link the guanine N3 or N2, adenine N3, and cytosine and thymine O2 from opposite strands, such that the bridges span two adjacent base pairs (Fig. 12, left). Six water molecules in the second hydration shell then coordinate to those of the first hydration shell with direct contacts to the DNA, thus conferring them with nearly tetrahedral coordination.[116] The ribose 4′-oxygens that line the minor groove stabilize the hydration spine, either through direct hydrogen bonds or by creating a polar environment.[117] It is surprising how little the presence of the methyl groups of the carbocyclic thymidines in the central region of the modified duplex affects the first hydration

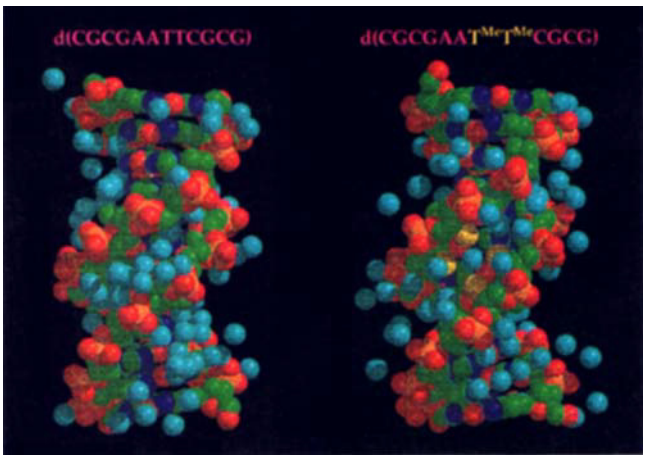

Fig. 12. Hydration of the minor groove in the B-DNA duplexes $[(d(CGCGAATTCGCG)]_2$ (left) and $[d(CGCGAAT^{Me}T^{Me}CGCG)]_2$ (right). Water molecules are represented as blue spheres and the CH_3 carbon atoms of the α-substituents in the modified thymidine residues are highlighted in yellow. The spine of hydration is visible as a chain of water molecules from the first and second hydration shell running down the minor groove in the modified duplex. The view of the central portion of the spine in the native dodecamer is slightly obstructed by water molecules of higher hydration spheres without contacts to the DNA.

shell. As in the native dodecamer, a water molecule bridges the O2 oxygens of residues $T^{Me}(7)$ and $T^{Me}(19)$. This water molecule is sealed off from the outer part of the minor groove by the four methyl groups, one of which forms a contact of 3.12 Å to the water molecule (Fig. 12, right). Two water molecules flanking the central water unit and bridging residues $T^{Me}(8)$ and A(18) as well as A(6) and $T^{Me}(20)$ are also conserved, as is the entire hydration pattern at the floor of the minor groove. However, the lipophilic patch formed by the methyl groups in the center of the minor groove leads to displacement of the water molecules of the second hydration shell that link the three water molecules in the center. In the B-DNA duplex, both the vector defined by the 6′-α-methyl carbon atoms of residues $T^{Me}(7)$ and $T^{Me}(20)$ and the vector defined by those carbons in $T^{Me}(8)$ and $T^{Me}(19)$ are roughly perpendicular to the direction of the minor groove. Thus, the distances between the methyl carbons of these residues across the groove are 1.21 and 0.87 Å, respectively (after subtraction of 4 Å, the sum of the van der Waals radii of methyl groups). The corresponding intrastrand distances between the methyl carbons of residues $T^{Me}(7)$ and $T^{Me}(8)$ and residues $T^{Me}(19)$ and $T^{Me}(20)$ are 1.03 and 0.53 Å, respectively.

The structure demonstrates that 6′-α-substituted carbocyclic nucleotides can mimic the furanosyl conformation in a duplex with B-type geometry. Insertion of isolated 6′-α-methylated building blocks into DNA could destabilize the duplex by distorting the global hydration motif. However, contiguous stretches of ten 6′-α-methylated carbocyclic pyrimidines resulted in duplexes with slightly elevated melting temperatures per incorporated residue compared with that after insertion of isolated analogs ($\Delta T_m = -1.3$ °C vs. -1.7 °C, complement DNA).[139, 142] This cooperative relative stability increase may arise from the release of water molecules in the vicinity of the methyl substituents and the near van der Waals contacts between methyl groups of adjacent intrastrand residues.

7. 2′-O-Methylated RNA

2′-O-Alkylation[40, 62, 143] and 2′-alkyl substitution[144] lead to oligonucleotides with improved metabolic stability. Heteroduplexes composed of 2′-O-alkylated RNA and natural RNA are more stable than those composed of DNA and RNA, and smaller substituents such as methyl, ethyl, and allyl are more stabilizing than longer chain alkyls.[39, 42] The 2′-hydroxyl group of RNA contributes to the thermodynamic stability of the RNA duplex, both enthalpically by improvement of hydration and entropically by conformational preorganization of the ribose.

The crystal structure of the A-RNA duplex $[r(C_4G_4)]_2$ at high resolution[103] and its comparison with the crystal structure of the A-DNA duplex with identical sequence[145, 146] have provided evidence for the superb hydration of the RNA duplex as a result of the 2′-hydroxyl groups in the minor groove (Fig. 13).

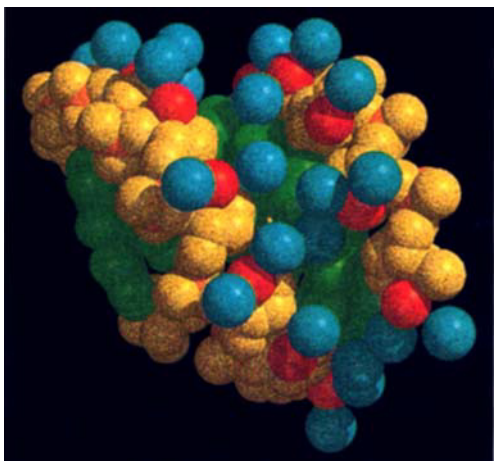

Fig. 13. Hydration of the 2′-hydroxyl groups in the minor groove of the RNA duplex $[r(C_4G_4)]_2$. Each of the water molecules (cyan, partly hidden) lies within 3.4 Å of a 2′-oxygen (red). Phosphorus atoms are orange, the remaining atoms in the ribose–phosphate backbone are yellow, and base atoms are green.

They form hydrogen bonds to two water molecules on average, and most of them serve as donors in an additional internal hydrogen bond to the 4′-oxygen of the adjacent ribose in the 5′ → 3′ direction.

The thermodynamics of hybridization for $r(C_4G_4)$ and $d(C_4G_4)$ were calculated from temperature-dependent UV-spectroscopic data. Perhaps surprisingly, the higher thermodynamic stability of the RNA duplex compared with that of the DNA duplex is not based on a more favorable entropy term, which would be a consequence of the conformational preorganization of the ribose–phosphate backbone in single-stranded RNA for an A-form duplex. Instead, the enthalpy for duplex formation for RNA is more than 30 kcal mol^{-1} higher than for DNA, consistent with the much better hydration of the RNA observed in the crystal (see 2′-OH hydration in Fig. 13). DNA duplex formation may cause a net loss of water molecules, whereas the overall number of water molecules may not be too different in the case of two RNA single strands and an RNA duplex. The very minor loss of hydration (or perhaps even slight increase) for RNA upon duplexation (entropically unfavorable) opposes

Table 2. Thermodynamic data for $r(C_4G_4)$ and $d(C_4G_4)$ based on temperature-dependent UV-hyperchromicity measurements [a].

Oligomer	T_m [°C]	ΔG [kcal mol^{-1}]	ΔH [kcal mol^{-1}]	$-T\cdot\Delta S$ [kcal mol^{-1}]
$d(C_4G_4)$	44.6	−8.4	−54.0	+45.6
$r(C_4G_4)$	70.1	−15.5	−85.1	+69.6

[a] The T_m values were measured in 10 mM sodium cacodylate (pH 7), 100 mM NaCl, 0.1 mM EDTA, at strand concentrations of 8.2 μM. Thermodynamic data are given for 37 °C.

the enthalpy gains due to bound water as well as the contribution from the preorganization of the single strand, which should favorably influence the entropy term. Nevertheless, the gains in enthalpy are higher than the losses in entropy, and the ΔG for duplex formation with RNA is roughly twice that of duplex formation with DNA (Table 2). It is interesting in this context that oligonucleotides containing 2′-alkoxy-substituted carbocyclic building blocks lacking the *gauche* interaction between the 2′-substituent and the 4′-ribose oxygen show reduced RNA-binding affinity relative to that of the corresponding DNA oligonucleotides.[57] Thus, the greater rigidity of RNA relative to DNA due to the *gauche* interaction between O2′ and O4′ in the sugar–phosphate backbone and the resulting entropic advantage for duplex formation are of crucial importance for the higher thermodynamic stability of RNA and 2′-*O*-Me-RNA.

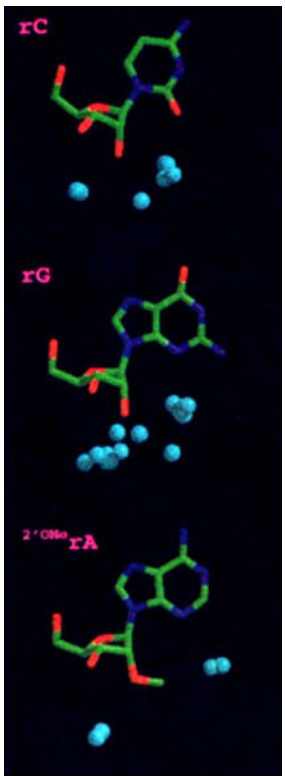

Fig. 14. Consensus hydration pattern of the minor groove in the vicinity of rC (top), rG (middle), and 2′-*O*-Me-rA (bottom). To generate each of the rC and rG pictures, the appropriate eight nucleosides in the $[r(C_4G_4)]_2$ crystal structure (replaced here with a nucleoside with a consensus conformation) and the water molecules around them were superimposed. The hydration pattern of $^{2'OMe}$rA is based on the hydration of the two modified adenosines observed in the crystal structure of a chimeric DNA:2′-*O*-Me RNA decamer duplex [106].

In the crystal structure of the decamer duplex $[d(GCGT)^{O2'Me}r(A)d(TACGC)]_2$, which contains 2′-*O*-methylated adenosines, both methoxy oxygens form a hydrogen bond to only one water molecule.[106] Thus, methylation of the 2′-hydroxyl group leads to a reduced hydration compared with that of native RNA (where 2′-hydroxyl groups are most often bound to two water molecules), and, in addition, disrupts the internal hydrogen bond often observed between O2′ and O4′ of the adjacent intrastrand ribose. The consensus patterns of minor groove hydration for cytidine and guanosine based on the $[r(C_4G_4)]_2$ crystal structure are depicted in the upper portion of Figure 14. There, the 2′-hydroxyl groups stabilize a continous band of water molecules across the groove, which are arranged more or less within the planes defined by the G–C base pairs and link backbones and bases (Fig. 13, foreground). For most of the G–C base pairs, one of the two water molecules hydrogen bonded to the 2′-oxygen atoms is located at the border of the minor groove and forms a bridge between O2′ and the phosphate group. The other water molecule then links O2′ to N3 of guanosine or to O2 of cytidine (Fig. 14). These water molecules are in turn bridged by a fifth water, which normally also forms a hydrogen bond to N2 of guanosine (not included in Fig. 13, as these water molecules do not interact directly with 2′-oxygens).

In the arrangement of water molecules around 2′-O-methylated adenosines it is apparent that the water molecule formerly linking O2′ to N3 (in analogy to G in the RNA duplex) is shifted to the center of the groove by the methoxy group (Fig. 14, bottom). Both the crystal structure and solution NMR experiments[71] provide evidence that the methoxy substituents point into the minor groove, resulting in an approximate *trans* conformation of the C2′–C3′ and O2′–CH_3 bonds. Accordingly, 2′-O-methylation of RNA seems to distort minor groove hydration at the local and the global level, suggesting that the superior stability of 2′-*O*-Me RNA could be mainly entropy driven. This is supported by the even higher thermodynamic stability of hybrids formed between 2′-deoxy-2′-fluorooligonucleotides and RNA.[42, 147] Although hydrogen bonding to covalently bound fluorine atoms has been invoked,[148] fluorine (in contrast to the fluoride anion) is an extremely poor hydrogen bond acceptor.[149] The strong RNA affinity of oligodeoxynucleotides with uniform 2′-fluoro substitution is therefore unlikely to be accounted for by enthalpic stabilization through hydration. However, electronegativity effects that stabilize the C3′-*endo* sugar pucker provide an important contribution to the exceptional RNA affinity.[99] Taken together, the structural and thermodynamic data support the view that 2′-*O*-Me RNA may combine an entropic stabilization similar to that of DNA through loss of water upon duplex formation with the entropic stabilization of RNA through conformational preorganization of the single strand. Additional stability may be provided through hydrophobic contacts between closely spaced O2′-substituents along the strand.[106] Subtle tuning between the gain in entropy and the loss in enthalpy as a consequence of altering the hydration may well be involved in the highly stabilizing effects of a methyl group at C5 in pyrimidines[150] and the exceptional RNA affinity of oligonucleotides comprising pyrimidines with propyne substituents at the C5 position.[62]

8. Sequence-Specific Cleavage of RNA

Hetero duplexes composed of RNA and almost all oligonucleotide analogs with modified sugar and/or phosphate moieties fail to activate the natural mRNA degradation pathway mediated by RNase H. The enzyme cleaves the RNA strand in DNA·RNA hybrids, and the only analogs that do not prevent recognition of the hetero substrate by the enzyme are phosphorothioates, phosphorodithioates, and those with base modifications affecting the major groove (for example 5-propynepyrimidines).[24] This failure to induce RNA degradation may con-

stitute a serious limitation for the therapeutic application of antisense compounds. Functionalized RNAs that can recognize a specific mRNA region and efficiently cleave it,[151] as well as unmodified and chemically modified hammerhead-type ribozymes[13, 41, 152, 153] may prove more potent as antisense therapeutics.

In the ribozyme-catalyzed cleavage of RNA through transesterification of phosphodiesters, the backbone is preoriented for an S_N2-type displacement. Thus, the incoming 2′-OH group and 5′-OH leaving group must both occupy apical positions in the trigonal-bipyramidal transition state formed by the nucleophile and the phosphate group with the scissile P–O5′ bond.[154–156] In an intact A-RNA duplex, the relative positions of the 2′-OH and the adjacent 5′-phosphate group preclude an in-line attack. However, distortions in the backbone geometry around single- or multiple-base bulges appear to provide the conformational freedom necessary for efficient strand cleavage. Quantitative cleavage of an RNA strand was observed at the phosphate adjacent to a "bulged" or unpaired nucleotide in the presence of moderate amounts of Mg^{2+}.[157] The products that result from cutting the 3′-5′-phosphodiester bond between the bulged and adjacent nucleotides in a 5′ → 3′ direction are a cyclic 2′,3′-phosphodiester and a free 5′-hydroxyl group, exactly the same products obtained in the cleavage reaction catalyzed by hammerhead-type ribozymes.[158]

We have determined the crystal structure of a self-complementary RNA–DNA chimera with single adenosine bulges at a resolution of 2.8 Å (Fig. 15).[160] In the crystal the fragment adopts crystallographic twofold symmetry and both adenosines extrude from the duplex (Fig. 16). The deoxyriboses of the bulged nucleotides A(8) and A(19) as well as A(6), T(7), A(17), and A(18) adopt C2′-*endo* puckers, while all others display the C3′-*endo* conformation of A-RNA. The backbone perturbations brought about by the unpaired adenosines kink the fragment by 20° and cause a drastic opening of the narrow major groove to about twice its normal width.

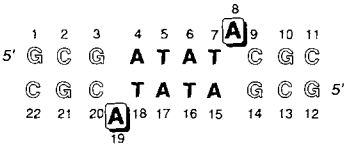

Fig. 15. Sequence of the self-complementary RNA–DNA chimera (units of RNA in outlined letters, those of DNA in filled letters) having two bulged (unpaired) adenosine residues, which was studied by X-ray crystallography. The central portion of the 11mer was originally left as DNA in order to conserve some features of a fully base-paired RNA–DNA chimera that had previously yielded high-resolution crystals [159], and to prevent strand cleavage between residues A(8) and C(9) (or A(19) and C(20)) during attempted crystallization in the presence of divalent metal cations.

In molecular modeling studies based on the crystal structure of this RNA–DNA chimera, a 2′-OH group was introduced at the deoxyribose of the bulged adenosine. As can be seen in Figure 17 (bottom), this hydroxyl group is relatively far removed from the scissile P–O5′ bond (O2′–P 4.2 Å). In addition, it lies approximately within the plane defined by the phosphate oxygens O1P, O2P, and O3′. Thus, the hypothetical O2′-P-O5′ angle of 90° would disfavor cleavage of the phosphodiester bond (Fig. 17, bottom). However, if the C2′-*endo* conformation at the ribose of the bulge residue is flipped into a C3′-*endo* pucker,

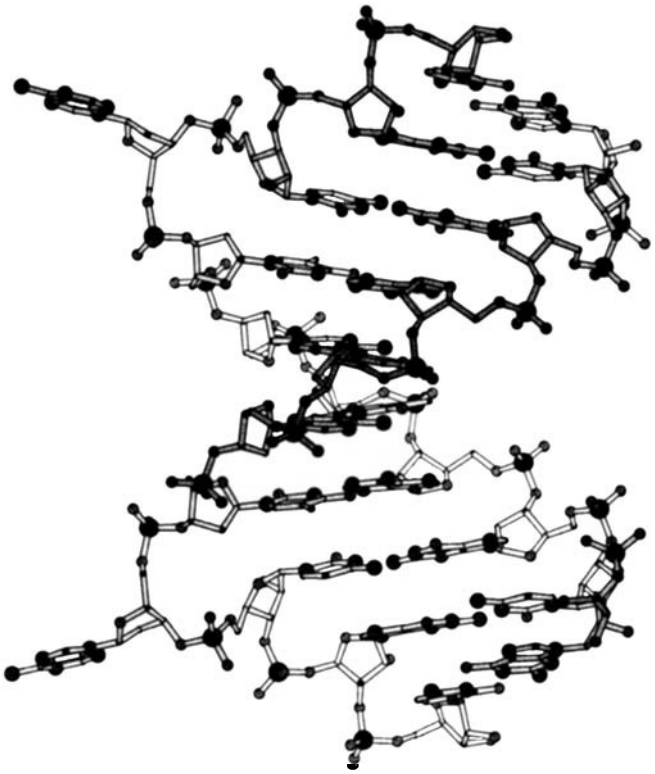

Fig. 16. Overall conformation of the A-RNA-like duplex containing bulged adenosines. Phosphorus atoms are filled circles and darker portions are closer to the viewer. Bulged adenosines are important RNA secondary structure elements and are involved in RNA folding, protein–RNA interactions, and splicing of group I and II introns as well as nuclear pre-mRNA [161–165].

a roughly apical arrangement of the 2′-OH results (O2′-P 3.6 Å, O2′-P-O5′ 150°; Fig. 17, top). This demonstrates that apical positions of incoming and leaving groups at the trigonal-bipyramidal intermediate can be achieved relatively easily as a result of local conformational rearrangements of the backbone around the bulged nucleotide, and is consistent with the efficient metal-assisted cleavage at such sites. The P-$O^{Si}\cdots O^{Re}$-P distance of 3.95 Å for residues C(9) and G(10) adjacent to the bulged nucleotide in the 5′-direction in the crystal structure is the shortest one in the entire duplex, and lies well below the usual intrastrand phosphate–phosphate contacts in A-type duplexes (Fig. 17). These closely spaced phosphate groups may provide a binding site for a Mg^{2+} ion that could activate the phosphate group for the nucleophilic attack and stabilize the 5′-hydroxyl leaving group. It is interesting that in the structure of a second crystal form, determined at a resolution of 1.83 Å,[160] the RNA–DNA chimeric fragment displays a conformation in the region of the bulged nucleotide that is very similar to the one in the modeled structure. In this structure the sugar of the bulged adenosine adopts a C3′-*endo* conformation and the added 2′-OH group assumes a nearly apical orientation relative to the phosphate group (O2′–P 3.8 Å, O2′-P-O5′ 145°).

9. Summary and Outlook

Progress in understanding of nucleic acid structure has always been intimately linked to the advances in the chemical synthesis of DNA and RNA. When milligram amounts of highly pure

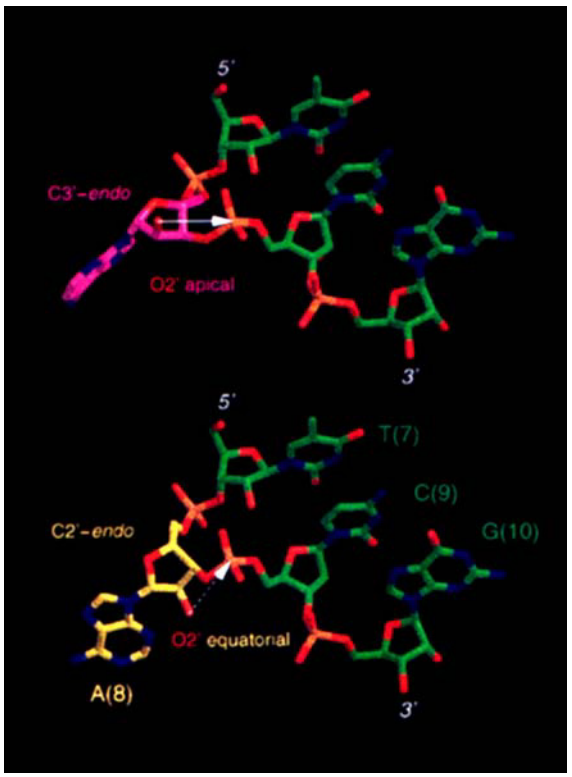

Fig. 17. Backbone conformation around the adenosine bulge (yellow) as observed in the crystal structure (bottom). Modeled backbone conformation around the adenosine bulge (purple) by changing the conformation of the sugar pucker from C2'-*endo* to C3'-*endo* (top). Solid and dashed arrows indicate the vectors between the adenosine 2'-OH, which is depicted here but missing from the crystal structure, and the phosphorus of the 3'-phosphate. The short distance between the phosphate oxygens O^{Si} and O^{Re} of residues C(9) and G(10), respectively, is visible in the foreground.

oligodeoxynucleotides became available in the early eighties, the way was paved for the first high-resolution crystal structures of DNA fragments. In somewhat more than a decade over a hundred crystal structures have given insight into many structural aspects of the double helix. Similar success with RNA has long been hampered by the difficulties encountered in developing synthesis protocols for the large-scale production of oligoribonucleotides. These have now largely been overcome and a dramatic rise in the number of RNA structures in the next years is foreseeable.

The challenge of advancing the antisense technique beyond its use as a research tool toward therapeutic applications has catalyzed the generation of an astounding variety of synthetic nucleic acid analogs. Many of them show improved resistance to cellular nuclease degradation over that of their natural counterparts. Several analogs combine higher chemical stability with increased RNA affinity.[51, 62, 166] However, with very few exceptions, such as the first-generation phosphorothioate analogs, modifications block the natural mRNA degradation pathway based on RNase H. Modified oligonucleotides that form stable complexes with newly transcribed RNA at nuclear sites and do not prevent recruitment of RNase H appear to be particularly effective in shutting down mRNA translation.[167]

Detailed three-dimensional structures provide clues to the origins of the changes in thermodynamic stability incurred by chemical modifications of DNA and RNA. A comparison of the high-resolution crystal structures of a DNA octamer and an RNA octamer duplex with identical sequences illustrates that double-helical DNA and RNA differ fundamentally in their degrees of hydration; the RNA duplex is more extensively hydrated as a result of the additional ribose 2'-hydroxyl groups. Consequently, with respect to bound H_2O, RNA duplex formation is favored enthalpically but disfavored entropically relative to DNA duplexation. The higher rigidity of the ribose moiety contributes positively to the overall thermodynamic stability of the RNA duplex. Hydration changes and the ensuing trade-off between enthalpy and entropy are mostly overlooked in the analysis of the thermodynamic stability data of nucleic acid analogs.[127] Because hydration makes an important contribution to the relative stabilities of native DNA and RNA, it would seem that changes in the solvation as a consequence of chemical modifications are a crucial factor in the altered thermodynamic stability of DNA and RNA analogs. This view is supported by the changes in hydration evident in the crystal structures of derivatives formed by introduction of methyl groups at the 2'-oxygen (2'-*O*-Me-RNA) and the 6'-carbon (carbocyclic DNA). Somewhat simplified, these results point to an equilibration or occasional overcompensation (2'-O-substituted RNA) of the enthalpy losses caused by the altered or reduced hydration in the vicinity of short-chain alkyl groups or heteroatom substituents by the entropy gains due to water loss. The close spacing of such substituents in the minor groove of the A-form duplex is likely to stabilize duplex formation, while longer chain alkyl groups, or in general bulky lipophilic substituents, disrupt hydration in such a way that the enthalpy loss becomes dominant. Hydration effects are probably also involved in the stabilization exerted by substituents at pyrimidine C5 (for example methyl or propyne); stacking and interactions between substituents provide additional contributions.

In addition to providing feedback for the design of further nucleic acid analogs for antisense applications, systematic study of the structures of chemically modified nucleic acids promises deeper insight into the properties of the native DNA and RNA molecules. Just as point mutations with proteins in combination with structural work have permitted the assessment of the individual influences of amino acids in folding and catalysis, specifically modified nucleic acids allow one to analyze the importance of various parameters for the overall structures of DNA and RNA. Thus, analogs may be helpful for an improved understanding of bending, interactions between proteins and nucleic acids, and a variety of other issues.

I wish to thank my collaborators in our laboratory, P. Lubini, S. Portmann, A. Roughton, and C. Richert, as well as those from outside institutions, C. Leumann (University of Berne), K.-H. Altmann, M. Blommers, D. Hüsken, and H. Moser (CIBA, Basel), N. Usman (Ribozyme Pharmaceuticals Inc., Boulder, USA), and F. K. Winkler (Hoffmann LaRoche, Basel) for their contributions and stimulating discussions. I am grateful to A. Roughton for his comments on the manuscript, and I would like to thank the ETH Zürich, the Organic Chemistry Laboratory, The Ciba-Geigy-Jubiläums-Stiftung, and CIBA for their financial support.

Received: July 19, 1995 [A 1231E]
German version: *Angew. Chem.* **1996**, *108*, 2020–2036

[1] P. J. Green, O. Pines, M. Inouye, *Annu. Rev. Biochem.* **1986**, *55*, 569–597.
[2] R. W. Simons, N. Kleckner, *Annu. Rev. Genet.* **1988**, *22*, 567.
[3] H. M. Weintraub, *Sci. Am.* **1990**, *262(1)*, 34–40.
[4] Y. Eguchi, T. Itoh, J. Tomizawa, *Annu. Rev. Biochem.* **1991**, *60*, 631–652.
[5] J. Tomizawa, *Cell* **1984**, *38*, 861–870.
[6] J. P. Marino, R. S. Gregorian, Jr., G. Csankovszki, D. M. Crothers, *Science* **1995**, *268*, 1448–1454.
[7] P. C. Zamecnik, M. L. Stephenson, *Proc. Natl. Acad. Sci. U. S. A.* **1978**, *75*, 280–284.
[8] M. L. Stephenson, P. C. Zamecnik, *ibid.* **1978**, *75*, 285–288.
[9] H. E. Moser, P. B. Dervan, *Science* **1987**, *238*, 645–650.
[10] T. Le Doan, L. Perronault, D. Praseuth, N. Habhoub, J. L. Decout, N. T. Thuong, J. L. Homme, C. Hélène, *Nucleic Acids Res.* **1987**, *15*, 7749–7760.
[11] J.-S. Sun, C. Hélène, *Curr. Opin. Struct. Biol.* **1993**, *3*, 345–356; N. T. Thuong, C. Hélène, *Angew. Chem.* **1993**, *105*, 697–723; *Angew. Chem. Int. Ed. Engl.* **1993**, *32*, 666–690.
[12] G. A. Prody, J. T. Bakos, J. M. Buzayan, I. R. Schneider, G. Bruening, *Science* **1986**, *231*, 1577–1580; A. C. Forster, R. H. Symons, *Cell* **1987**, *49*, 211–220; O. C. Uhlenbeck, *Nature* **1987**, *328*, 596–600.
[13] T. R. Cech, *Curr. Opin. Struct. Biol.* **1992**, *2*, 605–609; N. Usman, J. McSniggen, *Ann. Rep. Med. Chem.* **1995**, *30*, 285–294.
[14] C. A. Stein, J. S. Cohen, *Cancer Res.* **1988**, *48*, 2659–2668.
[15] J. Goodchild, *Bioconj. Chem.* **1990**, *1*, 165–187.
[16] C. Hélène, J.-J. Toulmé, *Biochim. Biophys. Acta* **1990**, *1049*, 99–125.
[17] E. Uhlmann, A. Peyman, *Chem. Rev.* **1990**, *90*, 543–584.
[18] P. Cook, *Anti-Cancer Drug Design* **1991**, *6*, 585.
[19] C. Hélène, *Anti-Cancer Drug Design* **1991**, *6*, 569–584.
[20] J. A. H. Murray, *Antisense RNA and DNA, Modern Cell Biology, Vol. 11*, Wiley-Liss, New York, **1992**.
[21] S. T. Crooke, *Curr. Opinion Biotechn.* **1992**, *3*, 656–661.
[22] R. Tullis, E. Wilkinson, J. Caravaca-Trujillo, *Biotechn. Int.* **1992**, 79–89.
[23] *Antisense Research and Applications* (Eds.: S. T. Crooke, B. Lebleu), CRC Press, Boca Raton, FL, **1993**.
[24] J. F. Milligan, M. D. Matteucci, J. C. Martin, *J. Med. Chem.* **1993**, 36, 1923–1937.
[25] H. E. Moser in *Perspectives in Medicinal Chemistry* (Eds.: B. Testa, W. Furrer, E. Kyburz, R. Giger), Helvetica Chimica Acta, Basel, **1993**, pp. 275–297, and references therein.
[26] E. Uhlmann, A. Peyman in *Methods in Molecular Biology* (Ed.: S. Agrawal), Humana, Clifton, NJ, **1993**, pp. 355–390.
[27] R. S. Varma, *Synlett* **1993**, 621–637.
[28] J. S. Cohen, M. E. Hogan, *Sci. Am.* **1994**, *Dec.*, 50–55.
[29] *Modified Oligonucleotides* (Ed.: G. L. Trainor), *Bioorg. Med. Chem. Lett.* **1994**, *4*, 965–1085.
[30] M. Z. Ratajczak, A. M. Gewirtz in *Nucleic Acids and Molecular Biology, Vol. 8* (Eds.: F. Eckstein, D. M. J. Lilley) Springer, Berlin, **1994**, pp. 298–326.
[31] R. W. Wagner, *Science* **1994**, *372*, 333–335.
[32] „Carbohydrate Modifications in Antisense Research": *ACS Symp. Ser.* **1994**, *580*.
[33] A. De Mesmaeker, K.-H. Altmann, A. Waldner, S. Wendeborn, *Curr. Opin. Struct. Biol.* **1995**, *5*, 343–355.
[34] J. A. Walder, *Biotechn. Int.* **1992**, 67–71.
[35] F. Eckstein, *Ann. Rev. Biochem.* **1986**, *54*, 367–402.
[36] G. Zon, *Biotechn. Int.* **1992**, 119–124.
[37] K. K. Chacko, K. Lindner, W. Saenger, P. S. Miller, *Nucleic Acids Res.* **1983**, *11*, 2801–2814.
[38] P. S. Miller, C. H. Agris, L. Aurelian, K. R. Blake, A. Murakami, M. P. Reddy, S. A. Spitz, P. O. P. Ts'o, *Biochimie* **1985**, *67*, 769–776.
[39] H. Inoue, Y. Hayase, A. Imura, S. Iwai, K. Miura, E. Ohtsuka, *Nucleic Acids Res.* **1987**, *15*, 6131–6148.
[40] A. M. Ibarren, B. S. Sproat, P. Neuner, I. Sulston, U. Ryder, A. I. Lamond, *Proc. Natl. Acad. Sci. USA* **1990**, 87, 7747–7751.
[41] J. Goodchild, *Nucleic Acids Res.* **1992**, *20*, 4607–4612, and references therein.
[42] E. A. Lesnik, C. J. Guinosso, A. M. Kawasaki, H. Sasmor, M. Zounes, L. L. Cummins, D. J. Ecker, P. D. Cook, S. M. Freier, *Biochemistry* **1993**, *32*, 7832–7838.
[43] X. Cao, M. D. Matteucci, *Tetrahedron Lett.* **1994**, *35*, 2325–2328.
[44] A. De Mesmaeker, J. Lebreton, A. Waldner, V. Fritsch, R. M. Wolf, S. M. Freier, *Synlett* **1993**, 733–736.
[45] C. V. C. Prasad, T. J. Caulfield, C. P. Prouty, A. K. Saha, W. C. Schairer, A. Yawman, D. A. Upson, L. I. Kruse, *Biorg. Med. Chem. Lett.* **1995**, *5*, 411–414.
[46] J. Lebreton, A. De Mesmaeker, A. Waldner, *Synlett* **1994**, 54–56.
[47] R. J. Jones, K.-Y. Lin, J. F. Milligan, S. Wadwani, M. D. Matteucci, *J. Org. Chem.* **1993**, *58*, 2983–2991.
[48] K.-I. Lin, J. S. Pudlo, R. J. Jones, N. Bischofberger, M. D. Matteucci, B. Fröhler, *Bioorg. Med. Chem. Lett.* **1994**, *4*, 1061–1064.
[49] a) R. O. Dempcy, K. A. Browne, T. C. Bruice, *J. Am. Chem. Soc.* **1995**, *117*, 6140–6141; b) R. O. Dempcy, K. A. Browne, T. C. Bruice, *Proc. Natl. Acad. Sci. USA* **1995**, *92*, 6097–6101.
[50] a) A. K. Saha, T. J. Caulfield, C. Hobbs, D. A. Upson, C. Waychunas, A. M. Yawman, *J. Org. Chem.* **1995**, *60*, 788–789; b) L. Beigelman, A. Karpeisky, N. Usman, *Nucleosides Nucleotides* **1995**, *14*, 901–905.
[51] a) S. M. Gryaznov, D. H. Lloyd, J.-K. Chen, R. G. Schultz, L. A. DeDionisio, L. Ratmeyer, W. D. Wilson, *Proc. Natl. Acad. Sci. USA* **1995**, *92*, 5798–5802; b) J.-K. Chen, R. G. Schultz, D. H. Lloyd, S. M. Gryaznov, *Nucleic Acids Res.* **1995**, *23*, 2661–2668.
[52] W. S. Marshall, M. H. Caruthers, *Science* **1993**, *259*, 1564–1570.
[53] B. Meng, S. H. Kawai, D. Wang, G. Just, P. A. Giannaris, M. J. Dahma, *Angew. Chem.* **1993**, *105*, 733–735; *Angew. Chem. Int. Ed. Engl.* **1993**, *32*, 729–731.
[54] E. B. McElroy, R. Bandaru, J. Huang, T. S. Widlanski, *Bioorg. Med. Chem. Lett.* **1994**, *4*, 1071–1076.
[55] Z. Huang, K. C. Schneider, S. A. Benner, *J. Org. Chem.* **1991**, *56*, 3869–3882.
[56] B. C. Froehler, D. J. Ricca, *J. Am. Chem. Soc.* **1992**, *114*, 8320–8322.
[57] K.-H. Altmann, M.-O. Bévierre, A. De Mesmaeker, H. E. Moser, *Biorg. Med. Chem. Lett.* **1995**, *5*, 431–436.
[58] A. Garbesi, M. L. Capobianco, F. P. Colonna, L. Tondelli, F. Acramone, G. Manzini, C. W. Hilbers, J. M. E. Aelen, M. J. J. Blommers, *Nucleic Acids Res.* **1993**, *21*, 4159–4165.
[59] A. Eschenmoser, E. Loewenthal, *Chem. Soc. Rev.* **1992**, 1–16.
[60] A. Eschenmoser in *Proceedings of the Robert A. Welch Foundation, Vol. 37*, The Robert A. Welch Foundation, Houston, TX, **1993**, pp. 201–235.
[61] P. Herdewijn, H. De Winter, B. Doboszewski, I. Verheggen, K. Augustyns, C. Hendrix, T. Saison-Behmoaras, C. De Ranter, A. Van Aerschot in ref. [32], pp. 80–99.
[62] R. W. Wagner, M. D. Matteucci, J. G. Lewis, A. J. Gutierrez, C. Moulds, B. C. Froehler, *Science* **1993**, *260*, 1510–1513.
[63] P. E. Nielsen, M. Egholm, O. Buchardt, *Bioconj. Chem.* **1994**, *5*, 3–7.
[64] A. De Mesmaeker, A. Waldner, J. Lebreton, P. Hoffmann, V. Fritsch, R. M. Wolf, S. M. Freier, *Angew Chem.* **1994**, *106*, 237–240; *Angew. Chem. Int. Ed. Engl.* **1994**, *33*, 226–229.
[65] V. Fritsch, A. De Mesmaeker, A. Waldner, J. Lebreton, M. J. J. Blommers, R. M. Wolf, *Bioorg. Med. Chem.* **1995**, *3*, 321–335.
[66] X. Gao, F. K. Brown, P. Jeffs, N. Bischofberger, K.-Y. Lin, A. J. Pipe, S. A. Noble, *Biochemistry* **1992**, *31*, 6228–6236.
[67] J. M. Veal, F. K. Brown, *J. Am. Chem. Soc.* **1995**, *117*, 1873–1880.
[68] X. Gao, P. W. Jeffs, *J. Biomol. NMR* **1994**, *4*, 17–34.
[69] A. Waldner, A. De Mesmaeker, J. Lebreton, V. Fritsch, R. M. Wolf, *Synlett* **1994**, 57–61.
[70] Y. Cho, F. C. Zhu, B. A. Luxon, D. G. Gorenstein, *J. Biomol. Struct. Dyn.* **1993**, *11*, 685–701.
[71] M. J. J. Blommers, U. Pieles, A. De Mesmaeker, *Nucleic Acids Res.* **1994**, *22*, 4187–4194.
[72] H. Robinson, K.-E. Jung, C. Switzer, A. H.-J. Wang, *J. Am. Chem. Soc.* **1995**, *117*, 837–838.
[73] S. C. Brown, S. A. Thomson, J. M. Veal, D. G. Davis, *Science* **1994**, *265*, 777–780.
[74] M. Leijon, A. Gräslund, P. E. Nielsen, O. Buchardt, B. Nordén, S. M. Kristensen, M. Eriksson, *Biochemistry* **1994**, *33*, 9820–9825.
[75] L. Betts, J. A. Josey, J. M. Veal, S. R. Jordan, *Science* **1995**, *270*, 1838–1841.
[76] R. H. Griffey, E. Lesnik, S. Freier, Y. S. Sanghvi, K. Teng, A. Kawasaki, C. Guinosso, P. Wheeler, V. Mohan, P. D. Cook in ref. [32], pp. 212–224.
[77] B. Honig, A. Nicholls, *Science* **1995**, *268*, 1144–1149, and references therein.
[78] J. K. Strauss, L. J. Maher III, *Science* **1994**, *266*, 1829–1834.
[79] K. Ezaz-Nikpay, G. L. Verdine, *Chem. Biol.* **1994**, *1*, 235–240.
[80] S. A. Wolfe, A. E. Ferentz, V. Grantcharova, M. E. A. Churchill, G. L. Verdine, *Chem. Biol.* **1995**, *2*, 213–221.
[81] J. R. Wyatt, I. Tinoco, Jr. in *The RNA World* (Hrsg.: R. F. Gesteland, J. F. Atkins), Cold Spring Harbor Laboratory Press, Cold Spring Harbor, NY, **1993**, pp. 465–496.
[82] A. Rich, *Gene* **1993**, *195*, 99–109.
[83] K. Yanagi, G. G. Privé, R. E. Dickerson, *J. Mol. Biol.* **1991**, *217*, 201–214.
[84] W. Saenger, W. N. Hunter, O. Kennard, *Nature* **1986**, *324*, 385–388.
[85] H. M. Berman, *Curr. Opin. Struct. Biol.* **1991**, *1*, 423–427.
[86] J. Doucet, J.-P. Benoit, W. B. T. Cruse, T. Prange, O. Kennard, *Nature* **1989**, *337*, 190–192.
[87] Z. Shakked, G. Guerstein-Guzikevich, M. Eisenstein, F. Frolow, D. Rabinovich, *Nature* **1989**, *342*, 456–460.
[88] S. Jain, M. J. Sundaralingam, *J. Biol. Chem.* **1989**, *264*, 12780–12784.
[89] A. Lipanov, M. L. Kopka, M. Kaczor-Grzeskowiak, J. Quintana, R. E. Dickerson, *Biochemistry* **1993**, *32*, 1373–1389.
[90] L. Nekludova, C. O. Pabo, *Proc. Natl. Acad. Sci. USA* **1994**, *91*, 6948–6952.
[91] O. Kennard, W. N. Hunter, *Angew. Chem.* **1991**, *103*, 1280–1304, *Angew. Chem. Int. Ed. Engl.* **1991**, *30*, 1254–1277.
[92] R. E. Dickerson in *Methods in Enzymology, Vol. 211* (Eds.: D. M. J. Lilley, J. E. Dahlberg), Academic Press, San Diego, **1992**, pp. 67–111.
[93] L. Joshua-Tor, J. L. Sussman, *Curr. Opin. Struct. Biol.* **1993**, *3*, 323–335.
[94] M. Egli in *Structure Correlation* (Eds.: H.-B. Bürgi, J. D. Dunitz), VCH, New York, **1994**, pp. 705–749.

[95] A. Rich in *The Chemical Bond: Structure and Dynamics* (Ed.: A. Zewail), Academic Press, New York, **1992**, pp. 31–85.
[96] P. B. Sigler, *Proc. Robert A. Welch Found.* **1993**, *37*, pp. 63–76.
[97] T. A. Steitz, *Structural Studies of Protein-Nucleic Acid Interaction*, Cambridge University Press, Cambridge, **1993**.
[98] *Curr. Opin. Struct. Biol.* **1994**, *4*, 1–66.
[99] W. Saenger, *Principles of Nucleic Acid Structure*, 1st ed., Springer, New York, **1986**.
[100] H. M. Berman, W. K. Olson, D. L. Beveridge, J. Westbrook, A. Gelbin, T. Demeny, S.-H. Hsieh, A. R. Srinivasan, B. Schneider, *Biophys. J.* **1992**, *63*, 751–759.
[101] K. B. Hall, L. W. McLaughlin, *Biochemistry* **1991**, *30*, 10606–10613.
[102] M. Egli, S. Portmann, D. Tracz, C. Workman, N. Usman, *Acta Crystallogr. Sect. D* **1995**, *51*, 1065–1070
[103] S. Portmann, N. Usman, M. Egli, *Biochemistry* **1995**, *34*, 7569–7575; M. Egli, S. Portmann, N. Usman, *ibid.* **1996**, *35*, 8489–8494.
[104] M. Egli, N. Usman, S. Zhang, A. Rich, *Proc. Natl. Acad. Sci. USA* **1992**, *89*, 534–538.
[105] M. Egli, N. Usman, A. Rich, *Biochemistry* **1993**, *32*, 3221–3237.
[106] P. Lubini, W. Zürcher, M. Egli, *Chem. Biol.* **1994**, *1*, 39–45.
[107] R. Wing, H. Drew, T. Takano, C. Broka, S. Tanaka, K. Itakura, R. E. Dickerson, *Nature* **1980**, *287*, 755–758.
[108] A.-H. Wang, Y.-G. Gao in *Methods, Vol. 1* (Eds.: J. N. Abelson, M. I. Simon), Academic Press, San Diego, **1990**, pp. 91–99.
[109] A. C. Dock-Bregeon, D. Moras in *Crystallization of Nucleic Acids and Proteins* (Eds.: A. Ducruix, R. Giegé), Oxford University Press, Oxford, **1992**, pp. 145–174.
[110] J. Jancarik, S.-H. Kim, *J. Appl. Crystallogr.* **1991**, *24*, 409–411.
[111] *Hampton Research Crystallization News* **1995**, *5*, No. 1.
[112] J. A. Doudna, C Grosshans, A. Gooding, C. E. Kundrot, *Proc. Natl. Acad. Sci. USA* **1993**, *90*, 7829–7833.
[113] W. G. Scott, J. T. Finch, R. Grenfell, J. Fogg, T. Smith, M. J. Gait, A. Klug, *J. Mol. Biol.* **1995**, 250, 327–332.
[114] K. J. Baeyens, J. Jancarik, S. R. Holbrook, *Acta Crystallogr. Sect. D* **1994**, *50*, 764–767.
[115] R. V. Gessner, G. J. Quigley, M. Egli, *J. Mol. Biol.* **1994**, *236*, 1154–1168.
[116] H. R. Drew, R. E. Dickerson, *J. Mol. Biol.* **1981**, *151*, 535–556.
[117] M. L. Kopka, A. V. Fratini, H. R. Drew, R. E. Dickerson, *J. Mol. Biol.* **1983**, *163*, 129–146.
[118] K. C. Schneider, S. A. Benner, *J. Am. Chem. Soc.* **1990**, *112*, 453–455.
[119] J. Hunziker, H.-R. Roth, M. Böhringer, A. Giger, U. Diedrichsen, M. Göbel, R. Krishnan, B. Jaun, C. Leumann, A. Eschenmoser, *Helv. Chim. Acta* **1993**, *76*, 259–352.
[120] R. J. Jones, S. Swaminathan, J. F. Milligan, S. Wadwani, B. C. Froehler, M. D. Matteucci, *J. Am. Chem. Soc.* **1993**, *115*, 9816–9817.
[121] K.-H. Altmann, R. Kesselring, E. Francotte, G. Rihs, *Tetrahedron Lett.* **1994**, *35*, 2331–2334.
[122] K.-H. Altmann, R. Imwinkelried, R. Kesselring, G. Rihs, *Tetrahedron Lett.* **1994**, *35*, 7625–7628.
[123] M. Tarköy, M. Bolli, C. Leumann, *Helv. Chim. Acta* **1994**, *77*, 716–744.
[124] M. Egli, P. Lubini, M. Bolli, M. Dobler, C. Leumann, *J. Am. Chem. Soc.* **1993**, *115*, 5855–5856.
[125] P. Lubini, M. Egli in *Structural Biology: The State of the Art, Proceedings of the Eighth Conversation, Vol. 2* (Eds.: R. H. Sarma, M. H. Sarma), Adenine Press, Schenectady, NY, **1994**, pp. 155–175.
[126] K. Gehring, J.-L. Leroy, M. Guéron, *Nature* **1993**, *363*, 561–565; L. Chen, L. Cai, X. Zhang, A. Rich, *Biochemistry* **1994**, *33*, 13540–13546; C. H. Kang, I. Berger, C. Lockshin, R. Ratliff, R. Moyzis, A. Rich, *Proc. Natl. Acad. Sci. USA* **1994**, *91*, 11636–11640; J.-L. Leroy, M. Guéron, *Structure* **1995**, *3*, 101–120; I. Berger, C. H. Kang, A. Fredian, R. Ratliff, R. Moyzis, A. Rich, *Nature Struct. Biol.* **1995**, *2*, 416–425; C. H. Kang, I. Berger, C. Lockshin, R. Ratliff, R. Moyzis, A. Rich, *Proc. Natl. Acad. Sci. USA* **1995**, *92*, 3874–3878.
[127] I. Berger, M. Egli, A. Rich, *Proc. Natl. Acad. Sci. USA* **1996**, *93*, in press.
[128] D. M. Crothers, *Science* **1994**, *266*, 1819–1820, and references therein.
[129] Z. Huang, K. C. Schneider, S. A. Benner in *Antisense Nucleotide Analogs* (Ed.: S. Agrawal), Humana Press, Totawa, NJ, **1993**, pp. 315–353.
[130] C. Richert, A. L. Roughton, S. A. Benner, *J. Am. Chem. Soc.* **1996**, *118*, 4518–4531.
[131] A. L. Roughton, S. Portmann, S. A. Benner, M. Egli, *J. Am. Chem. Soc.* **1995**, *117*, 7249–7250.
[132] R. O. Day, N. C. Seeman, J. M. Rosenberg, A. Rich, *Proc. Natl. Acad. Sci. USA* **1973**, *70*, 849–853.
[133] J. M. Rosenberg, N. C. Seeman, R. O. Day, A. Rich, *J. Mol. Biol.* **1976**, *104*, 145–167.
[134] N. P. Johnson, T. Schleich, *Biochemistry* **1974**, *13*, 981–987.
[135] R. R. Breaker, G. R. Gough, P. T. Gilham, *Biochemistry* **1993**, *32*, 9125–9128.
[136] S. P. Collingwood, A. D. Baxter, *Synlett* **1995**, 703–705.
[137] B. Hyrup, C. Richert, T. Schulte-Herbrüggen, S. A. Benner, M. Egli, *Nucleic Acids Res.* **1995**, *23*, 2427–2433.
[138] Review: S. L. Beaucage, R. P. Iyer, *Tetrahedron* **1993**, *49*, 6123–6194.
[139] S. Portmann, K.-H. Altmann, N. Reynes, M. Egli, *J. Am. Chem. Soc.*, submitted.
[140] R. E. Dickerson, H. R. Drew, *J. Mol. Biol.* **1981**, *149*, 761–786.
[141] H. R. Drew, R. M. Wing, T. Takano, C. Broka, S. Tanaka, K. Itakura, R. E. Dickerson, *Proc. Natl. Acad. Sci. USA* **1981**, *78*, 2179–2183.
[142] K.-H. Altmann CIBA AG, personal communication.
[143] B. S. Sproat, A. I. Lamond, B. Beijer, P. Neuner, U. Ryder, *Nucleic Acids Res.* **1989**, *17*, 3373–3386.
[144] C. Schmit, M.-O. Bévierre, A. De Mesmaeker, K.-H. Altmann, *Bioorg. Med. Chem. Lett.* **1994**, *4*, 1969–1974.
[145] T. E. Haran, Z. Shakked, A. H.-J. Wang, A. Rich, *J. Biomol. Struct. Dyn.* **1987**, *5*, 199–217.
[146] M. Eisenstein, Z. Shakked, *J. Mol. Biol.* **1995**, *248*, 662–678.
[147] A. M. Kawasaki, M. D. Casper, S. M. Freier, E. A. Lesnik, M. C. Zounes, L. L. Cummins, C. Gonzalez, P. D. Cook, *J. Med. Chem.* **1993**, *36*, 831–841.
[148] C. Mattos, B. Rasmussen, X. Ding, G. A. Petsko, D. Ringe, *Nature Struct. Biol.* **1994**, *1*, 55–58.
[149] R. Taylor, J. D. Dunitz, unpublished results.
[150] S. Wang, E. T. Kool, *Biochemistry* **1995**, *34*, 4125–4132.
[151] J. Hall, D. Hüsken, U. Pieles, H. E. Moser, R. Häner, *Chem. Biol.* **1994**, *1*, 185–190, and references therein.
[152] N. Usman, R. Cedergren, *Trends Biochem. Sci.* **1992**, *17*, 334–339, and references therein.
[153] N. Usman, D. T. Stinchcomb, *Nucleic Acids Mol. Biol.* **1995**, *10*, 243–264, and references therein.
[154] F. H. Westheimer, *Acc. Chem. Res.* **1968**, *1*, 70–78.
[155] D. A. Usher, A. H. McHale, *Proc. Natl. Acad. Sci. USA* **1976**, *73*, 1149–1153.
[156] R. S. Brown, J. C. Dervan, A. Klug, *Biochemistry* **1985**, *24*, 4785–4801.
[157] D. Hüsken, G. Goodall, R. Häner, H. E. Moser, unpublished results.
[158] H. W. Pley, K. M. Flaherty, D. B. McKay, *Nature* **1994**, *372*, 68–74.
[159] A. H.-J. Wang, S. Fujii, J. H. van Boom, G. A. van der Marel, S. A. A. van Boeckel, A. Rich, *Nature* **1982**, *299*, 601–604.
[160] S. Portmann, S. Grimm, C. Workman, N. Usman, M. Egli, *Chem. Biol.* **1996**, *3*, 173–184.
[161] H.-N. Wu, O. C. Uhlenbeck, *Biochemistry* **1987**, *26*, 8221–8227.
[162] F. Michel, M. Hanna, R. Green, D. P. Bartel, J. W. Szostak, *Nature* **1989**, *342*, 391–395.
[163] A. Jacquier, *Trends Biochem. Sci.* **1990**, *15*, 351–354.
[164] K. Valegård, J. B. Murray, P. G. Stockley, N. J. Stonehouse, L. Liljas, *Nature* **1994**, *371*, 623–626.
[165] C. C. Query, M. J. Moore, P. A. Sharp, *Genes Dev.* **1994**, *8*, 587–597.
[166] K. H. Altmann, N. M. Dean, D. Fabbro, S. M. Freier, T. Geiger, R. Häner, D. Hüsken, P. Martin, B. P. Monia, M. Müller, F. Natt, P. Nicklin, J. Phillips, U. Pieles, H. Sasmor, H. E. Moser, *Chimia* **1996**, *50*, 168–176.
[167] C. Moulds, J. G. Lewis, B. C. Fröhler, D. Grant, T. Huang, J. F. Milligan, M. D. Matteucci, R. W. Wagner, *Biochemistry* **1995**, *34*, 5044–5053.

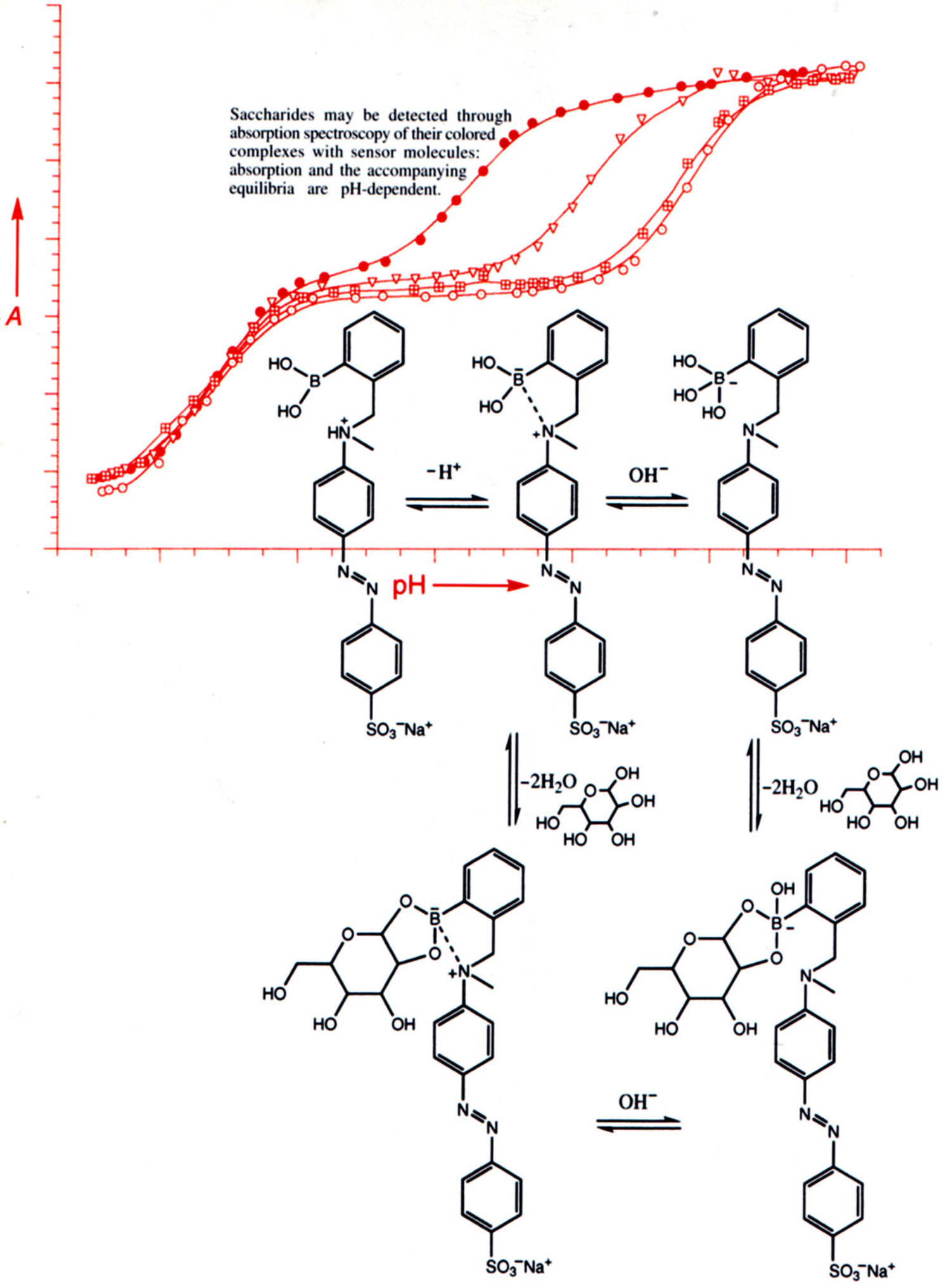
Saccharides may be detected through absorption spectroscopy of their colored complexes with sensor molecules: absorption and the accompanying equilibria are pH-dependent.
A
pH
-H+
OH-
-2H2O
-2H2O
OH-

Saccharide Sensing with Molecular Receptors Based on Boronic Acid

Tony D. James, K. R. A. Samankumara Sandanayake, and Seiji Shinkai*

The lock-and-key principle of natural systems is based on complex interactions like hydrogen bonding. Many synthetic systems that attempt to mimic natural systems have also used hydrogen bonding as the main binding force and have met with great success in non-hydrogen-bonding solvents that do not compete with the guest for the binding pocket. In contrast, natural systems function in water, a very competitive solvent. Synthetic hydrogen-bonding systems may yet evolve to be successful in water. If this transition can not be made, synthetic answers can nevertheless take inspiration from nature without slavishly following the blue print. This is not an attempt to re-invent the "lock": a new locking mechanism merely replaces the existing one. The inspiration might be the view of the hydrogen bond as an easily reversible "covalent" bond. Screening the literature we rediscovered boronic acids, which have been known for over 100 years. Conveniently, boronic acids rapidly and reversibly form cyclic esters with diols in basic aqueous media. Saccharides and other related "keys" contain a contiguous array of cyclic alcohols. In this work we hope to demonstrate that saccharide "keys" and boronic acid "locks" can open the door to a new and exciting field of research.

Keywords: boronic acids · fluorescence · electron transfer · saccharides · molecular recognition

1. Introduction

For many years boron-containing compounds have been important in organic synthesis.[1] However, only recently have aromatic boronic acid derivatives been employed in the construction of receptors for molecules such as saccharides.

Phenylboronic acid was first synthesized by Michaelis and Becker in 1880,[2] but 74 years passed before the first binding studies of diols (or saccharides) with boronic acid were published: in 1954 Kuivila et al. noticed that boronic acids solubilized saccharides and polyols, and they postulated the formation of a cyclic ester.[3] This result agreed with the known ability of borates to form complexes with polyhydroxyl compounds.[4] Subsequently it was found that arsenite and tellurate also formed complexes with polyols.[5] The first quantitative evaluation of interactions between saccharides and boronic acid were published by Lorand and Edwards in 1959.[6]

Despite this, the structure of the boronic acid and saccharide complex in aqueous solution is still in dispute.[7] Boronic acids form covalent bonds with 1,2- or 1,3-diols to generate five- or six-membered cyclic esters in nonaqueous or basic aqueous media (Scheme 1). The rigid, vicinal *cis* diols of saccharides form more stable cyclic esters than simple acyclic diols such as ethylene glycol. With saccharides the formation of a particular cyclic ester is complicated by the possibility of pyranose-to-furanose isomerization of the saccharide moiety. The selectivity of phenylboronic acid (**1**) towards saccharides was determined by Lorand and Edwards[6] (Table 1). This selectivity order seems to be common to all monoboronic acids and will be referred to throughout this review.

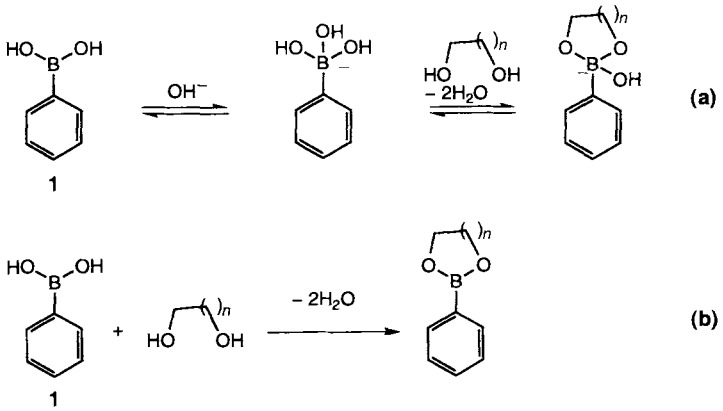

Scheme 1. Ester formation with boronic acids. Reaction (a) in basic, aqueous milieu; reaction (b) in aprotic milieu in the presence of a dehydrating agent.

The interest in the recognition of biologically important molecular species by synthetic molecular receptors has gained momentum recently. The function of many of these receptors, including several that recognize carbohydrates,[9-10] is based on hydrogen-bonding interactions.[8-10] The efficiency of such interactions has been well demonstrated in nonaqueous systems,

[*] Prof. S. Shinkai, Dr. T. D. James, Dr. K. R. A. S. Sandanayake
Shinkai Chemirecognics Project, JRDC
2432-3 Aikawa, Kurume
Fukuoka 830 (Japan)
Fax: Int. code +(92)632-4357

Table 1. Stability constants ($\lg K_a$) for the polyol-**1** complexes.

Polyol	$\lg K_a$
D-fructose	3.64
D-galactose	2.44
D-mannose	2.23
D-glucose	2.04
ethylene glycol	0.44

but in aqueous media competitive hydrogen bonding by the solvent is a serious drawback. Boronic acid readily forms covalent interactions with saccharides in aqueous media, and these represent an important alternative binding force in the recognition of saccharides and related molecular species. Although much progress in the construction and design of sensors based on boronic acids has been made, future development will require a greater understanding of the structural and electronic properties of boronic acids.

As the chemistry of saccharides and related molecular species play a significant role in the metabolic pathways of living organisms, detecting the presence and concentration of biologically important sugars (e.g., glucose, fructose, galactose) in aqueous solution is necessary in a variety of medicinal and industrial contexts. The recognition of D-glucose is of particular interest, since the breakdown of glucose transport in humans has been correlated with diseases such as renal glycosuria,[11, 12] cystic fibrosis,[13] diabetes,[14, 15] and also cancer.[16] Industrial applications range from the monitoring of fermenting processes to the establishment of the enantiomeric purity of synthetic drugs. Current enzymatic detection methods for sugars offer specificity for only a few saccharides; additionally, enzyme-based sensors are unstable in harsh conditions. Stable saccharide receptors based on boronic acid can act as saccharide sensors that are selective and sensitive for a particular saccharide.

The development of boronic acid based molecular receptors has been hampered by synthetic difficulties: Since boronic acids can exist as a mixture of acid and anhydride, analytical difficulties arise. Elemental analyses of boronic acid derivatives are complicated by incombustible residues.[17] The cleavage of boronic acids by copper salts,[18] silver salts,[17] and even by hot water have been reported.[17] This review will not discuss these synthetic aspects, and will instead provide a survey of the development of saccharide sensors based on boronic acid.

2. Saccharide Sensing with Circular Dichroism (CD) Measurements

2.1. Homogeneous Systems

Chiroptical properties, known since the mid-nineteenth century, play an important role in analysis in the food and drug industries. Increasingly strict regulations have applied pressure on industry to produce enantiomerically pure drugs because of the potentially devastating effects of the wrong enantiomer. Moreover, CD measurements are useful for the detection and

T. D. James

K. R. A. S. Sandanayake

S. Shinkai

Seiji Shinkai was born in Fukuoka Prefecture, Japan, in 1944 and received his PhD in 1972 from Kyushu University, where he became a lecturer soon afterwards. After postdoctoral work at the University of California, Santa Barbara, with Thomas C. Bruice, he joined Kyushu University in 1975 and became full professor there in 1988. Currently he is also the director of Shinkai Chemirecognics Project (a government-owned project under the Japanese Research Development Corporation (JRDC)). His research interests focus on host–guest chemistry, molecular recognition, liquid crystals, and enzyme models.

K. R. A. Samankumara Sandanayake was born in 1961 in Colombo, Sri Lanka. He received his B. S. in 1985 from the University of Colombo, and his PhD in 1989 from the Queens University of Belfast under A. P. de Silva on fluorescent macrocyclic sensors for alkali and other cations. After postdoctoral work at the University of Liverpool with Professor I. O. Sutherland on chromoionophoric molecular sensors, he joined the Shinkai Chemirecognics Project in 1993. His research interests include host–guest chemistry, molecular design and recognition, and polymers.

Tony D. James was born in Broseley, Shropshire, England in 1964. He received his B. Sc. in 1986 from the University of East Anglia after returning from a one year exchange with the University of Massachusetts. He received his PhD from the University of Victoria under T. M. Fyles on structure–activity studies of ion channel mimics in 1991. He is currently a postdoctoral fellow at the Chemirecognics Project. His research interests include molecular recognition, molecular assemblies, and molecular machines.

the optical purity of a sample. However, the expensive equipment required for CD measurements hampers the practical applications of this method.

The CD properties displayed because of chiral induction of molecular complexes containing chiral guest species such as saccharides provide an important method to determine the chirality of the guest. This is significant for nonchromophoric host molecules.

The presence of hydroxyl groups with only slight reactivity differences creates problems in designing saccharide receptors. On the other hand, the high number of hydroxyl groups is an advantage if these hydroxyl groups are used in the recognition/binding process. When two boronic acid units are arranged in a suitable orientation in a molecule (as in **2**), a saccharide may be bound in a 1:1 complex through the molecule's head and tail boronic acid groups. (Scheme 2). The cooperative binding by two units to monosaccharides and some disaccharides in basic aqueous media creates a rigid cyclic complex. The asymmetric immobilization of two chromophoric benzene rings by ring closure with saccharides can be "read" by CD spectroscopy.[19-21] D- and L-saccharides give positive and negative exciton coupling, respectively (Fig. 1); the highest association constant is 19000 $dm^3 mol^{-1}$ for glucose. Among the D-saccharides tested, D-galactose was the only saccharide to show a negative exciton coupling in the CD spectrum. Table 2 summarizes the CD data and association constants of different saccharide complexes with **2**. These results imply that the absolute configuration of saccharides can be conveniently predicted from the sign of the CD spectra of **2**. The 1,2-diol is widely accepted as the primary binding site of α-glucose with boronic acid (Fig. 1).[6] The pyranose structure of the D-glucose diboronic acid complex (**2**) was suggested by ^{1}H NMR spectroscopy.[20] However, recent ^{11}B, ^{13}C, and ^{1}H NMR investigations indicated that the complex contains the furanose form of D-glucose.[7]

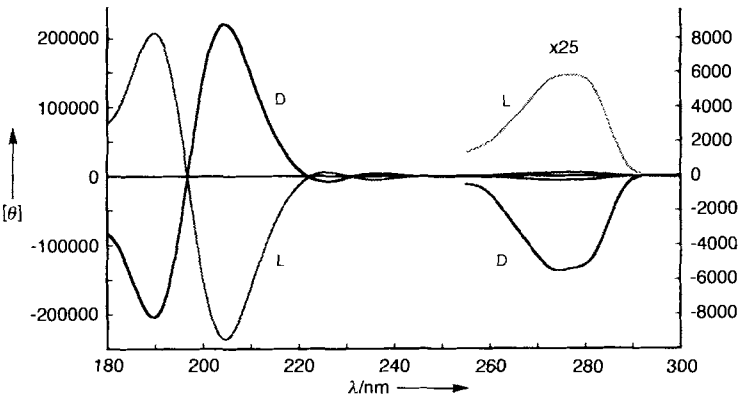

Fig. 1. CD spectra of **2** in the presence of D-glucose (D) and L-glucose (L): c(glucose) = 2.00×10^{-3} mol dm^{-3}, c(**2**) = 1.00×10^{-3} mol dm^{-3}, pH 11.3 with 0.10 mol dm^{-3} carbonate buffer, 25 °C; [θ]: molar ellipticity [° cm^2 $dmol^{-1}$].

Table 2. Absorption and CD maxima of complexes of saccharides with **2** [a].

Saccharide	UV λ_{max} [nm]	CD λ_{max} [nm]	CD $[\theta]_{max}$ [b] [° cm^2 $dmol^{-1}$]	Stoichiometry	K [dm^3 mol^{-1}]
D-glucose	274	275	−5300	1:1	19000
		205	+231000		
	200	190	−214000		
D-mannose	272	274	−400	1:1	60
		205	+69000		
	200	191	−23000		
D-galactose	273	276	+410	1:1	2200
		205	−22000		
	200	191	+19000		
D-talose	272	275	−3700	1:1	4600
		205	+247000		
		190	−196000		
D-fructose	274	[c]	[c]	–	–
	200	[c]	[c]		

[a] 25 °C, c(**2**) = 1.00×10^{-3} or 2.00×10^{-3} mol dm^{-3}, pH 11.3 with 0.10 mol dm^{-3} carbonate buffer. [b] $[\theta]_{max}$ values are calculated for complete formation of a 1:1 complex. [c] No perceptible CD band could be detected.

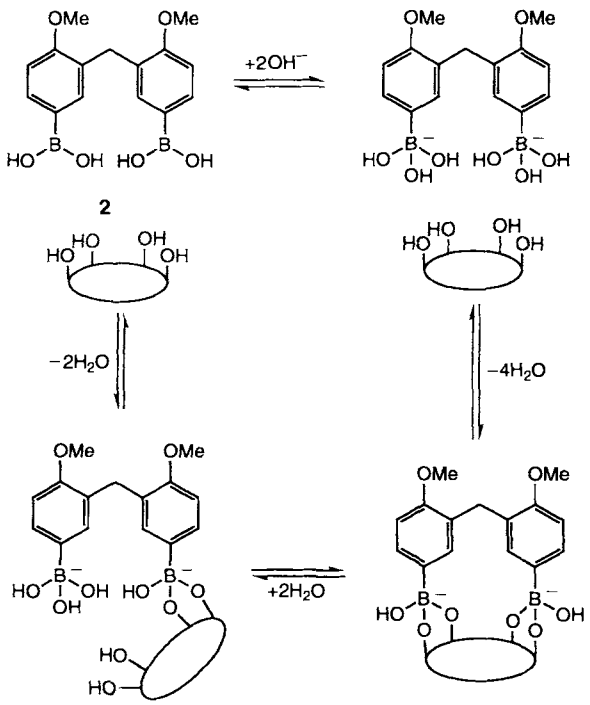

Scheme 2. Formation of the 1:1 complex between a monosaccharide and boronic acid **2**.

Diboronic acid **3** has a greater distance between the two boronic acid moieties and was expected to associate strongly with disaccharides.[21,22] However, association constants for disaccharides were much smaller than those for the complex formed between monosaccharides and **2**. CPK models revealed that the distance between the two boronic acids in **3** is shorter than the distance between the head and tail hydroxyl groups of the disaccharides. Accordingly, the CD activity was much weaker and was inadequate for the estimation of association constants. The Fe^{2+} complex (as $FeCl_2$) with the related diboronic acid **4** gave CD-active saccharide complexes.[23] The CD activity

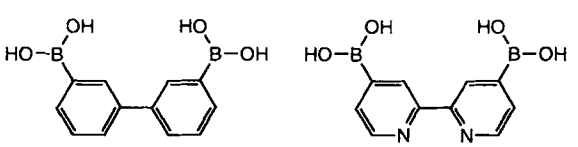

3 **4**

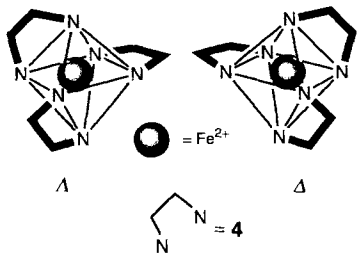

of **4** was derived from the asymmetric immobilization of the two pyridine units on saccharide binding. The Fe^{2+}-**4** complex gave a CD band in the region of the metal-to-ligand charge transfer band. The assignment of *Δ* or *Λ* complexes depended on the saccharide in the complex. For example, the D-maltose complex adopted *Λ* chirality, whereas the D-cellobiose complex adopted *Δ* chirality. The 3,3'-stilbenediboronic acid species **6** similarly gave a CD-active species upon disaccharide complexation.[24] Diboronic acid **5** gave better complexes with disaccharides.[25] The extended chromophore facilitates the detection of CD bands, and the allosteric switching of selectivity by *cis-trans* isomerization of **5** has been investigated.

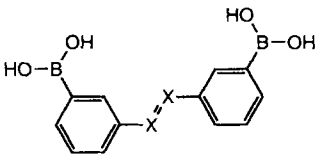

5, X = N
6, X = CH

Nature relies on allosteric (or cooperative) interactions in many biological functions, for instance, the transport of sugars across a cell membrane. In an attempt to mimic these functions, a saccharide-binding diboronic acid unit was combined with a simple crown ether. The strong cooperative binding of **2** prompted the design of such an allosteric system (**7**).[26] The

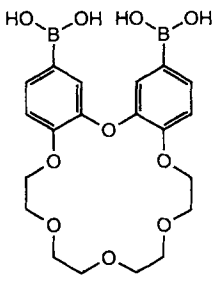

7

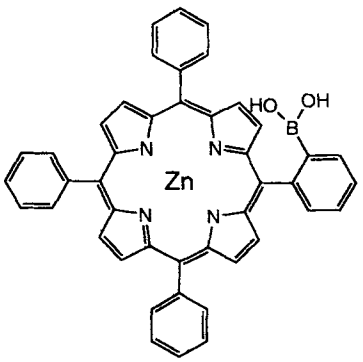

8

change in the angle between two phenyl rings of **2** by some secondary effect contols the sugar binding ability of **2**. Crown ether **7**, with a very similar binding site to **2**, exhibits an even larger association constant for glucose (31 000 $dm^3 mol^{-1}$) in basic $MeOH/H_2O$ solutions (according to CD measurements), since the framework is more flexible with regard to the rotation of the phenyl rings. The binding of metal ions to the crown ether was observed by ^1H NMR spectroscopy. It induces a twist in the crown ether resulting in negative allosterism. Figure 2 shows the decrease of the CD intensity of the D-allose–**7** complex with increasing metal ion concentration.

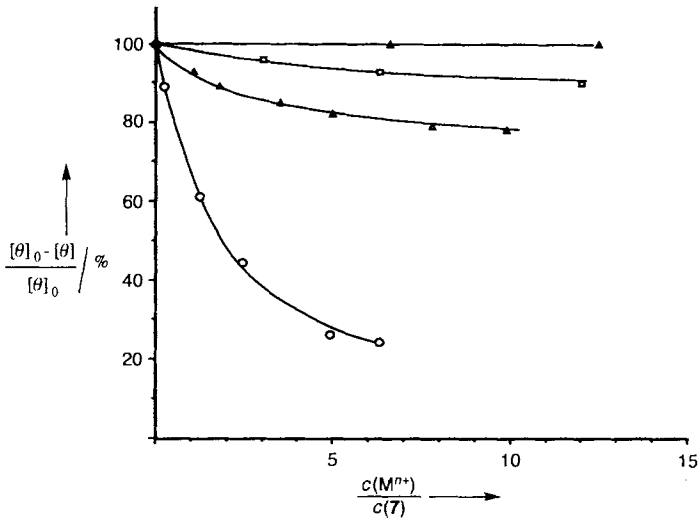

Fig. 2. Decrease in the CD intensity of the D-allose–**7** complex in the presence of metal perchlorates: ○ Ca^{2+}, △ K^+, □ Mg^{2+}, ▲ [Li^+, Na^+, Rb^+, Cs^+]. $c(7) = 1.63 \times 10^{-3}$ mol dm^{-3}, pH = 11.6 with 0.2 % choline hydroxide as the base in 9/1 CH_3OH/H_2O at 25 °C; $[\theta]_0$ and $[\theta]$ are the CD intensity in the absence or presence of metal salt, respectively.

Glucose phosphates are important molecular species in energy storage processes. The metalloporphyrin derivative **8** with a boronic acid appendage selectively distinguishes glucose-6-phosphate from glucose-1-phosphates.[27] The two point binding of glucose-6-phosphate creates a rigid complex that gives a strong exciton coupling signal in the CD spectrum. It is assumed that the strong binding by the primary 1,2-diol binding site of glucose to the boronic acid on one hand, and the subsequent secondary interaction between the phosphate residue and metal center on the other, result in the high affinity for glucose-6-phosphate. The replacement of the 1-hydroxyl group, which is part of the primary binding site of glucose, by a phosphate unit in glucose-1-phosphate weakens the interaction between the saccharide and boronic acid, and hence affects the overall strength of the complex. Binding of phosphate to the metal center was revealed by ^{31}P NMR peak shifts. CD exciton coupling peaks were not found for either metal-free **8** with glucose derivatives or for **8** with glucose itself, which indicates the importance of the two point binding.

2.2. Heterogeneous Systems

Some chiral molecules are known to form chiral, helical aggregates.[28] Chirality can also be induced in aggregates of nonchiral molecules by interactions with chiral species.[29] The chiral, helical aggregates that are formed when aggregates of a nonchiral tetraboronic acid derivative **9** are treated with monosaccharides[30] can be detected by CD spectroscopy. Furthermore, the sign of the exciton coupling of the sugar-complexed aggregate can be predicted by the sugar-induced, chiral orientation of the complex. The chromophoric boronic acid derivative **10** was also found to aggregate in mixed solvents (water/dimethyl formamide).[31] The aggregate was CD active on addition of glucose.

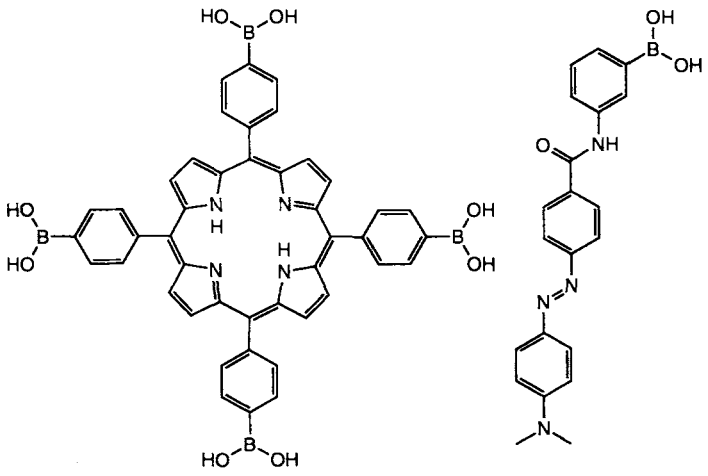

9 10

3. Saccharide Sensing with Absorption Spectroscopy

3.1. Homogeneous Systems

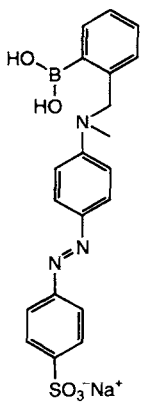

11

Although dyes containing boronic acid residues have been known for a long time,[32] the effect of saccharides on the color of these compounds has not been investigated until recently. The molecular internal-charge-transfer sensor **11**[33] is based on the intramolecular interaction between the boronic acid unit and the tertiary amine.[34] The adjacent amine creates a basic environment around the boronic acid moiety, which facilitates the boronic acid saccharide interaction and lowers the working pH of the sensor molecule.[35] The electronic changes associated with the pK_a changes of the boronic acid unit due to the formation of the boronic acid–saccharide complex[6] are directly transmitted to the neighboring amine moiety, thus causing the CT band in the spectrum of the chromophore to shift. The absorption vs. pH profile for **11** in aqueous media with different saccharides is given in Figure 3. The equilibrium processes in different pH regions and the most important species involved are depicted in Scheme 3. The pK_a value dependent on the boron–nitrogen interaction in **11** shifts on addition of saccharides. The pK_a shift was largest for fructose ($\Delta pK_a = 3.31$) and smallest for simple diols such as ethylene glycol ($\Delta pK_a \approx 0$).

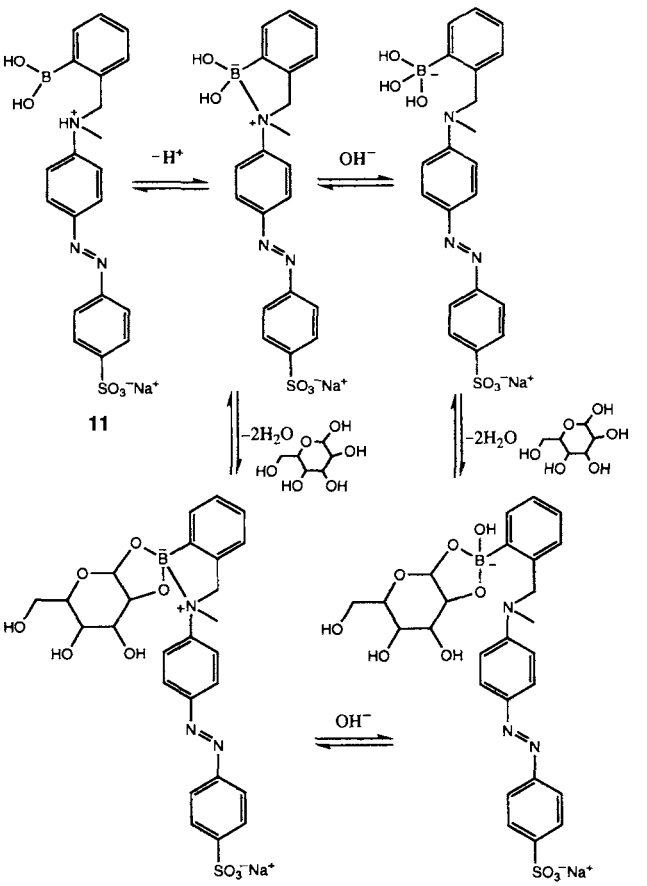

Scheme 3. Formation of the complex between **11** and saccharide at different pH values.

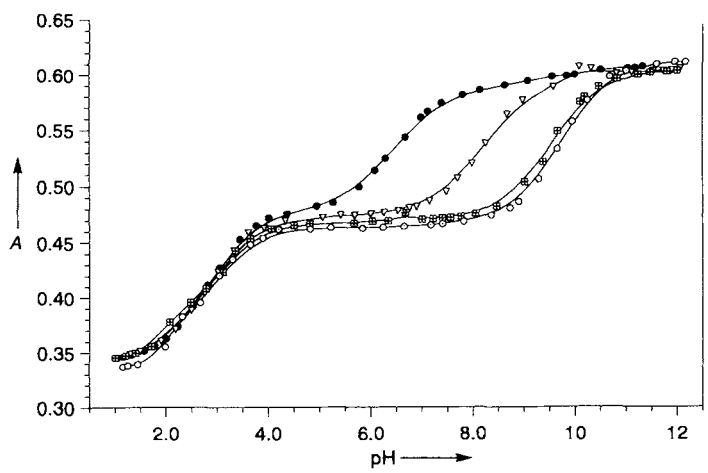

Fig. 3. Changes in absorption in the spectra of **11** (λ_{max} = 468 nm) at different pH values in the presence of 0.05 mol dm^{-3} NaCl and 0.05 mol dm^{-3} D-fructose ●, D-glucose ▽, ethylene glycol ⊞, and without saccharide ⊙.

To date, only small color changes have been achieved when saccharides form complexes with boronic acids. With the aid of better chromophores and better receptors it will be possible to develop selective and sensitive color sensors. Such sensory systems will have widespread applications in industry. For example, it should be possible to provide cheap and stable "test strips" for the detection of blood glucose.

3.2. Liquid Crystalline Systems

Liquid crystals composed of chiral molecules may possess helical structures in which the pitch determines the color of the liquid crystal. The change in pitch induced by inclusion of molecules results in visible color changes, and the spectral shifts can reflect the absolute configuration of such species. A liquid crystalline composite including cholesteryl boronic acid **12** changes color upon introduction of saccharides.[36] The pitch of the

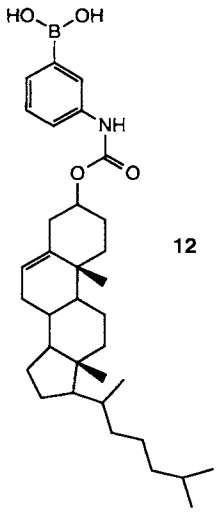

12

liquid crystal directly reflects the chirality of the bound sugar. For example, the green uncomplexed composite turned red upon introduction of D-glucose and blue upon introduction of L-glucose. A direct correlation between the color and the relative position of the saccharide ring when bound to the boronic acid moieties has been proposed.

As with the absorption spectroscopic techniques this system may find applications in test strips. Unfortunately, the response time may be a serious drawback: to be recognized the saccharide in solution must diffuse from the aqueous layer into the cholesteric liquid crystal layer of the test strip.

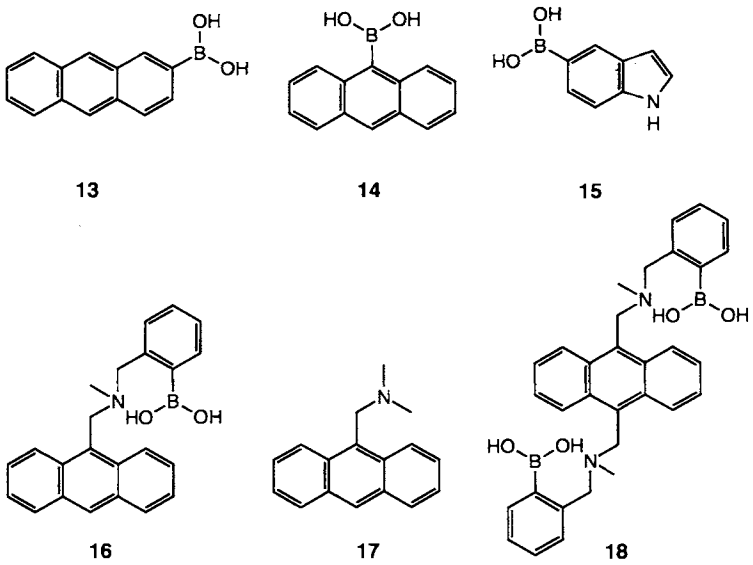

13 14 15 16 17 18

3.3. Heterogeneous Systems

Color changes upon introduction of saccharides have been observed in molecular aggregates of **10** in a DMF/water mixed-solvent system.[31] These changes appear to be due to the deaggregation process induced by saccharide binding.

4. Saccharide Sensing with Fluorescence Spectroscopy

An advantage of fluorescence sensors for saccharides is the inherent sensitivity of the fluorescence technique. Because only small amounts of a sensor are required (typically 10^{-6} M), the synthetic costs of such sensors can be offset. Moreover, fluorescence spectrometers are widely available and inexpensive. Fluorescence sensors have also been applied in continuous monitoring with optical fibers for intracellular mapping with confocal microscopy.

4.1. Homogeneous Systems

4.1.1. PET systems

Photoinduced electron transfer (PET) has been widely used as the preferred tool in fluorescent sensor design for atomic and molecular species.[37, 38] PET sensors generally consist of a fluorophore and a receptor linked by a short spacer. The changes in redox potential of the receptor upon guest binding can alter the PET process and generate changes in the fluorescence. The fluorescence of **13** and **14** was quenched by saccharide binding to the boronic acid moiety.[39] The extent of the pK_a shift for **13** induced by the presence of the saccharide in the medium was in line with the inherent selectivity of phenylboronic acid.[6] The PET from the boronate anion is considered to be the source of the fluorescence quenching. However, PET was not efficient although the boronate anion is directly bound to the chromophore (I(with saccharide)/I_0(without saccharide)$\approx$0.7). Catechol derivatives bind to **13** and **14** with even higher affinity, and the PET from the catechol moiety further increased the fluorescence quenching of the anthracene group.

Similarly, 5-indolylboronic acid (**15**) showed fluorescence quenching upon complexation with oligosaccharides.[40] In the pK_a values determined with ^{11}B NMR shifts were consistent with the fluorescence studies. The stability constants of complexes of **15** with monosaccharides correlated with the inherent selectivity of phenylboronic acid for the sugars.[6] The stability constants of oligosaccharides, on the other hand, were generally lower than predicted on these grounds, although higher oligomers were more stable than lower oligomers because of a secondary interaction with the indole N–H.

The lack of sufficiently large electronic changes in the boronic acid or the saccharide moiety upon complexation has hampered the design of fluorescent sensors based on the interaction between boronic acid and saccharide. Boronic acid binds saccharide only at pH values high enough to create a boronate anion. To overcome these disadvantages fluorescence sensor **16** was designed, based on the structure of **17**.[41] The neighboring group participation of the amine group that lowers the working pH of the sensor molecule[35] also provides an electron-rich center for PET.[37, 42] Fluorescence titration of **16** in aqueous media gives rise to a very high pK_a shift together with a very high fluorescence "switch-on" factor on saccharide binding. The increased acidity of the boronic acid moiety strengthens the boron–nitrogen bond and effectively suppresses the PET process. Figure 4 shows the pH titration of **16** in aqueous media with and without saccharides. The very large pK_a shift enables saccharide sensing over a wide pH. The selectivity of **16** is in line with that observed for other phenylboronic acids.[6]

As glucose possesses at least two binding sites that differ from those in other monosaccharides, it should be possible to selectively bind glucose. This has been achieved in the cleftlike structure of **18**[43, 44] with even higher "switch-on" factors than for **16** (Table 3). Upon 1:1 binding of glucose to the large macrocyclic structure **18** the monosaccharide is situated close to the anthracene aromatic face. The most important species involved in the equilibrium process are shown in Scheme 4. The C3 proton of D-glucose, in particular, points towards the π electrons of the anthracene moiety and consequently gives a very large para-

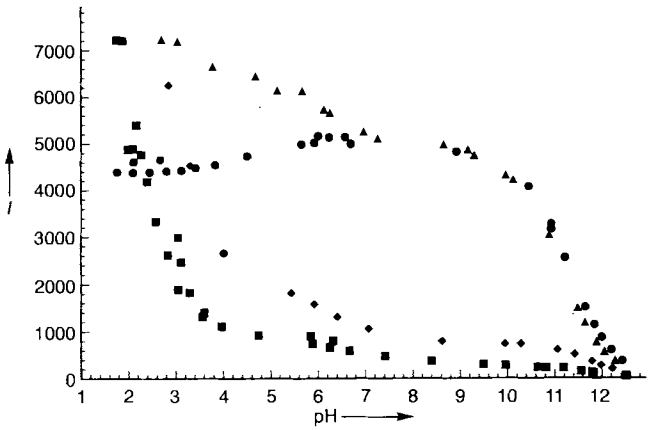

Fig. 4. Relative fluorescence intensity I versus pH profile of **16** at 25 °C; 1.2×10^{-5} mol dm^{-3} **16** in 0.05 mol dm^{-3} sodium chloride solution. Saccharide or ethylene glycol: $c = 0.05$ mol dm^{-3}; ■ only **16**, ● with D-glucose, ▲ D-fructose, ◆ ethylene glycol.

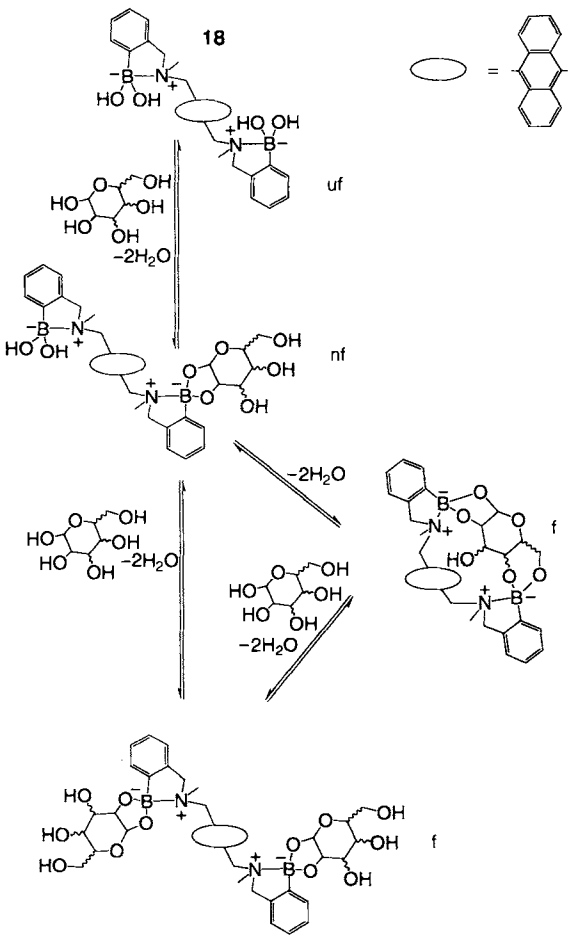

Scheme 4. Formation of the complex between glucose and **18**; f: fluorescent, nf: nonfluorescent.

magnetic shift in the ^{1}H NMR spectrum (Fig. 5). Similar paramagnetic shifts have also been observed in complexes of related PET sensor **19** and α,ω-alkanediyldiammonium ions.[45] The existence of a 1:1 complex of **18** and D-glucose was further confirmed by mass spectrometry. Such cooperative binding of saccharides, specifically glucose, occurs at very low saccharide concentrations. Due to the requirements for PET, noncyclic 1:1

Table 3. Stability constants ($\lg K_a$) for the monosaccharide and ethylene glycol complexes with boronic acids **16**, **18**, and **20**. pH = 7.77 (0.05 mol dm^{-3} phosphate buffer).

	16 [a]	**18** [a]	**20** [b]
D-glucose	1.8	3.6	3.3
D-fructose	3.0	2.5	[c]
D-allose	2.5	2.8	2.9
D-galactose	2.2	2.2	2.9
ethylene glycol	0.4	0.2	−0.5

[a] Measurements in MeOH/H_2O (1/2). [b] Measurements in MeOH/H_2O (2/1). [c] The plot of relative fluorescence intensity vs. saccharide concentration could not be analyzed precisely by a simple Benesi–Hildebrand type equation with the assumption that a 1:1 complex formed.

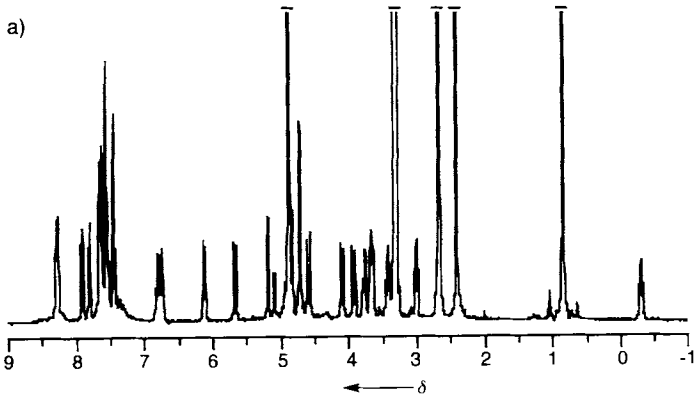

b)

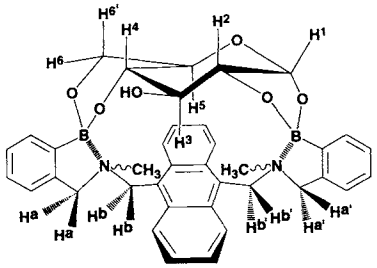

	δ
H1	5.18
H2	3.01
H3	-0.30
H4	2.68 (masked)
H5	3.43
2 H6	3.73
2 Ha or 2 Ha'	3.93 and 4.85 (masked)
2 Ha or 2 Ha'	4.10 and 4.60
2 Hb or 2 Hb'	5.66 and 6.80
2 Hb or 2 Hb'	6.13 and 6.78
CH_3 or H_3C'	2.42
CH_3 or H_3C'	2.68
Solvent	
CH_3OH	3.30
CH_3OH	4.89
Protecting group	
$(CH_3)_2C(CH_2OH)_2$	0.85
$(CH_3)_2C(CH_2OH)_2$	3.40
$(CH_3)_2C(CH_2OH)_2$	4.89

Fig. 5. ^{1}H NMR spectrum (a) and assignments (b) of the 1:1 complex of D-glucose and **18**. The protecting groups were cleaved under the NMR conditions.

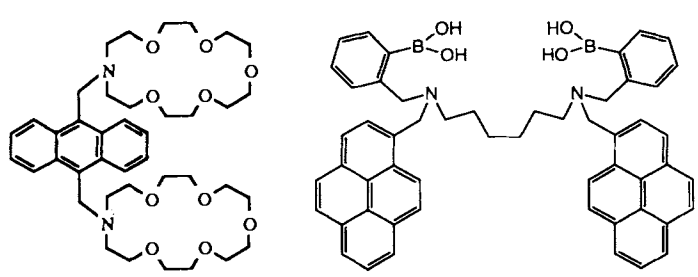

19 **20**

complexes could not be detected by fluorescence spectroscopy; only the 1:1 cyclic complexes and 1:2 complexes give fluorescent signals. In human blood three main monosaccharides are present: D-glucose(0.3–1.0 mM), D-fructose (≤0.1 mM) and D-galactose (≤0.1 mM). Competitive binding studies show that **18** is suitable for the detection of glucose at physiological levels.

Diboronic acid derivative **20**, which has a flexible spacer between the two boronic acids, behaves similarly to **18**.[46] Pyrene fluorophores capable of forming excimers give information on both the saccharide concentration and the structure of the complex. The 1:1 binding of a saccharide to **20** leads to an increase in fluorescence intensity over that of the monomer. This increase was produced partially by less excimer formation and partially by the increased overall fluorescence quantum yield because of the suppression of the PET process. The 1:2 binding of **20** to saccharides, on the other hand, increased the excimer:monomer fluorescence intensity ratio. In all cases the formation of a 1:1 complex was observed at low saccharide concentrations, while the predominant complex changed to 1:2 as the saccharide concentration increased. The selectivity of **20** was found to be similar to that of **18** as shown in Table 3. However, the higher concentration of methanol used in the measurements leads to somewhat lower stability constants than for **18**.

The success of these molecular PET systems prompted the design of **21** (*R* and *S*) for chiral recognition of monosaccharides.[47] Work by Irie et al. on the control of intermolecular chiral 1,1'-binapthyl fluorescence quenching by chiral amines[48] and by Cram et al. on the use of 1,1'-binaphthyl in the recognition of chiral amino acids[49] were the inspiration behind the design of **21**. Chiral recognition of saccharides by **21** utilizes both steric and electronic factors. In 1:1 complexes of **21** and D or L saccharides the asymmetric immobilization of the amine groups, which orients them differently relative to the binaphthyl moiety, leads to a difference in PET behavior. This difference is manifested in the maximum fluorescence intensity of the complex. Steric factors arising from the chiral binaphthyl building block are chiefly reflected by the stability constant of the complex. However, the interdependency of electronic and steric factors is not excluded. Figure 6

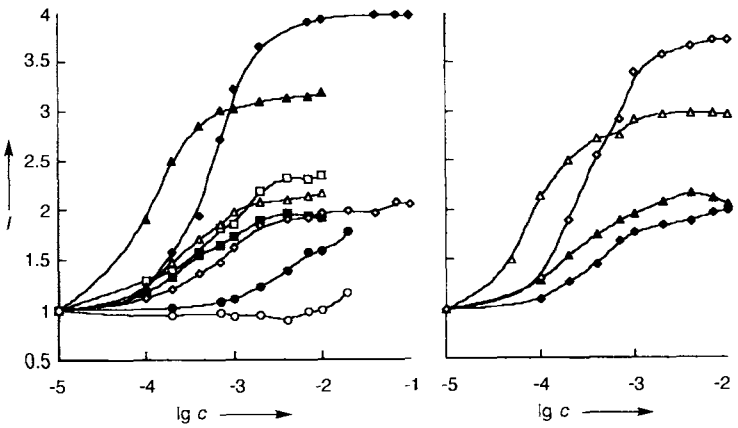

Fig. 6. Relative fluorescence intensity *I* of (*R*)-**21** (left) and (*S*)-**21** (right) versus lg *c*(saccharide) at 25 °C; 1.0×10^{-5} mol dm^{-3} **21** in MeOH/H_2O (1/2) at pH 7.77, λ_{ex} = 289 nm, λ_{em} = 358 nm. ◆ D-glucose, ◇ L-glucose, ■ D-galactose, □ L-galactose, ▲ D-fructose, △ L-fructose, ● D-mannose, ○ L-mannose.

Table 4. Stability constants and fluorescence enhancements for complexes of (*R*)- and (*S*)-**21** with D and L saccharides at pH 7.77 (0.05 mol dm^{-3} phosphate buffer, MeOH/H_2O (1/2)).

Saccharide	lg *K*(D) (±0.05)	lg *K*(L) (±0.05)	I_{em}(D)/I_{em}(L) [b]
fructose	4.0 (3.7)	3.5 (4.0)	1.47 (0.69)
glucose	3.3 (3.4)	3.1 (3.5)	1.93 (0.53)
galactose	3.1	3.3	0.82
mannose	<2.4	–	–

[a] In each case the value for (*S*)-**21** is given in parentheses. [b] I_{em}: fluorescence intensity.

shows the curves for titrations of **21** (*R* and *S* isomers) with D and L saccharides. This new molecular cleft, with a longer spacer unit than that in the anthracene-based diboronic acid **18**, gave the best chiral recognition for fructose. D-fructose was bound best by (*R*)-**21**, which gave rise to a large fluorescence increase. Table 4 shows the stability constants for some D and L monosaccharides. Though chiral recognition of saccharides employing hydrogen bonding by polyhydroxy compounds has been reported,[10] discrimination of isomers in aqueous media by fluorescence, as far as we are aware, had not been achieved before. In this system a combination of steric and electronic factors contributed to the chiral discrimination. Competitive studies with D and L monosaccharides show that selective detection of saccharide isomers is possible with **21**. The availability of both *R* and *S* isomers of this molecular sensor is an important advantage, since concomitant detection of both the D and the L saccharide is possible.

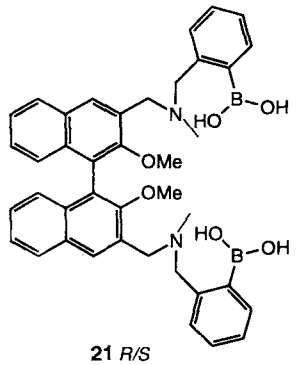

21 *R/S*

4.1.2 *Non-PET Systems*

Disturbing the electron donor or acceptor site of a chromophoric molecule can change its fluorescence properties. This phenomenon has been utilized in the design of fluorescent ionic and neutral compounds.[50] The coumarinium derivative **22** was designed for fluorescence mapping[51] of saccharides in biological samples.[52] The strengthening of the boron–nitrogen bond on saccharide binding was assumed to influence the coumarine internal charge transfer (ICT) chromophore. However, only small fluorescence spectral changes were found on titration of monosaccharides with **22**. In addition, the association constants for simple monosaccharides reveal that the saccharide complexes are considerable less stable. Steric factors together with low basicity of the amino group of **22** are counted as the reasons for this decreased stability.

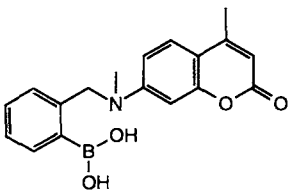

22

As shown above, diboronic acids can bind monosaccharides selectively, and if the binding is 1:1 a rigid molecular complex

is formed.[20–26] This rigidification effect can also be utilized in designing fluorescence sensors for disaccharides. Diboronic acid species **6** selectively forms cyclic complexes with disaccharides in basic aqueous media, which alter the fluorescence properties of the sensor molecule.[24] Excited stilbene is quenched by radiationless decay as a result of rotation of the ethylene double bond. Obstruction of this rotation leads to increased fluorescence.[53] The rigidification of **6** on binding disaccharide therefore increases the stilbene fluorescence. In particular, **6** shows higher selectivity for the disaccharide melibiose than for other common disaccharides and some trisaccharides (Fig. 7). Small

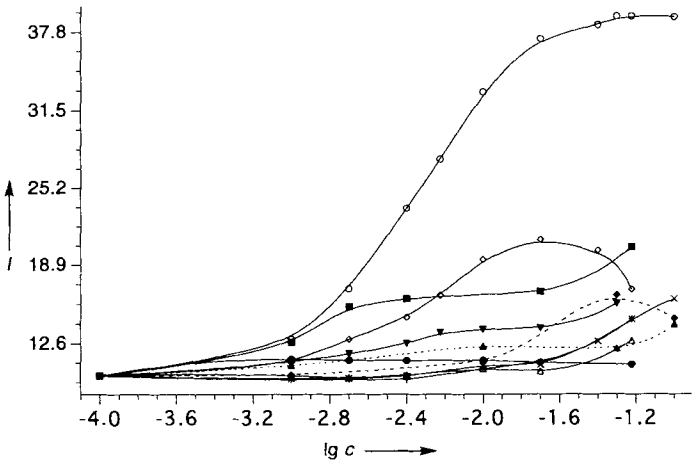

Fig. 7. Fluorescence titration of stilbenediboronic acid **6** (1.0×10^{-5} mol dm^{-3}) at pH 10.6 (0.1 mol dm^{-3} sodium carbonate/sodium bicarbonate buffer) as a function of lg c(disaccharide) (λ_{ex} = 310 nm, λ_{em} = 358 nm); I = relative fluorescence intensity. ○ D-(+)-melibiose, ▼ isomaltose, ◇ gentiobiose, × D-(+)-lactose, +D-(+)-maltose, △ D-(+)-saccharose, ● D-(+)-trehalose, ■ maltotriose, ◆ D-(+)-glucose (dashed line); ▲ D-(+)-mannose (dotted line).

increases of fluorescence intensity found at high concentrations of monosaccharides are believed to derive from 1:2 complex, in which the rotation is restricted by solvent molecules. Increasing viscosity at high saccharide concentration is also believed to increase stilbene fluorescence.[54]

Aggregates of fluorescent molecules do not exhibit fluorescence chiefly because of concentration quenching. Molecular forces which deaggregate such systems can therefore can cause an increase in the fluorescence intensity. Aggregates of porphyrin **23** formed in DMF/water could be dispersed by the

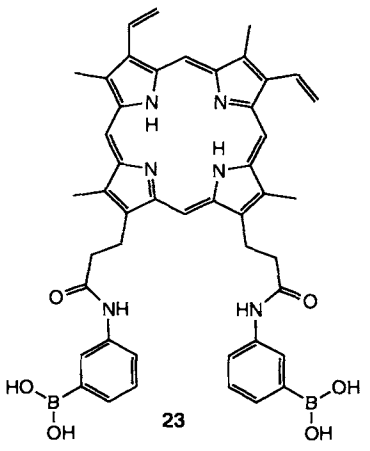

23

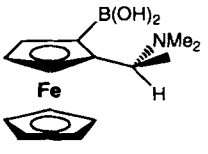

24

introduction of saccharides,[55] which leads to a very large fluorescence increase. Some selectivity has been observed in this process.

Important from a practical viewpoint is that only those of the fluorescent sensors mentioned above that contain a nitrogen atom adjacent to the boronic acid unit are applicable for physiological glucose detection, since they have a large working pH range, including physiological pH (approximately 7.7).

5. Saccharide Sensing with Electrochemical Detection

Electrochemical detection of saccharides by enzymatic decomposition of sugars is well known.[56] Boronic acid based electroactive saccharide receptors could provide selectivity for a range of saccharides. Chiral ferroceneboronic acid derivatives (−)-**24** and (+)-**24** have been synthesized and tested for electrochemical detection of monosaccharides.[57] D-Fructose, D-mannitol and D-sorbitol gave stability constants of 210, 150, and 500 mol^{-1} dm^3, respectively, with (−)-**24** in methanol/water solution. However, no significant chiral discrimination has yet been achieved with (+)- and (−)-**24**, and the field of electrochemical recognition by receptors based on boronic acid remains unexplored.

6. Saccharide Sensing at the Air/Water Interface

Molecular assemblies of monolayers and their properties have been well established.[58] The unique characteristics of Langmuir–Blodgett (LB) films have drawn particular attention. The pressure of an LB film sensitively reflects the interaction between its individual constituents on the surface and the guests in the aqueous subphase. The diboronic acids **25** and **26** (n = 16) were prepared in order to demonstrate the effect of

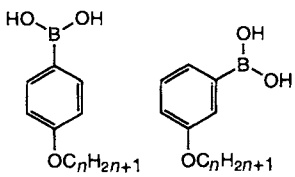

25

26

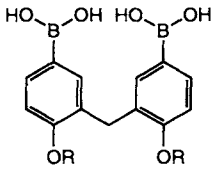

27 **a**, R = methyl
b, R = 2-octyldodecyl
c, R = 4-*tert*-butylbenzyl
d, R = geranyl

saccharide binding at the air/water interface.[59] The reactivity of the boronic acids was tested by solvent extraction methods (solid/solvent, neutral solvent/solvent, and basic solvent/solvent extraction). The ease of extraction of both compounds by the saccharides decreased in the order D-fructose > D-glucose > D-maltose > D-saccharose. Both the irreproducible pressure–area (π-A) isotherms and the crystalline nature of the monolayer indicated that monolayers formed by **25** were unstable. The *meta*-isomer, **26**, on the other hand, gave very reproducible re-

sults. The π-A isotherm of **26** was affected by the introduction of saccharide into the subphase at pH 10. Fructose was found to give the highest effect upon complexation (Fig. 8). The chiral cholesteryl boronic acid derivative **12**, which should selectively recognize chiral isomers of fructose, behaved similarly.[60]

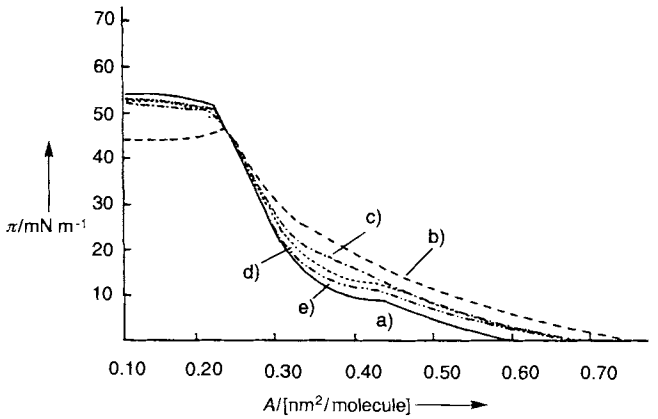

Fig. 8. Influence of saccharide on the π-A isotherms of a monolayer of **26**. The saccharide concentration in the subphase (pH 10.0 with 0.20 mol dm^{-3} carbonate buffer) is 10 mmol dm^{-3}. a) No saccharide, b) D-fructose, c) D-glucose, d) D-maltose, e) D-saccharose.

The influence of quaternized amines on the saccharide binding has also been investigated.[61] They facilitate the saccharide detection by the monolayer at neutral pH, probably because ammonium ions located close to the boronate acid enhance its deprotonation. The binding of saccharides to the diboronic acid derivatives **27a–d** on monolayers has also been investigated and found to be similar to that in homogeneous solutions.[62, 63] Molecular recognition in this system also seems to be facilitated by nearby ammonium cations.[63]

7. Saccharide Transport Through Membranes

Efficient transport of saccharide-related, water-soluble, synthetic drugs into cells through the membrane is critical to the future development of drugs. Many biomimetic systems capable of transporting neutral molecules are known, although examples of systems that can transport such species actively are rare.[64]

As formation of the anionic boronate is favored in alkaline pH and disfavored at acidic pH, glucose can be actively transported by a pH gradient. According to this principle, boronic acid and its derivatives have been used as a carrier in the transport of saccharide through membranes.[65] In saccharide transport by phenylboronic acid derivatives, the phenylboronate ions are accompanied by the lipophilic trioctylmethylammonium cation (TOMA).[65] Saccharide-related biologically important molecular species such as uridine can also be effectively transported in this way.[66, 67] The assistance of F^- ions in saccharide transport has been described by Smith et al.[68] Formation of phenylfluoroboronate[69] was proposed as the reason for this observation. Thus saccharide-related molecular species can be actively transported at neutral pH with a fluoride ion gradient. Interestingly, other halogens do not assist in transport through a membrane. The incorporation of a cationic charge into the boronic acid, as in the pyridinium derivatives **28**, could waive the requirement of an accompanying ammonium cation. Indeed, the strongly acidic pyridiniumboronic acid **28c**

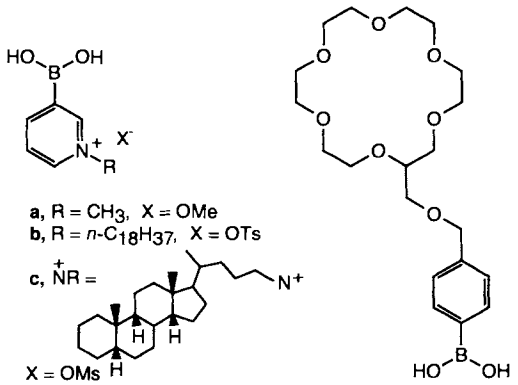

28 **29**

transports saccharide-related species through membranes.[70] The transport of dopamine and its derivatives by the molecular receptor **29** has been reported recently.[71] The cooperative binding by two types of receptor sites is possible in this case. Transport of amino acid derivatives by boronic acid also has been reported.[72]

8. Miscellaneous Applications

Boronic acid derivatives are known to inhibit certain enzymes.[73] For instance, phenylboronic acid inhibits the enzymatic hydrolysis of *N*-benzoyl-L-tyrosine-*p*-nitroanilide by α-chymotrypsin.[74] The inhibitory effect was intensified by the introduction of monosaccharides into the medium. The efficiency of the inhibition by monosaccharides decreases in the following order: D-talose > D-fructose > D-glucose > D-mannose > D-galactose; this differs from the usual order of affinity of phenylboronic acid for monosaccharides. Moreover, the D isomer is more effective than the L isomer. In a separate investigation it was also found that tripodal agents such as **30** can be complexed to boronic acid to regenerate the enzyme activity, thus providing a means of controlling the enzyme activity.[75]

Saccharide-based polymers that retain the inherent chirality of sugars may lead to organized structures such as helices. Diboronic acid **31** has been polymerized with simple monosaccharides or tetrahydroxy compounds.[76] The CD activity of the polymer differs from that of the monomeric structure **32** and is indicative of some type of organized structure. It is impossible to determine whether this polymer has regular head-to-tail or tail-to-head structure. However, the possibility of polymer formation with a C_2-symmetric chiral polyol could provide a means of structure elucidation.

Polymers prepared by imprinting with templates have been used in molecular recognition.[77] Complexes between boronic acid and saccharide have been utilized in this manner to imprint saccharide binding sites into highly cross-linked polymers.[77]

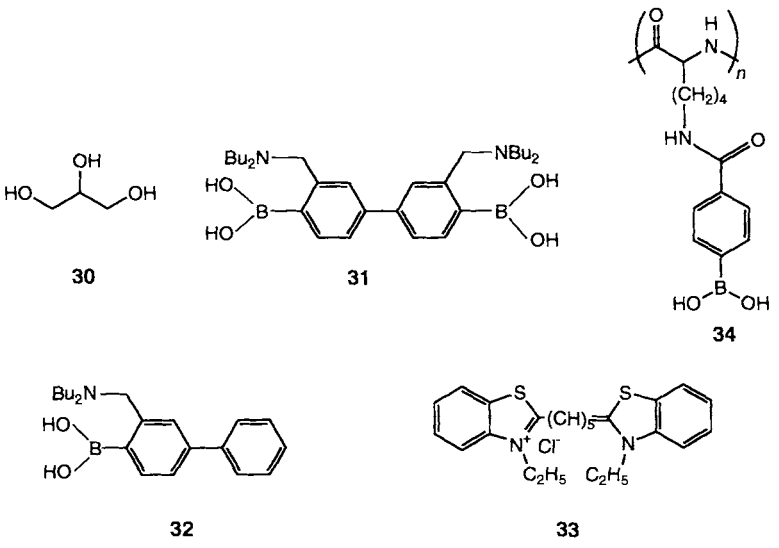

Such systems could be used in the separation of saccharide species.[35, 78]

Poly(D- and L-)lysine modified with boronic acid moieties respond to saccharides by altering the helical structure of the polymer. The helix-coil transition of the polypeptide is induced by subtle forces such as hydrogen bonding, dipole–dipole interactions, and electrostatic repulsion.[79] The boronic acid appended polylysine formed complexes with monosaccharides and altered the pH dependency of the helix-coil transition.[80]

Large ionic dyes are known to form organized inclusion complexes with poly(α-amino acids).[81] The formation of such inclusion complexes of cynene dye **33** with boronic acid appended polylysine is promoted by saccharide binding to the boronic acid moiety.[82] The formation of a boronate anion was facilitated by the inclusion of the cynene dye in a chiral manner and could be monitored by CD spectroscopy. More interestingly, the color of the polymeric assembly changed upon the introduction of saccharides. As an example, increasing D-fructose concentration from 0 to 2.00 mmol dm^{-3} changed the color of the solution from light blue to purple. The change of material properties upon introduction of saccharide related species could be used in molecular sensors and in polymeric materials with interesting physical properties.

9. Conclusions

The interest in boronic acid based molecular receptors for saccharides has grown tremendously during last few years. We believe that this relatively new field will attract the attention of many scientists in the years to come. However, a deeper understanding of the chemistry of boron-containing compounds is imperative for further advances in the development of boronic acid related saccharide receptors and sensing devices.

TDJ would like to thank Dr L. Sarson and Dr P. Linnane for helpful advice and discussions made during the preparation of this manuscript.

Received: April 25
Revised version: November 13, 1995 [A 113 IE]
German version: *Angew. Chem.* **1996**, *108*, 2038–2050

[1] a) M. Christophe, *Tetrahedron* **1994**, *50*, 12521; b) M. F. Lappert, *Chem. Rev.* **1956**, *56*, 959.
[2] a) A. Michaelis, P. Becker, *Ber. Dtsch. Chem. Ges.* **1880**, *13*, 58; b) *ibid.*, **1880**, *15*, 180.
[3] H. G. Kuivila, A. H. Keough, E. J. Soboczenski, *J. Org. Chem.* **1954**, *19*, 780.
[4] a) J. Böesken, V. Rossem, *Recl. Trav. Chim. Pays-Bas Belg.* **1912**, *30*, 392; b) J. Böesken, *Ber. Dtsch. Chem. Ges.* **1913**, *46*, 2612.
[5] G. L. Roy, A. L. Laferriere, J. O. Edwards, *J. Inorg. Nucl. Chem.* **1957**, *114*(4), 106.
[6] J. P. Lorand, J. D. Edwards, *J. Org. Chem.* **1959**, *24*, 769.
[7] J. C. Norrild, H. Eggert, *J. Am. Chem. Soc.* **1995**, *117*, 1479, and references therein.
[8] General hydrogen-bonding systems: a) J. Rebek, Jr., *Angew. Chem.* **1990**, *102*, 261; *Angew. Chem. Int. Ed. Engl.* **1990**, *29*, 245; b) A. D. Hamilton, D. van Engen, *J. Am. Chem. Soc.* **1987**, *109*, 5035; c) S. Goswami, A. D. Hamilton, *ibid.* **1989**, *111*, 3425; d) T. R. Kelly, P. M. Maguire, *ibid.* **1987**, *109*, 6549; e) T. R. Kelly, C. Zhao, G. J. Bridger, *ibid.* **1989**, *111*, 3744; f) M. C. Etter, T. W. Paunto, *ibid.* **1988**, *110*, 5896; g) M. C. Etter, D. A. Adsmond, *J. Chem. Soc. Chem. Commun.* **1990**, 589; h) V. Hedge, P. Madhukar, J. D. Madura, R. P. Thummel, *J. Am. Chem. Soc.* **1990**, *112*, 4549; i) T. W. Bell, L. Liu, *ibid.* **1988**, *110*, 3673; j) H. Furuta, J. L. Sessler, *ibid.* **1991**, *113*, 4706; k) A. Galan, D. Andreu, A. M. Echavarren, P. Prados, J. de Mendoza, *ibid.* **1992**, *114*, 1511.
[9] Hydrogen-bonding systems for saccharide and related compounds: a) Y. Aoyama, Y. Tanaka, S. Sugahara, *J. Am. Chem. Soc.* **1989**, *111*, 5397; b) Y. Tanaka, Y. Ubukata, Y. Aoyama, *Chem. Lett.* **1989**, 1905; c) Y. Kikuchi, Y. Tanaka, S. Sutarto, K. Kobayashi, H. Toi, Y. Aoyama, *J. Am. Chem. Soc.* **1992**, *114*, 10302; d) K. Kobayashi, Y. Asakawa, Y. Kato, Y. Aoyama, *ibid.* **1992**, *114*, 10307; e) R. P. Bonar-Law, A. P. Davis, B. A. Murray, *Angew. Chem.* **1990**, *102*, 1497; *Angew. Chem. Int. Ed. Engl.* **1990**, *29*, 1407; f) N. Greenspoon, E. Wachtel, *J. Am. Chem. Soc.* **1991**, *113*, 7233; g) K. Kano, K. Yoshiyasu, S. Hashimoto, *J. Chem. Soc. Chem. Commun.* **1988**, 801; h) C.-Y. Huang, L. A. Cabell, V. Lynch, E. V. Anslyn, *J. Am. Chem. Soc.* **1992**, *114*, 1900; i) C.-Y. Huang, L. A. Cabell, E. V. Anslyn, *ibid.* **1994**, *116*, 2778; j) A. V. Eliseev, H. J. Schneider, *ibid.* **1994**, *116*, 6081; k) P. B. Savage, S. H. Gellman, *ibid.* **1993**, *115*, 10448; l) G. Das, A. D. Hamilton, *ibid.* **1994**, *116*, 11139; m) J. M. Coteron, C. Vicent, C. Bosso, S. Penades, *ibid.* **1993**, *115*, 10066; n) Y. Kikuchi, K. Kobayashi, Y. Aoyama, *ibid.* **1992**, *114*, 1351.
[10] Hydrogen-bonding systems for the chiral recognition of saccharides: a) R. P. Bonar-Law, J. K. M. Sanders, *J. Am. Chem. Soc.* **1995**, *117*, 259; b) K. M. Bhattarai, R. P. Bonar-Law, A. P. Davis, B. A. Murray, *J. Chem. Soc. Chem. Commun.* **1992**, 752; c) R. Liu, W. C. Still, *Tetrahedron Lett.* **1993**, *34*, 2573; d) J. Cuntze, L. Owens, V. Aleazar, P. Seiler, F. Diederich, *Helv. Chim. Acta* **1995**, *78*, 367.
[11] L. J. Elsaa, L. E. Rosenberg, *J. Clin. Invest.* **1969**, *48*, 1845.
[12] S. De Marchi, E. Cecchin, A. Basil, G. Proto, W. Donadon, A. Jengo, D. Schinella, A. Jus, D. Villalta, P. De Paoli, G. Santini, F. Tesio, *Am. J. Nephrol.* **1984**, *4*, 280.
[13] P. Baxter, J. Goldhill, P. T. Hardcastle, C. J. Taylor, *Gut.* **1990**, *31*, 817.
[14] H. Yasuda, T. Kurokawa, Y. Fuji, A. Yamashita, S. Ishibashi, *Biochim. Biophys. Acta* **1990**, *1021*, 114.
[15] R. N. Fedoak, M. D. Gershon, M. Field, *Gastroenterology* **1989**, *96*, 37.
[16] T. Yamamoto, Y. Seino, H. Fukumoto, G. Koh, H. Yano, N. Inagaki, Y. Yamada, K. Inoue, T. Manabe, H. Imura, *Biochem. Biophys. Res. Commun.* **1990**, *170*, 223.
[17] W. Seaman, J. R. Johnson, *J. Am. Chem. Soc.* **1931**, *53*, 711.
[18] A. D. Donald, F. Challenger, *J. Chem. Soc.* **1930**, 2171.
[19] K. Tsukagoshi, S. Shinkai, *J. Org. Chem.* **1991**, *56*, 4089.
[20] Y. Shiomi, M. Saisho, K. Tsukagoshi, S. Shinkai, *J. Chem. Soc. Perkin Trans. 1* **1993**, 2111.
[21] Y. Shiomi, K. Kondo, M. Saisho, T. Harada, K. Tsukagoshi, S. Shinkai, *Sup. Mol. Chem.* **1993**, *2*, 11.
[22] K. Kondo, Y. Shiomi, M. Saisho, T. Harada, S. Shinkai, *Tetrahedron* **1992**, *48*, 8239.
[23] K. Nakashima, S. Shinkai, *Chem. Lett.* **1994**, 1267.
[24] K. R. A. S. Sandanayake, K. Nakashima, S. Shinkai, *J. Chem. Soc. Chem. Commun.* **1994**, 1621.
[25] T. D. James, Y. Shiomi, K. Kondo, S. Shinkai, presented at the XVIIIth International Symposium on Macrocyclic Chemistry **1993**. University of Twente, Enschede, The Netherlands, Abstract 94.
[26] G. Deng, T. D. James, S. Shinkai, *J. Am. Chem. Soc.* **1994**, *116*, 4567.
[27] T. Imada, K. Kijima, M. Takeuchi, S. Shinkai, *Tetrahedron Lett.* **1995**, *36*, 2093.
[28] R. G. Weiss, *Tetrahedron* **1988**, *44*, 3413.
[29] a) T. D. James, H. Kawabata, R. Ludwig, K. Murata, S. Shinkai, *Tetrahedron* **1995**, *51*, 555; b) T. D. James, K. Murata, T. Harada, K. Ueda, S. Shinkai, *Chem. Lett.* **1994**, 273.

[30] I. Imada, M. Murakami, S. Shinkai, *J. Chem. Soc. Chem. Commun.* **1994**, 1557.
[31] T. Nagasaki, H. Shinmori, S. Shinkai, *Tetrahedron Lett.* **1994**, *35*, 2201.
[32] a) H. R. Snyder, C. Weaver, *J. Am. Chem. Soc.* **1948**, *70*, 232; b) H. R. Snyder, S. L. Meisel, *ibid.* **1948**, *70*, 774; c) H. Gilman, L. Santucci, D. Swayampati, R. Ranck, *ibid.* **1957**, *79*, 2898.
[33] K. R. A. S. Sandanayake, S. Shinkai, *J. Chem. Soc. Chem. Commun.* **1994**, 1083.
[34] a) H. R. Snyder, M. S. Konecky, W. J. Jennarz, *J. Am. Chem. Soc.* **1958**, *80*, 3611; b) R. L. Letsinger, S. H. Dandegaonker, *ibid.* **1959**, *81*, 498; c) R. T. Hawkins, H. R. Snyder, *ibid.* **1960**, *82*, 3863.
[35] a) G. Wulff, *Pure Appl. Chem.* **1982**, *54*, 2093; b) G. Wulff, W. Dederichs, R. Grotstollen, C. Jupe in *Affinity Chromatography and Related Techniques* (Eds.: T. C. J. Gribnau, J. Visser, R. J. F. Nivard), Elsevier, Amsterdam, **1982**, S. 207.
[36] T. D. James, T. Harada, S. Shinkai, *J. Chem. Soc. Chem. Commun.* **1993**, 857.
[37] a) A. J. Bryan, A. P. de Silva, S. A. de Silva, R. A. D. Rupasingha, K. R. A. S. Sandanayake, *Biosensors* **1989**, *4*, 169; b) R. Bissel, A. P. de Silva, H. Q. N. Gunaratna, P. L. M. Lynch, G. E. M. Maguire, K. R. A. S. Sandanayake, *Chem. Soc. Rev.* **1992**, *21*, 187; c) T. D. James, P. Linnane, S. Shinkai, *J. Chem. Soc. Chem. Commun.* **1996**, 281.
[38] A. W. Czarnik, *Fluorescent Chemosensors Ion and Molecular Recognition*, ACS Books, Washington, **1993**; A. W. Czarnik, *Acc. Chem. Res.* **1994**, *27*, 302.
[39] J.-Y. Yoon, A. W. Czarnik, *J. Am. Chem. Soc.* **1992**, *114*, 5874; *Bioorg. Med. Chem.* **1993**, *1*, 267.
[40] Y. Nagai, K. Kobayashi, H. Toi, Y. Aoyama, *Bull. Chem. Soc. Jpn.* **1993**, *66*, 2965.
[41] T. D. James, K. R. A. S. Sandanayake, S. Shinkai, *J. Chem. Soc. Chem. Commun.* **1994**, 477.
[42] A. P. de Silva, R. A. D. Rupasingha, *J. Chem. Soc. Chem. Commun.* **1985**, 1669.
[43] Cleft-type receptors have been extensively studied by J. Rebek, Jr., *Acc. Chem. Res.* **1990**, *23*, 339.
[44] T. D. James, K. R. A. S. Sandanayake, S. Shinkai, *Angew. Chem.* **1994**, *106*, 2287; *Angew. Chem. Int. Ed. Engl.* **1994**, *33*, 2207.
[45] A. P. de Silva, K. R. A. S. Sandanayake, *Angew. Chem.* **1990**, *102*, 1159; *Angew. Chem. Int. Ed. Engl.* **1990**, *29*, 1173.
[46] K. R. A. S. Sandanayake, T. D. James, S. Shinkai, *Chem. Lett.* **1995**, 503.
[47] T. D. James, K. R. A. S. Sandanayake, S. Shinkai, *Nature* **1995**, *374*, 345.
[48] M. Irie, T. Yorozu, K. Hayashi, *J. Am. Chem. Soc.* **1978**, *100*, 2236.
[49] D. J. Cram, *Angew. Chem.* **1986**, *98*, 1041; *Angew. Chem. Int. Ed. Engl.* **1986**, *25*, 1039.
[50] B. Valuer, E. Bardez, *Chem. Br.* **1995**, *31*(3), 216.
[51] A. Minta, J. P. Y. Joseph, R. Y. Tsien, *J. Biol. Chem.* **1989**, *264*, 817.
[52] K. R. A. S. Sandanayake, S. Imazu, T. D. James, M. Mikami, S. Shinkai, *Chem. Lett.* **1995**, 139.
[53] N. J. Turro, *Modern Molecular Photochemistry*, Benjamin, Menlo Park, CA, USA, **1978**.
[54] Cf. Ref. [25], and references therein.
[55] a) H. Murakami, T. Nagasaki, I. Hamachi, S. Shinkai, *Tetrahedron Lett.* **1993**, *34*, 6273; b) *J. Chem. Soc. Perkin Trans. 2* **1994**, 975.
[56] W. Schuhmann, H.-L. Schmidt, *Adv. Biosensors* **1992**, *2*, 79.
[57] A. Ori, S. Shinkai, presented at the Annual Chemical Congress, Kyoto, **1995**, Abstract 3G212.
[58] A. Laschewsky, *Angew. Chem. Adv. Mater.* **1989**, *101*, 1606; *Angew. Chem. Int. Ed. Engl. Adv. Mater.* **1989**, *28*, 1574; *Adv. Mater.* **1989**, 392.
[59] S. Shinkai, K. Tsukagoshi, Y. Ishikawa, T. Kunitake, *J. Chem. Soc. Chem.Commun.* **1991**, 1039.
[60] R. Ludwig, T. Harada, K. Ueda, T. D. James, S. Shinkai, *J. Chem. Soc. Perkin Trans. 2* **1994**, 697.
[61] R. Ludwig, K. Ariga, S. Shinkai, *Chem. Lett.* **1993**, 1413.
[62] R. Ludwig, Y. Shiomi, S. Shinkai, *Langmuir* **1994**, *10*, 3195.
[63] C. Dusemund, M. Mikami, S. Shinkai, *Chem. Lett.* **1995**, 157.
[64] *Liquid Membranes: Chemical Applications*, (Eds. T. Araki, H. Tsukube), CRC press, Boca Raton, FL, USA, **1990**.
[65] T. Shinbo, K. Nishimura, T. Yamaguchi, M. Sugiura, *J. Chem. Soc. Chem. Commun.* **1986**, 349.
[66] B. F. Grotjohn, A. W. Czarnik, *Tetrahedron Lett.* **1989**, *30*, 2325.
[67] G. T. Morin, M. P. Hughes, M.-F. Paugam, B. D. Smith, *J. Am. Chem. Soc.* **1994**, *116*, 8895.
[68] M.-F. Paugam, B. D. Smith, *Tetrahedron Lett.* **1993**, *34*, 3723.
[69] a) L. Maya, *Inorg. Chem.* **1976**, *15*, 2179; b) R. E. Mesmer, A. C. Rutenberg, *ibid.* **1973**, *12*, 699; c) A. K. Sengupta, S. K. Mukherjee, *J. Ind. Chem. Soc.* **1970**, *47*, 679; d) C. Dusmond, K. R. A. S. Sandanayake, *J. Chem. Soc. Chem. Commun.* **1995**, 333.
[70] L. M. Mohler, A. W. Czarnik, *J. Am. Chem. Soc.* **1993**, *115*, 2998.
[71] M.-F. Paugam, L. S. Valencia, B. Boggess, B. D. Smith, *J. Am. Chem. Soc.* **1994**, *116*, 11203.
[72] L. M. Mohler, A. W. Czarnik, *J. Am. Chem. Soc.* **1993**, *115*, 7037.
[73] a) J. C. Powers, H. J. Wade, *Proteinase Inhibitors*, Elsevier, Amsterdam, **1986**; b) M. Philipp, M. L. Bender, *Proc. Natl. Acad. Sci, USA* **1971**, *68*, 478; c) C. A. Kettner, A. B. Shenvi, *J. Biol. Chem.* **1984**, *259*, 15106.
[74] H. Suenaga, K. Nakashima, S. Shinkai, *J. Chem. Soc. Chem. Commun.* **1995**, 29.
[75] H. Suenaga, K. Nakashima, M. Mikami, S. Shinkai, *Chem. Lett.* **1995**, 73.
[76] M. Mikami, S. Shinkai, *J. Chem. Soc. Chem. Commun.* **1995**, 153.
[77] G. Wulff, *Polymeric Reagents and Catalysts (ACS Symp. Ser.* **1986**, *308*, 186); *Angew. Chem.* **1995**, *107*, 1958; *Angew. Chem. Int. Ed. Engl.* **1995**, *34*, 1812.
[78] G. Wulff, W. Vesper, *J. Chromatogr.* **1978**, *9*, 4396.
[79] H. A. Scheraga, *Chem. Rev.* **1971**, *71*, 195.
[80] T. Nagasaki, T. Kimura, S. Arimori, S. Shinkai, *Chem. Lett.* **1994**, 1495.
[81] a) H. Ihara, M. Shibata, C. Hirayama, *Chem. Lett.* **1992**, 1731; b) L. Stryer, E. R. Blout, *J. Am. Chem. Soc.* **1961**, *83*, 1411; c) M. Hatano, M. Yoneyama, Y. Sata, Y. Kawamura, *Biopolymers* **1973**, *12*, 2423.
[82] T. Kimura, T. Takeuchi, T. Nagasaki, S. Shinkai, *Tetrahedron Lett.* **1995**, *36*, 559.

π-Pyrrole–Metal Complexes—The Missing Coordination Mode for Metal–Porphyrin Interactions**

Mathias O. Senge*

The ability of tetrapyrrole systems to coordinate metals is one of the most widely studied areas of porphyrin chemistry. Metalloporphyrins are important natural compounds involved in electron transfer, respiration, and photosynthesis and are gaining industrial importance as catalysts. For a detailed understanding of the mechanisms of catalytic processes performed by metalloporphyrins a thorough study of the interactions between metals and (metallo)porphyrins is necessary.

In theory, four principle coordination modes are possible for metal–porphyrin interactions (Scheme 1): metal σ bonding by

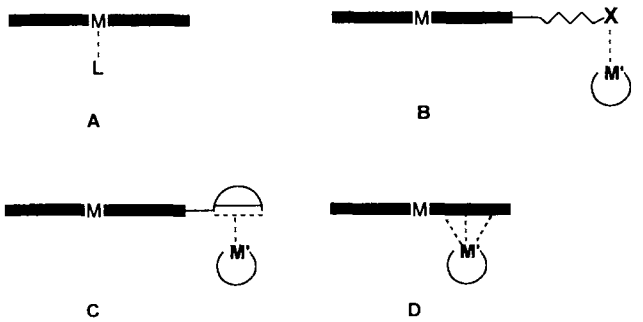

Scheme 1. Types of possible metal–porphyrin interactions.

either the pyrrole nitrogen atoms (A) or through peripheral side chain functionalities (B), and π bonding to metals either through peripheral aromatic systems (C) or by direct involvement of the aromatic porphyrin π system (D).

The best-known coordination type is derived from the intrinsic capability of free base porphyrins to complex almost any known metal ion with the pyrrole nitrogen atoms to yield metalloporphyrins by the formation of N-metal σ bonds.[1] This area of metalloporphyrin chemistry is well developed and encompasses not only the simple chelation of metal centers but also the investigation of metal–metal bonding and organometallic systems. In the latter case the M–C bonds are formed to carbon centers in the axial positions of the metalloporphyrin (type A). So far organometallic porphyrin chemistry has been restricted to this type of "axial coordination chemistry".[2]

Examples for metal coordination by the porphyrin by using functionalities other than the central N atoms are much more scarce. Three different binding motifs have been described for coordination type B. 1) Suitable peripheral substituents may be introduced to establish a second metal chelation site in close vicinity to the metal center of the metalloporphyrin.[3] 2) When heteroatom functionalities are present at the porphyrin periphery, these may serve as ligands for another metal.[4] 3) In a similar manner, the central metal of one metalloporphyrin of type B may form bonds with a second metalloporphyrin by interaction of the heteroatom and the metal, yielding polymeric[5a] or self-organized systems.[5b,c] Typical examples are porphyrins with *meso*-pyridyl or *meso*-nitro substituents as well as chlorophyll-type aggregates.

The structure types A and B are characterized by σ bonds to the metal. In a similar manner, two coordination modes are conceivable that involve π bonding to the metal center. The first example in which the π system of a peripheral substituent of a porphyrin participated in coordination to metal centers was described in 1970 by Gogan and Siddiqui (Scheme 1, type C).[6a] Reaction of zinc(II)tetraphenylporphyrin [Zn^{II}(tpp)] with hexacarbonylchromium(0) yielded the tricarbonylchromium arene complex **1**, in which the tricarbonylchromium(0) species is π-bonded to a *meso*-phenyl substituent. The corresponding [Zn^{II}(tpp){$Cr(CO)_3$}$_2$] complex was also characterized. The second example for type C are ferrocenyl porphyrins, which were prepared directly by reacting pyrrole with suitable aldehydes under the conditions applied by Adler. For instance, use of ferrocenylaldehyde yielded tetraferrocenylporphyrin **2**,[6b] while 4-ferrocenylbenzaldehyde gave tetra(4-ferrocenylphenyl)porphyrin **3**.[6c] Unfortunately, no definite structural data are available for any of these interesting compounds to date.

Examples for coordination type D (Fig. 1), in which the aromatic system of the porphyrin forms π bonds to metal centers, were unknown until recently. In contrast to this the organometallic chemistry of "simple" pyrrole compounds is much better developed. Although N-heterocycles seem to prefer η^1 coordination with metal–nitrogen σ bonds, there are a number of compounds with η^5-heteroatom–metal π bonds.

Most known pyrrole π complexes are obtained from the corresponding azacyclopentadienylanion, which is isoelectronic to cyclopentadienyl (Cp).[7–11] Sandwich complexes with one

[*] Dr. M. O. Senge
Institut für Organische Chemie (WE02) der Freie Universität
Takustrasse 3, D-14195 Berlin (Germany)
Fax: Int. code +(30)838-4248
e-mail: mosenge@chemie.fu-berlin.de

[**] I thank the the Deutsche Forschungsgemeinschaft and the Fonds der chemischen Industrie for their support.

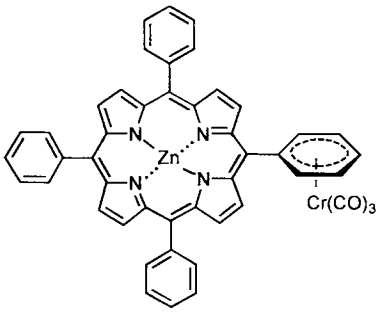

1

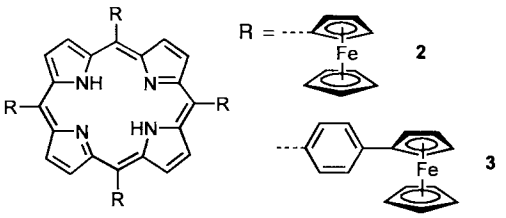

2 3

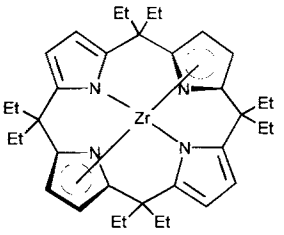

9

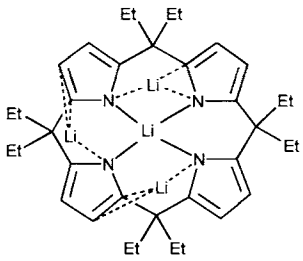

10

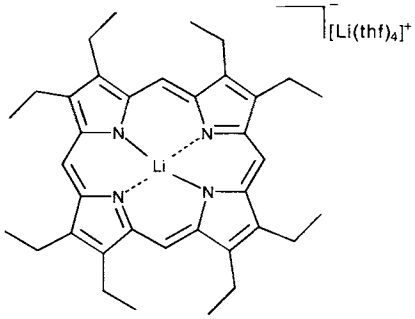

11

(**4**)[8a,c] or two (**5**)[8b,c] η^5-pyrrolyl groups as well as tricarbonyl(η^5-pyrrolyl) complexes (**6**)[9a] and carborane-stabilized η^5-pyrrolyl double and triple-decker compounds have been prepared.[10] In most cases, stable products of the diazametallocene structure type **5** were obtained only after shielding the nonbonding lone pairs of electrons on the nitrogen atom, for example, by employing sterically demanding α-substituents or by using N-alkylated derivatives.[8, 11] Nevertheless, some π-pyrrole complexes with the neutral pyrrole ligand (**7**) are known,[7, 9e] as are species that contain both nitrogen–metal σ and π bonding (**8**).[9d] An interesting combination of the structure type A with

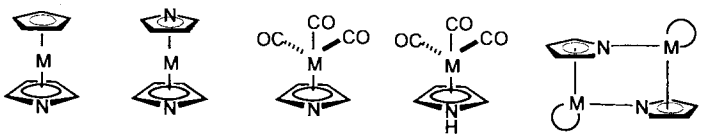

4 5 6 7 8

an azaferrocene (**5**) has been achieved in an Fe^{II}-porphyrin, which is bisaxially coordinated by the pyrrole nitrogen aotms of azaferrocene.[12]

An intermediary position between organometallic derivatives of pyrrole and those of porphyrins is adopted by metal complexes of porphyrinogens. Porphyrinogens are formally hexahydroporphyrins with four isolated pyrrole units separated by sp^3-hybridized carbon atoms. Such systems have been investigated in detail by Floriani and co-workers.[13] The recurring structural theme in transition metal complexes of octaethylporphyrinogen is the formation of both metal–nitrogen σ bonds and metal–(η^5-pyrrolyl) π bonds, which is facilitated by the free rotation of pyrrole rings around the C_m-C_a bonds, for example as shown for the Zr derivative **9**.[13] The intrinsic differences between the porphyrinogen and the porphyrin ligand are also made evident by a comparison of the respective lithium derivatives **10** and **11**.[14] While the porphyrin derivative **11** consists of a $[Li(thf)_4]^+$ ion and a lithium porphyrin anion, in which the lithium atom is bonded to the four pyrrole nitrogen atoms,[14b] the porphyrinogen complex **10** contains three coordination modes for the four lithium atoms. One lithium atom is bonded solely by the pyrrole nitrogen atoms, while the other three are η^2-bonded to a pyrrole ring (either to a C_a-C_b or $N-C_a$ unit) and σ-bonded to another pyrrole nitrogen atom.[14a]

The first example of the coordination type D (π bonding between the aromatic porphyrin system and a metal) has now been described by Rauchfuss et al.[15] Treatment of [(2,3,7,8,12,13,17,18-octaethylporphyrinato)nickel(II)] [Ni^{II}(oep)] with the arenophiles [(cymene)Ru]$(BF_4)_2$ or [(cymene)Ru]-$(F_3CSO_3)_2$, (cymene = *p*-isopropyltoluene) in CH_2Cl_2 at room temperature yielded a green complex of the composition [{(cymene)Ru}Ni^{II}(oep)]$(BF_4)_2$ (**12**). The single-crystal X-ray analysis clearly showed a sandwich-type structure with (η^6-cymene)Ru(η^5-pyrrole) π bonding involving one of the four pyrrole subunits. The planes of the arene and the π-bound pyrrole ring are almost coplanar and show structural characteristics similar to those found for the complex cation [(η^6-cymene)Ru(η^5-C_4Me_4N)]$^{2+}$.[16] These results were confirmed by NMR spectroscopy, which also indicated a considerably decreased ring current in **12**. This novel type of sandwich complex is air-stable; however, even weakly coordinating solvents like acetonitrile dissociate the complex under liberation of [Ni^{II}(oep)].

Similar arene complexes were formed by reacting [Ni^{II}(oep)] with [(cymene)Os]$^{2+}$ or [(Cp*)Ir]$^{2+}$ (Cp* = C_5Me_5). Reaction of [Zn^{II}(oep)] with these reagents gave rise to compounds **13** and **14**, respectively. The latter compound contained a [(η^5-Cp*)-Ir(η^5-pyrrole)] structural motif, opening a way to combine the rich organometallic chemistry of cyclopentadienyl derivatives with that of porphyrins. The results achieved to date indicate that metalloporphyrins seem to be capable of binding only one [(arene)M]$^{2+}$ unit, since reaction with excess arenophile yielded only the 1:1 adducts.

 © VCH Verlagsgesellschaft mbH, D-69451 Weinheim, 1996 0570-0833/96/3517-1924 $ 15.00+.25/0

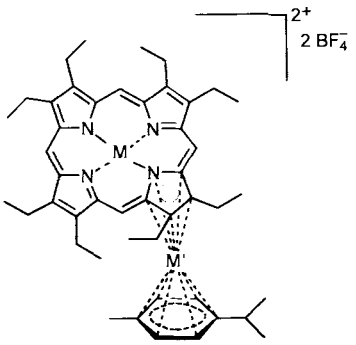

12 M = Ni, M' = Ru
13 M = Zn, M' = Os

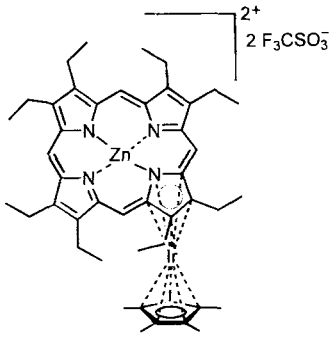

14

The spectroscopic characteristics of the products are quite different from those of the porphyrin starting materials. For instance, the UV/vis spectra showed line broadening and bathochromic shifts of the absorption bands. Very characteristic was the formation of a long wavelength band around 680–770 nm [depending on the $[(arene)M]^{2+}$ unit] similar to those found for chlorins. The coordination of $[(arene)M]^{2+}$ completely quenched the fluorescence of $[Zn^{II}(oep)]$. Thus, clearly π complexation has a strong effect on the metalloporphyrin properties. Further investigation of these and related compounds might help to unravel the mechanism of catalytic processes involving metal–metalloporphyrin interactions.

German version: *Angew. Chem.* **1996**, *108*, 2051–2053

Keywords: arene complexes · porphyrinoids · π-pyrrole complexes · sandwich compounds

[1] a) J. W. Buchler in *The Porphyrins Vol. 1*, (Ed. D. Dolphin), Academic Press, New York, **1978**, p. 389; b) W. R. Scheidt, Y. J. Lee, *Struct. Bonding (Berlin)* **1987**, *64*, 1.

[2] P. J. Brothers, J. P. Collman, *Acc. Chem. Res.* **1986**, *19*, 209; R. Guilard, C. Lecomte, K. M. Kadish, *Struct. Bonding (Berlin)* **1987**, *64*, 205; J. W. Buchler, C. Dreher, F. M. Künzel, *ibid.* **1995**, *84*, 1; R. Guilard, K. M. Kadish, *Chem. Rev.* **1988**, *88*, 1121.

[3] a) M. J. Gunter, L. N. Mander, G. M. Laughlin, K. S. Murray, K. J. Berry, P. E. Clark, D. A. Buckingham, *J. Am. Chem. Soc.* **1980**, *102*, 1470; b) S. J. Rodgers, C. A. Koch, J. R. Tate, C. A. Reed, C. W. Eigenbrot, W. R. Scheidt, *Inorg. Chem.* **1987**, *26*, 3647.

[4] C. Franco, G. McLendon, *Inorg. Chem.* **1984**, *23*, 2370; B. F. Abrahams, B. F. Hoskins, R. Robson, *J. Am. Chem. Soc.* **1991**, *113*, 3606.

[5] a) A. M. Shachter, E. B. Fleischer, R. C. Haltiwanger, *J. Chem. Soc. Chem. Commun.* **1988**, 960; M. O. Senge, K. M. Smith, *ibid.* **1994**, 923; b) S. Anderson, H. L. Anderson, A. Bashall, M. McPartlin, J. K. M. Sanders, *Angew. Chem.* **1995**, *107*, 1196; *Angew. Chem. Int. Ed. Engl.* **1995**, *34*, 1096; c) H. Tamiaki, T. Miyatake, R. Tanikaga, A. R. Holzwarth, K. Schaffner, *ibid.* **1996**, *108*, 810; and **1996**, *35*, 772.

[6] a) N. J. Gogan, Z. U. Siddiqui, *Chem. Commun.* **1970**, 284; *Can. J. Chem.* **1972**, *50*, 720; b) R. G. Wollmann, D. N. Hendrickson, *Inorg. Chem.* **1977**, *16*, 3079; c) E. S. Schmidt, T. S. Calderwood, T. C. Bruice, *ibid.* **1986**, *25*, 3718.

[7] Reviews: D. L. Kershner, F. Basolo, *Coord. Chem. Rev.* **1987**, *79*, 279; N. Kuhn, *Bull. Soc. Chim. Belge* **1990**, *99*, 707.

[8] a) R. B. King, M. B. Bisnette, *Inorg. Chem.* **1964**, *3*, 796; b) N. Kuhn, K. Jendral, R. Boese, D. Bläser, *Chem. Ber.* **1991**, *124*, 87; H. Schumann, J. Winterfeld, H. Hemling, N. Kuhn, *ibid.* **1993**, *126*, 2657; N. Kuhn, M. Köckerling, S. Stubenrauch, D. Bläser, R. Boese, *J. Chem. Soc. Chem. Commun.* **1991**, 1368; N. Kuhn, G. Henkel, S. Stubenrauch, *Angew. Chem.* **1992**, *104*, 766; *Angew. Chem. Int. Ed. Engl.* **1992**, *31*, 778; W. J. Kelly, W. E. Parthun, *Organometallics* **1992**, *11*, 4348; N. Kuhn, G. Henkel, J. Kreutzberg, S. Stubenrauch, C. Janiak, *J. Organomet. Chem.* **1993**, *456*, 97; c) M.-G. A. Shvekhgeimer, *Russ. Chem. Rev.* **1996**, *65*, 41.

[9] a) K. K. Joshi, P. L. Pauson, *Proc. Chem. Soc.* **1962**, 362; W. A Herrmann, I. Schweitzer, P. S. Skell, M. L. Ziegler, K. Weidenhammer, B. Nuber, *Chem. Ber.* **1978**, *111*, 2423; N. Kuhn, S. Stubenrauch, R. Boese, D. Bläser, *J. Organomet. Chem.* **1992**, *440*, 289; b) J. Zakrzewski, *ibid.* **1987**, *326*, C17; H. Felkin, J. Zakrzewski, *J. Am. Chem. Soc.* **1985**, *107*, 3374; c) K. Öfele, E. Dotzauer, *J. Organomet. Chem.* **1971**, *30*, 211; d) N. Kuhn, E.-M. Horn, R. Boese, D. Bläser, *Chem. Ber.* **1989**, *122*, 2275; N. Kuhn, G. Henkel, J. Kreutzberg, *Angew. Chem.* **1990**, *102*, 1179, *Angew. Chem. Int. Ed. Engl.* **1990**, *29*, 1143.

[10] K. J. Chase, R. F. Bryan, M. K. Woode, R. N. Grimes, *Organometallics* **1991**, *10*, 2631.

[11] N. Kuhn, J. Kreutzberg, E.-M. Lampe, D. Bläser, R. Boese, *J. Organomet. Chem.* **1993**, *458*, 125.

[12] J. Zakrzewski, M. Cesario, J. Guilhem, C. Giannotti, *J. Chem. Soc. Dalton Trans.* **1992**, 3059.

[13] a) Review: C. Floriani, *Pure Appl. Chem.* **1996**, *68*, 1; b) S. Isoz, C. Floriani, K. Schenk, A. Chiesi-Villa, C. Rizzoli, *Organometallics* **1996**, *15*, 337.

[14] a) S. De Angelis, E. Solari, C. Floriani, A. Chiesi-Villa, C. Rizzoli, *J. Chem. Soc. Dalton Trans.* **1994**, 2467; b) J. Arnold, D. Y. Dawson, C. G. Hoffman, *J. Am. Chem. Soc.* **1993**, *115*, 2707.

[15] K. K. Dailey, G. P. A. Yap, A. L. Rheingold, T. B. Rauchfuss, *Angew. Chem.* **1996**, *108*, 1985; *Angew. Chem. Int. Ed. Engl.* **1996**, *35*, 1833.

[16] F. Kvietok, V. Allured, M. Rakowski DuBois, *Organometallics* **1994**, *13*, 60.

 © *VCH Verlagsgesellschaft mbH, D-69451 Weinheim, 1996* *0570-0833/96/3517-1925 $ 15.00+.25/0*

A Novel Approach for Clarifying the Reaction Mechanism of Retaining Glycoside Hydrolases

Arnold E. Stütz*

Glycoside hydrolases (glycosidases) are abundant and very important enzymes which degrade poly- and oligosaccharides into monomers or cleave bonds between sugars and non-carbohydrate aglycons. From the degradation of starch to the highly organized and complex process of glycoprotein trimming, glycosidases have many functions essential for the existance and survival of living systems.

Several types of these enzymes have been defined based on their modes of action.[1] Exoglycosidases attack the nonreducing end of a saccharide, while endoglycosidases act somewhere along the polysaccharide chain. In degradation with retaining glycosidases the configuration at the anomeric center is conserved in the product, due to two inversion steps. In contrast, inverting glycosidases mediate a single hydrolysis step with inversion at C-1. In order to fully understand the catalytic properties of glycosidases and to design efficient and highly selective inhibitors for diagnostic as well as therapeutic purposes, their mechanisms have been extensively investigated over the past decades.

Despite extensive efforts it has not been possible to crystallize most of these enzymes, for example numerous interesting exoglycosidases, in order to elucidate their structures and the three-dimensional features of their active sites. Thus, their mechanisms of action have been investigated by indirect methods exploiting substrate analogues such as bromoconduritols, imino sugars, glycosyl fluorides, and related substances as competitive or noncompetitive inhibitors.[2] Mechanistic considerations have been based on work by Koshland[3] and the determination of the structure of hen-egg lysozyme, a small endohexosaminidase, by Phillips and co-workers.[4] According to their results, the reaction follows the pathway depicted in Scheme 1. A catalytically active carboxylic acid function in the active site protonates the glycoside. Subsequently, a carboxylate of the enzyme positioned at the opposite side of the sugar ring stabilizes the cyclic oxocarbonium-like transition state by formation of a covalent bond and inversion of the configuration at the anomeric carbon. This covalently bound glycosyl–enzyme intermediate can be formed from both directions via oxocarbonium-like transition states. Finally, in the hydrolysis step, attack of water at the anomeric center releases the glycoside. For many years it had been generally agreed upon that lysozymes in particular and retaining glycosidases in general had evolved to catalyze the formation of such a cyclic oxocarbonium-like species.[1, 2]

In 1985, on the basis of glycosidase inhibition by imino sugar derivatives, Fleet suggested that glycosidases may follow a reaction pathway in which in the first step the endocyclic bond

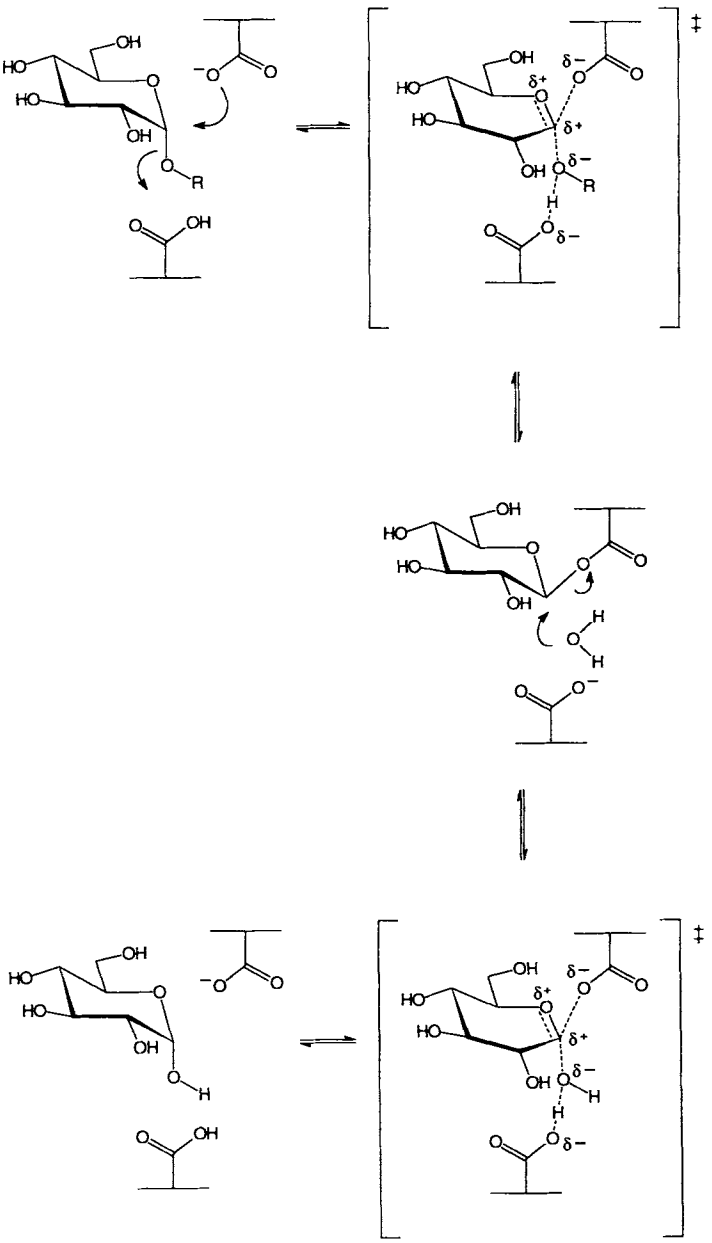

Scheme 1. Mechanism of enzyme-catalyzed glycoside hydrolysis proposed by Phillips et al.

between the ring oxygen and the anomeric carbon is cleaved to form an open-chain intermediate[5] (Scheme 2). Such an intermediate was also deemed to be feasable in an invigorating contribution from Post and Karplus[6] on the mechanism of hen-egg lysozyme. This conclusion was based on the experimentally observed absence of substrate distortions on binding with this enzyme,[4] an observation also commented on by Sinnott[1] and Legler,[2] and further supported by molecular dynamics simula-

[*] Univ.-Doz. Dipl.-Ing. Dr. A. E. Stütz
Institut für Organische Chemie der Technischen Universität
Stremayrgasse 16, A-8010 Graz (Austria)
Fax: Int. code +(316)873-8740
e-mail: stuetz@orgc.tu-graz.ac.at

 © VCH Verlagsgesellschaft mbH, D-69451 Weinheim, 1996 0570-0833/96/3517-1926 $ 15.00+.25/0

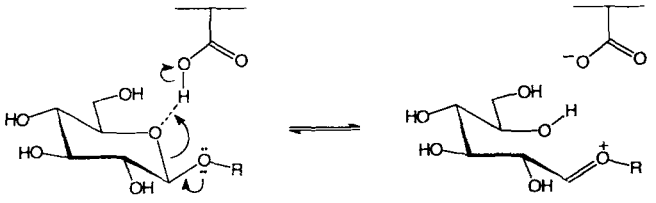

Scheme 2. Mechanism of enzyme-catalyzed glycoside hydrolysis proposed by Fleet.

tions combining the concept of "least molecular motions" with the theory of stereoelectronic control.[7] In this approach, the departure of a leaving group from a tetrahedral carbon center, which is functionalized by one or more heteroatoms, is assisted by the antiperiplanar arrangement of the lone pairs of electrons of the heteroatom(s).[8] An example of this type of mechanism is the nonenzymatic, Lewis acid catalyzed reaction of protected α- and β-glucopyranosides with various nucleophiles in an inert solvent; open-chain derivatives were isolated as the kinetically controlled products.[9]

These findings and conclusions prompted a discussion that continues even today. There are strong arguments against the endocyclic bond fission such as the fact that the enzymatic hydrolysis of glycopyranosyl fluorides or glycosyl pyridinium derivatives is not compatible[1] with this mechanism (Scheme 3).

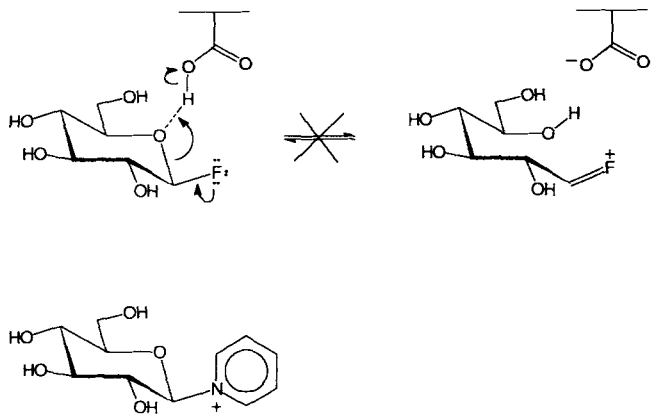

Scheme 3. The hydrolysis of glycopyranosyl fluoride and glycosylpyridinium derivatives does not follow the mechanism proposed by Fleet.

Furthermore, conduritol B epoxide was shown to be opened by both an α-[2, 10] and a β-glucosidase[2, 11] at the oxirane carbon equivalent to C-1 in the naturally occurring substrate and not at the alternative carbon position mimicking O-5 (Scheme 4). Nevertheless, it cannot yet be entirely excluded that during their evolution some glycosidases may have adjusted to changes in the relative basicities of ring oxygen O-5 and anomeric oxygen O-1 as well as to the particular aglycon such that either of these

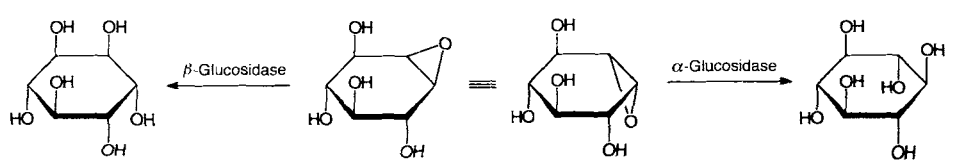

Scheme 4. Conduritol B epoxide is opened at C-1 by both α- and β-glucosidase.

two reaction pathways, which at first glance appear mutually exclusive, are available.

In an attempt to elucidate important mechanistic aspects of retaining glycoside hydrolases, Withers and co-workers synthesized and tested 2-deoxy-2-fluoroglucopyranosyl fluorides[12, 13] and 2-deoxy-2,2-difluoroglucopyranosides[14] as substrate analogues (Scheme 5). The fluorine substituents at C-2 inductively

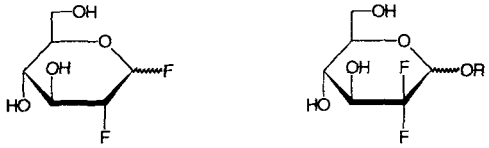

Scheme 5. 2-Deoxy-2-fluoroglucopyranosyl fluoride and 2-deoxy-2,2-difluoroglucopyranoside.

destabilize the developing positive charge at the vicinal anomeric carbon and thus extend the lifetime of the corresponding glycosyl–enzyme adduct. Though this approach worked well with β-glucosidases, it did not meet with success with various α-glucosidases, which require the original substituent at C-2 for proper recognition and binding.[15] Therefore, *N*-acetylhexosaminidases, for example, which require substrates having an acetylamino group at C-2, cannot be investigated with inhibitors of this type.

Recently, in an innovative contribution, McCarter and Withers have overcome these problems by introducing 5-fluoro-D-glucopyranosyl fluorides **1** and **2** as the first representatives of

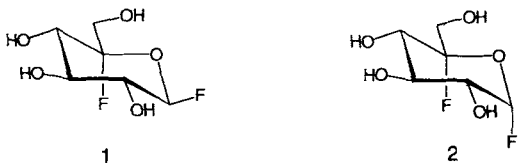

1 **2**

a novel class of "pseudo-substrates".[16] In the course of their investigation exciting new evidence was found in support of the classic mechanism originally proposed by Phillips and coworkers.

Following the approach of Ferrier and Tyler,[17] the two anomers **1** and **2** were synthesized by a simple and elegant route. In these stable new compounds the fluorine atom at C-5 replaces a slightly smaller axial hydrogen atom and does not interfere with the steric and electronic requirements important in recognition and binding. This is an advantage over 2-deoxy-2-fluoroglycopyranosyl fluorides, in which fluorine atom at C-2 in some instances takes the position of an essential hydroxyl or acetylamino group of the natural substrate. 5-Fluoro-β-glucopyranosyl fluoride **1** was shown be a strong inhibitor of the β-glucosidase from *Agrobacterium faecalis*. In marked contrast to results with 2-deoxyfluoro sugars, 5-fluoro-α-glucopyranosyl fluoride **2** turned out to be one of the most powerful inhibitors of α-glucosi-

dase from yeast known to date, hence proving the viability and efficiency of this new approach.

As one of the highlights in this report, an electron spray mass spectrum of the β-glucosidase inactivated by compound **1** showed that the mass of the protein had increased by 181 units, equivalent to one defined fluoroglucopyranosyl moiety attached to the catalytic site. This interesting and telling result provides strong, particularly direct support for the classic mechanism of action of this retaining glycoside hydrolase. Cleavage of an endocyclic C–O bond would have generated an unstable geminal fluorohydrin, which would have released hydrogen fluoride forming a 5-oxo sugar species. If this intermediate would be bound to the enzyme at all, the mass of the complex would be distinctly and measurably different. Consequently, exocyclic bond fission is definitely operative at least in this case.

Clearly, due to the versatility of the approach, 5-fluorohexopyranosyl fluorides and analogous derivatives modified at the anomeric center will be accessible and can serve as useful probes for studying the mechanisms of a large variety of glycosyl hydrolases. In terms of understanding complex bioorganic processes and evolutionary aspects of glycoside hydrolases, it will be exciting to learn whether all glycosidase-catalyzed hydrolysis reactions follow the same reaction pathway as that originally proposed for lysozymes, whether enzymes catalyzing endocyclic bond cleavage can be found with the aid of novel designed pseudo-substrates, and even whether certain enzymes can choose either mechanism, as was suggested in a recent review.[18]

German version: *Angew. Chem.* **1996**, *108*, 2054–2056

Keywords: enzyme inhibitors · fluoro sugars · glycosidases

[1] M. L. Sinnott, *Chem. Rev.* **1990**, *90*, 1171–1202.
[2] G. Legler, *Adv. Carbohydr. Chem. Biochem.* **1990**, *48*, 319–384.
[3] D. E. Koshland, Jr., *Biol. Rev.* **1953**, *28*, 416–436; see also his review: *Angew. Chem.* **1994**, *106*, 2468–2472; *Angew. Chem. Int. Ed. Engl.* **1994**, *33*, 2375–2378.
[4] C. C. F. Blake, L. N. Johnson, G. A. Mair, A. T. C. North, D. C. Phillips, V. R. Sharma, *Proc. R. Soc. London Ser. B* **1967**, *167*, 378–385.
[5] G. W. J. Fleet, *Tetrahedron Lett.* **1985**, *26*, 5073–5076.
[6] C. B. Post, M. Karplus, *J. Am. Chem. Soc.* **1986**, *108*, 1317–1319.
[7] P. Deslongchamps, *Stereoelectronic Effects in Organic Chemistry*, Pergamon, Oxford, **1983**.
[8] A. J. Kirby, *Acc. Chem. Res.* **1984**, *17*, 305–311; see also his review: *Angew. Chem.* **1996**, *108*, 770–790; *Angew. Chem. Int. Ed. Engl.* **1996**, *35*, 706–724.
[9] Y. Guidon, P. C. Anderson, *Tetrahedron Lett.* **1987**, *28*, 2485–2488.
[10] H. Braun, G. Legler, J. Deshusses, G. Semenza, *Biochim. Biophys. Acta* **1977**, *483*, 135–140.
[11] G. Legler, S. N. Hasnain, *Hoppe-Seylers Z. Physiol. Chem.* **1970**, *351*, 25–31.
[12] S. G. Withers, K. Rupitz, I. P. Street, *J. Biol. Chem.* **1988**, *263*, 7929–7932.
[13] I. P. Street, J. B. Kempton, S. G. Withers, *Biochemistry* **1992**, *31*, 9970–9978.
[14] C. Braun, G. D. Brayer, S. G. Withers, *J. Biol. Chem.* **1995**, *270*, 26778–26781.
[15] J. D. McCarter, M. J. Adam, C. Braun, M. Namchuk, D. Tull, S. G. Withers, *Carbohydr. Res.* **1993**, *249*, 77–90.
[16] J. D. McCarter, S. G. Withers, *J. Am. Chem. Soc.* **1996**, *118*, 241–242.
[17] R. J. Ferrier, P. Tyler, *J. Chem. Soc. Perkin Trans. 1* **1980**, 1528–1534.
[18] R. W. Franck, *Bioorg. Chem.* **1992**, *20*, 77–88.

Time is money...

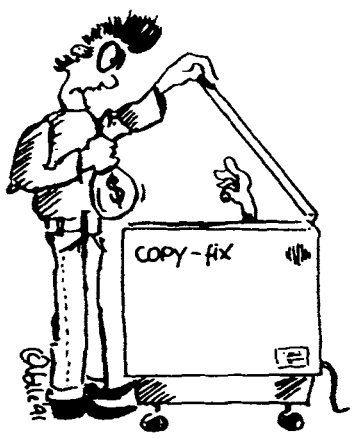

Save both by starting a personal subscription to *Angewandte Chemie* (now with *Chemistry - A European Journal*). At 9¢ per page you can't go wrong. With your own private copy you can read the "hot" articles before they cool, and waste less time in front of the copier.

Order now!
An order form can be found on the last page of this issue.

 © VCH Verlagsgesellschaft mbH, D-69451 Weinheim, 1996 0570-0833/96/3517-1928 $ 15.00+.25/0

Thermodynamically Controlled Self-Assembly of Pseudorotaxanes and Pseudopolyrotaxanes with Different Recognition Motifs Operating Self-Selectively**

Peter R. Ashton, Peter T. Glink,
M.-Victoria Martínez-Díaz, J. Fraser Stoddart,*
Andrew J. P. White, and David J. Williams

The emergence of self-assembly[1] as a new force in chemical synthesis has led to the appearance of numerous novel molecular assemblies[2] and supramolecular arrays.[3] These structures and superstructures, which are not readily accessible by conventional synthetic methodologies alone, rely on the programming of certain recognition motifs with sufficient information to allow them to interact attractively and selectively as a result of highly stabilizing noncovalent bonding interactions. One particularly successful self-assembling system is that arising[4] from the 1:1 association between π-electron deficient bipyridinium dications like paraquat $\mathbf{1}^{2+}$ and macrocyclic polyethers such as bis-*para*-phenylene[34]crown-10 (**BPP34C10**) containing π-

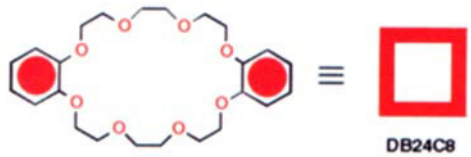

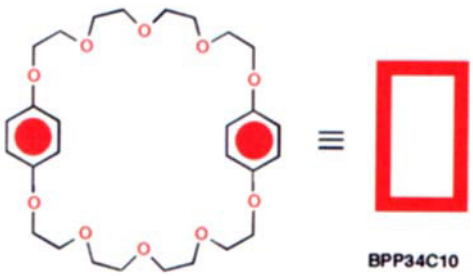

electron rich hydroquinone rings. This system, which can be instructed to operate under kinetic as well as thermodynamic control,[5] has been employed in the self-assembly of pseudorotaxanes,[6] rotaxanes,[7] and catenanes.[8] The requisite molecular recognition depends on π–π stacking augmented by [C–H···O] hydrogen bonding and [C–H···π] interactions. Only last year, a new self-assembling system, which is extremely efficient at producing inclusion complexes with pseudorotaxane-like geometries,[9, 10] emerged on the scene. It relies on the ability of secondary dialkylammonium ion centers, like those in $(\mathbf{2}\text{-H})^+$ and $(\mathbf{3}\text{-H}_2)^{2+}$, to form inclusion complexes with crown ethers, such as dibenzo[24]crown-8 (**DB24C8**) and **BPP34C10**, as a result of primarily [N^+–H···O] and [C–H···O] hydrogen bonding, occasionally supplemented by π–π stacking. The stoi-

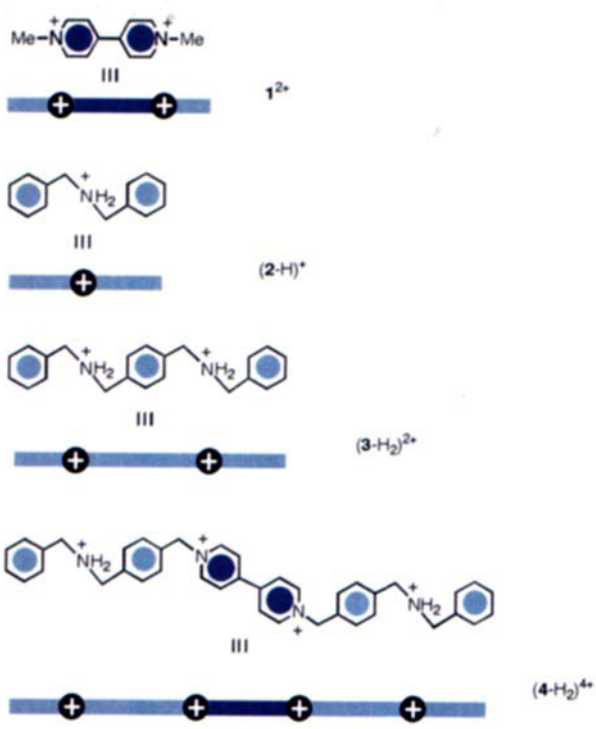

chiometries of the complexes are variable and are dictated by the ability of these thermodynamically fashioned supramolecular arrays to maximize their noncovalent bonding interactions (Scheme 1).

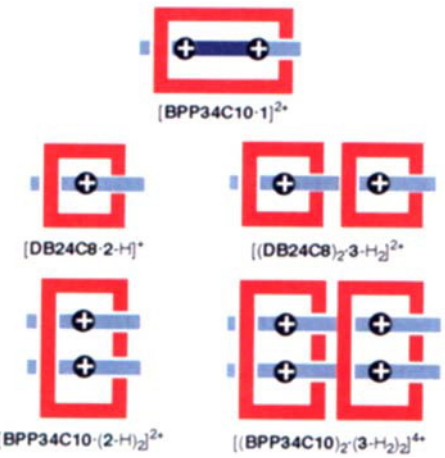

Scheme 1. Cartoon representations of the types of pseudorotaxanes that have been characterized previously.

We pose the following questions: What if the rodlike oligocations contained both a bipyridinium unit and NH_2^+ cationic centers? Would they self-assemble selectively and predictably with **DB24C8** and **BPP34C10** in a complementary manner? Here, we report the preparation of the tetracation $(\mathbf{4}\text{-H}_2)^{4+}$ and its complexation with **BPP34C10** and **DB24C8** and with a mixture of these two crown ethers, as probed by X-ray crystallography, NMR spectroscopy, and mass spectrometry.

The salt $\mathbf{4}\text{-H}_2\cdot 4\,PF_6$ was obtained, after counterion exchange, from the reaction of an excess of the hydrochloride salt of *N*-benzyl-*para*-chloromethylbenzylamine[11] with 4,4′-bipyridine in Me_2SO. Orange single crystals suitable for X-ray crystallog-

[*] Prof. J. F. Stoddart, Dr. M.-V. Martínez-Díaz, Dr. P. T. Glink, P. R. Ashton
School of Chemistry, University of Birmingham
Edgbaston, GB-Birmingham B152TT (UK)
Fax: Int. code +(121)414-3531
e-mail: j.f.stoddart@bham.ac.uk
Dr. D. J. Williams, Dr. A. J. P. White
Chemical Crystallography Laboratory
Department of Chemistry, Imperial College, London (UK)

[**] This research was supported by the Ministerio de Educación y Ciencia in Spain (postdoctoral fellowship to M.-V. M.-D.) and by the ZENECA Strategic Research Fund, the Wolfson Foundation, the Biotechnology and Biological Sciences Research Council, and the Engineering and Physical Sciences Research Council in the United Kingdom.

raphy[12] were obtained from a solution of **BPP34C10** and **4**-$H_2 \cdot 4PF_6$ (4:1 molar ratio) in $MeCN/CH_2Cl_2$ (1:1, v/v), which was layered with *n*-hexane. X-ray structural analysis[13] of a crystal revealed the formation of a complex with an empirical 2:1 stoichiometry, i.e. $[(\mathbf{BPP34C10})_2 \cdot \mathbf{4}\text{-}H_2 \cdot 4PF_6]_n$, in which each $(\mathbf{4}\text{-}H_2)^{4+}$ tetracation is threaded through three **BPP34C10** molecules (Fig. 1). The complex has crystallographic

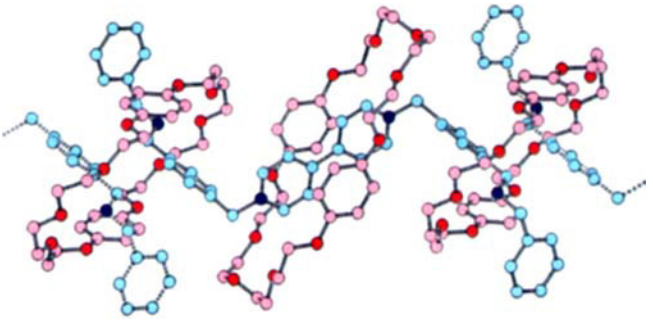

Fig. 1. Ball-and-stick representation of the solid-state structure of the C_i-symmetric "2:1 complex" formed between **BPP34C10** and $(\mathbf{4}\text{-}H_2)^{4+}$. The broken bonds represent portions of lattice-translated tetracationic threads. The π-electron deficient bipyridinium unit is sandwiched between the two hydroquinone rings of the central **BPP34C10** macrocycle (π···π stacking separation of 3.39 Å); the N···N axis of the bipyridinium unit forms an angle of ca. 30° with the OC_6H_4O axes of the hydroquinone rings. Further stabilization is achieved by [C–H···O] hydrogen bonds between one of the hydrogen atoms on each bipyridinium CH_2 group in $(\mathbf{4}\text{-}H_2)^{4+}$ and the central oxygen atoms of the polyether linkages in **BPP34C10**: the [C···O] and [H···O] distances are 3.26 and 2.30 Å, respectively, and the C-H-O angle is 173°. The tetracations are bound to the terminal **BPP34C10** macrocycles through $[N^+-H\cdots O]$ hydrogen bonds between the NH_2^+ centers and the second and fourth oxygen atoms of each polyether linkage: the $[N^+\cdots O]$ and [H···O] distances are 2.94, 2.89, and 1.99, 2.01 Å, respectively, and the N^+-H···O angles are 166 and 151°. The distance between the pair of cothreaded NH_2^+ centers is 8.6 Å, and the separation between the parallel hydroquinone rings in each terminal **BPP34C10** molecule is 6.66 Å (centroid···centroid separation of 6.91 Å).

C_i symmetry; the π-electronsandwich the π-electron deficient bipyridinium unit in the center of the tetracation (cf. $[\mathbf{BPP34C10} \cdot \mathbf{1}]^{2+}$, Scheme 1), while the other two crown ether molecules are positioned around each of the terminal NH_2^+ centers (Fig. 2). Additionally, the terminal dibenzylammonium ion centers are threaded centrosymmetrically with respect to each other through these latter **BPP34C10** molecules in a fashion similar to that observed[9] for the 1:2 complex formed between **BPP34C10** and **2**-H·PF_6 (Scheme 1), producing a pseudopolyrotaxane superstructure (Fig. 2). The pseudopolyrotax-

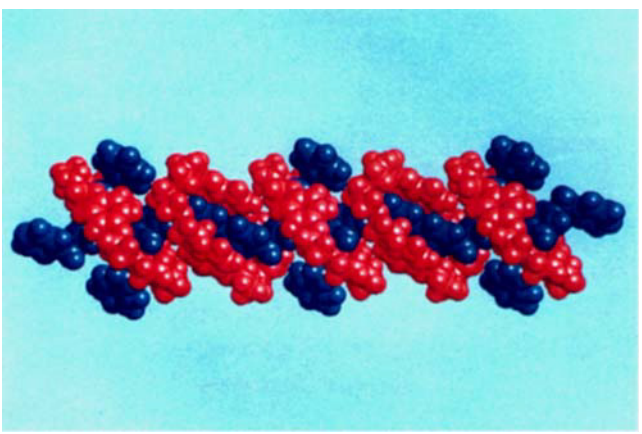

Fig. 2. Space-filling representation of the solid-state structure of a portion of the pseudopolyrotaxane $[(\mathbf{BPP34C10})_2 \cdot \mathbf{4}\text{-}H_2]_n^{4+}$. The **BPP34C10** macrocycle is depicted in red and the threadlike tetracationic component in blue.

ane[14] is stabilized by $[N^+-H\cdots O]$ and [C–H···O] hydrogen bonds as well as by arene–arene π–π stacking interactions.

Crystals of the "2:1 complex" $[(\mathbf{BPP34C10})_2 \cdot \mathbf{4}\text{-}H_2 \cdot 4PF_6]_n$ were also analyzed by liquid secondary ion mass spectrometry (LSIMS),[15] which showed evidence only for a 1:1 complex with intense peaks at *m/z* 1549, 1403, and 1257, corresponding to the loss of one, two, and three PF_6^- ions, respectively, from this species. By contrast, the ^{1}H NMR spectra are markedly dependent upon both the absolute and relative concentrations of the crown ether and the salt. When **BPP34C10** and **4**-$H_2 \cdot 4PF_6$ are present in CD_3COCD_3 in equimolar concentrations, it is the signals for the protons on the bipyridinium unit which experience the largest upfield shifts in this orange-colored solution. However, the addition of a fourfold molar excess of **BPP34C10** relative to **4**-$H_2 \cdot 4PF_6$ leads to small but significant upfield shifts for the $CH_2NH_2^+CH_2$ methylene protons, indicating that, under these conditions,[16] both the terminal dibenzylammonium ion centers and the bipyridinium unit are complexed by **BPP34C10** macrocycles.

The propensity for **4**-$H_2 \cdot 4PF_6$ to form inclusion complexes with the smaller **DB24C8** macrocycle was also investigated by ^{1}H NMR spectroscopy and mass spectrometry. Addition of two molar equivalents of **DB24C8** to a solution of **4**-$H_2 \cdot 4PF_6$ in CD_3COCD_3 resulted in a pale yellow solution. Its ^{1}H NMR spectrum suggested selective complexation of the dibenzylammonium ion centers by the **DB24C8** macrocycles since the signals for the $CH_2NH_2^+CH_2$ methylene and bipyridinium CH_2 and αCH protons of the bound $(\mathbf{4}\text{-}H_2)^{4+}$ tetracation were shifted significantly upfield. On the other hand, the resonances associated with the bipyridinium βCH protons were hardly influenced at all upon complexation, suggesting that it is indeed the NH_2^+ ion centers which are complexed by this crown ether. The spectrum showed separate sets of signals for free **DB24C8**, free **4**-$H_2 \cdot 4PF_6$, and the 2:1 complex $[(\mathbf{DB24C8})_2 \cdot \mathbf{4}\text{-}H_2][PF_6]_4$, indicating slow complexation/decomplexation on the ^{1}H NMR timescale at room temperature (cf. the behavior of $[\mathbf{DB24C8} \cdot \mathbf{2}\text{-}H][PF_6]$ in a variety of solvents[9]). On increasing the molar excess of **DB24C8** in the CD_3COCD_3 solution to sixfold, only signals corresponding to the excess free crown ether and the 2:1 complex were observed[17] in the ^{1}H NMR spectrum. LSIMS[15] confirmed the presence of such a complex with peaks at *m/z* 1910 and 1765 arising from loss of one and two PF_6^- ions, respectively, from the 2:1 complex.

Finally, we investigated the complexation of the $(\mathbf{4}\text{-}H_2)^{4+}$ tetracation by a mixture of **BPP34C10** and **DB24C8**. Orange crystals suitable for X-ray crystallography[12] were obtained from a solution of **DB24C8**, **BPP34C10**, and **4**-$H_2 \cdot 4PF_6$ (6:4:1 molar ratio) in Me_2CO which was layered with *n*-hexane. X-ray crystal structure analysis[18] reveals the formation of the expected 2:1:1 complex (Fig. 3). The central π-electron deficient bipyridinium unit of the tetracation is sandwiched between the π-electron donating hydroquinone rings of the larger **BPP34C10** macrocycle (cf. $[\mathbf{BPP34C10} \cdot \mathbf{1}]^{2+}$, Scheme 1), while the two terminal dibenzylammonium ion centers are encircled by the smaller **DB24C8** macrocycles (cf. $[\mathbf{DB24C8} \cdot \mathbf{2}\text{-}H]^+$ and $[(\mathbf{DB24C8})_2 \cdot \mathbf{3}\text{-}H_2]^{2+}$, Scheme 1). The overall structure has close to a C_i-symmetric arrangement which is broken only by the adoption of an *anti* geometry by one of the $CH_2OC_6H_4OCH_2$ units in the **BPP34C10** and a *syn* geometry for the other. In the case of the bipyridinium·**BPP34C10** recognition site, stabilization is achieved by a combination of π–π stacking and [C–H···O] hydrogen bonding interactions. In the case of the two $CH_2NH_2^+CH_2$·**DB24C8** recognition sites, stabilization arises principally from a mixture of $[N^+-H\cdots O]$ and [C–H···O] hydrogen bonding involving hydrogen atoms on

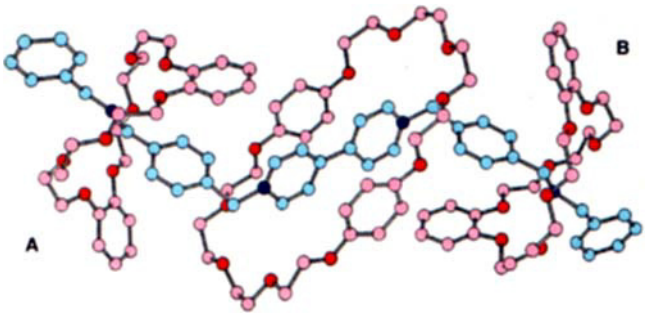

Fig. 3. Ball-and-stick representation of the solid-state structure of the asymmetric 2:1:1 complex formed between **DB24C8**, **BPP34C10**, and $(\mathbf{4}\text{-}H_2)^{4+}$. The distances associated with the $\pi-\pi$ stacking interaction between the bipyridinium unit and the approximately parallel (6° tilt) hydroquinone rings of the **BPP34C10** macrocycle are 3.48 and 3.54 Å. The N···N axis of the former is tilted by ca. 24° to the mean plane of the hydroquinone ring oxygen atoms. Stabilizing [C–H···O] hydrogen bonds are from one of the hydrogen atoms on each bipyridinium CH_2 group in $(\mathbf{4}\text{-}H_2)^{4+}$ to the central oxygen atoms in the polyether linkages in **BPP34C10**: the [C···O] and [H···O] distances are 3.19, 3.28 and 2.27, 2.33 Å, respectively, and the C-H···O angles are 161 and 173°. The $[N^+-H\cdots O]$ and [C–H···O] hydrogen bonding, involving the $CH_2NH_2^+$ centers and the terminal **DB24C8** macrocycles, although essentially the same for both sites (A and B), constitutes an extremely complex pattern. Although the conformations of the two **DB24C8** macrocycles are very similar, there are small differences in the "cleft angles" between the catechol rings: 70° in A and 73° in B. The associated centroid–centroid separations between the catechol rings are 9.23 Å in A and 9.39 Å in B. At end A, the mean separation between the planes of the phenyl rings associated with the terminal benzyl groups in the supramolecular structure shown in Figure 4 is 3.77 Å with a centroid–centroid separation of 4.48 Å, while, at end B, the comparable distances are 3.66 and 3.88 Å, respectively.

the NH_2^+ ion centers and on their adjacent *para*-xylyl methylene groups. As a consequence of the lack of symmetry of the complex, these terminal recognition sites—identified as A and B sites in Figure 3—are not identical. Both of the NH_2^+ hydrogen atoms are involved in bifurcated hydrogen bonds, one to both aryl oxygen atoms of one of the catechol units and the other to the adjacent second and third oxygen atoms of one of the polyether chains in **DB24C8**. One of the *para*-xylyl methylene hydrogen atoms is hydrogen bonded to one of the oxygen atoms of the other catechol unit. In the case of both the A and B sites, the *para*-xylyl units are inclined toward one of the catechol rings of the **DB24C8** macrocycle by about 20° and the distances are too large for any significant $\pi-\pi$ stabilization. In the 2:1:1 pseudorotaxane complex $[(\mathbf{DB24C8})_2\cdot\mathbf{BPP34C10}\cdot\mathbf{4}\text{-}H_2][PF_6]_4$, although there is no double threading of the terminal **DB24C8** macrocycles by the tetracation to produce an intimately linked pseudorotaxane superstructure, both terminal benzyl groups are arranged in a parallel overlapping $\pi-\pi$ stacking relationship with their centrosymmetrically related counterparts. The combination of these intercomplex $\pi-\pi$ interactions, coupled with the intracomplex noncovalent bonding interactions, results in the formation of a loosely bound pseudopolyrotaxane superstructure (Fig. 4).

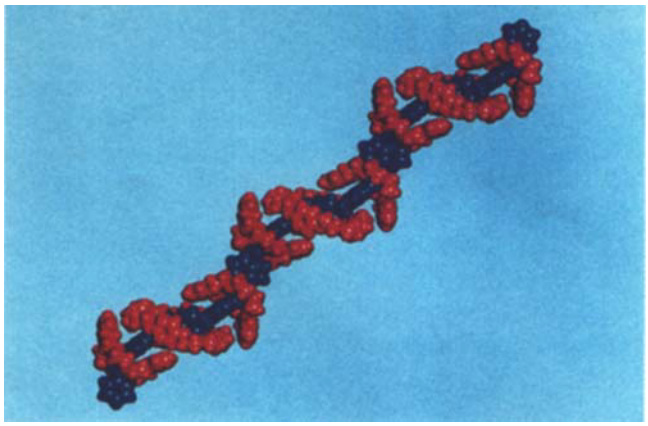

Fig. 4. Space-filling representation of the solid-state structure of a portion of the pseudopolyrotaxane-like $[(\mathbf{DB24C8})_2\cdot\mathbf{BPP34C10}\cdot\mathbf{4}\text{-}H_2]_n^{4+}$ superstructure. The **DB24C8** and **BPP34C10** macrocycles are depicted in red and the threadlike tetracationic component in blue.

LSI mass spectrometry[15] indicates the very high integrity of the 2:1:1 complex. Intense peaks are observed at *m/z* 2592, 2447, and 2301, corresponding to the supramolecular ion, $[(\mathbf{DB24C8})_2\cdot\mathbf{BPP34C10}\cdot\mathbf{4}\text{-}H_2][PF_6]_4$ and the ions resulting from the loss of one and two PF_6^- ions, respectively. Also, in an ^1H NMR experiment at room temperature[19] a solution of $\mathbf{4}\text{-}H_2\cdot 4PF_6$, a fourfold molar excess of **DB24C8**, and a sixfold molar excess of **BPP34C10** in CD_3COCD_3 produces signals only for the 2:1:1 complex, as well as those for the free crown ethers.

This research has established the principle of thermodynamically controlled self-assembly of matching components in an equilibrium situation where three different molecular recognition motifs experience self-selection, according to a recognition pattern that is entirely in line with expectation. It is evident that bipyridinium units and dibenzylammonium centers bind strongly with the **BPP34C10** and **DB24C8** macrocycles, respectively. The binding of dibenzylammonium ion centers, singly or in pairs by **BPP34C10**, is very much weaker in Me_2CO, and

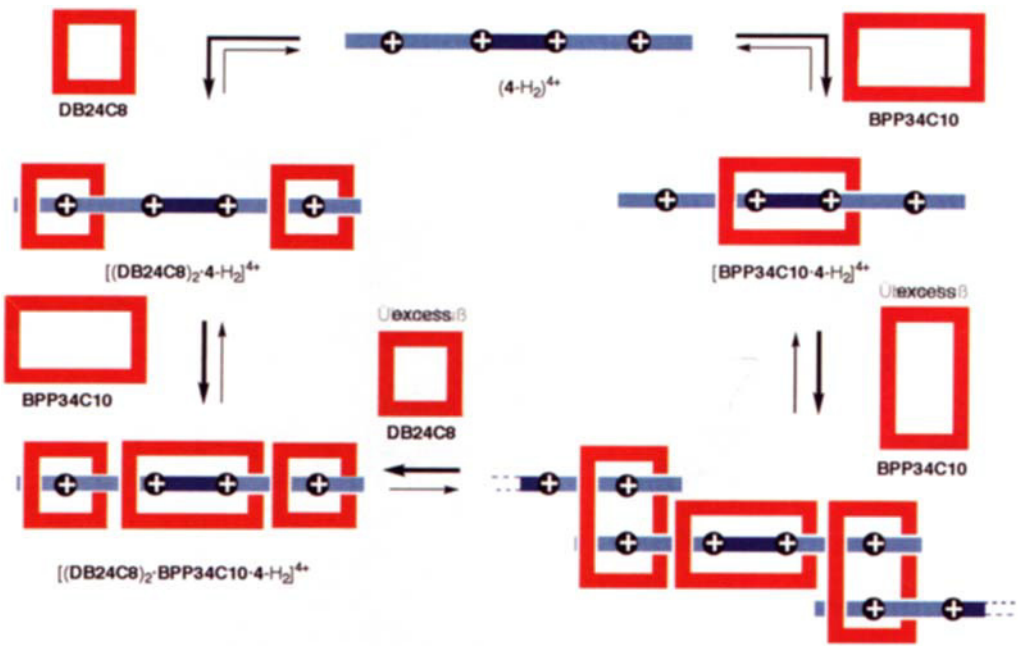

Scheme 2. The equilibrium processes of self-selection operating between the tetracation $(\mathbf{4}\text{-}H_2)^{4+}$ and the two crown ethers **DB24C8** and **BPP34C10**.

DB24C8 has very little affinity—at least in a threading sense—for bipyridinium units. The selection exercised by the $(\mathbf{4}\text{-}H_2)^{4+}$ tetracation in solution toward **DB24C8** and **BPP34C10**, individually and together in both short supply and in excess, is summarized in Scheme 2.

Experimental Procedure

4-$H_2\cdot 4PF_6$: A solution of 4,4'-bipyridine (72 mg, 0.46 mmol) in Me_2SO (5 mL) was added to a warm solution of the HCl salt (520 mg, 1.84 mmol) of *N*-benzyl-*para*-chloromethylbenzylamine [11] in Me_2SO (5 mL). The reaction mixture was stirred under reflux for 2 d. A white precipitate formed and was filtered off after the suspension had been cooled down to room temperature. The solid **4**-$H_2\cdot 4Cl$ was rinsed with DMF and Et_2O before being dissolved in H_2O. A saturated aqueous solution of NH_4PF_6 was added until no further precipitation occurred. The white solid **4**-$H_2\cdot 4PF_6$ was filtered off and dried (330 mg, 62%, m.p. 240 °C with decomp). Positive-ion LSIMS: *m/z* 1013 $[M-PF_6]^+$; ^{1}H NMR (CD_3COCD_3): δ = 4.63 (s, 4H), 4.70 (s, 4H), 6.21 (s, 4H), 7.40–7.50 (m, 6H), 7.50–7.60 (m, 4H), 7.73 (s, 8H), 8.77 (d, 4H), 9.44 (d, 4H).

Received: March 1, 1996 [Z8888IE]
German version: *Angew. Chem.* **1996**, *108*, 2058–2061

Keywords: crown ethers · crystal engineering · molecular recognition · rotaxanes · self-assembly

[1] a) J. S. Lindsey, *New J. Chem.* **1991**, *15*, 153–180; b) G. M. Whitesides, J. P. Mathias, C. T. Seto, *Science* **1991**, *254*, 1312–1319; c) G. M. Whitesides, E. E. Simanek, J. P. Mathias, C. T. Seto, D. N. Chin, M. Mammen, D. M. Gordon, *Acc. Chem. Res.* **1995**, *28*, 37–44; d) D. Philp, J. F. Stoddart, *Synlett* **1991**, 445–458; *Angew. Chem.* **1996**, *108*, 1155–1196; *Angew. Chem. Int. Ed. Engl.* **1996**, *35*, 1242–1286.

[2] a) J. C. Chambron, C. O. Dietrich-Buchecker, J.-P. Sauvage, *Top. Curr. Chem.* **1993**, *165*, 131–162; b) D. B. Amabilino, J. F. Stoddart, *Chem. Rev.* **1995**, *95*, 2725–2828.

[3] J.-M. Lehn, *Supramolecular Chemistry: Concepts and Perspectives*, VCH, Weinheim, **1995**.

[4] J. F. Stoddart, *Chem. Br.* **1991**, *27*, 714–718.

[5] D. B. Amabilino, P. R. Ashton, L. Pérez-García, J. F. Stoddart, *Angew. Chem.* **1995**, *107*, 2569–2572; *Angew. Chem. Int. Ed. Engl.* **1995**, *34*, 2378–2380.

[6] Since the molecular components of a pseudorotaxane are held together only by their mutual noncovalent bonding interactions, they behave like inclusion complexes and so are formed under thermodynamic control. See D. B. Amabilino, P. L. Anelli, P. R. Ashton, G. R. Brown, E. Córdova, L. A. Godínez, W. Hayes, A. E. Kaifer, D. Philp, A. M. Z. Slawin, N. Spencer, J. F. Stoddart, M. S. Tolley, D. J. Williams, *J. Am. Chem. Soc.* **1995**, *117*, 11142–11170.

[7] The formation of rotaxanes by the slippage procedure provides a good example of thermodynamically controlled self-assembly. See P. R. Ashton, R. Ballardini, V. Balzani, M. T. Gandolfi, D. Philp, L. Prodi, F. M. Raymo, M. V. Reddington, N. Spencer, J. F. Stoddart, M. Venturi, D. J. Williams, *J. Am. Chem. Soc.* **1996**, *118*, 4931–4951.

[8] For catenane formation as an example of kinetic selection during self-assembly, see a) P. R. Ashton, T. T. Goodnow, A. E. Kaifer, M. V. Reddington, A. M. Z. Slawin, N. Spencer, J. F. Stoddart, C. Vicent, D. J. Williams, *Angew. Chem.* **1989**, *101*, 1404–1408; *Angew. Chem. Int. Ed. Engl.* **1989**, *28*, 1396–1399; b) D. B. Amabilino, P. R. Ashton, C. L. Brown, E. Córdova, L. A. Godínez, T. T. Goodnow, A. E. Kaifer, S. P. Newton, D. Philp, M. Pietraszkiewz, F. M. Raymo, A. S. Reder, M. T. Rutland, A. M. Z. Slawin, N. Spencer, J. F. Stoddart, D. J. Williams, *J. Am. Chem. Soc.* **1995**, *117*, 1271–1293.

[9] a) P. R. Ashton, P. J. Campbell, E. J. T. Chrystal, P. T. Glink, S. Menzer, D. Philp, N. Spencer, J. F. Stoddart, P. A. Tasker, D. J. Williams, *Angew. Chem.* **1995**, *107*, 1997–2001; *Angew. Chem. Int. Ed. Engl.* **1995**, *34*, 1865–1869; b) P. R. Ashton, E. J. T. Chrystal, P. T. Glink, S. Menzer, C. Schiavo, J. F. Stoddart, P. A. Tasker, D. J. Williams, *ibid.* **1995**, *107*, 2001–2004 and **1995**, *34*, 1869–1871; c) P. R. Ashton, E. J. T. Chrystal, P. T. Glink, S. Menzer, C. Schiavo, N. Spencer, J. F. Stoddart, P. A. Tasker, A. J. P. White, D. J. Williams, *Chem. Eur. J.* **1996**, *2*, 709–728.

[10] Rotaxanes have been self-assembled from functionalized secondary dialkylammonium salts and **DB24C8**. See a) A. G. Kolchinski, D. H. Busch, N. W. Alcock, *J. Chem. Soc. Chem. Commun.* **1995**, 1289–1291; b) P. R. Ashton, P. T. Glink, J. F. Stoddart, P. A. Tasker, A. J. P. White, D. J. Williams, *Chem. Eur. J.* **1996**, *2*, 729–736.

[11] The HCl salt of benzyl-*para*-chloromethylbenzylamine was prepared in four steps from the commercially available starting materials benzylamine and methyl 4-formylbenzoate. Condensation of these two compounds in MeOH afforded the imine, which was reduced in situ with an excess of $NaBH_4$ to give the secondary amine. After reduction of the ester function with $LiAlH_4$ in Et_2O and subsequent reaction of the alcohol with an excess of $SOCl_2$, the HCl salt was obtained in good yield overall (58%).

[12] Siemens P4/RA diffractometer, ω scans, $Cu_{K\alpha}$ radiation (graphite monochromator). The structures were solved by direct methods and refined anisotropically. Crystallographic data (excluding structure factors) for the structures reported in this paper have been deposited with the Cambridge Crystallographic Data Centre as supplementary publication no. CCDC-179-87. Copies of the data can be obtained free of charge on application to The Director, CCDC, 12 Union Road, Cambridge CB2 1EZ, UK (fax: Int. code +(1223)336-033; e-mail: teched@chemcrys.can.ac.uk).

[13] Crystal data for [(**BPP34C10**)$_2\cdot$**4**-H_2][PF_6]$_4\cdot$X [12] (X represents unidentified solvent fragments wherein electron density has been allowed for by distributing six carbon atoms over twelve partial occupancy sites): triclinic, space group $P\bar{1}$, a = 12.603(1), b = 13.276(1), c = 17.983(3) Å, α = 85.00(1), β = 82.26(1), γ = 66.61(1)°, V = 2734.6(4) Å^3, Z = 1 (the complex has crystallographic C_i symmetry), ρ_{calcd} = 1.399 g cm^{-3}, $\mu(Cu_{K\alpha})$ = 15.9 cm^{-1}, T = 183 K, 6850 independent reflections measured, 4971 observed reflections with [$|F_o| > 4\sigma(|F_o|)$, $2\theta \le 110°$] refined on F^2 to R_1 = 0.080, wR_2 = 0.212.

[14] Inspection of the packing of the pseudopolyrotaxane chains does not reveal any strong $\pi-\pi$, [C–H$\cdots\pi$], or [C–H$\cdots$O] interactions between the pseudopolyrotaxanes. The only proximal relationship of note is an approach of the terminal benzyl rings of adjacent threads, suggesting the possibility of cross-linking. However, although the interplanar separation between the terminal benzyl groups is favorable at 3.1 Å, the centroid–centroid separation of 5.3 Å is much too large for any significant $\pi-\pi$ interaction. For a discussion of the term pseudopolyrotaxane, see D. B. Amabilino, I. W. Parsons, J. F. Stoddart, *Trends Polym. Sci.* **1994**, *2*, 146–152.

[15] LSI mass spectra were obtained from a VG Zabspec mass spectrometer equipped with a cesium ion source. Samples were dissolved in a small volume (ca. 1 μL) of *meta*-nitrobenzyl alcohol, which had previously been coated on to a stainless steel probe tip, and spectra were recorded in the positive-ion mode at a scan speed of 10 s per decade.

[16] When **BPP34C10** is present in fourfold molar excess relative to **4**-$H_2\cdot 4PF_6$ (3.3 mM) in CD_3COCD_3, $\Delta\delta$ values (with reference to the free salt) of -0.20, -0.41, -0.04, and $-0.03/-0.05$ are observed in the ^{1}H NMR spectrum for the bipyridinium αCH, βCH, and CH_2 protons and the $CH_2NH_2^+CH_2$ protons, respectively.

[17] When **DB24C8** is present in sixfold molar excess relative to **4**-$H_2\cdot 4PF_6$ (3.3 mM) in CD_3COCD_3, $\Delta\delta$ values (with reference to the free salt) of -0.21, -0.05, -0.30, and $+0.18/+0.16$ are observed in the ^{1}H NMR spectrum for the bipyridinium αCH, βCH, and CH_2 protons and the $CH_2NH_2^+CH_2$ protons, respectively. The 2:1 stoichiometry of the complex [(**DB24C8**)$_2\cdot$**4**-H_2][PF_6]$_4$ was established by integration under the conditions of slow exchange which prevail on the ^{1}H NMR timescale at room temperature.

[18] Crystal data for [(**DB24C8**)$_2\cdot$**BPP34C10**$\cdot$**4**-H_2][PF_6]$_4\cdot 3Me_2CO\cdot H_2O$ [12]: triclinic, space group $P\bar{1}$, a = 13.220(1), b = 22.352(2), c = 23.943(2) Å, α = 87.91(1), β = 78.50(1), γ = 81.99(1)°, V = 6864.9(9) Å^3, Z = 2, ρ_{calcd} = 1.347 g cm^{-3}, $\mu(Cu_{K\alpha})$ = 14.2 cm^{-1}, T = 203 K, 17104 independent reflections accumulated from two crystals of similar overall dimensions, 11145 observed reflections with [$|F_o| > 4\sigma(|F_o|)$, $2\theta \le 110°$] refined on F^2 to R_1 = 0.092, wR_2 = 0.228.

[19] When **DB24C8** and **BPP34C10** are present in four- and sixfold molar excesses, respectively, relative to **4**-$H_2\cdot 4PF_6$ (3.3 mM) in CD_3COCD_3, $\Delta\delta$ values (with reference to the free salt) of -0.35, -0.55, -0.19, and $+0.22/+0.12$ are observed in the ^{1}H NMR spectrum for the bipyridinium αCH, βCH, and CH_2 protons and $CH_2NH_2^+CH_2$ protons, respectively. The 2:1:1 stoichiometry of the complex [(**DB24C8**)$_2\cdot$**BPP34C10**$\cdot$**4**-H_2][PF_6]$_4$ was established by integration under the conditions of slow exchange which prevail on the ^{1}H NMR timescale at room temperature.

 © VCH Verlagsgesellschaft mbH, D-69451 Weinheim, 1996 0570-0833/96/3517-1933 $ 15.00+.25/0

Hf_7P_4: A New Binary Phosphide Synthesized by a Surprising Route**

Holger Kleinke and Hugo F. Franzen*

Dedicated to Professor Hans Georg von Schnering on the occasion of his 65th birthday

Despite numerous investigations of binary, ternary, and even quaternary pnictides and chalcogenides of the early transition metals, new binary compounds in these systems can still be found. Most recently, for example, Zr_2P,[1] $Zr_{1+x}Te_2$,[2] Hf_2Se_3,[3] Hf_3Te_2,[4] Nb_2Te_3,[2] Ta_3S_2,[5] Ta_2Se,[6] Ta_2Te_3,[7] and Ta_6Te_5[8] have been synthesized. Thereby, the differences between the metal-rich chemistry of Hf and Zr as well as between Nb and Ta became more and more apparent: none of these compounds have a counterpart among the corresponding homologous metal atom of the other period, and the stoichiometric equivalent phosphides Zr_2P[1] and Hf_2P[9] (or Nb_2P[10] and Ta_2P[11]) crystallize in different structure types; the same is also true for Nb_2Te_3 and Ta_2Te_3, as well as for Zr_2S[12] and Hf_2S.[13] As for some ternary Nb/Ta sulfides[14] and tellurides,[15] the 5d metal atoms prefer the positions with the higher metal–metal bond order. Similarly, the binary chalcogenides of the 5d metal atoms form structures with more metal–metal contacts (compare for example Zr_2S with Hf_2S, and Nb_2Te_3 with Ta_2Te_3).

It was therefore surprising to find that Hf_7P_4[16] is isostructural to Zr_7P_4.[19] Hf_7P_4 was prepared by arc-melting of Hf, Fe, and HfP in the ratio of 5:2:4 by using techniques previously described.[20] The powder diagram obtained from the ground bulk sample contained only the reflections of Hf_7P_4, $HfFe_2$, and Hf_4FeP, which is consistent with a reaction according to Equation (a).

$$5\,Hf + 2\,Fe + 4\,HfP \longrightarrow 6/7\,Hf_7P_4 + 5/7\,HfFe_2 + 4/7\,H_4FeP \qquad (a)$$

Single crystals of Hf_7P_4 were obtained after heating the bulk sample in an induction furnace at a temperature of 1400 °C for six hours. This shows that Hf_7P_4 is thermodynamically stable; its synthesis is only kinetically impeded. Our attempts to prepare Hf_7P_4 without the addition of Fe led only to mixtures of Hf_2P[10] and Hf_3P_2.[21] Thus, since the EDS (*E*lectron *D*ispersive *S*pectroscopy) investigation of the measured single crystal did not show a measurable amount of Fe, we conclude that there is no Fe incorporation into the structure of Hf_7P_4, which is in agreement with the uniformity of the equivalent temperature factors of the structure model of Hf_7P_4. Since the largest void in the structure is surrounded by four Hf and two P atoms at distances of about 2.2 Å, (partial) occupation of this void by iron can be excluded for steric reasons: a Hf–Fe distance of 2.2 Å would correspond to a bond order of 4.7 according to Pauling's Equation (b), using $r_{Hf} = 1.452$ Å and $r_{Fe} = 1.170$ Å

$$d(n) = d(1) - 0.6 \lg n \qquad (b)$$

(n = bond order).[22] Besides the results of the EDS investigation, a statistical presence of other heteroatoms is most unlikely for the following reasons: 1) The high yield argues against significant amounts of impurities in Hf_7P_4. 2) After the arc-melting had been carried out under an argon atmosphere, the annealing was performed under residual pressure of 10^{-7} Torr, thus significant incorporation of heteroatoms is impossible. In addition, if one takes into consideration a stabilization of Hf_7P_4 by oxygen, whereever it might come from, an analysis of the voids in the structure does not show any probable positions for oxygen: either the Hf–O distances would be too short (< 1.76 Å in the Hf_6 octahedra, compared to Hf–O bonds of 2.05 Å in the structure of monoclinic HfO_2)[23] or P–O distances less than 2.4 Å would occur. The latter is very unlikely when P and O are considered as anions with filled shells. In any case, no significant electron density was found in the considered voids.

However, the presence of Fe, which acts as a flux, seems to be essential for the formation of Hf_7P_4. This is presumably the reason why, in spite of studies of the formation of Hf-rich binary[24] and ternary phosphides,[25] the existence of Hf_7P_4 has not been demonstrated up to now. Although the technique of adding a flux material to prepare suitable crystals of metal-rich compounds has been applied successfully in the synthesis of Hf_3Te_2 (using KCl)[4] and Zr_2S (using Cr),[26] most of the previously mentioned pnictides and chalcogenides were prepared by reducing a more metal-poor compound with the corresponding metal, or from the elements directly, which led to very small crystals in most cases. To our knowledge, the synthesis of Hf_7P_4 is the first example in which the use of a flux material has enabled the synthesis of a metal-rich phosphide that has eluded synthesis without using flux.

Hf_7P_4 crystallizes in the Nb_7P_4 structure type, consisting of fragments of the body-centered cubic packing of Hf. The four crystallographically different P atoms are located in singly, two- and three-capped trigonal Hf prisms, and the Hf–P bonds range between 2.57(2) and 3.24(2) Å. Alternatively, this structure can be described in terms of condensed fragments of the M_6X_8 cluster type.[27] Two different variations of the condensed M_6X_8 cluster occur in the structure of Hf_7P_4, both kinds are condensed through common vertex atoms to form infinite chains running parallel to [010]: a Hf_5 fragment of the Hf_6P_8 cluster, in which one Hf atom in the basal plane of the octahedron is missing, is situated between two crystallographically independent Hf_6P_8 octahedra, connected through equatorial Hf atoms to form zigzag chains parallel to [101]. These chains are highlighted by bold lines in Figure 1. Furthermore, these chains are intercon-

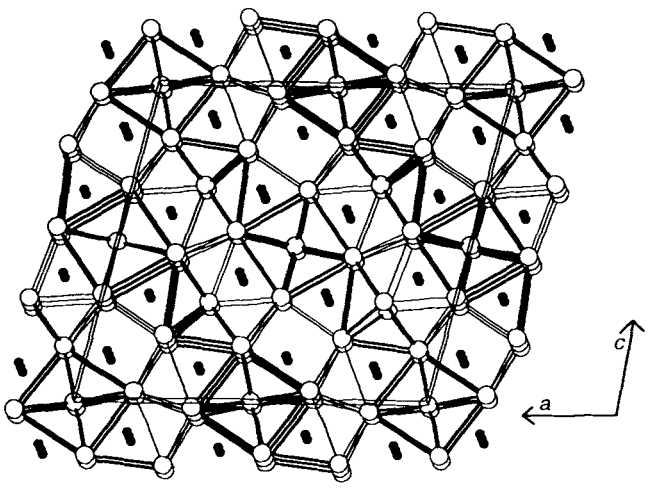

Fig. 1. Projection of the structure of Hf_7P_4 along [010], the Hf_5 and Hf_6 cluster units are highlighted. Small, black circles: P; large, white circles: Hf.

[*] Prof. Dr. H. F. Franzen, Dr. H. Kleinke
Ames Laboratory - DOE, Iowa State University
Ames, IA 50011 (USA)
Fax: Int. code +(515) 294 5718
e-mail: franzen@ameslab.gov

[**] H. K. thanks the Deutsche Forschungsgemeinschaft for financial support of this work. The Ames Laboratory is operated for the US Department of Energy by Iowa State University under Contract No. D-7405-Eng-82. This research was also supported by the Office of the Basic Energy Sciences, Materials Science Division, Department of Energy.

nected by common P atoms and Hf–Hf bonds between the cluster units. Thus, all Hf atoms are either part of the Hf_5 or of the Hf_6 units.

The shortest Hf–Hf bonds occur between the apical and basal atoms of the condensed cluster units (ranging from 3.025(3) to 3.194(2) Å), whereas the distances within the equatorial planes are significantly longer (ranging between 3.437(4) and 3.684(4) Å). As can be seen by the length of the *b* axis, the octahedra are tetragonally compressed, and the Hf–Hf distances between the vertices are 3.5209(9) Å. Therefore a consideration of these units as centered cubes is appropriate, but this model should not be taken too far because the Hf–Hf distances between the cubic units (varying from 3.223(4) to 3.413(4) Å) are even shorter than those within the cubes.

Most unusually, in comparison with other metal-rich systems of neighboring 4d and 5d elements, this metal-rich compound is isostructural to its 4d homologue Zr_7P_4,[19] although, based upon prior comparison of Group 4 and 5 homologues,[28] Hf should prefer a structure with more metal–metal bonding than in the Zr compound.

The observed contraction of the unit cell volume of almost 5% from Zr_7P_4 to Hf_7P_4 cannot be explained only by the different radii of Zr and Hf (1.452 vs. 1.442 Å).[22] Although the differences between the three different crystallographic axes vary between 1 and 3% (*b* axis), no significant trend is observed among the different interatomic interactions. The greatest deviations occur in the Hf–Hf separations parallel to [010], which correspond to the length of *b* and therefore have only weak bonding character. All other types of bonds are about 1.5% smaller in case of Hf_7P_4.

To investigate the consequences of the cell contraction, we calculated the Pauling bond orders with Equation (b)[22] for Zr_7P_4 and Hf_7P_4, and the Mulliken overlap populations (MOP) for Hf_7P_4 and for theoretical Hf_7P_4 with the cell dimensions and atomic positions of Zr_7P_4 by using the extended Hückel method.[29] The parameters for Hf and P were taken from the literature.[4, 30]

The calculated COOP curve (crystal orbital overlap population) consists of two well-separated parts (excluding the phosphorus 3s orbitals below the energy window): at lower energy, between -14.5 and -12 eV, the 3p states of P dominate, leading, by mixing with Hf 6s, 6p and 5d states, to strong bonding Hf–P interactions, whereas in the region of the Fermi level E_F mainly the Hf d bonding states occur. In contrast to more metal-rich compounds[31] not all metal–metal bonding states are filled (Fig. 2).

The calculated COOPs of Zr_7P_4 and Nb_7P_4 (parameters taken from literature)[32] are very similar. Because of the higher electronegativity of Nb its d block is shifted to lower energies and thus overlaps with the 3p block of P. The higher number of valence electrons leads not only to completely filled Nb–Nb bonding states, but also to the occupancy of some antibonding states (Fig. 3). Altogether, the Nb–Nb and Nb–P overlap populations are significantly larger than those of Hf_7P_4.

After the cell contraction from Zr_7P_4 to Hf_7P_4, all atomic sites show the same trend, that is, the metal–metal overlap populations increase by 2.8% from theoretical Hf_7P_4 in the Zr_7P_4 structure (average total $MOP_{Hf-Hf} = 0.996$) compared to those calculated for the structure model of Hf_7P_4 (average $MOP_{Hf-Hf} = 1.024$), and an increase is also found for the metal–nonmetal overlap population (0.948 vs. 0.964, corresponding to an increase of 1.7%). Accordingly, the averaged Pauling metal–metal bond orders changed from 2.56 (Zr_7P_4) to 2.77 (Hf_7P_4) and the metal–P bond orders from 2.44 to 2.70, indicating that

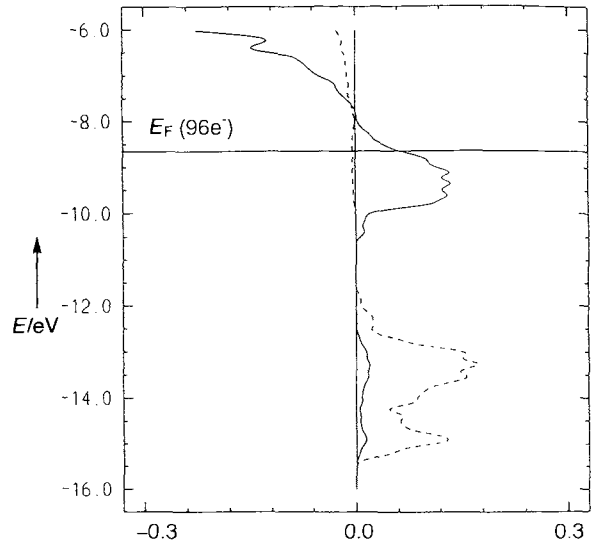

Fig. 2. COOP curve of Hf_7P_4; solid line: Hf–Hf; dashed line: Hf–P interactions. The left half of the diagram covers the antibonding, the right half the bonding interactions.

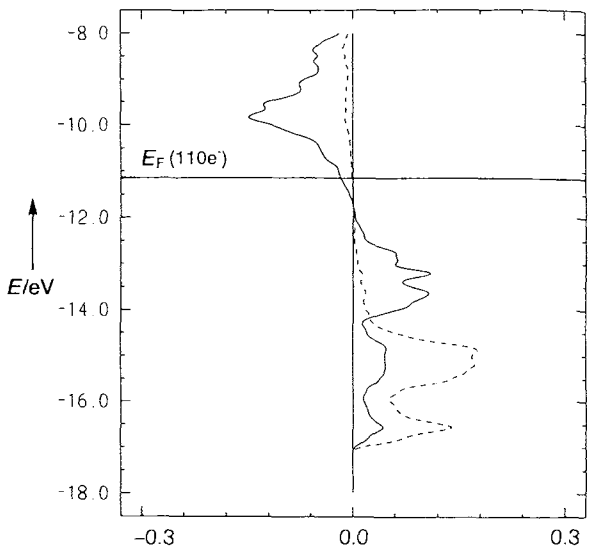

Fig. 3. COOP curve of Nb_7P_4; solid line: Nb–Nb; dashed line: Nb–P interactions. The left half of the diagram covers the antibonding, the right half the bonding interactions.

the cell contraction is not caused by the smaller radius of Hf alone.

The higher metal–metal bond order in the structure of Hf_7P_4 can be explained by the greater extension of the 5d orbitals as well as by the electron concentration rules of Brewer and Engel.[33] According to Brewer and Engel, the s and p conduction electrons determine the structure, and Zr and Hf tend in body-centered cubic structures to the configurations of $d^{2.7}sp^{0.3}$ and $d^{2.5}sp^{0.5}$, respectively; thus, the higher ratio of s and p electrons of Hf enables Hf to form stronger metal–metal bonds.

On the other hand, the increase of metal–metal bonding leads to a lower energy of bonding orbitals centered on Hf, which in turn leads to a higher "back-bonding" covalent character of the Hf–P bonds, corresponding to the higher overlap population. In other words, Hf is more electronegative than Zr and thus forms more covalent M–P interactions.

 © VCH Verlagsgesellschaft mbH, D-69451 Weinheim, 1996 0570-0833/96/3517-1935 $ 15.00+.25/0

Relativistic effects in general lead to a radial contraction of the s and p orbitals and to an expansion of the d orbitals;[34] this is particularly true in the case of Hf because of the increase of relativistic effects with Z^2.[35] The result is a volume contraction of the Hf phosphide because of its smaller, structure-determining s and p orbitals. However, since the radii used for calculating the bond orders are based on experimental results, and the experiments are necessarily relativistic, relativistic effects are included by comparisons based on radii. Therefore, the significant higher bond orders of Hf_7P_4 indicate that relativistic effects alone are not responsible for the observed cell contraction.

All viewpoints complement one another and lead to the conclusion that compared with Zr, Hf will be more strongly bonded to itself in metal-rich compounds and more covalently bonded to the nonmetal. In general, these conclusions should also be true for the structural differences of metal-rich compounds of Nb and Ta. In summary, the general trend in the different bonding behavior of Zr and Hf, observed in many examples with very different crystal structures, can also be studied based on isostructural compounds like Zr_7P_4 and Hf_7P_4.

Received: March 14, 1996 [Z89271E]
German version: *Angew. Chem.* **1996**, *108*, 2062–2064

Keywords: hafnium compounds · orbital populations · phosphorus compounds · solid-state structures

[1] P.-J. Ahlzén, S. Rundqvist, *Z. Kristallogr.* **1989**, *189*, 117–124.
[2] H. Kleinke, W. Tremel, *25. Hauptversammlung der Gesellschaft Deutscher Chemiker* (Münster) **1995**, Abstr. Pap. p. 240.
[3] I. M. Schewe-Miller, V. G. Young, Jr., *J. Alloys Compd.* **1994**, *216*, 113–115.
[4] R. L. Abdon, T. Hughbanks, *Angew. Chem.* **1994**, *106*, 2414–2416; *Angew. Chem. Int. Ed. Engl.* **1994**, *33*, 2328–2330.
[5] H. Wada, M. Onada, *Mater. Res. Bull.* **1989**, *24*, 191–196; S.-J. Kim, K. S. Nanjundaswamy, T. Hughbanks, *Inorg. Chem.* **1991**, *30*, 159–164.
[6] B. Harbrecht, *Angew. Chem.* **1989**, *101*, 1696–1698; *Angew. Chem. Int. Ed. Engl.* **1989**, *28*, 1660–1662.
[7] M. Conrad, B. Harbrecht, *J. Alloys Compd.* **1992**, *187*, 181–192.
[8] M. Conrad, B. Harbrecht, *IVth Eur. Conf. Solid State Chem.* (Dresden) **1992**, Abstr. Pap. p. 324.
[9] T. Lundström, N.-O. Ersson, *Acta Chem. Scand.* **1968**, *22*, 1801–1808.
[10] Y. B. Kuzma, S. V. Orishchin, Y. F. Lomnitskaya, T. Glov'jak, *Dopov. Akad. Nauk Ukr. RSR Ser. B: Geol. Khim. Biol. Nauki* **1988**, *2*, 47–49.
[11] A. Nylund, *Acta Chem. Scand.* **1966**, *20*, 2393–2401.
[12] B. R. Conard, H. F. Franzen, *High Temp. Sci.* **1971**, *3*, 49–55.
[13] H. F. Franzen, J. Graham, *Z. Kristallogr.* **1966**, *123*, 133–138.
[14] X. Yao, H. F. Franzen, *J. Solid State Chem.* **1990**, *86*, 88–93; *J. Am. Chem. Soc.* **1991**, *113*, 1426–1427; *J. Alloys Compd.* **1992**, *182*, 299–312; X. Yao, G. J. Miller, H. F. Franzen, *ibid.* **1992**, *183*, 7–17; K. S. Nanjundaswamy, T. Hughbanks, *J. Solid State Chem.* **1992**, *98*, 278–290.
[15] H. Kleinke, W. Tremel, *Z. Kristallogr. Suppl.* **1992**, *7*, 139.
[16] Crystal structure analysis of Hf_7P_4: lattice constants for the monoclinic cell (space group $C2/m$) were obtained from Guinier powder patterns under vacuum (50 reflections, $Cu_{K\alpha}$): $a = 15.488(5)$, $b = 3.526(1)$, $c = 14.553(5)$ Å, $\beta = 104.83(3)°$, $V = 768.3(8)$ Å^3, and from refinements of 14 centered reflections with the AFC6R diffractometer (RIGAKU, 23 °C, $Mo_{K\alpha}$): $a = 15.654(6)$, $b = 3.5209(9)$, $c = 14.596(7)$ Å, $\beta = 104.43(3)°$, $V = 779(1)$ Å^3. Experimental details of data collection: $Z = 4$, $\rho = 11.872$ g cm^{-3}, $\mu = 940.89$ cm^{-1}, $2\theta_{max} = 70°$, min./max transmission: 0.61/1.37. Refinements and absorption correction (Ψ scan, followed by DIFABS [17]) were carried out using the TEXSAN program package [18]. Final residual values are $R(F) = 0.058$, $Rw = 0.056$, GOF = 1.386 with 669 independent observed reflections ($I > 3\sigma(I)$) and 57 variables. Further details of the crystal structure investigation may be obtained from the Fachinformationszentrum Karlsruhe, D-76344 Eggenstein-Leopoldshafen (Germany), on quoting the depository number CSD-405208.
[17] N. Walker, D. Stuart, *Acta Crystallogr. Sect. A* **1983**, *39*, 159–166.
[18] TEXSAN: *Single Crystal Structure Analysis Software*, Version 5.0, Molecular Structure Corporation, The Woodlands, TX, USA, **1989**.
[19] P.-J. Ahlzén, S. Rundqvist, *Z. Kristallogr.* **1989**, *189*, 149–153.
[20] H. Kleinke, H. F. Franzen, *Z. Anorg. Allg. Chem.* **1996**, in press.
[21] T. Lundström, *Acta Chem. Scand.* **1968**, *22*, 2191–2199.
[22] L. Pauling, *The Nature of the Chemical Bond*, 3rd ed., Cornell University Press, Ithaca, NY, **1948**.
[23] C. E. Curtis, L. M. Doney, J. R. Johnson, *J. Am. Ceram. Soc.* **1954**, *37*, 458–465.
[24] T. Lundström, P. Tansuriwongs, *Acta Chem. Scand.* **1968**, *22*, 704–705.
[25] G. J. Miller, J. Cheng, *Inorg. Chem.* **1995**, *34*, 2962–2968; J. Cheng, H. F. Franzen, *J. Solid State Chem.* **1996**, *121*, 362–371.
[26] X. Yao, H. F. Franzen, *J. Less-Common Met.* **1988**, *142*, L27–L29.
[27] A. Simon, *Angew. Chem.* **1981**, *93*, 23–44; *Angew. Chem. Int. Ed. Engl.* **1981**, *20*, 1–22.
[28] H. F. Franzen, M. Köckerling, *Prog. Solid State Chem.* **1995**, *23*, 265–289.
[29] R. Hoffmann, *J. Chem. Phys.* **1963**, *39*, 1397–1412; M.-H. Whangbo, R. Hoffmann, *J. Am. Chem. Soc.* **1978**, *100*, 6093–6098; R. Hoffmann, *Angew. Chem.* **1987**, *99*, 871–906; *Angew. Chem. Int. Ed. Engl.* **1987**, *26*, 846–878.
[30] E. Clementi, C. Roetti, *At. Data Nucl. Data Tables* **1974**, *14*, 177–478.
[31] T. Hughbanks, *Prog. Solid State Chem.* **1989**, *19*, 329–372.
[32] R. H. Summerville, R. Hoffmann, *J. Am. Chem. Soc.* **1976**, *98*, 7240–7255.
[33] L. Brewer in *Alloying* (Eds.: J. L. Walter, M. R. Jackson, C. T. Sims), ASM International, Metal Park, OH, **1988**, Chapter 1.
[34] P. Pykkö, *Chem. Rev.* **1988**, *88*, 563–594.
[35] P. Pykkö, J. G. Snijders, E. J. Baerends, *Chem. Phys. Lett.* **1981**, *83*, 432–436.

Photoinduced Energy and Electron Transfer in Supramolecular Porphyrin Assemblies**

Christopher A. Hunter* and Robert K. Hyde

Nature uses complex arrays of chromophores to trap solar energy and convert it into the chemical potential that drives the chemistry of photosynthetic organisms.[1] These chromophores are all noncovalently attached to a protein scaffold which holds them at the right separation and orientation for fast energy and unidirectional electron transfer, so that the solar energy conversion process proceeds with a high quantum yield. If we are to mimic the functional properties of these systems, it is likely that we will have to develop strategies for the construction of similarly large but structurally well-defined multichromophore arrays.[2–4] Hydrogen bonding has been successfully employed in the construction of photoactive supramolecular assemblies, but these complexes are relatively unstable with association constants in the region of 10^3 M^{-1}, and this limits the concentration range over which they can be studied as well as their ultimate utility.[3] Complexes assembled through porphyrin coordination chemistry suffer from the same problem, and this has hampered detailed analysis of their photochemical properties.[4] We describe here a new approach that overcomes this problem: the use of cooperative coordination interactions to generate very stable self-assembled chromophore arrays.[5] The porphyrin units employed in these arrays are shown in Scheme 1.

The design of the two complexes shown in Figure 1 is based on the structure of a self-assembling porphyrin "dimer" which we described recently.[6, 7] Zn_2-**2** contains a naphthalenediimide group that can act as an electron acceptor in photoinduced electron transfer reactions with porphyrins.[8] Zn_2-**3** has the same overall dimensions as Zn_2-**2** but has in place of the naphthalenediimide a terephthaloyl diamide, which has a much higher reduction potential and therefore cannot act as an electron acceptor: for our purposes, it behaves as an inert spacer. H_2-**1** is a rigid bifunctional ligand of appropriate dimensions to bridge the two zinc centers in the porphyrin "dimers" as shown in Figure 1.

[*] Dr. C. A. Hunter, R. K. Hyde
Krebs Institute for Biomolecular Science, Department of Chemistry
University of Sheffield
Sheffield S3 7HF (UK)

[**] We thank the Lister Institute (C. A. H.), the University of Sheffield, and Zeneca Specialities (R. K. H) for financial support.

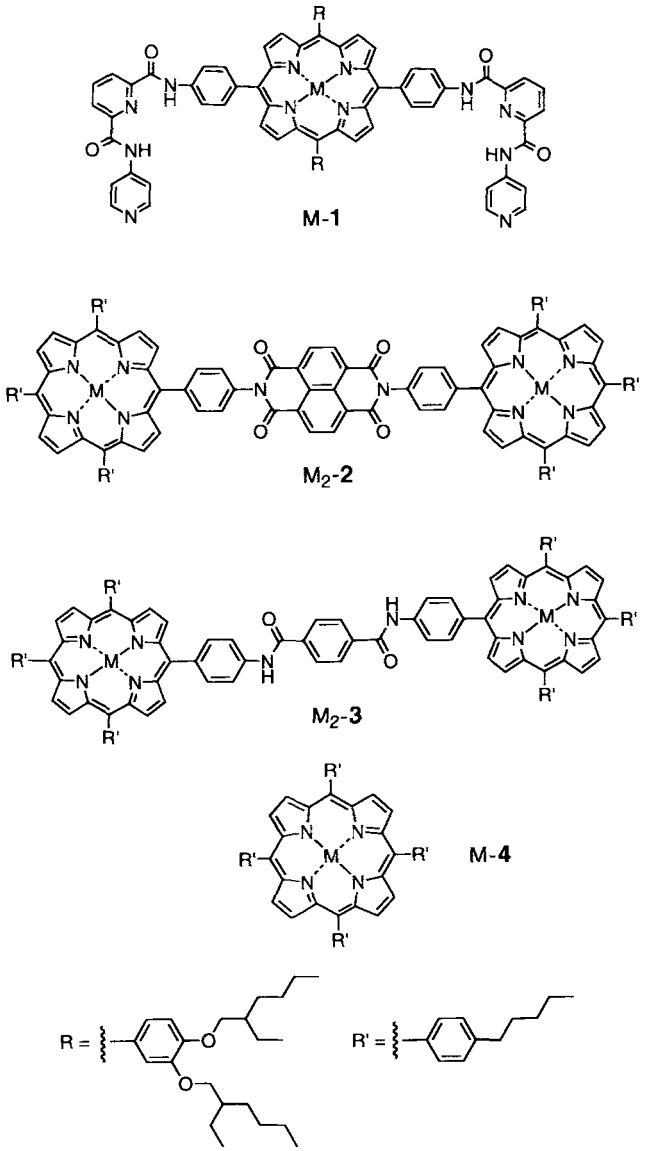

Scheme 1. Porphyrin units used in the construction of the new assemblies. M = H_2, Zn.

On mixing H_2-**1** with either Zn_2-**2** or Zn_2-**3** in organic solvents, exceptionally stable 1:1 complexes formed. Evidence for the structures comes from the following measurements (all in chloroform).

1) Vapor phase osmometry (VPO). The effective relative molecular masses in solution for the pure compounds and equimolar mixtures in solution are listed in Table 1. The results clearly show the presence of discrete 1:1 complexes for both H_2-**1**·Zn_2-**2** and H_2-**1**·Zn_2-**3**.

Table 1. Relative molecular masses in chloroform solution determined by vapor phase osmometry.

Compound(s)	Conc. [mM]	Expt.	Calcd.
H_2-**1**	1.50	1570±150	1606
Zn_2-**2**	1.50	1900±190	2038
Zn_2-**3**	1.50	1880±190	1934
H_2-**1** + Zn_2-**3** (1:1)	0.75	3500±350	3644
H_2-**1** + Zn_2-**3** (1:1)	0.75	3460±350	3540

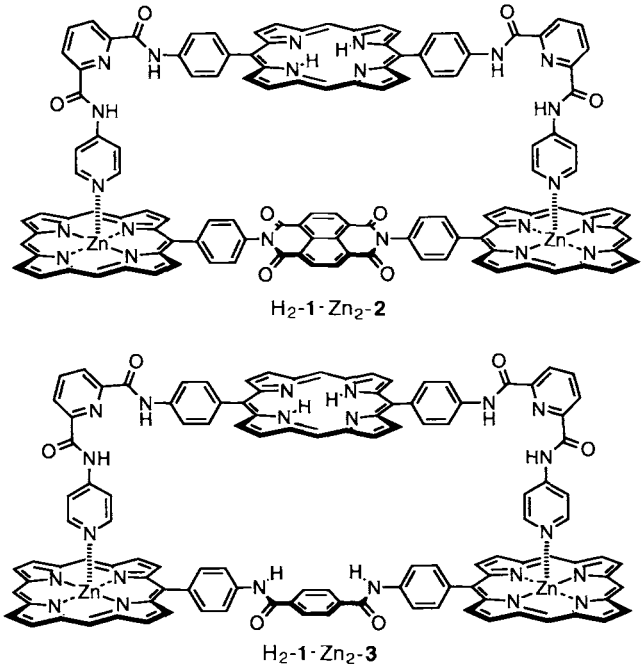

Fig. 1. Structural formulas of the complexes H_2-**1**·Zn_2-**2** and H_2-**1**·Zn_2-**3**. The *meso* substituents are omitted for clarity.

2) ^{1}H NMR spectra. On addition of one equivalent of H_2-**1** to Zn_2-**2** and to Zn_2-**3**, the ^{1}H NMR chemical shifts of several signals changed substantially. The signals of the pyridine a and b protons of H_2-**1** moved 6.0 and 2.5 ppm upfield, respectively, which indicates that they lie over the ring current on the face of a porphyrin π-system. These shifts are diagnostic of a coordination interaction between pyridine and the zinc porphyrin, and their magnitude shows that every pyridine group in the sample is fully bound to a zinc porphyrin under these conditions.[6]

3) UV/Vis absorption spectra. The wavelengths of the H_2-**1**, Zn_2-**2**, and Zn_2-**3** Soret bands are 426, 424, and 424 nm, respectively. However, UV/Vis absorption spectra recorded at 10^{-6} M for 1:1 mixtures of H_2-**1** + Zn_2-**2** and H_2-**1** + Zn_2-**3** both showed a Soret band at 430 nm. This red shift is characteristic of the formation of a zinc porphyrin/pyridine complex: the Soret band of Zn-**4** moves from 422 to 430 nm on coordination of pyridine.[6] Thus in a 1:1 mixture of H_2-**1** and Zn_2-**2** at 10^{-6} M every zinc porphyrin in the sample is coordinated to a pyridine ligand (the same is true for the mixture of H_2-**1** and Zn_2-**3**).

4) Dilution studies. The ^{1}H NMR and UV/Vis absorption spectra of both complexes do not change over the accessible concentration range (10^{-7} to 10^{-2} M); in other words, the complexes remain fully assembled down to concentrations below 10^{-7} M. These complexes are remarkably stable compared to simple zinc porphyrins, which have stability constants in the region of 10^3 M^{-1}, and shows that cooperative self-assembly is taking place.[6]

The spectroscopic results indicate that the structures of the complexes are closed: all of the coordination sites are occupied and there are no free end groups. Thus the complexes are macrocyclic, which also accounts for the observed cooperativity. The only possible structures consistent with these observations and the VPO results are those in Figure 1.

The fluorescence spectra of 1:1 mixtures of H_2-**1** + Zn_2-**2** and H_2-**1** + Zn_2-**3** in dichloromethane are also characteristic of fully bound zinc porphyrin/pyridine complexes at concentrations of

10^{-7} M. However, on dilution both complexes dissociated at a concentration of about 10^{-8} M. Since Zn_2-**2** does not fluoresce (vide infra), the stability constant of the H_2-**1**·Zn_2-**2** complex could be determined by fluorescence titration methods (Fig. 2).

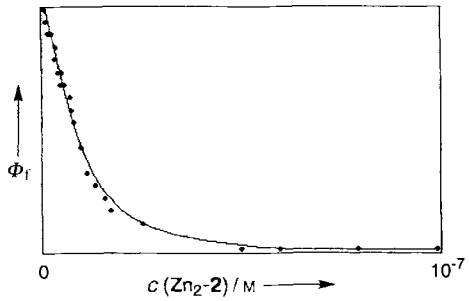

Fig. 2. Fluorescence titration curve for the binding of Zn_2-**2** to H_2-**1** in dichloromethane. The vertical scale is in arbitrary units. H_2-**1** (10^{-9} M) was selectively excited at 520 nm and the emission at 650 nm was recorded. Zn_2-**2** has negligible fluorescent emission at this wavelength at the concentrations used. The curve is the best fit of the 1:1 binding isotherm used to determine the association constant.

The titration data are approximated very well with an isotherm for 1:1 binding, confirming the VPO results. The stability constant for this complex is $3 \pm 1 \times 10^8\ M^{-1}$, which is very close to the value previously determined for the self-assembled "dimer" on which the design of these complexes were based.[6]

Evidence for electron and energy transfer processes in the complexes was also obtained from the fluorescence spectra. Compared with the Zn-**4** and Zn_2-**3**, Zn_2-**2** has a very weak fluorescent emission at 600 nm. The UV/Vis absorption spectrum of Zn_2-**2** is essentially the sum of the absorption spectra of the two component chromophores, Zn-**4** and **5**, which shows

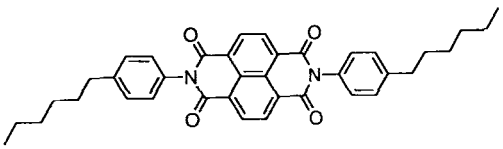

5

that there is little electronic interaction between the π-systems in the ground state. Thus we ascribe the quenching of the porphyrin emission in Zn_2-**2** to efficient intramolecular electron transfer from the excited singlet state of the porphyrin to the naphthalenediimide.[8]

In the H_2-**1**·Zn_2-**2** complex at a concentration of 10^{-6} M, the intensity of the fluorescent emission from H_2-**1** at 650 nm is 70% less than that of free H_2-**1** (see Fig. 2). Addition of 10^{-6} M **7** and 10^{-6} M Zn-**4** to H_2-**1** caused no change in the fluorescence spectrum. We therefore attribute the fluorescence quenching in the H_2-**1**·Zn_2-**2** assembly to intracomplex electron transfer from the H_2-**1** excited singlet state to the naphthalenediimide electron acceptor. The shortest bonded connection between the chromophores is 24 bonds or roughly 35 Å, whereas the separation of the chromophores in space is 10 Å at most. Thus it is probable that the pathway for the electron transfer is through space or through the solvent occupying the space between the two chromophores. The weak fluorescent emission of Zn_2-**2** is not significantly altered on complexation, which means that fast electron transfer from the zinc porphyrin to the naphthalenediimide also takes place in the complex. The photoinduced electron transfer reactions that take place in the H_2-**1**·Zn_2-**2** complex are summarized in Figure 3a.

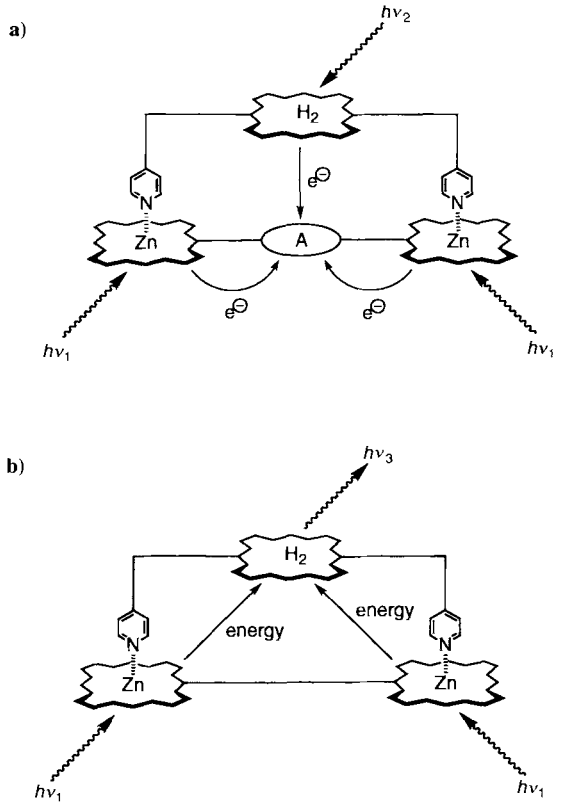

Fig. 3. a) The electron transfer processes assumed for the H_2-**1**·Zn_2-**2** complex. b) The energy transfer process assumed for the H_2-**1**·Zn_2-**3** complex. A = naphthalenediimide acceptor, H_2 = free-base porphyrin in H_2-**1**.

The H_2-**1**·Zn_2-**3** complex was prepared as a control, since it is formed by self-assembly but no electron transfer processes can occur. However, this complex also showed some interesting photochemistry. The intensity of the Zn_2-**3** fluorescent emission in this complex is significantly reduced. This is most clearly seen in Figure 4, which shows the emission spectra for a 1:1 mixture

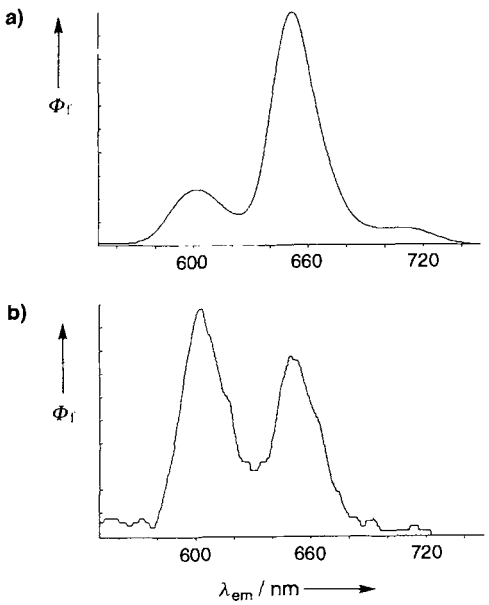

Fig. 4. Fluorescence spectra of a 1:1 mixture of H_2-**1** and Zn_2-**3** in dichloromethane at concentrations of 5×10^{-7} M (a) and 2×10^{-9} M (b); excitation at 426 nm. H_2-**1** fluoresces at 650 nm and Zn_2-**3** fluoresces at 600 nm.

of Zn_2-**3** and H_2-**1** at high concentration (complexed) and low concentration (uncomplexed). In addition, the intensity of the H_2-**1** fluorescent emission increases on adding Zn_2-**3**. Figure 5 shows that the emission from H_2-**1** in the complex is unaffected when the free-base porphyrin is selectively excited at 520 nm;

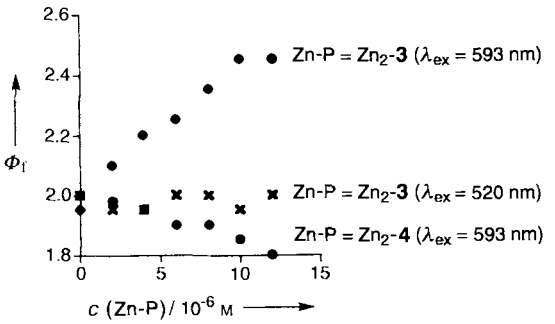

Fig. 5. Fluorescence titration data for the binding of Zn_2-**3** and of Zn-**4** to H_2-**1** (10^{-5} M) in dichloromethane. The vertical scale is in arbitrary units. The emission at 720 nm, which is exclusively due to H_2-**1**, was recorded. The excitation wavelengths are indicated: H_2-**1** absorbs at 520 and 593 nm; Zn_2-**3** absorbs at 593 nm only.

however, excitation at 593 nm, which excites both the zinc and free-base porphyrins, increases the intensity of the free-base emission. Addition of Zn-**4**, which does not complex to H_2-**1** at these concentrations, does not alter the free-base emission. We attribute this to energy transfer from the zinc porphyrins to the free-base porphyrin (Fig. 3b).

The approach described here is a powerful method for the construction of stable complex arrays of chromophores with well-defined three-dimensional structures. These systems represent a significant improvement over related noncovalent complexes, because they remain fully assembled at concentrations as low as 10^{-8} M, and the proportion of uncomplexed chromophore is negligible at higher concentrations. This will greatly facilitate detailed photophysical studies of their properties, and the preliminary fluorescence measurements reported here suggest that this will be a fruitful area for model studies of electron and energy transfer reactions in structurally well-defined yet complex architectures.

Received: January 22, 1996 [Z8740IE]
German version: *Angew. Chem.* **1996**, *108*, 2064–2067

Keywords: electron transfer · photochemistry · porphyrinoids

[1] G. McDermott, S. M. Prince, A. A. Freer, A. M. Hawthornethwaite-Lawless, M. Z. Papiz, R. J. Cogdell, N. W. Isaacs, *Nature* **1995**, *374*, 517; J. Deisenhofer, O. Epp, K. Miki, R. Huber, H. Michel, *Nature* **1985**, *318*, 618; G. Feher, J. P. Allen, M. Y. Okamura, D. C. Rees, *Nature* **1989**, *339*, 111.

[2] For an example of a light-harvesting model system, see: J. Seth, V. Palaniappan, T. E. Johnson, S. Prathapan, J. S. Lindsey, D. F. Bocian, *J. Am. Chem. Soc.* **1994**, *116*, 10578.

[3] For examples of models of photosynthetic reaction centers with covalent bonds, see: M. R. Wasielewski, *Chem. Rev.* **1992**, *92*, 435; D. Gust, T. A. Moore, A. L. Moore, *Acc. Chem. Res.* **1993**, *26*, 198; H. Kurreck, M. Huber, *Angew. Chem.* **1995**, *107*, 929; *Angew. Chem. Int. Ed. Engl.* **1995**, *34*, 849; Y. Sakata, H. Tsue, M. P. O'Neil, G. P. Wiederrecht, M. R. Wasielewski, *J. Am. Chem. Soc.* **1994**, *116*, 6904; H. Tamiaki, K. Nomura, K. Maruyama, *Bull. Chem. Soc. Jpn.* **1994**, *67*, 1863; J. C. Chambron, S. Chardonnoblat, A. Harriman, V. Heitz, J. P. Sauvage, *Pure Appl. Chem.* **1993**, *65*, 2343; J. Zaleski, W. Wu, C. K. Chang, G. E. Leroi, R. I. Cukier, D. G. Nocera, *Chem. Phys.* **1993**, *176*, 483; A. Osuka, S. Marumo, N. Mataga, S. Taniguchi, T. Okada, I. Yamazaki, Y. Nishimura, T. Ohno, K. Nozaki, *J. Am. Chem. Soc.* **1996**, *118*, 155.

[4] For examples of photoactive chromophore arrays constructed through hydrogen bonding, see: J. L. Sessler, B. Wang, A. Harriman, *J. Am. Chem. Soc.* **1993**, *115*, 10418; *ibid.* **1995**, *117*, 704; J. A. Roberts, J. P. Kirby, D. G. Nocera, *ibid.* **1995**, *117*, 8051; C. M. Drain, K. C. Russell, J. M. Lehn, *Chem. Comm.* **1996**, 337.

[5] For examples of models of the reaction center constructed with coordination chemistry, see: A. Harriman, F. Odobel, J. P. Sauvage, *J. Am. Chem. Soc.* **1995**, *117*, 9461; H. L. Anderson, C. A. Hunter, J. K. M. Sanders, *J. Chem. Soc. Chem. Comm.* **1989**, 226; C. A. Hunter, J. K. M. Sanders, G. S. Beddard, S. Evans, *ibid.* **1989**, 1765; U. Rempel, B. von Maltzan, C. von Borczyskowski, *Pure Appl. Chem.* **1993**, *65*, 2343.

[6] C. A. Hunter, L. D. Sarson, *Angew. Chem.* **1994**, *106*, 2424; *Angew. Chem. Int. Ed.* **1994**, *33*, 2313.

[7] The synthesis and characterization of these compounds will be described elsewhere.

[8] M. P. O'Neil, M. P. Niemczyk, W. A. Svec, D. Gosztola, G. L. Gaines, M. R. Wasielewski, *Science* **1992**, *257*, 63–65.

Peptide Nucleic Acids (PNAs) Containing Thymine Monomers Derived from Chiral Amino Acids: Hybridization and Solubility Properties of D-Lysine PNA**

Gerald Haaima, Anders Lohse, Ole Buchardt, and Peter E. Nielsen*

Peptide nucleic acids (PNAs) are DNA mimics containing an achiral, uncharged pseudopeptide backbone.[1–4] PNAs bind strongly and sequence-specifically to both single-stranded DNA and RNA[5,6] as well as to double-stranded DNA.[7,8] Furthermore, PNAs are both chemically and biologically stable.[9] These properties make PNAs attractive leads for the development of gene therapeutics[10–15] and biomolecular tools.[16] The original PNA backbone consists of *N*-(2-aminoethyl)glycine units; the nucleobases are attached to the glycine nitrogens through methylene carbonyl linkers (Scheme 1).[1–4] A number of modified PNAs have been prepared. Extension of the PNA backbone by the insertion of methylene units proved to be deleterious to the DNA-mimicking properties.[16] Introduction of chirality into the backbone has been also been studied, and the results

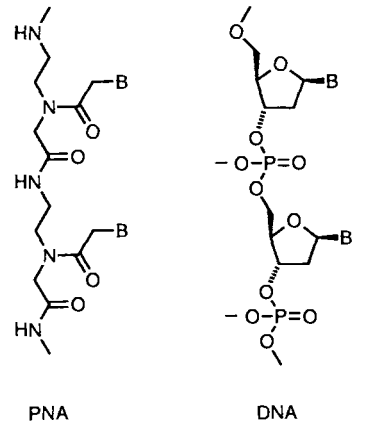

Scheme 1. Comparison of the backbones of DNA and PNA. B = nucleobases adenine, cytosine, guanine, and thymine.

[*] Prof. Dr. P. E. Nielsen
Center for Biomolecular Recognition
Department of Medical Biochemistry and Genetics
The Panum Institute
Blegdamsvej 3, DK-2200 N Copenhagen (Denmark)
Fax: Int. code +(313)96042
e-mail: penpanum@biobase.dk
Dr. G. Haaima, A. Lohse, Prof. Dr. O. Buchardt[+]
Center for Biomolecular Recognition
Department of Chemistry, University of Copenhagen
Universitetsparken 5, DK-2100 Copenhagen N (Denmark)

[+] Deceased

[**] This work was supported by the Danish National Research Foundation and ISIS Pharmaceuticals. We thank Annette W. Jørgensen and Margit Jørgensen for their technical assistance.

indicate that chirality arising from methyl groups incorporated at various positions along the backbone hardly affects the hybridization properties.[17, 18] However, it is not known whether larger substituents can be accommodated (although NMR studies on PNA–RNA[6] and PNA–DNA duplexes[19] indicate no steric interference of such substituents).

The question of accommodating functionality (and chirality) in the PNA backbone can be answered by constructing PNA monomers from α-amino acids other than glycine. This functionality would provide opportunities to tailor the hybridization behavior of PNA. Other properties such as solubility and cell penetration could also be improved. Finally, functional groups on the PNA backbone could provide convenient attachment points for various biologically active ligands.

We report here on the synthesis of PNA monomers from D- and L-lysine, D- and L-serine, D-glutamic acid, L-aspartic acid, and L-isoleucine with thymine as the nucleobase, as well as the preparation of PNA decamers containing three such monomers. Furthermore, we show that the change in thermal stability of PNA–DNA and PNA–RNA duplexes is −3.0 to +1.0 K per introduced monomer relative to the stability of the original glycine backbone; the D-lysine derivative is the only monomer with a stabilizing effect. Finally, discrimination of mismatched base pairs is generally improved when the monomers are introduced, and the D-lysine monomer is shown to increase the solubility of the PNA oligomer in water.

The synthesis of the chiral PNA monomers containing thymine as the nucleobase is outlined in Scheme 2. The synthetic route is analogous to that used for regular PNA monomers.[21]

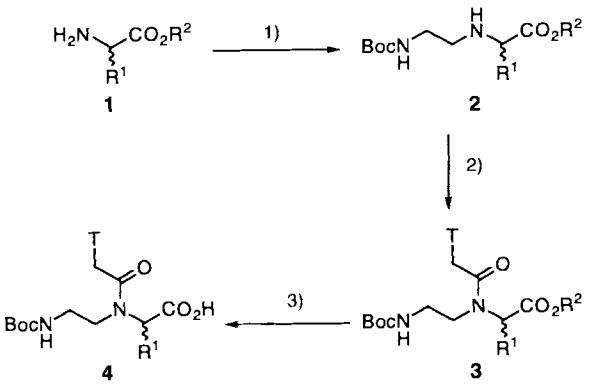

Scheme 2. Synthesis of the chiral PNA monomers **4a–g**. 1) $BocNHCH_2CHO$, $NaCNBH_3$; 2) thymin-1-yl-acetic acid, DCC. DhbtOH, DIEA, DMF, 40 °C; 3) for the benzyl ester: H_2, 10% Pd/C, MeOH, 1 h; for the allyl ester: $[Pd(PPh_3)_4]$, morpholine, THF, 30 min. Abbreviations are explained in ref. [20]. See also Table 1.

The protecting group chemistry used at the side chain and α-carboxyl group (Table 1) was designed to maintain the integrity of the stereogenic center during synthesis and subsequent oligomerization.[22] The α-carboxyl group was protected as an allyl ester,[22] a protecting group compatible with those used for the A, C, and G nucleobases of PNA.[21]

Table 1. Amino acids and protecting groups employed and overall yields for the PNAs synthesized according to Scheme 2.

Series	Amino acid	Stereo-chemistry	R^1	R^2	Overall yield [%]
a	Ile	L	*sec*-Bu	benzyl	49
b	Ser	L	CH_2OBn	allyl	44
c	Ser	D	CH_2OBn	allyl	41
d	Asp	L	CH_2CO_2cHex	benzyl	42
e	Glu	D	$CH_2CH_2CO_2Bn$	allyl	46
f	Lys	L	$(CH_2)_4NH$-2-ClZ	allyl	45
g	Lys	D	$(CH_2)_4NH$-2-ClZ	allyl	42

Duplex-forming PNA oligomers were synthesized on MBHA resin following a modified Merrifield solid-phase peptide synthesis.[24] The oligomer sequence was H-$GT_XAGAT_XCACT_X$-$(Lys)NH_2$, where T_X represents the new T monomers.[25] An L-lysine amino acid was included at the beginning of the sequence to facilitate comparisons with previously reported PNAs, except for oligomers incorporating monomers with carboxylic acid side chains. Deprotection and cleavage from the resin were achieved with anhydrous HF or by the "low/high" TFMSA method.[26] All oligomers were purified by HPLC and characterized by MALDI-TOF and/or FAB mass spectrometry.[27]

The thermal stabilities of complexes between the new PNA oligomers and complementary DNA and RNA oligomers were measured (Table 2). The results clearly show that the glycine units in the PNA backbone can be replaced by chiral amino acids with only a moderate loss of stability and, in some cases, an increase in DNA hybridization potency. Furthermore, as is observed for alanine-based PNAs,[17] D-amino acids appear to be better accommodated in the backbone of a PNA–DNA duplex (compare L- versus D-lysine and L- versus D-serine, Table 2). The introduction of negatively charged side chains in the backbone (for example glutamic and aspartic acid) decreases hybridization potency, while a positively charged side chain (L- and D-lysine, Table 2) has a beneficial effect on the DNA hybridization properties of PNA; an increase in T_m of roughly 1 K per lysine unit was observed. A similar increase is found in

Table 2. Melting temperatures [°C] of PNA–DNA and PNA–RNA duplexes [a, b].

Backbone [c]	[f]	T_m (DNA, antiparallel)	ΔT_m DNA [e]	T_m (DNA, parallel)	T_m (RNA)	ΔT_m (RNA) [e]
Gly	$LysNH_2$	52	–	38	55	–
Gly	NH_2	49	–	38	54	–
L-Lys	$LysNH_2$	49	−1.0	41	51	−1.3
D-Lys	$LysNH_2$	55	+1.0	40	55	0
L-Ser	$LysNH_2$	49	−1.0	37	52	−1.0
D-Ser	$LysNH_2$	50	−0.6	38	52	−1.0
D-Glu	NH_2	42	−2.3	28	[d]	[d]
L-Asp	NH_2	38	−3.3	33	[d]	[d]
L-Ile	$LysNH_2$	44	−2.6	38	46	−3.0

[a] Measured in aqueous buffer containing 100 mM NaCl, 10 mM phosphate, 0.1 mM EDTA, pH 7.0; heating rate: 1 K min^{-1}. UV absorbance measured at 254 nm. [b] The PNA sequence was H-$GT_XAGAT_XCACT_X$-R (R = NH_2 or L-$LysNH_2$). The complementary DNA sequence was 5′-d(AGTGATCTAC) for the antiparallel complex and 5′-d(CATCTAGTGA) for the parallel complex. [c] The backbone at the T_X position was constructed with the monomer derived from the indicated amino acid. [d] Not determined. [e] Increase or decrease in T_m [K] per chiral monomer (antiparallel orientation). [f] C-terminal amino acid.

oligonucleotides derived from aminoalkylphosphates.[28, 29] Hybridization of the PNAs to RNA led to similar thermal stabilities; however, the introduction of substituents to PNA resulted in a larger relative destabilization. Thus in this case no change in T_m was observed upon introduction of the D-lysine monomer. As previously noted for the glycine PNA,[5] the PNAs tested here show distinct directional preferences in binding: they bind better to an antiparallel DNA target than to parallel DNA.

We also studied the effect of a single mismatched base pair (T_{PNA}–$G_{DNA/RNA}$) in the middle of the duplex (Table 3). We found that PNAs containing a chiral amino acid discriminate better against base pair mismatches than glycine PNA does.

Table 3. Melting temperatures T_m [°C] of PNA–DNA and PNA–RNA duplexes with one mismatched base pair[a,b].

Backbone [c]	[f]	T_m (DNA)	ΔT_m (DNA) [e]	T_m (RNA)	ΔT_m (RNA) [e]
Gly	$LysNH_2$	37	−15	46	−9
L-Lys	$LysNH_2$	35	−14	40	−11
D-Lys	$LysNH_2$	36	−19	43	−12
D-Glu	NH_2	28	−20	[d]	[d]
L-Ile	$LysNH_2$	28	−16	36	−10
D-Ser	NH_2	33	−17	43	−9

[a] Measured in aqueous buffer containing 100 mM NaCl, 10 mM phosphate, 0.1 mM EDTA, pH 7.0; heating rate: 1 K min^{-1}. UV absorbance measured at 254 nm. [b] The PNA sequence was H-GT$_X$AGAT$_X$CACT$_X$-R (R = NH_2 or L-$LysNH_2$). The complementary DNA sequence with a single mismatched base was 5′-d(AGTGGTCTAC) (antiparallel orientation). [c] The backbone at the T_X position was constructed with the monomer derived from the indicated amino acid. [d] Not determined. [e] Increase or decrease in T_m [K] for the PNA–DNA duplex (antiparallel orientation). ΔT_m for the corresponding DNA–DNA duplex with a base mismatch: 10 K. [f] C-terminal amino acid.

Since the sequence selectivity is increased for both the D- and the L-amino acids, this discrimination is most likely a consequence of the bulky substituent in the α-position, which makes it difficult for the backbone to adopt the conformation required to accommodate the mispaired bases in the helix. Interestingly, the PNA containing D-lysine monomers displays a high sequence specificity ($\Delta T_m = -19$ K), which is approximately equal to that observed for the PNA incorporating D-glutamic acid ($\Delta T_m = -20$ K). Thus the electrostatic attraction between the anionic DNA strand and the cationic PNA apparently does not decrease sequence discrimination.

In general, very purine-rich PNAs are less water-soluble than fully purine–pyramidine mixed sequence PNAs. In order to examine whether the introduction of charged units in the PNA backbone leads to increased solubility, we synthesized the PNA dodecamer H-AGAGTGAGTGAG-NH_2 with T monomers attached to either a glycine or D-lysine backbone, and prepared a saturated solution of the PNA in 140 mM KCl and 10 mM sodium phosphate at pH 7.0 and 37 °C. While the all-glycine PNA was soluble up to a concentration of 40 mM, the D-lysine PNA was five times more soluble (200 mM). Naturally an even greater effect on the solubility is expected if more PNA units contain lysine monomers.

We have shown that PNAs with chiral funtionalized backbones retain strong DNA and RNA hybridization properties. This should provide unique opportunities (not possible with oligonucleotides) to prepare PNAs with specific physical and chemical properties, for example for pharmaceutical applications and for preparing PNA conjugates. For instance, amphiphilic and amphipatic PNAs are both easily constructed. Finally, amino acid functionalized PNAs are formally genuine chimera between proteins and nucleic acids, as functionalities of both are combined. In addition, the monomers may find interesting applications in amide-based combinatorial chemistry.[30]

Experimental Procedure

The general procedure is illustrated by the preparation of monomer **4b** derived from L-serine.

1b: To a stirred solution of L-BocSer(OBn)OH (5.00 g, 16.93 mmol) in dry DMF (60 mL) was added Cs_2CO_3 (5.52 g, 16.94 mmol). After 15 min allyl bromide (4.10 g, 33.88 mmol) was added and the reaction mixture stirred for a further 45 min. The inorganic salts were removed by filtration and the DMF was removed under reduced pressure. The residue was partitioned between ethyl acetate and saturated aqueous $NaHCO_3$. The aqueous layer was extracted several times with ethyl acetate and the combined organic layers were dried (Na_2SO_4). After removal of the solvent under reduced pressure, the light yellow residue was dissolved in benzene (50 mL) and pTSA·H_2O (3.33 g, 17.5 mmol) added. The solution was heated at reflux for 1 h, the volume was reduced to 10 mL, and crystallization was induced by slow addition of diethyl ether. Filtration of the solid material and recrystallization from methanol/diethyl ether afforded 5.68 g (82%) of white crystals (**1b**·pTSA). M.p. 81–82 °C; $[\alpha]_D^{20} = -4.8$ ($c = 5$ in MeOH); ^{1}H NMR ([D$_6$]DMSO, 400 MHz, DMSO reference): $\delta = 8.59$ (br. s, 3H), 7.43 (m, 5H), 7.57, 7.26 (ABq, $J_{AB} = 7.9$ Hz, 4H), 5.97 (m, 1H), 5.44 (m, 1H), 5.34 (dm, $J_{cis} = 10.5$, 1.5 Hz, 1H), 4.78 (m, 2H), 4.66, 4.57 (ABq, $J_{AB} = 12.3$ Hz, 2H), 4.52 (t, $J = 3.5$ Hz, 1H), 3.96 (dd, $J = 10.6$, 3.9 Hz, 1H), 2.37 (s, 3H); ^{13}C NMR ([D$_6$]DMSO): $\delta = 167.37$, 137.67, 137.27, 131.61, 128.29, 128.05, 127.76, 127.70, 118.48, 72.51, 67.30, 66.10, 52.58, 20.82; Anal. calcd. for $C_{20}H_{25}NO_6S$: C 58.95, H 6.18, N 3.36; found: C 58.70, H 6.17, N 3.44.

2b: A solution of **1b** (4.50 g, 11.04 mmol, which was freed from pTSA salts by multiple extraction of a solution of **1b** in aqueous $NaHCO_3$ with CH_2Cl_2) in methanol (40 mL) precooled to 0 °C was treated with Boc-aminoacetaldehyde (2.14 g, 13.28 mmol). The mixture was stirred at 0 °C for 30 min, after which acetic acid (0.75 mL) and sodium cyanoborohydride (0.37 g, 5.89 mmol) were added sequentially. After 30 min solvent was removed under reduced pressure and the resulting oil diluted with ethyl acetate (200 mL). After washing with saturated aqueous $NaHCO_3$ (1 × 100 mL) and brine (100 mL), the organic layer was dried (Na_2SO_4) and the solvent evaporated under reduced pressure to produce a colorless oil. An ethereal solution (80 mL) of this oil was cooled to −20 °C and treated with an equivalent of dry ethereal HCl (1.5 M). Dry hexanes (80 mL) were added and the solid hydrochloride salt was isolated by filtration. Crystallization from methanol/diethyl ether/hexanes produced 3.72 g (91%) of white crystals (**2b**·HCl). M.p. 120–121 °C; $[\alpha]_D^{20} = -11.1$ ($c = 5$ in MeOH);^{1}H NMR ([D$_6$]DMSO): $\delta = 10.22$ (br. s, 1H), 9.60 (br. s, 1H), 7.40 (m, 5H), 7.21 (t, $J = 5.3$ Hz, 1H), 5.96 (m, 1H), 5.43 (dm, $J_{trans} = 17.2$, $J_{gem} = 1.5$ Hz, 1H), 5.32 (dm, $J_{cis} = 10.6$, $J_{gem} = 1.5$ Hz, 1H), 4.78 (m, 2H), 4.68, 4.56 (ABq, $J_{AB} = 12.0$ Hz, 2H), 4.59 (m, 1H), 4.20 (dd, $J = 10.8$, 2.8 Hz, 1H), 4.00 (dd, $J = 10.8$, 3.1 Hz, 1H), 3.42 (m, 2H), 3.14 (m, 2H), 1.46 (s, 9H); ^{13}C NMR ([D$_6$]DMSO): $\delta = 166.78$, 155.77, 137.26, 131.58, 128.29, 127.76, 127.73, 118.55, 78.30, 72.50, 66.33, 66.20, 58.96, 46.21, 36.38, 28.21; Anal. calcd. for $C_{20}H_{31}ClN_2O_5$: C 57.89, H 7.53, N 6.75, Cl 8.54; found: C 57.61, H 7.64, N 6.60, Cl 8.7

3b: To a stirred solution of DhbtOH (2.20 g, 13.5 mmol) and thymin-1-yl-acetic acid (2.48 g, 13.5 mmol) in DMF (40 mL) was added DCC (2.92 g, 14.2 mmol). After 1 h **2b**·HCl (2.50 g, 6.74 mmol) and DIEA (0.88 g, 6.8 mmol) were added. The reaction mixture was stirred at 40 °C until the reaction was complete (typically 15 h). The DMF was evaporated under reduced pressure, the yellow residue taken up in ethyl acetate (120 mL), and the dicyclohexylurea removed by filtration. The organic layer was washed successively with saturated aqueous $NaHCO_3$ (1 × 100 mL), half saturated aqueous $KHSO_4$ (1 × 100 mL), and brine (1 × 100 mL), and then dried with Na_2SO_4. The solvent was removed under reduced pressure to give a light yellow foam, which was purified by silca gel chromatography (2/1 ethyl acetate/hexanes). Further purification by dissolving the product in ethyl acetate (5 mL), adding diethyl ether (100 mL), and stirring overnight afforded 2.04 g (58%) of the analytically pure product. $[\alpha]_D^{20} = -5.2$ ($c = 3$ in MeOH); ^{1}H NMR ([D$_6$]DMSO) (data for the major rotamer only): $\delta = 11.35$ (s, 1H), 7.41 (m, 6H), 6.90 (m, 1H), 5.94 (m, 2H), 5.36 (dd, $J = 17.3$, 1,5 Hz, 1H), 5.26 (dd, $J = 10.5$, 1.5 Hz, 1H), 4.68 (m, 6H), 1.83 (br. s, 3H), 1.47 (s, 9H); ^{13}C NMR ([D$_6$]DMSO): $\delta = 168.27$, 167.43, 164.32, 155.69, 150.92, 142.00, 137.96, 132.25, 128.26, 127.50, 117.69, 108.06, 78.06, 72.21, 67.43, 65.03, 59.76, 47.85, 46.79, 28.19, 11.91; Anal. calcd. for $C_{27}H_{36}N_4O_8$: C 59.55, H 6.66, N 10.29; found: C 59.40, H 6.65, N 10.29.

4b: A solution of ester **3b** (0.50 g, 0.92 mmol) and morpholine (0.80 mL, 9.2 mmol) in THF (9 mL) was treated with [Pd(PPh$_3$)$_4$] (10.6 mg, 0.09 mmol). After 30 min the solvent was removed under reduced pressure and the resulting foam taken up in ethyl acetate (30 mL) and washed with brine (set at pH 3 with aqueous $KHSO_4$). The aqueous layer was further extracted with ethyl acetate (6 × 15 mL) and the combined organic layers washed with brine and dried (Na_2SO_4). The solvent was removed to give a light yellow foam, which was dissolved in ethyl acetate and precipitated by slow addition of hexane. After filtration and drying under high vacuum, 0.386 g (83%) of a white solid was obtained. $[\alpha]_D^{20} = -35.3$ ($c = 3$ in MeOH); ^{1}H NMR ([D$_6$]DMSO): $\delta = 11.28$ (s, 1H), 7.41 (m, 6H), 6.85 (m, 1H),

4.66–4.49 (m, 4H), 3.85 (m, 2H), 1.75 (br. s, 3H), 1.38 (s, 9H); ^{13}C NMR ([D$_6$]DMSO): δ = 167.98, 166.93, 164.39, 155.63, 151.04, 142.09, 138.47, 132.04, 131.54, 128.25, 127.49, 107.94, 77.80, 71.92, 68.14, 61.71, 48.45, 38.19, 28.30, 11.91; FAB HRMS: *m/z* calcd. for $C_{24}H_{33}N_4O_8$: 505.2298; found: 505.2324.

Received: September 1, 1995
Revised version: May 20, 1995 [Z 8359 IE]
German version: *Angew. Chem.* **1996**, *108*, 2068–2070

Keywords: DNA hybridization · peptide nucleic acids

[1] P. E. Nielsen, M. Egholm, R. H. Berg, O. Buchardt, *Science* **1991**, *254*, 1497.
[2] M. Egholm, O. Buchardt, P. E. Nielsen, R. H. Berg, *J. Am. Chem. Soc.* **1992**, *114*, 1895.
[3] M. Egholm, O. Buchardt, P. E. Nielsen, R. H. Berg, *J. Am. Chem. Soc.* **1992**, *114*, 9677.
[4] M. Egholm, C. Behrens, L. Christensen, R. H. Berg, P. E. Nielsen, O. Buchardt, *J. Chem. Soc. Chem. Commun.* **1993**, 800.
[5] M. Egholm, O. Buchhardt, L. Christensen, C. Behrens, S. M. Freier, D. A. Driver, R. H. Berg, S. K. Kim, B. Nordén, P. E. Nielsen, *Nature* **1993**, *365*, 566.
[6] S. C. Brown, S. A. Thomson, J. M. Veal, D. G. Davis, *Science* **1994**, *265*, 777.
[7] D. Y. Cherny, B. P. Belotserkovskii, M. D. Frank-Kamenetskii, M. Egholm, O. Buchardt, R. H. Berg, P. E. Nielsen, *Proc. Natl. Acad. Sci USA* **1993**, *90*, 1667.
[8] P. E. Nielsen, M. Egholm, O. Buchardt, *J. Mol. Recognit.* **1994**, *7*, 165.
[9] V. V. Demidov, V. N. Potaman, M. D. Frank-Kamenetskii, M. Egholm, O. Buchardt, S. H. Sönnichsen, P. E. Nielsen, *Biochem. Pharmacol.* **1994**, *48*, 1310.
[10] P. E. Nielsen, M. Egholm, R. H. Berg, O. Buchardt in *Antisense Research and Development* (Eds.: S. Crooke, B. Lebleu), CRC Press, Boca Raton, FL, USA, **1993**, p. 363.
[11] J. C. Hanvey, N. J. Peffer, J. E. Bisi, S. A. Thomson, R. Cadilla, J. A. Josey, D. J. Ricca, C. F. Hassman, M. A. Bonham, K. G. Au, S. G. Carter, D. A. Bruckenstein, A. L. Boyd, S. A. Noble, L. E. Babiss, *Science* **1992**, *258*, 1481.
[12] P. E. Nielsen, M. Egholm, O. Buchardt, *Gene* **1994**, *149*, 139.
[13] M. A. Bonham, S. Brown, A. L. Boyd, P. H. Brown, D. A. Bruckenstein, J. C. Hanvey, S. A. Thomsen, A. Pipe, F. Hassman, J. E. Bisi, B. C. Froehler, M. D. Matteucci, R. W. Wagner, S. A. Noble, L. E. Babiss, *Nucleic Acids Res.* **1995**, *23*, 1197.
[14] P. E. Nielsen, *Annu. Rev. Biophys. Biomol. Struct.* **1995**, 167.
[15] A. DeMesmaeker, K.-M. Altman, A. Waldner, S. Wendeborn, *Curr. Opin. Struct. Biol.* **1995**, *5*, 343.
[16] B. Hyrup, M. Egholm, P. E. Nielsen, P. Wittung, B. Nordén, B. O. Buchardt, *J. Am. Chem. Soc.* **1994**, *116*, 7964.
[17] K. L. Dueholm, K. H. Petersen, D. K. Jensen, M. Egholm, P. E. Nielsen, O. Buchardt, *Biomed. Chem. Lett.* **1994**, *4*, 1077.
[18] L. Kosynkina, W. Wang, T. C. Liang, *Tetrahedron Lett.* **1994**, *35*, 5173.
[19] M. Eriksson, P. E. Nielsen, *Nature Struct. Biol.* **1996**, *3*, 410.
[20] Boc = *tert*-butoxycarbonyl, Bz = benzyl, cHex = cyclohexyl, 2-ClZ = (2-chlorobenzyloxy)carbonyl, DCC = dicyclohexylcarbodiimide, DhbtOH = 2,3-dihydro-3-hydroxy-4-oxo-1,2,3-benzotriazine, DIEA = diisopropylethylamine, DMF = dimethylformamide, MBHA = methylbenzhydrylamine, pTSA = *para*-toluenesulfonic acid.
[21] K. L. Dueholm, M. Egholm, C. Behrens, L. Christensen, H. H. Hansen, T. Vulpius, K. H. Petersen, R. H. Berg, P. E. Nielsen, O. Buchardt, *J. Org. Chem* **1994**, *59*, 5767.
[22] The enantiomeric purity of the L-Ser (**2b**), L-Glu (**2e**), and L-Lys (**2f**) monomers was determined as follows: The monomer was first coupled to racemic L-isoleucine methyl ester and then to optically pure L-isoleucine methyl ester; HPLC analysis of the products indicated an enantiomeric purity of >90%.
[23] S. Friedrich-Bochnitschek, H. T. Waldmann, H. Kunz, *J. Org. Chem.* **1989**, *54*, 751.
[24] J. P. Tam, W. F. Heath, R. B. Merrifield, *J. Am. Chem. Soc.* **1986**, *108*, 5242.
[25] The following nomenclature is used: In H-ACGT-LysNH_2, H denotes the free N-terminus, and A, C, G, and T stand for the *N*-A-acetyl, *N*-C-acetyl, *N*-G-acetyl, and *N*-T-acetyl-*N*-(2-aminoethyl)glycine units, respectively.
[26] L. Christensen, R. Fitzpatrick, B. Gildea, K. H. Petersen, H. F. Hansen, T. M. Koch, M. Egholm, O. Buchardt, P. E. Nielsen, J. Coull, R. H. Berg, *J. Pept. Sci.* **1995**, *3*, 175.
[27] FAB MS analysis: calcd (found): L-Ile 3021.4 (3023.7); L-Ser 2943.2 (2945.2); D-Ser 2943.2 (2945.3); D-Glu 2941.2 (2942.4), L-Lys 2937.3 (2938.5); D-Lys 3066.4 (3068.7).
[28] R. L. Letsinger, C. N. Singman, G. Histand, M. Salunkhe, *J. Am. Chem. Soc.* **1988**, *110*, 4470.
[29] R. Fathi, Q. Huang, G. Coppola, W. Delany, R. Teasdale, A. M. Krieg, A. F. Cook, *Nucleic Acids Res.* **1994**, *22*, 5416.
[30] P. E. Nielsen, *Methods Enzymol.* **1996**, *267*, 426.

A Stable Methyl Phosphane Oxide/Lithium Amide Complex: a Structural and MO Calculational Investigation of the Mechanism of Proton Abstraction by Alkali Metal Reagents**

David R. Armstrong, Matthew G. Davidson, Robert P. Davies, Helen J. Mitchell, Rachel M. Oakley, Paul R. Raithby, Ronald Snaith,* and Stuart Warren

Lithium alkyls $(RLi)_n$, lithium amides $(R_2NLi)_n$, and their complexes are used extensively in organic synthesis to deprotonate E–H units (E = C, N, O etc.).[1] How such proton abstractions occur is not well understood, although in many cases the preliminary step is presumed to be coordination of the organic compound (through one or more of its functionalities) to the lithium reagent.[2] Presumably also, in such a complex the E–H bond will be in reasonable proximity to the anionic center of the reagent, so facilitating proton transfer and formation of an E–Li bond. Here we describe a species that to some extent tests these presumptions. The methyl phosphane oxide $Ph_2P(=O)CH_3$, which is known to be lithiated by *n*BuLi (and also by *t*BuLi and iPr_2NLi (LDA)) in THF at −78 °C as the first step in Horner–Wittig reactions,[3] is *not* lithiated by lithium bis(trimethylsilyl)amide $(Me_3Si)_2NLi$. Instead, compound **1**

$[(Me_3Si)_2NLi{\cdot}O{=}P(CH_3)Ph_2]_n$ **1**

(n = 2 in the solid state), a complex of the two reagents is isolated. Examination of the structure of **1** indicates why deprotonation is blocked. Prompted by this experimental finding, we report also a MO calculational study of the mechanics and energetics of deprotonation within a related model system, $H_2NLi{\cdot}O{=}P(CH_3)H_2$.

Mixing $Ph_2P(=O)CH_3$ and $(Me_3Si)_2NLi$ in toluene/hexane gave a pale yellow solution at room temperature. Crystals of **1** were obtained in high yield on chilling this solution; a similar yield was gained even after prior heating of the solution to 80 °C for several hours. Adduct **1** was fully characterized by elemental analysis and NMR spectroscopy (see Experimental Procedure), and its solid-state structure was solved by X-ray crystallography[4] (Fig. 1). The observed aggregation of **1** to form a dimer is in itself not surprising. Solid $[(Me_3Si)_2NLi]_n$ is a ring trimer (n = 3), whereas its 1:1 complexes with monodentate Lewis bases such as Et_2O are dimers.[2, 5] Thus $Ph_2P(=O)CH_3$ acts simply as such a Lewis base even though it is a reasonably acidic molecule, deprotonated by reagents such as *n*BuLi at low temperatures. The view of **1** in Figure 1 gives some preliminary stereochemical indication as to why deprotonation is blocked; it shows also the (to us, inexplicable) *cis* arrangement of the methyl groups on the phosphane oxides.[6]

Several published crystal structures are relevant to the discussion of the structure of **1**. Most of them are species obtained after treating the organic compound (for example an amine, an imine, or an enolizable ketone) with a deficiency (less than

[*] Dr. R. Snaith, Dr. M. G. Davidson, R. P. Davies, H. J. Mitchell, R. M. Oakley, Dr. P. R. Raithby, Dr. S. Warren
Department of Chemistry, University of Cambridge
Lensfield Road, Cambridge CB2 1EW (UK)
Fax: Int. code +(1223)336-632
Dr. D. R. Armstrong
Department of Pure and Applied Chemistry
University of Strathclyde, Glasgow (UK)

[**] This work was supported by the UK Engineering and Physical Sciences Research Council (R. P. D., H. J. M.), St. John's College, Cambridge (research fellowship, M. G. D.), Rhône-Poulenc-Rorer (H. J. M.), and The Royal Society (low-temperature X-ray diffraction apparatus, P. R. R.).

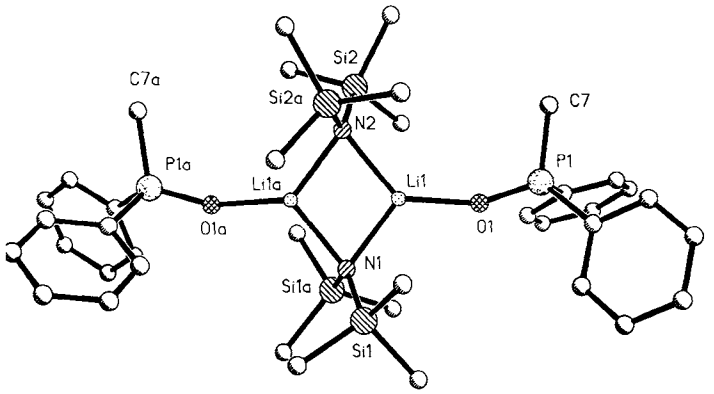

Fig. 1. The molecular structure of **1** in the crystal shown perpendicular to the Li_2N_2 ring (hydrogen atoms omitted for clarity).

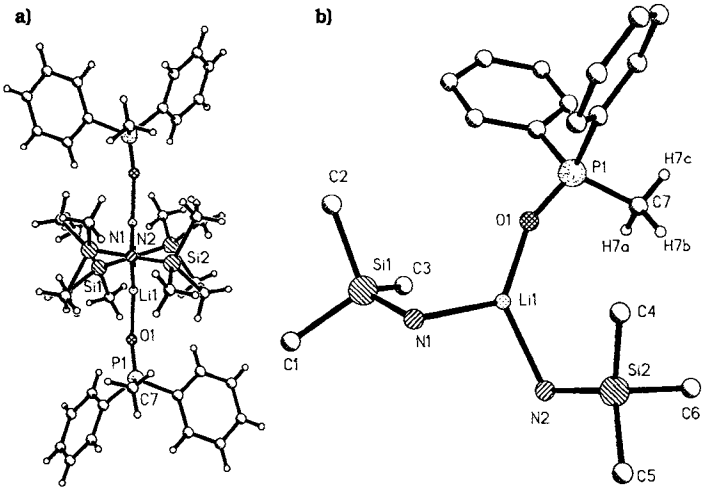

Fig. 2. a) The molecular structure of **1** in the crystal highlighting the relative positions of the $(P)CH_3$ groups and the N centers of the Li_2N_2 ring. b) One-half of the dimer of **1** showing the relative positions of the $(P)CH_3$ and $NSi(CH_3)_3$ groups.

one equivalent) of the metalating reagent. The excess, intact organic precursor then acts as a Lewis base towards the metalated compound, for example as in the monomer [Ph(2-Pyr)NLi]·HMPA·[HN(2-Pyr)Ph] (2-Pyr = 2-pyridyl, HMPA = hexamethylphosphoric triamide),[7a] the tetrameric ladder $[C_5H_{10}NLi \cdot HNC_5H_{10}]_4$ ($C_5H_{10}NH$ = piperidine),[7b] and the tetrameric cubanes $(t\mathrm{Bu_2C{=}NNa})_4 \cdot (HN{=}Ct\mathrm{Bu_2})_2$[7c] and $[t\mathrm{BuC}(=CH_2)ONa \cdot O{=}C(t\mathrm{Bu})CH_3]_4$.[7d] However, all these examples hint at a propagation mechanism: some of the organic precursor has been metalated, whilst the remainder coordinates to the metalation product and awaits subsequent metalation. The case of **1** is fundamentally different. Here, the reactants $Ph_2P(=O)CH_3$ and $(Me_3Si)_2NLi$, taken in 1:1 ratio, do not react but simply form an adduct. This result thus indicates what an initiation step in a deprotonation might be, namely coordination of the wholly intact organic precursor to the metalating reagent. Given this, the only published structure directly relevant to **1** is that of the complex between $(Me_3Si)_2NLi$ and the potentially enolizable ester *tert*-butyl isobutyrate, $[(Me_3Si)_2NLi \cdot O{=}C(t\mathrm{Bu})OCHMe_2]_2$.[8] Here, the failure of the components to react was attributed to the unfavorable position of the enol hydrogen atom, which points directly towards the basic nitrogen; if this hydrogen atom were to be abstracted, delocalization of resulting negative charge into the adjacent carbonyl π orbitals would not be possible. For **1**, however, we ascribe the failure to react to a rather simpler (and probably more general) reason. As Figure 2a makes clear, none of the methyl C–H bonds of the phosphane oxide can approach the negatively polarized N atom of the lithium amide component (key bond angles: Li-O-P 157.7(3)° and O-P-CH_3 112.9(2)°]. Any such proximity is prevented by the large and extensive Me_3Si substituents. In particular, one of the silyl methyl groups is placed between the $N^{\delta-}$ center and the phosphane methyl group (Fig. 2b; one half of the dimer of **1** is shown).

In view of the isolation of **1**, we carried out ab initio calculations to probe how H_2NLi would deprotonate $O{=}P(CH_3)H_2$, and what the energetics of such a reaction would be. All calculations were conducted with the 6-31G basis set (plus, where relevant, a set of d orbitals on phosphorus)[9] by means of the program GAMESS.[10] Species were optimized without imposed geometric constraints, and absolute energies are reported.[11] The precursors—$O{=}P(CH_3)H_2$ and H_2NLi—and the potential products—$LiOP(CH_2)H_2$, a planar ring with both Li–O and Li–C bonds, and NH_3—were optimized first. Formation of the complex $H_2P(CH_3)O \cdot LiNH_2$ (Fig. 3a) is highly favorable; the complex is 32.3 kcal mol^{-1} lower in energy than the

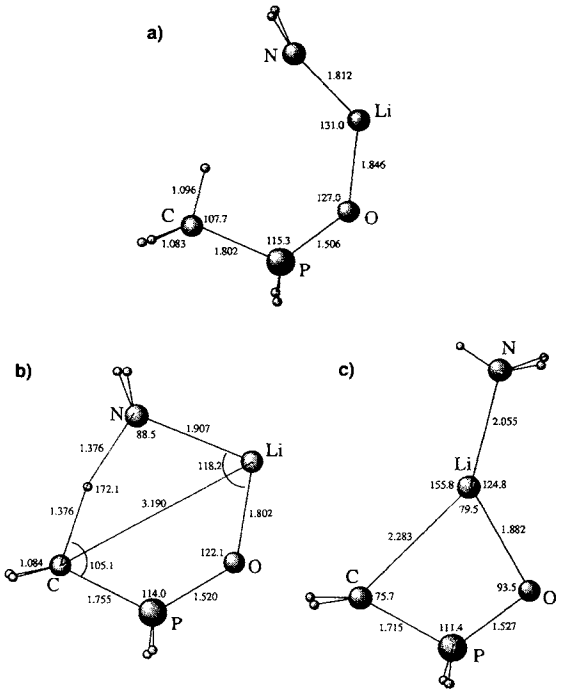

Fig. 3. Structures optimized by ab initio calculations (bond lengths in Å, bond angles in degrees) for a) the initial complex between $H_2P(CH_3)O$ and $LiNH_2$, b) the transition state for proton transfer from CH_3 to NH_2^-, and c) the resulting NH_3 complex of $H_2P(CH_2)OLi$.

separate components. Rotation of the CH_3 group is barrier-free (< 0.1 kcal mol^{-1}), so that none or one or two of its H atoms can point towards the H_2N unit. In the configuration shown in Figure 3a, the $(C)H \cdots N(H_2)$ and $(H_3)C \cdots Li$ distances are 2.368 and 3.383 Å, respectively. The calculated transition state for proton transfer is shown in Figure 3b. Here the transferable methyl proton is equidistant (1.376 Å) between C and N in a near-linear (C-H-N 172.1°) arrangement, it is significantly polarized (charge +0.44, cf. +0.17 for the remaining CH_2 protons), and the Li–C bond is beginning to form ($Li \cdots C$ 3.190 Å). Progression from the reactants' complex to this transition state requires an energy increase of only 8.7 kcal mol^{-1}. It is accomplished almost exclusively by a decrease in the O-Li-N angle (131.0° in the complex, 118.2° in the transition

state) and much of this reflects movement of the Li–N unit towards the carbon atom; the P-O-Li angle decreases from 127.0 to 122.1°, whereas the OPC angle changes little (115.3 to 114.0°). Complete proton transfer affords an ammonia complex of the lithiated phosphane oxide (Fig. 3c). This is 16.5 kcal mol^{-1} lower in energy than the transition state and so 7.8 kcal mol^{-1} more stable than the initial reactant complex. The complexation of NH_3 to the lithiated phosphane oxide is associated with a stabilization of 23.8 kcal mol^{-1}.

These calculational results quantify (to our knowledge, for the first time) the energetics of proton transfer from an acidic organic compound to a lithium reagent, and may have significance on several counts. 1) When the organic compound contains an electronegative functionality, its complexation to the lithium reagent seems a likely first step. 2) The activation energy for proton transfer is quite low in the model we have used; however, this is the least sterically demanding system possible. Progression to the transition state appears to require for the most part movement of the anionic center of the lithium reagent towards the acidic organic center. One would readily expect that this activation energy would be prohibitively high when groups on one or both centers are large (as found for **1**). 3) For lithium amide reagents in particular, the initial product of deprotonation is likely to be an amine complex (witness here the quite strong complexation of NH_3 to the lithiated phosphane oxide). Several post-enolization amine/lithium enolate complexes have been detected,[12] and this "secondary amine effect" can influence the subsequent reactivity of the lithium enolate.[13] It can also result in reprotonation of the enolate by the attached amine, so reducing final yields.[12a, 13a, c, 14] In our model calculations the step from the initial reactant amide complex to the ammonia-complexed product affords a modest 7.8 kcal mol^{-1} drop in energy. Within this step, the more substantial NH_3 complexation energy (23.8 kcal mol^{-1}) plays a determining role. Thus, poorly complexing amines such as $(Me_3Si)_2NH$[13, 14] might well affect the position of the equilibrium between the reactant amide complex and the amine-complexed product. The failure of $(Me_3Si)_2NLi$ to lithiate $Ph_2P(=O)CH_3$ might therefore be due to this phenomenon rather than due to the precise stereochemical features of the isolated product **1**.

Calculations have also been carried out on the model dimers $[H_2NLi\cdot O{=}P(CH_3)H_2]_2$, which are more akin to **1**. The findings are in line with those recorded above for the monomer and will be reported in a full paper.

Experimental Procedure

Synthesis of **1**: Solid methyldiphenylphosphane oxide (0.54 g, 2.5 mmol) and lithium bis(trimethylsilyl)amide (0.42 g, 2.5 mmol) were taken up together in chilled hexane/toluene (5 mL/5 mL). Brief warming of the resulting white suspension afforded a pale yellow solution, which was chilled (5 °C, 2 d) to give colorless crystalline blocks of **1**. First batch yield: 0.68 g, 71%; m.p. 148–152°C; satisfactory analysis for $C_{19}H_{31}LiNOPSi_2$; ^1H NMR (C_6D_6, 250 MHz, 25 °C): $\delta = 7.58$(m, 4H), 7.09 (m, 6H), 1.62 (d, $J = 13.2$ Hz, 3H, $Ph_2P(O)CH_3$), 0.56 (s, 18H, LiN[Si(CH_3)$_3$]$_2$).

Received: January 25, 1996 [Z 8753 IE]
German version: *Angew. Chem.* **1996**, *108*, 2071–2073

Keywords: ab initio calculations · amides · lithium compounds · phosphorus compounds · solid-state structures

[1] a) B. J. Wakefield, *Organolithium Methods*, Academic Press, New York, **1988**; b) M. Fieser, *Reagents for Organic Synthesis, Vol. 15*, Wiley-Interscience, New York, **1990**; c) L. Brandsma, *Preparative Polar Organometallic Chemistry, Vol 2*, Springer, Berlin, **1990**; d) P. G. Williard in *Comprehensive Organic Synthesis, Vol. 1* (Eds.: B. M. Trost, I. Fleming), Pergamon, New York, **1991**.

[2] a) K. Gregory, P. von R. Schleyer, R. Snaith, *Adv. Inorg. Chem.* **1991**, *37*, 47–142; b) A. Sekigushi, Y. Sugai, K. Ebata, C. Kabuto, H. Sakurai, *J. Am. Chem. Soc.* **1993**, *115*, 1144–1146.

[3] a) A. D. Buss, S. Warren, *J. Chem. Soc. Perkin Trans. 1* **1985**, 2307–2325; b) A. D. Buss, N. Greeves, R. Mason, S. Warren, *ibid.* **1987**, 2569–2577; c) J. Clayden, S. Warren, *Angew. Chem.* **1996**, *108*, 261–291; *Angew. Chem. Int. Ed. Engl.* **1996**, *35*, 241–270; d) D. R. Armstrong, D. Barr, M. G. Davidson, G. Hutton, P. O'Brien, R. Snaith, S. Warren, *Tetrahedron Lett.* **1996**, submitted.

[4] X-ray crystal data for **1**: $C_{38}H_{62}Li_2N_2O_2P_2Si_4$, $M = 767.08$, monoclinic, space group $C2/c$, $a = 23.217(5)$, $b = 11.181(2)$, $c = 18.351(4)$ Å, $\beta = 105.98(3)°$, $V = 4580(2)$ Å^3, $F(000) = 1648$, $\lambda(Mo_{K\alpha}) = 0.71073$ Å, $\mu(Mo_{K\alpha}) = 0.231$ mm^{-1}, $T = 153(2)$ K, $Z = 4$, $\rho_{calcd} = 1.113$ Mg m^{-3}. Data were collected on a Stoe-Siemens diffractometer in the range $3.56° \le \theta \le 22.50°$ (3330 reflections collected, 2969 independent ($R_{int} = 0.0556$)). The structure was solved by direct methods, and refinement, based on F^2, was by full-matrix least-squares techniques (SHELXL93, G. M. Sheldrick, Universität Göttingen); all non-hydrogen atoms were refined anisotropically, and hydrogen atoms were included in calculated positions and allowed to ride on the relevant carbon atom. Final residuals were $R1 = 0.0517$ for 2320 unique data with $I > 2\sigma(I)$, and $wR2 = 0.181$ (all data). Crystallographic data (excluding structure factors) for the structure reported in this paper have been deposited with the Cambridge Crystallographic Data Centre as supplementary publication no. CCDC-179-42. Copies of the data can be obtained free of charge on application to The Director, CCDC, 12 Union Road, Cambridge CB2 1EZ, UK (fax: Int. code +(1223)336-033; e-mail: teched@chemcrys.cam.ac.uk).

[5] a) R. E. Mulvey, *Chem. Soc. Rev.* **1991**, *20*, 167–209; b) D. Mootz, A. Zinnius, B. Böttcher, *Angew. Chem.* **1969**, *81*, 398–399; *Angew. Chem. Int. Ed. Engl.* **1969**, *8*, 378–379; c) M. F. Lappert, M. J. Slade, A. Singh, J. L. Atwood, R. D. Rogers, R. Shakir, *J. Am. Chem. Soc.* **1983**, *105*, 302–304; d) L. M. Engelhardt, B. S. Jolly, P. C. Junk, C. L. Raston, B. W. Skelton, A. H. White, *Aust. J. Chem.* **1986**, *39*, 1337–1345.

[6] In the closely related structure of $[(Me_3Si)_2NLi\cdot O{=}PPh_3]_2$ two of the phenyl groups have the expected *trans* configuration with respect to the $(NLi)_2$ ring: M. G. Davidson, unpublished results.

[7] a) D. Barr, W. Clegg, R. E. Mulvey, R. Snaith, *J. Chem. Soc. Chem. Commun.* **1984**, 469–470; b) G. Boche, I. Langlotz, M. Marsch, K. Harms, N. E. S. Nudelman, *Angew. Chem.* **1992**, *104*, 1239–1240; *Angew. Chem. Int. Ed. Engl.* **1992**, *31*, 1205–1207; c) W. Clegg, M. MacGregor, R. E. Mulvey, P. A. O'Neil, *ibid.* **1992**, *104*, 74 and **1992**, *31*, 93–95; d) P. G. Williard, G. B. Carpenter, *J. Am. Chem. Soc.* **1992**, *108*, 462–468.

[8] P. G. Williard, Q.-L. Liu, L. Lochmann, *J. Am. Chem. Soc.* **1992**, *114*, 348–350.

[9] a) W. J. Hehre, R. Ditchfield, J. A. Pople, *J. Chem. Phys.* **1972**, *56*, 2257–2261; b) P. C. Hariharan, J. A. Pople, *Theor. Chim. Acta* **1973**, *28*, 213–222; c) J. D. Dill, J. A. Pople, *J. Chem. Phys.* **1975**, *62*, 2921–2923.

[10] a) M. Dupuis, D. Spangler, J. J. Wendoloski, GAMESS NRCC Software Catalogue, Program No. 2 GOI, *Vol. 1*, **1980**; b) M. F. Guest, J. Kendrick, S. A. Pope, GAMESS Documentation, Daresbury Laboratory, Warrington, UK, **1983**; c) M. F. Guest, P. Fantucci, R. J. Harrison, J. Kendrick, J. H. van Lenthe, K. Schoeffel, P. Sherwood, GAMESS-UK Daresbury (CFS Ltd, **1993**).

[11] Absolute energies [a.u.] of optimized species: $O{=}P(CH_3)H_2$ −456.326246, H_2NLi −63.030536, reactant complex $H_2P(CH_3)O\cdot LiNH_2$ −519.408105, transition state for proton transfer −519.394259, lithiated phosphane oxide $LiOP(CH_2)H_2$ −463.217090, NH_3 −56.165521, NH_3 complex of the lithiated phosphane oxide −519.420488.

[12] a) T. Laube, J. D. Dunitz, D. Seebach, *Helv. Chim. Acta* **1985**, *68*, 1373–1393; b) R. A. Wanat, D. B. Collum, G. Van Duyne, J. Clardy, R. T. DePue, *J. Am. Chem. Soc.* **1986**, *108*, 3415–3422; c) S. Buchholz, K. Harms, W. Massa, G. Boche, *Angew. Chem.* **1989**, *101*, 57–58; *Angew. Chem. Int. Ed. Engl.* **1989**, *28*, 72–73.

[13] a) D. Seebach, *Angew. Chem.* **1988**, *100*, 1685–1715; *Angew. Chem. Int. Ed. Engl.* **1988**, *27*, 1624–1654; b) D. B. Collum, *Acc. Chem. Res.* **1993**, *26*, 227–234; c) R. Polt, D. Seebach, *J. Am. Chem. Soc.* **1989**, *111*, 2622–2632; d) F. E. Romesberg, M. P. Bernstein, J. H. Gilchrist, A. T. Harrison, D. J. Fuller, D. B. Collum, *ibid.* **1993**, *115*, 3475–3483.

[14] P. A. Magriotis, K. D. Kim, *J. Am. Chem. Soc.* **1993**, *115*, 2972–2973.

 © VCH Verlagsgesellschaft mbH, D-69451 Weinheim, 1996 0570-0833/96/3517-1944 $ 15.00+.25/0

Regioisomeric Effects on the Excited State Processes of a Cyclodextrin Modified with a Lumophore**

Mark A. Mortellaro, Wanda K. Hartmann, and Daniel G. Nocera*

Supramolecular topologies may be exploited to engender novel physical and chemical processes. Of the many diverse architectures offered by supramolecules,[1] the cylindrical cavities of cyclodextrins (CDs) have been intensively investigated. The six, seven, or eight $\alpha(1\rightarrow4)$ linked D-glucose units (α-, β-, and γ-CD, respectively) of these cyclic oligosaccharides allow for water solubility while maintaining a hydrophobic interior suitable for substrate binding. The hydroxyl groups on the outer rims of the CD offer a site for the derivitization that might promote biomimetic transformations on substrates included within the cavity.[2] Typically the primary hydroxyls provide the most convenient points of attachment to the CD, because the reactivity of the secondary hydroxyl groups is diminished. However, when CDs are derivatized on the primary and secondary OH groups with the same functional group,[3-5] substantial differences in thermal reactivity have been observed.

In recent years, the use of CDs to control molecular processes has been extended to reaction pathways proceeding through excited states. As a complement to the macromolecular fluorescent schemes designed for ion sensing,[6] lumophores have been appended[7, 8] onto CDs to afford supramolecules that produce a luminescent signal upon association of neutral substrates. An important and outstanding issue in the design of photoactive CD supramolecules is whether regioisomeric effects on reactivity, so prominent in ground state processes, are manifested in excited state processes as well. The synthesis of photoactive CD regioisomers is rare,[9] and to date no significant differences have been observed in the photophysics or photochemistry of these congeners. We now report an unusual example of differences in the excited state properties of regioisomers and in the chemistry of a bromonaphthalene lumophore appended to the primary (**1**) and secondary OH groups (**2**) of β-cyclodextrin.

Compounds **1** and **2** were prepared in one step from the reaction of β-CD with 1-bromo-2-bromomethylnaphthalene and sodium hydride [Eq. (a)]. The sites of attachment of the bromonaphthalene lumophore to the CD are clearly distinguished by ^{13}C NMR data (see Experimental Procedure). The carbon resonance at $\delta = 69.5$ in the spectrum of **1** is indicative of alkylation at a primary C6 hydroxyl. For regioisomer **2**, the appearance of a carbon resonance at $\delta = 80.1$ attests to alkylation at the secondary face of the β-CD; the downfield shift of the C4′ signal ($\delta = 81.6$) identifies reaction at the more acidic C2 hydroxyl group, which is the usual site of reaction under strongly basic conditions.[10] The emission spectra of **1** and **2** in aqueous, air-saturated solutions are presented in Figure 1. Whereas both molecules fluoresce at about 350 nm with nearly equal quantum yields, the phosphorescence of **2** at 530 nm is more than 10^2 times more intense than that observed for an equimolar solution of **1** ($\phi_e^{530}(\mathbf{1}) \leq 10^{-4}$; $\phi_e^{530}(\mathbf{2}) = 0.05$ in aerated H_2O; $\phi_e^{530}(\mathbf{1}$ and $\mathbf{2}) \approx 0.06$ in the absence of oxygen). Furthermore, deoxygenation of these solutions by freeze-pump-thaw or nitrogen purging results in a dramatic increase in the phosphorescence intensity of **1** but only a slight increase in the phosphorescence of **2**; the fluorescence intensity of both compounds is largely unaffected by deoxygenation. These results suggest that whereas the bromonaphthalene moiety of **2** is protected from oxygen quenching, the bromonaphthalene moiety of **1** is not.

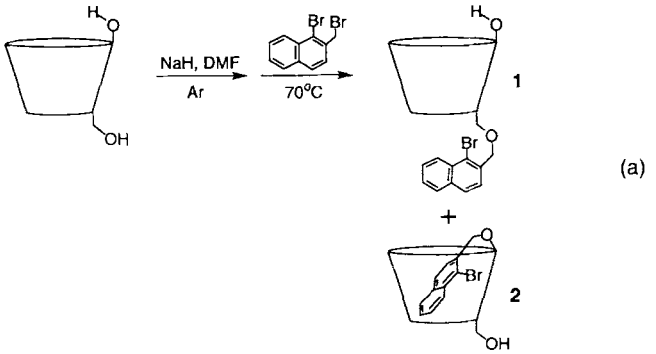

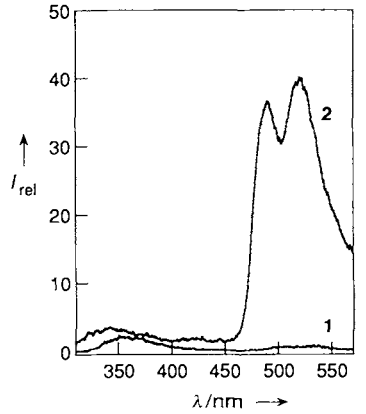

Fig. 1. Emission spectra of of **1** and **2** (each 1.0×10^{-4} M) in air-saturated, aqueous solution (excitation wavelength $\lambda_{ex} = 290$ nm).

The disparate luminescence properties of regioisomers **1** and **2** may be ascribed to the latter's forming an intramolecular complex in which the appended bromonaphthalene is protected from oxygen as a result of inclusion within the CD cavity. To assess this conjecture, we studied the phosphorescence quenching of **2** by oxygen in the presence of dodecyltrimethylammonium bromide (DTAB), which is a water-soluble, organic substrate that forms inclusion complexes with β-cyclodextrin.[11] Titration of an aqueous solution of **2** with DTAB results in the decrease of emission intensity at 520 nm (Fig. 2). The phosphorescence intensity approaches zero as the concentration of DTAB increases (the concentration of DTAB was maintained below the critical micelle concentration of 5–15 mM). A least squares fit[12] of the dependence of the phosphorescence intensity on DTAB concentration at 22 °C yields a K_{assoc} value of $1600 \pm 160\ M^{-1}$, which is greater than the association of DTAB to β-CD.[11]

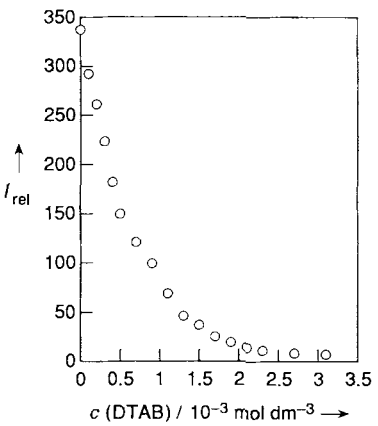

Fig. 2. Relative phosphorescence intensity at 520 nm of an air-saturated, aqueous solution of **2** (concentration 5.0×10^{-5} M) as function of the concentration of DTAB ($\lambda_{ex} = 290$ nm).

[*] Prof. D. G. Nocera, Dr. M. A. Mortellaro, W. K. Hartmann
Department of Chemistry and Center for Fundamental Materials Research
Michigan State University
East Lansing, MI 48824 (USA)
Fax: Int. code +(517)353-1793
e-mail: nocera@slater.cem.msu.edu

[**] Financial support for this work was provided by the Air Force Office of Scientific Research (F49620-94-1-0170) and the Center for Sensor Materials, a Materials Research Science and Engineering Center sponsored by the National Science Foundation (DMR-9400417).

Cyclodextrins modified on the secondary face show a greater tendency to bind aromatic residues owing to additional hydrophobic interactions and solvent shielding.[13] The increased stability of **2** therefore results in an attenuated binding of DTAB to the CD cup. These titration results can be attributed to the quenching of 1-bromonaphthalene phosphorescence when the lumophore is forced outside the CD cavity by the addition of a competitive guest.

To define the quenching kinetics of **1** and **2** better, the water-soluble solid, $[Co(NH_3)_6]Cl_3$, was employed as a quencher of bromonaphthalene phosphorescence in deoxygenated solution.[14] Table 1 lists the rate constants k_q for luminescence quenching in the systems **1**, **2**, **2** in the presence of DTAB and free 1-bromonaphthalene (1-BrNp), and the binary complex formed between 1-BrNp and glucosyl-β-CD (1-BrNp/Gβ-CD).[15] The rate constants were determined from Stern–Volmer analysis of phosphorescence decay as a function of the concentration of $[Co(NH_3)_6]^{3+}$; all plots are linear and exhibit an intercept of unity. Several important conclusions can be drawn from the data in Table 1. First, the large and similar rate

Table 1. Rate constants k_q for the luminescence quenching by $[Co(NH_3)_6]^{3+}$ in systems containing bromonaphthalene and/or β-cyclodextrin, in deaerated aqueous solution at 25 °C [a].

Compound	$k_q/M^{-1}s^{-1}$
2	1.5×10^3
1-BrNp/Gβ-CD [b]	1.9×10^6
1	8.2×10^7
2/DTAB	1.7×10^8
1-BrNp [c]	1.8×10^8

[a] Emission lifetimes were measured at 520 nm; excitation wavelength 309 nm. [b] A binary complex formed from glucosyl-β-CD and 1-BrNp (Ref. [15]). [c] 1-BrNp in methanol/water (1/1).

constants for the luminescence quenching of **1** and 1-BrNp indicate that the bromonaphthalene moiety of **1** is afforded no protection by the CD cavity but is exposed to bulk solution. Since the inclusion of 1-BrNp into β-CD circumvents luminescence quenching by $[Co(NH_3)_6]^{3+}$, as is observed for the 1-BrNp/Gβ-CD binary complex, these data are consistent with the inability of **1** to form an intramolecular inclusion complex.[16] Second, the quenching of **2** is 10^4 times slower than that of **1**. However, when **2** is saturated with DTAB, the resultant complex is quenched by $[Co(NH_3)_6]^{3+}$ with a rate constant commensurate with that observed for **1** and for free 1-BrNp in solution. We interpret these results as evidence that the bromonaphthalene moiety of **2** includes within the cyclodextrin cavity by intramolecular complexation and that addition of the competitive guest DTAB displaces the bromonaphthalene moiety from the CD, where it is quenched at rates approaching the diffusion-controlled limit.

Examination of CPK molecular models suggest that whereas the side of β-CD with secondary OH groups is wide enough for an appended bromonaphthalene to enter the cavity, the side with primary OH groups is too narrow for unimpeded intramolecular inclusion to occur. Consequently, only derivative **2** forms an intramolecular complex in which its appended bromonaphthalene lies inside the cyclodextrin cavity, giving rise to novel room temperature phosphorescence in oxygenated and aqueous environments. These results show that regioisomeric effects can control reactions of the excited state of photoactive CDs. Such issues will play an especially prominent role in the design of CD-based supramolecules for optical sensing, especially those that derive their function from equilibria of appended lumophores inside and outside the CD cup.

Experimental Procedure

β-Cyclodextrin (1.00 g, 0.881 mmol, dried at 120 °C in vacuo overnight) and NaH (38.0 mg, 0.95 mmol, 60% in mineral oil) were stirred in anhydrous DMF (40 mL) overnight under a stream of argon. 1-Bromo-2-bromomethylnaphthalene (292 mg, 0.973 mmol) was added, and the solution heated to about 70 °C under argon for 5 h. This solution was poured into 450 mL of acetone, and the resulting precipitate was washed with an additional 100 mL of acetone. ^{1}H NMR analysis of this sample indicated the presence of a 1:1 mixture of **1** and **2** in about 60% yield along with unchanged β-CD. This solid mixture was stirred in 20 mL of water for 30 minutes, filtered, washed with 10 mL of water, and the aqueous solutions were combined. Within 12 h, a white precipitate of pure **2** (82 mg, 6.9%) was isolated from the filtrate. Semipreparative reverse phase HPLC of the remaining crude material on a C-18 column with elution with a step gradient of 20% CH_3CN(aq) to 30% CH_3CN(aq) afforded pure **1** and **2**. Physical data for **1**: ^{1}H NMR (300 MHz, [D$_6$]DMSO): δ = 8.22 (d, 1H; ArH), 8.00 (d, 2H; ArH), 7.70 (d, 2H; ArH), 7.60 (t, 1H; ArH), 5.95–5.65 (br, 14H; C2-OH, C3-OH), 4.88 (d, 1H; H-1′), 4.8 (s, 6H; H-1), 4.78 (s, 2H; $ArCH_2$), 4.60–4.40 (br, 6H; C6-OH), 3.89–3.80 (m, 2H), 3.72–3.15 (m, 42H); ^{13}C NMR (500 MHz, [D$_6$]DMSO): δ = 136.2 (ArH), 133.5 (ArH), 131.2 (ArH), 128.3 (ArH), 127.8 (ArH), 127.7 (ArH), 126.6 (ArH), 126.1 (2 × ArH), 120.9 (ArH), 102.4 (Cl′), 101.9 (C1), 82.2 (C4′), 81.5 (C4), 73.0–72.0 (C2, C3, C5), 70.5 ($ArCH_2$), 69.5 (C6′), 59.9 (C6): FABMS: m/z 1376.0 [M^+ + Na]. Physical data for **2**: ^{1}H NMR (300 MHz, [D$_6$]DMSO): δ = 8.25 (d, 1H; ArH), 8.02 (dd, 2H; ArH), 7.82 (d, 1H; ArH), 7.71 (t, 1H; ArH), 7.65 (t, 1H; ArH), 6.10–5.60 (br, 13H; C2-OH, C3-OH), 5.14 (s, 2H; $ArCH_2$), 5.10 (s, 1H; H-1′), 4.85 (s, 6H; H-1), 4.59–4.35 (br, 7H, C6-OH), 3.95 (t, 2H), 3.90–3.15 (m, 42H); ^{13}C NMR (500 MHz, [D$_6$]DMSO): δ = 135.3 (ArH), 133.4 (ArH), 130.9 (ArH), 128.0 (ArH), 127.6 (ArH), 127.5 (ArH), 126.5 (ArH), 126.4 (ArH), 126.0 (ArH), 121.5 (ArH), 101.6 (C1), 99.6 (C1′), 81.6 (C4′), 81.1 (C4), 80.1 (C2′), 72.8–71.4 (C2, C3, C5, $ArCH_2$), 59.5 (C6); FABMS: m/z 1353.8 [M^+], 1376.4 [M^+ + Na].

Received: March 11, 1996 [Z 8919 IE]
German version: *Angew. Chem.* **1996**, *108*, 2073–2075

Keywords: cyclodextrins · host–guest chemistry · luminescence quenching · phosphorescence

[1] J.-M. Lehn, *Supramolecular Chemistry*, VCH, Weinheim, **1995**, *Angew. Chem.* **1988**, *100*, 91; *Angew. Chem. Int. Ed. Engl.* **1988**, *27*, 89.
[2] a) R. Breslow, *Acc. Chem. Res.* **1995**, *28*, 146; b) G. Wenz, *Angew. Chem.* **1994**, *106*, 851; *Angew. Chem. Int. Ed. Engl.* **1994**, *33*, 803; c) I. Tabushi, *Acc. Chem. Res.* **1982**, *15*, 66.
[3] a) R. Breslow, A. W. Czarnik, *J. Am. Chem. Soc.* **1983**, *105*, 1390; b) R. Breslow, M. Hammond, M. Lauer, *ibid.* **1980**, *102*, 421.
[4] K. A. Martin, M. A. Mortellaro, R. W. Sweger, L. E. Fikes, D. T. Winn, S. C. Clary, M. P. Johnson, A. W. Czarnik, *J. Am. Chem. Soc.* **1995**, *117*, 10443.
[5] a) K. R. Rao, T. N. Srinivasan, N. Bhanumathi, P. B. Sathur, *J. Chem. Soc. Chem. Commun.* **1990**, 10; b) F. Cramer, G. Mackensen, *Angew. Chem.* **1966**, *78*, 641; *Angew. Chem. Int. Ed. Engl.* **1966**, *5*, 601.
[6] a) L. Fabbrizzi, A. Poggi, *Chem. Soc. Rev.* **1995**, 197; b) A. W. Czarnik, *Acc. Chem. Res.* **1994**, *27*, 302; c) *Fluorescent Chemosensors for Ion and Molecular Recognition* (*ACS Symp. Ser.* **1993**, 538).
[7] a) D. G. Nocera, *New Sci.* **1996**, *149*, 24; b) M. A. Mortellaro, D. G. Nocera, *ChemTech* **1996**, *26*, 17; c) Z. Pikramenou, J.-A. Yu, R. B. Lessard, A. Ponce, P. A. Wong, D. G. Nocera, *Coord. Chem. Rev.* **1994**, *132*, 181; d) M. A. Mortellaro, D. G. Nocera, *J. Am. Chem. Soc.* **1996**, *118*, 7414.
[8] a) See A. Ueno in Ref. [6c], p. 74; b) R. Deschenaux, T. Ruch, P.-F. Deschenaux, A. Juris, R. Ziessel, *Helv. Chim. Acta* **1995**, *78*, 619; c) M. Nakamura, A. Ikeda, N. Ise, T. Ikeda, H. Ikeda, F. Toda, A. Ueno, *J. Chem. Soc. Chem. Commun.* **1995**, 721.
[9] a) M. N. Berberan-Santos, J. Canceill, J.-C. Brochon, L. Jullien, J.-M. Lehn, J. Pouget, P. Tauc, B. Valeur, *J. Am. Chem. Soc.* **1992**, *114*, 6427; b) A. Ueno, I. Suzuki, T. Osa, *ibid.* **1989**, *111*, 6391.
[10] D. Rong, V. T. D' Souza *Tetrahedron Lett.* **1990**, *31*, 4275.
[11] J. W. Park, K. H. Park, *J. Inclusion Phenom. Mol. Recog. Chem.* **1994**, *17*, 277.
[12] K. A. Connor, *Binding Constants*, Wiley, New York, **1987**, 341.
[13] E. van Dienst, B. H. M. Snellink, I. von Piekartz, J. F. J. Engbersen, D. N. Reinhoudt, *J. Chem. Soc. Chem. Commun.* **1995**, 1151.
[14] N. J. Turro, T. Okube, C.-J. Chung, *J. Am. Chem. Soc.* **1982**, *104*, 1789.
[15] a) W. K. Hartmann, M. H. B. Gray, A. Ponce, D. G. Nocera, P. A. Wong, *Inorg. Chim. Acta* **1996**, *243*, 239; b) A. Ponce, P. A. Wong, J. J. Way, D. G. Nocera, *J. Phys. Chem.* **1993**, *97*, 11137.
[16] At the concentration of our complexes (50 μm), the extent of the association of BrNp to β-CD is too small (K_{assoc} = 700 M^{-1} [15]) for intermolecular complexes to be observed.

A Three-Dimensional Molecular Ferrimagnet Based on Ferricyanide and $[Ni(tren)]^{2+}$ Building Blocks**

M. Salah El Fallah, Eva Rentschler, Andrea Caneschi, Roberta Sessoli, and Dante Gatteschi*

Prussian blue analogues are components of a large variety of magnets, some of which are magnetically ordered at high temperatures.[1-10] The origin of the magnetic behavior is associated with the three-dimensional structure of the compounds, in which the metal ions are connected by efficient cyanide bridges that transmit strong ferro- or antiferromagnetic interactions. These materials can be considered as molecular-based magnets because they can be synthesized by applying the techniques of molecular chemistry, but they more closely resemble ionic magnets in terms of the possibility of tuning the magnetic properties. In fact they can only be varied by altering the pairs of interacting metal ions, like in ionic lattices, while for molecular magnets the tuning can be achieved by varying the organic part of the molecule.

Recently several research groups have employed a hybrid approach, in which $[M(CN)_6]^{n-}$ building blocks have been combined with transition metal ion complexes in order to exploit the features of the ligands to give different structures. For instance, $[Ni(en)_2]_3[Fe(CN)_6]_2 \cdot 2H_2O$[11] (en = ethylenediamine) and $[Ni(pn)_2]_2[Fe(CN)_6]ClO_4 \cdot 2H_2O$[12] (pn = propylenediamine) have been obtained as variations of $Ni^{II}_3[Fe^{III}(CN)_6]_2$, which have a rope-ladder or a two-dimensional structure. Both compounds seem to undergo magnetic phase transitions at lower temperatures than the Prussian blue analogue. We have now found that by using the nickel complex of the tetradentate ligand tris(2-aminoethyl)amine) (tren) the compound $[Ni(tren)]_3[Fe(CN)_6]_2 \cdot 6H_2O$ **1** is obtained, which has a three-dimensional structure and orders to a bulk ferrimagnet at about 8 K.

The structure of **1** was determined by X-ray structure analysis.[13] The asymmetric unit contains four iron ions, which are localized at the special equivalent positions (1/2,0,0), (0,0,0), (0,1/2,0), and (1/2,0,1/2), connected to nickel ions by bridging cyanide groups (Figs. 1 and 2). The Ni–Fe separations range between 4.958(2) and 5.119(3) Å. Each Ni^{II} center is octahedrally coordinated by four nitrogen atoms of the tren ligand and two nitrogen atoms of cyanide groups. The Ni–N distances range between 2.08(1) and 2.13(1) Å for Ni–N(tren) and between 2.01(1) and 2.15(1) Å for Ni–N(CN). The Fe–C distances range from 1.91(1) to 1.97(1) Å, whereas, as expected, the Fe-C-N bond angles only vary in the small range between 175(1) and 179(1)°. The Ni-N-C bond angles, on the other hand, deviate significantly from linearity and lie between 149(1) and 177(1)°. There are two types of $[Fe(CN)_6]^{3-}$ groups, one bridges four $[Ni(tren)]^{2+}$ groups, the other only two; we have labeled these as $Fe_\square$ and Fe_Λ, respectively. The three-dimensional structure of **1** can be described by Ni–Fe chains parallel to the three cell axes. As can be seen from Figure 2, the chains parallel to the *a* axis are built up from Ni–$Fe_\square$ units, whereas the chains parallel to the *b* axis and the *c* axis are composed of -Ni-$Fe_\square$-Ni-Fe_Λ-Ni- units. Each $Fe_\square$ group belongs to two different orthogonal chains.

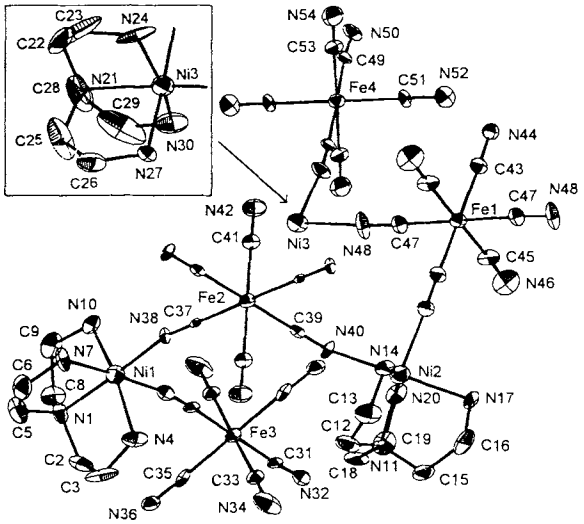

Fig. 1. ORTEP plot of the structure of **1** (without H_2O molecules). Selected distances [Å] and angles [°] (standard deviation in parentheses): Ni1–N38 2.042(11), Ni1–N32 2.055(11), Ni2–N44 2.056(11), Ni2–N40 2.149(11), Ni3–N48 2.008(12), Ni3–N50 2.061(11), Fe1–C45 1.91(2), Fe1–C47 1.913(14), Fe1–C43 1.946(14), Fe2–C41 1.945(14), Fe2–C37 1.950(13), Fe2–C39 1.965(14), Fe3–C35 1.915(14), Fe3–C31 1.921(13), Fe3–C33 1.933(2), Fe4–C51 1.905(13), Fe4–C53 1.928(14), Fe4–C49 1.931(14); C31-N32-Ni1 171.4(10), C37-N38-Ni1 165.6(9), C39-N40-Ni2 148.7(9), C43-N44-Ni2 163.3(10), C47-N48-Ni3 177.5(13), C49-N50-Ni3 170.0(10), N38-Ni1-N32 91.0(4), N44-Ni2-N40 89.4(4), N48-Ni3-N50 89.8(4), N46-C45-Fe1 179(2), N48-C47-Fe1 175.2(13), N44-C43-Fe1 176.3(11), N40-C39-Fe2 169.8(10), N42-C41-Fe2 179.3(11), N38-C37-Fe2 177.8(9), N32-C31-Fe3 177.2(10), N36-C35-Fe3 177.6(11), N34-C33-Fe3 178.1(11), N54-C53-Fe4 178.0(12), N52-C51-Fe4 178.3(11), N50-C49-Fe4 174.5(11).

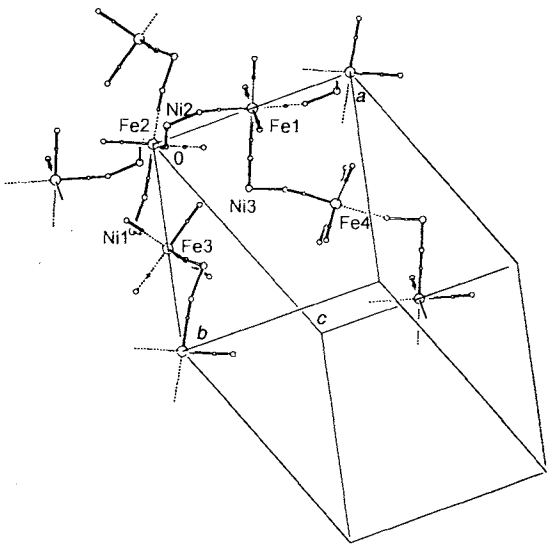

Fig. 2. Simplified cell-packing diagram of the building blocks of $[Ni(tren)]_3[Fe(CN)_6]_2$, in which only the Ni, Fe, and CN groups are shown for clarity.

The magnetic behavior of **1** in a field of 1 T[14] is shown in Figure 3. The $\chi_M T$ value of 4.96 emu mol^{-1} K at 225 K, which is close to the value expected for uncoupled Ni_3Fe_2 (4.88 emu mol^{-1} K with $g_{Ni} = 2.3$ and $g_{Fe} = 2.2$), increases gradually with decreasing temperature to reach a maximum of 12.19 emu mol^{-1} K at about 8.4 K and then decreases below this temperature. The same behavior has been observed in many compounds like $[Ni(en)_2]_3[Fe(CN)_6]_2 \cdot 2H_2O$ and $[Ni(pn)_2]_2$-

[*] Prof. D. Gatteschi, Dr. M. S. El Fallah, Dr. E. Rentschler, Dr. A. Caneschi, Dr. R. Sessoli
Dipartimento di Chimica, Università degli Studi di Firenze
Via Maragliano, 75/77, I-50144 Firenze (Italy)
Fax: Int. code +(55)354845
e-mail: gattesch@chimat1.chim1.unifi.it

[**] The Grant of Consorzio Interuniversitario Nazionale per la Chimica dei Materiali (INCM) and the Human Capital and Mobility Grant ERBCHICT940957 are gratefully acknowledged. tren = tris(2-aminoethyl)amine.

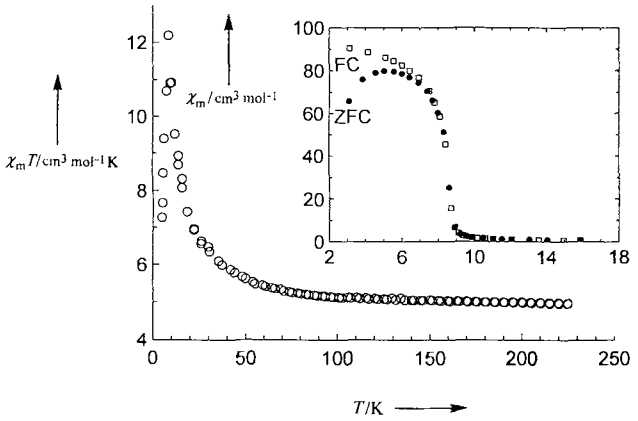

Fig. 3. Plot of $\chi_m T$ vs. T of a polycrystalline sample of **1** at an applied field of 1 T. The χT curves at zero-field-cooled (ZFC) and field-cooled (FC) magnetization are shown in the insert.

$[Fe(CN)_6]ClO_4 \cdot 2H_2O$, which order ferromagnetically[11, 12] at a maximum critical temperature of about 10 K. The ferromagnetic interaction between the Fe^{III} and Ni^{II} ions has been rationalized by the strict orthogonality of the magnetic orbitals of the Ni^{II} and the low-spin Fe^{III} centers.

In order to characterize the magnetic ordering of **1**, the magnetization has been measured between 3 and 16 K (see insert in Fig. 3). The zero-field-cooled (ZFC) magnetization, measured by cooling the sample under zero field and then warming it up under an applied field of 80 G, shows a maximum at 5.5 K and decreases rapidly above 8 K with increasing temperature. When the sample is cooled down again, the curve diverges below 8 K, tending to a plateau, thus confirming the transition to a magnetically ordered phase.

The course of the reduced magnetization $M/N\mu_\beta$ (Fig. 4) shows a spontaneous magnetization close to zero field, which reaches a value of 1.98. This corresponds to an $S = 1$ spin state.

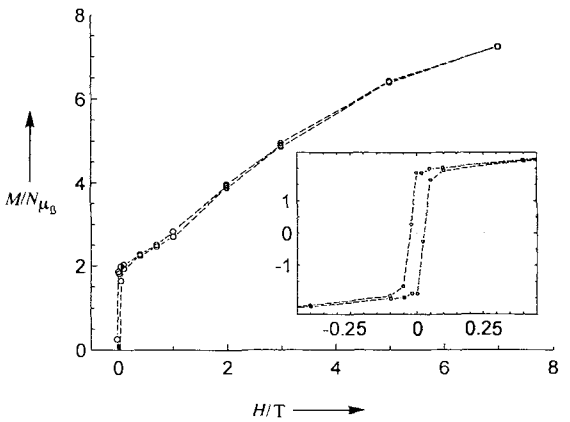

Fig. 4. Plot of $M/N\mu_\beta$ vs. H of a polycrystalline sample of **1** at 3 K. The hysteresis loop is shown in the insert.

When the applied field is increased to 1 T, the magnetization curve increases slower than expected. Above 1 T the curve becomes steeper and reaches a value of 7.2 at 7 T. A hysteresis loop was observed with a coercive field smaller than 30 G. This seems to indicate a small magnetic anisotropy and the absence of irreversible movements of the domain walls, which, had they been present, would have led to large hysteresis effects.[15]

The rapid saturation of the magnetization at a value of $S = 1$ in low field, the sharp increase in fields of about 2 T, and the slow increase for higher fields suggest ferrimagnetic order. This is determined by a weak antiferromagnetic interaction, which is flipped by external fields larger than 1 T. Ni–Fe interactions are normally ferromagnetic; however, taking into account the structural parameters of **1**, we find that the bond lengths of one CN^- bridging group (C39, N40) to the metal ions Fe2 and Ni2 is elongated with respect to the others. If we assume that at very low field the alternating -Ni-$Fe_\square$-Ni-Fe_Λ-Ni- chains are already ferromagnetically ordered and Ni2 and Fe2 are very weakly antiferromagnetically coupled, a noncompensated spin of $S = 1$ is obtained, which is in agreement with the observed value of 1.98 for the reduced magnetization.

Compound **1** is an example of a three-dimensional molecular ferrimagnet; however, since the three-dimensional lattice arises from the interaction of chains, the magnetic connectivity is low and the critical temperture is lower than in $Ni^{II}_3[Fe^{III}(CN)_6]_2 \cdot xH_2O$.[5] The weak interaction, which is mediated by one CN^- group, further depresses the critical temperature.

Experimental Procedure

To a solution of $Ni(ClO_4)_2 \cdot 6H_2O$ (3 mmol) in water (50 mL) was added tren (3 mmol). After the mixture had been stirred for a few minutes, the resulting solution was mixed with potassium ferricyanide (2 mmol) dissolved in water (30 mL). Slow evaporation of the resulting solution gave crystals suitable for X-ray diffraction. The elemental analysis gave satisfactory results.

Received: March 28, 1996 [Z 8982 IE]
German version: *Angew. Chem.* **1996**, *108*, 2081–2083

Keywords: ferrimagnetism · iron compounds · magnetic properties · nickel compounds

[1] F. Herren, P. Fischer, A. Lüdi, W. Hälg, *Inorg. Chem.* **1980**, *19*, 956.
[2] R. Klenze, B. Kanellakopulos, G. Trageser, H. H. Eysel, *J. Chem. Phys.* **1980**, *72*, 5819.
[3] W. D. Griebler, D. Babel, *Z. Naturforsch. B*, **1982**, *37*, 832.
[4] W. Kurtz, D. Babel, *Solid State Commun.* **1983**, *48*, 277.
[5] V. Gadet, M. Bujoli-Doeuff, L. Force, M. Verdaguer, K. E. Malkhi, A. Deroy, J. P. Besse, C. Chappert, P. Veillet, J. P. Renard, P. Beauvillain, in *Magnetic Molecular Materials, Vol. 198*, (Eds.: D. Gatteschi, O. Kahn, J. S. Miller, F. Palacio), *NATO ASI Series E*, Plenum, New York, **1991**, p. 281.
[6] V. Gadet, T. Mallah, I. Castro, M. Verdaguer, *J. Am. Chem. Soc.* **1992**, *114*, 9213.
[7] T. Mallah, M. Thièbaut, M. Verdaguer, P. Veillet, *Science* **1993**, *262*, 1554.
[8] W. R. Entley, G. S. Girolami, *Inorg. Chem.* **1994**, *33*, 5165; *ibid.* **1995**, *34*, 2262.
[9] T. Mallah, S. Ferlay, C. Auberger, C. Hélary, F. L'Hermite, R. Ouahès, J. Vaissermann, M. Verdaguer, P. Veillet, *Mol. Cryst. Liq. Cryst.* **1995**, *273*, 141.
[10] W. R. Entley, C. R. Treadway, G. S. Girolami, *Mol. Cryst., Liq. Cryst.* **1995**, *273*, 153.
[11] M. Ohba, N. Maruoono, H. Okawa, T. Enoki, J. M. Latour, *J. Am. Chem. Soc.* **1994**, *116*, 11566.
[12] M. Ohba, H. Okawa, T. Ito, A. Ohto, *J. Chem. Soc. Chem. Commun.* **1995**, 1545.
[13] Crystal data for **1**: $M_r = 1146.90$, triclinic, $P\bar{1}$ $a = 14.205(5)$, $b = 14.665(5)$, $c = 15.318(5)$ Å, $\alpha = 63.170(5)$, $\beta = 82.740(5)$, $\gamma = 80.280(5)°$, $V = 2802(2)$ Å^3, $F(000) = 1196$, $Z = 2$, $\rho_{calcd} = 1.359$ gcm^{-3}, $\mu = 5.638$ mm^{-1}, crystal size = $0.2 \times 0.2 \times 0.4$, $T = 25\,°C$, scan type ω-2θ, $4.30 < \theta_{max} < 49.94$. 4908 reflections were measured, of which 4680 were independent ($R_{int} = 0.0859$), 4678 applying the condition $I > 4\sigma(I)$. All data were corrected for Lorentz and polarization effects. An empirical absorption correction was applied to collected intensities using the DIFABS program (max./min. = 1.2/0.8) [16]. The crystal structure was solved by direct methods using the SIR92 program [17]. Refinement was carried out by using the SHELX93 computer program [18]. The position of the H atoms not assigned to water were computed and refined with an overall isotropic factor, using a riding model. All non-H atoms were treated anisotropically. Disorder among a significant portion of water molecules was evidenced by large temperature factors obtained in the least-squares refinements. Refinement of the multipliers of the disordered water molecules yielded a complex model for the disorder which involved three-quarter, one-half, and one-quarter occupancies of several water positions. The sum was determined to be six water molecules. Final refinement leads to $R_1 = 0.0787$, $wR_2 = 0.2282$ (all data),

max./min. residual electron density: 0.64/ − 0.52 e Å^{-3}. Crystallographic data (excluding structure factors) for the structure reported in this paper have been deposited with the Cambridge Crystallographic Data Centre as supplementary publication no. CCDC-179-63. Copies of the data can be obtained free of charge on application to The Director, CCDC, 12 Union Road, Cambridge CB2 1EZ, UK (fax: Int. code +(1223) 336-033; e-mail: teched@chemcrys.cam.ac.uk).

[14] The magnetic measurements of the polycrystalline sample were carried out using a Métronique *MSO3 SQUID magnetometer*. The contribution of the sample holder was determined separately in the same temperature range and field. Diamagnetic corrections were estimated from Pascal's constants.

[15] A. H. Morrish in *The Physical Principles of Magnetism*, Wiley, **1965**, p. 382.

[16] N. Walker, D. Stuart, *Acta Cryst. Sect. A* **1983**, *39*, 158–166.

[17] A. Altomare, G. Cascarano, C. Giacovazzo, A. Cuagliardi, *J. Appl. Crystallogr.* **1994**, *27*, 1045.

[18] G. M. Sheldrick, SHELXL-93, Universität Göttingen, **1993**.

Prominent Gelation and Chiral Aggregation of Alkylamides Derived from *trans*-1,2-Diaminocyclohexane

Kenji Hanabusa,* Manabu Yamada, Mutsumi Kimura, and Hirofusa Shirai

The design of building blocks that can assemble into supramolecules of nanoscale dimensions has received a great deal of attention.[1, 2] We have been investigating gelling agents for hardening organic fluids, and have become particularly interested in self-complementary molecules in which functional binding groups of one molecule interact with complementary groups of a neighboring molecule,[3–6] since our previous results indicate that self-complementary interactions, which lead to macromolecule-like aggregates, are essential for gelation. Herein we report on the remarkable gelation ability of alkylamides derived from *trans*-1,2-diaminocyclohexane and the resulting chiral aggregates in organic solvent.

Several recent reports have described the thermoreversible gelling properties of low molecular weight organic compounds.[7–13] We have studied gelling agents that form thermoreversible physical gels; the main driving forces of these reactions are intermolecular hydrogen bonding and van der Waals interactions. Three important features for development of gelling agent are 1) the existence of intermolecular interactions for building up macromolecule-like aggregates, 2) the occurrence of intertwining of the aggregates, and 3) the presence of some factor for preventing the crystallization of the metastable gel. We have now focused on a simple diamide compound, **1**, in the expectation that it may form interlocked macromolecule-like aggregates as a result of two cooperating noncovalent forces, the intermolecular hydrogen bonding between the amide groups of adjacent molecules and the hydrophobic interaction of the long hydrocarbon tails. The (1*R*,2*R*)-1,2-cyclohexane derivative **1** was prepared by the reaction of (1*R*,2*R*)-(−)-1,2-diaminocyclohexane and lauroyl chloride in THF in the presence of triethylamine.

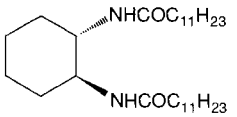

1 *trans (1R, 2R)*
2 *trans (1S, 2S)*

[*] Associate Prof. K. Hanabusa, M. Yamada, Dr. M. Kimura, Prof. H. Shirai
Department of Functional Polymer Science
Faculty of Textile Science & Technology, Shinshu University
Ueda, Nagano 386 (Japan)
Fax: Int. code +(268)24-7248
e-mail: hanaken@giptc.shinshu-u.ac.jp

A typical procedure for testing the gelation is as follows: A weighed sample of **1** was mixed with an organic liquid (1 mL) in a septum-capped test tube and the mixture was heated until the solid dissolved. The resulting solution was cooled at 25 °C for 1 h and then the gelation was checked visually. Once the gel is formed, it is stable and the tube can be inverted without changing the shape of the gel. The resulting gels were so stable that they were not converted to viscoelastic fluids or crystals even after six months. The minimum gel concentrations of **1** necessary for gelation are summarized in Table 1. Surprisingly, **1** can form physical gels and harden a wide variety of organic fluids, including hydrocarbons, alcohols, ketones, esters, ethers, aprotic polar compounds, aromatic compounds, mineral oils, and edible oils. The only other universal gelling agent of this kind known to date is the octadecylamide of *N*-benzyloxycarbonyl-L-valyl-L-valine.[7] For example, the amounts of **1** necessary to gel one liter of hexane, ethanol, ethyl acetate, acetonitrile, tetrachloromethane, toluene, and *N*,*N*-dimethylformamide are 6 g, 33 g, 8 g, 5 g, 23 g, 12 g, and 10 g, respectively. This means that one molecule of **1** interacts with about 600 molecules of hexane, 200 molecules of ethanol, 600 molecules of ethyl acetate, 1800 molecules of acetonitrile, 200 molecules of tetrachloromethane, 400 molecules of toluene, and 600 molecules of *N*,*N*-dimethylformamide. It is important to note that the corresponding *cis* isomer prepared from *cis*-1,2-diaminocyclohexane forms no gels with any of the liquids. Furthermore, the racemate consisting of **1** and the *S*,*S*-enantiomer **2** only formed an unstable gel, which was converted to cocrystals after several hours, though **2** itself revealed the same gelation behavior as **1**. The introduction of a hydrophobic group longer than hexanoyl into (1*R*,2*R*)-(−)-1,2-diaminocyclohexane is essential for gelation, since gels fail to form when the chain of the lipophilic tail group is shortened to four carbon atoms.

Table 1. Minimum gel concentration *c* of **1** (in g per L solvent) necessary for gelation at 25 °C.

Solvent	*c* (**1**)	Solvent	*c* (**1**)
hexane	6	1,4-dioxane	12
cyclohexane	11	benzene	20
methanol	20	toluene	12
ethanol	33	chlorobenzene	22
1-propanol	44	nitrobenzene	12
2-propanol	40	dimethylsulfoxide	12
ethyl acetate	8	N,N-dimethylformamide	10
acetone	10	N,N-dimethylacetamide	11
2-butanone	15	soybean oil	7
cyclohexanone	13	kerosene	7
acetonitrile	5	light oil	8
pyridine	25	silicone oil	2
tetrachloromethane	23	liquid paraffin	3

The FT-IR spectrum of a cyclohexane gel formed by **1** or **2** is characterized by broad bands at 3279 and 1637 cm^{-1}, which are assigned to N–H and C=O intermolecular hydrogen bonding stretching vibrations, respectively. The FT-IR spectrum of **1** in KBr also contains bands in these regions at 3286 and 1638 cm^{-1}, indicating the presence of similar hydrogen bonding. These spectroscopic results are consistent with what one would expect if association by self-complementary intermolecular hydrogen bonding occurs between two equatorially positioned amide units of **1** in both the gel and the solid, thus forming long sequences of hydrogen bonds. The FT-IR spectrum of a homogeneous cyclohexane solution of the *cis* isomer of **1** showed broad bands at 3300 and 1671 cm^{-1}, which can be

 © VCH Verlagsgesellschaft mbH, D-69451 Weinheim, 1996 0570-0833/96/3517-1949 $ 15.00+.25/0

assigned to groups not undergoing hydrogen bonding. The data for the *cis* isomer can be explained by taking into account that macromolecule-like aggregates fail to form because the amide unit in an axial position cannot form hydrogen bonds; thus, the *cis* isomer has no gelation ability.

The sol–gel process of **1** is temperature-dependent; the minimum gel concentrations necessary to form the gel increase with temperature. From the sol–gel phase diagram, in which the minimum gel concentration is plotted against temperature, the thermodynamic parameters[14] for the sol to gel of **1** in toluene are calculated as follows: $\Delta H(40\,^{\circ}C) = -65\,kJ\,mol^{-1}$ and $\Delta S(40\,^{\circ}C) = -160\,J\,K^{-1}\,mol^{-1}$. These values indicate that the enthalpic contribution compensates for the undesirable entropic change in the gelation. The value of ΔH suggests that two hydrogen bonds per molecule are formed when the gel is built up in toluene. The thermodynamic parameters are consistent with the FT-IR spectroscopic findings.

To study the chiral structure of the aggregate in the gel, circular dichroism (CD) spectra were measured. The CD spectra of loose gels (1 mM; 0.0677 wt %) for **1** and **2** in acetonitrile are shown in Figure 1. Importantly, for the interpretation, it was

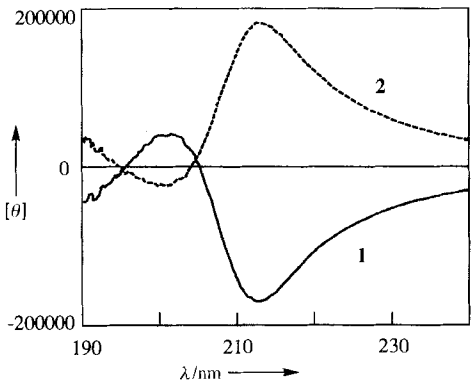

Fig. 1. CD spectra of **1** and **2** in acetonitrile; c (**1**) = c (**2**) = 1.0 mM. The molar ellipticity $[\theta]$ is given in $^{\circ}cm^2\,dmol^{-1}$. $T = 20\,^{\circ}C$.

confirmed that the contributions of linear dichroism (LD) spectra to the true CD spectra were almost negligible. The CD spectrum of **1** at 20 °C exhibited markedly strong peaks for the amide unit: $[\theta]_{201} = +4.20 \times 10^4$ and $[\theta]_{213} = -1.73 \times 10^5\,^{\circ}cm^2\,dmol^{-1}$. The corresponding values for the *S,S*-enantiomer **2** are $[\theta]_{201} = -2.69 \times 10^4$ and $[\theta]_{213} = +1.82 \times 10^5\,^{\circ}cm^2\,dmol^{-1}$. These strong peaks decreased with increasing temperature and disappeared at 50 °C as the loose gel was transformed to an isotropic solution. The disappearance of the CD signal in the isotropic solution led us to conclude that the CD bands originate from a chiral aggregate of **1** and not from a chiral conformation of **1**. Considering that such a much-enhanced CD is derived from exciton coupling among the organized chromophore, the observed CD indicates that the aggregate formed from **1** is cooperatively organized for helical stacking.

The results of CD spectroscopic studies prompted us to investigate the chiral aggregate by electron microscopy. In fact, helical superstructures built up from chiral low molecular weight compounds were observed by electron microscopy[15–19] and optical microscopy.[20, 21] The transmission electron micrographs (TEMs) of a **1**-acetonitrile gel negatively stained by osmic acid are shown in Figure 2. Numerous intertwined aggregates were formed from helical fibers with widths of 40–70 nm. The helicity of fibers was always right-handed for **1**, and left-

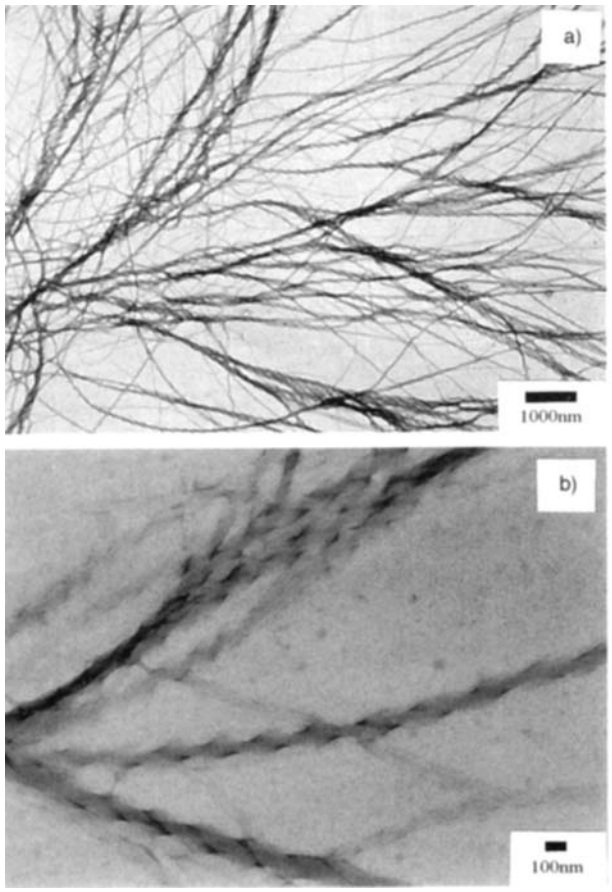

Fig. 2. TEM images of a loose **1**-acetonitrile gel (1 mM **1**) stained by osmic acid. Magnification: a) × 7000, b) × 30000.

handed for the *S,S*-enantiomer **2**. The pitches of the helices in Figure 2 are very similar (ca. 150 nm, Fig. 2b). It is unknown at this time whether the helical fiber observed in the TEM represents the "unit" of helical structure causing the strong CD band.

Molecular modeling studies suggest that the two equatorial amide-NH and amide-CO of **1** can direct themselves antiparallel to each other and perpendicular to the cyclohexyl ring, therefore, an extended molecular tape (for example **3**) stabilized by two intermolecular hydrogen bonds between each molecule is formed. The resulting asymmetric tape may be responsible for the chiral superstructure observed in the CD spectra and the TEM images. It is assumed that the tapelike molecular aggregates are formed by intermolecular hydrogen bonding. Subsequently these are interlocked through van der Waals interactions and transformed to the helical fiberlike aggregates, which finally immobilize the organic fluids.

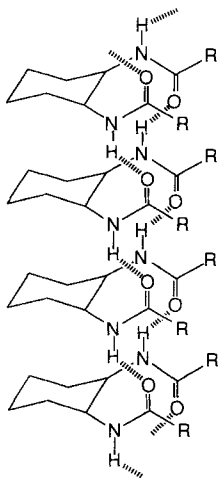

3

Received: March 11, 1996 [Z 8917 IE]
German version: *Angew. Chem.* **1996**, *108*, 2086–2088

Keywords: amides · gelation · hydrogen bonds · supramolecular chemistry

[1] F. Vögtle, *Supramolecular Chemistry*, Wiley, Chichester, **1991**.
[2] J.-M. Lehn, *Supramolecular Chemistry: Concepts and Perspectives*, VCH, Weinheim, **1995**.
[3] M. Reza, J. R. Granja, R. A. Milligan, D. E. McRee, N. Khazanovich, *Nature* **1993**, *366*, 324.
[4] S. Hanessian, A. Gomtsyan, M. Simard, S. Roelens, *J. Am. Chem. Soc.* **1994**, *116*, 4495.
[5] S. J. Geib, C. Vicent, E. Fan, A. D. Hamilton, *Angew. Chem.* **1993**, *105*, 83; *Angew. Chem. Int. Ed. Engl.* **1993**, *32*, 119.
[6] E. Fan, J. Yang, S. J. Geib, T. C. Stoner, M. D. Hopkins, D. Hamilton, *J. Chem. Soc. Chem. Commun.* **1995**, 1251.
[7] K. Hanabusa, J. Tange, Y. Taguchi, T. Koyama, H. Shirai, *J. Chem. Soc. Chem. Commun.* **1993**, 390.
[8] K. Hanabusa, Y. Matsumoto, T. Miki, T. Koyama, H. Shirai, *J. Chem. Soc. Chem. Commun.* **1994**, 1401 and references therein.
[9] K. Hanabusa, Y. Naka, T. Koyama, H. Shirai, *J. Chem. Soc. Chem. Commun.* **1994**, 2683.
[10] M. Jokic, J. Makarevic, M. Zinic, *J. Chem. Soc. Chem. Commun.* **1995**, 1723.
[11] H. T. Stock, N. J. Turner, R. McCague, *J. Chem. Soc. Chem. Commun.* **1995**, 2063.
[12] P. Terech, I. Furman, R. G. Weiss, *J. Phys. Chem.* **1995**, *99*, 9558.
[13] F. M. Menger, Y. Yamasaki, K. K. Catlin, T. Nishimi, *Angew. Chem.* **1995**, *107*, 616; *Angew. Chem. Int. Ed. Engl.* **1995**, *34*, 585.
[14] J. E. Eldridge, J. D. Ferry, *J. Phys. Chem.* **1954**, *58*, 992.
[15] T. Tachibana, S. Kitagawa, H. Takeno, *Bull. Chem. Soc. Jpn.* **1970**, *43*, 2418.
[16] N. Nakashima, S. Asakuma, J.-M. Kim, T. Kunitake, *Chem. Lett.* **1984**, 1709.
[17] P. Terech, R. H. Wade, *J. Colloid Interface Sci.* **1988**, *125*, 542.
[18] H. Yanagawa, Y. Ogawa, H. Fukuta, K. Tsuno, *J. Am. Chem. Soc.* **1989**, *111*, 4567.
[19] J.-H. Fuhrhop, C. Boettcher, *J. Am. Chem. Soc.* **1990**, *112*, 1768.
[20] N. Nakashima, S. Asakuma, T. Kunitake, *J. Am. Chem. Soc.* **1985**, *107*, 509.
[21] T. Shimizu, M. Hato, *Thin Solid Films*, **1989**, *180*, 179.

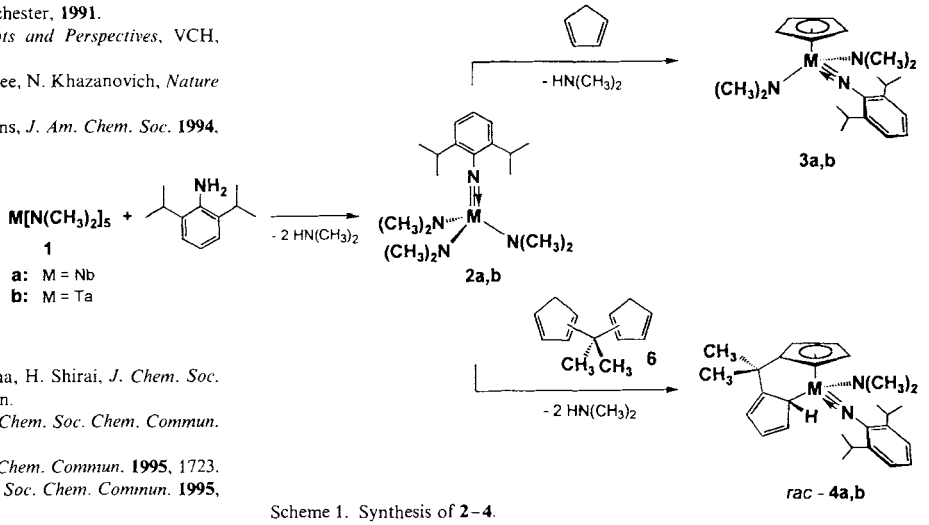

Scheme 1. Synthesis of **2**–**4**.

tion of two equivalents of amine in the reaction of di(2,6-isopropyl)aniline with pentakis(dimethylamido)niobium **1a** and -tantalum **1b** (Scheme 1). The single-crystal X-ray structure analysis of the niobium derivative **2a**[6] exhibits a pyramidal geometry of the NbN_4 core (Fig. 1) with three almost planar metal amide groups. The metal–nitrogen distances reflect the individual bonding situations (Nb–N_{imide}: 179.4(2) pm; Nb–N_{amide}: 197.4(2)–202.3(2) pm).

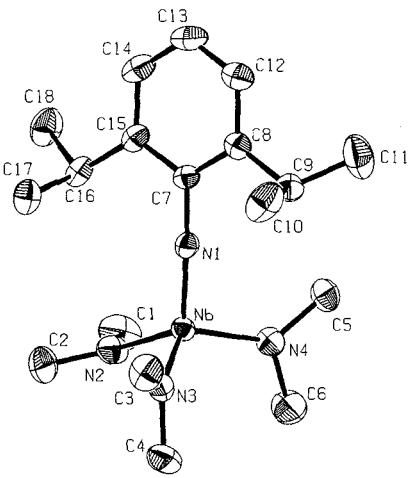

Fig. 1. ORTEP drawing of the crystal and molecular structure of **2a**. Thermal ellipsoids are at the 50% probability level. Selected bond lengths [pm] and angles [°]: Nb–N1 179.4(2), Nb–N2 202.3(2), Nb–N3 197.4(2), Nb–N4 197.9(2); N1-Nb-N2 116.6(1) N1-Nb-N3 108.1(1), Nb-N1-C7 167.4(2).

When the complexes **2a,b** are treated with cyclopentadienyl in toluene, dimethylamine is eliminated and the η^5-cyclopentadienyl complexes **3a,b** are obtained in >70% yield (Scheme 1); cleavage of one further equivalent of amine could not be forced, even with an excess of the CH-acidic ligand.[7]

However, *two* of the amido ligands in **2a,b** can be exchanged for a doubly deprotonated hydrocarbon in boiling toluene by using the diprotic 2,2-bis(cyclopentadienyl)propane (**6**) as ligand precursor (Scheme 1). The resulting products **4a** and **4b** were obtained as orange and yellow crystals, respectively, and proved[8] to be thermally surprisingly stable (decomp. ≫200 °C), but highly sensitive to moisture.

Structure Dynamics in Novel *ansa*-Metallocenes of Niobium and Tantalum**

Wolfgang A. Herrmann,* Walter Baratta, and Eberhardt Herdtweck

Dedicated to Professor Rudolf Taube on the occasion of his 65th birthday

ansa-Metallocenes of zirconium have founded a new era of industrial polyolefin chemistry.[1] However, whereas a large number of zirconocene derivatives have been synthesized since the first publication in this area,[2] most[3] derivatives of the neighboring elements niobium and tantalum have remained unknown. An extended redox chemistry, resulting from the combination of high-valent metals (Nb^V, Ta^V) with π-unsaturated organic ligands, complicates the access to this class of compounds, which serve as possible catalysts for the polymerization of olefins.[4] We report herein on novel niobocene and tantalocene derivatives with bridged cyclopentadienyl ligands and show that additional strong donor ligands are essential for the existence of these compounds.

The new trisamido complexes **2a** and **2b** of the imido-type[5] can be obtained in 79% and 86% yield, respectively, by elimina-

[*] Prof. Dr. W. A. Herrmann, Dr. W. Baratta, Dr. E. Herdtweck
Anorganisch-chemisches Institut der Technischen Universität München
Lichtenbergstrasse 4, D-85747 Garching (Germany)
Fax: Int. code +(89)289-1-3473

[**] Multiple Bonds between Main Group Elements and Transition Metals, Part 156. This work was generously supported by the Alexander-von-Humboldt-Stiftung (research scholarship for W. B.), the Bayerische Forschungsstiftung (IPDS structure analysis), and the Volkswagenstiftung. Part 155: W. A. Herrmann, J. D. G. Correia, G. R. J. Artus, R. W. Fischer, C. C. Romão, *J. Organomet. Chem.*, in press.

A single-crystal X-ray structure analysis[9] of the niobium derivative **4a** revealed a pseudo-tetrahedral geometry at the Nb center; the structurally most interesting feature is the $\eta^1:\eta^5$ coordination of the metallocene-forming hydrocarbon ligand (Fig. 2). The dimethylamido and the (nearly linearly coordinated) arylimido ligand show no remarkable bonding modes ($\sphericalangle$Nb-N2-C3 = 167.4(1)°), but the *ansa*-ligand forms an asymmetric bridge in which the two bonds to the metal are almost perpendicular to the N1-Nb-N2 plane. One of the cyclopentadienyl rings is π-coordinated (average Nb–C(15–19) distance: 246.3 pm), while the other is η^1-coordinated to the metal (Nb–C27 229.1(2) pm). A crystallographic study of the analogous tantalum compound **4b** confirmed the structural characteristics observed for **4a**.

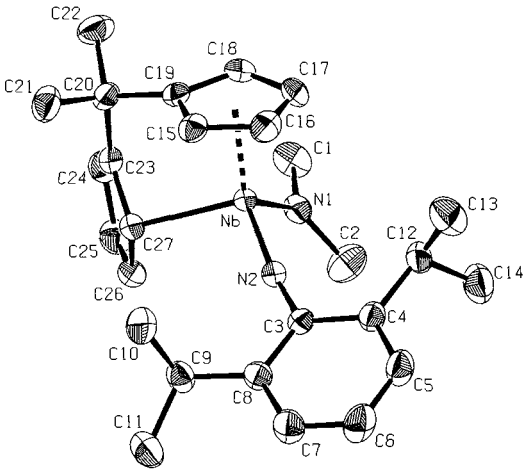

Fig. 2. ORTEP drawing of the crystal and molecular structure of **4a**. Thermal ellipsoids are at the 50% probability level. Selected bond lengths [pm] and angles [°]: Nb–N1 197.4(2), Nb–N2 178.6(2), Nb···C23 289.7(2), Nb···C24 369.0(2), Nb···C25 379.1(2), Nb···C26 308.2(2), Nb–C27 229.1(2), Nb–Cp(centroid) 215.0, N2–C3 138.9(2); N1-Nb-N2 102.13(7), N1-Nb-C27 105.04(7), N2-Nb-C27 102.78(7), Cp(centroid)-Nb-N1 122.4, Cp(centroid)-Nb-N2 119.6, Cp(centroid)-Nb-C27 102.5, Nb-N2-C3 167.4(1). Cp(centroid) corresponds to the calculated center of the π-coordinated ring ligand C(15–19).

The η^1-coordinated cyclopentadienyl ligand shows exactly the C–C bond length variations expected for a 1,3-diene system: short distances for C23–C24 and C25–C26, and long distances for the remaining three interligand bonds. The angle formed between the centroid of the planar ring C(23–27) and the single bond (C27–Nb) to the metal center is 111°.

The results of NMR experiments confirmed that the coordination of the *ansa*-ligand was maintained in solution until −80 °C. However, an $\eta^1:\eta^5 \rightleftharpoons \eta^5:\eta^1$ coordination exchange equilibrium was observed with a rather low activation barrier [Eq. (a)] evidently because of the minor changes in the ring geometry associated with the exchange process. The fluctuational equilibration of **4a,b** leads to a (*S,R*)/(*R,S*) racemate.

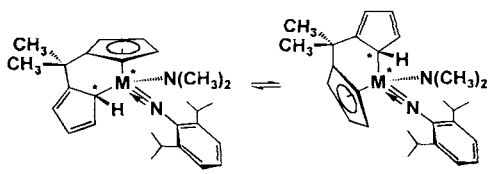

(a)

Consecutive reactions performed with the metallocenes **4a,b** provoke slight modifications in the coordination, but do not change the overall structure of the complexes. A quantitative amide/chloride exchange is achieved by the use of chlorotrimethylsilane [Eq. (b)]. The resulting complexes **5a,b** exhibit $\eta^5:\eta^5$-metallocene structures (based on NMR spectroscopy, and a single-crystal X-ray structure analysis[10]), which is further proof that the chloro ligand is a poorer π donor than the amido ligand. Treatment of **4a** with $[HNMe_3][B(C_6H_5)_4]$ leads to the new cationic complex $[ansa\text{-}(\eta^5:\eta^5\text{-}C_5H_4\text{-}CMe_2\text{-}C_5H_4)\text{-}Nb(=NR)(HNMe_2)]^+$, which has also been isolated and characterized by ^1H and ^{13}C NMR and FAB-MS.

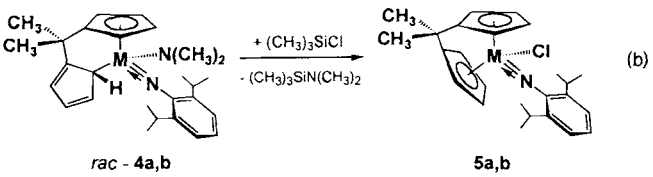

(b)

rac - **4a,b** **5a,b**

Like the conventional chloro systems, amide derivatives of zirconocene complexes are catalytically active in stereoregular propene polymerization. Therefore, the niobocene and tantalocene complexes described herein for the first time provide realistic prerequisites for catalytic applications. In particular, the use of the readily accessible arylimido complexes **2a,b** as precursors holds promise as a generalized synthetic route to niobocene and tantalocene complexes. Importantly, disadvantages arising from the notorious redox chemistry of homoleptic, high-valent metal amides like **1a,b**[11] are overcome by our synthetic concept.

Experimental Procedure

4a: A solution of 2,2-bis(cyclopentadienyl)propane (480 mg, 2.78 mmol) in toluene (20 mL) was added dropwise to a solution of tris(dimethylamido)(2,6-diisopropylphenylimido)niobium(v) (**2a**) (1092 mg, 2.72 mmol) in toluene (10 mL) at −30 °C. The solution was then allowed to warm up to 20 °C and then heated to reflux for 3 h. The volatiles were removed in vacuo and the oily residue was redissolved in *n*-pentane (6 mL). An orange solid (**4a**) precipitated at −78 °C and was dried in vacuo. Yield 980 mg (74%). The tantalocene derivative **4b** was prepared analogously (yield 59%).

Received: March 25, 1996 [Z8967IE]
German version: *Angew. Chem.* **1996**, *108*, 2098–2100

Keywords: catalysis · niobium compounds · sandwich complexes · tantalum compounds

[1] Recent reviews: a) A. M. Thayer, *Chem. Eng. News* **1995**, *73* (No. 37), 15–20; b) *Ziegler Catalysts* (Eds.: G. Fink, R. Mülhaupt, H.-H. Brintzinger), Springer, Berlin, **1995**; c) W. Kaminsky, A. Ahlers, N. Möller-Lindenhof, *Angew. Chem.* **1989**, *101*, 1304; *Angew. Chem. Int. Ed. Engl.* **1989**, *28*, 1216; d) J. Okuda, *Nachr. Chem. Tech. Lab.* **1993**, *41*, 8; e) T. N. Doman, T. K. Hollis, B. Bosnich, *J. Am. Chem. Soc.* **1995**, *117*, 1352.

[2] W. Kaminsky, K. Külper, H.-H. Brintzinger, F. R. W. P. Wild, *Angew. Chem.* **1985**, *97*, 507; *Angew. Chem. Int. Ed. Engl.* **1985**, *24*, 507.

[3] A. N. Chernega, M. L. H. Green, A. G. Suárez, *Can. J. Chem.* **1995**, *73*, 1157.

[4] a) K. Mashima, S. Fujikawa, A. Nakamura, *J. Am. Chem. Soc.* **1993**, *115*, 10990; b) K. Mashima, S. Fujikawa, Y. Tanaka, H. Urata, T. Oshiki, E. Tanaka, A. Nakamura, *Organometallics* **1995**, *14*, 2633.

[5] **2a**: ^1H NMR (400 MHz, C_6D_6, 25 °C, TMS): $\delta = 1.37$ (d, 12H; $^3J(H,H) = 7.0$ Hz; $CH(CH_3)_2$), 3.13 (s, 18H; $N(CH_3)_2$), 4.21 (sept, 2H; $^3J(H,H) = 6.8$ Hz; $CH(CH_3)_2$), 7.02 (t, 1H; $^3J(H,H) = 7.5$ Hz, *p*-C_6H_3), 7.16 (d, 2H; $^3J(H,H) = 7.5$ Hz, *m*-C_6H_3); $^{13}C\{^1H\}$ NMR (100.4 MHz, C_6D_6, 25 °C, TMS): $\delta = 24.1$ ($CH(CH_3)_2$), 28.5 ($CH(CH_3)_2$), 46.2 ($N(CH_3)_2$), 122.6 (*m*-C_6H_3), 122.9 (*p*-C_6H_3), 142.2 (*o*-C_6H_3), 152.8 (*ipso*-C_6H_3). **2b**: ^1H NMR (400 MHz, C_6D_6, 25 °C, TMS): $\delta = 1.40$ (d, 12H; $^3J(H,H) = 6.7$ Hz; $CH(CH_3)_2$), 3.15 (s, 18H; $N(CH_3)_2$), 4.20 (sept, 2H; $^3J(H,H) = 7.0$ Hz; $CH(CH_3)_2$), 7.02 (t, 1H; $^3J(H,H) = 8.1$ Hz, *p*-C_6H_3), 7.24 (d, 2H; $^3J(H,H) = 7.9$ Hz, *m*-C_6H_3); $^{13}C\{^1H\}$ NMR (100.4 MHz, C_6D_6, 25 °C, TMS): $\delta = 24.2$ ($CH(CH_3)_2$), 28.3 ($CH(CH_3)_2$), 45.2 ($N(CH_3)_2$), 121.9 (*p*-C_6H_3), 122.3 (*m*-C_6H_3), 142.7 (*o*-C_6H_3), 153.1 (*ipso*-C_6H_3).

 © VCH Verlagsgesellschaft mbH, D-69451 Weinheim, 1996 0570-0833/96/3517-1952 $ 15.00+.25/0

[6] Single crystals of **2a** were obtained from *n*-pentane at −78 °C. $C_{18}H_{35}N_4Nb$, $M_r = 400.41$, yellow block (0.51 × 0.43 × 0.38 mm), triclinic, space group $P\bar{1}$ (no. 2), $a = 885.9(1)$, $b = 1065.5(1)$, $c = 1276.7(1)$ pm, $\alpha = 70.47(1)$, $\beta = 85.49(1)$, $\gamma = 70.58(1)$, $V = 1070.4(2) \times 10^6$ pm^3, $Z = 2$, $\rho_{calcd} = 1.242$ g cm^{-3}; $F_{000} = 424$; $\mu = 5.7$ cm^{-1}. IPDS (STOE & CIE), $Mo_{K\alpha}$, $\lambda = 71.073$ pm, oscillation, 3 min per image, 11965 intensities were collected at $T = -100$ °C. After LP and combined decomposition and absorption correction 3446 ($R_{int} = 0.0273(F_o^2)$) were considered as independent reflections. The structure was solved by a combination of direct methods and difference-Fourier syntheses (STRUX-V, SIR-92, SHELXS-93, full matrix). All heavy atoms were refined with anisotropic, all H atoms with isotropic displacement parameters, convergence at $R1 = \Sigma(||F_o| - |F_c||)/\Sigma|F_o| = 0.0255$, $wR2 = [\Sigma w(F_o^2 - F_c^2)^2/\Sigma w(F_o^2)^2]^{1/2} = 0.0680$ [$w^{-1} = \sigma^2(F_o^2) + (0.0417\ P)^2 + 0.57\ P$ mit $P = (F_o^2 + 2F_c^2)/3$], $GOF = 1.070$ for 3446 reflections [$I > 0.0\sigma(I)$] and 348 variables. A final difference-Fourier synthesis remained without remarkable features ($e_{min\ max} = +0.30/-0.38$ e Å^{-3}) [9].

[7] **3a**: ^{1}H NMR (400 MHz, C_6D_6, 25 °C, TMS): $\delta = 1.29$ (d, 12H; $^3J(H,H) = 6.7$ Hz; $CH(CH_3)_2$), 3.22 (s, 12H; $N(CH_3)_2$), 4.11 (sept, 2H; $^3J(H,H) = 7.0$ Hz; $CH(CH_3)_2$), 5.92 (s, 5H; C_5H_5), 6.97 (t, 1H; $^3J(H,H) = 7.3$ Hz, p-C_6H_3), 7.11 (d, 2H; $^3J(H,H) = 7.3$ Hz, m-C_6H_3); $^{13}C\{^1H\}$ NMR (100.4 MHz, C_6D_6, 25 °C, TMS): $\delta = 24.7$ ($CH(CH_3)_2$), 27.4 ($CH(CH_3)_2$), 52.1 ($N(CH_3)_2$), 108.2 (C_5H_5), 122.9 (m-C_6H_3), 123.1 (p-C_6H_3), 143.0 (o-C_6H_3), 152.8 (*ipso*-C_6H_3).

[8] **4a**: ^{1}H NMR (400 MHz, C_6D_6, 25 °C, TMS): $\delta = 1.31$ (d, 12H; $^3J(H,H) = 7.0$ Hz; $CH(CH_3)_2$), 1.55 (s, 3H; $C(CH_3)_2$), 1.58 (s, 3H; $C(CH_3)_2$), 2.88 (s, 6H; $N(CH_3)_2$), 4.04 (sept, 2H; $^3J(H,H) = 7.0$ Hz; $CH(CH_3)_2$), 5.48 (s, 2H; C_5H_4), 5.53 (s, 2H; C_5H_4), 6.18 (s, 4H; C_5H_4), 6.96 (t, 1H; $^3J(H,H) = 7.5$ Hz, p-C_6H_3), 7.09 (d, 2H; $^3J(H,H) = 7.5$ Hz, m-C_6H_3); $^{13}C\{^1H\}$ NMR (100.4 MHz, C_6D_6, 25 °C, TMS): $\delta = 24.4$ ($CH(CH_3)_2$), 25.2 ($C(CH_3)_2$), 28.1 ($CH(CH_3)_2$), 28.4 ($C(CH_3)_2$), 36.3 ($C(CH_3)_2$), 54.2 ($N(CH_3)_2$), 90.9, 106.7, 112.5, 114.0 (C_5H_4), 122.9 (m-C_6H_3), 123.8 (p-C_6H_3), 142.8 (*ipso*-C_5H_4), 143.2 (o-C_6H_3), 152.6 (*ipso*-C_6H_3). **4b**: ^{1}H NMR (400 MHz, C_6D_6, 70 °C, TMS): $\delta = 1.32$ (d, 12H; $^3J(H,H) = 7.3$ Hz; $CH(CH_3)_2$), 1.49 (s, 3H; $C(CH_3)_2$), 1.58 (s, 3H; $C(CH_3)_2$), 2.93 (s, 6H; $N(CH_3)_2$), 3.99 (sept, 2H; $^3J(H,H) = 7.0$ Hz; $CH(CH_3)_2$), 5.01 (s, 2H; C_5H_4), 5.51 (m, 2H; C_5H_4), 6.08 (m, 2H; C_5H_4), 6.28 (m, 2H; C_5H_4), 6.91 (t, 1H; $^3J(H,H) = 7.6$ Hz, p-C_6H_3), 7.15 (d, 2H; $^3J(H,H) = 8.0$ Hz, m-C_6H_3). $^{13}C\{^1H\}$ NMR (100.4 MHz, C_6D_6, 70 °C, TMS): $\delta = 24.4$ ($CH(CH_3)_2$), 25.5 ($C(CH_3)_2$), 28.1 ($CH(CH_3)_2$), 29.4 ($C(CH_3)_2$), 36.4 ($C(CH_3)_2$), 53.3 ($N(CH_3)_2$), 89.4, 108.3, 113.2, 116.1 (C_5H_4), 122.4 (m-C_6H_3), 123.1 (p-C_6H_3), 143.7 (o-C_6H_3), 145.3 (*ipso*-C_5H_4), 152.2 (*ipso*-C_6H_3).

[9] Single crystals of **4a** were obtained from *n*-heptane at −30 °C. $C_{27}H_{37}N_2Nb$, $M_r = 482.51$, orange plate (0.39 × 0.38 × 0.31 mm), monoclinic, space group $P2_1n$ (no. 14), $a = 1000.3(1)$, $b = 2186.1(1)$, $c = 1153.1(1)$ pm, $\beta = 95.29(1)°$, $V = 2510.8(4) \times 10^6$ pm^3, $Z = 4$, $\rho_{calcd} = 1.276$ g cm^{-3}, $F_{000} = 1016$, $\mu = 4.9$ cm^{-1}. IPDS (STOE & CIE), $Mo_{K\alpha}$, $\lambda = 71.073$ pm, oscillation, 2.5 min per image, 18328 intensities were collected at $T = -50$ °C. After LP correction 4322 ($R_{int} = 0.0215(F_o^2)$) were considered independent reflections. The structure was solved by a combination of direct methods and difference-Fourier syntheses (STRUX-V, SIR-92, SHELXS-93, full matrix). All heavy atoms were refined with anisotropic, all H atoms with isotropic displacement parameters; convergence at $R1 = \Sigma(||F_o| - |F_c||)/\Sigma|F_o| = 0.0295$ $wR2 = [\Sigma w(F_o^2 - F_c^2)^2/\Sigma w(F_o^2)^2]^{1/2} = 0.0649$ [$w^{-1} = \sigma^2(F_o^2) + (0.0476\ P)^2 + 0.14\ P$, mit $P = (F_o^2 + 2F_c^2)/3$], $GOF = 1.072$ for all 4322 reflections [$I > 0.0\sigma(I)$] and 419 variables. A final difference-Fourier synthesis remained without remarkable features ($e_{min\ max} = +0.30/-0.38$ e Å^{-3}). Further details of the crystal structure investigations may be obtained from the Fachinformationszentrum Karlsruhe, D-76344 Eggenstein-Leopoldshafen (Germany), on quoting the depository numbers CSD-405082 (**2a**) and CSD-405083 (**4a**).

[10] **5a**: ^{1}H NMR (400 MHz, C_6D_6, 25 °C, TMS): $\delta = 1.00$ (s, 3H; $C(CH_3)_2$), 1.32 (s, 3H; $C(CH_3)_2$), 1.33 (d, 12H; $^3J(H,H) = 7.0$ Hz; $CH(CH_3)_2$), 3.89 (sept, 2H; $^3J(H,H) = 7.0$ Hz; $CH(CH_3)_2$), 5.51 (pseudo q, 2H; $J(H,H) = 2$ Hz; C_5H_4), 5.85 (pseudo q, 2H; $J(H,H) = 2$ Hz; C_5H_4), 6.03 (pseudo q, 2H; $J(H,H) = 3$ Hz; C_5H_4), 6.30 (pseudo q, 2H; $J(H,H) = 3$ Hz; C_5H_4), 6.85 (t, 1H; $^3J(H,H) = 7.5$ Hz, p-C_6H_3), 7.06 (d, 2H; $^3J(H,H) = 7.5$ Hz, m-C_6H_3); $^{13}C\{^1H\}$ NMR (100.4 MHz, C_6D_6, 25 °C, TMS): $\delta = 22.1$ ($C(CH_3)_2$), 24.1 ($C(CH_3)_2$), 24.4 ($CH(CH_3)_2$), 27.7 ($CH(CH_3)_2$), 36.4 ($C(CH_3)_2$), 95.4, 105.7, 115.4, 118.3 (C_5H_4), 122.6 (m-C_6H_3), 123.1 (p-C_6H_3), 139.8 (*ipso*-C_5H_4), 140.9 (o-C_6H_3), 154.5 (*ipso*-C_6H_3). **5b**: triclinic space group $P\bar{1}$ (no. 2), $a = 951.4(1)$, $b = 1071.9(1)$, $c = 1138.5(1)$ pm, $\alpha = 76.44(1)$, $\beta = 83.16(1)$, $\gamma = 80.36(1)$. Detailed description of the synthesis and structure: W. A. Herrmann, W. Baratta, E. Herdtweck, *Organometallics* **1996**, in press.

[11] a) A. D. Jenkis, M. F. Lappert, R. C. Srivastava, *J. Organomet. Chem.* **1970**, *23*, 165; b) J. S. Basi, D. C. Bradley, M. H. Chisholm, *J. Chem. Soc. A* **1971**, 1433.

Glycocoating of Oligovalent Amines: Synthesis of Thiourea-Bridged Cluster Glycosides from Glycosyl Isothiocyanates**

Thisbe K. Lindhorst* and Christoffer Kieburg

Many cell adhesion phenomena are based on the specific interactions of carbohydrates and proteins.[1] Important examples include the transfer of leucocytes to areas of acute or chronic inflammation, which is initiated by the interaction of selectins with the sialyl Lewis^x tetrasaccharide,[2] and the phagocytosis of bacteria, which is prompted by carbohydrate–protein interactions.[3] Microbial adhesion is in many cases also dependent on the recognition of carbohydrates on the surface of the host cells by specific lectins.[4] The so-called mannose-binding protein (MBP),[5] an acute phase protein of immune response, recognizes a broad array of oligosaccharide moieties on the surface of bacteria, which it is able to distinguish from its own sugar epitopes.[6] There is even evidence that carohydrate–lectin interactions are a key requirement for processes leading to neuronal outgrowth.[7]

Suitable glycomimetics that are able to compete with or even perform better than the naturally occurring carbohydrate ligands are needed for the elucidation and manipulation of carbohydrate–protein interactions.[8] For this purpose the clustering of glycosides has proved to be advantageous in many instances, as the multipresentation of specific sugar epitopes in one molecule can result in remarkably increased avidities in the adhesion systems examined.[9] This phenomenon has been termed the cluster effect and was first shown for the galectin on hepatocytes.[10] Since then the clustering of glycosides has been examined in particular for the inhibition of the influenza virus hemagglutinin.[11] Copolymerization reactions[12] or telomerizations[13] have often been used to incorporate several oligosaccharides; meanwhile an increasing number of dendrimers has appeared as core molecules for the synthesis of clustered glycosides with exactly defined structures.[14] Recently the clustering of the sialyl Lewis^x tetrasaccharide has been also investigated for the control of leucocyte trafficking.[15]

We have lately described a facile method for the preparation of glycosyl isothiocyanates, which gives access to these versatile carbohydrate derivatives on a multigramm scale.[16] We now demonstrate that glycosyl isothiocyantes are ideally suited for the preparation of cluster glycosides. The ease of the transformation of isothiocyanates and amines to thiourea derivatives can generally be applied to the reaction of glycosyl isothiocyanates with oligovalent, multibranched amines to yield oligoantennary, thiourea-bridged glycoconjugates directly.

We have tested the reaction with the trivalent tris(2-aminoethyl)amine (**1**) and mono- as well as disaccharide glycosyl isothiocyanates of different configurations and obtained the triantennary products in very good yields. The sugar units can be deprotected easily in a Zémplen reaction with sodium methanolate in methanol without attack on the thiourea bridges (Scheme 1). Thus the acetylated *gluco*-, *manno*-, *galacto*-, *cellobio*-, and *lacto*-configurated glycosyl isothiocyanates were

[*] Dr. T. K. Lindhorst, C. Kieburg
Institut für Organische Chemie der Universität
Martin-Luther-King-Platz 6, D-20146 Hamburg (Germany)
Fax: Int. code +(40) 4123-4325
e-mail: tklind@chemie.uni-hamburg.de

[**] This work was funded by the Deutsche Forschungsgemeinschaft and the Fonds der Chemischen Industrie. We wish to thank Prof. J. Thiem for his valuable support. We thank Dr. V. Havlicek for the electrospray-MS experiments, Dipl. Chem. A. Jacob for the MALDI-TOF-spectrum, and Dr. V. Sinnwell for the high temperature NMR measurements.

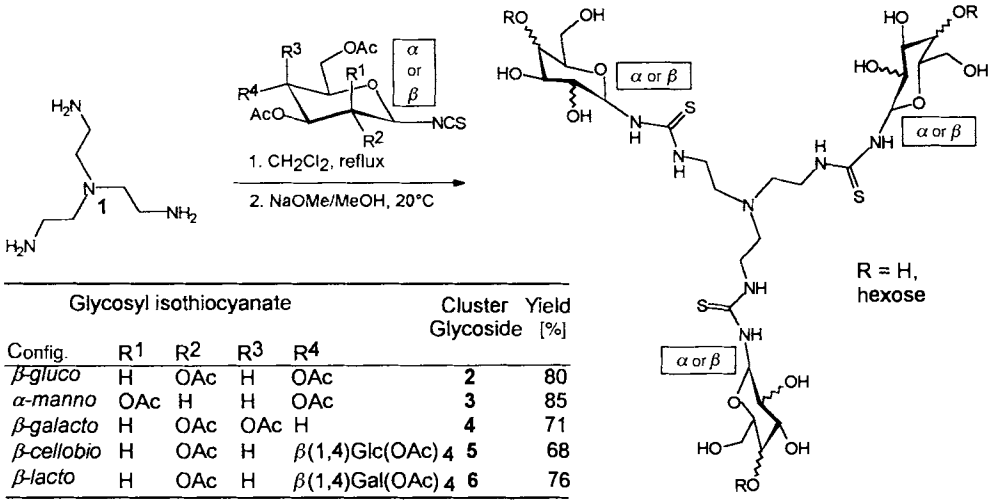

Glycosyl isothiocyanate					Cluster Glycoside	Yield [%]
Config.	R^1	R^2	R^3	R^4		
β-gluco	H	OAc	H	OAc	**2**	80
α-manno	OAc	H	H	OAc	**3**	85
β-galacto	H	OAc	OAc	H	**4**	71
β-cellobio	H	OAc	H	β(1,4)Glc(OAc)4	**5**	68
β-lacto	H	OAc	H	β(1,4)Gal(OAc)4	**6**	76

Scheme 1. Reaction of tris(2-aminoethyl)amine (**1**) with glycosyl isothiocyanates to yield triantennary thiourea-bridged cluster glycosides **2**–**6**.

converted in two steps into the tris(2-glycosylthiourea-ethyl)-amines **2**–**6** in overall yields of 70–85%.[17]

The anomeric sugar configuration is determined by the glycosyl isothiocyanate used and does not change during the reaction. However, the base-catalyzed O → N migration of the acyl groups from the acetyl-protected glycosyl isothiocyanates onto the amino termini of the core molecules was troublesome. If the reaction was not carried out carefully enough, only the divalent bis(glycosylthiourea) cluster was formed, while the third amino group was acetylated and therefore blocked. This unwanted side reaction resulted in lower yields and structural defects in the periphery of the cluster. It was suppressed by an appropriate reaction procedure: a diluted solution of the oligovalent core molecule was added dropwise to a solution of the glycosyl isothiocyanate in dichloromethane at reflux temperature.

This method can also be applied to the synthesis of higher branched clusters, in which dendritic polyamines serve as suitable core molecules. These core molecules are easily obtained by the exhaustive Michael addition of methyl acrylate to initial amines and the subsequent amidation of the resulting esters with an excess of ethylenediamine to afford amidoamines. The reiteration of this two step reaction sequence results in the doubling of peripheral animo funtionalities; thus higher branched structures are assembled in each developing generation. This construction principle leads to the so-called PAMAM (polyamidoamine) dendrimers as in the work of Tomalia et al.[18] In this way the hexavalent amine **8** was synthesized from tris(2-aminoethyl)amine (**1**) as well as the tetravalent amine **7** and the next octaantennary generation **9** starting from ethylenediamine.

For the synthesis of bigger clusters we focused on the application of mannosyl isothiocyanate for the coupling reaction, as we were especially interested in clustered mannosides for the investigation of mannose-sensitive adhesion systems.[19] As expected 2,3,4,6-tetra-*O*-acetyl-α-D-mannosyl isothiocyanate reacted easily with the tetrafunctional amine **7** to give the tetraantennary cluster **10**, with the hexafunctional core **8** to yield the hexaantennary conjugate **11**, and with the octavalent dendrimer **9** to afford the octaantennary cluster mannoside **12** in very good yields of 76, 69, and 55%, respectively. The reaction can be carried out following the same basic protocol for a variety of clusters. Bigger clusters have to be dissolved in DMF instead of dichloromethane, and the reaction times lengthened. The purification of all presented products was successfully performed on

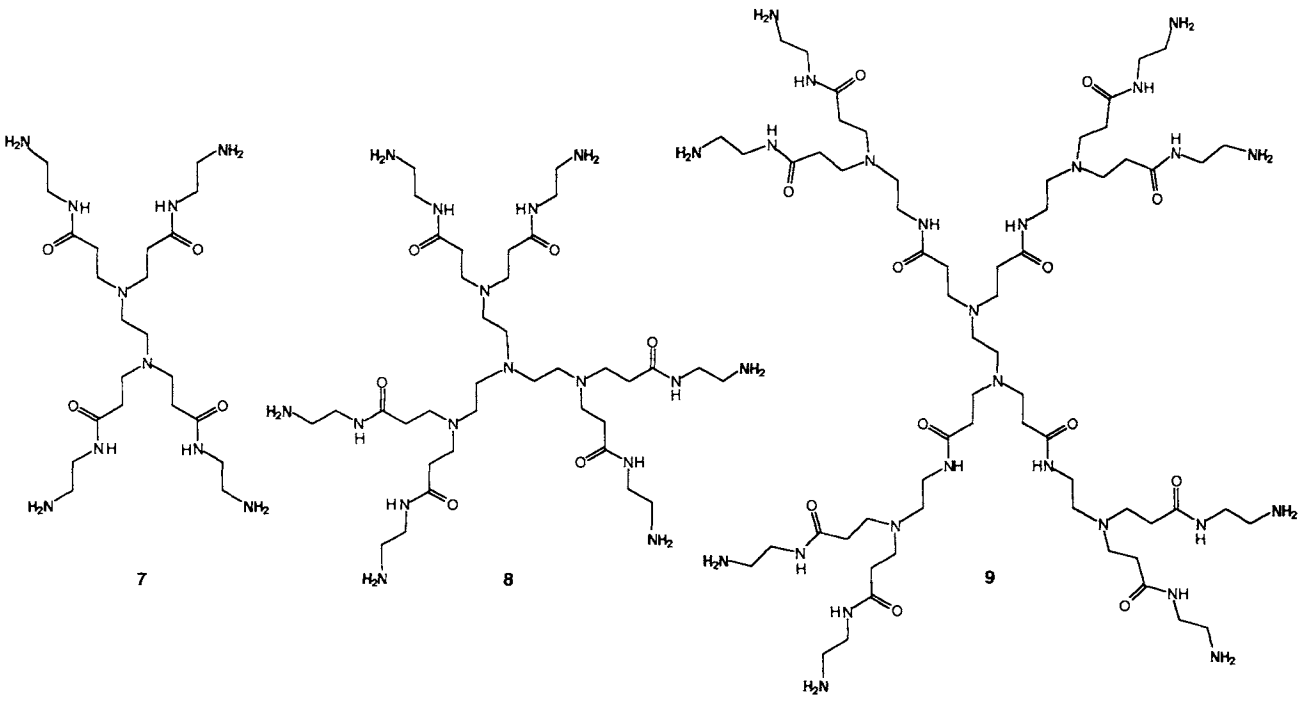

 © VCH Verlagsgesellschaft mbH, D-69451 Weinheim, 1996 0570-0833/96/3517-1954 $ 15.00+.25/0

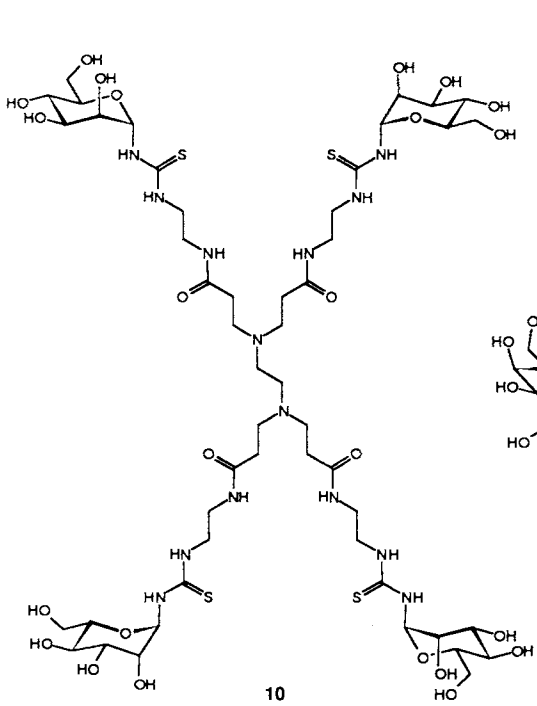

10

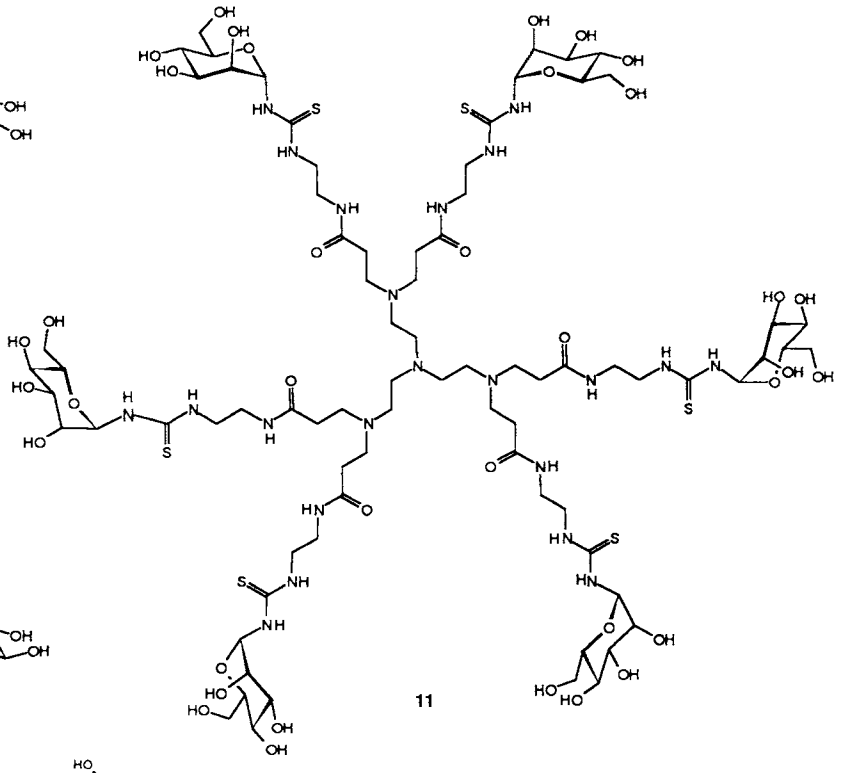

11

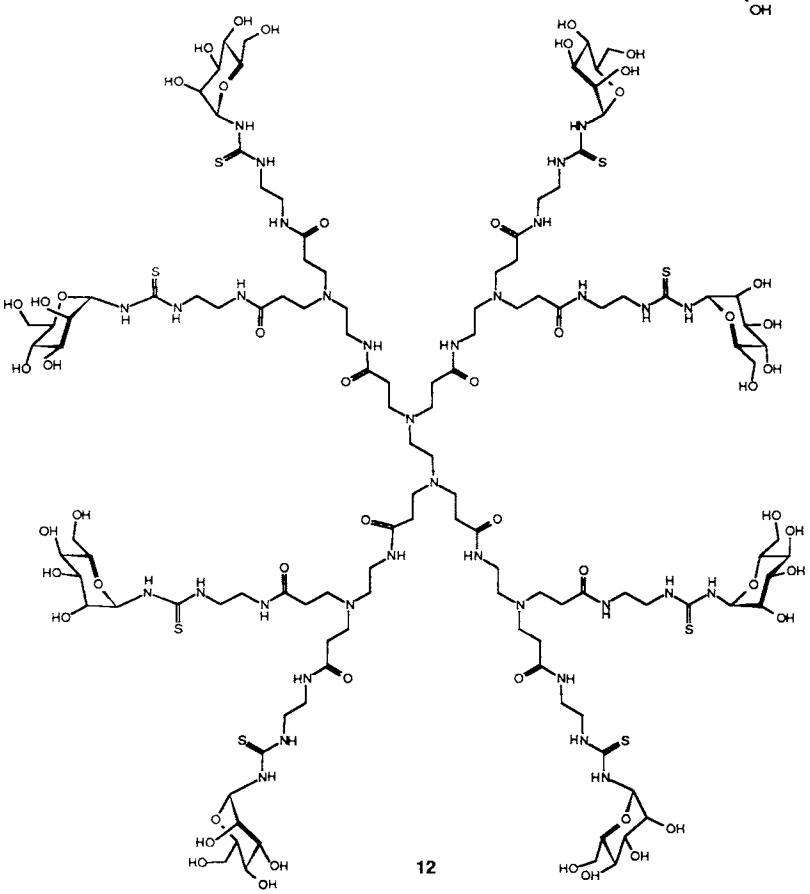

12

Table 1. Selected ^1H and ^{13}C NMR shifts of the glycoclusters **10**–**12** in D_2O.

	10 δ	**11** δ	**12** δ
^1H NMR (400 MHz):			
glycosyl H-1	5.37 (4H)	5.37 (6H)	5.37 (8H)
CH_2 groups	3.62 (8H)	3.66 (6H)	3.65 (16H)
of the core region	3.32 (8H)	3.30 (6H)	3.31 (24H)
	2.86 (8H)	2.75 (9H)	2.99 (12H)
	2.72 (4H)	2.62 (3H)	2.90 (16H)
	2.43 (8H)	2.23 (6H)	2.73 (8H)
			2.51 (8H)
			2.41 (16H)
^{13}C NMR (69.89 MHz):			
C=S	182.62	182.67	182.60
C=O	174.75	175.28	175.01
glycosyl C-1	82.70	82.78	82.72
CH_2 groups	50.11	51.35	51.89
of the core region	49.28	49.70	49.97
	44.41	49.45	49.60
	39.32	44.47	49.19
	32.33	39.34	44.43
		33.03	39.26
			37.04
			32.69
			31.97

silica gel. The acetylated compounds yielded glasses; the water-soluble, deprotected cluster glycosides were obtained as white powders after lyophylization.

All products were examined by means of ^1H and ^{13}C NMR spectroscopy and mass spectrometry. The NMR spectra show a single signal pattern for all sugar units; the ratios of the integrals for these signals and for the signals of the methylene protons of the core are correct for each product as formulated. The NMR spectra of the acetylated clusters were recorded in DMSO, where the required number of NH resonances for every compound were observed between $\delta = 7.2$ and 9.5.

 © VCH Verlagsgesellschaft mbH, D-69451 Weinheim, 1996 0570-0833/96/3517-1955 $ 15.00+.25/0

The dynamic behavior of the aliphatic core chains resulted in signal broadening in the ^{1}H NMR spectra of the synthesized cluster glycosides, especially for the thioamide protons, the methylene peaks of the core region, and the anomeric protons of the sugar antennae. For the same reason some signals in the ^{13}C spectrum, for example the signals related to the methylene groups were hardly or not at all detected when the spectrum was recorded at room temperature. These effects were less intense for the deprotected compounds and when D_2O was used as the solvent. High-temperature measurements led to an improved resolution of the multiplets in the ^{1}H NMR and to the detection of the complete signal pattern in the carbon spectrum (Table 1). In the case of the octaantennary compound **12**, the methylene carbon atoms of the central ethylenediamine moiety can only be seen with a highly concentrated sample.

MALDI-TOF mass spectrometry was a well-suited method for the mass analysis of the largest cluster **12** (M_r = 3199.69 g mol^{-1}). The protonated molecular ion peak was the only signal in the MALDI-TOF MS spectrum of **12**.

We have shown here that glycosyl isothiocyanates can be linked with dendritic polyamines to give thiourea-bridged cluster glycosides with defined structures. The method requires simple starting materials, two reaction steps only, and easily permits the variation of the carbohydrate epitopes, as well as the number of branches, by choice of different core molecules. It facilitates the rapid preparation of cluster glycosides of different kinds on a multigramm scale.

Experimental Procedure

12: A solution of generation 1 PAMAM dendrimer **9** (40 mg, 0.028 mmol) in DMF (10 mL) was added dropwise to 2,3,4,6,-tetra-*O*-acetyl-α-mannopyranosyl isothiocyanate (122 mg, 0.31 mmol, 11.2 equiv) in dichloromethane (50 mL) at reflux temperature. It was stirred at reflux for 6 h, then the solvent was removed by distillation, and the residual syrup was purified by flash column chromatography (silica gel 0.04–0.063 mm; CH_2Cl_2/MeOH, 9/1). The acetylated reaction product was dissolved in dry methanol (80 mL), and the solution was adjusted to pH 8–9 with a freshly prepared 1 N sodium methanolate solution. The reaction mixture was stirred at 40 °C until the reaction was complete, then it was neutralized with ion exchange resin (Dowex, H^+ W50x8), and the ion exchanger was filtered off and washed with water. The resulting solution was distilled to remove the methanol and lyophilization. The octaantennary cluster mannoside **12** was obtained as a white lyophilizate (49 mg, 0.015 mmol).

Received: March 21, 1996 [Z 8961 IE]
German version: *Angew. Chem.* **1996**, *108*, 2083–2086

Keywords: dendrimers · glycoconjugates · glycosyl thioureas

[1] a) M. Fukuda, *Bioorg. Med. Chem.* **1995**, *3*, 207–215; b) Y. C. Lee, R. T. Lee, *Acc. Chem. Res.* **1995**, *26*, 323–327.
[2] A. Giannis, *Angew. Chem.* **1994**, *106*, 188–191; *Angew. Chem. Int. Ed. Engl.* **1994**, *33*, 178–181.
[3] I. Ofek, N. Sharon, *Infect. Immun.* **1988**, *56*, 539–547.
[4] a) N. Sharon, *FEBS Lett.* **1987**, *217*, 145–157; b) K.-A. Karlsson, *Ann. Rev. Biochem.* **1989**, *58*, 309–350; c) *Curr. Opin. Struct. Biol.* **1995**, *5*, 622–635.
[5] a) W. I. Weis, R. Kahn, R. Fourme, K. Drickamer, W. A. Hendrickson, *Science* **1991**, *254*, 1608–1615; b) M. W. Turner, *Biochem. Soc. Trans.* **1994**, *22*, 88–94.
[6] a) R. A. B. Ezekowitz, *Curr. Biol.* **1992**, *2*, 147–149; b) J. G. Raynes, *Biochem. Soc. Trans.* **1994**, *22*, 69–74.
[7] T. Feizi, *TIBS* **1994**, *19*, 233–234.
[8] Y. C. Lee, *Biochem. Soc. Trans.* **1993**, *21*, 460–463.
[9] a) S. A. DeFrees, F. C. A. Gaeta, *J. Am. Chem. Soc.* **1993**, *115*, 7549–7550; b) E. S. Litscher, K. Juntunen, A. Seppo, L. Penttilä, R. Niemalä, O. Renkonen, P. M. Wassarman, *Biochemistry* **1995**, *34*, 4662–4669.
[10] a) D. T. Connolly, R. R. Townsend, K. Kawaguchi, W. R. Bell, Y. C. Lee, *J. Biol. Chem.* **1982**, *257*, 939–945; b) Y. C. Lee, R. R. Townsend, M. R. Hardy, J. Lönngren, J. Arnarp, M. Haraldsson, H. Lönn, *ibid.* **1983**, *258*, 199–202; c) E. A. L. Biessen, D. M. Beuting, H. C. P. F. Roelen, G. A. van de Marel, J. H. van Boom, T. J. C. van Berkel, *J. Med. Chem.* **1995**, *38*, 1538–1546.
[11] a) S. Sabesan, J. Ø. Duus, S. Neira, P. Domaille, S. Kelm, J. C. Paulson, K. Bock, *J. Am. Chem. Soc.* **1992**, *114*, 8363–8375; b) C. Unverzagt, S. Kelm, J. C. Paulson, *Carbohydr. Res.* **1994**, *251*, 285–301.
[12] a) A. Spaltenstein, G. M. Whitesides, *J. Am. Chem. Soc.* **1991**, *113*, 686–687; b) K. H. Mortell, M. Gingras, L. L. Kiessling, *ibid.* **1994**, *116*, 12053-12054.
[13] a) S. Aravind, W. K. C. Park, S. Brochu, R. Roy, *Tetrahedron Lett.* **1994**, *35*, 7739–7742; b) W. K. C. Park, S. Aravind, A. Romanowska, J. Renaud, R. Roy, *Methods Enzymol.* **1994**, *242*, 294–304; c) R. Roy, D. Zanini, S. J. Mennier, A. Romanowska, *ACS Symp. Ser.* **1994**, *560*, 104–119.
[14] a) R. Roy, D. Zanini, S. J. Meunier, A. Romanowska, *J. Chem. Soc. Chem. Commun.* **1993**, 1869–1872; b) T. Toyokuni, A. K. Singhal, *Chem. Soc. Rev.* **1995**, 231–242; c) R. Roy, W. K. C. Park, Q. Wu, S.-N. Wang, *Tetrahedron Lett.* **1995**, *36*, 4377–4380; d) D. Zanini, W. K. C. Park, R. Roy, *ibid.* **1995**, *36*, 7383–7386; e) K. Aoi, K. Itoh, M. Okada, *Macromolecules* **1995**, *28*, 5391–5393; f) N. Jayaraman, S. A. Nepogodiev, J. F. Stoddart, *Abstr. Pap. Eurocarb VIII* (Seville) **1995**, A-148; g) R. Roy in *Modern Methods in Carbohydrate Synthesis* (Eds.: S. H. Khan, R. A. O'Neill), Harwood, Amsterdam, **1996**, pp. 378–402.
[15] a) G. Kretzschmar, U. Sprengard, H. Kunz, E. Bartnik, W. Schmidt, A. Toepfer, B. Hörsch, M. Krause, D. Seiffge, *Tetrahedron* **1995**, *51*, 13015–13030; b) U. Sprengard, M. Schudok, W. Schmidt, G. Kretzschmar, H. Kunz, *Angew. Chem.* **1996**, *108*, 359–362; *Angew. Chem. Int. Ed. Engl.* **1996**, *35*, 321–324.
[16] T. K. Lindhorst, C. Kieburg, *Synthesis* **1995**, 1228–1230.
[17] Tris[2-(2,3,4,6-tetra-*O*-acetyl-α-D-mannopyranosyl)thiourea-ethyl]amine-($C_{51}H_{75}N_7O_{27}S_3$): FAB-MS: *m/z*: 1314 ($M+H^+$), 1336 ($M+Na^+$); $[\alpha]_D^{20}$ = +50.4 (*c* = 1.0 in CH_2Cl_2); ^{1}H NMR (400 MHz, DMSO): δ = 8.75 (d, 3H, NHCH), 7.61 (br. s, 3H, $NHCH_2$), 5.95 (dd, 3H, H-1), 5.39 (dd, 3H, H-3), 5.11 (m, 6H, H-2, H-4), 4.18 (dd, 3H, H-6), 4.00 (dd, 3H, H-6'), 3.89 (ddd, 3H, H-5), 3.60 (d, 6H, CH_2NH), 2.72 (t, 6H, CH_2N), 2.13, 2.02, 2.01, 1.97 (je s, je 9H, 12OAc) J(NH,H1) = 8.0, J(2,3) = 3.5, J(3,4) = 9.7, J(4,5) = 9.6, J(5,6) = 5.1, J(5,6') = 2.5, J(6,6') = 12.2 Hz; ^{13}C NMR (62.89 MHz, DMSO): δ = 182.84 (C=S), 170.03, 169.64, 169.61, 169.39 (C=O), 79.20 (C-1), 69.28, 68.98, 68.43, 66.09 (C-2, C-3, C-4, C-5), 62.01 (C-6), 52.08 (CH_2N), 41.99 (CH_2NH), 20.62, 20.57, 20.45, 20.43 ($COCH_3$). Tris[2-(α-D-mannopyranosyl)thioureaethyl]amine **3** ($C_{27}H_{51}N_7O_{15}S_3$): Electrospray MS: *m/z*: 810 ($M+H^+$); $[\alpha]_D^{20}$ = +91.5 (*c* = 1.0 in H_2O); ^{1}H NMR (400 MHz, D_2O): δ = 5.55 (br. s, 3H, H-1), 4.08 (br. s, 3H, H-2), 3.89–3.86 (m, 6H, H-3, H-6), 3.78 (dd, 3H, H-6'), 3.74–3.69 (m, 9H, H-4, CH_2NH), 3.57 (ddd, 3H, H-5), 2.87 (t, 6H, CH_2N); J(3,4) = 9.1, J(4,5) = 9.1, J(5,6) = 2.1, J(5,6') = 6.4, J(6,6') = 12.2 Hz; ^{13}C NMR (62.89 MHz, D_2O): δ = 181.94 (C=S), 82.84 (C-1), 74.02, 70.94, 69.95, 67.72 (C-2, C-3, C-4, C-5), 61.27 (C-6), 52.78 (CH_2N), 43.11 (CH_2NH); J(H1,C1) = 165 Hz.
[18] D. A. Tomalia, A. M. Naylor, W. A. Goddard III, *Angew. Chem.* **1990**, *102*, 119–157; *Angew. Chem. Int. Ed. Engl.* **1990**, *29*, 113–151.
[19] In collaboration with the research center in Borstel we are currently testing the dependence of the inhibitory properties of cluster mannosides in the agglutination of type 1 fimbriae from *Escherichia coli* and yeast cells on the structure and number of antennae of the examined compounds (cf. N. Firon, S. Ashkenazi, D. Mirelman, I. Ofek, N. Sharon, *Infect. Immun.* **1987**, *55*, 472–476). In addition, cluster mannosides are needed for the investigation of the biological functions of glycoproteins from the CD66 gene cluster (cf. S. L. Sauter, S. M. Rutherford, C. Wagener, J. E. Shively, S. A. Hefta, *J. Biol. Chem.* **1993**, *268*, 15510–15516).

Synthesis of a Water-Soluble Conjugated [3]Rotaxane**

Sally Anderson* and Harry L. Anderson*

Organic molecules with extended conjugated π-systems have many potential applications, for example as dyes for nonlinear optics and in electroluminescent displays.[1] However, the small HOMO–LUMO energy gaps that are responsible for the special electronic properties of these compounds also make them reactive, so chemical instability often limits the usefulness of

[*] Dr. S. Anderson, Dr. H. L. Anderson
University of Oxford, Dyson Perrins Laboratory
South Parks Road, GB-Oxford OX1 3QY (UK)
Fax: Int. code +(1865)275-674
e-mail: harry.anderson@dyson.ox.ac.uk

[**] This work was supported by an Award to Newly Appointed Science Lecturers from the Nuffield Foundation and by a gift of trimethylsilyacetylene from Farchan Laboratories (Florida, USA). S. A. gratefully acknowledges a research fellowship and generous support from Trinity College, Cambridge.

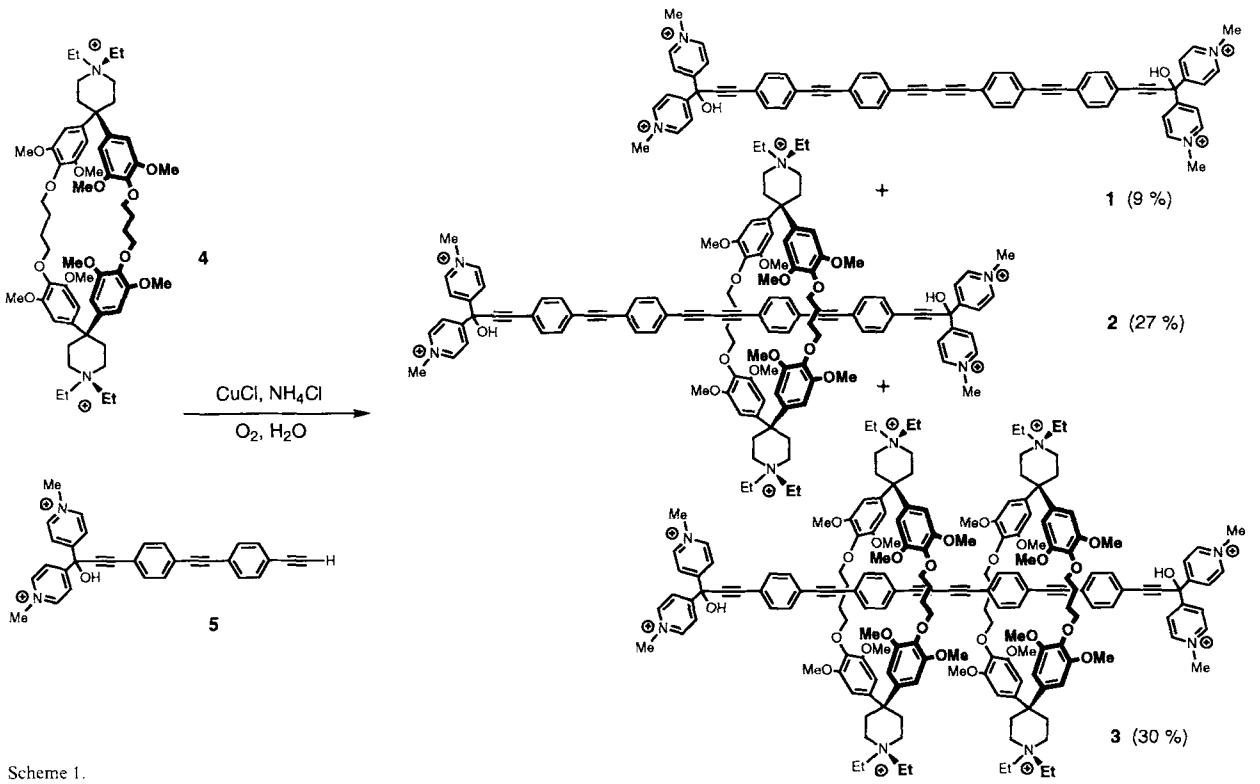

Scheme 1.

these materials. The threading of a conjugated dumbbell through one or more macrocycles to form a rotaxane should protect the π-system from attack. Rotaxane formation may also protect the excited state of the chromophore from quenchers and thus increase its fluorescence efficiency, which could be relevant to electroluminescent applications. Here we present a synthetic approach to conjugated rotaxanes in which the hydrophobic effect is used to direct rotaxane formation. Comparison of the "naked" dumbbell **1** with its [2]rotaxane **2** and [3]rotaxane **3** shows that threading macrocycles increases its fluorescence yield.

Many rotaxanes have been synthesized[2] but this is the first synthesis of rotaxanes with conjugated backbones.[3] We chose to use the hydrophobic effect to direct the formation of our rotaxanes because, as most of the monomers used for synthesizing conjugated structures are hydrophobic, this avoids the need to build specific binding sites into our components. Many water-soluble macrocycles bind 1,4-disubstituted benzenes in water.[4] We chose to use Diederich's cyclophane **4** because of its convenient solubility, binding properties, and synthesis.[5] Our approach was to couple the stopper **5**[6] in the presence of one equivalent of **4** as shown in Scheme 1.

^{1}H NMR titrations showed that **5**·2Cl forms a stable complex with macrocycle **4**·2Cl in water, despite the fact that both units are dications.[7] Complexation is accompanied by large upfield shifts in the ^{1}H NMR signals of the aromatic protons of **5** ($\Delta\delta_{sat}$ = 0.13, 0.49, 1.72, and 2.04 ppm for H_C, H_D, H_F and H_G; for assignments see Fig. 1). In contrast, the pyridine resonances are not significantly shifted ($\Delta\delta_{sat} < 0.015$ ppm), indicating that only the phenylene ethynylene region of **5** binds inside the cavity of the cyclophane. Job plot analysis confirmed the 1:1 stoichiometry. The binding constant at 298 K is $(4.1 \pm 0.5) \times 10^4\ M^{-1}$. Titrations at several temperatures between 298 and 348 K gave a linear van't Hoff plot with ΔH and $T\Delta S_{298}$ of 12 and 6 kcal mol^{-1}, respectively, showing that the hydrophobic binding is enthalpically driven as is typical for receptors of this type.[5, 8]

Glaser coupling[9] of a 1:1 mixture of **5** and **4** at 3 mM concentration in water (Scheme 1) gave a product mixture containing 38% [3]rotaxane **3**, 36% [2]rotaxane **2**, and 26% dumbbell **1**.[10] These compounds were isolated after chromatography and recrystallization as PF_6^- salts in yields of 30, 27, and 9%, respectively. The ratio of [3]rotaxane to dumbbell is less than that predicted based on the stability of the **4**·**5** complex; its binding constant of $4.1 \times 10^4\ M^{-1}$ implies that at 3 mM concentration 91% of the stoppers should be bound to cyclophane, whereas the yields indicate that only 56% of the stoppers are bound to **4** when they couple. This implies that binding under coupling conditions is weaker than in pure water or that free **5** couples faster than the **4**·**5** complex.

The structures of the [3]rotaxane **3** and the [2]rotaxane **2** were established by mass spectrometry and by ^{1}H and ^{13}C NMR spectroscopy (Table 1). The electrospray ionization mass spectrum (ESI-MS) of **3**·8PF_6 in acetonitrile shows peaks at *m/z* 360.2, 411.5, and 479.9 due to M^{8+}, $(M - H)^{7+}$, and $(M - 2H)^{6+}$, as well as a peak at *m/z* 500.5 due to $\mathbf{4}^{2+}$ formed by fragmentation of **3** during electrospray ionization.[11]

The ^{1}H NMR spectrum of the [3]rotaxane **3**·8Cl in D_2O (Fig. 1) was fully assigned by NOESY and COSY experiments. Many NOEs were observed within the dumbbell, within the cyclophane, and between the two components;[12] some of these are illustrated in Figure 1. Both the NOEs and the large upshield shift of the $H_{F/G}$ resonance ($\Delta\delta$ = 1.97 ppm) show that the cyclophanes prefer to reside on the central phenylene rings, away from the stoppers. The rims of the cyclophane are nonequivalent in **3** so the diastereotopic protons of the methylenes in the $O(CH_2)_4O$ chain, such as H_N, give pairs of multiplets. However, the aromatic H_E and methoxy H_I protons of the cyclophane give rise to singlets at room temperature, showing that the aromatic rings of the cyclophane are rotating fast on the

 © VCH Verlagsgesellschaft mbH, D-69451 Weinheim, 1996 0570-0833/96/3517-1957 $ 15.00+.25/0

Table 1. Selected physical data for the new compounds.

1·4Cl: ^{1}H NMR (500 MHz, D_2O): $\delta = 8.89$ (d, $J = 6.7$ Hz, 8H), 8.43 (d, $J = 7.0$ Hz, 8H), 7.68 (s, 8H), 7.65 (s, 8H), 4.42 (s, 12H); UV/Vis (H_2O): λmax (ε) [nm] = 354 (7.7×10^4 M^{-1}cm^{-1}). **1**·4PF_6: ^{13}C NMR (125 MHz, 1:1 CD_3OD:$(CD_3)_2CO$): $\delta = 161.1$, 147.5, 133.5, 133.1, 132.73, 132.68, 126.1, 125.3, 124.9, 122.5, 121.8, 92.0 [b], 90.8, 88.7, 82.8, 76.1, 73.0, 48 [a]; ESI$^+$ MS: m/z 219.8 ($[M - 4PF_6]^{4+}$, $C_{62}H_{46}N_4O_2$ requires 219.8)

2·6Cl: ^{1}H NMR (500 MHz, D_2O): $\delta = 8.94$ (d, $J = 6.9$ Hz, 8H), 8.48 (d, $J = 6.9$ Hz, 8H), 7.67 (q, AB, $J = 8.4$ Hz, 8H), 6.92 (s, 8H), 6.76 (q, AB, $J = 8.2$ Hz, 8H), 4.46 (s, 12H), 3.86 (s, 24H), 3.30–3.60 (m, 24H), 2.70–3.10 (m, 8H), 1.60–1.70 (m, 8H), 1.31 (t, $J = 7.0$ Hz, 12H); UV/Vis (H_2O): λmax (ε) [nm] = 354 (7.8×10^4 M^{-1}cm^{-1}). **2**·6PF_6: ^{13}C NMR (125 MHz, 1:1 CD_3OD:$(CD_3)_2CO$): $\delta = 161.1$, 154.8 [b], 147.5, 136.9, 133.2 [b], 132.6, 132.4, 126.1, 125.1, 124.2, 121.9, 121.7, 104.3, 91.93, 91.88, 90.8, 88.8, 82.8, 76.0, 73.1, 72.7 [b], 56.6 [b], 48 [a], 44.2, 30 [a], 26.6, 7.3; ESI$^+$ MS: m/z 313.4, ($[M - 6PF_6]^{6+}$, $C_{120}H_{130}N_6O_{14}$ requires 313.4), 375.8 ($[M - H - 6PF_6]^{5+}$, $C_{120}H_{129}N_6O_{14}$ requires 375.8); Anal. calcd for $C_{120}H_{130}N_6O_{14}P_6F_{36}$: C 52.40, H 4.77, N 3.06; found: C 52.67, H 5.08, N 3.09

3·8Cl: ^{1}H NMR (500 MHz, D_2O): $\delta = 8.94$ (d, $J = 6.9$ Hz, 8H), 8.48 (d, $J = 6.9$ Hz, 8H), 7.76 (d, $J = 8.2$ Hz, 4H), 7.54 (d, $J = 8.2$ Hz, 4H), 6.90 (s, 16H), 5.68 (s, 8H) [b], 4.46 (s, 12H), 3.83 (s, 48H), 3.60–3.43 (m, 48H), 3.20–2.80 (m, 16H), 1.80–1.50 (m, 16H), 1.31 (t, $J = 6.9$ Hz, 24H); UV/Vis (H_2O): λmax (ε) [nm] = 356 (7.7×10^4 M^{-1}cm^{-1}). **3**·8PF_6: ^{13}C NMR (125 MHz, 1:1 CD_3OD:$(CD_3)_2CO$): $\delta = 161.0$, 154.7 [b], 147.7, 136.9, 133.0, 132.7, 132.5, 132.1, 126.1, 124.9, 123.6, 121.3, 121.2, 104.2, 91.9, 91.6, 90.8, 88.6, 82.6, 75.8, 73.1, 72.6 [b], 56.6 [b], 48 [a], 44.1, 30 [a], 26.6, 7.4; ESI$^+$ MS: m/z 360.2 ($[M - 8PF_6]^{8+}$, $C_{178}H_{214}N_8O_{26}$ requires 360.2), 411.5 ($[M - H - 8PF_6]^{7+}$ $C_{178}H_{213}N_8O_{26}$ requires 411.6), 479.9 ($[M - 2H - 8PF_6]^{6+}$, $C_{178}H_{212}N_8O_{26}$ requires 480.0); Anal. calcd for $C_{178}H_{214}N_8O_{26}P_8F_{48}$: C 52.89, H 5.35, N 2.77; found: C 53.18, H 5.41, N 2.80

4·2Cl: ^{1}H NMR (300 MHz, D_2O): $\delta = 6.47$ (s, 8H), 3.73 (m, 8H), 3.49 (s, 24H), 3.21 (m, 16H), 2.59 (m, 8H), 1.46 (m, 8H), 1.08 (t, $J = 7$ Hz, 12H); ^{13}C NMR (125 MHz, D_2O): $\delta = 153.6$ [b], 134.6, 104.4, 73.0 [b], 56.5, 55.7, 44.0, 29.1, 25.6, 6.9; ESI$^+$ MS: m/z 500.7 ($[M - 2Cl]^{2+}$, $C_{58}H_{84}N_2O_{12}$ requires 500.7); Anal. calcd for $C_{58}H_{84}N_2O_{12}Cl_2 \cdot 0.5H_2O$: C 64.40, H 7.94, N 2.59; found: C 64.35, H 8.39, N 2.59

[a] Signal hidden by solvent resonance. [b] Two overlapping signals.

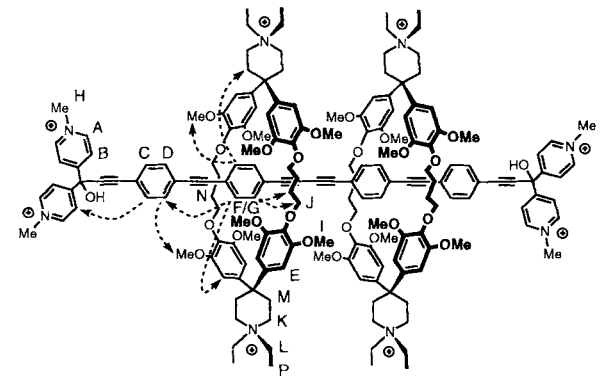

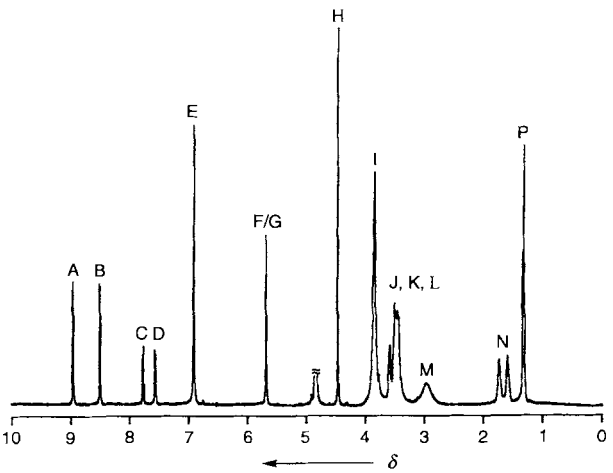

Fig. 1. 500 MHz ^{1}H NMR spectrum of **3**·8Cl in D_2O. The broken arrows indicate some negative NOEs that were important for the structure assignment. The truncated peak is due to HOD.

chemical shift timescale. At 278 K this process is slow and split signals are observed. In the ^{1}H NMR spectrum of the [2]rotaxane **2** the rims of the cyclophane are equivalent and there are only two phenylene environments, which implies that the cyclophane shuttles rapidly along the dumbbell at room temperature;[13] the signals are broader at 278 K but the shuttling process does not go into slow exchange.[14]

The electronic absorption and emission spectra of **1**, **2**, and **3** are compared in Figure 2. The absorption spectra in the 300–400 nm region are very similar because the cyclophane does not absorb significantly at wavelengths greater than 250 nm.

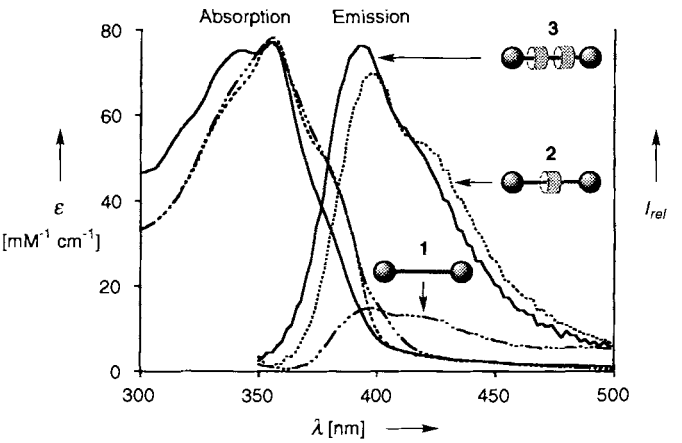

Fig. 2. UV absorption and emission (excitation 300 nm) spectra for **3**·8Cl (– –), **2**·6Cl (· · ·), and **1**·4Cl (– · · · –) in water at 20 °C at 1.0 μM concentration.

All three compounds show emission at around 400 nm when they are excited at 300 nm, but the emission intensity of **3** and **2** is about six times greater than that of **1**. The presence of the cyclophane rings in these rotaxanes appears to increase the fluorescence efficiency of the dumbbell by hindering quenching and increasing the kinetic stability of the excited state.[15] We plan to apply this methodology to synthesize conjugated polyrotaxanes as "insulated molecular wires", in which the macrocycles increase the kinetic stability of the ground state.

Experimental Procedure

1, **2**, and **3**: A solution of **4**·2Cl (210 mg, 0.196 mmol) and **5**·2Cl (100 mg, 0.196 mmol) in water (15 mL) was added to a solution of copper(I)chloride (12.9 g, 0.13 mol) and ammonium chloride (20.92 g, 0.39 mol) in water (50 mL), and the mixture was stirred under oxygen for 48 h [9]. The reaction was quenched by the addition of hydrochloric acid (50 mL, 2 N). NH_4PF_6 was added to the resulting green solution until no further precipitation occurred, and the solid product was collected by centrifugation. The crude product mixture was analyzed at this stage [10], and the three components were separated by flash column chromatography on silica eluting with methanol/2 N aqueous ammonium chloride/nitromethane [13] (7:2:1 v:v) for dumbbell **1** and [2]rotaxane **2**. The polarity was increased to methanol/2 N aqueous ammonium chloride/nitromethane (5:3:2 v:v) to elute the [3]rotaxane **3**. Each fraction was then treated with excess NH_4PF_6 to precipitate the cationic product. Each product was then recrystallized from methanol/acetone (1:1) by layering with diethyl ether, and then dried under vacuum to yield [3]rotaxane **3**·8PF 120 mg (30%), **2**·6PF_6 57 mg (27%), and dumbbell **1**·4PF_6 13 mg (9%).

Received: March 21, 1996 [Z89571E]
German version: *Angew. Chem.* **1996**, *108*, 2075–2078

Keywords: alkynes · cyclophanes · luminescence · molecular wires · supramolecular chemistry

[1] J. L. Brédas, *Adv. Mater.* **1995**, 7, 263–274; N. C. Greenham, S. C. Moratti, D. D. C. Bradley, R. H. Friend, A. B. Holmes, *Nature* **1993**, *365*, 628–630; U. Scherf, K. Müllen, *Synthesis* **1992**, 23–38; *Conjugated Polymers* (Eds.: J. L. Brédas, R. Silbey), Kluwer Academic, Dordrecht, **1991**; O. A. Patil, A. J. Heeger, F. Wudl, *Chem. Rev.* **1988**, *88*, 183–200.

[2] Rotaxanes were first prepared by solid-phase synthesis (I. T. Harrison, S. Harrison, *J. Am. Chem. Soc.* **1967**, *89*, 5723–5724) and by directed synthesis (G. Schill, H. Zollenkopf, *Liebigs Ann. Chem.* **1969**, *721*, 53–74). For an early use of the hydrophobic effect to direct rotaxane synthesis see H. Ogino, *J. Am. Chem. Soc.* **1981**, *103*, 1303–1304. For some recent rotaxanes see: a) D. B. Amabilino, J. F. Stoddart, *Chem. Rev.* **1995**, *95*, 2725–2828; b) H. W. Gibson, S. Liu, P. Lecavalier, C. Wu, Y. X. Shen, *J. Am. Chem. Soc.* **1995**, *117*, 852–874; c) F. Diederich, C. Dietrich-Buchecker, J.-F. Nierengarten, J.-P. Sauvage, *J. Chem. Soc. Chem. Commun.* **1995**, 781–782; d) F. Vögtle, M. Händel, S. Meier, S. Ottens-Hildebrandt, F. Ott, T. Schmidt, *Liebigs Ann.* **1995**, 739–743; e) A. C. Benniston, A. Harriman, V. M. Lynch, *J. Am. Chem. Soc.* **1995**, *117*, 5275–5291; f) G. Wenz, *Angew. Chem.* **1994**, *106*, 851–870; *Angew. Chem. Int. Ed. Engl.* **1994**, *33*, 803–822; g) A. Harada, J. Li, M. Kamachi, *J. Am. Chem. Soc.* **1994**, *116*, 3192–3196; *Nature* **1992**, *356*, 325–327; h) G. Wenz, B. Keller, *Angew. Chem.* **1992**, *104*, 201–204; *Angew. Chem. Int. Ed. Engl.* **1992**, *31*, 197–199; i) R. S. Wylie, D. H. Macartney, *J. Am. Chem. Soc.* **1992**, *114*, 3136–3138; j) R. Isnin, A. E. Kaifer, *ibid.* **1991**, *113*, 8188–8190.

[3] A conjugated pseudorotaxane has been reported: H. Sleiman, P. Baxter, J.-M. Lehn, K. Rissanen, *J. Chem. Soc. Chem. Commun.* **1995**, 715–716. Swager et al. have also synthesized conjugated polypseudorotaxanes in which the macrocycles are part of the covalent backbone: Q. Zhou, T. M. Swager, *J. Am. Chem. Soc.* **1995**, *117*, 12593–12602. The [2]- and [3]rotaxanes reported by J.-C. Chambron, V. Heitz, J.-P. Sauvage, *J. Am. Chem. Soc.* **1993**, *115*, 12378–12384 do not have a conjugated backbone because the aryl substituents on the porphyrins tend to lie perpendicular to the plane of the porphyrin.

[4] a) F. Diederich, *Cyclophanes*, Royal Society of Chemistry, Cambridge, **1991**; F. Diederich, *Angew. Chem.* **1988**, *100*, 372–396; *Angew. Chem. Int. Ed. Engl.* **1988**, *27*, 362–386; b) C. Seel, F. Vögtle, *ibid.* **1992**, *104*, 542–563 and **1992**, *31*, 528–549; c) J. M. Coterón, C. Vicent, C. Bosso, S. Penadés, *J. Am. Chem. Soc.* **1993**, *115*, 10066–10076; d) F. M. Menger, K. K. Catlin, *Angew. Chem.* **1995**, *107*, 2330–2333; *Angew. Chem. Int. Ed. Engl.* **1995**, *34*, 2147–2150; e) R. M. Izatt, K. Pawlak, J. S. Bradshaw, R. L. Bruening, *Chem. Rev.* **1995**, *95*, 2529–2586.

[5] S. B. Ferguson, E. M. Sanford, E. M. Seward, F. Diederich, *J. Am. Chem. Soc.* **1991**, *113*, 5410–5419. The preparation of **4** followed the published procedure except for the last two steps; we used DIBAL-H to reduce the amides to tertiary amines and then quaternized with ethyl iodide. See B. R. Peterson, T. Mordasini-Denti, F. Diederich, *Chem. Biol.* **1995**, *2*, 139–146.

[6] Stopper **5** was synthesized from di(4-pyridyl) ketone (F. L. Minn, C. L. Trichilo, C. R. Hurt, N. Filipescu, *J. Am. Chem. Soc.* **1970**, *92*, 3600–3610) by reaction with ethynylmagnesium bromide and extension by Heck coupling. The synthesis will be reported in detail elsewhere.

[7] NMR dilution experiments showed that the critical aggregation concentrations for **4** and **5** in water are both >1 mM at 298 K. Titration of **4** and **5** was carried out at 0.1 mM **5** and 0–0.6 mM **4**, leading to $>95\%$ saturation at the end of the titration. $\Delta\delta_{sat} = \delta_{free} - \delta_{bound}$.

[8] D. B. Smithrud, T. B. Wyman, F. Diederich, *J. Am. Chem. Soc.* **1991**, *113*, 5420–5426; S. B. Ferguson, E. M. Seward, F. Diederich, E. M. Sanford, A. Chou, P. Inocencio-Szweda, C. B. Knobler, *J. Org. Chem.* **1988**, *53*, 5593–5595.

[9] Our Glaser coupling conditions are derived from those of J. B. Armitage, E. R. H. Jones, M. C. Whiting, *J. Chem. Soc.* **1952**, 2014–2018.

[10] The ratios of **1**:**2**:**3** were determined by integration of the ^{1}H NMR spectrum of the crude reaction mixture. No other products were detected.

[11] The amount of fragmentation of **3** to give **4** increased with increasing cone voltage. ESI MS measurements were carried out on a VG-Bio Q instrument. We are very grateful to Dr R. T. Aplin for recording these mass spectra.

[12] The NOEs from H_C to H_B and from H_D to $H_{F,G}$ were small and could be detected reliably only with a double pulsed field gradient spin echo-Gradient NOESY experiment. We are very grateful to Dr T. D. W. Claridge for measuring these spectra.

[13] This behavior contrasts with that of some of Stoddart's molecular shuttles, which exhibit slow translational isomerism: D. B. Amabilino, P.-L. Anelli, P. R. Ashton, G. R. Brown, E. Córdova, L. A. Godínez, W. Hayes, A. E. Kaifer, D. Philp, A. M. Z. Slawin, N. Spencer, J. F. Stoddart, M. S. Tolley, D. J. Williams, *J. Am. Chem. Soc.* **1995**, *117*, 11142–11170.

[14] The ^{1}H NMR spectra of **2**·6Cl in [D$_4$]methanol give evidence of fast exchange down to 193 K. Cyclophane aryl rotation in **3**·8PF$_6$ in [D$_4$]methanol/[D$_6$]acetone gives rise to fast exchange evident in ^{1}H NMR spectra down to 233 K. The dynamic behavior of both rotaxanes is diminished in water due to hydrophobic binding between the cyclophane and the dumbbell.

[15] The fluorescence yields of **1**·4Cl, **2**·6Cl, and **3**·8Cl in water were measured by comparison with anthracene in cyclohexane as 0.04, 0.2, and 0.2%, respectively. See: *CRC Handbook of Organic Photochemistry*, (Ed.: J. C. Scaiano), CRC Press, Boca Raton **1989**. These quantum yields are independent of concentration for concentrations of less than 5 μM. The enhanced fluorescence of these rotaxanes appears to be similar to that of cyclodextrin complexes. See R. Corradini, A. Dossena, R. Marchelli, A. Panagia, G. Sartor, M. Saviano, A. Lombardi, V. Pavone, *Chem. Eur. J.* **1996**, *2*, 373–381; M. Hoshino, M. Imamura, *J. Phys. Chem.* **1981**, *85*, 1820–1823; F. Cramer, W. Saenger, H.-C. Spatz, *J. Am. Chem. Soc.* **1967**, *89*, 14–20.

Organoplatinum Building Blocks for One-Dimensional Hydrogen-Bonded Polymeric Structures

Philip J. Davies, Nora Veldman, David M. Grove, Anthony L. Spek, Bert T. G. Lutz, and Gerard van Koten*

The exploitation of the hydrogen bond in the assembly of molecules in the solid state is a topic of current interest.[1] Crystal packing of molecules can take place in a very precise manner, since the hydrogen bonds introduce a high degree of directionality and confer unique properties on the resulting molecular material.

We set out to synthesize organoplatinum complexes possessing hydrogen-bond donor (D) and hydrogen-bond acceptor (A) groups at either end of the molecule, separated by a rigid aryl spacer (**1**, Fig. 1). These features could then promote self-orga-

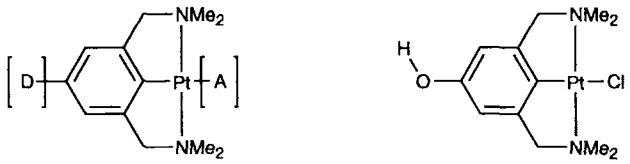

1 **2**

Fig. 1. Complex **2** possesses both hydrogen-bond donor [D] and hydrogen-bond acceptor [A] groups.

nization in the solid state through intermolecular hydrogen bonding to form a self-assembled organometallic polymeric structure containing directed, noncovalent bonds. Here we present primarily the synthesis and solid-state structure of the *para*-hydroxyaryldiamineplatinum complex **2**. This complex has all the properties required for the formation of intermolecular hydrogen bonds, namely a *para*-hydroxyl group and a potential hydrogen bond acceptor in the chloride ligand.

The synthetic strategy relies on initial synthesis of the required organic ligand (**3**) (Scheme 1) in which the hydroxyl group is protected as its *tert*-butyldimethylsilyl (TBDMS) ether.[2] The ligand **3** was isolated in 45% yield based on the starting compound, 5-hydroxyisophthalic acid.

Reaction of **3** with *n*-butyllithium in hexane afforded **4** (Scheme 2) in which exclusively the position *ortho* to both CH_2NMe_2 arms was lithiated. This was established by quenching a sample of the lithiated compound with D_2O and deducing the position of deuterium incorporation by ^{1}H NMR spectroscopy. We propose a dimeric structure for **3** in both the solid state and in solution, based on studies of similar species.[3]

[*] Prof. Dr. G. van Koten, Dr. P. J. Davies, Dr. D. M. Grove
Department of Metal-Mediated Synthesis, Debye Institute, Utrecht University
Padualaan 8, NL-3584 CH Utrecht (The Netherlands)
Fax: Int. code +(30)252-3615
e-mail: vankoten@xray.chem.ruu.nl

Dr. A. L. Spek, N. Veldman
Bijvoet Center for Biomolecular Research, Utrecht University (The Netherlands)

B. T. G. Lutz
Department of Analytical Molecular Spectrometry, Utrecht University (The Netherlands)

[**] This work was supported in part (A. L. S. and N. V.) by the Netherlands Foundation of Chemical Research (SON) with financial aid from the Netherlands Organization for Scientific Research (NWO). The Royal Society of London is thanked for the award of an ESEP Fellowship to P. J. D.

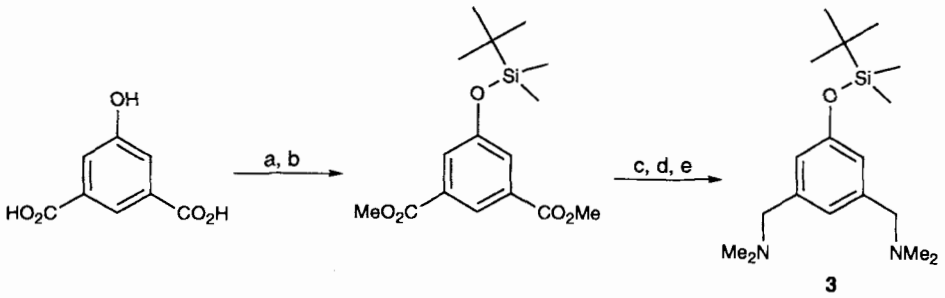

Scheme 1. Synthesis of the TBDMS-protected aryldiamine ligand **3** [2b]. a) MeOH, H_2SO_4, Δ; b) *t*BuMe$_2$SiCl, NEt_3, THF, Δ; c) $LiAlH_4$, Et_2O; d) $MeSO_2Cl$, NEt_3, CH_2Cl_2, Δ; e) $NHMe_2 \cdot HCl$, NEt_3, DMF.

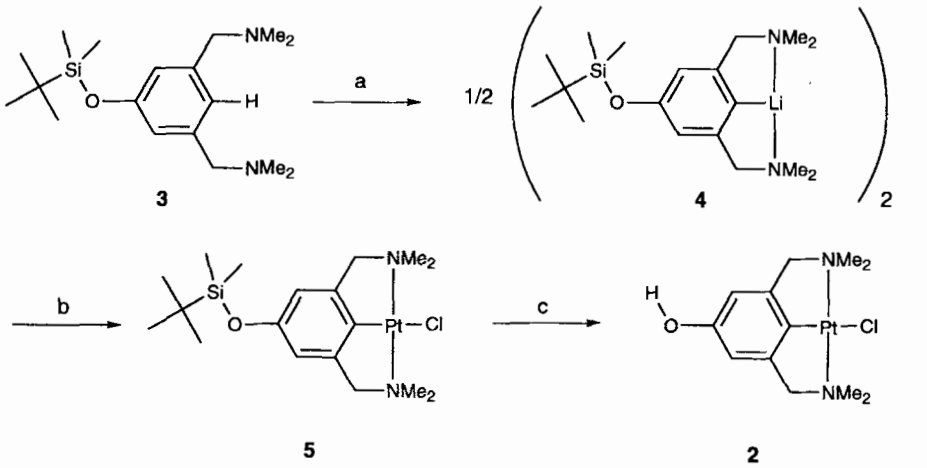

Scheme 2. Lithiation, transmetalation, and deprotection of the aryldiamine ligand **3**. a) *n*BuLi, C_6H_{14}, −78 °C; b) $[PtCl_2(SEt_2)_2]$, Et_2O; c) NBu_4F, THF, H_2O.

Transmetalation of **4** with $[PtCl_2(SEt_2)_2]$ afforded the protected aryldiamineplatinum complex **5**. Reaction of **5** with tetrabutylammonium fluoride trihydrate in THF/water then afforded the *para*-hydroxyaryldiamineplatinum complex **2**.

Complex **2** self-assembles to form, in the solid state, neutral, linear, regularly repeating, one dimensional arrays through the formation of intermolecular hydrogen bonds from the phenolic hydrogen atom to the chloride ligand of an adjacent molecule of **2** (Fig. 2).[4] A cooperative hydrogen bonding motif in which oxygen acts as both hydrogen bond donor and acceptor is not observed. All aryldiamineplatinum molecules align in the same direction in each polymer chain as a consequence of the hydrogen bonding. An equal number of individual polymer chains are, however, oriented in opposite directions, and macroscopic directionality throughout the whole crystal is therefore cancelled out. The hydroxyl hydrogen atom was located in the difference Fourier map and included in the refinement. The environment around the oxygen atom has been examined for close C–H···O contacts, and none shorter than 2.600(14) Å (O1···H9b) were found, that is, only one type of hydrogen bond motif is present. Variable-temperature infrared spectroscopic studies of **2** have been carried out to obtain further insight into the nature of the intermolecular hydrogen bonding. In the solid state at ambient temperature (296 K, Poflu mull) an O–H stretching band at 3284 cm^{-1} shows a red-shift upon cooling (3277 cm^{-1} at 180 K and 3270 cm^{-1} at 87 K), a phenomenon characteristic of hydrogen bonding (Fig. 3).[5] This temperature effect is due to a strengthening of the intermolecular hydrogen bond on cooling with concomitant weakening of the O–H bond. Shoulders on each side of the OH band originate from coupling interactions with lattice vibrations, which occur at low wavenumber (<150 cm^{-1}).[6] Upon cooling, the intensities of the shoulders decrease and that of the O–H mode increases significantly; this behavior is characteristic of hydrogen bonding. An IR spectrum of **2** in chloroform solution at 296 K shows a non-hydrogen-bonded O–H mode at 3598 cm^{-1}, which can be assigned to an unassociated phenolic hydroxyl group.[7] In this spectrum there is also a residual hydrogen-bonded O–H mode at 3284 cm^{-1}. This indicates that, even in solution, there is a degree of hydrogen bonding present that can lead to the formation of dimers or higher oligomers. It is possible to calculate an approximate hydrogen-bond enthalpy (ΔH°) from the difference in stretching frequency between the O–H bond observed in the solution spectrum and that in the solid-state spectrum;[8] the value of −22.7 kJ mol^{-1} obtained is indicative of a moderately strong hydrogen bond.

Here we have demonstrated the usefulness of the intermolecular hydrogen bond in the self-assembly of an organometallic compound in the solid state to form one-dimensional polymeric structures. Research is currently in progress to introduce chiral, identi-

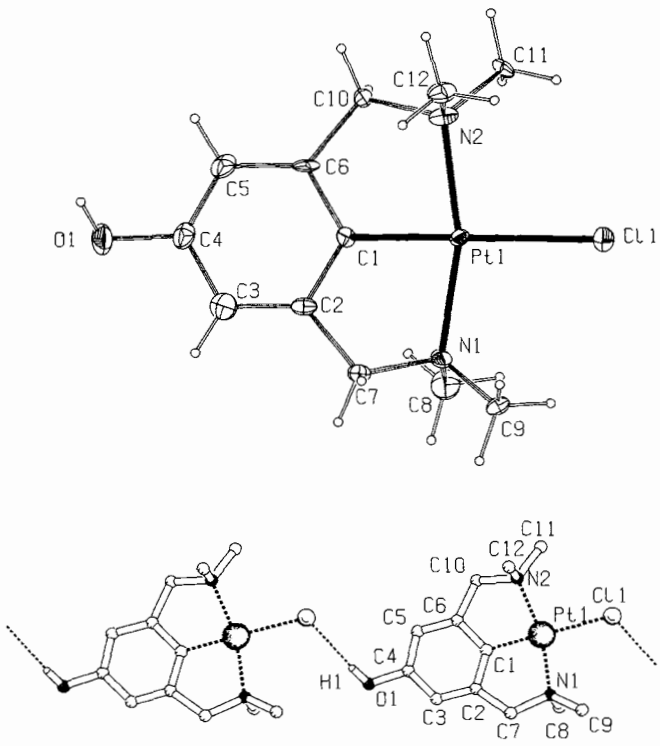

Fig. 2. Top: ORTEP plot of the structure of **2** in the solid state. Bottom: PLUTON plot showing two molecules of **2** linked by an intermolecular hydrogen bond where the hydrogen bond donor is O and the hydrogen bond acceptor is Cl. Selected bond lengths [Å] and angles [°]: Pt1–Cl1 2.434(2), Pt1–C1 1.915(9), O1–H1 0.84(13), Cl1···H1 2.32(13); Cl1···H1–O1 161(15), Pt1–Cl1···H1 115(3).

 © VCH Verlagsgesellschaft mbH, D-69451 Weinheim, 1996 0570-0833/96/3517-1960 $ 15.00+.25/0

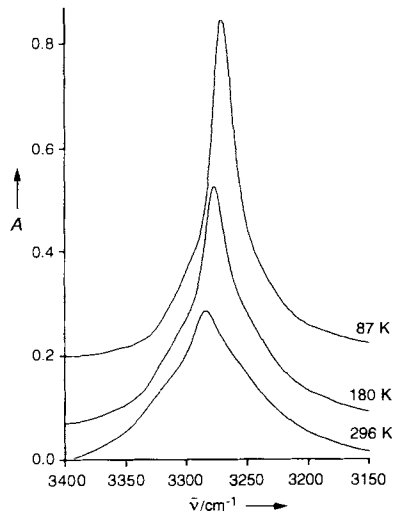

Fig. 3. The variable-temperature, solid-state infrared spectrum of **2** showing the O–H stretching region. The spectra are offset along the y axis for clarity; hence the units for the absorbance (A) are arbitrary.

cally configurated substituents into the aryldiamine skeleton to give a noncentrosymmetric space group on crystallization, as this could give rise to desirable macroscopic properties such as optical nonlinearity.

Experimental Procedure

2: Tetrabutylammonium fluoride trihydrate (0.076 g, 0.24 mmol) was dissolved in THF (20 mL). The chloroplatinum compound **5** (0.131 g, 0.24 mmol) was added as a solid, and the mixture was stirred for 2 h at room temperature. Water (0.2 mL) was then added, and the reaction mixture stirred at room temperature for another 12 h. The precipitate that formed was collected by filtration, washed with hexane, and dried in vacuo to yield a colorless solid (0.060 g, 58%). A water-free sample for elemental analysis was obtained by drying the sample in vacuo over calcium oxide. Single crystals suitable for X-ray crystallography were grown by slow evaporation of a solution of **2** in dichloromethane/dimethylsulfoxide. Elemental analysis: calcd for $C_{12}H_{19}ClN_2OPt$: C 32.92, H 4.37, N 6.40%; found: C 33.06, H 4.42, N 6.36%; ^{1}H NMR (200 MHz, [D$_1$]chloroform/[D$_6$]DMSO, 25 °C, TMS): $\delta = 2.55$ (s, ^3J(Pt,H) = 37.4 Hz, 12H, NMe_2), 3.49 (s, ^3J(Pt,H) = 45.8 Hz, 4H, CH_2), 5.88 (s, 2H, aromatic), 8.00 (s, 1H, OH); ^{13}C NMR (50 MHz, [D$_1$]chloroform/[D$_6$]DMSO, 25 °C, TMS): $\delta = 154.3$ (C_{para}), 143.4 (^2J(Pt,C) = 81.0 Hz, C_{ortho}), 133.1 (^1J(Pt,C) not observed, C_{ipso}), 106.7 (^3J(Pt,C) = 38.3 Hz, C_{meta}), 77.3 (^2J(Pt,C) = 62.0 Hz, CH_2), 54.0 (^2J(Pt,C) = 15.0 Hz, NMe_2).

Received: April 29, 1996 [Z 8884 IE]
German version: *Angew. Chem.* **1996**, *108*, 2078–2081

Keywords: crystal engineering · hydrogen bonds · organometallic polymers · platinum compounds · self-assembly

[1] G. R. Desiraju, *Angew. Chem.* **1995**, *107*, 2541; *Angew. Chem. Int. Ed. Engl.* **1995**, *34*, 2311; D. Braga, F. Grepioni, P. Sabatino, G. R. Desiraju, *Organometallics* **1994**, *13*, 3532; S. B. Copp, K. T. Holman, J. O. S. Sangster, S. Subramanian, M. J. Zaworotko, *J. Chem. Soc. Dalton Trans.* **1995**, 2233; F. J. Hoogesteger, L. W. Jenneskens, H. Kooijman, N. Veldman, A. L. Spek, *Tetrahedron* **1996**, *52*, 1773; J. Bernstein, R. E. Davis, L. Shimoni, N-L. Chang, *Angew. Chem.* **1995**, *107*, 1689; *Angew. Chem. Int. Ed. Engl.* **1995**, *34*, 1555.

[2] a) We thank Professor D. N. Reinhoudt for communicating the details for the steps a, b, c, and d (Scheme 1) (cf. Step a: 5-(OH)C_6H_3-1,3-$(CO_2H)_2$ (0.22 mol), MeOH (250 mL), H_2SO_4 (4.6 mL), Δ, 12 h, 99% (recrystallized from MeOH); step b: 5-(OH)C_6H_3-1,3-$(CO_2Me)_2$ (48.0 mmol), THF (100 mL), *t*$BuMe_2SiCl$ (50.0 mmol), NEt_3 (75.0 mmol), Δ, 4 h, 69% (recrystallized from MeOH); step c: 5-(*t*$BuOSiMe_2$)C_6H_3-1,3-$(CO_2Me)_2$ (21.0 mmol), Et_2O (150 mL), $LiAlH_4$ (43.0 mmol), room temperature (RT), 20 h, 82%; step d: 5-(*t*$BuOSiMe_2$)C_6H_3-1,3-$(CH_2OH)_2$ (21.0 mmol), CH_2Cl_2 (150 mL), $MeSO_2Cl$ (49.0 mmol), NEt_3 (49.0 mmol), Δ, 12 h, 89%; step e: 5-(*t*$BuOSiMe_2$)C_6H_3-1,3-$(CH_2Cl)_2$ (17.0 mmol), DMF (130 mL), $Me_2HN\cdot HCl$ (0.31 mol), NEt_3 (0.73 mol), RT, 18 h, 91%. W. T. S. Huck, F. C. J. M. van Veggel, B. L. Kropman, D. H. A. Blank, E. G. Keim, M. M. A. Smithers, D. N. Reinhoudt, *J. Am. Chem. Soc.* **1995**, *117*, 8293).

[3] J. T. B. H. Jastrzebski, G. van Koten, M. Konijn, C. H. Stam, *J. Am. Chem. Soc.* **1982**, *104*, 5490.

[4] Crystal data for **2**: $C_{12}H_{19}ClN_2OPt$, $M_r = 437.83$, colorless, transparent, needle-shaped crystals (0.63 × 0.05 × 0.05 mm), orthorhombic, space group $Pna2_1$ (no.33) with $a = 24.2238(14)$, $b = 10.1986(8)$, $c = 5.4483(14)$ Å, $V = 1346.0(4)$ Å^3, $Z = 4$, $\rho_{calcd} = 2.161$ g cm^{-3}, $F(000) = 832$, $\mu(Mo_{K\alpha}) = 106.1$ cm^{-1}, 6631 reflections measured, 2936 independent ($1.7° < \theta < 27.5°$, ω scan, $\Delta\omega = 0.87 + 0.35 \tan\theta$, $T = 150$ K, $Mo_{K\alpha}$ radiation, graphite monochromator, $\lambda = 0.71073$ Å) on an Enraf-Nonius CAD4-T diffractometer on a rotating anode. Data were corrected for Lorentzian polarization and for a linear decay of 8% of the reference reflections (212, 220, 2$\bar{2}$0) during 13 h of X-ray exposure time; empirical absorption correction (DIFABS) applied as implemented in PLATON (transmission range 0.579–1.000). The structure was solved by Patterson methods and subsequent difference Fourier techniques (DIRDIF-92). Refinement on F^2 was carried out by full-matrix least-squares techniques (SHELXL-93); no observance criterion was applied during refinement. Final $R1$ value 0.0376, for 2340 reflections with $F_o > 4.0\sigma(F_o)$, $wR2 = 0.0793$ for 2934 data, $w = 1/[\sigma^2(F_o^2) + (0.0311P)^2]$, where $P = (\mathrm{Max}(F_o^2, 0) + 2 \times F_c^2)/3$, $S = 1.024$, for 161 parameters. Maximum and minimum residual density: 0.84, −1.08 e Å^{-3}. All non-hydrogen atoms were refined with anisotropic thermal parameters. The hydrogen atoms were refined with a fixed isotropic thermal parameter related to the value of the equivalent isotropic thermal parameter of their carrier atoms, by a factor of 1.5 for the methyl groups, and 1.2 for the other hydrogen atoms. The hydroxyl hydrogen was found in the difference Fourier map and allowed to refine freely. Weights were refined in the final refinement cycles. Crystallographic data (excluding structure factors) for the structure reported in this paper have been deposited with the Cambridge Crystallographic Data Centre as supplementary publication no. CCDC-179-70. Copies of the data can be obtained free of charge on application to The Director, CCDC, 12 Union Road, Cambridge CB2 1EZ, UK (Fax: Int. code Int. +(1223)336-033; e-mail: teched@chemcrys.cam.ac.uk).

[5] Infrared studies have also been carried out on a KBr disc. In this case, partial halogen exchange occurs as evidenced by the appearance of a new O–H band at 3309 cm^{-1} (90 K), which was assigned to the Pt-Br···H–O hydrogen bond motif; the intensity of this new band increases as a function of the grinding time. This phenomenon does not, however, occur with KCl discs, which is in accord with the proposed explanation. The shift to higher wavenumber relative to the Pt–Cl···H–O motif indicates that the hydrogen bond to bromide is weaker.

[6] C. Sandorfy in *The Hydrogen Bond, Vol. 2* (Eds.: P. Schuster, G. Zundel, C. Sandorfy), North-Holland, Amsterdam, **1976**, p. 613.

[7] D. Lin-Vien, N. B. Colthup, W. G. Fateley, J. G. Grasselli, *The Handbook of Infrared and Raman Characteristic Frequencies of Organic Molecules*, Academic Press, Boston, **1991**, p. 45.

[8] The equation employed was $\Delta H^\circ = -1.28(\Delta\nu)^{1.2}$. See, for example, S. G. Kazarian, P. A. Hamley, M. Poliakoff, *J. Am. Chem. Soc.* **1993**, *115*, 9069.

Coordination Chemistry of Polyoxometalates: Rational Synthesis of the Mixed Organosilyl Derivatives of Trivacant Polyoxotungstates α-A-$[PW_9O_{34}(t\mathrm{BuSiO})_3(\mathrm{RSi})]^{3-}$ and α-B-$[AsW_9O_{33}(t\mathrm{BuSiO})_3(\mathrm{HSi})]^{3-}$**

Agnès Mazeaud, Najib Ammari, Francis Robert, and René Thouvenot*

Derivatized polyoxometalates are expected to play an increasingly greater role in catalysis, chemotherapy, and molecular science.[1] In particular, heteropolyoxometalates with an organic, organometalloid, or organometallic group anchored to the oxometalate backbone are attractive precursors for the synthesis of organic–inorganic hybrid materials. They were among the very first organometallic derivatives of polyoxometalates to be reported.[2, 3a, 3b, 4a] A number of organotin derivatives of the Lindqvist,[5] Keggin,[3, 4] and Dawson-type[4] structures have now been characterized. In contrast, organosilicon derivatives have received comparatively less attention. However, "Keggin-type" derivatives of general formula $[SiW_{11}O_{40}(RSi)_2]^{4-}$

[*] Dr. R. Thouvenot, A. Mazeaud, Dr. N. Ammari, F. Robert
Laboratoire de Chimie des Métaux de Transition
URA CNRS 419, case 42, Université Pierre et Marie Curie
4 Place Jussieu, F-75252 Paris Cedex 05, (France)
Fax: Int. code +(1)44273841
e-mail: rth@ccr.jussieu.fr

[**] This work was supported by the Centre National de la Recherche Scientifique.

(R = Et, $CH{=}CH_2$, $N{\equiv}N(CH_2)_3$, Ph, $C_{10}H_{21}$), in which an $(RSi)_2O^{4+}$ unit replaces a WO^{4+} unit, have been described.[3a, 6] We are currently investigating the reactions of chlorosilanes with trivacant polyoxotungstates.[7] Under phase-transfer conditions, dichlorosilanes, R_2SiCl_2, react with α-A-$[XW_9O_{34}]^{n-}$ ions (X = Si, $n = 10$, X = P, $n = 9$) to give the ions **1** and **2**,

α-A-$[SiW_9O_{34}(R_2Si)_3]^{4-}$ **1a**: R = Me, **1b**: R = Ph

α-A-$[PW_9O_{34}(R_2Si)_3]^{3-}$ **2a**: R = Me, **2b**: R = Ph

respectively, which have been characterized by multinuclear NMR spectroscopy.[7a] The proposed structure with C_{3v} symmetry has been confirmed by the X-ray analysis of $(nBu_4N)_4$-**1a**.[7c] Under similar conditions, reactions with trichlorosilanes, $RSiCl_3$, yield the ions **3** and **4**, respectively. The structure of **3**

α-A-$[SiW_9O_{34}(RSiO)_3(RSi)]^{4-}$ **3a**: R = H, **3b**: R = Me

3c: R = Et, **3d**: R = *n*Bu

α-A-$[PW_9O_{34}(RSiO)_3(RSi)]^{3-}$ **4a**: R = H, **4b**: R = Me

4c: R = Et, **4d**: R = *n*Bu

(C_{3v} symmetry proposed on the basis of a thorough multinuclear NMR study of **3a**)[7b] has been confirmed by the X-ray analysis of α-A-$(nBu_4N)_3(Me_2NH_2)$-**3c**.[7c] These studies have now been extended to some other chlorosilanes, for example $tBuSiCl_3$, and other trivacant polyoxotungstates, for example α-B-$[HAsW_9O_{33}]^{8-}$.

Whereas $nBuSiCl_3$ reacts with α-A-$[PW_9O_{34}]^{9-}$ ions to give **4d**, the analogous reaction with $tBuSiCl_3$ yields only **5** pre-

α-A-$[PW_9O_{34}(tBuSiOH)_3]^{3-}$ **5**

sumably because of steric crowding. The ion **7** has been obtained in a similar manner by reacting $tBuSiCl_3$ with α-B-$[HAsW_9O_{33}]^{8-}$ ions. The two ions **5** and **7** have been characterized by X-ray crystallography as their tetrabutylammonium salts.[8] Both anions display approximate C_{3v} symmetry and the structure of the parent trivacant polyoxotungstate is retained.[9] Each of the three chemically equivalent *t*BuSi(OH) units is attached to the polyoxotungstate backbone through two W-O-Si bridges (Fig. 1). The difference in composition between organosilicon and organotin derivatives, for example α-A-$[PW_9O_{34}(tBuSiOH)_3]^{4-}$ vs. $[\{\alpha\text{-A-}(PW_9O_{34})\}_2(PhSnOH_2)_3]^{9-}$[3d] or $[\{\beta\text{-A-}(PW_9O_{34})\}_2(PhSnOH)_3]^{12-}$[4b] can be ascribed to different coordination preferences between Si and Sn. ^{29}Si and ^{183}W NMR data indicate that the structures of **5** and **7** are maintained in solution (Tables 1 and 2).

The "open-structure" anions **5** and **7** react cleanly with $RSiCl_3$ in DMF to yield **6** and **8**, respectively. In the first case, the

α-A-$[PW_9O_{34}(tBuSiO)_3(RSi)]^{3-}$ **6a**: R = H, **6b**: R = Me, **6c**: R = Et

6d: R = $CH{=}CH_2$,

6e: R = CH_2-CH_2-CH_2Cl

α-B-$[AsW_9O_{33}(tBuSiOH)_3]^{3-}$ **7**

α-B-$[AsW_9O_{33}(tBuSiO)_3(RSi)]^{3-}$ **8a**: R = H

reaction has been monitored by ^{31}P NMR spectroscopy, and the reactivity of $RSiCl_3$ has been seen to decrease in the order: H > Me > Et. The ions **6** and **8** have been characterized by multi-

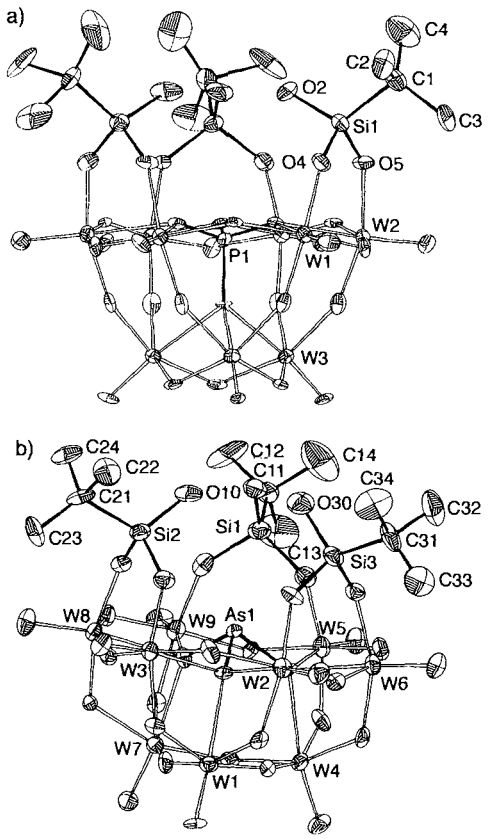

Fig. 1. a) Crystal structure of **5**. Selected distances [Å] and angles [°] (mean values): W–O_{term} 1.67, W–O(W) (corner-sharing) 1.90, W–O(W) (edge-sharing) 1.92, W–O(Si) 1.92, W–O(P) 2.36, Si–O(W) 1.64, Si–O(H) 1.68; W-O-Si, 138.2, W-O-W (corner-sharing) 152.1, W-O-W (edge-sharing) 122.6; b) Crystal structure of **7**. Selected distances [Å] and angles [°] (mean values): W–O_{term} 1.69, W–O(W) (corner-sharing) 1.90, W–O(W) (edge-sharing) 1.91, W–O(Si) 1.88, W–O(As) 2.34, Si–O(W) 1.66, Si–O(H) 1.63; W-O-Si, 139.8, W-O-W (corner-sharing) 152.3, W-O-W (edge-sharing) 122.6.

Table 1. NMR data of **5** and **6a–e** (solvent: DMF/[D_6]DMSO).

	$\delta^{31}P$	$\delta^{29}Si$		$\delta^{183}W$ [a]	
		*t*BuSi [b]	RSi [c]	3 W [d]	6 W [e]
5	−15.9	−46.42	–	−81.2	−156.4
6a	−16.91	−59.06	−96.86	−77.8	−153.7
		$^3J_{Si-H}$ = 3.8 Hz [f]	$^1J_{Si-H}$ = 299.7 Hz		
6b	−16.8	−60.16	−80.08	−80.0	−154.5
			$^2J_{Si-H}$ = 8.8 Hz		
6c	−16.78	−60.21	−80.24	−78.0	−155.7
6d	−16.74	−59.63	−94.12	−78.7	−155.5
			J_{Si-H} = 9.7 Hz		
6e	−17	−60.07	−81.90	−77.9	−155.9

[a] Tungsten–tungsten coupling about 22 Hz. [b] Complex multiplet (^3J(Si,H) ca. 6.7 Hz); tungsten satellite signals in proton-decoupled spectra (^2J(Si,W) ca. 7 Hz). [c] More or less complex multiplet, depending on R: **6a**, doublet; **6b**, quartet; **6d**, pseudo quintet. [d] Doublet (^2J(P,W) ca. 1 Hz). [e] Doublet (^2J(P,W) ca. 1.6 Hz). [f] doublet in selectively decoupled spectrum (coupling with *H*Si).

Table 2. NMR data of **7** and **8a** (solvent: DMF/[D_6]DMSO).

	$\delta^{29}Si$		$\delta^{183}W$ [a]	
	*t*BuSi [b]	RSi	3 W	6 W
7	−44.56	–	−127.1	−132.7
8a	−55.51	−90.66 (d)	−125.3	−136.4
		$^1J_{Si-H}$ = 308.8 Hz		

[a] Tungsten–tungsten coupling about 9 Hz. [b] Complex multiplet (^3J(Si,H) ca. 6.7 Hz); tungsten satellite signals in proton-decoupled spectra (^2J(Si,W) ca. 9.5 Hz).

 © VCH Verlagsgesellschaft mbH, D-69451 Weinheim, 1996 0570-0833/96/3517-1962 $ 15.00+.25/0

nuclear NMR spectroscopy (Tables 1 and 2). The ion **6a** provides a typical example. Its ^{29}Si NMR spectrum in solution exhibits two signals with a multiplicity of 3:1 (Fig. 2). The low-frequency doublet (1Si, $\delta = -96.86$, $^{1}J_{Si,H} = 299.7$ Hz) is assigned to the silicon center of the capping group HSi, and the high-frequency signal (3Si, $\delta = -59.06$) appears as a poorly resolved multiplet due to coupling with the nine protons of the *t*Bu group ($^{3}J_{Si,H}$ ca. 6.7 Hz) and to the one H atom of the capping HSi group: this signal reduces to a doublet ($^{3}J_{Si,H} = 3.8$ Hz) in the selectively decoupled spectrum (Fig. 2b).

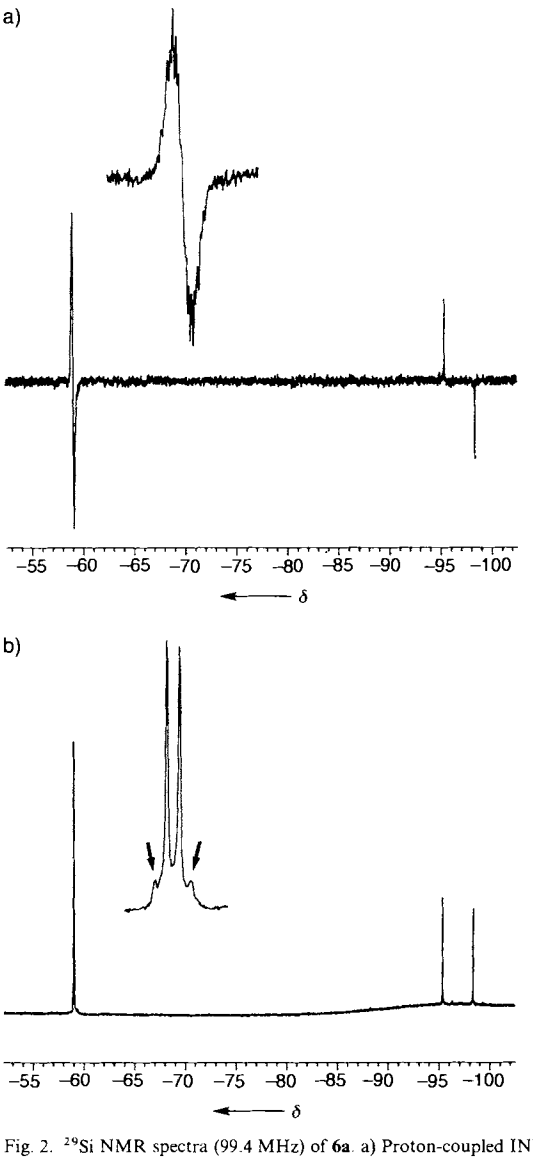

Fig. 2. ^{29}Si NMR spectra (99.4 MHz) of **6a**. a) Proton-coupled INEPT spectrum, with abscissa expansion of the high-frequency *t*BuSi signal. b) Inverse-gated selectively decoupled spectrum, with abscissa expansion of the high-frequency *t*BuSi signal showing the tungsten satellite signals (arrows).

Tungsten satellite signals appear around the high-frequency signal in the proton-decoupled spectrum ($^{2}J_{Si,W}$ ca. 7 Hz). The ^{183}W NMR spectrum of **6a** displays two signals with a multiplicity of 2:1 and a mutual coupling $^{2}J_{W,W}$ of about 22 Hz (Fig. 3); in addition, each line is split into a doublet due to coupling with the phosphorus atom ($^{2}J_{P,W} \approx 1.6$ and 1 Hz, respectively). Taken together these data are consistent with a "closed-structure" with C_{3v} symmetry, similar to that of **3**.[7b]

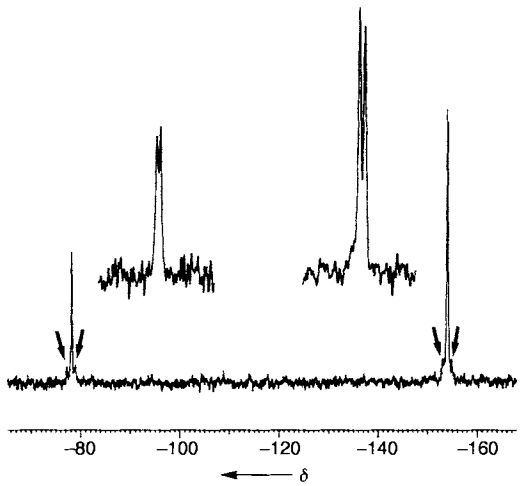

Fig. 3. ^{183}W NMR (12.5 MHz) spectrum of **6a**. Tungsten satellite signals are marked by arrows. The abscissa expansions (after resolution enhancement) clearly show the doublet structure due to the $^{2}J(W,P)$ couplings.

The characterization of **5** and **7**, and the formation of **6** and **8** from **5** and **7**, respectively, support the reaction pathway shown in Scheme 1 for the reactivity of trichlorosilanes with trivacant polyoxotungstates.

$$3\,RSiCl_3 + 9\,H_2O \longrightarrow 3\,RSi(OH)_3 + 9\,HCl$$

$$\alpha\text{-A-}[PW_9O_{34}]^{9-} + 3\,RSi(OH)_3 \longrightarrow \alpha\text{-A-}[PW_9O_{34}(RSiOH)_3]^{3-} + 6\,OH^- \text{ (heterogeneous)}$$

$$\alpha\text{-A-}[PW_9O_{34}(RSiOH)_3]^{3-} + R'SiCl_3 \longrightarrow \alpha\text{-A-}[PW_9O_{34}(RSiO)_3(R'Si)]^{3-} + 3\,HCl \text{ (homogeneous)}.$$

Scheme 1.

These results open up new perspectives in the chemistry of organosilicon derivatives of polyoxotungstates. Indeed, it may be possible to construct interconnected polyoxometalate networks through reaction of "open-structure" species, such as **5** and **7**, with polysilanes. These reactions are currently under investigation.

Experimental Procedure

$(n\text{Bu}_4\text{N})_3$-**5**·0.5 MeCN: To a well-stirred suspension of α-A-$K_9[PW_9O_{34}]\cdot 16H_2O$ [10a] (10 g, 3.48 mmol) in dry MeCN (200 mL) under argon were added solid $n\text{Bu}_4\text{NBr}$ (6 g, 18.6 mmol) and then *t*BuSiCl$_3$ (2.1 g, 10.1 mmol); the mixture was stirred overnight at 0 °C. After separation of the white solid (KCl + KBr), white crystals of $(n\text{Bu}_4\text{N})_3$-**5** formed upon slow evaporation of the resulting solution in an open vessel at room temperature. The crude compound was recrystallized from MeCN. Yield: 7.8 g (67 %). Compound $(n\text{Bu}_4\text{N})_3$-**7** was similarly obtained in 60 % yield from α-B-$K_8[HAsW_9O_{33}]\cdot x H_2O$ [10b].

$(n\text{Bu}_4\text{N})_3$-**6a**: **5** (3 g, 0.91 mmol) was dissolved in dry DMF (10 mL) under argon and $HSiCl_3$ (0.2 mL, 2 mmol) was added. The solution was stirred overnight at room temperature and then was set aside. White crystals of $(n\text{Bu}_4\text{N})_3$-**6a** formed within a few days. Yield: 1.43 g (70 %). $(n\text{Bu}_4\text{N})_3$-**6b**–**e** were similarly obtained from $MeSiCl_3$, $EtSiCl_3$, $CH_2{=}CHSiCl_3$ and $CH_2ClCH_2CH_2SiCl_3$, respectively, and $(n\text{Bu}_4\text{N})_3$-**8a** was similarly prepared by reaction of $HSiCl_3$ on $(n\text{Bu}_4\text{N})_3$-**7**.

Received: March 5, 1996 [Z 8897 IE]
German version: *Angew. Chem.* **1996**, *108*, 2089–2091

Keywords: NMR spectroscopy · polyoxometalates · silicon compounds · tungsten compounds

[1] *Polyoxometalates: From Platonic Solids to Anti-Retroviral Activity*, (Eds.: M. T. Pope, A. Müller), Kluwer, Dordrecht, **1994**.
[2] R. K. C. Ho, W. G. Klemperer, *J. Am. Chem. Soc.* **1978**, *100*, 6772.
[3] a) W. H. Knoth, *J. Am. Chem. Soc.* **1979**,*101*, 759; b) W. H. Knoth, *ibid.* **1979**, *101*, 2211; c) P. J. Domaille, W. H. Knoth, *Inorg. Chem.* **1983**, *22*, 818; d) W. H. Knoth, P. J. Domaille, R. D. Farlee, *Organometallics* **1985**, *4*, 62.
[4] a) F. Zonnevijlle, M. T. Pope, *J. Am. Chem. Soc.* **1979**, *101*, 2731; b) F. Xin, M. T. Pope, *Organometallics* **1994**, *13*, 4881.
[5] B. Krebs, R. Klein in *Polyoxometalates: From Platonic Solids to Anti-Retroviral Activity*, (Eds.: M. T. Pope, A. Müller), Kluwer, Dordrecht, **1994**, p. 41.
[6] P. Judeinstein, C. Deprun, L. Nadjo, *J. Chem. Soc. Dalton Trans.* **1991**, 1991.
[7] a) N. Ammari, Thesis, Université Pierre et Marie Curie, Paris, **1993**; b) N. Ammari, G. Hervé, R. Thouvenot, *New J. Chem.* **1991**, *15*, 607; c) N. Ammari, F. Robert, R. Thouvenot, unpublished results.
[8] Crystal data of $(n\mathrm{Bu_4N})_3$-**5**·0.5 MeCN: rhombohedric, space group $R\bar{3}c$, $M_r = 3284.16$, $Z = 6$, $a = b = 22.420(2)$, $c = 35.807(8)$ Å, $V = 15586(82)$ Å^3, $\rho_{calc} = 2.10$ g cm^{-3}, $1 < \theta < 25$, $\lambda(\mathrm{Mo_{K\alpha}}) = 0.71069$ Å, $\mu = 102.5$ cm^{-1}; 3042 unique reflections collected; 348 parameters refined; $R = 0.042$, $R_w = 0.046$ ($w = 1.0$) for 1861 reflections with $I > 3\sigma(I)$. Crystal data of $(n\mathrm{Bu_4N})_3$-**7**: monoclinic, space group $P2_1/c$, $M_r = 3291.6$, $Z = 4$, $a = 14.518(5)$, $b = 27.017(7)$, $c = 26.626(7)$ Å, $\beta = 96.51(2)°$, $V = 10376(29)$ Å^3, $\rho_{calc} = 2.11$ g cm^{-3}, $1 < \theta < 25$, $\lambda(\mathrm{Mo_{K\alpha}}) = 0.71069$ Å, $\mu = 105.7$ cm^{-1}; 18132 unique reflections collected; 1011 parameters refined; $R = 0.059$, $R_w = 0.064$ ($w = 1.0$) for 5308 reflections with $I > 3\sigma(I)$. Both structures were solved by direct methods; final refinements were carried out with anisotropic thermal parameters for all atoms except for the molecule of MeCN in $(n\mathrm{Bu_4N})_3$-**5**·0.5 MeCN; hydrogen atoms were not introduced. Further details of the crystal structure investigations may be obtained from the Fachinformationszentrum Karlsruhe, D-76344 Eggenstein-Leopoldshafen (Germany), on quoting the depository numbers CSD-391005, and CSD-391006.
[9] The anion **5** is also obtained starting from β-A-$\mathrm{Na_8H[PW_9O_{34}]}\cdot x\mathrm{H_2O}$ (R. Massart, R. Contant, J.-M. Fruchart, J.-P. Ciabrini, M. Fournier, *Inorg. Chem.* **1977**, *16*, 2916), which, in this case, implies the $\beta \rightarrow \alpha$ isomerization of the tungstophosphate framework during the reaction.
[10] a) R. Contant, *Can. J. Chem.* **1987**, *65*, 568; b) α-B-$\mathrm{K_8[HAsW_9O_{33}]}\cdot x\mathrm{H_2O}$ was prepared by following the procedure described for α-B-$\mathrm{Na_8[HAsW_9O_{33}]}\cdot x\mathrm{H_2O}$, except that KCl was added to the solution prior to the crystallization of the sodium salt: M. Leyrie, Thesis, Université Pierre et Marie Curie, **1984**.

Photoinduced Electron Transfer between Multifunctional Porphyrin and Ubiquinone Analogues Linked by Several Hydrogen-Bonding Interactions**

Takashi Hayashi,* Takashi Miyahara, Shigeichi Kumazaki, Hisanobu Ogoshi,* and Keitaro Yoshihara

In the last decade, electron transfer (ET) has received a great deal of attention due partly to its importance in biological systems. Particularly, the quinone–linker–porphyrin triad seems to be one of the most suitable combinations to elucidate the mechanism of ET, and many unique porphyrin–quinone compounds have been designed and discussed.[1, 2] However, studies on noncovalently linked porphyrin–quinone systems with specific donor–acceptor interactions such as hydrogen bonding remain quite limited,[3, 4] although in nature ET often proceeds in an assembly of several chromophores that are noncovalently connected.[5] Recently we reported the molecular recognition of face-to-face pairing between porphyrin and ubiquinone through several hydrogen bonds.[6] In this paper, we wish to report the intracomplex ET for specific porphyrin–quinone complexes in which weak chemical interactions hold the donor and acceptor in a cofacial orientation.

We prepared two zinc porphyrins, zinc(II) *meso*-α,α,α,α-tetra(2-hydroxy-1-naphthyl)porphyrin (**1**) and zinc(II) *meso*-α,α,α,α-tetra(7-hydroxy-1-naphthyl)porphyrin (**2**) from each free-base porphyrin.[6a, d, 7] The face-to-face interaction between zinc porphyrin and tetramethoxy-*p*-benzoquinone (**3**) has been characterized by ^{1}H NMR and visible absorption spectroscopy,

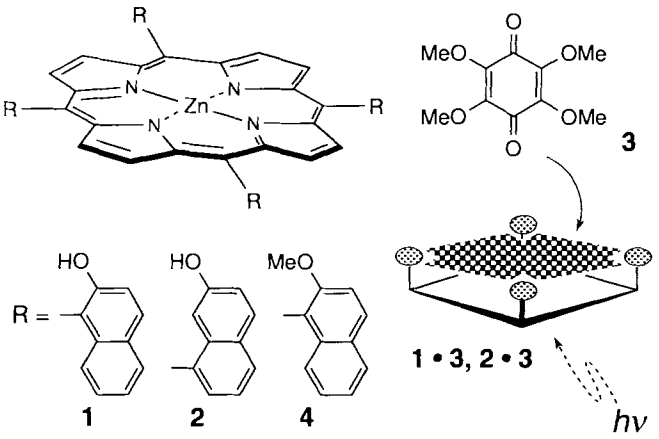

and these affinities were determined by titrimetric measurement of visible spectra in the region of 550–700 nm which gave clear isosbestic points ($K_a(\mathbf{1}\cdot\mathbf{3}) = 2.5 \times 10^5\ \mathrm{M}^{-1}$ and $K_a(\mathbf{2}\cdot\mathbf{3}) = 2.2 \times 10^3\ \mathrm{M}^{-1}$ in toluene at 298 K). The Stern–Volmer plots indicate efficient fluorescence quenching of **1** and **2** in the low concentration range of quinone ($c(\mathbf{3}) < 5 \times 10^{-3}$ M). In contrast, no fluorescence quenching of zinc(II) *meso*-α,α,α,α-tetra(2-methoxy-1-naphthyl)porphyrin (**4**) was detected in the same concentration range of quinone. These findings indicate that static quenching of fluorescence of **1** and **2** occurs by ET from the photoexcited state to **3** in the face-to-face mode. From CPK molecular models the distances between porphyrin and the quinone rings are estimated to be 3.5 (for **1**·**3**) and 6.0 Å (for **2**·**3**).[8]

The time-resolved fluorescence measurements of **1** and **2** in dry toluene reveal monoexponential decay with a lifetime of 2.0 ± 0.1 and 2.2 ± 0.1 ns, respectively.[9] Figure 1a shows the transient absorption spectra of **1** excited by dye laser pulses (570 nm, fwhm ≤ 3 ps).[10] The spectra display a broad excited state absorption in the 615–750 nm region with a dip at 650 nm due to stimulated emission. These features are characteristic of a zinc porphyrin singlet excited state. There was no substantial change in the spectra recorded with between 5 and 45 ps delays after excitation by a laser pulse, which is consistent with the lifetime of the fluorescence. Qualitatively similar results were obtained for **2**.

The transient absorption spectra of **1** and **2** in the presence of **3** (Fig. 1b) show a significant time-dependent positive absorption at 640 nm, which is distinctly different from those without **3** (Fig. 1a). The spectra are characteristic of zinc porphyrin

[*] Dr. T. Hayashi, Prof. H. Ogoshi, T. Miyahara
Department of Synthetic Chemistry and Biological Chemistry
Faculty of Engineering, Kyoto University
Kyoto 606-01 (Japan)
Fax: Int. code +(75)753-4979
S. Kumazaki, Prof. K. Yoshihara
Institute for Molecular Science, Okazaki, Aichi 444 (Japan)

[**] This work was supported by a Grant-in-Aid for Specially Promoted Research (No. 04101003) from the Japanese Ministry of Education, Science, and Culture.

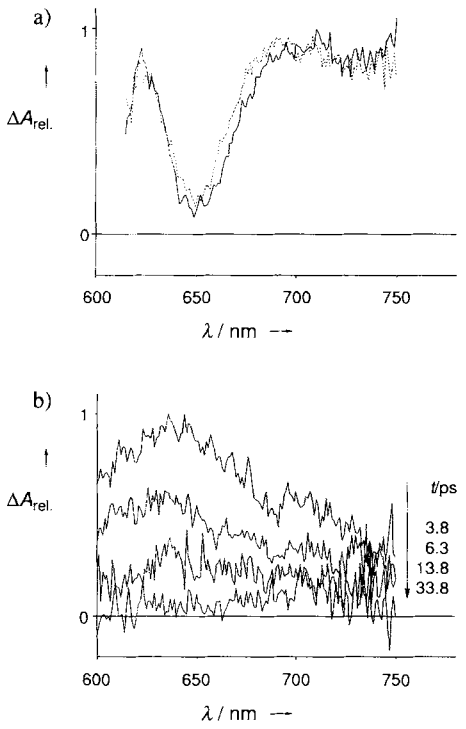

Fig. 1. a) The transient spectra upon excitation (570 nm) of porphyrin **1** in toluene (1.69×10^{-4} M) at 5.0 ps (solid line) and 45.0 ps (broken line) delays. b) Transient spectra of the porphyrin **1** (1.69×10^{-4} M) at 3.8, 6.3, 13.8, and 33.8 ps after excitation at 570 nm in the presence of quinone **3** (8.94×10^{-3} M) in toluene, showing the disappearance of the cation radical.

cation radical.[5b, 11, 12] Immediately after the excitation, the spectra are already free of the dip at 650 nm characteristic of excited state of zinc porphyrin. Forward ET rate constants were estimated to be greater than or equal to 4×10^{11} s^{-1} (limited by the pulse width and signal-to-noise ratio) for both samples. The decays of the radical pairs monitored at 650 nm (Fig. 2)

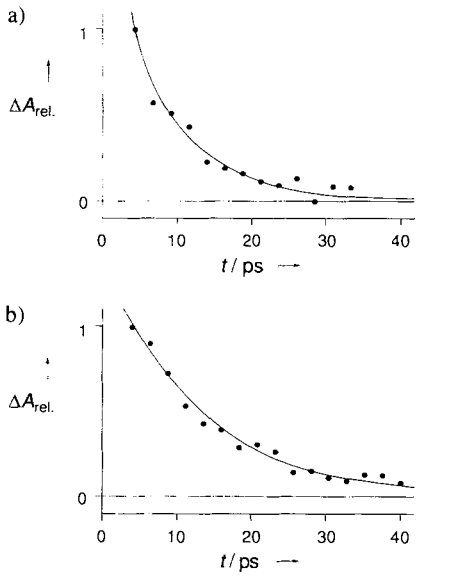

Fig. 2. Transient absorption kinetics after the full rise of the signal at 650 ± 2 nm for **1** (1.69×10^{-4} M) (a) and **2** (2.36×10^{-4} M) (b) in toluene following a 570 nm laser flash in the presence of **3** (concentration for (a) 8.94×10^{-3} M and for (b) 9.33×10^{-3} M).

were fitted to monoexponential curves with time constants of $(1.1 \pm 0.4) \times 10^{11}$ s^{-1} for **1** and $(6.8 \pm 0.3) \times 10^{10}$ s^{-1} for **2**. In contrast, the transient absorption spectra of zinc(II) *meso*-α,α,α,α-tetra(2-methoxy-1-naphthyl)porphyrin (**4**) even in the presence of a large excess of **3** exhibited no radical species (data not shown).

In conclusion, our present work demonstrates the first example of an ET complete in the picosecond range between zinc porphyrin and quinone linked in face-to-face mode by specific noncovalent interaction. The forward and backward ET rate constants in this work are at least as large as those reported in covalently bridged porphyrin–quinone systems.[13] The rate of ET is not limited by diffusion processes of donor or acceptor, and the association by hydrogen bonding seems to be stable during the period of excitation, charge separation, and recombination processes. Further work on the kinetics of ET reaction to elucidate the mechanism by use of different quinones and porphyrins is in progress.

Received: May 6, 1996 [Z 8905 IE]
German version: *Angew. Chem.* **1996**, *108*, 2096–2098

Keywords: electron transfer · hydrogen bonding · molecular recognition · porphyrinoids · quinones

[1] Recent reviews on ET in covalently linked porphyrin–quinone compounds: a) H. Kurreck, M. Huber, *Angew. Chem.* **1995**, *107*, 929; *Angew. Chem. Int. Ed. Engl.* **1995**, *34*, 849; b) M. R. Wasielewski, *Chem. Rev.* **1992**, *92*, 435; c) J. L. Sessler, *Isr. J. Chem.* **1992**, *32*, 449; d) V. V. Borovkov, R. P. Evstigneeva, L. N. Strekova, E. I. Filippovich, *Russ. Chem. Rev.* **1989**, *58*, 602.

[2] ET in quinone-capped porphyrins: a) J. S. Lindsey, D. C. Mauzerall, H. Linschitz, *J. Am. Chem. Soc.* **1983**, *105*, 6528; b) J. S. Lindsey, J. K. Delaney, D C. Mauzerall, H. Linschitz, *ibid.* **1988**, *110*, 3610; c) J. K. Delaney, D. C. Mauzerall, J. S. Lindsey, *ibid.* **1990**, *112*, 957; d) C. Krieger, J. Weiser, H. A. Staab, *Tetrahedron Lett.* **1985**, *26*, 6055; e) D. Mauzerall, J. Weiser, H. Staab, *Tetrahedron* **1989**, *45*, 4807; f) H. A. Staab, J. Weiser, E. Baumann, *Chem. Ber.* **1992**, *125*, 2275; g) W. F. R. Klann, F. Laermer, T. Elsaesser, E. Baumann, M. Futscher, H. A. Staab, *Chem. Phys. Lett.* **1992**, *190*, 567; h) F. Pöllinger, H. Heitele, M. E. Michel-Beyerle, C. Anders, M. Futscher, H. A. Staab, *ibid.* **1992**, *198*, 645; i) H. Heitele, F. Pöllinger, T. Häberle, M. E. Michel-Beyerle, H. A. Staab, *J. Phys. Chem.* **1994**, *98*, 7402; j) P. Leighton, J. K. M. Sanders, *J. Chem. Soc. Chem. Commun.* **1985**, 24; k) M. P. Irvine, R. J. Harrison, G. S. Beddard, P. Leighton, J. K. M. Sanders, *J. Chem. Phys.* **1986**, *104*, 315; l) A. Osuka, K. Maruyama, S. Hirayama, *Tetrahedron*, **1989**, *45*, 4815.

[3] a) Y. Aoyama, M. Asakawa, Y. Matsui, H. Ogoshi, *J. Am. Chem. Soc.* **1991**, *113*, 6233; b) Y. Kuroda, M. Ito, T. Sera, H. Ogoshi, *ibid.* **1993**, *115*, 7003.

[4] a) A. Harriman, Y. Kubo, J. L. Sessler, *J. Am. Chem. Soc.* **1992**, *114*, 388; b) J. L. Sessler, B. Wang, A. Harriman, *ibid.* **1993**, *115*, 10418; c) A. Berman, E. S. Izraeli, H. Levanon, B. Wang, J. L. Sessler, *ibid.* **1995**, *117*, 8252.

[5] a) P. Tecilla, R. P. Dixon, G. Slobodkin, D. S. Alavi, D. H. Waldeck, A. D. Hamilton, *J. Am. Chem. Soc.* **1990**, *112*, 9408; b) C. Turró, C. K. Chang, G. E. Leroi, R. I. Cukier, D. G. Nocera, *ibid.* **1992**, *114*, 4013; c) J. A. Roberts, J. P. Kirby, D. G. Nocera, *ibid.* **1995**, *117*, 8051; d) P. J. F. deRege, S. A. Williams, M. J. Therien, *Science* **1995**, *269*, 1409; e) A. Osuka, H. Shiratori, R. Yoneshima, T. Okada, S. Taniguchi, N. Mataga, *Chem. Lett.* **1995**, 913; f) T. Hayashi, T. Takimura, H. Ogoshi, *J. Am. Chem. Soc.* **1995**, *117*, 11606.

[6] a) T. Hayashi, T. Miyahara, N. Hashizume, H. Ogoshi, *J. Am. Chem. Soc.* **1993**, *115*, 2049; b) T. Hayashi, T. Asai, H. Hokazono, H. Ogoshi, *ibid.* **1993**, *115*, 12210; c) T. Hayashi, T. Miyahara, Y. Aoyama, M. Kobayashi, H. Ogoshi, *Pure Appl. Chem.* **1994**, *66*, 797; d) T. Hayashi, T. Miyahara, Y. Aoyama, M. Nonoguchi, H. Ogoshi, *Chem. Lett.* **1994**, 1749.

[7] **1**: M.p. >300 °C; ^{1}H NMR (500 MHz, $C_2D_2Cl_4$, 25 °C): δ = 8.70 (s, 8H), 8.26 (d, J = 9.2 Hz, 4H), 8.06 (d, J = 8.3 Hz, 4H), 7.63 (d, J = 8.9 Hz, 4H), 7.36 (dd, J = 6.7, 8.2 Hz, 4H), 7.07 (d, J = 7.0, 8.2 Hz, 4H), 6.93 (d, J = 8.2 Hz, 4H), 4.97 (s, 4H); UV/Vis (toluene): λ_{max} (ε) = 430 (1.42×10^5), 550 nm (1.30×10^4); fluorescence (toluene): λ_{em} = 600, 645 nm; MS(FAB): calcd. for $C_{60}H_{36}N_4O_4Zn$: m/z = 940.2028, found 940.2027. **2**: M.p. >300 °C; ^{1}H NMR (500 MHz, C_6D_6 25 °C): δ = 8.74 (s, 8H), 8.23 (dd, J = 1.2, 7.0 Hz, 4H), 7.97 (d, J = 8.2 Hz, 4H), 7.53 (dd, J = 6.9, 8.1 Hz, 4H), 7.07 (d, J = 7.0, 8.2 Hz, 4H), 6.50 (s, 4H); UV/Vis (toluene): λ_{max} (ε) = 428 (1.57×10^5), 550 nm (9.36×10^3); fluorescence (toluene): λ_{em} = 596, 644 nm; MS(FAB): calcd for $C_{60}H_{36}N_4O_4Zn$: m/z = 940.2028, found 940.2039. **4**: M.p. >300 °C;

^{1}H NMR (500 MHz, $CDCl_3$, 25 °C): δ = 8.51 (s, 8H), 8.26 (d, J = 9.0 Hz, 4H), 8.00 (d, J = 8.2 Hz, 4H), 7.69 (d, J = 9.2 Hz, 4H), 7.29 (ddd, J = 8.3, 6.6, 1.2 Hz, 4H), 6.98 (ddd, J = 8.6, 6.7, 1.2 Hz, 4H), 6.91 (d, J = 8.1 Hz, 4H), 3.63 (s, 12H); UV/Vis (toluene): λ_{abs} (ε) = 429 (3.12×10^5), 551 nm (1.59×10^4); fluorescence (toluene): λ_{em} = 599, 645 nm; MS(FAB): calcd for $C_{64}H_{44}N_4O_4Zn$: m/z = 996.2654, found 996.2696.

[8] According to the X-ray crystal structure analysis of free base of **1** and **3** complex, the face-to-face distance between the porphyrin and the quinone is 3.3 Å.

[9] The lifetimes were obtained on a Hamamatsu Picosecond Lifetime Measuring System type C4780, Hamamatsu Photonics equipped with a N_2 laser-pumped dye laser, LN100C2, Laser Photonics INC (λ_{ex} = 550 nm).

[10] The measurement system consisting of laser and transient absorption spectrometer was described previously [14]. The excitation laser was operated at 10 Hz, the center wavelength was at 570 nm, and the single pulse energy for excitation was 300–500 μJ. The absorbance change was proportional to the excitation pulse energy in the energy range studied. The sample was flowed by peristatic pumping in a cell (10 mm light path) in which pump and probe pulses overlapped at an angle of 5°. The magic angle polarization condition was selected. No difference was observed in absorption spectra of the sample after the measurement. The instrumental response time, which was measured by 10–90% rise time of oxazine 750 in ethanol, was 5 ± 1 ps.

[11] M. R. Wasielewski, M. P. Niemczyk, *J. Am. Chem. Soc.* **1984**, *106*, 5043.

[12] J. Fajer, D. C. Borg, A. Forman, D. Dolphin, R. H. Felton, *J. Am. Chem. Soc.* **1970**, *92*, 3451.

[13] For example, in 5,15-[3,6-dimethoxy-*p*-benzoquinone-1,4-diylbis(4,1-butanediyl-2,1-benzeno)]-2,3,7,8,12,13,17,18-octamethylporphyrin, ET rate constants of $k_{CS} = 1\times10^{11}\ s^{-1}$ and $k_{CR} = 3.9\times10^{10}\ s^{-1}$ in toluene, measured by fluorescence lifetime have been reported [2i].

[14] S. Kumazaki, M. Iwaki, I. Ikegami, H. Kandori, K. Yoshihara, S. Itoh, *J. Phys. Chem.* **1994**, *98*, 11220.

Reactions of β,γ- and γ,δ-Unsaturated Esters with the Reagent Ti(O*i*Pr)$_4$/2*i*PrMgCl: Formation of β-Titanated Esters, β-Titanated Cyclobutanones, and Acyltitanium Compounds

Aleksandr Kasatkin, Takanori Yamazaki, and Fumie Sato*

Recently, we have found that substituted allylmalonic esters undergo deallylation on treatment with complex **1**,[1] which

$[(\eta^2\text{-}CH_3CHCH)Ti(OiPr)_2]$ **1**

is readily generated in situ from Ti(O*i*Pr)$_4$ and two equivalents of *i*PrMgCl. This reaction thus makes it possible to use the allyl group as a protective group for the acidic hydrogen of malonic esters.[2] The plausible mechanism of the deallylation involves the exchange of the coordinated propene ligand in **1** with an olefinic moiety of the substrate and subsequent β-elimination of malonate carbanion.

With these results in hand, we anticipated that the reaction of **1** with substituted propargylmalonic esters **2** would result in depropargylation.[3] However, treatment of diethyl 2-butynylmethylmalonate (**2a**) with **1** followed by hydrolysis afforded the olefinic ester **3a** in addition to the expected depropargylation product **4** [Eq. (a) and entry 1 in Table 1]. Similarly, diethyl

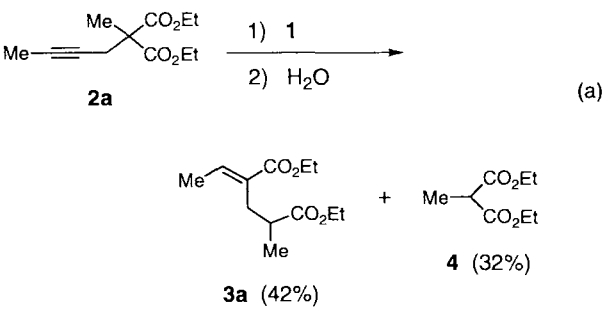

Table 1. Reaction of **1** with β,γ- and γ,δ-unsaturated esters [a].

Entry	Substrate	Product, yields [%] (in parantheses) [b]	
	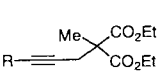	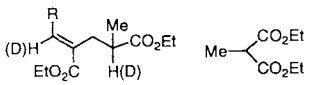	
1	**2a**: R = Me	**3a** (42) [c]	**4** (32) [d]
2	**2b**: R = Hex	**3b** (45)	**4** (34) [d]
3	**2c**: R = Ph	**3c** (46)	**4** (31) [d]
	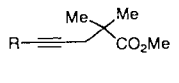	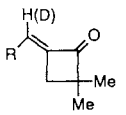	
4	**8a**: R = Hex	**10a** (68) [c]	
5	**8b**: R = Ph	**10b** (77)	
	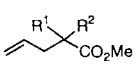	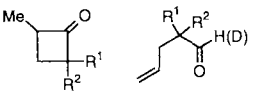	
6	**11a**: R^1 = H, R^2 = $PhCH_2$	**13a** (12) [e]	**12a** (48) [c]
7	**11b**: R^1 = Me, R^2 = $PhCH_2$	**13b** (60) [e]	**12b** (21)
8	**11c**: R^1 = Me, R^2 = OAc	**13c** (63) [e]	
9	**11d**: R^1 = Me, R^2 = $N(CH_2Ph)_2$	**13d** (83) [e]	
10	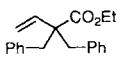	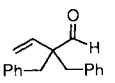	
	16	**17** (80)	

[a] All reactions were carried out with 2.0 equiv Ti(O*i*Pr)$_4$ and 4.0 equiv *i*PrMgCl in Et_2O between −45 and −40 °C (1 h). [b] Yields of isolated products based on starting unsaturated esters unless stated otherwise. [c] Deuterolysis of the reaction mixture gave the product with > 95% D incorporation. [d] According to ^{1}H NMR data of the crude product using an internal standard. [e] Combined yield of diastereomers according to ^{1}H NMR analysis.

methyl(propargyl)malonates **2b,c** provided mixtures of **4** and the corresponding diethyl α-alkylideneglutarates **3b,c** (entries 2 and 3 in Table 1). This new reductive rearrangement of propargylmalonates into α-alkylideneglutarates can be explained by the mechanism shown in Scheme 1. The titanacyclopropene intermediate **5**[4] generated from **1** and **2** undergoes intramolecular carbonyl addition to give **6**; subsequent cleavage of the cyclobutane ring then gives **7** through elimination of the titanium enolate. The presence of the alkenyltitanium compounds **7** in the reaction mixture was confirmed by deuterolysis to afford doubly deuterated **3a** with >95% D incorporation at both the alkenyl and α-positions (entry 1 in Table 1). Although the yields of **3** are only moderate, the high synthetic utility of the products and the easy access to the starting compounds make this methodology promising.[5] Furthermore, the opportunity for

[*] Prof. F. Sato, Dr. A. Kasatkin, T. Yamazaki
Department of Biomolecular Engineering
Tokyo Institute of Technology
4259 Nagatsuta-cho
Midori-ku, Yokohama, Kanagawa 226 (Japan)
Fax: Int. code +(45)924-5826
e-mail: fsato@bio.titech.ac.jp

[+] On leave from Institute of Organic Chemistry, Ufa Research Center, Russian Academy of Sciences.

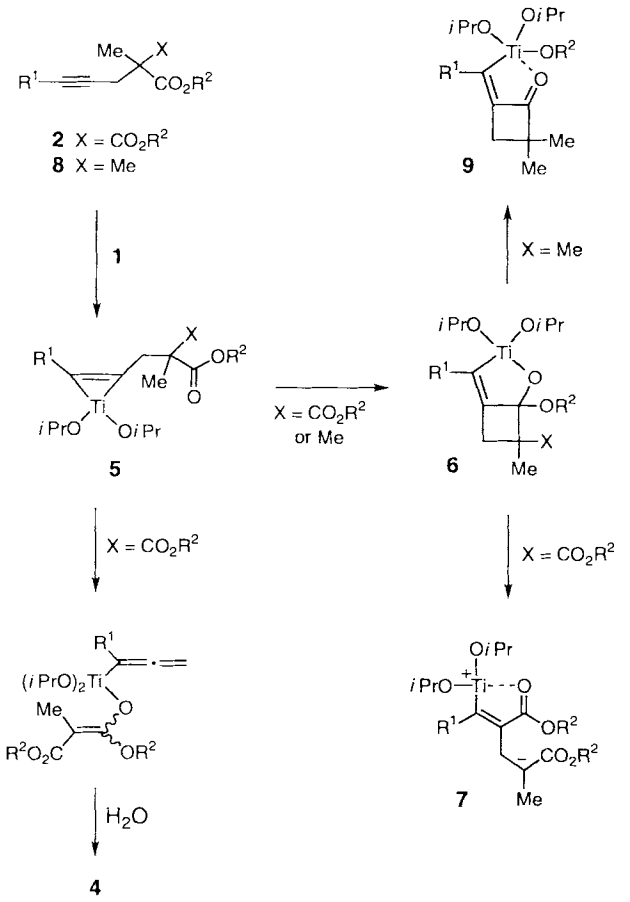

Scheme 1.

functionalization through manipulation of the carbon–titanium bonds in **7** serves to enhance the attractiveness of the reaction.[6]

Since the generation of relatively stable titanium enolate derivatives seems to be essential for the present rearrangement, we anticipated that alkynyl monoesters **8** would give the corresponding alkenyltitanium compounds **9**, which have a cyclobutanone unit, via **6** through an intramolecular nucleophilic acyl substitution (INAS) reaction as shown in Scheme 1.[7] As expected, the reactions of **1** with the alkynyl esters **8a,b** furnished after hydrolysis the α-alkylidenecyclobutanones **10a,b** in high yield (entries 4 and 5 in Table 1). Deuterolysis of the reaction mixture obtained from **8a** gave deuterated **10a** (entry 4).

Next, we investigated the reaction of **1** with methyl 2-benzyl-4-pentenoate (**11a**) and anticipated formation of the corresponding INAS product (β-titanated cyclobutanone). To our surprise, the reaction afforded mainly 2-benzyl-4-pentenal (**12a**) in addition to the expected cyclobutanone **13a** [Eq. (b) and entry 6 in Table 1]. Similarly, the α,α-disubstituted ester **11b** gave a mixture of cyclobutanone **13b** and γ,δ-unsaturated aldehyde **12b** (entry 7). The formation of **12** can be explained by ring-opening of the expected β-titanated cyclobutanone **14** to give the acyltitanium compound **15** as shown in Scheme 2.[8, 9]

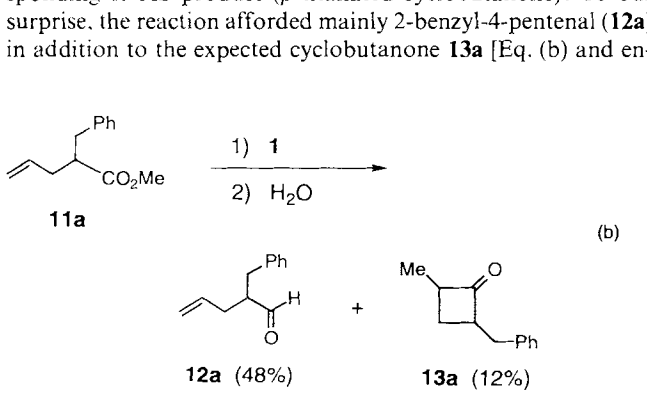

(b)

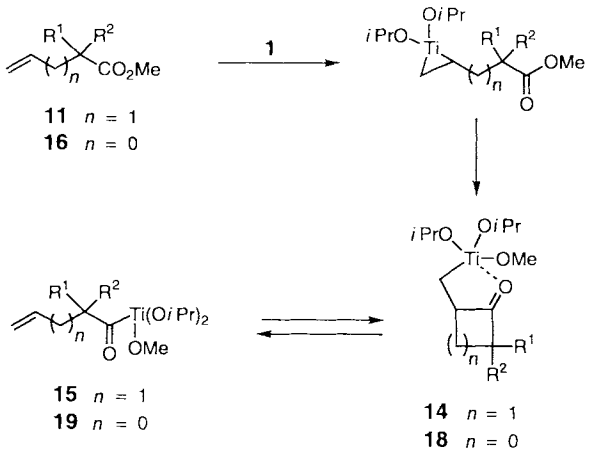

Scheme 2.

In accordance with this explanation, deuterolysis of the reaction mixture led to deuterated **12a** with >95% D incorporation (entry 6 in Table 1). The reaction of **1** with the α-heteroatom substituted esters **11c,d**, however, afforded only the corresponding cyclobutanones **13c,d** in high yield (entries 8 and 9). Although the factors influencing the equilibrium between **14** and **15** are not clear at this time, the smooth preparation of α-O- and α-N-substituted cyclobutanones from readily accessible starting compounds is noteworthy from a synthetic point of view.[10] The reaction of **1** with the vinylic ester **16**, in which the double bond and the ester group are separated by one less carbon than in substrates **11**, however, afforded the β,γ-unsaturated aldehyde **17** exclusively (Scheme 2 and entry 10 in Table 1). Complete ring-opening of the β-titanated cyclopropanone **18** yielding **19** reflects the higher strain of the three-membered cycloalkanone fragment compared to that of the four-membered unit in **14**.[8, 11]

Experimental Procedure

The following procedures for preparation of **3a**, **4** (entry 1 in Table 1) and **12b**, **13b** (entry 7) are representative.

3a, **4**: To a solution of $Ti(OiPr)_4$ (284 mg, 1.00 mmol) and **2a** (113 mg, 0.50 mmol) in Et_2O (7.5 mL) was added dropwise *i*PrMgCl (1.53 mL, 1.31 M in ether, 2.00 mmol) at −50 °C. The reaction mixture was stirred at −45 to −40 °C for 1 h and hydrolyzed by addition of 1 N HCl (3.0 mL). After warming up to 20 °C and stirring for 15 min, the organic layer was separated and the aqueous layer was extracted with ether. The combined organic layers were dried over $MgSO_4$ and concentrated under reduced pressure. The yield of **4** (32%) was determined by ^1H NMR analysis of the crude reaction mixture with trichloroethylene as an internal standard. After separation by column chromatography (silica gel, hexane:ether = 6:1), **3a** (47 mg, 0.21 mmol) was isolated in 42% yield as a colorless oil. ^1H NMR (300 MHz, $CDCl_3$): $\delta = 1.17$ (d, $J = 7.5$ Hz, 3H), 1.28 (t, $J = 7.1$ Hz, 3H), 1.32 (t, $J = 7.1$ Hz, 3H), 1.84 (d, $J = 7.5$ Hz, 3H), 2.42 (dd, $J = 15.7$, 8.3 Hz, 1H), 2.70 (m, 2H), 4.10 (q, $J = 7.1$ Hz, 2H), 4.19 (q, $J = 7.1$ Hz, 2H), 6.96 (q, $J = 7.5$ Hz, 1H); ^{13}C NMR (300 MHz, $CDCl_3$): $\delta = 14.13$, 14.17, 14.42, 16.73, 30.23, 38.80, 60.17, 60.32, 130.77, 139.09, 167.37, 176.19.

12b, **13b**: To a solution of $Ti(OiPr)_4$ (284 mg, 1.00 mmol) and **11b** (109 mg, 0.50 mmol) in Et_2O (7.5 mL) was added dropwise *i*PrMgCl (1.35 mL, 1.48 M in ether, 2.00 mmol) at −50 °C. The reaction mixture was stirred at −45 to −40 °C for 1 h, then a solution of water (1.2 mL) in THF (30 mL) was added. After warming up to 20 °C and stirring for 30 min, the organic layer was decanted and the white solid was washed thoroughly with ether. The combined organic layers were dried

 © VCH Verlagsgesellschaft mbH, D-69451 Weinheim, 1996 0570-0833/96/3517-1967 $ 15.00+.25/0

over $MgSO_4$ and concentrated under reduced pressure. After separation by column chromatography (silica gel, hexane:EtOAc = 20:1), **12b** (20 mg, 0.11 mmol) and **13b** (56 mg, 0.30 mmol) were isolated in 21 and 60% yield, respectively, as colorless oils. **12b**: ^{1}H NMR (300 MHz, $CDCl_3$): δ = 1.03 (s, 3H), 2.19 (dd, J = 15.0, 7.1 Hz, 1H), 2.37 (dd, J = 15.0, 7.5 Hz, 1H), 2.75, 2.88 (d, J = 14.3 Hz, 2H), 5.10 (m, 2H), 5.74 (m, 1H), 7.05–7.35 (m, 5H), 9.60 (s, 1H). **13b** (55:45 mixture of diastereoisomers): ^{1}H NMR (300 MHz, $CDCl_3$): δ = 0.88, 1.10 (d, J = 7.1 Hz, 3H), 1.19, 1.25 (s, 3H), 1.32, 1.65 (dd, J = 10.5, 7.1 Hz, 1H), 1.94, 2.32, (dd, J = 10.4, 9.7 Hz, 1H), 2.65, 2.72, 2.91, 2.97 (d, J = 14.3 Hz, 2H), 2.77, 3.29 (m, 1H), 7.10–7.35 (m, 5H); ^{13}C NMR (300 MHz, $CDCl_3$): δ = 13.00, 14.25, 21.77, 22.60, 31.67, 32.20, 41.58, 42.76, 49.02, 50.39, 62.28, 62.55, 126.32, 126.40, 128.16, 128.25, 129.77, 130.13, 137.57, 137.85, 218.20.

Received: April 4, 1996 [Z 9007 IE]
German version: *Angew. Chem.* **1996**, *108*, 2091–2093

Keywords: alkenes · alkynes · cyclizations · cyclobutanones · titanium compounds

[1] A. Kasatkin, T. Nakagawa, S. Okamoto, F. Sato, *J. Am. Chem. Soc.* **1995**, *117*, 3881; O. G. Kulinkovich, S. V. Sviridov, D. A. Vasilevskii, *Synthesis* **1991**, 234.

[2] T. Yamazaki, A. Kasatkin, Y. Kawanaka, F. Sato, *J. Org. Chem.* **1996**, *61*, 2266.

[3] T. Nakagawa, A. Kasatkin, F. Sato, *Tetrahedron Lett.* **1995**, *36*, 3207.

[4] K. Harada, H. Urabe, F. Sato, *Tetrahedron Lett.* **1995**, *36*, 3203.

[5] For preparation of the compounds of type **3** and their application in organic synthesis, see: H. Stetter, K. Marten, *Liebigs Ann. Chem.* **1982**, 240; H. Amri, M. Rambaud, J. Villieras, *Tetrahedron Lett.* **1989**, *30*, 7381; A. M. Moiseenkov, B. Ceskis, N. A. Shapiro, G. A. Stashina, V. M. Zhulin, *Izv. Akad. Nauk SSSR Ser. Khim.* **1990**, 595; S. E. Drewes, N. D. Emslie, N. Karodia, G. Loizou, *Synth. Commun.* **1990**, *20*, 1437; J. Tanaka, S. Kanemasa, Y. Ninomiya, O. Tsuge, *Bull. Chem. Soc. Jpn* **1990**, *63*, 466.

[6] We found that **7** reacts with PhCHO selectively at the titanium enolate moiety to furnish after hydrolysis the corresponding α-alkylidene-α′-(hydroxybenzyl)-glutarates.

[7] A. Kasatkin, S. Okamoto, F. Sato, *Tetrahedron Lett.* **1995**, *36*, 6075; S. Okamoto, A. Kasatkin, P. K. Zubaidha, F. Sato, *J. Am. Chem. Soc.* **1996**, *118*, 2208.

[8] Ring-opening of (cyclopropylmethyl)- and (cyclobutylmethyl)titanium derivatives to give 3-butenyl- and 4-pentenyltitanium complexes, respectively, has been reported, see: H. Lehmkuhl, S. Fustero, *Liebigs Ann. Chem.* **1980**, 1361.

[9] Synthesis of acyltitanium compounds having cyclopentadienyl ligands has been reported, see: G. Fachinetti, C. Floriani, *J. Organomet. Chem.* **1974**, *71*, C5; G. Fachinetti, C. Floriani, H. Stoeckli-Evans, *J. Chem. Soc. Dalton Trans.* **1977**, 2297; L. B. Kool, M. D. Rausch, H. G. Alt, M. Herberhold, B. Honold, U. Thewalt, *J. Organomet. Chem.* **1987**, *320*, 37.

[10] For reviews on synthesis and reactions of cyclobutanones, see: D. Bellus, B. Ernst, *Angew. Chem.* **1988**, *100*, 820; *Angew. Chem. Int. Ed. Engl.* **1988**, *27*, 797; B. M. Trost, *Top. Curr. Chem.* **1986**, *133*, 3; H. N. C. Wong, K.-L. Lau, K.-F. Tam, *ibid.* **1986**, *133*, 83.

[11] Treatment of diethyl methyl(vinyl)malonate with **1** afforded after hydrolysis diethyl 2,3-dimethylsuccinate in 76% yield. The mechanism is presumably similar to that shown in Scheme 1 (**2** → **7**).

Enhancing DNA Triple Helix Stability at Neutral pH by the Use of Oligonucleotides Containing a More Basic Deoxycytidine Analog**

Stefan Hildbrand and Christian Leumann*

High-affinity, sequence-specific recognition of double-stranded DNA by oligonucleotide analogs is important in the selective control of gene expression.[1] Triple-helix formation of oligodeoxynucleotides with duplex DNA according to the py–pu:py binding motif,[2] however, is hampered at neutral pH because the cytosine residues in the third strand must be protonated. The pK_a of this base in the corresponding free nucleoside is 4.3. In the past, attempts to overcome this obstacle mainly focused on the design and use of (deoxy)ribonucleosides carrying charge-neutral bases that display a H-bonding pattern isomorphous to that of N^3-protonated cytosine. Examples of such altered bases investigated in triple-helix formation include pseudoisocytosine,[3] the "base P",[4] 4-amino-5-methyl-2,6-[1*H*,3*H*]-pyrimidione,[5] 8-oxoadenine[6] and its N^6-methyl derivative,[7] N^7-deoxyguanine,[8] and the base "pyrazine-ADD".[9]

In an alternative approach to increase the affinity of oligonucleotides to target DNA at neutral pH, the cytidine nucleosides could be replaced by analogs that ideally were completely protonated at physiological pH. A limited increase in basicity can be achieved by replacing the furanose sugar in 2′-deoxycytidine by the corresponding carbocyclic sugar. Carbocyclic 5-methyldeoxycytidine is more basic than 5-methyldeoxycytidine by 0.45 pK_a units.[10] Oligonucleotides containing this analog showed increased triple-helix stability by 3.9 °C per substitution (relative to 5-methyldeoxycytidine). The more obvious way to increase basicity consists in replacing the base cytosine by an aromatic heterocycle that is intrinsically more readily protonated. Oligonucleotides containing 6-amino-2′-*O*-methylcytidine (pK_a = 6.8) were therefore recently prepared and incorporated into oligonucleotides.[11] Their pairing to duplex DNA, however, was inhibited, most probably as a result of unfavorable conformational properties around the nucleosidic bond in this 2,6-substituted pyrimidine nucleoside.

In our design of a more readily protonated cytosine substitute we started from the basic idea that replacement of the nitrogen atom N^1 in the pyrimidine ring by carbon and concomitant removal of the 2-oxo function should result in a more basic pyridine derivative without perturbing the hydrogen-bonding pattern relevant for triple-helix formation. This concept seemed to be applicable because of the relative differences in basicity for 4-aminopyrimidine (pK_a = 5.71) and the analogous heterocycle 2-aminopyridine (pK_a = 6.86), containing only one ring nitrogen.[12] Here we report on the synthesis of the target C-nucleoside analogs **5** and **7**, as well as on the incorporation of **7** into oligonucleotides and their properties with respect to binding to double-stranded DNA. Although an alternative synthesis of the C-nucleoside **7** recently appeared in the literature,[13] the concept of using **7** as a protonated cytidine equivalent in oligonucleotides is unprecedented.

Our synthesis of the C-nucleosides **5** and **7** (Fig. 1) starting from the readily obtainable 2,3,5-tri-*O*-benzyl-*D*-ribono-1,4-lactone (**3**)[14] and the commercially available 2-amino-

[*] Dipl. Chem. S. Hildbrand, Prof. C. Leumann
Institut für organische Chemie der Universität
Freiestrasse 3, CH-3012 Bern (Switzerland)
Fax: Int. code +(31)631-3422

[**] This work was supported by the Schweizerische Nationalfonds zur Förderung der wissenschaftlichen Forschung and by Ciba-Geigy AG Basel.

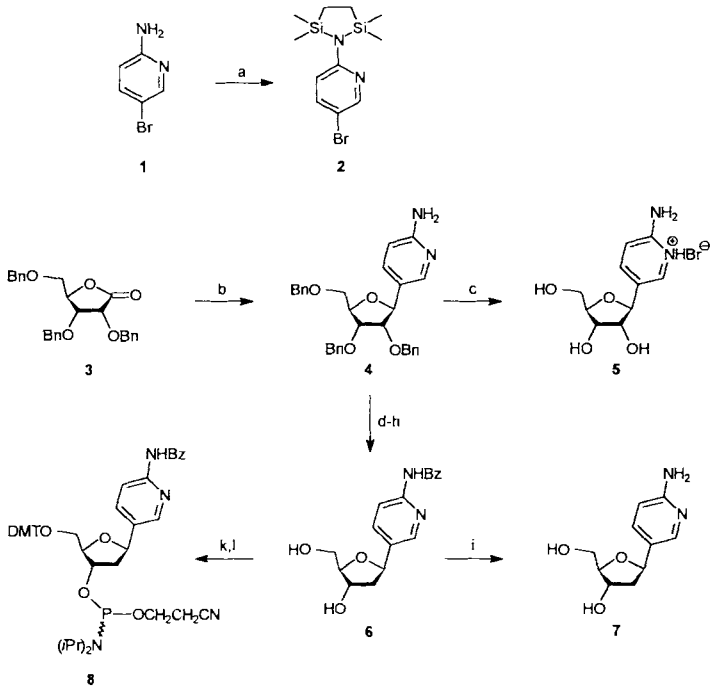

Fig. 1. a) *n*BuLi (2 equiv), $Cl(Me)_2SiCH_2CH_2Si(Me)_2Cl$ (1 equiv), THF, −75 °C, 2.5 h, 68%; b) **2** (1.8 equiv), *n*BuLi (1.7 equiv), THF, −75 °C, 3 h, −75 °C → 0 °C, 4 h, then Et_3SiH (5 equiv), $BF_3 \cdot Et_2O$ (5 equiv), CH_2Cl_2, −75 °C → room temperature (RT), 12 h, 64%; c) 0.15 M BBr_3 in CH_2Cl_2, −75 °C, 3 h, 71%; d) BzCl (1.3 equiv), pyridine, CH_2Cl_2, RT, 24 h, then 0.4 M BBr_3 in CH_2Cl_2, −75 °C, 4 h, 70%; e) $(Cl(iPr)_2Si)_2O$ (1.2 equiv), pyridine, RT, 5 h, 75%; f) *p*-TolOC(S)Cl (1.6 equiv), 4-dimethylaminopyridine (2.2 equiv), CH_3CN, RT, 25 h, 81%; g) azobisisobutyronitril (0.1 equiv), nBu_3SnH (1.5 equiv), toluene, 80 °C, 4 h, 84%; h) tetra-*n*-butylammonium fluoride (2 equiv), THF, RT, 1.5 h, 86%; i) $MeNH_2$ solution (40% in H_2O), 70 °C, 25 h, 83%; k) dimethoxytrityl chloride (1.2 equiv), pyridine, RT, 3.5 h, 84%; l) $(NCCH_2CH_2O)(iPr_2N)PCl$ (1.5 equiv), $Et(iPr)_2N$ (3 equiv) THF, RT, 2 h, 81%.

5-bromopyridine (**1**) essentially followed the syntheses of C-glycosides by Krohn et al.[15] and Kraus et al.[16] Protection of the amino group in **1** with 1,2-bis(chlorodimethylsilyl)ethane lead to compound **2**, which was suitable for coupling with the sugar component. In situ bromo–lithium exchange in **2** with *n*-BuLi at −75° furnished the nucleophile, which readily added to the lactone **3**. The resulting mixture of hemiacetals was subsequently reduced with $Et_3SiH/BF_3 \cdot Et_2O$ to provide **4** (only β-configured isomer was obtained), which after debenzylation with BBr_3 yielded the ribonucleoside **5** in its hydrobromide form. The corresponding N-protected 2′-deoxynucleoside was obtained from **4** in five consecutive steps starting with benzoylation of the exo amino group, followed by debenzylation, selective protection of the 3′ and 5′ hydroxyl group, subsequent removal of the 2′ hydroxyl group by Barton chemistry, and finally desilylation to give **6**. Compound **6** was then either converted into the phosphoramidite building block **8** by standard methods[17] or to the free 2′-deoxynucleoside **7** by treatment with 40% aqueous CH_3NH_2. The ^1H NMR data of **7** were identical to those already reported.[13]

The pK_a values of the cytidine nucleoside analogs are 6.15 for the ribonucleoside **5** and 6.26 for the deoxyribonucleoside **7**.[18] These values are about 0.6 pK_a units lower than that reported for 2-aminopyridine but more importantly, about two pK_a units higher than that of natural cytidine. As expected, the difference in the basicity of **5** and **7** is only 0.1 pK_a unit, thus confirming that the presence or absence of a hydroxyl group on C(2′) in the ribose ring has negligible influence on the pK_a of these C-nucleosides.

target duplex (21-mer)

5′-d(GCT**AAAAAGAGAGAGA**TCG)

3′-d(CGA**TTTTTCTCTCTCT**AGC)

9 5′-d(TTTTTCTCTCTCT)

10 5′-d(TTTTTCT**X**TCTCTCT)

11 5′-d(TTTTT**X**T**X**T**X**T**X**T)

12 5′-d(TTTTT^{Me}CT^{Me}CT^{Me}CT^{Me}CT^{Me}CT)

Fig. 2. Sequences of the 21-mer target DNA-duplex and the oligonucleotides **9**–**12** for triple-helix formation (X = 7; ^{Me}C = 5-methyldeoxycytidine).

Once the building block **8** had been prepared, the oligonucleotides **10** and **11** (Fig. 2) were synthesized on a solid support according to standard phosphoramidite chemistry.[19] Coupling efficiencies were estimated from trityl assays and were in the range of 95% per step (including those with the phosphoramidite **8**). After chain assembly and final detritylation the oligomers were detached from the solid support and freed from protecting groups with 25% NH_3 (55 °C, 12 h), followed by 40% aqueous CH_3NH_2 (70 °C, 26 h). Methylamine treatment was absolutely necessary because of the poor ammonolysis of the benzoyl group in residues of **6**. The crude material obtained in this manner was purified by DEAE ion exchange chromatography (DEAE = diethylaminoethyl), its purity determined by reversed phase HPLC and the structural integrity of the oligomers analyzed by matrix-assisted laser desorption ionization—time of flight (MALDI-TOF) mass spectrometry.[20] The oligonucleotides **9** and **12** were prepared for comparison.

Binding to duplex DNA was monitored by UV melting curves in the pH interval 6.0–8.0 and at salt concentrations of 200 mM and 1 M NaCl. Melting transition data (T_m) for third-strand dissociation of **9**–**12** from the chosen target 21-mer duplex (Fig. 2) are summarized in Table 1. Representative melting curves

Table 1. T_m values [°C] and hyperchromicity [%] (in parentheses) of the dissociation of the third strand **9**–**12** from UV-melting curves (λ = 260 nm). Triple helix concentration 1.5–1.7 μM in 10 mM NaH_2PO_4.

Strand	200 mM NaCl [a]				1 M NaCl [b]			
	pH 6.0	pH 7.0	pH 7.5	pH 8.0	pH 6.0	pH 7.0	pH 7.5	pH 8.0
9	42.5 (10)	20.3 (3)	9.8 (2)	<4	42.9 (10)	20.7 (8)	13.0 (6)	4.0 (3)
10	44.3 (9)	25.7 (3)	15.3 (2)	7.8 (1)	47.2 (10)	26.3 (7)	16.4 (6)	8.0 (4)
11	50.3 (11)	39.0 (6)	31.3 (4)	23.1 (3)	[c]	43.4 (5)	33.2 (4)	28.5 (4)
12	53.3 (12)	31.5 (5)	20.1 (2)	12.2 (1)	55.1 (11)	31.4 (7)	21.2 (6)	12.5 (5)

[a] T_m of target duplex melting: 61 ± 1 °C. [b] T_m of target duplex melting: 69 ± 1 °C. [c] Only one T_m value for triplex and duplex melting (69.4 °C) was observed.

(pH 7.5, 200 mM NaCl) are depicted in Figure 3.[21] From the data in Table 1 it becomes clear that oligomer **11**, in which all cytosine bases were replaced by the 2-aminopyridyl residue, shows a dramatic increase in T_m relative to **9** incorporating the natural base cytosine, and **12** containing 5-methylcytosine. The increase in stability relative to the controls is most pronounced at pH > 7.0. Even replacement of only one deoxycytidine residue has a strong stabilizing effect as can be seen from the binding data of **10**. The average increase in T_m per residue at pH 7.5 is 4.3 K relative to cytosine and 2.2 K relative to 5-methylcytosine. Interestingly, replacement of only one residue, as in **10**, has a stronger effect on triplex stability than expected from the average values.

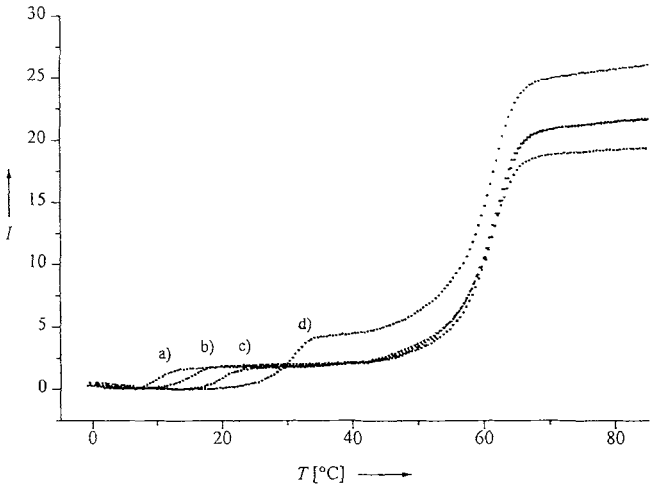

Fig. 3. UV-melting curves ($\lambda = 260$ nm) of **9** (a), **10** (b), **11** (d), and **12** (c) with the target duplex sequence (T_m of the duplex 61 ± 1 °C). Conditions: 10 mM NaH_2PO_4, 200 mM NaCl, pH 7.5; triplex concentration 1.5–1.7 μM. I = hyperchromicity (%).

The results clearly demonstrate that the nucleoside analog **7**, due to its enhanced basicity relative to natural cytidine, is an excellent substitute for the latter in DNA duplex recognition at physiological pH through the py:pu–py motif. Furthermore, the lack of the 2-oxo function present in cytidine does not perturb third-strand binding in the major groove of DNA. This opens the possibility for chemical modifications of the base in **7** at positions 2 and 5 (cytidine numbering) for various purposes, for example, further increasing the pK_a, optimizing stacking properties, or attachment of functional units.

Received: April 9, 1996 [Z 8961 IE]
German version: *Angew. Chem.* **1996**, *108*, 2100–2102

Keywords: C-nucleosides · cytidine analogs · DNA · oligonucleotides · triple helices

[1] N. T. Thuong, C. Hélène, *Angew. Chemie*, **1993**, *105*, 697–723; *Angew. Chemie Int. Ed. Engl.* **1993**, *33*, 666–690.
[2] G. Felsenfeld, D. R. Davies, A. Rich, *J. Am. Chem. Soc.* **1957**, *79*, 2023–2024; H. E. Moser, P. B. Dervan, *Science*, **1987**, *238*, 645–650; J.-C. François, T. Saison-Behmoaras, C. Hélène, *Nucleic Acids Res.* **1988**, *16*, 11431–11440.
[3] A. Ono, P. O. P. Ts'o, L.-S. Kan, *J. Am. Chem. Soc.* **1991**, *113*, 4032–4033; A. Ono, P. O. P. Ts'o, L.-S. Kan, *J. Org. Chem.* **1992**, *57*, 3225–3230.
[4] J. S. Koh, P. B. Dervan, *J. Am. Chem. Soc.* **1992**, *114*, 1470–1478; E. S. Priestley, P. B. Dervan, *ibid.* **1995**, *117*, 4761–4765.
[5] a) G. Xiang, W. Soussou, L. W. McLaughlin, *J. Am. Chem. Soc.* **1994**, *116*, 11155–11156; b) R. Berressem, J. W. Engels, *Nucleic Acids Res.* **1995**, *23*, 3465–3472; c) G. Xiang, R. Bogacki, L. W. McLaughlin, *ibid.* **1996**, *24*, 1963–1970.
[6] P. S. Miller, P. Bhan, C. D. Cushman, T. L. Trapane, *Biochemistry*, **1992**, *31*, 6788–6793; M. C. Jetter, F. W. Hobbs, *ibid.* **1993**, *32*, 3249–3254; E. C. Davison, K. Johnsson, *Nucleosides Nucleotides* **1993**, *12*, 237–243.
[7] S. L. Young, S. H. Krawczyk, M. D. Matteucci, J. J. Toole, *Proc. Natl. Acad. Sci. USA* **1991**, *88*, 10023–10026; S. H. Krawczyk, J. F. Milligan, S. Wadwani, C. Moulds, B. C. Froehler, M. D. Matteucci, *ibid.*, **1992**, *89*, 3761–3764.
[8] J. Hunziker, E. S. Priestley, H. Brunar, P. B. Dervan, *J. Am. Chem. Soc.* **1995**, *117*, 2661–2662.
[9] U. von Krosigk, S. A. Benner, *J. Am. Chem. Soc.* **1995**, *117*, 5361–5362.
[10] B. C. Froehler, D. J. Ricca, *J. Am. Chem. Soc.* **1992**, *114*, 8320–8322.
[11] J. S. Pudlo, S. Wadwani, J. F. Milligan, M. D. Matteucci, *Bioorg. Med. Chem. Lett.* **1994**, *4*, 1025–1028.
[12] A. Albert, R. Goldacre, J. Phillips, *J. Chem. Soc.* **1948**, 2240–2249.
[13] H.-P. Hsieh, L. W. McLaughlin, *J. Org. Chem.* **1995**, *60*, 5356–5359.
[14] W. Timpe, K. Dax, N. Wolf, H. Weidmann, *Carbohydr. Res.* **1975**, *39*, 53–60.
[15] K. Krohn, H. Heins, K. Wielckens, *J. Med. Chem.* **1992**, *35*, 511–517.
[16] G. A. Kraus, M. T. Molina, *J. Org. Chem.* **1988**, *53*, 752–753.
[17] ^1H and ^{31}P NMR data of **8** (diastereomeric mixture): ^1H NMR (500 MHz, $CDCl_3$): $\delta = 1.10$ (d, $J = 6.8$ Hz, 3H), 1.16–1.21 (m, 9H), 1.99–2.09 (m, 1H), 2.34 (dd, $J = 13.0$, 5.1 Hz, 0.5H), 2.44 (dd, $J = 13.0$, 4.9 Hz, 0.5H), 2.46 (t, $J = 6.5$ Hz, 1H), 2.62 (t, $J = 6.5$ Hz, 1H), 3.23–3.36 (m, 2H), 3.54–3.67 (m, 2H), 3.67–3.90 (m, 2H), 3.784, 3.786, 3.789, 3.792 (4s, 6H), 4.22–4.29 (m, 1H), 4.51–4.58 (m, 1H), 5.14–5.19 (m, 1H), 6.80–6.85 (m, 4H), 7.18–7.24 (m, 1H), 7.26–7.31 (m, 2H); 7.33–7.37 (m, 4H); 7.44–7.52 (m, 4H); 7.54–7.59 (m, 1H); 7.78–7.82 (m, 1H), 7.92 (s, 1H), 7.93 (s, 1H), 8.29–8.32 (m, 1H), 8.359, 8.364 (2d, $J = 8.5$ Hz, 1H), 8.71, 8.72 (2s, NH). ^{31}P NMR (202 MHz, $CDCl_3$): $\delta(PPh_3 = 0)$: 154.00, 154.12.
[18] pK_a values were determined by titration with 0.1 M NaOH and 0.1 M HCl respectively at 25 °C in H_2O. We thank the analytical department of Ciba-Geigy AG, Basel for performing these measurements.
[19] Oligonucleotide synthesis was performed on a DNA synthesizer (Pharmacia Gene Assembler Special). Reagents and concentrations of the phosphoramidites were as for the synthesis of natural DNA oligomers. The only change made to the usual synthesis cycle was the prolongation of the coupling time to 6 min. Syntheses were performed in the trityl off mode on a 1.3 μmol scale.
[20] Ion exchange HPLC of oligomers **10** and **11**: column: Nucleogen DEAE 60-7 (Macherey & Nagel); mobile phase A: 20 mM NaH_2PO_4, pH 3.9, in H_2O/CH_3CN (4/1), B: A + 1 M NaCl; gradient: 35–65% B in 35 min (55 °C), flow: 1 mL min^{-1}; **10**: $t_R = 17.9$ min; **11**: $t_R = 11.5$ min; MALDI-TOF MS (*m/z*): **10**: calcd (monoanionic form) 4407.9; found 4407.9; **11**: calcd (monoanionic form) 4340.0; found 4340.4.
[21] Melting curves were recorded for a consecutive heating-cooling-heating protocol with a linear gradient of 1 K min^{-1}. Consecutive heating cycles were superimposable while cooling cycles showed slight hysteresis for the dissociation of the third strands **9**–**12**.

Stereoselective Insertion of Ketenes into O,O-Acetals: Synthesis of β-Alkoxy Esters and 1,4-Dioxepan-5-ones

Johann Mulzer,* Dirk Trauner, and Jan W. Bats

Lewis acid (LA) mediated aldol additions of carboxylic acid derivatives can be performed either by the reaction of ketene acetals with aldehydes and ketones (path A; Mukaiyama aldol addition[1]) or with acetals (path B[2]). Path B can be regarded as the insertion of **1** in one of the C–O bonds of **2** followed by hydrolysis of the resulting orthoester **3** to yield β-alkoxy ester **4**.

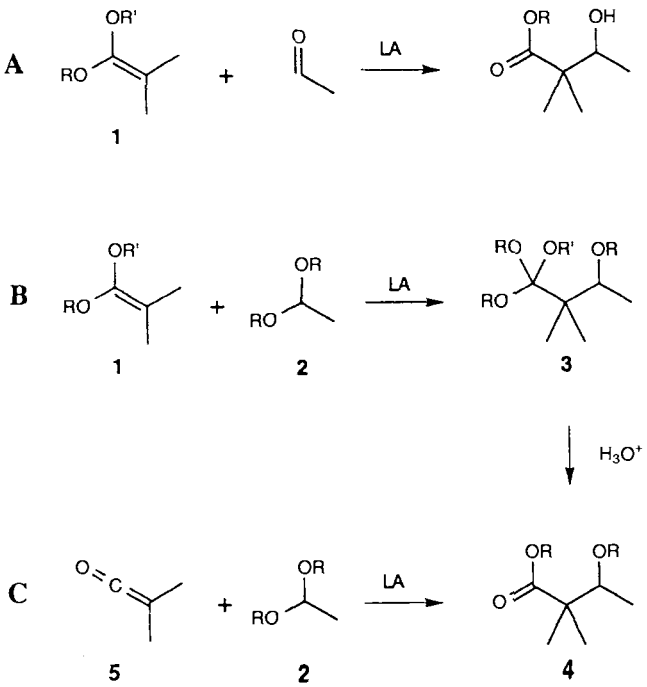

[*] Prof. Dr. J. Mulzer, Dipl.-Chem. D. Trauner, Dr. J. W. Bats
Institut für Organische Chemie der Universität
Marie-Curie-Strasse 11, D-60439 Frankfurt am Main (Germany)
Fax: Int. code +(69)798-29464

A logical extension would be a reaction in which ketene **5** instead of ketene acetal **1** directly inserts into one of the C–O bonds of acetal **2** (path C). Known examples of reaction C are largely restricted to unsubstituted ketene and acyclic aldehyde acetals.[3]

We used the experimentally convenient Staudinger conditions,[4] which have not been employed in this context before, to generate the ketene and the necessary Lewis acid, $ZnCl_2$, simultaneously. Thus dichloroketene was prepared in situ from trichloroacetyl chloride and commercially available zinc–copper couple and treated with 1,3-dioxolanes **6a–g** to yield the corresponding 6,6-dichloro-1,4-dioxepan-5-ones **7a–g** (Table 1).

Table 1. Reaction of dichloroketene with 1,3-dioxolanes.

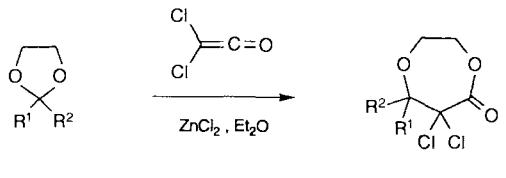

6a-g **7a-g**

6, 7	R^1	R^2	Yield [%] [a]
a	H	H	7
b	CH_3	CH_3	48
c		$-(CH_2)_4-$	74
d		$-(CH_2)_5-$	71
e	9-anthryl	H	18 [b]
f	C_6H_5	H	82
g	*p*-$MeOC_6H_4$	H	92

[a] Not optimized. [b] Prone to elimination.

1,3-Dioxanes like **8** also underwent the reaction. The product, the achiral, eight-membered 1,5-dioxocan-2-one **9**, displays four broadened methyl signals in its ^{13}C and ^1H NMR spectra,[5] indicating slow conformational interconversion.

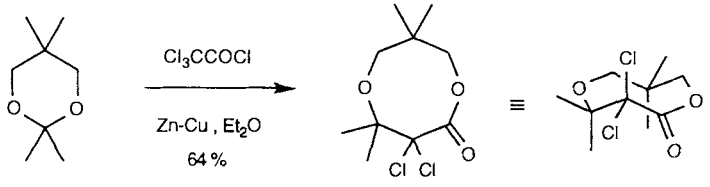

8 **9**

The variability of the ketene component **11** was investigated with anisaldehyde dimethyl acetal **10** (Table 2). The first step in the ketene insertion[6] is probably the nucleophilic attack of an acetal oxygen on the ketene, which is activated by the Lewis acid. The dipolar intermediate **13** is formed, which dissociates into enolate **14a** and carboxonium ion **14b** (a zwitterion in the case of cyclic acetals). These components recombine to give the α,β-alkoxyester **15**.

Accordingly, the rate of the reaction is strongly dependent on the inductive and mesomeric effects exerted by the substituents R^1 and R^2. Since di- and polymerization of the ketenes dominate with decreasing rate of the insertion, the yields also reflect this electronic influence. The parent 1,3-dioxolane **6a** gave dioxepanone **7a** in only 7% yield (Table 1), whereas the *p*-anisyl-substituted compound **6g** furnished **7g** in 92% yield. Doubly

Table 2. Reaction of **10** with ketenes **11a–f**.

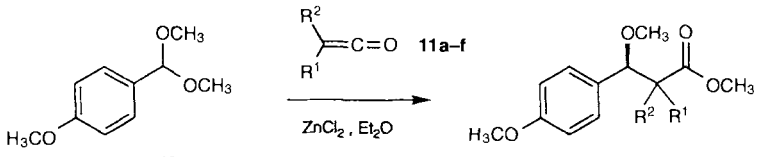

10 **12a–f**

11, 12	R^1	R^2	Yield [%] [a]
a	Cl	Cl	94
b	H	H	42
c	CH_3	CH_3	42
d	CH_3	H	41 [b]
e	C_6H_5	H	28 [b]
f	C_6H_5	C_6H_5	67

[a] Not optimized. [b] Combined yield of diastereomers.

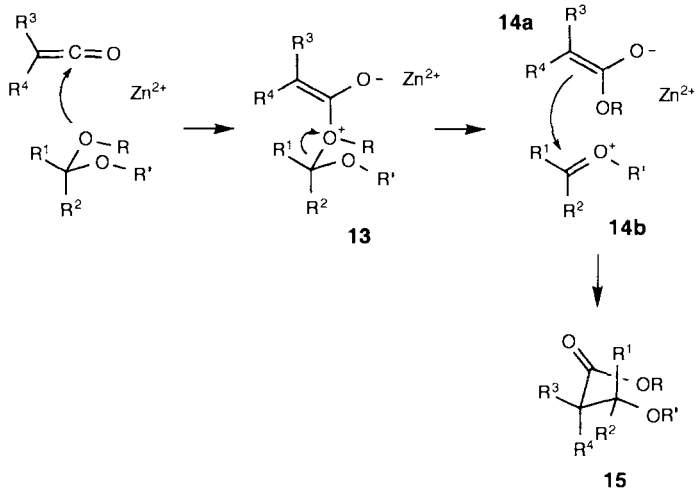

alkylated dioxolanes **6b–d** also reacted with good yields. Sterically hindered substrates, for example camphor ethylene ketal, did not react for the reasons mentioned above.

The ketene substituents have less influence on the reaction. The strongly electrophilic dichloroketene **11a** gave the best yield (94%) of insertion product **12a** (Table 2). Ketene itself (**11b**) furnished **12b** in 42% yield under the chosen conditions. Even monosubstituted ketenes, which have a strong tendency to di- or polymerize, like methylketene **11d** or phenylketene **11e**, underwent the reaction. The aldol-type products **12d** and **12e** were formed in modest yields as 3:1 and 2.2:1 mixtures of diastereomers, respectively. Sterically hindered diphenylketene (**11f**) also inserted cleanly, probably due to its low tendency to dimerize.

For an asymmetric version of the ketene insertion we chose the chiral dioxolane **16** (Table 3), which displays a nonstereogenic chirotopic acetal center. Reaction of **16** with ketenes **17a–d** led to compounds **18a–d** with >95% stereoselectivity. The structures of **18a–d** were elucidated by crystal structure analysis[7] and NMR spectroscopy (NOESY). Comparably high stereoselectivities have been observed in analogous reactions with silyl ketene acetals.[8] Products **18a** und **18b** were formed as the sole detectable isomers. In the case of both **18c** and **18d**, a second diastereomer was isolated in less than 5% yield (based on **18c,d**); the structures of these side products were not fully secured. Products **18b–d** contain the structural element of an *anti*-configurated aldol, and all four compounds **18** display the same relative configuration at the benzylic center with

Table 3. Reaction of ketenes with chiral dioxolane **16**.

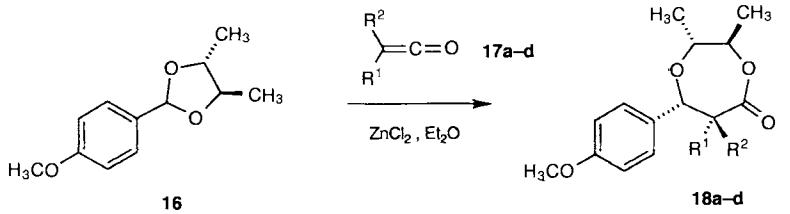

17, 18	R^1	R^2	*d.e.* [%]	Yield [%] [a]
a	Cl	Cl	>95	82
b	H	Cl	>95	60
c	H	CH_3	91	58
d	H	C_6H_5	92	55

[a] Combined yield of diastereomers, not optimized.

respect to the two preexisting stereocenters. The induced diastereoselectivity is quantitative; the simple diastereoselectivity is high. The crystal structure of compound **18c** is shown in Figure 1.

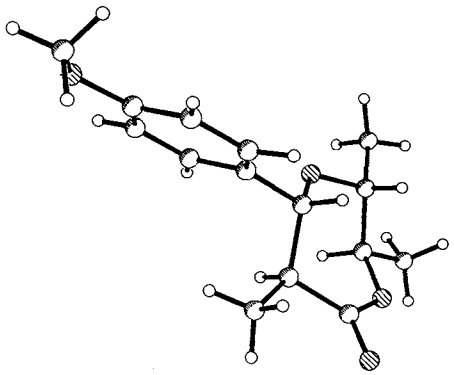

Fig. 1. Crystal structure of **18c**. The oxygen atoms are hatched.

Attack of either oxygen of dioxolane **16** on the ketene leads to the same intermediate of type **14**. Since monosubstituted ketenes such as methyl ketene (**17c**) are attacked by nucleophiles in the plane of the molecule and preferentially on the side opposite to the substituent,[8] the (*Z*) enolate is selectively formed. The seven-membered transition state **19b–d** leading to the main diastereomer **18b–d** is presumably favored as a consequence of the pseudo-equatorial positions of all four residues, which are also observed in the product (Fig. 1).

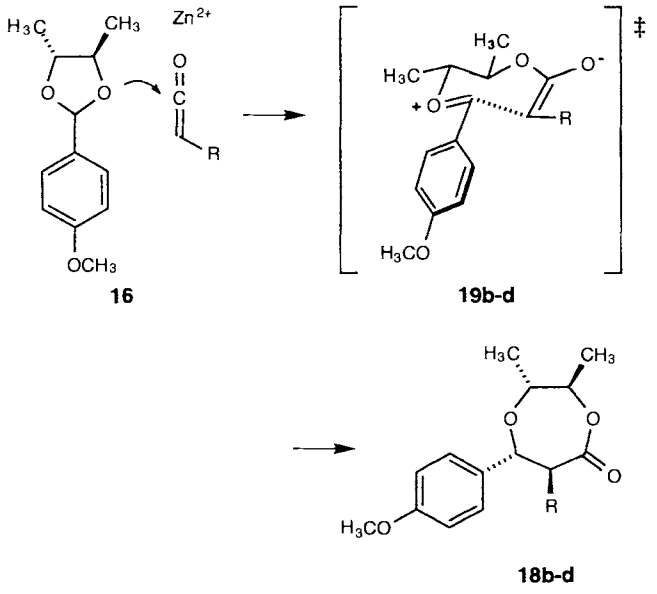

Experimental Procedure

A solution of trichloroacetyl chloride (1.5 mL, 13 mmol) in anhydrous ether (25 mL) was added dropwise within 1 h to a mixture of **16** (1 g, 4.5 mmol) and Zn–Cu couple (1 g, 15 mmol) in refluxing anhydrous ether (25 mL). The mixture was refluxed for an additional hour and stirred at room temperature for ca. 15 h. Subsequently, it was diluted with ether (50 mL), filtered, and extracted twice with water (50 mL), once with saturated bicarbonate solution (50 mL), and twice with brine (50 mL). The organic phase was dried ($MgSO_4$) and concentrated to dryness. The residue was purified by column chromatography (silica; hexanes:ethyl acetate = 10:1; $R_F = 0.2$) to yield 1.15 g (82%) of diastereomerically pure **18a** as colorless crystals [5].

Received: February 19, 1996 [Z 8835 IE]
German version: *Angew. Chem.* **1996**, *108*, 2093–2095

Keywords: acetals · aldol additions · dioxepanones · ketenes

[1] a) T. Mukaiyama, M. Murakami, *Synthesis* **1987**, 1043; b) T. Mukaiyama, *Org. React. (N.Y.)* **1982**, *28*, 203.

[2] a) W. S. Johnson, C. Edington, J. D. Elliott, I. R. Silverman, *J. Am. Chem. Soc.* **1984**, *106*, 7588; b) J. M. McNamara, Y. Kishi, *ibid.* **1982**, *104*, 7371; b) Review: C. Gennari in *Comprehensive Organic Synthesis, Vol. 2* (Ed.: B. M. Trost), Pergamon, Oxford, **1991**, Chapter 2.4.

[3] a) P. B. Rasmussen, S. Bøwadt, *Synthesis* **1989**, 114; b) C. D. Hurd, R. D. Kimbrough, Jr., *J. Am. Chem. Soc.* **1961**, *83*, 236; c) F. Šorm, J. Smrt, *Chem. Listy* **1953**, *47*, 413; d) Review: E. Schaumann, S. Scheiblich in *Houben-Weyl, Methoden der Organischen Chemie, Bd. E15*, Teil 3 (Eds.: H. Hagemann, D. Klamann), Thieme, Stuttgart, **1993**, p. 2453; e) H. Eck, *Chem. Ztg.* **1973**, *97*, 629.

[4] a) H. Staudinger, *Chem. Ber.* **1905**, *38*, 1735; b) C. C. McCarney, R. S. Ward, *J. Chem. Soc. Perkin Trans. 1* **1975**, 1600; c) P. W. Jeffs, G. Molina, M. W. Cass, N. A. Cortese, *J. Org. Chem.* **1982**, *47*, 3871.

[5] Selected spectroscopic data for **9** and **18a**: **9**: ^{1}H NMR (250 MHz, $CDCl_3$): $\delta = 0.72$ (s, 3H), 1.22 (s, 3H), 1.55 (s, 3H), 1.56 (s, 3H), 3.22 (d, 1H, $J = 12.2$ Hz), 3.48 (d, 1H, $J = 12.2$ Hz), 3.90 (d, 1H, $J = 10$ Hz), 4.70 (d, 1H, $J = 10$ Hz); ^{13}C NMR (63 MHz, $CDCl_3$): $\delta = 21.14$, 21.58, 22.21, 26.18, 39.33, 71.37, 80.40, 85.88, 89.04, 169.31; all signals are very broad. **18a**: ^{1}H NMR (250 MHz, $CDCl_3$): $\delta = 1.23$ (d, 3H, $J = 6.4$ Hz), 1.40 (d, 3H, $J = 6.5$ Hz), 3.74 (dq, 1H, $J = 6.4$, 8.5 Hz), 4.79 (dq, 1H, $J = 6.5$, 8.5 Hz), 4.82 (s, 1H), 6.91 (dd, 1H, $J = 6.7$, 2.1 Hz); 7.44 (dd, 1H, $J = 2.1$, 6.7 Hz); ^{13}C NMR (63 MHz, $CDCl_3$): $\delta = 17.93$, 17.98, 55.14, 83.81, 86.34, 86.45, 87.71, 113.03, 128.24, 129.38, 159.92, 166.88.

[6] Cf. C. D. Hurd, R. D. Kimbrough, Jr., *J. Am. Chem. Soc.* **1961**, *83*, 236.

[7] Crystal structure analysis of compounds **18a**, **18c**, und **18d**: Enraf-Nonius CAD4 diffractometer; $Cu_{K\alpha}$ radiation; room temperature; empirical absorption correction based on Ψ-scans; Structure elucidation by direct methods using SIR92; Hydrogen atom positions determined from difference densities and refined with isotropic temperature factors; C, O, and Cl atoms anisotropic. **18a**: $C_{14}H_{16}Cl_2O_4$, orthorhombic, space group $P2_12_12_1$; $a = 6.0120(7)$, $b = 7.2430(5)$, $c = 34.812(2)$ Å; $V = 1515.9(4)$ Å^3; $Z = 4$; $\rho_{calcd} = 1.399$ g cm^{-3}; $\mu = 40.2$ cm^{-1}; Quadrant to $2\theta = 120°$; 2128 reflections with $I > 0$; 246 parameters refined, $R = 0.037$, $R_w = 0.045$; Residual electron density between -0.17 and $+0.26$ e Å^{-3}. **18c**: $C_{15}H_{20}O_4$, orthorhombic, space group $P2_12_12_1$; $a = 6.3224(7)$, $b = 9.635(1)$, $c = 23.543(2)$ Å; $V = 1434.1(5)$ Å^3; $Z = 4$; $\rho_{calcd} = 1.224$ g cm^{-3}; $\mu = 6.8$ cm^{-1}; Quadrant to $2\theta = 130°$; 2774 reflections with $I > 0$; 253 parameters refined, $R = 0.042$, $R_w = 0.056$; Residual electron density between -0.11 and $+0.14$ e Å^{-3}. **18d**: $C_{20}H_{22}O_4$, orthorhombic, space group $P2_12_12_1$; $a = 8.3584(5)$, $b = 8.6305(6)$, $c = 25.007(2)$ Å; $V = 1803.9(4)$ Å^3; $Z = 4$; $\rho_{calcd} = 1.202$ g cm^{-3}; $\mu = 6.4$ cm^{-1}; 3 octands to $2\theta = 130°$; 4536 reflections with $I > 0$; 306 parameters refined; $R = 0.035$; $R_w = 0.043$; Residual electron density between -0.09 and $+0.12$ e Å^{-3}. Crystallographic data (excluding structure factors) for the structures reported in this paper have been deposited with the Cambridge Crystallographic Data Centre as supplementary publication no. CCDC-179-69. Copies of the data can be obtained free of charge on application to The Director, CCDC, 12 Union Road, Cambridge CB2 1EZ, UK (fax: Int. code +(1223) 336-033; e-mail: teched@chemcrys.cam.ac.uk).

[8] F. P. Cossio, J. M. Ugalde, X. Lopez, B. Lecea, C. Palomo, *J. Am. Chem. Soc.* **1993**, *115*, 995.

 © VCH Verlagsgesellschaft mbH, D-69451 Weinheim, 1996 0570-0833/96/3517-1972 $ 15.00+.25/0

An Unsymmetrical Dinuclear Iron(III) Complex with Peroxidase Properties**

Burkhard Eulering, Michael Schmidt,
Ulrich Pinkernell, Uwe Karst, and Bernt Krebs*

Dedicated to Professor Hans Georg von Schnering on the occasion of his 65th birthday

The use of heptadentate dinucleating ligands is a promising strategy for the synthesis of dinuclear iron complexes that serve as model compounds for metalloproteins. To imitate the respective active sites as well as possible, unsymmetrical ligands are required. The crystallization of the corresponding unsymmetrical iron complexes has proven to be extremely difficult, and to date only two examples, both based on the use of μ-phenoxo-bridged ligands, have been described. Latour et al. have successfully synthesized an unsymmetrical $Fe^{II}Fe^{III}$ complex with terminal phenolato coordination as a model for purple acid phosphatases[1] and also prepared a semimet-hemerythrin analogue.[2] We report here on the synthesis and X-ray structure analysis of the first unsymmetrical μ-alkoxo-bridged dinuclear iron complex and on its peroxidase activity.

Compound **1** was synthesized by reacting the unsymmetrical hexadentate chelating ligand *N*-methyl-*N*,*N*′,*N*′-tris(2-benzimidazolylmethyl)-2-hydroxy-1,3-diaminopropane (Hmtbpo)[3] with equimolar amounts of $Fe(ClO_4)_3 \cdot 9H_2O$, $FeCl_3$, and $NaO_2As(CH_3)_2 \cdot 3H_2O$ in methanol.

$[Fe_2(mtbpo)\{O_2As(CH_3)_2\}Cl_2(CH_3OH)](ClO_4)_2 \cdot 4CH_3OH$ **1**

Hmtbpo =

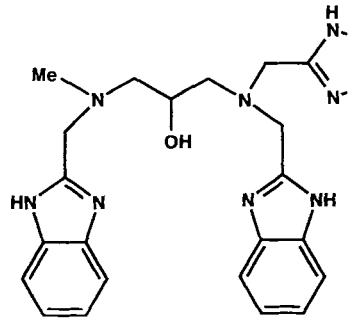

The X-ray structure analysis shows that (Fig. 1) the metal centers in **1** are linked by a dimethylarsinato-*O*,*O*′ bridge and by the deprotonated alkoxo oxygen atom O1. This results in a (μ-alkoxo)(μ-dimethylarsinato)diiron(III) center, which was also recently reported in a complex with the symmetrical heptadentate chelating ligand *N*,*N*,*N*′,*N*′-tetrakis(2-benzimidazolylmethyl)-2-hydroxy-1,3-diaminopropane (Htbpo).[5] Complex **1** is a structural model for the active site of the arsenato inhibitor complex of the purple acid phosphatase ($Fe^{III}Fe^{III}$ form) from porcine uterus (uteroferrin), since both the type of bridging and the number of arsenato groups in **1** correspond to the postulated situation in uteroferrin. The environment of Fe1 in the complex

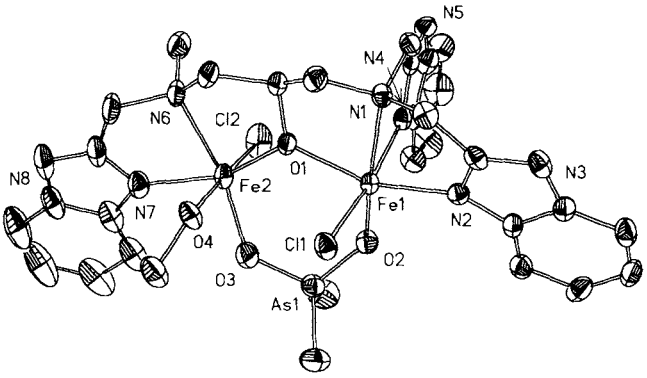

Fig. 1. Structure of one of the crystallographically independent cations $[Fe_2(mtbpo)\{O_2As(CH_3)_2\}Cl_2(CH_3OH)]^{2+}$ of **1** in the crystal. Selected distances [Å] and interatomic angle [°]: Fe1 ··· Fe2 3.535(1), Fe1 ··· As1 3.269(1), Fe2 ··· As1 3.297(1), Fe1–Cl1 2.367(1), Fe1–O1 2.021(2), Fe1–O2 1.906(3), Fe1–N1 2.309(3), Fe1–N2 2.075(3), Fe1–N4 2.102(3), Fe2–Cl2 2.261(1), Fe2–O1 1.972(2), Fe2–O3 1.912(3), Fe2–O4 2.247(3), Fe2–N6 2.268(3), Fe2–N7 2.066(3), As1–O2 1.694(3), As1–O3 1.689(3); Fe1-O1-Fe2 124.5(1).

cation of **1** is completed by the facial coordination of two benzimidazole nitrogen atoms, a tertiary nonaromatic nitrogen donor atom of the ligand $mtbpo^-$, and a chloro ligand. The distorted octahedral coordination at Fe2 is completed by two nitrogen donor atoms of the ligand $mtbpo^-$, a chloro ligand, and a methanol group. Thus, different coordination spheres are obtained for the two iron atoms: Fe1 is surrounded by a N_3O_2Cl and Fe2 by a N_2O_3Cl donor set. The Fe ··· Fe and Fe ··· As distances in **1** with average values for both crystallographically independent complex cations of 3.54 Å and 3.28 Å, respectively, are in the same order of magnitude as those of the complex with the symmetrical ligand Htbpo (3.58 and 3.31 Å, respectively).[5]

The catalytic properties of **1** in oxidations have been investigated by using hydrogen peroxide. The reaction of H_2O_2 and **1** in methanol can be monitored photometrically. A peroxide adduct is formed that is stable over several hours and that has an absorption maximum at 578 nm. The labile chloro ligands at Fe1 and Fe2 and the methanol ligand at Fe2 are coordination partners that can be substituted easily by H_2O_2. Complex **1** exhibits very limited catalase properties (catalytic decomposition of H_2O_2 to O_2 and H_2O). In contrast, the high stability of the adduct suggested that **1** may be suitable to activate peroxides for oxidations.

In the study of this peroxidase behavior, we observed the catalytic oxidation according to Equation (a). The diammoni-

$$H_2O_2 + \text{substrate}_{red} \longrightarrow H_2O + \text{substrate}_{ox} \quad \text{(a)}$$

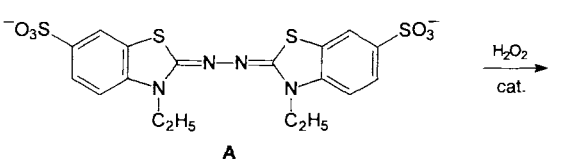

A

(b)

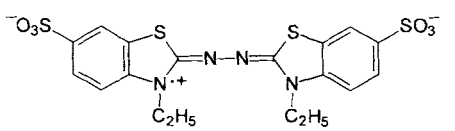

D

[*] Prof. Dr. B. Krebs, Dr. B. Eulering, Dipl.-Chem. M. Schmidt
Anorganisch-chemisches Institut der Universität
Wilhelm-Klemm-Strasse 8, D-48149 Münster (Germany)
Fax: Int code +(251)838366
e-mail: krebs@uni-muenster.de
Dipl.-Chem. U. Pinkernell, Dr. U. Karst
Lehrstuhl für Analytische Chemie der Universität
Wilhelm-Klemm-Strasse 8, D-48149 Münster (Germany)

[**] This work was supported by the Deutsche Forschungsgemeinschaft and the Fonds der Chemischen Industrie.

um salt of 2,2'-azinobis-(3-ethylbenzothiazoline-6-sulfonic acid) (ABTS) proved to be particularly suitable as substrate; it is commonly applied for the quantification of the enzymatic activity of peroxidases. The reduced form of ABTS is colorless; in contrast, when ABTS is oxidized to the radical cation, several characteristic absorption bands appear at 415, 650, 735, and 815 nm, and the resulting solution is green. Similar investigations have been performed with iron–porphyrin complexes.[8] Peroxidase properties of dinuclear complexes, however, have not been observed yet.

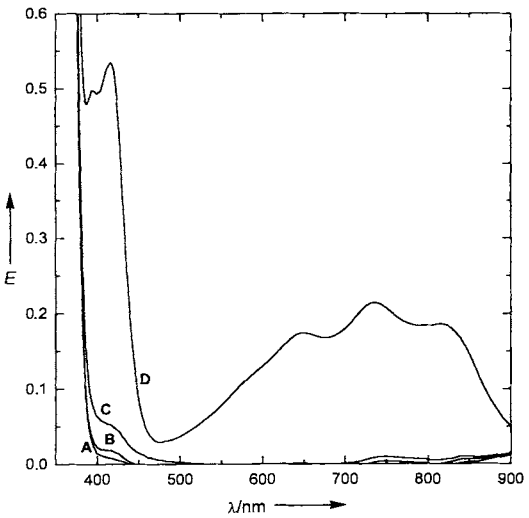

Fig. 2. UV/Vis absorption spectra of ABTS (A), ABTS + H_2O_2 (B), ABTS + **1** (C), ABTS + **1** + H_2O_2 (D), each recorded 10 min after mixing the solutions.

In the reaction of ABTS with H_2O_2 in the presence of **1**, the characteristic absorption bands of $ABTS^{\cdot+}$ were established immediately after mixing (Fig. 2). Without **1**, the oxidation of ABTS by H_2O_2 did not occur. The further oxidation to the corresponding dication[7] was also not observed. Thus, **1** can be considered as a functional model for peroxidase.

Experimental Procedure

1: $Fe(ClO_4)_3 \cdot 9H_2O$ (0.104 g, 0.20 mmol) and $FeCl_3$ (0.033 g, 0.20 mmol) were dissolved in methanol (5 mL) and added to a solution of Hmtbpo (0.1 g, 0.20 mmol) in methanol (5 mL). Sodium dimethylarsinate (0.043 g) in methanol (5 mL) was added to the deep red solution. The red product crystallized after a few days. Correct elemental analysis. UV/vis (methanol): λ_{max} (ε[L mol^{-1} cm^{-1}]) = 211 (38210), 240 (23660), 271 (26530), 278 (24430), 351 nm (4860). Cyclic voltammogram (in acetonitrile with 0.1 M tetrabutylammonium perchlorate; three-component system: mercury disk working electrodes, platinum wire auxiliary electrodes, and a Ag/AgCl 3 M NaCl reference electrode): quasi-reversible one electron transfer transition at −830 mV. Magnetic susceptiblity (SQUID measurement, 5.1–299.5 K) [9]: $H = -2JS_1S_2$ ($S_1 = S_2 = 5/2$): J [cm^{-1}]: −10.8(1). Mössbauer spectra at 4.2 K (doublet) [9]: δ [mm s^{-1}], ΔE_Q [mm s^{-1}]: 0.34, 0.27.

Oxidation of ABTS with H_2O_2 in the presence of **1**: An aqueous solution of ABTS (50 μL; 5 mg mL^{-1}) and a methanolic solution of **1** (10 μL; 1 mmol L^{-1}) were added to water (3 mL). The oxidation of ABTS starts immediately after addition of an aqueous solution of H_2O_2 (50 μL; 10 M).

Received: March 18, 1996 [Z8943IE]
German version: *Angew. Chem.* **1996**, *108*, 2102–2104

Keywords: complexes with oxygen ligands · enzyme models · iron compounds · oxidations

[1] E. Bernard, W. Moneta, J. Laugier, S. Chardon-Noblat, A. Deronzier, J.-P. Tuchagues, J.-M. Latour, *Angew. Chem.* **1994**, *106*, 914–917; *Angew. Chem. Int. Ed. Engl.* **1994**, *33*, 887–889.

[2] W. Kanda, W. Moneta, M. Bardet, E. Bernard, N. Debaecker, J. Laugier, A. Bousseksou, S. Chardon-Noblat, J.-M. Latour, *Angew. Chem.* **1995**, *107*, 625–628; *Angew. Chem. Int. Ed. Engl.* **1995**, *34*, 588–590.

[3] The ligand Hmtbpo can be synthesized by the reaction of an aqueous, alkaline solution of iminodiacetic acid with an equimolar amount of epichlorohydrine, followed by subsequent reaction with an alkaline solution of sarcosine. The ligand is obtained by the reaction of the free acid with 1,2-phenylenediamine. A complete description of the synthesis and characterization of the ligand will be described elsewhere [10]. The synthesis of the N-methyl derivative of the ligand Hmtbpo was recently achieved by another synthetic route [11].

[4] Crystal structure of **1**: crystal dimensions 0.25 × 0.28 × 0.18 mm, triclinic, $P\bar{1}$, $a = 14.184(3)$, $b = 16.381(3)$, $c = 24.054(3)$ Å, $\alpha = 75.70(3)$, $\beta = 86.54(3)$, $\gamma = 68.56(3)$, $V = 5038$ Å^3, $Z = 4$, $\rho_{calcd} = 1.545$ g cm^{-3}, $2\theta_{max} = 54°$, $Mo_{K\alpha}$ radiation ($\lambda = 0.71073$ Å), ω scan, $T = 150$ K, 21685 symmetry-independent reflections of which 11885 had $I > 2\sigma(I)$, 21679 reflections were used in the refinement, no absorption correction ($\mu = 1.51$ mm^{-1}, max./min. transmission: 0.762/0.686), the structure was solved by using Patterson methods (SHELXS-86, G. M. Sheldrick, **1990**), refinement on F^2 (SHELXS-93, G. M. Sheldrick, **1993**), 1364 independent parameters, calculation of the H atoms in ideal postions, $R1 = 0.0438$ ($I > 2\sigma(I)$), $wR2 = 0.1029$ (all data), max. residual electron density 0.82 e A^{-3}. Perchlorate anions and two solvate molecules are disordered. Crystallographic data (excluding structure factors) for the structure reported in this paper have been deposited with the Cambridge Crystallographic Data Centre as supplementary publication no. CCDC-179-68. Copies of the data can be obtained free of charge on application to The Director, CCDC, 12 Union Road, Cambridge CB2 1EZ, UK (fax: Int. code +(1223) 336-033; e-mail: teched@chemcrys.cam.ac.uk).

[5] B. Eulering, F. Ahlers, F. Zippel, M. Schmidt, H.-F. Nolting, B. Krebs, *J. Chem. Soc. Chem. Commun.* **1995**, 1305–1307.

[6] A. E. True, R. C. Scarrow, C. R. Randall, R. C. Holz, L. Que, Jr., *J. Am. Chem. Soc.* **1993**, *115*, 4246–4255.

[7] S. Hünig, H. Balli, H. Conrad, A. Schott, *Justus Liebigs Ann. Chem.* **1964**, *676*, 36–51.

[8] M. F. Zipplies, W. A. Lee, T. C. Bruice, *J. Am. Chem. Soc.* **1986**, *108*, 4433–4445.

[9] We thank Dr. M. Windhaus, R. Müllmann, and Prof. W. Müller-Warmuth (Institut für Physikalische Chemie, Münster) for support during the measurement of the Mössbauer data and K. Griesar and Prof. W. Haase (Technische Hochschule, Darmstadt) for the magnetic susceptibility measurements.

[10] D. Volkmer, B. Hommerich, K. Griesar, W. Haase, B. Krebs, *Inorg. Chem.* **1996**, *35*, 3792–3803.

[11] J. H. Satcher, Jr., M. W. Droege, T. M. R. Weakley, R. T. Taylor, *Inorg. Chem.* **1995**, *34*, 3317–3328.

Cationic Iridium(III) Carbonyl Complexes: $[Ir(CO)_6]^{3+}$ and $[Ir(CO)_5Cl]^{2+}$**

Christian Bach, Helge Willner,* Changqing Wang, Steven J. Rettig, James Trotter, and Friedhelm Aubke*

Neutral homoleptic carbonyl complexes of iridium such as the tetranuclear cluster $[Ir_4(CO)_{12}]$ have been known for some time.[1–3] More recently the highly reduced carbonylate $[Ir(CO)_3]^{3-}$ was reported,[4] and it has since become a challenge to synthesize the homoleptic carbonyl cations $[Ir(CO)_6]^{3+}$. Its existence as a thermally stable species would complete a series of carbonyl cations of the 5d block metals that stretches from linear $[Au(CO)_2]^+$[5] over square-planar $[Pt(CO)_4]^{2+}$[6] to octahedral $[Ir(CO)_6]^{3+}$. We report here the synthesis and spectroscopic characterization of $[Ir(CO)_6][Sb_2F_{11}]_3$ and the molecular structure determination of $[Ir(CO)_5Cl][Sb_2F_{11}]_2$.

[*] Prof. Dr. H. Willner, Dipl.-Chem. C. Bach
Institut für Anorganische Chemie der Universität
Callinstrasse 9, D-30167 Hannover (Germany)
Fax: Int. code +(511) 762 3006
e-mail: willner@mbox.acc.uni-hannover.de
Prof. Dr. F. Aubke, Dr. C. Wang, Dr. S. J. Rettig, Prof. Dr. J. Trotter
Department of Chemistry, The University of British Columbia
Vancouver B.C. V6T 1Z1 (Canada)

[**] Financial support by National Science and Engineering Research Council (J. T. and F. A.), Deutsche Forschungsgemeinschaft (H. W.), NATO (H. W. and F. A.), and the Alexander-von-Humboldt-Foundation (F. A.) is gratefully acknowledged. We are thankful to the Degussa Company for a gift of Ir metal powder.

Since $[Au(CO)_2][Sb_2F_{11}]$[5] and $[Pt(CO)_4][Sb_2F_{11}]_2$[6] are obtained from the fluorosulfate precursors $[Au(CO)SO_3F]$[7] and *cis*-$[Pt(CO)_2(SO_3F)_2]$,[8] respectively, by solvolysis in liquid SbF_5 under a CO pressure of about 1 atm, the recent discovery of $[Ir(CO)_3(SO_3F)_3]$[9] provides a promising starting material for the synthesis of $[Ir(CO)_6][Sb_2F_{11}]_3$. Our recent report on the compounds $[M(CO)_6][Sb_2F_{11}]_2$, M = Ru or Os,[10] suggests that in addition to the well-known cations $[M(CO)_6]^+$ (M = Mn, Tc, and Re)[11] multiply charged homoleptic octahedral metal carbonyl cations exist and display unexpectedly high thermal stabilities. The molecular structure of $[Hg(CO)_2][Sb_2F_{11}]_2$[12] indicates that the $[Sb_2F_{11}]^-$ ion plays an important role in stabilizing the linear $[Hg(CO)_2]^{2+}$ ion through $SbF\cdots CO$ secondary contacts. The use of liquid antimony(v) fluoride as reaction medium for (reductive) carbonylations has been reviewed very recently.[13]

While the synthesis of $[Ir(CO)_3(SO_3F)_3]$[9] proceeds smoothly, the preparation of the starting material $[Ir(SO_3F)_3]$ by metal oxidation with $S_2O_6F_2$ in HSO_3F at 120–140 °C[14] is more difficult. Hence only small amounts (250 mg) of $[Ir(SO_3F)_3]$ are available for a subsequent carbonylation to $[Ir(CO)_3(SO_3F)_3]$. Solvolysis of $[Ir(CO)_3(SO_3F)_3]$ in an excess of SbF_5 under a CO atmosphere at 60 °C produces an inseparable mixture of $[Ir(CO)_6][Sb_2F_{11}]_3$ and at least one other species, judging by the complexity of the vibrational spectra in the CO region. When crystalline *mer*-$[Ir(CO)_3(SO_3F)_3]$[9] was dissolved in magic acid (65 mol% SbF_5 in HSO_3F) at 25 °C under 0.5 atm CO and the solution was allowed to stand for about nine weeks, pale yellow crystals form, which were identified by X-ray single-crystal diffraction as $[Ir(CO)_5Cl][Sb_2F_{11}]_2$[15] (Fig. 1). Fluorochloro-

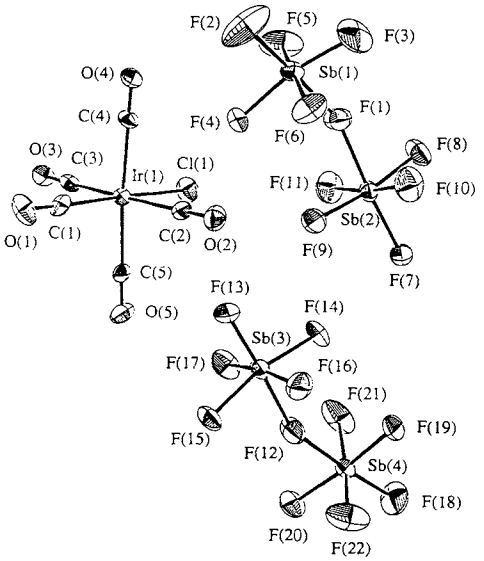

Fig. 1. Molecular structure of $[Ir(CO)_5Cl][Sb_2F_{11}]_2$ (50% probability thermal ellipsoids are shown).

carbon grease is considered to be the most likely source for the chloride ion.

The $[Ir(CO)_5Cl]^{2+}$ ion is unique in carbonyl complex chemistry. $[Fe(CO)_5Cl]^+$[16] and the isoelectronic species $[Re(CO)_5Cl]$[1–3] provide remotely related precedents. The Ir–C distances of 202(2) pm are long compared to the q_u value of 189.8 pm, which was calculated based on 148 examples.[17a] As expected, the C–O distances of 108(2) pm are very short, but the large standard deviations do not permit a meaningful discussion. Both sets of data are comparable within standard deviations to those reported for *mer*-$[Ir(CO)_3(SO_3F)_3]$[9] and for $[Ir(CO)_3F_3]$ from EXAFS data.[17b] As found for *mer*-$[Ir(CO)_3(SO_3F)_3]$[9] and for $[Hg(CO)_2][Sb_2F_{11}]_2$[12] there are significant secondary interionic $SbF\cdots CO$ contacts (ca. 280 pm, two for each C atom), which are less than the sum of the van der Waals radii (317 pm).[18]

These interionic interactions are comparable in strength but not in number to those found for $[Hg(CO)_2][Sb_2F_{11}]_2$, in which the C atoms of the linear $[Hg(CO)_2]^{2+}$ ion appear to be more accessible and where four interionic $SbF\cdots CO$ contacts are observed.[12] Consequently the Sb-F_b-Sb angle of 147.6(3)° in the anion $[Sb_2F_{11}]^-$ is more acute in the mercury compound than in $[Ir(CO)_5Cl][Sb_2F_{11}]_2$ (153.2(6)° and 156.2(6)°). Reduced secondary interionic interactions within the iridium compound are also reflected in the Sb–F distances, which range from 178 to 188 pm. The corresponding bondlengths in $[Hg(CO)_2][Sb_2F_{11}]_2$ lie between 185 and 189 pm.[12]

Since the synthesis of $[Ir(SO_3F)_3]$ is difficult[9, 14] and $IrCl_3$ is found to be unreactive in SbF_5 when CO is also present, a different synthetic approach to $[Ir(CO)_6][Sb_2F_{11}]_3$ was developed: the reductive carbonylation of IrF_6 in SbF_5 [Eq. (a)].

$$2\,IrF_6 + 12\,SbF_5 + 15\,CO \xrightarrow[60\,^\circ C,\ 12\ h]{SbF_5(l)} 2\,[Ir(CO)_6][Sb_2F_{11}]_3 + 3\,COF_2 \qquad (a)$$

IrF_6 was prepared by fluorination of iridium metal powder at 250 °C by a published procedure.[19] The white, extremely moisture-sensitive complex $[Ir(CO)_6][Sb_2F_{11}]_3$ remained after removal of all volatiles in vacuo. The isotopomer $[Ir(^{13}CO)_6][Sb_2F_{11}]_3$ was obtained in an identical manner by using ^{13}CO. The product was identified by the mass balance of the reaction, by its vibrational spectra, and by the ^{13}C MAS NMR spectrum (Table 1).[20]

The vibrational data for $[Ir(CO)_6][Sb_2F_{11}]_3$ and its ^{13}C isotopomer clearly indicate that the $[Ir(CO)_6]^{3+}$ ion is strictly octahedral. Consistent with this finding, a single line resonance at $\delta = 121$ is found in the ^{13}C MAS NMR spectrum, and coupling to either ^{191}Ir or ^{193}Ir (both with a nuclear spin of 3/2) is not observed.

With the inclusion of the two carbonylates $[Hf(CO)_6]^{2-}$[4] and $[Ta(CO)_6]^-$[21] a correlation of spectroscopic properties for six octahedral carbonyl species ranging from $[Hf(CO)_6]^{2-}$ to $[Ir(CO)_6]^{3+}$ is now possible (Table 1). In addition to the ^{13}C

Table 1. Vibrational spectra ($\tilde{\nu}_{CO}$ region), force constants f_{CO}, and ^{13}C chemical shifts for homoleptic, isoelectronic, and octahedral $[M(CO)_6]$ species of the 5d block metals.

	$[Hf(CO)_6]^{2-}$	$[Ta(CO)_6]^-$	$[W(CO)_6]$	$[Re(CO)_6]^+$	$[Os(CO)_6]^{2+}$	$[Ir(CO)_6]^{3+}$
$\tilde{\nu}(a_{1g})$/cm^{-1}			2115 [e]	2197 [g]	2259 [i]	2295
$\tilde{\nu}(e_g)$/cm^{-1}			1998 [e]	2122 [g]	2218 [i]	2276
$\tilde{\nu}(f_{1u})$/cm^{-1}	1757 [a]	1850 [c]	1977 [e]	2085 [g]	2190 [i]	2254
f_{CO}/$\times 10^2$ Nm^{-1}			17.0 [f]	18.1 [f]	19.8 [f]	20.8 [f]
$\delta(^{13}C)$	244 [b]	211 [d]	192 [d]	171 [h]	147 [i]	121

[a] J. E. Ellis, K. M. Chi, *J. Am. Chem. Soc.* **1990**, *112*, 6022–6025. [b] Reference [4]. [c] H. Siebert, *Anwendungen der Schwingungsspektroskopie in der anorganischen Chemie*, Springer, Berlin, **1966**. [d] B. E. Mann, *J. Chem. Soc. Dalton Trans.* **1973**, 2012–2015. [e] Reference [22]. [f] Obtained by using the Cotton–Kraihanzel method: F. A. Cotton, C. S. Kraihanzel, *J. Am. Chem. Soc.* **1962**, *84*, 4432–4438. [g] Reference [23]. [h] This work, measured as $[Re(CO)_6][Sb_2F_{11}]$. [i] Reference [10].

chemical shifts, the frequencies of the asymmetric CO stretches $\tilde{\nu}_{CO}(f_{1u})$ are given in Table 1, because Raman spectra have so far not been reported for the two carbonylate anions. For the remaining four molecular species from $[W(CO)_6]$ to $[Ir(CO)_6]^{3+}$ complete vibrational data are available.[10, 20–23]

The trend shown by the f_{1u} vibrations, that the CO bond strength increases with increasing formal charge of the metal, is quantified by the increasing stretching force constants f_{CO} (Table 1). The value of the force constant for $[Ir(CO)_6]^{3+}$ (20.8×10^2 Nm^{-1}) is only slightly below that for $[Hg(CO)_2]^{2+}$ (21.0×10^2 Nm^{-1})[12] and that for HCO^+ (21.3×10^2 Nm^{-1}).[5] The ^{13}C chemical shift of $\delta = 121$ is the lowest that has been measured for carbonyl complexes. The rather smooth trend in both $\tilde{\nu}^{CO}(f_{1u})$ and ^{13}C chemical shifts illustrates that for the six isostructural and isoelectronic $(d^6)[M(CO)_6]$ species π back donation gradually decreases with a concomitant increase in σ donation as the formal charge on the metal gradually increases from -2 to $+3$. For $[Ir(CO)_6]^{3+}$, π back bonding makes only a small, insignificant contribution to the Ir–CO bonding. A similar correlation can be made for carbonyl derivatives of iridium where $\tilde{\nu}_{CO}$ for terminal CO groups increases from 1642 cm^{-1} for $[Ir(CO)_3]^{3-}$[14] to 2295 cm^{-1} for the a_{1g} mode of $[Ir(CO)_6]^{3+}$. Both trends clearly demonstrate the great versatility of the CO ligand, which coordinates to metallic centers of formal charges from -3 to $+3$ form stable metal carbonyl species.

As more cationic carbonyl complexes like $[M(CO)_6]^{2+}$ (M = Ru, Os)[10], $[Ir(CO)_5Cl]^{2+}$, and $[Ir(CO)_6]^{3+}$ become known, together with accurate structural and vibrational data, and as smooth correlations between the formal charge on the metal and the bonding characteristics in the CO ligands emerge, it becomes increasingly obvious that any arbitrary subdivision using vague terms like "classical" and "nonclassical (σ-only)" carbonyl complexes as proposed sometime ago for the thermally unstable $[Ag(CO)_n]^+$ ($n = 1, 2$) species[24] is incorrect, inappropriate, and unnecessary. The first metal carbonyl derivative $[Pt(CO)_2Cl_2]$ reported in 1868[25] with an average $\tilde{\nu}_{CO}$ value of 2175 cm^{-1} [well above that (2143 cm^{-1}) for free CO[26]] would be assigned "nonclassical", which is in our view absurd.

Received: April 17, 1996 [Z 9046 IE]
German version: *Angew. Chem.* **1996**, *108*, 2104–2106

Keywords: carbonyl complexes · iridium compounds · IR spectroscopy · structure elucidation

[1] F. A. Cotton, G. Wilkinson, *Advanced Inorganic Chemistry*, 5th ed., Wiley & Sons, New York, **1988**, p. 58 and 1035.
[2] F. P. Pruchnik, *Organometallic Chemistry of Transition Elements*, Plenum Press, New York, **1990**, p. 23.
[3] H. Werner, *Angew. Chem.* **1990**, *102*, 1109–1121; *Angew. Chem. Int. Ed. Engl.* **1990**, *29*, 1077–1089.
[4] J. E. Ellis, *Adv. Organomet. Chem.* **1990**, *31*, 1–51.
[5] H. Willner, J. Schaebs, G. Hwang, F. Mistry, R. Jones, J. Trotter, F. Aubke, *J. Am. Chem. Soc.* **1992**, *114*, 8972–8980.
[6] G. Hwang, C. Wang, F. Aubke, M. Bodenbinder, H. Willner, *Can. J. Chem.* **1993**, *71*, 532–536.
[7] H. Willner, F. Aubke, *Inorg. Chem.* **1990**, *29*, 2195–2200.
[8] G. Hwang, C. Wang, M. Bodenbinder, H. Willner, F. Aubke, *J. Fluorine Chem.* **1994**, *66*, 159–166.
[9] C. Wang, A. R. Lewis, R. J. Batchelor, F. W. B. Einstein, H. Willner, F. Aubke, *Inorg. Chem.* **1996**, *35*, 1279–1285.
[10] C. Wang, B. Bley, G. Balzer-Jöllenbeck, A. R. Lewis, S. C. Siu, H. Willner, F. Aubke, *J. Chem. Soc. Chem. Commun.* **1995**, 2071–2072.
[11] a) E. W. Abel, S. P. Tyfield, *Adv. Organomet. Chem.* **1970**, *8*, 117–165; b) W. Beck, K. Sünkel, *Chem. Rev.* **1988**, *88*, 1405–1421.
[12] M. Bodenbinder, G. Balzer-Jöllenbeck, H. Willner, R. J. Batchelor, F. W. B. Einstein, C. Wang, F. Aubke, *Inorg. Chem.* **1996**, *35*, 82–92.
[13] C. Wang, G. Hwang, S. C. Siu, B. Bley, M. Bodenbinder, C. Bach, H. Willner, F. Aubke, *Eur. J. Inorg. Solid State Chem.*, in press.
[14] K. C. Lee, F. Aubke, *J. Fluorine Chem.* **1982**, *19*, 501–516.
[15] Colorless, irregular crystal, $0.20 \times 0.40 \times 0.45$ mm, monoclinic, $P2_1$ (No. 4), $a = 9.868(2)$, $b = 12.585(2)$, $c = 10.499(2)$ Å, $\beta = 106.59(2)°$, $V = 1226.5(4)$ Å^3, $Z = 2$, $\rho_{calc.} = 3.446$ g cm^{-3}, $Mo_{K\alpha}$ ($\lambda = 0.71069$ Å), ω 2θ scans at 21 °C, 4829 reflections to $2\theta = 65°$, unique 4604, the data were corrected for *Lp*, linear decay (12.3%), absorption ($\mu = 100.6$ cm^{-1}, ψ scans, relative transmission factors: 0.314–1.000), and secondary extinction (Zachariasen type, isotropic, coefficient $= 1.05(3) \times 10^{-6}$). The structure was solved by the Patterson method and was refined by full-matrix least-squares procedures (on *F*, all atoms anisotropic) to $R = 0.032$ and $wR = 0.031$ (343 prameters, 3218 reflections with $I \geq 3\sigma(I)$). A parallel refinement of the mirror-image structure gave significantly higher residuals; the *R* and *wR* factors ratios were 1.17 and 1.19, respectively. Residual density: -1.16 to $+1.12$ e Å^{-3} (near Ir). All calculations performed using TeXsan (Molecular Structure Corporation, The Woodlands, TX, USA, 1995). Further details of the crystal structure investigation may be obtained from Fachinformationszentrum Karlsruhe, D-76344 Eggenstein-Leopoldshafen (Germany) on quoting the depository number CSD-405106.
[16] L. Iqbal, T. C. Waddington, *J. Chem. Soc. (A)* **1968**, 2958–2961.
[17] a) A. G. Orpen, L. Brammer, F. H. Allen, O. Kennard, D. G. Watson, R. Taylor, *J. Chem. Soc. Dalton Trans.* **1989**, S1–S83; b) S. A. Brewer, A. K. Brisdon, J. H. Holloway, E. G. Hope, L. A. Peck, P. G. Watson, *ibid.* **1995**, 2945–2948.
[18] A. Bondi, *J. Phys. Chem.* **1964**, *4*, 441–451.
[19] O. Ruff, J. Fischer, *Z. Anorg. Allg. Chem.* **1929**, *179*, 161–185.
[20] Characterization of $[Ir(CO)_6][Sb_2F_{11}]_3$: white, hygroscopic solid, >120 °C (decomp.); molecular mass expected: 1717.7 g mol^{-1}, molecular mass found: 1632.5 g mol^{-1}; vibrational data in [cm^{-1}], data for $[Ir(^{13}CO)_6][Sb_2F_{11}]_3$ are given in parentheses: Raman: 2295 s (2241), 2276 s (2222), 729 w (728), 699 m (699), 668 vs (668), 641 vs (640), 604 s (604), 581 m (580), 555 m (555), 428 w (422), 289 m (289), 232 w (232), 138 m-w (136); IR: 2254 s (2203), 689 vs (689), 663 vs (664), 636 vs (635), 573 m-w (572), 531 s (513), 480 w; ^{13}C MAS NMR: $\delta = 121$.
[21] F. Calderazzo, U. Englert, G. Pampaloni, G. Pelliziana, R. Zamboni, *Inorg. Chem.* **1983**, *22*, 1865–1870.
[22] L. H. Jones, R. S. McDowell, M. Goldblatt, *Inorg. Chem.* **1969**, *8*, 2349–2363.
[23] E. W. Abel, R. A. N. McLean, S. P. Tyfield, P. S. Braterman, A. P. Walker, P. J. Hendra, *J. Mol. Spectrosc.* **1969**, *30*, 29–50.
[24] P. K. Hurlburt, J. J. Rack, J. S. Luck, S. F. Dec, J. D. Webb, O. P. Andersen, S. H. Strauss, *J. Am. Chem. Soc.* **1994**, *116*, 10003–10014.
[25] P. Schützenberger, *Bull. Soc. Chim. Fr.* **1868**, *10*, 188–192.
[26] J. Browning, P. L. Goggin, R. J. Goodfellow, M. J. Morton, A. J. M. Rattray, B. F. Taylor, J. Mink, *J. Chem. Soc. Dalton Trans.* **1977**, 2061–2067.

Achieving Stable, Reverse Water-in-Fluorocarbon Emulsions**

Véronique M. Sadtler, Marie Pierre Krafft, and Jean G. Riess*

Macroemulsions are thermodynamically unstable systems that tend to separate irreversibly into the component phases upon aging. Their kinetic stability can, however, be increased by counteracting the processes by which they break down, that is, coalescence and molecular diffusion (Ostwald ripening).[1] Preparing stable water-in-fluorocarbon "reverse" emulsions is a stimulating challenge from both fundamental and applied standpoints.

Fluorocarbons are unique due to the extreme position of fluorine in the Periodic Table.[2] Liquid fluorocarbons display very

[*] Prof. J. G. Riess, V. M. Sadtler, Dr. M. P. Krafft
Unité de Chimie Moléculaire, associée au CNRS
Université de Nice-Sophia Antipolis, Faculté des Sciences
F-06108 Nice Cedex 2 (France)
Fax: Int. code +92 07 61 44
e-mail: mpk@naxos.unice.fr

[**] This work was supported by Alliance Pharmaceutical Corp. and ATTA (*A*pplications et *T*ransferts de *T*echnologies *A*vancées). We thank Dr. L. Zarif and Dr. R. Follana (Centre de Transfusion Sanguine des Alpes Maritimes) for the toxicity tests, and Dr. A. Kabalnov (Alliance) for helpful discussions.

weak intermolecular (van der Waals) interactions, and this results in the lowest possible associative character.[3] Water-in-fluorocarbon emulsions are thus a most unnatural combination of the least associated of liquids with one of the most strongly associated ones. Their formation and stabilization presuppose that very high interfacial tensions have been overcome.

Molecular diffusion was shown to be the predominant mechanism of particle size increase in direct, fluorocarbon-in-water emulsions.[4] We have now found that the same mechanism is effective for water-in-fluorocarbon emulsions. According to the Lifshitz–Slyozov equation [Eq. (a)][5] that describes this

$$v = \mathrm{d}(\bar{a}^3)/\mathrm{d}t = 8\gamma_i CDV_m/9RT \qquad \text{(a)}$$

mechanism, the rate v of particle volume increase ($\bar{a}$ = average radius of the particle) over time t through molecular diffusion is proportional to the molar volume of the dispersed phase (V_m), to the interfacial tension γ_i between continuous and dispersed phase, and to the solubility and diffusivity coefficients (C and D) of the dispersed phase in the continuous phase.

Molecular diffusion of water through the continuous fluorocarbon phase in a reverse water-in-fluorocarbon emulsion is expected to be faster than that of the same fluorocarbon through water, on two accounts: 1) although no data appear to be available on mutual solubilities of water and fluorocarbons, water should be more soluble in the fluorocarbon than vice versa because of its smaller molar volume and the easier formation of holes capable of hosting the water molecules in the loosely associated fluorocarbon. According to Hildebrand's theory, the solubility of water in a fluorocarbon is actually expected to be higher by several orders of magnitude than that of the same fluorocarbon in water, as it varies exponentially with the molar volume.[6] 2) The diffusivity of water in the fluorocarbon should also be larger than that of the fluorocarbon in water as indicated by the Hayduk–Laudie equation, although the difference is not expected to be as great.[7] Coalescence of water droplets in a fluorocarbon phase should be favored by the large difference in densities and by the higher fluidity of the fluorocarbons utilized here relative to that of water.

In spite of these unfavorable premises we have prepared stable water-in-fluorocarbon emulsions with submicrometer particles and a narrow size distribution. The key to meeting this challenge lay in the selection of an effective surfactant system. Because the continuous phase is fluorinated, the surfactant needs to have definite affinity for fluorocarbons, and hence needs to be fluorinated. A number of single- and double-chain perfluoroalkyl surfactants, among those that have been synthesized in this laboratory in recent years,[8] were therefore screened. Their modular molecular design allows stepwise modifications of their hydrophilic, lipophilic, and fluorophilic properties, which, in turn, have a considerable impact on their ability to form and stabilize colloidal systems.

Potential applications of reverse fluorocarbon emulsions can be envisaged in pulmonary administration of drugs and other agents. The agents to be delivered (which include surfactants, antibodies, antioxidants, steroids, nucleic acids, vasoactive agents, and cytotoxic drugs) are usually insoluble in fluorocarbons in significant amounts. Contrary to the presently investigated dispersions of micronized solid drugs in liquid fluorocarbons,[9] water-in-fluorocarbon emulsions should allow uniform, reproducible distribution of the agents, including to the deeper parts of the lungs; this presupposes, however, that emulsion stability has been achieved. Controlled release and reduced toxicity are also expected; in the hydrocarbon series, for example, water-in-oil emulsions of doxorubicin that allowed controlled delivery of the drug have been prepared, and fewer side-effects were experienced than with dispersions of solids.[10]

Perfluorooctyl bromide and perfluorooctylethane were chosen for this study, because they satisfy the criteria required for liquid breathing, a procedure investigated for treatment of acute respiratory distress. The former compound is in Phase II/III clinical trials for this procedure;[11] its fluorocarbon-in-water emulsions are in Phase II clinical trials as injectable oxygen carriers (blood substitutes).[12] The emulsifying agent utilized for the reverse fluorocarbon emulsions was eventually selected from a homologous series of fluorinated surfactants (*F*n*C*m*DMP*) derived from dimorpholinophosphate.[13]

$C_nF_{2n+1}(CH_2)_mOP(O)[N(CH_2CH_2)_2O]_2$

FnCmDMP; $n = 4, 6, 8, 10$ and $m = 2, 5, 11$

FnCmDMP are indeed highly fluorophilic; the potential for spontaneous formation of membranes with low curvature is indicated by the presence of elongated rather than spherical self-assemblies when dispersed in water.[14] Various spacer (m) and fluorocarbon chain lengths (n) were investigated. The best results, that is, the obtention of stable emulsions with small droplet size and long shelf-life, were achieved with F8C11DMP. It is noteworthy that no stable reverse emulsions could be prepared with the phospholipids used to prepare direct fluorocarbon-in-water emulsions, nor with the hydrocarbon dimorpholinophosphate $C_{15}H_{31}OP(O)[N(CH_2CH_2)_2O]_2$.

The preparation of the reverse fluorocarbon emulsions involved first the dispersion of the perfluoroalkylated surfactant in the fluorocarbon, followed by the addition of the aqueous phase, which may contain an active component. Emulsification was initiated with a low-energy mixer and completed with a high-pressure mechanical homogenizer. A series of water-in-fluorocarbon emulsions was thus prepared with water contents ranging from 1 to 30% v/v.

A typical example of a reverse emulsion containing perfluorooctyl bromide (95% v/v), NaCl (2.5% solution in water; 5% v/v), and F8C11DMP (2% w/v) was prepared as follows: F8C11DMP (40 mg) was dispersed in perfluorooctyl bromide (1.9 mL) by gentle stirring. The aqueous 2.5% solution of NaCl (0.1 mL) was added to the fluorocarbon phase, and the mixture was shaken by hand. The resulting coarse pre-emulsion was homogenized under high pressure (Emulsiflex B3, Avestin, 4.1×10^7 Pa, 12 cycles); the temperature was maintained below 40 °C.

The final emulsion was highly fluid and bluish. The average particle diameter, as measured by photosedimentation (Horiba Capa 700) immediately after preparation, was 0.15 ± 0.01 μm; this emulsion was stable enough to withstand heat sterilization conditions (121 °C, 15 min, 15 $N m^{-2}$) without significant particle size increase (0.16 ± 0.02 μm). As an alternative, the emulsion can also be filtered through a 0.22 μm sterilizing membrane without detectable change (0.15 ± 0.01 μm). The reverse nature of the water-in-fluorocarbon emulsion is unequivocally supported by the high fluidity (comparable to that of the fluorocarbon), by the absence of electrical conduction, and by the fact that the emulsions can easily be diluted with a fluorocarbon but not with water. The possibility of having reverse surfactant vesicles was excluded by an epifluorescence microscopy experiment in which 5,6-carboxyfluorescein was incorporated into the aqueous phase (2×10^{-3} M); it clearly showed uniformly fluorescent droplets rather than the fluorescent rim that was seen in the case of reverse vesicles.[15] Furthermore, as much as 30% by weight (45% by volume) of water can be incorporated into our reverse emulsions, with a surfactant/water ratio as low as 0.03

by weight, which is definitely incompatible with the formation of reverse vesicles.

The shelf stability of the reverse fluorocarbon emulsions was monitored at 25 °C by photosedimentation. After about 4.5 months, the average particle diameter of the above emulsion was still only 0.27 ± 0.02 μm, and the particle size distribution remained reasonably narrow as shown in Figure 1. That the

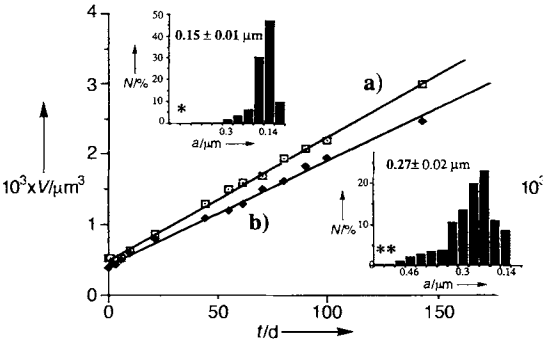

Fig. 1. Linear variation with time of the average volume V of water droplets at 25 °C in a reverse water-in-fluorocarbon emulsion (95% v/v perfluorooctyl bromide, 5% v/v saline, 2% (perfluorooctyl)undecyldimorpholinophosphate F8C11DMP) after heating at 121 °C for 15 min (a) and after filtration on a 0.22 μm sterilizing membrane (b). Insets: Size distribution histograms measured for the heated emulsion immediately after preparation (*) and after 140 days at 25 °C (**). N = percentage of particles with radius a. The quoted values give the average radii $\bar{a}$.

mechanism of particle growth in reverse fluorocarbon emulsions is molecular diffusion is strongly indicated by the following findings: a) the average volume of the water droplets increases linearly with time, as seen in Figure 1 for both heated and filtered emulsions; b) the distribution function, that is, the ratio $a_i/\bar{a}$ of particle radius a_i to the mean radius $\bar{a}$, is time-in variant;[4, 5] and c) the addition of NaCl contributes to stabilizing the emulsions by reducing the solubility of water in the fluorocarbon.

A series of drugs, including antibiotics (doxycycline, gentamycin, erythromycin), vasoactive bronchodilators (epinephrine, tolazoline), mucolytic agents (acetyl cysteine), antituberculosis agents (ethambutol, pyrazinamide), cholinergic (acetylcholine chloride), glucocorticoid (prednisone), and antitumor agents (cyclophosphamide), could be incorporated into such reverse fluorocarbon emulsions without inducing significant loss of stability.

For example, a reverse fluorocarbon emulsion otherwise formulated as in the example given above was prepared by adding 0.1 mL (5% v/v) of an aqueous solution of tolazoline (3% w/v in a 2.5% aqueous solution of NaCl). The average particle size, as measured by photosedimentation was 0.15 μm after preparation, 0.17 μm after heat-sterilization, and 0.23 μm after a month at 25 °C.

Preliminary toxicity data on water-in-fluorocarbon emulsions are encouraging. Intravenous administration of a dispersion of F8C11DMP in NaCl (0.9% solution) showed no acute toxicity at concentrations as high as $2\,g\,kg^{-1}$ body weight in mice (limit of protocol; all ten animals treated survived) indicating an i.v. LD_{50} value greater than $2\,g\,kg^{-1}$. Intraperitoneal administration of the same compound dispersed in perfluorooctyl bromide yielded an i.p. LD_{50} value around $4\,g\,kg^{-1}$. In the case of F8C2DMP all ten animals survived a $2\,g\,kg^{-1}$ body weight dose i.p. No hemolytic activity was detected either for these surfactants. A reverse emulsion (perfluorooctyl bromide, 95% v/v; NaCl 0.9% in water, 5% v/v; F8C11DMP, 1% w/v) was injected intraperitoneally into 10 mice (25 mL kg^{-1} body weight); after one month all the animals were still alive; no significant perturbation in their growth or behavior was observed during this period.

Received: February 1, 1996
Revised version: May 13, 1996 [Z8777IE]
German version: *Angew. Chem.* **1996**, *108*, 2106–2108

Keywords: drug delivery · emulsions · fluorocarbons · surfactants

[1] *Encyclopedia of Emulsion Technology, Vol. 1* (Ed.: P. Becher), M. Dekker, New York, **1983**.
[2] R. E. Banks, in *Fluorine in Medicine* (Eds.: R. E. Banks, K. C. Lowe), Rapra Technology Ltd., Shawbury, **1994**; B. Smart, in *Organofluorine Chemistry: Principles and Commercial Applications*, (Ed.: R. E. Banks), Plenum Press, New York, **1994**; J. G. Riess, *New J. Chem.* **1995**, *19*, 893–911.
[3] T. M. Reed III, in *Fluorine Chemistry, Vol. 5* (Ed.: J. H. Simmons), Academic Press, New York, **1964**, p. 133; P. Mukerjee, T. Handa, *J. Phys. Chem.* **1981**, *85*, 2298–2303.
[4] S. S. Davis, H. P. Round, T. S. Purewal, *J. Colloid Interface Sci.* **1981**, *80*, 508–511; A. S. Kabalnov, Y. D. Aprosin, O. B. Pavlova-Verevkina, A. V. Pertzov, E. D. Shchukin, *Kolloidn. Zh.* **1986**, *48*, 27–32; L. Trevino, L. Solé-Violan, P. Daumur, B. Devallez, M. Postel, J. G. Riess, *New J. Chem.* **1993**, *17*, 275–278.
[5] I. M. Lifshitz, V. V. Slyozov, *Sov. Phys. JETP (Engl. Transl.)* **1959**, *35*, 331–339; L. C. Wagner, *Z. Elektrochem.* **1961**, *65*, 581–591.
[6] Hildebrand's theory allows a qualitative estimation of the solubilities $C_{1\cdot2}$ and $C_{2\cdot1}$ of two liquids 1 and 2 in each other using the following simplified equations: $-RT\ln C_{1\cdot2} \approx V_{m1}(\delta_1 - \delta_2)^2$ and $-RT\ln C_{2\cdot1} \approx V_{m2}(\delta_1 - \delta_2)^2$, where δ_1 and δ_2 are the solubility parameters, and V_{m1} and V_{m2} are the molar volumes. See *Regular and Related Solutions* (Eds.: J. H. Hildebrand, J. M. Prausnitz, R. L. Scott), Van Nostrand Reinhold, New York, **1970**.
[7] The diffusivity coefficient can be estimated by a form of the Stokes–Einstein equation for small molecules, for example the Hayduk–Laudie equation: $D \approx V_m^{-0.589}$ (W. Hayduk, H. Laudie, *AIChE J.* **1974**, *20*, 611–615).
[8] J. Greiner, J. G. Riess, P. Vierling, in *Organofluorine Compounds in Medicinal Chemistry and Biomedical Applications* (Eds.: R. Filler, T. Kobayashi, L. M. Yagupolski), Elsevier, **1993** p. 339; J. G. Riess, M. P. Krafft, L. Zarif, *Mat. Res. Soc. Bull.* **1996**, in press.
[9] M. R. Wolfson, J. S. Greenspan, T. H. Shaffer, *Pediatr. Res.* **1992**, *29*, 336A; T. H. Shaffer, M. R. Wolfson, J. S. Greenspan, S. D. Rubenstein, R. G. Stern in *Proceed. Vth Intl. Symp. Blood Substitutes* (San Diego, March **1993**), Vol. I (Ed.: T. M. S. Chang, J. G. Riess, R. M. Winslow), in *Artif. Cells, Blood Substitutes, Immob. Biotech.* **1994**, *22*, 315–326.
[10] S. Fukushima, M. Nishida, T. Shibuta, K. Juni, M. Nakano, N. Uchara, T. Ohkuma, Y. Yamashita, M. Takahashi, *J. Pharmacobio-Dyn.* **1986**, *9*, s–17.
[11] R. B. Hirschl, T. Pranikoff, P. Gauger, R. J. Schreiner, R. Dechert, R. H. Bartlett, *Lancet* **1995**, *346*, 1201–1202.
[12] P. E. Keipert, *Artif. Cells, Blood Substitutes, Immob. Biotech.* **1995**, *23*, 381–394; T. F. Zuck, J. G. Riess, *Crit. Rev. Clin. Lab. Sci.* **1994**, 295–324; J. A. Wahr, A. Trouwborst, R. K. Spence, C. P. Henny, A. C. Cernaianu, G. P. Graziano, K. K. Tremper, K. E. Flaim, P. E. Keipert, N. S. Faithfull, J. J. Clymer, *Anesth. Analg. (Paris)* **1996**, *82*, 103–107.
[13] M. P. Krafft, P. Vierling, J. G. Riess, *Eur. J. Med. Chem.* **1991**, *26*, 545–550.
[14] F. Giulieri, M. P. Krafft, J. G. Riess, *Angew. Chem.* **1994**, *106*, 1583–1584; *Angew. Chem. Int. Ed. Engl.* **1994**, *33*, 1514–1515.
[15] H. Kunieda, K. Nakamura, U. Olsson, B. Lindman, *J. Phys. Chem.* **1993**, 97, 9525–9531.

 © VCH Verlagsgesellschaft mbH, D-69451 Weinheim, 1996 0570-0833/96/3517-1978 $ 15.00+.25/0

Ruthenium-Catalyzed Metathesis of Polymer-Bound Olefins**

Matthias Schuster, Josef Pernerstorfer, and Siegfried Blechert*

Olefin metathesis has experienced a remarkable renaissance through the development of catalysts[1] that remain active even in the presence of many functional groups. This impetus is reflected in the numerous publications on ring closing and ring opening metathesis, and cross metathesis.[2, 3] Since the development of combinatorial synthesis,[4] in particular with the aim of discovering drugs, much interest is devoted to efficient synthesis processes on solid phases. We therefore studied metathesis reactions of polymer-bound, functionalized olefins. Here we present some ruthenium-catalyzed olefin metatheses with polymer-bound olefins. Whereas the examples of ring closing metathesis of diolefins suggest applications in the construction of functionalizable heterocyclic frameworks, cross metathesis between a polymer-bound and a dissolved olefin is an interesting concept for the catalytic immobilization.

Figure 1 shows the results of the ruthenium-catalyzed ring closing metathesis of a series of diolefins. After gel-phase ^{13}C NMR spectra[5] revealed that the tentacle-polymer-bound diallyl amide **2**[6] could be converted into **3** in high yield with **1a**[1a]

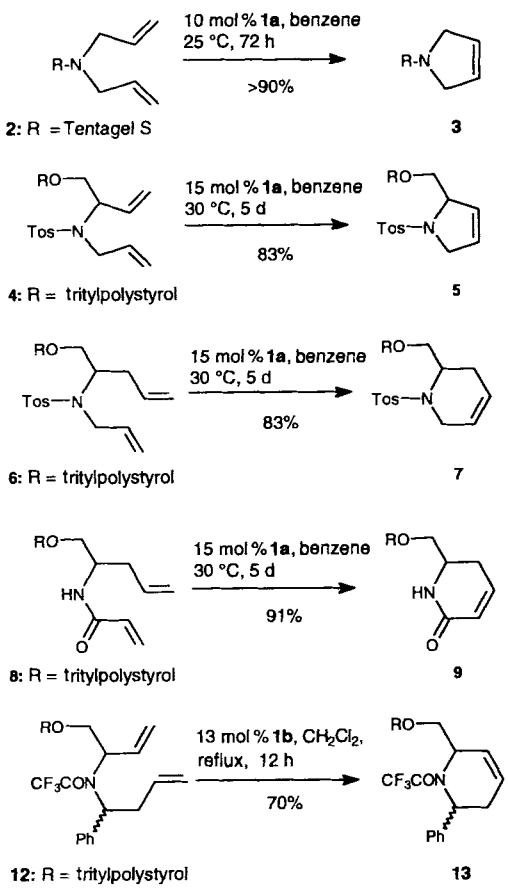

Fig. 1. Results of the ruthenium-catalyzed ring closing metathesis of polymer-bound substrates.

$[Cl_2(PCy_3)_2Ru{=}CH{-}CH{=}CPh_2]$ **1a**

(Cy = cyclohexyl), the following experiments were performed on the inexpensive polystyrene resins. Olefins **4** and **6** were obtained by *N*-allylation of polymer-bound racemic *N*-tosyl-*C*-vinylglycinol and *N*-tosyl-*C*-allylglycinol, respectively, in quantitative yield;[7] olefin **8** was prepared by binding *N*-acryloyl-*C*-allylglycinol to chlorotritylpolystyrene.[8] The loading in all cases was between 0.4 and 0.6 mmol g^{-1} resin.[9] The quoted yields were determined by HPLC analysis of the metathesis products obtained by acid cleavage from the trityl resin. The distinctly faster transformation of **12** into **13** in high yields catalyzed by **1b**[1b] emphasizes that α,α′-substituted nitrogen

$[Cl_2(PCy_3)_2Ru{=}CHPh]$ **1b**

heterocycles, which are ubiquitous in nature as bioactive compounds, are also accessible in polymer-bound form. After acid cleavage of **13** and subsequent basic workup of the soluble product, 2-hydroxymethyl-6-phenyl-1,2,5,6-tetrahydropyridine (**13b**) was isolated in an overall yield of 60%, based on **10**, with a *syn-anti* ratio of 3:5 and characterized.[10] The sequential preparation of the metathesis precursor **12** from polymer-bound *C*-vinylglycinol, benzaldehyde, and allyllithium (Scheme 1) should make α,α′-substituted hydropyridines readily accessible by variation of the components.

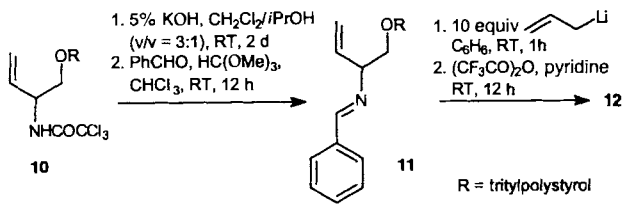

Scheme 1. RT = room temperature.

Besides ring closure reactions, intermolecular metathesis reactions between two different olefins interest us. In the course of such reactions the cross metathesis competes with the dimerization of the two starting alkenes. We hoped to prevent the dimerization by binding one of the olefin components to a polymer and thus also to achieve better reaction control. Since both tritylpolystyrene-bound 4-pentenol and allyl alcohol dimerize on the polymer surface by macrocyclic ring closure under metathesis conditions,[11] sterically demanding hydroxyolefins were immobilized and subjected to metathesis. In the case of polymer-bound *N*-trichloroacetyl-*C*-vinylglycinol (**10**), although as expected no dimerization was observed, the ruthenium-catalyzed metathesis gave only slight conversion despite higher catalyst concentrations. On use of the less sterically demanding *N*-Boc-*N*-allylglycinol (**14**), a slow dimerization was detected at a loading of 0.6 mmol g^{-1} polymer, which could, however, be suppressed by reducing the loading to 0.2 mmol g^{-1} polymer. All experiments were therefore performed with this loading. The results of binding a series of olefins to **14**, as well as to the isomeric *N*-Boc-*C*-allylglycinol resin **19** are summarized in Figure 2.[12] *cis*-Hexene was used as only slightly volatile propene equivalent. The examples demonstrate that cross metathesis between soluble and immobilized olefins can be

[*] Prof. Dr. S. Blechert, Dr. M. Schuster, Dipl.-Ing. J. Pernerstorfer
Institut für Organische Chemie der Technischen Universität Berlin
Strasse des 17. Juni 135, D-10623 Berlin (Germany)
Fax: Int. code +(30)3142-3619
e-mail: paul@wap0105.chem.tu-berlin.de

[**] This work was supported by the Fonds der Chemischen Industrie.

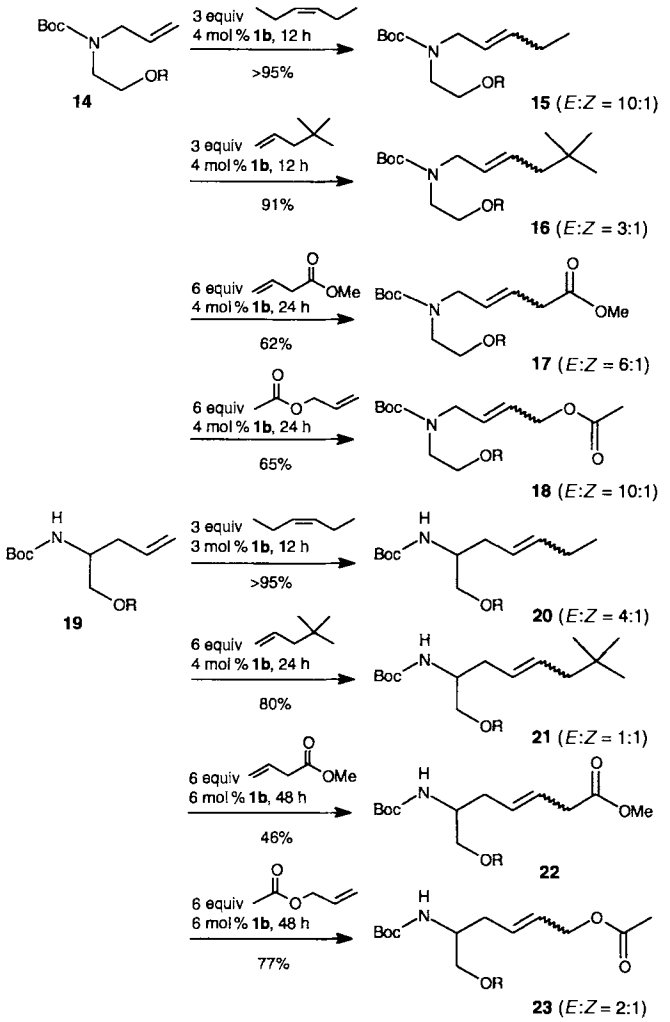

Figure 2. Results of the catalytic immobilization of olefins on tritylpolystyrene-bound *N*-Boc-*N*-allylglycinol (**14**) and *N*-Boc-*C*-allylglycinol (**19**). Boc = *tert*-butoxycarbonyl.

performed in viable yields. This reaction is interesting, because it enables a catalytic immobilization of dissolved compounds by C,C bond linkage. The tolerance of the applied catalysts to nitrogen- and oxygen-containing functional groups suggests that very diverse substrates can be coupled with this principle.

Experimental Procedure

General procedure for ruthenium-catalyzed ring closing metathesis: Under exclusion of moisture and air the tritylpolystyrene-bound diolefin (200–500 mg) was treated with the catalyst in the given solvent (10 mL g^{-1} resin). At the end of the reaction the resin was washed five times alternately with chloroform and methanol. For the cleavage the resin was suspended in a solution of trifluoroacetic acid (25% in chloroform) and shaken for 5 min. After addition of methanol (1 mL) and 5 min shaking, the liquid phase was separated off, and the resin again washed twice with 2 mL portions of a mixture of chloroform and methanol (1:1 v/v). The liquid phases were combined and concentrated under vacuum. The conversion was determined by analytical reversed-phase HPLC or GC. Finally the metathesis product was purified by chromatography and characterized.

General procedure for the ruthenium-catalyzed cross metathesis [12]: After addition of the soluble olefins the reactions were performed as already described. The catalyst was added in two steps, at the beginning of the reaction and after half the quoted reaction time had elapsed. After thorough washing the polymer was suspended in chloroform (10 mL g^{-1} resin). After addition of a drop of trifluoroacetic acid (intense red coloration of the globules of resin), the mixture was briefly shaken, and the reaction quenched with methanol (2 mL g^{-1} resin). After two subsequent washings with chloroform/methanol (1:1 v/v) the liquid phases were combined, treated with saturated $NaHCO_3$ solution and extracted three times with chloroform. Thin-layer chromatography confirmed that the urethane function was retained in the process of cleaving the product from the resin. The products were purified by chromatography and characterized.

Received: October 16, 1995
Revised version: May 10, 1996 [Z8477IE]
German version: *Angew. Chem.* **1996**, *108*, 2111–2112

Keywords: catalysis · heterocycles · metathesis · ruthenium compounds · solid-phase syntheses

[1] a) S. T. Nguyen, R. H. Grubbs, J. W. Ziller, *J. Am. Chem. Soc.* **1993**, *115*, 9858; b) P. Schwab, M. B. France, J. W. Ziller, R. H. Grubbs, *Angew. Chem.* **1995**, *107*, 2179; *Angew. Chem. Int. Ed. Engl.* **1995**, *34*, 2039.

[2] a) H.-G. Schmalz, *Angew. Chem.* **1995**, *107*, 1981; *Angew. Chem. Int. Ed. Engl.* **1995**, *34*, 1833; b) R. H. Grubbs, S. J. Miller, G. C. Fu, *Acc. Chem. Res.* **1995**, *28*, 446.

[3] Ring closing metathesis: a) A. F. Houri, Z. Xu, D. Cogan, A. H. Hoveyda, *J. Am. Chem. Soc.* **1995**, *117*, 2943; b) C. M. Huwe, O. C. Kiehl, S. Blechert, *Synlett* **1996**, 65; ring opening metathesis: c) M. F. Schneider, S. Blechert, *Angew. Chem.* **1996**, *108*, 479; *Angew. Chem. Int. Ed. Engl.* **1996**, *35*, 410; cross metathesis: d) W. E. Crowe, D. R. Goldberg, Z. J. Zhang, *Tetrahedron Lett.* **1996**, *13*, 2117.

[4] Recent reviews on combinatorial chemistry: a) J. S. Früchtel, G. Jung, *Angew. Chem.* **1996**, *108*, 19; *Angew. Chem. Int. Ed. Engl.* **1996**, *35*, 17; b) M. A. Gallop, R. W. Barrett, W. J. Dower, S. P. A. Fodor, E. M. Gordon, *J. Med. Chem.* **1994**, *37*, 1233; c) *ibid.* **1994**, *37*, 1385.

[5] Physical and spectroscopic properties of tentacle polymers: E. Bayer, *Angew. Chem.* **1991**, *103*, 117; *Angew. Chem. Int. Ed. Engl.* **1991**, *30*, 113.

[6] Preparation of **2**: Tentagel S *N*-hydroxysuccinimide ester (Rapp Polymers, Tübingen) was treated with diallyl amine in dichloromethane. Tentagel S is a polystyrene–polyethyleneglycol block copolymer.

[7] N-Allylations adapted from C. M. Huwe, S. Blechert, *Tetrahedron Lett.* **1995**, *36*, 1621.

[8] Chlorotritylpolystyrene resin was prepared and modified according to J. M. J. Frechet, L. J. Nuyens, *Can. J. Chem.* **1976**, *54*, 926.

[9] Loading was determined by a comparison by HPLC or GC of the filtrate after cleavage with trifluoroacetic acid from a defined amount of resin (5–20 mg) with a standard solution of the authentic compound.

[10] Compound **13** was treated several times with trifluoroacetic acid (10% solution in dichloromethane). The combined extracts were treated with methanol and an excess of K_2CO_3, shaken, and washed with water. The organic phase was dried over $MgSO_4$, filtered, and concentrated under vacuum. Compound **13b** was isolated by chromatography in an overall yield of 60% and characterized. The assignment of the diastereomers was achieved by NOE measurements. Selected spectroscopic data: **13b**-*syn*: ^{1}H NMR (400 MHz, $CDCl_3$): $\delta = 7.44-7.24$ (m, 5H), 5.94–6.01 (m, 1H), 5.63 (ddd, 1H, $J = 10$ Hz, 4 Hz, 2 Hz), 3.97 (dd, 1H, $J = 10$ Hz, 5 Hz), 3.82–3.76 (m, 1H), 3.69 (dd, 1H, $J = 10.5$ Hz, 3.5 Hz), 3.60 (dd, 1H, $J = 10.5$ Hz, 5 Hz), 2.31–2.15 (m, 2H); ^{13}C NMR (50.32 MHz, $CDCl_3$): $\delta = 144.5$ (C), 128.5 (CH), 128.0 (CH), 127.4 (CH), 127.0 (CH), 126.7 (CH), 65.8 (CH_2), 57.6 (CH), 57.1 (CH), 34.5 (CH_2); MS: *m/z* (%) 189 (0.5) [M^+], 188 (2), 170 (2), 158 (100), 141 (18), 131 (8), 115 (17), 106 (35), 91 (32), 77 (12), 65 (5), 55 (7); high resolution MS: calcd. for $C_{12}H_{14}NO$ [M^+-H]: 188.1075, found: 188.1075. **13b**-*anti*: ^{1}H NMR (400 MHz, $CDCl_3$): $\delta = 7.42-7.24$ (m, 5H), 6.05–5.98 (m, 1H), 5.69 (ddd, 1H, $J = 10$ Hz, 4 Hz, 2.5 Hz), 3.96 (dd, 1H, $J = 10$ Hz, 4 Hz), 3.61–3.48 (m, 3H), 2.38–2.19 (m, 2H); ^{13}C NMR (50.32 MHz, $CDCl_3$): $\delta = 143.7$ (C), 128.5 (CH), 127.9 (CH), 127.2 (CH), 126.6 (CH), 126.1 (CH), 62.9 (CH_2), 55.1 (CH), 50.9 (CH), 32.6 (CH_2); MS: *m/z* (%) 189 (0.5) [M^+], 188 (1), 170 (2), 158 (100), 141 (18), 131 (6), 115 (15), 104 (10), 91 (25), 77 (7), 65 (6), 53 (4); high resolution MS: calcd. for $C_{12}H_{14}NO$ [M^+-H]: 188.1075, found: 188.1075.

[11] The corresponding dimers, 4-octenediol and 2-butenediol, were isolated after cleavage from the resin as *E*/*Z* mixtures.

[12] The quoted amounts of catalyst refer to the components in solution. After acid cleavage the yield, based on the immobilized components, was determined by GC. The *E*/*Z* rations were likewise determined by gas chromatography, and the isomers, purified by chromatography on silica gel, were assigned by ^{1}H NMR spectroscopy.

Dioxygen Activation by a Manganese Complex Containing a Schiff Base: Selective Oxidation of an Imino to an Amido Group within the Salophen Ligand and Formation of a Hydroxy-Bridged Mn^{III}-Polymer**

Emma Gallo, Euro Solari, Nazzareno Re, Carlo Floriani,* Angiola Chiesi-Villa, and Corrado Rizzoli

The manganese-assisted oxygen transfer from dioxygen to substrates remains a rather uncommon process,[1] even though investigations on the interaction of manganese with dioxygen are very extensive over several classes of complexes.[2] However, the reactions are carried out in situ on poorly defined products that were not previously isolated and under protic conditions. The products of such reactions are almost exclusively μ-oxo complexes,[3] which are supposed to be reactive oxidizing agents. The oxygen transfer ability belongs essentially to the [Mn=O] functionality,[4] formed from oxidizing agents other than dioxygen, or to much rarer peroxo-[5] or superoxomanganese[6] derivatives, which come from dioxygen.

Tetradentate Schiff bases, particularly those having the salen skeleton (H_2salen = bis(salicylidene)ethylenediamine),[7] were ligands of choice in this field, whereas only minor attention was given to the salophen dianion[8] (H_2salophen = N,N'-*o*-phenylenebis(salicylideneimine)).

This report concerns the reaction the Schiff base (SB) complexes depicted in Scheme 1 with dioxygen under very controlled conditions. The reaction products vary, depending on the solvent (*n*-hexane, thf, or pyridine).

The reaction of **1** and **3** with oxygen in hydrocarbon solvents or thf gave polymeric **5** and **6**, respectively, which underwent cleavage to **7** and **8** when pyridine was added. However, the reaction of **2** and **4** with oxygen in pyridine led directly to **7** and **8**, which formed in a yield consistently lower than 50% at a constant O_2 uptake in the Mn/O_2 molar ratio of 2/1.[10] Even when the reaction is run in pyridine, these data support the intermediacy of **5** and **6** and rule out the further oxidative conversion of the undetected monomeric hydroxy-Mn moiety. In pyridine the oxygenation of **2** and **4**, which have been isolated from neat pyridine and structurally characterized as dimers, probably occurs on the dimeric form. We proposed that the formation of a superoxo complex is followed by hydrogen abstraction from the imino carbon (Scheme 2). The cleavage of the resulting hydroperoxo moiety generates a Mn-O· radical which couples with the radical at the imino carbon. The reaction very probably occurs intramolecularly within the dimer. Although the relatively slow oxygenation of **1** and **3** was carried out both at -78 and $-40\,^{\circ}C$, we were unable to detect any peroxo-type intermediate in the UV/Vis spectrum. The overall result of the dioxygen reaction with **1** and **3** is the conversion of one imino group of the dimer into an amido with the concurrent formation of a OH-bridged Mn^{III} dimer.

$[\{Mn(SB)(L)\}_2]$

1 [9]: SB = salophen, L = thf
2: SB = salophen, L = pyridine (py)
3: SB = 3,5-*t*Bu salophen, L = thf
4: SB = 3,5-*t*Bu salophen, L = py

Scheme 1. 3,5-*t*Busalophen = dianion of *N,N*-*o*-phenylene-bis(3,5-di-*tert*-butylsalicylidenimine).

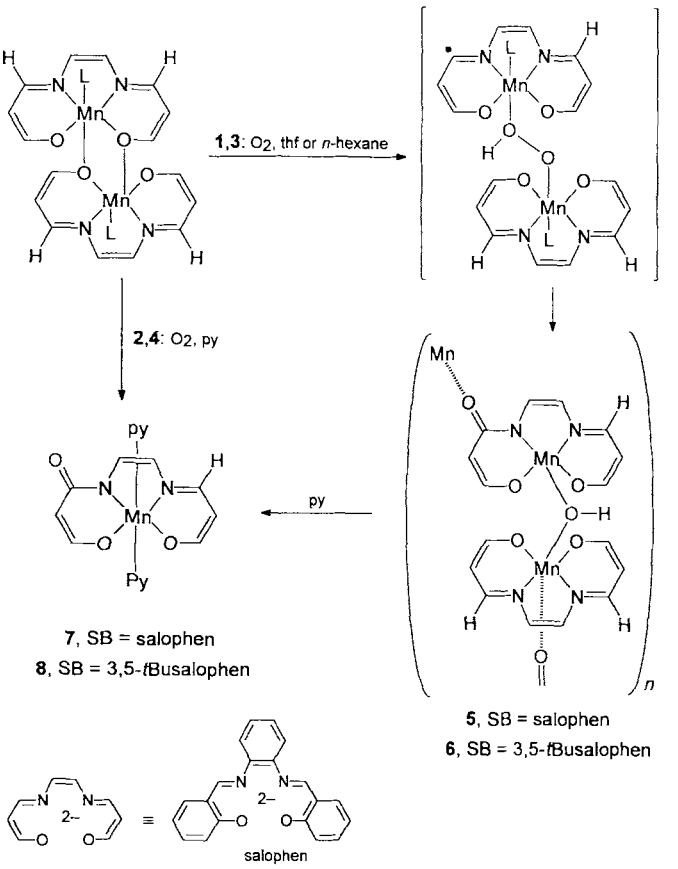

Scheme 2.

Complexes **2** and **6**–**8** have been structurally characterized, but details are given only for **6**,[11] which is a rare[12] Mn^{III} dimer bridged by a single hydroxy group. Its structure is shown in Figure 1. The hydroxy group asymmetrically bridges the two Mn^{III} atoms [unit A: Mn1–O4 2.009(8) Å; unit B: Mn1–O4 2.082(8) Å], and the Mn–O distances are much longer than those of corresponding oxo-bridged analogues [1.78–1.84 Å]. The coupling constant for **6** ($-24.0\ cm^{-1}$) shows a significant antiferromagnetic coupling between the two Mn^{III} units ($S = 2$) within the dimer, in agreement with the wide Mn-O-Mn angle [Mn1(unit A)-O4-Mn1(unit B) 147.2(4)°], whereas the interdimer coupling is irrelevant. The coupling constant value is close to that found in the single (μ-hydroxy)Mn^{III}–Mn^{III} dimer reported very recently.[12] Besides the electronic properties, a major reason for the difference between the salophen and salen skeletons stems from the much more rigid, square-planar coordination that the salophen imposes on the metal. Thus, for the case of salophen, the evolution of a superoxo and subsequently peroxo type of intermediate to a *cis* bis-μ-oxo arrangement becomes much less favorable, since other evolution pathways are possible.

[*] Prof. Dr. C. Floriani, Dr. E. Gallo, Dr. E. Solari
Institut de Chimie Minérale et Analytique
Université de Lausanne
BCH, CH-1015 Lausanne (Switzerland)
Fax: Int. code +(21)692-3905
e-mail: carlo.floriani@icma.unil.ch
Dr. N. Re
Dipartimento di Chimica, Università di Perugia (Italy)
Prof. Dr. A. Chiesi-Villa, Dr. C. Rizzoli
Dipartimento di Chimica, Università di Parma (Italy)

[**] This work was supported by the Fonds National Suisse de la Recherche Scientifique (Grant. No. 20-40268.94).

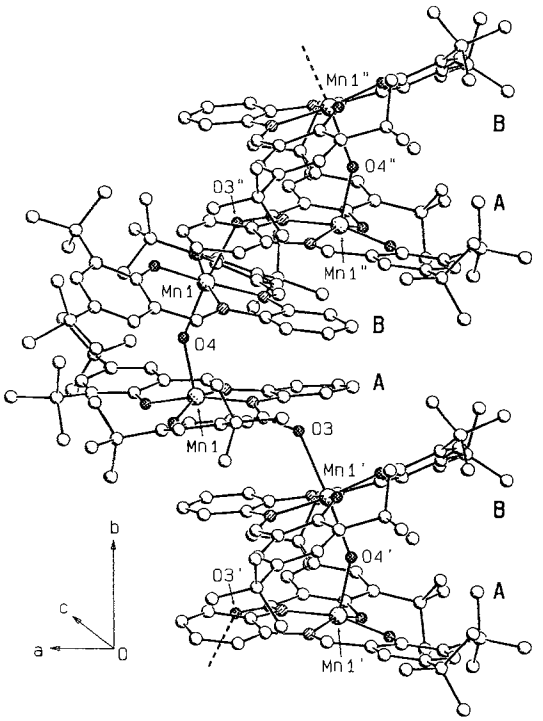

Fig. 1. SCHAKAL view of the chaining of complex **6** along the [010] direction. Selected bond lengths [Å] and angles [°] for moiety A [B in square brackets]: Mn1–O4, 2.009(8) [2.082(8)]; Mn1B–O3″, 2.373(7); O3–C7, 1.257(10); N1–C7, 1.343(12) [1.292(14)]; N2–C14, 1.291(12) [1.292(13)]. Selected bond angles [°]: C7-O3-Mn1B′, 132.6(6); Mn1A-O4-Mn1B, 147.2(4). Disorder omitted for clarity. Prime and double prime denote a transformation from x,y,z to $-x, -0.5+y, 0.5-z$ and $-x, 0.5+y, 0.5-z$, respectively.

The reactions with **1** and **3** have been carried out under strictly nonprotic conditions. Thus, the imino hydrogen plays a major role as a source of peroxo hydrogen. By replacing the hydrogen atom at the imino functionality with a methyl group as in **9**,[9]

[Mn(Me–salophen)(thf)]$_2$ **9**

a very different reaction pathway was observed, which also varied depending on the nature of the solvent. In fact, the reaction of O_2 with **9** in thf was strikingly different from that with **1** and **3**. The O_2:Mn ratio changes from 0.5:1 for **1** and **3** to 1:1 for **9**.[10] Therefore, in the case of **9**, we propose the formation of a superoxo species, which in the absence of the imine proton cannot evolve in the same manner as for **1** and **3**.[13] We should also emphasize that, in general, the genesis of the OH ligand in manganese complexes is from either hydrolysis[14] or protonation of μ-oxo compounds[15] rather than from the activation of a carbon–hydrogen bond.

Experimental Procedure

6: **4** (2.01 g, 1.51 mmol) was dissolved in thf (100 mL), nitrogen was removed from the red solution by evacuation, and oxygen dried over P_2O_5 was allowed to enter at room temperature. The resulting brown solution was stirred for 12 h at room temperature under an oxygen atmosphere. The mixture was then evaporated to dryness, and the resulting brown solid extracted with Et_2O (50 ml). The extract was filtered to collect the product and the resulting red solid was then dried in vacuo (65%). Elemental analysis calcd for $[C_{72}H_{92}Mn_2N_4O_6]_n$: C 70.92, H 7.60, N 4.59; found: C 70.53, H 7.76, N 4.17. Recrystallization of the powder from heptane yielded red crystals suitable for X-ray diffraction. IR (Nujol): $\tilde{\nu}$ = 1602(s), 1576(m), 1548(w), 1525(s) 1419(w), 1358(m), 1315(m), 1256(m), 1172(m), 836(m), 741(s), 540(m) cm^{-1}.

8: **6** (1.04 g, 0.85 mmol) was dissolved in pyridine (30 mL), and the resulting red solution was stirred for 12 h at room temperature and then evaporated to dryness. The residue was extracted with Et_2O (50 ml) to give a suspension of the red solid product in Et_2O. The product was then filtered off and dried in vacuo (31%). Recrystallization of the powder from Et_2O:pyridine (90:10) yielded red crystals suitable for X-ray diffraction. Elemental analysis calcd for $C_{46}H_{55}MnN_4O_3$: C 72.04, H 7.23, N 7.31; found: C 71.57, H 7.30, N 7.08. μ = 4.63 μ_B at 293 K.

Received: February 29, 1996 [Z8881IE]
German version: *Angew. Chem.* **1996**, *108*, 2113–2115

Keywords: complexes with nitrogen ligands · manganese compounds · oxygen activation · Schiff base complexes

[1] a) T. Mukaiyama, T. Yamada, T. Nagata, K Imagawa, *Chem. Lett.* **1993**, 327–330; b) T. Nagata, K. Imagawa, T. Yamada, T. Mukaiyama, *ibid.* **1994**, 1259–1262; c) K. Imagawa, T. Nagata, T. Yamada, T. Mukaiyama, *ibid.* **1995**, 335–336; d) F. M. MacDonnel, N. L. P. Fackler, C. Stern, T. V. O'Halloran, *J. Am. Chem. Soc.* **1994**, *116*, 7431–7432.

[2] a) W. M. Coleman, L. T. Taylor, *Coord. Chem. Rev.* **1980**, *32*, 1–31; b) C. P. Horwitz, G. C. Dailey, *Comments Inorg. Chem.* **1993**, *14*, 283–319; c) V. L. Pecoraro, M. J. Baldwin, A. Gelasco, *Chem. Rev.* **1994**, *94*, 807–826.

[3] a) J. W. Gohdes, W. H. Armstrong, *Inorg. Chem.* **1992**, *31*, 368–373; b) A. Gelasco, V. L. Pecoraro, *J. Am. Chem. Soc.* **1993**, *115*, 7928–7929; c) C. A. Kipke, M. J. Scott, J. W. Gohdes, W. H. Armstrong, *Inorg. Chem.* **1990**, *29*, 2193; d) C. P. Horwitz, Y. Ciringh, *Inorg. Chim. Acta* **1994**, *225*, 191–200.

[4] a) M. K. Stern, J. T. Groves in *Manganese Redox Enzymes* (Ed.: V. L. Pecoraro), VCH, New York, **1992**, Chapter 11; b) R. D. Arasasingham, G. X. He, T. C. Bruice, *J. Am. Chem. Soc.* **1993**, *115*, 7985–7991; c) J. T. Groves, M. K. Stern, *ibid.* **1988**, *110*, 8628–8638; d) T. J. Collins, R. D. Powell, C. Slebodnick, E. S. Uffelman, *ibid.* **1990**, *112*, 899–901; e) T. J. Collins, S. W. Gordon-Wylie, *ibid.* **1989**, *111*, 4511–4513.

[5] a) W. M. Coleman, L. T. Taylor, *Inorg. Chim. Acta* **1978**, *30*, L291–L293; b) N. Kitajima, H. Komatsuzaki, S. Hikichi, M. Osawa, Y. Moro-oka, *J. Am. Chem. Soc.* **1994**, *116*, 11596; c) U. Bossek, T. Weyhermüller, K. Wieghardt, B. Nuber, J. Weiss, *ibid.* **1990**, *112*, 6387; d) E. J. Larson, V. L. Pecoraro, *ibid.* **1991**, *113*, 3810; e) R. Bhula, G. J. Gainsford, D. C. Weatherburn, *ibid.* **1988**, *110*, 7550; f) R. B. VanAtta, C. E. Strouse, L. K. Hanson, J. S. Valentine, *ibid.* **1987**, *109*, 1425.

[6] C. J. Weschler, B. M. Hoffman, F. Basolo, *J. Am. Chem. Soc.* **1975**, *97*, 5278–5280.

[7] a) T. Yarino, T. Matsushita, I. Masuda, K. Shiura, *J. Chem. Soc. Chem. Commun.* **1970**, 1317; b) J. H. Burness, J. G. Dillard, L. T. Taylor, *Inorg. Nucl. Chem. Lett.* **1974**, *10*, 387; c) E. N. Jacobsen in *Comprehensive Organometallic Chemistry II, Vol. 12* (Eds.: E. W. Abel, F. G. A. Stone, G. Wilkinson), Pergamon, New York, **1995**, Chapter 11.1; d) E. N. Jacobsen in *Catalytic Asymmetric Synthesis* (Ed.: I. Ojima), VCH, New York, **1993**; e) E. N. Jacobsen, W. Zhang, A. R. Muci, J. R. Ecker, L. Deng, *J. Am. Chem. Soc.* **1991**, *113*, 7063–7064; f) J. F. Larrow, E. N. Jacobsen, *J. Org. Chem.* **1994**, *59*, 1939; g) W. Zhang, N. H. Lee, E. N. Jacobsen, *J. Am. Chem. Soc.* **1994**, *116*, 425–426; h) L. Deng, E. N. Jacobsen, *J. Org. Chem.* **1992**, *57*, 4320–4323; i) B. D. Brandes, E. N. Jacobsen, *ibid.* **1994**, *59*, 4378–4380; j) T. Katzuki, *Coord. Chem. Rev.* **1995**, *140*, 189–214; k) H. Sasaki, R. Irie, T. Katsuki, *Synlett* **1993**, 300–302; l) N. Hosoya, A. Hatayama, R. Irie, H. Sasaki, T. Katsuki, *Tetrahedron* **1994**, *50*, 4311–4322.

[8] a) W. M. Colemann, R. K. Bogges, J. M. Hughes, L. T. Taylor, *Inorg. Chem.* **1981**, *20*, 1253–1258; b) R. K. Bogges, J. W. Hughes, W. M. Coleman, L. T. Taylor, *Inorg. Chim. Acta* **1980**, *38*, 183–189; c) C. J. Boreham, B. Chiswell, *ibid.* **1977**, *24*, 77.

[9] Complexes **1** and **9** have been prepared according to E. Gallo, E. Solari, C. Floriani, N. Re, A. Chiesi-Villa, C. Rizzoli, *J. Am. Chem. Soc.* **1993**, *115*, 9850–9851 (see Ref. [3]).

[10] O_2 uptake has been measured in thf and py at 298 K, according to a modified version of the apparatus reported in F. A. Cotton, F. Calderazzo, *Inorg. Chem.* **1962**, *1*, 30. The expected error in the O_2 uptake volume is lower than 5%.

[11] Crystal data for **6**: $C_{72}H_{92}Mn_2N_4O_6 \cdot 2C_6H_{14}$, M = 1391.8, monoclinic, space group $P2_1/c$, a = 17.395(4), b = 13.083(3), c = 34.904(6) Å, β = 103.61(2)°, V = 7720(3) Å^3, Z = 4, ρ_{calcd} = 1.197 g cm^{-3}, $F(000)$ = 3000, $Cu_{K\alpha}$ radiation (λ = 1.54178 Å), μ = 30.72 cm^{-1}; crystal dimensions 0.15 × 0.27 × 0.38 mm. The structure was solved by the heavy atom method and anisotropically refined for all the non-H atoms except for those affected by disorder. One butyl group (C33 ··· C36) in unit A was found to be disordered over two positions with a site occupation factor of 0.5 on isotropic refinement. The two *n*-hexane solvent molecules of crystallization showed high isotropic thermal parameters indicating the presence of disorder. The best fit was obtained on isotropic refinement by splitting the C2, C3, C10, and C11 atoms over two positions with site occupation factors of 0.6 and 0.4, respectively. The H4 hydrogen atom associated with the hydroxo group was located from a difference Fourier map and isotropically refined. All the other hydrogen atoms except those associated with disordered atoms (which were ignored) were located from difference Fourier maps or put in geometrically calculated positions and introduced as

fixed contributors in the last stage of refinement (U_{iso} = 0.08 Å^2). During the refinement the C–C bond distances within the disordered butyl group and *n*-hexane molecules were constrained to be 1.54(1) Å. For 5086 unique observed reflections [$I > 2\sigma(I)$] of a total of 11 208 collected at T = 173 K on a Rigaku AFC6S diffractometer ($6 > 2\theta > 140°$) and corrected for absorption, R is 0.073 ($wR2$ = 0.178). All calculations were carried out on an IBM PS2/80 Personal Computer and an ENCORE E91 computer. Crystallographic data (excluding structure factors) for the structure reported in this paper have been deposited with the Cambridge Crystallographic Data Centre, as supplementary publication no. CCDC-179-62. Copies of the data can be obtained free of charge on application to the Director, CCDC, 12 Union Road, Cambridge CB2 1EZ (UK) (Fax: Int. code +(1223)336-033; e-mail: teched@chemcrys.cam.ac.uk).

[12] B. Cheng, F. Cukiernik, P. H. Fries, J.-C. Marchon, W. R. Scheidt, *Inorg. Chem.* **1995**, *34*, 4627.

[13] Work in progress.

[14] a) R. T. Stibrany, S. M. Gorun, *Angew. Chem.* **1990**, *102*, 1195–1197; *Angew. Chem. Int. Ed. Engl.* **1990**, *29*, 1156–1158; b) S. Pal, M. K. Chan, W. H. Armstrong, *J. Am. Chem. Soc.* **1992**, *114*, 6398; c) K. Wieghardt, K. U. Bossek, B. Nuber, J. Weiss, J. Bonvoisin, M. Corbella, S. E. Vitols, J. J. Girerd, *ibid.* **1988**, *110*, 7398; d) H. S. Maslen, N. T. Waters, *J. Chem. Soc. Chem. Commun.* **1973**, 760–761; e) N. Kitajima, U. P. Singh, H. Amagai, M. Osawa, Y. Moro-oka, *J. Am. Chem. Soc.* **1991**, *113*, 7757.

[15] a) A. Niemann, K. U. Bossek, K. Wieghardt, C. Butzlaff, A. X. Trautwein, B. Nuber, *Angew. Chem.* **1992**, *104*, 345–347; *Angew. Chem. Int. Ed. Engl.* **1992**, *31*, 311–313; b) M. J. Baldwin, T. L. Stemmler, P. Riggs-Gelasco, M. L. Kirk, J. E. Penner-Hann, V. L. Pecoraro, *J. Am. Chem. Soc.* **1994**, *116*, 11349; c) E. J. Larson, P. J. Riggs, J. E. Penner-Hahn, V. L. Pecoraro, *J. Chem. Soc. Chem. Commun.* **1992**, 102; d) K. S. Hagen, T. D. Westmoreland, M. J. Scott, W. H. Armstrong, *J. Am. Chem. Soc.* **1989**, *111*, 1907.

$BaYbSi_4N_7$—Unexpected Structural Possibilities in Nitridosilicates**

Hubert Huppertz and Wolfgang Schnick*

Dedicated to Professor Hans Georg von Schnering on the occasion of his 65th birthday

Recently we developed a novel synthetic approach to ternary nitridosilicates by reacting alkaline earth or rare earth metals with silicon diimide in a specially developed high-frequency (HF) furnace.[1–3] These reactions may be interpreted as the dissolution of an electropositive metal in a nitrido-analogous, polymeric acid accompanied by the evolution of hydrogen [Eqs. (a) and (b)]. A specific advantage of this method is the possibility of varying the metals and the fact that preparative amounts of nitridosilicates are accessible as coarse crystalline and single-phase products in short reaction times.[4]

$$2M + 5Si(NH)_2 \xrightarrow[\text{HF-furnace}]{1500–1650\,^\circ C} M_2[Si_5N_8] + N_2 + 5H_2 \quad (a)$$
M = Ca, Sr, Ba

$$3M' + 6Si(NH)_2 \xrightarrow[\text{HF-furnace}]{1650\,^\circ C} M'_3[Si_6N_{11}] + {}^1/_2\,N_2 + 6H_2 \quad (b)$$
M' = Ce, Pr

SiO_4 and SiN_4 tetrahedra are characteristic structural elements in oxo- and nitridosilicates, respectively. These tetrahedra are connected through corner-sharing to give network structures. In oxosilicates a maximum cross linkage is reached in silicon dioxide, in which the molar ratio of tetrahedral centers to bridging atoms is Si:O = 1:2. All bridging atoms ($O^{[2]}$) are bonded to two Si atoms. In nitridosilicates built up from the SiN_4 tetrahedra, bridging atoms ($N^{[3]}$) were found for molar ratio of Si:N > 1:2 for the first time. These bridging atoms each connect three silicon atoms (for instance $^3_\infty[(Si_6^{[4]}N_9^{[2]}N_2^{[3]})^{9-}]$ and $^3_\infty[(Si_5^{[4]}N_4^{[2]}N_4^{[3]})^{4-}]$).

Accordingly, nitridosilicates extend the structural possibilities of silicates and lead with a molar ratio Si:N > 1:2 to higher condensed network structures, for which there are no analogues in the oxosilicates. The maximum cross linking is reached in Si_3N_4,[5] in which according to $^3_\infty[Si_3^{[4]}N_4^{[3]}]$ all nitrogen atoms ($N^{[3]}$) are connected to three Si atoms.

In the Si–N networks we have examined to date, no nitrogen atoms simultaneously connected to four Si tetrahedral centers ($N^{[4]}$) were observed. In condensed tetrahedral structures such a structure motif is only expected to occur when the molar ratio of tetrahedral centers T to bridging atoms X lies in the range of $1.0 \geq T:X \geq 0.75$. In the case of nitridosilicates(IV), this would require partial cationic Si–N structures, which have not been observed so far.[6] Herein we report on $BaYbSi_4N_7$, the first compound in which one nitrogen atom connects four silicon atoms (cf. Scheme 1).

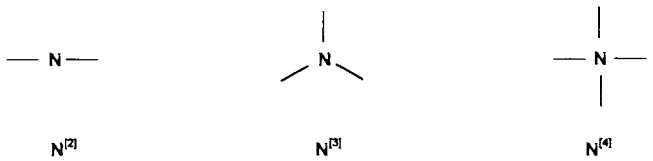

Scheme 1. In nitridosilicates, nitrogen atoms covalently connect two, three, or four Si tetrahedral centers.

The new nitridosilicate $BaYbSi_4N_7$ was synthesized by reacting stoichiometric amounts[7] of Ba and Yb metal with silicon diimide $Si(NH)_2$ in a HF furnace[1] under nitrogen atmosphere [Eq. (c)]. This process leads to the formation of $BaYbSi_4N_7$ as a single-phase,[8] coarse crystalline, colorless solid. Similar to all the other nitridosilicates we have synthesized so far, $BaYbSi_4N_7$ is stable up to 1600 °C and resistant to hot acids and alkalines.

$$Ba + Yb + 4Si(NH)_2 \xrightarrow[\text{HF-furnace}]{900–1650\,^\circ C,\ 18\,h} BaYbSi_4N_7 + {}^1/_2\,N_2 + 4H_2 \quad (c)$$

According to the X-ray structure determination on single crystals,[9] $BaYbSi_4N_7$ contains a network structure of corner-sharing SiN_4 tetrahedra $^3_\infty[(Si_4^{[4]}N_6^{[2]}N^{[4]})^{5-}]$. Although a stoichiometric ratio of Si:N = 4:7 should lead to $^3_\infty[(Si_4^{[4]}N_5^{[2]}N_2^{[3]})^{5-}]$, no $N^{[3]}$ atoms were found. Instead, there is a corresponding number of $N^{[4]}$ bridges, which connect four Si tetrahedral centers. As expected the bond lengths to the $N^{[4]}$ atoms in $BaYbSi_4N_7$ are significantly longer (Si–N: 188–196 pm) than those to the $N^{[2]}$ atoms (Si–N: 170–172 pm).

The Si–N network structure in $BaYbSi_4N_7$ is built up from starlike $[N(SiN_3)_4]$ building blocks (Fig. 1). By connecting these groups through common

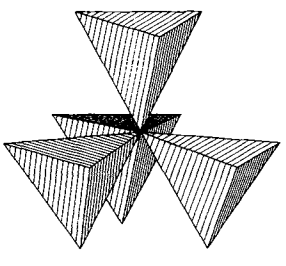

Fig. 1. Four SiN_4 tetrahedra are connected through a common nitrogen atom to give a $[N(SiN_3)_4]$ building block. The entire network structure of $BaYbSi_4N_7$ is built up by these starlike-shaped building blocks.

[*] Prof. Dr. W. Schnick, Dipl.-Chem. H. Huppertz
Laboratorium für Anorganische Chemie der Universität
D-95440 Bayreuth (Germany)
Fax: Int. code +(921)55-2788
e-mail: wolfgang.schnick@uni-bayreuth.de

[**] This work was supported by the Fonds der Chemischen Industrie and the Deutsche Forschungsgemeinschaft (Schwerpunktprogramm "Nitridobrücken", project SCHN 377/7-1 and 2, and the Gottfried Wilhelm Leibniz program).

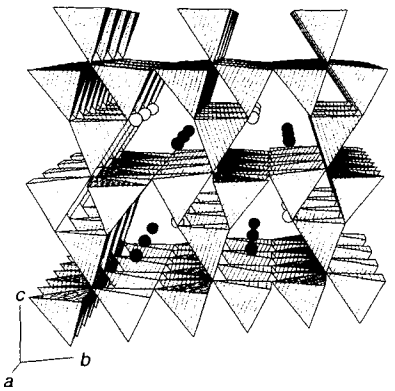

Fig. 2. Crystal structure of $BaYbSi_4N_7$. The SiN_4 tetrahedra are shown as closed polyhedra, the Ba^{2+} ions as grey and the Yb^{3+} ions as black spheres.

N atoms a stacking variant of the wurtzite-analogous aluminum nitride structure type is formed (Fig. 2). Systematic elimination of tetrahedra from this arrangement along [100], leads to the formation of sechser ring channels, in which the Ba^{2+} and Yb^{3+} are positioned. The Ba^{2+} and Yb^{3+} metal ions show anticuboctahedral and octahedral coordination, respectively, by nitrogen atoms of the Si_4N_7 network. The Ba–N and Yb–N contact distances (298–305 pm and 229–231 pm) approximately correspond to the sum of the ionic radii.[10]

$BaYbSi_4N_7$ provides the first example of $N^{[4]}$ connections between four Si tetrahedral centers. This extends the structural possibilities in nitridosilicates by a surprising dimension. Thoroughly cross-linked Si–N network structures, particularly in highly condensed nitridosilicates (Si:N $>1:2$), should be possible for which attractive material properties (high mechanical, thermal, and chemical stability) can be predicted. While the structural chemistry of oxosilicates is limited to terminal oxygen atoms and simple bridging $O^{[2]}$ atoms, the nitridosilicates show extended structural possibilities with $N^{[2]}$, $N^{[3]}$, and $N^{[4]}$ connections of Si tetrahedral centers. These variations have not as yet been found in oxosilicates and may not be possible with silicon and oxygen.[11]

Received: May 2, 1996 [Z9088IE]
German version: *Angew. Chem.* **1996**, *108*, 2115–2116

Keywords: high-temperature synthesis · network structures · nitridosilicates · silicates · structure elucidation

[1] T. Schlieper, W. Schnick, *Z. Anorg. Allg. Chem.* **1995**, *621*, 1037.
[2] T. Schlieper, W. Milius, W. Schnick, *Z. Anorg. Allg. Chem.* **1995**, *621*, 1380.
[3] T. Schlieper, W. Schnick, *Z. Anorg. Allg. Chem.* **1995**, *621*, 1535.
[4] Meanwhile some rare earth nitridosilicates $Ln_3Si_6N_{11}$ (Ln = La, Ce, Pr, Nd) and $LnSi_3N_5$ (Ln = Ce, Pr, Nd) are synthesized by reaction of the silicides $LnSi_2$ and "$LnSi_3$" with N_2: M. Woike, W. Jeitschko, *Inorg. Chem.* **1995**, *34*, 5105. A problem with this procedure is the avoidance of metallic impurities.
[5] W. Schnick, *Angew. Chem.* **1993**, *105*, 846; *Angew. Chem. Int. Ed. Engl.* **1993**, *32*, 806.
[6] Well-known examples for $N^{[4]}$ connections in nitrides are BN and AlN.
[7] In a typical charge 1 mmol of the metals were thoroughly mixed with $Si(NH)_2$ under inert gas atmosphere in a glove box and transferred in a tungsten crucible into the HF reactor. Under nitrogen atmosphere the reaction mixture was slowly heated up to 1650 °C, maintained at that temperature for 2 h, and then cooled down to 1400 °C within 15 h. At the end of the reaction the product was quenched to room temperature.
[8] The composition of $BaYbSi_4N_7$ was confirmed to be in agreement with the structure analysis by energy dispersive X-ray microanalysis (Ba,Yb,Si) and quantitative determination by Pascher (Remagen). The absence of hydrogen (NH) was checked by IR spectroscopy.
[9] $BaYbSi_4N_7$: $P6_3mc$, $a = 603.07(2)$, $c = 981.98(4)$ pm, $Z = 2$, Siemens P4 diffractometer, $Mo_{K\alpha}$ radiation, graphite monochromator, $F(000) = 462.0$, $\mu(Mo_{K\alpha}) = 22.07\ mm^{-1}$, ω scan, 11456 measured reflections in the range $2° \le 2\theta \le 95°$, 1144 unique reflections with $F_o^2 \ge 0\sigma(F_o^2)$, empirical absorption correction (ψ scans), $R_{int} = 0.0728$, the crystal structure was solved by direct methods (SHELXTL-Plus, Vers. 5.03) and anisotropically refined by a least-squares procedure against F^2 with all data, 32 refined parameters, $R1 = 0.0210$, $wR2 = 0.0475$, GOF = 1.06. The absolute structure was determined, Flack parameter $x = 0.151(8)$. Further details of the crystal structure investigation may be obtained from the Fachinformationszentrum Karlsruhe, D-76344 Eggenstein-Leopoldshafen (Germany), on quoting the depository number CSD-405194.
[10] W. H. Baur, *Crystallogr. Rev.* **1987**, *1*, 59.
[11] Indeed there are $O^{[3]}$ connections in stishovite according to $^3_\infty[Si^{[6]}O^{[3]}_2]$ but at the same time the coordination number of the Si atoms in this high-pressure modification is raised from four to six. Also compare: F. Liebau, *Structural Chemistry of Silicates*, Springer, Berlin, **1985**.

LUCY—A Program for Structure Elucidation from NMR Correlation Experiments**

Christoph Steinbeck*

With the introduction of gradient-supported NMR spectroscopy, the time and effort required to record two-dimensional C,H correlations has now reached such a level that they can be considered as routine applications. Thus, long-range C,H correlation (HMBC[1]), long appreciated as a very valuable tool for determining the constitution, is also widely available. The idea of using this spectroscopic information for computer-supported, automated structure elucidation was close at hand. Although Lindley et al.[2] demonstrated the use of 2D information in a computer program for generating structures as early as 1983, it was not until the beginning of the 1990s that useful attempts in CASE systems (*c*omputer *a*ssisted *s*tructure *e*lucidation) were published.

We now introduce the program LUCY with which one can determine the constitution of an unknown compound based on the results of an HMBC experiment by using a standard personal computer. The information required for this task is the empirical formula, the broadband-decoupled ^{13}C, the DEPT-90, the DEPT-135, and the C,H COSY spectra (HMQC,[3] HSQC[4]). The H,H COSY diagram is optional, but useful. Here $^3J_{H,H}$ couplings are used exclusively. Evaluation of the DEPT spectrum and the C,H COSY diagram permits the user to exclude geminal coupling in the H,H COSY spectrum for diastereotopic protons of CH_2 groups. Furthermore, statements can be made as to whether or not a C atom is attached to a heteroatom, as evidenced by its chemical shift or its C,H coupling constants.

The authors of programs that use 1D NMR, mass, and IR spectra for structure elucidation have also reported recently on the use of HMBC data.[5, 6] However, new modules were always added to existing systems. LUCY, on the other hand, has been specifically designed to make use of HMBC data.

Our process uses these data to generate larger fragments of the carbon skeleton already in the first step of the structure elucidation. The CH_x ($x = 0-3$) fragments and the heteroatoms obtained from the DEPT experiments are combined in a recur-

[*] Dr. C. Steinbeck
Department of Chemistry, Tufts University
62 Talbot Avenue, Medford, MA 02155 (USA)
Fax: Int. code +(617) 627-3443
e-mail: stein@microvirus.chem.tufts.edu

[**] My particular gratitude goes to Prof. Dr. E. Breitmaier for the original idea and the stimulation to carry out this project.

 © VCH Verlagsgesellschaft mbH, D-69451 Weinheim, 1996 0570-0833/96/3517-1984 $ 15.00+.25/0

sive process [analyse coloc( )] to give all possible interpretations of the long-range C,H coupling in question. The use of $^3J_{H,H}$ couplings leads to a marked reduction in the number of combinations to be carried out. The algorithm is based on the hypothesis that the HMBC cross signals are representations of $^2J_{C,H}$ or $^3J_{C,H}$ couplings. Two atoms C_A and B (where B can be a carbon atom or a heteroatom bearing a proton) between which a correlation $C_A \rightarrow B{-}H$ exists, are connected to each other either directly ($^2J_{C,H}$) or through an optional heavy atom in the matrix ($^3J_{C,H}$). $^4J_{C,H}$ Couplings have not been considered, which appears to be justified given the statistical rarity of such cross signals and the enormous increase in computing time that would result were these couplings taken into account. Generation of these fragments from HMBC data leads to an extremely effective limitation in the number of solutions and the time required for structure elucidation is considerably reduced in comparison with that required for one based on selected HMBC data *after* the structure generation. In this way, a selection by applying other rules can be largely avoided.

During evaluation of the HMBC data, if a valid interpretation (in terms of the rules defined above) of all HMBC signals is found, the structure generator make bond( ) is used to complete the connectivity matrix. The resulting structure is subjected by the routine test global( ) to a number of user-defined selection criteria (for example, exclusion of rings of a certain size) and then displayed as a structure formula (an algorithm[8] developed by Ugi is used for the display).

The program consists of two parts (Fig. 1). The user interface LUCY (structure e*LUCI*dation), which runs under MS-Windows 3.1, Windows 95, and Windows NT, allows the convenient

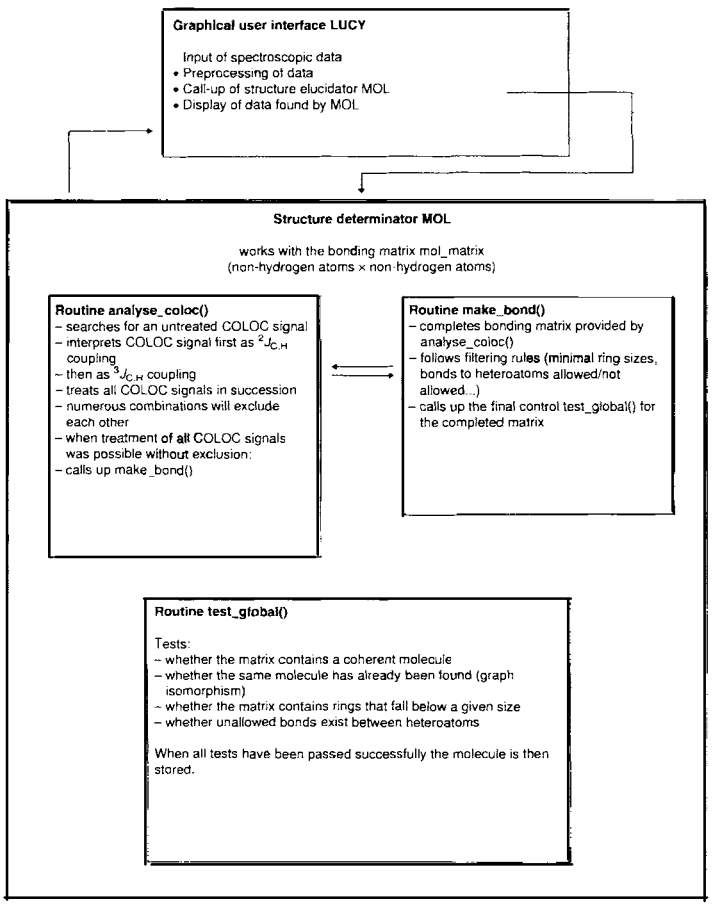

Fig. 1. Structure of the program LUCY.

introduction of data, whilst the calculation is carried out by the module MOL. Every modern PC (minimum requirement: an Intel 80486 processor) can be used. The structure elucidation can be transferred to another computer, for example, a work station, because the program can be divided into two parts.

The performance of the system is demonstrated with two examples. In 1991 Munk and Christie[5] determined the structure of monochaetin ($C_{18}H_{20}O_5$) by using DEPT, H,H COSY, and C,H COSY spectra, together with long-range C,H correlation with the system COCOA/INFER2D. The constitution of this fungal metabolite had already been elucidated in 1986 by conventional means.[7] Munk and Christie obtained six structures, including the correct one.

The same experimental data[5] were used for a structure elucidation with LUCY (Table 1, Fig. 2). The program effected a

Table 1. Data used for calculating the monochaetin structure [a]

Atom	DEPT	δ_C	C,H-COSY cross signal with δ_H	HMBC cross signal with δ_H	H,H-COSY cross signal with δ_H [b]
C-1	C	205.94		4.05, 3.76, 1.11	
C-2	C	191.77		1.32	
C-3	C	169.10		4.05	
C-4	C	158.52		6.79, 6.02, 2.13	
C-5	C	145.52		6.79, 6.02	
C-6	CH	143.30	6.79	3.76	
C-7	C	116.22		6.79, 6.02, 5.29, 3.76	
C-8	CH	107.04	6.02	5.29, 2.13	
C-9	CH	105.73	5.29	6.02	
C-10	C	82.55		5.29, 3.76, 1.32	
C-11	CH	52.13	4.05	3.76	3.76
C-12	CH	46.70	3.19	1.11	1.81/1.48, 1.11
C-13	CH	43.66	3.76	4.05, 1.32	4.05
C-14	CH_2	26.27	1.81/1.48	1.11	3.19, 0.97
C-15	CH_3	19.49	2.13	6.02	
C-16	CH_3	18.92	1.32	3.76	
C-17	CH_3	14.39	1.11		3.19
C-18	CH_3	11.45	0.97		1.81/1.48

[a] The shifts of the diastereotopic protons, which belong to the same CH_2 group, are separated by a backslash. [b] The δ values in the column H,H COSY are the coordinates of the cross signals, for which the matching values can be found in the column C,H COSY. This is also valid for the data given in Table 2.

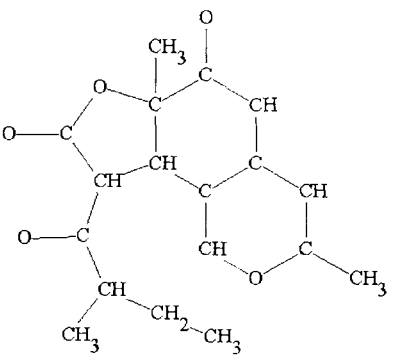

Fig. 2. Results calculated with LUCY on the monochaetin problem

minimal preprocessing in which it assigned, on the basis of the ^{13}C chemical shift, the signal at $\delta_C = 169$ to a carboxylic acid derivative (COO function) and the signals at $\delta_C = 205$ and $\delta_C = 191$ to two keto functions (>C=O). This preprocessing cannot be switched off at the moment, but can be adjusted. LUCY obtained the correct structure as the only result within about one minute using Windows95 with a Pentium PC operating at 100 MHz.

 © VCH Verlagsgesellschaft mbH, D-69451 Weinheim, 1996 0570-0833/96/3517-1985 $ 15.00+.25/0

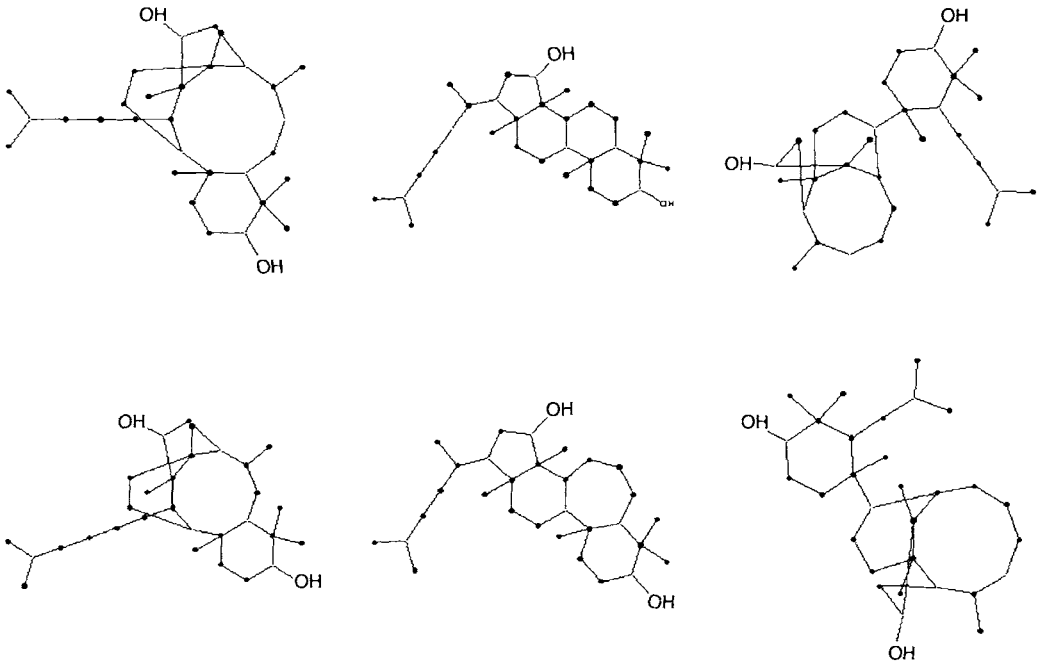

Fig. 3. Results calculated with LUCY on the polycarpol problem. Only connectivities are shown, not bond orders.

Table 2. Data used for calculating the polycarpol structure.

Atom	DEPT	δ_C	C,H-COSY cross signal with δ_H	HMBC cross signal with δ_H	H,H-COSY cross signal with δ_H [a]
C-1	C	146.0		6.00, 2.00/2.26, 1.01	
C-2	C	142.0		5.30, 1.04	
C-3	C	131.0		1.66, 1.60	
C-4	CH	125.5	5.20	1.66, 1.60	
C-5	CH	122.0	6.00	2.05/2.14	2.05/2.14
C-6	CH	116.3	5.30	2.00/2.26	2.00/2.26
C-7	CH	79.0	3.15		1.68
C-8	CH	74.8	4.30	1.04	1.83/1.93
C-9	C	52.5		1.04, 0.64	
C-10	CH	49.7	1.14	1.00, 1.01, 0.91	
C-11	CH	49.3	1.65	0.87, 0.64	1.83/1.93
C-12	C	44.4		5.30, 1.65, 1.04, 0.64	
C-13	CH_2	39.8	1.83/1.93		4.30, 1.65
C-14	C	39.0		1.14, 1.00, 1.68, 0.91	
C-15	CH_2	38.8	2.00/2.26	0.64	5.30
C-16	C	37.7		1.14, 1.68, 1.01	
C-17	CH_2	36.8	1.07/1.45	0.87	
C-18	CH	36.4	1.32	0.87	0.87
C-19	CH_2	36.3	1.38/1.92	1.01	1.68
C-20	CH_3	28.3	1.00	0.91	
C-21	CH_2	27.9	1.68		3.15, 1.38/1.92
C-22	CH_3	25.9	1.66	1.60	
C-23	CH_2	25.3	2.00		
C-24	CH_2	23.3	2.05/2.14		6.00
C-25	CH_3	23.0	1.01	1.14	
C-26	CH_3	18.7	0.87		1.32
C-27	CH_3	17.8	1.60	1.66	
C-28	CH_3	17.5	1.04		
C-29	CH_3	16.1	0.64	1.65, 2.00/2.26	
C-30	CH_3	16.0	0.91	1.14, 1.00	

[a] See footnote [b] in Table 1.

The program is being tested on numerous other examples in the course of our daily work.[10] Figure 3 shows the six solutions to the polycarpol problem[9] calculated by LUCY with data from Table 2, the largest matrix tested by us to date. The program requires two hours for the calculation (same conditions as above).

Received: February 9, 1996 [Z 8801 IE]
German version: *Angew. Chem.* **1996**, *108*, 2108–2110

Keywords: computer chemistry · NMR spectroscopy · structure elucidation

[1] M. F. Summers, L. G. Marzilli, A. Bax, *J. Am. Chem. Soc.* **1986**, *108*, 4285.
[2] M. R. Lindley, J. N. Shoolery, D. H. Smith, C. Djerassi, *Org. Magn. Reson.* **1983**, *21*, 405.
[3] A. Bax, R. Griffey, B. L. Hawkins, *J. Am. Chem. Soc.* **1983**, *105*, 7188; A. Bax, M. F. Summers, *ibid.* **1986**, *108*, 2093.
[4] G. Bodenhausen, D. J. Ruben, *Chem. Phys. Lett.* **1980**, *69*, 185.
[5] B. D. Christie, M. E. Munk, *J. Am. Chem. Soc.* **1991**, *113*, 3750.
[6] C. Peng, S. Yuan, C. Zheng, *J. Chem. Inf. Comput. Sci.* **1995**, *35*, 539.
[7] P. Steyn, R. J. Vleggaar, *J. Chem. Soc. Perkin Trans. 1* **1986**, 1975.
[8] K. Bley, J. Brandt, A. Dengler, R. Frank, I. Ugi, *J. Chem. Res.* **1991** (M), 2601.
[9] V. Hellwig, Diplomarbeit, Universität Bonn **1994**.
[10] E. Breitmaier, *Vom NMR-Spektrum zur Strukturformel organischer Verbindungen*, 2nd ed., Teubner, Stuttgart, **1992**; Wiley, **1993** (English translation); Maruzen, **1995** (Japanese translation).

An Unusually Stable Pentaethynylcyclopentadienyl Radical**

Norbert Jux, Karoly Holczer,* and Yves Rubin*

A major research goal of fullerene chemistry has been to encapsulate atoms or metal ions within the carbon framework of C_{60}.[1,2] Schwarz et al. and Saunders et al. have shown that inert gases like helium can be inserted into fullerenes, albeit with

[*] Prof. Y. Rubin, Dr. N. Jux
Department of Chemistry and Biochemistry
University of California, Los Angeles
Los Angeles, CA 90095-1569 (USA)
Fax: Int. code + (310) 206-7649
e-mail: rubin@chem.ucla.edu
Prof. K. Holczer
Department of Physics
University of California, Los Angeles
Los Angeles, CA 90095 (USA)

[**] This work was supported by the U. S. Office of Naval Research (N00014-94-1-0534). K. H. thanks the National Science Foundation for an instrumentation grant (DMR-9404166) and for support of a Bruker ESP380e spectrometer equipped with a 360D Dice ENDOR unit. N. J. thanks the Deutsche Forschungsgemeinschaft for a postdoctoral fellowship.

low efficiency, to give $He@C_{60}$.[3] Endohedral metal complexes of fullerenes are generated by evaporation of carbon rods filled with lanthanide oxides or nitrides yielding, for example, $La@C_{82}$.[2] A significant limitation of this procedure is that none of these compounds can be obtained in reasonable amounts, and so far no endohedral transition metal complexes of C_{60} itself (**1**, $M@C_{60}$) have been isolated.[4] The properties of the latter are potentially the most rewarding with regard to their superconductivity, ferromagnetism, and other interesting physical properties.

As part of a three-front approach to a rational synthesis of endohedral metal fullerene complexes such as **1** based on the multiple bond reorganization of alkyne-rich cyclophanes,[5–8] we have been investigating ways to incorporate the metal early on in the synthesis in the form of the D_{5h}-symmetric metallocene cyclophane **5**, isomeric to $M@C_{60}$ **1** (Scheme 1). Although we do not expect to isolate **5**, it may be an intermediate in flash vacuum pyrolytic or solution-phase reactions of the decakis-

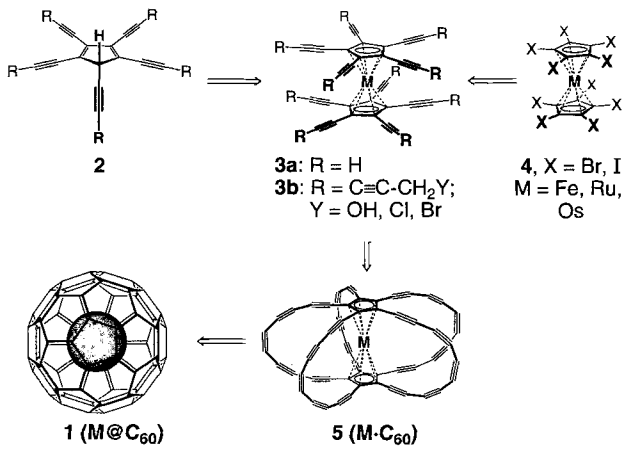

Scheme 1.

(1,3-pentadiynyl)metallocenes **3b**. The logical precursor of **5** is the decaethynylmetallocene **3a**, but little is known about this class of compounds. Bunz et al. have reported the synthesis of the half-sandwich pentaethynylcymantrenes (cymantrene = $CpMn(CO)_3$) through alkynylation of the corresponding pentaiodide.[9] In our hands similar ethynylation reactions of the decahalogenated precursors **4** have failed so far.[10] An alternate approach to decaethynylmetallocene **3a** is by deprotonation of a pentaethynylcyclopentadiene **2** and reaction with a metal halide.

In pursuit of this goal, we have developed a straightforward approach to the alcohols **10a–e**, halides **11a–c**, and the tautomeric fulvene-allenes **12a**, **12e**, and **13**. The preparation and characterization of the surprisingly stable pentaethynylcyclopentadienyl radical **14** is also presented.

1,1-Dimethoxy-2,3,4,5-tetrabromocyclopentadiene (**6**)[11] was ethynylated with various substituted acetylenes using a modified Sonogashira reaction (Scheme 2).[12] Substituents on acetylene include the trimethylsilyl (TMS), triethylsilyl (TES), triisopropylsilyl (TIPS), *tert*-butyldimethylsilyl (TBS), *tert*-butyl, phenyl, and 4-dimethylaminophenyl groups. The resulting ketals are obtained as yellow (**7a–e**), orange (**7f**), or red (**7g**)

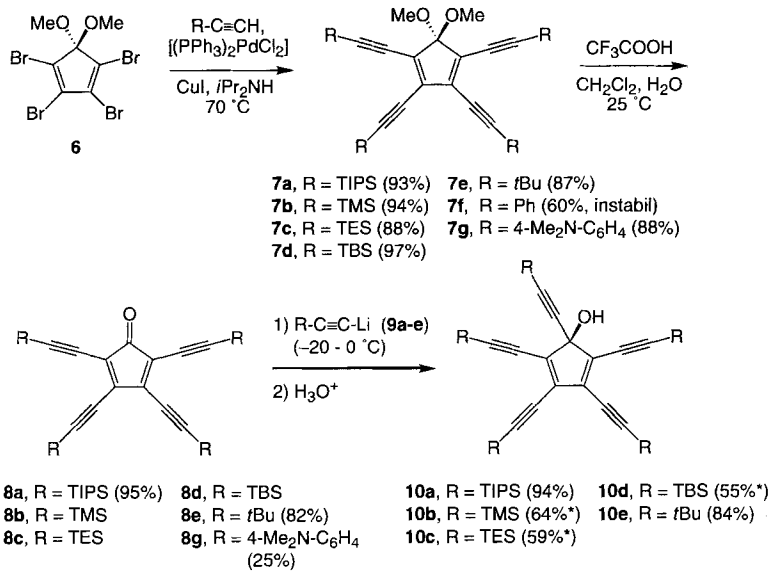

Scheme 2. Preparation of the pentaethynylcyclopentadienols **10a–e**; the yields marked with an asterisk are based on corresponding ketals.

crystals and are highly fluorescent in solution. The compounds we describe here are limited mainly to those protected with the triisopropylsilyl group (TIPS), because of the large kinetic stability it provides them (Table 1). However, the same reactions have been carried out on most of the other members of this series without significant alterations.

Acidic cleavage of the ketals **7a–e** and **7g** with trifluoroacetic acid/water (9:1) in CH_2Cl_2 afforded the cyclopentadienones

Table 1. Selected physical data for compounds **7a**, **8a**, **10a**, **12a**, **13**, and **14**.

7a: M.p. 116–118 °C; ^{1}H NMR (400 MHz, $CDCl_3$): δ = 1.09–1.14 (m, 84H), 3.48 (s, 6H); ^{13}C NMR (100 MHz, $CDCl_3$): δ = 11.26 (2C), 18.62, 18.72, 51.75, 99.14, 101.05, 103.51, 108.06, 109.11, 130.31, 132.04; IR (KBr): $\tilde{\nu}$ = 2146, 2116 cm^{-1}; HR-MS (FAB): *m/z* 846.6017 (M^+), calcd for $C_{51}H_{90}O_2Si_4$: 846.6018; UV/Vis (cyclohexane): λ_{max} (ε) = 287 nm (44500), 421 (8400), 404 (9600).

8a: M.p. 156–158 °C (decomp); ^{1}H NMR (400 MHz, $CDCl_3$): δ = 1.09–1.16 (m, 84H); ^{13}C NMR (100 MHz, $CDCl_3$): δ = 11.19, 11.21, 18.62, 18.68, 97.99, 99.41, 107.98, 116.46, 118.94, 139.82, 191.40; IR (KBr): $\tilde{\nu}$ = 2150, 2126, 1728 cm^{-1}; HR-MS (FAB): *m/z* 801.5683 (M^+ + H), calcd for $C_{49}H_{85}OSi_4$: 801.5677; UV/Vis (cyclohexane): λ_{max} (ε) = 282 nm (27500), 343 (10000), 555 (1600).

10a: M.p. 120–122 °C; ^{1}H NMR (400 MHz, $CDCl_3$): δ = 1.06–1.10 (m, 105H), 2.49 (s, 1H); ^{13}C NMR (100 MHz, $CDCl_3$): δ = 11.11, 11.20, 11.25, 18.65 (2C), 18.71, 79.19, 86.75, 99.22, 99.91, 102.22, 103.04, 105.77, 129.51, 135.57; IR (KBr): $\tilde{\nu}$ = 3588, 2136 cm^{-1}; HR-MS (FAB): *m/z* 983.7161 (M^+ + H), calcd for $C_{60}H_{107}OSi_5$: 983.7168; UV/Vis (cyclohexane): λ_{max} (ε) = 278 nm (37600), 288 (57000), 399 (9600), 415 (8900).

12a: M.p. 214–216 °C (decomp); ^{1}H NMR (400 MHz, $CDCl_3$): δ = 1.09–1.16 (m, 105H); ^{13}C NMR (100 MHz, $CDCl_3$): δ = 11.48, 11.51, 11.83, 18.59, 18.74, 18.78, 84.68, 100.31, 100.33, 101.48, 102.54, 114.30, 122.96, 130.28; IR (KBr): $\tilde{\nu}$ = 2136, 1911 cm^{-1}; HR-MS (FAB): *m/z* 1046.6250 (M^+), calcd. for $C_{60}H_{105}{}^{81}BrSi_5$: 1046.6225; UV/Vis (cyclohexane): λ_{max} (ε) = 255 nm (26900), 302 (39500), 332 (15800), 377 (16800), 390 (16600), 511 (1900), 636 (520).

13: M.p. 258–260 °C; ^{1}H NMR (400 MHz, $CDCl_3$): δ = 1.08–1.19 (m, 105H), 5.88 (s, 1H); ^{13}C NMR (100 MHz, $CDCl_3$): δ = 11.41, 11.47, 11.91, 18.51, 18.75, 18.78, 18.80, 18.81 (more than three signals due to hindered rotation), 81.39 (^1J(C,H) = 154.7 Hz), 99.12, 99.48, 100.73, 100.98, 109.40 (^3J(C,H) = 7.7 Hz), 123.96, 127.26, 207.41 (^2J(C,H) = 8.1 Hz); IR (KBr): $\tilde{\nu}$ = 2136, 1901 cm^{-1}; HR-MS (FAB): *m/z* 967.7249 (M^-), calcd for $C_{60}H_{107}Si_5$: 967.7219; UV/Vis (cyclohexane): λ_{max} (ε) = 297 nm (46800), 300 (41900), 327 (16900), 358 (16000), 375 (18300), 394 (14600), 466 (4600), 638 (30).

14: M.p. > 145 °C (decomp); ^{1}H NMR (400 MHz, C_6D_6): δ = 2.86 (br. s, 90H), 1.37 (s, 15H); IR (KBr): $\tilde{\nu}$ = 2126, 1896 cm^{-1}; HR-MS (FAB): *m/z* 966.7131 (M^+ + H), calcd for $C_{60}H_{106}Si_5$: 966.7141; UV/Vis (cyclohexane): λ_{max} (ε) = 289 nm (46800), 308 (41400), 421 (4000), 529 (1200), 564 (3100), 595 (6100), 614 (4100), 640 (14200).

8a–e and **8g**. The TIPS and *tert*-butyl derivatives **8a** and **8e** are stable purple crystalline solids which show no tendency to dimerize, while the other ketones can be stored only in dilute solution.[13,14] Reaction of **8a–e** with the corresponding lithiated acetylenes **9a–e** gave the stable alcohols **10a–e**. These alcohols could be converted smoothly to either the chlorinated pentaethynylcyclopentadienes **11a–c** or their brominated fulvene-allene tautomers **12a** and **12e**, depending on whether $SOCl_2$ or $SOBr_2$ was used (Scheme 3).

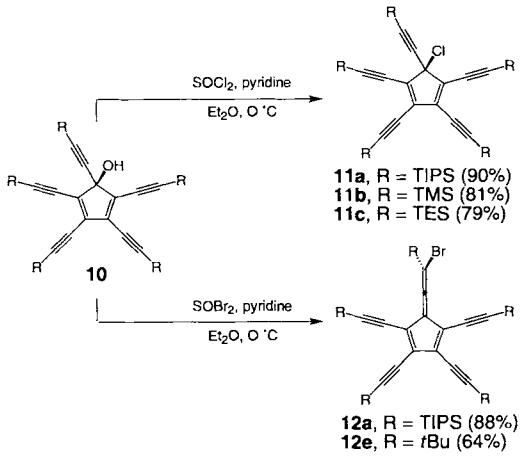

Scheme 3. Formation of the halogenated pentaethynylcyclopentadienes **11a–c** and their fulvene-allene tautomers **12a** and **12e**.

On addition of *n*-butyllithium to bromide **12a** (Scheme 4) in THF or Et_2O at $-78\,^{\circ}C$ the red color of the fulvene-allene disappeared and a yellow suspension of the lithium salt formed. Addition of anhydrous iron(II) chloride did not lead to the formation of the ferrocene **3a** (M = Fe). Instead, quenching of the reaction mixture with saturated NH_4Cl gave the dehalogenated fulvene-allene **13** rather than the cyclopentadiene tautomer **2** (R = TIPS). In another attempt to prepare the ferrocene **3a**

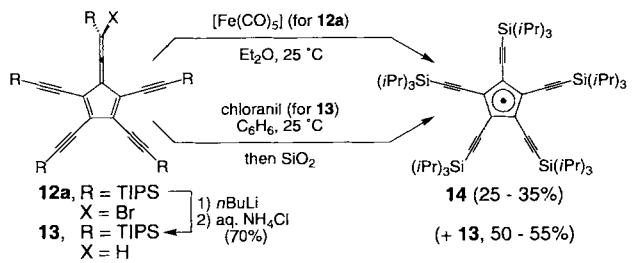

Scheme 4.

(M = Fe), bromide **12a** was treated with $[Fe(CO)_5]$[15] in ether at $25\,^{\circ}C$ to yield a new compound with an intense blue-green color, along with some orange-red **13**. Column chromatography on silica gel with hexanes in air gave the surprisingly stable cyclopentadienyl radical **14**.[16] Alternatively, radical **14** was prepared by oxidation of fulvene-allene **13** with chloranil or 2,3-dichloro-5,6-dicyanobenzoquinone (DDQ) in benzene at $25\,^{\circ}C$; interestingly this reaction required treatment with silica gel to induce formation of the radical.[17]

The surprising stability of radical **14** is in striking contrast with that of pentaaryl- or pentaisopropylcyclopentadienyl radicals,[16] which, although stable at $25\,^{\circ}C$, are all described as being highly sensitive to oxygen. Remarkably, radical **14** is stable in contact with air for weeks in the solid state and for days in hexane solution. This stability is even more peculiar because the steric shielding provided by the aryl or isopropyl substituents around the cyclopentadienyl radical must be considerably greater than that in the pentaethynyl system **14**, where the cyclopentadienyl ring remains very accessible to small molecules like oxygen.

The ^1H NMR spectrum of **14** shows two broad signals at $\delta = 2.86$ (90H; 350 Hz half-width) and $\delta = 1.37$ (15H) indicating the effect of the paramagnetic system on the proton resonances of the remote TIPS hydrogens. These two signals are well-separated in contrast to the usual TIPS-C≡C resonances which coincide at $\delta = 1.1$. The signal at $\delta = 2.86$ is shifted about 1.8 ppm downfield, indicating the effect of the paramagnetic system on the methyl protons of the TIPS groups. The paramagnetic shielding in **14** is less pronounced than that in the pentaisopropylcyclopentadienyl radical[16b,c] due to the larger distances of the CH and CH_3 groups from the radical center in the pentaethynylated system.

Confirmation of the radical nature of **14** was provided by an intense (unresolved) ESR signal at $25\,^{\circ}C$ in methylcyclohexane (MCH). For further evaluation of the structure of **14**, we performed a hyperfine-correlated ENDOR (HYEND) experiment (ENDOR = electron nuclear double resonance) at 20 K (Fig. 1).[18] This method is applicable to disordered spin systems

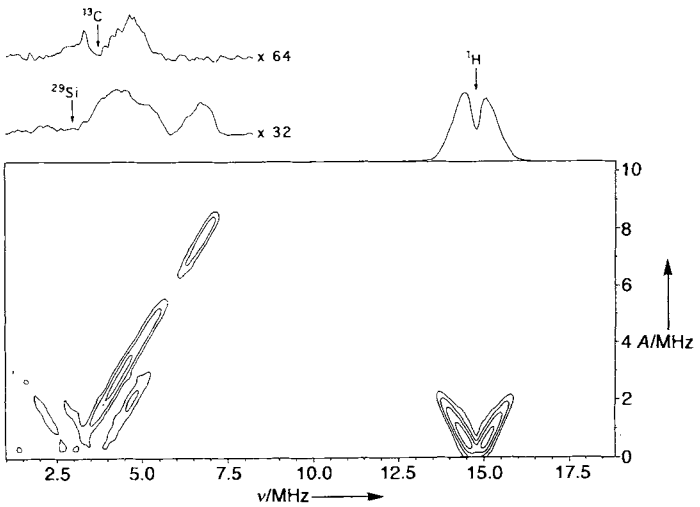

Fig. 1. Hyperfine-correlated ENDOR (HYEND) spectrum of radical **14** in methylcyclohexane at 20 K. The signals in the 1–8 MHz portion on the ENDOR axis are represented at 32 times higher intensity than those in the right-hand portion, and the corresponding projections are multiplied by 32 and 64 for ^{29}Si and ^{13}C, respectively. The spin flip angle of the applied radio-frequency pulses drop linearly below ≈3 MHz, resulting in an artificial loss of signal intensity. ν = ENDOR frequency, A = hyperfine splitting.

such as frozen solutions, and correlates hyperfine splitting to the nuclear transition frequencies in a 2D experiment. HYEND allows the separation of the ENDOR contributions of the three spin-active nuclei (^1H, ^{13}C, and ^{29}Si), the distinction of ^{13}C and ^{29}Si being especially important. These signals are centered around the free Larmor frequencies for these elements on the ENDOR frequency scale (^1H, 14.902 MHz; ^{13}C, 3.748 MHz; ^{29}Si, 2.963 MHz at 0.35 T); the projections show their separated ENDOR spectra. Note that the integrated intensities[19] are compatible with the elemental composition of **14** and the natural abundances of these elements. Interestingly, the silicon signal

 © VCH Verlagsgesellschaft mbH, D-69451 Weinheim, 1996 0570-0833/96/3517-1988 $ 15.00+.25/0

is split into two parts with integration ratios close to 4:1. The higher frequency part can be assigned to a silicon atom with high spin density, that is, to a hyperfine tensor with an isotropic part of about 8 MHz. The remaining broad contribution does not allow us to distinguish between the other four silicon atoms; assuming similar anisotropy, the isotropic part can vary between 2 and 4 MHz, implying two to four times less spin density on these atoms. This indicates that the D_{5h} structure of the radical is Jahn–Teller distorted in the MCH matrix at 20 K in favor of the C_s-symmetric equilibrium structure **14a** (Scheme 5).

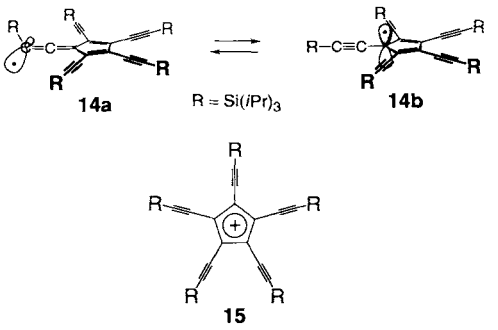

Scheme 5.

Strain release by bringing one of the bulky TIPS groups out of plane from the other four, occurring by passing from equilibrium form **14b** to **14a**, could be one factor accounting for this observation. Permanent Jahn–Teller distortion was also observed for the pentafluorocyclopentadienyl radical, but only below 8 K.[20]

The UV/Vis spectrum of radical **14** shows strong, sharp absorption bands with vibrational fine structure in the long-wavelength region (Fig. 2), whereas the corresponding ketone **8a**

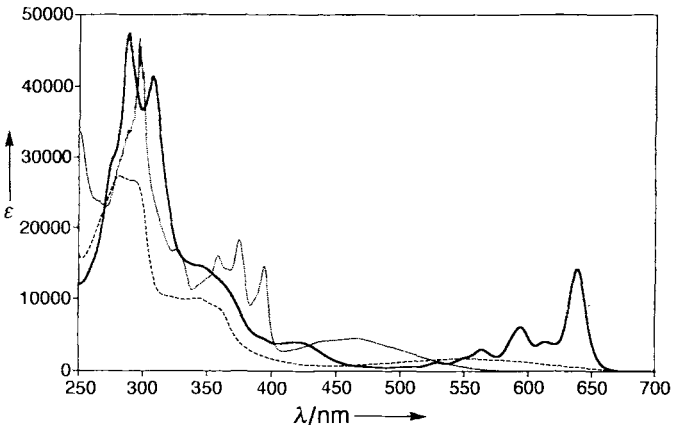

Fig. 2. UV/Vis absorption spectra of compounds **8a** (– – –), **13** (——), and **14** (——).

and fulvene-allene **13** have broad visible absorptions, implying that **14** has a more rigid structure in solution at 25 °C. The highly structured visible absorption region for radical **14** differs from the broad bands centered around 580 nm observed for the pentaarylcyclopentadienyl radicals,[16a,d,21] where the out-of-plane aryl rings are subject to bond rotation affecting conjugation.

The considerable bulk of the TIPS groups in the anion corresponding to **14** prevents coupling of two units to form a metallocene **3** (R = TIPS)[16c] even with larger metals such as Sn or Pb,[16d,22] and further studies will determine if smaller end groups can be used for that purpose. Cyclic voltammetry of radical **14** (CH_2Cl_2, 0.1 M $[nBu_4N][PF_6]$, 100 mVs^{-1}) reveals that it has a remarkable propensity to lose one electron to form the potentially antiaromatic cation **15** ($E_{ox1/2}$ = 0.15 V vs Fc/Fc^+). The pentaisopropylcyclopentadienyl radical is somewhat harder to oxidize ($E_{ox1/2}$ = 0.58 V).[16b] The facile oxidation of **14** reflects a significant propargylic/allenic resonance stabilization by the silylalkyne moieties. We believe that the cyclopentadienyl cation **15** should be stable at room temperature, and the isolation and characterization of this unusual species will be the subject of further studies.

Experimental Procedure

7a: Ketal **6** (4.42 g, 10 mmol) [11], $[(PPh_3)_2PdCl_2]$ (560 mg, 0.8 mmol), CuI (300 mg, 1.6 mmol), and $(iPr)_3Si\text{-}C\equiv CH$ (8.21 g, 45 mmol) were added in this order to 200 mL of degassed $(iPr)_2NH$. The mixture was heated at 70 °C for 12 h under argon. After evaporation of the solvent, the residue was dissolved in CH_2Cl_2 and filtered through silica gel. Column chromatography (SiO_2, hexanes/CH_2Cl_2 5:1) and recrystallization from CH_2Cl_2/methanol afforded **7a** as yellow needles (7.88 g, 93%).

8a: A solution of ketal **7a** (6.78 g, 8 mmol) in 400 mL of CH_2Cl_2 was allowed to react with was treated with CF_3COOH (20 mL) and H_2O (5 mL) for 30 min. After aqueous workup, the organic layer was washed with aq. $NaHCO_3$, dried over $MgSO_4$, and concentrated to dryness. Column chromatography (SiO_2, hexanes/CH_2Cl_2 5:1) and recrystallization from CH_2Cl_2/methanol afforded **8a** as small purple needles (6.09 g, 95%).

10a: *n*-Butyllithium (5.5 mmol) was added to a solution of $(iPr)_3Si\text{-}C\equiv CH$ (1.0 g, 5.5 mmol) in dry Et_2O (50 mL) at 0 °C. The reaction mixture was stirred 30 min, then a solution of ketone **8a** (4.01 g, 5 mmol) in Et_2O (100 mL) was added dropwise at 0 °C. The reaction mixture was stirred for a further 1 h then treated with sat. NH_4Cl. The organic layer was washed with H_2O and dried ($MgSO_4$). Evaporation of the solvent, column chromatography (SiO_2, CH_2Cl_2/hexanes 3:1), and recrystallization from hexanes afforded **10a** as yellow needles (4.62 g, 94%).

12a: $SOBr_2$ (0.842 g, 4.05 mmol) was added dropwise to a solution of alcohol **10a** (3.94 g, 4 mmol) and pyridine (0.316 g, 4 mmol) in dry Et_2O at 0 °C. The reaction mixture was stirred for 30 min then quenched with H_2O. The organic layer was treated with 2 M HCl, washed with H_2O, and dried ($MgSO_4$). Evaporation of the solvent, column chromatography (SiO_2, hexanes), and recrystallization from CH_2Cl_2/methanol afforded **12a** as shiny purple needles (3.68 g, 88%).

13: *n-Butyllithium (1 mmol) was added to a solution of bromide* **12a** *(1.05 g,* 1 mmol) in dry Et_2O (50 mL) at −78 °C. After 30 min the reaction mixture was treated with sat. NH_4Cl, and the organic layer was washed with H_2O and dried ($MgSO_4$). Evaporation of the solvent, column chromatography (SiO_2, hexanes), and recrystallization from CH_2Cl_2/methanol afforded **13** as small red needles (678 mg, 70%).

14: a) $[Fe(CO)_5]$ (294 mg, 1.5 mmol) was added to a solution of **12a** (523 mg, 0.5 mmol) in dry, degassed Et_2O. After 4 h the solvent was removed and the residue dissolved in hexanes. Column chromatography (SiO_2, hexanes) gave **14** as blue-green waxy crystals (170 mg, 35%) in addition to **13** (242 mg, 50%).
b) Chloranil (1.23 g, 5 mmol) was added to a solution of **13** (968 mg, 1 mmol) in benzene (50 mL). The reaction mixture was stirred for 2 h at 25 °C, poured onto silica gel, and extracted with hexanes. Evaporation of the solvent and column chromatography (SiO_2, hexanes) afforded **14** (339 mg, 35%) in addition to **13** (483 mg, 50%).

Received: March 29, 1996 [Z8958IE]
German version: *Angew. Chem.* **1996**, *108*, 2116–2120

Keywords: alkynes · cyclopentanes · ENDOR spectroscopy · fullerenes · radicals

[1] J. R. Heath, S. C. O'Brien, Q. Zhang, Y. Liu, R. F. Curl, H. W. Kroto, F. K. Tittel, R. E. Smalley, *J. Am. Chem. Soc.* **1985**, *107*, 7779–7780.
[2] F. T. Edelmann, *Angew. Chem.* **1995**, *107*, 1071–1075; *Angew. Chem. Int. Ed. Engl.* **1995**, *34*, 981–985, and references therein.
[3] a) T. Weiske, H. Schwarz, *Angew. Chem.* **1992**, *104*, 639–640; *Angew. Chem. Int. Ed. Engl.* **1992**, *31*, 605–606; b) M. Saunders, H. A. Jimenez-Vazquez, R. J. Cross, S. Mroczkowski, M. L. Gross, D. E. Giblin, R. J. Poreda, *J. Am. Chem. Soc.* **1994**, *116*, 2193–2194.
[4] $Ca@C_{60}$ is highly sensitive to O_2 and water: Y. Kubozono, T. Ohta, T. Hayashibara, H. Maeda, H. Ishida, S. Kashino, K. Oshima, H. Yamazaki, S. Ukita, T. Sogabe, *Chem. Lett.* **1995**, 457–458.
[5] Y. Rubin, T. C. Parker, S. I. Khan, C. L. Holliman, S. W. McElvany, *J. Am. Chem. Soc.* **1996**, *118*, 5303–5304.
[6] a) Y. Rubin, M. Kahr, C. B. Knobler, F. Diederich, C. L. Wilkins, *J. Am. Chem. Soc.* **1991**, *113*, 495–500; b) S. W. McElvany, M. M. Ross, N. S. Goroff, F. Diederich, *Science* **1993**, *259*, 1594–1596; c) N. S. Goroff, *Acc. Chem. Res.* **1996**, *29*, 77–83.

[7] G. von Helden, N. G. Gotts, M. T. Bowers, *Nature* **1993**, *363*, 60–63.
[8] a) D. E. Clemmer, M. F. Jarrold, *J. Am. Chem. Soc.* **1995**, *117*, 8841–8850; b) J. Hunter, J. Fye, M. F. Jarrold, *Science* **1993**, *260*, 784–786.
[9] a) U. H. F. Bunz, V. Enkelmann, J. Räder, *Organometallics* **1993**, *12*, 4745–4747; b) U. H. F. Bunz, V. Enkelmann, *ibid.* **1994**, *13*, 3823–3833; c) U. H. F. Bunz, V. Enkelmann, F. Beer, *ibid.* **1995**, *14*, 2490–2495.
[10] Y. H. Han, M. J. Heeg, C. H. Winter, *Organometallics* **1994**, *13*, 3009–3019.
[11] R. G. Pews, C. W. Roberts, C. R. Hand, *Tetrahedron* **1970**, 1711–1717. The preparation of C_5Br_6 should be repeated in Et_2O rather than petroleum ether for reliable yields, see: F. Straus, L. Kollek, W. Heyn, *Ber. Dtsch. Chem. Ges. B* **1930**, *63*, 1868–1885.
[12] K. Sonogashira, Y. Tohda, N. Hagihara, *Tetrahedron Lett.* **1975**, 4467–4470.
[13] M. E. Ogliaruso, M. G. Romanelli, E. I. Becker, *Chem. Rev.* **1965**, *65*, 261–367, and references therein.
[14] Since cyclopentadienones are excellent dienophiles, we have investigated the reaction of **8a** and **8e** with several alkynes including dimethyl acetylenedicarboxylate, 3-hexyne, diphenylacetylene, diphenylbutadiyne, and 1,6-bis(trimethylsilyl)-1,3,5-hexatriyne. This work will be reported in a separate paper for their use as precursors to graphynes. See: a) F. Diederich, Y. Rubin, *Angew. Chem.* **1992**, *104*, 1123–1146; *Angew. Chem. Int. Ed. Engl.* **1992**, *31*, 1101–1123; b) F. Diederich, *Nature* **1994**, *369*, 199–207.
[15] For the formation of decaphenylferrocene under similar conditions, see: H. Schumann, A. Lentz, R. Weimann, J. Pickardt, *Angew. Chem.* **1994**, *106*, 1827–1829; *Angew. Chem. Int. Ed. Engl.* **1994**, *33*, 1731–1733.
[16] For other stable cyclopentadienyl radicals, see: a) K. Ziegler, B. Schnell, *Liebigs Ann. Chem.* **1925**, *445*, 266–282; b) H. Sitzmann, R. Boese, *Angew. Chem.* **1991**, *103*, 1027–1029; *Angew. Chem. Int. Ed. Engl.* **1991**, *30*, 971–973; c) H. Sitzmann, H. Bock, R. Boese, T. Dezember, Z. Havlas, W. Kaim, M. Moscherosch, L. Zanathy, *J. Am. Chem. Soc.* **1993**, *115*, 12003–12009; d) R. H. Lowack, K. P. C. Vollhardt, *J. Organomet. Chem.* **1994**, *476*, 25–32.
[17] The ^{13}C NMR spectrum of the 1:1 complex formed between **13** and chloranil shows only those two components. We are currently investigating the mechanism of the formation of **14** in the presence of silica gel.
[18] G. Jeschke, A. Schweiger, *Chem. Phys. Lett.* **1995**, *246*, 431–438.
[19] Instrumental artifacts such as the linear drop of nuclear nutation angle below ca. 3 MHz must be taken into account.
[20] T. Chen, H. H. Günthard, *Chem. Phys.* **1985**, *97*, 187–203.
[21] K. Ziegler, L. Ewald, *Liebigs Ann. Chem.* **1929**, *473*, 163–193.
[22] a) M. J. Heeg, C. Janiak, J. J. Zuckerman, *J. Am. Chem. Soc.* **1984**, *106*, 4259–4261; b) C. Janiak, H. Schumann, C. Stader, B. Wrackmeyer, J. J. Zuckerman, *Chem. Ber.* **1988**, *121*, 1745–1751.

1,2-Diboretanides: Homoaromatic 2π-Electron Compounds with High Inversion Barriers**

Dirk Steiner, Heinz-Jürgen Winkler, Christian Balzereit, Thorsten Happel, Matthias Hofmann, Govindan Subramanian, Paul von Ragué Schleyer, Werner Massa, and Armin Berndt*

Dedicated to Professor Kurt Dehnicke on the occasion of his 65th birthday

1,2-Diboretanes with amino substitutents on the boron atoms have the classical structures **1**.[1] When such π-donor groups are absent the nonclassical form **2**, which contains two three-center-two-electron (3c,2e) bonds, is more stable.[2] We describe herein the corresponding anions of **1** and **2**, 1,2-diboretanides **3**, which have one 3c,2e bond and serve as a link between classical and nonclassical 1,2-diboretanes (Scheme 1).

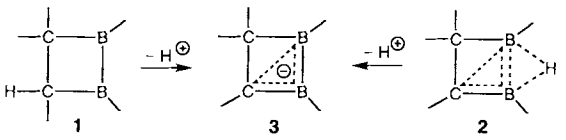

Scheme 1.

The lithium 1,2-diboretanide **3a** is formed by the reaction of the nonclassical 1,2-diboretane **2a**[2] or of the chloroborylborirane **4**[3] with lithium in diethyl ether (Scheme 2). Compound **2a** can be obtained almost quantitatively from the methyleneborane **5**[4] in two steps. Treatment of **5** with $NaHBEt_3$ in toluene gives the hydride adduct **6**, which is then allowed to react with cyclopentadiene to yield **2a**. The constitution of **3a** is deduced from the NMR data (Table 1) by means of the NMR/GIAO/ab initio method.[5] Note the agreement of the chemical shifts of the framework atoms with values computed at the GIAO-MP2/tzp level for unsubstituted **3u** and **3u'** (Table 2).[6] Figure 1 shows the structure of **3a** in the crystal.[7]

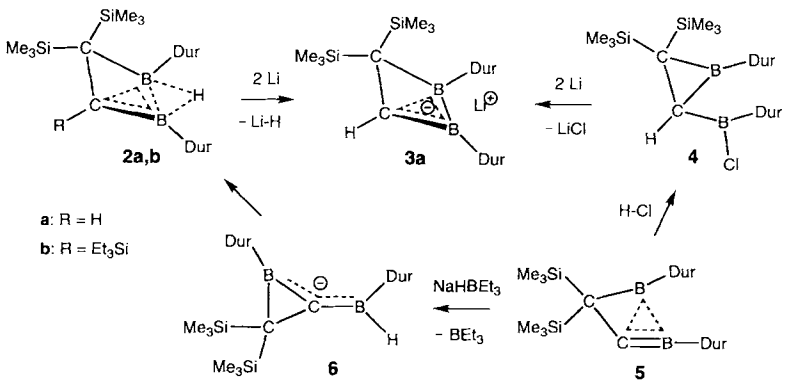

Scheme 2.

The geometry of the four-membered ring in the 1,2-diboretanide **3a** strongly resembles those of the nonclassical 1,2-diboretanes **2u** and **2b**;[2] the lithium ion coordinated by one di-

Table 1. Some physical properties of compounds **3a** and **6**.

3a: Solid, m.p. 157 °C (decomp.), yield: 75%. ^1H NMR (300 MHz, C_6D_6, 25 °C): δ = 0.09, 0.32 (each s, each 9H, $SiMe_3$), 2.05, 2.14, 2.28, 2.43, 2.61 (each s, total of 24H, *o*- and *m*-CH_3), 4.69 (s, 1H, CHB), 6.72, 6.77 (each s, each 1H, *p*-H); ^{13}C NMR (125 MHz, C_6D_6, 25 °C): δ = 1.6, 2.7 (each q, each 3C, each $(CH_3)_3Si$), 19.8, 20.5, 20.8, 21.0, 21.3, 21.5 (each q, total of 8 C, *o*- and *m*-CH_3), 32.0 (br. s, 1 C, CSi_2), 84.8 (br. d, 1 C, CHB, ^1J(C,H) = 161 Hz), 130.0, 131.7, 132.5, 133.9, 134.1, 137.1, 137.4 (total of 10 C, *o*-, *m*- and *p*-C), 139.2, 146.5 (each br. s, each 1 C, each *ipso*-C); ^{11}B NMR (96 MHz, C_6D_6, 25 °C): δ = 5, 58.

6: yellow solid, m.p. 170 °C (decomp.), yield ca. 90%. ^1H NMR (500 MHz, [D$_8$]THF, −30 °C): δ = −0.02 (s, 18H, $SiMe_3$), 2.07, 2.10, 2.27, 2.38 (each s, each 6H, *o*- and *m*-CH_3), 5.65 (br. s, 1H, BH), 6.48, 6.70 (each s, each 1H, *p*-H); ^{13}C NMR (125 MHz, [D$_8$]THF, −30 °C): δ = 2.0 (q, 6C, $SiMe_3$), 19.5, 20.6, 20.8, 21.0 (each q, each 2C, *o*- and *m*-CH_3), 106.1, (br. s, 1 C, BCB), 127.1, 132.0 (each d, each 1 C, *p*-C), 130.1, 131.4, 134.8, 142.5 (each s, each 2C, *o*- and *m*-C), 138.1, 155.8 (each br. s, each 1 C, *ipso*-C), the signal of the C atom carrying the trimethylsilyl groups could not be observed; ^{11}B NMR (96 MHz, [D$_8$]toluene, 25 °C): δ = 44 ($\nu_{1/2}$ = ca. 2600 Hz).

[*] Prof. Dr. A. Berndt, Dr. D. Steiner, Dr. H.-J. Winkler, Dr. C. Balzereit, T. Happel, Prof. Dr. W. Massa
Fachbereich Chemie der Universität
D-35032 Marburg (Germany)
Fax: Int. code +(6421)28 89 17
Dr. M. Hofmann, Dr. G. Subramanian, Prof. Dr. P. von R. Schleyer
Computer-Chemie-Centrum des Instituts für Organische Chemie der Universität Erlangen-Nürnberg (Germany)

[**] This work was supported by the Deutsche Forschungsgemeinschaft and the Fonds der Chemischen Industrie. G. S. gratefully acknowledges a postdoctoral fellowship from the Alexander-von-Humboldt-Stiftung.

Table 2. Experimental (**2a**, **3a**) and computed (**2u**, **3u'**, **3u**) [a] chemical shifts of framework atoms, and distances [pm].

	2a	**2u**	**3a**	**3u'**	**3u**
$\delta(^{11}B1)$	5.0	−2.6	5.0	−3.8	−1.3
$\delta(^{11}B2)$	44.0	43.5	58.0	53.8	60.8
$\delta(^{13}C3)$	73.8	71.2	84.8	90.4	72.6
$\delta(^{13}C4)$	30.6	24.2	32.0	28.9	27.9
B1-B2		171.7	165.5(4)	162.2	161.3
B2-C3		146.4	146.0(4)	148.4	149.1
C3-C4		150.0	154.2(4)	149.9	151.1
C4-B1		157.0	162.9(4)	158.2	159.7
B1-C3		170.5	171.1(4)	171.8	174.9

[a] MP2(FU) 6-31G*-optimized geometries. ^{11}B and ^{13}C NMR computations with GIAO-MP2 tzp.

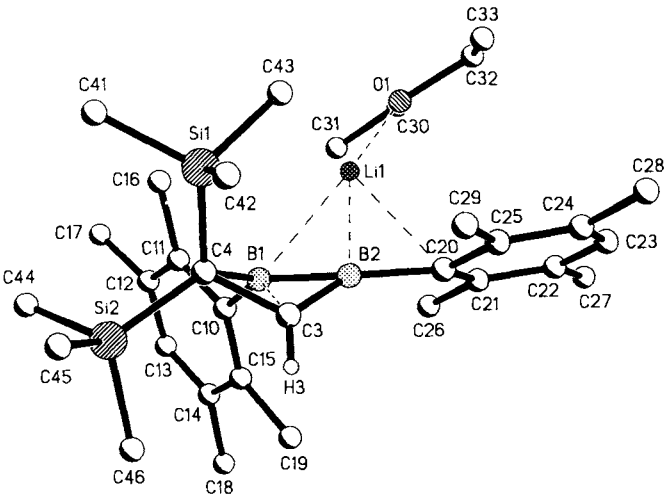

Fig. 1 Structure of **3a** in the crystal. Important interatomic distances [pm] and angles [°]: B1–B2 165.5(4), B1–C3 171.1(4), B1–C4 162.9(4), B1–C10 160.9(4), B2–C3 146.0(4), B2–C20 157.8(4), C3–C4 154.2(4), Li1–B1 250.8(7), Li1–B2 224.6(7), Li1–C20 259.8(7), Li1–O1 187.2(6), C4–Si1 186.2(2), C4–Si2 187.9(3); B2-B1-C4 97.5(2), B2-B1-C10 136.1(2), C4-B1-C10 123.1(2), B1-B2-C3 66.3(2), B1-B2-C20 151.8(2), C3-B2-C20 138.7(2), B2-C3-C4 110.7(2), C3-C4-B1 65.2(2), Si1-C4-Si2 116.7(1). Folding angle at B1–C3 140.0(2).

ethyl ether molecule adopts the position of the bridging H atom in **2u** and **2b**. However, the B1–B2 distance of 165.5(4) pm in **3a** (computed[8] to be 162.2 pm for **3u'**, Table 2) is considerably shorter than the corresponding distances in **2b** (179.9(3) pm) and **2u** (171.7 pm): the interaction of the B–B bond with the Li^+ ion in **3a** is electrostatic, whereas that with the H^+ ion in **2b** and **2u** is multicenter covalent. The Wiberg bond indices (WBIs) and charges obtained by natural population analysis (NPA) of the HF/6-31G* wavefunction clearly characterize the B-H-B bridge as a covalent 3c,2e bond, while the Li^+ ion in **3u'** is bound essentially electrostatically (Fig. 2).

The short B1–C3 distance (**3a**: 171.1(4) pm, **3u'**: 171.8 pm) and the corresponding WBI (0.528) indicate a strong 1,3-interaction, which also is consistent with the high barrier of ring inversion of **3a**. Two sharp signals for the geminal trimethylsilyl groups in the ^1H and ^{13}C NMR spectra at 25 °C broaden at higher temperatures. The barrier of 19.5 kcal mol^{-1}, determined from the coalescence temperature (130 °C in [D_{10}]*o*-xylene) in the ^1H NMR spectrum and the difference of the chemical shifts at slow exchange ($\Delta\delta = 100$ Hz), is considerably higher than all barriers reported for the homoaromatic 2π-electron compounds **7**–**9** (Fig. 3).[9]

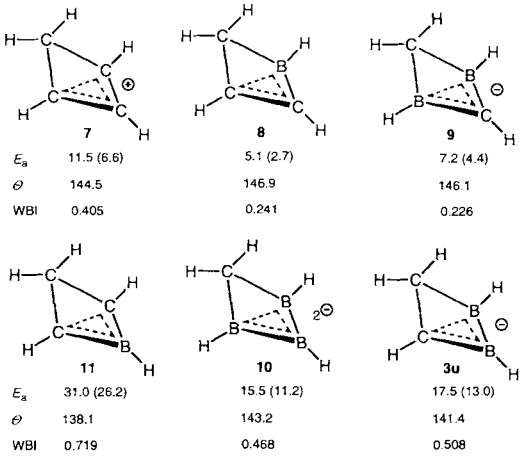

Fig. 3. MP2(FU)/6-31G*//MP2(FU)/6-31G* + ZPE inversion barriers E_a [kcal mol^{-1}], dihedral angles θ [°], and Wiberg bond indices (WBIs) for isoelectronic homoaromatic 2π-electron compounds. Inversion barriers at B3LYP/6-311 + G**//B3LYP/6-311 + G** + ZPE level are given in parentheses for comparison.

MP2/6-31G* calculations gave inversion barriers of 17.5 and 20.4 kcal mol^{-1} (Fig. 3) for the unsubstituted **3u** and **3u'**, respectively. Hence, such high barriers are characteristic for 1,2-diboretanides. Two related members of the family of homoaromatic 2π-electron compounds are still unknown, the homotriborirane dianion **10** and the borabicyclobutane **11**; their computed barriers are 15.5 and 31.0 kcal mol^{-1}, respectively (Fig. 3).

The inversion barriers given in Figure 3 reflect the degree of cyclic delocalization and the magnitude of homoaromaticity in the four-membered rings. The barriers correlate both with the folding angles between the two planes of the three-membered rings (correlation coefficient 0.98) and with the WBI of the transannular bonds (correlation coefficient 0.96).

Received: April 12, 1996 [Z 9019 IE]
German version: *Angew. Chem.* **1996**, *108*, 2123–2125

Keywords: ab initio calculations · boron compounds · heterocycles · homoaromaticity · strained rings

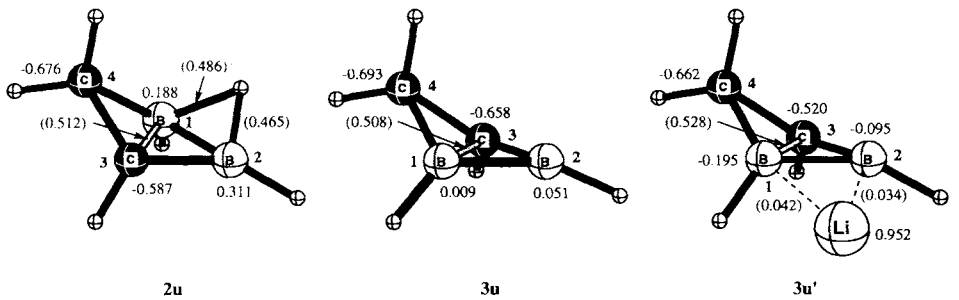

Fig. 2. Natural population analysis (NPA) charges and Wiberg bond indices (WBIs, in parentheses) for **2u**, **3u**, and **3u'** at the MP2(FU)/6-31G* level.

[1] A. Krämer, J.-K. Uhm, E. S. Garner, A. Pritzkow, W. Siebert, *Z. Naturforsch. B* **1990**, *45*, 1019–1021; R. Littger, H. Nöth, M. Thomann, M. Wagner, *Angew. Chem.* **1993**, *105*, 275–277; *Angew. Chem. Int. Ed. Engl.* **1993**, *32*, 295–297; W. Maringgele, A. Heine, M. Noltemeyer, A. Meller, *J. Organomet. Chem.* **1994**, *468*, 25–35.

[2] D. Steiner, C. Balzereit, H.-J. Winkler, N. Stamatis, M. Hofmann, P. von R. Schleyer, W. Massa, A. Berndt, *Angew. Chem.* **1994**, *106*, 2391–2394, *Angew. Chem. Int. Ed. Engl.* **1994**, *33*, 2303–2306.

[3] P. Willershausen, G. Schmidt-Lukasch, C. Kybart, J. Allwohn, W. Massa, M. L. McKee, P. von R. Schleyer, A. Berndt, *Angew. Chem.* **1992**, *104*, 1417–1420, *Angew. Chem. Int. Ed. Engl.* **1992**, *31*, 1384–1386.

[4] A. Berndt, *Angew. Chem.* **1993**, *105*, 1034–1058; *Angew. Chem. Int. Ed. Engl.* **1993**, *32*, 985–1009, and references therein.

[5] The generally good agreement between measured and computed chemical shifts for (carba)boranes has been shown previously: ^{11}B: M. Bühl, P. von R. Schleyer, *J. Am. Chem. Soc.* **1992**, *114*, 477–491. ^{13}C: M. Bühl, J. Gauss, M. Hofmann, P. von R. Schleyer, *ibid.* **1993**, *115*, 12385–12390. M. Diaz, J. Jaballas, J. Arias, H. Lee, T. Onak, *ibid.* **1996**, *118*, 4405–4410, and references therein.

[6] GIAO-MP2: a) J. Gauss, *Chem. Phys. Lett.* **1992**, *191*, 614; b) J. Gauss, *J. Chem. Phys.* **1993**, *99*, 3629–3643. The method was implemented in ACESII: ACESII is an ab initio program system written by J. F. Stanton, J. Gauss, J. D. Watts, W. J. Lauderdale, R. J. Bartlett, *Quantum Theory Project*, University of Florida, FL, USA, **1991**, **1992**). The abreviation tzp stands for "triple zeta plus polarization" basis sets: A. Schäfer, H. Horn, R. Ahlrichs, *J. Chem. Phys.* **1992**, *97*, 2571–2577.

[7] X-ray structure analysis: colorless crystals of **3a** ($C_{28}H_{45}B_2Si_2Li\cdot Et_2O$) were investigated with a four-circle diffractometer (CAD4, Enraf-Nonius) at −70 °C with $Cu_{K\alpha}$ radiation ($\lambda = 154.178$ pm). Crystal dimensions $0.6 \times 0.3 \times 0.3$ mm^3, monoclinic, space group $P2_1/c$, $Z = 4$, $a = 1287.5(3)$, $b = 1536.0(3)$, $c = 1745.2(3)$ pm, $\beta = 90.88(3)°$, $V = 3450.9 \times 10^{-30}$ m^3, $\rho_{calc} = 1.040$ g cm^{-3}; a total of 4630 reflections were measured up to $2\theta = 110°$ with $\omega/2\theta$ scans; 4329 independent reflections were used after LP correction in subsequent calculations; no absorption correction ($\mu = 10.7$ cm^{-1}). The structure was solved by direct methods and refined with full matrix against the F^2 data. Some of the H atoms could be localized from difference Fourier syntheses, the rest were calculated. Anisotropic temperature factors were used for all other atoms. $wR_2 = 0.1489$ resulted, corresponding to $R = 0.0517$ for 3614 reflections $> 4\sigma(F_o)$, the maximum residual electron density was 0.31 e Å^{-3}. Crystallographic data (excluding structure factors) for the structure(s) reported in this paper have been deposited with the Cambridge Crystallographic Data Centre as supplementary publication no. CCDC-179-67. Copies of the data can be obtained free of charge on application to The Director, CCDC, 12 Union Road, Cambridge CB2 1EZ, UK (fax: Int. code +(1223) 336-033; e-mail: teched(@ chemcrys.cam.ac.uk).

[8] MP2(FU)/6-31G* geometries computed with *Gaussian 94*; M. J. Frisch, G. W. Trucks, H. B. Schlegel, P. M. W. Gill, B. G. Johnson, M. A. Robb, J. R. Cheeseman, T. Keith, J. A. Petersson, J. A. Montgomery, K. Raghavachari, M. A. Al-Laham, V. G. Zakrzewski, J. Y. Ortiz, J. B. Foresman, J. Cioslowski, B. B. Stefanov, A. Nanayakkara, M. Challcombe, C. Y. Peng, P. Y. Ayala, W. Chen, M. W. Wong, J. L. Andres, E. S. Replogle, R. Gomperts, R. L. Martin, D. J. Fox, J. S. Binkley, D. J. DeFrees, J. Baker, J. J. P. Stewart, M. Head-Gordon, C. Gonzalez, J. A. Pople, Gaussian Inc., Pittsburgh, PA, USA, **1995**.

[9] P. Willershausen, C. Kybart, N. Stamatis, W. Massa, M. Bühl, P. von R. Schleyer, A. Berndt, *Angew. Chem.* **1992**, *104*, 1278–1280; *Angew. Chem. Int. Ed. Engl.* **1992**, *31* 1238–1240, and references therein; S. Sieber, P. von R. Schleyer, A. H. Otto, J. Gauss, F. Reichel, D. Cremer, *J. Phys. Org. Chem.* **1993**, *6*, 445–464.

Enantioselective Hydrogenations on Platinum Colloids**

Helmut Bönnemann* and Gerhard A. Braun

Metal colloids with dimensions of a few nanometers are important for catalysis research because of their high proportion of surface atoms.[1] These colloids can either be employed as catalysts in quasi-homogeneous phases[2] or serve as precursors for heterogeneous catalysts.[3] Their stabilization in solution at concentrations necessary for catalysis is achieved by polymers,[4] ligands,[5] or surfactants.[6] In several cases it was possible to show that the stabilizer affects the catalytic selectivity.[7] Herein, we report on a chiral induction by the stabilizer in a colloid-catalyzed hydrogenation. Using as an example a platinum sol stabilized by the protonated alkaloid dihydrocinchonidine (DHCin), we examined the influence of the stabilizer on the enantioselective hydrogenation of ethylpyruvate to (*R*)-ethyllactate [Eq. (a)] in a quasi-homogeneous phase.

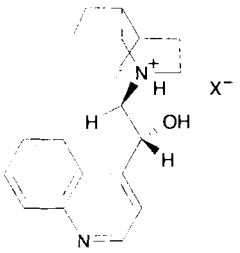

DHCin · HX:
X = Cl, AcO, HCO_2

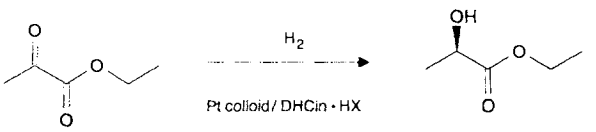

(a)

The enantioselective hydrogenation of α-oxoesters on heterogeneous platinum catalysts in the presence of cinchona alkaloids was reported for the first time by Y. Orito.[8] Over the last few years, these chirally modified heterogeneous catalysts have been systematically studied with respect to catalyst preparation,[9a] catalyst structure,[9b, c, d] reaction conditions,[9e, f, g] and kinetics.[9h, i] The structure of the modifier has been varied,[10a] and the interaction between the substrate and the alkaloid has been modeled.[10b, c]

In order to synthesize colloidal platinum, an aqueous solution of a platinum salt is reduced in the presence of protonated DHCin. The normally water-insoluble alkaloid is initially transformed into the water-soluble hydroformate, and then added by syringe to an aqueous platinum tetrachloride solution. The formate reacts to yield carbon dioxide, and the resulting platinum sol (**2**) is stabilized by the hydrochloride of DHCin [Eq. (b)].

$$PtCl_4 + (2-n)\ DHCin\cdot HCO_2H + n\ HCO_2H \rightarrow Pt_{colloid}\ [DHCinH^+\ Cl^-]_{2-n} + (2+n)\ HCl + 2\ CO_2 \quad \text{(b)}$$

2

$n = 0$–1.75

[*] Prof. Dr. H. Bönnemann, Dipl.-Chem. G. A. Braun
Max-Planck-Institut für Kohlenforschung
Kaiser-Wilhelm-Platz 1, D-45470 Mülheim an der Ruhr (Germany)
Fax: Int. code +(208)3062983

[**] This work is part of the planned thesis of G. Braun, RWTH Aachen. It was supported by the Bundesministerium für Bildung, Forschung, Technologie, und Wissenschaft, Bonn (FKZ 03 D 00007 A2), and the Funds der chemischen Industrie, Frankfurt. We thank Dr. Helmut Cölfen, Max-Planck-Institut für Kolloid- und Grenzflächenforschung/Teltow-Seehof, for the studies employing the analytical ultracentrifuge.

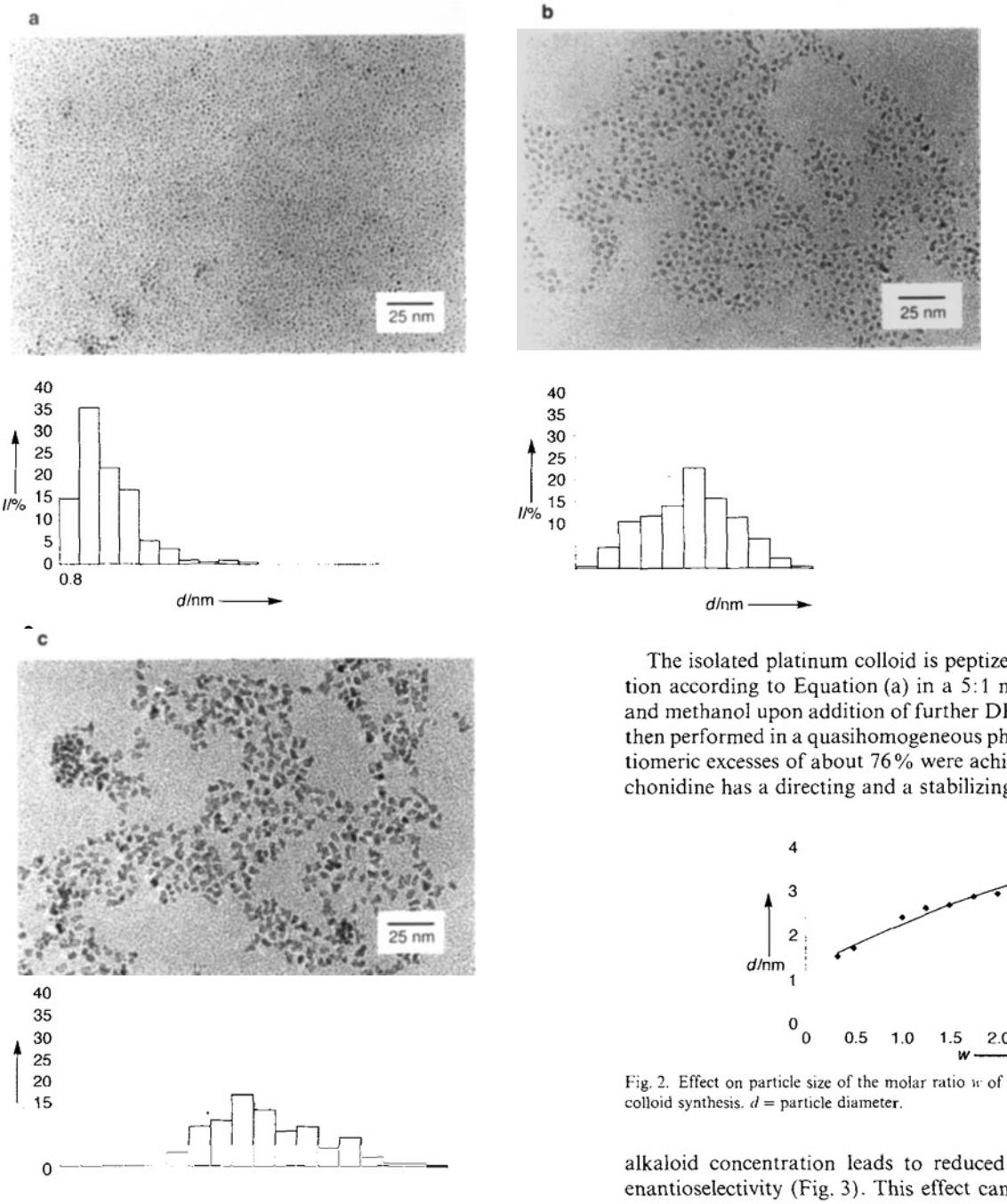

Fig. 1. Particle size distribution of DHCin-stabilized platinum colloids as a function of stabilizer concentration. Molar ratios of platinum to DHCin during the synthesis: a) 0.5, b) 1.25, c) 3.5. The distribution was determined by measuring at least 230 particles at different locations in the sample. d = particle diameter; I = relative abundance.

The colloids were examined by high-resolution electron microscopy (Fig. 1).[11] The molar ratio of platinum to dihydrocinchonidine during the synthesis determines the size of the resulting colloid; the particle size can by varied from 1.5 to 4 nm (Fig. 2).

The platinum sol (**2**) is precipitated by using sodium hydrogencarbonate, filtered off, washed, taken up in dilute acetic acid, and finally freeze-dried. The resulting black powder can be stored in the air and can be completely peptized in water or acetic acid upon the addition of methanol. The isolated platinum colloids exhibit a metal content of 40–50% by weight and are virtually free of chlorine.

The isolated platinum colloid is peptized for the hydrogenation according to Equation (a) in a 5:1 mixture of acetic acid and methanol upon addition of further DHCin. The catalysis is then performed in a quasihomogeneous phase. In general, enantiomeric excesses of about 76% were achieved.[12] Dihydrocinchonidine has a directing and a stabilizing effect: a decrease in

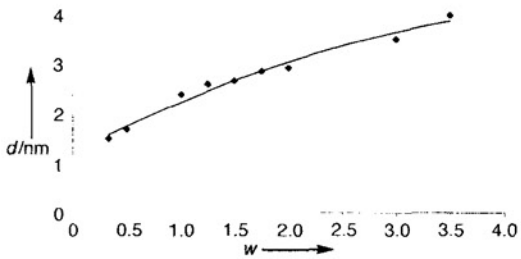

Fig. 2. Effect on particle size of the molar ratio w of platinum to DHCin during colloid synthesis. d = particle diameter.

alkaloid concentration leads to reduced activity at constant enantioselectivity (Fig. 3). This effect can be attributed to the agglomeration of the colloid in solution, which can be demonstrated by UV/Vis spectroscopic studies.[13] This agglomeration reduces only the accessible surface area, while the chiral induction at the remaining catalytically active sites is not affected. In

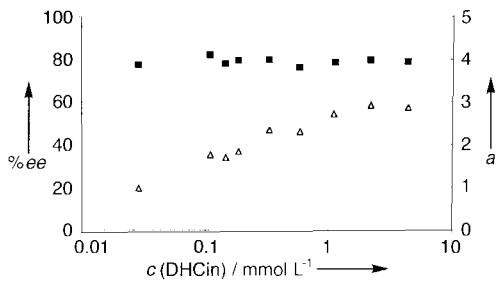

Fig. 3. Activity a (△) of colloidal platinum and enantiomeric excess (■) during the hydrogenation reaction (a) as a function of the concentration c of DHCin in the reaction medium [16].

order to avoid this agglomeration during catalysis, DHCin was added in 25 molar excess to platinum. UV/Vis spectroscopy, electron microscopy, and analytical ultracentrifuge studies before and after the reaction showed that under these conditions, no agglomeration takes place.[14] Thermostatically controlled glass reactors with flow breakers and gas addition stirrers were used for the hydrogenation. These reactors yield a very good material transport from the gas phase into the liquid. The hydrogenation was performed at 12 °C under atmospheric pressure; the course of the reaction was monitored by observing the consumption of hydrogen. Table 1 lists the colloid catalysts employed, their selectivities, as well as the turnover frequencies (TOF).

Table 1. Enantiomeric excess and TOF values for the catalytic hydrogenation according to Equation (a) on DHCin-stabilized platinum colloids of varying particle sizes.

w [a]	d_{TEM} [nm] [b]	d_s [nm] [c]	Dispersion [d]	TOF [s^{-1}]	% *ee*
0.5	1.5	2.0	0.57	1.1	76
1.25	2.6	3.0	0.38	1.1	74
3.5	3.9	4.7	0.22	0.9	78

[a] w is the molar ratio of platinum to DHCin during colloid synthesis. [b] d_{TEM} is the average particle diameter as determined by transmission electron microscopy. [c] d_s is the mean particle diameter, as averaged over the entire surface [15]. [d] The dispersion of the particles was calculated as outlined in ref. [15].

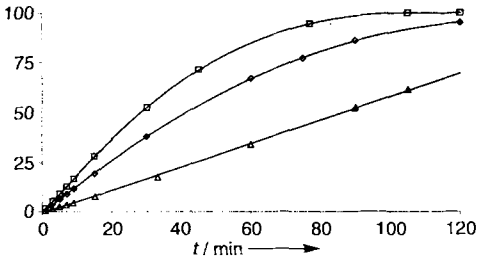

Fig. 4. Hydrogenation of ethylpyruvate on DHCin-stabilized platinum colloids of varying sizes. ▵: d_{TEM} = 3.9 nm, ◇: d_{TEM} = 2.6 nm, □: d_{TEM} = 1.5 nm [16]. The turnover [%] is plotted on the ordinate axis.

The activity of DHCin-stabilized platinum colloids decreases with increasing particle sizes (Fig. 4) as a result of decreasing dispersion. The dispersion is defined as the ratio of the number of surface atoms to the total number of atoms. It was calculated by using a surface density of platinum atoms estimated according to the method by Scholten et al.[15] and their mean diameter, as averaged over the entire surface. For the calculation of the TOF, all surface atoms were assumed to be catalytically active. The particle size had *no* effect on the TOF (Table 1) or on the enantiomeric excess (76 ± 2 % *ee*). The use of heterogeneous catalysts, on the other hand, has been reported to be associated with a distinct structure sensitivity.[9b]

DHCin-stabilized platinum colloids can be adsorbed on activated charcoal and silica. The thus obtained carrier catalysts show, for the hydrogenation according to Equation (a) at a hydrogen pressure of 100 bar in acetic acid, enantioselectivities (80 % *ee*) comparable to those reported for modified conventional heterogeneous catalysts.[9]

Experimental Procedure

Synthesis of the platinum colloid: Into a 250 mL two-neck flask, previously rinsed with aqua regia and a H_2SO_4/H_2O_2 mixture, was placed $PtCl_4$ (0.208 g, 0.6 mmol) dissolved in distilled water (160 mL). The flask was fitted with a reflux condenser and a septum, and the mixture was heated to reflux in an oil bath. During the synthesis, the bath temperature was maintained at 140 °C (± 5 °C). A solution of dihydrocinchonidine (0.355 g, 1.2 mmol) in 0.1 M aqueous formic acid (15 mL) was added rapidly by syringe. Initially, the reaction mixture became turbid and began to turn black after a few minutes. About ten minutes after the color change to black, the reaction was complete. The reaction mixture was poured into a saturated $NaHCO_3$ solution (200 mL), and the resulting precipitate was removed by a G4 fritted glass filter. The residue was washed first with a half-saturated $NaHCO_3$ solution (400 mL), then with water. The black solid was taken up in 1 M acetic acid (50 mL), and subsequently freeze-dried to remove the solvent. In this way a black powder (0.216 g) was obtained, which could be completely peptized in water and acetic acid/methanol. The metal content was found to be 41 % by weight, which indicated a yield of 71 % based on platinum. The chlorine content was below 0.5 % by weight. For the preparation of colloids with different particle sizes, the amount of platinum salt used was kept constant, while the amount of dihydrocinchonidine was reduced.

Enantioselective hydrogenation of ethylpyruvate on platinum colloids: Dihydrocinchonidine (150 mg) was dissolved in a 5:1 mixture of acetic acid and methanol (70 mL). Subsequently, platinum colloid (10 mg; particle size 1.5 nm, 41 % platinum by weight) was peptized in this solution and the dispersion was treated for 90 min in an ultrasonic bath. The resulting catalyst dispersion was a clear yellow-brown liquid. This liquid was cooled to 12 °C in a closed reactor fitted with a stirrer, degassed three times, and finally saturated with hydrogen. Using a hydrogen counterflow, ethylpyruvate (5 mL, 48 mmol) was added. The reaction was initiated by turning on the stirrer at a speed of 2000 revolutions per minute and was performed at atmospheric pressure. The course of the reaction was monitored by using the hydrogen consumption as an indicator; the reaction was complete after 120 minutes. The enantiomeric excess was determined by gas chromatography (6-*tert*-butyldimethylsilyl-2,3-dimethyl-β-cyclodextrin/SE54 as stationary phase) to be 76 % *ee*.

Received: February 8, 1996
Revised version: May 7, 1996 [Z8796IE]
German version: *Angew. Chem.* **1996**, *108*, 2120–2123

Keywords: asymmetric synthesis · catalysis · hydrogenation · platinum compounds

[1] J. S. Bradley in *Clusters and Colloids* (Ed.: G. Schmid), VCH, Weinheim, **1994**, Chapter 6.
[2] a) W. Hückel, *Katalyse mit kolloidalen Metallen*, Akademische Verlagsgesellschaft, Leipzig, **1927**; b) A. Behr, N. Döring, S. Durowicz-Heil, B. Ellenberg, C. Kozik, C. Lohr, H. Schmidke, *Fat. Sci. Technol.* **1993**, *95*, 2–12.
[3] a) G. C. Bond, *Trans. Faraday Soc.* **1956**, *52*, 1235; b) J. Turkevich, G. Kim, *Science* **1970**, *169*, 873; c) M. Boutonnet, J. Kizling, V. Mintsa-Eya, A. Choplin, R. Touroude, G. Maire, P. Stenius, *J. Catal.* **1987**, *103*, 95–104; d) H. Bönnemann, R. Brinkmann, W. Brijoux, E. Dinjus, T. Joussen, B. Korall, *Angew. Chem.* **1991**, *103*, 1344–1346; *Angew. Chem. Int. Ed. Engl.* **1991**, *30*, 804–806; e) H. Bönnemann, W. Brijoux, R. Brinkmann, E. Dinjus, R. Fretzen, T. Joussen, B. Korall, *J. Mol. Catal.* **1992**, *74*, 323; f) D. G. Duff, T. Mallat, M. Schneider, A. Baiker, *Appl. Catal. A* **1995**, *133*, 133–148; g) M. T. Reetz, S. A. Quaiser, R. Breinbauer, B. Tesche, *Angew. Chem.* **1995**, *107*, 2956; *Angew. Chem. Int. Ed. Engl.* **1995**, *34*, 2956.
[4] a) H. Hirai, Y. Nakao, N. J. Toshima, *J. Macromol. Sci. Chem.* **1978**, *A 12*, 1117–1141; b) D. G. Duff, P. P. Edwards, J. Evans, J. T. Gauntlett, D. A. Jefferson, B. F. G. Johnson, A. J. Kirkland, D. J. Smith, *Angew. Chem.* **1989**, *101*, 610; *Angew. Chem. Int. Ed. Engl.* **1989**, *28*, 590–593; c) M. Antonietti, E. Wenz, L. Bronstein, M. Seregina, *Adv. Mater.* **1995**, *7*, 1000–1005.
[5] G. Schmid, *Chem. Rev.* **1992**, *92*, 1709–1727.
[6] a) G. V. Lisichkin, A. Ya. Yuffa, V. Yu. Khinchagashvii, *Russ. J. Phys. Chem.* **1976**, *50*, 1285; b) J. Kiwi, M. Grätzel, *J. Am. Chem. Soc.* **1979**, *101*, 7214; c) J. Blum, Y. Sasson, A. Zoran, *J. Mol. Catal.* **1981**, *11*, 293; d) M. Boutonnet, J. Kizling, P. Stenius, G. Maire, *Colloids Surf.* **1982**, *5*, 209; e) N. Toshima, T. Takahashi, H. Hirai, *Chem. Lett.* **1985**, 1245; f) J. Wiesner, A. Wokaun, H. Hoffmann, *Prog. Colloid Polym. Sci.* **1988**, *76*, 271; g) H. Bönnemann, W. Brijoux, T. Joussen, *Angew. Chem.* **1990**, *102*, 324–326; *Angew. Chem. Int. Ed. Engl.* **1990**, *29*, 273; h) N. Toshima, T. Takahashi, *Bull. Chem. Soc. Jpn.* **1992**, *65*, 400–409; i) M. T. Reetz, W. Helbig, *J. Am. Chem. Soc.* **1994**, *116*, 7401–7402.
[7] a) M. Ohtaki, N. Toshima, M. Komiyama, H. Hirai, *Bull. Chem. Soc. Jpn.* **1990**, *63*, 1433–1440; b) K. Nasar, F. Fache, M. Lemaire, J.-C. Béziat, M. Besson, P. Gallezot, *J. Mol. Catal.* **1994**, *87*, 107–115.
[8] Y. Orito, S. Imai, S. Niwa, *Nippon Kagaku Kaishi* **1979**, 1118.
[9] a) J. T. Wehrli, A. Baiker, D. M. Monti, H. U. Blaser, *J. Mol. Catal.* **1990**, *61*, 207–226; b) H. U. Blaser, H. P. Jalett, D. M. Monti, A. Baiker, J. T. Wehrli, *Stud. Surf. Sci. Catal.* **1991**, *67*, 147–155; c) M. Garland, H. P. Jalett, H. U. Blaser, *ibid.* **1991**, *59*, 177–184; d) J. T. Wehrli, A. Baiker, D. M. Monti, H. U. Blaser, *J. Mol. Catal.* **1989**, *49*, 195–203; e) H. U. Blaser, H. P. Jalett, D. M. Monti, J. F. Reber, J. T. Wehrli, *Stud. Surf. Sci. Catal.* **1988**, *41*, 153–163; f) J. T. Wehrli, A. Baiker, D. M. Monti, H. U. Blaser, H. P. Jalett, *J. Mol. Catal.* **1989**, *57*, 245–257; g) H. U. Blaser, H. P. Jalett, J. Wiehl, *ibid.* **1991**, *68*, 215–

222; h) M. Garland, H. U. Blaser, *J. Am. Chem. Soc.* **1990**, *112*, 7048–7050; i) U. K. Singh, R. N. Landau, Y. Sun, C. LeBlond, D. G. Blackmond, S. K. Tanielyan, R. L. Augustine, *J. Catal.* **1995**, *154*, 91–97.

[10] a) B. Minder, T. Mallat, A. Baiker, G. Wang, T. Heinz, A. Pfaltz, *J. Catal.* **1995**, *154*, 371–378; b) O. Schwalm, J. Weber, B. Minder, A. Baiker, *Catal. Lett.* **1994**, *23*, 271–279; c) K. E. Simons, P. A. Meheux, S. P. Griffiths, J. M. Sutherland, P. Johnston, P. B. Wells, A. F. Carley, M. K. Rajumon, M. W. Roberts, A. Ibbotson, *Recl. Trav. Chim. Pays-Bas* **1994**, *113*, 465–474.

[11] The electron microscope studies were performed with a Hitachi high-resolution transmission electron microscope, type HF 2000. The TEM samples were prepared by peptizing the colloid in water, followed by a dropwise addition of the solution onto a copper sample mesh covered with carbon. The colloidal dispersion was removed after two minutes using cellulose and the sample was transferred to the microscope. We thank the electron microscopy department of the Max-Planck-Institut für Kohlenforschung for the critical discussion of these results.

[12] a) After the study reported herein was completed, we received a personal communication form H. U. Blaser (October 5, 1995) that polyvinylpyrrolidone (PVP)-stabilized platinum colloids yield 65% *ee* for reaction (a) (at a hydrogen pressure of 100 bar and with 2-propanol as solvent). b) Collier et al. report the enantioselective hydrogenation of ethylpyruvate (up to 40% *ee* at 17% turnover) on 2-butanone-stabilized platinum colloids after the addition of DHCin. The colloids were prepared by metal evaporation and are highly agglomerated: P. J. Collier, T. Goulding, J. A. Iggo, R. Whyman in *Chiral Reactions in Heterogeneous Catalysis* (Eds.: G. Jannes, V. Dubois), Plenum Press, New York, **1995**, 105.

[13] The absorption of metal sols in the UV/Vis range is determined by the shape and size of the metal particles. The agglomeration of the colloids was confirmed by UV/Vis spectroscopy. More details about the UV/Vis spectroscopy of metal sols can be found in G. D. Duff, P. P. Edwards, B. F. G. Johnson, *J. Phys. Chem.* **1995**, *99*, 15934–15944, and references therein.

[14] The TEM studies on the agglomeration of the colloids during catalysis were performed by conserving 5 mL of the reaction solution from before and after the reaction in an aqueous solution of the polymer PVP. Details regarding the conservation of metal colloids in PVP can be found in the literature cited in ref. [13].

[15] The surface density of platinum atoms in the colloid is $\rho_s = 1.25 \times 10^{19}$ atoms per m^2, assuming equal proportions of (100), (110), and (111) surfaces: J. J. F. Scholten, A. P. Pijpers, A. M. L. Hustings, *Catal. Rev. Sci. Eng.* **1985**, *27*, 151–206. The surface-averaged diameter d_s is obtained from the expression $d_s = \sum_i n_i d_i^3 (\sum_i n_i d_i^2)^{-1}$, where n_i is the number of particles having the diameter d_i. The dispersion is calculated from $D = 6fM(\rho\sigma N d)^{-1}$, where f is the percentage of the freely accessible surface of the particle, M the relative atomic mass of platinum, ρ the density of platinum, $\sigma = \rho_s^{-1}$ the mean surface area occupied by an atom, and N is Avogadro's number: J. L. Lemaitre, P. G. Menon, F. Delannay in *Characterization of Heterogeneous Catalysts* (Ed.: F. Delannay), Dekker, New York, **1984**, 299.

[16] The hydrogenation according to Equation (a) was performed in all cases using colloidal platinum metal (ca. 4 mg), AcOH/MeOH (70 mL), and ethylpyruvate (5 mL). For the calculation of the activity a, the consumption of hydrogen per minute (in mL) was compared to the mass of platinum (in mg) employed. The hydrogen consumption during the first ten minutes of the hydrogenation reaction was used as the basis for this calculation.

Corrigendum

In the communication "Discovery of Chiral Catalysts through Ligand Diversity: Ti-Catalyzed Enantioselective Addition of TMSCN to *meso* Epoxides" by M. L. Snapper, A. H. Hoveyda, et al. (*Angew. Chem. Int. Ed. Engl.* **1996**, *35*, 1668–1671) the entries in Table 1 under the column heading "Ligand" were inadvertantly cut off. Table entries 1, 3, and 5 were obtained with ligand **10**, entries 2, 4, and 6 with ligand **15**.

Furthermore, the citations in the text beyond no. 10 are incorrect. On page 1670 they should read "...as yellow crystalline solids.[11] In a manner similar to "positional scanning",[12]..." On page 1671 the passages should be "...enantioselectivity is improved from 40 to 86% *ee*.[13]" and in the Experimental Procedure at the top of the second column "...subjected to a ninhydrin test[14]...".

 © VCH Verlagsgesellschaft mbH, D-69451 Weinheim, 1996 0570-0833/96/3517-1995 $ 15.00+.25/0

A New Angle on Asymmetric Synthesis

Stereoselective Synthesis. By *R. S. Atkinson*. Wiley, Chichester, 1995. 529 pp., paperback £29.95.—ISBN 0-471-95250-8/0-471-95419-5

The subject of stereoselective synthesis has recently inspired quite a number of authors. In the case of the book *Stereoselective Synthesis* by R. S. Atkinson, published last year in a first edition, we even find that there are "cousins" with the same name: the Houben-Weyl volumes E 21 a–f and a book by M. Nógrádi, both of which bear the same title.

A glance at the contents of this latest addition to the family shows that it covers all the subject areas expected in a work of this size (see below). The description of each class of reactions begins with a precise explanation of the underlying principle, based on mechanistic considerations and a transition state model, and this is followed by a detailed discussion with suitable examples. This should provide the reader with a thorough understanding of the causes of the observed stereoselectivity.

When it comes to the arrangement of the subject matter the author takes a more exotic line than in his choice of title, as will appear below. One of the main purposes of the book is to promote a new way of classifying stereoselective reactions. This is based on comparing the number of chiral centers formed in the product molecule with the number that were present in the starting molecule, resulting in a classification into five reaction types from 0 to IV. A reaction of type 0 does not form any new chiral centers, whereas a type I reaction involves the breaking of one bond at a chiral center and the stereoselective formation of one new bond. Type II reactions are those in which two or more chiral centers are formed simultaneously from achiral reagent molecules (e.g., simple diastereoselection). In type III reactions one or several stereocenters are formed under the influence of an already existing stereocenter. The latter reactions are further divided into several different sub-groups (types $III_{s.c.}$, $III'_{s.c.}$, $III_{r.c.}$, $III_{s.c./r.c.}$, and $III_{cat.enant.}$). Type IV reactions are those in which no chiral centers are generated but diastereomers can be formed (e.g, diastereoselective formation of an enolate). Last but not least, it is also necessary to introduce type II/III reactions, which do not fit clearly into the above groups. The system has other weaknesses, which are particularly well illustrated by the fact that the author himself has not consistently followed this classification as a basis for the structure of the book! Instead of devoting one chapter to each reaction type with subdivisions where necessary, the author has arranged the contents in 16 chapters, all of equal status. In some cases a chapter corresponds to a single type, whereas elsewhere one reaction type is distributed through up to eight chapters!

Chapter 1 explains the meanings of the terms used in the book, such as chemo-, regio-, diastereo-, and enantioselectivity, chirality, prochirality, homotopy, enantiotopy, and diastereotopy. In Chapter 2 the author briefly explains the system of classification mentioned above (which is treated in greater depth in the later chapters). Chapter 3 is concerned with reactions of type 0. The most important part of this chapter is a table listing enantiomerically pure compounds that are readily obtainable. The author decribes how these can be converted into other enantiomerically pure synthetic building blocks in which the chiral centers are retained. Still following a logical sequence, Chapter 4 deals with type I reactions, beginning with inversion by means of S_N2 reactions and continuing through double inversion (equivalent to retention of configuration) and 1,2-rearrangements, both with inversion and with retention of configuration, and leading finally to Still's carbanions with a stable configuration. In Chapter 5 we find the first deviation from the system of classification, since instead of type II reactions this is devoted to some special type $III_{s.c.}$ reactions. Specific reactions discussed here are 1,3 chirality transfers via S_N2' reactions, [2,3]-sigmatropic and [3,3]-sigmatropic rearrangements, and the ene reaction.

Type II reactions are now taken up in Chapter 6, in which the discussion covers 1,2-additions to olefins, electrocyclic reactions, Diels-Alder reactions, and 1,3-dipolar cycloadditions. Even here, however, the author is innovative, introducing the terms "inherent diastereoselectivity" and "occasional diastereoselectivity", which have never appeared previously. In Chapter 7 the topic of "occasional diastereoselectivity" is treated in more detail, discussing as examples photochemical [2+2]-cycloadditions, photochemical 1,3-additions of arenes, 1,3-diyl additions, palladium-catalyzed trimethylenemethane additions to olefins, and again [2,3]- and [3,3]-sigmatropic rearrangements.

Chapter 8 deals with the aldol addition and related reactions (still belonging to type II). Type III reactions are then treated, along with others, in Chapters 9-12. Here we again find mentions of nearly all types of reactions in which asymmetric induction is known to occur, ranging from epoxidation through alkylation reactions to carbonyl addition reactions. For the first time the author explains the concepts of $A_{1,2}$- and $A_{1,3}$-strain, already mentioned several times in earlier discussions. Chapter 13 treats the hybrid type II/III reactions along with [4+2]-cycloadditions, 1,3-dipolar cycloadditions, aldol additions, and [3,3]-sigmatropic rearrangements.

Chapter 14 returns to type III reactions, and provides examples of catalytic enantioselective reactions (type $III_{cat.enant.}$). Particular topics treated here are the Sharpless epoxidation, CBS reduction of ketones, homogeneously catalyzed hydrogenations, chiral Lewis acids for Diels-Alder and ene reactions, the Sharpless dihydroxylation, cyclopropanation reactions, carbonyl additions, and Michael additions. Type $III_{s.c./r.c.}$ reactions are covered in Chapter 15, which explains double stereo-differentiation and the meaning of terms such as "matched" and "mismatched".

This section contains book reviews and a list of new books received by the editor. Book reviews are written by invitation from the editor. Suggestions for books to be reviewed and for book reviewers are welcome. Publishers should send brochures or (better) books to the editorial office: Redaktion Angewandte Chemie, Postfach 101161, D-69451 Weinheim, Germany. The editor reserves the right of selecting which books will be reviewed. Uninvited books not chosen for review will not be returned.

The sixteenth and final chapter is again concerned with type III reactions. Here the focus of attention is the distinction between enantiotopic and diastereotopic atoms or groups. In addition about 19 pages are devoted to the use of enzymes in stereoselective synthesis.

At the end of each chapter there is a summary of the most important points occupying about half a page. There is an adequate index containing about 500 entries which include all the important keywords. However, it is annoying that for some keywords not all the relevant page-numbers are listed; for example, the entry for the Diels-Alder reaction fails to refer to page 477. Altogether there are about 700 literature citations extending up to 1992.

The author's use of the word "echt", presumably borrowed from German, as in "the design of *echt* type $III_{r.c.}$ reactions" (p. 361) struck me as odd. Apart from a few minor inconsistencies of the kind that always slip through in the first edition of any book, I have found only three serious errors: on pages 217, 233, etc. allyl metal compounds are repeatedly referred to as "alkenyl metal compounds"; in Scheme 14b on page 372 the wrong olefin is shown; thirdly, instead of *syn* and *anti* as introduced by Masamune, the prefixes *cis* and *trans* are incorrectly used.

In any discussions involving stereochemistry the quality of the structural diagrams is of paramount importance. The perspective formula diagrams used here for the transition states are clear, but the mushroom-like appearance of the oxygen atoms at the ends of the backward-directed bonds (e.g. on p. 27) takes a little getting used to. The "lassos" that are occasionally shown around bonds whose movement is indicated by arrows (e.g. on p. 81) convey an odd sense of urgency.

The author's decision to abandon the usual order of presentation, based on either the stereoselective synthesis of a particular class of compounds or the stereochemical aspects of individual reactions (e.g. the Diels-Alder reaction), has its disadvantages. For example, it results in the various stereochemical aspects of the Diels-Alder reaction being treated in a fragmented way in seven different chapters. The numerous cross-references to other chapters are therefore really essential. On the other hand, the arrangement of the subject matter adopted here emphasizes principles of stereoselection that are common to different reactions, which has the advantage of focusing the reader's attention on an interesting new perspective and helping him or her to discover new relationships. Thus, on pages 148ff the common features linking the epoxidation, aziridination, and cyclopropanation of alkenes are discussed, then the reactive properties of the compounds concerned are correlated with those of intermediates in the halogenation of alkenes and of sulfonium and selenium ions in three-membered rings. However, as explained above this interesting sequence of topics is not directly derived from the proposed new system of classification, and therefore the usefulness of the latter is called into question.

To sum up, the above inconsistency means that the book is not very suitable for newcomers to the subject of stereoselective synthesis; on the other hand, for readers who already have a basic knowledge of the subject it offers new ideas and insights. It remains to be seen whether this attempt at a new classification of stereoselective reactions will gain acceptance.

A. Stephen K. Hashmi
Institut für Organische Chemie
der Universität Frankfurt/Main
(Germany)

Analytical Electrochemistry. By *J. Wang*. VCH Publishers, New York, 1994. 193 pp., hardcover $ 59.95.—ISBN 1-56081-575-2

It is pleasing to note that during the last few years the VCH group has devoted much effort, with considerable success, to remedying the relative neglect of electrochemistry in the available literature. Examples of successes in this field are the new series *Frontiers in Electrochemistry*, the journal *Electroanalysis*, and several monographs. The latest monograph from this publishing house is devoted to the very interesting and highly topical area of analytical electrochemistry, where new methods, especially the use of electrochemical sensors, are becoming increasingly important. The choice of this currently highly interesting topic, together with the expertise of the publishers in this field and the high reputation of the author, hold out to users of the methods and to students the promise of an interesting and valuable book. Regrettably, however, the reality does not quite come up to these expectations.

Already in the first short chapter on the fundamentals we find that there is no treatment of the electrochemical potential nor of equilibrium considerations. In the sections on kinetics one occasionally comes across mathematical equations that are incomplete, derivations that are not quite correct, and statements that are rather superficial. The poor quality of the figures is especially noticeable. The potential is shown increasing either from right to left or in the opposite sense depending on the original source. Dimensions are only partly standardized, and the symbols used for the same quantity vary from page to page. For example, A is first introduced to represent the electrode surface area, but two pages later is unashamedly used as a probability factor. Several examples of computations are given, which at first seems impressive, but is less helpful than expected: whereas the user's difficulties are most likely to be concerned with dimensions and orders of magnitude, the computational problem of electroanalysis (e.g. on p. 103) is cleverly reduced to the dimensionless problem of the rule of three.

Chapter 2 is mainly concerned with potential-controlled methods. Here the practitioner will find a collection of information on important instruments, relationships, and new systems. This presentation is a considerable step forward compared with the more conventional books by Plambeck and others. Chapter 3 contains much valuable practical information, including even the addresses of equipment suppliers. The sections on modern electrodes are also very useful; aspects such as special modifications, microelectrodes, and methods for producing these are included. A chapter on potentiometry is followed by a discussion of biosensors and chemical sensors; this is interesting and up-to-date, but not very systematic. The last 30 pages describe many new developments, in areas ranging from cyclovoltammetry to scanning tunneling microscopy. The information on the role of electrochemistry as a modern tool of interfacial science is useful, but is not easy to understand if one is not familiar with the principles.

Thus the book presents in an unusual way both the successful and the less successful aspects of applied research in this area. For the practitioner it has a certain value as a source of information. On the other hand, the reader who wishes to gain an understanding of the fundamentals of electroanalysis and modern electrochemistry will be better served by the more established works on the subject.

Joachim Walter Schultze
Institut für Physikalische Chemie
und Elektrochemie
der Universität Düsseldorf (Germany)

 © VCH Verlagsgesellschaft mbH, D-69451 Weinheim, 1996 0570-0833/96/3517-1998 $ 15.00+.25/0

Multidimensional Solid-State NMR and Polymers. By *K. Schmidt-Rohr* and *H. W. Spiess*. Academic Press, London, 1994. 478 pp., hardcover $ 65.00—ISBN 0-12-626630-1

Klaus Schmidt-Rohr and Hans Wolfgang Spiess have certainly written an impressive monograph. While always keeping polymers in mind, they clearly put the emphasis on the methodology of modern solid-state NMR, much of which has originated in the last decade in the laboratory of H. W. Spiess. Accordingly, the heading of Chapter two is "principles of NMR of Organic Solids", and only a short descriptive chapter is devoted specifically to the structure and dynamics of solid polymers.

One may ask, as the authors also do, for whom the book is written. Actually, the intention is to address a broad readership including beginners in solid-state NMR, typically students starting their work for a diploma or master's degree in a solid-state NMR laboratory. Although K. S.-R. and H. W. S. have tried to provide a self-contained text which can be read without constantly being forced to consult the cited literature (statement in the preface), I think that a beginner will need guidance for the study of this monograph, and I hasten to add: why not—after all it is through the interplay between reading, discussing, and doing experiments oneself that one's learning in science progresses.

With guidance, the beginner will recognize that from this monograph she or he can learn all that is needed to thoroughly understand spin gymnastics, Fourier theory in one and two dimensions, and all about the magic of magic-angle sample spinning, including the facts that it really is advantageous to introduce a bewilderingly large number of different reference frames and seemingly complicated functions, and that DOR and DAS, beautiful as they are conceptually and technically, have only limited applications. No word, though, about Floquet theory.

For the reader with some experience the monograph will prove to be a mine of treasures where countless "experiments", serving a wide range of purposes in polymer science and elsewhere, can be found. (Note that the usage of the word experiment is quite different in NMR from that in, for example, high energy physics. In NMR, already a new pulse sequence which can be implemented through the keyboard of a commercial spectrometer is termed a new "experiment".) The practitioner in the laboratory will appreciate the numerous helpful remarks on very practical everyday problems.

The expert will enjoy the fresh approach by the authors to some simple questions and the deep thought they give to some classical problems. For example, how many of us know whether our pulses rotate the nuclear magnetization to the left or to the right? K. S.-R. and H. W. S. at least *care*. They make considerable efforts to clarify important concepts and terms that are often carelessly used. Examples are the distinctions between homogeneous and inhomogeneous line-broadening, homogeneous and inhomogeneous Hamiltonians, and coherent and stochastic processes.

Much consideration is given to the question of the basic information content of various multidimensional spectra. In this context the reader leans about the usefulness of various joint and conditional probabilities, and that certain multidimensional spectra will exactly correspond to them. The close relationship between exchange NMR spectra and correlation functions in neutron scattering is discussed. Everyone who has performed a multidimensional solid-state NMR experiment would be well advised to consult this monograph as to whether or not the information contained in the spectra has been fully recognized and correctly interpreted. And this advice is certainly also pertinent to those who have questions about a material, be it a polymer or not, and wonder what kind of NMR experiment might give the answer. Even more: the monograph provides guidance to ask the right questions in the first place.

The sections and chapter on spin diffusion and its applications for characterizing polymers and polymer blends are particular highlights. It is refreshing to see that the monograph even serves as a platform for scientific controversy. Here one becomes very conscious of the personal involvement of K. S.-R. and of how much original work he has contributed to the subject.

I am sure that the monograph will soon become a standard reference source, a *classic*, simply "the SRS". It will be a *must* for all who work in solid-state NMR. I am the happy owner of two copies, one for the bedside and one for the office.

Ulrich Haeberlen
Max-Planck-Institut für
Medizinische Forschung
Heidelberg (Germany)

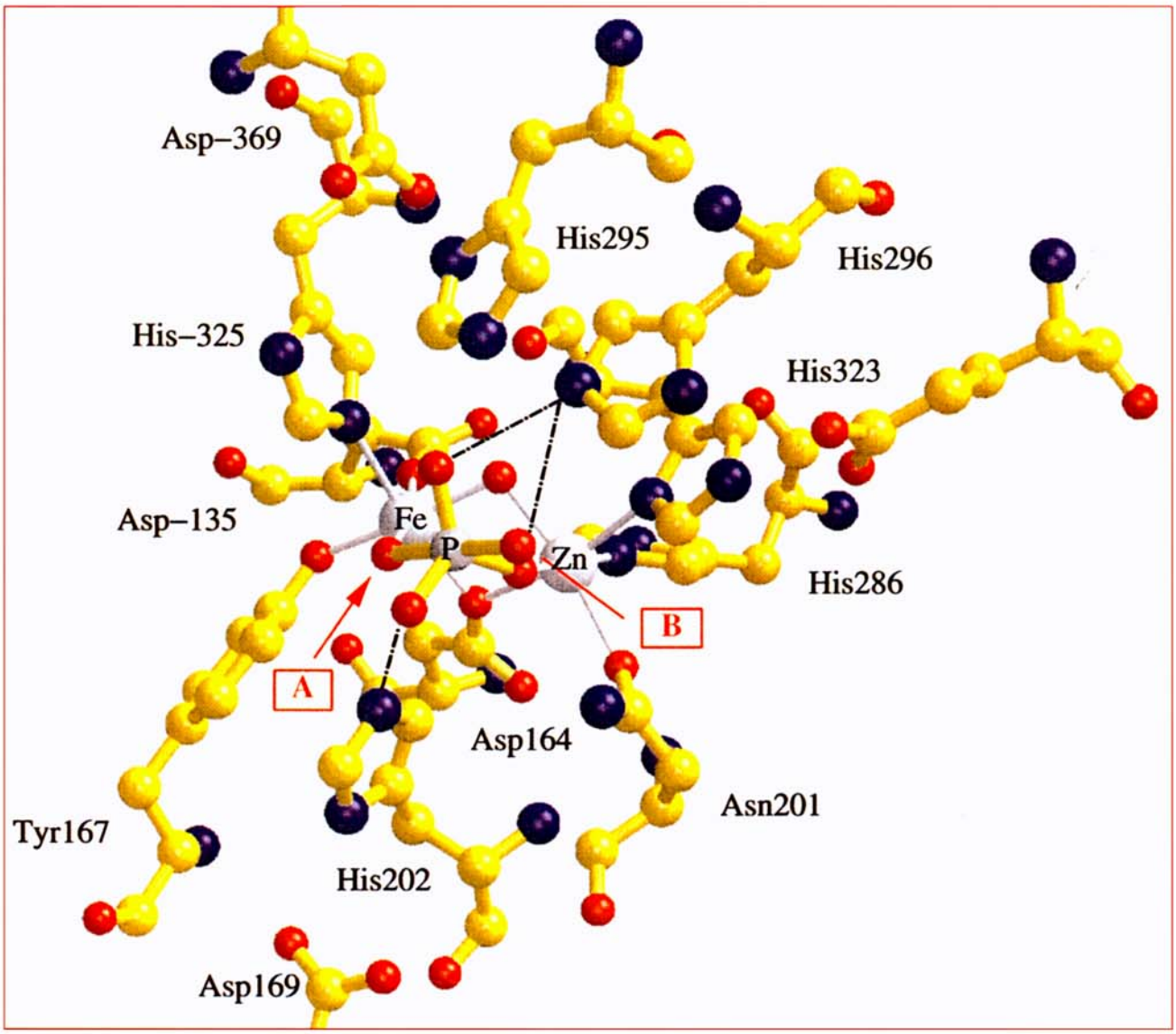

View of the pentacovalent transition state that is presumed for the reaction catalyzed by purple acid phosphatase. A labels the nucleophile attacking the phosphorus atom of the substrate and B denotes the oxygen atom of the leaving alcoholate group. For clarity only the ester oxygen atom of the alcohol group is shown.

Two-Metal Ion Catalysis in Enzymatic Acyl- and Phosphoryl-Transfer Reactions

Norbert Sträter, William N. Lipscomb,* Thomas Klabunde, and Bernt Krebs*

Numerous studies, both in enzymatic and nonenzymatic catalysis, have been undertaken to understand the way by which metal ions, especially zinc ions, promote the hydrolysis of phosphate ester and amide bonds. Hydrolases containing one metal ion in the active site, termed mononuclear metallohydrolases, such as carboxypeptidase A and thermolysin were among the first enzymes to have their structures unraveled by X-ray crystallography. In recent years an increasing number of metalloenzymes have been identified that use two or more adjacent metal ions in the catalysis of phosphoryl-transfer reactions (R-OPO_3 + R′-OH → R′-OPO_3 + R-OH; in the case of the phosphatase reaction R′-OH is a water molecule) and carbonyl-transfer reactions, for example, in peptidases or other amidases. These dinuclear metalloenzymes catalyze a great variety of these reactions, including hydrolytic cleavage of phospho-mono-, -di- and -triester bonds, phosphoanhydride bonds as well as of peptide bonds or urea. In addition, the formation of the phosphodiester bond of RNA and DNA by polymerases is catalyzed by a two-metal ion mechanism. A remarkable diversity is also seen in the structures of the active sites of these di- and trinuclear metalloenzymes, even for enzymes that catalyze very similar reactions. The determination of the structure of a substrate, product, stable intermediate, or a reaction coordinate analogue compound bound to an active or inactivated enzyme is a powerful approach to investigate mechanistic details of enzyme action. Such studies have been applied to several of the metalloenzymes reviewed in this article; together with many other biochemical studies they provide a growing body of information on how the two (or more) metal ions cooperate to achieve efficient catalysis.

Keywords: catalysis · enzymatic catalysis · metallohydrolases

1. Introduction

Enzymes containing two metal ions separated by about 3 to 5 Å in the active site, termed dinuclear metalloenzymes, catalyze a wide variety of chemical reactions in nature. Prominent examples are the dinuclear iron proteins hemerythrin, ribonucleotide reductase, and methane monooxygenase,[1] or the copper proteins superoxide dismutase, hemocyanin, tyrosinase, and cytochrome c oxidase, all of which are involved in transport or activation of oxygen. Examples for nonredox-active dinuclear metalloenzymes include enolase, xylose isomerase, and arginase. An active role in catalysis (or oxygen binding in the case of hemerythrin and hemocyanin) has been assigned to both metal ions, and none of the closely neighboring metal ions seems to have a purely structural role. Increasing numbers of dinuclear metalloenzymes that catalyze hydrolytic reactions are now recognized (Table 1). However, it has only been in the last few years that detailed three-dimensional structural information became available for some of these enzymes.

Two-metal ion catalysis is now found in several biological transfer reactions of phosphoryl and acyl or other carbonyl groups, mostly to water molecules (phosphatases, peptidases, amidases). In view of the similarities of these reactions a comparative review of the presumed reaction mechanisms and their structural basis seems desirable. Therefore the scope of this article covers structural and mechanistic aspects of the catalysis of metalloenzymes that utilize two or more catalytic metal ions in phosphoryl- and carbonyl-transfer reactions. No limitation is made to a specific metal ion (e.g. Zn^{2+}) employed for catalysis in vivo, especially since for most of these enzymes activity is seen with several divalent metal ions. The enzymes are discussed and compared mainly on the basis of structural investigations, including also kinetic and spectroscopic results of relevance to the two-metal ion mechanism. Considering the number of enzymes included here, it is evident that a comprehensive coverage of the available literature on each one could not be achieved. However, for most of these enzymes a recent and more comprehensive review article is cited. We also regret that studies on small-molecule dinuclear metallocatalysts, many of which were

[*] Prof. Dr. W. N. Lipscomb, Dr. N. Sträter
Department of Chemistry and Chemical Biology
Harvard University
12 Oxford Street, Cambridge, MA 02138 (USA)
Fax: Int. code +(617) 495-3330
e-mail: lipscomb@chemistry.harvard.edu
Prof. Dr. B. Krebs, Dr. T. Klabunde
Institut für Anorganische Chemie der Universität
Wilhelm-Klemm-Strasse 8, D-48149 Münster (Germany)
Fax: Int. code +(251) 838366
e-mail: krebs@nwz.uni-muenster.de

Table 1. Abbreviations, metal ions present in vivo, and metal · · · metal distances (with type of metal bound in the structure determination in parentheses) for the enzymes reviewed in this article. M indicates that any of the ions Mn^{2+}, Mg^{2+}, or Zn^{2+} could be the active metal ions in vivo.

Enzyme	Abbr.	Metal ions present	Distance [Å]
alkaline phosphatase	AP	Zn1, Zn2, Mg3	4.1 (Zn1 · · · Zn2)
purple acid phosphatase	PAP	Fe, Zn (Fe, Fe)	3.1 (Fe1 · · · Zn2)
Ser/Thr protein phosphatase 1	PP-1	Fe, Zn (?)	3.3 (Mn1 · · · Mn2), 4.0 (Fe1 · · · Mn2)
calcineurin	PP-2B	Fe, Zn	3.0 (Fe1 · · · Zn2) 3.1 (Fe1 · · · Zn2)
DNA polymerase β	pol-β	M, M	4.7 [a] (MgA · · · MgB)
3′,5′-exonuclease of DNA polymerase I	(pol-I)	M, M	3.9 [a] (ZnA · · · MgB)
ribonuclease H (HIV-RT)	RNase H	M, M	≈4 (Mn · · · Mn)
fructose-1,6-diphosphatase	FBP	M, M	3.7 [a] (Mn1 · · · Mn2)
inositol monophosphatase	IMP	M, M	3.9 [a] (Mn1 · · · Mn2)
inositol polyphosphate 1-phosphatase	IPP	M, M	3.9 (Mn1 · · · Mn2)
phospholipase C	PLC	Zn1, Zn2, Zn3	3.3 (Zn1 · · · Zn3)
nuclease P1	P1	Zn1, Zn2, Zn3	3.2 (Zn1 · · · Zn3)
(*S*)-adenosylmethionine synthetase	AMS	M, M	5 [a] (Mg1 · · · Mg2)
glutamine synthetase	GLS	Mg, Mg	5.8 (Mn1 · · · Mn2)
phosphotriesterase	PTE	Zn, Zn	3.8 (Cd1 · · · Cd2)
leucine aminopeptidase	LAP	Zn, Zn	3.0 (Zn1 · · · Zn2)
Aeromonas proteolytica aminopeptidase	AAP	Zn, Zn	3.5 (Zn1 · · · Zn2)
methionine aminopeptidase	MAP	Co, Co (?)	2.9 (Co1 · · · Co2)
urease		Ni, Ni	3.5 (Ni1 · · · Ni2)

[a] The distance could not be observed in the structure of the unliganded enzyme because two metal ions bind only in the presence of substrates, products, or inhibitors.

synthesized as structural or functional models for the enzymes discussed here, could not be included. For zinc enzymes containing two or more adjacent metal ions, termed cocatalytic zinc motifs, a recent analysis with respect to their structural and biochemical properties is available.[2]

2. Phosphoryl-Transfer Reactions

Phosphoryl-transfer mechanisms have been intensively studied both in enzymatic and nonenzymatic reactions because of their fundamental biological importance. Consequently, several comprehensive reviews are available on these reactions in general[3–5] and on the role of metal ions.[6] A main step in the classification of an enzyme-catalyzed phosphoryl-transfer reaction concerns the question of whether the reaction proceeds via a covalent phosphoenzyme intermediate or whether the phosphoryl group is directly transferred to the final acceptor. Provided that each elementary step yields an inversion of the chiral

N. Sträter

W. N. Lipscomb

T. Klabunde

B. Krebs

Norbert Sträter was born in Soest, Germany, in 1965. He studied Chemistry at the University of Münster, Germany, and obtained his PhD in 1994. In the group of Bernt Krebs he worked on the X-ray crystal structure of purple acid phosphatase. As a postdoctoral researcher in the laboratory of William N. Lipscomb at Harvard he is currently studying the two-metal ion mechanisms of leucine aminopeptidase and aminopeptidase A by X-ray crystallography.

William N. Lipscomb was born in Cleveland, Ohio, in 1919. After obtaining his BS in Chemistry at the University of Kentucky, he earned a PhD in Chemistry at the California Institute of Technology for X-ray and electron diffraction studies in the group of Linus Pauling. He then joined the faculty of the University of Minnesota, where he studied the structure and bonding of volatile boron hydrides by low-temperature single-crystal X-ray diffraction. He pursued this work after 1959, when he became Professor of Chemistry at Harvard, and was awarded the Nobel Prize in Chemistry in 1976 for these research studies. X-ray studies on enzyme structure and function, focussing on metalloenzymes and allosteric enzymes, started in 1962. His research on metalloenzymes has included work on carboxypeptidase A, carbonic anhydrase, leucine aminopeptidase, and fructose-1,6-bisphosphatase.

Thomas Klabunde was born in Lüdenscheid, Germany, in 1968. After studying Chemistry at the University of Münster, Germany, he joined the group of Bernt Krebs. He obtained his PhD in 1996 for biochemical and crystallographic studies on purple acid phosphatase and has now joined the research group of James C. Sacchettini at Texas A & M University for postdoctoral research in crystallography.

Bernt Krebs was born in 1938 in Gotha, Germany. He studied Chemistry at the University of Göttingen, Germany, and received his PhD in 1965 for studies on the crystal structure and chemistry of trithiocarbonic acid under supervision of G. Gattow. Thereafter followed postdoctoral research at Brookhaven National Laboratory (X-ray and neutron diffraction on biological macromolecules), Habilitation in Inorganic Chemistry in Göttingen, and faculty positions in Kiel, Bielefeld, and Münster, where he has been a full Professor since 1977. His primary research interests include chemical and structural studies on thio- and seleno-compounds, chalcogen halides, chalcogenide solid-state compounds, transition metal oxygen compounds, cis-platinum analogues, and metalloproteins as well as model complexes for these metalloproteins.

configuration around the phosphorus atom (see below), a direct transfer would result in an inverted configuration, whereas one phosphoenzyme intermediate would yield a retention of the configuration, and so forth. Of the nucleophilic amino acid side chains available to the enzyme to form a phosphoenzyme intermediate, histidine, serine, threonine, cysteine, and tyrosine are known to become phosphorylated. However, aspartate, glutamate, and lysine may also act as nucleophiles. An enzyme-bound intermediate may be trapped at a certain pH or in a metal-exchanged enzyme form, as was shown for Cd-substituted alkaline phosphatase.[7]

A second main characteristic of the mechanism concerns the nature of each elementary step. Each displacement step may proceed either by a largely dissociative mechanism via a metaphosphate-like intermediate[8] or by an associative pathway through a pentacoordinate intermediate or transition state (Fig. 1). Both possibilities have been demonstrated to occur in nonenzymatic phosphoryl-transfer reactions.[3, 9, 10]

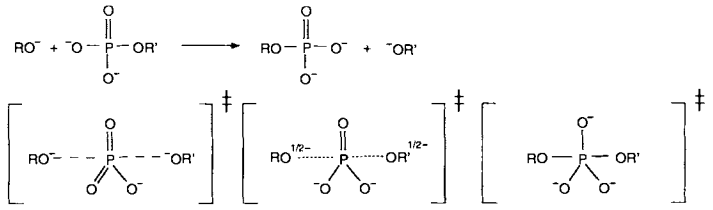

Fig. 1. Phosphoryl-transfer reaction of a phosphomonoester dianion with a deprotonated nucleophile (top). Structure of the transition state for a dissociative (bottom left), intermediate (bottom middle), and associative (bottom right) mechanism.

Inversion of the configuration around the phosphorus atom is a characteristic of an associative in-line S_N2 displacement step as long as no rearrangement of the ligands in the pentacoordinate intermediate takes place. Whereas such rearrangements like the Berry pseudo-rotation[10] are possible in nonenzymatic reactions, they have not been observed in enzymatic catalysis so far.

The experimental differentiation between a reaction pathway via a short-lived metaphosphate-like intermediate and an associative pathway is extremely difficult. If the rate constant can be determined as a function of the pK_a value of the attacking nucleophile or the leaving group, a plot of $\lg(k)$ against pK_a usually yields a linear relationship (Brønsted plot).[11] A large dependence of the rate constant on the nucleophilicity of the attacking group can be expected for an associative mechanism, whereas no dependence is expected for a purely dissociative pathway. Both pathways are influenced by the nucleophilicity of the leaving group.

It is evident from Figure 1 that the bond order to the equatorial phosphoryl oxygen atoms changes for an associative and a dissociative pathway in the transition state relative to the ground state. Isotopic substitution of these oxygen atoms can thus influence the rate constant.[9, 12, 13] Substitution of ^{18}O in an associative pathway will slow down the reaction (normal secondary isotope effect), whereas the same substitution leads to a rate enhancement for dissociative mechanisms (inverse secondary isotope effect). Likewise, the influence of an isotopic substitution of the ester oxygen atom can indicate the degree of bond cleavage in the transition state.[12, 13] Studies on the isotope effect have been applied to the reactions catalyzed by alkaline phosphatase, calcineurin, and phosphotriesterase (see Sections 2.1, 2.2.2, and 2.9).

In addition, a number of well-founded considerations have been put forward by various authors on the basis of the energetics of enzymatic catalysis to assess the factors favoring each pathway. These criteria operate mainly on the interactions between enzyme and substrate and between enzyme and transition state or intermediate and can thus most thoroughly be applied on the basis of a detailed structural analysis, preferably of complexes of the enzyme with reaction coordinate analogues. One structural consideration concerns the distance between the intermediate and the final acceptor: Since even a stabilized metaphosphate intermediate is a highly reactive chemical species it has to be separated by a minimum distance from the enzyme-bound nucleophile in order to be stable for a limited lifetime. Mildvan and Fry[14] estimated that a distance of more than 4.9 Å is necessary for a dissociative path.

Several significant conclusions can be drawn from studying the possible interactions between the participating reactants (Fig. 2). Because of the high reactivity of a metaphosphate intermediate, an activation of the attacking nucleophile is not necessary and would favor an associative pathway. Activation of the leaving group promotes both pathways and is thus of little diagnostic use, although it has a greater influence on a metaphosphate path. Interaction of the equatorial phosphoryl oxygen atoms with positively charged amino acid side chains or metal ions stabilizes the intermediate of both pathways by reducing the negative charge on the oxygen atoms. However, it becomes apparent from Figure 1 that an associative pathway increases the negative charge on the equatorial oxygen atoms of the intermediate, whereas in a dissociative pathway the magnitude of the negative charge of the metaphosphate intermediate is reduced compared to that of the substrate. The interaction of metal ions or positively charged amino acid side chains with the phosphoryl oxygen atoms thus stabilizes the substrate more than it stabilizes a metaphosphate intermediate, so that the metaphosphate ion is destabilized relative to the ground state by these interactions, whereas the pentacoordinate intermediate is stabilized relative to the ground state. Neglecting the influence of the different geometrical structures of ground state and transition state (see below), electrostatic interactions of the equatorial phosphoryl oxygen atoms with positively charged species may therefore favor an associative pathway.

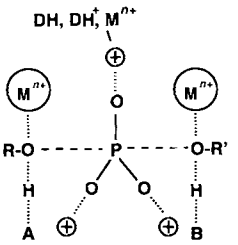

Fig. 2. Possible interactions in the stabilization of a transition state of an in-line displacement step for a phosphomonoester with metal ions (M^{n+}), general acids (AH), general bases (B), and hydrogen-bond donors (DH). OR is the leaving group and OR' the incoming nucleophile.

Partly because of the aforementioned reasons most authors assume an associative phosphoryl-transfer mechanism, since positively charged metal ions or amino acid side chains are frequently found in interaction with the phosphoryl oxygen atoms in enzyme active sites. However, the nonenzymatic hy-

drolysis of phosphomonoesters, of phosphodiesters,[5] and of the γ-phosphoryl group of ATP[15] takes place largely or in part via a metaphosphate pathway in solution. Does an enzyme change the dissociative character of these reactions by employing metal ions or positively charged side chains in catalysis, or does it enhance catalysis by further stabilizing the same transition state of the reaction in solution? Metal ions evidently do not change the transition state character of nonenzymatic reactions and they have little effect on the rate constant.[15, 16] Thus, it was argued that coordination of metal ions to the phosphoryl oxygen atoms has a much smaller effect than generally assumed and does not change the character of the transition state.[15] Also, the metal ions are usually coordinated by one or more negatively charged ligands (most often carboxylate groups), which can reduce the overall charge toward neutrality. The role of the metal ions may primarily be to achieve a favorable orientation of the reactants. Furthermore, the assumption that a metaphosphate-like transition state is destabilized relative to the substrate in a positively charged electrostatic field neglects geometrical factors such as the different structures of the tetrahedral phosphate group of the substrate and of the trigonal-planar metaphosphate. These factors could result in a stabilization of a metaphosphate by a more perfect fit of the intermediate to the enzyme active site. Orbital interactions, in particular, may be very sensitive to the complementary geometry of intermediate and active site.

Figure 2 summarizes possible interactions of protein groups and metal cofactors in the stabilization of a transition state of a phosphoryl-transfer reaction. Metal ions (M^{n+}) lower the pK_a value of the nucleophile (HOR') such that it can be deprotonated to the much stronger nucleophile OR'^-, possibly with the help of a general base B (B = Glu^-, Asp^-, His) as a proton acceptor. Expulsion of the leaving group (OR^-) is facilitated by protonation by a general acid AH (AH = Glu, Asp, His^+) and/or by reducing the nucleophilicity of OR^- by metal coordination. The energy of the transition state can be minimized by interaction of the equatorial phosphoryl oxygen atoms with hydrogen-bond donors DH (DH = amide NH, Thr, Ser, Tyr, Cys, Asn, Gln, His, H_2O), which may also be positively charged (DH^+: His^+, Arg^+, Lys^+), or with metal ions.

2.1. Alkaline Phosphatase

Alkaline phosphatase (AP) is certainly the most intensely studied enzyme of all dinuclear metallohydrolases described in this article.[17] The enzyme is a nonspecific phosphomonoesterase found in prokaryotes and eukaryotes. Hydrolysis to produce free inorganic phosphate competes with the transfer of the phosphoryl group to other alcohols, for example 2-amino-2-(hydroxymethyl)-1,3-propanediol (Tris), if present in the buffer. Although its specific function in mammals is not known at present, the biological importance is indicated by the widespread use of AP activity in human serum as an enzymatic signal for a variety of disease states.

The homodimeric AP (94 kDa) from *E. coli* contains two Zn^{2+} and one Mg^{2+} ion in each active site. Activity has a sigmoid pH-rate profile with a pK_a of 7.5 which involves a change in the rate-determining step from release of phosphate at high pH to dephosphorylation at low pH.[18, 19]

The reaction proceeds via a phosphoenzyme intermediate (E–P), in which Ser-102 is phosphorylated (Scheme 1).[18, 20] This intermediate could be isolated at acid pH (below 5.5), where the

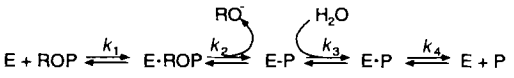

Scheme 1. Reaction pathway for the hydrolysis of phosphate esters by alkaline phosphatase.

E–P$\rightleftharpoons$E·P equilibrium favors the phosphorylated intermediate. E·ROP and E·P refer to the noncovalent complexes with substrate and product, respectively. R can vary from a methyl group to a large protein molecule with almost no influence on the overall reaction constant k_{cat} as long as the pK_a value of the leaving group is less than 10.[21] This finding reflects the fact that the dissociation of P_i, the product phosphate, is the rate-limiting step at alkaline pH, as demonstrated by a variety of NMR spectroscopic methods.[22, 17] In addition, at pH 8.0 the overall second-order rate constant k_{cat}/K_m for the hydrolysis of phosphate esters was found to be dependent on the viscosity of the solution, indicating that the maximum activity of AP is also limited by the diffusion-controlled encounter with the substrate.[23]

The alkaline phosphatase reaction proceeds with retention of configuration around the phosphorus atom.[24] This result suggested that the reaction consists of two in-line S_N2 nucleophilic attacks: the first by Ser-OH (or Ser-O^-) on the substrate and the second by solvent H_2O (or OH^-) on the phosphoserine intermediate. Brønsted correlations that probe the nature of the transition state have been applied by different groups and have yielded conflicting results. The first such study on AP revealed a small value of $\beta_{lg} = -0.2$ for a series of aryl and alkyl monoesters.[25] A β_{lg} value of -0.6 for the leaving group was determined for a series of phosphomonoesters with a pK_a value of less than 15 for the alcohol group.[21] The fact that this value was found to be only -0.3 for a mutant in which the nucleophilic serine residue was mutated to a cysteine residue was, together with the 50-fold lower rate constant for this mutant, interpreted as indicative of a largely associative phosphorylation step. In contrast, a β_{lg} value of -0.8 for a series of aryl phosphorothiolates led, in comparison with a value of β_{lg} of -1.1 for the nonenzymatic reaction that is known to follow a dissociative pathway, to the suggestion that there is considerable dissociative character in both enzymatic and nonenzymatic transition states.[26] An inverse secondary ^{18}O kinetic isotope effect on the hydrolysis of glucose 6-phosphate by AP also indicated a dissociative mechanism.[27] Studies on the isotope effects using *p*-nitrophenyl phosphate as substrate yielded values near unity, indicating that a nonchemical step is rate-limiting for the hydrolysis of this substrate.[28]

The metal atoms in native Zn1-Zn2-Mg3-AP can be exchanged for various divalent metal ions.[17] The native enzyme has maximal activity, but the Mg^{2+} ion in binding site 3 has only a minor influence on the activity of bacterial APs.[17, 29] However, the presence of magnesium in this binding site influences the activity in mammalian APs, possibly because a histidine

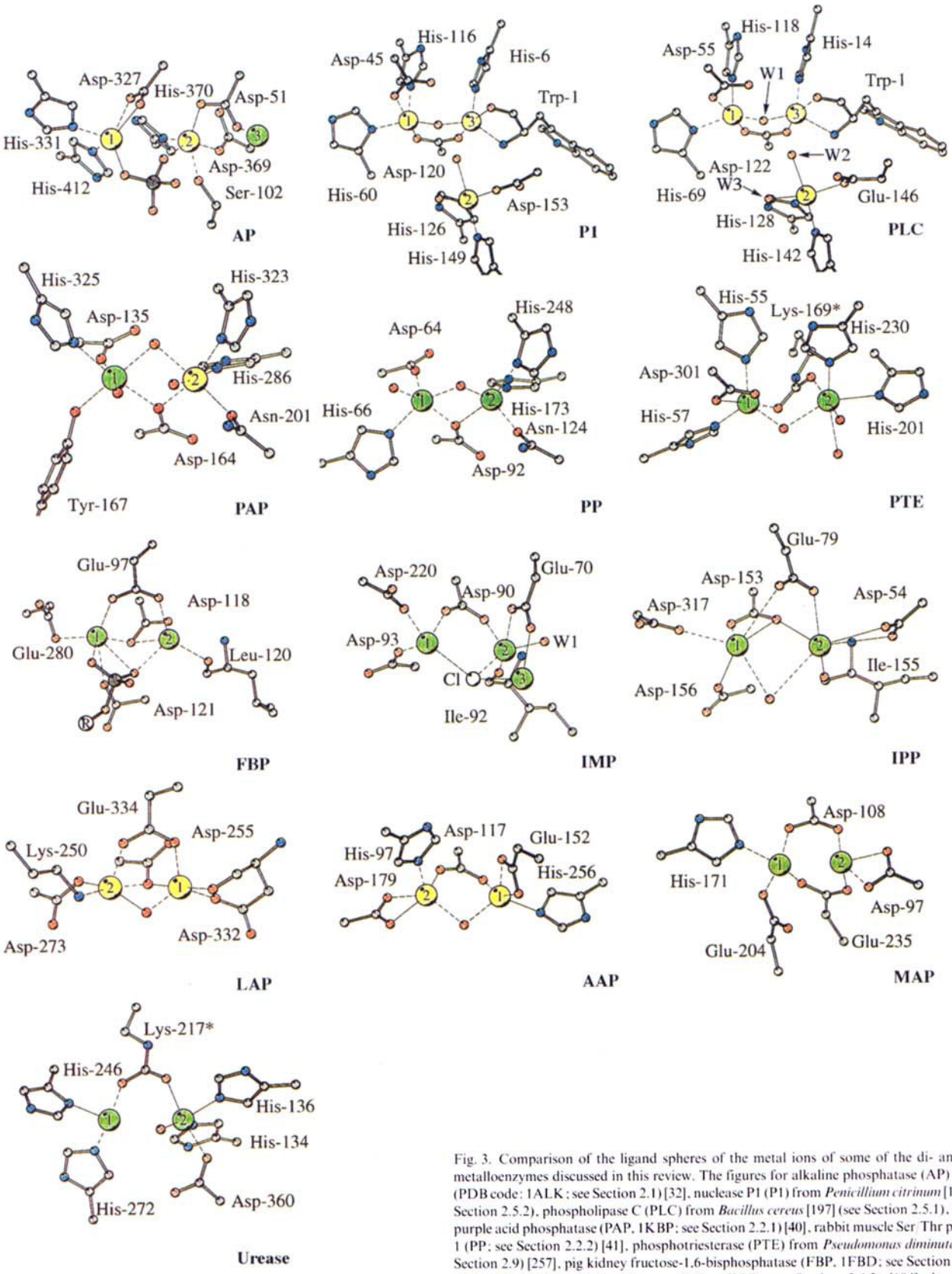

Fig. 3. Comparison of the ligand spheres of the metal ions of some of the di- and trinuclear metalloenzymes discussed in this review. The figures for alkaline phosphatase (AP) from *E. coli* (PDB code: 1ALK; see Section 2.1) [32], nuclease P1 (P1) from *Penicillium citrinum* [196, 212] (see Section 2.5.2), phospholipase C (PLC) from *Bacillus cereus* [197] (see Section 2.5.1), kidney bean purple acid phosphatase (PAP, 1KBP; see Section 2.2.1) [40], rabbit muscle Ser/Thr phosphatase-1 (PP; see Section 2.2.2) [41], phosphotriesterase (PTE) from *Pseudomonas diminuta* (1PSC; see Section 2.9) [257], pig kidney fructose-1,6-bisphosphatase (FBP, 1FBD; see Section 2.4.1) [169], human inositol monophosphatase (IMP, 1IMC; see Section 2.4.2) [184], bovine inositol polyphosphate 1-phosphatase (IPP, 1INP; see Section 2.4.3) [151], bovine lens leucine aminopeptidase (LAP, 1LAM; see Section 3.1.1) [284, 286], aminopeptidase (AAP) from *Aeromonas proteolytica* (1AMP; see Section 3.1.2) [292], methionine aminopeptidase (MAP) from *E. coli* (1MAT; see Section 3.1.3) [300], and urease (1KAU; see Section 3.2) [260] have been generated from the atom coordinates. Zinc ions are shown in yellow, all other metal ions in green [320], carbon atoms in grey, oxygen atoms in red, and nitrogen atoms in blue.

residue in the mammalian enzymes replaces a Asp-153.[30] The exchange of one or both of the zinc ions in sites 1 and 2 by Mg^{2+}, Co^{2+}, or Mn^{2+} ions results in a considerably reduced activity. Substitution of Zn^{2+} by Cd^{2+} has a drastic effect on the dephosphorylation of E–P, and allows the isolation of the E–P intermediate.[7] This finding can be readily explained by the diminished ability of the "softer" and larger Cd^{2+} ion to generate an OH^- nucleophile or to stabilize the transition state.

Structures of native AP at 2.8 Å resolution, of the complex with phosphate (E·P) at 2.0 Å resolution, and of the Cd-substituted enzyme with covalently bound phosphate (E–P) at 2.5 Å resolution have been determined.[31, 32] The structure of the native enzyme complexed with phosphate at 2.0 Å resolution provided the most detailed insight into the active site structure (Figs. 3 and 4). The Zn1 center is pentacoordinated by His-331,

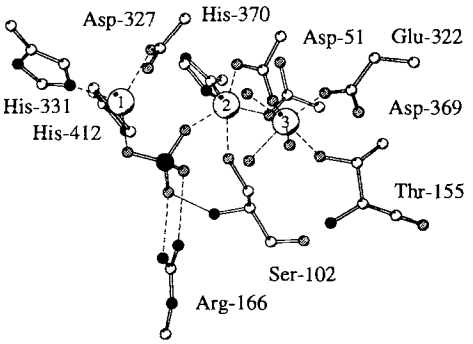

Fig. 4. Structure of the active site of the alkaline phosphatase with a bound phosphate ion (generated from the coordinate file 1ALK) [32]. The Ser-102 side chain, which is modeled in coordination to Zn2, is disordered in this structure (see Fig. 6). Sites 1 and 2 are occupied by Zn^{2+} and site 3 binds Mg^{2+}.

His-412, the two carboxylate oxygen atoms of Asp-327, and one oxygen atom of the phosphate group. Several water molecules were found in the active site region but no water coordination to Zn1 was reported. Water relaxation measurements[33] as well as ^{113}Cd and ^{35}Cl NMR data[34] suggested that one or two water molecules are coordinated to the site 1 metal in the absence of phosphate. The Zn2 center is coordinated tetrahedrally by an oxygen atom of His-370, two oxygen atoms of monodentate carboxylate side chains (Asp-51 and Asp-369), and another oxygen atom of the phosphate group. Thus, the phosphate ion bidentately bridges the two zinc ions. The other two phosphate oxygen atoms are tightly held by the guanidinium group of Arg-166. Asp-51, Glu-322, Thr-155, and three water molecules coordinate Mg at site 3. Asp-51 bidentately bridges Zn2 and Mg3. The distances between the metal ions are 4.1 Å between Zn1 and Zn2, 4.8 Å between Zn2 and Mg3, and 7.1 Å between Zn1 and Mg3.[35] The side chain of the Ser-102 residue was found to be disordered. This structure serves as a model for the product complex E·P as well as for the complex with bound substrate (E·ROP), since the enzyme evidently builds no specific interactions to the leaving group.

Exchange of the two zinc ions by cadmium ions enabled the structural characterization of the E–P intermediate at pH 7.5 at 2.5 Å resolution.[32] Figure 5 shows a schematic drawing of the interactions of the phosphorylated Ser-102 side chain with the

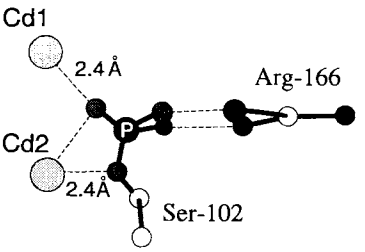

Fig. 5. Schematic drawing of the interactions in the phosphoserine intermediate of the Cd Cd form of alkaline phosphatase [32]. This structure is also considered to model the binding mode of the phosphorylated Ser-102 side chain to a catalytically active Zn Zn cluster (see Fig. 6).

cadmium ions and Arg-166. A similar model is considered to be applicable for the zinc ions.

The substrate probably binds to both zinc ions with its ester oxygen atom coordinated to Zn1 and opposite to Ser-102 (Fig. 6b).[32, 17] Coordination of the serine oxygen atom to Zn2 facilitates deprotonation of this side chain to yield the attacking Ser-O^- nucleophile. The Zn1 center activates the leaving alcohol group. After the phosphoenzyme intermediate (E–P) has formed (Fig. 6d), the alkoxide leaves and its coordination site

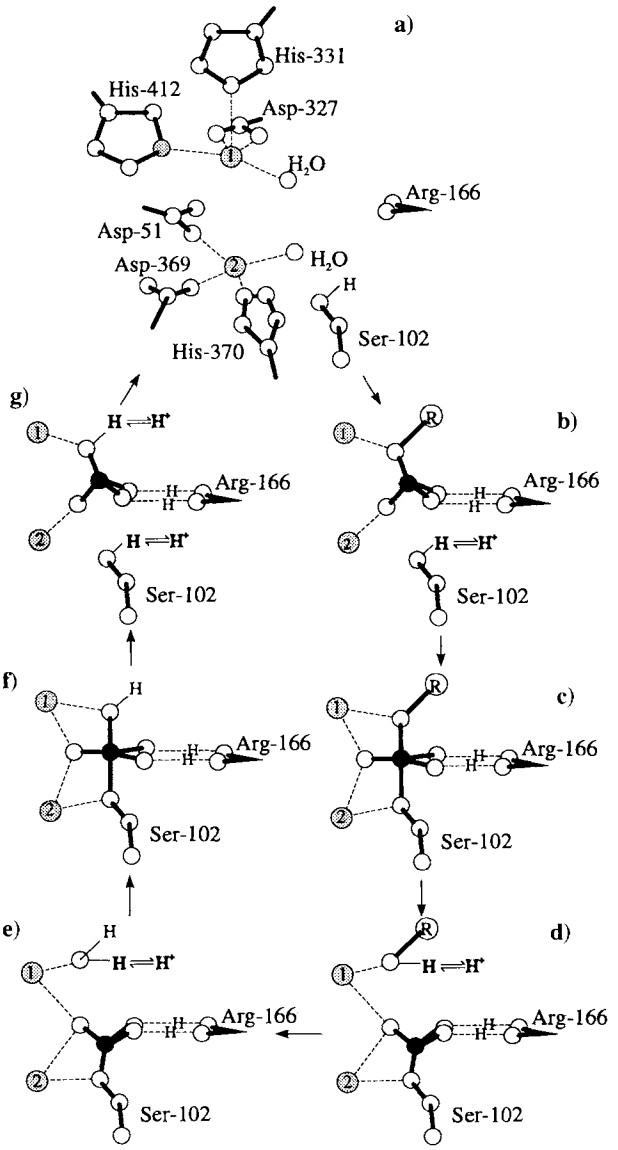

Fig. 6. Proposed mechanism for the hydrolysis of a phosphomonoester by alkaline phosphatase on the basis of the X-ray crystal structures [32] and biochemical data.

on Zn1 is substituted by a water molecule that dissociates a proton to form the Zn-OH^- nucleophile for the hydrolysis of the phosphoserine intermediate (Fig. 6e). The structure of this intermediate is known from the X-ray crystal structural analysis. Dephosphorylation of the E–P intermediate occurs in a displacement step in which the two metal ions have reversed roles: the oxygen atom of the leaving group (Ser-O^-) is now activated by Zn2 and the remaining oxygen atoms are coordinated to both metal ions or hydrogen-bonded to Arg-166 in order to enhance the electrophilicity of the phosphorus atom.

Besides the two metal ions the side chains of Ser-102 and Arg-166 evidently play major roles in AP catalysis. Mutation of Ser-102 to the nonnucleophilic residues alanine or leucine resulted in a greatly reduced activity in the hydrolysis of phosphate monoesters.[36] Values for $k_{cat} \approx 1/1000$ and $\approx 1/500$ of the wild-type activity were determined for both mutant forms, respectively, with only a minor influence on K_m. Although the activity of these mutants is significantly reduced, the hydrolysis of *p*-nitrophenylphosphate is still enhanced by a factor of about 10^7 compared to the rate for the uncatalyzed reaction.[36] Hydrolysis by these mutants probably proceeds by a different mechanism, for example, by direct attack of a zinc-activated water molecule similar to mechanisms seen in other phosphatases. Replacement of Arg-166 against serine, alanine, lysine, and glutamine demonstrated that Arg-166 is important for activity but not essential.[37] Loss of Arg-166 results in an increase of K_m and in a diminished k_{cat} (2.4% of wild-type for R166A).

The proposed mechanism contains dissociative character in the activation of the leaving group by one metal ion; however, the nucleophile is also activated by deprotonation by a metal ion. A remarkably unique feature of the AP mechanism is the reversed role of the two metal ions in the two displacement steps: the second step of the reaction is almost a mirror image of the first step.

2.2. Family of $\beta\alpha\beta\alpha\beta$ Metallophosphoesterases

Even before any structural information for the purple acid phosphatases (PAPs) or the Ser/Thr protein phosphatases (PPs) were available, a phosphoesterase signature motif, DX[G/H]-$(X)_n$-GDXX[Y/X]-$(X)_n$-GNH[E/D] (motif A), had been identified in a large group of phosphoesterases (Fig. 7). This motif is found in the sequences of PAP, the PPs, diadenosine tetraphosphatases, exonucleases, 5′-nucleotidases, sphingomyelin phosphodiesterases, and other phosphoesterases.[38,39] In these enzymes the core structure is formed by two sandwiched β-sheets with the metals located at the C-termini of central parallel strands as shown by the X-ray crystal structures of PAP[40] and the PPs.[41–44] In kidney bean PAP, motif A contains four of the metal coordinating residues: Asp-135, Asp-164, Tyr-167, and Asn-201. In all other phosphoesterases the tyrosine residue of the second loop appears to be exchanged, and the corresponding position in the coordination sphere is filled by the histidine residue of the first loop (which is a glycine in PAP). Based on the structure of PAP, sequence alignments revealed a second signature motif (motif B), H-$(X)_n$-[G/A]HX[H/X], comprising His-286, His-323, and His-325 in PAP.[45]

2.2.1. Purple Acid Phosphatase

Purple acid phosphatases (PAPs) represent a group of widely distributed phosphomonoesterases characterized by their low pH-optima, by their insensitivity to tartrate inhibition, and by their intense purple color, which results from a tyrosine → Fe^{III} charge transfer. A role in degradative biological processes such as in the phagocytosis of aged erythrocytes[46] and in active bone resorption[47] has been implicated for the mammalian PAPs, possibly including phosphorylated proteins as substrates. The monomeric 35-kDa mammalian PAPs all contain a Fe^{III}–Fe^{II} center in their active form. This diiron center has attracted considerable interest and is now spectroscopically well characterized by Mössbauer,[48,49] EPR,[48,50–53] NMR,[53,54] EXAFS,[55] magnetic,[48,56,57] electrochemical,[58] and resonance Raman[59] studies. Most of these studies used bovine spleen PAP and porcine uterus PAP (also known as uteroferrin), which share a sequence homology of 90%.

In contrast to the mammalian PAPs, the divalent metal binding site in kidney bean PAP is occupied by zinc.[60] This plant enzyme is a homodimeric glycoprotein (111 kDa) with a disul-

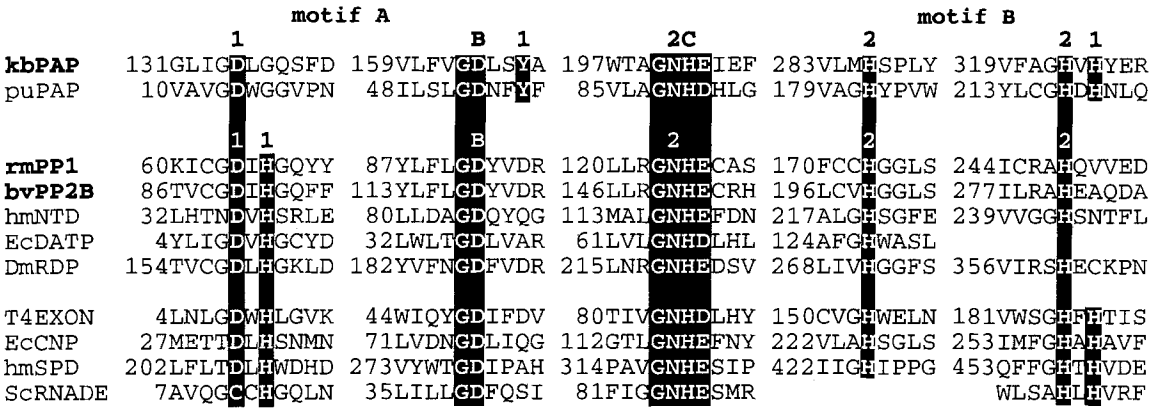

Fig. 7. Sequence alignment of the metal-coordinating motifs of some members of the family of $\beta\alpha\beta\alpha\beta$ metallophosphoesterases (more complete analyses can be found in refs. [38,39,45]). The sequences of kidney bean PAP (kbPAP), rabbit muscle PP1 (rmPP1), and bovine calcineurin (bvPP2B), for which X-ray crystal structures are available, are aligned to those of porcine uterus PAP (puPAP), human 5′-nucleotidase (hmNTD), *E. coli* diadenosine tetraphosphatase (EcDATP), *Drosophila melanogaster* retinal degeneration protein (DmRDP), bacteriophage T4 exonuclease protein GP47 (T4EXON), *E. coli* 2′,3′-cyclic nucleotide 2′-phosphodiesterase (EcCNP), human sphingomyelin phosphodiesterase (hmSPD), *Saccharomyces cerevisiae* RNA debranching enzyme (ScRNADE). Those residues coordinated to metal ions 1 and 2, as well as the bridging apartate (B) and the conserved catalytic histidine (C) are marked. Motif A comprises the first three blocks and motif B the last two blocks.

fide bridge connecting both monomers.[60, 61] The zinc ion in kidney bean PAP can be exchanged against other divalent metal ions, yielding almost the same (Fe^{2+} or Co^{2+}) or reduced activity.[62] After exchange of Zn^{2+} for Fe^{2+} the kidney bean enzyme shows nearly identical spectroscopic and kinetic behavior to the mammalian PAPs.[62, 63] In spite of a low overall sequence homology, significant local sequence similarities could be identified especially in the regions of active site residues, suggesting that the mammalian enzymes and kidney bean PAP are evolutionary related and have a similar three-dimensional core structure.[64] In addition, all metal-ligating residues are conserved between the plant and mammalian PAPs.

A small antiferromagnetic coupling constant in the mixed-valent iron center ($S = 1/2$) has been revealed by the temperature dependence of the intensities of the EPR signals,[48] and by ^1H NMR spectroscopic[65] and magnetic susceptibility[56] measurements. This small coupling constant suggests the presence of a μ-hydroxo bridge, but not a μ-oxo bridge. The oxidized enzyme displays stronger antiferromagnetic coupling; however, the existence of a μ-oxo bridge in the $Fe^{III}-Fe^{III}$ enzyme is still not clear.

The existence of water molecules coordinated to the dinuclear cluster has been demonstrated by electron spin echo envelope modulation (ESEEM) spectroscopy and electron nuclear double resonance (ENDOR) spectroscopy,[51] and by electrochemical[58] studies. Based on the observed decrease of the activity at lower pH values, as well as on the pH-dependence of the EPR spectra a solvent molecule bound to the ferric iron with an apparent pK of around 4.5 has been proposed.[50] Stopped flow measurements on uteroferrin indicate a rapid binding of phosphate to the Fe^{2+} center.[66, 67] For substrates a similar fast binding to the Fe^{2+} center is proposed and the Fe^{3+}-bound hydroxide ion can attack the phosphorus atom of the substrate. A direct in-line transfer of the phospho group to the water molecule is supported by the inversion of the absolute configuration around the phosphorus atom for phosphomonoester hydrolysis by PAP.[68] Furthermore, a recent study found no evidence for the formation of a phosphoenzyme intermediate.[69]

The X-ray crystal structure of kidney bean PAP at 2.9 Å resolution showed the Fe^{3+} ion to be coordinated by Tyr-167, His-325, and Asp135, whereas the Zn^{2+} center is ligated by His-286, His-323, and the amide oxygen atom of Asn-201 (see Fig. 3, Section 2.1).[40] Also, Asp-164 monodentately bridges the two metal ions, which are 3.1 Å apart. Although positions of water molecules could not be determined in the X-ray crystal structure because of the moderate resolution, the authors placed three exogeneous ligands into the coordination sphere of the dinuclear metal cluster based on biochemical evidence (see above) and the observed coordination geometry:[40] the presumed OH^- nucleophile bound to the Fe^{3+} center, a terminal water molecule coordinated to the Zn^{2+} center, and a μ-hydroxo bridge (see Fig. 3, Section 2.1). The coordination sphere of the Fe^{3+} ion is then almost perfectly octahedral and that of the Zn^{2+} ion matches a more distorted octahedron. An X-ray crystal structure of kidney bean PAP in the presence of phosphate showed that the phosphate ion bidentately bridges the two metal ions (Fig. 8).[45] The two noncoordinated phosphate oxygen atoms are hydrogen-bonded to His-202 and His-296, which move by about 1 Å relative to their positions in the phosphate-free enzyme.

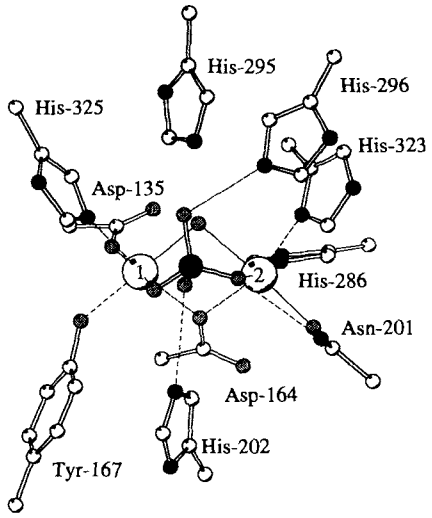

Fig. 8. Structure of the active site of PAP with a bound phosphate ion (generated from coordinate file 4KBP) [45]. The Fe^{3+} ion is bound to site 1 and the Zn^{2+} ion to site 2. The position of the bridging water molecule was not determined from the X-ray crystal data; it was modeled on the basis of biochemical evidence and the observed coordination geometry.

In a plausible mechanism (Fig. 9)[40, 50, 66] the phosphate group of the substrate binds to the divalent metal ion, which together with the histidine ligands preorients the phosphate group and enhances the electrophilicity of the phosphorus center. Then a nucleophilic attack occurs by the hydroxide ligand bound to the Fe^{3+} center, and the configuration at the phosphorus center is inverted through a pentacoordinate transition state in which the leaving group and the attacking nucleophile are in the apical positions. In addition to the metal ions the protonated side chains of His-202 and His-296 reduce the energy of the pentacovalent transition state through the formation of hydrogen bonds. After a small movement, His-295 may also interact with the substrate and His-296 may then protonate the leaving alcohol group.

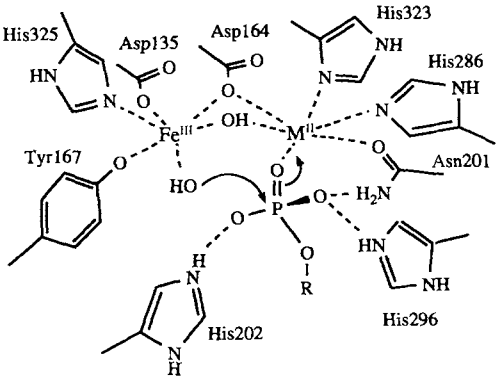

Fig. 9. Substrate binding mode and attack of the Fe^{3+}-bound nucleophile for the proposed reaction mechanism of phosphomonoester hydrolysis by PAP [40, 45, 50, 66].

2.2.2. *Serine/Threonine Protein Phosphatases*

Protein phosphorylation plays a cardinal role in regulating many cellular processes in eukaryotes. The phosphorylation of a protein is a dynamic process controlled by protein kinases and protein phosphatases (PPs). The serine/threonine phosphatases are unrelated in sequence and structure to the tyrosine phosphatases, and have been classified into four groups (1, 2A, 2B, 2C) on the basis of their biochemical properties.[70] Protein phosphatases 1, 2A, 2B (also known as calcineurin) have highly homologous catalytic domains,[38] but differ in their interactions with regulatory subunits and in their substrate specificity.[71]

Calcineurin, a heterodimer of a catalytic 60-kDa subunit (calcineurin A) and a 19-kDa calmodulin-like regulatory subunit (calcineurin B), is activated by several divalent metal ions,[72, 73] but the native enzyme probably contains a dinuclear Fe–Zn center in the active site.[72] Conflicting results have been reported concerning the oxidation state of the iron ion.[74] Manganese-activated calcineurin exhibits a broad pH-optimum around 7.[75] A solvent isotope effect of 1.35 in deuterated water on V_{max}/K_m is consistent with one or two proton transfer steps in the enzyme reaction.[76] Furthermore, several kinetic and chemical data support a mechanism without the formation of a phosphoenzyme intermediate.[75–77]

X-ray crystal structure analyses for Ser/Thr protein phosphatases are now available for the catalytic subunit of rabbit muscle PP-1 complexed with the toxin microcystin (2.1 Å resolution),[41] for human PP-1 and its complex with tungstate (both 2.5 Å resolution),[44] for bovine brain calcineurin complexed with the immunophilin-immunosuppressant FKBP12-FK506 complex (2.5 Å resolution),[42] and for human calcineurin with and without bound FKBP12-FK506 (3.5 and 2.1 Å resolution, respectively).[43] In agreement with the substantial sequence homologies between these proteins the overall folding architecture of the homologous domains of the three structures seems to be the same.

In the crystal structure of rabbit PP-1 both metal sites are probably occupied by Mn^{2+} ions, which is required to restore the full activity of the recombinant protein and was present in the crystallization buffer.[41, 78] However, a recent study indicates that PP1, like calcineurin, might be a Fe–Zn metalloenzyme in vivo.[79] Metal ion 1 is coordinated by Asp-64, His-66, and Asp-92, metal ion 2 by Asp-92, Asn-124, His-173, and His-248 (Fig. 3, Section 2.1 and 10).[41] Two exogeneous solvent molecules, one coordinated to metal ion 1 and one bridging the two metal ions, provide two additional ligands for the metal ions. A third water molecule has been located at a larger distance of 3.4 Å to metal ion 2. The coordination geometries of the two metal ions, which are 3.3 Å apart, are approximately square-pyramidal for site 1 and trigonal-bipyramidal for site 2. Proton-induced X-ray emission (PIXE) spectroscopy data and the X-ray crystal structure indicate that in human PP-1 metal site 1 contains iron and site 2 manganese.[44] Interestingly, the metal–metal distance for unliganded human PP-1 was refined to 4.0 Å on the basis of a data set collected on a frozen crystal in the presence of 30% glycerol. In the complex with tungstate this distance is reduced to 3.5 Å.

A very similar arrangement of the metal-ligating protein residues has been found in the two calcineurin structures.[42, 43]

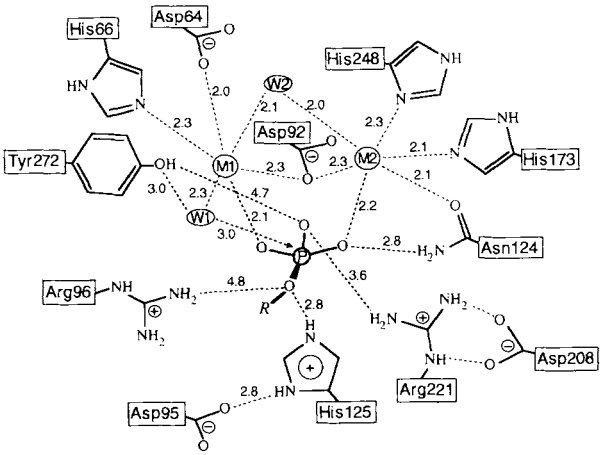

Fig. 10. Active site structure of rabbit muscle PP-1 and modeled binding mode of a phosphomonoester [41]. W1 might be the nucleophile that attacks the phosphorus center. A similar bidentate binding mode (as proposed here for the substrate) of a tungstate ion to the metal ions was determined for human PP-1 [44]. The latter structure implied that also W2 might be the nucleophile. His-125 could protonate the leaving group in both mechanisms.

Here the distance between the two metal ions was refined to 3.0 Å for the enzyme from bovine brain and to 3.1 Å for human calcineurin. In both calcineurin structures metal ion 1 has been modeled as an iron ion and metal ion 2 as a zinc ion, based on the homology to PAP. A phosphate ion, which was present in the crystallization buffer, bidentately bridges the two metal ions in the bovine calcineurin structure.[42] Furthermore, there is a weak electron density feature consistent with a water molecule bridging the two metal centers. In human calcineurin, three metal-bound water molecules were found: a bridging water molecule and a Fe^{3+}-bound water molecule similar to those found in PP-1 and an additional Fe^{3+}-bound water molecule, which is also hydrogen-bonded to His-151 (Fig. 11). This latter water molecule is not seen in the PP-1 structure, possibly because the nearby bound microcystin inhibitor sterically precludes binding

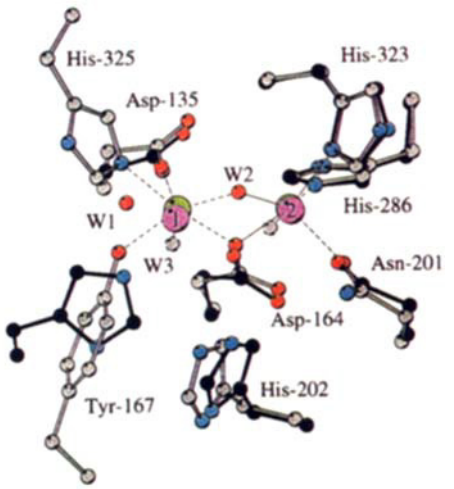

Fig. 11. Superposition of the dimetal clusters and the catalytic histidine residues of rabbit PP-1 (C atoms black) [41] and PAP (C atoms grey) [40]. Labels for the protein side chains and metal-coordinating bonds are only shown for PAP. The Fe^{3+} ion binds to site 1 and the Zn^{2+} ion to site 2 in kidney bean PAP. The water molecules W1 and W2 shown in red (labeled as in Fig. 10) belong to PP-1. The two terminal metal-bound water molecules shown in grey are proposed to be present as ligands in PAP in addition to a bridging water molecule at the position of W2.

of this water. A bidentate bridging binding mode to the dimetal center was found for a tungstate ion bound to human PP-1.[44]

Mutational analysis on Ser/Thr phosphatases has been employed on the smallest family member, the bacteriophage λPP.[39] Mutation of the catalytic histidine residue (marked C in Fig. 7) that is proposed to interact with the substrate phosphate group has a deleterious effect on activity, decreasing k_{cat} by a factor of 10^5. Mutagenesis of one of the two arginine residues in the active site (Arg-53 in PP-1) supports a role for this residue in binding of the substrate and stabilization of the transition state.

In spite of the similarity of the active site structures of the three Ser/Thr phosphatase structures, the putative reaction mechanisms discussed by the authors differ considerably. In the bovine calcineurin structure the μ-hydroxo bridge is within 2.9 Å of the phosphorus atom of the bidentately bound phosphate and colinear with one of the P–O bonds. Assuming that the substrate phosphate group binds in the same way as a phosphate ion does to the active site, the bridging hydroxide ion (W2 in Fig. 11) could be the attacking nucleophile in an in-line mechanism.[42] A similar mechanism based on the tungstate binding mode is assumed by Egloff et al.[44] The negative charge of the intermediate is supposed to be stabilized by interactions with both metal ions, and by Arg-122 and Arg-254, which were found to be in hydrogen-bonding distance with two of the phosphate oxygen atoms. His-151, which is hydrogen-bonded to the most solvent-exposed oxygen atom, is proposed to protonate the leaving alcohol group. A similar assistance of the corresponding two arginine residues and the conserved histidine residue in stabilization of the transition state and protonation of the leaving group is also proposed in an alternative mechanism (see Fig. 10).[41] The substrate phosphate group is assumed to bind in a bidentate way. However, based on the modeled binding mode of the phosphate group an in-line attack of the terminal water molecule W1 coordinated to M1 is discussed. A third alternative assumes that water molecule W3 in Figure 11 is the catalytically active nucleophile.[43] The catalytically active histidine residue may act here as a general base to accept a proton from this iron-coordinated water molecule.

2.2.3. Comparison of the Structures of Purple Acid Phosphatase and the Ser/Thr Protein Phosphatase

Superposition of the active sites of kidney bean PAP and rabbit PP-1 shows that the conserved ligands of the metal ions and also the catalytically active histidine residue (His-202 in PAP) have identical conformations and superimpose very well (see Fig. 11). The Fe^{3+}-coordinated tyrosine group is replaced by a histidine group in the Ser/Thr PPs and the position of the Fe^{3+}-bound histidine group in PAP is occupied by a water molecule (W1) in PP-1 and in the calcineurin structures. The bridging water molecule proposed for PAP probably also has a similar position to that of the bridging water in the PPs (W2). One additional water molecule has been proposed to occupy the sixth ligand position at each of the two metal ions in PAP. This sixth ligand to Fe^{3+} is indeed seen in the human calcineurin structure (W3). In bovine calcineurin this position is occupied by the bound phosphate group, whereas in rabbit PP-1 this position is empty, possibly due to the influence of the nearby bound inhibitor microcystin. The zinc ions are only five-coordinate in all PP structures. The main differences between the structures of the active sites of PAP and the PPs are thus the additional water molecule at Fe in the PPs, which is substituted by a histidine residue in PAP, and the presence of two arginine groups in the PPs, which might interact with the phosphate group. His-295 and His-296 in PAP might serve similar roles.

Phosphate as the reaction product as well as the analogue inhibitor tungstate bind in a bidentate bridging mode to both metal ions, as seen in structures of PAP, bovine calcineurin, and human PP1. Several possible mechanisms have been proposed for PAP and the PPs, differing mainly in the substrate binding mode and the identity of the water nucleophile, which may be any one of the water molecules W1, W2, and W3 as seen in the human calcineurin structure. All mechanisms proposed for the PPs assume that the substrate binds in the same bidentate bridging mode as seen in product–enzyme complexes, whereas in PAP the substrate is assumed to bind monodentately to the divalent metal ion. It therefore remains to be seen if PAP and the Ser/Thr PPs, despite the similarity of the structures of their active sites, actually employ a different mechanism in catalysis.

2.3. RNA and DNA Polymerases and Other Nucleotidyl-Transferases

Their role in the faithful transmission of genetic information make the RNA and DNA polymerases some of the most important enzymes for all living organisms.[80, 81] These enzymes often contain one or more nuclease activities besides the polymerase activity. DNA polymerase I from *E. coli*, for example, catalyzes template-directed DNA synthesis, 3′,5′-DNA hydrolysis, and 5′,3′-DNA hydrolysis on three separate domains of one polypeptide chain of 103 kDa. All three activities are dependent on divalent metal ions. Furthermore, the polymerase and 3′,5′-exonuclease activity and possibly also the 5′,3′-nuclease activity are accomplished by a two-metal ion mechanism (see below). Human immunodeficiency virus 1 reverse transcriptase (HIV-RT) also contains, besides the polymerase active site, ribonuclease H (RNase H) activity. It remains to be shown whether RNase H and HIV-RT from *E. coli* or other organisms, use one or two metal ions in catalysis.

In addition to the activities present on the polymerases a two-metal ion mechanism is discussed for other nucleotidyl-transferases, such as the restriction endonucleases. A common characteristic of all these active sites is the low metal-binding affinity in the absence of substrates. The two metal ions are bound through two or three carboxylate side chains upon substrate binding. This feature distinguishes these enzymes from other nucleases such as nuclease P1.

However, a word of caution is appropriate here concerning the question of whether or not all these enzymes mentioned in this section actually use two metal ions. In most cases the presence of some conserved carboxylate side chains and a requirement for divalent metal ions is, sometimes together with a homology to another enzyme which presumably uses two metal ions for catalysis, the only evidence for a two-metal ion mechanism. Studies of metal binding to the apoenzyme have led to conflicting results in some cases, possibly because of the use of crystallographic difference Fourier techniques in the location of

metal ions without further refinement. Biochemical and crystallographic studies with substrate analogues or products in the presence of various metal ions may clarify more mechanistic details. Considering that many enzymes catalyze a similar nucleotidyl-transfer reaction with only one or no metal ion it may well be that some of the enzymes discussed here use only one metal and a free carboxylate side chain to act as a general base.

2.3.1. *Polymerase Active Sites*

Several structures of enzymes containing a polymerase active site have been determined to date, including the Klenow fragment of *E. coli* DNA polymerase I (pol-I),[82-87] reverse transcriptase from the human immunodeficiency virus HIV-1 (HIV-RT),[88-91] rat DNA polymerase-β (pol-β),[92-94] bacteriophage T7 RNA polymerase (pol-T7),[95] and *Thermus aquaticus* DNA polymerase (*Taq* pol).[96] Although these polymerases are of significantly different size and complexity and some of them show very limited or no overall sequence homology,[97] the core catalytical units of all polymerases show a strikingly similar molecular architecture.[81, 91, 96, 98, 99] Sequence alignments among many polymerases revealed the presence of three similar sequence motifs A–C containing three highly conserved carboxylate residues and a lysine group.[81, 100] However, pol-β is most likely not related to the other polymerases by a common ancestor.

What role do these carboxylic acid side chains play in the polymerase mechanism? Site-directed mutagenesis of many of the conserved amino acids demonstrated that mutations of these three carboxylate groups of motifs A and C cause the most dramatic effect on catalytic activity.[101, 102] A crystal structure of HIV-RT complexed with an oligonucleotide showed that the 3′-hydroxyl group of the DNA primer terminus binds near the three catalytic aspartate side chains.[89] Divalent metal ions, especially Mn^{2+} and Mg^{2+} ions, are known to activate polymerase activity.[103-105] Some polymerases, including *E. coli* RNA polymerase, contain tightly bound zinc ions, but also need other divalent cations as activators.[103, 106] The nature of the metal ion also influences the fidelity of the polymerase reaction.[107, 108] As a result, some metal ions, like Mn^{2+} and Ni^{2+}, are considered to be mutagenic or carcinogenic. The Mg^{2+} ion might therefore be the active metal ion in vivo for most polymerases.[104, 108]

Based on kinetic and magnetic resonance studies of metal ion and substrate binding to pol I, a two-metal ion mechanism has been proposed for the polymerase reaction.[103, 109, 110] Indeed, the crystal structure of rat pol-β complexed with a DNA template-primer and dideoxycytidine triphosphate (ddCTP) in the presence of 10 mM $MgCl_2$ showed two metal ions coordinated to the three conserved carboxylate groups.[93] ddCTP lacks the nucleophilic 3′-OH group of the natural 2′-deoxycytidine 5′-triphosphate (dCTP) substrate; thus, after one catalytic cycle of incorporation of this polymerase inhibitor into the growing primer strand, no 3′-OH group of the primer is available for the next catalytic cycle. In the X-ray crystal structure the 3′-carbon atom of the primer strand, which would bear the nucleophilic hydroxyl group in a catalytically active arrangement, and the phosphate groups of ddCTP are bound in the immediate vicinity of the metal ions (Fig. 12). The magnesium ion B (Mg B), which is near the 3′-carbon atom of the primer strand, is coordinated by Asp-256, Asp-190, Asp-192, one of the nonesterified phosphoryl oxygen atoms of the α-phosphate of ddCTP, and possibly a water molecule (Fig. 12). In the complex with an intact

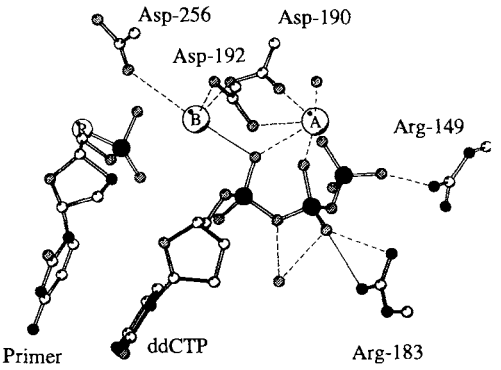

Fig. 12. Binding mode of ddCTP and the 3′-ddCTP of the primer strand to the dimetal cluster of pol-β (generated from coordinate file 2BPF) [93]. The carbon atom shown in black of the 3′-ddCTP group of the primer bears the nucleophilic 3′-OH group in a catalytically active arrangement with a normal dNTP nucleotide instead of ddCTP at the 3′-primer end.

primer terminus, the 3′-OH group of the primer would probably also be coordinated to Mg B. The magnesium ion A (Mg A) is liganded by Asp-190, Asp-192, three phosphoryl oxygen atoms of the α-, β-, and γ-phosphate groups of ddCTP, and one water molecule (Fig. 12). Both metal ions, which are 4.7 Å apart, have a distinct coordination sphere that cannot be easily described in terms of more symmetrical coordination polyhedrons. Also, the coordination sphere of Mg B is characterized by a number of relatively long metal–ligand distances. Interestingly, in this structure there are no protein side chains interacting with the oxygen atoms of the α-phosphate group. The transition state may thus be solely stabilized by the metal ions, water molecules in the region of the active site, and weaker van der Waals forces.

The structure of rat pol-β was also independently solved by another group.[92] Soaking experiments with Mn^{2+} ions revealed two metal ion binding sites in the native enzyme[111] and in a complex with 2′-deoxythymidine 5′-triphosphate (dTTP). Surprisingly, both metal ions were described as being coordinated by only one bidentate bridging carboxylate chain (Asp-190) in the native enzyme, but these structures have not been refined at this stage. Most of the other polymerase structures[82-96] also have either been determined in the absence of divalent metal ions in the crystallization buffer and thus contain no bound metal ions, or the metal-ion binding sites have not yet been fully refined. We will thus not describe these structures here, since more detailed results may be expected in the near future.

On the basis of the rat pol-β structure a polymerase mechanism has been proposed in which Mg B helps to deprotonate the primer 3′-OH nucleophile and stabilizes the transition state by coordination to one of the equatorial phosphoryl oxygen atoms (Fig. 13).[93] In this mechanism Mg A is neither involved in the stabilization of the pentacoordinate transition state nor in the activation of the leaving group by coordination to the oxygen

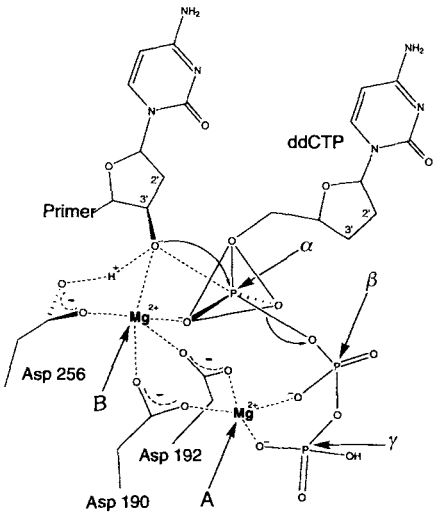

Fig. 13. Mechanism for the polymerase reaction as proposed on the basis of the ternary complex of pol-β, DNA primer, and ddCTP as shown in Fig. 12 [93]. In a similar alternative polymerase mechanism [112] the Mg^{2+} ion at site A also participates in the activation of the leaving group by coordinating to the anhydride oxygen atom between the α- and β-phosphate groups.

atom between the α- and the β-phosphate groups. Instead, Mg A binds and orients the β- and γ-phosphate groups. In an alternative polymerase mechanism, which resembles that of one in-line displacement step in AP, Mg A has additional interactions to one of the equatorial phosphoryl oxygen atoms and to the bridging oxygen atom of the leaving group in the transition state.[112] So far, all stereochemical studies have found an inversion of the phosphorus configuration in the polymerase reaction,[113] in agreement with the proposed one-step in-line mechanisms. A role in the polymerase mechanism could be demonstrated by mutagenesis studies for several active site residues, including the conserved lysine side chain of motif B.[101, 114]

2.3.2. 3',5'-Exonuclease Active Site of DNA Polymerase I

The Klenow fragment of *E. coli* DNA polymerase I contains besides the polymerase activity also a 3',5'-exonuclease active site, which is located about 33 Å away from the polymerase active site.[82, 115–117] The two active sites function independently and have separate binding sites for DNA. The exonuclease activity serves to remove polymerase errors by excision of mismatched base pairs. Other polymerases also contain homologous domains that have 3',5'-exonuclease activity.[97, 118] A number of crystallographic studies make the exonuclease reaction pathway one of the best-studied two-metal ion mechanisms by structural means.[81–86, 110, 117]

The exonuclease reaction takes place with inversion of the configuration around the phosphorus atom,[119] consistent with one in-line displacement step. Divalent metal ions (Mg^{2+}, Mn^{2+}, Zn^{2+}, or Co^{2+}) are essential for exonuclease activity,[120] and two metal-binding sites were located in crystal structures of the enzyme complexed with the products 2'-deoxycytidine monophosphate (dCMP) or 2'-deoxythymidine monophosphate (dTMP).[84, 85] The presence of more than one metal binding site was also implicated by NMR spectroscopic studies[105] and by a cooperative effect of metal binding on the exonuclease activity.[120] In the dTMP–product complex these two metal ions are 3.9 Å apart and are bidentately bridged by Asp-355 and by one of the phosphoryl oxygen atoms (Fig. 14). Site A has a distorted tetrahedral ligand sphere, whereas the metal ion in site B is octahedrally coordinated. The complex was crystallized in the presence of 20 mM $MgSO_4$ and 1 mM $ZnSO_4$ and it was shown that under these conditions a Zn A – Mg B site is formed,[85] consistent with the preferred coordination geometries of zinc and magnesium.

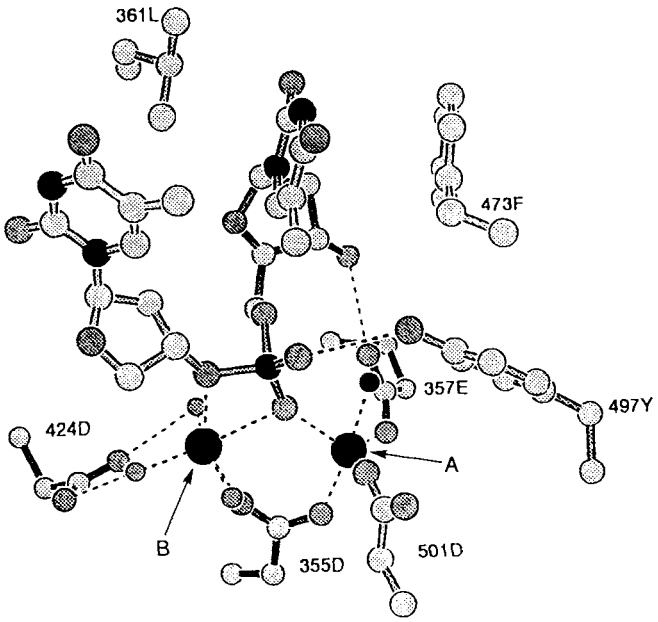

Fig. 14. A dinucleoside phosphate bound to the 3',5'-exonuclease active site of pol-I (taken from ref. [85]). The coordinates of the dinucleoside phosphate are taken from the structure analysis of the inactive D424A mutant enzyme, with an Mg^{2+} ion in site A, no metal ion in site B, and with a bound tetranucleotide. These coordinates are shown together with the structure of the protein with two bound metal ions taken from a complex of the wild-type enzyme with dTMP (dTMP not shown). The water molecule (in black) coordinated to the metal ion in site A is well positioned for attack on the phosphorus atom.

Metal binding site B is not occupied in the absence of bound dNMP in the native enzyme crystallized in the presence of divalent metal ions.[82, 85] This finding suggests that metal ions bind to site B together with or after substrate binding to form a catalytically active complex. In contrast, metal binding site A is occupied also in the native enzyme when crystallized in the presence of metal ions, and has a strong preference to bind zinc ions.[82, 85] Mutation of the site B ligand Asp-424 to alanine yielded an inactive enzyme with no metal bound to site B.[82, 84] This inactive mutant allowed the structure determination of a complex with a bound tetranucleotide $(dT)_4$ substrate in the presence of Mg^{2+} ions bound to site A (Fig. 14).[85] The 3'-terminal nucleotide of the tetranucleotide binds in the same way as dTMP of the product complex.

Assuming that the substrate binding mode in the catalytically active complex in the presence of a metal ion in site B is the same as that found in the structure with bound $(dT)_4$, this study provides detailed insight into the arrangement of the reactants prior to the transition state (Fig. 14). The water molecule coordinated to metal ion A is opposite to the leaving group and

therefore in an ideal position for the nucleophilic attack. Both metal ions are coordinated to one of the nonesterified phosphoryl oxygen atoms and metal ion B is also coordinated to the oxygen atom of the leaving group. A remarkable result of the crystallographic study of the substrate binding in the D424A mutant is that the loss of metal ion B results in an almost complete loss of activity (of at least five orders of magnitude),[84] even though the electrophilic phosphorus atom is presumably still correctly positioned and activated by metal ion A with respect to the nucleophile bound to metal ion A. This finding stresses the importance of the stabilization of the transition state and the activation of the leaving group by metal ion B.

Figure 15 shows a plausible mechanism for the exonuclease reaction. The roles of the metal ions resemble those in each

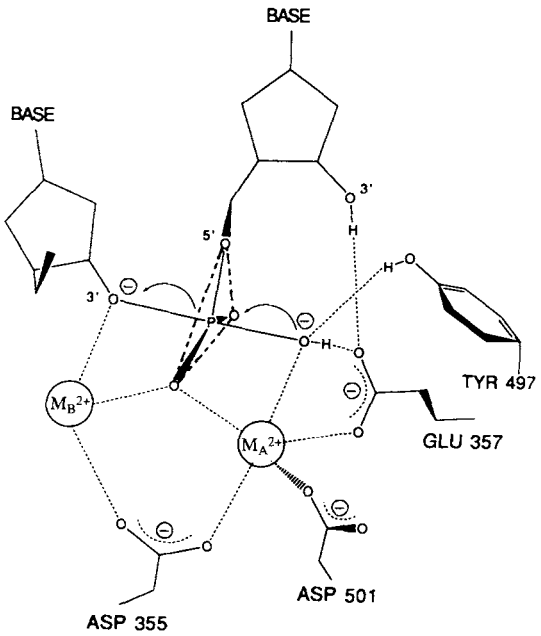

Fig. 15. Proposed interactions of the transition state with the protein for the 3',5'-exonuclease reaction of pol-I [85].

displacement step in AP. Metal ion A helps to generate the attacking hydroxide ion nucleophile, which is further stabilized by hydrogen bond interactions with Glu-357 and Tyr-497. Since Glu-357 is also coordinated to metal ion A, its pK_a value is lowered and it is not assumed to act as a general base. This assumption is supported by structure–energy calculations that make use of the empirical valence bond method.[121] Also, Tyr-497 is unlikely to function as a proton acceptor since its mutation to a phenylalanine residue resulted in a similar dependence of the rate on the pH value as in the native enzyme, and in only a modest reduction in activity.[116] A remarkable feature of this mechanism in contrast to that of alkaline phosphatase is that no protein side chains have significant roles in the stabilization of the transition state similar to that of Arg-166 in AP. The main task of the protein ligands seems to be the binding and orientation of the two metal ions and of the reactants. This mechanism is thus consistent with the finding that mutations of Asp-355, Asp-424, and Asp-501 have the largest effects on exonuclease activity.[116]

2.3.3. 5',3'-Nuclease Activity of the Polymerase from *Thermus aquaticus*

Thermus aquaticus DNA polymerase (*Taq* pol), famous for its use in the polymerase chain reaction,[122] is homologous to pol-I and also contains a 5',3'-nuclease activity in its N-terminal domain, but no 3',5'-exonuclease activity. The crystal structure of *Taq* pol revealed one metal binding site I, when the crystals were soaked in a solution containing Zn^{2+} ions (1 mM).[96] Soaking the crystals in a solution containing Mn^{2+} ions (20 mM) revealed two additional metal binding sites, II and III. I and II are 5 Å apart, whereas III is displaced by 10 Å from I and from II. The metal-containing structures have not yet been fully refined and are therefore not described here in more detail. However, the localization of two adjacent metal binding sites in the 5',3'-nuclease domain of *Taq* pol suggests that this activity might also use two metal ions in catalysis.

2.3.4. Ribonuclease H

HIV-RT possesses ribonuclease H (RNase H)[123] activity, acting as an endonuclease to degrade the viral RNA template strand during DNA synthesis.[124] The RNase H active site is located on a separate domain of the 66-kDa subunit; the distance to the polymerase active site is about 60 Å.[81, 88] The crystal structure of the isolated domain, which is stable but devoid of catalytic activity,[125] was determined at 2.4 Å resolution.[126, 127] Divalent metal ions are essential for RNase H activity.[128] In the presence of a solution of $MnCl_2$ (45 mM) two metal ion binding sites, which are approximately 4 Å apart, were located in 2.8 Å difference electron density maps (Fig. 16).[126] The side chains of Asp-443, Glu-478, Asp-498, and Asp-549 are near the two metal ions. These four carboxylate groups were also found to be highly conserved among retroviruses.[129]

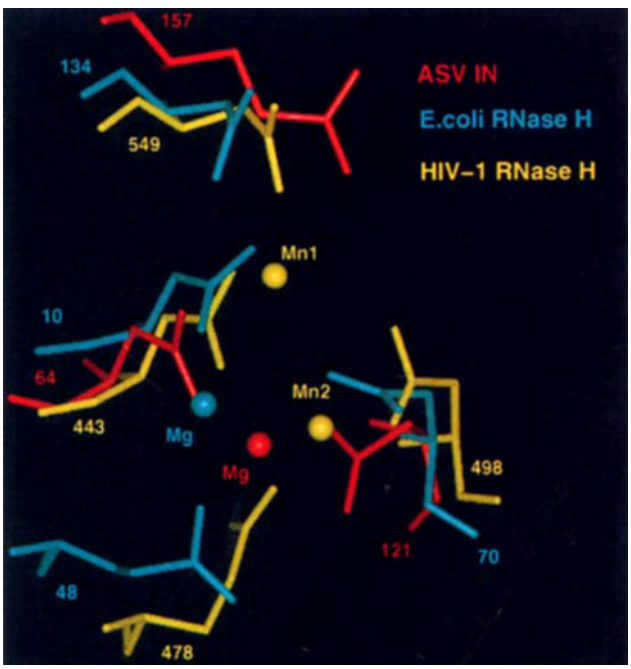

Fig. 16. Comparison of the metal ion binding sites in *Avian sarcoma* virus integrase (red) and RNase H from *E. coli* (blue) and HIV-1 (yellow) (taken from ref. [136])

The RNase H domain of HIV-RT displays significant sequence and structural homology to *E. coli* RNase H.[130,131] The residues Asp-443, Glu-478, Asp-498, and Asp-549 of HIV-RT RNase H that coordinate the metal ions correspond to Asp-10, Glu-48, Asp-70, and Asp-134 of *E. coli* RNase H. Mutagenesis of Asp-10, Glu-48, and Asp-70 of the bacterial enzyme also resulted in a significant loss of activity.[132] In contrast to the viral enzyme, only one Mg^{2+} binding site was found in *E. coli* RNase H by crystallographic[131] and NMR spectroscopic[133] studies (Fig. 16), even in the presence of nucleotides. These results support a one-metal ion mechanism for RNase H, in which one carboxylate side chain serves as a general base to deprotonate a water nucleophile and the metal ion coordinates to the two nonesterified phosphoryl oxygen atoms of the polynucleotide.[131] Thus, the question as to whether RNase uses one or two metal ions in catalysis, or if homologous RNases have different reaction mechanisms, remains open.

The crystal structures of the integrases from HIV-1[134] and *avian sarcoma* virus (ASV),[135,136] bacteriophage Mu transposase, MuA,[137] as well as the Holliday junction resolvase RuvC from *E. coli*[138] show a structural similarity to RNase H from HIV and *E. coli*.[139] Three highly conserved carboxylate side chains in their active sites and the fact that all enzymes depend on divalent metal ions, mainly Mg^{2+} and Mn^{2+} ions, for activity suggest that these nucleotidyl-transferases need one or more metal ions for activity. One metal ion binds to ASV integrase in the presence of Mg^{2+} or Mn^{2+} ions, close to the homologous metal ion position in *E. coli* RNase H (Fig. 16).[136] More detailed insight into the catalytic pathways of these enzymes can be expected for the future, when more structures with bound substrate analogues or products in the presence of metal ions become available.

2.3.5. *Restriction Endonucleases*

Restriction endonucleases, which cut the phosphodiester bond of DNA at specific sequences, require Mg^{2+} ions as a cofactor for catalysis. There is also biochemical and structural evidence that these nucleases, which show conserved carboxylate residues in the active site region, despite weak or no primary sequence homologies, might employ a two-metal ion mechanism.[140-143] The crystal structure of an enzyme–product–Mg^{2+} ion complex of *Eco*RV endonuclease showed the presence in the active site of two adjacent magnesium ions, which were bidentately bridged by the product phosphate group.[141,144] Also, the structures of *Eco*RI,[145] *Pvu*II,[146] *Bam*HI,[140] and *Cfr*10I[143] support a possible two-metal ion mechanism based on structural similarities of the active sites, although some differences exist (see ref. [143] for a superposition).

2.3.6. *Ribozymes*

Despite the absence of functional groups that have pK_a values and chemical properties similar to protein amino acid side chains, RNA can catalyze chemical reactions, for example as a nuclease or in RNA splicing.[147] The requirement for divalent metal ions and a comparison to other nucleases utilizing a two-metal ion mechanism led to the hypothesis that these RNA enzymes also catalyze nucleic acid hydrolysis or RNA splicing with the help of two metal ions.[148]

2.4. The Lithium-Sensitive Metallophosphatases Fructose-1,6-bisphosphatase, Inositol Monophosphatase, and Inositol Polyphosphatase

The three structurally characterized phosphatases fructose-1,6-bisphosphatase (FBP), inositol monophosphatase (IMP), and inositol polyphosphatase (IPP) form a group of distinctly related enzymes. FBP was the first enzyme of this group to have its three-dimensional structure unraveled by X-ray crystallography.[149] This structure analysis revealed a characteristic fold of five layers of secondary structural elements of alternating $\alpha\beta\alpha\beta\alpha$, which was later also found in the structures of IMP[150] and IPP.[151] The structural similarity also extends to the active sites, where all but one (which is an Asp/Glu exchange) of the metal binding residues are conserved.[152] These conserved residues have been grouped into three motifs, which contain the ligands of the metal ions and other active site residues (Fig. 17).[152,153] All three enzymes also share common bio-

```
          motif A          motif B          motif C
            B 21             1                2
FBP  115VCFDPLDGSSN 279YECNPMAYVMEKAGG 96SEED
IMP   87WIIDPIDGTTN 219WDVAGAGIIVTEAGG 69GEES
IPP  151W-VDPLLSTYQ 316WDSCAAHAILRAMGG 78GEES
```

Fig. 17. Sequence alignment for three homologous motifs containing the metal-ligating residues in FBP, IMP, and IPP (for a list of additional homologous proteins see refs. [152, 322]). The weak homology extends to a core structure of five α-helices and 11 β-strands. Those residues coordinated to the metal ions 1 and 2 and the bridging aspartate side chain (B) are marked.

chemical characteristics, such as their sensitivity to inhibition by monovalent ions, especially lithium, and their dependence on divalent cations for activity. Although active enzyme forms are observed in the presence of several ions, including Zn^{2+} and Mn^{2+} ions, the metal binding constants as well as the much higher concentration of magnesium in the cell favor magnesium as the bound metal ion in vivo; however, FBP may prefer zinc ions.[154]

2.4.1. *Fructose-1,6-Bisphosphatase*

Fructose-1,6-bisphosphatase (FBP) is a key regulatory enzyme in the gluconeogenic pathway.[155-157] It converts D-fructose-1,6-bisphosphate to D-fructose-6-phosphate with maximum activity at pH 7.6 for the rabbit liver enzyme. The presence of divalent metal ions (Mg^{2+}, Mn^{2+}, Zn^{2+}, or Co^{2+}) is essential for catalytic activity.[154,156,158-160] One to three zinc binding sites were found in each monomer in the presence or absence of substrate, product, or their analogues.[154,159,161] One Mn^{2+} ion binds per monomer in the absence of substrate, whereas two metal ions bind in the presence of substrate or analogues.[159,162] Consistent with one in-line displacement step, the hydrolysis takes place with inversion of the configuration at the phosphorus atom.[163]

Substrate fructose-1,6-bisphosphate exists in solution as a mixture of 15% α-form, 81% β-form, 2% keto form, and 1.3% *gem*-diol (Fig. 18).[164] Rapid quench kinetic studies indicate that the α-anomer is the real substrate.[165] In contrast, 2,5-anhydro-D-mannitol-1,6-bisphosphate (AhM-1,6-P_2), a β-substrate analogue inhibitor (Fig. 18), displays a 20-fold lower inhibition constant toward FBP than does the corresponding α-analogue inhibitor.[166]

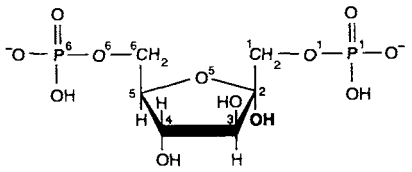

Fig. 18. Structure of the α-anomer of fructose-1,6-bisphosphate. In the analogue inhibitor AhG-1,6-P_2 the 2-OH group (printed bold) is replaced by a hydrogen atom. In the β-anomer and its analogue AhM-1,6-P_2 the chiral configuration around C2 is inverted.

The mammalian enzymes are regulated by adenosine monophosphate (AMP) at an allosteric site and by fructose-2,6-bisphosphate at the active site. Crystal structures of FBP from pig kidney,[149, 167–171] human liver,[172] and spinach chloroplast[173] are available. The 144-kDa pig kidney enzyme is a homotetramer of 222 symmetry. One side chain of the neighboring monomer, Arg-243, contributes to substrate binding at the interface between two monomers.

In the crystal structure of the complex from Mn–Mn FBP and the α-analogue inhibitor the two metal ions are separated by 3.7 Å and are bridged by two bidentate carboxylate groups of Glu-97 and Asp-118, and bidentately by the 1'-phosphate group of the inhibitor (Fig. 19 and Fig. 3, Section 2.1).[169] Other ligands of the metal ions are Glu-280 to Mn1 and the backbone carbonyl group of Leu-120 to Mn2. Disregarding metal-coordinated water molecules, which could not be located in the 2.9 Å electron density maps, the coordination spheres around both metal ions match a distorted tetrahedron. In addition to the bonds to the metal center one of the phosphoryl oxygen atoms of the inhibitor's 1-phosphate group interacts with the Arg-276 side chain, and the ester oxygen atom forms a hydrogen bond to the NH group of Gly-122 (Fig. 19). In the absence of metal ions,

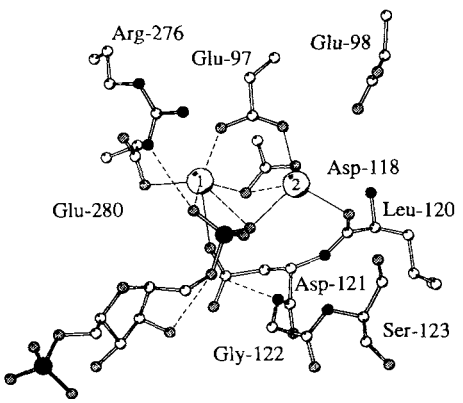

Fig. 19. Substrate analogue inhibitor AhG-1,6-P_2 (see Fig. 18) bound to the active site of FBP (generated from coordinate file 1FBD) [169].

the substrate fructose-1,6-bisphosphate in the α-form binds in a similar way as AhG-1,6-P_2, indicating that this inhibitor provides a good model for the binding mode of the substrate.

In the presence of Zn^{2+} or Mn^{2+} ions, two binding sites were found for the unliganded enzyme, one of which is identical to metal ion site 1, while the second metal ion site, designated as metal ion site 3, is near but different from metal ion site 2 found in the presence of substrate analogue.[172] The binding mode of the product was revealed by a crystal structure analysis of FBP cocrystallized with fructose-6-phosphate and Mn^{2+} or Zn^{2+} ions.[155] Under these conditions only the metal ion site 1 is occupied, and no metal binding is observed at site 2 or site 3. These results suggest that binding of Mn^{2+} or Zn^{2+} ions to metal ion site 2 requires the presence of the 1-phosphate group of the substrate, and that binding to metal ion site 3 is inhibited by the presence of substrate analogue or product. Thus, the first metal ion and the substrate bind independently to the active site, followed by binding of the second metal ion. It also seems likely that after hydrolysis the metal ion at site 2 leaves the active site before the product.

A putative mechanism assumes that the substrate binds in a bidentate bridging mode, as observed in the crystal structure with the AhG-1,6-P_2 inhibitor. The two metal ions M_1 and M_2 orient the substrate for attack of the nucleophile and stabilize the transition state (Fig. 20).[169] Deprotonation of the water

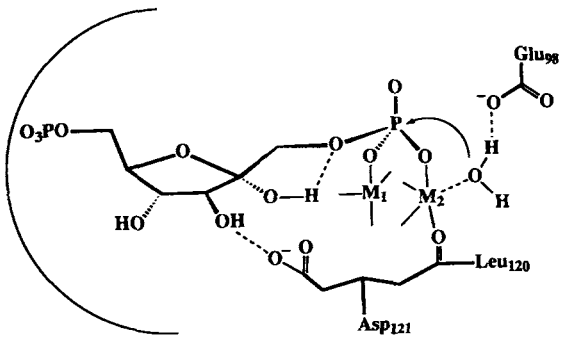

Fig. 20. Substrate binding mode and attack of a water molecule coordinated to the metal ion M_2 in the proposed mechanism for FBP [169].

nucleophile is facilitated by coordination to the metal ion M_2 and by interaction with Glu-98, which acts as a general base. Additional interactions of protein residues with other substrate atoms orient the substrate in a conformation in which the 2-hydroxyl group can interact with the ester oxygen atom of the 1-phosphate group. The importance of this interaction for catalysis is demonstrated by the resistance of substrates lacking the 2-hydroxyl group to enzymatic cleavage.[166] In addition, the backbone NH group of Gly-122 and the side chain of Arg-276 might play a role in the stabilization of the transition state. In agreement with the X-ray crystallographic studies, mutational analysis showed that substitution of Arg-276 by methionine reduces k_{cat} to less than 1%,[175] whereas Asn-212, Arg-243, Tyr-244, Tyr-264, and Lys-274 are primarily involved in substrate binding.[176] A mutation of the catalytic base Glu-98 to glutamine reduces k_{cat}/K_m 12000-fold.[177]

Binding of AMP to the allosteric site, 28 Å away from the active site, results in the catalytically inactive T-form of the

enzyme. The allosteric transition is accompanied by a 15–17° rotation of the two dimers of the tetramer relative to each other.[168] As a result, a displacement of residues Glu-97, Asp-118, and Leu-120 takes place, which also displaces metal ion 2 by 1.4 Å.[171] This metal ion is thereby no longer appropriately positioned to coordinate to the 1-phosphate group of the substrate in a catalytically productive position. In addition, FBP activity is modified by monovalent ions: K^+ and Tl^+ ions are activators, whereas Li^+ ions are inhibitors.[178] The activators bind to three positions in the active site, two of which are very close to the catalytic metal binding sites 1 and 2.[170] The third binding site is 3.8 Å away from one of the oxygen atoms of the substrate's 1-phosphate group and may be the activation site. Interestingly, in the absence of K^+ or Tl^+ ions, site 3 is occupied by the guanidinium group of Arg-276. The activators might therefore substitute efficiently for Arg-276 in catalysis.[170] The Li^+ ion inhibits FBP by binding to site 1; this finding provides a model for the role of lithium in treatment of manic depression, in which it inhibits inositol monophosphatase (see Section 2.4.2).

2.4.2. *Inositol Monophosphatase*

Inositol monophosphatase (IMP) participates in the phosphatidylinositol cell signaling pathway by hydrolyzing the inositol monophosphates Ins(1)P, Ins(3)P, and Ins(4)P to give *myo*-inositol.[179] Since human IMP is inhibited by therapeutically relevant concentrations (0.5–1.0 mM) of lithium ions, the putative role of the enzyme in the lithium therapy of manic depression has raised considerable interest.

IMP requires the presence of Mg^{2+} ions for activity, though other divalent metal ions such as Mn^{2+}, Zn^{2+}, and Co^{2+} also promote catalysis.[180, 181] The cooperative binding behavior of the Mg^{2+} ion to IMP with a Hill coefficient of 1.9 was originally interpreted on the basis of two nonadjacent metal binding sites in the homodimeric IMP (molecular mass 60 kDa).[182, 183] On the basis of the X-ray crystal structure analysis[184] and metal titration experiments,[181] these results have now been reinterpreted in the light of a cooperative binding to two adjacent metal binding sites within each active site. The fact that the structurally homologous bovine inositol polyphosphatase, despite its monomeric structure, also shows cooperative metal binding supports this view.[151, 185] IMP catalyzes the exchange of ^{18}O from H_2O to phosphate only in the presence of inositol,[183] indicating that the reaction does not proceed via a phosphoenzyme intermediate. In addition, attempts to isolate such an intermediate failed,[183, 186] and the X-ray crystal structures show no suitable nucleophilic side chain positioned to attack the phosphoryl group.[150]

Several crystal structures of IMP have been determined in the presence of different metal ions and substrate analogues in order to characterize the reaction pathway and the mode of lithium inhibition.[150, 184, 187] The structure of the free (unliganded) enzyme in the presence of manganese ions revealed three metal ion binding sites (see Fig. 3, Section 2.1).[184] The Mn1 and Mn2 ions are 3.9 Å apart and bridged bidentately by Asp-90.[45] Mn2 is further coordinated by Glu-70, the backbone oxygen atom of Ile-92, one terminal water molecule (W1), and a chloride ion which is at a distance of about 2.8 Å from all three metal ions. Additional ligands to Mn1 are Asp-93 and Asp-220. Besides $O_\varepsilon 1$ of Glu-70 and the chloride ion there are only three water ligands present in the coordination sphere of the metal ion at site 3. This site is not occupied in the product complex with phosphate and is probably a very low affinity binding site, which is not involved in catalysis.

In addition to the structure of the free enzyme, structures of complexes with either of the D- or L-form of *myo*-inositol 1-phosphate[187] and with product phosphate[184] contributed detailed insight into the catalytic pathway. Both substrate molecules could be bound to an enzyme inactivated by the presence of Gd^{3+} and Li^+ ions in the crystallization buffer. The Gd^{3+} ion binds to the metal binding site 2 and the Li^+ ion probably to site 1.[188] Figure 21 shows a superposition of the binding

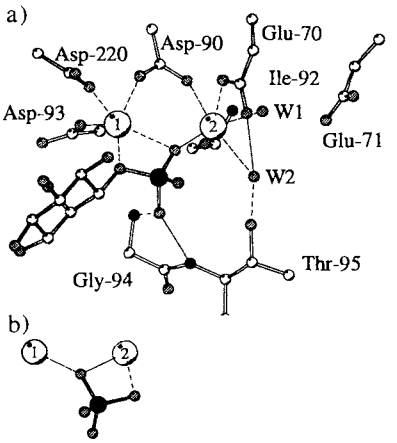

Fig. 21. a) Superposition of the binding mode of D-Ins(1)P as seen in Li1-Gd2 inactivated IMP onto the structure of the active Mn1–Mn2 enzyme (generated from coordinate files 1IMA and 1IMC) [184, 321]. Water molecule W2 is proposed to be the nucleophile coordinated to the metal ion in the mechanism of IMP [184]. b) Binding mode of a phosphate ion to Mn1–Mn2 IMP (PDB file 1IMD).

mode of the substrate D-Ins(1)P complexed to the inactivated enzyme onto the structure of active Mn–Mn IMP, thus yielding a plausible model of the catalytically productive substrate binding mode.[187] The phosphate group interacts with the metal ions, the backbone NH groups of Gly-94 and Thr-95, and two water molecules. A phosphate ion binds to Mn-Mn IMP such that the phosphate group is inverted compared to the substrate (Fig. 21).[184] Such an inverted binding mode of the product phosphate ion can be expected after attack on the substrate phosphate group by a water nucleophile apical to the inositol leaving group.

The wealth of biochemical and structural data available for IMP catalysis has been interpreted to be consistent with a direct displacement mechanism in which W2, the water molecule coordinated to the site 2 metal ion, is the nucleophile.[179, 181] This water molecule is also stabilized by hydrogen bonds to Glu-70 and Thr-95. The importance of Thr-95 for catalysis was demonstrated by mutation of this residue to an alanine, which reduced the enzyme activity by a factor of 14000.[189] Also, mutation of Glu-70 to a glutamine, which may not affect the enzyme's metal binding ability, resulted in a 7000-fold reduction in activity. The metal ion at site 1 possibly binds after the substrate is bound, since some of its ligands are substrate atoms: the two phosphate

oxygen atoms and possibly the 6-OH group of inositol, as suggested by modeling studies on the mechanism.[181] The importance of the 6-hydroxy group of the substrate in the mechanism has also been implicated by the inability of IMP to cleave 6-deoxyinositol 1-phosphate.[190] Stabilization of the transition state might be achieved by the interaction of the equatorial phosphoryl oxygen atoms with both metal ions and with the backbone NH groups of Gly-94 and Thr-95. The release of the leaving group may be facilitated by coordination of the esterified oxygen atom to the metal ion at site 2.

2.4.3. Inositol Polyphosphate 1-Phosphatase

Inositol polyphosphate 1-phosphatase (IPP) is another enzyme of the phosphatidylinositol signaling pathway[191] that removes the 1-phosphate from inositol 1,4-bisphosphate and inositol 1,3,4-trisphosphate.[192, 193] IPP requires Mg^{2+} ions for activity and is inhibited by lithium and calcium ions.[185, 192] Binding of magnesium ions shows cooperativity that has a Hill coefficient of 1.9, indicating the presence of two or more binding sites for Mg^{2+} ions.

The crystal structure analysis of bovine IPP at a resolution of 2.3 Å in the presence of magnesium ions showed two metal binding sites separated by 3.9 Å.[151] Both metal ions have an unusual coordination sphere with very long metal–ligand distances (see Fig. 3, Section 2.1). Only two ligands are less than 3 Å away from the coordinated metal. If one generously defines a ligand sphere of 4 Å around the metal ions, both magnesium ions are surrounded by six ligands in a distorted octahedral fashion. As in IMP, a crystal structure of the enzyme complexed with Gd^{3+} ions showed that this cation is located at metal binding site 1. The hydroxyl group of Thr-158, which is highly conserved between the phosphatases of this group, is hydrogen-bonded to the water molecule near the two Mg^{2+} ions and to the nearby side chain of Lys-37. Both residues are essential for catalytic activity, as demonstrated by mutagenesis studies.[194]

2.4.4. Comparison of the Structures of the Active Sites of Fructose 1,6-Bisphosphatase, Inositol Monophosphatase, and Inositol Polyphosphatase

A superposition of the active sites of FBP, IMP, and IPP based on the C_α coordinates of the five conserved coordinating ligands (see Fig. 17) and the two metal ions shows that these residues superimpose with (root mean square) deviations of 0.7–0.8 Å (Fig. 22).[195] Thus, the conserved side chains and the metal ions within this protein family show larger positional deviations than the conserved residues in PAP and the PPs (see Fig. 11). However, most of the residues have similar conformations, and they coordinate to the metal ions in a similar way. Glu-280 in FBP has a different conformation than it has in the homologous residues in IMP and IPP. Although the ligands are similarly arranged in the three proteins, the displacements of ligands and metal ions lead to some unusually long metal–ligand distances in IPP. Similar positions occur for Glu-98 in FBP, which is proposed to act as a general base, and the homologous glutamate side chains in IMP and IPP.

For FBP and IMP models of the substrate binding mode could be derived from co-crystal structures containing a bound substrate analogue, or a substrate bound to the inactivated enzyme (Figs. 19 and 21, respectively). These studies implicate a different binding mode of the substrate for the two enzymes: in FBP the phosphoryl group binds in a bidentate fashion through two nonesterified oxygen atoms, whereas in IMP one metal ion interacts with the ester oxygen atom of the leaving group, reminiscent of one displacement step in AP. Despite the significant structural homology of the active sites and the similarity of the catalyzed reactions, the two enzymes might therefore employ different mechanisms.

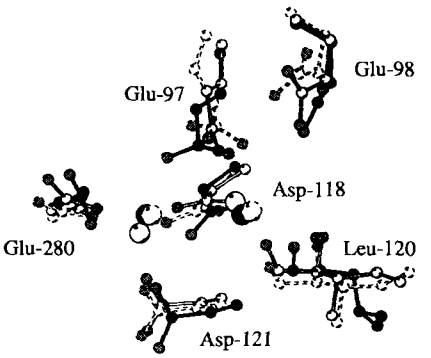

Fig. 22. Superposition of the active sites of FBP (C atoms black), IMP (C atoms white), and IPP (broken lines) [195]. The labels refer to the residues in FBP.

2.5. The Trinuclear Zinc Phosphodiesterases Phospholipase C and P1 Nuclease

Although phospholipase C (PLC) from *Bacillus cereus* and P1 nuclease (P1) from *Penicillium citrinium* display only low sequence homology in the zinc binding regions, the crystal structure analysis of P1[196] revealed a structure of similar fold and active site arrangement as found previously in phospholipase C.[197] By using 145 C_α atoms, the two structures can be superimposed with a (root mean square) deviation of 1.8 Å. They show 18% sequence homology in the superimposed regions.[196] The arrangement of the zinc ions and their coordination sphere including the positions of the three water molecules is very similar, and all ligands are conserved with the exception of Asp-153, which is Glu-146 in PLC (see Fig. 3, Section 2.1).

2.5.1. Phospholipase C

Phospholipase C (PLC) hydrolyses phosphatidylinositol and phosphatidylcholine and participates in the generation of second messengers in mammalian cells. The monomeric 28-kDa PLC from *Bacillus cereus*[198] is similar to the mammalian enzymes, and serves as a model for the hitherto less-characterized mammalian PLCs.[199] Determination of its metal content as well as removal and exchange of the metal ions characterized *B. cereus* PLC as a zinc enzyme containing two tightly bound zinc ions per molecule.[200] A third zinc ion was revealed by the X-ray crystal structure (1.5 Å resolution) of PLC.[197] The zinc ions can be exchanged for cobalt, manganese, and magnesium ions to give enzymes of reduced activity and altered substrate specificity.[200, 201] Spectroscopic studies indicated that in the cobalt(II)-substituted enzyme, two metal ions are present in a

distorted octahedral environment.[202] However, in the X-ray crystal structure of the native enzyme, all three zinc ions have a distorted trigonal-bipyramidal environment (see Fig. 3, Section 2.1).[197] The three metal ions are relatively close together: Zn1–Zn3 3.3, Zn1–Zn2 6.0, and Zn2–Zn3 4.7 Å. Zn1 and Zn3 are bridged bidentately by Asp-122 and by a water molecule (W1). Zn1 is further coordinated by His-69, His-118, and Asp-55. The ligand sphere of Zn3 is completed by His-14 and by the backbone carbonyl oxygen atom and the terminal amino group of Trp-1. Zn2 is coordinated by His-142, His-128, Glu-146, and two water molecules (W2 and W3).

In addition to the structure of the native enzyme the three-dimensional structures of complexes with a phospholipid substrate analogue, phosphate, iodate, iodide, and Tris have been determined.[203–205] In the phosphonyl group of a nonhydrolyzable substrate analogue inhibitor,[206] one of the ester oxygen atoms of the substrate's phosphate group is replaced with a methylene group. This analogue binds such that one of the free phosphonyl oxygen atoms bridges Zn1 and Zn3, whereas the other phosphonyl oxygen atom is coordinated to Zn2 (Fig. 23).[203] All three water ligands to the metal cluster are

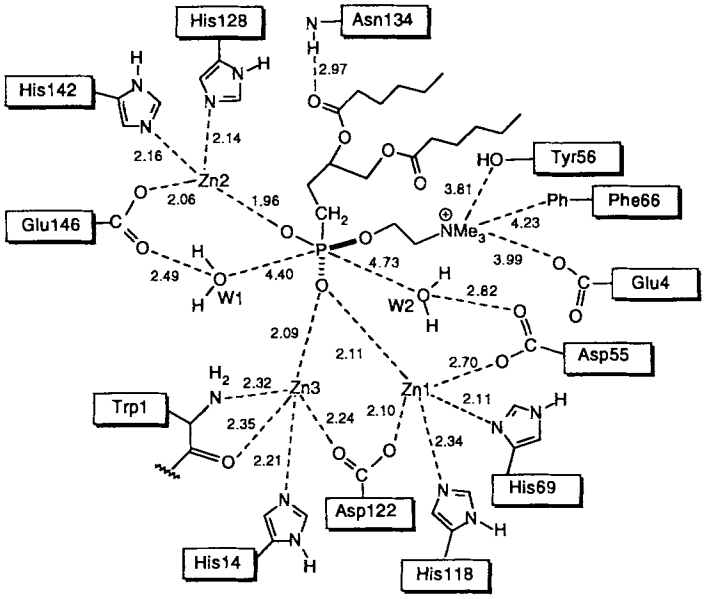

Fig. 23. Schematic drawing of the binding mode of the substrate analogue inhibitor 3(*S*),4-dihexanoyloxybutyl-1-phosphonylcholine to the active site of PLC (taken from ref. [206]; bond lengths given in [Å]). The labeling of the water molecules W1 and W2 does not correspond to that in Fig. 3.

displaced upon inhibitor binding, since the 1.9 Å electron density maps give no indication of zinc-coordinated water molecules. It was therefore proposed that the nucleophile is not generated by coordination to one of the zinc ions. A water molecule, which is 4.4 Å from the phosphorus atom and in an apical position to the diacylglycerol leaving group, may function as the water nucleophile. This water molecule is hydrogen-bonded to one carboxylate oxygen atom of the Zn2-coordinated Glu-146, which is proposed to function as a general base. All three zinc ions probably play a role in the stabilization of the transition state, but in this mechanism these zinc ions do not participate in the generation of the nucleophile, but possibly in the activation of the leaving group. There are no protein side chains positioned to protonate the diacylglycerol leaving group or interacting with the phosphoryl oxygen atoms, except for the metal-coordinated Asp-55 and Glu-146 side chains. Thus, all three metal ions evidently play a dominant role in catalysis by PLC. A computational evaluation of the binding energy of the substrate in different conformations to the enzyme yielded a different proposal for the substrate binding mode.[207] Here, the substrate binds to Zn2 and the nucleophile is the Zn1–Zn3 bridging water molecule. This study suggests that the binding mode of the substrate analogue inhibitor (Fig. 23) might not model the catalytically productive substrate binding. A phosphate ion binds like the phosphonyl group of the substrate analogue to all three zinc ions.[204]

2.5.2. *Nuclease P1*

Nuclease P1 (P1) is a phosphodiesterase that cleaves the bond between the 3′-hydroxyl and 5′-phosphate group of preferably single-stranded RNA and DNA under inversion of the configuration at the phosphorus center.[208] P1 also acts as a phosphomonoesterase on the 3′-terminal phosphate group of a (poly)nucleotide,[209] thus generating 5′-mononucleotides as the final cleavage products. Both activities require the presence of three zinc ions per molecule and are rather unspecific with respect to the nucleotide sequence.[210] The X-ray crystal structure of the monomeric 36-kDa *Penicillium citrinium* P1 nuclease was solved at a resolution of 2.8 Å.[196] Three zinc ions were found in the active site of P1, which are 3.2 Å (Zn1–Zn3), 5.8 Å (Zn1–Zn2), and 4.7 Å (Zn2–Zn3) apart (see Fig. 3, Section 2.1). All three zinc ions have three oxygen and two nitrogen ligands in a trigonal-bipyramidal coordination geometry.

To determine the substrate binding mode the crystal structure analysis of P1 liganded with the (*R*)-diastereomer of the thiophosphodinucleotide dA·P(S)·dA, a supposedly uncleavable substrate analogue,[211] was determined at 3.0 Å resolution.[196] This compound binds to two sites, which are about 20 Å apart, but for both binding sites only one mononucleotide could be found in the electron density map. The second half of the dinucleotide is presumably disordered or was cleaved off by the enzyme (Fig. 24).[212] The phosphate group of the mononucleotide is coordinated to Zn2 and has no contacts to the other two zinc ions. Arg-48 is hydrogen-bonded to one or two phosphate oxygen atoms. In contrast to the presumed substrate binding mode to PLC on the basis of the PLC-inhibitor complexes,[203, 204] the phosphate group of the mononucleotide binds differently to P1 than to PLC. Therefore, the authors discuss a different reaction mechanism for P1, in which one of the two Zn2-coordinated water molecules is the nucleophile.[196] However, more recent results suggest that the water molecule bridging Zn1 and Zn3 is the nucleophile.[212] This mechanism is thus similar to that for PLC which was proposed on the basis of the computational study (see Section 2.5.1).[207] Arg-48 and Zn2 evidently stabilize the transition state and/or activate the leaving group.

Nuclease P1 shows 50% sequence identity to nuclease S1 from *Aspergillus oryzae*. Nuclease S1 also needs three zinc ions for activity,[213] and the nuclease activity inverts the configuration at the phosphorus atom.[214] The two nucleases might therefore employ similar mechanisms for phosphate ester hydrolysis.

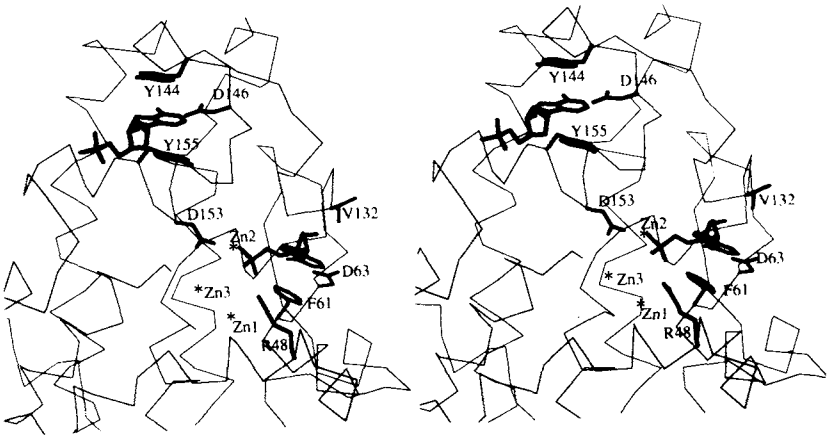

Fig. 24. Stereoview of two mononucleotide binding sites of the nuclease P1 (taken from ref. [196]).

2.6. Inorganic Pyrophosphatase and the *Mut*T Enzyme

The cleavage of pyrophosphate shifts the equilibrium of several, mainly ATP-dependent, biosynthetic reactions, including protein, DNA and RNA synthesis towards the products. This hydrolysis reaction is catalyzed by inorganic pyrophosphatase (IPY) in the presence of divalent metal ions.[215] Highest activity is seen with Mg^{2+} ions, but Mn^{2+}, Zn^{2+}, and Co^{2+} ions also promote catalysis.[216] The best studied IPYs are those from *E. coli* and yeast, *Saccharomyces cerevisiae*. X-ray crystal structures are available for the homohexameric *E. coli* enzyme,[217–219] the homodimeric yeast IPY,[220] and for the homohexameric IPY from *Thermus thermophilus*.[221] The structures of the homologous monomers of all three IPYs show a great similarity (for a superposition see reference [219]).[222] Furthermore, the catalytic mechanisms of the enzymes from *E. coli* and yeast seem to be very similar.

Inversion of the configuration around the phosphorus atom indicates a direct phosphoryl-transfer to the water molecule, in which the first phosphate released from the enzyme contains the oxygen atom from the solvent.[223] Studies on *E. coli* IPY showed that three to five Mg^{2+} ions participate in the reaction, depending on the protonation state of the enzyme.[224] Yeast IPY binds two Mn^{2+} ions per subunit in the free enzyme and three Mn^{2+} ions in the presence of phosphate.[225] Mutational analysis of residues in the active site of the *E. coli* enzyme showed that these mutations influence the activity by increasing the pK_a value of a catalytically important basic group.[226] This group probably is a metal-bound hydroxide ion nucleophile.

In the X-ray crystal structure of yeast IPY with three Mn^{2+} ions and two phosphate ions (P1 and P2), M1 is coordinated by Glu-58 and one oxygen atom of P2, M2 by Asp-116, Asp-119, Glu-48, and P2, and M3 by Asp-114, Asp-151, one oxygen atom each from P1 and P2, and by one water molecule.[220] M2 and M3 are 3.5 Å apart, whereas M1 is separated by 4.2 Å and 5.3 Å from M2 and M3, respectively. Three positively charged side chains, Lys-56, Lys-153, and Arg-77, are near the two phosphate groups and might assist in substrate binding and transition state stabilization.

Mechanistically related to IPY is the *Mut*T enzyme, a pyrophosphohydrolase of 129 residues, that catalyzes the hydrolysis of nucleoside triphosphates to nucleoside monophosphates and pyrophosphate. The structure determined by NMR spectroscopy of the *Mut*T protein, which requires two divalent cations for activity,[227] shows a cluster of five glutamate residues (41, 53, 56, 57, and 98), which might bind one or both metal ions.[228] More detailed information on the metal binding sites is not yet available. *Mut*T and IPY have a similar $\alpha + \beta$ fold, although they show no significant sequence homology.

2.7. (*S*)-Adenosylmethionine Synthetase

(*S*)-adenosylmethionine synthetase (AMS) catalyzes the formation of the sulfonium compound (*S*)-adenosylmethionine (AdoMet), which serves as an important methylation reagent in biological systems, from L-methionine and ATP (Fig. 25).[229] This synthesis proceeds by a unique two-step process: in the first step the complete tripolyphosphate chain of ATP is displaced by methionine to yield AdoMet and tripolyphosphate (PPP_i). Kinetic isotope effects characterized this step as an S_N2-type reaction with attack of the sulfur nucleophile at the C5′ of ATP. In a second step tripolyphosphate is hydrolyzed to pyrophosphate (PP_i) and phosphate (P_i) before AdoMet leaves the active site first.[230]

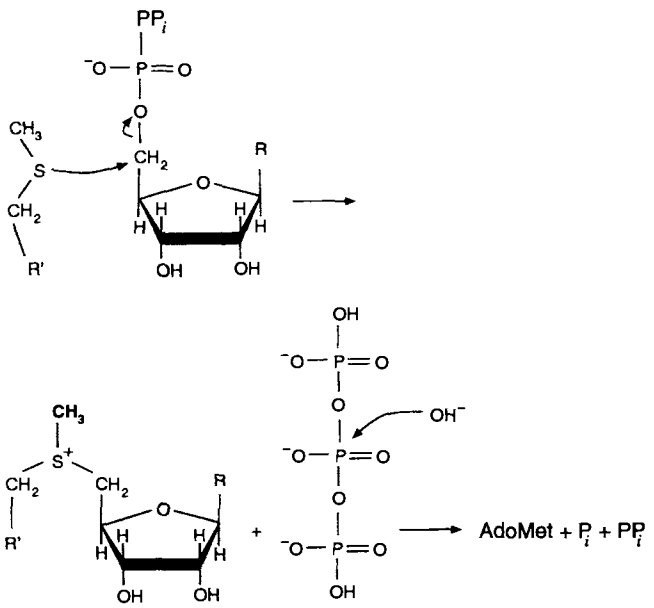

Fig. 25. Two-step reaction catalyzed by AMS. R′ denotes the missing part of methionine group and R is the adenyl group of ATP.

Divalent metal ions (Mg^{2+}, Mn^{2+}, Zn^{2+}, Co^{2+}, or Ni^{2+}) are required for AMS activity.[231] Since a vanadyl cation (VO^{2+}) binds to these divalent metal sites, it could be used as a spectroscopic probe.[232] In addition, a spatial proximity of two Mn^{2+} binding sites was demonstated by EPR spectroscopy.[233]

Monovalent cations (mainly K^+) also activate AMS. According to ^{205}Tl NMR spectra, Tl^+ ions bound to this monovalent site were not influenced by the presence of methionine, an ATP analogue, or pyrophosphate, indicating that substrates and products do not coordinate to the monovalent metal activator.[234] Binding of two phosphate ions to the dimetal center was implicated by the inhibition profile of this product.[230]

In good agreement with these biochemical results the 3.0 Å X-ray crystal structure of AMS in the presence of Mg^{2+}, K^+, and phosphate ions showed two magnesium sites, which are 5 Å apart, and one potassium ion in the active site.[235] The two divalent metal ions are bridged by two phosphate ions such that each metal ion is coordinated to two oxygen atoms of one phosphate and to one oxygen atom of the other phosphate. In addition, crystal structures of the enzyme with ADP and phosphate and with pyrophosphate and phosphate have been determined in the presence of Mg^{2+} ions.[236] In all of these structures two Mg^{2+} ions were found in the active site. ADP and phosphate, which were products of AMS-catalyzed cleavage of ATP, bind such that all three phosphate groups bridge the two metal ions in a bidentate fashion (Fig. 26). Further ligands are Asp-A271 to Mg1 and Asp-B16 to Mg2 (A and B refer to different subunits of the homotetramer). The positively charged side chains of His-B14, Lys-B165, Lys-A265, Arg-B244, and Lys-B245 interact with the products and thus may play important catalytic roles.

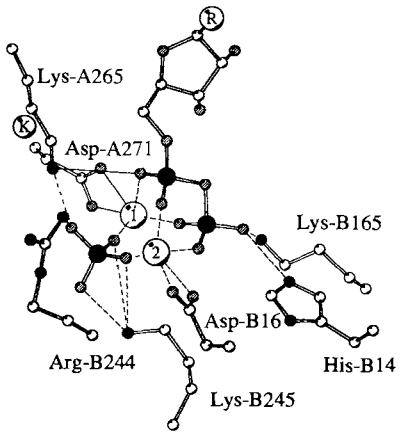

Fig. 26. Structure of ADP and phosphate bound to the active site of AMS [236]. R denotes the adenyl group of ADP.

The current data clearly implicate a two-metal ion mechanism for one or both steps of the reaction pathway of AMS. A possible mechanism of the second step, the hydrolysis of triphosphate, includes a role of Lys-265 in the protonation of the α-β-bridging oxygen atom and subsequently in the deprotonation of the water nucleophile.[236] However, further biochemical and structural studies are needed in order to clarify details of the unusual two-step catalysis of this enzyme.

2.8. Glutamine Synthetase

Glutamine synthetase (GLS) catalyzes the synthesis of glutamine from ammonia, glutamate, and ATP (Fig. 27). The reaction takes place via an enzyme-bound tetrahedral intermediate.[237] Divalent metal ions (Mg^{2+}, Mn^{2+}) are necessary for activity.[238] X-ray crystal structures of native GLS from *Salmonella typhimurium* and of complexes with substrate, product, and intermediate analogue compounds, including L-methionine-*S*-sulfoximine phosphorylated by the enzyme, yielded structural models for several stages of the reaction pathway (Fig. 28).[239, 240]

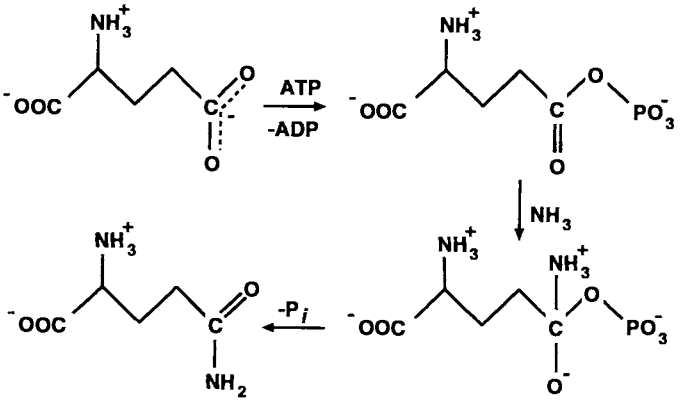

Fig. 27. Reaction catalyzed by glutamine synthetase.

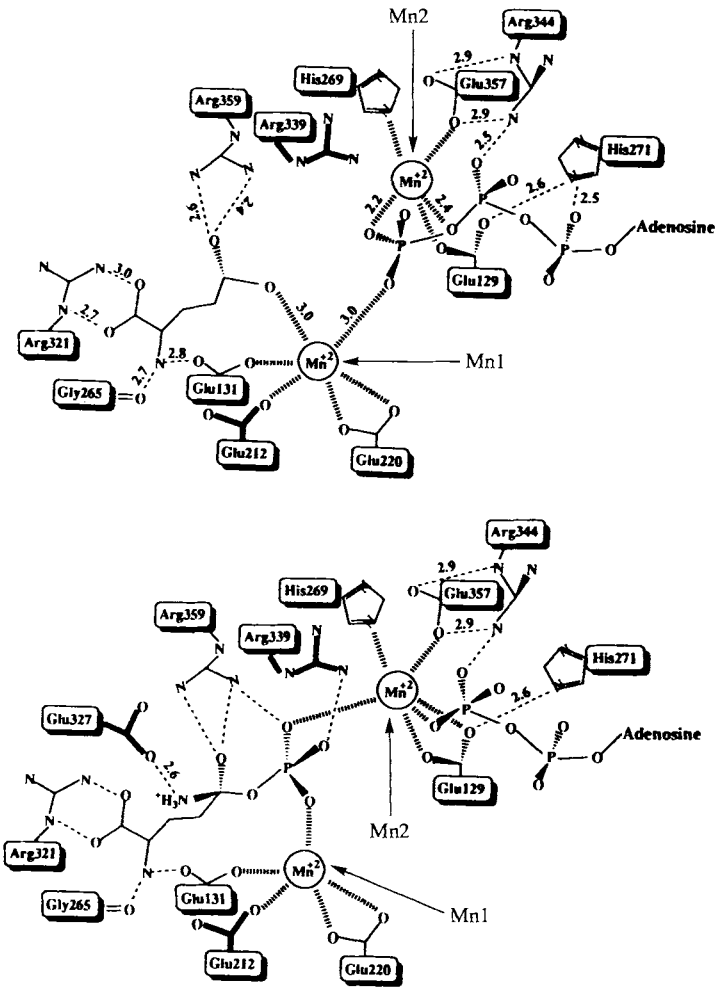

Fig. 28. Structural models for the phosphoryl-transfer step of the reaction pathway of glutamine synthetase (taken from ref. [240]).

Mn1, which is coordinated by three glutamate residues (131, 212, and 220), binds the nucleophilic carboxylate group of the substrate glutamate. The γ-phosphoryl group of ATP is polarized by both metal ions, but more strongly by Mn2, which has His-269, Glu-357, and Glu-129 as protein ligands (Fig. 28 top). The two metal ions are 5.8 Å apart, consistent with spectroscopic results.[241] Mn2 also activates the AMP leaving group. After the phosphoryl group has been transferred to the substrate carboxylate group, an ammonium ion attacks the carboxylate carbon atom, and the tetrahedral intermediate is formed (Fig. 28 bottom). In the last step the phosphate group leaves by cleavage of the carbon–oxygen bond. Arg-339 and Arg-359 may stabilize the transition-state of the phosphoryl-transfer reaction. Mutation of either of these two arginine residues severely diminishes the catalytic activity.[242] Interestingly, GLS also catalyses the arsenolysis of glutamine, probably by a mechanism in which phosphate is replaced by arsenate in the reversal of glutamine synthesis.

2.9. Phosphotriesterase

Organophosphate triesters are not naturally occurring compounds, but they are released in quantities on the order of millions of kilograms every year into nature by man's use as pesticides and insecticides. In addition, several nerve agents belong to this group of compounds and are stockpiled as chemical warfare agents. Resistance of some insects to insecticides and the degradation of pesticides by soil microbes led to the detection of phosphotriesterases that catalyze hydrolysis of many organophosphate triesters.[243–245] The enzyme from the soil bacteria *Pseudomonas diminuta* is by far the best characterized phosphotriesterase (PTE). It is a 39-kDa monomeric metalloprotein that exhibits a fairly broad substrate specificity and hydrolyzes P–O, P–F, P–CN, and P–S bonds between the phosphorus center and the leaving group.[244, 246] However, phosphomonoesters and phosphodiesters are not cleaved by PTE.[247] Although PTE shows comparable activity with Zn^{2+}, Co^{2+}, Ni^{2+}, Cd^{2+}, or Mn^{2+} ions in the active site, its binding affinity for metal ions and atomic absorption measurements on the native enzyme indicate that it is a dinuclear zinc enzyme in vivo.[244, 248] The environment of the metal ions has been characterized by EPR[249] and ^{113}Cd NMR spectroscopy [250] as a mixed N,O ligand sphere with one or more ligands bridging the two metal ions. Some of these ligands as well as other active site residues were identified as histidine residues by the use of histidine-modifying agents and by mutagenesis studies.[251, 252]

Hydrolysis of phosphotriesters by PTE occurs upon inversion of the configuration at the phosphorus atom, consistent with an in-line displacement reaction.[253] The pH-dependence of the activity indicates that one ionizable residue with a pK_a value of 6.1 plays a role in the mechanism of the catalysis.[251] Brønsted plots on the influence of the pK_a value of the leaving group on the rate constants, which yielded β values around -1.8,[254] as well as primary and secondary ^{18}O isotope effects[255] indicate a largely broken bond to the leaving group in the transition state (very late transition state). Although the PTE-catalyzed reaction is thus not as associative as the alkaline hydrolysis in solution, these data were interpreted as consistent with an S_N2-like concerted associative mechanism in both enzymatic and nonenzymatic hydrolysis of phosphotriesters.

Crystal structures of the apoenzyme[256] and the Cd–Cd form[257] revealed the molecular structure of the enzyme and the active site. The two cadmium ions are 3.8 Å apart and are located at the C-terminus of the β-strands of the α/β-barrel structure. The two metal ions are bridged by the carbamylated side chain of Lys-169 and by a water molecule (see Fig. 3, Section 2.1). In the structure of the apoenzyme[256] Lys-169 is not carbamylated. It has been subsequently demonstrated that CO_2 is required for the assembly of the two-metal site.[258] A carbamylated lysine side chain has also been found as a ligand to magnesium in ribulose-1,5-bisphosphate carboxylase/oxygenase[259] and as a bidentate bridging ligand to the two nickel ions in urease.[260] Cd1 is further coordinated by His-55, His-57, and Asp-301 in a trigonal-bipyramidal geometry, whereas Cd2 is also coordinated by His-201, His-230, and two terminal water molecules. Interestingly, assembly of the dinuclear cluster in PTE also induces drastic changes in the course of the polypeptide chain in some regions, yielding a (root mean square) deviation of 3.4 Å for the superposition of the C_α atoms of the apoenzyme and the holoenzyme.

3. Acyl- and Other Carbonyl-Transfer Reactions

Carbonyl-transfer reactions share many features with the chemistry of phosphoryl-transfer. In principle, an associative mechanism via a tetrahedral *gem*-diolate intermediate and a dissociative pathway via an acylium ion ($R-CO^+$), which is assumed to be an intermediate in the mechanism of Friedel–Crafts acylation,[261] are possible.[262] However, due to the polarity and electrophilicity of the carbonyl group nucleophilic substitutions via a tetrahedral transition state or intermediate dominate in enzymatic and nonenzymatic reactions of carbonyl compounds. Isotope effects and structure–activity correlations support such a tetrahedral transition state structure.[13]

3.1. Aminopeptidases

Aminopeptidases are ubiquitous in nature and are of critical biological and medical importance because of their key role in protein modification and degradation, and in the metabolism of biologically active peptides.[263, 264] These enzymes catalyze the hydrolysis of amino acid residues from the amino terminus of a peptide and generally have a broad substrate specificity. X-ray crystal structures are available for three aminopeptidases: leucine aminopeptidase, aminopeptidase from *Aeromonas proteolytica*, and methionine aminopeptidase. These three proteins have no detectable sequence homology, and thus constitute different prototypes of proteolytic enzymes.

A number of natural and synthetic reaction coordinate analogue inhibitors have been characterized for aminopeptidases. These inhibitors can be used to study mechanistical aspects of the hydrolytic reaction by biochemical and structural means. Examples include bestatin and amastatin,[265, 266] aminoboronates,[267, 268] aminophosphonates,[269] aminoaldehydes,[270] methyl ketones,[271] chloromethyl ketones,[272] and

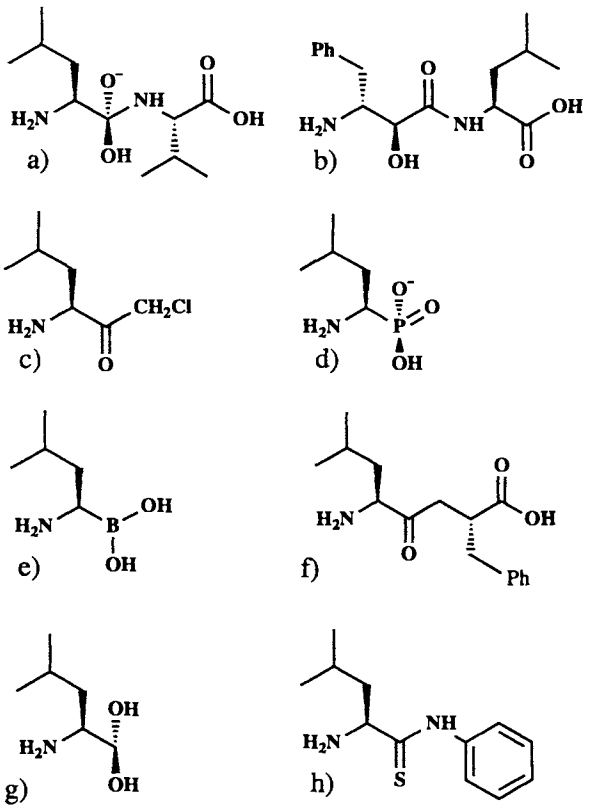

Fig. 29. Structures of a putative *gem*-diol intermediate for hydrolysis of substrate L-leucyl-L-leucine (a) and some reaction coordinate analogue inhibitors for aminopeptidases. The inhibition constants for porcine kidney LAP are: bestatin (b), 0.6 nM [265]; DL-leucylchloromethylketone (c), 12 μM [323]; L-leucylphosphonic acid (d), 0.23 μM [324]; DL-leucylboronic acid (e), 20 nM (IC_{50}) [267]; L-Leu-CO-CH_2-(DL)Phe (f), 57 μM [273]; L-leucinal (g), 60 nM [325]; L-leucylthioanilide (h), 0.19 mM [274].

peptides containing a ketomethylene amide bond replacement[273] as transition state analogues of an associative acyl-transfer reaction (Fig. 29). Thionopeptides may serve as substrate analogue compounds.[274]

3.1.1. Leucine Aminopeptidase

A number of biochemical and X-ray crystal structural studies make leucine aminopeptidase (LAP) currently the best characterized aminopeptidase containing a dinuclear metal center.[275] Bovine lens LAP is a hexameric enzyme with a molecular mass of 324 kDa and shows maximum activity at pH 8–9. Each of the six identical 54-kDa subunits contains two zinc ions[276] that are essential for catalytic activity and display different exchange kinetics. The readily exchangeable site 1 binds Zn^{2+}, Mn^{2+}, Mg^{2+}, or Co^{2+} ions[276–279] and has been identified as Zn1 in the X-ray crystal structure by the structure determination of the Zn^{2+}–Mg^{2+} metallohybrid enzyme.[280] The zinc ion in the tight binding site 2 can be exchanged for a Co^{2+} ion only when both binding sites are not occupied.[278, 279] In contrast to some earlier results, it is now apparent that metal substitution in both binding sites significantly affects both K_m and k_{cat}.[279] Thus, both metal ions participate in substrate binding and activation, including a possible role in the activation of the nucleophile. Although Mg^{2+} and Mn^{2+} ions hyperactivate LAP,[281] the enzyme has a significantly higher affinity for Zn^{2+} than for Mn^{2+} or Mg^{2+} ions,[277] and the isolated enzyme contains zinc ions.[282] Bovine LAP shows 31% sequence identity to aminopeptidase A from *E. coli*,[283] which serves a role as an accessory protein in Xer site-specific recombination in *E. coli*. The homology is 52% in the catalytic domains and all active site residues are conserved between LAP and aminopeptidase A.

The X-ray crystal structure of bovine lens LAP at a resolution of 1.6 Å showed that the two zinc ions are 3.0 Å apart and are bridged bidentately by Glu-334, monodentately by Asp-255, and by an exogenous water or hydroxide ion ligand (see Fig. 3, Section 2.1).[284–286] Further ligands are one carboxylate and the carbonyl oxygen atom of Asp-332 to Zn1, and Asp-273 and the amino group of Lys-250 to Zn2. Both zinc ions are thus five-coordinate in an arrangement best described as octahedral with one vacant position.

X-ray crystal structures of LAP with four transition state analogues have been determined: the natural inhibitors bestatin[285, 287] and amastatin,[288] L-leucinephosphonic acid,[289] and L-leucinal.[286] All transition state analogues bind in a similar way to the active site of LAP (Fig. 30). Even bestatin, which has a D-configuration at the N-terminal phenylalanine residue and contains an additional carbonyl group next to the hydroxyl group (Fig. 29), differs in its binding mode only by the absence of a fourth coordination bond to Zn1. Together these structures provide a reasonable model for the binding mode of the transition state. In all of these inhibitor structures the terminal amino group is coordinated to Zn2. Upon binding of the inhibitor, the zinc–zinc distance widens to about 3.3 Å, but no rearrangements of the ligand spheres of the metal ions take place.

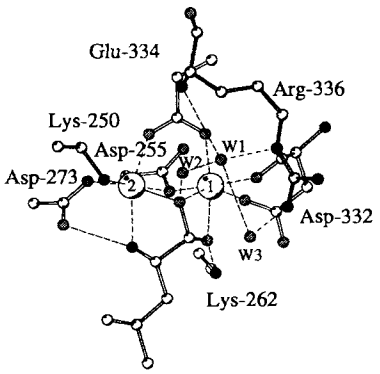

Fig. 30. Binding mode of the transition state analogue inhibitor L-leucinal to the active site of LAP (generated from coordinate file 1LAN) [286]. Binding sites 1 and 2 are occupied by zinc ions.

Leucinal resembles the presumed tetrahedral *gem*-diolate intermediate of an associative acyl-transfer mechanism more closely than do any of the other inhibitors. The positions of the two *gem*-diol oxygen atoms of the hydrated aldehyde group probably correspond to the positions of the two *gem*-diol oxygen atoms of the intermediate (Fig. 30). One of these oxygen atoms bridges the two metal ions, whereas the other oxygen atom is coordinated only to Zn1. The binding modes of bestatin and amastatin, which show the peptide leaving group in a position pointing away from the dizinc center toward the central solvent channel of the LAP hexamer, are in agreement with this model of the intermediate binding mode. There are no protein residues in the active site positioned to act as a general base. Furthermore, the X-ray crystal structure of the unliganded enzyme[286] at 1.6 Å resolution showed that only one exogenous solvent ligand is coordinated to the dizinc cluster: a water or hydroxide ion ligand that symmetrically bridges the two metal

ions (see Fig. 3, Section 2.1). The position of this water ligand is identical to the position of the bridging oxygen ligands in the inhibitor structures.

Based on the X-ray crystal structures and the biochemical data a reaction mechanism was proposed in which the bridging hydroxide ion acts as the nucleophile (Fig. 31).[286, 289] In this mechanism both metal ions participate in substrate binding and

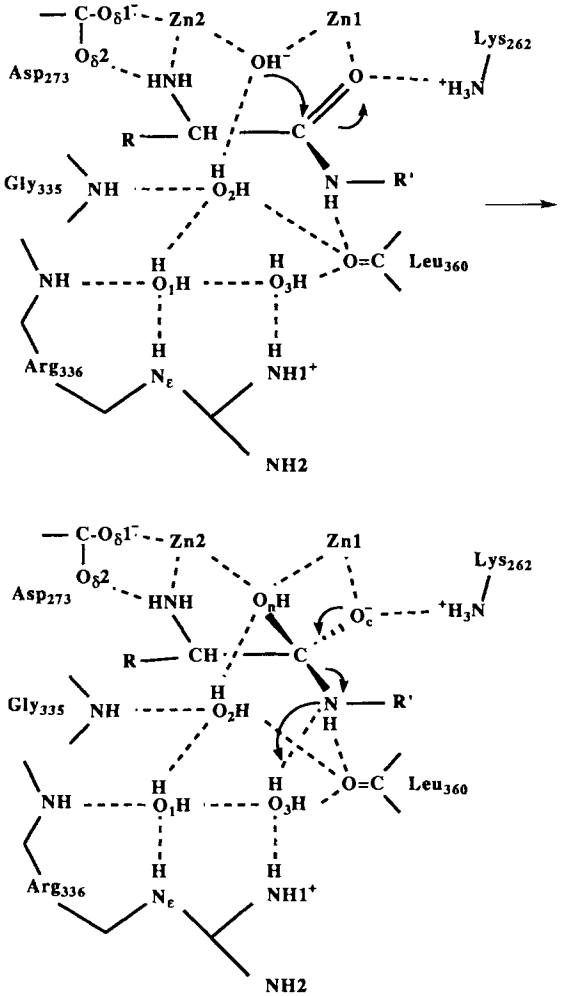

Fig. 31. Reaction mechanism proposed for LAP based on X-ray crystal structures and biochemical evidence [286].

in catalysis. Zn2 binds the terminal amino group, activates the water nucleophile, and stabilizes the transition state. Zn1 polarizes the carbonyl group, activates the water nucleophile, and stabilizes the transition state by coordination to both *gem*-diolate oxygen atoms. In addition, two amino acid side chains probably play an important role in catalysis: Lys-262 in the polarization of the carbonyl group and in the stabilization of the transition state, and Arg-336, which interacts with the substrate and intermediate through three water molecules. These water molecules may lower the transition state energy through the formation of hydrogen bonds. One of these water molecules probably protonates the leaving group (see also Section 3.1.4).

3.1.2. *Aminopeptidase from Aeromonas proteolytica*

In contrast to the mammalian aminopeptidases, *Aeromonas proteolytica* aminopeptidase (AAP) is a small monomeric protein (29.5 kDa).[290] As isolated from the bacteria, APP contains two zinc ions. In addition to Zn^{2+} ions, Co^{2+}, Ni^{2+}, and Cu^{2+} ions are capable of restoring activity to the inactive apoenzyme.[291] These metal exchanged enzymes display a higher activity towards certain substrates than does the native Zn–Zn enzyme. An even higher hyperactivity is obtained for the mixed Ni–Zn and Cu–Zn forms of AAP. Again, the hyperactivation strongly depends on the type of the substrate and on the order of metal addition: the more active forms were obtained by adding one equivalent of Cu^{2+} or Ni^{2+} ions before adding Zn^{2+} ions, consistent with the existence of two nonidentical metal binding sites. As in LAP, substitutions of both metal ions influence both k_{cat} and K_m.

The X-ray crystal structure analysis (1.8 Å resolution) of the Zn–Zn form of unliganded AAP showed the presence of two zinc ions, 3.5 Å apart.[292] Both Asp-117 (bidentate) and a water molecule bridge the two zinc ions, which are five-coordinate if one includes the slightly more distant second carboxylate oxygen atoms of Glu-152 to Zn1 (2.4 Å) and Asp-179 to Zn2 (2.3 Å) (see Fig. 3, Section 2.1). In addition to the bridging ligands Zn1 is coordinated by Glu-152 and His-256, and Zn2 by His-97 and Asp-179. A striking feature of this metal center is the similarity of the coordination spheres of the two zinc ions. The bridging water molecule is hydrogen-bonded at a distance of 3.3 Å to the carboxylate group of Glu-151.

3.1.3. *Methionine Aminopeptidase*

Most proteins are synthesized beginning with methionine (in eukaryotes) or formylmethionine (in prokaryotes) at the N-terminus. Removal of the N-terminal methionine group may be catalyzed by methionine aminopeptidase (MAP), depending on the identity of the adjacent residue. MAPs purified from different mammalian and microbial sources display similar substrate specificities, showing cleavage when the penultimate residue is small.[293, 294] For MAP isolated from several of these sources, the enzyme, which requires divalent metal ions, is most active in the presence of cobalt ions. However, it remains to be shown whether MAP is a cobalt enzyme in vivo. MAP is a soluble monomer with optimal activity at neutral pH. The prokaryotic and yeast MAPs display a significant degree of sequence homology, and all ligands are conserved, with the exception of a replacement of a glutamate residue for a glutamine residue in yeast MAP. Furthermore, sequence comparisons among other proteins indicated that aminopeptidase P,[295] proline dipeptidase,[296] and p67[297] have a similar fold as that of MAP and probably also contain a two-metal active site.[298, 299]

The X-ray crystal structure analysis (2.4 Å resolution)[300] of *E. coli* MAP[293] revealed the presence of two metal ions separated by 2.9 Å. These metal ions are located at the center of the central curved antiparallel β-sheet of the mixed α/β structure. Residues Glu-235 and Asp-108 bridge the two metal ions bidentately (see Fig. 3, Section 2.1). Further ligands are Glu-204 and His-171 to Co1 and both carboxylate oxygen atoms of Asp-97 to Co2. Thus, Co1 and Co2 both have four protein ligands. The coordination geometry of both metal ions may be described as

octahedral, in which one of the vacant ligand positions is occupied sterically by the other cobalt ion.[300] Weak electron density features suggest that solvent ligands may occupy the remaining two ligand positions, one at each cobalt ion. These water ligands would then interact with His-178 or Thr-99, which may thus also play important roles in the catalysis. The short distance between the two metal ions may, alternatively, permit a bridging water molecule or hydroxide ion.

3.1.4. Comparison of the Aminopeptidase Structures

AAP and the carboxy-terminal, catalytic domain of LAP have similar folds, despite only insignificant sequence homology.[292] However, this similarity does not extend to the precise location or structure of the active site. The metal coordination spheres of the two zinc aminopeptidases are significantly different. Also, the active site cavity in AAP contains neither a lysine nor an arginine side chain, in order to serve similar roles as Lys-262 and Arg-336 in LAP. A common feature of AAP and LAP is the presence of a dinuclear metal center, which contains one water ligand bridging the two metal ions. In addition, both metal ions in both structures are five-coordinate, thus having a vacant ligand position at each zinc ion. The two active sites may thus be superimposed on the basis of the zinc ions and the bridging water molecule, in such a way that the more buried Zn2 of AAP is superimposed onto the more buried Zn2 of LAP, which also coordinates the amino terminus of the substrate (superposition not shown). Interestingly, this superposition also maps the hydrophobic binding pocket for the N-terminal side chain of LAP onto the presumed specificity pocket for this residue of AAP. In detail, Met-270, Met-454, and Thr-359 of LAP have similar positions as Met-180, Phe-244, and Met-242 of AAP, respectively. Furthermore, the carboxylate group of Glu-151 of AAP is at a position that is occupied by water molecules or a carbonate ion near Arg-336 in the structures of LAP. There is indirect evidence that two of these water molecules in LAP are actually a $H_3O_2^-$ ion stabilized in the active site of LAP to serve a functional role.[286] This role could be similar to that of Glu-151 in AAP, including a function as a general base. However, Lys-262 of LAP has no similar residue in AAP in this superposition, since the side chain of Ile-255 takes its place in AAP.

Both metal ions in MAP also have four protein ligands, similar to the situation in AAP and LAP. Unfortunately, the crystallographic resolution did not allow an unambiguous determination of coordinated water molecules. Whether AAP, LAP, and MAP employ similar reaction mechanisms despite the pronounced differences in their metal coordination geometries and active site structures remains to be shown, for example by structure determination of suitable enzyme-inhibitor complexes.

3.2. Urease

Urease is a metalloenzyme that catalyses the hydrolysis of urea to ammonia and carbamate.[301–304] This enzyme allows bacteria, fungi, and higher plants to use urea as a nitrogen source. In 1975 urease was identified as the first nickel metalloenzyme,[305] and nickel has since been found in all ureases characterized so far. Thus, nickel evidently has a unique role in the catalysis by urease. Considering the similarity of urea hydrolysis to other hydrolytic reactions, it is surprising that this role can not be fulfilled by other more readily available divalent "hydrolytic ions" such as zinc, cobalt, magnesium, manganese, or iron ions. Indeed, Zn^{2+}, Cu^{2+}, and Co^{2+} ions do not restore activity to the apoenzyme of the urease from *Klebsiella aerogenes*.[306] Only the Mn protein possesses 2% of the activity of the Ni-activated apoprotein. Spectroscopic studies and titration experiments with a tight-binding inhibitor further characterized the active site as a dinuclear nickel center.[307, 308] Urease is also interesting because of its selectivity in the assembly of the metal ion center: several accessory proteins, encoded by adjacent genes of the urease gene cluster in bacteria,[302, 309] are needed to incorporate nickel into the apoenzyme in vivo. Furthermore, the discovery that carbon dioxide is necessary for nickel binding to urease[310] can now be readily explained by the presence of a carbamylated lysine side chain as a ligand to both metal ions.[260] Nickel binding and the carbamylation of this lysine residue (Lys-217) is a synergistic process; in the apoenzyme Lys-217 is not carbamylated despite the presence of CO_2.[260]

Crystals of urease from the jack bean were obtained in 1926 by Sumner.[311] These were the first crystals of a then recognized enzyme. This crystallization was an historic landmark in enzymology, because it demonstrated that enzymes are well-defined chemical compounds. The crystal structure[260] (2.2 Å resolution) of urease from *Klebsiella aerogenes*[312] shows a tightly associated trimer of $(\alpha\beta\gamma)_3$ stoichiometry. Since other ureases share about 50% sequence homology with the enzyme from *K. aerogenes* possibly all known ureases have a similar trimeric structure.[260] The two nickel ions are 3.5 Å apart and bridged bidentately by the carbamylated Lys-217 side chain (see Fig. 3). Further ligands to the metal ions are His-246 and His-272 to Ni1, and His-134, His-136, Asp-360, and a water molecule to Ni2. Thus, Ni1 is coordinated by three ligands in a tetrahedral geometry in which one ligand is missing. The coordination geometry of Ni2 may be described as a distorted trigonal bipyramid.

The side chains of His-219, Cys-319, and His-320 delineate—among other residues—a putative urea binding pocket.[260] Chemical modification and mutagenesis studies demonstrated that these three residues influence the catalytic efficiency.[313–315] Site-directed mutagenesis of His-219 suggested a role of this residue in substrate binding, whereas His-320 was proposed to act as a general base.[314] Cys-319 is not essential for activity but its mutation or modification to larger side chains can greatly reduce the activity.[313]

A mechanism has been proposed for catalysis by urease in which one nickel ion binds the hydroxide ion nucleophile and the other nickel ion binds and polarizes the carbonyl group of the substrate (Fig. 32).[316] The X-ray crystal structure of urease supports this model in

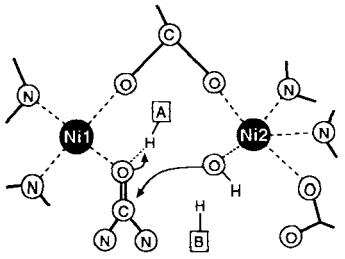

Fig. 32. Mechanism proposed for urease based on biochemical data and the X-ray crystal structure [260, 304, 316] A = general acid, B = general base.

that the Ni2-coordinated water molecule (or hydroxide ion) may be the nucleophile, and Ni1 has a vacant ligand position to coordinate the carbonyl oxygen atom.[260] Furthermore, His-219 would then be within hydrogen-bonding distance to the carbonyl oxygen atom, and thus able to assist in polarizing the carbonyl group and stabilizing the negatively charged tetrahedral intermediate, which is formed after the attack of the hydroxide ion. Except for $O_\delta 1$ of the Ni1-coordinated Asp-360 side chain there is no other residue in a position to function as a general base. For structural studies with mechanism-based inhibitors, a number a suitable compounds have been shown to inhibit urease. Phosphate inhibits urease in a strongly pH-dependent way.[307, 317] Boric and boronic acids are also possible reaction coordinate analogues, but it is not clear whether they bind as substrate analogues with a trigonal planar $R-B(OH)_2$ group or as transition state analogues as tetrahedral $R-B(OH)_3^-$ ions.[307, 318] Another strong binding inhibitor is phenylphosphorodiamidate, inhibiting *K. aerogenes* urease with an overall dissociation constant of 94 pM.[307]

The urease structure revealed a striking similarity[260] of its $(\alpha\beta)_8$ barrel in the catalytic α domain to that in adenosine deaminase (ADA), a mononuclear zinc enzyme.[319] This homology also extends to the location of the active site: Ni2 has a position close to Zn in ADA and three of the Ni2 ligands in urease coordinate in a way which is similar to the corresponding ligands of zinc in ADA (Fig. 33). Also, the position of the water

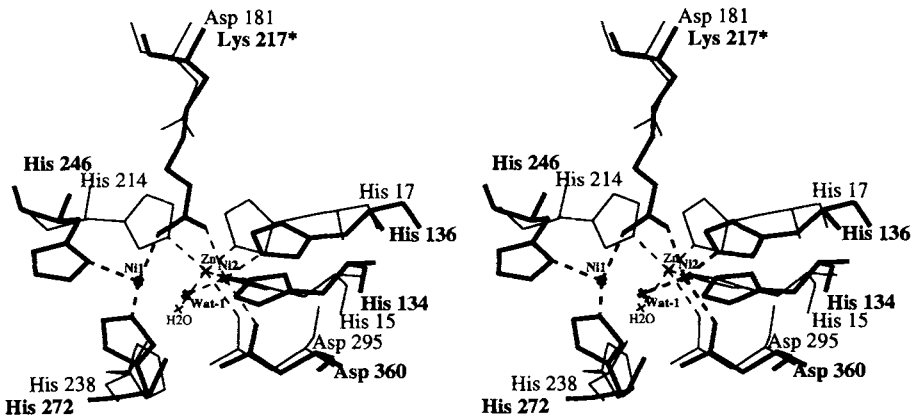

Fig. 33. Superposition of the active site structures of urease (bold lines) and the mononuclear zinc enzyme adenosine deaminase (thin lines) (taken from ref. [260]).

(or hydroxide ion) nucleophile is similar in these two enzymes. One of the ligands to Ni1 in urease, His-246, has a different position in ADA (His-214) in which it is coordinated to zinc. The relationship between ADA and urease provides an instructive example of how a dinuclear metal center (here of urease) has evolved from a possible ancestor protein containing a mononuclear metal site (here similar to ADA). It was proposed that the mutation to and carbamylation of Lys-217, which is an aspartate residue in ADA, was necessary to provide a side chain long enough to bridge the two metal ions (the corresponding Asp-181 side chain in ADA is not metal-coordinated).[260]

4. A Common Structural or Mechanistic Theme?

The two adjacent metal ions are in most cases separated by a distance of between 3 and 4 Å (this is also true for the centers containing three metal ions if we consider only the two closest metal atoms in these centers). A longer distance is seen in structures of pol-β (4.7 Å),[93] 5′-nuclease of *Taq* pol (5 Å),[96] AMS (5 Å), and GLS (5.8 Å).[235, 240] In these three enzymes both metal binding sites have a very low binding affinity for metal ions, or are only occupied in the presence of substrate or analogues (as seen in the structures). Usually one or more bridging carboxylate side chains or carbamylated lysine residues facilitate the assembly of such a di- or trinuclear metal cluster. No such bridge is seen in the dimetal centers of AP, AMS, and GLS. In contrast to those enzymes in which at least one of the bridging carboxylate groups is bidentate, PAP and the PPs contain only one monodentate metal-bridging carboxylate side chain. A great diversity is seen in the type of ligands and the geometry of the coordination spheres of the metal ions, even in enzymes that catalyze similar or identical reactions, such as the aminopeptidases. With respect to the zinc enzymes, a tendency to coordination numbers higher than four (three protein ligands and one water nucleophile), as seen in many mononuclear zinc hydrolases, is noted.[2]

For some enzymes reviewed in this article, structures could be obtained with substrates, products, intermediates, or reaction coordinate analogue compounds bound to the active site. These yield reasonable models for the possible interactions activating the reactants and stabilizing the transition state. These studies indicate that in all of the metalloenzymes containing two adjacent metal ions in the active site, both metal ions participate in catalysis, and none of them serves a mere structural role. Also, in the phosphodiesterases P1 and PLC, all three metal ions are probably involved in the binding and activation of the reactants. However, the magnesium ion in AP probably serves a more indirect role in catalysis. AP is also unique among all enzymes discussed here in its two-step mechanism with the formation of a phosphoenzyme intermediate. All other enzymes evidently directly transfer the phosphoryl group to the water molecule (or the acceptor) in one in-line displacement step. However, the mechanism of each of the two displacement steps in AP is a prototype of a two-metal ion mechanism, which is also thought to be realized in a similar form in other enzymes (see below). A possible pitfall in the determination of the substrate binding mode by the use of phosphate or substrate analogues containing a phosphate group is that the binding mode of the inhibitor might resemble a product binding mode or might be a thermodynamically most stable binding mode, but not the catalytically productive substrate binding mode (see Sections 2.2.1–2.2.3 and 2.5.1).

Table 2 shows that each of the possible interactions of the reactants with metal ions or protein residues as mentioned in

Table 2. Residues that activate the nucleophile or leaving group, or stabilize the transition state (or intermediate) as implicated from suitable enzyme-inhibitor structures. M = metal ion.

Enzyme	Transition state stabilization	Leaving group activation	Nucleophile activation
AP	Zn1, Zn2, Arg-166, NH_{102}	Zn1 / Zn2 [a]	Zn2 / Zn1 [a]
PAP	M^{II}, His-202, His-296	His-296	Fe^{III}
PP-1	Zn2, Fe1	His-125	Fe1, or Fe1 and Zn2
Pol-β	MgB	(H_2O)	MgB, Asp-256 [b, c]
Pol-I	Mg1, Mg2	Mg2	Mg1
EXO	M_A, M_B	M_B	M_A, Glu-357 [b], Tyr-497
FBP	M1, M2, Arg-276	2'-OH of the substrate, NH_{122}	M2, Glu-98 [c]
IMP	M1, M2, NH_{94}, NH_{95}, (H_2O)	M2	M1, Glu-70 [b, c], Thr-95
PLC	Zn1, Zn2, Zn3	Zn2 (?)	Glu-146 [b, c]
P1	Zn2, Arg-48	Zn2 (?)	Zn1 and Zn3, or Zn2
GLS	Mg1, Mg2, Arg-339, Arg-359	Mg2	Mg1
LAP	Zn1, Zn2, Lys-262, (H_2O)	(H_2O)	Zn1 and Zn2

[a] In the first/second phosphoryl-transfer step. [b] Ligand at metal ion. [c] The residue is proposed to act as a general base (proton acceptor).

Section 2 (see Fig. 2) is thought to be realized in one or more of the presumed two-metal ion mechanisms. In the mechanisms of AP, PAP, the PPs, FBP, and LAP positively charged side chains (Arg, His, or Lys) evidently participate in the stablization of the transition state in addition to the metal ions. In contrast, in the polymerases, 3',5'-exonuclease, IMP, and PLC the metal ions appear to provide most of the transition state stabilization alone, since no other protein residues are positioned to interact with the phosphoryl oxygen atoms. In IMP, two backbone NH groups may also help in the stabilization of the transition state.

For all di- and trinuclear metalloenzymes discussed here, a metal ion is proposed to help in the deprotonation of the nucleophile. For LAP, the Ser/Thr PPs, and nuclease P1, a deprotonation of the nucleophile by two metal ions is discussed (metal-ion-bridging nucleophile). Since two metal ions may lower the pK_a value of a coordinated water molecule even more than one metal ion, such a bridging water molecule may be deprotonated more easily without the help of a protein residue acting as a general base. However, the Lewis acidity of the metal ion(s), modulated by the coordinating ligands, should be strong enough to just generate a metal-bound hydroxide ion at the pH value of the natural enzyme environment, but not stronger since the Lewis acidity will also reduce the nucleophilicity of the generated hydroxide ion. An open question remains on the issue as to whether a carboxylate group coordinated to a metal ion is likely to accept a proton from the nucleophile, as proposed for the mechanisms of pol-β and IMP. A computational study on the 3',5'-exonuclease activity of pol I indicated that the Glu-357 side chain coordinated to the metal ion is unlikely to become protonated during the reaction, since the basicity of a carboxylate group is significantly lowered by metal coordination.[150] Also, an activation of the leaving group by metal ions or protein side chains is proposed for most enzymes (Table 2). Often water molecules are seen at hydrogen-bonding distance to phosphoryl or ester oxygen atoms (e.g. in IMP, or pol-β), or to the *gem*-diolate oxygen atoms of the transition state analogue inhibitors for LAP. These water molecules may also significantly stabilize the transition state or protonate the leaving group. Such catalytically important water molecules may be present in X-ray crystal structures, although at lower resolution (greater than about 2.5 Å) they may not be seen in the electron density maps.

The data in Table 2 indicates that both metal ions play a dominant role in most of the the catalytic pathways. In an attempt to simplify the proposed two-metal ion phosphoryl-transfer mechanisms we might therefore compare them on the basis of the binding mode of the reactants to the metal ions, as shown in Figure 34, in which all interactions with other protein residues are neglected. A substrate binding mode, in which one metal ion generates the deprotonated nucleophile and the other metal ion activates the leaving group and both metal ions polarize the phosphoryl group, is implicated for both displacement steps of AP, as well as for IMP, 3',5'-exonuclease, and as one possibility for the RNA/DNA polymerases (Fig. 34a). This kind of mechanism is supported by several structural studies for these enzymes and thus appears to be a prevalent two-metal mechanism. A mechanism, in which one metal ion binds the substrate phosphoryl group and the other metal ion deprotonates the nucleophile is discussed for PAP, and in a modified form as one possibility for P1, assuming that the nucleophile is the water molecule that bridges Zn1 and Zn3 (Fig. 34b). In a third alternative substrate binding mode, the phosphoryl group bridges the two metal ions in a bidentate fashion (Figs. 34c and d). The nucleophile might be a terminal ligand to one metal ion, as proposed for FBP and for PP-1, or a bridging water molecule, one possibility for the mechanism of the Ser/Thr PPs.

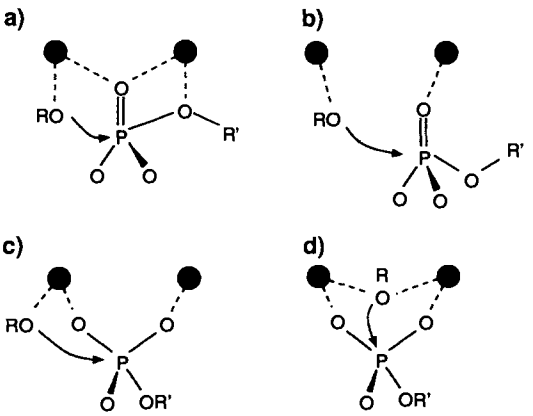

Fig. 34. Simplified scheme showing four possible binding modes of a phosphomonoester and a nucleophile to a dimetal center. In mechanisms a) and b) the substrate binds monodentate bridging or terminal with one nonbridging phosphoryl oxygen atom to the metal ions, whereas in mechanisms c) and d) the substrate binding mode is bidentate bridging.

We do not know how close these mechanistic models approach the actual reaction pathways, nor do we know the extent that further structural or other studies will modify these proposed mechanisms. Nevertheless, it appears as if significantly different mechanisms can be achieved with a two-metal ion arrangement. Even for evolutionary related enzymes, such as PAP and the PPs, FBP and IMP, or P1 and PLC, differences in the pathways with respect to the identity of the nucleophile or the substrate binding mode are observed or at least implicated or possible. We know that three-dimensional structures are more conserved than protein sequences, but it remains to be shown how well enzyme mechanisms are conserved.

We are grateful to Hazel Holden, Fusao Takusagawa, Dietrich Suck, Edward Hough, Sissel Hansen, Zdenek Hostomsky, Andy Karplus, Stephen Martin, Alexander Wlodawer, Harold Wyckoff, Tom Steitz, Jonathan Goldberg, and John Kuriyan for providing figures and coordinates for the generation of figures prior to release by the Protein Data Bank. Huguette Pelletier, Fusao Takusagawa, and Dietrich Suck are thanked for sharing results before publication and for helpful comments. B. K., N. S., and T. K. thank Herbert Witzel for advice and many helpful discussions. Research in the laboratories of the authors was supported by grants NIH GM06920 to W. N. L. and DFG 406/13/15 and BMFT(BMBF) 05648PMA to B. K. N. S. thanks the Deutsche Forschungsgemeinschaft for financial support.

Received: March 12, 1996 [A157IE]
German version: *Angew. Chem.* **1996**, *108*, 2158–2191

[1] R. G. Wilkins, *Chem. Soc. Rev.* **1992**, *21*, 171; J. B. Vincent, G. L. Olivier-Lilley, B. A. Averill, *Chem. Rev.* **1990**, *90*, 1447; P. Nordlund, H. Eklund, *Curr. Opin. Struct. Biol.* **1995**, *5*, 758.
[2] B. L. Vallee, D. S. Auld, *Proc. Natl. Acad. Sci. USA* **1993**, *90*, 2715; B. L. Vallee, D. S. Auld, *Biochemistry* **1993**, *32*, 6493.
[3] a) J. R. Knowles, *Annu. Rev. Biochem.* **1980**, *49*, 877; b) S. J. Benkovic, K. J. Schray in *The Enzymes, Vol. 8*, 3rd ed. (Ed.: P. D. Boyer), Academic Press, New York, **1973**, pp. 201–238; c) J. A. Gerlt in *The Enzymes, Vol. 20*, 3rd ed. (Ed.: D. S. Sigman), Academic Press, San Diego, **1992**, pp. 95–139.
[4] J. B. Vincent, M. W. Crowder, B. A. Averill, *Trends Biochem. Sci.* **1992**, *17*, 105; D. Gani, J. Wilkie, *Chem. Soc. Rev.* **1995**, *24*, 55.
[5] S. J. Benkovic, K. J. Schray in *Transition States of Biochemical Processes, Vol. 1*, 1st ed. (Ed.: R. D. Gandour), Plenum, New York, **1978**, pp. 493–527; G. J. Thatcher, R. Kluger, *Adv. Phys. Org. Chem.* **1989**, *25*, 99.
[6] J. J. Villafranca, T. Nowak in ref. [3c], pp. 63–94; A. S. Mildvan, C. M. Grisham, *Struct. Bonding (Berlin)* **1974**, *20*, 1; A. S. Mildvan, *Adv. Enzymol.* **1979**, *49*, 103; B. S. Cooperman, *Met. Ions Biol. Syst.* **1976**, *5*, 79–126.
[7] J. F. Chlebowski, J. E. Coleman, *J. Biol. Chem.* **1976**, *251*, 1202; J. F. Chlebowski, I. M. Armitage, P. P. Tusa, J. E. Coleman, *ibid.* **1976**, *251*, 1207.
[8] A. J. Kirby, W. P. Jencks, *J. Am. Chem. Soc.* **1965**, *87*, 3209; W. W. Butcher, F. H. Westheimer, *ibid.* **1955**, *77*, 2420.
[9] W. W. Cleland, *FASEB J.* **1990**, *4*, 2899.
[10] F. H. Westheimer *Acc. Chem. Res.* **1968**, *1*, 70.
[11] A. Williams, *Adv. Phys. Org. Chem.* **1992**, *27*, 1; W. P. Jencks, *Catalysis in Chemistry and Enzymology*, McGraw-Hill, New York, **1969**.
[12] W. W. Cleland, *Bioorg. Chem.* **1987**, *15*, 283.
[13] W. W. Cleland, A. C. Hengge, *FASEB J.* **1995**, *9*, 1585.
[14] A. S. Mildvan, D. C. Fry, *Adv. Enzymol.* **1987**, *59*, 241.
[15] S. J. Admiraal, D. Herschlag, *Chem. Biol.* **1995**, *2*, 729.
[16] D. Herschlag, W. P. Jencks, *J. Am. Chem. Soc.* **1987**, *109*, 4665; R. M. Milburn, M. Gautam-Basak, R. Tribolet, H. Sigel, *ibid.* **1985**, *107*, 3315; P. E. Amsler, H. Sigel, *Eur. J. Biochem.* **1976**, *63*, 569; M. Tetas, J. M. Lowenstein, *Biochemistry* **1963**, *2*, 350; L. B. Nanninga, *J. Phys. Chem.* **1957**, *61*, 1144.
[17] J. E. Coleman, *Annu. Rev. Biophys. Biomol. Struct.* **1992**, *21*, 441.
[18] H. N. Fernley, P. G. Walker, *Nature* **1966**, *212*, 1435.
[19] W. N. Aldridge, T. E. Barman, H. Gutfreund, *Biochem. J.* **1964**, *92*, 23C.
[20] J. H. Schwartz, A. M. Crestfield, F. Lipmann, *Proc. Natl. Acad. Sci. USA* **1963**, *49*, 723.; J. H. Schwartz, F. Lipmann, *ibid.* **1961**, *47*, 1996; L. Engström, *Biochim. Biophys. Acta* **1962**, *52*, 604.
[21] R. Han, J. E. Coleman, *Biochemistry* **1995**, *34*, 4238.
[22] P. Gettins, M. Metzler, J. E. Coleman, *J. Biol. Chem.* **1985**, *260*, 2875; W. E. Hull, S. E. Halford, H. Gutfreund, B. D. Sykes, *Biochemistry* **1976**, *15*, 1547; W. Bloch, M. J. Schlesinger, *J. Biol. Chem.* **1973**, *248*, 5794.
[23] T. T. Simopoulos, W. P. Jencks, *Biochemistry* **1994**, *33*, 10375.
[24] S. R. Jones, L. A. Kindman, J. R. Knowles, *Nature* **1978**, *275*, 564.
[25] A. D. Hall, A. Williams, *Biochemistry* **1986**, *25*, 4784.
[26] F. Hollfelder, D. Herschlag, *Biochemistry* **1995**, *34*, 12255.
[27] P. M. Weiss, W. W. Cleland, *J. Am. Chem. Soc.* **1989**, *111*, 1928.
[28] A. C. Hengge, W. A. Edens, H. Elsing, *J. Am. Chem. Soc.* **1994**, *116*, 5045.
[29] R. A. Anderson, W. F. Bosron, F. S. Kennedy, B. L. Vallee, *Proc. Natl. Acad. Sci. USA* **1975**, *72*, 2989.
[30] J. E. Murphy, X. Xu, E. R. Kantrowitz, *J. Biol. Chem.* **1993**, *268*, 21497; J. E. Murphy, T. T. Tibbitts, E. R. Kantrowitz, *J. Mol. Biol.* **1995**, *253*, 604; J. E. Murphy, E. R. Kantrowitz, *Mol. Microbiol.* **1994**, *12*, 351; C. M. Janeway, X. Xu, J. E. Murphy, A. Chaidaroglou, E. R. Kantrowitz, *Biochemistry* **1993**, *32*, 1601.
[31] J. M. Sowadski, M. D. Handschumacher, H. Murthy, B. A. Foster, H. W. Wyckoff, *J. Mol. Biol.* **1985**, *186*, 417.
[32] E. E. Kim, H. W. Wyckoff, *J. Mol. Biol.* **1991**, *218*, 449.
[33] C. Schulz, I. Bertini, M. S. Viezzoli, R. D. Brown III, S. H. Koenig, J. E. Coleman, *Inorg. Chem.* **1989**, *28*, 1490.
[34] P. Gettins, J. E. Coleman, *J. Biol. Chem.* **1984**, *259*, 11036.
[35] These distances are averaged between the two independent monomers within the asymmetric unit.
[36] J. E. Butler-Ransohoff, S. E. Rokita, D. A. Kendall, J. A. Banzon, K. S. Carano, E. Kaiser, A. R. Matlin, *J. Org. Chem.* **1992**, *57*, 142.
[37] A. Chaidaroglou, D. J. Brezinski, S. A. Middleton, E. R. Kantrowitz, *Biochemistry* **1988**, *27*, 8338; J. E. Butler-Ransohoff, D. A. Kendall, E. Kaiser, *Proc. Natl. Acad. Sci. USA* **1988**, *85*, 4276.
[38] E. V. Koonin, *Protein Sci.* **1994**, *3*, 356; G. J. Barton, P. T. Cohen, D. Barford, *Eur. J. Biochem.* **1994**, *220*, 225.
[39] S. Zhuo, J. C. Clemens, R. L. Stone, J. E. Dixon, *J. Biol. Chem.* **1994**, *269*, 26234.
[40] N. Sträter, T. Klabunde, P. Tucker, H. Witzel, B. Krebs, *Science* **1995**, *268*, 1489.
[41] J. Goldberg, H. Huang, Y. Kwon, P. Greengard, A. C. Nairn, J. Kuriyan, *Nature* **1995**, *376*, 745.
[42] J. P. Griffith, J. L. Kim, E. E. Kim, M. D. Sintchak, J. A. Thomson, M. J. Fitzgibbon, M. A. Fleming, P. R. Caron, K. Hsiao, M. A. Navia, *Cell* **1995**, *82*, 507.
[43] C. R. Kissinger, H. E. Parge, D. R. Knighton, C. T. Lewis, L. A. Pelletier, A. Tempczyk, V. J. Kalish, K. D. Tucker, R. E. Showalter, E. W. Moomaw, L. N. Gastinel, N. Habuka, X. Chen, F. Maldonado, J. E. Barker, R. Bacquet, J. E. Villafranca, *Nature* **1995**, *378*, 641.
[44] M. Egloff, P. T. Cohen, P. Reinemer, D. Barford, *J. Mol. Biol.* **1995**, *254*, 942.
[45] T. Klabunde, N. Sträter, R. Fröhlich, H. Witzel, B. Krebs, *J. Mol. Biol.* **1996**, *259*, 737.
[46] J. Schindelmeiser, D. Münstermann, H. Witzel, *Histochemistry* **1987**, *87*, 13; J. Schindelmeiser, P. Schewe, T. Zonka, D. Münstermann, *ibid.* **1989**, *92*, 81.
[47] M. Zaidi, B. Moonga, D. W. Moss, I. MacIntyre, *Biochem. Biophys. Res. Commun.* **1989**, *159*, 68; K. W. Lau, T. K. Freeman, D. J. Baylink, *J. Biol. Chem.* **1987**, *262*, 1389.
[48] B. A. Averill, J. C. Davis, S. Burman, T. Zirino, J. Sanders-Loehr, T. M. Loehr, J. T. Sage, P. G. Debrunner, *J. Am. Chem. Soc.* **1987**, *109*, 3760.
[49] J. W. Pyrz, J. T. Sage, P. G. Debrunner, L. Que, Jr., *J. Biol. Chem.* **1986**, *261*, 11015.
[50] M. Dietrich, D. Münstermann, H. Suerbaum, H. Witzel, *Eur. J. Biochem.* **1991**, *199*, 105.
[51] K. Doi, J. McCracken, J. Peisach, P. Aisen, *J. Biol. Chem.* **1988**, *263*, 5757.
[52] J. B. Vincent, M. W. Crowder, B. A. Averill, *Biochemistry* **1991**, *30*, 3025; D. C. Crans, C. M. Simone, R. C. Holz, L. Que, Jr., *ibid.* **1992**, *31*, 11731; M. W. Crowder, J. B. Vincent, B. A. Averill, *Biochemistry* **1992**, *31*, 9603; E. P. Day, S. S. David, J. Peterson, W. R. Dunham, J. J. Bonvoisin, R. H. Sands, L. Que, Jr., *J. Biol. Chem.* **1988**, *263*, 15561; J. C. Davis, B. A. Averill, *Proc. Natl. Acad. Sci. USA* **1982**, *79*, 4623.
[53] K. Doi, R. Gupta, P. Aisen, *J. Biol. Chem.* **1987**, *262*, 6982.
[54] Z. Wang, L. Ming, L. Que, Jr., J. B. Vincent, M. W. Crowder, B. A. Averill, *Biochemistry* **1992**, *31*, 5263; R. C. Holz, L. Que, Jr., L. Ming, *J. Am. Chem. Soc.* **1992**, *114*, 4434.
[55] S. M. Kauzlarich, B. K. Teo, T. Zirino, S. Burman, J. C. Davis, B. A. Averill, *Inorg. Chem.* **1986**, *25*, 2781; A. E. True, R. C. Scarrow, C. R. Randall, R. C. Holz, L. Que, Jr., *J. Am. Chem. Soc.* **1993**, *115*, 4246.
[56] S. Gehring, P. Fleischhauer, W. Haase, M. Dietrich, H. Witzel, *Biol. Chem. Hoppe-Seyler* **1990**, *371*, 786.
[57] E. Sinn, C. J. O'Connor, *Inorg. Chim. Acta* **1983**, *78*, L13.
[58] D. L. Wang, R. C. Holz, S. S. David, L. Que, Jr., M. T. Stankovich, *Biochemistry* **1991**, *30*, 8187.
[59] B. C. Antanaitis, T. Strekas, P. Aisen, *J. Biol. Chem.* **1982**, *257*, 3766; M. P. Allen, A. H. Yamada, F. H. Carpenter, *Biochemistry* **1983**, *22*, 3778.
[60] J. L. Beck, L. A. McConachie, A. C. Summors, W. N. Arnold, J. De Jersey, B. Zerner, *Biochim. Biophys. Acta* **1986**, *869*, 61.
[61] N. Sträter, R. Fröhlich, A. Schiemann, B. Krebs, M. Körner, H. Suerbaum, H. Witzel, *J. Mol. Biol.* **1992**, *224*, 511; B. Stahl, T. Klabunde, H. Witzel, B. Krebs, M. Steup, M. Karas, F. Hillenkamp, *Eur. J. Biochem.* **1994**, *220*, 321.
[62] J. L. Beck, M. J. McArthur, J. de Jersey, B. Zerner, *Inorg. Chim. Acta* **1988**, *153*, 39.
[63] H. Suerbaum, M. Körner, H. Witzel, E. Althaus, B. Mosel, W. Müller-Warmuth, *Eur. J. Biochem.* **1993**, *214*, 313; J. L. Beck, J. de Jersey, B. Zerner, M. P. Hendrich, P. G. Debrunner, *J. Am. Chem. Soc.* **1988**, *110*, 3317.
[64] T. Klabunde, N. Sträter, B. Krebs, H. Witzel, *FEBS Lett.* **1995**, *367*, 56.
[65] R. B. Lauffer, B. C. Antanaitis, P. Aisen, L. Que, Jr, *J. Biol. Chem.* **1983**, *258*, 14212.
[66] M. A. Aquino, J. Lim, A. Sykes, *J. Chem. Soc. Dalton Trans.* **1992**, 2135.
[67] M. A. Aquino, J. Lim, A. Sykes, *J. Chem. Soc. Dalton Trans.* **1994**, 429.
[68] E. G. Mueller, M. W. Crowder, B. A. Averill, J. R. Knowles, *J. Am. Chem. Soc.* **1993**, *115*, 2974.
[69] C. J. Wynne, S. E. Hamilton, D. A. Dionysius, J. L. Beck, J. De Jersey, *Arch. Biochem. Biophys.* **1995**, *319*, 133.
[70] P. Cohen, *Annu. Rev. Biochem.* **1989**, *58*, 453; C. B. Klee, G. F. Draetta, M. J. Hubbard, *Adv. Enzymol.* **1988**, *61*, 149; S. Shenolikar, *Annu. Rev. Cell Biol.*

1994, *10*, 55; S. Wera, B. A. Hemmings, *Biochem. J.* **1995**, *311*, 17; D. L. Lohse, J. M. Denu, J. E. Dixon, *Structure* **1995**, *3*, 987; W. P. Taylor, T. S. Widlanski, *Chem. Biol.* **1995**, *2*, 713; L. M. Ballou, E. H. Fischer in *The Enzymes*, *Vol. 17*, 3rd ed. (Eds.: P. D. Boyer, E. G. Krebs), Academic Press, Orlando, **1986**, p. 311; D. Barford, *Curr. Opin. Struct. Biol.* **1995**, *5*, 728.

[71] T. S. Ingebritsen, P. Cohen, *Eur. J. Biochem.* **1983**, *132*, 255.

[72] M. M. King, C. Y. Huang, *J. Biol. Chem.* **1984**, *259*, 8847.

[73] D. J. Wolff, D. W. Sved, *J. Biol. Chem.* **1985**, *260*, 4195; C. J. Pallen, J. H. Wang, *ibid.* **1984**, *259*, 6134; R. C. Gupta, R. L. Khandelwal, P. V. Sulakhe, *FEBS Lett.* **1984**, *169*, 251.

[74] K. F. Qin, S. Khangulov, C. Liu, C. Y. Huang, *FASEB J.* **1995**, *9*, A1347; L. Yu, A. Haddy, F. Rusnak, *J. Am. Chem. Soc.* **1995**, *117*, 10147.

[75] B. L. Martin, D. J. Graves, *J. Biol. Chem.* **1986**, *261*, 14545.

[76] B. L. Martin, D. J. Graves, *Biochim. Biophys. Acta* **1994**, *1206*, 136.

[77] B. Martin, C. J. Pallen, J. H. Wang, D. J. Graves, *J. Biol. Chem.* **1985**, *260*, 14932.

[78] D. R. Alessi, A. J. Street, P. Cohen, P. T. Cohen, *Eur. J. Biochem.* **1993**, *213*, 1055.

[79] Y. Chu, E. Y. Lee, K. K. Schlender, *J. Biol. Chem.* **1996**, *271*, 2574.

[80] T. S. Wang, *Annu. Rev. Biochem.* **1991**, *60*, 513; K. J. Marians, *ibid.* **1992**, *61*, 673.

[81] C. M. Joyce, T. A. Steitz, *Annu. Rev. Biochem.* **1994**, *63*, 777.

[82] D. L. Ollis, P. Brick, R. Hamlin, N. G. Xuong, T. A. Steitz, *Nature* **1985**, *313*, 762.

[83] P. S. Freemont, J. M. Friedman, L. S. Beese, M. R. Sanderson, T. A. Steitz, *Proc. Natl. Acad. Sci. USA* **1988**, *85*, 8924.

[84] V. Derbyshire, P. S. Freemont, M. R. Sanderson, L. Beese, J. M. Friedman, C. M. Joyce, T. A. Steitz, *Science* **1988**, *240*, 199.

[85] L. S. Beese, T. A. Steitz, *EMBO J.* **1991**, *10*, 25.

[86] L. S. Beese, V. Derbyshire, T. A. Steitz, *Science* **1993**, *260*, 352.

[87] L. S. Beese, J. M. Friedman, T. A. Steitz, *Biochemistry* **1993**, *32*, 14095.

[88] L. A. Kohlstaedt, J. Wang, J. M. Friedman, P. A. Rice, T. A. Steitz, *Science* **1992**, *256*, 1783.

[89] A. Jacobo-Molina, J. Ding, R. G. Nanni, A. D. Clark, X. Lu, C. Tantillo, R. L. Williams, G. Kamer, A. L. Ferris, P. Clark, A. Hizi, S. H. Hughes, E. Arnold, *Proc. Natl. Acad. Sci. USA* **1993**, *90*, 6320.

[90] S. J. Smerdon, J. Jäger, J. Wang, L. A. Kohlstaedt, A. J. Chirino, J. M. Friedman, P. A. Rice, T. A. Steitz, *Proc. Natl. Acad. Sci. USA* **1994**, *91*, 3911; J. Wang, S. J. Smerdon, J. Jäger, L. A. Kohlstaedt, P. A. Rice, J. M. Friedman, T. A. Steitz, *ibid.* **1994**, *91*, 7242; P. H. Patel, A. Jacobo-Molina, J. Ding, C. Tantillo, A. D. Clark, Jr., R. Raag, R. G. Nanni, S. H. Hughes, E. Arnold, *Biochemistry* **1995**, *34*, 5351; R. Esnouf, J. Ren, C. Ross, Y. Jones, D. Stammers, D. Stuart, *Nat. Struct. Biol.* **1995**, *2*, 303.

[91] D. W. Rodgers, S. J. Gamblin, B. A. Harris, S. Ray, J. S. Culp, B. Hellmig, D. J. Woolf, C. Debouck, S. C. Harrison, *Proc. Natl. Acad. Sci. USA* **1995**, *92*, 1222.

[92] J. F. Davies II, R. J. Almassy, Z. Hostomska, R. Ferre, Z. Hostomsky, *Cell* **1994**, *76*, 1123.

[93] H. Pelletier, M. R. Sawaya, A. Kumar, S. H. Wilson, J. Kraut, *Science* **1994**, *264*, 1891.

[94] M. R. Sawaya, H. Pelletier, A. Kumar, S. H. Wilson, J. Kraut, *Science* **1994**, *264*, 1930.

[95] R. Sousa, Y. Chung, J. P. Rose, B. Wang, *Nature* **1993**, *364*, 593.

[96] Y. Kim, S. H. Eom, J. Wang, D. Lee, S. W. Suh, T. A. Steitz, *Nature* **1995**, *376*, 612.

[97] L. Blanco, A. Bernad, M. A. Blasco, M. Salas, *Gene* **1991**, *100*, 27; O. Poch, I. Sauvaget, M. Delarue, N. Tordo, *EMBO J.* **1989**, *8*, 3867; D. K. Braithwaite, J. Ito, *Nucleic Acids Res.* **1993**, *21*, 787; M. Delarue, O. Poch, N. Tordo, D. Moras, P. Argos, *Protein Eng.: Proc. Int. Conf. Protein Eng. 2nd* **1990**, *3*, 461.

[98] E. Arnold, J. Ding, S. H. Hughes, Z. Hostomsky, *Curr. Opin. Struct. Biol.* **1995**, *5*, 27.

[99] T. A. Steitz, S. Smerdon, J. Jäger, J. Wang, L. A. Kohlstaedt, J. M. Friedman, L. S. Beese, P. A. Rice, *Cold Spring Harbor Symp. Quant. Biol.* **1993**, *63*, 495.

[100] C. M. Joyce, X. Sun, N. D. Grindley, *J. Biol. Chem.* **1992**, *267*, 24485.

[101] A. H. Polesky, M. E. Dahlberg, S. J. Benkovic, N. D. Grindley, C. M. Joyce, *J. Biol. Chem.* **1992**, *267*, 8417; A. H. Polesky, T. A. Steitz, N. D. Grindley, C. M. Joyce, *ibid.* **1990**, *265*, 14579; W. C. Copeland, T. S. Wang, *ibid.* **1993**, *268*, 11028; A. Bernad, J. M. Lazaro, M. Salas, L. Blanco, *Proc. Natl. Acad. Sci. USA* **1990**, *87*, 4610; S. Sankar, A. G. Porter, *J. Biol. Chem.* **1992**, *267*, 10168; M. A. Blasco, J. M. Lazaro, L. Blanco, M. Salas, *ibid.* **1993**, *268*, 24106; G. Jung, M. C. Leavitt, M. Schultz, J. Ito, *Biochem. Biophys. Res. Commun.* **1990**, *170*, 1294.

[102] K. L. Menge, Z. Hostomsky, B. R. Nodes, G. O. Hudson, S. Rahmati, E. W. Moomaw, R. J. Almassy, Z. Hostomska, *Biochemistry* **1995**, *34*, 15934.

[103] A. S. Mildvan, L. A. Loeb, *CRC Crit. Rev. Biochem.* **1979**, *6*, 219.

[104] F. Focher, A. Verri, G. Maga, S. Spadari, U. Hübscher, *FEBS Lett.* **1990**, *259*, 349.

[105] G. P. Mullen, E. H. Serpersu, L. J. Ferrin, L. A. Loeb, A. S. Mildvan, *J. Biol. Chem.* **1990**, *265*, 14327; S. Tabor, C. C. Richardson, *Proc. Natl. Acad. Sci. USA* **1989**, *86*, 4076.

[106] D. Solaiman, F. Y. Wu, *Biochemistry* **1985**, *24*, 5077; D. P. Giedroc, J. E. Coleman, *Biochemistry* **1986**, *25*, 4969; L. J. Ferrin, A. S. Mildvan, L. A. Loeb, *Biochem. Biophys. Res. Commun.* **1983**, *112*, 723.

[107] M. F. Goodman, S. Creighton, L. B. Bloom, J. Petruska, *Crit. Rev. Biochem. Mol. Biol.* **1993**, *28*, 83; M. D. Lai, K. L. Beattie, *Mutat. Res.* **1988**, *198*, 27; W. S. El-Deiry, A. G. So, K. M. Downey, *Biochemistry* **1988**, *27*, 546; G. G. Hillebrand, K. L. Beattie, *Nucleic Acids Res.* **1984**, *12*, 3173; S. K. Niyogi, R. P. Feldman, *ibid.* **1981**, *9*, 2615; H. Pelletier, M. R. Sawaya, W. Wolfle, S. H. Wilson, J. Kraut, *Biochemistry*, submitted (two papers).

[108] N. T. Christie, D. M. Tummolo, *Biol. Trace Elem. Res.* **1989**, *21*, 3.

[109] J. P. Slater, I. Tamir, L. A. Loeb, A. S. Mildvan, *J. Biol. Chem.* **1972**, *247*, 6784.

[110] T. A. Steitz, *Curr. Opin. Struct. Biol.* **1993**, *3*, 31.

[111] Pelletier et al., UCSF, note that they could not reproduce this metal binding behavior in 31 kDa apo-enzyme crystals of pol-β (unpublished results, [107]).

[112] T. A. Steitz, S. J. Smerdon, J. Jäger, C. M. Joyce, *Science* **1994**, *266*, 2022.

[113] R. S. Brody, S. Adler, P. Modrich, W. J. Stec, Z. J. Leznikowski, P. A. Frey, *Biochemistry* **1982**, *21*, 2570; P. M. Burgers, F. Eckstein, *J. Biol. Chem.* **1979**, *254*, 6889; P. J. Romaniuk, F. Eckstein, *ibid.* **1982**, *257*, 7684; R. S. Brody, P. A. Frey, *Biochemistry* **1981**, *20*, 1245; P. A. Bartlett, F. Eckstein, *J. Biol. Chem.* **1982**, *257*, 8879; S. Hopkins, P. A. Furman, G. R. Painter, *Biochem. Biophys. Res. Commun.* **1989**, *163*, 106.

[114] P. A. Osumi-Davis, M. C. de Aguilera, R. W. Woody, A. Woody, *J. Mol. Biol.* **1992**, *226*, 37; I. Joung, M. S. Horwitz, J. A. Engler, *Virology* **1991**, *184*, 235; Q. Dong, W. C. Copeland, T. S. Wang, *J. Biol. Chem.* **1993**, *268*, 24163.

[115] P. S. Freemont, D. L. Ollis, T. A. Steitz, C. M. Joyce, *Proteins* **1986**, *1*, 66.

[116] V. Derbyshire, N. D. Grindley, C. M. Joyce, *EMBO J.* **1991**, *10*, 17.

[117] C. M. Joyce, T. A. Steitz, *Trends Biochem. Sci.* **1987**, *12*, 288.

[118] J. A. Esteban, M. S. Soengas, M. Salas, L. Blanco, *J. Biol. Chem.* **1994**, *269*, 31946; A. Bernad, L. Blanco, J. M. Lazaro, G. Martin, M. Salas, *Cell* **1989**, *59*, 219; L. J. Reha-Krantz, *Gene* **1992**, *112*, 133.

[119] A. P. Gupta, S. J. Benkovic, *Biochemistry* **1984**, *23*, 5874.

[120] I. R. Lehman, C. C. Richardson, *J. Biol. Chem.* **1964**, *239*, 233; H. Han, J. M. Rifkind, A. S. Mildvan, *Biochemistry* **1991**, *30*, 11104.

[121] M. Fothergill, M. F. Goodman, J. Petruska, A. Warshel, *J. Am. Chem. Soc.* **1995**, *117*, 11619.

[122] R. K. Saiki, D. H. Gelfand, S. Stoffel, S. J. Scharf, R. Higuchi, G. T. Horn, K. B. Mullis, H. A. Ehrlich, *Science* **1988**, *239*, 487.

[123] R. J. Crouch, *New Biol.* **1990**, *2*, 771.

[124] F. Oyama, R. Kikuchi, R. J. Crouch, T. Uchida, *J. Biol. Chem.* **1989**, *264*, 18808; M. S. Krug, S. L. Berger, *Proc. Natl. Acad. Sci. USA* **1989**, *86*, 3539.

[125] Z. Hostomsky, Z. Hostomska, G. O. Hudson, E. W. Moomaw, B. R. Nodes, *Proc. Natl. Acad. Sci. USA* **1991**, *88*, 1148.

[126] J. F. Davies, Z. Hostomska, Z. Hostomsky, S. R. Jordan, D. A. Matthews, *Science* **1991**, *252*, 88.

[127] A crystal structure of an active RNase H domain of HIV-RT was obtained later by D. Chattopadhyay, B. C. Finzel, S. H. Munson, D. B. Evans, S. K. Sharma, N. A. Strakalaitis, D. P. Brunner, F. M. Eckenrode, Z. Dauter, Ch. Betzel, H. M. Einspahr, *Acta Crystallogr. Sect. D* **1993**, *49*, 423. No divalent metal ions are bound to the enzyme in this structure determination.

[128] M. Starnes, Y. Cheng, *J. Biol. Chem.* **1989**, *264*, 7073.

[129] R. F. Doolittle, D. Feng, M. S. Johnson, M. A. McClure, *Q. Rev. Biol.* **1989**, *64*, 1.

[130] M. S. Johnson, M. A. McClure, D. Feng, J. Gray, R. F. Doolittle, *Proc. Natl. Acad. Sci. USA* **1986**, *83*, 7648; W. Yang, W. A. Hendrickson, R. J. Crouch, Y. Satow, *Science* **1990**, *249*, 1398; K. Katayanagi, M. Miyagawa, M. Matsushima, M. Ishikawa, S. Kanaya, M. Ikehara, T. Matsuzaki, K. Morikawa, *Nature* **1990**, *347*, 306.

[131] K. Katayanagi, M. Miyagawa, M. Matsushima, M. Ishikawa, S. Kanaya, H. Nakamura, M. Ikehara, T. Matsuzaki, K. Morikawa, *J. Mol. Biol.* **1992**, *223*, 1029; K. Katayanagi, M. Okumura, K. Morikawa, *Proteins* **1993**, *17*, 337.

[132] S. Kanaya, A. Kohara, Y. Miura, A. Sekiguchi, S. Iwai, H. Inoue, E. Ohtsuka, M. Ikehara, *J. Biol. Chem.* **1990**, *265*, 4615.

[133] H. W. Huang, J. A. Cowan, *Eur. J. Biochem.* **1994**, *219*, 253.

[134] F. Dyda, A. B. Hickman, T. M. Jenkins, A. Engelman, R. Craigie, D. R. Davies, *Science* **1994**, *266*, 1981.

[135] G. Bujacz, M. Jaskolski, J. Alexandratos, A. Wlodawer, G. Merkel, R. A. Katz, A. M. Skalka, *J. Mol. Biol.* **1995**, *253*, 333.

[136] G. Bujacz, M. Jaskolski, J. Alexandratos, A. Wlodawer, G. Merkel, R. A. Katz, A. M. Skalka, *Structure* **1996**, *4*, 89.

[137] P. Rice, K. Mizuuchi, *Cell* **1995**, *82*, 209.

[138] M. Ariyoshi, D. G. Vassylyev, H. Iwasaki, H. Nakamura, H. Shinagawa, K. Morikawa, *Cell* **1994**, *78*, 1063.

[139] W. Yang, T. A. Steitz, *Structure* **1995**, *3*, 131.

[140] M. Newman, T. Strzelecka, L. F. Dorner, I. Schildkraut, A. K. Aggarwal, *Science* **1995**, *269*, 656.

[141] D. Kostrewa, F. K. Winkler, *Biochemistry* **1995**, *34*, 683.

[142] I. Vipond, G. S. Baldwin, S. E. Halford, *Biochemistry* **1995**, *34*, 697; G. S. Baldwin, I. Vipond, S. E. Halford, *ibid.* **1995**, *34*, 705.
[143] D. Bozic, S. Grazulis, V. Siksnys, R. Huber, *J. Mol. Biol.* **1996**, *255*, 176.
[144] F. K. Winkler, D. W. Banner, C. Oefner, D. Tsernoglou, R. S. Brown, S. P. Heathman, R. K. Bryan, P. D. Martin, K. Petratos, K. S. Wilson, *EMBO J.* **1993**, *12*, 1781.
[145] Y. Kim, J. C. Grable, P. J. Choi, P. Greene, J. M. Rosenberg, *Science* **1990**, *249*, 1307.
[146] X. Cheng, K. Balendiran, I. Schildkraut, J. E. Anderson, *EMBO J.* **1994**, *13*, 3927.
[147] S. Altman, *Angew. Chem.* **1990**, *102*, 735; *Angew. Chem. Int. Ed. Engl.* **1990**, *29*, 749; T. R. Cech, *ibid.* **1990**, *102*, 745 and **1990**, *29*, 759; B. L. Iverson, *Chem. Biol.* **1995**, *2*, 67; T. R. Cech, A. J. Zaug, P. J. Grabowski, *Cell* **1981**, *27*, 487; C. Guerrier-Takada, K. Gardiner, T. Marsh, N. Pace, S. Altman, *ibid.* **1983**, *35*, 849.
[148] T. A. Steitz, J. A. Steitz, *Proc. Natl. Acad. Sci. USA* **1993**, *90*, 6498; J. A. Piccirilli, J. S. Vyle, M. H. Caruthers, T. R. Cech, *Nature* **1993**, *361*, 85; T. Shimayama, S. Nishikawa, K. Taira, *FEBS Lett.* **1995**, *368*, 304.
[149] H. Ke, C. M. Thorpe, B. A. Seaton, F. Marcus, W. N. Lipscomb, *Proc. Natl. Acad. Sci. USA* **1989**, *86*, 1475.
[150] R. Bone, J. P. Springer, J. R. Atack, *Proc. Natl. Acad. Sci. USA* **1992**, *89*, 10031; M. Fothergill, M. F. Goodman, J. Petruska, A. Warshel, *J. Am. Chem. Soc.* **1995**, *117*, 11619.
[151] J. D. York, J. W. Ponder, Z. Chen, F. Matthews, P. W. Majerus, *Biochemistry* **1994**, *33*, 13164.
[152] Y. Zhang, J. Liang, W. N. Lipscomb, *Biochem. Biophys. Res. Commun.* **1993**, *190*, 1080.
[153] A. F. Neuwald, J. D. York, P. W. Majerus, *FEBS Lett.* **1991**, *294*, 16; R. E. Diehl, P. Whiting, J. Potter, N. Gee, C. I. Ragan, D. Linemeyer, R. Schoepfer, C. Bennett, R. A. Dixon, *J. Biol. Chem.* **1990**, *265*, 5946; J. D. York, J. W. Ponder, P. W. Majerus, *Proc. Natl. Acad. Sci. USA* **1995**, *92*, 5149.
[154] P. A. Benkovic, C. A. Caperelli, M. M. de Maine, S. J. Benkovic, *Proc. Natl. Acad. Sci. USA* **1978**, *75*, 2185.
[155] J. Liang, Y. Zhang, S. Huang, H. Ke, W. N. Lipscomb, *Proc. Robert A. Welch Found. Conf. Chem. Res.* **1992**, *36*, 57.
[156] S. J. Benkovic, M. M. de Maine, *Adv. Enzymol.* **1982**, *53*, 45.
[157] S. J. Pilkis, T. H. Claus, P. D. Kountz, M. El-Maghrabi in *The Enzymes, Vol. 18*, 3rd ed. (Eds.: P. D. Boyer, E. G. Krebs), Academic Press, Orlando, **1987**, p. 3.
[158] G. Gomori, *J. Biol. Chem.* **1943**, *148*, 139; H. G. Nimmo, K. F. Tipton, *Biochem. J.* **1975**, *145*, 323.
[159] C. B. Libby, W. A. Frey, J. J. Villafranca, S. J. Benkovic, *J. Biol. Chem.* **1975**, *250*, 7564; S. Pontremoli, E. Melloni, F. Salamino, B. Sparatore, B. L. Horecker, *Arch. Biochem. Biophys.* **1978**, *188*, 90.
[160] S. Pontremoli, B. Sparatore, F. Salamino, E. Melloni, B. L. Horecker, *Arch. Biochem. Biophys.* **1979**, *194*, 481.
[161] F. O. Pedrosa, S. Pontremoli, B. L. Horecker, *Proc. Natl. Acad. Sci. USA* **1977**, *74*, 2742; G. A. Tejwani, F. O. Pedrosa, S. Pontremoli, B. L. Horecker, *ibid.* **1976**, *73*, 2692; T. Ikeda, K. Kimura, T. Hama, N. Tamaki, *J. Biochem.* **1980**, *87*, 179.
[162] S. Pontremoli, E. Grazi, A. Accorsi, *Biochem. Biophys. Res. Commun.* **1969**, *37*, 597; E. Grazi, A. Accorsi, S. Pontremoli, *J. Biol. Chem.* **1971**, *246*, 6651; P. A. Benkovic, W. A. Frey, S. J. Benkovic, *Arch. Biochem. Biophys.* **1978**, *191*, 719.
[163] P. L. Domanico, J. F. Rahil, S. J. Benkovic, *Biochemistry* **1985**, *24*, 1623.
[164] S. J. Benkovic, J. L. Engle, A. S. Mildvan, *Biochem. Biophys. Res. Commun.* **1972**, *47*, 852; T. A. Koerner, Jr., L. W. Cary, N. S. Bhacca, E. S. Younathan, *ibid.* **1973**, *51*, 543; C. F. Midelfort, R. K. Gupta, I. A. Rose, *Biochemistry* **1976**, *15*, 2178.
[165] W. A. Frey, R. Fishbein, M. M. de Maine, S. J. Benkovic, *ibid.* **1977**, *16*, 2479.
[166] C. J. Marcus, *J. Biol. Chem.* **1976**, *251*, 2963.
[167] H. Ke, C. M. Thorpe, B. A. Seaton, W. N. Lipscomb, F. Marcus, *J. Mol. Biol.* **1989**, *212*, 513; H. Ke, Y. Zhang, W. N. Lipscomb, *Proc. Natl. Acad. Sci. USA* **1990**, *87*, 5243; H. Ke, Y. Zhang, J. Liang, W. N. Lipscomb, *ibid.* **1991**, *88*, 2989; J. Liang, S. Huang, Y. Zhang, H. Ke, W. N. Lipscomb, *ibid.* **1992**, *89*, 2404.
[168] H. Ke, J. Liang, Y. Zhang, W. N. Lipscomb, *Biochemistry* **1991**, *30*, 4412; J. Liang, Y. Zhang, S. Huang, W. N. Lipscomb, *Proc. Natl. Acad. Sci. USA* **1993**, *90*, 2132.
[169] Y. Zhang, J. Liang, S. Huang, H. Ke, W. N. Lipscomb, *Biochemistry* **1993**, *32*, 1844.
170] V. Villeret, S. Huang, H. J. Fromm, W. N. Lipscomb, *Proc. Natl. Acad. Sci. USA* **1995**, *92*, 8916.
[171] V. Villeret, S. Huang, Y. Zhang, W. N. Lipscomb, *Biochemistry* **1995**, *34*, 4307.
[172] M. Gidh-Jain, Y. Zhang, P. D. van Poelje, J. Liang, S. Huang, J. Kim, J. T. Elliott, M. D. Erion, S. J. Pilkis, M. R. El-Maghrabi, W. N. Lipscomb, *J. Biol. Chem.* **1994**, *269*, 27732.
[173] V. Villeret, S. Huang, Y. Zhang, Y. Xue, W. N. Lipscomb, *Biochemistry* **1995**, *34*, 4299.
[174] H. Ke, W. N. Lipscomb, Harvard University, unpublished results.
[175] R. Zhang, H. J. Fromm, *Biochemistry* **1995**, *34*, 8190.
[176] L. Shyur, R. Zhang, H. J. Fromm, *Arch. Biochem. Biophys.* **1995**, *319*, 123; M. Chen, L. Chen, H. J. Fromm, *J. Biol. Chem.* **1994**, *269*, 5554; L. Chen, R. Hegde, M. Chen, H. J. Fromm, *Arch. Biochem. Biophys.* **1993**, *307*, 350; R. Zhang, L. Chen, V. Villeret, H. J. Fromm, *J. Biol. Chem.* **1995**, *270*, 54; M. El-Maghrabi, M. Gidh-Jain, L. R. Austin, S. J. Pilkis, *ibid.* **1993**, *268*, 9466; M. El-Maghrabi, L. R. Austin, J. J. Correia, S. J. Pilkis, *ibid.* **1992**, *267*, 6526; M. Gidh-Jain, Y. Zhang, P. D. van Poelje, J. Liang, S. Huang, J. Kim, J. T. Elliot, M. D. Erion, S. J. Pilkis, M. El-Maghrabi, W. N. Lipscomb, *ibid.* **1994**, *269*, 27732.
[177] N. Kelley, E. L. Giroux, G. Lu, E. R. Kantrowitz, *Biochem. Biophys. Res. Commun.* **1996**, *219*, 848.
[178] E. Hubert, J. Villanueva, A. Gonzalez, F. Marcus, *Arch. Biochem. Biophys.* **1970**, *138*, 590; W. J. Black, A. Van Tol, J. Fernando, B. L. Horecker, *ibid.* **1972**, *151*, 576; G. Colombo, F. Marcus, *J. Biol. Chem.* **1973**, *248*, 2743; K. Nakashima, S. Tuboi, *ibid.* **1976**, *251*, 4315; F. Marcus, M. M. Hosey, *ibid.* **1980**, *255*, 2481.
[179] J. R. Atack, H. B. Broughton, S. J. Pollack, *FEBS Lett.* **1995**, *361*, 1.
[180] F. Strasser, P. D. Pelton, A. J. Ganzhorn, *Biochem. J.* **1995**, *307*, 585.
[181] S. J. Pollack, J. R. Atack, M. R. Knowles, G. McAllister, C. Ragan, R. Baker, S. R. Fletcher, L. L. Iversen, H. B. Broughton, *Proc. Natl. Acad. Sci. USA* **1994**, *91*, 5766.
[182] A. J. Ganzhorn, M. Chanal, *Biochemistry* **1990**, *29*, 6065.
[183] A. P. Leech, G. R. Baker, J. K. Shute, M. A. Cohen, D. Gani, *Eur. J. Biochem.* **1993**, *212*, 693.
[184] R. Bone, L. Frank, J. P. Springer, J. R. Atack, *Biochemistry* **1994**, *33*, 9468.
[185] R. C. Inhorn, P. W. Majerus, *J. Biol. Chem.* **1987**, *262*, 15946.
[186] J. K. Shute, R. Baker, D. C. Billington, D. Gani, *J. Chem. Soc. Chem. Commun.* **1988**, 626.
[187] R. Bone, L. Frank, J. P. Springer, S. J. Pollack, S. Osborne, J. R. Atack, M. R. Knowles, G. McAllister, C. Ragan, H. B. Broughton, R. Baker, S. R. Fletcher, *Biochemistry* **1994**, *33*, 9460.
[188] Due to its low scattering power lithium is difficult to detect in protein crystal structures.
[189] S. J. Pollack, M. R. Knowles, J. R. Atack, H. B. Broughton, I. Ragan, S. Osborne, G. McAllister, *Eur. J. Biochem.* **1993**, *217*, 281.
[190] R. Baker, J. J. Kulagowski, D. C. Billington, P. D. Leeson, I. C. Lennon, N. Liverton, *J. Chem. Soc. Chem. Commun.* **1989**, 1383.
[191] B. V. Potter, D. Lampe, *Angew. Chem.* **1995**, *107*, 2085; *Angew. Chem. Int. Ed. Engl.* **1995**, *34*, 1933; P. W. Majerus, T. S. Ross, T. W. Cunningham, K. K. Caldwell, A. B. Jefferson, V. S. Bansal, *Cell* **1990**, *63*, 459; P. W. Majerus, *Annu. Rev. Biochem.* **1992**, *61*, 225.
[192] R. C. Inhorn, P. W. Majerus, *J. Biol. Chem.* **1988**, *263*, 14559.
[193] R. C. Inhorn, V. S. Bansal, P. W. Majerus, *Proc. Natl. Acad. Sci. USA* **1987**, *84*, 2170.
[194] J. D. York, J. E. Saffitz, P. W. Majerus, *J. Biol. Chem.* **1994**, *269*, 19992.
[195] The active sites were superimposed on the basis of the C_α coordinates of only those homologous residues that are shown in the figure and the two metal ions using a least-squares algorithm implemented in the program O: T. A. Jones, M. Kjeldgaard in *From First Map to Final Model. Proceedings of the CCP4 Study Weekend* (Eds. S. Bailey, R. Hubbard, D. Waller), Daresbury Laboratory, Warrington, **1994**, p. 1.
[196] A. Volbeda, A. Lahm, F. Sakiyama, D. Suck, *EMBO J.* **1991**, *10*, 1607.
[197] E. Hough, L. K. Hansen, B. Birknes, K. Jynge, S. Hansen, A. Hordvik, C. Little, E. Dodson, Z. Derewenda, *Nature* **1989**, *338*, 357.
[198] A. C. Ottolenghi, *Biochim. Biophys. Acta* **1965**, *106*, 510.
[199] M. A. Clark, R. G. Shorr, J. S. Bomalaski, *Biochem. Biophys. Res. Commun.* **1986**, *140*, 114.
[200] C. Little, A. Otnaess, *Biochim. Biophys. Acta* **1975**, *391*, 326; C. Little, *Acta Chem. Scand. B* **1981**, *35*, 39.
[201] C. Little, S. Aakre, M. G. Rumsby, K. Gwarsha, *Biochem. J.* **1982**, *207*, 117; A. Otnaess, *FEBS Lett.* **1980**, *114*, 202.
[202] R. Bicknell, G. R. Hanson, B. Holmquist, *Biochemistry* **1986**, *25*, 4219.
[203] S. Hansen, E. Hough, L. A. Svensson, Y. Wong, S. F. Martin, *J. Mol. Biol.* **1993**, *234*, 179.
[204] S. Hansen, L. K. Hansen, E. Hough, *J. Mol. Biol.* **1992**, *225*, 543.
[205] S. Hansen, L. K. Hansen, E. Hough, *J. Mol. Biol.* **1993**, *231*, 870.
[206] S. F. Martin, Y. Wong, A. S. Wagman, *J. Org. Chem.* **1994**, *59*, 4821.
[207] S. Sundell, S. Hansen, E. Hough, *Protein Eng.: Proc. Int. Conf. Protein Eng. 2nd* **1994**, 7, 571.
[208] K. Shishido, T. Ando in *Nucleases* (Eds.: S. M. Linn, R. J. Roberts), Spring Harbor Laboratory Press, New York, **1982**, p. 155; B. V. Potter, B. A. Connolly, F. Eckstein, *Biochemistry* **1983**, *22*, 1369; D. Suck in *Molecular Structure and Life* (Eds.: T. Kyogaku, Y. Nishimura), CRC, Boca Raton, FL, **1992**, p. 141; M. A. Chaudhry, M. Weinfeld, *Nucleic Acids Res.* **1995**, *23*, 3805; H. C. Box, E. E. Budzinski, M. S. Evans, J. B. French, A. E. Maccubbin, *Biochim. Biophys. Acta* **1993**, *1161*, 291.
[209] M. Fujimoto, A. Kuninaka, H. Yoshino, *Agr. Biol. Chem.* **1974**, *38*, 785.
[210] M. Fujimoto, A. Kuninaka, H. Yoshino, *Agr. Biol. Chem.* **1974**, *38*, 1555; M. Fujimoto, K. Fujiyama, A. Kuninaka, H. Yoshino, *ibid.* **1974**, *38*, 2141; M. Fujimoto, A. Kuninaka, H. Yoshino, *ibid.* **1975**, *39*, 1991; *ibid.* **1975**, *39*, 2145.
[211] S. Spitzer, F. Eckstein, *Nucleic Acids Res.* **1988**, *16*, 11691.

[212] D. Suck, EMBL Heidelberg, personal communication. The coordinates used to generate the nuclease P1 active site in Figure 3 are of the orthorhombic crystal form of *Penicillium citrinium* nuclease P1 [193].
[213] K. Shishido, N. Habuka, *Biochim. Biophys. Acta* **1986**, *884*, 215.
[214] B. V. Potter, P. J. Romaniuk, F. Eckstein, *J. Biol. Chem.* **1983**, *258*, 1758.
[215] B. S. Cooperman, *Methods Enzymol.* **1982**, *87*, 526; R. Lahti, *Microbiol. Rev.* **1983**, *47*, 169.
[216] K. M. Welsh, A. Jacobyansky, B. Springs, B. S. Cooperman, *Biochemistry* **1983**, *22*, 2243.
[217] J. Kankare, T. Salminen, R. Lahti, B. S. Cooperman, A. B. Baykov, A. Goldman, *Acta Crystallogr. Sect. D* **1996**, *52*, 551; J. Kankare, G. S. Neal, T. Salminen, T. Glumhoff, B. S. Cooperman, R. Lahti, A. Goldman, *Protein Eng.: Proc. Int. Conf. Protein Eng. 2nd* **1994**, *7*, 823; V. Yu. Oganessyan, S. A. Kurilova, N. N. Vorobyeva, T. I. Nazarova, A. N. Popov, A. A. Lebedev, S. M. Avaeva, E. H. Harutyunyan, *FEBS Lett.* **1994**, *348*, 301.
[218] J. Kankare, T. Salminen, R. Lahti, B. S. Cooperman, A. A. Baykov, A. Goldman, *Biochemistry* **1996**, *35*, 4670.
[219] E. G. Harutyunyan, V. Yu. Oganesyan, N. N. Oganesyan, S. S. Terzyan, A. N. Popov, S. V. Rubinskii, B. K. Vainshtein, T. I. Nazarova, S. A. Kurilova, N. N. Vorob'eva, S. M. Avaeva, *Crystallogr. Rep.* **1996**, *41*, 77 (*Kristallografiya* **1996**, *41*, 96).
[220] N. Y. Chirgadze, I. P. Kuranova, N. A. Nevskaya, A. V. Teplyakov, K. Wilson, B. V. Strokopytov, E. G. Arutyunyan, V. Khene, *Sov. Phys. Crystallogr.* ***Engl. Transl.*** **1991**, *36*, 72 (*Kristallografiya* **1991**, *36*, 128).
[221] A. Teplyakov, G. Obmolova, K. S. Wilson, K. Ishii, H. Kaji, T. Samejima, I. Kuranova, *Protein Sci.* **1994**, *3*, 1098.
[222] B. S. Cooperman, A. A. Baykov, R. Lahti, *Trends Biochem. Sci.* **1992**, *17*, 262.
[223] M. A. Gonzalez, M. R. Webb, K. M. Welsh, B. S. Cooperman, *Biochemistry* **1984**, *23*, 797.
[224] A. A. Baykov, T. Hyytia, S. E. Volk, V. N. Kasho, A. V. Vener, A. Goldman, R. Lahti, B. S. Cooperman, *Biochemistry* **1996**, *35*, 4655.
[225] W. B. Knight, D. Dunaway-Mariano, S. C. Ranson, J. J. Villafranca, *J. Biol. Chem.* **1984**, *259*, 2886.
[226] T. Salminen, J. Käpylä, P. Heikinheimo, J. Kankare, A. Goldman, J. Heinonen, A. A. Baykov, B. S. Cooperman, R. Lahti, *Biochemistry* **1995**, *34*, 782.
[227] D. N. Frick, D. J. Weber, C. Abeygunawardana, A. G. Gittis, M. J. Bessman, A. S. Mildvan, *Biochemistry* **1995**, *34*, 5577.
[228] C. Abeygunawardana, D. J. Weber, A. G. Gittis, D. N. Frick, J. Lin, A.-F. Miller, M. J. Bessman, A. S. Mildvan, *Biochemistry* **1995**, *34*, 14997.
[229] G. D. Markham, E. W. Hafner, C. W. Tabor, H. Tabor, *Methods Enzymol.* **1983**, *94*, 219.
[230] M. Kotb, N. M. Kredich, *Biochim. Biophys. Acta* **1990**, *1039*, 253.
[231] S. H. Mudd, G. L. Cantoni, *J. Biol. Chem.* **1958**, *231*, 481.
[232] C. Zhang, G. D. Markham, R. LoBrutto, *Biochemistry* **1993**, *32*, 9866; G. D. Markham, *ibid.* **1984**, *23*, 470.
[233] G. D. Markham, *J. Biol. Chem.* **1981**, *256*, 1903.
[234] G. D. Markham, *J. Biol. Chem.* **1986**, *261*, 1507.
[235] F. Takusagawa, S. Kamitori, S. Misaki, G. D. Markham, *J. Biol. Chem.* **1996**, *271*, 136.
[236] F. Takusagawa, S. Kamitori, G. D. Markham, *Biochemistry* **1996**, *35*, 2568.
[237] T. D. Meek, J. J. Villafranca, *Biochemistry* **1980**, *19*, 5513; R. E. Weisbrod, A. Meister, *J. Biol. Chem.* **1973**, *248*, 3997.
[238] L. M. Abell, J. J. Villafranca, *Biochemistry* **1991**, *30*, 1413.
[239] M. M. Yamashita, R. J. Almassy, C. A. Janson, D. Cascio, D. Eisenberg, *J. Biol. Chem.* **1989**, *264*, 17681; S. Liaw, C. Pan, D. Eisenberg, *Proc. Natl. Acad. Sci. USA* **1993**, *90*, 4996; R. J. Almassy, C. A. Janson, R. Hamlin, N. H. Xuong, D. Eisenberg, *Nature* **1986**, *323*, 304; S. Liaw, G. Jun, D. Eisenberg, *Biochemistry* **1994**, *33*, 11184.
[240] S. Liaw, D. Eisenberg, *Biochemistry* **1994**, *33*, 675.
[241] J. J. Villafranca, M. S. Balakrishnan, F. C. Wedler *Biochem. Biophys. Res. Commun.* **1977**, *75*, 464.
[242] A. M. Dhalla, B. Li, M. F. Alibhai, K. J. Yost, J. M. Hemmingsen, W. M. Atkins, J. Schineller, J. J. Villafranca, *Protein Sci.* **1994**, *3*, 476.
[243] M. Watanabe, S. Takebe, K. Kobashi, *Chem. Pharm. Bull.* **1991**, *39*, 980; D. P. Dumas, J. R. Wild, F. M. Raushel, *Experientia* **1990**, *46*, 729.
[244] D. P. Dumas, S. R. Caldwell, J. R. Wild, F. M. Raushel, *J. Biol. Chem.* **1989**, *264*, 19659.
[245] T. S. Scanlan, R. C. Reid, *Chem. Biol.* **1995**, *2*, 71.
[246] K. Lai, N. J. Stolowich, J. R. Wild, *Arch. Biochem. Biophys.* **1995**, *318*, 59; D. P. Dumas, H. D. Durst, W. G. Landis, F. M. Raushel, J. R. Wild, *Arch. Biochem. Biophys.* **1990**, *277*, 155.
[247] W. J. Donarski, D. P. Dumas, D. P. Heitmeyer, V. E. Lewis, F. M. Raushel, *Biochemistry* **1989**, *28*, 4650.
[248] G. A. Omburo, J. M. Kuo, L. S. Mullins, F. M. Raushel, *J. Biol. Chem.* **1992**, *267*, 13278.
[249] M. Y. Chae, G. A. Omburo, P. A. Lindahl, F. M. Raushel, *Arch. Biochem. Biophys.* **1995**, *316*, 765.
[250] G. A. Omburo, L. S. Mullins, F. M. Raushel, *Biochemistry* **1993**, *32*, 9148.
[251] D. P. Duma, F. M. Raushel, *J. Biol. Chem.* **1990**, *265*, 21498.
[252] J. A. Banzon, J. M. Kuo, D. R. Fischer, P. J. Stang, F. M. Raushel, *Biochemistry* **1995**, *34*, 750; K. Lai, K. I. Dave, J. R. Wild, *J. Biol. Chem.* **1994**, *269*, 16579.
[253] V. E. Lewis, W. J. Donarski, J. R. Wild, F. M. Raushel, *Biochemistry* **1988**, *27*, 1591.
[254] S. R. Caldwell, J. R. Newcomb, K. A. Schlecht, F. M. Raushel, *Biochemistry* **1991**, *30*, 7438.
[255] S. R. Caldwell, F. M. Raushel, P. M. Weiss, W. W. Cleland, *Biochemistry* **1991**, *30*, 7444.
[256] M. M. Benning, J. M. Kuo, F. M. Raushel, H. M. Holden, *Biochemistry* **1994**, *33*, 15001.
[257] M. M. Benning, J. M. Kuo, F. M. Raushel, H. M. Holden, *Biochemistry* **1995**, *34*, 7973.
[258] S. Hong, J. M. Kuo, L. S. Mullins, F. M. Raushel, *J. Am. Chem. Soc.* **1995**, *117*, 7580.
[259] T. Lundqvist, G. Schneider, *Biochemistry* **1991**, *30*, 904; G. H. Lorimer, M. R. Badger, T. J. Andrews, *ibid.* **1976**, *15*, 529.
[260] E. Jabri, M. B. Carr, R. P. Hausinger, P. A. Karplus, *Science* **1995**, *268*, 998.
[261] R. T. Morrison, R. N. Boyd, *Organic Chemistry*, 5th ed., Allyn and Bacon, Boston, **1987**, p. 768.
[262] a) *Enzyme Mechanisms* (Eds.: M. Page, A. Williams), The Royal Society of Chemistry, London, **1987**; b) A. Williams in ref. [262a], p. 123; c) D. S. Auld in ref. [262a] p. 240.
[263] A. Taylor, *Trends Biochem. Sci.* **1993**, *18*, 167.
[264] A. Taylor, *FASEB J.* **1993**, *7*, 290.
[265] S. H. Wilkes, J. M. Prescott, *J. Biol. Chem.* **1985**, *260*, 13154.
[266] A. Taylor, C. Z. Peltier, F. J. Torre, N. Hakamian, *Biochemistry* **1993**, *32*, 784.
[267] A. B. Shenvi, *Biochemistry* **1986**, *25*, 1286.
[268] J. O. Baker, J. M. Prescott, *Biochem. Biophys. Res. Commun.* **1985**, *130*, 1154.
[269] B. Lejczak, P. Kafarski, J. Zygmunt, *Biochemistry* **1989**, *28*, 3549; P. P. Giannousis, P. A. Bartlett, *J. Med. Chem.* **1987**, *30*, 1603.
[270] L. Andersson, J. MacNeela, R. Wolfenden, *Biochemistry* **1985**, *24*, 330; L. Frick, R. Wolfenden, *Biochim. Biophys. Acta* **1985**, *829*, 311.
[271] C. Kettner, G. I. Glover, J. M. Prescott, *Arch. Biochem. Biophys.* **1974**, *165*, 739.
[272] P. L. Birch, H. A. El-Obeid, M. Akhtar, *Arch. Biochem. Biophys.* **1972**, *148*, 447.
[273] S. L. Harbeson, D. H. Rich, *J. Med. Chem.* **1989**, *32*, 1378.
[274] R. E. Beattie, D. T. Elmore, C. H. Williams, D. J. Guthrie, *Biochem. J.* **1987**, *245*, 285.
[275] H. Kim, W. N. Lipscomb, *Adv. Enzymol.* **1994**, *68*, 153; R. J. Delange, E. L. Smith in *The Enzymes*, *Vol. 3*, 3rd ed. (Ed.: P. D. Boyer), Academic Press, New York, **1971**, p. 81; E. L. Smith, R. L. Hill in *The Enzymes*, *Vol. 4*, 2nd ed. (Eds.: P. D. Boyer, H. Lardy, K. Myrbäck), Academic Press, New York, **1960**, p. 37.
[276] F. H. Carpenter, J. M. Vahl, *J. Biol. Chem.* **1973**, *248*, 294.
[277] G. A. Thompson, F. H. Carpenter, *J. Biol. Chem.* **1976**, *251*, 53.
[278] G. A. Thompson, F. H. Carpenter, *J. Biol. Chem.* **1976**, *251*, 1618.
[279] M. P. Allen, A. H. Yamada, F. H. Carpenter, *Biochemistry* **1983**, *22*, 3778.
[280] H. Kim, W. N. Lipscomb, *Proc. Natl. Acad. Sci. USA* **1993**, *90*, 5006.
[281] J. Berger, M. J. Johnson, *J. Biol. Chem.* **1939**, *130*, 641; M. J. Johnson, G. Johnson, W. H. Peterson, *ibid.* **1936**, *116*, 515; E. L. Smith, D. H. Spackman, *ibid.* **1955**, *212*, 271; E. L. Smith, *ibid.* **1946**, *163*, 15; H. E. Van Wart, S. H. Lin, *Biochemistry* **1981**, *20*, 5682.
[282] S. Himmelhoch, *Arch. Biochem. Biophys.* **1969**, *134*, 597.
[283] C. J. Stirling, S. D. Colloms, J. F. Collins, G. Szatmari, D. J. Sherratt, *EMBO J.* **1989**, *8*, 1623; R. McCulloch, M. E. Burke, D. J. Sherratt, *Mol. Microbiol.* **1994**, *12*, 241.
[284] S. K. Burley, P. R. David, A. Taylor, W. N. Lipscomb, *Proc. Natl. Acad. Sci. USA* **1990**, *87*, 6878.
[285] S. K. Burley, P. R. David, R. M. Sweet, A. Taylor, W. N. Lipscomb, *J. Mol. Biol.* **1992**, *224*, 113.
[286] N. Sträter, W. N. Lipscomb, *Biochemistry* **1995**, *34*, 14792.
[287] S. K. Burley, P. R. David, W. N. Lipscomb, *Proc. Natl. Acad. Sci. USA* **1991**, *88*, 6916.
[288] H. Kim, W. N. Lipscomb, *Biochemistry* **1993**, *32*, 8465.
[289] N. Sträter, W. N. Lipscomb, *Biochemistry* **1995**, *34*, 9200.
[290] J. M. Prescott, S. H. Wilkes, *Methods Enzymol.* **1976**, *45*, 530; J. M. Prescott, S. H. Wilkes, F. W. Wagner, K. J. Wilson, *J. Biol. Chem.* **1971**, *246*, 1756; J. M. Prescott, S. H. Wilkes, *Methods Enzymol.* **1976**, *45*, 530.
[291] M. E. Bayliss, J. M. Prescott, *Biochemistry* **1986**, *25*, 8113; J. M. Prescott, F. W. Wagner, B. Holmquist, B. L. Vallee, *Biochem. Biophys. Res. Commun.* **1983**, *114*, 646; J. M. Prescott, F. W. Wagner, B. Holmquist, B. L. Vallee, *Biochemistry* **1985**, *24*, 5350.
[292] B. Chevrier, C. Schalk, H. D'Orchymont, J. Rondeau, D. Moras, C. Tarnus, *Structure* **1994**, *2*, 283.
[293] A. Ben-Bassat, K. Bauer, S. Y. Chang, K. Myambo, A. Boosman, S. Chang, *J. Bacteriol.* **1987**, *169*, 751.
[294] C. G. Miller, K. L. Strauch, A. M. Kukral, J. L. Miller, P. T. Wingfield, G. J. Mazzei, R. C. Werlen, P. Graber, N. R. Movva, *Proc. Natl. Acad. Sci. USA* **1987**, *84*, 2718; R. L. Kendall, R. A. Bradshaw, *J. Biol. Chem.* **1992**, *267*,

20667; R. P. Moerschell, Y. Hosokawa, S. Tsunasawa, F. Sherman, *J. Biol. Chem.* **1990**, *265*, 19638; P. H. Hirel, M. J. Schmitter, P. Dessen, G. Fayat, S. Blanquet, *Proc. Natl. Acad. Sci. USA* **1989**, 86, 8247.
[295] M. J. Butler, A. Bergeron, G. Soostmeyer, T. Zimny, L. T. Malek, *Gene* **1993**, *123*, 115.
[296] F. Endo, A. Tanoue, H. Nakai, Y. Indo, K. Titani, I. Matsuda, *J. Biol. Chem.* **1989**, *264*, 4476.
[297] S. Wu, S. Gupta, N. Chatterjee, R. E. Hileman, T. G. Kinzy, N. D. Denslow, W. C. Merrick, D. Chakrabarti, J. C. Osterman, N. K. Gupta, *J. Biol. Chem.* **1993**, *268*, 10796.
[298] J. F. Bazan, L. H. Weaver, S. L. Roderick, R. Huber, B. W. Matthews, *Proc. Natl. Acad. Sci. USA* **1994**, *91*, 2473.
[299] S. M. Arfin, R. L. Kendall, L. Hall, L. H. Weaver, A. E. Stewart, B. W. Matthews, R. A. Bradshaw, *Proc. Natl. Acad. Sci. USA* **1995**, *92*, 7714.
[300] S. L. Roderick, B. W. Matthews, *Biochemistry* **1993**, *32*, 3907.
[301] N. E. Dixon, C. Gazzola, R. L. Blakeley, B. Zerner, *Science* **1976**, *191*, 1144.
[302] C. M. Collins, S. E. D'Orazio, *Mol. Microbiol.* **1993**, *9*, 907.
[303] C. T. Walsh, W. H. Orme-Johnson, *Biochemistry* **1987**, *26*, 4901; R. L. Blakeley, J. A. Hinds, H. E. Kunze, E. C. Webb, B. Zerner, *ibid.* **1969**, *8*, 1991.
[304] S. J. Lippard, *Science* **1995**, *268*, 996.
[305] N. E. Dixon, C. Gazzola, R. L. Blakeley, B. Zerner, *J. Am. Chem. Soc.* **1975**, *97*, 4131.
[306] I.-S. Park, R. P. Hausinger, *Biochemistry* **1996**, *35*, 5345.
[307] M. J. Todd, R. P. Hausinger, *J. Biol. Chem.* **1989**, *264*, 15835.
[308] M. G. Finnegan, A. T. Kowal, M. T. Werth, P. A. Clark, D. E. Wilcox, M. K. Johnson, *J. Am. Chem. Soc.* **1991**, *113*, 4030; S. S. Hasnain, B. Piggott, *Biochem. Biophys. Res. Commun.* **1983**, *112*, 279; L. Alagna, S. S. Hasnain, B. Piggott, D. J. Williams, *Biochem. J.* **1984**, *220*, 591; S. Wang, M. H. Lee, R. P. Hausinger, P. A. Clark, D. E. Wilcox, R. A. Scott, *Inorg. Chem.* **1994**, *33*, 1589.
[309] S. B. Mulrooney, R. P. Hausinger, *J. Bacteriol.* **1990**, *172*, 5837; M. H. Lee, S. B. Mulrooney, M. J. Renner, Y. Markowicz, R. P. Hausinger, *J. Bacteriol.* **1992**, *174*, 4324; I. S. Park, M. B. Carr, R. P. Hausinger, *Proc. Natl. Acad. Sci. USA* **1994**, *91*, 3233.
[310] I. S. Park, R. P. Hausinger, *Science* **1995**, *267*, 1156.
[311] J. B. Sumner, *J. Biol. Chem.* **1926**, *69*, 435.
[312] M. J. Todd, R. P. Hausinger, *J. Biol. Chem.* **1987**, *262*, 5963.
[313] P. R. Martin, R. P. Hausinger, *J. Biol. Chem.* **1992**, *267*, 20024; M. J. Todd, R. P. Hausinger, *ibid.* **1991**, *266*, 24327.
[314] I. Park, R. P. Hausinger, *Protein Sci.* **1993**, *2*, 1034.
[315] I. S. Park, R. P. Hausinger, *J. Protein Chem.* **1993**, *12*, 51.
[316] N. E. Dixon, P. W. Riddles, C. Gazzola, R. L. Blakeley, B. Zerner, *Can. J. Biochem.* **1980**, *58*, 1335.
[317] K. M. Harmon, C. Niemann, *J. Biol. Chem.* **1949**, *177*, 601.
[318] J. M. Breitenbach, R. P. Hausinger, *Biochem. J.* **1988**, *250*, 917.
[319] D. K. Wilson, F. B. Rudolph, F. A. Quiocho, *Science* **1991**, *252*, 1278.
[320] The coloring scheme refers to the assumed metal ion content in vivo (see Table 1).
[321] Note that in order to match the numbers of the homologous sites in FBP and IPP the numbers of the two metal ion binding sites in IMP are different from the ones used in the paper describing this structure [208].
[322] A. F. Neuwald, J. D. York, P. W. Majerus, *FEBS Lett.* **1991**, *294*, 16; R. E. Diehl, P. Whiting, J. Potter, N. Gee, C. I. Ragan, D. Linemeyer, R. Schoepfer, C. Bennett, R. A. Dixon, J. Biol. Chem. **1990**, *265*, 5946; J. D. York, J. W. Ponder, P. W. Majerus, *Proc. Natl. Acad. Sci. USA* **1995**, *92*, 5149.
[323] P. L. Birch, H. A. El-Obeid, M. Akhtar, *Arch. Biochem. Biophys.* **1972**, *148*, 447.
[324] P. P. Giannousis, P. A. Bartlett, *J. Med. Chem.* **1987**, *30*, 1603.
[325] L. Andersson, T. C. Isley, R. Wolfenden, *Biochemistry* **1982**, *21*, 4177.

VCH Weinheim, New York
Akademie Verlag
Ernst & Sohn
ACADEMY GROUP LTD
Verlag Helvetica Chimica Acta
SIEMENS, Publicis MCD Verlag
Chemical Concepts
VCH Software
VCH PUBLISHING GROUP
Information available on Internet
www.vchgroup.de

Orthogonal Stability

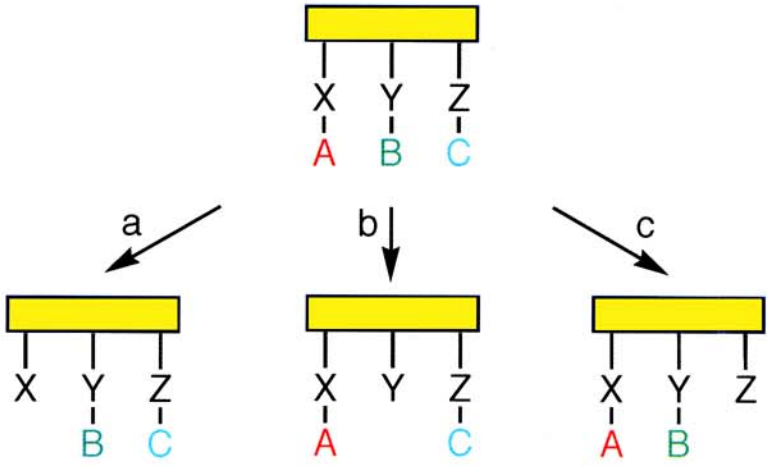

Modulated Lability

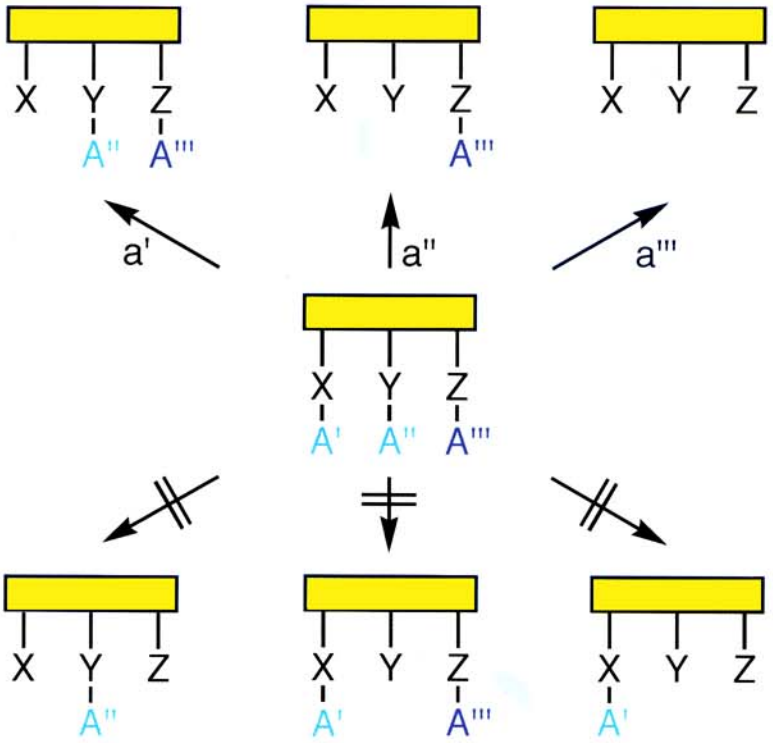

Orthogonal stability and modulated lability are protecting group strategies often employed in combination in complex syntheses.

Protecting Group Strategies in Organic Synthesis

Michael Schelhaas and Herbert Waldmann*

Dedicated to Professor Leopold Horner on the occasion of his 85th birthday

The choice of protecting groups is one of the decisive factors in the successful realization of a complex, demanding synthetic project. The protecting groups used influence the length and efficiency of the synthesis and are often responsible for its success or failure. A wide range of blocking groups are currently available for the different functional groups; however, an overall strategy combining these different masking techniques in an advantageous and reliable manner has never been proposed or at best only for individual cases. This review attempts to make a contribution to filling this gap. First a very short overview of the most commonly used protecting groups will be given, in which they are classified according to their lability and not according to the functional group they protect. This classification clarifies coherent concepts for the development of blocking strategies. On the basis of this brief summary reliable strategies will then be illustrated and developed with selected examples from the recent literature by which protecting groups may be combined successfully and advantageously in synthetic projects of differing degrees of complexity and difficulty.

Keywords: protecting groups · retrosynthetic analyses · synthetic methods · total syntheses

1. Introduction

Today, organic synthesis has reached a remarkable level of competence and even the most complex molecules are accessible.[1] The prerequisites for this success are both the availability of a wide range of efficient synthetic methods[2] and reagents,[3] and the fact that "retrosynthetic analysis"[4] can provide a framework for the design of a synthetic strategy leading to the desired product in the most efficient and logical way.

These strategies include tactics for the construction of the molecular framework, for the establishment of the absolute configuration of any stereocenters present, for the efficient formation of rings, and for the reduction of the number of synthetic steps. The complex synthetic intermediates and products contain, in general, a multiplicity of functional groups, most of which must be blocked and, at an appropriate point in the synthesis, liberated. The correct choice of protecting groups is often decisive for the realization of the overall operation. This is exemplified by the recently published total synthesis of the mitomycin analog FR-900482. In model studies Danishefsky et al. had shown that the basic skeleton of this natural product can be accessed by $FeCl_3$-mediated opening of the epoxide in **1** (Scheme 1).[5] However, the synthesis could not be concluded successfully, because cleavage of the methyl ether was accompanied by decomposition of the aziridine. To avoid this problematic situation, the hydroxyl groups in **2** were not protected as methyl ethers but rather as benzyl and methoxymethyl ethers. Unfortunately, after this seemingly innocuous[6] alteration in the protecting group pattern, the selective $FeCl_3$-mediated cleavage of the oxirane failed owing to the higher lability of the newly introduced ether functions. The authors were forced to find an entirely new reagent to complete the synthesis.[6]

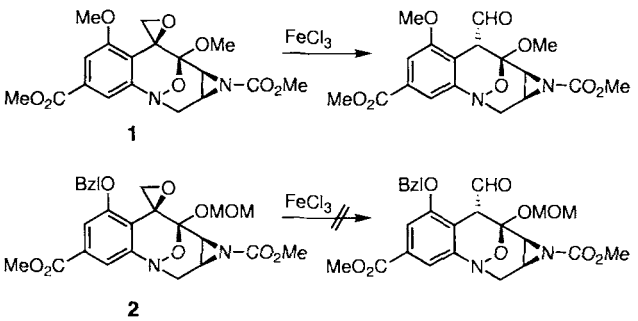

Scheme 1. Protecting group problems in the synthesis of mitomycin analog FR-900482 by S. Danishefsky et al. [5]. MOM = methoxymethyl, Bzl = benzyl.

Another unexpected protecting group problem appeared during the total synthesis of taxol, again by Danishefsky et al.[7] The advanced intermediate **3** was converted into the epoxide **4**, but the robust *tert*-butyldimethylsilyl (TBDMS) ether could not be removed in the next steps (Scheme 2). Thus the TBDMS in **3** was replaced by the more labile triethylsilyl (TES) ether. Compound **5** was converted into the corresponding epoxide **6**, which was then successfully transformed into the complex natural

[*] Prof. Dr. H. Waldmann, Dipl.-Chem. M. Schelhaas
Institut für Organische Chemie der Universität Karlsruhe
Richard-Willstätter-Allee 2, D-76128 Karlsruhe (Germany)
Fax: Int. code +(721)608-4825
e-mail: waldmann@ochhades.chemie.uni-karlsruhe.de

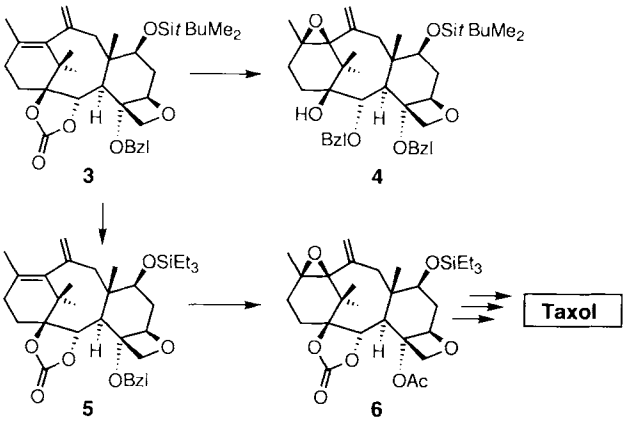

Scheme 2. Protecting group problems in the synthesis of taxol by S. Danishefsky et al. [7].

product. The TES group was removed only after construction of the correctly functionalized polycycle.

These examples make it obvious that a successful synthesis requires both basic retrosynthetic planning and a separate protecting group strategy that takes into account different requirements such as the lability of the intermediates and of the reagents to be used.

As a consequence of the great importance of protecting groups in organic chemistry, a multitude of blocking techniques have been developed for a wide range of functional groups. Here the chemist has numerous choices. However, when giving a detailed description of a successfully completed total synthesis, authors rarely comment on why they selected particular protecting group patterns.[8] Similarly, in the monographs[9, 10] and reviews[11] concerning protecting group chemistry, the emphasis lies in the presentation of the various possibilities that exist for the blocking and deprotection of the function in question. Strategies that can be used to combine protecting groups in appropriate ways and that have proved their capability and reliability in complex syntheses have never been published or only for isolated cases.[12] The protecting groups will be classified according to their lability (for a more comprehensive treatment see refs. [9–11]) instead according to the functional group they block. This has the advantage that the sensitivity of the compounds to be protected and the required reaction conditions can be accounted for in the planning of a synthesis.

Experience shows that the critical parameters are generally the stability and the cleavage of the protecting group rather than its introduction. For most of the typically required functional groups, protecting groups are known that are labile under different, often alternative, conditions. Furthermore, unified concepts for the development of new blocking possibilities become clear as a consequence of this approach. As an example, the N-*tert*-butyloxycarbonyl (Boc) group, the *tert*-butyl ester, and the *tert*-butyl ether can be cleaved under acidic conditions, the trimethylsilylethoxycarbonyl (Teoc) group and the trimethylsilylethyl (TMSE) ether are cleaved by fluoride ions through β-elimination, and allyloxycarbonyl (Aloc) urethane, allyl (All) ester, allyl ether, and 5-methylene-1,3-dioxane acetal,[13] which is used for the protection of carbonyl groups, can all be removed by noble metal catalyzed reactions. Following this short overview, selected examples from the recent literature will be used to illustrate proven strategies for the successful and advantageous combination of protecting groups in synthetic projects of varying complexity and difficulty. This review should provide simple guidelines for the the development of successful tactics and strategies for organic synthesis.

2. Lability and Cleavage of Protecting Groups

For a protecting group to find wide application in organic synthesis, it must fulfill several criteria. In particular, it must

be introduced into the molecule to be protected under mild conditions in a selective manner and in high yield; functional groups other than that to be protected must not be attacked.

H. Waldmann

M. Schelhaas

Herbert Waldmann was born in 1957, studied chemistry at the University of Mainz, and received his doctorate in 1985 under the supervision of Horst Kunz. After a postdoctoral appointment at Harvard University with George Whitesides, he returned to the University of Mainz in 1986 and completed his habilitation in 1991. He was Professor of Organic Chemistry at the University of Bonn from 1991 to 1993 before taking up a chair of Organic Chemistry at the University of Karlsruhe. His work has been recognized by the award of the Friedrich-Weygand-Preis, the Dozentenstipendium of the Fonds der Chemischen Industrie, and the Carl-Duisberg-Preis of the Gesellschaft Deutscher Chemiker. His research encompasses diastereo- and enantioselective synthesis, the chemistry of peptides, carbohydrates, and alkaloids, and the use of enzymes in organic synthesis. One of his current research topics is the preparation of new tools by the methods of organic chemistry for addressing biological questions such as the control of signal transduction.

Michael Schelhaas was born in 1967, studied chemistry at the University of Bonn, and completed his degree in 1993. He then moved to Karlsruhe with Herbert Waldmann's group, where he is currently working on his doctoral thesis in the field of chemoenzymatic syntheses of lipid-modified peptide conjugates. He won the Heinrich-Hörlein-Preis for his degree and the Wolf-und-Sohn-Preis for further work.

be stable under all the conditions used during the synthesis, including those of the purification steps, up to the step in which the protecting group is removed, it should, as far as possible, have a stabilizing effect on the molecule and should suppress racemization or epimerization.
- be cleavable under very mild conditions in a highly selective manner and in high yield; other protecting groups present in the molecule and unprotected functionalities should not be affected by the cleavage conditions.

In addition to these minimum requirements, the protecting group should also
- be introduced and removed with the help of readily available reagents, such that in both transformations the products can be easily purified.
- introduce no additional stereocenters.
- lend the protected intermediates advantageous physical properties; for example the compounds should be easily crystallized and/or readily soluble.

Only a few protecting groups meet all of these demands, and in most cases a compromise must be found, in which the most important criteria are addressed. In most cases guaranteeing that the protecting group is very stable and, at the same time, readily liberated (an apparent contradiction) is the crucial problem and overshadows the requirements for efficient introduction and the provision of desirable physical and chemical properties. In the next sections the most important protecting groups will be presented briefly according to their lability and their ease of cleavage.

2.1. Acid-Labile Protecting Groups[9-11]

The cleavage of protecting groups by acid-mediated hydrolysis is one of the best established methods in protecting group chemistry and forms one of the central pillars of the subject. Nevertheless, only those protecting groups that can be removed under sufficiently mild (but not too mild) conditions find widespread use.

2.1.1. Acetal Protecting Groups

Acetals are formed and cleaved under acid catalysis. They are generally stable towards nucleophiles and bases, and are thus suitable for the protection of alcohols, diols, and carbonyl compounds. Furthermore, N,N- and N,O-acetals are utilized for the protection of amino groups.

Cyclic O,O-acetals can be considered as protecting groups for either carbonyl groups or diols, depending on which component is of interest. Carbonyl groups are normally protected as the 1,3-dioxolane or -dioxane by condensation with ethylene glycol or propylene glycol (Scheme 3). Similarly, 1,2- and 1,3-diols are masked by reaction with acetone, (substituted) benzaldehyde, and cyclic ketones (cyclopentanone, cyclohexanone, cycloheptanone) as isopropylidene, (substituted) benzylidene, and cycloalkylidene acetals. Recently, the dispiroketal (DISPOKE)[14] and the cyclohexane-1,2-diacetal (CDA) groups[15] have been proposed as two promising new acetal protecting groups (see Section 5).

Acyclic O,O-acetals are normally used for the protection of alcohols. Most commonly used are the tetrahydropyranyl (THP),

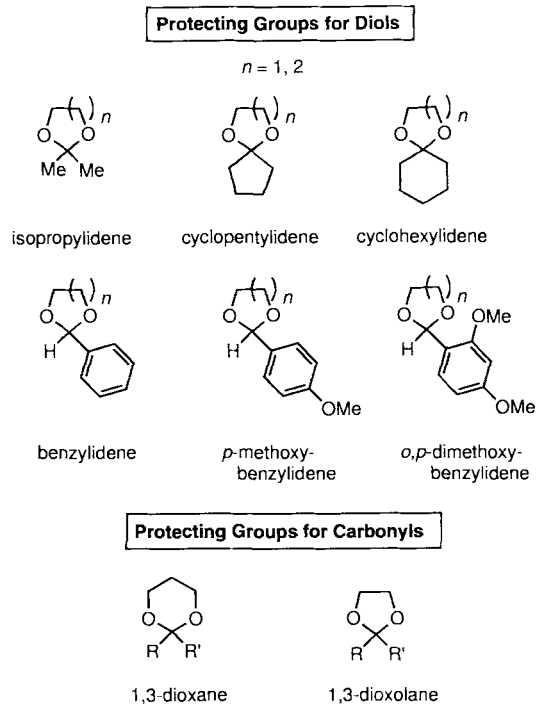

Scheme 3. Examples of cyclic O,O-acetals as protecting groups for 1,2-diols, 1,3-diols, and carbonyl compounds.

the methoxymethyl (MOM), the benzyloxymethyl (BOM), and the methoxyethoxymethyl (MEM) protecting groups (Scheme 4). They can be cleaved readily under mildly acid conditions, and their complexing ability can also be used to control the stereochemical course of a transformation (see Section 3.5).

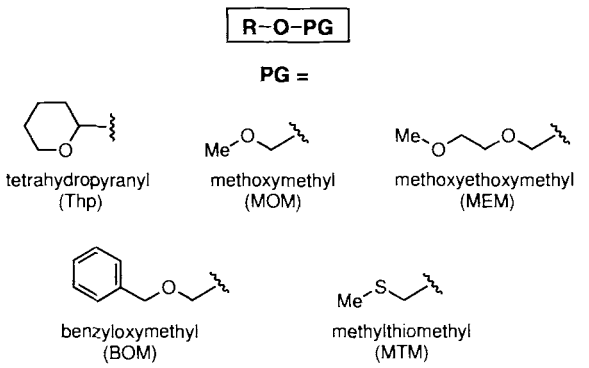

Scheme 4. Examples of acyclic O,O-acetals and O,S-acetals as protecting groups for alcohols.

2.1.2. Formation of Stabilized Cations

The second large class of acid-labile protecting groups is characterized by the formation of stabilized cations upon cleavage. The *tert*-butyl ether along with the corresponding ester and urethane (Boc protecting group) are examples of this class, which find use in the protection of alcohols, thiols, amines, and carboxylic acids (Scheme 5). In each case, their cleavage liberates the *tert*-butyl cation. By analogy, benzyl cations are generated on the cleavage of benzyl protecting groups, which are also common blocking groups for hydroxyl groups, thiols, esters, and amino groups. By introduction of additional substituents,

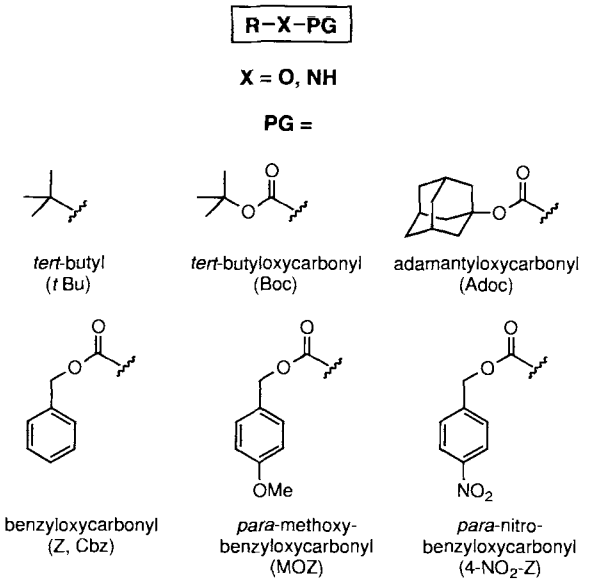

Scheme 5. Examples of acid-labile protecting groups that are cleaved with formation of stabilized cations.

the stability of the cation can be increased or reduced, and thereby the acid sensitivity of the protecting group can be fine-tuned. Thus, the adamantyloxycarbonyl (Adoc) and the *para*-methoxybenzyloxycarbonyl (MOZ) groups are more acid-labile than the respective parent Boc and Z groups. The 4-NO_2-Z group is, however, significantly more stable than the Z-urethane. It should be noted that the silyl ether protecting groups, which are usually removed by treatment with fluoride ion (see Section 2.3), are also labile under mild acidic conditions.

2.2. Base-Labile Protecting Groups[9–11]

The removal of protecting functions under basic conditions is also one of the tried-and-true methods in protecting group chemistry. On the basis of mechanistic considerations, two categories can be distinguished: basic hydrolysis and based-induced β-elimination.

2.2.1. Basic Hydrolysis

This method applies to practically all esters, with the exception of the *tert*-butyl ester mentioned in Section 2.1.2. Carboxylic acids are typically protected as (substituted) alkyl esters. Alcohols are often esterified with acetic acid, benzoic acid, or pivalic acid (Scheme 6). The rate of hydrolysis can be modified by adjusting steric and electronic factors. For example, trifluoroacetate can be removed selectively in the presence of acetate, and acetate can be cleaved in the presence of pivalate.

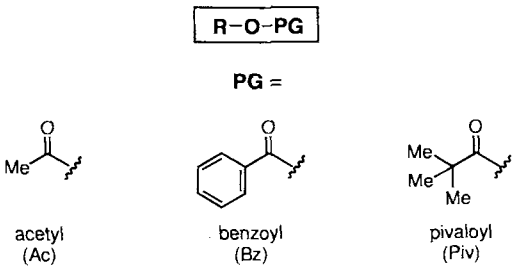

Scheme 6. Examples of base-labile acyl protecting groups.

Basic cleavage of amides to liberate amines is only seldom used on account of the generally harsh conditions required. The phthaloyl group is one exception; it can be cleaved with hydrazine under mildly basic conditions. Again, it should be noted that the silyl ethers can be removed by basic hydrolysis (however, see Section 2.3).

2.2.2. Cleavage by Base-Induced β-Elimination

Protecting groups such as the fluorenylmethoxycarbonyl (Fmoc) urethane, which has established itself as one of the standard protecting functions for amino groups in solution-phase and solid-phase peptide synthesis, and the phenylsulfonylethyl group are cleaved by the abstraction of an acidic proton and subsequent β-elimination, with the formation of a vinyl system (Scheme 7). Direct attack of the base on a carbonyl function is thus avoided. This type of protecting group has found many applications.

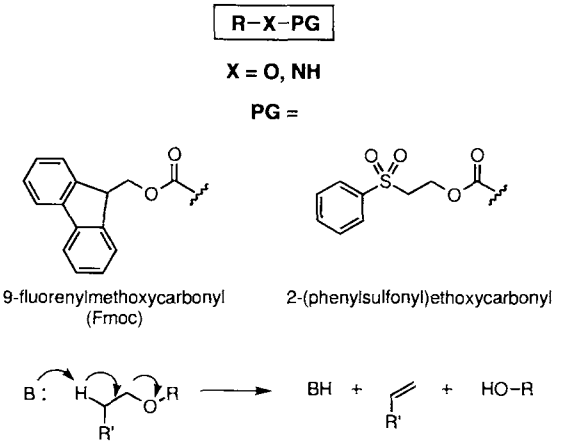

Scheme 7. Examples of protecting groups that are cleaved by β-elimination.

2.3. Fluoride-Labile Protecting Groups[9–11]

Silyl protecting groups can be cleaved by treatment with fluoride ion under conditions that affect nearly no other functionalities. They thus make up an essential chapter in protecting group chemistry (Scheme 8). Variation of the substituents on silicon allows modification of their stability towards acids and bases, as well as the selectivity of the cleavage with fluoride ion (see Section 3.2.2 and Scheme 37). A simple rule of thumb holds—the greater the steric demand, the higher the stability. Alcohols are typically protected as trialkylsilyl ethers; the order of stability for the ethers is TMS < TES < TBDMS < TIPS[16] $\approx$ thexyl. For particularly challenging cases, a further level of fine-tuning can be achieved with, for example, isopropyldimethylsilyl,[17] diisopropylmethylsilyl,[18] and diethylisopropylsilyl (DEIPS)[19] groups. 1,3-Diols can be masked as silanediyl derivatives (see also Scheme 44) or by introduction of the tetraisopropyldisiloxane-1,3-diyl (TIPDS) group. Silyl groups are rarely used for the protection of esters and amines due to the high lability of the resulting derivatives (the STABASE protecting group[20] for amines is an exception, see Scheme 8). For this purpose, trialkylsilylethyl esters and carbamates have been

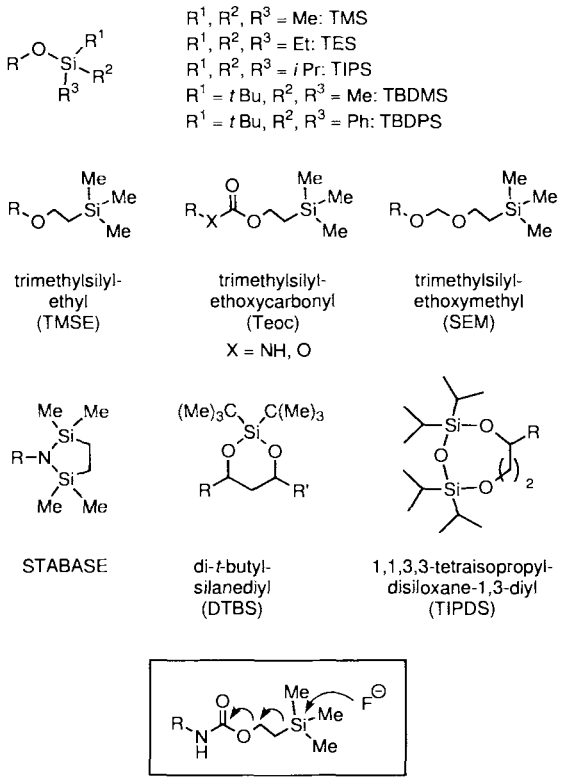

Scheme 8. Examples of protecting groups that are cleaved with fluoride ions.

developed, which can be removed by fluoride ion promoted fragmentation analogous to the previously described β-elimination (Section 2.2.2; Scheme 8). The same principle is also behind the trimethylsilylethyl (TMSE) and trimethylsilylethoxymethyl (SEM) protecting groups for alcohols.

2.4. Enzyme-Labile Protecting Groups[21, 22]

In many cases the selective removal of different acyl protecting groups from amines and alcohols and the targeted deblocking of carboxylic acids under mild conditions is most readily achieved with biocatalysts. Enzymes typically function in the pH range 5–9 and at room temperature; they may display a high specificity for the structures they recognize and the reactions they catalyze, and at the same time they may tolerate a wide range of substrates. Thus enzymes enable the targeted removal of protecting groups (which may in principle also be removed by classical chemical methods) under mild conditions and with a chemo- and regioselectivity that is hardly, if at all, possible by classical chemical techniques. Although the development of enzymatic protecting group techniques has been intensively studied only in the last few years, a number of interesting enzyme-labile protecting groups have been developed for organic synthesis (Scheme 9). Thus, for example, the phenylacet (PhAc) amide[23] and the 4-acetoxybenzyloxycarbonyl (AcOz) urethane[24] have been used as enzyme-labile protecting functions for amino groups, and carboxylic acids can be selectively demasked through enzyme-mediated cleavage of heptyl[25] and choline esters.[26] Hydroxyl groups protected as the acetate, benzoate, butyrate, and even pivalate can be liberated enzymatically.[21, 22] In this way such conversions can be carried out in

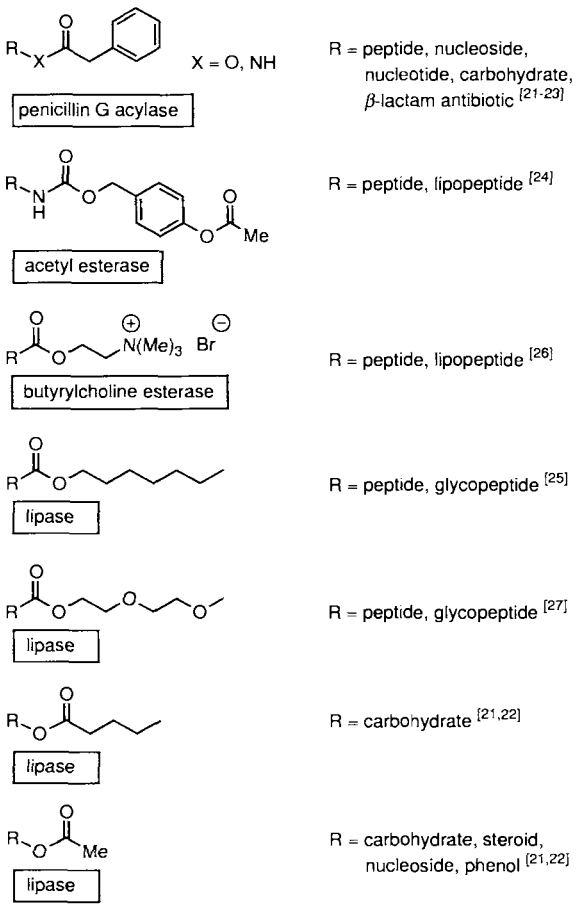

Scheme 9. Selected enzyme-labile protecting groups.

polyfunctional carbohydrates, nucleosides, steroids, alkaloids, and phenolic natural products, often with astonishingly high regioselectivity not achievable with classical chemical techniques. The ability of enzymes to function in organic solvents opens up new possibilities for the introduction of protecting groups.

2.5. Reduction-Labile Protecting Groups[9–11]

Reductive conditions can be used to cleave a variety of protecting groups that are used more or less frequently in organic synthesis.

2.5.1. Cleavage by Hydrogenolysis

Benzyl groups, which can be present as ethers, esters, urethanes, carbonates, or benzylidene acetals, and are used for the protection of alcohols, carboxylic acids, amines, and diols, can be removed under mild conditions by hydrogenolysis. The rate of hydrogenolysis can be influenced by introducing electron-donating or -accepting substituents in the aromatic ring. Benzyl groups are frequently used.

2.5.2. Cleavage by Reductive Elimination

Protecting groups of the 2-haloethyl type can be cleaved by a mechanism involving the donation of electrons into the carbon–halogen bond, leading to a fragmentation corresponding to the β-elimination discussed in Sections 2.2.2 and 2.3 (Scheme 10).

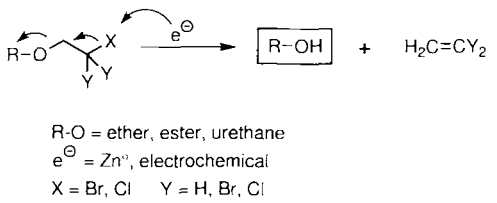

Scheme 10. 2-Haloethyl protecting groups that can be cleaved by reduction.

Zinc is the preferred electron donor, but electrochemical methods are also successfully used.

The reduction of, for instance, ester protecting groups with complex hydrides, reagents that also will attack a pivalate ester, is rarely used, owing to the poor selectivity of these reagents. An exception worth mentioning is the regioselective opening of benzylidene acetals in carbohydrate chemistry[28] (Scheme 11). The

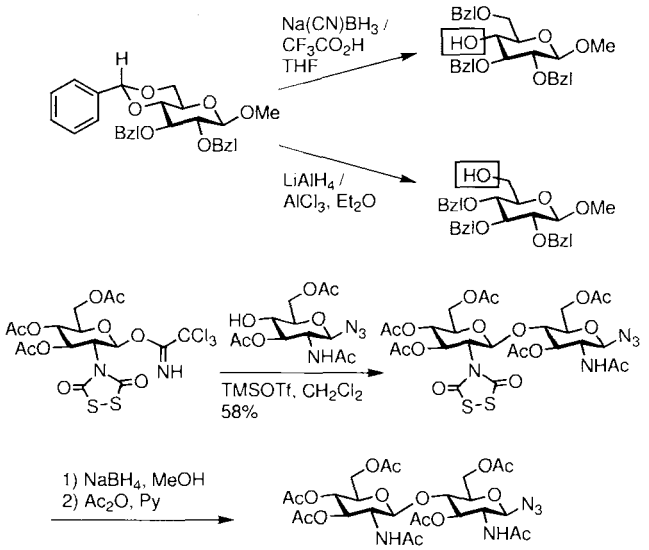

Scheme 11. Regioselective opening of benzylidene acetals and reductive cleavage of the dithiasuccinimide (Dts) protecting group in carbohydrate chemistry.

reductive cleavage of disulfides with thiols or complex hydrides is also seldom used. However, an interesting application of this deblocking technique for the liberation of amino groups from dithiasuccinimides (Dts protecting group) in saccharide synthesis was recently published[29] (Scheme 11).

2.6. Oxidation-Labile Protecting Groups[9-11]

The choice of oxidation-labile protecting groups is very limited. The 4-methoxybenzyl (Mpm) and the more labile 2,4-dimethoxybenzyl (Dmpm) ethers have proved their worth as reagents in the synthesis of complex molecules. Both of these functions are easily removed under mild conditions with dichlorodicyanoquinone (DDQ) or with cerium(IV) ammonium nitrate (CAN) (Scheme 12), or under acidic conditions (see Section 2.1.1).

It is also worth mentioning that S,S-acetals of carbonyl compounds, such as 1,3-dithianes, can be cleaved after oxidation of the sulfur (Scheme 12).

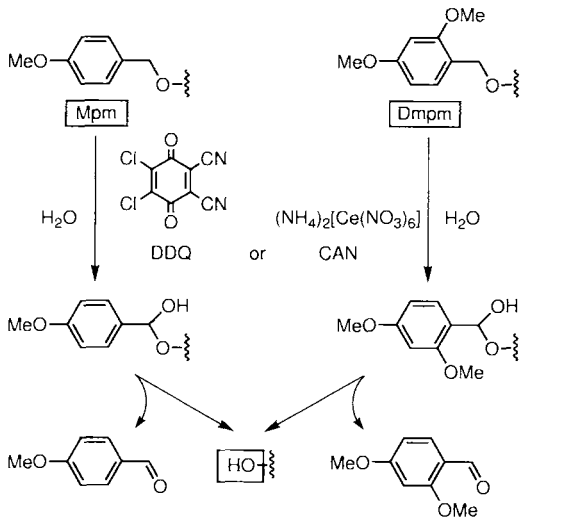

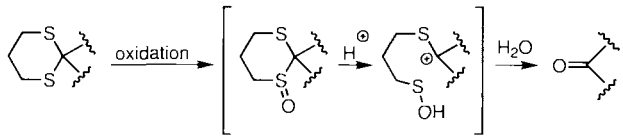

Scheme 12. Examples of oxidation-labile protecting groups.

2.7. Cleavage of Protecting Groups Assisted by Heavy Metal Salts or Complexes[9-11]

The activation of protecting groups with noble metals often offers an advantageous alternative for the targeted deblocking of functional groups. Thus, carbonyl compounds masked as 1,3-dithianes can be hydrolytically regenerated easily by treatment with stoichiometric amounts of Hg^{II}, Ag^{I}, Cu^{II}, or Tl^{III} salts or alternatively by reaction with other electrophiles or by oxidation of the sulfur (see Section 2.6).

Catalytic amounts of Rh^{I}, Ir^{II}, and Pd^{0} complexes and even Pd–C suffice for the removal of protecting groups containing the allyl group. Thus, allyl ethers in carbohydrates and peptides can be selectively isomerized to the acid-labile prop-1-enyl system through the action of catalytic quantities of Pd–C or Rh^{I}, or Ir^{II} complexes. Hydrolysis of this group is achieved under mild conditions. (Scheme 13). The allyloxycarbonyl (Aloc)

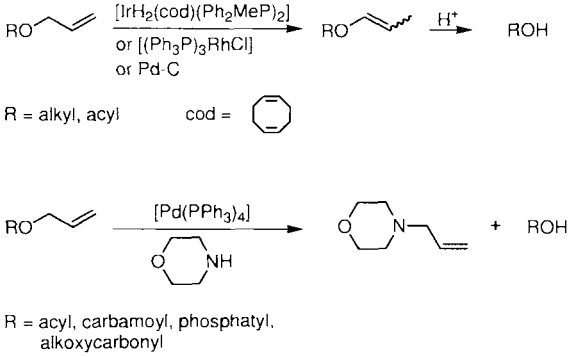

Scheme 13. Cleavage of allyl ethers, allyl esters, allyl urethanes, and allyl carbonates by using heavy metal complexes.

group, allyl esters, and allyl phosphates can be cleaved under mild conditions by Pd^0-mediated allyl transfer to a variety of nucleophiles such as amines and C–H-acidic compounds (Scheme 13). As a consequence of its ready removal and its compatibility with a range of other functional groups, the allyl protecting group has become established in protecting group chemistry and is finding increasing application in the synthesis of complex natural products (see Sections 3.1.3, Schemes 23–27). 1,3-Dithianes and allyl protecting groups can also be viewed "two-stage" protecting groups (see Section 2.9).

2.8. Photolabile Protecting Groups[9–11]

Photolabile protecting groups contain a chromophore of high chemical stability that can be selectively activated by irradiation with light of a suitable wavelength. Of the many known photolabile protecting groups, the *o*-nitrobenzyl group[30] has been used repeatedly in the form of ethers, esters, carbonates, carbamates, and acetals (Scheme 14, see also Section 3.1.5). Two

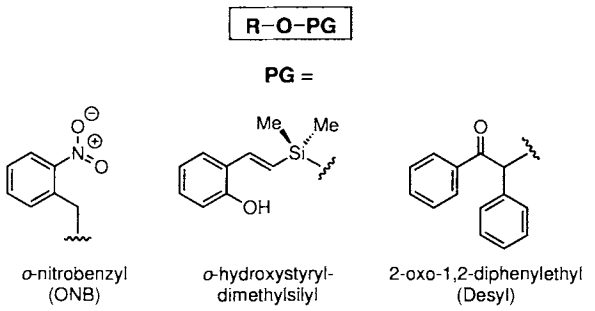

Scheme 14. Examples of photolabile protecting groups.

further interesting photolabile protecting groups are the 2-oxo-1,2-diphenylethyl (Desyl) group[31] and the *o*-hydroxystyryldimethylsilyl group[32] (Scheme 14). Photolabile protecting groups can be cleaved under mild conditions with light of a suitable wavelength, and highly selective cleavage in the presence of other functional groups is possible by the choice of an appropriate chromophore. Despite these advantages, photolabile protecting groups are used much less frequently than other types of protecting groups.

2.9. "Two-Stage" and "Safety-Catch" Protecting Groups

The inherent (and deliberately employed) reactivity of, for example, acid- and base-labile protecting groups is often the source of undesired side reactions. Thus, masking can be (partially) lost at the wrong point in the synthesis. If several protecting groups of comparable reactivity are present in one molecule, selective removal of a single protecting group can be difficult. This problem can be avoided by the use of protecting functions that initially exist in a chemically stable form and can be converted into a labile group when their cleavage is required; these are the "two-stage" protecting groups.[33] Examples include the methylthioethyl (Mte) and the 1,3-dithianylmethoxycarbonyl (Dmoc) groups, which are insensitive towards acid and base, but which, after oxidation of the sulfur to sulfone, fragment by

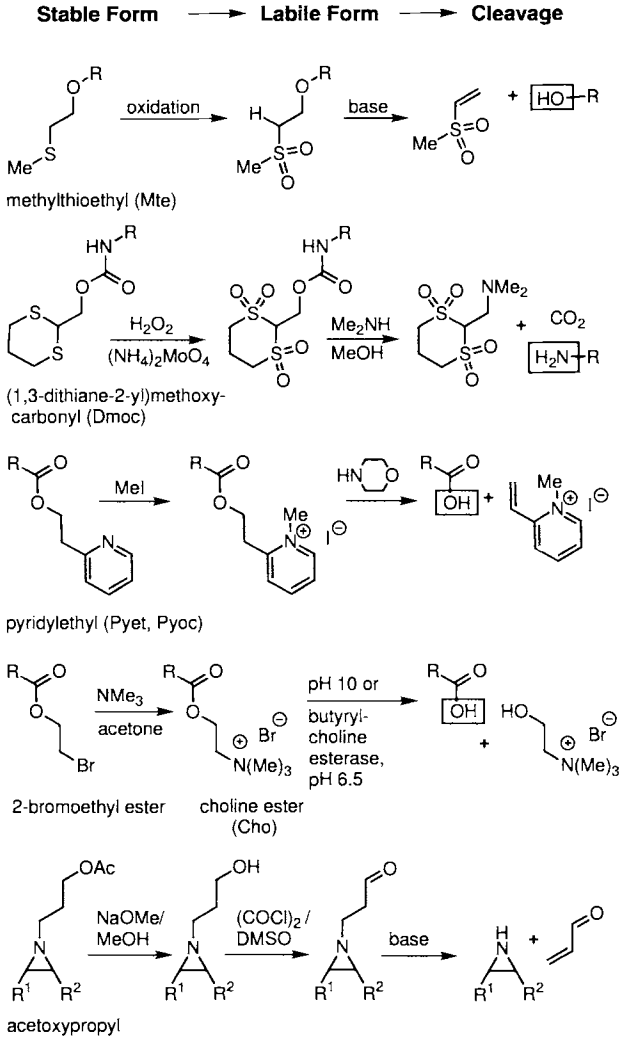

Scheme 15. Selected "two-stage" protecting groups.

base-induced β-elimination (Scheme 15). The same principle applies to the 2- and 4-pyridylethyl protecting groups, which, after alkylation of the pyridine nitrogen, can be cleaved even with morpholine (Scheme 15). 2-Bromoethyl esters can be transformed into salts of the corresponding choline esters by reaction with trimethylamine. The protecting group can then be cleaved either with base or under milder conditions with the enzyme butyrylcholine esterase (see Sections 2.4 and 3.1.4). Removal of another interesting protecting group, the acetoxypropyl protecting group for amines, requires hydrolysis of the acetate, subsequent oxidation of the liberated hydroxyl group to give the aldehyde, and finally base-induced elimination (Scheme 15). This proved to be a useful alternative to classical acyl protecting groups in the total synthesis of mitomycin C.[34] Other examples of this method of protecting group cleavage are 1) the removal of 1,3-dithianes by reaction with electrophiles (or oxidation of sulfur) and subsequent hydrolysis (see Sections 2.6 and 2.7), and 2) the removal of allyl groups by a) isomerization of the allyl system followed by acid hydrolysis or by b) formation of a π-allylpalladium complex and subsequent reaction with a nucleophile (see Sections 2.7 and 3.1.3).

Closely related to the two-stage protecting groups are the "safety-catch" protecting groups.[35] In these systems a chemi-

cally stable precursor is introduced, which is converted into an activated intermediate directly before cleavage. In this case no additional reagent, such as a base or a nucleophile, is required in order to remove the protecting groups. The activated intermediate itself carries a reactive functional group, typically a nucleophile, which intramolecularly attacks the bond to the blocked function and thus causes the cleavage of the protecting group. Several examples of this technique are presented in Scheme 16. Thus, reduction of the nitro-substituted aromatic

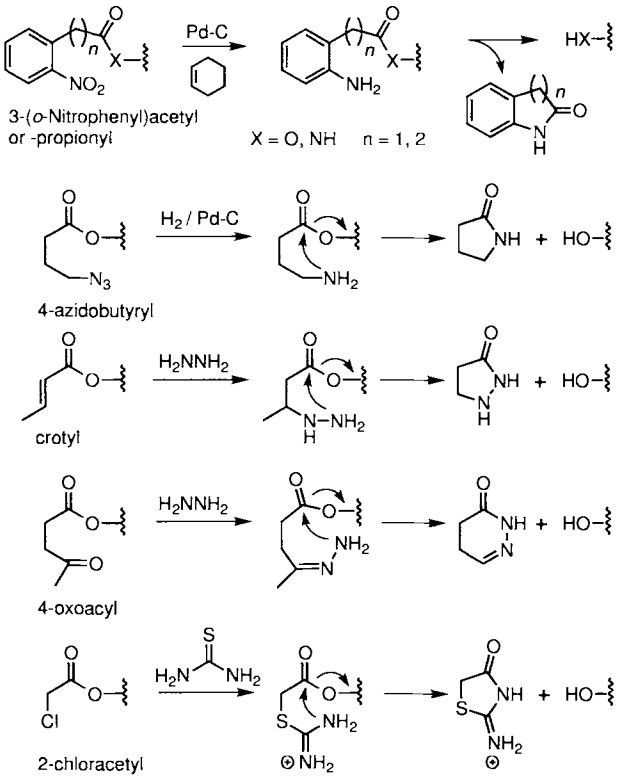

Scheme 16. Selected "safety-catch" protecting groups.

precursor generates the aniline derivative, which then cyclizes to give the amide with liberation of the deprotected functional group. The same principle applies for azidobutyrates. Crotyl and 4-oxoacyl protecting groups react with hydrazine by addition to the α,β-unsaturated system and by formation of a hydrazone, respectively, thereby placing the nucleophile in the correct position. Analogously, chloroacetates are converted to substituted α-thioacetates by reaction with thiourea; subsequent cyclization releases the unprotected functional group.

3. Strategies for the Choice of Protecting Groups

When a synthesis is planned, the choice of suitable protecting groups is inseparable from the consideration of how one will construct the basic structure of the target molecule and how the stereochemistry will be established. The first step in planning a synthesis is the retrosynthetic analysis of the target molecule, which designates the fragments containing the groups to be protected. On the basis of the inherent lability of these intermediates one can, even at this early stage, already exclude certain protecting group strategies. For example, if a fragment contains a C–C double bond, one would not consider using benzyl ethers or esters as protecting groups, which must be removed by hydrogenolysis. After a successful analysis, concrete reactions, the required reagents, and protecting groups are chosen simultaneously. Functional groups, which, after they are introduced or formed, should remain blocked throughout the entire synthesis, will be protected with permanent protecting groups, whereas those that will be liberated at an early stage in the synthesis will be blocked with temporary protecting groups. In practice, it is often neccessary to try out alternative approaches in the course of the synthesis. One must remain alert to the fact that in such cases other protecting groups may be required. For example, if an aldol reaction is planned and strong base is required to deprotonate the carbonyl compound, any protecting groups required should be base-stable but may be acid-labile. However, if this aldol reaction does not prove satisfactory, for example because of low or undesired stereoselectivity, an alternative would be Mukaiyama's variant of the aldol reaction, in which the corresponding silyl enol ether is activated by a Lewis acid (such a case has been described by Reetz et al.[36]). Now the requirements for successful protecting groups would be completely reversed, and exchange of the previously used protecting groups for others might thus be required. It should be noted that the type of blocking can also affect the course of the planned synthesis (see Section 3.5). This example illustrates that each synthetic alternative (here an aldol reaction under basic or acidic conditions) can require its own pattern of protecting groups (base-stable or acid-stable as the case may be).

In the development of a protecting group strategy two fundamental concepts are available (Scheme 17):

- the use of orthogonally stable protecting groups
- the use of protecting groups with modulated lability

The principle of orthogonal stability[37] requires that only those protecting functions should be used that can be cleaved under (as a rule totally) different reaction conditions without affecting the other functions present (Scheme 17). For example, three protecting groups A, B, and C, which are attacked by acid, by base, and by hydrogenolysis, respectively, could therefore be selectively removed in any sequence at any point in a synthesis.

In following the principle of modulated lability, the protecting groups are all sensitive to one set of conditions, but to differing extents. Consider three protecting groups A', A'' and A''', all of which are acid-labile. The most acid-sensitive group, A', can be removed without affecting the other two. However, the least labile A''' cannot be removed selectively in the presence of one or both of the others (Scheme 17).

A strategy based upon the concept of orthogonal stability guarantees a great degree of flexibility in the execution of a synthesis. However, it is often not possible to find and use the requisite number of orthogonally stable protecting groups, particularly in the case of multifunctional molecules, since cleavage of one protecting group requires not only the stability of all the other protecting groups but also of the masked molecule itself under a wide range of reaction conditions. Additionally, in the last steps of a synthesis it is often not necessary that all protecting groups have strictly orthogonal stability, since only a few groups must be selectively liberated and a series of selective

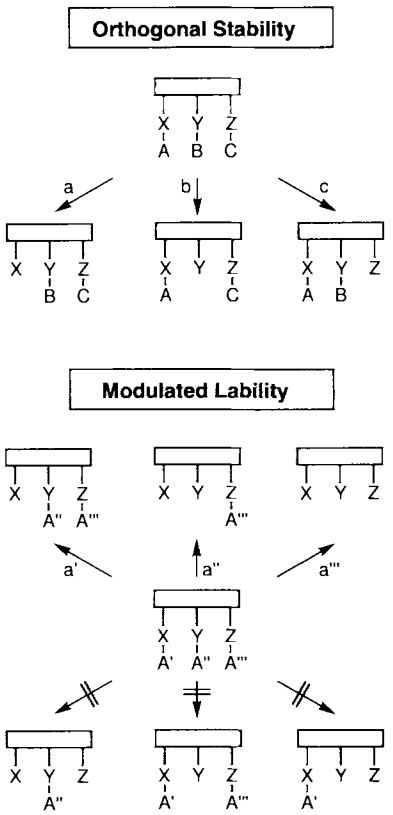

Scheme 17. Orthogonal stability and moldulated lability as basic concepts for the development of protecting group strategies.

deblockings extend the synthesis significantly. These disadvantages do not exist if one uses a set of protecting groups of similar but modulated stability. In practice, a combination of the two strategies is often employed, in which the earlier stages rely more heavily on orthogonal stability and in the latter stages the concept of similar lability is more important.

These two fundamental strategies can be augmented by auxiliary strategies, including:
- the earliest possible unification of a protecting group pattern
- the introduction of "stand-ins"
- the use of protecting groups to direct reactions.

3.1. The Use of Orthogonally Stable Protecting Groups

The protecting groups discussed in Section 2 of differing lability can be used in a wide variety of combinations. In this case again, there are numerous possibilities. A general answer to the question of the most convenient combinations is not available. However, from the many published syntheses one can sift out some combinations that have proved effective time and again.

3.1.1. Acid Hydrolysis/Base Hydrolysis/Hydrogenolysis

The combination of acid-labile, base-labile, and hydrogenolytically labile protecting groups is a frequently used protecting group strategy. In oligonucleotide chemistry, for instance, the acid-labile dimethoxytrityl ether is typically used to protect hydroxyl functions, base-labile amides mask the amino groups of the nucleobases, and base-labile phosphate esters block the phosphate groups (Scheme 18). Similarly, in solid-

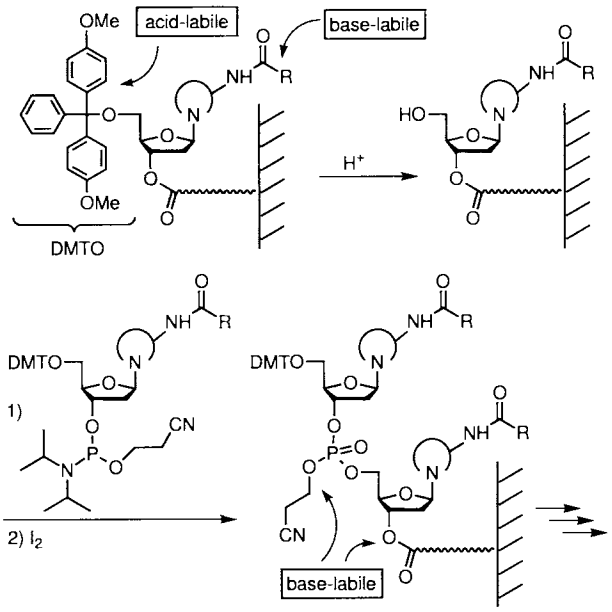

Scheme 18. Oligonucleotide synthesis with acid-labile alcohol protecting groups and base-labile linkers and amino protecting groups. R = phenyl, isobutyl, etc.

phase peptide synthesis the base-labile Fmoc group is frequently used to block the N-terminus, while an acid-sensitive function links the C-terminal carboxylic acid and the polymeric carrier (that is, an acid-labile, polymeric protecting group). The orthogonal stability of all three types of protecting groups has, for example, been employed in the synthesis of a precursor of the dolastatin cytostatics by R. C. Kelly et al. (Scheme 19).[38a]

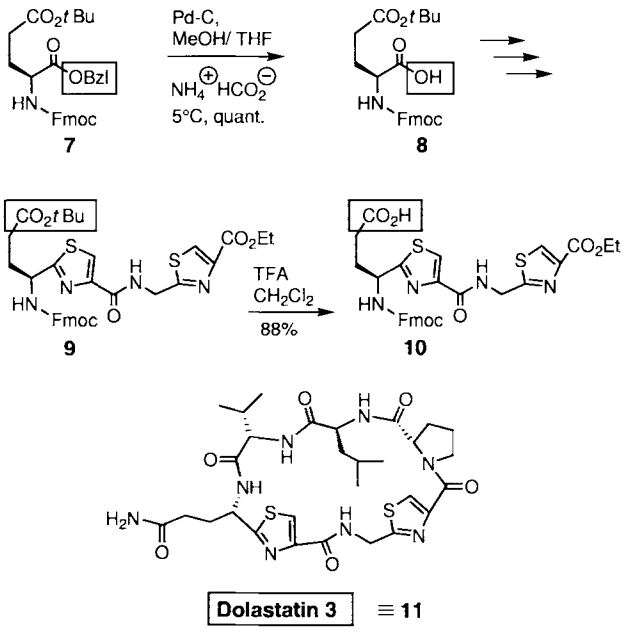

Scheme 19. The combination of acid-labile, base-labile, and reduction-labile protecting groups in the synthesis of a precursor of dolastatin 3 (**11**) by R. C. Kelly et al. [38a].

selectively protected glutamic acid derivative **7** the α-benzyl ester was selectively removed by hydrogenolysis and then the desired bisthiazole unit was constructed. Acid-mediated cleavage of the γ-*tert*-butyl ester in **9** opened up the possibility of converting the γ-carboxyl group of glutamic acid into the amide. In both steps the Fmoc group remained intact. This group can be removed under basic conditions, if required, and the amino acid N-terminus can be extended.[38b]

Among the classical combinations of protecting groups is the simultaneous use of acid-labile acetals for the protection of carbonyl groups or 1,2-diols, base-labile esters, and reductively cleavable benzyl groups. This strategy is often used, particularly in the field of carbohydrate chemistry, as illustrated by the synthesis of the dimeric Lewis^x antigen described by R. R. Schmidt et al. (Scheme 20).[39] In this case, the isopropylidene group of

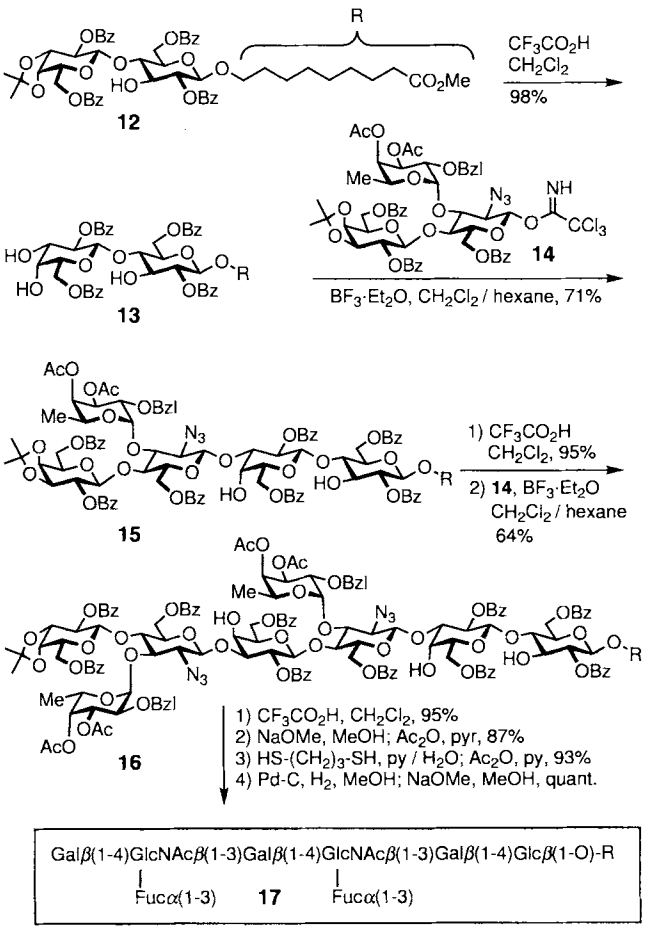

Scheme 20. Synthesis of the dimeric Lewis^x antigen by R. R. Schmidt et al. [39].

the lactoside **12** was initially removed by acid hydrolysis. Of the two liberated hydroxyl groups present in **13**, only the equatorial reacts in the subsequent glycosylation with the activated trisaccharide **14**. A combination of base-labile esters (acetate and benzoate), a benzyl ether, and, again an acid-labile acetal are present in the resulting pentasaccharide **15**. The benzyl group in the fucose unit of **15** ensures that the correct stereochemistry is produced in the introduction of this monosaccharide (see also Section 3.5); the acetates increase the stability of the O-fucosidic bond towards acidic conditions.[40] The acetal protecting group was again selectively removed from the complex pentasaccharide **15** by acidic hydrolysis. This made possible repeated glycosylation with the trisaccharide unit **14**, leading to the complete octasaccharide **16**. Finally, all the protecting groups were successively removed from **16**.

As demonstrated in this example, acetals are commonly employed as temporary protecting groups, whereas benzyl and acyl protecting functions are preferred as permanent protecting groups. When all such groups are removed to give the target compound, the acyl groups are typically removed before the benzyl ethers, in order to minimize steric hindrance in the final heterogeneous catalytic hydrogenolysis. For this reason, it can be advisable to exchange benzyl for acyl protecting groups as early in the synthesis as possible (see Section 3.3).

Examples of alcohols protected as acyclic O,O-acetals are given in Schemes 40, 45, and 50. Oxidation-labile and acid-labile protecting groups can also be advantageously combined. In the example in Scheme 41 the oxidatively cleavable (but also acid-labile) Mpm and Dmpm ethers were combined with an acid-labile dimethyl acetal.

3.1.2. Fluoride-Labile Protecting Groups in Combination with Oxidation-Labile Functions

The 4-methoxybenzyl (Mpm) and 2,4-dimethoxybenzyl (Dmpm) ether groups, which are cleaved by oxidation to quinone methides, can be favorably combined with a range of different protecting groups. Their combination with fluoride-labile silyl ethers has proved to be particularly effective. This combination rarely gives problems, since the substituted benzyl ethers are completely inert towards the fluoride ion. The

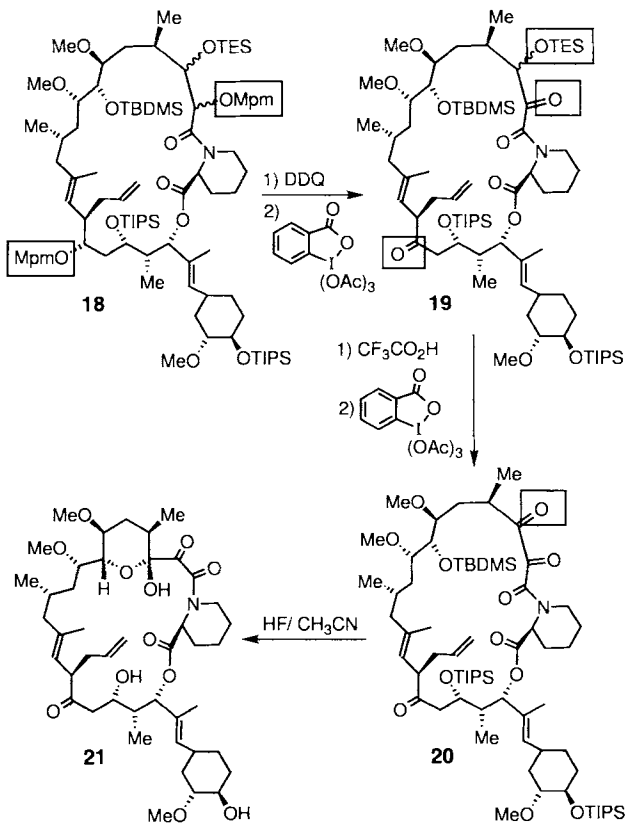

Scheme 21. Final transformations in the synthesis of the immunosuppressant FK506 (**21**) by S. L. Schreiber et al. [41].

oxidants DDQ and CAN (see Section 2.3), which are used for the oxidative cleavage of the Mpm and Dmpm groups, can in the worst case attack only the most labile silyl ethers such as the TMS group, which is seldom used in any case due to its high hydrolytic lability.

An illustration of the use of Mpm ethers in concert with various silyl ethers is provided by the synthesis of the immunosuppressant FK506 (**21**) by S. L. Schreiber et al. (Scheme 21).[41] Two hydroxyl groups are masked as substituted benzyl ethers and four others as different silyl ethers in the advanced intermediate **18**. Oxidation with DDQ cleaved the alkoxybenzyl ethers selectively, and the hydroxyl group thus liberated was then oxidized with Dess–Martin periodinane to give the corresponding diketone **19**. Of the various silyl groups in **19** (for a discussion of their relative stabilities see Section 3.2.2), the most labile was removed by treatment with acid and the selectively demasked hydroxyl group was then oxidized to give triketone **20** (see Section 3.4 for the strategy of masking carbonyl groups by the temporary introduction of hydroxyl groups as "stand-ins"). The synthesis was completed by the simultaneous cleavage of the remaining silyl groups.

The combination of Mpm and silyl ethers also proved its worth in the synthesis of the immunosuppressant rapamycin by K. C. Nicolaou et al. (Scheme 22).[42] In this case, the hydroxyl group in the product obtained from the Cr^{II}-mediated addition of vinyl iodide **23** to aldehyde **22** was blocked as a TIPS ether. The TBDMS group was cleaved selectively (see Section 3.2.2) and the deblocked hydroxyl group was oxidized to give aldehyde **25**, which enabled a subsequent aldol reaction (**25** → **26**). Intermediate **26** carries both Mpm groups and a TIPS ether, and the methoxybenzyl ethers were selectively removed by oxidation. The resulting diol **27** was oxidized to provide the dicarbonyl compound **28**. The TIPS ether remained intact in this reaction sequence and was removed only at the end of the synthesis.

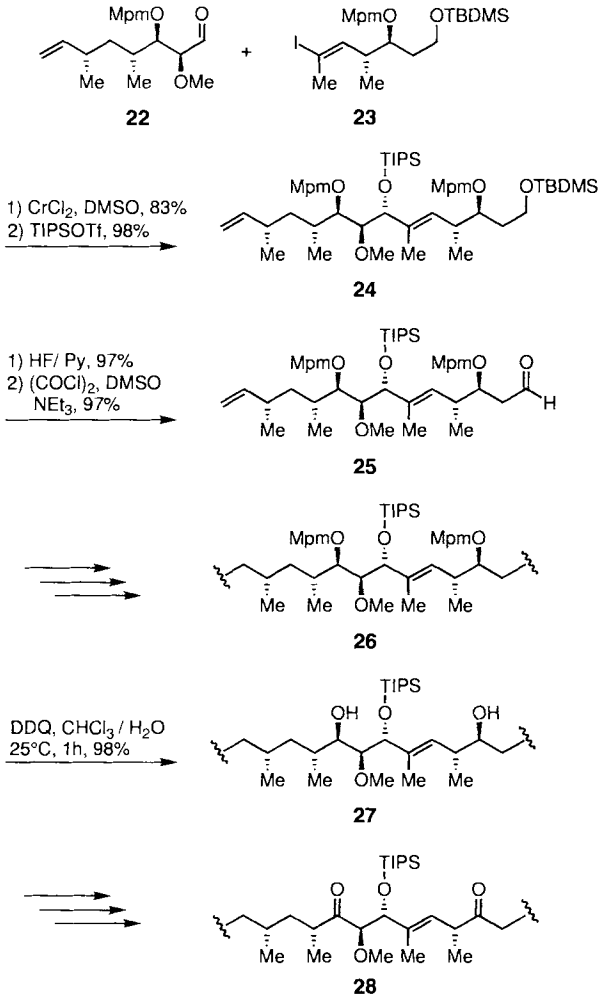

Scheme 22. Sections of the synthesis of the immunosuppressant rapamycin by K. C. Nicolaou et al. [42].

3.1.3. *Allyl Groups with Acid- and Base-Labile Protecting Groups*

Allyl groups can be profitably utilized in combination with a wide variety of other protecting groups, in particular acid- and base-labile blocking groups, as they are readily cleaved by means of Pd-, Rh-, and Ir-catalyzed reactions (see Section 2.7). Carboxylic acids, amines, and alcohols can be blocked as allyl esters, allyl urethanes, allyl ethers, and allyl carbonates. In the past ten years the increasing number of examples in which allylic groups are removed in crucial deblocking steps proves that this protecting group has assumed a permanent position in protecting group chemistry.

One of the first demonstrations of the effectiveness of allyl protecting groups in the synthesis of complex molecules was provided by the synthesis of glycopeptide **32** by H. Kunz et al. (Scheme 23).[43] The allyl group in the glycosylated allyl ester of asparagine **29** was transferred to morpholine in almost quantitative yield in a Pd^0-catalyzed reaction. Neither the acid-labile *tert*-butylurethane, nor the glycosidic bond, nor the base-labile

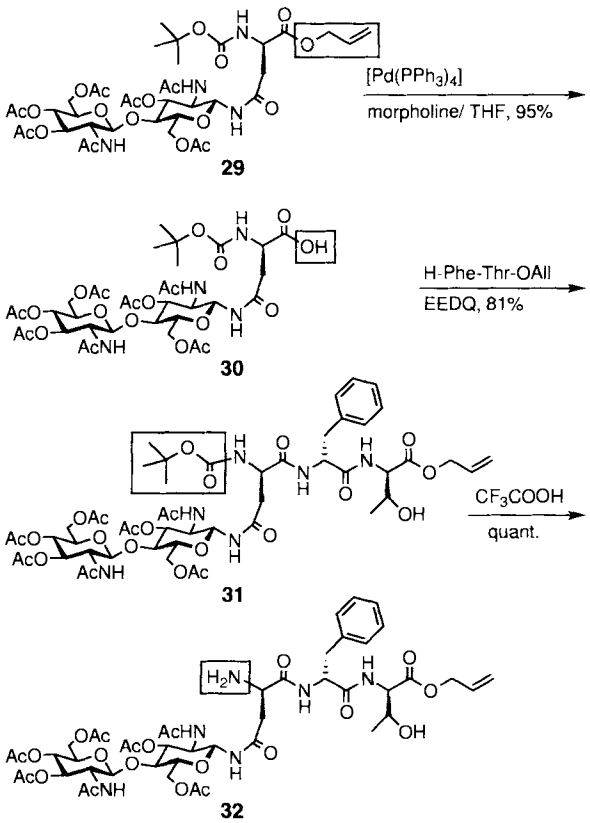

Scheme 23. Application of allyl esters in a glycopeptide synthesis by H. Kunz et al. [43]. EEDQ = ethyl-2-ethoxy-1,2-dihydroquinoline-1-carboxylate.

acetates of the carbohydrate moiety were attacked under these conditions.

The especially mild conditions for the cleavage of allyl esters were also used to advantage by S. Danishefsky et al. in the synthesis of the immunosuppressant rapamycin[44] (Scheme 24). Attempts to activate the carboxyl group in the advanced intermediate **33** prior to a condensation reaction resulted in lactonization at the tertiary OH group of the tetrahydropyranyl

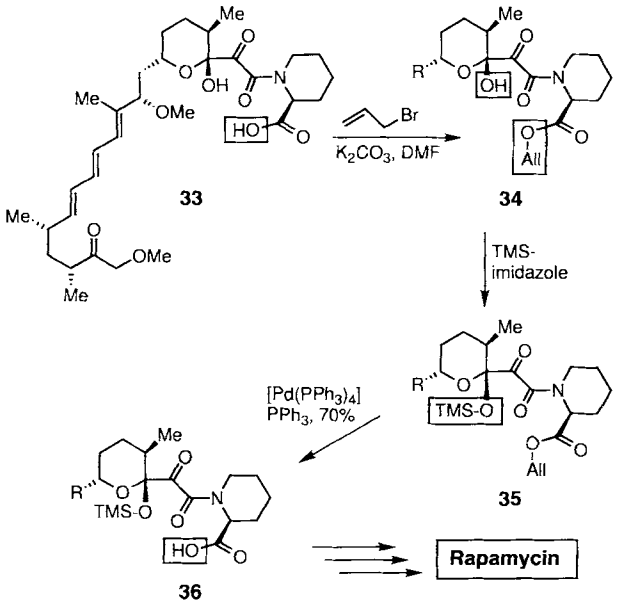

Scheme 24. Section of the synthesis of rapamycin by S. Danishefsky et al. [44].

ring. The OH group therefore had to be protected. To avoid side reactions, it was necessary to mask the carboxylic acid as an allyl ester and then to silylate the remaining free hydroxyl group in **34**, leading to the doubly protected **35**. At this point the carboxyl group could be deprotected. The Pd^0-mediated removal of the allyl ester in **35** proceeded under such gentle conditions that neither the complex molecular framework (including the α-ketoamide) nor the acid- and base-labile TMS ether were lost or damaged.

R. Noyori et al. relied on allyl groups to protect amines and phosphates in the preparation of oligonucleotides[45] (Scheme 25). They employed O-allyl-masked phosphoroamidites as condensation reagents and allyloxycarbonyl (Aloc) protected nucleobases for the construction of oligonucleotides **37** on the solid phase. When the synthesis was complete, all of the allyl protecting groups in the polymer-bound oligonucleotide were removed in a single step. The DNA oligomers **38** thus obtained, which are still bound to the polymer carrier, can be used directly for biological tests or can be cleaved from the solid phase. In one example, the simultaneous cleavage of 104 allyl groups led to the 60mer **39** in an overall yield of 25% and in high purity. (When conventional protecting groups were used an overall yield of 6% was obtained.)

Blechert et al. incorporated the targeted cleavage of an allyl carbonate into the synthesis of a biologically active analog of the antitumor alkaloid taxol[46] (Scheme 26). The allyl carbonate in **40** was cleaved in almost quantitative yield without attack at the ketal or ring expansion by fragmentation of the base-labile β-hydroxyketone unit.

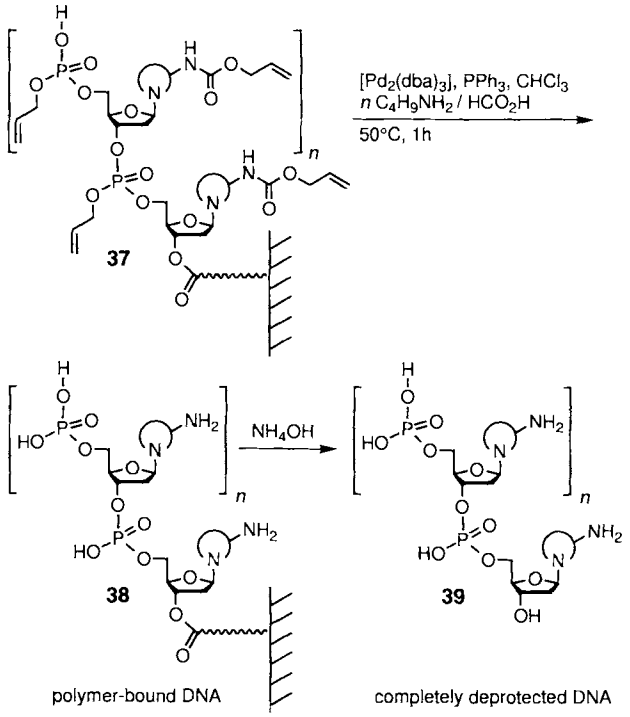

Scheme 25. Application of allyl protecting groups in the synthesis of oligonucleotides by R. Noyori et al. [45]. dba = dibenzylideneacetone.

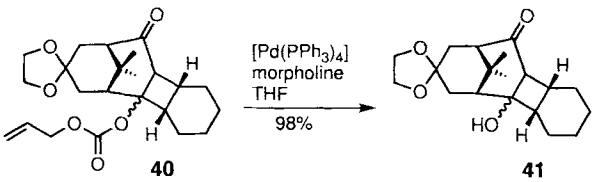

Scheme 26. Cleavage of an allyl carbonate in the synthesis of a taxol analog by S. Blechert et al. [46].

The selective cleavage of an allyl ether was employed by D. A. Evans in the synthesis of vancomycin[47] (Scheme 27). The Boc group in peptide **42** was specifically removed with retention of

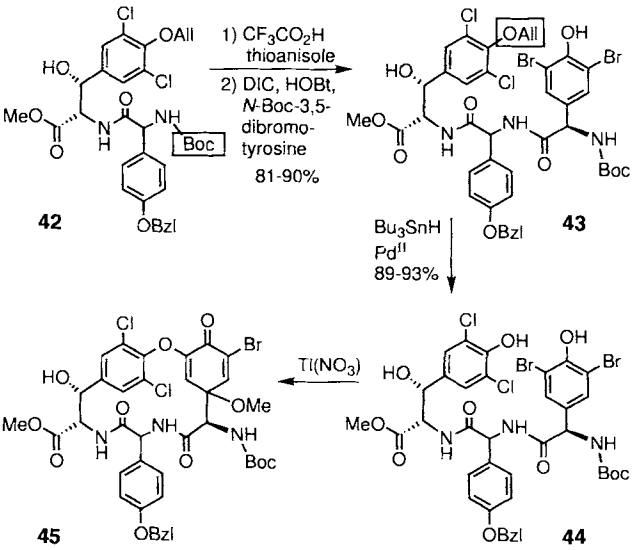

Scheme 27. Section of the synthesis of vancomycin by D. A. Evans et al. [47]. DIC = diisopropylcarbodiimide, HOBt = 1-hydroxybenzotriazole.

the phenolic allyl ether, thus enabling selective extension of the amino acid chain to give **43**. Removal of the allyl group under mild conditions provided phenol **44**, and subsequent oxidative ring closure yielded the cyclic product **45**.

3.1.4. Enzyme-Labile Protecting Groups with Acid- and Base-Labile Groups

Owing to the often distinct chemo-, regio-, and stereoselectivity of enzyme-mediated transformations, enzyme-labile protecting groups can be combined with other protecting groups that can be removed by classical chemical techniques (see Section 2.4). Enzyme-catalyzed reactions are invaluable especially when

- the substrate is so labile that only the most gentle deblocking methods are tolerated.
- the chemo-, regio-, and stereoselectivity of the enzyme imparts orthogonality to protecting groups which, under classical deblocking methodology, would have similar or even inverted lability.

Both principles were utilized in the chemoenzymatic synthesis of the S-palmitoylated and S-farnesylated C-terminal lipohexapeptide of the human N-Ras protein **49**[24, 26] (Scheme 28). This type of modified lipoprotein cannot be deblocked under basic conditions because the labile palmitic acid thioester group would be preferentially hydrolyzed. Under acidic conditions the double bonds of the farnesyl moiety are attacked. However, the C-terminus of the peptide chain was successfully deprotected by selective enzymatic hydrolysis of the choline ester in **46** without attack on the palmitic acid thioester. The observed chemoselectivity here is exactly opposite to that found in the nonenzymatic conversion. Extension of the peptide chain in **47** with the farnesylated tripeptide **48** yielded the desired lipopeptide **49**. Alternatively, the N-terminal AcOZ protecting group in **52** could be removed by lipase-initiated spontaneous fragmentation under neutral conditions and without attack on the C–C double bonds. After extension of the peptide chain in **48** with a further AcOZ-protected dipeptide and enzymatic deprotection, the lipopentapeptide **51** was obtained, which afforded the acid- and base-labile Ras peptide **49** after treatment with the S-palmitoylated cysteine **50**. In these enzyme-catalyzed deprotections of urethane protecting groups, the biocatalyst differentiates between the C-terminal methyl ester and the aryl acetate incorporated in the urethane group.

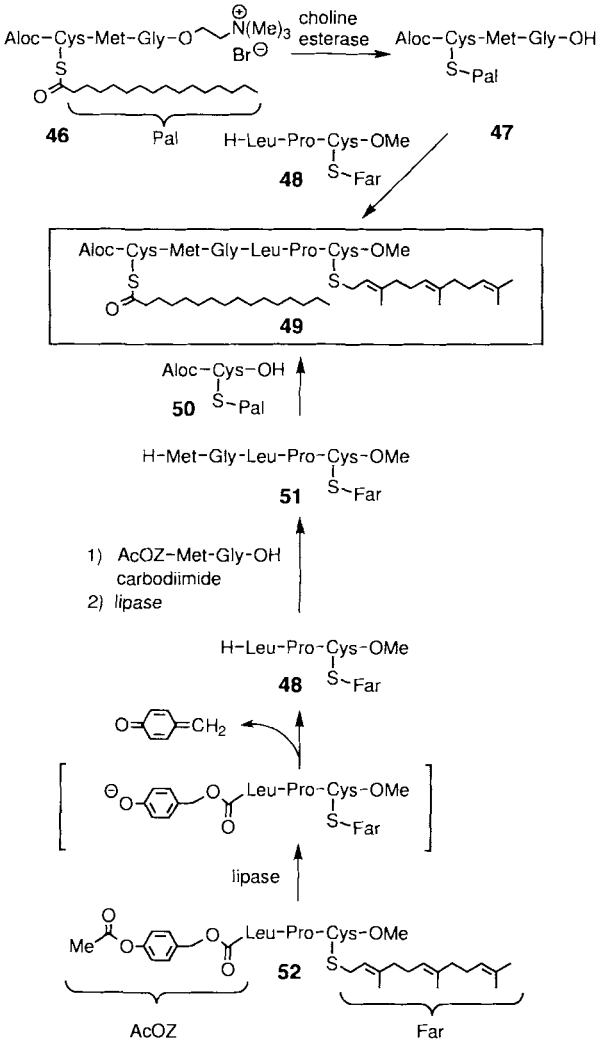

Scheme 28. Chemoenzymatic synthesis of the S-palmitoylated and S-farnesylated C-terminal lipohexapeptide of the human N-Ras protein by H. Waldmann et al. [24, 26].

The advantageous properties of the enzyme-labile protecting groups also makes possible the chemoenzymatic synthesis of base- and acid-sensitive O-glycopeptides.[48, 49] Thus, the C-terminal heptyl ester of the glycosylated serine derivative **53** could be selectively cleaved by lipase-mediated hydrolysis[48] (Scheme 29). Glycopeptide **54** was condensed with an N-terminal deblocked glycodipeptide to give **55**, and enzymatic removal of the heptyl ester was still efficient. Compound **56**, accessible in this way in high yield, was subsequently extended to provide the glycohexapeptide **57**. This compound represents a characteristic

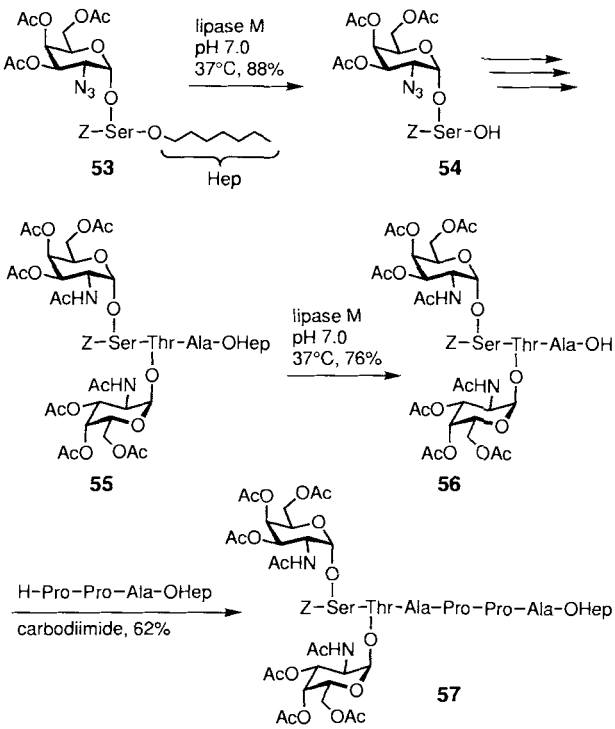

Scheme 29. C-terminal enzymatic deprotection of glycopeptide heptyl esters by H. Waldmann and H. Kunz et al. [48].

fragment of a tumor-associated antigen that appears on the surface of human breast cancer cells.

Selective N-terminal cleavage of a phenylacetoxybenzyloxycarbonyl (PhAcOZ) urethane group (analogous to the AcOZ group) in O-glycopeptides was accomplished by action of penicillin G acylase[49] (Scheme 30). The enzymatic cleavage of this

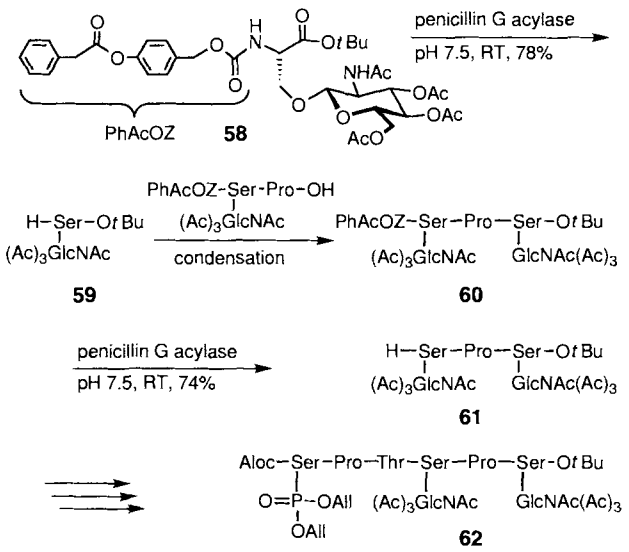

Scheme 30. Use of the enzyme-labile PhAcOZ group in the synthesis of a hexapeptide sequence of a partially processed RNA polymerase by H. Waldmann et al. [49]. RT = room temperature.

urethane protecting group in **58** yielded **59**, which was condensed with a further glycosylated dipeptide to give **60**. The N-terminal protecting group in **60** was removed enzymatically in a selective manner, and the peptide **61** thus liberated was finally converted into the phosphorylated and glycosylated peptide conjugate **62**, a characteristic sequence of a partially processed RNA polymerase. In the enzymatic transformations described in Schemes 29 and 30, no undesired attack on the acetate esters in the carbohydrates was observed, and neither β-elimination of the carbohydrate moiety nor anomerization of the glycosidic bonds take place.[48–50]

The stereoselectivity of enzyme-mediated reactions can also be used advantageously for the preparation of specifically functionalized and protected synthetic intermediates. An example of this is the desymmetrization of the *meso* diacetate **63** in the enantioselective synthesis of the indole alkaloid (−)-anthirin (**66**) by G. Lesma et al.[51] (Scheme 31). Diester **63** was converted into the monoprotected diol **64** with essentially complete selectivity by treatment with porcine pancreatic lipase. The configuration remained intact throughout the construction of the target compound **66** via intermediate **65**. Further applications[52] of such biocatalyzed transformations include syntheses of showdomycin,[53] biotin,[54] an analog of thromboxane A_2,[55] rhizoxin,[56] neplanocin A,[57] nicardipin,[58] chrysanthemic acid, permethric acid and caronic acid,[59] rifamycin,[60] compactin,[61] (+)-disparlure,[62] and aphanorphin.[63]

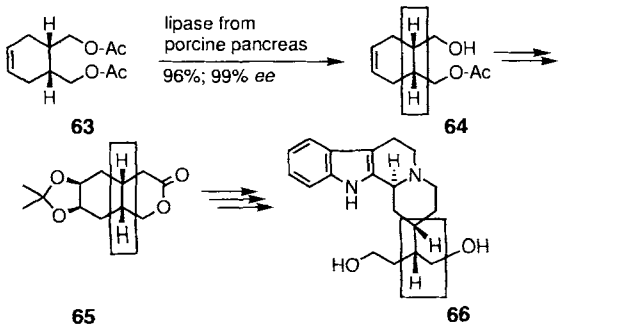

Scheme 31. Example of an enzymatic conversion in the synthesis of (−)-anthirin (**66**) by G. Lesma et al. [51].

3.1.5. *Photolabile Protecting Groups with Other Protecting Groups*

The cleavage of protecting groups by irradiation with light of a suitable wavelength lends itself well to an orthogonal protection strategy.[64] Many other protecting groups are not affected by these conditions, and thus no particularly advantageous combinations have emerged. One of the most impressive applications of this technique is found in the synthesis of the enediyne antitumor antibiotic calicheamicin γ_1^I by K. C. Nicolaou et al.[65] (Scheme 32). To activate the complex oligosaccharide of

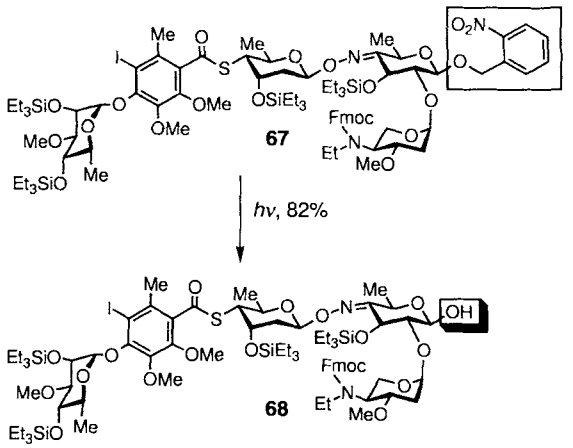

Scheme 32. Application of a photolabile *o*-nitrobenzyl protecting group in the synthesis of calicheamicin γ_1^I by K. C. Nicolaou et al. [65].

the natural product towards the coupling reaction with the aglycone, the anomeric center of the terminal carbohydrate part of the fully protected intermediate **67** had to be liberated. The *o*-nitrobenzyl ether function proved to be a suitable protecting group. Due to its high stability, it could be introduced at an early point in the synthesis and remained intact even under drastic conditions such as treatment with methoxide, tetrabutylammonium fluoride, bromine, and diisobutylaluminum hydride. However, it was easily cleaved from **67** in high yield by photolytic conditions, under which the oxime group, the glycosidic bond, the thioester, the Fmoc group, and the silyl ether all remained intact.

The rate and selectivity of the photochemical deblocking is also an integral part of the "caging" technique used in biological studies[66] (Scheme 33). In this context a inactive substrate such as **69** having a photolabile protecting group is introduced into a biological system, for example, a cell. The protecting group is removed by an intense flash of light and the active compound, in this case **70**, is thereby liberated. The advantage of this method is the precise triggering of the deprotection and libera-

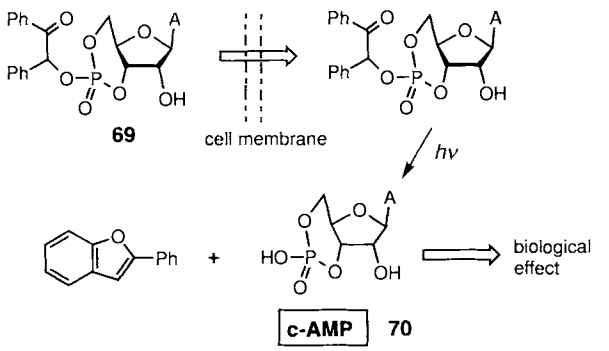

Scheme 33. Application of a photolabile protecting group in the "caging" method. A = adenine.

tion of the active species, making pharmacokinetics measureable, even for fast processes. The prerequisite for the use of the "caging" technique is that the photodecomposition products have minimal toxicity. The required excitation wavelength and intensity should also not damage the cell. The photolabile protecting group most frequently employed in synthesis is the *o*-nitrobenzyl group. Since the photochemical cleavage of this species leads to the production of the toxic *o*-nitrobenzaldehyde, other photolabile groups such as 1-pyrenylethyl[67] and the benzoin group[68] are commonly used for biological applications (see Scheme 33). An exception was described by W. Mäntele et al.,[69] who monitored the progress of a reaction by following the decomposition of an *aci*-nitro intermediate by IR spectroscopy.

Although photochemically cleavable protecting groups offer many advantages, their use is restricted since the substance to be deblocked may not itself contain any photoexcitable functional groups. For this reason this protecting group strategy was not widely applied for a long time. In more recent developments, for example the establishment of anchor groups in combinatorial chemistry (see Section 5), photolabile protecting groups may play an increasingly important role.

3.2. Protecting Groups with Modulated Lability

Protecting groups with modulated lability are often utilized in organic synthesis, although they do not provide the same degree of safety offered by orthogonally stable functions. In particular, this strategy is applied when several of the same type of functional group are present in the molecule to be protected for which an insufficient number of orthogonal groups is available, or when the removal of the most stable protecting group could lead to undesired side reactions. In principle, protecting groups of modulated lability can be developed for each of the classes discussed in Section 2. Acid-labile, base-labile, and fluoride-labile protecting groups have proved to be particularly suitable; oxidatively cleavable functions have more limited scope. The modulated lability of many protecting groups can be referred to in, for example, ref. [9].

3.2.1. Modulated Acid- or Base-Lability

In many cases acetals have different labilities towards acids. For instance, acyclic acetals are more sensitive than their cyclic equivalents to acidic conditions. This property was utilized by R. Ellison et al. in the synthesis of a prostaglandin precursor[70] (Scheme 34). The selective removal of the dimethyl acetal in **71** proceeded in almost quantitative yield and provided the liberated aldehyde **72**, which was used in chain extension. After the removal of the dithiane group, **73** was ready for ring closure, which yielded the desired functionalized prostaglandin precursor **74**.

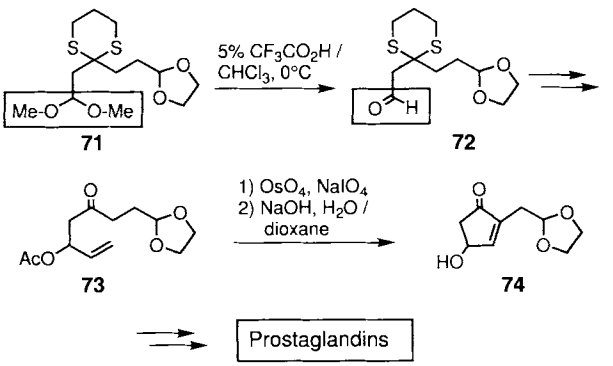

Scheme 34. Use of acid-labile protecting groups with modulated lability in the synthesis of a prostaglandin precursor by R. Ellison et al. [70].

The principle of using protecting groups with modulated acid-lability has found repeated application in peptide chemistry (see Sections 2 and 4). This is exemplified by the synthesis of human insulin carried out by P. Sieber et al.[71] and sketched in Scheme 35. Compound **75** bears three protecting groups of

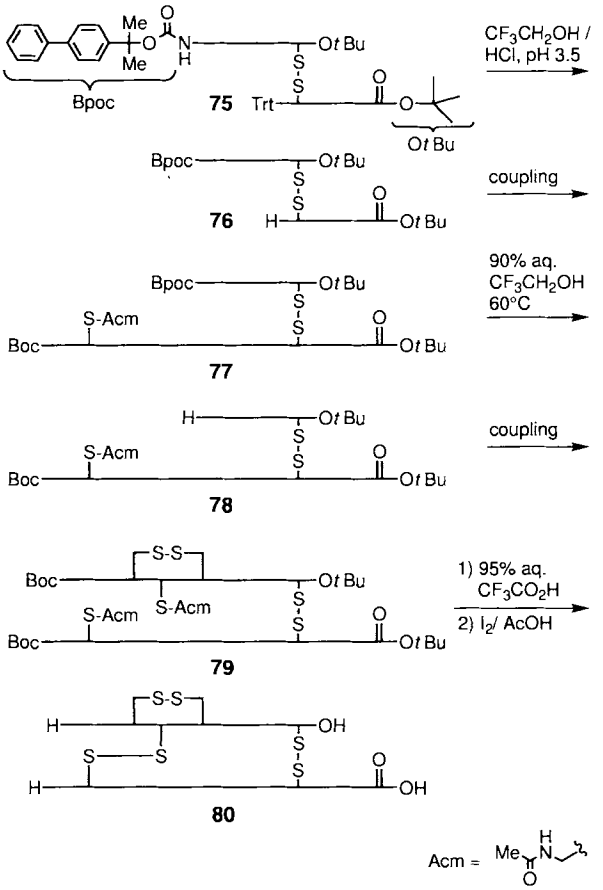

Scheme 35. Use of acid-labile protecting groups with modulated lability in the synthesis of human insulin by P. Sieber et al. [71].

varying lability—the *tert*-butyl ester and the Bpoc and trityl (Trt) groups. First the trityl group was removed selectively in the presence of the Bpoc group, which is likewise very acid-sensitive. After extension of the B chain (**76** → **77**), the Bpoc group was selectively removed. The A chain was completed by coupling **78** with a similarly Boc-protected peptide. All the *tert*-butyl protecting groups in **79** were then simultaneously cleaved. After the cysteine side chain was deblocked, ring closure provided insulin **80**.

While the synthesis shown in Scheme 35 proves that this methodology can be quite successful, it has not found widespread use in peptide chemistry due to the potential of losing protecting groups required later in the synthesis. Owing to their greater reliability, orthogonal protecting strategies are generally preferred.

The modulated based-lability of two urethane protecting groups was used by K. C. Nicolaou et al. in the synthesis of a calicheamicin–dynemicin hybrid[72] (Scheme 36). The 2-fluorenylmethoxycarbonyl (Fmoc) group was removed from the complex glycoside **81** by treatment with diethylamine, without attack at the similarly base-labile 2-phenylsulfonylethoxycarbonyl (Psec) group. The cleavage of this group under basic conditions later triggered the liberation of the "warhead", which is buried in the dynemicin aglycone of **82**.

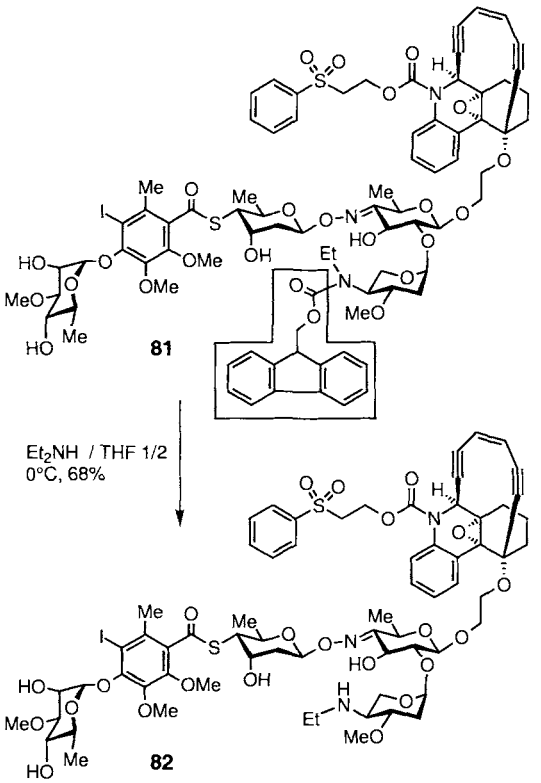

Scheme 36. Use of amino protecting groups of differing lability in the synthesis of a calicheamicin–dynemicin hybrid by K. C. Nicolaou et al. [72].

3.2.2. *Modulated Lability of Silyl Protecting Groups*

The lability of silyl groups towards acids, bases, and fluoride ions can be specifically tuned by varying the substituents on silicon. Scheme 37 indicates the relative rates of hydrolysis of various silyl ethers under acidic and basic conditions. (The order of the cleavage rates on treatment with fluoride ions is similar.) As a consequence of this range of activities, silyl ethers with modulated solvolytic activity are now commonly used in synthesis.

Relative stability of silyl ethers	R–O–SiR'$_3$
Acidolysis:	R'$_3$Si: Me_3Si (1) < Et_3Si (64) < tBuMe$_2$Si (20000) < iPr$_3$Si (700000) < tBuPh$_2$Si (5000000)
Basic solvolysis:	R'$_3$Si: Me_3Si (1) < Et_3Si (10-100) < tBuMe$_2$Si ≈ tBuPh$_2$Si (20000) < iPr$_3$Si (100000)

Scheme 37. Relative rates of hydrolysis for silyl ethers R–O–SiR'$_3$ (k_{rel}^{-1}).

tert-Butyldimethylsilyl (TBDMS) ethers can be cleaved with, for example, tetrabutylammonium fluoride (TBAF), while the cleavage of the more stable triisopropylsilyl (TIPS) and the *tert*-butyldiphenylsilyl (TBDPS) protecting groups requires solutions of HF in pyridine, acetonitrile, or even water.

These clear differences in reactivity were employed by Danishefsky et al. in the synthesis of the immunosuppressant rapamycin[44] (Scheme 38). When intermediate **83**, which con-

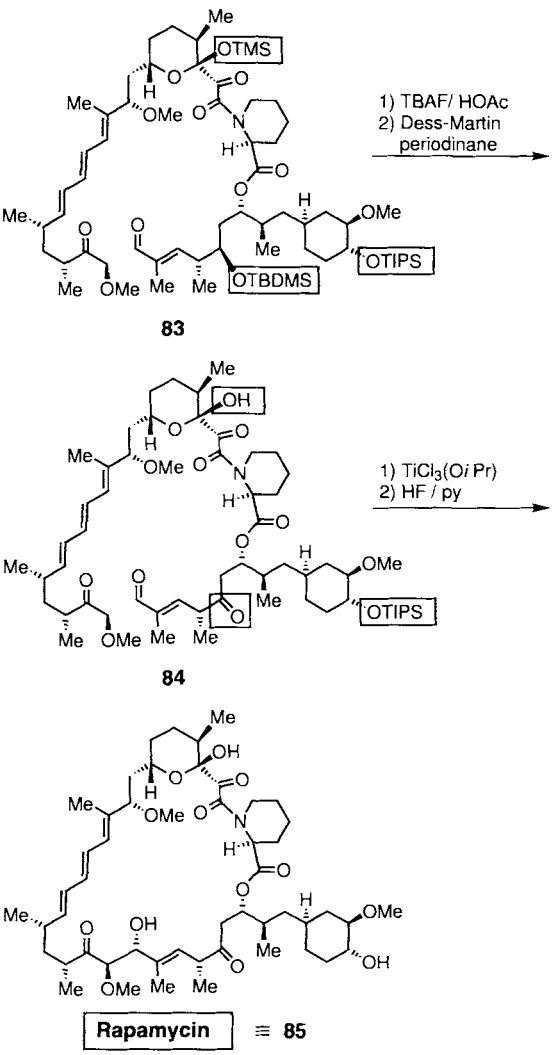

Scheme 38. Use of silyl protecting groups of modulated lability in the synthesis of rapamycin (**85**) by S. Danishefsky et al. [44].

tains a TMS, a TBDMS, and a TIPS ether, was treated with TBAF, the TMS and the TBDMS ethers were cleaved, but the TIPS ether remained intact. After oxidation of the liberated secondary hydroxyl group, the macrocyclic ring was closed, and finally the TIPS ether in the cyclohexane moiety in **84** was cleaved with a solution of HF in pyridine to yield the natural product **85**.

The different stabilities of silyl ethers was also utilized by K. C. Nicolaou et al.[42] in their synthesis of rapamycin. Scheme 22 indicates that treatment of **24** with HF/pyridine removed only the TBDMS protecting group, while the TIPS-protected secondary hydroxyl group remained intact. A similar strategy was used in the last steps of this synthesis (Scheme 39).

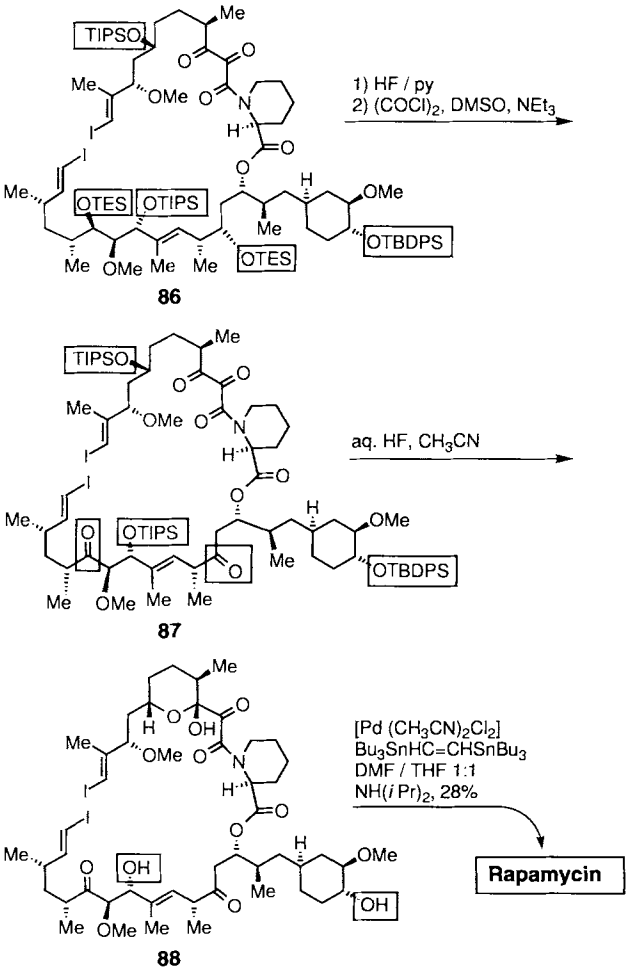

Scheme 39. Use of silyl protecting groups of modulated lability in the synthesis of rapamycin by K. C. Nicolaou et al. [42].

Of the five silyl protecting groups present in **86**, only the TES ethers were cleaved by HF/pyridine. Thus the selective oxidation of the liberated secondary hydroxyl groups to give the corresponding carbonyl groups could be carried out. The remaining, more stable silyl ethers were cleaved by treatment with HF in CH_3CN/H_2O, and the synthesis was subsequently concluded by Pd^0-mediated coupling of the two vinyl iodides.

The differing acid sensitivity of silyl ethers allowed S. Schreiber et al. to selectively deblock an advanced intermediate in the synthesis of FK506[41] (Scheme 21). Macrocycle **19** contains TIPS, TBDMS, and TES protecting groups, of which only the TES group was removed by treatment with aqueous trifluoroacetic acid, allowing the selective oxidation of only one of the four hydroxyl groups.

R. A. Holton et al. took advantage of the varying lability of silyl ethers towards both bases and different sources of fluoride ions in the synthesis of the antitumor agent taxol[73] (Scheme 40). Thus, treatment of **89** with acetic acid cleaved only

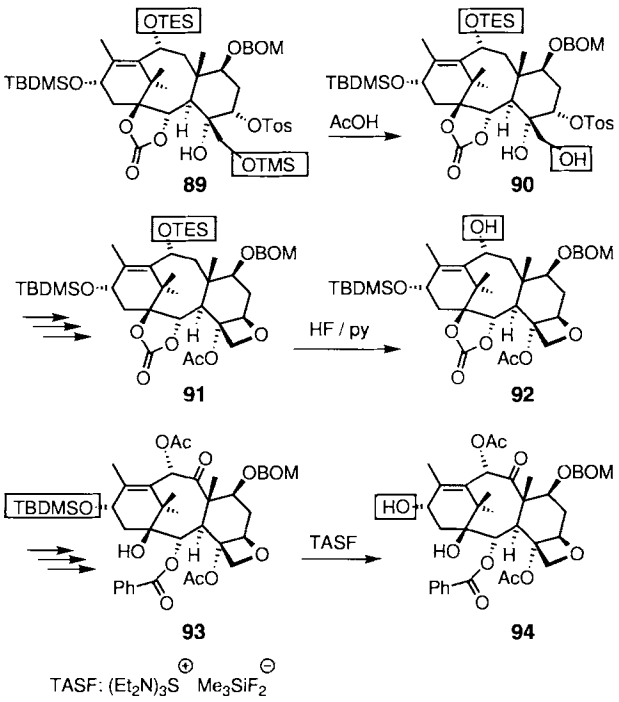

Scheme 40. Use of silyl protecting groups of modulated lability in the synthesis of taxol by R. A. Holton et al. [73].

the TMS ether; the other acid-labile groups, the BOM acetal and the other silyl groups, remained intact. After transformation of **90** into the oxetane **91**, the TES group was selectively removed by treatment with HF/pyridine. The central eight-membered ring was oxygenated as required in the position adjacent to the free hydroxyl group. Finally, the remaining TBDMS protecting group was removed with the reagent TASF (see Scheme 40; this conversion failed with TBAF) to allow the attachment of the side chain.

3.2.3. Modulated Oxidation-Lability

The oxidation-labile Mpm and Dmpm ethers (see Section 2.6) are attacked at different rates by dichlorodicyanoquinone (DDQ) at 0–5 °C. This modulated lability can be employed advantageously in the synthesis of polyfunctional target compounds, including those containing C–C double bonds. Thus, in the course of a total synthesis of methynolide (**98**), O. Yonemitsu et al. cleaved the more electron-rich, and therefore more easily oxidized Dmpm group in **95** in the presence of an Mpm group by treatment with DDQ at 0 °C (Scheme 41).[74, 75] The hydroxyl group in **96** thus liberated was then oxidized to the

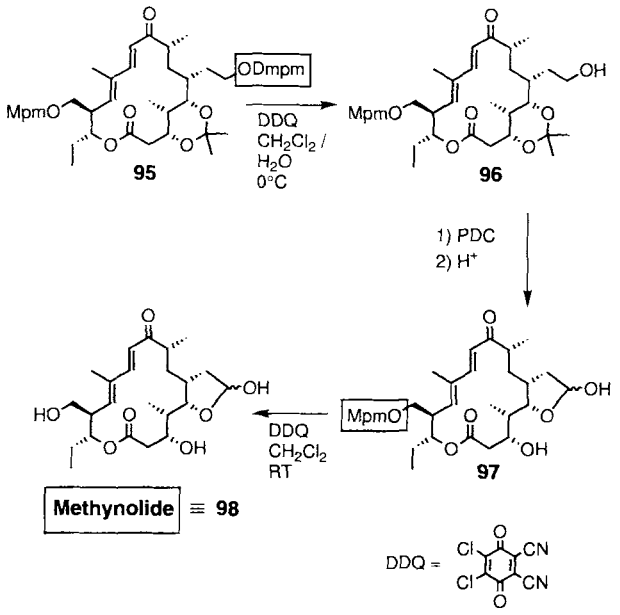

Scheme 41. Selective oxidative cleavage of the Dmpm group in the presence of the Mpm group in the synthesis of methynolide (**98**) by O. Yonemitsu et al. [74, 75]. PDC = pyridinium dichromate. RT = room temperature.

aldehyde, which cyclized to give the hemiacetal **97** following the acid-catalyzed hydrolysis of the adjacent acetal protecting group. Finally, the desired natural product was obtained by oxidative cleavage of the Mpm ether at room temperature.

Such fine-tuning of lability through the introduction of substituents can also be achieved for other types of protecting groups. Thus, for example, when a nitrophenyl substituent is attached to the allyl system of an allyloxycarbonyl (Aloc) group, cleavage of the resulting 4-nitrophenylallyl (Noc) urethane with Pd^0 and Rh^I catalysts is significantly slower than that of the simple unsubstituted allyl protecting groups.[76] As can be seen from Scheme 42, the allyl ester in dipeptide **99** can be cleaved selectively without attack on the Noc group.

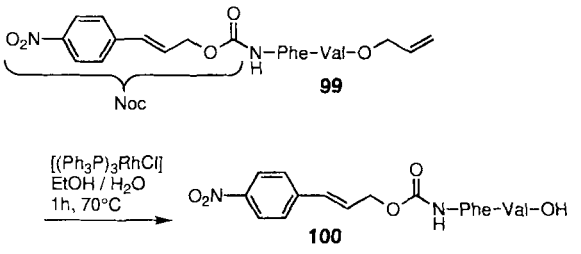

Scheme 42. Selective cleavage of an unsubstituted allyl ester in the presence of a nitrophenylallyl group by H. Kunz et al. [76].

3.3. Unification of Protecting Groups

In the construction of polyfunctional molecules the tactic of using several protecting groups that must be removed under drastically different reaction conditions can lead to problems in the late stages of a synthesis, for example after successful construction of the molecular framework. First, the molecule must be stable under all of the conditions used for deblocking. This stipulation must be made in the selection of protecting groups for each subunit in the whole molecule. It is thus possible that only a few—and under certain circumstances too few—of the available protecting groups fulfill this criterium. Second, such a strategy can lead to a significant increase in the number of steps required at the end of the synthesis, even to the point that the associated losses become crippling.

To avoid these problems, the following strategy is often followed, in particular in complex multistep syntheses. As early as possible in the synthesis, protecting groups are used that can be removed under the same conditions in order to unify the protecting group pattern as much as possible. For example, intermediates having a single type of protecting group can be designed and used from the beginning of a synthesis, thus automatically simplifying the problem. This strategy cannot be used if specific reactivities in the intermediates are eliminated in the course of the synthesis, or the directing effect of particular protecting groups is required (see Section 3.5). Then protecting groups in the intermediates must be removed and replaced with others that correspond to the type remaining in the molecule. Under certain conditions this can increase the length of the

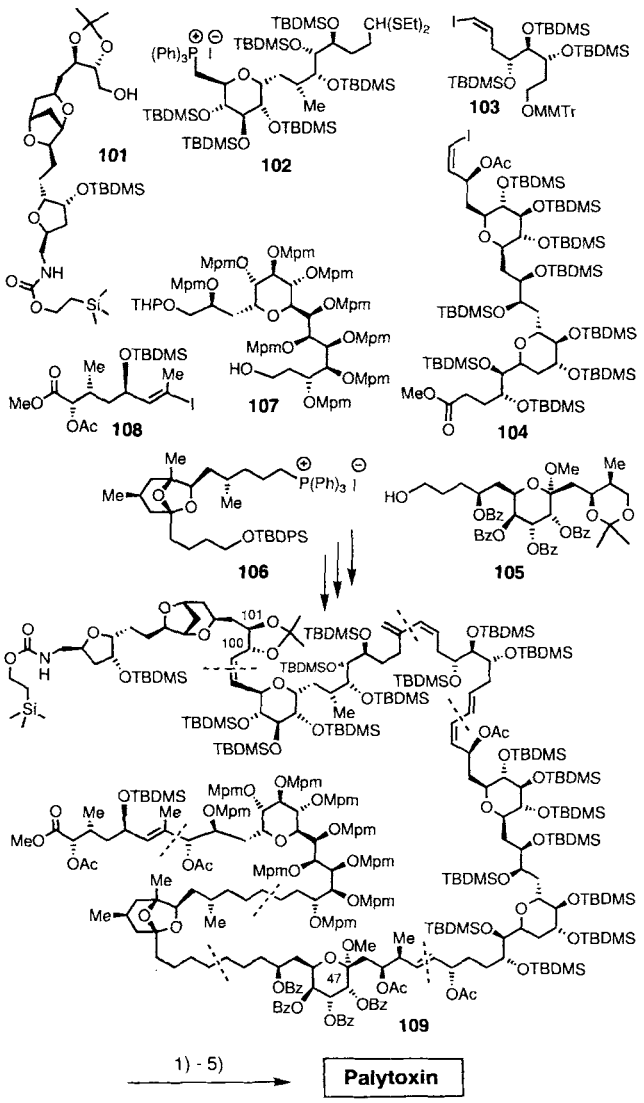

Scheme 43. Part of the synthesis of palytoxin by Y. Kishi et al. [77]. 1) DDQ, tBuOH/CH_2Cl_2, room temperature (RT), then Ac_2O, DMAP in pyridine; 2) $HClO_4$ (1.18 N) in THF, 25 °C, 8 d; 3) 0.08 N LiOH, H_2O/THF (1:2:8), 25 °C, 20 h; 4) nBu$_4$NF in THF, 22 °C, 20 h; 5) AcOH/H_2O (1:9), RT, 12 h.

synthesis; however, the risk of losses is shifted toward earlier stages in the synthesis with the simpler and more readily available early intermediates.

The strategy of creating the uniformly protected intermediates, which can be completely deblocked in only a few steps at the end of the synthesis, was followed by Y. Kishi et al. in the synthesis of the marine natural product palytoxin[77] (Scheme 43). The size of the molecule, sheer number of groups needing protection, and the long list of synthetic problems to be overcome made it very difficult to use only one type of protecting group. Intermediate **109** (Scheme 43) contains the complete and still completely protected molecular framework of palytoxin, which was formed by the coupling of fragments **101**–**108**. In **101**, **102**, **103**, and **104** the protecting groups are almost exclusively fluoride-labile, **105** and **108** incorporate esters of differing base-lability, and in **107** the hydroxyl groups are protected as oxidation-labile Mpm ethers. In addition, it was necessary to protect the hemiacetal at C-47 and the diol unit at C-100 and C-101 as acid-labile acetals. This significant unification of the types of protecting groups enabled efficient deblocking in only five steps at the end of this extremely arduous synthesis (Scheme 43).

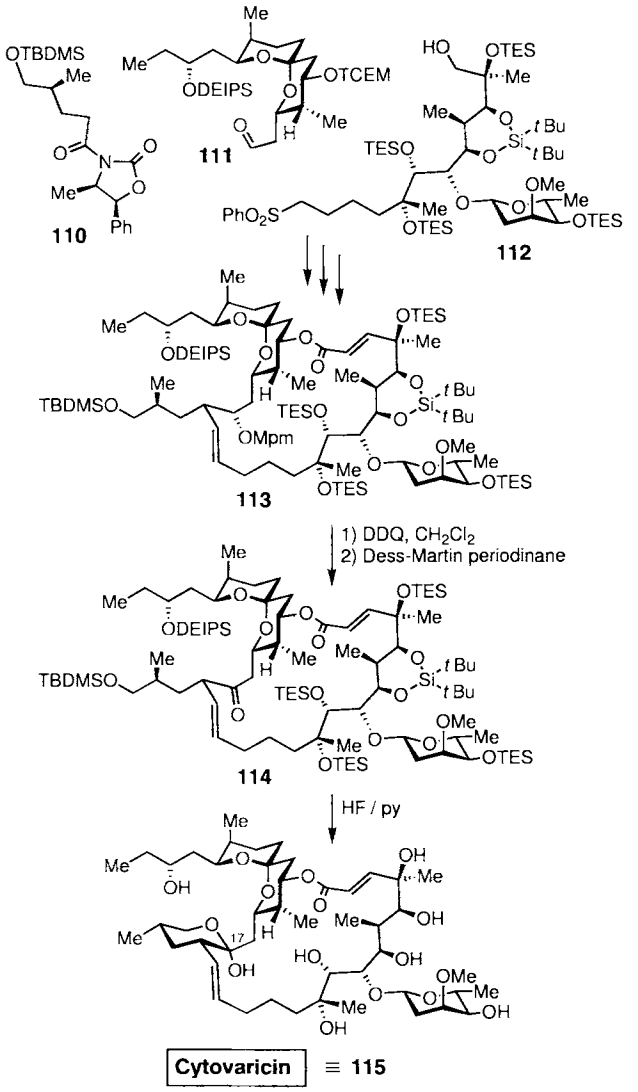

Scheme 44. Synthesis of cytovaricin (**115**) by D. A. Evans et al. [78]. DEIPS = diethylisopropylsilyl, TCEM = trichloroethoxymethyl.

The strategy of choosing all the permanent protecting groups from the same class was demonstrated by D. A. Evans et al. in the synthesis of cytovaricin (**115**)[78] (Scheme 44). The intermediates **110**–**112** used to construct the protected form of the natural product **114** carried exclusively silyl protecting groups, all of which were removed in high yield in a single step at the end of the synthesis. The conditions required were so mild that the hemiacetal formed at C-17 remained stable and did not lose water and form a diene.

S. Danishefsky et al. used the same principle in the synthesis of the enediyne antibiotic dynemicin A[79] (Scheme 45). Thus

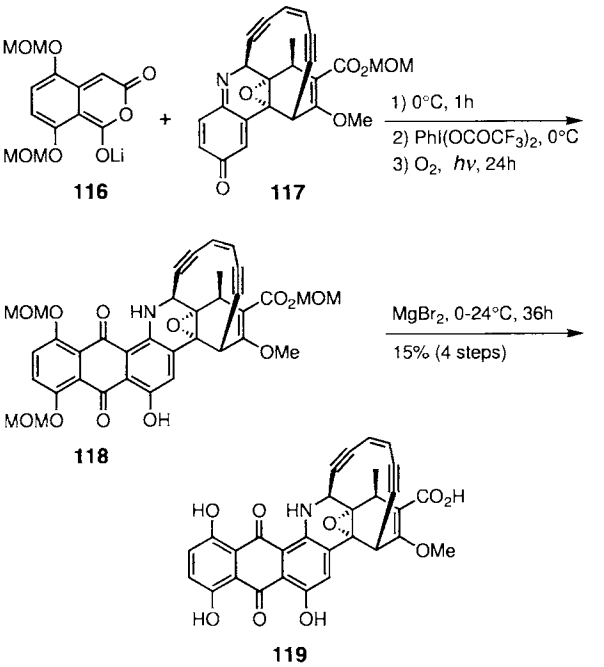

Scheme 45. Use of a single type of protecting group in the synthesis of dynemicin by S. Danishefsky et al. [79]. MOM = methoxymethyl.

116 and **117** were fused to give compound **118** with three MOM acetal protecting groups, from which the sensitive natural product **119** was liberated.

The protecting group pattern of an advanced intermediate was changed by K. C. Nicolaou et al. in the synthesis of calicheamicin γ_1^I[65] (Scheme 46). The complex glycoside **123** was formed from the predominantly acyl-protected unit **120** and the intermediates **121** and **122**. After the coupling, the acetates were transformed into silyl ethers, which were cleaved in the same step as the silyl ethers originating from **121** and **122** by treatment with HF/pyridine in almost quantitative yield.

In the synthesis of the glycosphingolipid Gb_3 (**130**), K. C. Nicolaou et al.[80] swapped the reduction-sensitive benzyl ethers for the base-labile acetates and thus unified the pattern of protecting groups (Scheme 47). Because the galactosylfluoride **125** carried benzyl groups, its coupling with the partially deblocked glycosyl acceptor **126** yielded the trisaccharide **127** predominantly as the α-anomer. Intermediate **126** carried acyl protecting groups, guaranteeing a high degree of β-selectivity in the introduction of the sphingosine group (see also Section 3.5). At the stage of trisaccharide **127** the benzyl protecting groups were

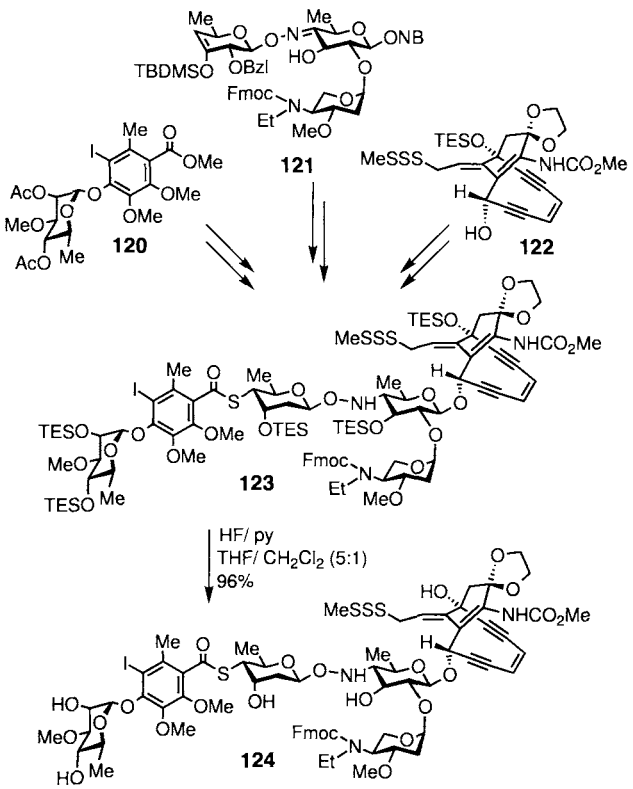

Scheme 46. Change in the pattern of protecting groups in the synthesis of calicheamicin γ_1^1 by K. C. Nicolaou et al. [80]. NB = nitrobenzyl.

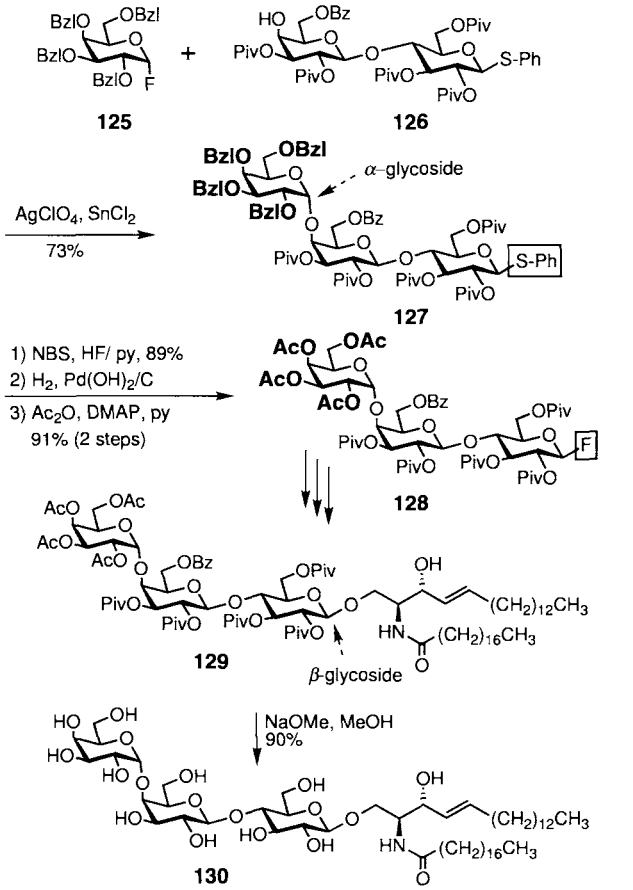

Scheme 47. Unification of the protecting group pattern in the synthesis of the glycosphingolipid Gb_3 (**130**) by K. C. Nicolaou et al. [81].

removed by hydrogenolysis and the hydroxyl groups thus liberated were immediately protected as acetates. The complete trisaccharide unit thus contained exclusively base-labile acyl protecting groups, which, at the end of the synthesis, were removed simultaneously in high yield. This strategy also proved to be very effective in the construction of the trimeric Lewis^x nonasaccharide.[81]

3.4. Introduction of "Stand-Ins"

In the synthesis of polyfunctional compounds, two factors can make the choice of protecting group strategy particularly difficult: the lability of the intermediates and the fact that sufficiently different enough protecting groups might not be available for a given type of functional group. Aldehydes and ketones are generally protected as thioacetals or O,O-acetals. An example of this is given by the synthesis of FK506 by S. Schreiber et al.,[41] a section of which is shown in Scheme 48. The terminal aldehyde was masked as a 1,3-dithiane in **131**; however, all attempts to liberate the protected carbonyl group by established methods afforded the desired product in very low

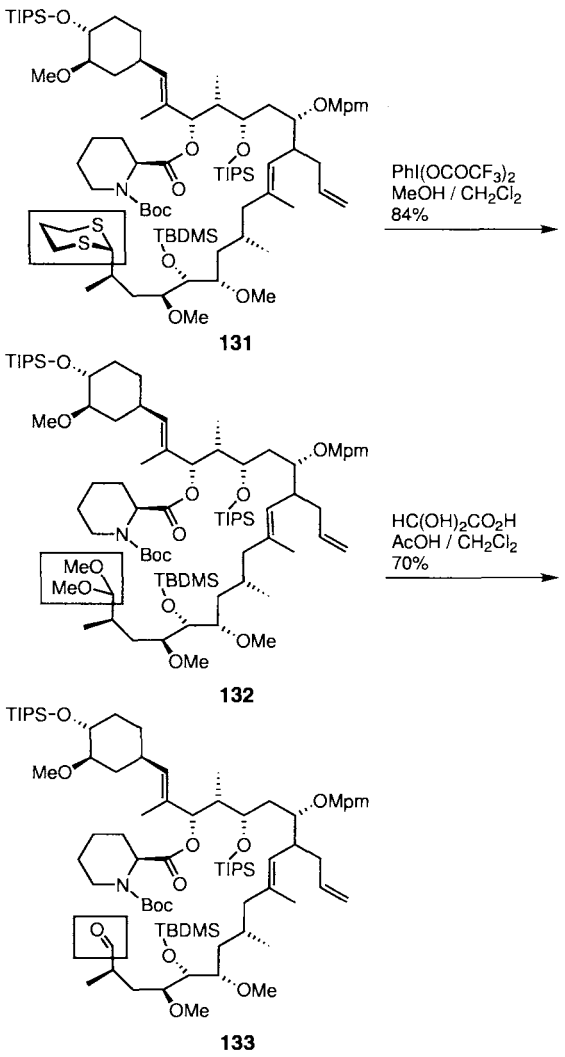

Scheme 48. Application of 1,3-dithiane and dimethyl acetal protecting groups in the synthesis of the immunosuppressant FK506 by S. L. Schreiber et al. [41].

yields. Only dethioacetalization employing a hypervalent iodine reagent as a mild oxidant gave satisfactory results. Even so, the aldehyde thus liberated was not isolated directly in the free state, but rather as the dimethyl acetal **132**. This very sensitive compound yielded **133** with the free aldehyde group after transacetalization with glyoxylic acid under mildly acidic conditions. This approach is practically identical to that employed by T. K. Jones et al. in the synthesis of FK506.[82]

The example just given illustrates that, despite the effectiveness of thioacetals and acetals as protecting groups, the conditions necessary for their removal often hinder their use. 1,3-Diols can also be protected as silylene derivatives, which are useful replacements for the acid-labile acetals (see **114** in Scheme 44). When such choices are not available, a completely different tactic must be used.

In one increasingly popular alternative strategy a "stand-in" is introduced for the required functional group. In the case of a carbonyl group, a masked alcohol can be used, which can be deprotected and subsequently oxidized to give the required aldehyde or ketone. Although a further protecting group must be introduced in following this strategy, many more masking groups are established for the hydroxyl function.

This methodology is illustrated by the synthesis of FK506 by S. Schreiber et al.[41] sketched out in Scheme 21. The very sensitive and reactive tricarbonyl unit in **20** was constructed right at the end of the synthesis by the deprotection and oxidation of the corresponding hydroxyl groups. The successive deblocking and oxidation prevented the formation of mixtures of products resulting from incomplete oxidation. TES- and Mpm-protected hydroxyl groups were employed as the "stand-ins" for the carbonyl groups, while the hydroxyl groups found in the final product (**20**) were masked as TIPS and TBDMS ethers.

Similarly, in the synthesis of rapamycin by S. Danishefsky et al.[44] (Scheme 38) at a step close to the end of the synthesis, one of the three protected hydroxyl groups in **83** is selectively deblocked and oxidized to give a carbonyl group.

D. A. Evans et al. also used this strategy in the synthesis of cytovaricin[47] (Scheme 44). The hydroxyl group to be oxidized in **113** was present as the Mpm ether, whereas all other alcohols were blocked as silyl ethers. After cleavage of the benzylic protecting group with DDQ, the required carbonyl group was formed and finally the silyl groups removed. This approach was necessary because the hemiacetal formed in the last step is very sensitive (see Section 3.3.).

3.5. The Influence of Protecting Groups on the Course of Syntheses

One factor that should always be taken into account when planning a protecting group strategy is the potential of the protecting group, under certain circumstances, to actively influence the course of the synthesis.

For example, the ability (or lack of) of a protecting function to complex metal ions can be utilized to direct the stereochemical course of a reaction. This use of "(non)chelating" protecting groups is one of the best established tools of asymmetric synthesis.[83] Such an effect was used by J. Mulzer et al.[84] in the synthesis of erythronolide B (Scheme 49). The diastereomeric

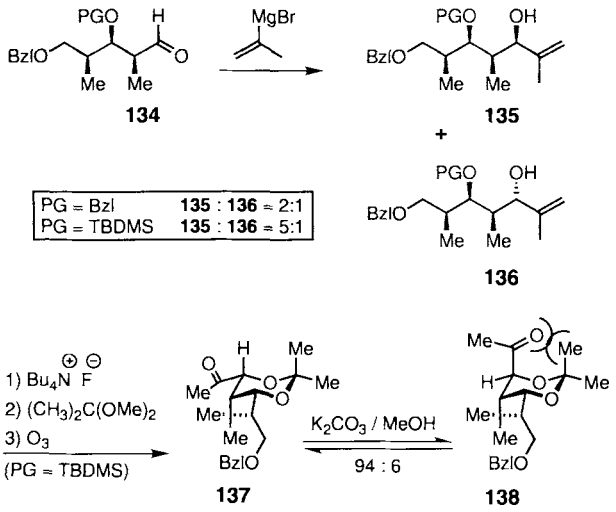

Scheme 49. Stereochemical directing effects of protecting groups in the synthesis of erythronolide B by J. Mulzer et al. [84].

ratio of **135** and **136** formed from the addition of propenylmagnesium bromide to the aldehyde **134** was dependent upon the type of ether function present in **134**. When the secondary hydroxyl group was protected as its benzyl ether, this ratio was 2:1; however, the corresponding silyl ether led to a 5:1 ratio of **135** and **136**. The silyl group hindered the formation of a 1,3-chelate leading to *anti*-**136** and favored the development of a Felkin–Anh transition state leading to the *syn*-diol. The diastereomeric ratio could be increased further by manipulation of the protecting groups. The mixture of **135** and **136** was converted to the acetonides **137** and **138**. An unfavorable 1,3-diaxial interaction of the ketone with one of the methyl groups of the acetal protecting group came into play in **138**, which meant that **138** could be equilibrated to the more stable **137** by treatment with K_2CO_3 in methanol.

BOM, MOM, and MEM ethers are typically used as chelating protecting groups (see Section 2.1.1.). Thus, for example, M. Isobe et al. employed the directing effect of a MEM group for the stereoselective construction of a precursor to maytansin[85] (Scheme 50). In the reaction of **139** with methyllithium, the oxygen atoms of the protecting group complex the lithium cation and thus force the attack of the organometallic reagent onto the *Re* side of the double bond in the vinyl sulfone.

The directing effect of protecting groups is typically used in the synthesis of oligosaccharides, where the course of the glyco-

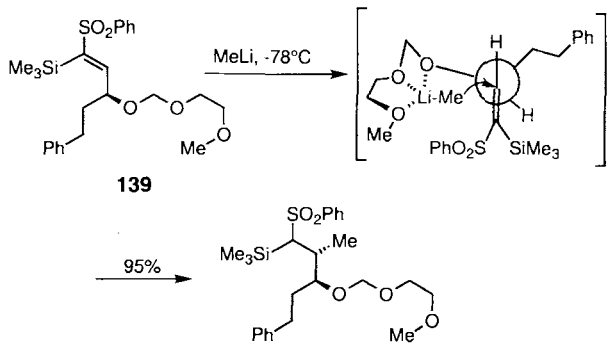

Scheme 50. Directing influence of the MEM protecting group in the synthesis of a precursor of maytansin by M. Isobe et al. [85].

sylation can be affected. In glycosyl donors such as **140** (Scheme 51) the ester function in the 2-position shields the underside of the glycosyl cation **142** formed during the glycosylation reaction. Thus, the glycosyl acceptor **143** attacks from above to form the β-glycoside **144**.[86] If the 2-position of the

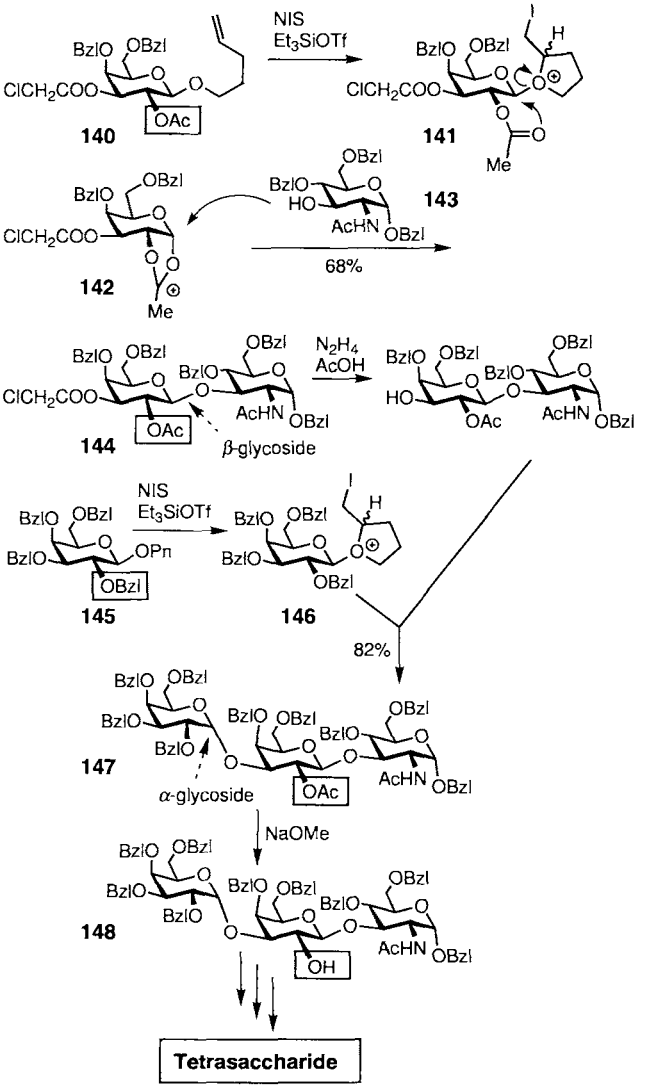

Scheme 51. Control over α/β-selectivity by choice of suitable protecting groups in the synthesis of the blood group B tetrasaccharide by B. Fraser-Reid et al. [86]. Pn = pentenyl, NIS = *N*-iodosuccinimide.

glycosyl donor is not blocked by an acyl group capable of neighboring group participation, as is the case in the benzyl-protected donor **145**, then the α-glycoside, in this case **147**, is preferentially formed. This directing effect was used highly effectively by B. Fraser-Reid et al. in the synthesis of **147**, en route to the tetrasaccharide characteristic of the human blood group B. A further example is given in the preparation of the Gb_3 glycolipid by K. C. Nicolaou et al. sketched in Scheme 47.

The type of protecting group determines not only the stereochemical course of glycoside synthesis, but also affects the reactivity of the glycosyl donor. Since esters are better electron acceptors than ethers, the formation of glycosyl cations is less favored from an acyl-protected glycosyl donor like **140** than from an alkyl-protected donor such as **145**. The nucleophilicity of the leaving group at the anomeric center is also less in the ester case than in the alkyl-protected system. To characterize this finding, B. Fraser-Reid et al. described these acyl-masked glycosyl donors as "disarmed" with respect to activation by electrophiles, while alkyl-masked donors were viewed as being "armed".[87] This concept of armed/disarmed groups has proved useful for a wide variety of different glycosyl donors.

4. The Best Protecting Group Is No Protecting Group

The examples discussed in the foregoing sections illustrate the capabilities of the protecting group techniques available today and indicate that protecting groups can also be used to influence the course of reactions. Nevertheless, an unavoidable consequence of the introduction and removal of protecting groups is that the synthesis is lengthened, and that the use of protecting groups is thus often seen as "unproductive".[84]

The number of protecting group manipulations can be kept to a minimum through the use of the differences in reactivity of similar or identical functional groups. In certain cases this can determine the course of the entire synthesis and the chosen protecting group pattern. This approach is chosen again and again in the synthesis of glycosides, for example, because reliable information is available concerning the reactivity of the various hydroxyl groups in carbohydrates. R. R. Schmidt et al. applied this strategy in the synthesis of the dimeric Lewis^x determinant illustrated in Scheme 20.[39] In **12** and **15**, the hydroxyl groups at C-3 and C-4 of the terminal carbohydrate were protected together as an acetal. After cleavage of the isopropylidene acetals of **12** and **15**, the glycosyl donor **14** reacted regioselectively in both cases with the equatorial groups at C-3 to give the pentasaccharide **15** and the octasaccharide **16**, respectively. The introduction of a protecting group at C-4 was thus unneccessary. R. R. Schmidt et al.[88] also utilized the difference in reactivity of the C-3 and C-4 hydroxyl groups in the syntheses of the tri- and tetrameric Lewis^x glycosphingolipids.

Differences in the reactivity of functional groups have also been utilized in the synthesis of oligopeptides. An example of this tactic of "minimal protection" was also used in impressive fashion by R. Hirschmann and D. F. Veber et al.[89] in the synthesis of the S-protein of ribonuclease A. This peptide consists of 103 amino acids and contains all of the trifunctional amino acids with the exception of tryptophan. As indicated in Scheme 52 for the masked 21–40 fragment **149**, only the ε-amino groups of lysine and the β-mercapto group of the cysteine were masked, while the side chains of arginine, aspartic acid, and the hydroxyamino acids serine, threonine, and tyrosine remained unprotected. This strategy stands in contrast to the concept of "maximum protection", in which the maximum number of functional groups are masked in order to avoid side reactions. E. Wünsch et al. followed this strategy in the synthesis of the peptide hormone glucagon[90] and protected the side chains of all the hydroxyamino acids, histidine, lysine, and aspartic acid with acid-labile protecting groups. The resulting 7–15 intermediate **150** (Scheme 52) indicates that a distinctly greater effort must be made to prepare such synthetic intermediates than is demanded by the "minimal protection" tactic.

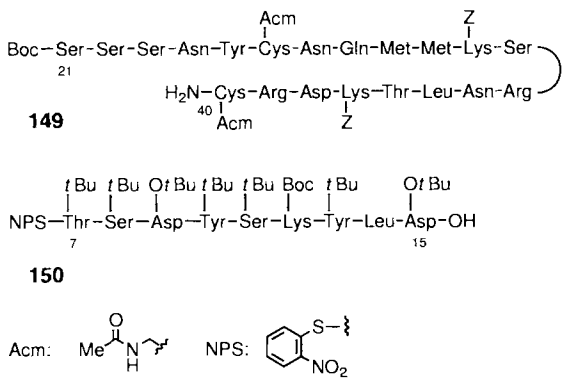

Scheme 52. The "minimal protection" tactic in the synthesis of the S-protein of ribonuclease A (21–40 fragment **149**) by R. Hirschmann and D. F. Veber et al. [89] and the "maximum protection" tactic in the synthesis of glucagon (7–15 fragment **150**) by E. Wünsch et al. [90].

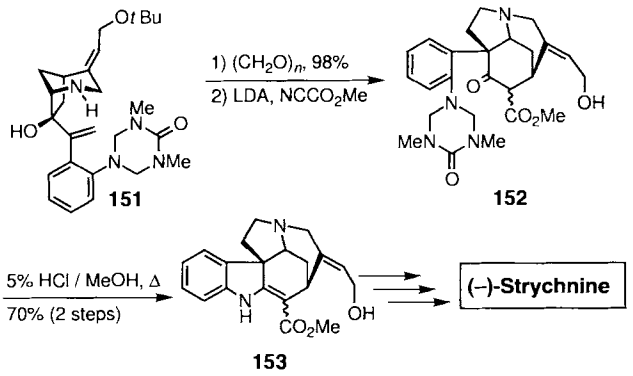

Scheme 53. Use of the triazone protecting group in the synthesis of strychnine by L. E. Overman et al. [92].

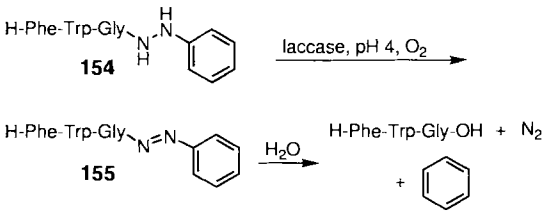

Scheme 54. Enzymatic cleavage of phenylhydrazides from peptides by A. N. Semonov et al. [93].

While the danger of side reactions is greater when one uses minimal protection, and the number of compatible coupling techniques is reduced, the tactic of maximum protection has the disadvantage that losses in yield can occur during the removal of protecting groups, and that the protected peptide fragments are often poorly soluble or difficult to purify.

5. New Developments

Most of the protecting groups discussed in Sections 2 through 4 have been known for some time. Their usefulness has been demonstrated in a multitude of complex syntheses and they can be considered to be well-established[10, 11] (this conclusion cannot yet be drawn for the enzyme-labile protecting groups). Nevertheless, the development of new protecting group techniques and the improvement of existing methods continues to be the subject of intensive research in organic synthesis. The following trends can be distinguished from the large number of new developments.

5.1. Development of Protecting Groups with New Lability/Stability

New developments on protecting groups with modulated reactivity have been described for silyl ethers, in particular (see Section 2.3), but new acid-labile groups have also been successfully developed and applied. An example is the triazone protecting group for amines developed by S. Knapp et al.,[91] which blocks two N–H positions and can be easily cleaved with dilute acid. This protecting group was essential in studies by L. E. Overman et al.[92] on the synthesis of the strychnine alkaloids, as illustrated by the synthesis of strychnine itself (Scheme 53). In the precursor **151** the amino group of the aniline was masked as a triazone, which, after a domino sequence consisting of Mannich reaction and aza-Claisen rearrangement, could be removed from **152**, enabling the subsequent ring closure to give **153**. If the *tert*-butylurethane (Boc) group or a pivalinamide is used in place of the triazone, the selective cleavage is not successful.

The application of biocatalysts has given the area of orthogonally stable protecting groups new impetus. An example of this is given in Scheme 54. Peptides such as **154**, which carry a phenylhydrazide at the C-terminus, are oxidized by the enzyme laccase to give the diimide, in this case **155**, which spontaneously hydrolyzes and liberates the desired peptide.[93] Phenylhydrazides can be cleaved by classical chemical methods only under much more drastic conditions.

5.2. Development of Protecting Groups that Induce Alternative Selectivities in Reactions

The number of blocking/deblocking steps in a synthesis can be reduced by employing protecting groups which, upon introduction, can distinguish between several functional groups of similar reactivity. Examples of such protecting groups are the recently developed dispiroketal (DISPOKE) and cyclohexane-1,2-diacetal (CDA) protecting groups,[14, 15, 94] which selectively mask diequatorial 1,2-diols. In the synthesis of the trisaccharide unit **161** of a streptococcal antigen, the two OH groups in the 3- and 4-positions of the glycosyl acceptor **156** were selectively blocked and thus the axial hydroxyl group at C-2 was made available for the coupling reaction with the glycosyl donor **158** (Scheme 55).[15] The disaccharide **159** thus formed was ready for a further glycosylation; its coupling with **160** and subsequent cleavage of the CDA and the benzyl groups completed an efficient synthesis of the trisaccharide **161**.

The development of reagents for the introduction of protecting groups under alternative conditions is of great interest. Recent results in this area include the introduction of allyl, benzyl, and *tert*-butyl ethers via the corresponding trichloroacetimidate[95] under acidic, rather than the usual basic, conditions. The formation of benzylidene acetals, normally introduced under acidic conditions, with the help of benzylidene-1,2-dibromide under basic conditions[96] is also a valuable alternative.

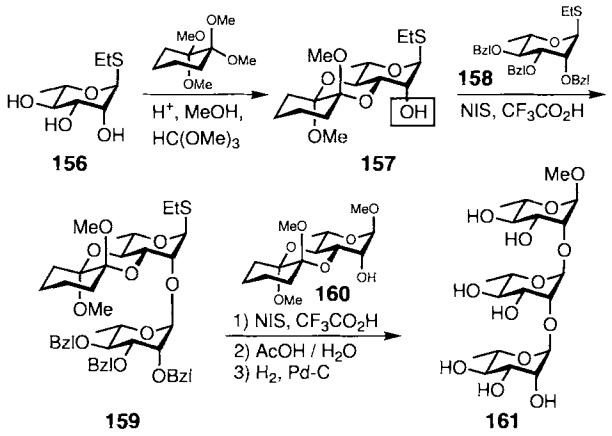

Scheme 55. Synthesis of a rhamnotrisaccharide by S. V. Ley et al. [15] using the CDA protecting group. NIS = *N*-iodosuccinimide.

5.3. Development of Protecting Groups that Can Be Converted into Activated Groups

If it is possible to use a protecting group that can be converted into a form that actually activates the molecule for the next transformation, then protecting groups become more than just a "necessary evil" and can be seen to play an active, positive role.

An example of the successful realization of such a principle is given by the use of protecting groups based on *o*-phenylenediamine[97] in peptide synthesis (Scheme 56). Under basic conditions peptide derivatives such as **162** react at the urethane function to form 1-acylbenzimidazolin-2-ones such as **163**. These activated compounds can then be coupled directly with amino acid esters and peptide esters. A further example is the use of *n*-pentenyl groups in carbohydrate chemistry[98] (see Section 3.5, Scheme 51). In **140** and **145** the anomeric center is protected as a pentenyl ether. Treatment with *N*-iodosuccinimide and triethylsilyl triflate converts the stable, protected **140** and **145** into the activated glycosyl donors **141** and **146**, respectively.

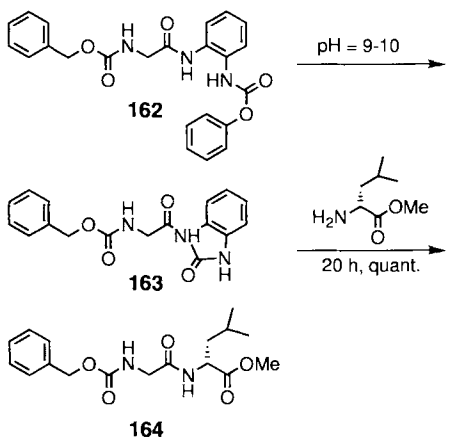

Scheme 56. Use of protecting groups capable of activation based on *o*-phenylenediamine in the synthesis of peptides by R. Pascal et al. [97].

If the principle of converting protecting groups to activating groups can also be applied to doubly orthogonal systems, then one would have a very effective tool for the synthesis of oligomers. T. Ogawa et al.[99] have recently described such a system for the construction of oligosaccharides. They exploited the possibility of orthogonally activating thioglycosides and glycosyl fluorides (Scheme 57). The thioglycosides **165** and **169** were converted into reactive glycosyl donors with *N*-iodosuccinimide and trifluoromethane sulfonic acid or with silver(I) trifluoroacetate. The configuration of the anomeric center of the fluorosugar remained stable under these conditions. However, when bis(cyclopentadienyl)hafnium dichloride and silver(I) perchlorate were used, only the glycosyl fluorides **167** and **171** were activated. This switchable activation and direct glycosylation allows a rapid and elegant synthesis of oligosaccharides. The strategy is highly efficient, and it can be expected that further combinations of protecting groups capable of orthogonal activation will find use.

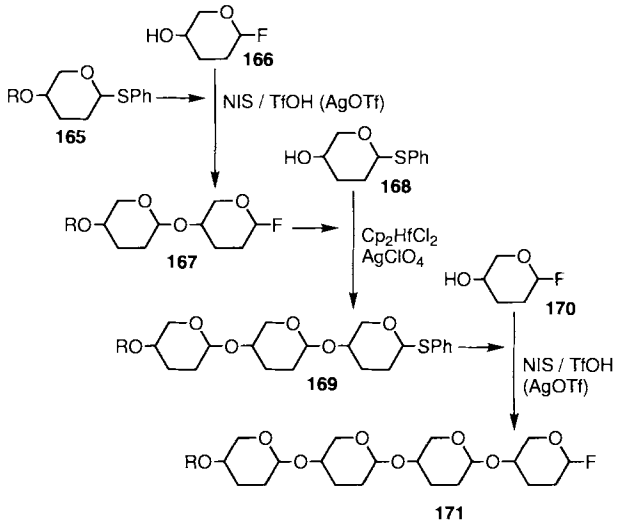

Scheme 57. Construction of oligsaccharides by T. Ogawa et al. [99] using orthogonal activation. NIS = *N*-iodosuccinimde, TfOH = trifluoromethanesulfonic acid.

5.4. Development of New Anchor Groups for Solid-Phase Synthesis

In the synthesis of oligopeptides and nucleotides on polymeric supports, the terminal monomer is attached to the solid phase by an anchor group. The anchor groups are generally derived from protecting groups developed for solution-phase applications. Solid-phase synthesis can thus be understood as synthesis with polymer-modified protecting groups.

Synthesis on polymeric supports has found particular interest due to the development of combinatorial chemistry.[100] The anchor groups used in solid-phase oligopeptide and nucleotide chemistry often cannot be directly applied to the synthesis of other types of compounds. With the growing application of combinatorial techniques, the demand for new anchor groups will increase, which will be defined by the requirements of combinatorial chemistry in general, as well as by the properties of the target compounds. A representative example is given by the

work of S. Fodor et al.,[101] who have combined modern protecting group chemistry with photolithographic methods for the parallel synthesis of oligopeptides and oligonucleotides on spatially well-defined regions of a solid support (Scheme 58). The

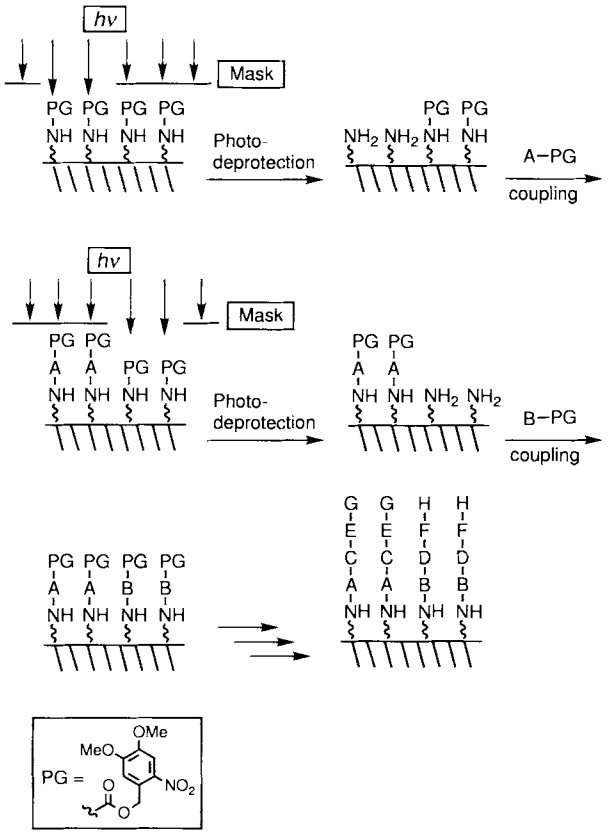

Scheme 58. Light-directed parallel synthesis of oligomers developed by S. P. A. Fodor et al. [101].

surface of the support was initially derivatized with photolabile protected amino functions. Certain areas of the surface were then covered with a mask and the whole was then irradiated. Only the protecting groups in uncovered areas of the surface were removed, leaving free amino functions. These were chemically coupled with photolabile animo acid derivatives. By using another mask, other regions can be selectively deblocked and converted. This process allows a defined sequence to be prepared on a given area of the surface.

6. Outlook

The continuous development of new protecting group techniques over the last decades resulted in most of the strategies discussed in this review and has contributed substantially to the impressive achievements in organic synthesis today. The successful applications of the silyl and allyl protecting groups in complex syntheses are particularly good examples. The authors are of the opinion that the potential of biocatalysts is equally vast. Basic methods relying on these systems have been developed in many areas and all that is lacking is definitive proof of their performance in demanding synthesis.

The development of more efficient protecting group techniques, relying, for example, on differences in reactivity between similar functional groups (see Section 4) and on new reagents with alternative reactivities, stabilities, and selectivities, continues to be the focus of attention (see Section 5) and will certainly lead to new protecting group strategies. Protecting group chemistry will thus continue to provide organic synthesis with great impetus in the future and open up new possibilities.

The basis and motivation for this review was research carried out at the Universities of Mainz, Bonn, and Karlsruhe aimed at developing and establishing enzymatically cleavable protecting groups (see ref. [21]). Active participants in this work were (in alphabetic order): Peter Braun, Alain Cotté, Stephanie Gabold, Simone Glomsda, Axel Heuser, Volker Jungmann, Thomas Kappes, Bruno Klaholz, Karsten Kuhn, Edgar Nägele, Torsten Pohl, Armin Reidel, Jörg Sander, Bernd Sauerbrei, Michael Schelhaas, Dagmar Sebastian, and Paul Stöber. We are grateful to the Deutsche Forschungsgemeinschaft, the Fonds der Chemischen Industrie, the Bundesministerium für Bildung und Forschung, BASF AG, Boehringer Mannheim GmbH, and Degussa AG for funding our research.

Received: December 15, 1995
Revised version: March 11, 1996 [A145IE]
German version: *Angew. Chem.* **1996**, *108*, 2192–2219
Translated by Dr. D. Macquarrie, York (UK)

[1] K. C. Nicolaou, E. J. Sorensen, *Classics in Total Synthesis; Targets, Strategies, Methods*, VCH, Weinheim, **1996**.
[2] *Comprehensive Organic Synthesis*, Vol. 1–8 (Eds.: B. M. Trost, I. Fleming), Pergamon, Oxford, **1991**.
[3] *Encyclopedia of Reagents for Organic Chemistry* (Ed.: L. A. Paquette), Wiley, New York, **1995**.
[4] E. J. Corey, X.-M. Cheng, *The Logic of Chemical Synthesis*, Wiley, New York, **1989**.
[5] K. F. McClure, S. J. Danishefsky, *J. Am. Chem. Soc.* **1993**, *115*, 6094–6100.
[6] J. M. Schkeryantz, S. J. Danishefsky, *J. Am. Chem. Soc.* **1995**, *117*, 4722–4723.
[7] J. J. Masters, J. T. Link, L. B. Snyder, W. B. Young, S. J. Danishefsky, *Angew. Chem.* **1995**, *107*, 1886–1888; *Angew. Chem. Int. Ed. Engl.* **1995**, *34*, 1723–1726.
[8] Peptide and nucleotide chemistry are, however, exceptions. The most advantageous combinations of protecting groups and strategies for the synthesis of oligopeptides and oligonucleotides have often been commented on in the relevant publications and textbooks (for examples see Schemes 35 and 52). Because the types of functions requiring protection in these classes of compounds is limited and the number of reactions to be carried out is restricted, the problem is more easily defined in this area of synthesis than in the stereoselective synthesis of a complex natural product. For discussions of protecting group strategy in peptide synthesis see for examples refs. [35, 37], and references therein, or J. Jones, *The Chemical Synthesis of Peptides*, Clarendon, Oxford, **1992**; *Method in Molecular Biology, Vol. 35: Peptide Synthesis Protocols* (Eds.: M. W. Pennington, B. M. Dunn), Humana Press, Totowa, NJ (USA), **1994**; S. Sakakibara, *Biopolymers (Peptide Science)* **1994**, *37*, 17–28.
[9] T. W. Greene, P. G. M. Wuts, *Protective Groups in Organic Chemistry*, 2nd ed., Wiley, New York, **1991**.
[10] P. J. Kocienski, *Protecting Groups*, 1st ed., Thieme, Stuttgart, **1994**.
[11] H. Kunz, H. Waldmann in *Comprehensive Organic Synthesis, Vol. 6* (Eds.: B. M. Trost, I. Fleming, E. Winterfeldt), Pergamon, Oxford, **1991**, pp. 631–701.
[12] In the introduction in ref. [9] the choice of protecting groups in the total synthesis of palytoxin by Kishi et al. [77] is discussed (see also Section 3.3). The synthesis of dihydroerythronolide by R. W. Hoffmann et al. (R. Stürmer, K. Ritter, R. W. Hoffmann, *Angew. Chem.* **1993**, *105*, 112–114; *Angew. Chem. Int. Ed. Engl.* **1993**, *32*, 101–103) was also analyzed from this point of view in ref. [10].
[13] E. J. Corey, J. W. Suggs, *Tetrahedron Lett.* **1975**, 3775–3778.
[14] S. V. Ley, M. Woods, A. Zanossi-Gerosa, *Synthesis* **1992**, 52–54.
[15] a) S. V. Ley, H. M. W. Priepke, S. L. Warriner, *Angew. Chem.* **1994**, *106*, 2410–2412; *Angew. Chem. Int. Ed. Engl.* **1994**, *33*, 2290; b) S. V. Ley, H. M. W. Priepke, *ibid.* **1994**, *106*, 2412–2414 and **1994**, *33*, 2292.
[16] C. Rücker, *Chem. Rev.* **1995**, *95*, 1009–1064.
[17] E. J. Corey, R. K. Varma, *J. Am. Chem. Soc.* **1971**, *93*, 7319–7320.

[18] K. K. Ogilvie, E. A. Thompson, M. A. Quilliam, J. B. Westmore, *Tetrahedron Lett.* **1974**, 2865–2868.
[19] K. Toshima, S. Mukaiyama, M. Kinoshita, K. Tatsuta, *Tetrahedron Lett.* **1989**, *30*, 6413–6416.
[20] S. Djuric, J. Venit, P. Magnus, *Tetrahedron Lett.* **1981**, *22*, 1787–1790; R. P. Bonar-Law, A. P. Davis, B. J. Dorgan, *ibid.* **1990**, *31*, 6721–6728.
[21] a) H. Waldmann, D. Sebastian, *Chem. Rev.* **1994**, *94*, 911–937; b) A. Reidel, H. Waldmann, *J. Prakt. Chem.* **1993**, *335*, 109–127; c) T. Pohl, E. Nägele, H. Waldmann, *Catalysis Today* **1994**, *22*, 407–426; d) H. Waldmann in [22], Vol. 2, pp. 851–886.
[22] *Enzyme Catalysis in Organic Chemistry* (Eds.: K. Drauz, H. Waldmann), VCH, Weinheim, **1995**.
[23] H. Waldmann, *Tetrahedron Lett.* **1988**, *29*, 1131–1134; *Liebigs Ann. Chem.* **1988**, 1175–1180.
[24] H. Waldmann, E. Nägele, *Angew. Chem.* **1995**, *107*, 2425–2428; *Angew. Chem. Int. Ed. Engl.* **1995**, *34*, 2259–2262.
[25] a) P. Braun, H. Waldmann, W. Vogt, H. Kunz, *Synlett* **1990**, 105–107; b) *Liebigs Ann. Chem.* **1991**, 165–170.
[26] M. Schelhaas, S. Glomsda, M. Hänsler, H.-D. Jakubke, H. Waldmann, *Angew. Chem.* **1996**, *108*, 82–85; *Angew. Chem. Int. Ed. Engl.* **1996**, *35*, 106–109.
[27] H. Kunz, D. Kowalczyk, P. Braun, *Angew. Chem.* **1994**, *106*, 353–355; *Angew. Chem. Int. Ed. Engl.* **1994**, *33*, 336–339.
[28] a) P. Fügedi, A. Liptak, P. Nanasi, *Carbohydr. Res.* **1982**, *104*, 55–67; b) P. J. Garegg, H. Hultberg, S. Wallin, *ibid.* **1982**, *108*, 97–101.
[29] a) G. Barany, R. B. Merrifield, *J. Am. Chem. Soc.* **1977**, *99*, 7363–7365; b) E. Meinjohanns, M. Meldal, H. Paulsen, K. Bock, *J. Chem. Soc. Perkin Trans. 1* **1995**, 405–415.
[30] J. A. Barltrop, P. J. Plant, P. Schofield, *Chem. Commun.* **1966**, 822–823.
[31] a) J. C. Sheehan, R. M. Wilson, A. W. J. Oxford, *J. Am. Chem. Soc.* **1971**, *93*, 7222–7728; b) R. S. Givens, Ph. S. Athey, B. Matuszewski, L. W. Kueper III, J.-Y. Xue, T. Fister, *ibid.* **1993**, *115*, 6001–6012.
[32] M. C. Pirrung, Y. R. Lee, *J. Org. Chem.* **1993**, *58*, 6961–6963.
[33] a) A. T. Tesser, I. C. Balvert-Geers, *Int. J. Pept. Protein Res.* **1975**, *7*, 295–305; b) G. G. J. Verhart, G. I. Tesser, *Recl. Trav. Chim. Pays-Bas* **1988**, *107*, 621–626.
[34] a) F. Nakatsubo, T. Fukuyama, A. J. Cocuzza, Y. Kishi, *J. Am. Chem. Soc.* **1977**, *99*, 8115–8116; b) *Tetrahedron Lett.* **1977**, 4295–4298.
[35] J. Rudinger, *Pure Appl. Chem.* **1963**, *7*, 335–362; recent review: M. Patek, *Int. J. Pept. Protein Res.* **1993**, *42*, 97–117.
[36] M. T. Reetz, M. W. Drewes, A. Schmitz, *Angew. Chem.* **1987**, *99*, 1186–1188; *Angew. Chem. Int. Ed. Engl.* **1987**, *26*, 1141–1143.
[37] R. B. Merrifield, *Pept., Proc. Am. Pept. Symp., 5th* **1977**, 488.
[38] a) R. C. Kelly, I. Gebhard, N. Wicnienski, *J. Org. Chem.* **1986**, *51*, 4590–4594; b) G. R. Pettit, Y. Kamano, C. W. Holzapfel, W. J. van Zyl, A. A. Tuinman, C. L. Herald, L. Baczynskyj, J. M. Schmidt, *J. Am. Chem. Soc.* **1987**, *109*, 7581–7582.
[39] R. Windmüller, R. R. Schmidt, *Tetrahedron Lett.* **1994**, *35*, 7927–7930.
[40] H. Kunz, C. Unverzagt, *Angew. Chem.* **1988**, *100*, 1763–1765; *Angew. Chem. Int. Ed. Engl.* **1988**, *27*, 1697–1699.
[41] M. Nakatsuka, J. A. Ragan, T. Sammakia, D. B. Smith, D. E. Uehling, S. L. Schreiber, *J. Am. Chem. Soc.* **1990**, *112*, 5583–5601.
[42] a) A. D. Piscopio, N. Minowa, T. K. Chakraborty, K. Koide, P. Bertinato, K. C. Nicolaou, *J. Chem. Soc. Chem. Commun.* **1993**, 617–618; *ibid.* **1993**, 619–622; b) K. C. Nicolaou, T. K. Chakraborty, A. D. Piscopio, N. Minowa, P. Bertinato, *J. Am. Chem. Soc.* **1993**, *115*, 4419–4420.
[43] H. Kunz, H. Waldmann, *Angew. Chem.* **1985**, *97*, 885–887; *Angew. Chem. Int. Ed. Engl.* **1985**, *24*, 883–885.
[44] C. M. Hayward, D. Yohannes, S. J. Danishefski, *J. Am. Chem. Soc.* **1993**, *115*, 9345–9346.
[45] Y. Hayakawa, S. Wakabayashi, H. Kato, R. Noyori, *J. Am. Chem. Soc.* **1990**, *112*, 1691–1696.
[46] S. Blechert, A. Kleine-Klausing, *Angew. Chem.* **1991**, *103*, 428–429; *Angew. Chem. Int. Ed. Engl.* **1991**, *30*, 412–414.
[47] D. A. Evans, J. A. Ellman, K. M. DeVries, *J. Am. Chem. Soc.* **1989**, *111*, 8912–8914.
[48] P. Braun, H. Waldmann, H. Kunz, *Synlett* **1992**, 39–40; *Bioorg. Med. Chem.* **1993**, *1*, 197–207.
[49] T. Pohl, H. Waldmann, *Angew. Chem.* **1996**, *108*, 1829–1832; *Angew. Chem. Int. Ed. Engl.* **1996**, *35*, 1720–1723.
[50] H. Kunz, *Angew. Chem.* **1987**, *99*, 297–311; *Angew. Chem. Int. Ed. Engl.* **1987**, *26*, 294–308.
[51] B. Danieli, G. Lesma, M. Mauro, G. Palmisano, D. Passarella, *Tetrahedron* **1994**, *50*, 8837–8852.
[52] A. L. Margolin, *Enzyme Microb. Technol.* **1993**, *5*, 266–280; K. Mori, *Synlett* **1995**, 1097–1109.
[53] M. Ohno, Y. Ito, M. Arita, T. Shibata, K. Adachi, H. Sawai, *Tetrahedron* **1984**, *40*, 145–152.
[54] S. Iruchijima, K. Hasegawa, G. Tsuchihashi, *Agric. Biol. Chem.* **1982**, *46*, 1907–1910.
[55] J. Fried, V. John, M. J. Szwedo, Jr., C.-K. Chen, C. O'Yang, T. A. Morinelli, A. K. Okwu, P. V. Halushka, *J. Am. Chem. Soc.* **1989**, *111*, 4510–4511.
[56] S. Kobayashi, M. Nakada, M. Ohno, *Pure Appl. Chem.* **1993**, *64*, 1121–1124.
[57] M. Arita, K. Adachi, Y. Ito, H. Sawai, M. Ohno, *J. Am. Chem. Soc.* **1983**, *105*, 4049–4055.
[58] X. K. Holdgrun, C. J. Sih, *Tetrahedron Lett.* **1991**, *32*, 3465–3468.
[59] M. Schneider, M. Engel, H. Boensmann, *Angew. Chem.* **1984**, *96*, 52–54; *Angew. Chem. Int. Ed. Engl.* **1984**, *23*, 64–66.
[60] P. Mohr, N. Waespe-Sarceivic, C. Tamm, K. Gawronska, J. K. Gawronski, *Helv. Chim. Acta* **1983**, *66*, 2501–2511.
[61] K. J. Harris, Q.-M. Gu, Y. E. Shih, G. Girdaukas, C. J. Sih, *Tetrahedron Lett.* **1991**, *32*, 3941–3944.
[62] J.-L. Brevet, K. Mori, *Synthesis* **1992**, 1007–1012.
[63] K. O. Hallinan, T. Honda, *Tetrahedron* **1995**, *51*, 12211–12216.
[64] a) V. R. N. Pillai, *Synthesis* **1980**, 1–26; b) *Org. Photochem.* **1987**, 225; c) U. Zehavi, *Adv. Carbohydr. Chem. Biochem.* **1988**, *46*, 179–204.
[65] a) R. D. Groneberg, T. Miyazaki, N. A. Stylianides, T. J. Schulze, W. Stahl, E. P. Schreiner, T. Suzuki, A. L. Schmith, K. C. Nicolaou, *J. Am. Chem. Soc.* **1993**, *115*, 7593–7611; b) A. L. Schmith, E. N. Pitsinos, C.-H. Hwang, Y. Mizuno, H. Saitomo, G. R. Scarlato, T. Suzuki, K. C. Nicolaou, *ibid.* **1993**, *115*, 7612–7624; c) K. C. Nicolaou, M. Nakada, K. Shibayama, E. N. Pitsinos, H. Saimoto, Y. Mizuno, K.-U. Baldenius, A. L. Schmith, *ibid.* **1993**, *115*, 7625–7635.
[66] S. R. Adams, J. P. Y. Kao, R. Y. Tsien, *J. Am. Chem. Soc.* **1989**, *111*, 7957–7968.
[67] M. C. Pirrung, S. W. Shuey, *J. Org. Chem.* **1994**, *59*, 3890–3897.
[68] R. S. Givens, P. S. Athey, L. W. Kueper III, B. Matuszewski, J.-Y. Xue, *J. Am. Chem. Soc.* **1992**, *114*, 8708–8710.
[69] A. Barth, K. Hauser, W. Mäntele, J. E. T. Corrie, D. R. Trentham, *J. Am. Chem. Soc.* **1995**, *117*, 10311–10316.
[70] R. A. Ellison, E. R. Lukenbach, C. W. Chiu, *Tetrahedron Lett.* **1975**, 499–502.
[71] P. Sieber, B. Kamber, A. Hartmann, A. Jöhl, B. Riniker, W. Rittel, *Helv. Chim. Acta* **1974**, *57*, 2617–2621.
[72] K. C. Nicolaou, E. P. Schreiner, Y. Iwabuchi, T. Suzuki, *Angew. Chem.* **1992**, *104*, 317–319; *Angew. Chem. Int. Ed. Engl.* **1992**, *31*, 340–342.
[73] a) R. A. Holton, C. Somoza, H.-B. Kim, F. Liang, R. J. Biedinger, P. D. Boatman, M. Shindo, C. C. Smith, S. Kim, H. Nadizadeh, Y. Suzuki, C. Tao, P. Vu, S. Tang, P. Zhang, K. K. Murthi, L. N. Gentile, J. H. Liu, *J. Am. Chem. Soc.* **1994**, *116*, 1597–1598, 1599–1600.
[74] K. Horita, T. Yoshioka, T. Tanaka, Y. Oikawa, O. Yonemitsu, *Tetrahedron* **1986**, *42*, 3021–3028.
[75] T. Tanaka, Y. Oikawa, T. Hamada, O. Yonemitsu, *Tetrahedron Lett.* **1986**, *27*, 3651–3654.
[76] H. Kunz, J. März, *Angew. Chem.* **1988**, *100*, 1424–1425; *Angew. Chem. Int. Ed. Engl.* **1988**, *27*, 1375–1376.
[77] a) R. W. Armstrong, J. M. Beau, S. H. Cheon, W. J. Christ, H. Fujioka, W. H. Ham, L. D. Hawkins, H. Jin, S. H. Kang, Y. Kishi, M. J. Martinelli, W. D. McWhorter, Jr., M. Mizuno, M. Nakata, A. E. Stutz, F. X. Talamas, M. Taniguchi, J. A. Tino, K. Ueda, J. I. Uenishi, J. B. White, M. Yonaga, *J. Am. Chem. Soc.* **1989**, *111*, 7525–7530, 7530–7533.
[78] D. A. Evans, S. W. Kaldor, T. K. Jones, J. Cardy, T. J. Stout, *J. Am. Chem. Soc.* **1990**, *112*, 7001–7031.
[79] M. D. Shair, T.-Y. Yoon, S. J. Danishefsky, *Angew. Chem.* **1995**, *107*, 1883–1885; *Angew. Chem. Int. Ed. Engl.* **1995**, *34*, 1720–1723.
[80] a) K. C. Nicolaou, T. J. Caulfield, H. Kataoka, T. Kumazawa, *J. Am. Chem. Soc.* **1988**, *110*, 7910–7912; b) K. C. Nicolaou, *Chemtracts – Org. Chem.* **1991**, *4*, 181–198.
[81] K. C. Nicolaou, T. J. Caulfield, H. Kataoka, N. A. Stylianides, *J. Am. Chem. Soc.* **1990**, *112*, 3693–3695.
[82] T. K. Jones, S. G. Mills, R. A. Reamer, D. Askin, R. Desmond, R. P. Volante, I. Shinkai, *J. Am. Chem. Soc.* **1989**, *111*, 1157–1159.
[83] For example, see: M. Nogrady, *Stereoselective Synthesis*, 2nd ed., VCH, Weinheim, **1994**.
[84] J. Mulzer, H. M. Kirstein, J. Buschmann, C. Lehmann, P. J. Luger, *J. Am. Chem. Soc.* **1991**, *113*, 910–923.
[85] M. Isobe, M. Kitamura, T. Goto, *Tetrahedron Lett.* **1979**, 3465–3468.
[86] U. E. Udodong, C. S. Rao, B. Fraser-Reid, *Tetrahedron* **1992**, *48*, 4713–4724.
[87] a) D. R. Mootoo, P. Konradsson, U. Udodong, B. Fraser-Reid, *J. Am. Chem. Soc.* **1988**, *110*, 5583–5584; b) B. Fraser-Reid, U. E. Udodong, Z. Wu, H. Ottoson, R. Merrit, C. S. Rao, C. Roberts, *Synlett* **1992**, 927–942.
[88] A. Toepfer, W. Kinzy, R. R. Schmidt, *Liebigs Ann. Chem.* **1994**, 449–464.
[89] R. G. Denkewalter, D. F. Veber, F. W. Holly, R. Hirschmann, *J. Am. Chem. Soc.* **1969**, *91*, 502–503.
[90] a) E. Wünsch, G. Wendlberger, *Chem. Ber.* **1968**, *101*, 341–345; b) *ibid.* **1968**, *101*, 3659–3663.
[91] a) S. Knapp, J. J. Hale, M. Bastos, F. S. Gibson, *Tetrahedron Lett.* **1990**, *31*, 2109–2112; b) S. Knapp, J. J. Hale, M. Bastos, A. Molina, K. Y. Chen, *J. Org. Chem.* **1992**, *57*, 6239–6256.

[92] a) S. R. Angle, J. M. Fevig, S. D. Knight, R. W. Marquis, Jr., L. E. Overman, *J. Am. Chem. Soc.* **1993**, *115*, 3966–3976; b) S. D. Knight, L. E. Overman, G. Pairaudeau, *ibid.* **1993**, *115*, 9293–9294; c) *ibid.* **1995**, *117*, 5776–5788.
[93] A. N. Semenov, I. V. Lomonosova, V. I. Berezin, M. I. Titov, *Biotech. Bioeng.* **1993**, *42*, 1137–1141.
[94] Short review: T. Ziegler, *Angew. Chem.* **1994**, *106*, 2362–2365; *Angew. Chem. Int. Ed. Engl.* **1994**, *33*, 2272–2275.
[95] a) T. Iverson, D. R. Bundle, *J. Chem. Soc. Chem. Commun.* **1981**, 1240–1241; b) H.-P. Wessel, T. Iverson, D. R. Bundle, *J. Chem. Soc. Perkin Trans. 1* **1985**, 2247–2250.
[96] a) H. G. Fletcher, Jr., *Methods Carbohydr. Chem.* **1963**, *2*, 307; b) M. E. Evans, *ibid.* **1980**, *8*, 313–315; c) P. J. Caregg, C. G. Swahn, *Acta Chem. Scand.* **1972**, *26*, 3895–3901.
[97] R. Pascal, D. Chauvey, R. Sola, *Tetrahedron Lett.* **1994**, *35*, 6291–6294.
[98] a) B. Fraser-Reid, P. Konradsson, D. R. Mootoo, U. Udodong, *J. Chem. Soc. Chem. Commun.* **1988**, 823–825.
[99] O. Kanie, Y. Ito, T. Ogawa, *J. Am. Chem. Soc.* **1994**, *116*, 12073–12074; H. Paulsen, *Angew. Chem.* **1995**, *107*, 1562–1564; *Angew. Chem. Int. Ed. Engl.* **1995**, *34*, 1432–1434.
[100] a) M. A. Gallop, R. W. Barrett, W. J. Dower, S. P. A. Fodor, E. M. Gordon, *J. Med. Chem.* **1994**, *37*, 1233–1251; b) *ibid.* **1994**, *37*, 1385–1401.
[101] S. P. A. Fodor, J. L. Read, M. C. Pirrung, L. Stryer, A. Tsai Lu, D. Solas, *Science* **1994**, *251*, 767–773; see also: G. v. Kiedrowski, *Angew. Chem.* **1991**, *103*, 839–840; *Angew. Chem. Int. Ed. Engl.* **1991**, *30*, 822.

Time is money...

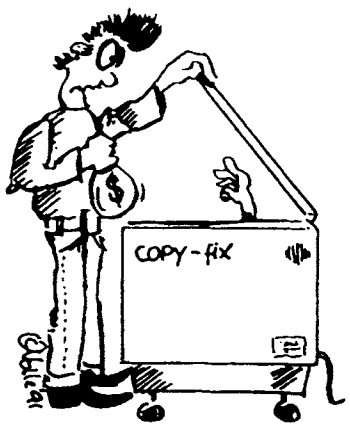

Save both by starting a personal subscription to *Angewandte Chemie* (now with *Chemistry - A European Journal*). At 9¢ per page you can't go wrong. With your own private copy you can read the "hot" articles before they cool, and waste less time in front of the copier.

Order now!
An order form can be found on the last page of this issue.

The New Inductees in the "Hall of Phane"—No Phane, No Gain

Graham J. Bodwell*

Since their emergence as a distinct class of compounds in the 1950s, the general appeal of cyclophanes has shown no signs of waning. They possess unusual and aesthetically pleasing structures. They pose unique synthetic challenges. They undergo interesting conformational processes. They exhibit peculiar chemical reactivity, spectroscopic properties, and physical properties. They can also be designed to be chiral. From the ever smaller and more strained cyclophanes to the ever larger and more complex cyclophanes, chemists continue to push back the frontiers of all aspects of this captivating field of chemistry.

The [*n*]cyclophanes are the archetypal small cyclophanes; of these, the [*n*]paracyclophanes have received by far the most attention. A detailed computational study of [4]paracyclophane,[1] which has only been prepared as a transient species by matrix isolation,[2] was recently reported. An energy difference of 9 kcal mol^{-1} between it and its Dewar benzene isomer was predicted. This paper also provides a comprehensive summary of the literature of the [*n*]paracylophanes. [5]Paracyclophane, which exists as the minor component of an equilibrium with its valence isomeric Dewar benzene, is the smallest member of this series to exhibit sufficient stability to be studied directly.[3] To further stabilize the [5]paracyclophane unit, Bickelhaupt et al.[4] recently synthesized a benzoannelated version, namely [5](1,4)-naphthalenophane **2** (Scheme 1). Even though this compound also exists in equilibrium with the Dewar naphthalene **2** from which it was produced, the proportion of the cyclophane (35% of the mixture) is higher than in any previously reported photochemical aromatization of a Dewar isomer. A particularly interesting feature of this system is that two bridge conformers (**2** and **2'**) are observed in solution in a ratio of 95:5. Unfortunately, despite considerable effort, assignment of the two conformers was not possible.

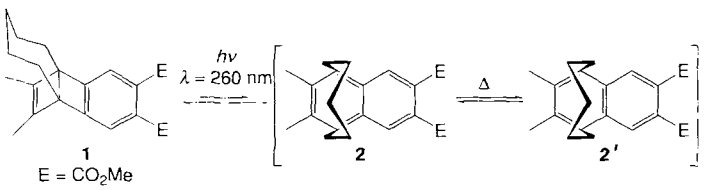

Scheme 1. Synthesis of the benzoannelated [5](1,4)naphthalenophane **2** by Bickelhaupt et al. [4].

Over the years, a number of [*n*]cyclophanes based on polycyclic aromatic hydrocarbons have been prepared.[5] However, the limits to which any of these systems can be bent has not been systematically investigated. Hafner's [*n*](1,6)- (**4**) and [*n*](2,6)-azulenophanes (**5**, $n = 11-13$) are a promising step in this direction.[6] They were produced by an intramolecular azulene-forming reaction of the 4-(ω-cyclopentadienylalkyl)-1-methylpyridinium salts **3** (Scheme 2). The crystal structure of [13](2,6)-azulenophane **5** ($n = 13$) revealed a 3.7° angle between the mean planes of the two rings. Hopefully, lower homologues of this series will soon be prepared.

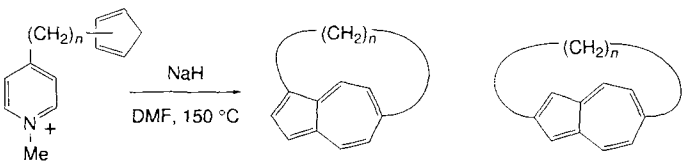

Scheme 2. Synthesis of the [*n*](1,6)- and [*n*](2,6)azulenophanes **4** and **5** by Hafner et al. [6].

Our group were able to impart much greater deviations from planarity in the pyrene framework.[7] The remarkably distorted 1,8-dioxa[8](2,7)pyrenophane **7** was prepared by the valence isomerization and dehydrogenation of the tethered [2.2]metacyclophanediene **6** (Scheme 3). In the crystal the overall bend is nearly 90°. The curvature of the aromatic surface approximates that expected for a fragment of the D_{6h}-symmetric C_{84} molecule. Bond angles of up to 119° were observed in the aliphatic bridge, as well as a very high field proton resonance at $\delta = -1.47$. Although the next smaller member of this series, [7](2,7)pyrenophane, could not be prepared in this way, this compound has since been isolated.[8]

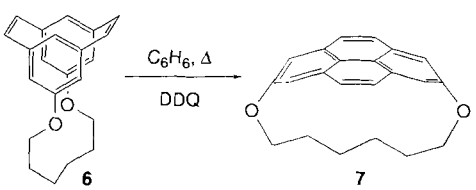

Scheme 3. Synthesis of the 1,8-dioxa[8](2,7)pyrenophane **7** from [2.2]metacyclophanediene **6** by Bodwell et al. [7]; DDQ = 2,3-dichloro-5,6-dicyanobenzoquinone.

[*] Dr. G. J. Bodwell
Department of Chemistry
Memorial University of Newfoundland
St. John's, NF A1B 3X7 (Canada)
Fax: Int. code +(709)737-3702
e-mail: gbodwell@morgan.ucs.mun.ca

It has long been known that appropriately substituted [2.2]paracyclophanes are chiral, chemically stable, and do not racemize under normal reaction conditions. Considering these seemingly ideal prerequisites for use in chiral synthesis, it is surprising that only three examples have appeared in the literature, all of them in recent years (Scheme 4). Reich et al. employed [2.2]paracyclophane-substituted selenides such as **8** to achieve chirality transfer through [2,3]sigmatropic rearrangements of the selenoxide. Using this methodology, he was able to synthesize optically active linalool **9** (*S*:*R* ratio = 5:1).[9] Yanada, Yoneda et al. constructed the deazaflavinophane **10**, which exhibits complete regioselectivity when oxidized or reduced, for example, in the reduction with $NaBD_4$ to afford **11**.[10] Belokon, Rozenberg et al. used scalemic 4-formyl-5-hydroxy[2.2]paracyclophane (**12**) in the synthesis of α-amino acids (*ee* = 45–98%).[11] An alternate synthesis of **12** was more recently reported by Hopf and Barrett.[12] Another interesting advance in the area of chiral cyclophanes was the synthesis of the homochiral [2.2]paracyclophane amino acids **13** and **14**.[13]

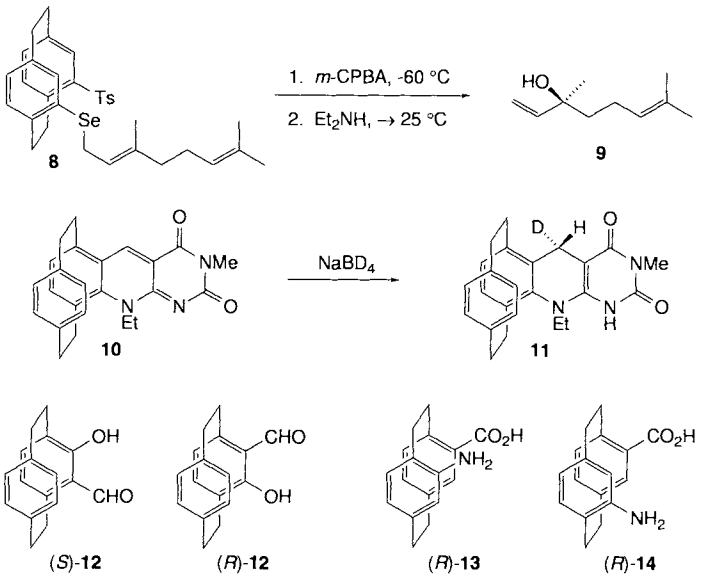

Scheme 4. Examples of the application of chiral [2.2]paracyclophanes in organic synthesis.

Many cyclophanes are conformationally mobile, and the study of their behavior in solution has proved to be one of their most intriguing features. A particularly striking example is the conformational analysis of [4.4]paracyclophane derivative **17**, synthesized by Fukazawa et al.[14] through a photoinduced double $S_{RN}1$ reaction of the precursors **15** and **16** (Scheme 5). Signals due to three conformers appear in the low temperature ^1H NMR spectrum of **17**. The crystal structure of the major conformer corresponded to the calculated lowest energy conformer. When crystals of **17** were dissolved in precooled (−80 °C) solvent, the ^1H NMR spectrum of the resulting solution exhibited signals arising only from the major conformer of the previous mixture.

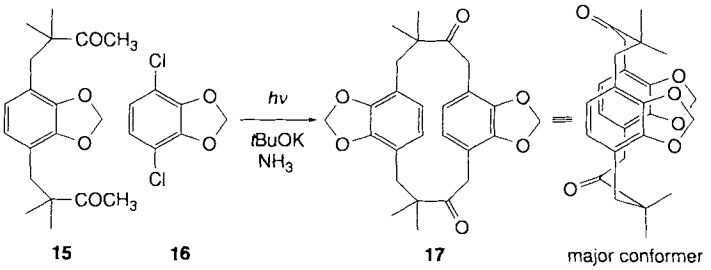

Scheme 5. Synthesis of the [4.4]paracyclophane derivative **17** by Fukazawa et al. [14].

The [6.6]paracyclophanetetrayne **20** was synthesized by Hopf et al. by the reaction of dibromide **18** with $Bu_3SnSiMe_3$ (Scheme 6).[15] The intermediacy of the novel cumulated *para*-quinodimethane **19** was invoked. Reaction of the *ortho*-substituted isomer **21** under the same conditions presumably gave the intermediate **22** to yield the highly strained 3,4-benzocyclooct-3-en-1,5-diyne **23**.

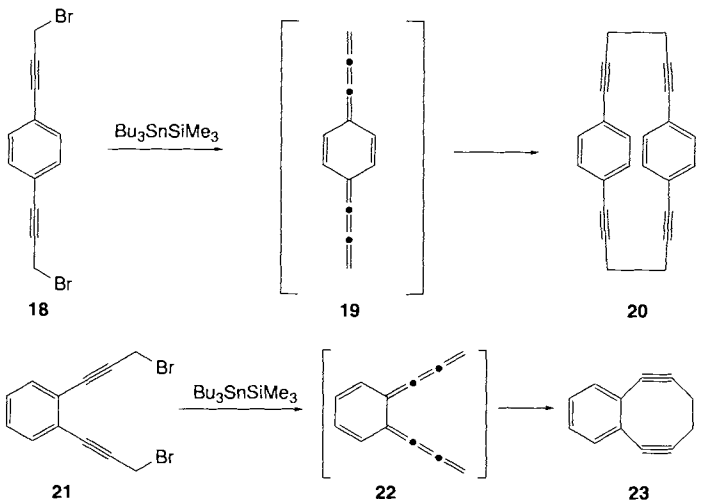

Scheme 6. Synthesis of the [6.6]paracyclophanetetrayne **20** and 3,4-benzocyclooctene-1,5-diyne **23** by Hopf et al. [15].

Seventeen years after Boekelheide et al.'s landmark synthesis of $[2_6](1,2,3,4,5,6)$cyclophane (termed superphane),[16] Shinmyozu et al. very recently described the synthesis of the homologous $[3_6](1,2,3,4,5,6)$cyclophane **27** (Scheme 7).[17] Formation of the final bridge of this "molecular pinwheel" was accom-

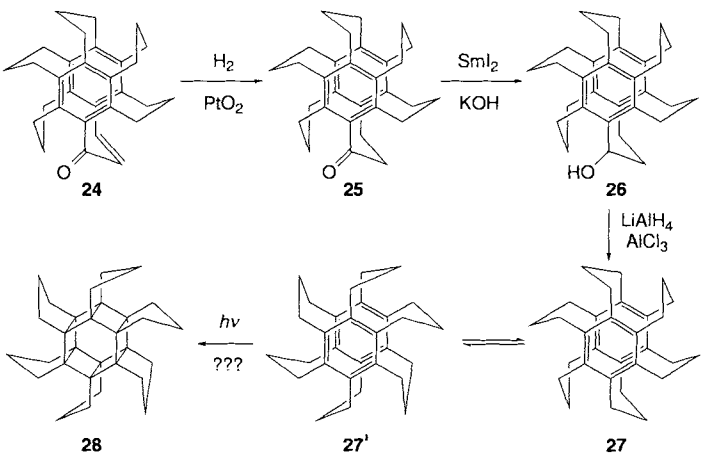

Scheme 7. Synthesis of the $[3_6](1,2,3,4,5,6)$cyclophane **27** by Shinmyozu et al. [17].

plished with an intramolecular aldol condensation. While the double bond of enone **24** could be easily hydrogenated, the carbonyl of the resulting ketone **25** proved to be quite inert towards reduction. The action of SmI_2/1 M KOH finally yielded the alcohol **26**, which on treatment with $LiAlH_4/AlCl_3$ afforded cyclophane **27**. The well averaged ^1H NMR signals of the bridge protons are consistent with a correlated inversion of all six trimethylene bridges in solution at room temperature. News about whether this molecule fulfills predictions[18] of a photochemical isomerization to the [6]prismane derivative **28** is eagerly awaited.

Tani et al. recently described the coupling of the tetrabromide **29** with the tetraselenocyanate **30** to give the parallel and crossed tetraselenabiphenylophanes **31** and **32** in a ratio of 1:3 (Scheme 8).[19] The thia analogue of **32** was synthesized earlier

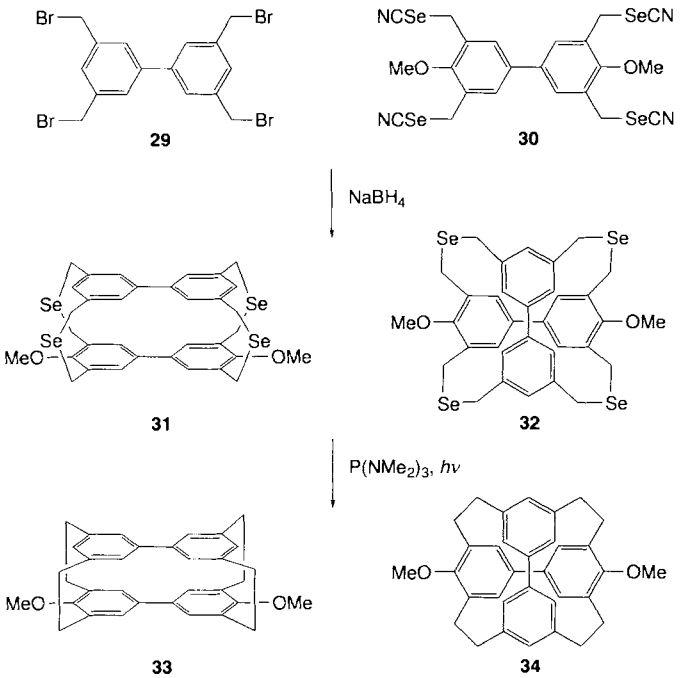

Scheme 8. Synthesis and deselenation of the tetraselenaphenylophanes **31** and **32** by Tani et al. [19].

through a thiol-bromide coupling,[20] but the isomer corresponding to **31** was not formed. While the thia analogue of **32** could not be desulfurated, **31** and **32** were successfully deselenated in 40–50% yield upon photolysis in the presence of $P(NMe_2)_3$ to give the structurally interesting bridge-contracted phanes **33** and **34**.

The *in*-cyclophanes **35**–**37** described by Pascal, Jr, et al. are excellent vehicles for the study of functional group interactions resulting from enforced proximity (Scheme 9). While original work was directed towards compounds containing alkane CH groups projected towards the center of an aromatic ring (for example **35**, $\delta_H = -4.03$),[21] it now includes second row elements. Silaphane **36**[22] exhibits a proton resonance at ($\delta = 1.04$), some 5 ppm upfield from that of an acyclic model compound. In addition there is a 280 cm^{-1} hypsochromic shift of the infrared Si–H stretching frequency arising from steric compression. For the phosphaphane **37**,[22] which is resistant to

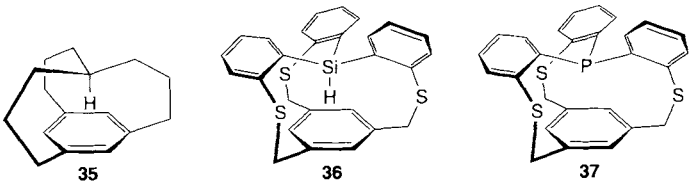

Scheme 9. Examples of *in*-cyclophanes.

protonation with HBr, the ^{13}C and ^{31}P NMR spectra indicate that there is an electronic interaction between the phosphane P atom and the basal ring. However, the presence of a bonding attraction between them could not be determined. Subsequent functionalization of the basal ring with a nitro or amino substituent enabled HPLC resolution of the enantiomers, which exhibit exceptionally high optical activity.[23]

Vögtle's group continues to produce a steady stream of fascinating cyclophanes. Among these are the nanometer-scale molecular ribbons **38** (Scheme 10), which were synthesized with an iterative approach.[24] The longest yet, ribbon **38** ($n = 5$), has seven layers. The conversion of some of these ribbons into molecular belts such as **39**–**41** has also been described.[25] Cyclic

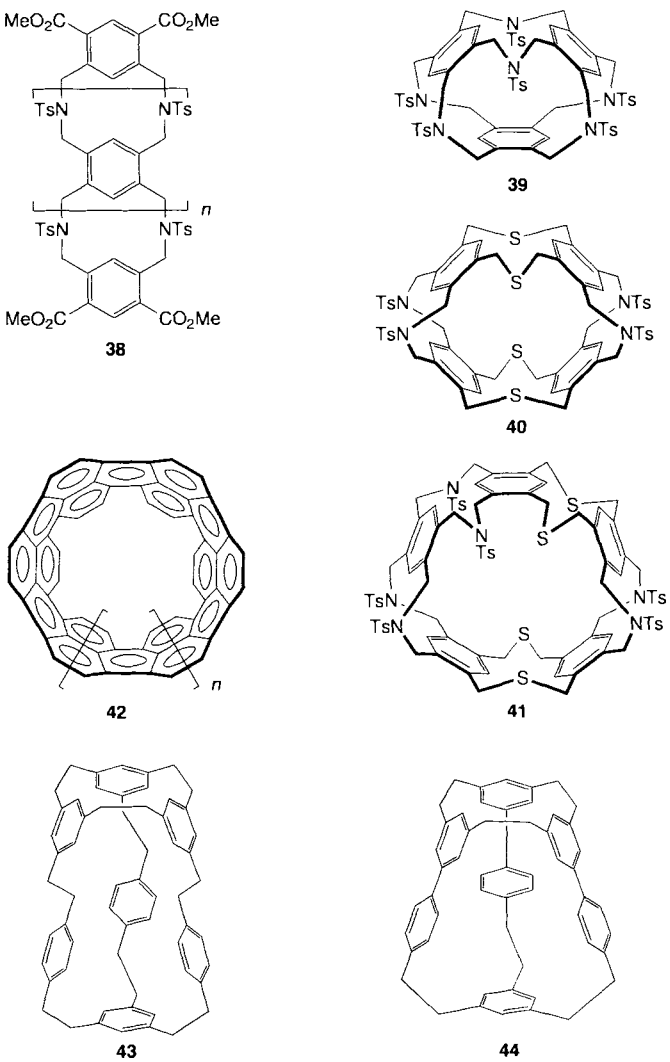

Scheme 10. Examples of cyclophanes in ribbon and belt form.

side-products containing up to 40 (!) benzene rings were observed by Plasma Desorption Mass Spectrometry, although none of these higher oligomers has been isolated. Conversion of these macrocycles into fully aromatic belts **42** should provide an entry to nanotube fullerene fragments. The "spheriphanes" **43** and **44** were also prepared by the same group.[26] Spheriphane **43** exhibits a high affinity for silver cations and, by virtue of its sixty carbon framework, may serve as a direct precursor to C_{60}.[27]

One of the most spectacular cyclophanes to be prepared in recent years is the "Kuratowski cyclophane" **45** (Scheme 11).[28] This nanodimensional multicyclophane is the

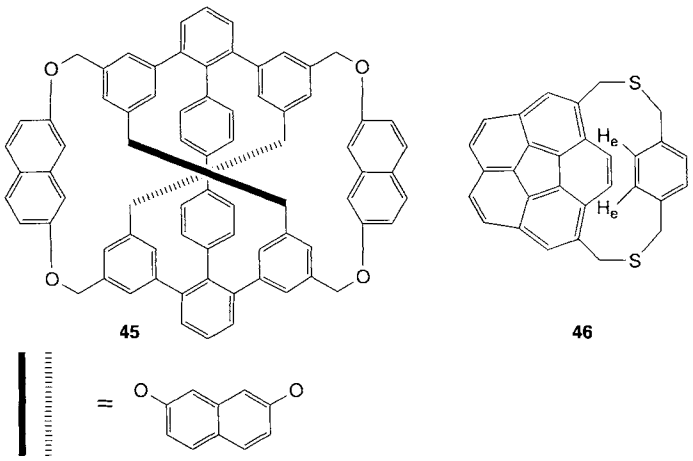

Scheme 11. The "Kuratowski-cyclophane" **45** [28] and the first corannulenocyclophane, **46** [29].

first example of an achiral molecule possessing nonplanar $K_{3,3}$ topology. The straightforward synthesis of this intricately entwined macrocyclophane should pave the way to a new family of molecules possessing novel architecture and vast dimensions. A further contribution from Siegel's group is the synthesis of the first corannulene cyclophane **46**.[29] A striking feature of its ^{1}H NMR spectrum is the *endo* aromatic protons (H_e) of the benzene ring, which are positioned almost directly over the center of the corannulene system, appear at remarkably high field ($\delta = 1.89$). Furthermore, since no peak broadening was observed up to 148 °C, dynamic conformational processes in the thioether bridges and bowl-to-bowl inversion of the corannulene moiety both have lower limits of 18 ± 1 kcal mol^{-1}.

From its rudimentary beginnings over four decades ago, cyclophane chemistry has developed into an ever-evolving, multifaceted discipline that overlaps with many other areas of chemistry. A rough cross-section of some of the recent developments in the mainstream of this field, as highlighted here, certainly attests to that.

German version: *Angew. Chem.* **1996**, *108*, 2221–2224

Keywords: arenes · cyclophanes · hydrocarbons · polycycles · strained rings

[1] B. Ma, H. M. Sulzbach, R. B. Remington, H. F. Schaefer III, *J. Am. Chem. Soc.* **1995**, *117*, 8392–8400.

[2] G. B. M. Kostermans, M. Bobeldijk, W. H. de Wolf, F. Bickelhaupt, *J. Am. Chem. Soc.* **1987**, *109*, 2471–2475; T. Tsuji, S. Nishida, *ibid.* **1988**, *110*, 2157–2164; F. Bickelhaupt, *Pure Appl. Chem.* **1990**, *62*, 373–382.

[3] L. W. Jenneskens, F. J. J. de Kanter, P. A. Kraakman, L. A. M. Turkenburg, W. E. Koolhaas, W. H. de Wolf, F. Bickelhaupt, Y. Tobe, K. Kakiuchi, Y. Odaira, *J. Am. Chem. Soc.* **1985**, *107*, 3716–3717.

[4] D. S. van Es, F. J. J. de Kanter, W. H. de Wolf, F. Bickelhaupt, *Angew. Chem.* **1995**, *107*, 2728–2730; *Angew. Chem. Int. Ed. Engl.* **1995**, *34*, 2553–2555.

[5] For some examples, see J. A. Reiss in *Cyclophanes, Vol II* (Eds.: P. M. Keehn, S. M. Rosenfeld), Academic Press, New York, **1983**, p. 443–484.

[6] P. Schuchmann, K. Hafner, *Tetrahedron Lett.* **1995**, *36*, 2603–2606.

[7] G. J. Bodwell, J. N. Bridson, T. J. Houghton, J. W. J. Kennedy, M. R. Mannion, *Angew. Chem.* **1996**, *108*, 1418–1420; *Angew. Chem. Int. Ed. Engl.* **1996**, *35*, 1320–1321.

[8] G. J. Bodwell, T. J. Houghton, J. W. J. Kennedy, M. R. Mannion, unpublished results.

[9] H. J. Reich, Y. E. Yelm, *J. Org. Chem.* **1991**, *56*, 5672–5679.

[10] R. Yanada, H. Higashikawa, Y. Mura, T. Taga, F. Yoneda, *Tetrahedron Asymmetry* **1992**, *3*, 1387–1390.

[11] D. Y. Antonov, Y. N. Belokon, N. S. Ikonnikov, S. A. Orlova, A. P. Pisarevsky, N. I. Raevski, V. I. Rozenberg, E. V. Sergeeva, Y. T. Struchkov, V. I. Tararov, E. V. Vorontsov, *J. Chem. Soc. Perkin Trans. 1* **1995**, 1873–1879.

[12] H. Hopf, D. G. Barrett, *Liebigs Ann.* **1995**, 449–451.

[13] A. Pelter, R. A. N. C. Crump, H. Kidwell, *Tetrahedron Lett.* **1996**, *37*, 1273–1276.

[14] Y. Fukazawa, H. Kitayama, K. Yasuhara, K. Yoshimura, S. Usui, *J. Org. Chem.* **1995**, *60*, 1696–1703.

[15] H. Hopf, P. G. Jones, P. Bubenitschek, C. Werner, *Angew. Chem.* **1995**, *107*, 2592–2594; *Angew. Chem. Int. Ed. Engl.* **1995**, *34*, 2367–2368.

[16] Y. Sekine, M. Brown, V. Boekelheide, *J. Am. Chem. Soc.* **1979**, *101*, 3126–3127; Y. Sekine, V. Boekelheide, *ibid.* **1981**, *103*, 1777–1785.

[17] Y. Sakamoto, N. Miyoshi, T. Shinmyozu, *Angew. Chem.* **1996**, *108*, 585–586; *Angew. Chem. Int. Ed. Engl.* **1996**, *35*, 549–550; see also T. Shinmyozu, S. Kusumoto, S. Nomura, H. Kawase, T. Inazu, *Chem. Ber.* **1993**, *126*, 1815–1818.

[18] O. J. Cha, E. Osawa, S. Park, *J. Mol. Struct.* **1993**, *300*, 73–81.

[19] K. Tani, H. Seo, M. Maeda, K. Imagawa, N. Nishiwaki, M. Ariga, Y. Tohda, H. Higuchi, H. Kuma, *Tetrahedron Lett.* **1995**, *36*, 1883–1886.

[20] F. Vögtle, G. Hohner, E. Weber, *J. Chem. Soc. Chem. Commun.* **1973**, 366–367; K. Matsumoto, M. Kugimiya, *Z. Kristallogr.* **1975**, *141*, 260–274.

[21] R. A. Pascal, Jr., R. B. Grossman, D. Van Engen, *J. Am. Chem. Soc.* **1987**, *109*, 6878–6880. See also R. A. Pascal, Jr., C. G. Winans, D. Van Engen, *ibid.* **1989**, *111*, 3007–3111; A. Pascal Jr., R. B. Grossman, *J. Org. Chem.* **1987**, *52*, 4616–4617.

[22] R. P. L'Esperance, A. P. West, Jr., D. Van Engen, R. A. Pascal, Jr., *J. Am. Chem. Soc.* **1991**, *113*, 2672–2676.

[23] A. P. West, Jr., N. Smyth, C. M. Craml, D. M. Ho, R. A. Pascal Jr., *J. Org. Chem.* **1993**, *58*, 3502–3506.

[24] S. Breidenbach, S. Ohren, M. Nieger, F. Vögtle, *J. Chem. Soc., Chem. Commun.* **1995**, 1237–1238; S. Breidenbach, S. Ohren, F. Vögtle, *Chem. Eur. J.* **1996**, *2*, 832–837.

[25] W. Josten, D. Karbach, M. Nieger, F. Vögtle, K. Hägele, M. Svoboda, M. Przybylski, *Chem. Ber.* **1994**, *127*, 767–777; W. Josten, S. Neumann, F. Vögtle, M. Nieger, K. Hägele, M. Przybylski, F. Beer, K. Müllen, *ibid.* **1994**, *127*, 2089–2096; A. Schröder, D. Karbach, R. Güther, F. Vögtle, *ibid.* **1992**, *125*, 1881–1887.

[26] J. Gross, G. Harder, F. Vögtle, H. Stephan, K. Gloe, *Angew. Chem.* **1995**, *107*, 523–526; *Angew. Chem. Int. Ed. Engl.* **1995**, *34*, 481–484.

[27] R. Taylor, G. J. Langley, H. W. Kroto, D. R. M. Walton, *Nature (London)* **1993**, *366*, 728–731; F. T. Edelmann, *Angew. Chem.* **1995**, *107*, 1071–1075; *Angew. Chem. Int. Ed. Engl.* **1995**, *34*, 981–985.; cf. Y. Rubin, T. C. Parker, S. I. Khan, C. L. Holliman, S. W. McElvany, *J. Am. Chem. Soc.* **1996**, *118*, 5308–5309.

[28] C.-T. Chen, P. Gantzel, J. S. Siegel, K. K. Baldridge, R. B. English, D. M. Ho, *Angew. Chem.* **1995**, *107*, 2870–2873; *Angew. Chem. Int. Ed. Engl.* **1995**, *34*, 2657–2660.

[29] T. J. Seiders, K. K. Baldridge, J. S. Siegel, *J. Am. Chem. Soc.* **1996**, *118*, 2754–2755.

 © VCH Verlagsgesellschaft mbH, D-69451 Weinheim, 1996 0570-0833/96/3518-2088 $ 15.00+.25/0

"Strangelove" in Cluster Chemistry: A New Class of Open-Shell Transition Metal Clusters

Lutz H. Gade*

The way we view (and teach!) transition metal cluster chemistry is based on its partition into the two paradigms of metal–metal-bonded systems, as established by the pioneering work of Cotton, Dahl, Lewis, Chini, and others:[1] "The two general types of metal cluster compounds, which may be loosely called the 'lower halide' type and the 'carbonyl' type, differ from each other in many ways, and there is little in the way of chemical reactions to interrelate them."[2] The exceptional cases in which complex fragments of the two regimes are directly bonded to each other have attracted some attention but on the whole remained at the margin of an otherwise mature field of research.

One such class of compounds comprising the so-called "early-late heterobimetallics" that contain unsupported metal–metal bonds has received increasing attention over the past decade and is a field of research that is rapidly expanding.[3] Another type of metal–metal bonded compounds, which occupies the gap between the two regimes of "classical" clusters, is *formally* composed of cationic transition metal centers stabilized by "hard" donor ligands that are directly bonded to carbonylmetalate fragments. The first well-characterized example of such a species were reported by Fachinetti and co-workers almost a decade ago[4, 5] and stemmed from a variation of the well-known redox disproportionations that some metal carbonyls undergo in the presence of donor bases. Although such reactions were among the first to be studied in the early days of metal carbonyl chemistry,[6] by careful control of the stoichiometry and reaction conditions a hitherto undiscovered class of metal–metal-bonded compounds emerged. From the reactions of $[Fe(CO)_5]$ and $[Co_2(CO)_8]$ with pyridine the truly remarkable complexes $[\{(py)_2FeFe(CO)_4\}_2]$ (**1**)[4] and $[(py)_3CoCo(CO)_4]^+$ (**2**)[5] could be isolated and structurally characterized.

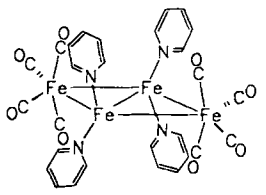

1

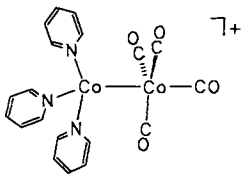

2

Both complexes **1** and **2** are paramagnetic and highly electron-deficient on the basis of EAN-electron counting, and their reactivity indicated that they dissociate heterolytically in solution. In their first reports Fachinetti et al. therefore interpreted them as "homonuclear ion-pair clusters"; however, an Extended Hückel Molecular Orbital study (EHMO) of **1** published a few years later supported the notion of essentially covalent donor–acceptor metal–metal bonding with almost equal charge distribution between the $\{(py)_2Fe\}$ and $\{(CO)_4Fe\}$ centers.[7] The good match of the donor and acceptor capabilities of the two metal fragments is responsible for this bonding situation, which is not unlike that of equally dissimilar complex fragments directly bonded to each other in, for instance, $[(R_2N)_3TiFeCp(CO)_2]$.[8]

This earlier work has most recently received renewed attention due to the remarkable results from the treatment of another neutral metal carbonyl, $[Mn_2(CO)_{10}]$, with the Lewis acid $AlMe_3$ in the polar donor solvent THF (Scheme 1).[9] Depending on the reaction conditions chosen the products of redox disproportionations that Whittlesey et al. identified were $[Mn(thf)_6][\{Mn(CO)_5\}_2]$ (**3**), $[(thf)_2Mn\{Mn(CO)_5\}_2]$ (**4**), and $[Mn\{Mn_7(thf)_6(CO)_{12}\}_2]$ (**5**).

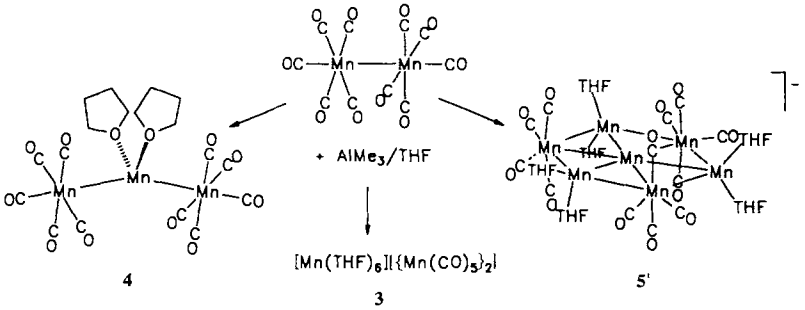

Scheme 1. Products of the disproportionation reaction of $[Mn_2(CO)_{10}]$ in THF in the presence of $AlMe_3$. **5'** is the anionic cluster fragment in **5**.

While the trinuclear cluster **4** is related to **2**, complex **5** turned out to be a high-nuclearity cluster. A crystal structure analysis of the latter revealed a metal–metal-bonded array unique in metal cluster chemistry (Fig. 1). The compound may be viewed as consisting of two $[Mn_7(thf)_6(CO)_{12}]$ units, each containing an almost planar metal core. These are coordinated through isocarbonyl linkages to a central manganese atom that has an octahedral coordination geometry.

The most remarkable feature of the structure is the central unligated manganese atom of the Mn_7 moiety, which is surrounded by a hexagonal planar arrangement of alternating $Mn(thf)_2$ and $Mn(CO)_4$ fragments. The planar cluster structure is reminiscent of the hexagonal planar compound $[Ni\{PtBu_3\}_6]$[10] and the pentagonal dianion $[In\{Mn(CO)_4\}_5]^{2-}$ (Fig. 2).[11] Hoffmann et al. have offered a qualitative rationale for the bonding in these interesting complexes based on the isolobal relationship between RP and $Mn(CO)_4$.[12] However, the presence of $Mn(thf)_2$ fragments linking the $Mn(CO)_4$ units

[*] Dr. L. H. Gade
Institut für Anorganische Chemie der Universität
Am Hubland, D-97074 Würzburg (Germany)
Fax: Int. code +(931)888-4605

 © VCH Verlagsgesellschaft mbH, D-69451 Weinheim, 1996 0570-0833/96/3518-2089 $ 15.00+.25/0

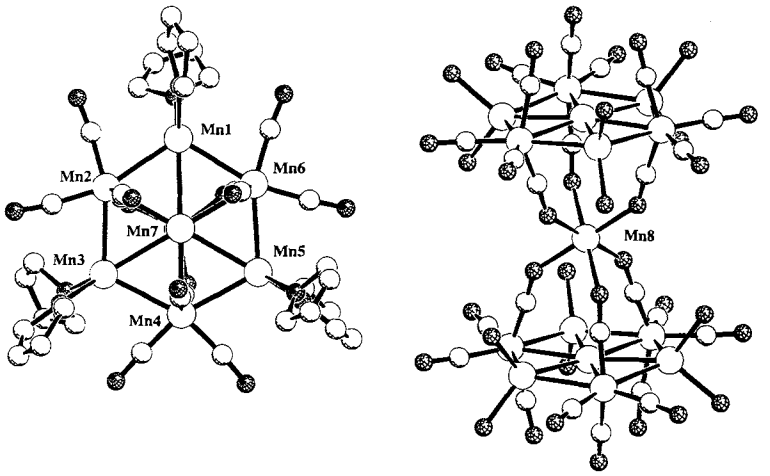

Fig. 1. Molecular structure of **5** in the crystal. Left: view of the virtually planar $[Mn_7(thf)_6(CO)_{12}]$ cluster monoanions. Right: view of the whole aggregate with the central Mn^{2+} ion octahedrally coordinated by six isocarbonyl ligands through the O atoms.

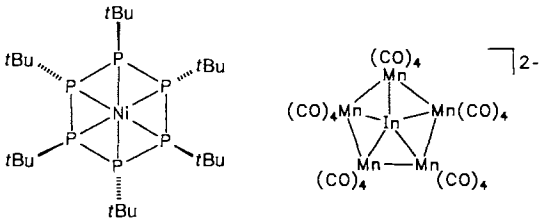

Fig. 2. Molecular structures of $[Ni(PtBu]_6]$ (left) and $[In\{Mn(CO)_4\}_5]^{2-}$ (right).

present in **5** makes an analysis of the bonding along the same lines less straightforward.

There is strong evidence from infrared spectroscopy that the aggregate observed in the crystal dissociates in solution, partially breaking down to $[Mn(CO)_4]^{3-}$ units. The isolation of **3** and **4** from reaction mixtures containing $[Mn\{Mn_7(thf)_6(CO)_{12}\}_2]$ suggests that these clusters form from the ions $[Mn(thf)_6]^{2+}$ and $[Mn(CO)_5]^-$, which are the products of a redox disproportionation of $[Mn_2(CO)_{10}]$ in THF[13] and which aggregate upon simultaneous displacement of THF and CO.

The planar manganese cluster may serve as a starting material in the synthesis of heterometallic clusters, as was also shown by Whittlesey and Harakas.[14] From the reaction of **5** with $[Fe(CO)_5]$ the MnFe-heterobimetallic analogue of **1**, $[(thf)_2MnFe(CO)_4]_2$ (**6**) could be isolated in moderate yield.

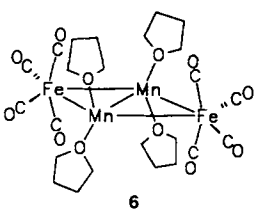

6

Whereas the magnetic behavior of **1** is consistent with a triplet ground state, the more open-shell complex **6** appears to have a quintet ground state. This implies the presence of substantial covalent bonding between the metal centers in **6** involving three of the five valence d-electrons of the Mn centers. Comparison of the position of the ν(CO) infrared bands of the $Fe(CO)_4$ units in both compounds reveals (not unexpectedly!) a somewhat more polar nature of **6**.

With the structural characterization of **1**, **2**, and **4**–**6** a new type of open-shell transition metal cluster is emerging. Whittlesey proposed the term xenophilic ("stranger-loving") for this class of clusters to characterize the nature of the combining complex fragments. A more detailed theoretical investigation into their metal–metal bonding is clearly required to categorize them meaningfully.

The thermal lability of these systems in solution and their partial break down in polar solvents have thus far prevented the development of their reaction chemistry. In pursuing the aim of stabilizing such polynuclear complexes the focus will be on the fragments containing the Werner-type coordination sphere, since they are the primary points of attack in solution. As in the chemistry of early-late heterobimetallics[3g, h] the judicious choice of, for example, chelating ligands, which stabilize these metal centers kinetically (without causing complete dissociation into solvent separated ion pairs!), may provide the entry into the systematic development of this area of cluster chemistry. Modern coordination chemistry offers a whole armory of ligands for that purpose!

German version: *Angew. Chem.* **1996**, *108*, 2225–2226

Keywords: carbonyl complexes · clusters · metal–metal bonds · redox disproportionations

[1] See, for example, a) F. A. Cotton, *Q. Rev* **1966**, *20*, 389; b) J. Lewis, R. S. Nyholm, *Sci. Prog. (London)* **1964**, *208*, 557; c) P. Chini, G. Longoni, V. G. Albano, *Adv. Organomet. Chem.* **1976**, *14*, 285.

[2] F. A. Cotton, G. Wilkinson, *Advanced Inorganic Chemistry*, 5th ed., Wiley, New York **1988**, p. 1053.

[3] a) C. P. Casey, R. F. Jordan, A. L. Rheingold, *J. Am. Chem. Soc.* **1983**, *105*, 665; b) *Organometallics* **1984**, *3*, 504; c) C. P. Casey, *J. Organomet. Chem.* **1990**, *400*, 205; c) W. S. Sartain, J. P. Selegue, *J. Am. Chem. Soc.* **1985**, *107*, 5818; d) *Organometallics* **1987**, *6*, 1812; e) *ibid.* **1989**, *8*, 2153; f) D. Selent, R. Beckhaus, J. Pickart, *ibid.* **1993**, *12*, 2857; g) S. Friedrich, H. Memmler, L. H. Gade, W.-S. Li, M. McPartlin, *Angew. Chem.* **1994**, *106*, 705; *Angew. Chem. Int Ed. Engl.* **1994**, *33*, 676; h) B. Findeis, M. Schubart, C. Platzek, L. H. Gade, I. J. Scowen, M. McPartlin, *Chem. Commun.* **1996**, 219.

[4] G. Fachinetti, G. Fochi, T. Funaioli, P. F. Zanazzi, *J. Chem. Soc. Chem. Commun.* **1987**, 89.

[5] G. Fachinetti, G. Fochi, T. Funaioli, P. F. Zanazzi, *Angew. Chem.* **1987**, *99*, 681; *Angew. Chem. Int. Ed. Engl.* **1987**, *26*, 680.

[6] See, for example, W. Hieber, F. Sonnenkalb, *Ber. Dtsch. Chem. Ges.* **1928**, *61*, 558 and references therein. For a historical account, see W. Hieber, *Adv. Organomet. Chem.* **1970**, *8*, 1.

[7] C. Mealli, D. M. Proserpio, G. Fachinetti, T. Funaioli, G. Fochi, P. F. Zanazzi, *Inorg. Chem.* **1989**, *28*, 1122.

[8] G. Jansen, C. E. Housecroft, personal communication.

[9] G. Kong, G. N. Harakas, B. R. Whittlesey, *J. Am. Chem. Soc.* **1995**, *117*, 3502.

[10] R. Ahlrichs, D. Fenske, H. Oesen, U. Schneider, *Angew. Chem.* **1992**, *104*, 312; *Angew. Chem. Int. Ed. Engl.* **1992**, *31*, 323.

[11] M. Schollenberger, B. Nuber, M. L. Ziegler, *Angew. Chem.* **1992**, *104*, 329; *Angew. Chem. Int. Ed. Engl.* **1992**, *31*, 350.

[12] H. Tang, D. M. Hoffman, T. A. Albright, H. Deng, R. Hoffmann, *Angew. Chem.* **1993**, *105*, 1682; *Angew. Chem. Int. Ed. Engl.* **1993**, *32*, 1616.

[13] It should be noted that $[Mn_2(CO)_{10}]$ can undergo photochemically induced redox disproportionation in THF to yield $[Mn(thf)_6]^{2+}$ and $[Mn(CO)_5]^-$: B. K. Nicholson, *J. Organomet. Chem.* **1979**, *169*, 185.

[14] G. N. Harakas, B. R. Whittlesey, *J. Am. Chem. Soc.* **1996**, *118*, 3210.

 © VCH Verlagsgesellschaft mbH, D-69451 Weinheim, 1996 0570-0833/96/3518-2090 $ 15.00+.25/0

Nanostructured Metal Oxide Clusters by Oxidation of Stabilized Metal Clusters with Air

Manfred T. Reetz,* Stefan A. Quaiser, Martin Winter, Jörg A. Becker, Rolf Schäfer, Ulrich Stimming, Andrea Marmann, Roland Vogel, and Toyohiko Konno

Dedicated to Professor Heinz A. Staab on the occasion of his 70th birthday

Nanostructured metal sulfides and oxides are useful as catalysts in organic and inorganic chemistry, and as materials with special electronic and optical properties.[1] The size-dependent semiconductor properties of these materials are of special interest in microelectronics (quantum dots). Metal chalcogenides are usually obtainable by precipitation or sol–gel processes, in which a wide variety of compounds, for example, polyphosphate, can be used as stabilizers.[1, 2] Although there are several interesting approaches to control the particle size of metal sulfides and oxides in the nanometer range, it is usually necessary to use chromatographic enrichment to obtain monodisperse materials.[1]

We have recently described two electrochemical methods for preparing $R_4N^+X^-$-stabilized metal and bimetal clusters.[3, 4] In some cases it was possible to control the size of the clusters within the range 1.5–6 nm by varing the current density and solvent.[3, 5] It was shown by high resolution transmission electron microscopy (HRTEM) and scanning tunneling microscopy (STM) that the metal clusters are stabilized by a monomolecular layer of the ammonium salt.[6] We now report that in the case of fairly readily oxidizable metals such as cobalt, iron, or nickel the $R_4N^+X^-$-stabilized clusters can be quantitatively converted into the corresponding nanostructured metal oxide clusters (Scheme 1).

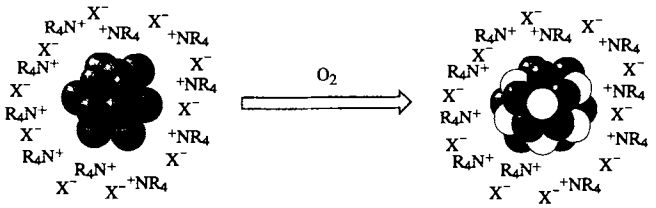

Scheme 1. Idealized representation of the oxidation of $(C_8H_{17})_4N^+X^-$-stabilized metal clusters with O_2 (dark spheres, metal atoms; light spheres, oxygen atoms).

If a 0.5 M solution of $(C_8H_{17})_4N^+Br^-$-stabilized cobalt clusters[7] (3.6 nm mean diameter by TEM) is allowed under exclusion of moisture to react slowly with oxygen, the color of the solution changes from blackish-brown to olive-green within a few hours. To exclude the possibility that only a surface layer of oxide on the cobalt clusters is formed, the progress of the oxidation reaction was monitored by measuring the oxygen consumption. Accordingly, the amount of oxygen consumed turned out to be exactly that required for the stoichiometric formation of cobalt(II) oxide.[8] The UV/Vis spectra of the material before and after the reaction with O_2 also indicate complete oxidation (Fig. 1). The solution of Co clusters shows unstructured absorption in the UV/Vis spectrum (359–800 nm), increasing with increasing wavelength, which is typical for metal clusters (Fig. 1a). This decreases by a factor of 10 during the course of the oxidation, and additional bands appear between 600 and 750 nm (Fig. 1b).

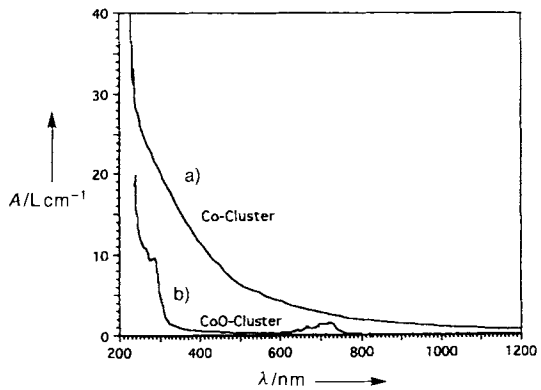

Fig. 1. UV Vis spectra of $(C_8H_{17})_4N^+Br^-$-stabilized Co clusters (a) and CoO clusters (b) in THF.

To obtain a better insight into the oxidation process, the magnetic properties of the Co clusters were investigated. Since $R_4N^+Br^-$-stabilized Co clusters are superparamagnetic,[7] this property should change during the oxidation. Indeed, the magnetic susceptibility, as measured by a magnetic (Gouy) balance, falls away completely during the course of the reaction with O_2 (Fig. 2), parallel to the O_2 uptake.[9] After complete oxidation the THF solution of CoO clusters is diamagnetic.

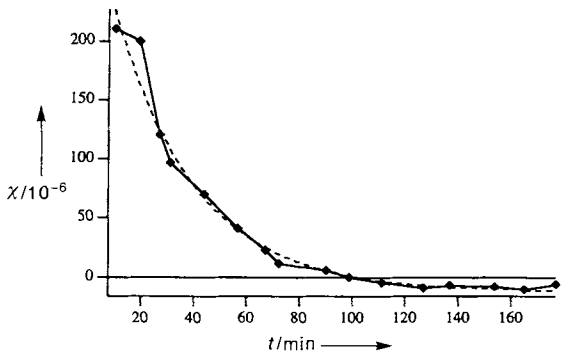

Fig. 2. Change of magnetic susceptibility χ with time in the reaction of $(C_8H_{17})_4N^+Br^-$-stabilized Co clusters in THF with air (◆, —); exponential interpolation (- - -).

For further characterization, the cobalt oxide clusters were investigated by HRTEM. In the TEM images (Fig. 3) single clusters are visible, which are similar in mean diameter and shape to the Co clusters in their initial state.[10] The lattice planes are also clearly visible. In the electron diffraction image the diffraction rings characteristic of nanocrystalline materials can be identified (Fig. 3 inset). Analysis of these revealed the presence of a face-centered cubic structure. Of the known bulk

[*] Prof. M. T. Reetz, Dr. S. A. Quaiser, Dipl.-Chem. M. Winter
Max-Planck-Institut für Kohlenforschung
Kaiser-Wilhelm-Platz 1, D-45470 Mülheim an der Ruhr (Germany)
Fax: Int. code +(208)3062-985
Dr. habil. J. A. Becker, Dipl.-Chem. R. Schäfer
Fachbereich Physikalische Chemie der Universität Marburg (Germany)
Prof. U. Stimming, Dipl.-Chem. A. Marmann, Dr. R. Vogel
Forschungszentrum Jülich GmbH, Institut für Energieverfahrenstechnik
Jülich (Germany)
Dr. T. Konno
Institute of Metals Research, Tohoku University, Sendai (Japan)

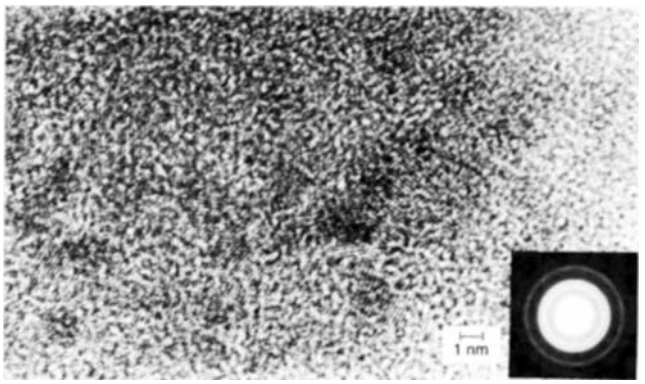

Fig. 3. TEM image of oxidized Co clusters. The inset shows the electron diffraction image.

cobalt oxides CoO, Co_2O_3, and Co_3O_4, only the unit cell of the monoxide is face-centered cubic. The lattice constant found from the electron diffraction rings (Fig. 3 inset) was found to be 4.249 Å, which agrees well with the known value for bulk CoO (4.2495 Å).[11, 12]

To answer the question whether the cobalt oxide clusters in solution are in fact stabilized by a layer of ammonium salt (Scheme 1),[13] an STM study was carried out. The oxidized metal clusters were deposited on a specially prepared, faceted gold surface[6] by dip coating. The STM image shows that the cobalt oxide clusters are located on the steps of the surface (Fig. 4). The clusters have an average diameter of 6.0 nm. As the corresponding TEM images for the metal oxide core gave a diameter of approximately 3.6 nm, the result of the combined STM/TEM study is consistent with the existence of a stabilized outer layer of surfactant.[6]

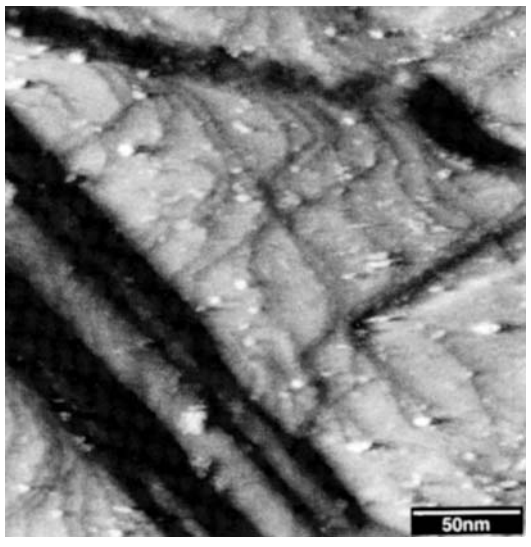

Fig. 4. STM image of CoO clusters.

If solutions of CoO clusters are allowed to come into contact with moisture in the air, light green precipitates are formed. TEM images reveal particles 100 nm to several millimeters in size formed by agglomeration of cobalt oxide clusters.

Both the preformed Co clusters and the CoO clusters can be immobilized on solid supports. For example, if dried Al_2O_3 pellets (Johnson Matthey 11838) are immersed in solutions of Co clusters in THF, the clusters become efficiently fixed onto the support. Within 45 min the impregnation is complete, as shown by photographs of sections of the pellets (Fig. 5, top). During and after the immobilization, the Co clusters are oxidized by air, resulting in an olive-green coloration. Fixation of preformed CoO clusters on a support proceeds differently, penetration being only slight even after 45 min, (less than 200 μm; Fig. 5, bottom). This corresponds to a morphology that is desirable for shell catalysts.[14, 15] It is likely that the Co clusters do not migrate very far into the pores of the Al_2O_3 particles on a microscopic scale (cortexlike morphology),[14] although this still needs to be clarified.

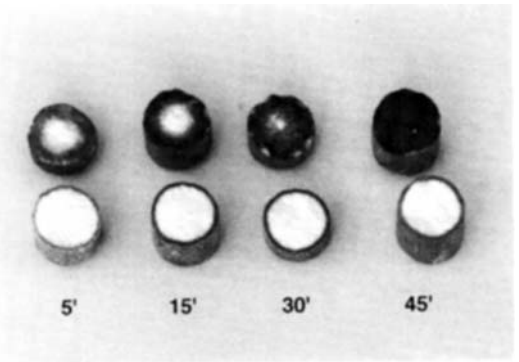

Fig. 5. Section through Al_2O_3 pellets (diameter 3.2 mm) after immersion in 0.5 M THF solution of $(C_8H_{17})_4N^+Br^-$-stabilized Co clusters (top) and CoO clusters (bottom) for 5, 15, 30, and 45 min.

Other readily oxidizable $R_4N^+X^-$-stabilized metal clusters can also be converted by oxygen into the corresponding metal oxide clusters without forming insoluble bulk metal oxides. Examples include $(C_8H_{17})_4N^+Br^-$-stabilized iron oxide clusters (2–3 nm) and nickel oxide clusters (2–3 nm), which respectively form reddish-brown and green solutions in THF. Finally, bimetal clusters (for example, Fe/Co)[3] can also be oxidized by oxygen. The exact characterization of these materials and their possible use in catalysis are subjects of further investigation.

Received: March 19, 1996 [Z89491E]
German version: *Angew. Chem.* **1996**, *108*, 2228–2230

Keywords: clusters · cobalt compounds · magnetic properties · nanostructures · scanning tunneling microscopy

[1] H. Weller, *Angew. Chem.* **1993**, *105*, 43; *Angew. Chem. Int. Ed. Engl.* **1993**, *32*, 41; A. Henglein, *Ber. Bunsenges. Phys. Chem.* **1995**, *99*, 903; G. Nimtz, P. Marquard, H. Gleiter, *J. Cryst. Growth* **1988**, *86*, 66.

[2] A. Fojtik, H. Weller, U. Koch, A. Henglein, *Ber. Bunsenges. Phys. Chem.* **1984**, *88*, 969.

[3] M. T. Reetz, W. Helbig, *J. Am. Chem. Soc.* **1994**, *116*, 7401; M. T. Reetz, S. A. Quaiser, *Angew. Chem.* **1995**, *107*, 2461; *Angew. Chem. Int. Ed. Engl.* **1995**, *34*, 2240; M. T. Reetz, W. Helbig, S. A. Quaiser, *Chem. Mater.* **1995**, *7*, 2227.

[4] $R_4N^+X^-$-stabilized metal clusters have been known for a long time: J. Kiwi, M. Grätzel, *J. Am. Chem. Soc.* **1979**, *101*, 7214; J. Blum, Y. Sasson, A. Zoran, *J. Mol. Catal.* **1981**, *11*, 293; M. Boutonnet, J. Kizling, P. Stenius, G. Maire, *Colloids Surf.* **1982**, *5*, 209; N. Toshima, T. Takahashi, H. Hirai, *Chem. Lett.* **1985**, 1245; M. Boutonnet, J. Kizling, R. Touroude, G. Maire, P. Stenius, *Appl. Catal.* **1986**, *20*, 163; K. Meguro, M. Toriyuka, K. Esumi, *Bull. Chem. Soc. Jpn.* **1988**, *61*, 341; J. Wiesner, A. Wokaun, H. Hoffmann, *Prog. Coll. Polym. Sci.* **1988**, *76*, 271; N. Satoh, K. Kimura, *Bull. Chem. Soc. Jpn.* **1989**, *62*, 1758; H. Bönnemann, W. Brijoux, R. Brinkmann, E. Dinjus, T. Joussen, B. Korall, *Angew. Chem.* **1991**, *103*, 1344; *Angew. Chem. Int. Ed. Engl.* **1991**, *30*, 1312; N. Toshima, T. Takahashi, *Bull. Chem. Soc. Jpn.* **1992**, *65*, 400.

[5] M. T. Reetz, R. Breinbauer, M. Winter, unpublished results.

[6] M. T. Reetz, W. Helbig, S. A. Quaiser, U. Stimming, N. Breuer, R. Vogel, *Science* **1995**, *267*, 367.
[7] J. A. Becker, R. Schäfer, R. Festag, W. Ruland, J. H. Wendorff, J. Pebler, S. A. Quaiser, W. Helbig, M. T. Reetz, *J. Chem. Phys.* **1995**, *103*, 2520.
[8] It is also possible intentionally to oxidize the Co clusters partially with substoichiometric amounts of O_2.
[9] We thank C. Herwig, H. Petersen, S. Zahn, and M. Becker (University of Marburg) for performing the measurements.
[10] A slight increase in particle size (by about 18%, estimated from the properties of bulk Co and CoO) would be expected, but such small differences cannot be detected with certainty within the limits of accuracy of the TEM analysis.
[11] N. C. Trombs, H. P. Rooksby, *Nature* **1950**, *165*, 412.
[12] In bulk CoO the proportion of cobalt is usually substoichiometric because of lattice defects, and the required charge neutralization is achieved by an increase in the oxidation state of a few cobalt ions in the lattice from +2 to +3. This material is thus a homeotopic mixed crystal of CoO and a little (green) Co_2O_3 (N. Wiberg, *Lehrbuch der Anorganischen Chemie*, de Gruyter, Berlin, 91st–100th ed., **1985**, p. 127, 1148). We cannot exclude the presence of small amounts of Co_2O_3 in the CoO clusters. Interestingly, the electron diffraction images show the presence of not only Co and CoO but also Co_2O_3 (corundum structure, hexagonal close packing) in the samples obtained by partial oxidation (extent, for example, 50%) [8].
[13] Some surfactant-stabilized metal oxides in microemulsions are known: J. B. Nagy, A. Claerbout in *Surfactants in Solution, Vol. 11* (Eds.: K. L. Mittal, D. O. Shah), Plenum, New York, **1991**, p. 363; J. B. Nagy, *Colloids Surfaces* **1989**, *35*, 201; A. Claerbout, J. B. Nagy, *Stud. Surf. Sci. Catal.* **1991**, *63*, 705. See also N. Moumen, M. P. Pilini, *Chem. Mater.* **1996**, *8*, 1128, and references therein.
[14] M. T. Reetz, S. A. Quaiser, R. Breinbauer, B. Tesche, *Angew. Chem.* **1995**, *107*, 2956; *Angew. Chem. Int. Ed. Engl.* **1995**, *34*, 2728.
[15] E. F. Gallei, H.-P. Neumann, *Chem. Ing. Tech.* **1994**, *66*, 924.

Chiral Metallocalix[4]arenes: Resolution by Diastereomeric Tungsten(VI) Alkoxides**

Bing Xu, Partrick J. Carroll, and Timothy M. Swager*

Efficient preparations of chiral supramolecular systems are critical to the design of new materials and catalysts. Calixarenes[1] present one of the most versatile platforms for the construction of supramolecular receptor assemblies with well-defined structures and specific functions.[2] Recent applications include the use of calixarenes as highly specific ligands,[3] sensors,[4] nonlinear optical chromophores,[5] porous monolayers,[6] and bowlic liquid crystals.[7] Chiral calix[4]-arenes have been produced by unsymmetric substitution of the lower rim,[8] by the addition of chiral appendages,[9] and by the incorporation of unsymmetric substitution patterns on the phenyl rings.[10] *meta*-Substituted systems with C_4 symmetry of the latter type have been prepared as racemates,[10b] and a route to analogs with a variety of functional groups has recently been reported.[11] In spite of the interest in chiral calix[4]arenes, few resolutions have been developed. We have been investigating transition metal containing calix[4]arenes[12] with rigid well-defined receptor cavities for the development of supramolecular materials and catalysts. We report herein the first resolution of chiral metallocalix[4]arenes. This method makes use of tungsten alkoxides,[13] which may be efficiently transformed into Lewis acidic oxotungsten(VI) calix[4]arene complexes or dichlorotungsten(VI) calix[4]arenes.[7a, 12a]

Among many resolution methods, we have concentrated on the use of diastereomeric intermediates to resolve the chiral metallocalix[4]arenes. Since the racemic $R_4W{=}O$ complex can be considered as a conceptual analog of a $R_2C{=}O$, the complex $R_4W(OR^*)_2$ was chosen to provide separable diastereomers similar to classical resolutions of chiral ketones via diastereomeric ketals. After separation, removal of the alkoxy groups produces resolved enantiomers. To test the accessibility and stability of cyclic tungsten(VI) calix[4]arene alkoxides,[14] we synthesized *trans*-1,2-cyclohexanediol-based chelates to produce complexes **2a** and **2b**. Two synthetic procedures were developed (Scheme 1). In one route, dichlorotungsten(VI) *p*-*t*Bu-calix[4]-arene (**1a**) was heated to reflux with doubly deprotonated cyclohexanediol in toluene for four hours to give **2a** in 96% yield. Alternatively, oxotungsten(VI) calix[4]arene (**1b**) is transformed to **2b** in 10% yield when treated with silylated cyclohexanediol in refluxing toluene for two days. The

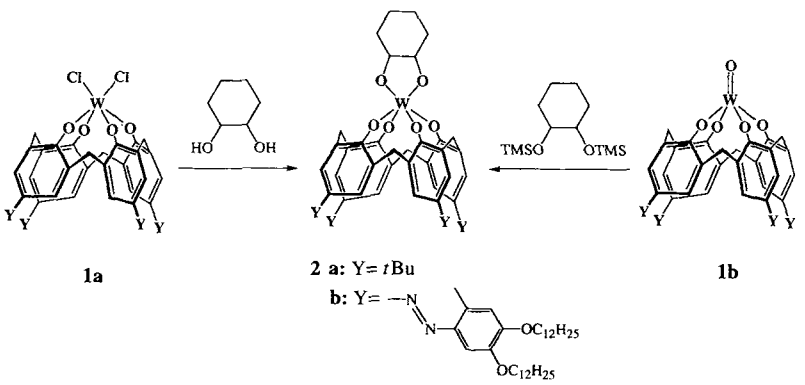

Scheme 1. Synthesis of **2**.

^{1}H NMR spectra displayed by these calix[4]arenes are diagnostic for the formation of **2**. Due to lower symmetry of **2**, the methylene groups of the calix[4]arene core are inequivalent and produce two sets of coupled geminal protons for a total of four doublets. Both **2a** and **2b** can be purified by chromatography on a silica gel column without any decomposition.

With methods to prepare tungsten(VI) dialkoxy calix[4]arenes in hand, we endeavored to synthesize diastereomeric complexes in which both the calix[4]arene and dialkoxy ligands are chiral (Scheme 2). We employed 3,4-dimethylcalix[4]arene, which had been previously reported by Böhmer et al., since it has an interesting inherently chiral structure with C_4 symmetry.[10b] Reaction of 3,4-dimethylcalix[4]arene with WCl_6 in benzene produced the dichlorotungsten(VI) complex **3** in 81% yield. The ^{1}H NMR spectrum contained four doublets for the calix[4]arene methylene protons, which is consistent with **3** having a elliptical cone conformation with C_2 symmetry.[12a] Racemic **3** reacts with (1*S*,2*S*)-*trans*-1,2-cyclohexanediol under the same conditions used to prepare **2a** to give a mixture of the diastereomers **4** and **5**. The diastereomeric relationship is apparent from the ^{1}H NMR resonances for the methylene protons (eight doublets, Fig. 1). The two diastereomers **4** and **5** can be separated by

[*] Prof. T. M. Swager,[+] Dr. B. Xu,[+] Dr. P. J. Carroll
Department of Chemistry
University of Pennsylvania
Philadelphia, PA 19104-6323 (USA)
[+] New address:
Department of Chemistry
Massachusetts Institute of Technology
Cambridge, MA 02139 (USA)
Fax: Int. code +(617)253-7929
[**] This work was supported by the Office of Naval Research and a Camille and Henry Dreyfus Teacher Scholar Award.

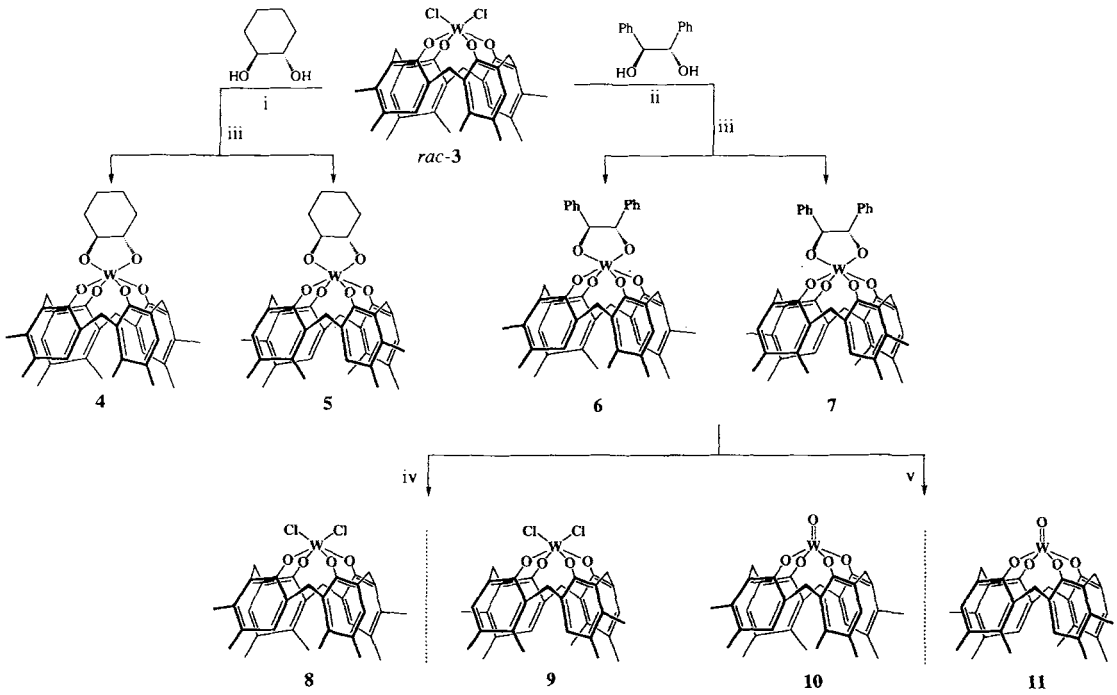

Scheme 2. Conditions: i) *n*BuLi, toluene, 4 h, 96%; ii) *n*BuLi, toluene, 4 h, 75%; iii) HPLC; iv) $AlCl_3$, $CHCl_3$, reflux, 3 min, 98%; v) trimethylsilyl triflate (TMSOTf), toluene, reflux overnight, 76%.

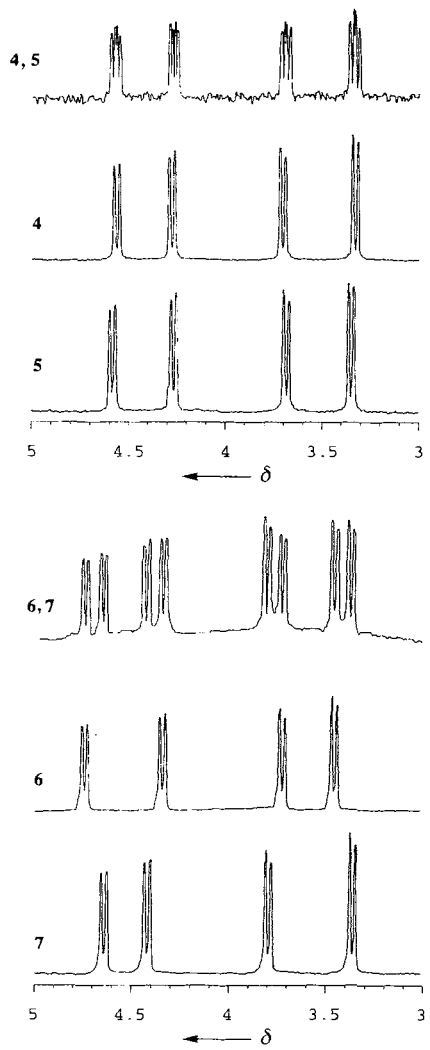

Fig. 1. ^{1}H NMR spectra of the characteristic calix[4]arene methylene protons of the diastereomeric mixtures (**4**, **5** and **6**, **7**), the first components from HPLC (**4** and **6**), and the second components from HPLC (**5** and **7**).

chromatography on silica gel (HPLC; eluent, *n*-hexane:CH_2Cl_2 3:1), and each compound has the expected four methylene doublets (Fig. 1).

After separation of **4** and **5**, we tried to complete the resolution and produce pure enantiomers **8** and **9** or oxo analogs **10** and **11**. However, a variety of deprotection protocols (H_2O, HCl, $AlCl_3$, BBr_3) proved ineffective. This difficulty is likely due to the inert nature of the W–O′ bond, which is considered to be very strong.[14c] We considered that a more productive approach would use dialkoxy groups in which the C–O bond may be cleaved. We prepared a (*S*,*S*)-(−)-hydrobenzoin-based diastereomeric mixture, **6** and **7**, in 75% yield (Scheme 2). Similar to **4** and **5**, the diagnostic calix[4]arene methylene protons of the diastereomeric mixture display eight pairs of doublets in the ^{1}H NMR spectrum. However, in this case we observe a greater dispersion in chemical shift (Fig. 1), which suggests that **6** and **7** have larger variations in their properties. Indeed their chromatography properties reflect this; **6** and **7** are more easily separated (silica: flash or HPLC) than **4** and **5**.

In order to assign the absolute configuration of the chiral tungsten(VI) calixarenes, we performed a crystal structure determination[15a] of compound **7** (the second component from the HPLC separation). In the crystal structure (Fig. 2), the tungsten(VI) center is approximately octahedral,[15b] and the calix[4]arene phenyl rings define an elliptical cone similar to that reported for dichlorotungsten(VI) *p*-*t*Bu-calix[4]arene.[12a] Crystals of **7** exhibit a noncentrosymmetric highly polar structure (Fig. 3).

The higher reactivity of the C–O bonds facilitates the transformation of **6** and **7** to enantiomeric metallocalix[4]arenes. Indeed, **6** and **7** are converted to the respective dichlorotungsten(VI) complexes **8** and **9** in near quantitative yield when treated with excess $AlCl_3$ (in refluxing $CHCl_3$, 3 min). The short reaction time was necessary since **8** and **9** were observed to decompose with longer reaction times. The CD spectra of compounds **8** and **9** are mirror images (Fig. 4), thereby confirming that they are indeed optical isomers. The strong Cotton effects observed

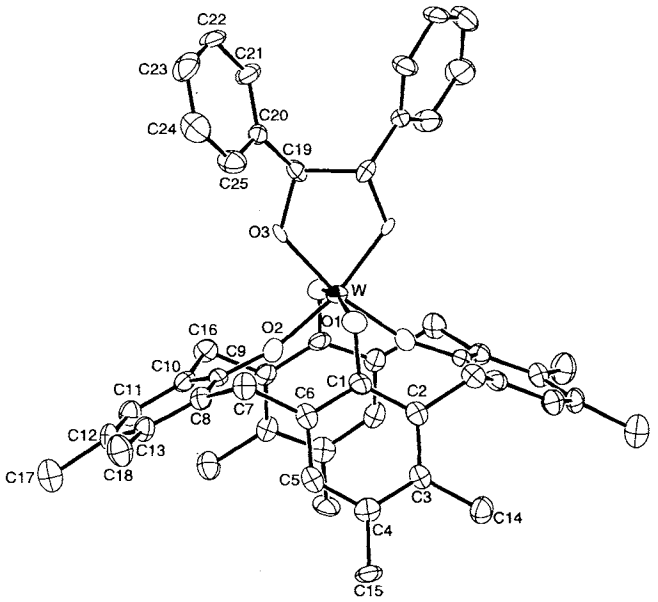

Fig. 2. X-ray structure of compound 7 [15b].

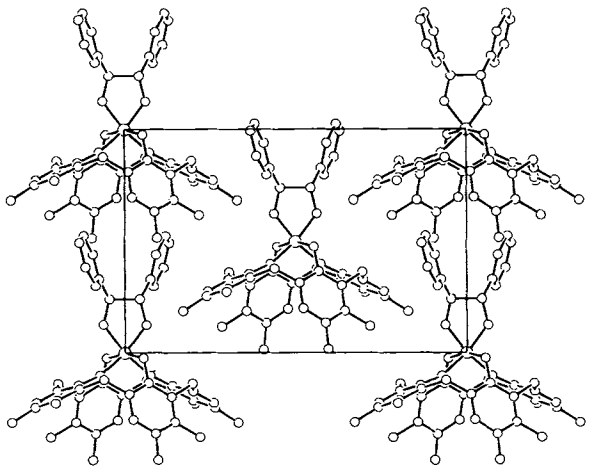

Fig. 3. Crystal packing of 7.

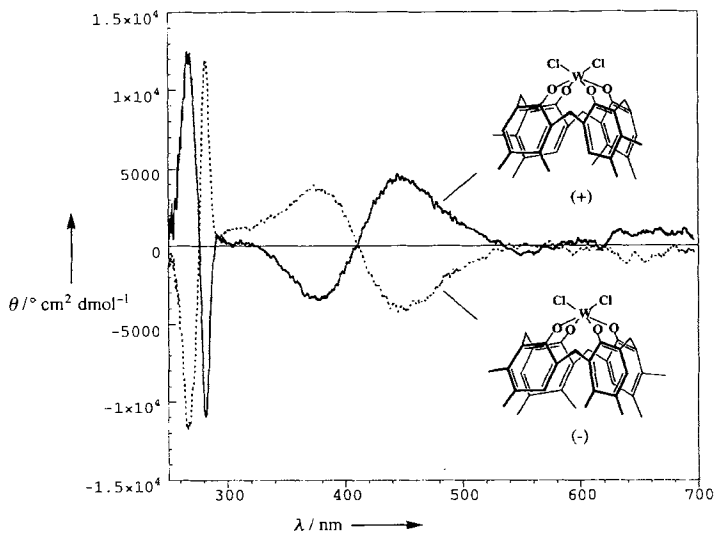

Fig. 4. CD spectra of resolved **8** and **9**.

at 250–300 nm are similar to what has been observed in other optically pure chiral calix[4]arenes[17] and likely result from exciton coupling of the aromatic chromophores.[16] The Cotton effects at 375–450 nm are most probably ligand–metal charge transfer in character. At λ_{max} (280 nm), θ is quite large (+12540), indicating that these chiral metallocalix[4]arenes have very strong rotary power. On the basis of the X-ray structure of **7**, we can assign the absolute configurations of **8** and **9** (Fig. 4).

To prepare Lewis acidic chiral oxotungsten(VI) calix[4]arenes with C_4 symmetry, we first investigated the method applied by Floriani et al.[12a] for the transformation of the dichlorotungsten(VI) group of **3** to an oxotungsten group. However, in contrast to other dichlorotungsten calix[4]arenes such as **1a**, which is hydrolytically sensitive, **3** has remarkably high stability and is even stable to chromatography on silica. To prepare oxotungsten calix[4]arenes **10** and **11**, we treated **6** and **7** with trimethylsilyl triflate followed by an aqueous workup (Scheme 2). Presumably, the initial product is a ditriflate, which is hydrolyzed to give the oxo compound. The calix[4]arene methylene protons in the ^{1}H NMR spectrum collapse to a pair of doublets at $\delta = 4.55$ and 3.59, indicating the C_4 symmetry of compounds **10** and **11**. The CD spectra of **10** and **11** again indicate that these complexes are optical isomers (Fig. 5). It is also interesting to note that **10** and **11** have yet stronger rotary power than **8** and **9** ($\theta = +45100$ at 265 nm (λ_{max})). The absolute configurations of **10** and **11** are shown in Figure 5.

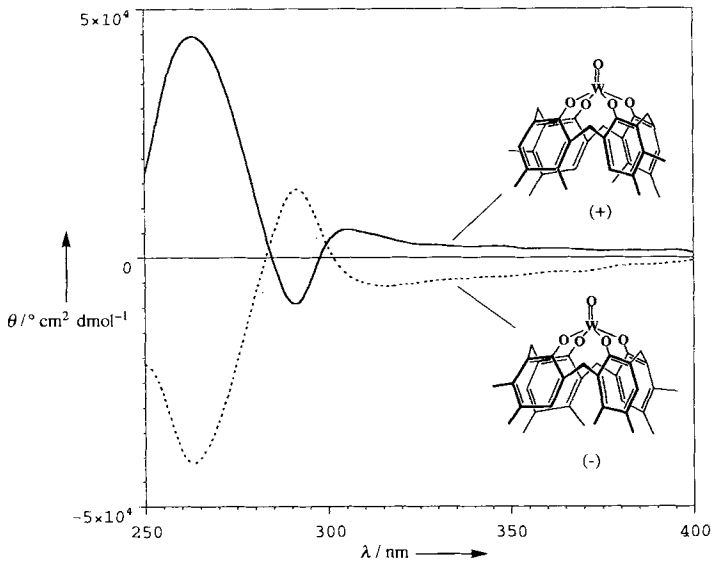

Fig. 5. CD spectra of optical isomers of **10** and **11**.

In summary, we have demonstrated the first resolution of metallocalix[4]arenes. The Lewis acidity and rigid chiral cavity of the oxotungsten(VI) calix[4]arenes present opportunities for the development of catalytic and liquid crystalline systems. Such applications are the subject of ongoing investigations in our laboratory.

Experimental Procedure

2a: *trans*-1,2-Cyclohexanediol (0.064 g, 0.56 mmol) in dry toluene (20 mL) was treated with *n*BuLi (1.1 mL, 1.6M) at room temperature under an argon atmosphere. After the solution had been stirred for 1 h, it was transferred to a suspension of dichlorotungsten(VI) *p*-*t*Bu-calix[4]arene (0.56g, 0.56 mmol) in toluene [12a]. The resulting dark purple suspension was heated to reflux for 4 h to give a clear orange-red solution. After the toluene had been evaporated, the residue was

purified by flash chromatography (*n*-hexane:dichloromethane 3:1) to give an orange solid (0.51 g, 96%). positive-ion FABMS: *m/z*: 943 [*M* + 1]; ^{1}H NMR (CDCl$_3$, 200 MHz): δ = 1.18 (s, 18H, *t*Bu), 1.29 (s, 18H, *t*Bu), 1.30 (m, 2H, CH$_2$), 1.71 (m, 2H, CH$_2$), 1.85 (m, 2H, CH$_2$), 2.16 (m, 2H, CH$_2$), 3.30 (dd, ^2J = 14.02, ^3J = 4.02 Hz, 4H, ArCH$_2$Ar), 4.62 (dd, ^2J = 13.38, ^3J = 5.08 Hz, 4H, ArCH$_2$Ar), 5.17 (m, 2H, OCH), 7.01 (s, 4H, ArH), 7.18 (s, 4H, ArH).

2b: *trans*-1,2-Cyclohexanediol (0.022g, 0.19 mmol) was dissolved in THF (5 mL) under an argon atmosphere, excess TMSCl (0.2 mL) and Et$_3$N (0.2 mL) were added at room temperature. The reaction mixture was allowed to stir until TLC showed the disappearance of cyclohexanediol, then THF, excess TMSCl, and Et$_3$N were removed under reduced pressure. Then **1b** (0.40 g, 0.171 mmol) [7a] in dry toluene (20 mL) was added to the residue, and the reaction mixture was heated to reflux for two days. Purification by flash chromatography (*n*-hexane:dichloromethane 3:1) gave an orange-red solid 50 mg (10%). Positive-ion FABMS: *m/z*: 2666 [*M* + 1], ^{1}H NMR (CDCl$_3$, 250 MHz): δ = 0.85 (t, 24H, CH$_3$), 1.10–2.00 (m, 166H, alkyl and CH$_2$), 2.20–2.30 (m, 2H, CH$_2$), 2.56 (s, 6H, ArCH$_3$), 2.74 (s, 6H, ArCH$_3$), 3.63 (dd, ^2J = 13.52, ^3J = 4.52 Hz, 4H, ArCH$_2$Ar), 3.89 (t, 4H, OCH$_2$), 3.97 (t, 4H, OCH$_2$), 4.00–4.10 (m, 8H, OCH$_2$), 4.71 (dd, ^2J = 13.62, ^3J = 6.42 Hz, 4H, ArCH$_2$Ar), 5.35–5.45 (m, 2H, OCH), 6.65 (s, 2H, ArH), 6.79 (s, 2H, ArH), 7.11 (s, 2H, ArH), 7.36 (s, 2H, ArH), 7.67 (s, 4H, ArH), 7.88 (s, 4H, ArH).

3: 3,4-Dimethylcalix[4]arene (0.501 g, 0.93 mmol) [10b] and WCl$_6$ (0.40 g, 1.0 mmol) were stirred in dry benzene (10 mL) overnight. After the solvent had been removed, the residue was purified by flash chromatography (*n*-hexane:dichloromethane 3:1) to give **3** as dark purple product (0.59 g, 81%). positive-ion FABMS: *m/z*: 787 [*M* + 1], ^{1}H NMR (CDCl$_3$, 500 MHz): δ = 2.06 (s, 6H, CH$_3$), 2.37 (s, 6H, CH$_3$), 2.39 (s, 6H, CH$_3$), 2.58 (s, 6H, CH$_3$), 3.52 (d, ^2J = 14.19 Hz, 2H, ArCH$_2$Ar), 3.91 (d, ^2J = 14.19 Hz, 2H, ArCH$_2$Ar), 4.43 (d, ^2J = 14.16 Hz, 2H, ArCH$_2$Ar), 4.70 (d, ^2J = 14.17 Hz, 2H, ArCH$_2$Ar), 6.83 (s, 2H, ArH), 7.13 (s, 2H, ArH).

4 and **5**: These compounds were prepared in 92% yield by using the same procedure as for **2a**. Positive-ion FABMS: *m/z*: 831 [*M* + 1]. The mixture was separated by HPLC to give **4** and **5**. (Rainin preparative silica column, *n*-hexane:dichloromethane 3:1, flow rate 20 mL min^{-1}). First component: ^{1}H NMR (CDCl$_3$, 500 MHz): δ = 1.36 (m, 2H, CH$_2$), 1.70 (m, 2H, CH$_2$), 1.84 (m, 2H, CH$_2$), 2.06 (s, 6H, CH$_3$), 2.15 (m, 2H, CH$_2$), 2.17 (s, 6H, CH$_3$), 2.353 (s, 6H, CH$_3$), 2.347 (s, 6H, CH$_3$), 3.33 (d, ^{2}J = 13.79 Hz, 2H, ArCH$_2$Ar), 3.71 (d, ^2J = 13.8 Hz, 2H, ArCH$_2$Ar), 4.28 (d, ^2J = 13.83Hz, 2H, ArCH$_2$Ar), 4.57 (d, ^2J = 13.68 Hz, 2H, ArCH$_2$Ar), 5.17 (m, 2H, OCH), 6.76 (s, 2H, ArH), 7.01 (s, 2H, ArH); second component: ^{1}H NMR (CDCl$_3$, 500 MHz): δ = 1.36 (m, 2H, CH$_2$), 1.71 (m, 2H, CH$_2$), 1.85 (m, 2H, CH$_2$), 2.07 (s, 6H, CH$_3$), 2.15 (m, 2H, CH$_2$), 2.17 (s, 6H, CH$_3$), 2.354 (s, 6H, CH$_3$), 2.344 (s, 6H, CH$_3$), 3.35 (d, ^2J = 13.80 Hz, 2H, ArCH$_2$Ar), 3.69 (d, ^2J = 13.80 Hz, 2H, ArCH$_2$Ar), 4.27 (d, ^2J = 13.77 Hz, 2H, ArCH$_2$Ar), 4.59 (d, ^2J = 13.78 Hz, 2H, ArCH$_2$Ar), 5.16 (m, 2H, OCH), 6.75 (s, 2H, ArH), 7.01 (s, 2H, ArH).

6 and **7**: These compounds were also prepared by the same procedure as for **2a** (75% yield). positive-ion FABMS: *m/z*: 929 [*M* + 1]. Again separation by HPLC (*n*-hexane:dichloromethane 3:1) afforded **6** and **7**. First component: ^{1}H NMR (CDCl$_3$, 500 MHz): δ = 2.09 (s, 6H, CH$_3$), 2.20 (s, 6H, CH$_3$), 2.325 (s, 6H, CH$_3$), 2.344 (s, 6H, CH$_3$), 3.45 (d, ^2J = 13.91 Hz, 2H, ArCH$_2$Ar), 3.72 (d, ^2J = 13.81 Hz, 2H, ArCH$_2$Ar), 4.34 (d, ^2J = 13.83 Hz, 2H, ArCH$_2$Ar), 4.74 (d, ^2J = 13.79 Hz, 2H, ArCH$_2$Ar), 6.52 (s, 2H, ArH), 6.80 (s, 2H, ArH), 7.02 (s, 2H, ArH), 7.29–7.38 (m, 10H, ArH); second component: ^{1}H NMR (CDCl$_3$, 500 MHz): δ = 2.08 (s, 6H, CH$_3$), 2.20 (s, 6H, CH$_3$), 2.334 (s, 6H, CH$_3$), 2.345 (s, 6H, CH$_3$), 3.36 (d, ^2J = 13.84 Hz, 2H, ArCH$_2$Ar), 3.79 (d, ^2J = 13.86 Hz, 2H, ArCH$_2$Ar), 4.42 (d, ^2J = 13.94 Hz, 2H, ArCH$_2$Ar), 4.64 (d, ^2J = 13.72 Hz, 2H, ArCH$_2$Ar), 6.51 (s, 2H, ArH), 6.81 (s, 2H, ArH), 6.99 (s, 2H, ArH), 7.29–7.38 (m, 10H, ArH).

8 and **9**: Compound **6** (or **7**) (1.2 mg) was dissolved in CHCl$_3$ (2 mL), then AlCl$_3$ (10 mg) was quickly added to the solution, and the solution was heated to reflux for about 3 min, upon which the color of the solution changed from orange to dark purple. The reaction was quenched with water (0.5 mL) and dried under reduced pressure. The residue was purified by HPLC (*n*-hexane:dichloromethane 3:1) to give the dichlorotungsten(VI) calix[4]arene (1 mg) **8** (or **9**), as a dark purple solid (98%). Positive-ion FABMS: *m/z*: 787 [*M* + 1], ^{1}H NMR (CDCl$_3$, 500 MHz): δ = 2.06 (s, 6H, CH$_3$), 2.36 (s, 6H, CH$_3$), 2.39 (s, 6H, CH$_3$), 2.58 (s, 6H, CH$_3$), 3.52 (d, ^2J = 14.20 Hz, 2H, ArCH$_2$Ar), 3.91 (d, ^2J = 14.19 Hz, 2H, ArCH$_2$Ar), 4.43 (d, ^2J = 14.11 Hz, 2H, ArCH$_2$Ar), 4.70 (d, ^2J = 14.17 Hz, 2H, ArCH$_2$Ar), 6.83 (s, 2H, ArH), 7.13 (s, 2H, ArH).

10 and **11**: Excess trimethylsilyl triflate was added to a solution containing compound **6** (or **7**) (2 mg) in toluene (10 mL). The solution changed from orange to red-orange under heating to reflux overnight under argon. The reaction was quenched with water (1 mL) and neutralized by the addition of triethylamine. The solvent was removed and the residue was purified by flash chromatography (AcOH:CH$_2$Cl$_2$ 5:95) to give the oxotungsten(VI) calix[4]arene **10** (or **11**) (1 mg) as a yellow solid (76%). Positive-ion FABMS: *m/z*: 733 [*M* + 1], ^{1}H NMR (CDCl$_3$, 500 MHz): δ = 2.14 (s, 12H, CH$_3$), 2.31 (s, 12H, CH$_3$), 3.59 (d, ^2J = 13.46 Hz, 4H, ArCH$_2$Ar), 4.55 (d, ^2J = 13.40 Hz, 4H, ArCH$_2$Ar), 7.04 (s, 4H, ArH).

Received: April 15, 1996 [Z 9038 IE]
German version: *Angew. Chem.* **1996**, *108*, 2238–2242

Keywords: calixarenes · enantiomeric resolution · NMR spectroscopy · tungsten compounds

[1] a) C. D. Gutsche, *Aldrichimica Acta.* **1995**, *28(1)*, 3; b) *Calixarenes 50th Anniversary*; (Eds.: J. Vicens, Z. Asfari, J. M. Harrowfield), Kluwer, Dordrecht, **1994**; c) C. D. Gutsche, *Calixarenes*, The Royal Society of Chemistry, Cambridge, England, **1989**; d) *Calixarenes: A Versatile Class of Macrocyclic Compounds* (Eds.: V. Böhmer, J. Vicens), Kluwer, Dordrecht, **1991**.

[2] a) V. Böhmer, *Angew. Chem.* **1995**, *107*, 785; *Angew. Chem. Int. Ed. Engl.* **1995**, *34*, 713, and references therein; b) E. van Dienst, W. I. I. Bakker, J. F. J. Engbersen, W. Verboom, D. N. Reinhoudt, *Pure Appl. Chem.* **1993**, *65*, 387.

[3] For a few examples see: a) Z. Brzozka, B. Lammerink, D. N. Reinhoudt, E. Ghidini, R. Ungaro, *J. Chem. Soc. Perkin Trans. 2.* **1993**, 1037; b) Y. Morzherin, D. M. Rudkevich, W. Verboom, D. N. Reinhoudt, *J. Org. Chem.* **1993**, *58*, 7602; c) P. L. H. M. Cobben, R. J. M. Egberink, J. G. Bomer, P. Bergveld, W. Verboom, D. N. Reinhoudt, *J. Am. Chem. Soc.* **1992**, *114*, 10573; d) Z. Asfari, J. M. Harrowfield, M. I. Ogden, J. Vicens, A. H. White, *Angew. Chem.* **1991**, *103*, 887; *Angew. Chem. Int. Ed. Engl.* **1991**, *30*, 854; e) for a recent review: see ref. [2a].

[4] a) R. Grigg, J. M. Holmes, S. K. Jones, W. D. J. A. Norbert, *J. Chem. Soc. Chem. Commun.* **1994**, 185. b) M. J. Marsella, R. J. Newland, P. J. Carroll, T. M. Swager, *J. Am. Chem. Soc.* **1995**, *117*, 9842, and references therein..

[5] E. Kelderman, L. Derhaeg, G. J. T. Heesink, W. Verboom, J. F. J. Engbersen, N. F. van Hulst, A. Persoons, D. N. Reinhoudt, *Angew. Chem.* **1992**, *104*, 1107; *Angew. Chem. Int. Ed. Engl.* **1992**, *31*, 1075.

[6] a) P. Dedek, V. Janout, S. L. Regen, *J. Org. Chem.* **1993**, *58*, 6553; b) M. Conner, V. Janout, S. L. Regen, *J. Am. Chem. Soc.* **1993**, *115*, 1178; c) M. A. Markowitz, V. Janout, D. G. Castner, S. L. Regen, *ibid.* **1989**, *111*, 8192; d) W. Lee, R. A. Hendel, P. Dedek, V. Janout, S. L. Regen, *ibid.* **1995**, *117*, 6793.

[7] a) B. Xu, T. M. Swager, *J. Am. Chem. Soc.* **1993**, *115*, 1159; b) *ibid.* **1995**, *117*, 5011; c) See T. M. Swager, B. Xu, in ref. [1b], and references therein; d) T. Komori, S. Shinkai, *Chem. Lett.*, **1993**, 1455.

[8] a) K. Iwamato, H. Shimizu, K. Araki, S. Shinkai, *J. Am. Chem. Soc.* **1993**, *115*, 3997; b) G. Ferguson, J. F. Gallagher, L. Glunta, P. Neri, S. Pappalardo, M. Parisi, *J. Org. Chem.* **1994**, *59*, 42; c) S. Pappalardo, G. Ferguson, P. Neri, C. Rocco, *ibid.* **1995**, *60*, 4576, and references therein.

[9] a) P. Neri, A. Bottino, C. Geraci, M. Piattelli, *Tetrahedron Asymm.* **1996**, *7*, 17, and reference therein; b) A. Marra, M.-C. Scherrmann, A. Dondoni, A. Casnati, P. Minari, R. Ungaro, *Angew. Chem.* **1994**, *106*, 2533; *Angew. Chem. Int. Ed. Engl.* **1994**, *33*, 2479; c) C. D. Gutsche, K. C. Nam, *J. Am. Chem. Soc.* **1988**, *110*, 6153; d) C. Loeber, D. Matt, P. Briard, D. Grandjean, *J. Chem. Soc. Dalton. Trans.* **1996**, 513.

[10] a) For a review, V. Böhmer, D. Krat, in ref. [1b]; b) G. D. Andreetti, V. Böhmer, J. G. Jordon, M. Tabatabai, F. Ugozzoli, W. Vogt, A. Wolff, *J. Org. Chem.* **1993**, *58*, 4023; c) W. Verboom, P. J. Bodewes, G. van Essen, P. Timmerman, G. J. Van Hummel, S. Harkema, D. N. Reinhoudt, *Tetrahedron*, **1995**, *51*, 499.

[11] D.-K. Fu, B. Xu, T. M. Swager, *J. Org. Chem.* **1996**, *61*, 802.

[12] For the recent examples of metallocalix[4]arenes see: a) F. Corazza, C. Floriani, A. Chiesi-Villa, C. Rizzoli, *Inorg. Chem.* **1991**, *30*, 4465; b) F. Corazza, C. Floriani, A. Chiesi-Villa, C. Guastini, *J. Chem. Soc., Chem. Commun.* **1990**, 640; c) B. R. Cameron, F. C. J. M. Van Veggel, D. N. Reinhoudt, *J. Org. Chem.* **1995**, *60*, 2802; d) J. A. Acho, T. Ren, J. W. Yun, S. J. Lippard, *Inorg. Chem.* **1995**, *34*, 5226; e) J. A. Acho, L. H. Doerrer, S. J. Lippard, *ibid.* **1995**, *34*, 2542; f) V. C. Gibson, C. Redshaw, W. Clegg, M. R. J. Elsegood, *J. Chem. Soc. Chem. Commun.* **1995**, 2371; g) L. Giannini, E. Solari, A. Zanottigerosa, C. Floriani, A. Chiesivilla, C. Rizzoli, *Angew. Chem.* **1996**, *108*, 79; *Angew. Chem. Int. Ed. Engl.* **1996**, *35*, 85, and references therein.

[13] Tungsten alkoxycalixarenes were recently reported: A. Zanotti-Gerosa, E. Solari, L. Giannini, C. Floriani, A. Chiesi-Villa, C. Rizzoli, *J. Chem. Soc. Chem. Commun.* **1996**, 119.

[14] For a general discussion of tungsten alkoxides see: a) Z. Dori, in *Comprehensive Coordination Chemistry*, (Eds.: G. Wilkinson, R. D. Gillard, J. A. McCleverty), Pergamon, England, **1987**; b) W. A. Nugent, J. M. Mayer, *Metal-Ligand Multiple Bonds*, Wiley, New York, **1988**; c) J. M. Mayer, *Polyhedron*, **1995**, *14*, 3273.

[15] Crystallographic data (excluding structure factors) for the structure(s) reported in this paper have been deposited with the Cambridge Crystallographic Data Centre as supplementary publication no. CCDC-179-73. Copies of the data can be obtained free of charge on application to The Director, CCDC, 12 Union Road, Cambridge CB2 1EZ, UK (fax: Int. code +(1223) 336-033; e-mail: teched@ chemcrys.cam.ac.uk).

[16] C. Andraud, C. Garcia, A. Collet, in *Circular Dichroism*, (Eds.: K. Nakanishi, N. Berova, R. W. Woody), VCH, New York, **1994**.

[17] a) S. T. Pickard, W. H. Pirkle, M. Tabatabai, W. Vogt, V. Böhmer, *Chirality*, **1993**, *5*, 310; b) S. Shinkai, T. Arimura, H. Kawabata, H. Murakami, K. Araki, K. Iwamoto, T. Matsuda, *J. Chem. Soc. Chem. Commun.* **1990**, 1734.

 © VCH Verlagsgesellschaft mbH, D-69451 Weinheim, 1996 0570-0833/96/3518-2097 $ 15.00+.25/0

Boron–Carbon Chains Stabilized in Rare Earth Metallic Frameworks

Denis Ansel, Josef Bauer,* François Bonhomme, Ghania Boucekkine, Gilles Frapper, Patrick Gougeon, Jean-François Halet,* Jean-Yves Saillard,* and Bachir Zouchoune

Ternary and higher order phases comprising a rare earth metal, boron, and carbon show a particularly rich and varied structural chemistry. These structure types can be classified in three different families according to the dimensionality of the boron–carbon sublattice: two-dimensional (2D) networks, one-dimensional (1D) zigzag chains, or finite, linear units of various lengths.[1] Such compounds are attractive not only as new materials with interesting physical properties, but also simply as solid-state analogues of molecular organic and organometallic compounds containing all-carbon ligands.[2]

Finite boron–carbon units stabilized in metallic lattices are rather scarce and limited in length to three or four atoms as demonstrated in the metal- and carbon-rich compounds Sc_2BC_2,[3] $Ce_5B_2C_6$,[4] $La_3BC_2Br_2$, and $Ce_6B_2C_3Br_3$.[5] We report herein on the characterization of chains with up to 13 atoms that are contained in new cerium, lanthanum, and neodynium boride carbide materials. $La_{15}B_{14}C_{19}$, $M_{10}B_9C_{12}$ (M = La, Ce, Nd), and $Ce_5B_4C_5$ are obtained as lustrous black pellets by arc melting and subsequent annealing of the elements for several days.[6]

In all compounds, the metallic sublattice can be described as resulting from an irregular stacking of slightly corrugated 2D square nets, which gives rise to a three-dimensional (3D) framework with metal–metal separations between 3.40 and 4.10 Å.[9] This leads to the formation of small channels of different sizes in which roughly linear B_xC_y units are inserted (Fig. 1). Two kinds of eleven-membered units, B_4C_7 and B_5C_6, are embedded in the structure of $La_{15}B_{14}C_{19}$, corresponding to the formula $La_{15}(B_4C_7)(B_5C_6)_2$. $Ce_{10}B_9C_{12}$ contains a thirteen-membered B_5C_8 chain (the longest so far observed in these materials) and an eight-membered B_4C_4 chain, corresponding to the $Ce_{10}(B_5C_8)(B_4C_4)$ formula. $Ce_5B_4C_5$ contains eight-membered B_4C_4 and six-membered B_3C_3 units, in addition to single C atoms and the already known BC_2 group, giving rise to the formula $Ce_{10}(B_4C_4)(B_3C_3)(BC_2)(C)$. These tightly bonded boron–carbon "molecules" and their metal environments are shown in Figures 2–4. The boron atoms are generally attached to two carbon atoms and often located in a distorted cube of metal atoms, whereas the carbon atoms are generally accomodated in $[M_4B_2]$ or $[M_5B]$ octahedra.[11] The B–B, B–C, and C–C bond lengths vary between 1.57 and 1.68, 1.43 and 1.58, and 1.33 and 1.35 Å, respectively. They suggest some double-bond character.[3–5] The associated bond angles vary from 180° to about 140° (Figs. 2–4).

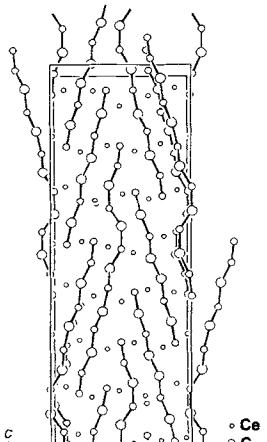

Fig. 1. Unit cell of $Ce_{10}B_9C_{12}$.

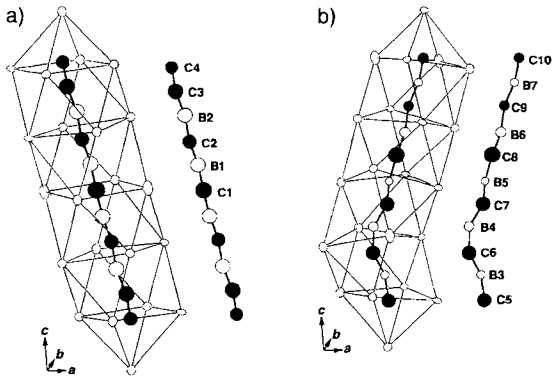

Fig. 2. Environments of the centrosymmetric B_4C_7 (a) and noncentrosymmetric B_5C_6 (b) chains in $La_{15}B_{14}C_{19}$. Selected interatomic distances [Å] and angles [°]: B_4C_7: C1–B1 1.46(3), C2–B1 1.46(4), C2–B2 1.47(3), C3–B2 1.51(4), C3–C4 1.35(3); B1-C1-B1′ 180, C1-B1-C2 167(2), B1-C2-B2 162(2), C2-B2-C3 160(3), C4-C3-B2 164(3); B_5C_6: C5–B3 1.44(3), C6–B3 1.50(3), C6–B4 1.50(3), C7–B4 1.50(3), C7–B5 1.40(3), C8–B5 1.51(3), C8–B6 1.58(3), C9–B6 1.49(3), C9–B7 1.49(3), C10–B7 1.43(3); C5-B3-C6 153(2), B3-C6-B4 148(2), C6-B4-C7 149(2), B4-C7-B5 153(2), C7-B5-C8 157(2), B5-C8-B6 148(2), C8-B6-C9 145(2), B6-C9-B7 156(2), C9-B7-C10 163(2).

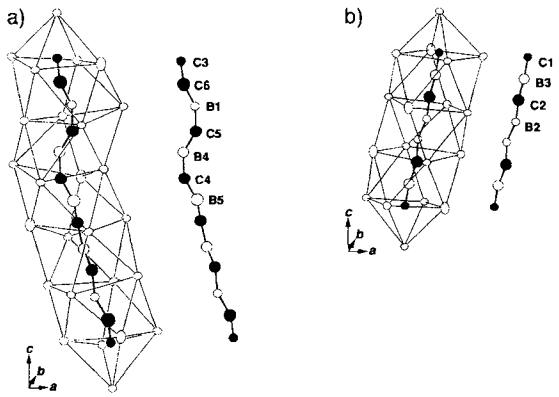

Fig. 3. Environments of the centrosymmetric B_5C_8 (a) and B_4C_4 (b) chains in $Ce_{10}B_9C_{12}$. Selected interatomic distances [Å] and angles [°]: B_5C_8: C3–C6 1.33(2), C6–B1 1.52(2), B1–C5 1.51(2), C5–B4 1.49(2), B4–C4 1.55(2), C4–B5 1.44(1); C3-C6-B1 156(2), C6-B1-C5 151(1), B1-C5-B4 145(2), C5-B4-C4 148(2), B4-C4-B5 149(2), C4-B5-C4′ 146(2); B_4C_4: C1–B3 1.46(2), B3–C2 1.53(2), C2–B2 1.41(2), B2–B2′ 1.57(3); C1-B3-C2 167(2), B3-C2-B2 158(2), C2-B2-B2′ 152(2).

Previous theoretical studies on rare earth metal boride carbides have shown that their structures can be rationalized within the approximation of a purely ionic bonding mode between the metal and the nonmetal centers.[1, 3, 12–14] For instance, Sc_2BC_2 can be described in a first approximation as being built of $(BC_2)^{5-}$ ions surrounded by not fully oxidized $Sc^{2.5+}$ ions.[3] The same approach is used here to tackle the chemical bonding in the new materials $La_{15}B_{14}C_{19}$, $Ce_{10}B_9C_{12}$, and $Ce_5B_4C_5$.

The first question that arises concerns the assignment of formal ionic charges to account for the cumulene-like character of

[*] Dr. J. Bauer, Dr. J.-F. Halet, Prof. J.-Y. Saillard, Dr. D. Ansel, F. Bonhomme, Prof. G. Boucekkine, Dr. G. Frapper, Dr. P. Gougeon, B. Zouchoune
Laboratoire de Chimie du Solide et Inorganique Moléculaire
URA CNRS 1495
Université de Rennes 1, F-35042 Rennes (France)
Fax: Int. code +02 99 63 57 04
e-mail: halet@univ-rennes1.fr; saillard@univ-rennes1.fr

[**] B. Zouchoune (permanent address: Institut de Chimie, Université de Constantine, Route de Aïn-el-Bey, Constantine, Algeria) and G. Boucekkine (permanent address: Laboratoire de Chimie Théorique, USTHB, BP 31, El Alia, 16111 Bab Ezzouar, Alger, Algeria) are grateful to the Ministère Français des Affaires Etrangères for a research grant (MAE 90 MDU 136 and MAE 94 MDU 309, respectively). G. Frapper thanks the Région Bretagne for a predoctoral fellowship (1992–1995).

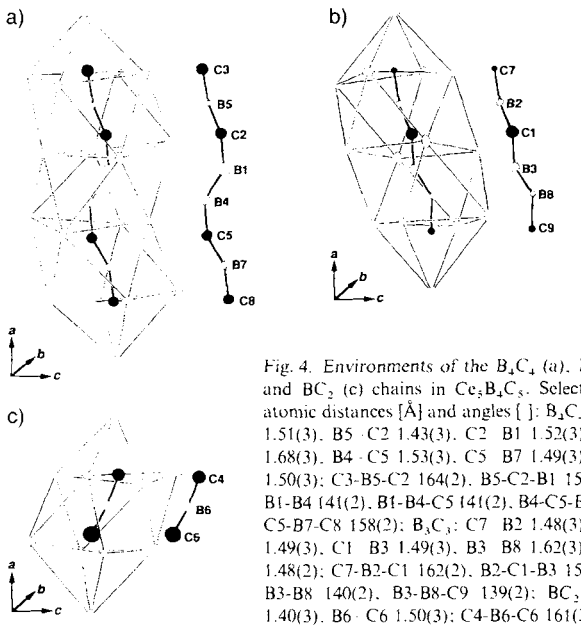

Fig. 4. Environments of the B_4C_4 (a), B_3C_3 (b), and BC_2 (c) chains in $Ce_5B_4C_5$. Selected interatomic distances [Å] and angles [°]: B_4C_4: C3–B5 1.51(3), B5–C2 1.43(3), C2–B1 1.52(3), B1–B4 1.68(3), B4–C5 1.53(3), C5–B7 1.49(3), B7–C8 1.50(3); C3-B5-C2 164(2), B5-C2-B1 158(2), C2-B1-B4 141(2), B1-B4-C5 141(2), B4-C5-B7 154(2), C5-B7-C8 158(2); B_3C_3: C7–B2 1.48(3), B2–C1 1.49(3), C1–B3 1.49(3), B3–B8 1.62(3), B8–C9 1.48(2); C7-B2-C1 162(2), B2-C1-B3 152(2), C1-B3-B8 140(2), B3-B8-C9 139(2); BC_2: C4–B6 1.40(3), B6–C6 1.50(3); C4-B6-C6 161(2).

the boron–carbon units in these materials. The usual oxidation state for the La and Ce is 3+, but can be lower as demonstrated for Sc in Sc_2BC_2.[3] In this compound the formal charge of 5− was found to be the energetically most favorable for an isolated BC_2 unit, since this provides a large HOMO/LUMO gap separating the low-lying bonding and nonbonding levels from the high-lying antibonding levels. The extended Hückel molecular orbital[15] (EHMO) diagrams of the various B_xC_y groups encountered in $La_{15}B_{14}C_{19}$, $Ce_{10}B_9C_{12}$, and $Ce_5B_4C_5$ are shown in Figure 5; they are based on averaged linearized geometries. As for the BC_2 case, only one favored electron count, which leads to a significant HOMO/LUMO gap and corresponds to $[B_5C_6]^{9-}$, is possible for B_5C_6. In the case of the B_3C_3 and the B_4C_4 units two, and for the B_4C_7 and B_5C_8 units four π-type orbitals of intermediate energy (~9 eV) lie in the middle of a large energy gap. This is a typical situation for the existence of a range of possible electron counts corresponding to a partial or complete occupation of these intermediate levels.

A clearer answer to the question concerning which of the possible electron counts is closer to the real situation in $La_{15}B_{14}C_{19}$, $Ce_{10}B_9C_{12}$, and $Ce_5B_4C_5$ can be gained by analyzing the band structure of these materials, calculated within the extended Hückel tight-binding (EHTB) formalism.[16] This analysis reveals that in all of these compounds, the states lying in the vicinity (above and below) of the Fermi level (ε_F) result from the overlap of the bottom of the metallic d band with bands generated by the intermediate MOs of the B_3C_3, B_4C_4, B_4C_7, or B_5C_8 units. This is exemplified by the density of states (DOS) of $Ce_{10}B_9C_{12}$ shown in Figure 6. The analysis of the states around ε_F reveals a significant participation of all the components (Ce, B_4C_4, and B_5C_8). The contributions from B_4C_4 and B_5C_8 come essentially from their $3\pi_u$ and $4\pi_g + 4\pi_u$ levels, respectively. It follows that the intermediate levels of the B_4C_4 and B_5C_8 units in $Ce_{10}B_9C_{12}$ are calculated to be roughly half-occupied. A similar situation is found for the other chains B_3C_3, B_4C_4, and B_4C_7 in $Ce_5B_4C_5$ and $La_{15}B_{14}C_{19}$. This leads to the approximate formal charges $(B_3C_3)^{7-}$, $(B_4C_4)^{8-}$, $(B_5C_6)^{9-}$, and $(B_5C_8)^{9-}$. By assuming these charges, the EHMO Mulliken overlap populations calculated on the isolated anions are in reasonably good agreement with the observed bond lengths.

Geometry optimization with ab initio calculations[17] has been also performed on $(BC_2)^{5-}$, $(B_3C_3)^{7-}$, $(B_4C_4)^{8-}$, $(B_5C_6)^{9-}$, and $(B_5C_8)^{9-}$ to ascertain the proposed assignment of the anionic charges. A cumulene-like character (formal double bonds along the chains) is confirmed for these charges.[18] As mentioned previously, the nonmetal chains encountered in these new rare earth metal boride carbides are not rigourously linear. Deviation from linearity is well-established in organic cumulene and cumulenone molecules.[19] It is known that a small bending of these molecules is not costly in energy and is facilitated as they become longer.[19] The same phenomenon might occur for the boron–carbon "molecules". Larger distortion is observed experimentally for the longest B–C chains. For instance, ab initio calculations on a bent and linear $(BC_2)^{5-}$ ion show almost no change in the B–C distances (ca. 1.50 Å) and only a small increase of the total energy (0.59 eV) for a C-B-C bending angle of 150° compared to 180°.[20] Clearly, small constraints of the surrounding metal matrix must be sufficient to allow a small distortion of the B–C chains without modifying their electronic structure too much.

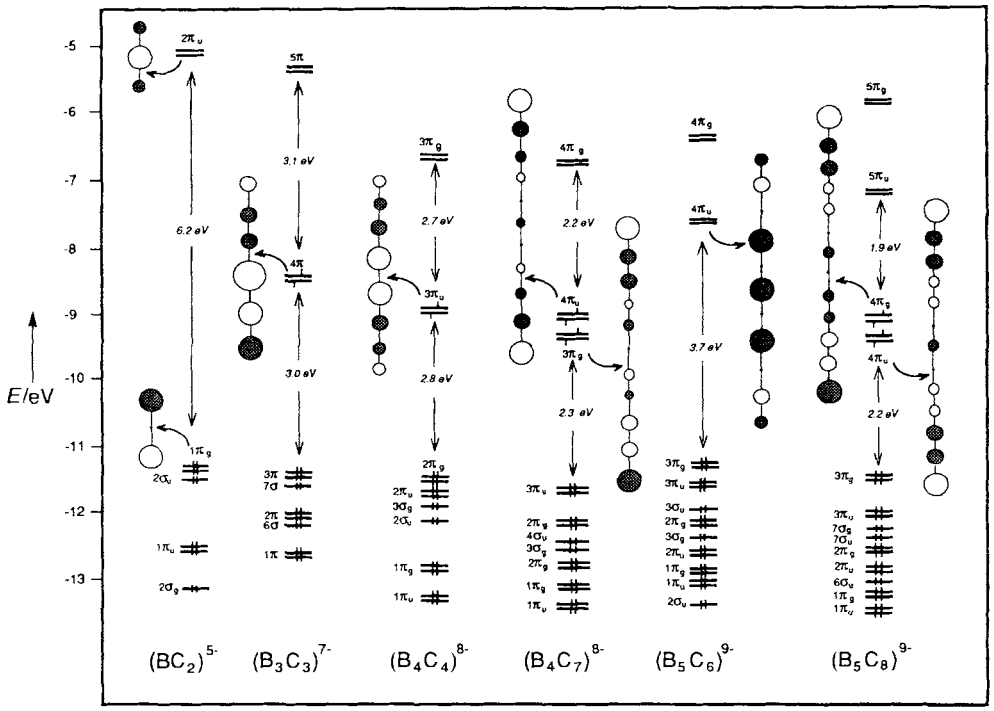

Fig. 5. EHMO diagrams of the boron-carbon units $(BC_2)^{5-}$, $(B_3C_3)^{7-}$, $(B_4C_4)^{8-}$, $(B_4C_7)^{8-}$, $(B_5C_6)^{9-}$, and $(B_5C_8)^{9-}$ (linear models of $C_{\infty v}$ or $D_{\infty h}$ symmetry were assumed).

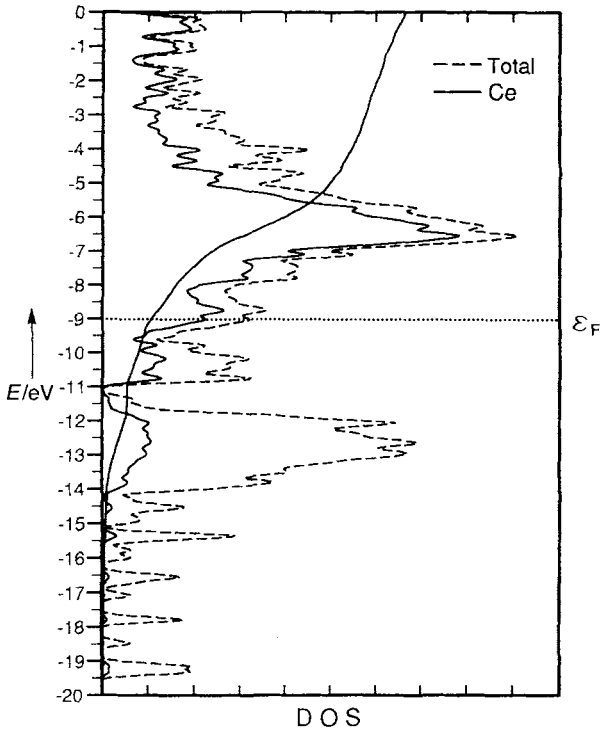

Fig. 6. Total density of states (solid line) and metal contribution (dashed line) for $Ce_{10}B_9C_{12}$ obtained from EHTB calculations.

Within the first-order approximation of an ionic model, $La_{15}B_{14}C_{19}$, $Ce_{10}B_9C_{12}$, and $Ce_5B_4C_5$ can then be written as $(La^{1.73+})_{15}(B_4C_7)^{8-}[(B_5C_6)^{9-}]_2$, $(Ce^{1.7+})_{10}(B_4C_4)^{8-}(B_5C_8)^{9-}$, and $(Ce^{2.4+})_{10}(BC_2)^{5-}(B_3C_3)^{7-}(B_4C_4)^{8-}(C^{4-})$, respectively. Similarly, Sc_2BC_2,[3] and $Ce_5B_2C_6$[4] can be written as $(Sc^{+2.5})_2(BC_2)^{5-}$ and $(Ce^{2.8+})_5[(BC_2)^{5-}]_2(C_2)^{4-}$, respectively. It is noteworthy that all the B_xC_y anions are isoelectronic to cumulene- or carbyne-like C_x^{4-} anions, satisfying the octet rule, some of which such as C_2^{4-} and C_3^{4-} have been characterized in the solid state.[10] The question of the stability of rare earth metal-boron-carbon phases containing oligomeric or polymeric chains longer than 13 atoms remains open.[21]

Significant covalent interaction occurs between the metallic framework and the boron–carbon units. This is exemplified by the significant metallic participation below ε_F in the states generated by the occupied levels of the $(BC_2)^{5-}$, $(B_3C_3)^{7-}$, $(B_4C_4)^{8-}$, $(B_5C_6)^{9-}$, and $(B_5C_8)^{9-}$ ions (see Fig. 6 for the example of $Ce_{10}B_9C_{12}$). Such an interaction is associated with an electron transfer into the empty levels of the metallic d band. This reduces somewhat the anionic charge on the boron–carbon "ligands" trapped in the metallic matrix, consequently contributing to their stabilization.[22]

Since the metal atoms are not fully oxidized and their band structures exhibit the same features as that described in Figure 6 for $Ce_{10}B_9C_{12}$, all these new materials are expected to exhibit metallic properties.[23] They do not show any superconducting properties, despite the coexistence of metallic and nonmetallic states around ε_F, which might favor such properties as observed in related compounds such as $La_5B_2C_6$[4] or $LuNi_2B_2C$.[24]

Received: March 25, 1996 [Z 8971 IE]
German version: *Angew. Chem.* **1996**, *108*, 2245–2248

Keywords: ab initio calculations · boron compounds · lanthanides · solid-state structures

[1] F. Wiitkar, S. Kahlal, J.-F. Halet, J.-Y. Saillard, J. Bauer, P. Rogl, *J. Am. Chem. Soc.* **1994**, *116*, 251.
[2] See for instance F. Diederich, Y. Rubin, *Angew. Chem.* **1992**, *104*, 1123; *Angew. Chem. Int. Ed. Engl.* **1992**, *31*, 1101.
[3] J.-F. Halet, J.-Y. Saillard, J. Bauer, *J. Less-Common Met.* **1990**, *158*, 239. See also: A. C. Switendick, *10th Int. Conf. Solid Compd. Trans. Elem.* Munster, Germany, 21–25 March **1991**.
[4] J. Bauer, O. Bars, *J. Less-Common Met.* **1982**, *83*, 17; *ibid.* **1983**, *95*, 267.
[5] H. Mattausch, A. Simon, *Angew. Chem.* **1995**, *107*, 1764; *Angew. Chem. Int. Ed. Engl.* **1995**, *34*, 1633.
[6] Preparation: Cold-pressed pellets of different mixtures of powders prepared from commercially available pure elements were arc-melted in a water-cooled copper furnace under purified argon. They were turned over and remelted several times to ensure homogeneity. Subsequent annealing at 1000 °C for four days was carried out with a high-frequency furnace under purified argon. Single crystals of $La_{15}B_{14}C_{19}$, $Ce_{10}B_9C_{12}$, and $Ce_5B_4C_5$ were obtained from slowly cooled samples. Crystallographic data: $La_{15}B_{14}C_{19}$, $P2_1/c$, $a = 8.671$ (3), $b = 8.656(1)$, $c = 19.953$ (8) Å, $\beta = 94.45(1)°$ $V = 1493.2$ (8) Å^3, $Z = 2$, $\mu = 210.53$ cm^{-1}, $R(F) = 0.036$, $R_w(F) = 0.049$ (based on 1941 reflections with $I > 3\sigma(I)$). $Ce_{10}B_9C_{12}$, $P4_12_12$, $a = 8.4785(7)$, $c = 25.350(4)$ Å, $V = 1822.3(3)$ Å^3, $Z = 4$, $\mu = 248.41$ cm^{-1}, $R(F) = 0.028$, $R_w(F) = 0.039$ (based on 1247 reflections with $I > 2\sigma(I)$). $Ce_5B_4C_5$, $Pna2_1$, $a = 24.426(5)$, $b = 8.4636(7)$, $c = 8.5007(7)$ Å, $V = 1757.3(4)$ Å^3, $Z = 4$, $\mu = 257.59$ cm^{-1}, $R(F) = 0.040$, $R_w(F) = 0.042$ (based on 1755 reflections with $I > 2\sigma(I)$). Data were collected at room temperature on an Enraf-Nonius CAD-4 diffractometer equipped with graphite-monochromatized $Mo_{K\alpha}$ radiation ($\lambda = 0.71073$ Å). Accurate cell parameters were obtained by least-squares refinement of the setting angles of 25 reflections. Structures were solved with the aid of MULTAN 11/82 [7] and subsequent difference Fourier syntheses. All the calculations were performed with the SDP programs [8]. Further details of the crystal structure investigations may be obtained from the Fachinformationszentrum Karlsruhe, D-76344, Eggenstein-Leopoldshafen, on quoting the depository numbers CSD-402368 ($Ce_5B_4C_5$), CSD-402387 ($Ce_{10}B_9C_{12}$), and CSD-402390 ($La_{15}B_{14}C_{19}$).
[7] P. Main, S. Fiske, S. E. Hull, L. Lessinger, G. Germain, J.-P. Declercq, M. M. Woolfson, MULTAN 82, Universities of York, England, and Louvain, Belgium, **1982**. MULTAN 82 is a system of computer programs for the automatic solution of crystal structures from X-ray diffraction data.
[8] B. A. Frenz, Enraf-Nonius SDP-Plus Structure Determination Package, version 3.0. Enraf–Nonius, Delft, The Netherlands, **1985**.
[9] The unit cell parameters a and b in $La_{15}B_{14}C_{19}$, a in $Ce_{10}B_9C_{12}$, and b and c in $Ce_5B_4C_5$, are nearly identical and comparable to those measured in $La_5B_2C_6$ [4]. The stacking parameter (c in $La_{15}B_{14}C_{19}$ and $Ce_{10}B_9C_{12}$, a in $Ce_5B_4C_5$) depends only on the number of metal layers (separated by ca. 3 Å) needed to accomodate the boron–carbon anions. They can be derived from the defect NaCl structure of the rare earth metal monocarbides as in Sc_3C_4 for instance [10].
[10] a) R. Pöttgen, W. Jeitschko, *Inorg. Chem.* **1991**, *30*, 427; b) H.-J. Meyer, R. Hoffmann, *Z. Anorg. Allg. Chem.* **1992**,*607*, 57.
[11] The assignment of boron or carbon to a particular atomic position was based on structural considerations and confirmed by our calculations.
[12] F. Wiitkar, S. Kahlal, J.-F. Halet, J.-Y. Saillard, J. Bauer, P. Rogl, *Inorg. Chem.* **1995**, *34*, 1248.
[13] F. Wiitkar, J.-F. Halet, J.-Y. Saillard, P. Rogl, J. Bauer, *Inorg. Chem.* **1994**, *33*, 1297.
[14] J. K. Burdett, E. Canadell, T. Hughbanks, *J. Am. Chem. Soc.* **1986**, *108*, 3971.
[15] R. Hoffmann, *J. Chem. Phys.* **1963**, *39*, 1397. The exponent (ζ) and the valence shell ionization potential (H_{ii} in eV) were respectively: 1.3, −15.2 for B 2s; 1.3, −8.5 for B 2p; 1.625, −21.4 for C 2s; 1.625, −11.4 for C 2p.
[16] M.-H. Whangbo, R. Hoffmann, *J. Am. Chem. Soc.* **1978**, *100*, 6093. The exponent (ζ) and the valence shell ionization potential (H_{ii} in eV) were respectively: 2.14, −7.67 for La 6s; 2.08, −5.01 for La 6p. The H_{ii} value for La 5d was set equal to −8.21. A linear combination of two Slater-type orbitals of exponents $\zeta_1 = 3.78$, $\zeta_2 = 1.38$ with weighting coefficients $c_1 = 0.7765$, $c_2 = 0.4586$ was used to represent the 5d atomic orbitals of La. The La parameters were taken in all calculations. The crystal structures of $La_{15}B_{14}C_{19}$, $Ce_{10}B_9C_{12}$, and $Ce_5B_4C_5$ were used for the calculations.
[17] M. J. Frisch, G. W. Trucks, M. Head-Gordon, P. M. W. Gill, M. W. Wong, J. B. Foresman, B. G. Johnson, H. B. Schlegel, M. A. Robb, E. S. Replogle, R. Gomperts, J. L. Andres, K. Raghavachari, J. S. Binkley, C. Gonzales, R. L. Martin, D. J. Fox, D. J. Defrees, J. Baker, J. J. P. Stewart, J. A. Pople, Gaussian 92, Revision C, Gaussian Inc. Pittsburgh, PA, **1992**.
[18] Geometries were optimized at the HF and MP2 level using a 6-31G* basis set. In order to mimic the cationic environment, calculations were carried out with Na^+ ions described by an effective core pseudopotential (see G. Frapper, J.-F. Halet, J.-Y. Saillard, F. Volatron, *J. Phys. Chem.* **1995**, *99*, 12164).
[19] See for instance: C. Liang, L. C. Allen, *J. Am. Chem. Soc.* **1991**, *113*, 1873, and references therein.
[20] G. Frapper, G. Boucekkine, B. Zouchoune: J.-F. Halet, J.-Y. Saillard, unpublished results.

 © VCH Verlagsgesellschaft mbH, D-69451 Weinheim, 1996 0570-0833/96/3518-2100 $ 15.00+.25/0

[21] The synthesis and characterization of one-dimensional carbyne has been claimed. See for example: a) A. M. Sladkov, *Soviet Sci. Rev. Sect. B* **1981**, *3*, 75; b) R. B. Heiman, J. Kleiman, N. M. Salansky, *Nature* **1983**, *306*, 164; c) K. Akagi, M. Nishiguchi, H. Shirakawa, Y. Furukawa, I. Harada, *Synt. Met.* **1987**, *17*, 557; d) K. Yamada, K. Kunishige, A. B. Sawaoka, *Naturwissenschaften* **1991**, *78*, 450, and references therein.

[22] The EHTB computed atomic net charges are the following: $(La^{1.19+})_{15}(B_4C_7)^{6.67-}$ $[(B_5C_6)^{5.59-}]_2$ for $La_{15}B_{14}C_{19}$, $(Ce^{1.12+})_{10}$ $(B_4C_4)^{4.2-}$ $(B_5C_8)^{7.00-}$ for $Ce_{10}B_9C_{12}$, and $(Ce^{1.33+})_{10}(C)^{2.31-}$ $(BC_2)^{2.72-}$ $(B_3C_3)^{3.72-}$ $(B_4C_4)^{4.51-}$ for $Ce_5B_4C_5$.

[23] Preliminary electrical resistivity measurements indicate that $La_{15}B_{14}C_{19}$, $Ce_{10}B_9C_{12}$, and $Ce_5B_4C_5$ are good metallic conductors. According to magnetic susceptibility measurements, no superconductivity is observed down to 2 K (H. Noël, personal communication).

[24] See for instance: a) J. K. Burdett, S. Sevov, *Inorg. Chem.* **1994**, *33*, 3857; b) J.-F. Halet, *ibid.* **1994**, *33*, 4173. c) G. Miller, *J. Am. Chem. Soc.* **1994**, *116*, 6332.

Regio- and Diastereoselective Bisfunctionalization of C_{60} and Enantioselective Synthesis of a C_{60} Derivative with a Chiral Addition Pattern**

Jean-François Nierengarten, Volker Gramlich, Francesca Cardullo, and François Diederich*

Although a rich variety of methods for the preparation of covalent monoadducts of C_{60} are known,[1] the development of selective routes to isomerically pure multiple adducts of the fullerene is still in its infancy.[2–4] We recently described a versatile strategy for the regioselective preparation of specific bis-through hexakisadducts of C_{60} based on the concept of tether-directed remote functionalization.[4] We now report a similar, yet much simpler, direct bisfunctionalization of C_{60} based on a cyclization reaction of the carbon sphere with bis(malonate) derivatives in a double Bingel addition.[5] A short synthetic route led to a variety of specific fullerene bisadducts with high regio- and diastereoselectivity. Starting from optically pure bis(malonate) derivatives, the new method also permitted the preparation of enantiomerically pure bis(cyclopropanated) C_{60} derivatives whose chirality results exclusively from the addition pattern.[6, 7]

During the synthesis of precursors to polytriacetylenes with pendant C_{60} moieties,[8] we found that reaction of C_{60} with bis(2-bromomalonates) **3a** and **3b**, which were prepared in two steps from the corresponding diols **1a,b**[9] via **2a,b** (Scheme 1), yielded the macrocyclic bisadducts **4** and **5**, respectively, resulting from double Bingel addition to one carbon sphere (Table 1, Fig. 1). Since the linker between the two malonate moieties in **3a,b** acted as a directing tether, the bisfunctionalization of C_{60} was highly regioselective and only one of the possible isomeric bisadducts was formed in 16% (**4**) and 10% (**5**) yield. The general character of this facile methodology for the selective preparation of C_{60} bisadducts was subsequently established by

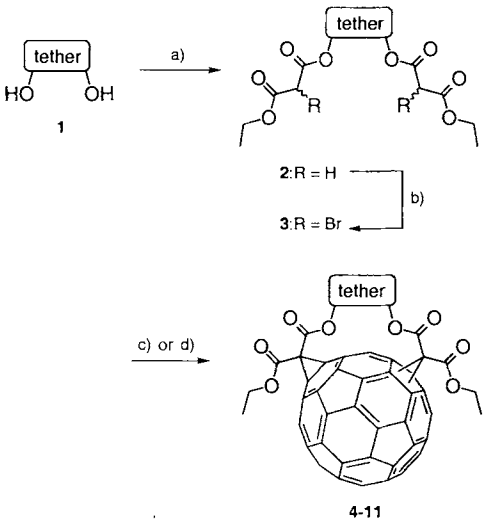

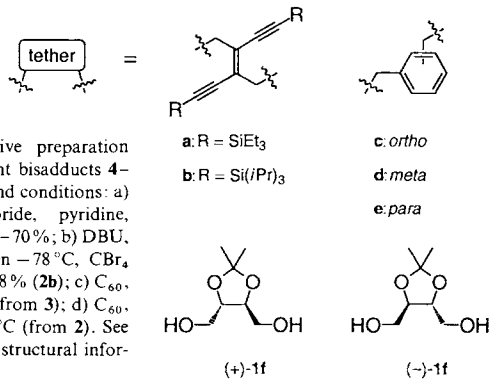

Scheme 1. Regioselective preparation of macrocyclic covalent bisadducts **4**–**11** of C_{60}. Reagents and conditions: a) ethyl malonyl chloride, pyridine, CH_2Cl_2, 0 to 20 °C, 60–70%; b) DBU, THF, 0 to 20 °C, then −78 °C, CBr_4 (2 equiv), 52% (**2a**), 48% (**2b**); c) C_{60}, DBU, toluene, 20 °C (from **3**); d) C_{60}, DBU, I_2, toluene, 20 °C (from **2**). See Table 1 for additional structural information and yields.

Table 1. The diols and derived bis(malonate) derivatives, which were used in the addition to C_{60}, along with the addition products. All products are out–out stereoisomers [a].

Diol	Bis(malonate)	Bisadduct (symmetry, add. pattern, yield) [b]
1a	**3a**	**4** (C_1, *cis*-2, 16%)
1b	**3b**	**5** (C_1, *cis*-2, 10%)
1c	**2c**	**6** (C_s, *cis*-2, 33%)
1d	**2d**	**7** (C_s, *cis*-2, 32%)
1e	**2e**	**8** (C_s, *trans*-4, 33%)
		9 (C_1, *e*, 8%)
(+)-**1f**	(−)-**2f**	**10a** (C_1, *cis*-2, 20%)
		11a (C_2, *cis*-3, 13%)
(−)-**1f**	(+)-**2f**	**10b** (C_1, *cis*-2, 21%)
		11b (C_2, *cis*-3, 15%)

[a] All new compounds were fully characterized by ^1H and ^{13}C NMR, UV/Vis, FT-IR, FAB-MS data, and, except for **9**, by elemental analysis. [b] For the position notation in the bisaddition patterns, see ref. [3a] and Fig. 1. For identical addends, a second attack into *e-face* or *e-edge* positions leads to identical products [4c].

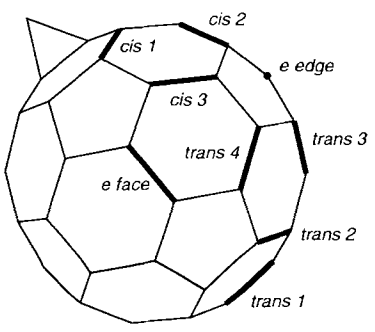

Fig. 1. Position notation for bisadducts of C_{60}.

[*] Prof. F. Diederich, Dr. J.-F. Nierengarten, Dott.-Chim. F. Cardullo
Laboratorium für Organische Chemie, ETH-Zentrum
Universitätstrasse 16, CH-8092 Zürich (Switzerland).
Fax: Int. code +(1)632-1109
Dr. V. Gramlich
Laboratorium für Kristallographie, ETH-Zentrum
Sonneggstrasse 5, CH-8092 Zürich (Switzerland).

[**] This work was supported by the Swiss National Science Foundation and by a postdoctoral fellowship (Human Capital and Mobility) from the EU (J.-F. N.). We thank Dr. M. Sebova and J. Cuntze for NMR measurements, T. Granier for help with the CD measurements, and A. Herrmann for help in the HPLC analysis.

starting from the three isomeric benzenedimethanols **1c–e**. In a typical procedure, diols **1c–e** were treated with ethyl malonyl chloride in the presence of pyridine in CH_2Cl_2 at 20 °C to give the bis(ethyl malonyl) derivatives **2c–e**, respectively, in 60–70% yield. The corresponding halomalonates were prepared in situ with iodine,[10] and the one-pot reaction of C_{60} with compounds **2c–e**, I_2, and 1,8-diazabicyclo[5.4.0]undec-7-ene (DBU) in toluene at 20 °C afforded the corresponding bisadducts **6–9** (Scheme 1 and Table 1).

For each macrocyclic bisadduct **4–9**, the relative position of the two cyclopropane rings on the C_{60} surface was determined based on the molecular symmetry (Table 1) deduced from the ^1H and ^{13}C NMR spectra as well as on its UV/Vis spectra. Stepwise double Bingel reaction with diethyl 2-bromomalonate had previously been shown by Hirsch and co-workers to yield a total of seven out of eight possible regioisomers, with the *trans*-3-and *e*-isomers (Table 1, Fig. 1) being the dominant products.[3a] They found that the UV/Vis spectra of the bisadducts are highly dependent on the addition pattern and characteristic for each regioisomer. The UV/Vis spectra (CH_2Cl_2) of **4–9** are totally consistent with those previously reported for the analogous tetraethyl esters.[3a, 3e]

In theory, each cyclic regioisomer could form as a mixture of different diastereoisomers, depending on how the two ethoxycarbonyl residues at the two methano bridge C atoms are oriented with respect to each other (in–in, in–out, and out–out isomerism).[11] Actually, for cyclic bisadducts such as **6–9** with a simple symmetrical linker, there exist, in theory, 37 possible different constitutional isomers and stereoisomers. Nevertheless, bisadducts **4–9** were all isolated either as achiral, isomerically pure compounds or as single racemic mixtures; therefore, the second intramolecular Bingel addition occurs not only regio- but also diastereoselectively. Because of the length of the linker between the two cyclopropane rings, only the out–out diastereoisomer appeared reasonable for the bisadducts **8** and **9**. Two C_s-symmetrical *cis*-2 diastereoisomers (in–in and out–out) are possible for **6** and **7**.[11] Due to the additional chirality arising from the presence of the *trans*-alkene fragment in the macrocyclic bridges, four different C_1-symmetrical *cis*-2 diastereoisomers are possible for **4** and **5**. However, steric considerations based on molecular and computer modeling indicated that the two cyclopropane rings on the C_{60} surface in all *cis*-2 bisadducts should be linked in a similar (out–out) manner to that determined by X-ray crystal structure analysis for compound **6** (Fig. 2a).[12] The crystal packing analysis showed that the molecules are assembled in a dimeric arrangement (Fig. 2b). The phenyl ring of one molecule is stacked above the C_{60} moiety of the second molecule at an intermolecular distance of 3.30 Å between the center of the aromatic ring and the closest C_{60} C atom.[13] Noteworthy are the two short intermolecular $C(sp^3)$–$H\cdots O$ contacts between the benzylic CH and the ester C=O groups of neighboring molecules ($H\cdots O$ distance: 2.68 Å; C-$H\cdots O$ angle: 139.4°).[14]

Using the same methodology, the two enantiomeric *cis*-2 bisadducts **10a** and **10b** as well as the two enantiomeric *cis*-3 bisadducts **11a** and **11b** were prepared from the commercially available optically pure diols (+)- and (−)-**1f**, respectively (Scheme 1, Table 1). The cyclization reaction is highly diastereoselective and only one of the possible diastereoisomers could be detected in each case.[15] The *cis*-3 addition pattern on the C_{60} surface is chiral;[7] therefore transesterification (K_2CO_3, EtOH/THF) of **11a** yielded the *cis*-3 tetraethyl ester **12** as an enantiomerically pure compound (Fig. 3). The other enantiomer *ent*-**12** was prepared in a similar way starting from **11b**. The circular dichroism (CD) spectra of the two enantiomers (^fC and ^fA; f = fullerene, *C* = clockwise, *A* = anticlockwise)[16] are depicted in Figure 3. As previously described, the CD spectra show pronounced Cotton effects due to strong chiroptical contributions from the chirally functionalized fullerene chromophore.[6, 16] The enantiomeric excess (*ee*) determined by HPLC[17] was higher than 97% for both enantiomers of **12**.

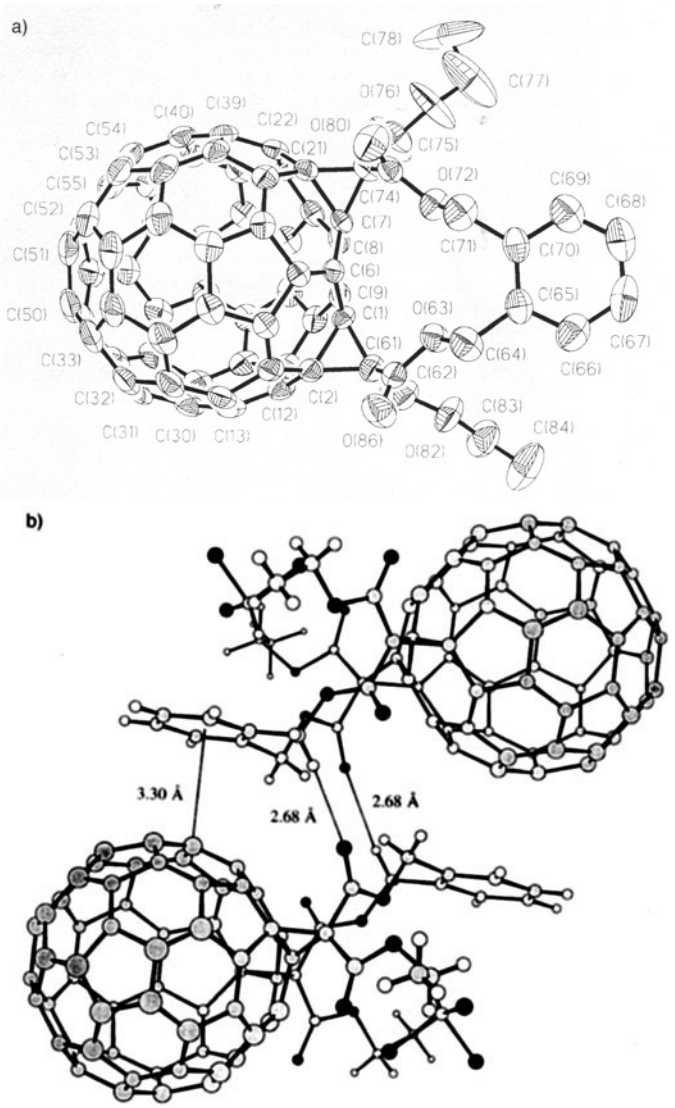

Fig. 2. a) X-ray crystal structure of **6**. The $CHCl_3$ molecule located in the crystal lattice has been omitted. b) Crystal packing of **6** showing the face-to-face dimeric arrangement of the C_{60} derivatives. Each pair of molecules is surrounded on top and bottom by cocrystallized $CHCl_3$ molecules (shown in dark).

With similar efficiency to that of the asymmetric Sharpless dihydroxylation of C_{60},[6] the addition of the chirally tethered bismalonate enables an enantioselective synthesis of optically active C_{60} bisadducts in which the chirality results exclusively from the addition pattern. Additionally, it should be noted that all macrocyclic C_{60} bisadducts described above are topologically nontrivial molecules; in other words, they cannot be represented by planar molecular graphs.[18]

Experimental Procedure

Preparation of **10b**, **11b**, and *ent*-**12**: DBU (0.43 mL, 2.913 mmol) was added under Ar at 20 °C to a stirred solution of C_{60} (350 mg, 0.485 mmol), I_2 (271 mg, 1.068 mmol), and (+)-**2f** (208 mg, 0.534 mmol) in toluene (700 mL). The mixture was stirred for 7 h, and filtered over a plug of silica, first with toluene to remove the unreacted C_{60}, then with CH_2Cl_2/MeOH 99:1. Column chromatography (SiO_2)

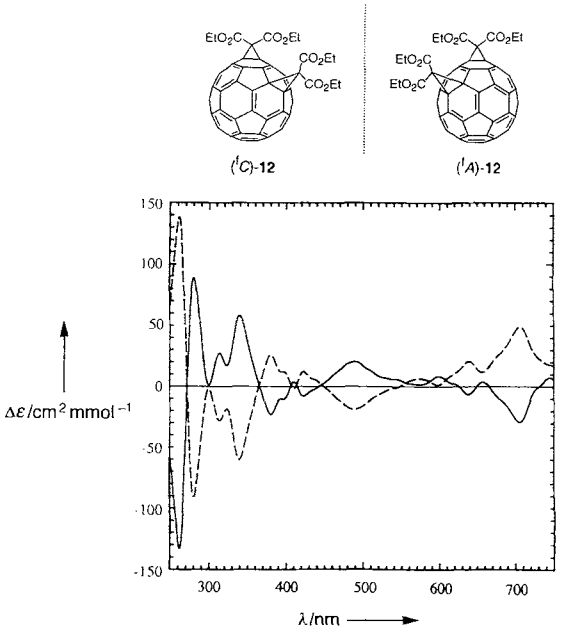

Fig. 3. CD spectra for both enantiomers of tetraethyl ester **12** in CH_2Cl_2 ($c = 0.8 \times 10^{-5}$ M). Solid line: enantiomer resulting from the transesterification of **11a**; dashed line: enantiomer resulting from the transesterification of **11b**.

eluting with CH_2Cl_2/hexane 9:1 followed by precipitation from CH_2Cl_2/hexane yielded **10b** (114 mg, 21%). Dark red solid, m.p. >280 °C; UV/Vis (CH_2Cl_2): λ_{max} (ε) = 258 (108500), 320 (sh, 32500), 374 (sh, 10700), 437 (2700), 468 (2300); ^{1}H NMR ($CDCl_3$, 500 MHz): δ = 1.36 (t, J = 7.1 Hz, 3H), 1.37 (t, J = 7.1 Hz, 3H), 1.46 (s, 3H), 1.47 (s, 3H), 4.05 (m, 1H), 4.15 (m, 1H), 4.22 (m, 1H), 4.33–4.47 (m, 4H), 4.60 (m, 1H), 4.84 (m, 1H), 4.98 (m, 1H); ^{13}C NMR ($CDCl_3$, 125 MHz): δ = 14.12, 14.13, 28.48, 28.55, 48.90 (2C), 63.46 (2C), 66.89, 67.08, 67.16 (2C), 70.10, 70.17, 78.25, 78.29, 111.35, 133.55, 137.55, 137.73, 137.83, 138.06, 138.33, 138.48, 138.55, 140.92, 140.95, 141.30, 141.33, 141.88, 142.09, 142.42, 142.45, 143.15, 143.20, 143.64, 143.66, 143.89, 143.94, 144.19, 144.25, 144.39, 144.57, 144.58, 144.69, 144.72, 144.90, 145.03, 145.18, 145.19, 145.21, 145.31, 145.33, 145.35, 145.64, 145.71, 145.75, 145.77, 146.00, 146.04, 146.15, 146.19, 147.33, 147.43, 147.53, 149.38, 149.51, 162.63, 162.68, 162.92, 162.99; FAB-MS (*meta*-nitrobenzyl alcohol (NOBA)): m/z: 1107 (100, MH^+), 720 (42, C_{60}^+).

Elution with CH_2Cl_2 followed by precipitation from CH_2Cl_2/hexane yielded **11b** (84 mg, 15%). Brown solid, m.p. >280 °C; UV/Vis (CH_2Cl_2): λ_{max} (ε) = 255 (110200), 317 (36400), 399 (sh, 4750), 408 (sh, 4000), 454 (1800), 468 (1750), 697 (280), 632 (490); ^{1}H NMR ($CDCl_3$, 500 MHz): δ = 1.44 (t, J = 7.1 Hz, 6H), 1.50 (s, 6H), 4.31–4.36 (m, 2H), 4.39–4.44 (m, 2H), 4.44–4.57 (m, 4H), 4.70–4.75 (m, 2H); ^{13}C NMR ($CDCl_3$, 125 MHz): δ = 14.16, 27.70, 48.82, 63.54, 64.80, 68.90, 71.75, 75.77, 109.75, 129.92, 136.11, 139.15, 139.42, 140.97, 141.00, 141.06, 141.65, 141.80, 142.17, 142.35, 143.61, 143.63, 144.18, 144.37, 144.43, 144.68, 144.87, 145.00, 145.04, 145.18, 145.20, 145.32, 145.56, 145.63, 146.43, 146.66, 163.25, 163.36; FAB-MS (NOBA): m/z: 1107 (100, MH^+), 720 (18, C_{60}^+).

K_2CO_3 (314 mg, 2.276 mmol) was added to a stirred solution of **11b** (35 mg, 0.031 mmol) in THF/EtOH 1:1 (34 mL) under Ar. The mixture was stirred at 20 °C for 1.5 h, then filtered, and evaporated to dryness. Column chromatography (SiO_2, toluene) followed by precipitation from CH_2Cl_2/hexane yielded *ent*-**12** (28 mg, 83%). Brown solid, m.p. >280 °C; UV/Vis, IR, ^{1}H NMR, and mass spectra identical to those of *rac*-**12** previously prepared by Hirsch and co-workers [3a,e].

Received: May 30, 1996 [Z91701E]
German version: *Angew. Chem.* **1996**, *108*, 2242–2244

Keywords: asymmetric syntheses · fullerenes

[1] a) A. Hirsch, *The Chemistry of the Fullerenes*, Thieme, Stuttgart, **1994**; b) F. Diederich, C. Thilgen, *Science* **1996**, *271*, 317–323; c) "Fullerene Chemistry, Tetrahedron Symposia-In-Print Number 60": *Tetrahedron*, **1996**, *52*, 4925–5262.

[2] a) P. J. Fagan, J. C. Calabrese, B. Malone, *J. Am. Chem. Soc.* **1991**, *113*, 9408–9409; b) J. M. Hawkins, A. Meyer, T. A. Lewis, U. Bunz, R. Nunlist, G. E. Ball, T. W. Ebbesen, K. Tanigaki, *ibid.* **1992**, *114*, 7954–7955; c) M. Tsuda, T. Ishida, T. Nogami, S. Kurono, M. Ohashi, *J. Chem. Soc. Chem. Commun.* **1993**, 1296–1298; d) C. C. Henderson, C. M. Rohlfing, R. A. Assink, P. A. Cahill, *Angew. Chem.* **1994**, *106*, 803–805; *Angew. Chem. Int. Ed. Engl.* **1994**, *33*, 786–788; e) H. W. Kroto, R. Taylor, D. R. M. Walton, *Pure Appl. Chem.* **1994**, *66*, 2091–2094; f) A. L. Balch, B. Cullison, W. R. Fawcett, A. S. Ginwalla, M. M. Olmstead, K. Winkler, *J. Chem. Soc. Chem. Commun.* **1995**, 2287–2288; g) T. Hamano, T. Mashino, M. Hirobe, *ibid.* **1995**, 1537–1538; h) B. Kräutler, J. Maynollo, *Angew. Chem.* **1995**, *107*, 69–71; *Angew. Chem. Int. Ed. Engl.* **1995**, *34*, 87–88; i) J. C. Hummelen, M. Prato, F. Wudl, *J. Am. Chem. Soc.* **1995**, *117*, 7003–7004; j) S. R. Wilson, Q. Lu, *Tetrahedron Lett.* **1995**, *36*, 5707–5710; k) B. Kräutler, T. Müller, J. Maynollo, K. Gruber, C. Kratky, P. Ochsenbein, D. Schwarzenbach, H.-B. Bürgi, *Angew. Chem.* **1996**, *108*, 1294–1296; *Angew. Chem. Int. Ed. Engl.* **1996**, *35*, 1203–1206.

[3] a) A. Hirsch, I. Lamparth, H. R. Karfunkel, *Angew. Chem.* **1994**, *106*, 453–455; *Angew. Chem. Int. Ed. Engl.* **1994**, *33*, 437–438; b) A. Hirsch, I. Lamparth, T. Grösser, H. R. Karfunkel, *J. Am. Chem. Soc.* **1994**, *116*, 9385–9386; c) T. Grösser, M. Prato, V. Lucchini, A. Hirsch, F. Wudl, *Angew. Chem.* **1995**, *107*, 1462–1464; *Angew. Chem. Int. Ed. Engl.* **1995**, *34*, 1343–1345; d) I. Lamparth, C. Maichle-Mössmer, A. Hirsch, *ibid* **1995**, *107*, 1755–1757 and **1995**, *34*, 1607–1609; e) A. Hirsch, Habilitationsschrift, Universität Tübingen, **1994**.

[4] a) L. Isaacs, R. F. Haldimann, F. Diederich, *Angew. Chem.* **1994**, *106*, 2434–2437; *Angew. Chem. Int. Ed. Engl.* **1994**, *33*, 2339–2342; b) C. Boudon, J.-P. Gisselbrecht, M. Gross, L. Isaacs, H. L. Anderson, R. Faust, F. Diederich, *Helv. Chim. Acta* **1995**, *78*, 1334–1344; c) L. Isaacs, P. Seiler, F. Diederich, *Angew. Chem.* **1995**, *107*, 1636–1639; *Angew. Chem. Int. Ed. Engl.* **1995**, *34*, 1466–1469; d) F. Cardullo, L. Isaacs, F. Diederich, J.-P. Gisselbrecht, C. Boudon, M. Gross, *J. Chem. Soc. Chem. Commun.* **1996**, 797–799.

[5] C. Bingel, *Chem. Ber.* **1993**, *126*, 1957–1959.

[6] J. M. Hawkins, A. Meyer, M. Nambu, *J. Am. Chem. Soc.* **1993**, *115*, 9844–9845.

[7] F. Diederich, C. Thilgen, A. Herrmann, *Nachr. Chem. Tech. Lab.* **1996**, *44*, 9–16.

[8] J.-F. Nierengarten, F. Diederich, unpublished results.

[9] a) J. Anthony, A. M. Boldi, Y. Rubin, M. Hobi, V. Gramlich, C. B. Knobler, P. Seiler, F. Diederich, *Helv. Chim. Acta* **1995**, *78*, 13–45; b) J.-F. Nierengarten, M. Schreiber, F. Diederich, V. Gramlich, *New J. Chem.* **1996**, in press.

[10] C. Bingel, presentation at the meeting New Perspectives in Fullerene Chemistry and Physics, Rome (Italy), **1994**.

[11] For the concept of in–in, in–out, and out–out stereoisomerism, see G. Quinkert, E. Egert, C. Griesinger, *Aspekte der Organischen Chemie: Struktur*, VHCA, Basel, **1995**, p. 28. For *cis*-1, *cis*-2, and *trans*-4 bisadducts, there exist two C_s-symmetrical (in–in, out–out) and one C_1-symmetrical (in–out) isomers. For *cis*-3, *trans*-2, and *trans*-3 bisadducts, two C_2-symmetrical (in–in, out–out) and one C_1-symmetrical (in–out) isomers can form. The *e* bisaddition yields two C_1-symmetrical isomers (out–out, in–out), and *trans*-1 addition gives one C_{2h}-symmetrical (out–out) and one C_2-symmetrical (in–out) isomer. Taking into consideration the pairs of enantiomers in C_1- and C_2-symmetrical compounds, a total of 37 bisadducts can theoretically be formed.

[12] X-ray crystal data for **6** ($C_{78}H_{18}O_8 \cdot CHCl_3$, M_r = 1202.3): dark red prisms of **6** were obtained by slow diffusion of hexane in a $CHCl_3$/benzene solution of **6**. Monoclinic space group $P2_1/c$, Z = 4, ρ_{calcd} = 1.688 g cm^{-3}, a = 17.469(14), b = 14.471(9), c = 19.51(2) Å, β = 106.41(7)°, V = 4732(7) Å^3, Picker-Stoe diffractometer, $Cu_{K\alpha}$ radiation using ω scans, λ = 1.54178 Å. The structure was solved by the PATSEE method and refined by full-matrix least-squares analysis (SHELXTL PLUS; heavy atoms anisotropic, H atoms fixed, whereby H positions are based on stereochemical considerations) to give $R(F)$ = 0.0637 and $R_w(F)$ = 0.0925 for 811 variables and 3984 observed reflexions with $F > 4.0\sigma(F)$ and $3.0 \le 2\theta \le 100°$. Crystallographic data (excluding structure factors) for the structure reported in this paper have been deposited with the Cambridge Crystallographic Data Centre as supplementary publication no. CCDC-179-92. Copies of the data can be obtained free of charge on application to The Director, CCDC, 12 Union Road, Cambridge CB21EZ, UK (Telefax: Int. code +(1223)336-033; e-mail: teched@chemcrys.cam.ac.uk).

[13] a) M. F. Meidine, P. B. Hitchcock, H. W. Kroto, R. Taylor, D. R. M. Walton, *J. Chem. Soc. Chem. Commun.* **1992**, 1534–1537; b) A. L. Balch, J. W. Lee, B. C. Noll, M. M. Olmstead, *J. Chem. Soc. Chem. Commun.* **1993**, 56–58.

[14] For C–H···O interactions in the crystals of fullerene adducts, see P. Seiler, L. Isaacs, F. Diederich, *Helv. Chim. Acta* **1996**, *79*, 1047–1058.

[15] In these reactions, two diastereoisomeric out–out *cis*-3 products are possible due to the chiral addition pattern; however, the very high asymmetric induction in the second intramolecular Bingel addition leads to the formation of **11a** or **11b** only.

[16] For the introduction of the stereochemical descriptors ^{t}*A* and ^{t}*C* for fullerenes with chiral addition patterns, see A. Herrmann, M. Rüttimann, C. Thilgen, F. Diederich, *Helv. Chim. Acta* **1995**, *78*, 1673–1704.

[17] Eluent: hexane/CH_2Cl_2 7:3; column (*S,S*)-Whelk-01, Regis Chemical Company, Morton Grove, IL, USA.

[18] J.-C. Chambron, C. O. Dietrich-Buchecker, J.-P. Sauvage, *Top. Curr. Chem.* **1993**, *165*, 131–162.

Thioenols from Peptidyl Cysteines: Oxidative Decarboxylation of a ^{13}C-Labeled Substrate**

Christoph Kempter, Thomas Kupke, Dietmar Kaiser, Jörg W. Metzger, and Günther Jung*

Dedicated to Professor Anton Rieker on the occasion of his 65th birthday

Epidermin, a tetracyclic peptide antibiotic with therapeutic activity against acne, is produced by the Gram-positive bacterium *Staphylococcus epidermidis*. It contains the uncommon amino acids 2,3-didehydroaminobutyric acid, *meso*-lanthionine, β-methyllanthionine, and C-terminal *S*-[(*Z*)-2-aminovinyl]-D-cysteine.[1] The prepeptide EpiA, consisting of 52 amino acids, is synthesized ribosomally and transformed into the biologically active 22mer peptide by posttranslational modifications. These modification reactions comprise oxidative decarboxylation, dehydration, formation of four thioether bridges, and cleavage of the leader peptide[2] (Fig. 1). Complementation studies of epidermin-negative mutants and DNA sequencing have revealed that the genes *epiB*, *epiC*, *epiD*, and *epiP* encode the enzymes for the biosynthesis of epidermin.[3] The enzyme EpiD has been isolated and characterized. In this novel flavoprotein (20.8 kDa) flavinmononucleotide (FMN) is a noncovalently bound coenzyme that reacts with the precursor peptide EpiA under reducing conditions.[4] The modified polypeptide exhibits increased hydrophobicity, increased absorbance at 260 nm, and a decrease in molecular mass by 46 Da relative to the starting polypeptide.[5] EpiD catalyzes the oxidative decarboxylation ($-H_2$, $-CO_2$) of the C-terminal cysteine residue of EpiA and thus takes part in the formation of *S*-[(*Z*)-2-aminovinyl]-D-cysteine (Scheme 1). Although the mechanism

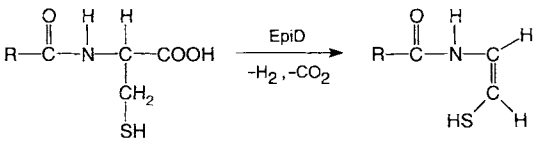

Scheme 1.

has not yet been studied in detail, it can be assumed that the first step is the oxidation leading to the formation of the double bond followed by decarboxylation to form the thioenol.[5] Flavin coenzyme that has been reduced during the reaction is reoxidized probably by aerial oxygen.

The substrate specificity of the new enzyme has been investigated by using synthetic peptides and peptide libraries.[6] It was found that peptides with the C-terminal consensus sequence AA1-AA2-Cys (AA1 = Val/Ile/Leu/(Met)/Phe/Tyr/Trp; AA2 = Ala/Ser/Val/Thr/Cys/(Ile, Leu)) show a decrease in molecular mass of 46 Da after reaction with EpiD.[7] The MS–MS fragmentation pattern of the substrate Ser-Phe-Asn-Ser-Tyr-Thr-Cys after reaction with EpiD revealed that only the C-terminal cysteine was modified, presumably by conversion into a C-terminal thioenol by oxidative decarboxylation. In this paper, we report on the structure determination of the product of this unusual enzymatic reaction.

The heptapeptide SFNSYTC was prepared by solid-phase synthesis with fluorenylmethoxycarbonyl/*tert*-butyl protecting groups.[8] After treatment with 5,5′-dithiobis(2-nitrobenzoic acid) (Ellman's reagent), both the purified peptide and the peptide modified by EpiD showed an increase in molecular mass by 197 Da in the electrospray ionization mass spectrum (ESI-MS). This corresponds to the formation of asymmetric disulfides from the thiol groups of the peptide and of 5-thio-2-nitrobenzoic acid. These disulfides could be reduced by addition of *n*-propanethiol and partly converted into the asymmetric disulfide with *n*-propanethiol. The addition of Ellman's reagent to the assumed double bond in the product, which would lead to an increase in molecular mass by 199 Da, has not been observed.

Previous two-dimensional NMR experiments failed to help in determining the structure of the peptides obtained by modification of SFNSYCC and SFNSYTC, because the products are not stable long enough in solution. According to ESI-MS experiments, the thioenol derivatives are substantially degraded after only one hour. Since the modification product of the peptide SFNSYTC turned out to be more stable than SFNSYCC, a peptide with the C-terminal sequence Thr-Cys was used in the subsequent NMR experiments as a substrate for EpiD. The enzymatic reaction was carried out in the NMR spectrometer, enabling us to monitor the process and to observe the unstable reaction product in situ. Due to the complexity of the spectra, the introduction of a ^{13}C isotope in the cysteine was necessary in order to extract the interesting signals by heteronuclear correlation experiments. Hence, the peptide KKSFNSYTC was synthesized by solid-phase synthesis using cysteine labeled with ^{13}C

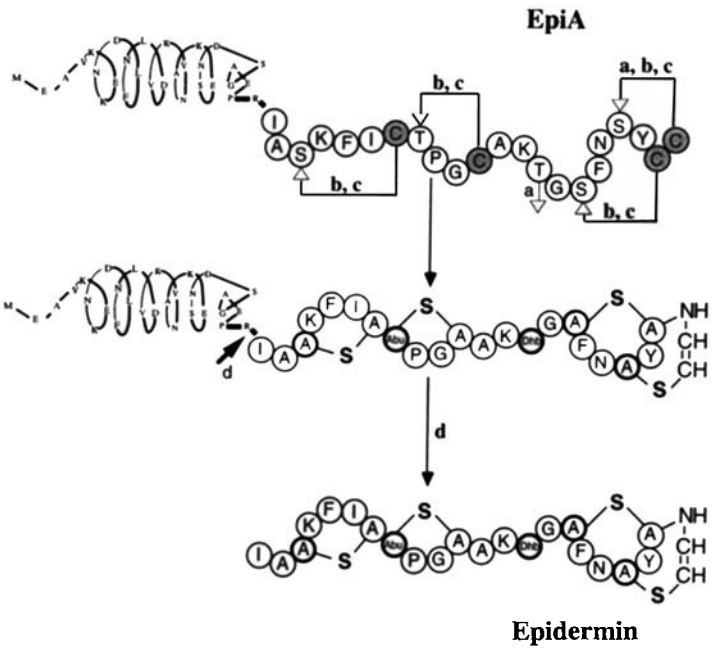

Fig. 1. Model of the biosynthesis of epidermin. The ribosomally synthesized prepeptide EpiA is converted into the antimicrobially active, tetracyclic lantibiotic epidermin by the following posttranslational modifications: a) oxidative decarboxylation of the C-terminal cysteine residue, b) dehydration of serine and threonine residues, c) formation of thioether bridges (lanthionine and β-methyllanthionine), and d) cleavage of the leader peptide (30 residues). Abu = 2-aminobutyric acid; Dhb = α,β-didehydrobutyric acid; cysteine residues are shaded in gray, modified amino acids are marked with bold circles.

[*] Prof. Dr. G. Jung, Dipl.-Chem. C. Kempter, Dipl.-Chem. D. Kaiser, Prof. Dr. J. W. Metzger
Institut für Organische Chemie der Universität
Auf der Morgenstelle 18, D-72076 Tübingen (Germany)
Fax: Int. code +(7071)29-6925
e-mail: guenther.jung@uni-tuebingen.de
Dr. T. Kupke
Mikrobielle Genetik, Universität Tübingen
Waldhäuserstrasse 70/8, D-72076 Tübingen (Germany)

[**] This work was supported by the Deutsche Forschungsgemeinschaft (SFB 323).

at the β-carbon atom. The two lysine residues at the N-terminus were introduced to increase the solubility of the substrate in water.

Two crosspeaks at $\delta(^1H) = 2.83$, $\delta(^{13}C) = 29.1$, and $\delta(^1H) = 3.58$, $\delta(^{13}C) = 63.3$ occur in the HSQC spectrum[9] of the starting peptide KKSFNSYTC. The first signal is due to the ^{13}C-labeled β-carbon, while the second stems from the methyl groups in tris(hydroxymethyl)aminomethane (Tris buffer). In the one-dimensional ^{13}C NMR spectrum of the starting peptide, there are two peaks for the β-carbon atom at $\delta = 29.1$ and 29.2 from the two epimers, which cannot be resolved in the two-dimensional experiment. After only 15 min a third signal emerges at $\delta(^1H) = 6.01$ and $\delta(^{13}C) = 120.5$, the intensity of which increases over time. Figures 2 and 3 show projections of the HSQC spectra onto the F2 (^1H) and F1 (^{13}C) axes, respectively, recorded over a period of 825 min; an increase in intensity of the product signal is clearly visible. Because of the high substrate concentration, the enzymatic reaction is slower than in previous experiments (substrate inhibition). On the other hand, the constant supply of new product in this experiment gives the impression that the product is fairly stable. After 16 h a HSQC-TOCSY experiment[10] was conducted to determine the chemical shift of the α-proton in the cysteine residue. The spectrum shows an additional signal at $\delta(^{13}C) = 120.5$ and $\delta(^1H) = 6.59$. The observed chemical shifts for H_α and H_β ($\delta = 6.59$ and 6.01, respectively) as well as for C_β ($\delta = 120.5$) are characteristic of a double bond. The NMR data, the MS–MS experiments, the observed reaction product with Ellman's reagent, and the fact that the difference in mass between starting material and product is 46 Da, all indicate that the product contains a C-terminal thioenol. The (Z) configuration of the double bond in the reaction product was determined from the ^3J coupling constant of H_α and H_β. In the 1D ^1H NMR spectrum the signal for the β-proton at $\delta(^1H) = 6.01$ is a doublet of doublets with the coupling constants $^1J(H_\beta, C_\beta) = 170$ Hz and $^3J(H_\alpha, H_\beta) = 7.3$ Hz, which is typical for a double bond with (Z) configuration and comparable to the coupling constant observed in epidermin[1] (Fig. 4).

After 16 h the ^{13}C spectrum still contains two signals at $\delta = 29.1$ and 29.2; however, the latter signal has only about 50% of its initial intensity, and after 40 h this signal vanishes completely. Therefore the enzyme EpiD only modifies the epimer with L-cysteine. In this spectrum no signal was evident in the region around $\delta = 250$, which is the typical ^{13}C chemical shift for a carbon atom in a thioaldehyde. In contrast to the corresponding enols, the thermodynamic stability of the thioenols is similar to that of the thioaldehydes and they tautomerize only slowly.[11]

After the unusual thioenol in the modified peptide had been proved, one question still remained: What are the degradation products of the initially formed thioenols? With the present NMR and MS data no distinct conclusions are possible, because the concentration of the secondary products is too low to be detected by NMR spectroscopy.

The present results imply that in the biosynthesis of epidermin the oxidative decarboxylation of the precursor protein takes place before and not, as previously assumed,[2] after the formation of the thioether bridges. Work is in progress to fully label the novel enzyme EpiD with ^{13}C and ^{15}N in order to determine the three-dimensional solution structure of the enzyme and the enzyme–substrate complex by NMR spectroscopy. It is safe to assume that the posttranslational modification described in this work also occurs during the biosynthesis of the natural epidermin analogues gallidermin,[12] mersacidin (a novel inhibitor of the biosynthesis of cell walls),[13] and the new peptide antibiotic cypemycin.[14]

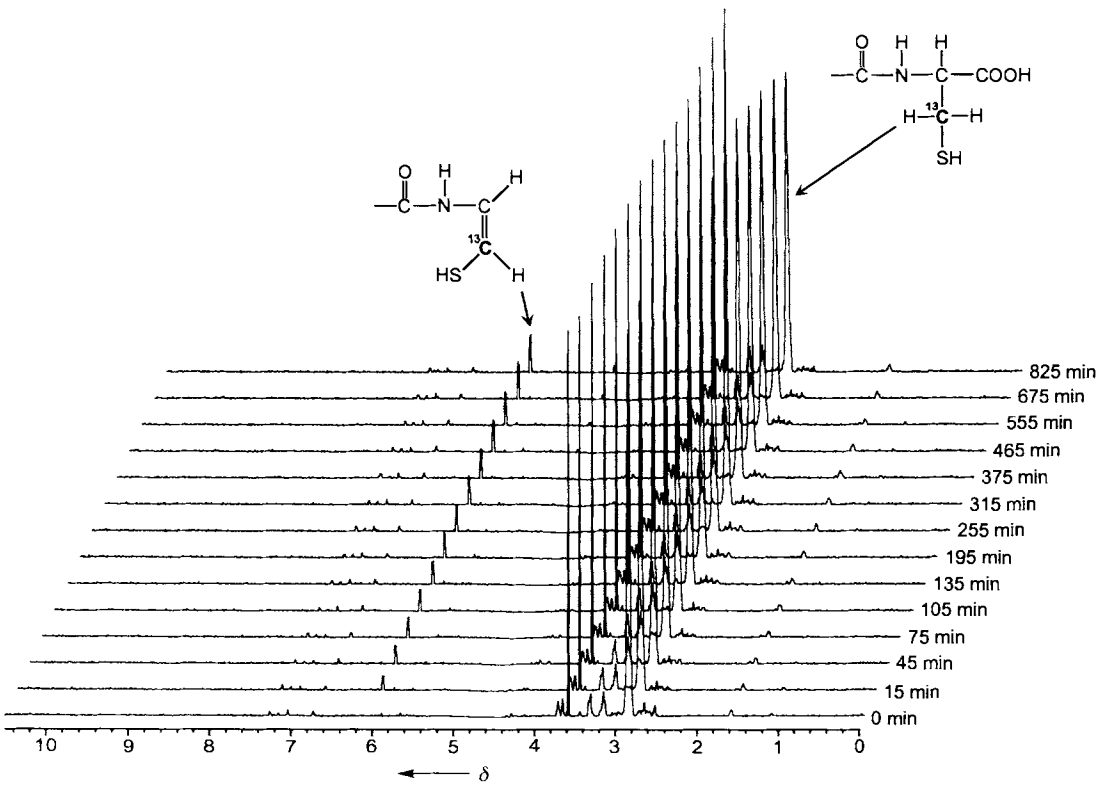

Fig. 2. Reaction of the labeled substrate KKSFNSYTC with the enzyme EpiD. Shown are projections along the F2 (^1H) axis of the HSQC spectra recorded during the course of the reaction. The product signal at $\delta(^1H) = 6.01$ increases in intensity with time. The signal at $\delta(^1H) = 2.83$ corresponds to the protons at the ^{13}C-labeled C_β atom of cysteine. The signal at $\delta(^1H) = 3.58$ stems from the methyl groups of the Tris buffer.

 © VCH Verlagsgesellschaft mbH, D-69451 Weinheim, 1996 0570-0833/96/3518-2105 $ 15.00+.25/0

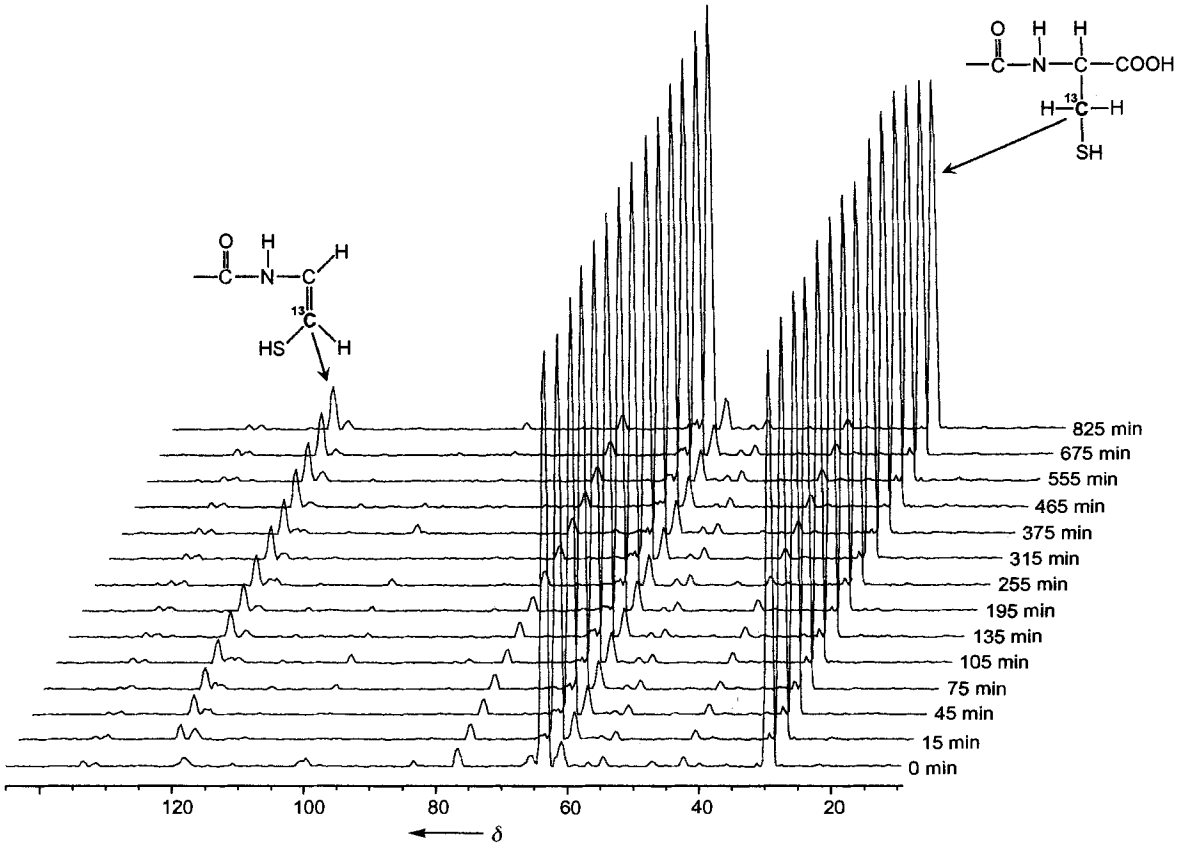

Fig. 3. Reaction of the labeled substrate KKSFNSYTC with the enzyme EpiD. Shown are the projections along the F1 (^{13}C) axis of the HSQC spectra recorded during the course of the reaction. The product signal at $\delta(^{13}C) = 120.5$ increases in intensity with time. The signal at $\delta(^{13}C) = 29.1$ corresponds to the C_β atom of the cysteine residue in the starting material, while the signal at $\delta(^{13}C) = 63.3$ can be assigned to the methyl groups of the Tris buffer.

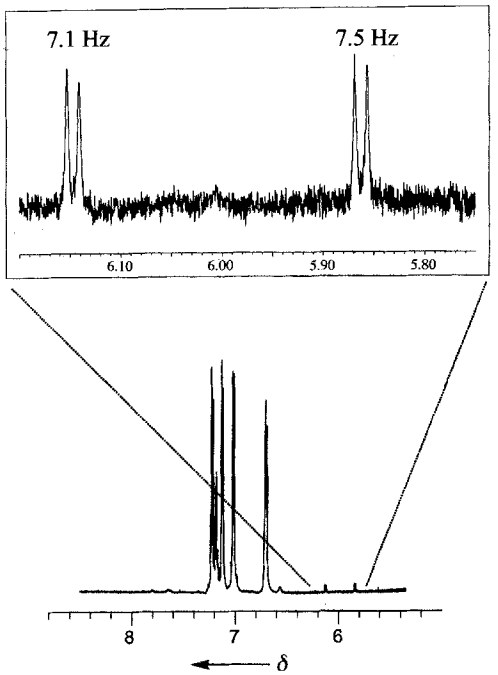

Fig. 4. ^1H NMR spectrum of the reaction mixture of KKSFNSYTC and EpiD after 16 h. The signal at $\delta(^1H) = 6.01$ corresponds to the proton at the C_β atom of the former C-terminal cysteine after the modification by EpiD; the signal is a doublet of doublets with the coupling constants of $^3J(H_\alpha,H_\beta) = 7.3$ Hz and $^1J(H_\beta,C_\beta) = 170$ Hz. The homonuclear coupling constant of 7.3 Hz between H_α and H_β is typical for a double bond with (*Z*) configuration in the reaction product [1, 3, 15].

Experimental Procedure

DL-Cysteine was purchased from Isocom (Landshut, Germany) and trimethoxybenzaldehyde from Aldrich (Steinheim, Germany). N,S-protected 3-^{13}C-labeled DL-cysteine was synthesized as follows: The thiol group of DL-cysteine (3-^{13}C) was protected with a 2,4,6-trimethoxybenzyl (Tmob) group by reaction with 2,4,6-trimethoxybenzaldehyde in the presence of trifluoroacetic acid [16]. The amino group was protected by reaction with 9-fluorenylmethyloxycarbonyl-*O*-succinimide (Fmoc-OSu) in a solution of Na_2CO_3 in H_2O/THF. Fmoc-3-[^{13}C]-DL-Cys(Tmob) was attached to 2-chlorotrityl chloride resin and the peptide KKSFNSYTC synthesized with a peptide synthesizer (MultiSynTech, Bochum). Fmoc-protected amino acids were coupled with diisopropylcarbodiimide/1-hydroxybenzotriazole (DIC/HOBT) (1:1). The enzyme EpiD was purified after overexpression in *Escherichia coli* as described in ref. [4].

ESI-MS and MS–MS spectra were recorded on an API III triple-quadrupole mass spectrometer (Sciex, Thornhill, Canada). The NMR experiments were performed at 305 K on a AMX600 spectrometer (Bruker, Karlsruhe) equipped with a $^{13}C,^{15}N$ triple resonance probe at a proton frequency of 600.13 MHz. The nonapeptide KKSFNSYTC (2.7 mg) labeled with ^{13}C at C_β of the cysteine residue was dissolved in 20 mM Tris buffer (Tris/HCl, pH 8.0, 0.5 mL) containing 10 mM dithiothreitol and 10% D_2O. This solution was transferred to an NMR tube and 6 μg of EpiD was added. HSQC spectra, with a measuring time of 10 min each, were recorded every 20 min over the course of the enzymatic reaction.

Received: March 25, 1996 [Z 8968 IE]
German version: *Angew. Chem.* **1996**, *108*, 2235–2238

Keywords: biosyntheses · decarboxylations · epidermin · peptides · sulfur compounds

[1] a) H. Allgaier, G. Jung, R.-G. Werner, U. Schneider, H. Zähner, *Angew. Chem.* **1985**, *97*, 1052–1054; *Angew. Chem. Int. Ed. Engl.* **1985**, *24*, 1051–1053; b) H. Allgaier, G. Jung, R.-G. Werner, U. Schneider, H. Zähner, *Eur. J. Biochem.* **1986**, *160*, 9–22.

[2] N. Schnell, K.-D. Entian, U. Schneider, F. Götz, H. Zähner, R. Kellner, G. Jung, *Nature* **1988**, *333*, 276–278.
[3] a) J. Augustin, R. Rosenstein, B. Wieland, U. Schneider, N. Schnell, G. Engelke, K.-D. Entian, F. Götz, *Eur. J. Biochem.* **1992**, *204*, 1149–1154; b) N. Schnell, G. Engelke, J. Augustin, R. Rosenstein, V. Ungermann, F. Götz, K.-D. Entian, *ibid.* **1992**, *204*, 57–68.
[4] T. Kupke, S. Stevanovic, H.-G. Sahl, F. Götz, *J. Bacteriol.* **1992**, *174*, 5354–5361.
[5] T. Kupke, C. Kempter, V. Gnau, G. Jung, F. Götz, *J. Biol. Chem.* **1994**, *269*, 5653–5659.
[6] *Combinatorial Peptide and Non-peptide Libraries* (Ed.: G. Jung), VCH, Weinheim, **1996**.
[7] T. Kupke, C. Kempter, G. Jung, F. Götz, *J. Biol. Chem.* **1995**, *270*, 11282–11289.
[8] Review: G. B. Fields, R. L. Noble, *Int. J. Pept. Res.* **1990**, *35*, 161–214.
[9] L. Lerner, A. Bax, *J. Magn. Reson.* **1986**, *69*, 375–380.
[10] G. Bodenhausen, D. J. Reuben, *Chem. Phys. Lett.* **1980**, *69*, 185–188.
[11] A.-M. Le Nocher, P. Metzner, *Tetrahedron Lett.* **1992**, *41*, 6151–6154.
[12] a) R. Kellner, G. Jung, T. Hörner, H. Zähner, N. Schnell, K.-D. Entian, F. Götz, *Eur. J. Biochem.* **1988**, *177*, 53–59; b) S. Freund, G. Jung, O. Gutbrod, G. Folkers, W. A. Gibbons in ref. [15b], pp. 91–102.
[13] H. Kogler, M. Baud, H. W. Fehlhaber, C. Griesinger, W. Schubert, U. Teetz in ref. [15b], pp. 159–170.
[14] a) Y. Minami, K. Yoshida, R. Azuma, A. Urakawa, T. Kawauchi, T. Otani, K. Komiyama, S. Omura, *Tetrahedron Lett.* **1994**, *35*, 8001–8004; b) K. Komiyama, K. Otoguro, T. Segawa, K. Shiomi, H. Yang, Y. Takahashi, M. Hayashi, T. Otani, S. Omura, *J. Antibiot.* **1993**, *46*, 1666–1671.
[15] Reviews: a) G. Jung, *Angew. Chem.* **1991**, *103*, 1067–1084; *Angew. Chem. Int. Ed. Engl.* **1991**, *30*, 1051–1068; b) *Nisin and Novel Lantibiotics* (Eds.: G. Jung, H.-G. Sahl), Escom, Leiden, **1991**; c) R. Jack, F. Götz, G. Jung in *Biotechnology 7*, VCH, Weinheim, in press.
[16] M. C. Munson, C. Garcia-Echeverria, F. Albericio, G. Barany, *J. Org. Chem.* **1992**, *57*, 3031–3018.

First Characterization of a Titanium Enolate Radical Cation in Solution: Carbon–Carbon Bond Formation and the Kinetics of the Mesolytic Ti–O Bond Cleavage**

Michael Schmittel* and Rolf Söllner

Ever since their first successful use in 1981[1] titanium enolates have had an important standing as versatile synthetic carbon nucleophiles in stereoselective aldol[2] and Michael reactions,[3] in particular because they allow for higher stereoselectivites than lithium enolates. Most importantly, the incorporation of chiral ligands at the titanium center opened the way for enantioselective aldol reactions with excellent *ee* values.[4] Surprisingly, the umpolung of titanium enolates through one-electron oxidations is hitherto completely unknown,[5] although such radical cations should offer interesting electrophilic features that could be exploited in carbon–carbon bond formation, quite in analogy to the recent chemistry of silyl[6] and stannyl[7] enol ether radical cations. Here we report for the first time on titanium enolate radical cations in solution, their characterization by cyclic voltammetry and ESR, as well as on the kinetics of the mesolytic[8] Ti–O bond cleavage. In addition, our exploratory investigations reveal that oxidative carbon–carbon bond formation from titanium enolates is possible.

In view of the significance of titanium enolates in organic synthesis it is quite astonishing how little is known about their structural and spectroscopic properties. The lack of data is mainly because these reactive compounds are usually prepared in situ and have only been isolated in a few cases,[9] as a result of their high sensitivity toward hydrolysis. Hence, a pivotal prerequisite for our investigations on the corresponding radical cations was the availability of stable and pure titanium enolates, a problem that could be solved by using some well-known stabilizing structural motifs from the design of simple stable enols.[10] Accordingly, we have synthesized the sterically shielded model compounds **T1**–**T3** as well as the sterically unimpeded **T4**.[5a]

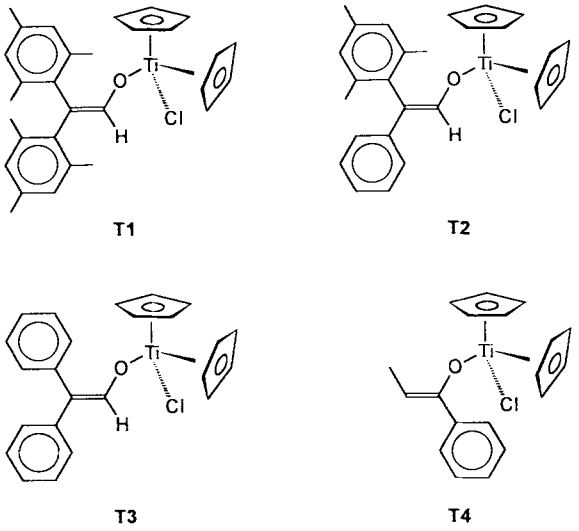

T1 **T2** **T3** **T4**

The novel titanium enolates **T1**–**T3** were prepared in analytically pure form in 32–53% yield as dark red solids from the corresponding stable enol or carbonyl precursor by quantitative deprotonation with sodium hydride followed by reaction with dichlorotitanocene in tetrahydrofuran at room temperature.

While **T4** could only be handled under rigorous exclusion of water in Schlenk glassware, **T1**–**T3** exhibited a remarkable stability against hydrolysis. For instance, **T1** could be exposed to atmospheric water and oxygen for three months without significant decomposition.

In standard cyclic voltammetry (cv) investigations irreversible oxidation waves were monitored for titanium enolates **T1**–**T4** in acetonitrile at a scan rate of 100 mVs^{-1} (Table 1); they indicated that a rapid follow-up reaction occurred. The oxidation potentials E_{pa} (0.4–0.6 V vs. Fc[11]) are in a range where chemical one-electron oxidations should easily be realized in the pres-

Table 1. Oxidation potentials E_{pa} and half-wave potentials $E_{1/2}$ of titanium enolates determined by cyclic voltammetry (potentials referred to the ferrocene/ferrocenium redox couple; electrolyte: tetra-*n*-butylammonium hexafluorophosphate).

Titanium enolate	E_{pa} [a]	$E_{1/2}$
T1	+ 0.44	+ 0.50 [b]
T2	+ 0.44	
T3	+ 0.40	+ 0.49 [c]
T4	+ 0.54	

[a] In acetonitrile at v = 100 mVs^{-1}. [b] In dichloromethane at v = 100 Vs^{-1}. [c] In dichloromethane at v = 1000 Vs^{-1}.

[*] Prof. Dr. M. Schmittel, Dipl. Chem. R. Söllner
Institut für Organische Chemie der Universität
Am Hubland, D-97074 Würzburg (Germany)
Fax: Int. code + (931)888-4606
e-mail: mjls@chemie.uni-wuerzburg.de

[**] Electroactive Protecting Groups and Reaction Units, Part 3. This research was supported financially by the Volkswagen-Stiftung and the Deutsche Forschungsgemeinschaft (SFB 347, Selective reactions of metal activated molecules). We thank Dr. G. Gescheidt, Basel for support in interpreting the ESR spectra. For Part 2, see Ref. [16]. For the term mesolytic, see Ref. [8].

 © VCH Verlagsgesellschaft mbH, D-69451 Weinheim, 1996 0570-0833/96/3518-2107 $ 15.00+.25/0

ence of many other common functional groups.[12] For **T1** and **T3** the thermodynamic half-wave potentials $E_{1/2}$ were determined with fast scan cyclic voltammetry at ultramicro electrodes; for instance, **T1** exhibited a reversible wave in dichloromethane at scan rates v greater than 20 Vs^{-1}.

Besides the first oxidation wave at $E_{pa1} = 0.44$ V, titanium enolate **T1** displays an additional irreversible oxidation wave (at $v = 100\ mVs^{-1}$) at $E_{pa2} = 1.08$ V[13] that is caused by the benzofuran **B1** (Scheme 1),[14] formed as product of the one-elec-

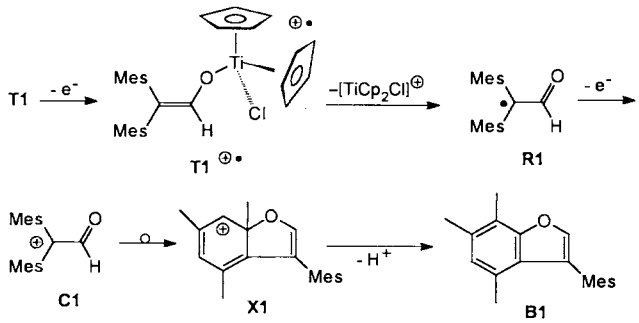

Scheme 1. Mechanism of the formation of the benzofuran. On 1,2-methyl-migration with proton loss **X1** forms **B1**. Mes = mesityl.

tron oxidation of **T1** already on the time scale of the cv run. In order to support this assignment, we oxidized **T1** with 200 mol% of $[Fe(phen)_3](PF_6)_3$ (phen = 1,10-phenanthroline), a well defined outer-sphere one-electron oxidant, and obtained benzofuran **B1** in 93% yield. The cyclic voltammogram of **B1** indeed exhibited an irreversible oxidation wave at $E_{pa} = 1.06$ V. The formation of product **B1** clearly indicates that a clean Ti–O bond cleavage must have taken place in the course of the one-electron oxidation. The most likely mechanism, following the pathways of the corresponding enol[15] and silyl enol ether[16] oxidations, is depicted in Scheme 1. The alternative mechanism (that is, direct cyclization within $\mathbf{T1}^{+\bullet}$) can be excluded on steric grounds.

Another mesolytic cleavage pathway[17] involving fragmentation of $\mathbf{T1}^{+\bullet}$ directly to **C1** and $Ti^{III}Cp_2Cl$ could be postulated. However, such a cleavage mode seems highly implausible, because the oxidation potential of $Ti^{III}Cp_2Cl$ ($E_{pa} = -0.68$ V)[18] is much lower than that of **R1** ($E_{pa} = +0.37$ V).[19]

Since chiral titanium enolate radical cations can potentially be used in enantioselective carbon–carbon bond formation (Scheme 2), it was important to investigate the kinetics of the

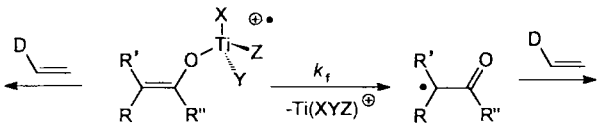

Scheme 2. Conceivable reaction pathways of the titanium enolate radical cations. D = donor.

Ti–O bond cleavage process. Obviously, if the Ti–O bond fragmentation (k_f) is too rapid, α-carbonyl radical intermediates and not the desired chiral titanium enolate radical cations would be the pivotal species in the bond formation process.

Consequently, we determined the rate of Ti–O bond rupture in $\mathbf{T1}^{+\bullet}$ in acetonitrile using cv with scan rates between 200 and 3000 Vs^{-1}. According to the method of Nicholson and Shain,[20] a first-order rate constant of $k_f = 850\ s^{-1}$ was obtained for the fragmentation in acetonitrile at room temperature on applying a working curve for an $EC_{irr}E$ mechanism[21] (electron transfer/chemical reaction/electron transfer). This rate constant is similar to that of the O–$SiMe_2t$Bu fragmentation in silyl enol ether radical cations ($k_f = 1300\ s^{-1}$).[22] Notably, O–$SiMe_2t$Bu silyl enol ethers have already been used successfully in oxidative C–C couplings.[6]

The first ESR spectra of titanium enolate radical cations,[23] generated through one-electron oxidation of the neutral precursors **T1**–**T3** with tris(*p*-bromophenyl)aminium hexachloroantimonate in dichloromethane, were recorded at −100 °C. Whereas for $\mathbf{T1}^{+\bullet}$ ($g = 2.0043$) only unresolved spectra were obtained in spite of measurements at different concentrations, the spectra of $\mathbf{T2}^{+\bullet}$ ($g = 2.0036$) and $\mathbf{T3}^{+\bullet}$ ($g = 2.0038$) exhibited hyperfine splitting caused through mesityl, phenyl, and vinyl hydrogen atoms. No spin density seems to reside on the titanocene fragment, which qualifies such radical cations as electrophilic radicals that are most likely to react at the β-carbon.

While such carbon–carbon bond formation is highly unlikely with $\mathbf{T1}^{+\bullet}$ due to the extreme steric shielding of the β-carbon, one-electron oxidation of **T4** with 100 mol% of $[Fe(phen)_3](PF_6)_3$ in acetonitrile gave rise to dimer **5** (64%, *meso*:D,L = 1:1, Scheme 3). Although some mechanistic details of this new carbon–carbon bond formation reaction are open to discussion, cv investigations suggest that C–C bond formation is much more rapid than Ti–O bond cleavage in $\mathbf{T4}^{+\bullet}$.[24] Therefore, the dimerization most likely is initiated by the nucleophilic attack of **T4** on the titanium enolate radical cation $\mathbf{T4}^{+\bullet}$.

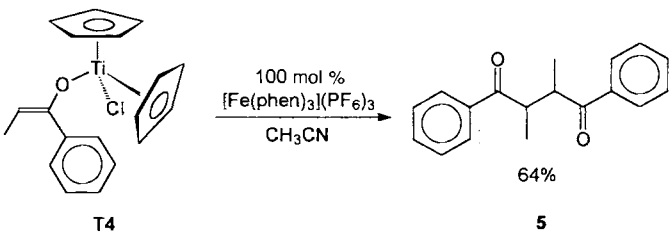

Scheme 3. Synthesis of **5** by dimerization.

In summary, we have synthesized three remarkably stable titanium enolates and investigated for the first time titanium enolate radical cations in solution. Since the mesolytic Ti–O bond cleavage is rather slow, sterically unshielded titanium enolate radical cations (for example, $\mathbf{T4}^{+\bullet}$) undergo direct carbon–carbon bond formation processes with π-nucleophiles.

Received: April 15, 1996 [Z90301E]
German version: *Angew. Chem.* **1996**, *108*, 2248–2250

Keywords: cyclic voltammetry · electron transfer · radical cations · titanium enolates

[1] M. T. Reetz, R. Peter, *Tetrahedron Lett.* **1981**, *22*, 4691–4694.
[2] a) A. Choudhury, E. R. Thornton, *Tetrahedron* **1992**, *48*, 5701–5708; b) D. A. Evans, F. Urpi, T. C. Somers, J. S. Clark, M. T. Bilodeau, *J. Am. Chem. Soc.* **1990**, *112*, 8215–8216; c) S. Shirodkar, M. Nerz-Stormes, E. R. Thornton, *Tetrahedron Lett.* **1990**, *31*, 4699–4702; d) M. P. Bonner, E. R. Thornton, *J. Am. Chem. Soc.* **1991**, *113*, 1299–1308; e) D. A. Evans, D. L. Rieger, M. T. Bilodeau, F. Urpi, *ibid.* **1991**, *113*, 1047–1049.
[3] D. A. Evans, M. T. Bilodeau, T. C. Somers, J. Clardy, D. Cherry, Y. Kato, *J. Org. Chem.* **1991**, *56*, 5750–5752.
[4] a) R. O. Duthaler, P. Herold, W. Lottenbach, K. Oertle, M. Riediker, *Angew. Chem.* **1989**, *101*, 490–491; *Angew. Chem. Int. Ed. Engl.* **1989**, *28*, 495–496; b) R. O. Duthaler, A. Hafner, *Chem. Rev.* **1992**, *92*, 807–832.
[5] Oxidation reactions of titanium enolates are rather scarce; the only known examples report on reactions with oxygen-transfer reagents: a) W. Adam, M. Müller, F. Prechtl, *J. Org. Chem.* **1994**, *59*, 2358–2364; b) M. Schulz, R. Kluge, M. Schüßler, G. Hoffmann, *Tetrahedron* **1995**, *51*, 3175–3180.
[6] a) A. B. Paolobelli, D. Latini, R. Ruzziconi, *Tetrahedron Lett.* **1993**, *34*, 721–724; b) B. B. Snider, T. Kwon, *J. Org. Chem.* **1992**, *57*, 2399–2410; c) A.

Heidbreder, J. Mattay, *Tetrahedron Lett.* **1992**, *33*, 1973–1976; d) H. J. Schäfer in: *Organic Electrochemistry*, 3rd ed. (Eds.: H. Lund, M. M. Baizer), Dekker, New York **1991**, 949–1027; e) B. B. Snider, T. Kwon, *J. Org. Chem.* **1990**, *55*, 4786–4788; f) E. Baciocchi, A. Casu, R. Ruzziconi, *Tetrahedron Lett.* **1989**, *30*, 3707–3710.

[7] Y. Kohno, K. Narasaka, *Bull. Chem. Soc. Jpn.* **1995**, *68*, 322–329.

[8] The expression mesolytic was coined by Maslak and will be used throughout this paper: P. Maslak, J. N. Narvaez, *Angew. Chem.* **1990**, *102*, 302–304; *Angew. Chem. Int. Ed. Engl.* **1990**, *29*, 283–285.

[9] a) M. D. Curtis, S. Thanedar, W. M. Butler, *Organometallics* **1984**, *3*, 1855–1859; b) C. P. Gibson, D. S. Bem, *J. Organomet. Chem.* **1991**, *414*, 23–32; c) P. Veya, C. Floriani, A. Chiesi-Villa, C. Rizzoli, *Organometallics* **1993**, *12*, 4892–4898; d) R. Beckhaus, I. Strauß, T. Wagner, *J. Organomet. Chem.* **1994**, *464*, 155–161; e) P. Veya, P. G. Cozzi, C. Floriani, A. Chiesi-Villa, C. Rizzoli, *Organometallics* **1995**, *14*, 4101–4108.

[10] H. Hart, Z. Rappoport, S. E. Biali in *The Chemistry of Enols* (Ed.: Z. Rappoport), Wiley, Chichester, **1990**, Chap. 8.

[11] All potentials are referred to the ferrocene/ferrocenium (Fc) redox couple unless otherwise noted. Addition of + 0.39 V yields values referred to SCE.

[12] For the preparative application of such a strategy it would be desirable not to isolate the titanium enolates, but to oxidize them selectively in the presence of other compounds.

[13] In presence of 2,6-di-*tert*-butylpyridine. Without addition of base an additional oxidation wave was observed at $E_{pa3} = 0.65$ V that could be readily assigned to the oxidation of the corresponding dimesitylethenol formed by proton-induced hydrolysis of the titanium enolate.

[14] M. Schmittel, M. Röck, *Chem. Ber.* **1992**, *125*, 1611–1620.

[15] M. Schmittel, G. Gescheidt, M. Röck, *Angew. Chem.* **1994**, *106*, 2056–2058; *Angew. Chem. Int. Ed. Engl.* **1994**, *33*, 1961–1963.

[16] M. Schmittel, M. Keller, A. Burghart, *J. Chem. Soc. Perkin Trans. 2* **1995**, 2327–2333.

[17] M. Schmittel, J. Heinze, H. Trenkle, *J. Org. Chem.* **1995**, *60*, 2726–2733.

[18] S. V. Kukharenko, G. L. Solveichik, V. V. Strelets, *Bull. Acad. Sci USSR, Div. Chem. Sci. (Engl. Transl.)* **1986**, *35*, 926–932.

[19] M. Röck, M. Schmittel, *J. Chem. Soc. Chem. Commun.* **1993**, 1739–1741.

[20] R. S. Nicholson, I. Shain, *Anal. Chem.* **1964**, *36*, 706–723.

[21] The working curve was simulated according to an $EC_{irr}E$ mechanism with parameters obtained from cv measurements.

[22] M. Schmittel, M. Levis, unpublished results.

[23] The signals of $\mathbf{T1}^{+\bullet}$ and $\mathbf{T2}^{+\bullet}$ persisted for several hours, whereas that of $\mathbf{T3}^{+\bullet}$ decayed within 1 hour.

[24] Thermochemical cycle calculations[17] indicate that the free energy for the Ti-O-bond cleavage in $\mathbf{T1}^{+\bullet}$–$\mathbf{T4}^{+\bullet}$ should differ by less than 2 kcal mol^{-1} as a consequence of the small differences in the oxidation potentials of the titanium enolates. Accordingly, the kinetics of the mesolytic bond cleavage is not expected to differ vastly. Nevertheless, **T1** is reversibly oxidized at scan rates greater than 20 Vs^{-1}, whereas **T4** shows no sign of reversibility at scan rates smaller than 40000 Vs^{-1}, which is indicative of an alternative follow-up reaction, for example, dimerization.

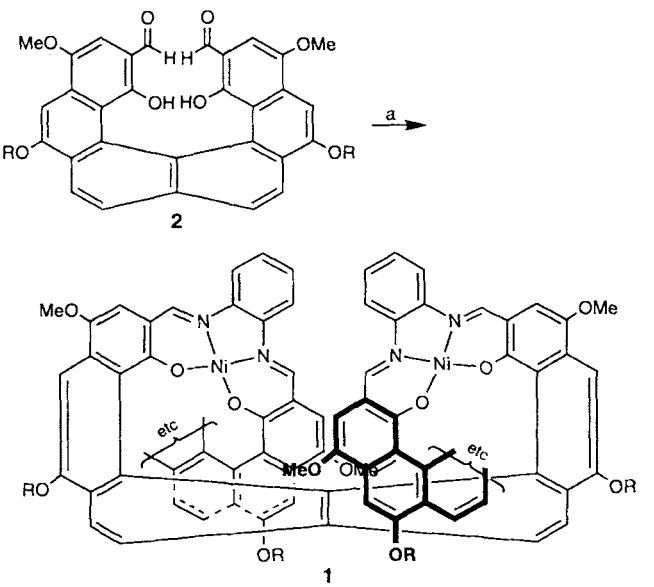

Scheme 1. Synthesis of the helical conjugated ladder polymer **1**. a) *o*-phenylenediamine in refluxing ethanol, then $Ni(OAc)_2$ in refluxing THF/EtOH (95%). R = CH_2CH_2OnBu.

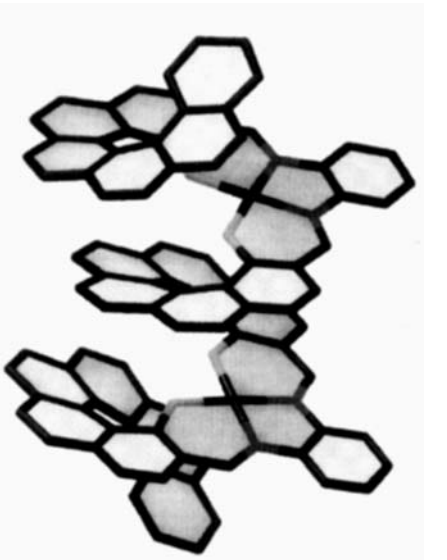

Fig. 1. A portion of structure **1**, consisting of three helicene rings and two salophens. The side chains have been deleted for clarity.

Synthesis of a Helical Conjugated Ladder Polymer**

Yujia Dai, Thomas J. Katz,* and David A. Nichols

Reported here is the synthesis of the first polymer (**1**) with an unbroken network of double bonds that winds in one direction along a helix.[1, 2] The key step is the union of a [6]helicene possessing salicylaldehyde functionality at each end, 1,2-phenylenediamine, and nickel acetate (Scheme 1). In the resulting structure (Fig. 1) "nickel salophen"[5, 6] units bind adjacent helicenes,[7] provide a conjugated link from one ring system to the next, and constrain the p-orbitals of the rings they unite to be nearly parallel.[8] Unlike other ladder polymers,[9] **1** is chiral, and unlike other optically active conjugated polymers (such as polythiophenes), its helical shape is preserved by unaggregated molecules in solution.[10]

Helical bis(salicylaldehyde) **2**, which was used for the experiments, was synthesized from optically active helical bis(quinone) **3**[11] by the procedures outlined in Scheme 2. Noteworthy is the selectivity of two steps, the addition of HBr that converts **3** into **4**[12, 13] and the removal of half the acetate functions that converts **5** into **6**.[4]

The dark red product **1** that formed in the reaction shown in Scheme 1 was purified by dissolution in CH_2Cl_2 and precipitation by the addition of hexane. The material is soluble in $CHCl_3$, CH_2Cl_2, THF, benzene, acetone, and CH_3OH. Thus it does not suffer the insolubility that is a major deficit of many planar ladder polymers.[9]

[*] Prof. T. J. Katz, Dr. Y. Dai, D. A. Nichols
Department of Chemistry, Columbia University
New York, NY 10027 (USA)
Fax: Int. code + (212) 932-1289
e-mail: tjk1@columbia.edu

[**] This work was supported by grants from The National Science Foundation (CHE92-24634) and The Kanagawa Academy of Science and Technology. We thank Dr. Y. Itagaki (Suntory Institute for Bioorganic Research, Osaka, Japan) for the mass spectrum of **1**, Dr. James C. Carnahan (General Electric Co., Schenectedy, New York) for its GPC analysis, and Dr. Ullrich Scherf for informing us of his related work on ladder polymers.

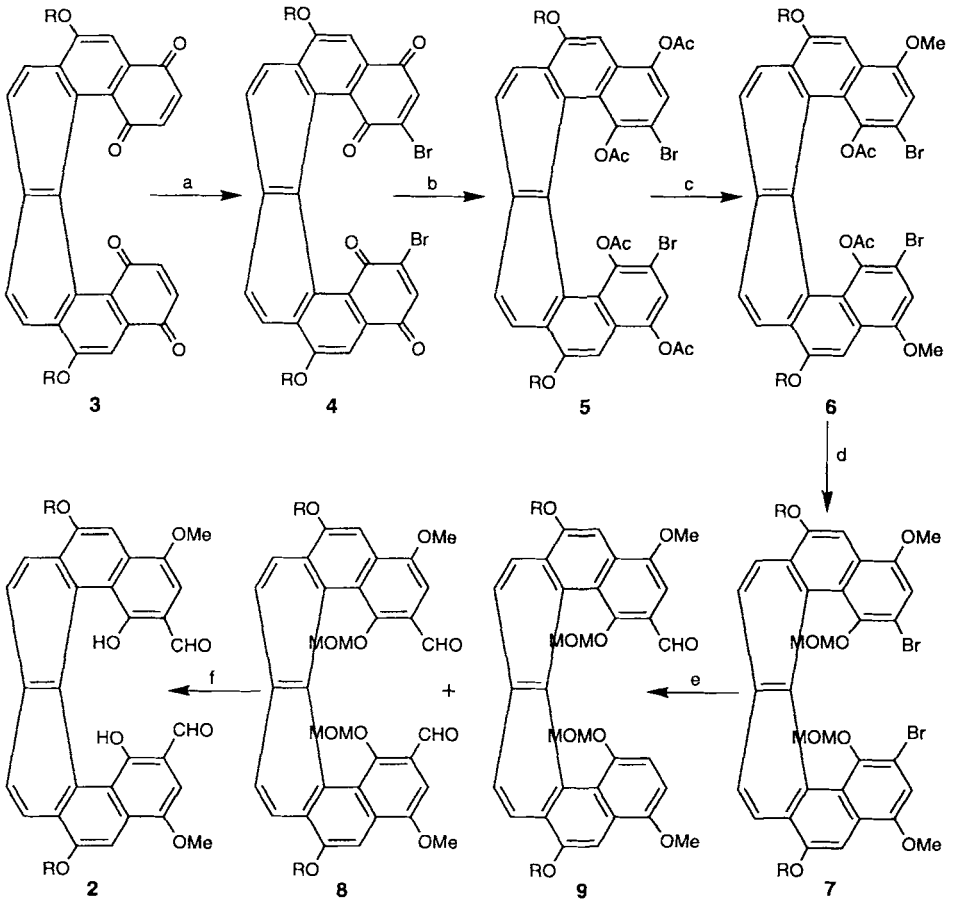

Scheme 2. Route to optically active helical bis(salicylaldehyde) **2**. a) HBr in $EtCO_2H$, then chloranil (25–30%); b) $Na_2S_2O_4$, nBu_4NBr, H_2O/CH_2Cl_2, then Ac_2O, Et_3N, CH_2Cl_2 (78–82%); c) K_2CO_3, MeOH, 25 °C, then MeI, K_2CO_3, acetone, reflux (81%); d) KO*t*Bu, THF, 25 °C, then $MeOCH_2Cl$ (MOMCl), THF, 25 °C (92%); e) *n*BuLi, THF, −78 °C, then Me_2NCHO, −78 → 25 °C (80% **8**, 16% **9**); f) H_2SO_4, HOAc, H_2O, 60 °C (100%). R = CH_2CH_2OnBu.

Evidence that the product has structure **1** includes the following. 1) The procedure used is expected to give this structure.[6, 7a–c] 2) The ^1H NMR spectrum of the product in $CDCl_3$ shows four clearly defined broad peaks—broad, probably, because of the viscosity. The signal intensities are those required[14] and their positions are, with the exception of the resonances of the outermost portions of the side chains,[15] shifted upfield, most likely by electron currents in nearby rings,[16] by $\Delta\delta \approx 1$ from their positions in the spectra of **2** and of nickel salophen itself. The intensities of resonances related to the CHO and OH resonances in **2** are tiny. 3) The ^{13}C NMR spectrum of **1** in $CDCl_3$, although it consists of broad and multiple peaks (presumably because the material is a mixture of oligomers and because in small polymers some carbons are nearer the ends while others are nearer the middle), exhibits resonances that match those of **2**, with these differences: the aldehyde resonance, which in **2** appears at $\delta = 193.7$, is barely visible, and one of the low-field resonances of **2** (attributable to the carbon next to the phenoxide $C_{ar}-O^-$) is shifted.[17] Resonances at $\delta = 124$ and 143 may be attributable to the phenylene moiety. 4) The infrared spectrum of **1** (KBr) shows a band at 1596 cm^{-1}, appropriate for the C=N stretch of a nickel salophen.[18] No bands are evident for either a C=O or an OH stretching absorption. 5) The Matrix-Assisted Laser Desorption/Ionization Time-of-Flight (MALDI-TOF) mass spectrum[19] consists of two peaks separated by 90.0 ± 0.2 Da that repeat ten times with decreasing intensity at intervals of 837.6 ± 0.2 Da. This last figure is exactly the mass of the repeat unit of **1** ($C_{48}H_{46}N_2NiO_8$).

The mass spectrum also identifies the end groups. The repeating motif of two peaks distinguishes two series of polymers. The signal for the lowest mass member of one series corresponds to ($2 + NiO \cdot H_2O$), implying that one end has the *o*-hydroxybenzaldehyde functionality of **2** and the other the functionality of its hydroxynickel salt. The ions of the second, and probably predominant,[20] series have the additional mass (90.1) of one phenylenediamine unit less water, expected for a Schiff base derivatives. Two small but prominent resonances in the ^1H NMR spectrum of the oligomers, at $\delta = 4.6$ and 4.5, are at lower fields than the other OCH_2 resonances and at a position characteristic of the hydrogens on one of the OCH_2 groups in precursor **2** (undoubtedly the one closest to the benzene rings). Their integration suggests that the number average molecular mass is approximately 7000.[23] This agrees with the value $M_n \approx 7400$ obtained by GPC analysis of a solution in THF and the assumption that a published correction applies that relates the molecular masses of certain rigid rod polymers and polystyrenes.[24, 25]

The optical properties of **1** (Fig. 2) differ from those of simpler molecules. The feature at longest wavelength in the UV spectrum (in CH_2Cl_2) is a band at 594 nm, with $\varepsilon = 9300$. Although its position corresponds to that of d–d transitions in simple salophens,[26] the intensity (calculated per unit monomer concentration as if the polymer were infinite)[27] is roughly 60 times larger. Accordingly, we suppose the peak to be related to the "metal-to-ligand" charge transfer band of nickel salophen, but shifted to longer wavelength by 114 nm from its position in the spectrum of the parent compound (480 nm),[26b, 28] possibly because the energy of the HOMO is raised by the electron-donating substituents. The circular dichroism (CD) at this wavelength is very large. At the maximum at longest wavelength

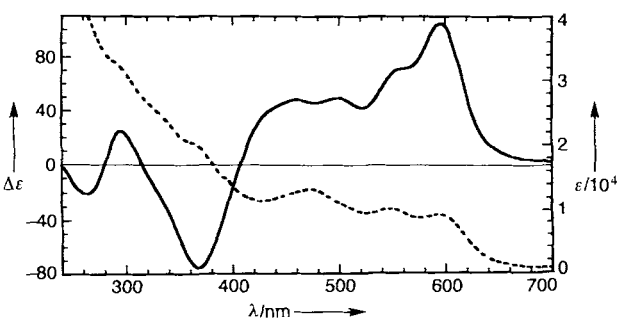

Fig. 2. CD (—) and UV (- - -) spectra of **1** in CH_2Cl_2.

 © VCH Verlagsgesellschaft mbH, D-69451 Weinheim, 1996 0570-0833/96/3518-2110 $ 15.00+.25/0

(595 nm, there is no exciton splitting), $\Delta\varepsilon$[27] is 105, much higher than the value of around 3 shown by the simpler metal Schiff base complexes studied previously.[26b, 29, 30]

Received: April 29, 1996 [Z 9074 IE]
German version: *Angew. Chem.* **1996**, *108*, 2230–2232

Keywords: helical structures · polymers · Schiff base complexes

[1] Another is described by Fiesel, Huber, and Scherf in this issue: R. Fiesel, J. Huber, U. Scherf, *Angew. Chem.* **1996**, *108*, 2233–2234; *Angew. Chem. Int. Ed. Engl.* **1996**, *35*, 2111–2113.
[2] Polymeric helical metallocenes [3] and aggregates of helical molecules [4] are related materials that were synthesized earlier.
[3] T. J. Katz, A. Sudhakar, M. F. Teasley, A. M. Gilbert, W. E. Geiger, M. P. Robben, M. Wuensch, M. D. Ward, *J. Am. Chem. Soc.* **1993**, *115*, 3182.
[4] C. Nuckolls, T. J. Katz, L. Castellanos, *J. Am. Chem. Soc.* **1996**, *118*, 3767.
[5] Nickel *N,N'*-bis(*o*-oxybenzylidene)phenylenediamine or (*N,N'*-disalicylidene-1,2-phenylenediaminato)nickel(II) or *N,N',O,O'*-{2,2'-[1,2-phenylenebis(nitrilomethylidyne)]bis(phenolato)}(2 −) nickel.
[6] a) P. Pfeiffer, E. Breith, E. Lübbe, T. Tsumaki, *Ann. Chem.* **1933**, *503*, 84; b) R. H. Holm, G. W. Everett, Jr., A. Chakravorty, *Prog. Inorg. Chem.* **1966**, *7*, 83; c) J. Costamagna, J. Vargas, R. Latorre, A. Alvarado, G. Mena, *Coord. Chem. Rev.* **1992**, *119*, 67.
[7] Links between metals and either salophens, other Schiff bases, or salicylaldehyde oximes have been studied before to construct polymers. a) H. Chen, J. A. Cronin, R. D. Archer, *Inorg. Chem.* **1995**, *34*, 2306, and references therein; b) R. D. Archer, *Coord. Chem. Rev.* **1993**, *128*, 49; c) R. Müller, D. Wöhrle, *Makromol. Chem.* **1976**, *177*, 2241; d) M. J. S. Dewar, A. M. Talati, *J. Am. Chem. Soc.* **1964**, *86*, 1592.
[8] A. Radha, M. Seshasayee, K. Ramalingam, G. Aravamudan, *Acta Crystallogr. Sect. C Cryst. Struct. Commun.* **1985**, *41*, 1169, and references therein.
[9] a) U. Scherf, K. Müllen, *Adv. Polym. Sci.* **1995**, *123*, 1; b) A.-D. Schlüter, *Adv. Mater.* **1991**, *3*, 282; c) L. Yu, M. Chen, L. R. Dalton, *Chem. Mater.* **1990**, *2*, 649.
[10] a) M. M. Bouman, E. E. Havinga, R. A. J. Janssen, E. W. Meijer, *Mol. Cryst. Liq. Cryst.* **1994**, *256*, 439; B. M. W. Langeveld-Voss, R. A. J. Janssen, M. P. T. Christiaans, S. C. J. Meskers, H. P. J. M. Dekkers, E. W. Meijer, *J. Am. Chem. Soc.* **1996**, *118*, 4908; c) G. Bidan, S. Guillerez, V. Sorokin, *Adv. Mater.* **1996**, *8*, 157; d) J. S. Moore, C. B. Gorman, R. H. Grubbs, *J. Am. Chem. Soc.* **1991**, *113*, 1704; e) Q.-S. Hu, D. Vitharana, G.-Y. Liu, V. Jain, M. W. Wagaman, L. Zhang, T. R. Lee, L. Pu, *Macromolecules* **1996**, *29*, 1082.
[11] a) N. D. Willmore, L. Liu, T. J. Katz, *Angew. Chem.* **1992**, *104*, 1081; *Angew. Chem. Int. Ed. Engl.* **1992**, *31*, 1093; b) N. D. Willmore, Ph.D. Dissertation, Columbia University, **1994**.
[12] HBr in $EtCO_2H$ adds bromine selectively to the 2-carbon of 6-methoxynaphthoquinone. Air, the oxidant in those experiments, was unsatisfactory here. D. W. Cameron, G. I. Feutrill, P. G. Griffiths, *Aust. J. Chem.* **1981**, *34*, 1513.
[13] In the case of bis(quinone) **3**, N. D. Willmore [11b] and A. L. Rheingold showed that prolinol adds selectively to the "inner" carbons, giving a nitrogen analogue of **4**.
[14] The signals at $\delta = 8.3-6.6$, 6.4–5.0, 4.7–2.3, and 2.0–0.6 have intensity ratios of 4.0:3.0:8.3:7.7, appropriate for hydrogens on six aromatic positions and one CH=N, on nine aliphatic positions next to oxygen, and on seven other aliphatic positions.
[15] The propyl resonances are shifted from their position in **2** by $\Delta\delta < 0.2$.
[16] Because the shifts are only to high fields, contact with unpaired spins cannot be the origin. a) D. R. Eaton, W. D. Phillips, D. J. Caldwell, *J. Am. Chem. Soc.* **1963**, *85*, 397; b) ref. [6b].
[17] Possibly to higher field by $\Delta\delta \approx 4$.
[18] Our figure for nickel salophen is 1609 cm^{-1}. a) M. R. Mahmoud, S. A. Ibrahim, N. M. Ismail, *Monatsh. Chem.* **1985**, *116*, 167; b) R. Nagar, R. C. Sharma, R. K. Parashar, *Spectrochim. Acta Part A* **1990**, *46*, 401.
[19] The matrix was 2,5-dihydroxybenzoic acid. Observed are M^+ ions. See F. Hellenkamp, M. Karas, R. C. Beavis, B. T. Chait, *Anal. Chem.* **1991**, *63*, 1193A.
[20] This is implied by the elemental analysis for nitrogen. Calcd. for $C_{378}H_{368}N_{14}Ni_8O_{68}$ (corresponding to the first series $M_r = 6664$): C 68.12, H 5.57, N 2.94, Ni 6.95%; Found: C 64.51, H 5.24, N 3.89, Ni 7.99. Calcd for $C_{384}H_{374}N_{16}Ni_8O_{67}$ (corresponding to the second series $M_r = 6755$): C 68.28, H 5.58, N 3.32, Ni 6.95. (CHN analyses were conducted by Desert Analytics, Tucson, AZ; the Ni analysis by Galbraith Laboratories, Knoxville, TN. In refs. [21, 22] analyses for carbon in five highly unsaturated polymers were too low by 3.2 ± 1.3% (absolute values).
[21] J. J. Lamba, J. M. Tour, *J. Am. Chem. Soc.* **1994**, *116*, 11723.
[22] M. B. Goldfinger, T. M. Swager, *J. Am. Chem. Soc.* **1994**, *116*, 7895.
[23] If the distinction of the OCH_2 groups that give rise to this resonance in the oligomers is their location on the outer end of the caps, where they are not flanked by an adjoining helicene (and there is one such group at the cap to each end), the intensity (0.24 protons per [6]helicene unit) implies that the average chain contains 8.3 helicene units. If both $ArOCH_2$ groups at each end give rise to this resonance, the average molecule would be twice as large. M_n would be approximately 14000.
[24] J. S. Schumm, D. L. Pearson, J. M. Tour, *Angew. Chem.* **1994**, *106*, 1445; *Angew. Chem. Int. Ed. Engl.* **1994**, *33*, 1360.
[25] Absorption (254 nm) detector. The chromatogram is bimodal. There is a large peak, with $M_n = 29000$ (corrected, $M_w/M_n = 8.3$), and one that is one-ninth as large, with $M_n = 1000$ (corrected, $M_w/M_n = 1.2$).
[26] a) S. M. Crawford *Spectrochim. Acta* **1963**, *19*, 255; b) B. Bosnich, *J. Am. Chem. Soc.* **1968**, *90*, 627.
[27] The concentration, 0.0189 gL^{-1}, was considered to be 2.26×10^{-5} M.
[28] S. Di Bella, I. Fragalà, I. Ledoux, T. J. Marks, *J. Am. Chem. Soc.* **1995**, *117*, 9481.
[29] a) R. S. Downing, F. L. Urbach, *J. Am. Chem. Soc.* **1970**, *92* 5861; b) J. P. Costes, J. M. Dominguez-Vera, J. P. Laurent, *Polyhedron* **1995**, *14*, 2179; c) A. Pasini, M. Gullotti, R. Ugo, *J. Chem. Soc. Dalton Trans.* **1977**, 346; d) R. D. Peacock, B. Stewart, *Coord. Chem. Rev.* **1982**, *46*, 129.
[30] $[\alpha]_D = +4900$ ddeg$cm^2 g^{-1}$ ($c = 8.6 \times 10^{-4}$ gL^{-1} in CH_2Cl_2).

Synthesis of an Optically Active Poly(*para*-phenylene) Ladder Polymer**

Rainer Fiesel, Joachim Huber, and Ullrich Scherf*

The synthesis of optically active conjugated polymers is an exciting challenge from the point of view of both the synthesis itself and also its potential for applications based on nonlinear optical and chiroptical effects.[1] If, in addition, these materials are efficient luminophores, they are also of importance for generating polarized photo- and electroluminescence. Until now, such compounds have usually been synthesized by introducing chiral side groups, which induced a helical formation of the single-stranded main polymer chain.[1, 2] We describe here a new approach to the preparation of optically active conjugated polymers such as **1**, in which planar chirality elements (cyclophane building blocks) are bonded together to form flat nonhelical poly(*para*-phenylene) (PPP) ladder polymers.

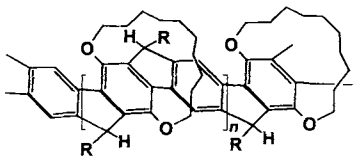

1

The achiral analogs of **1** (PPP ladder polymers LPPP with two alkyl or alkoxy substituents instead of the $OC_{10}H_{20}O$ bridges) have been thoroughly described.[3] They are characterized by unusual optical and electronic properties such as extremely small Stokes shifts (about 30 meV[4]) and high photoluminescence quantum yields,[5] and can be used as emitter materials in light-emitting diodes.[6]

[*] Dr. U. Scherf, Dr. R. Fiesel, Dr. J. Huber
Max-Planck-Institut für Polymerforschung
Ackermannweg 10, D-55128 Mainz (Germany)
Fax: Int. code +(6131)379100
e-mail: scherf@max.mpip-mainz.mpg.de

[**] This work was supported by the Deutsche Forschungsgemeinschaft. Our thanks are also due to Prof. Dr. K. Müllen for his wide-ranging and generous support, Prof. Dr. G. Wulff for carrying out the CD measurements, and Dr. K. Cabrera for her help in the separation of enantiomers.

A decisive factor in the realization of our idea was the use of the $OC_{10}H_{20}O$-bridged diboronic acid **2** as one of the monomer components. We first considered the synthesis of the ladder polymer **1**, which contains these $OC_{10}H_{20}O$ bridges, with racemic **2** as the starting material (Scheme 1). The diboronic

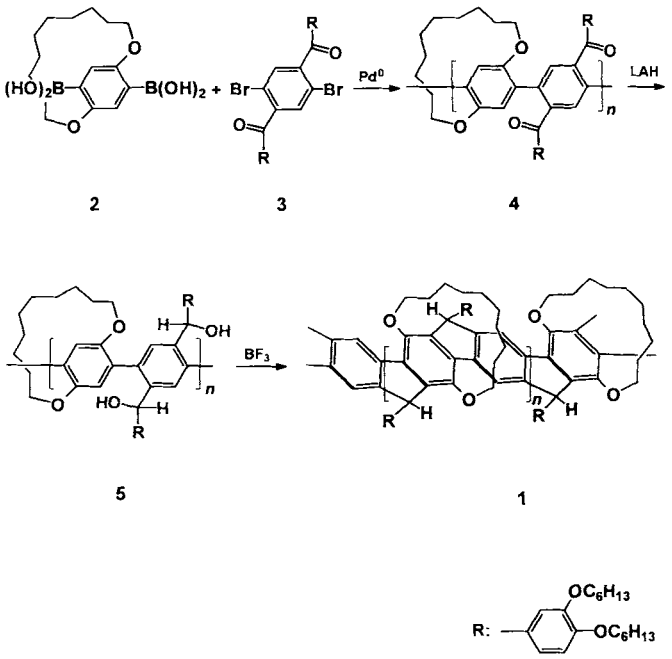

2 3 4 5 1

Scheme 1. Preparation of the $OC_{10}H_{20}O$-bridged PPP ladder polymer **1**.

acid **2** is treated with the terephthalophenone **3** to form the single-stranded PPP derivative **4** in a Suzuki aryl–aryl coupling reaction.[7] The coupling, which is catalyzed by $[Pd^0(PPh_3)_4]$, takes place in a two-phase reaction medium (THF/aqueous sodium carbonate solution). The subsequent cyclization to give the ladder polymer is carried out in a two-stage polymer-analogous reaction, the first stage of which is the reduction of the ketone functions with lithium aluminum hydride (LAH) to form **5**. This is followed the formation of **1** by ring closure, a reaction catalyzed by boron trifluoride etherate (analogous to the Friedel–Crafts reaction).[3] The transformation from the open-chain colorless **5** to the deep yellow ladder polymer **1** is accompanied by a drastic bathochromic shift of the long-wavelength absorption maximum λ_{max}.[3]

The ladder polymer **1**, with its unequivocal structure, can be prepared in yields of greater than 90% and with a molecular mass M_n of 12000–13000 (approximately 28 phenylene units in the main chain).[8] The course of the polymer-analogous cyclization of **5** to **1** was monitored by ^{13}C NMR spectroscopy. The signal from the secondary alcohol group disappears completely at $\delta = 72.5$, and the signal from the newly formed methylene bridge of **1** appears at $\delta = 53.1$. Besides the six signals from the aliphatic side chains, the $ArOCH_2$ methylene carbon atoms ($\delta = 69.8$, 70.1) are characteristic. Eleven signals for nonequivalent arene carbon atoms also appear.[8]

The diboronic acid monomer **2** is prepared in four steps (Scheme 2) from 1,4-benzoquinone. This is reductively brominated to give 2,5-dibromohydroquinone, which is treated with α,ω-dibromodecane to give the half-ether **6**. The intramolecular cyclization of **6** (at high dilution) gives a 58% yield of the dibromocyclophane **7**,[9] which, after twofold metalation with butyllithium, is treated with trimethyl borate to form **2**.[10]

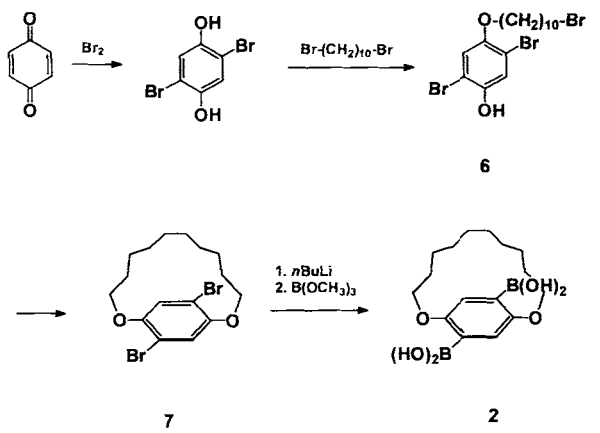

6 7 2

Scheme 2. Preparation of the cyclophanediboronic acid **2**.

Because partial racemization takes place on formation of **2** from enantiomerically pure **7**,[11] we had separate the enantiomers at the stage of the diboronic acid **2** before synthesizing the optically active ladder polymers (+)-**1** and (−)-**1**, whose *ansa* substituents ($OC_{10}H_{20}O$) are located entirely on one side of the molecule. However, separation on cellulose triacetate by liquid chromatography, which is possible with the dibromide **7**,[11,12] was not successful with **2**. A suitable chiral phase, a β-cyclodextrin-modified silica gel (Chiradex, Merck), was found to be surprisingly efficient for the preparative separation of the enantiomers of **2**. This good separation can be explained by the formation of cyclodextrin/**2** inclusion compounds by hydrogen bonding.[13] Both enantiomers of **2** are obtained in high optical purity, namely 100% (+) and 97% (−) (Fig. 1). The absolute configurations of (+)-**2** and (−)-**2** can be assigned, as the structure of (+)-**7** has been determined from anomalous X-ray dispersion.[14]

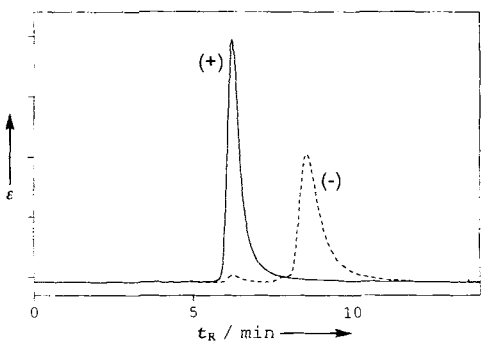

Fig. 1. Chromatograms for the determination of the enantiomeric purities of (+)-**2** and (−)-**2** [analytical separation; column material: Chiradex (Merck); solvent: methanol/water, (50/50)]. t_R = retention time, ε = absorption coefficient (310 nm).

The chiral ladder polymers (+)-**1** and (−)-**1** were obtained from the pure enantiomers of **2**.[15] Figure 2 shows the optical absorption and CD spectra of (+)-**1**. The extremely high chiroptical activity (molar ellipticity $\theta = 2.2 \times 10^6$ rad cm^2 mol^{-1}) in the long-wavelength $\pi-\pi^*$ absorption band ($\lambda_{max} \approx 461$ nm) is striking.[16] The resulting anisotropy factor $g = \Delta\varepsilon/\varepsilon$ is approximately 0.003, and is therefore only one order of magnitude less than the maximum value so far reported for chiral conjugated polymers ($g = 0.02$ for chiral aggregates of a polythiophene with a helical structure[17]). The CD spectra of (+)-**1** and

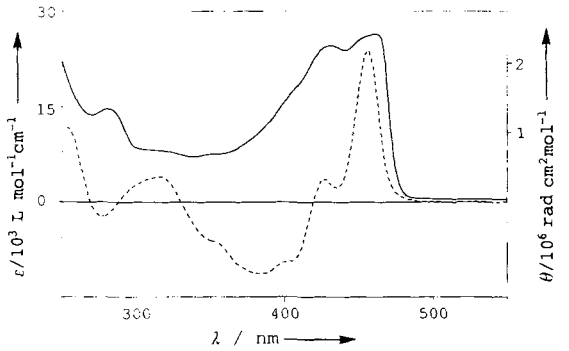

Fig. 2. UV/Vis spectrum (*continuous line*, ε = *absorption coefficient*) and CD spectrum (broken line, θ = molar ellipticity) of (+)-**1** (in dichloromethane).

(−)-**1** are mirror images of each other, the only slight differences between them being in the relative intensities of the bands.

Remarkably, hitherto only compounds of helical structure and their chiral aggregates had been considered as candidates that might display such high chiroptical activities.[1, 2, 17, 18] The cause of the surprisingly high activity of the ladder polymer **1**, whose structure is undoubtedly nonhelical, is to be investigated by temperature-dependent CD measurements and by the synthesis and characterization of model oligomers.[19]

The polymer **1**, like the achiral LPPP parent system,[20] shows very intense photoluminescence both in solution and in the solid state. This is the starting point for measurements of circular polarized luminescence (CPL) after both photoelectric and electric excitation. The detection of polarized electroluminescence in organic materials has not so far been reported. An obviously very promising candidate for this is **1**.

Received: May 31, 1996 [Z 9178 IE]
German version: *Angew. Chem.* **1996**, *108*, 2233–2234

Keywords: chirality · circular dichroism · polymers

[1] a) R. L. Elsenbaumer, H. Eckardt, Z. Iqbal, J. Toth, R. H. Baughman, *Mol. Cryst. Liq. Cryst.* **1985**, *118*, 111; b) M. M. Bouman, E. E. Havinga, R. A. J. Janssen, E. W. Meijer, *ibid.* **1994**, *256*, 439; c) J. S. Moore, C. B. Gorman, R. H. Grubbs, *J. Am. Chem. Soc.* **1991**, *113*, 1704.

[2] a) T. Aoki, M. Kokai, K. Shinohara, E. Oikawa, *Chem. Lett.* **1993**, 2009; b) M. Yamaguchi, K. Omata, M. Hirama, *ibid.* **1992**, 2261.

[3] a) U. Scherf, K. Müllen, *Makromol. Chem. Rapid Commun.* **1991**, *12*, 489; b) *Adv. Polym. Sci.* **1995**, *123*, 1.

[4] U. Lemmer, S. Heun, R. F. Mahrt, U. Scherf, M. Hopmeier, U. Siegner, E. O. Göbel, K. Müllen, H. Bässler, *Chem. Phys. Lett.* **1995**, *240*, 373.

[5] J. Stampfl, W. Graupner, G. Leising, U. Scherf, *J. Lumin.* **1995**, *63*, 117.

[6] J. Grüner, H. F. Wittmann, P. J. Hamer, R. H. Friend, J. Huber, U. Scherf, K. Müllen, S. C. Moratti, A. B. Holmes, *Synth. Met.* **1994**, *67*, 181.

[7] a) M. Miyaura, T. Yanagi, A. Suzuki, *Synth. Commun.* **1981**, *11*, 513; b) A.-D. Schlüter, G. Wegner, *Acta Polymer.* **1993**, *44*, 59.

[8] **1**: ^{13}C NMR (1,1,2,2-$C_2D_2Cl_4$, 60 °C; 125 MHz): δ = 14.4, 22.9, 26.1, 29.9, 32.0, 33.2, 53.1, 69.8, 70.1, 106.4, 115.7, 121.3, 129.9, 132.3, 134.1, 137.3, 139.4, 141.7, 148.5, 149.5; C,H analysis ($(C_{60}H_{82}O_6)_n$, $n \times 899.31$): calcd: C 80.13, H 9.19; found: C 79.34, H 9.11; UV/Vis: λ_{max} (ε) = 461 nm (26400 L mol^{-1} cm^{-1}); M_n = 12200, M_w = 24000 for (+/−)-**1** (prepared from *rac*-**2**); M_n = 12300, M_w = 28000 for (+)-**1**; M_n = 12200, M_w = 24600 for (−)-**1**.

[9] A. Lüttringhaus, H. Gralheer, *Ann.* **1942**, *550*, 67.

[10] J. Huber, U. Scherf, *Macromol. Rapid Commun.* **1994**, *15*, 897.

[11] a) J. Huber, Dissertation, Universität Mainz, **1996**; b) R. Fiesel, Diplomarbeit, Universität Mainz, **1996**; c) J. Huber, R. Fiesel, U. Scherf, *Macromol. Chem. Phys.*, unpublished results.

[12] G. Hesse, R. Hagel, *Liebigs Ann. Chem.* **1976**, 996.

[13] Separation conditions: Chiradex (Merck); column dimensions: 250 × 50; particle size: 10 μm; solvent: methanol/water (50/50); flow rate: 15 mL min^{-1}; charge: 50 mg **2** in 5 mL methanol per separation run; using automated separation, 1–2 g **2** can be separated per day [11].

[14] (+)-**7** has the absolute configuration p(*R*) [11]. As only part of **2** is racemized during the conversion from **7**, it must be concluded that (−)-**2** and (+)-**2** have the configurations p(*R*) and p(*S*), respectively.

[15] From p(*R*)-(+)-**7**, p(*R*)-(−)-**2** is formed in the monomer synthesis, and (+)-**1** is formed from this by polycondensation and a polymer-analogous cyclization.

[16] The molar optical rotation of (+)-**1** is 594 rad cm^2 damol^{-1}.

[17] B. M. V. Langenveld-Voss, R. A. J. Janssen, M. P. T. Christiaans, S. C. J. Meskers, H. P. J. M. Dekkers, E. W. Meijer, *J. Am. Chem. Soc.* **1996**, *118*, 4908.

[18] C. Nuckolls, T. J. Katz, L. Castellanos, *J. Am. Chem. Soc.* **1996**, *118*, 3767.

[19] Here we concentrate on the determination of the configuration of the new stereogenic centers of the methylene bridges (ArCHRAr'); a diastereoselective ring closure process to give an all-*trans* configuration of R relative to the cyclophane bridges could offer a plausible approach to the elucidation of the chiroptical activity.

[20] The PL quantum yields of known LPPPs, depending on the substitution pattern of the peripheral solubilizing side groups, are 65–80% (in solution, dichloromethane) and 10–25% (in the solid state [film]) [5]. The PL quantum yield of **1** is currently being determined.

Synergy between Magnetic Interaction and Spin Crossover in an Iron(III) Complex with an Organic Radical as Ligand

Jean-Pascal Sutter, Mohammed Fettouhi, Licun Li, Cécile Michaut, Lahcène Ouahab,* and Olivier Kahn*

Molecular magnetism is a novel and very active field of research that deals with the chemical and physical properties of molecular assemblies with open-shell units.[1] Two of the most important phenomena in molecular magnetism are the magnetic interaction between two spin carriers and spin crossover. We have been studying these two phenomena from both experimental and theoretical viewpoints for a few years. Here we report on the first compound in which the two phenomena occur in a synergistic way. This compound is bis(*cis*-1,2-dicyano-1,2-ethylenedithiolato)[2-(*para*-*N*-methylpyridinium)-4,4,5,5-tetramethylimidazoline-1-oxyl]iron(III) (**1**), abbreviated hereafter as [(rad)Fe(mnt)$_2$], in which rad$^+$ stands for 2-(*para*-*N*-methylpyridinium)-4,4,5,5-tetramethylimidazoline-1-oxyl, and mnt^{2-} for *cis*-1,2-dicyano-1,2-ethylenedithiolato.

Compound **1** was prepared by reacting the iodide **3** with sodium bis(*cis*-1,2-dicyano-1,2-ethylenedithiolato)iron(III) (Scheme 1).

The molecular structure of **1** is shown in Figure 1.[2, 3] The rad$^+$ unit is linked to the iron atom of [Fe(mnt)$_2$]$^-$ through the oxygen atom of the nitroxide group. The iron atom adopts square-pyramidal coordination, as observed for all the other five-coordinate bis(dithiolene) complexes;[4–9] the oxygen atom of rad$^+$ occupies the apical position. The Fe–S bond lengths are in the range 2.235(2)–2.250(2) Å, and the Fe–O bond length is 2.056(5) Å. The Fe-O1-N5 angle around the nitroxide group is 119.7(3)°. The iron atom is pulled out of the S_4 mean plane toward the apical position by Δ = 0.427(1) Å; this

[*] Dr. L. Ouahab, Dr. M. Fettouhi, Dr. C. Michaut
Laboratoire de Chimie du Solide et Inorganique
Moléculaire, URA CNRS no 1495
Université de Rennes 1, F-35042 Rennes (France)
Fax: Int. code +99383487
e-mail: ouahab@univ-rennes1.fr
Prof. O. Kahn, Dr. J. P. Sutter, L. Li
Laboratoire des Sciences Moléculaires
Institut de Chimie de la Matière Condensée de Bordeaux
UPR CNRS no 9048, F-33608 Pessac (France)
Fax: Int. code +56842649
e-mail: kahn@icmcb.u-bordeaux.fr

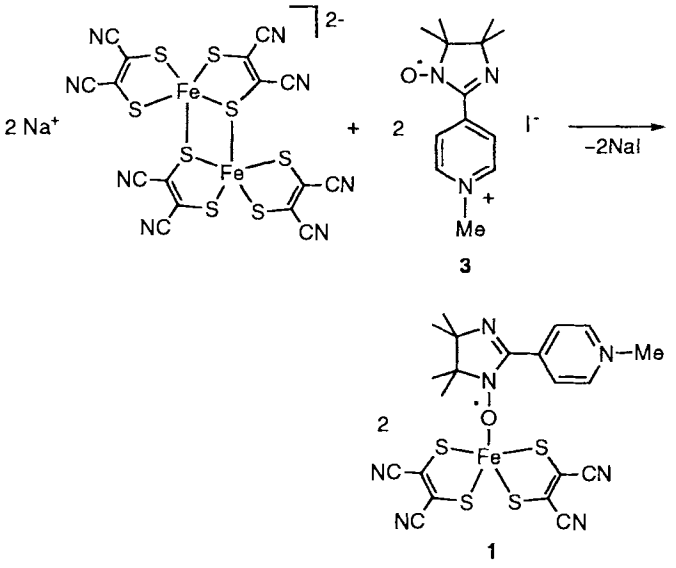

Scheme 1.

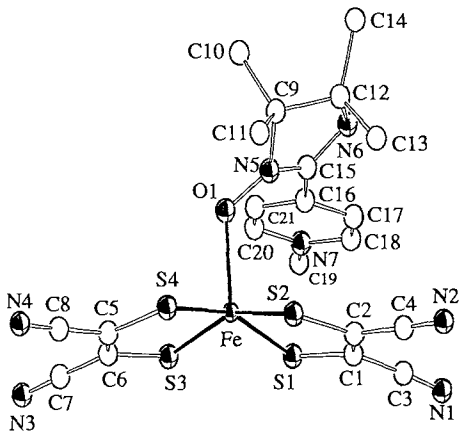

Fig. 1. Molecular structure of **1**.

value is close to that in the five-coordinate (S_4O) anionic species $\{Ph_3POFe[S_2C_2(CF_3)_2]_2\}^-$ with Fe–O = 1.957 Å and Δ = 0.434 Å.[8] The O1-N5-C15-N6 mean plane of the imino-nitroxide group makes dihedral angles of 43.6(5)° with the Fe-S1-S2-C1-C2 mean plane, and 36.7(6)° with the pyridine ring. Within the crystal lattice, the molecules are arranged in such a way that the $[Fe(mnt)]^-$ moieties are face-to-face and the rad^+ moieties are side-to-side, thus leading to the formation of columns (Fig. 2). The shortest intermolecular Fe···Fe and Fe···S separations are 5.000(2) and 4.524(4) Å, respectively, and the shortest O···O and O···N intermolecular separations between the imino-nitroxide groups are 4.703(6) and 5.357(6) Å, respectively. All the intermolecular contacts are large, thus the [(rad)-$Fe(mnt)_2$] units can be considered as being magnetically isolated within the crystal lattice.

The magnetic properties of **1** warrant a thorough investigation. The temperature dependence of both the product $\chi_m T$ and the molar magnetic susceptibility χ_m are represented in Figure 3. $\chi_m T$ is 2.33 $cm^3 K mol^{-1}$ at room temperature and remains essentially constant as the temperature is lowered to about 100 K, then decreases more and more rapidly as the temperature is lowered further, and eventually tends to zero as T approaches absolute zero. As for the magnetic susceptibility, χ_m shows a well-pronounced rounded maximum at T = 9.5 K.

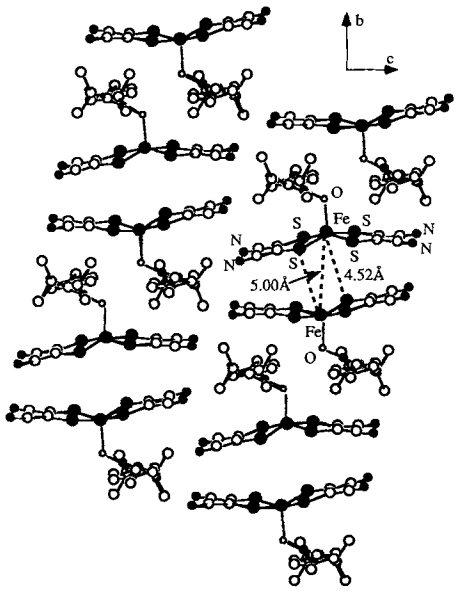

Fig. 2. Crystal structure of **1** showing the face-to-face $[Fe(mnt)]^-$ columns.

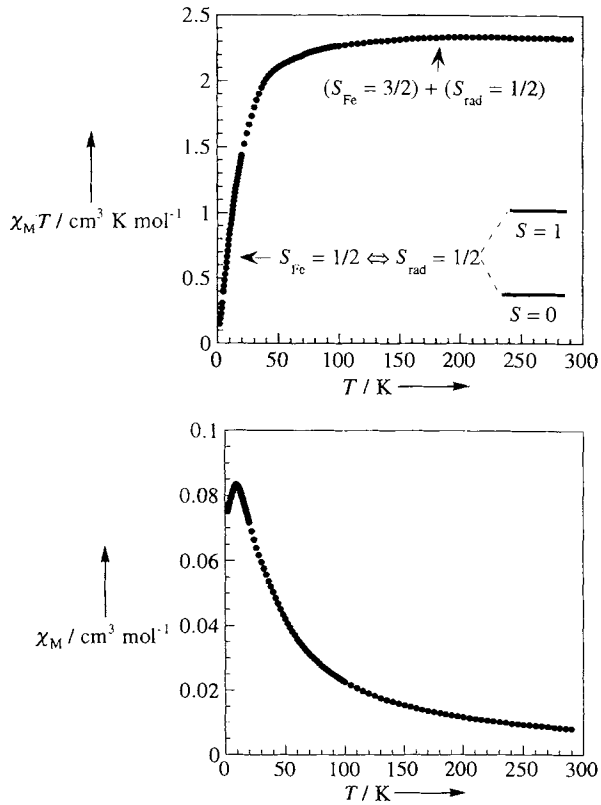

Fig. 3. Temperature dependence of $\chi_m T$ (top) and χ_m (bottom) for **1**. The applied magnetic field was 2 kOe.

To interpret these magnetic data, we will initially consider the range 100 K < T < 300 K, and then that with T < 100 K. In the high-temperature range, the magnetic susceptibility closely follows the Curie law ($\chi_m T$ = constant), which means that either the thermal energy kT is much larger than any interaction parameter between the rad^+ and $[Fe(mnt)_2]^-$ moieties, or only one molecular state is thermally populated in this temperature range. This latter hypothesis can be ruled out. Indeed, all the possible molecular states have an integer spin, and none of them

 © VCH Verlagsgesellschaft mbH, D-69451 Weinheim, 1996 0570-0833/96/3518-2114 $ 15.00+.25/0

can lead to a $\chi_m T$ value of 2.33 $cm^3 K mol$. This $\chi_m T$ value is therefore the sum of the two contributions arising from each of the moieties. The rad^+ moiety carries a spin $S_{rad} = 1/2$, and its contribution to the $\chi_m T$ value is 0.38 $cm^3 K mol^{-1}$;[1] thus, the contribution of $[Fe(mnt)_2]^-$ is 1.95 $cm^3 K mol^{-1}$, which exactly corresponds to what is expected for a spin quartet state, $S_{Fe} = 3/2$. In summary, the magnetic properties of the compound at high temperature correspond to the superposition of $S_{rad} = 1/2$ and $S_{Fe} = 3/2$ local states. The magnetic interaction between these two local states, which gives rise to $S = 1$ and $S = 2$ molecular states, is too small to be detectable in this temperature range.

Let us now consider the low-temperature range. The maximum in the χ_m versus T plot together with the low-temperature limit of $\chi_m T$ unambiguously indicates that the ground state of **1** is a spin singlet, $S = 0$. This nonmagnetic state can only arise from an antiferromagnetic interaction between $S_{rad} = 1/2$ and $S_{Fe} = 1/2$ local states. In other words, at low temperature the local ground state of the $[Fe(mnt)_2]^-$ moiety is a spin doublet, and not a spin quartet anymore. This moiety exhibits a spin crossover between $S_{Fe} = 3/2$ and $S_{Fe} = 1/2$ states. This very unusual magnetic behavior is shown schematically in the plot of $\chi_m T$ versus T in Figure 3.

One of the problems at hand concerning **1** is to see whether it is possible to simulate its magnetic properties. If the intermolecular interactions are neglected, the molar fraction of Fe^{III} ions in the $S_{Fe} = 3/2$ local state, $x_{S = 3/2}$, may be written according to Equation (a),[1] in which ΔH is the change in enthalpy between

$$x_{S = 3/2} = \frac{1}{1 + \exp\left[\frac{\Delta H}{R}\left(\frac{1}{T} - \frac{1}{T_{1/2}}\right)\right]} \quad (a)$$

the $S_{Fe} = 3/2$ and $S_{Fe} = 1/2$ local states, R the gas constant, and $T_{1/2}$ the inversion temperature for which $x_{S = 3/2} = 0.5$. The molar magnetic susceptibility may then be expressed according to Equation (b), in which $\chi[S_{Fe} = 1/2]$ and $\chi[S_{Fe} = 3/2]$ are the

$$\chi_M = (1 - x_{S = 3/2})\chi[S_{Fe} = 1/2] + x_{S = 3/2}\chi[S_{Fe} = 3/2] \quad (b)$$

molar magnetic susceptibilities for **1** when the Fe^{III} ion is in the $S_{Fe} = 1/2$ and $S_{Fe} = 3/2$ local state, respectively. It follows that χ_m may be according to Equation (c),[1] in which g is an average

$$\chi_M = \frac{2N\beta^2 g^2}{kT}\left\{\frac{(1 - x_{S = 3/2})}{3 + \exp(-J_{1/2}/kT)} + \frac{x_{S = 3/2}[1 + 5\exp(2J_{3/2}/kT)]}{3 + 5\exp(2J_{3/2}/kT)}\right\} \quad (c)$$

value of the Zeeman factor for all the spin carriers, and $J_{1/2}$ and $J_{3/2}$ are the rad-Fe interaction parameters when the Fe^{III} ion is in the $S_{Fe} = 1/2$ and $S_{Fe} = 3/2$ local state, respectively (the Hamiltonian operators for the interactions are defined as $-J_{1/2}\boldsymbol{S}_{rad}\cdot\boldsymbol{S}_{Fe(S = 1/2)}$ and $-J_{3/2}\boldsymbol{S}_{rad}\cdot\boldsymbol{S}_{Fe(S = 3/2)}$, respectively). Expressions such as Equations (a) and (c) can perfectly reproduce the experimental susceptibility data. However, the number of parameters involved in the model is too large to allow an unambiguous determination of their values. In any case, both the $J_{1/2}$ and $J_{3/2}$ interaction parameters are found to be rather small; $J_{1/2}$ is of the order of $-15\ cm^{-1}$. These small values may be easily rationalized in terms of orbital interactions between the $[Fe(mnt)_2]^-$ and rad^+ moieties. For instance, in the low-spin $S_{Fe} = 1/2$ local state, the unpaired electron arising from the Fe^{III} ion occupies a yz- or zx-type orbital; the z axis is colinear with the apical Fe–O direction. The overlap density between such an orbital and the singly occupied π^* orbital of the radical cation is certainly very weak in any point of space.[1]

As expected, the X-band powder EPR spectrum is strongly temperature dependent. At 9.5 K, which is the temperature of the maximum of the susceptibility, the spectrum is characteristic of a triplet state with a zero-field splitting parameter D smaller than the incident radiation. D was found to be approximately 0.15 cm^{-1}.[10] This spectrum also shows well-pronounced half-field transitions. The intensity of the triplet state signal decreases as T drops below 9.5 K.

The occurrence of an $S_{Fe} = 3/2$ intermediate spin ground state for square-pyramidal Fe^{III} species is well documented. Such a situation, for instance, has been found in halogenobis(diethyldithiocarbamato)iron(III) compounds, in which a $\chi_m T$ value of 1.90 $cm^3 K mol^{-1}$ has been determined down to 10 K.[11–14] In other respects, spin doublet–spin quartet crossovers have already been observed for a few five-coordinate iron(III) complexes, for instance for [Fe(salen)(NO)] (salen = *N*,*N*′-ethylenebis(salicylideneiminato)[15, 16] and [Fe(tmc)(NO)](BF_4) (tmc = 1,4,8,11-tetramethyl-1,4,8,11-tetraazacyclotetradecane).[17] Finally, recently a large number of metal–radical compounds have been found to exhibit ferro- or antiferromagnetic intramolecular interactions.[18–20] What is entirely novel as far as [(rad)Fe(mnt)$_2$] is concerned, is that three facets of molecular magnetism, namely intermediate spin state, spin crossover, and magnetic interaction, occur simultaneously within a single compound.

Experimental Procedure

3: A solution of 2-(*para*-pyridyl)-4,4,5,5-tetramethylimidazoline-1-oxyl-3-oxide [21] (3.51 g, 15 mmol) in CH_2Cl_2 (15 mL) was added to a suspension of $NaNO_2$ (2.62 g, 38 mmol) in CH_2Cl_2 (70 mL) and CH_3COOH (8.6 mL, 150 mmol). The reaction mixture was heated to reflux for 5 min to give a bright orange solution. After filtration and neutralization with aqueous $NaHCO_3$, the organic layer was washed with water, and the aqueous phase extracted with CH_2Cl_2 (20 mL). The combined organic phase was dried over Na_2SO_4. The solution was concentrated and chromatographed over a short alumina column. Elution with a solution of CH_2Cl_2/acetone (85/15 in volume) afforded an orange fraction. The solvent was removed in vacuo and addition of hexane (10 mL) to the residue afforded the neutral 2-(*para*-pyridyl)imino-nitroxide **2** as a crystalline solid (2.20 g, 67%). IR(KBr): $\tilde{\nu}[cm^{-1}]$ = 2979, 1594, 1534, 1453, 1279, 1198, 836, 658. The quaternarization was achieved by heating a solution of **2** (2.20 g, 10 mmol) and MeI (3.8 mL, 60 mmol) in THF (25 mL) to 45 °C for 3 h. After the mixture had been cooled, the deep red suspension was filtered, the solid washed with Et_2O, and dried in vacuo to yield **3** (2.57 g, 71%) as a crystalline red solid. Anal. calcd for $C_{13}H_{19}N_3OI$: C 43.35, H 5.32, N 11.66, O 4.44; found: C 43.36, H 5.37, N 11.56, O 4.90. IR(KBr): $\nu[cm^{-1}]$ = 2980, 1644, 1546, 1458, 1278, 1190, 850, 649.

1: A suspension of **3** (75.6 mg, 0.21 mmol) in THF (8 mL) was added dropwise to a solution of Na[Fe(mnt)$_2$] [22] (71.8 mg, 0.2 mmol) in THF (8 mL). The resulting mixture was stirred at room temperature for 30 min. After filtration, Et_2O (20 mL) was slowly added. The precipitate was collected by filtration, washed with water and Et_2O, and dried in vacuo to yield **1** (35 mg, 31%) as a brown solid. Anal. calcd for $C_{21}H_{19}N_7OS_4Fe$: C 44.29, H 3.36, N 17.22, S 22.52, Fe 9.81; found: C 45.0, H 3.62, N 16.28, S 22.46, Fe 8.88. IR(KBr): $\tilde{\nu}[cm^{-1}]$ = 3247, 2976, 2203, 1637, 1490, 1148, 1108.

Surprisingly, the best-shaped single crystals of **1** were obtained in a very low yield by reaction of Na[Fe(mnt)$_2$] with 2-(*para*-*N*-Me-pyridinium)-4,4,5,5-tetramethylimidazoline-1-oxyl-3-oxide in ethanol. During this reaction, a very small amount of the nitronyl-nitroxide radical cation is reduced to the imino-nitroxide radical cation.

Received: March 11, 1996 [Z8912IE]
German version: *Angew. Chem.* **1996**, *108*, 2250–2253

Keywords: iron compounds · magnetic properties · radical cations · spin crossover

 © VCH Verlagsgesellschaft mbH, D-69451 Weinheim, 1996 0570-0833/96/3518-2115 $ 15.00+.25/0

[1] O. Kahn, *Molecular Magnetism*, VCH, New York, **1993**.
[2] Crystal data for **1**, $M_r = 569.54$, space group $P\bar{1}$, $a = 9.290(2)$, $b = 11.922(3)$, $c = 12.360(2)$ Å, $\alpha = 73.95(2)$, $\beta = 84.69(2)$, $\gamma = 71.64(2)^\circ$, $V = 1248.5(5)$ Å^3, $Z = 2$, $\mu(Mo_{K\alpha}) = 9.52$ cm^{-1}, $T = 293$ K, 5210 data collected on an Enraf-Nonius CAD4 diffractometer equipped with a graphite-monochromated $Mo_{K\alpha}$ ($\lambda = 0.71073$ Å) radiation, 4574 independent reflections and 1733 observed with $I > 6\sigma(I)$ were considered, $R = 0.035$ and $R_w = 0.047$. The structure was solved by direct methods and successive Fourier difference synthesis. The refinements (on F) were performed by the full-matrix least squares method [H atoms placed at computed positions were not refined]. All the calculations were performed on a MicroVAX 3100 with the Molen programs [9]. Crystallographic data (excluding structure factors) for the structure(s) reported in this paper have been deposited with the Cambridge Crystallographic Data Centre as supplementary publication no. CCDC-179-72. Copies of the data can be obtained free of charge on application to The Director, CCDC, 12 Union Road, Cambridge CB2 1EZ, UK (fax: Int. code +(1223) 336-033; e-mail: teched@chemcrys.cam.ac.uk).
[3] Crystal Structure Analysis, Molecular Enraf-Nonius (MolEN)1990, Delft Instruments, The Netherlands.
[4] R. Williams, E. Billing, J. H. Waters, H. B. Gray, *J. Am. Chem. Soc.* **1966**, *88*, 43.
[5] N. Schrauzer, R. P. Mayweg, H. W. Finck, W. J. Heinrich, *J. Am. Chem. Soc.* **1966**, *88*, 4604.
[6] N. G. Connelly, J. A. McCleverty, C. J. Winscom, *Nature*, **1967**, *216*, 999;
[7] A. L. Balch, *Inorg. Chem.*, **1967**, *6*, 2158.
[8] E. F. Epstein, I. Bernal, A. L. Balch, *Chem. Commun*, **1970**, 136.
[9] G. B. Carpenter, G. S. Clark, A. L. Rieger, D. A. Sweigart, *J. Chem. Soc. Dalton Trans.* **1994**, 2903.
[10] E. Wasserman, L. C. Snyder, W. A. Yager, *J. Chem. Phys.* **1964**, *41*, 1763.
[11] B. F. Hoskins, R. L. Martin, A. H. White *Nature (London)* **1966**, *211*, 627.
[12] G. E. Chapps, S. W. McCann, H. H. Wickman, R. C. Sherwood, *J. Chem. Phys.* **1974**, *60*, 990.
[13] P. Ganguli, R. Marathe, S. Mitra, *Inorg. Chem.* **1975**, *14*, 970.
[14] H. H. Wickman, *J. Chem. Phys.* **1972**, *56*, 976.
[15] K. J. Haller, P. L. Johnson, R. D. Feltham, J. H. Enemark, J. R. Ferraro, L. J. Basile, *Inorg. Chim. Acta* **1979**, *33*, 119.
[16] F. V. Wells, S. W. McCann, H. H. Wickman, S. L. Kessel, D. N. Hendrickson, R. D. Feltham, *Inorg. Chem.* **1982**, *21*, 2306.
[17] K. D. Hodges, R. G. Wollmann, S. L. Kessel, D. N. Hendrickson, D. G. Van Derveer, E. K. Barefield, *J. Am. Chem. Soc.* **1979**, *101*, 906.
[18] Y. Pei, A. Lang, P. Bergerat, O. Kahn, M. Fettouhi, L. Ouahab, *Inorg. Chem.* **1996**, *35*, 193.
[19] D. Gatteschi, *Adv. Mater.* **1994**, *6*, 635.
[20] A. Caneschi, D. Gatteschi, R. Sessoli, P. Rey, *Acc. Chem. Res.* **1989**, *22*, 392.
[21] E. F. Ullman, J. H. Osiecki, D. G. B. Boocock, R. Darey, *J. Am. Chem. Soc.* **1972**, *94*, 7049.
[22] A. Davison, H. R. Holm, *Inorg. Synth.* **1967**, *10*, 8.

Proton-Controlled Switching of Luminescence in Lanthanide Complexes in Aqueous Solution: pH Sensors Based on Long-Lived Emission**

A. Prasanna de Silva,* H. Q. Nimal Gunaratne, and Terence E. Rice

Luminescent lanthanide complexes[1] are finding increasing use as labels for immunoassays in clinical diagnostic procedures.[2] One reason for this success is the length of their luminescence lifetimes (ms range), which permits easy temporal resolution from the short-lived (ns range) fluorescence background commonly present in biological systems. Now we show how lanthanide f–f luminescence can be exploited for the design of sensors that preserve the special features found in luminescent labels.

We[3] and others[4] have developed "fluorophore–spacer–receptor" systems which operate as ion sensors by ion-induced suppression of Photoinduced Electron Transfer (PET) from the receptor to the fluorophore. So it was a direct, logical progression to replace the organic fluorophore with a luminescent lanthanide complex. The terpyridyl derivative **4**[1r, 2f] is particularly suitable as a ligand since, besides its straightforward synthesis and its near-ultraviolet absorption, it should have a relatively electron-deficient π-system when complexed to lanthanide ions. We first modified **4** by introducing simple amino groups in the side chains, which should serve as both proton receptors and electron donors in the PET process. Of course, the PET sensor principle can be applied to many other analytes besides protons.[3, 4]

Compound **1** was converted to the desired ligand **3** according to Scheme 1. The changes in the UV absorbance A of **3** on addition of lanthanide salts were analyzed according to Equation (a)[3] to yield the binding constants β, which are listed in

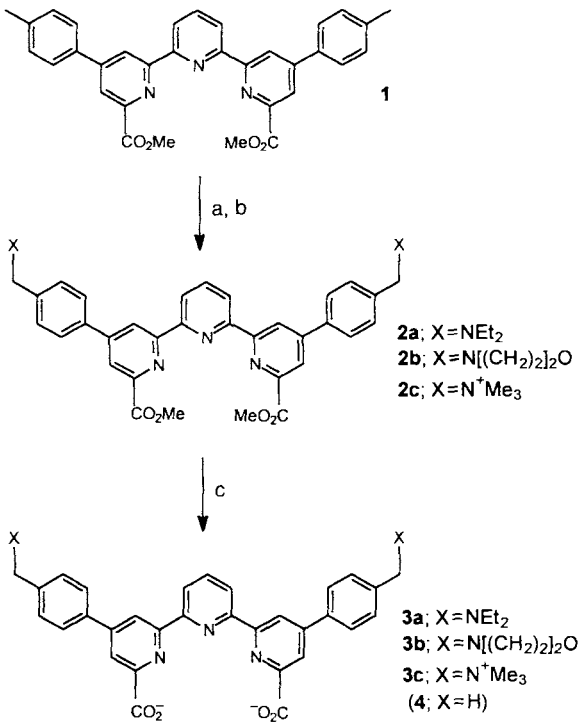

Scheme 1. Reagents: a) *N*-Bromosuccinimide, dichloromethane; b) Et_2NH, $HN[(CH_2)_2]_2O$, or Me_3N; c) KOH. The structures are drawn in the metal-complexing conformation even though in the conformation of the free ligand the pyridyl dipoles are opposite to each other [13].

$$\lg[(A - A_{min})/(A_{max} - A)] = \lg[(Ln^+)_{total} - (\mathbf{3})_{total}(A - A_{min})/(A_{max} - A)] + \lg\beta \quad (a)$$

Table 1. Given the magnitude of β (roughly 10^6 at pH 6.0), mixtures of ligand **3** and lanthanide salt in hundredfold excess were used to generate the complex **3**·Ln in situ. pH Titrations of these sensor solutions resulted in small but measurable changes in the UV absorption spectra, which yielded pK_a values for the side chain amino groups (Table 1) after analysis with Equation (b).[5] Dramatic changes were found in the delayed

$$\lg[(A_{max} - A)/(A - A_{min})] = \mp pH \pm pK_a \quad (b)$$

[*] Dr. A. P. de Silva, Dr. H. Q. N. Gunaratne, T. E. Rice
School of Chemistry, Queen's University
Belfast BT9 5AG (UK)
Fax: Int. code +(1232)382117

[**] We thank SERC/EPSRC (UK) and the Department of Education in Northern Ireland for support.

Table 1. Optical and ion-coordination parameters of lanthanide complexes of **3a**–**c** [a, b].

	3a·Tb	**3a**·Eu	**3b**·Tb	**3b**·Eu	**3c**·Tb	**3c**·Eu
$\lg\beta$ [c]	5.8	5.8	6.2	6.2	5.8	6.2
pK_a [d]	7.2	7.6	5.3	5.5	-	-
ϕ_{Lum}(acid) [e]	0.49	0.1	0.51	0.1	0.52	0.11
ϕ_{Lum}(base) [e]	0.03	0.06	0.05	0.08	0.46	0.11
LE [f]	16	1.5	10	1.3	1.1	1
pK'_a [g]	6.8	7.5	4.9	5.8	n.a.	n.a.
τ_{Lum}/ms(acid) [h]	0.62	0.25	0.65	0.25	0.64	0.26
q [i]	4.2	3.7	4.2	3.7	4.2	3.8

[a] 10^{-6} M **3a**–**c**·Ln in aerated H_2O at 22.0 °C. Lanthanide salts were used as chlorides. All of the complexes **3a**–**c**·Tb and **3a**–**c**·Eu have essentially identical UV absorption spectra with λ_{Abs} ($\lg\varepsilon$) values of 285 nm (4.74), 335 nm (4.43), and 345 nm (4.44) at pH 6.0 (ε in units of $M^{-1}cm^{-1}$). The free ligands **3a**–**c** also have essentially identical UV absorption spectra with λ_{Abs} ($\lg\varepsilon$) values of 245 nm (4.81), 272 nm (sh) (4.65), and 330 nm (sh) (3.9). Luminescence measured with a delay time of 0.1 and 0.1 ms; gate time of 0.5 and 1.5 ms for the Tb and Eu complexes, respectively. Under our conditions, the principal emission of **3a**–**c**·Eu is at 617 nm (due to the $^5D_0 \rightarrow {}^7F_2$ transition), whereas **3a**–**c**·Tb shows emission mainly at 544 nm and also at 493 nm (due to the $^5D_4 \rightarrow {}^7F_5$ and $^5D_4 \rightarrow {}^7F_6$ transitions, respectively). Corrected excitation spectra obtained during the recording of these principal emissions are very similar in shape to the corresponding absorption spectra in all cases. Due to the hydration number (q) of ca. 4, it is not surprising that hydrolytic effects at or near the metal center predominate at pH > 8. This results in luminescence decreases in both Tb and Eu systems as the pH is increased, except that the Eu cases show an increase at intermediate stages. Therefore our studies were restricted to the pH range 3 to 8. Deaeration caused 4–10% increases in the luminescence intensity of **3a**–**c**·Tb, whereas **3a**–**c**·Eu showed <2% change. Preliminary analysis of the temperature dependence of luminescence intensity[14] for **3a**–**c**·Tb yielded activation energies of 2–8 kcal mol^{-1}. The luminescence of **3a**–**c**·Eu showed virtually no temperature effect. [b] Spectral data for ligands **2a**–**c** will be presented in a full paper. [c] Obtained by analyzing the UV spectral changes seen during Eu^{3+} and Tb^{3+} variation with Equation (a) (pH 6.0). However it must be noted that the behavior is nonideal, as may be expected in such highly charged systems[15]. [d] Obtained by analyzing the small but measurable changes in the UV absorption spectra of **3**·Ln during pH variation according to Equation (b). The protonation of the two amino groups cannot be distinguished. The pK_a values have an uncertainty of ±0.2 pH units. These pK_a values are expected to be in close agreement with the pK'_a values[3]. [e] Obtained by comparison of corrected luminescence emission spectra with that of **4**·Eu[1r, 2f] and the ternary Tb complex with EDTA and sulfosalicylic acid[16] for the Eu and Tb cases, respectively. [f] Luminescence enhancement factor induced by protons = ϕ_{Lum}(acid)/ϕ_{Lum}(base). [g] Obtained by analyzing luminescence quantum yield (ϕ_{Lum}) vs pH profiles (Fig. 2), according to Equation (c). The pK'_a value corresponds to the protonation of the second amino group following the first, since both amines must be blocked before luminescence can be recovered[15]. However the corresponding pK'_a values do not differ by very much since the two amino groups behave nearly independently[17]. This is not unexpected owing to their large spatial separation and the 1,3 connections of the intervening aromatic rings. The pK'_a values have an uncertainty of ±0.1 pH units. [h] Determined by analyzing the luminescence intensity (I_t) vs delay time (τ) profile according to the equation $2.3\lg(I_t/I_{t,0}) = -\tau/\tau_{Lum}$[10]. [i] Hydration number obtained from the equation $(1/\tau_{Lum;H_2O}) - (1/\tau_{Lum;D_2O}) = (q/A)$ [18], where A is 4.2 and 1.05 for Tb and Eu, respectively.

luminescence spectra of **3a**·Tb and **3b**·Tb during pH titration (Fig. 1). These complexes show proton-induced luminescence enhancement factors (LE) of 16 and 10, respectively, without

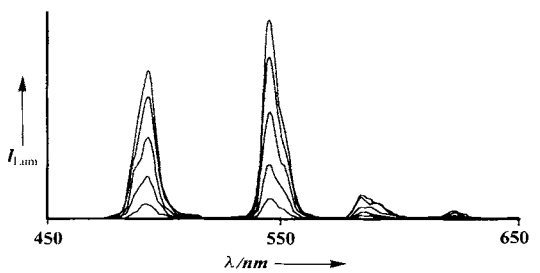

Fig. 1. Uncorrected delayed luminescence spectra of sensor **3b**·Tb as a function of pH. The pH values are (in order of decreasing intensity) 3.2, 4.4, 5.0, 5.6, 6.5.

any shift in the wavelengths of the emission bands or in their relative heights.

$$\lg[(\phi_{Lum;max} - \phi_{Lum})/(\phi_{Lum} - \phi_{Lum;min})] = pH - pK'_a \quad (c)$$

These delayed luminescence measurements completely reject intrinsic fluorescence. We note that ϕ_{Lum} vs. pH profiles (Fig. 2)

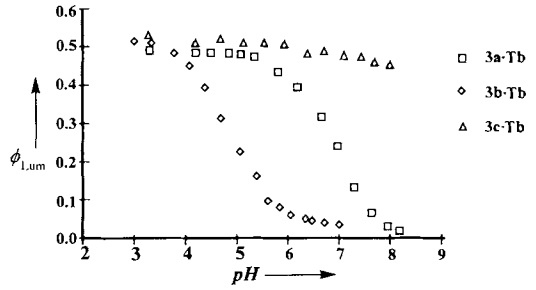

Fig. 2. Luminescence quantum yield ϕ_{Lum} versus pH for sensors **3a**·Tb, **3b**·Tb, and model compound **3c**·Tb.

are dictated by the nature of the side chain X as expected, with **3c**·Tb showing essentially pH-independent luminescence over the pH range 3–8. This also rules out any collapse of the sensor complex by hydrolysis over the pH range 3–8, since hydrolysis would remove the sensitizer/antenna effect of the ligand and extinguish the terbium luminescence. Protonation of the ligating atoms and subsequent dissociation of the complexes can also lead to pH dependence of luminescence,[1n] but this is not suitable for use in a unimolecular sensor.

Interestingly, the complexes **3a**·Eu and **3b**·Eu participate only weakly in PET processes despite the fact that aqua and edta complexes (edta = ethylenediaminetetraacetate) of Eu^{3+} are more easily reduced than those of Tb^{3+}.[6] On the other hand, because luminescence lifetimes τ_{Lum} of **3**·Eu are shorter than those of their Tb counterparts, the efficiency of the PET activity would be expected to be reduced. A further consideration is that the PET process can potentially intervene before the transfer of energy from the ligand excited state (singlet or triplet) to the lanthanide ion. This is important since previous PET sensors concern PET to or from singlet excited states of relatively high energy and nanosecond lifetime.[3, 4] In the present cases, the ligand π-electron system is spatially closer than the lanthanide ion to the electron-donating amino group in the side chain,[7] though the role of the intervening π-systems in controlling the PET rate must also be considered.[8] The π-systems in the Tb complexes appear to be marginally more electron-deficient than in **3a**·Eu and **3b**·Eu under our conditions, as judged by the relative pK'_a or pK_a values of the side chain amino groups. This should encourage more efficient PET to the π-system in **3a**·Tb and **3b**·Tb. Perhaps the most important clues to the different behavior of the Tb and Eu complexes lie in the fact that **3**·Tb shows a) a small but measurable luminescence quenching with oxygen and b) a small but measurable decrease of luminescence at increasing temperatures. The effects of oxygen and temperature on the luminescence of **3**·Eu are both negligible. Several Tb complexes are known to display more drastic examples of such effects,[1b–d] due to the equilibration of the Tb $^5D_4$ state with a ligand-centered ππ* triplet state of slightly higher energy. This situation is clearly present in **3**·Tb though to a relatively small extent (which is fortunate for the application of **3a**·Tb and **3b**·Tb as pH sensors). Thus the ligand-centered triplet state in

3·Tb would be expected to have a longer lifetime than 3·Eu. Conceptually related situations are found in E-type delayed fluorescence, for example.[9] Of course PET processes from the side chain amino group would be much more efficient when such longer lived excited states are involved.

In conclusion, we have demonstrated the pH sensing action of 3·Tb by means of its delayed luminescence. We have also developed "message in a bottle" systems which exploit room-temperature phosphorescence of all-organic π-electron systems for ion sensing.[10] These are complementary to lanthanide complexes reported here. Taken together, these sensors, which exploit relatively long-lived luminescence in the millisecond domain, should have significant potential for real-time (> ms) ion monitoring in intrinsically fluorescent environments. The relatively long emission lifetimes should also permit easy analysis of luminescence decays, which can allow ion sensing without any complications from variations in optical path, sensor concentration, and quenchers in these microenvironments.[11] A further interesting aspect of selectivity in the design of supramolecular systems like 3·Tb involves the use of a terpyridyl receptor for Tb^{3+} ions, which serves as the antenna–lumophore combination, whereas the side chain amino groups serve as receptors for the proton analyte.[12]

Received: December 19, 1995
Revised version: May 28, 1996 [Z8668IE]
German version: *Angew. Chem.* **1996**, *108*, 2253–2255

Keywords: electron transfer · lanthanides · luminescence · sensors

[1] Leading references: a) N. Sabbatini, M. Guardigli, I. Manet, R. Ungaro, A. Casnati, R. Ziessel, G. Ulrich, Z. Asfari, J.-M. Lehn, *Pure Appl. Chem.* **1995**, *67*, 135; b) N. Sabbatini, M. Guardigli, F. Bolletta, I. Manet, R. Ziessel, *Angew. Chem.* **1994**, *106*, 1543; *Angew. Chem. Int. Ed. Engl.* **1994**, *33*, 1501; c) N. Sabbatini, M. Guardigli, I. Manet, F. Bolletta, R. Ziessel, *Inorg. Chem.* **1994**, *33*, 955; d) N. Sabbatini, M. Guardigli, J.-M. Lehn, *Coord. Chem. Rev.* **1993**, *123*, 201; e) S. T. Frey, M. L. Gong, W. deW. Horrocks, *Inorg. Chem.* **1994**, *33*, 3229; f) V.-M. Mukkala, J. J. Kankare, *Helv. Chim. Acta* **1992**, *75*, 1579; g) M. Pietraszkiewicz, J. Karpiuk, A. K. Rout, *Pure Appl. Chem.* **1993**, *65*, 563; h) N. Sato, M. Goto, S. Matsumoto, S. Shinkai, *Tetrahedron Lett.* **1993**, *34*, 4847; i) N. Sato, S. Shinkai, *J. Chem. Soc. Perkin Trans. 2* **1993**, 621; j) M. J. Remuinan, H. Roman, M. T. Alonso, J. C. Rodriguez-Ubis, *ibid.* **1993**, 1099; k) M. Murru, D. Parker, G. Williams, A. Beeby, *J. Chem. Soc. Chem. Commun.* **1993**, 1116; l) J. Coates, P. G. Sammes, R. M. West, *ibid.* **1994**, 1107; m) J. Coates, P. G. Sammes, G. Yahioglu, R. M. West, A. J. Garman, *ibid.* **1994**, 2311; n) P. G. Sammes, G. Yahioglu, G. D. Yearwood, *ibid.* **1992**, 1282; o) H. Hoshino, S. Utsumi, T. Yotsuyanagi, *Talanta* **1994**, *41*, 93; p) A. K. Saha, K. Kross, E. D. Kloszewski, D. A. Upson, J. L. Toner, R. A. Snow, C. D. V. Black, V. D. Desai, *J. Am. Chem. Soc.* **1993**, *115*, 11032; q) C. Piguet, A. F. Williams, G. Bernardinelli, J.-C. G. Bunzli, *Inorg. Chem.* **1993**, *32*, 4139; r) J. L. Toner (Eastman Kodak). USP **1989**, 4837169; s) M. Sowinska, M.-T. Le Bris, B. Valeur, *J. Photochem. Photobiol. A* **1991**, *60*, 383.

[2] a) V. Balzani, F. Scandola, *Supramolecular Photochemistry*, Ellis-Horwood, Chichester, **1990**; b) J.-M. Lehn, *Supramolecular Chemistry*, VCH, Weinheim, **1995**; c) A. Mayer, S. Neuenhofer, *Angew. Chem.* **1994**, *106*, 1097; *Angew. Chem. Int. Ed. Engl.* **1994**, *33*, 1044; d) J.-C. G. Bunzli in *Lanthanide Probes in Life, Chemical and Earth Sciences* (Eds.: J.-C. G. Bunzli, G. R. Choppin), Elsevier, Amsterdam, **1989**, Chapter 7; e) I. Hemmila, *Clin. Chem.* **1985**, *31*, 359; f) J. L. Toner in *Inclusion Phenomena and Molecular Recognition* (Ed.: J. L. Atwood), Plenum, New York, **1990**, p. 185; g) I. Hemmila, *Applications of Fluorescence in Immunoassays*, Wiley, New York, **1991**.

[3] A. J. Bryan, A. P. de Silva, S. A. de Silva, R. A. D. D. Rupasinghe, K. R. A. S. Sandanayake, *Biosensors* **1989**, *4*, 169; R. A. Bissell, A. P. de Silva, H. Q. N. Gunaratne, P. L. M. Lynch, G. E. M. Maguire, K. R. A. S. Sandanayake, *Chem. Soc. Rev.* **1992**, *21*, 187; R. A. Bissell, A. P. de Silva, H. Q. N. Gunaratne, P. L. M. Lynch, G. E. M. Maguire, C. P. McCoy, K. R. A. S. Sandanayake, *Top. Curr. Chem.* **1993**, *168*, 223.

[4] A. W. Czarnik, *Adv. Supramol. Chem.* **1993**, *3*, 131; A. W. Czarnik, *Acc. Chem. Res.* **1994**, *27*, 302; L. Fabrizzi, A. Poggi, *Chem. Soc. Rev.* **1995**, *24*, 197; R. Y. Tsien, *Chem. Eng. News* **1994**, *72* (29), 34. See also: T. D. James, P. Linnane, S. Shinkai, *J. Chem. Soc. Chem. Commun.* **1996**, 281.

[5] K. Connors, *Binding Constants. The Measurement of Complex Stability*, Wiley, New York, **1987**.

[6] A. Abu-Saleh, C. F. Meares, *Photochem. Photobiol.* **1984**, *39*, 763.

[7] G. L. Closs, J. R. Miller, *Science* **1988**, *240*, 440; G. McLendon, *Chem. Rev.* **1992**, *92*, 481; J. R. Winkler, H. B. Gray, *Chem. Rev.* **1992**, *92*, 369; J. W. Verhoewen, *Pure Appl. Chem.* **1990**, *62*, 1585.

[8] S. Higashida, H. Tsue, K. Sugiura, T. Kaneda, Y. Tanaka, S. Taniguchi, T. Okada, *Chem. Lett.* **1995**, 515; A. M. Brun, S. J. Atherton, A. Harriman, V. Heitz, J.-P. Sauvage, *J. Am. Chem. Soc.* **1992**, *114*, 4632; G. Gust, T. A. Moore, A. L. Moore, *Acc. Chem. Res.* **1993**, *26*, 198.

[9] C. A. Parker, *Adv. Photochem.* **1964**, *2*, 305.

[10] R. A. Bissell, A. P. de Silva, *J. Chem. Soc. Chem. Commun.* **1991**, 1148.

[11] S. Draxler, M. E. Lippitsch, I. Klimant, H. Kraus, O. S. Wolfbeis, *J. Phys. Chem.* **1995**, *99*, 3162. See also: H. Szmacinski, J. R. Lakowicz, *ACS Symp. Ser.* **1993**, *538*, 196.

[12] Similar selectivities in bireceptor systems have given rise to "AND" logic gates: A. P. de Silva, H. Q. N. Gunaratne, C. P. McCoy, *Nature* **1993**, *364*, 42.

[13] G. S. Hanan, J.-M. Lehn, N. Kyritsakas, J. Fischer, *J. Chem. Soc. Chem. Commun.* **1995**, 765.

[14] J. Grimshaw, A. P. de Silva, *J. Chem. Soc. Perkin Trans. 2* **1983**, 1679.

[15] A. P. de Silva, K. R. A. S. Sandanayake, *Angew. Chem.* **1990**, *102*, 1159; *Angew. Chem. Int. Ed. Engl.* **1990**, *29*, 1173.

[16] R. G. Charles, E. P. Riedel, *J. Inorg. Nucl. Chem.* **1966**, *28*, 527.

[17] A. P. de Silva, R. A. D. D. Rupasinghe, *J. Chem. Soc. Chem. Commun.* **1985**, 1669.

[18] W. DeW. Horrocks, D. R. Sudnick, *Acc. Chem. Res.* **1981**, *14*, 384.

Maximum Functionalization of Metallocenes: Decaallylferrocene and Derivatives**

Peter Jutzi,* Christoph Batz, Beate Neumann, and Hans-Georg Stammler

Multiply functionalized metallocenes are very attractive molecules for a variety of reasons.[1] The steric and electronic properties of the parent compounds can be significantly altered by substitution at the metallocene framework. The presence of suitable substituents in the side chain enables the incorporation of the corresponding metallocenes in polymers,[2] the preparation of discotic liquid crystals,[3] or, in the context of the dendrimer strategy, the construction of highly branched systems. Furthermore, functionalization with redox building blocks could concievably lead to electron storage systems capable of simultaneously transfering several electrons at the same potential. Special properties have been predicted for such molecular electron reservoirs;[4] they are already in use for the modification of electrodes[5] and in electrochemical sensors.[6] In this context, the decafunctionalization of a metallocene is a particularly attractive goal.

Among the metallocenes, ferrocene has the largest number of known derivatives.[7] The only known decasubstituted ferrocene[8–11] capable of incorporating additional functionalities at the periphery is decabenzylferrocene, which can be additionally functionalized by Friedel–Crafts substitutions.[3] However, a disadvantage here is that the substitution reaction frequently affords mixtures comprising *ortho*- and *para*-substituted products. In this context, the route described by Astruc et al. is of special interest: starting from sandwich compounds multiple basic alkylation affords, among other complexes, hexasubstituted ferrocenyl complexes.[12, 13]

[*] Prof. Dr. P. Jutzi, Dipl.-Chem. C. Batz, B. Neumann, Dr. H.-G. Stammler
Fakultät für Chemie, Lehrstuhl für Anorganische Chemie II der Universität
D-33501 Bielefeld (Germany)
Fax: Int. code + (521)106-6026

[**] We thank Dipl.-Ing. K. Hägele (Research group Prof. Przybylski, Universität Konstanz) for recording the FAB-MS spectra.

Herein we report the synthesis of the decaallylferrocene **1**, which can be readily transformed by simple subsequent reactions to yield a wide variety of functionalized ($(n \times 10)$-fold) derivatives. The key compound for the synthesis of **1** (Scheme 1)

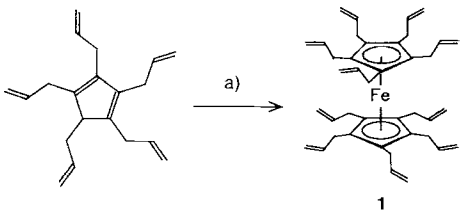

1

Scheme 1. a) 1. KH, THF; 2. $FeCl_2$ (0.5 equiv), THF, room temperature, 3 d.

is 1,2,3,4,5-pentaallylcyclopentadiene, which is prepared from cyclopentadiene and allyl bromide in a one-pot synthesis.[14] Subsequent treatment of potassium pentaallylcyclopentadienide[14] with iron(II) chloride in THF gave the decaallylferrocene **1** using standard procedures at room temperature. Product **1** is obtained as small, orange crystals; however, these crystals are not suitable for a single-crystal X-ray structure analysis. Compound **1** is air- and moisture-stable and dissolves readily in all common organic solvents; however, in polar solvents such as THF or chloroform, it decomposes slowly to give a deep red compound, which has not yet been fully characterized. Compound **1** is electrochemically oxidized in a reversible process at a potential of $E_{1/2} = 0.144$ V.[15] This value lies between those for unsubstituted ferrocene (0.337 V)[15] and decamethylferrocene (-0.163 V),[15] a finding that can be explained by steric effects and in light of the smaller inductive effect exerted by the allyl groups in comparsion to that exerted by the methyl substituents. The direct comparison with octaallylferrocene **5**, which is obtained analogously to **1** from potassium tetraallylcyclopentadienide,[14] shows that inductive effects alone cannot sufficiently explain the value of the redox potential of ferrocenes with sterically demanding substitutents.[16] The redox potential of **5** was determined to be $E_{1/2} = 0.100$ V;[15] thus, in comparison with that of **1** it is cathodically and not anodically shifted.

Chemical oxidation of **1** with $NOBF_4$ led to the decaallylferrocenium salt **2** (Scheme 2), which is very soluble in polar solvents and crystallizes from CH_3CN as blue-green needles.

Figure 1 shows the structure of the cation of **2** in the crystal.[17] The allyl groups point away from the center of the molecule in a "spider-leg-like" arrangement without a directional preference for the position of the terminal double bond. The Fe–Cp(centroid) distance of 1.715 Å is of the same magnitude as in similarly substituted ferrocenium cations.[16a, 18] Interesting, and unusual for decasubstituted ferrocene, is the almost eclipsed arrangement of the two Cp rings (twist angle 15°).

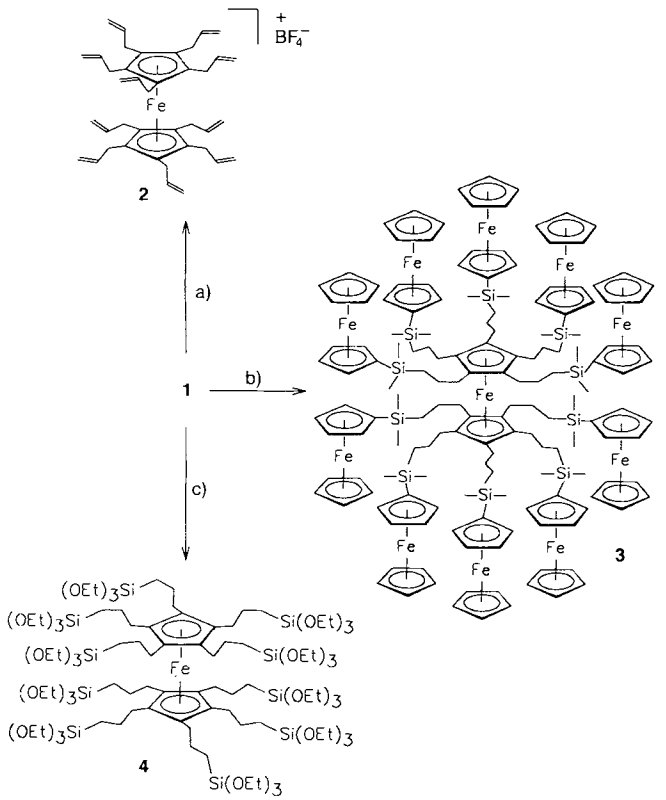

Scheme 2. a) $NOBF_4$, CH_3CN, room temperature; b) $HSi(Me_2)Fe$ (10 equiv), Karstedt-cat. (1% solution in toluene), xylene, room temperature, 1 d; c) $HSi(OEt)_3$ (excess), Karstedt-cat. (1% solution in toluene), toluene, reflux, 1 d.

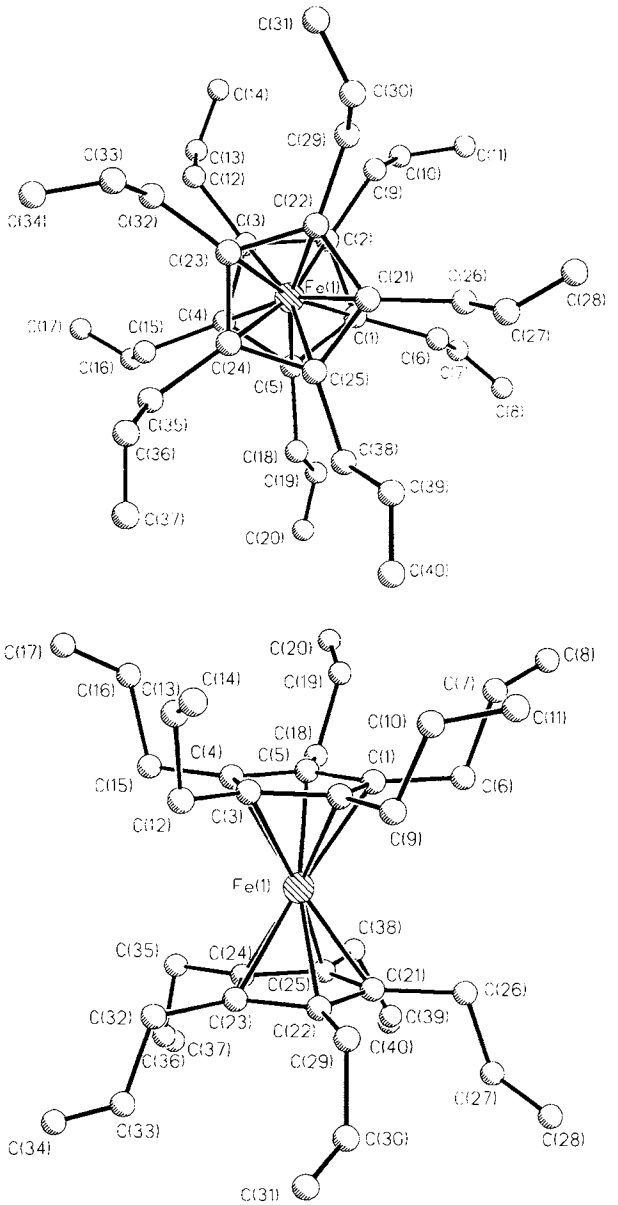

Fig. 1. Top view (top) and side view (bottom) of the cation of **2** in the crystal.

The platinum-catalyzed hydrosilylation of **1** with ten equivalents of dimethylsilylferrocene in xylene led almost quantitatively to the decaferrocenyl ferrocene **3** (Scheme 2) as an orange, waxy solid, which readily dissolves in polar and aromatic solvents. The absence of signals for the vinylic H and C atoms in the ^1H and ^{13}C NMR spectra, respectively, confirms the decasubstitution as does the detection of the molecular ion in the FAB-MS spectrum. The NMR spectra of **3** also show signals attributable to the α-hydrosilylation product (Table 1), which is formed in about 10% yield. This implies that on average one of the ten outer ferrocenyl moieties is bound to the core not by a propanediyl chain but by an isomeric methylethanediyl chain.

Table 1. Selected physical data for **1** and **3**–**5**.

1: ^1H NMR [a]: $\delta = 2.94$ (d, 2H, $^3J = 6.7$ Hz), 4.80–5.05 (m, 2H), 5.62–5.75 (m, 1H); ^{13}C NMR [a]: $\delta = 30.25$ (Fc-CH_2), 82.33 (C_5R_5), 114.96 (=CH_2), 137.96 (-CH=); MS (70 eV): *m/z* (%): 586 (100) [M^+], 546 (2) [$M^+ - C_3H_4$], 321 (2.5) [$C_5(C_3H_5)_5Fe^+$]

3: ^1H NMR [a]: $\delta = 0.19$ [c]/0.22 (2s, 60H, $SiCH_3$), 0.57 (s, 3H, CH_3 [c]), 0.65–0.80 (m, 20H, $SiCH_2$), 1.20–1.35 (m, 20H, $SiCH_2CH_2$), 1.97–2.12 (m, 20H, C_5CH_2), 4.08/4.10 (2s), 4.05–4.08 (m), 4.29 (m) (in total 90H, Fc-H); ^{13}C NMR [b] (C_6D_6): $\delta = -2.57$ [c], −1.47 ($SiCH_3$), 19.12, 28.24, 31.41 (($CH_2)_3$), 9.71 (CH_3 [c]), 68.53 (C_5H_5), 71.10, 73.40 (C_4H_4CSi), 71.20 (C_4H_4CSi), 83.8 (C_5R_5); ^{29}Si NMR [b]: $\delta = -2.8$, −0.5 [c]; FAB-MS [d]: *m/z* (%): 3029 (100) [$M^+ + H$], 2786 (89) [$M^+ - FcSiMe_2$], 2543 (37) [$M^+ - 2 \times FcSiMe_2$], 1514 (15) [M^{2+}], 1169 (58), 927 (46)

4: ^1H NMR [b]: $\delta = 0.52$ (CH_3 [c]), 1.19 (m, 2H, $SiCH_2$), 1.33 (m, 2H, $SiCH_2CH_2$), 2.12 (m, 2H, C_5CH_2), 1.21 (t, $^3J = 6.9$ Hz, 9H, OCH_2CH_3), 3.79 (q, $^3J = 6.9$ Hz, 6H, OCH_2CH_3); ^{13}C NMR [b]: $\delta = 11.95, 25.80, 29.99$ (($CH_2)_3$), 11.4 (CH_3 [c]), 82.81 (C_5R_5), 18.37, 58.18 (OEt), 17.96, 59.10 (OEt [c]); ^{29}Si NMR [b] (C_6D_6): $\delta = -45.43$; FAB-MS [d]: *m/z* (%): 2228 (90) [M^+], 2065 (100) [$M^+ - Si(OEt)_3$], 1901 (60) [$M^+ - 2Si(OEt)_3$], 1141 (37) [$FeC_5R_5^+$]

5: ^1H NMR [a] (C_6D_6): $\delta = 2.85$–2.91 (m, 16H, Fc-CH_2R), 3.65 (s, 2H, C_5R_4H), 4.91–5.05 (m, 16H), 5.76–5.96 (m, 8H); ^{13}C NMR [b]: $\delta = 30.17/31.49$ ($FcCH_2$), 82.19/83.88 (C_5R_4H), 114.78/114.90 (=CH_2), 137.52/137.84 (-CH=); MS (70 eV): *m/z* (%): 506 (100) [M^+]

[a] ^1H NMR: 300.1 MHz, ^{13}C NMR: 75.47 MHz, ^{29}Si NMR: 59.59 MHz; unless otherwise stated: $CDCl_3$, 25 °C. [b] ^1H NMR: 500.1 MHz, ^{13}C NMR: 125.7 MHz, ^{29}Si NMR: 99.4 MHz; unless otherwise stated: $CDCl_3$, 25 °C. [c] Signal corresponding to the α-hydrosilylation product. [d] Matrix: 3-nitrobenzyl alcohol.

The cyclovoltammetric studies of **3** show that the outer ferrocenyl moieties, which can be reversibly ($I_a/I_c \approx 1$) oxidized at $E_{1/2} = 0.40$ V (vs. Ag/AgCl), are equivalent. Furthermore, a second wave with an intensity of approximately one-twelfth of that of the dominant wave is easily discernible and attributed to the central ferrocenyl moiety ($E_{1/2} = -0.10$ V vs. Ag/AgCl) (Fig. 2). The fact that the observed ratio of intensities is not exactly 1:10 is attributed to adsorption phenomena on the electrode surface.

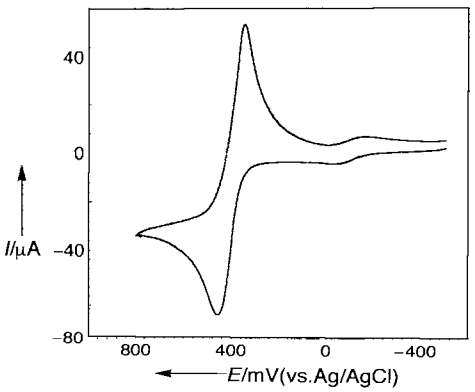

Fig. 2. Cyclovoltammogram of **3** in CH_2Cl_2 (ca. 8.8×10^{-4} mol L^{-1}, conducting electrolyte: 0.1 mol L^{-1} nBu_4NPF_6, 20 °C, Au disc electrode, scan rate 50 mVs^{-1}.

Hydrosilylation of **1** with triethoxysilane afforded the 30-fold ethoxy-substituted ferrocene **4** (Scheme 2). However, compared to the synthesis of **3**, the reaction mixture needs to be stirred for a longer period of time and heated to achieve complete addition to the ten double bonds. Here, too, the α-hydrosilylation product is formed in about 10% yield. Cyclovoltammetric studies of **4** gave a potential of $E_{1/2} = -0.055$ V (vs. Ag/AgCl) with a peak separation of $\Delta E_p = 87.6$ mV (for conditions see cyclovoltammogram of **3**).

Decaallylferrocene is an ideal substrate for further ($n \times 10$)-fold functionalization in the context of the dendrimer strategy. Hydrosilylation is one of several easily applicable reactions for the assembly of starlike organometallic molecules that can serve as building blocks for redox-active polymers (e.g. by a sol–gel process) or as molecular multielectron reservoirs. The strategy presented herein should also be suitable for the synthesis of other metallocene or cyclopentadienyl-metal compounds; it allows, generally speaking, the preparation of highly functionalized compounds.

Experimental Procedure

1: Potassium pentaallylcyclopentadienide (0.611 g, 2.00 mmol) and $FeCl_2 \cdot THF_{1.4}$ (0.303 g, 1.33 mmol) were added to THF (50 mL) at room temperature, and the resulting mixture was stirred for 3 d. The solvent was removed under vacuum and the residue was extracted with hexane. After the mixture had been filtered, the solution was concentrated and allowed to crystallize at 0 °C. Yield: 0.37 g (63%) of orange needles, m.p. 195 °C.

2: A mixture of **1** (130 mg, 0.222 mmol) and $NOBF_4$ (40 mg, 0.342 mmol) was treated with acetonitrile (5 mL), and stirred at room temperature for 12 h. The solution was concentrated and then stored under a diethyl ether atmosphere for several days, which led to the crystallization of blue-green needles of **2**. Yield: 0.13 g (87%). m.p. ≈ 350 °C (decomp.).

3: To a solution of **1** (0.10 g, 0.170 mmol) in xylene (10 mL) was added a 1% solution of the Karstedt catalyst in toluene (0.5 mL). Air was briefly passed through the solution, and then dimethylferrocenylsilane (1.00 g, 4.09 mmol) in a small amount of xylene was added dropwise. The mixture was stirred overnight at 20 °C, and then the solvent and excess ferrocenylsilane were removed under high vacuum. The residue was purified by flash chromatography (toluene, silica gel) to **3** as a dark orange, waxy solid. Yield: 0.43 g (82%).

4: To a solution of **1** (0.20 g, 0.340 mmol) in toluene (10 mL) was added a 1% solution of the Karstedt catalyst in toluene (0.8 mL). Air was briefly passed through the solution, and then an excess of triethoxysilane (2 mL) was added dropwise to the mixture. The reaction mixture was stirred for 48 h at 100 °C and then filtered through charcoal. The solvent and excess triethoxysilane were removed under high vacuum to afford **4** as a dark brown, viscous oil. Yield: 0.74 g (90%).

5: Compound **5** was prepared analogously to **1** from potassium tetraallylcyclopentadienide [14] (8.00 g, 30.2 mmol). Yield: 9.20 g (60%) as a dark orange oil.

Received: March 11, 1996 [Z8914IE]
German version: *Angew. Chem.* **1996**, *108*, 2272–2274

Keywords: dendrimers · hydrosilylations · iron compounds · sandwich complexes

[1] a) D. Astruc, *Electron Transfer and Radical Processes in Transition Metal Chemistry*, 1st ed., VCH, New York, **1995**; b) C. Janiak, H. Schumann, *Adv. Organomet. Chem.* **1991**, *33*, 291–390; c) J. Okuda, *Top. Curr. Chem.* **1991**, *160*, 97–146.

[2] a) P. Jutzi, T. Heidemann, B. Neumann, H. G. Stammler, *J. Organomet. Chem.* **1994**, *472*, 27–38; b) K. E. Gonsalves, X. Chen in ref. [7], pp. 497–530.

[3] H. Schumann, K. Sühring, R. Weimann, *J. Organomet. Chem.* **1995**, *496*, C5–C8.

[4] a) A. J. Bard, *Nature* **1995**, *374*, 13; b) D. Astruc, *New J. Chem.* **1992**, *16*, 305.

[5] B. Alonso, M. Morán, C. M. Casado, F. Lobete, J. Losada, I. Cuadrado, *Chem. Mater.* **1995**, *7*, 1440–1442.

[6] P. D. Hale, T. Inagaki, H. I. Karan, Y. Okamoto, T. A. Skothein, *J. Am. Chem. Soc.* **1989**, *111*, 3482.

[7] *Ferrocenes* (Eds.: A. Togni, T. Hayashi), VCH, Weinheim, **1995**.

[8] Hitherto known $FeC_{10}R_{10}$: a) R = Me: R. B. King, M. B. Bisnette, *J. Organomet. Chem.* **1967**, *8*, 287; b) R = Et: K. Schlögl, M. Peterlik, *Monatsh. Chem.* **1962**, *93*, 1328; c) R = Ph: H. Schumann, A. Lentz, R. Weimann, J. Pickardt, *Angew. Chem.* **1994**, *106*, 1827–1829; *Angew. Chem. Int. Ed. Engl.* **1994**, *33*, 1731–1733; d) R = Bz: H. Schumann, C. Janiak, R. D. Köhn, J. Loebel, A. Dietrich, *J. Organomet. Chem.* **1989**, *365*, 137–150; M. D. Rausch, W. M. Tsai, J. W. Chambers, R. D. Rogers, H. G. Alt, *Organometallics* **1989**, *8*, 816–821.

[9] F. L. Hedberg, H. Rosenberg, *J. Am. Chem. Soc.* **1973**, *95*, 870–875.

[10] a) V. I. Boev, A. V. Dombrovskii, *Zh. Obschch. Khim.* **1977**, *47*, 727–728; Y.-H. Han, M. J. Heeg, C. H. Winter, *Organometallics* **1994**, *13*, 3009–3019.

[11] Ferrocenes substituted with functional (organic) groups are unknown; the corresponding cyclopentadienes (e.g. $(CN)_5C_5H$) are poor complexing ligands for electronic reasons [1b]. Decahalogen-substituted ferrocenes can be prepared by repeated metalation/ chlorination [9] and permercuration [10]. However, little is known about the substitution chemistry of these compounds.

[12] a) J.-L. Fillaut, J. Lanares, D. Astruc, *Angew. Chem.* **1994**, *106*, 2540–2542; *Angew. Chem. Int. Ed. Engl.* **1994**, *33*, 2460–2462; b) F. Moulines, D. Astruc, *ibid.* **1988**, *100*, 1394–1396 bzw. **1988**, *27*, 1347–1349.

[13] D. Buchholz, B. Gloaguen, J.-L. Fillaut, M. Cotrait, D. Astruc, *Chem. Eur. J.* **1995**, *1*, 374–381.

[14] The synthesis of pentaallylcyclopentadiene parallels that of iPr_5C_5H: H. Sitzmann, *Z. Naturforsch. B* **1989**, *44*, 1293–1297; improved synthesis: E. V. Dehmlow, C. Bollmann, *ibid.* **1993**, *48*, 457–460. Following destillation (b.p. 65 °C, 0.03 mbar) a mixture containing all three possible isomers is obtained. Tetraallylcyclopentadiene can also be isolated as an isomeric mixture from a different fraction. The C–H acidic isomers can be separated by conversion to their potassium salts. 1,2,3,4,5-pentaallylcyclopentadiene: ^{13}C NMR ($CDCl_3$, 75.43 MHz): δ = 51.6, 138.0, 140.6 (C_5R_5), 30.3, 31.3, 31.8 (CH_2), 134.0–137.7 (3 signals, $CH{=}CH_2$), 114.6–115.9 (3 signals, $CH{=}CH_2$). Further information regarding the synthesis and additional analytical data: C. Batz, P. Jutzi, *Synthesis*, in press.

[15] Average potential ($E_{1/2}$) vs. saturated calomel electrode (SCE), cyclovoltammetry, 0.1 M $NaClO_4$ solution in CH_3CN, disk electrode (Au), scan rate 50 mVs^{-1}.

[16] a) P. Zanello, A. Cinquantini, S. Mangani, G. Opromolla, L. Pardi, C. Janiak, M. D. Rausch, *J. Organomet. Chem.* **1994**, *471*, 171–177; b) M. P. Castellani, J. M. Wright, S. J. Geib, A. L. Rheingold, W. C. Trogler, *Organometallics* **1986**, *5*, 1116–1120.

[17] $C_{40}H_{50}BF_4Fe \cdot CH_3CN$ **2**: M_r = 714.51, crystal dimensions 0.25 × 0.4 × 0.5 mm^3, monoclinic, $P2_1/n$, a = 21.340(7), b = 11.595(4), c = 16.558(5) Å, β = 72.69(2)°, V = 3912(2) $Å^3$, Z = 4, ρ_{calcd} = 1.213 gcm^{-3}, μ = 0.433 mm^{-1}, Siemens-P2-diffractometer, ω scans, $Mo_{K\alpha}$ = 0.71073 Å, graphite monochromator, T = 173 K, 3.0° ≤ 2θ ≤ 50.0°, 7035 measured reflections of which 6850 were independent (R_{int} = 0.0243), structure solution by direct methods (SHELXTL PLUS), structure refinement with SHELXL-93, semiempirical absorption correction with ψ scans (min./max. transmission 0.494/0.527), max. residual electron density 0.7 e $Å^{-3}$, $R(F)$ 0.0726 for 4206 reflections with $I > 2\sigma I$, $wR(F^2)$ = 0.2333 for all 6839 reflections ($w = 1/[\sigma^2(F_o)^2 + (0.0940P)^2 + 9.2791P]$ with $P = (F_o^2 + 2F_c^2)/3$), full-matrix least-squares refinement of F^2 (441 parameters) with the constraint that all double bonds of allylic groups are of approximately equal length (169 restraints). All non-hydrogen atoms were refined anisotropically with the exception of six disordered carbon atoms, which were refined isotropically. Hydrogen atoms were considered in calculated positions with the 1.2 × U_{eq} value of the corresponding carbon atom. The hydrogen atoms of acetonitrile were refined with the 1.5 × U_{eq} value of the C(42) atom assuming idealized symmetry and C–H bond lengths as well as free rotation along the C(41)–C(42) axis. Further details of the crystal structure investigations may be obtained from the Fachinformationszentrum Karlsruhe, D-76344 Eggenstein-Leopoldshafen (Germany), on quoting the depository number CSD-405264.

[18] K. M. Chi, J. C. Calabrese, W. M. Reiff, J. S. Miller, *Organometallics* **1991**, *10*, 688–693.

First-Generation Tethered [2.2]Metacyclophanes—Prototypes of Molecular Devices**

Graham J. Bodwell,* Tom J. Houghton, Jason W. J. Kennedy, and Michael R. Mannion*

It has long since been established that the preferred conformation of [2.2]metacyclophanes is *anti*.[1] Indeed *syn*-[2.2]-metacyclophanes are relatively uncommon, as they isomerize thermally to their *anti* counterparts.[2–4] Substantial kinetic stabilization of the *syn* conformer has been achieved by introducing substituents at the internal positions.[3] The same is true, but to a lesser extent, for bridge substituents.[4] Alternately, the fusion of small rings to the bridges can fix the [2.2]-metacyclophane framework in the *syn* conformation,[5] as can the presence of a third bridge as in **1c**.[6]

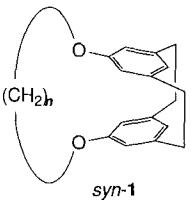

syn-**1**

With respect to this latter approach, we became interested in the [*n*.2.2](1,3,5)-cyclophanes **1** because of the fascinating possibilities that they present.

First of all, it was envisaged that the conformational preference of these "tethered [2.2]metacyclophanes" would be determined by the length of the tether. A very long tether should not significantly influence the system and thus allow the [2.2]metacyclophane to behave as though it were absent; in other words, the *anti* conformation should be adopted and the two aromatic rings should be parallel (**1A**). As the length of the tether decreases, the strain in the *anti* conformer should increase, thereby lowering the difference in energy between the *anti* and *syn* conformers. In addition, the aromatic rings should now be tilted with respect to one another (**1B**). Accordingly, the internal proton of the "inner" ring will

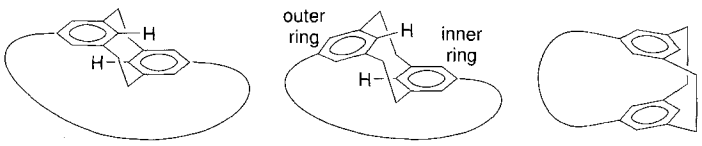

1A **1B** **1C**

have moved further into the shielding cone of the "outer" ring than in the previous case. Exceptionally high-field ^1H NMR resonances are thus anticipated. At the same time the internal proton of the outer ring will have moved away from the shielding cone of the inner ring. Continuing to decrease the length of the tether will eventually render the *anti* conformer less stable than *syn* (**1C**). However, at some intermediate tether length, the two conformers may be close enough in energy to coexist. Modifying the constitution of the tether should ultimately provide a means of "fine-tuning" the system.

Given that *syn*-[2.2]metacyclophane itself undergoes facile isomerization to its *anti* conformer at 0 °C,[3] it does not seem unreasonable to expect an energy barrier between the two conformers low enough to allow them to interconvert at room tem-

[*] Dr. G. J. Bodwell, M. R. Mannion, T. J. Houghton, J. W. J. Kennedy
Department of Chemistry, Memorial University of Newfoundland
St. John's, NF, A1B 3X7 (Canada)
Fax: Int. code +(709) 737-3702
e-mail: gbodwell@morgan.ucs.mun.ca

[**] Tethered [2.2]Metacyclophanes, Part 1. Support of this work from the Natural Sciences and Engineering Research Council (NSERC) of Canada is gratefully acknowledged.

perature. However, the two conformers do have markedly different structures and their interconversion will clearly involve considerable molecular reorganization, which should serve to heighten the energy barrier between them. The *syn* conformer possesses a cavity in which guest molecules or ions might be accommodated, while the *anti* conformer does not. Thus, great potential exists for the development of molecular devices based on this isomerization. Appropriate functionalization of the tether may eventually allow the system to be customized for selected guests. We now report the synthesis and conformational behavior of members of the first generation of tethered [2.2]metacyclophanes.

The dithiacyclophanes **2a–c** were prepared in analogy to a lower homologue in this series[7] by using Na_2S/Al_2O_3[8] to couple the appropriate tetrabromides (Scheme 1). Oxidation of

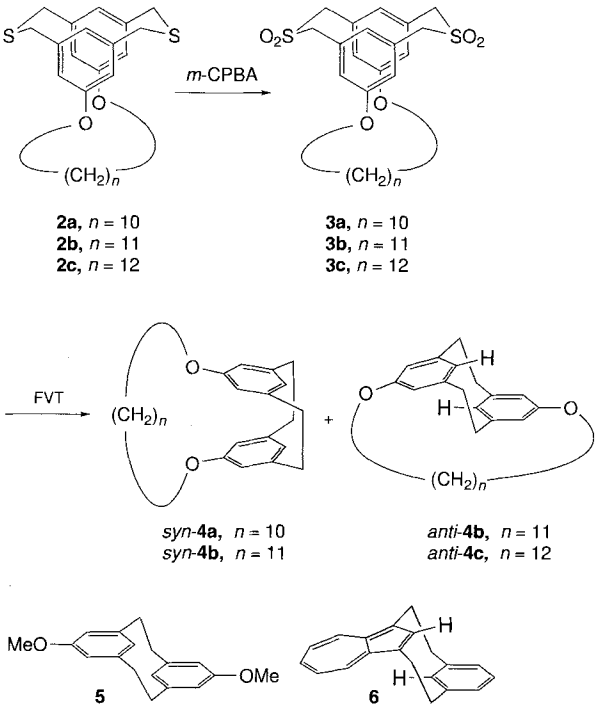

Scheme 1. Synthesis of tethered [2.2]metacyclophanes **4a–c**. FVT = flash vacuum thermolysis.

2a–c with *m*-chloroperoxybenzoic acid (*m*-CPBA) afforded the remarkably soluble bissulfones **3a–c** (95–100%), and these were thermolyzed in vacuo to give the tethered [2.2]metacyclophanes **4a–c** in 45–69% yield. Compound **4a** (12-atom tether, 54%) was obtained exclusively as the *syn* conformer. The ^1H and ^{13}C NMR spectra (Table 1) indicate the presence of two planes of symmetry. The signals of the internal aromatic protons are observed at $\delta = 6.19$. In contrast, compound **4c** (14-atom tether, 45%) was isolated exclusively as the *anti* conformer. The ^1H and ^{13}C NMR spectra (Table 1) indicate the presence of a single plane of symmetry, and signals of the internal aromatic protons are observed at $\delta = 4.83$ and 3.30. The higher field signal is arbitrarily assigned to the internal proton of the inner ring. With *anti*-5,13-dimethoxy[2.2]metacyclophane **5**[9] as a reference compound ($\delta(H_i) = 4.08$), $\Delta\delta$ values for the two internal protons are -0.75 (outer ring) and 0.78 (inner ring). The highest field signals of the tether are observed at $\delta = 0.50$.

The 300 MHz ^1H NMR spectrum (Table 1) of the crude pyrolysate of **3b** (13-atom tether) indicated the presence of both

Table 1. ^1H and ^{13}C NMR data for **4a–c** and **5** [a].

syn-**4a**: $\delta_H = 6.19$ (s, 2H), 5.99 (d, $J = 1.2$ Hz, 4H), 3.67 (t, $J = 5.9$ Hz, 4H), 3.08 (AA'BB' half spectrum, 4H), 2.80 (AA'BB' half spectrum, 4H), 1.69 (m, 4H), 1.40 (m, 12H); $\delta_C = 159.2, 138.9, 131.1, 112.7, 66.6, 35.6, 28.7, 26.9, 26.2, 24.7$

syn-**4b**: $\delta_H = 6.17$ (s, 2H), 5.99, (s, 4H), 3.66 (t, $J = 6.6$ Hz, 4H), 3.06 (AA'BB' half spectrum, 4H), 2.80 (AA'BB' half spectrum, 4H), 1.66 (m, 4H), 1.38 (m, 14H); $\delta_C = 159.1, 139.0, 131.1, 112.9, 67.5, 35.6, 28.5, 26.7, 26.4, 24.4$

anti-**4b**: $\delta_H = 6.83$ (d, $J = 1.1$ Hz, 2H), 6.67 (s, 2H), 5.07 (s, 1H), 4.30 (t, $J = 6.2$ Hz, 2H), 4.11 (t, $J = 5.4$ Hz, 2H), 3.13 (ABXY part spectrum, 2H), 3.03 (s, 1H), 2.92 (ABXY part spectrum, 2H), 2.32 (ABXY part spectrum, 2H), 2.09 (ABXY part spectrum, 2H), 1.69, (m, 2H), 1.46 (m, 2H), 1.18 (m, 2H), 0.93 (m, 2H), 0.76 (m, 4H), 0.53 (m, 4H), 0.37 (m, 2H); $\delta_C = 160.6, 157.5, 143.8, 136.2, 134.7, 129.1, 117.7, 117.4, 72.2, 70.1, 41.5, 39.5, 30.4, 29.9, 29.9, 29.5, 29.1, 28.1, 27.6, 26.2, 26.0$

anti-**4c**: $\delta_H = 6.76$ (s, 2H), 6.68 (s, 2H), 4.83 (s, 1H), 4.32 (t, $J = 6.0$ Hz, 2H), 4.18 (t, $J = 5.1$ Hz, 2H), 3.30 (s, 1H), 3.10 (ABXY part spectrum, 2H), 2.94 (ABXY part spectrum, 2H), 2.25 (ABXY part spectrum, 2H), 2.07 (ABXY part spectrum, 2H), 1.70 (m, 2H), 1.52 (m, 2H), 1.31 (m, 2H), 1.07 (m, 2H), 0.81 (m, 8H), 0.50 (m, 4H); $\delta_C = 159.5, 158.9, 143.0, 137.1, 133.4, 129.3, 116.5, 115.9, 70.7, 68.5, 41.6, 39.9, 30.3, 30.2, 29.9, 29.8, 29.6, 29.0, 28.2, 28.1, 26.1, 24.9$

anti-**5**: $\delta_H = 6.62$ (d, $J = 1.2$ Hz, 4H), 4.08 (t, $J = 1.0$ Hz, 2H), 3.83 (s, 6H), 3.01 (AA'XX' half spectrum, 4H), 2.13 (AA'XX' half spectrum, 4H); $\delta_C = 160.5, 140.5, 129.5, 110.7, 55.3, 41.0$

[a] ^1H NMR: 300 MHz, $CDCl_3$, TMS; ^{13}C NMR: 75 MHz, $CDCl_3$, TMS.

syn-**4b** and *anti*-**4b** in a ratio of roughly 2.5:1. The significant difference in their R_f values (SiO_2, 1:1 CH_2Cl_2:hexanes, R_f(*syn*-**4b**) = 0.40, R_f(*anti*-**4b**) = 0.25) allowed for straightforward chromatographic separation. The yields of isolated products were 20% (*syn*-**4b**) and 49% (*anti*-**4b**). The ^1H NMR signals of the internal protons of *syn*-**4b** are observed at $\delta = 6.17$, whereas those of *anti*-**4b** appear at $\delta = 5.07$ (outer ring) and 3.03 (inner ring). These chemical shifts are very similar to those observed in azulenophane **6**,[10] for which Mitchell[2] invoked a tilting effect akin to that in **1B**. Compared to **5**, the $\Delta\delta$ values are -0.99 (outer ring) and 1.05 (inner ring). The highest field protons of the tether are observed at $\delta = 0.37$. The conformers interconvert slowly at room temperature as seen by the gradual appearance over time of peaks corresponding to the other conformer in the ^1H NMR spectra of the original solutions of the pure conformers.[11] The equilibrium *anti*:*syn* ratio at room temperature is approximately 5.9:1, as determined by integration of the low-field aromatic signals. This ratio corresponds to a free energy difference of roughly 1.1 kcal mol^{-1}. Also worthy of note is that the isomerization of *anti*-**4b** to *syn*-**4b** is only the second documented instance of an *anti*-to-*syn* isomerization of a [2.2]metacyclophane derivative.[12]

We have established that a tether of 13 sp^3-hydridized atoms renders the two conformers of these tethered [2.2]metacyclophanes nearly equal in energy and that their interconversion takes place slowly at room temperature. Compound **4b** is thus a prototype of a molecular device, the development of which we are now actively pursuing.

Experimental Procedure

General procedure for the thermolysis of sulfones **3a–c** [13]: A solution of the bissulfone (200–300 mg per run) in CH_2Cl_2 (ca. 40 mL) in a 100 mL round-bottomed flask was evaporated on a rotary evaporator to leave a thin coating of the substrate on the surface of the flask. A cold finger was attached to the flask and high vacuum (ca. 10^{-1} mm Hg) with a nitrogen bleed was applied. The flask was then heated with a full Bunsen burner flame. The sublimate was washed back into the flask with CH_2Cl_2 and the procedure was repeated. The combined sublimate and residue thus obtained were chromatographed on SiO_2 with CH_2Cl_2:hexanes (1:4 to 1:1 gradient) as eluent to afford the products.

Received: March 8, 1996
Revised version: June 5, 1996 [Z8911IE]
German version: *Angew. Chem.* **1996**, *108*, 2280–2281

Keywords: cyclophanes · isomerizations

[1] C. J. Brown, *J. Chem. Soc.* **1953**, 3278–3285; Y. Kai, N. Yasuoka, N. Kasai, *Acta Crystallogr. Sect. B* **1977**, *33*, 754–761.
[2] For comprehensive discussions of *syn*/*anti* isomerism in [2.2]metacyclophanes, see R. H. Mitchell in *Cyclophanes, Vol 1*, (Eds.: P. M. Keehn, S. M. Rosenfeld), Academic Press, New York, **1983**, p. 239–310; F. Vögtle, *Cyclophan-Chemie*, Teubner, Stuttgart, **1990**; F. N. Diederich, *Cyclophanes*, Royal Society of Chemistry, London, **1991**.
[3] R. H. Mitchell, T. K. Vinod, G. W. Bushnell, *J. Am. Chem. Soc.* **1990**, *112*, 3487–3497.
[4] D. Kamp, V. Boekelheide, *J. Org. Chem.* **1978**, *43*, 3470–3475; R. H. Mitchell, G. J. Bodwell, T. K. Vinod, K. S. Weerawarna, *Tetrahedron Lett.* **1988**, *29*, 3287–3290.
[5] H. Meier, *Angew. Chem.* **1992**, *104*, 1425–1447; *Angew. Chem. Int. Ed. Engl.* **1992**, *31*, 1399–1420, and references therein; J. Nishimura, Y. Horikoshi, Y. Wada, H. Takahashi, M. Sato, *J. Am. Chem. Soc.* **1991**, *113*, 3485–3489, and references therein.
[6] V. Boekelheide, R. A. Hollins, *J. Am. Chem. Soc.* **1973**, *95*, 3201–3208.
[7] G. J. Bodwell, J. N. Bridson, T. J. Houghton, J. W. J. Kennedy, M. R. Mannion, *Angew. Chem.* **1996**, *108*, 1418–1420; *Angew. Chem. Int. Ed. Engl.* **1996**, *35*, 1320–1321.
[8] G. J. Bodwell, T. J. Houghton, H. E. Koury, B. Yarlagadda, *Synlett* **1995**, 751–752.
[9] This compound was prepared in an analogous fashion to **4a**–**c**.
[10] Y. Nesumi, T. Nakazawa, I. Murata, *Chem. Lett.* **1979**, 771–774.
[11] A full account of the thermodynamic parameters of this and related systems will be reported elsewhere.
[12] For the only other example of an *anti*-to-*syn* isomerization, see Y.-H. Lai, Z.-L. Zhou, *J. Org. Chem.* **1994**, *59*, 8275–8278.
[13] Oven techniques (H. A. Staab, M. Haenel, *Chem. Ber.* **1973**, *106*, 2190–2202) may ultimately prove to be a superior method for the thermolysis, but the procedure described here is straightforward, repeatable, gives acceptable yields, and does not require specialty equipment.

A Novel Catalyst with a Cuboidal $PdMo_3S_4$ Core for the Cyclization of Alkynoic Acids to Enol Lactones**

Takanori Wakabayashi, Youichi Ishii, Kazunari Ishikawa, and Masanobu Hidai*

Transition metal sulfide clusters with a cuboidal core or related structure have been found in the active sites of several metalloproteins such as nitrogenase, aconitase, and ferredoxin.[1] In order to elucidate the functions of these unique sulfide cluster structures, which are considered to be responsible for the functions of these proteins, considerable attention has been paid to the synthesis and characterization of model systems, that is cuboidal sulfide clusters containing mainly the first row transition metals.[2] Sulfide clusters of this kind have so far found little application as catalysts for organic synthesis.[3] Thus, in this context, we have prepared sulfide clusters containing metals from Group 10, which might function as catalytically active centers, and have recently synthesized and fully characterized a novel mixed-metal sulfide cluster with a cuboidal core $[PdMo_3S_4(tacn)_3Cl](PF_6)_3$ (**1**; tacn = 1,4,7-triazacyclononane).[4] Cluster **1** catalyzes the selective *trans*-addition of alcohols or carboxylic acids to acetylenes conjugated with electron-withdrawing group(s).[4b, 5] Here we report that cluster **1** is a highly effective catalyst for the cyclization of 3-, 4-, and 5-alkynoic acids to the corresponding enol lactones under very mild conditions.

Convenient and selective synthesis of enol lactones has attracted a great deal of interest because of their biological importance, and the cyclization of readily available alkynoic acids provides one of the most attractive and straightforward synthetic routes to enol lactones. Palladium and rhodium complexes such as $[PdCl_2(PhCN)_2]$ (**2**)[6] and $[RhCl(cycphos)]_2$ (**3**; cycphos = 1,2-bis(dicyclohexylphosphanyl)ethane),[7] as well as several silver[8] and mercury[9] salts have been reported to effect the lactonization of alkynoic acids. However, the catalytic activities of these monometallic catalysts are not necessarily satisfactory. For example, the cyclization of 5-hexynoic acid catalyzed by $PdCl_2$ in CH_3CN gives only a moderate yield of 6-methylene-tetrahydro-2-pyrone even under reflux,[6a] while the same reaction using **3** as the catalyst proceeds at room temperature but very sluggishly (turnover number (TON) = 21 after 50 h; where TON = mol of product per mol of catalyst).[7]

In contrast to the above catalytic systems, cluster **1** is very catalytically active in the lactonization of alkynoic acids in the presence of a small amount of NEt_3 (3 mol%) under mild conditions (20–40 °C, in acetonitrile). Figure 1 illustrates the time

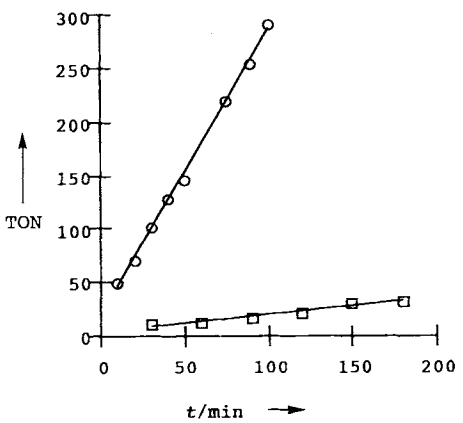

Fig. 1. Time dependence of the TON in the cyclization of **4g** catalyzed by **1** (○) and **2** (□) at 20 °C.

dependence of the TON in the cyclization of 2,2-dimethyl-5-hexynoic acid (**4g**) catalyzed by **1** and **2** at 20 °C to give 3,3-dimethyl-6-methylene-2-pyrone [Eq. (a)]. Kinetic measurements indicated that the reaction catalyzed by **1** is first order with respect to the concentration of both **1** and NEt_3. By comparing the slope of the two curves, the catalytic activity of **1** was evaluated to be 17 times higher than that of **2**. No noticeable decrease in the activity of **1** was observed during the measurement. Furthermore, the UV/Vis spectrum of the reaction solution showed no appreciable change during the catalysis, and

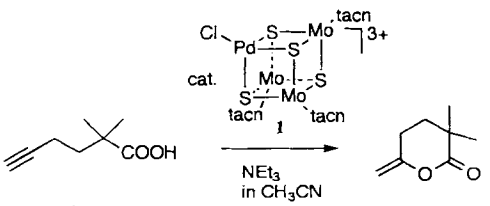

(a)

[*] Prof. M. Hidai, T. Wakabayashi, Dr. Y. Ishii, K. Ishikawa
Department of Chemistry and Biotechnology
Graduate School of Engineering
The University of Tokyo
Hongo, Bunkyo-ku, Tokyo 113 (Japan)
Telefax: Int. code +(3)5800-6945

[**] This work was supported by the Ministry of Education, Science and Culture of Japan.

dilution of the reaction mixture with 1 N aqueous HCl after the reaction reproduced UV/Vis λ_{max} and ε values (463 nm (0.89×10^3), 580 nm (1.36×10^3)) essentially identical to those of **1** in CH_3CN/1 N aqueous HCl. These observations strongly support that the cluster structure of **1** is retained throughout the catalysis and that the active catalyst is a cuboidal cluster species closely related to **1**. It is noteworthy that the palladium center embedded in the molybdenum–sulfide cluster core provides a much more efficient reaction site than mononuclear palladium catalysts. γ-Lactone formation proceeded much faster than the cyclization to δ-lactones. Cluster **1** was found to be 12 times more active than **2** for the cyclization of 2,2-dimethyl-4-pentynoic acid at 20 °C. When 4-pentynoic acid (**4a**) was used as the substrate, the TON reached 100000 after 19 h at 40 °C.

The results of the catalytic cyclization of various alkynoic acids with **1** are summarized in Table 1.[10] 5-Alkynoic acids gave the corresponding δ-lactones, while 3- and 4-alkynoic acids afforded the corresponding γ-lactones as the single product, except for the reaction of 4-hexynoic acid (**4d**), which produced a mixture of γ- and δ-lactones. These reactions proceeded very rapidly under mild conditions. However, the lactonization of 6-heptynoic acid (**4h**) to the corresponding ε-lactone was rather slow and the yield was low even in CH_3CN under reflux conditions in the presence of 50 mol% of NEt_3. Mechanistically, the catalytic cycle is considered to involve intramolecular nucleophilic attack of a carboxylate anion on the C≡C bond of an acetylene coordinated to the palladium center of the cuboidal core, followed by the protonolysis of the resulting vinylpalladium species. This mechanism is basically similar to that proposed for mononuclear metal catalysts. In fact, the stereoselectivity and the ratio of the γ- and δ-lactones found in the reaction of **4d** with complex **1** is closely related to those obtained with complex **3**.[7] Although the catalytic transformation of the substrate by **1** is assumed to proceed only at the palladium center, it is particularly interesting that the palladium atom incorporated into the cuboidal sulfide cluster exhibits significantly enhanced catalytic activity in comparison with mononuclear palladium complexes.

Finally, it should also be pointed out that the above cyclization can be conducted in water, owing to the good solubility and stability of **1** in this medium. Treatment of dipropargylmalonic acid (**4i**) with catalytic amounts of **1** (0.1 mol%) and NEt_3 (1 mol%) in water led to the quick precipitation of the corresponding enol γ-lactone, which amounted to 76% yield after 10 min at 20 °C. A similar reaction catalyzed by $PdCl_2$/NaCl afforded the γ-lactone only in 8.6% yield. The catalytic activity of **1** is also considerably higher than mononuclear palladium species in aqueous media as well. Transformations of organic molecules catalyzed by metal complexes using water as solvent are of current interest in organic synthesis from an economical and environmental point of view.[11] Cluster **1** is expected to provide a new type of intrinsically water-soluble metal complex catalyst.

Table 1. Lactonization of alkynoic acids with **1** as catalyst [a].

Substrate		t [h]	Product	Yield [%] [b]
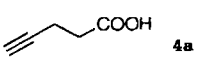	**4a**	6 min 19 [c]	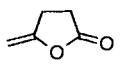	77 (100) 97
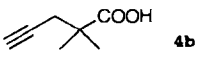	**4b**	1 min	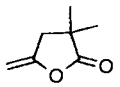	68 (98)
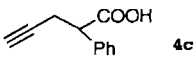	**4c**	2	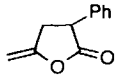	99
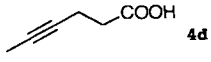	**4d**	4	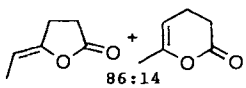 86:14	87
	4e	2	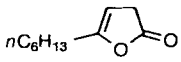	62
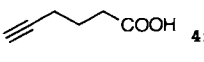	**4f**	3 [d]	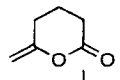	86
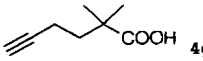	**4g**	2	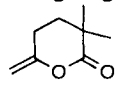	87 (98)
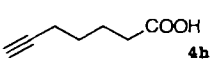	**4h**	10 [e]	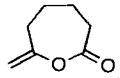	28
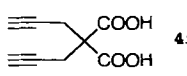	**4i**	1 [d]	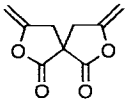	81

[a] Reaction conditions: **4** (3 mmol), NEt_3 (0.1 mmol), **1** (0.01 mmol), MeCN (5 mL), room temperature. [b] Yield of isolated product. The yield determined by GC is given in parentheses. [c] **4a** (0.1 mol), NEt_3 (1 mmol), **1** (1 μmol), 40 °C. [d] 40 °C. [e] **4i** (2 mmol), NEt_3 (1 mmol), reflux.

Experimental Procedure

The following procedure is representative for the catalytic conversion of alkynoic acids to the corresponding enol lactones. 2,2-Dimethyl-5-hexynoic acid (0.42 g, 3.0 mmol), NEt_3 (0.10 mmol, 10.5 mg), and **1** (0.010 mmol, 13.9 mg) were dissolved in acetonitrile (5 mL), and the resulting violet solution was kept at 20 °C. After 2 h, the GC analysis of the reaction mixture indicated that 3,3-dimethyl-6-methylene-2-pyrone was formed in 98% yield. Ether (25 mL) and hexane (25 mL) were added to the mixture, and the resultant violet precipitate was removed by filtration. The colorless filtrate was evaporated to dryness, and the residual oil was further purified by bulb-to-bulb distillation (100 °C/2 mmHg) to give pure 3,3-dimethyl-6-methylene-2-pyrone in 87% yield.

Received: April 10, 1996 [Z90141E]
German version: *Angew. Chem.* **1996**, *108*, 2268–2269

Keywords: catalysis · cyclizations · lactones · molybdenum compounds · palladium compounds

[1] J. J. R. Frausto da Silva, R. J. P. Williams, *The Biological Chemistry of the Elements*, Clarendon Press, Oxford, **1991**.
[2] S. Harris, *Polyhedron* **1989**, *8*, 2843.
[3] M. Rakowski Dubois, *Chem. Rev.* **1989**, *89*, 1.
[4] a) T. Murata, H. Gao, Y. Mizobe, F. Nakano, S. Motomura, T. Tanase, S. Yano, M. Hidai, *J. Am. Chem. Soc.* **1992**, *114*, 8287; b) T. Murata, Y. Mizobe, H. Gao, Y. Ishii, T. Wakabayashi, F. Nakano, T. Tanase, S. Yano, M. Hidai, I. Echizen, H. Nanikawa, S. Motomura, *ibid.* **1994**, *116*, 3389.
[5] T. Wakabayashi, Y. Ishii, T. Murata, Y. Mizobe, M. Hidai, *Tetrahedron Lett.* **1995**, *36*, 5585.
[6] a) C. Lambert, K. Utimoto, H. Nozaki, *Tetrahedron Lett.* **1984**, *25*, 5323. For modified enol lactone synthesis; b) N. Yanagihara, C. Lambert, K. Iritani, K. Utimoto, H. Nozaki, *J. Am. Chem. Soc.* **1986**, *108*, 2753; c) T. Tsuda, Y. Ohashi, N. Nagahama, R. Sumiya, T. Saegusa, *J. Org. Chem.* **1988**, *53*, 2650; d) A. Arcadi, A. Burini, S. Cacchi, M. Delmastro, F. Marinelli B. R. Pietroni, *ibid.* **1992**, *57*, 976; e) X. Lu, X. Huang, S. Ma, *Tetrahedron Lett.* **1993**, *34*, 5963.
[7] D. M. T. Chan, T. B. Marder, D. Milstein, N. J. Taylor, *J. Am. Chem. Soc.* **1987**, *109*, 6385.
[8] a) T.-T. Jong, P. G. Williard, J. P. Porwoll, *J. Org. Chem.* **1984**, *49*, 735; b) P. Pale, J. Chuche, *Tetrahedron Lett.* **1987**, *28*, 6447; c) V. Dalla, P. Pale, *ibid.* **1994**, *35*, 3525.
[9] a) S. W. Rollinson, R. A. Amos, J. A. Katzenellenbogen, *J. Am. Chem. Soc.* **1981**, *103*, 4114; b) G. A. Krafft, J. A. Katzenellenbogen, *ibid.* **1981**, *103*, 5459; c) M. Yamamoto, *J. Chem. Soc., Perkin Trans. 1* **1981**, 582; d) A. Jellal, J. Grimaldi, M. Santelli, *Tetrahedron Lett.* **1984**, *25*, 3179; e) M. J. Sofia, J. A. Katzenellenbogen, *J. Org. Chem.* **1985**, *50*, 2331; f) R. W. Spencer, T. F. Tam, E. Thomas, W. J. Robinson, A. Krantz, *J. Am. Chem. Soc.* **1986**, *108*, 5589.
[10] Cluster **1** was not effective for the catalytic intermolecular addition of carboxylic acids to unactivated acetylenes [5].
[11] D. M. Roundhill, *Adv. Organomet. Chem.* **1995**, *38*, 155.

Palladium-Catalyzed Carbonylative Cyclization Cascades with Iododienes and -trienes**

Christophe Copéret, Shengming Ma, and Ei-ichi Negishi*

In memory of Wolfgang Oppolzer

We report here on a novel palladium-catalyzed cyclization cascade proceeding by carbonylation of ω-iododienes and -trienes. In this cascade, multiple carbon–carbon bonds are formed by acylpalladation cyclization,[1] with incorporation of CO in each cyclization step. The use of CO as a one-carbon unit enables the novel cyclization cascade with an angular mode of ring fusion (Scheme 1).[2]

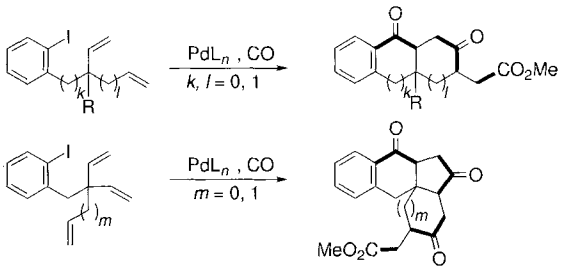

Scheme 1. Acylpalladation cascades with an angular mode of ring fusion.

We have previously reported a series of studies delineating the scope of ring-forming acylpalladation.[3] Despite these acylpalladation reactions giving monocycles and related polymerization processes proceeding by acylpalladation,[4] no acylpalladation cascade forming polycycles appeared to be known. This prompted us to explore the feasibility of this type of reaction cascade and its applicability to the formation of five- and six-membered bicycles and polycycles. With these goals in minds, iododienes and -trienes **1a–e**[5] were subjected to palladium-catalyzed carbonylative cyclization under previously described conditions[3b] (CO (40 atm), $[Pd(PPh_3)_2Cl_2]$ (5 mol%), MeOH (4 equiv), NEt_3 (4 equiv), acetonitrile/benzene (1/1)). The results are summarized in Table 1.

The compounds **1a–c** gave the corresponding tricyclic compounds **2a–c** in good yields as a mixture of diastereomers with no sign of products arising from premature esterification.[6] Of the four possible diastereomers, only two were detected for **2b** and **2c** (Scheme 2). The major diastereomers of **2b** and **2c** showed strong NOE cross-peaks between 3-H, 9a-H, and 3a-CH_2R', strongly pointing to a *cis* ring junction and a *trans* relationship between the (methoxycarbonyl)methyl substituent and the $R'CH_2$ group. Moreover, the minor diastereomer of **2b** was shown by X-ray crystal structure analysis[7] to be the epimer with the (methoxycarbonyl)methyl substituent *cis* to the R group. In contrast, tricycle **2a** was obtained as an inseparable mixture of three diastereomers.

Table 1. Acylpalladation cascade of alkenes [a].

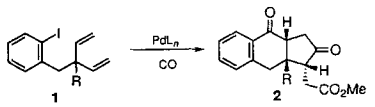

1 2

Starting cmpd.	R	T[°C]	t[h]	Prod. [b]	Yield [%][c]	d.r. [d]	Other products
1a	CH_3	95	8	**2a**	70	2:2:1	–
1b	CH_2OMe	95	14	**2b**	72	2:1	–
1c	2-heptynyl	95	6	**2c**	54	2:1	–
1d	allyl	95	10	**2d**	58	5:1	**3** (12%) [e]
1e	vinyl	95	8	**2e**	35	4:1	**4** (12%) [f]
1e [g]	vinyl	95	8	**2e**	39	4:1	**4** (22%) [f]

[a] Solvent CH_3CN/C_6H_6, if not specified otherwise. [b] Major product shown in the reaction. [c] Yield of isolated product. [d] Ratio of the major diastereomers; the other isomers are present in <5%. [e] Isomeric purity: 88±2%, >98% after recrystallization. [f] Isomeric purity: >98%. [g] Solvent C_6H_6.

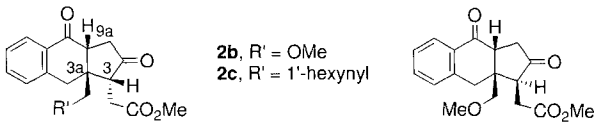

Scheme 2. The major isomers of **2b** and **2c** (left) characterized by NOE experiments, and the minor diastereomer of **2b** (right) characterized by X-ray structure analysis.

The absence of premature trapping products in the reaction of **1a–c** prompted us to investigate the corresponding reaction with iodotrienes for a tricyclization cascade. Under the previously described conditions, **1d** gave **2d** (58%, 5:1 mixture of diastereomers) and **3** (12%, 88±2% stereoisomeric purity); the structure of **3** was firmly established by X-ray crystallography.[8] The formation of **3**, albeit in low yield, is remarkable, as it involves the formation of seven carbon–carbon bonds.[9] The corresponding reaction of **1e** proceeded similarly producing a mixture of **2e** (35%, 4:1 mixture of diastereomers) and **4** (12%, >95% isomerically pure).[10] The use of a less polar solvent,

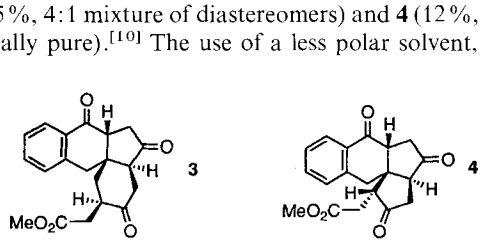

benzene, improved the yield of **4** to 22%. Further attempts to improve the yield of tricyclization are currently underway. It may be worth pointing out that the previously developed cascade with a linear mode of ring fusion[2b] involving noncarbonylative carbopalladation is not applicable to the synthesis of angularly fused polycyclic structures consisting of five- and six-membered rings. The present carbonylative procedure makes this feasible through the incorporation of CO as a one-carbon component.

Having demonstrated the feasibility of the [6-5]-cyclization cascade and its extension to the [6-5-5]- and [6-5-6]-cascades with angular ring fusion,[11] we then examined the possibility of the [5-5]-, [5-6]-, and [6-6]-cyclization cascades. Under the standard conditions, **5** gave compounds **6** (40%) and **7** (38%) both as roughly 1:1 mixtures of diastereomers. This reaction is in sharp contrast with those of **1a–e**, where premature trapping after the first cyclization was not observed. Presumably, a mixture of the *cis*- and *trans*-cyclized intermediates **8a** and **8b** is formed. The intermediate **8a** could readily cyclize to give **6**,

[*] Prof. E. Negishi, C. Copéret, S. Ma
Department of Chemistry, Purdue University
West Lafayette, IN 47907 (USA)
Fax: Int. code +(317)494-0239
e-mail: negishi@ev3.chem.purdue.edu

[**] This research was supported by the U. S. National Institutes of Health (GM 36792). C. C. was a Purdue Research Foundation Graduate Research Fellow (1993–1994). We are grateful to Dr. P. E. Fanwick for X-ray crystallography, Dr. D. V. Carlson, Purdue Chemistry Department NMR Facilities, for technical assistance, and Johnson Matthey for kindly providing $PdCl_2$. We acknowledge that Dr. T. Sugihara was involved in some related aspects of this research.

while **8b**, in which the two substituents are *trans* to each other, would preferentially react with MeOH to give **7** rather than the strained *trans*-bicyclo[3.3.0]octane ring system.[12] Finally, under the standard conditions, **9** and **10** gave **11** (54%, 2:1 mixture of diastereomers) and **12** (38%, 2:1:1 mixture of diastereomers) along with their respective products arising from premature trapping, **13** (14%) and **14** (34%). We have recently shown that

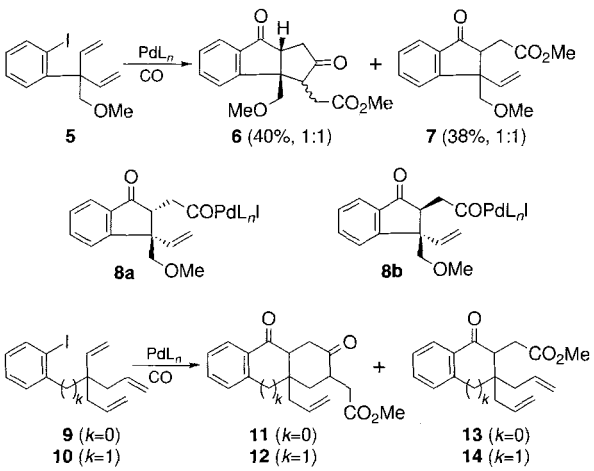

the formation of five-membered rings by acylpalladation is faster than that of six-membered rings.[3b] Consequently, if a six-membered ring is formed in the second cyclization, premature esterification would become a serious side reaction. Generally speaking, the relative effectiveness of the carbonylative cyclization cascade reactions as judged by product yields and ratios is as follows: [6-5]- > [5-6]- > [5-5]- ≥ [6-6]-cascades.

Received: May 14, 1996 [Z9119IE]
German version: *Angew. Chem.* **1996**, *108*, 2255–2257

Keywords: carbonylations · cascade reactions · catalysis · cyclizations · palladium compounds

[1] Acylpalladation can be defined as the addition of the acyl–palladium bond to alkenes and alkynes.

[2] Carbopalladation cascade processes yielding cyclic products have been divided into several categories according to their modes of cyclization: a) E. Negishi, *Pure Appl. Chem* **1992**, *74*, 323; b) L. E. Overman, *ibid.* **1992**, *74*, 1813; c) For some more recent reviews, see: A. de Meijere, F. E. Meyer, *Angew. Chem.* **1994**, *106*, 2473; *Angew. Chem. Int. Ed. Engl.* **1994**, *33*, 2379; E. Negishi, C. Copéret, S. Ma, F. Liu, S.-Y. Liou, *Chem. Rev.* **1996**, *96*, 365.

[3] a) For seminal papers, see: J. A. Miller, E. Negishi, *J. Am. Chem. Soc.* **1983**, *105*, 6761; J. M. Tour, E. Negishi, *ibid.* **1985**, *107*, 8289; b) For recent comprehensive studies, see: E. Negishi, C. Copéret, S. Ma, T. Mita, T. Sugihara, J. M. Tour, *ibid.* **1996**, *118*, 5904; E. Negishi, S. Ma, J. Amanfu, C. Copéret, J. A. Miller, J. M. Tour, *ibid.* **1996**, *118*, 5919.

[4] Copolymerization of alkenes and CO proceeds by a series of intermolecular acylpalladation reactions without ring closure. a) For seminal papers, see: J. Tsuji, S. Hosaka, *J. Polym. Lett.* **1965**, *3*, 705; A. Sen, T. W. Lai, *J. Am. Chem. Soc.* **1982**, *104*, 3520; b) For recent reviews, see: A. Sen, *Acc. Chem. Res.* **1993**, *26*, 303; E. Drent, P. H. M. Budzelaar, *Chem. Rev.* **1996**, *96*, 663.

[5] Synthesis of **1a**: Ethyl crotonate was alkylated with 2-iodobenzyl bromide to give ethyl 2-(2-iodobenzyl)-3-butenoate. This compound was then alkylated according to the same procedure with MeI to give the corresponding esters. Reduction of the ester group with *i*Bu$_2$AlH followed by oxidation with pyridinium chlorochromate/Celite and olefination with CH_2=PPh_3 gave **1a**. For the α-alkylation of esters, see: J. L. Herrmann, G. H. Kieczykowski, R. H. Schlessinger *Tetrahedron Lett.* **1973**, 2433.

[6] Analysis of the ^{1}H NMR spectrum of the crude reaction mixture.

[7] Crystallographic data (excluding structure factors) for the structures reported in this paper have been deposited with the Cambridge Crystallographic Data Center as supplementary publication no. CCDC-179-84. Copies of the data can be obtained free of charge on application to The Director, CCDC, 12 Union Road, Cambridge CB21EZ, UK (fax: Int. code +(1223)336-033; e-mail: teched@chemcrys.cam.ac.uk).

[8] Crystals of **3** were obtained from MeOH/pentane; ref. [7].

[9] For examples of cyclization cascades with the formation of five carbon–carbon bonds: a) B. M. Trost, Y. Shi, *J. Am. Chem. Soc.* **1991**, *113*, 701; b) T. Sugihara, C. Copéret, Z. Owczarczyk, L. S. Harring, E. Negishi, *ibid.* **1994**, *116*, 7923.

[10] The configuration of **4** was established by ^{1}H,^{1}H-COSY, gf-HMQC, gf-HMBC, and NOESY experiments, and further confirmed by X-ray crystallography [7]. For a reference on NMR techniques, see H. Günther, *NMR Spectroscopy. Basic Principles, Concepts, and Applications in Chemistry*, 2nd ed., Wiley, Chichester, **1995**.

[11] The numbers in square brackets refer to the size of each ring formed during the cascade reaction in the order of their formation.

[12] For some examples of transition metal promoted synthesis of *trans*-bicyclo[3.3.0]octanes: a) C. J. Rousset, D. R. Swanson, F. Lamaty, E. Negishi, *Tetrahedron Lett.* **1989**, *30*, 5105; b) W. A. Nugent, D. F. Taber, *J. Am. Chem. Soc.* **1989**, *111*, 6435; c) E. Negishi, D. Choueiry, T. B. Nguyen, D. R. Swanson, N. Suzuki, T. Takahashi, *ibid.* **1994**, *116*, 9761.

Bis(guanidinium) Alcohols as Models of Staphylococcal Nuclease: Substrate Binding through Ion Pair Complexes and Fast Phosphoryl Transfer Reactions**

Marc-Steffen Muche and Michael W. Göbel*

In memory of Wolfgang Oppolzer

For the past few years our interest has focused on the synthesis of simple, non-peptidic molecules that mimic structural and functional aspects of staphylococcal nuclease.[1, 2] The active site of this enzyme contains two arginine units, which, in conjunction with a calcium ion, lead to the electrophilic activation of phosphodiester substrates for hydrolysis.[3] The most important factor for catalysis is the optimal complexation of the pentacoordinated transition state structures by the guanidinium groups.[4] Scheme 1 illustrates our working hypothesis for the construction of metal-free "synthetic phosphodiesterases"[5, 6] along the lines of staphylococcal nuclease.

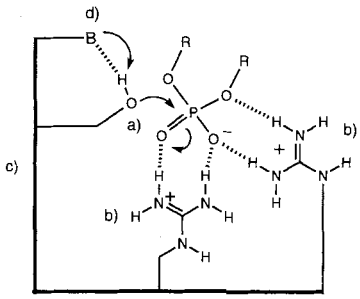

Scheme 1. Construction principle behind a synthetic phosphodiesterase. a) Nucleophile; b) guanidinium ions which contribute to the electrostatic stabilization of the transition state and to the protonation of the leaving group; c) supporting molecular framework; d) base which activates the nucleophile (not yet realized).

Since translating Scheme 1 into concrete chemical structures is not simple, we have examined individual aspects of the problem. We first studied the phosphorylation of monocationic alcohols of type **1**.[2a, d, e] Compound **1** and phosphodiesters form ion pair complexes reversibly, in which facile phosphoryl transfer to the hydroxyl

[*] Prof. Dr. M. W. Göbel, Dipl.-Chem. M.-S. Muche
Département de Chimie Organique, Université de Genève
30 quai Ernest-Ansermet, CH-1211 Genève 4 (Switzerland)
Fax: Int. code +(22)328-7396
e-mail: michael.goebel@chiorg.unige.ch

[**] This work was supported by the Fonds der Chemischen Industrie, by the Deutsche Forschungsgemeinschaft, and by the Schweizerischer Nationalfonds zur Förderung der wissenschaftlichen Forschung. We thank André Pinto and Philippe Kamalaprija for recording the ^{31}P NMR spectra.

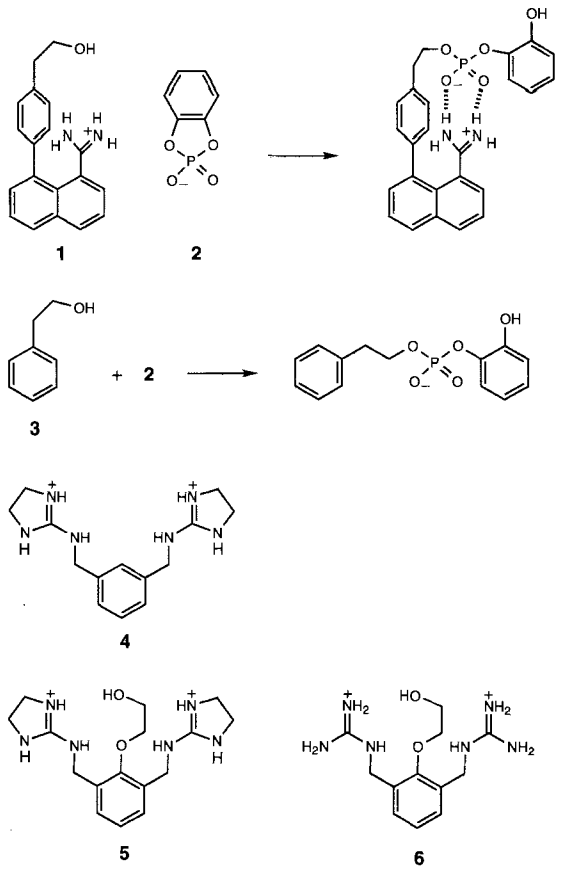

group occurs. Phosphorylation of **1** with cyclophosphate **2** is 2700 times faster than that of the uncharged alcohol **3**.[2a, d] This acceleration is explained not only by the close proximity of nucleophile and substrate in the ion pair (**1**·**2**); electrophilic activation of the phosphodiester through coordination to the amidinium ion also plays a role. This effect is observed for a variety of mono-, bis-, and tris(guanidinium) compounds.[2b, c] Thus, the rate of phosphorylation of **3** with **2** is increased by a factor of almost 5000 in the presence of bis(guanidinium) ion **4**. Compound **4** and related species are also effective catalysts for other phosphoryl transfer reactions.[7, 8] In an attempt to combine the structural characteristics of alcohol **1** and dication **4** we have now prepared compounds **5** and **6** and have studied their reaction with cyclophosphate **2**.

The syntheses of **5** and **6** are outlined in Scheme 2. The incorporation of a second cationic unit proved to increase both the reaction rates (see below) and the strength of substrate binding. ^{31}P NMR titration of **2** with **5** in the absence of base led to an association constant K_a of 2900($\pm$800) M^{-1} (DMF/[D$_7$]DMF = 2:1, 30 °C). The association constant of the ion pair (**1**·**2**) has a modest value of 190 M^{-1}. When base is added to a mixture of **2** and **5**, the hydroxyl group is phosphorylated readily giving **9** in high yield (DMF, 0.25 M diisopropylethylamine, 30 °C; Scheme 3). Compound **9**, isolable as the monopicrate salt, was characterized by ^{1}H and ^{31}P NMR spectroscopy, ESI mass spectrometry, and elemental analysis. In contrast to the phosphorylation of **1**, formation of **9** is reversible. In experiments conducted with a range of initial concentrations, equilibrium was achieved with an equilibrium constant of almost 150 M^{-1} at conversions between and 60 and 94% (Table 1, Fig. 1). The reverse reaction of **9** leading to cyclophosphate **2** can be observed directly by ^{31}P NMR spectroscopy.

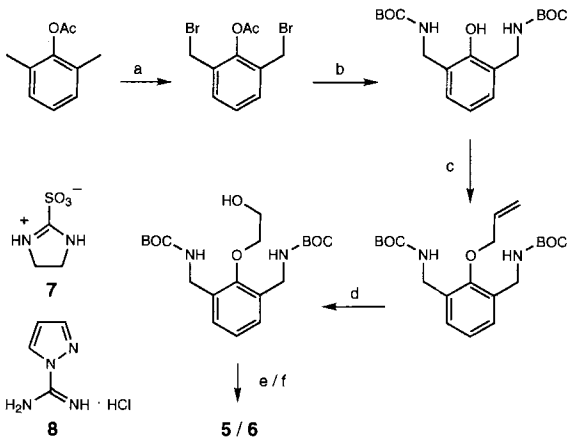

Scheme 2. Synthesis of bis(guanidinium) alcohols **5** and **6**. a) *N*-bromosuccinimide (NBS), HCO_2Me, azoisobutyronitrile (AIBN), Δ, *hν*, 3 h, 69%. b) 1. $NaN(CHO)_2$, *N*,*N*-dimethylformamide (DMF), 80 °C, 3 h; 2. 3 M HCl, Δ, 7 h; 3. $(BOC)_2O$, (BOC = *tert*-butoxycarbonyl), dioxane, aq. NaOH, room temperature (RT), 16 h, 80%. c. Allyl bromide, Cs_2CO_3, DMF, 80 °C, 2 h, >95%. d) 1. O_3, MeOH, −90 °C; 2. $NaBH_4$, RT, 16 h, 75%. e) 1. HCl, MeOH, RT, 2 h; 2. **7** [11], MeOH, H_2O, NEt_3, RT, 16 h; 3. picric acid, >95%. f) 1. HCl, MeOH, RT, 2 h; 2. **8** [12], MeOH, H_2O, NEt_3, RT, 16 h; 3. picric acid, 70%.

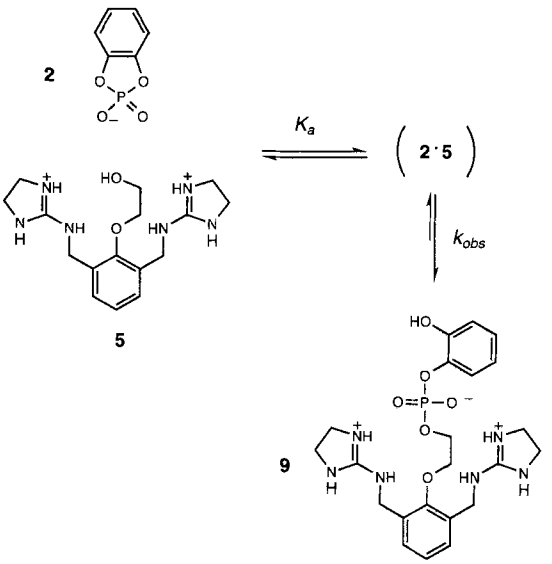

Scheme 3. Phosphorylation of **5** to give **9** via the intermediate ion pair (**2**·**5**). Counterions employed: picrate, tetramethylguanidinium.

Table 1. Phosphorylation of bis(guanidinium) alcohol **5** to give **9**. Equilibrium concentration of **9** and pseudo-first-order rate constants depend on the starting concentrations c_0(**2**) and c_0(**5**). DMF, 0.25 M diisopropylethylamine, 30 °C; counterions: picrate, tetramethylguanidinium.

c_0(**2**)	c_0(**5**)	c(**9**)	k_{obs}
0.025 M	0.025 M	0.015 M	
0.075 M	0.025 M	0.022 M	
0.05 M	0.05 M	0.033 M	4.6×10^{-3} min^{-1}
0.15 M	0.05 M	0.047 M	8.0×10^{-3} min^{-1}

The kinetics of the forward reaction were determined by ^{31}P NMR spectroscopy and by HPLC (Table 1). For c_0(**5**) = 0.05 M and c_0(**2**) = 0.15 M the pseudo-first-order rate constant of the bis(guanidinium) compound **5** (k_{obs} = 8.0($\pm$1)$\times10^{-3}$ min^{-1}) far exceeds the values of all other alcohols we have examined up to now. Compound **5** is phosphorylated 800 times faster than

 © VCH Verlagsgesellschaft mbH, D-69451 Weinheim, 1996 0570-0833/96/3518-2127 $ 15.00+.25/0

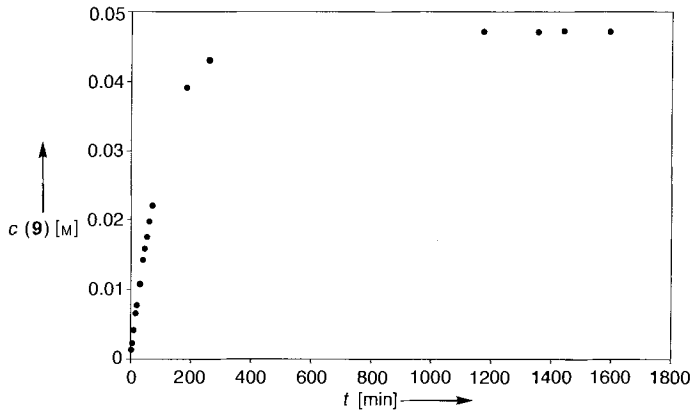

Fig. 1. Plot of the phosphorylation of **5** to give **9** versus time (c_0(**2**) = 0.15 M, c_0(**5**) = 0.05 M, DMF, 0.25 M diisopropylethylamine, 30 °C). An equilibrium is established.

the monocation **1** ($k_{obs} = 9.9 \times 10^{-6}$ min^{-1}). To compare **5** with the uncharged alcohol **3** ($k_2 = 2.4 \times 10^{-7}$ M^{-1} min^{-1}) a formal second-order rate constant can be derived ($k_{2obs} = k_{obs}/c_0$(**2**)). According to this, in the experiment with c_0(**2**) = c_0(**5**) = 0.05 M, the phosphorylation of **5** is 380000 times faster than the reaction of phenylethanol. At high dilution the limiting value of k_{2obs} is determined by $K_a k_1$. The maximum acceleration factor of 10^8, which can in theory be obtained when $k_{obs} = k_1$, is too high, because k_{obs} depends significantly on the starting concentration of alcohol **5**.[9] An acceleration factor of 10^6 to 10^7 is more realistic.

As previously observed with compound **4**,[2b] the replacement of the heterocyclic cations by unsubstituted guanidinium groups (**5** → **6**) also leads to a marked loss in reactivity of the dicationic alcohols. For the phosphorylation of **6** a value of $k_{obs} = 7.5(\pm 1) \times 10^{-4}$ min^{-1} was determined (c_0(**6**) = 0.05 M, c_0(**2**) = 0.15 M, DMF, 0.25 M diisopropylethylamine, 30 °C). The superiority of the 2-aminoimidazolinium ions over guanidinium groups is probably related to their higher acidity, as potentiometric titrations of **5** and **6** indicate. This enhanced acidity could affect the rate of reaction in two ways: a) The transition state in the addition step could be stabilized more effectively by stronger hydrogen bonding (or even protonation?). b) During the elimination the protonation of the leaving group could be facilitated.

Base concentrations of 0.25 M still appear to suffice for some deprotonation of the cations in **5**. This is evident from slight shifts in the NMR signals. Thus it cannot be excluded that the heterocycles function as general bases. N-Phosphorylated intermediates, the main products of the reaction with bis(4-nitrophenyl) phosphate, cannot be detected in even trace amounts in the ^{31}P NMR spectra of reaction mixtures of **2** and **5**. If they exist at all, they must be short-lived.

In view of the strained structure of cyclophosphate **2**, the reversibility of its reaction with **5** is remarkable. A structural aspect can be considered as a possible explanation in addition to the increased acidity of the glycolic hydroxyl group. According to molecular models, an ideal arrangement of cations and anion (four NH···O hydrogen bonds) is possible in the complex of **2** and **5** together with a correct orientation of the nucleophile. However, the hydroxylated side chain is so short that the phosphoryl group in product **9** is pulled out of the optimal position. As a result the ground state of **9** is thermodynamically destabilized, and only high-energy substrates can react.[10] Thus optimizing the side chain structure of **5** will be among the most important measures for achieving the tremendous acceleration effects obtained with cyclophosphate **2** with nonactivated phosphodiesters as well.

Experimental Procedure

4,5-Dihydro-1*H*-imidazolium 2-sulfonate (**7**) [11]: A suspension of *N*,*N*′-ethylenethiourea (2.5 g, 24.5 mmol) in 30 mL of water was treated with sodium molybdate dihydrate (18 mg, 0.075 mmol, 0.003 equiv) and cooled to 0 °C in an ice bath. To the suspension was added dropwise (temperature ≤ 5 °C) 15% hydrogen peroxide solution (16.8 mL, 74 mmol, 3 equiv). After the addition was complete, the ice bath was removed and the reaction mixture allowed to warm to roughly 20 °C. After a further 90 min the reaction solution was diluted with 50 mL of methanol and stored in a refrigerator for about 12 h. 1.56 g (42%) of **7** crystallized. M.p. 142 °C (decomp; water/methanol). ^{1}H NMR (270 MHz, [D$_6$]DMSO): δ = 3.86 (s, 4H, ethylene CH$_2$), 10.38 (br. s, 2H, NH). $C_3H_6N_2O_3S$ (150.16): calcd: C 24.00, H 4.03, N 18.66; found: C 24.10, H 4.19, N 18.46.

5: The BOC-protected alcohol (306 mg, 0.77 mmol) was dissolved in 2 mL of methanol and treated with 2 mL of methanolic hydrochloric acid. After 2 h the reaction mixture was concentrated to dryness under vacuum to give a colorless solid. This residue was dissolved in methanol/water/triethylamine (1:1:1; 6 mL), compound **7** (255 mg, 1.7 mmol, 2.2 equiv) was added, and the reaction mixture was stirred at about 20 °C for 12 h. The reaction mixture was diluted with 4 mL of 1 M sodium hydroxide and extracted twice with CH_2Cl_2. The aqueous phase was concentrated to half of its volume under vacuum, acidified with 2 M hydrochloric acid (pH 3–4), and concentrated to dryness. The dried solid residue was heated at reflux in 5 mL of methanol, the resulting mixture cooled and filtered. This procedure was repeated two more times. Water was added to the combined filtrates until a clear solution formed. A solution of picric acid (2 equiv) in methanol was added; then water was added until the solution became cloudy. The precipitating product was redissolved on heating. Slow cooling and crystallization afforded 590 mg (97%) of **5** (bispicrate). M.p. 196 °C (methanol/water). ^{1}H NMR (270 MHz, [D$_6$]DMSO): δ = 3.62 (s, 8H, ethylene CH$_2$), 3.76 (m, 2H, CH$_2$), 3.89 (t, J = 4.4 Hz, 2H, CH$_2$), 4.45 (d, J = 6.0 Hz, 4H, benzylic CH$_2$), 5.28 (br. s, 1H, OH), 7.23 (m, 3H, aromatic H), 7.45–8.45 (br. s, 4H, guanidine H), 8.51 (t , J = 6.0 Hz, 2H, benzyl NH), 8.60 (s, 4H, picrate H). $C_{28}H_{30}N_{12}O_{16}$ (790.62): calcd: C 42.54, H 3.82, N 21.26; found: C 42.58, H 4.06, N 21.49.

Received: March 21, 1996 [Z 8958 IE]
German version: *Angew. Chem.* **1996**, *108*, 2263–2265

Keywords: enzyme mimetics · guanidines · molecular recognition · phosphorylations

[1] Review: A. J. Kirby, *Angew. Chem.* **1996**, *108*, 770–790; *Angew. Chem. Int. Ed. Engl.* **1996**, *35*, 705–724.

[2] a) M. W. Göbel, J. W. Bats, G. Dürner, *Angew. Chem.* **1992**, *104*, 217–218; *Angew. Chem. Int. Ed. Engl.* **1992**, *31*, 207–209; b) R. Groß, G. Dürner, M. W. Göbel, *Liebigs Ann. Chem.* **1994**, 49–58; c) R. Groß, J. W. Bats, M. W. Göbel, *ibid.* **1994**, 205–210; d) G. Müller, G. Dürner, J. W. Bats, M. W. Göbel, *ibid.* **1994**, 1075–1092; e) D. Reckenbeil, J. W. Bats, G. Dürner, M. W. Göbel, *ibid.* **1994**, 1219–1229.

[3] F. A. Cotton, E. E. Hazen, Jr., M. J. Legg, *Proc. Natl. Acad. Sci. USA* **1979**, *76*, 2551–2555.

[4] E. H. Serpersu, D. Shortle, A. S. Mildvan, *Biochemistry* **1987**, *26*, 1289–1300; J. K. Judice, T. R. Gamble, E. C. Murphy, A. M. de Vos, P. G. Schultz, *Science* **1993**, *261*, 1578–1581; J. Åqvist, A. Warshel, *Biochemistry* **1989**, *28*, 4680–4689.

[5] Recent examples of metal ion mediated hydrolysis of phosphodiesters: B. Linkletter, J. Chin, *Angew. Chem.* **1995**, *107*, 529–531; *Angew. Chem. Int. Ed. Engl.* **1995**, *34*, 472–474; D. Wahnon, A. M. Lebuis, J. Chin, *ibid.* **1995**, *107*, 2594–2597 and **1995**, *34*, 2412–2414; B. K. Takasaki, J. Chin, *J. Am. Chem. Soc.* **1995**, *117*, 8582–8585; M. J. Young, J. Chin, *ibid.* **1995**, *117*, 10577–10578; M. Komiyama, N. Takeda, Y. Takahashi, H. Uchida, T. Shiiba, T. Kodama, M. Yashiro, *J. Chem. Soc. Perkin Trans. 2* **1995**, 269–274; M. Komiyama, N. Takeda, T. Shiiba, Y. Takahashi, Y. Matsumoto, M. Yashiro, *Nucleosides Nucleotides* **1994**, *13*, 1297–1309; M. Komiyama, *J. Biochem. (Tokyo)* **1995**, *118*, 665–670; E. Kövári, J. Heitker, R. Krämer, *J. Chem. Soc. Chem. Commun.* **1995**, 1205–1206; J. Rammo, R. Hettich, A. Roigk, H.-J. Schneider, *ibid.* **1996**, 105–107; R. Breslow, B. L. Zhang, *J. Am. Chem. Soc.* **1994**, *116*, 7893–7894; J. Hall, D. Hüsken, U. Pieles, H. E. Moser, R. Häner, *Chem. Biol.* **1994**, *1*, 185–190; J. K. Bashkin, E. I. Frolova, U. S. Sampath, *J. Am. Chem. Soc.* **1994**, *116*, 5981–5982; D. Magda, R. A. Miller, J. L. Sessler, B. L. Iverson, *ibid.* **1994**, *116*, 7439–7440; A. Tsubouchi, T. C. Bruice, *ibid.* **1994**, *116*, 11614–11615; A. Tsubouchi, T. C. Bruice, *ibid.* **1995**, *117*, 7399–7411; L. M. T. Schnaith, R. S. Hanson, L. Que, Jr., *Proc. Natl. Acad. Sci. USA* **1994**, *91*, 569–573. For further references see [2].

[6] Reactions of metal-coordinated alcohols comparable to the phosphorylation of **1**: M. J. Young, D. Wahnon, R. C. Hynes, J. Chin, *J. Am. Chem. Soc.* **1995**,

117, 9441–9447; E. Kimura, Y. Kodama, T. Koike, M. Shiro, *ibid.* **1995**, *117*, 8304–8311; I. O. Kady, B. Tan, Z. Ho, T. Scarborough, *J. Chem. Soc. Chem. Commun.* **1995**, 1137–1138; J. R. Morrow, K. Aures, D. Eppstein, *ibid.* **1995**, 2431–2432.

[7] V. Jubian, R. P. Dixon, A. D. Hamilton, *J. Am. Chem. Soc.* **1992**, *114*, 1120–1121; J. Smith, K. Ariga, E. V. Anslyn, *ibid.* **1993**, *115*, 362–364; V. Jubian, A. Veronese, R. P. Dixon, A. D. Hamilton, *Angew. Chem.* **1995**, *107*, 1343–1345; *Angew. Chem. Int. Ed. Engl.* **1995**, *34*, 1237–1239; M. W. Hosseini, A. J. Blakker, J.-M. Lehn, *J. Am. Chem. Soc.* **1990**, *112*, 3896–3904; B. Barbier, A. Brack, *ibid.* **1992**, *114*, 3511–3515.

[8] Complexation of phosphates by bis(guanidines) and related compounds: B. Dietrich, D. L. Fyles, T. M. Fyles, J.-M. Lehn, *Helv. Chim. Acta* **1979**, *62*, 2763–2787; R. P. Dixon, S. J. Geib, A. D. Hamilton, *J. Am. Chem. Soc.* **1992**, *114*, 365–366; D. M. Kneeland, K. Ariga, V. M. Lynch, C.-Y. Huang, E. V. Anslyn, *ibid.* **1993**, *115*, 10042–10055; F. Chu, L. S. Flatt, E. V. Anslyn, *ibid.* **1994**, *116*, 4194–4204; V. Král, H. Furuta, K. Shreder, V. Lynch, J. L. Sessler, *ibid.* **1996**, *118*, 1595–1607; B. L. Iverson, K. Shreder, V. Král, P. Sansom, V. Lynch, J. L. Sessler, *ibid.* **1996**, *118*, 1608–1616; W. Peschke, F. P. Schmidtchen, *Tetrahedron Lett.* **1995**, 5155–5158; G. Deslongchamps, A. Galán, J. de Mendoza, J. Rebek, Jr., *Angew. Chem.* **1992**, *104*, 58–60; *Angew. Chem. Int. Ed. Engl.* **1992**, *31*, 61–63.

[9] A superposition of first and higher order reaction channels was also evident in the case of the amidinium alcohol **1**. Here, k_1 was determined exactly by extrapolating k_{obs} to $c_0(1) = 0$ [2d]. This has not yet been successful with **5**.

[10] F. M. Menger, M. Ladika, *J. Am. Chem. Soc.* **1987**, *109*, 3145–3146.

[11] C. A. Maryanoff, J. N. Plampin, R. C. Stanzione, US 4,656,291, **1988**; *Chem. Abstr.* **1988**, *108*, 21911.

[12] M. S. Bernatowicz, Y. Wu, G. R. Matsueda, *J. Org. Chem.* **1992**, *57*, 2497–2502.

Dibromine Monoxide, Br_2O, and Bromine Dioxide, OBrO: Spectroscopic Properties, Molecular Structures, and Harmonic Force Fields**

Holger S. P. Müller,* Charles E. Miller, and Edward A. Cohen

The halogen oxides show great variations in structural parameters and other physical as well as chemical properties. Over a dozen chlorine oxides are known, and many of them are quite well characterized. Bromine oxides are unstable at room temperature; thus few of them are known.[1] Even fewer have been studied structurally, generally in the solid state. Structure determinations of free molecules have been confined to the BrO radical.[2]

Recently the chlorine and bromine oxides have attracted considerable attention because of their implication in reaction cycles leading to the destruction of atmospheric ozone. Of particular importance are the catalytic cycles involving ClO and BrO. Recently, bromine dioxide, OBrO, has been observed in the bromine-sensitized photodecomposition of O_3.[3, 4]

Dibromine monoxide, Br_2O, was obtained in low yields from the reaction of Br_2 with HgO.[5] Bromine dioxide was first reported by Schwarz and Schmeisser as an egg-yellow deposit from a Br_2/O_2 discharge.[6] The stoichiometry of the oxide was deduced by quantitative analysis. Its controlled decomposition below 0 °C enabled Schmeisser and Wiele to obtain pure Br_2O.[7] Later, Schmeisser and Jörger reported that the ozonolysis of Br_2 in cooled CCl_3F solution yielded OBrO.[8] In contrast, Seppelt et al. obtained single crystals of orange Br_2O_3[9] and colorless Br_2O_5[10] from that reaction but found no evidence for molecular OBrO. OBrO was detected during mass spectrometric investigations of the $O + Br_2$ reaction system,[11] ESR studies of X-ray irradiated perbromates,[12] and UV/Vis spectroscopic investigations of the $Br + O_3$ reaction system.[3, 4] The ν_1[13] and ν_3[13, 14] stretching fundamentals of the oxide were observed in Ar matrices.

Studies on Br_2O included determination of the melting point,[7] the solution[5c] and gas-phase UV/Vis spectra,[15] the solid-state Raman spectrum,[16] the solid-state structure from EXAFS (*e*xtended *X*-ray *a*bsorption *f*ine *s*tructure) data,[17] and the heat of formation.[15] The symmetric stretching vibration ν_1[14] or both stretching modes[17, 18] were observed in Ar[14, 18] or N_2 matrices.[17]

We have observed the rotational spectra of the triatomic oxides Br_2O and OBrO in the millimeter- and submillimeter-wave regions using the spectrometer described in reference [19]. We report here some of the fundamental spectroscopic constants as well as derived properties such as structure and harmonic force field.

Initially, Br_2O was obtained when Br_2 was passed through a column of HgO at room temperature, and the products were flowed through the microwave absorption cell. Although the yields were low, in agreement with earlier work,[5] many transitions were observed with no or little signal averaging.

OBrO was formed when the reaction products of an O_2 discharge plus Br_2 were condensed onto the wall of the microwave absorption cell at −20 °C. After the flow of O_2 and Br_2 was stopped, spectra of the vapor were recorded while pumping on the condensate. The identity of the product on the wall is not clear. It might be OBrO, a more complex bromine oxide, or a mixture of oxides that decompose slowly to yield OBrO. At low temperatures (≈ −20 °C) and pressures (≈0.1 Pa) essentially all absorption features were due to OBrO, although weak features of BrO were also seen. The amount of OBrO increased at higher temperatures because of a larger vapor pressure or an enhanced decomposition of its precursor. The BrO/OBrO ratio increased as well, possibly because of decomposition of OBrO. Strong absorptions of Br_2O were also seen at higher pressures (reduced flow rate) and higher temperatures. This method was subsequently used for further study of Br_2O.

The hyperfine patterns of $^{79}Br_2O$ and $^{81}Br_2O$ are consistent with their C_{2v} symmetry, whereas $^{79/81}Br_2O$ has C_s symmetry. At low J or K_a quantum numbers the splittings between single hyperfine components can be several tens of MHz, and the patterns often are complex. At high J and K_a quantum numbers usually several components overlap and symmetric triplets or quartets, or even single lines are seen, as shown in Figure 1. Additional complications arise from perturbations of the quadrupole patterns due to effects of the off-diagonal quadrupole coupling constant χ_{ab}.

The OBrO rotational spectrum is that of a C_{2v}-symmetric molecule in the $^2B_1$ electronic ground state, as is that of OClO. In general, each rotational transition is observable as a doublet of quartets. This is illustrated in Figure 2 for a transition with rather small splittings. The doublets indicate the presence of an unpaired electron, the quartets are due to one nucleus with spin 3/2 (^{79}Br or ^{81}Br).

A large number of lines was observed for Br_2O (>700) and OBrO (>1400), resulting in the precise determination of

[*] Dr. H. S. P. Müller, Dr. C. E. Miller, Dr. E. A. Cohen
Jet Propulsion Laboratory
California Institute of Technology
Mail Stop 183–301
4800 Oak Grove Drive, Pasadena, CA 91109-8099 (USA)
Fax: Int. code +(818)3548460
e-mail: hspm@spec.jpl.nasa.gov

[**] H. S. P. M. and C. E. M. thank the National Research Council for NRC-NASA Resident Research Associateships. The research was performed at the Jet Propulsion Laboratory, California Institute of Technology, under a contract with the National Aeronautics and Space Administration.

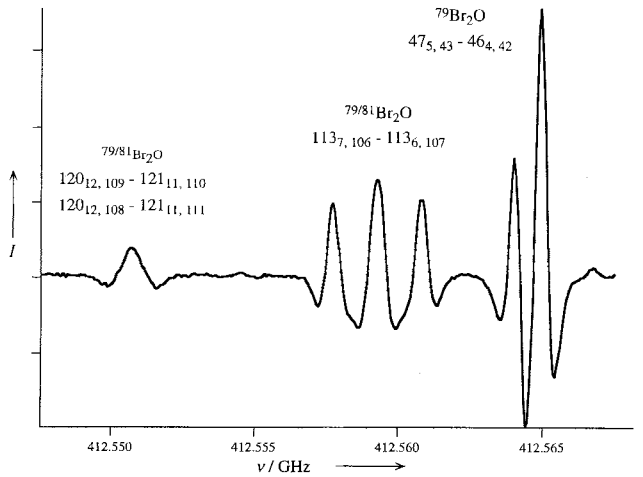

Fig. 1. Section from the submillimeter spectrum of Br_2O, which demonstrates significant intensity and quadrupole splitting for high J transitions. The asymmetric pattern of the $47_{5,43} - 46_{4,42}$ transition is caused by the off-diagonal quadrupole coupling constant χ_{ab}. I = intensity in arbitrary units.

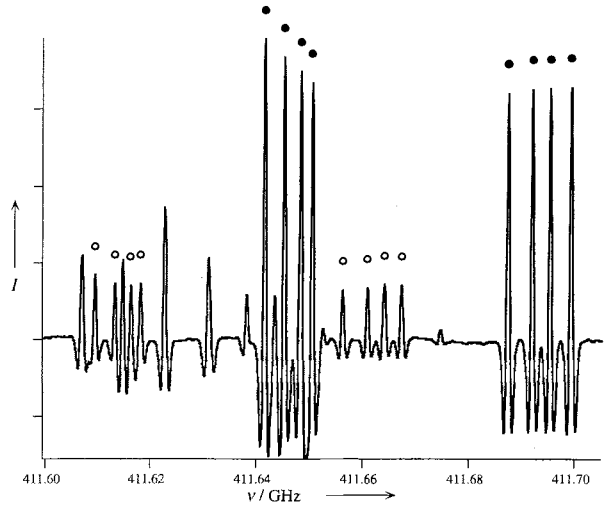

Fig. 2. Section from the submillimeter spectrum of the bromine dioxide radical. The $31_{1,30} - 30_{2,29}$ transition of $O^{81}BrO$ in the ground vibrational state (filled circles) and of $O^{79}BrO$ in the first excited bending mode (open circles) are indicated. In general each transition appears as a doublet of quartets; see text for details.

rotational, centrifugal distortion, fine (OBrO only), and Br hyperfine structure constants as well as distortion terms on fine and some hyperfine constants. Rotational and quartic centrifugal distortion constants for the vibrational ground state are given in Table 1 for $^{79}Br_2O$ and $O^{79}BrO$.

Table 1. Rotational [MHz] and quartic centrifugal distortion constants [a] [kHz] of $^{79}Br_2O$ and $O^{79}BrO$ in the ground vibrational states.

Parameter	$^{79}Br_2O$	$O^{79}BrO$
A	33220.6172 (64)	28024.51786 (111)
B	1368.30433 (29)	8233.17265 (32)
C	1313.37607 (39)	6345.43314 (32)
D_J	0.285030 (82)	7.13486 (48)
D_{JK}	−19.1365 (26)	−70.6925 (33)
D_K	1051.319 (126)	714.380 (27)
$1000\ d_1$	−19.6723 (124)	−2637.543 (124)
$1000\ d_2$	−0.3533 (29)	−156.555 (53)

[a] Numbers in parentheses are two standard deviations in units of the least significant figures. Watson's S reduction is used in the representation I^r [20].

The principal planar moments have been used to calculate the r_0 structural parameters. They are given with data for the related chlorine compounds in Table 2. The structural parameters of different isotopomers agree well within the quoted digits. However, structural ambiguities due to vibrational effects are of up to the order of ±0.2 pm and 0.2° for Br_2O and ±0.15 pm and 0.25° for OBrO.[20] The equilibrium (r_e) structures of Br_2O and OBrO have not been determined. For both molecules the r_e bond lengths are about 0.5 pm smaller than the r_0 parameters, as estimated from the changes of related molecules; the r_e bond angles are expected to agree with the r_0 data to within the uncertainties ascribed to vibrational effects.

Table 2. Structural parameters [pm, °] [a] and harmonic force constants [N m^{-1}] of Br_2O and OBrO in comparison with related chlorine compounds.

Parameter	Br_2O [a]	Cl_2O [b,c]	OBrO[a]	OClO[b,d]
r	184.29 (20)	169.59	164.91 (15)	146.984
α	112.24 (20)	110.88	114.44 (25)	117.403
f_r	288.2	294.9	530.5	711.0
f_α	103.3	123.7	99.5	137.2
f_{rr}	38.7	50.4	−3.1	−25.0
f_r	29.6	31.2	−4.1	−2.7

[a] This work; r_0 structure with estimated upper limits for uncertainties, see text. [b] Equilibrium structure. [c] Ref. [21]. [d] Refs. [22,23].

The present structural parameters of Br_2O support the EXAFS results (185 (1) pm and 112 (2)°) for the molecular solid.[17] However, the present values are more precise and refer to the free molecule. The changes in structural parameters are smaller from Cl_2O to Br_2O than from Cl_2O to F_2O, which is in agreement with the corresponding results in the HOBr, HOCl, HOF series.[1]

The differences in bond lengths are smaller between Br_2O and Cl_2O (14.2 pm) than between OBrO and OClO (17.4 pm). This can be explained by the decreased tendency of Br compared to Cl to form double bonds. For both chlorine oxides, known r_e values were employed, for the two bromine oxides the estimates of r_e.

The quartic distortion constants have been used to calculate the harmonic force fields for both bromine oxides. Vibrational data for Br_2O were taken from reference [18]. The force constants are also given in Table 2 together with those of related molecules.

The stretching force constants f_r of Br_2O and Cl_2O are remarkably similar, possibly a reflection of the pure single-bond character. The larger stretching force constants and shorter bond lengths in OBrO and OClO compared to those of Br_2O and Cl_2O are indicative of substantial double-bond character in the dioxides.

For Br_2O both f_α and $f_{r\alpha}$ and the values of the quartic centrifugal distortion constants are strongly interdependent. The present force field indicates a value of 180 cm^{-1} for the ν_2 band center, which may be compared to 197 cm^{-1} observed for the solid.[16]

We have observed the ν_3 band of OBrO in the gas phase (Fig. 3). The Q-branch feature of $O^{79}BrO$ at 848.6 cm^{-1} and the isotopic shift of 2.4 cm^{-1} agree well with values from the force field (851.2 and 2.35 cm^{-1}) as does the position of the ν_1 band in an argon matrix (794.6 versus 794.1 cm^{-1} from reference [13]). The calculated isotopic shift for ν_1 is 1.15 cm^{-1}; an observed splitting of 2.9 cm^{-1} is more likely due to a matrix effect; see for example reference [23], where these effects have

 © VCH Verlagsgesellschaft mbH, D-69451 Weinheim, 1996 0570-0833/96/3518-2130 $ 15.00+.25/0

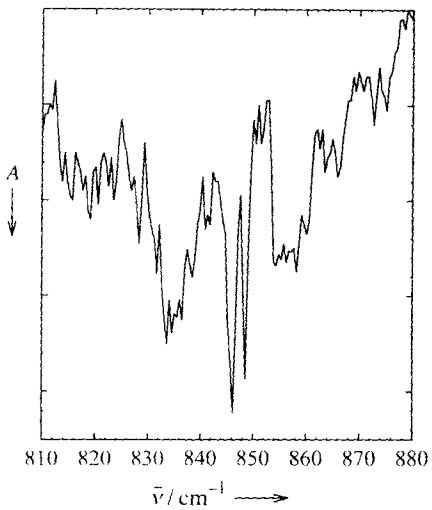

Fig. 3. The IR spectrum of gaseous OBrO in the region of the ν_3 fundamental, which shows PQR branch structure (resolution: 1 cm^{-1}).

been studied in detail for OClO. Although the bending mode has not yet been observed directly, our calculated value of 311 cm^{-1} for $O^{79}BrO$ is consistent with relative intensities observed for rotational transitions in the ground state compared to those in the $\nu_2 = 1$ state (Fig. 2).

The principal Br quadrupole constants of Br_2O have been obtained by diagonalization of the quadrupole tensor. The value $\chi_{zz} = 928$ MHz is close to that of Br_2 (810 MHz[24]), indicating a predominantly covalent Br–O bond.[20] Contributions from ionic forms Br^+OBr^- and BrO^-Br^+ are about 12% and π bonding is almost negligible (ca. 2%). The ionic character is slightly larger than in BrCl (9%)[25] and essentially the same as in HOBr,[26] which is consistent with the view that the OX group (X = H, halogen) is slightly more electronegative than the Cl atom. The quadrupolar z axis differs substantially from the Br–O bond (by ca. 2.4°; Fig. 4). If one would assume the z axis to be identical with the Br–O bond, one would derive an ionic character of about 45% for the Br–O bond in Br_2O, exceeding that of BrF (35%),[27] and a substantial degree of π bonding.

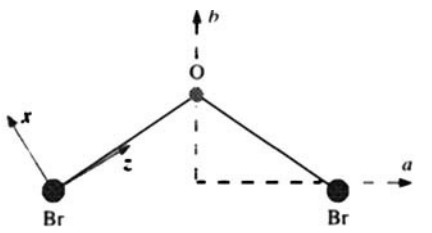

Fig. 4. The principal inertial (dashed arrows) and quadrupole axis systems (solid arrows) of Br_2O ($c \equiv y$ is perpendicular to the molecular plane).

Although a detailed discussion of the fine and hyperfine structure constants is beyond the scope of a brief communication, it should be noted that earlier ESR results[12] are consistent with those of this study. Thus, the conclusion given in reference [12] that, as in OClO, half of the spin-density is at the halogen atom, and essentially all of this in the p-orbital perpendicular to the molecular plane, remains unchanged.

In conclusion, we have used the $O + Br_2$ reaction system to study Br_2O and the OBrO radical. The presence of a mixture of bromine oxides under certain conditions indicates complex secondary chemistry that may be of atmospheric importance. We are currently investigating the spectroscopy and kinetics of these interesting molecules.

Received: April 20, 1996
Revised version: June 3, 1996 [Z 9058 IE]
German version: *Angew. Chem.* **1996**, *108*, 2285–2288

Keywords: bromine oxides · halogen compounds · radicals · spectroscopy · structure elucidation

[1] R. P. Wayne, G. Poulet, P. Biggs, J. P. Burrows, R. A. Cox, P. J. Crutzen, G. D. Hayman, M. E. Jenkin, G. Le Bras, G. K. Moortgat, U. Platt, R. N. Schindler, *Atmos. Envir.* **1995**, *29*, 2677–2881.
[2] E. A. Cohen, H. M. Pickett, M. Geller, *J. Mol. Spectrosc.* **1981**, *87*, 459, and references therein.
[3] a) O. V. Rattigan, R. L. Jones, R. A. Cox, *Chem. Phys. Lett.* **1994**, *230*, 121; b) *J. Chem. Soc. Faraday Trans.* **1995**, *91*, 4189.
[4] D. M. Rowley, M. H. Harwood, R. A. Freshwater, R. L. Jones, *J. Phys. Chem.* **1996**, *100*, 3020.
[5] a) E. Zintl, G. Rienäcker, *Ber. Dtsch. Chem. Ges. B* **1930**, *63*, 1098; W. Brenschede, H. J. Schumacher, b) *Z. Phys. Chem. Sect. B* **1935**, *29*, 356; c) *Z. Anorg. Allg. Chem.* **1936**, *226*, 370.
[6] R. Schwarz, M. Schmeisser, *Ber. Dtsch. Chem. Ges. B* **1937**, *70*, 1163.
[7] a) R. Schwarz, H. Wiele, *Naturwissenschaften* **1938**, *26*, 742; b) *J. Prakt. Chem.* **1939**, *152*, 157.
[8] M. Schmeisser, K. Jörger, *Angew. Chem.* **1959**, *71*, 523.
[9] R. Kuschel, K. Seppelt, *Angew. Chem.* **1993**, *105*, 1734; *Angew. Chem. Int. Ed. Engl.* **1993**, *32*, 1632.
[10] D. Leopold, K. Seppelt, *Angew. Chem.* **1994**, *106*, 1043; *Angew. Chem. Int. Ed. Engl.* **1994**, *33*, 975.
[11] N. I. Butkovskaya, I. I. Morozov, V. L. Tal'rose, E. S. Vasiliev, *Chem. Phys.* **1983**, *79*, 21.
[12] a) J. R. Byberg, *J. Chem. Phys.* **1971**, *55*, 4867; b) *ibid.* **1986**, *85*, 4790; c) J. R. Byberg, J. Linderberg, *Chem. Phys. Lett.* **1975**, *33*, 612.
[13] G. Maier, A. Bothur, *Z. Anorg. Allg. Chem.* **1995**, *621*, 743.
[14] D. E. Tevault, N. Walker, R. R. Smardzewski, W. B. Fox, *J. Phys. Chem.* **1978**, *82*, 2733.
[15] J. J. Orlando, J. B. Burkholder, *J. Phys. Chem.* **1995**, *99*, 1143.
[16] C. Campbell, J. P. M. Jones, J. J. Turner, *Chem. Commun.* **1968**, 888.
[17] W. Levason, J. S. Ogden, M. D. Spicer, N. A. Young, *J. Am. Chem. Soc.* **1990**, *112*, 1019.
[18] S. D. Allen, M. Poliakoff, J. J. Turner, *J. Mol. Struct.* **1987**, *157*, 1.
[19] M. Birk, R. R. Friedl, E. A. Cohen, H. M. Pickett, S. P. Sander, *J. Chem. Phys.* **1989**, *91*, 6588.
[20] W. Gordy, R. L. Cook, *Microwave Molecular Spectra*, 3rd ed., Wiley, New York, **1984**.
[21] M. Sugie, M. Ayabe, H. Takeo, C. Matsumura, *J. Mol. Struct.* **1995**, *352/353*, 259.
[22] K. Miyazaki, M. Tanoura, K. Tanaka, T. Tanaka, *J. Mol. Spectrosc.* **1986**, *116*, 435.
[23] H. S. P. Müller, H. Willner, *J. Phys. Chem.* **1993**, *97*, 10589, and references therein.
[24] N. Bettin, H. Knöckel, E. Tiemann, *Chem. Phys. Lett.* **1980**, *80*, 386.
[25] A. C. Legon, J. C. Thorn, *Chem. Phys. Lett.* **1993**, *215*, 554.
[26] Y. Koga, H. Takeo, S. Kondo, M. Sugie, C. Matsumura, G. A. McRae, E. A. Cohen, *J. Mol. Spectrosc.* **1989**, *138*, 467.
[27] H. S. P. Müller, M. C. L. Gerry, *J. Chem. Phys.* **1995**, *103*, 577.

 © VCH Verlagsgesellschaft mbH, D-69451 Weinheim, 1996 0570-0833/96/3518-2131 $ 15.00+.25/0

Enzyme-Catalyzed Formation of Carboxybiotin as Proved by the Measurement of $^{15}N,^{13}C$ and $^{13}C,^{13}C$ Spin–Spin Coupling**

Stefan Berger,* Annett Braune, Wolfgang Buckel,* Ulrich Härtel, and Man-Ling Lee

Dedicated to Professor Anton Rieker on the occasion of his 65th birthday

The action of biotin as a prosthetic group in carboxylating, transcarboxylating, and decarboxylating enzymes is well-known; however, the detailed mechanism of the conversion of biotin (**1**) into carboxybiotin (**2**) is still the subject of intense debate.[1] Even the proof for the occurrence of carboxybiotin during these reactions is only indirect and has been addressed very recently by the synthesis of "crippled" biotin, in which the nitrogen atom 1'-N was replaced by carbon.[2] By in situ methylation of the unstable **2** (obtained with ^{14}C-labeled hydrogen carbonate) with diazomethane, F. Lynen and co-workers were able to compare the reaction product with authentic methoxycarbonylbiotin methyl ester (**3**) and thus could show the likelihood of **2** during the enzymatic process.[3] The direct nonenzymatic synthesis of **2**, however, has to our knowledge not been demonstrated to date. We could show that **2**, when obtained by base-catalyzed hydrolysis of **3** under NMR control at 5 °C, decarboxylates within a few minutes;[4] however, a half-life of 103 min has been reported for analogous enzymatic processes.[5]

In order to obtain a better understanding of the action of biotin as a prosthetic group[6] and proof of the occurrence of **2** during the enzymatic reaction we have synthesized [1'-^{15}N]-(**1a**)[7] and [2'-^{13}C]biotin (**1b**).[8] By applying the carboxytransferase subunit GcdA of the biotin-dependent sodium ion pump glutaconyl-CoA decarboxylase (EC 4.1.1.70) for catalysis of the carboxylation of free **1b** via (*E*)-glutaconyl-CoA (**4**) to form crotonyl-CoA (**5**), we could observe a transient signal at $\delta = 160.4$. The time dependence of this signal is shown in Figure 1 and the data was fitted with a curve corresponding to the equation for consecutive reactions using one first order rate constant for the formation and one for the decarboxylation of **2**. However, the occurrence of one transient signal alone, considering background signals, impurities etc., is certainly not convincing proof of an intermediate product.

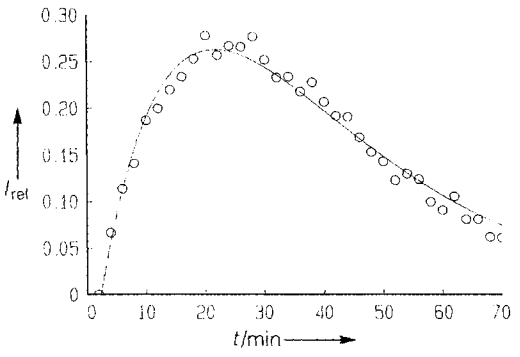

Fig. 1. Time dependence of the intensity of the 2'-^{13}C signal of carboxybiotin (**2**) during the reaction of **1b** with glutaconyl-CoA catalyzed by the carboxytransferase subunit GcdA (I_{rel} = relative intensity).

We therefore considered the use of ^{13}C-labeled glutaconyl-CoA (**4**) in this reaction. With **1b** one would expect two transient signals stemming from the newly formed product **2b**, which in addition display a $^2J(C,C)$ spin–spin coupling constant. With **1a** one would expect one transient signal displaying a $^1J(C,N)$ spin–spin coupling constant, unequivocally demonstrating that a C–N bond is formed in the enzyme-catalyzed reaction.

The synthesis of [1-^{13}C]glutaconic acid (**4a**) was unexpectedly difficult due to label scrambling and other complications. [1,5-$^{13}C_2$]Glutaconic acid (**4b**), however, was readily accessible in three steps starting from 1,3-dibromopropane-2-ol.[9] The additional ^{13}C label proved to be helpful, since the final acetate formed in the reaction [cf. Eq. (a)] could be observed.

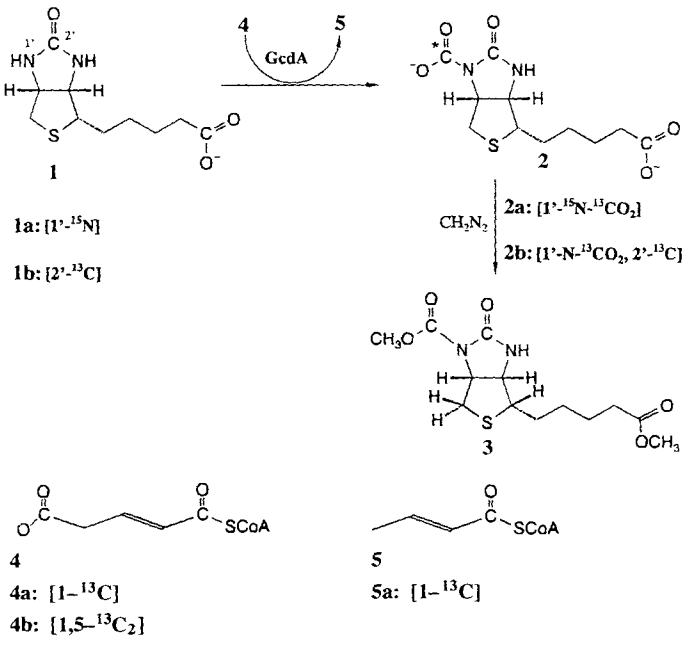

Scheme 1. Carboxylation of labeled biotin (**1**) by (*E*)-glutaconyl-CoA (**4**) in the presence of the carboxytransferase subunit GdcA of glutoconyl CoA-decarboxylase.

The enzyme system used in the experiments was composed of the carboxytransferase subunit GcdA of glutaconyl CoA-decarboxylase from *Acidaminococcus fermentans*[10] and a mixture of auxiliary enzymes prepared from the same organism.[11] GcdA was obtained by overexpression of its gene *gcdA* harbored in the vector pJF118HE in *Escherichia coli* DH5α.[10b] GcdA from cell extracts was purified by two successive rounds of anion exchange chromatography.[12] The enzyme mixture contained glutaconate CoA-transferase (EC 2.8.3.12), crotonase [(*E*)-2-butenoyl CoA-hydratase, EC 4.1.2.17], 3-hydroxybutyryl CoA-dehydrogenase (EC 1.1.1.35), thiolase (acetyl-CoA *C*-acetyltransferase, EC 2.3.1.9), and phosphate acetyltransferase (EC 2.3.1.8). Hence, the system was able to convert glutaconate and biotin in phosphate buffer (pH 7.0) in the presence of NAD and catalytic amounts of acetylphosphate and CoASH, via the intermediates glutaconyl-CoA, crotonyl-CoA, (*S*)-3-hydroxybutyryl-CoA, acetoacetyl-CoA, and acetyl-CoA, into carboxy-

[*] Prof. Dr. S. Berger, Dr. M.-L. Lee
Fachbereich Chemie der Universität
D-35032 Marburg (Germany)
Fax: Int. code +(6421)288917
e-mail: berger@ps1515.chemie.uni-marburg.de
Prof. Dr. W. Buckel, Dipl.-Biol. A. Braune, Dr. U. Härtel
Fachbereich Biologie der Universität
D-35032 Marburg (Germany)

[**] This work was supported by the Deutsche Forschungsgemeinschaft and the Fonds der Chemischen Industrie.

biotin, acetate, and acetylphosphate [Eq. (a)]. Finally carboxybiotin spontaneously decarboxylated to biotin and CO_2 [half-life ca. 13 min, Eq. (b)].

$$\text{glutaconate}^{2-} + \text{biotin}^{-} + H_2O + NAD^{+} + HPO_4^{2-} \longrightarrow \text{carboxybiotin}^{2-} + \text{acetate}^{-} + \text{acetylphosphate}^{2-} + NADH + H^{+} \quad (a)$$

$$\text{carboxybiotin}^{2-} + H^{+} \longrightarrow \text{biotin}^{-} + CO_2 \quad (b)$$

The experiments, which were carried out at room temperature with a Bruker AMX-500 spectrometer, fully confirmed the mechanism originally proposed by F. Lynen. ^{13}C NMR spectra were continuously recorded; each was accumulated over 2 min. Initial spectra obtained from a solution containing the incubation mixture and **1a** or **1b** but without the carboxytransferase subunit GcdA displayed only the signals of the labeled starting materials. An induction period of several minutes was observed after addition of GcdA, depending on the enzyme preparation. Figure 2 shows the transient signals, which first increased in intensity, reached a maximum after about half an hour, and then decreased and disappeared. In Figure 2a (with **1a**) a $^{13}C,^{15}N$ spin–spin coupling constant of 17.8 Hz is evident; in Figure 2b (with **1b**) a $^{13}C,^{13}C$ spin–spin coupling constant of 3.1 Hz can be seen. Both coupling constants are fully consistent with values in similar chemical environments.[13, 14]

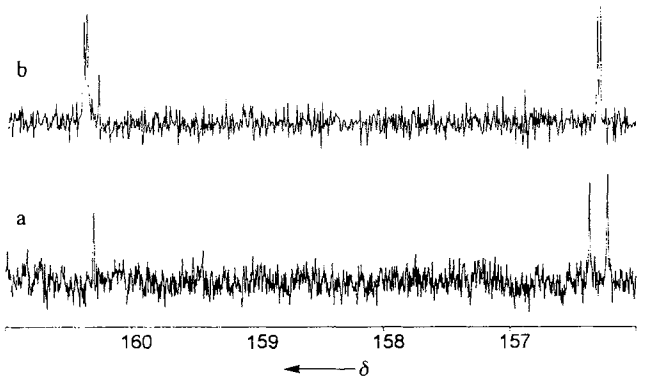

Fig. 2. Expansion of the 125 MHz ^{13}C NMR spectra of a) [1′-^{15}N-$^{13}CO_2$]carboxybiotin (**2a**) and b) [1′-N-$^{13}CO_2$,2′-^{13}C]carboxybiotin (**2b**) formed during the reaction of **1a** and **1b**, respectively, with the carboxytransferase subunit GcdA.

The method demonstrated here is also generally applicable,[15] provided that the two species that are linked by the new chemical bond can be synthesized with appropriate labels. Thus formation of a chemical bond can be proved unequivocally.

Experimental Procedure

The incubation mixture for the experiment on which Figure 1 is based contained in a total volume of 750 μL: 100 mM potassium phosphate (pH 7.0), 10% ^2H_2O, 27 mM glutaconate, 24 mM *d*-[2′-^{13}C]biotin (**1b**), 6.3 mM NAD^+, 2.1 mM acetylphosphate, 4.8 mM CoASH, 30 mM dioxane, 330 μg GcdA, and 500 μg auxiliary enzymes. The incubation mixtures for the experiments on which Figure 2 is based were essentially identical to that providing Figure 1, but unlabeled glutaconate was replaced by [1,5-$^{13}C_2$]glutaconate, and the incubation mixture for Figure 2a contained *d*-[1′-^{15}N]biotin instead of *d*-[2′-^{13}C]biotin. Since the total synthesis of [1′-^{15}N]biotin yielded the racemate [7], the biological occurring *d*-enantiomer (**1a**) was separated from the *l*-enantiomer by HPLC on a chiral column [16].

Received: April 15, 1996
Revised version: May 29, 1996 [Z9029IE]
German version: *Angew. Chem.* **1996**, *108*, 2259–2261

Keywords: biotin · carboxylations · enzyme mechanisms · NMR spectroscopy

[1] S. E. Polakis, R. B. Guchhait, E. E. Zwergel, M. D. Lane, *J. Biol. Chem.* **1974**, *249*, 6657–6667; R. Kluger, P. P. Davis, P. D. Adawadkar, *J. Am. Chem. Soc.* **1979**, *101*, 5995–6000; P. A. Tipton, W. W. Cleland, *Biochemistry* **1988**, *27*, 4325–4331; T. Ogita, J. R. Knowles, *ibid.* **1988**, *27*, 8028–8033; N. F. B. Phillips, M. A. Snoswell, A. Chapman-Smith, D. B. Keech, J. C. Wallace, *ibid.* **1992**, *31*, 9445–9450; D. J. Kuo, E. A. Rose, *J. Am. Chem. Soc.* **1993**, *115*, 387–390; H. Martini, J. Rétey, *Angew. Chem.* **1993**, *105*, 287–289; *Angew. Chem. Int. Ed. Engl.* **1993**, *32*, 278–280.
[2] S. A. Henderson, J. O'Connor, A. R. Rendina, G. P. Savage, G. W. Simpson, *Aust. J. Chem.* **1995**, *48*, 1907–1916.
[3] F. Lynen, J. Knappe, E. Lorch, G. Jütting, E. Ringelmann, *Angew. Chem.* **1959**, *71*, 481–486; F. Lynen, J. Knappe, E. Lorch, G. Jütting, E. Ringelmann, J. P. Lachance, *Biochem. Z.* **1961**, *335*, 123–167; J. Knappe, E. Ringelmann, F. Lynen, *ibid.* **1961**, *335*, 168–176.
[4] W. A. Etzel, Dissertation, Universität Marburg, **1990**.
[5] P. A. Tipton, W. W. Cleland, *J. Am. Chem. Soc.* **1988**, *110*, 5566–5869.
[6] K. Bendrat, S. Berger, W. Buckel, W. A. Etzel, K. H. Röhm, *FEBS Lett.* **1990**, *277*, 156–158.
[7] M.-L. Lee, S. Berger, *J. Labelled Compd. Radiopharm.* **1992**, *31*, 1065–1070.
[8] W. A. Etzel, S. Berger, *J. Labelled Compd. Radiopharm.* **1990**, *28*, 977–982.
[9] M.-L. Lee, Dissertation, Universität Marburg, **1993**.
[10] a) W. Buckel, H. Liedtke, *Eur. J. Biochem.* **1986**, *156*, 251–257; b) K. Bendrat, W. Buckel, *ibid.* **1993**, *211*, 697–702.
[11] W. Buckel, *Methods Enzymol.* **1986**, *125*, 547–558.
[12] A. Braune, K. Bendrat, W. Buckel, unpublished results.
[13] H.-O. Kalinowski, S. Berger, S. Braun, *Carbon-13 NMR Spectroscopy*, Wiley, Chichester, **1988**.
[14] S. Berger, S. Braun, H.-O. Kalinowski, *NMR-Spektroskopie von Nichtmetallen*, Vol. 2, Thieme, Stuttgart, **1992**.
[15] a) E. J. Mueller, E. Meyer, J. Rudolph, V. J. Davisson, J. Stubbe, *Biochemistry* **1994**, *33*, 2270–2278; b) B. T. Golding, P. K. Slaich, G. Kennedy, C. Bleasdale, W. P. Watson, *Chem. Res. Toxicol.* **1996**, *9*, 147–157.
[16] K. Steinbach, S. Berger, unpublished results.

The Reaction of White Phosphorus with Lithium (Trimethylsilyl)diazomethanide: Direct Access to a New, Aromatic 1,2,3,4-Diazadiphosphole Ring

Claude Charrier, Nicole Maigrot, Louis Ricard, Pascal Le Floch, and François Mathey*

All of the possible polyphosphacyclopentadienide ions $[R_nC_nP_{5-n}]^-$ have been described,[1] and all but one of these can be prepared in a pure form and in preparative quantitities by specific syntheses. The only exception are the tetraphosphacyclopentadienides $[RCP_4]^-$, whose parent ion has been characterized by Baudler et al. as a minor by-product of the reaction of white phosphorus with sodium in diglyme.[2] We reasoned that the reaction of the synthetic equivalent of a $[RC]^-$ fragment with P_4 might provide a simple route to the $[RCP_4]^-$ ion, because of the driving force of this reaction provided by the aromatic stabilization of the final five-membered ring.[3] Thus, we decided to investigate the reaction of lithium (trimethylsilyl)diazomethanide with P_4. As expected, the reaction proceeded cleanly; however, the sole product was the previously unknown 1,2,3,4-diazadiphospholide anion **2**, which results from a formal [3+2] cycloaddition between [P≡P] and the diazomethyl anion **1** (Scheme 1).

The lithium salt of **2** displays a very characteristic ^{31}P NMR spectrum (81.01 MHz, C_6D_6+[D$_8$]THF, 25 °C, 85% H_3PO_4): $\delta = +352.5$ (d, $^1J(P,P) = 457$ Hz; P3), +231 (d, P4), and the negative ion mass spectrum confirms the formula of **2**: *m/z* (%)

[*] Prof. Dr. F. Mathey, Dr. C. Charrier, N. Maigrot, Dr. L. Ricard, Dr. P. Le Floch
Laboratoire "Hétéroéléments et Coordination" URA 1499 CNRS
DCPH, Ecole Polytechnique, F-91128 Palaiseau Cedex (France)
Fax: Int. code +(1) 69 33 39 90

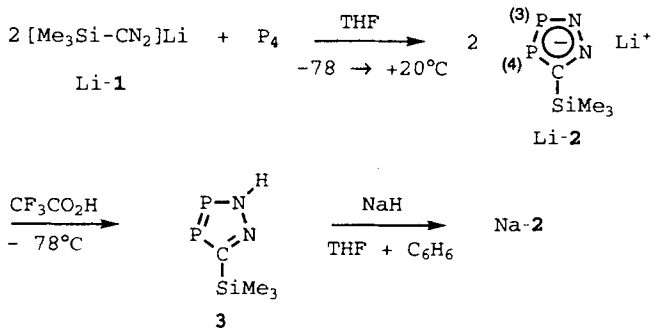

Scheme 1.

175(100) [M^-]. The protonation of **2** by trifluoroacetic acid at low temperature cleanly affords the stable 2*H*-1,2,3,4-diazadiphosphole **3**, which can be purified by chromatography on silica gel. The X-ray crystal structure analysis of **3** (Fig. 1)[4] shows that the ring is planar and that the proton resides on the nitrogen atom adjacent to the P=P unit. The double bonds are fairly well localized: the lengths of the P=P and C=N bonds are 2.07 and 1.32 Å, respectively, and these lengths are very similar to those of the corresponding bonds in a series of heterophospholes.[5] The two molecules of the asymmetric unit are connected by a N–H···N hydrogen bond, and their two planes are almost orthogonal (87.92±0.07°). The NMR parameters of **2** and **3** are surprisingly similar: **2**: $\delta(^{13}C) = 185.2$ (dd, $^1J(C,P) = 107$, $^2J(C,P) = 10$ Hz, C5); **3**: (C_6D_6): $\delta(^{13}C) = 184.45$ (d, $^1J(C,P) = 105$ Hz, C5); δ +345.8 (d, $^1J(P,P) = 489$ Hz; P3), +245 (d, P4). This resemblance suggests the existence of an equilibrium such as **3** ⇌ **2** + H^+. In C_6D_6, the signal of the proton of **3** indeed appears at $\delta = 11.4$, suggesting some weak acidic character. Consequently, **3** may be easily deprotonated by a weak base such as sodium hydride to give the sodium salt of **2** in a pure form (see Scheme 1).

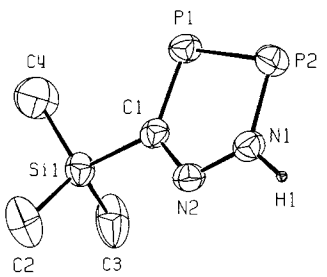

Fig. 1. Molecular structure of **3** (benzene solvate) (methyl hydrogen atoms omitted for clarity) [7]. Significant bond lengths [Å] and angles [°]: P1–P2 2.0706(6), P1–C1 1.768(2), P2–N1 1.670(1), N1–N2 1.357(2), N1–H1 0.89(2), N2–C1 1.320(2), C1–Si1 1.896(2); P2-P1-C1 92.10(5), P1-P2-N1 93.53(5), P2-N1-N2 121.7(1), P2-N1-H1 119(1), N2-N1-H1 118(1), N1-N2-C1 113.6(1), P1-C1-N2 119.1(1), P1-C1-Si1 123.39(9), N2-C1-Si1 117.5(1).

After the discoveries of pentaphosphaferrocenes by Scherer et al.[6] and the pentaphospholide ion by Baudler et al.,[2] this work underlines that white phosphorus can be an interesting starting material for the synthesis of new aromatic polyphosphorus compounds. We are currently investigating the reactivity of **2**.

Experimental Procedure

White phosphorus (2.17 g, 17.5 mmol) was dissolved in dry THF (80 mL) at 35 °C. The solution was cooled to −78 °C and a solution of lithium (trimethylsilyl)diazomethanide ((52 mmol), obtained by reaction of 1.6 M *n*BuLi in hexane with Me_3SiCHN_2 in Et_2O at −78 °C) was added dropwise. After 1 h at −78 °C, the solution was allowed to warm to room temperature and stirred for 2 h. The P_4 resonance signal completely disappeared from the ^{31}P NMR spectrum of the crude reaction solution, and only the AX system corresponding to the lithium salt of **2** was visible. Protonation of Li-**2** with trifluoroacetic acid (35 mmol) was then performed at −78 °C. The solution was evaporated at room temperature and the residue was chromatographed on silica gel with hexane/benzene 40:60 as the eluent. Traces of white phosphorus were eluted first, then the product **3** was collected: yield 1.48 g (24%), pale yellow crystals, m.p. 87 °C (benzene). ^1H NMR (200.13 MHz, C_6D_6, 25 °C, TMS): $\delta = 0.66$ (s, 9H, Me_3Si), 11.4 (s broad, 1H, NH); ^{13}C NMR (50.32 MHz, C_6D_6, 25 °C, TMS): $\delta = 0.2$ (d, $^3J(C,P) = 2.8$ Hz, Me), 184.5 (d, $^1J(C,P) = 105$ Hz, P-C-N); MS (CI, 70 eV): *m/z* (%): 176(7) [M^+], 161(13) [M^+ − Me], 149(15), 73(100) [Me_3Si^+].

The deprotonation of **3** was carried out in benzene/THF at −30 °C with one equivalent of NaH. After the mixture was allowed to warm to room temperature, the pure sodium salt of **2** was obtained: ^1H NMR (200.13 MHz, C_6D_6 + [D_8]THF, 25 °C, TMS): $\delta = 0.45$ (s, Me); ^{13}C NMR (50.32 MHz, C_6D_6 + [D_8]THF, 25 °C, TMS): $\delta = 1.4$ (s, Me), 185.2 (dd, $^1J(C,P) = 107$ Hz, $^2J(C,P) = 10$ Hz, P-C-N); MS (NCI, 70 eV): *m/z* (%): 175(100) [M^-], 160(35) [M^- − Me].

Received: April 29, 1996 [Z 9073 IE]
German version: *Angew. Chem.* **1996**, *108*, 2282–2283

Keywords: aromaticity · heterocycles · lithium compounds phosphorus compounds

[1] For recent reviews, see : F. Mathey, *Coord. Chem. Rev.* **1994**, *137*, 1; F. Mathey in *Stereoselective Reactions of Metal-activated Molecules* (Eds.: H. Werner, J. Sundermeyer), Vieweg, Braunschweig, **1995**, pp. 173–181.
[2] M. Baudler, D. Düster, D. Ouzounis, *Z. Anorg. Allg. Chem.* **1987**, *544*, 87.
[3] E. J. Padma Malar, *J. Org. Chem.* **1992**, *57*, 3694.
[4] X-ray structure determination for **3**: Crystals of **3**, $C_4H_{10}N_2P_2Si \cdot 0.25C_6H_6$ were grown from a cold solution of the compound in benzene. Data were collected at −150±0.5 °C on an Enraf Nonius CAD4 diffractometer using graphite-monochromated $Cu_{K\alpha}$ radiation ($\lambda = 1.54184$ Å). The crystal structure was solved and refined with the Enraf Nonius MOLEN package. The compound crystallizes in space group *C*2/*c* (no. 15), $a = 20.723(2)$, $b = 9.967(1)$, $c = 20.626(2)$ Å, $\beta = 91.50(1)°$; $V = 4258.8(1.3)$ Å^3, $Z = 16$, $\rho_{calc} = 1.221$ g cm^{-3}, $\mu = 44.3$ cm^{-1}, $F(000) = 1640$. A total of 3479 unique reflections were collected in the range $2° \le 2\theta \le 120.0°$, of which 668 were considered as unobserved ($F^2 < 3.0\sigma(F^2)$); 2811 reflections were used for solving and refining the structure. Direct methods yielded a solution for all atoms. The NH hydrogen atoms were refined with isotropic temperature factors and the methyl and benzene hydrogen atoms were included as riding atoms in the final stages of least-squares refinement while using anisotropic temperature factors for all other atoms. A nonPoisson weighting scheme was applied with a *p* factor of 0.08. The final agreement factors were $R = 0.039$, $R_w = 0.081$, GOF = 1.81. Crystallographic data (excluding structure factors) for the structure(s) reported in this paper have been deposited with the Cambridge Crystallographic Data Centre as supplementary publication no. CCDC-179-74. Copies of the data can be obtained free of charge on application to The Director, CCDC, 12 Union Road, Cambridge CB2 1EZ, UK (fax: Int. code +(1223) 336-033; e-mail: teched@chemcrys.cam.ac.uk).
[5] A. Schmidpeter, K. Karaghiosoff in *Multiple Bonds and Low Coordination in Phosphorus Chemistry* (Eds.: M. Regitz, O. J. Scherer), Thieme, Stuttgart, **1990**, pp. 258–286.
[6] O. J. Scherer, T. Brück, *Angew. Chem.* **1987**, *99*, 59; *Angew. Chem. Int. Ed. Engl.* **1987**, *26*, 59.
[7] Figure 1 was prepared using ORTEP-III (Oak Ridge Thermal Ellipsoid Plot Program), by Carroll K. Johnson and Michael N. Burnett, Oak Ridge National Laboratory.

$[Cu_4Mn_4(SiC_3H_7)_{12}S]^{2-}$, a Novel Octanuclear Heterometallic Complex Consisting of a Metal Cube with an Interstitial μ_4-Sulfide Ion and Edge-Bridging Thiolate Ligands**

Hans-Oscar Stephan, Mercouri G. Kanatzidis, and Gerald Henkel*

Dedicated to Professor Peter Sartori on the occasion of his 65th birthday

Transition metal complexes with thiolate ligands have been intensively studied for about 25 years;[1] however, surprisingly few reports have emerged on heterometallic compounds.[2-4] Such species would be of particular interest with respect to their molecular structures and chemical properties because of reactivity patterns that originate from the combination of different metal atoms.

To determine the synthetic conditions under which mixed-metal thiolates may form, we have investigated the reactivity of well-defined metal thiolate precursors towards heterometal sources such as simple metal halides. This approach towards cluster build-up has been shown to be successful for the formation of homometallic systems such as $[Fe_4(SPh)_6Cl_4]^{2-}$[5] and $[Mn_4(SiC_3H_7)_6Cl_4]^{2-}$[6] as well as for the synthesis of the heterometallic complexes $[Cu_6In_3(SEt)_{16}]^{-}$[3a] and $[(PPh_3)_2CuIn(SEt)_4]$.[3b] The latter species is the only well-characterized single-source precursor to the semiconductor $CuInS_2$.

We report herein on the synthesis, structure, and magnetic properties of the novel octanuclear mixed-metal thiolate complex **2**, which is formed in the reaction of $(Me_4N)_2[Mn_2(SiC_3H_7)_6]$[6] with two equivalents of CuCl in acetonitrile at room temperature and can be isolated as the double salt of **1**.

$(Me_4N)_6[MnCl_4]_2[Cu_4Mn_4(SiC_3H_7)_{12}S]$ **1**

$[Cu_4Mn_4(SiC_3H_7)_{12}S]^{2-}$ **2**

Compound **1** is also accessible by a solvothermal reaction of the reagents in a 1:2.5 molar ratio (Mn:Cu compound) in acetonitrile at 80 °C. In both cases, a yellow microcrystalline byproduct is formed, which still has not been identified.[7]

According to the results of an X-ray crystal structure analysis,[8] **1** contains $[MnCl_4]^{2-}$ ions and the octanuclear anion **2**, whose charges are balanced by $(Me_4N)^+$ counterions. The structure of **2** is shown in Figure 1. The novel cage compound **2** contains a distorted Cu_4Mn_4 cube (mean edge length 3.092 Å), which is composed of two interpenetrating Cu_4 and Mn_4 tetrahedra of slightly different size. The center of this cube is occupied by a μ_4-S atom, which binds to the manganese atoms with a mean distance of 2.475 Å.

Because of the slightly longer edge lengths in the Cu_4 tetrahedron, the Cu–S distances are 2.853 Å (av) in length and thus

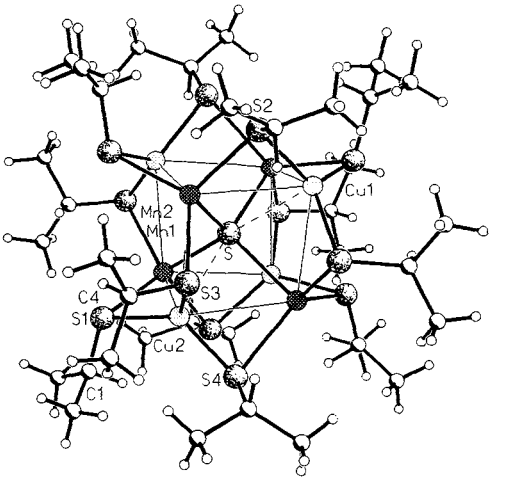

Fig. 1. Structure of **2** in crystals of **1**. Selected distances [Å] and angles [°] (mean values): Mn···S 2.506, Cu···S 2.200, Cu···S 2.853, Mn···Cu 3.092; S-Mn-S 108.8, S-Cu-S 118.6.

nonbonding in nature. In addition, each metal atom binds to three outer thiolate ligands, leading to distorted tetrahedral (manganese) or distorted trigonal-planar (copper) coordination sites. The average metal–sulfur bond lengths of 2.506 and 2.200 Å lie in the range expected for tetrahedral MnS_4[6] and trigonal-planar CuS_3[9] units, respectively.

Since each thiolate ligand is bonded to a manganese and a copper atom simultaneously, all the edges of the central metal cube in **2** are bridged by sulfur atoms. The bridging S atoms define a slightly distorted S_{12} icosahedron (Fig. 2), possibly as

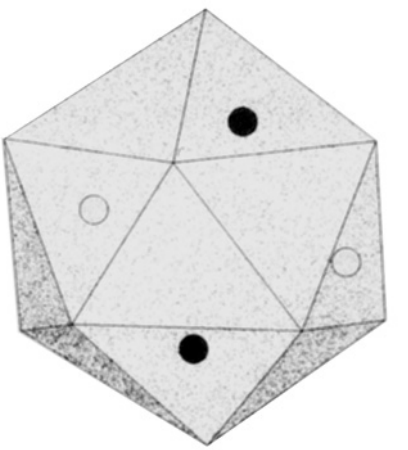

Fig. 2. Schematic representation of the $Mn_4Cu_4S_{13}$ core of **2**, showing the icosahedral arrangement of sulfur atoms.

a result of the steric requirements of the isopropyl groups. Evidently a cuboctahedral arrangement of the sulfur atoms is less favorable in this case. Taking a Mn_2Cu_2 face of the metal cube as a reference plane, the four bridging ligands thus divide equally into two sets with S–C vectors parallel and normal to the plane. As a result, the α-carbon atoms form a slightly distorted cuboctahedron.

Viewed in a different way, **2** can be considered to contain the unusual complex anion $[Mn_4(SR)_{12}S]^{6-}$, which is composed of four tetrahedral MnS_4 units sharing one common vertex. Its Mn_4S_{13} core is a minimal fragment of the cubic closest packed sphalerite-type structure, consisting of one sulfide ion surround-

[*] Prof. Dr. G. Henkel, Dr. H.-O. Stephan
Fachgebiet Anorganische Chemie der Universität
Lotharstrasse 1, D-47048 Duisburg (Germany)
Fax: Int. code +(203)3792110
e-mail: biohenkel@uni-duisburg.de
Prof. Dr. M. G. Kanatzidis
Department of Chemistry, Michigan State University
East Lansing, MI 48824 (USA)

[**] This work has been supported by the Deutsche Forschungsgemeinschaft (DFG), the Bundesministerium für Bildung, Wissenschaft, Forschung und Technologie (BMBF), and the Fonds der Chemischen Industrie. H.-O. S. thanks the DFG for a postdoctoral fellowship. We thank Prof. Cowen for his help and many fruitful discussions of the magnetic properties of the title compound.

ed by the complete set of 12 direct sulfur neighbors. This fragment is stabilized here for the first time as a discrete entity in a molecular complex. Other complexes containing related M_4X_{13} units as constituents of more extended M–X cores (X = S, Se) are $[Cd_{17}(SPh)_{28}(\mu_4\text{-}S)_4]^{2-}$[10] and $[Cd_8(SePh)_{16}(\mu_4\text{-}S)]^{2-}$.[11] The S_{12} polyhedron in **2** deviates slightly from the regular cuboctahedron of the sphalerite-type structure by small rotations of the atoms forming the triangular faces about their normals. The Mn^{II} ions occupy one half of the tetrahedral holes of the S_{13} fragment (T^+ set), whereas the Cu^I ions lie on triangular faces of the remaining S_4 tetrahedra (T^- set).

To our knowledge, **2** is the first complex anion that contains a metal cube with edge-bridging thiolate ligands and an interstitial μ_4-S ion. However, there are several reports on cubane complexes with thiolate-bridged Cu^I_8 skeletons and trigonal-planar Cu^IS_3 coordination centers of general composition $[Cu^{II}_6Cu^I_8(SC(Me)_2R)_{12}Cl]^{n+}$ (R = CH_2NH_2, $n = 7$ [12]; R = CO_2^-, $n = -5$;[13] R = $CH(NH_2)CO_2^-$, $n = -5$[14]), whose centers are occupied by chloride ions. In these compounds, both thiolate and amine (or carboxylate) donor functions bind to additional Cu^{II} atoms in the outer periphery of the cube. Very recently, a sulfur-bridged Cu^I_8 cube with trigonal-planar coordination of the copper atoms and an interstitial μ_8-S ion in the compound $[Cu_8(S_2P\{OiC_3H_7\}_2)_6(\mu_8\text{-}S)]$ has been reported.[15] Interestingly, similar complexes with such centered metal cubes and tetrahedrally coordinated divalent metal ions are not yet known.[16]

The metal–chalcogen framework of $[Cd_8(SePh)_{16}(\mu_4\text{-}S)]^{2-}$[11] is a rearranged extension of the framework of **2** with four additional chalcogenolate ligands. They add to the trigonal-planar coordination sites, resulting in a second set of tetrahedrally coordinated divalent metal atoms, which now are placed on the outside of the Se_{12} icosahedron.

Magnetic susceptibilities of **1** have been recorded in the temperature range from 5 to 300 K, and the Curie–Weiss law is obeyed between 200 and 300 K with $\theta = -32$ K (Fig. 3). The overall magnetic behavior is dominated by the strongly paramagnetic $[MnCl_4]^{2-}$ ions.

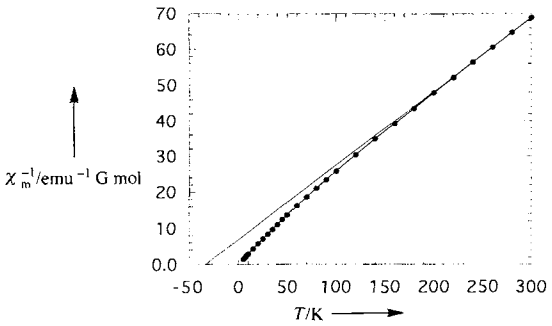

Fig. 3. Plot of the temperature dependence of the molar magnetic susceptibility of **1**.

Attempts to subtract these contributions by simply assuming perfect noninteracting paramagnets with $\mu_{eff} = 5.92\ \mu_B$ gave physically unreasonable susceptibilities for **2** at low temperatures. This observation implies that the $[MnCl_4]^{2-}$ ions interact weakly antiferromagnetically with the manganese sites in **2** and/or with themselves. Despite these limitations, however, it is possible to gain insight into the magnetic properties of **2** at higher temperatures up to about 200 K, since the weak interactions caused by the $[MnCl_4]^{2-}$ ions can then be neglected because they are small compared to the magnetic exchange interactions within complex **2**.[17] At room temperature, μ_{eff} of **1** is calculated to be 11.1 μ_B. The theoretical value for six uncoupled Mn^{2+} centers is 14.5 μ_B, indicating that the manganese atoms in **2** are antiferromagnetically coupled. This behavior is also typical for the complex ions $[Mn_4Te_4(TeiC_3H_7)_4]^{4-}$ [18] and $[Mn_2(SPh)_6]^{2-}$.[19]

In summary, we have described the synthesis and some properties of the novel octanuclear mixed-metal complex ion $[Cu_4Mn_4(SiC_3H_7)_{12}S]^{2-}$, which possesses a cubane-like Mn_4Cu_4 arrangement. This compound belongs to a new class of mixed sulfide–thiolate complexes and is the first example of a metal cube with an interstitial μ_4-S ligand.

Experimental Procedure

All manipulations were carried out in gloveboxes or with Schlenk techniques under nitrogen.

1: $(Me_4N)_2[Mn_2(SiC_3H_7)_6]$ [6] (1.42 g, 2 mmol) was dissolved in acetonitrile (50 mL). Solid CuCl (0.40 g, 4 mmol) was added to the red solution to give a yellow solution, which was stirred for 24 h. A small amount of an insoluble material was filtered off and the solution was layered with an equal volume of diethyl ether after reduction of its volume to ⅓ of its initial value. During the course of several days, orange-yellow crystals of **1** deposited along with a yellow by-product. Yield: 65% (based on Cl); C, H, N, S analysis of **1**: found (%): C 32.08, H 7.00, N 3.74, S 18.56; calc. (%): C 32.19, H 6.92, N 3.80, S 18.65.

Alternatively, **1** was accessible as follows: $(Me_4N)_2[Mn_2(SiC_3H_7)_6]$ (159 mg, 0.23 mmol) was mixed with CuCl (57 mg, 0.58 mmol), ground, and loaded into a thickwall pyrex tube. After addition of acetonitrile (1 mL), the tube was frozen with liquid nitrogen and sealed under vacuum. After 3 d at 80 °C, orange-yellow hexagonal plates were deposited together with a yellow by-product.

Received: March 19, 1996 [Z8933IE]
German version: *Angew. Chem.* **1996**, *108*, 2257–2259

Keywords: copper compounds · magnetic properties · manganese compounds · sulfur compounds

[1] B. Krebs, G. Henkel, *Angew. Chem.* **1991**, *103*, 785; *Angew. Chem. Int. Ed. Engl.* **1991**, *30*, 769.

[2] $[Au_2Ag_4(SCH_2CH_2S)_4]^{2-}$, $[Au_2Cu_4(SCH_2CH_2S)_4]^{2-}$, $[Au_3Cu_3(SCH_2CH_2S)_4]^{2-}$, $[Cu_4(SCH_2CH_2S)_3]^{2-}$, and $[Ag_9(SCH_2CH_2S)_6]^{3-}$: G. Henkel, B. Krebs, P. Betz, H. Fietz, K. Saatkamp, *Angew. Chem.* **1988**, *100*, 1373; *Angew. Chem. Int. Ed. Engl.* **1988**, *27*, 1326.

[3] a) $[Cu_6In_3(SEt)_{16}]^-$: W. Hirpo, S. Dhingra, M. G. Kanatzidis, *J. Chem. Soc. Chem. Commun.* **1992**, 557; b) $[(PPh_3)_2CuIn(SEt)_4]$: W. Hirpo, S. Dhingra, A. Sutorik, M. G. Kanatzidis, *J. Am. Chem. Soc.* **1993**, *115*, 1597.

[4] $[Eu_2M_2(SPh)_8(py)_6]$ (M = Cd, Hg) and $[Eu_2Zn_2(SPh)_8(thf)_6]$: M. Brewer, J. Lee, J. G. Brennan, *Inorg. Chem.* **1995**, *34*, 5919.

[5] D. Coucouvanis, M. Kanatzidis, E. Simhon, N. C. Baenziger, *J. Am. Chem. Soc.* **1982**, *104*, 6264.

[6] H.-O. Stephan, G. Henkel, *Polyhedron*, **1996**, *15*, 501.

[7] Microanalysis (EDS method) and the odorous smell upon hydrolysis in air indicate that this material is a copper thiolate complex.

[8] Crystal structure analysis of **1**: Siemens P4RA four-circle diffractometer, $Mo_{K\alpha}$ radiation ($\lambda = 0.71073$ Å), graphite monochromator, rotating anode generator, scintillation counter, 150 K, empirical absorption corrections, SHELXTL-PLUS programs, direct methods, least-squares refinement; $C_{60}H_{156}Cl_8Cu_4Mn_6N_6S_{13}$, $M_r = 2246.09$, trigonal, space group $P\bar{3}1m$, $a = 14.814(9)$, $c = 14.164(7)$ Å, $V = 2691.91$ Å^3, $Z = 1$, $\rho_{calc} = 1.386$ g cm^{-3}, $\mu(Mo_{K\alpha}) = 1.94$ mm^{-1}, crystal dimensions about $0.65 \times 0.37 \times 0.33$ mm, ω scan, $2\theta_{max} = 54°$, 9373 reflections, of which 1536 are independent ($R_{merge} = 0.031$), R (R_w) = 0.0610 (0.0562) for 1288 observed reflections ($I > 2\sigma(I)$), 147 variables, all non-hydrogen atoms anisotropic, H atoms calculated at idealized positions, fixed and refined with one common temperature factor, one scaling factor, and one isotropic extinction parameter. Anion **2** possesses a threefold rotation axis passing through Mn1, S, and Cu1 (see Fig. 1), but the crystallographic point symmetry is $\bar{3}m$. The resulting disorder could be readily resolved and the structure was successfully refined by restricting the mean M–S bond lengths of chemically equivalent metal sites to be equal within 2σ. Further details of the crystal structure investigation may be obtained from the Fachinformationszentrum Karlsruhe, D-76344 Eggenstein-Leopoldshafen (Germany), on quoting the depository number CSD-59401.

[9] G. A. Bowmaker, G. R. Clark, J. K. Seadon, I. G. Dance, *Polyhedron* **1984**, *5*, 535.

[10] G. S. H. Lee, D. C. Craig, I. Ma, M. L. Scudder, T. D. Bailey, I. G. Dance, *J. Am. Chem. Soc.* **1988**, *110*, 4863.
[11] G. S. H. Lee, K. J. Fisher, D. C. Craig, M. L. Scudder, I. G. Dance, *J. Am. Chem. Soc.* **1990**, *112*, 6435.
[12] H. J. Schugar, C. Ou, J. A. Thich, J. A. Potenza, R. A. Lalancette, W. Furey, Jr., *J. Am. Chem. Soc.* **1976**, *98*, 3047; H. J. Schugar, C. Ou, J. A. Thich, J. A. Potenza, T. R. Felthouse, M. S. Haddad, D. N. Hendrickson, W. Furey, Jr., R. A. Lalancette, *Inorg. Chem.* **1980**, *19*, 543.
[13] P. J. M. W. L. Birker, *Inorg. Chem.* **1979**, *18*, 3502.
[14] P. J. M. W. L. Birker, H. C. Freeman, *J. Am. Chem. Soc.* **1977**, *99*, 6890; *J. Chem. Soc., Chem. Commun.* **1976**, 312.
[15] C. W. Liu, T. Stubbs, R. J. Staples, J. P. Fackler, Jr., *J. Am. Chem. Soc.* **1995**, *117*, 9778.
[16] In the complex ion $[Cd_8(SC_2H_4OH)_{12}(\mu_8\text{-}I)]^{3+}$, the coordination numbers of the cadmium atoms range from five to seven: H. B. Bürgi, H. Gehrer, P. Strickler, F. K. Winkler, *Helv. Chim. Acta* **1977**, *59*, 2558.
[17] For comparison, the magnetic behavior of $(Me_4N)_2[MnCl_4]$ and $(Et_4N)_2[MnCl_4]$ was also studied. $(Et_4N)_2[MnCl_4]$ ($\mu_{eff} = 5.91\ \mu_B$) behaves almost like a perfect paramagnet over the entire temperature range. In contrast, the manganese atoms in $(Me_4N)_2[MnCl_4]$ are weakly antiferromagnetically coupled, with μ_{eff} ranging from 5.1 μ_B (5 K) to the ideal value for isolated centers of 5.91 μ_B (300 K). In this compound, the shortest Mn···Mn contact is estimated to be 7.8 Å. ($(Me_4N)_2[MnCl_4]$ is isotypic with $(Me_4N)_2[ZnCl_4]$: *Acta Crystallogr.* **1959**, *12*, 611.) In crystals of **1**, this distance compares well with the shortest separations between the Mn atoms in $[MnCl_4]^{2-}$ and the Mn sites in **2** (8.6 Å) as well as those between the $[MnCl_4]^{2-}$ ions (8.5 Å). Thus, it is reasonable to assume that the $[MnCl_4]^{2-}$ ions in **1** act as pure paramagnets at room temperature, as they do in $(Me_4N)_2[MnCl_4]$.
[18] H.-O. Stephan, C. Chen, G. Henkel, K. Griesar, W. Haase, *J. Chem. Soc. Chem. Commun.* **1993**, 886.
[19] H.-O. Stephan, K. Griesar, W. Haase, G. Henkel, *Z. Naturforsch. B* **1994**, *49*, 1620.

Spiro-Surfactants and -Phospholipids: Synthesis and Properties**

Fredric M. Menger* and Julia Ding

Although a micelle cross-section is often pictured as the "spokes of a wheel",[1] the micelle is in fact highly disorganized and replete with bent chains. Persuasive arguments for "brush-heap" organization range from theoretical work[2] to binding studies[3] to our ^{13}C-labeling experiments.[4] It is interesting, from an historical standpoint, that G. S. Hartley wrote in 1936, "The symmetrical asterick form...has no physical basis and is drawn for no other reason than that the human mind is an organizing instrument and finds unorganized processes uncongenial. It is easier to speak in a sentence than in a jumble of words."[5] Unfortunately, for reasons of artistic convenience, the so-called Hartley model has evolved into the "spokes of a wheel" structure. Current textbooks portraying such a model[6] perpetuate what Hartley disclaimed decades ago and, to compound matters, fix his name to it.

Recently, while musing over the disorganization of micellar chains, we asked ourselves a set of intriguing questions: What would happen if the chains of a surfactant were indeed forced to remain unbent? Would micelles even form? If micelles did form, how would their critical micelle concentrations compare with those of conventional surfactants? To answer these questions, we required a means with which to rigidify hydrocarbon chains. Introducing unsaturation might seem like the most obvious way of preventing free rotation, but this possibility was dismissed owing to uncertainty as to how electronic factors (π–π repulsion etc.) would affect micelle formation. It was necessary, clearly, to retain chains that were fully populated with sp^3 carbons. This was accomplished with the spiro systems **1** and **2** shown below. The spiro chain is vaguely reminiscent of [*n*]staffanes[7] with a main difference that the former is completely devoid of any free rotations. As described below, spiro chains were also attached to phospholipids.

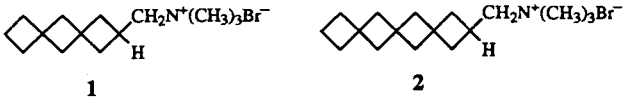

1 **2**

The 13-step synthesis of surfactant **1** is presented in Scheme 1. Construction of the spirocyclobutanes was based upon past work of Rice and Grogan[8] and Buchta and Geibel.[9] Compound **3** was either prepared by means of a Perkin cycliza-

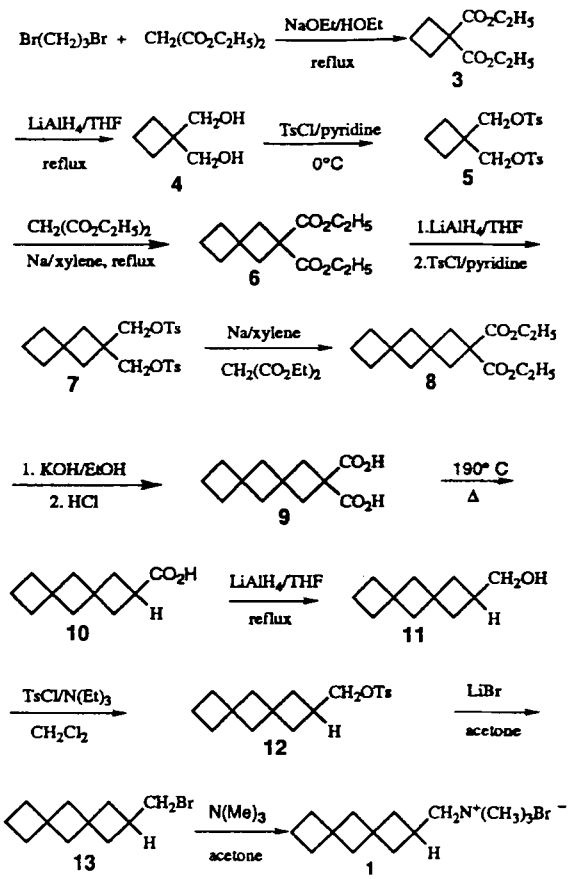

Scheme 1. Synthesis of spiro-surfactant **1**.

tion[10] or purchased (Aldrich). Reduction of the diester to dialcohol **4**[4] with $LiAlH_4$ (96%) and ditosylation (90%) gave **5** from which **6** was formed (60%) in a second Perkin reaction. Note that cyclizations with sodium alkoxide failed (< 10%), so that Na/xylene was used throughout. Repetition of the sequence on **6** produced **7** and **8**. It then remained only to convert the diester of **8** into a trimethylammoniummethyl group. This was achieved by saponifying the diester to dicarboxylic acid **9** (100%), which was decarboxylated to monocarboxylic acid **10** at 175 °C (80%). Reduction gave alcohol **11** (100%). Preparation of primary bromide **13** directly from **11** proved difficult. Neither bromination with PBr_3/pyridine nor with Br_2/Ph_3P/imidazole was satisfactory. Ultimately, success (81%) was attained by treating the corresponding tosylate with LiBr/acetone. Surfactant **1** was formed by allowing **13** to react at 80 °C (sealed tube) with trimethylamine in aqueous acetone. The final

[*] Prof. F. M. Menger, J. Ding
Department of Chemistry, Emory University
Atlanta, GA 30322 (USA)
Fax: Int. code +(404)727-6586

[**] This work was supported by the U. S. National Institutes of Health.

product, obtained in a 7.5% overall yield, was characterized by ^1H and ^{13}C NMR spectroscopy and by high-resolution FAB mass spectrometry.

A 16-step synthesis of surfactant **2** (2.4% overall yield) began with **8** in Scheme 1 and continued by construction of the fourth cyclobutane ring in the usual manner. Once the four-ring analog of **8** was in hand, the chemistry corresponding to **8**→**1** was followed identically. Product **2** was characterized by ^1H and ^{13}C NMR spectroscopy and by high-resolution FAB mass spectrometry. In addition, an X-ray structure of a crystalline intermediate (the ditosylate of the tetracyclic diol) affirmed the presence of the four spiro-linked rings.

Aqueous solutions of **1** and **2** at room temperature (25 °C) were investigated tensiometrically in order to detect possible micelle formation. Conventional surfactants are known to lower the surface tension steadily as the concentration is increased below the critical micelle concentration (CMC). Upon reaching the CMC, the plot levels off since the molecules prefer to enter the micelles rather than the air/water interface. (In fact, the point at which this occurs defines the CMC.) This general behavior was observed with **1** as seen in Figure 1. An approximate CMC of 0.14 M for **1** turns out to be identical to the CMC for linear $[C_8H_{17}N(CH_3)_3]^+Br^-$ with a similar chain length.[11] On the other hand, the CMC is 3.3 times larger than that of $[C_{11}H_{23}N(CH_3)_3]^+Br^-$, a conventional surfactant[11] with the same number of chain-carbons as **1**. Clearly, the propensity of **1** to form micelles relative to its total number of chain-carbons is substantially less than normal. Micelle formation might be impaired by the rigidity of the spiro system. Alternatively, the surfactant's compactness and buried quaternary carbons might

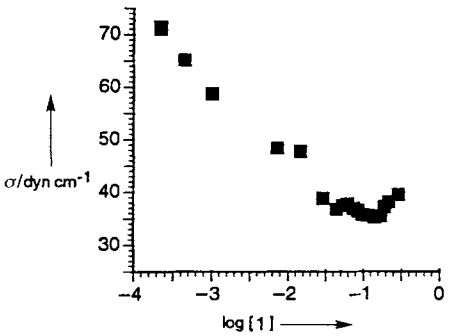

Fig. 1. Plot of surface tension σ as a function of the logarithm of the concentration of spiro-surfactant **1** [mol L^{-1}] in water at 25 °C.

reduce hydrocarbon–water contact of the monomer and thus diminish the hydrophobic forces that drive micelle formation.

Surfactant **2** lowers the surface tension effectively to less than 33 dyn cm^{-2} (Fig. 2). If a CMC exists, it must clearly exceed

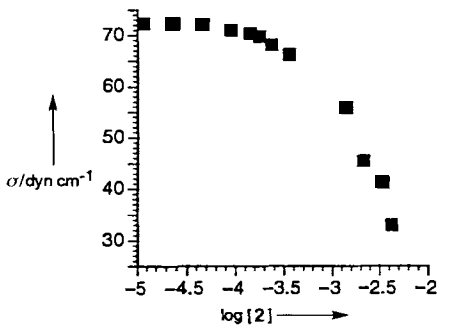

Fig. 2. Plot of surface tension σ as a function of the logarithm of the concentration of spiro-surfactant **2** [mol L^{-1}] in water at 25 °C.

4.4×10^{-3} M (at which point our experiments ceased owing to lack of compound). The surface tension plot is anomalous in that it displays convex curvature and little change in surface tension at low concentrations. It is difficult to deduce anything conclusive here except that the spiro system has a profound effect upon the ability of the surfactant to self-assemble. Note that the presence of a CMC for **1** or **2** says nothing about the size and shape of the aggregates. Dynamic light scattering, used to address this issue, revealed that the micelle hydrodynamic diameters fall far below the detection limits of the Nicomp Model 370 laser (about 40 Å). One can conclude, therefore, that the micelles are small aggregates (perhaps only 10–20 molecules) owing, presumably, to the difficulty of packing the rigid chains into a space-filled sphere. Vesicular bilayers (which were a distinct possibility because the width of the spiro system approaches that of a double-chain) are also ruled out by the light-scattering data.

Several standard methods for preparing phospholipids **14** and **15** failed to give satisfactory yields with our hard-won spiro

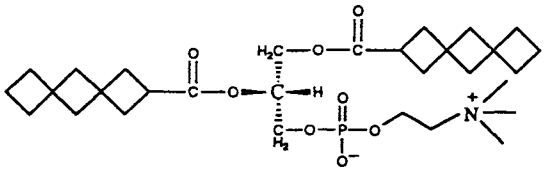

14

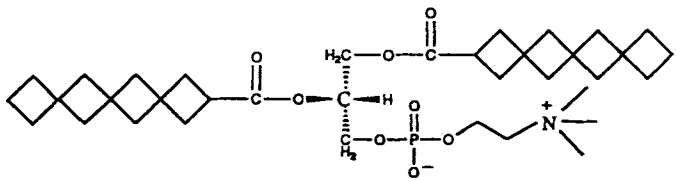

15

compounds. These included acylation of sn-glycero-3-phosphocholine ($CdCl_2$ complex) with: spirocarboxylic acid/DCC/DMAP; spirocarboxylic acid/TFA; spirocarboxylic acid anhydride/DMAP; and spiroacylimidazolide in DMSO. Ultimately, phospholipids **14** and **15** were obtained via the spirocarboxylic acid chlorides (made from the carboxylic acids and $SOCl_2$ at −20 °C) plus pyridine in $CHCl_3$ (25 °C, 14 h). Combined yields for the two steps, following purification by column chromatography, ranged from 40–75%.

Dynamic light-scattering studies were carried out on thin films of lipids **14** and **15**, which had been deposited on glass from a solution in $CHCl_3$/MeOH and then bath-sonicated in pH 7.0 buffer at 60 °C for 30 min. The resulting vesicles were polydisperse, ranging in diameter from 200–500 Å for **14** and from 500–1300 Å for **15**. Differential scanning calorimetry (Hart Scientific DSC II) showed no detectable phase transition from −20 to 110 °C (0.5 mg lipid in 0.5 mL water or ethylene glycol/water with a scan rate of 10 K h^{-1}). Absence of an endothermic transition most likely stems from the spiro units being conformationally immobile. Conventional lipids, by contrast, undergo a thermally induced conversion from an ordered gel phase into a liquid-crystalline state replete with *gauche* linkages. It will be interesting to elaborate the transport properties of our unusual rigidified membranes.

Synthetic organic chemistry would seem to offer special opportunities for lipid chemists to explore their field. Indeed, this was the philosophy that steered the above work as well as previ-

 © VCH Verlagsgesellschaft mbH, D-69451 Weinheim, 1996 0570-0833/96/3518-2138 $ 15.00+.25/0

ous syntheses of novel lipids.[12-15] It should be noted, finally, that surfactants **1** and **2** are among a growing list of new surfactants that violate the Israelachvili notions about how simple geometric factors control aggregate morphology.[16] On the face of it, the alkyl chains of **1** and **2** would seem too broad for micelle formation.

Received: April 12, 1996 [Z 9024 IE]
German version: *Angew. Chem.* **1996**, *108*, 2266–2268

Keywords: micelles · spiro compounds · surfactants

[1] K. Goodling, K. Johnson, L. Lefkowitz, B. W. Williams, *J. Chem. Ed.* **1994** *71*, A8–A12.
[2] B. Smit, K. Esselink, P. A. J. Hilbers, N. M. van Os, L. A. M. Rupert, I. Szleifer *Langmuir* **1993**, *9*, 9–11.
[3] D. G. Whitten, J. C. Russell, T. K. Foreman, R. H. Schmehl, J. Bonilha, A. M. Braun, W. Sobol in *Proceedings of the 26th OHOLO Conference, Zichron, Israel* (Eds.: B. S. Green, Y. Ashani, D. Chipman), Elsevier, Amsterdam, **1982**.
[4] F. M. Menger, D. W. Carnahan, *J. Am. Chem. Soc.* **1986**, *108*, 1297–1298.
[5] G. S. Hartley, *Aqueous Solutions of Paraffin-chain Salts. A Study of Micelle Formation*, Herman, Paris, **1936**.
[6] H. R. Horton, L. A. Moran, R. S. Ochs, J. D. Rawn, K. G. Scrimgeour, *Principles of Biochemistry*, 2nd ed., Prentice Hall, **1996**, p. 35. Many other current biochemistry texts likewise present micelles with totally linear chains.
[7] G. S. Murthy, K. Hassentück, V. M. Lynch, J. Michl, *J. Am. Chem. Soc.* **1989**, *111*, 7262–7264.
[8] L. M. Rice, C. H. Grogan, *J. Org. Chem.* **1961**, *26*, 54–58.
[9] E. Buchta, K. Geibel, *Liebigs Ann. Chem.* **1961**, *648*, 36–50.
[10] C. M. Sharts, A. H. McLeod, *J. Org. Chem.* **1965**, *30*, 3308–3312.
[11] H. B. Klevens, *J. Phys. Colloid Chem.* **1948**, *52*, 130–148.
[12] F. M. Menger, X. Y. Chen, *Tetrahedron Lett.* **1996**, *37*, 323–326.
[13] F. M. Menger, A. V. Eliseev, *Langmuir* **1995**, *11*, 1855–1857.
[14] F. M. Menger, Y. Yamasaki, *J. Am. Chem. Soc.* **1993**, *115*, 3840–3841.
[15] F. M. Menger, P. Aikens, *Angew. Chem.* **1992**, *104*, 919–921; *Angew. Chem. Int. Ed. Engl.* **1992**, *31*, 898–300.
[16] J. N. Israelachvili, *Intermolecular and Surface Forces*, Academic Press, London, **1985**, p. 251.

Synthesis of Water-Soluble Inclusion Compounds from Polyamides and Cyclodextrins by Solid-State Polycondensation

Marc Boris Steinbrunn and Gerhard Wenz*

Polyamides have of large practical significance because of their high form stability and high melting points. Due to strong intermolecular hydrogen bonding, these polymers are insoluble in most solvents except, for instance, in concentrated sulfuric acid.[1] Polyamides are produced technically by ring opening polymerization of the respective lactam or by bulk polycondensation of the salts formed from the amine and acid components (AH-salt) at high temperatures.[2] We now describe a method for the formation of water-soluble polymeric inclusion compounds by the polycondensation of crystalline AH-salts in the presence of cyclodextrins.

Cyclodextrins are cyclic oligomers of amylose consisting of six, seven, or eight glucose building blocks (α-, β-, and γ-cyclodextrin, respectively; **1a–1c**).[3] The inclusion of cyclodextrins in polymers was first investigated with polyethylene glycols.[4] These polymeric inclusion compounds are not water-soluble, and they dissolve in strong polar solvents only upon dissociation. The first soluble cyclodextrin inclusion compounds in polymers were obtained in our group from water-soluble poly(iminooligomethylene) compounds and ionenes.[5]

Previously the inclusion of polyamides in cyclodextrins was attempted by employing phase boundary polycondensation of diamines with dicarboxylic acid dichlorides in the presence of β-cyclodextrin.[6] The resulting products, however, were not soluble in water, which is probably due to a low coverage of the polyamide chain by cyclodextrin. With the method described herein, it is possible to obtain high coverage by solid-state polycondensation in the crystal array of the host molecule (Scheme 1). Polymerizations occurring in host crystals (clathrates) are well-established; to date, however, cyclic compounds have not been used as the matrix.[7] Cyclic matrices offer the advantage of maintaining the supramolecular order, even after dissolution of the polymeric product.

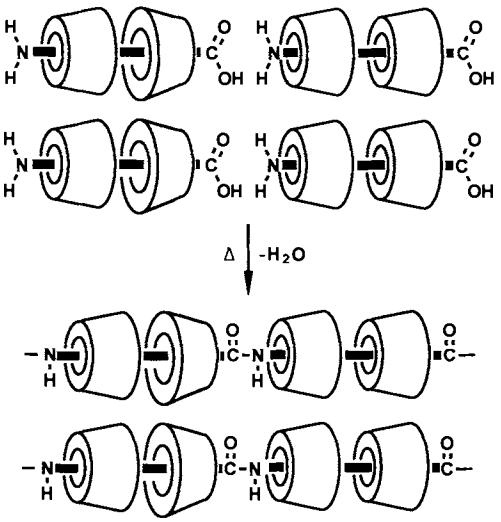

Scheme 1. Polycondensation of α,ω-amino acids in the cyclodextrin channel.

The α,ω-amino acids **2–5** that were used as reactive guest compounds were dissolved with **1a** in hot water, and the resulting solution was then rapidly cooled, upon which the inclusion compounds crystallized in high yields (Table 1). Depending on the molar ratio between the host and guest, 11-aminoundecanoic acid **2** is surrounded by either one or two cyclodextrins. The stoichiometry was determined by integration of the ^{1}H NMR signal of H-1 of the host **1a** and H-c through H-h of

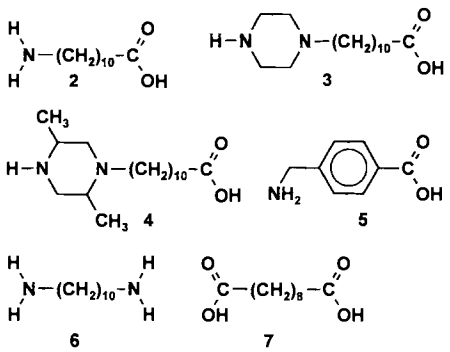

[*] Prof. Dr. G. Wenz, Dipl.-Chem. M. B. Steinbrunn
Polymer-Institut der Universität
Hertzstrasse 16, D-76187 Karlsruhe (Germany)
Fax: Int. code +(721)608-4421
e-mail: cg07@uw70.rz.uni-karlsruhe.de

[**] This work was supported by the BMBF (BEO 22/0310059A). We thank Prof. Dr. M. Ballauff for the use of the X-ray powder diffractometer and M. Hartenstein for his assistance.

Table 1. Preparation of the monomeric inclusion compounds.

Guest	Host	Host:Guest[a]	Inclusion cmpd.	Host:Guest[b]	Yield [%]
2	**1a**	1:1	**2·1a**	1:1	53
2	**1a**	2:1–10:1	**2·(1a)$_2$**	2:1	65
3	**1a**	2:1	**3·(1a)$_2$**	2:1	56
4	**1a**	2:1	**4·(1a)$_2$**	2:1	17
5	**1b**	1:1	**5·1b**	1:1	67
6, **7**	**1a**	2:1	**6·7·(1a)$_4$**	4:2	38

[a] Initial ratio. [b] In the inclusion compound.

the guest **2** (Fig. 1a). The splitting of signals for H-c through H-h show that the guest molecule **2** is indeed present in the inner portion of the host molecule **1a**. The microcalorimetric titration of **2** with **1a** revealed a stepwise inclusion with binding constants $K_1 = 4850\,M^{-1}$ and $K_2 = 507\,M^{-1}$.[8] Similarly, a crystalline ternary inclusion compound with defined 1:1:4 stoichiometry was also obtained when α,ω-diamine **6**, α,ω-dicarboxylic acid **7**, and **1a** were allowed to crystallize together.

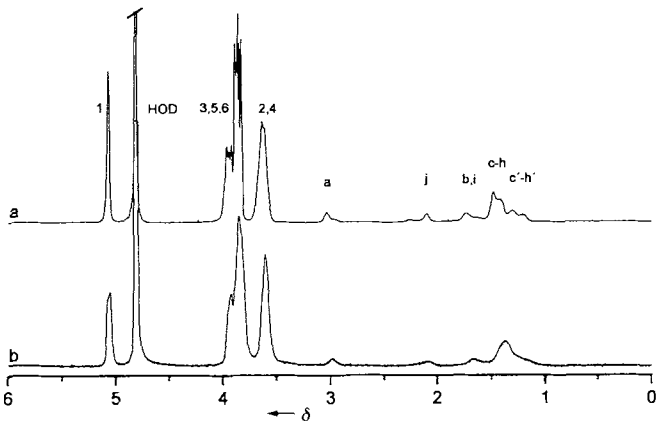

Fig. 1. ^{1}H NMR spectra of **2·(1a)$_2$** in D_2O a) before and b) after polycondensation.

The polycondensation of amino and acid groups requires a channellike packing of the cyclodextrins. The X-ray powder diffractograms of the inclusion compounds in Table 1 strongly support such a channellike packing (Fig. 2). In particular, the reflections at $2\theta = 19.63°$ ($d = 4.53$ Å) match those of known channellike inclusion compounds.[4] Only the inclusion compound **5·1b** is an exception.

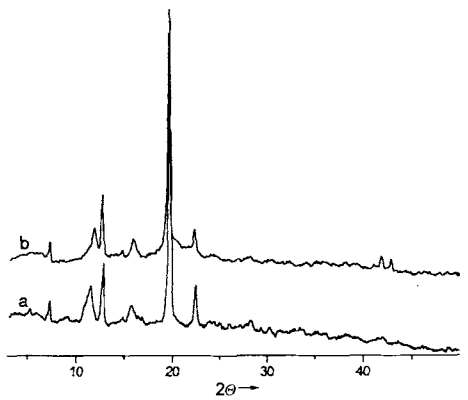

Fig. 2. X-ray powder diffractograms of **2·(1a)$_2$** in D_2O a) before and b) after polycondensation.

The polycondensation was carried out by annealing the microcrystalline inclusion compounds at 150–250 °C under vacuum. The formation of the amide can be monitored by IR spectroscopy (Fig. 3). The yield of the polyamide was independently

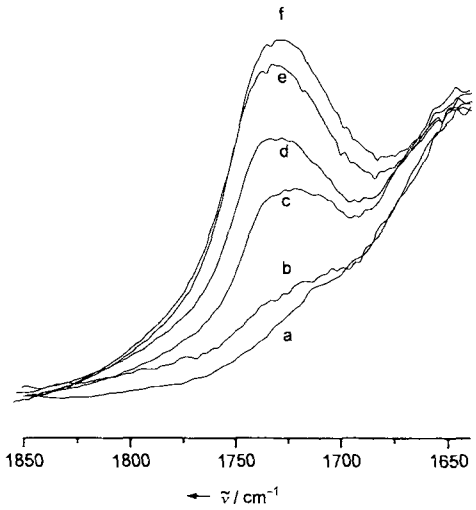

Fig. 3. IR spectra (section) of **2·(1a)$_2$** a) before and after annealing for 4 h at b) 200, c) 210, d) 220, e) 230, and f) 240 °C.

determined gravimetrically after hydrolysis of the cyclodextrin, which furthermore showed that the rate of reaction is strongly temperature-dependent: the condensation occurs at temperatures above 200 °C, a further temperature increase rapidly accelerates the polycondensation, and above 250 °C the cyclodextrin decomposes. The polycondensation of **2·(1a)$_2$** is nearly quantitative at 220 °C (Fig 4).

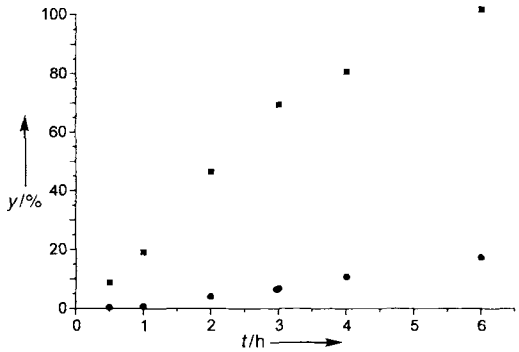

Fig. 4. Conversion y of the polycondensation of **2·(1a)$_2$** as a function of the annealing time t at 200 (●) and at 220 °C (■).

No polycondensation was observed in the case of **5·1b**. It is possible that the reactive groups are too distant from one another due to the herringbone type packing of **5·1b**. Further indications for a kind of topochemical control like that found for the solid-state polymerization of diacetylenes[9] have yet to be established. It would be interesting to investigate the impact of the alkyl chain length on the reactivity.

Based on the X-ray powder diffractogram of the product, the crystalline order is maintained during the polycondensation (Fig. 2b). An orientation reversal of the monomers can therefore be excluded. The high conversions obtained are indicative for a strictly alternating sequence of amino and acid groups in

the cyclodextrin channel, which can only be explained by strong intermolecular interactions.

Very surprising was our observation that these polyamide inclusion compounds are water-soluble. The ^{1}H NMR spectrum of $[2\cdot(\mathbf{1a})_2]_n$ in D_2O (Fig. 1b) shows the signals of cyclodextrin and polyamide. Although these are slightly broader than the corresponding signals of the monomers, they indicate the existence of a real solution. The signals of $[2\cdot(\mathbf{1a})_2]_n$ in [D$_6$]DMSO/CD$_3$COOD are better resolved, and the sharp signal for H-1 of **1a** proves that the C_6-symmetry of the α-cyclodextrin has been retained. Thus a reaction between the guest and cyclodextrin can be ruled out. The integration supports a coverage of the polyamide chain with two cyclodextrin units per repeating unit. This very high coverage explains the good solubility.

If the solution of the polyamide inclusion compound $[2\cdot(\mathbf{1a})_2]_n$ is allowed to stand for several hours, a precipitate forms in which the cyclodextrin content is reduced by 30% with respect to $[2\cdot(\mathbf{1a})_2]_n$. Apparently, the solubilizing cyclodextrins slowly unthread, with the result that free polymer chain ends can aggregate to allow the inclusion compound to precipitate. Due to the lack of mobility, the rings that are still threaded cannot slip off. The inclusion compound of polymer $[4\cdot(\mathbf{1a})_2]_n$ is soluble in water for an unlimited time. Thus the methyl substituents of the piperazine moiety seem to prevent the rings from slipping off the polymer chain.

The pure polyamides were isolated by cleaving the threaded cyclodextrins with dilute HCl. The yields of the pure polyamides, for example, polyamide-11 from $[2\cdot(\mathbf{1a})_2]_n$, was greater than 90%. The molecular masses were determined by gel permeation chromatography after N-trifluoroacylation.[10] The molecular mass of $M_w = 4500\ \mathrm{g\,mol^{-1}}$, which was obtained for **2**, corresponds to about 16 repeating units.[11]

With this solid-state polycondensation it is, in principle, possible to synthesize polyrotaxanes on any scale. Furthermore, this methodology might be applicable for the synthesis of rigid-chain, aromatic polyamides. Due to their good water-solubility, polymeric inclusion compounds could, for instance, be used for the coating of metals, polymers or textile surfaces with polyamides. Composite materials of the polyamide inclusion compounds and hydrophilic polymers, such as starch, might also be obtained.

Experimental Procedure

General: The ^{1}H NMR spectra were obtained at 400 MHz, and the X-ray powder diffractograms performed on a Siemens-WAXS-S-5000 diffractometer at 22 °C.

$[2\cdot(\mathbf{1a})_2]$: **2** (5 g, 24.9 mmol) and **1a** (125 g, 129 mmol) were dissolved in water (250 mL) and heated to 80 °C upon stirring. The clear solution was then quickly cooled to 5 °C. The resulting white precipitate was filtered, washed with water (400 mL), and dried in vacuo. Yield: 39.8 g (65%). ^{1}H NMR ([D$_6$]DMSO/CD$_3$COOD, 10:1): $\delta = 4.78$ (d, ^3J(H,H) = 1.73 Hz, 12H, H-1), 3.74 (t, ^3J(H,H) = 7.9 Hz, 12H, H-3), 3.63 (m, 36H, H-5, H-6), 3.37 (t, ^3J(H,H) = 7.86 Hz, 12H, H-4), 3.26 (dd, ^3J(H-1,H-2) = 1.73, ^3J(H-2,H-3) = 7.86 Hz, 12H, H-2), 2.73 (t, ^3J(H,H) = 7.38 Hz, 1.7H, H-a), 2.15 (t, ^3J(H,H) = 7.39 Hz, 1.7H, H-j), 1.47 (m, 3.7H, H-b, H-i), 1.225 (s, 12H, H-c through H-h); IR (KBr): $\tilde{\nu}$ = 3408 s, 2925 s, 1635 m, 1410 w, 1362 w, 1291 w, 1246 w, 1202 w, 1162 s, 1095 s, 938 m cm^{-1}.

$[2\cdot(\mathbf{1a})_2]_n$: $[2\cdot(\mathbf{1a})_2]$ (203 mg) was tempered at 230 °C and 0.1 mbar for 5 h. Yield: 196 mg (97.4%), light brown powder. ^{1}H NMR ([D$_6$]DMSO/CD$_3$COOD, 10/1): $\delta = 4.78$ (d, ^3J(H,H) = 1.73 Hz, 12H, H-1), 3.74 (t, ^3J(H,H) = 7.9 Hz, 12H, H-3), 3.62 (m, 36H, H-5, H-6), 3.36 (t, ^3J(H,H) = 7.86 Hz, 12H, H-4), 3.26 (dd, ^3J(H-1,H-2) = 1.73, ^3J(H-2,H-3) = 7.86 Hz, 12H, H-2), 2.98 (t, ^3J(H,H) = 7.38 Hz, 1.7H, H-a), 2.13 (t, ^3J(H,H) = 7.39 Hz, 1.7H, H-j), 1.44 (m, 3.7H, H-b, H-i), 1.35–1.15 (br., 12H, H-c through H-h); IR (KBr): $\tilde{\nu}$ = 3399 s, 2925 s, 2362 w, 1733 m, 1646 m, 1410 w, 1362 w, 1161 s, 1087 s, 938 m cm^{-1}; elemental analysis (%): calcd: C 46.83, H 6.68, N 0.66; found: C 46.61, H 6.96, N 1.14.

$(\mathbf{2})_n$: $[2\cdot(\mathbf{1a})_2]_n$ (1.172 g) was stirred in 1%HCl (60 mL) at 80 °C for 25 h. The resulting precipitate was filtered and washed several times with water and methanol. Yield: 103.1 mg (93.9%). For the molecular mass determination, $(\mathbf{2})_n$ (90 mg, 0.49 mmol) was added to absolute CH_2Cl_2 (15 mL) and stirred with trifluoroacetic anhydride (0.21 g, 1.0 mmol) at 25 °C for 24 h [10]. After removal of the solvent by distillation, the residue was dried at 0.1 mbar. Yield: 139 mg (96%) N-trifluoroacylated nylon-11. The soluble product was subjected to size exclusion chromatography on Styralgel columns (Waters, calibration with polystyrene standards [10]) in absolute THF.

Received: March 21, 1996
Revised version: June 3, 1996 [Z 8956 IE]
German version: *Angew. Chem.* **1996**, *108*, 2274–2277

Keywords: cyclodextrins · host–guest chemistry · polyamides · solid-state reactions

[1] Additional suitable solvents include solutions of LiCl in DMF and $CaCl_2$ in methanol. Polyamides can also be dissolved by chemical modification: R. Vieweg in *Kunststoff-Handbuch, Bd. VI (Polyamide)* (Ed.: A. Müller), Hanser, München, **1966**, pp. 392 and 489.

[2] H. Rinke, E. Istel, *Methoden Org. Chem. (Houben Weyl) 4th ed. 1952–, Vol. 14/2*, **1963**, pp. 99–193.

[3] G. Wenz, *Angew. Chem.* **1994**, *106*, 851–870; *Angew. Chem. Int. Ed. Engl.* **1994**, *33*, 803–822.

[4] A. Harada, M. Kamachi, *Macromolecules* **1990**, *23*, 2821–2823; A. Harada, J. Li, M. Kamachi, *ibid.* **1994**, *27*, 4538–4543.

[5] G. Wenz, B. Keller, *Angew. Chem.* **1992**, *104*, 201–204; *Angew. Chem. Int. Ed. Engl.* **1992**, *31*, 197–199; *Polym. Prep. Am. Chem. Soc. Div. Polym. Chem.* **1993**, *34*, 62–64.

[6] N. Ogata, K. Sanui, J. Wada, *J. Polym. Sci. Polym. Lett. Ed.* **1976**, *14*, 459–462.

[7] To date, urea, thiourea, deoxycholic acid and perhydrotriphenylene have been used as matrices: M. Farina, U. Pedretti, M. T. Gramegna, G. Audisio, *Macromolecules* **1970**, *3*, 475–480; M. Miyata in *Polymerization in Organized Media* (Eds.: C. M. Paleos), Gordon & Breach, Philadelphia, **1992**, pp. 327–367.

[8] M. Kremm, S. Wehrle, G. Wenz, unpublished results.

[9] G. Wegner, *Z. Naturforsch. B* **1969**, *24*, 824; G. Wenz, G. Wegner, *Mol. Cryst. Liq. Cryst.* **1983**, *96*, 99–108.

[10] E. Jakobi, Dissertation, Mainz, **1980**, 129–158; K. Weisskopf, Dissertation, Mainz, **1983**, 47–61, 130–131.

[11] The relatively low molecular mass has to be considered a minimal value since a small portion of polyamide **2** could not be dissolved.

Molecular Recognition of Cyanide by a Dicopper(II) Macrocyclic Ionophore: Construction of a Cyanide-Selective Liquid-Membrane Electrode

Benedikt Ahlers, Karl Cammann,* Sabine Warzeska, and Roland Krämer*

Over the years various types of synthetic receptors for the efficient and selective binding of anions have been developed.[1] A particularly interesting application of such compounds is their use as ionophores in potentiometric sensors.[2] There are only few examples of anion-selective microelectrodes that are based on the specific interaction of the target anion with a transition metal complex. Lipophilic metalloporphyrins[3] and alkyltin compounds[4] are selective carriers for various anions in liquid-membrane electrodes; they show a correlation between the selectivity sequence of the electrode and the strength of the coordinative bond between metal and anion.

[*] Prof. Dr. K. Cammann, Dipl.-Chem. B. Ahlers
Institut für Chemo- und Biosensorik
Mendelstrasse 7, D-48149 Münster (Germany)
Fax: Int. code + (251)980-2802
Dr. R. Krämer, Dipl.-Chem. S. Warzeska
Anorganisch-Chemisches Institut der Universität
Wilhelm-Klemm-Strasse 8, D-48149 Münster (Germany)
Fax: Int. code + (251)83-8366
e-mail: kramerr@vnwz01.uni-muenster.de

[**] This work was supported by the Deutsche Forschungsgemeinschaft and the Fonds der Chemischen Industrie.

Here we present the first potentiometric anion sensor in which the dinuclear metal complex of a polyaza macrocycle acts as an ion-selective ionophore. Complexes of macrocycles that have two sites for ligation to metal centers coordinate bridging anions in a shape-selective, molecular recognition process.[5]

The lipophilic bis(tridentate) macrocycles L^1 and L^2 are readily available by alkylation of the secondary amino groups of a previously described ligand.[6] For a comparative study the related monotopic ligand L^3 was prepared by Schiff base condensation of pyridine-2,6-dicarbaldehyde and benzylamine, followed by $NaBH_4$ reduction of the imino groups. The crystalline complexes $[(L^1)Cu_2(NO_3)_4]$, $[(L^2)Cu_2(NO_3)_4]$,[7] and $[(L^3)Cu(NO_3)_2]$ were obtained by reaction of the ligands with $Cu(NO_3)_2 \cdot 3H_2O$ in appropriate stoichiometry.

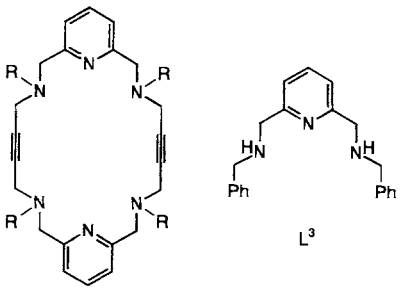

L^1: R = $C_{16}H_{33}$
L^2: R = CH_2Ph

L^3

To our knowledge the reaction of macrocyclic dicopper(II) complexes with cyanide, particularly in solution, has not yet been studied in detail. The green microcrystalline complexes $[(L^n)Cu_2(\mu\text{-}CN)(NO_3)_3]$ are obtained from $[(L^n)Cu_2(NO_3)_4]$ ($n = 1, 2$) and KCN (1 equiv). A weak ν(CN) infrared band at 2205 cm^{-1} for $[(L^1)Cu_2(\mu\text{-}CN)(NO_3)_3]$ and at 2208 cm^{-1} for $[(L^2)Cu_2(\mu\text{-}CN)(NO_3)_3]$ indicate the presence of bridging cyanide.[8] The crystal structure of the cyano-bridged dicopper(II) compound of a related ligand[9] with ν(CN) at 2235 cm^{-1}

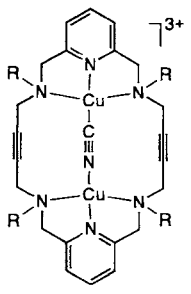

$[(L^n)Cu_2(\mu\text{-}CN)]^{3+}$

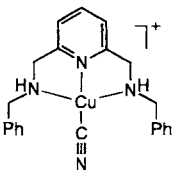

$[(L^3)Cu(CN)]^+$

demonstrates that CN^- fits well into the central cavity defined by the relatively rigid macrocyclic framework. The cleft between the alkyne spacers is only about 6 Å wide,[6,9] which should disfavor the incorporation of bulkier (for example tetrahedral) anions for steric reasons. Addition of KCN to $[(L^3)Cu(NO_3)_2]$ yields purple $[(L^3)Cu(CN)(NO_3)]$. The rather strong ν(CN) infrared band of this complex at 2127 cm^{-1} is typical for terminally coordinated cyano ligands.[8a]

In MeOH–MeCN (1:1 v/v) solution blue $[(L^1)Cu_2]^{4+}$ (λ_{max} = 647 nm, ε_{647} = 480 $M^{-1}cm^{-1}$, ε_{400} = 290 $M^{-1}cm^{-1}$) is smoothly converted into blue-green $[(L^1)Cu_2(\mu\text{-}CN)]^{3+}$ (λ_{max} = 617 nm, ε_{617} = 550 $M^{-1}cm^{-1}$, ε_{400} = 1200 $M^{-1}cm^{-1}$) by titration with between 0 and 1 equivalent of cyanide (isosbestic point at 665 nm). Similarly, blue $[(L^2)Cu_2]^{4+}$ (λ_{max} = 656 nm, ε_{656} = 590 $M^{-1}cm^{-1}$, ε_{400} = 340 $M^{-1}cm^{-1}$) forms green $[(L^2)Cu_2(\mu\text{-}CN)]^{3+}$ (λ_{max} = 635 nm, ε_{635} = 680 $M^{-1}cm^{-1}$, ε_{400} = 1100 $M^{-1}cm^{-1}$), with an isosbestic point at 670 nm. The mononuclear complex $[(L^3)Cu]^{2+}$ (λ_{max} = 635 nm, ε = 220 $M^{-1}cm^{-1}$) reacts with between 0 and 1 equivalent of cyanide to yield purple $[(L^3)Cu(CN)]^+$ (λ_{max} = 580 nm, ε = 280 $M^{-1}cm^{-1}$, isosbestic point at 630 nm). Smooth formation of 1:1 complexes shows that the first cyanide molecule is bound with high affinity in all cases.[10] Further changes in the spectra on addition of more than one equivalent of KCN indicate coordination of more than one CN^- ion to the complexes. Thus, for 1–3 equivalents of cyanide the green solutions of the dinuclear complexes turn blue again, due to a significant decrease of 400 nm absorbance.

Evidence for the particularly efficient binding of bridging cyanide is given by the behavior of the complexes on treatment with strong acid. In a MeOH–MeCN solution (1:1 v/v) of $[(L^n)Cu_2(\mu\text{-}CN)]^{3+}$ (1 mM) λ_{max} and ε of the optical band remain unchanged upon addition of 3 equivalents of *p*-toluenesulfonic acid (TsOH) (with a very large excess of TsOH the complexes are decomposed by ligand protonation rather than by release of HCN). In contrast, treatment of $[(L^3)Cu(CN)]^+$ (λ_{max} = 580 nm) with TsOH results in protonation of coordinated cyanide to produce 70% $[(L^3)Cu]^{2+}$ (λ_{max} = 635 nm) on addition of one equivalent of TsOH and 90% $[(L^3)Cu]^{2+}$ on addition of two. Also, TsOH removes the second coordinated cyanide molecule in $[(L^n)Cu_2(CN)_2]^{2+}$ to give 55% $[(L^n)Cu_2(\mu\text{-}CN)]^{3+}$ (1 equiv. TsOH) and 80% $[(L^n)Cu_2(\mu\text{-}CN)]^{3+}$ (2 equiv. TsOH). Based on these observations we can estimate the relative affinities of the complexes for bridging and terminal cyanide ligands. The binding constant of $[(L^n)Cu_2]^{4+}$ for bridging cyanide is at least 10^2 times larger than that of $[(L^3)Cu]^+$ or $[(L^n)Cu_2(\mu\text{-}CN)]^{3+}$ for terminal cyanide.[11] It is well known that dinuclear macrocyclic copper(II) complexes have a much higher affinity for bridging anions of appropriate geometry than related mononuclear complexes.[12]

In the presence of excess cyanide $[(L^n)Cu_2]^{4+}$ ($n = 1,2$) is more stable against reduction than $[(L^3)Cu]^{2+}$. In a MeOH–MeCN solution (1:1 v/v) containing 5 mM KCN the optical absorbance of the dinuclear complex (1 mM) is unchanged for 3 min whereas reduction of Cu^{II} to Cu^{I} in the mononuclear complex (1 mM) is indicated by a complete disappearence of the absorbance around 600 nm in the same period of time.

Application of $[(L^n)Cu_2(NO_3)_4]$ ($n = 1, 2$), $[(L^3)Cu(NO_3)_2]$ and L^2 as ion-selective materials in liquid-membrane electrodes was studied by measuring the potentiometric behavior. The compounds were embedded into a plastisized PVC-membrane (PVC/*o*-nitrophenyl octyl ether/ionophore in a 33/66/1 ratio).[2a] The membranes containing $[(L^n)Cu_2(NO_3)_4]$ and $[(L^3)Cu(NO_3)_2]$ were light blue and transparent when kept in H_2O. Apparently, the $C_{16}H_{33}$ and CH_2Ph substituents anchor the complexes in the lipophilic membrane phase and prevent loss to the aqueous solution.

The membranes were implemented into a potentiometric measuring setup and the potential differences referred to a Ag/AgCl reference electrode were determined.[2a] The electrodes containing $[(L^n)Cu_2(NO_3)_4]$ exhibited fast and reversible near-Nernstian response to aqueous cyanide solutions at pH 10 with a linear working range for cyanide concentrations between 10^{-5} to 10^{-2} M. The response to CN^- is highly selective, in particular for $[(L^1)Cu_2(NO_3)_4]$ (Fig. 1). Alternating current impendance measurements[13] confirmed the interaction of membranes con-

 © VCH Verlagsgesellschaft mbH, D-69451 Weinheim, 1996 0570-0833/96/3518-2142 $ 15.00+.25/0

taining $[(L^2)Cu_2(NO_3)_4]$ with cyanide ions. The bulk membrane resistance changed by a factor of 4 on exposure to 1 mM KCN solution in a 0.1 M $Ca(NO_3)_2$ background electrolyte. Furthermore, the bright blue membrane adopts the bright green color of $[(L^2)Cu_2(\mu\text{-}CN)(NO_3)_3]$ when kept in 0.1 M cyanide solution for 5 h.[14]

Electrodes based on $[(L^3)Cu(NO_3)_2]$ or L^1 show only a slight sensitivity to cyanide ions and behave more or less as typical anion exchangers with a selectivity pattern dependent on the lipophilicity of the sample anions (Fig. 1).[2a] Although formation of $[(L^3)Cu(CN)(NO_3)]$ is indicated by the purple color of the membrane after exposure to 0.1 M KCN, cyanide affinity of the mononuclear complex appears to be too weak to induce a selective response.

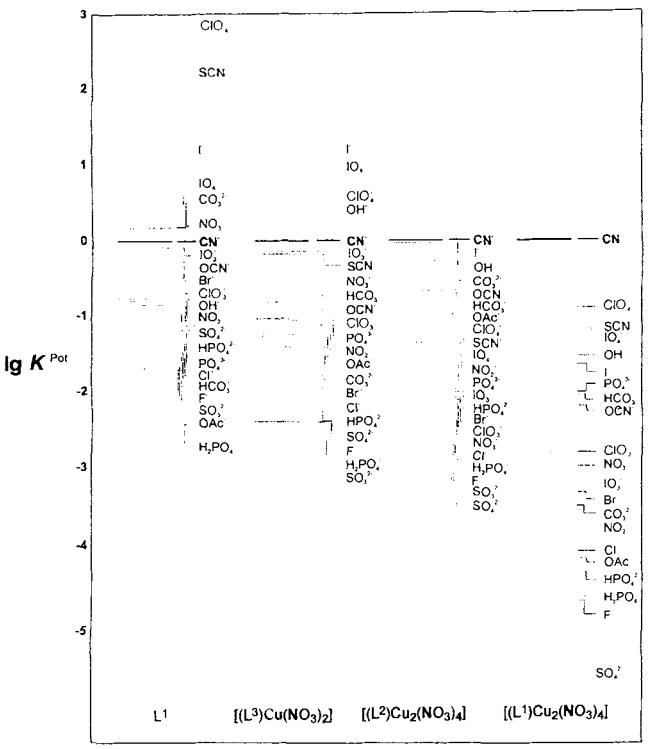

Fig. 1. Selectivity coefficients lg $K^{Pot}_{CN^-,A^-}$ of a membrane electrode containing ionophores $[(L^1)Cu_2(NO_3)_4]$, $[(L^2)Cu_2(NO_3)_4]$, $[(L^3)Cu(NO_3)_2]$, and L^2, determined according to the FIM-method.[2a] The selectivity coefficient is given by the weighting factor (K^{Pot}_{ij}) in the Nicolsky Eisenmann equation $\left(E = E^0_i + \frac{2.3\,RT}{z_i F}\,\lg\left[a_i + \sum_j K^{Pot}_{ij}\cdot(a_j)^{z_i/z_j}\right]\right)$.

In conclusion, the first cyanide-selective electrode based on a molecular recognition process was constructed. Dinuclear metal complexes of lipophilic macrocycles represent a novel class of ionophore in liquid-membrane electrodes. By variation of the metal ion and of the macrocyclic framework selective carriers for many different target anions should be available.

Received: April 10, 1995 [Z 90121E]
German version: *Angew. Chem.* **1996**, *108*, 2270–2271

Keywords: copper compounds · cyanides · electrodes · macrocycles · molecular recognition

[1] Reviews: J.-M. Lehn, *Pure Appl. Chem.*, **1978**, *50*, 871–892; *Acc. Chem. Res.*, **1978**, *11*, 49; *Science*, **1985**, *227*, 849–856; F. P. Schmidtchen, *Nachr. Chem. Tech. Lab.* **1988**, *36*, 8–17; F. Vögtle, H. Sieger, W. M. Müller, *Topics Curr. Chem.* **1981**, *98*, 107–161; J.-L. Pierre, P. Baret, *Bull. Soc. Chim. Fr.* **1983**, 367–380; B. Dietrich, *Pure Appl. Chem.*, **1993**, *65*, 1457–1464.

[2] a) K. Cammann, H. Galster, *Das Arbeiten mit ionenselektiven Elektroden*, Springer, Berlin, Heidelberg, **1996**; b) W. E. Morf, *The Principles of Ion Selective Electrodes and of Membrane Transport*, Elsevier, Amsterdam, **1981**; c) J. F. J. Engbersen, D. N. Reinhoudt, *Analusis* **1994**, *22*, M16–M18.

[3] Examples: P. Schulthess, D. Amman, B. Kräutler, C. Caderas, R. Stepánek, W. Simon, *Anal. Chem.* **1985**, *57*, 1397–1401; D. Amman, M. Huser, B. Kräutler, B. Rusterholz, P. Schulthess, B. Lindemann, E. Halder, W. Simon, *Helv. Chim. Acta*, **1986**, *69*, 849–854.

[4] S. A. Glazier, M. A. Arnold, *Anal. Chem.* **1988**, *60*, 2540.

[5] J.-M. Lehn, *Pure Appl. Chem.* **1980**, *52*, 2441–2460.

[6] S. Warzeska, R. Krämer, *Chem. Ber.* **1995**, *128*, 115–119.

[7] $[(L^2)Cu_2(NO_3)_4]$ was characterized by X-ray crystallography. Each Cu center is five-coordinate and ligated by three N atoms of a tridentate subunit of L^2 and two O atoms of two different nitrate ions in a distorted square-pyramidal fashion.

[8] a) D. M. Duggan, R. G. Jungst, K. R. Mann, G. D. Stucky, D. N. Hendrickson, *J. Am. Chem. Soc.* **1974**, *11*, 3443–3450; b) O. P. Anderson, A. B. Packard, M. Wicholas, *Inorg. Chem.* **1976**, *15*, 1613–1618.

[9] S. Warzeska, R. Krämer, *J. Chem. Soc. Chem. Commun.* **1996**, 499–500. A mixed valence Cu^{II} Cu^{I} macrocyclic complex containing bridging cyanide has been reported previously: Y. Agnus, J. P. Gisselbrecht, R. Louis, B. Metz, *J. Am. Chem. Soc.* **1989**, *111*, 1494–1496.

[10] The copper ion in $[(L^3)Cu]^{2+}$ most likely adopts a square-pyramidal coordination with two vacant coordination sites, one in the equatorial and one in the axial position. In this type of complex equatorial coordination of cyanide is strongly preferred over axial coordination: E. J. Billo, *Inorg. Nucl. Chem. Lett.* **1977**, *13*, 673–677.

[11] Based on 10% error for the spectrophotometrically determined complex concentrations.

[12] R. J. Motekaitis, A. E. Martell, B. Dietrich, J.-M. Lehn, *Inorg. Chem.* **1984**, *23*, 1588–1591; S. Kida, I. Murase, C. Harada, L. Daizeng, M. Mikuriya, *Bull. Chem. Soc. Jpn.* **1986**, *59*, 2595; A. Evers, R. D. Hancock, I. Murase, *Inorg. Chem.* **1986**, *25*, 2160–2163.

[13] G. Horvai, E. Graf, K. Toth, E. Pungor, R. P. Buck, *Anal. Chem.* **1986**, *58*, 2741.

[14] It was not possible to follow complexation of cyanide by direct investigation of the PVC-membranes with standard UV/Vis or IR spectroscopic methods. Absorbances of the complexes are too weak and are superimposed by background absorbance of the membrane.

Structure-Directed Synthesis under Thermodynamic Control: Macrocyclic Trimers from Cinchona Alkaloids**

Stuart J. Rowan, Paul A. Brady, and Jeremy K. M. Sanders*

Covalent organic structures have traditionally been synthesized through kinetically controlled irreversible reactions, whereas noncovalent supramolecular assemblies are generally constructed with thermodynamically controlled reversible interactions.[1,2] Irreversible reactions lack the ability to proofread and repair "incorrect" bond formation, while supramolecular assemblies tend to lack the robust character associated with covalent bonds, so we have been exploring the synthetic potential of covalent chemistry under reversible conditions.[3] We now report the exceptionally efficient synthesis under thermodynamic control of macrocyclic trimers from new supramolecular building blocks derived from the cinchona alkaloids quinine (**1a**) and cinchonidine (**1b**).

[*] Prof. Dr. J. K. M. Sanders, Dr. S. J. Rowan, P. A. Brady
Cambridge Centre for Molecular Recognition
University Chemical Laboratory
Lensfield Road, GB-Cambridge CB2 1EW (UK)
Fax: Int. code +(1223) 336017
e-mail: jkms@cam.ac.uk

[**] We thank the Engineering and Physical Science Research Council, Merck, Sharp, and Dohme, and Rhône-Poulenc-Rorer for financial support, and the EPSRC Mass Spectrometry Service in Swansea for mass spectra.

Cinchona alkaloids have recently received much attention in the field of asymmetric synthesis.[4] For example, quinine and its derivatives have been widely used in the Sharpless dihydroxylation reaction.[5] Despite all this interest, however, there has been little use of this building block in supramolecular or macrocyclic chemistry. Notable exceptions include its use as a chiral resolution agent, where quinine forms an inclusion complex with binaphthols,[6] and as a quinine-derived macrocycle, prepared by Corey and Noe[7] for use as a more rigid ligand in the Sharpless dihydroxylation reaction.

The size and relatively concave shape of quinine, together with the functionality present in the natural product, make it attractive for macrocycle synthesis. As our thermodynamic cyclizations are transesterifications,[3] we require a hydroxyl group at one end of the molecule and an ester elsewhere. There is already a hydroxyl group present at the 9-position of quinine, but an ester group had to be introduced into the system. This was achieved by modifying the vinyl group in five steps (Scheme 1)[8] to give the methyl ester **2a**. Starting with the natural product **1a** the hydroxyl group at the 9-position was protected with a *tert*-butyldimethylsilyl (TBDMS) group by reaction with Et_3N/(4-dimethylamino)pyridine (DMAP) and TBDMSCl to give **3a** in 99% yield. Hydroboration of the vinyl group with five equivalents of $BH_3 \cdot THF$ in diglyme, followed by oxidation with $Me_3NO \cdot 2H_2O$[9] yielded the terminal alcohol **4a** in 87% yield.[10] Subsequent oxidation of this alcohol with Jones' reagent gave the acid **5a** in 62% yield, which was esterified with MeOH/HCl conc. to furnish **6a** in 97% yield. Finally, deprotection by cleaving the TBDMS group with TBAF/THF yielded the monomer **2a** in 66% yield. Overall the final monomeric building block was synthesized in a 34% yield from the starting natural product. The cinchonidine monomer **2b** was prepared in an analogous manner starting from natural cinchonidine (**1b**).

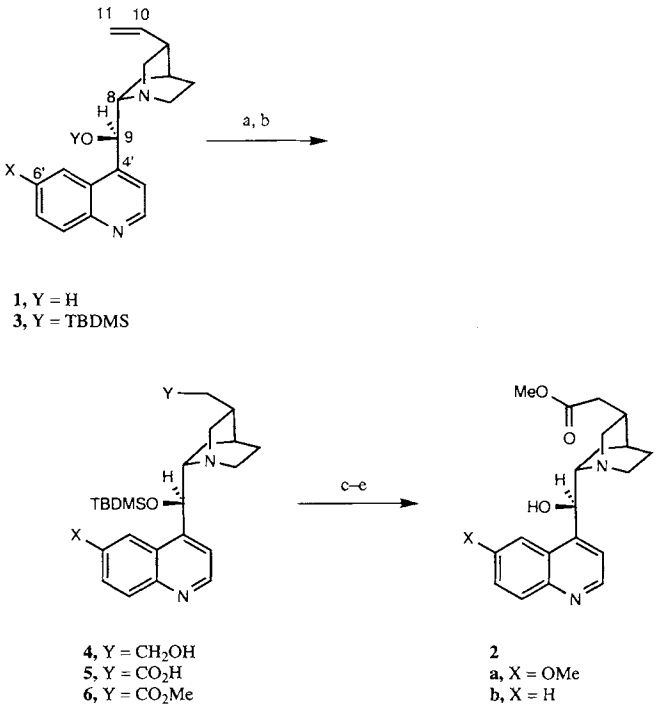

Scheme 1. a) TBDMSCl, Et_3N, DMAP, DMF, room temperature; b) 1. 5 equiv $BH_3 \cdot THF$, diglyme, 0 °C, 2. Me_3NO, 100 °C; c) Jones' reagent, acetone, room temperature; d) MeOH, $HCl_{conc.}$, room temperature; e) TBAF, THF, room temperature.

Thermodynamic cyclizations of **2a** were carried out by utilizing a procedure similar to that reported previously[3] (Scheme 2). The catayst (5% KOMe/[18]crown-6) was added to a refluxing solution (5 mM) of **2a** in toluene, with azeotropic removal of the methanol produced. Initially, the extent of the reaction was followed by HPLC;[11] recently, electrospray mass spectrometry (ESMS) has proved to be a more powerful probe for following the oligomerization. Remarkably, the cyclization of **2a** gave virtually a single product: the cyclic trimer **7a** was formed in high yield (about 90% by NMR and 84% isolated yield). The reaction was virtually complete after 20 min and no significant change in distribution was seen in the following 160 minutes. Cyclization of **2b** results in the corresponding trimer **7b** in excellent yield.

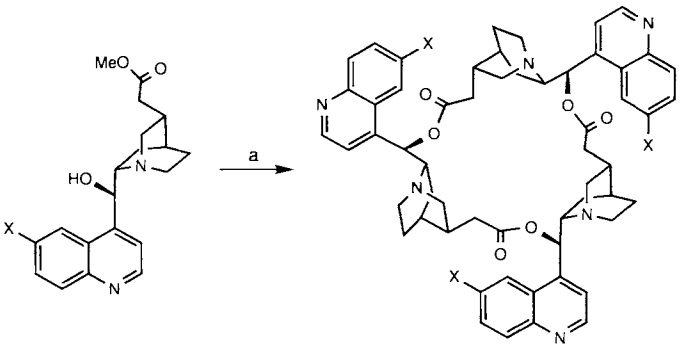

Scheme 2. a) KOMe, [18]crown-6, toluene, reflux.

To demonstrate that the apparent trimer was the single product rather than a mixture of cyclic oligomers with indistinguishable NMR, MS, and HPLC characteristics, the linear dimer, trimer, and tetramer were synthesized by independent synthetic routes and subjected to cyclization under Yamaguchi-type kinetic conditions. The linear dimer and tetramer each gave the cyclic tetramer, which was indeed spectroscopically different from cyclic trimer;[12] attempts to build CPK models of the cyclic dimer suggested that this dimer would be kinetic inaccessible. Cyclization[13] of the monomer unit was also carried out under kinetic control. This yielded a mixture of cyclic trimer (37%), tetramer (23%), and other higher oligomers (40%) (according to ^1H NMR spectra). These results show that although the cyclic dimer is not kinetically accessible, higher oligomers can be formed. The narrow distribution observed in the thermodynamic reaction is thus not due to kinetic inaccessibility of the other cyclic oligomers.

Proof was then sought that the cyclization was a reversible process. To this end a mixture of the two preformed trimers **7a** and **7b** was subjected to the reaction conditions,[14] and the resulting solution was assayed by ESMS[15] after quenching with aqueous buffer (pH 7) and extraction into ethyl acetate. As Figure 1 demonstrates all four possible trimers (containing 0, 1, 2, or 3 methoxyl groups) are present, a result that is consistent only with reversible breakdown and reformation of the initial trimers. The heterotrimers appear almost immediately (20 s), and after only 2 minutes there is already a ratio of over 2:1 (heterotrimer: homotrimer). The statistically expected 3:1 is

 © VCH Verlagsgesellschaft mbH, D-69451 Weinheim, 1996 0570-0833/96/3518-2144 $ 15.00+.25/0

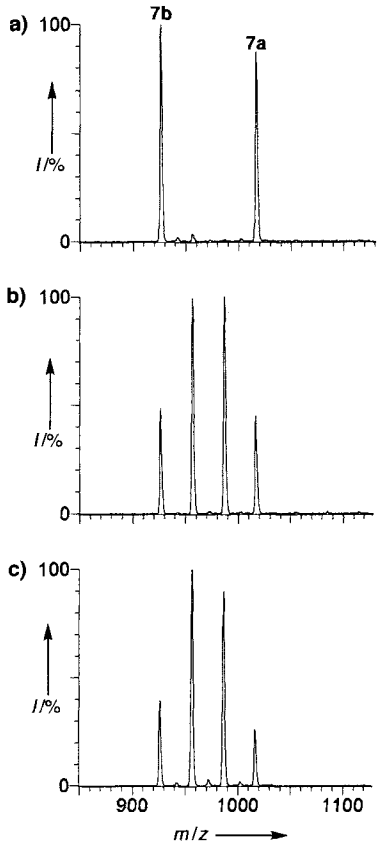

Fig. 1. Molecular ion region of the ES mass spectra of the reaction of quinine trimer (**7a**) and cinchonidine trimer (**7b**) before any catalyst was added (a), and 2 (b) and 10 minutes (c) after addition. The four peaks correspond to trimers without 6′-OMe groups (**7b**: *m/z* 925) and with one (*m/z* 955), two (*m/z* 985), or three 6′-OMe groups (**7a** 1015). The deviation from the expected 1:1 peak intensities in (a) and from 1:3:3:1 in (c) results mainly from the slight excess of **7b** used (9.5 mg, 1.03×10^{-5} mol for **7b**, 9.8 mg, 9.7×10^{-6} mol for **7a**).

reached within 10 minutes and persists beyond 1 hour.

The narrow product distributions in these cinchona alkaloid cyclizations contrast with the broader distributions observed in the cholate series,[3] when the same cyclization conditions are used, a result that must be due to a different balance of the statistical and enthalpic factors in the two systems. In the cholate series, steroid cores are linked by flexible four-carbon units, which apparently allow considerable dispersity in the ring size distribution (mainly dimer, trimer, tetramer, pentamer). In the cinchona series, rigid quinuclidine cores are connected by a flexible two-carbon unit (C_{10} and C_{11}), with some further rotation possible around the C_8-C_9 and $C_9-C_{4'}$ bonds. This rotation, however, turns out to be unexpectedly restricted: ^{1}H NMR spectra of compounds **3a–6a** show splitting of both the $(CH_3)_3CSi$ and CH_3Si proton resonances, which suggests that rotation of the bonds around the C9 carbon atom is hindered, presumably due to the bulky quinoline unit. This is also seen in the cinchonidine series **3b–6b**, although broadening of these signals suggests faster rotation due to the removal of the 6′-OMe group. The overall effect is that trimer is by far the most favored product in this reaction, with only trace amounts of the higher oligomers and no detectable dimer.

We have now shown that the thermodynamic transesterification reaction is applicable to systems other than cholates and that our new alkaloid-derived building blocks are preorganized to give cyclic trimers even though they appear to have many degrees of rotational freedom available.[16] This work is now being extended to investigate mixtures of building blocks and the effects of potential templates.

Experimental Procedure

KOMe · [18]crown-6 [17]: KOMe in methanol (0.513 mL, 0.78 M, 0.40 mmol), freshly prepared from potassium metal and methanol, was added to [18]crown-6 (106 mg, 0.40 mmol). Dried toluene (1 mL) was then added, and the mixture concentrated under reduced pressure to about 0.5 mL. More toluene (1 mL) was added, and the mixture was again concentrated under reduced pressure to 0.5 mL. This was repeated once more to ensure that all the methanol had been removed azeotropically. The catalyst mixture was then diluted with toluene (about 1.5 mL), and the solution filtered under inert atmosphere to give a KOMe · [18]crown-6 toluene solution of about 0.015–0.03 M (determined by titration).

7a: Monomer **2a** (10 mg, 2.703×10^{-5} mol) was added to a round-bottomed flask attached to a soxhlet extractor that contained molecular sieves (4 Å) and then dissolved in toluene (5.4 mL). This solution was refluxed for 30 min to remove all water from the system, and then the KOMe · [18]crown-6 catalyst solution (45 μL, 0.03 M, 1.35×10^{-6} mol) was added. To work up the reaction, the mixture was added to aqueous buffer (pH 7) and extracted with ethyl acetate. The compound was purified by column chromatography on silica (graduated elution with ethyl acetate/methanol (10/0, 9/1, 8/2, ... etc.)) to obtain **7a**. Yield. 7.7 mg (84%). TLC ethyl acetate/methanol (1/1) $R_f = 0.17$. ^{1}H NMR (400 MHz, $CDCl_3$): $\delta = 1.35$ (dd, $J = 13.4$, 7.9 Hz, 3H), 1.57 (m, 3H), 1.76 (m, 3H), 1.90 (br s, 3H), 1.97–2.18 (m, 9H), 2.24 (m, 3H), 2.62 (m, 6H), 2.99 (dd, $J = 11.2$, 14.7 Hz, 3H), 3.11 (dd, $J = 14.7$, 11.2 Hz, 3H), 3.43 (dd, $J = 18.4$, 9.0 Hz, 3H), 3.97 (s, 9H), 6.53 (d, $J = 10.6$, 3H), 7.37 (m, 6H), 7.53 (d, $J = 2.6$ Hz, 3H), 8.01 (d, $J = 9.2$ Hz, 3H), 8.76 (d, $J = 4.5$,3H); ^{13}C NMR (100 MHz, $CDCl_3$): $\delta = 24.39$, 25.79, 28.17, 31.96, 38.50, 41.77, 55.71, 56.65, 59.42, 72.09, 102.26, 119.63, 121.24, 127.78, 131.88, 143.69, 144.88, 147.55, 157.88, 171.88. FAB-MS: *m/z*: 1015 $[M+H^+]$. ES-MS: *m/z*: 1015 $[MH^+]$, 508 $[MH_2^{2+}]$, 339 $[MH_3^{3+}]$.

Received: March 18, 1996
Revised version: June 3, 1996 [Z 8941IE]
German version: *Angew. Chem.* **1996**, *108*, 2283–2285

Keywords: alkaloids · cyclizations · macrocycles · mass spectrometry

[1] C. A. Hunter, *Angew. Chem.* **1995**, *107*, 1181; *Angew. Chem. Int. Ed. Engl.* **1995**, *34*, 1079–1081.
[2] a) P. Baxter, J. M. Lehn, A. DeCian, J. Fischer, *Angew. Chem.* **1993**, *105*, 92; *Angew. Chem. Int. Ed. Engl.* **1993**, *32*, 69–72; b) P. Baxter, J. M. Lehn, J. Fischer, M. T. Youinou, *ibid.* **1994**, *106*, 2432 bzw. **1994**, *33*, 2284–2287; c) X. Chi, A. J. Guerin, R. A. Haycock, C. A. Hunter, L. D. Sarson, *J. Chem. Soc. Chem. Commun.* **1995**, 2563–2566, 2567–2569; d) M. Fujita, S. Nagao, K. Ogura, *J. Am. Chem. Soc.* **1995**, *117*, 1649–1650; e) P. J. Stang, K. Chen, A. M. Arif, *ibid.* **1995**, *117*, 8793–8797.
[3] P. A. Brady, R. P. Bonar-Law, S. J. Rowan, C. J. Suckling, J. K. M. Sanders, *Chem. Commun.* **1996**, 319–320.
[4] H. Wynberg in *Topics in Stereochemistry, Vol. 16* (Eds.: E. L. Eliel, S. H. Wilen, N. L. Allinger), Interscience, New York, **1986**, pp. 87–129.
[5] a) H. C. Kolb, M. S. Van Nieuwenhze, K. B. Sharpless, *Chem. Rev.* **1994**, *94*, 2483–2547; b) H. Becker, K. B. Sharpless, *Angew. Chem.* **1996**, *108*, 447–449; *Angew. Chem. Int. Ed. Engl.* **1996**, *35*, 448–451.
[6] J. Reeder, P. P. Castro, C. B. Knobler, E. Martinborough, L. Owens, F. Diederich, *J. Org. Chem.* **1994**, *59*, 3151–3160.
[7] E. J. Corey, M. C. Noe, *J. Am. Chem. Soc.* **1993**, *115*, 12579–12580.
[8] All new compounds were characterized by ^{1}H and ^{13}C NMR and mass spectrometry.
[9] a) G. W. Kabalka, S. W. Slayden, *J. Organomet. Chem.* **1977**, *125*, 273–280; b) G. W. Kabalka, H. C. Hedgecock, Jr., *J. Org. Chem.* **1975**, *40*, 1776–1779.
[10] As commercial quinine from Aldrich or Lancaster contains 10% dihydroquinine, this yield is based on the actual amount of quinine used.
[11] Dichloromethane/methanol (containing 1% triethylamine) mixtures, Hewlett Packard 1050 system, 25 cm × 4 mm Spherisorb S5W normal phase column, detection by a Hewlett Packard HP1050 Diode Array UV detector.
[12] Selected spectroscopic data of cyclic tetramer: ^{1}H NMR (400 MHz, $CDCl_3$). $\delta = 6.45$ (d, $J = 9.3$ Hz, 4H); ES-MS: *m/z* 1353 $[MH^+]$, 677 $[MH_2^{2+}]$, 452 $[MH_3^{3+}]$, 339 $[MH_4^{4+}]$. Full experimental and spectroscopic details will be published elsewhere.
[13] S. J. Rowan, P. A. Brady, J. K. M. Sanders, *Tetrahedron Lett.* **1996**, *37*, 6013–6016.
[14] The reaction procedure is the same as before, but 15 mol % catalyst with respect to the trimers was used which corresponds to 5% per monomer unit.
[15] Positive-ion ES mass spectra were obtained on a VG BioQ triple quadrupole apparatus with a mass-to-charge (*m/z*) range of up to 4000 (VG Bio Tech Ltd, Altrincham, UK). The electrospray source was heated to 70 °C. The sampling cone voltage (V_c) was at 105 V to reduce the amount of multiply charged ions observed. The samples were introduced into the mass spectrometer source with an LC pump (Shimadzu LC-9A LC pump) at a flow rate of 4 μL min^{-1} of acetonitrile/water (1/1). Calibration was performed with protonated horse myoglobin. Scanning was performed from *m/z* 200 to 1500 in 10s. The data system was operated as a multichannel analyzer, and several scans were summed to obtain the final spectrum. Samples for ES-MS were prepared by taking aliquots from the reaction, injecting into pH 7 buffer, and extracting with ethyl acetate. The organic phase was dried (with $MgSO_4$) and concentrated to dryness by evaporation. The residue was then dissolved in acetonitrile water (1/1) and injected into the mass spectrometer.
[16] A similar narrow distribution has recently been observed by Shea and co-workers, in the cyclization of their spirocatechols with phenyltriethoxysilane to give the rigid cyclic tetramer, but they did not comment on the origin of the selectivity: J. H. Small, D. J. McCord, J. Greaves, K. J. Shea, *J. Am. Chem. Soc.* **1995**, *117*, 11588–11589.
[17] This is a modification of the Pederson method: C. J. Pedersen, *J. Am. Chem. Soc.* **1967**, *89*, 7017–7036.

 © VCH Verlagsgesellschaft mbH, D-69451 Weinheim, 1996 0570-0833/96/3518-2145 $ 15.00+.25/0

Controlling the Course of Nucleophilic Additions to *ortho*-Substituted (η^6-Anisole)tricarbonylchromium Complexes: Dienol Ether Formation versus *tele*-Substitution**

Hans-Günther Schmalz,* and Kurt Schellhaas

(η^6-Arene)tricarbonylchromium complexes, which were first described in 1958 by Fischer und Öfele,[1] enjoy a multifarious potential for organic synthesis,[2] and the chemistry of this class of compounds has been the subject of intense investigation for many years.[3] With our research we want to contribute to the acceptance of chiral arenetricarbonylchromium complexes as building blocks for the enantioselective synthesis of bioactive compounds.[4] For this purpose we pursue novel synthetic concepts based on the specific reactivity pattern of arenetricarbonylchromium complexes, and we take synthetically relevant cases as occasion to explore and tame the often subtle reactivity of these complexes and to adapt it to other synthetic applications.[5]

Recently, we aimed to synthesize the marine natural product (+)-ptilocaulin (**1**)[6, 7] following the strategy sketched in Scheme 1.[8] As the key step of the projected reaction sequence, we intended to convert complex **3**, which is accessible from anisoletricarbonylchromium (**5**), into the enone **2** by reaction with the C_1-nucleophile **4**—according to a transformation discovered by Semmelhack.[9, 10]

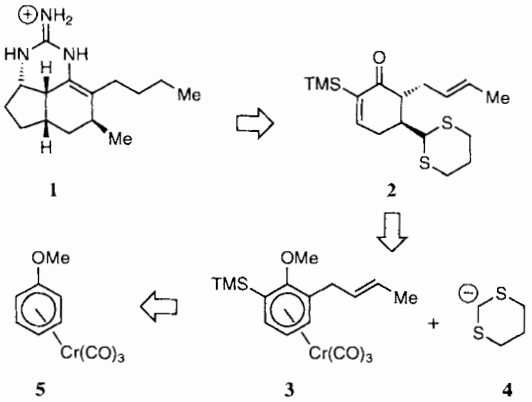

Scheme 1. Retrosynthetic analysis of (+)-ptilocaulin (**1**).

In contrast to all expectations, our initial attempts to achieve the conversion of **3** into **2** failed completely and led to the insight that in contrast to **5** *ortho*-substituted anisoletricarbonylchromium derivatives behave unusually, giving rise to *tele*-substituted products (e.g. **9**; see below) under the routine reaction conditions (nucleophile addition followed by protonation).[8] However, we have now succeeded in finding conditions that effectively suppress the *tele*-substitution. We report here (among other things) on the successful synthesis of the (optically active) enone **2** and demonstrate that the transformation of **3** into **2** occurs under chirality transfer without loss of stereochemical information.

[*] Prof. Dr. H.-G. Schmalz, Dipl.-Chem. K. Schellhaas
Institut für Organische Chemie der Technischen Universität
Strasse des 17. Juni 135, D-10623 Berlin (Germany)
Fax: Int. code +(30) 314-21105
e-mail: schmalz@wap0109.chem.tu-berlin.de

[**] This work was supported by the Volkswagenstiftung (Project I 69907) and the Fonds der Chemischen Industrie (among other things through a graduate scholarship award to K. S.). We thank the Chemetall GmbH for gifts of chemicals and Prof. M. F. Semmelhack, Princeton, for a valuable discussion.

Following the route described previously,[8] the regio- and enantioselective preparation of complex **3** was accomplished in appealing yield after optimization of all individual steps (Scheme 2).[11] Starting from the prochiral complex **5**, enantioselective deprotonation/silylation[12, 13] provides the monosilylated derivative **6** (91% *ee*[14]), which in turn is converted into complex **3** through *ortho*-deprotonation and Cu-mediated alkylation.[15]

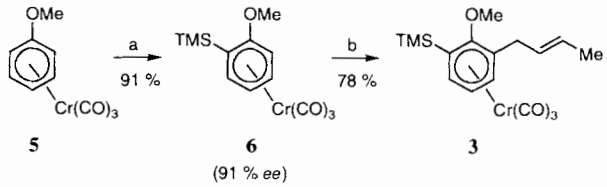

Scheme 2. Preparation of the optically active complex **3**. a) Li*N*[(*S*)-CHMePh]$_2$, TMSCl (6 equiv), THF, −100 °C, 10 min; b) *n*BuLi, THF, −60 → −20 °C, then CuCl (1.1 equiv), −50 → 0 °C, then $BrCH_2CH{=}CHCH_3$ (2 equiv), −30 → 0 °C, 2 h.

In order to prepare the enone **2**, complex **3** was treated with 2-lithio-1,1-dithiane (Li-**4**) in THF in the presence of hexamethylphosphoric triamide (HMPA) as cosolvent to give the anionic intermediate **7**, which on addition of HCl-free chlorotrimethylsilane (TMSCl), extractive workup, and oxidative decomplexation afforded a mixture containing the dienol ether **8** as the major product.[16] After acidic hydrolysis of the dienol ether moiety, the diastereomerically pure, crystalline enone **2** was isolated in 53% yield (based on **3**) (Scheme 3).[17] The enantiomeric purity of the product was greater than 95% *ee*,[14] indicating that the chirality transfer from the planar-chiral metal complex structure to the chirality center in β-position to the carbonyl function in **2** has occurred without racemization.

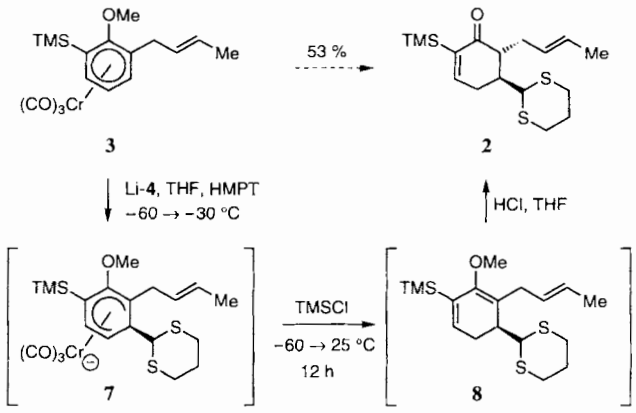

Scheme 3. Preparation of the enone **2** from the chiral complex **3**.

With this new procedure, the enantioselective synthesis of the highly functionalized ptilocaulin precursor **2** is now possible in only four steps from anisole. To demonstrate that the method is not limited to a single case, we have prepared the enone *rac*-**10**.[18] It should be emphasized that the *tele*-substituted product

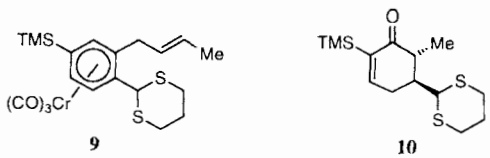

9 is formed only in trace amounts under the reaction conditions described, in contrast to all other conditions tested so far (see below), where **9** always appears as the major product.

The results obtained so far provide the following picture (Scheme 4): the anionic η^5-complex **12**, which results from the stereospecific *anti*-addition of the nucelophile to the less hindered *meta*-position of the *ortho*-substituted anisoletricarbonylchromium substrate **11**, may react further by two different

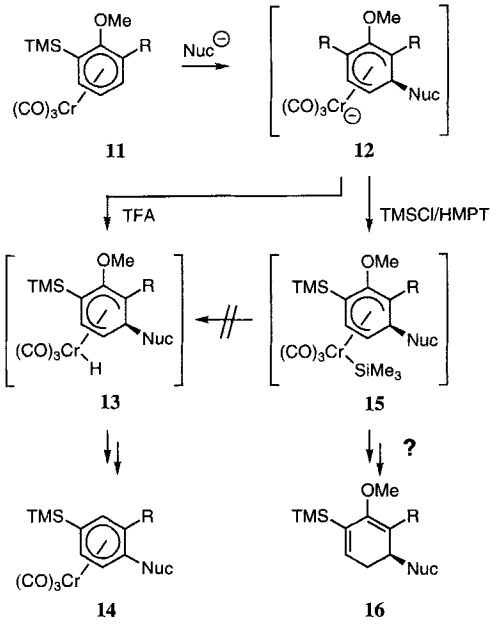

Scheme 4. *anti*-Addition of a nucleophile (Nuc$^{\ominus}$) to **11** and protonation or silylation of the intermediate **12**.

modes depending on the reaction conditions. On addition of trifluoroacetic acid (TFA), protonation takes place primarily at the chromium atom (→ **13**),[9] which leads under elimination of methanol to the *tele*-substituted product (**14**),[8] probably according to the mechanism formulated by Rose et al.[19, 20] If **12** is treated with TMSCl in the presence of HMPA, however, the reaction takes a completely different course. We assume that the silylation initially takes place at the chromium atom.[21] The conversion of the resulting species **15** into the dienol ether **16** then occurs by a still unknown mechanism, however, without passing through an intermediate of type **13**, from which the *tele*-substituted product would arise. When the anionic intermediate *rac*-**7** was treated either with Bu_3SnCl followed by TFA or with $BF_3 \cdot Et_2O$, *rac*-**9** was isolated after hydrolytic workup as the sole product.[22] Also remarkable is the fact that *tele*-substitution proceeds with particular efficiency if the primary nucleophilic addition product *rac*-**7** is treated with $EtAlCl_2$. In this case the *tele*-substitution occurs even before hydrolysis of the reaction mixture (under aprotic conditions!) (Scheme 5).[23]

The protocols reported herein allow effective control of the outcome of nucleophilic additions to *ortho*-substituted anisoletricarbonylchromium derivatives of type **11**. Either dienol ether of type **16** (or the cyclohexenone derivatives) or *tele*-substituted products of type **14** can now be selectively prepared as required. Current efforts in our laboratory are directed towards the completion of the synthesis of (+)-ptilocaulin and the exploration of the scope and limitations of our general method.

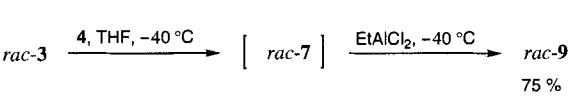

Scheme 5. $EtAlCl_2$-mediated *tele*-substitution.

Experimental Procedure

All reactions were performed in anhydrous solvents in an atmosphere of argon.

6: To a solution of (*S*,*S*)-di(1-phenylethyl)amine (272 mg, 1.1 mmol) in THF (30 mL) at −70 °C was added *n*BuLi (0.74 mL, 1.16 mmol, 1.56 M in hexane), and stirring was continued for 1 h while warming to −40 °C. Then into the vigorously stirred solution at −100 °C was injected first TMSCl (0.83 mL, 6.6 mmol) immediately followed by the rapid injection of a solution of **5** (269 mg, 1.1 mmol) in 3 mL of THF. After 10 min the cooling bath was removed, and the reaction mixture was diluted with *t*BuOMe and washed twice with 2N HCl, and then with saturated aqueous solutions of $NaHCO_3$ and NaCl. The dried (K_2CO_3) organic solution was evaporated in vacuo, and the crude product was purified on a chromatotron (eluent: hexane/ethyl acetate 5/1) to give 318 mg (1.01 mmol, 91%) of compound **6** (91% *ee* [14]) as a greenish-yellow powder. M.p. 99–100 °C; $[\alpha]_D^{20} = -209$ ($c = 1.0$ in $CHCl_3$); FT-IR (KBr): $\tilde{\nu} = 1942, 1885, 1865, 1842\ cm^{-1}$; ^1H NMR (400 MHz, $CDCl_3$): $\delta = 0.31$ (s, 9H), 3.73 (s, 3H), 4.79 (t, $J = 6$ Hz, 1H), 4.97 (d, $J = 7$ Hz, 1H), 5.57 (dd, $J = 6$, 1.5 Hz, 1H), 5.68 (pseudo dt, $J_t = 6$ Hz, $J_d = 1.5$ Hz, 1H); ^{13}C NMR (67.5 MHz, $CDCl_3$): $\delta = -0.7$(q), 55.3(q), 73.4(d), 85.0(d), 88.8(s), 95.9(d), 101.8(d), 147.5(s), 233.2(s).

3: To a solution of **6** (275 mg, 0.869 mmol) in THF (10 mL) at −60 °C was added *n*BuLi (0.59 mL, 0.913 mmol, 1.56 M in hexane), and stirring was continued for 1 h while warming to −20 °C. After cooling to −50 °C, CuCl (98 mg, 0.986 mmol) was added. While the mixture was stirred for 1.5 h and allowed to warm to 0 °C, it slowly turned greenish-black. The solution was then cooled to −50 °C, treated with crotyl bromide (0.18 ml, 1.74 mmol), and stirred for 2 h at 0 °C. The reaction mixture was then diluted with *t*BuOMe and washed several times with small portions of 2N HCl (until the green color of the aqueous layer no longer intensified). The organic solution was washed with saturated aqueous solutions of $NaHCO_3$ and NaCl, dried (K_2CO_3), and the solvent was removed in vacuo to give an orange oil. Purification on the chromatotron (hexane/ethyl acetate 10/1) afforded 252 mg (0.68 mmol, 78%) of complex **3** as a dark yellow oil, which solidified upon standing. An analytical sample was crystallized from hexane at −18 °C: M.p. 55–56 °C; $[\alpha]_D^{20} = -190$ ($c = 1.0$ in $CHCl_3$); FT-IR (KBr): $\tilde{\nu} = 1960, 1883\ cm^{-1}$; ^1H NMR (400 MHz, $CDCl_3$): $\delta = 0.36$ (s, 9H), 1.75 (dd, $J = 6$, 1 Hz, 3H), 3.19 (d, $J = 6$ Hz, 2H), 3.74 (s, 3H), 4.88 (t, $J = 6.5$ Hz, 1H), 5.40 (dd, $J = 6.5$, 1.5 Hz, 1H), 5.50–5.67 (m, 3H); ^{13}C NMR (67.5 MHz, $CDCl_3$): $\delta = 0.1$(q), 17.9(q), 32.1(t), 62.8(q), 87.8(d), 92.6(s), 97.2(d), 99.6(d), 103.9(s), 127.8(d), 129.1(d), 146.6(s), 233.6(s).

2: To a solution of 1,3-dithiane (71 mg 0.594 mmol) in THF (1 mL) and HMPA (0.94 mL) at −60 °C was added a 1.56 M solution (0.38 mL) of *n*BuLi in hexane, and stirring was continued for 1.5 h while warming to −30 °C. At −70 °C a solution of complex **3** (200 mg, 0.54 mmol) in THF (2 mL) was added dropwise over a period of 5 min, and the mixture was allowed to warm slowly to −30 °C within 2 h. At this point freshly distilled TMSCl (0.68 mL, 5.4 mmol) was added, and the mixture was stirred for 12 h at 25 °C before it was diluted with *t*BuOMe and washed twice with 2N HCl. The organic layer was then exposed to the sunlight and air until it decolorized completely, and washed with saturated aqueous solutions of $NaHCO_3$ and NaCl. The dried (K_2CO_3) solution was filtered through a pad of Celite, and the solvent was removed in vacuo to give a clear, slightly yellow oil (dienol ether), which was dissolved in a mixture of THF (20 mL) and 2N HCl (10 mL) and heated for 1 h to 80 °C. The cooled mixture was diluted with *t*BuOMe, washed as described above, and dried with $MgSO_4$. After removal of the solvent, the crude product was purified on the chromatotron (hexane/ethyl acetate 10/1) to yield 98 mg (0.287 mmol; 53%) of the enone **2** as a colorless solid. An analytical sample was crystallized from hexane at −18 °C. M.p. 157 °C; $[\alpha]_D^{20} = 46$ ($c = 0.4$ in $CHCl_3$); FT-IR (KBr): $\tilde{\nu} = 1660, 1593, 1245, 839$; ^1H NMR (400 MHz, $CDCl_3$): $\delta = 0.10$ (s, 9H), 1.60 (d, $J = 4.5$ Hz, 3H), 1.87 (m, 1H), 2.03–2.19 (m, 2H), 2.22–2.34 (m, 2H), 2.51 (m, 1H), 2.69–2.89 (m, 6H), 4.05 (d, $J = 9$ Hz, 1H), 5.27–5.40 (m, 2H), 6.99 (dd, $J = 5$, 3 Hz, 1H); ^{13}C NMR (100 MHz, $CDCl_3$): $\delta = -1.5$(q), 17.8(q), 25.8(t), 28.3(t), 29.3(t), 29.7(t), 29.8(t), 40.6(d), 48.6(d), 49.2(d), 127.0(d), 127.8(d), 140.5(s), 154.5(d), 203.9(s); HR-MS: $m/z = 340.13508$ (as calculated for $C_{17}H_{28}OS_2Si$).

rac-**9**: To a solution of 1,3-dithiane (71 mg, 0.594 mmol) in THF (2 mL) at −60 °C was added a 1.56 M solution of *n*BuLi (0.38 mL, 0.594 mmol) in hexane. Stirring was continued for 2.5 h (→ −20 °C), the mixture was recooled to −60 °C, and a solution of *rac*-**3** (200 mg, 0.54 mmol) in THF (2 mL) was added dropwise over a period of 5 min. After 2.5 h (−60 → −30 °C) the mixture was cooled to −78 °C, and a 1 M solution of $EtAlCl_2$ (1.62 mL, 1.62 mmol) in hexane was added dropwise. The mixture was stirred for 2 h at −78 °C, quenched by careful addition of 2N HCl, and diluted with *t*BuOMe. The organic layer was washed with 2N HCl, saturated aqueous $NaHCO_3$ and brine, and dried with K_2CO_3, and the solvent was removed in vacuo. Chromatography (chromatotron; hexane/ethyl acetate 10/1) gave 186 mg of *rac*-**9** 0.406 mmol; 75%) besides some starting material (*rac*-**3**). An analytical sample of *rac*-**9** was crystallized from hexane at −18 °C. M.p. 120 °C; ^1H NMR (400 MHz, C_6D_6): $\delta = 0.23$ (s, 9H), 1.42 (m, 1H), 1.60 (m, 1H), 1.64 (d, $J = 3$ Hz, 3H), 2.26 (m, 1H), 2.45–2.58 (m, 3H), 3.14, 3.44 (each dd, $J = 8$, 3.5 Hz, 1H), 4.76

(d, $J = 3$ Hz, 1H), 5.07 (s, 1H), 5.15 (s, 1H), 5.52, 5.65 (each m, 1H), 5.86 (d, $J = 3$ Hz, 1H). For further characteristic data of *rac*-**9** see ref. [8].

Received: March 15, 1996 [Z 8928IE]
German version: *Angew. Chem.* **1996**, *108*, 2277–2280

Keywords: arene complexes · asymmetric syntheses · chromium compounds · nucleophilic additions

[1] E. O. Fischer, K. Öfele, *Z. Naturforsch. B* **1958**, *13*, 458.
[2] Review: L. S. Hegedus, *Transition Metals in the Synthesis of Complex Organic Molecules*, University Science Books, Mill Valley **1994**, Chapter 10.
[3] Selected recent work: a) E. P. Kündig, A. Ripa, R. Liu, G. Bernardinelli, *J. Org. Chem.* **1994**, *59*, 4773; b) K. Kamikawa, T. Watanabe, M. Uemura, *ibid.* **1996**, *61*, 1375; c) M. Brands, H. G. Wey, J. Bruckmann, C. Krüger, H. Butenschön, *Chem. Eur. J.* **1996**, *2*, 182.
[4] a) H.-G. Schmalz, J. Hollander, M. Arnold, G. Dürner, *Tetrahedron Lett.* **1993**, *34*, 6259; b) H.-G. Schmalz, M. Arnold, J. Hollander, J. W. Bats, *Angew. Chem.* **1994**, *106*, 77; *Angew. Chem. Int. Ed. Engl.* **1994**, *33*, 109; c) H.-G. Schmalz, A. Schwarz, G. Dürner, *Tetrahedron Lett.* **1994**, *35*, 6861; d) H.-G. Schmalz, A. Majdalani, T. Geller, J. Hollander, J. W. Bats, *ibid.* **1995**, *36*, 4777.
[5] An example is the radical cyclization of arenetricarbonylchromium complexes discovered recently in our laboratory: a) H.-G. Schmalz, S. Siegel, J. W. Bats, *Angew. Chem.* **1995**, *107*, 2597; *Angew. Chem. Int. Ed. Engl.* **1995**, *34*, 2383; b) H.-G. Schmalz, S. Siegel, A. Schwarz, *Tetrahedron Lett.* **1996**, *37*, 2947.
[6] Isolation and structure elucidation: G. C. Harbour, A. A. Thymiak, K. L. Rinehart, Jr., P. D. Shaw, R. G. Hughes, Jr., S. A. Mizsak, J. H. Coats, G. E. Zurenko, L. H. Li, S. L. Kuentzel, *J. Am. Chem. Soc.* **1981**, *103*, 5604.
[7] Synthetic work: a) B. B Snider, W. C. Faith, *Tetrahedron Lett.* **1983**, *24*, 861; b) *J. Am. Chem. Soc.* **1984**, *106*, 1443; c) W. R. Roush, A. E. Walts, *ibid.* **1984**, *106*, 721; d) A. E. Walts, W. R. Roush, *Tetrahedron* **1985**, *41*, 3463; e) T. Uyehara, T. Furuta, Y. Kabasawa, J. Yamada, T. Kato, *J. Chem. Soc. Chem. Commun.* **1986**, 539; f) T. Uyehara, T. Furuta, Y. Kabasawa, J. Yamada, T. Kato, Y. Yamamoto, *J. Org. Chem.* **1988**, *53*, 3669; g) A. Hassner, K. S. K. Murthy, *Tetrahedron Lett.* **1986**, *27*, 1407; h) M. Asaoka, M. Sakurai, H. Takei, *ibid.* **1990**, *31*, 4759.
[8] H.-G. Schmalz, K. Schellhaas, *Tetrahedron Lett.* **1995**, *36*, 5511.
[9] a) M. F. Semmelhack, J. J. Harrison, Y. Thebtaranonth, *J. Org. Chem.* **1979**, *44*, 3275; b) M. F. Semmelhack, H. T. Hall, Jr., R. Farina, M. Yoshifuji, G. Clark, T. Bargar, K. Hirotsu, J. Clardy, *J. Am. Chem. Soc.* **1979**, *101*, 3535; c) M. F. Semmelhack, G. R. Clark, J. L. Garcia, J. J. Harrison, Y. Thebtaranonth, W. Wulff, A. Yamashita, *Tetrahedron* **1981**, *37*, 3957; d) M. F. Semmelhack in *Comprehensive Organometallic Chemistry II, Vol. 12* (Eds.: E. W. Abel, F. G. A. Stone, G. Wilkinson), Pergamon, NY, **1995**, p. 979; e) for an application in a synthesis of (±)-acorenone B (preparation of a spirocyclic, 5,5-disubstituted cyclohexenone derivative) see: e) M. F. Semmelhack, A. Yamashita, *J. Am. Chem. Soc.* **1980**, *102*, 5924.
[10] For a review on nucleophilic additions to arene complexes, see M. F. Semmelhack in *Comprehensive Organic Synthesis, Vol. 4* (Eds.: B. M. Trost, I. Fleming), Pergamon, Oxford, **1991**, p. 517.
[11] All new compounds were characterized by the usual spectroscopic methods and gave correct elemental analyses.
[12] a) D. A. Price, N. S. Simpkins, A. M. MacLeod, A. P. Watt, *J. Org. Chem.* **1994**, *59*, 1961; b) *Tetrahedron Lett.* **1994**, *35*, 6159; c) H.-G. Schmalz, K. Schellhaas, *ibid.* **1995**, *36*, 5515.
[13] The enantioselectivity of the reaction was enhanced over that of earlier procedures [12] by reducing the reaction temperature. The absolute configuration given for **6** is based on the assignment of Simpkins [12a].
[14] The enantiomeric excesses were determined by HPLC on a Chiralcel OJ-column (Diacel). The separation conditions were optimized with racemic samples.
[15] a) M. F. Semmelhack, A. Zask, *J. Am. Chem. Soc.* **1983**, *105*, 2034; for a different procedure for the preparation of *rac*-**3**, see b) M. F. Semmelhack, J. Bisaha, M. Czarny, *ibid.* **1979**, *101*, 768.
[16] After extractive workup, the crude product (dienol ether) still contains significant amounts of (undefined) chromium complexes. A complete decomplexation is achieved by exposing the yellow solution to the sunlight for some time. Thereafter, GLC-MS and ^{1}H NMR analysis of the product mixture indicates that **8** is the major component (beside small amounts of **2**, some decomplexed **9**, and several unidentified by-products).
[17] The *trans*-configuration of **2** follows from the ^{1}H NMR coupling constants; the signals were assigned by means of a COSY spectrum.
[18] This product was obtained under analogous conditions in a yield comparable to that of **2**; for *rac*-**10**: m.p. 98 °C (hexane); FT-IR (KBr): $\tilde{\nu} = 1652$, 1597, 1343, 1246, 841 (s) cm^{-1}; ^{1}H NMR (400 MHz, $CDCl_3$): $\delta = 0.12$ (s, 9H), 1.05 (d, $J = 7$ Hz, 3H), 1.89 (m, 1H), 2.09 (m, 1H), 2.26 (ddd, $J = 20$, 10, 2 Hz, 1H), 2.45 (pseudo sept., $J = 5$ Hz, 1H), 2.69–2.91 (m, 6H), 4.00 (d, $J = 10$ Hz, 1H), 7.06 (pseudo dd, $J = 5$, 2 Hz, 1H); ^{13}C NMR (67.5 MHz, $CDCl_3$): $\delta = -0.7$ (q), 10.3 (q), 25.9 (t), 28.3 (t), 29.7 (t), 29.8 (t), 41.1 (d), 42.9 (d), 49.3 (d), 140.2 (s), 155.5 (d), 205.1 (s); HR-MS: $m/z = 300.10378$ as calcd. for $C_{14}H_{24}OS_2Si$.
[19] a) J.-C. Boutonnet, F. Rose-Munch, E. Rose, *Tetrahedron Lett.* **1985**, *26*, 3989; b) J. P. Djukic, F. Rose-Munch, E. Rose, F. Simon, Y. Dromzee, *Organometallics* **1995**, *14*, 2027, and references therein.
[20] There are several examples of nucleophilic *tele*- and *cine*-substitutions (S_NAr reactions) to $Cr(CO)_3$-complexed arenes [10], but only in very few cases does a methoxy group act as a leaving group. See, for instance, refs. [4b, 8, 19b].
[21] It is known that the reaction of anionic η^5-complexes of type **12** with Ph_3SnCl may lead to (isolable) stannylated products with a structure similar to **15**: E. P. Kündig, A. F. Cunningham, Jr., P. Paglia, D. P. Simmons, G. Bernardinelli, *Helv. Chim. Acta.* **1990**, *73*, 386.
[22] In these cases, a characteristic red color of the reaction mixture appeared, which is also observed when TFA is added to solutions of anionic intermediates of type **12**.
[23] This was secured by ^{1}H NMR spectroscopy of a sample that had been removed under exclusion of air (prior to the hydrolysis of the reaction mixture), freed from all volatile components in vacuo, and redissolved in C_6D_6.

Cyclopeptide Libraries as New Chiral Selectors in Capillary Electrophoresis

Günther Jung,* Heike Hofstetter, Susanne Feiertag, Dieter Stoll, Oliver Hofstetter, Karl-Heinz Wiesmüller, and Volker Schurig*

For the chromatographic separation of enantiomers a single chiral selector is added to the mobile phase or used as stationary phase. Multicomponent chiral selectors have been applied rarely, for example in inclusion gas chromatography[1] and in complexation gas chromatography.[2] Combinatorial chemistry[3] furnishes defined libraries that may be utilized as novel multicomponent chiral additives for the mobile phase or as multicomponent chiral stationary phases in pressure-driven or electrically driven separation systems. Thus, the time-consuming screening of a multitude of individual potential chiral selectors can be avoided by employing a selector library. Sublibraries with reduced heterogeneity can be employed to identify the components with the best selector properties. The search for the most efficient selectors is indicated because each component is highly dilute. Yet the use of the whole library may prove beneficial if cooperative effects between the components affect the enantioselectivity.

Capillary electrophoresis with chiral additives in the mobile phase is an efficient technique for separating water-soluble enantiomers in small sample volumes. Enantiomeric resolution has been achieved with proteins such as bovine serum albumin (BSA),[4] orosomucoid,[5] ovomucoid,[6, 7] caseine,[7] and cellulase[8] as well as with cyclic structures such as the macrocyclic antibiotics vancomycin and rifamycin B,[9, 10] crown ethers,[11] and cyclodextrins[12] serving as single chiral selectors. The mechanisms of retention and enantiodifferentiation by proteins and peptides are not yet well-understood.[13] However, the selector systems described here, which are based on cyclopeptides, may provide first hints. Firstly, as the structures of conformationally constrained cyclopeptides in solution can be determined

[*] Prof. Dr. G. Jung, Prof. Dr. V. Schurig, Dipl.-Chem. H. Hofstetter, Dipl.-Biochem. O. Hofstetter
Institut für Organische Chemie der Universität
Auf der Morgenstelle 18, D-72076 Tübingen (Germany)
Fax: Int. code +(7071) 29-6925
e-mail: guenther.jung@tuebingen.de
Dr. S. Feiertag, Dipl.-Chem. D. Stoll, Dr. K.-H. Wiesmüller
Naturwissenschaftliches und Medizinisches Institut
an der Universität Tübingen, D-72762 Reutlingen (Germany)

quickly by two-dimensional NMR spectroscopy, it should be possible to study the mechanisms of chiral recognition on the molecular level in systematic studies. Secondly, cyclopeptide libraries of high molecular diversity can be obtained by including structural variation. For example, by using the nearly 200 commercially available amino acids of defined chirality, $200^6 = 64 \times 10^{12}$ individual cyclohexapeptides are accessible. The number of cyclopeptides can be further increased by varying the ring size and by including nonpeptidic compounds, derivatives with side chain and backbone modifications, and selected building blocks with inverted chirality.

We describe here a new approach to enantiomeric resolution in which highly complex synthetic cyclohexapeptide libraries are used as chiral selectors. Three randomly chosen sublibraries were added to the mobile phase in capillary electrophoresis. These peptide libraries consist of $18^3 = 5832$ individual cyclohexapeptides which are synthesized as a mixture.[14, 15] Each sublibrary has the general formula c(OOXXXO) and is characterized by defined positions (O) and three random positions (X), which represent a mixture of 18 of the genetically encoded amino acids except cysteine and tryptophan. The synthesis of the cyclopeptide libraries is highly reproducible[14] as analyzed by electrospray mass spectrometry.[16–18]

c(DFXXXa): A 10 mM solution of the cyclopeptide library c(DFXXXa) in phosphate buffer (pH 7.4) was used to discriminate between two enantiomeric DNP-amino acids (DNP=2,4-dinitrophenyl) and Tröger's base (Table 1). The separations were performed at 20 kV. Due to very high plate numbers, Tröger's base could be separated with high efficiency despite the low separation factor α, and good resolution R_s resulted (Fig. 1a). The (+) enantiomer eluted first. The enantiomers of DNP-glutamic acid could be separated with higher selectivity and higher resolution R_s (Fig. 1b). The L enantiomer eluted first. The separation factor α of DNP-aspartic acid is lower than that of DNP-glutamic acid and baseline resolution was not achieved (Table 1), again the L enantiomer eluted first.

Table 1. Chromatographic data for the separation of enantiomers using cyclohexapeptide libraries (10 mM) in phosphate buffer pH 7.4 (20 mM); N = plate number.

Selector and selectand	α	R_S	N_1	N_2
c(DFXXXa)				
DNP-glutamic acid	1.05	3.82	40000	88000
DNP-aspartic acid	1.01	1.08	175000	133000
Tröger's base	1.01	2.94	358000	369000
c(RKXXXa)				
DNP-glutamic acid	1.13	7.2	79000	65000
c(RMXXXa)				
Fmoc-glutamic acid	1.04	1.91	22300	9430

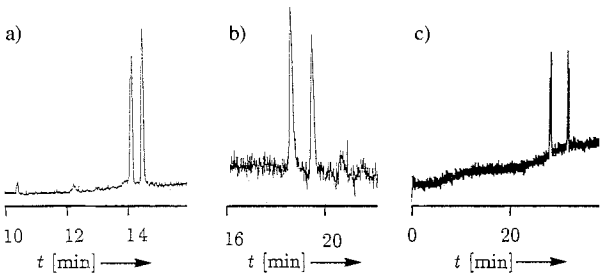

Fig. 1. Enantiomeric resolution of a) Tröger's base with c(DFXXXa), b) DNP-D,L-glutamic acid with c(DFXXXa), and c) DNP-D,L-glutamic acid with c(RKXXXa). Conditions: 10 mM cyclopeptide library c(OOXXXO) in phosphate buffer pH 7.4 (20 mM), capillary 50 µm i.d. × 50 cm effective length, 20 kV for (a) and (b), −10 kV for (c); detection at 260 nm for (a) and 340 nm for (b) and (c).

c(RKXXXa): By using a 10 mM solution of the cyclopeptide library c(RKXXXa) in phosphate buffer (pH 7.4) two enantiomers of DNP-glutamic acid could be separated (Fig. 1c). The experiments wer performed with inverse polarity at −10 kV. The separation factor α is much higher than that with the c(DFXXXa) library, and the resolution R_s is significantly improved (Table 1).

c(RMXXXa): By using a 10 mM solution of the cyclic hexapeptide library c(RMXXXa), separation of the enantiomers of Fmoc-glutamic acid (Fmoc = 9-fluorenylmethoxycarbonyl) was possible. The separation factor α is high, but the resolution R_s is rather low (Table 1). The experiments were performed at −10 kV.

These three examples demonstrate that cyclic hexapeptide libraries dissolved in the electrolyte solution can be used as chiral selectors in capillary electrophoresis. With this approach it may be possible to screen for the most effective selectors for a given enantiomeric resolution. If a mixture proves suitable, the active subunit responsible for efficient chiral separation can be pinpointed by synthesizing sublibraries of lower diversity, and several individual selectors may be precisely defined. Studies along this line are currently in progress.

Experimental Procedure

Apparatus und chemicals: Capillary electrophoresis was performed using the capillary electrophoresis system PRINCE (Bischoff, Leonberg, Germany) and one manufactured by Grom (Herrenberg, Germany), both equipped with on-line UV detectors. The cyclic hexapeptide libraries were synthesized according to ref. [14] and characterized by amino acid analysis and mass spectrometry [15, 16]. One-letter codes for these amino acids: a = D-alanine, D = L-aspartic acid, F = L-phenylalanine, K = L-lysine, M = L-methionine, R = L-arginine, X = all natural amino acids except cysteine and tryptophan. DNP-glutamic acid was purchased from Sigma (Deisenhofen, Germany), Fmoc-glutamic acid from Orpegen (Heidelberg, Germany), Tröger's base from Fluka (Neu-Ulm, Germany), DNP-aspartic acid was prepared according to ref. [19]. Water was purified with a Waters Millipore System Q (Eschborn, Germany).

Preparation of capillary columns and separations: The separations were performed in 50 µm i.d. fused-silica capillaries (Ziemer, Mannheim, Germany) with an effective length of 50 cm and a total length of 67 cm. Solutions of the peptide libraries c(DFXXXa), c(RKXXXa), and c(RMXXXa) (6.6 mg mL^{-1}) were prepared with phosphate buffer (pH 7.4, 20 mM), resulting in a total concentration of 10 mM. The solution was microfiltered (45 µm pore size; Macherey-Nagel, Düren, Germany). The capillaries were pretreated with 0.1 N NaOH for 15 min, then rinsed with water for 10 min and buffer for 10 min. This procedure was repeated after every five runs to remove peptides adsorbed to the wall of the column. Injection was performed hydrodynamically or electrokinetically. Depending on the library investigated, the experiments were carried out at +20 kv or −10 kV. The DNP-amino acids were detected at 340 nm, Tröger's base at 260 nm. The enantiomeric resolution was verified by injection of the pure enantiomers, and the elution order was determined by spiking the racemate with single enantiomers. The separation factor α was determined from $\alpha = t'_{R2}/t'_{R1}$, where t'_{R1} is the migration time of the first and t'_{R2} of the second eluted enantiomer. Water was used as a dead-time maker.

Received: November 22, 1995 [Z 8577 IE]
Publication delayed at authors' request
German version: *Angew. Chem.* **1996**, *108*, 2261–2263

Keywords: capillary electrophoresis · chirality · combinatorial chemistry · compound libraries · peptides

[1] V. Schurig, H.-P. Nowotny, *Angew. Chem.* **1990**, *102*, 969; *Angew. Chem. Int. Ed. Engl.* **1990**, *29*, 939.
[2] V. Schurig in *Bioflavour '87* (Ed.: P. Schreier), de Gruyter, Berlin, **1987**, p. 35.
[3] a) *Combinatorial Peptide and Nonpeptide Libraries* (Ed.: G. Jung), VCH, Weinheim, **1996**; b) J. Früchtel, G. Jung, *Angew. Chem.* **1996**, *108*, 19; *Angew. Chem. Int. Ed. Engl.* **1996**, *35*, 17.
[4] K. Jinno, Y. Saito, Y.-L. Chen, G. Luehr, J. Archer, C. J. Fetzer, W. R. Biggs, *J. Microcolumn. Sep.* **1993**, *5*, 135.
[5] S. Busch, J. C. Kraak, H. Poppe, *J. Chromatogr.* **1993**, *635*, 199.

 © VCH Verlagsgesellschaft mbH, D-69451 Weinheim, 1996 0570-0833/96/3518-2149 $ 15.00+.25/0

[6] Y. Ishimama, Y. Oda, N. Asakawa, Y. Yoshida, T. Sato, *J. Chromatogr.* **1994**, *666*, 193.
[7] D. Wistuba, H. Diebold, V. Schurig, *J. Microcolumn. Sep.* **1995**, *7*, 17.
[8] L. Valcheva, G. Pettersson, S. Hjerten, *J. Chromatogr.* **1993**, *638*, 263.
[9] D. W. Armstrong, Y. Tang, S. Chen, Y. Zhou, C. Bagwill, J. R. Chen, *Anal. Chem.* **1994**, *66*, 1473.
[10] D. W. Armstrong, K. Rundlett, G.-L. Reid, *Anal. Chem.* **1994**, *66*, 1690.
[11] R. Kuhn, D. Riester, B. Fleckenstein, K.-H. Wiesmüller, *J. Chromatogr.* **1995**, *716*, 371.
[12] B. Chankvetadze, G. Endresz, G. Blaschke, *Electrophoresis (Weinheim Fed. Repub. Ger.)* **1994**, *15*, 804.
[13] S. Allenmark, S. Andersson, *J. Chromatogr.* **1994**, *666*, 167.
[14] K.-H. Wiesmüller, S. Feiertag, B. Fleckenstein, S. Kienle, D. Stoll, M. Herrmann, G. Jung in ref. [3a], p. 203.
[15] G. Jung, A. G. Beck-Sickinger, *Angew. Chem.* **1992**, *104*, 375; *Angew. Chem. Int. Ed. Engl.* **1992**, *31*, 367.
[16] J. W. Metzger, K.-H. Wiesmüller, V. Gnau, J. Brünjes, G. Jung, *Angew. Chem.* **1993**, *105*, 901; *Angew. Chem. Int. Ed. Engl.* **1993**, *32*, 894.
[17] J. W. Metzger, C. Kempter, K.-H. Wiesmüller, G. Jung, *Anal. Biochem.* **1994**, *219*, 261.
[18] S. Feiertag, K.-H. Wiesmüller, G. J. Nicholson, G. Jung in *Peptides, Structure, Chemistry and Biology, Proc. 14th Am. Pept. Symp.* (Eds.: P. T. P. Kaumaya, R. S. Hodges), Mayflower Scientific, Kingswinford, UK, **1996**, 693.
[19] K. R. Rao, H. A. Sober, *J. Am. Chem. Soc.* **1954**, *76*, 1328.

Synthesis and Structure of a Unique Monomeric σ-Bonded Aryllithium Compound Stabilized by a Weak Li–Benzene π Interaction**

Berthold Schiemenz and Philip P. Power*

Alkyl and aryllithium compounds that feature Li–C σ bonds are of major importance in both inorganic and organic chemistry.[1] Their structures[2] may be divided into two broad classes: a) uncomplexed species that are normally observed to have electron-poor, associated, frameworks and b) species complexed to Lewis bases (almost exclusively ethers or tertiary amines) that may have either associated or unassociated structures. The number of structures of organolithium compounds that are complexed by Lewis bases and contain Li–C σ bonds is now quite large,[2] whereas those for uncomplexed LiR species are limited to about a dozen examples[3, 4] most of which are alkyllithium compounds.[3] Many of these structures, for example $(LiiPr)_6$,[3c] $(LinBu)_6$,[3d] $(LitBu)_4$,[3d] and $[LiC(SiMe_3)_3]_2$,[3i] have been reported in a recent surge of interest in this area. In contrast, uncomplexed homoleptic organolithium compounds with lithium–aryl σ bonds have hardly been studied.[4] The only two currently known examples are $(LiTrip)_4$ and $(LiC_6H_3\text{-}2,6\text{-}Mes_2)_2$ (Trip = 2,4,6-$iPr_3C_6H_2$, Mes = 2,4,6-$Me_3C_6H_2$).[5a] In addition, two related, mixed aryllithium/lithium phosphide and aryllithium/alkyllithium complexes $(LiPHMes^*LiMes^*)_2$[5b] and $(LiMes^*LinBu)_2$ (Mes^* = 2,4,6-$tBu_3C_6H_2$),[5a] respectively, have also been structurally characterized. The structures of all these compounds are quite clearly different from those of alkyllithium compounds.[5] A further point of interest is that no monomeric σ-bonded aryllithium or alkyllithium compounds have been structurally characterized in the solid state without coordination of the Li^+ ion by Lewis bases.[2] In this regard we have become interested in the use of very sterically demanding *ortho*-substituted terphenyl ligands[4] in attempts to synthesize the first examples of Lewis base free monomeric organolithium compounds. Here we describe the isolation of two new aryllithium compounds, the dimer **1** (Dipp = 2,6-$iPr_2C_6H_3$) and the benzene-complexed species **2**, which has a unique monomeric structure with a Li–C(aryl) σ bond, stabilized only by steric effects and by the weakly coordinating benzene ligand.

$(LiC_6H_3\text{-}2,6\text{-}Dipp_2)_2$ **1** $C_6H_6\cdot LiC_6H_3\text{-}2,6\text{-}Trip_2$ **2**

Compounds **1** and **2** were synthesized in good yield by treatment of the appropriate aryl iodide with one equivalent of *n*Bu-Li in hexane (see Experimental Procedure). They were characterized by ^1H, ^{13}C, and ^7Li NMR spectroscopy, and X-ray quality crystals were grown from solutions in toluene (**1**) or benzene (**2**). The structures[6] of **1** and **2** are illustrated in Figures 1 and 2, respectively. In **1** each Li^+ ion is bound η^1 to the central phenyl ring of one 2,6-$Dipp_2C_6H_3$ group and η^6 to an *ortho*-Dipp substituent of the other 2,6-$Dipp_2C_6H_3$ aryl ligand. Thus **1** differs structurally from $(LiC_6H_3\text{-}2,6\text{-}Mes_2)_2$,[5a] or $[LiC(SiMe_3)_3]_2$,[3i] which have symmetric C-(μ-Li)$_2$-C bridges. The average Li–C(η^1) distance is 2.068(6) Å, the Li···C(η^6) distances range from 2.366(7) to 2.534(6) Å, and there are no close approaches between the lithium ions and the cocrystallized toluene molecules. The coordination sphere of the lithium ions is slightly distorted: for instance, the angles between the Li–C(*ipso*) bonds and the C(*ipso*)···C(*para*) vectors are 16.7° for Li1 and 21.0° for Li2. In addition, the Li–C(*ipso*) bonds subtend angles of 5.0° and 4.1° to the normals of the aromatic rings that contain C7 and C49, respectively. These distortions are undoubtedly a result of the crowded nature of the dimeric structure.

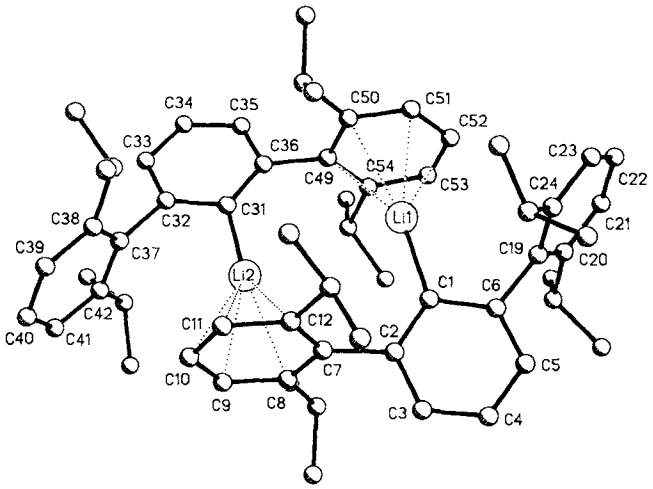

Fig. 1. Crystal structure of **1** (H atoms are not shown). Important bond lengths [Å] and angles [°]: Li1–C1 2.067(6), Li2–C31 2.069(6), Li1···C49–C54 2.534(6), 2.528(6), 2.426(6), 2.372(7), 2.366(7), 2.435(6), Li2···C7–C12 2.526(6), 2.464(6), 2.390(7), 2.385(7), 2.418(6), 2.504(6); C2-C1-C6 113.6(3), C32-C31-C36 113.7(3).

Further examination of the structure of **1** suggested that the presence of *para*-*i*Pr groups on the *ortho*-aromatic ring substituents (e.g. at C10 or C52) would result in steric interactions with the aromatic moieties that contain C37 or C19. This fea-

[*] Prof. P. P. Power, Dr. B. Schiemenz
Department of Chemistry
University of California
Davis, CA 95616, (USA)
Fax: Int. code +(916)752-8995

[**] This work was supported by the National Science Foundation and the Donors of the Petroleum Research Fund administered by the American Chemical Society. We are also grateful for the award of DAAD/NATO Fellowship to B. S.

ture, together with the weakness (vide infra) of the Li–C(η^6) bonds (ca. 2.46 Å), led to the conclusion that the use of *ortho*-Trip rather than *ortho*-Dipp rings might effect dissociation to a monomeric structure. The structure of **2** (Fig. 2) showed that this hypothesis was essentially correct. The lithium ion is bound η^1 to the *ipso*-carbon atom of the 2,6-Trip$_2$C$_6$H$_3$ group and has an Li–C1 distance of 2.03(2) Å, which is identical to the corresponding distance found in the vapor phase structure of monomeric LiCH(SiMe$_3$)$_2$.[3h] The lithium ion is also bound η^6 to a benzene solvent molecule with an average Li···C distance of 2.35(2) Å. The C–C bonds in the benzene ring are 1.42(2) Å.

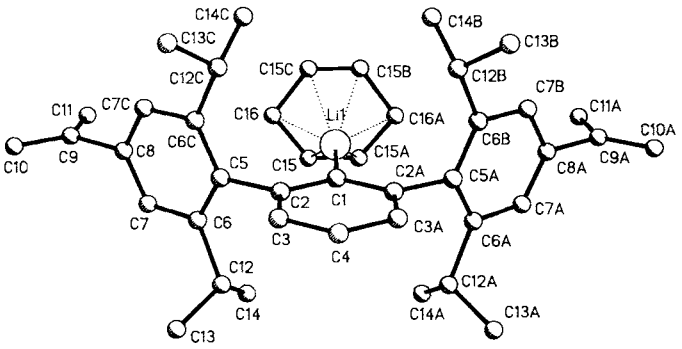

Fig. 2. Crystal structure of **2** (H atoms are not shown). Important bond lengths [Å] and angles [°]: Li1–C1 2.03(2), Li1···C15 2.36(2), Li1···C16 2.33(2), C15–C16 1.42(2); C2-C1-C2a 115.0(9).

Compound **2** is the first instance of an organometallic species in which a Li$^+$ ion interacts with a free benzene molecule in an η^6 fashion.[7] Although η^6 coordination between benzene or neutral, benzene-like rings, is well established for various main group ions[8] and the heavier alkali metals,[9, 10] it is rare for lithium and is only observed when a chelating arrangement of aromatic rings is present as, for example, in LiMesBCB(Mes)-[CH(2,3,5,6-Me$_4$C$_6$H)]$_2$[11] or [{LiN(Mes)}$_2$SiMe$_2$]$_2$,[11b] where the Li···C distances fall within the narrow range between 2.32 and 2.39 Å (cf. 2.46 Å observed in **1**).

The most important feature of the structure of **2** is not the η^6 coordination of the Li$^+$ ion with benzene, however. The structure is unique owing to the fact that it is the first example of a monomeric σ-bonded organolithium species in the solid state that is stabilized only by steric effects and by weak solvation. Thus far it has not been possible to detect the Li–η^6(aryl) complexation in either **1** or **2** by ^{1}H or ^{13}C NMR spectroscopy. The addition of Et$_2$O to **1** or **2** results in the displacement of the Li···C(η^6) ring interactions and the formation of 1:1 complexes. The species Et$_2$OLiC$_6$H$_3$-2,6-Trip$_2$ is monomeric and has been structurally characterized.[12]

In summary, the novel structure of **2** shows that monomeric organolithium species can be obtained in the solid state by using sterically demanding and weakly solvating ligands (or solvents). Moreover, the Li–C bond length in **2** is identical to the Li–C distance in LiCH(SiMe$_3$)$_2$, which contains a one-coordinate lithium ion and whose structure has been determined in the vapor phase.[3h] These results are consistent with relatively weak solvation by benzene.

Experimental Procedure

All manipulations were carried out under anaerobic and anhydrous conditions. The synthesis [12] of 2,6-Dipp$_2$C$_6$H$_3$I and 2,6-Trip$_2$C$_6$H$_3$I were carried out by modification of the procedure for 2,6-Mes$_2$C$_6$H$_3$I [13].

1: Finely powdered 2,6-Dipp$_2$C$_6$H$_3$I (2.70 g, 5 mmol) was dissolved in hexane (50 mL) and the solution was cooled to −15 °C and then treated with *n*BuLi (3.13 mL, 5 mmol of a 1.6 M solution in hexane). The solution was allowed to warm slowly to room temperature over 6 h and then stirred for a further 8 h. A colorless precipitate of **1** was formed that was allowed to settle. The solvents were removed by cannula, and the product was washed with hexane (10 mL) and dried under reduced pressure. Yield: 1.90 g (94%); m.p. 182–185 °C (decomp.). ^{1}H NMR (C_6D_6): δ = 1.125 (d, 12H, *o*-CH(CH_3)$_2$), ^3J(H,H) = 6.9 Hz, 3.21 (sept, 2H, *o*-CH(CH$_3$)$_2$), ^3J(H,H) = 6.9 Hz, 6.95–7.3 (m, several aromatic H). ^{13}C NMR (C_6D_6): δ = 24.17 (*o*-CH(CH_3)$_2$), 25.02 (*o*-CH(CH_3)$_2$), 30.02 (*m*-CH(CH$_3$)$_2$), 122.41 (*m*-Dipp), 122.70 (*m*-Ph), 123.25 (*p*-Ph), 125.84 (*p*-Dipp), 146.33 (*i*-Dipp), 147.11 (*o*-Dipp), 150.26 (*o*-Ph). ^{7}Li NMR (C_6D_6): δ = −4.08. Colorless crystals of **1** suitable for X-ray crystallography were obtained by dissolving the colorless powder in toluene (20 mL), reducing the volume to about 10 mL, and cooling in a freezer for 3 days at −20 °C. Yield: 1.53 g (68%).

2: Finely powdered 2,6-Trip$_2$C$_6$H$_3$I (2.43 g, 4 mmol) was suspended in a mixture of benzene (5 mL) and hexane (50 mL), and the mixture was cooled to −15 °C and then treated with *n*BuLi (2.5 mL, 4 mmol of a 1.6 M solution in hexane) with rapid stirring. The solution was allowed to warm to room temperature over 6 h and then stirred for a further 4 h. The finely divided suspension was allowed to settle and the supernatant liquid was removed by cannula. The colorless precipitate was dissolved in benzene (50 mL) to give a pale yellow solution. Filtration, concentration to incipient crystallization at 50 °C, and slow cooling to about 10 °C in a refrigerator yielded 1.4 g (62%) of large colorless plates of **2**. M.p. 174–176 °C (decomp.). ^{1}H NMR (C_6D_6): δ = 1.14 (d, 12H, *p*-CH(CH_3)$_2$, ^3J(H,H) = 6.9 Hz, 1.22 (d, 12H, *o*-CH(CH_3)$_2$), $^3J_{HH}$ = 6.9 Hz, 1.37 (d, 12H, *o*-CH(CH_3)$_2$), ^3J(H,H) = 6.9 Hz, 2.95 (sept, 2H, *p*-CH(CH$_3$)$_2$), ^3J(H,H) = 6.9 Hz, 3.24 (sept, 4H, *o*-CH(CH$_3$)$_2$), ^3J(H,H) = 6.9 Hz, 7.15 (s, C_6H_6), 7.16 (s, 4H, *m*-Trip), 7.19 (d,2H, *m*-Ph), ^3J(H,H) = 6.6 Hz, 7.29 (t, 1H, *p*-Ph), ^3J(H,H) = 6.6 Hz. ^{13}C NMR (C_6D_6): δ = 24.30 (*o*-CH(CH_3)$_2$), 24.80 (*p*-CH(CH_3)$_2$), 25.07 (*o*-CH(CH_3)$_2$), 30.10 (*o*-CH(CH$_3$)$_2$), 34.95 (*p*-CH(CH$_3$)$_2$), 119.96 (*m*-Trip), 122.49 (*m*-Ph), 123.16 (*p*-Ph), 128.53 (C_6H_6), 145.76 (*i*-Trip), 146.67 (*o*-Trip), 147.96 (*p*-Trip), 150.40 (*m*-Ph), 177.89 (*i*-Ph). ^{7}Li NMR (C_6D_6): δ = −3.97.

Received: February 9, 1996
Revised version: April 16, 1996 [Z8805IE]
German version: *Angew. Chem.* **1996**, *108*, 2288–2290

Keywords: lithium compounds · solid-state structures

[1] G. E. Coates, K. Wade, *Organometallic Compounds*, Methuen, London, **1967**; J. L. Wardell in *Comprehensive Organometallic Chemistry Vol. 1* (Eds.: E. W. Abel, F. G. A. Stone, G. Wilkinson), Pergamon, New York, **1982**, Chapter 2.

[2] W. N. Setzer, P. von R. Schleyer, *Adv. Organomet. Chem.* **1985**, *24*, 353; M. A. Beswick, D. S. Wright in *Comprehensive Organometallic Chemistry II, Vol. 1*, (Eds.: F. G. A. Stone, E. W. Abel, G. Wilkinson), Pergamon, New York, **1995**, Chapter 1.

[3] The presently known uncomplexed alkyllithium structures: a) (LiMe)$_4$: E. Weiss, E. C. A. Lucken, *J. Organomet. Chem.* **1964**, *2*, 197; b) (LiEt)$_6$: H. Dietrich, *J. Organomet. Chem.* **1981**, *205*, 291; c) (Li*i*Pr)$_4$: U. Siemeling, T. Redecker, B. Neumann, H.-G. Stammler, *J. Am. Chem. Soc.* **1994**, *116*, 5507; d) (Li*n*Bu)$_6$ and (Li*t*Bu)$_4$: T. Kottke, D. Stalke, *Angew. Chem.* **1993**, *105*, 619; *Angew. Chem. Int. Ed. Engl.* **1993**, *32*, 580; e) [LiCH$_2$(*c*-CHCMe$_2$CMe$_2$)]$_4$: A. Maercker, M. Bsata, W. Buchmeier, B. Engelen, *Chem. Ber.* **1984**, *117*, 2547; f) [Li(*c*-C$_6$H$_{11}$)]$_6$·2C$_6$H$_6$: R. Zerger, W. Rhine, G. Stucky, *J. Am. Chem. Soc.* **1974**, *96*, 6048; g) (LiCH$_2$SiMe$_3$)$_6$: B. Tecle, A. F. Maqsudur Rahman, J. P. Oliver, *J. Organomet. Chem.* **1986**, *317*, 267; h) [LiCH(SiMe$_3$)$_2$]$_2$: J. L. Atwood, T. Fjelberg, M. F. Lappert, N. T. Luong Thi, R. Shakir, A. J. Thorne, *J. Chem. Soc. Chem. Commun.* **1984**, 1163; i) [LiC(SiMe$_3$)$_3$]$_2$, W. Hiller, M. Layh, W. Uhl, *Angew. Chem.* **1991**, *103*, 339; *Angew. Chem. Int. Ed. Engl.* **1991**, *30*, 324.

[4] The structures of a large number of uncomplexed aryllithium salts of cyclic compounds with anionic delocalized π-electron systems and Li–C π interactions have been reported. None of these have involved Li–C σ bonding to the aromatic ring, however. See ref. [2] for further discussions.

[5] The structures of (LiTrip)$_4$, (LiC$_6$H$_3$-2,6-Mes$_2$)$_2$ and the mixed alkyl/aryllithium compounds (LiMes*Li*n*Bu)$_2$ are described in the following: a) K. Ruhlandt-Senge, J. J. Ellison, R. J. Wehmschulte, F. Pauer, P. P. Power, *J. Am. Chem. Soc.* **1993**, *115*, 11353. The compounds display a variety of σ and π interactions with the aryl groups. The (LiTrip)$_4$ and (LiMes*Li*n*Bu)$_2$ (Mes* = 2,4,6-*t*Bu$_3$C$_6$H$_2$) structures feature almost planar Li$_4$ arrays (cf. tetrahedral Li$_4$ arrays in (LiMe)$_4$, (LiEt)$_4$, and (Li*t*Bu)$_4$). In contrast, the structure of (LiC$_6$H$_3$-2,6-Mes$_2$)$_2$ is dimeric with Li–C interactions involving only the *ipso*-carbon atoms of the central and mesityl aromatic rings. The structure of the mixed lithium phosphide/aryllithium compound (LiPHMes*LiMes*)$_2$ also displays η^1-P/η^6-C and η^1-C/η^6-C coordination modes similar to these compounds; b) S. Kurz, E. Hey-Hawkins, *Organometallics* **1992**, *11*, 2729.

 © VCH Verlagsgesellschaft mbH, D-69451 Weinheim, 1996 0570-0833/96/3518-2151 $ 15.00+.25/0

[6] Crystal data for $1 \cdot C_7H_8$ and **2** ($T = 130$ K, $Cu_{K\alpha}$ ($\lambda = 1.54178$ Å): $1 \cdot C_7H_8$, $C_{67}H_{82}Li_2$, $M = 901.2$, $a = 19.906(6)$, $b = 18.120(6)$, $c = 17.251(4)$ Å, $\beta = 114.49(2)°$, monoclinic, $Z = 4$, space group $P2_1/c$, R = 0.074 for 5758 ($I > 2\sigma(I)$) data; **2**, $C_{42}H_{50}Li$, $M = 561.76$, $a = 10.929(2)$, $b = 14.097(3)$, $c = 24.581(5)$ Å, orthorhombic, $Z = 4$, space group $Cmcm$, $R = 0.102$ for 1379 ($I > 2\sigma(I)$) data. Compound **1** has no crystallographically imposed symmetry and crystallized with a disordered toluene molecule (0.5:0.5 occupancy in two orientations) in each asymmetric unit. The data for **2** require that the molecule has two mirror planes at right angles to each other along the C(1)—C(4) axis, one of which contains the plane of the C(1) ring. Crystals of **2** undergo phase changes and/or crack upon cooling below about −20 °C. They also desolvate, and this behavior, along with the disorder in the *para*-*i*Pr groups resulted in a data set that was not of the very highest quality (cf. high thermal parameters for some atoms and $R = 0.102$). Nonetheless, the structure quality is more than sufficient to substantiate the arguments made. Crystallographic data (excluding structure factors) for the structure(s) reported in this paper have been deposited with the Cambridge Crystallographic Data Centre as supplementary publication no. CCDC-179-80. Copies of the data can be obtained free of charge on application to The Director, CCDC, 12 Union Road, Cambridge CB2 1EZ, UK (fax: Int. code +(1223) 336-033; e-mail: teched@chemcrys.cam.ac.uk).

[7] Some Li–C, σ-bonded, organoalkali metal salts that can be obtained from solutions in benzene may contain benzene of crystallization or benzene that has weak η^1–η^2 (but not η^6) interactions with the metal. An early example of such a species is the classic structure of cyclohexyllithium [3f], which crystallizes as the hexamer $(C_6H_{11})_6 \cdot 2C_6H_2$, and contains two benzene molecules of crystallization.

[8] a) H. Schmidbaur, *Angew. Chem.* **1985**, *97*, 893; *Angew. Chem. Int. Ed. Engl.* **1985**, *24*, 893; b) P. Jutzi, *Adv. Organomet. Chem.* **1986**, *26*, 217.

[9] C. Schade, P. von R. Schleyer, *Adv. Organomet. Chem.* **1987**, *27*, 169.

[10] C. Eaborn, P. B. Hitchcock, K. Izod, J. D. Smith, *Angew. Chem.* **1995**, *107*, 756; *Angew. Chem. Int. Ed. Engl.* **1995**, *34*, 687.

[11] a) M. Pilz, J. Allwohn, P. Willershausen, W. Massa, A. Berndt, *Angew. Chem.* **1990**, *102*, 1085; *Angew. Chem. Int. Ed. Engl.* **1990**, *29*, 1030; b) H. Chen, R. A. Bartlett, H. V. R. Dias, M. M. Olmstead, P. P. Power, *Inorg. Chem.* **1991**, *30*, 2487.

[12] B. Schiemenz, P. P. Power, *Organometallics*, **1996**, *15*, 958.

[13] C. F. Du, H. Hart, K. D. Ng, *J. Org. Chem.* **1986**, *51*, 3162.

Troubleshooting... with VCH books!

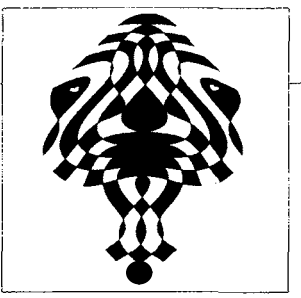

Neuhoff, V.
Scientists in Conference The Congress Organizer's Handbook
1987. X, 223 pages.
Hardcover. DM 68.00
ISBN 3-527-26579-1

Do you have to organize a conference? Well, sometimes, this can't be avoided. But you don't want to get crushed by the wheels of paperwork? And you want to stay in your budget? Then this handy little book is your survival kit!

Schoenfeld, R.
The Chemist's English Third, revised edition with Say It in English, Please!
1990. XII, 195 pages with 9 figures.
Hardcover. DM 48.00
ISBN 3-527-28003-0

"Recommended without qualification; and a suitable gift for friends."
Chemical and Engineering News

"The book might well serve as a prescribed text for PhD students."
Nature

Ebel, H.F. /Bliefert, C. / Russey, W.
The Art of Scientific Writing
From Student Reports to Professional Publications in Chemistry and Related Fields
1990. XIX, 493 pages with 27 figures and 16 tables.
Softcover. DM 52.00
ISBN 3-527-26677-1

First of all, here we have a highly readable text on scientific communication - with all its ramifications from writing the most effective text to getting it published. Never before has so much information on scientific writing been assembled in a single book.

To order please contact your bookseller or:
VCH, P.O. Box 10 11 61,
D-69451 Weinheim,
Telefax (0) 62 01 - 60 61 84
VCH, Hardstrasse 10, P.O. Box,
CH-4020 Basel
VCH, 8 Wellington Court,
Cambridge CB1 1HZ, UK
VCH, 303 N.W. 12th Avenue,
Deerfield Beach, FL 33442-1788,
USA
toll-free: 1-800-367-8249 or
fax: 1-800-367-8247
VCH, Eikow Building,
10-9 Hongo 1-chome, Bunkyo-ku,
Tokyo 113

VCH

 © VCH Verlagsgesellschaft mbH, D-69451 Weinheim, 1996 0570-0833/96/3518-2152 $ 15.00+.25/0

Everything You Wanted to Know about Ketenes but Were Afraid to Ask

Ketenes. By *T. T. Tidwell*. Wiley, New York, 1995. 665 pp., hardcover £ 70.00.–ISBN 0-471-57580-1

Following earlier works on ketenes, notably the classic monograph by Staudinger (1912) and the well-known reviews by Patai (1964 and 1980) and in Houben-Weyl (1968 and 1993), we now have a new up-to-date monograph by Tidwell. The first part (51 pp.) is concerned with the structure, bonding, and thermochemistry of ketenes. Aspects covered in the first chapter include orbital treatments and the latest ab initio methods, and energy calculations related to protonation, substituent effects, and stabilization of fulvenones and fulvenes, with detailed tables where appropriate. This is followed by a chapter on structure determination, in which experimentally determined bond lengths and angles are compared with calculated values. Tables giving CC, CO and CF bond lengths and angles optimized by HF/6-31G* calculations are included. These are followed by spectroscopic and physical data, including ^{13}C and ^{1}H NMR data for a large number of ketenes (and some recently measured ^{17}O chemical shifts), data from UV and photoelectron spectra, and IR spectra (including tables comparing observed and calculated CO band positions). The chapter ends with data on dipole moments, mass spectra, and gas-phase ion chemistry, including some very recent results.

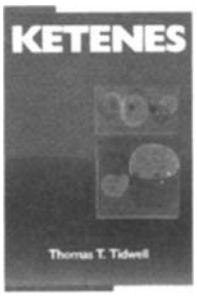

The second part (47 pp.) describes the preparation of ketenes, starting with the classical synthetic routes. In addition to the best known routes (thermolysis of diketenes, pyrolysis of carboxylic acids and anhydrides, and the methods starting from acyl halides, esters, α-halogenated carboxylic acids, or diazoketenes), the author describes recently developed photochemical and thermolytic methods, and syntheses starting from alkenylcarbene-metal complexes.

The following section is the longest (294 pp.), and contains detailed descriptions of all types of ketenes, with numerous tables listing the methods of preparation, CAS numbers, and key literature references. The types of compounds covered include C-substituted ketenes (substituents: aryl, alkyl, alkenyl, alkynyl, cyano, cyclopropyl, acyl, imidoyl, cumulenyl, and fulvenones), N-, O-, and halogen-substituted ketenes, Si-, Ge-, Sn-, P-, As-, S-, and metal-substituted ketenes, bisketenes, ketenyl radicals, anions, and cations, and lastly cumulenones. The value of the book lies largely in this important central part.

The last part (211 pp.) deals with the reactions of ketenes (oxidations, reductions, photochemical and thermolytic reactions, nucleophilic and electrophilic additions to ketenes, free radical reactions, and polymerizations. As expected, considerable space is given to cycloaddition reactions of ketenes, with particular emphasis on the [2+2]-cycloadditions originally discovered by Staudinger, the [3+2]- and [4+2]-cycloadditions, and intramolecular cycloadditions, e.g. involving the carbonyl groups. The preparative methods described are accompanied by semiempirical and ab-initio calculations, discussions of the role of transition states, and stereochemical considerations. A separate subsection (5.4.1.3) is devoted to the mechanism of the addition of ketenes to alkenes; this includes tables listing rate constants for the reaction, and results from MP2/6-31G* and AM1 calculations of the transition states. The chapter ends by describing cycloadditions to N = N, N = O and N = S = O groups. 1,3-Dipolar and [4+2]-cycloadditions offer a route to many interesting types of heterocycles with a variety of applications. Intramolecular cycloadditions are attracting growing interest as novel synthetic stages, and have been discussed in three recent reviews containing recent examples of their use. The section of this book on nucleophilic additions includes a useful discussion of theoretical aspects (calculations of energy profiles and of hydration kinetics). Wittig reactions of ketenes yield allenes. Aza-Wittig reactions are only mentioned briefly, and it would have been useful to give more references on these.

I found very few errors in the monograph. It is definitely recommended, especially for its treatment of theoretical ideas and for the central chapter on the different types of ketenes with many informative tables. It lists over 2500 literature references, which are arranged in a clear and readily accessible form under the individual section headings. The index is rather meager, and it could have been enlarged to great advantage by filling the six blank pages at the end of the book. The structural formulas drawn by Pat Woodcock are large and clear; however, they are not always accurate, and the use of different styles of formulas and standards within a scheme is rather clumsy and inappropriate for a book in this price class, especially since better formula-drawing programs than ChemDraw are now available (e.g., ChemWindow).

To summarize, by its lucid, well-written, and well constructed presentation this book provides a quickly assimilable and authoritative introduction to, and up-to-date treatment of, the chemistry and theoretical aspects of ketenes. It can be thoroughly recommended for everyone involved in academic or industrial research with an interest in this class of compounds.

Heinrich Wamhoff
Institut für Organische Chemie
und Biochemie
der Friedrich-Wilhelms-Universität Bonn
Bonn (Germany)

This section contains book reviews and a list of new books received by the editor. Book reviews are written by invitation from the editor. Suggestions for books to be reviewed and for book reviewers are welcome. Publishers should send brochures or (better) books to the editorial office: Redaktion Angewandte Chemie, Postfach 101161, D-69451 Weinheim, Germany. The editor reserves the right of selecting which books will be reviewed. Uninvited books not chosen for review will not be returned.

Diazo Chemistry II. Aliphatic, Inorganic and Organometallic Compounds. By *H. Zollinger*. VCH Verlagsgesellschaft, Weinheim, 1995. 522 pp., hardcover DM 198.00.—ISBN 3-527-29222-5

Part II of this splendid monograph by Heinrich Zollinger covers aliphatic, inorganic, and organometallic diazo compounds, and, as the author explains in the introduction, its publication alongside Part I (aromatic and heteroaromatic diazo compounds) now brings together the long separated "sisters and cousins". It can be said at the outset that these two volumes certainly belong together, and the combined work is undoubtedly one of the best ever surveys of the many and remarkably varied aspects of diazo compounds.

The structure of Part II closely follows that of Part I; the author avoids unnecessary repetition of the general discussions in Part I while also not assuming too much prior knowledge. The 11 chapters treat every aspect of the chemistry of the compounds defined in the title, with comprehensive coverage of the literature up to the fall of 1994, supplemented by extensive footnotes referring to more recent work.

Chapter 1 (10 pp.) briefly outlines the history of developments in aliphatic diazo compounds and explains the recommended system of nomenclature. Chapter 2 (84 pp.) contains a very thorough and precise description of existing methods for preparing such compounds together with discussions of alternative possibilities. The author first explains the general principles of the preparative methods, then describes each individual method in turn with many examples. The methods based on diazo transfer reactions are treated especially thoroughly.

In Chapter 3 (25 pp.) inorganic diazo compounds are treated in greater detail, with special emphasis on metal complexes with N_2 ligands and diazo derivatives of boron hydrides. This chapter also includes a concise and informative survey of the chemistry of nitrogen fixation.

Chapter 4 (23 pp.) and Chapter 5 (45 pp.) are concerned with mechanistic and kinetic aspects of "aliphatic" diazotization reactions. Topics discussed include the nitrosylation of alkyl amines, the mechanisms involved in the diazoalkane synthesis, the carcinogenicity of *N*-nitrosamines, and the structure of aliphatic diazo compounds. On the latter topic there is a useful critical discussion of the large amount of spectroscopic data and theoretical results on this class of compounds, which is not available elsewhere in such a concise form.

As one expects, much space is devoted to the reactions of aliphatic diazo and diazonium compounds. Chapter 6 (49 pp.) deals with reactions in which the N_2 fragment remains intact. Here the author devotes special attention to 1,3-dipolar cycloadditions, and gives convincing evidence of the great potential value of such reactions for organic synthesis. Chapter 7 (64 pp.) discusses the often complicated situations that occur in dediazotization reactions involving diazonium intermediates. The mechanistic aspects of deamination and its synthetic applications are explained in precise detail.

The large and important group of dediazotization reactions that proceed via carbenes and carbenoids are treated in Chapter 8 (77 pp.). In discussing every aspect of the reactions of diazo compounds of carbenes the author again presents an amazing wealth of information. As well as the classical applications in organic synthesis (including the Wolff rearrangement and the Arndt-Eistert synthesis) the chapter covers recent developments such as the addition of diazo compounds to fullerenes and applications in enantioselective syntheses. The part of the book concerned with reactions is completed by Chapter 9 (37 pp.), which collects together various other reactions of aliphatic diazo compounds, such as electrophilic and nucleophilic substitutions at the α-carbon atom, electron transfer processes, and redox reactions.

In Chapter 10 (34 pp.) the author discusses the complexation of diazonium and diazo compounds with main-group and transition metals. Here one is again impressed by the comprehensive nature of this monograph. Chapter 11 is an epilog in which the author rounds off the two-volume work on diazo compounds with a broad survey of the historical development, extending from the original discovery by Peter Griess to the organometallic diazo compounds. The book is completed by a list of literature citations and a very comprehensive index, which facilitates using the work as a reference source.

In common with the first part (*Diazo Chemistry I*) this second volume too is a must for all chemists with an interest in diazo compounds, and their personal libraries should include both volumes. Moreover, the excellent presentation of the contents and the high standard of writing make both books a pleasure to read.

Thomas Ziegler
Institut für Organische Chemie und
Isotopenforschung
der Universität Stuttgart (Germany)

Modern Acetylene Chemistry. Edited by *P. J. Stang* and *F. Diederich*. VCH Verlagsgesellschaft, Weinheim, 1995. 506 pp., hardcover DM 168.00.—ISBN 3-527-29084-2

This book fills a gap that has existed for about twenty years. Everyone who has observed and experienced the renaissance of acetylene chemistry during the past 10–15 years has been aware of the lack of a comprehensive source of information on the subject.

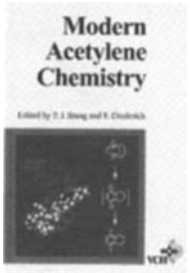

The editors of the book, both of whom have themselves made important contributions to acetylene chemistry, have succeeded in persuading nearly every prominent researcher in the field to contribute an article, with the result that practically all modern aspects of compounds containing triple bonds are discussed. In the introductory chapter D. A. Plattner, V. Li, and K. N. Houk describe the latest developments in the theoretical treatment of acetylenes, diacetylenes, polyacetylenes, and linear and cyclic C_n species with *n*-values from 2 to 18. Other articles report on cyano- and halogen-substituted acetylenes (Ch. 2, H. Hopf and B. Witulski), alkynyl-iodonium salts (Ch. 3, P. J. Stang), and phosphaalkynes (Ch. 6, M. Regitz, A. Hoffmann, and U. Bergsträsser). The synthesis and reactive properties of the alkynyl-iodonium salts are treated very comprehensively, whereas in Chapters 2 and 6, after describing the synthesis of the compounds and their general reactive properties, attention is concentrated on a few special areas, such as the reaction of cyanoacetylenes with cyclophane derivatives, the use of iodoacetylenes in natural products syntheses, and the reactions of phosphaacetylenes yielding phosphorus-carbon cage compounds. Chapter 4, by G. G. Melikyan and K. M. Nicholas, is a general survey of the synthesis and reactions of metal-alkyne-π-complexes. The binuclear dicobalt-hexacarbonyl-alkyne complexes and the corresponding propargylium complexes that are described here also appear again in other chapters as synthetic building blocks. For example, the former are used in the Pauson–Khand reaction for synthesizing cyclopentenones from alkynes, alkenes, and carbon monoxide, as described in thorough detail by J. A. Casalnuovo and N. E. Schore in Chapter 5. The first part of this chapter

 © VCH Verlagsgesellschaft mbH, D-69451 Weinheim, 1996 0570-0833/96/3518-2154 $ 15.00+.25/0

deals with the reactions of alkynes with Fischer carbene complexes (including the Dötz reaction), which yield naphtholes, indenes, cyclobutenones, cyclopentenones, and other compounds. Chapter 7 contains a detailed survey of the "new" enediyne antibiotics, whose effectiveness depends on the Bergman cycloaromatization reaction. The diradicals formed in this reaction abstract hydrogen atoms from specific sites in the DNA. This leads to the break-up of the DNA single strand, or even of the double strand, and finally to the death of the cell. K. C. Nicolaou and A. L. Smith, discuss the structures and modes of action of the compound classes known up to now, and describe several total syntheses and some extensive studies aimed at preparing synthetic analogs. In Chapter 8 R. Gleiter and R. Merger report on the synthesis of strained cyclic alkynes and polyynes and discuss how the strain in these compounds affects their spectroscopic properties and reactivities. Of special interest here are the transannular reactions and the formation of superphanes by complexed cyclobutadienes. Chapter 10 on "Polyacetylenes" (E. J. Ginsburg, C. B. Gorman, R. H. Grubbs) and Chapter 11 on "Acetylenic Compounds as Building Blocks for High-Spin Molecules and Molecular Assemblies" (H. Iwamura, K. Matsuda) are of special interest to materials scientists.

The remaining three chapters treat various types of triple-bonded compounds in a systematic sequence that strikes one as almost playful. L. T. Scott and M. J. Cooney describe the synthesis of macrocyclic polyynes in which the acetylene and butadiyne units are separated by isopropylidene or cyclopropylidene groups. Other compounds of this general type have different bridging groups: sulfide, *tert*-butylphosphinediyl, or dimethylsilanediyl. In Chapter 12 J. K. Young and J. S. Moore describe their strategy for preparing dendrimers and macrocycles of phenylacetylene. In these each acetylene unit is flanked by two benzene rings, which in turn are linked at the *meta* and *para* or at the *meta* and *meta'* positions to continue the acetylene chain. For reasons of solubility the dendrimers have 3,3'-di-*t*-butylphenyl groups at the ends of the branches. In the ring compounds the continuation of the chain can also take place from the *ortho* positions of the flanking phenyl groups. In the last chapter F. Diederich begins by describing his three syntheses aimed at approaching as nearly as possible to the compounds cyclo-C_{18}, cyclo-C_{24}, and cyclo-C_{30}. This is followed by his syntheses of tetraethynylethenes, in which the four acetylenic end-groups are either protected by silyl groups or have their protection selectively removed. It is thus possible by a Glaser-Hay coupling reaction to prepare perethynylated dehydroannulenes, expanded radialenes, and oligomeric diyne chains.

As can be seen from this selection of topics, which is far from exhaustive, the book covers practically all aspects of current developments in acetylene chemistry (although this reviewer would have liked to see a contribution from K. P. C. Vollhardt also included). Twelve of the chapters fit fairly well into the overall scheme of the book—the only exception is the article on the enediyne antibiotics. Notwithstanding the great interest that this class of compounds holds for chemists and medical scientists, one must question whether the many approaches to their synthesis, even including, for example, that of the sugar fragment in some enediyne antibiotics, really belongs in a book on acetylenes. Despite the large number of authors the individual articles are very consistent in style, presumably because of clear guidance by the editors. In each chapter a brief introduction is followed in turn by information on synthesis, properties, and reactions. The chapter ends with additional comments (usually descriptions of a number of experiments), followed by an extensive collection of references, which also affords access to earlier work on other aspects of acetylene chemistry that are not covered in the main text.

The book is handsomely produced with a cover design showing – in a model – an enediyne antibiotic molecule entering a fold in the DNA strand, alongside a formula scheme for the Bergman cycloaromatization. There are very few printing errors that annoy one (example: in Table 8-3 the transannular distance is given as 2.09 Å instead of 2.909 Å). However, the author index needs to be thoroughly revised, as it lists only authors who are mentioned in the text, with the result that, for example, Nicolaou appears three times (including, exceptionally, the page number of his contribution to the work), whereas Regitz appears only once and Gleiter not at all.

However, this minor criticism certainly does not detract from the value of the book. It should be on every acetylene chemist's bookshelf, and will be an indispensable source for preparing lectures in advanced chemistry courses.

Gerhard Himbert
Fachbereich Chemie
der Universität Kaiserslautern (Germany)

 © *VCH Verlagsgesellschaft mbH, D-69451 Weinheim, 1996* 0570-0833/96/3518-2155 $ 15.00+.25 0

Embryogenesis of zebra fish up
to an age of 19 hours

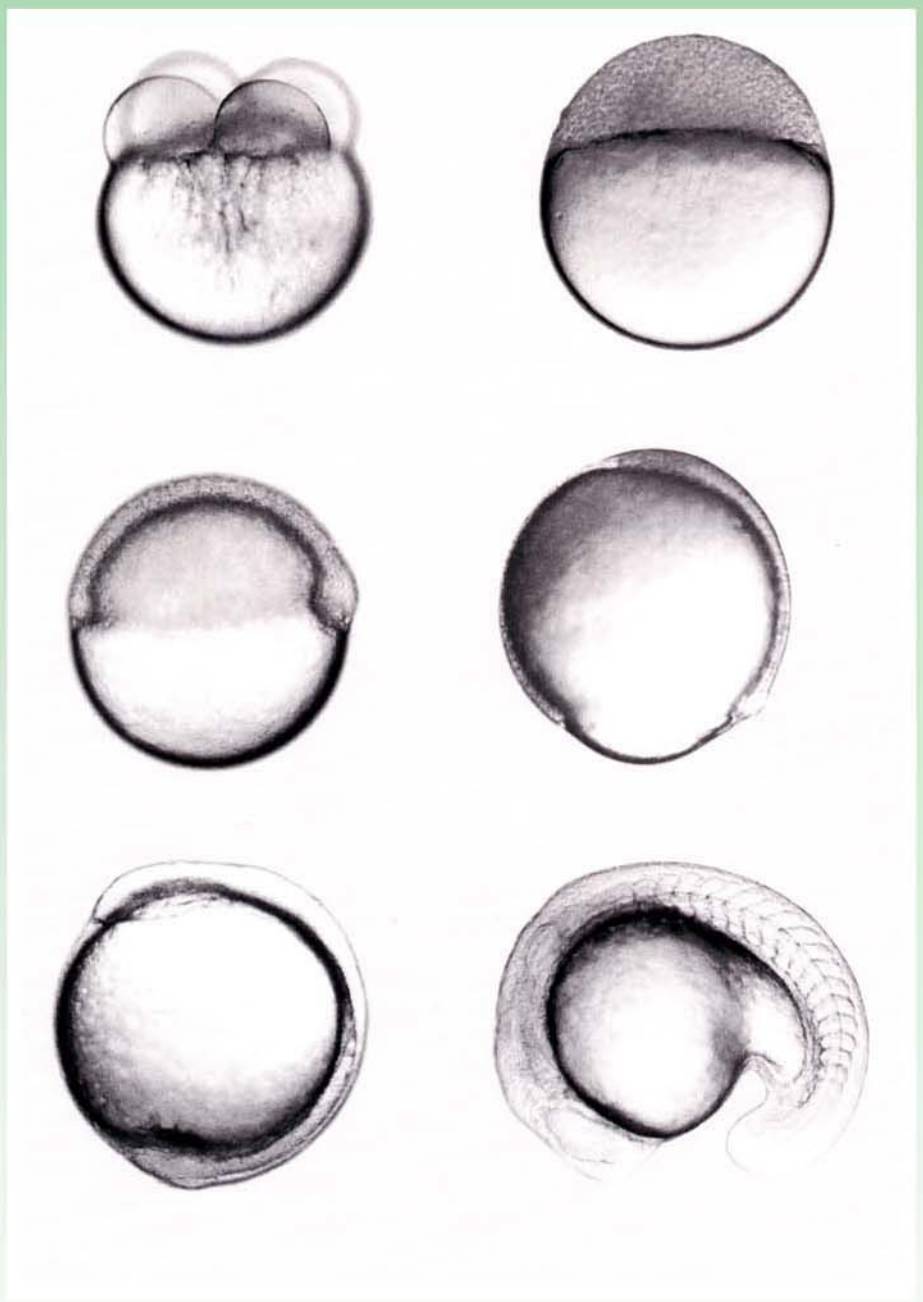

Studies of embryonic development

The Identification of Genes Controlling Development in Flies and Fishes (Nobel Lecture)**

Christiane Nüsslein-Volhard*

In the life of animals, complex forms alternate with simple ones. An individual develops from a simple one-celled egg that bears no resemblance to the complex structure and pattern displayed in the juvenile or adult form. The process of embryonic development, with its highly ordered increase in complexity accompanied by perfect reproducibility, is controlled by a subset of the animal's genes. Animals have a large number of genes. The exact number is not known for any multicellular organism, nor is it known how many and which are required for the development of complexity, pattern, and shape during embryogenesis. Identifying these genes and understanding their functions is a major issue in biological research.

Genes can be detected by mutations, changes that affect their function. Compared with other experimental approaches, mutations provide a uniquely powerful tool for studying the role of individual components in development. Primarily, only a single component, the gene product, is removed or altered, while the remainder of the organism is left intact. The function of a gene can be deduced from the mutant phenotype, the way the animal develops in the absence of the primary gene product. The mutant phenotype provides most useful information about a gene function. Genes with similar phenotypes are likely to have similar functions, and their products are likely to cooperate in a developmental process.

Mutations occur spontaneously at a low rate, but their frequency can be increased by application of X-rays or chemicals that alter the DNA sequence. This property was first used to systematically score for mutations affecting processes of interest in bacteria and fungi.[1-3] Mutations affecting developmental processes had been collected in *Drosophila melanogaster* more or less fortuitously, starting with the bithorax mutation by Bridges in 1922.[4] In addition, a small number of embryonic mutants including *notch* had been described in detail by D. Poulson and collaborators.[5] In the 1970s, more systematic approaches were started. In the nematode *Caenorhabditis elegans* screens were begun by S. Brenner for mutations that alter the stereotyped pattern of postembryonic development.[6] E. Lewis at the California Institute of Technology collected a number of mutations causing homeotic transformations in the adult and the larva of *Drosophila*.[7] In 1979, Eric Wieschaus and I, at that time at the European Molecular Biology Laboratory (EMBL) in Heidelberg, had developed methods for the large-scale screening for embryonic lethal mutations in *Drosophila*. The screening procedure focused on the segmented pattern of the larval epidermis.[8] In this and subsequent screens, a number of new genes acting in the embryo and required for the formation of a morphologically normal larva were discovered.[9-11] Similar screens in several laboratories have led to the identification of genes that are expressed by the maternal genome, and whose products, laid down in the unfertilized egg, control the expression of the zygotic genes.[12-16] The subsequent phenotypic analysis and molecular cloning of many of these genes, and investigation of the interactions of their products, resulted in a rather complete general picture of the mechanisms establishing the anteroposterior and the dorsoventral axis of the early embryo.[17-19] These mechanisms now provide a useful paradigm for the development of complexity from a simply shaped egg cell.

Drosophila is a fly and as such has rather special properties. It is no more or less "special" than a worm or a frog, but in many respects very different from those animals. Therefore it was not clear a priori to what extent the results obtained with *Drosophila* could be generalized, and how much we could learn from them for an understanding of the development of other animals, in particular, vertebrate species. Knowledge of vertebrate embryogenesis had been collected predominantly in experiments with frogs[20] and chickens, but only to a very limited extent by genetic approaches. Because of the small size and the turgor under which *Drosophila* embryos develop, transplantation of tissues as done in frogs and chickens is hardly possible in *Drosophila*, and the power of systematic mutant searches for the analysis of complex processes, although highly desirable, cannot readily be applied to most vertebrates. Therefore, the description and understanding of the development of animals from the two phyla—arthropods with *Drosophila*, and vertebrates with frogs and chickens, mice and man—were on such different levels that for a long time a comparison seemed almost pointless. However, the development of recombinant DNA technology and with it the cloning of genes on a large scale allowed a comparison of genes from different organisms on the basis of DNA (or protein) sequences. Two most important findings emerged from these studies:

[*] Prof. C. Nüsslein-Volhard
Max-Planck-Institut für Entwicklungsbiologie, Abteilung Genetik
Spemannstrasse 35, D-72076 Tübingen (Germany)
Fax: Int. code +(7071) 601-384
e-mail: derbio3@fservl.mpib-tuebingen.mpg.de

[**] Copyright© The Nobel Foundation 1996. We thank the Nobel Foundation, Stockholm, for permission to print this lecture.

1. The biochemical function of *Drosophila* gene products, in many cases, could be deduced from a comparison of their amino acid sequences with those of related and well-characterized proteins from other organisms such as mammals, bacteria, and yeast. This revealed that many of the components controlling development are members of well-known classes of proteins, such as transcription factors, protein kinases, and secreted signaling molecules or receptors.

2. In many instances, the similarity between *Drosophila* and vertebrate proteins was found not to be restricted to their biochemical properties, but to extend to a true homology of function in a developmental process. This homology is apparent both in similar expression patterns and in the phenotypes obtained by eliminating the gene function by homologous recombination in mice. These studies lead to the surprising conclusion that the basic features of body organization, such as specification along the anteroposterior axis and polarity of gastrulation, are apparently conserved in organisms of different animal phyla.[21, 22] This conservation suggests the existence of a common basic body plan, originating from common evolutionary ancestors, the first bilaterally symmetrical organisms.

The investigation of genes discovered by their homology to *Drosophila* genes is now one of the most successful approaches to understanding the genetic control of vertebrate development. Although the elegant method of homologous recombination in the mouse allows the introduction of mutations into the chromosomal copy of any previously cloned gene,[23] there is no way of predicting which genes are indispensable in development and will therefore give an informative phenotype in "knock out" mice. An important reason for the success of the homology approach is based on the fact that the *Drosophila* genes in question represent a small fraction of the animal's genes, which were selected, through mutagenesis experiments, as being crucial and indispensable in development. Their vertebrate homologs often also have unique functions, as revealed in the mouse.[24]

Approaches based on the homology between invertebrate and vertebrate genes focus on conserved properties and therefore select against the features that make these animals different. Vertebrates have acquired specific structures and novel mechanisms during evolution. In order to identify genes affecting such functions, it is necessary to conduct mutagenesis screens directly in a vertebrate organism. Therefore, several laboratories have established methods for using the zebra fish as a model organism to analyze the genetic control of embryonic development in a vertebrate.[25–28]

In this lecture I would like to discuss the *Drosophila* screens and their most important results as well as their limitations. I will compare them with the results of a large-scale screen for mutations affecting development and pattern in the zebra fish recently performed in my laboratory in Tübingen.[29]

The *Drosophila* Mutant Screens

As a model organism for genetic studies of development, *Drosophila* has a long tradition and is by far the best established organism available.[30] Also, it proved to be quite well-suited for studying embryology. Some properties of *Drosophila* are listed in Table 1. Its small number of chromosomes enabled the development of many genetic tools such as balancer chromosomes carrying multiple inversions which prevent recombination, visible markers that allow the scoring for the absence or presence of particular progeny, and conditional lethal or sterile mutations making selection systems possible. These tools were invaluable in systematic mutagenesis screens for mutations causing lethality or sterility (Fig. 1). In combination with the giant chromosomes that provide a physical measure for the number of genes, it is possible, in *Drosophila*, to determine rather accurately the

Table 1. Properties of *Drosophila melanogaster* and *Danio rerio* for genetic and embryological research.

	Drosophila	*Danio*
Adult size	4 mm	40 mm
Space requirement	1000 per liter	10 per liter
Generation time	14 days	3 months
Lifetime	6 weeks	1–2 years
Egg size	0.15 × 0.5 mm	0.8 mm
Embryonic development	24 h	48 h
Fecundity	50 eggs per day per female	200 eggs per week per female
Number of chromosomes	4	25
Advantages for genetic research	polytene chromosomes marker mutants balancer chromosomes conditional lethal mutants	in vitro fertilization haploid development homozygous fish freezing of sperm
Advantages for embryological research	mechanical hatching cuticle preparations external segmentation	external fertilization synchronous development optically clear embryo

Christiane Nüsslein-Volhard began her academic career with a degree in biochemistry. Following studies of transcription in bacteria, she directed her attention in the mid-1970s at the University of Basel (Switzerland) to studies of the fruit fly Drosophila. In 1978 she worked together with Eric Wieschaus as group leaders at the European Molecular Biology Laboratory in Heidelberg (Germany), where they studied genes affecting embryological patterning. For the past ten years C. Nüsslein-Volhard has been Director of the Department of Genetics at the Max Planck Institute for Developmental Biology in Tübingen (Germany). In 1995 she received the Nobel Prize for Physiology and Medicine along with Eric Wieschaus and the geneticist Edward B. Lewis.

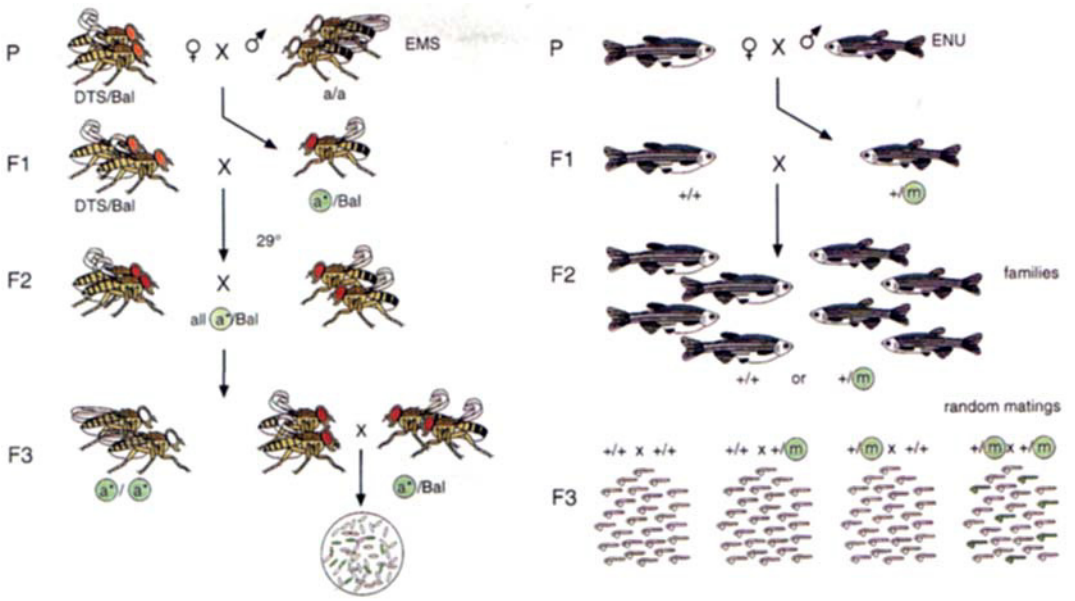

Fig. 1. Crossing schemes for isolating mutants with embryonic visible phenotypes in *Drosophila melanogaster* (left) and *Danio rerio* (right). EMS: treatment of sperm with ethyl methyl sulfonate, ENU: treatment of spermatogonia with ethylnitroso urea, DTS: dominant temperature-sensitive, Bal: balancer chromosomes. In *Drosophila*, eye colors and wing shape are markers used to distinguish carrier animals from noncarriers, which are inevitably produced in the crosses required for inbreeding. They also are useful for determining whether a lethal mutation was induced (absence of white-eyed progeny in the F3 generation). Marking and selecting systems, such as balancers, recessive mutations, and dominant temperature-sensitive mutants, useful for selection, are available for each major chromosome, but it is not easy to do screens for the entire genome all at once, because the multitude of markers significantly affects viability. *Drosophila* larvae hatch mechanically, a process that is very sensitive to perturbations. A large fraction of lethal mutations prevent hatching, although most of them do not visibly affect the embryonic pattern. Mutant embryos can be separated as unhatched from their normal siblings. In the zebra fish, the large number of chromosomes makes the development of marking systems impracticable. Instead, the entire genome is scored at once, and in each generation, carriers must be recognized by the production of mutant progeny with a visible phenotype. Mutations causing lethality without a visible mutant phenotype cannot readily be detected. In the F3 generation, only a quarter of the crosses will yield mutant embryos (25% of all embryos), as only half of the F2 fish share a particular mutation. But there is no way to distinguish carriers from noncarriers.

total number of genes essential for survival and fertility. About 5000 genes mutate to lethality. The number of genes required for fertility is less well-defined, but is probably not more than one thousand. However, the total number of genes, defined as transcription units, is much larger, about 20000. This also means that in *Drosophila* the majority of the genes do not have indispensable functions. A large fraction, about one-third of all lethal mutations, cause a failure of the embryo to hatch (embryonic lethality); however, only about ten percent of these mutations show an easily detectable and specific morphological phenotype in the unhatched differentiated larvae.

The *Drosophila* larva displays a clear axial organization with many landmarks of position and polarity, which are provided by the external cuticle shed by the larval epidermis (Fig. 2). This larval skin is derived from a large portion of the embryonic fate map, while the remainder of the blastoderm largely gives rise to internal organs which are less visible in the living embryo. Whereas an excellent and simple fixation technique was available for the skin, at the time of the mutant screens there were no efficient methods for visualizing the internal organs, which are hidden by the opaque yolk. This problem has since been overcome by the development of molecular probes and antibodies, and a number of screens have used these for the detection of mutants, albeit every screen for a rather limited range of phenotypes. The properties and advantages of *Drosophila* for the genetic analysis of embryonic pattern formation are summarized in Table 1.

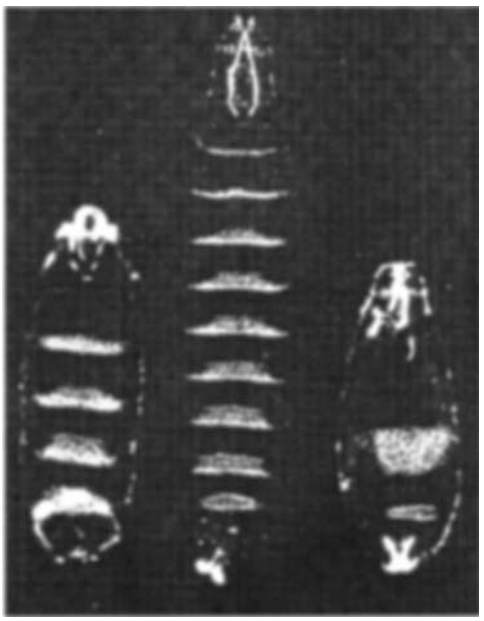

Fig. 2. The cuticular pattern of segmentation mutants. The picture shows the ventral view of a normal larva (middle), a mutant *paired* larva (left), and a *knirps* larva (right). *paired* is a pair-rule gene, and mutants produce approximately half the normal number of segments, every other segment is deleted. *knirps* belongs to the gap class of segmentation genes; most of the abdominal segments, marked by the prominent denticle belts seen in the normal larva, are deleted. Anterior is at the top of the picture.

In the Heidelberg screens[9–11] we collected mutants detectable by a distinct and significant deviation from normal patterning of the cuticle. These mutants, after complementation tests, defined about 130 genes distributed randomly over the three major chromosomes. Using similar scoring criteria, screens for maternal mutants defining about 30 genes were per-

formed in several laboratories.[12-16] Without molecular markers, most of the mutant phenotypes could not readily be analyzed and interpreted at the time. We used rather pragmatic criteria both for screening and characterizing the mutant embryos. By similarity in phenotype, several groups of genes were recognized that probably affect the same or related developmental processes. Subsequent phenotypic and genetic analysis, followed by the molecular cloning of the genes, frequently supported this notion. The groups of genes identified in the mutant screens are shown in Table 2.

Table 2. The *Drosophila* gene classes.

Class	Subclass	Genes	Cloned	Vertebrate homologs
maternal	anterior	4	4	0
	posterior	8	6	2
	terminal	6	3	1
	dorsoventral	12	12	3
zygotic	gap	9	7	1
	pair-rule	8	8	4
	segment polarity	13	8	6
	homeotic	11	9	7
	head morphology	10	4	0
	dorsalized	4	4	3
	ventralized	6	5	2
	dorsal holes	8	6	3
	others	8	2	0
	neuralized	6	6	2
	midline	5	5	1
	epithelia	4	2	2
	cell cycle	6	4	0
	denticles and hairs	4	1	0
	pigmentation	5	3	1
	tracheae	2	0	0
	hyperactive	4	1	0

In our screens, we put great emphasis on completeness, in other words, on the saturation of the genome with mutants detectable by our criteria. Several lines of evidence, such as allele frequency and comparison with phenotypes of deletion mutants, supported the notion that the majority of genes that mutate to a phenotype visible in the larval cuticle had been discovered in our screens. As an additional generation of inbreeding is required, the screens for maternal mutants were more demanding and difficult than those for embryonic lethals. Therefore, it is likely that the degree of saturation for the maternal genes is not as high as that for the zygotically expressed genes. Although the screens were successful in identifying many important genes, and screening more lines would not have significantly increased the number of genes discovered, we were aware of a number of severe intrinsic limitations of our approach.

Genetic Redundancy

At the time, the viewpoint held amongst most *Drosophila* geneticists was that genes not mutating to lethality or sterility were almost not worth studying. There was the tacit assumption that the great majority of all genes were essential for survival or fertility. Concern about redundancy and duplicated genes was a later issue, as it depended on the physical isolation of a gene by cloning, whereas in "precloning times" a gene was only detectable by a mutation causing a phenotype. However, we took redundancy as a theoretical possibility into account. Among the segmentation genes, a number of cases of gene duplications have been fortuitously discovered during the molecular analysis. As methods of reversed genetics are not generally applicable in *Drosophila*, the proportion of redundant genes cannot readily be determined. It is not at all clear why some genes are duplicated and others are not.

Maternal and Zygotic Contribution

Another limitation we were more concerned about was that genes whose products were required both maternally and zygotically would be difficult to detect in mutant screens. In cases where the product is provided maternally, the zygotic phenotype may not represent the complete lack of function. This concern applied in particular to the maternal mutants: in cases of additional functions in the embryo, mutations in genes with important maternal functions might be lethal zygotically and would therefore not be discovered in maternal screens. A number of such cases have been found. To this day, the genes required both maternally and in the zygote are not easily accessible to investigations of function.

Axis Determination in *Drosophila*

A large fraction of the genes identified in both the zygotic and the maternal screens affect either the anteroposterior or the dorsoventral axis. The pattern of the larva is composed of a series of segments that change their character from anterior to posterior. Nonsegmented terminal structures are located at both ends. The pattern also displays a clear dorsoventral difference, although the ventralmost (mesoderm) and dorsalmost (amnioserosa) structures of the embryonic fate map are not represented in the epidermal pattern.

The Anteroposterior Axis

We defined three classes of zygotic segmentation genes, which we called gap genes, pair-rule genes, and segment polarity genes.[8] In mutant embryos of the gap genes, large unique regions are deleted. In pair-rule mutants, deletions in the pattern affect homologous regions in every other segment (Fig. 2), while every segment shows a defect in mutants of the class of segment polarity genes. The phenotypes suggested that the process of segmentation involves at least three levels of spatial organization: Processes beginning during oogenesis define the large unique regions requiring the gap gene function, and the gap genes in turn control a repeat pattern with the periodicity of double segments. Finally, the individual segments are established as developmental units in response to the action of the pair-rule genes.[8]

The subsequent molecular analysis of the properties and function of the segmentation genes was carried out in many laboratories. In these studies, the method of producing transgenic flies by P element induced germline transformation, developed by

Alan Spradling and Gerald Rubin, opened up a rich repertoire of powerful approaches.[31] Many of the segmentation genes are transcription factors that control the expression domains of other segmentation genes, either within the same or of the downstream class. The pattern of expression of many segmentation genes in the first approximation corresponds to the deletion pattern displayed in cuticle preparations.[18] During early embryogenesis, a series of such molecular prepatterns, composed of the expression domains of transcription factors, which are the products of the segmentation genes, is formed. The gap genes are expressed in large unique regions early in embryogenesis; their expression patterns are controlled by maternally provided transcription factors.[18] The earliest metameric pattern, that of the pair-rule genes, has seven stripes that are each determined by the action and interaction of a particular combination of gap gene products.[32, 33] The pair-rule genes finally control the pattern of more than 14 stripes preceding the formation of the morphological pattern, the segments[34] (Fig. 3).

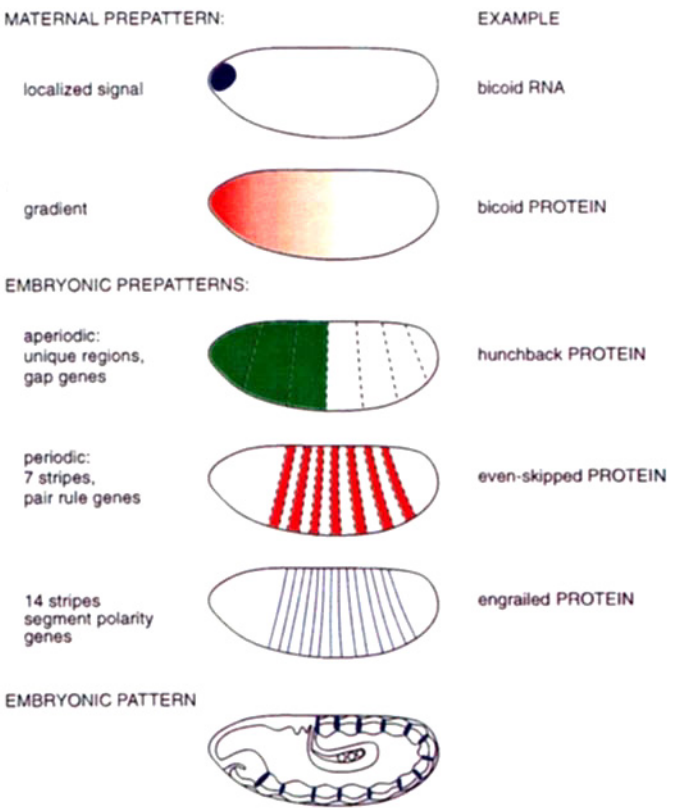

Fig. 3. The hierarchy of genes establishing the anteroposterior pattern in *Drosophila melanogaster*. In every tier, the distribution of the protein product of one representative gene of its class is shown in color. Anterior is on the left, ventral is at the bottom in each picture.

The identification and analysis of the maternal genes affecting the segmentation pattern revealed that the anteroposterior axis is controlled by three groups of genes, each independently determining a subset of the pattern, the segmented anterior or posterior, or the unsegmented terminal regions of the embryo.[35–37] Although the molecular processes by which the three groups function are largely different, they share some common features. Spatial signals are produced that are localized at the anterior or posterior egg pole. In each group, a series of molecular interactions finally results in the formation of a transcription factor gradient spanning a substantial portion of the egg length; the highest concentration is located at the site of the localized signal (Fig. 2).[38] These transcription factor gradients determine the expression of the gap genes in a concentration-dependent manner, thereby defining the first subregions of the embryo.

The Dorsoventral Axis

Two classes of zygotic genes have been identified, mutation of which cause a dorsalized or ventralized phenotype.[39] in *Drosophila*, the mesoderm is formed during gastrulation in the ventral region of the egg; its formation depends on the expression domain of two zygotic transcription factors. The refinement of the dorsoventral pattern on the dorsal side involves a long-range signaling process, unlike the series of prepatterns of transcription factors observed along the anteroposterior axis.[40] The maternal control of the dorsoventral pattern is achieved by only one group of genes that establish a nuclear localization gradient, with its maximum at the ventral side, of a transcription factor that functions both as a repressor of dorsally expressed genes and an activator of ventrally expressed genes.[17, 19] The first zygotic expression pattern divides the embryo into at least three domains along the dorsoventral axis.

Molecular Mechanisms of Pattern Formation

Despite the limitations of the mutant screens discussed above, the collection of genes within each phenotypic group and thus of components of a developmental pathway appears to be relatively complete. In several instances, the molecular interactions of the components within and between pathways have been elucidated in some detail. These examples show how complex patterns can develop from a small set of independently localized signals. A principal mechanism by which spatial complexity is increased is based on concentration gradients of morphogens, molecules that elicit different responses at different concentrations. An example of this mechanism has been discovered by studying the maternal control of the expression pattern of the gap gene *hunchback* by the morphogenic protein Bicoid.[41–43] Bicoid is the transcription factor determining the anterior pattern; it is distributed in a concentration gradient with its maximum at the anterior pole of the egg and controls the transcription of several target genes in a concentration-dependent manner. Morphogen gradients can be formed by diffusion of the protein translated from a localized mRNA source, as in the case of the anterior and posterior maternal gradients (Fig. 2).[35, 37] In other cases, gradients are apparently produced by diffusion in the extracellular space.[44] Their spatial distribution is communicated to the interior of the egg cell through a ligand/receptor-based signal transduction mechanism.[45] In the case of the dorsoventral axis, this mechanism results in the formation of a nuclear localization gradient of the initially equally distributed transcription factor Dorsal.[46, 47] During segmentation, the series of transcription factor patterns with increasing spatial complexity develops by concentration-dependent transcriptional ac-

tivation and repression, involving combinations of transcription factors.[18] The determination of the final molecular prepattern depends on short-range signaling between adjacent cells.[34, 48] This pattern immediately precedes the first morphological changes occurring during segment differentiation.

Limitations of the *Drosophila* Screens

The mechanisms by which axes are established in *Drosophila* are among the best understood examples of pattern formation to date. Because of some special features of early development in the *Drosophila* embryo, they may, however, not always have an immediate parallel in other animal classes. This restriction applies in particular to the processes requiring diffusion in a syncytial embryo, as in the case of the formation of the Bicoid gradient. On the other hand, examples such as the formation of gradients by diffusion in the extracellular space, signal transduction, and the establishment of a nuclear localization gradient, as in the case of Dorsal, may prove to have analogies in pattern-forming processes in multicellular tissues. The genetic analysis of pattern formation in *Drosophila* teaches us about the logic of pattern formation in a complex system. It also led to the discovery of some basic mechanisms that allow an increase in complexity during the development of multicellular organisms. On the other hand, many aspects of animal development, in particular the formation of organs and their functions, have not been studied as thoroughly in *Drosophila*. The reason for this restriction is the fact that we relied on the epidermal pattern in scoring mutant phenotypes in our screens. Obviously, this limitation was very apparent to us, although we tried to use it to our advantage. It limited, with rigid criteria, the number of genes we were concerned with. However, many mutations could not be recovered by the scoring of the cuticular pattern alone. To this day, a systematic screen for *Drosophila* mutants with defects in inner organs has not been performed; however, a number of genes with particular functions in inner organs have been identified in special screens using specific molecular probes[49] or by other means such as the very powerful enhancer trap screens.[50, 51] A crude classification of the *Drosophila* genes discovered in the Heidelberg screens is presented in Table 2. To date more than 60% of them have been cloned.

Many *Drosophila* genes have been shown to have homologs in vertebrates. This homology is not restricted to amino acid sequence and to their biochemical function, but extends to the biological role played in development. This remarkable conservation came as a great surprise. It had been neither predicted nor expected. One of the first indications came with the discovery of the *hox* gene clusters in vertebrates, and the conservation of the colinearity of their expression domains with the chromosomal location.[22, 52] This was soon followed by the isolation of homologs in vertebrates of other homeobox-containing genes, and it now seems that a large fraction of the *Drosophila* genes that we found in our screens have vertebrate homologs. It is difficult to give an estimate of this fraction, because not in all cases have homologs been sought. However, it may be significant that of the maternal genes very few are known so far to have vertebrate homologs (Table 2). This may reflect the very great differences observed in very early development between vertebrates and invertebrates. A large fraction of the vertebrate homologs of *Drosophila* genes have been shown to play an important role in pattern formation in the mouse. Important patterning pathways appear to be conserved, such as the signaling pathway involving TGF-β-like growth factors, and homologs of *hedgehog* and *wingless*.[21, 53, 54] Most of the components of such pathways have been detected by phenotypes visible in the segmented pattern of the *Drosophila* larva. In the vertebrate body organization they are not always required in this context. For example, genes involved in segmentation in *Drosophila* also participate in patterning the brain and limbs in *Drosophila* as well as in vertebrates. Although the collection of the *Drosophila* pattern genes provides a rich source for the study of some aspects of vertebrate development, this sample is strongly biased and probably provides only a small fraction of the genes controlling patterning in vertebrate embryos. In order to obtain a more complete collection of those genes, a direct screen for mutations in a vertebrate organism is required.

The Zebra Fish Screen

The zebra fish, *Danio rerio*, was selected as a potential model for genetic research by the late George Streisinger.[28] In the past 20 years a number of useful methods have been developed for its breeding and genetic analysis, as well as for the investigation of its embryonic development.[25–27] It is interesting to compare characteristics of flies and fishes with regard to genetic and embryological research. Obviously the long generation time and space requirement for rearing zebra fish make large-scale genetic screens difficult. In addition because of technical and logistical problems in running large numbers of aquaria, working with fish is more costly and labor-intensive than with flies. On the other hand, compared to mice, the more traditional vertebrate organism used in genetic research, zebra fish offer the advantages of extrauterine development and high fecundity. With fish, in vitro fertilization, haploid development of embryos until the larval stage, diploidization, and the freezing of sperm samples is possible (Table 1). These techniques are invaluable in the maintenance and analysis of a large number of mutants, and are not possible with flies. The greatest advantage of the zebra fish, however, lies in the nature of its embryonic development. Zebra fish eggs are fertilized synchronously, they develop rapidly outside the maternal organism, and, most importantly, they are initially completely transparent. This allows the observation of the development of many tissues and organs directly in the living embryo and at subsequent stages without the necessity of fixing, clearing, and staining[55] (Fig. 4).

The early embryogenesis of zebra fish is very different from that of flies. A period of rapid synchronous cleavages results in a three-dimensional mass of cells, unlike the two-dimensional blastoderm formed by the *Drosophila* embryo. Gastrulation in the fish involves several morphogenetic movements such as involution of mesendodermal regions and dorsal convergence.[55] Although these movements appear very different, they might be related to the invagination of mesodermal and endodermal anlagen, and ventral condensation and extension of the germ band in the *Drosophila* embryo. They result in a multilayered

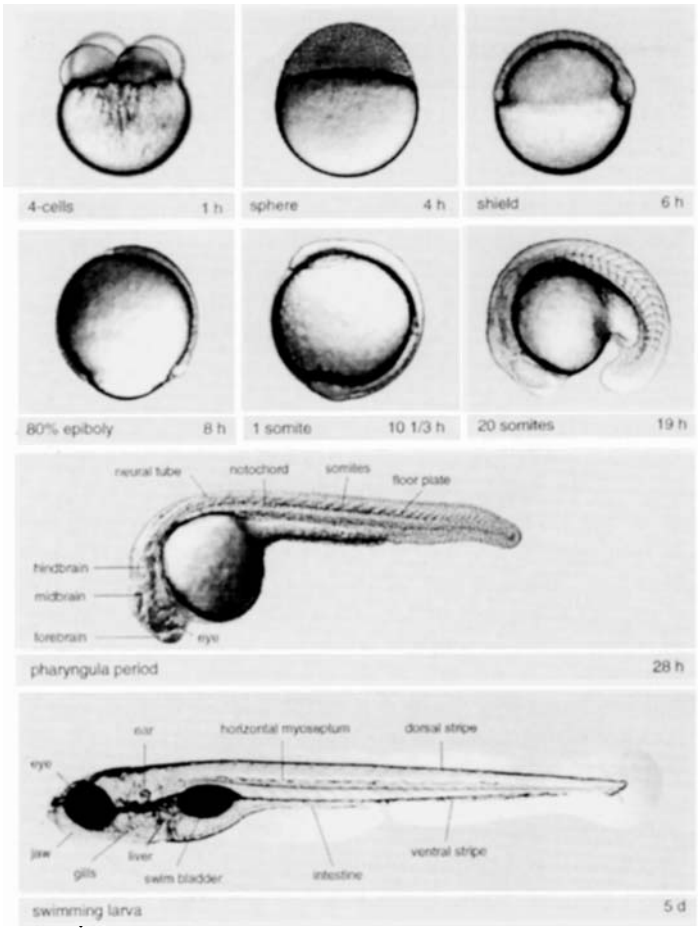

Fig. 4. Embryonic development of the zebra fish. Photographs of live embryos at different ages. With the exception of the swimming larva, the embryos were dissected out of the chorion. In the early embryos, the dorsal side is on the right. In the pharyngula and swimming larva, the dorsal side is up and the anterior to the left. Characteristic structures scored in the mutant screen are indicated. Stages are given according to ref. [55].

embryo, the pharyngula or phylotypic stage, which displays the typical vertebrate body organization (Fig. 4).

While in the *Drosophila* embryo fate mapping studies allow the construction of two-dimensional maps of the early gastrula with distinct and clearly separated anlagen, in the fish the fate of cells within particular gastrula regions is much less precisely predictable. The fish gastrula is multilayered. Large regions that later develop into different organs or tissues overlap and are superimposed. This difference may reflect quite distinct developmental mechanisms determining fate of cells in the fish and fly embryo. A comparison of fly and fish fate maps reveals further dramatic differences between the relative size occupied by the anlagen for various organs. For example in the fish the brain anlage occupies a very large fraction of the gastrula, while the epidermis is rather inconspicuous, compared to its dominance in the fly map. To a certain extent, the sizes of the anlagen reflect the importance and visibility of the structures that can be scored in a mutant screen.

The crossing scheme used to make mutants with phenotypes visible in the embryo or early fish larva is displayed in Figure 1. Treatment of fish spermatogonia with ethylnitrosourea (ENU) has been used for mutagenesis with a similar efficiency as that obtained by treatment of fly sperm with ethyl methyl sulfonate (EMS) (about one mutation per gene per 1000 genomes).[26] In contrast to the fly screens, in the fish no markers can be used to help distinguish carrier from noncarrier fish in the F2 generation. Therefore, to detect a mutation induced by the treatment of parental males, a number of crosses have to be set up, of which only 25% on average yield progeny that are homozygous for a mutation. As fish hatch enzymatically, most homozygous mutant embryos also hatch, and therefore, with few exceptions, they cannot be recognized as nonhatchers, a useful way to identify mutant embryos in the *Drosophila* screens. Mutant fish embryos can be recognized by their phenotypes only. The lack of markers and preselection is compensated somewhat by the fact that the entire genome is scored at once and not chromosome by chromosome. In the case of the fly, three separate screens on a total of more than 20000 inbred families were performed to obtain about 600 mutants in 130 genes.[9-11] For the fish, 3100 families were screened, with an average of 4.2 crosses, corresponding to the screening of 3800 genomes (Fig. 1).[29] As the breeding of such a large number of fish families is necessary to achieve a reasonable degree of saturation for any given phenotypic trait, this screen was the collaborative effort of 12 scientists. We screened as many different phenotypic traits as could be efficiently scored. We isolated a total of 1200 mutants, of which to date about 900 have been characterized both phenotypically and genetically. They define 350 genes, of which 150 have more than one allele.[29]

The different developmental features of the fish embryo were scored at different times in development, as the structures and organs became visible with age (Fig. 4). On the second day of development, the somites, notochord, and brain were scored, while after hatching heart, blood, musculature, fins, eye, ear, and other features were studied. Fish of the larval stage, the latest time scored, almost one week old, have a complete set of internal organs, liver, gut, pancreas, kidney, can see and respond to stimuli, and are pigmented with three types of pigment cells. They still display a pigment pattern characteristic for the larval stage, and the fin structure does not yet completely correspond to that of the adult fish (Fig. 4). Some structural features of the fish are recognized readily and unequivocally, while others are less conspicuous and therefore abnormalities may not always have been detected. The high degree of complexity, which is far more than that displayed in the cuticular pattern of the fly larva, allows a much broader spectrum of organs and tissues to be investigated, but it also sets considerable demands on the skill and expertise of the experimenter. The recognition of a particular phenotype is greatly enhanced if an interpretation of the phenotype is available, or if it has been seen before. Many mutants have rather general defects; they have not been kept for analysis.[29] Mutants with complex or subtle phenotypes resembling rather general defects are not always recognized as interesting or interpreted correctly. This means that the degree of saturation varies among different phenotypic classes (Table 3). On average it is certainly less than that achieved in the fly screens.

Based on their predominant phenotypic traits, the genes can be classified in a large number of groups with similar phenotypes. Classification of each mutant depends on the interpretation of its phenotype, and this in turn on the degree of phenotypic analysis that can be performed. In the fish, a number of

Table 3. The zebra fish gene classes.

Class	Subclass	Genes	Alleles	Alleles/gene
early	epiboly, arrest	11	16	1.5
	ventralized	2	4	2
	dorsalized	5	16	3
	others	13	19	1.5
mesoderm	notochord	15	67	4.5
	somites	8	26	3.2
CNS	brain	19	37	1.9
	midline	10	19	1.9
organs	blood	9	23	2.6
	heart, circulation	22	28	1.4
	liver, gut	6	6	1
	muscles	18	63	3.5
	eye	8	11	1.4
	ear	19	46	2.3
	fins	13	60	4.6
neural crest	pigment pattern	10	39	3.9
	pigment cells	61	150	2.5
	jaw and gill arches	17	30	1.8
motility	reduced	15	50	3.3
	abnormal	15	53	3.5

molecular probes are available that serve as markers for particular regions at specific developmental times. The expression patterns of such markers were very useful in characterizing many of the mutant phenotypes. The classes of fish genes identified by the mutants are shown in Table 3. A small number of classes have a parallel among the classes of fly genes, while the majority of phenotypes are novel. The collection of the fish gene classes is so different from that of the fly genes that a comparison is possible only in selected cases. With regard to the most prominent classes of fly genes, gastrulation and segmentation, however, a small number of fish genes might have similarities to fly processes.

The Zebra Fish Gene Classes

Gastrulation is affected in two gene groups, the phenotypes of which display a partial dorsalization or ventralization.[56, 57] In *dino* mutant embryos, dorsal anterior structures are reduced, while ventral posterior structures are increased in size. This results in embryos with small heads and large tails. The effect is most pronounced in the structures derived from the most ventral position in the fate map: the blood and ventral tail fin, which is increased in number in *dino*. By using molecular markers that are expressed before gastrulation in a polar manner, it is apparent that the fate map is distorted already at an early point in fish embryogenesis (Fig. 5A). As suggested by a characteristic duplication of the ventral tail fin, mutants in the *mercedes* gene have a role in the same process[56] (Fig. 5K). A phenotype complementary to that of *dino* and *mercedes* is displayed in mutants in a number of genes with a dorsalized phenotype; *swirl* embryos, for example, have much enlarged paraxial mesoderm; the forming somites encircle the entire embryo (Fig. 5F) and ventrally derived structures such as blood and the ventral tail fin are reduced or lacking entirely.[57] These groups of genes are reminiscent of genes with dorsalizing and ventralizing phenotypes also observed in *Drosophila*. For genes of both groups, homologs in the frog and fish have been cloned and shown to be expressed at opposite regions of the blastula.[58–61] These and other observations led to the revival of an old theory postulating that the orientation of the dorsoventral axis in invertebrates is inverted compared to that of vertebrates.[62–64] The fish genes are likely to provide components in these conserved pathways.

An interest in the mechanism of segmentation in vertebrates was an important incentive for the mutant screens in fish. In contrast to flies, which have a clearly segmented ectoderm, in fish the mesoderm is the primary vertebrate tissue that is organized in a metameric pattern. We did not find many genes in the fish that have similarities to fly segmentation genes. The closest are mutants in which the somites, the earliest visible repetitive structures formed in the fish embryo after ten hours of development, are fused. Five genes have a phenotype with fused somites (Fig. 5B, M, N).[65] The somite pattern in the fish embryo is much less complex than the segment pattern of the *Drosophila* larva. However, the vertebrate that develop in postlarval stages in mutant fish display characteristic mirror duplications (Fig. 5N), albeit less striking and regular than the phenotypes of the segment polarity genes in the fly, with which they may be compared. No genes with obvious resemblance to gap or pair-rule genes have been detected in the fish screens. Using molecular approaches, no clear homologs to the gap genes could be detected so far, and the homologs of the pair-rule genes do not seem to be expressed in a pair-rule fashion.[59] The failure to find mutations resembling the gap and pair-rule mutations in the fish may mean that the formation of metameric patterns differs between *Drosophila* and most other animals. On the other hand, it may be the result of redundancy.

Other mutations affect the dorsoventral subdivision of the somites by the horizontal myoseptum. Some of these also lack the notochord, while in others the notochord is apparently normal. The notochord is a vertebrate-specific structure. The gene *no tail*, a fish homolog of the mouse *brachyury* or *T* gene, is expressed in the notochord (Fig. 5C)[66, 67] (a homolog in *Drosophila* is expressed in the hindgut[68]), and mutations in *no tail* as well as in three other genes required for notochord formation have been identified (Fig. 5C).[69, 70] The structure of the somites in fish is thought to be dependent on signals derived from the notochord. The genes affecting somite subdivision by the horizontal myoseptum might represent members of these signaling processes (Fig. 5G). Their products may be involved in producing or receiving the signals.[65] For these genes, homologous processes in *Drosophila* are not obvious.

A large number of the fish genes affect structures and functions of the central nervous system and sensory organs (Table 3). This class is poorly represented in the fly screen. In our screen several aspects of CNS development have been scored. For the neurogenic genes of *Drosophila*, such as *notch* and *delta*, homologs have been detected in the vertebrate by molecular means,[71] and in our screen at least one gene with neurogenic features, *white tail*, has been found. Mutant embryos display a considerable multiplication of primary neurons at the expense of secondary neurons and certain types of glial cells (Fig. 5E).[72] Another class of genes affect structures along the midline in all three germlayers. In the mutants, the eyes are often fused. Mutant embryos display a lack of structures derived from axial mesoderm and ventral regions of the spinal cord or brain.

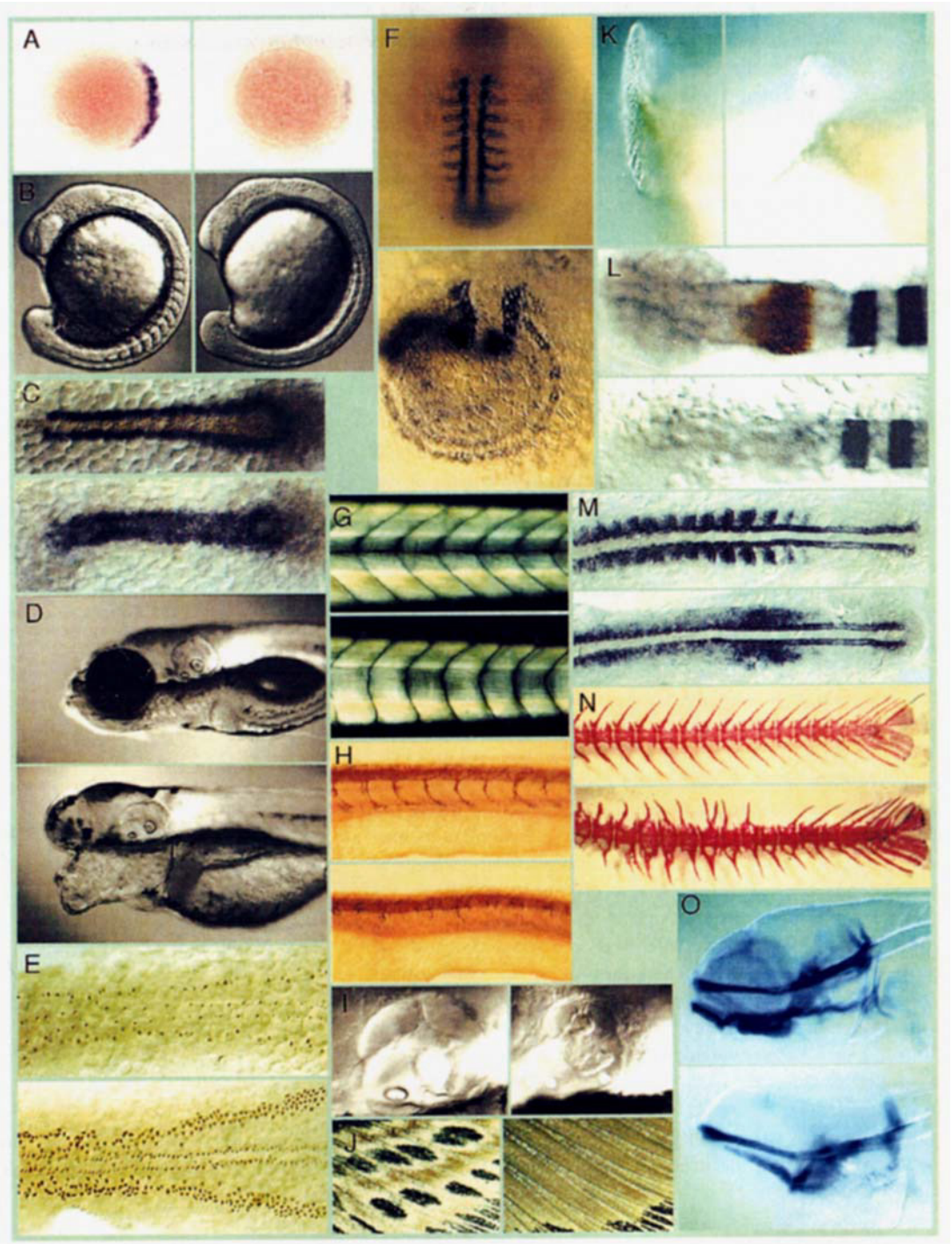

Fig. 5. Zebra fish mutants. In the pairs of panels, a wildtype embryo is shown together with a mutant embryo, which is to the right or below the wildtype. The anterior is on the left and the dorsal side up, except when otherwise noted. A) *dino*, fkd 3 in situ hybridization, shield stage. Optical section through the germ ring, dorsal right [56]. B) *fused somites*, living embryos, 12 somites stage [65]. C) *floating head*, myoD in situ hybridization, the brown staining in the wildtype marks the notochord with ntl antibody, dorsal view [69]. D) *masterblind*, living, swimming larval stage [76]. E) *white tail*, islet 1 antibody, 8 somite stage, dorsal view [72]. F) *swirl*, myoD in situ hybridization, 8 somite stage, anterior up [57]. G) *you*, living, swimming larva [65]. H) *diwanka*, znp-1 antibody, pharyngula [78]. I) *van gogh*, living, swimming larva [79]. J) *leopard, obelix*, adult fin [29]. K) *mercedes*, swimming larva, view on tail fin [56]. L) *no isthmus*, brown: 4D9 (Eng) antibody, blue: Krox 20, 8 somite stage, dorsal view [80]. M, N) *fused somites*, M myoD in situ hybridization, 14 somites, dorsal view, N) skeletal staining, adult [65]. O) *sucker* alcian blue staining of cartilage, swimming larva [81].

In some mutants the pathfinding of nerves across the midline is impaired. The most prominent and longest known representative of this class of genes is *cyclops*.[73] The eyes of mutant embryos are fused anteriorly, and the floorplate, the ventral region of the spinal cord, is lacking. There are several new members of this class of genes including *diwanka* (Fig. 5H) and *chameleon*.[74] It will be interesting to see whether the mutations that delete the midline structures (the ventral portion of the neuroectoderm and head in *Drosophila*) such as *spitz* and others[75] are homologous to the fish midline genes.

The brain morphology is affected in a number of mutants of which only some will be mentioned here. The forebrain, including the olfactory placodes and eyes, are deleted in the mutant *masterblind* (Fig. 5D). The analysis with molecular markers re-

vealed that the region that normally would develop into forebrain, instead develops into more posterior structures, similar to a homeotic transformation.[76] The midbrain–hindbrain boundary is absent in mutants of two genes, *no isthmus and* acerebellar. The *no isthmus* gene (Fig. 5L), which is also required for the formation of the kidney, is homologous to one of the *pax* genes, a family of genes first identified in the mouse by their homology to the *Drosophila* segmentation gene *paired*.[77]

A large number of zebra fish mutant classes do not have parallels in our *Drosophila* mutant collection. They will only be summarized briefly here. Of particular interest regarding their potential for medical research are mutants affecting inner organs. A number of genes affecting blood formation and circulation as well as the heart, structures easily scorable in the first two days of fish embryogenesis, have been identified. Mutants affected in organs developing later, such as liver, pancreas, and kidney, are less well-represented. Differentiation defects or degeneration of the musculature are displayed in embryos mutant for a number of genes. In addition, sensory organs such as eye and ear (Fig. 5) are affected in a number of mutants. A large number of genes are required for the formation of structures derived from the neural crest. The largest class are genes required for pigmentation, that is, pigment cell formation and pigment pattern, and a number of genes affect portions of the jaw (Fig. 5O) or branchial arches, structures specific to vertebrates (Table 3). We also isolated mutants with specific defects in motility of the larva. Mutant larvae fail to respond to touch, show reduced or no motility, and display spastic or circling behavior, as well as defects in the reciprocal inhibition across the midline of muscular contractions. In a small number of mutants, defects in the outgrowth of motoneurons were observed.[78] In *Drosophila*, our screens did not permit the recovery of motility mutants, although immotile larval phenotypes could be recognized in principle by an abnormal distortion of the larval cuticle in the unhatched embryo. Fortuitously, a small group of four genes of *Drosophila* was detected in which larvae were hyperactive, sometimes turning around in the egg case (Table 2).[9–11] These phenotypes in addition showed defective head skeleton differentiation; they have not yet been analyzed in detail.

Conclusions

Genetic research on axis determination in the *Drosophila* embryo has provided perhaps the most complete understanding of pattern formation to date. The elegance and efficiency with which mutations can be isolated and genes can be manipulated in this organism will permit further important discoveries concerning a number of basic processes of cell and developmental biology. However, mechanisms in the fly are, in several instances, likely to be unique to this specialized organism. While the approach of using fly genes to find homologs in vertebrates is a very powerful one, it emphasizes the similarities between these clearly different organisms. To understand vertebrate development, genes specific to vertebrates must be investigated in addition to those common to both flies and fishes. To find and elucidate these differences, the mutants discovered in the zebra fish will provide an important entry point for the investigation of fundamental biological and medical problems with genetic tools.

I would like to thank my collaborators, past and present, for their contributions and for their skill, understanding, thoughtfulness, brilliance, patience, enthusiasm, and support. I also wish to thank Siegfried Roth, Stefan Schulte-Merker, Stefan Meyer, Darren Gilmour, Nancy Hopkins, Peter Overath, Michael Granato, and Judith Kimble for suggestions and help with the manuscript.

Received: April 25, 1996 [A 165 IE]
German version: *Angew. Chem.* **1996**, *108*, 2316–2328

Keywords: *Drosophila* · fruit flies · genes · Nobel lecture

[1] D. J. Beadle, E. Tatum, Nobel lecture, **1958**.
[2] L. Hartwell, *J. Cell Biol.* **1978**, *77*, 627–637.
[3] F. Jacob, J. Monod, *J. Mol. Biol.* **1961**, *3*, 318–356.
[4] D. L. Lindsley, E. H. Grell, *Genetic variations of Drosophila melanogaster*, Carnegie Inst. Wash., Publ. 627, Washington, **1968**.
[5] T. R. F. Wright, *Adv. Genet.* **1970**, *15*, 262–395.
[6] S. Brenner, *Genetics* **1974**, *77*, 71–94.
[7] E. B. Lewis, *Nature* **1978**, *276*, 565–570.
[8] C. Nüsslein-Volhard, E. Wieschaus, *Nature* **1980**, *287*, 795–801.
[9] G. Jürgens, E. Wieschaus, C. Nüsslein-Volhard, H. Kluding, *Wilhelm Roux's Arch. Dev. Biol.* **1984**, *193*, 283–295.
[10] C. Nüsslein-Volhard, E. Wieschaus, H. Kluding, *Wilhelm Roux's Arch. Dev. Biol.* **1984**, *193*, 267–282.
[11] E. Wieschaus, C. Nüsslein-Volhard, G. Jürgens, *Wilhelm Roux's Arch. Dev. Biol.* **1984**, *193*, 296–307.
[12] K. V. Anderson, C. Nüsslein-Volhard, *Nature* **1984**, *311*, 223–227.
[13] M. Gans, C. Audit, M. Masson, *Genetics* **1975**, *81*, 683–704.
[14] C. Nüsslein-Volhard, H. G. Frohnhöfer, R. Lehmann, *Science* **1987**, *238*, 1675–1681.
[15] C. Nüsslein-Volhard, G. Jürgens, R. Lehman, K. Anderson, unpublished results.
[16] T. Schüpbach, E. Wieschaus, *Genetics* **1989**, *121*, 101–117.
[17] a) R. Chasan, K. V. Anderson in ref. [17b], pp. 387–424; b) *The Development of Drosophila melanogaster, Vol. 1* (Eds.: M. Bate, A. Martinez-Arias), CSH Laboratory Press, New York, **1993**.
[18] M. J. Pankratz, H. Jäckle in ref. [17b], pp. 467–516.
[19] D. St. Johnston, C. Nüsslein-Volhard, *Cell* **1992**, *68*, 201–219.
[20] H. Spemann, Nobel lecture **1933**.
[21] B. L. M. Hogan, M. Blessing, G. E. Winnier, N. Suzuki, M. C. Jones, *Development (Cambridge, UK)* (Suppl.) **1994**, 53–60.
[22] J. R. Manak, M. P. Scott, *Development (Cambridge, UK)* (Suppl.) **1994**, 61–77.
[23] S. L. Mansour, K. R. Thomas, M. R. Capecchi, *Nature* **1988**, *336*, 348–352.
[24] R. Nusse, H. E. Varmus, *Cell* **1992**, *69*, 1073–1087.
[25] C. B. Kimmel, *Trends Genet.* **1989**, *5*, 283–288.
[26] M. C. Mullins, M. Hammerschmidt, P. Haffter, C. Nüsslein-Volhard, *Curr. Biol.* **1994**, *4*, 189–202.
[27] L. Solnica-Krezel, A. F. Schier, W. Driever, *Genetics* **1994**, *136*, 1401–1420.
[28] G. Streisinger, C. Walker, N. Dower, D. Knauber, F. Singer, *Nature* **1981**, *291*, 293–296.
[29] P. Haffter, M. Granato, M. Brand, M. C. Mullins, M. Hammerschmidt, D. A. Kane, J. Odenthal, F. J. M. van Eeden, Y.-J. Jiang, C.-P. Heisenberg, R. N. Kelsh, M. Furutani-Seiki, E. D. Vogelsang, U. Schach, C. Fabian, C. Nüsslein-Volhard, *Development (Cambridge, UK)* **1996**, *23*, 1–36.
[30] T. H. Morgan, Nobel lecture **1933**.
[31] A. C. Spradling, G. M. Rubin, *Science* **1982**, *218*, 341–347.
[32] K. Howard, P. Ingham, C. Rushlow, *Genes & Dev.* **1988**, *2*, 1037–1046.
[33] S. Small, R. Kraut, T. Hoey, R. Warrior, M. Levine, *Genes Dev.* **1991**, *5*, 827–839.
[34] A. Martinez-Arias in ref. [17b], pp. 517–608.
[35] W. Driever in ref. [17b], pp. 301–324.
[36] F. Sprenger, C. Nüsslein-Volhard in ref. [17b], pp. 365–386.
[37] D. St. Johnston in ref. [17b], pp. 325–363.
[38] C. Nüsslein-Volhard, *Development (Cambridge, UK)* (Suppl.) **1991**, 1–10.
[39] K. Arora, C. Nüsslein-Volhard, *Development (Cambridge, UK)* **1992**, *114*, 1003–1024.
[40] E. L. Ferguson, K. V. Anderson, *Cell* **1992**, *71*, 451–461.
[41] W. Driever, C. Nüsslein-Volhard, *Cell* **1988a**, *54*, 83–93.
[42] W. Driever, C. Nüsslein-Volhard, *Cell* **1988b**, *54*, 95–104.

[43] G. Struhl, K. Struhl, P. M. Macdonald, *Cell* **1989**, *57*, 1259–1273.
[44] D. Stein, S. Roth, E. Vogelsang, C. Nüsslein-Volhard, *Cell* **1991**, *65*, 725–735.
[45] D. Morisato, K. V. Anderson, *Cell* **1994**, *76*, 677–688.
[46] S. Roth, D. Stein, C. Nüsslein-Volhard, *Cell* **1989**, *59*, 1189–1202.
[47] C. A. Rushlow, K. Han, J. L. Manley, M. Levine, *Cell* **1989**, *59*, 1165–1177.
[48] P. W. Ingham, A. Martinez-Arias, *Cell* **1992**, *68*, 221–235.
[49] D. Van Vactor, H. Sink, D. Fambrough, R. Tsoo, C. S. Goodman, *Cell* **1993**, *73*, 1137–1153.
[50] H. J. Bellen, C. J. O'Kane, C. Wilson, U. Grossniklaus, R. K. Pearson, W. J. Gehring, *Genes & Dev.* **1989**, *3*, 1288–1300.
[51] Y. N. Jan, L. Y. Jan, *Trends Neurosci.* **1990**, *13*, 493–498.
[52] S. J. Gaunt, P. T. Sharpe, D. Duboule, *Development (Cambridge, UK)* (Suppl.) **1988**, 169–179.
[53] S. Krauss, J.-P. Concordet, P. W. Ingham, *Cell* **1993**, *75*, 1431–1444.
[54] R. W. Padgett, R. D. St. Johnston, W. M. Gelbart, *Nature* **1987**, *325*, 81–84.
[55] C. B. Kimmel, W. W. Ballard, S. R. Kimmel, B. Ullmann, T. Schilling, *Dev. Dyn.* **1995**, *203*, 253–310.
[56] M. Hammerschmidt, F. Pelegri, D. A. Kane, M. C. Mullins, G. Beuchle, M. Brand, M. Furutani-Seiki, M. Granato, P. Haffter, C.-P. Heisenberg, Y.-J. Jiang, R. N. Kelsh, J. Odenthal, F. J. M. van Eeden, R. M. Warga, C. Nüsslein-Volhard, *Development (Cambridge, UK)* **1996**, *123*, 129–142.
[57] M. C. Mullins, M. Hammerschmidt, D. A. Kane, J. Odenthal, M. Brand, M. Furutani-Seiki, M. Granato, P. Haffter, C.-P. Heisenberg, Y.-J. Jiang, R. N. Kelsh, F. J. M. van Eeden, C. Nüsslein-Volhard, *Development (Cambridge, UK)* **1996**, *123*, 81–93.
[58] L. Dale, G. Howes, J. C. Smith, *Development (Cambridge, UK)* **1992**, *115*, 573–585.
[59] J. S. Joly, C. Joly, S. Schulte-Merker, H. Boulekbache, H. Condamine, *Development (Cambridge, UK)* **1993**, *119*, 1261–1275.
[60] C. M. Jones, K. M. Lyons, P. M. Lapan, C. V. E. Wright, B. L. M. Hogan, *Development (Cambridge, UK)* **1992**, *115*, 639–647.
[61] Y. Sasai, B. Lu, H. Steinbeisser, D. Geissert, L. K. Gont, E. M. De Robertis, *Cell* **1994**, *79*, 779–790.
[62] D. Arendt, K. Nübler-Jung, *Nature* **1994**, *371*, 26.
[63] E. Geoffroy St.-Hilaire, *Mem. Mus. Hist. Nat.* **1822**, *9*, 89–119.
[64] S. Holley, P. Jackson, Y. Sasai, B. Lu, E. M. De Robertis, F. Hoffmann, E. Ferguson, *Nature* **1995**, *376*, 249–253.
[65] F. J. M. van Eeden, M. Granato, U. Schach, M. Brand, M. Furutani-Seiki, P. Haffter, M. Hammerschmidt, C.-P. Heisenberg, Y.-J. Jiang, D. A. Kane, R. N. Kelsh, M. C. Mullins, J. Odenthal, R. M. Warga, M. L. Allende, E. S. Weinberg, C. Nüsslein-Volhard, *Development (Cambridge, UK)* **1996**, *123*, 153–164.
[66] M. E. Halpern, R. K. Ho, C. Walker, C. B. Kimmel, *Cell* **1993**, *75*, 99–111.
[67] S. Schulte-Merker, F. J. M. van Eeden, M. E. Halpern, C. B. Kimmel, C. Nüsslein-Volhard, *Development (Cambridge, UK)* **1994**, *120*, 1009–1015.
[68] A. Kispert, B. G. Herrmann, M. Leptin, R. Reuter, *Genes Dev.* **1994**, *8*, 2137–2150.
[69] J. Odenthal, P. Haffter, E. Vogelsang, M. Brand, F. J. M. van Eeden, M. Furutani-Seiki, M. Granato, M. Hammerschmidt, C.-P. Heisenberg, Y.-J. Jiang, D. A. Kane, R. N. Kelsh, M. C. Mullins, R. M. Warga, M. L. Allende, E. S. Weinberg, C. Nüsslein-Volhard, *Development (Cambridge, UK)* **1996**, *123*, 103–115.
[70] W. S. Talbot, B. Trevarrow, M. E. Halpern, A. E. Melby, G. Farr, J. H. Postlethwait, T. Jowett, C. B. Kimmel, D. Kimelman, *Nature* **1995**, *378*, 150–157.
[71] C. Bierkamp, J. A. Campos-Ortega, *Mech. Dev.* **1993**, *43*, 87–100.
[72] Y.-J. Jiang, M. Brand, C.-P. Heisenberg, D. Beuchle, M. Furutani-Seiki, R. N. Kelsh, R. M. Warga, M. Granato, P. Haffter, M. Hammerschmidt, D. A. Kane, M. C. Mullins, J. Odenthal, F. J. M. van Eeden, C. Nüsslein-Volhard, *Development (Cambridge, UK)* **1996**, *123*, 205–216.
[73] K. Hatta, C. B. Kimmel, R. K. Ho, C. Walker, *Nature* **1991**, *350*, 339–341.
[74] M. Brand, C.-P. Heisenberg, R. M. Warga, F. Pelegri, R. O. Karlstrom, D. Beuchle, A. Picker, Y.-J. Jiang, M. Furutani-Seiki, F. J. M. van Eeden, M. Granato, P. Haffter, M. Hammerschmidt, D. A. Kane, R. N. Kelsh, M. C. Mullins, J. Odenthal, C. Nüsslein-Volhard, *Development (Cambridge, UK)* **1996**, *123*, 129–142.
[75] U. Mayer, C. Nüsslein-Volhard, *Genes Dev.* **1988**, *2*, 1496–511.
[76] C.-P. Heisenberg, M. Brand, Y.-J. Jiang, R. M. Warga, D. Beuchle, F. J. M. van Eeden, M. Furutani-Seiki, M. Granato, P. Haffter, M. Hammerschmidt, D. A. Kane, R. N. Kelsh, M. C. Mullins, J. Odenthal, C. Nüsslein-Volhard, *Development (Cambridge, UK)* **1996**, *123*, 191–203.
[77] U. Deutsch, G. R. Dressler, P. Gruss, *Cell* **1988**, *53*, 617–625.
[78] M. Granato, F. J. M. van Eeden, U. Schach, T. Trowe, M. Brand, M. Furutani-Seiki, P. Haffter, M. Hammerschmidt, C.-P Heisenberg, Y.-J. Jiang, D. A. Kane, R. N. Kelsh, M. C. Mullins, J. Odenthal, C. Nüsslein-Volhard, *Development (Cambridge, UK)* **1996**, *123*, 399–403.
[79] T. T. Whitfield, M. Granato, F. J. M. van Eeden, U. Schach, M. Brand, M. Furutani-Seiki, P. Haffter, M. Hammerschmidt, C.-P. Heisenberg, Y.-J. Jiang, D. A. Kane, R. N. Kelsh, M. C. Mullins, J. Odenthal, C. Nüsslein-Volhard, *Development (Cambridge, UK)* **1996**, *123*, 241–254.
[80] M. Brand, C.-P. Heisenberg, Y.-J. Jiang, D. Beuchle, M. Furutani-Seiki, M. Granato, P. Haffter, M. Hammerschmidt, D. A. Kane, R. N. Kelsh, M. C. Mullins, J. Odenthal, F. J. M. van Eeden, C. Nüsslein-Volhard, *Development (Cambridge, UK)* **1996**, *123*, 179–190.
[81] T. Piotrowski, T. F. Schilling, M. Brand, Y.-J. Jiang, C.-P. Heisenberg, D. Beuchle, H. Grandel, F. J. M. van Eeden, M. Furutani-Seiki, M. Granato, P. Haffter, M. Hammerschmidt, D. A. Kane, R. N. Kelsh, M. C. Mullins, J. Odenthal, R. M. Warga, C. Nüsslein-Volhard, *Development (Cambridge, UK)* **1996**, *123*, 345–356.

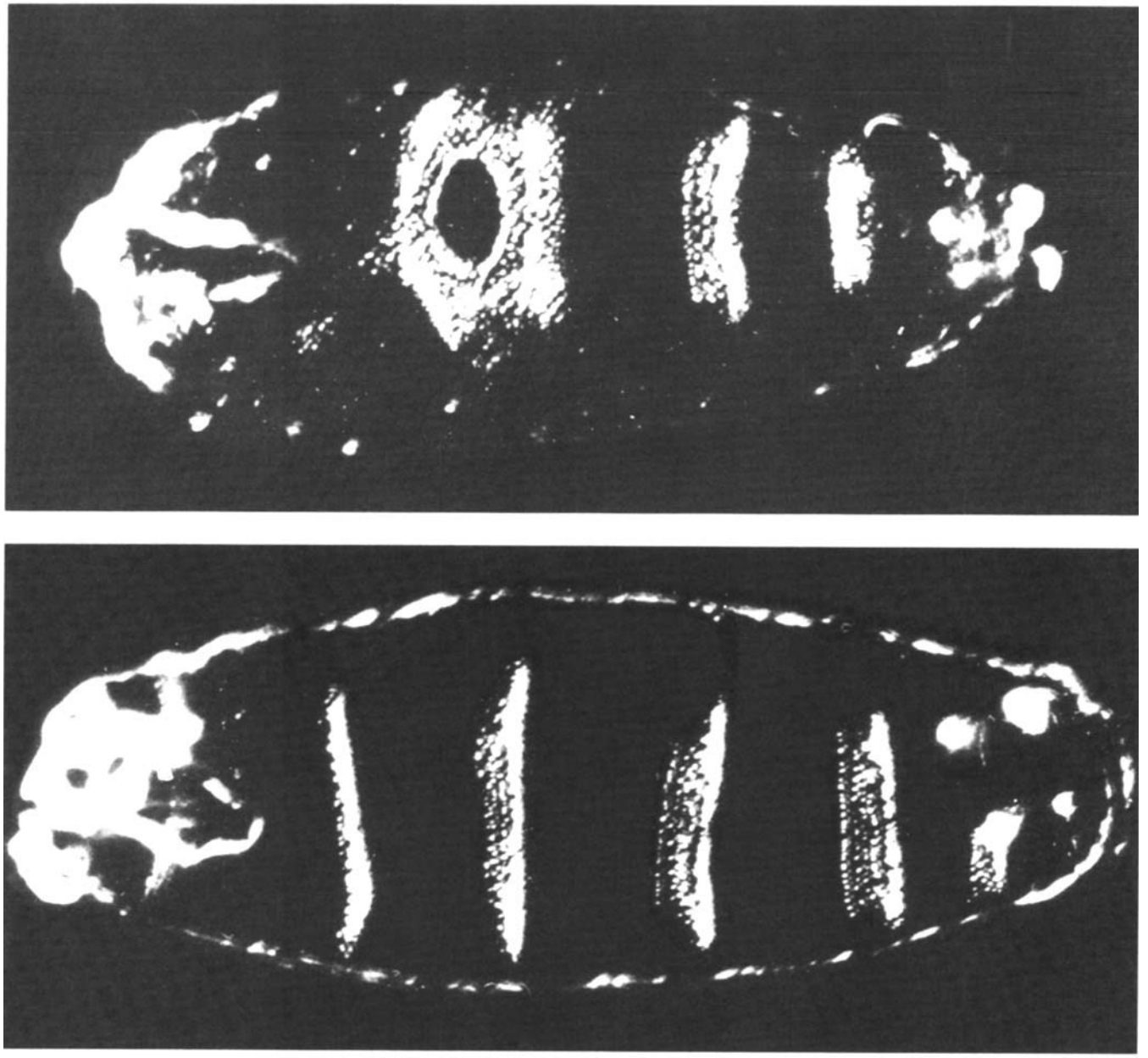

The size and spacing of the pattern deletions in mutant embryos at the end of development were used to group segmentation genes into three classes–gap, pair-rule, and segment polarity genes. One mutant embryo is shown for each class.

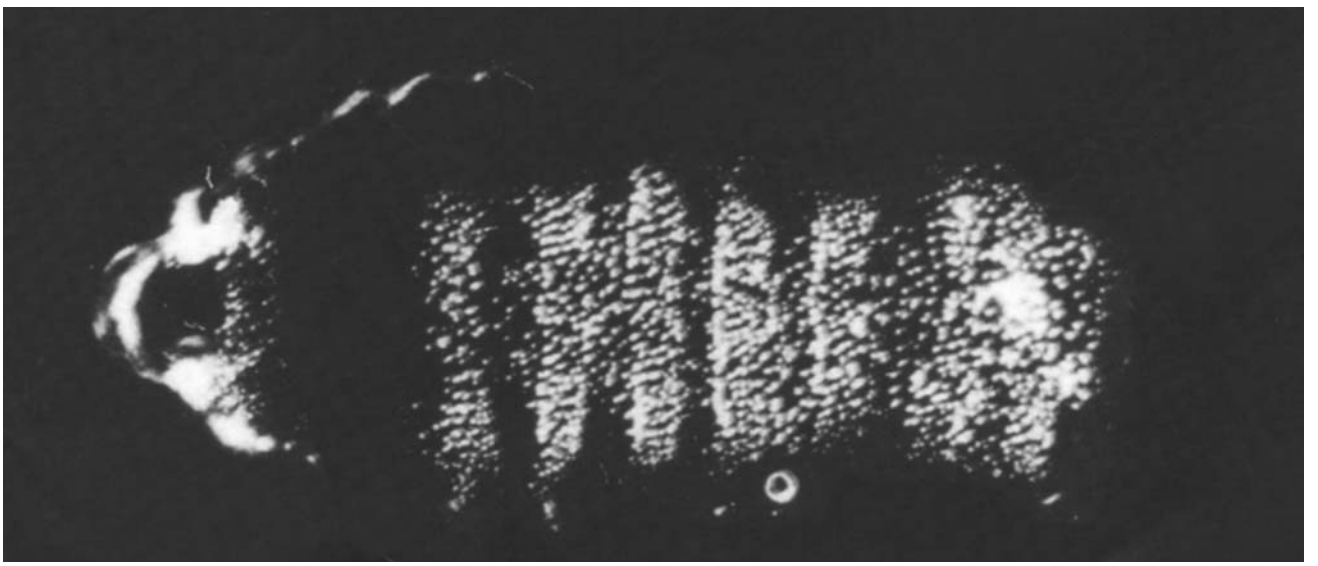

From Molecular Patterns to Morphogenesis—The Lessons from Studies on the Fruit Fly *Drosophila* (Nobel Lecture)**

Eric Wieschaus*

During development, cells in an embryo face two major tasks. First, they must be programmed to form specific parts of the body, and second, they must realize those fates by altering their shape, position, and patterns of gene expression. Both the determination of cell fate and the corresponding alterations in form occur progressively during development. The organism that results from this process contains a wide variety of different cell types and functions, arranged in a complex spatial pattern. In the fruit fly *Drosophila* this final pattern is achieved about 20 hours after fertilization, when the embryo has formed a larva of 40000 cells. The most obvious external feature of this larva is a segmentally repeated pattern of hairs and denticles secreted by the underlying epidermis. Beneath these hypodermal cells is a complex array of muscles also arranged in a segmentally repeated fashion. Internal to this somatic musculature are other mesodermal ddrivatives, as well as equally complex structures and organs of endodermal origin. By following the development of individual cells, it has been possible to trace the precursors for each structure in the differentiated larva back to the earliest cellular stages in the embryo.[1, 2] In *Drosophila* this stage (the blastoderm) consists of an oblong embryo about half a millimeter in length, with about 100 cells along the future anterior–posterior axis and 40 cells along the dorsal–ventral axis. The epidermis is formed by cells on the lateral side of the embryo, the muscles and other mesodermal derivatives are formed from a stripe of cells on the ventral side of the blastoderm, and the endodermal cells arise from two groups of precursors at the anterior and posterior ends of the embryo.

At the blastoderm stage, all of these cells are similar in size and morphology. A few minutes later, at the onset of gastrulation, the mesodermal precursors initiate cell shape changes that carry them into the interior of the embryo.[3] Similar changes in cellular morphology then internalize the endodermal cells. These morphogenetic movements are the first of many examples in which cells in an embryo change their shape in response to the developmental programs that control their fate. The large size of cells at gastrulation and the rapidity of these changes give gastrulation a particularly strong visual impact. The cellular mechanisms underlying these movements, however, utilize many of the same cytoskeletal and adhesive structures found in all cells. The pathway between a particular cell fate decision and the mechanisms controlling cell form have not yet been worked out in detail in any organism.

The past 15 years have seen remarkable advances in our understanding of how the changing pattern of gene activity in the *Drosophila* embryo directs cells to their final fates. These advances have been produced by an unheralded combination of molecular biology and classical genetics. At this point many of the genes that control cell fate have been cloned and their basic cellular roles are understood. In principle, this information provides an ideal starting point to address how cell fate is translated into cell form. This has proven more difficult, largely because the genetic strategies that work so well in elucidating cell fates have met unanticipated obstacles in the elucidation of cell form. Here I would like to review the general picture that has emerged from our studies on *Drosophila* about how genes control cell fate in the *Drosophila* embryo, and examine how the activity of those genes might be related to the constantly changing form of the embryo.

The Heidelberg Mutagenesis Screens

It was to address both cell fate and cell form Christiane Nüsslein-Volhard and I began the mutagenesis experiments honored in Stockholm. In the 1970s when we were finishing our graduate studies in Basel and Tübingen, it was clear that cell development, like all processes in living cells, depended on genes and gene products. Not only was the relationship between DNA, RNA, and protein known, but the analysis of several bacterial operons made it clear that gene activities could be controlled temporally and spatially. Almost everyone believed that such temporal and spatial control might explain the sequence of events giving rise to embryonic pattern. The analysis of such genes seemed formidable, however. Molecular cloning was in its infancy and there were no obvious tools for analyzing single genes in higher eukaryotes. What made the matter worse was the enormous diversity of genes and gene products present in an embryo. RNA complexity experiments estimated the number of different RNA species to be between 10000 and 50000.[4] These RNAs were expressed at varying levels and in a changing pattern as the embryo progressed through various stages. How

[*] Prof. E. Wieschaus
Department of Molecular Biology, Princeton University
Princeton, NJ 08544 (USA)
Fax: Int. code +$$(609)$$258-1547

[**] Copyright' The Nobel Foundation 1996. We thank the Nobel Foundation, Stockholm, for permission to print this lecture.

was one ever to sort out which gene products were essential for particular steps in development? How could the relevant genes and proteins be identified? To Christiane Nüsslein-Volhard and me, the genetic techniques that had been established in *Drosophila* over the preceding sixty years seemed to offer the best approach.

The particular mutagenesis strategy we adopted depended on two facts established about the *Drosophila* genome in the early 1970s. First, mutagenesis experiments involving small, cytologically defined chromosomal regions[5] suggested that, regardless of the total molecular complexity of the *Drosophila* genome, only about 5000 genes present in the DNA were essential for viability under laboratory conditions. This number set an upper limit on the genes essential for embryonic development. Second, a detailed analysis of flies monosomic or trisomic for various genomic regions[6] suggested that although flies are normally diploid, a single copy of most genes was sufficient for viability. This meant that most mutations leading to loss of function would be recessive and could therefore be maintained in heterozygous stocks. These two observations suggested that the requirements for gene activity during *Drosophila* embryogenesis could be surveyed in large-scale (but limited) mutagenesis experiments. If transcription of a gene was essential for embryonic development, homozygous embryos should develop abnormally when that gene was eliminated. If the gene played a specific role in patterning or cell fate, most structures in the affected embryo would be normal and the defects limited to specific regions of the body or specific tissues. Based on these defects, it should be possible to reconstruct the normal function of each gene. In that view, all that was required for a thorough survey of development was to make enough mutant lines and to be able to recognize defects by looking at embryos.

Because flies are diploid and most mutations are recessive, the mutagenesis scheme we settled on involved establishing inbred lines from single individuals carrying mutagenized chromosomes (Fig. 1). In two generations, this inbreeding produces homozygotes whose development can be compared with that of their heterozygous siblings. To obtain mutations in most or all genes in the genome, we had to establish enough mutagenized lines to hit most genes several times. Although Christiane and I carried out preliminary mutagenesis runs ourselves, the final experiments were extremely labor-intensive and were completed with the help of Gerd Jürgens and Hildegard Kluding.[7–10]

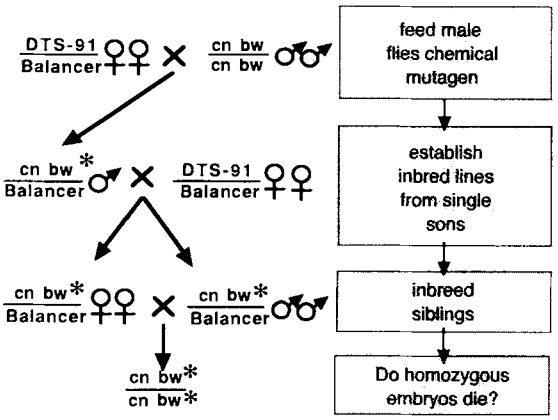

Fig. 1. Mutagenesis scheme used in Heidelberg to identify mutations on the second chromosome causing lethality in homozygous embryos. Similar crossing schemes were used for the third chromosome and the X chromosome.

Over the course of a year, from the fall of 1979 to the summer of 1980, we established 27000 inbred lines. These lines contained an estimated 18000 independently induced mutations, each causing lethality at some point during the life cycle of the animal (Table 1). Only about a quarter of these lethal mutations prevented homozygous embryos from hatching to the larval stage,

Table 1. Results of Heidelberg mutagenesis experiments [a].

Total lines established and tested	26978
Lethal mutations	18136
Mutations causing embryonic lethality	4332
Mutations causing embryonic phenotypes	580
Complementation groups (genes)	139

[a] Numbers given are totals for experiments on the X chromosome and the two major autosomes. The number of mutations in the various classes have been corrected by using the Poisson distribution to account for those lines containing multiple mutations.

and only about 2.5% caused visible alteration of the external morphology of the embryo. These 580 mutations could be assigned by complementation tests to one of 139 different genes. The small final number of genes was an important result, since it meant that each gene could be characterized in some detail. By examining mutant embryos from the various stocks, Christiane

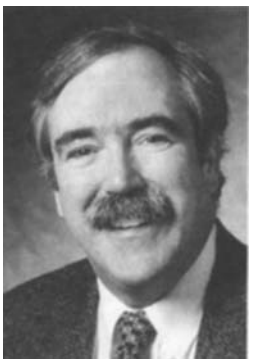

Eric Wieschaus was born in South Bend, IN (USA), in 1947 and grew up in Birmingham, AL. He did his undergraduate work at the University of Notre Dame and obtained his Masters degree and PhD degree from Yale University. A significant fraction of his graduate and postdoctoral research was carried out in Basel and Zurich (Switzerland). In 1978 he moved to the European Molecular Biology Laboratory in Heidelberg (Germany), where in collaboration with Christiane Nüsslein-Volhard he began the mutagenesis experiments that were recognized with the 1995 Nobel Prize for Medicine and Physiology. He is a fellow of the American Academy of Arts and Sciences and a member of the National Academy of Sciences. Since 1981 he has lived in New Jersey, where he is the Squibb Professor of Molecular Biology at Princeton University.

and I were able to establish a general picture of how gene activity in the embryo directs the development of individual cells.

In all species, many of the gene products present in the embryo are supplied by the mother during oogenesis. These include most RNAs and proteins needed for normal cell functions during early stages, as well as certain "inhomogeneities" that are used to define the initial cell axis. In our experiments, homozygous embryos are derived from mothers that have a wild-type allele. Consequently, the Heidelberg mutagenesis screens missed all maternally supplied gene products. The 139 genes identified represent only those genes whose products must be supplied by the embryo's own transcription. We therefore explained the large number of the RNA and protein species in the embryo as largely derived from maternal supplies.

The fact that zygotically required transcripts were relatively rare suggested that they might play specialized roles in development. One possibility was that zygotic transcription allows particular gene products to be expressed in one cell and not in its immediate neighbors, only at particular times. This would contrast with the ubiquitous distribution generally observed for maternally derived transcripts. In this view, the embryo would use transcription to elaborate differences between adjacent cell populations, differences that would ultimately account for the variety of cell fates and cell behaviors observed in the embryo after the blastoderm stage.

The Heidelberg Collection of Mutants: A Survey of Zygotic Gene Activities

One historical coincidence that contributed to the significance of the Heidelberg screens was the almost simultaneous development of molecular techniques that allowed genes to be cloned based on their genetic position. After we had published our experiments, a number of labs studying *Drosophila* began a concerted effort to clone the genes identified by the mutations. This effort has continued over the past ten years and is still going on today. Of the 139 lines that produce phenotypes, 20 were single hits, had relatively nondescript phenotypes, and were never given names or further characterized. Most were eventually lost. Of the remaining 119, an informal survey of the *Drosophila* database indicates that 75 have been cloned and their expression patterns examined in embryos. These molecular analyses along with the phenotypic descriptions begun in Heidelberg have generated an increasingly detailed view of the kind of functions supplied by zygotic transcripts in the *Drosophila* embryo.

In general, the greatest insights into developmental mechanism came when number of different Heidelberg genes could be grouped together because they affected the same developmental process. Sometimes, as in the series of segmentation mutants,[7] peculiarities of the phenotype of individual genes suggested regulatory hierarchies between members of the group (Fig. 2). In other cases (for example *armadillo* and *wingless*[11]), homogeneous phenotypic groups pointed to unanticipated relationships between previously characterized proteins.

One of the most striking features of the Heidelberg collection of mutants was the specificity of the phenotypes. For a given line, certain cell types or regions are affected in the mutant embryo, while other cell types and regions are normal. This

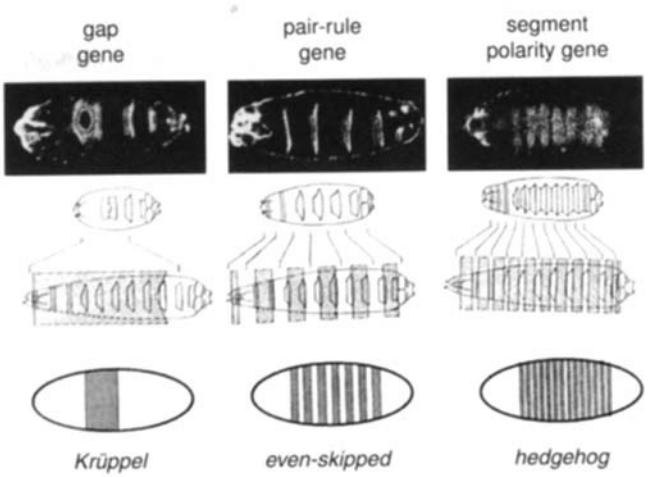

Fig. 2. Phenotypes of mutations affecting segmental pattern. The size and spacing of the pattern deletions in mutant embryos at the end of development allows extrapolation back to requirements for gene activities at the blastoderm stage. Segmentation genes can be grouped into three classes: mutations in gap genes show large contiguous deletions in the pattern; mutations in pair-rule genes show pattern deletions spaced at double segment intervals; and mutations in segment polarity genes cause pattern deletions in each segment. One example is shown for each class.

phenotypic specificity was reinforced by molecular data once the various Heidelberg genes had been cloned. Most genes show highly regulated patterns of expression such that transcripts accumulate only in those regions and cell types where they are needed. Defects associated with a given mutant stock are generally different from those of other stocks, and expression patterns show a corresponding diversity. The two observations together suggest that most of the genes play unique roles at morphologically distinct steps in development.

Mutants usually affect areas of the embryo, rather than specific cell types. These areas generally do not correspond to obvious subdivisions and could not have been predicted based on morphological considerations alone. Obvious examples of these regional specificities are the genes affecting segmentation: one could not have predicted the domains of gap gene expression, the existence of pair-rule phenotypes, or the precise structures duplicated in segment polarity mutants. Because the region affected by a particular gene ultimately gives rise to a variety of different cell types, the genes seem to define positions or spatial coordinates rather than tissues or organs.

Genes often are used several times during embryonic development. Most segmentation genes for example, are used later in the nervous system and in other tissues as well (for example the gene *Krüppel* in the Malpighian tubules[12]). This pleiotropy is not limited to genes controlling segmental pattern. Many of the genes controlling dorsal–ventral patterning at the blastoderm stage are used again at specific times in development. Even a gene like *twist*, which ultimately seems specific for muscle differentiation, shows a more complicated, broader expression pattern at the blastoderm stage, suggesting that it plays a role in determining ventral fates in general, rather than specific mesodermal identities. These features make it difficult to relate early expression patterns of particular genes to final qualities of differentiation. Again, it is consistent with a role for the genes in programming regions or fates, rather than defining differentiated cell types per se.

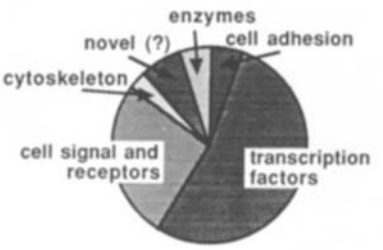

Fig. 3. Cellular functions of Heidelberg mutations. Based on the sequence of 75 cloned genes, most of the loci identified in Heidelberg encode transcription factors, or cell signals and receptors.

More that half of the 75 cloned genes encode transcription factors, judging from the presence of DNA binding motifs and/or their homology to known vertebrate or yeast transcription factors (Fig. 3). Their DNA binding properties might allow them to control expression of many different target genes. If used at various stages of development and in different combination with other genes, they might therefore affect a variety of different developmental pathways. Most of the cloned genes that are not transcription factors are cell surface signals or receptors. Some of these signaling factors may have immediate consequences for cell behavior (see below), but most of this signaling ultimately feeds back on positional identities not directly related to final differentiated states.

Genes Missed in the Heidelberg Screens: The Control of Cell Form

During the period when patterns of cell fate are being established, the embryo undergoes dramatic morphological changes. The final stages of cleavage (that is, nuclear division) occur when the embryo is still a syncytium. Once the number of nuclei have reached 6000, they stop dividing and cell membranes are pulled down between individual nuclei. This process of cellularization requires a major reorganization of the embryonic cytoskeleton and takes about an hour. When it is completed, the embryo consists of 6000 individual cells that are still morphologically identical. They are, however, molecularly different, due to expression of many of the 139 genes and transcription factors described in the previous section. At the onset of gastrulation, these differences are translated into changes of cell shape that result in the invagination of mesoderm or endoderm during gastrulation. Overall, the 90 minutes from completion of cleavage through early gastrulation represent the major period of morphological transformation that occurs in the *Drosophila* embryo.

What is the relationship between these morphological changes and the genes that were identified in the Heidelberg screens? When embryos from each of the 139 mutant stocks were examined, we found that even mutants with phenotypes identified very early in development showed no morphological defects before the onset of gastulation. This suggested that the products of the Heidelberg genes were irrelevant for the early morphological events of cleavage and cellularization, and were only required when cells in individual regions of the embryos began their regionally specific cell shape changes. One way to test this was to block all new RNA synthesis by injecting early embryos with drugs that inhibit RNA polymerase. To our consternation, work by Arking and Parente[13] as well as by Edgar et al.[14] indicated that such treatment causes embryos to become abnormal at the onset of cellularization, an hour before the earliest defects produced by any of the Heidelberg mutants. These experiments provided the first suggestion that the Heidelberg screens may have missed early acting, morphologically important genes.

To identify such genes, we developed a system of translocation crosses to generate embryos deficient for defined chromosomal regions.[15, 16] By using this system, we were able to work our way through the entire genome in a small number of crosses, examining potential mutants at early stages to detect relatively subtle deviations in morphology. These experiments identified seven regions (or genes) that together account for the defects observed in drug-treated embryos. These genes were identified because of their effects on early morphology rather than on viability or overall pattern at the end of embryonic development. They therefore represent a different sampling of the transcriptional requirements than the Heidelberg loci. Three of these seven genes have now been cloned.[17–19] Unlike the Heidelberg mutants, they do not encode transcription factors or components of a cell signaling system. Instead all three are cytoplasmic proteins associated with the cytoskeleton.[19, 20]

Genes affecting morphology during gastrulation also appear to have been missed in the Heidelberg screens.[3] For example, the two Heidelberg genes absolutely required for mesodermal programming are *twist* and *snail*. Both have been cloned and have been shown to encode transcription factors.[21, 22] Immediately before gastrulation, these genes are expressed in the nuclei of mesodermal precursors on the ventral side of the blastoderm. When either gene is mutated, no cells are programmed to mesodermal fates and no ventral furrow forms. Thus, *twist* and *snail* not only direct blastoderm cells to a mesodermal cell fate, they have an immediate read-out in terms of mesodermal cell behavior. Since they are transciption factors, they must do this by controlling the expression of other genes.

What are these downstream target genes? If they produced phenotypes visible in the final cuticle, such genes would have been detected in the Heidelberg screens. One candidate for such a target is *folded gastrulation* (*fog*). In *fog* mutant embryos, the cell shape changes of the ventral furrow are delayed and uncoordinated. Wild-type cells in the ventral furrow express *fog* immediately before changing their shape.[23] When ectopically expressed outside the ventral furrow primordium, *fog* is capable of eliciting those same initial cell shape changes, even in cells that lack *twist* or *snail* or any other factors normally affecting mesodermal fate.[24] All this makes *folded gastrulation* an excellent downstream target for *twist* and *snail*, one whose expression might account for the cell shape changes associated with mesodermal programming.

fog is the only Heidelberg gene (other than *twist* and *snail*) that affects ventral furrow formation. Because *fog* embryos make slow uncoordinated invaginations, whereas *twist* or *snail* embryos make no ventral furrow at all, *fog* cannot be the only target of *twist* and *snail*. Other genes not detected in Heidelberg must account for the difference between the *twist*, *snail*, and *fog* phenotypes, and for the delayed mesodermal invagination that still occurs in *fog* mutants. These target genes may not have been detected in Heidelberg because they may not be essential for mesoderm invagination, as long as the embryo has a wild-type allele of *fog*. They might, however, have been detected if mutant

embryos had been scored directly for morphological defects during gastrulation itself. Given the large number of stocks examined, this was not possible in the Heidelberg mutagenesis experiments. On the other hand, the relevant chromosomal regions might be identified by using translocation crosses, since only a small number of such crosses are needed to examine the effects of most chromosomal regions. Ongoing experiments of this kind in my lab suggest that there are regions that affect ventral furrow formation in ways that cannot be explained by any Heidelberg genes. Most of these morphological effects appear to be transient and similar to the case in *fog* mutant embryos; embryos that are deleted for these genes eventually internalize their mesoderm. It is therefore possible that point mutations in the genes responsible for these early morphological effects may not cause lethality or easily visible effects on final morphology.

The Relationship between Cell Fate and Cell Form

The efficiency with which mutagenesis screens identify mutations affecting cell fate but not cell form may point to a difference in the way the two processes are controlled. The existence of mutations affecting cell fate suggests that patterning functions are not redundant; each gene is absolutely essential for normal development. If only single, nonredundant factors control cell fate, ambiguity in determined states might be avoided. In this view, a precise cell-by-cell pattern of gene expression may not be as important as having at least some cells unambiguously programmed to each fate. Once a cell choice has been made, it must be realized in morphological terms. At this point there may be an enormous advantage for redundancy, since multiple pathways might ensure that a particular fate, once chosen, is actually achieved. This redundancy need not be total; elimination of a single target pathway may causes subtle deviations in the process similar in magnitude to the defects observed in the ventral furrows of *fog* embryos. In this view, cell shape changes at gastrulation would be the summed effect of various targets, each of which would be necessary for the characteristic wild-type morphology, but not for the final outcome itself.

Developmental biologists are a diverse lot; some are more interested cell fate and patterning, others in morphogenesis. Those interested in pattern might focus on genes like *twist* and *snail*, since their expression at the blastoderm stage determines the ventral cells to become mesoderm (Fig. 4 left). In this view, genes like *fog* would be just one of many downstream regulators. On the other hand, the cell shape changes that occur in mesodermal cells during ventral furrow formation are not restricted to gastrulation. Moreover, genes like *fog* are expressed in other stages and other primordia, not under control of *twist* and *snail*. Thus from the standpoint of the cellular morphology, genes like *fog* become the central players (Fig. 4 right). *fog*-Dependent cell shape changes may be activated in a variety of different developmental programs by a variety of different cell fate genes, but its role in cellular behavior would be conserved.

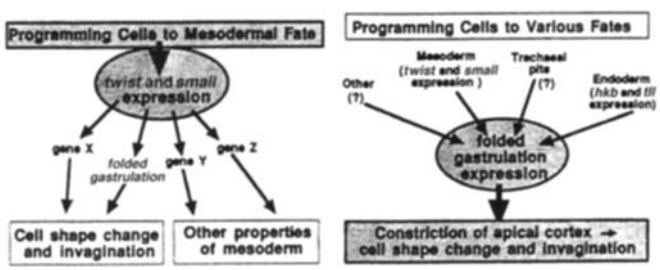

Fig. 4. Contrasting views of development. The left-hand side emphasizes programming of cells to specific cell fates; the right-hand side emphasizes the cellular mechanisms that produce changes in morphology.

Conclusions: The Powers and Limitations of the Genetic Approach

Mutagenesis experiments are a mixture of random and biased elements. Perhaps their strongest advantage is that we scientists have very little control over the kind of mutations produced. Mutations occur randomly throughout the genome, eliminating genes whether or not they have anything to do with the process of interest. This means that the production of mutants is usually not affected by biases about the kinds of molecules involved or the underlying mechanisms. Success depends on the experimenter's ability to sort through the mutations obtained and to recognize and interpret phenotypes of interest. It is this second step that introduces the major bias, in that it depends on the scientist's response to mutant phenotypes and on his or her ability to understand the nature of the defect and the proper context in which it can be described. Because we used a dual-observation microscope, Christiane and I were often simultaneously confronted with particular phenotype for the first time. It was not always easy to agree about defects or to decide why a particular stock was interesting. Because they were often the product of intense discussions, our final descriptions benefitted from a dual input. However, Christiane and I were both primarily interested in spatial patterns and gross morphological aspects of embryogenesis. Mutations affecting finer aspects of cell differentiation were certainly produced in Heidelberg, but even if they had caused embryonic lethality, they would have been discarded.

In addition to the bias introduced by experimenters, genetic screens are inherently biased by the organism. *Drosophila* embryos develop rapidly and most gene products are supplied by maternal rather than zygotic transcriptions. Development is highly regulative and cell signaling pathways ensure that a constant final morphology is achieved even when starting situations are different. One obvious limitation of the Heidelberg screen is that even though we were interested in broad aspects of morphology and early changes in cell shape, we scored only final differentiation, and there only cuticle pattern. Because the hypodermal cells that secrete cuticle represent such a large fraction of the blastoderm, we assumed that it would be not be possible to cause morphological changes at gastrulation without altering final morphology. Our later experiments suggest that this may not be true. Thus although we were not necessarily biased between mutations affecting cell fate and cell form, most genes actually detected altered fate, perhaps because effects on form in *Drosophila* are often more transient.

It is possible that different results would have been obtained had we chosen a different organism. One is curious whether

nematodes, which show an extraordinarily constant lineages, would be more subject to subtle perturbations in the movement and positioning of cells than *Drosophila*. Development in vertebrates, on the other hand, has been shown to be much more variable in terms of cell lineage and much more regulative in achieving constant final morphologies. In that respect, the ongoing screens for mutants in zebra fish and mice may produce a spectrum of genes more similar to that of *Drosophila*.

Of course, one of the important lessons from the Heidelberg experiments is that such speculations generally have little predictive value. The phenotypes and genes actually obtained by a particular mutagenesis protocol will only be known once the experiments are done. The same lesson applies to the ongoing analysis of *Drosophila* development. In spite of enormous advances made in understanding cell fates, we do not yet know how those programs produce constant morphology and structure. The morphologies assumed by *Drosophila* cells are often very similar to those in vertebrates. Moreover, the molecules and therefore the underlying mechanisms have probably been conserved over the course of evolution. By bridging the connection between cell fate and cell form in *Drosophila*, we may therefore also reinforce the bridges that connect developmental studies in all different organisms.

Received: March 4, 1996 [A 154 IE]
German version: *Angew. Chem.* **1996**, *108*, 2330–2337

Keywords: *Drosophila* · embryonic development · fruit flies · Noble lecture

[1] "Histogenesis, organogenes and differentiation in the embryo of *Drosophila melanogaster* (Meigen)": D. F. Poulson in *Biology of Drosophila* (Ed.: M. Demerec), Wiley, New York, **1950**, pp. 168–274.

[2] J. A. Campos-Ortega, V. Hartenstein, *The Embryonic Development of Drosophila melanogaster*, Springer, Berlin, **1985**.

[3] Review: "*Drosophila* Gastrulation: from Pattern Formation to Morphogenesis": M. Leptin, *Annu. Rev. Cell Dev Biol.* **1995**, *11*, 189–212.

[4] E. Davidson, *Gene Activity in Early Development*, Academic Press, Orlando, FL **1986**.

[5] "The anatomy and function of a segment of the X-chromosome of *Drosophila melanogaster*": B. H., Judd, M. W. Shen, T. C. Kaufman, *Genetics* **1972**, *71*, 139–156.

[6] "Segmental aneuploidy and the genetic gross structure of the *Drosophila* genome": D. L. Lindsley, L. Sandler, B. S. Baker, A. T. C. Carpenter, R. E. Denell, J. C. Hall, P. C. Jacobs, G. L. G. Miklos, B. K. Davis, R. C. Gethmann, R. W. Hardy, A. Hessler, S. M. Miller, H. Nozawa, D. M. Parry, M. Gould-Somero, *Genetics* **1972**, *71*, 157–184.

[7] "Mutations affecting segment number and polarity in *Drosophila*": C. Nüsslein-Volhard, E. Wieschaus, *Nature* **1980**, *287*, 795–801.

[8] "Mutations affecting the pattern of the larval cuticle in *Drosophila melanogaster*. I. Zygotic loci on the second chromosome": C. Nüsslein-Volhard, E. Wieschaus, H. Kluding, *Roux's Arch. Dev. Biol.* **1984**, *193*, 267–282.

[9] "Mutations affecting the pattern of the larval cuticle in *Drosophila melanogaster*. II. Zygotic loci on the third chromosome": G. Jürgens, H. Kluding, C. Nüsslein-Volhard, E. Wieschaus, *Roux's Arch. Dev. Biol.* **1984**, *193*, 283–295.

[10] "Mutations affecting the pattern of the larval cuticle in *Drosophila melanogaster*. III. Zygotic loci on the X chromosome and the fourth chromosome": E. Wieschaus, C. Nüsslein-Volhard, G. Jürgens, *Roux's Arch. Dev. Biol.* **1984**, *193*, 296–307.

[11] "Spatial expression of the *Drosophila* segment polarity gene *armadillo* is posttranscriptionally regulated by *wingless*": B. Riggleman, P. Schedl, E. Wieschaus, *Cell* **1990**, *63*, 549–560.

[12] "Spatial and temporal patterns of *Krüppel* gene expression in early *Drosophila* embryos": D. Knipple, C. Seifert, U. B. Rosenberg, A. Preiss, H. Jäckle, *Nature* **1985**, *317*, 40–44.

[13] "Effects of RNA inhibitors on the development of *Drosophila* embryos permeabilized by a new technique": R. Arking, A. Parente, *J. Exp. Zool.* **1980**, *212*, 183–194.

[14] "Cell cycle control by the nucleo-cytoplasmic ratio in early *Drosophila* development": B. A. Edgar, C. P. Kiehle, G. Schubiger, *Cell* **1986**, *44*, 365–372.

[15] "Requirements for autosomal gene activity during precellular stages of *Drosophila melanogaster*": P. T. Merrill, D. Sweeton, E. Wieschaus, *Development* **1988**, *104*, 495–509.

[16] "Requirements for X-linked zygotic gene activity during cellularization of early *Drosophila* embryos": E. Wischaus, D. Sweeton, *Development* **1988**, *104*, 483–493.

[17] "The spatial distribution of a blastoderm stage-specific mRNA from the *serendipity* locus of *Drosophila melanogaster*": A. James, A. Vincent, *Devel. Biol.* **1986**, *118*, 474–479.

[18] "The *Drosophila* cellularization gene *nullo* produces a blastoderm-specific transcript whose levels respond to the nucleocytoplasmic ratio": L. S. Rose, E. Wischaus, *Genes Development* **1992**, *6*, 1255–1268.

[19] "*bottleneck* acts as a regulator of the microfilament network governing cellularization of the *Drosophila* embryo": E. D. Schejter, E. Wieschaus, *Cell* **1993**, *75*, 373–385.

[20] "The *nullo* protein is a component of the actin-myosin network that mediates cellularization in *Drosophila melanogaster* embryos": M. A. Postner, E. Wieschaus, *J. Cell Science* **1994**, *107*, 1863–1873.

[21] "The *Drosophila* development gene *snail* encodes a protein with nucleic acid binding fingers": J.-L. Boulay, C. Dennefeld, A. Alberga, *Nature* **1987**, *330*, 395–398.

[22] "Sequence of the *twist* gene and nuclear localization of its protein in endomesodermal cells of early *Drosophila* embryos": B. Thisse, C. Stoetzel, C. Gorostiza-Thisse, F. Perrin-Schmitt, *EMBO J.* **1988**, *7*, 2175–2183.

[23] "A putative cell signal encoded by the *folded gastrulation* gene coordinates cell shape changes during *Drosophila* gastrulation": M. E. Costa, T. Wilson, E. Wieschaus, *Cell* **1994**, *76*, 1075–1089.

[24] "*Folded gastrulation* is upstream of *concertina* in a pathway that mediates apical flattening and constriction": P. Morize, M. Costa, S. Parks, E. Wischaus, unpublished results.

Crystal Packing and Molecular Geometry

J. Jens Wolff*

It is still not possible to deduce the packing of a molecular crystal from the structure of its constituent molecules. Crystal engineering, the often-stressed construction of crystal structures at will, in general remains an unrealized vision. While great strides have definitely been made since the pioneering work of Kitaigorodsky, neither computational methods[1] for the calculation of packing structures, nor experimental studies[2] can analyze this paradigm of molecular recognition in a completely satisfactory manner. This comes as no surprise—crystal packing is determined by a great number of factors, with the van der Waals energy as the dominant term. Even quite small energy differences may drastically alter a packing pattern. Parallels may be drawn to stereoselective synthesis where small differences in energies, which are more than often the sum of different effects, decide the success or failure of a particular reaction. Recurring ordering motifs in the structures of molecular crystals have at least been identified for crystals of aromatic hydrocarbons.[3a] In this class of compounds, the possible intermolecular interactions[3b] are restricted to the van der Waals type, and the molecular shape, since the occurrence of different conformers is limited,[3c] restricts the number of possible packing patterns to a few types (see Fig. 1). Even in this area, surprises are still possible as exemplified by the structural analysis of **1**, which unexpectedly crystallizes in a γ-type rather than a sandwich pattern.[3d]

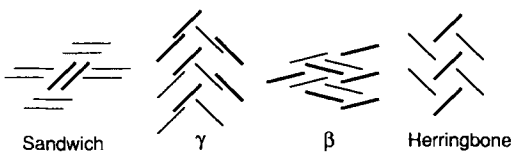

Fig. 1. Frequently occurring packing patterns for aromatic hydrocarbons.

Structures with strongly directional intermolecular interactions like hydrogen bonds have also been investigated frequently.[4] This approach is akin to successful supramolecular chemistry in solution which frequently draws upon hydrogen bonds as the organizing element.[5] The statistical analysis of the contents of the Cambridge Crystallographic Database[6] has made it possible to identify a multitude of further intermolecular interactions in crystals like CH···O and Cl···Cl contacts.[2] However, it may be difficult to decide for a given case to what extent these interactions really determine the observed structure.

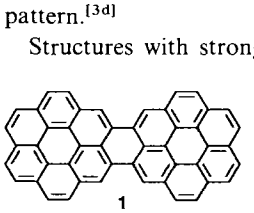

1

Special problems are presented by the phenomenon of polymorphism,[7] which arises when one molecule crystallizes in two or more geometrically different structures that are close in energy. Polymorphs may not even always be obtained reproducibly.[8] Preoccupation with the problem of polymorphism is not necessarily esoteric. For example, the acid blocker ranitidine (**2**), the active constituent of the best-selling drug worldwide in 1992, exists in two polymorphic forms of which only one is bioaccessible. Several lawsuits against the manufacturers of generic drugs, all won by the patent holder, centered around the protectability of the active polymorph, which had been discovered seven years later than the inactive form.[9]

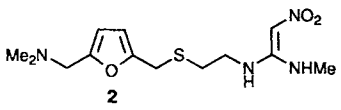

2

Clearly, the mode of molecular packing determines the practical value of a material not only in solid-state organic syntheses[10] but also in all areas of applied research that depend on the solid-state properties of molecular crystals. Many organic pigments occur in different polymorphic forms that have different optical properties, for example quinacridone (**3**), which exists in orange to violet modifications, and copper phthalocyanine.[11] The use of crystalline materials for second-order nonlinear optics[12] requires the NLO-phores at least to crystallize in noncentrosymmetric space groups—not a trivial problem to solve, because about three-quarters of all nonchiral organic compounds adopt centric space groups in the solid state.[13] Likewise, materials with special electric[14] or (ferro-)magnetic[15] properties require well-defined molecular arrangements.

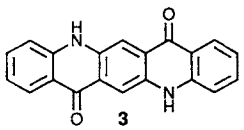

3

Polymorphic forms often occur for molecules with high conformational mobility. Frequently in different polymorphs quite different conformers are observed. At present, this interplay between packing pattern on one hand and molecular conformation on the other is also little understood. Outside the realm of crystallography, it is still common to consider one molecular

[*] Priv.-Doz. Dr. J. J. Wolff
Organisch-chemisches Institut der Universität
Im Neuenheimer Feld 270, D-69120 Heidelberg (Germany)
Fax: Int. code +(6221)544205
e-mail: wolff@donar.oci.uni-heidelberg.de

structure elucidated by diffraction methods as *the* structure of the molecule; in other words, this structure is implicitly looked upon as that of the nonperturbed, isolated molecule in the gas phase. Molecular parameters that do not agree with this perception are thought to arise from "crystal packing forces". Only in rare cases may these forces be approximately quantified. Methods available for studying these crystal fields are: the comparison with data observed or computed for the gas-phase structure, the comparison of crystallographically independent molecules within the same crystal, and the comparison of molecular parameters for different polymorphic crystal forms. Unfortunately, most molecules are either not volatile enough or too complex in structure for sufficient information to be obtained from spectroscopic methods in the gas phase. For many molecules only one crystal form with crystallographically identical molecules is obtained (or studied). Four examples taken from the recent literature (apart from the review articles cited) qualitatively illustrate the state of the art in this area, with its successes as well as its problems: a systematic study of a class of compounds and examples of structures distorted by ionic interactions, of conformational polymorphism, and of structure-dependent photochromism.

For the study of the influence of crystal packing on molecular parameters it is advantageous to use molecules with high polarizabilities and conformational mobilities. Recently, Glaser et al. have tried to employ the azines **5** as probes for the quantification of crystal packing forces.[16] Schiff bases like **4** had already proven valuable in the studies of conformational polymorphism by Bernstein,[7d] who found crystal packing effects on the order of 2 kJ mol^{-1} for the rotamers that occur in the polymorphic forms of **4**. Seventeen azines of acetophenone (**5**) were investigated. The results show that the *gauche* conformation around the N–N bond favored for the gas-phase structure according to ab initio calculations may be altered by packing effects. In some crystals the *trans* arrangement is found. However, the expectation of push–pull effects on the molecular conformation (e.g. for X = MeO and Y = CN) could not be substantiated, since the molecular parameters of symmetrically substituted compounds do not differ appreciably from those with push–pull sub-stitution. Likewise, the crystal packing effects observed could be explained solely on the basis of van der Waals contributions to the packing energy without invoking any polar contributions.

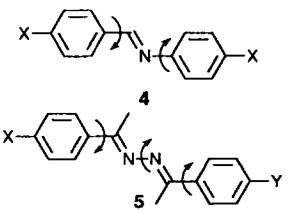

Dähne and Reck[17] succeeded in distorting the equalized C–C bond lengths along the chain of the cyanine **6** in the solid state to a maximum alternation of 0.02 Å, an effect that had not been encountered before with small counterions like tetrafluoroborate. The sterically demanding tetraphenylborate ion requires a good van der Waals contact for optimum packing. As a consequence, the distribution of negative charge in the vicinity of the cyanine cation becomes quite unsymmetrical, which leads to a much greater distortion as would be expected for a corresponding point charge.

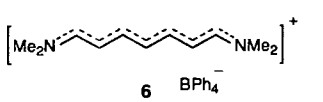

Conformational polymorphism was observed with **7**.[18a] Two different rotamers with respect to the C–N bond are found in two polymorphs which, due to the different ability for conjugation with the π-system, also differ in the pyramidality at the nitrogen atom and in the *ipso* angles of the benzene rings. PM3 calculations indicated that the conformers are very close in energy; the differences in the packing energies between the polymorphs fall into the range of about 4 kJ mol^{-1}. Similar effects on the molecular structure had been found before for **8** for which two C–N rotamers coexist in the same crystal.[18b]

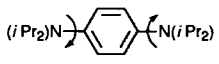

7

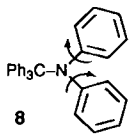

8

Crystals of **9**, a member of a class of compounds known to be photochromic, exist in two polymorphic forms of which only one shows photochromic behavior.[19] The arrangement of **9** in the polymorphs shows distinct differences. The inactivity of the first polymorph was ascribed to the short intermolecular contacts between the molecules, which could lead to the deactivation of the excited state and thus impede the proton transfer. This study also highlights the far-reaching consequences that even extremely subtle changes in molecular shape may have on crystallization: even deuteration of the methylene group of **9** markedly changes the ratio in which the two polymorphs occur.

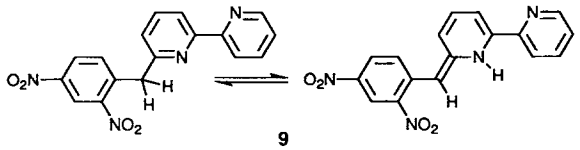

9

Especially this last observation could leave doubts whether an ab initio description of the packing of organic molecular crystals will ever be possible. Certainly, a precise quantificiation of the influence of crystal fields[20] on the molecular conformation will be very useful. On the other hand, the nucleation and the kinetics of growth of molecular crystals[21] will have to be studied intensely, for example by observation of the integration of contaminants into the crystal lattice; optically anomalous crystals[2b] are suitable candidates for studies of this kind. Reducing the problem of crystallization from three to two dimensions, as offered by the investigation of the self-organization of monomolecular layers on surfaces, also promises decisive progress.

German version: *Angew. Chem.* **1996**, *108*, 2339–2341

Keywords: crystal engineering · packing forces · polymorphism · structure predictions

[1] a) A. Kitaigorodsky, *Molecular Crystals and Molecules*, Academic Press, New York, **1973**; b) A. Gavezzotti, *J. Am. Chem. Soc.* **1991**, *113*, 4622; *Acc. Chem. Res.* **1994**, *27*, 309; c) H. R. Karfunkel, R. J. Gdanitz, *J. Comput. Chem.* **1992**, *13*, 1171; d) A. M. Chaka, R. Zaniewski, W. Youngs, C. Tessier, G. Klopman, *Acta Crystallogr. Sect. B* **1996**, *52*, 165. e) For prediction of polymorphs: D. E. Williams, *Acta Crystallogr. Sect. A* **1996**, *52*, 326. f) More recent search algorithms improve the efficiency of the procedures substantially: P. Erk, Ludwigshafen, private communication. Computational methods are of great importance for structure determinations from powder diagrams.

[2] a) G. R. Desiraju, *Angew. Chem.* **1995**, *107*, 2541; *Angew. Chem. Int. Ed. Engl.* **1995**, *34*, 2328. The parallels drawn there between organic synthesis and the synthesis of crystal structures may also be found in: b) B. Kahr, J. M. McBride,

 © VCH Verlagsgesellschaft mbH, D-69451 Weinheim, 1996 0570-0833/96/3519-2196 $ 15.00+.25/0

Angew. Chem. **1992**, *104*, 1; *Angew. Chem. Int. Ed. Engl.* **1992**, *31*, 1. c) For the influence of weak hydrogen bonds on crystal structures, see also: T. Steiner, W. Saenger, *J. Chem. Soc. Chem. Commun.* **1995**, 2087.

[3] a) G. R. Desiraju, A. Gavezzotti, *Acta Crystallogr. Sect. B* **1989**, *45*, 473. The similarities in the packing of aromatic molecules are also demonstrated by the success of increment systems to compute thermodynamic data: K. Nass, D. Lenoir, A. Kettrup, *Angew. Chem.* **1995**, *107*, 1865; *Angew. Chem. Int. Ed. Engl.* **1995**, *34*, 1735. b) For the well-understood interaction (molecular recognition) between aromatic π-systems, see: C. A. Hunter, *Chem. Soc. Rev.* **1994**, *23*, 101; A. W. Schwabacher, Z. Shuhog, W. Davy, *J. Am. Chem. Soc.* **1993**, *115*, 6995; F. Cozzi, F. Ponzini, R. Annunziata, M. Cinquini, J. S. Siegel, *Angew. Chem.* **1995**, *107*, 1092; *Angew. Chem. Int. Ed. Engl.* **1995**, *34*, 1019; R. Laatikainen, J. Ratilainen, R. Sebastian, H. Santa, *J. Am. Chem. Soc.* **1995**, *117*, 11006. c) Even the introduction of one degree of rotational freedom, as in the polyphenyls, leads to crystallographically unpleasant problems like incommensurate phases: J. L. Baudour, *Acta Crystallogr. Sect. B* **1991**, *47*, 935, and references therein; d) R. Goddard, M. W. Haenel, W. C. Herndon, C. Krüger, M. Zander, *J. Am. Chem. Soc.* **1995**, *117*, 30, and references therein.

[4] a) J. Bernstein, R. E. Davis, L. Shimoni, N.-L. Chang, *Angew. Chem.* **1995**, *107*, 1689; *Angew. Chem. Int. Ed. Engl.* **1995**, *34*, 1545; b) A. D. Burrows, C.-W. Chan, M. M. Chowdhry, J. E. McGrady, D. M. P. Mingos, *Chem. Soc. Rev.* **1995**, *24*, 329; C. B. Aakeröy, K. R. Seddon, *ibid.* **1993**, *22*, 397; c) M. C. Etter, S. M. Reutzel, *J. Am. Chem. Soc.* **1991**, *113*, 2586; M. C. Etter, *Acc. Chem. Res.* **1990**, *23*, 120.

[5] H. Schneider, *Angew. Chem.* **1991**, *103*, 1419; *Angew. Chem. Int. Ed. Engl.* **1991**, *30*, 1417; G. M. Whitesides, E. E. Simanek, J. P. Mathias, C. T. Seto, D. N. Chin, M. Mammen, D. M. Gordon, *Acc. Chem. Res.* **1995**, *28*, 37; E. Fan, J. Yang, S. J. Geib, T. C. Stoner, M. D. Hopkins, A. D. Hamilton, *J. Chem. Soc. Chem. Commun.* **1995**, 251.

[6] a) *Structure Correlation* (Eds.: H.-B. Bürgi, J. D. Dunitz), VCH, Weinheim, **1994**; b) F. H. Allen, O. Kennard, D. G. Watson in [6a], pp. 71–110; c) R. Taylor, F. H. Allen, in [6a], pp. 111–161.

[7] a) One of the pioneers in this area was Hantzsch, whose observations on "chromoisomerism", that is, polymorphs with different spectral properties, are still frequently perused (though rarely cited): A. Hantzsch, *Justus Liebigs Ann. Chem.* **1931**, *492*, 65; b) A. Gavezzotti, G. Filippini, *J. Am. Chem. Soc.* **1995**, *117*, 12299; c) J. D. Dunitz, *Pure Appl. Chem.* **1991**, *63*, 177; *Acta Crystallogr. Sect. B*, **1995**, *51*, 619; d) I. Bar, J. Bernstein, *Tetrahedron* **1987**, *43*, 1299; J. Bernstein, in *Accurate Molecular Structures* (Eds.: A. Domenicano, I. Hargittai), Oxford University Press, New York, **1992**, pp. 469–497; J. Bernstein, in *Organic Solid State Chemistry* (Ed.: G. R. Desiraju) Elsevier, Amsterdam, **1987**, pp. 471–518; e) J. H. Matthews, I. C. Paul, D. Y. Curtin, *J. Chem. Soc. Perkin Trans 2* **1991**, 113; D. Y. Curtin, I. C. Paul, *Chem. Rev.* **1981**, *81*, 525; f) Cosolvate: E. Weber, S. Finge, I. Csöregh, *J. Org. Chem.* **1991**, *56*, 7281; *Top. Curr. Chem.* **1987**, *140* and **1988**, *149*. h) For crystallization in general, see: J. Hulliger, *Angew. Chem.* **1994**, *106*, 151; *Angew. Chem. Int. Ed. Engl.* **1994**, *33*, 143.

[8] Several cases of (seemingly) disappearing polymorphs are discussed by: J. D. Dunitz, J. Bernstein, *Acc. Chem. Res.* **1995**, *28*, 193.

[9] C. Leadbeater, *Financial Times*, April 9, 1991.

[10] Cf. references in: J. J. Wolff, *Angew. Chem.* **1995**, *107*, 2407; *Angew. Chem. Int. Ed. Engl.* **1995**, *34*, 2225. For some recent cases, see also: F. Toda, *Acc. Chem. Res.* **1995**, *28*, 480; M. Smrčina, Š. Vyskočil, V. Hanuš, M. Polášek, V. Langer, B. G. M. Chew, D. B. Zax, H. Verrier, K. Harper, T. A. Claxton, P. Kočovský, *J. Am. Chem. Soc.* **1996**, *118*, 487.

[11] W. Herbst, K. Hunger, *Industrielle organische Pigmente*, 2nd vol., VCH, Weinheim, **1995**, p. 468; H. Zollinger, *Color Chemistry*, 2nd ed., VCH, Weinheim, **1991**, p. 240ff. A recent example taken from the area of organic dyes is given by: S. J. Bonafede, M. D. Ward, *J. Am. Chem. Soc.* **1995**, *117*, 7853.

[12] Special issue devoted to NLO: *Chem. Rev.* **1994**, 94, 1–278; *Nonlinear Optical Properties of Organic Molecules and Crystals* (Eds.: D. S. Chemla, J. Zyss, Academic Press, Orlando, FL (USA), **1987**.

[13] For the problem of centrosymmetric space groups, see: A. J. C. Wilson, *Acta Crystallogr. Sect. A* **1990**, *46*, 742; G. R. Desiraju, *Crystal Engineering—The Design of Organic Solids*, Materials Science Monographs 54, Elsevier, Amsterdam, **1989**, Chapter 8; C. P. Brock, J. D. Dunitz, *Chem. Mater.* **1994**, *6*, 1118. For the correlation between molecular dipole moment and the formation of centric space groups, see: J. K. Whitesell, R. E. Davis, L. L. Saunders, R. J. Wilson, J. P. Feagins, *J. Am. Chem. Soc.* **1991**, *113*, 3267.

[14] M. R. Bryce, *Chem. Soc. Rev.* **1991**, *20*, 355; F. J. Adrian, D. O. Cowan, *Chem. Eng. News* **1992**, *70*(51), 24.

[15] J. S. Miller, A. J. Epstein, *Angew. Chem.* **1994**, *106*, 399; *Angew. Chem. Int. Ed. Engl.* **1994**, *33*, 385.

[16] G. Shiahuy Chen, J. K. Wilbur, C. L. Barnes, R. Glaser, *J. Chem. Soc. Perkin Trans 2* **1995**, 2311, and references therein. The criteria of high polarizability and conformational lability are also fulfilled by benzene derivatives that are threefold substituted with strong donors and acceptors which tend to form cosolvates (pseudopolymorphs): J. J. Wolff, H. Irngartinger, F. Gredel, I. Bolocan, *Chem. Ber.* **1993**, *126*, 2127.

[17] L. Dähne, G. Reck, *Angew. Chem.* **1995**, *107*, 735; *Angew. Chem. Int. Ed. Engl.* **1995**, *34*, 690. For differences in N=N bond lengths that arise through the coordination of boron-containing anions, see the analysis of a diazenium salt with eight crystallographically independent molecules in the unit cell: S. F. Nelsen, H. Chang, J. J. Wolff, D. R. Powell, *J. Org. Chem.* **1994**, *59*, 6558.

[18] a) H. Bock, I. Göbel, C. Näther, Z. Havlas, A. Gavezzotti, G. Filippini, *Angew. Chem.* **1993**, *105*, 1823; *Angew. Chem. Int. Ed. Engl.* **1993**, *32*, 1755; b) M. Kaftory, in *Acyclic Organonitrogen Stereodynamics* (Eds.: J. B. Lambert, Y. Takeuchi), VCH, New York, **1992**, p. 263; A. Domenicano, A. Vaciago, *Acta Crystallogr. Sect. B* **1979**, 35, 1382.

[19] Y. Eichen, J.-M. Lehn, M. Schwerl, D. Haarer, J. Fischer, A. DeCian, A. Corval, H. P. Trommsdorff, *Angew. Chem.* **1995**, *107*, 2753; *Angew. Chem. Int. Ed. Engl.* **1995**, *34*, 2530.

[20] For theoretical strategies to model the electrostatic influence on the molecular conformations in crystals, see, for example: P. Popelier, A. T. H. Leustra, C. van Alsenoy, H. J. Geise, *J. Am. Chem. Soc.* **1989**, *111*, 5658.

[21] I. Weissbuch, L. Addadi, M. Lahav, L. Leiserowitz, *Science* **1991**, *253*, 637.

 © *VCH Verlagsgesellschaft mbH, D-69451 Weinheim, 1996* *0570-0833/96/3519-2197 $ 15.00+.25/0*

The Tricks of Ribosomal Elongation Factors**

Knud H. Nierhaus*

Elongation factors (EF) catalyze protein biosynthesis. Two classes of elongation factors can be differentiated: EF-Tu and EF-G in eubacteria and EF-1 and EF-2 in archaebacteria and eukaryotes. They can adopt at least two conformations; one when bound to GDP and another when bound to GTP. In addition, EF-Tu (EF-1) can have still other ligands.

The crystal structures of the various forms in which EF-Tu can appear[1-5] and those of EF-G with and without GDP[6, 7] have afforded exciting insights into the functions of elongation factors as well as into ribosomal mechanisms. The biggest surprise came from the crystal structure of the ternary complex aminoacyl-tRNA·EF-Tu·GTP.[4] Before we discuss the structures and some of the functional implications we will turn briefly to the process of protein biosynthesis.

In all cells ribosomes translate genetic information stored as nucleic acid (DNA or RNA) into proteins. The nucleic acids are composed of four building blocks, the nucleotides. A sequence of three nucleotides (codon) defines unequivocally one unit of a protein, an amino acid. Both nucleic acids and proteins are nonbranched molecules.

The information storage format is almost exclusively DNA; only some important virus families such as HIV store the protein sequences as RNA. To convert the information of a gene into a protein sequence, the corresponding region of the DNA is transcribed into an mRNA (transcription). The sum of all mRNAs of a cell describes the actual synthesis program for cell proteins, the central importance of which is evident—more than 99.9% of all enzymes are proteins. The synthesis program can be regulated and adjusted to changing conditions; that is the importance of this circumstantial transcription procedure: The storage medium, DNA, is very long-lived (many years), whereas the mRNA is short-lived, and thus can be easily regulated (half-life of seconds to minutes. One of the most stable mRNAs is that from globin in erythrocytes with a half-life of about 100 days.)

A ribosome "walks" in codon "steps" along an mRNA and synthesizes the corresponding protein. The ribosome cannot read the codons itself but makes use of transfer RNAs (tRNAs). tRNAs are L-shaped molecules that carry an amino acid at the end of their short arm and expose three nucleotides at the end of their long arm. The three nucleotides are complementary to the codon that codes for the corresponding amino acid. The exposed trinucleotide is therefore called an anticodon. The one-codon movement of the ribosome along the mRNA is called a translocation.

During elongation, the extension of the growing peptide chain amino acid by amino acid, there are at least two tRNAs on the ribosome. Before translocation the tRNAs are present at the A and P regions, respectively. "A" stands for aminoacyl-tRNA and "P" for peptidyl-tRNA (Fig. 1). After translocation the tRNAs are in the ribosomal P and E regions. "E" stands for exit, since the tRNA liberated from its acyl residue is released from this region of the ribosome during the subsequent occupation of the A region. The ribosomal states before (Pre) or after translocation (Post) are the main states of the active ribosome, which are separated by high energy barriers (about 80 to 90 kJ mol^{-1}[8]). The Post state is probably lower in energy than the Pre state. This is indicated by the fact that after peptide-bond formation incubation at 37 °C for a couple of minutes is sufficient to promote translocation from the Pre to the Post state in the absence of the translocation factor EF-G and GTP (spontaneous translocation[9]). In contrast, a reverse translocation has been never observed with an isolated Post state; however, a Post state can be converted into a Pre state in the presence of an A-region ligand such as *N*-acetyl-Phe-tRNA even in the absence of EF-Tu and GTP.

The elongation factors lower the activation barrier separating the two main states of the ribosome and thus dramatically accelerate protein synthesis by more than 10^4-fold. In this way they resemble enzymes, which also lower the activation energy of a reaction and lead to enormous acceleration factors of 10^6 to 10^{12}. But enzymes accelerate a reaction only until equilibrium is reached; in other words, one enzyme can catalyze both the forward and the back reaction. An elongation factor can do more: it accelerates a reaction and determines the direction of reaction as well. For example, EF-Tu catalyzes the Post → Pre transition and EF-G the Pre → Post transition. For this reason there are two elongation factors, one for each direction of reaction. Only the higher fungi such as yeast or *Candida albicans* require a third factor, EF-3, which is an E-region factor and essential for protein synthesis.[10]

Both universal elongation factors EF-Tu and EF-G are prototypes of the large superfamily of the G-proteins which regulate important processes of the cell. G-proteins are GTPases and pass through a basic GTPase cycle.[11] They can bind GTP and GDP and thus assume an "ON" and "OFF" conformation. In the "ON" conformation (GTP is bound) a G-protein can bind a protein or a complex and trigger a distinct reaction. Then the GTPase center of the G-protein is activated, the terminal phosphate residue is cleaved such that GDP is now bound, and the G-protein adopts an "OFF" conformation and dissociates from the protein or complex. A new cycle begins after the GDP has been regenerated to GTP.

Figure 1 shows the GTPase cycles of EF-G and EF-Tu which bind in the "ON" conformation to the ribosome. EF-G follows the most simple scheme possible for a G-protein. The EF-G·GTP complex binds to a ribosome which is in the Pre state and which carries the peptidyl-tRNA in the A region after peptidyl transfer. EF-G lowers the activation energy between the Pre and Post states of the ribosome (Fig. 1). Since the Post state is apparently lower in energy, the ribosome assumes this state

[*] Prof. Dr. K. H. Nierhaus
Max-Planck-Institut für Molekulare Genetik, AG Ribosomen
Ihnestrasse 73, D-14195 Berlin (Germany)
Fax: Int. code +(30)8413-1380
e-mail: nierhauskh@mpimg-berlin-dahlem.mpg.de

[**] I thank Eva Philippi for the drawings.

 © VCH Verlagsgesellschaft mbH, D-69451 Weinheim, 1996 0570-0833/96/3519-2198 $ 15.00+.25/0

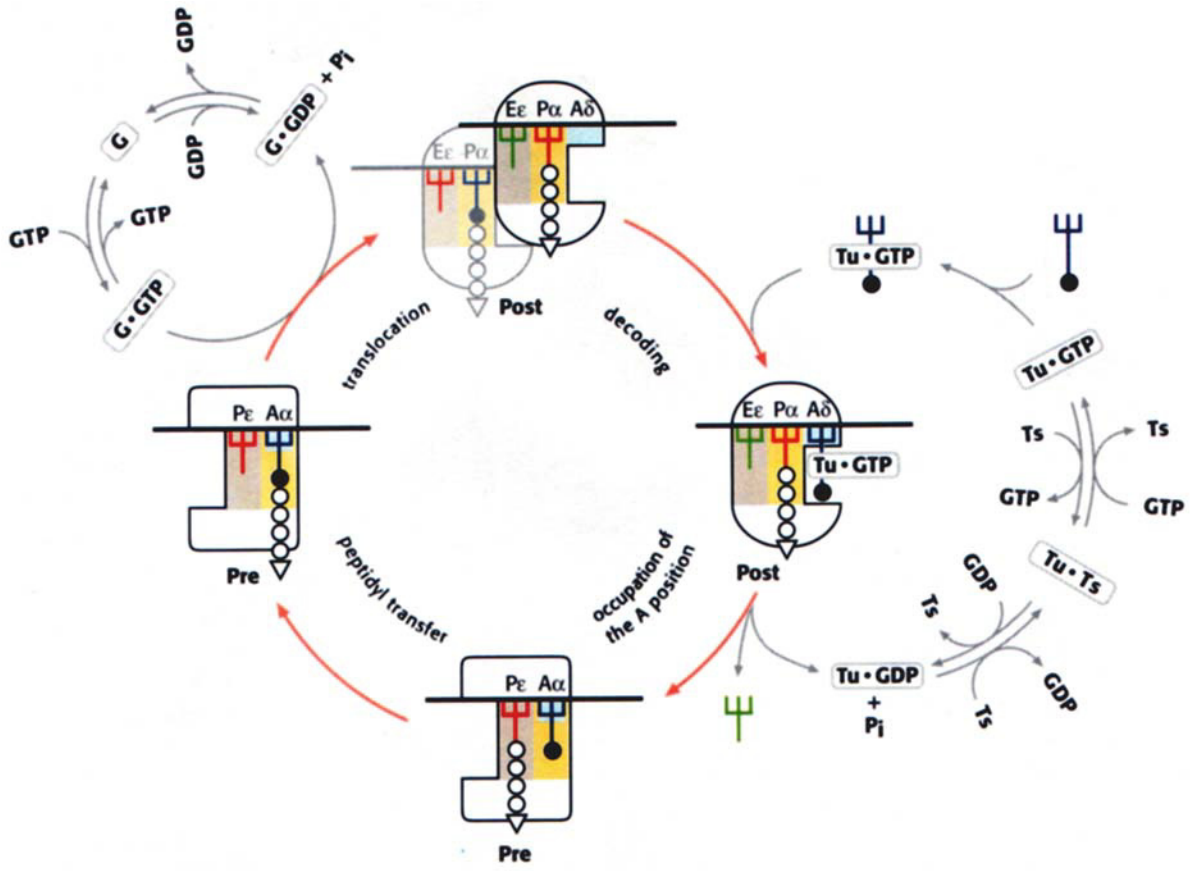

Fig. 1. The ribosomal elongation cycle (middle) and the GTPase cycles of the elongation factors EF-Tu (abbreviated as Tu, right) and EF-G (abbreviated as G, left). The elongation cycle is shown along the lines of the α–ε model, according to which the two tRNAs on the ribosome are bound to a movable domain of the ribosome. This movable domain contains two binding sites α and ε. The binding sites expose the tRNAs at the A and P regions of the ribosome in the Pre state and carries the tRNAs to the P and E regions, respectively, during translocation, thus establishing the Post state. In addition the decoding center δ is fixed at the A region; it overlaps with the α site in the the Pre state but stands alone in the Post state.

and now carries the peptidyl-tRNA at the P region and the deacylated tRNA at the E region. After the ribosome activates the GTPase center by means of an unknown mechanism, the resulting EF-G·GDP assumes the "OFF" conformation and dissociates from the ribosome. The activation barrier is raised again and keeps the ribosome stable in the Post state.

EF-G has a very low affinity to both GTP and GDP (2.7×10^4 M^{-1}[12] and 2.5×10^5 M^{-1},[13] respectively) so that the actual concentrations of GTP and GDP in the cell (ca. 1 mM and 0.1 mM, respectively[14]) are sufficient to replace GDP by GTP without the help of an additional factor, thus enabling the next round of an EF-G cycle.

The situation with EF-Tu is more complicated since EF-Tu·GTP alone cannot bind to the ribosome. It must first bind to an aminoacyl-tRNA and then form the ternary complex aminoacyl-tRNA·EF-Tu·GTP. This is a consequence of the second essential task of EF-Tu besides catalyzing the Post → Pre transition, namely to carry an aminoacyl-tRNA to the ribosome.

At this point, the X-ray crystal structure of the ternary complex (Fig. 2A[4]) is quite surprising. The ribosome is thought to use more than once the codon–anticodon interaction (proofreading) in order to achieve the accuracy of about one error per 1000 incorporated amino acids. Proposed proofreading mechanisms assume that EF-Tu uses the energy released during the hydrolysis of GTP for driving the proofreading process.[15] However, the crystal structure of the ternary complex demonstrates that EF-Tu binds the aminoacyl-tRNA at the short arm of the tRNA about 50 Å away from the anticodon (Fig. 2A), and thus EF-Tu hardly has a chance to interfere with the mechanism of codon–anticodon interaction. This conclusion is in accord with the results of recent investigations,[16] which suggest that the recognition (initial binding) of a correct codon–anticodon interaction in the ribosomal decoding center δ raises sufficient energy to explain the accuracy of 1:1000 of protein synthesis without the assumption of a proofreading mechanism. This explanation significantly simplifies the hypothesis for the selection of the correct ternary complex.

Accordingly it is probable that the correctness of the codon–anticodon interaction is checked at the decoding center δ without the participation of EF-Tu. In this view the considerable binding energy of EF-Tu and the aminoacyl-tRNA outside the anticodon region is exploited to drive the transition to the pretranslocational state only after the decoding has been completed successfully. It is generally accepted that replicases and trancriptases, which synthesize DNA and RNA, respectively, probe the stereochemoical correctness of base pairing in the course of nucleic acid synthesis and that these enzymes achieve an accuracy of better than 1:10000 without proofreading.[17]

The biggest surprise is that the X-ray crystal structures of the ternary complex and EF-G·GDP are very similar (cf. Figs. 2A

 © VCH Verlagsgesellschaft mbH, D-69451 Weinheim, 1996 0570-0833/96/3519-2199 $ 15.00+.25/0

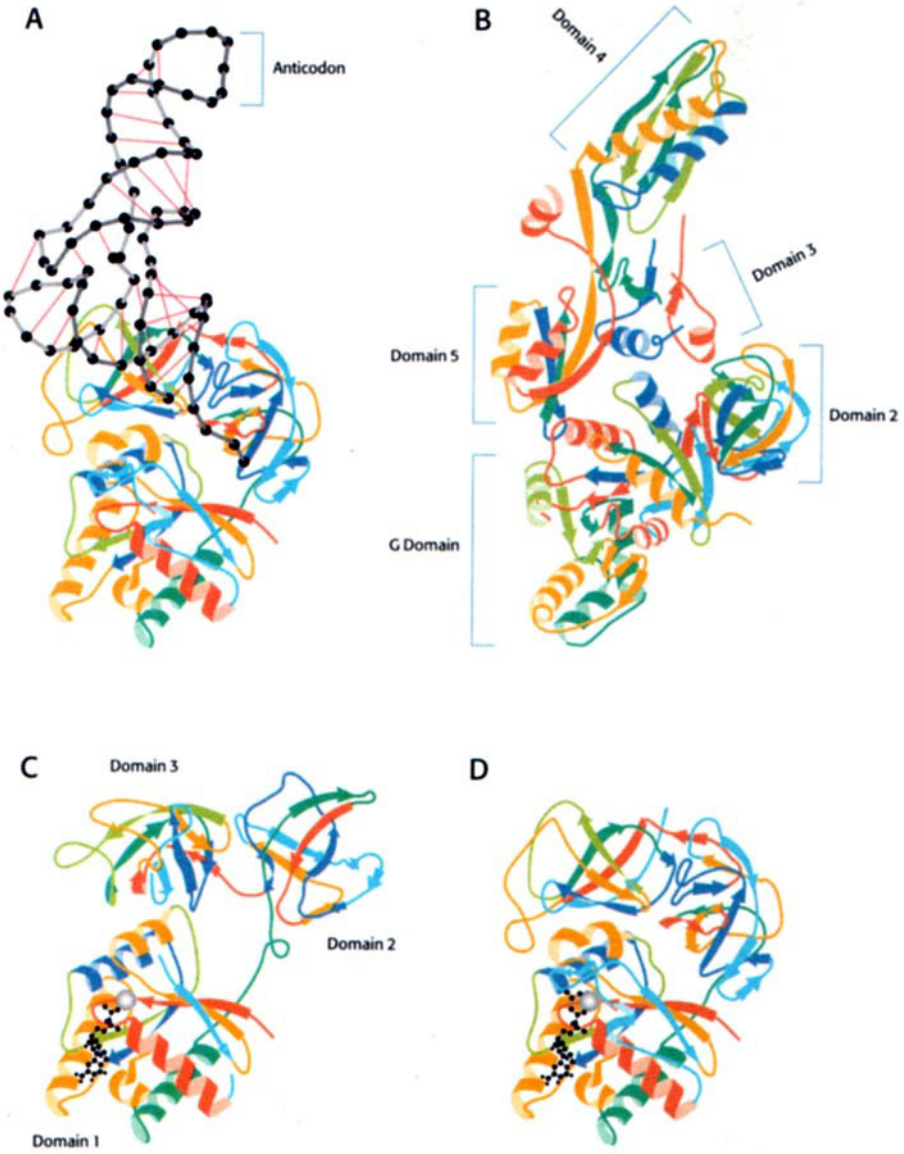

Fig. 2. X-ray crystal stuctures of elongation factors. A: Ternary complex Phe-tRNA·EF-Tu·GTP, adapted from refs. [4, 21]. B: EF-G from *T. thermophilus*, adapted from refs. [6, 7]. C and D: EF-Tu·GDP and EF-Tu·GTP, respectively. The *E. coli* sequence of EF-Tu has been modeled in analogy to the structure of EF-Tu·GTP from *Thermus thermophilus* [2]. GDP and GTP are represented as black ball-and-stick models. The Mg^{2+} ion important for the GTP/GDP binding is shown as a gray sphere; adapted from ref. [21].

and B)! The EF-G structure shows five domains (Fig. 2B); domains three to five imitate the structure of the tRNA component of the ternary complex! This is a surprising example of molecular mimicry. The ribosome model shown in Figure 1 suggests the following interpretation:[18] After EF-G·GTP has established the Post state of the ribosome, the domains of EF-G mimicking a tRNA bind to the vacant decoding center. This simple action prevents a reverse translocation of the ribosome into the Pre state as long as the presence of EF-G on the ribosome keeps the energy barrier between the two ribozome states low. After the hydrolysis of GTP, EF-G·GDP dissociates from the ribosome, the activation energy is raised again, and the ribosome is held in the Post state until the next ternary complex has finished decoding.

After EF-Tu has triggered the Pre state of the ribozyme, the ribosome activates the GTPase center of EF-Tu, probably by a similar mechanism to that in the case of EF-G. The resulting EF-Tu·GDP adopts the "OFF" conformation and dissociates from the ribosome. The structure of the "OFF" conformation of EF-Tu·GDP is more open than that of EF-Tu·GTP (cf. Figs. 2C and 2B). Upon cleavage of GTP, domains 2 and 3 move away from domain 1 as a block, and domain 2 departs from domain 1 by astonishing 40 Å.

In striking contrast to EF-G, the factor EF-Tu binds GDP with high affinity ($6 \times 10^8\ M^{-1}$) and GTP with ten times less affinity (which is still relatively high).[19] The consequence is that the concentrations of GDP and GTP in the cell do not influence the binding of the guanosine nucleotides to EF-Tu. Therefore, the special factor EF-Ts exists which regenerates EF-Tu·GTP from EF-Tu·GDP; this factor binds to EF-Tu·GDP and mediates the replacement of GDP with GTP.

The X-ray crystal structure of EF-Tu·EF-Ts[5] demonstrates that the complex is not a heterodimer as expected but rather a tetramer. In the tetramer both EF-Ts units have distinct contact areas, whereas the EF-Tu molecules hardly touch each other. Accordingly, the structure of the tetramer is best described as EF-Tu·$(EF\text{-}Ts)_2$·EF-Tu. The motif Thr-Asp-Phe-Val82, which is conserved in all structures of EF-Ts known, plays a dominant role in the replacement of GDP. The amino acids Asp80-Phe81 press into the GDP binding site and displace three amino acids of EF-Tu, which stabilize two H_2O molecules. Both water molecules are coordinated to a Mg^{2+} ion which is essential for the affinity of Ef-Tu to GDP. The disruption of the Mg^{2+} binding site causes the loss of GDP, which now can be replaced by GTP. These reactions are reversible, but for effective protein synthesis GDP must be replaced by GTP and not vice versa. The direction of the GTPase cycle (Fig. 1) is determined by the practically irreversible formation of the ternary complex, which removes EF-Tu·GTP from the equilibrium reactions.[20]

The X-ray crystal structures discussed here have afforded surprising insights into the functions of elongation factors and of G-proteins in general. The strucures shed some light on ribosomal mechanisms such as decoding and give an exciting example of molecular mimicry. Yet the ribosome, the most complicated complex in the cell, is not well understood. Exactly how the ribosome activates the GTPase centers of the elongation factors and by which mechanisms elongation fac-

 © VCH Verlagsgesellschaft mbH, D-69451 Weinheim, 1996 0570-0833/96/3519-2200 $ 15.00+.25/0

tors lower the activation barriers separating ribosome states is not known.

German version: *Angew. Chem.* **1996**, *108*, 2342–2345

Keywords: elongation factors · G-proteins · protein biosynthesis · protein structures · ribosomes

[1] M. Kjeldgaard, J. Nyborg, *J. Mol. Biol.* **1992**, *223*, 721–742.
[2] H. Berchtold, L. Reshetnikova, C. O. A. Reiser, N. K. Schirmer, M. Sprinzl, R. Hilgenfeld, *Nature* **1993**, *365*, 126–132.
[3] M. Kjeldgaard, P. Nissen, S. Thirup, J. Nyborg, *Structure* **1993**, *1*, 35–50.
[4] P. Nissen, M. Kjeldgaard, S. Thirup, G. Polekhina, L. Reshetnikova, B. F. C. Clark, J. Nyborg, *Science* **1995**, *270*, 1464–1472.
[5] T. Kawashima, C. Berthet-Colominas, M. Wulff, S. Cusack, R. Leberman, *Nature* **1996**, *379*, 511–518.
[6] J. Czworkowski, T. J. Wang, T. A. Steitz, P. B. Moore, *EMBO J.* **1994**, *13*, 3661–3668.
[7] A. Ævarsson, E. Brazhnikov, M. Garber, J. Zheltonosova, Y. Chirgadze, S. Al-karadaghi, L. A. Svensson, A. Liljas, *EMBO J.* **1994**, *13*, 3669–3677.
[8] S. Schilling-Bartetzko, A. Bartetzko, K. H. Nierhaus, *J. Biol. Chem.* **1992**, *267*, 4703–4712.
[9] K. Bergemann, K. H. Nierhaus, *J. Biol. Chem.* **1983**, *258*, 15105–15113.
[10] F. J. Triana-Alonso, K. Chakraburtty, K. H. Nierhaus, *J. Biol. Chem.* **1995**, *270*, 20473–20478.
[11] H. R. Bourne, D. A. Sanders, F. McCormick, *Nature* **1991**, *349*, 117–127.
[12] M. S. Rohrbach, J. W. Bodley, *Biochemistry* **1976**, *15*, 4565–4569.
[13] O. G. Baca, M. S. Rohrbach, J. W. Bodley, *Biochemistry* **1976**, *15*, 4570–4574.
[14] J. Neuhard, P. Nygaard, in *Escherichia coli and Salmonella Typhimurium, Cellular and Molecular Biology* (Eds.: F. Neidhart, J. L. Ingraham, K. B. Low, B. Magasanik, M. Schaechter, H. E. Umbarger), American Society of Microbiology, Washington, **1987**, pp. 445–473.
[15] C. G. Kurland, *Trends Biochem. Sci.* **1987**, *12*, 126–128.
[16] A. P. Potapov, F. J. Triana-Alonso, K. H. Nierhaus, *J. Biol. Chem.* **1995**, *270*, 17680–17684.
[17] H. Echols, M. F. Goodman, *Annu. Rev. Biochem.* **1991**, *60*, 477–511.
[18] K. H. Nierhaus, *Nature* **1996**, *379*, 491–492.
[19] A. Wagner, I. Simon, M. Sprinzl, R. S. Goody, *Biochemistry* **1995**, *34*, 12535–12542.
[20] G. Romero, V. Chau, R. L. Biltonen, *J. Biol. Chem.* **1985**, *260*, 6167–6174.
[21] K. Abel, F. Jurnak, *Structure* **1996**, *4*, 229–238.

Hexameric, almost planar aggregates of compound **1**, which are formed from building blocks (red, blue) that exhibit hydrogen bonding codes like nucleobases, overlap in the crystal. More about this fascinating planned self-assembly is reported by M. Mascal et al. on the following pages.

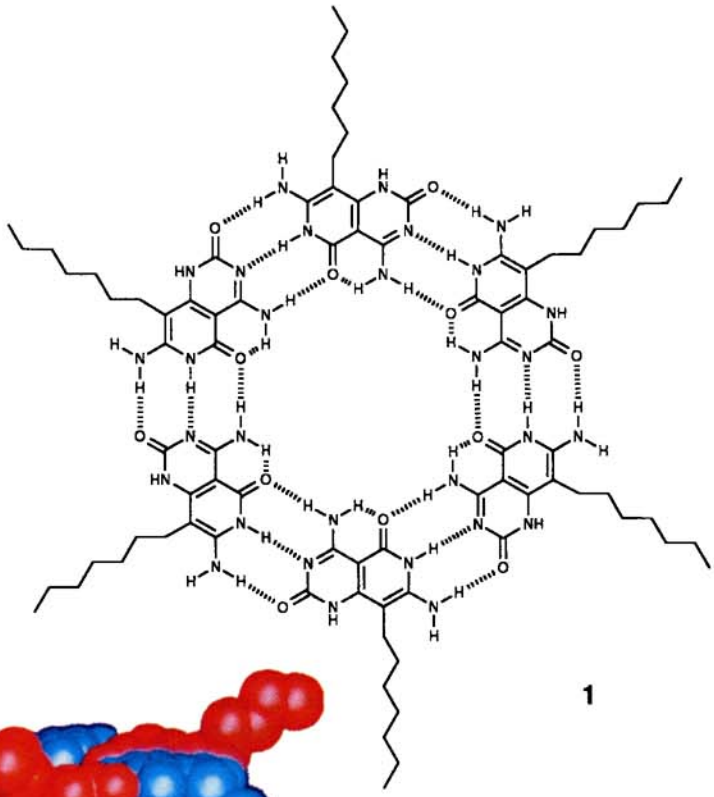

1

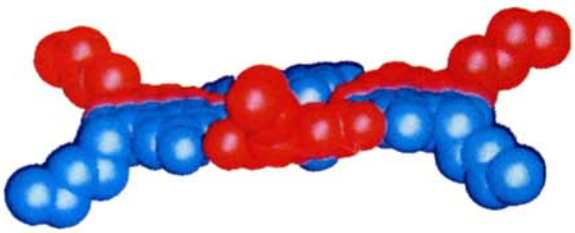

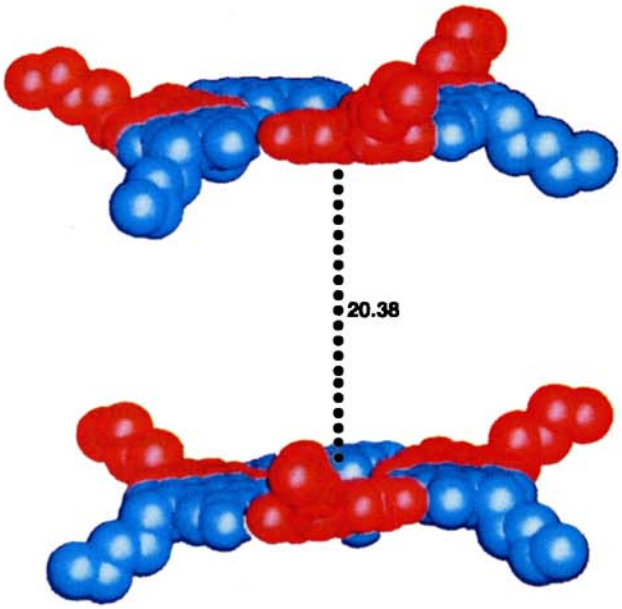

 © VCH Verlagsgesellschaft mbH, D.-69451 Weinheim, 1996 0570-0833/96/3519-2203 $ 15.00 + .25/0

Programming a Hydrogen-Bonding Code for the Specific Generation of a Supermacrocycle**

Mark Mascal,* Nicholas M. Hext, Ralf Warmuth, Madeleine H. Moore, and Johan P. Turkenburg

The organization of matter brought about through noncovalent forces makes feats of molecular engineering possible that are virtually unthinkable from a covalent perspective. The natural world provides numerous examples of this, and yet benchtop efforts to master the behavior of molecules, apart from those immediately derived from natural systems, have been modest. The challenge lies both in the realm of information and in chemical synthesis: The conceptualization of an organized state of matter is intimately linked with the design of real components that possess the steric and functional information necessary to translate concept into substance.[1] Much of the work done along these lines has been devoted to the use of hydrogen bonds as the design principle,[2] and the structures expressed have spanned the range of dimensions, from diamondoid[3] and dendrimeric[4] (three-dimensional), to sheets (two-dimensional),[5] to various descriptions of chains,[6,7] helices,[8] and even tubes (one-dimensional).[9] Interestingly, an acknowledged challenge has been to *restrict* the dimensionality to effectively "zero",[10-12] such that the structure qualifies as a discrete, nanoscale species and not simply a crystal motif. Recently, this has taken the form of the cyclic hexameric aggregate based on the melamine (**1**)–cyanuric acid (**2**) cocrystal originally reported by Lehn et al.[6] and Whitesides et al.[7] Because the hydrogen bonding donor (D)-acceptor (A) patterns (or codes) are centrosymmetric in **1** and **2**, an ambiguity arises in the expression of the information,[13] leading to two distinct infinite chain structures besides the cyclic hexamer.[14] Although all three states of aggregation have been obtained by careful control of the steric demands of the components, the high-fidelity matching of hydrogen-bonding information which would lead exclusively to a "supermacrocycle" remained elusive.

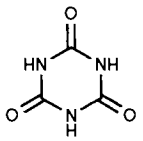

1

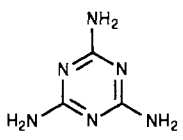

2

We now report the synthesis of a DNA-base hybrid purpose-designed to function exclusively as the cornerpiece of a hexagon: The combination of the A-A-D sequence of cytosine and the complementary D-D-A sequence of guanine at an angle of 120° to each other in pyrido[4,3-*d*]pyrimidine **3**, leads to the assembly of independent hexagonal aggregates $\mathbf{3}_6$ in the solid state (Scheme 1). This is purely the result of the communication of programmed, hydrogen-bonding information.

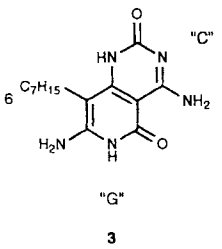

3

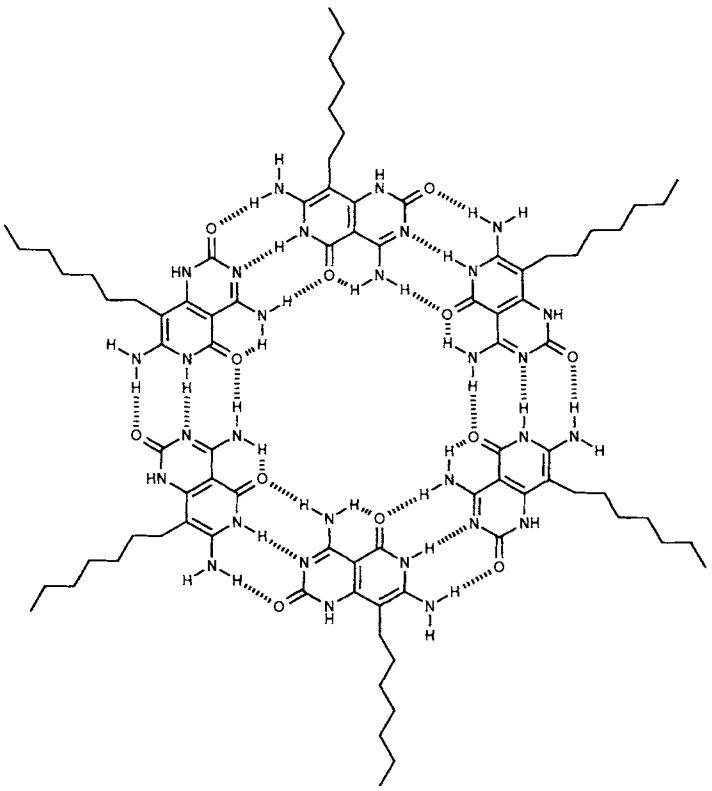

Scheme 1. The enforced self-assembly of molecules of **3** into a hexamer.

Subunit **3** was synthesized in five steps from the commercially available, inexpensive malononitrile dimer **4** (Scheme 2). Experience had shown that the final product would require a tail-group for solubility purposes,[15] and thus **4** was first alkylated by treatment with heptyl bromide and base to give **5** (71%). Cyclization with sodium methoxide gave the pyridine **6** (69%) together with the regioisomer that results from attack at the wrong cyano group (19%). Selective protection of the amino group in the 2-position was accomplished by deprotonation and subsequent treatment with dimethyl carbonate to give **7** (85%). The most difficult step proved to be formation of the second ring. After much trial-and-error, it was found that reaction of **7** with chlorosulfonyl isocyanate gave bicycle **8** in a modest 15% yield. The simultaneous demasking of both the amino and latent carbonyl functions with trimethylsilyl iodide (TMSI) proceeded smoothly to give the target material **3** in 73% yield.

The preparation of solutions of **3** in warm DMSO[16] results after several hours in the deposition of large, clear crystals of cubic habit, which show no extinction of plane-polarized light. X-ray structural data collected[17] by using synchrotron radiation indicated that **3** crystallized in the very rare cubic space group $Ia\bar{3}d$ (number 230), which possesses the highest symmetry of all space groups.[18] The unit cell contains 96 molecules of **3** and has a total volume of over 100000 Å^3. The programmed hexagonal motif (Fig. 1) can clearly be seen in the view of the

[*] Dr. M. Mascal, Dr. N. M. Hext, Dr. R. Warmuth
Department of Chemistry
University of Nottingham
Nottingham, NG72RD (UK)
Fax: Int. code +(115)9513564
e-mail: PCZMM@vax.ccc.nottingham.ac.uk
Dr. M. H. Moore, Dr. J. P. Turkenburg
Department of Chemistry
University of York
Heslington, York, YO1 5DD (UK)

[**] This research was supported by the BBSRC and the Materials Group of the EPSRC. We thank A. M. Z. Slawin, D. Hibbs, O. V. Shishkin, and especially A. J. Blake for attempts to collect data and advice on crystallographic matters.

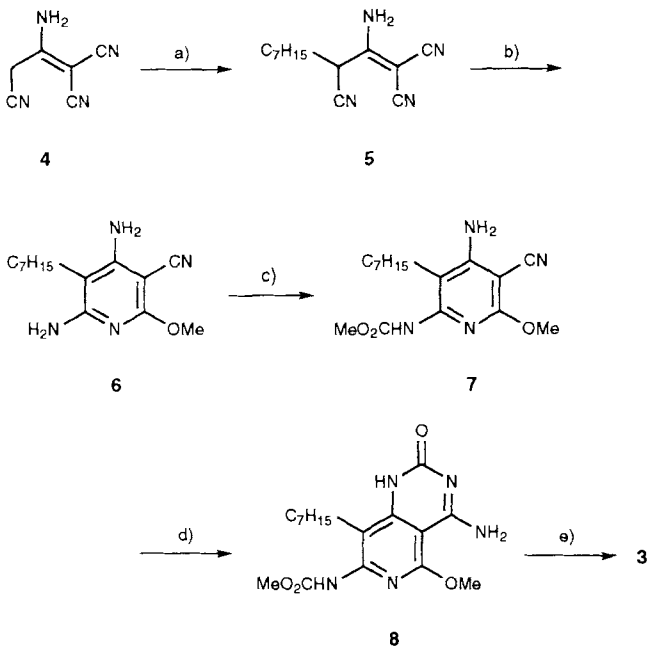

Scheme 2. a) iPr_2EtN, $C_7H_{15}Br$, $nBu_4N^+I^-$, 1,2-dimethoxyethane (DME), Δ; b) NaOMe, MeOH, Δ; c) *t*BuLi, $(MeO)_2CO$, THF, −78 °C to room temperature; d) $ClSO_2NCO$, CH_2Cl_2; e) TMSCl, NaI, MeCN, Δ.

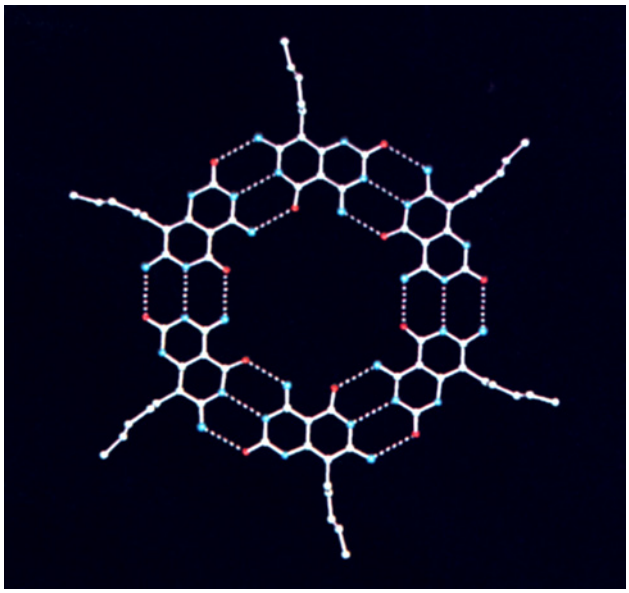

Fig. 1. The hexagonal motif $\mathbf{3}_6$ taken from the crystal structure.

unit cell (Fig. 2). The macrocycle is assembled through 18 intermolecular hydrogen bonds, (O···N (outer) 2.80, N···N 2.91, and O···N (inner) 2.91 Å); six additional intramolecular hydrogen bonds are observed between N5-H and O2 (N···O 2.66 Å). It is worth noting that the AAD–DDA interactions present in $\mathbf{3}_6$ are known to be more effective than those in **1**·**2** (ADA–DAD), the latter possessing stability constants in solution two orders of magnitude inferior to typical C–G pairs.[19]

An important feature of this structure is that the hexamers coincide with each other to describe channels with a diameter of 10.5 Å that extend through the crystal (Fig. 2). Alternate $\mathbf{3}_6$ units are rotated 24.3° in the plane of the hexagon and translated 20 Å down a perpendicular threefold axis that runs parallel to the body diagonals. The maximum deviation of the ring atoms from the plane of the hexamer is ±0.2 Å. The C_7 alkyl chains, however, extend above and below the plane in an alternating up–down arrangement related by an S_6 axis. Although the rigid core of **3** is well ordered, the alkyl chain shows dramatic progressive disorder with increasing distance from the ring atom (Fig. 3), such that the last two carbon atoms could not be located. The crystal has a calculated density of only 0.479 g cm^{-3} based on the empirical formula, which indicates that the void space (ca. 65% of the crystal) is occupied mainly by liquid solvent,[20] although partial occupancy of two solvent molecules per molecule of **3** can be modeled on the data. The presence of this solvent in the crystal prevented low-temperature data collection, but even taking this and the disorder in the structure into account, refinement gave an *R* value of 0.152 (for all $I \geq 2\sigma(I)$ data). This compares to values for the "rosette" reported by Whiteside et al. (0.112)[14d] and for the channel-forming macrocycle (0.176) reported by Moore et al.[5d]

In conclusion, we have demonstrated the value of a high-level information approach in imposing a predetermined state of order on molecular crystal components. An independent study of a related molecule has

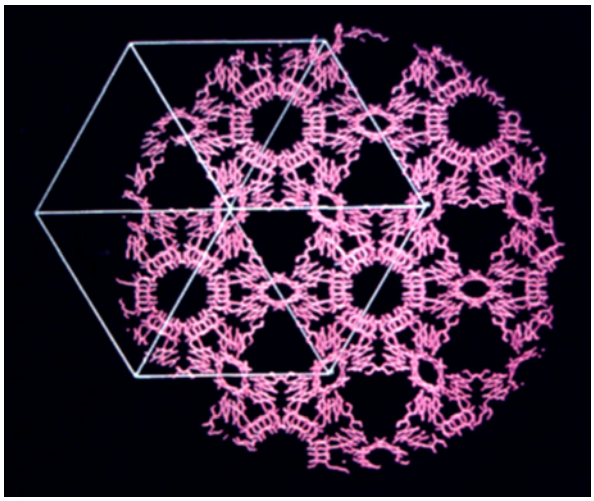

Fig. 2. A view of the cell of **3** along a body diagonal.

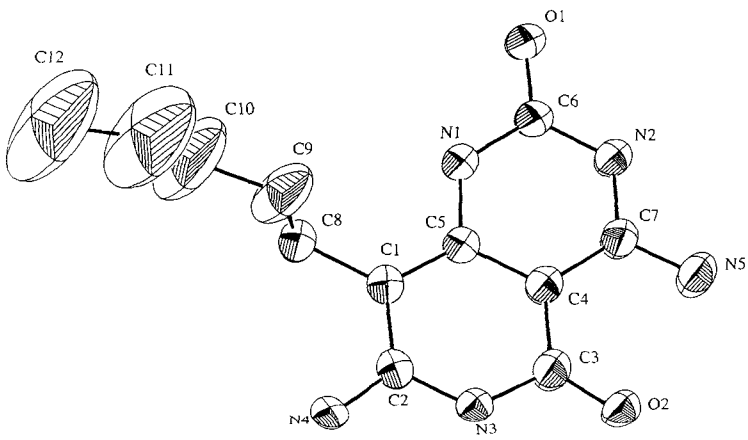

Fig. 3. An ORTEP view of **3** showing 20% ellipsoids.

provided evidence for the existence of such order also in the solution state.[21] We foresee applications of precision self-assembly to the targeted fabrication of organized states of matter of ever increasing complexity from systems of components of advanced synthetic and informational sophistication. Efforts on our part are now being directed towards the inclathration of complementary species in the channel voids of $\mathbf{3}_6$, as well as the elaboration of the periphery for the exploitation of this effective means of generating hexagonal order.

Received: April 12, 1996 [Z9023IE]
German version: *Angew. Chem.* **1996**, *108*, 2347–2350

Keywords: channel structures · hydrogen bonds · self-assembly

[1] a) M. Mascal, *Contemp. Org. Synth.* **1994**, *1*, 31; b) D. S. Lawrence, T. Jiang, M. Levett, *Chem. Rev.* **1995**, *95*, 2229; c) G. R. Desiraju, *Angew. Chem.* **1995**, *107*, 2541; *Angew. Chem. Int. Ed. Engl.* **1995**, *34*, 2311; d) J.-M. Lehn, *Supramolecular Chemistry*, VCH, Weinheim, **1995**, and references therein.

[2] a) M. C. Etter, *Acc. Chem. Res.* **1990**, *23*, 120; b) *J. Phys. Chem.* **1991**, *95*, 4601; c) C. B. Aakeröy, K. R. Seddon, *Chem. Soc. Rev.* **1993**, *22*, 397; d) J. C. MacDonald, G. M. Whitesides, *Chem. Rev.* **1994**, *94*, 2383; e) J. Bernstein, R. E. Davis, L. Shimoni, N.-L. Chang, *Angew. Chem.* **1995**, *107*, 1687; *Angew. Chem. Int. Ed. Engl.* **1995**, *34*, 1555, and references therein.

[3] a) O. Ermer, L. Lindenberg, *Helv. Chim. Acta* **1991**, *74*, 825; b) X. Wang, M. Simard, J. D. Wuest, *J. Am. Chem. Soc.* **1994**, *116*, 12119.

[4] S. C. Zimmerman, F. Zeng, D. E. C. Reichert, S. V. Kolotuchin, *Science* **1996**, *271*, 1095.

[5] a) D. J. Duchamp, R. E. Marsh, *Acta Crystallogr. Sect. B* **1969**, *25*, 5; b) F. Garcia-Tellado, S. J. Geib, S. Goswami, A. D. Hamilton, *J. Am. Chem. Soc.* **1991**, *113*, 9265; c) Y.-L. Chang, M.-A. West, F. W. Fowler, J. W. Lauher, *ibid.* **1993**, *115*, 5991; d) D. Venkataraman, S. Lee, J. Zhang, J. S. Moore, *Nature* **1994**, *371*, 591; e) S. V. Kolotuchin, E. F. Fenlon, S. R. Wilson, C. J. Loweth, S. C. Zimmerman, *Angew. Chem.* **1995**, *107*, 2873; *Angew. Chem. Int. Ed. Engl.* **1995**, *34*, 2564.

[6] J.-M. Lehn, M. Mascal, A. DeCian, J. Fischer, *J. Chem. Soc. Chem. Commun.* **1990**, 479.

[7] J. A. Zerkowski, C. T. Seto, D. A. Wierda, G. M. Whitesides, *J. Am. Chem. Soc.* **1990**, *112*, 9025.

[8] a) C. Fouquey, J.-M. Lehn, A. Levelut, *Adv. Mater.* **1990**, *2*, 254; b) S. J. Geib, C. Vincent, E. Fan, A. D. Hamilton, *Angew. Chem.* **1993**, *105*, 83; *Angew. Chem. Int. Ed. Engl.* **1993**, *32*, 119.

[9] J. D. Hartgerink, J. R. Granja, R. A. Milligan, M. R. Ghadiri, *J. Am. Chem. Soc.* **1996**, *118*, 43, and references therein.

[10] a) G. M. Whitesides, J. P. Mathias, C. T. Seto, *Science* **1992**, *254*, 1312; b) G. M. Whitesides, E. E. Simanek, J. P. Mathias, C. T. Seto, D. N. Chin, M. Mammen, D. M. Gordon, *Acc. Chem. Res.* **1995**, *28*, 37.

[11] a) J. Yang, E. Fan, S. J. Geib, A. D. Hamilton, *J. Am. Chem. Soc.* **1993**, *115*, 5314, and references therein; b) Y. Yang, J.-L. Marendaz, S. J. Geib, A. D. Hamilton, *Tetrahedron Lett.* **1994**, *35*, 3665.

[12] a) R. Wyler, J. de Mendoza, J. Rebek, Jr., *Angew. Chem.* **1993**, *105*, 1820; *Angew. Chem. Int. Ed. Engl.* **1993**, *32*, 1699; b) C. Valdés, U. P. Spitz, L. M. Toledo, S. W. Kubik, J. Rebek, Jr., *J. Am. Chem. Soc.* **1995**, *117*, 12733.

[13] For a related system see: N. Kimizuka, T. Kawasaki, K. Hirata, T. Kunitake, *J. Am. Chem. Soc.* **1995**, *117*, 6360.

[14] a) J. A. Zerkowski, G. M. Whitesides, *J. Am. Chem. Soc.* **1994**, *116*, 4298; b) J. A. Zerkowski, J. P. Mathias, G. M. Whitesides, *ibid.* **1994**, *116*, 4305; c) J. P. Mathias, E. E. Simanek, J. A. Zerkowski, C. T. Seto, G. M. Whitesides, *ibid.* **1994**, *116*, 4316; d) J. A. Zerkowski, C. T. Seto, G. M. Whitesides, *ibid.* **1992**, *114*, 5473.

[15] A version of **3** synthesized without the tailgroup did not dissolve to an appreciable extent in any solvent.

[16] Compound **3** also gave crystals of similar appearance from DMF and DMF/DMSO mixtures. The possibility that powerful H-bond accepting solvents such as these could interfere with the assembly process was considered, but the experience has been that interbase H-bonding tends to win out over competition: J.-M. Lehn, M. Mascal, A. DeCian, J. Fischer, *J. Chem. Soc. Perkin Trans 2* **1992**, 461.

[17] X-ray structure analysis of **3**: $C_{13.42}H_{14}N_5O_{2.71}S_{0.71}$ ($M_r = 311.34$), crystal dimensions $0.7 \times 0.4 \times 0.3$ mm; cubic, space group $Ia\bar{3}d$ (no. 230), $a = 46.980(5)$ Å, $V = 103691(19)$ Å^3, $Z = 96$, $\rho_{calc} = 0.479$ g cm^{-3}, $\lambda = 0.8700$ Å, $T = 293$ K, $F(000) = 15600$. A total of 72292 reflections were measured in the range 10–0.9 Å, $0 \le h \le 27$, $4 \le k \le 50$, $0 \le l \le 35$ at the CCLRC Daresbury Laboratory Synchrotron Radiation Source, station 9.6, using a MAR image plate detector. Merging gave 5725 unique data (overall $R_{int} = 0.057$). No correction for absorption or decay was applied. The structure was solved by direct methods in SHELXS-86. Refinement was carried out against F^2 in SHELXL-93 using all 5725 reflections. Hydrogen atoms were placed in calculated positions on the appropriate N atoms and on the first four C atoms of the alkyl chain. All non-hydrogen atoms were refined anisotropically and hydrogen atoms were refined by using a riding model (C–H = 0.97, N–H = 0.86 Å) with $U_{iso}(H) = 1.2U_{eq}(C, N)$. Full-matrix least squares refinement of 247 parameters gave $R_F = 0.1701$ [$R_F = 0.1523$ on $I \ge 2\sigma(I)$ data] and $S = 1.723$. Although the overall solution is satisfactory, we are continuing to investigate the distribution of the remaining solvent molecules. Crystallographic data (excluding structure factors) for the structure reported in this paper have been deposited with the Cambridge Crystallographic Data Centre as supplementary publication no. CCDC-179-90. Copies of the data can be obtained free of charge on application to The Director, CCDC, 12 Union Road, Cambridge CB2 1EZ, UK (fax: Int. code +(1223) 336-033; e-mail: teched@chemcrys.cam.ac.uk).

[18] This is the first report of an all-organic molecule in this space group. Only two other molecules in $Ia\bar{3}d$ are identified in a search of the Cambridge Crystallographic Database (F. H. Allen, J. E. Davies, J. J. Galloy, O. Johnson, O. Kennard, C. F. Macrae, E. M. Mitchell, G. F. Mitchell, J. M. Smith, D. G. Watson, *J. Chem. Info. Comput. Sci.* **1991**, *31*, 187).

[19] J. Pranata, S. G. Wierschke, W. L. Jorgensen, *J. Am. Chem. Soc.* **1991**, *113*, 2810.

[20] The actual density of the crystals is greater than that of DMSO (1.1 g cm^{-3}), in which they are not buoyant.

[21] A. Marsh, M. Silvestri, J.-M. Lehn, *Chem. Commun.* **1996**, 1527.

A Neutral, Triple-Helical, Trinuclear, Oxo-Centered Mixed-Valence Iron Complex**

Rolf W. Saalfrank,* Stefan Trummer, Harald Krautscheid, Volker Schünemann, Alfred X. Trautwein, Stefan Hien, Christian Stadler, and Jörg Daub

In memory of Gerrit L'abbé

Programming and self-assembly are key concepts underlying the design of supramolecular systems.[1] Hitherto, interest has focused on the synthesis of helicates,[2] catenanes,[3] knots,[3] and cages,[4] as well as coordination polymers.[5] However, it is in principle possible to generate a larger variety of structures selectively by using appropriate ligands and metal ions.[4, 6]

Our interest in polynuclear supramolecular iron complexes mainly stems from the importance of oxo-centered polyiron aggregates as model compounds for iron–oxo proteins, oxidation catalysts, and corrosion inhibitors.[7] In principle, oxo-centered complexes related to $[Fe_3O(O_2CR)_6(H_2O)_3]$[7] with doubly negatively charged, pentadentate, tritopic ligands L should

[*] Prof. Dr. R. W. Saalfrank, Dipl.-Chem. S. Trummer
Institut für Organische Chemie der Universität Erlangen-Nürnberg
Henkestrasse 42, D-91054 Erlangen (Germany)
Fax: Int. code +(9131)85-6864
Dr. H. Krautscheid[+]
Institut für Anorganische Chemie der Universität Karlsruhe (Germany)
Dr. V. Schünemann, Prof. Dr. A. X. Trautwein[++]
Institut für Physik der Medizinischen Universität Lübeck (Germany)
Dr. S. Hien, Dipl.-Chem. C. Stadler, Prof. Dr. J. Daub[+++]
Institut für Organische Chemie der Universität Regensburg (Germany)

[+] Single-crystal X-ray diffraction analysis.

[++] Mössbauer spectra.

[+++] Electrochemistry.

[**] Chelate Complexes, Part 7. This work was supported by the Deutsche Forschungsgemeinschaft, the Volkswagen-Stiftung, and the Fonds der Chemischen Industrie. We are grateful to Prof. Dr. K.-P. Zeller, Universität Tübingen, for recording the numerous FAB-MS spectra. This work was initially conceived, while R. W. S. was occupying a chair at the Universität München. Part 6: R. W. Saalfrank, R. Harbig, J. Nachtrab, W. Bauer, K.-P. Zeller, D. Stalke, M. Teichert, *Chem. Eur. J.* **1996**, *2*, no. 11.

be accessible. This hypothesis is confirmed for $[Fe_3OL_3]$ by space-filling models.

We therefore doubly deprotonated H_2L (**1**)[8] at 20 °C with triethylamine, treated the corresponding dianion L^{2-} with a solution of iron(III) chloride, and after workup isolated dark green crystals. According to the microanalysis and FAB-MS data (FAB = fast atom bombardment) the product formed was a trinuclear iron chelate complex of the composition $[Fe_3OL_3]$ (**2**).

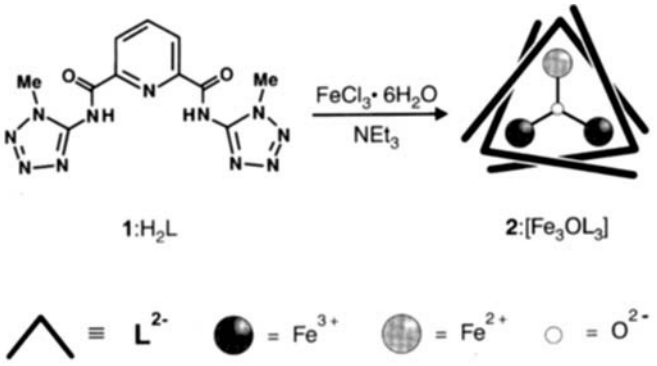

The oxygen atom in this formula apparently stems from deprotonated water of crystallization. Consequently an excess of triethylamine leads to higher yields. Furthermore under these conditions the water-soluble mononuclear by-product $[FeL_2]^-$ is formed only in small amounts.[9]

As the ^1H and ^{13}C NMR spectra of **2** do not enable unequivocal structure determination, we carried out an X-ray crystallographic analysis of the complex.[10] Compound **2** is present in the crystal as a neutral, trinuclear, iron chelate complex (Fig. 1).

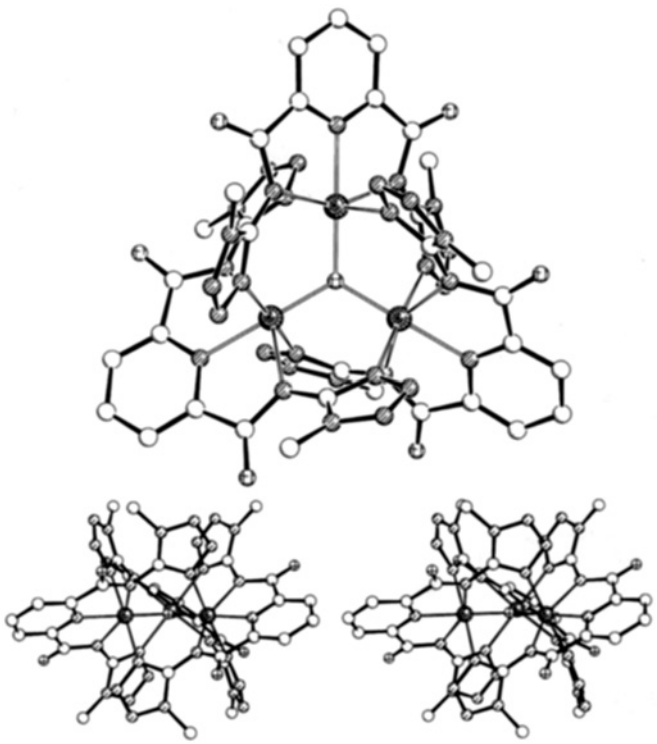

Fig. 1. Crystal structure of **2** (SCHAKAL representation). Top: view along the crystallographic C_3 axis perpendicular to the triangular plane. Bottom: stereorepresentation of a side view (for clarity H atoms have been omitted; C atoms shaded, N atoms hatched, O atoms cross-hatched, Fe atoms radially hatched). Selected bond lengths [Å] and angles [°]: (μ_3-O)-Fe 1.886(1), pyridine-N-Fe 2.070(3), amide-N-Fe 2.105(3), tetrazole-N-Fe 2.176(4); Fe-(μ_3-O)-Fe 120.0, (μ_3-O)-Fe-pyridine-N 180.0.

The core of complex **2** is generated by an equilateral triangle with a μ_3-O^{2-} ion in the center and three iron ions in the corners. Each of the three doubly negatively charged pentadentate ligands L (H_2L = **1**) links three metal centers. As a result all iron ions are distorted octahedrally, coordinated to five N donors and to a μ_3-O-ligand shared by the three iron atoms. The iron centers of the racemic complex $[Fe_3OL_3]$ (**2**) are homochiral. Since the tetrazolyl donors of the tritopic ligands attack neighboring iron ions at opposite sides of the (Fe,Fe,Fe)-triangular plain, a triple-helical, D_3-symmetric arrangement results (Fig. 2).[11]

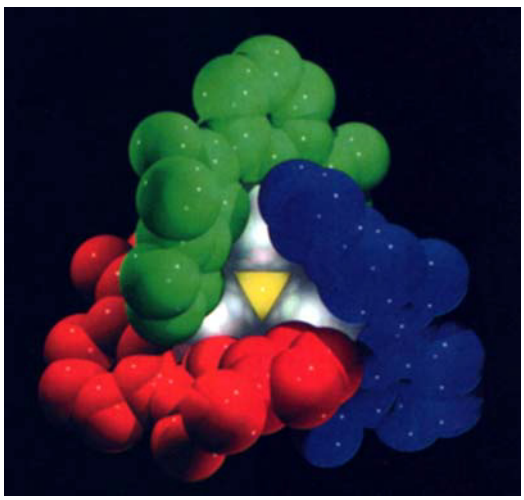

Fig. 2. Space-filling model of **2**; view along the C_3 axis perpendicular to the Fe,Fe,Fe triangular plane. To show the triple helix clearly, each ligand (H atoms omitted) is presented in a different color; oxygen atom yellow, iron atoms light gray.

The lack of a counterion implies intramolecular charge compensation and therefore mixed-valence character for $[Fe_3OL_3]$ (**2**). This is unambiguously confirmed by a Mössbauer spectrum of a powder sample of **2** recorded at 4.2 K. The spectrum exhibits two quadrupolar doublets with a peak area ratio of 1:2 (Fig. 3). The doublet with a quadrupolar splitting of ΔE_Q = 2.64(1) mm s^{-1} and an isomeric shift of δ = 0.95(1) mm s^{-1} is consistent with a high-spin iron(II) species (relative percentage: 33.7%), whereas the doublet with a quadrupolar splitting of ΔE_Q = 1.83(1) mm s^{-1} and an isomeric shift of δ = 0.53(1) mm s^{-1} is consistent with a high-spin iron(III) species

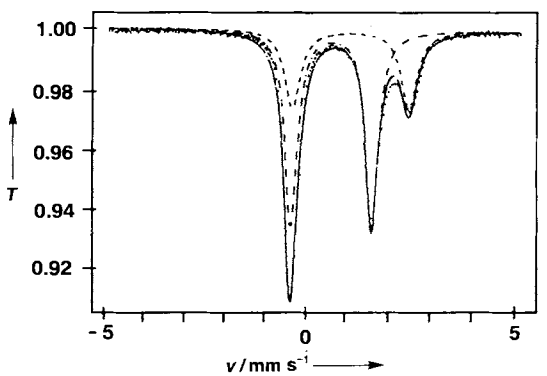

Fig. 3. Mössbauer spectrum of a powder sample of **2** recorded at 4.2 K. The connecting line is the result of an adjustment with two doublets of Lorentz lines. T = relative transmission, v = relative velocity.

 © VCH Verlagsgesellschaft mbH, D-69451 Weinheim, 1996 0570-0833/96/3519-2207 $ 15.00+.25/0

(relative percentage: 66.3%). It may thus be deduced that the mixed-valent trinuclear complex **2** is formed by two Fe^{III} ions and one Fe^{II} ion.

Under aprotic conditions[12] cyclic voltammetric investigation of the redox-active iron centers of neutral $[(Fe^{III})_2Fe^{II}OL_3]$ (**2**) shows two reversible one-electron transfer processes (chart speed 250 mVs^{-1}, Fig. 4). The half-wave potential $E_{1/2}$ =

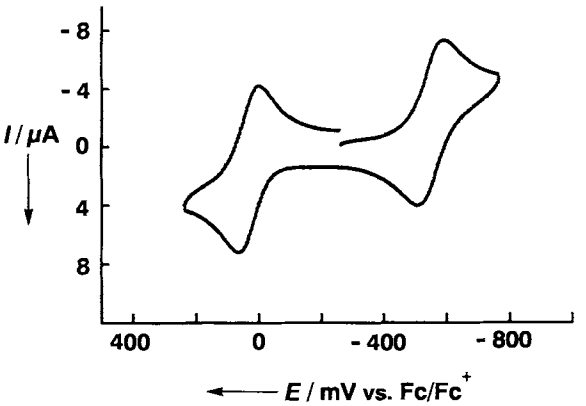

Fig. 4. Cyclic voltammogram of **2** in acetonitrile/0.1 M tetrabutylammonium hexafluorophosphate, scan rate 250 mVs^{-1}.

− 550 mV corresponds to the redox process $[(Fe^{III})_2Fe^{II}OL_3]/[Fe^{III}(Fe^{II})_2OL_3]^-$, whereas the oxidation of $[(Fe^{III})_2Fe^{II}OL_3]$ (**2**) to $[(Fe^{III})_3OL_3]^+$ occurs at $E_{1/2}$ = + 30 mV. In the reductive region at the peak potential $E_{1/2}$ = −1120 mV a further quasi-reversible pair of signals is recorded (not shown), which can be assigned to the all iron(II) species. However, this signal is not stable in a multisweep experiment, which is due to gradual decomposition of the dianion.

We will report elsewhere on the catalytic potential of $[Fe_3OL_3]$ (**2**) for the oxidation of olefins by hydrogen peroxide, and also by molecular oxygen.

Experimental Procedure

2: General procedure: To a solution of **1** (3 mmol, 988 mg) in 300 mL THF was added triethylamine (1.2 mL, 9 mmol, 911 mg) and a solution of $FeCl_3 \cdot 6H_2O$ (3 mmol, 811 mg) in 20 mL THF. The dark green mixture was stirred for 12 h at 20 °C, warmed to 66 °C during 3d, cooled to 20 °C, and filtered. The solvent was removed under vacuum, and the solid residue was dissolved in 150 mL trichlormethane. $[FeL_2]^-$ was removed by washing the organic phase eight times with 150 mL portions of warm water (40 °C). The organic layer was separated, dried over sodium sulfate, and concentrated to 30 mL. The product was crystallized by adding 50 mL of hexane, filtered off, and dried under vacuum (oil pump). Yield: 502 mg (43%), correct elemental analysis; m.p. >250 °C (decomp.); IR (KBr): $\tilde{\nu}$ = 1657, 1528, 1448 cm^{-1} (C=O, C=N, C=C, N=N); FAB-MS (3-nitrobenzylalcohol matrix): *m/z* (%): 1167.2 (100) $[M^+ + 2H]$.

Received: March 28, 1996 [Z8981IE]
German version: *Angew. Chem.* **1996**, *108*, 2350–2352

Keywords: chelate complexes · complexes with oxygen ligands · iron compounds · supramolecular chemistry

[1] D. Philp, J. F. Stoddart, *Angew. Chem.* **1996**, *108*, 1243–1286; *Angew. Chem. Int. Ed. Engl.* **1996**, *35*, 1154–1196; J.-M. Lehn, *Supramolecular Chemistry*, VCH, Weinheim, **1995**, Chap. 9, p. 139–197.

[2] J.-M. Lehn, *Angew. Chem.* **1988**, *100*, 91–116; *Angew. Chem. Int. Ed. Engl.* **1988**, *27*, 89–112; *ibid.* **1990**, *102*, 1347–1362 and **1990**, *29*, 1304–1319; E. J. Enemark, T. D. P. Stack, *ibid.* **1995**, *107*, 1082–1084 and **1995**, *34*, 996–1000; E. C. Constable, A. J. Edwards, P. R. Raithby, J. V. Walker, *ibid.* **1993**, *105*, 1486–1486 and **1993**, *32*, 1465–1467; G. Bernardinelli, C. Piguet, A. F. Williams, *ibid.* **1992**, *104*, 1626–1628 and **1992**, *31*, 1622–1624; R. Krämer, J.-M. Lehn, A. De Cian, J. Fischer, *ibid.* **1993**, *105*, 764–767 and **1993**, *32*, 703–706; K. T. Potts, C. P. Horwitz, A. Fessak, M. Keshavarz-K, K. E. Nash, P. J. Toscano, *J. Am. Chem. Soc.* **1993**, *115*, 10444–10445; C. Piguet, G. Hopfgartner, A. F. Williams, J.-C. G. Bünzli, *J. Chem. Soc. Chem. Commun.* **1995**, 491–493; A. L. Airey, G. F. Swiegers, A. C. Willis, S. B. Wild, *ibid.* **1995**, 695–696.

[3] C. O. Dietrich-Buchecker, J.-P. Sauvage, *Bioorganic Chemistry Frontiers, Vol. 2*, Springer, Berlin, **1991**, p. 195–248; C. O. Dietrich-Buchecker, B. Frommberger, I. Lüer, J.-P. Sauvage, F. Vögtle, *Angew. Chem.* **1993**, *105*, 1526–1529; *Angew. Chem. Int. Ed. Engl.* **1993**, *32*, 1434–1437.

[4] R. W. Saalfrank, R. Burak, S. Reihs, N. Löw, F. Hampel, H.-D. Stachel, J. Lentmaier, K. Peters, E. M. Peters·H, G. von Schnering, *Angew. Chem.* **1995**, *107*, 1085–1087; *Angew. Chem. Int. Ed. Engl.* **1995**, *34*, 993–995; R. W. Saalfrank, R. Burak, A. Breit, D. Stalke, R. Herbst-Irmer, J. Daub, M. Porsch, E. Bill, M. Müther, A. X. Trautwein, *ibid.* **1994**, *106*, 1697–1699 and **1994**, *33*, 1621–1623; R. W. Saalfrank, B. Hörner, D. Stalke, J. Salbeck, *ibid.* **1993**, *105*, 1223–1225 and **1993**, *32*, 1179–1182; P. Baxter, J.-M. Lehn, A. De Cian, J. Fischer, *ibid.* **1993**, *105*, 92–95 and **1993**, *32*, 69–72.

[5] G. Denti, S. Serroni, S. Campagna, A. Juris, M. Ciano, V. Balzani in *Perspectives in Coordination Chemistry* (Eds.: A. F. Williams, C. Floriani, A. E. Merbach), VHCA, Basel, and VCH, Weinheim, **1992**, p.153; S. Subramanian, M. J. Zaworotko, *Angew. Chem.* **1995**, *107*, 2295–2297; *Angew. Chem. Int. Ed. Engl.* **1995**, *34*, 2127–2129; R. W. Saalfrank, C.-J. Lurz, K. Schobert, O. Struck, E. Bill, A. X. Trautwein, *ibid.* **1991**, *103*, 1499–1501 and **1991**, *30*, 1494–1496; R. W. Saalfrank, O. Struck, M. G. Davidson, R. Snaith, *Chem. Ber.* **1994**, *127*, 2489–2492; R. W. Saalfrank, Struck, K. Peters, H. G. von Schnering, *Inorg. Chim. Acta.* **1994**, 222, 5–11; R. W. Saalfrank, K. Schobert, S. Trummer, A. Wolski, *Z. Naturforsch.* **1995**, **50 b**, 642–648.

[6] P. N. W. Baxter, J.-M. Lehn, J. Fischer, M.-T. Youinou, *Angew. Chem.* **1994**, *106*, 2432–2434; *Angew. Chem. Int. Ed. Engl.* **1994**, *33*, 2284–2287; S. Rüttimann, G. Bernardinelli, A. F. Williams, *ibid.* **1993**, *105*, 432–434 and **1993**, *32*, 392–394.

[7] S. J. Lippard, J. M. Berg, *Bioanorganische Chemie*, Spektrum Akademischer Verlag, Heidelberg **1995**, Chap. 5, p. 136 ff.; S. M. Gorun, G. C. Papaefthymiou, R. B. Frankel, S. J. Lippard, *J. Am. Chem. Soc.* **1987**, *109*, 4244–4255; S. J. Lippard, *Angew. Chem.* **1988**, *100*, 353–371; *Angew. Chem. Int. Ed. Engl.* **1988**, *27*, 344–361; K. Wieghardt, K. Pohl, I. Jibril, G. Huttner, *ibid.* **1984**, *96*, 66–67 and **1984**, *23*, 77–78.

[8] Synthesis of H_2L **1** according to A. G. Oertli, W. R. Meyer, U. W. Suter, *Helv. Chim. Acta* **1992**, *75*, 184–189.

[9] Details of the structure of anion $[FeL_2]^-$ will be reported elsewhere.

[10] Crystal structure analyses: **2**·6$CHCl_3$: $C_{39}H_{33}Cl_{18}Fe_3N_{33}O_7$, M = 1881.63. Crystal dimensions: 0.30 × 0.20 × 0.15 mm, trigonal, space group $R\bar{3}c$ (No. 167), a = 2341.8(9), c = 2273.6 (7) pm, V = 10798(7) × 10^6 pm^3, Z = 6, ρ_{calcd} = 1.736 gcm^{-3}. Diffractometer: STOE STADI IV. radiation: $Mo_{K\alpha}$, λ = 71.069 pm, T = 200 K. Programs: SHELXS-86, SHELXL-93 [13]; graphite monochromator. Measurement details: ω scan; range: $1.5° \le \theta \le 25°$; section of the reciprocal lattice: h = − 27 to 13, k = 0 to 27, l = 0 to 23. Of 3954 measured intensities, 2067 reflections are independent, 1583 with $I > 2\sigma(I)$. Linear absorption coefficient: 1.335 mm^{-1}; absorption correction: Ψ scans. Refined parameters: 160; $R1$ = 0.056 (observed reflections); $wR2$ = 0.163 (all data). Due to space group symmetry all Fe atoms in **2** are equivalent. The $CHCl_3$ molecule is disordered. Crystallographic data (excluding structure factors) for the structure reported in this paper have been deposited with the Cambridge Crystallographic Data Centre as supplementary publication no. CCDC-179-106. Copies of the data may be obtained free of charge on application to The Director, CCDC, 12 Union Road, Cambridge CB2 1EZ, UK (Fax: Int. code +(1223) 336-033; e-mail: teched@chemcrys.cam.ac.uk).

[11] For the subject of circular, chiral supramolecular systems through linkage of three metal ions by one ligand see: B. Hasenknopf, J.-M. Lehn, B. O. Kneisel, G. Baum. D. Fenske, *Angew. Chem.* **1996**, *108*, 1987–1990; *Angew. Chem. Int. Ed. Engl.* **1996**, *35*, 1838–1840.

[12] Amel System 5000. Ungraduated cell with Pt plate electrodes and a Ag/AgCl pseudo reference electrode. Potential measured vs. Fc/Fc^+.

[13] SHELXS-86; G. M. Sheldrick, C. Krüger, P. Goddard, *Crystallographic Computing 3*, Oxford University Press, Oxford, **1985**, p. 175. G. M. Sheldrick, SHELXL-93, Program for structure refinement, Göttingen, **1993**.

 © VCH Verlagsgesellschaft mbH, D-69451 Weinheim, 1996 0570-0833/96/3519-2208 $ 15.00+.25/0

The First Metallacrown Ether Sandwich Complex**

Rolf W. Saalfrank,* Norbert Löw, Frank Hampel, and Hans-Dietrich Stachel

For some time we have been working in the field of cage compounds such as $[NH_4 \subset Fe_4L_6^1]$ (**1**), originating by the spontaneous self-assembly of preprogrammed bis(bidentate) bridging ligands and suitable metal ions.[1, 2] A notable feature of these tetranuclear adamantanoid endoreceptor complexes is their topological equivalence to cryptates (**2**).[2]

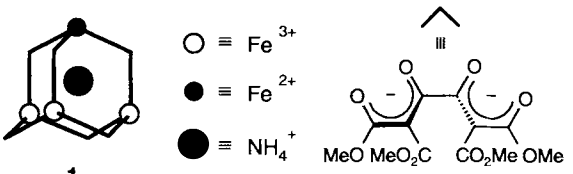

1 L^1

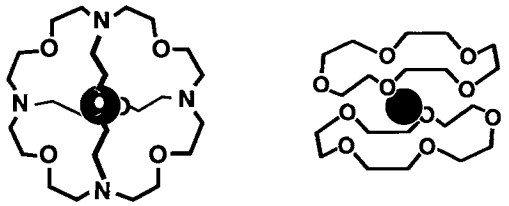

2 3

In principle, metallacrown ethers, [2]-metallacryptands, and [3]-metallacryptands[3] should exist parallel to the corresponding crown ethers, [2]-cryptands, and [3]-cryptands.[4] We were convinced that the analogy perceived between **1** and **2** is not a special case, but that the use of properly tailored ligands should give access to other metallatopomers. In order to test this hypothesis we treated dialkyl ketipinates **4a,b**[5] or tetraketone **4c**[6] with copper(II) chloride and aqueous ammonia or potassium hydroxide in methanol, obtaining dark green crystals in each case. The microanalytical data and FAB-MS spectra (FAB = fast atom bombardment) gave initial indications that the products were hexanuclear copper chelate compounds (**5**) of the general composition $[MOH(Cu_3L_3^2)_2]\cdot 6HOR^2$, constituting host guest systems topologically equivalent to well-known organocrown ether sandwich complexes **3** [for example, $KI(benzo[15]crown\text{-}5)_2$].[7] In principle, the composition of a coronate is dependent on the cavity diameter of the host. Correspondence between the size of host and guest leads to complexes with 1:1 stoichiometry, whereas "oversize" cations result in sandwich complexes with 2:1 stoichiometry.

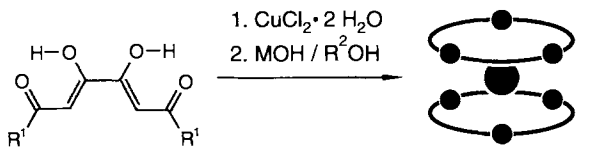

4 5

4, 5	R^1	R^2	M
a	O*t*Bu	Me	NH_4^+
b	OE*t*	H	NH_4^+
c	*t*Bu	H	K^+

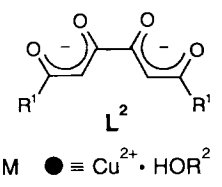

To obtain an unambiguous characterization of the molecular structure of the metallacoronates, we carried out an X-ray crystallographic structure analysis of complex $[NH_4OH(Cu_3L_3^2)_2]\cdot 6HOMe$ (**5a**).[8] According to this analysis, **5a** is indeed present as a metallacrown ether sandwich complex (Fig. 1).

The cation **5a** consists of two identical, neutral, 15-membered trimetallacrown-6 building blocks, twisted relative to each other by 60°. The ammonium ion in the center is sandwiched by the

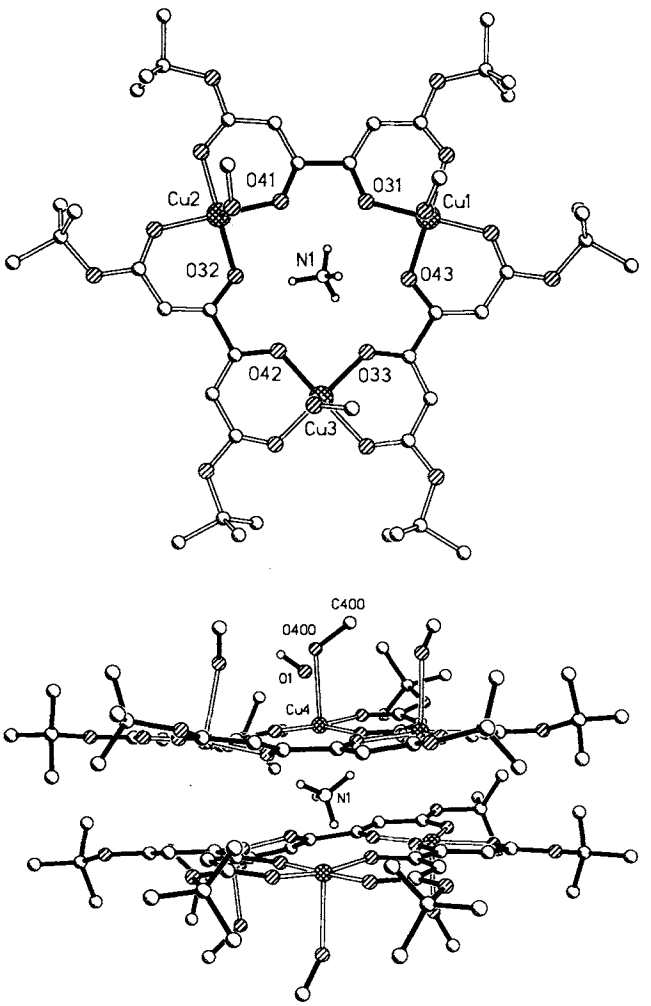

Fig. 1. Top: Structure of one 15-membered trimetallacrown-6 unit of sandwich complex **5a**, including the ammonium ion (top view: H atoms omitted, O atoms hatched, Cu atoms double hatched, C atoms shaded, N atom and ammonium-H atoms empty; counterion omitted). Bottom: Structure of **5a** (side view with counterion).

[*] Prof. Dr. R. W. Saalfrank, Dipl.-Chem. N. Löw, Dr. F. Hampel
Institut für Organische Chemie der Universität Erlangen-Nürnberg
Henkestrasse 42, D-91054 Erlangen (Germany)
Fax: Int. code +(9131)85-6864
Prof. Dr. H.-D. Stachel
Institut für Pharmazie und Lebensmittelchemie der Universität München (Germany)

[**] Chelate Complexes, Part 8. This work was supported by the Deutschen Forschungsgemeinschaft and the Fonds der Chemischen Industrie. We thank Prof. Dr. K.-P. Zeller, University of Tübingen, for the FAB mass spectra. This work was initially conceived while R. W. S. was deputizing a chair at the Universität München. Part 7: R. W. Saalfrank, S. Trummer, H. Krautscheid, V. Schünemann, A. X. Trautwein, S. Hien, C. Stadler, J. Daub, *Angew. Chem.* **1996**, *108*, 2350–2352; *Angew. Chem. Int. Ed. Engl.* **1996**, *35*, 2206–2208.

two metallacrowns C ($\bar{d}_{C-C}$ = 375 pm). The copper(II) ions of the metallacoronands occupy the corners of two equilateral triangles ($\bar{d}_{Cu-Cu}$ = 620 pm). The copper ions are linked by bis(bidentate) di-*tert*-butyl ketipinate dianions L^2 [H_2L^2 = **4a**]. Each of the copper(II) ions is coordinated in a square-planar fashion by four O-donors. Coordination of methanol leads to a tetragonal-pyramidal oxygen environment for all copper centers. The counterion of cation $[NH_4(Cu_3L_3^2)_2]^+ \cdot 6$HOMe (**5a**) is a hydroxide ion, hydrogen-bonded to methanol.[9] Neglecting the resulting loss in symmetry, and assuming spherical symmetry for the ammonium ion, the cation **5a** has C_{6h} symmetry (Fig. 2).

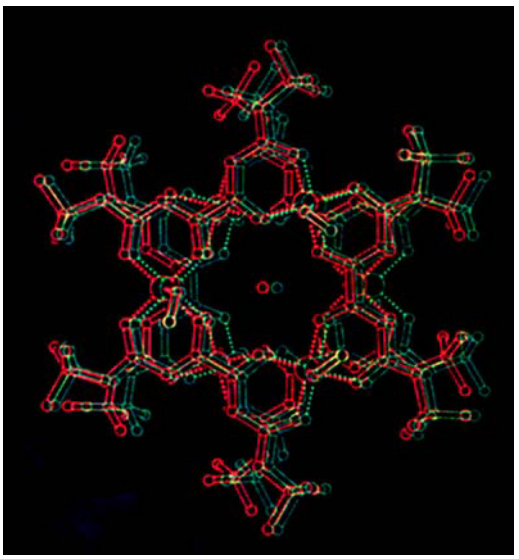

Fig. 2. Red-green stereoview of cation **5a** (top view: H atoms omitted).

Preliminary experiments indicate that use of Na^+ instead of K^+[10] or NH_4^+ leads to 1:1 metallacoronates $[\{NaCu^{II}Cl_2(Cu_3^{II}L_3^2)\}_2]$, which perpetuates the analogy with the well known organocrown ether chemistry.

Experimental Procedure

5: General procedure: Aqueous ammonia (2 mL, 12%) or potassium hydroxide (2 mL, 2N) was added dropwise to a solution of copper(II) chloride dihydrate (1.0 mmol, 171 mg) and the appropriate bis-1,3-dioxo ligand **4** (1.0 mmol) in methanol (100 mL) until no more turbidity was observed. To achieve complete precipitation of the products, water (200 mL) was added. The products were filtered off and dried under vacuum (oil pump). All new compounds gave correct elemental analyses.

5a: Yield of dark green crystals from methanol: 265 mg (69%); decomp. above 155 C; IR ($CHBr_3$): $\tilde{\nu}$ = 3300 cm^{-1} (OH), 3200 (NH), 1602, (C⋯O), 1499 (C = C); FAB-MS (3-nitrobenzyl alcohol matrix = *m*-NBA): *m/z* (%): 2103 (100) $[NH_4^+ \subset Cu_6L_6^2 - 2H]$.

5b: Yield of green microcrystals: 210 mg (67%); decomp. above 175 C; IR ($CHBr_3$): $\tilde{\nu}$ = 3420 cm^{-1} (OH), 3190 (NH), 1600 (C⋯O), 1500 (C=C); FAB-MS (*m*-NBA): *m/z* (%): 1768 (48) $[NH_4^+ \subset Cu_6L_6^2]$.

5c: yield of green microcrystals: 153 mg (45%); decomp. above 154 C; IR ($CHBr_3$): $\tilde{\nu}$ = 3360 cm^{-1} (OH), 1565 (C⋯O), 1500 (C=C); FAB-MS (*m*-NBA): *m/z* (%): 1934 (10) $[K^+ \subset Cu_6L_6^2]$, 986 (100) $[K^+ \subset Cu_3L_3^2]$.

Received: April 1, 1996 [Z 8988 IE]
German version: *Angew. Chem.* **1996**, *108*, 2353–2354

Keywords: copper compounds · crown ethers · metallacrown ethers · sandwich complexes · supramolecular chemistry

[1] D. Philp, J. F. Stoddart, *Angew. Chem.* **1996**, *108*, 1243–1286; *Angew. Chem. Int. Ed. Engl.* **1996**, *35*, 1154–1196; B. Hasenknopf, J.-M. Lehn, B. O. Kneisel, G. Baum, D. Fenske, *ibid.* **1996**, *108*, 1987–1990 and **1996**, *35*, 1838–1840; J.-M. Lehn, ibid. **1988**, *100*, 91–116 and **1988**, *27*, 89–112; J.-M. Lehn, *ibid.* **1990**, *102*, 1347–1362 and **1990**, *29*, 1304–1319; I. Cragg-Hine, M. G. Davidson, O. Kocian, F. S. Mair, E. Pohl, P. R. Raithby, R. Snaith, N. Spencer, J. F. Stoddart, *ibid.* **1993**, *105*, 1254–1256 and **1993**, *32*, 1182–1184; M. Simard, D. Su, J. D. Wuest, *J. Am. Chem. Soc.* **1991**, *113*, 4696–4698.

[2] R. W. Saalfrank, A. Stark, K. Peters, H. G. von Schnering, *Angew. Chem.* **1988**, *100*, 878–880; *Angew. Chem. Int. Ed. Engl.* **1988**, *27*, 851–853; R. W. Saalfrank, R. Burak, S. Reihs, N. Löw, F. Hampel, H.-D. Stachel, J. Lentmaeier, K. Peters, E. M. Peters, H. G. von Schnering, *ibid.* **1995**, *107*, 1085–1087 and **1995**, *34*, 993–995; R. W. Saalfrank, R. Burak, A. Breit, D. Stalke, R. Herbst-Irmer, J. Daub, M. Porsch, E. Bill, M. Müther, A. X. Trautwein, *ibid.* **1994**, *106*, 1697–1699 and **1994**, *33*, 1621–1623; R. W. Saalfrank, A. Dresel, B. Hörner, O. Struck, H. Maid, *Mol. Cryst. Liq. Cryst.* **1994**, *240*, 39–52.

[3] A. J. Blake, R. O. Gould, C. M. Grand, P. E. Y. Milne, D. Reed, R. E. P. Winpenny, *Angew. Chem.* **1994**, *106*, 208–210; *Angew. Chem. Int. Ed. Engl.* **1994**, *33*, 195–197; B. R. Gibney, D. P. Kessissoglou, J. W. Kampf, V. L. Pecoraro, *Inorg. Chem.* **1994**, *33*, 4840–4849; D. P. Kessissoglou, J. W. Kampf, V. L. Pecoraro, *Polyhedron* **1994**, *13*, 1379–1391; M. S. Lah, B. R. Gibney, D. L. Tierney, J. E. Penner-Hahn, V. L. Pecoraro, *J. Am. Chem. Soc.* **1993**, *115*, 5857–5858.

[4] C. J. Pedersen, *J. Am. Chem. Soc.* **1967**, *89*, 2495–3496; J.-M. Lehn, *Supramolecular Chemistry*, VCH, Weinheim, **1995**, p. 17 ff.; G. Gokel, *Crown Ethers and Cryptands* in *Monographs in Supramolecular Chemistry* (Ed.: J. F. Stoddart), Black Bear Press, Cambridge, **1991**, p. 64 ff.; F. Vögtle, *Supramolekulare Chemie*, Teubner, Stuttgart, **1992**, p. 45 ff.; "Crown-Type Compounds—An Introductory Overview": E. Weber, F. Vögtle, *Top. Curr. Chem.*, Springer, Berlin, **1981**, *98*, 1–41.

[5] H.-D. Stachel, *Arch. Pharm. Ber. Dtsch. Pharm. Ges.* **1962**, *295*, 735–744; H.-D. Stachel, M. Jungkenn, C. Koser-Gnoss, H. Poschenrieder, J. Redlin, *Liebigs Ann. Chem.* **1994**, 961–964.

[6] J. L. Finar, *J. Chem Soc.* **1955**, 1205–1208.

[7] P. R. Mallinson, M. R. Truter, *J. Chem. Soc. Perkin Trans. 2* **1972**, 1818–1823; A. J. Layton, P. R. Mallinson, D. G. Parsons, M. R. Truter, *J. Chem. Soc. Chem. Commun.* **1973**, 694–695.

[8] **5a**: $C_{90}H_{149}Cu_6NO_{43}$, M = 2314.43. Crystal dimensions: 0.30 × 0.30 × 0.2 mm^3, triclinic, space group $P\bar{1}$, a = 1561.2 (3), b = 1874.8 (4), c = 2448.6 (5) pm, V = 6333(2) × 10^6 pm^3, Z = 2, ρ_{calcd} = 1.298 $g\,cm^{-3}$. Diffractometer: Enraf-Nonius CAD4-MACH3, $Mo_{K\alpha}$ radiation (λ = 71.073 pm), T = 193(2) K, graphite monochromator. Measurement details: omega/theta scan; range 2.36° ≤ θ ≤ 22.48°; section of reciprocal lattice: −16 ≤ h ≤ 16, −19 ≤ k ≤ 20, −26 ≤ l ≤ 0. Number of measured intensities: 16964; number of independent reflections: 16496; number of reflections with $F > 4\sigma(F)$: 6898. Linear absorption coefficient: 1.070 mm^{-1}. Absorption correction: Ψ scan. Ratio of F/parameters: 1355. The structure was solved by direct methods using SHELXTL Plus 4.11. Refinement with all data (1355 parameters) by full-matrix least-sqares on F^2 using SHELXL93 (G. M. Sheldrick, Göttingen 1993). All non-hydrogen atoms were refined anisotropically; the hydrogen atoms were fixed in idealized positions using a riding model. Final R values: $R1$ = 0.0773 for $F > 4\sigma(F)$ and $wR2$ = 0.2993 (all data) with $R1 = \sum|F_o - F_c| / \sum F_o$ and $wR2 = \sum w|(F_o^2 - F_c^2)^2| / \sigma w(F_o^2)^2)^{0.5}$; largest peak (1.156 e $Å^{-3}$) and hole (−0.805 e $Å^{-3}$). Crystallographic data (excluding structure factors) for the structure reported in this paper have been deposited with the Cambridge Crystallographic Data Centre as supplementary publication no. CCDC-179-105. Copies of the data can be obtained free of charge on application to The Director, CCDC, 12 Union Road, Cambridge CB2 1EZ, UK (fax: Int. code +(1223) 336-033; e-mail: teched@chemcrys.cam.ac.uk).

[9] The positions of the hydrogen atoms could not be determined by the data set obtained. Therefore an exact assignment of the tautomeric variants [CuHOMe/OH] or [CuOMe/H_2O] is not possible.

[10] Note added in proof (4. 9. 96): According to an X-ray crystallographic structure analysis, complex $[KOH(Cu_3L_3^2)_2] \cdot 6$ HOMe is isostructural to **5a**.

Highly Selective Epoxidation Catalysts Derived from Intrazeolite Trimethyltriazacyclononane–Manganese Complexes**

Dirk E. De Vos, Julia L. Meinershagen, and Thomas Bein*

Dedicated to Professor Galen D. Stucky on the occasion of his 60th birthday

Over the last few years the development of zeolite-based catalysts for the liquid-phase oxidation of hydrocarbons has been a field of active research, and several interesting systems have been discovered.[1–8] However, the selectivities of these systems in the epoxidation of olefins may be limited by acid-catalyzed or other side reactions. This is particularly true with Ti-β and $[Mn(bpy)_2]^{2+}$–NaY catalysts (bpy = 2,2′-bypridine). Furthermore, the epoxides are frequently subject to solvolysis,[1, 3] or large amounts of less desirable products are formed, for example phenylacetaldehyde and benzaldehyde in the case of the oxidation of styrene.[8]

We now report on a novel zeolite-based catalyst, a manganese faujasite containing the cyclic triamine 1,4,7-trimethyl-1,4,7-triazacyclononane (tmtacn). This material catalyzes the oxidation of numerous olefins with H_2O_2, yielding epoxides with only minimal by-product formation. We also report on the characteristics of the corresponding homogeneously catalyzed reaction, which allows us to outline the effect of the heterogenization on the catalytic activity.

The zeolite-based oxidation catalysts were prepared by reacting a Mn^{II}NaY zeolite (0.8 wt% Mn, or about one metal ion per four supercages), dehydrated at 250 °C, with the polyamine ligand for 10 h at 150 °C under an inert atmosphere and occasional shaking. A polyamine to Mn molar ratio of 2.2 was found to be optimal for an efficient diffusion of the ligand into the zeolite pores. Homogeneous catalysts were prepared in situ by adding the ligand, dissolved in the organic reaction solvent, and $MnSO_4 \cdot H_2O$, dissolved in water, to the reaction mixture. All chemicals used were commercial products, with the exception of tmtacn and 1,4,7-triazacyclononane (tacn), which were prepared by known procedures.[9] Numerous epoxides were synthesized as reference compounds through the peracid method and identified through gas chromatograpy/mass spectrometry (GC/MS) and ^{1}H NMR spectroscopy.

Before the adsorption of the ligand by the Mn zeolite, X-band ESR spectroscopy shows the characteristic six-line signal of Mn^{II} with a total width of about 500 G, which is typical for an oxygen-coordinated Mn ion in zeolites (Fig. 1a).[10] After sorption of the ligand into the zeolite host, the intensity of this signal strongly decreases at the expense of a new Mn^{II} signal, which extends over a much wider field range, and displays a recognizable fine splitting (Fig. 1b).[11] We recently observed similar spectra for Mn^{II} ions in different A zeolites.[12] From the spectrum, the zero-field splitting parameter D can be estimated to amount to $0.06 \pm 0.015\ cm^{-1}$. Such a fine splitting is characteristic for a departure of the crystal field around Mn from cubic symmetry, with preservation of an at least threefold symmetry axis.[13] As the formation of complexes with two tmtacn ligands

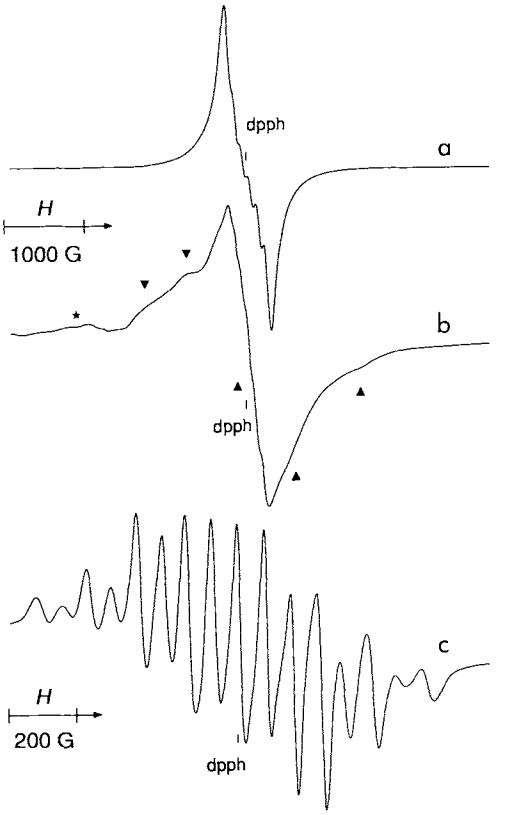

Fig. 1. X-band ESR spectra (9.44 GHz) of Mn in a) Mn^{II}NaY, before ligand adsorption, 298 K; b) $[Mn^{II}(tmtacn)]^{2+}$–NaY, under a dry N_2 atmosphere, 298 K; c) $[Mn(tmtacn)]^{2+}$–NaY, exposed for 2 h to H_2O_2 in the concentrations of catalytic experiments (see Table 1), recorded at 8 K. In a) only the central $M_S = +1/2 \rightarrow -1/2$ transition of the Mn fine structure is resolved, indicating that the symmetry of the all-oxygen Mn environment is close to cubic. The reaction with the tmtacn ligand in b) reduces the local symmetry to axially symmetric; the non-central fine transitions (involving $M_S = \pm 3/2$ and $M_S = \pm 5/2$) now also contribute to the spectrum. The resulting five fine lines ($\Delta M_S = \pm 1$) are roughly spaced by the distance D and have been marked (∇) in the spectrum. At lower magnetic field in b), half-field transitions ($\Delta M_S = \pm 2$) are observed (*). In the H_2O_2 oxidized sample c), a sixteen-line signal of the Mn^{III}–Mn^{IV} dinuclear complex is observed. dpph = 1,1-diphenyl-2-picrylhydrazyl (as reference).

per Mn ion is unlikely for steric reasons,[14] we ascribe the new ESR signal to the formation of the $[Mn(tmtacn)]^{2+}$ complex. This chelation is not observed with smaller pore MnNa-ZSM-5 or MnNa-A zeolites that have pore openings of 0.53 and 0.41 nm, respectively, which implies that the chelation in the large-pore NaY zeolite is essentially intraporous. This $[Mn(tmtacn)]^{2+}$–NaY material is used as the catalyst precursor in the catalytic reactions.

The selective epoxidation activity of the $[Mn(tmtacn)]^{2+}$–NaY zeolite is somewhat surprising. Complexes of manganese and tmtacn ligands have been observed to activate H_2O_2 at room temperature, for example for bleaching and for epoxidations.[15, 16] However, bleaching is often associated with a) the production of reactive particles such as $(OH)^{\cdot}$, $(OOH)^{\cdot}$, or singlet oxygen ($^1O_2$), which may cause the formation of side products in epoxidations, and with b) disproportionation of the peroxide to molecular oxygen and water, which leads to a reduction of the selectivity of the oxidant.[17] It is therefore understandable that the reported epoxidation of styrenes with homogeneous Mn–tmtacn catalysts requires an at least 100-fold excess of the oxidant.[15]

In our initial experiments with the zeolite-based $[Mn(tmtacn)]^{2+}$–NaY catalyst, we adopted the same conditions as used for the homogeneous epoxidation (aqueous methanol,

[*] Prof. Dr. T. Bein, Dr. D. E. De Vos, J. L. Meinershagen
Purdue University
Department of Chemistry
West Lafayette, IN 47907 (USA)
Fax: Int. code +(317)494-0239
e-mail: tbein@chem.purdue.edu

[**] This work was supported by a grant from the U. S. Department of Energy.

 © VCH Verlagsgesellschaft mbH, D-69451 Weinheim, 1996 0570-0833/96/3519-2211 $ 15.00+.25/0

room temperature)[15] except that the oxidant to substrate ratio was 1:1. The epoxide yields of these reactions were very low (<1%). However, three major modifications of the procedure resulted in highly improved epoxide yields, even at close to stoichiometric H_2O_2:olefin ratios (Table 1): a) cooling the reaction mixture to 273 K or below, b) gradual peroxide addition, and c) use of acetone as a solvent. The latter produces a dramatic effect, not only for the zeolite-catalyzed reaction but also for the homogeneous reaction. For a discussion of the effect of acetone see reference [21]. The combined effects of these modifications result in a marked reduction of the undesired oxidant disproportionation, and an increase of the epoxide yield by a factor of 50.

Table 1. Effect of solvents and temperature on the epoxidation of styrene and cyclohexene with H_2O_2, catalyzed by the $[Mn(tmtacn)]^{2+}$–NaY zeolite or by homogeneous Mn–tmtacn complexes [a].

Catalyst	Substrate	T[K]	Solvent	Olefin conversion [%]	Epoxide selectivity [%] [b]
$[Mn(tmtacn)]^{2+}$–NaY					
	styrene	298	methanol	0.4	100
		298	acetone	7.0	99.1
		273	methanol	1.5	100
		273	acetone	19.3	97.7
	cyclohexene	298	methanol	0.3	100
		298	acetone	6.8	97.2
		273	methanol	2.1	100
		273	acetone	25.3	95.4
		273	acetone	47.2[c]	94.7
Mn^{II} + tmtacn					
	styrene	298	methanol	1.5	100
		273	acetone	47.1	97.8
	cyclohexene	298	methanol	1.4	100
		273	acetone	55.3	84 [d]

[a] Reaction conditions: olefin (1 mmol), H_2O_2 (1 mmol; as a 30 wt.% aqueous solution, gradually added), solvent (1 g), $[Mn(tmtacn)]^{2+}$–NaY solid catalyst (0.025 g). For homogeneous catalysis, tmtacn (22 μmol) and Mn^{II} (10 μmol) were consecutively added in organic solvent and water (0.1 mL), respectively. The homogeneous reaction conditions were chosen to match the heterogeneous experiments; they are not optimized (see ref. [21]). H_2O_2 consumption was usually complete within 12 h or less. [b] Remaining products: benzaldehyde (in case of styrene), (*E*)-1,2-cyclohexanediol (in case of cyclohexene). [c] A second aliquot of H_2O_2 (1 mmol) was added after 6 h. [d] Allylic cyclohexene oxidation products: 7%.

This yield increase does not affect the selectivity of the oxidation process. With the $[Mn(tmtacn)]^{2+}$–NaY system, side products in the reactions of styrene, cyclohexene, and *cis*-2-hexene (not listed) are minimal, if observed at all (Table 1). Products of double-bond cleavage, such as benzaldehyde, account for less than 3% of the products in the case of the oxidation of styrene. Remarkably, in the oxidation of cyclohexene with zeolite catalysts, no cyclohexenyl-2-hydroperoxide, cyclohex-2-enol, or cyclohex-2-enone was detected. This indicates that under these conditions, (HOO)$^{\bullet}$ or (HO)$^{\bullet}$ radicals, or other reactive O species, such as $^1O_2$, play no major role in the formation of cyclohexene oxidation products.[18] Epoxide solvolysis is also minimal. While in the related homogeneous systems an alkaline aqueous buffer may play a role in preventing this side reaction,[15] the excess amine adsorbed on the zeolite catalyst seems to quench effectively any acidity of the zeolite surface. This is a marked advantage of our material over catalysts such as Ti-β and $[Mn(bpy)_2]^{2+}$–faujasite; in these materials the surface pH is intrinsically acidic and further reactions of epoxides are the rule rather than the exception.[1, 3]

The structure of the tmtacn ligand seems to fulfill an essential role in making the Mn ion suited for the selective epoxidation. With the unmethylated tacn as ligand, only vigorous decomposition of the H_2O_2 oxidant is observed, resulting in the formation of the products in extremely low yields. While the methylation might protect the amine ligand against oxidation, an alternative explanation for this dramatic difference is that the methyl groups provide a hydrophobic wrapping around the Mn ion (Fig. 2). This lipophilic shield around the Mn ion probably favors the adsorption of an olefin at the peroxide-activated Mn ion, retarding the approach of new peroxide molecules and thus the catalytic H_2O_2 decomposition.

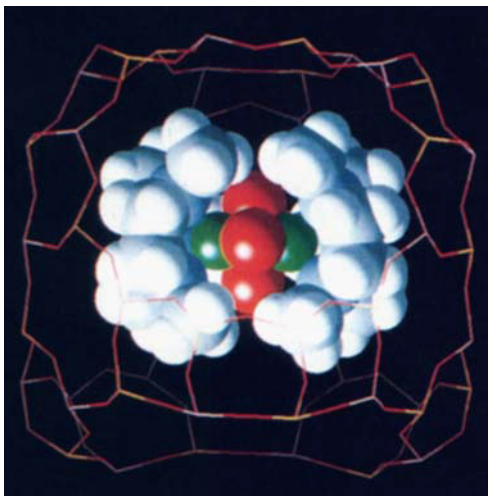

Fig. 2. Computer model (Cerius², Molecular Simulations Inc.) of a dinuclear complex of Mn and tmtacn in the supercage of a Y zeolite (Mn = green; O = red, N = blue; C = gray;, H = white).

While with the homogeneous catalyst the reaction starts almost instantaneously, an induction period is observed with $[Mn(tmtacn)]^{2+}$–NaY. In the ESR spectrum (Fig. 1c), this period corresponds to the appearance of a 16-line signal with a hyperfine constant $A = 78$ G, which is typical for a Mn^{III}–Mn^{IV} dinuclear complex.[19] Although other ESR-silent species could have formed, the correlation between the induction period and the appearance of the Mn^{III}–Mn^{IV} dinuclear complex suggests that catalysis occurs in conditions that promote oxidative formation of dinuclear Mn complexes in the cavitities of the Y zeolite. Analogous spectra are not observed when MnNa-ZSM-5 or MnNa-A zeolites treated with tmtacn are contacted with H_2O_2. This failure to observe dinuclear complexes in smaller pore zeolites suggests that for the Y zeolite, the dinuclear complexes are largely confined to the inner surface. Such complexes can contain manganese in its +IV oxidation state, in which state the metal is known to have the capacity to act as an oxygen-transferring species.

The spatial interaction between a NaY supercage and a dinuclear Mn-tmtacn complex, such as $[(tmtacn)Mn^{III}\text{-}O_2(OH)\text{-}Mn^{IV}(tmtacn)]^{2+}$, was studied by molecular modeling.[20] These complexes appear to have the appropriate dimensions to reside in the large faujasite cage, suggesting their steric entrapment inside these supercages (Fig. 2). The proposed intrazeolitic complexation of the Mn^{II} ion by tmtacn, and the consecutive formation of the larger dinuclear complexes upon addition of H_2O_2, are schematically represented in Scheme 1. The zeolite-confined character of the $[Mn(tmtacn)]^{2+}$–NaY catalysis was ultimately confirmed by a filtration experiment. Two styrene oxidations were run under identical conditions, in one case, however, the catalyst powder was removed from the reaction after about 5% conversion. While in the other reaction an oxide yield of 20%

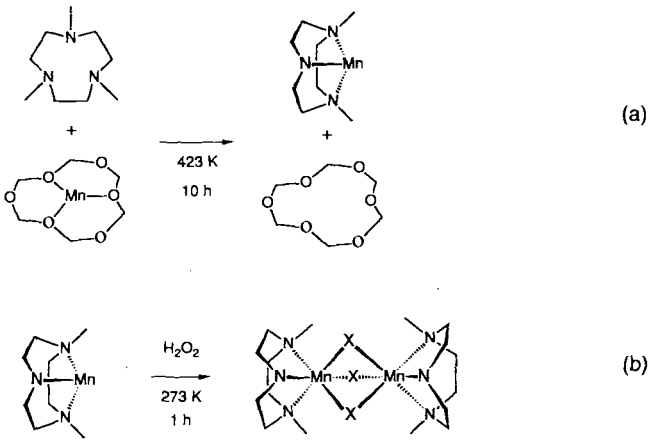

Scheme 1. Proposed reactions of Mn ions and tmtacn ligands in zeolite Y. Reaction a: In the chelation reaction, the Mn^{II} ion leaves an all-zeolite coordination, for example on a six-membered ring, to form a mononuclear $[Mn^{II}(tmtacn)]^{2+}$ chelate complex. Reaction b: The interaction of $[Mn^{II}(tmtacn)]^{2+}$–NaY with H_2O_2 in a water/acetone medium leads to intrazeolite formation of Mn^{III}–Mn^{IV} dinuclear complexes or other dimerization products (X = O^{2-}, OH^-, or other oxygen bridges).

was eventually obtained, the increase of the oxide yield stopped in the vial without catalyst.

In summary, the intrazeolite assembly of manganese complexes with cyclic amine ligands leads to novel catalytic materials for highly selective epoxidation. Dramatic effects of the ligand structure and of the solvent on the reactivity, as well as the patterns of substrate and product selectivity,[21] support the emerging picture of a sterically crowded, ligand-embedded active site in the cages of zeolite Y.

Received: March 19, 1996 [Z 8945 IE]
German version: *Angew. Chem.* **1996**, *108*, 2355–2357

Keywords: catalysis · complexes with nitrogen ligands · epoxidations · zeolites

[1] A. Corma, M. A. Camblor, P. Esteve, A. Martinez, J. Pérez-Pariente, *J. Catal.* **1994**, *145*, 151.
[2] K. M. Reddy, A. V. Ramaswamy, P. Ratnasamy, *J. Catal.* **1993**, *143*, 275.
[3] P. P. Knops Gerrits, D. E. De Vos, F. Thibault-Starzyk, P. A. Jacobs, *Nature* **1994**, *369*, 543.
[4] R. F. Parton, I. F. Vankelecom, M. J. Casselman, C. P. Bezoukhanova, J. B. Uytterhoeven, P. A. Jacobs, *Nature* **1994**, *370*, 541; T. Maschmeyer, F. Rey, G. Sankar, J. M. Thomas, *ibid.* **1995**, *378*, 159.
[5] K. J. Balkus, M. Eissa, R. Levado, *J. Am. Chem. Soc.* **1995**, *117*, 10753.
[6] N. Herron, G. D. Stucky, C. A. Tolman, *J. Chem. Soc. Chem. Commun.* **1986**, 1521.
[7] M. G. Clerici, P. Ingallina, *J. Catal.* **1993**, *140*, 71.
[8] S. B. Kumar, S. P. Mirajkar, G. C. G. Pais, P. Kumar, R. Kumar, *J. Catal.* **1995**, *156*, 163.
[9] G. H. Searle, R. J. Geue, *Austr. J. Chem.* **1984**, *37*, 959; K. Wieghardt, P. Chaudhuri, B. Nuber, J. Weiss, *Inorg. Chem.* **1982**, *21*, 3086.
[10] T. I. Barry, L. A. Lay, *Nature* **1965**, *208*, 1312.
[11] B. Bleaney, D. J. E. Ingram, *Proc. Royal Soc. London A* **1951**, *205*, 336.
[12] D. E. De Vos, B. M. Weckhuysen, T. Bein, *J. Am. Chem. Soc.* in press.
[13] A. Abragam, B. Bleaney, *Electron Paramagnetic Resonance of Transition Ions*, Clarendon Press, Oxford, **1970**.
[14] P. Chaudhuri, K. Wieghardt, *Prog. Inorg. Chem.* **1987**, *35*, 329.
[15] R. Hage, J. E. Iburg, J. Kerschner, J. H. Koek, E. L. M. Lempers, R. J. Martens, U. S. Racherla, S. W. Russell, T. Swarthoff, M. R. P. van Vliet, J. B. Warnaar, L. van der Wolf, B. Krijnen, *Nature* **1994**, *369*, 637.
[16] S. H. Jureller, J. L. Kerschner, R. Humphreys, (Unilever), US Patent 5329024, **1994**.
[17] K. M. Thompson, W. P. Griffith, M. Spiro, *J. Chem. Soc. Faraday Trans.* **1993**, *89*, 1203; ibid. **1993**, *89*, 4035.
[18] A. A. Frimer, *Singlet Oxygen, Vol. 2*, CRC Press, Boca Raton, Florida, **1985**; R. A. Sheldon, J. K. Kochi, *Metal-Catalyzed Oxidation of Organic Compounds*, Academic Press, New York, **1981**.
[19] K. Wieghardt, U. Bossek, L. Zsolnai, G. Huttner, G. Blondin, J.-J. Girerd, F. Babonneau, *J. Chem. Soc. Chem. Commun.* **1987**, 651; R. Hage, B. Krijnen, J. B. Warnaar, F. Hartl, D. J. Stufkens, T. L. Snoeck, *Inorg. Chem.* **1995**, *34*, 4973.
[20] Molecular modeling was performed with the Cerius² Software from Molecular Simulations Inc. Plausible coordinates for a dimeric complex of Mn and tmtacn were obtained from K. Wieghardt, U. Bossek, B. Nuber, J. Weiss, J. Bonvoisin, M. Corbella, S. E. Vitols, J. J. Girerd, *J. Am. Chem. Soc.* **1988**, *110*, 7398.
[21] D. E. De Vos, T. Bein, *Chem. Commun.* **1996**, 917; *J. Organomet. Chem.* in press.

Toward the Design of Porous Organic Solids: Modular Honeycomb Grids Sustained by Anions of Trimesic Acid**

Rosa E. Melendez, C. V. Krishnamohan Sharma, Michael J. Zaworotko,* Carey Bauer, and Robin D. Rogers

The concept of design or crystal engineering of functional solids relies upon controlling the topology of crystal packing through exploitation of forces that range in the continuum from weak hydrogen bonds to covalent bonds.[1, 2] In the context of porosity, a particularly relevant functional property given the commercial importance of zeolites, it is becoming increasingly clear that even noncovalent interactions can be directional and strong enough to generate and sustain porosity.[3] Several research groups have recently demonstrated that a modular strategy to crystal engineering can propagate molecular symmetry into crystalline architecture or even space group symmetry.[4–9] Unfortunately, two- (2D) and three-dimensional (3D) frameworks typically fail to realize their full potential for porosity because of interpenetration or self-inclusion of identical frameworks.[4b, 7a, 9] In such a context, trimesic acid (1,3,5-benzenetricarboxylic acid, H_3TMA) is prototypal since it *predictably* self-assembles through the well-known carboxylic acid dimer motif into an interpenetrating honeycomb grid with 11 Å cavities.[6, 10, 11] We report herein on two compounds that illustrate two alternate modular strategies to propagate the trigonal symmetry of H_3TMA: the ammonium salt **1** forms a neutral honeycomb grid and the ammonium salt **2** has an anionic honeycomb grid based upon hydrogenbiscarboxylate hydrogen bonds.

$[NH_2(c\text{-}C_6H_{11})_2]_3[TMA]$ **1**

$[NH_2(CH_3)_2]_{12}[H_3TMA][H_2TMA]_3[HTMA]_3[TMA]$ **2**

Compounds **1** and **2**, which contain the fully and 50% deprotonated forms of H_3TMA, respectively, predictably self-assemble into honeycomb grids because of their trigonal symmetry

[*] Prof. M. Zaworotko, R. E. Melendez, Dr. C. V. K. Sharma
Department of Chemistry
Saint Mary's University
Halifax, Nova Scotia, B3H 3C3 (Canada)
e-mail: mzaworot@science.stmarys.ca
Fax: Int. code + (902) 420 5261
Dr. C. Bauer, Prof. R. D. Rogers
Department of Chemistry, Northern Illinois University
DeKalb, IL, 60115-2862 (USA)

[**] We gratefully acknowledge financial support from the National Science and Engineering Research Council (NSERC) and the Environmental Science and Technology Alliance of Canada (ESTAC). Trimesic acid = 1,3,5-benzenetricarboxylic acid.

 © VCH Verlagsgesellschaft mbH, D-69451 Weinheim, 1996 0570-0833/96/3519-2213 $ 15.00+.25/0

and the number and complementarity of their hydrogen bonding sites.[12] At first sight the secondary ammonium cations in compound **1** might appear to be unsuitable for facilitating propagation of the trigonal symmetry of H_3TMA or its derivatives to the crystal structure. However, as Scheme 1 reveals, there are

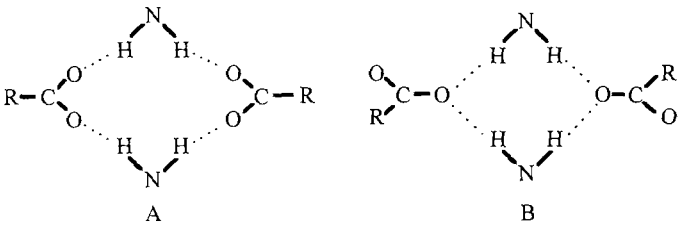

A B

Scheme 1.

two common motifs that occur between secondary ammonium cations and carboxylate anions,[13] both of which would readily propagate TMA^{3-} into a honeycomb grid (Scheme 2). For

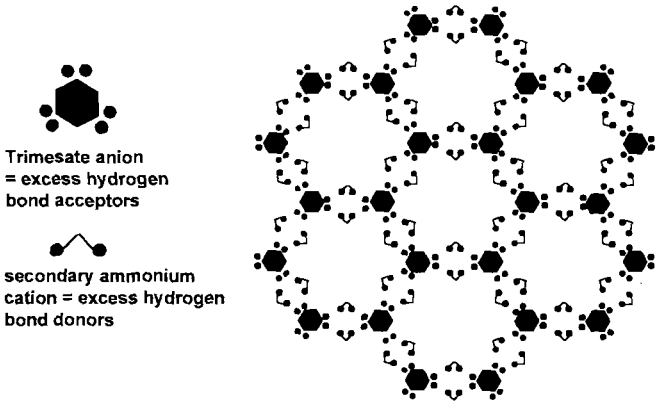

Scheme 2.

compound **2**, the hierarchy of hydrogen bond strengths prevents the cation from influencing the honeycomb structure that would result from self-assembly of hydrogenbiscarboxylate moieties (Scheme 3).[14]

The noncentrosymmetric crystal structure of **1**[15] reveals that the hexagonal network has an effective internal diameter of 12.7 Å. The TMA^{3-} ions are bridged by ammonium ion "spacers" in motif **B** (Scheme 1 N···O, 2.725(9), 2.837(11), 2.755(10), 2.763(10) Å, Fig. 1). The cyclohexyl groups of the ammonium ions project above and below the plane of the honeycomb sheets and almost close the cavities, thereby precluding interpenetration of the type observed in H_3TMA. The carboxylate oxygen atoms of one of the two crystallographically independent TMA^{3-} ions are hydrogen-bonded (O···O 2.727(8) Å) to three clathrated MeOH molecules that lie outside the cavity. The hydrophobic cavity enclosed by the cyclohexyl moieties contains disordered solvent molecules[15] and is reminiscent of "carceplexes".[16]

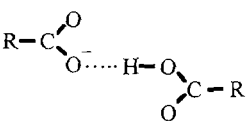

Scheme 3.

Compound **2** crystallizes as an anionic honeycomb grid. It is effectively a cocrystal of H_3TMA and, remarkably, all three of its possible deprotonated forms: H_2TMA^-, $HTMA^{2-}$, and TMA^{3-}. These components self-assemble through strong O–H···O^- hydrogen bonds to form two independent honeycomb anionic grids: $H_3TMA \cdot 3HTMA^{2-}$ and $3H_2TMA^- \cdot TMA^{3-}$ (Fig. 2).[17] The formulation of the grids was determined after hydrogen atom location and careful examination of the C–O bond lengths within the carboxylate moieties.[18] The O···O distances of the hydrogen bonds in these two sheets (2.551(5) and 2.524(5) Å, 2.535(5) and 2.523(5) Å) are contracted by 0.1 Å compared to those in H_3TMA, thereby affording a distorted hexagon with an effective internal diameter of 10.4 Å. The cations cross link adjacent hexagonal sheets (N···O, 2.711(6) to 2.808(7) Å) by donating hydrogen bonds to CO_2^- ions rather than to CO_2H moieties. This would be expected based upon the hierarchy of the donor–acceptor strengths of the hydrogen bonds of these functional groups.

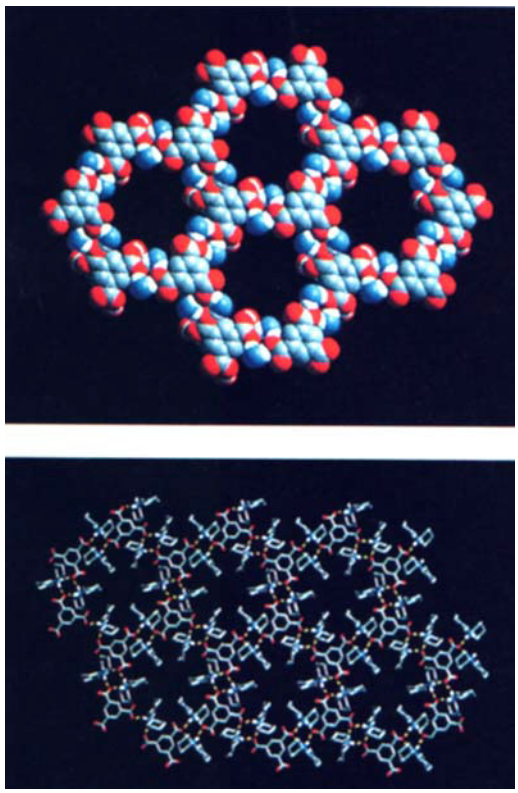

Fig. 1. Crystal structure of **1**: Top: A space-filling model of the honeycomb grid in **1**. Trimesate anions are bridged by cations through motif B (Scheme 1). Cyclohexyl groups are omitted for the sake of clarity. Bottom: A view perpendicular to the honeycomb grid, cyclohexyl groups of the cations project above and below the grid and preclude interpenetration by capping the cavity.

In summary, the crystal structures of **1** and **2** illustrate the inherent advantages of modular approaches to crystal engineering: facile synthesis, fine tuneable functional properties (i.e. cavity size), eschewing of interpenetration. Furthermore, the ionic hydrogen bonds[12] afford solids that are readily crystallized from solution yet, relative to many organic compounds, high melting. Compound **2** further illustrates that pK_a values derived from solution can be misleading in the context of predicting the location of protons in hydrogen-bonded cocrystals and/or salts.[14a] We anticipate that compounds **1** and **2** are prototypes for two new classes of host matrix based upon derivatives of H_3TMA and are presently investigating the generality of this modular strategy and the ability of such solids to selectively enclathrate moderately sized guests.

Received: March 27, 1996 [Z8980IE]
German version: *Angew. Chem.* **1996**, *108*, 2357–2359

 © VCH Verlagsgesellschaft mbH, D-69451 Weinheim, 1996 0570-0833/96/3519-2214 $ 15.00+.25/0

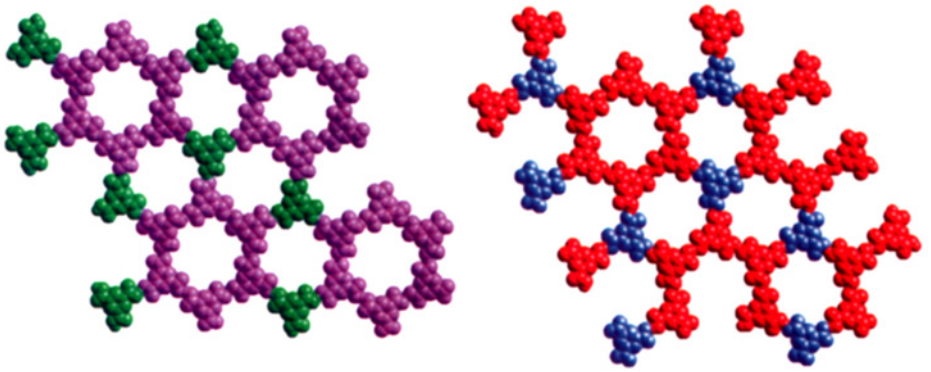

Fig. 2. The two independent honeycomb grids in **2**. Left: Grid consists of H_3TMA molecules (green) and $HTMA^{2-}$ ions (magenta) in the ratio 1:3; right: Grid consists of TMA^{3-} ions (blue) and H_2TMA^- ions (red) in the ratio 1:3. The grids are sustained by O–H···O$^-$ bis(carboxylate) hydrogen bonding. Cations, omitted for the sake of clarity, fill the void space of the cavities and cross link parallel honeycomb grids.

Keywords: crystal engineering · hydrogen bonds · solid-state structures · trimesic acid

[1] G. R. Desiraju, *Crystal Engineering, The Design of Organic Solids*, Elsevier, Amsterdam, **1989**.

[2] a) B. F. Hoskins, R. Robson, *J. Am. Chem. Soc.* **1990**, *112*, 1546; b) J.-M. Lehn, *Angew. Chem.* **1990**, *102*, 1347; *Angew. Chem. Int. Ed. Engl.* **1990**, *29*, 1304; c) P. R. Ashton, C. G. Claessens, W. Hayes, S. Menzer, J. F. Stoddart, A. J. P. White, D. J. Williams, *Angew. Chem.* **1995**, *107*, 1994; *Angew. Chem. Int. Ed. Engl.* **1995**, *34*, 1862.

[3] Organic crystals tend to close-pack with packing coefficients in the range 0.65–0.77 [1]. However, symmetrical and rigid hydrogen bonding networks often afford less dense open structures (e.g. trimesic acid, urea, hydroquinone, and Dianin's compound) that are stabilized by enclathration of guest molecules or interpenetration. The effective cavity diameter in H_3TMA (11 Å) is determined by calculating internuclear O···O distances across the hexagon, and subtracting the van der Waal's radius of the oxygen atom. Although synthetic zeolites can have comparable or larger pores, those in naturally occuring inorganic zeolites are typically smaller than 5 Å.

[4] a) G. B. Gardner, D. Venkataraman, J. S. Moore, S. Lee, *Nature* **1995**, *374*, 792; b) K. A. Hirsch, D. Venkataraman, S. R. Wilson, J. S. Moore, S. Lee, *J. Chem. Soc. Chem. Commun.* **1995**, 2199.

[5] O. M. Yaghi, G. Li, H. Li, *Nature* **1995**, *378*, 703.

[6] S. V. Kolotuchin, E. E. Fenlon, S. R. Wilson, C. J. Loweth, S. C. Zimmerman, *Angew. Chem.* **1995**, *107*, 2873; *Angew. Chem. Int. Ed. Engl.* **1995**, *34*, 2654.

[7] a) M. J. Zaworotko, *Chem. Soc. Rev.* **1994**, 283; b) S. Subramanian, M. J. Zaworotko, *Angew. Chem.* **1995**, *107*, 2295; *Angew. Chem. Int. Ed. Engl.* **1995**, *34*, 2127.

[8] B. F. Abrahams, B. F. Hoskins, D. M. Michail, R. Robson, *Nature* **1994**, *369*, 727.

[9] a) O. Ermer, *J. Am. Chem. Soc.* **1988**, *110*, 3747; b) O. Ermer, A. Eling, *Angew. Chem.* **1988**, *100*, 856; *Angew. Chem. Int. Ed. Engl.* **1988**, *27*, 829.

[10] F. H. Herbstein, *Top. Curr. Chem.* **1987**, *140*, 107

[11] H_3TMA eschews interpenetration if guest molecules fit efficiently into the hexagonal framework: F. H. Herbstein, M. Kapon, G. M. Reisner, *J. Incl. Phen.* **1987**, *5*, 211.

[12] However, $HTMA^{2-}$ and H_2TMA^- salts do not sustain honeycomb grids: R. E. Melendez, M. J. Zaworotko, *Supramolecular Chem.* in press.

[13] A Cambridge Structural Database (CSD, version V5.09) analysis of primary and secondary ammonium-carboxylate salts revealed the occurrence of three possible motifs (N···O ≤ 3.0 Å, N–H···O ≤ 90–180°, *R* factor ≤ 0.010). Of 723 compounds studied, motifs A, $R_4^4(8)$, and B, $R_4^2(8)$, were found in 101 and 511 compounds, respectively. A third motif, $R_4^3(8)$, occurs less frequently, and is a combination of A and B.

[14] a) M. C. Etter, *Acc. Chem. Res.* **1990**, *32*, 120; b) C. B. Aakeroy, K. R. Seddon, *Chem. Soc. Rev.* **1993**, 397.

[15] Trimesic acid was treated with *N*,*N*-dicyclohexylamine in a molar ratio of 1:3 in MeOH to give **1**. Hexagonal crystals of **1** were obtained from a 1:1 mixture of 1-butanol and MeOH. Crystals lose solvent and crystallinity at 45 °C and sublime above 240 °C. Crystal structure data for **1**: $[NH_2(cyclo\text{-}C_6H_{11})_2]_3[C_6H_3(CO_2)_3]\cdot x$MeOH, hexagonal, $P6_3$, $a = 17.6903(3)$, $b = 17.6767(6)$, $V = 4790.7(2)$ Å^3, $Z = 6$, $\rho_{calcd} = 1.121$ Mg m^{-3}. 2495 reflections of 3952 with $I_{net} > 3F$ were measured at 173 K on a Siemens SMART CCD area detector using the 2θ scan mode. Three MeOH molecules are hydrogen-bonded to the grid outside the cavity and there appear to be several disordered MeOH molecules within the honeycomb. The latter could not be readily resolved. Final *R* factors of $R_f = 0.057$ and $R_w = 0.055$ were obtained.
Crystallographic data (excluding structure factors) for the structure reported in this paper have been deposited with the Cambridge Crystallographic Data Centre as supplementary publication no. CCDC-179-76. Copies of the data can be obtained free of charge on application to The Director, CCDC, 12 Union Road, Cambridge CB2 1EZ, UK (fax: Int. code +(1223) 336-033; e-mail: teched@chemcrys.cam.ac.uk).

[16] a) D. J. Cram, *Nature* **1992**, *356*, 29; b) M. E. Tanner, C. B. Knobler, D. J. Cram, *J. Org. Chem.* **1992**, *57*, 40.

[17] Crystals of **2** were formed serendipitously from attempted cocrystallization of 4,4'-bipyridine and trimesic acid in dimethyl formamide (DMF). Compound **2** crystallized over a period of two months at room temperature, presumably by decomposition of DMF, m.p. > 300 °C. Crystal structure data for **2**: $[NH_2(CH_3)_2]_{12}[C_6H_3(CO_2H)(CO_2)_2]_3\cdot[C_6H_3(CO_2)_3]$, trigonal, $R\bar{3}$, $a = 33.412(5)$, $b = 17.465(3)$, $V = 16885(4)$ Å^3, $Z = 18$, $\rho_{calcd} = 1.311$ Mg m^{-3}. 2766 reflections of 4889 with $I_{net} > 3F$ were measured at 290 K on an Enraf-Nonius CAD4 diffractometer using the ω scan mode, final *R* factors of $R_f = 0.053$ and $R_w = 0.049$ were obtained [15].

[18] L. Leiserowitz, *Acta Crystallogr. Sect. B* **1976**, *32*, 775.

Synthesis and Structure of the Nanoclusters $[Hg_{32}Se_{14}(SePh)_{36}]$, $[Cd_{32}Se_{14}(SePh)_{36}(PPh_3)_4]$, $[P(Et)_2(Ph)C_4H_8OSiMe_3]_5[Cd_{18}I_{17}(PSiMe_3)_{12}]$, and $[N(Et)_3C_4H_8OSiMe_3]_5[Cd_{18}I_{17}(PSiMe_3)_{12}]$**

Silke Behrens, Marco Bettenhausen, Anne C. Deveson, Andreas Eichhöfer, Dieter Fenske,* Almut Lohde, and Ulrike Woggon

Nanoclusters and colloids from the semiconducting II–V and II–VI compounds are particularly interesting with respect to their optical and electronic properties in comparison to those of the solid bulk materials.[1] The influence of the size of the molecules and particles in the nanometer scale plays an important role in determining the band-gap ("size quantization effect"). An exact interpretation of the measured effects is made more difficult by a size distribution of the particles, which is usually found to be the case for colloids. The synthesis and structural characterization of cluster molecules with a defined size and structure provide an interesting approach to this class of compounds.[2]

In the case of the cadmium chalcogenide clusters, the largest structurally characterized clusters reported to date are **1a**[3] and **1b**.[4] We have already isolated and structurally characterized

[*] Prof. Dr. D. Fenske, Dipl.-Chem. S. Behrens, Dipl.-Chem. M. Bettenhausen, Dr. A. C. Deveson, Dr. A. Eichhöfer
Institut für Anorganische Chemie der Universität
Engesserstrasse, Gebäude-Nr. 30.45, D-76128 Karlsruhe (Germany)
Fax: Int. code +(721)661921
e-mail: eich@achbm6.chemie.uni-karlsruhe.de
A. Lohde, Dr. U. Woggon
Institut für Angewandte Physik der Universität Karlsruhe (Germany)

[**] This work was supported by the Deutsche Forschungsgemeinschaft (SFB 195 "Lokalisierung von Elektronen in makroskopischen und mikroskopischen Systemen") and the Bundesministerium für Bildung und Forschung (BMBF).

a large number of copper chalcogenide clusters,[5] amongst which is one of the largest known characterized clusters $[Cu_{146}Se_{76}(PPh_3)_{30}]$.[6] Herein we describe the first synthesis and structural characterization of mercury and cadmium selenide clusters as well as cadmium phosphide clusters **2**–**5** [Eqs. (a)–(e)].

$[Cd_{32}S_{14}(SPh)_{36}]\cdot 4DMF$ **1a**

$[Cd_{32}S_{14}(SCH_2CH(OH)CH_3)_{36}]\cdot 4H_2O$ **1b**

The reaction of $[Fe(CO)_4(HgCl)_2]$ with $PhSeSiMe_3$ in toluene [Eq. (a)] gave a red solution from which a mixture of yellow

$$[Fe(CO)_4(HgCl)_2] \xrightarrow[\text{toluene}]{PhSeSiMe_3} [Hg_{32}Se_{14}(SePh)_{36}]_{cub} + [Hg(SePh)_2] \quad \text{(a)}$$

2a

crystals of $[Hg(SePh)_2]$ and red crystals of **2a** were formed after a few days. Figures 1 and 2 show the molecular structure of the $Hg_{32}Se_{50}$ cluster of **2a**. The compound crystallizes in the cubic space group $P23$, and the cluster molecules possess T symmetry.

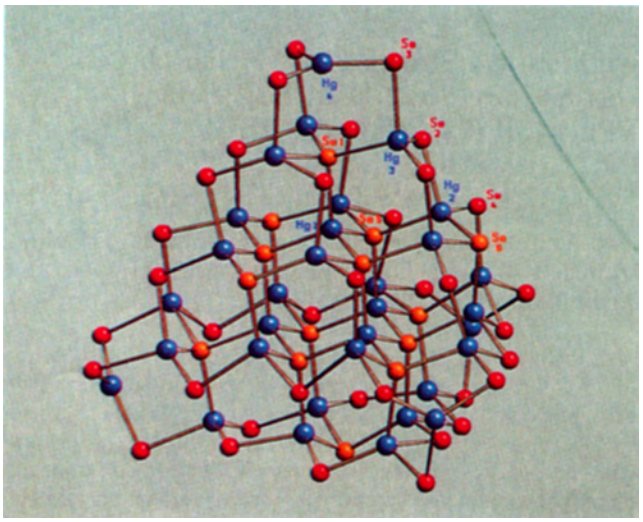

Fig. 1. Molecular structure of the $Hg_{32}Se_{50}$ cluster of **2a**. Hg: blue; Se^{2-}: orange; Se from $SePh^-$: red. Selected bond lengths [pm] and angles [°] (deviations ±0.3 pm and ±0.1°): Hg(1,2,3)–Se: 257.5–269.9, Hg4–Se3: 256.7; Se-Hg(1,2,3)-Se 91.0–130.1 (distorted tetrahedral coordination by Se); sum of the angles at Hg4 (trigonal planar coordination by Se): 360.0°

The core of the cluster, which comprises 13 HgSe adamantane cages, is a section of the sphalerite structure, which is also found in HgSe.[7] The corners of the cluster are made up of barrelanoid HgSe cages that are characteristic of the wurzite structure of HgSe. The Hg atoms Hg1–Hg3 have distorted tetrahedral environments, coordinated by the Se atoms of SePh (red) and Se ligands (orange) (Se-Hg-Se: 91.0(1)–130.1(1)°). The four Hg atoms Hg4 at the corners of the tetrahedral cluster have almost trigonal-planar coordination from the three Se atoms of the SePh ligands (Se-Hg-Se: 120.0(1)°). This is very remarkable because these Hg atoms are not sterically shielded by the phenyl groups (Fig. 2). The diameter of **2a** is thus about 2400 pm. The

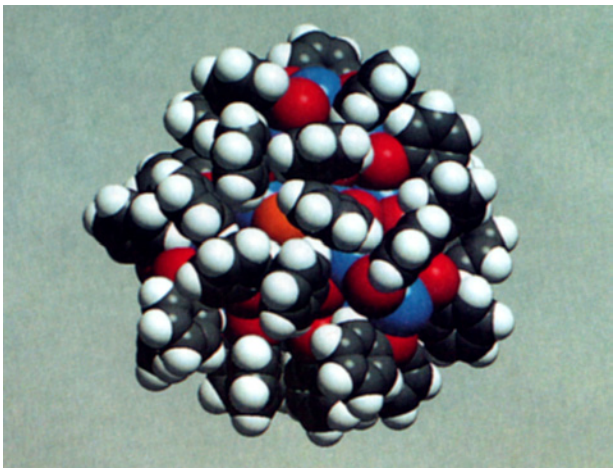

Fig. 2. Space-filling model of **2a**. Hg: blue; Se^{2-}: orange; Se from $SePh^-$: red; C: grey; H: white.

Hg–Se bond lengths lie between 256.7 and 269.9(3) pm, which correspond to those distances in HgSe (262 pm).[8] The structure of **2a** resembles that of the reported cadmium sulfide clusters[3, 4] and also that of the cadmium selenide cluster **3** (see below). However in these structures the cadmium atoms at the corners of the cluster have tetrahedral environments through additional coordination of solvent molecules or phosphane ligands.

The reaction of $HgCl_2$ with $PhSeSiMe_3$ in toluene [Eq. (b)], and subsequent layering of the red reaction solution with heptane, resulted in the formation of red needlelike crystals of **2b**,

$$HgCl_2 \xrightarrow[\text{toluene/heptane}]{PhSeSiMe_3} [Hg_{32}Se_{14}(SePh)_{36}]_{trig} + [Hg(SePh)_2] \quad \text{(b)}$$

2b

which have the same empirical formula as **2a**, but crystallize in the trigonal space group $P3_2$. The two modifications differ only in the packing of the cluster molecule in the crystal (Fig. 3). The arrangement of the cluster molecules in **2a** is such that channels with a diameter of about 700 pm are formed.

The red color of the crystals shows that the electronic structure of the cluster differs from that of the black semimetal HgSe in the macroscopic state ($\Delta E_g = -$ -0.06 eV at 300 K).[9] To obtain a more accurate analysis of the optical and electronic properties of compounds **2a** and **2b**, the absorption and luminescence spectra were measured. The absorption spectrum of **2b**, recorded in the solid state on a glass slide layered with indium tin oxide at 10 K, shows two maxima at 539 nm (2.3 eV) and 496 nm (2.5 eV) (Fig. 4). The luminescence spectrum of this sample (dotted line in Fig. 4), measured with an excitation wavelength of 436 nm at 10 K, shows a maximum at 670 nm (1.85 eV). The red solution of **2b** in THF shows weak maxima at 549 nm (2.26 eV) and 504 nm (2.46 eV) in the absorption spectrum at room temperature. In comparison to the absorption maxima of the Cd_{32} clusters,[3, 4] those for **2b** show a strong shift to larger wavelengths.

Treatment of $[CdCl_2(PPh_3)_2]$ with $PhSeSiMe_3$ in acetone afforded colorless crystals of **3** [Eq. (c)]. In analogy to the struc-

 © VCH Verlagsgesellschaft mbH, D-69451 Weinheim, 1996 0570-0833/96/3519-2216 $ 15.00+.25/0

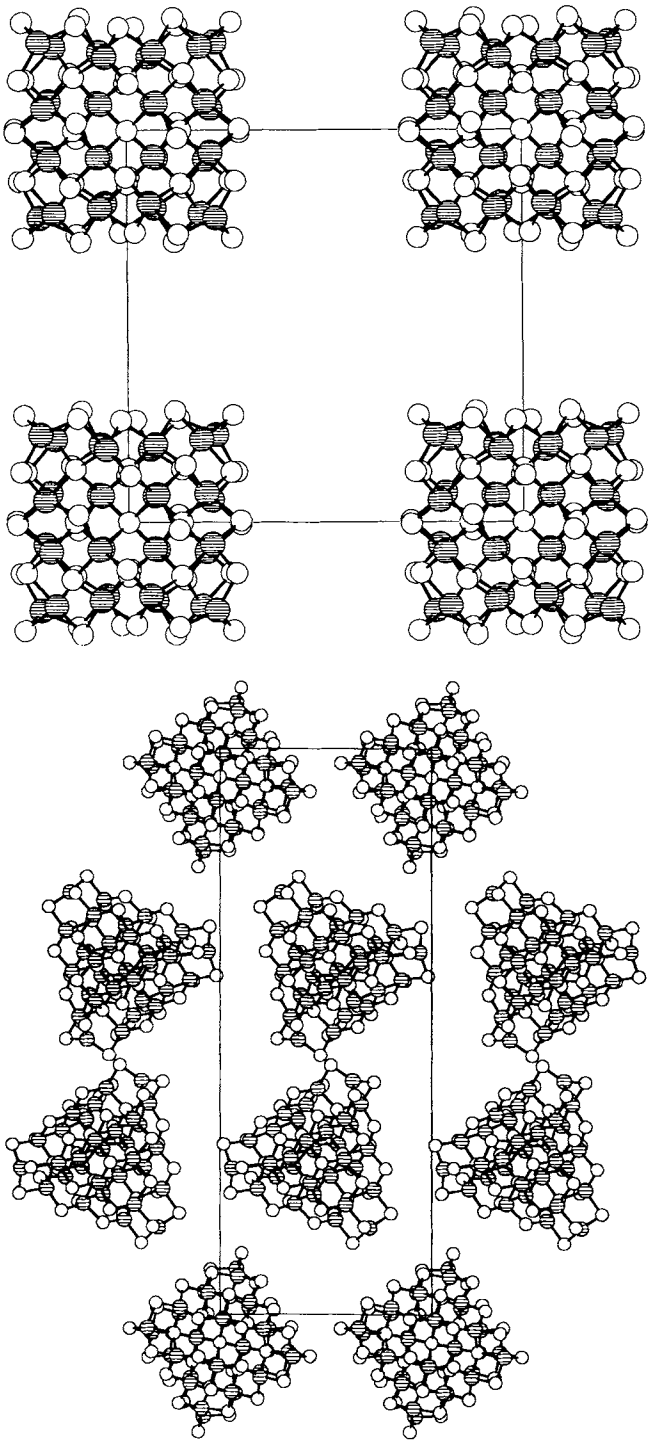

Fig. 3. Arrangement of the clusters **2a** (above) and **2b** (below) in the crystal (without C and H atoms). Hg: ◎; Se: ○.

tures of **2a** and **2b**, the skeleton of the $Cd_{32}Se_{50}$ cluster is built up from two characteristic structural units; the center of the cluster is of the sphalerite type and the corners of the cluster are formed by wurzite-analogous cages. The Cd atoms have distorted tetrahedral environments, coordinated by Se atoms from the SePh and Se ligands and by the P atoms of the PPh_3 ligands (Se-Cd-Se: 89.0–126.9(1)°, Se-Cd-P: 96.1–109.5(2)°). The Cd–Se bond lengths lie between 255.9 and 267.9(3) pm. This is comparable to the bulk material CdSe (zinc blende structure) in which the Cd–Se bond length is 262 pm.[10]

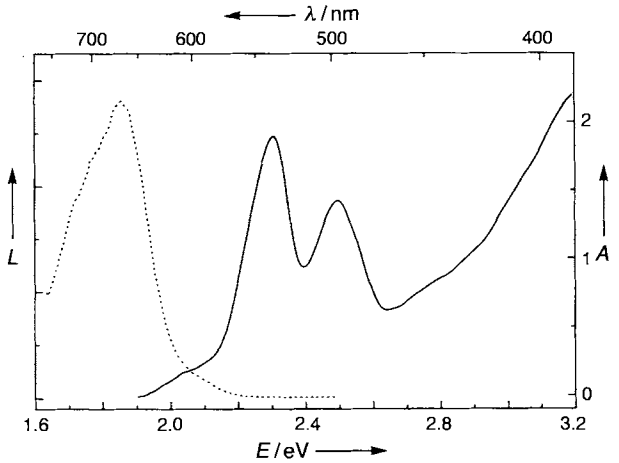

Fig. 4. Absorption (full line) and luminescence spectra (dotted line) of **2b** in the solid state on an indium tin oxide layered glass holder at 10 K. A = absorption. L = luminescence.

The reaction of CdI_2 with PEt_2Ph and $P(SiMe_3)_3$ in THF [Eq. (d)] led to the formation of a pale yellow solution, which

$$CdI_2 + 2\,PEt_2Ph + P(SiMe_3)_3 \xrightarrow[-\,ISiMe_3]{THF\,/\,RT} [PEt_2(Ph)C_4H_8OSiMe_3]_5[Cd_{18}I_{17}(PSiMe_3)_{12}] \quad \textbf{4} \qquad (d)$$

when layered with hexane produced a yellow oil (of unknown composition) and colorless, strongly refracting crystals of **4**. The analogous cluster anion also crystallized from the reaction of CdI_2 with NEt_3 and $P(SiMe_3)_3$ in THF as the compound **5** [Eq. (e)]. In both structures the cations were particularly diffi-

$$CdI_2 + NEt_3 + P(SiMe_3)_3 \xrightarrow[-\,ISiMe_3]{THF\,/\,RT} [NEt_3C_4H_8OSiMe_3]_5[Cd_{18}I_{17}(PSiMe_3)_{12}] \quad \textbf{5} \qquad (e)$$

cult to refine in the difference Fourier analysis such that for each structure only three of the cations could be localized. The two missing cations are highly disordered. The formation of the cations can be ascribed to the cleavage of THF molecules by reactive $SiMe_3$ groups, which then can attack the tertiary phosphane or amine, leading to the formation of C–P or C–N bonds, respectively.

Complex **4** crystallizes in the chiral space group $P2_12_12_1$, **5** in $P\bar{1}$. The structure of the cluster anion of **4** and **5** is shown in Figure 5 (the data for **4** are discussed). The 18 Cd atoms are μ_3-bridged by the P atoms of the 12 $PSiMe_3$ groups and the eight I atoms I10–I17, in such a way that a spherical cluster is formed. The terminal I atoms I1–I9 are coordinated to the Cd atoms Cd1–Cd9. Apart from Cd12, Cd16, and Cd17, which are coordinated by I and P atoms in a distorted trigonal planar environment, all other Cd atoms have near tetrahedral coordination. The Cd–I distances lie between 300.7 and 329.1(2) pm for the bridging I atoms and between 271.0 and 284.9(8) pm for the terminal I atoms. The Cd–P bond lengths range between 244.8 and 255.5(5) pm.

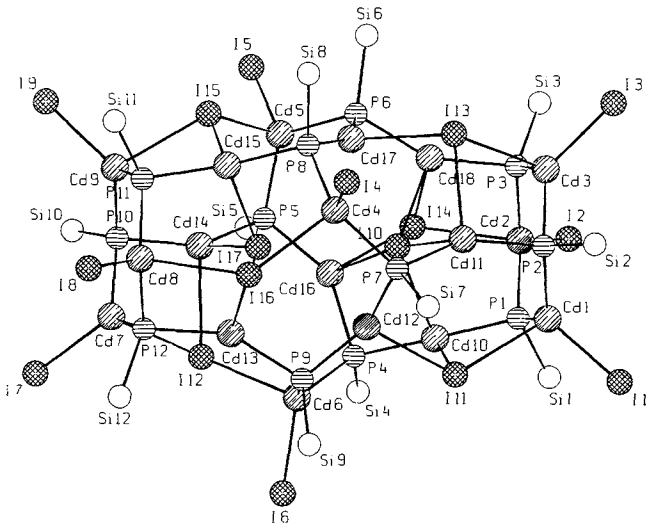

Fig. 5. Molecular structure of the cluster anion of **4** and **5**.

The cluster anions of **4** and **5** do not show any resemblance to any known bulk material structure of cadmium phosphides[11] or cadmium iodophosphides.[12] However, one might expect that the presence of the halogen atoms and the reactive $PSiMe_3$ groups could well lead to further reaction and that aggregation of the clusters to form the above-mentioned cadmium iodophosphides might be possible. Cadmium halogenophosphides are semiconductors in their macroscopic states. Sections of the solid-state structure in the form of ligand-stabilized cluster molecules would be very interesting with regard to investigations of larger quantum effects, as observed for the Q-Cd_3P_2 particles.[11]

Experimental Procedure

Preparation of compounds **2**–**5** (all steps were performed under a nitrogen atmosphere and absolute solvents were used).

2a: $PhSeSiMe_3$ (0.38 mL, 1.50 mmol) was added to a suspension of $[Fe(CO)_4(HgCl)_2]$ (0.48 g, 0.75 mmol) in toluene (25 mL). From the resulting clear red solution a yellow precipitate quickly formed. After a few days red cubes of **2a** crystallized.

2b: $PhSeSiMe_3$ (0.37 mL, 1.48 mmol) was added dropwise to a suspension of $HgCl_2$ (0.2 g, 0.74 mmol) in toluene (25 mL). The resulting clear red solution was layered with heptane and within a few hours the solution lightened in color and yellow crystals of $Hg(SePh)_2$ and red needlelike crystals of **2b** were formed.

3: $PhSeSiMe_3$ (0.46 mL, 1.86 mmol) was added to a suspension of $CdCl_2(PPh_3)_2$ (0.33 g, 0.47 mmol) in acetone (25 mL). This produced a clear, pale yellow solution, from which colorless rhomboids of **3** crystallized.

4 and **5**: A solution of CdI_2 (0.36 g 0.98 mmol) in THF (50 mL) was treated with PEt_2Ph (0.32 g, 1.96 mmol) (for **4**) or NEt_3 (0.1 g, 0.99 mmol) (for **5**). $P(SiMe_3)_3$ (0.5 g, 1.99 mmol) was added to the clear solutions. Layering the pale yellow reaction mixtures with hexane resulted in the formation of colorless crystals of **4** and **5** after three days.

Received: April 10, 1996
Revised version: July 10, 1996 [Z 9010 IE]
German version: *Angew. Chem.* **1996**, *108*, 2360–2363

Keywords: cadmium compounds · clusters · nanostructures · mercury compounds · silicon compounds

[1] H. Weller, *Angew. Chem.* **1996**, *108*, 1159; *Angew. Chem. Int. Ed. Engl.* **1996**, *35*, 1079; *ibid.* **1993**, *105*, 43 and **1993**, *32*, 41; *Adv. Mater.* **1993**, *5*, 88.

[2] I. Dance, K. Fisher, *Prog. Inorg. Chem.* **1994**, *41*, 637.

[3] N. Herron, J. C. Calabrese, W. E. Farneth, Y. Wang, *Science* **1993**, *259*, 1426.

[4] T. Vossmeier, G. Reck, B. Schulz, L. Katsikas, H. Weller, *J. Am. Chem. Soc.* **1995**, *117*, 12881.

[5] D. Fenske, J.-C. Steck, *Angew. Chem.* **1993**, *105*, 1364; *Angew. Chem. Int. Ed. Engl.* **1993**, *32*, 238; S. Dehnen, A. Schäfer, D. Fenske, R. Ahlrichs, *ibid.* **1994**, *106*, 786 and **1994**, *33*, 746; S. Dehnen, D. Fenske, *ibid.* **1994**, *106*, 2369 and **1994**, *33*, 2287.

[6] H. Krautscheid, D. Fenske, G. Baum, M. Semmelmann, *Angew. Chem.* **1993**, *105*, 1364; *Angew. Chem. Int. Ed. Engl.* **1993**, *33*, 1303.

[7] Crystal structure analysis data: STOE IPDS diffractometer, Siemens rotating anode, $Mo_{K\alpha}$, 180 K (**2a**, **2b**) and 200 K (**3**–**5**). **2a**: $a = 2224.5(3)$ pm, $V = 11008(2) \times 10^6$ pm^3; space group $P23$ (No. 195), $Z = 1$, $\mu(Mo_{K\alpha}) = 15.3$ mm^{-1}, $2\theta_{max} = 45°$; 29085 reflections of which 4816 were independent, 4035 observed with $I > 2\sigma(I)$, 94 parameters (Hg, Se anisotropically, and C isotropically refined; the phenyl rings, some of which were highly disordered, were refined as rigid groups with idealized geometry, some of them with a common U(eq) value for the whole ring), $R = 0.054$, max. residual electron density 1.89 e Å^{-3}. There are probably solvent molecules also in the unit cell, but these cannot be refined due to high disorder. **2b**: $a = 2275.3(3)$, $c = 5302.0(11)$ pm, $V = 23772(7) \times 10^6$ pm^3; space group $P3_2$ (No. 145), $Z = 3$, $\mu(Mo_{K\alpha}) = 21.2$ mm^{-1}, $2\theta_{max} = 45°$; 50168 reflections of which 33565 were independent, 21430 observed with $I > 2\sigma(I)$, 1106 parameters (Hg, Se anisotropically, and C isotropically refined; the phenyl rings, some of which were highly disordered, were refined as rigid groups, some of them with a common U(eq) value for the whole ring), $R = 0.113$, max. residual electron density 2.24 e Å^{-3}. There are probably solvent molecules also in the unit cell, but these cannot be refined due to high disorder. **3**: $a = 2534.05(76)$, $b = 6813.53(94)$, $c = 2540.53(36)$ pm, $\beta = 113.519(20)°$, $V = 40220(14) \times 10^6$ pm^3; space group $P2_1/n$ (No. 14), $Z = 4$, $\mu(Mo_{K\alpha}) = 6.229$ mm^{-1}, $2\theta_{max} = 42°$, 134694 reflections of which 40678 were independent, 27073 observed with $I > 2\sigma(I)$, parameters 1333 (Cd, Se, P anisotropically, and C isotropically refined, the phenyl rings, some of which were highly disordered, were refined as rigid groups. One of the μ_2Se atoms has a very high temperature factor and it is not possible to locate the attached phenyl ring. It is possible that this could be a Cl^- ion), $R = 0.0868$, max. residual electron density 1.65 e Å^{-3}. It was not possible to find all the C atoms of the phenyl rings in the Fourier difference map. **4**: $a = 2422.2(5)$, $b = 3132.1(6)$, $c = 3673.7(7)$ pm, $V = 27871(10) \times 10^6$ pm^3; space group $P2_12_12_1$ (No. 19), $Z = 4$, $|E^2 - 1| = 0.748$, $\mu(Mo_{K\alpha}) = 3.43$ mm^{-1}, $2\theta_{max} = 45°$; 85711 reflections of which 36240 were independent, 31559 observed with $I > 2\sigma(I)$, 1113 parameters (Cd, I, P, Si in the cluster anion were refined anisotropically), $R = 0.061$, max. residual electron density 2.02 e Å^{-3}, the Flack parameter has a value of 0.38(3), which is an indication of an inversion twin. However this parameter cannot be taken as conclusive as not all of the atoms could be found in the Fourier difference map. **5**: $a = 2041.3(6)$, $b = 2341.7(8)$, $c = 2830.4(9)$ pm, $\alpha = 91.08(3)$, $\beta = 96.58(3)$, $\gamma = 113.43(2)°$, $V = 12301.45(5) \times 10^6$ pm^3; space group $P\bar{1}$ (No.2), $Z = 2$, $\mu(Mo_{K\alpha}) = 3.84$ mm^{-1}, $2\theta_{max} = 45°$; 37934 reflections of which 26189 were independent, 16340 observed with $I > 2\sigma(I)$, 1019 parameters (Cd, I, P, Si in the cluster anion were refined anisotropically), $R = 0.083$, max. residual electron density 2.18 e Å^{-3}. Due to high disorder it was not possible to find all the atoms in the Fourier difference map. Further details of the crystal structure investigations may be obtained from the Fachinformationszentrum Karlsruhe, 76344 Eggenstein-Leopoldshafen (Germany), on quoting the depository numbers CSD-405068 (**2a**), CSD-405069 (**2b**), CSD-405470 (**3**), CSD-405070 (**4**), and CSD-405071 (**5**).

[8] W. F. de Jong, *Z. Kristallogr.* **1926**, *63*, 466.

[9] *Landolt-Börnstein, Gruppe III: Kristall- und Festkörperphysik, Band 17: Halbleiter* (Gesamtherausgabe: O. Madelung), Springer, Berlin, **1982**, p. 236.

[10] V. M. Goldschmidt, *Geochemische Verteilungsgesetze der Elemente, Band 8: Untersuchungen über Bau und Eigenschaften von Krystallen* (Ed.: J. Dybwad), Oslo, **1927**

[11] a) R. Juza, K. Bär, *Z. Anorg. Allgem. Chem.* **1956**, *283*, 230; b) H. Krebs, K.-H. Müller, G. Zürn, *ibid.* **1956**, *285*, 15; c) M. von Stackelberg, R. Paulus, *Z. Physik. Chem. B* **1935**, *28*, 427.

[12] a) M. K. Chaled, *Dissertation*, Universität Bonn **1975**; b) P. C. Donohue, *J. Solid State Chem.* **1972**, *5*, 71.

 © VCH Verlagsgesellschaft mbH, D-69451 Weinheim, 1996 0570-0833/96/3519-2218 $ 15.00+.25/0

The Mechanism of Class II, Metal-Dependent Aldolases**

Wolf-Dieter Fessner,* Achim Schneider, Heike Held, Gudrun Sinerius, Christiane Walter, Mark Hixon, and John V. Schloss*

Dedicated to Professor Horst Prinzbach on the occasion of his 65th birthday

The four distinct dihydroxyacetone phosphate dependent aldolases[1, 2] enjoy increasing interest for preparative asymmetric synthesis because of their capacity to build up two new stereogenic centers with high chiral induction.[3] While all DHAP aldolases have a very broad substrate tolerance for the aldol acceptor substrate, they appear to have a high substrate specificity for dihydroxyacetone phosphate (DHAP) as the aldol donor, and only few isosteric replacements of the phosphate ester moiety are tolerated.[4] Diastereoselectivity may be limited for certain cases in the control of the stereocenter at C-4, which points to occasional inverse binding of the aldehyde carbonyl group.[2e] Certainly, a detailed understanding of the contributions of active site residues in substrate recognition and in the catalytic event is highly desirable to further improve the predictive value of the method.

Aldolases have been divided into two classes according to their mode of donor activation.[5] Class I aldolases achieve stereospecific deprotonation of the substrate by means of covalent linkage to an active site lysine residue (imine/enamine formation), while class II aldolases utilize transition metal ions (usually Zn^{2+}) as essential Lewis acid cofactors to facilitate deprotonation (Fig. 1). For the class I FruA,[2] despite extensive efforts using modern techniques of enzymology, site-directed mutagenesis, and protein crystallography,[6] a conclusive model that accounts for the function of the active site residues in the individual steps of catalysis is advancing very slowly.[7] In particular, no structure with bound substrates or inhibitors is yet available.

Based on work with the class II FruA from yeast, several early hypotheses for the mechanism of Zn-dependent aldolases have been developed. According to ESR and NMR relaxation rate measurements on the Mn^{2+}-substituted holoenzyme, DHAP is bound through its phosphate group,[8] and the carbonyl is polarized by Zn^{2+} through an intervening imidazole ring (Fig. 1, **A**).[9] Subsequent FT-IR and deuterium exchange studies with native yeast aldolase[10] led to the conclusion that aldehyde activation occurs by an additional direct coordination of the carbonyl (Fig. 1, **B**). Recently, Dreyer and Schulz[11a] reported the X-ray structure for FucA (2.13 Å resolution), the first of a class II aldolase. The active site, which is located at the interface

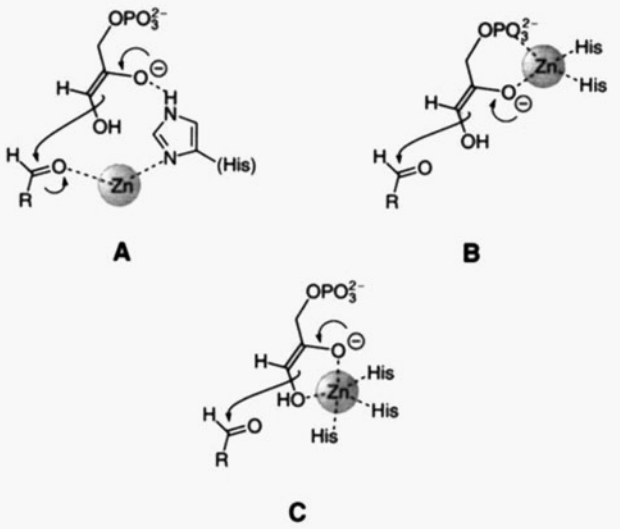

Fig. 1. Hypothetical mechanisms for catalysis by type II aldolases. **A**: Enolate stabilization by proton relay[9] and aldehyde activation by Zn^{2+}[10]. **B**: Enolate stabilization by coordination of Zn^{2+} to the carbonyl and phosphate groups[8]. **C**: Enediolate stabilization by chelate coordination to Zn^{2+}.

between two subunits of the homotetramer, contains the catalytically active Zn^{2+} ion tightly coordinated by three N^{ε} atoms of histidine residues (His92, His94, His155; Fig. 1, **C**). Thus, all previous mechanistic hypotheses must be rejected in light of the steric restraints imposed on the Zn^{2+} ion, which precludes coordination of more than a single substrate, and on its histidine ligands, which cannot act as a proton relay between bound substrates.

Under the slightly alkaline conditions required for FucA crystallization, the natural substrate L-fuculose 1-phosphate **1** (Scheme 1) cannot be used for X-ray analysis of the enzyme–ligand complex because it is cleaved to give the labile DHAP and

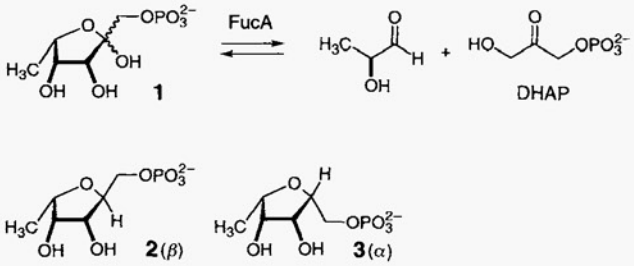

Scheme 1. Natural substrate **1** of FucA and the structurally related compounds **2** and **3**.

L-lactaldehyde. For stable substrate mimics in soaking or cocrystallization studies, we first focused on the synthesis of the structurally related anhydroalditol derivatives **2** and **3** as potential inhibitors; as they lack the anomeric hydroxyl group of **1**, ring opening and cleavage is not possible. Fucitol 1-phosphate was included as a potential mimic of the open-chain form.

L-Fuculose (**4**, obtained by enzymatic dephosphorylation of **1**[12]) was acetylated to provide a mixture of acetates **5**–**7**, from which the major product, triacetate **5** (61%), could be separated by distribution between water–ether and back extraction (Scheme 2). Silane reduction cleanly afforded a mixture of anhydroalditol esters **8** and **9** ($\geq 10:1$, 89%), which were deprotected and separated by column chromatography on Ca^{2+}-loaded ion exchange resin. Regioselective acetalization of the

[*] Prof. Dr. W.-D. Fessner, Dr. A. Schneider, Dipl.-Chem. H. Held, Dr. G. Sinerius, Dr. C. Walter
Institut für Organische Chemie der Technischen Hochschule
Professor-Pirlet-Strasse 1, D-52056 Aachen (Germany)
Fax: Int. code +(241)8888-385
e-mail: fessner@rwth-aachen.de
Prof. Dr. J. V. Schloss, M. Hixon
Department of Medicinal Chemistry, University of Kansas
Lawrence, KS 66045 (USA)
Fax: Int. code +(913)864 4503
e-mail: schloss@kuhub.cc.ukans.edu

[**] Enzymes in Organic Synthesis, Part 12. This work was supported by the Deutsche Forschungsgemeinschaft (Grants Fe 244/6-1 and SFB380/B25 to W. D. F.), and by the U. S. National Institutes of Health (Grants GM48568 and GM07775 to J. V. S.). We thank Prof. Dr. G. E. Schulz and Dr. M. Dreyer (University of Freiburg) for sharing their X-ray data prior to publication (see ref. [11b]). Part 11: [4b].

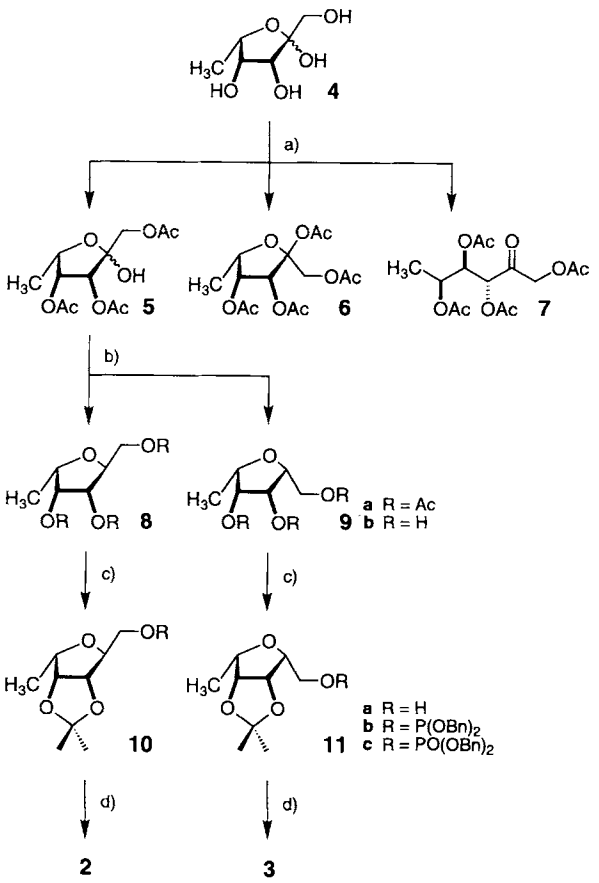

Scheme 2. Synthesis of FucA inhibitors. a) Ac_2O/pyridine, 93% **5**–**7** (ratio 61:17:22); b) $Et_3SiH/BF_3/(CH_2Cl)_2$, 89% **8a**/**9a** (ratio 10:1), then K_2CO_3/MeOH, 93% **8b**/**9b**; c) acetone/H_2SO_4, $Et_2NP(OBn)_2$/THF, H_2O_2, 69% **10c** (48% **11c**) for three steps; d) H_2/Pd–C/EtOH, Dowex 50W H^+/H_2O/EtOH at room temperature, 94% **2** (90% **3**).

vic-diol (**10a**, **11a**) was followed by phosphitylation/oxidation to afford the primary dibenzyl phosphate esters **10c** and **11c**, respectively, from which the target compounds were liberated by hydrogenolysis and acid-catalyzed removal of the acetal. Purification by ion-exchange chromatography provided crystalline phosphates **2** and **3** as the bis(cyclohexylammonium) salts (14% and 2% overall yield from **4**, respectively). In kinetic studies only analog **2** showed detectable FucA inhibition, albeit with low affinity (K_i = 22 mM), which indicates that the aldolase selectively binds the more abundant β-anomer of the natural substrate **1** (K_m = 0.7 mM; $\alpha:\beta$ = 2:5). In addition, the higher affinities of *sn*-glycerol 3-phosphate (K_i = 6 mM) and phosphoglycolate ($K_i \approx$ 10 mM) point to the importance of the missing anomeric OH group for specific binding. The need for the correct configuration at the anomeric center is underscored by the fact that no significant inhibition was observed for the enantiomeric *sn*-glycerol 1-phosphate or for D-glycerate 3-phosphate. The low affinity for L-fucitol 1-phosphate (K_i = 70 mM) may be interpreted as an indication of weak binding by the open-chain form of **1**.

Deprotonation of DHAP at C-3 yields an enediolate intermediate **12** closely resembling phosphoglycolohydroxamate **13** (Fig. 2). Indeed, **13** was found not only to be a potent inhibitor of FucA (K_i = 4 μM), but also a strong inhibitor of each of the class II aldolases tested so far (Table 1). Apparently the hydroxamate very effectively mimics the catalytic intermediate or transition state common to these enzymes, and seems to be bound by all Zn^{2+}-dependent aldolases in a very similar fashion.

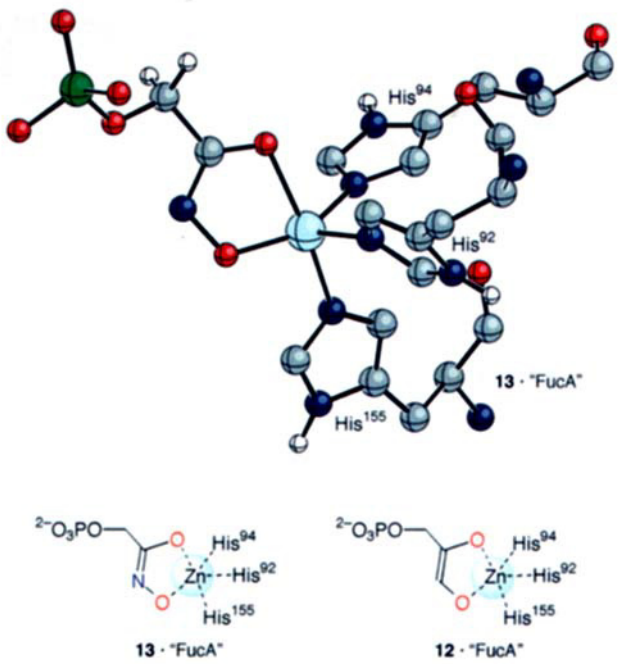

Fig. 2. Coordination of Zn^{2+} in the active site of FucA complexed with phosphoglycolohydroxamate (**13**) as determined by X-ray structure analysis[11b].

Table 1. Inhibition of zinc-dependent aldolases[a].

Enzyme [2]	Substrate K_m [M]	**13** K_i [M]	Phosphoglycolate K_i [M]
FucA	1.5×10^{-3}	$3.1 \pm 0.9 \times 10^{-6}$	$> 10 \times 10^{-3}$
RhuA	1.6×10^{-3}	$120 \pm 12 \times 10^{-9}$	$260 \pm 46 \times 10^{-6}$
FruA	6.2×10^{-6}	$15 \pm 2.5 \times 10^{-9}$	$130 \pm 26 \times 10^{-9}$

[a] Standard assays[2, 12] were based on the rate of DHAP formation from cleavage of the corresponding natural substrates by the aldolase (0.01 U), which was determined by consumption of NADH (0.2 mM) in the presence of glycerol phosphate dehydrogenase (5 U). Inhibition kinetics were determined by varying the concentrations of aldolase substrate and inhibitors. The inhibitor concentrations were chosen such that they bracketed the IC_{50} value for the aldolase at that substrate concentration. Inhibition was competitive for FucA, whereas **13** displayed slow binding kinetics with FruA and RhuA.

Very recently an X-ray structure has been determined for the complex of FucA and the substrate analog **13** (Fig. 2).[11b] The analysis reveals that the inhibitor forms a bidentate chelate in which both the enol and hydroxamate oxygens are coordinated to the Zn^{2+} ion. These results clearly indicate a role for Zn^{2+} in stabilizing the enediolate. Indeed, hydroxamates typically act as chelators in simple metal complexes[13] in which the hydroxamic acid group is in the anionic rather than the protonated form.[14] Bidentate binding of a DHAP ligand also helps to explain the natural preference of metal-dependent aldolases for an active site Zn^{2+} ion (which can be exchanged for Co^{2+} to yield highly active catalysts) because zinc (like cobalt) readily adapts to trigonal-bipyramidal coordination and is able to change its coordination state far more easily than other metals.[15] Also, zinc(II) is the most common Lewis acid in bioinorganic chemistry.

Thus, based on these considerations we propose a different catalytic cycle for FucA, with general implications for other metalloaldolases (Scheme 3). In direction of synthesis, DHAP enters as the first substrate and coordinates in an extended conformation to zinc through both hydroxyl and carbonyl oxygens initially in ground state complexes and then in intermediate

 © VCH Verlagsgesellschaft mbH, D-69451 Weinheim, 1996 0570-0833/96/3519-2220 $ 15.00+.25/0

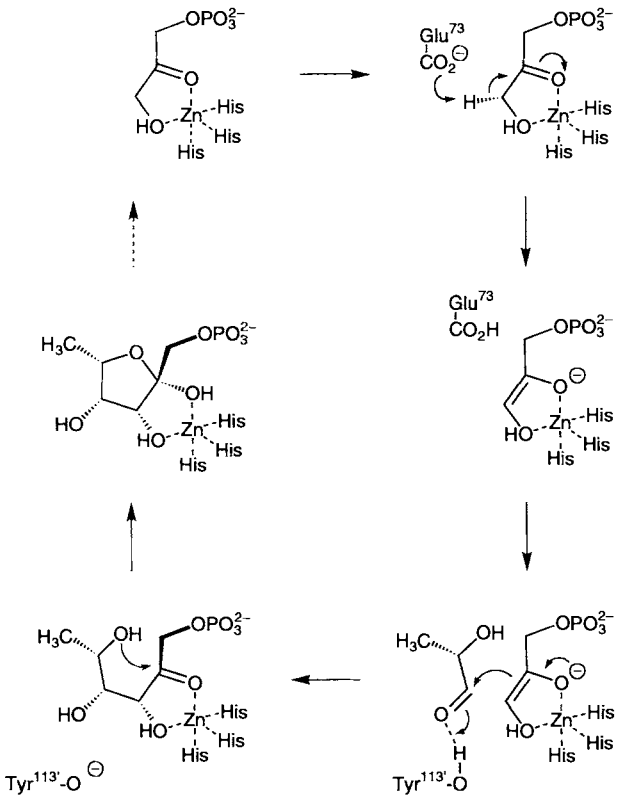

Scheme 3. Proposed catalytic cycle of FucA in direction of synthesis indicating relevant protein–substrate interactions.

states. Polarization of the carbonyl bond increases the acidity of the hydroxymethylene hydrogens and facilitates abstraction of the *pro-R* proton by a general base, which probably is Glu73. The phosphate group is rigidly held by a number of contacts to backbone amides and polar residues, most likely in order to suppress the facile enediolate fragmentation from an orthogonal conformation. Consequently, its proposed function as an intrinsic base becomes highly implausible.[16] The nucleophilic *cis*-enediolate attacks the *Si* face of an incoming lactaldehyde carbonyl, assisted by Tyr113′, which can donate a proton to stabilize the developing charge. This hydrogen bond is responsible for the asymmetric induction at C-4, while the shielding of the *Si* face of the DHAP enediolate by the protein assures the correct stereochemistry at C-3 of the product. Liberation of the product from the catalyst may be induced directly by restoring the carbonyl originating from DHAP, or may be preceded by ring closure from attack of the hydroxyl group introduced by lactaldehyde. Proton exchange with (or without) solvent prepares for the next catalytic cycle.

Previous hypotheses were based primarily on studies of enzyme–substrate interactions in the ground state, whereas our current model relies on inhibition studies and data from X-ray structure analyses with inhibitors that resemble the catalytic intermediate and/or transition state. While this model successfully explains all key stereochemical issues and the influence of the catalyst on the rate-limiting steps, it currently does not explain the high enantioselectivity for 2-hydroxyaldehydes,[12] because **13** is a model for DHAP only.

A detailed understanding of the events of molecular recognition in aldolase–substrate interactions during catalysis should develop and enable further progress, for example in the development of selective inhibitors of class I versus class II FruA enzymes for therapeutic purposes, in the design of new substrate analogs to enhance the spectrum of potential preparative applications, and in rational protein engineering towards an altered substrate tolerance and novel catalytic functions.

Received: May 15, 1996 [Z9126IE]
German version: *Angew. Chem.* **1996**, *108*, 2366–2369

Keywords: aldolases · enediols · enzyme inhibitors · enzyme mechanisms

[1] W.-D. Fessner, in *Microbial Reagents in Organic Synthesis* (Ed.: S. Servi), Kluwer, Dordrecht, **1992**, pp. 43–55.

[2] Abbreviations used: D-fructose 1,6-bisphosphate aldolase (FruA, EC 4.1.2.13); D-tagatose 1,6-bisphosphate aldolase (TagA, EC 4.1.2.n); L-fuculose 1-phosphate aldolase (FucA, EC 4.1.2.17); L-rhamnulose 1-phosphate aldolase (RhuA, EC 4.1.2.19). All four stereochemically complementary Zn^{2+}-dependent DHAP aldolases (class II) are found, for example, in *Escherichia coli*[1]. The enzymes are commercially available (except for TagA) or can be isolated from recombinant strains: a) C. H. von der Osten, A. J. Sinskey, C. F. Barbas, R. L. Pederson, Y. F. Wang, C.-H. Wong, *J. Am. Chem. Soc.* **1989**, *111*, 3924–3927; b) A. Ozaki, E. J. Toone, C. H. von der Osten, A. J. Sinskey, G. M. Whitesides, *ibid.* **1990**, *112*, 4970–4971; c) W.-D. Fessner, G. Sinerius, A. Schneider, M. Dreyer, G. E. Schulz, J. Badia, J. Aguilar, *Angew. Chem.* **1991**, *103*, 596–599; *Angew. Chem. Int. Ed. Engl.* **1991**, *30*, 555–558.

[3] C.-H. Wong, G. M. Whitesides, *Enzymes in Synthetic Organic Chemistry*, Pergamon, Oxford, **1994**; W.-D. Fessner, C. Walter, *Top. Curr. Chem.* **1996**, in press.

[4] a) W.-D. Fessner, G. Sinerius, *Angew. Chem.* **1994**, *106*, 217–220; *Angew. Chem. Int. Ed. Engl.* **1994**, *33*, 209–212; b) H.-L. Arth, G. Sinerius, W.-D. Fessner, *Liebigs Ann.* **1995**, 2037–2042; c) D. Stribling, *Biochem. J.* **1974**, *141*, 725–728.

[5] B. L. Horecker, O. Tsolas, C. Y. Lai, in *The Enzymes, Vol. VII* (Ed.: P. D. Boyer), Academic Press, New York, **1972**, pp. 213–258.

[6] J. Sygusch, D. Beaudry, M. Allaire, *Proc. Natl. Acad. Sci. USA* **1987**, *84*, 7846–7850; S. J. Gamblin, G. J. Davies, J. M. Grimes, R. M. Jackson, J. A. Littlechild, H. C. Watson, *J. Mol. Biol.* **1991**, *219*, 573–576; G. Hester, O. Brenner-Holzach, F. A. Rossi, M. Struck-Donatz, K. H. Winterhalter, J. D. G. Smit, K. Piontek, *FEBS Lett.* **1991**, *292*, 237–242.

[7] J. A. Littlechild, H. C. Watson, *Trends Biochem. Sci.* **1993**, *18*, 36–39; A. J. Morris, D. R. Tolan, *J. Biol. Chem.* **1993**, *268*, 1095–1100; *Biochemistry* **1994**, *33*, 12291–12297.

[8] A. S. Mildvan, R. D. Kobes, W. J. Rutter, *Biochemistry* **1971**, *10*, 1191–1204; K. D. Collins, *J. Biol. Chem.* **1974**, *249*, 136–142. Hydroxamate **13** was prepared by a modification of this literature procedure.

[9] G. M. Smith, A. S. Mildvan, E. T. Harper, *Biochemistry* **1980**, *19*, 1248–1255; G. M. Smith, A. S. Mildvan, *ibid.* **1981**, *20*, 4340–4346; B. S. Szwergold, K. Ugurbil, T. R. Brown, *Arch. Biochem. Biophys.* **1995**, *317*, 244–252.

[10] J. G. Belasco, J. R. Knowles, *Biochemistry* **1983**, *22*, 122–129; J. T. Kadonaga, J. R. Knowles, *ibid.* **1983**, *22*, 130–136.

[11] a) M. K. Dreyer, G. E. Schulz, *J. Mol. Biol.* **1993**, *231*, 549–553; b) M. K. Dreyer, Dissertation, Universität Freiburg **1995**.

[12] W.-D. Fessner, A. Schneider, O. Eyrisch, G. Sinerius, J. Badia, *Tetrahedron Asymmetry* **1993**, *4*, 1183–1192; W.-D. Fessner, J. Badia, O. Eyrisch, A. Schneider, G. Sinerius, *Tetrahedron Lett.* **1992**, *33*, 5231–5234.

[13] S. Göttlicher, P. Ochsenreiter, *Chem. Ber.* **1974**, *107*, 391–397. Related pentacoordinate complexes of hydroxamate inhibitors to catalytic zinc have been determined for several metalloproteases: M. A. Holmes, B. W. Matthews, *Biochemistry* **1981**, *20*, 6912–6920; A. F. Monzingo, B. W. Matthews, *ibid.* **1984**, *23*, 5724–5729; M. F. Browner, W. W. Smith, A. L. Castelhano, *ibid.* **1995**, *34*, 6602–6610; F. Grams, M. Crimmin, L. Hinnes, P. Huxley, M. Pieper, H. Tschesche, W. Bode, *ibid.* **1995**, *34*, 14012–14020; J. C. Spurlino, A. M. Smallwood, D. D. Carlton, T. M. Banks, K. J. Vavra, J. S. Johnson, E. R. Cook, J. Falvo, R. C. Wahl, T. A. Pulvino, J. J. Wendoloski, D. L. Smith, *Proteins* **1994**, *19*, 98–109; F. Grams, P. Reinemer, J. C. Powers, T. Kleine, M. Pieper, H. Tschesche, R. Huber, W. Bode, *Eur. J. Biochem.* **1995**, *228*, 830–841.

[14] A. Zalkin, J. D. Forrester, D. H. Templeton, *J. Am. Chem. Soc.* **1966**, *88*, 1810–1814; L. Bauer, O. Exner, *Angew. Chem.* **1974**, *86*, 419–428; *Angew. Chem. Int. Ed. Engl.* **1974**, *13*, 376–384.

[15] I. Bertini, C. Luchinat, in *Bioinorganic Chemistry* (Eds.: I. Bertini, H. B. Gray, S. J. Lippard, J. S. Valentine), University Science Books, Mill Valley, CA, USA, **1993**, pp. 37–106.

[16] R. A. Periana, R. Motiu-DeGrood, Y. Chiang, D. J. Hupe, *J. Am. Chem. Soc.* **1980**, *102*, 3923–3927.

 © VCH Verlagsgesellschaft mbH, D-69451 Weinheim, 1996 0570-0833/96/3519-2221 $ 15.00+.25/0

The Design and Synthesis of a Scaffold for Combinatorial Chemistry Based on Bile Acid

Günther Wess,* Klaus Bock, Horst Kleine, Michael Kurz, Wolfgang Guba, Horst Hemmerle, Eloisa Lopez-Calle, Karl-Heinz Baringhaus, Heiner Glombik, Alfons Enhsen, and Werner Kramer

Combinatorial chemistry opens up new possibilities for research in medicinal chemistry in both the search for lead structures and their rapid optimization.[1] Nevertheless, though many peptides are already the first milestones along this path, the optimization of sequences suitable for their combinatorial synthesis is still hardly a straightforward task.[2] The synthesis strategy must take into account the compatibility and interplay of the spacers between resin and molecular scaffold, the protecting groups, and the derivatization reactions. The number, diversity and availability of nonpeptidic scaffolds is, at present, still very limited. The design of new and structurally highly diversified nonpeptide scaffolds is a prerequisite for encompassing the widest possible range of structures.[3] We are interested in conformationally fixed amino acid units, which can be used in a variety of ways, both to generate compound libraries and to optimize targeted lead structures by means of parallel synthesis. In particular these structural elements should replace peptide sequences and/or pre-organize pharmacophores or other residues.[4, 6]

We report here on the amino acid equivalent **1**, which contains a *cis*-decalin partial structure (**2**) within a bile acid skeleton and, formally, mimics a tetrapeptide. In the form of derivative **3** it should be highly suitable for combinatorial syntheses. In **1** the two *cis*-related OH functions on the α-face of chenodeoxycholic acid (**4**) are used. Separated in each case by a spacer, the

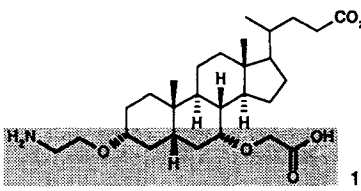

1

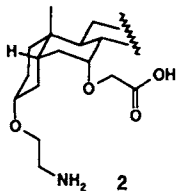

2

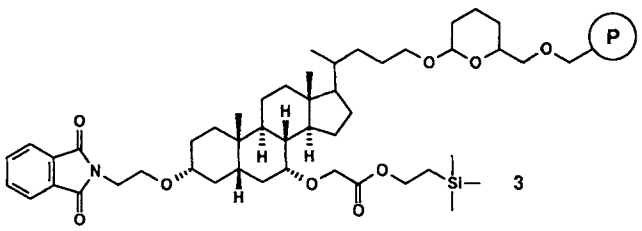

3

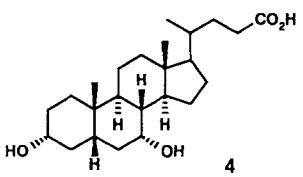

4

C-7 atom bears a carboxy substituent and the C-3 atom an amino group. In previous work with bile acids[5] the functions on C-3 and C-7 were the same and used either as OH groups in the form of esters or amino groups in the form of amides. In contrast to this we use different functional groups connected through spacers to C-3 and C-7 as well as an OH-group on C-24.

In **3** both the amino groups and the carboxy groups are protected but may be deprotected at any time under mild conditions on the solid support. The acid-labile tetrahydropyranyl unit acts as the connector to the polymer support.[7] After separation from the resin under very mild conditions, the C-24 alcohol is obtained, which can be easily purified and derivatized.

The synthesis of **3** is shown in Scheme 1. Preparative, selective allylation of bile acids and bile acid esters at the hydroxy groups has hitherto been a problem.[8] The use of allyl bromide/diisopropylethylamine gave satisfactory yields of the allylated product in only a few cases. Selective monoalkylation of the 3-OH-group always required protecting groups on 7-OH and 12-OH. In addition during the alkylation of 7-OH and 12-OH the other functions had to be protected, and long reaction times were necessary. We found that in allyl bromide/DMF (1/1) in the presence of powdered potassium hydroxide and with controlled temperature (10–20 °C, 8 h), allyl 3-allylchenodeoxycholate was formed selectively. Reduction of this ester with lithium aluminum hydride gave alcohol **5**, which was selectively benzylated with benzyl bromide/DMF/KOH. The 7-OH group was subsequently allylated.

Since the phthalimido group is a stable protecting group in the presence of many reagents, we chose the Gabriel synthesis[9] for the introduction of the amino function. The coupling of **10** with the polymer support was accomplished by the Ellman procedure.[7] For the coupling in dichloroethane with pyridinium-*p*-toluenesulfonate (PPTS; 18 h reflux), 1.5 g of polymer support was used (more than 2.25 mmol) and 2.65 g of the coupled product was obtained. The chlorine content, determined argentometrically after decomposition, was less than 0.76%.

The investigation of the acid conditions for cleavage from the polymer support proved that the trimethylsilylethyl group was very sensitive. The cleavage took place smoothly and without decomposition in THF with hydrochloric acid in diethyl ether (4 h, room temperature; Scheme 2). To optimize the reaction conditions the products were cleaved from the resin (THF, HCl/Et_2O, room temperature), chromatographed, and analyzed spectroscopically. The conversion of **3** to the free amine **11** under classical Gabriel conditions (hydrazinolysis)[9] did not occur; a side reaction is the formation of the carboxylic acid hydrazide from the trimethylsilyl ester. However, compound **11** is formed smoothly when **3** is treated with methylhydrazine in THF/ethanol at room temperature and is easily acylated to form **13**. Trimethylsilyl ester **3** was converted to the carboxylic acid **12** by treatment with tetrabutylammonium fluoride in DMF. Derivatization to amides was carried out with dicyclohexylcarbodiimide/1-hydroxy-1*H*-benzotriazole (DCC/HOBT)[10] in dichloromethane. Each 250 mg of **3** yielded 50 mg of **13** and 65 mg of **14** after chromatographic purification.

A library of 40 compounds of type **15** was prepared based on these results.[11]

To verify that **1** was suitable as a β-turn mimetic, the cyclic compound **16**,[16] which contains D-Pro-Ala, was prepared. This resembles a cyclic hexapeptide in which four of the amino acids have been replaced by the skeleton **1**. The interproton distances in **16** were determined from ROESY NMR spectra in $CDCl_3$ and DMSO. In DMSO two conformers, which differed in the conformation of the peptide bond between the skeleton and D-Pro, were present as an equilibrium mixture, whereas in

[*] Dr. G. Wess, K. Bock, H. Kleine, Dr. M. Kurz, Dr. W. Guba, Dr. H. Hemmerle, Dr. E. Lopez-Calle, Dr. K.-H. Baringhaus, Dr. H. Glombik, Dr. A. Enhsen, Dr. W. Kramer
Zentrale Pharma-Forschung, Hoechst AG, D-65926 Frankfurt (Germany)
Fax: Int. code +(69)331399

 © VCH Verlagsgesellschaft mbH, D-69451 Weinheim, 1996 0570-0833/96/3519-2222 $ 15.00+.25/0

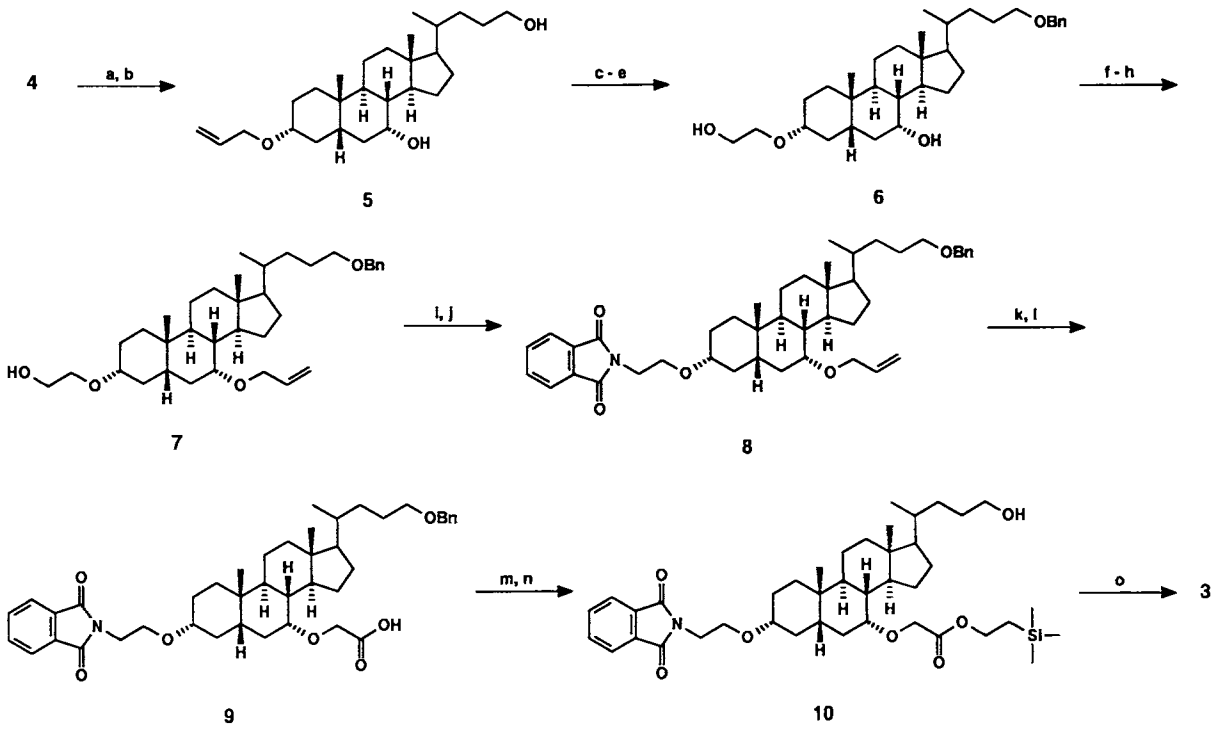

Scheme 1. Synthesis of **10** and its binding to the solid phase. a) Allyl bromide/DMF (1/1), powdered KOH, 10–20 °C, 8 h (81%); b) $LiAlH_4$, THF, 50 °C, 1 h (98%); c) $PhCH_2Br$/DMF (1/5), powdered KOH, −10 → 0 °C, 3 h (85%); d) $OsO_4/NaIO_4$, Et_2O/H_2O (1/1), room temperature (RT), 4 h (crude, quant.); e) $NaBH_4$, Et_2O/EtOH (3/1), RT, 1 h (83%); f) *t*BuMe$_2$SiCl, 4-(dimethylamino)pyridine (DMAP), CH_2Cl_2, RT, 4 h (95%); g) allyl bromide/DMF (1/1), powdered KOH, 0 °C, 3 h (94%); h) Bu_4NF, THF, RT, 3 h (crude, quant.); i) CH_3SO_2Cl, pyridine, 0 °C → RT, 2 h (95%); j) potassium phthalimide salt, DMF, 70 °C, 3 h (97%); k) $OsO_4/NaIO_4$, Et_2O/H_2O (1/1), RT, 8 h (crude, quant.); l) pyridinium dichromate, DMF, 70 °C, 5 h (79%); m) HOBT, DCC, DMAP, CH_2Cl_2, RT, 15 min, then $Me_3SiCH_2CH_2OH$, RT, 2 h (91%); n) H_2, Pd/C 10%, ethyl acetate, normal pressure, RT, 4 h (87%); o) spacer polymer [7b], PPTS, $ClCH_2CH_2Cl$, reflux, 18 h.

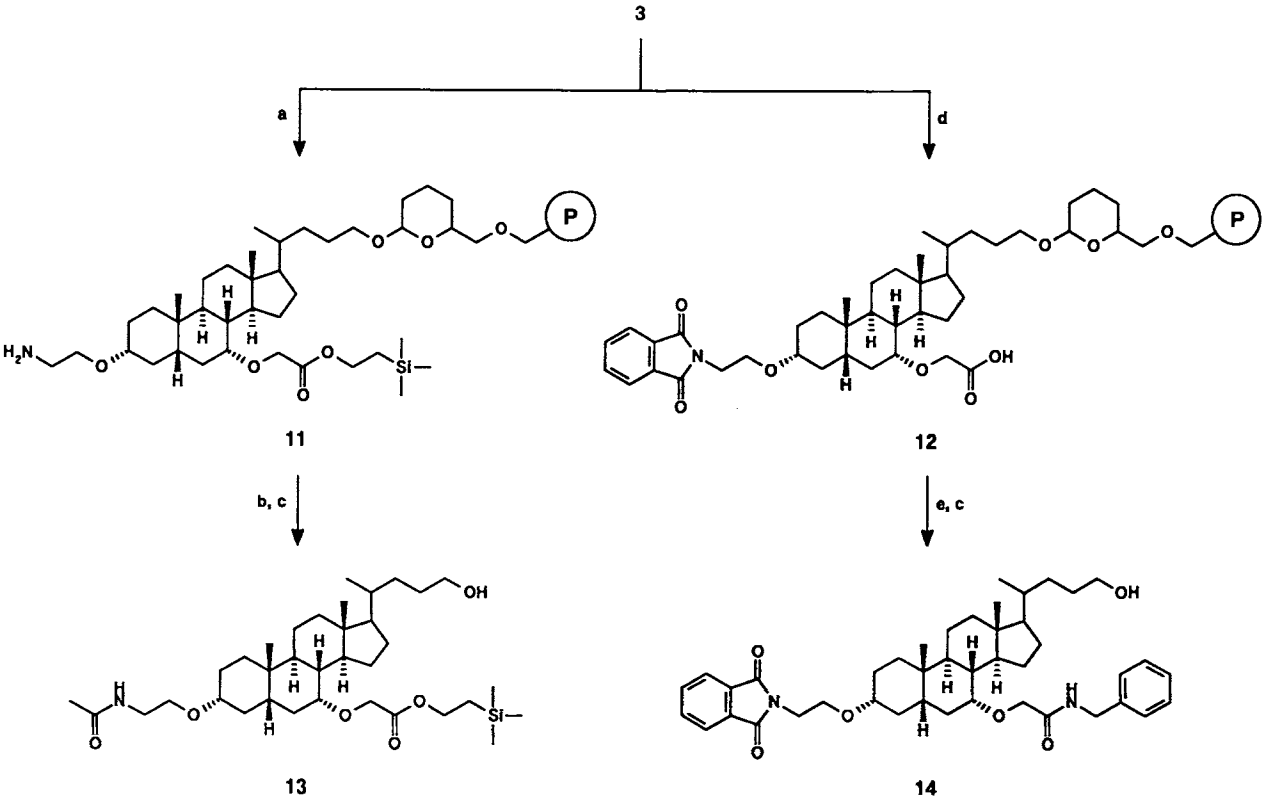

Scheme 2. Solid-phase reactions and release. a) $MeNHNH_2$/THF/EtOH (1/6/1), RT, 18 h; b) $(CH_3CO)_2O$, pyridine, CH_2Cl_2, RT, 12 h; c) HCl/Et_2O, THF, 4 h; d) Bu_4NF, DMF, RT, 12 h; e) HOBT, DCC, CH_2Cl_2, RT, 1 h, then $PhCH_2NH_2$, RT, 4 h. Ⓟ = polymer support.

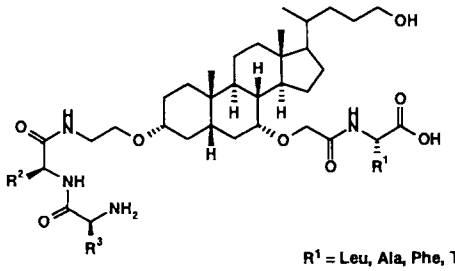

R^1 = Leu, Ala, Phe, Tyr, Asp
R^2 = Phe, Pro
R^3 = Trp, Ala, Ser, Pro

15

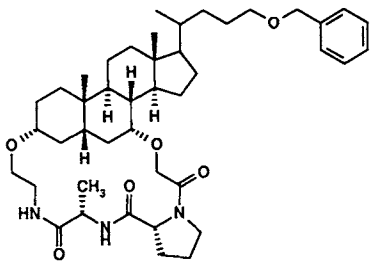

16

$CDCl_3$ only the *trans*-conformer was present. The distances obtained experimentally were used for a three-dimensional structure refinement by distance geometry and molecular dynamic simulations in both $CDCl_3$ and DMSO. In Figure 1 the structure of **16** is compared with that of a cyclic hexapeptide with two β-II'-turns. It is clear that the bile acid moiety occupies the positions i to $i+3$ of the upper β-turn of the hexapeptide. In contrast to the previously known turn mimetics, which usually replace positions $i+1$ and $i+2$ of a β-loop, we have here a β-turn mimetic that corresponds to a complete β-turn and enables a chain extension unambiguously in the direction of the N- and C- terminus.

Thus **1** makes available a novel scaffold for the design of combinatorial compound libraries which includes structures other than those of the previously used turn-mimetics. In addition the bile acid scaffold **1** exhibits a compact hydrophobic surface, which, if built into active peptidic substances, could have beneficial effects on their pharmacokinetic properties. We are currently synthesizing model compounds to investigate the β-fold-inducing effects of **1**. Compound libraries derived from **1** are being biologically tested for the synthesis of various targets.

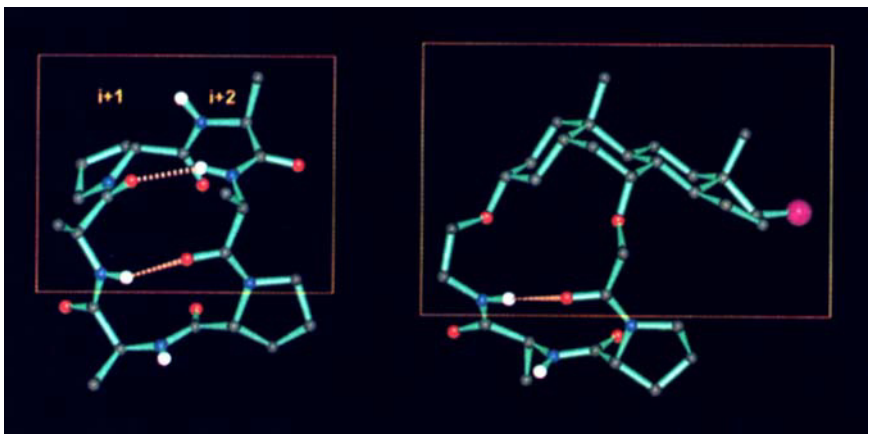

Fig. 1. Comparison of the three-dimensional structure of **16** (right) and cyclo(D-pro-Ala-Ala)$_2$ (left) [13]. The framed areas each correspond to a β-turn.

Received: January 30, 1996
Revised version: June 7, 1996 [Z 8768 IE]
German version: *Angew. Chem.* **1996**, *108*, 2363–2366

Keywords: bile acids · combinatorial chemistry · peptide mimetics · solid-phase syntheses

[1] a) M. A. Gallop, R. W. Barrett, W. J. Dower, S. P. A. Fodor, E. M. Gordon, *J. Med. Chem.* **1994**, *37*, 1233; b) E. M. Gordon, R. W. Barrett, W. J. Dower, S. P. A. Fodor, M. A. Gallop, *ibid.* **1994**, *37*, 1385; c) J. A. Ellman, *Chemtracts* **1995**, *8*, 1; M. C. Pirrung, *ibid.* **1995**, *8*, 5; A. W. Czarnik, *ibid.* **1995**, *8*, 13; d) L. A. Mitscher, *ibid.* **1995**, *8*, 19; e) M. C. Desai, R. N. Zuckermann, W. H. Moos, *Drug Dev. Res.* **1994**, *33*, 174.

[2] a) C. Gennari, H. P. Nestler, B. Solom, W. C. Still, *Angew. Chem.* **1995**, *107*, 1892; *Angew. Chem. Int. Ed. Engl.* **1995**, *34*, 1763; b) G. T. Wang, S. Li, N. Wideburg, G. A. Krafft, D. J. Kempf, *J. Med. Chem.* **1995**, *38*, 2995.

[3] E. J. Martin, J. M. Blaney, M. A. Siani, D. C. Spellmeyer, A. K. Wong, W. H. Moos, *J. Med. Chem.* **1995**, *38*, 1431.

[4] a) A. Giannis, T. Kolter, *Angew. Chem.* **1993**, *105*, 1303; *Angew. Chem. Int. Ed. Engl.* **1993**, *32*, 1244; b) D. P. Fairlie, G. Abbenante, D. R. March, *Curr. Med. Chem.* **1995**, *2*, 654; c) R. M. J. Liskamp, *Angew. Chem.* **1994**, *106*, 661; *Angew. Chem. Int. Ed. Engl.* **1994**, *33*, 633.

[5] a) M. Lebl, V. Krchnak, N. F. Sepetor, B. Seligman, P. Strob, S. Felder, K. S. Lam, *Peptide Sci.* **1995**, *37*, 177; b) R. Boyce, G. Li, H. P. Nestler, T. Suenaga, W. C. Still, *J. Am. Chem. Soc.* **1994**, *116*, 7955.

[6] a) R. Hirschmann, P. A. Sprengeler, I. Kawasaki, J. W. Leahy, W. C. Shakespeare, A. B. Schmith, *Tetrahedron* **1993**, *49*, 3665; b) H. Diaz, J. W. Kelly, *Tetrahedron Lett.* **1991**, *32*, 5725; c) J. B. Ball, R. A. Hughes, P. F. Alewood, P. R. Andrews, *Tetrahedron* **1993**, *49*, 3567.

[7] a) E. K. Kick, J. A. Ellman, *J. Med. Chem.* **1995**, *38*, 1427; b) L. A. Thompson, J. A. Ellman, *Tetrahedron Lett.* **1994**, *35*, 9333.

[8] a) G. Wess, W. Kramer, S. Bartmann, A. Enhsen, H. Glombik, S. Müllner, K. Bock, A. Dries, H. Kleine, W. Schmitt, *Tetrahedron Lett.* **1992**, *33*, 195; b) A. P. Davis, P. J. Dorgan, E. R. Mageean, *J. Chem. Soc. Chem. Commun.* **1993**, 492.

[9] M. S. Gibson, R. W. Bradshaw, *Angew. Chem.* **1968**, *80*, 986; *Angew. Chem. Int. Ed. Engl.* **1968**, *7*, 919.

[10] W. König, R. Geiger, *Chem. Ber.* **1970**, *103*, 788.

[11] The carboxylic acid function of **3** was deprotected and separately coupled with each of five different *tert*-butyl-protected amino acids (HOBT, DCC, CH_2Cl_2). After regeneration from the phthalimide ($MeNHNH_2$) the amino group was coupled with Fmoc-protected (Fmoc = fluorenylmethoxycarbonyl) amino acids (*O*-((ethoxycarbonyl)cyanomethylenamino)-*N*,*N*,*N*',*N*'tetramethyluronium tetrafluoroborate (TOTU), DMF). Finally the Fmoc groups were cleaved (piperidine) and subjected to reaction with other amino acids (Fmoc derivatives, TOTU). After cleavage from the resin and deprotection (trifluoroacetic acid (TFA), CH_2Cl_2, Et_3SiH), the products were obtained as their trifluoroacetates. Filtration through aluminum oxide (EtOAc, MeOH, H_2O, HOAc) provided the free compounds **15** in yields of 50–90% and a purity of 50–90% (determined by HPLC).

[12] Compound **9** was treated with the *tert*-butyl ester hydrochloide of D-proline (HOBT, DCCI, $EtNiPr_2$) and finally deprotected with TFA/H_2O (98/2). Reaction of the free acid with the *tert*-butyl ester hydrochloride of L-alanine (HOBT, DCC, $EtNiPr_2$), cleavage with TFA/H_2O (98/2) to form the acid, phthalimide cleavage with $MeOH/H_2NNH_2$ and finally cyclization with pentafluorophenol (DCC, CH_2Cl_2, high dilution) provides **16** in excellent yield (92%).

[13] M. Kurz, Dissertation, Technische Universität München, **1991**.

Synthesis and Crystal Structure of the $[Ni_{32}C_6(CO)_{36}]^{6-}$ Hexaanion: An Extended Fragment of the $M_{23}C_6$ Lattice Stabilized in a Shell of Edge-Bridging Carbonyl Ligands**

Francesca Calderoni, Francesco Demartin, M. Carmela Iapalucci, and Giuliano Longoni*

Transition metal carbonyl clusters of high nuclearity are often closely related to fragments of a metal lattice; more rarely, clusters that can be considered as an extended fragment of the lattice of a binary compound have been stabilized in a ligand shell, although some important examples of this type of cluster are known.[1, 2] Metal carbonyl clusters that exhibit the above behavior are of interest since they may provide a molecular approach to new materials,[3] and may be used as models for both experimental[4] and theoretical studies.[5]

Several years ago we reported the synthesis and crystal structure of the nickel carbide cluster **1** and its corresponding hexaanion **2**;[6] the $Ni_{32}C_6$ inner core of **1** is closely related to the

$[HNi_{38}C_6(CO)_{42}]^{5-}$ **1**

$M_{32}C_6$ truncated-octahedral fragment that is present in the $M_{23}C_6$ lattice, for example, in $Cr_{23}C_6$.[7] The method for preparing these clusters was improved recently, and thus it has now been possible to study their reactivity. As part of these reactivity studies we report here on the synthesis and crystal structure of the new $[Ni_{32}C_6(\mu\text{-}CO)_{36}]^{6-}$ hexaanion **3**, which consists of the above-mentioned $M_{32}C_6$ fragment stabilized in a shell of 36 edge-bridging carbonyl groups.

Compound **3** was obtained by degradation of **2** with carbon monoxide at atmospheric pressure [Eq. (a)], or by thermal decomposition of $[Ni_{10}C_2(CO)_{16}]^{2-}$ (**4**)[8] in diglyme at 110 °C under a nitrogen atmosphere [Eq. (b)].

$$\underset{\mathbf{2}}{[Ni_{38}C_6(CO)_{42}]^{6-}} + 18\,CO \underset{}{\overset{\text{MeCN, CO (1 atm)}}{\rightleftharpoons}} \underset{\mathbf{3}}{[Ni_{32}C_6(CO)_{36}]^{6-}} + 6\,[Ni(CO)_4] \quad \text{(a)}$$

Equilibrium (a) was shifted to the right by removal of $[Ni(CO)_4]$ under vacuum and re-exposure of the solution to a carbon monoxide atmosphere. The appearance of $[Ni(CO)_4]$ and a change in the pattern of the carbonyl absorption bands of **2** (1992 s, 1877 s, 1862 s cm^{-1}) was observed when the reaction was monitored by IR spectroscopy.[6] As the reaction proceeds, the absorption band attributed to the terminal carbonyl groups (1992 cm^{-1}) becomes progressively less intense, and the two bands attributed to the edge-bridging carbonyl ligands collapse into a single absorption band that is shifted to a slightly higher wavenumber. The intermediate IR patterns suggest the possible formation of $[Ni_{38-x}C_6(CO)_{42-x}]^{6-}$ ($x = 1-5$) species by stepwise elimination of Ni(CO) moieties. All $[Ni_{38-x}C_6(CO)_{42-x}]^{6-}$ ($x = 0-6$) clusters would constantly have $6n + 19$ filled valence orbitals, and thus, each member of the series should be possible both from a steric and electronic standpoint. A known example of such behavior is provided by the $[Ni_{34}C_4(CO)_{38}]^{6-}$ and $[Ni_{35}C_4(CO)_{39}]^{6-}$ pair of compounds.[9] The final product **3** shows a single sharp carbonyl absorption band at 1889 cm^{-1}.

Alternately, **3** can be obtained by thermal decomposition of **4** in diglyme, which proceeds approximately according to Equation (b).

$$5\,\underset{\mathbf{4}}{[Ni_{10}C_2(CO)_{16}]^{2-}} \xrightarrow{\Delta,\ 110\,^\circ C} \underset{\mathbf{5}}{[Ni_{16}C_4(CO)_{23}]^{4-}} + \underset{\mathbf{3}}{[Ni_{32}C_6(CO)_{36}]^{6-}} + 2\,[Ni(CO)_4] + 13\,CO \quad \text{(b)}$$

Owing to their very low solubility, the salts of **3** separate out, together with some insoluble inorganic material, from the reaction solution containing **5**.[10] The quaternary ammonium and phosphonium salts have been purified by extraction in MeCN and crystallized by layering the extracts with diisopropyl ether.

The unit cell of the $[PPh_3Me]_6$ salt of **3** contains one cluster anion located on a crystallographic inversion center, six cations, and four acetonitrile molecules.[11] The structure of **3**, which shows an overall idealized O_h symmetry, is shown in Figure 1.

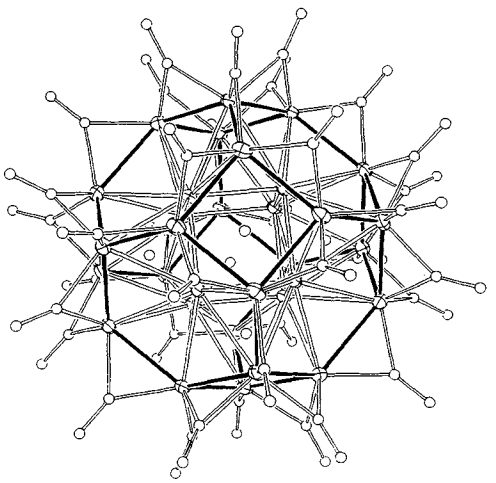

Fig. 1. Crystal structure of **3** (the Ni–Ni bonds in black highlight the outer Ni_{24} truncated-octahedron; $Ni-C_{carbide}$ bonds have been omitted for clarity).

The truncated octahedral $Ni_{32}C_6$ framework of **3** is identical to the corresponding fragment in **1**, and reveals very close interatomic separations. The structure contains an inner, empty Ni_8 cube (av Ni–Ni = 2.397 Å) whose six faces are capped by carbon atoms, which describe a C_6 octahedron without bonding interactions between the C atoms. This inner Ni_8C_6 moiety is surrounded by a truncated-octahedral Ni_{24} shell (av Ni–Ni = 2.461 Å). The Ni atoms of the Ni_{24} shell are arranged in such a way that they generate six square-antiprismatic cavities, in which the six carbide-C atoms (av Ni–C = 2.062 Å) are located. Each Ni atom of the inner cube lies approximately 0.93 Å below the center of each hexagonal face of the outer Ni_{24} shell (av $Ni_{inner}-Ni_{outer}$ = 2.634 Å) and is 12-coordinate; they are within bonding distances from six Ni atoms of the outer shell, three Ni atoms of the inner cube, and three carbide-C atoms.

The solid-state structure of **3** has exclusively edge-bridging carbonyl groups (av Ni–C = 1.917; av C–O = 1.152 Å), which span all Ni–Ni edges of the outer Ni_{24} shell. This structural feature is reminiscent of CO chemisorbed at low coverage on metal surfaces.[12] The solution IR spectrum of **3** reveals that this arrangement of the carbonyl ligands is also retained in

[*] Prof. G. Longoni, Dr. F. Calderoni, Dr. M. C. Iapalucci
Dipartimento di Chimica Fisica ed Inorganica
viale Risorgimento 4, I-40136 Bologna (Italy)
Fax: Int. code +(51)6443690
e-mail: longoni@ms.fci.unibo.it
Prof. F. Demartin
Dipartimento di Chimica Strutturale e Stereochimica Inorganica, Milano (Italy)

[**] This work was supported by the Ministero dell'Università e della Ricerca Scientifica e Tecnologica (MURST). G. L. is grateful to the Human Capital Mobility program of EEC for a grant.

solution. As a result, a $Ni_{32}C_6^{6-}$ molecular ion, which is identical to the $Cr_{32}C_6$ building unit of the $Cr_{23}C_6$ carbide,[7, 13] has now been stabilized in a shell of 36 carbonyl ligands. The isolation and characterization of **3** also substantiates the linear combination of Guassian type orbitals–local density functional (LCGTO-LDF) study previously carried out on a $[Ni_{32}C_6(CO)_{36}]^{n-}$ model compound.[16]

The space-filling model in Figure 2 illustrates an interesting feature of **3**: the structure shows eight distorted hexagonal cup-shaped hollows formed by consecutive concentric rings of oxygen, carbon, and nickel atoms, and ending with an unique nickel atom belonging to the inner cube. We are currently investigating the possibility of placing sterically less demanding molecules in these cup-shaped hollows, as well as the potential use of **3** as a molecular precursor for the preparation of the unknown $Ni_{23}C_6$ alloy.

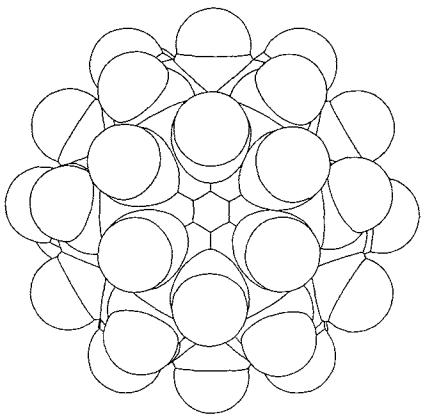

Fig. 2. Space-filling model of **3** illustrating one of the eight cup-shaped hollows.

Experimental Procedure

A solution of $[PPh_3Me]_6$-**2** (350 mg, 0.067 mmol) in acetonitrile (20 mL) was stirred under a CO atmosphere for 15 min and then evaporated under vacuum to dryness. The residue was dissolved in acetonitrile (20 mL) and stirred under a CO atmosphere for 10 min and then dried under vacuum. The resulting dark brown residue was extracted with acetonitrile (20 mL) and filtered. Precipitation by layering the extract with diisopropyl ether (40 mL) gave black crystals of $[PPh_3Me]_6[Ni_{32}C_6(CO)_{36}]\cdot 4$ MeCN (210 mg, 0.043 mmol). The salt is soluble in acetone, acetonitrile, and dimethyl sulfoxide, insoluble in THF, alcohols, and nonpolar solvents (ν_{CO} in MeCN at 1889 cm^{-1}). Elemental analysis for $[PPh_3Me]_6[Ni_{32}C_6(CO)_{36}]\cdot 4$ MeCN: calcd C 41.08, H 2.50, N 1.17; found C 40.86, H 2.41, N 1.14.

Received: April 25, 1996 [Z 9069 IE]
German version: *Angew. Chem.* **1996**, *108*, 2393–2394

Keywords: carbides · carbonyl complexes · clusters · nickel compounds

[1] G. Longoni, M. C. Iapalucci in *Clusters and Colloids: From Theory to Applications* (Ed.: G. Schmid), VCH, Weinheim, **1994**, p. 91.
[2] I. Dance, K. Fischer, *Prog. Inorg. Chem.* **1994**, *41*, 637.
[3] L. C. Roof, J. W. Kolis, *Chem. Rev.* **1993**, *93*, 1037.
[4] J. M. van Ruitenbeek, D. A. van Leeuwen, L. J. de Jongh in *Physics and Chemistry of Metal Cluster Compounds, Vol. 18* (Ed.: L. J. de Jongh), Kluwer, Dordrecht, **1994**, p. 277.
[5] N. Rösch, G. Pacchioni in *Clusters and Colloids: From Theory to Applications*, (Ed.: G. Schmid), VCH, Weinheim, **1994**, p. 5.
[6] A. Ceriotti, A. Fait, G. Longoni, G. Piro, F. Demartin, M. Manassero, N. Masciocchi, M. Sansoni, *J. Am. Chem. Soc.* **1986**, *108*, 8091.
[7] A. L. Bowman, G. P. Arnold, E. K. Storms, N. G. Neresov, *Acta Crystallogr. Sect. B*, **1972**, *28*, 3102.
[8] A. Ceriotti, G. Longoni, M. Manassero, N. Masciocchi, L. Resconi, M. Sansoni, *J. Chem. Soc. Chem. Commun.* **1985**, 181.
[9] A. Ceriotti, A. Fait, G. Longoni, G. Piro, L. Resconi, F. Demartin, M. Manassero, N. Masciocchi, M. Sansoni, *J. Am. Chem. Soc.* **1986**, *108*, 5370.
[10] A. Ceriotti, G. Longoni, M. Manassero, N. Masciocchi, G. Piro, L. Resconi, M. Sansoni, *J. Chem. Soc. Chem. Commun.* **1985**, 1402.
[11] Crystal data for $[PPh_3Me]_6[Ni_{32}C_6(CO)_{36}]\cdot 4$ MeCN: triclinic, space group $P\bar{1}$ (No. 2), $a = 15.974(3)$, $b = 17.474(3)$, $c = 18.200(4)$ Å, $\alpha = 61.37(2)$, $\beta = 69.31(2)$, $\gamma = 72.35(2)°$, $V = 4115(1)$ Å^3, $Z = 1$, $\rho_{calcd} = 1.93$ g cm^{-3}, $Mo_{K\alpha}$ radiation ($\lambda = 0.71073$ Å), $\mu(Mo_{K\alpha}) = 37.1$ cm^{-1}, $T = 298$ K. 14585 reflections with $3° < \theta < 25°$ were measured on a CAD4 diffractometer at room temperature using a crystal with approximate dimensions $0.20 \times 0.15 \times 0.35$ mm. Data were corrected for Lorentz-polarization and absorption effects (empirical absorption, transmission factors in the range 0.56–1.00). The structure was solved by direct methods (SIR 89) and refined by using 10639 independent reflections having $I > 3\sigma(I)$. Anisotropic displacement parameters were assigned to all non-hydrogen atoms. The final R value was 0.033 ($R_w = 0.043$). Crystallographic data (excluding structure factors) for the structure(s) reported in this paper have been deposited with the Cambridge Crystallographic Data Centre as supplementary publication no. CCDC-179-79. Copies of the data can be obtained free of charge on application to The Director, CCDC, 12 Union Road, Cambridge CB2 1EZ, UK (fax: Int. code +(1223) 336-033; e-mail: teched@chemcrys.cam.ac.uk).
[12] G. Ertl in *Metal Clusters in Catalysis, Vol. 29* (Eds.: B. C. Gates, L. Guczi, H. Knözinger), Elsevier, Amsterdam, **1986**, p. 577.
[13] The $Cr_{23}C_6$ alloy has a *Fm3m* structure [7], which conforms to the No. 24 of Andreini's space-filling combination of polyhedra [14,15]. It derives from a three-dimensional sequence of fused $Cr_{32}C_6$ truncated octahedra and Cr_{13}-centered cuboctahedra; this architecture generates truncated tetrahedra that are centered by further chromium atoms.
[14] A. Andreini, *Mem. Soc. Ital. Sci.* **1907**, *14*, 75.
[15] A. F. Wells, *Three-Dimensional Nets and Polyhedra*, Wiley, New York, **1977**, p. 145.
[16] N. Rösch, L. Ackermann, G. Pacchioni, *J. Am. Chem. Soc.* **1992**, *114*, 3549.

The Aluminocenium Cation $[Al(C_5H_5)_2]^+$: A Highly Effective Initiator for the Cationic Polymerization of Isobutene**

Manfred Bochmann* and David M. Dawson

Dedicated to Professor Sir Geoffrey Wilkinson on the occasion of his 75th birthday

The role of aluminum reagents as Lewis acids and as activators for olefin polymerization catalysts is well documented.[1] Very little is known, however, about the chemistry of cationic organoaluminum compounds $[AlR_2]^+$ for which very high Lewis acidity can be expected. Some donor-stablized cationic complexes such as $[AlMe_2(crown)]^+$, $[(EtAl)_2(diazacrown)]^{2+}$, and $[Al\{C(SiMe_3)_2py\}_2]^+$ have been structurally characterized,[2, 3] and recently Schnöckel et al. reported the formation of the decamethylaluminocenium cation $[AlCp_2^*]^+$ by the disproportionation of $[AlCp^*]_4$ in the presence of $AlCl_3$ ($Cp^* = C_5Me_5$).[4] The reactivity of such cationic organoaluminum complexes has to our knowledge not been explored. We report here the synthesis of the unsubstituted aluminocenium cation, $[AlCp_2]^+$, ($Cp = C_5H_5$) and its reactivity as an initiator for cationic polymerizations.

[*] Prof. M. Bochmann, Dr. D. M. Dawson
School of Chemistry
University of Leeds
Leeds, LS2 9JT (UK)
Fax: Int. code +(113) 233 6401
e-mail: M. Bochmann@chem.leeds.ac.uk

[**] This work was supported by the Engineering and Physical Sciences Research Council and Bayer AG, Leverkusen. We are grateful to Dr. W. Obrecht and Dr. G. Langstein (Bayer AG) for helpful discussions.

The reaction of $[AlCp_2Me]$ (**1**)[5] with $B(C_6F_5)_3$ (**2**) in dichloromethane at low temperature, followed by evaporation of the solvent affords the white microcrystalline solid **3** [Eq. (a)].[6] Compound **3** is sparingly soluble in warm benzene

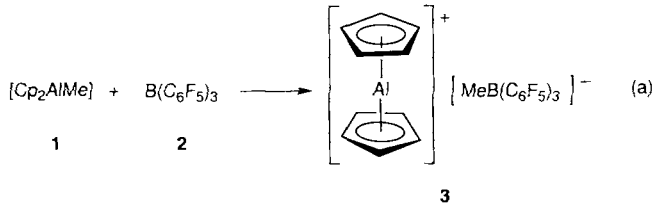

or toluene but dissolves rapidly in cold dichloromethane. Over the temperature range from -80 to $-20\,^{\circ}C$, solutions of **3** in CD_2Cl_2 show two singlets in the ^1H NMR spectrum at $\delta = 7.05$ and 0.55, consistent with the formation of the solvated ion pair $[AlCp_2]^+[MeB(C_6F_5)_3]^-$. These solutions decompose rapidly on warming them to $20\,^{\circ}C$. The ^{27}Al NMR spectrum recorded at $-60\,^{\circ}C$ for the reaction of **1** with **2** shows that the broad signal for **1** at $\delta = 72.7$ (half-width ca. 250 Hz) is replaced by a new sharp peak at $\delta = -126.4$ (half-width 30 Hz). This value is in excellent agreement with the calculated chemical shift for the $[Al(\eta^5\text{-}Cp)_2]^+$ ion ($\delta = -130.0$).[4]

1:1 mixtures of **1** and **2** in $[D_8]$toluene at $20\,^{\circ}C$ show very similar ^1H and ^{27}Al NMR spectra. The limited solubility of the reaction product in toluene leads to the formation of two phases on cooling. Although the formation of the methyl-bridged isomer $[Cp_2Al(\mu\text{-}Me)B(C_6F_5)_3]$ might reasonably be expected in less polar solvents, conclusive evidence for this was not found.

Even in the solid state **3** is highly air- and moisture-sensitive. Unfortunately crystals suitable for X-ray diffraction could not be obtained. Although **1** has been shown to contain η^2-coordinated Cp rings in the crystal and is highly fluxional in solution, the $[AlCp_2]^+$ ion most likely possesses a metallocene-type structure with η^5-bound Cp ligands. This assumption is supported by the structure of $[Al(\eta^5\text{-}Cp^*)_2]^+$, the close agreement of the observed ^{27}Al chemical shift with the one calculated assuming a D_{5d} symmetry, the narrow half-width of the ^{27}Al signal, which is typical for a highly symmetric ligand environment for Al, as well as the sandwich structures of the isoelectronic magnesiocene $[MgCp_2]$ and related Group 2 cyclopentadienyl complexes.[7] An increase in hapticity from η^1 to η^5 on forming a more Lewis acidic cationic metal center from a neutral cyclopentadienyl complex is also a common feature of boron cyclopentadienyl complexes.[8]

Starting point for the synthesis of $[AlCp_2]^+$ was the search for highly Lewis acidic compounds as initiators for carbocationic polymerizations. Compound **3** is indeed a highly active initiator for the polymerization of isobutene and isobutene–isoprene copolymerizations [Eq. (b)]. Such copolymerizations to butyl rubber are carried out on an industrial scale by using a heterogeneous initiator based on $AlCl_3$ in chloromethane at between -95 and $-100\,^{\circ}C$.[9, 10] The need to recycle large amounts of chlorinated solvents and the high energy requirements of such a low-temperature process make cleaner, less energy intensive alternatives that can be operated at higher temperatures highly desirable.

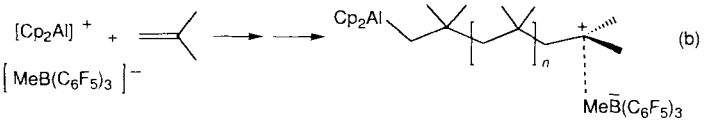

The activity of **3** as an initiator for the polymerization of isobutene has been studied over a temperature range of $-78\,^{\circ}C$ to $-25\,^{\circ}C$. The reactions proceed in dichloromethane as well as in saturated hydrocarbons. Neither **1** nor **2** on their own was found to polymerize isobutene.[11] Whereas an excess of **2** over **1** has no effect on polymer yield or molecular weight, an excess of **1** over **2** retards the polymerization. The results for isobutene homopolymerizations are given in Table 1. As expected for carbocationic polymerizations, the polymer molecular weights increase with decreasing temperature, from $M_w \approx 3 \times 10^5$ at $-30\,^{\circ}C$ to 1.8×10^6 at $-70\,^{\circ}C$, with narrow polydispersities.[12]

Table 1. Isobutene homopolymerizations initiated with **3** [a].

Entry	**1** [μmol]	**2** [μmol]	T [°C]	t [min]	Yield [g]	M_w $\times 10^{-3}$	M_w/M_n
1 [b]	40	40	−78	10	0.63	731	3.0
2 [c]	38	38	−78	10	0.28	1340	3.0
3	50	50	−70	10	0.30	1800	2.8
4	100	50	−70	10	0.02	820	3.4
5	50	50	−50	10	0.18	618	2.0
6	50	50	−30	10	0.08	318	1.8
7	50	100	−30	10	0.03	337	1.8
8	50	50	−25	10	0.05	289	1.6

[a] For reaction conditions see Experimental Procedure. Entries 3–8: Polymerizations were carried out in the presence of 1.5 mL dichloromethane. [b] Solvent: toluene (1.5 mL). [c] Solvent: methylcyclohexane (1.5 mL).

Compound **3** also initiates the copolymerization of isobutene with 2–5 vol% of isoprene, at typical reaction temperatures of -78 to $-50\,^{\circ}C$. For example, the reaction with 5% isoprene at $-70\,^{\circ}C$ gave a polymer with $M_w = 7.8 \times 10^5$ and $M_w/M_n = 3.3$. The polymer contained about 2.7% isoprene units with a 1,4-*trans* structure; there was no evidence for 1,4-*cis* or 1,2-incorporation within NMR detection limits.[13] Similar reactions with 2 vol% isoprene at $-50\,^{\circ}C$ gave copolymers with $M_w \approx 2 \times 10^5$.

It is likely that the relatively high molecular weights obtained in these reactions are not least due to the weakly basic nature of the counteranion used in this system. Isobutene homo- and copolymerizations are usually carried out with a mixture of a Lewis acidic metal halide MX_n and an alkyl halide RX capable of generating a carbocation, resulting in the formation of $R^+[MX_{n+1}]^-$. Self-ionization of the Lewis acid to $[MX_{n-1}]^+[MX_{n+1}]^-$ has also been suggested, although there is so far no direct evidence for species such as $[AlX_2]^+$ in polymerization systems.[14] Complex halide anions $[MX_{n+1}]^-$ possess rather limited stability and are prone to loss of X^- ions, which may lead to halide incorporation into the polymer and may assist deprotonation and chain transfer. In the present case we make use of the stability and very low basicity of perfluorophenylborates to generate a well-defined polymerization initiator system free of halide anions.[15, 16]

Experimental Procedure

All reactions were carried out under strictly dry and anaerobic conditions. NMR spectra were measured on JEOL EX270 and Bruker DPX300 spectrometers (reference: tetramethylsilane: ^1H and ^{13}C; $[Al(H_2O)_6]^{3+}$: ^{27}Al). Isobutene was dried over $Et_2AlOC_6H_{13}$ and recondensed; isoprene was dried over calcium hydride and distilled from sodium prior to use.

3: To a solution of **1** (400 mg, 2.3 mmol) in dichloromethane (10 mL) at $-78\,^{\circ}C$ was added **2** (1.2 g, 2.3 mmol). The mixture was stirred for 15 min, and the solution allowed to warm to $0\,^{\circ}C$ whilst the solvent was removed in vacuo. The off-white solid residue was washed with light petroleum and dried to give **3** (1.6 g, 2.3 mmol, 99%). Elemental analysis: Found: C 50.13, H 1.90, F 41.2%; calc.: C 50.87, H 1.90,

F 41.6%; ^{1}H NMR (CD_2Cl_2, −60 °C): δ = 0.55 (s, 3H, Me-B), 7.05 (s, 10H, Cp); ^{13}C NMR (CD_2Cl_2, −20 °C): δ = 10.5 (s, br, Me-B), 114.5 (s, Cp); ^{27}Al NMR (CD_2Cl_2, −20 °C): δ = −126.35; ([D$_8$]toluene, 20 °C): δ = −128.3 (half-width ca. 30 Hz).

(Co-)Polymerizations were carried out in an all-glass reactor, which was flame-dried in vacuo. Isobutene (10 mL) was condensed into the reaction vessel and magnetically stirred at 1000 rpm to allow it to equilibrate at the appropriate temperature. This was followed by injection of **2** (50 μmol) in 1 mL of solvent (cf. Table 1). The mixture was stirred for 1 min before **1** (50 μmol) in 0.5 mL solvent were injected. Polymerization took place instantaneously. The polymerization was terminated by injecting 0.5 mL methanol, and the polymer precipitated by the addition of further methanol. The product was filtered and dried in an oven at 60 °C. For copolymerizations the condensation of isobutene was followed by an injection of 2–5 vol% isoprene.

Received: February 21, 1996 [Z 8845 IE]
German version: *Angew. Chem.* **1996**, *108*, 2371–2373

Keywords: aluminum compounds · isobutenes · polymerizations · sandwich complexes

[1] J. J. Eisch in *Comprehensive Organometallic Chemistry, Vol 1* (Eds.: G. Wilkinson, F. G. A. Stone, E. W. Abel), Pergamon, **1982**, p. 555ff; *Comprehensive Organometallic Chemistry II, Vol. 1*, Pergamon, **1995**, p. 431ff.

[2] S. G. Bott, A. Alvanipour, S. D. Morley, D. A. Atwood, C. Mitchell Means, A. W. Coleman, J. L. Atwood, *Angew. Chem.* **1987**, *99*, 476; *Angew. Chem. Int. Ed. Engl.* **1987**, *26*, 485; H. G. Richey, G. L. Bergstresser, *Organometallics* **1988**, *7*, 1459; M. F. Self, W. T. Pennington, J. A. Laske, G. H. Robinson, *ibid* **1991**, *10*, 36.

[3] L. M. Engelhardt, U. Kynast, C. L. Raston, A. H. White, *Angew. Chem.* **1987**, *99*, 702; *Angew. Chem. Int. Ed. Engl.* **1987**, *26*, 681.

[4] C. Dohmeier, H. Schnöckel, C. Robl, U. Schneider, R. Ahlrichs, *Angew. Chem.* **1993**, *105*, 1714; *Angew. Chem. Int. Ed. Engl.* **1993**, *32*, 1655.

[5] J. Stadelhofer, J. Weidlein, A. Haaland, *J. Organomet. Chem.* **1975**, *84*, C1; J. D. Fisher, M. Y. Mei, R. Willet, P. J. Shapiro, *Organometallics* **1994**, *13*, 3324. In this reference a ^{13}C NMR signal at δ = 14.05 is quoted for Al-CH_3. In our experience pure, petroleum ether free $AlCp_2Me$ does not exhibit such a resonance.

[6] The reaction of **1** with $[CPh_3][B(C_6F_5)_4]$ proceeds similarly but is less clean and appears to involve abstraction of Cp as well as methyl anions by $[CPh_3]^+$.

[7] W. Bünder, E. Weiss, *J. Organomet. Chem.* **1975**, *92*, 1; T. P. Hanusa, *Polyhedron* **1990**, *9*, 1345.

[8] P. Jutzi, A. Seufert, *J. Organomet. Chem.* **1978**, *161*, C5; P. Jutzi, A. Seufert, W. Buchner, *Chem. Ber.* **1979**, **112**, 2488.

[9] I. M. Campbell, *Introduction to Synthetic Polymers*, Oxford University Press, Oxford **1994**, p. 130.

[10] J. P. Kennedy, B. Iván, *Designed Polymers by Carbocationic Macromolecular Engineering*, Hanser, Munich **1991**.

[11] In the presence of moisture **2** gives the acidic hydrate $B(C_6F_5)_3 \cdot H_2O$, which results in H^+-initiated formation of polyisobutene of variable molecular weight. Traces of moisture lead to very small amounts of high molecular weight polyisobutene (M_w = ca. $2-3 \times 10^6$), typical for very low initiator concentrations.

[12] Very similar polymerization results were obtained with the system [Al-Cp(R)Cl]/**2** (R = Me, Et). Monitoring the reaction between [AlCpMeCl] and **2** in CD_2Cl_2 at −73 °C shows the formation of $[AlCp_2]^+$ as the only identifiable product, evidently formed by Cp ligand exchange.

[13] J. L. White, T. D. Shaffer, C. J. Ruff, J. P. Cross, *Macromolecules* **1995**, *28*, 3290.

[14] L. Balogh, Z. Fodor, T. Kelen, R. Faust, *Macromolecules* **1994**, *27*, 4648. Dialkylaluminum cations have been generated in the gas phase: R. Srinivas, D. Sülzle, H. Schwarz, *J. Am. Chem. Soc.* **1990**, *112*, 8334.

[15] M. Bochmann, *Angew. Chem.* **1992**, *104*, 1206; *Angew. Chem. Int. Ed. Engl.* **1992**, *31*, 1181. For the use of metal alkyl/$B(C_6F_5)_3$ systems in Ziegler-type olefin polymerizations see for example X. Yang, C. L. Stern, T. J. Marks, *J. Am. Chem. Soc.* **1991**, *113*, 3623; *ibid.* **1994**, *116*, 10015; M. Bochmann, *J. Chem. Soc., Dalton Trans.* **1996**, 255, and references therein.

[16] Since this work was started, the cationic polymerization of isobutene with a [Cp*$TiMe_3$]/$B(C_6F_5)_3$ initiator system has been reported: F. Barsan, M. C. Baird, *J. Chem. Soc. Chem. Commun.* **1995**, 1065. The polyisobutene molecular weights reported for this system, which range from 3×10^4 (−20 °C) to 2×10^5 (−78 °C), are significantly lower than those obtained here with $[AlCp_2]^+$.

From $1\sigma^4,2\sigma^2$ to $1\sigma^4,2\sigma^n$-Diphosphetes (n = 3–6): The Surprising Persistence of the P–P bond**

Muriel Sanchez, Régis Réau, Françoise Dahan, Manfred Regitz, and Guy Bertrand*

Dedicated to Professor Miha Tišler on the occasion of his 70th birthday

The phosphanylidene-σ^4-phosphorane **A** was reported by Burg and Mahler in 1961.[1] It was the first example of a two-coordinate phosphorus atom in a neutral molecule, but more importantly, this compound opened the way to a variety of new types of P–P bonding beyond the classical ones (**B**–**D**) accepted

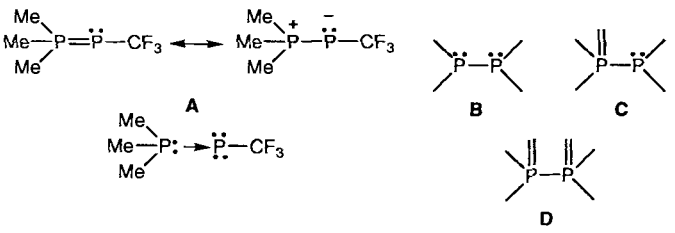

at that time.[2] Among other resonance forms, **A** can be regarded as a phosphane complex of a phosphinidene (phosphanediyl) unit.[3] Since phosphinidene units feature a phosphorus atom with the lowest possible coordination number, it is surprising that they have not been used more frequently to prepare phosphorus derivatives with much higher coordination states.[4] Very recently, we reported the synthesis of the $1\sigma^4,2\sigma^2$-diphosphete **1**,[5] a cyclic phosphanylidene-σ^4-phosphorane, and herein we report the conversion of the low-coordinate phosphorus center of **1** into a succession of higher coordinate phosphorus centers; the P–P interaction and the cyclic structure is retained throughout this series.

One of the rare examples of reactivity known for derivatives of type **A** is methylation.[3, 6] Thus, heterocycle **1** was treated with methyl triflate, which led to the cationic $1\sigma^4,2\sigma^3$-diphosphete **2** in 95% yield (Scheme 1); selective spectroscopic data are given in Table 1. The cyclic structure is supported by the high-field shift of the ^{31}P NMR resonance of the PMe unit (δ = + 54.9), the small $^2J(PNCH)$ coupling constants (5.2 and 4.8 Hz) typical of a diisopropylamino-substituted σ^4-phosphorus atom,[7] and by the multiplicity of the ^{1}H (δ = 1.84, dd, J(P,H) = 19.1 and 4.9 Hz) and ^{13}C NMR (δ = 11.26, dd, J(P,C) = 42.0 and 8.5 Hz) signals of the P-methyl group. Note the relatively small value of J(P,P) (107.4 Hz), which results from superimposition of the ^1J and ^3J coupling constants.

[*] Dr. G. Bertrand, M. Sanchez, Dr. R. Réau, Dr. F. Dahan
Laboratoire de Chimie de Coordination du CNRS
205, route de Narbonne, F-31077 Toulouse Cédex (France)
Fax: Int. code +61 55 30 03
e-mail: gbertran@lcctoul.lcc-toulouse.fr
Prof. Dr. M. Regitz
Fachbereich Chemie der Universität Kaiserslautern (Germany)

[**] This work was supported by the Centre National de Recherche Scientifique (CNRS), the Fonds der Chemischen Industrie (Graduiertenkolleg Phosphor), and the Deutsche Forschungsgemeinschaft. Editorial note: According to IUPAC recommendations, when ring atoms display a connectivity that differs from their standard bonding number, the actual bonding number is expressed as an arabic superscript to the Greek letter lambda following immediately after the appropriate locant. In this communication, however, contrary to this recommendation the Greek letter sigma has been applied to highlight the structural connection between the compounds **1**–**6**. The superscript, here gives the number of σ bonds starting from the ring phosphorus atoms.

Table 1. Selected NMR data for compounds **1**–**6** (coupling constants in Hz) [a].

	$\delta(N_2P)$	δ(P)	J(P,P)	$^3J(PNCH)$	$^2J(PNCH)$	δ CSiMe$_3$	(J(P,C))	δ C*t*Bu	(J(P,C))
1	+49.2	+58.4	201	13.6	5.6	105.7	(36.8; 4.2)	224.3	(54.9; 9.9)
2	+40.2	+54.9	107	10.9	5.2–4.8	151.7	(36.6; 9.5)	193.7	(23.0; 0)
3	+39.2	+117.1	246	–	4–2.7	158.5	(28.5; 12.5)	202.4	(51.8; 15.3)
4	+59.2	+83.2	47	10.0	3.0	135.5	(25.6; 18.3)	194.9	(53.3; 22.6)
5	+117.0	+25.2	36	10.0	8–3.6	142.2	(44.2; 26.5)	209.9	(85.0; 7.6)
6	+131.3	– 65.4	122	8.1	4.3–4.5	130.5	(39.2; 13.9)	207.0	(89.1; 120.4)

[a] Correct elemental analyses or/and mass spectra were obtained for compounds **2**–**6**.

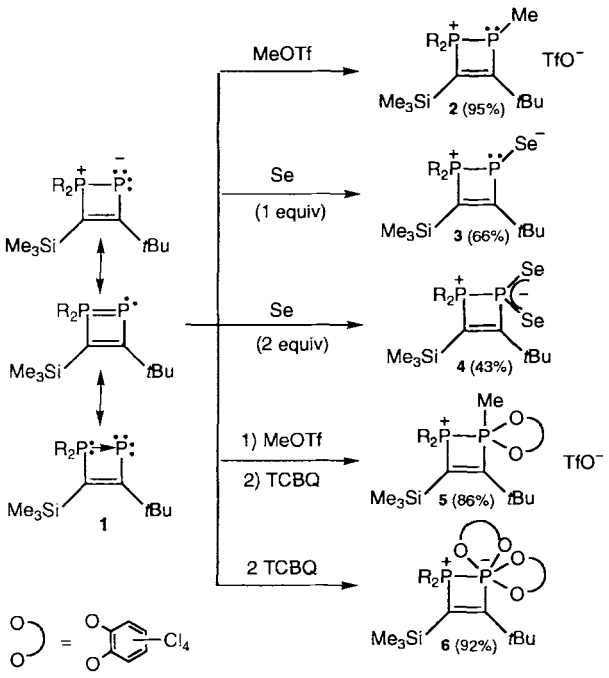

Scheme 1. Synthesis of $1\sigma^4,2\sigma^n$-diphosphetes (n = 3–6) **2**–**6** from **1**. R = iPr$_2$N, Tf = CF_3SO_2, TCBQ = tetrachloro-*o*-benzoquinone.

The reaction of **1** with one equivalent of elemental selenium afforded the zwitterionic $1\sigma^4,2\sigma^3$-diphosphete **3** as an orange oil in 66% yield (Scheme 1). The best indications of its cyclic structure are given by the small $^2J(PNCH)$ coupling constants (4.0 and 2.7 Hz) and by the very low-field position[5] of the ^{13}C NMR signals of both ring carbon atoms (δ = 158.5 and 202.4).

A smooth reaction occurred when two equivalents of elemental selenium were added to **1**, affording the corresponding $1\sigma^4,2\sigma^4$-diphosphete **4** in 43% yield as a yellow oil (Scheme 1). Apart from the J(P,P) coupling constant (**3**: 246 Hz; **4**: 47 Hz), which is not relevant for the discussion, as mentioned above, the main difference between the spectroscopic data for **3** and **4** lies in the ^{77}Se NMR spectra (**3**: δ = – 63.0, ^1J(P,Se) = 487 Hz; **4**: δ = + 264.8, ^1J(P,Se) = 699 Hz).

For compounds **1**–**4**, ring strain is a destabilizing factor. Although ring opening through breaking the P–P bond would generate a stable phosphane on one side, a rather unstable low-coordinate phosphorus moiety[8] (a phosphinidene, a phosphenium ion, a selenoxophosphane, and a diselenoxophosphorane, respectively) would be generated on the other. If P–P bond cleavage led to stable phosphorus entities on both sides, one might expect that ring cleavage would occur. Surprisingly then, derivative **2** reacts with one equivalent of tetrachloro-*o*-benzoquinone (TCBQ) to produce the cationic $1\sigma^4,2\sigma^5$-diphosphete **5** (86% yield) as an orange oil, and addition of two equivalents of TCBQ to $1\sigma^4,2\sigma^2$-diphosphete **1** affords the $1\sigma^4,2\sigma^6$-diphosphete **6** (92% yield) as colorless crystals (Scheme 1). In addition to the arguments already used for compounds **2**–**4**, a strong indicator of a P–P bond in **5** and **6** is given by the low-field ^{31}P NMR signals of the amino-substituted phosphorus (**5**: δ = +115.5; **6**: δ = +131.5), which are inconsistent with free phosphanes. The cyclic structure has been confirmed by a single-crystal X-ray diffraction study[9] of compound **6** (Fig. 1).

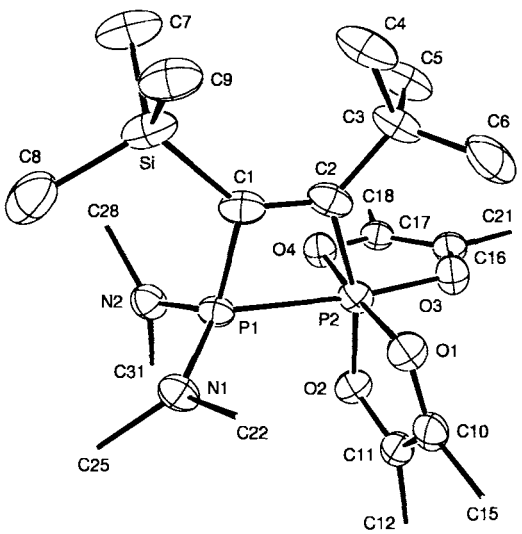

Fig. 1. Crystal structure of **6** (ORTEP view). The CH_3 groups of the diisopropylamino group and a section of the catecholate rings have been omitted for clarity. Selected bond lengths [Å] and angles [°]: P1–P2 2.2962(6), P2–C2 1.921(2), C2–C1 1.355(3), C1–P1 1.823(2); C1-P1-P2 79.66(7), P1-P2-C2 71.34(6), P1-P2-O3 173.09(5), O1-P2-O4 173.01(7), O2-P2-C2 165.44(7), P2-C2-C1 107.5(1), C1-C2-C3 129.2(2), C2-C1-P1 101.4(2), C2-C1-Si 136.1(2), P1-C1-C2-P2 1.9(2).

The P–P bond length of 2.2962 (6) Å is in the range of normal P–P single bonds (2.20–2.35 Å);[10] the P2 atom has a slightly distorted square-planar, bipyramidal coordination sphere, typical for hexacoordinate phosphorus.[11]

While P–P interactions between phosphanes and electron-poor polyfluorophosphoranes have been observed,[12] in marked contrast, several *cis*-1-phosphino-2-phosphonioethene derivatives exist, and none of them features a P–P interaction (P–P distances >3 Å).[13] The persistence of the P–P bond in derivatives **5** and **6** might be due to the steric repulsion between the bulky Me_3Si and *t*Bu groups, which induces small P1-C1-C2 (101.4(2)°) and P2-C2-C1 (107.5(1)°) angles. This study raises the question of a possible P–P interaction in compounds such as **7**.[14] In other words, can *cis*-$1\sigma^3,2\sigma^3$-diphosphorus-substi-

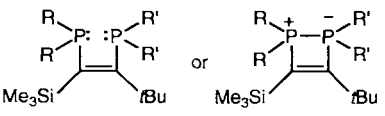

7

tuted ethene derivatives be forced to form four-membered heterocycles with a P–P bond?

Experimental Procedure

In a typical experiment, a solution of **1** (0.29 g, 0.70 mmol) in CH_2Cl_2 (1 mL) at −78 °C was added dropwise to a solution of TCBQ (0.34 g, 1.40 mmol) in CH_2Cl_2 (2 mL). The solution was allowed to warm to room temperature, and the solvent was removed under vacuum. The product was extracted from the residue with pentane (3 × 6 mL). Compound **6** was obtained from a solution in CH_2Cl_2 at −30 °C as colorless crystals (m.p. 223 °C), yield: 0.58 g (92%).

2: Orange oil from a CH_2Cl_2/pentane solution, yield: 0.34 g (95%); **3** and **4**: THF instead of CH_2Cl_2, sonication 10 min for **3** (orange oil, yield: 0.43 g (66%)) and 1 h for **4** (yellow oil, yield: 0.33 g (43%)); **5** (orange oil from a THF/pentane solution, yield: 0.41 g (86%)).

Received: April 9, 1996 [Z 9001 IE]
German version: *Angew. Chem.* **1996**, *108*, 2386–2388

Keywords: heterocycles · phosphorus compounds

[1] A. B. Burg, W. Mahler, *J. Am. Chem. Soc.* **1961**, *83*, 2388–2389.
[2] A. H. Cowley, *Chem. Rev.* **1965**, *65*, 617–634.
[3] A. Schmidpeter in *Multiple Bonds and Low Coordination in Phosphorus Chemistry* (Eds.: M. Regitz, O. J. Scherer), Thieme, Stuttgart, **1990**, pp. 338–351 and references therein.
[4] For reviews on phosphinidenes, see: a) F. Mathey, *Angew. Chem.* **1987**, *99*, 285–296; *Angew. Chem. Int. Ed. Engl.* **1987**, *26*, 275–286; b) A. H. Cowley, A. R. Barron, *Acc. Chem. Res.* **1988**, *21*, 81–87; c) F. Mathey, in *Multiple Bonds and Low Coordination in Phosphorus Chemistry* (Eds.: M. Regitz, O. J. Scherer), Thieme, Stuttgart, **1990**, pp. 33–47; d) G. Huttner, H. Lang, *ibid.*, pp. 48–57; e) G. Huttner, K. Evertz, *Acc. Chem. Res.* **1986**, *19*, 406–413; f) G. Huttner, K. Knoll, *Angew. Chem.* **1987**, *99*, 765–782; *Angew. Chem. Int. Ed. Engl.* **1987**, *26*, 743–760.
[5] R. Armbrust, M. Sanchez, R. Réau, U. Bergsträsser, M. Regitz, G. Bertrand, *J. Am. Chem. Soc.* **1995**, *117*, 10785–10786.
[6] A. B. Burg, K. K. Joshi, J. F. Nixon, *J. Am. Chem. Soc.* **1966**, *88*, 31–37.
[7] R. W. Reed, G. Bertrand, in *Phosphorus-31 NMR Spectral Properties in Compound Characterization and Structural Analysis* (Eds.: L. D. Quin, J. G. Verkade), VCH, New York, **1994**, pp. 189–200.
[8] *Multiple Bonds and Low Coordination in Phosphorus Chemistry* (Eds.: M. Regitz, O. J. Scherer), Thieme, Stuttgart **1990**.
[9] X-ray structure data for **6**: $C_{33}H_{46}Cl_8N_2O_4P_2Si$, monoclinic, space group $P2_1/c$ (No 14), $a = 11.0616(12)$, $b = 18.620(2)$, $c = 20.7035(15)$ Å, $\beta = 97.477(7)°$, $V = 4227.9$ Å^3, $\rho_{calcd} = 1.427$ g cm^{-3}, $Z = 4$. Data were collected on an Enraf-Nonius CAD4 diffractometer at 293 K with ω-2θ scans with $Mo_K\alpha$ radiation ($\lambda = 0.71073$ Å). A total of 8724 reflections were collected up to $2\theta = 52°$, of which 5023 were observed [$F_o^2 > 2\sigma(F_o^2)$]. The solution and refinement on F_o^2, with SHELXL-93, of the structure gave R(obs) = 0.0324, [R(all) = 0.0886] and Rw(obs) = 0.0774 [Rw(all) = 0.0878]. Further details of the crystal structure investigation can be obtained from the Fachinformationszentrum Karlsruhe, D-76344 Eggenstein-Leopoldshafen (Germany), on quoting the depository number CSD-405413.
[10] L. Lamandé, K. Dillon, R. Wolf, *Phosphorus, Sulfur, Silicon Relat. Elem.* **1995**, *103*, 1–24.
[11] R. Luckenbach in *Methoden Org. Chem. (Houben-Weyl) 4th. Ed. 1952-, Vol. E2*, (Ed.: M. Regitz), **1982**, pp. 897–907.
[12] a) W. S. Sheldrick, J. A. Gibson, G. V. Röschenthaler, *Z. Naturforsch. B* **1978**, *33*, 1102–1105; b) C. W. Schultz, R. W. Rudolph, *J. Am. Chem. Soc.* **1971**, *93*, 1898–1903.
[13] a) H. Schmidbaur, C. Paschalidis, O. Steigelmann, D. L. Wilkinson, G. Müller, *Chem. Ber.* **1989**, *122*, 1857–1861; b) N. K. Roberts, B. W. Skelton, A. H. White, *J. Chem. Soc. Dalton Trans* **1980**, 1567–1571.
[14] a) R. W. Alder, D. D. Ellis, J. K. Hogg, A. Martin, A. G. Orpen, P. N. Taylor, *Chem. Commun.* **1996**, 537–538; b) interactions between phosphanes and amines have already been reported: C. Chuit, R. J. P. Corriu, P. Monforte, C. Reyé, J. P. Declercq, A. Dubourg, *Angew. Chem.* **1993**, *105*, 1529–1531; *Angew. Chem. Int. Ed. Engl.* **1993**, *32*, 1430–1432.

Microporous Mixed Oxides—Catalysts with Tunable Surface Polarity**

Stephan Klein and Wilhelm F. Maier*

The optimization of reaction conditions and heterogeneous catalysts is still of central importance for the improvement of selectivity in chemical production processes. The surface polarity of the catalysts has so far played a minor role. There is no detailed knowledge on the correlation of catalytic reactions and surface polarity or on catalysts whose surface polarity can be adjusted at will over a wide range, irrespective of the catalytically active centers. Here we show for the first time the preparation of microporous mixed oxide catalysts with controlled surface polarity and demonstrate their effect on selected selective oxidation reactions.

Isolated Ti^{4+} sites in an SiO_2 matrix are active centers for the selective oxidation of organic substrates with peroxides.[1] Whereas crystalline Ti zeolites like TS-1 are catalysts for selective oxidations with aqueous hydrogen peroxide but cannot utilize organic hydroperoxides such as *tert*-butylhydroperoxide (TBHP), amorphous TiO_2–SiO_2 oxides are excellent catalysts for selective oxidation with TBHP, but not with hydrogen peroxide.[2] These differences in the catalytic behavior are attributed to the difference in surface polarity of hydrophobic silicalites and hydrophilic, amorphous mixed oxides, as well as to geometric limitations in the formation of the transition state. The only exception is a TiO_2–SiO_2 oxide of unknown surface polarity and bimodal pore size distribution, which was recently reported to be active for the oxidation of arenes with hydrogen peroxide.[3]

As we have shown recently, SiO_2-based amorphous, microporous mixed oxides (AMM), prepared by an optimized sol–gel procedure in the absence of template molecules or hydrothermal synthesis conditions, are capable of catalyzing acidic and redox[4] reactions shape-selectively.[5] This synthesis concept has now been expanded to include the preparation of microporous mixed oxides, where the number of Si atoms carrying a covalently bound alkyl group is freely variable.[6] These nonhydrolyzable alkyl groups formally replace a hydroxyl group in the mixed oxide and therefore affect the surface polarity of the final catalyst.

In the following, these amorphous microporous mixed oxides are named AMM-M_x(Si-alkyl)$_y$Si. Here Si stands for the matrix materials SiO_2, x for the content of catalytically active metal oxide M (in atom %) and (Si-alkyl)$_y$ for the content (atom %) of alkyltrialkoxysilane in the Si matrix. A material named AMM-$Ti_1(SiMe)_{25}Si$ therefore has the composition of $1\,TiO_2 : 25\,H_3C\text{-}SiO_{1.5} : 74\,SiO_2$. Besides the already mentioned catalyst containing 1% Ti, any desired extent of Ti, as well as Al, Zr, Sn, and V can also be incorporated in those hybrid oxides; thus the metal as well as the alkyl content can be varied over a wide range.[7]

In the following we describe our studies on TiO_2-containg mixed oxides to illustrate the behavior of such alkyl-containing compounds. Argon adsorption–desorption isotherms con-

[*] Prof. Dr. W. F. Maier, Dr. S. Klein
Max-Planck-Institut für Kohlenforschung
Kaiser-Wilhelm Platz 1, D-45470 Mülheim an der Ruhr (Germany)
Fax: Int. code +(208)306-2987
e-mail: maier@dsa.mpi-muelheim.mpg.de

[**] S. K. thanks the Fonds der Chemischen Industrie for a stipend, and W. F. M. the Fonds der Chemischen Industrie and Hoechst AG for support. We thank Prof. J. A. Martens (CUK Leuven) for discussions and a sample of TS-1 catalyst (1% Ti).

firmed the identical narrow micropore distribution already found in alkyl-free AMM materials.[4, 5, 8] The maxima of the pore size distribution (method of Horváth and Kawazoe) of the alkyl-containing mixed oxides (0.7 nm pore diameter) lie in the range of large-pore zeolites, comparable to the alkyl-free reference samples. The narrowness of the pore-size distribution decreases slightly with increasing methyl content in the series AMM-$Ti_1(SiMe)_ySi$ with $0 < y < 45$ (Table 1), whereas high surface areas remain a constant feature. Because the materials are all microporous, the absolute BET values from Table 1 are only

Table 1. Specific surface S_{BET}, maxima of pore size distribution D_{max} (method of Horváth - Kawazoe) and width at half height δ of the distributions of the AMM-$Ti_1(SiMe)_xSi$ materials. The values were obtained from Ar adsorption isotherms at 77 K.

Material AMM-	S_{BET} [m_2g^{-1}]	D_{max} [nm]	δ [nm]
Ti_1Si	585	0.73	0.12
$Ti_1(SiMe)_5Si$	489	0.74	0.07
$Ti_1(SiMe)_{10}Si$	627	0.73	0.06
$Ti_1(SiMe)_{15}Si$	527	0.73	0.09
$Ti_1(SiMe)_{20}Si$	545	0.72	0.07
$Ti_1(SiMe)_{25}Si$	532	0.73	0.11
$Ti_1(SiMe)_{30}Si$	539	0.74	0.36
$Ti_1(SiMe)_{35}Si$	575	0.74	0.35
$Ti_1(SiMe)_{40}Si$	625	0.73	0.30
$Ti_1(SiMe)_{45}Si$	574	0.72	0.20
$Ti_1(SiMe)_{50}Si$	580	0.73	0.17

important for mutual comparison and should be treated with caution. No microcrystalline areas could be detected by high resolution transmission electron microscopy. The amorphous structure of the materials must thus extend into the subnanometer region. Comparison of the elemental composition obtained from selected-area EDX-analysis (energy dispersive X-ray emission) of large and small sample areas in the nm to µm range confirms the high homogeneity of the mixed oxides already observed in the above mentioned spectroscopic studies and excludes the presence of domains. As in the methyl-free AMM-TiSi materials,[5] despite a very low Ti content a distinct IR band in DRIFT (diffuse-reflectance infrared Fourier Transform)/spectroscopic studies at 960 cm^{-1} in the AMM-$Ti_1(SiMe)_ySi$ materials confirm the isomorphic substitution of Si by Ti and thus the presence of atomically isolated Ti centers (Fig. 1). This band is absent in the Ti-free AMM-Si materials.

The incorporation of the methyl groups into the materials could be confirmed directly by DRIFT spectroscopy: the characteristic band of the structural CH_3-Si[9] unit was observed at 1280 cm^{-1}.[10] The signal intensity, which correlates with the y value of the AMM-$Ti_1(SiMe)_ySi$ (Fig. 1) did not change to 773 K. The presence of these stable methyl groups affects especially the surface polarity of these glasses. In analogy to a method employed by Weitkamp et al.[11] the polarity of materials was quantified by competitive gas-phase adsorption of octane–water mixtures.[12] From the loading x_i, obtained from the breakthrough curves of the two components, the modified hydrophobicity index $HI^* = x_{octane}/x_{water}$ was calculated as a measure of the relative affinity of the sample for these sorbates. Hydrophobic materials like Ti-silicalites of the MFI type have high HI* values greater than 1 and thus a tendency to absorb hydrocarbons, while hydrophilic materials like amorphous TiO_2–SiO_2 mixed oxides of similar composition have HI* values smaller than 1 and a preference for water absorption.

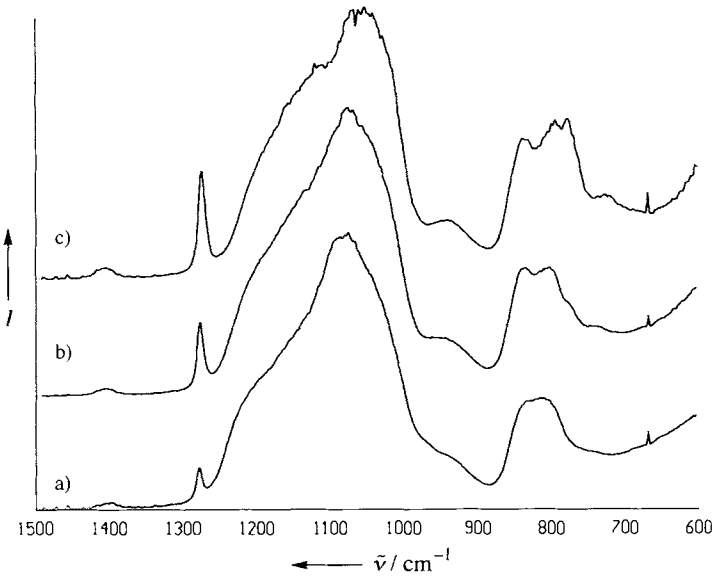

Fig. 1. DRIFT spectra of a) AMM-$Ti_1(SiMe)_{10}Si$, b) AMM-$Ti_1(SiMe)_{25}Si$, and c) AMM-$Ti_1(SiMe)_{45}Si$. The in situ measurements were performed at 303 K with calcined samples under inert atmosphere.

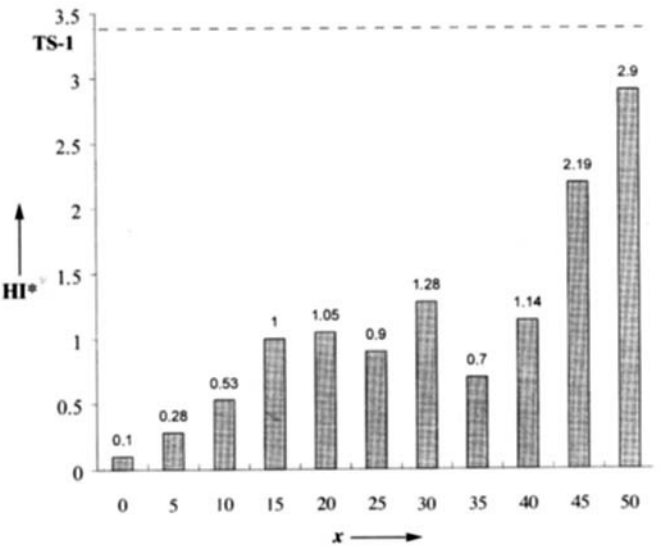

Fig. 2. The hydrophobicity index $HI^* = x_{octane}/x_{water}$ on AMM-$Ti_1(SiMe)_xSi$ as function of x. The loadings were obtained from the breakthrough curves of octane and water by competitive absorption experiments in the gas phase at 308 K.

As documented in Figure 2, the synthesis principle presented here builds a catalyst class in which the surface polarity is controlled by the number of cocondensed CH_3Si components only. The polarity can therefore be varied from hydrophilic to hydrophobic while maintaining a constant oxide composition and pore architecture.

All our observations point to a narrow correlation between catalyst surface polarity and its activity for peroxide-mediated selective oxidation reactions. As already reported, AMM-Ti_xSi materials are good catalysts for the epoxidation of olefins with a limiting concentration of TBHP.[4] During the reactions a rapid, reproducible deactivation is observed at longer reaction times or higher conversions preventing quantitative conversion (Fig. 3a). This is explained by reversible blocking (autoretardation) of catalysts through the enrichment of the reaction mixture with polar components (for example, epoxide, alcohol, water, by-products).[13] By washing with solvent and drying below the

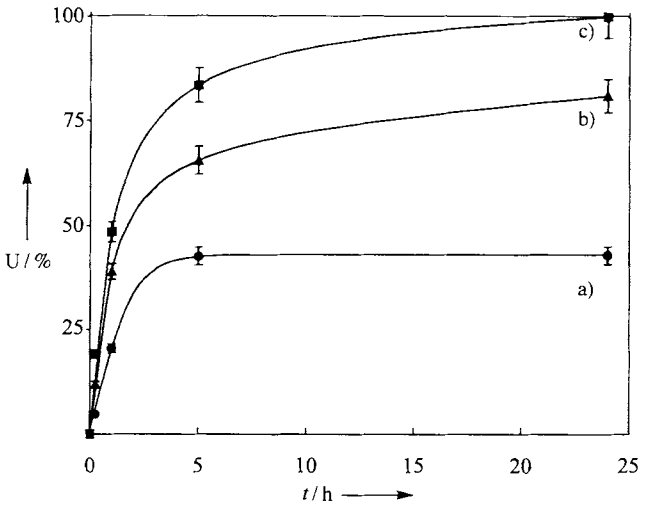

Fig. 3. Conversion–time curves (based on TBHP) of the epoxidation of 1-octene with a) AMM-Ti_1Si, b) AMM-$Ti_1(SiMe)_{25}Si$, and c) AMM-$Ti_1(SiMe)_{45}Si$. Reactions were performed in a batch reactor at 353 K with 15 mmol 1-octene, 3 mmol TBHP (3 M in isooctane), and 50 mg catalyst.

temperature of calcination, the deactivated catalyst can be completely and repeatedly regenerated. As can be seen from Figure 3b and c, the deactivation can be overcome by using more hydrophobic AMM-$Ti_1(SiMe)_ySi$ materials, and quantitative conversion is obtained at high selectivity for the first time at $y = 45\%$. We assume that in the hydrophobic mixed oxides the pores are not filled with hydrophilic components, and mass transport, even at high concentrations of polar components, is not hindered. These methyl-containing catalysts can also be regenerated thermally and reused without recognizable activity loss. The methyl groups are stable at these oxidative reaction conditions. DRIFT studies show that the used catalysts are identical to the fresh materials.

Besides the limitation of alkene conversion with TBHP because of catalyst deactivation, other disadvantages in the catalytic behavior of the mixed oxides in olefin epoxidation with TBHP can be avoided with the methylated AMM-materials. For example, the large 1,5,9-*t*,*t*,*t*-cyclododecatriene is not oxidized by TBHP with the hydrophilic AMM-Ti_xSi catalysts. Under identical reaction conditions[14] quantitative conversion to the monoepoxide is obtained with AMM-$Ti_x(SiMe)_ySi$ materials. The hydrophobicity of the methyl-containing glasses seems to facilitate the diffusion of the nonpolar triene, but the slightly increased pore size with increasing methyl content may also contribute to the improved reactivity of the system.

The most obvious effect of the surface polarity, however, is the successful catalysis of selective oxidation reactions with hydrogen peroxide. Like redox molecular sieves, the AMM-$Ti_1(SiMe)_ySi$ materials catalyze the selective oxidation of nonpolar hydrocarbons whose oxyfunctionalization with H_2O_2 could not be achieved with the methyl-free AMM-Ti_xSi materials. Besides the oxidation of olefins and hydrocarbons the oxidation of primary alcohols to the corresponding aldehydes, the oxidation of alkylarenes, and the ammoxidation of ketones has been performed (Fig. 4, Table 2).

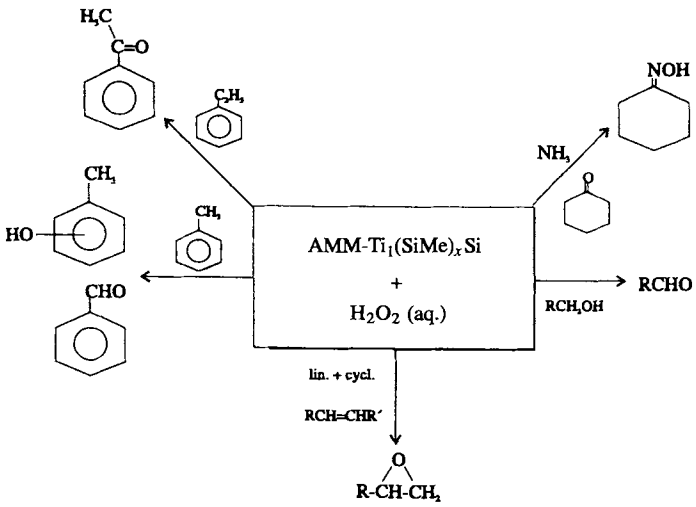

Fig. 4. Schematic overview of selective oxidations with aqueous hydrogen peroxide on AMM-$Ti_1(SiMe)_xSi$ catalysts.

The activity of the catalysts in the oxidation of polar substrates like ethanol shows no dependence on surface polarity. There is little difference in activity and selectivity between TS-1 and the AMM-$Ti_1(SiMe)_ySi$ materials with various methyl contents.

The selective oxidation of alkylarenes behaves quite differently. The toluene conversion shows a clear dependence on the catalyst polarity. The highest conversion is obtained with the most hydrophobic TS-1 zeolites, which furnish cresols as major products, whereas the AMM-$Ti_1(SiMe)_ySi$ materials catalyze exclusively side-chain oxidation (benzaldehyde, benzyl alcohol, benzyl hydroperoxide) and produce almost no cresols.

As with TS-1, AMM-$Ti_1(SiMe)_ySi$ materials oxidize ethylbenzene predominantly at the side chain, but they show higher conversion and selectivities to yield acetophenone and 2-phenylethanol. Aside from the smaller pore size of TS-1, the extreme hydrophobicities (HI* = 3.3) both of TS-1 and of AMM-

Table 2. Conversions [%] and selectivities [%] (in parentheses) for the selective oxidation of organic substrates with aqeous hydrogen peroxide on Ti-containing oxide catalysts of varying polarity.

Substrate (Product) HI*	Ti_1Si 0.1	$Ti_1(SiMe)_{25}Si$ 0.9	$Ti_1(SiMe)_{30}Si$ 1,3	AMM- $Ti_1(SiMe)_{40}Si$ 1.1	$Ti_1(SiMe)_{45}Si$ 2.2	$Ti_1(SiMe)_{50}Si$ 2.9	TS-1 3.3	Blank –
ethanol [a] (acetaldehyde)	9.7 (89.0)	8.8 (89.9)	10.1 (86.0)	13.5 (92.0)	14.8 (92.0)	9.0 (93.0	13.1 (93.8)	–
toluene [b] (benzaldehyde + benzyl alcohol + benzyl hydroperoxide)	0.4 (85.2)	2.8 (90.8)	–	–	4.3 (97.6)	–	7.5 (87.0 [e])	–
ethylbenzene [b] (acetophenone)	5.1 (72.3)	–	–	6.8 (72.1)	–	4.2 (67.2)	1.1 (43.7)	–
cyclohexene [c] (epoxycyclohexane)	5.9 (69.7)	15.7 (66.2)	24.0 (57.8)	8.3 (63.9)	7.4 (68.9)	7.3 (54.5)	4.4 (38.8)	1.3 (70.0)
cyclohexanone [d] (cyclohexanonoxime)	64.4 (0.8)	50.5 (1.8)	–	31.0 (9.1)	–	–	56.8 (20.0)	20.8 (1.0)

[a] 21.0 mmol ethanol, 7.0 mmol H_2O_2 (25% solution), 2.4 g catalyst per mol substrate, $T = 318$ K, $t = 18$ h. [b] 13.6 mmol alkylbenzene, 5 mmol H_2O_2 (25% solution), 20 g catalyst per mol substrate, 3 mL acetonitrile, $T = 353$ K, $t = 20$ h. [c] 2.0 mmol cyclohexene, 4.0 mmol H_2O_2 (25%), 10 g catalyst mol^{-1} substrate, 2 mL methanol, $T = 323$ K, $t = 5$ h. [d] 5.0 mmol cyclohexanone, 5.0 mmol H_2O_2 (25% solution, addition over 4 h by syringe pump), 7.5 mmol NH_3(aq.), 10.1 g catalyst per mol substrate, $T = 333$ K, $t = 6$ h. Discontinuous reaction conditions in batch reactors (9 mL volume). [e] Cresols. HI* = hydrobicity index.

 © VCH Verlagsgesellschaft mbH, D-69451 Weinheim, 1996 0570-0833/96/3519-2232 $ 15.00+.25/0

$Ti_1(SiMe)_{50}Si$ (HI* = 2.9) result in a less efficient catalysis for this reaction. More optimal parameters seem to be provided by the more balanced affinities to polar and nonpolar compounds of AMM-$Ti_1(SiMe)_{40}Si$ (HI* = 1.1).

AMM-$Ti_1(SiMe)_ySi$ is an excellent catalyst for the epoxidation of the reactive cyclohexene with H_2O_2; the activity is dependent on y and reaches a maximum for catalysts with balanced surface polarity ($HI^* \approx 1$, $y = 25-35$). Cyclohexene conversions exceed those of TS-1 by a factor of 4 to 5. Neither hydrophobic catalysts like TS-1 or AMM-$Ti_1(SiMe)_{50}Si$ nor the hydrophilic AMM-Ti_1Si can provide such optimal reactivity; their conversion is only sligthly higher than that of the uncatalyzed reaction. While the poor reactivity of TS-1 in cyclohexene epoxidation may partly be attributed to hindered diffusion because of small pore size, all AMM-$Ti_1(SiMe)_ySi$ materials have pores large enough for unhindered reactions of cyclohexene. Thus the change in surface polarity is most likely the rate-determining factor with the AMM-materials.

The ammoxidation of ketones to oximes with H_2O_2/NH_3 most likely proceeds through an intermediate formation of hydroxylamines at Ti^{4+} centers followed by oxime formation.[15] Under the reaction conditions reported in the literature,[15] we did not observe the activity and selectivity attributed to TS-1. Like with all other catalysts studied, bis(cyclohexylamine)-peroxide was the main product, indicative of a primary classical imination of the ketone followed by oxidation. However, the difference in product distribution obtained with the AMM-$Ti_1(SiMe)_ySi$ catalysts and the TS-1 show that variation of surface polarity again affects the chemical reaction. Although the AMM catalysts could not match either the activity or the selectivity of TS-1 in this reaction, a clear trend to increasing oxime selectivity with increasing hydrophobicity is evident.

With selected examples we have shown that amorphous microporous mixed oxides with adjustable surface polarity can be used for various selective oxidation reactions with polar aqueous hydrogen peroxide as well as with nonpolar TBHP. The well-known conflict in the catalytic behavior between amorphous Ti–Si mixed oxides and crystalline oxides is therefore resolved. The results document for the first time that a precisely adjusted surface polarity is as important as the presence of catalytically active sites in such microporous catalysts with high surface areas. Apparently there is an optimal surface polarity for a given reaction mixture, which affects not only reaction rate and selectivity but also conversion and catalyst lifetime. It must be assumed that there are many examples for which catalyst inactivity in a specific reaction is not an intrinsic problem of the catalytically active centers, but is attributable to the wrong surface polarity of the catalyst for the reaction conditions chosen.

The sol–gel synthesis of AMM catalysts described here allows for the first time adjustment of the monomodal microporosity, elemental composition, and surface polarity of the final catalyst material in a one-step procedure. Such catalysts can be much better tuned to the selected reaction conditions than all traditional catalysts. This sol–gel synthesis of the AMM catalysts is a new example of successful catalyst design. In contrast to zeolites, in which the surface polarity is fixed by the Al content and the pore system by the zeolite type, the extended preparation concept of the AMM catalysts offers the opportunity of adjusting the surface polarity of the catalysts precisely to the reaction of interest without affecting reaction conditions like concentration or type of solvent in the reaction mixture.

Received: February 9, 1996 [Z 8810 IE]
German version: *Angew. Chem.* **1996**, *108*, 2376–2379

Keywords: catalysis · metal oxides · oxidations · silicon compounds · titanium compounds

[1] B. Notari, *Catal. Today* **1993**, *18*, 163.
[2] C. B. Khouw, C. B. Dartt, J. A. Labinger, M. E. Davis, *J. Catal.* **1994**, *149*, 195.
[3] A. Keshavaraja, V. Ramaswamy, H. S. Soni, A. V. Ramaswamy, R. Ratnasamy, *J. Catal.* **1995**, *157*, 501.
[4] S. Klein, J. A. Martens, R. Parton, K. Vercruysse, P. A. Jacobs, W. F. Maier, *Catal. Lett.* **1996**, *38*, 209.
[5] W. F. Maier, J. A. Martens, S. Klein, J. Heilmann, R. Parton, K. Vercruysse, P. A. Jacobs, *Angew. Chem.* **1996**, *108*, 222; *Angew. Chem. Int. Ed. Engl.* **1996**, *35*, 180.
[6] The preparation procedure starts with the acid-catalyzed copolycondensation of tetraethoxysilane (TEOS), methyltriethoxysilane (MTES), and titanium tetraisopropoxide (TIPOT). In a typical reaction (AMM-$Ti_1(SiMe)_{25}Si$) ethanol (150 mmol) is added to a stirred mixture of TEOS (37.1 mmol), MTES (12.4 mmol), and TIPOT (0.5 mmol). Hydrolysis is obtained by dropwise addition of HCl (8 N, 2.2 mL). After about 3 days, gelation of the loosely covered sol–gel reaction mixture takes place. The gels are then calcined under inert atmosphere: The gels are heated at 0.5 K min^{-1} to 338 K, kept there for 5 h, then heated at 0.2 K min^{-1} to the final temperature of 523 K, and kept there for 5 h. After cooling to room temperature (1 K min^{-1}) the glasses are milled, and the sieve fraction smaller than 10 μm was used for catalysis.
[7] S. Klein, *Dissertation*, Universität Gesamthochschule Essen, **1996**.
[8] W. F. Maier, I.-C. Tilgner, M. Wiedorn, H.-C. Ko, *Adv. Mater.* **1993**, *10*, 726.
[9] V. Raman, O. P. Bahl, N. K. Jha, *J. Mater. Sci. Lett.* **1988**, *12*, 1188.
[10] For confirmation of covalent methyl group incorporation the mixed oxides have been studied on a BRUKER IFS 48 IR spectrometer under diffuse reflection conditons. The finely powdered sample (20 mg) was mixed with a ten times larger amount of KBr and in a HARRICK HVC environmental cell (mounted with a diffuse-reflectance unit, type HARRICK DRA-XX) and heated over 15 h at 773 K in a slow stream of Ar. The measurement was done at room temperature under an inert atmosphere (Ar) with a spectral resolution of 2 cm^{-1}. After substraction of the KBr background the spectra were plotted as the Kubelka–Munk function for diffuse reflectance spectroscopy.
[11] a) R. Glöckler, J. Weitkamp, *5th German Workshop on Zeolites*, Universität Leipzig, March 14–16, **1993**; b) J. Weitkamp, P. Kleinschmit, A. Kiss, C. H. Berke in: *Proc. 9th Intern. Zeolite Conference*, Montreal, July 5–10, **1992**; c) C. H. Berke, A. Kiss, P. Kleinschmit, J. Weitkamp, *Chem. Ing. Tech.* **1991**, *64*, 623.
[12] The catalyst sample was heated at 673 K for 12 h under a stream of Ar. Then a stream of Ar containing defined, comparable water and octane concentrations was used to load the sample (water and octane flow rates of about 20 mg h^{-1} were controlled by mass flow meters; Ar saturation temperature 298 K, loading temperature 308 K). The breakthrough curves of the individual components were obtained by on-line gas chromatography. Numerical integration of the normalized breakthrough curves provided the loading of water and octane. After correction for the background behavior of the total reactor the hydrophobicity index HI* was obtained as the ratio x_{octane}/x_{water}.
[13] R. A. Sheldon, J. A. Van Doorn, *J. Catal.* **1973**, *31*, 427.
[14] Olefin (15 mmol) in isooctane (2 mL) was treated with *tert*-butylhydroperoxide (3 mmol, 3 M in isooctane) in a batch reactor in the presence of 50 mg catalyst. The reaction temperature was 353 K; the reaction time 20 h.
[15] a) Z. Tvarůžková, K. Habersberger, N. Zilkova, P. Jirů , *Appl. Catal.* **1991**, *A 79*, 105; b) A. Thangaraj, S. Sivasanker, P. Ratnasamy, *J. Catal.* **1991**, *131*, 394.

 © VCH Verlagsgesellschaft mbH, D-69451 Weinheim, 1996 0570-0833/96/3519-2233 $ 15.00+.25/0

Isolation and Characterization of the Dimetallofullerene $Ce_2@C_{80}$

Junqi Ding and Shihe Yang*

The availability of pure metallofullerenes in milligram quantities has allowed a number of metallofullerenes to be characterized by a variety of spectroscopic means.[1] Although there have been some studies on $Sc_n@C_{2n}$,[2] the main research effort has been directed towards metallofullerenes of the type $M@C_{82}$ with a single encaged metal atom.[1] The first soluble dimetallofullerene, $La_2@C_{80}$, was reported soon after the method of synthesizing fullerenes on the macroscopic scale was developed.[3] Most recently, Achiba et al. described the first isolation and electrochemical studies of $La_2@C_{80}$.[4] This dimetallofullerene was found to be an even better electron acceptor than any metallofullerene of the type $M@C_{82}$. The first derivatization of $La_2@C_{80}$ has also been achieved by the same group.[5] Calculations have predicted that the I_h isomer of C_{80} should be able to accommodate two La atoms to form a thermodynamically and kinetically stable endohedral fullerene.[4, 6] The remarkable stability of $La_2@C_{80}$ comes from the fact that all six valence electrons of the two La atoms are transferred to the C_{80} cage; these six electrons are just enough to form a closed-shell electronic structure for the carbon cage with a large HOMO–LUMO gap. However, direct experimental confirmation for the oxidation states of the metal atoms inside the carbon cage has not yet been available.

We have recently reported a technique for the efficient separation of $Ce@C_{82}$ and also its spectroscopic characterization.[6, 7] Ce was shown to have an oxidation state of III.[8] This new method also allowed separation and characterization of the new dimetallofullerene $Ce_2@C_{80}$, which like $Ce@C_{82}$ was detected in previous laser desorption mass spectrometry experiments.[9] We report here on the separation of $Ce_2@C_{80}$ and on its characterization by UV-Vis-NIR absorption spectroscopy and X-ray photoelectron spectroscopy (XPS).

The high purity of $Ce_2@C_{80}$ isolated by HPLC can be seen from the negative-ion desorption chemical ionization (DCI) mass spectrum shown in Figure 1; a purity of >99% can be estimated.

Figure 2 shows the UV-Vis-NIR absorption spectrum of $Ce_2@C_{80}$ in the wavelength range of 300 to 2100 nm. The spectrum exhibits a monotonically decreasing absorption coefficient with increasing wavelength without well-defined, sharp features. This relatively featureless spectrum is in contrast to those of the empty fullerenes[10] as well as of the monometallofullerenes.[1c] Whetten et al. proposed that in $La_2@C_{80}$ the C_{80} cage has I_h symmetry, resulting in overall D_{2h} symmetry for the dimetallofullerene.[3, 9, 11] This is supported by a recent theoretical calculation.[6] In this and earlier work[5] it was demonstrated that $La_2@C_{80}$ can be formally represented by $La_2^{3+}@C_{80}^{6-}$, forming a closed-shell electronic structure with a HOMO–LUMO gap larger than that of $M@C_{82}$ (M = rare earth metal). As will be shown below, C_{80} in $Ce_2@C_{80}$ also acquires the six valence electrons from the two Ce atoms, presumably resulting

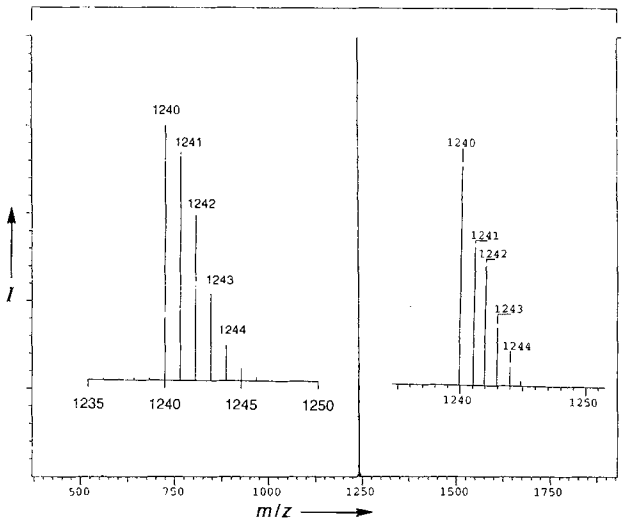

Fig. 1. Methane DCI negative-ion mass spectrum of the $Ce_2@C_{80}$ sample after HPLC separation. The insets show the calculated (left) and observed (right) isotopic distributions for $Ce_2@C_{80}$. I = intensity (arbitrary units).

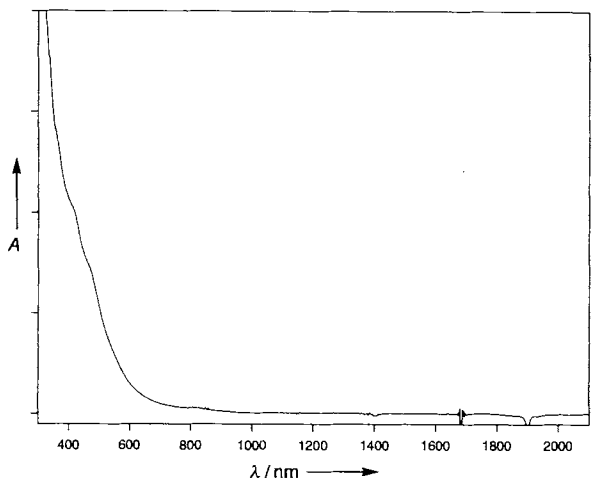

Fig. 2. UV-Vis-NIR absorption spectrum of $Ce_2@C_{80}$ in toluene. A = absorption (arbitrary units).

in the same electronic configuration as that of $La_2@C_{80}$. The closed-shell electronic structure of C_{80}^{6-} in $Ce_2@C_{80}$ is likely to account for the absence of NIR absorption peaks in the spectrum of $Ce_2@C_{80}$.

Figure 3 shows the XPS spectrum of $Ce_2@C_{80}$ in the region of the Ce $3d_{3/2}$ and $3d_{5/2}$ core levels. The spectrum is quite similar to that of $Ce@C_{82}$ with two main features for the $3d_{3/2}$ and $3d_{5/2}$ levels in order of decreasing binding energy.[8] Both features show a strong peak and a weak shoulder. For the $3d_{5/2}$ feature, the stronger peak at higher binding energy (886.57 eV) can be explained by the screening of only the surrounding fullerene orbitals, while the weak shoulder at lower binding energy (881.83 eV) may be accounted for by screening arising from charge transfer to the empty 4f shell.[12]

It is known that Ce^{4+} has a characteristic XPS (3d) peak at a binding energy of approximately 914 eV arising from a transition to the $3d^94f^0$ final state.[13] The intensity of this peak has been used for estimating Ce^{4+} concentration.[14] Since we did not observe this characteristic peak, we can rule out the presence of Ce^{4+} in $Ce_2@C_{80}$. As no characteristic peak for Ce^{2+} is known in the 3d core level region, we cannot rule out Ce^{2+} in the same way. However, the location and shape of the Ce(3d)

[*] Prof. S. Yang, J. Ding
Department of Chemistry
Hong Kong University of Science and Technology
Clear Water Bay, Kowloon (Hong Kong)
Fax: Int. code +(2358)1594

[**] The authors would like to thank the Department of Chemistry at HKUST for its support for the fullerene project. This work was supported by an RGC Grant (HKUST601/95P) administrated by the UGC of Hong Kong. The assistance of L.-T. Weng is acknowledged.

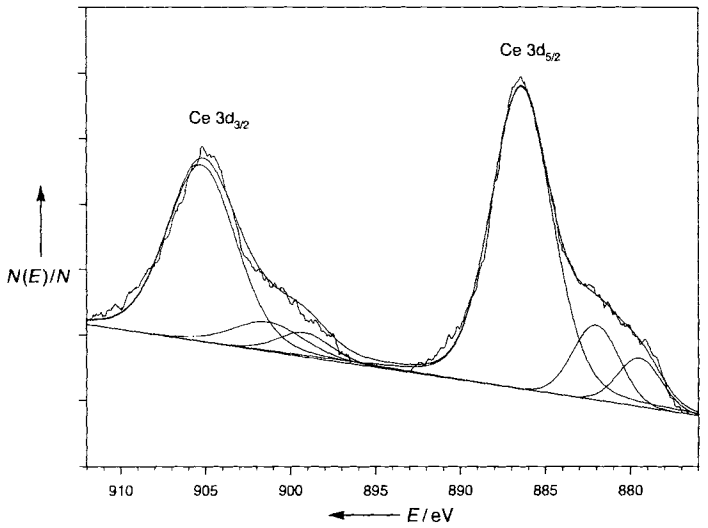

Fig. 3. XPS spectrum of $Ce_2@C_{80}$ on a gold substrate in the core level region of Ce(3d). The smooth line results from a least-square fitting of the spectral peaks using a linear baseline. The occurrence of two features ($3d_{3/2}$: signal at higher energy; $3d_{5/2}$: signal at lower energy) is due to spin–orbital splitting of the 3d core level. E = binding energy. $N(E)/N$ = photoelectron signal intensity (arbitrary units).

peak in the XPS spectrum of $Ce_2@C_{80}$ are rather similar to those of cerium trihalides,[15] suggesting that the oxidation state of Ce is III. The ratio of the intensities of the peaks at higher and lower energies is known to be very sensitive to the electronegativity of the ligands.[16] Our analysis shows that the electronegativity of the fullerene cage is somewhat less than that of chlorine. This conclusion is similar to that we drew for $Ce@C_{82}$[8] and Weaver et al. reported for $La@C_{82}$.[17]

In fact, the XPS spectram of $Ce_2@C_{80}$ is at first glance almost identical to that of $Ce@C_{82}$; however, for $Ce_2@C_{80}$ the curve-fitting can be improved by assuming more peaks. For example, Figure 3 shows the curve obtained by assuming one extra small peak at a lower binding energy. The approximation may be further improved by assuming small peaks at the high binding energy side of the two strong peaks. The presence of a few extra small peaks in addition to the strong peak and weak shoulder characteristic of Ce^{3+} may signify the interaction between the two Ce atoms in the carbon cage. Further studies are required to support this hypothesis.

We have reported the first successful separation of the new endohedral dimetallofullerene $Ce_2@C_{80}$ and its UV-Vis-NIR absorption and XPS spectra. The UV-Vis-NIR spectrum exhibits monotonically decreasing absorption as a function of wavelength without any sharp absorption features. The XPS spectrum suggests that the Ce atoms encaged in C_{80} are in the form of Ce^{3+}. This implies that in the cage one valence electron remains on each metal atom. The nature of their spin–spin coupling within the carbon cage constitutes a fascinating subject for future research.

Experimental Procedure

The procedures for isolating the metallofullerenes have been described previously[7]. Soot containing metallofullerenes was produced by the standard arc vaporization method using a composite anode which contains graphite and cerium in its oxide or carbide form. The rod was then subjected to a DC contact-arc discharge as an anode under an He atmosphere of 50 Torr. The soot was collected and extracted for 8 h in a Soxhlet extractor with *N*,*N*-dimethylformamide (DMF, 99.9%, BDH). After removal of the DMF by evaporation, a black powder (ca. 1% of the soot) was obtained. The soluble fraction was dissolved in toluene and injected into an HPLC. A buckyprep column (4.6 mm × 250 mm; Cosmosil, Nacalai Tesque Inc.) similar to a PYE column was used, and toluene served as the mobile phase. The injection volume was 1 mL and the elution rate was 1 mL min^{-1}. The sample of $Ce_2@C_{80}$ collected from HPLC was analyzed by DCI negative-ion mass spectrometry (Finnigan TSQ7000).

The UV-Vis-NIR absorption spectrum of $Ce_2@C_{80}$ in toluene was recorded with a Perkin-Elmer spectrometer (Lambda 19). For the XPS study, we prepared a $Ce_2@C_{80}$ film on a polycrystalline Au substrate. To clean the Au surface, we heated a small piece of gold foil with a natural gas torch, dipped it in methanol, and dried it in N_2 gas. Several drops of a concentrated solution of $Ce_2@C_{80}$ in toluene were transferred to the Au foil. The evaporation of the solvent left a uniform film of $Ce_2@C_{80}$, which was was dried and washed with *n*-hexane. An XPS measurement was taken using monochromatized $Al_{K\alpha}$ radiation ($h\nu$ = 1486.6 eV) with an energy resolution of roughly 0.6 eV (Perkin-Elmer PHI 5600).

Received: March 7, 1996 [Z8908IE]
German version: *Angew. Chem.* **1996**, *108*, 2369–2371

Keywords: cerium compounds · fullerenes · metallofullerenes · spectroscopy

[1] a) F. T. Edelmann, *Angew. Chem.* **1995**, *107*, 1071; *Angew. Chem. Int. Engl.* **1995**, *34*, 981; b) D. S. Bethune, R. D. Johnson, J. R. Salem, M. S. de Vries, C. S. Yannoni, *Nature* **1993**, *366*, 123; c) D. Fuchs, H. Rietschel, R. H. Michel, M. Benz, A. Fischer, M. M. Kappes in *Physics and Chemistry of Fullerenes and Fullerene Derivatives Proc. IWEPNM 95*, (Eds.: J. Fink, H. Kuzmani, M. Mehring, S. Roth), World Scientific, Singapore, **1995**, p. 105.

[2] R. Beyers, C.-H. Chiang, R. D. Johnson, J. R. Salem, M. S. de Vries, C. S. Yannoni, D. S. Bethune, H. C. Dorn, P. Burbank, K. Harich, S. Stevenson, *Nature* **1994**, *370*, 196; P. H. M. van Loosdrecht, R. D. Johnson, D. S. Bethune, H. C. Dorn, P. Burbank, S. Stevenson, *Phys. Rev. Lett.* **1994**, *73*, 3425; H. Shinohara, H. Yamaguchi, N. Hayashi, H. Sato, M. Ohkohchi, Y. Ando, Y. Saito, *J. Phys. Chem.* **1993**, *97*, 4259; H. Shinohara, N. Hayashi, H. Sato, Y. Saito, X.-D. Wang, T. Hashizume, T. Sakurai, *J. Phys. Chem.* **1993**, *97*, 13438.

[3] M. M. Alvarez, E. G. Gillan, K. Holczer, R. B. Kaner, K. S. Min, R. L. Whetten, *J. Phys. Chem.* **1991**, *95*, 10561.

[4] T. Suzuki, Y. Maruyama, T. Kato, K. Kikuchi, Y. Nakao, Y. Achiba, K. Kobayachi, S. Nagase, *Angew. Chem.* **1995**, *107*, 1228; *Angew. Chem. Int. Ed. Engl.* **1995**, *34*, 1094.

[5] T. Akasaka, S. Nagase, K. Kobayashi, T. Suzuki, T. Kato, K. Kikuchi, Y. Achiba, K. Yamamoto, H. Funasaka, T. Takahashi, *Angew. Chem.* **1995**, *107* 2303; *Angew. Chem. Int. Ed. Engl.* **1995**, *34*, 2139.

[6] K. Kobayashi, S. Nagase, T. Akasaka, *Chem. Phys. Lett.* **1995**, 245, 230.

[7] J. Q. Ding, S. H. Yang, *Chem. Mater.* in press.

[8] J. Q. Ding, L. Weng, S. H. Yang, *J. Phys. Chem.* **1996**, *100*, 11120.

[9] E. G. Gillan, C. Yertzian, K. S. Min, M. M. Alvarez, R. L. Whetten, R. B. Kaner, *J. Phys. Chem.* **1992**, *96* 6869.

[10] K. Kikuchi, N. Nakahara, T. Wakabayashi, M. Honda, H. Matsumiya, T. Moriwaki, S. Suzuki, H. Shiromaru, K. Saito, K. Yamauchi, I. Ikemoto, Y. Achiba, *Chem. Phys. Lett.* **1992**, *188*, 177.

[11] C. Yeretzian, K. Hansen, M. M. Alvarez, K. S. Min, E. G. Gillan, K. Holczer, R. B. Kaner, R. L. Whetten, *Chem. Phys. Lett.* **1992**, *196*, 337.

[12] a) W. D. Schneider, B. Delley, E. Wuilloud, J.-M. Imer, Y. Baer, *Phys. Rev. B. Condens. Matter* **1985**, *32*, 6819; b) S. Imada, T. Jo, *Physica Scripta* **1990**, *41*, 115.

[13] a) A. Fujimori, *Phys. Rev. B Condens. Matter* **1983**, 27, 3992; b) *ibid.* **1983**, *28*, 2281.

[14] J. Z. Shyu, W. H. Weber, H. S. Gandhi, *J. Phys. Chem.* **1988**, *92*, 4964.

[15] S. Suzuki, T. Ishii, T. Sagawa, *J. Phys. Soc. Jpn.* **1974**, *37*, 1334.

[16] S. Imada, T. Jo, *J. Phys. Soc. Jpn.* **1989**, *58*, 2665.

[17] J. H. Weaver, Y. Chai, G. H. Kroll, C. Jin, T. R. Ohno, R. E. Haufler, T. Guo, J. M. Alford, J. Conceicao, L. P. F. Chibante, A. Jain, G. Palmer, R. E. Smalley, *Chem. Phys. Lett.* **1992**, *190*, 460.

Heavy Element π Donation Is Not Less Effective**

Jürgen Kapp, Christian Schade, Ahmed M. El-Nahasa, and Paul von Ragué Schleyer*

Very strong cation stabilization results from π conjugation, for example, from the interaction between empty carbon 2p orbitals and the lone pairs on nitrogen- or oxygen-based substituents.[1-3] How do the heavier group 15–17 substituent lone pair donors compare with their lighter analogs? It has been recognized for some time that π overlap arising from elements of different rows is *not* reduced due to differences in the p-orbital extensions.[4]

Conclusions from previous work are contradictory. While the amino group is the most stabilizing π-donor substituent, it is not clear if sulfur or oxygen is the better π donor.[5-11] The σ_p^+ constants, PhO = −0.62, PhS = −0.54, and PhSe = −0.47 are not very different but show a progression down the group.[12, 13] The trend in the calculated hydride affinities of $^+CH_2XH$ (X = O, S, Se, Te) is similar, with a sharp difference between oxygen and sulfur.[11] However, earlier ab initio calculations gave methyl stabilization energies [Eq. (a)] in the order OH > SeH > SH (52.6, 41.7, and 31.8 kcal mol^{-1}, respectively).[14]

$$CH_3XH_n + CH_3^+ \longrightarrow {}^+CH_2XH_n + CH_4 \qquad \text{(a)}$$

Pioneering mass spectrometric investigations by Taft, Martin, and Lampe,[2] as well as more recent experiments,[3] gave α-halomethyl cation stabilization energies that *increase* down the group: F < Cl < Br < I. In contrast, the halogen σ_p^+ constants (F = −0.07, Cl = 0.11, Br = 0.15, and I = 0.14) reveal the same trend as the chalcogen series.[15]

According to the ab initio investigation ten years ago by Bernardi et al. differences between methyl stabilization energies of second and third period lone pair donors are small within a group but more pronounced along a row.[9] We have now extended the previous studies by examining all group 15–17 π donors from the first five rows at high ab initio levels. Our objective was to compare the methyl-stabilizing effects of the lighter with the heavier elements. Schematic representations of the structures examined are given in Figure 1: neutral parent systems **15**, **15p** with planar XH_2 units (group 15), **16** (group 16), and **17** (group 17) as well as cationic species **15**$^+$, **16**$^+$, and **17**$^+$.

All structures were optimized at the restricted MP2-FC level of theory.[16] Refined energies were obtained in QCISD(T) single point calculations on the MP2-optimized structures. The GAUSSIAN94 program was employed with standard basis sets for molecules containing elements from hydrogen through chlorine during optimizations, frequency runs (6-31 + G*), and single point calculations (6-31 + + G**). Pseudopotentials (PSP) were used to replace the core electrons of systems with heavier elements: a four valence electron (Ve) PSP for carbon and 5–7 Ve PSP for Se–Br and Te–I together with the corresponding DZ + P basis sets.[17, 18] Atomic charges as well as bond orders and orbital occupancies were obtained from QCISD(T)-single point calculations according to Reed and Weinhold's NBO analysis.[19]

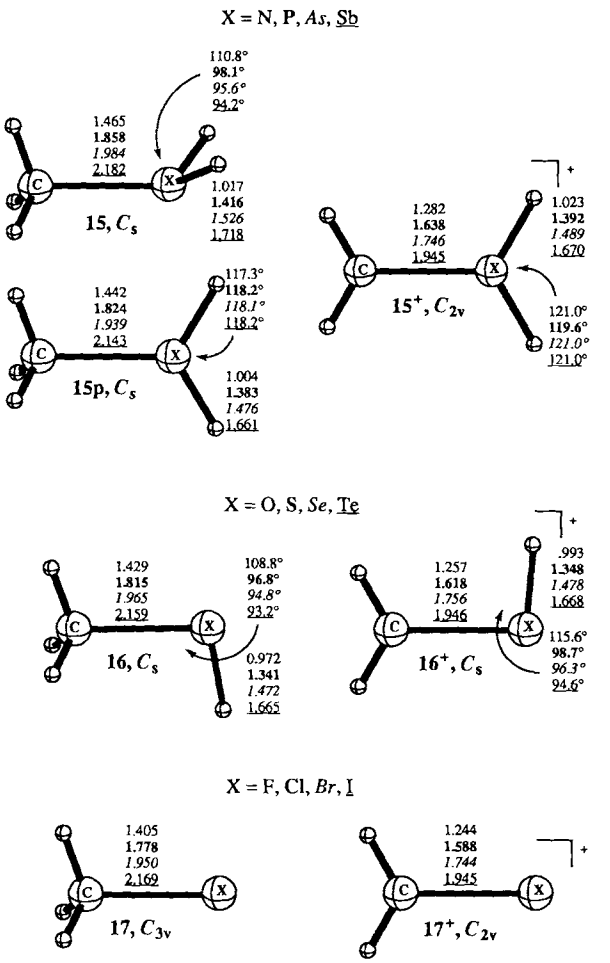

Fig. 1. Schematic representations of the structures of the neutral molecules and the cations together with selected bond lengths [Å] and angles [°]. **15p**: planar XH_2 group.

The $^+CH_2-XH_2$ cations (X = N, P, As, Sb) prefer planar structures **15**$^+$. Their isodesmic methyl stabilization energies (MSEs) [Eq. (a)] decrease in a stepwise fashion from 94 kcal mol^{-1} for NH_2 to 45 kcal mol^{-1} for SbH_2 (Table 1, column 1); although large, these MSEs are reduced due to the "cost" of planarizing the XH_2 substituents (Table 1, column 2).[20] The inversion barriers of ammonia and amines are quite low, relative to those of phosphines, arsines, and the corresponding compounds of the heavier pnictogens. The apparently superior ability of nitrogen to act as a π donor is due, in part, to the ease in achieving the optimum planar configurations with sp^2 hybridization.[4a]

However, we were interested in the *inherent* π donor ability of the heavy group 15 elements, although the idealized π interactions may have little practical relevance. The complicating influence of planarization can be eliminated and a better assessment of the "pure" π interaction be obtained by employing *planar* CXH_2 conformers **15p** of the reference CH_3XH_2 systems in Equation (a). These π stabilization energies (πSE, boldface in Table 1, column 3) are much larger than the MSEs for X = P, As, and Sb. Surprisingly, the πSEs are nearly the same for N, P, As, and Sb! In contrast, the chalcogen substituents (and, of course, the halogens) do not suffer the planarization problem. In the most favorable geometry, a pure p-orbital lone pair is

[*] Prof. Dr. P. von R. Schleyer, Dipl.-Chem. J. Kapp, Dr. A. M. El-Nahas[+]
Computer Chemie Centrum
Institut für Organische Chemie der Universität Erlangen-Nürnberg
Henkestrasse 42, D-91054 Erlangen (Germany)
Fax: Int. code +(9131)859132
e-mail: pvrs@organik.uni-erlangen.de
Dr. C. Schade
BASF AG, D-67056 Ludwigshafen (Germany)
[+] Present address: Chemistry Department, Faculty of Science El-Menoufia University, Shebin El-Kom (Egypt)

[**] The research in Erlangen was supported by the Deutsche Forschungsgemeinschaft, by the Fonds der Chemischen Industrie, and by the Convex Computer Corporation. J. K. gratefully acknowledges a grant from the Studienstiftung des Deutschen Volkes

Table 1. Stabilization and planarization energies as well as rotational barriers [kcal mol^{-1}].

Species	(1) MSE [b] calc.	exp. [d]	(2) XH_2-planarization **15 → 15p**	(3) πSE [c]	(4) XH_n-rotation (90°)
CH_3NH_2			4.23		
$CH_2NH_2^+$	−93.94	−95±0.6		**−98.18**	77.95
CH_3PH_2			35.54		
$CH_2PH_2^+$	−61.38			**−96.93**	97.70
CH_3AsH_2			45.10		
$CH_2AsH_2^+$	−50.68			**−95.79**	95.74
CH_3SbH_2			48.42		
$CH_2SbH_2^+$	−45.19			**−93.61**	[e]
CH_2OH^+	−59.73	−63±0.6		**−59.73**	[f]
CH_2SH^+	−63.69	−68±0.6		**−63.69**	51.97
CH_2SeH^+	−63.29			**−63.29**	[g]
CH_2TeH^+	−66.24			**−66.24**	[g]
CH_2F^+	−17.96	−21±0.5		**−17.96**	
CH_2Cl^+	−31.29	−30±0.6		**−31.29**	
CH_2Br^+	−31.81	−36±0.8		**−31.81**	
CH_2I^+	−38.14	−37±0.7 [h]		**−38.14**	

[a] All calculated energies at QCISD(T)/DZ + + PP//MP2(FC)/DZ + P inclusive of ZPE-correction. [b] Group 15: relative **15**. [c] Group 15: relative **15p**, for groups 16/17: MSE = πSE. [d] Ref. [3]. [e] Not stable due to intramolecular electron transfer. [f] Adopts C_{2v} symmetry. [g] Hydride shift under formation of H-bridged H_3CX^+. [h] a) L. Andrews, J. M. Dyke, N. Jonathan, N. Keddar, A. Morris, *J. Phys. Chem.* **1984**, *88*, 1950; b) J. J. DeCorpo, D. A. Bafus, J. L. Franklin, *J. Chem. Thermodyn.* **1971**, *3*, 125.

available for electron donation to the carbocation center. Indeed, the πSEs (which are identical to the MSEs for groups 16 and 17) are nearly the same for a given group, following the pnictogen >chalcogen >halogen order (Table 1, column 3)!

The calculated MSE values are in reasonable agreement with the experimentally determined values (Table 1, column 1).[2, 3] However, a complete set of MSE values is available only for group 17. These and the computed values increase from about 20 kcal mol^{-1} for F to nearly double that for I. In contrast to some previous findings,[5, 8, 9, 11] the heavier chalcogens are better π donors than oxygen, although the range of MSE values in group 16, 59 to 66 kcal mol^{-1}, is much smaller than that in group 17.

Sigma inductive effects, which also are present, can be assessed by means of Allred–Rochow electronegativity correlations. However, the πSEs [Eq. (a)] for each group reveal little electronegativity influence (Fig. 2). These results demonstrate

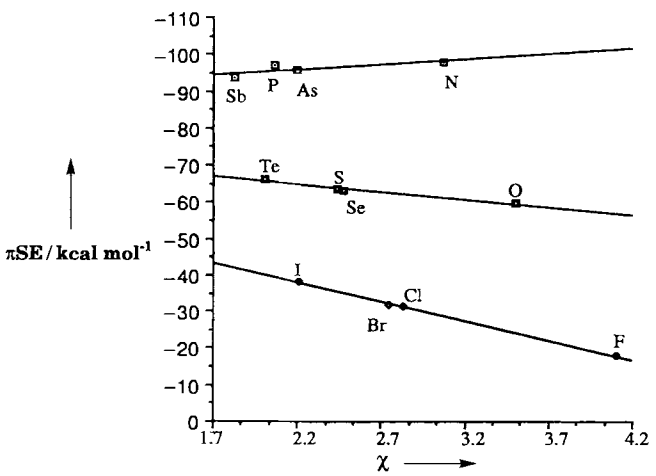

Fig. 2. $^+CH_2-XH_2$ π Stabilization energies πSE [kcal mol^{-1}] [QCISD(T)/DZ + + PP//MP2/DZ + P + ZPE, [Eq. (a)], see Table 1, column 3] versus the electronegativity χ of X.

that π interactions between the very strong π acceptor CH_2^+ and adjacent p-lone pairs do not depend on the row of the substituent. Hence, the higher period heteroatoms are just as effective π donors as their first row counterparts as assumed by Bernardi et al.[9] In group 15, most of the reduced net-stabilization and the reversed MSE variation (N >P >As >Sb) arises from the energetically costly XH_2 planarization of **15 → 15p**.[8–10, 20]

The barriers for the 90° rotation of the planar XH_2 fragments of group 15 cations also reveal strong π interactions between the carbon 2p orbital and the substituent lone pairs (Table 1, column 4): they increase from 78.0 kcal mol^{-1} (X = N) to 97.7 (X = P) and 95.7 kcal mol^{-1} (X = As), indicating powerful π bonding in the $^+CH_2-XH_2$ ground states of similar magnitude.[21]

The energies of the 90° rotation of the X–H group (X = O–Te) also should indicate the magnitude of the π interactions. However, only the rotated structure of the sulfur compound, which is 52 kcal mol^{-1} less stable than planar ^+H_2CSH (Table 1, column 4), could be located. In contrast, 90° rotated ^+H_2COH optimized directly to a C_{2v} symmetric structure with a linear C-O-H group. Hence, oxygen is readily capable of adopting an sp-hybridization with *two* p-lone pairs in the transition state (compare the small NH_2 planarization barrier) and of acting as a double-sided π donor.[22] The rotated conformers of $^+H_2CSeH$ and $^+H_2CTeH$ rearrange to H-bridged structures, which can be regarded as side-on protonated $H_2Se{=}O$ and $H_2Te{=}O$.

Natural atomic charges and orbital populations also reflect strong π interactions in all cations: while the σ-charge transfer between X and C depends on the heteroatom electronegativity, significant charge density is transferred to the formally empty carbon 2p orbital through the π bonds (0.32 e$^-$, X = F, to 1.01 e$^-$, X = Sb). Other interactions, for example, hyperconjugation between σ_{X-H} bonds or X lone pairs and σ^*_{C-H} bonds, are of minor importance. A detailed examination of the hyperconjugation contributions[23] reveals that the magnitudes of these interactions are similar in CH_3-XH_n and $^+CH_2-XH_n$ and cancel in Equation (a). The insignificant differences remaining are dominated by the π effects. Bond orders and atomic charges suggest that these cations are represented adequately by iniumion resonance structures $CH_2{=}XH_n^+$. The C–X Wiberg bond indices (WBI) are of similar magnitude for all cations (1.5–1.75); only $^+H_2C-F$ has a slightly lower WBI (1.23).

Likewise, all cation C–X bond lengths are reduced in comparison to the CH_3-XH_n reference compounds. There is an excellent correlation between C–X distances in the neutral molecules and in the cations [Figs. 1 and 3, [Eq. (b)]!

$$d_{C-X^+} = 0.92\ d_{C-X} - 6.2\ \text{pm} \qquad \text{(b)}$$

Consequently, the C–X bond shortening going from the neutral to the corresponding cation is *not* related to the πSE magnitudes. For example, the C–X bond lengths in the CH_3SbH_2, CH_3TeH, and CH_3I set (214.3, 215.9, and 216.9 pm, respectively) and those in the $^+CH_2SbH_2$, $^+CH_2TeH$, and $^+CH_2I$ set (194.5, 194.6, and 194.5 pm, respectively) are both nearly the same, despite the very large πSE differences.

While π interaction between a lone pair and the vacant orbital of an adjacent carbocation center is well recognized to be strongly stabilizing, we find that the magnitude depends on the period to a remarkably small extent. In contrast to the still common misconception that 2p-3/4/5p overlap is ineffective, our comparison emphasizes that the *inherent* π donor capabilities of the heavier elements are as large as or larger than their second row counterparts.

Received: March 19, 1996 [Z8947IE]
German version: *Angew. Chem.* **1996**, *108*, 2373–2376

 © VCH Verlagsgesellschaft mbH, D-69451 Weinheim, 1996 0570-0833/96/3519-2237 $ 15.00+.25/0

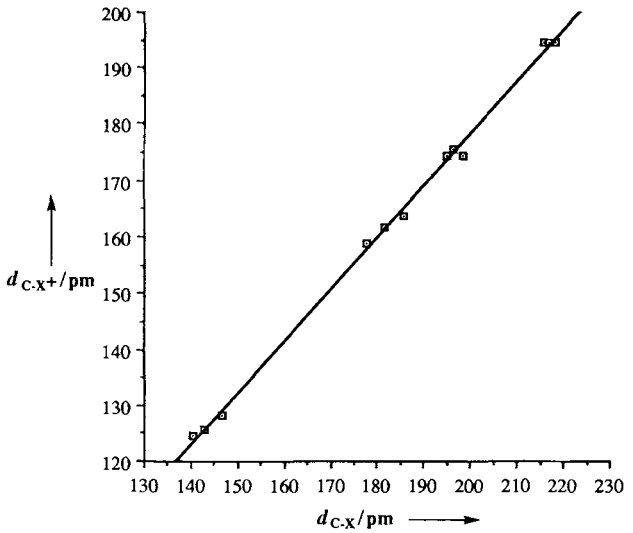

Fig. 3. C–X Bond lengths [pm] in cations ($d_{C\text{-}X^+}$) as a function of those in neutral compounds ($d_{C\text{-}X}$) [MP2/DZ + P, see Fig. 1].

Keywords: ab initio calculations · carbocations · conjugation · theoretical chemistry

[1] a) *Carbonium Ions, Vol I-V* (Eds.: G. A. Olah, P. von R. Schleyer), Wiley, New York, **1976**; b) P. Vogel, *Carbocation Chemistry*, Elsevier: Amsterdam, **1985**; c) *Methoden Org. Chem. (Houben-Weyl), 4th ed. Vol. E19c*, (Ed.: M. Hanack), **1990**; d) M. Saunders, H. A. Jiménez-Vázquez, *Chem. Rev.* **1991**, *91*, 375.

[2] R. W. Taft, R. H. Martin, F. W. Lampe, *J. Am. Chem. Soc.* **1965**, *87*, 2490.

[3] S. G. Lias, J. E. Bartmess, J. F. Liebman, J. L. Holmes, R. D. Levin, W. G. Mallard, *J. Phys. Chem. Ref. Data*, Suppl. 1, **1988**.

[4] a) W. Kutzelnigg, *Angew. Chem.* **1984**, *96*, 262; *Angew. Chem. Int. Ed. Engl.* **1984**, *23*, 272; b) M. W. Schmidt, P. N. Truong, M. S. Gordon, *J. Am. Chem. Soc.* **1987**, *109*, 5217.

[5] Y. Apeloig, M. Karni, *J. Chem. Soc. Perkin Trans. 2* **1988**, 625.

[6] J. K. Pau, M. B. Ruggera, J. K. Kim, M. C. Caserio, *J. Am. Chem. Soc.* **1978**, *100*, 4242.

[7] P. von R. Schleyer, *Pure Appl. Chem.* **1987**, *59*, 1647.

[8] J. C. White, R. J. Cave, E. R. Davidson, *J. Am. Chem. Soc.* **1988**, *110*, 6308

[9] F. Bernardi, A. Bottoni, A. Venturini, *J. Am. Chem. Soc.* **1986**, *108*, 5395.

[10] A. M. Aissani, J. C. Baum, R. F. Langler, J. L. Ginsburg, *Can. J. Chem.* **1986**, *64*, 532.

[11] P. G. Jasien, W. J. Stevens, *J. Chem. Phys.* **1985**, *83*, 2984.

[12] R. A. McClelland, M. Leung, *J. Org. Chem.* **1980**, *45*, 187. Substituents with a lone pair at the atom attached to a benzene ring can interact with an unsaturated atom in the *para* position of the ring (resonance stabilization). A set of special substituent constants, denoted σ_p^+, has been defined based on the solvolysis of *tert*-cumyl chlorides. More negative values of σ_p^+ indicated a stronger stabilization of the intermediate carbocation center (i.e. faster solvolysis).

[13] V. J. Nowlan, T. T. Tidwell, *Acc. Chem. Res.* **1977**, *10*, 252.

[14] C. F. Rodriquez, A. C. Hopkinson, *J. Mol. Struct.* **1987**, *152*, 55.

[15] C. D. Johnson, *The Hammett Equation*, University Press, Cambridge, **1973**, p33.

[16] W. J. Hehre, L. Radom, P. von R. Schleyer, J. A. Pople, *Ab Initio Molecular Orbital Theory*, Wiley, New York, **1986**.

[17] A. Bergner, M. Dolg, W. Küchle, H. Stoll, H. Preuss, *Mol. Phys.* **1993**, *80*, 1431.

[18] d-Polarization functions taken from *Gaussian Basis Sets for Molecular Calculations*, (Ed.: S. Huzinaga), Elsevier, New York, **1984**.

[19] A. E. Reed, L. A. Curtis, F. Weinhold, *Chem. Rev.* **1988**, *88*, 899.

[20] C. Schade, P. von R. Schleyer, *J. Chem. Soc. Chem. Commun.* **1987**, 1399.

[21] The rotated C_{2v} structure of $^+CH_2\text{–}SbH_2$ is exceptional as intramolecular electron transfer occurred to form $^{\cdot}CH_2\text{–}SbH_2^+$ due to the large C–Sb electronegativity difference. The singlet biradical character of this species cannot be described adequately by one-determinant procedures such as MP2.

[22] The different behavior of S and O in the perpendicular rotation transition states of the isoelectronic H_2BXH systems was examined by: a) E. Magnusson, *Austr. J. Chem.* **1986**, *39*, 735; b) M. T. Ashby, N. A. Sheshtawy, *Organometallics* **1994**, *13*, 236. However, the H_2B group is a weaker π acceptor than ^+H_2C; therefore, the H_2BOH transition state does not adopt C_{2v} symmetry.

[23] Obtained from the second-order perturbation analysis of the wavefunction in the NBO procedure.

The First Demonstration of Molecular Queuing in Pseudo[*n*]polyrotaxanes: A Novel Variant of Supramolecular Motion**

Philip E. Mason, Ian W. Parsons,* and Malcolm S. Tolley

Pseudo[*n*]polyrotaxanes and to a lesser extent poly[*n*]rotaxanes are now well-established features of the supramolecular scene, following pioneering work by, inter alia, the groups of Wenz, Harada, Gibson, and Stoddart.[1] A particularly characteristic feature expected for pseudo[*n*]polyrotaxanes (Fig. 1), since generally the ring components cannot pass each other along the thread, is that the movement of rings is restricted by queuing as they shuffle along the central thread and eventually escape into solution. Here we report the first unequivocally identified example of such motion in supramolecular chemistry.

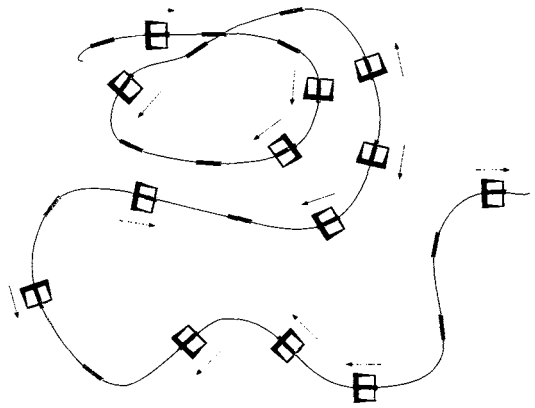

Fig. 1. Schematic representation of a pseudo[*n*]polyrotaxane.

The molecules studied in the present investigation (Scheme 1) readily self-assemble in solution[2] to provide straightforward representatives of this very simple supramolecular architecture. They are the electron-poor cyclophane **1** (Scheme 1), which moves onto, off, and along a central polymeric thread (**2**) containing alternating electron-rich 1,5-dioxonaphthalene and 1,4-dioxobenzene sites, with which **1** complexes.

For simplification we consider **1** simply as a ring and the polymer molecule as a sequence of n discrete stations, S_1 to S_n (which may or may not equate to single arene units), with each station able to accommodate only one ring. Rings threaded onto the same chain cannot pass each other, and the probability of an individual station bearing a ring is x.

We concentrate upon a particular ring complexed on the station S_m and its chances of escaping by way of the nearer end of the chain at S_1. If this ring encounters another complexed ring, it will be unable to pass and thus unable to escape into solution. Clearly, the chances of finding no other rings in attaining the chain end will be $(1 - x)^{(m-1)}$, and if the last step is equivalent the final result will be $(1 - x)^m$. The rate of intersite hopping has

[*] Dr. I. W. Parsons, P. E. Mason, M. S. Tolley
School of Chemistry, University of Birmingham
Edgbaston, Birmingham B15 2TT (UK)
Fax: Int. code +(121)414-4403
e-mail: parsonsiw@vms1.bham.ac.uk

[**] This work was supported by the Engineering and Physical Science Research Council (EPSRC). We also thank the University of Birmingham and the EPSRC for providing spectroscopic facilities.

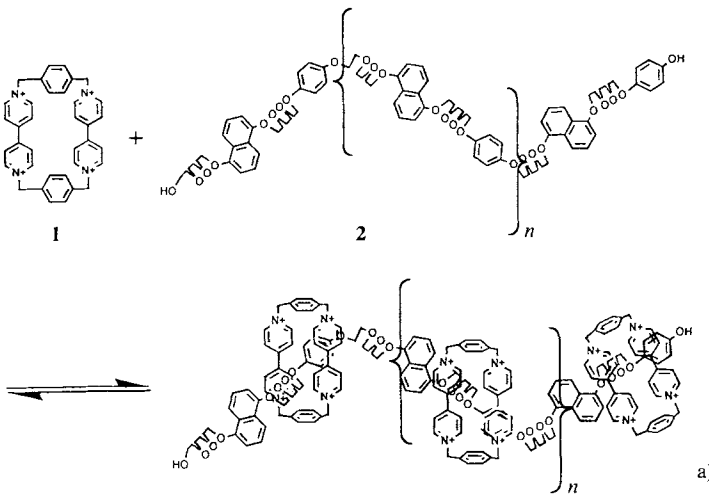

Scheme 1. Formation of the pseudo[*n*]polyrotaxane from cyclophane **1** and polymer **2**. Counterion PF_6^-.

been measured for a two-station [2]rotaxane chemically similar to the species studied here;[3] at room temperature there will be approximately 2500 hops per second between arene sites. In the system studied here x has been varied from 0.05 to 0.5.

We may define two possible ring types (states). Type A rings are in rapid exchange on the NMR timescale between existence in the solution and complexation onto a polymer chain. Type B rings are similarly in exchange, but the exchange is slow on the NMR timescale.

We can distinguish spectroscopically between **1** moving freely in solution and **1** bound onto the polymer chain by threading. The ^{1}H NMR signals arising from both the α and β protons on the 4,4′-bipyridyl unit of **1** (Fig. 2) are known to change their chemical shift values on inclusion of an aromatic guest.[4, 5] Similar results have also been reported for the signals due to the hydrogens on the guest molecules[6] and for the analogous ^{13}C NMR signals.[7] Our discussions here are limited to the ^{1}H NMR signals.

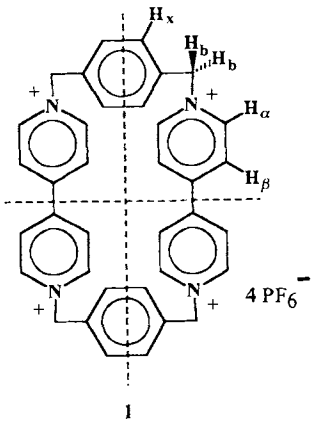

Fig. 2. Labeling of the protons of **1**.

NMR signals due to particular protons exchanging between one state and another coalesce when the lifetime of the states τ is sufficiently short. For each particular proton type the explicit condition is described by Equation (a).[8]

$$\tau \leq (2^{1/2})(\pi\Delta\nu)^{-1} \qquad \text{(a)}$$

In general, since the chemical shifts of, for example, the α protons in [D$_6$]DMSO above its freezing point (Fig. 2) will be the same (or at least very similar) for all threaded **1**, a single α-proton peak will arise for all the threaded **1** molecules that escape from the thread too slowly to satisfy the above condition (that is, which are type B rings). The remaining type A molecules will give, in the usual way,[9] a coalesced NMR peak at a chemical shift that is a weighted average. Thus, with fixed concentrations of species the temperature at which a particular type of proton in **1** will give rise to a single NMR peak (in other words **1** is exclusively type A) will depend upon the value of $\Delta\nu$, the molecular weight and molecular weight distribution of the polymer, x, and the rate of intersite hopping.

The result of increasing the total concentration of **1** will be complex. The rate of exchange of bound and free **1**, as it is strongly dependent upon x, will decrease markedly. The proportion of type B rings will thus certainly increase, but the exact result depends strongly upon a number of factors. Later we use this particular effect to demonstrate "molecular queuing".

The polymers were prepared by the sequence shown in Scheme 2 by reaction of hydroquinone with an excess of the

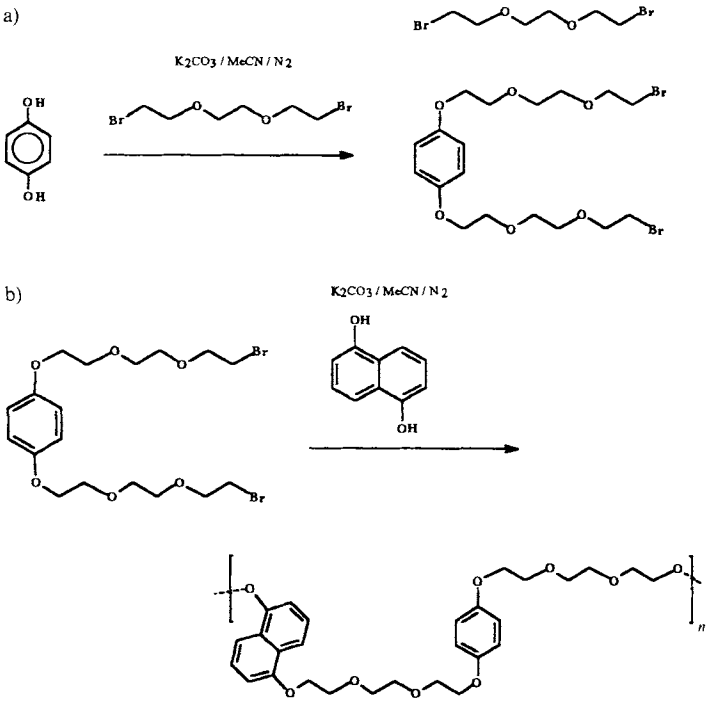

Scheme 2. Synthesis of polymer **2**. a) and b) heated at reflux for 4 h. Higher oligomers are also formed in step a).

dibromide, isolation of the hydroquinone bis(ω-bromo)ether, and finally reaction of this intermediate with naphthalene-1,5-diol under basic conditions. The resulting alternating copolymer's general architecture, aryl groups separated by polyether chains, is designed to mimic the existing successful chemistry of rotaxanes and catenanes[10] based on **1**. Three polymers prepared by this method showed number average molecular weights of 3600, 6100, and 12000 (M_w/M_n of 2.1, 2.5, and 3.3, respectively) by size exclusion chromatography (*N*-methylpyrrolidinone (NMP) solvent, polymethyl methacrylate standards). These M_n values correspond to approximately 7, 12, and 24 polymer repeat units.

For experimental reasons the NMR studies were conducted with [D$_6$]DMSO as the solvent rather than the more usual[11] acetonitrile. Figure 3 shows ambient temperature 300 MHz spectra of the polymer (M_n = 6100), **1**, and a 1:1 (**1**:polymer repeat unit) mixture of the two in DMSO. For simplicity and brevity, in the description of the last spectrum we concentrate on the changes in the signals at $\delta > 9$, both of which we assign (by COSY and spin transfer experiments) to the α protons of **1**.

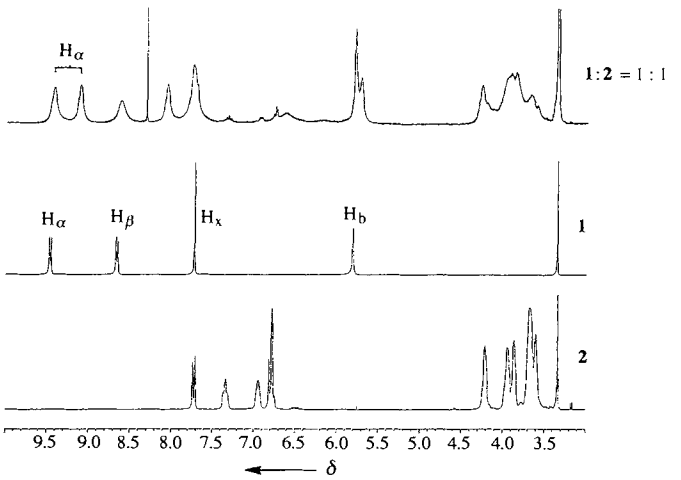

Fig. 3. Sections of the ^{1}H NMR spectra (300 MHz) of polymer **2** (M_n = 6100) (top), cyclophane **1** (middle), and a 1:1 mixture (ratio of cyclophane to polymer repeat unit) (bottom) in [D$_6$]DMSO.

There are two peaks, one at $\delta \approx 9.1$ and one at $\delta \approx 9.4$, and the fact that the upfield peak decreases rapidly in intensity as the temperature rises (Fig. 4) leads to the natural presumption that the first of these corresponds to **1** bound to the polymer, and the second to free **1**. However, this interpretation is false, as will be shown by using the (simplified) theoretical framework given above.

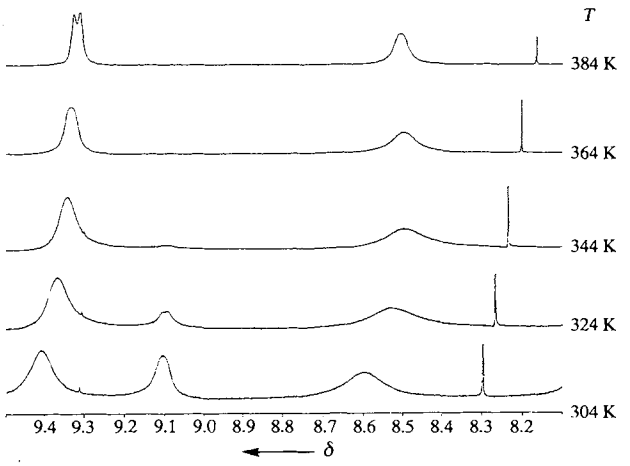

Fig. 4. Sections of the ^{1}H NMR spectra (300 MHz) of a solution containing a 1:1 mixture of **1** and **2** (M_n = 6100) (ratio of cyclophane to polymer repeat unit) in [D$_6$]DMSO at 304, 324, 344, 364, and 384 K. The sharp singlet arises from $CHCl_3$.

The two signals at $\delta > 9$ are indeed due to two different types of **1**, but they are type A and type B rings. Thus, it is perfectly possible to obtain only a single (type A) peak around δ = 9.1–9.4 whilst **1** is complexed to a substantial degree by threading on the polymer chain.

Clearly, this model predicts that the ratio of these two peaks will be dependent upon the field strength of the NMR spectrometer used. The peak at $\delta \approx 9.4$ should decrease with increasing field, since $\Delta\nu$ will thus increase. The chemical shift of this signal will also change with field, since it is an average between species of changing concentrations. Also, increasing the average polymer molecular weight (without changing the total concentration of polymer repeat unit) will result in an intensity increase for the peak at $\delta \approx 9.1$ at the expense of the peak at $\delta \approx 9.4$, and vice versa. If the concentration of **1** is increased while that of the polymer is fixed, the rings will progessively change from all type A to a mixture of types A and B, as molecular queuing makes escape from the centers of the longer chains impossible within the NMR timescale. (For even modest molecular weight polymers it may be impossible to achieve a regime in which **1** is exclusively of type A.) We have performed these experiments and here report the results.

A solution containing **1** (11.0 mg) and the polymer with M_n = 6100 (4.98 mg), which corresponds to a 1:1 ratio of **1** to the polymer repeat unit,[12] was prepared in [D$_6$]DMSO (0.700 mL; the concentration of each component is thus 14.3 mM) and its ^{1}H NMR spectrum recorded at 295 K at 90, 300, and 400 MHz (Fig. 5). The integrations of the signals due to the α protons and the derived fractions of bound and free **1**[13] are shown in Table 1.

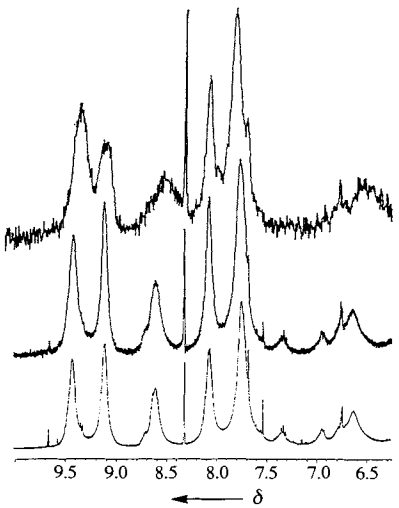

Fig. 5. Sections of the ^{1}H NMR spectra of a solution containing a 1:1 mixture of **1** and **2** (M_n = 6100) (ratio of polymer repeat unit to cyclophane) in [D$_6$]DMSO recorded at 90 (top), 300 (middle), and 400 MHz (bottom).

Table 1. Fractions of type A and type B cyclophane units, as determined by the integration of the α protons.

Spectrometer frequency [MHz]	δ (Type A)	δ (Type B)	Fraction of type A (fast exchange)	Fraction of type B (slow exchange)	Fraction in solution	Fraction bound
90 [a]	9.35	9.10	0.62	0.38	0.41	0.59
300	9.41	9.11	0.52	0.48	0.43	0.57
400	9.42	9.12	0.50	0.50	0.44	0.56

[a] Broad overlapping peaks in the 90 MHz spectrum make precise chemical shifts and integrals difficult to measure.

The results are closely in line with the predictions: as the observation frequency increases the intensity of the lower field signal decreases relative to that of the higher field signal, and its chemical shift changes. Within reasonable bounds of error this change in chemical shift is consistent with constant instantaneous fractions of bound and free **1**, as would be expected. We emphasize here that these results cannot possibly be explained by assigning one signal to bound **1** and one to free **1**.

To demonstrate molecular queuing we have kept the total concentration of polymer constant and varied the amount of **1** in solution. In the ^{1}H NMR spectra in Figure 6 the concentra-

 © VCH Verlagsgesellschaft mbH, D-69451 Weinheim, 1996 0570-0833/96/3519-2240 $ 15.00+.25/0 Angew. Chem. Int. Ed. Engl 1996 35 No 19

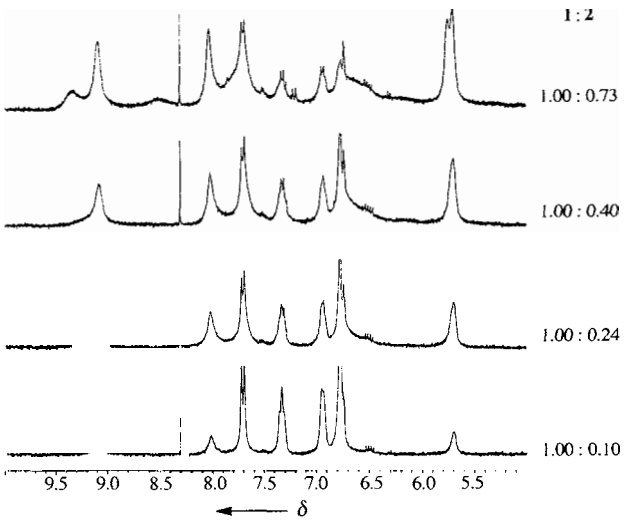

Fig. 6. Sections of the ^{1}H NMR spectra of a solution containing the shown ratios of **1** to the polymer repeat unit in **2** (M_n = 6100) in [D_6]DMSO. The sharp singlet arises from $CHCl_3$.

tion ratio varies from 0.1 to 0.73. In the first case only one peak is visible for the α protons, presumably type A species. As the concentration of **1** increases, a second peak makes its appearance, as expected, as the value of x rises to the point at which some of the **1** molecules, on the longer polymer chains, no longer exchange freely on the NMR timescale and thus become type B. At the same time the type A species spend a higher proportion of their time in solution.

These observations clearly demonstrate molecular queuing: the only reasonable explanation for the emergence and behavior of the second peak is that the rings of **1** complexed onto the polymer chain near the ends prevent the escape of rings complexed near the centers of the longer chains within the NMR time period. In mixtures with lower concentrations of **1** the rings spend nearly all of their time complexed to the polymer and their α protons have a chemical shift close to $\delta = 9.10$. As the concentration of **1** increases, the chemical shift of the type A species changes towards $\delta = 9.48$, whilst the proportion of the type B rings increases and retains a chemical shift of $\delta \approx 9.10$.

Three separate [D_6]DMSO solutions, each containing the same concentration of the polymer repeat unit and **1** (1:1) were prepared from the three polymers, and ^{1}H NMR spectra (300 MHz) were then recorded at 295 K for all three. Table 2 summarizes the findings, which are consistent with the present

Table 2. The effect of the polymer molecular weight on the relative amounts of type A and type B cyclophanes in otherwise identical solutions.

T [K]	M_r	δ (Type A)	δ (Type B)	Integral (Type A)	Integral (Type B)
295	3600	9.400	9.113	64	36
295	6100	9.418	9.105	55	45
295	12000	9.420	9.104	49	51

hypothesis. The lowest molecular weight polymer shows the greatest intensity ratio of the peak at $\delta \approx 9.4$ (due to rapid exchange) to that at $\delta = 9.10$.

A variable-temperature 400 MHz study also supports this. For the polymer with M_n = 3600 the signal of the type B protons disappears between 324 and 344 K, for the polymer with M_n = 6100 between 344 and 364 K, and for the polymer with M_n = 12000 between 364 and 384 K. At each temperature studied the three solutions showed a very similar fraction of free and complexed **1**, which generally decreased slowly as the temperature increased.

In this work we have for the first time experimentally demonstrated the existence of molecular queuing as molecules of **1** move along polymeric threads, and have shown that a simple model of this behavior serves to predict the main features of the changes wrought by altering the concentration of **1**, polymer molecular weight, and temperature. Crucially, the model's verisimilitude is confirmed by its correct prediction of the effect of changing the NMR observation frequency.

Received: January 11, 1996 [Z87141E]
German version: *Angew. Chem.* **1996**, *108*, 2405–2408

Keywords: cyclophanes · polymers · rotaxanes · supramolecular chemistry

[1] See A. Harada, J. Li, T. Nakamitsu, M. Kamachi, *J. Org. Chem.* **1993**, *58*, 7524–7528; A. Harada, J. Li, M. Kamachi, *J. Am. Chem. Soc.* **1994**, *116*, 3192–3196; G. Wenz, E. Vonderbey, L. Schmidt, *Angew. Chem.* **1992**, *104*, 758; *Angew. Chem. Int. Ed. Engl.* **1992**, *31*, 783–785; G. Wenz, F. Wolf, M. Wagner, S. Kubik, *New J. Chem.* **1993**, *17*, 729–738; X. Shen, D. Xie, H. W. Gibson, *J. Am. Chem. Soc.* **1994**, *116*, 537–548; H. W. Gibson, H. Marand, *Adv. Mater.* **1993**, *5*, 11–21; H. W. Gibson, S. Liu, P. Lecavalier, C. Wu, Y. Shen, *J. Am. Chem. Soc.* **1995**, *117*, 859–874. For a fairly recent review, see D. B. Amabilino, I. W. Parsons, J. F. Stoddart, *Trends. Polym. Sci.* **1994**, *2*, 146–152.

[2] P. L. Anelli, P. R. Ashton, R. Ballardini, V. Balzani, M. Delgado, M. T. Gandolfi, T. T. Goodnow, A. E. Kaifer, D. Philp, M. Pietraszkiewicz, L. Prodi, M. V. Reddington, A. M. Z. Slawin, N. Spencer, J. F. Stoddart, C. Vincent, D. J. Williams, *J. Am. Chem. Soc.* **1992**, *114*, 193–218.

[3] P. L. Anelli, N. Spencer, J. F. Stoddart, *J. Am. Chem. Soc.* **1991**, *113*, 5131–5133.

[4] P. R. Ashton, D. Philp, N. Spencer, J. F. Stoddart, D. J. Williams, *J. Chem. Soc. Chem. Commun.* **1994**, 181–184.

[5] P. R. Ashton, M. R. Johnston, J. F. Stoddart, M. S. Tolley, J. W. Wheeler, *J. Chem. Soc. Chem. Commun.* **1992**, 1128–1131.

[6] P. R. Ashton, T. T. Goodnow, A. E. Kaifer, M. V. Reddington, A. M. Z. Slawin, N. Spencer, J. F. Stoddart, C. Vincent, D. J. Williams, *Angew. Chem.* **1989**, *101*, 1404; *Angew. Chem. Int. Ed. Engl.* **1989**, *28*, 1396–1399.

[7] D. Philp, PhD Thesis, University of Birmingham, **1994**, pp. 126–131

[8] P. W. Atkins, *Physical Chemistry*, 4th ed., Oxford University Press, **1990**, pp. 553–555; J. A. Pople, W. G. Schneider, H. J. Bernstein, *High-Resolution Nuclear Magnetic Resonance*, 1st ed., **1959**, pp. 218–225.

[9] B. Odell, M. V. Reddington, A. M. Z. Slawin, N. Spencer, J. F. Stoddart, D. J. Williams, *Angew. Chem.* **1988**, *100*, 1605; *Angew. Chem. Int. Ed. Engl.* **1988**, *27*, 1547–1550; P. R. Ashton, B. Odell, M. V. Reddington, A. M. Z. Slawin, J. F. Stoddart, D. J. Williams, *ibid.* **1988**, *100*, 1608 and **1988**, *27*, 1550–1553.

[10] D. B. Amabalino, P. R. Ashton, C. L. Brown, E. Cordova, L. A. Godinez, T. T. Goodnow, A. E. Kaifer, S. P. Newton, M. Pietraszkiewicz, D. Philp, F. M. Raymo, A. S. Reder, M. T. Rutland, A. M. Z. Slawin, N. Spencer, J. F. Stoddart, D. J. Williams, *J. Am. Chem. Soc.* **1995**, *117*, 1271–1293.

[11] P. R. Ashton, L. Perez-Garcia, J. F. Stoddart, A. J. P. White, D. J. Williams, *Angew. Chem.* **1995**, *107*, 607; *Angew. Chem. Int. Ed. Engl.* **1995**, *34*, 571–573.

[12] Solutions were prepared by removal of solvents from carefully dispensed quantities of volumetric solutions of the cyclophane in MeCN and the polymer in $CHCl_3$. This material was then dissolved in 0.700 mL of [D_6]DMSO

[13] The chemical shift of α protons on the free cyclophanes in [D_6]DMSO is δ = 9.48 (δf) and that for α protons on the bound cyclophanes is taken to be δ = 9.10 (δb). For the 90 MHz spectrum the chemical shift of the α protons of a type A cyclophane is 9.35. This is an average arising from the following: fraction of free type A cyclophanes × δf + fraction of bound type A cyclophanes × δb = 9.35; fraction of type A that are free = 0.66 (F); fraction of type A that are bound = 0.34 (C); Total fraction of bound cyclophanes = [(C × integral of type A α protons + integral of type B α protons)/(total integral of all α protons)] = 0.41.

A Triphosphete and a Spirocyclic Cation with a PP_4 Skeleton and a 10e Spiro P Atom

Hans H. Karsch,* Eva Witt, and F. Ekkehardt Hahn

A particularly wide variety of suitable redox processes are available for the formation of P–P bonds. For example, from the reaction of white phosphorus with phosphanes and phosphanides Schmidpeter et al. obtained cyclic and acyclic triphosphenium ions containing phosphorus(I) centers with eight electrons.[1] Diphosphinomethanides are particularly suitable for the synthesis of heterocycles containing a P_3 unit; they can react with PCl_3 to yield heterocycles with eight-,[1] seven-, or six-membered rings.[2] However, in the reaction of PCl_3 with $Li[C(PMe_2)_2(SiMe_3)]$ it was not possible to completely rule out the formation of an as yet unknown four-membered ring system (triphosphete) rather than an eight-membered ring.[2]

1,2-Diphosphetenes,[3] 1,2,3-triphosphetenes,[4] and 1,3-diphosphetes[5] have been known for some time. In order to discover whether an eight- or a four-membered ring was formed, we exchanged the methyl substituents on the phosphorus atoms of the phosphinomethanide for phenyl groups [Eq. (a)]. Indeed,

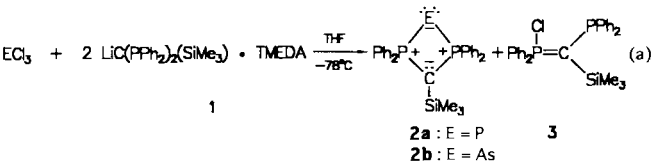

(a)

the four-membered ring compounds **2a,b** were obtained as colorless crystals from pentane, and were unequivocally characterized by elemental analysis and by mass and NMR spectra. If **2a** is formulated with formal charges, then the phosphanide nature of the divalent phosphorus atom (oxidation state +I) is evident and in agreement with the observed high-field ^{31}P NMR shift ($\delta = -86.31$). The course of the reaction can be easily understood in terms of Li/Cl exchange, subsequent elimination of LiCl, and a further substitution step. In this last step the behavior of **2a** differs from that of the methylated compound,[2] because Ph_2P-PPh_2 coupling of the phosphinomethanides as the pertinent redox step is obviously not feasible for steric reasons.[6]

If $SbCl_3$ and $BiCl_3$ are treated with **1** in an analogous manner, then the *P*-chloromethylenephosphorane **3** is obtained along with elemental antimony and bismuth, respectively. An alternative method, based on the Schmidpeter procedure,[1] yields **2a** from white phosphorus and **1**. Although only produced in moderate yields (30%), it is free of **3**. The stoichiometry was chosen based on the (hypothetical) formation of Li_3P_7 [Eq. (b)].[7]

(b)

X-ray structural analysis[8] of the isotypic compounds **2a,b** revealed that they both crystallize in the space group $P\bar{1}$ and contain two independent, but very similar molecules in the unit cell (Fig. 1). The four-membered rings are not completely planar: P3a and As1a project out of the C1a-P1a-P2a plane by 0.148(1) and 0.177(1) Å, respectively. The most striking features are the bond angles P1a-P3a(As1a)-P2a, the smallest found so far for divalent phosphorus (arsenic), and the relatively short nonbonding P1a–P2a distance, particularly in **2a**.[9] The structural parameters, especially the almost identical P1a–P3a(As1a) and P2a–P3a(As1a) bond lengths, suggest a representation as a cyclic bis(ylide) as expressed in the heteropolar notation in Equation (a).[10] Alternatively, **2a,b** can be regarded as an internally donor-stabilized phosphinidene and arsinidene, respectively. Further, a representation derived from a P^I phosphenium ion[11b] or a phosphanide ion[11] can also be considered.[12] Less convincing is a description as a cycloheterobutadiene (cf. ref.[5]) with a λ^5P-$\lambda^3P(As)\lambda^5P$ structural element. Another novel feature of **2a,b** is that these are the first bis(organo)-substituted examples of 1,3-diphosphonium four-membered rings.[26]

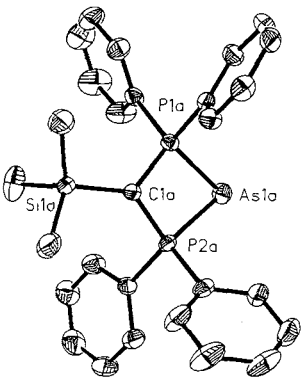

Fig. 1. Crystal structure of **2b** (the asymmetric unit contains two molecules that are identical within the limits of error). **2a** crystallizes isomorphously (exchange of As1a,b by P3a,b). Selected bond lengths [Å] and angles [°] of molecule a [molecule b] in **2a**: P1-P3 2.1489(5) [2.1526(5)], P2-P3 2.1530(6) [2.1488(5)], P1-C1 1.729(1) [1.738(1)], P2-C1 1.738(1) [1.733(1)], P1...P2 2.5483(5) [2.5347(5)]; P1-C1-P2 94.64(7) [93.83(7)], C1-P1-P3 96.44(5) [96.77(5)], C1-P2-P3 96.03(5) [97.07(5)], P1-P3-P2 72.65(2) [72.21(2)]. **2b** molecule a [molecule b]: P1-As1 2.2710(7) [2.2729(7)], P2-As1 2.2692(7) [2.2681(7)], P1-C1 1.741(2) [1.740(2)], P2-C1 1.731(2) [1.730(2)], P1...P2 2.6008(9) [2.5868(9)]; P1-C1-P2 97.0(1) [96.4(1)], C1-P1-As1 96.21(8) [96.78(8)], C1-P2-As1 96.59(8) [97.27(8)], P1-As1-P2 69.90(2) [69.45(2)].

The small P1a-P3a(As1a)-P2a angle may lead to special reactivity, for example high nucleophilicity. However, large amounts of **2a,b** could not be obtained free of **3**, so that reactions of **2a,b** as nucleophiles have not yet been successful. In order to use this "disadvantage" positively, an equivalent amount of $NaBPh_4$ was added to the mixture of **2a** and **3** obtained according to Equation (a). Here **3** is converted in situ into the cation **3a**,[13] which is then attacked by the nucleophilic **2a** to yield the spirocyclic phosphorus(III) cation **4** with a PP_4 backbone [Eq. (c)].

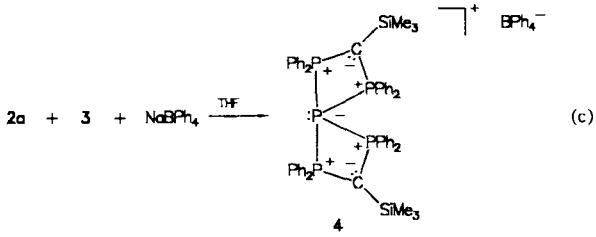

(c)

Pale yellow crystals of **4**-BPh_4 were obtained from THF. X-ray structural analysis[14] confirmed the structure deduced from the $^{31}P\{^1H\}$ NMR spectrum (see below) (Fig. 2). As in phosphonium ions, the central phosphorus atom is tetravalent; however, it does not have a (distorted) tetrahedral environment, but exhibits a distorted pseudo-trigonal-bipyramidal frame-

[*] Prof. Dr. H. H. Karsch, Dipl.-Chem. E. Witt
Anorganisch-chemisches Institut der Technischen Universität München
Lichtenbergstrasse 4, D-85747 Garching (Germany)
Fax: Int. code +(89)2891-4421
Prof. F. E. Hahn
Institut für Anorganische und Analytische Chemie der Freien Universität
Fabeckstrasse 34–36, D-14195 Berlin (Germany)

 © VCH Verlagsgesellschaft mbH, D-69451 Weinheim, 1996 0570-0833/96/3519-2242 $ 15.00+.25/0

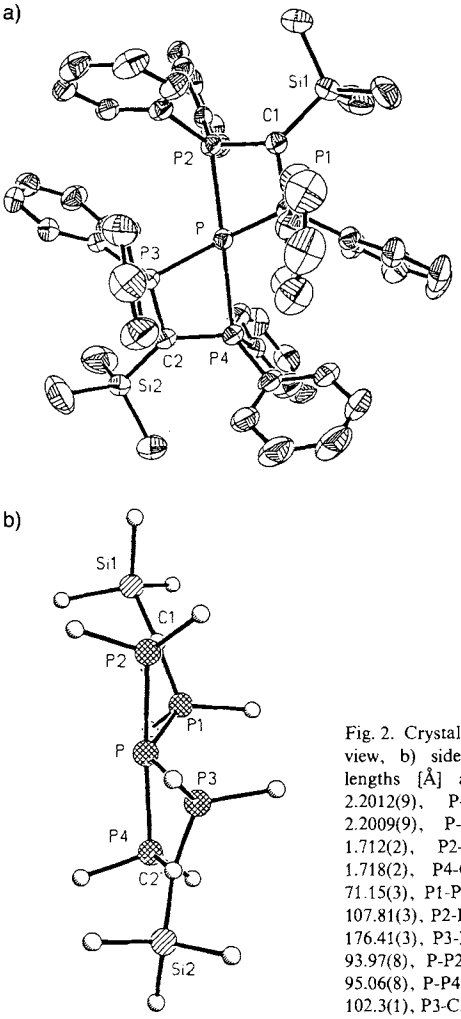

Fig. 2. Crystal structure of **4**. a) Front view, b) side view. Selected bond lengths [Å] and angles [°]: P-P1 2.2012(9), P-P2 2.4077(8), P-P3 2.2009(9), P-P4 2.4616(9), P1-C1 1.712(2), P2-C1 1.737(2), P3-C2 1.718(2), P4-C2 1.733(2); P1-P-P2 71.15(3), P1-P-P3 125.12(4), P1-P-P4 107.81(3), P2-P-P3 107.22(3), P2-P-P4 176.41(3), P3-P-P4 70.41(3), P-P1-C1 93.97(8), P-P2-C1 86.46(8), P-P3-C2 95.06(8), P-P4-C2 85.98(9), P1-C1-P2 102.3(1), P3-C2-P4 102.8(1).

work (Fig. 2a,b). The free equatorial position indicates the presence of a lone pair. Thus **4** can be included in a series, in general terms, of electronically isovalent element(II) compounds $E[C(PMe_2)_2(SiMe_3)]_2$ **5** (E = Si,[15] Ge,[16] Sn,[17] Pb[18]), with a formal isoelectronic exchange of Si by P^+. Therefore, following this type of notation, **4** can be regarded as a double phosphane adduct of a phosphenium ion (in short, a ten-electron phosphenium ion). In contrast to simple phosphenium ions (e.g. $[(R_2N)_2P]^+$, six electrons[19a]) or simple base adducts of ions of the type $[R_3N-PR'_2]X$[19b, 20] and $[R_3P-PR'_2]X$[21] (eight electrons), the chelate function of the two diphosphinomethanide ligands in **4** leads to ten electrons on the central P atom.[22] Therefore, it is possible to describe **4** as a tetraonio-substituted phosphoranide[23] with partial charge compensation by two internal carbanion functions. Although the phosphenium formalism represents the charge correctly and establishes the analogy to the systems listed above, the phosphoranide formalism describes the nature of the central phosphorus atom more accurately. Therefore, both representations are useful and should be used in conjunction.

As in the compounds **5**, the axial P–P bonds in **4** are not only longer than the equatorial P–P bonds, which are both equal in length, but they also differ slightly. The bond length differences Δd $P-P_{ax}$ and $P-P_{eq}$ (0.21 and 0.26 Å, ca. 8%) lie in the usual range for this geometry.

The chelate four-membered rings are not planar here either; the deviation of C1 from the P1-P-P2 plane amounts to 0.480(2), that of C2 from the P3-P-P4 plane, 0.467(3) Å. However, at both C1 and C2 the sum of the angles is 360°. The ring strain in the two chelate four-membered rings in **4** has a different effect on the bond angles than that expressed in compounds **5**. Not only the P2-P-P4 but also the P1-P-P3 angles are greatly expanded. Thus the P2-P-P4 axis is almost linear, whilst P1 and P3 are very clearly distorted out of the equatorial "plane" of the pseudo-trigonal-bipyramidal framework. The reason for this could lie in the interactions of the bulky phenyl groups (methyl groups in **5**).

The $^{31}P\{^1H\}$ NMR spectra of **4** in solution reveal a rapid scrambling of the equatorial and axial positions at room temperature. The signal of the central phosphorus atom is, as in **2a**, shifted to high field ($\delta = -76.26$). The average "coupling constant" $^1J(P,P)$ of 137.3 Hz is about half of that found in **2a**. On cooling to −107 °C this scrambling process is essentially frozen; an A_2B_2M spin system can be observed.

Tetravalent phosphorus(III) compounds, in which the phosphorus has ten electrons with one lone pair, have only been achieved with phosphoranide ions.[23] Compound **4** is novel as an illustration of one of the possible types of bonding in P–P systems.[24] PP_4 skeletons—be they cationic, neutral, or anionic—have not been detected to date. The formation of the novel type of structure in **4** is obviously a consequence of the nucleophilic behavior of the triphosphete **2a** and the amphiphilic character of "diphosphino carbocations" such as **3a**.

Experimental Procedure

All work was carried out under exclusion of air and moisture in an inert atmosphere of N_2.

2a: To a solution of **1**[25] (2.66 g, 4.6 mmol) in 30 mL of THF at −78 °C was added PCl_3 (0.15 mL, 1.72 mmol) by pipette. The mixture was slowly warmed to room temperature and stirred for 12 h before the solvent was removed in vacuo. The residual orange foam was extracted with pentane (2 × 40 mL). Slow evaporation of the combined pentane extracts at room temperature furnished orange crystals of **2a** (0.31 g, 37%). $^{31}P\{^1H\}$ NMR (C_6D_6, 20 °C): AB_2 spin system: $\delta P_A = -86.31$; $\delta P_B = 20.18$; $J(P_A,P_B) = 261.0$ Hz. MS(CI): $m/z = 487$ ($M^+ + 1$, 100%). ^{31}P NMR spectroscopy of the remaining oil indicates **3** along with $HC(PPh_2)_2(SiMe_3)$. $^{31}P\{^1H\}$ NMR (C_6D_6, 20 °C) of **3**: AB spin system: $\delta P_A = 0.15$; $\delta P_B = 70.15$ ($J = 164.0$ Hz).

2b: To a solution of **1** (1.76 g, 3.04 mmol) in 30 mL of THF at −90 °C was added dropwise $AsCl_3$ (0.11 mL, 1.31 mmol) in 15 mL of THF. The mixture was slowly warmed to room temperature and stirred for 12 h. The solvent was evaporated in vacuo and the residue extracted with pentane (3 × 30 mL). Evaporation of the combined pentane extracts at room temperature yielded a precipitate of product **2b** as a red crystalline solid (0.32 g, 46%). $^{31}P\{^1H\}$ NMR (C_6D_6, 20 °C): δP: −0.51, s. MS(CI): $m/z = 530$ (M^+, 100%).

4-BF_4: To a mixture of **3** (0.403 g, 0.82 mmol) and **2a** (0.398 g, 0.82 mmol) in 35 mL of THF at −78 °C was added dry $NaBPh_4$ (0.281 g, 0.82 mmol). The mixture was warmed to room temperature and stirred for 10 h before the solvent was removed by evaporation (room temperature)). Extraction with pentane gave traces of **3** and $HC(PPh_2)_2(SiMe_3)$. Extraction with THF yielded a yellow-orange oil, which when left to stand for 5 d at room temperature gave a precipitate of orange crystals of **4** (0.40 g, 39%). $^{31}P\{^1H\}$ NMR (C_6D_6 + THF, 20 °C): AB_4 spin system: $\delta P_A = -76.26$, $\delta P_B = 37.73$, $J(P_A,P_B) = 137.3$ Hz; ($C_6D_5CD_3$ + THF, −107 °C): A_2B_2M spin system: $\delta P_A = 44.39$; $\delta P_B = 26.25$; $\delta P_M = -83.71$; $J(P_A,P_B) = 172.0$ Hz, $J(P_A,P_M) = 86.0$ Hz, $J(P_B,P_M) = 172.0$ Hz.

Received: February 23. 1996 [Z8852IE]
German version:. *Angew. Chem.* **1996**, *108*, 2380–2382

Keywords: heterocycles · low-valent compounds · phosphorus compounds · redox processes

[1] a) A. Schmidpeter, G. Burget, *Phosphorus Sulfur Relat. Elem.* **1985**, *22*, 323–335; b) A.Schmidpeter, S. Lochschmidt, W. S. Sheldrick, *Angew. Chem.* **1985**, *97*, 214–215; *Angew. Chem. Int. Ed. Engl.* **1985**, *24*, 226–227; c) A. Schmidpeter, F. Steinmüller, W. S. Sheldrick, *Z. Anorg. Allg. Chem.* **1989**, *579*, 158–172.

[2] a) E = P: H. H. Karsch, E. Witt, A. Schneider, E. Herdtweck, M. Heckel, *Angew. Chem.* **1995**, *107*, 628–631; *Angew. Chem. Int. Ed. Engl.* **1995**, *34*, 557–560; b) E = As: H. H. Karsch, A. Schier, *J. Chem. Soc. Chem. Commun.* **1994**, 2703–2704.

[3] G. Becker, W. Becker, G. Uhl, *Z. Anorg. Allg. Chem.* **1984**, *518*, 21–35.

[4] H. Pucknat, J. Grobe, D. Le Van, B. Broschk, M. Hegemann, B. Krebs, M. Läge, *Chem. Eur. J.* **1996**, *2*, 208–213.

[5] a) B. Neumüller, E. Fluck, *Phosphorus Sulfur Relat. Elem.* **1986**, *29*, 23–29; b) H. H. Karsch, T. Rupprich, M. Heckel, *Chem. Ber.* **1995**, *128*, 959–961; c) H. Keller, G. Maas, M. Regitz, *Tetrahedron Lett.* **1986**, *27*, 1903–1906; d) A dicationic analog also exists: J. Weiss, B. Nuber, *Z. Anorg. Allg. Chem.* **1981**, *473*, 101–106, and references therein.

[6] This P–P coupling determines the reaction of the P-methyl-substituted phosphinomethanide and leads eventually to the isolable bis(ylide): $(Me_2P)(Me_3Si)C{=}PMe_2\text{-}PMe_2{=}C(SiMe_3)(PMe_2)$: H. H. Karsch, B. Deubelly, G. Müller, *J. Chem. Soc. Chem. Commun.* **1988**, 517–518. In contrast to earlier reports (H. H. Karsch, B. Deubelly, G. Grauvogel, G. Müller, *J. Organomet. Chem.* **1993**, *459*, 95–105), this step can be ruled out for the analog with phenyl substituents. See also: P. Braunstein, R. Hasselbring, A. DeCian. J. Fischer, *Bull. Soc. Chim. Fr.* **1995**, *132*, 691–695. Accordingly, **3** does not react with excess **1** under the present conditions, as can be demonstrated independently.

[7] Since the reduced phosphorus species was not identified, the formulation in Equation (b) as Li_3P_7 only reflects the chosen stochiometry and is also in agreement with the corresponding formulation in ref.[1].

[8] Crystal structure determinations: Crystals of **2a** and **2b** were obtained by recrystallization from pentane. **2a** [**2b**]: $C_{28}H_{29}P_3Si$ [$C_{28}H_{29}AsP_2Si$], triclinic [triclinic], space group $P\bar{1}$ [$P\bar{1}$], $a = 9.606(1)$ [9.687(1)], $b = 16.227(1)$ [16.317(1)], $c = 17.172(1)$ [17.274(1) Å, $\alpha = 106.30(2)$ [106.35(1)], $\beta = 90.13(2)$ [90.34(1)], $\gamma = 93.12(2)$ [92.55(1)]°, $V = 2564.9(9)$ [2616.9(3)] Å^3, $Z = 4$ [4] (each contains two independent molecules in the asymmetric unit), $\rho_{calcd} = 1.260$ [1.346] g cm^{-3}, $Mo_{K\alpha}$ radiation ($\lambda = 0.71073$ Å), $\mu(Mo_{K\alpha}) = 2.86$ [14.81] cm^{-1}. 11157 [9108] independent reflections measured with $\omega - 2\theta$ scans at $-120(2)$ [$-68(2)$] °C in the 2θ range [°] 2–54 [3–50]. Structure solution using direct methods, refinement of the positional parameters of all the non-hydrogen atoms with anisotropic thermal parameters, hydrogen atoms on calculated positions with $B_H[U_H] = 1.3\, B_{eq.C}$ [1.2–1.5 $U_{eq.C}$]. Refinement of the positional parameters with MolEN versus F (for **2a**) and with SHELXL-93 versus F^2 (for **2b**). $R = 0.0287$ [0.0311], $R_w = 0.0480$ [0.0747] for 8849 [7116] structural factors $F_o^2 \geq 3\sigma(F_o^2)$ [$F_o \geq 4\sigma(F_o)$] and 577 [583] variables. Further details of the crystal structure investigation may be obtained from the Fachinformationszentrum Karlsruhe, D-76344 Eggenstein-Leopoldshafen (Germany) on quoting the depository number CSD-59325.

[9] This short nonbonding distance is typical for many diphosphinomethanide complexes. For example in $Br_2B[C(PMe_2)_2(SiMe_3)]$ it is 2.59(1) Å: H. H. Karsch, K. Zellner, A. Schier, unpublished results. Because of the interaction of the carbanion-like C atoms, this distance is even shorter in 1,3-diphosphetes e.g. 2.39 Å in $[C_9H_{14}N_2P(C_7H_{19}Si_2)_2]_2P_2[C(SiMe_3)]_2$ [5b].

[10] Here the extent of a possible delocalization of charges in the sense of heteroallyl cation/P anion is not considered, cf.: G. Alcaraz, A. Baceiredo, M. Niger, W. W. Schoeller, G. Bertrand, *Inorg. Chem.* **1996**, *35*, 2458–2462.

[11] Twofold coordination of a P atom with (formally) two lone pairs as in R_2P^-.

[12] This representation takes account of the (otherwise obsolete) assignment of the oxidation state of +1 between two identical elements for the bivalent P and As atoms.

[13] *P*-Chloro-methylenephosphoranes have been reported: O. I. Kolodyazhnyi, *Russ. Chem. Rev.* **1991**, *60*, 391–409; R. Appel, J. Peters, R. Schmitz, *Z. anorg. allg. Chem.* **1981**, *475*, 18–26. They can be converted into the cation e.g. with $AlCl_3$: N. Burford, R. E. v. H. Spenze, R. D. Rogers, *J. Am. Chem. Soc.* **1989**, *111*, 5006–5008; H. Grützmacher, H. Pritzkow, *Angew. Chem.* **1992**, *104*, 92–94, *Angew. Chem. Int. Ed. Engl.* **1992**, *31*, 99–101. However, C-phosphino-substituted *P*-chloro-methylenephosphoranes such as **3** and its cations, for example $[(Ph_2P)_2C(SiMe_3)]^+$ **3a**, have not yet been reported. **3a** cannot be detected by spectroscopy when **3** is treated with $NaBPh_4$. On the other hand, **4** is also produced in the reaction of a mixture of **2a** and **3** with $GeCl_2$; the counterion is $[GeCl_3]^-$. This proves that the presence of a (strong) nucleophile is essential for the abstraction of chloride from **3**. However, the reaction of **3** with the strong chloride acceptor $AlCl_3$ produces a new species, whose ^{31}P NMR signal appears at $\delta = 67.26$ and can be attributed to the "diphosphino carbocation" **3a**. A unequivocal identification of **3a** has yet to be achieved.

[14] Crystal structure determination of **4**-BPh_4: crystals of were obtained by recrystallization from THF. $C_{80}H_{78}BP_5Si_2$, monoclinic, space group $P2_1/c$, $a = 14.817(1)$, $b = 18.639(1)$, $c = 25.665(2)$ Å, $\beta = 94.08(1)°$, $V = 7070.0(8)$ Å^3, $Z = 4$, $\rho_{calcd} = 1.185$ g cm^{-3}, $Mo_{K\alpha}$ radiation ($\lambda = 0.71073$ Å), $\mu(Mo_{K\alpha}) = 20.6$ cm^{-1}. 12373 independent reflections measured with ω scans at $-68(2)$ °C in the 2θ range [°] 3–50. Structure solution using direct methods, refinement of the positional parameters of all the non-hydrogen atoms with anisotropic thermal parameters, hydrogen atoms on calculated positions with $U_H = 1.2$–$1.5\, U_{eq.C}$. Refinement of the positional parameters with SHELXL-93 versus F^2. $R = 0.0403$, $R_w = 0.0950$ for 8783 structural factors $F_o \geq 4\sigma(F_o)$] and 799 variables. Further details of the crystal structure investigation may be obtained from the Fachinformationszentrum Karlsruhe, D-76344 Eggenstein-Leopoldshafen (Germany) on quoting the depository number CSD-59325.

[15] H. H. Karsch, U. Keller, S. Gamper, G. Müller, *Angew. Chem.* **1990**, *102*, 297–298, *Angew. Chem. Int. Ed. Engl.* **1990**, *29*, 295–296.

[16] H. H. Karsch, B. Deubelly, G. Hanika, J. Riede, G. Müller, *J. Organomet. Chem.* **1988**, *344*, 153–161.

[17] H. H. Karsch, A. Appelt, G. Müller, *Angew. Chem.* **1985**, *97*, 404–406, *Angew. Chem. Int. Ed. Eng.* **1985**, *24*, 402–404.

[18] H. H. Karsch, G. Baumgartner, still unpublished (**1991**), for $Pb[C(PPh_2)_2\text{-}(SiMe_3)]_2$ see: A. L. Balch, D. E. Oram, *Inorg. Chem.* **1987**, *26*, 1906–1912.

[19] a) A. H. Cowley, M. C. Cushner, J. S. Szobota, *J. Am. Chem. Soc.* **1978**, *100*, 7784–7786. b) M. Sanchez, M. R. Mazières, L. Lamandé, R. Wolf in *Multiple Bonds and Low Coordination in Phosphorus Chemistry* (Eds.: M. Regitz, O. J. Scherer), Thieme, Stuttgart, **1990**, p. 129.

[20] a) G. Bouhadir, R. W. Reed, R. Réau, G. Bertrand, *Heteroat. Chem.* **1995**, *Vol. 6*, 371–375. b) R. Weiss, S. Engel, *Angew. Chem.* **1992**, *104*, 239–240, *Angew. Chem. Int. Ed. Engl.* **1992**, *31*, 216–217.

[21] a) F. Sh. Shagvaleev, T. V. Zykova, R. I. Tarasova, T. Sh. Sitdikova, V. V. Moskva, *J. Gen. Chem.* **1990**, *60*, 1585–1589, and references therein; *Zh. Obsch. Khim.* **1990**, *60*, 1775–1779, and references therein; b) N. Burford, P. Losier, S. V. Sereda, T. S. Cameron, G. Wu, *J. Am. Chem. Soc.* **1994**, *116*, 6474–6475; and references therein.

[22] This does not conflict with the representation using formal charges, in which the central phosphorus atom is assigned a negative formal charge. For example, in the "triphosphenium ion" $[Ph_3P\text{-}\bar{P}PPh_3]^+$ [1b] the phosphorus has a negative formal charge. The representation as a phosphane–base adduct of a triono-substituted phosphane [20a] with partial charge compensation by two carbanion functions is very artificial. However, it does illustrate that **4** can also be regarded as the first phosphane–phosphane adduct—if only for very specific phosphanes.

[23] K. B. Dillon, *Chem. Rev.* **1994**, *94*, 1441–1456.

[24] L. Lamandé, K. Dillon, R. Wolf, *Phosphorus, Sulfur Silicon Relat. Elem.* **1995**, *103*, 1–24.

[25] H. H. Karsch, G. Grauvogl, P. Mikulcik, P. Bissinger, G. Müller, *J. Organomet. Chem.* **1994**, *465*, 65–71.

[26] Note added in proof (August 15, 1996): Accordingly, in the first report on tetraphosphete derivatives published since submission of this manuscript the phosphonium centers each bear two amino groups: W. Frank, V. Petry, E. Gerwalin, G. J. Reiss, *Angew. Chem.* **1996**, *108*, 1616–1618; *Angew. Chem. Int. Ed. Engl.* **1996**, *35*, 1512–1514.

Donor/Acceptor Complexes in Hydrogen-Bonded Networks: pH-Dependent Self-Organization**

Hans Bock,* Wolfgang Seitz, Mark Sievert, Markus Kleine, and Jan W. Bats

Donor/acceptor complexes $\{D^{\delta+} \cdots A^{\delta-}\}$[1, 2] between donor molecules of low ionization energy, which also function as Lewis bases, nucleophiles, or reducing reagents, and electron-deficient acceptor molecules with their properties as Lewis acids, electrophiles, or oxidizing reagents are kept together by weak Coulomb interactions and can be intermediates in microscopic pathways of substitution or redox reactions.[1d, 2] Their fascinating color is due to the long-wavelength excitation into short-lived charge transfer (CT) states $\{D^{\bullet+} \cdots A^{\bullet-}\}$.[1a] Structural analysis of mixed-stack aggregates between six-membered ring donors and acceptors, which can be specifically crystallized,[2c–g] proves that in their ground states, all bond lengths and angles of the components remain unchanged on π-complexation. Attempts to increase the π-interaction by shortening the donor···acceptor distance, thereby generating recognizable structure perturbations, have been the starting point for the

[*] Prof. Dr. H. Bock, Dr. W. Seitz, Dipl.-Chem. M. Sievert, Dipl.-Chem. M. Kleine, Dr. J. W. Bats
Institut für Anorganische Chemie der Universität
Marie-Curie-Strasse 11, D-60439 Frankfurt (Germany)
Fax: Int. code +(69) 798-29188

[**] Interactions in Molecular Crystals, Part 90. This project has been supported by the Adolf-Messer-Stiftung, the Deutsche Forschungsgemeinschaft, the State of Hesse, and the Fonds der Chemischen Industrie. Part 89: H. Bock, K. Ziemer, C. Näther, H. Schödel, M. Kleine, M. Sievert, *Z. Naturforsch. B* **1996**, *51*, in press.

crystallization of donor/acceptor complexes in hydrogen-bonded networks illustrated by the following examples.[3]

1) In molecular crystals of donor/acceptor complexes exhibiting a herringbone pattern, the lattice can be planarized by additional hydrogen bonds:[2a] this is demonstrated by an exchange of the acceptor 1,2,4,5-tetracyanobenzene by the likewise tetracyano-substituted hydroquinone (Fig. 1), which, depending on the basicity of the hydrogen-bond partner, either forms a network with $-CN\cdots HO-$ ($pK_B \approx -11$) or $>NH_2^+\cdots {}^-O-$ contacts ($pK_B \approx 8$) involving cooperative effects of about 2 kJ mol^{-1} (10%) or 18 kJ mol^{-1} (32%),[4] respectively.

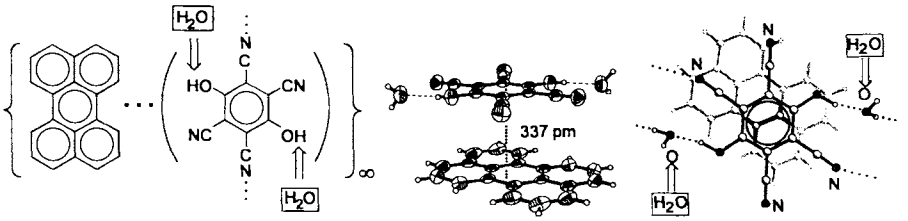

Fig. 2. Single-crystal structure of the donor/acceptor complex {perylene $\cdots$ tetracyanohydroquinone$(H_2O)_2\}_\infty$: side view (50% thermal ellipsoids) and top view; cf. {pyrene $\cdots$ 1,2,4,5-tetracyanobenzene$\}_\infty$, Fig. 1, and text.

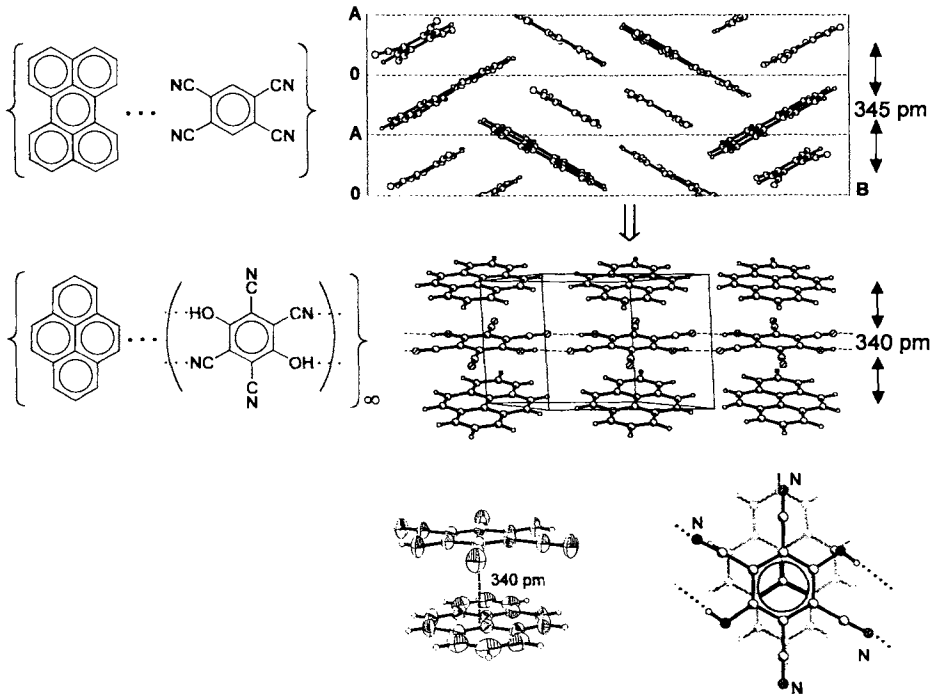

Fig. 1. Single-crystal structures of the donor/acceptor complexes {perylene $\cdots$ 1,2,4,5-tetracyanobenzene} and {pyrene $\cdots$ tetracyanohydroquinone} exhibiting lattices with either herringbone pattern or parallel layers flattened by hydrogen bonds, shown in side view (50% thermal ellipsoids) and top view (cf. text).

The herringbone pattern[1b] of the complex {perylene $\cdots$ 1,2,4,5-tetracyanobenzene}[2a] is leveled in {pyrene $\cdots$ 1,2,4,5-tetracyanohydroquinone}[5] by four additional $-CN\cdots HO-$ hydrogen bonds; simultaneously the interplanar donor $\cdots$ acceptor π-distance is shortened by 5 pm to double the van der Waals π-radius ($2\times 170 = 340$ pm).[3a] Nevertheless, no significant structural changes due to the complex formation are evident in either the donor or acceptor components. PM3/CI and AM1/CI calculations[2g] based on the crystal structure data, which approximately reproduce the long-wavelength CT-excitations of the violet or dark red dichloromethane solutions at 19000 and 21000 cm^{-1}, respectively, predict only charge transfer contributions of less than 0.1 electrons for the ground states of the individual complexes. Charge-inflicted structural perturbations, therefore, are not to be expected.

2) Crystallization of the donor/acceptor complex between perylene and tetracyanohydroquinone from a hot acetic acid solution[6] surprisingly yields the doubly hydrated polymer {perylene $\cdots$ tetracyanohydroquinone$(H_2O)_2\}_\infty$ (Fig. 2).

Lattice incorporation of two water molecules stretches the N–O distance between the hydrogen-bond pair $(CN\cdots HO-)_2$ of the pyrene adduct from 265 pm to 565 pm in the analogous perylene complex containing the contact pairs $(-CN\cdots HO-(H)\cdots HO-)_2$. Despite the comparable interplanar π-distances of 340 and 337 pm, respectively, which correspond to twice the standard van der Waals π-radius of 340 pm, the π-overlap of the polycyclic hydrocarbon donor with the tetracyanohydroquinone six-membered ring change drastically (Fig. 1 and 2). In the pyrene complex a trigonal C center and in the perylene one ring-connecting C_2 fragment is superimposed by the arene ring. Because pyrene also contains a central CC bond and perylene trigonal C centers, the energy differences between the specific overlap possibilities of six-membered rings, which are probably only small, will be explored by density functional calculations for selected model compounds,[2b] as in the case of benzene dimers in the gas phase.[7] Until proven otherwise, dominant packing effects have to be assumed, which even for small differences in lattice sublimation energies,[8] are known to determine the crystal structures. Both π-overlap situations, however, require more space for perylene (Fig. 2), and therefore the hydrate stretching of the polymer chain under comparable crystallization conditions is an interesting variation resulting from insertion of donor/acceptor complexes in hydrogen-bonded networks.

3) A third possibility of incorporating donor molecules into H-bonded layers of the acceptor tetracyanohydroquinone is observed in the complex {tetracyanohydroquinone anion $\cdots$ *N,N'*-tetramethylbenzidinium dication$(H_2O)_2\}_\infty$ (Fig. 3).[2g] Proton transfer from two hydroquinone molecules yields doubly protonated tetramethylbenzidinium dications, which are connected by hydrogen bonds to the polymer chains of likewise H-bonded tetracyanohydroquinone monoanions (Fig. 3; all H experimentally detected). After proton exchange between the donor and acceptor functions, relatively long, interplanar {benzidine$^{2+}\cdots$ hydroquinone$^-$} π-distances of 360 pm result (Fig. 3) in contrast to those of only 335 pm between the hydroquinone anions, which are arranged parallel to each other, presumably due to lattice packing. In the different hydrogen bonds the heterocenters are separated by 246 pm for $O(H)\cdots {}^-O$, 272 pm for $N^+(H)\cdots O$, and 290 pm for $N\cdots(H)O$, and form

 © VCH Verlagsgesellschaft mbH, D-69451 Weinheim, 1996 0570-0833/96/3519-2245 $ 15.00+.25/0

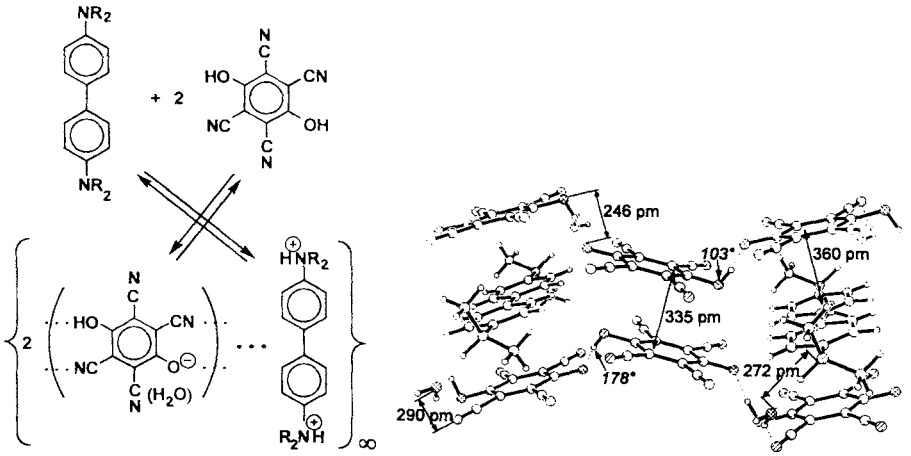

Fig. 3. Scheme for the proton transfer between *N,N'*-tetramethylbenzidine and tetracyanohydroquinone, as well as the single-crystal structure of the resulting donor/acceptor complex in a polymeric hydrogen-bonded network (cf. text).

an overall energetically favorable hydrogen-bonded network.[1b, 3c, d, 9]

Clearly, donor/acceptor complexes in hydrogen-bonded networks provide additional aspects for novel materials. The three examples presented—flattened, alternate layers of donors and acceptors (1), stretching of the hydrogen-bonded network by hydrate water inclusion for incorporation of larger π-donor molecules (2), and exchange of donor and acceptor functions by protonation/deprotonation equilibria (3)—should stimulate further exploration of the many facets of this pH-dependent molecular self-organization.

Received: September 21, 1995
Revised version: May 17, 1996 [Z 8416 IE]
German version: *Angew. Chem.* **1996**, *108*, 2382–2384

Keywords: donor–acceptor complexes · hydrogen bonds · self-assembly · structure elucidation

[5] Crystallization of the 1:1-Complex {pyrene···tetracyanohydroquinone}: 2,3,5,6-Tetracyanohydroquinone (210 mg, 1 mmol) in conc. acetic acid (10 mL) was heated to boiling together with a solution of pyrene (202 mg, 1 mmol) in dichloromethane (15 mL). On slow cooling of the dark yellow solution and evaporation of about two-thirds of the solvent mixture at 200 mbar, dark red blocks, which are best kept in the solution under argon, crystallize within three days. Crystal structure: crystal dimensions $0.12 \times 0.20 \times 0.25$ mm; $C_{26}H_{12}N_4O_2$ ($M_r = 412.41$ g mol^{-1}); $a = 709.2(1)$, $b = 837.8(1)$, $c = 866.4(2)$ pm, $\alpha = 112.92(1)$, $\beta = 92.86(1)$, $\gamma = 92.08(1)°$, $V = 472.7(3) \times 10^6$ pm^3, $Z = 1$, $\rho_{calcd} = 1.449$ g cm^{-3} (room temperature), $\mu(Cu_{K\alpha}) = 0.77$ mm^{-1}, triclinic, space group $P\bar{1}$ (No. 2). Enraf-Nonius CAD-4 diffractometer, graphite monochromator, 1502 reflections in the range $2° < 2\theta < 120°$, of which 1360 are independent with $I > 2\sigma(I)$. Structure determination by direct methods (SHELXTL-PLUS) and (SHELXL93), $N = 1360$, $N_P = 147$, $R = 0.0378$, $wR2 = 0.1083$, $w = 1/[\sigma^2(F_o^2) + (0.0604\,P)^2 + 0.10\,P]$ with $P = (\mathrm{Max}(F_o^2,0) + 2F_c^2)/3$. Residual electron density: max. 0.18 e Å^{-3}, min. -0.14 e Å^{-3}, GOF = 1.070. The C, N, and O positions are anisotropically refined; the hydrogens are geometrically ideally positioned and refined with the riding model and isotropic fixed displacement parameters. See also [10].

[6] Crystallization of the 1:1-complex {perylene···tetracyanohydroquinone$(H_2O)_2$}: 2,3,5,6-Tetracyanohydroquinone (210 mg, 1 mmol) in conc. acetic acid (10 mL) was heated to boiling together with a solution of perylene (252 mg, 1 mmol) in dichloromethane (10 mL). On slow cooling of the yellow solution and evaporation of about two-thirds of the solvent mixture at 200 mbar, black needles, which are best kept in the solution under argon, crystallize within 3 days. Crystal structure: Crystal dimensions $0.07 \times 0.07 \times 0.95$ mm; $C_{30}H_{18}N_4O_4$ ($M_r = 516.0$ g mol^{-1}); $a = 1055.3(1)$, $b = 720.8(1)$, $c = 1566.3(2)$ pm, $\alpha = \gamma = 90°$, $\beta = 99.42(1)°$, $V = 1175.4(4) \times 10^6$ pm^3, $Z = 2$, $\rho_{calcd} = 1.408$ g cm^{-3} (room temperature), $\mu(Cu_{K\alpha}) = 0.79$ mm^{-1}, monoclinic, space group $P2_1/n$ (No. 14). ENRAF-NONIUS CAD-4 diffractometer, graphite monochromator, 4349 reflections in the range $2° < 2\theta < 130°$, of which 1915 are independent with $I > 2\sigma(I)$. Structure determination by direct methods (SHELXTL-PLUS) and (SHELXL93), $N = 1915$, $N_P = 182$, $R = 0.0363$, $wR2 = 0.1050$, $w = 1/[\sigma^2(F_o^2) + (0.0617\,P)^2 + 0.17\,P]$ with $P = (\mathrm{Max}(F_o^2,0) + 2F_c^2)/3$. Residual electron density: max. 0.20 e Å^{-3}, min. -0.12 e Å^{-3}, GOF = 1.047. The C, N, and O positions are anisotropically refined; the hydrogen centers are geometrically ideally positioned and refined with a riding model and fixed isotropic displacement parameters. The hydrogens of the hydrate water are isotropically freely refined.

[7] B. P. Hobza, H. L. Selzle, W. Schlag, *J. Am. Chem. Soc.* **1994**, *116*, 3506.
[8] H. Bock, A. Rauschenbach, C. Näther, Z. Havlas, A. Gavezzotti, G. Filippini, *Angew. Chem.* **1995**, *107*, 120; *Angew. Chem. Int. Ed. Engl.* **1995**, *34*, 76.
[9] Cf., for example G. A. Jeffrey, W. Saenger *Hydrogen Bonding in Biological Structures*, Springer, Heidelberg, **1992**; A. F. Wells, *Structural Inorganic Chemistry*, 5. ed. Clarendon Press, Oxford **1987**, S. 355–376; J. Emsley, *Chem. Soc. Rev.* **1980**, *9*, 91–124; R. Taylor, O. Kennard, *Acc. Chem. Res.* **1984**, *17*, 320; R. Desiraju, *ibid.* **1991**, *24*, 290.
[10] Further details of the crystal structure investigations may be obtained from the Fachinformationszentrum Karlsruhe, D-76344 Eggenstein-Leopoldshafen (Germany), on quoting the depository numbers CSD-391036 and CSD-391037.

[1] The following selected reviews illustrate the multifaceted aspects of donor/acceptor complexes: a) electronic spectra: R. Foster, *Organic Charge Transfer Complexes*, Academic Press, London, **1969**; G. Briegleb, *Elektronen-Donator/Acceptor-Komplexe*, Springer, Berlin, **1961**; b) structures: G. R. Desiraju, *Crystal Engineering*, Elsevier, Amsterdam, **1989**; c) reactivity: J. K. Kochi, *Pure Appl. Chem.* **1991**, *63*, 255; d) intermediates in substitution or redox reactions: W. Kaim, *Nachr. Chem. Techn. Lab.* **1984**, *32*, 436; L. Eberson, *Electron Transfer Reactions in Organic Chemistry*, Springer, Berlin, **1987**, and references in each.
[2] Investigations of donor/acceptor complexes by our group: a) H. Bock, *Mol. Cryst. Liq. Cryst.* **1994**, *240*, 155; b) H. Bock, Z. Havlas, A. Rauschenbach, C. Näther, M. Kleine, *J. Chem. Soc. Chem. Commun.* **1996**, 2345; c) H. Bock, A. Rauschenbach, C. Näther, M. Kleine, J. W. Bats, *Phosphorus, Sulfur, Silicon Rel. Elem.* **1996**, *101*, 234; d) H. Bock, M. Kleine, *Z. Phys. Chem.* **1996**, in press; e) H. Bock, M. Sievert, H. Schödel, M. Kleine, *Z. Naturforsch. B* **1996**, 51, in press; f) H. Bock, K. Ziemer, C. Näther, H. Schödel, M. Kleine, M. Sievert, *ibid.* **1996**, *51*, in press; g) unpublished results: Ph.D. Dissertations of W. Seitz, A. Rauschenbach, K. Ziemer, Universität Frankfurt, **1995**, M. Kleine, Dissertation Universität Frankfurt, **1996**.
[3] Summaries of own investigations on hydrogen bonds: a) H. Bock, K. Ruppert, C. Näther, Z. Havlas, H.-F. Herrmann, C. Arad, I. Göbel, A. John, J. Meuret, S. Nick, A. Rauschenbach, W. Seitz, T. Vaupel, B. Solouki, *Angew. Chem.* **1992**, 104, 564; *Angew. Chem. Int. Ed. Engl.* **1992**, *31*, 550; b) H. Bock, *Mol. Cryst. Liq. Cryst.* **1994**, *240*, 155; c) H. Bock, *Phosphorus, Sulfur, Silicon, Rel. Elem.* **1994**, *87*, 23; d) *Akad. Wiss. Lit. Mainz, Abh. Math.-Naturw. Klasse* **1995**, 1 (F. Steiner Verlag, Stuttgart, **1995**) and the references in each.
[4] H. Bock, W. Seitz, Z. Havlas, J. W. Bats, *Angew. Chem.* **1993**, *105*, 410; *Angew. Chem. Int. Ed. Engl.* **1993**, *32*, 411.

A New Chiral, Cationic β-Amino Alcohol Equivalent: A Variable Approach to Enantiomerically Pure Building Blocks for Hydroxyethylene Isosters

Karsten Danielmeier, Kerstin Schierle, and Eberhard Steckhan*

β-Amino alcohols are structure elements of many important peptidomimetics.[1] Numerous compounds with this subunit were synthesized in the last few years and function as inhibitors of aspartic proteases[2] such as renin[3] and HIV protease.[4] In addition to C_2-symmetric inhibitors developed by Kempf et al.,[5] hydroxyethylene isosters (HDI) have received increasing attention (Scheme 1).[4a]

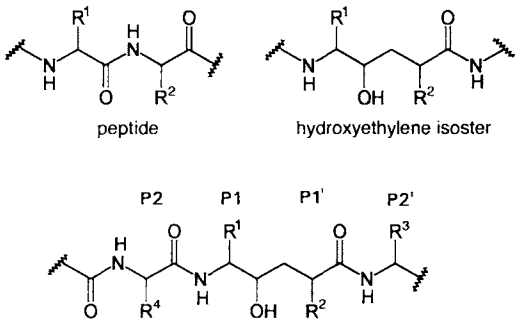

Scheme 1. Peptide and analogous hydroxyethylene isoster (top); P-nomenclature (below).

Since the pioneering work of Szelke et al.[6] a number of approaches to these compounds have been reported.[7] Often the 2,3-epoxypropylamine **1** is used as a key building block.[8, 9] Generally, **1** is synthesized from α-amino acids, for example, via chiral α-amino aldehyde[10] intermediates. The scope of these methods is limited because the substituents in the P1 position of the HDI structure are determined by the amino acid employed.[11] A hydrophobic residue in this P1 position is advantageous for achieving the optimum fit for the active center of the enzyme and thus a high inhibiting effect of the substance.[3a] Therefore, a more variable approach to the key building block that is not limited by the α-substituent of the amino acid remains an important goal. Herein we present an efficient pathway to a variable building block for chiral β-amino alcohols. We show that a variety of hydrophobic residues can be introduced easily in the P1 position of the HDI structure by using a new cationic β-amino alcohol equivalent that is not derived from α-amino acids.[12]

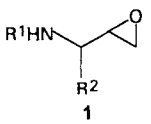

1

Starting from (*S*)-5-chloromethyl-oxazolidin-2-one (**2**),[13a] which is easily accessible from L-malic acid ((*R*)-5-chloromethyl-oxazolidin-2-one is available from D-malic acid), (4*RS*,5*S*)-5-chloromethyl-4-methoxy-oxazolidin-2-one (**3**) can be obtained by direct anodic oxidation in a *trans*/*cis* ratio of 5:1 in 76% yield[13b] (quasi-divided cell; anode: graphite; cathode: Pt wire; current density: 50 mA cm^{-2}; supporting electrolyte: sodium benzene sulfonate (0.1 M); solvent: methanol; $T = -10\,^{\circ}C$; c (**2**) = 2.53 mol L^{-1}). Compound **3** can be synthesized on a 10 g scale and stored at +4 °C without decomposition. This *N*,*O*-acetal is a stable form of an *N*-acyliminium ion that additionally can be further functionalized at the chloromethyl substituent in a variety of ways. Amidoalkylation reactions with **3** through exchange of the methoxy group for different nucleophiles led with high diastereoselectivity to the corresponding *trans*-disubstituted oxazolidinones **4** (Scheme 2, Table 1), which are cyclic carbamates of the desired β-amino alcohols.

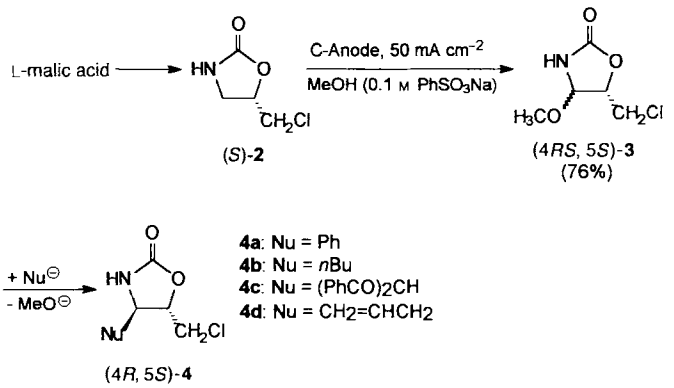

Scheme 2.

Table 1. Nucleophilic exchange reactions with *N*,*O*-acetal **3**.

Nucleophile (Nu)	Lewis acid	Product [e]	Yield [%] [g]	*trans*:*cis*
Ph_3Cu_2Li	$BF_3 \cdot OEt_2$ [a]	**4a** [19]	62	>12:1
nBu_3Cu_2Li	$BF_3 \cdot OEt_2$ [a]	**4b**	59	>20:1
$nBuCu \cdot Me_2S$	$BF_3 \cdot OEt_2$ [b]	**4b**	52	7:1
dibenzoylmethane	TFA [c]	**4c** [f]	47	6:1
allyltrimethylsilane	$TiCl_4$ [d]	**4d**	79	>15:1

[a] According to Zietlow et al. [15a] the cuprate is generated at −50 °C, the Lewis acid and the substrate dissolved in absolute THF are added at −78 °C. [b] According to Wistrand and Skrinjar [17] *n*-butylcuprate is generated from one equiv Cu-Br·Me_2S and one equiv *n*BuLi, then the Lewis acid and the substrate are added. [c] According to Herborn et al. [18], first the nucleophile in dichloromethane is added, then 10 equiv TFA at 0 °C are added, and the solution is stirred for 24 h at room temperature. [d] The substrate is dissolved in dichloromethane, 2 equiv $TiCl_4$ is added at −10 °C, and the solution is treated dropwise with 1.1 equiv allyltrimethylsilane in dichloromethane. After the solution has been warmed to room temperature, it is stirred for 10 h. [e] All products were characterized by ^{13}C NMR (DEPT), ^1H NMR (NOE), IR spectroscopy, MS, high-resolution MS, and CHN analysis. An example is given in ref. [19]. [f] The product is not stable. [g] Except **4c** (*cis*/*trans*-mixture) isolated yields are for pure *trans* products.

After simple purification by column chromatography the *trans* isomers are isolated in enantiomerically pure form (GC). The relative configuration was determined by using NOE difference spectroscopy. Different cuprates, dibenzoyl methane as an example of a CH-acidic nucleophile, and allyltrimethylsilane in a Sakurai reaction[14] have been selected as nucleophiles. The best results for cuprates were obtained by using mixtures of R_3Cu_2Li and $BF_3 \cdot OEt_2$.[15, 16] But the desired products can also be obtained by amidoalkylation with nBuCu·$(H_3C)_2S$/

[*] Prof. Dr. E. Steckhan, Dr. K. Danielmeier,[+] Dipl.-Chem. K. Schierle
Institut für Organische Chemie und Biochemie der Universität
Gerhard-Domagk-Strasse 1, D-53121 Bonn (Germany)
Fax: Int. code +(228)73-5683
e-mail: steckhan@uni-bonn.de

[+] New address:
Bayer AG, Zentrale Forschung
D-51368 Leverkusen (Germany)

[**] This work was supported by the Deutsche Forschungsgemeinschaft (Ste 227/19-1), the Fonds der Chemischen Industrie, and BASF Aktiengesellschaft. K. D. thanks the Fritz-ter-Meer-Stiftung, the Theodor-Laymann-Stiftung, the Heinrich-Hörlein-Stiftung, and the state of Nordrhein-Westfalen for fellowships.

$BF_3 \cdot OEt_2$,[17] although with a lower diastereoselectivity. Remarkably, substitution at the chloro function was not detected in any example. The resulting chiral 5-chloromethyl-oxazolidin-2-ones **4** can be easily converted into the desired chiral 2,3-epoxypropylamines **1**. Using **4a**[19] as an example, the epoxide is obtained spontaneously after ring opening. To achieve this, initially the N-Boc-protected compound **5a** is formed from **4a** with Boc_2O (1 equiv) and catalytic amounts of DMAP (16 mol%) in absolute THF (0.5 h at 0 °C, 10 h at room temperature). The subsequent ring opening by LiOH (5 equiv) in methanol (1 h at room temperature, 10 mL) leads directly to the protected *threo*-(1*R*,2*S*)-1-phenyl-2,3-epoxypropylamine **1a**[20] enantomerically pure in 68% yield (Scheme 3). The enantiomeric purity was established by NMR spectroscopy in the presence of a chiral shift reagent and comparison with racemic **1a**.

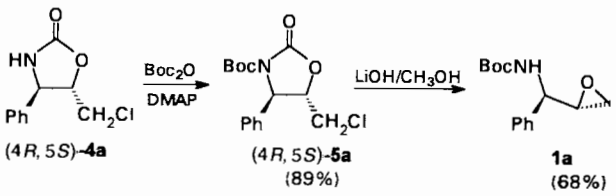

Scheme 3.

The applicability of (4*RS*,5*R*)- and (4*RS*,5*S*)-5-chloromethyl-4-methoxy-oxazolidin-2-one as variable functionalizable chiral, cationic β-amino alcohol equivalent for the generation of interesting target molecules has been demonstrated by the synthesis of 4-substituted, chiral 5-chloromethyl-oxazolidin-2-ones **4** and their easy transformation to epoxides **1**, exemplified by **1a**. The application of the synthesis to other compounds of pharmacological interest like derivatives of β-blockers, and the use of functionalized nucleophiles are currently under investigation.

Received: April 9, 1996 [Z9003IE]
German version: *Angew. Chem.* **1996**, *108*, 2397–2399

Keywords: alkylations · amino alcohols · epoxidations · peptide isosters

[1] a) J. Gante, *Angew. Chem.* **1994**, *106*, 1780–1802; *Angew. Chem. Int. Ed. Engl.* **1994**, *33*, 1699–1721; b) A. Giannis, T. Kolter, *ibid.* **1993**, *105*, 1303–1326 and **1993**, *32*, 1244–1267.

[2] C. U. T. Hellen, H.-G. Kräusslich, E. Wimmer, *Biochemistry* **1989**, *28*, 9881–9890.

[3] a) D. Dhanoa, W. H. Parsons, W. J. Greenlee, A. A. Patchett, *Tetrahedron Lett.* **1992**, *33*, 1725–1728; b) D. V. Patel, K. Rielly-Gauvin, D. E. Ryono, C. A. Free, S. A. Smith, E. W. Petrillo Jr., *J. Med. Chem.* **1993**, *36*, 2431–2447; c) A. M. Doherty, J. S. Kaltenbronn, J. P. Hudspeth, J. P. Repine, W. H. Roark, I. Sircar, F. J. Tinney, C. J. Connolly, J. C. Hodges, M. D. Taylor, B. L. Batley, M. J. Ryan, A. D. Essenburg, S. T. Rapundalo, R. E. Weishaar, C. Humblet, E. A. Lunney, *ibid.* **1991**, *34*, 1258–1271.

[4] a) D. Dorsch, P. Raddatz, C.-J. Schmitges, K. von der Helm, F. Rippmann, *Kontakte (Darmstadt)* **1993**(2), 48–56; b) J. R. Huff, *J. Med. Chem.* **1991**, *34*, 2305–2314; c) M. Lang, J. Roessel, *Arch. Pharm. (Weinheim, Ger.)* **1993**, *326*, 921–924; d) A. Wlodawer, J. W. Ericson, *Ann. Rev. Biochem.* **1993**, *62*, 543–585.

[5] a) D. J. Kempf, L. Codacovi, X. C. Wang, W. E. Kohlbrenner, N. E. Wideburg, A. Saldivar, S. Vasavanonda, K. C. Marsh, P. Bryant, H. L. Sham, B. E. Green, D. A. Betebenner, J. Erickson, D. W. Norbeck, *J. Med. Chem.* **1993**, *36*, 320–330; b) D. J. Kempf, K. C. Marsh, L. Fino, L. Codacovi, P. Bryant, A. Craig-Kennard, H. L. Sham, C. Zhao, S. Vasavanonda, W. E. Kohlbrenner, *Bioorg. Med. Chem.* **1994**, *2*, 847–858.

[6] M. Szelke, D. M. Jones, B. Atarsh, A. Hallet, B. J. Leckie, *Pept. Stud. Funct. Proc. Am. Pept. Symp. 8th* **1983**, 579–582.

[7] a) R. Henning, *Nachr. Chem. Tech. Lab.* **1990**, *38*, 460–464; b) K. E. Harding, M. T. Coleman, L. T. Liu, *Tetrahedron Lett.* **1991**, *32*, 3795–3798; c) D. J. Plata, M. R. Leanna, H. E. Morton, *ibid.* **1991**, *32*, 3623–3626; d) J. V. N. Vara Prasad, D. H. Rich, *ibid.* **1991**, *32*, 5857–5860; e) *ibid.* **1990**, *31*, 1803–1806; f) H. Sasai, W. S. Kim, T. Suzuki, M. Shibasaki, M. Mitsuda, J. Hasegawa, T. Ohashi, *ibid.* **1994**, *35*, 6123–6126.

[8] B. E. Evans, K. E. Rittle, C. F. Hommnick, J. P. Springerm J. Hirshfield, D. F. Veber, *J. Org. Chem.* **1985**, *50*, 4615–4625.

[9] a) J. R. Luly, J. F. Dellaria, J. J. Plattner, J. L. Soderquist, N. Yi, *J. Org. Chem.* **1987**, *52*, 1487–1492; b) P. L. Beaulieu, D. Wernic, J. S. Duceppe, Y. Guidon, *Tetrahedron Lett.* **1995**, *36*, 3317–3320; c) J. S. Ng, C. A. Przybyla, C. Liu, J. C. Yen, F. W. Muellner, C. L. Weyker, *Tetrahedron* **1995**, *51*, 6397–6410; d) J. C. Barrish, E. Gordon, M. Alam, P.-F. Lang, G. S. Bisacchi, P. Chen, P. T. W. Cheng, A. W. Fritz, J. A. Greytok, M. A. Hermsmeier, W. G. Humphreys, K. A. Lis, M. A. Marella, Z. Merchant, T. Mitt, R. A. Morrison, M. T. Obermeier, J. Pluscec, M. Skoog, W. A. Slusarchyk, S. H. Spergel, J. M. Stevenson, C.-Q. Sun, J. E. Sundeen, P. Taunk, J. A. Tino, B. M. Warrack, R. J. Colonno, R. Zahler, *J. Med. Chem.* **1994**, *37*, 1758–1768; e) B. E. Green, X. Chen, D. W. Norbeck, D. J. Kempf, *Synlett* **1995**, 613–614.

[10] a) M. T. Reetz, M. W. Drewes, A. Schmitz, *Angew. Chem.* **1987**, *99*, 1186–1188; *Angew. Chem. Int. Ed. Engl.* **1987**, *26*, 1141–1143; b) M. T. Reetz, *ibid.* **1991**, *103*, 1559–1573 and **1991**, *30*, 1531–1545.

[11] An exception is described by Larchevêque et al.; L. Pégorier, Y. Petit, M. Larchevêque, *J. Chem. Soc. Chem. Commun.* **1994**, 633–634.

[12] Examples of alternative syntheses of chiral amino alcohols and amino alcohol equivalents: a) D. Xu, K. B. Sharpless, *Tetrahedron Lett.* **1993**, *34*, 951–952; b) T. Franz, M. Hein, U. Veith, V. Jäger, E.-M. Peters, K. Peters, H. G. von Schnering, *Angew. Chem.* **1994**, *106*, 1308–1311; *Angew. Chem. Int. Ed. Engl.* **1994**, *33*, 1298–1301; c) T. Ishizuka, S. Ishibuchi, T. Kunieda, *Tetrahedron* **1993**, *49*, 1841–1852; d) G. Li, H.-T. Chang, K. B. Sharpless, *Angew. Chem.* **1996**, *108*, 449–452, *Angew. Chem. Int. Ed. Engl.* **1996**, *35*, 451–454.

[13] a) K. Danielmeier, E. Steckhan, *Tetrahedron: Asymmetry* **1995**, *6*, 1181–1190; b) K. Danielmeier, K. Schierle, E. Steckhan, *Tetrahedron*, **1996**, *52*, 9743–9754.

[14] H. Sakurai, *Pure Appl. Chem.* **1982**, *54*, 1–22.

[15] a) P. Brungs, K. Danielmeier, J. Jakobi, C. Nothhelfer, A. Stahl, A. Zietlow, E. Steckhan, *J. Chim. Phys. Phys. Chim. Biol.* **1996**, *93*, 575–590; b) E. Steckhan, P. Brungs, A. Zietlow, A. Stahl, B. Lewall, G. Kardassis, A. Papadopoulos in *Modern Methodology in Organic Synthesis* (Ed.: T. Shono), Kodansha/VCH, Tokyo, Weinheim, **1992**, pp. 323–337.

[16] Y. Yamamoto, H. Sato, J. Yamada, *Synlett* **1991**, 339–341.

[17] a) M. Skrinjar, L. G. Wistrand, *Tetrahedron Lett.* **1990**, *31*, 1775–1778; b) L. G. Wistrand, M. Skrinjar, *Tetrahedron* **1991**, *47*, 573–582.

[18] C. Herborn, A. Zietlow, E. Steckhan, *Angew. Chem.* **1989**, *101*, 1392–1394; *Angew. Chem. Int. Ed. Engl.* **1989**, *28*, 1399–1401.

[19] Analytical data for (4*R*,5*S*)-**4a**: ^{1}H NMR (200 MHz, $CDCl_3$): $\delta = 7.47-7.22$ (m, 5H), 6.75 (s, 1H), 4.82 (dd, $^3J = 5.3$, 0.3 Hz, 1H), 4.52 (ddd, $^3J = 5.3$, 4.8, 3.8 Hz, 1H), 3.78 (dd, $^2J = 10.0$, $^3J = 4.8$ Hz, 1H), 3.70 (dd, $^2J = 10.0$, $^3J = 3.8$ Hz, 1H); ^{13}C NMR (50.3 MHz, $CDCl_3$): $\delta = 158.6$, 139.1, 129.2, 128.9, 126.1, 82.7, 59.1, 39.2; IR (NaCl): $\tilde{\nu} = 3264$, 3150, 2999, 2947, 1750, 1457, 1237, 1075, 1072, 930, 701 cm^{-1}; MS (70 eV): *m/z* (%): 211 (10), 176 (100), 133 (18), 105 (55), 104 (68), 91 (28), 77 (37); high-resolution MS ($C_{10}H_{10}ClNO_2$): calc. 211.0401, found 211.0399; $[\alpha]_D^{25} = +30$ ($c = 1$ in CH_2Cl_2).

[20] Analytical data for (1*R*,2*S*)-**1a**: ^{1}H NMR (400 MHz, $CDCl_3$): $\delta = 7.45-7.19$ (m, 5H), 4.90 (s, 2H, 2.72 (dd, $^3J = 4.7$, 4.0 Hz, 1H), 2.67 (dd, $^3J = 4.7$, 2.7 Hz, 1H), 1.35 (s, 9H); ^{13}C NMR (100.6 MHz, $CDCl_3$): $\delta = 155.4$, 140.2, 128.8, 127.9, 127.2, 79.9, 53.9, 53.1, 44.3, 28.3; IR (NaCl): $\tilde{\nu} = 3333$, 3040, 2983, 1684, 1528, 1253, 1166, 862, 702 cm^{-1}; MS (70 eV): *m/z* (%): 206 (42), 150 (98), 106 (92), 57 (100); MS (FAB, thioglycerin): *m/z*: 250 ($M^+ + H$), 194, 150; C,H,N analysis ($C_{14}H_{19}NO_3 \cdot H_2O$): calc. C 62.90, H 7.92, N 5.24; found C 63.22, H 7.59, N 5.36.

 © VCH Verlagsgesellschaft mbH, D-69451 Weinheim, 1996 0570-0833/96/3519-2248 $ 15.00+.25/0

The Nature of the Starter Unit for the Rapamycin Polyketide Synthase**

Philip A. S. Lowden, Günter A. Böhm, James Staunton,* and Peter F. Leadlay

Rapamycin, FK 506, and FK 520 are structurally similar macrolide natural products of streptomycetes. Their potent immunosuppressant properties have stimulated great interest in their total synthesis[1] and in the molecular basis for their biological activity.[2] The therapeutic potential of structural analogues has also prompted research into the production of chemically modified rapamycins.[3]

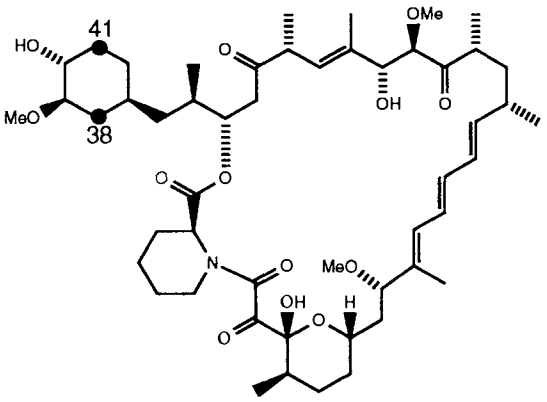

Rapamycin

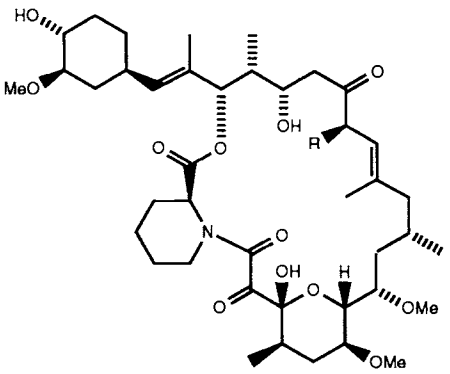

FK 506, R = 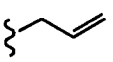

FK 520, R = Et

Biosynthetic experiments have confirmed that rapamycin is a polyketide.[4] Rapid progress has recently been made in the manipulation of complex polyketide biosynthesis to produce unnatural metabolites,[5] so a detailed knowledge of rapamycin biosynthesis at the genetic and enzymological level should provide the means to produce novel rapamycin derivatives by genetic engineering of the biosynthetic enzymes. The complete DNA sequence of the rapamycin polyketide synthase has been established.[6] Like erythromycin[7] the core of rapamycin is assembled by a modular type I polyketide synthase (PKS). In all there are 14 chain extension modules, and these are housed in three giant (M = 660–1070 kDa) multimodular polypeptides. The modules for chain initiation and termination differ markedly from those of the erythromycin PKS. Termination is effected by a specialized multidomain protein (pipecolate incorporating enzyme), which is thought to incorporate a pipecolate unit and then perform macrocyclization.[6] Chain initiation, the subject of the current report, also seems to be carried out differently than for erythromycin. Instead of an acyl transferase domain and an acyl carrier protein domain, which together transfer the starter acid from the thiol of CoA to the active thiol of the first keto–acyl synthase domain, the starter loading module of the rapamycin PKS contains a domain with amino acid sequence similarity to carboxylic acid-CoA ligases (CL), and an adjacent domain with potential for enoyl reductase activity (ER).[6] Further sequencing in our laboratory has recently shown that a putative acyl carrier protein domain lies between the ER and the keto–acyl synthase domain of the first extension module.

The nonstandard character of the starter loading module in the rapamycin PKS reflects the unusual nature of the substituted cyclohexane ring at the start of the polyketide chain in rapamycin, FK 506, and FK 520. Feeding studies with ^{13}C-labeled shikimic acid have shown that this is the source of the carbon atoms of the cyclohexane ring in rapamycin[8] and FK 520,[9] and O-methylation has been shown to occur post-PKS for FK 506.[10] A biosynthetic pathway to the starter unit can be envisaged from shikimic acid (**1**) via dehydration to **2** and reduction via **3** to dihydroxycyclohexanecarboxylic acid (**4**) (Scheme 1), which would be activated as a thioester to initiate polyketide chain extension. This pathway is related to that which has been elucidated for cyclohexanecarboxylic acid in

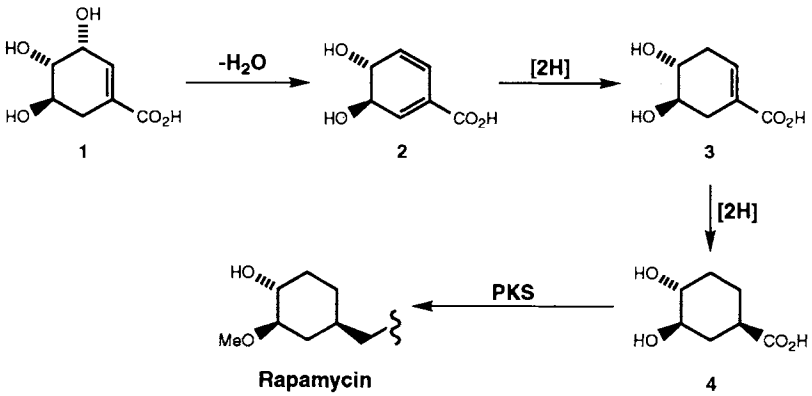

Scheme 1. Proposed pathway from shikimic acid (**1**) to the rapamycin starter unit **4**.

cyclohexyl fatty acids in *Alicyclobacillus acidocaldarius*[11] and in ansatrienin A from *Streptomyces collinus*.[12] The early steps of this pathway have been confirmed for FK 520,[9] but the intermediacy of the saturated dihydroxycyclohexanecarboxylic acid **4** has not been studied until now.

Before undertaking genetic engineering of the rapamycin PKS, we wished to use in vivo studies to confirm the identity of the starter acid for the PKS as **4**. The putative precursor was synthesized with four ^2H labels (**4a**), since incorporation into

[*] Dr. J. Staunton, P. A. S. Lowden, Dr. G. A. Böhm
Department of Chemistry, University of Cambridge
Lensfield Road, Cambridge CB2 1EW (UK)
Fax: Int. code +(1223) 336913
e-mail: js24@cus.cam.ac.uk
Dr. P. F. Leadlay
Department of Biochemistry
University of Cambridge
Tennis Court Road, Cambridge CB2 1QW (UK)

[**] This research was supported by the Wellcome Trust. P.A.S.L. thanks the Engineering and Physical Sciences Research Council for a studentship.

 © VCH Verlagsgesellschaft mbH, D-69451 Weinheim, 1996 0570-0833/96/3519-2249 $ 15.00+.25/0

rapamycin would result in easily identifiable changes in the mass spectrum, and a characteristic ^2H NMR spectrum. The synthesis was modeled on methods developed by Ireland et al. and Corey et al.[13] in synthetic approaches toward FK 506 (Scheme 2).

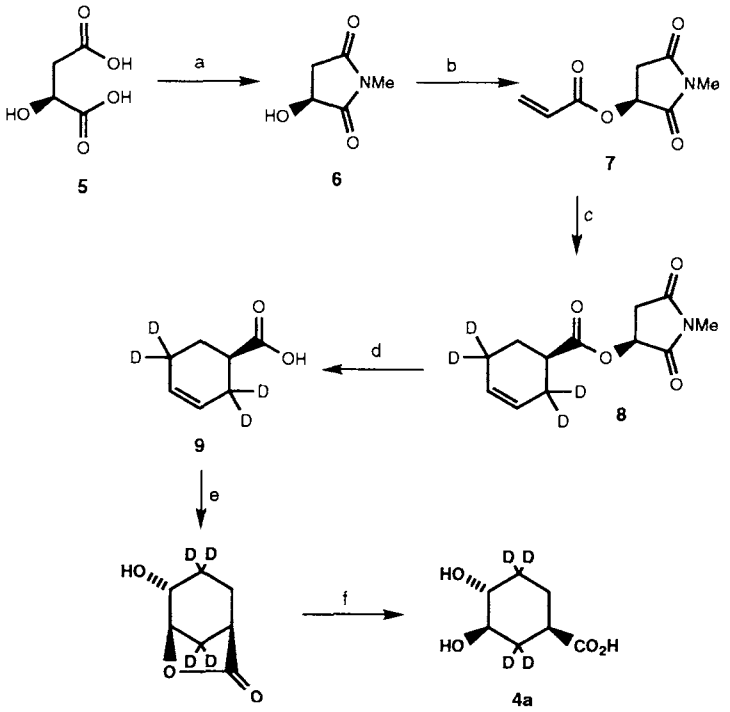

Scheme 2. Synthesis of labeled precursor **4a**. a) 1. $MeNH_2$, 2. Heating in xylene at reflux (55%); b) Et_3N, acryloyl chloride, −30 °C (56%); c) $TiCl_4$, $^2H_4$-butadiene, 0 °C (93%); d) LiOH, H_2O_2 (82%); e) 1. mCPBA, 2. Et_3N, 55 °C (60%); f) KOH, H_2O, THF (100%).

L-Malic acid (**5**) was condensed with methylamine to give imide **6**, which was acylated with acryloyl chloride to give **7**, which acted as a dienophile in a $TiCl_4$-promoted asymmetric Diels–Alder reaction with tetradeuterobutadiene (obtained by thermal decomposition of commercially available butadiene-2,2,5,5-$^2H_4$-sulfone) to afford a single diastereoisomer of Diels–Alder adduct **8**. The chiral auxiliary was removed by treatment with lithium hydroxide and hydrogen peroxide to give labeled (1*R*)-cyclohex-3-enecarboxylic acid (**9**) in 84% *ee*. Hydroxylactonization was achieved by treatment with *meta*-chloroperoxybenzoic acid (mCPBA), then triethylamine, followed by hydrolysis to afford the $^2H_4$-dihydroxycyclohexanecarboxylic acid **4a**.

This acid was fed to a growing culture (1 L) of *Streptomyces hygroscopicus* (ATCC 29253) in two 0.5 mM portions at 24 h and 48 h after inoculation. After a total of four days, the mycelia were collected, extracted with methanol, and the rapamycin (0.01 mM) purified by reverse-phase HPLC. The electrospray mass spectrum of the isolated rapamycin showed peaks at the expected masses for the unlabeled compound at 936.5 Da (Na^+ adduct), and 952.5 Da (K^+ adduct). Associated with each peak was another peak four mass units higher, due to the presence of rapamycin labeled with four deuteriums. These additional peaks were not observed in extracts of unlabeled rapamycin. Accurate mass analysis of the peak at 940.5 Da using fast atom bombardment (FAB) confirmed its derivation from the sodium adduct of tetradeuterorapamycin. Comparison of the peak intensities showed that 44% of the rapamycin was labeled. ^2H NMR analysis of the labeled rapamycin gave a spectrum that could be assigned to rapamycin in which the expected positions were equally enriched with deuterium (Table 1). The combination of the mass spectrometric and NMR evidence establishes the intact incorporation of the labeled precursor into the predicted site. A larger scale (3 L) repeat experiment gave similar results.

Table 1. ^2H NMR data for labeled rapamycin in $CHCl_3$ at 61.4 MHz. Chemical shifts (δ values) are given relative to the TMS signal. The published chemical shifts are of major and minor amide rotamers, respectively. Line widths were $\Delta\delta$ = 0.2–0.4.

Observed δ	Relative intensity	Assignment	Published δ [14]
2.01	2	38-H (eq)	2.10, 2.09
		41-H (eq)	1.99, 1.97
1.26	1	41-H (ax)	1.33, 1.30
0.64	1	38-H (ax)	0.68, 0.64

The high level of incorporation of **4a** into rapamycin demonstrates that it can compete effectively with the endogenous flow of unlabeled precursors. We conclude therefore that the saturated acid **4** is acceptable as a substrate for the CL domain. By comparison with known carboxylic acid-CoA ligases, we believe that it is activated as an acyl-adenylate. Transfer to the thiol of the first keto–acyl synthase domain may occur directly, or it may be mediated by the thiol of the 4′-phosphopantetheine prosthetic group on the nearby putative ACP domain of the PKS (Scheme 3). However, the existence of the putative ER domain next to the ligase suggests that the normal substrate of the PKS may be the unsaturated derivative **3**. This may be reduced prior to activation by the CL, in which case **4** would be the natural substrate for the CL. However, if **3** is activated before reduction, the incorporation of **4** would reflect a relaxed

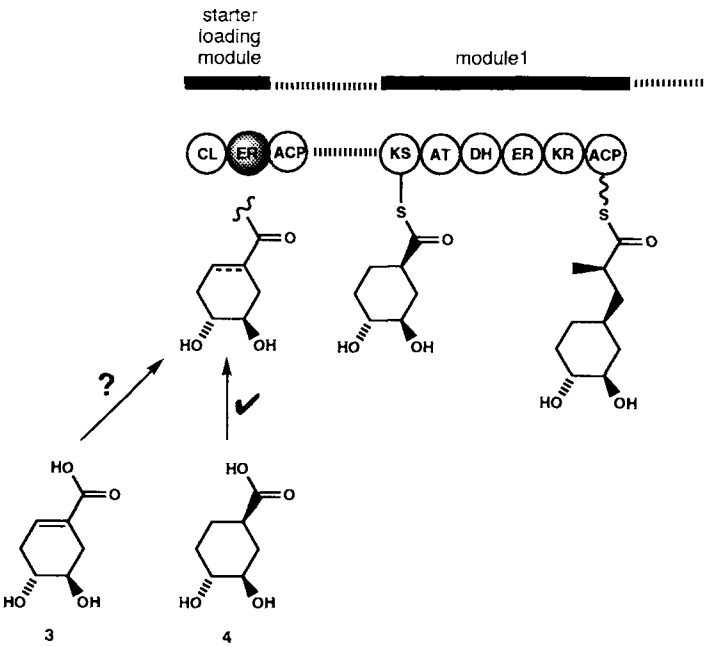

Scheme 3. Relationship of the feeding results to the predicted organization of the rapamycin polyketide synthase (PKS). The N terminus of the first multienzyme polypeptide is shown with the linear arrangement of the predicted catalytically active domains. CL: carboxylic acid ligase, ER: enoyl reductase, ACP: acyl carrier protein, KS: keto–acyl synthase, AT: acyl transferase, DH: dehydratase, KR: ketoreductase.

 © VCH Verlagsgesellschaft mbH, D-69451 Weinheim, 1996 0570-0833/96/3519-2250 $ 15.00+.25/0

specificity in the CL domain, with encouraging implications for the in vivo production of structural analogues of rapamycin differing in the starter unit.

Received: April 15, 1996 [Z9031IE]
German version: *Angew. Chem.* **1996**, *108*, 2395–2397

Keywords: biosyntheses · polyketides · rapamycin

[1] K. C. Nicolaou, A. D. Piscopio, P. Bertinato, T. K. Chakraborty, N. Minowa, K. Koide, *Chem. Eur. J.* **1995**, *1*, 318–333, and references therein; A. B. Smith, S. M. Condon, J. A. McCauley, J. L. Leazer, J. W. Leahy, R. E. Maleczka, *J. Am. Chem. Soc.* **1995**, *117*, 5407–5408.
[2] F. J. Dumont, Q. X. Su, *Life Sci.* **1995**, *58*, 373–395, and references therein.
[3] J. I. Luengo, D. S. Yamashita, D. Dunnington,. A. K. Beck., L. W. Rozamus, H.-K. Yen, M. J. Bossard, M. A. Levy, A. Hand, T. Newman-Tarr, A. Badger, L. Faucette, R. K. Johnson, K. D'Alessio, T. Porter, A. Y. L. Shu, R. Heys, J. Choi, P. Kongsaerce, J. Clardy, D. A. Holt, *Chem. Biol.* **1995**, *2*, 471–481; H. Nishida, T. Sakakibara, F. Aoki, T. Saito, K. Ichikawa, T. Inagaki, Y. Kojima, Y. Yamauchi, L. H. Huang, M. A. Guadliana, T. Kaneko, N. Kojima, *J. Antibiot.* **1995**, *48*, 657–666.
[4] N. L. Paiva, A. L. Demain, M. F. Roberts, *J. Nat. Prods.* **1991**, *54*, 167–177.
[5] S. Donadio, J. B. McAlpine, P. J. Sheldon, M. Jackson, L. Katz, *Proc. Natl. Acad. Sci. USA* **1993**, *90*, 7119–7123; K. E. H. Wiesmann, J. Cortés, M. J. B. Brown, A. L. Cutter, J. Staunton, P. F. Leadlay, *Chem. Biol.* **1995**, *2*, 583–589; C. M. Kao, G. Luo, L. Katz, D. E. Cane, C. Khosla, *J. Am. Chem. Soc.* **1995**, *117*, 9105–9106; R. McDaniel, S. Ebert-Khosla, D. A. Hopwood, C. Khosla, *Nature* **1995**, *375*, 549–554.
[6] T. Schwecke, J. F. Aparicio, I. Molnár, A. König, L. E. Khaw, S. F. Haydock, M. Oliynyk, P. Caffrey, J. Cortés, J. B. Lester, G. A. Böhm, J. Staunton, P. F. Leadlay, *Proc. Natl. Acad. Sci. USA* **1995**, *92*, 7839–7843; J. F. Aparicio, I. Molnár, T. Schwecke, A. König, S. F. Haydock, L. E. Khaw, J. Staunton, P. F. Leadlay, *Gene* **1996**, *169*, 9–16.
[7] J. Cortés, S. F. Haydock, G. A. Roberts, D. J. Bevitt, P. F. Leadlay, *Nature* **1990**, *348*, 176–178; S. Donadio, M. J. Staver, J. B. McAlpine, S. J. Swanson, L. Katz, *Science* **1991**, *252*, 675–679.
[8] N. L. Paiva, M. F. Roberts, A. L. Demain, *J. Ind. Microbiol.* **1993**, *12*, 423–428.
[9] K. W. Wallace, K. A. Reynolds, K. Koch, H. A. I. McArthur, M. S. Brown, R. G. Wax, B. S. Moore, *J. Am. Chem. Soc.* **1994**, *116*, 11600–11601.
[10] A. Shafiee, H. Motamedi, T. Chen, *Eur. J. Biochem.* **1994**, *225*, 755–764.
[11] B. S. Moore, K. Poralla, H. G. Floss, *J. Am. Chem. Soc.* **1993**, *115*, 5267–5274.
[12] B. S. Moore, H. Cho, R. Casati, E. Kennedy, K. A. Reynolds, U. Mocek, J. M. Beale, H. G. Floss, *J. Am. Chem. Soc.* **1993**, *115*, 5254–5266.
[13] R. E. Ireland, T. K. Highsmith, L. D. Gegnas, J. L. Gleason, *J. Org. Chem.* **1992**, *57*, 5071–5073; E. J. Corey, H. Huang, *Tetrahedron Lett.* **1989**, *30*, 5235–5238.
[14] J. B. McAlpine, S. J. Swanson, M. Jackson, D. N. Whittern, *J. Antibiot.* **1991**, *44*, 688–690.

[Rh(7-SPh-8-Me-7,8-$C_2B_9H_{10}$)(PPh_3)$_2$]: A New Rhodacarborane with Enhanced Activity in the Hydrogenation of 1-Alkenes**

Francesc Teixidor, Miquel A. Flores, Clara Viñas,* Raikko Kivekäs, and Reijo Sillanpää

The use of rhodacarboranes as homogeneous catalysts for the hydrogenation and isomerization of alkenes was first reported by Hawthorne and co-workers,[1] and their utility was later extended to other catalytic transformations.[2] A thorough mechanistic study[3] attributed the catalytic activity to the formation of B–Rh^{III}–H species by the oxidative addition of terminal B–H bonds to Rh^{I} centers in *exo-nido*-rhodacarborane derivatives. Besides, the formation of nonactive *closo*-rhodacarborane tautomers and the involvement in the catalytic cycle of B–H–Rh^{I} species attached to the less active "lower belt" of the carborane framework[3] were two reasons proposed to account for the lower activity of some of the catalysts tested (Fig. 1). For these

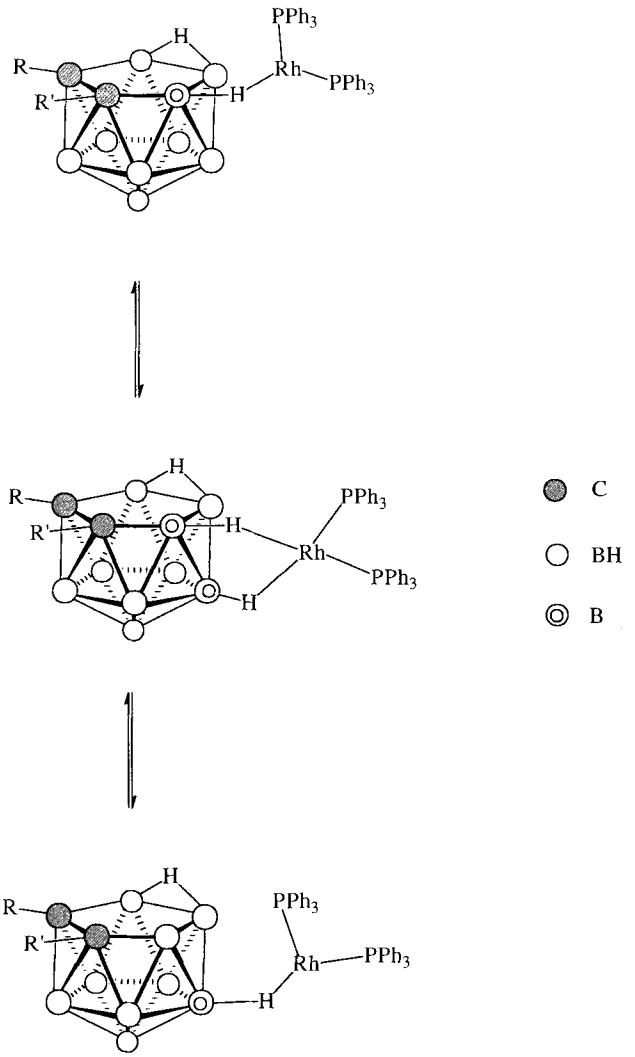

Fig. 1. Simplified description of lower belt (bottom)/upper belt (top) B–H–Rh equilibrium. R and R′ represent arbitrary alkyl or aryl groups.

reasons, two features of *exo*-monothiocarborane ligands (Fig. 2) prompted us to consider the study of their rhodium complexes: 1) the ability of such ligands to form the necessary B–H–M interactions and 2) the presence of the thioether moiety bonded to an open-face carbon atom.[4] The latter would hinder the formation of catalytically undesirable *closo* tautomers[5] and, in addition, would favor the formation of more reactive upper belt B–H–Rh^{I} species. Here we wish to report the synthesis of the first *exo*-monothiocarboranerhodium complex and its enhanced activity in the hydrogenation of 1-hexene.

Attempts to prepare [Rh(7-SPh-8-Me-7,8-$C_2B_9H_{10}$)(PPh_3)$_2$] (**1**) by heating (NMe_4)[7-SPh-8-Me-$C_2B_9H_{10}$] (NMe_4-**2**) and [RhCl(PPh_3)$_3$] at reflux in ethanol were unsuccessful and gave [RhCl(CO)(PPh_3)$_2$] as the main product. Treatment of [RhCl-

[*] Dr. C. Viñas, Dr. F. Teixidor, M. A. Flores
Institut de Ciència de Materials de Barcelona (CSIC)
Campus de la U. A. B., E-08193 Bellaterra (Spain)
Fax: Int. code +(3)5805729
e-mail: clara@icmab.es
Dr. R. Kivekäs
Department of Chemistry, University of Helsinki (Finland)
Dr. R. Sillanpää
Department of Chemistry, University of Turku (Finland)

[**] This work was supported by CIRIT (Project QFN92-4313). We also gratefully acknowledge the Academy of Finland for financial support and the Oskar Öflund Foundation for a grant.

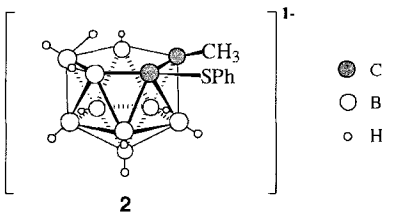

2

Fig. 2. *Exo-nido*-monothiocarborane ligand **2**.

$(PPh_3)_3$] with an ethanolic solution of $AgClO_4$ and subsequent reaction with NMe_4-**2** also had little success. However, reaction of the cesium salt of **2** with Wilkinson's catalyst in toluene/ethanol (8/1) at room temperature[6] resulted in the isolation of **1** as a bright red solid in 91% yield.

The IR spectrum of **1** exhibited an intense absorption at 2527 cm^{-1} characteristic of the B–H stretching of *nido*-carboranes, along with bands associated to PPh_3 and one additional band at 2112 cm^{-1} that could be attributed to B–H–Rh bridges. The $^{11}B\{^1H\}$ NMR spectrum of **1** contained eight resonances in the ratio 1:2:1:1:1:1:1:1. The $^1H\{^{11}B\}$ NMR spectrum displayed a broad resonance centered at $\delta = -4.55$ confirming the existence of B–H–Rh interactions. The remaining carborane protons appeared as a broad resonance between $\delta = 2.3$ and -0.1, and one resonance found at $\delta = -2.69$ was assigned to the B–H–B bridge. A complex series of resonances centered at $\delta = 7.4$, characteristic of phenyl protons, and a singlet at $\delta = 1.48$ assigned to the methyl protons were also observed. Finally, the $^{31}P\{^1H\}$ NMR spectrum revealed only a relatively broad doublet centered at $\delta = 42.8$ ($^1J_{Rh,P} = 176$ Hz). Low temperature (−94 °C) $^{31}P\{^1H\}$ NMR spectra (Fig. 3) exhibited two doublets of doublets centered at $\delta = 41.2$ ($^1J_{Rh,P} = 165$ Hz, $^2J_{P,P} = 40$ Hz) and $\delta = 44.0$ ($^1J_{Rh,P} = 187$ Hz, $^2J_{P,P} = 40$ Hz) characteristic of two *cis* phosphorus atoms. Variable temperature $^1H\{^{11}B\}$ NMR spectra recorded in the range between 25 °C and −94 °C exhibited a small upfield shift of the B–H–Rh resonance from $\delta = -4.55$ to −4.84. The spectroscopic data and elemental analysis are consistent with an *exo-nido*-carborane rhodium complex containing two mutually *cis* PPh_3 ligands. The variable temperature NMR experiments suggest that only one isomer exists in solution, and its PPh_3 ligands exchange readily on the NMR time scale at ambient temperatures. To determine unambiguously the nature of the interaction between the $[Rh(PPh_3)_2]^+$ fragment and the carborane cage, an X-ray crystallographic[7] study was necessary. The simplified drawing of **1** is shown in Figure 4. The carborane cage forms a chelate with the metal through a S–Rh bond and a B(11)–H–Rh bond (B(11) belongs to the cluster's open face). Two PPh_3 ligands complete the coordination sphere of the rhodium center.

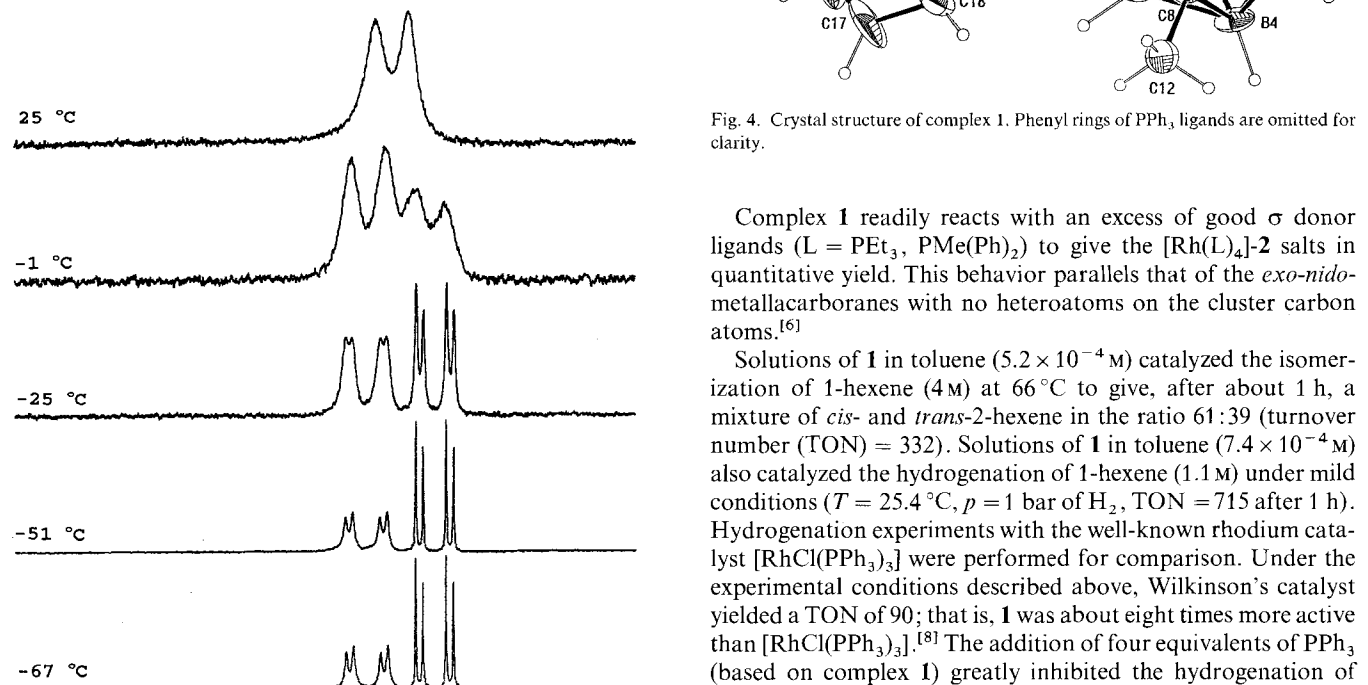

Fig. 3. Variable temperature $^{31}P\{^1H\}$ NMR spectra of complex **1** in CD_2Cl_2.

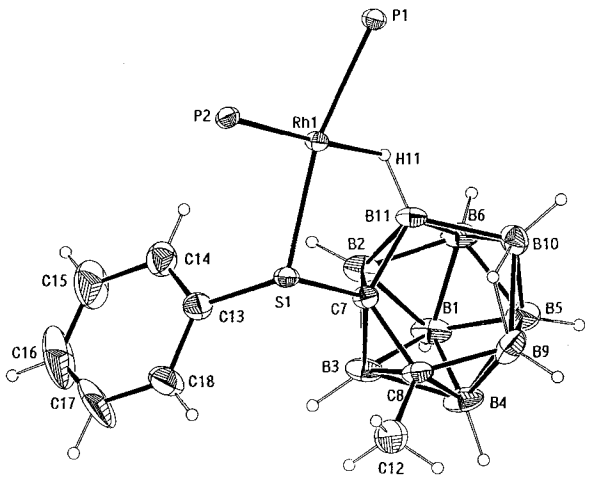

Fig. 4. Crystal structure of complex **1**. Phenyl rings of PPh_3 ligands are omitted for clarity.

Complex **1** readily reacts with an excess of good σ donor ligands (L = PEt_3, $PMe(Ph)_2$) to give the $[Rh(L)_4]$-**2** salts in quantitative yield. This behavior parallels that of the *exo-nido*-metallacarboranes with no heteroatoms on the cluster carbon atoms.[6]

Solutions of **1** in toluene (5.2×10^{-4} M) catalyzed the isomerization of 1-hexene (4 M) at 66 °C to give, after about 1 h, a mixture of *cis*- and *trans*-2-hexene in the ratio 61:39 (turnover number (TON) = 332). Solutions of **1** in toluene (7.4×10^{-4} M) also catalyzed the hydrogenation of 1-hexene (1.1 M) under mild conditions ($T = 25.4$ °C, $p = 1$ bar of H_2, TON = 715 after 1 h). Hydrogenation experiments with the well-known rhodium catalyst $[RhCl(PPh_3)_3]$ were performed for comparison. Under the experimental conditions described above, Wilkinson's catalyst yielded a TON of 90; that is, **1** was about eight times more active than $[RhCl(PPh_3)_3]$.[8] The addition of four equivalents of PPh_3 (based on complex **1**) greatly inhibited the hydrogenation of 1-hexene, which is a common feature in phosphane-containing catalysts. Hydrogenation of internal alkenes (e.g. cyclohexene) with complex **1** proceeded much more slowly than that of terminal ones.

Complex **1** could be recovered quantitatively upon completion of the catalytic reactions as shown by $^1H\{^{11}B\}$, $^{11}B\{^1H\}$, and $^{31}P\{^1H\}$ NMR spectroscopy. Lifetime studies at high pressure in THF ([**1**] = 2.1×10^{-4} M, [1-hexene] = 7.6 M, $p = 45$ bar,

$T = 25\,^{\circ}C$, $t = 3.5$ h) also showed that complex **1** is able to perform more than 36000 turnovers[9] (yield 99.9%) without loss of activity.

In order to rule out the participation in the catalysis of free, solvated $[Rh(PPh_3)_2]^+$ or similar cationic species formed by dissociation of complex **1**, two independent experiments were made. First, the addition of four equivalents of Cs-**2** did not alter the rate of reaction, which suggests that the common ion effect is absent. Second, hydrogenation experiments with added D_2O provided further evidence to eliminate this hypothesis. If $[Rh(PPh_3)_2]^+$ or a related species were present, partially deuterated hexane would be found.[10] By GC-MS analysis it was shown that the hexane formed in the reaction was not deuterium-enriched.

The first *exo*-monothiocarborane rhodium complex has been synthesized, and it catalyzed the hydrogenation of 1-hexene eight times faster than Wilkinson's catalyst. The thioether group directly bonded to the cluster's open face enables discrimination between upper and lower belt B–H groups, leading to the formation of a B(11)–H–Rh bond. This supports the initial hypothesis that the favoring of an *exo-nido* upper-belt form would readily enhance the hydrogenation activity of a rhodacarborane molecule.

Experimental Procedure

1: $[RhCl(PPh_3)_3]$ (203 mg, 0.22 mmol) was added to a solution of Cs[7-SPh-8-Me-7,8-$C_2B_9H_{10}$] (90 mg, 0.23 mmol) in toluene/ethanol (8/1, 28 mL) under N_2 atmosphere. The solution was stirred at room temperature for 18 h until a red precipitate formed. THF was added until the red solid dissolved to give an orange solution and a white precipitate of CsCl, which was removed by filtration through Celite. The orange filtrate was concentrated in vacuo to 5 mL, and ethanol (20 mL) was added. The resulting red solid was isolated by filtration, washed with ethanol (2 × 5 mL) and ether (2 × 5 mL), and dried in vacuo. Yield: 176 mg (91%). If a lower volume of toluene is used in the synthesis, the product precipitates as an orange solid which, upon stirring, is slowly converted into the red crystalline form. IR(KBr): $\tilde{\nu} = 2527$ (s, BH), 2112 cm^{-1} (B–H–Rh); $^1H\{^{11}B\}$ NMR (300 MHz, CD_2Cl_2, 25 °C, TMS): $\delta = 7.66-7.11$ (m, 35H, aryl), 2.3–0.1 (br, BH), 1.48 (s, 3H, CH_3), −2.69 (br, 1H, BHB), −4.55 (br, 1H, BHRh); $^1H\{^{11}B\}$ NMR (300 MHz, CD_2Cl_2, −94 °C, TMS): $\delta = -4.84$ (br, 1H, B–H–Rh); $^{11}B\{^1H\}$ NMR (96.3 MHz, CD_2Cl_2, 25 °C, $Et_2O{\cdot}BF_3$): $\delta = -6.1$(1B), −9.2(2B), −12.2(1B), −16.5(1B), −21.0(1B), −22.9(1B), −27.4(1B), −34.3(1B); $^{31}P\{^1H\}$ NMR (121.5 MHz, CD_2Cl_2, 25 °C, 85% H_3PO_4): $\delta = 42.8$ (br d, $^1J(Rh,P) = 176$ Hz); $^{31}P\{^1H\}$ NMR (121.5 MHz, CD_2Cl_2, −94 C, 85% H_3PO_4): $\delta = 41.2$ (dd, $^1J(Rh,P) = 165$ Hz, $^2J(P,P) = 40$ Hz), 44.0 ($^1J(Rh,P) = 187$ Hz, $^2J(P,P) = 40$ Hz). Elemental analysis for $C_{45}H_{48}B_9P_2SRh$: calcd: C 61.20, H 5.48, S 3.60; found: C 61.15, H 5.44, S 3.07.

Received: July 12, 1996
Revised version: June 11, 1996 [Z8194IE]
German version: *Angew. Chem.* **1996**, *108*, 2388–2391

Keywords: boron compounds · catalysis · hydrogenations · rhodium compounds

[1] T. E. Paxson, M. F. Hawthorne, *J. Am. Chem. Soc.* **1974**, *96*, 4674–4677.
[2] Examples: a) H. C. Kang, M. F. Hawthorne, *Organometallics* **1990**, *9*, 2327–2332. Other catalytic applications of metallacarboranes: b) A. Demonceau, E. Saive, Y. de Froidmont, A. F. Noels, A. J. Hubert, *Tetrahedron Lett.* **1992**, *33*, 2009–2012; c) B. Pirotte, A. Felekidis, M. Fontaine, A. Demonceau, A. F. Noels, J. Delarge, *ibid* **1993**, *34*, 1471–1474.
[3] J. A. Belmont, J. Soto, R. E. King, A. J. Donaldson, J. D. Hewes, M. F. Hawthorne, *J. Am. Chem. Soc.* **1989**, *111*, 7475–7486, and references therein.
[4] a) F. Teixidor, J. Casabó, A. M. Romerosa, C. Viñas, J. Rius, C. Miravitlles, *J. Am Chem. Soc.* **1991**, *113*, 9895–9896; b) F. Teixidor, C. Viñas, J. Casabó, A. M. Romerosa, J. Rius, C. Miravitlles, *Organometallics* **1994**, *13*, 914–919.
[5] R. T. Baker, M. S. Delaney, R. E. King, C. B. Knobler, J. A. Long, T. B. Marder, T. E. Paxson, R. G. Teller, M. F. Hawthorne, *J. Am. Chem. Soc.* **1984**, *106*, 2965–2978.
[6] J. A. Long, T. B. Marder, P. E. Behnken, M. F. Hawthorne, *J. Am. Chem. Soc.* **1984**, *106*, 2979–2989.
[7] Structure analysis of **1** ($C_{45}H_{48}B_9P_2SRh$, $M_r = 883.08$): $0.04 \times 0.22 \times 0.30$ mm^3, orthorhombic, space group *Pbca*, $a = 20.819(5)$, $b = 21.154(4)$, $c = 20.516(4)$ Å, $V = 9035(4)$ $Å^3$, $Z = 8$, $\rho_{calcd} = 1.298$ $g\,cm^{-3}$; data were collected at $T = 294$ K with $Mo_{K\alpha}$ radiation ($\lambda = 0.71069$ Å); scan method $\omega/2\theta$; 7560 independent reflections with $2\theta_{max} = 50°$ were collected, of which 3424 with $|F| > 4\sigma(F)$ were used in the refinement. Lorentzian polarization and absorption corrections were performed [$\mu(Mo_{K\alpha}) = 5.3$ cm^{-1}, empirical ψ scan, $T = 0.84–1.00$]. The structure was solved with the SHELXS86 program and refined with the Xtal3.2 program; 552 parameters. The methyl group was refined as a rigid group with group isotropic U; coordinates of H(B) were refined and the rest of the H atoms at calculated positions [C–H = 0.95, $U(H) = 1.2 \times U$ of the host atom]. The structure was refined against $|F|$ to $R(F) = 0.054$, $wR(F_0) = 0.052$; min. and max. residual electron densities were −0.4 and 0.5 e $Å^{-3}$. Crystallographic data (excluding structure factors) for the structures reported in this paper have been deposited with the Cambridge Crystallographic Data Centre as supplementary publication no. CCDC-179-77. Copies of the data can be obtained free of charge on application to The Director, CCDC, 12 Union Road, Cambridge CB2 1EZ, UK (fax: int. code +(1223) 336-033; e-mail: teched@chemcrys.cam.ac.uk).
[8] Yields represent averaged values for three runs.
[9] This is the TON that we can obtain with the volume of our reactor. However, the real maximum number seems to far exceed this figure.
[10] R. R. Schrock, J. A. Osborn, *J. Am. Chem. Soc.* **1976**, *98*, 2134–2142.

Bimetallic Hydroformylation Catalysis: In Situ Characterization of a Dinuclear Rhodium(II) Dihydrido Complex with the Largest Rh–H NMR Coupling Constant**

Rhonda C. Matthews, Donna K. Howell, Wei-Jun Peng, Spencer G. Train, W. Dale Treleaven, and George G. Stanley*

The ability of two or more metal centers to cooperate in heterogeneous catalytic reactions is quite common and well established.[1] Bi- or polymetallic cooperativity in homogeneous catalysis, however, is much rarer and far less well understood.[2] Perhaps the most dramatic example of bimetallic cooperativity in homogeneous catalysis is the homobimetallic rhodium complex *rac*-$[Rh_2(nbd)_2(et,ph\text{-}P4)](BF_4)_2$ **1** (nbd = norbornadiene; et,ph-P4 = $(Et_2PCH_2CH_2)P(Ph)CH_2P(Ph)CH_2CH_2PEt_2$), which is a precursor for a highly active and regioselective catalyst for the hydroformylation of 1-alkenes.[3, 4] The originally proposed mechanism for this novel catalyst started with the neutral Rh^I carbonyl hydrido bimetallic complex *rac*-$[Rh_2H_2(CO)_2(et,ph\text{-}P4)]$,[3] in direct analogy with monometallic hydroformylation catalysts that have the generic formula $[RhH(CO)(P_2)]$ (P_2 = two monodentate or one chelating bis(phosphane) ligand).[5] Further reaction and spectroscopic studies have demonstrated, however, that the neutral bimetallic complex *rac*-$[Rh_2H_2(CO)_2(et,ph\text{-}P4)]$ is actually a very poor hydroformylation catalyst.[6] We report here the results of in situ spectroscopic studies that demonstrate that the active catalyst is actually the highly unusual dicationic bimetallic Rh^{II} complex *rac*-$[Rh_2H_2(\mu\text{-}CO)_2(CO)_2(et,ph\text{-}P4)](BF_4)_2$.

In situ FT-IR studies were carried out using complex **1** and *rac*-$[Rh_2(CO)_4(et,ph\text{-}P4)](BF_4)_2$ (**2**-$(BF_4)_2$), which generate the

[*] Prof. G. G. Stanley, R. C. Matthews, D. K. Howell, Dr. W.-J. Peng, S. G. Train, Dr. W. D. Treleaven
Department of Chemistry, Louisiana State University
Baton Rouge, LA 70803-1804 (USA)
Fax: Int. code +(504)388-3458
e-mail: george.stanley@chemgate.chem.lsu.edu

[**] This research was supported by the National Science Foundation (predoctoral fellowship for R. C. M; grant CHE-9201051) as well as by the Louisiana Educational Quality Support Fund. We are also grateful to Hoechst Celanese for generous donations of $[Rh(acac)(CO)_2]$, and to Prof. Richard Eisenberg and Dr. Brian Cleary (University of Rochester) for initial assistance in obtaining $^1H\{^{31}P\}$ NMR spectra of **4**.

 © VCH Verlagsgesellschaft mbH, D-69451 Weinheim, 1996 0570-0833/96/3519-2253 $ 15.00+.25/0

same catalytically active species and give identical spectroscopic results (Fig. 1). The FT-IR spectra of **2**-$(BF_4)_2$ under CO (1 bar, 22 °C) is shown in Figure 1a. The $\tilde{\nu}_{CO}$ IR bands for **2**-$(BF_4)_2$ (2058 and 2006 cm^{-1}) compare well to those of other known $[Rh(CO)_2(P_2)]^+$ complexes (P_2 = chelating phosphane).[7] The ^{31}P NMR spectrum of **2**-$(BF_4)_2$ is also consistent with the proposed chelated symmetrical structure.

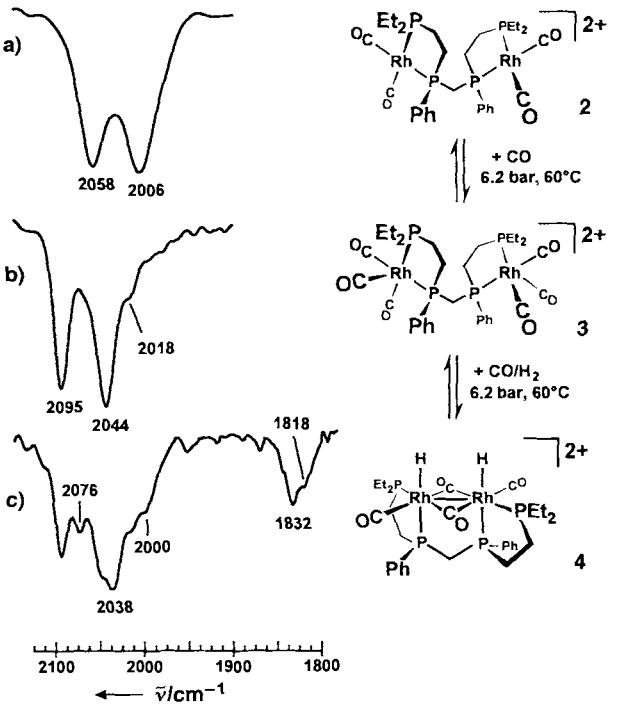

Fig. 1. In situ FT-IR spectra in acetone of a) *rac*-$[Rh_2(CO)_4(et,ph\text{-}P4)]^{2+}$ (**2**) (22 °C, 1 bar CO); b) *rac*-$[Rh_2(CO)_6(et,ph\text{-}P4)]^{2+}$ (**3**) formed when **2** is placed under 6.2 bar of CO at 60 °C; c) **3** under 6.2 bar of H_2/CO at 60 °C. Spectrum c) is a roughly equal mixture of **3** and **4**. There are also several other currently uncharacterized minor components, probably Rh^I and Rh^{III} bimetallic hydrido carbonyl complexes.

The reaction of **2** with excess CO produces the bimetallic hexacarbonyl complex *rac*-$[Rh_2(CO)_6(et,ph\text{-}P4)]^{2+}$ **3** (Fig. 1b). The addition of one additional carbonyl ligand to each rhodium center in the conversion of **2** → **3** leads to the expected shift to higher energies (by 37 cm^{-1}) for the carbonyl bands. Studies with different CO pressures indicate that **3** is stable under about 3.1 bar of CO; lower CO pressures result in CO loss and a shift back to **2**. ^{31}P NMR studies support the proposed symmetrical chelated structure and confirm a very facile equilibrium between **2** and **3** that is dependent on CO pressure.

Placing **2** under H_2/CO (4.1–13.8 bar, 20–90 °C) generates a new equilibrium mixture that contains the hexacarbonyl bimetallic complex **3** and several new hydrido species as indicated by ^1H, ^{31}P NMR, and FT-IR spectroscopy. D_2/CO studies demonstrate that all major IR bands in the region between 2200 and 1700 cm^{-1} (Fig. 1c) are due to carbonyl ligands; Rh-H/D bands are either very weak or not present. Most notable in the FT-IR spectrum is the presence of relatively intense bridging CO bands at 1832 and 1818 cm^{-1}.[8]

The in situ ^1H and $^{31}P\{^1H\}$ NMR spectra of **1** and **2**-$(BF_4)_2$ under H_2/CO (13.8 bar) at 22 °C clearly demonstrate that mainly complex **3** (92%) is present; in addition there are at least four metal carbonyl hydrido complexes, two of which are in dynamic exchange and have broad ^1H (δ = −9.8, −11.6) and ^{31}P resonances (δ = 66, 74), while the other two have relatively static (slow exchange) and well-defined ^1H NMR peaks (δ = −9.0, (dq), −18.5 (pseudo-decet). On increasing the temperature, the hydrido complex with the signal at δ = −9.0 becomes dominant (≈ 80% of the observable hydrido complexes at 90 °C) and has a simple ^{31}P and ^1H NMR spectrum, indicating a symmetrical bimetallic structure. The region of the ^1H NMR spectrum in which the hydride hydrogen atoms for this complex appear is given in Figure 2a. The ^1H and ^{31}P NMR, as well as the IR spectra do not change (apart from that the concentration of alkene decreases and that of the aldehyde product increases) on addition of 1-hexene and initiation of hydroformylation catalysis, indicating that the rate-determining step is the loss of CO and/or addition of alkene to the catalyst.

We propose the dicationic complex *rac*-$[Rh_2H_2(\mu\text{-}CO)_2(CO)_2(et,ph\text{-}P4)]^{2+}$ **4** as the active catalyst. This is an 18-electron Rh^{II} complex with a Rh–Rh bond and an edge-sharing bioctahedral structure. While there are many examples of dinuclear Rh^{II} compounds with a metal–metal bond,[9] edge-sharing bioctahedral structures are extremely rare. Theoretical studies have predicted that d^7–d^7 bioctahedral dimers with acceptor bridging ligands should have a M–M bond.[10]

The two dinuclear Rh^{II} complexes most closely related to **4** are $[Rh_2(\mu\text{-}CO)(\mu\text{-}Cl)Cl_2(dppm)_2(MeOH)]^+$ (dppm = bis(diphenylphosphano)methane), which has been structurally characterized and needs one additional terminal ligand to achieve a full edge-sharing bioctahedral coordination geometry,[11] and $[Rh_2H_2(\mu\text{-}H)_2(tripod)_2]$ (tripod = $MeC(CH_2PPh_2)_3$) that has been proposed to have a full edge-sharing bioctahedral structure, but for which there is scant spectroscopic or structural data.[12] There are also several examples of Rh^{II} complexes with one or three bridging hydrido ligands.[13] $[Rh_2(\mu\text{-}H)_3(H)(PR_3)_4]$ (R = O*i*Pr, *i*Pr) complexes have also been characterized, but both have been assigned as mixed-valent Rh^I/Rh^{III} compounds.[14] However, none of these Rh^{II} hydrido complexes have been demonstrated to be highly efficient hydroformylation catalysts like **4**.

The hydride coupling constants for the doublet of pseudo-quartets (Fig. 2a) have been determined by ^{31}P-decoupled ^1H NMR spectroscopy (Fig. 2b). The large coupling constant

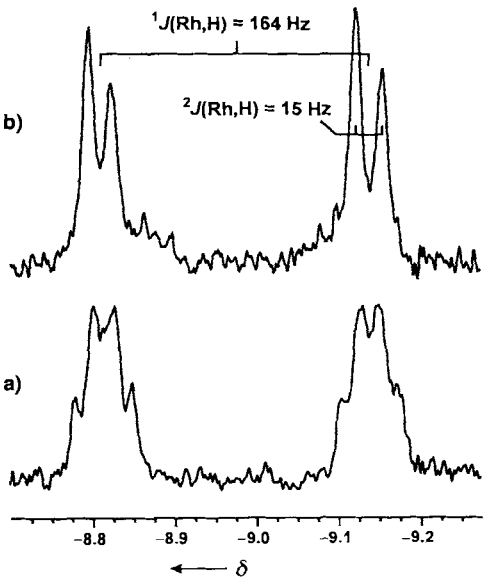

Fig. 2. a) Hydrido region of the in situ 500 MHz ^1H NMR spectrum of **4** (13.8 bar H_2/CO, 22 °C); b) broadband phosphorus-decoupled $^1H\{^{31}P\}$ NMR spectrum of **4** under the same conditions.

 © VCH Verlagsgesellschaft mbH, D-69451 Weinheim, 1996 0570-0833/96/3519-2254 $ 15.00+.25/0

of 164 Hz is *not* caused by *trans* ^2J(P,H) coupling, as seen in virtually all other H-Rh^{I}Rh^{III}-P complexes, but rather, is due to ^1J(Rh,H) coupling![15] There are hundreds of rhodium hydrido complexes known and their ^1J(Rh,H) coupling constants are typically small and vary from almost 0 to 50.8 Hz.[16] The ^1J(Rh,H) coupling constant of **4** (164 Hz), therefore, is by far the largest value ever seen. Large ^1J(Rh,H) coupling constants may be a distinctive feature of bimetallic Rh^{II} complexes with terminal hydrido ligands, though further examples are clearly needed to confirm this idea.

The pseudo-quartet arises from roughly equal *cis*- and *trans*-^2J(P,H) as well as ^2J(Rh,H) coupling constants of about 15 Hz. While *cis*-^2J(P,H) and ^2J(Rh,H) coupling values of 15 Hz are reasonable, this value might appear to be too small for a *trans*-^2J(P,H) coupling constant. This is an important point for elucidatng the exact structure of **4**. While there can be little doubt about the overall symmetric geometry, or the arrangement of the phosphane and bridging carbonyl ligands, the exact placement of the terminal carbonyl and hydrido ligands can be questioned. The essentially equal ^2J(P,H) coupling constants could, therefore, indicate that the hydrido ligand should be *cis* to both of the phosphane groups, placing the terminal carbonyl ligand *trans* to the internal phosphane group of the et,ph-P4 ligand (**4***).

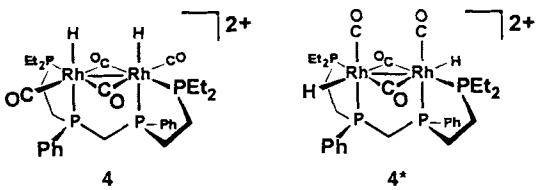

4 **4***

A number of arguments provide strong support for the proposed structure of **4**. While *trans*-^2J(P,H) coupling constants in Rh^{I}Rh^{III} complexes are virtually always large,[17] the extraordinarily strong ^1J(Rh,H) coupling present in this dinuclear Rh^{II} hydrido complex could be attenuating the normal *trans*-^2J(P,H) interaction. In normal lantern-type dinuclear Rh^{II} compounds (e.g., $[Rh_2(O_2CR)_4]$) the ligands in axial sites *trans* to the Rh–Rh single bond are relatively labile.[9] When this D_{4h}-symmetric structure is transformed to an edge-sharing bioctahedral structure, the labile character of the axial ligands seems to be retained. In both $[Rh_2(\mu\text{-CO})(\mu\text{-Cl})Cl_2(dppm)_2(MeOH)]^+$ and $[Rh_2(\mu\text{-H})(\mu\text{-Cl})Cl_3(dppm)_2]$ one of these "axial" sites is empty.[11a, 13a] In our structural assignment for **4** we are placing the more labile CO ligands in these more weakly binding "axial" sites. It is unlikely that strongly binding hydrido ligands would occupy these positions.

Further evidence for the proposed structure of **4** comes from nuclear Overhauser effect (NOE) ^{1}H NMR experiments. Molecular modeling studies on **4** indicate that the *ortho*-hydrogen atoms on the phenyl ring are 4.4 to 5.1 Å from the hydrido ligand; for **4*** they are considerably closer (2.3–3.0 Å). The NOE ^{1}H NMR experiments on the catalyst solution demonstrate only a weak interaction between the hydrido ligands ($\delta = -9.0$) and the *ortho*-hydrogen atoms, which fits well with the expected contact distance of 4.4–5.1 Å. Finally, we know that **4** readily reductively eliminates H_2, but this should be more difficult for **4*** where one has a *trans*-like separation of the hydrido ligands.

The dicationic charge and the Rh^{II} oxidation state offer an excellent explanation for the remarkable hydroformylation activity and regioselectivity of **4**. There are no other examples of active and highly regioselective monometallic hydroformylation catalysts that have mainly alkylated, strongly donating phosphane ligands (like et,ph-P4). The reason for this is well understood. The presence of two electron-donating alkylated phosphane ligands increases the electron density on the rhodium center leading to increased π-backdonation and stronger Rh–CO bonding. This stabilizes the unreactive five-coordinate 18-electron complexes $[RhH(CO)_2(P_2)]$ and $[Rh(acyl)(CO)_2(P_2)]$ (P_2 = two monodentate or one chelating bisphosphane). Facile CO (or phosphane) dissociation is needed to generate the reactive four-coordinate 16-electron complexes needed to allow coordination of alkene or H_2 to start and/or to finish the hydroformylation catalytic cycle. The fact that **4** is a dication and the rhodium centers are in the +II oxidation state compensates for the strongly donating et,ph-P4 ligand. This makes the terminal CO ligands labile enough to allow good catalytic activity.

The high aldehyde regioselectivity of this catalyst (linear:branched = 28:1 for 1-hexene)[3] is a result of the rigid dinuclear structure of **4** and the favorable steric effects at the et,ph-P4 ligand. When an alkene coordinates to a typical monometallic square-planar rhodium hydroformylation catalyst, the other ligands bend away to form a trigonal bipyramid (or square pyramid), which is the least congested coordination geometry. This geometric reorganization results from electronic orbital rehybridization on the metal center and causes the steric directing groups on the phosphane ligands to swing away from the incoming alkene substrate. This, in turn, reduces the steric effectiveness of the phosphane ligand for orienting the alkene to insert properly into the Rh–H bond to give the desired linear alkyl intermediate species.

The catalyst **4**, however, cannot be distorted in this way on alkene coordination because the Rh–Rh bond and bridging carbonyl ligands prevent any significant movement of the ligand environment away from the alkene. Minimizing the geometric reorganization about the rhodium center maximizes the steric effect of the et,ph-P4 ligand, directing the alkene insertion into the M–H bond to form a linear alkyl group, which goes on to form the linear aldehyde. In agreement with our original proposed mechanism,[3] we still believe that an intramolecular hydride transfer plays a key role at the end of the catalytic cycle to reductively eliminate the aldehyde product and regenerate the Rh^{I} bimetallic complex **3** (or **2**).

Experimental Procedure

All synthetic procedures were carried out under an inert atmosphere with Schlenk techniques or glove boxes. FT-IR spectra were recorded on a Perkin-Elmer 1760 instrument using GRAMS/386 data collection and processing software (Galactic Software), and the NMR spectra were collected on Bruker ARX-300 or AMX-500 instruments.

2-$(BF_4)_2$: $HBF_4 \cdot OEt_2$ (0.81 g, 5.0 mmol) was added to a solution of $[Rh(acac)(CO)_2]$ (1.29 g, 5.0 mmol; acac = acetyl acetonate) in CH_2Cl_2 (30 mL) and stirred. Then *rac*-et,ph-P4 (1.16 g, 2.5 mmol in 5 mL of CH_2Cl_2) was added, which led to a red solution. The volume was reduced to about 10 mL by vacuum evaporation. CO gas was then bubbled through the solution for 5 min. The concentrated solution was then added dropwise to diethyl ether (100 mL) and stirred. The resulting red solution and precipitate were cooled to −32 °C, which afforded a red powder. Yield: 2.1 g, 90%. IR (acetone, 1 bar of CO): $\tilde{\nu}_{CO}$ = 2058 (vs), 2006 (vs) cm^{-1}; $^{31}P\{^1H\}$ NMR (124 MHz, [D$_6$]acetone, 1 bar CO, H_3PO_4): δ = 69.9 (dd, ^1J(Rh,P) = 112, ^2J(P,P) = 25 Hz, terminal P atoms), 53.5 (dd, ^1J(Rh,P) = 127, ^2J(P,P) = 25 Hz, internal P atoms). Anal. calcd for $C_{29}H_{40}P_4Rh_2B_2F_8O_4$ (M_r = 955.95): C 36.43, H 4.22; found: C 36.51, H 4.22.

3-$(BF_4)_2$: IR (acetone, 6.2 bar CO, 60 °C): $\tilde{\nu}_{CO}$ = 2095 (vs), 2044 (vs) cm^{-1}; $^{31}P\{^1H\}$ NMR (124 MHz, CD_2Cl_2, 6.9–13.8 bar CO, 22 °C, H_3PO_4): δ = 70.2 (dd, ^1J(Rh,P) = 107, ^2J(P,P) = 26.5 Hz, terminal P atoms), 59.2 (d, ^1J(Rh,P) = 117.8 Hz, internal P atoms).

4-$(BF_4)_2$: IR (acetone, 6.2 bar H_2/CO, 60 °C): $\tilde{\nu}_{CO}$ = 2095 (s), 2076 (m), 2044 (sh), 2038 (vs), 2018 (sh), 2000 (sh), 1832 (m), 1818 (m) cm^{-1}; ^{1}H NMR (500 MHz, CD_2Cl_2, 6.9–13.8 bar H_2/CO, 22 °C, TMS): δ = −9.0 (dq, ^1J(Rh,H) = 164, ^2J(Rh,H) = 15, ^2J(P,H) = 15 Hz); $^{31}P\{^1H\}$ NMR (124 MHz, CD_2Cl_2, 13.8 bar H_2/

 © VCH Verlagsgesellschaft mbH, D-69451 Weinheim, 1996 0570-0833/96/3519-2255 $ 15.00+.25/0

CO, 22 °C, H_3PO_4): $\delta = 72.5$ (d, $^1J(Rh,P) = 158$ Hz, terminal P atoms), 60.8 (d, $^1J(Rh,P) = 158$ Hz, internal P atoms).

In situ FT-IR studies: A SpectraTech external sample bench was attached to the spectrometer equipped with a SpectraTech circle reaction cell (CRC) using a ZnSe crystal rod. Instrument parameters: 25 scans, resolution 4 cm^{-1}, scan speed 1.0 $cm\,s^{-1}$, scan range 4000–800 cm^{-1} (for data collection range narrowed to 2500–1400 cm^{-1}). Under these conditions we get an energy reading of 18000 to 20000 counts through the empty CRC cell; concentration of the catalyst precursor (**1** or **2**): 30–40 mM (in acetone).

In situ NMR studies: A high-pressure 5 mm NMR tube (Wilmad model 524-PV-6) with a Teflon valve was used for studying the catalyst solutions. The threads of valve were wrapped with Teflon tape to make better seals and minimize the chance of the valve being blown out of the tube. Due to the small gas volume in the NMR tube, the slow gas diffusion and reaction, and the high concentration (30–120 mM) of catalyst precursor present (**1** or **2**), the tube was shaken reasonably vigorously for at least 30–60 minutes while the tube was open to the H_2/CO gas mixture. Compound **1** is only moderately soluble in acetone giving a maximum concentration at room temperature of ≈30–40 mM; **1** is very soluble in CD_2Cl_2 giving a maximum concentration of ≈ 140 mM, but there is a considerably lower equilibrium concentration of the catalytically active complex **4** present in this solvent at room temperature.

Received: June 4, 1996 [Z9192IE]
German version: *Angew. Chem.* **1996**, *108*, 2402–2405

Keywords: cooperativity · homogenous catalysis · hydroformylations · rhodium compounds

[1] a) G. A. Somorjai, *Prog. Surf. Sci.* **1995**, *50*, 3; b) S. M. George, *Chem. Rev.* **1995**, *95*, 475; c) D. F. Shriver, *J. Cluster Sci.* **1992**, *3*, 459; d) G. A. Somorjai, *Perspect. Catal.* **1992**, 147; e) B. Walther, *Z. Chem.* **1989**, *29*, 117; f) P. J. Denny, D. A. Whan, *Catalysis (London)* **1978**, *2*, 46.

[2] a) R. D. Adams, T. S. Barnard, Z. Li, W. Wu, J. Yamamoto, *J. Am. Chem. Soc.* **1994**, *116*, 9103; b) A. Tsubouchi, T. C. Bruice, *ibid.* **1994**, *116*, 11614; c) N. Zhang, C. M. Mann, P. A. Shapley, *ibid.* **1988**, *110*, 6591; d) J. P. Collman, J. A. Belmont, J. I. Brauman, *ibid.* **1983**, *105*, 7288; e) M. J. Don, M. G. Richman, *J. Mol. Catal.* **1992**, *73*, 181; f) M. Hidai, A. Fukuoka, Y. Koyasu, Y. Uchida, *ibid.* **1986**, *35*, 29; g) G. Suss-Fink, G. Herrmann, *J. Chem. Soc. Chem. Commun.* **1985**, 735.

[3] M. E. Broussard, B. Juma, S. G. Train, W. J. Peng, S. A. Laneman, G. G. Stanley, *Science* **1993**, *260*, 1784.

[4] G. Süss-Fink, *Angew. Chem.* **1994**, *106*, 71; *Angew. Chem. Int. Ed. Engl.* **1994**, *33*, 67.

[5] a) B. Cornils in *New Syntheses with Carbon Monoxide* (Ed.: J. Falbe), Springer, Berlin, **1980**, p. 1; b) I. Tkatchenko in *Comprehensive Organometallic Chemistry, Vol. 8* (Eds.: G. Wilkinson, F. G. A. Stone, E. W. Abel), Pergamon, Oxford, **1982**, p. 101; c) G. G. Stanley in *Encyclopedia of Inorganic Chemistry, Vol. 2* (Ed.: R. B. King), Wiley, London, **1994**, p. 575.

[6] W. J. Peng, F. R. Fronczek, G. G. Stanley, *Chem. Commun.* submitted.

[7] a) P. Albano, M. Aresta, *J. Organomet. Chem.* **1980**, *190*, 243; b) D. P. Fairlie, B. Bosnich, *Organometallics* **1988**, *7*, 946; c) S. H. Bergens, D. P. Fairlie, B. Bosnich, *ibid.* **1990**, *9*, 566; d) A. Del Zotto, L. Costella, A. Mezzetti, P. Rigo, *J. Organomet. Chem.* **1991**, *414*, 109.

[8] We have collected other FT-IR spectra that more clearly show the splitting of the band for the bridging CO molecule.

[9] F. A. Cotton, R. A. Walton, *Multiple Bonds Between Metal Atoms*, Oxford, New York, **1993**, p. 431–501, and references therein.

[10] S. Shaik, R. Hoffmann, C. R. Fisel, R. H. Summerville, *J. Am. Chem. Soc.* **1980**, *102*, 4555.

[11] a) F. A. Cotton, C. T. Eagle, A. C. Price, *Inorg. Chem.* **1988**, *27*, 4362; b) L. J. Tortorelli, P. W. Tinsley, C. Woods, C. J. Janke, *Polyhedron* **1988**, *7*, 315; c) C. Woods, L. J. Tortorelli, *ibid.* **1988**, *7*, 1751.

[12] C. Bianchini, A. Meli, F. Laschi, J. A. Ramirez, P. Zanello, A. Vacca, *Inorg. Chem.* **1988**, *27*, 4429.

[13] a) B. R. Sutherland, M. Cowie, *Inorg. Chem.* **1984**, *23*, 1290; b) C. Bianchini, F. Laschi, D. Masi, C. Mealli, A. Meli, F. M. Ottaviani, D. M. Proserpio, M. Sabat, P. Zanello, *ibid.* **1989**, *28*, 2552; c) S. L. Schiavo, G. Bruno, F. Nicolo, P. Piraino, F. Faraone, *Organometallics* **1985**, *4*, 2091.

[14] a) A. J. Sivak, E. L. Muetterties, *J. Am. Chem. Soc.* **1979**, *101*, 4878; b) D. L. Thorn, J. A. Ibers, *Adv. Chem. Ser.* **1982**, *196*, 117.

[15] This coupling has been confirmed at a variety of different ^1H NMR frequencies (250, 300, 400, and 500 MHz), different temperatures (− 20 to +60 °C), and by both broadband and selective ^{31}P decoupling experiments. We have not, as yet, been able to perform a ^{103}Rh-decoupled ^1H NMR experiment.

[16] H. Werner, M. Baum, D. Schneider, B. Windmuller, *Organometallics* **1994**, *13*, 1089.

[17] Rhodium hydridophosphite ($P(OR)_3$) complexes can have lower *trans* $^2J(P,H)$ coupling constants: R. R. Burch, E. L. Muetterties, A. J. Schultz, E. G. Gebert, J. M. Williams, *J. Am. Chem. Soc.* **1981**, *103*, 5517.

Proximate, Synperiplanar Diazene/Diazene Substrates: N=N/N=NO and ON=N/N=NO Photometathesis Reactions**

Kai Exner, Dirk Hochstrate, Manfred Keller, Frank-Gerrit Klärner, and Horst Prinzbach*

Dedicated to Professor Michael Hanack on the occasion of his 65th birthday

Studies of transannular π,π-interactions in neutral systems[1] (through-space vs. through-bond conjugation, σ-homoaromaticity, [2 + 2] photocycloaddition) as well as in four-center–three-electron (4c/3e) radical cations and 4c/2e dications[2] have greatly profited from homoconjugated bichromophores with the rigid skeleton **A**: At nearly synperiplanar orientation of the chromophores—benzo/ene, benzo/benzo,[3] ene/diazene,[4–6] benzo/diazene[7, 8]—the transannular distance *d* and interorbital angle ω were gradually modified. Investigations with bisdiazenes of this type (**A**, X = N) are scarce for the simple reason that such substrates are hardly accessible.[9–11] For the [2 + 2] photocycloaddition, particularly under stereoelectronic (*d*, ω) and energetic aspects ($\Delta\Delta H_f^\circ$), calculations (Table 1)[12]

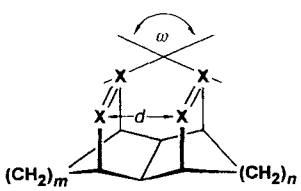

A

Table 1. Calculated geometric [a] and energetic [a,b] data for bisdiazenes (dienes) of type **A** [X = N (CH)].

	$A_{2,2}$	$A_{1,2}$	$A_{1,1}$
d [Å]	2.93 (2.89)	2.87 (2.83)	2.83 (2.79)
ω [°]	166.3 (167.6)	171.5 (172.3)	176.4 (176.5)
$\Delta\Delta H_f^\circ$	108 (− 13.7)	88 (− 22.2)	70 (− 29.5)

[a] Data for X = N calculated by AM1, for X = CH by MM2. [b] Reaction enthalpies for the [2 + 2] cycloadditions [kcal mol^{-1}].

make the homologs with $m = n = 1$ ($A_{1,1}$) the "first choice", followed by those with $m = 1$, $n = 2$ ($A_{1,2}$) and $m = n = 2$ ($A_{2,2}$). This assessment, however, holds only if N_2 elimination, particularly in the diazabicyclo[2.2.1]heptene (DBH) subunit

DBH

$\Phi(-N_2) = 1.00$
$\lambda(\varepsilon) = 341$ nm (420)
IP = 8.96 eV

DBO

$\Phi(-N_2) = 0.02$
$\lambda(\varepsilon) = 378$ nm (187)
IP = 8.32 eV

[*] Prof. Dr. H. Prinzbach, Dipl.-Chem. K. Exner, Dr. M. Keller
Chemisches Laboratorium der Universität
Institut für Organische Chemie und Biochemie
Albertstrasse 21, D-79104 Freiburg (Germany)
Fax: Int. code +(761)203-5987

Prof. Dr. F.-G. Klärner, Dr. D. Hochstrate
Institut für Organische Chemie der Universität–Gesamthochschule
Universitätsstrasse 5, D-45117 Essen (Germany)
Fax: Int. code +(201)183-3082

[**] Photochemical Transformations, Part 80. This work was supported by the Deutsche Forschungsgemeinschaft, the Fonds der Chemischen Industrie, and the BASF AG. K. E. thanks the Studienstiftung des deutschen Volkes for a stipend and Dr. N. Bahr for stimulating discussions. We thank Prof. Dr. G. Seitz for generous support [16], Dr. D. Hunkler for NMR, and Dr. J. Wörth for MS measurements. Part 79: ref. [3a].

(cf. diazabicyclo[2.2.2]octene (DBO)[13]), does not proceed much faster than the cycloaddition.[14] Indeed, for some $\mathbf{A}_{1,1}$-, $\mathbf{A}_{1,2}$-, and $\mathbf{A}_{2,2}$-ene/diazene and -benzo/diazene systems, [2+2] cycloaddition dominates.[6, 8]

So far, only $\mathbf{A}_{2,2}$-bisdiazenes ("third choice") were available for studies.[9] Herein we present the synthesis, X-ray structural data, and photochemical results on $\mathbf{A}_{1,2}$-bisdiazenes ("second choice").[15]

The synthesis (Scheme 1) starts with the cycloaddition of tetramethyl-4*H*-pyrazole (**1**)[4] and a mixture of 2,5-dimethoxy-2,5-dihydrofurans (**2**). After attempts to perform the reaction at temperatures up to 150 °C by using microwave irradiation

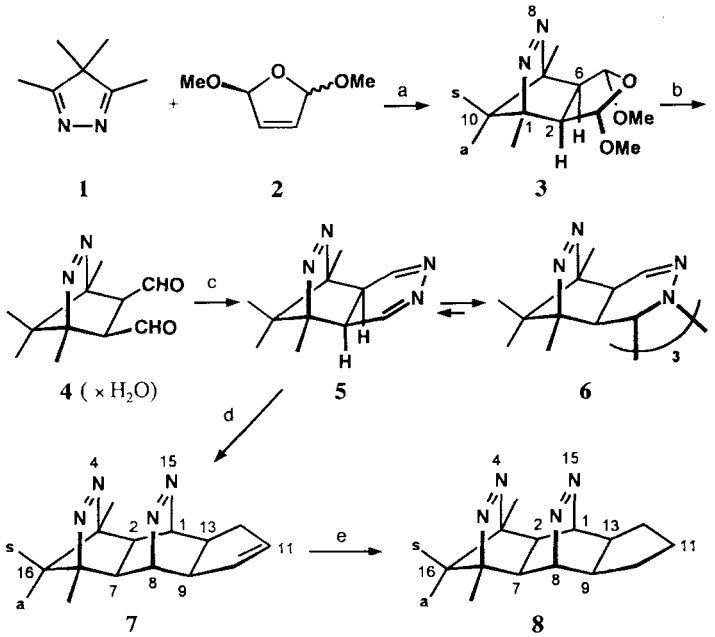

Scheme 1. a) 10 kbar, 110 °C, 3 d, 74%; b) 0.22% H_2SO_4, reflux, 10 min; c) extraction with CH_2Cl_2, K_2CO_3, N_2H_4 anhydrous (10 equiv), 95–98%; d) cyclopentadiene, CH_2Cl_2, CF_3COOH (1.0 equiv based on **5**), 4 °C, 18 h, 48–52% based on **3**; e) MeOH, Pd/C (10%), 1 atm H_2, 90%.

(700 W, 3 min, decomposition) and by standard activation with trifluoroacetic acid (TFA) or lithium perchlorate had failed (decomposition of **2**),[16] high pressure was applied (10.0 kbar, 115 °C, 3 d, toluene, strict absence of any acid traces).[17] The C_s-symmetric *1*:*1* adduct **3** was obtained as the single product (*trans*-**2** was not converted) in 74% yield (gram scale) after chromatographic workup [m.p. 94 °C; λ_{max} (ε) (CH_3CN) = 197 (1335), 358 nm (195); *endo* addition confirmed by NOE experiments]. After acid-catalyzed hydrolysis of **3** in aqueous solution, the dialdehyde **4** was treated (without isolation) with hydrazine to provide the dihydropyridazine **5** nearly quantitatively in the form of its trimer **6** (stereoisomers, ^{1}H NMR).[4, 5] From the acid-catalyzed addition of cyclopentadiene[4] to **5**, only (TLC, ^{1}H NMR) the desired *exo*-1:1 adduct **7** was secured [48–52% based on **3**; yellowish plates, m.p. 273 °C (decomp.); NOEs between 16-Me_a/2-H/7-H and 2-H/7-H/9-H/13-H; λ_{max}(ε) (CH_3CN) = 213 (3140), 233 (1785), 367 nm (433)]. Catalytic hydrogenation of the C–C double bond in **7** gave **8** together with hydrazines **9** and **11** (see Scheme 2); after reoxidation of the latter (by bubbling air through the solution in the presence of a palladium catalyst) **8** was isolated by chromatography in 90% yield.[15] The n → π* band for **7** and **8** at about 370 nm can be considered as a superposition of the [2.2.1]/[2.2.2] absorp-

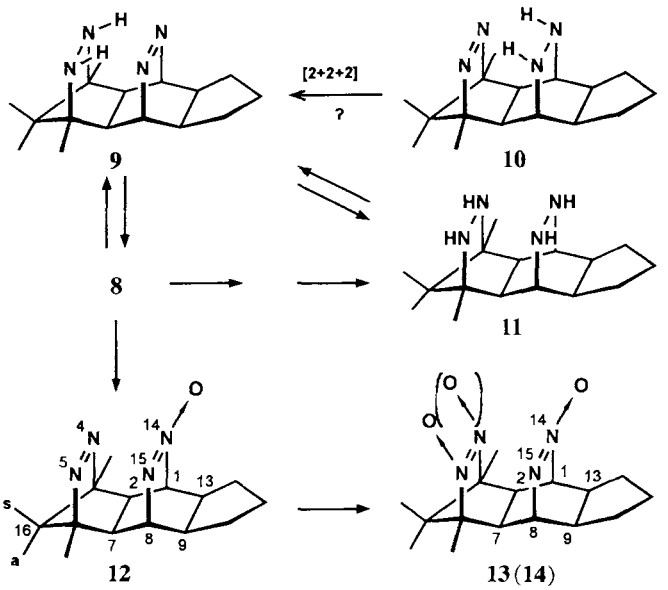

Scheme 2. Reactions with **8**.

tions at 358 and 384 nm. The bisdiazenes **7** and **8** remained unaltered in boiling benzene for a longer period of time (5–7 h). The catalytic hydrogenation of **8** to the bishydrazine **11** (Pt, MeOH, 1 atm H_2, room temperature) presumably started with the more strained N4–N5 double bond to give **9** as the sole detectable monohydrazine; dehydrogenation of **11** upon exposure to air occurred faster at the NH14–NH15 unit to produce **9** as an intermediate on the way to **8** (there is interest in **10** as a substrate for the as yet unknown dyotropic HNNH/N=N hydrogen transfer). Dimethyl dioxirane (DMDO, CH_2Cl_2, room temperature) neatly differentiated the two N–N double bonds of **8** to give only (TLC, ^{1}H NMR) the N14-oxide **12** [colorless crystals, m.p. 265 °C (decomp.); 94%]. The distinction from the N4-oxide is primarily based on the influence of the N–O bond on the 1-H(C) chemical shifts (e.g. $\delta_{C-1/C-8}$ = 64.2 in **8** and 74.0/58.1 in **12**); the 16s(16a)-CH_3 shifts (δ = 0.47 (0.83)) are only slightly influenced; the mass spectrum [chemical ionization (CI) with NH_3] exhibits a relatively intensive peak for the pyrazole **1**. In the UV spectrum (CH_3CN) the distinct N=NO(π,π*) maximum at 246 nm [ε = 3580; n,π*: 367 nm (370)] suggests a transannular N=N/N=NO interaction (cf. the maximum at 230 nm for an "undisturbed" [2.2.2]-N=NO chromophore, like that of DBO oxide[18, 19]).[20] Further oxidation of **12** with DMDO led to the dioxides *anti*-**13** and *syn*-**14** as a nonseparable mixture (ca. 3.9:1) [colorless crystals, λ_{max}(ε) (CH_3CN) = 228 nm (9920)]. Their differentiation on the basis of the spectral data is not unequivocal, and rests on analogy[7, 9] and on the typically divergent photochemical behavior.

Crystals of **8** suitable for X-ray analysis were obtained by diffusion of ether vapor into a solution of **8** in $CHCl_3$.[21] The four N atoms form a plane with a N_2/N_2 distance (*d*) of 2.822 Å and an interorbital angle (ω) of 174.2° (Fig. 1). The cyclopentane unit is disordered. The nonbonding distances given in Figure 1 as well as model considerations and AM1 calculations[22] suggest a considerable buttressing effect by the methyl groups (16s-, 16a-CH_3) and, to a minor extent, by the cyclopentane hydrogen atoms, which forces the N–N double bonds closer together. The transannular distance and interorbital angle are indeed "better" than that for the $\mathbf{A}_{2,2}$ analogue (2.88/2.82 Å, 168.6°).[7]

 © VCH Verlagsgesellschaft mbH, D-69451 Weinheim, 1996 0570-0833/96/3519-2257 $ 15.00+.25/0

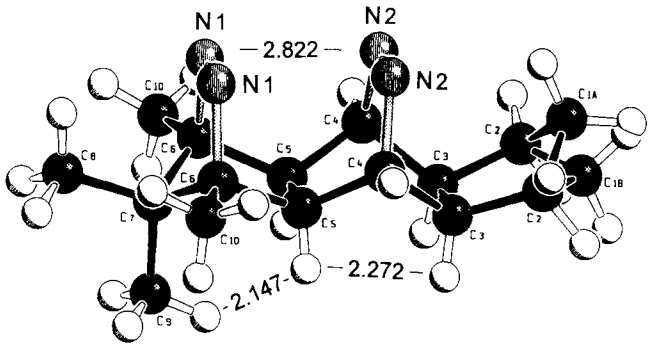

Fig. 1. Crystal structure of **8** (the numbering does not correspond to IUPAC-nomenclature).

When **8** was exposed to various direct irradiation conditions between −78 °C and +30 °C (254 nm, Rayonet RUL 2537, daylight, $CHCl_3$, MeOH, or CH_3CN) only N_2 extrusion could be detected.[22] Analogous direct, monochromatic irradiation of monoxide **12** (254 nm, CH_3CN or MeOH) again caused, yet not exclusively, denitrogenation (Scheme 3): After about 75% conversion the product mixture contained, besides oligomeric material, **16** (49%), **18** (7%), possibly traces of **19**, and the metathesis isomer **17** (2–4%), which was characterized after enrichment by preparative TLC; the more flexible "open" skeleton of **17** [λ_{max} = 238 (π,π^*, NNO), 343 nm (n,π^*, NN)] is distinguished from that of **12** ($J_{1,2(7,8)} < 1.5$ Hz) for example by the $^1H,^1H$ coupling constants (**17**: $J_{4,15\ (10,14)} = 6.5-7.5$ Hz) and by the lack of peaks for [4 + 2] cycloreversion fragments in the mass spectrum.

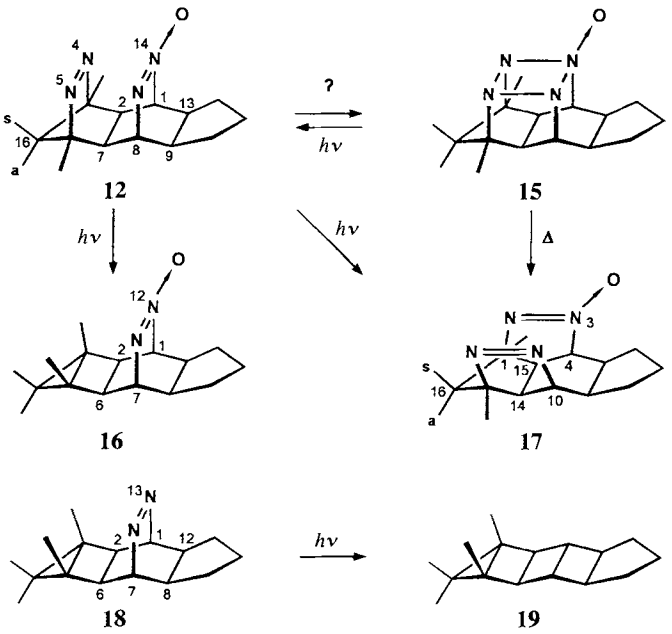

Scheme 3. Reaction products of the monochromatic irradiation of **12**.

The picture changed significantly with the dioxides *anti*-**13**/*syn*-**14** (mixture) in that standard direct, monochromatic irradiation (254 nm, MeOH) gave rise to notable discrepancy in the rate of conversion and a high degree of metathesis; after about 50% conversion of *anti*-**13**—only 3% of *syn*-**14** was consumed—based on the conversion, 29–31% of the metathetical dioxide **21** and 1–2% of its isomer **22** (of unclear origin[23]) were present, together with other trace components and oligomeric material (in control experiments **21** was slowly decomposed) (Scheme 4). The UV spectra of **13** and **21** (purified by HPLC) are very similar; there are, as for the pair **12** and **17**, typical differences in the NMR and MS spectra (e.g. $J_{1,13} = J_{8,9} = 1.6$ Hz, $J_{1,2} = J_{7,8} = 1.6$ Hz vs. $J_{4,5} = J_{4,15} = 6.4$ Hz, $J_{9,10} = J_{10,14} = 6.3$ Hz; low-field shift of the CH_{3s}-C16 signal from $\delta = 0.74$ (**13**) to 1.43 (**21**); no retro [4 + 2] fragmentation pattern). When several experiments were carefully monitored between −78 °C and room temperature, no [2+2] photocycloadduct (**20**) nor any intermediate such as the [6+6] photocycloadduct could be seen.

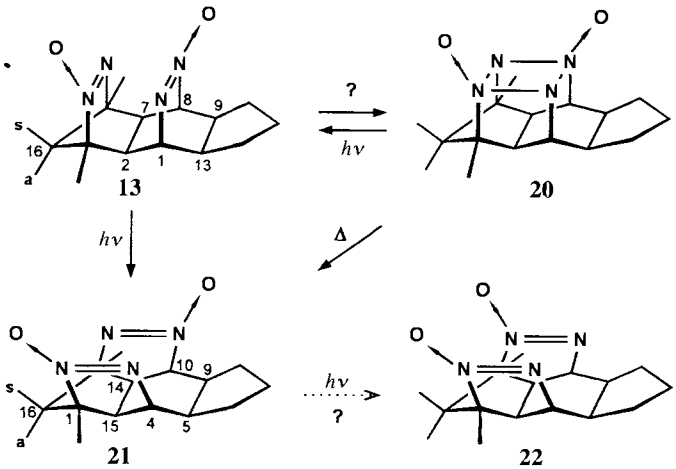

Scheme 4. Reaction products of the monochromatic irradiation of **13**.

To conclude, in **8** (and **7**) the stereoelectronic and energetic prerequisites for a diazene/diazene [2+2] photocycloaddition are better than ever; nevertheless, denitrogenation remained the exclusive stabilization pathway. N-oxidation favors cycloaddition but has its price in product complexity and thermal lability of the resulting intermediate tetraazetidine oxides.[19, 24] Whether the latter can be directly observed or even isolated in low-temperature matrix experiments is currently under investigation. Doubts are justified whether the stereoelectronic advantages (Table 1) ascribed to "first choice" $\mathbf{A}_{1,1}$ skeletons—as nicely documented in the homologous benzo/benzo series **A** (X=X = C_6H_4[3])—will strongly favor N=N/N=N photocycloaddition over N_2 elimination.

Received: June 14, 1996 [Z 9022 IE]
German version: *Angew. Chem.* **1996**, *108*, 2399–2402

Keywords: cycloadditions · diazenes · metathesis · photochemistry · polycycles

[1] H.-D. Martin, B. Mayer, *Angew. Chem.* **1983**, *95*, 281; *Angew. Chem. Int. Ed. Engl.* **1983**, *22*, 283; J. J. Wolff, *ibid.* **1995**, *107*, 2409 and **1995**, *34*, 2225, and references therein.

[2] H. Prinzbach, G. Gescheidt, H.-D. Martin, R. Herges, J. Heinze, G. K. Surya Prakash, G. A. Olah, *Pure Appl. Chem.* **1995**, *67*, 673, and references therein.

[3] a) T. Mathew, M. Keller, D. Hunkler, H. Prinzbach, *Tetrahedron Lett.* **1996**, *37*, 4491; b) H. Prinzbach, G. Sedelmeier, C. Krüger, R. Goddard, H.-D. Martin, R. Gleiter, *Angew. Chem.* **1978**, *90*, 297; *Angew. Chem. Int. Ed. Engl.* **1978**, *17*, 271; G. Sedelmeier, W.-D. Fessner, C. Grund, P. R. Spurr, H. Fritz, H. Prinzbach, *Tetrahedron Lett.* **1986**, *27*, 1277.

[4] W. Berning, S. Hünig, *Angew. Chem.* **1977**, *89*, 825; *Angew. Chem. Int. Ed. Engl.* **1977**, *16*, 777; S. Hünig, P. Kraft, *J. Prakt. Chem.* **1990**, *332*, 133; S. Hünig, P. Kraft, F.-G. Klärner, U. Artschwager-Perl, K. Peters, H.-G. von Schnering, *Liebigs Ann.* **1995**, 351, and references therein.

[5] S. F. Nelsen, M. R. Willi, *J. Org. Chem.* **1984**, *49*, 1, and references therein; J. Kettenring, D. Ginsburg, *Tetrahedron* **1984**, *40*, 5269; G. Fischer, D. Hunkler, H. Prinzbach, G. Rihs, H. Fritz, *Tetrahedron Lett.* **1984**, *25*, 2459; W. Marterer, H. Prinzbach, G. Rihs, J. Wirz, J. Lecoultre, E. Heilbronner, *Helv. Chim. Acta* **1988**, *71*, 1937; for "orthogonal" azo/enes see: K.-H. Lehr, R. Hildebrand, H. Fritz, L. Knothe, C. Krüger, H. Prinzbach, *Chem. Ber.* **1982**, *115*, 1875.

[6] L. A. Paquette, R. V. C. Carr, P. Charumilind, J. F. Blount, *J. Org. Chem.* **1980**, *45*, 4922; K. Beck, S. Hünig, *Chem. Ber.* **1987**, *120*, 477; B. Albert, W. Berning, C. Burschka, S. Hünig, F. Prokschy, *ibid.* **1984**, *117*, 1465.

[7] G. Fischer, E. Beckmann, H. Prinzbach, G. Rihs, J. Wirz, *Tetrahedron Lett.* **1986**, *27*, 1273.

[8] K. Beck, S. Hünig, *Angew. Chem.* **1986**, *98*, 193; *Angew. Chem. Int. Ed. Engl.* **1986**, *25*, 187.

[9] H. Prinzbach, G. Fischer, G. Rihs, G. Sedelmeier, E. Heilbronner, Z. Yang, *Tetrahedron Lett.* **1982**, *22*, 1251; E. Beckmann, N. Bahr, H. Prinzbach, *ibid.* **1990**, *31*, 1125; N. Bahr, E. Beckmann, K. Mathauer, D. Hunkler, M. Keller, H. Prinzbach, H. Vahrenkamp, *Chem. Ber.* **1993**, *126*, 429.

[10] J. M. Mellor, N. M. Smith, *J. Chem. Res. Synop.* **1985**, 60; J. M. Mellor, R. Pathirana, N. M. Smith, *J. Chem. Soc. Perkin Trans. 1* **1988**, 2501.

[11] G. Ritter, G. Häfelinger, E. Lüddecke, H. Rau, *J. Am. Chem. Soc.* **1989**, *111*, 4627; E. Tauer, K.-H. Grellmann, A. Heinrich, *Chem. Ber.* **1991**, *124*, 2053.

[12] AM1: M. J. S. Dewar, E. G. Zoebisch, E. F. Healy, J. J. P. Stewart, *J. Am. Chem. Soc.* **1985**, *107*, 3902; MM2: N. L. Allinger, H. C. Flanagan, *J. Comput. Chem.* **1983**, *4*, 399. For AM1 calculations MOPAC 6.0 was used.

[13] P. S. Engel, *Chem. Rev.* **1980**, *80*, 99; M. A. Anderson, C. B. Grissom, *J. Am. Chem. Soc.* **1995**, *117*, 5041, and references therein.

[14] W. Adam, O. De Lucci, *Angew. Chem.* **1980**, *92*, 815; *Angew. Chem. Int. Ed. Engl.* **1980**, *19*, 762; W. Adam, G. Fragale, D. Klapstein, W. M. Nau, J. Wirz, *J. Am. Chem. Soc.* **1995**, *117*, 12578.

[15] The new compounds have been fully characterized (^{1}H and ^{13}C NMR, IR, UV, MS). **8**: yellowish plates; m.p.: 266 °C (decomp.); R_f ($CHCl_3$/MeOH 10/1) = 0.48; ^{1}H NMR (400 MHz, $CDCl_3$): δ = 5.20 (s, 2 H, 1-H, 8-H), 2.20 (m, 2 H, 9-H, 13-H), 1.96 (s, 2 H, 2-H, 7-H), 1.73 (m, 2 H, 10a-H, 12a-H), 1.60 (s, 6 H, 3-Me, 6-Me), 1.33 (m, 3 H, 10s-H, 11a-H, 12a-H), 1.14 (m, 1 H, 11s-H), 0.78 (s, 3 H, 16a-Me), 0.39 (s, 3 H, 16s-Me); ^{13}C NMR (100.6 MHz, $CDCl_3$): δ = 88.4 (C-3, C-6), 64.2 (C-1, C-8), 59.7 (C-16), 45.2 (C-9, C-13), 39.8 (C-2, C-7), 29.8 (C-10, C-12), 26.2 (C-11), 17.1 (16a-Me), 15.4 (16s-Me), 11.4 (3-Me, 6-Me); IR (KBr): $\tilde{\nu}$ = 2958, 2867, 1445, 1282 cm^{-1}; UV (CH_3CN): $\lambda_{max}(\varepsilon)$ = 212 (1500), 234 (1580), 368 nm (435); MS (CI, NH_3, 170 eV): *m/z* (%): 397 (4) $[M+1+H]^+$, 290 (19) $[M+NH_4]^+$, 273 (100) $[M+H]^+$, 245 (59) $[M-N_2+H]^+$, 125 (93) $[1+H]^+$; elemental analysis: $C_{16}H_{24}N_4$, calc: C 70.55, H 8.88, N 20.57; found: C 70.54, H 8.79, N 20.47; **21**: R_f ($CHCl_3$/MeOH 10/1) = 0.59; ^{1}H NMR (400 MHz, CD_3CN): δ = 4.71 (dd, J(4,5) = J(4,15) = 6.4 Hz, 1 H, 4-H*), 4.33 (dd, J(9,10) = J(10,14) = 6.3 Hz, 1 H, 10-H*), 2.87–2.78 (m, 2 H, 14-H, 15-H), 2.70–2.61 (m, 1 H, 6s-H*), 2.58–2.49 (m, 1 H, 5-H*), 2.44–2.35 (m, 1 H, 9-H*), 2.00 (m, 4 H), 1.48–1.36 (m, 1 H), 1.43 (s, 3 H, 16s-Me), 1.39 (s, 3 H, 13-Me*), 1.20 (s, 3 H, 1-Me*); ^{13}C NMR (100.6 MHz, CD_3CN): δ = 78.7 (C-4*), 65.4 (C-10*), 45.3/45.1 (C-5/C-9), 37.8/37.7 (C-14/C-15), 30.9/28.3/26.8 (C-6/C-7/C-8), 24.3 (16s-Me), 17.4/17.0/16.98 (16a-Me/1-Me/13-Me); IR (KBr): $\tilde{\nu}$ = 2978, 2940, 2862, 1509 (NNO), 1499 (NNO), 1367, 1263, 1073 cm^{-1}; UV (CH_3CN): λ_{max} (ε) = 225 nm (11570); MS (CI, isobutane, 170 eV): *m/z* (%): 305 (100) $[M+H]^+$, 289 (21) $[M+H-O]^+$, 261 (8) $[M+H-N_2O]^+$. Assignment of ^{1}H and ^{13}C NMR signals is based on NOE, ^{1}H/^{1}H COSY, and selective ^{1}H/^{13}C decoupling experiments. Assignments marked by * may be interchanged as a whole set.

[16] In analogy the more reactive 4,4-dimethoxy-3,5-bistrifluoromethyl-4*H*-pyrazole (C. Gerninghaus, A. Kümmel, G. Seitz, *Chem. Ber.* **1993**, *126*, 733) underwent addition with *cis*-**2** in boiling chlorobenzene (ca. 30% yield); however, neat hydrolysis of the adduct to the corresponding dialdehyde could not be effected. Cf. N. Bahr, Dissertation, University of Freiburg, **1994**.

[17] The high-pressure experiments were performed in a 14 kbar apparatus containing a 100 mL autoclave (A. Hofer, Mülheim/Ruhr, Germany). The reaction mixture was sealed in a PTFE tube pretreated with Et_3N. The Diels–Alder reaction of **1** with **2** is accelerated by high pressure to an extent comparable to the acceleration of the reaction of **1** with norbornadiene (130.1 °C: $\Delta V^{\neq}$ = −41 cm^{3}mol^{-1}); cf. K. Beck, S. Hünig, F.-G. Klärner, P. Kraft, U. Artschwager-Perl, *Chem. Ber.* **1987**, *120*, 2041.

[18] J. P. Snyder, V. T. Bandurco, F. Darack, H. Olsen, *J. Am. Chem. Soc.* **1974**, *96*, 5158.

[19] G. Fischer, Dissertation, University of Freiburg, **1987**.

[20] One of the remarkable chemical consequences of the special N=N/N=N arrangement in **8** is the stability of the 1,2,4,5-perhydrotetrazine formed after twofold methylation of **11** and base treatment in the presence of oxygen.

[21] Crystal data for **8**: Monoclinic system, space group $P2_1/m$, unit cell dimensions a = 6.1041(4), b = 10.8204(8), c = 11.4023(8) Å, β = 98.052(3)°, V = 745.68(9) Å^3, Z = 2, ρ_{calc} = 1.213 Mg m^{-3}, crystal dimensions 0.22 × 0.20 × 0.10 mm, θ range 3.92–72.93°, λ = 1.54178 Å, collected reflections 1652, independent reflections 1576, no absorption correction, full-matrix least-squares refinement on F^2, 1573 data, 156 parameters, final indices ($I > 2\sigma(I)$): R = 0.0503, R_w^2 = 0.1691. Of the two conformers **8A** and **8B** (4:1), the minor one (**B**) shows an enhanced isotropic displacement parameter U(eq, **8B**)/U(eq, **8A**) = 1.8; according to AM1 calculations **8B** corresponds to a plateau on the potential energy surface lying 0.2 kcal mol^{-1} above **8A**. Further details of the crystal structure investigation may be obtained from the Fachinformationszentrum Karlsruhe, D-76344 Eggenstein-Leopoldshafen (Germany), on quoting the depository number CSD-404417.

[22] K. Exner, Dissertation, University of Freiburg.

[23] A. Albini, M. Alpegiani, *Chem. Rev.* **1984**, *84*, 43.

[24] Compare the rapid fragmentation of oxidized 1,2-diazetidines [5] and 1,2,3-triaziridines: W. Marterer, O. Klingler, R. Thiergardt, E. Beckmann, H. Fritz, H. Prinzbach, *Chem. Ber.* **1991**, *124*, 621.

Stereoselective Synthesis of Steroids with the Heck Reaction**

Lutz F. Tietze,* Thomas Nöbel, and Maurus Spescha

Dedicated to Professor Michael Hanack on the occasion of his 65th birthday

Steroids present an attractive synthetic goal because of their biological activity and pharmacological applications. Despite the large number of known synthetic methods,[1] there is a continuous demand for new approaches that are short, generally applicable, and allow access to compounds with novel structures like **1b**. We now describe a new strategy based on the synthesis of the B-ring of the steroid structure by a double Heck reaction[2] between (*Z*)-(2-bromoethenyl)bromobenzene (**2b**) and the hexahydro-1*H*-indene derivative **3**,[3] which can be synthesized in a few steps from the ketone **4**[4] by an intramolecular Pd-catalyzed rearrangement of an allyl formate.[3] With this procedure the otherwise difficult *trans*-annelation of **3** is achieved in a stereoselective way.

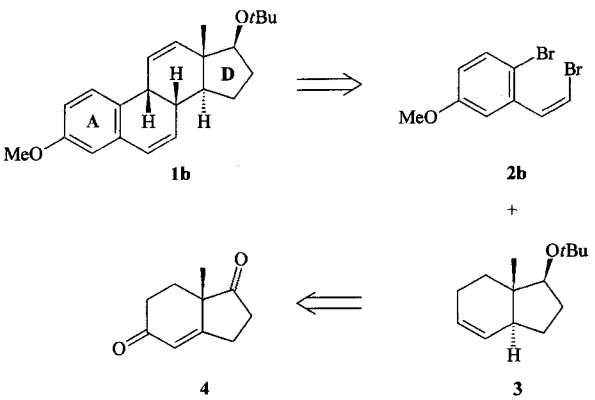

Scheme 1. Retrosynthesis of **1b**.

Our initial investigations of the Heck reaction of **3** with iodobenzene (**5a**) using a catalytic amount of Pd^0 revealed that the bond formation at C-4 in **3** proceeds with high regio- and stereoselectivity in *anti*-position to the angular methyl group (Scheme 2).[5] Thus, the 4-phenyl derivatives **6a** and **7a** were

[*] Prof. Dr. L. F. Tietze, Dipl.-Chem. T. Nöbel, Dr. M. Spescha
Institut für Organische Chemie der Universität
Tammannstrasse 2, D-37077 Göttingen (Germany)
Fax: Int. code +(551) 39-9476

[**] This work was supported by the Deutsche Forschungsgemeinschaft (Sonderforschungsbereich 416) and the Fonds der Chemischen Industrie. We thank the Schering AG for providing a hydrindenone derivative.

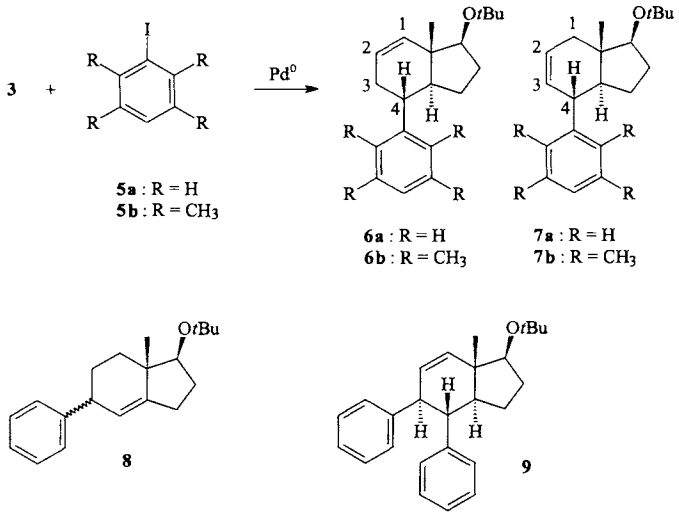

Scheme 2. Heck reaction of **3** with **5**.

formed in 39% and 27% yield, respectively, and the regioisomer **8** was obtained in 16% yield;[6] at slightly elevated temperatures and in the presence of Ag_2CO_3, the diphenyl derivative **9** was also obtained (**6a**: 37%; **7a**: 26%; **8**: 8%; **9**: 4%).[7] Stereoisomers of **6** and **7** could not be identified. When the more sterically demanding 3-iodotetramethylbenzene **5b** were used in the Heck reaction with **3**, the C-4 arylated products **6b** and **7b** were formed exclusively in 90% yield and 1:1 ratio.[8] The primary products **7a** and **7b** presumably isomerize to **6a** and **6b**; the addition of silver salts[9] did not prevent the isomerization.[10]

The construction of the steroid system required the introduction of two additional carbon atoms; therefore, the Heck reactions of **3** with (*Z*)-(2-bromoethenyl)benzene[11] (**10**) and (*E*)-(2-iodoethenyl)benzene[12] (**11**) were carried out; they exhibited high regio- and stereoselectivities similar to those obtained in the transformations with **5** (Scheme 3). At a conversion of about

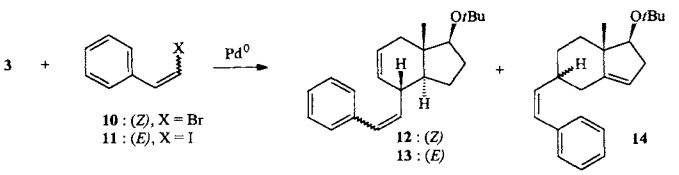

Scheme 3. Heck reaction of **3** with **10** as well as **11**.

50%, **12** and **14** were obtained in 78% and 8% yield,[13] respectively, from the reaction of **3** and **10**, and **13** was isolated exclusively from **3** and **11** in a yield of 91%.[14] The (*Z*)-(2-bromoethenyl)bromobenzenes **2a** and **2b** as well as the (*Z*)-(2-bromoethenyl)iodobenzenes **2c** and **2d** were used for the synthesis of the estrone derivatives **1a** and **1b** (Scheme 4). Assuming that the haloethenyl substituent in **2** is more reactive than the haloarene, we expected a selective coupling to C-4 in **3**. However, the difference in reactivity in **2c** and **2d** proved to be insufficient; furthermore, in the presence of Ag_3PO_4,[15] an I/Br exchange occurred at the arene.

In contrast, the reactions of **3** with **2a** and **2b** proceeded in a highly selective fashion and resulted in the nearly exclusive formation of **15a** and **15b** in 66% and 50% yield, respectively.[16, 17] In each case 30% of **3** could be recovered. The subsequent cyclization of **15a** and **15b** under Heck reaction conditions afforded the estrone derivatives **1a** and **1b**[18] in 85% and 99% yield, respectively.[19, 20] The best results were obtained when the palladacycle recently described by Herrmann, Beller et al.[21] was used as the catalyst.

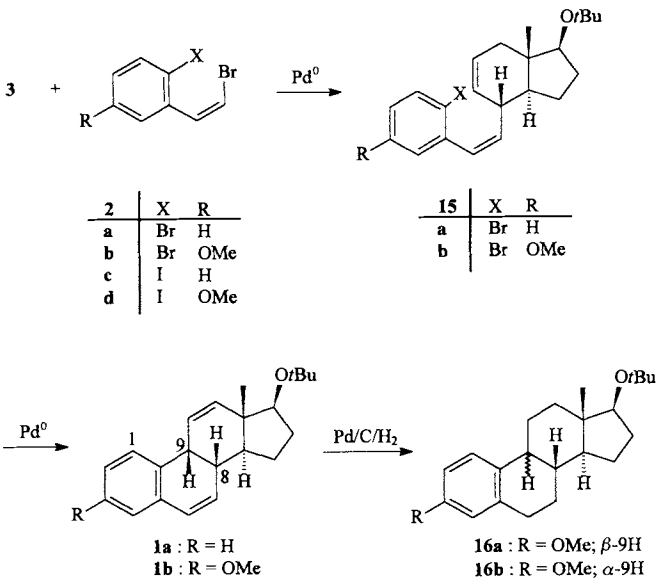

Scheme 4. Double Heck reaction of **3** with **2**.

The transformation can also be carried out as a domino reaction[22] without the isolation of **15a** and **15b**.[23] Hydrogenation of **1b** in the presence of Pd/C led to the estradiol derivatives **16a** and **16b** in 63% and 13% yield, respectively.[24]

The relative configuration of the stereogenic centers C-8 and C-9 in **1a** and **1b** was determined by 1H-1H NOESY experiments. The hitherto unknown estrone derivatives **1a** and **1b** could be used as starting materials for numerous novel steroids, for instance by hydroxylation, epoxidation, halogenation, or ene reaction. Moreover, a large number of compounds can be synthesized by variation of the hexahydro-1*H*-indene **3** and the (bromoethenyl)bromobenzene **2**. Thus, this novel Pd-catalyzed annelation of **3** provides a general and efficient access to steroidal systems.

Experimental Procedure

1b: A solution of **15b** (182 mg, 0.43 mmol), nBu$_4$NOAc (327 mg, 1.09 mmol), and *trans*-di(μ-acetato)-bis[*o*-(di-*o*-tolylphosphino)benzyl]dipalladium(II) [21] (8.1 mg, 2.0 mol%) in DMF/CH_3CN/H_2O (1/1/0.2, 5 mL) was heated for 4.5 h at 115 °C. After cooling, H_2O (30 mL) was added, and the resulting mixture was extracted with Et_2O (2 × 50 mL). Washing the combined ether layers with a saturated NaCl solution, drying over $MgSO_4$, concentration in vacuo, and subsequent purification by column chromatography (PE/CH_2Cl_2 = 3/1) afforded 145 mg (99%) of **1b**.

Received: May 7, 1996 [Z9103]
German version: *Angew. Chem.* **1996**, *108*, 2385–2386

Keywords: domino reactions · estrones · Heck reactions · steroids · synthetic methods

[1] F. J. Zeelen, *Nat. Prod. Rep.* **1994**, *11*, 607.
[2] Reviews: E. Negishi, C. Coperet, S. Ma, S. Liou, F. Liu, *Chem. Rev.* **1996**, *96*, 365; W. Cabri, I. Candiani, *Acc. Chem. Res.* **1995**, *28*, 2; A. de Meijere, F. E. Meyer, *Angew. Chem.* **1994**, *106*, 2473; *Angew. Chem. Int. Ed. Engl.* **1994**, *33*, 2379. R. F. Heck, *Palladium Reagents in Organic Synthesis*, Academic Press, London, **1985**.
[3] a) T. Mandai, T. Matsumoto, M. Kawada, J. Tsuji, *Tetrahedron* **1994**, *49*, 5483; b) L. F. Tietze, P. S. V. Subba Rao, *Synlett* **1993**, 291.

[4] Z. G. Hajos, D. R. Parrish, *J. Org. Chem.* **1974**, *39*, 1615; U. Eder, G. Sauer, R. Wiechert, *Angew. Chem.* **1971**, *83*, 492; *Angew. Chem. Int. Ed. Engl.* **1971**, *10*, 496.
[5] a) R. C. Larock, W. H. Gong, *J. Org. Chem.* **1989**, *54*, 2047; b) R. C. Larock, B. E. Baker, *Tetrahedron Lett.* **1988**, *29*, 905; c) T. Jeffery, *ibid.* **1985**, *26*, 2667.
[6] 3 mol% $Pd(OAc)_2$, 2.0 equiv KOAc, 1.0 equiv nBu_4NCl, 2.0 equiv **5a**, DMF, 80 °C, 80 h.
[7] 10 mol% $Pd(OAc)_2$, 22 mol% PPh_3, 2.5 equiv Ag_2CO_3, 2.0 equiv **5a**, DMF, 110 °C, 60 h.
[8] 5 mol% $Pd(OAc)_2$, 3.0 equiv KOAc, 1.0 equiv nBu_4NCl, 2.0 equiv **5b**, DMF, 90 °C, 43 h.
[9] 5 mol% $Pd(OAc)_2$, 2.0 equiv Ag_3PO_4, 2.0 equiv **5b**, DMF, 90 °C, 64 h; **6b**: **7b** 2/1.
[10] L. F. Tietze, R. Schimpf, *Chem. Ber.* **1994**, *127*, 2235; *Angew. Chem. Int. Ed. Engl.* **1994**, *33*, 1089.
[11] S. J. Cristol, W. P. Norris, *J. Am. Chem. Soc.* **1953**, *75*, 2645.
[12] G. Zweifel, C. C. Whitney, *J. Am. Chem. Soc.* **1967**, *89*, 2753.
[13] 10 mol% $Pd(OAc)_2$, 22 mol% PPh_3, 2.5 equiv Ag_3PO_4, 21.4 equiv **10**, DMF, 110 °C, 60 h.
[14] 10 mol% $Pd(OAc)_2$, 2.5 equiv Ag_3PO_4, 1.7 equiv **11**, DMF, 80 °C, 60 h.
[15] 10 mol% $[Pd(PPh_3)_4]$, 2.0 equiv Ag_3PO_4, 1.5 equiv **2d**, DMF, 120 °C, 63 h.
[16] 10 mol% $Pd(OAc)_2$, 22 mol% PPh_3, 2.5 equiv nBu_4NOAc, 2.0 equiv **2a**, DMF/CH_3CN 1/1, 60 °C, 60 h.
[17] 10 mol% $Pd(OAc)_2$, 21 mol% PPh_3, 2.5 equiv nBu_4NOAc, 0.5 equiv **2b**, DMF/CH_3CN/H_2O 1/1/0.2, 60 °C, 60 h.
[18] **1b**: ^1H NMR (500 MHz, $CDCl_3$): $\delta = 0.86$ (s, 3H, 13-CH_3), 1.10 (s, 9H, 17-O*t*Bu), 1.35-1.50 (m, 3H, 15-H_a, 15-H_b, 16-H_a), 1.65-1.75 (m, 1H, 14-H), 1.81-1.92 (m, 1H, 16-H_b), 2.64 (ddd, $J = 11.7, 6.7, 6.4$ Hz, 1H, 8-H), 3.46 (dd, $J = 6.5, 6.4$ Hz, 1H, 17-H), 3.67 (dd, $J = 6.4, 4.5$ Hz, 1H, 9-H), 3.77 (s, 3H, 3-OCH_3), 5.90 (dd, $J = 9.8, 6.7$ Hz, 1H, 7-H), 6.03 (d, $J = 9.9$ Hz, 1H, 12-H), 6.11 (dd, $J = 9.9, 4.5$ Hz, 1H, 11-H), 6.32 (d, $J = 9.8$ Hz, 1H, 6-H9, 6.54 (d, $J = 2.8$ Hz, 1H, 4-H), 6.68 (dd, $J = 8.3, 2.8$ Hz, 1H, 2-H), 7.17 (d, $J = 8.3$ Hz, 1H, 1-H).
[19] 12 mol% $(Pd(OAc)_2$, 24 mol% PPh_3, 1.3 equiv Ag_3PO_4, DMF, 60 h, 115 °C.
[20] 2.0 mol% *trans*-di(μ-acetato)-bis[*o*-(di-*o*-tolyphosphino)-benzyl]dipalladium(II), 2.5 equiv nBu_4NOAc, DMF/CH_3CN/H_2O 1/1/0.2, 4.5 h, 115 °C.
[21] W. A. Herrmann, C. Broßmer, K. Öfele, C.-P. Reisinger, T. Priermeier, M. Beller, H. Fischer, *Angew. Chem.* **1995**, *107*, 1989; *Angew. Chem. Int. Ed. Engl.* **1995**, *34*, 1844.
[22] a) L. F. Tietze, *Chem. Rev.* **1996**, 115; b) L. F. Tietze, U. Beifuß, *Angew. Chem.* **1993**, *105*, 137; *Angew. Chem. Int. Ed. Engl.* **1993**, *32*, 131.
[23] 2.5 mol% *trans*-di(μ-acetato)-bis[*o*-(di-*o*-tolylphosphino)-benzyl]dipalladium(II), 2.5 equiv nBu_4NOAc, DMF/CH_3CN/H_2O 1/1/0.2, 168 h, 60 °C, **3**/**2b** 1/1; 35% yield not optimized; 30% **3** could be recovered.
[24] 10 mol% Pd/C, MeOH/ethyl acetate 1/1, 3 bar H_2, 18 h, room temperature.

Diastereo- and Enantioselective Synthesis of C_2-Symmetric, Protected 1,*n*-Diamines from Dialdehydes**

Dieter Enders* and Michaela Meiers

Diastereo- and enantiomerically pure diamines have a wide range of applications in organic synthesis and are characteristic structural features of numerous interesting target molecules. In particular vicinal C_2-symmetric diamines are of importance in asymmetric synthesis. They serve as chiral reagents[1] and chiral auxiliaries[2] and also as ligands[3] and ligand building blocks[4, 5] in transition metal catalyzed asymmetric synthesis. In this context salen complexes that can be employed with different transition metals are particularly well-known.[5] A class of C_2-symmetric molecules that has been found to efficiently inhibit HIV-protease contains 1,*n*-diamino functions ($n = 3-5$) as a structural feature.[6] Because of the great interest in C_2-symmetric diamines, several stereoselective syntheses have been developed; however, the majority lead to vicinal diamines.[7, 8] For this reason, we focused our attention on devising a flexible, highly diastereo- and enantioselective approach to C_2-symmetric diamines.

The retrosynthesis of diamines **A** lead to the 1,*n*-diamine synthons **B** which have an a^1-reactivity with regard to the amino group and nucleophiles (Nu). Enantiomerically pure dialdehydehydrazones **C** can be used as synthetic equivalents for **B**.

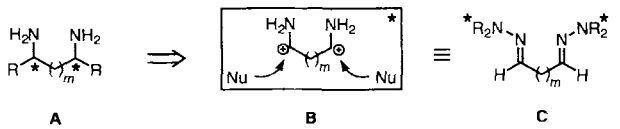

The SAMP/RAMP method has already been successfully employed for the generation of amino functions.[9, 10] The key step is the diastereoselective addition of organometallic reagents to the C=N bond of the enantiomerically pure hydrazone. Beside organolithium compounds and Grignard compounds in toluene,[11] organocerium compounds[12] proved to be particularly well-suited for the addition. We now report a flexible, diastereo- and enantioselective synthesis of N-protected diamines **A**.

Dialdehydes **1** can be converted into the corresponding bis-SAMP-hydrazones (*S,S*)-**2** in good yields by reaction with the chiral auxiliary SAMP[9] (Scheme 1). In the case of succinic dialdehyde, the dialdehyde is first liberated from 2,5-dimethoxytetrahydrofuran and then treated with SAMP. The bis-SAMP-hydrazones are treated with eight equivalents of an organocerium compound[13] formed in situ at low temperatures and the resulting lithium hydrazides then trapped with 24 equivalents of propionyl chloride (PropCl) or methyl chloroformate (MocCl)

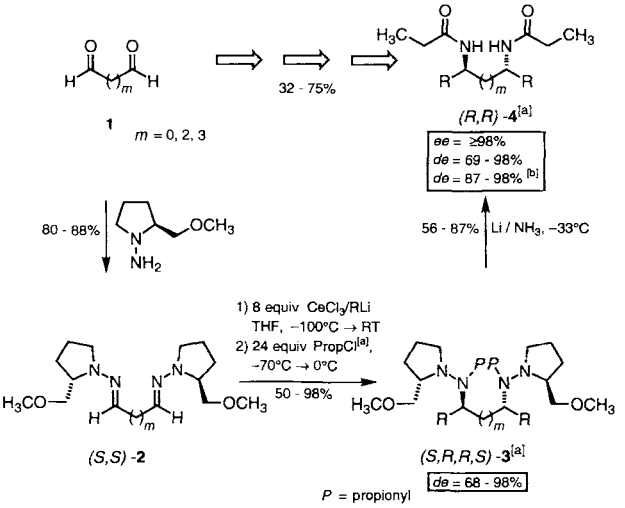

Scheme 1. Diastereo- and enantioselective synthesis of N-protected 1,*n*-diamines **4**. [a] For the synthesis of **3b**, methyl chloroformate was used as trapping reagent. The absolute configurations of **3f** and **4f** were determined to be (*S,S,S,S*) and (*S,S*), respectively. [b] After chromatography.

[*] Prof. Dr. D. Enders, Dipl.-Chem. M. Meiers
Institut für Organische Chemie der Technischen Hochschule
Professor-Pirlet-Strasse 1, D-52074 Aachen (Germany)
Fax: Int. code +(241)8888-127
e-mail: enders@rwth-aachen.de

[**] This work was supported by the Deutsche Forschungsgemeinschaft (Leibniz prize) and the Fonds der Chemischen Industrie. We are obliged to the companies Degussa AG, BASF AG, Bayer AG, Hoechst AG, and Wacker Chemie for donations of chemicals.

in the case of **3b**. After aqueous workup and chromatographic purification the N-protected hydrazines **3** are obtained in moderate to excellent yields (50–98%) with moderate to very high diastereomeric excesses (*de* = 68–98%) (Table 1).

Table 1. N-protected 1,*n*-bishydrazines **3** prepared by nucleophilic 1,2-addition to bis-SAMP-hydrazones **2**.

3	*n*	R	Yield [%]	*de* [a] [%]	$[\alpha]_D^{25}$ (c, $CHCl_3$)	Config. [b]
a	2	Me	50	98	−89.9 (0.91)	(*S,R,R,S*)
b [c]	4	Me	93	[d]	−85.8 (0.93)	(*S,R,R,S*)
c	4	*n*Bu	98	68	−52.2 (1.16)	(*S,R,R,S*)
d	4	nC_6H_{13}	91	69	−49.2 (1.09)	(*S,R,R,S*)
e	5	Me	98	94	−63.0 (0.96)	(*S,R,R,S*)
f	5	Bn [e]	98	[d]	+17.8 (0.99)	(*S,S,S,S*)

[a] The *de* values were determined by gas chromatography (SE-54, FID) from (*S,R,R,S*)/(*S,R,S,S*)-**3**. [b] Configuration of the major diastereomer. [c] Trapped with MocCl. [d] The *de* value could not be determined by either gas chromatography or by NMR spectroscopy. [e] $BnMgCl/CeCl_3$ was used as the nucleophile.

The activated N–N bond is reductively cleaved without racemization by using lithium in liquid ammonia.[14] After purification by column chromatography and, if necessary, removal of the *meso* compound, the N-protected diamines **4** are obtained in moderate to good yields (56–87%) with high diastereomeric excesses (*de* = 87–98%) and very high enantiomeric excesses (*ee* ≥ 98%) (Scheme 1). The total yield (**1** to **4**) over three steps is 32–75% (Table 2).[15]

Table 2. N-protected 1,*n*-diamines **4** prepared by N–N bond cleavage of the 1,*n*-bishydrazines **3** using lithium in liquid ammonia.

4	*n*	R	Yield [%]	*de* [a] [%]	*ee* [b] [%]	$[\alpha]_D^{25}$ (c, $CHCl_3$)	Config. [c]
a	2	Me	73	98	≥98	+65.5 (0.91)	(*R,R*)
b [d]	4	Me	56	87	≥98	+20.3 (1.02)	(*R,R*)
c	4	*n*Bu	63	91 [e]	≥98	+35.1 (1.03)	(*R,R*)
d	4	nC_6H_{13}	65	98 [e]	≥96	+25.5 (0.55)	(*R,R*)
e	5	Me	87	94	≥98	−15.5 (1.06)	(*R,R*)
f	5	Bn	81	88 [f]	≥98 [f]	−30.9 (1.02)	(*S,S*)

[a] The *de* values were determined by gas chromatography (SE-54, FID). [b] According to GC analysis on chiral stationary phases, for **4b** by GC analysis of the propionyl-protected compound, for **4d** according to NMR shift experiments[16]. [c] According to correlation of the optical rotation with literature data[17]. [d] Moc-protected diamine obtained by cleavage of **3b**. [e] After separation of the diastereomers by column chromatography. [f] The *de* and *ee* values were determined by HPLC separation on a chiral stationary phases[16].

The diastereomeric excesses were determined by gas chromatography (GC) and by HPLC, the enantiomeric excesses by gas chromatography and HPLC using chiral stationary phases (CSP) and by ^1H NMR shift experiments.[16] The chiral amine (*S*)-2-methoxymethylpyrrolidine (SMP) can be recovered after cleavage of the N–N bond and converted back into the chiral auxiliary SAMP.[9] The absolute configuration was determined by comparing the optical rotation of (2*R*,3*R*)-2,3-diacetamidobutane, which can be prepared according to the same procedure using acetylchloride for trapping the lithium hydrazide and subsequent bond cleavage, with literature data. The absolute configurations were thus found to be (*R,R*) for **4a–e** and (*S,S*) for **4f**, assuming a uniform reaction mechanism for all examples.[17] This is in agreement with the relative topicity typical for the 1,2-addition to SAMP-hydrazones.

The method presented here makes possible the diastereo- and enantioselective synthesis of N-protected, C_2-symmetric diamines, since both the nucleophiles as well as the separation of the amino functions can be varied.

Experimental Procedure

Preparation of the N-protected bishydrazines **3**: Cerium trichloride heptahydrate (8 mmol) was dehydrated for 2 h at 140 °C and 0.1 Torr with cautious stirring. After cooling, the flask was filled with argon and the solid suspended in THF (35 mL) at room temperature for 2 h, during which ultrasound was applied for 1 h. The colorless suspension was cooled to −70 °C and then a solution of the organolithium reagent (8 mmol) was added slowly; in the case of **3f** a solution of benzylmagnesium chloride (8 mmol) was added. The suspension turned an intense yellow color and was stirred for another 2 h then cooled to −100 °C. The resulting organocerium reagent was treated with a solution of bishydrazone (*S,S*)-**2** (1 mmol) in 6 mL of THF, and then the reaction mixture was allowed to warm up slowly over about 15 h. The solution was again cooled to −70 °C and propionyl chloride (24 mmol) was added. The solution was stirred for 0.5 h at this temperature and for another hour at 0 °C. Alternatively, methyl chloroformate (24 mmol) was added at 0 °C and the solution stirred for 20 h at room temperature. The reaction was terminated by addition of a saturated $NaHCO_3$ solution (20 mL). The organic layer was separated and the residue extracted with ether (4 × 25 mL). The combined organic layers were then dried over $MgSO_4$ and the solvent removed on a rotary evaporator. After purification of the yellow-brown crude products by chromatography (SiO_2, ether/petroleum ether 1:1 to 4:1), colorless to light-yellow viscous oils were obtained.

Cleavage of the N–N bond to afford the N-protected diamines **4**: Lithium (4.8 mmol) was dissolved in liquid ammonia (25 mL) at −70 °C. Then a solution of the hydrazides **3** (0.5 mmol) in THF (5 mL) was added. The cooling bath was removed and the solution allowed to warm up to reflux for 3 h. Ammonium chloride (9.6 mmol) was then carefully added in order to terminate the reaction. After the ammonia had evaporated, the residue was extracted with CH_2Cl_2 (3 × 20 mL) and filtered. After removal of the solvent on a rotary evaporator and purification of the colorless, highly viscous oils by chromatography (SiO_2, ether/MeOH 8:1 to 20:1), colorless solids were obtained.

Received: May 13, 1996 [Z9115IE]
German version: *Angew. Chem.* **1996**, *108*, 2391–2393

Keywords: asymmetric syntheses · diamines · hydrazones · nucleophilic additions · synthetic methods

[1] a) S. Hanessian, D. Delorme, S. Beaudoin, Y. Leblanc, *J. Am. Chem. Soc.* **1984**, *106*, 5754; b) E. J. Corey, *Pure Appl. Chem.* **1990**, *62*, 1209, and references therein; c) E. J. Corey, S. S. Kim, *J. Am. Chem. Soc.* **1990**, *112*, 4976; d) V. J. Blazis, K. J. Koeller, C. D. Spilling, *Tetrahedron: Asymmetry* **1994**, *5*, 499.

[2] a) S. G. Davies, A. A. Mortlock, *Tetrahedron* **1993**, *49*, 4419; b) S. G. Davies, G. B. Evans, A. A. Mortlock, *Tetrahedron: Asymmetry* **1994**, *5*, 585; c) A. Alexakis, R. Sedrani, N. Lensen, P. Mageney in *Organic Synthesis via Organometallics* (Eds.: D. Enders, H.-J. Gais, W. Keim), Vieweg, Braunschweig, **1993**, p. 1; d) A. Alexakis, N. Lensen, J.-P. Tranchier, P. Mangeney, J. Feneau-Dupont, J. P. Declercq, *Synthesis* **1995**, 1038; e) A. Alexakis, T. Kanger, P. Mangeney, F. Rose-Munch, A. Perrotey, E. Rose, *Tetrahedron: Asymmetry* **1995**, *6*, 47; f) A. Alexakis, J.-P. Tranchier, N. Lensen, P. Mangeney, *J. Am. Chem. Soc.* **1995**, *117*, 10767; g) A. Alexakis, P. Mangeney, N. Lensen, J.-P. Tranchier, R. Gosmini, S. Raussou, *Pure Appl. Chem.* **1996**, *68*, 531.

[3] Latest examples: a) A. Fujii, S. Hashiguchi, N. Uematsu, T. Ikariya, R. Noyori, *J. Am. Chem. Soc.* **1996**, *118*, 2521; b) Y. Nishibayashi, Y. Arikawa, K. Ohe, S. Uemura, *J. Org. Chem.* **1996**, *61*, 1172; c) T. Ohkuma, H. Ooka, S. Hashiguchi, T. Ikariya, R. Noyori, *J. Am. Chem. Soc.* **1995**, *117*, 2675; d) A. Alexakis, T. Kanger, P. Mangeney, R. Rose-Munch, A. Perrotey, E. Rose, *Tetrahedron: Asymmetry* **1995**, *6*, 2135; e) P. Gamez, F. Fache, M. Lemaire, *ibid.* **1995**, *6*, 705; f) M. Nakajima, K. Tomioka, K. Koga, *Tetrahedron* **1993**, *49*, 9735.

[4] Latest examples: a) J.-X. Gao, T. Ikariya, R. Noyori, *Organometallics* **1996**, *15*, 1087; b) B. M. Trost, Z. Shi, *J. Am. Chem. Soc.* **1996**, *118*, 3037; c) B. M. Trost, R. C. Bunt, *Angew. Chem.* **1996**, *108*, 70; *Angew. Chem. Int. Ed. Engl.* **1996**, *35*, 70; d) X. Zhang, C. Guo, *Tetrahedron Lett.* **1995**, *36*, 4947; e) S. E. Denmark, B. L. Christenson, S. P. O'Connor, *ibid.* **1995**, *36*, 2219; f) A. Vaupel, P. Knochel, *ibid.* **1995**, *36*, 231; g) H. Takahashi, M. Yoshioka, M. Shibasaki, M. Ohno, N. Imai, S. Kobayashi, *Tetrahedron* **1995**, *51*, 12013.

[5] Reviews: a) E. N. Jacobsen in *Catalytic Asymmetric Synthesis* (Ed.: I. Ojima), VCH, New York, **1993**, p. 159; b) T. Katsuki, *Coord. Chem. Rev.* **1995**, *140*, 189; latest examples: c) Y. Belokon, N. Ikonnikov, M. Moscalenko, M. North, S. Orlova, V. Tararov, L. Yashkina, *Tetrahedron: Asymmetry* **1996**, *7*, 851; d) B. B. De, B. B. Lohray, S. Sivaram, P. K. Dhal, *ibid.* **1995**, *6*, 2105; e) B. D. Brandes, E. N. Jacobsen, *Tetrahedron Lett.* **1995**, *36*, 5123; f) D. Mikame, T. Hamada, R. Irie, T. Katsuki, *Synlett* **1995**, 827; g) K. G. Rasmussen, D. S. Thomsen, K. A. Joergensen, *J. Chem. Soc. Perkin Trans. 1* **1995**, 2009; h) T. Nagata, K. Yorozu, T. Yamada, T. Mukaiyama, *Angew. Chem.* **1995**, *107*, 2309;

Angew. Chem. Int. Ed. Engl. **1995**, *34*, 2145; i) P. Pie-Tikäinen, *Tetrahedron Lett.* **1995**, *36*, 319; j) E. N. Jacobsen, L. Deng, Y. Furukawa, L. E. Martinez, *Tetrahedron* **1994**, *50*, 4323.

[6] Review: a) J. W. Erickson, *Perspectives in Drug Discovery and Design* **1993**, *1*, 109; recent examples: b) M. E. Pierce, G. D. Harris, Q. Islam, L. A. Radesca, L. Storace, R. E. Waltermire, E. Wat, P. K. Jadhav, G. C. Emmett, *J. Org. Chem.* **1996**, *61*, 444; c) L. T. Rossano, Y. S. Lo, L. Anzalone, Y.-C. Lee, D. J. Meloni, J. R. Moore, T. M. Gale, J. F. Arnett, *Tetrahedron Lett.* **1995**, *36*, 4967; d) P. K. Jadhav, F. J. Woerner, *ibid.* **1995**, *36*, 6383; e) G. T. Wang, S. Li, N. Wideburg, G. A. Krafft, D. J. Kempf, *J. Med. Chem.* **1995**, *38*, 2995; f) B. Kammermeier, G. Beck, D. Jacobi, H. Jendralla, *Angew. Chem.* **1994**, *106*, 719; *Angew. Chem. Int. Ed. Engl.* **1994**, *33*, 685; g) M. V. Hosur, T. N. Bhat, D. J. Kempf, E. T. Baldwin, B. Liu, S. Gulnik, N. W. Wideburg, D. W. Norbeck, K. Appelt, J. W. Erickson, *J. Am. Chem. Soc.* **1994**, *116*, 847; h) W. R. Baker, S. L. Condon, *J. Org. Chem.* **1993**, *58*, 3277; i) D. Enders, U. Jegelka, B. Dücker, *Angew. Chem.* **1993**, *105*, 423; *Angew. Chem. Int. Ed. Engl.* **1993**, *32*, 423.

[7] Stereoselective synthesis of vicinal C_2-symmetric diamines by nucleophilic 1,2-addition to C=N bonds: a) M. T. Reetz, R. Jaeger, R. Drewlies, M. Hübel, *Angew. Chem.* **1991**, *103*, 76; *Angew. Chem. Int. Ed. Engl.* **1991**, *30*, 103; b) W. L. Neumann, M. M. Rogic, T. J. Dunn, *Tetrahedron Lett.* **1991**, *32*, 5865; c) K. Bambridge, M. J. Begley, N. S. Simpkins, *ibid.* **1994**, *35*, 3391; latest examples: d) M. Bruncko, T.-A. V. Khuong, K. B. Sharpless, *Angew. Chem.* **1996**, *108*, 453, *Angew. Chem. Int. Ed. Engl.* **1996**, *35*, 454; e) N. Kise, K. Kashiwagi, M. Watanabe, J-i. Yoshida, *J. Org. Chem.* **1996**, *61*, 428; f) P. F. Richardson, L. T. J. Nelson, K. B. Sharpless, *Tetrahedron Lett.* **1995**, *36*, 9241; g) M. Shimizu, M. Kamei, T. Fujisawa, *ibid.* **1995**, *36*, 8607; h) B. Baruah, D. Prajapati, J. S. Sandhu, *ibid.* **1995**, *36*, 6747; i) M. Shimizu, T. Iida, T. Fujisawa, *Chem. Lett.* **1995**, 609; j) E. J. Corey, D.-H. Lee, S. Sarshar, *Tetrahedron: Asymmetry* **1995**, *6*, 3.

[8] Stereoselective synthesis of C_2-symmetric 1,3-diamines: a) S. E. Denmark, J.-H. Kim, *Synthesis* **1992**, 229; b) D. Pini, A. Mastantuono, G. Uccello-Barretta, A. Iuliano, P. Salvadori, *Tetrahedron* **1993**, *49*, 9613.

[9] Reviews of the SAMP/RAMP method: a) D. Enders in *Asymmetric Synthesis, Vol. 3B* (Ed.: J. D. Morrison), Academic Press, Orlando, FL, USA, **1984**, p. 275; b) D. Enders, P. Fey, H. Kipphardt, *Org. Synth.* **1987**, *65*, 173; c) D. Enders, M. Klatt in *Encyclopedia of Reagents for Organic Synthesis* (Ed.: L. A. Paquette), Wiley, New York, **1995**, p. 178.

[10] Recent examples for the 1,2-addition to hydrazones: a) D. Enders, J. Schankat, M. Klatt, *Synlett* **1994**, 795, and references therein; b) D. Enders, U. Reinhold, *Angew. Chem.* **1995**, *107*, 1332; *Angew. Chem. Int. Ed. Engl.* **1995**, *34*, 1219; c) D. Enders, U. Reinhold, *Liebigs Ann.* **1996**, 11.

[11] A. Alexakis, N. Lensen, J.-P. Tranchier, P. Mangeney, *J. Org. Chem.* **1992**, *57*, 4563.

[12] a) G. A. Molander, *Chem. Rev.* **1992**, 29; b) D. Enders, R. Funk, M. Klatt, G. Raabe, E. R. Hovestreydt, *Angew. Chem.* **1993**, *105*, 418; *Angew. Chem. Int. Ed. Engl.* **1993**, *32*, 418; c) S. E. Denmark, O. Nicaise, *Synlett* **1993**, 359.

[13] a) T. Imamoto, N. Takiyama, K. Nakamura, *Tetrahedron Lett.* **1985**, *26*, 4763; b) T. Imamoto, Y. Sugiura, *J. Organomet. Chem.* **1985**, *C21*, 285; c)T. Imamoto, Y. Sugiura, N. Takiyama, *Tetrahedron Lett.* **1984**, *25*, 4233; d) T. Imamoto, T. Kusumoto, Y. Tawarayama, Y. Sugiura, T. Mita, Y. Hatanaka, M. Yokoyama, *J. Org. Chem.* **1984**, *49*, 3904.

[14] a) C. Nübling, *Dissertation*, Technical University of Aachen, **1987**; b) S. E. Denmark, O. Nicaise, J. P. Edwards, *J. Org. Chem.* **1990**, *55*, 6219.

[15] All new compounds gave appropriate spectroscopic data (IR, NMR, MS) and correct elemental analyses or high-resolution mass spectra (HRMS).

[16] CSP for **4a–c** and **4e**: XE-60-S-valine-S-X-phenylethylamide, carrier gas hydrogen, chiral HPLC for **4f** using (S,S)-Whelk-O, eluent cyclohexane/isopropanol. (−)-(*R*)-1-(9-anthryl)-2,2,2-trifluoroethanol was used as chiral cosolvent in the NMR shift experiments. The racemates were prepared analogously from the bis(dimethylhydrazones).

[17] M. H. Nantz, D. A. Lee, D. M. Bender, A. H. Roohi, *J. Org. Chem.* **1992**, *57*, 6653; optical rotation for (2*R*,3*R*)-2,3-diacetamidobutane $[\alpha]_D^{25} = +44.9$ ($c = 0.049$ in butanone), lit.: $[\alpha]_D^{25} = +54.7$ ($c = 0.098$ in butanone); m.p. 195 °C, lit.: 203.7–204.3 °C.

Always a Good Starting Point

Houben-Weyl. (Methods of Organic Chemistry) Vol. E21 1–10, Stereoselective Synthesis. Workbench Edition. Edited by *G. Helmchen, R. W. Hoffmann, J. Mulzer* and *E. Schaumann*. Thieme, Stuttgart, 1996. 6304 pp., paperback DM 3600,00.—ISBN 3-13-106123-3; Hardcover: Vol. E21a–e. Thieme, Stuttgart, 1995. a) 1168 pp., DM 2840,00.—ISBN 3-13-219504-9; b) 1150 pp., DM 2340,00.—ISBN 3-13-797904-8; c) 1078 pp., DM 2500,00.—ISBN 3-13-798004-1; d) 1200 pp., DM 2770,00.—ISBN 3-13-100114-3; e) 900 pp., DM 2100,00.—ISBN 3-13-100124-0; f) 843 pp., DM 1600,00.—ISBN 3-13-102794-0

In the program of the well-known German reference work Houben-Weyl a five-volume series entitled "Stereoselective Synthesis" is fortunately now available as an English edition, which gives a complete overview over this field of chemistry. Virtually all topics of stereoselective synthesis are covered and represented in depth by more than 100 top-class authors. Both editors and authors have obviously put in great effort to produce a book of great value for chemists involved in stereoselective synthesis and stereoselective catalysis.

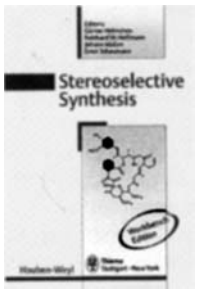

The chapters are mainly organized by the kind of bond formed or broken during the reaction, enabling the reader to spot specific reactions easily rather than products. A separate index facilitates the search for certain types of products. Thus these well-written books provide the natural product chemist with the ideal reference work in which he can find both product and reaction types.

After an excellent introduction into basic principles of stereochemistry and stereoselective synthesis, including nomenclature, separation, and analysis, chapters about the stereoselective synthesis of compounds with axial chirality and the formation of chiral compounds by bond disconnection follow.

After this the biggest chapter of the series (more than 2500 pages) starts, covering stereoselective synthesis by the formation of carbon–carbon bonds. Reactions of organometallic compounds, of all types of enolates, additions to carbonyls and to C–C double bonds as well as allylic substitution reactions, radical reactions, and pericyclic reactions form the main parts of this major chapter. In the remaining two volumes of the series methods for the stereoselective formation of C–H, C–Hal, C–O, C–S, C–Se, C–Te, C–N, C–P, C–Si, and C–Sn bonds are described. Substrate-induced, reagent-induced, and auxilliary-induced stereoselectivity are included in the chapters of this valuable series. As enzymatic methods are discussed in detail too, these books represent a complete work on stereoselective synthesis.

Each article is well written. Mechanistic backgrounds as well as explanations about the origin of stereoselectivity are briefly discussed where necessary and precede the well-selected examples given. The effect is to focus the attention on the specific topic.

Due to the great number of authors and reactions, some overlap seems to be inevitable; however, this concerns mainly the theoretical background of the reactions, and makes the separate articles easy to follow and a joy to read. The tabulated data and the representative experimental procedures given make these books both practical and informative for scientists working in a laboratory, too. Mistakes are extremely rare and only minor. Where they occur, they do in no way influence the clear, logical line of argumentation in this book. The high standards of these volumes are reflected in the citation of well-chosen references, including 1995. They are thus an extremely up-to-date comprehensive reference source.

In summary these books represent the present state of the art of stereoselective synthesis and are an invaluable source of information and references. They can be highly recommended and are definitely the best starting point for obtaining information about the reactions covered in these volumes. They should therefore not be missing from any chemistry library.

Masakatsu Shibasaki
University of Tokyo (Japan)

100 and more Basic NMR Experiments. A Practical Course. By *S. Braun, H.-O. Kalinowski* and *S. Berger*. VCH Verlagsgesellschaft, Weinheim, 1996. xii, 418 pp., paperback DM 68.00.—ISBN 3-527-29091-5

This book by Braun, Kalinowski, and Berger is the sixth joint production from these authors, following their ^{13}C *NMR-Spektroskopie* and the four volumes of *NMR-Spektroskopie von Nichtmetallen* [English-language versions: *Carbon-13 NMR Spectroscopy* (1988), and the soon forthcoming single-volume *NMR Spectroscopy of the Non-Metallic Elements*.] The present work is a collection of laboratory procedures, the NMR spectroscopist's equivalent of the organic chemist's preparative handbook, which aims to teach the user how to perform NMR experiments. Thus it is a guide through the bewildering variety of available NMR techniques, and is intended for both average and more advanced users of NMR spectrometers.

The 12 chapters cover a wide range, from the basic operations with an NMR spectrometer up to the latest multipulse experiments. The individual experiments are described in detail in subchapters which follow a standard pattern: first the purpose of the experiment, then some key literature references, the pulse sequence

This section contains book reviews and a list of new books received by the editor. Book reviews are written by invitation from the editor. Suggestions for books to be reviewed and for book reviewers are welcome. Publishers should send brochures or (better) books to the Redaktion Angewandte Chemie, Postfach 101161, D-69451 Weinheim, Federal Republic of Germany. The editor reserves the right of selecting which books will be reviewed. Uninvited books not chosen for review will not be returned.

and phase cycle, the spectrometer settings and conditions appropriate for a specific sample solution, the processing of the recorded data, typical results including an actual spectrum (reproduced in excellent quality), and additional information about the method. Each subchapter is self-contained, so that the reader can concentrate on the method in hand without needing to have read the previous sections.

The first five chapters are concerned with basic spectrometer procedures such as tuning the probe-head, optimizing the magnetic field homogeneity, determining the pulse length, and carrying out simple NMR experiments, including recording ^{1}H and ^{13}C spectra under standard conditions, decoupling techniques, and dynamic NMR measurements. In Chapter 6 the reader learns about multiplicity selection methods (spectral "editing"), including the APT, INEPT, and DEPT techniques, about pulse sequences used as building blocks in more complicated sequences (the BIRD filter, etc.), and about methods for suppressing the water signal. Chapter 7 is devoted to experiments using selective pulses, and Chapter 8 to the use of auxiliary reagents and to quantitative measurements. Chapter 9 introduces heteronuclear NMR spectroscopy. The topics of the last three chapters are two-dimensional methods (including H,H shift correlations, C,H correlation methods using either ^{13}C or ^{1}H detection, and others), NMR experiments with pulsed field gradients, and 3D NMR experiments. The book ends with two appendices, the first listing the different names used by various instrument manufacturers to describe the recording parameters, and the second explaining the basic rules of the product operator formalism.

The authors have included here the most important and frequently used NMR methods, and their choice of experiments is appropriate for the intended readership. However, in the chapter on heteronuclear NMR spectroscopy we would have expected to find examples of measurements on ^{31}P, certainly a much more important nuclide than ^{11}B and ^{17}O, which are chosen here. Chapters 6 ("1D Multipulse Sequences") and 10 ("The Second Dimension") are especially well constructed from a teaching standpoint. All the experiments described in the book use only compounds that are readily available. In the 3D H,C,P correlation experiment the potential applications of the technique could have been demonstrated more convincingly by choosing, instead of triphenylphosphine, a compound having more than one chemical shift value in each dimension.

The methods are described in a clearly understandable way which should enable readers to perform the experiments without serious problems. However, those with little practical experience of NMR spectrometers may have a few difficulties with processing the data, especially if they are using a spectrometer of a different make from that of the authors, this despite the translations of technical terms in the appendix. Also, readers with less theoretical background would be better able to understand the pulse sequences if these were explained using the magnetization vector picture wherever possible, rather than the product operator formalism.

This book dealing with the practical aspects of carrying out NMR experiments fills a gap between the operating manuals provided by instrument manufacturers and the mainly theoretically-orientated books on the subject. It can be thoroughly recommended for purchasing by every NMR laboratory.

Kerstin Ibrom
Königstein im Taunus

Ludger Ernst
NMR-Laboratorium
der Chemischen Institute
der Technischen-Universität
Braunschweig
Braunschweig (Germany)

Solving Problems with NMR Spectroscopy. By *A.-u. Rahman* and *M. I. Choudhary*. Academic Press, San Diego, 1996. xvi, 430 pp., paperback $ 34.95.—ISBN 0-12-066320-1

The purpose of this book, according to the authors, is to provide research chemists with the practical knowledge needed to use NMR methods for determining the structures of organic molecules. They have been especially concerned to avoid making it too technical, and wherever possible they have described the underlying principles of the experiments in non-mathematical language. Like the book by Braun et al. which is reviewed above, it is concerned with the practical details of carrying out NMR experiments, but here there is more emphasis on analyzing the results.

The book begins with a long chapter (98 pp.) on the fundamentals of modern NMR spectroscopy. Aspects covered include the most important parts of the spectrometer, basic operations with the instrument, the effects of radiofrequency pulses on the magnetization vector, processing of the experimental data, and technical points related to these. Chapter 2 (57 pp.) is concerned with spin-echo and polarization transfer methods, with particular attention to the APT, INEPT, and DEPT techniques. Chapter 3 (37 pp.) introduces the basic principles of two-dimensional NMR spectroscopy, explaining how the data are recorded and subsequently processed, but not yet going so far as to describe specific experiments. In Chapter 4 (25 pp.) the authors discuss the nuclear Overhauser effect (NOE) and the practical aspects of recording NOE difference spectra. The real core of the book is Chapter 5 (131 pp.), which is devoted to various important 2D NMR experiments. These include the recording of homonuclear and heteronuclear *J*-resolved spectra, homonuclear and heteronuclear chemical shift correlation experiments, 2D nuclear Overhauser experiments (NOESY, ROESY, HOESY) and exchange spectroscopy (EXSY), the 2D TOCSY and INADEQUATE experiments, and heteronuclear correlation experiments with proton detection (HMQC, HMBC). Chapter 6 (19 pp.) introduces the principles of 3D NMR spectroscopy and describes a few of the many types of experiments that are possible. Chapter 7 (26 pp.), on recent developments in NMR spectroscopy, is mainly concerned with experiments using frequency-selective excitation pulses, with a brief mention of the use of pulsed field gradients for suppressing unwanted coherences. Lastly, Chapter 8 (19 pp.) considers how one should approach the problem of determining an unknown molecular structure, giving general recommendations as to which experiments should be performed and in what order, together with the analysis of the results. The authors then describe the sequence of events in a structural analysis, using two examples from their own research, a lupinine alkaloid and a steroid alkaloid. The book ends with a glossary of technical terms used in NMR spectroscopy (10 pp.) and a subject index of similar length.

The text is in general easy to read and understand, and gives good explanations of the most important NMR techniques in current use. However, it is not completely clear which readers the book is intended for. Beginners without any previous knowledge will find that many of the descriptions are not sufficiently detailed, whereas for experienced NMR users much of the information is superfluous. The book does not fully live up to the promise of its title. To solve structural problems without any previous knowledge of chemical shifts and coupling con-

 © VCH Verlagsgesellschaft mbH, D-69451 Weinheim, 1996 0570-0833/96/3519-2266 $ 15.00+.25/0

stants, neither of which is discussed in the book, may often be possible in principle, but is usually not the most efficient approach. Also some important older and well-established techniques, such as spin decoupling, are not discussed. A more honest title for the book would be something like "Modern NMR Spectroscopic Techniques".

The inclusion of exercise problems with answers in each chapter is a welcome feature. Unfortunately, however, the questions posed are not always very useful from a learning standpoint (example: "The signal-to-noise ratio can be increased by [applying] proper apodization functions. What would happen without apodization?"), and occasionally they suggest a whimsical attitude on the part of the authors. For example, to the question of what type of probe-head is most suitable for a group of preparative chemists where the problem of insufficient sample does not arise, the answer given is "a probe-head for 10-15 mm sample tubes". The book's most serious shortcoming is that many of the figures are of very poor quality. This applies especially to the reproduction of spectra, a few of which have obviously been drawn by hand. Many of the 2D spectra are much too small. Occasionally the one-dimensional spectrum is missing from one of the axes, or is shown on such a small scale that only methyl group singlets are adequately reproduced (4 mm height!), with the result that no coupling multiplets can be recognized, since they would only be a fraction of a millimeter in height. This happens even on pages whose space is not fully used. The book would have been much improved by using a larger format and taking greater care with the layout. It needs to be thoroughly reworked.

Ludger Ernst
NMR-Laboratorium
der Chemischen Institute
der Technischen Universität
Braunschweig
Braunschweig (Germany)

Kerstin Ibrom
Königstein im Taunus (Germany)

Unimolecular Reactions. Second edition. By *K. A. Holbrook, M. J. Pilling* and *S. H. Robertson*. Wiley, Chichester, 1996. 417 pp., hardcover £ 90.00.—ISBN 0-471-92268-4

The subject of unimolecular reactions has undergone much development in the last few decades. Many new types of experiments have been carried out, affording insights that could scarcely have been imagined 30 years ago. It has become possible to make remarkably precise measurements on reactions of practical importance. Alongside these advances, theoretical methods now allow one to analyze the fundamental processes with improving quantitative reliability. Consequently, monographs and review articles dealing with this fast-moving field soon become outdated. It is therefore very pleasing that K. A. Holbrook, M. J. Pilling, and S. H. Robertson have now produced a thoroughly revised and significantly enlarged new edition of *Unimolecular Reactions*, first published in 1972 under the authorship of P. J. Robinson and K. A. Holbrook. In that first edition, "Robinson and Holbrook" contained an excellent introduction to the application of the HRRKM theory, the statistical theory of unimolecular reactions developed by Hinshelwood, Rice, Ramsperger, Kassel, and Marcus, together with a detailed compilation of experimental data on classical reactions. At that time this was the most detailed introduction to the practical application of the RRKM theory available in the literature. However, in recent years it had become seriously outdated because the many later developments were not covered.

Thermal and nonthermal unimolecular reactions are often studied under conditions in which the reaction rate is determined solely or partly by intermolecular energy exchange through collisions. In retrospect it seems surprising that for many years the details of this process received so little attention. The new edition of this book remedies that omission by including descriptions based on the fundamental equations. Nevertheless, perhaps an even more detailed treatment of the energy transfer process would have conveyed a better understanding of its characteristics.

The new numerical algorithms for calculating densities of states and numbers of states are treated in detail in this book, so that the statistical analyses of the RRKM theory can be carried to completion. Thus, even a beginner should have no difficulty in learning how to treat reactions involving rigid activated complexes, for which the classical RRKM theory was mainly developed. The new edition also includes a detailed treatment of reactions involving nonrigid activated complexes. The description and comparison of the different variants of theoretical treatments of the transition state is excellent and useful. In view of this it is even more surprising that the phase space theory, which represents the limiting case of completely flexible transition states, and makes it easy to correctly take into account the conservation of angular momentum in the reaction, is almost completely ignored. To have included a treatment of this limiting case would have helped the reader to understand the detailed description of the statistical adiabatic channel model.

The book contains a wealth of information about current experimental and theoretical studies in this field. The descriptions of the kinds of investigations now possible are illustrated by informative examples, thus providing the beginner with an excellent introduction and the more advanced researcher with many stimulating ideas. It retains the spirit of the original "Robinson and Holbrook", while also bringing the treatment up to date. If the book had been completely rewritten from the start, there would probably have been some changes of emphasis. It would then have been possible to devote more space to topics such as the breakdown of molecular ions, bimolecular complex-forming reactions of neutral or charged species, trajectory calculations, calculations of adiabatic channel potentials made possible by the latest methods, anharmonic densities of states, and (as already mentioned above) phase space theory. At the same time the treatment of the classical RRKM theory could be shortened. However, to do so would have resulted in a more bulky monograph than intended. Therefore the changes have been limited to a very successful updating of the original concept. The book is well suited as a text for further reading by advanced students, and will also serve the needs of reaction kineticists who intend to work on gas phase reactions.

Jürgen Troe
Institut für Physikalische Chemie
der Universität Göttingen (Germany)

 © VCH Verlagsgesellschaft mbH, D-69451 Weinheim, 1996 0570-0833/96/3519-2267 $ 15.00+.25/0

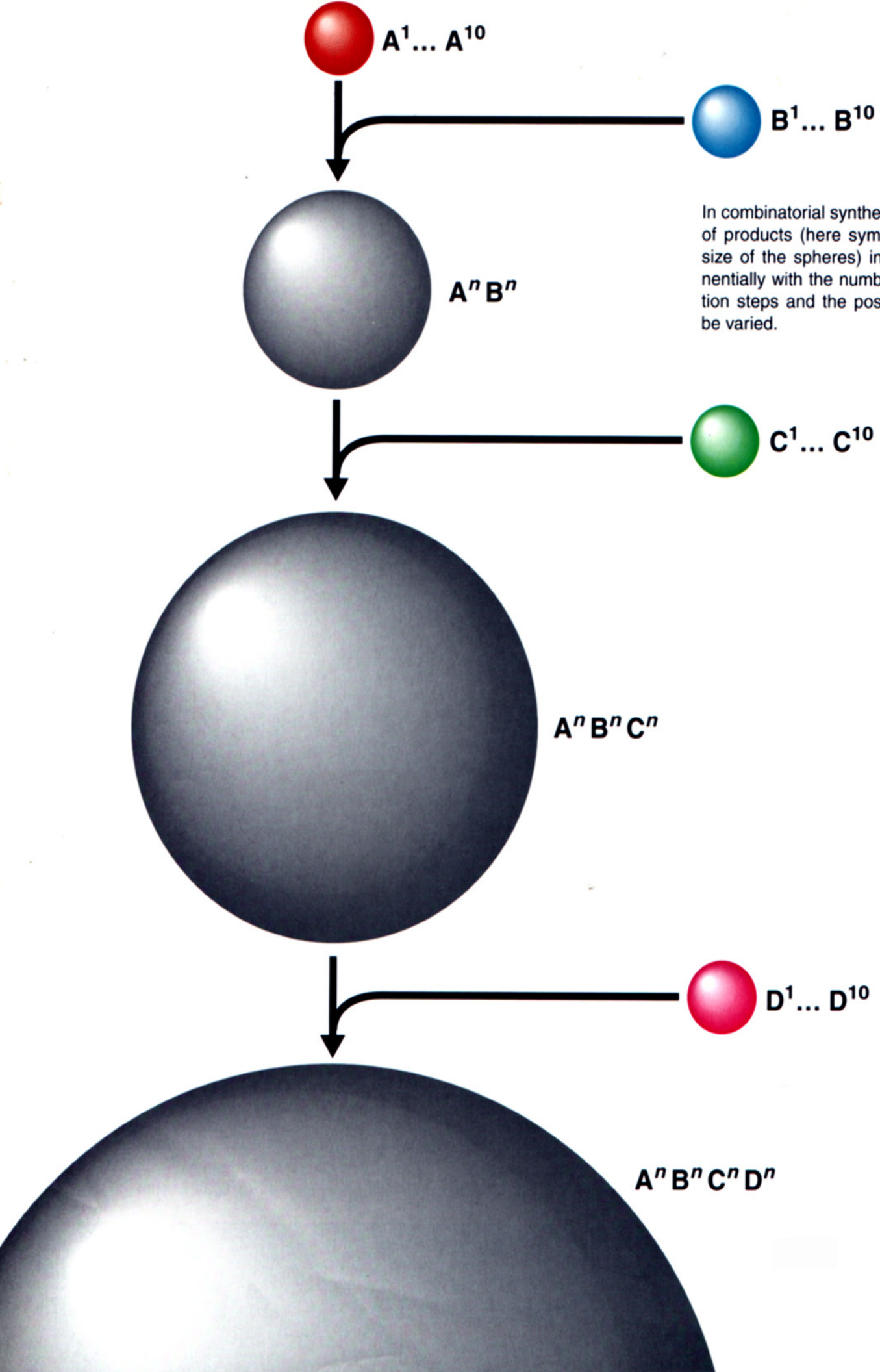

In combinatorial synthesis the number of products (here symbolized by the size of the spheres) increases exponentially with the number of the reaction steps and the positions that can be varied.

Combinatorial Synthesis of Small Organic Molecules

Friedhelm Balkenhohl,* Christoph von dem Bussche-Hünnefeld, Annegret Lansky, and Christian Zechel

Combinatorial synthesis has developed within a few years from a laboratory curiosity to a method that is taken seriously in drug research. Rapid progress in molecular biology and the resulting ability to determine the activity of new substances extremely efficiently have led to a change in paradigm for the synthesis of test compounds: in addition to the conventional procedure of synthesizing one substance *after* another, new methods allowing *simultaneous* creation of many structurally defined substances are becoming increasingly important. A characteristic of combinatorial synthesis is that a reaction is performed with *many* synthetic building blocks at once—in parallel or in a mixture— rather than with just *one* building block. All possible combinations are formed in each step, so that a large number of products, a so-called library, is obtained from only a few reactants. Several methods have been developed for combinatorial synthesis of small organic molecules, based on research into peptide library synthesis: single substances are produced by highly automated parallel syntheses, and special techniques enable targeted synthesis of mixtures with defined components. Many structures can be obtained by combinatorial synthesis, and the size of the libraries created ranges from a few individual compounds to many thousand substances in mixtures. This article gives an overview of the combinatorial syntheses of small organic molecules reported to date, performed both in solution and on a solid support. In addition, different techniques for identification of active compounds in mixtures are presented, together with ways to automate syntheses and process the large amounts of data produced. An overview of pioneering companies active in this area is also given. The final outlook attempts to predict the future development of this exponentially growing area and the influence of this new thinking in other areas of chemistry.

Keywords: automation · combinatorial chemistry · compound libraries · solid-phase synthesis · molecular diversity

"The more methodical people are, the greater the effects of coincidence."
Friedrich Dürrenmatt
(Translated from the German)

1. Introduction

1.1. The Role of Organic Synthesis in the Search for Active Compounds

Synthesis has been the backbone of organic chemistry since Wöhler's work on production of urea from ammonium cyanate. During the last hundred years chemists have been challenged time and again to new achievements by the products of nature. The total syntheses of, for instance, vitamin B_{12}, palytoxin, and taxol are impressive demonstrations of this.[1] Today, new, ever more selective methods enable synthesis of molecules of almost any complexity. However, despite all this progress, the goal of organic synthesis has remained the same: the most efficient and selective synthesis possible of a single target molecule of defined structure.

The synthesis of biologically active compounds has, up to the present time, been influenced by this aim: once a suitable target has been selected, it is synthesized, purified, characterized, and tested for activity. The activity is then optimized, partly by systematic and partly by intuitive variation of the initial structure. A new active substance is obtained by trial and error, and many thousand molecular variations must be synthesized before a marketable product is found. Even a well-equipped and efficient synthetic laboratory can hardly produce more than *one* substance per day at present. This is one of the main factors that makes development of new pharmaceuticals or crop protection agents a lengthy, and thus expensive, process.

Rapid progress in molecular biology and gene technology has brought about fundamental changes in biomedical research in the last ten years (Fig. 1).[2] Use of molecular biological methods to identify and prepare proteins (enzymes, receptors, ion channels) that are directly associated with medical symptoms is very important in drug research. Determination of the structure of these molecules has made it possible to understand diseases at the molecular level and has opened the door to rational drug

[*] Dr. F. Balkenhohl, Dr. C. von dem Bussche-Hünnefeld, Dr. A. Lansky, Dr. C. Zechel
BASF-Aktiengesellschaft
Hauptlaboratorium, ZHB/C-A 30
D-67056 Ludwigshafen (Germany)
Fax: Int. code + (621) 602-0440
e-mail: friedhelm.balkenhohl@zhb.x400.basf-ag.de

design. Of even greater importance is the use of these targets to design efficient test systems, since this enables *thousands* of substances (with suitable automation) to be screened per day. The in vitro activity can be reliably ascertained even with minute amounts of substance. This so-called "high-throughput screening" for identification of new lead structures requires a large number of structurally diverse test substances, and this is where the concept of traditional organic synthesis (synthesizing one compound after another) reaches its limits. Preparation of test substances becomes the bottleneck in the search for active compounds. The speed of synthesis, or more precisely, the number of substances synthesized per time unit, is a new dimension in organic synthesis (high-throughput synthesis), in addition to yield and selectivity. The future goal in drug discovery will be to synthesize many structurally diverse substances rapidly so that, in combination with high-throughput screening the search for new lead structures and their optimization can be accelerated.

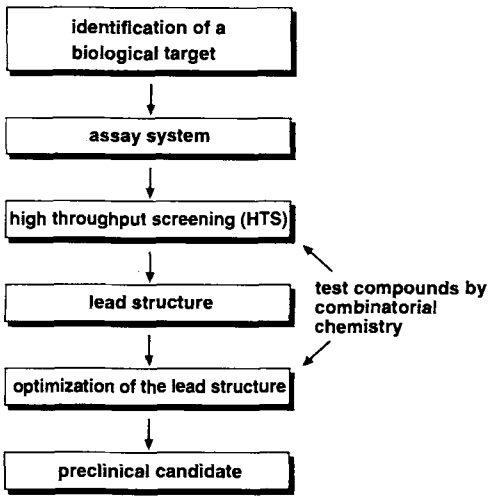

Fig. 1. The search for pharmaceuticals today.

C. von dem Bussche-Hünnefeld F. Balkenhohl A. Lansky C. Zechel

Friedhelm Balkenhohl, born in 1961 near Osnabrück (Germany), studied chemistry at the Universities of Göttingen and Hannover and finished his PhD in 1989 with Prof. E. Winterfeldt. The topic of his dissertation was the stereoselective synthesis of acceptor-substituted prostacyclins. After joining the main laboratory at BASF AG, he worked on the synthesis and process development of vitamins and their derivatives. Afterwards he investigated the use of enzyme-catalyzed reactions for the synthesis of optically active intermediates, such as amines. Since 1994 he has been the leader of the "combinational chemistry" research group.

Christoph von dem Bussche-Hünnefeld, born in 1964 in Koblenz (Germany), studied chemistry at the University of Bonn and the ETH, Zürich. His doctoral work on enantiomerically pure, fluorinated synthetic building blocks was completed in 1992 with Prof. D. Seebach. During a postdoctorial fellowship at the University of California, Los Angeles, he worked on the synthesis of cage compounds in the research group of Prof. D. J. Cram. In 1993 he joined the main laboratory at BASF AG (research area: crop-protection agents).

Annegret Lansky, born in 1965 in Offenbach am Main (Germany), studied chemistry at the Universities of Hamburg and Southampton (UK). She finished her PhD in 1992 at the University of Göttingen with Prof. A. de Meijere in the area of palladium-catalyzed multiple coupling. In 1993 she began working in the main laboratory at BASF AG, where she synthesized pharmaceutical products for the central nervous system.

Christian Zechel, born in 1958 in Berlin (Germany), studied chemistry at the University of Frankfurt am Main and finished his PhD in 1985 with Prof. H. Kessler. His dissertation was on homo- and heterodetic cyclic enkephalin analogues. During a subsequent postdoctoral fellowship with Prof. V. J. Hruby at the University of Arizona, Tucson he investigated the solid-phase synthesis of glucagon antagonists. Since 1986 he has been in the main laboratory at BASF AG and works on pharmaceutical products.

The authors have been working in the area of combinatorial chemistry in synthesis of biologically active compounds since 1994. At the center of their interest is the combinatorial synthesis of low molecular weight organic compounds on solid phase. In addition to identifying appropriate reaction sequences and synthesis of compound libraries, they are also working on automation and analytical methods for combinatorial chemistry.

1.2. The Principle of Combinatorial Organic Synthesis

The goal of combinatorial synthesis is to *simultaneously* produce many different products with defined structures.[3] The aim is no longer to produce a single, selected structure, but rather to find ways to produce many structures "in one go". Combinatorial synthesis takes its lead from nature, which succeeds in obtaining from only a few synthetic units (for example, the twenty amino acids) a large number of products with diverse functions (the peptides) by combinatorial principles. Combination of all the naturally occurring amino acids to all possible hexapeptides gives the astronomical number of $20^6 = 64\,000\,000$ substances!

Combinatorial chemistry is based on a principle that is both simple yet revolutionary: Instead of linking starting materials **A** and **B** to form one product **AB** (Fig. 2), different building blocks

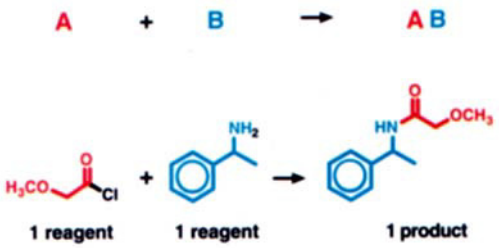

Fig. 2. Conventional organic synthesis.

of type **A** ($\mathbf{A}_1-\mathbf{A}_{10}$) are treated with different building blocks of type **B** ($\mathbf{B}_1-\mathbf{B}_{10}$) according to combinatorial principles; that is, each substance reacts with all other reactants (Fig. 3). This can take place in separate reaction vessels or compartments, or simultaneously in a mixture.

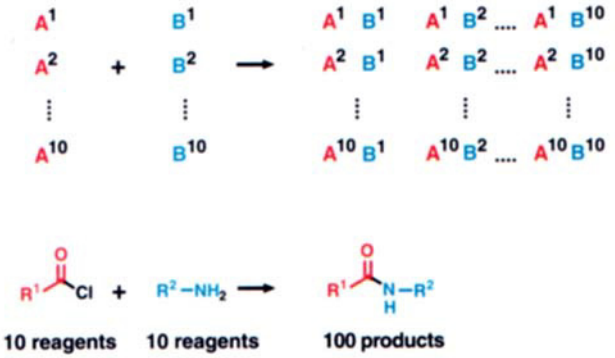

Fig. 3. Combinatorial organic synthesis.

In the above example, ten reagents of type **A** and ten reagents of type **B** give a hundred products in a combinatorial reaction. If we extend this principle of producing all possible combinations in each reaction to multiple-step syntheses, as is generally the case in drug discovery, we rapidly obtain a large number of products from only a few building blocks (Fig 4). For a three-step synthesis with ten building blocks each of type **A**, **B**, **C**, and **D**, we obtain 10 000 products.

The set of all the compounds produced in a combinatorial synthesis is known as a library, in analogy to other such collections.[4] Depending on the production method, a compound library created by combinatorial synthesis can comprise separate compounds or may be a mixture of defined composition.[5] In a multistep combinatorial synthesis, the size of such a library, which corresponds to the total number of all substances synthesized, is determined by the number of reactants or building blocks used per reaction (linear relation), and the number of reaction steps (exponential relation).

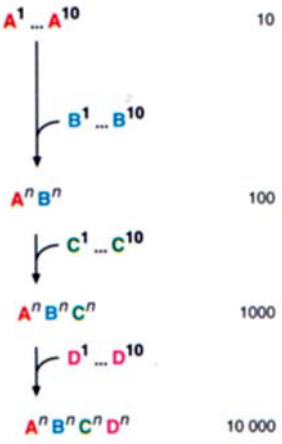

Fig. 4. Multiple-step combinatorial synthesis.

1.3. From Peptide Libraries...

That compound libraries could be created by combinatorial synthesis was first recognized by peptide chemists in the 1980s. Pioneers such as Geysen[6] (multipin method) and Houghten[7] (teabag method) led the way. They developed various methods for multiple (parallel) synthesis of peptides,[10] based on the techniques of solid-phase peptide synthesis according to Merrifield.[8, 9] Further progress was achieved in this field, among others by Frank[11] (spot synthesis) and Fodor et al.,[12] who achieved extreme miniaturization (VLSIPS method). However, combinatorial synthesis of peptides in the strict sense was made possible by the work of Furka and coworkers,[13–16] and this can be regarded as the "birth" of combinatorial chemistry. It was the use of the so-called "portioning-mixing method" ("split synthesis"[17] or the "divide-couple-and-recombine method"[18] as it was later named) that enabled technically simple and efficient synthesis of peptide libraries of almost any size[19] in the form of defined equimolar mixtures. A detailed description of this method, which is important for synthesis of libraries of small organic molecules, is given in Section 2.2.2.

1.4. ...to Small Organic Molecules

Peptides often have a number of disadvantages as drugs such as low bioavailability and ready proteolytic degradation. In addition, conversion of a peptide lead structure into a non-peptide structure is a lengthy and nontrivial undertaking. For this reason, in the last three years the focus of research in the field of combinatorial synthesis has been directed away from peptides towards libraries of "small organic molecules";[20–25] at the same time this research area has undergone a huge expansion. Until recently only a few pioneer companies and academic working groups were involved in combinatorial synthesis, whereas today probably all researching pharmaceutical firms and many academic groups are active in this field. The aim of this review is to present fundamental research on combinatorial synthesis of small organic molecules and to give a "snapshot" of this exponentially growing field. Peptides, oligonucleotides,

oligosaccharides, and pseudo-biological oligomers made up of repeating monomers (such as peptoids or oligocarbamates) are not included.[22, 24–26] The emphasis is on combinatorial synthesis,[5] regardless whether on solid phase or in solution. Syntheses of both mixtures and separate substances are included, as long as the procedure can be described as combinatorial (parallel syntheses under identical conditions according to combinatorial principles).

2. Design, Methods, and Techniques of Combinatorial Syntheses

2.1. Design

Various aspects must be considered when planning a combinatorial synthesis:

- Required is a sequence in which as many as possible of the reactions are bond-forming steps (C–C or C-heteroatom). The target molecule is thus formed by successive reactions with individual building blocks.
- The building blocks for these "construction" reactions must be available as structurally diverse sets.
- The biggest challenge, however, is the chemistry itself: Formation of a new linkage must succeed *irrespective* of the structure already synthesized and the synthetic building block to be linked; that is, the required product must be delivered with high yield and selectivity. This is, of course, the ideal, and one of the main tasks in combinatorial synthesis is to identify reaction sequences that allow the maximum variety in the building blocks ("high-fidelity reactions").
- The products should be as diverse as possible. This means that groups that can undergo noncovalent interactions (hydrophobic and ionic interactions, H-bonds) with a biological target molecule are presented in as many spatial configurations as possible (see Section 2.1.1).
- Finally, the reaction conditions for both the individual reactions and the whole sequence should be amenable to automation.

Peptide synthesis meets all these conditions. There is only a single coupling reaction that is repeated, namely formation of an amide from an activated acyl species and an amine. This reaction has been optimized over many years.

For synthesis of small organic molecules the range of application of each reaction in a chosen sequence must be examined on an individual basis. The aim is to maximize the range of application by suitable choice of reaction conditions or to identify suitable conditions for a particular set of diverse building blocks. Knowing the exact scope and limitations of each individual step in a given sequence enables a sensible choice of building blocks and thus a successful library synthesis.

Finally, there remains the question of strategy for efficient synthesis of the library (Fig. 5). Doubly functionalized monomer units are linked (**A**) in peptide synthesis, and the same is true for other oligomer syntheses. However, different strategies can be considered for synthesis of nonoligomeric small organic molecules. For example, one can start with a template that is already equipped with several functional groups. Different building blocks are attached through these groups, either in a series of separate steps or in one pot (**B**). Alternatively, one can use reactions that introduce a new functionality in the product, on which the next reaction step (**C**) takes place. The multicomponent reactions are an extreme example of this strategy in which intermediates immediately undergo further reactions under constant conditions. Examples of these different strategies and also some mixed strategies are described in the following sections.

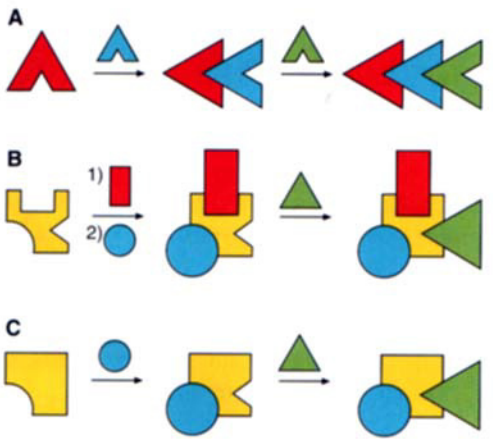

Fig. 5. Strategies for combinatorial synthesis.

2.1.1. Diversity

If one considers that the number of possible organic compounds with a molecular weight less than 750 is estimated at 10^{200},[27] it quickly becomes clear that, despite the great potential of combinatorial synthesis, it would be impossible to synthesize and test all potentially active compounds. Even in a perfect combinatorial synthesis with chemistry that, in principle, enables synthesis of libraries of any size ("virtual libraries"), there has to be a selection of the building blocks to be used and the products to be made.

Compound libraries are generally synthesized with the intention of later biological testing. The chance of finding active compounds in a library increases with the diversity and dissimilarity of the compounds in the library. The test substances should therefore be as "diverse" as possible with respect to the test system; diversity is therefore dependent on the structure of the molecular site of interaction. For example, the compounds thiorphan and *retro*-thiorphan not only have similar appearance at first glance but they also bind to the zinc proteases thermolysin and neutral endopeptidase (NEP) with almost identical affinity (Fig. 6).[28] One would accordingly class them as similar. However, at another site of action, the angiotensin-converting enzyme (ACE),[*] which is also a zinc protease, thiorphan binds about a factor of 100 more strongly than *retro*-thiorphan. Thiorphan and *retro*-thiorphan are therefore not similar relative to this enzyme.

Another example, the oligopeptide-binding protein from *Salmonella typhimurium*, puts the definition of diversity further into perspective (Fig. 7). This peptide binds dipeptides to pentapeptides without differentiation with a K_D of 10^{-6} M.[29] A library of di- to pentapeptides would therefore have no diversity in relation to this molecular target.

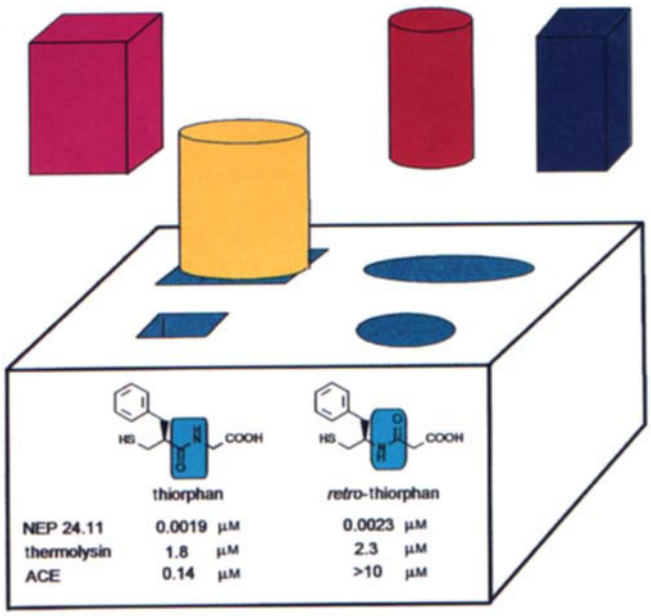

Fig. 6. As illustrated by the different activities of the inhibitors thiorphan and *retro*-thiorphan for these three metalloproteases, the similarity of any two molecules depends on the molecular target under consideration [28].

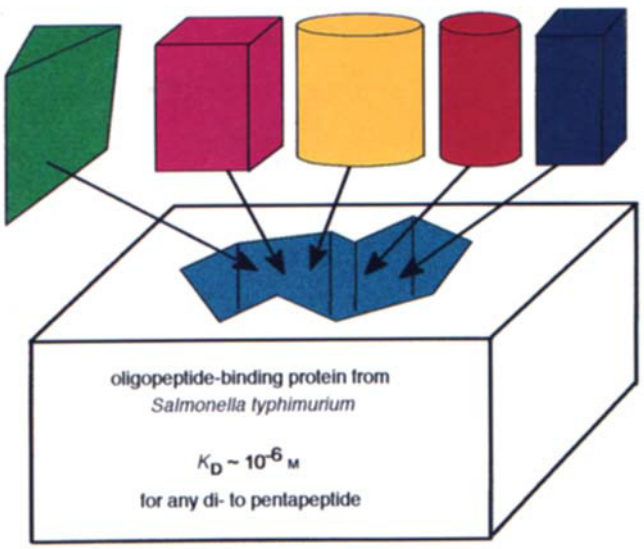

Fig. 7. The oligopeptide-binding protein from *S. typhimurium* binds all di- to pentapeptides with the same affinity [29]. A library of di- to pentapeptides would not have any diversity relative to this molecular target.

Expressing diversity with respect to the biological site of action may seem attractive, but this is not feasible in practice. The structure of the site of action is often unknown, particularly when searching for new lead structures, and a compound library should be tested on many different targets. It is thus much more useful to look for an abstract definition of diversity on an absolute scale when planning a combinatorial compound library. In the following, a collection of compounds will be defined as diverse if groups that can undergo noncovalent interactions with a receptor molecule are available in as many spatial configurations as possible, that is, if a multitude of different pharmacophoric patterns are represented.[30]

The method of Martin et al. of the firm Chiron is based on this definition of diversity. They present selected physical parameters in so-called "flowerplots" and use these to compare individual compounds graphically.[31]

A library suitable for the discovery of new lead structures should be made up of a large number of small organic molecules, which have a high degree of diversity ("random library"). However, if a known lead structure is to be optimized, or if information is available about the biological site of action, the library may have comparatively little diversity ("focused" or "biased library"; see, for example, refs. [32, 33] and Scheme 28).

2.1.2. Format

A library can comprise mixtures of low or high complexity or discrete individual compounds. The decision to use a particular format, that is, whether to test separate compounds or substance mixtures, influences both their synthesis and the procedure for biological testing. If mixtures are used, significantly more substances can be synthesized and tested per time unit. However, the synthesis must deliver all compounds in the mixture in approximately equimolar amounts. Potential problems with false positives and negatives are known in testing mixtures, and these depend on the composition of the mixture to be tested and on the test system used.[34] A common view is that one can afford to miss some active substances during screening because of the large number of test substances—a sufficient number of interesting substances will still be detected ("magic of numbers").[35] This can certainly be justified as long as no attempt is being made to determine structure–activity relationships. Experiments performed at the pharmaceutical company Pfizer[36] indicate that an optimal mixture complexity is about 20 substances per mixture. If more complex mixtures were used, detec-

[*] In this review the following abbreviations were used: Alloc: allyloxycarbonyl, Ac: acetyl, ACE: angiotensin conversion enzyme, 9-BBN: 9-borabicyclo[3.3.1]-nonane, Bn: benzyl, Boc: *tert*-butoxycarbonyl, BOP: 1-benzotriazolyloxytris-(dimethylamino)phosphonium hexafluorophosphate, Bpoc: 2-(biphenylyl-4-yl)propyl-2-oxycarbonyl, Bu: butyl, Bz: benzoyl, CDI: 1,1′-carbonyldiimidazole, mCPBA: *m*-chloroperoxybenzoic acid, DBL: dibutyltin laurate, DBU: diazabicyclo[5.4.0]undec-7-ene, DCC: dicyclohexylcarbodiimide, Dde: 1-(4,4-dimethyl-2,6-dioxocyclohexylidene)ethyl, DEAD: diethyl azodicarboxylate, DIBAH: diisobutylaluminum hydride, DIC: diisopropylcarbodiimide, DIPEA: diisopropylethylamine, DMA: dimethylacetamide, DMAP: dimethylaminopyridine, DME: 1,2-dimethoxyethane, DMF: dimethylformamide, DMS: dimethylsulfide, DMSO: dimethylsulfoxide, DMT: dimethoxytrityl, EDC: *N*-ethyl-*N*′-(3-dimethylaminopropyl)carbodiimide, EE: ethyl acetate, Et: ethyl, Fmoc: 9-fluorenylmethoxycarbonyl, HATU: *O*-(7-azabenzotriazol-1-yl)-*N*,*N*′,*N*″,*N*‴-tetramethyluronium hexafluorophosphate, HBTU: *O*-benzotriazol-1-yl-*N*,*N*′,*N*″,*N*‴-tetramethyluronium hexafluorophosphate, HOAt: 1-hydroxy-7-azabenzotriazole, HOBt: hydroxybenzotriazole, HTS: high-throughput screening, LAH: lithium aluminum hydride, LDA: lithium diisopropylamide, Lig: ligand, L-selectride: lithium tri-*sec*-butyl borohydride, Lys: lysine, Me: methyl, NMM: *N*-methylmorpholine, NMP: *N*-methylpyrrolidone, Nu: nucleophile, PBS: phosphate buffered saline (physiological saline), PDC: pyridinium dichromate, PEG: polyethylene glycol, Pfp: pentafluorophenyl, PG: protecting group, Ph: phenyl, Pip: piperidine, PipOAc: piperidinium acetate, PPTS: pyridinium *p*-toluenesulfonate, iPr: isopropyl, pTA: *p*-toluic acid, Py: pyridine, PyBOP: 1-benzotriazolyloxy-tris(pyrrolidino)phosphonium hexafluorophosphate, PyBroP: bromotris(pyrrolidino)phosphonium hexafluorophosphate, Py·SO_3: pyridine/SO_3 adduct, RT: room temperature, Su: succinimidyl, TBAF: tetrabutylammonium fluoride, TBS: *tert*-butyldimethylsilyl, TCAA: trichloracetic anhydride, TES: triethylsilyl: Tf: trifluoromethane sulfonyl, TFA: trifluoracetic acid, THF: tetrahydrofuran, TMG: tetramethylguanidine, TMS: trimethylsilyl, Trp: tryptophan, Trt: trityl, Ts: *p*-toluenesulfonyl.

tion of active compounds was no longer reliable, because the signal-to-noise factor deteriorated or false positives occurred.

Time saved by working with mixtures can, however, be partially or completely lost by the effort required for deconvolution, that is, new synthesis of less complex sublibraries or individual substances, if the active components can only be identified in this way. Since a compound library will ideally be used in a large number of tests, it is statistically possible that sooner or later each substance mixture will give a positive test result and will have to be broken down into its constituents. Taking an extreme view of the time expended long-term, it could be considered sensible to use separate substances from the beginning. However, libraries of separate compounds are unlikely to reach the size desirable for identification of lead structures. Very large libraries ($\gg 10000$ compounds) can only be efficiently produced as mixtures.

Experience shows that the optimization of lead structures yields numerous compounds displaying biological activity. In such a case it is better to use libraries of separate compounds from the start rather than to have to deconvolute all the mixtures later on. Here the reaction building blocks are selected more precisely and smaller libraries (<1000 compounds) are synthesized.

Whether the synthesis of separate compounds or mixtures will predominate is difficult to say at present. There are equally many examples of the two strategies, which will be presented in the following sections. It is unlikely that a general strategy will emerge in the future, since the choice of format will always depend on the particular problem in hand.

Another basic decision concerns investigation of the synthesized compound library in biological tests (Section 5): should the substances be tested in solution or on a support (as they are obtained initially in the case of solid-phase syntheses). The trend here is clearly to examine the test substances in solution. The results are not influenced by undesired interactions with the support, and above all, many assay systems that have already been established can be used.

2.2. Methods and Techniques of Combinatorial Synthesis

2.2.1. Synthesis in Solution; Synthesis on Solid Phase

In principle, combinatorial syntheses can be performed both in solution and on solid phase (Fig. 8). Small organic molecule synthesis on supports is nowhere near as well optimized as syntheses of peptides and nucleotides. Consequently, the effort required for development of such a synthesis is considerable. However, solid-phase synthesis has a number of advantages over conventional solution synthesis.

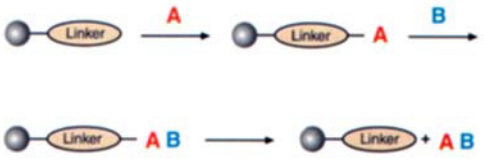

Fig. 8. Principle of solid-phase synthesis. Sphere = polymeric support, **A** = first building block, **B** = second building block, **AB** = product.

The reaction is accelerated by using an excess of the soluble reaction partner, and complete conversion can be achieved. Complex workup and purification steps are replaced by simple washing of the support at the end of each reaction. Thus, solid-phase synthesis enables full automation of all steps, even for multiple-step syntheses. It is therefore not surprising that a large proportion of combinatorial small organic molecule syntheses reported up to the present time were performed on supports. This has led to a renaissance of the solid-phase syntheses of organic molecules developed in the 1970s and 1980s, particularly those of Fréchet[37] and Leznoff,[38] and an abundance of classical organic synthetic reactions have since been carried out on solid supports.[26, 39, 40]

However, as seen from the comparison in Table 1, combinatorial synthesis in solution has advantages that should not be underestimated, especially since multiple-step organic synthesis on solid phase is still in its infancy at the moment. Combinatorial synthesis in solution does not require any additional reaction steps for linkage to or cleavage from a polymeric support. Stability and reactivity of linkers and resins do not have to be considered when choosing the reaction conditions. The biggest advantage is that the reaction conditions do not have to be adapted to the requirements of solid-phase synthesis. In addition, expensive functionalized polymeric supports are not required, and a relatively simple scale-up is possible. However, simple concepts for automated raw product purification will be important for the further development of combinatorial synthesis in solution. If side products or excess reagents could be reliably separated in this way, the number of useful reactions will be vastly increased. For this reason, combinatorial synthe-

Table 1. Comparison of combinatorial syntheses on solid phase and in solution.

Combinatorial synthesis	
On solid phase	In solution
Advantages	
Reagents can be used in excess without separation problems later, and thus reactions can be driven to completion.	All organic reactions can be used in principle
Purification of the product by washing the support	No adaption of known reaction conditions is required
Simple complete automation of reaction sequences	No additional reaction steps for linkage to and cleavage from the support
Split synthesis possible ("one bead, one compound")	Unlimited amounts of product can be produced
Pseudo-dilution	
Disadvantages:	
Not well developed → expenditure of time for development required	Reactants cannot be used in excess unless additional work is invested during purification
Additional reaction steps for linkage to and cleavage from the support	Automation of isolation and purification steps is difficult
Support and linker limit possible chemistry	
Methods for analytical monitoring of the reactions not well developed	

ses in solution are at the moment most common where only one or two steps are involved. In future, choice of solution or solid-phase synthesis will depend on the particular requirements. It may also make sense to combine solution and solid-phase reactions in a synthesis sequence, as described in recent work by Armstrong et al.[41] and Suto.[42]

2.2.2. *Synthesis of Separate Substances; Synthesis of Mixtures*

Both separate substances and defined mixtures can be synthesized according to combinatorial principles. Individual substances can be obtained by fast parallel syntheses, that is, n substances are synthesized in n reaction vessels. An efficient automated reaction process is a basic requirement for this.

Synthesis of defined mixtures requires procedures that deliver a large number of structurally defined compounds in equimolar amounts with as few reaction steps as possible. Thus mixtures of reactants could be used in each reaction step so that many reaction products are formed in one reaction vessel at the same time.

This is the usual procedure for combinatorial synthesis of mixtures in solution. However, for solid-phase synthesis this concept could be demonstrated convincingly only for synthesis of amide compounds in peptide libraries[43,44] or for synthesis of nucleotides.[45,46] Although this strategy was also employed initially for synthesis of small organic molecules,[47,48] only reactants with similar reactivity were used. Much larger differences in reactivity must usually be reckoned with in the synthesis of large libraries of small organic molecules. This may mean that certain reaction products are only formed to a lesser extent or not at all. Such reaction procedures also lack one of the big advantages of solid-phase synthesis, namely that reactants can be used in a large excess to drive the reaction to completion.

The problem of different reaction rates is elegantly avoided by the "split method" according to Furka et al.,[13-18] which furnishes an efficient synthesis of equimolar mixtures. As shown in Figure 9, the solid support is divided, for example, into three equal parts, and each of the three aliquots is treated with a

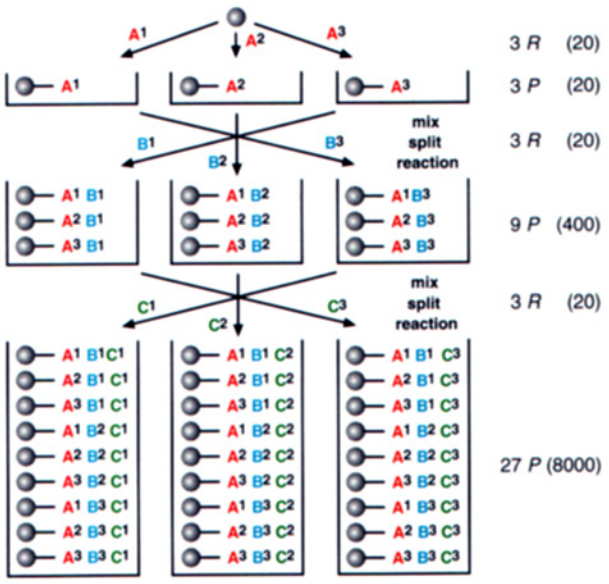

Fig. 9. Split method. Sphere = polymeric support; ***R*** gives the number of reactions performed in parallel, ***P*** is the number of different products [13-18].

synthetic unit of type **A**. The resulting product resins are mixed and divided anew, giving three mixtures in which the resin-linked components $\mathbf{A}^1$, $\mathbf{A}^2$, and $\mathbf{A}^3$ are present in equimolar amounts. These are treated with $\mathbf{B}^1$, $\mathbf{B}^2$, or $\mathbf{B}^3$, which gives nine defined products in total. Since there is only one reactant in solution in a reaction vessel at any one time that reacts with a large or small number of support-bound reaction partners depending on the synthesis plan, all reactions can proceed to completion despite possible differences in kinetics. Repetition of the cycle of division, reaction, and mixing gives, in a short time, large compound libraries in which all compounds are present in equimolar amounts. At the end of such a synthesis sequence, a compound library is obtained in which many copies of only one compound are present on each bead (one bead, one compound[17]). The obvious advantage is that 27 products are obtained in nine reaction steps with nine synthetic building blocks (in three mixtures of nine compounds each), whereas their synthesis as separate compounds would require 81 reaction steps.

All 8000 tripeptides obtained from the 20 natural amino acids can be synthesized in 20 mixtures of 400 compounds each in an analogous way using only 60 coupling reactions. These are quasi separate compounds as long as they are bound to the solid phase.

The number of all synthesized substances N is given in Equation (a), where n is the number of building blocks in each reaction (1,2, 3,... m) and m is the number of reaction steps in which new reaction building blocks are introduced.

$$N = n_1 \times n_2 \times n_3 \times \ldots n_m \qquad \text{(a)}$$

Burgess et al.[49] have thrown some light on the statistical aspects of the split method. In particular, they examined how many support particles have to be used in order that all desired compounds are present in the resulting library with a certain probability. They were able to show that with ten reactants per cycle and a total of five cycles (resulting in $10^5 = 100000$ substances), at least 500000 support particles must be used if 99% of all theoretically possible compounds are to be present in the library with 99% probability. For the commonly used synthetic resins, 1 g of support material corresponds to several million particles so that from a statistical point of view, libraries of the order of greater than 10^5 substances are possible in practice. Further statistical investigations of the split method were recently published by Zhao et al.[50] and Boutin and Fauchère.[51] A recent patent application from the company Pharmacopeia[52] describes an attempt to overcome a statistically unfavorable distribution by avoiding the mixing step in a common vessel. The support material is aliquoted from the current reaction vessel *directly* into the reaction vessel in which the next synthesis step should take place. However, synthesis of larger libraries then requires a large number of distribution steps. It is noteworthy that the split method in solution does not have this kind of statistical problem.

2.2.3. *Genetic Algorithms*

An interesting and not yet widespread approach to minimizing the number of substances to be synthesized is the use of genetic algorithms.[53] This evolutionary strategy is commonly used for efficient optimization of multiparameter systems[54]

and gives a good solution with high probability, if not necessarily the optimal solution. Using the genetic operations replication, mutation, and crossover, new solutions are generated from a set of the starting solutions, which have improved properties from generation to generation. Carrying this idea over to combinatorial synthesis, the aim is to optimize a desired substance characteristic such as biological activity whilst keeping the number of substances to be synthesized and tested as low as possible.

Weber et al.[55] used genetic algorithms to select the products to be synthesized with a four-component reaction, in order to obtain products with maximal biological activity from as few syntheses as possible. They created a library of 160000 virtual compounds by computational combination of 100 building blocks. All compounds were assigned a bit pattern (binary code) according to the building blocks they were composed of. These substance codes represented the genetic material. After parallel syntheses of 20 randomly selected reaction products, the bit patterns of these products were submitted to the genetic operations mentioned above. The new bit patterns obtained by this method coded for 20 new compounds, which were then synthesized. The biological activity was determined for the 40 compounds, and the 20 most active reaction products were selected, which now formed the parent generation for computation and synthesis of further substances. This process was carried out for 20 generations so that in total 400 (0.25% of the possible 160000) reaction products were synthesized and tested. The reaction products of the twentieth generation were 2000 times move active enzyme inhibitors than the compounds of the first generation. However, no comparison was made with the biological activity of 400 randomly selected reaction products. A further recent publication from Singh et al.[56] describes optimization of hexapeptide substrates of stromelysin by applying genetic algorithms. Model calculations of Sheridan et al.[57] show that genetic algorithms can be used for selection of suitable reagents for a combinatorial synthesis, that is, for designing a library.

2.2.4. Characterization of Test Substance Libraries

The procedure for characterization of test substance libraries depends on their format. If individual substances are produced in a parallel synthesis, the analysis is the same as for conventionally synthesized substances. The situation is similar if a compound library is synthesized by the split method. Since in this case, each particle only carries one substance (one bead, one compound), the analysis of such libraries can be reduced to that of the individual substances, as long as they are resin-bound. Since the amount of substance bound to a single support particle is usually of the order of several 100 pmol, mass spectroscopic methods are the methods of choice, despite recent progress in the fields of IR[58] and NMR spectroscopy.[59] Practical feasibility was first demonstrated with peptides,[60–62] also coupled with affinity capillary electrophoresis,[63] then with peptoids,[64] and recently with low molecular weight, non-peptide compounds.[65] Cleavage of the product-linker bond was either performed in a separate step before the measurement with trifluoroacetic acid vapor or photochemically,[61] or directly in the spectrometer under matrix-assisted, laser desorption-ionization time-of-flight (MALDI-TOF) conditions.[62]

If libraries are in the form of mixtures after cleavage from the support, a reliable analytical characterization is difficult and becomes impossible at a certain mixture complexity. The first reports of characterization of such libraries—likewise with mass spectroscopic methods—also come from the peptide field.[66] Combinatorial mixtures of low molecular weight organic molecules have also been characterized in this way since then.

Along these lines, Rebek's group examined how much of the theoretically possible product in a library synthesis was formed in solution, using combinations of different mass spectroscopic methods.[67] Meutermans et al. synthesized di- and tetrahydroisoquinolines on solid phase[47] and were able to show using ion spray MS that all the predicted compounds were present in the mixture after cleavage. Another variant, which gives reliable results particularly for characterization of smaller mixtures, is the coupling of HPLC and MS.

In addition to the *direct* methods of structural determination described above, there are also *indirect* methods, which are particularly advantageous when working with mixtures produced by split synthesis. Here, the structure is obtained by deciphering a code generated in parallel to the synthesis of the library, which represents a recording of the synthetic steps performed. Coded libraries are discussed in full in Section 5.5.

3. Combinatorial Synthesis in Solution

There are basically two strategies for combinatorial synthesis in solution. Some research groups use approaches involving synthesis of compound mixtures of varying complexity, whilst other groups use parallel synthesis, which gives a lower number of synthesized compounds but has advantages during characterization and determination of biological activity of the individual substances. Advantages and disadvantages of both strategies were discussed in Section 2.2.2.

3.1. Synthesis of Compound Mixtures

3.1.1. Random Synthesis

The synthesis of unwanted compound mixtures is a big problem in classical chemistry that every synthetic chemist has to confront. This explains the skepticism towards combinatorial chemistry often encountered especially with regard to random syntheses. The Maillard reaction[68] and research such as that of Chen and Radmer can be considered examples of random syntheses for creation of molecular diversity.[69] They treated an equimolar mixture of glucose, galactose, and inositol in pyridine with a subequimolar amount of sodium azide. According to their report, the oligomer content of the mixture obtained was increased from 14% to 27% by performing a further transformation with $Hg(CN)_2$, $HgBr_2$, and HgI_2. Subsequent reduction with hydrogen catalyzed by $Pd(OH)_2$ on carbon gave a wide variety of deoxysugars and aminoglycosides.

Since random syntheses are only a fringe area in combinatorial chemistry and are beset with major problems similar to those known from processing natural substance extracts, they will not be discussed further here.

3.1.2. One-Step Synthesis

The type of combinatorial syntheses in which per reaction step two molecules from only two different compound classes undergo a defined reaction or reaction sequence (such as acid chlorides with amines to amides) are more clear-cut than random syntheses. If sequential reactions are avoided, unwanted side products will not accumulate. However, this advantage is severely limited by the small number of products that can be obtained, since only two different components are incorporated in each molecule formed. Examples of this type of synthesis have been demonstrated by research groups at the laboratories of Duke University in the USA and at Glaxo Research and Development Ltd in Great Britain.[70, 71] They solved the problem of identification of biologically active compounds from the product mixture by using an elegant synthesis strategy. Pirrung et al. produced an "indexed combinatorial library" composed of 72 tetrahydroacridines[35] by condensing six cyanoanilines with twelve symmetrical cyclohexanones in one reaction step (Scheme 1).[71]

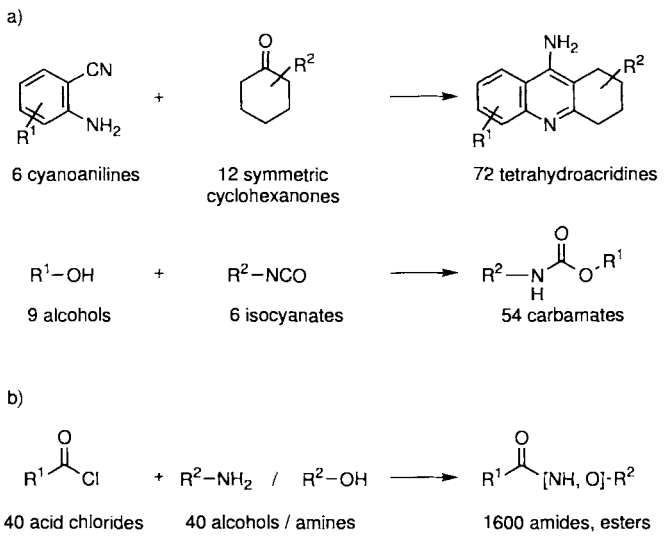

Scheme 1. Reactions used by Pirrung et al. [35, 71] (a) and Smith et al. [70] (b) for synthesis of indexed combinatorial compound libraries. The tetrahydroacridines are in 6 mixtures of 12 and 12 mixtures of 6 compounds [71]. The carbamates are 9 and 6 mixtures of 6 and 9 compounds, respectively [35], and the amides/esters are each 40 mixtures of 40 compounds [70].

The reactions were performed so that each of the six cyanoanilines was treated with a stoichiometric quantity of an equimolar mixture of the twelve cyclohexanone derivatives. Each cyclohexanone was also treated with a corresponding mixture of the amine components. Six mixtures of twelve components and twelve mixtures of six components were produced in total, in which the individual compounds in each mixture have half a molecule in common. In addition, each component appears in exactly two of these 18 mixtures. If a compound is biologically active, it will be detected in both of the mixtures that contain it (cf. Section 5.2). The same research group was able to use this method to identify acetylcholinesterase inhibitors in a carbamate library (Scheme 1).[35]

At about the same time as Pirring, Smith et al.[70] used this strategy to synthesize mixtures of esters or amides (Scheme 1) and investigated the biological activity of the mixtures with a wide range of molecular test systems. They were able to identify an inhibitor of the matrix metalloprotease-1 (MMP-1) and a neurokinin-NK_3 antagonist.

3.1.3. Two-Step Reaction Sequences

Storer of Glaxo Wellcome has worked on two-step combinatorial synthesis in solution.[72] He combined 50 amino acids, 80 carboxylic acids, and 40 amines to form a library of 160000 diamides, composed of 4000 mixtures each of 40 compounds. To achieve this, he first treated each of the 50 amino acids with a mixture of 40 amines. These 50 mixtures each of 40 compounds were subsequently treated with each of the 80 carboxylic acids. Although only 4000 reactions had to be performed rather than individual synthesis of all 160000 compounds, the use of synthesis robots was a big advantage here. This strategy saved reaction steps since, unlike in indexed libraries, each substance was not synthesized twice. However, if a mixture showed biological activity, all the individual components had to be synthesized separately for further investigation. Lead structures for different targets (HIV protease, neurokinin-1 receptor) have since been identified from this diamide library.[73]

3.1.4. Three-Step Reaction Sequences

For multiple step combinatorial synthesis sequences, MacLachlan has shown that heterocycle syntheses are possible, in addition to proven amidation reactions (Scheme 2).[74] By

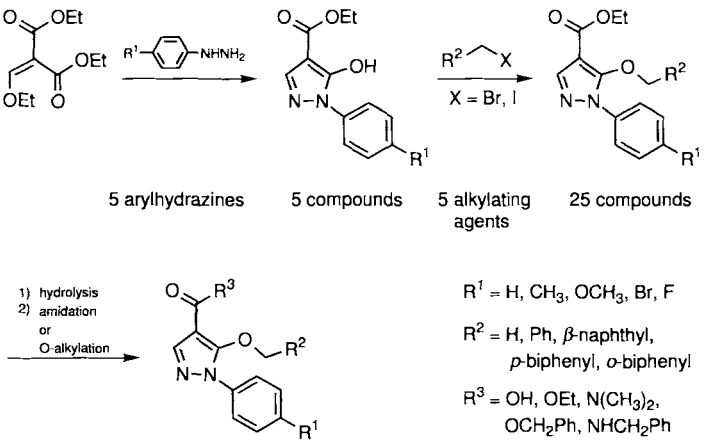

Scheme 2. Synthesis of a phenylpyrazole library [74]. The 125 pyrazole derivatives are obtained as 5 mixtures each of 25 compounds.

variation of three molecule segments, he was able to synthesize a pyrazole library of 125 compounds in a three-step phenylpyrazole synthesis. Careful choice of reaction conditions and clever selection of reagents was also important here. For example, allyl bromide could not be used as an alkylation reagent for the O-alkylation, since the Claisen rearrangement would otherwise predominate. MacLachlan's work is a good example of how more complicated reaction sequences can be performed combinatorially in solution. To determine the structure of a biological-

ly active compound obtained with this synthesis scheme, three (number of variable groups) times five (number of different variants per group) sublibraries are created. The first set of sublibraries is composed of 5 mixtures each of 25 substances, which each have a defined group R^1. The groups R^2 and R^3 are identified in a similar manner.

3.1.5. *One-Pot Syntheses*

Further multiple-step reaction sequences for production of molecule libraries have been reported by Rebek, Jr., and coworkers.[67, 75–80] The reactions used were restricted to the reliable formation of amides from amines and acid chlorides, and the reaction of isocyanates with amines. They were able to link four different groups to a central molecular scaffold simultaneously in a one-pot reaction and thereby obtained a large number of highly diverse compounds. The rigid xanthene- and cubanetetracarboxylic acid chlorides **1** and **2** as well as the more flexible tricarboxylic acid chloride **3** were used as the central scaffold for their amide libraries (Fig. 10). Either the rather

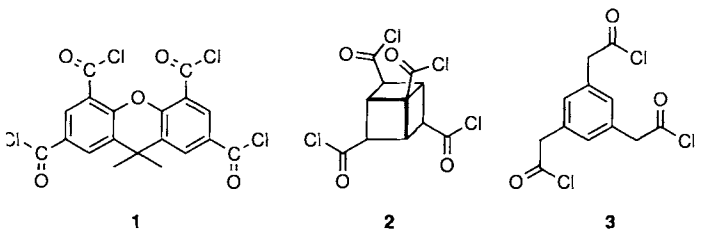

Fig. 10. Three central building blocks used by Rebek, Jr. et al. [75–80] for the synthesis of amide libraries.

more disc-shaped molecules (the derivatives of **1** and **3**) or the rather more spherical compounds (the derivatives of **2**) were obtained. At the same time, the distance between the reactive centers ensured that they had little steric influence on one another. The molecules were also chosen so that the reactivities of the functional groups were similar. To synthesize the library, templates **1**, **2**, or **3** were each treated with up to 21 amines.[75, 79, 80] The amine components chosen were mainly amino acid esters; one equivalent of an equimolar mixture of the individual amines was used.

The lower the symmetry of the central building block and the larger the number of its reactive centers, the higher the number of different products that can be formed. For example, reaction of the xanthene **1** with 4, 7, 12, and 19 amines theoretically gives mixtures of 136, 1225, 10440 and 65341 compounds (Fig. 11).

The question whether all possible reaction products are actually formed is of particular interest. HPLC chromatograms of libraries of varying complexity gave evidence that use of additional amines results in a larger number of compounds.[75] However, this question could only be answered convincingly on application of mass spectroscopic methods.[67, 77, 79] Since the analysis of a mixture of several thousand compounds is very difficult, examples of less complex libraries were synthesized by treating **4** with different sets of amines. Derivative **4** (Fig. 11) was chosen since steric interactions between the substituents at positions 4 and 5 of the xanthene, which would influence the reactivity at these positions, are unlikely. Reaction of **4** with sets

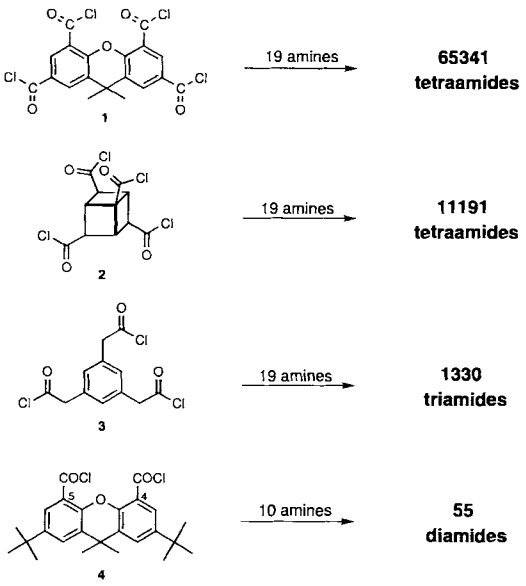

Fig. 11. Maximal number of compounds from various amide libraries. As the symmetry of the central scaffold increases, compound mixtures of lower complexity are obtained with the same number of amines [79].

of 8, 9, and 10 amines should give 36, 45, and 55 diamide products with this simplified molecular scaffold. Suitable choice of reagents ensured that the reaction products possible from different sets of amines had different molecular weights so that their examination by mass spectroscopy gave conclusive results. These showed that for the library of 36 compounds, about 85% of the expected compounds could be identified by their molecular ion peaks compared to 78% for the 55-compound library. The experiment also permitted identification of "problem candidates" among the amine components. For example, if the arginine derivative is excluded, 93% of the expected compounds were detected in the 55-compound library. These investigations showed that a large proportion of the predicted compounds are actually present in the mixture, if the individual components are carefully chosen. At the same time, analyses indicated that about a 10% fraction of the libraries were side products.

An extension of this concept was presented by Rebek, Jr., at the fall meeting of the American Chemical Society last year (Scheme 3).[78] By using the tetraisocyanate **6** instead of the

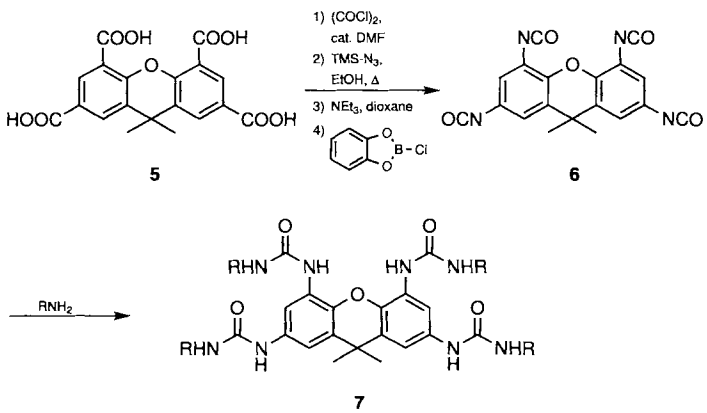

Scheme 3. Synthesis of the tetraisocyanate **6** as central building block for the urea derivatives **7** [78].

tetrachloride, urea derivatives are obtained—the reactivity of the isocyanate is so high that a 1.5-fold excess of amino acids can be used without preferential formation of any of the reaction products. This was demonstrated by examination of the reaction products of mixtures of glycine methyl ester and leucine *tert*-butyl ester with **6**.

A similar formulation was chosen by researchers at ISIS Pharmaceuticals. To increase the number of possible products, they used unsymmetrical linear and cyclic tri- and tetraamines such as azacyclophanes as templates. These were treated with acid chlorides, alkyl halides, and aldehydes.[81]

This kind of one-pot reaction enables very fast and efficient production of large substance mixtures from known reactions in solution. If the reaction components are available in highly structurally diverse forms—as is certainly the case for amines[82]—restriction to one reaction type need not result in compound libraries of reduced diversity. More serious is that only reactions that proceed reliably with reactants of very similar reactivity can be used, and that this method only permits synthesis of mixtures. This procedure has become less popular as the synthesis of large mixtures has decreased in importance.

Rebek, Jr., also presented a strategy for detection of biologically active compounds in a compound library[76, 79] and has used this to identify the trypsin inhibitor **8** ($K_i = (9 \pm 2) \times 10^{-6}$ M) (Fig. 12). The method of deconvolution used here is noteworthy in that it is not the most active compound mixture that dictates the choice of building blocks; rather the less active mixtures are used to set the exclusion criteria for the choice of building blocks.

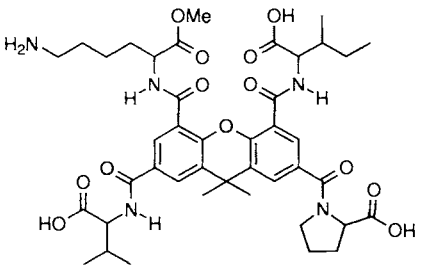

8

Fig. 12. Trypsin inhibitor found by screening a library that theoretically contains 65341 xanthenamides; $K_i = (9 \pm 2) \times 10^{-6}$ M [76].

An important limitation of this iterative process is that not necessarily the most active compounds are identified. However, Rebek, Jr., et al. presented a plausible hypothesis using computer simulation that—even if the compounds identified are not the most active—a compound which is an order of magnitude more active will not be missed.[79] Above all, groups of active compounds are identified, since a single active compound can scarcely be detected in a mixture of ten thousand inactive substances.

3.1.6. Multicomponent Reactions

The multicomponent reactions have a unique position in combinatorial synthesis of compound libraries.[83] A particular reaction *sequence* takes place after all reaction participants have been mixed. The difference from the work described by Rebek, Jr., et al. is that a sequence of reactions of different types are used. Ugi, a pioneer in this field, has been involved in multicomponent reactions for several decades.[84] As early as 1961 (that is, many years before the term combinatorial chemistry was coined) he and Steinbrückner pointed out that it should be possible to produce an enormous number of different compounds by multicomponent reactions: "Since such condensation reactions take place between four (in exceptional cases even more than four) components, the number of possibilities are very high. The use of merely ten compounds each of the four condensation components yields 10^4 combinations. It therefore seems expedient to determine the scope and limitations with respect to the individual components by studies on simple systems in which as many variables as possible are kept constant" (translated from the German).[85] It is therefore not surprising that, almost 35 years later, after the advent of combinatorial chemistry, Ugi and his co-workers were using "Ugi Chemistry" to create compound mixtures (Scheme 4).[86]

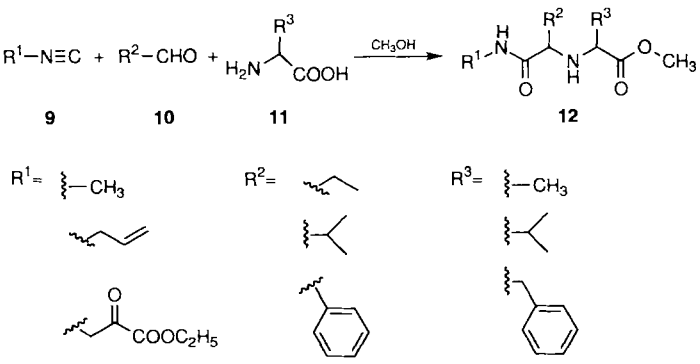

Scheme 4. A variation of the Ugi reaction. Starting from three isonitriles **9**, three aldehydes **10**, and three amino acids **11**, a substance mixture theoretically containing 54 compounds of type **12** is obtained [86].

By treating three amino acids (**11**) with three isonitriles (**9**) and three aldehydes (**10**) and methanol, they obtained a library of type **12**, theoretically composed of 54 compounds (if possible stereoisomers are counted as separate compounds). Since only 37 compounds were shown to exist by GC-MS analysis, three daughter libraries each of 18 compounds were created. Examination of these showed that almost all of the expected products were actually formed.[86] As one-pot reactions that are simple to perform, multicomponent reactions represent an efficient way of generating compound libraries, although the products may be formed at widely differing concentrations.[86] Based on many years of experience with these reactions, Ugi selected the starting materials so that they had similar reactivities. Careful choice of reagent also ensured that the products were formed with good yield and high purity. Under these conditions, a larger library of pyridine-2,6-dicarboxylic acid derivatives (**14**) with 8256 components was successfully synthesized (Scheme 5).[86]

Libraries of carbohydrate derivatives have also been produced with multicomponent reactions.[87] However, nowhere near all the expected products were formed. In addition to this

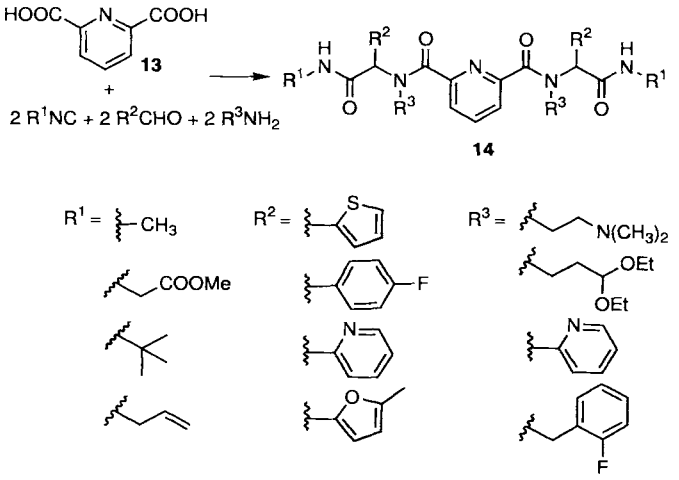

Scheme 5. Synthesis by a variation of the Ugi reaction [86] of a library theoretically containing 8256 pyridine dicarboxylic acid derivatives **14**.

particularly bad problem, large differences in concentration of the products were obtained.

Further examples of combinatorial syntheses with multicomponent reactions are given in the following section and in the section on combinatorial syntheses on solid phase (Section 4.3.3).

3.2. Parallel Syntheses of Single Compounds

To avoid the disadvantages already mentioned of synthesis of compound mixtures, several research groups have been involved in combinatorial synthesis of single compounds in solution. The most efficient synthesis possible of a large number of defined individual compounds through combinatorial principles is the aim here. The border between classical and combinatorial chemistry is therefore fluid for these types of reaction.

3.2.1. Multicomponent reactions

Like Ugi, Armstrong[88] and Holmes et al.[89] also employ multicomponent reactions for combinatorial synthesis but they generate single compounds (the work of Weber et al.[55] was described in Section 2.2.3). Whilst Holmes's work is mostly associated with optimization of a solid-phase synthesis, Armstrong has reported synthesis of a library of 64 α-acyloxyamides **18** by systematic combination of 8 aldehydes **15**, 8 carboxylic acids **16**, and an isonitrile **17** in a Passerini reaction (Scheme 6).

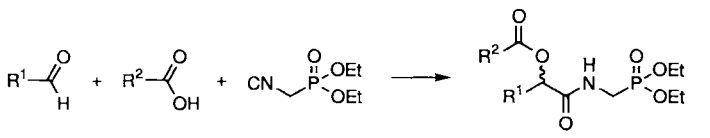

R^1 = C_2H_5, n-C_3H_7, n-C_6H_{13}, CH=CHCH$_3$, CH=CHPh, Ph, p-(H_3CO)Ph, p-$((H_3C)_2N)$Ph

R^2 = CH_3, CH=CH, CH_2CHCl_2, CH_2Ph, $CH(Ph)_2$, CH=CHPh, Ph, α-naphthyl

Scheme 6. Passerini reaction for synthesis of a library of 64 α-acyloxyamides **18** [88].

In each of the parallel reactions, one equivalent each of the acid and the isonitrile was treated with two equivalents of the aldehyde at room temperature. The products were worked up by simple evaporation of the reaction solution. Analysis of the reaction products by ^{1}H NMR spectroscopy gave a yield of about 80% based on converted isonitrile. Armstrong's synthesis of eight azinomycin analogues also with a Passerini reaction (see also Section 4.3.3) was certainly on the border between classical derivatization and combinatorial synthesis. Although interesting compounds were obtained, these were isomeric mixtures; in addition, workup of each product required chromatographic separation.

The restrictions on the starting materials limit creation of molecule libraries with the Passerini and Ugi reactions. Although many aldehydes, carboxylic acids, and amines of differing structures are commercially available, the number of available isonitriles is much smaller.

An interesting variation of the Ugi reaction has been presented by Armstrong and Keating.[41, 90] They used 1-isonitrilecyclohexene (**19**) as the isonitrile component in the Ugi reaction and thus obtained the cyclohexenamides **20**. These were converted into further derivatives by introduction of a fourth component of molecular diversity (Scheme 7). The carboxylic acids

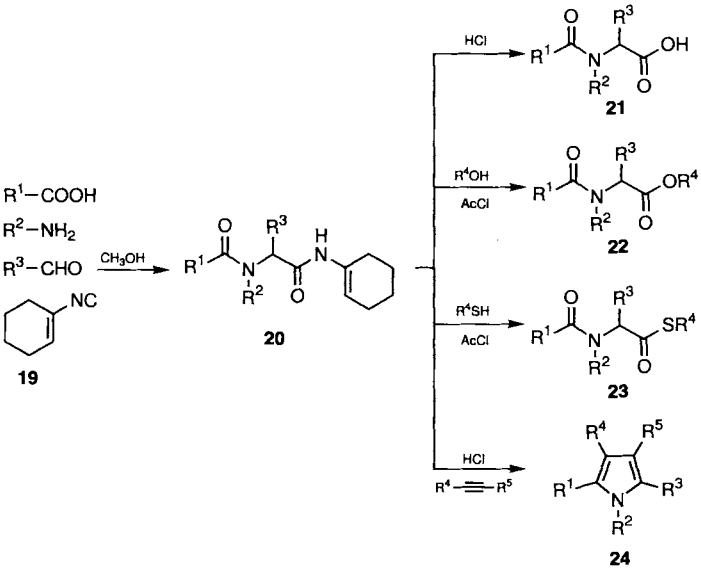

Scheme 7. The Ugi reaction with the isonitrile **19** gives the reactive enamide **20**. This can be converted by further reactions into different acid derivatives (**21**–**23**) or pyrroles (**24**) [41, 90].

21 were obtained by acid hydrolysis; alcoholysis of the reactive enamide with alcohols and mercaptanes gave the esters and thioesters **22** and **23**. Polymer-bound alcohols could also be used as the alcohol component. This so-called "resin capture" meant that the resulting esters **22** were available on a polymer support for further reactions. The pyrrole derivatives **24** were generated by [3 + 2] cycloadditions of electron-deficient alkynes on the Münchnones obtained by protonation of **20**. (A related, purely solid-phase synthesis has since been reported; see Scheme 35).[91] When anthranilic acid derivatives were used as the acid component in the Ugi reaction, the corresponding cyclohexenamides were cyclized to yield benzodiazepine derivatives.

Use of protected D-arabinose as the aldehyde component gave the corresponding lactone by cyclization of the enamide **20**.

3.2.2. *Classical Solution-Phase Reactions*

The most obvious approach for combinatorial single-substance synthesis of compound libraries is the performance of known reliable reactions in parallel. These must proceed very smoothly with high yield and preferably should not require any purification steps. In other words, any reagents remaining at the end of the reaction should be able to be removed by evaporation, as far as possible. These requirements are satisfied by so-called "snap reactions", for example as used to create compound libraries by the company ArQule (Scheme 8).[92, 93]

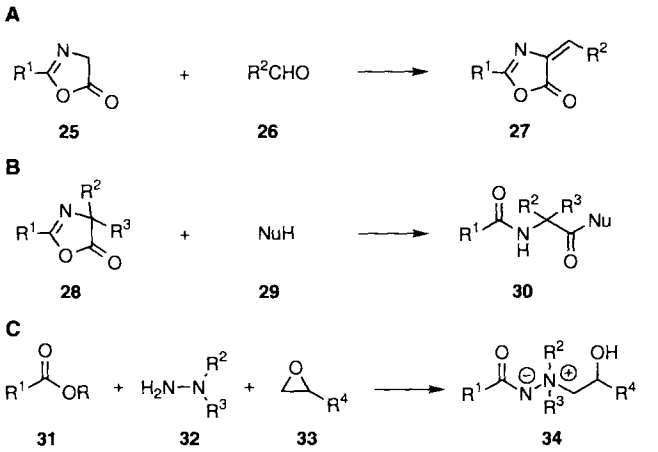

Scheme 8. Types of reaction used by the firm ArQule for production of compound libraries [92–94]. **A**: Knoevenagel condensation of oxazolones with aldehydes; **B**: reaction of oxazolones and nucleophiles (Nu) with ring opening; **C**: synthesis of aminimides.

By Knoevenagel condensation of oxazolone derivatives **25** with aldehydes **26**, the corresponding unsaturated compounds **27** were obtained, which with suitable choice of substituents enabled further functionalization, for example, by Michael addition (Scheme 8, **A**). Reaction of oxazolones **28** with nucleophiles **29** ran equally smoothly and led to the corresponding ring-opening products **30** (Scheme 8, **B**).[92] The aminimides **34** were another synthetic target. These can be used as peptide mimetics due to their high hydrolytic stability and improved solubility (Scheme 8, **C**).[94] Their synthesis was achieved by a 3-component reaction of ester **31**, hydrazine **32**, and epoxide **33**. Examples of libraries synthesized with this reaction include an aminimide library of type **35** composed of 5000 compounds, and a library of type **36** with 8000 compounds (Fig. 13).

Fig. 13. Structural types of individual compound libraries synthesized by the firm ArQule [92,93].

The Mannich reaction has also been used for library synthesis in solution. A library of 9000 aminophenols was produced from formaldehyde, phenols, and secondary amines.[95] Each of these three libraries were made up of single compounds synthesized on a 20 mg scale with a purity of greater than 80%. Examples of syntheses of smaller libraries each composed of 16 compounds are described in the patent literature.[96] However, both the aminimide synthesis and the Mannich reaction have since been transferred to the solid phase by ArQule researchers. The advantage gained is reported to be increased reliability of the reactions. In addition, it was noted that simpler, more uniform reaction conditions than in solution syntheses could be found for many different reactants in solid-phase syntheses.[97]

The choice of available reactions becomes much wider if simple workup steps can be used. Researchers at Panlabs[98] use excess reagents, deactivate the excess on completion of the reaction, and follow this with an extractive workup. Nevertheless, these reactions must run as quantitatively as possible. Some of the reactions used along these lines by Peterson and co-workers for combinatorial synthesis are shown in Figure 14.

Substrates	Reagents	Products
ROH	RCOCl	aldols, alcohols, amides,
RSH	ROCOCl	amines, (thio-)carbamates,
RNH_2	R_2NCOCl	(thio-)carbonates, (thio-)
$RCONH_2$	RSO_2Cl	esters, (thio-)ethers,
$RHNNH_2$	RCN	thiosulfates, urethanes,
RMgX	RCH_2X	ureas, hydrazones,
RCOR	RCHO	ketones, sulfonamides,
	RCOOH	sulfones
	RCOR	

Fig. 14. Substrates, reagents, and product classes chosen by the firm Panlabs for the synthesis of libraries of individual substances [98].

The basic difference of this procedure to the research described so far in this section is that only two building blocks are incorporated into the molecule to be synthesized. In addition, it should be pointed out that the compounds produced are crude products rather than pure substances. Seven reactions were therefore chosen to investigate the purity of the compounds, and reaction conditions were optimized for as wide a substrate spectrum as possible. With these seven reactions, 200 reaction products were produced from 40 substrates and 5 reagents, and about half of these were analyzed by mass spectrometry (Scheme 9). The analysis showed that the desired molecular ion was detected in over 92% of the samples examined. According to company reports, about 50000 compounds were produced by this method in 1995.

Panlabs researchers recently presented various two-step reactions for parallel synthesis of single compounds that extend the product diversity (for example, cyclic anhydride opening with amines and subsequent conversion into the unsymmetrical bisamide).[99] A cooperation was recently started between Panlabs and Tripos to optimize diversity of libraries obtained by this method.

A library of 4400 benzimidazole derivatives **38** synthesized as single compounds was also obtained by a two-step synthesis by Dhanoa of the company Alanex (Scheme 10).[100] A synthesizer developed by Alanex was used to produce the library.

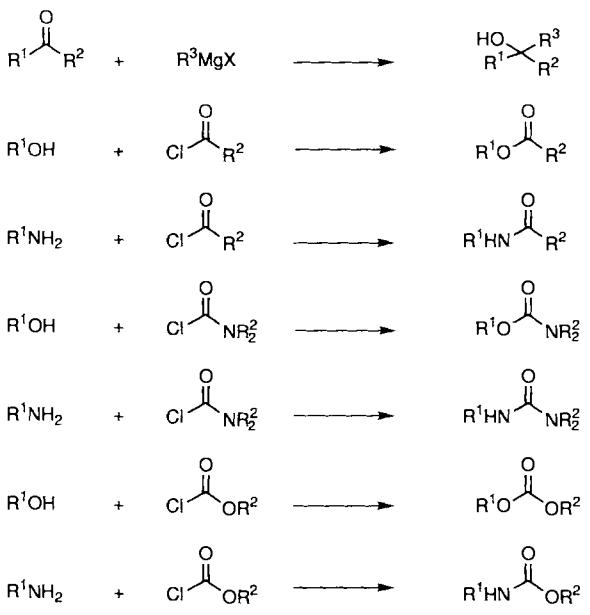

Scheme 9. Reactions used by the firm Panlabs in a validation study for synthesis of compound libraries. With these seven reactions, a library of 200 reaction products was obtained by parallel syntheses [98].

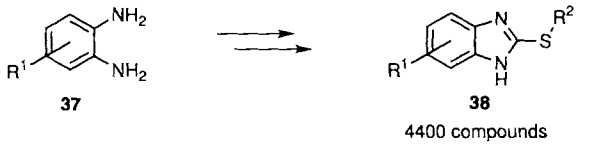

Scheme 10. With a two-step reaction sequence, a library of 4400 benzimidazole derivatives was synthesized from *o*-aminoanilines [100].

The firm Combichem has presented a library of 10000 conformationally flexible compounds as a library with a high degree of diversity. It is referred to by Combichem as a "universal library". Synthesis of a group of these compounds was recently reported by Tarby (Combichem) and Boger.[101] They converted templates **39** and **41** into the triamides **40** and **42** in three derivatization steps (Scheme 11). Purification was restricted to acidic and basic washing. Although the yields fluctuated between 3 and 89% for **40** and between 16 and 99% for **42**, the products were obtained with purities of greater than 85% and greater than 90%, respectively. The libraries synthesized so far are composed of 39 (**40**) and 125 compounds (**42**).

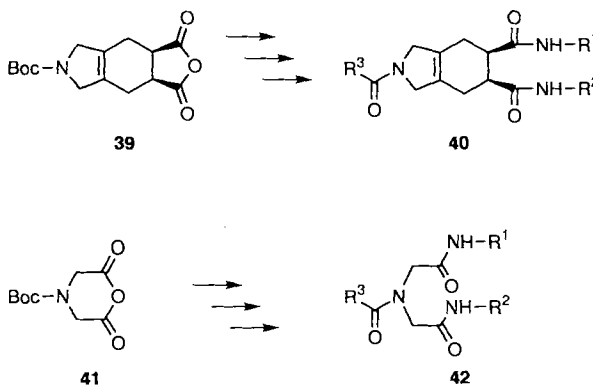

Scheme 11. Synthesis of substituted triamides (**40**, **42**) by successive derivatization of templates (**39**, **41**) [101].

Libraries of five-membered heterocycles (**46**, **49**, **52**) were recently reported by Merritt (Glaxo).[73] These were also produced as single substances by one- or two-step syntheses in solution (Scheme 12).

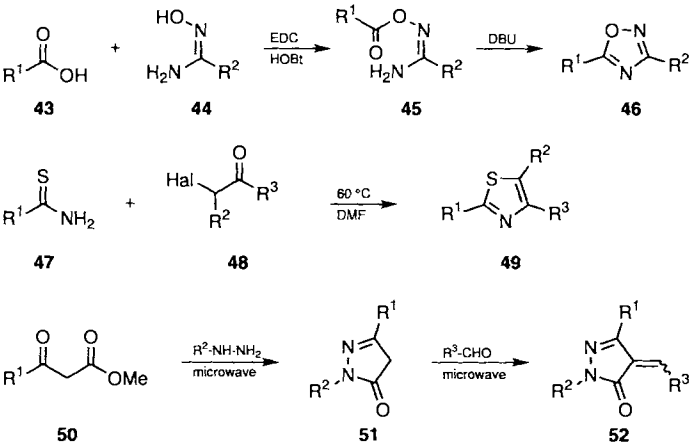

Scheme 12. Oxadiazoles (**46**), thiazoles (**49**), and pyrazolones (**52**) by combinatorial synthesis in solution [73].

Combination of synthesis in solution and on solid phase has already been mentioned as the strategy of Armstrong,[41, 90] who attached the product of a Ugi reaction to a polymer support during a further transformation (resin capture). Another example of combination of synthesis in solution and on solid phase was reported by Suto (Signal Pharmaceuticals).[42] The reaction was performed in solution with an excess of reagent, for example acid chloride, and the excess reagent was captured by addition of an appropriately functionalized resin, for example an aminomethylated resin ("reverse use of resin"). By-products can also be removed with this procedure if the synthesis is carefully planned (for example, free acids formed by hydrolysis).

3.2.3. *Synthesis on Soluble Polymers*

Synthesis in solution was chosen as the strategy for each of the library syntheses described so far. Some of the problems of solid-phase syntheses were thereby avoided, yet at the same time, the advantages of this method were sacrificed. For this reason, Janda et al.[102] employed a strategy from the work of Bayer and Mutter,[103] which combines the advantages of synthesis in solution with those of solid-phase syntheses. Polyethylene glycol (PEG) was used as the polymeric support. This polymer is soluble in many solvents yet can be precipitated as required by addition of a large amount of diethyl ether. The reactivity of free and PEG-bound substrates can differ in individual cases;[104] however, the reaction conditions determined for synthesis in solution can often be used. This saves having to adjust a synthesis to suit solid-phase conditions. Purification of the reaction mixture can be performed by precipitation and solid-phase extraction of the PEG derivative, making use of the good crystallization properties of PEG derivatives.

An arylsulfonamide library of six individual compounds was constructed as an example library, starting by linking the iso-

cyanate **53** to PEG monomethyl ether (Scheme 13). Subsequently, the sulfonic acid chloride **54** was treated with an amine to form sulfonamide **55**. The aniline derivative **56** was released by hydrolysis of the carbamate functionality with 0.5 M sodium hydroxide.

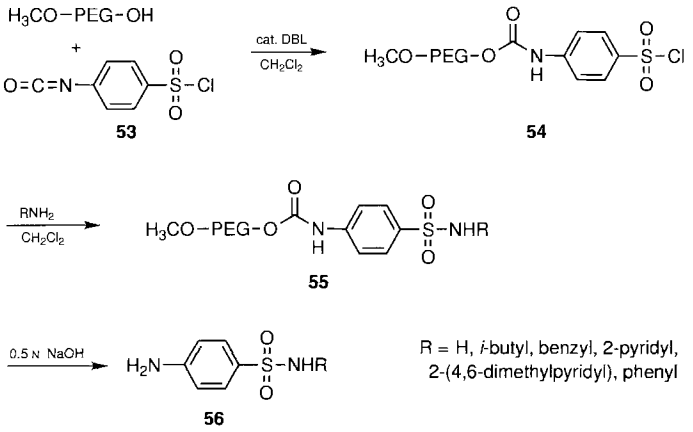

Scheme 13. Synthesis of sulfonamides on polyethylene glycol (PEG, M_r = 5000) as a soluble polymeric support [102].

Synthesis on soluble polymers was unable to compete with solid-phase syntheses in the field of peptide synthesis. It remains to be seen if this—also in view of the problems of automation—will be the case for combinatorial synthesis of small organic molecules.

4. Combinatorial Synthesis on Solid Phase

4.1. Linkers for Organic Solid-Phase Synthesis

During organic solid-phase synthesis, the molecules to be synthesized are bound to a polymeric support through a linker (see Fig. 8). This linker largely determines the conditions under which the product is released and thus the reaction conditions suitable for the synthesis. These aspects have been discussed in a review article recently published in this journal.[26]

The support used almost exclusively in combinatorial synthesis of low molecular weight organic compounds is polystyrene crosslinked with 1–2% divinylbenzene, which is also used in peptide synthesis. The most frequently used linkers also originate from peptide synthesis, and consequently, the reactants are almost always bound to the support by an ester or amide bond. The products are generally cleaved from the resin under acidic conditions and have an acid or amide function at the former linkage site, which is not always desirable. Reactions that take place under strongly acidic conditions are therefore not feasible, and the synthesis products must be stable under the same acidic conditions during cleavage. This requirement for compatibility of the linker with the reaction conditions and for product stability precludes the possibility of a "universal linker" for all syntheses. However, it can be expected that a repertoire of linkers will be available in the future, from which a linker suitable for any synthesis sequence can be selected. The first steps in this direction are described next.

Thompson and Ellman developed the new linker **57** based on the THP protective group, which is suitable for immobilization of alcohols.[105] Binding of the alcohol takes place under the usual conditions, and cleavage is most favorable with 95% aqueous trifluoroacetic acid (Scheme 14).

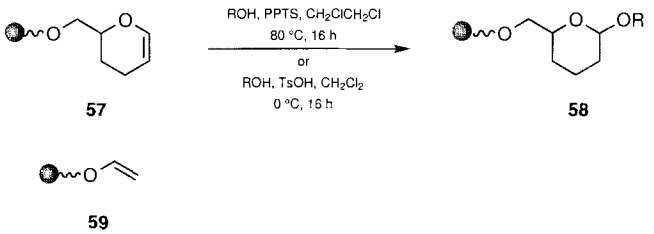

Scheme 14. The THP linker **57** from Ellman et al. [105] and the polymer-bound vinyl ether **59** proposed by Wang [106] enable direct linkage of alcohols to the support.

Polymer-bound vinyl ether **59**[106] reported by Wang is structurally related but more reactive due to less steric hindrance (Scheme 14). Linkers **60**–**65**[107–111] (Fig. 15, Scheme 15) described below are suitable for linking amines to the support. Compounds **60**, **61**,[107] and **62**[108] are derived from the benzyloxycarbonyl protective group. Trifluoroacetic acid is used to

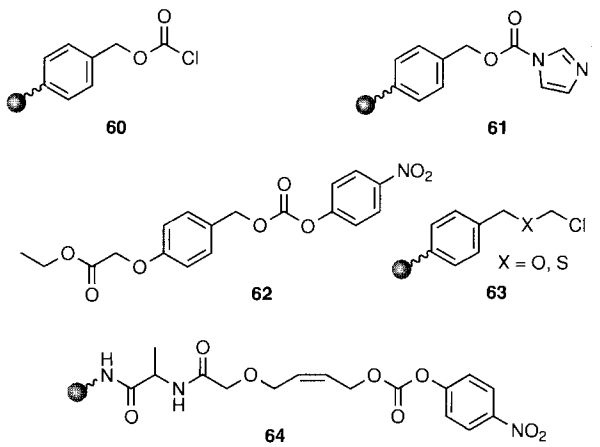

Fig. 15. Linkers for immobilization of amines. Linkers **60**, **61** [107], and **62** [108] are derived from the benzyloxycarbonyl group and are TFA-labile. The amine-linker conjugate is produced from **62** in solution and is linked to the aminomethyl resin after saponification of the ethyl ester. Linker **63** is suitable for linkage of carboxylic acids or (thio)phenols to the support [111]. Linker **64** [109] is based on the Alloc protective group, and cleavage is Pd-catalyzed.

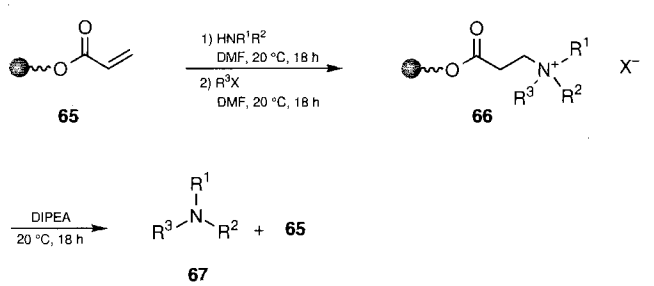

Scheme 15. Amine addition with a Michael reaction on the polymer-bound acrylic ester **65**. After the solid-phase synthesis, the product **67** is cleaved by Hofmann elimination, and **65** is recovered [110].

cleave the product from the solid phase. The cleavage is palladium-catalyzed for **64**,[109] whereas for **65**[110] the tertiary amine **67** is released by Hofmann elimination under mild conditions, thereby regenerating the polymer-bound acrylate **65** (Scheme 15).

Nucleophiles such as (thio)phenols or carboxylic acids can be immobilized with linker **63**[111] from SmithKline Beecham (Fig. 15). Cleavage occurs with 25% trifluoroacetic acid in CH_2Cl_2, for example.

Linkers based on the "safety catch" principle seem to be particularly promising for organic chemistry on solid phase, since they are compatible with many reaction conditions in the non-activated state. Backes and Ellman[112] used the acylsulfonamide linker **68** first described by Kenner[113] for synthesis of phenylacetic acid derivatives **70** (Schemes 16 and 71). Activation takes place by methylation of the sulfonamide

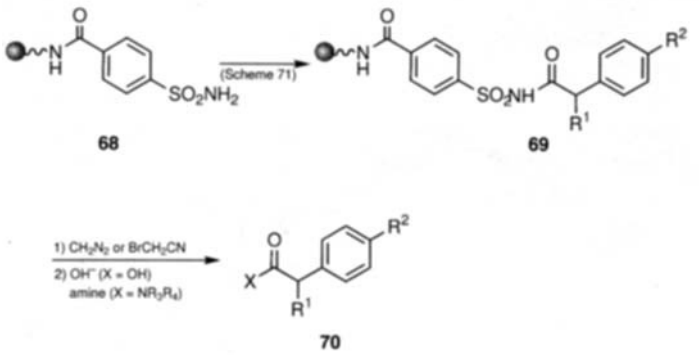

Scheme 16. Kenner's "safety catch linker" **68** [113] as used by Ellman et al. for synthesis of phenylacetic acid derivatives **70** [112, 114, 115].

nitrogen, and the resulting secondary sulfonamide can be nucleophilically cleaved under mild conditions. Anilines, however, are not sufficiently nucleophilic to bring about cleavage. This only takes place after activation of the sulfonamide bond by alkylation with bromo- or iodoacetonitrile.[114, 115]

Highly desirable linkers would not leave any functional groups behind in the target product of the combinatorial synthesis on cleavage. At the same time, the cleavage reagent should preferably be evaporable or easily separated (as in peptide synthesis), since workup that is complicated or difficult to automate is generally undesirable. These requirements are fulfilled by two chemically similar silyl linkers **71** and **73** (Scheme 17), which were developed independently by Ellman et al.[116] and Veber et al.[117] Somewhat complicated syntheses are required if these linkers are used, since the first synthetic building block cannot simply be coupled to the support-bound linker. Instead, conjugates of linker and starting material are first synthesized in solution and attached to the solid phase afterwards. This laborious synthesis has to be repeated for every new starting compound. Both silyl linkers are cleaved with trifluoroacetic acid or fluoride and do not leave any functional groups behind in the target molecule. This is also the case for the photochemically cleavable NpSSMpact linker **75**[118] (Scheme 18) developed by Sucholeiki. The linker molecules **78** described by Holmes et al.[119] and **81** from Geysen et al.[61] can also be cleaved photochemically (Scheme 19).

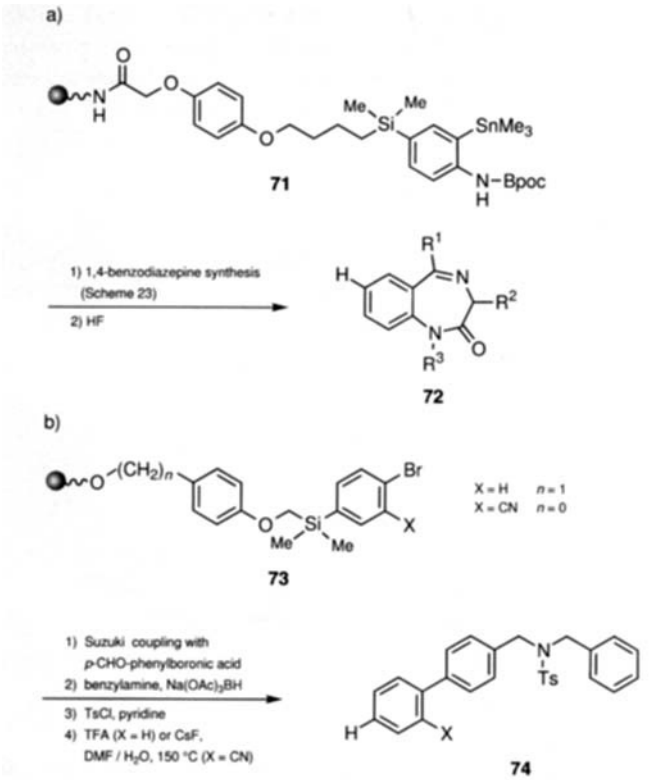

Scheme 17. Arylsilyl linkers **71** from Ellman et al. [116] and **73** from Veber et al. [117] that do not leave any functional groups in the product after cleavage.

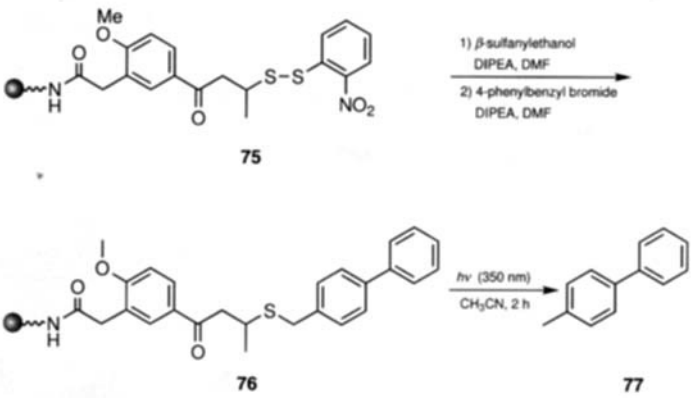

Scheme 18. Photochemically cleavable NpSSMpact linker **75** according to Sucholeiki et al. [118], used in the synthesis of biaryl templates (see Scheme 73).

If the linker can be cleaved selectively, cleavage can take place in aliquots rather than releasing all the compound bound to one resin particle at once. This is of interest for structural determination of biologically active components in substance mixtures, particularly in coded libraries (see Section 5.5). Selectively cleavable linkers known at present are only usable under peptide synthesis conditions. Lebl et al.[120] described linker systems such as **84** (Scheme 20). Activation by acidic cleavage of the Boc group and subsequent dioxopiperazine formation under neutral conditions releases the first aliquot, and nucleophilic ester cleavage gives the second aliquot, both in the form of the propanol amide **87**.

Bradley et al.[121] reported multiple linkers **89** that were obtained by derivatization of aminoethyl resin with equimolar

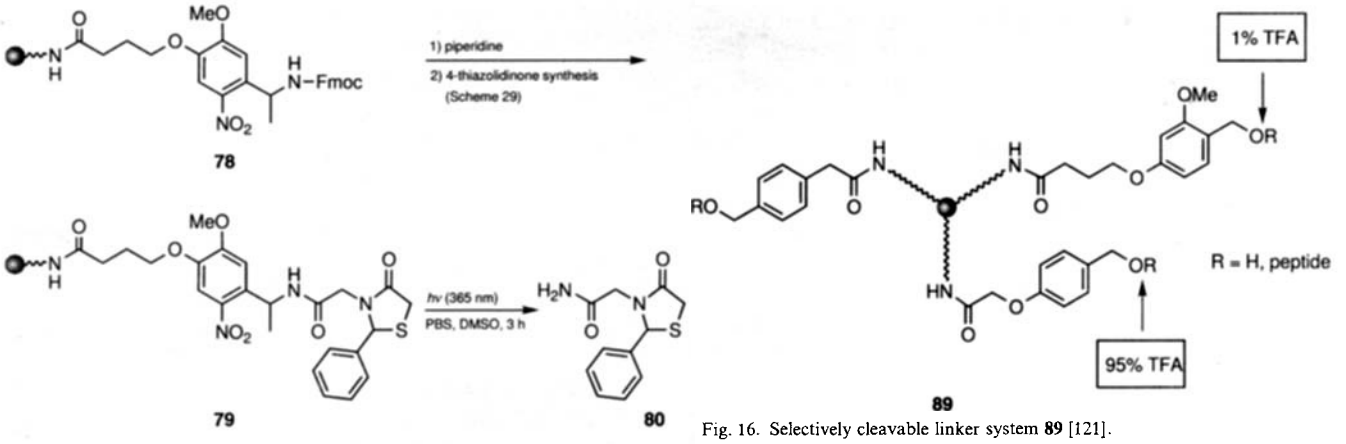

Fig. 16. Selectively cleavable linker system **89** [121].

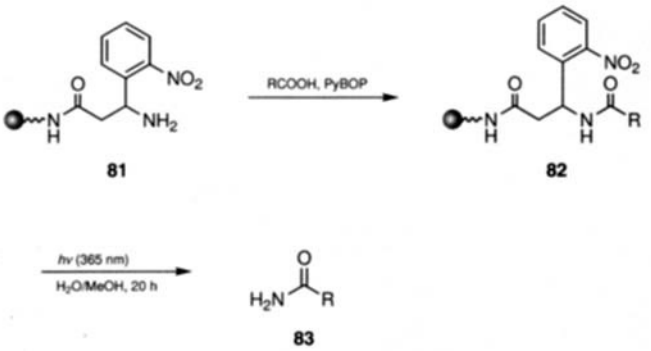

Scheme 19. Photolabile linkers **78** (Holmes et al. [119]) and **81** (Geysen et al. [61]).

amounts of linker molecules with differing acid lability (Fig. 16; R = H). After the synthesis (R = peptide), a third of the product is released with 1% trifluoroacetic acid, followed by the next third with 95% trifluoroacetic acid; the last third remains on the resin under these conditions.

Development of selectively cleavable linkers with wide applications in organic solid-phase synthesis is very difficult since the desired selectivity on aliquot cleavage must be compatible with the necessary orthogonality of the cleavage and synthesis conditions. A chemically much simpler solution has been developed by Baldwin et al.[122] of the firm Pharmacopeia. They used a photochemically cleavable *o*-nitrobenzyl linker[123] **90**, known from peptide chemistry, and achieved aliquoted cleavage by varying the irradiation time (Scheme 21).

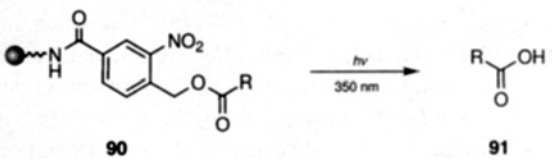

Scheme 21. Photolabile linker **90** used at Pharmacopeia for aliquoted cleavage of product [122].

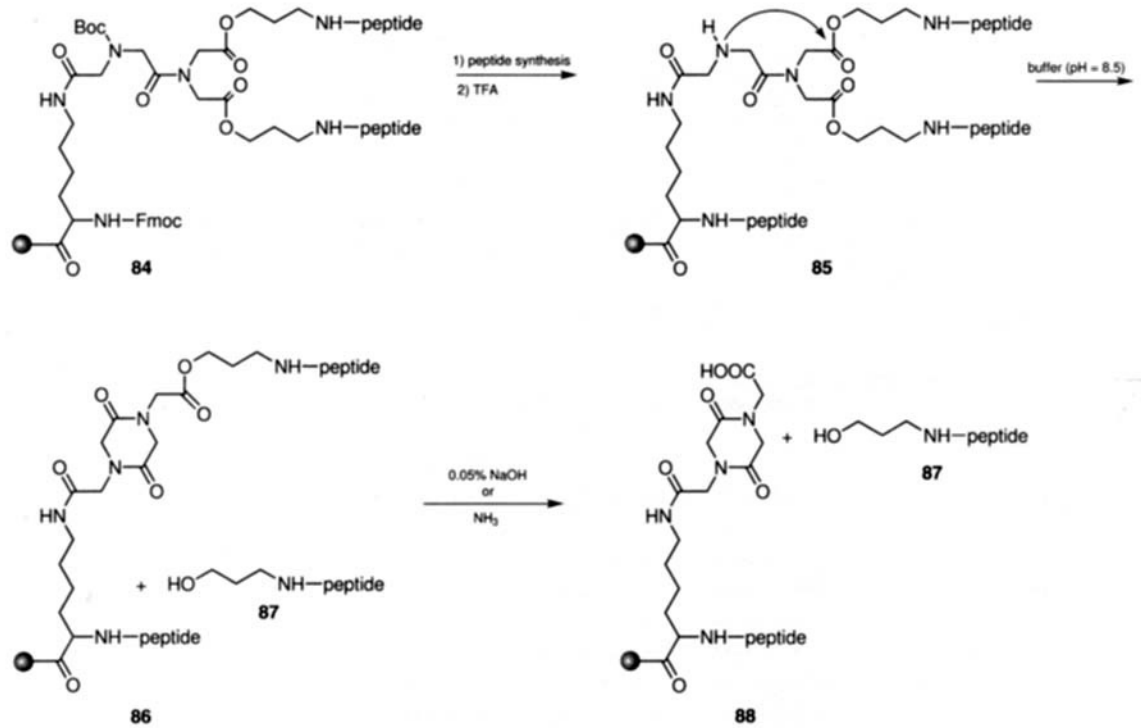

Scheme 20. Linker **84** developed by Selectide [120] that is cleaved in several steps.

In addition to those described here, linkers specially tailored to a particular synthesis are described in the literature. These linkers together with their respective synthesis sequences are described in the next section.

4.2. Synthesis by Ring Closure

4.2.1. Heterocycles

Experience has shown that compounds with biological activity are often derived from heterocyclic structures. It is therefore not surprising that this structural class has received special attention in combinatorial synthesis and that syntheses of heterocycles on solid phase have mushroomed. Small heterocycles, in particular, are used as rigid, highly functionalized molecular scaffolds.

4.2.1.1. Benzodiazepines and Derivatives

The foundation for solid-phase synthesis of non-oligomeric compound libraries was laid in 1992 with the 1,4-benzodiazepine syntheses of Ellman[124–126] and DeWitt et al.[127] (Parke Davis). This important class of heterocyclic pharmacophores is highly suitable for combinatorial syntheses, since the 1,4-benzodiazepine skeleton can be built up in two or three steps on the central, polymer-bound building block. The benzodiazepine synthesis of DeWitt et al. was based on a synthesis route developed by Camps in 1974,[128] in which amino acids bound to the solid phase (**92**) are treated either with 2-aminobenzophenones (synthesized beforehand in solution) or their imines **93** and are cyclized in the next step (Scheme 22).[129, 130] Diversity of the target compounds **95** is limited by the availability of the 2-aminobenzophenones.

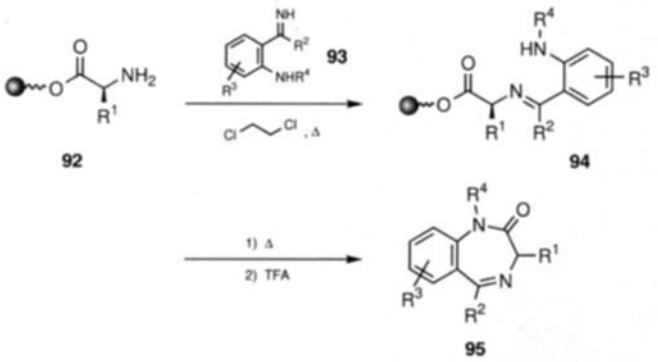

Scheme 22. Solid-phase synthesis of 1,4-benzodiazepines **95** by reaction of resin-bound amino acids **92** with imines **93** and subsequent cyclization [127, 129, 130].

The company Parke Davis used the so-called DIVERSOMER technology[130–132] to synthesize individual substances in a semiautomated parallel synthesis. The apparatus has fritted glass tubes as reaction vessels. Each of these tubes contains about 100 mg resin to which Fmoc-amino acids are bound through an anchor group. Based on previous validation experiments, the reaction times were chosen so that reaction with the least reactive benzophenonimine and subsequent cyclization was successful yet degradation of the benzodiazepine derived from tryptophan was minimal. At the end of the reaction, 40 benzodiazepines were obtained with yields between 9–63% with an average purity of greater than 60% (determined by ^{1}H NMR spectroscopy).

The new synthesis from Ellman et al.,[23, 133–135] in which the 2-aminoaryl ketones **96** are assembled on the solid phase by Stille coupling of protected 2-aminoarylstannanes **71** and acid chlorides, is much more flexible than previous solid-phase benzodiazepine syntheses. This route provides elegant access to hundreds of different 2-aminoaryl ketones **96**, since over 500 acid chlorides are commercially available. 1,4-Benzodiazepines **72** can be obtained by acylation with a series of Fmoc-protected α-amino acid fluorides, deprotection, and acid catalyzed cyclization, and these can be functionalized further by N-amide alkylation (Scheme 23). The 2-aminoarylstannanes **71** are first bound

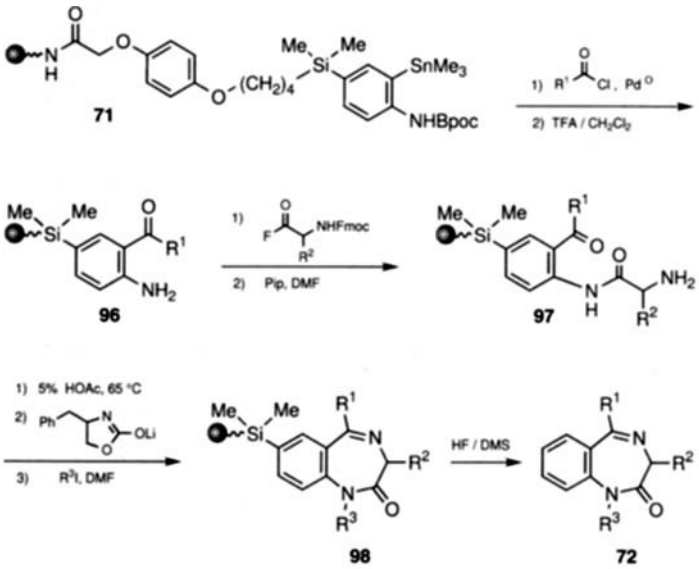

Scheme 23. 1,4-Benzodiazepine synthesis on solid phase to assemble 2-aminoaryl ketones **96** [133–136] by Stille coupling with use of a new silyl linker **71** [116].

to the support with a 4-(hydroxymethyl)phenoxyacetic acid ester linker, and the products can be cleaved after the end of the synthesis with trifluoroacetic acid to provide high-purity hydroxy-substituted benzophenones. This linker was recently modified with a silyl anchor that, after HF cleavage, only leaves a proton at the anchor site in the molecule instead of a functional group, which could interfere in biological tests.[114, 116] Extensive libraries of over 11000 compounds[136] have been synthesized on pins[6] and were examined, for example, for tyrosine kinase inhibition and binding to G-protein-coupled receptors, amongst other functions.

Another benzodiazepine synthesis was reported by Chenera et al. (SmithKline Beecham)[137] in which the benzophenones were also assembled on the solid phase by halogen–metal exchange and reaction with benzoyl chloride.

Successful 1,4-benzodiazepine syntheses certainly provided the impetus for the solid-phase syntheses of the closely related 1,4-benzodiazepine-2,5-diones published last year, and hopes are high that these will result in libraries of valuable lead compounds.[138] During the search for fibrinogen GPIIb/IIIa binding inhibitors, Phelan et al. (Genentech) developed a

four-step synthesis for 1,4-benzodiazepine-2,5-diones (**104**, Scheme 24).[139] β-Alanine-loaded Wang resin **99**[140] was converted with an iodoisatoic anhydride derivative **100** into benzamide **101**, which gave the benzodiazepinedione scaffold **103** after acylation with bromoacetic acid chloride and cyclization. Different basic nitrogen side chains were subsequently introduced at the C-7 position by palladium catalyzed coupling reactions.[141] The products were cleaved from the resin with trifluoroacetic acid and purified by reversed phase HPLC. The total yield over all steps was about 15%. No information is available about the size of the libraries or success during screening. As for many other reports on solid-phase syntheses and compound libraries, the applicability of the method is not discussed in this publication. The answer to the question "Which combinations of synthetic building blocks can reliably be used?" often remains the secret of the authors.

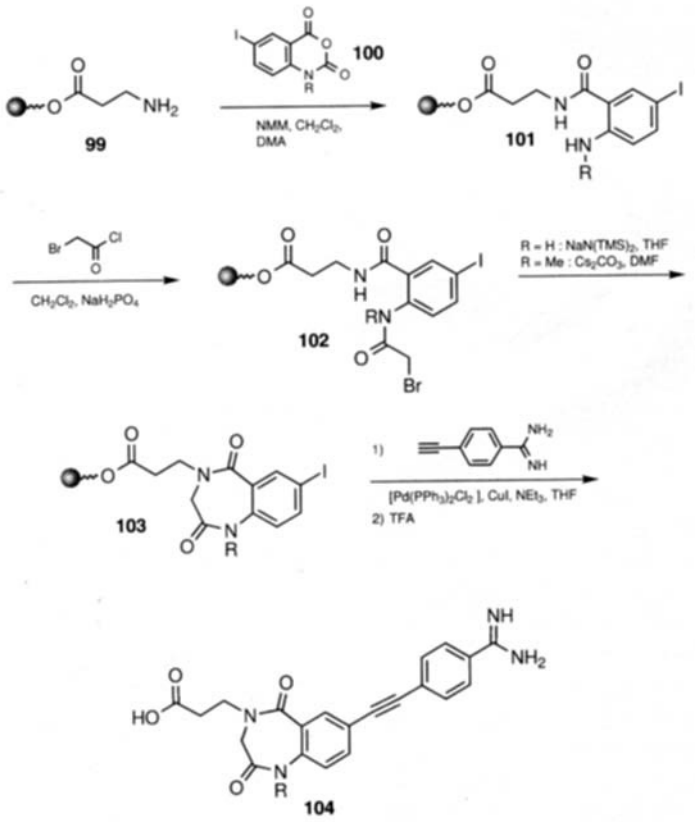

Scheme 24. Solid-phase synthesis of 1,4-benzodiazepine-2,5-diones **104**. Incorporation of basic side chains by palladium-catalyzed alkyne coupling [139].

In a benzodiazepinedione synthesis from Ellman et al.[22, 23, 142] the anthranilic acids **107** can be used as obtained commercially, since the reaction conditions do not require any protective groups (Scheme 25). α-Amino acid esters **106** are linked to dimethoxybenzaldehyde-functionalized Merrifield resin[8] **105** by reductive alkylation. Acylation of the secondary amine with anthranilic acid gives the tertiary amide **108**, which is cyclized and subsequently alkylated with lithium acetanilide in one step. A further functionalization is achieved by Suzuki coupling. Whilst in the aforementioned benzodiazepine syntheses the possibilities for variation of the aromatic substituents are limited (R^3 in Scheme 22), in this synthesis over 40 anthranilic acids can be used in the unprotected form. Racemization is observed neither during acylation nor during cyclization. The products **110** are obtained in 60–90% yield after column chromatography.

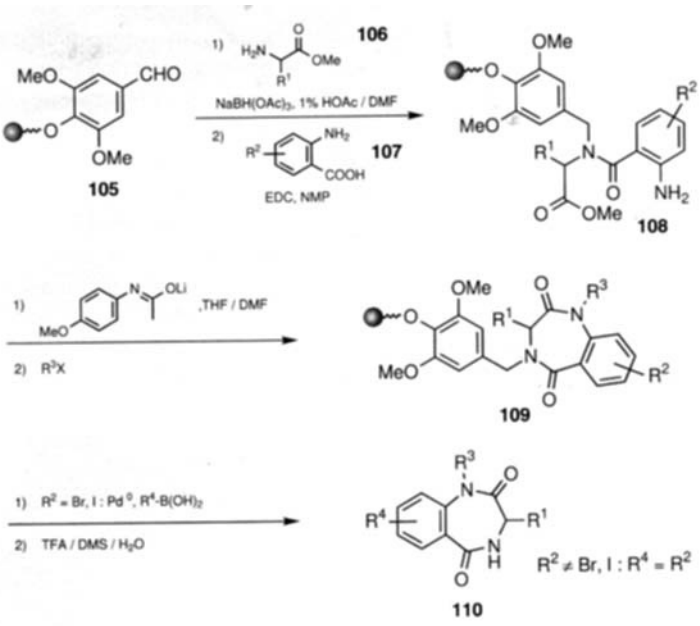

Scheme 25. Benzodiazepinedione synthesis on solid phase: reductive amination of support-bound benzaldehyde linker **105** with amino acid esters **106**, followed by acylation with anthranilic acids **107**, cyclization, and alkylation. Further derivatization by Suzuki reaction [142].

Another 1,4-benzodiazepine-2,5-dione synthesis originates from the laboratory of Goff and Zuckermann (Chiron),[143] who used the benzodiazepinedione unit to introduce a higher degree of diversity and rigidity in their peptoids (Scheme 26).[144] First, the peptoid part **112** is assembled according to established procedure,[145] and then acylation with an *o*-azidobenzoic acid chloride **113** prepares the way for an

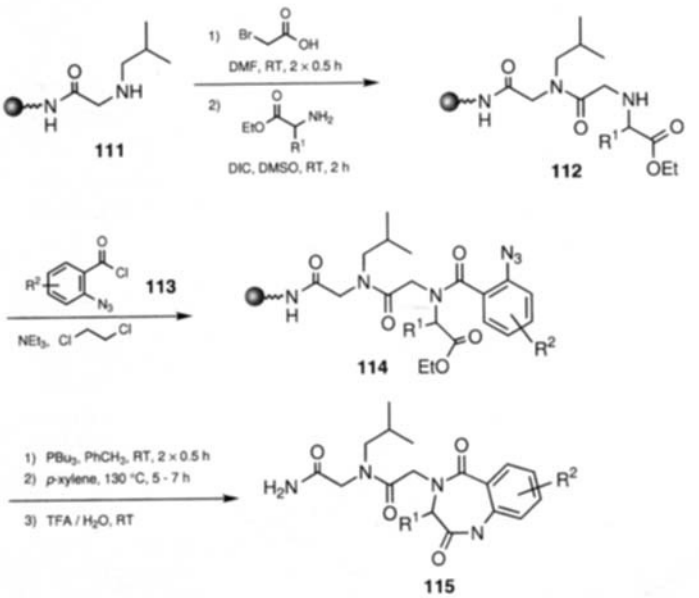

Scheme 26. Benzodiazepinedione synthesis according to Goff and Zuckermann [143]: acylation of the peptoid unit **112** [144, 145] with *o*-azidobenzoic acid chloride **113** and subsequent aza-Wittig reaction [146].

intramolecular aza-Wittig reaction. Initially, the iminophosphoranes are formed with tributylphosphane; they cyclize to the corresponding benzodiazepinediones **115** at 130 °C. Substituents on the arene offer further possibilities for derivatization. For example, a benzodiazepinedione was assembled with a triflate substituent, which was successfully used as a leaving group in a palladium-catalyzed reaction.[146] The products were obtained with 60–95% purity after cleavage (yield 34–90%). Construction of a large benzodiazepinedione library that aims for maximal diversity (!) is currently in progress.[143]

Pyrrolo-1,4-benzodiazepine-2,5-diones were also synthesized by aza-Wittig ring closure by Baldwin et al. (Pharmacopeia). However, no variation of residual groups was reported here; only the reaction of Fmoc-proline resin with unsubstituted *o*-azidobenzoyl chloride, cyclization, and cleavage.[147]

Aminobenzazepines were modified on BHA resin[148] by Chenera et al. (SmithKline Beecham) (Scheme 27).[137] First,

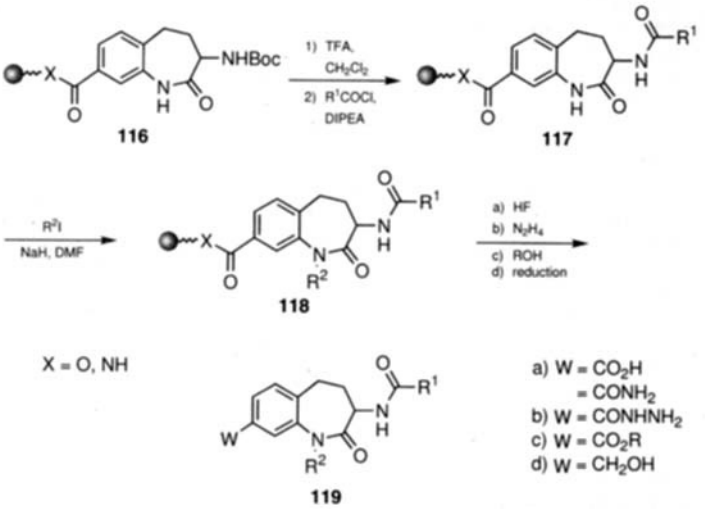

Scheme 27. Modification of 3-aminotetrahydrobenzazepinones **116** on benzhydrylamine resin. Cleavage under different conditions [137] is possible.

Boc-protected 3-amino-8-carboxytetrahydro-1*H*-1-benzazepine-2-one (**116**) was synthesized in solution (8 steps) and then bound to the polymer. After deprotection, the amino group was acylated and subsequently alkylated in DMF in the presence of sodium hydride. The finished products **119** were cleaved off the resin by acidolysis, reduction, transesterification, or hydrazinolysis.

4.2.1.2. Further Heterocycles (Cyclization on the Support)

If cyclization occurs prior to cleavage from the resin, the anchor group remains as a functionality within the molecule (see Section 4.1). This can be an acid group, an amide group, or a hydroxyl group, as exemplified by the benzodiazepines and benzodiazepinediones.

In the pyrrolidine synthesis described by Gallop and his colleagues at Affymax,[21, 32, 149] this is a carboxyl group, which is a desired element of the target structures (Scheme 28). This pyrrolidine synthesis is based upon a 1,3-dipolar cycloaddition of the support-bound azomethinylides obtained from the imines **120** under basic conditions. The imines are prepared by condensation of resin-bound amino acids with aromatic and heteroaromatic aldehydes in pure trimethylorthoformate as dehydrating solvent.[150] The substituted pyrrolidines **121** obtained after cycloaddition may be further acetylated at the nitrogen atom. In a search for new ACE inhibitors[151] a library of 500 sulfanylacyl prolines **122**, analogues of the hypotensive agent captopril, was prepared by the Split method.[13–18] After four iterative screening cycles for ACE inhibition and synthesis of partial libraries the active pyrrolidine **123** was identified, which also contains the sulfanylisobutyryl chain of captopril. It was shown that the diastereoisomer **123a** is three times more effective as an ACE inhibitor than captopril, whereas the other diastereoisomer **123b** exhibited only weak activity. The example of sulfanylacyl prolines demonstrates the possibilities a focused library offers in rapidly identifying new and even more active derivatives of a lead structure.

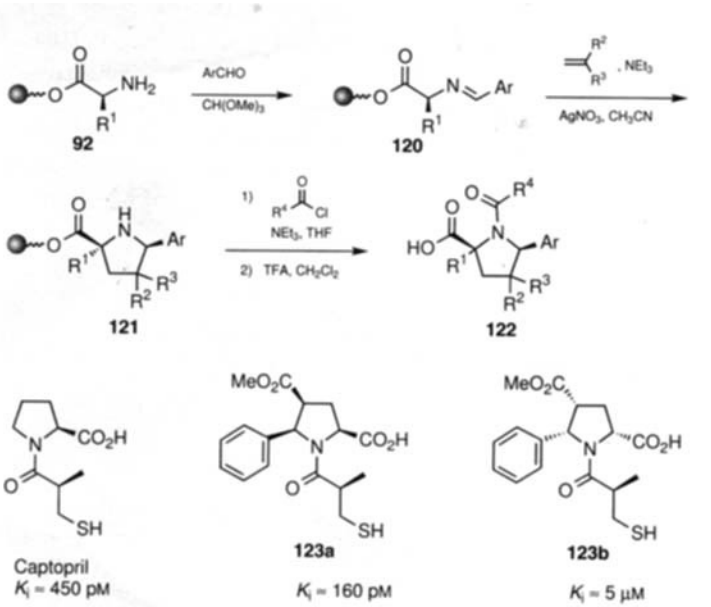

Scheme 28. Synthesis of pyrrolidines **122** by 1,3-dipolar cycloaddition of support-bound azomethinylides. Pyrrolidine **123a** was identified as a potential ACE inhibitor [32, 149].

Support-bound imines were also employed by Holmes et al. (Affymax) in the synthesis of 4-thiazolidinediones **126** and 4-metathiazanones **127**.[21, 89, 152] The three-component condensation of a primary amine **92**, an aldehyde **124**, and a sulfanylacetic or propionic acid **125**, which may also be carried out sequentially, affords the corresponding heterocycles **126** and **127** in a smooth reaction (Scheme 29). 4-Thiazolidinones are known for their inhibition of cyclooxygenase-1.[153] In this manner an active inhibitor was identified in a library of 3×125 compounds prepared with the split method.[154]

This synthesis is an example of a one-pot, multicomponent reaction on a solid phase, as in this case the intermediate products undergo further reaction directly and under constant reaction conditions. Multicomponent reactions on solid phases will be discussed in more detail in Section 4.3.3.

A third application of support-bound imines, recently demonstrated by Gallop et al., is the preparation of the β-lactams **130** by [2 + 2]-cycloaddition to ketenes.[21, 155] This solid-phase β-lactam synthesis was carried out on the extremely acid-labile Sasrin resin (Scheme 30).[156] As in the previously

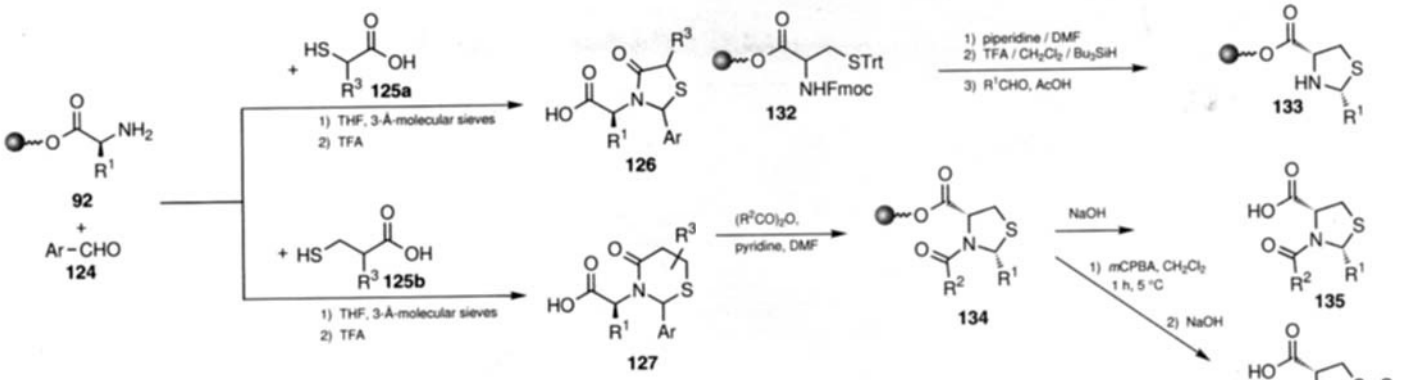

Scheme 29. 4-Thiazolidinones **126** and 4-metathiazanones **127** by three component condensation of a support-bound amine with aldehydes and sulfanylcarboxylic acids [89, 152].

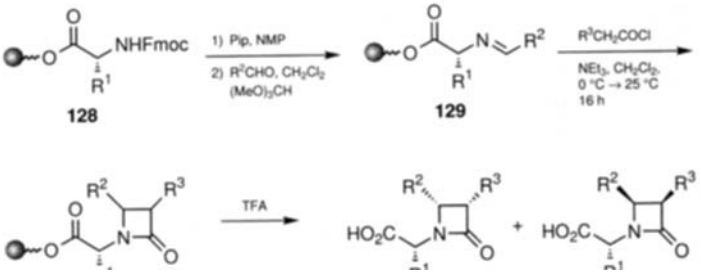

Scheme 30. β-Lactam synthesis by [2 + 2] cycloaddition of support-bound imine **129** with ketenes [155].

Scheme 31. Preparation of thiazolidines **135** by conversion of support-bound β-sulfanylalkylamines **132** with aldehydes. Oxidation to acid-stable sulfoxide analogues **136** [157].

described pyrrolidine synthesis, the resin-bound amino acids **128** were condensed quantitatively to the imines **129** by using a large excess of alkyl, aryl, or α,β-unsaturated aldehydes in a mixture of trimethylorthoformate and dichloromethane. Following thorough optimization studies, the [2 + 2]-cycloaddition was demonstrated only to take place by slow addition of acid chlorides to a suspension of the imine resin at 0 °C in the presence of triethylamine. By using a large excess of ketene in high concentration, even the cycloaddition of imines from sterically hindered amino acids (for example valine) could be carried out with full conversion. After cleavage of the resin and preparative HPLC purification, the β-lactams **131a/b** were isolated in yields of 55–97%. The β-lactam formation occurred with high *cis* selectivity, but showed only a slight stereoinduction by the asymmetric center of the amino acid. On the other hand, induction could be achieved with an optically active ketene. The synthesis of a small model library of 25 compounds showed that most β-lactams were formed in higher than 80% purity. The course of the reaction was observed with "magic angle spinning" ^{1}H NMR spectroscopy. Subsequently a library of several thousand different β-lactams was constructed, the purity of which was suitable for direct testing. The screening results will be reported shortly.

A solid-phase synthesis of thiazolidine derivatives **135** has been developed by Patek et al. (Selectide) (Scheme 31).[157] β-Sulfanylalkylamines such as the cystein derivative **132** react with aldehydes to form a series of thiazolidines **133**. N-acylation and subsequent alkaline hydrolysis form almost exclusively the (2*R*,4*R*)-stereoisomers **134**. Strongly electron-withdrawing substituents in the *para*-position of the aromatic ring reduce the rate of acylation so much that in this case no products are obtained. Thiazolidines with aliphatic substituents, on the other hand, are readily acylated under mild conditions. A number of the thiazolidines are too acid-labile to be cleaved successfully from the resin with TFA. Oxidation with *m*CPBA, however, opens a route to the acid-stable sulfoxide analogues **136**, which after cleavage from the resin are isolated analytically pure. Derivatives with the basic thiazolidine framework are known for their antimicrobial, antihypertensive, and antitumor activity; the biological test results have currently not been reported.

Baldwin and his colleagues at Pharmacopeia are studying the synthesis of binary encoded compound libraries.[158–161] In this variant of the split synthesis, which will discussed in more detail in Section 5.5, the beads are tagged with code molecules that allow the structures of the compounds synthesized on individual beads to be elucidated.[160] The syntheses were carried out on TentaGel resin[9, 162] bearing photolabile *o*-nitrobenzyl linkers. In the construction of a dihydrobenzopyran library (Scheme 32), three dihydroxyacetophenones were initially condensed under Mitsunobu conditions with the linker **137**, which had been coupled to the resin under normal coupling conditions. Following cyclization with seven aminoketones **140**, spirodihydrobenzopyrans were obtained, which, after derivatization of the nitrogen atom, were reduced to **143** with sodium borohydride or converted into dithiolanes **144**. Similar spirocyclics **142** are known in the patent literature as Class III antiarrythmics.[163] Overall 1143 compounds were obtained, which were tested for carboanhydrase inhibition, and a compound active in the nanomolar range was identified.[158, 159]

Similarly, the encoded acylpiperidine library **145** with 6727 compounds was prepared in a three-step sequence using the photolabile nitrobenzyl linker.[158, 159] Initially seven resin-bound piperidine carboxylic acids were coupled with 31 amino acids and subsequently derivatized with 31 acylating agents to form the corresponding carboxamides, carbamates, sulfonamides, and ureas (Fig. 17). The sulfonamide **146** was found to be a carboanhydrase inhibitor, which was active in the nanomolar range.

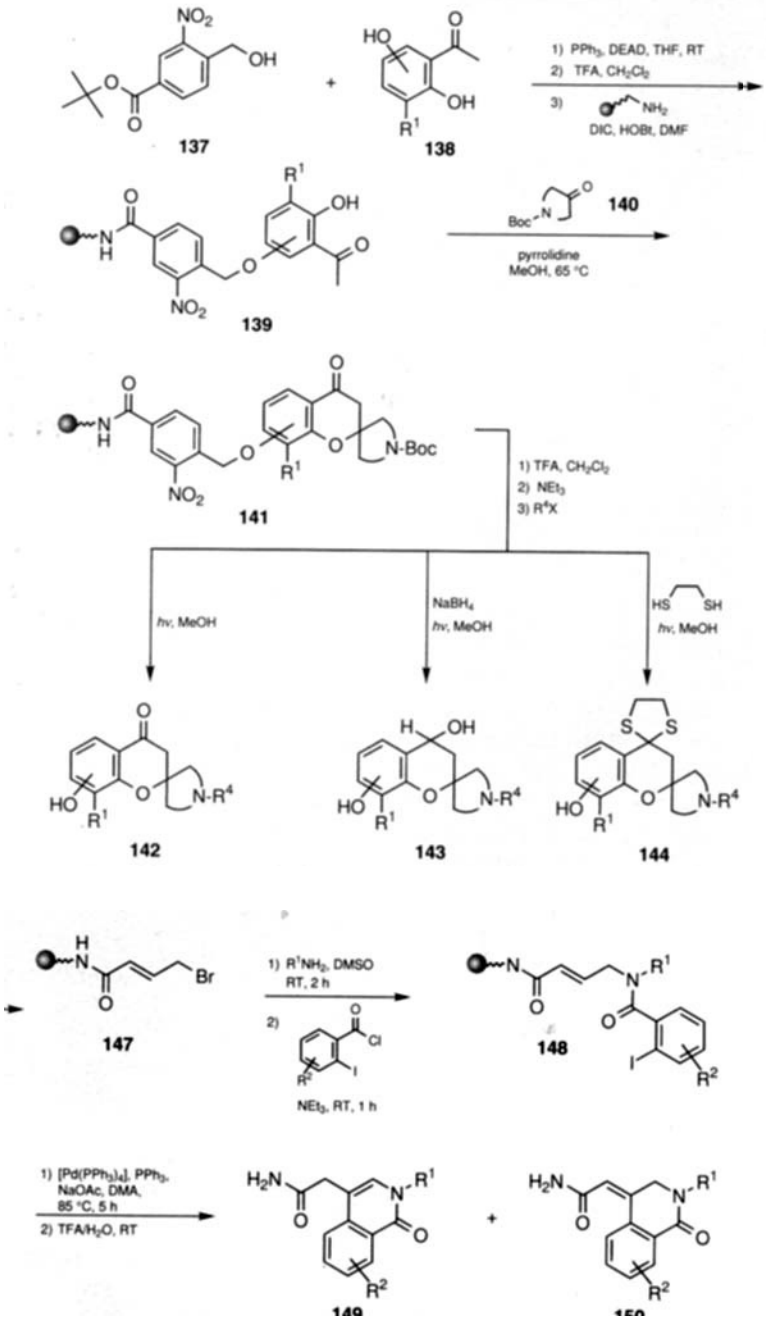

Fig. 17. Acylpiperidine library **145** containing 6727 compounds from which the carboanhydrase inhibitor **146** was identified during screening [158, 159].

Coded sulfonamide libraries obtained by combinatorial techniques and their use are also the subject of a recent patent application of Pharmacopeia.[161]

An intramolecular Heck reaction has been used by Goff and Zuckermann in the formation of 1(2*H*)-isoquinolinones (Scheme 33).[164] Acylation of a resin-bound secondary amine with *o*-iodobenzoyl chloride affords the amide **148**, which is capable of undergoing a Pd-catalyzed 6-*exo*-cyclization. Initially the 2*H*-isoquinolinone **150** is formed, which by readdition of PdH and subsequent elimination isomerizes to the thermodynamically favored 1*H*-isoquinolinone **149**. If **148** carries a substituent *ortho* to the iodine, this isomerization is totally or partially suppressed; in this case a mixture of **149** and **150** or

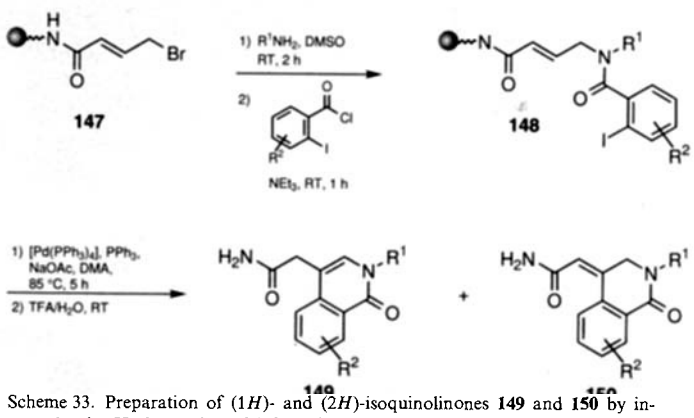

Scheme 33. Preparation of (1*H*)- and (2*H*)-isoquinolinones **149** and **150** by intramolecular Heck reaction of **148** [164].

exclusively **150** is obtained. After cleavage from the resin and freeze-drying, the products are isolated in good yields and with purities of 70 to 95%. Finally, a mixture of seven different peptoids **148** was cyclized. With HPLC-MS it was possible to identify all seven products, which were present in almost equimolar amounts. Apart from the initial necessity of preparing the *o*-iodobenzoic acids or the corresponding heterocyclic derivatives in solution, this reaction sequence offers rapid access to isoquinolinone systems.

Kiely[165] and Houghten[166] have published the tetrahydroisoquinolinone and quinazolinone libraries **153** and **156** (Scheme 34). In this synthesis, which is based upon a route

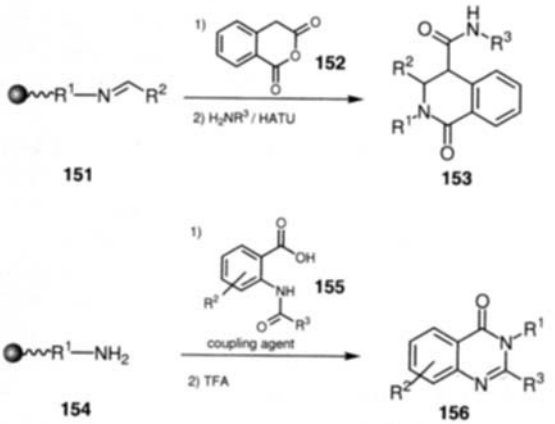

Scheme 34. Synthesis of substituted tetrahydroisoquinolinones **153** and quinazolinones **156** according to Kiely [165] and Houghten [166].

devised by Cushman,[167] the tetrahydroisoquinolinones **153** are obtained by conversion of the imines **151** prepared in situ with homophthalic anhydride **152**. Coupling of the free carboxylic acid with amines affords the tetrahydroisoquinolinone carboxamides **153**, which possess three independently variable substituents. Libraries consisting of theoretically 43472 or 367200 compounds (52 sublibraries of 836 compounds and 120 sublibraries of 3060 compounds, respectively) were prepared by this synthetic pathway. Testing of these sublibraries and subsequent deconvolution in a manner analogous to that used for peptide libraries (see Section 5.3) led to compounds with affinity for the σ-receptor and for κ- and μ-opiate receptors.

In the synthesis of the quinazolinones **156**, the immobilized amine **154** was coupled with *N*-acetylanthranilic acid **155** (R^3 = Me), and cyclization gave **156**. The C–H acidity of the R methyl group allows further chemistry; thus condensation with benzaldehydes to form the corresponding styryl compounds has been described. The currently largest quinazolinone libraries synthesized consist of 3185 compounds in subsets of 35 components each. Armstrong et al.[91] have synthesized the substituted pyrroles **159** in hitherto unsatisfactory yields (4–17%) by 1,3-dipolar cycloaddition of the münchnones **158** with esters of acetylenedicarboxylic acid (Scheme 35). The münchnones are formed under acidic conditions from the enamides **157**, which are in turn prepared by an Ugi four-component reaction.

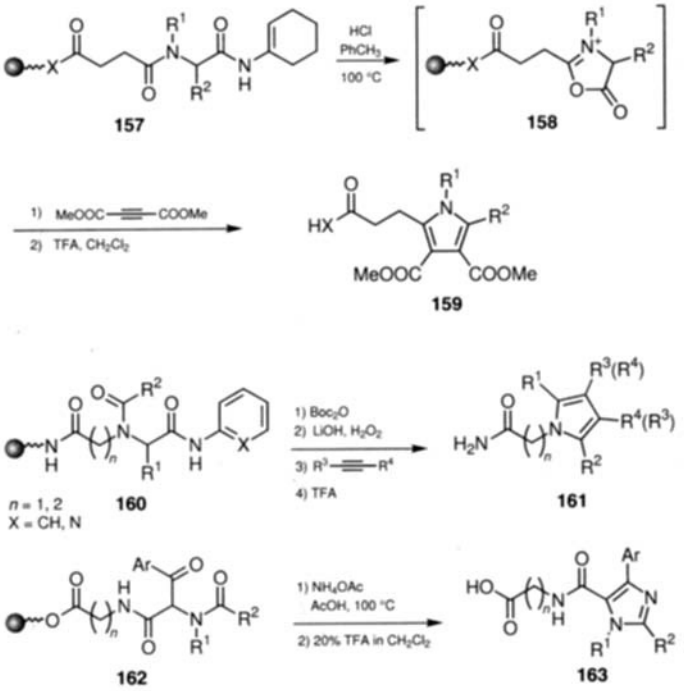

Scheme 35. Synthesis of pyrroles **159** and **161** and imidazoles **163** from α-(*N*-acyl-*N*-alkylamino)-β-ketoamides prepared by the Ugi reaction [91, 168, 169].

Mjalli et al. at Ontogen[168] also hydrolyzed the initial Ugi products **160**, and the intermediate münchnones were subsequently converted into the pyrroles **161** by cycloaddition with acetylenedicarboxylates (Scheme 35). They were obtained in high purity and in significantly better yields (27–72%) than in the previous work.[91] Mjalli and coworkers[169] also used the Ugi products **162** to synthesize imidazoles **163** (Scheme 35). Wang resin, which remarkably is stable under the cyclization conditions, was used as support. The products thus obtained were purified by preparative thin layer chromatography; the overall yield of Ugi reaction and cyclization lay between 16 and 56% based on the resin-bound isonitrile. It was demonstrated that the cyclization occurs in almost quantitative yields, and the Ugi reaction is the yield-determining step.

The same research group has described[170] another imidazole synthesis on Wang resin, which is based upon a known literature procedure.[171] Aldehydes, 1,2-diketones, ammonium acetate, and primary amines are used as synthetic building blocks. In two different procedures the resin-bound aldehydes **164** and **165** or the amine **167** were utilized (Scheme 36). In both cases the imidazoles **166** and **168** were obtained in very good yields (71–99%) and in very high purity (90–95%).

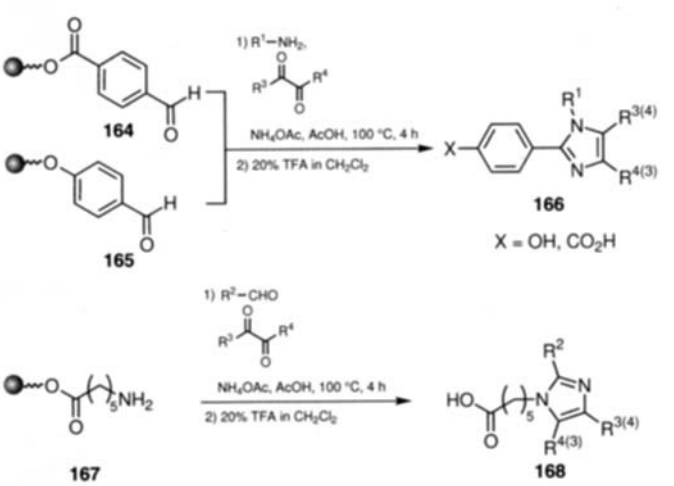

Scheme 36. Solid-phase synthesis of imidazoles **166** and **168** [170]. Either the aldehyde (top) or the amine component (bottom) can be bound to the support.

By aldol addition of support-bound hydroxynitrobenzaldehydes **169** with aryl methyl ketones, Ruhland and Künzer (Schering) have obtained the hydroxyketones **170**, which undergo reductive cyclization to give the corresponding quinoline *N*-oxides **171** (Scheme 37).[172] Deoxygenation with titanium trichloride affords the 2,6-disubstituted quinolines **172**, which may be cleaved from the resin by aminolysis.

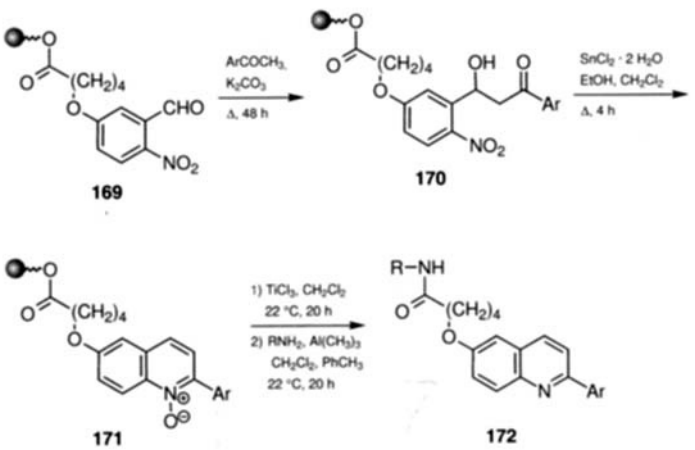

Scheme 37. Quinoline-*N*-oxides **171** were prepared by a reaction sequence of aldol reaction and subsequent reductive cyclization, giving quinolines **172** after deoxygenation [172].

The synthesis of dihydro- and tetrahydroisoquinolines by Bischler–Napieralski reaction has been achieved by Meutermans and Alewood (Scheme 38).[47] In this reaction resin-bound L-3,4-dimethoxyphenylalanine (**173**) is acylated with acetic acid derivatives and subsequently cyclized. Considerable

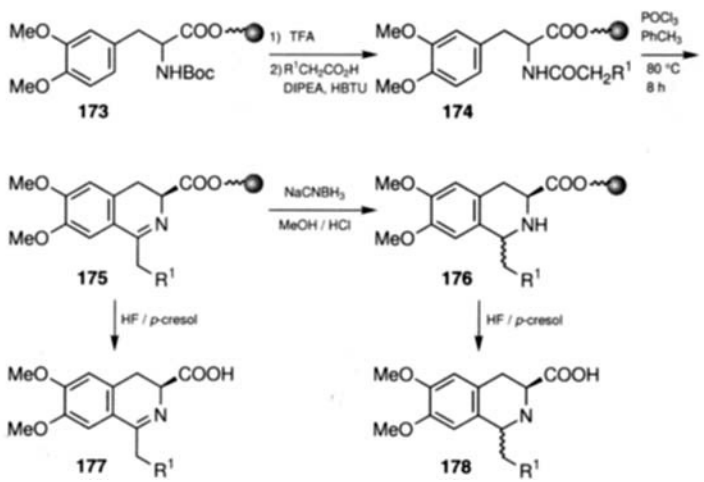

Scheme 38. Synthesis of dihydro- (**177**) and tetrahydroisoquinolines (**178**) by Bischler–Napieralski synthesis on solid phase [47].

optimization work was necessary to achieve the best results. Whereas reduction of the imine **175** with sodium cyanoborohydride was possible, the use of sodium borohydride led to undesirable premature cleavage from the resin. By using equimolar mixtures of eight different acetic acid derivatives in the acylation stage, well-defined mixtures of the target products **177** and **178** were obtained after cyclization and cleavage and characterized by ion-spray MS. It was not reported whether the products were also formed in equimolar amounts.

The formation of a six-membered nitrogen heterocycle was also achieved by Kaljuste and Undén in their synthesis of tetrahydro-β-carbolines **182** and **183**.[173] In this synthesis they use the Pictet–Spengler reaction on solid phase (Scheme 39). In a two stage procedure on Wang resin[140] an aminoalkylurethane linker (**180**) is initially formed[174] and acylated with Fmoc-tryptophan or reductively alkylated with Fmoc-tryptophanal followed after deprotection by condensation with a

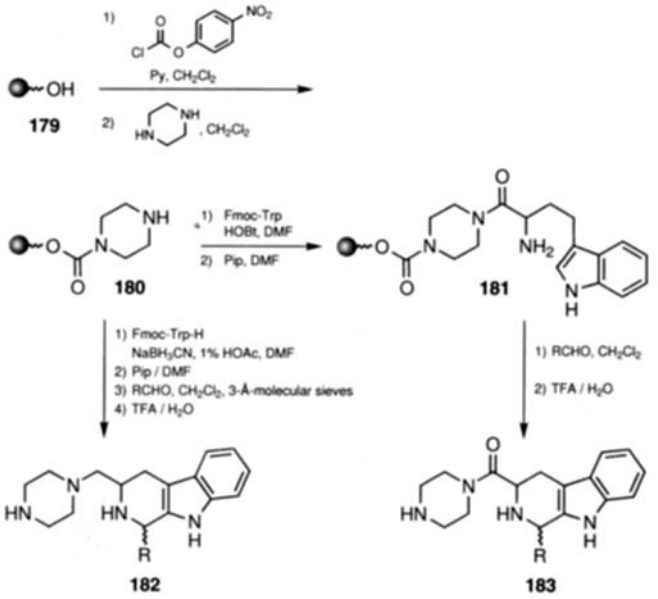

Scheme 39. Solid-phase synthesis of tetrahydro-β-carbolines **182** and **183** by Pictet–Spengler reaction [173].

large excess of different aldehydes. The tetrahydro-β-carbolines **182** and **183** are obtained in relatively high yields and high purity. Further derivatization on the nitrogen atom was not possible, since the secondary amino group in the 2-position could neither be reductively alkylated nor acylated with acid chlorides. N-protected aminoaldehydes could be used as aldehyde component, however, which allowed further acylation and reductive alkylation.

Yang (Merck) also used the Pictet–Spengler reaction for the construction of "druglike" molecules on solid phase.[175] Without using a linker he attached tryptophan directly to Merrifield resin. Following completion of the synthesis, the products were cleaved from the resin by aminolysis.

A procedure for the parallel synthesis of quinolones **187** of the ciprofloxazin type has been described by DeWitt et al.[130, 176] (Scheme 40). Here benzoylacetic acids were bound to Wang

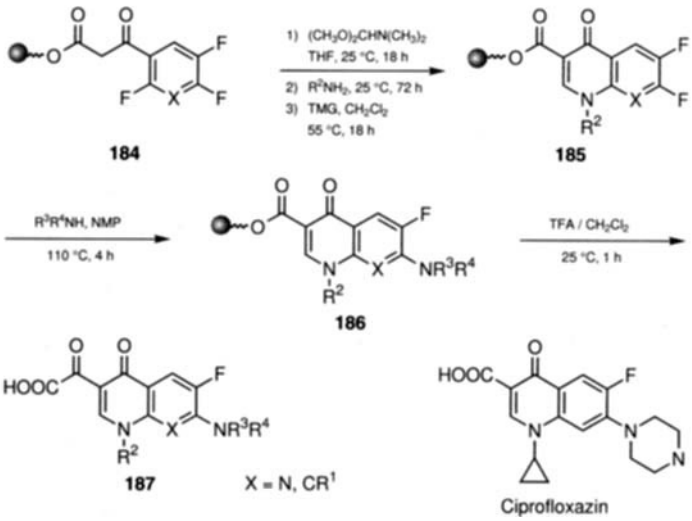

Scheme 40. Nucleophilic aromatic substitution to form ciprofloxazin-analogous quinolones **187** on solid phase [130, 176].

resin[140] by ester exchange. Following Knoevenagel condensation with dimethylformamide dimethylacetal, reaction of **184** with a series of amines produces a number of different enamines, which undergo cyclization by nucleophilic aromatic substitution. Further nucleophilic aromatic substitution allows replacement of a second fluorine atom by cyclic secondary amines. By combining three benzoylacetic acids, three primary amines, and four cyclic amines, a focused library of 36 compounds was obtained, amongst which ciprofloxazin itself was observed. It was not mentioned whether gyrase inhibitors more effective than ciprofloxazin were found.

Catecholamines with a semirigid molecular framework are familiar dopamine agonists and are used, for example, against Parkinson's disease. A synthesis of 3-substituted 1-aminomethyl-3,4-dihydro-5,6-dihydroxy-1*H*-2-benzopyrans (**195**) has been devised by DeWitt et al. (Scheme 41).[130] The aromatic diol was protected as a ketal, which served as linker. Initially a catechol ketal resin (**191**) was formed by hydrolysis and decarboxylation of a support-bound β-oxoester, followed by reaction with catechol. After *ortho*-metalation **191** was converted into **192** with

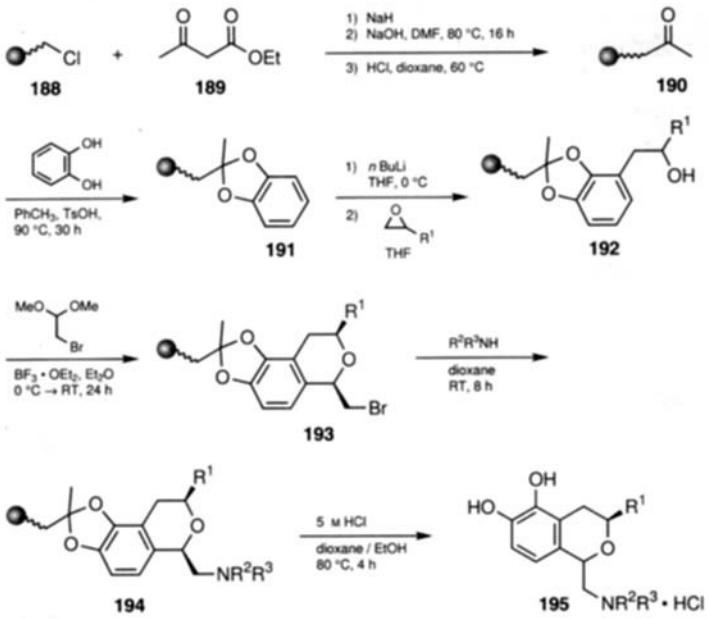

Scheme 41. Preparation of aminomethyldihydroxybenzopyrans **195** starting from a catechol ketal resin **191** [130].

styrene oxide or cyclohexylethylene oxide, and the pyran ring in **193** formed with bromoacetaldehyde dimethylacetal under Lewis acid catalysis. After substitution with amines, cleavage from the resin was undertaken. Only six examples of this sequence were described. Similarly, only very few examples are found in the same patent application describing the synthesis of pilocarpine analogues, isoindolone spirosuccinimides, and pyrazoles.

In the preparation of isoindolone spirosuccinimides[130] (**202**, Scheme 42) cyanoacetic acid bound to Wang resin (**196**) was condensed with 3-imino-1-oxoisoindolines **197**. After alkylation of the nitrogen atom and Michael addition of cyanide, **200** was hydrolyzed to the imide and concomitantly cleaved from the resin. The crude product **201** was then decarboxylated in glacial acetic acid. Spirosuccinimides of this structural type

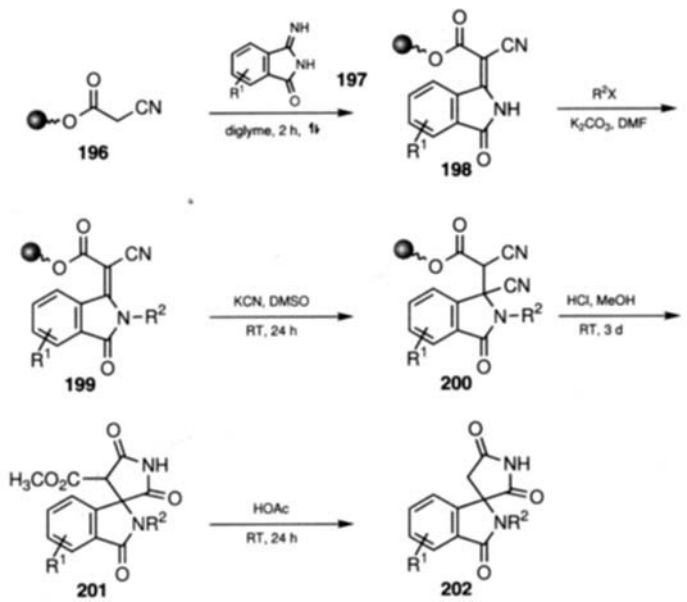

Scheme 42. Solid-phase synthesis of isoindolone spirosuccinimides **202** [130].

are known to be aldose reductase inhibitors and antidiabetics.[177]

In a classical pyrazole synthesis DeWitt at al. were able to prepare a number of tepoxaline derivatives (**205**) on a polymeric support (Scheme 43).[130] In this synthesis β-diketones linked to the solid phase were condensed with a number of different hydrazines to form the corresponding pyrazoles **204**, which were cleaved from the resin by aminolysis with hydroxylamines under reflux.

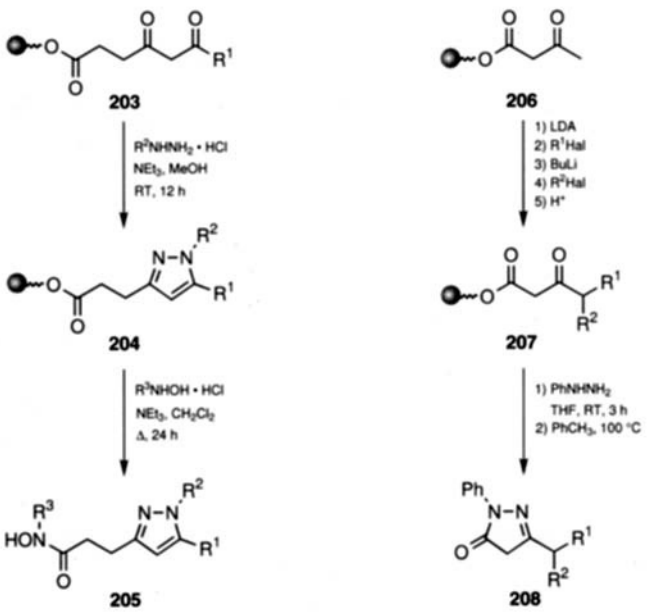

Scheme 43. Solid-phase pyrazole synthesis of tepoxaline derivatives **205** (cleavage from the resin by aminolysis with hydroxylamine [130]; tepoxaline: $R^1 = p\text{-}ClC_6H_4$, $R^2 = p\text{-}CH_3OC_6H_4$, $R^3 = CH_3$) and of pyrazolones **208** (cleavage at the cyclization step [179]).

The condensation of β-dicarbonyl compounds with hydrazines has also been used by Tietze et al. in the solid-phase synthesis of 1-phenylpyrazolones **208** (Scheme 43).[178] The β-oxoesters used were obtained by selective γ-alkylation of the polymer-bound acetoacetate **206**. Since cyclization occurs during the cleavage step, and only those intermediates with the correct structure are capable of cyclization, the desired pyrazolones are obtained in very high purity.

In a similar manner Felder et al. (Ciba-Geigy) were able to prepare a library of more than 10000 pyrazolones in a split synthesis (Scheme 44).[179] The β-diketone **210** was prepared by acylation of a resin-bound methyl ketone (**209**) with an ester in

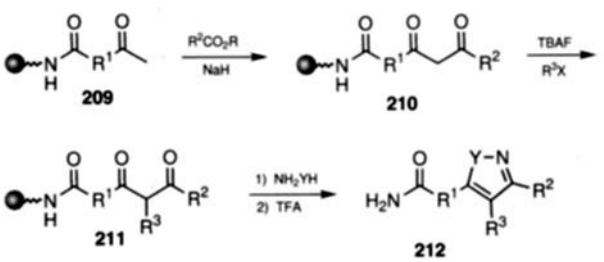

Scheme 44. Solid-phase synthesis of pyrazoles **212** (Y = NR^4) and isoxazoles **212** (Y = O) [180].

the presence of sodium hydride. The subsequent alkylation was successful in the presence of TBAF. The β-diketones **211** thus obtained were cyclized both to the pyrazoles (**212**, Y = NR^4) and to the isoxazoles (**212**, Y = O). A detailed study of the scope and limitations of this reaction sequence has been recently published.[180] A further pyrazole library with about 5000 compounds has been assembled in solution by Dhanoa[100] at Alanex.

The *N*-phenylimidazolyl acrylic acid library of Chenera et al. (SmithKline Beecham) has $5 \times 5 \times 5 = 125$ members (Scheme 45).[137] In this example, the solid support is the ion

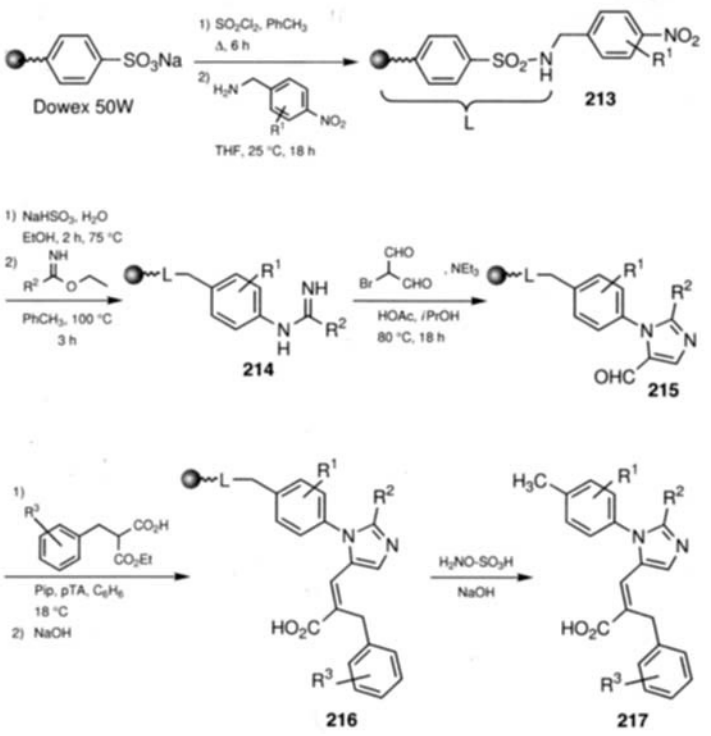

Scheme 45. Construction of a *N*-phenylimidazolyl acrylic acid library **217** through use of an ion-exchange resin with a reductively cleavable sulfonamide linker **214** [137].

exchange resin Dowex 50W. In order to ensure complete conversion a large excess of reagent was used in each reaction step. In the first step a nitrobenzylamine was bound to the resin as a sulfonamide and reduced to the aniline with sodium hydrogen sulfite. Treatment with iminoesters led to the resin-bound *N*-phenylamidines **214**, which were cyclized to the formylimidazolones **215** with bromomalonaldehyde. Conversion into the corresponding imidazolyl-5-acrylic acids **216** was achieved by a type of Knoevenagel condensation with monoethylbenzyl malonate under dehydrating conditions. After completion of the reaction, cleavage from the resin was achieved by reductive amination on heating with hydroxylamine-*O*-sulfonic acid in NaOH as reported by Nickon.[181]

4.2.1.3. Further Heterocycles (Cyclization during Cleavage from Support)

Many research groups are concerned with the development of supports that allow the mildest possible cleavage at the end of the synthesis. DeWitt and her colleagues at Parke–Davis are pursuing a somewhat different strategy in many of their syntheses; they are attempting to induce cleavage during the final cyclization step. This has a big advantage: reaction products that are not capable of cyclization and that arise from incomplete conversion in the earlier stages remain on the solid phase, so that purer products are obtained. Examples are the syntheses of 1,4-benzodiazepines illustrated in Scheme 22 and the pyrazolones **208** (Scheme 43). The same strategy was followed in the parallel synthesis of 40 hydantoins (Scheme 46).[129, 130]

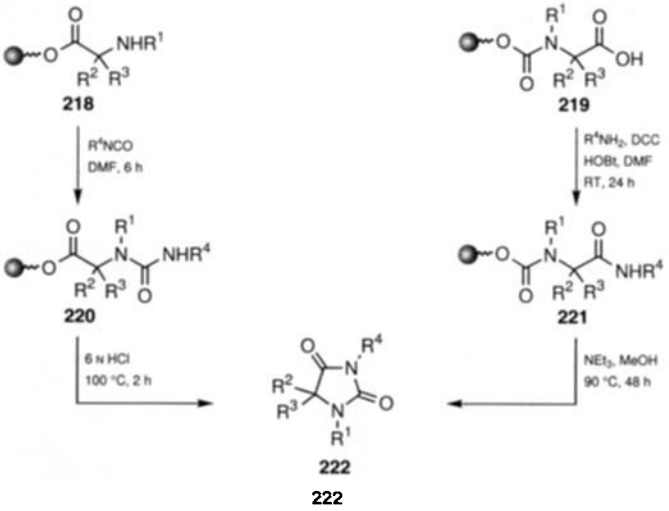

Scheme 46. Synthesis of hydantoins **222** by reaction of support-bound amino acids **218** and **219** with isocyanates and amines, respectively, and subsequent cyclization [129, 130].

Hydantoins represent the basic structure of a number of antiepileptics, of which phenytoin is still on the market. In the hydantoin synthesis, eight different C-terminally coupled amino acids (**218**) were first deprotected and then treated with five different isocyanates. Heating the ureas (**220**) in 6 N hydrochloric acid initiated cyclization to **222**; 39 individual compounds were obtained in yields of between 4 and 81%. To achieve a greater variation in the products the amino acids may be reductively alkylated with aldehydes prior to reaction with the isocyanates.[130]

Dressman et al. (Lilly Research Lab.) have described a further hydantoin synthesis in which the amino acids are N-terminally bound to a hydroxymethyl resin through a carbamate linker (Scheme 46).[182] After amide formation to form **221**, cyclization took place under basic conditions. In this way, a library of 800 individual compounds was constructed from 20 amino acids and 80 primary amines. This hydantoin synthesis, in which a wide variety of amines may be used, has the advantage over the previous synthesis in that numerous, readily available primary amines may be used in place of the isocyanates.

The Parke–Davis research group has developed a solid-phase synthesis of benzoisothiazolones, which are known[183] for their antibacterial, antimycotic, and antifungal properties (Scheme 47). In one example, a library of nine compounds of type **226** was constructed.[130, 184] Here, aromatic thiocarboxylic acids were bound to a Merrifield resin,[8] converted into active esters, and treated with amines to form **224**. After oxidation, the sulfoxides **225** were cyclized to the benziso-

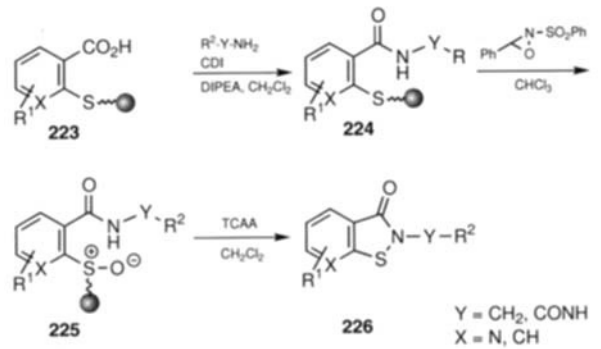

Scheme 47. Benzoisothiazolone synthesis by sulfoxide rearrangement of **225** during cleavage from the solid phase [129, 130].

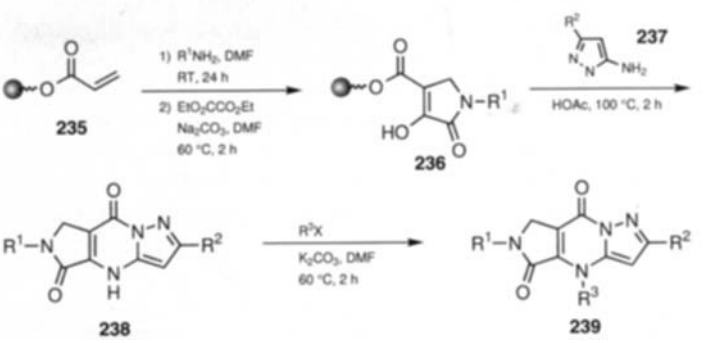

Scheme 49. Pyrimidinedione synthesis by formation of a pyrrolidinone **236** on solid phase, subsequent substitution with aminopyrazoles **237**, and cyclization during cleavage from the resin [130].

thiazolones **226** with trichloroacetic anhydride in a type of Pummerer-sulfoxide rearrangement.

β-Oxoesters may be formed on solid phase,[185] amongst other methods, by ester enolate acylation with Weinreb amides **228** (Scheme 48).[186] The β,δ-dioxoesters **230**, formed by further acylation, cyclize to pyrones **231** on heating in the presence of DMAP. The number of products produced by this method was not reported. Three examples of the preparation of tetrahydrohydroxypyranones **234** have also been described.[130] In a five-step synthesis starting from acrylic acid substituted resin **235**, the same authors have prepared the pyrrolidinones **236** by Michael addition with amines followed by cyclization with diethyl oxalate (Scheme 49). After substitution with 3-aminopyrazoles they cyclize on treatment with 5N HCl at 80°C, with concomitant cleavage from the resin to form the pyrimidinedione systems **238**, of which eight examples were described.[130] Pyrazolopyrrolopyrimidinediones of the type **239** are known to be inhibitors of cholesterol-*O*-acyltransferase (acylCoA inhibitors).[187]

In their synthesis of cyclic ethers, Kurth et al.[188] have also made use of the strategy of cleaving the target products from the polymeric support during the cyclization stage. In a five step synthesis the nitroolefin **241** was first prepared by nitroaldol condensation and then treated with a dienol in a Michael-type reaction. The β-nitroethers **242** thus formed were converted into nitrile oxides with phenylisocyanate and immediately transformed into the tetrahydrofuroisoxazolines **243** in an intramolecular 1,3-dipolar cycloaddition. Oxidative cleavage and electrophilic cyclization of these heterocyclic systems afforded selectively the cyclic ethers **244**, as illustrated in Scheme 50. All by-products formed during this reaction sequence remained bound to the solid phase. Although various reactions were

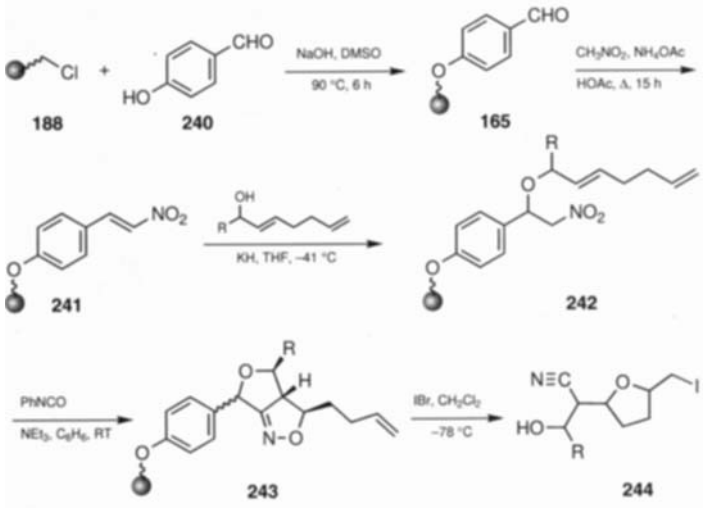

Scheme 50. Solid-phase synthesis of cyclic ethers **244** by the sequence nitroaldol condensation, Michael reaction, 1,3-dipolar cycloaddition, and subsequent oxidative cleavage from the resin by cyclization [188].

adapted for solid-phase synthesis in this reaction sequence, they are not ideally suited to library synthesis as only one moiety can be varied, since the achievable diversity of products is extremely low. The same applies to the γ-butyrolactone synthesis also developed by Kurth et al,[189] as here, too, only one substituent can be modified.

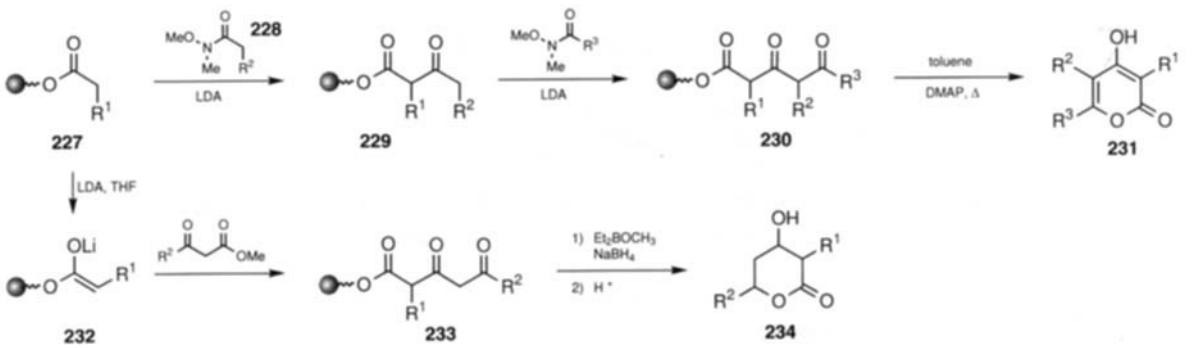

Scheme 48. Preparation of hydroxypyranones **231** on solid phase by synthesis of the β,δ-dioxoesters **230** on the resin by acylation with *N*-methoxy-*N*-methylamides **228** and cyclization during cleavage from the resin [185]. Hydroxy-δ-lactones **234** were obtained analogously by reduction before cleavage.

In contrast to the Kurth methodology, the solid-phase synthesis of a dioxopiperazine library **247** described by Gordon and Steele (Pfizer) fulfills the requirement laid down for combinatorial synthesis to a much greater extent.[190] With two readily available building blocks, amino acids and aldehydes, a heterocycle with three different substituents can be formed (Scheme 51). The key step is reductive alkylation with sodium

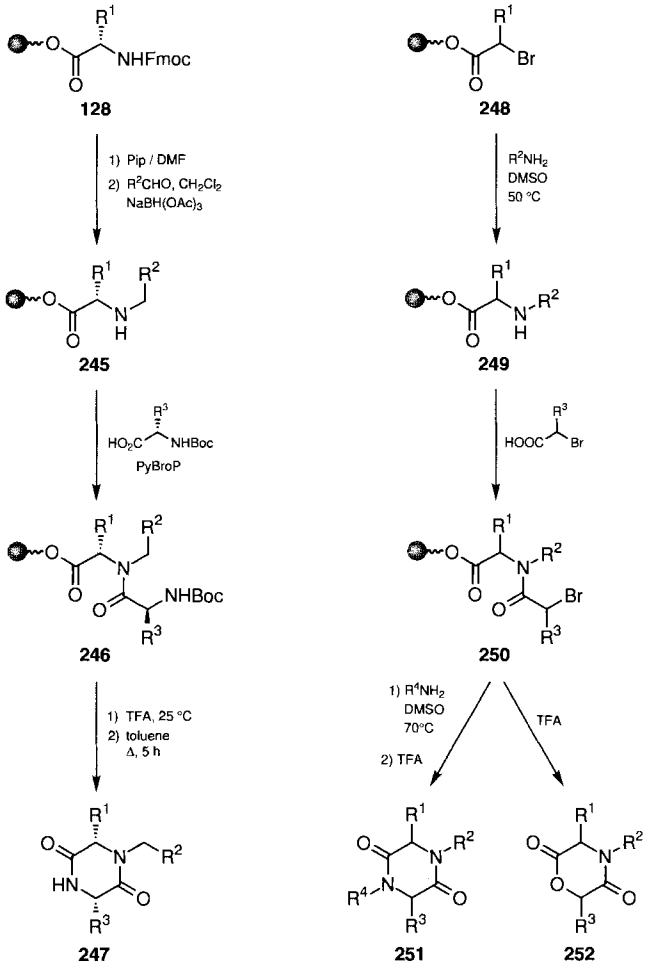

Scheme 51. Preparation of a dioxopiperazine library **147** by reaction of amino acids and aldehydes (Gordon, Steele [190]), and dioxopiperazines **251** and dioxomorpholines **252** from bromoacetic acids and amines (Spear et al. [191]).

triacetoxyborohydride, which allows the use of different amino acids and aldehydes. Acylation of the secondary amine **245** is difficult and requires repeated coupling with PyBroP to obtain complete conversion. As no cyclization occurs under cleavage conditions, heating in toluene for a short while is required after evaporation of the TFA. A model library with 10×100 compounds was constructed by the split method[13–18] and characterized by HPLC-MS. By iterative screening and deconvolution of the library, several dioxopiperazines that exhibited high affinity for the neurokinin-2 receptor were identified.

Starting from α-bromocarboxylic acids and amines Spear et al. (Chiron) synthesized a library of 22540 dioxopiperazines (**251**) in 23 mixtures, each containing 980 compounds (Scheme 51).[191] Similarly, starting from the same intermediates **250**, a library of dioxomorpholines **251** was also constructed.

Dioxopiperazines, also investigated by the research group at Affymax, are subject of a recently published patent application.[192]

4.2.2. Macrocycles

A library of macrocyclic β-turn mimetics **256** has been constructed by Virgilio and Ellman from α-amino acids, α-halocarboxylic acids, and ω-amino disulfides (Scheme 52).[134, 193, 194]

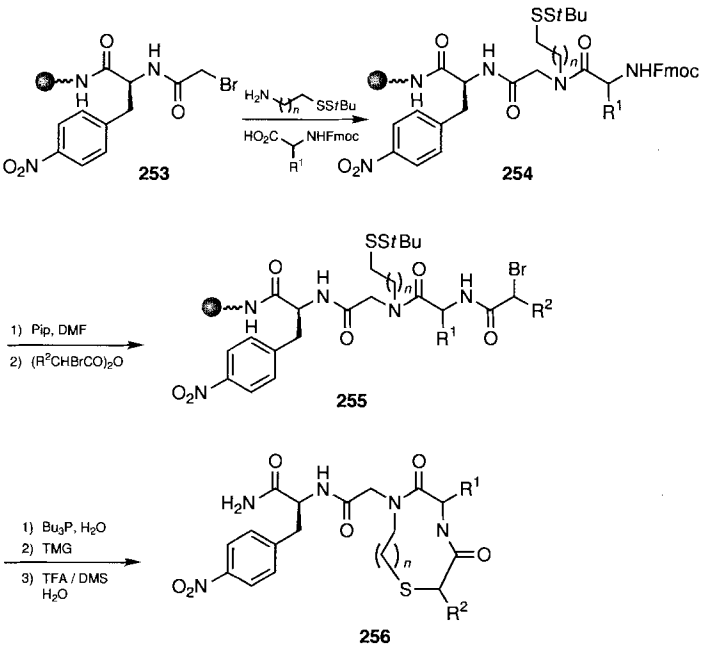

Scheme 52. Solid-phase synthesis of β-turn mimetics **256** from α-amino acids, α-halocarboxylic acids and ω-aminodisulfides [134, 193, 194].

Initially bromoacetic acid is coupled to support-bound *p*-nitrophenyl alanine, substituted with aminoalkyl disulfides, and coupled to **254** with an amino acid. Acylation with α-bromoacetic anhydride affords the precyclization product **255**. Deprotection with tributylphosphane in a 5:3:2 mixture of propanol, DMF, and water occurs successfully only on a TentaGel resin.[195] Cyclization to the nine and ten membered rings **256** occurs under strongly basic conditions in the above-mentioned solvent mixture. The β-turn mimetics, of which over 2000 examples have now been synthesized, are obtained after cleavage with TFA.[194]

Another interesting macrocyclization on a solid phase has been described by Hauske et al. (Arris, Scheme 53).[196, 197] An imidazolidine linker[107] **61** is first attached to a TentaGel support with CDI, which with diaminopropane gives an amino-functionalized resin containing an acid-labile carbamate linker. After coupling with lysine, β-alanine, and proline, *m*-iodobenzoic acid and acrylic acid are attached to the two amino termini of the tripeptides thus formed. The key step is an intramolecular Heck reaction that can only be successfully carried out on TentaGel resins, but not on conventional Merrifield resins. This macrocyclization occurs in solution at essentially "infinite" di-

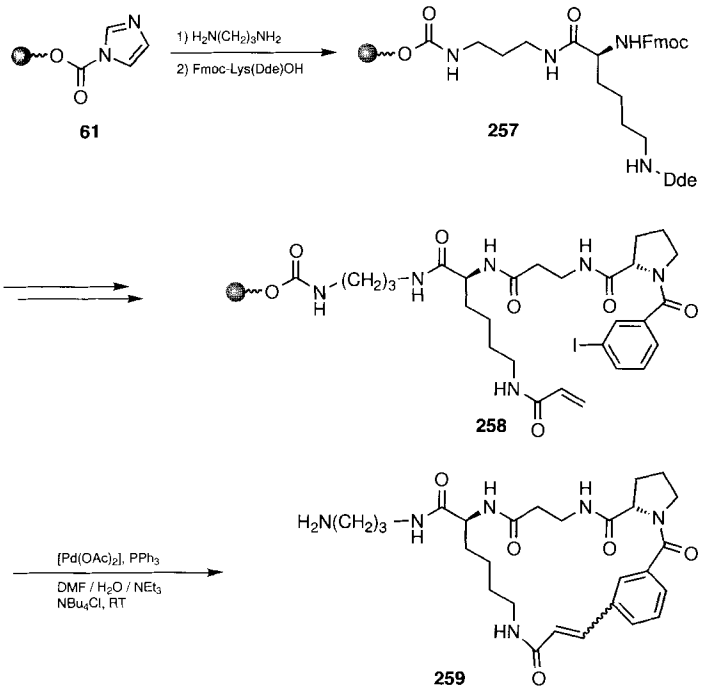

Scheme 53. Macrocyclization to **259** by an intramolecular Heck reaction on a solid phase [196].

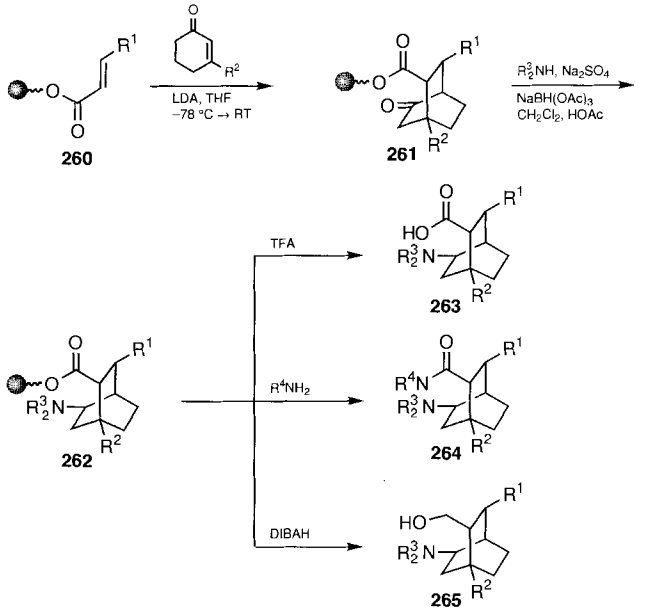

Scheme 54. Solid-phase synthesis of bicyclo[2.2.2]octanes **263**–**265** by tandem Michael addition and cleavage from the resin under different conditions [203].

lution, because of the pseudo-dilution on the solid phase, and is clearly independent of substituents and ring size: the 20–24 membered macrocycles **259** are obtained in high purity and in remarkable overall yields (75–85%). A library with 15 members was produced by the split method. Intramolecular Wadsworth–Emmons reactions[198] have also been used by Hauske et al. for macrocyclization.[196]

4.2.3. Carbocyclic Compounds

The construction of carbocyclic compounds by Diels–Alder reaction on solid support was originally investigated by Leznoff et al. in the 1980s.[199] More recent examples of a Diels–Alder reaction are the reaction of a C_{60} fullerene with cyclopentadiene bound to a solid phase,[200] which, as expected, is reversible on heating at 180 °C, and a diastereoselective reaction of aminofurans with acrylates[201] on the solid phase. The Pauson–Khand reaction of polymer-bound alkynes with norbornadiene and norbornenone is more efficient than in solution.[202] Both cycloadditions have undeniably "combinatorial" potential, although the authors were probably not thinking of compound libraries at that time.

Until now enolate anions on a solid phase have only been used in simple alkylation reactions. Ley et al. have used them in a tandem Michael addition for the solid-phase synthesis of bicyclo[2.2.2]octanes (**262**).[203] Here, polymer-bound acrylates **260** are treated with cyclohexenone enolates (Scheme 54). After reductive amination, the bicyclo[2.2.2]octanes **262** are cleaved from the resin under reductive conditions or by aminolysis or acidolysis. This reaction sequence offers great potential for synthesis of a library of high diversity. More than 250 different acrylates and enones are currently available commercially, and the palette of amines available for reductive amination is equally extensive. One awaits further reports from this group with great anticipation.

In a further example of support-bound carbocycle synthesis, Tietze and Steinmetz have recently published a stereoselective solid-phase synthesis of the cyclopentane and cyclohexane derivatives **271** and **272** that employs a domino Knoevenagel–ene reaction (Scheme 55).[48] A Merrifield resin modified with a propandiol linker (**L**) was used as support. Subsequent reaction with monomethyl malonoyl chloride afforded the polymer-bound malonate **267**, which, for the two-component domino reaction, was treated with the unsaturated aldehydes **268** in the presence of catalytic quantities of piperidinium acetate, fol-

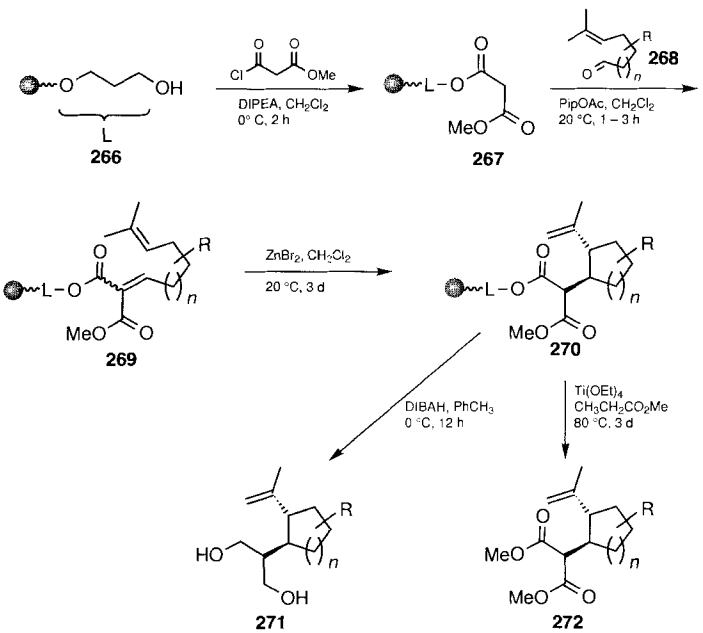

Scheme 55. Stereoselective solid-phase synthesis of cyclopentane and cyclohexane derivatives **271** and **272** by a domino Knoevenagel–ene reaction [48].

lowed by zinc chloride. Except with α-substituted aldehydes, the primary Knoevenagel condensation occurs without the addition of dehydrating agents. The cyclopentane and cyclohexane derivatives **270** obtained by a subsequent intramolecular ene reaction may be cleaved from the resin either by reduction or ester exchange. In either case the products were obtained not only in good yields (41–61%) and high purity (approximately 90%), but also with excellent diastereoselectivity. As expected, when geminally disubstituted aldehydes are used, only modest induced diastereoselectivity is observed. The authors did not prepare a sample library by split synthesis, but by simultaneous reaction of the polymer-bound malonate with six aldehydes in equimolar amounts (in each case 0.15 equivalents aldehyde per equivalent malonate) and subsequent by an ene reaction. With one exception, after reduction the corresponding diols could actually be obtained in almost equal concentrations. If, as here, mixtures are prepared without use of the split synthesis, one significant advantage of solid-phase synthesis is lost, namely the use of large reagent excesses. If the aldehydes used differ greatly in their reactivity, it is less likely all the compounds in the product mixture are present in equimolar amounts.

Currently these are the only carbocycle syntheses that have found application in combinatorial chemistry. It may be expected, however, that in the future the Diels–Alder and other reactions leading to carbocycles will find increasing use in library synthesis.

4.3. Further Library Syntheses

4.3.1. Modular Compound Libraries

In addition to numerous heterocyclic syntheses, several combinatorial syntheses have been described recently in which no central cyclic framework has been constructed.

A two stage aldol reduction sequence for the 1,3-diols **275** has been developed by Kurth et al. (Scheme 56).[33] The basic ele-

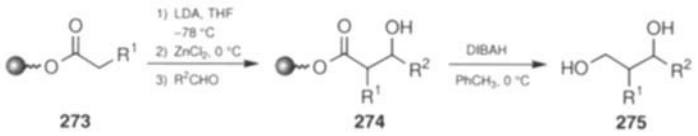

Scheme 56. Synthesis of 1,3-diols **275** by solid-phase aldol reaction and reductive cleavage from the resin [33].

ment is coupled to Merrifield resin by esterification, converted into the zinc enolate and finally into **274** with a series of aldehydes in an aldol reaction. Whereas treatment with lithium aluminum hydride led to considerable retroaldol reaction, the products were reductively cleaved from the resin with diisobutylaluminum hydride. The *threo* and *erythro* isomers of **275** were obtained in a 7:5 ratio and overall yield of 26%. The progress of the reaction was monitored by IR analysis of the polymer. A model library of 27 compounds in three mixtures was prepared by the split method, purified by thin layer chromatography, and tested for their activity as antioxidants.

By means of their synthesis of β-sulfanylketones, Kurth et al. have shown[204] how a series of well-known reactions may be linked together on the solid phase (Scheme 57): the sequence begins with monosubstitution of butanediol on Merrifield resin

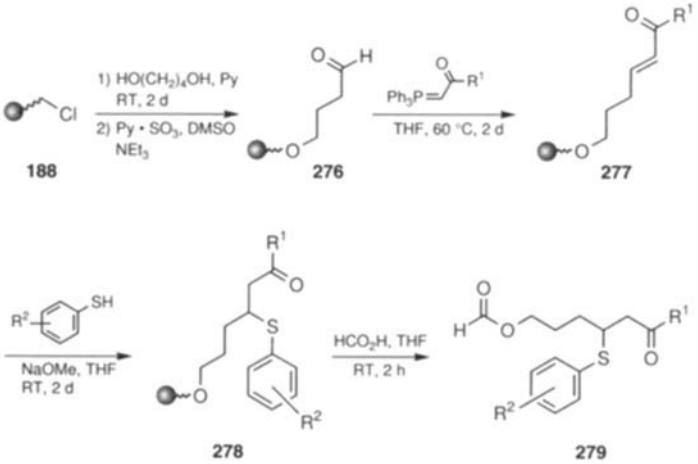

Scheme 57. Combination of several classical named reactions on solid phase. A Swern oxidation followed by a Wittig olefination with subsequent Michael reaction affords **279** [204].

188. The free hydroxyl group is oxidized with complex of sulfur trioxide and pyridine to give the aldehyde **276**, which is converted into the enones **277** in a Horner–Emmons reaction with a series of phosphoranes followed by the addition of thiophenols in a Michael type reaction. After a total reaction time of almost a week, the β-sulfanylketones **278** were cleaved from the resin with formic acid. The desired products are obtained in yields of about 20%. Here too, the course of the reaction was readily monitored by IR analysis. A small library of nine (3 × 3) compounds was prepared by the split-and-combine principles and characterized by gas chromatography. Biological testing was carried out both with the products cleaved from the resin and with the products still bound to the resin. Whether the identity of a polymer-bound compound could be determined form a single resin particle was also investigated. In this method, a single particle (200–400 mesh) was isolated under a microscope, incubated with the cleaving reagent, and analyzed by GC-MS. The structure of this and other support-bound compounds could be determined unambiguously. One problem is, however, the mechanical separation of a single resin particle. Therefore studies with larger polymer particles (20–40 mesh) are underway, as these can be separated simply without a microscope.

Dankwardt et al. (Syntex) have synthesized an aryl- and benzylpiperazine library of 190 compounds (38 × 5) by benzylation and alkylation of phenylpiperazines and investigated its biological activity.[205] However, the results of these tests have not been published.

A further *N*-arylpiperazine synthesis has been described by the research group at Parke–Davis (Scheme 58).[130] Chloropropionic and butyric acids were coupled to Wang resin and converted into **281** with arylpiperazines. The enolate produced with trityl lithium could be trapped with acid chlorides. Cleavage of the product **282** from the resin under decarboxylation

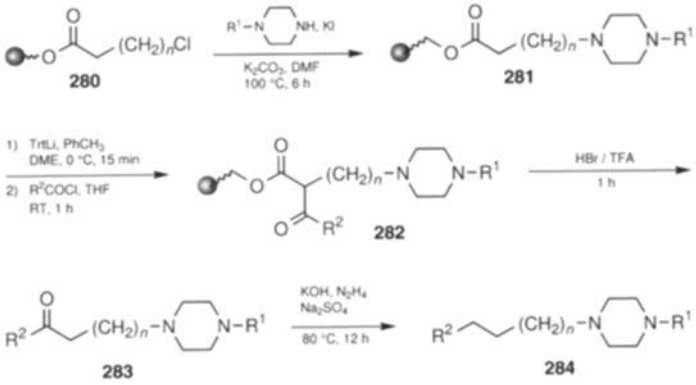

Scheme 58. Preparation of *N*-arylpiperazines **283** on solid phase. Cleavage from the resin and modified Wolff–Kischner reduction to **284** [130].

conditions was achieved by anhydrous HBr in trifluoroacetic acid. The compounds **283** thus obtained could then be reduced in a modified Wolff–Kishner reduction. In this way a library of 2×12 individual compounds was prepared, but because of the similarity of the building blocks used it exhibited only low diversity. However, further arylpiperazines should be available in an analogous manner.

Kobayashi et al. prepared silyl enol ethers **286** on solid phase from the thioesters **285** by reaction with trimethylsilyl triflate.[206] These react with imines in the presence of catalytic amounts of scandium triflate to form β-aminothioesters **287**, which may be reductively cleaved to the aminoalcohols **288** (Scheme 59).

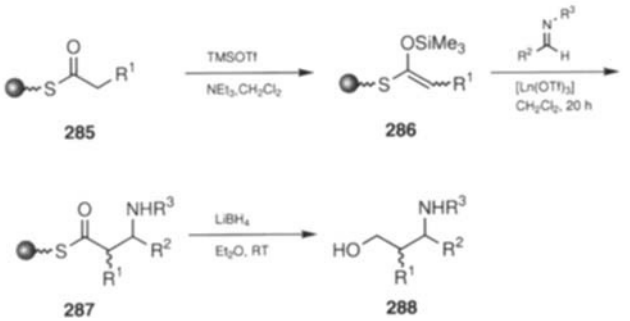

Scheme 59. Synthesis of β-amino acid derivatives **287** by reaction of silyl enol ethers **286** with imines [206].

Aspartyl- and metalloproteases can be inhibited by hydroxyethylamines. A solid-phase synthesis of hydroxyethylamines and hydroxyethyl ureas **294** has been described by Ellman et al. (Scheme 60).[134, 207] In this method the starting material **289**, previously used as an intermediate in the synthesis of a known HIV protease inhibitor, was coupled to the resin through a dihydropyran (DHP) linker. After replacement of the tosyl group by amines, conversion into the ureas **292** was achieved with isocyanates in the case of primary amines or otherwise with triphosgene and amines. The two-stage alternative is more universally applicable because of the better availability of primary amines. The azide **292** was reduced with a cocktail of thiophe-

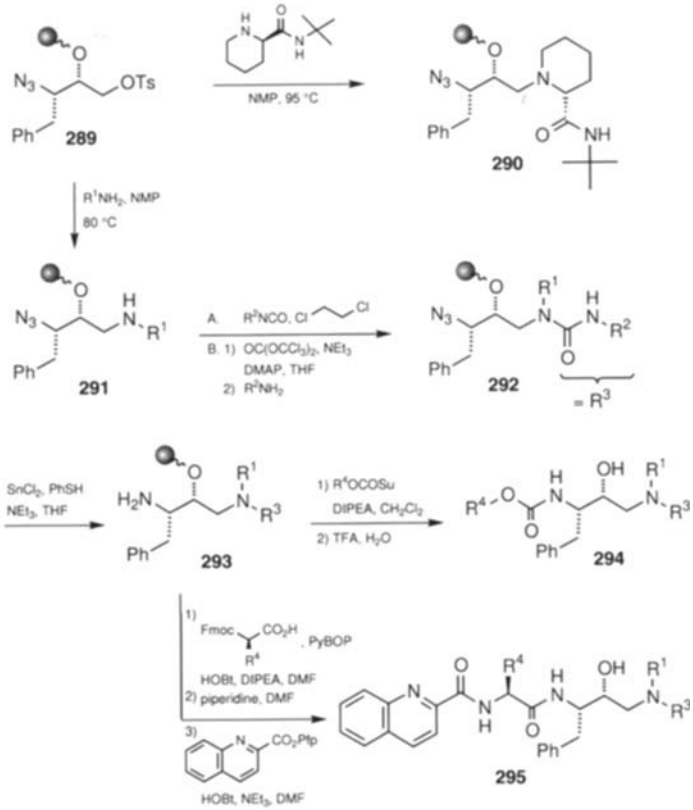

Scheme 60. Solid-phase synthesis of hydroxyethylamines and hydroxyethylureas. The key step is azide reduction with thiophenol/triethylamine/tin chloride to **193** [207].

nol/triethylamine/tin chloride[208] to yield the amine **293**, which could be acylated to the carbamate or amide. After cleavage with trifluoracetic acid and purification by column chromatography, the products were obtained analytically pure in 47–86% yield in this four- to six-stage synthesis.

Wang et al. (Abbott) proceeded in a similar manner.[209] The tosylated azide **289** was linked to benzhydryl resin by means of a bifunctional linker, and after deprotection of the two amino groups, the molecule could be extended on both sides with, for instance, carboxylic acids, sulfonyl chlorides, or isocyanates, to afford 300 individual compounds in an automated parallel synthesis. The products could only be cleaved from the resin under very drastic conditions and in purities of 20–50% in the diol series and 30–70% for the monoalcohol diamine derivative. Most of the impurities found contained linker fragments. The crude products were tested for HIV protease inhibition without further purification and gave IC_{50} values of less than 1 nM to 6.4 μM.

A solid phase variant of the Noyori three-component prostaglandin synthesis has been devised by Ellman et al. (Scheme 61).[210] After addition of alkylzinc derivatives to 4-hydroxy-2-cyclopentanones **298** bound to a resin, alkylation was carried out with alkyl triflates. This synthesis was originally performed with the DHP linker, but the cleavage conditions were not compatible with the target molecule. When the silyl linker **296** was used, the severe coupling conditions required that the hydroxypentane be protected with the dimethoxytrityl group. After two reaction stages the prostaglandin **299** was isolated diastereomerically pure in a yield higher than 50%. Fur-

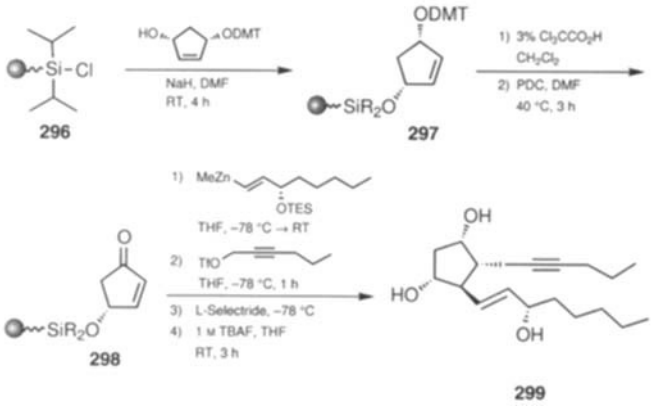

Scheme 61. Synthesis of prostaglandin **299** on solid phase by addition of an organozinc compound to resin-bound hydroxycyclopentenone **298** and alkylation with triflate [210].

thermore, the alkylation proceeded in only poor yield on Merrifield resin. A macroporous resin proved to be a better support for this reaction sequence.

Familiar problems of this prostaglandin synthesis are the low reactivity of the initially formed enolates as well as the danger of proton exchange and subsequent elimination of the alkoxy group to form the cyclopentenone, which in this case amounts to a cleavage from the resin. Ellman has recently introduced an alternative solid phase prostaglandin synthesis[211] to overcome this problem (Scheme 62).[134] A resin-bound iodocyclopentenone (**300**), formed in three steps from **297**, is treated with an organoborane under palladium catalysis. The introduction of the ω side chain is achieved by means of Michael addition of a cuprate.

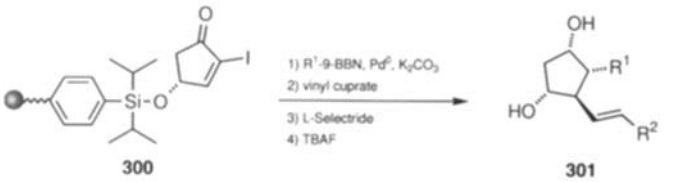

Scheme 62. Pd-mediated prostaglandin synthesis on solid phase [115b, 134].

A further reaction that proved its worth in the preparation of bicyclic prostaglandin analogues is the palladium-catalyzed three-component coupling of norbornene derivatives with bromo- or iodoolefins and alkynes.[212] Ellman has used this reaction in the solid-phase synthesis of the tropane derivatives **303** (Scheme 63).[134] Boronic acids may be coupled under these conditions in place of alkynes. Finally, after deprotection, **303** may be further derivatized on the nitrogen atom. Whether this reaction allows a wide variation in coupling partner (and hence the construction of large compound libraries) is currently being investigated.

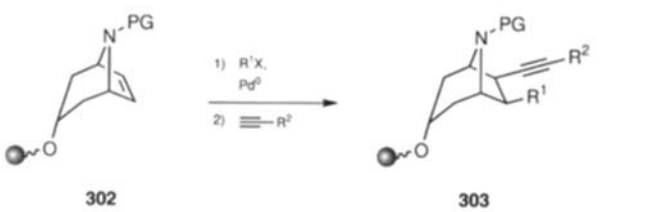

Scheme 63. Pd-mediated three-component coupling [115b, 134].

A strategy for the formation of diaminourea libraries **308** from amino acids, diamines, and amines has been developed by Hutchins and Chapman (Merck, Scheme 64).[213] The diamine unit serves to control conformatively the coupling of two molecular fragments. In this reaction, Fmoc-protected 4-(aminomethyl)benzoic acid is bound to Rink resin[214] and after deprotection is converted into the *p*-nitrophenyl carbamate.[215] The carbamate **305** forms the first urea bond with a series of unprotected primary diamines (**306**). The free amine is again converted into the nitrophenyl carbamate to allow the formation of the second urea bond with a number of amines. After cleavage with TFA the products were formed with a purity of greater than 90% and could thus be directly investigated for activity in solution. This method should be well suited for the construction of large compound libraries because of the ready availability of the reagents and the reliable chemistry.

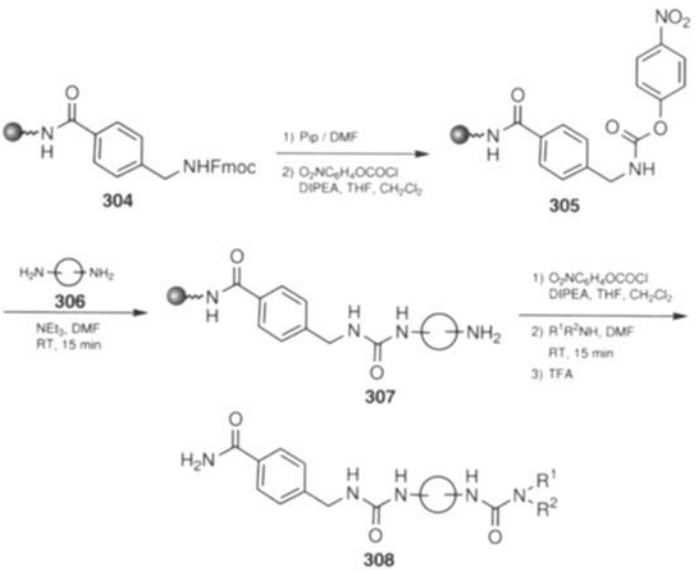

Scheme 64. Synthesis of diaminourea libraries **308** by combination of amino acids, diamines, and amines on solid phase [213].

There have been numerous reports of solid phase Mitsunobu reactions.[216, 217] Krchnák and his colleagues at Selectide have used the Mitsunobu reaction to prepare a model library of 4200 compounds of the type **312** from amino acids, hydroxyphenyl carboxylic acids and alcohols (Scheme 65).[218] Initially an Fmoc-protected amino acid (**309**) is linked to a TentaGel resin under Mitsunobu conditions and then coupled to phenolic carboxylic acids **310**. In the final step, the reaction is carried out with a series of alcohols and benzyl alcohols, again under Mitsunobu conditions. The products **312** can be cleaved from the resin by hydrolysis with NaOH. No satisfactory results were obtained if the reaction was carried out in *N*-methylmorpholine, which has been described as the solvent of choice for the reaction of resin-bound benzyl alcohol with phenols.[217] The model library constructed from a combination of 20 amino acids, 10 aromatic hydroxy acids, and 21 alcohols was tested in biological assays whilst bound to the resin. The results are to be published later.

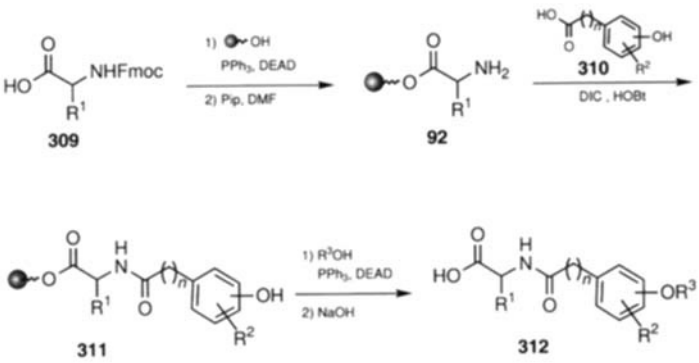

Scheme 65. Derivatization of phenolic carboxylic acids **310** to **312** by solid-phase Mitsunobu reactions [218].

4.3.2. Libraries by Derivatization of Templates

In this variant of library synthesis a template usually preformed in solution is coupled to the solid phase. There it serves as a central building block, its reactive groups being transformed during the course of the synthetic sequence.

A typical example is the bisamidophenol **317** of Pavia et al. (Sphinx):[219] the trifunctional 3-nitro-4-aminophenol (**314**) is coupled to a carboxylated resin[220] (**313**) and then acylated with acid chlorides or converted into ureas with isocyanates (Scheme 66). Finally the nitro group is reduced with tin dichloride in DMF, and the way is open for further conversions with acid chlorides, sulfonyl chlorides, or isocyanates. The products are cleaved by hydrolysis in amounts of 3–9 mg (15–45% overall yield) with purities of 60–80%. In this way a library of 600 individual compounds was prepared; it was tested in solution for protein kinase inhibition after cleavage from the resin. There are currently no reports of any lead structures having been found.

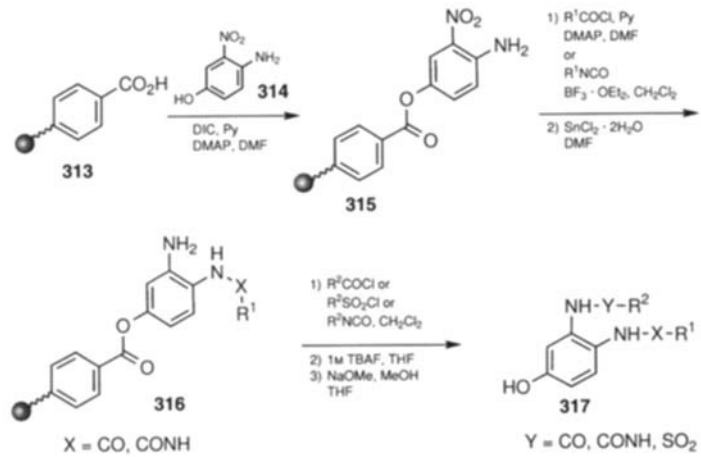

Scheme 66. Preparation of a bisbenzamidophenol library **317** by derivatization of 3-nitro-4-aminophenol **314** on polymeric support material **313** [219].

The procedure of Dankwardt et al. (Syntex) is similar.[221] Here too, a trifunctional building block, 3-amino-5-hydroxybenzoic acid (**319**), is coupled to resin and then derivatized (Scheme 67). The synthesis also starts with acylation of the amine, and the hydroxy function is concomitantly esterified. De-esterification was achieved with cesium carbonate[222] in DME, and the freed hydroxy function was further treated with alkyl halides and sulfonyl chlorides. Prior to library synthesis the scope and limitations of the reaction was first determined (criterium: greater than 70% product purity by HPLC). Each member of a model library of 5×5 compounds prepared by the split method was obtained with a purity of greater than 80 % (with less than 20% unalkylated material). To increase the diversity of the products the template was attached to the resin by means of an amino acid. Ultimately a library of 2001 (69×29) compounds (**322**) was formed (split synthesis), the biological activity of which is currently being investigated. "Fingerprints" of each mixture of 69 compounds were determined by analytical HPLC.

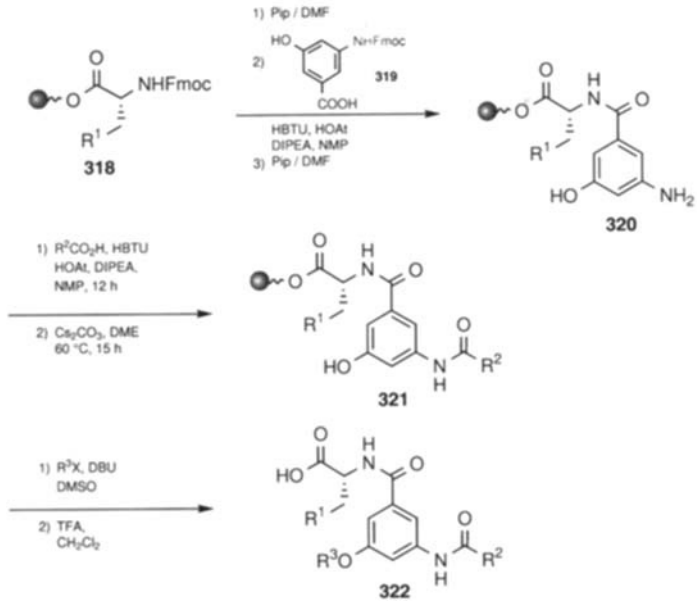

Scheme 67. Derivatization of N-protected 3-amino-5-hydroxybenzoic acid **319** to form libraries of the type **322** [221].

Researcher groups at both Affymax[223] and Selectide[224] have used the differential reactivities of the chlorine atoms of 2,4,6-trichloro-*s*-triazine (**324**) in a simple library synthesis (Scheme 68). A resin-bound amino acid (**323**) is initially treated with **324**, which smoothly causes monosubstitution of the trichlorotriazine. The remaining chlorine atoms are then sequentially substituted under more forcing conditions.

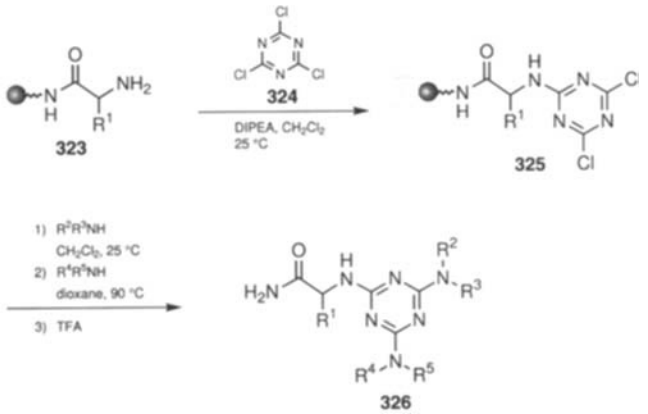

Scheme 68. Synthesis of a triazine library **326** [223, 224].

A simple bifunctional template has been derivatized by DeWitt et al. (Scheme 69).[130] Kornblum oxidation with sodium hydrogen carbonate in DMSO converted the Merrifield resin (**188**) into a support-bound benzaldehyde (**327**), which gave an

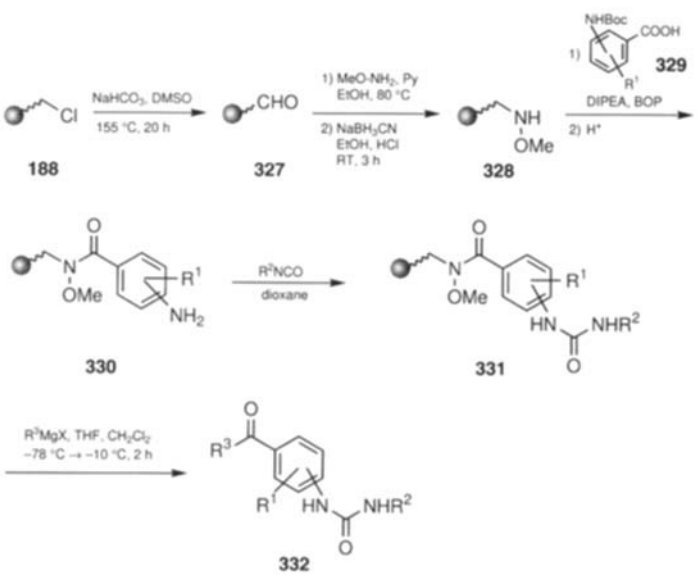

Scheme 69. Synthesis of the *O*-methylhydroxylamine resin **328** on which aminobenzoic acids **329** are converted into different ketoureas **332** [130].

O-methylhydroxylamine resin (**328**) by heating with hydroxylamine and subsequent reduction with sodium cyanoborohydride. Coupling with aminobenzoic acids **329** followed by reaction with isocyanates afforded the corresponding ureas **331**. Treatment with alkyl- and arylmagnesium bromides led to cleavage of ketoureas **332** from the resin.

Such resin-bound Weinreb amides have also been used recently by Armstrong et al. in the synthesis of aldehydes and ketones.[225] Here, too, cleavage with Grignard compounds gave the corresponding ketones, whereas aldehydes were formed by reduction with DIBAH or $LiAlH_4$.

In parallel syntheses, Green (Ariad Pharmaceuticals) has prepared 60 analogues of the tyrosine kinase inhibitor lavendustin (Scheme 70).[226] In this work, methoxyaniline **333** bound to Wang or Rink resin was initially reductively alkylated to **334** with substituted benzaldehydes and subsequently treated with benzyl bromides. The tertiary amines **335** were obtained in good yields and usually with high purity after cleavage from the resin with trifluoracetic acid or boron tribromide. Cleavage from Wang resin with boron tribromide has the advantage that the methyl phenyl ethers are also cleaved to give the free polyhydroxylated target compounds.

Tertiary amines have also been the interest of Flegelová and Pátek (Selectide).[227] They have obtained the substituted products **338** by palladium-catalyzed bisallylation (Scheme 70). The reaction conditions were optimized for each of six different templates.

Arylacetic acids have been derivatized by Ellman et al. with enol alkylation and subsequent Suzuki reaction (Scheme 71).[112, 134] Certain representatives of this class, for example ibuprofen, are cyclooxygenase inhibitors. 4-Bromo-

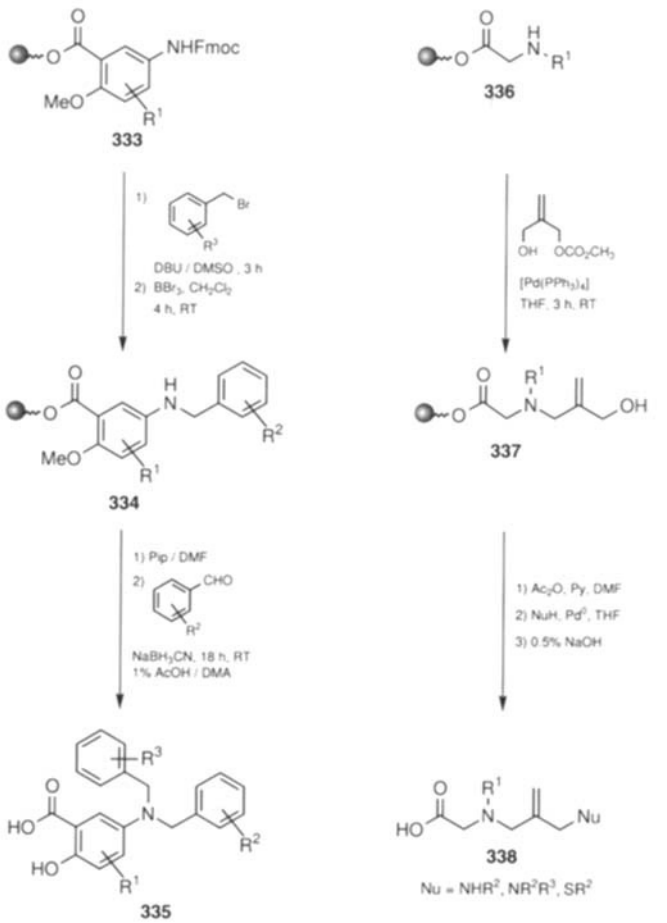

Scheme 70. Solid-phase synthesis of the tertiary amine **335** (lavendustin A analogues [226]) and **338** (products of a Pd-catalyzed bisallylation [227]).

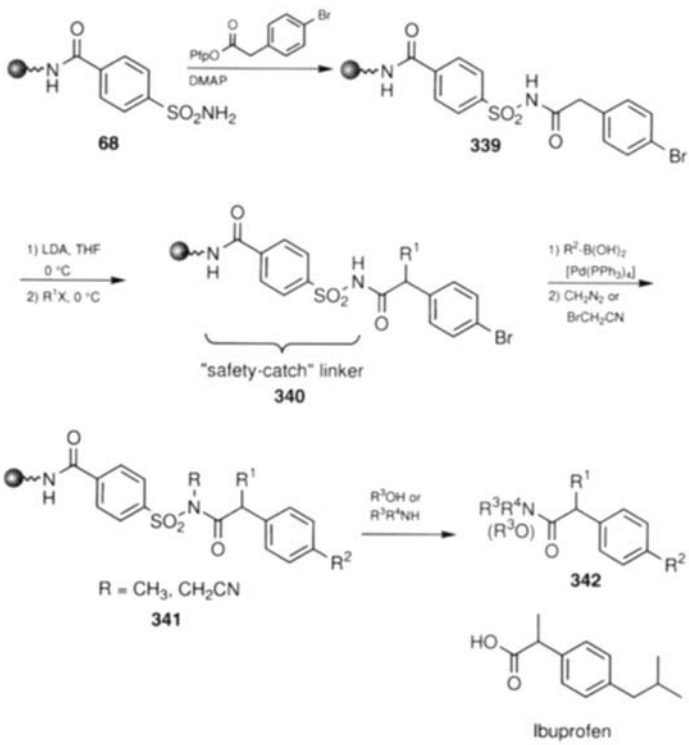

Scheme 71. Solid-phase synthesis of phenylacetic acid derivatives **342** by enolate alkylation and subsequent Suzuki reaction [112, 134] on use of the "safety catch" linker [113].

phenylacetic acid was linked to the resin through the rarely used but, under these reaction conditions, compatible "safety catch" linker.[113] The derivatives **340** were obtained by trapping the corresponding enolates with alkyl halides. A subsequent palladium-catalyzed conversion with alkyl-9-BBN derivatives or alkylboronic acids under Suzuki conditions yielded the coupled products **341**. Following N-methylation of the sulfonamide linker with diazomethane, cleavage from the resin was achieved with a series of reactive nucleophiles. Cleavage with weaker nucleophiles, such as aniline and primary amines succeeded only when the acylsulfonamide was activated by cyanomethyl substitution.[114, 115] A series of phenylacetic acids and amides **342** were obtained in high yields in a clean reaction sequence.

The cyclopentane template **343** was prepared in solution by Pátek et al. (Selectide) and derivatized on resin in a sequence of amide formation and protective group transformations (Scheme 72).[228] The completely substituted cyclopentanes **345** were obtained in high yields (83–90%) and purities (>90%).

The biphenyl library **349** was prepared at Sphinx Pharmaceuticals from trifunctional, alkoxy-protected biphenyl templates. These were prepared in solution, coupled to the resin, and there successively deprotected and converted into different alkoxy derivatives under modified Mitsunobu conditions (Scheme 73).[229] In a so-called "double combinatorial" procedure on a resin two aromatic templates were attached in a palladium-catalyzed coupling reaction (Scheme 73).[230] In this sequence, a protected dihydroxyarylstannane (Template 1, **351**)

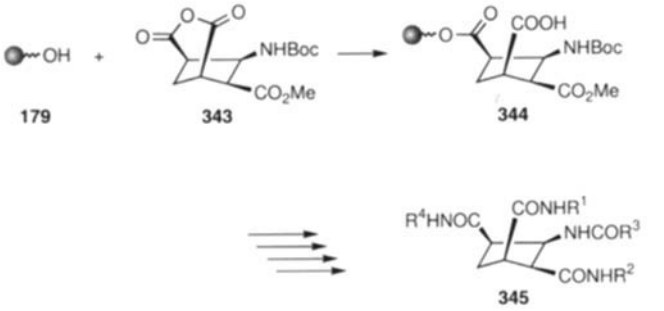

Scheme 72. Conversion of the cyclopentane template **343** into compounds of type **345** [228].

was linked to a resin through the "NpSSMpact linker"[188, 231], the hydroxyl groups sequentially deprotected and etherified, and further treated with protected dihydroxybromobenzene or dihydroxybromobenzyl chloride (Template 2, **353**) in a Stille coupling reaction. The two new hydroxy groups were also derivatized before the products were cleaved photochemically. If bromoaromatics are attached to the resin as the first template, these may be converted into the tolanes **357** with the phenylacetylenes **356** by palladium catalysis and then reduced to the *cis*-stilbenes under Lindlar catalysis or to the phenylethylbenzenes with palladium acetate. In this way two functionalized aromatic templates may be connected by different flexible C-bridges. Massive libraries may be constructed by this "double combinatorial" library synthesis. With only 10 alkyl bromides in each step, 10000 compounds are obtained in which the triple

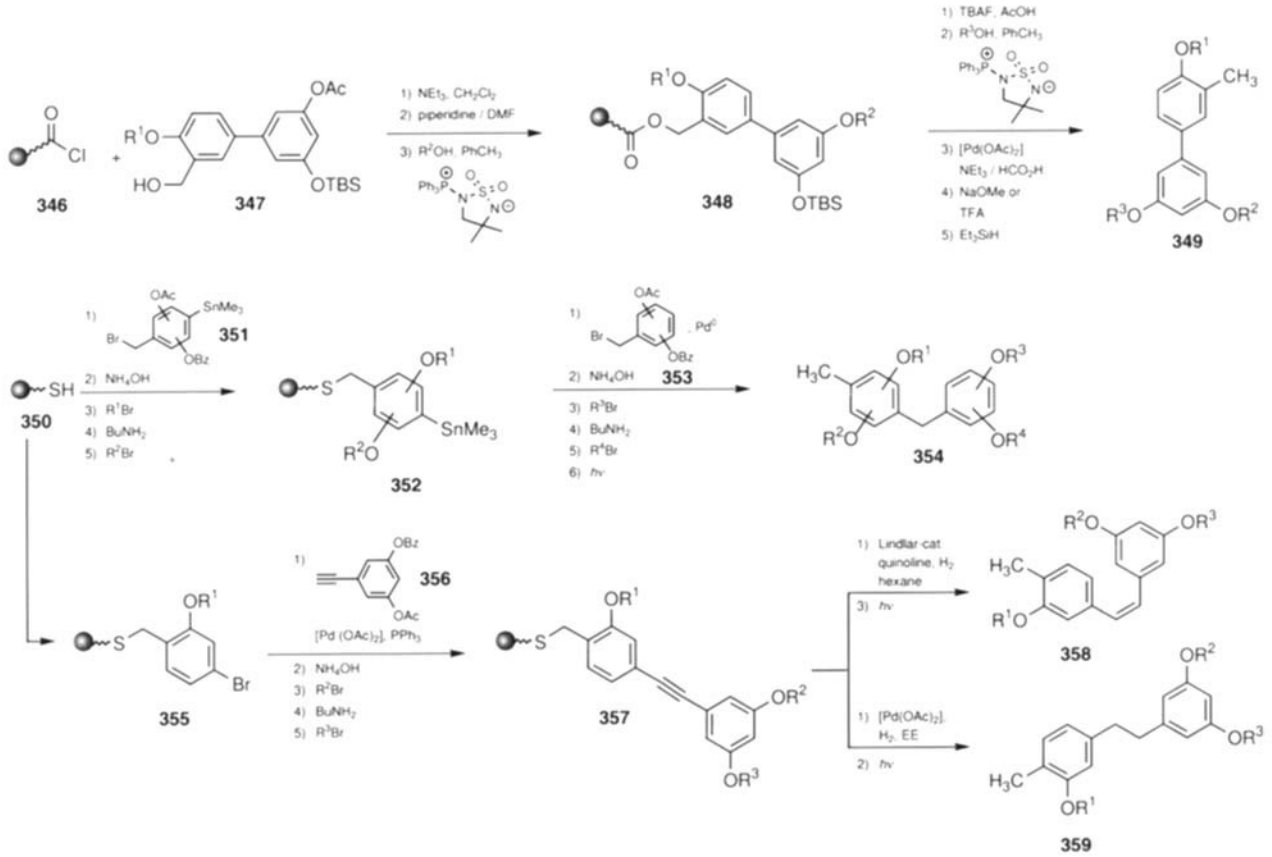

Scheme 73. Synthesis of "double combinatorial" libraries **349**, **358**, and **359** by palladium-catalyzed coupling and derivatization of two templates on a solid phase [229, 230].

bond can be partially or totally hydrogenated. Whether the biphenyls will become the templates of the 1990s—as predicted by the authors—remains to be seen.

4.3.3. *Libraries from Multicomponent Reactions*

In the syntheses previously described, the compound libraries were produced from the components by individual reaction steps in a linear synthesis. Particularly attractive, however, are reactions in which highly diverse libraries are produced in a one-pot reaction. These are multicomponent reactions[83, 84] that have previously been described in combinatorial syntheses in solution (c.f. Section 3.2.1). The Affymax thiazolidine synthesis[89] (Scheme 29) in which aldehydes and α-sulfanylcarboxylic acids were treated with amino acids in a single step was one example of a solid-phase multicomponent reaction.

The first solid-phase multicomponent reactions were the Ugi and Passerini reactions described by Armstrong et al.[88, 232] In the three component Passerini reaction, a carboxylic acid is condensed with an aldehyde and an isonitrile. In this manner azinomycin analogues inter alia could be formed (Scheme 74).

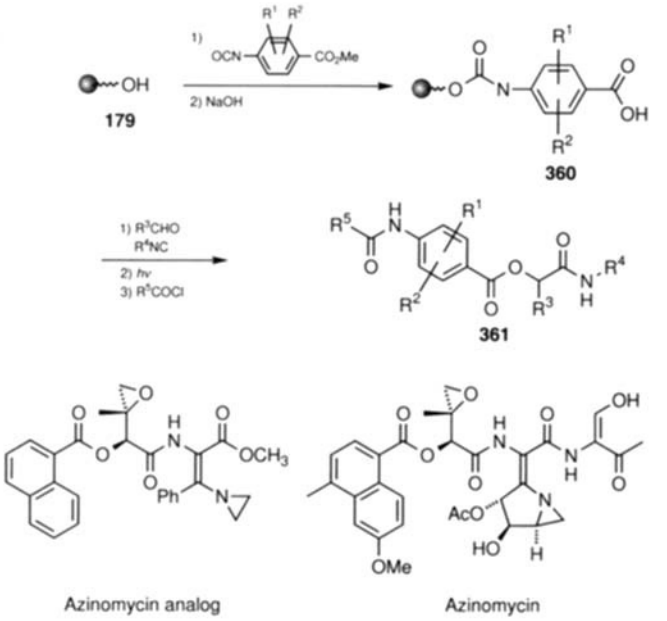

Scheme 74. Passerini three-component reaction on solid phase and preparation of azinomycin derivatives [232, 233].

In an Ugi reaction, Rink resin[124] was condensed to α-amidoamides with three further components. To expand the range of commercially available isonitriles, additional isonitriles were prepared by lithiation of benzyl isonitrile and trapping with alkyl halides. With corresponding automation large libraries may be constructed on resin and in solution, with these two types of reaction.

Similarly Rink resin has also been used as amine component in an Ugi reaction by Mjalli et al. of Ontogen,[234] who in this

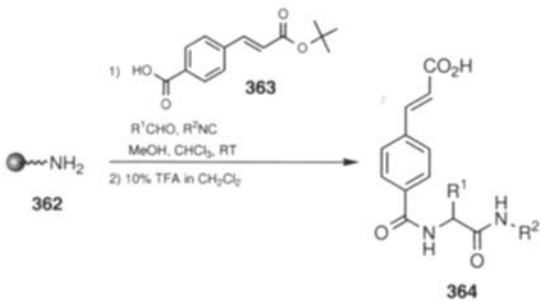

Scheme 75. Synthesis of cinnamic acid derivatives **364** by the Ugi reaction [234]. Rink resin **362** is used as amine component.

way obtained the cinnamic acid derivatives **364** in yields and purities of over 90% (Scheme 75). These compounds represent new lead structures for inhibitors of hematopoietic protein tyrosine phosphatases (HePTP). The most active compound (R^1 = phenyl, R^2 = benzyl) inhibited this enzyme with an IC_{50} value of 3.9 μM.

A further solid-phase four-component reaction developed by this research group started from resin-bound isonitriles **366**, phenyl glyoxals, primary amines, and carboxylic acids. The products, α-(*N*-acyl-*N*-alkylamino)-β-oxoamides **162** (Scheme 76), were subsequently cyclized to imidazoles.[169] The

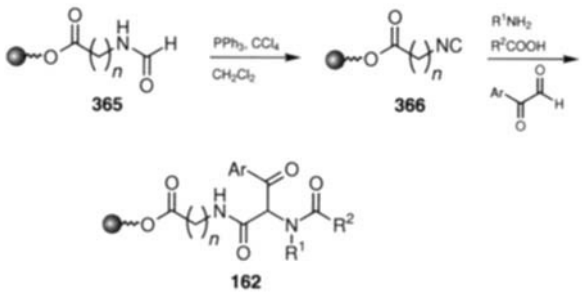

Scheme 76. Preparation of α-(*N*-acyl-*N*-alkylamino)-β-oxoamides **162** by the Ugi reaction [169]. The isonitrile **366** is produced on the solid support by dehydration of the formyl compound **365**.

required isonitriles were prepared directly on the solid support (Wang resin) by dehydration of N-formyl compounds. The Ugi reaction proceeded in moderate yields (about 50%), independent of the starting materials used; only on the use of aniline as amine component did the yield fall dramatically (16% after cyclization to the imidazole).

A further solid-phase three-component reaction has been recently reported by Wipf et al.[235] Dihydropyrimidines were obtained in high yields and purities by Biginelli condensation of β-oxoesters, aldehydes, and ureas (Scheme 77). In this sequence the resin-bound γ-aminobutyric acid (GABA) urea **367** is converted into the dihydropyrimidines **368** by heating with β-oxoesters and aldehydes under acid catalysis and isolated by simple filtration after cleavage of the benzyl ester with trifluoracetic acid. The individual products were obtained in high yields (67–98%) and excellent purity (>95%) in amounts of 10–20 mg. Since β-oxoesters are readily obtained in one step and many aldehydes

are commercially available, this reaction is applicable to the parallel synthesis of large compound libraries. The GABA linker increases the water solubility of the products and offers opportunity for further derivatization. Dihydropyrimidines are known for their wide-ranging biological effects, for instance, antiviral, antihypertensive, and antitumor activities, as well as calcium channel blockage, so libraries of this type may well contain interesting lead structures.

The Biginelli condensation has been carried out stepwise by Robinett (Arris Pharmaceuticals), who used the Atwal modification (basic conditions).[236] The conversion of Knoevenagel products with substituted thioureas affords thiosubstituted dihydropyrimidines **370**, which may be cleaved from the resin with formic acid (Scheme 77).

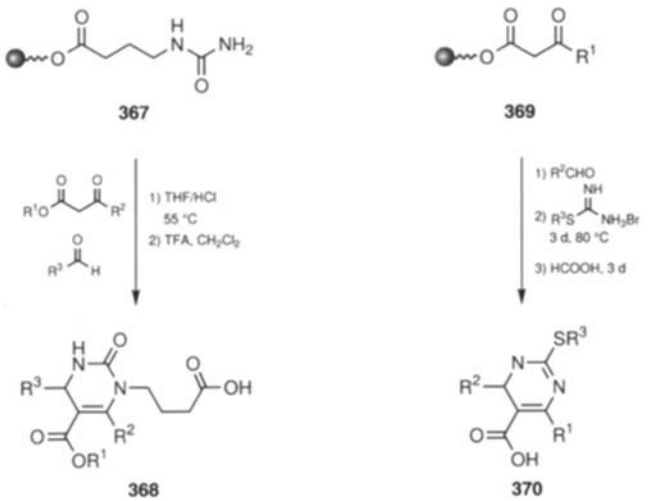

Scheme 77. Solid-phase Biginelli condensation of β-oxoesters, aldehydes, and ureas to form dihydropyrimidinones **368** [235] and synthesis of dihydropyrimidines **370** by the Atwal modification of the Biginelli reaction [236].

The Knoevenagel products **379** from β-oxoesters **377** and aldehydes **378** are ideal intermediates for the formation of a number of heterocycles (Scheme 78). Not only the thioureas **375**, but also the amidines **376**, guanidines **374**, or enaminoesters **380** may also be used as double donors to afford different pyrimidines **371**, dihydropyrimidines (**372**, **373**), and dihydropyridines **382**.

Syntheses of this type are being studied at a number of centers for their suitability for solid-phase combinatorial synthesis. Different strategies for coupling the starting building block to the solid phase are being pursued. Whereas the Chiron group starts with support-bound aldehydes, the Affymax group attaches the double donors (guanidines, enaminoesters[238]) or the β-oxoester to the solid phase, depending on the particular synthesis.[239] Resin-bound aldehydes have been used by Chiron in the synthesis of a number of heterocyclic systems (β-lactams, oxazoles, imidazoles, etc.).[237] The potential of classical heterocyclic syntheses for combinatorial chemistry is considerable; on one hand the compounds synthesized, for example dihydropyrimidines, are per se biologically active and on the other it should be possible to prepare a much greater variety of these compounds.

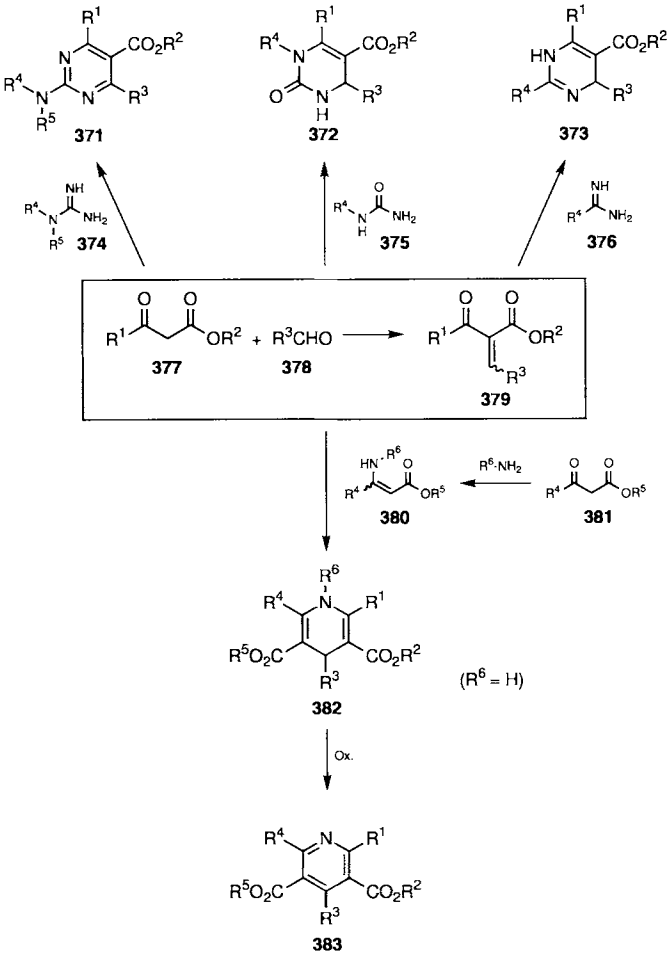

Scheme 78. Solid-phase synthesis of heterocycles starting from Knoevenagel products [237–239].

5. Structural Determination of Active Components in Libraries

Just as the substance library format determines the procedure for characterizing them, it is also critical in the analysis of the structure of the active compounds. If this is merely a question of a library of single compounds prepared by parallel synthesis, there is no problem in elucidating the structure of active compounds, since the site of synthesis is clearly associated with the structure being synthesized. Examples are the DIVERSOMER technique,[129, 130] photolithographic synthesis on a functionalized glass surface (VLSIPS[12]), and Ellman's synthesis[126] of benzodiazepine derivatives on a polyethylene pin matrix, which was used initially by Geysen et al. for epitope mapping.[6]

If the compound library prepared by combinatorial synthesis is tested in its support-bound form, those support particles that carry the active compounds are first sorted. Following cleavage from the support, the identity of the active substance can at least be reduced directly to a few alternative structures by mass spectrometric determination of the molecular weight (c.f. Section 2.2.4). In coded libraries the structure is determined indirectly by reading the code.

The most complicated situation for structural determination arises when mixtures are tested in solution. In these cases a

deconvolution procedure is usually required, or investigations must be carried out with indexed libraries.

In the following discussion the current methods used for structure determination during testing are reviewed. Published applications are mainly from the fields of peptides and nucleotides, but the principal procedures are essentially applicable to low molecular weight organic compounds.

5.1. Affinity Selection

Zuckermann et al. incubated peptide libraries with an antibody deficiency and, after elution of the few bound peptides, were able to elucidate the structures of the compounds of highest affinity by mass spectrometry and amino acid analysis.[240] An analogous application to low molecular weight compounds (the structures were, however, not published) has been recently reported.[241]

5.2. Indexed Libraries

In the synthesis of indexed (orthogonal) libraries, each starting material A^n is treated with an equimolar mixture of educts B^1-B^x, as is each educt B^m with A^1-A^y. Figure 18 illustrates schematically the formation of an indexed library from each of six reactants of type A (A^1-A^6) and type B (B^1-B^6).[35, 70, 71, 242] This synthetic procedure results in each compound being formed exactly twice, and every pair of mixtures has exactly one compound in common. The presence of an active compound must therefore result in activity in two mixtures. Moreover, this form of internal control allows the recognition of false positives. Assignment of activity to a certain structure is possible by simple comparison, that is, without time consuming deconvolution or new synthesis. As an example, the activity of the two mixtures $A^1-A^6B^3$ and $A^3B^1-B^6$ in Figure 18 indicates that compound A_3B_3 is active. An example of the synthesis of an indexed library is described in Section 3.1.2.

	A^1B^{1-6}	A^2B^{1-6}	A^3B^{1-6}	A^4B^{1-6}	A^5B^{1-6}	A^6B^{1-6}
$A^{1-6}B^1$						
$A^{1-6}B^2$						
$A^{1-6}B^3$			A^3B^3			
$A^{1-6}B^4$						
$A^{1-6}B^5$						
$A^{1-6}B^1$						

Fig. 18. Schematic representation of an orthogonal library (modified according to ref. [71]) synthesized from each of six components A and B. Each column and each row represents a compound mixture consisting of six components (for example, A^1B^1 to A^1B^6). The single compound responsible for the activity is derived from the correlation of two active mixtures (in this case A^3B^3).

5.3. Deconvolution

In conjunction with the split method for the preparation of equimolar mixtures of peptides, Furka[13] has outlined iterative procedures for the identification of active components (c.f. Section 2.2). A practical application to peptides bound to a solid phase has been described by Geysen,[44] and both Houghten et al.[18] and Ecker et al.[45, 46, 243, 244] were the first to report on the deconvolution of soluble peptide and oligonucleotide libraries. Initial literature examples indicate that this deconvolution method can also be used successfully for low molecular weight organic compounds, as exemplified by the pyrrolidine library described in Section 4.2.1.2.[32] This is illustrated diagrammatically in Figure 19.

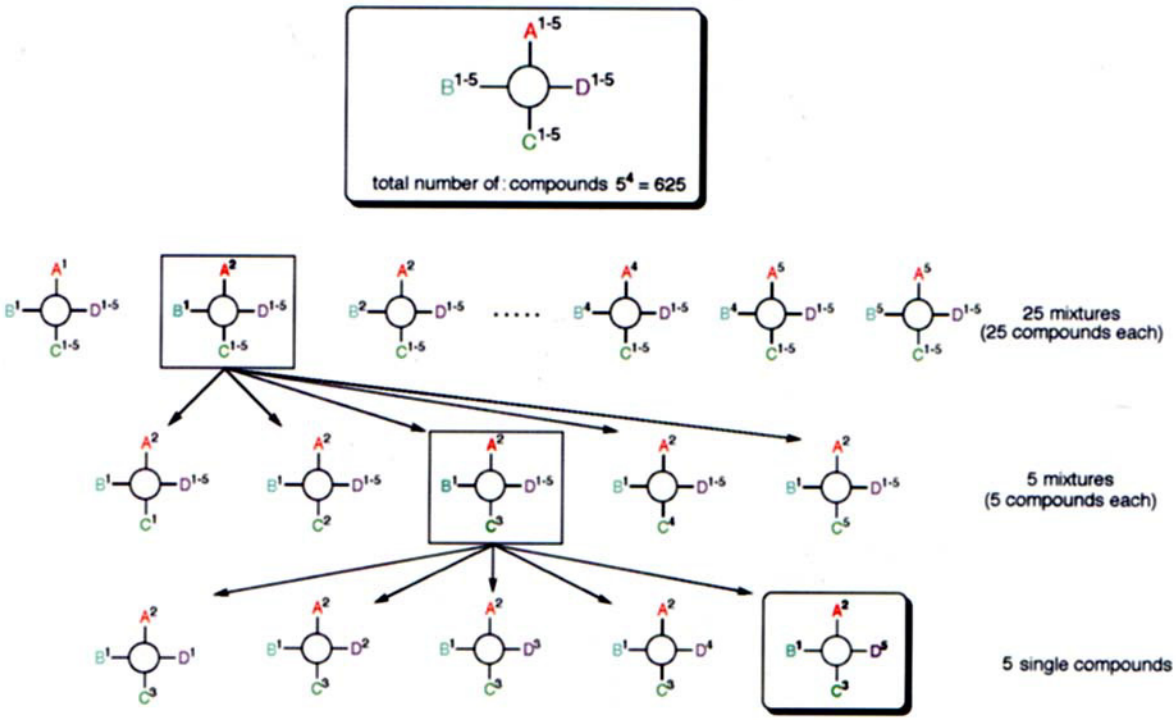

Fig. 19. Identification of the most active library component by deconvolution. In each case the most active libraries (framed) are further divided until finally the most active single compound $A^2B^1C^3D^5$ is uncovered.

A library consisting of low molecular weight organic compounds with four variable substituents (A–D) is treated formally as a tetrapeptide library. If there are, for example, five different possibilities for each substituent, the total library consists of $5^4 = 625$ compounds. In the first deconvolution round this total library can be synthesized in the form of 25 sublibraries each of 25 compounds in which in each case the substituents A and B are defined. The most active sublibrary contains the optimal combination of the substituents A and B. In Figure 19 this is the combination A^2B^1. On the basis of this result five further sublibraries in the form $A^2B^1C^nD^1-D^5$ are prepared. Each contains five compounds in which C is additionally defined. The optimal residue D is determined in the last step, the synthesis of the five individual compounds in the form $A^2B^1C^3D^n$. In the present example the most active compound is $A^2B^1C^3D^5$. One disadvantage of this iterative procedure is that the most active compound may not be necessarily found. However, Ecker et al.[243, 244] were able to show using a model calculation for oligonucleotides that even if not the most active, then at least one of only slightly less activity is selected. Moreover, it has since been demonstrated that the result is independent of the sequence in which the individual positions were iteratively optimized.[244] To what extent this may be applied to low molecular weight organic compounds is currently not clear.

Each test of the total library in another assay requires corresponding new syntheses of yet more sublibraries. In order to reduce the effort of new synthesis, Janda[102, 245] has used the procedure of recursive deconvolution. This method differs from the deconvolution described above in that an aliquot is held back after each cycle of the split synthesis. From active mixtures, similarly in one or more steps, the single active compound is identified. However, the new syntheses are not nearly so labor-intensive, because no new split syntheses are involved, merely the intermediates retained during the first split synthesis need to be elaborated further. Currently the only examples of this method of recursive deconvolution are in the peptide field.[102, 245] Application to low molecular weight organic compounds is plausible if the intermediates in the split synthesis are stable.

5.4. Positional Scanning

The noniterative method of "positional scanning" was realized for peptides by Houghten et al.[246] Using as example the library described in Section 5.3, Figure 20 illustrates how this may be carried out with low molecular weight compounds.

A total of $4 \times 5 = 20$ sublibraries in the form $A^1B^{1-5}C^{1-5}D^{1-5}$, $A^2B^{1-5}C^{1-5}D^{1-5}$, $A^3B^{1-5}C^{1-5}D^{1-5}$ to $A^{1-5}B^{1-5}C^{1-5}D^4$, $A^{1-5}B^{1-5}C^{1-5}D^5$ are synthesized. Thus for every substituent a complete library consisting of 5 sublibraries each of 125 compounds is prepared; that is, four syntheses of the total library are carried out. In the ideal situation, testing of these 4×5 sublibraries highlights immediately which substituents A–D are optimal. Thus Figure 20 illustrates how the results of the individual tests lead to the most active compound $A_2B_1C_3D_5$.

The advantage of positional scanning over deconvolution is that it is only necessary to carry out one library synthesis. However, if in one position there is no clear preference for a definitive substituent, all combinations of the preferred substituents must be synthesized in order to find the most active compound.

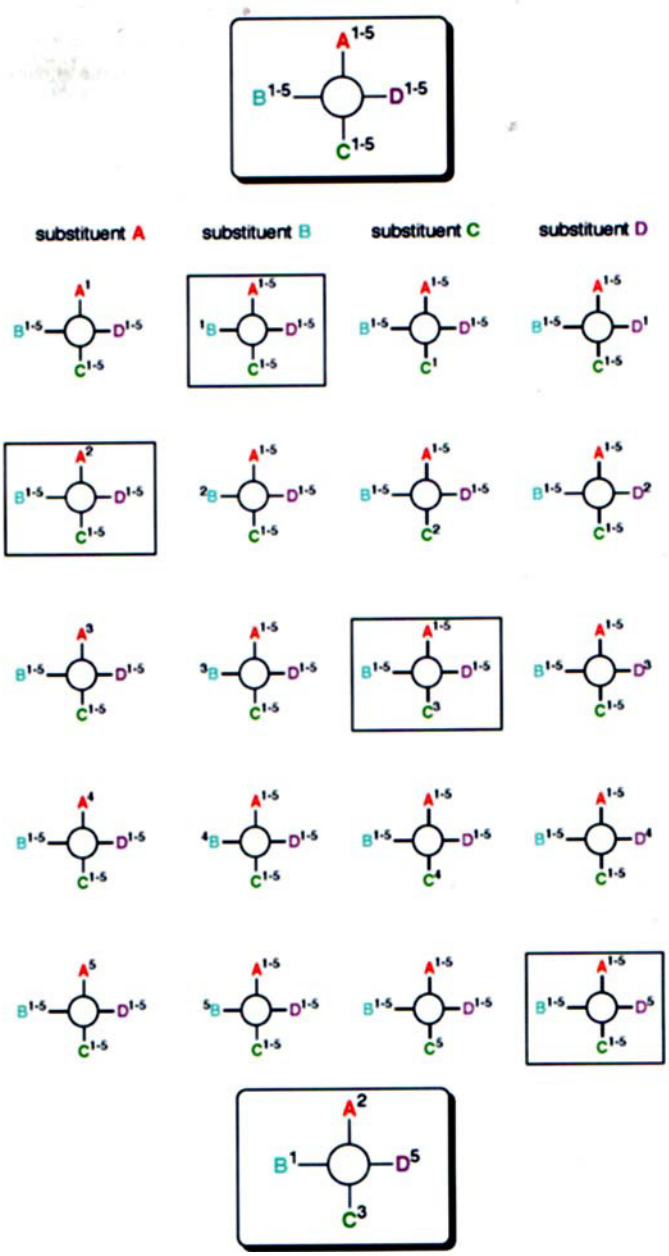

Fig. 20. Identification of the most active library component by the method of "positional scanning" (modified according to ref. [166]). The complete library is synthesized a total of four times, each time in the form of five sublibraries, and the activities of the 20 libraries thus obtained are determined. The most active libraries (framed) indicate the optimal substituents. In the illustrated example these are A^2, B^1, C^3, and D^5. The most active compound is thus $A^2B^1C^3D^5$.

5.5. Encoded Libraries

Inherent in the split synthesis ("one bead, one compound) is the problem of structural analysis of minute amounts of a substance (see Section 2.2.4). Whereas highly sensitive methods exist for the structural determination of peptides and nucleotides in the form of sequencing procedures, the direct struc-

tural determination of small amounts of low molecular weight organic compounds is comparatively less well developed. In this respect advances are to be expected in particular in mass spectrometric methods.

This problem is avoided with coded libraries,[247] in which instead of the structure of the test substance, the more accessible structure of a carefully selected—sequential or nonsequential (c.f. Section 5.5.1)—molecular code is determined. Each resin particle carries not only the respective product of the combinatorial synthesis, but also a record of the "synthetic history" in the form of this molecular code (Fig. 21). In this way, the

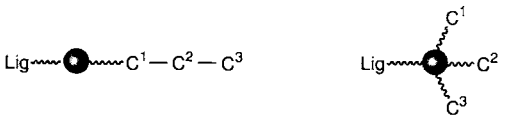

Fig. 21. In the normal case, a support particle in a coded library carries both the test substance (Lig) and the molecular codes (C^1, C^2, C^3). The code can be either sequential (left) or nonsequential (right).

reagents and the reaction conditions with which this particle has come into contact during the course of the reaction are coded. Consequently, such a procedure results in an increased complexity of synthesis. Caution must be observed, however, that the code molecules tolerate the reaction conditions used in the combinatorial synthesis and that the products of the combinatorial synthesis also remain inert during the coding reactions. This could limit the reactions available for a combinatorial synthesis.

In all cases, such a coding is of course valid only if the relationship between support, target molecules, and code molecules remains intact. This provides no problems if biological testing is carried out with the support-bound compound, not in solution. After testing and cleavage the active compound is identified by reading the code following cleavage.

However, the assay is usually carried out with dissolved material. Then, for efficient testing, cleavage of the synthetic product from the support must be able to be carried out in aliquots. Examples are the screening strategies followed by the companies Selectide[120] (Fig. 22) and Pharmacopeia.[122, 158] As Figure 22 illustrates, 500 resin particles, which can carry 500 different compounds ("one bead, one compound"), are placed in each

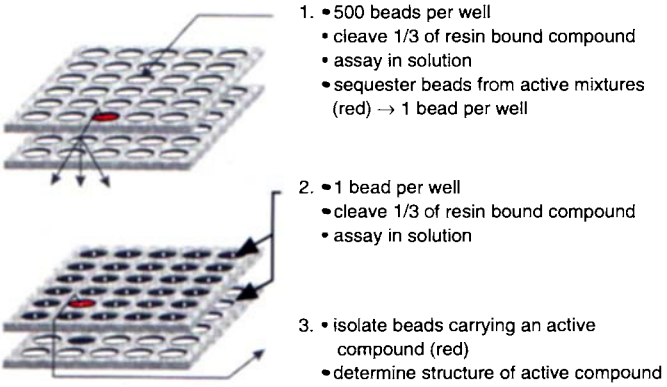

Fig. 22. Aliquot cleavage from the support and two stage testing of compound libraries (according to ref. [120c]). The procedure used by Pharmacopeia [122, 158] employs a photolabile linker and in Step 3 determines the structure of the active compounds by reading a code (see Scheme 79).

well of a microtiter plate. In the first step 1/3 of the respective compound is cleaved and transferred to a second microtiter plate. There the biological assay is then performed on dissolved substance. Since the mixtures in solution can be traced to the particle mixtures from which they were cleaved, sequestering of the particle mixtures from which the dissolved, active substance mixtures originated is possible. The individual compounds formed after cleavage of a further aliquot can be tested again and identified with the help of the resin-bound code ("single-bead assay").

In the future with the use of more effective microanalytical methods, structure determination by direct analysis of test compounds cleaved from the resin rather than by complex coding techniques should become feasible. A prerequisite for the use of these methods is, however, that an aliquot of material bound to a single resin particle is sufficient for the test. When this is guaranteed, this procedure offers ideal conditions for efficient testing.

5.5.1. Chemical Codes

The first chemical codes were peptide[248] and nucleotide[249] sequences synthesized in parallel for the construction of the library. Reading of this sequential code occurs serially by sequencing, possibly after amplification by the polymerase chain reaction (PCR) in the case of nucleotides. Unfortunately, the chemical instability of nucleotides severely limits the range of reaction conditions available for chemical synthesis.

A totally different and currently the most elegant chemical solution comes from Still et al.[160, 250] In the creation of a binary nonsequential code, they employed a number of halogenated aromatics that were coupled directly to the polymeric matrix through alkoxy spacers of varying lengths by a Rh-$(TFA)_2$-catalyzed carbene insertion reaction (Scheme 79). To

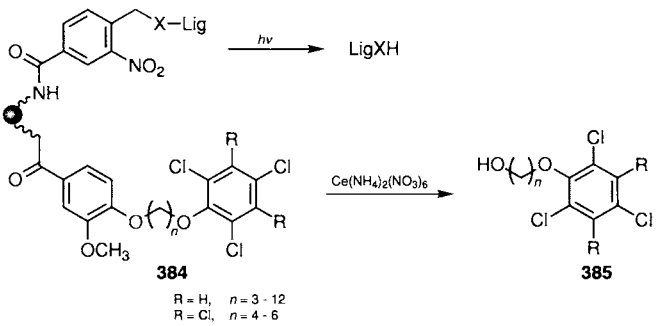

Scheme 79. Coding of compound libraries with halogenoaryloxy alcohols (according to ref. [252]). Lig = ligand.

read this code the coded aryloxyalcohols **385** were cleaved oxidatively and silylated. The presence (logic 1) or the absence (logic 0) of the different code molecules was determined by means of electron capture GC. The binary count obtained coded for the respective synthetic pathway.

The first application came again from the peptide area,[160] but more recently there have also been reports of binary coded libraries of non-peptide molecules[122, 158] (see also Section 4.2.1.2.).

A procedure very similar in principle to the Still method has been described recently by Gallop et al.[251] They used sec-

ondary amines as letters of a molecular code. Parallel to the synthesis of the test compound the oligoamide **388** was constructed from the code molecules (Scheme 80). For decoding, **388** was hydrolyzed with 6N HCl, and the secondary amines thus obtained converted into dansyl derivatives, which after HPLC separation were detected by fluorescence spectroscopy. In this way β-lactam and pyrrolidine libraries have been coded.[251]

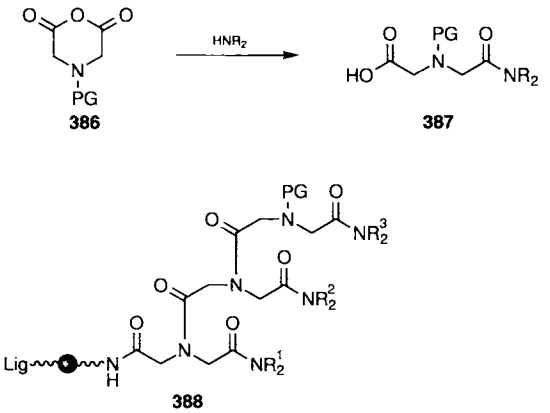

Scheme 80. Gallop et al. [251] use secondary amines as code molecules. Parallel to the synthesis of the test compound on the support, the coded oligoamide **388** is formed from the protected amino acids **387**. Hydrolysis regenerates the free secondary amines, which can be identified after conversion into the dansyl derivatives.

A recently published patent application from SmithKline Beecham describes the coding of libraries by labeling the solid-phase particles with fluorophores.[253] This method of labeling also allows sorting of the particles with a cell sorter, during or after the split synthesis.

5.5.2. *Nonchemical Coding*

Currently the only examples of nonchemical coding are the recent papers of Nicolaou et al.[255] and Moran et al.[256] The relevant synthesis steps are recorded on a storage chip which can be written or read by high-frequency signals. Since in both cases the work was carried out with a relatively low number of particles (de facto reaction vessels), the procedure at the present state of the art may be regarded as a high-tech version of the teabag method.[7] The viability of this method was also verified by the coding of peptide syntheses.

6. Automation and Data Processing

Solving the problems of synthesis is not the end of the matter. Only an integrated concept embracing chemistry, automation, electronic data processing, and high-capacity screening promises success. One extreme position is outlined in a patent recently granted to 3-Dimensional Pharmaceuticals:[257] In a *fully automated*, computer-controlled process, optimized structures are reported to be obtained in iterative cycles that include the synthesis of test compounds, their testing, and the analysis of the biological data thus obtained.

A review of the state of automation is given by DeWitt,[258] who has also been deeply involved in the development of the now commercially available DIVERSOMER technology.[127, 129, 131, 259] The currently marketed equipment[260] is derived from multiple peptide synthesizers and is still limited in scope. For this reason venture companies have developed their own synthesizers that are used solely for their own syntheses.[261] However, developments are in progress by instrument and automation companies,[262] so systems are expected to become available in the near future that will be constructed on a modular basis that can be adapted to a number of reaction conditions. In such a system, all liquid transfers (addition of solvents or reagents, washing steps) take place in a central module constructed around a pipetting robot. The charged reaction vessels are then transferred to special incubation modules, where they remain for the duration of the reaction, while the central module is again available for the preparation of further reactions.

Another concept[263] being followed by Combichem and Argonaut Technologies totally dispenses with the use of pipetting robots: in this fully closed system, reagent and solvent vessels are permanently interconnected with the reaction vessels by means of tubes and valves.

Because of the considerable amount of data collected, combinatorial chemistry is unthinkable without the support of electronic data processing.[264, 265]

The following applications have come to the fore:

- Software for control of the synthesizer.
- Selection of reagents by search of chemical databases such as the *Available Chemicals Directory* (ACD).[266]
- Support in the selection and optimization of reactions by searching reaction databases such as *REACCS*[266] or *Crossfire Plus*.[267] With *SPORE*[39] or the solid-phase synthesis database Synopsys,[39] there are now special reaction databases for organic solid-phase synthesis.
- Management of and searches in (virtual) compound libraries. In this context programmes such as *Project Library*,[266] *Legion*,[268], *Unity*,[268] or a programme package from Daylight[269] are available.

A significant challenge is presented by programs that go beyond mere administrative functions and allow intelligent selection of the compounds to be synthesized, thus aiming to achieve a maximum diversity with the minimum number of compounds.

Significant developments are to be expected in this area in the future. A start has already been made. The programs *Selector*,[268] *Jarpat*,[269] *C²-Diversity*,[271] and *Chem-X*[271] are commercially available for assessing diversity. *Chem-X* also enables library management.

7. Venture Companies in the Field of Combinatorial Chemistry

In the 1990s the possibility of producing compound libraries by combinatorial chemistry, thus accelerating dramatically the search for novel active compounds, has led to a veritable flood of company establishments, particularly in the USA. The prospect of a drastic reduction in development time and costs of new pharmaceuticals has given rise to a gold-rush mentality, the like of which has not been experienced in chemistry since the foundation of the dye industry at the close of the last century.

These venture companies have made a major contribution to the development in the techniques of combinatorial chemistry. Many of the currently described examples of combinatorial syntheses have been published by scientists from these small companies. Without attempting to discuss the strategies of these companies in detail, the following trends are apparent:

- All companies are involved with combinatorial synthesis on solid phase, some even exclusively.
- Most companies began with the synthesis of peptide libraries, but now all are developing combinatorial syntheses of small organic molecules.
- Many companies are involved with the development of new synthesizers.
- According to the size and format of the libraries produced, the spectrum extends from parallel synthesis of individual compounds (a few hundred products) to enormous (coded) peptide libraries generated with the split method.
- Testing is carried out predominantly in solution.

At present, besides the number of products, the design of a library (diversity criteria, inclusion of pharmacophore patterns) is coming increasingly to the fore.

Without any claim to completeness, Table 2 gives an over view of a few of these companies and gives information on more recent important acquisitions and cooperations.[273] The figures show quite clearly the considerable potential the established pharmaceutical industry sees in these new techniques.

8. Outlook

"Predictions are always difficult, particularly where the future is concerned."
Niels Bohr

Combinatorial synthesis of small organic molecules is without doubt still in its infancy. The syntheses currently described do indeed start from more than one building block or reactant

Table 2. Venture companies in the area of combinatorial chemistry; research cooperations and acquisitions.

Venture Company	Partner company [a]	Project	Investment volume [mil. US$] [b]	Time period
Affymax	Glaxo	acquisition	533	February 1995
Alanex	Novo Nordisk	diabetes	n.d.	April 1996
Ariad Pharmaceuticals	Hoechst Marion Roussel	cooperation in the area of osteoporosis	40	November 1995
ArQule	Abbott Laboratories	5-year contract, development of combinatorial libraries based on lead structures of Abbott	35	June 1995
ArQule	Pharmacia Biotech	cooperation in the field of separation technology	30	March 1995
ArQule	Solvay-Duphar	5-year contract	50	November 1995
Arris Pharmaceuticals	Bayer	5-year contract new protease inhibitors against inflammatory diseases	70	January 1995
Arris Pharmaceuticals	Pharmacia Biotech	5-year contract serine protease inhibitors	40	August 1995
Chiron	Ciba Geigy	non-exclusive access to Chiron's libraries	26	November 1995
Chiron	Dow Elanco	cooperation (new lead structures in the agricultural field)	n.d.	January 1996
Chiron	Japan Tobacco	non-exclusive access to Chiron's libraries	n.d.	March 1996
Chiron	Organon	research cooperation, technology transfer	n.d.	August 1996
CombiChem	PE Sciex	instrument development	n.d.	May 1996
CombiChem	Teijin	targeted libraries	10	April 1996
Houghten Pharmaceuticals	Procter & Gamble	3-year research cooperation	n.d.	May 1995
Houghten Pharmaceuticals	Novo Nordisk	diabetes, osteoporosis	4	February 1996
Ontogen	Boehringer Ingelheim	research cooperation	41.6	August 1996
Oxford Asymmetry	Pfizer	formation of a jointly owned subsidiary company: Oxford Diversity, development of new solid-phase chemistry	5.8	March 1995
Pharmacopeia	Schering-Plough	cancer and asthma pharmaceuticals	76	January 1995
Pharmacopeia	Berlex Laboratories	multiple sclerosis	20	February 1995
Pharmacopeia	Sandoz	research cooperation for the indication area CNS, cancer, transplantations, skin	100	October 1995
Pharmacopeia	Bayer	research cooperation	20	January 1996
Pharmacopeia	Daiichi Pharmaceutical	research cooperation	22	April 1996
Pharmacopeia	Organon	research cooperation	19	June 1996
Selectide	Marion Merrell Dow	acquisition, development project: factor Xa inhibitors	58	January 1995
Sphinx Pharmaceuticals	Eli Lilly	acquisition	75	March 1994
Tripos	Menarini	cooperation in the field of inflammation inhibitors	n.d.	October 1995
Tripos	Merck	software development	n.d.	November 1995
Tripos	Panlabs	software development	n.d.	February 1995

[a] Name at time of agreement. [b] n.d. = no details.

and may therefore be termed combinatorial, but the libraries produced are frequently very small (a few to several thousand compounds).

After initial hesitation, the community of preparative chemists has ventured into combinatorial chemistry, and it may be expected that this area, until now dominated by peptide chemists, will consequently enter a new and more vigorous development phase. It is precisely these synthetic chemists, accustomed to synthesizing a specific target product, who are finding the transition to combinatorial chemistry most difficult. It is their expertise, however, which will lead to significant advances in the planning of combinatorial syntheses. Currently, reaction sequences that will in each case allow the preparation of many thousands of compounds are being worked upon in many places. Whether the perfection of peptide synthesis and hence similarly large libraries will be achieved is questionable.

Intelligent selection of individual building blocks—supported by modeling—will play an increasingly important role in library design, so that these libraries, in spite of all the limitations imposed by chemistry, will have the largest diversity possible. It remains to be seen whether in this respect the high expectations are fulfilled. Large libraries in a format suitable for wide testing will only be achievable by solid-phase synthesis, for it is only solid-phase synthesis that allows automation of all steps in a multistage synthesis and the targeted synthesis of mixtures. It is for this reason that there will be significant advances in further methodology development of solid-phase synthesis.

This will lead to new resins and linkers that will be better suited to organic reactions than the currently used materials derived from peptide synthesis. There will never be a "miracle support" upon which any organic reaction can be carried out, possibly without adjustment problems, and which will finally release the final product at the touch of a button. Most probably a selection of resins and linkers will be available from which the combination most suitable for a particular synthesis can be chosen.

The repertoire of reactions able to be carried out in the solid phase will also be considerably expanded, and in the foreseeable future a wide know-how will be available in this area.

Even more importantly, new analytical methods will ensure that we will have a better understanding of the processes on the resin and be better able to predict many results. Both NMR spectroscopy on the resin and single-bead mass spectrometry[223] are already a reality. The significance of indirect analytical methods (such as coding) will decline with the possibility of *direct* determination of the structure of products on the resin.

Finally, synthesizers will be developed that allow automated, parallel implementation of many reactions on a small scale, both on the solid phase and in solution. Moreover, methods for automated product purification (such as solid-phase extraction and preparative HPLC) will find greater use.

Miniaturization and automation of organic synthesis can no longer be restrained and will lead to the rationalization of synthesis in many areas, even outside medicinal and agricultural chemistry. This can certainly be regarded as one of the first "results" of combinatorial chemistry. However, confirmation that combinatorial chemistry in its own right leads to an acceleration in the search for active compounds has not yet been forthcoming. It may certainly be assumed that—if the peptide libraries are included—more products have already been produced by combinatorial chemistry than by conventional syntheses. There are, however, currently very few products under or close to clinical investigation that have been identified with combinatorial techniques.[166, 274]

Meanwhile the first clouds have appeared in the otherwise deep blue sky of combinatorial synthesis of small organic molecules. Is it really sensible to seek enormous compound libraries of closely related molecules in mixtures? Should not combinatorial synthesis be better used to produce a few (<1000) single compounds where prior information on a target or lead structure can be used in the planning of syntheses ("structure-based combinatorial chemistry")? It is too early for a clear answer to these questions; however, the touch of realism that is now being added to the previous euphoria will do the area more good than harm. Questions such as "single compounds versus mixtures" or "solid phase versus solution" are currently being intensively discussed. A clear path has yet to emerge, and at present rather the task and the chemistry determine strategy (Table 3).

Table 3. Characteristics of combinatorial compound libraries

Lead structure search	Lead structure optimization
random libraries (screening libraries)	focused libraries (targeted libraries)
synthesis of diverse "druglike" compounds	lead structure:target determines chemistry
many targets	one target or target class
solid-phase synthesis	solid/solution-phase synthesis
split synthesis → "compound mixtures" ("one bead, one compound")	automated parallel synthesis → single compounds
$\geqslant 10000$ products	$\ll 10000$ products
<1 mg per product	>1 mg per product
testing of mixtures (with deconvolution) or of single compounds (with decoding)	procedure for screening optional

On one hand, therefore, the opportunities for combinatorial chemistry lie in the search for lead structures, where with the help of large, diverse libraries it should be possible to access structural classes that would otherwise remain unknown in the classical approach. Here solid-phase syntheses are indispensable, and mixtures (<50 compounds) are tolerated. Innovative screening technology and analytical methods will replace coding methods, particularly where they also restrict possible chemistry. On the other hand, combinatorial synthesis will accelerate lead structure optimization. Depending upon the structure to be modified, this can be carried out both on the solid phase and in solution ("high speed analoging"). Structure–activity relationships can then be determined by testing individual compounds.

Combinatorial synthesis will not replace, merely complement, conventional synthesis. Not all structures will be accessible by combinatorial chemistry. Nevertheless it will develop into a standard method in the search for active compounds, comparable with the screening of natural products and molecular modeling. Meanwhile hundreds of scientists worldwide are working to realize the vision of the automated synthesis of new active compounds. However, whether the "laboratory on a chip" will become the standard laboratory in the search for active compounds hangs in the balance.

The perspectives of combinatorial chemistry extend beyond the search for biologically active materials; wherever the discovery and optimization of compounds with certain definitive properties is the target, combinatorial synthesis will acquire a place. Examples which have been described include new catalysts[275] and ligands,[276] complexing agents, dyes, or superconductors.[277] A requirement is, in any case, the availability of an efficient test system with high-throughput and low-substance requirement. However, the chances that combinatorial synthesis will rapidly reach maturity are favorable.[278]

We thank F. Oldenburg and K. Stüber for efficient help in the preparation of the graphics and diagrams. We are grateful to our colleagues, Drs. H. Albrecht, S. Blank, K. Ditrich, P. Eckes, G. Klebe, I. Münster, M. Puhl, and G. Steiner for their review of the manuscript and for their numerous and valuable comments.

Received: March 15, 1996
Updated version: June 13, 1996 [A 158 IE]
German version: *Angew. Chem.* **1996**, *108*, 2436–2487

[1] a) K. C. Nicolaou, E. Sorensen, *Classics in Total Synthesis, Targets, Strategies, Methods*, VCH, Weinheim, **1996**; b) E. J. Corey, X.-M. Cheng, *The Logic of Chemical Synthesis*, Wiley, New York, **1989**.

[2] a) R. B. Silverman, J. Seydel, *Medizinische Chemie*, VCH, Weinheim, **1994**; b) *Medicinal Chemistry for the 21st Century* (Ed.: C. G. Wermuth), Blackwell, Oxford, **1992**.

[3] General introductions: a) *Combinatorial Libraries—Synthesis, Screening and Application Potential* (Ed.: R: Cortese), Walter de Gruyter, Berlin, **1996**; b) *Combinatorial Libraries: The Theory and Practice of Combinatorial Chemistry* (Ed.: R. A. Houghten), ESCOM, Leiden, **1995**; c) *Combinatorial Peptide and Non Peptide Libraries—a Handbook* (Ed.: G. Jung), VCH, Weinheim, **1996**; d) *Molecular Diversity and Combinatorial Chemistry: Libraries and Drug Discovery* (Eds.: I. Chaiken, K. Janda), ACS, Washington, **1996**.

[4] The word "*library*" is not used consistently in the literature. Often the term library is reserved for substance mixtures whereas collections of single compounds are called "*arrays*".

[5] The term *combinatorial synthesis* is strictly used only when different building blocks are treated in *one* reaction vessel, and mixtures are thus obtained. Since the boundary becomes blurred at the latest for the split synthesis (see refs. [13–15]), which also represents a compartmentalization ("one bead, one compound"), no differentiation will be made here.

[6] a) H. M. Geysen, R. H. Meloen, S. J. Barteling, *Proc. Natl. Acad. Sci. USA* **1984**, *81*, 3998–4002; b) H. M. Geysen, S. J. Barteling, R. H. Meloen, *ibid.* **1985**, *82*, 178–182; c) N. J. Maeji, R. M. Valerio, A. M. Bray, R. A. Campbell, H. M. Geysen, *Reactive Polymers* **1994**, *22*, 203–212.

[7] R. A. Houghten, *Proc. Natl. Acad. Sci. USA* **1985**, *82*, 5131–5135.

[8] R. B. Merrifield, *J. Am. Chem. Soc.* **1963**, *85*, 2149–2154.

[9] For the chemical synthesis of proteins, see E. Bayer, *Angew. Chem.* **1991**, *103*, 117–133; *Angew. Chem. Int. Ed. Engl.* **1991**, *30*, 113–129.

[10] a) Reviews: G. Jung, A. G. Beck-Sickinger, *Angew. Chem.* **1992**, *104*, 375–391; *Angew. Chem. Int. Ed. Engl.* **1992**, *31*, 367–383; b) H.-E. Radunz, *GIT Fachz. Lab.* **1992**, 869–873.

[11] R. Frank, *Tetrahedron* **1992**, *48*, 9217–9232.

[12] VLSIPS: very large scale immobilized polymer synthesis (photolithographic parallel synthesis); S. P. A. Fodor, J. L. Read, M. C. Pirrung, L. Stryer, A. T. Lu, D. Solas, *Science* **1991**, *251*, 767–773.

[13] "Studies on Possibilities of Systematic Searching for Pharmaceutically Useful Peptides": Á. Furka, notarized Document No. 36237/1982, Budapest, **1982**.

[14] a) Á. Furka, F. Sebestyen, M. Asgedom, G. Dibo, *Abstr. 14th Int. Congr. Biochem.*, Prague, **1988**, *5*, 47; b) *Abstr. 10th Int. Symp. Med. Chem.*, Budapest, **1988**, *9*, 288.

[15] a) Á. Furka, F. Sebestyen, M. Asgedom, G. Dibo, *Int. J. Pept. Prot. Res.* **1991**, *37*, 487–493; b) F. Sebestyen, G. Dibo, A. Kovacs, Á. Furka, *Bioorg. Med. Chem. Lett.* **1993**, *3*, 413–418.

[16] Á. Furka, *Drug Dev. Res.* **1995**, *36*, 1–12.

[17] K. S. Lam, S. E. Salmon, E. M. Hersh, V. J. Hruby, W. M. Kazmiersky, R. J. Knapp, *Nature (London)* **1991**, *354*, 82–84.

[18] R. A. Houghten, C. Pinilla, S. E. Blondelle, J. R. Appel, C. T. Dooley, J. H. Cuervo, *Nature (London)* **1991**, *354*, 84–86.

[19] For a review, see M. A. Gallop, R. W. Barrett, W. J. Dower, S. P. A. Fodor, E. M. Gordon, *J. Med. Chem.* **1994**, *37*, 1233–1251.

[20] Reviews: a) E. M. Gordon, R. W. Barrett, W. J. Dower, S. P. A. Fodor, M. A. Gallop, *J. Med. Chem.* **1994**, *37*, 1385–1401; b) E. M. Gordon, *Curr. Opin. Biotechnol.* **1995**, *6*, 624–631.

[21] E. M. Gordon, M. A. Gallop, D. V. Patel, *Acc. Chem. Res.* **1996**, *29*, 144–154.

[22] L. A. Thompson, J. A. Ellman, *Chem. Rev.* **1996**, *96*, 555–600.

[23] J. A. Ellman, *Acc. Chem. Res.* **1996**, *29*, 132–143.

[24] N. K. Terrett, M. Gardner, D. W. Gordon, R. J. Kobylecki, J. Steele, *Tetrahedron* **1995**, *51*, 8135–8173.

[25] E. R. Felder, *Chimia* **1994**, *48*, 531–541.

[26] Recent reviews: J. S. Früchtel, G. Jung, *Angew. Chem.* **1996**, *108*, 19–46; *Angew. Chem. Int. Ed. Engl.* **1996**, *35*, 17–42.

[27] "Pitfalls in Creating a Chemically Diverse Compound Screening Library": D. Weininger, cited by J. Bradshaw in a lecture at the conference "Synthetic Chemical Libraries in Drug Discovery", London, **1995**.

[28] B. P. Roques, F. Noble, V. Daugé, M.-C. Fournié-Zaluski, A. Beaumont, *Pharm. Rev.* **1993**, *45*, 87–146.

[29] J. R. H. Tame, G. N. Murshudov, E. J. Dodson, T. K. Neil, G. G. Dodson, C. F. Higgins, A. J. Wilkinson, *Science* **1994**, *264*, 1578–1581, and references therein.

[30] The authors thank Dr. H.-J. Böhm and Dr. G. Klebe, BASF AG, Ludwigshafen, for stimulating discussions on diversity and for Figs. 6 and 7.

[31] E. J. Martin, J. M. Blaney, M. A. Siani, D. C. Spellmeyer, A. K. Wong, W. H. Moos, *J. Med. Chem.* **1995**, *38*, 1431–1436.

[32] M. M. Murphy, J. R. Schullek, E. M. Gordon, M. A. Gallop, *J. Am. Chem. Soc.* **1995**, *117*, 7029–7030.

[33] M. J. Kurth, L. A. Ahlberg Randall, C. Chen, C. Melander, R. B. Miller, K. McAlister, G. Reitz, R. Kang, T. Nakatsu, C. Green, *J. Org. Chem.* **1994**, *59*, 5862–5864.

[34] M. H. Lyttle, *Drug Dev. Res.* **1995**, *35*, 230–236.

[35] M. C. Pirrung, J. Chen, *J. Am. Chem. Soc.* **1995**, *117*, 1240–1245.

[36] a) "Combinatorial Libraries in Practice": D. Brown, in a lecture at the conference "Synthetic Chemical Libraries in Drug Discovery", London, **1995**; b) N. K. Terrett, D. Bojanic, D. Brown, P. J. Bungay, M. Gardner, D. W. Gordon, C. J. Mayers, J. Steele, *Bioorg. Med. Chem. Lett.* **1995**, *5*, 917–922.

[37] J. M. Fréchet, *Tetrahedron* **1981**, *37*, 663–683.

[38] C. C. Leznoff, *Acc. Chem. Res.* **1978**, *11*, 327–333.

[39] An extensive review by product class and reactions on research published in the field of solid-phase synthesis of small organic molecules is contained in the brochure *Solid Phase Chemistry Publications* (January 1996 issue) published by the firm Chiron Mimitopes Pty Ltd., 11 Duerdin Street, Clayton, Victoria 3168 (Australia); fax: int. code +(3)9565-1199; e-mail: ianjames@cc.chiron.com. A database for computer searches for solid-phase reactions has recently become available. *Solid-Phase Organic Reaction Database* (SPORE), MDL Information Systems, 14600 Catalina Street, San Leandro, CA 94577 (USA); fax: int. code +(510)614-3652; e-mail: bobs@mdli.com. A further solid-phase synthesis database is currently being assembled by Synopsys Scientific Systems. Synopsis Scientific Systems, 175 Woodhouse Lane, Leeds LS2 3AR (UK); fax: int. code +(113)243-8733; e-mail: sales@synopsys.co.uk.

[40] Up-to-date tabulated overview: P. H. H. Hermkens, H. C. J. Ottenheim, D. Rees, *Tetrahedron* **1996**, *52*, 4527–4554.

[41] a) "Resin Capture Strategies to Small Molecule Pharmacophores": R. W. Armstrong, in a lecture at the conference "Synthesis of Small Molecules on Solid Phase", Basel, **1996**; b) T. A. Keating, R. W. Armstrong, *J. Am. Chem. Soc.* **1996**, *118*, 2574–2583.

[42] "Integrated Combinatorial Chemistry and High-Throughput Screening for the Discovery of NF-kB and AP-1 Inhibitors": M. J. Suto, in a lecture at the conference "Lead Generation and Optimization", New Orleans, LA, **1996**.

[43] a) J. M. Ostresh, J. H. Winkle, V. T. Hamashin, R. A. Houghten, *Biopolymers* **1994**, *34*, 1681–1689.

[44] H. M. Geysen, S. J. Rodda, T. J. Mason, *Mol. Immunol.* **1986**, *23*, 709–715.

[45] D. J. Ecker, T. A. Vickers, R. Hanecak, V. Driver, K. Anderson, *Nucleic Acids Res.* **1993**, *37*, 1385–1401.

[46] J. R. Wyatt, T. A. Vickers, J. L. Roberson, R. W. Buckheit, T. Klimkait, E. DeBaets, P. W. Davis, B. Rayner, J. L. Imbach, D. J. Ecker, *Proc. Natl. Acad. Sci. USA* **1994**, *91*, 1356–1360.

[47] W. D. F. Meutermans, P. F. Alewood, *Tetrahedron Lett.* **1995**, *36*, 7709–7712.

[48] L. F. Tietze, A. Steinmetz, *Angew. Chem.* **1996**, *108*, 682–683; *Angew. Chem. Int. Ed. Engl.* **1996**, *35*, 651–652.

[49] K. Burgess, A. I. Liaw, N. Wang, *J. Med. Chem.* **1994**, *37*, 2985–2987.

[50] P.-L. Zhao, R. Zambias, J. Bolognese, D. Boulton, K. Chapman, *Proc. Natl. Acad. Sci. USA* **1995**, *92*, 10212–10216.

[51] J. A. Boutin, A. L. Fauchère, *Trends in Pharmac. Sci* **1996**, *17*, 8–12.

[52] J. J. Baldwin, E. G. Horlbeck (Pharmacopeia), WO 95/35503, **1995**.

[53] P. Willett, *Trends Biotechnol.* **1995**, *13*, 516–521.

[54] D. E. Goldberg, *Genetic Algorithms in Search Optimization and Machine Learning*, Addison-Wesley, New York, **1989**.

[55] L. Weber, S. Wallbaum, C. Broger, K. Gubernator, *Angew. Chem.* **1995**, *107*, 2452–2454; *Angew. Chem. Int. Ed. Engl.* **1995**, *34*, 2280–2282.

[56] J. Singh, M. A. Ator, E. P. Jaeger, M. P. Allen, D. A. Whipple, J. E. Soloweij, S. Chowdhary, A. M. Treasurywala, *J. Am. Chem. Soc.* **1996**, *118*, 1669–1676.

[57] R. P. Sheridan, S. K. Kearsley, *J. Chem. Inf. Comput. Sci.* **1995**, *35*, 310–320.
[58] a) B. Yan, G. Kumaravel, *Tetrahedron* **1996**, *52*, 843–848; b) B. Yan, G. Kumaravel, H. Anjaria, A. Wu, R. C. Petter, C. F. Jewell, Jr., J. R. Wareing, *J. Org. Chem.* **1995**, *60*, 5736–5738.
[59] a) R. C. Anderson, J. P. Stokes, M. J. Shapiro, *Tetrahedron Lett.* **1995**, *36*, 5311–5314; b) G. C. Look, C. P. Holmes, J. P. Chinn, M. A. Gallop, *J. Org. Chem.* **1994**, *59*, 7588–7590; c) W. L. Fitch, G. Detre, C. P. Holmes, J. N. Shoolery, P. A. Keifer, *ibid.* **1994**, *59*, 7955–7956; d) R. C. Anderson, M. A. Jarema, M. J. Shapiro, J. P. Stokes, M. Ziliox, *ibid.* **1995**, *60*, 2650–2651; e) S. K. Sarkar, R. S. Garigapati, J. L. Adams, P. A. Keifer, *J. Am. Chem. Soc.* **1996**, *118*, 2305–2306; f) P. A. Keifer, *J. Org. Chem.* **1996**, *61*, 1558–1559; g) R. S. Garigipati, B. Adams, J. L. Adams, S. K. Sarkar, *ibid.* **1996**, *61*, 2911–1914; h) P. A. Keifer, L. Baltusis, D. M. Rice, A. A. Tymiak, J. N. Shoolery, *J. Magn. Reson. Ser. A* **1996**, *119*, 65–75.
[60] a) B. J. Egner, M. Cardno, M. Bradley, *J. Chem. Soc. Chem. Commun.* **1995**, 2163–2164; b) B. J. Egner, J. Langley, M. Bradley, *J. Org. Chem.* **1995**, *60*, 2652–2653; c) C. L. Brummel, I. N. W. Lee, Y. Zhou, S. J. Benkovic, N. Winograd, *Science* **1994**, *264*, 399–402; d) S. J. Benkovic, N. Winograd, Brummel, I. N. W. Lee (The Penn State Research Foundation), WO 95/25737, **1995**.
[61] B. B. Brown, D. S. Wagner, H. M. Geysen, *Mol. Diversity* **1995**, *1*, 4–12.
[62] M. C. Fitzgerald, K. Harris, C. G. Shevlin, G. Siuzdak, *Bioorg. Med. Chem. Lett.* **1996**, *6*, 979–982.
[63] Y.-H. Chu, D. P. Kirby, B. L. Karger, *J. Am. Chem. Soc.* **1995**, *117*, 5419–5420.
[64] R. A. Zambias, D. A. Boulton, P. R. Griffin, *Tetrahedron Lett.* **1994**, *35*, 4283–4286.
[65] a) N. J. Haskins; D. J. Hunter, A. J. Organ, S. S. Rahman; C. Thom, *Rapid Commun. Mass Spectrom.* **1995**, *9*, 1437–1440; b) C. L. Brummel, J. C. Vickerman, S. A. Garr, M. E. Hemling, G. D. Roberts, W. Johnson, J. Weinstock, D. Gaitanopoulos, S. J. Benkovic, N. Winograd, *Anal. Chem.* **1996**, *68*, 237–242.
[66] a) J. W. Metzger, K.-H. Wiesmüller, V. Gnau, J. Brünjes, G. Jung, *Angew. Chem.* **1993**, *105*, 901–903; *Angew. Chem. Int. Ed. Engl.* **1993**, *32*, 894–896; b) J. W. Metzger, C. Kempter, K.-H. Wiesmüller, G. Jung, *Anal. Biochem.* **1994**, *219*, 261–277; c) R. S. Youngquist, G. R. Fuentes, M. P. Lacey, T. Keough, *Rapid Commun. Mass Spectrom.* **1994**, *8*, 77–81; d) J. A. Boutin, P. Hennig, P.-H. Lambert, S. Bertin, L. Petit, J.-P. Mahieu, B. Serkiz, J. P. Volland, J.-L. Fauchère, *Anal. Biochem.* **1996**, *234*, 126–141.
[67] Y. Dunayevskiy, P. Vouros, T. Carell, E. A. Wintner, J. Rebek, Jr., *Anal. Chem.* **1995**, *67*, 2906–2915.
[68] L. C. Maillard, *Compt. Rend. Acad. Sci.* **1912**, *154*, 66–68; review: F. Ledl, E. Schleicher, *Angew. Chem.* **1990**, *102*, 597–626; *Angew. Chem. Int. Ed. Engl.* **1990**, *29*, 565–594.
[69] H. Chen, R. J. Radmer (Martek Biosciences Corporation), WO 95/21850, **1995**.
[70] P. W. Smith, J. Y. Q. Lai, A. R. Whittimgton, B. Cox, J. G. Houston, C. H. Stylli, M. N. Banks, P. R. Tiller, *Bioorg. Med. Chem. Lett.* **1994**, *4*, 2821–2824.
[71] M. C. Pirrung, J. H.-L. Chau, J. Chen, *Chem. Biol.* **1995**, *2*, 621–626.
[72] "Automated Solution Phase Synthesis: Opportunities in Drug Discovery": R. Storer, in a lecture at the conference "Synthetic Chemical Libraries in Drug Discovery", London, **1995**.
[73] "Solution phase multiple synthesis in drug discovery": A. Merritt, in a lecture at the conference "Molecular Diversity & Combinatorial Chemistry", San Diego, CA, **1996**.
[74] "Solution Phase Synthesis of Pyrazole Libraries": W. S. MacLachlan, in a lecture at the conference "Synthetic Chemical Libraries in Drug Discovery", London, **1995**.
[75] T. Carell, E. A. Wintner, A. Bashir-Hashemi, J. Rebek, Jr., *Angew. Chem.* **1994**, *106*, 2159–2162; *Angew. Chem. Int. Ed. Engl.* **1994**, *33*, 2159–2161.
[76] T. Carell, E. A. Wintner, J. Rebek, Jr., *Angew. Chem.* **1994**, *106*, 2162–2164; *Angew. Chem. Int. Ed. Engl.* **1994**, *33*, 2161–2164.
[77] "Scaffolds for Combinatorial Synthesis": T. Carell, E. A. Wintner, Y. Dunayevskiy, P. Vouros, J. Rebek, Jr., in a lecture at the conference "Synthetic Chemical Libraries in Drug Discovery", London, **1995**.
[78] "Solution-Phase Generation of Tetraurea Libraries": G. W. Shipps, Jr., U. P. Spitz, J. Rebek, Jr., in a lecture at the 210th ACS National Meeting, Chicago, **1995**, Abstract No. 342.
[79] T. Carell, E. A. Wintner, A. J. Sutherland, J. Rebek, Jr., Y. M. Dunayevskiy, P. Vouros, *Chem. Biol.* **1995**, *2*, 171–183.
[80] J. Rebek, Jr., T. Carell, E. A. Wintner (Massachusetts Institute of Technology), WO 95/19359, **1995**.
[81] "Nonstructure-Based Scaffolds for Generating Combinatorial Chemistry Libraries": P. D. Cook, in a lecture at the conference "Exploiting Molecular Diversity: Small Molecule Libraries For Drug Discovery", San Diego, CA, **1996**.
[82] Gasteiger et al. recently reported on evaluation of similarity of components of compound libraries using spatial autocorrelation functions and neural networks taking libraries created by Rebek, Jr., et al. as an example: J. Sadowski, M. Wagner, J. Gasteiger, *Angew. Chem.* **1995**, *107*, 2892–2895; Angew. *Chem. Int. Ed. Engl.* **1995**, *34*, 2674–2677.
[83] Review on the use of multicomponent reactions in combinatorial synthesis: R. W. Armstrong, A. P. Combs, P. A. Tempest, S. D. Brown, T. A. Keating, *Acc. Chem. Res.* **1996**, *29*, 123–131.
[84] General reviews on multicomponent reactions: a) G. Posner, *Chem. Rev.* **1986**, *86*, 831–844; b) I. Ugi, S. Lohberger, R. Karl in *Comprehensive Organic Synthesis, Vol. 2* (Eds.: B. M. Trost, I. Fleming), Pergamon, New York, **1991**, pp. 1083–1109; c) I. Ugi, A. Dömling, W. Hörl, *Endeavour* **1994**, *18*, 115–122.
[85] I. Ugi, C. Steinbrückner, *Chem. Ber.* **1961**, *94*, 734–742.
[86] a) "Formale Unterstützung bei Multikomponentenreaktionen – Automatisierung der Synthesechemie": I. Ugi, A. Dömling, B. Gruber, M. Heiligbrunner, C. Heiß, W. Hörl in *Software-Entwicklung in der Chemie—Proceedings of the 9th Workshop, Bitterfeld, 16.–18.11.1994* (Ed.: R. Moll), Gesellschaft Deutscher Chemiker, Frankfurt am Main, **1995**, pp. 113–128; b) "Multicomponent Reactions for Generation of Molecular Diversity": I. Ugi, A. Dömling, M. Goebel, B. Gruber, M. Heiligbrunner, C. Heiß, W. Hörl, presented at the conference "Small Molecular Libraries for Drug Discovery", La Jolla, CA, **1995**.
[87] M. Goebel, I. Ugi, *Tetrahedron Lett.* **1995**, *36*, 6043–6046.
[88] R. W. Armstrong (The Regents of the University of California), WO 95/02566, **1995**.
[89] C. P. Holmes, J. P. Chinn, G. C. Look, E. M. Gordon, M. A. Gallop, *J. Org. Chem.* **1995**, *60*, 7328–7333.
[90] T. A. Keating, R. W. Armstrong, *J. Am. Chem. Soc.* **1995**, *117*, 7842–7843.
[91] A. M. Strocker, T. A. Keating, P. A. Tempest, R. W. Armstrong, *Tetrahedron Lett.* **1996**, *37*, 1149–1152.
[92] a) "New Synthetic Technology for Generation of Molecular Diversity": J. C. Hogan, Jr., in a lecture at the conference "Small Molecular Libraries for Drug Discovery", La Jolla, CA, **1995**; b) J. C. Hogan, Jr. (Legomer Partners), WO 94/00509, **1994**.
[93] J. C. Hogan, Jr. (Legomer Partners), WO 94/01102, **1994**.
[94] E. Peisach, D. Casebier, S. L. Gallion, P. Furth, G. A. Petsko, J. C. Hogan Jr., D. Ringe, *Science* **1995**, *269*, 66–69.
[95] "Automated High-Throughput Synthesis and Analysis of Small Molecular Thematic Arrays": J. C. Hogan, in a lecture at the conference "Exploiting Molecular Diversity: Small Molecule Libraries For Drug Discovery", San Diego, CA, **1996**.
[96] a) J. C. Hogan, Jr. (ArQule), WO 95/18972, **1995**; b) J. C. Hogan, Jr., D. Casebier, P. Furth (ArQule Partners), WO 95/18186, **1995**.
[97] "Solid-Phase Synthesis of Novel Scaffolds": J. C. Hogan, in a lecture at the conference "Solid-Phase Synthesis: Developing Small Molecule Libraries", San Diego, CA, **1996**.
[98] "A Simple Approach to Small Molecule Synthetic Libraries": J. R. Peterson, in a lecture at the conference "Small Molecular Libraries for Drug Discovery", La Jolla, CA, **1995**.
[99] "Solution-Phase Synthesis of Small Molecule Libraries: Process and Automation": C. D. Garr, in a lecture at the conference "Exploiting Molecular Diversity: Small Molecule Libraries For Drug Discovery", San Diego, CA, **1996**.
[100] "Synthesis of Small Molecule Libraries for the Discovery of Novel G-Protein Coupled Receptor Antagonists": D. S. Dhanoa, in a lecture at the conference "Lead Generation and Optimization", New Orleans, LA, **1996**.
[101] a) "An Alternative to Solid-Phase Chemistry: The Solution-Phase Parallel Synthesis of Combinatorial Libraries": C. M. Tarby, in a lecture at the conference "Solid-Phase Synthesis: Developing Small Molecule Libraries", San Diego, CA, **1996**; b) D. L. Boger, C. M. Tarby, P. L. Myers, L. H. Caporale, *J. Am. Chem. Soc.* **1996**, *118*, 2109–2110; c) S. Cheng, D. D. Comer, J. P. Williams, P. L. Myers, D. L. Boger, *J. Am. Chem. Soc.* **1996**, *118*, 2567–2573; d) D. L. Boger (Scripps Research Institute), WO 96/03424, **1996**.
[102] a) H. Han, M. Wolfe, S. Brenner, K. D. Janda, *Proc. Natl. Acad. Sci. USA* **1995**, *92*, 6419–6423; b) S. Brenner (Combichem, Inc.), WO 95/16918, **1995**.
[103] E. Bayer, M. Mutter, *Nature (London)* **1972**, *237*, 512–513.
[104] D. E. Bergbreiter, T. Kimmel, J. W. Caraway, *Tetrahedron Lett.* **1995**, *36*, 4757–4760.
[105] L. A. Thompson, J. A. Ellman, *Tetrahedron Lett.* **1994**, *35*, 9333–9336.
[106] "Application of High-Throughput Parallel Synthesis for Leads Optimization and Expedient SAR": G. T. Wang, in a lecture at the conference "Exploiting Molecular Diversity: Small Molecule Libraries For Drug Discovery", San Diego, CA, **1996**.
[107] J. R. Hauske, P. Dorff, *Tetrahedron Lett.* **1995**, *36*, 1589–1592.
[108] I. R. Marsh, H. Smith, M. Bradley, *J. Chem. Soc. Chem. Commun.* **1996**, 941–942.
[109] K. Kaljuste, A. Undén, *Tetrahedron Lett.* **1996**, *37*, 3031–3034.
[110] J. R. Morphy, Z. Rankovic, D. C. Rees, *Tetrahedron Lett.* **1996**, *37*, 3209–3212.
[111] D. E. Gaitanopoulos, J. Weinstock (SmithKline Beecham Corporation), WO 95/34813, **1995**.
[112] B. J. Backes, J. A. Ellman, *J. Am. Chem. Soc.* **1994**, *116*, 11171–11172.
[113] G. W. Kenner, J. R. McDermott, R. C. Sheppard, *J. Chem. Soc. Chem. Commun.* **1971**, 636–637.

[114] B. J. Backes, A. A. Virgilio, J. A. Ellman, *J. Am. Chem. Soc.* **1996**, *118*, 3055–3056.

[115] a) B. J. Backes, J. A. Ellman, *Carbon-Carbon Bond-Forming Methods on Solid Support*, 209th ACS National Meeting, Anaheim, CA, **1995**, Poster ORGN 261; b) "Synthesis of Small Molecule Libraries": J. Ellman, in a lecture at the conference "Molecular Diversity & Combinatorial Chemistry", San Diego, CA, **1996**.

[116] M. J. Plunkett, J. A. Ellman, *J. Org. Chem.* **1995**, *60*, 6006–6007.

[117] B. Chenera, J. A. Finkelstein, D. F. Veber, *J. Am. Chem. Soc.* **1995**, *117*, 11999–12000.

[118] NpSSMpact = 2-methoxy-5-[2-{(2-nitrophenyl)dithio}-1-oxopropyl]phenylacetamide; for this photocleavable linker, see I. Sucholeiki, *Tetrahedron Lett.* **1994**, *35*, 7307–7310.

[119] a) C. P. Holmes, D. G. Jones, *J. Org. Chem.* **1995**, *60*, 2318–2319; b) C. P. Holmes (Affymax Technologies), WO 96/00378, **1995**.

[120] a) M. Lebl, M. Patek, P. Kocis, V. Krchnák, V. J. Hruby, S. E. Salmon, K. S. Lam, *Int. J. Pept. Prot. Res.* **1993**, *41*, 201–203; b) M. Lebl, K. S. Lam, P. Kocis, V. Krchnák, M. Patek, S. E. Salmon, V. J. Hruby, *Pept. 1992, Proc. 22nd Eur. Pept. Symp.* **1993**, 67–69; c) S. E. Salmon, K. S. Lam, M. Lebl, A. Kandola, P. S. Khattri, S. Wade, M. Patek, P. Kocis, V. Krchnák, D. Thorpe, S. Felder, *Proc. Natl. Acad. Sci. USA* **1993**, *90*, 11708–11712; d) P. Kocis, V. Krchnák, M. Lebl, *Tetrahedron Lett.* **1993**, *34*, 7251–7252; e) M. Lebl, V. Krchnák, P. Kocis (Selectide Corporation), WO 95/00165, **1995**.

[121] M. Cardno, M. Bradley, *Tetrahedron Lett.* **1996**, *37*, 135–138.

[122] J. J. Baldwin, J. J. Burbaum, I. Henderson, M. H. J. Ohlmeyer, *J. Am. Chem. Soc.* **1995**, *117*, 5588–5589.

[123] G. Barany, F. Albericio, *J. Am. Chem. Soc.* **1985**, *107*, 4936–4942.

[124] a) J. A. Ellman, US 588514, **1992**; b) J. A. Ellman, A. A. Virgilio (The Regents of the University of California), WO 94/06291, **1994**.

[125] J. A. Ellman, B. A. Bunin, *J. Am. Chem. Soc.* **1992**, *114*, 10997–10998.

[126] J. A. Ellman, B. A. Bunin, M. J. Plunkett, *Proc. Natl. Acad. Sci. USA* **1994**, *91*, 4708–4712.

[127] D. R. Cody, S. H. DeWitt, J. C. Hodges, J. S. Kiely, W. H. Moos, M. R. Pavia, B. D. Roth, M. C. Schroeder, C. J. Stankovic, US 5324483, **1993**.

[128] F. Camps, J. Castells, J. Pi, *Ann. Quim.* **1974**, *70*, 848–849.

[129] S. H. DeWitt, J. S. Kiely, C. J. Stankovic, M. C. Schroeder, D. M. R. Cody, M. R. Pavia, *Proc. Natl. Acad. Sci. USA* **1993**, *90*, 6909–6913.

[130] D. R. Cody, S. H. DeWitt, J. C. Hodges, B. D. Roth, M. C. Schroeder, C. J. Stankovic, W. H. Moos, M. R. Pavia, J. S. Kiely (Warner-Lambert Company), WO 94/08711, **1994**.

[131] S. H. DeWitt, M. C. Schroeder, C. J. Stankovic, J. E. Strode, A. W. Czarnik, *Drug Dev. Res.* **1994**, *33*, 116–124.

[132] S. H. DeWitt, A. W. Czarnik, *Acc. Chem. Res.* **1996**, *29*, 114–122.

[133] J. A. Ellman, M. J. Plunkett, *J. Am. Chem. Soc.* **1995**, *117*, 3306–3307.

[134] "The Solid Phase Synthesis of Complex Small Molecules": J. A. Ellman, in a lecture at the conference "Synthesis of Small Molecules on Solid Phase", Basel, **1996**.

[135] "Solid Phase Synthesis of Structurally Diverse 1,4-Benzodiazepine Derivatives Using the Stille Coupling Reaction": J. A. Ellman, M. J. Plunkett, 209th ACS National Meeting, Anaheim, CA, **1995**, Poster ORGN 267.

[136] a) "The Combinatorial Synthesis of 1,4-Benzodiazepine Libraries": J. A. Ellman, B. A. Bunin, 209th ACS National Meeting, Anaheim, CA, **1995**, Poster ORGN 266; b) "Advances in the Simultaneous Synthesis of Organic Compounds": J. A. Ellman, presented at the 209th ACS National Meeting, Anaheim, CA, **1995**.

[137] B. Chenera, J. Elliott, M. Moore (SmithKline Beecham), WO 95/16712, **1995**.

[138] Benzodiazepinediones are well known for their anticonvulsive and anxiolytic properties. A potential glycoprotein antagonist was recently discovered which has a benzodiazepinedione structure: R. S. McDowell, B. K. Blackburn, T. R. Gadek, L. R. McGee, T. Rawson, M. E. Reynolds, K. D. Robarge, T. C. Somers, E. D. Thorsett, M. Tischler, R. R. Wegg II, M. C. Venuti, *J. Am. Chem. Soc.* **1994**, *116*, 5077–5083.

[139] "Solid-Phase Synthesis of Fibrinogen-GPIIb/IIIa Binding Inhibitors": C. J. Phelan, B. K. Blackburn, T. R. Gadek, 209th ACS National Meeting, Anaheim, CA, **1995**, Poster ORGN 346.

[140] S.-S. Wang, *J. Am. Chem. Soc.* **1973**, *95*, 1328–1333.

[141] Palladium-catalyzed couplings on the solid phase: a) Heck reactions: K.-L. Yu, M. S. Deshpande, D. M. Vyas, *Tetrahedron Lett.* **1994**, *35*, 8919–8922; M. Hiroshige, J. R. Hauske, P. Zhou, *ibid.* **1995**, *36*, 4567–4570; b) Suzuki reaction: R. Frenette, R. W. Friesen, *ibid.* **1994**, *35*, 9177–9180; d) Stille reactions: M. S. Deshpande, *ibid.* **1994**, *35*, 5613–5614; Ref. [201].

[142] C. G. Boojamra, K. M. Burow, J. A. Ellman, *J. Org. Chem.* **1995**, *60*, 5742–5743.

[143] D. A. Goff, R. N. Zuckermann, *J. Org. Chem.* **1995**, *60*, 5744–5745.

[144] a) R. N. Zuckermann, E. J. Martin, D. C. Spellmeyer, G. B. Stauber, K. R. Shoemaker, J. M. Kerr, G. M. Figliozzi, D. A. Goff, M. A. Siani, R. J. Simon, S. C. Banville, E. G. Brown, L. Wang, L. S. Richter, W. H. Moos, *J. Am. Chem. Soc.* **1994**, *116*, 2678–2685; b) R. J. Simon, R. S. Kania, R. N. Zuckermann, V. D. Huebner, D. A. Jewell, S. C. Banville, S. Ng, L. Wang, S. Rosenberg, C. K. Marlowe, D. C. Spellmeyer, R. Tan, A. D. Frankel, D. V. Santi, F. E. Cohen, P. A. Bartlett, *Proc. Natl. Acad. Sci. USA* **1992**, *89*, 9367–9371.

[145] R. N. Zuckermann, J. M. Kerr, S. B. H. Kent, W. H. Moos, *J. Am. Chem. Soc.* **1992**, *114*, 10646–10647.

[146] Experimental details and data are not given for synthesis of the triflate benzodiazepinedione or for the products of the Suzuki coupling.

[147] "The Design of Small Molecule Combinatorial Libraries": J. J. Baldwin, in a lecture at the conference "Synthetic Chemical Libraries in Drug Discovery", London, **1995**.

[148] Benzhydrylamine-polystyrene resin.

[149] M. A. Gallop, M. A. Murphy (Affymax Technologies), WO 95/35278, **1995**.

[150] G. C. Look, M. M. Murphy, D. A. Campbell, M. A. Gallop, *Tetrahedron Lett.* **1995**, *36*, 2937–2940.

[151] Inhibitors of the angiotensin conversion enzyme.

[152] C. P. Holmes (Affymax Technologies), WO 96/00148, **1996**.

[153] D. A. Walsh, I. M. Uwaydah, US 5061720, **1991**.

[154] G. C. Look, J. R. Schullek, C. P. Holmes, J. P. Chinn, E. M. Gordon, M. A. Gallop, *Bioorg. Med. Chem. Lett.* **1996**, *6*, 707–712.

[155] B. Ruhland, A. Bhandari, E. M. Gordon, M. A. Gallop, *J. Am. Chem. Soc.* **1996**, *118*, 253–254.

[156] *SASRIN* = super acid sensitive resin; M. Mergler, R. Tanner, J. Gosteli, P. Grogg, *Tetrahedron Lett.* **1988**, *29*, 4005–4008.

[157] a) M. Pátek, B. Drake, M. Lebl, *Tetrahedron Lett.* **1995**, *36*, 2227–2230; b) "Solid Phase Synthesis of "Small" Organic Molecules Based on Thiazolidine Scaffold": M. Pátek, B. Drake, M. Lebl, 209th ACS National Meeting, Anaheim, CA, **1995**, Poster ORGN 461.

[158] J. J. Burbaum, M. H. J. Ohlmeyer, J. C. Reader, I. Henderson, L. W. Dillard, G. Li, T. L. Randle, N. H. Sigal, D. Chelsky, J. J. Baldwin, *Proc. Natl. Acad. Sci. USA* **1995**, *92*, 6027–6031.

[159] a) "Design, Synthesis and Use of Binary Encoded Synthetic Chemical Libraries": J. C. Chabala, in a lecture at the conference "Synthetic Chemical Libraries in Drug Discovery", London, **1995**; b) "Design, Synthesis and Use of Binary Encoded Small Molecule Libraries and Their Use in Elucidating Structure-Activity": J. C. Chabala, in a lecture at the conference "Conference on Exploiting Molecular Diversity, Small Molecule Libraries for Drug Discovery", La Jolla, CA, **1995**; c) J. J. Baldwin, J. C. Reader, L. W. Dillard, J. J. Burbaum (Pharmacopeia), WO 95/30642, **1995**.

[160] a) M. H. J. Ohlmeyer, R. N. Swanson, L. W. Dillard, J. C. Reader, G. Asouline, R. Kobayashi, M. Wigler, W. C. Still, *Proc. Natl. Acad. Sci. USA* **1993**, *90*, 10922–10926; b) P. Eckes, *Angew. Chem.* **1994**, *106*, 1649–1651; *Angew. Chem. Int. Ed. Engl.* **1994**, *33*, 1573–1575.

[161] J. J. Baldwin, M. H. J. Ohlmeyer, I. Henderson (Pharmacopeia), WO 95/24186, **1995**.

[162] a) E. Bayer, W. Rapp, *Chem. Pept. Prot.* **1986**, *3*, 3–8; b) E. Bayer, M. Dengler, B. Hemmasi, *Int. J. Pept. Res.* **1985**, *25*, 178–186.

[163] a) D. A. Claremon, G. S. Ponticello, H. G. Selnick (Merck & Co.), US 5439914, **1994**; b) J. J. Baldwin, D. A. Claremon, J. M. Elliott, G. S. Ponticello, D. C. Remy, H. G. Selnick (Merck & Co.), WO 94/18204, **1994**.

[164] D. A. Goff, R. N. Zuckermann, *J. Org. Chem.* **1995**, *60*, 5748–5749.

[165] "Solid-Phase Bound Imines: Synthesis of Heterocyclic Systems": J. S. Kiely, in a lecture at the conference "Solid-Phase Synthesis: Developing Small Molecule Libraries", San Diego, CA, **1996**.

[166] "Linear Arrays and Combinatorial Mixtures of Quinazolinones": R. A. Houghten, in a lecture at the conference "Exploiting Molecular Diversity: Small Molecule Libraries For Drug Discovery", San Diego, CA, **1996**.

[167] M. Cushman, E. J. Madaj, *J. Org. Chem.* **1987**, *52*, 907–915.

[168] A. M. M. Mjalli, S. Sarshar, T. J. Baiga, *Tetrahedron Lett.* **1996**, *37*, 2943–2946.

[169] C. Zhang, E. J. Moran, T. F. Woiwode, K. M. Short, A. M. M. Mjalli, *Tetrahedron Lett.* **1996**, *37*, 751–754.

[170] S. Sarshar, D. Siev, A. M. M. Mjalli, *Tetrahedron Lett.* **1996**, *37*, 835–838.

[171] B. Krieg, G. Manecke, *Z. Naturforschg. B* **1967**, *22*, 132–141.

[172] T. Ruhland, H. Künzer, *Tetrahedron Lett.* **1996**, *37*, 2757–2760.

[173] K. Kaljuste, A. Undén, *Tetrahedron Lett.* **1995**, *36*, 9211–9214.

[174] A similar resin has already been constructed along a more complicated route: G. Breipohl, J. Knolle, R. Geiger, *Tetrahedron Lett.* **1987**, *28*, 5647–5650.

[175] "Pictet-Spengler Reaction on Solid Support": L. Yang, presented at the 211th ACS National Meeting, New Orleans, LA, **1996**.

[176] a) "DIVERSOMER™ Technology: Recent Advances in the Generation of Chemical Diversity": S. H. DeWitt, in a lecture at the conference "Chemical Lead Generation in Drug Discovery", Cambridge, United Kingdom, **1995**; b) A. MacDonald, R. Ramage, S. H. DeWitt, E. Hogan, presented at the "Combinatorial Synthesis Symposium", Exeter, United Kingdom, **1995**; c) "Consideration of Solid Phase Synthesis with Reference to Quinolone Antibiotics": R. Ramage, in a lecture at the conference "Synthesis of Small Molecules on Solid Phase", Basel, **1996**.

[177] a) J. Wrobel, A. Dietrich, S. A. Woolson, J. Millen, M. McCaleb, M. C. Harrison, T. C. Hohmann, J. Sredy, D. Sullivan, *J. Med. Chem.* **1992**, *35*, 4613–4627; b) J. E. Wroel (American Home Products), US 4900739, **1988**.

[178] L. F. Tietze, A. Steinmetz, *Synlett* **1996**, 667–668.

[179] "Solid-Phase Synthesis of Five Membered Ring Heterocycles": A. L. Marzinzik, E. R. Felder, presented at the conference "Solid-Phase Synthesis: Developing Small Molecule Libraries", San Diego, CA, **1996**.

[180] A. L. Marzinzik, E. R. Felder, *Tetrahedron Lett.* **1996**, *37*, 1003–1006.

[181] A. Nickon, A. S. Hill, *J. Am. Chem. Soc.* **1964**, *86*, 1152–1158.

[182] B. A. Dressman, L. A. Spangle, S. W. Kaldor, *Tetrahedron Lett.* **1996**, *37*, 937–940.

[183] a) G. Massimo, F. Zani, E. Coghi, A. Belloti, P. Mazza, *Farmaco* **1990**, *45*, 439–446; b) C. Branca, G. Vaona, *Farmaco Ed. Sci.* **1971**, *26*, 1115–1117.

[184] "DIVERSOMER™ Technology: The Synthesis of Benzisothiazolones as Epidermal Growth Factor Receptor Tyrosine Kinase Inhibitors": M. C. Schroeder, A. J. Kraker, C. W. Moore, J. S. Kiely, S. H. DeWitt, A. W. Czarnik, 208th ACS National Meeting, Washington, DC, **1994**, Abstr. MEDI 239.

[185] "Parke Davis DIVERSOMER™ Technology. A Practical Approach to Parallel, Simultaneous Organic Synthesis": A. W. Czarnik, in a lecture at the conference "Synthetic Chemical Libraries in Drug Discovery", London, **1995**.

[186] β-Oxoester synthesis in solution: J. A. Turner, W. S. Jacks, *J. Org. Chem.* **1989**, *54*, 4229–4231.

[187] a) S. D. Larsen, F. P. Bell (Upjohn), WO 90/01031, **1990**; b) S. D. Larsen, C. H. Spilman, F. P. Bell, D. M. Dink, E. Martinsborough, G. J. Wilson, *J. Med. Chem.* **1991**, *34*, 1721–1727.

[188] a) X. Beebe, C. L. Chiappari, M. M. Olmstead, M. J. Kurth, N. E. Schore, *J. Org. Chem.* **1995**, *60*, 4204–4212; b) X. Beebe, N. E. Schore, M. J. Kurth, *ibid.* **1995**, *60*, 4196–4203; c) X. Beebe, N. E. Schore, M. J. Kurth, *J. Am. Chem. Soc.* **1992**, *114*, 10061–10062.

[189] H. S. Moon, N. E. Schore, M. J. Kurth, *Tetrahedron Lett.* **1994**, *35*, 8915–8918.

[190] D. W. Gordon, J. Steele, *Bioorg. Med. Chem. Lett.* **1995**, *5*, 47–50.

[191] B. O. Scott, A. C. Siegmund, C. K. Marlowe, Y. Pei, K. L. Spear, *Mol. Diversity* **1995**, *1*, 125–134.

[192] D. Campbell, M. A. Gallop, E. M. Gordon, G. C. Look, D. V. Patel, A. K. Szardenings (Affymax Technologies), WO 96/00391, **1996**.

[193] J. A. Ellman, A. A. Virgilio, *J. Am. Chem. Soc.* **1994**, *116*, 11580–11581.

[194] "Synthesis and Evaluation of a Library of β-Turn-Mimetics": J. A. Ellman, A. A. Virgilio, 209th ACS National Meeting, Anaheim, CA, **1995**, Poster ORGN 263.

[195] The TentaGel resin is suitable for reactions in polar medium because of its swelling properties.

[196] M. Hiroshige, J. R. Hauske, P. Zhou, *J. Am. Chem. Soc.* **1995**, *117*, 11590–11591.

[197] "New Linkers and Scaffolds—Molecular Design of Scaffolds and Side Chains and Their Application to Combinatorial Chemistry": J. R. Hauske, in a lecture at the conference "High Throughput Screening for Drug Discovery", San Diego, CA, **1995**.

[198] C. R. Johnson, B. Zhang, *Tetrahedron Lett.* **1995**, *36*, 9253–9256.

[199] V. Yedida, C. C. Leznoff, *Can. J. Chem.* **1980**, *58*, 1144–1150.

[200] K. I. Guhr, M. D. Greaves, V. M. Rotello, *J. Am. Chem. Soc.* **1994**, *116*, 5997–5998.

[201] R. H. Schlesinger, C. P. Bergstrom, *Tetrahedron Lett.* **1996**, *37*, 2133–2136.

[202] N. E. Schore, S. D. Najdi, *J. Am. Chem. Soc.* **1990**, *112*, 441–442.

[203] S. V. Ley, D. M. Mynett, W.-J. Koot, *Synlett* **1995**, 1017–1020.

[204] C. Chen, L. A. Ahlberg Randall, B. R. Miller, A. D. Jones, M. J. Kurth, *J. Am. Chem. Soc.* **1994**, *116*, 2661–2662.

[205] S. M. Dankwardt, S. R. Newman, J. L. Krstenansky, *Tetrahedron Lett.* **1995**, *36*, 4923–4926.

[206] S. Kobayashi, I. Hachiya, S. Suzuki, M. Moriwaki, *Tetrahedron Lett.* **1996**, *37*, 2809–2812.

[207] a) E. K. Kick, J. A. Ellman, *J. Med. Chem.* **1995**, *38*, 1427–1430; b) "Solid Phase Synthesis of Aspartic Acid Protease Inhibitors": 209th ACS National Meeting, Anaheim, CA, **1995**, Poster ORGN 265.

[208] M. Bartra, P. Romea, F. Urpf, J. Vilarrasa, *Tetrahedron* **1990**, *46*, 587–594.

[209] G. T. Wang, S. Li, N. Wideburg, G. A. Krafft, D. J. Kempf, *J. Med. Chem.* **1995**, *38*, 2995–3002.

[210] a) "The Solid Phase Synthesis of Prostaglandines": L. A. Thompson, J. A. Ellman, 209th ACS National Meeting, Anaheim, CA, **1995**, Poster ORGN 262; b) M. Suzuki, Y. Morita, H. Koyano, M. Koga, R. Noyori, *Tetrahedron* **1990**, *46*, 4809–4822.

[211] The corresponding synthesis in solution was described by C. R. Johnson, M. P. Braun, *J. Am. Chem. Soc.* **1993**, *115*, 11014–11015.

[212] a) R. C. Larock, US 4436934, **1981**; b) US 4658033, **1985**; R. C. Larock, S. Babu, *Tetrahedron Lett.* **1985**, *26*, 2763–2764; c) R. C. Larock, N. Narayanan, *Tetrahedron* **1988**, *44*, 6995–7000; S. Torii, H. Okumoto, T. Kotani, S. Nakayasu, H. Ozaki, *Tetrahedron Lett.* **1992**, *33*, 3503–3506; d) other fundamental work on three-component palladium catalysis: M. Catellani, G. P. Chiusoli, *Tetrahedron Lett.* **1982**, *23*, 4517–4520; M. Catellani, G. P. Chiusoli, A. Mari, *J. Organomet. Chem.* **1984**, *275*, 129–138.

[213] S. M. Hutchins, K. T. Chapman, *Tetrahedron Lett.* **1995**, *36*, 2583–2586.

[214] H. Rink, *Tetrahedron Lett.* **1987**, *28*, 3787–3790.

[215] Urea synthesis on support-bound *p*-nitrophenylcarbamate: S. M. Hutchins, K. T. Chapman, *Tetrahedron Lett.* **1994**, *35*, 4055–4058.

[216] a) T. A. Rano, K. T. Chapman, *Tetrahedron Lett.* **1995**, *36*, 3789–3792; b) R. M. Valerio, A. M. Bray, H. Patsiouras, *ibid.* **1996**, *37*, 3019–3022.

[217] L. S. Richter, T. R. Gadek, *Tetrahedron Lett.* **1994**, *35*, 4705–4706.

[218] a) V. Krchnák, Z. Flegelová, A. S. Weichsel, M. Lebl, *Tetrahedron Lett.* **1995**, *36*, 6193–6196; b) "Solid-phase Mitsunobu and Wittig Reactions and their Use for the Construction of Peptide and Non-Peptide Libraries": V. Krchnák, J. P. Vágner, Z. Flegelová, A. S. Weichsel, G. Barany, M. Lebl, presented at the 14th American Peptide Symposium, Columbus, OH, **1995**; c) "The Use of Synthetic Combinatorial Libraries to Discover, Develop SAR, and Optimize Novel Therapeutic Agents: A Tool for the Medicinal Chemist to Accelerate and Improve the Quality of the Drug Discovery Process": B. Seligmann, P. Strop, M. Lebl, N. Sepetov, V. Krchnák, M. Patek, O. Issakova, P. Safar, F. Al-Obeidi, A. Safarova, S. Stringer, A. Walser, J. Ostrem, P. Wildgoose, in a lecture at the conference "Synthetic Chemical Libraries in Drug Discovery", London, **1995**.

[219] H. V. Meyers, G. J. Dilley, T. L. Durgin, T. S. Powers, N. A. Winssinger, H. Zhu, M. R. Pavia, *Mol. Diversity* **1995**, *1(1)*, 13–20.

[220] M. J. Farall, J. M. J. Frechet, *J. Org. Chem.* **1976**, *41*, 3877–3882.

[221] S. M. Dankwardt, T. M. Phan, J. L. Krstenansky, *Mol. Diversity* **1995**, *1*, 113–120.

[222] On selective cleavage of aryl esters, see: H. E. Zaugg, *J. Org. Chem.* **1976**, *41*, 3419–3421.

[223] "Single Bead Mass Spectrometry for Qualitative Assurance of Solid Phase Libraries": W. L. Fitch, in a lecture at the conference "Molecular Diversity & Combinatorial Chemistry", San Diego, CA, **1996**.

[224] "Mixtures of Molecules vs. Mixtures of Pure Compounds on Polymeric Beads": M. Lebl, in a lecture at the conference "Exploiting Molecular Diversity: Small Molecule Libraries For Drug Discovery", San Diego, CA, **1996**.

[225] T. Q. Dinh, R. W. Armstrong, *Tetrahedron Lett.* **1996**, *37*, 1161–1164.

[226] J. Green, *J. Org. Chem.* **1995**, *60*, 4287–4290.

[227] "Bis-Allylic Templates for Pd^0-Catalyzed Combinatorial Synthesis of Tertiary Amines": Z. Flegelová, M. Pátek, presented at the 211th ACS National Meeting, New Orleans, LA, **1996**.

[228] M. Pátek, B. Drake, M. Lebl, *Tetrahedron Lett.* **1994**, *35*, 9169–9172.

[229] "Solid-Phase Synthetic Methods in Combinatorial Chemistry": I. Sucholeiki, in a lecture at the conference "High Throughput Screening for Drug Discovery", San Diego, CA, **1995**.

[230] M. R. Pavia, G. M. Whitesides, D. G. Hangauer, M. E. Hediger (Sphinx Pharmaceuticals Corporation), WO 95/04277, **1994**.

[231] F. W. Forman, I. Sucholeiki, *J. Org. Chem.* **1995**, *60*, 523–528.

[232] "SAR Studies of Antitumor Drugs Using a Combinatorial Screening Approach": R. W. Armstrong, in a lecture at the conference "Exploiting Molecular Diversity for Drug Discovery", San Diego, CA, **1994**.

[233] a) P. A. Tempest, S. D. Brown, R. W. Armstrong, *Angew. Chem.* **1996**, *108*, 689–691; *Angew. Chem. Int. Ed. Engl.* **1996**, *35*, 640–642; b) "Combinatorial Libraries Related to Natural Products": presented at the 209th ACS National Meeting, Anaheim, CA, **1995**, ORGN 145.

[234] X. Cao, E. J. Moran, D. Siev, A. Lio, C. Ohashi, A. M. M. Mjalli, *Bioorg. Med. Chem. Lett.* **1995**, *5*, 2953–2958.

[235] P. Wipf, A. Cunningham, *Tetrahedron Lett.* **1995**, *36*, 7819–7822.

[236] "Solid-Phase Synthesis of Dihydropyrimidine Combinatorial Libraries by the Atwal-Modifikation of the Biginelli Reaction": L. D. Robinett, presented at the 211th ACS National Meeting, New Orleans, LA, **1996**.

[237] a) "Strategy for the Synthesis of Heterocyclic Libraries for the Discovery of Lead Structures": M. C. Desai, in a lecture at the conference "Exploiting Molecular Diversity: Small Molecule Libraries For Drug Discovery", San Diego, CA, **1996**; b) "Articulating a General Strategy for the Solid-Supported Synthesis of Heterocycles: Application to the Generation of Molecular Diversity": J. M. Nuss, in a lecture at the conference "Solid-Phase Synthesis: Developing Small Molecule Libraries", San Diego, CA, **1996**.

[238] M. F. Gordeev, D. V. Patel, E. M. Gordon, *J. Org. Chem.* **1996**, *61*, 924–928.

[239] "Solid-Phase Combinatorial Synthesis of Small Molecule Libraries": D. V. Patel, in a lecture at the conference "Solid-Phase Synthesis: Developing Small Molecule Libraries", San Diego, CA, **1996**.

[240] R. N. Zuckermann, J. M. Kerr, M. A. Siani, S. C. Banville, D. V. Santi, *Proc. Natl. Acad. Sci. USA* **1992**, *89*, 4505–4509.

[241] "Rapid Lead Identification Using Affinity Selection and Mass Spectrometry": G. D. Dollinger, in a lecture at the conference "Synthetic Chemical Libraries in Drug Discovery", London, **1995**.

[242] B. Déprez, X. Williard, L. Bourel, L. H. Coste, F. Hyafil, F. A. Tartar, *J. Am. Chem. Soc.* **1995**, *117*, 5405–5406.

[243] S. M. Freier, D. A. M. Konings, J. R. Wyatt, D. J. Ecker, *J. Med. Chem.* **1995**, *38*, 344–352.

[244] "Unconventional Chemical Libraries and a Rigorous Evaluation of Pooling Strategies": D. Ecker, in a lecture at the conference "Molecular Diversity & Combinatorial Chemistry", San Diego, CA, **1996**.

[245] E. Erb, K. D. Janda, S. Brenner, *Proc. Natl. Acad. Sci. USA* **1994**, *91*, 11422–11426.

[246] a) R. A. Houghten, J. R. Appel, S. E. Blondelle, J. H. Cuervo, C. T. Dooley, C. Pinilla, *BioTechniques* **1992**, *13*, 412–421; b) C. T. Dooley, R. A. Houghten, *Life Sci.* **1993**, *52*, 1509–1517.

[247] a) S. Brenner, R. A. Lerner, *Proc. Natl. Acad. Sci. USA* **1992**, *89*, 5381–5383; b) K. D. Janda, *ibid.* **1994**, *91*, 10779–10785.

[248] a) J. M. Kerr, S. C. Banville, R. N. Zuckermann, *J. Am. Chem. Soc.* **1993**, *115*, 2529–2531; b) V. Nikolaev, A. Stierandova, V. Krchnák, B. Seligmann, K. S. Lam, S. E. Salmon, M. Lebl, *Pept. Res.* **1993**, *6*, 161–170; c) M. Lebl, K. S. Lam, S. E. Salmon, V. Krchnák, N. Sepetov, P. Kocis (Selectide Corporation), WO 94/28028, **1994**; d) E. Felder, H. Rink, I. T. W. Matthews (Ciba-Geigy AG), WO 95/16209, **1995**; e) E. R. Felder, G. Heizmann, I. T. Matthews, H. Rink, E. Spieser, *Mol. Diversity* **1995**, *1*, 109–112.

[249] a) J. Nielsen, S. Brenner, K. D. Janda, *J. Am. Chem. Soc.* **1993**, *115*, 9812–9813; b) M. C. Needels, D. G. Jones, E. H. Tate, G. L. Heinkel, L. M. Kochersperger, W. J. Dower, R. W. Barrett, M. A. Gallop, *Proc. Natl. Acad. Sci. USA* **1993**, *90*, 10700–10704.

[250] a) H. P. Nestler, P. A. Bartlett, W. C. Still, *J. Org. Chem.* **1994**, *59*, 4723–4724; b) W. C. Still, *Acc. Chem. Res.* **1996**, *29*, 155–163; W. C. Still, M. H. Wigler, M. H. J. Ohlmeyer (The Trustees of Columbia University in the City of New York), WO 95/28640, **1995**.

[251] a) Z.-J. Ni, D. MacLean, C. P. Holmes, M. M. Murphy, B. Ruhland, J. W. Jacobs, E. M. Gordon, M. A. Gallop, *J. Med. Chem.* **1996**, *39*, 1601–1608; b) "Integrating Automation and Encoding Technologies with Combinatorial Organic Synthesis for Drug Discovery": M. A. Gallop, in a lecture at the conference "Molecular Diversity & Combinatorial Chemistry", San Diego, CA, **1996**.

[252] J. C. Chabala, *Curr. Opin. Biotechnol.* **1995**, *6*, 632–639.

[253] D. S. Yamashita, J. Weinstock (SmithKline Beecham Corporation), WO 95/32425, **1995**.

[254] A labeling of the solid support with fluorophores was also described by Furka et al.: a) F. Sebestyén, G. Dibó, Á. Furka, *Pept. 1992 Proc. 22nd Eur. Pept. Symp.* **1993**, 63–64; b) E. Campian, F. Sebestyén, Á. Furka, *Innovation and Perspectives in Solid Phase Synthesis 1994* (Ed.: R. Epton), Mayflower, Birmingham, **1994**, pp. 469–472.

[255] K. C. Nicolaou, X.-Y. Xiao, Z. Parandoosh, A. Senyei, M. P. Nova, *Angew. Chem.* **1995**, *107*, 2476–2479; *Angew. Chem. Int. Ed. Engl.* **1995**, *34*, 2289–2291.

[256] E. J. Moran, S. Sarshar, J. F. Cargill, M. M. Shahbaz, A. Lio, A. M. M. Mjalli, R. W. Armstrong, *J. Am. Chem. Soc.* **1995**, *117*, 10787–10788.

[257] a) D. K. Agrafiotis, R. F. Bone, F. R. Salemme, R. M. Soll (3-Dimensional Pharmaceuticals), US 5463564, **1995**; b) "The Impact of Structural Data on the Design of Small Molecule libraries": T. L. Graybill, in a lecture at the conference "Exploiting Molecular Diversity: Small Molecule Libraries For Drug Discovery", San Diego, CA, **1996**.

[258] a) S. H. DeWitt, A. W. Czarnik, *Curr. Opin. Biotechnol.* **1995**, *6*, 640–645; b) A. W. Czarnik, S. H. DeWitt, *Chem. Br.* **1996**, *32*, 43–45

[259] This method is being developed further by DIVERSOMER Technologies, 2800 Plymouth Rd., Ann Arbor, MI 48105 (USA); fax: int. code +(313)998-2782; production and marketing: Chemglass, Inc., 3861 N. Mill Rd., Vineland, NJ 08360 (USA); fax: int. code +(800)922-4361.

[260] MultiSynTech, Müllensiefenstrasse 22, D-44894 Bochum (Germany); fax: int. code +(234)263-634. Advanced ChemTech, 5609 Fern Valley Rd., Louisville, KY 40228 (USA); fax: int. code +(502)968-1000.

[261] a) S. Borman, *Chem. Eng. News* **1996**, 29–54; b) "Automated Combinatorial Chemistry on Solid Phase": J. F. Cargill, R. R. Maiefski, B. E. Toyonaga, *Proc. 13th Int. Symp. Laboratory Automation Robotics 1995*, **1995**, 221–234; c) "An Integrated Drug Discovery Approach Incorporating Combinatorial Chemistry—The Role of Instrumentation": P. L. Myers, *ibid.* **1995**, 235–248.

[262] Appropriate instrumentation and automated procedures are under development, for example, at the following companies: Bohdan Automation Inc., 1500 McCormick Blvd., Mundelein, IL 60060 (USA); fax: int. code +(847)680-1199; The Technology Partnership plc, Melbourn Science Park Melbourn/Royston, Herts SG8 6EE (UK); fax: int. code +(1763)261582; TECAN U. S. SLT Labinstruments, P. O. Box 13953, Research Triangle Park, NC 27709 (USA); fax: int. code +(919)361-5201.

[263] Argonaut Technologies, Inc., 887 Industrial Road, Suite G, San Carlos, CA 94070 (USA); fax: int. code +(415)598-1359; CombiChem, Inc., 11099 N. Torrey Pines Road, Suite 200, La Jolla, CA 92037 (USA); fax: int. code +(619)453-3102.

[264] S. Goldby, *Scrip Mag.* **1995**, 6–7.

[265] a) J. H. Krieger, *Chem. Eng. News* **1996**, 67–73; b) P. Rees, *Sci. Comput. World* **1996**, 25–30.

[266] *ACD*, *REACCS*, and *Project Library* are products of the company MDL Information Systems, 14600 Catalina Street, San Leandro, CA 94577 (USA); fax: int. code +(510)614-3652, http://www.mdli.com.

[267] *Crossfire Plus* is a product of the company Beilstein Information Systems Inc., 15 Inverness Way East, P. O. Box 1154, Englewood, CO 80150 (USA); fax: int. code +303/792-2652, http://www.beilstein.com.

[268] *Legion*, *UNITY* and *Selector* are products of the company Tripos, 1699 South Hanley Road, St. Louis, MO 63144 (USA); fax: int. code +(314)647-9241.

[269] "A Database System for Combinatorial Synthesis Experiments": C. A. James, in a lecture at the conference "Synthetic Chemical Libraries in Drug Discovery", London, **1995**; *Jarpat* is a product of the company Daylight Chemical Information Systems Inc., 27401 Los Altos, Suite 370, Mission Viejo, CA 92691; fax: int. code +(714)367-0990; http://www.daylight.com.

[270] a) "Using pharmacophore diversity with protein targets of known structure": K. Davies, in a lecture at the conference "Molecular Diversity & Combinatorial Chemistry", San Diego, CA, **1996**; b) "Practical Information-Handling Issues in Molecular Diversity and Combinatorial Chemistry": R. D. Cramer, in a lecture at the conference "Molecular Diversity & Combinatorial Chemistry", San Diego, CA, **1996**; c) "Client-Server Software Tools for Combinatorial Information Storage and Experiment Planning": M. Bronzetti, in a lecture at the conference "Molecular Diversity & Combinatorial Chemistry", San Diego, CA, **1996**; d) "Diversity, Shmiversity: Is Your Library Any Good?": S. L. Teig, in a lecture at the conference "Exploiting Molecular Diversity: Small Molecule Libraries For Drug Discovery", San Diego, CA, **1996**.

[271] *C^2-Diversity* is a product of the company Biosym Technologies/Molecular Simulations, 9685 Scranton Road, San Diego, CA 92121; fax: int. code +(619)458-0136; http://www.biosym.com or http://www.msi.com; e-mail: solutions@biosym.com.

[272] *Chem-X* is a product of the company Chemical Design Ltd., Roundwell House, Cromwell Park, Chipping Norton, Oxon OX7 5SR (UK); fax: int. code +(1608)642244.

[273] On acquisitions and cooperations in the years 1992–1994, see "R & D Strategies: The Promise of Combinatorial Chemistry": R. Longman, *In Vivo int. code J. In Vivo Res.* **1994** (May), 23–31. For an up-to-date summary, see A. M. Thayer, *Chem. Eng. News* **1996**, 57–64. A collation of the firms and researchers active in the field of "molecular diversity" can be obtained from the Internet: http://vesta.pd.com. Here lists with publications and patents in this field can also be found, as well as the Internet edition of the Journal *Molecular Diversity*, with complete articles in the already accepted, but not yet printed form.

[274] "Parallel Synthesis of Small Molecule Libraries Using Aromatic Templates": H. V. Meyers, in a lecture at the conference "Molecular Diversity & Combinatorial Chemistry", San Diego, CA, **1996**.

[275] K. Burgess, H.-J. Lim, A. M. Porte, G. A. Sulikowski, *Angew. Chem.* **1996**, *108*, 192–194; *Angew. Chem. int. code Ed. Engl.* **1996**, *35*, 220–222.

[276] G. Liu, J. A. Ellman, *J. Org. Chem.* **1995**, *60*, 7712–7713.

[277] a) X.-D. Xiang, X. Sun, G. Biceno, Y. Lou, K.-A. Wang, H. Chang, W. G. Wallace-Freedman, S.-W. Chen, P. G. Schultz, *Science* **1995**, *268*, 1738–1740; b) G. Briceno, H. Chang, X. Sun, P. G. Schultz, X.-D. Xiang, *ibid.* **1995**, *270*, 273–275; c) L. C. Hsieh-Wilson, X.-D. Xiang, P. G. Schultz, *Acc. Chem. Res.* **1996**, *29*, 164–170.

[278] After submission of this review other publications on combinatorial synthesis of low molecular weight organic compounds have appeared; these added in proof present the state of the art as of September 1996 (lectures not included; some papers cited as lectures in the preceding references have now been published and have been included: a) new reviews: 1. "Applications of Small-Molecule Combinatorial Chemistry to Drug Discovery": D. V. Patel, E. M. Gordon, *Drug Discovery Today* **1996**, *1*, 134–144; 2) "Solution-phase synthesis in combinatorial chemistry: Applications in drug discovery": R. Storer, *Drug Discovery Today* **1996**, *1*, 248–254; 3) "Molecular Diversity and Libraries of Structures: Synthesis and Screening": M. Rinnová, M. Lebl, *Collect. Czech. Chem. Commun.* **1996**, *61*, 171–231; 4) "Combinatorial Organic Synthesis and Phase Separation: Back to the Future": D. P. Curran, *Chemtracts-Org. Chem.* **1996**, *9*, 75–87; 5) "Synthetic Library Techniques. Subjective (Biased and Generic) Thoughts and Views": V. Krchnák, M. Lebl, *Mol. Diversity* **1995**, *1*, 177–182. b) Section 2: 1)"Deconvolution of Combinatorial Libraries for Drug Discovery: Theoretical Comparison of Pooling Strategies": D. A. M. Konings, J. R. Wyatt, D. J. Ecker, S. M. Freier, *J. Med. Chem.* **1996**, *39*, 2710–2719; 2) "Deconvolution of Combinatorial Libraries for Drug Discovery: Experimental Comparison of Pooling Strategies": L. Wilson-Lingardo, P. W. Davis, D. J. Ecker, N. Hébert, O. Acevedo, K. Sprankle, T. Brennan, L. Schwarcz, S. M. Freier, J. R. Wyatt, *J. Med. Chem.* **1996**, *39*, 2720–2726; 3) "Measuring Diversity: Experimental Design of Combinatorial Libraries for Drug Discovery": T. M. Ross, A. B. Reitz, *Chemtracts-Org. Chem.* **1996**, *9*, 110–114; 4) "New Perspectives in Lead Generation II: Evaluating Molecular Diversity": M. J. Ashton, M. C. Jaye, J. S. Mason, *Drug. Discovery Today* **1996**, *1*, 71–78; 5) "Computer-Based Screening of Compound Databases for the Identification of New Leads": P. W. Finn, J. S. Mason, *Drug. Discovery Today* **1996**, *1*, 363–370; 6) "Neighborhood Behavior: A Useful Concept for Validation of "Molecular Diversity" Descriptors": D. E. Patterson, R. D. Cramer, A. M. Ferguson, R. D. Clark, L. E. Weinberger, *J. Med. Chem.* **1996**, *39*, 3049–3059; 7) "Assessing the Ability of Chemical Similarity Measures to Discriminate Between Active and Inactive Compounds": J. S. Delaney, *Mol. Diversity* **1996**, *2*, 217–222; 8) "^{19}F NMR Monitoring of a S_NAr Reaction on Solid Support": M. J. Shapiro, G. Kumaravel, R. C. Petter, R. Beveridge, *Tetrahedron Lett.* **1996**, *37*, 4671–4674; 9) "Magic Angle Spinning NMR: A Valuable Tool for Monitoring the Progress of Reactions in Solid Phase Synthesis": T. Wehler, J. Westman, *Tetrahedron*

Lett. **1996**, *37*, 4771–4774; 10) "Use of Spin Echo Magic Angle Spinning ^{1}H NMR in Reaction Monitoring in Combinatorial Organic Synthesis": R. S. Garigipati, B. Adams, J. L. Adams, S. K. Sarkar, *J. Org. Chem.* **1996**, *61*, 2911–2914; 11) "Use of FT-IR Internal Reflection Spectroscopy in Combinatorial Chemistry": H.-U. Gremlich, S. L. Berets, *Appl. Spectrosc.* **1996**, *50*, 532–536; 12) "Analytical Techniques for Combinatorial Chemistry: Quantitative Infrared Spectroscopic Measurements of Deuterium-Labeled Protecting Groups": K. Russell, D. C. Cole, F. M. McLaren, D. E. Pivonka, *J. Am. Chem. Soc.* **1996**, *118*, 7941–7945. c) Section 3: 1) "Solution and Solid Phase Synthesis of 5-Alkoxyhydantoin Libraries with a Three-Fold Functional Diversity": S. Hanessian, R.-Y. Yang, *Tetrahedron Lett.* **1996**, *37*, 5835–5838; 2) "A Convenient Procedure for the Solution Phase Preparation of 2-Aminothiazole Combinatorial Libraries": N. Bailey, A. W. Dean, D. B. Judd, D. Middlemiss, R. Storer, S. P. Watson, *Bioorg. Med. Chem. Lett.* **1996**, *6*, 1409–1414; 3) "Parallel Compound Synthesis: Methodology for Accelerating Drug Discovery": C. N. Selway, N. K. Terrett, *Bioorg. Med. Chem.* **1996**, *4*, 645–654; 4) "Solution Phase Generation of Tetraurea Libraries": G. W. Shipps, Jr., U. P. Spitz, J. Rebek, Jr., *Bioorg. Med. Chem.* **1996**, *4*, 655–657; 5) "A Solution Phase Strategy for the Synthesis of Chemical Libraries Containing Small Organic Molecules: A Universal and Dipeptide Mimetic Template": S. Cheng, C. M. Tarby, D. D. Comer, J. P. Williams, L. H. Caporale, P. L. Myers, D. L. Boger, *Bioorg. Med. Chem.* **1996**, *4*, 727–737. d) Section 4: 1) "A Linker That Allows Efficient Formation of Aliphatic C-H Bonds on Polymeric Support": K. W. Jung, X. Zhao, K. Janda, *Tetrahedron Lett.* **1996**, *37*, 6491–6494; 2) "Synthesis and Photolysis Properties of a Photolabile Linker Based on 3′-Methoxybenzoin": R. S. Rock, S. I. Chan, *J. Org. Chem.* **1996**, *61*, 1526–1529; 3) "A New Linker for Primary Amines Applicable to Combinatorial Approaches": W. Bannwarth, J. Huebscher, R. Barner, *Bioorg. Med. Chem. Lett.* **1996**, *6*, 1525–1528; 4) "A Universal Allyl Linker for Solid-Phase Synthesis": X. Zhang, R. A. Jones, *Tetrahedron Lett.* **1996**, *37*, 3789–3790; 5) "Facile Synthesis of an *o*-Nitrobenzyl Photolabile Linker for Combinatorial Chemistry": S. J. Teague, *Tetrahedron Lett.* **1996**, *37*, 5751–5754; 6) "The Impact of Polystyrene Resins in Solid-Phase Synthesis": A. A. MacDonald, S. H. DeWitt, S. Ghosh, E. M. Hogan, L. Kieras, A. W. Czarnik, R. Ramage, *Mol. Diversity* **1996**, *2*, 183–186; 7) "POEPOP and POEPS: Inert Polyethylene Glycol Crosslinked Polymeric Supports for Solid Synthesis": M. Renil, M. Meldal, *Tetrahedron Lett.* **1996**, *37*, 6185–6188; 8) "CLEAR: A Novel Family of Highly Cross-Linked Polymeric Supports for Solid-Phase Peptide Synthesis": M. Kempe, G. Barany, *J. Am. Chem. Soc.* **1996**, *118*, 7083–7093; 9) "The Solid-Phase Part of Supported Small-Molecule Synthesis": M. J. Kurth, *Chimia* **1996**, *50*, 261–266; 10) "Solid-Phase Synthesis of 1,3-Dialkyl Quinazoline-2,4-Diones": B. O. Buckman, R. Mohan, *Tetrahedron Lett.* **1996**, *37*, 4439–4442; 11) "Approaches to Combinatorial Synthesis of Heterocycles: Solid Phase Synthesis of Pyridines and Pyrido[2,3-d]pyrimidines": M. F. Gordeev, D. V. Patel, J. Wu, E. M. Gordon, *Tetrahedron Lett.* **1996**, *37*, 4643–4646; 12) "An Efficient Solid Phase Synthetic Route to 1,3-Disubstituted 2,4(1*H*, 3*H*)-Quinazolinediones Suitable for Combinatorial Synthesis": A. L. Smith, C. G. Thomson, P. D. Leeson, *Bioorg. Med. Chem. Lett.* **1996**, *6*, 1483–1486; 13) "Bifunctional Scaffolds as Templates for Synthetic Combinatorial Libraries": V. Krchnák, A. S. Weichsel, O. Issakova, K. S. Lam, M. Lebl, *Mol. Diversity* **1995**, *1*, 177–182; 14) "Solid Phase Synthesis of Benzimidazoles": G. B. Phillips, G. P. Wei, *Tetrahedron Lett.* **1996**, *37*, 4887–4890; 15) "Ruthenium-catalyzed Metathesis of Polymerbound Olefins": M. Schuster, J. Pernerstorfer, S. Blechert, *Angew. Chem.* **1996**, *108*, 2111–2112; *Angew. Chem. Int. Ed. Engl.* **1996**, *35*, 1979–1980; 16) "The Synthesis of 2-Oxopiperazines by Intramolecular Michael Addition on Solid Support": D. A. Goff, R. N. Zuckermann, *Tetrahedron Lett.* **1996**, *37*, 6247–6250; 17) "Combinatorial Method for the Synthesis of α-Hydroxy Phosphonates on Wang Resin": X. Cao, A. M. M. Mjalli, *Tetrahedron Lett.* **1996**, *37*, 6073–6076; 18) "Solid Phase Reductive Alkylation of Secondary Amines": N. M. Khan, V. Arumugam, S. Balasubramanian, *Tetrahedron Lett.* **1996**, *37*, 4819–4822; 19) "A Structure-Based Library Approach to Kinase Inhibitors": T. C. Norman, N. S. Gray, J. T. Koh, P. G. Schultz, *J. Am. Chem. Soc.* **1996**, *118*, 7030–7431; 20) "Solid-Phase Synthesis of 5,6-Dihydropyrimidine-2,4-diones": S. A Kolodziej, B. C. Hamper, *Tetrahedron Lett.* **1996**, *37*, 5277–5280; 21) "Combinatorial Modification of Natural Products: Preparation of Unencoced and Encoded Libraries of *Rauwolfia* Alkaloids": A. Atuegbu, D. Maclean, C. Nguyen, E. M. Gordon, J. W. Jacobs, *Bioorg. Med. Chem.* **1996**, *4*, 1097–1106; 22) "Synthesis of Tetrasubstituted Ethylenes on Solid Support via Resin Capture": S. D. Brown, R. W. Armstrong, *J. Am. Chem. Soc.* **1996**, *118*, 6331–6332; 23) "Fischer Indole Synthesis on a Solid Support": S. M. Hutchins, K. T. Chapman, *Tetrahedron Lett.* **1996**, *37*, 4869–4872; 24) "Solid Phase Synthesis of Tetrahydroisoquinolines and Tetrahydroimidazopyridines": S. M. Hutchins, K. T. Chapman, *Tetrahedron Lett.* **1996**, *37*, 4865–4868; 25) "A Combinatorial Method for the Solid Phase Synthesis of α-Amino Phosphonates and Phosphonic Acids": C. Zhang, A. M. M. Mjalli, *Tetrahedron Lett.* **1996**, *37*, 5457–5460; 26) "The Use of Anion Exchange Resins for the Synthesis of Combinatorial Libraries Containing Aryl and Heteroaryl Ethers": J. J. Parlow, *Tetrahedron Lett.* **1996**, *37*, 5257–5260; 27) "Aryl-Aryl Cross Coupling on a Solid Support using Zinc Organic Reagents and Palladium Catalysts": S. Marquiais, M. Arlt, *Tetrahedron Lett.* **1996**, *37*, 5491–5494; 28) "Pictet-Spengler Reaction on Solid Support": L. Yang, L. Guo, *Tetrahedron Lett.* **1996**, *37*, 5041–5044; 29) "Application of the Pictet-Spengler Reaction In Combinatorial Chemistry": J. P. Mayer, D. Bankaitis-Davis, J. Zhang, G. Beaton, K. Bjergarde, C. M. Andersen, B. A. Goodman, C. J. Herrera, *Tetrahedron Lett.* **1996**, *37*, 5633–5636; 30) "Aldol Reactions on Solid Phase. $Sc(OTf)_3$-Catalyzed Reactions of Polymer Supported Silyl Enol Ethers with Aldehydes Providing Convenient Methods for the Preparation of 1,3-Diol, β-Hydroxy Carboxylic Acid and β-Hydroxy Aldehyde Libraries": S. Kobayashi, I. Hachiya, M. Yasuda, *Tetrahedron Lett.* **1996**, *37*, 5569–5572; 31) "A Solid Phase Synthesis of Miconazole Analogs via an Iodoetherification Reaction": D. R. Tortolani, S. A. Biller, *Tetrahedron Lett.* **1996**, *37*, 5687–5690; 32) "Solid Phase Suzuki Coupling for C-C Bond Formation": J. W. Guiles, S. G. Johnson, W. V. Murray, *J. Org. Chem.* **1996**, *61*, 5169–5171; 33) "Solid-Phase Synthesis of Proline Analogs via a Three Component 1,3-Dipolar Cycloaddition": B. C. Hamper, D. R. Dukesherer, M. S. South, *Tetrahedron Lett.* **1996**, *37*, 3671–3674; 34) "Pictet-Spengler Reaction on Solid Support: Synthesis of 1,2,3,4-Tetrahydro-β-Carboline Libraries": R. Mohan, Y.-L. Chou, M. M. Morissey, *Tetrahedron Lett.* **1996**, *37*, 3963–3966; 35) "Solid-Phase Synthesis of Substituted 3-Aminothiophenes and 2-Methylene-2,3-dihydrothiazoles": F. Zaragoza, *Tetrahedron Lett.* **1996**, *37*, 6213–6216; 36) "Consideration of Solid Phase Synthesis with Reference to Quinolone Antibiotics": A. A. MacDonald, S. H. DeWitt, R. Ramage, *Chimia* **1996**, *50*, 258–260; 37) "Palladium-Mediated Three-Component Coupling Strategy for the Solid-Phase Synthesis of Tropane Derivatives": J. S. Koh, J. A. Ellman, *J. Org. Chem.* **1996**, *61*, 4494–4495; 38) "The Design and Synthesis of Substituted Biphenyl Libraries": M. R. Pavia, M. P. Cohen, G. J. Dillay, G. R. Dubuc, T. L. Durgin, F. W. Forman, M. E. Hediger, G. Milot, T. S. Powers, I. Sucholeiki, S. Zhou, D. G. Hangauer, *Bioorg. Med. Chem.* **1996**, *4*, 1097–1106; 39) "Structurally Homogenous and Heterogenous Synthetic Combinatorial Libraries": V. Krchnák, A. S. Weichsel, O. Issakova, K. S. Lam, M. Lebl, *Mol. Diversity* **1996**, *2*, 149–164; 40) "Discovery of a Herbicidal Lead Using Polymer-Bound Activated Esters in Generating A Combinatorial Library": J. J. Parlow, J. E. Normansell, *Mol. Diversity* **1996**, *2*, 266–269; 41) "Library Generation through Successive Substitution of Trichlorotriazines": M. Stankova, M. Lebl, *Mol. Diversity* **1996**, *2*, in press. d) Section 5: 1) "Microautoradiographic Identification of Receptor-Ligand Interactions in Bead-Supported Combinatorial Libraries": H. P. Nestler, H. Wennemers, R. Sherlock, D. L.-Y. Dong, *Bioorg. Med. Chem. Lett.* **1996**, *6*, 1327–1330; 2) "Screening Derivatized Peptide Libraries for Tight Binding Inhibitors to Carbonic Anhydrase II by Electrospray Ionization-Mass Spectrometry": J. Gao, X. Cheng, R. Chen, G. B. Sogal, J. E. Bruce, B. L. Schwartz, S. A. Hofstadler, G. A. Anderson, R. D. Smith, G. M. Whitesides, *J. Med. Chem.* **1996**, 39, 1949–1955; 3) "Affinity Capillary Electrophoresis-Mass Spectrometry for Screening Combinatorial Libraries": Y.-H. Chu, Y. M. Dunayevskiy, D. P. Kirby, P. Vouros, B. L. Karger, *J. Am. Chem. Soc.* **1996**, *118*, 7827–7835; 4) "Microchip Encoded Combinatorial Libraries: Generation of a Spatially Encoded Library from a Pool Synthesis": R. W. Armstrong, P. A. Tempest, J. F. Cargill, *Chimia* **1996**, *50*, 258–260. e) Section 6: 1) "Automating Combinatorial Chemistry: A Primer on Benchtop Robotic Systems": J. H. Hardin, F. R. Smietana, *Mol. Diversity* **1996**, *2*, 270–274. f) Section 8: 1) "The Discovery of Chiral Catalysts through Ligand Diversity: Ti-Catalyzed Enantioselective Addition of TMSCN to *meso* Epoxides": B. M. Cole, K. D. Shimizu, C. A. Krueger, J. P. A. Harrity, M. L. Snapper, A. H. Hoveyda, *Angew. Chem.* **1996**, *108*, 1776–1779; *Angew. Chem. Int. Ed. Engl.* **1996**, *35*, 1668–1671; 2) "The Combinatorial Synthesis of Chiral Phosphine Ligands": S. R. Gilbertson, X. Wang, *Tetrahedron Lett.* **1996**, *37*, 6475–6478.

Solid-State Chemistry: Restoring the Balance**

R. Schöllhorn*

Chemistry as a subject in science has two well-defined faces: a *static* face pertaining to the determination and description of the properties of a given material in terms of geometrical structure, electronic structure, chemical bonding, and physical properties, and a *dynamic* face describing any kind of time-dependent structural, compositional, or electronic reorganization in materials, in particular the *reactivity* as a functional property of chemical systems. In the area of solid-state and materials chemistry considerable progress has been achieved in the understanding of correlations between structure, bonding, and physical properties. However, understanding of the most important relationship between these static parameters and the dynamic aspects—the reactivity of solids—is far less developed.

This can be illustrated easily by analyzing (in a simplified fashion) the conventional art of synthesis in solid-state chemistry. Although synthesis is clearly an aspect of the dynamic face of chemistry, it is in fact performed essentially as a static game. If we consider the typical procedure [Eq. (a)], we find that the starting materials **A** and **B**, whose static properties are well-

$$\mathbf{A} + \mathbf{B} \longrightarrow \boxed{\text{"black box"}} \longrightarrow \mathbf{C} \qquad \text{(a)}$$

defined, are subject to certain experimental conditions based upon a combination of valuable practical experience, qualitative guidelines, intuition, and chance. This step is followed usually by a thorough examination and characterization of the static properties of the new product **C** in terms of averaged geometrical structure, chemical bonding, physical properties, and its relationship to related known materials. The next synthetic step then follows based in part upon the results of the previous experiment. The essential point here is that as a rule the "black box" located between **A**/**B** and **C** hiding the *dynamic* aspects of the chemistry involved, in other words the reaction mechanism, is not "opened" for good reasons.

The intelligent synthesis of new materials is without doubt a necessary and highly valuable task and a major source of innovation in solid-state and materials chemistry. Rational synthesis planning and modeling—essential aspects of molecular chemistry—are unfortunately hardly developed in this area with the exception of some specific domains.[1–6] In recent years "tailoring of materials" has become a fashionable term in solid-state chemistry and materials science. This promising expression suggests the existence of a predictive approach which does certainly not agree, however, with the actual reality and creates unjustified expectations about our present potential. We need to emphasize here the simple fact that without an appropriate knowledge of the contents of the "black box," that is, without a systematic investigation of *reaction mechanisms*, this ambitious goal clearly cannot be realized.

At this point we have to return to the statement made previously, that as a rule investigators avoid "opening the black box". This reality can be readily explained.

1. Most solid-state reaction mechanisms are rather complex, involving types of properties not usually found in molecular systems, for example collective behavior of solids, existence of structure-specific extended defects, and interface phenomena.
2. The detailed investigation of a single reaction mechanism in solid-state systems requires particular efforts in terms of manpower and time (frequently on the order of a decade); a combination of a large variety of specific preparative and analytical methods is frequently necessary in order to collect (mostly indirect) evidence and verify models.
3. The field is thus not attractive for younger scientists, who need rapid success to gain tenure in academic institutions and simultaneously will encounter problems in funding long-term projects under current policies in research funding. The natural trend will therefore favor synthesis-oriented short-term research projects.
4. As a consequence only a relatively small number of research groups work actively and systematically in this field, and in turn limited academic teaching staff serve to educate and motivate young scientists in this area.[6, 7]

The following paradoxical situation results: a research area representing one fundamental aspect of solid-state and materials chemistry, which is urgently required for the continued development of rational and economic synthesis strategies, has become necessarily neglected, in part for tactical reasons. We should agree that the time has come to make a serious effort to restore the balance.

German version: *Angew. Chem.* **1996**, *108*, 2493–2494

Keywords: materials science · solid-state chemistry

[*] Prof. Dr. R. Schöllhorn
Institut für Anorganische und Analytische Chemie
der Technischen Universität
Strasse des 17. Juni 135, D-10623 Berlin (Germany)
Fax: Int. code +(30)314-21106
e-mail: schoe@wap0209.chem.tu-berlin.de

[**] The topic "Synthesis Planning in Solid-State Chemistry" was recently addressed: J. C. Schön, M. Jansen, *Angew. Chem.* **1996**, *108*, 1358; *Angew. Chem. Int. Ed. Engl.* **1996**, *35*, 1286.

[1] H. Schäfer, *Angew. Chem.* **1971**, *83*, 35; *Angew. Chem. Int. Ed. Engl.* **1971**, *10*, 43.
[2] F. J. DiSalvo, *Science* **1990**, *247*, 649.
[3] G. D. Stucky, *Prog. Inorg. Chem.* **1992**, *40*, 99.
[4] A. K. Cheetham, *Science* **1994**, *264*, 794.
[5] R. Schlögl, *Angew. Chem.* **1994**, *106*, 319; *Angew. Chem. Int. Ed. Engl.* **1994**, *33*, 311.
[6] A. W. Sleight, *MRS Bull.* **1989**, *14*(9), 5.
[7] V. Boldyrev, *Adv. Mater.* **1992**, *4*, 70.

Asymmetric Two-Center Catalysis—Learning from Nature

Henning Steinhagen and Günter Helmchen*

Many catalytic systems contain one reaction center in a suitable ligand environment. During catalysis one reactant is bound to, oriented, and possibly activated by this center in such a way that another reactant can attack selectively and the product is formed. Also commonly encountered are systems in which several reactants are bound to one reaction center, usually a transition metal ion, and due to their positioning they react fast and selectively. We want to point out a new and very effective principle that has not yet been studied very thoroughly: two-center catalysis.[1] In this case the reactants are bound and oriented at two different centers, which often results in both high selectivity and reactivity. This principle will be illustrated here both with recent developments and results and with well-known examples.

Urease, an enzyme for the hydrolysis of urea, provides a clear example of the principle of two-center catalysis. In 1995 Jabri and co-workers obtained an X-ray crystal stucture at 2.2 Å resolution of the urease from *Klebsiella aerogenes*[2] on which Lippard based a mechanistic model[3] (Scheme 1). The two nickel ions participating in catalysis are bridged and placed into juxtaposition by an N-carboxylated lysine (Ni–Ni distance = 3.5 Å). The entering urea substrate is bound through its carbonyl group and spatially oriented by one of the Lewis-acidic nickel centers in such a way that a hydroxide ion from the second nickel center can be added very efficiently to the carbonyl carbon. Deprotonation of the H_2O coordinated to nickel is effected by an adjacent basic histidine side chain. The resultant carbamic acid dissociates into CO_2 and NH_3, which is essential for the bacterium. As a result of the cooperative effect of the two nickel centers, the reaction rate of the hydrolysis of urea with OH^- is enhanced by a factor of 10^{14}! An analogous principle is used by the carbonylating enzyme carbon monoxide dehydrogenase (CODH). Ragsdale et al. proved both a methyl–nickel and an iron–carbon monoxide unit by resonance Raman spectroscopy in carbon monoxide dehydrogenase from *Clostridium thermoaceticum*.[4] The formation of the acetyl–metal unit probably takes place by insertion of CO into the $Ni-CH_3$ bond.

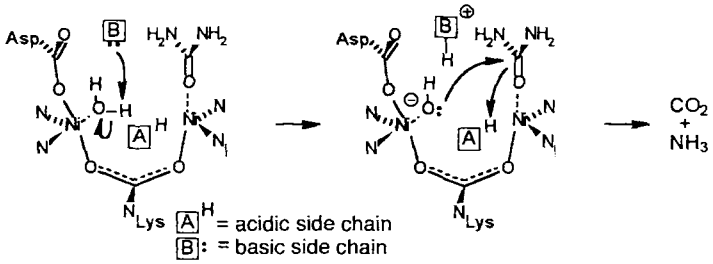

Scheme 1. Mechanism of two-center catalysis in the hydrolysis of urea by the urease enzyme of *Klebsiella aerogenes* (according to Lippard [3]); the nitrogen atoms coordinated to nickel stem from histidine. In all schemes only some of the charges are given.

A biomimetic model system for amide hydrolysis on the basis of two Cu^{2+} centers was reported by Karlin et al. in 1993.[5] Here the amide, in the example dimethylformamide, is bound to the carbonyl group and activated by one of the copper centers while a hydroxide ion is transferred by a second copper center (Scheme 2). Hydrolysis of dimethylformamide occurs within a few seconds and, thus, it is much faster than the uncatalyzed reaction, which does not proceed at room temperature.

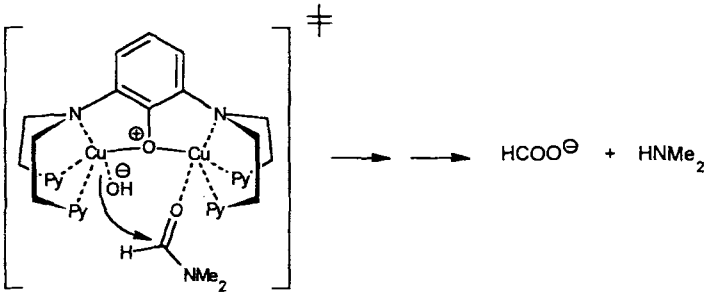

Scheme 2. Biomimetic system for the hydrolysis of amides (according to Karlin et al. [5]).

Over the last few years several examples have been reported in the field of asymmetric catalysis that are based on the interaction of two centers. Recently, the group of Shibasaki reported particularly impressive findings.[6–9] The new catalysts (Scheme 3) consist of a central metal ion (e.g. La^{3+}, Al^{3+}), three alkali metal ions (e.g. Li^+, Na^+, K^+), and three molecules of the chiral diphenol 1,1′-(*R*)- or 1,1′-(*S*)-binaphthol [(*R*)- or (*S*)-binol, respectively]. The catalysts exhibit basic (at the oxygen of M^2-O) as well as Lewis-acidic properties (at M^1 and M^2) and are therefore multifunctional catalysts. The complexes can be prepared easily; they are stable to air and moisture and are nontoxic according to Shibasaki. In addition, binol is easy to recover.[6b] These heterobimetallic M^1-M^2-binol complexes

[*] Prof. Dr. G. Helmchen, Dipl.-Chem. H. Steinhagen
Organisch-chemisches Institut der Universität
Im Neuenheimer Feld 270, D-69120 Heidelberg (Germany)
Fax: Int. code +(6221)54-4205
e-mail: en4@ix.urz.uni-heidelberg.de

 © VCH Verlagsgesellschaft mbH, D-69451 Weinheim, 1996 0570-0833/96/3520-2339 $ 15.00+.25/0

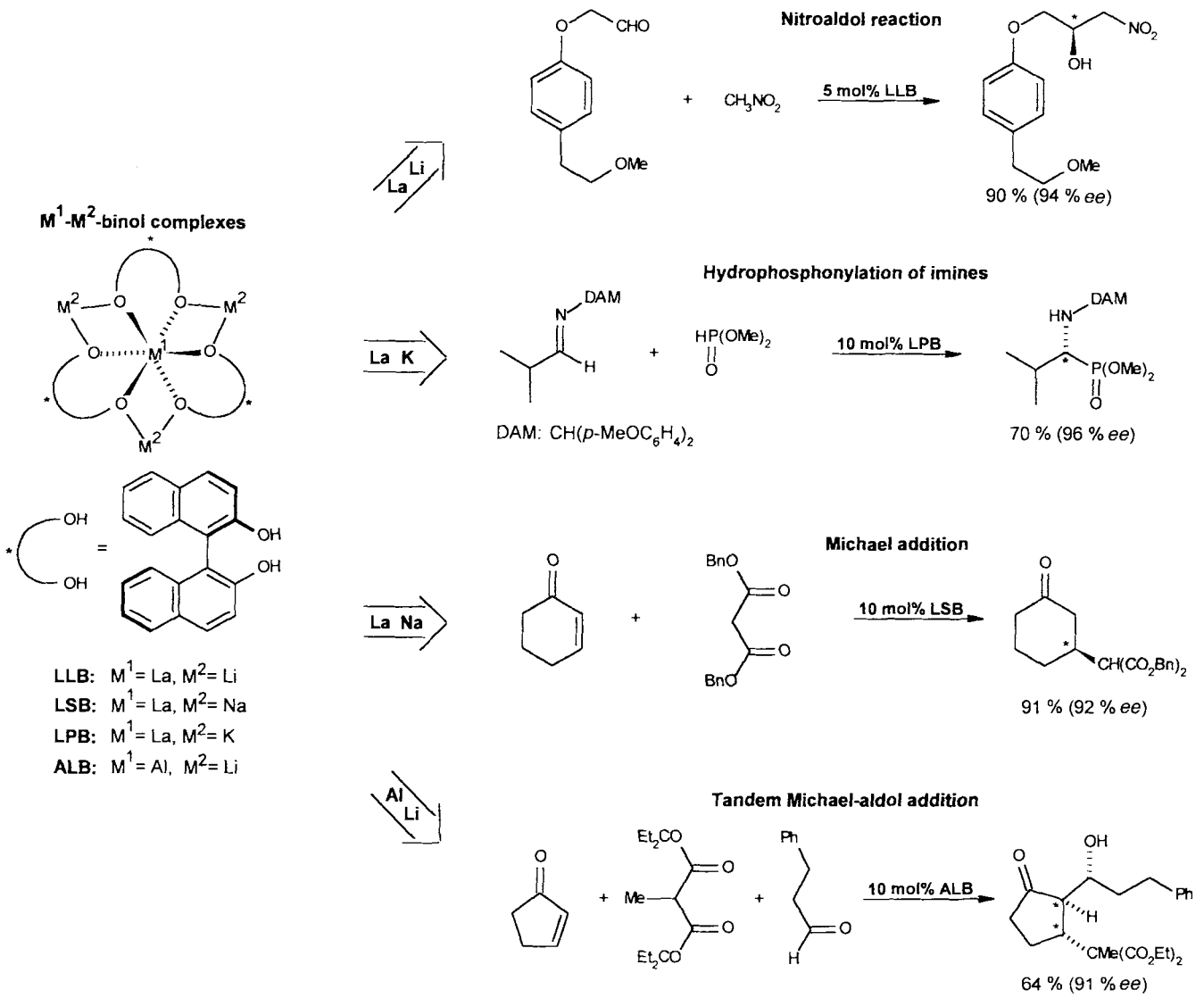

Scheme 3. Results of various reactions with specific M^1-M^2-binol complexes as catalysts (according to Shibasaki et al. [6–9]).

constitute a new class of widely applicable and versatile chiral catalysts. By careful choice of the metal centers, organic transformations of widely differing types can be catalyzed (Scheme 3).

The investigations of the Shibasaki group began with the asymmetric nitroaldol reaction.[6] When the La–Li–(*R*)-binol complex (**LLB**) was used as a catalyst, up to 94% *ee* and 90% yield were achieved[6e] (Scheme 3). By using a 6,6′-bis((trialkylsilyl)ethynyl)-substituted (*R*)-binol in the reaction of aldehydes with 2-nitroethanol, they even raised the enantiomeric excess to 97% and the yield to 97%.[6h] The nitroaldol reaction according to Shibasaki was applied both in the synthesis of the β-receptor blocking drugs (*S*)-Metoprolol,[6d] (*S*)-Pindolol,[6g] and (*S*)-Propanolol,[6c] and in the synthesis of phenylnorstatine, a building block used in the synthesis of the HIV protease inhibitor KNI-272.[6f]

Another reaction that can be catalyzed by metal–binol complexes is the asymmetric hydrophosphonylation of imines[8a] and aldehydes.[8b] This reaction is of great interest, because the products, α-amino- and α-hydroxyphosphonic acids, are potentially useful as enzyme inhibitors.[10] With the lanthanum–potassium–(*R*)-binol complex (**LPB**), it was possible to achieve enantiomeric excesses of up to 96% with yields of at most 70%[8a] (Scheme 3).

In search of further reactions that can be catalyzed by metal–binol complexes the Shibasaki group reported in 1994 the highest known enantiomeric excesses (95% *ee*, quantitative yield) for the catalytic asymmetric Michael addition.[7] In this case, not only the La–Na–(*R*)-binol complex (**LSB**) was an effective catalyst, but also the alkali-free La–(*S*)-binol complex (**LB**) (Scheme 3). The latest and most impressive discovery is a catalytic tandem Michael–aldol addition to cyclopentenones (Schemes 3, 4).[9] By varying the metals in the M^1-M^2-binol complexes, optimal conditions were found under which this multistep reaction proceeds with high selectivity (91% *ee*) and acceptable yield (64%). With regards to synthetic strategy, this reaction is a catalytic variant of a three-component coupling reaction developed in 1985 by Noyori et al. for the synthesis of prostaglandins.[11]

The mechanism according to Shibasaki (Scheme 4) clearly shows the different functions of the two metal centers in the Al–Li–(*R*)-binol complex (**ALB**) during catalysis. The nucleo-

 © VCH Verlagsgesellschaft mbH, D-69451 Weinheim, 1996 0570-0833/96/3520-2340 $ 15.00+.25/0

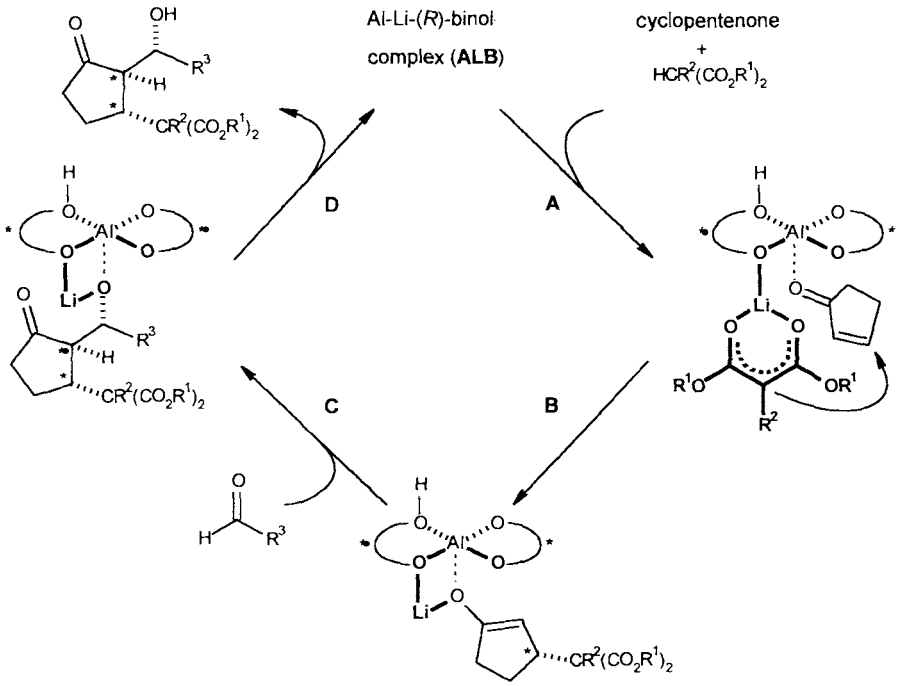

Scheme 4. Postulated catalytic cycle for the tandem Michael–aldol addition (according to Shibasaki et al. [9]).

phile to be transferred, malonate, is probably formed at the catalyst by deprotonation and is positioned by means of a Li bridge at the complex (**A**). In addition, cyclopentenone is bound and oriented at the Lewis-acidic Al^{3+} center. In the next step, the nucleophile attacks the substrate with enantioface-differentiation (**B**). The resultant enolate remains bound and positioned at the catalyst so that the subsequent aldol reaction (**C**) proceeds with both high selectivity and yield. Subsequently the products dissociate and new **ALB** enters the catalytic cycle (**D**). This system can be considered a "chemzyme" (*chem*ical en*zyme*)[12].

The catalysts developed by the Shibasaki group represent only one of several possible types of two-center catalysis. This is illustrated by the following classification (Scheme 5). The previously described systems belong to a particular class of the two-center catalysts (**A**) in which two Lewis-acidic centers (Z_a, Z_b) such as metal ions are available for binding after each catalytic cycle.[13] A second class (**B**) consists of catalysts that provide a Lewis-acidic (Z_a) as well as a Lewis-basic center (X). A second Lewis-acidic center (Z_b) is supplied by a reactant and appears in the product formed (see examples in Scheme 6).

In 1987 Corey, Bakshi, and Shibata introduced a very effective catalytic system for the reduction of prochiral ketones[12] based on the work of Itsuno. With oxazaborolidines as catalysts it is possible to obtain products with enantiomeric excesses of up to 99%. In this system the endocyclic, Lewis-acidic boron center B_a binds the carbonyl compound. The center atom B_b is provided by the stoichiometrically used reductant BH_3 and remains in the reaction product. With respect to two-center catalysis, B_a corresponds to the center Z_a; the second center is given by a Lewis-basic nitrogen to which the reactant BH_3 (Z_b) is bound (Scheme 6). In connection with this catalytic system terms like "molecular robot" and "chemzyme" were introduced.

On the basis of a discovery by Oguni et al.,[14] Noyori and co-workers were able to achieve enantiomeric excesses of up to 99% with chiral amino alcohols as ligands in the enantioselective addition of organozinc compounds to prochiral aldehydes (Scheme 6).[15] Again, only one metal ion (Zn_a) remains in the catalytic cycle; the second one is provided by the stoichiometrically added R_2Zn and replaced after each cycle. Thus, the two centers essential for the two-center catalysis are Zn_a and the endocyclic oxygen atom.

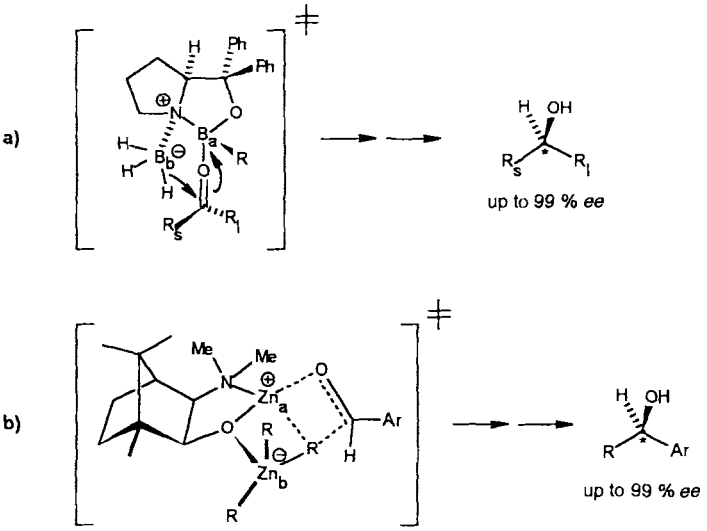

Scheme 6. Examples of two-center catalysis of type **B**: a) enantioselective reduction of prochiral ketones (according to Corey et al. [12]); b) enantioselective addition of R_2Zn to aldehydes (according to Noyori et al. [15]).

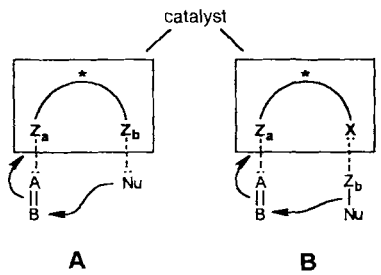

Scheme 5. Classification of two-center catalysts; A=B, Nu: reactants; Z_a, Z_b: Lewis-acidic centers; X: Lewis-basic centers.

The classification presented here should be regarded as a proposal, because with the relatively few examples available, setting up a final classification would be premature. This may be illustrated by an example taken from the copper-catalyzed 1,4-addition of Grignard reagents to α,β-unsaturated carbonyl compounds[16] (Scheme 7). Although the reaction seems to demonstrate two-center catalysis at first glance, it is a borderline

 © VCH Verlagsgesellschaft mbH, D-69451 Weinheim, 1996 0570-0833/96/3520-2341 $ 15.00+.25/0

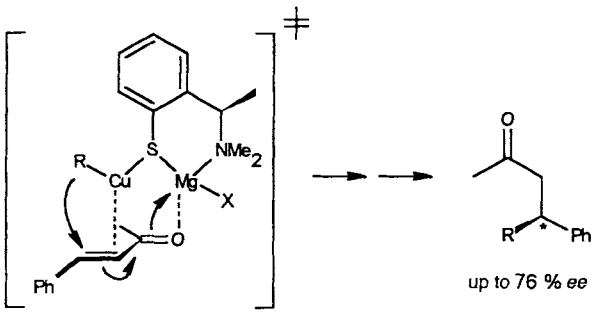

Scheme 7. Enantioselective 1,4-addition of RMgX to enones (according to van Koten et al. [16a]).

case. The enone is bound to the Cu^+ center through its double bond and also to the Mg^{2+} center through the carbonyl oxygen. The nucleophile is tranferred from the Cu^+ center. If one regards bonding and activation of the enone at the Mg^{2+} center as essential for catalysis, then the example would demonstrate two-center catalysis in the sense we have discussed. However, if one considers the Mg^{2+} center to take part only in spatial positioning and not in activation, the reaction would not be an example of two-center catalysis because both reactants are essentially attached to the Cu^+ center. This example shows the limits and the formal character of the classification because the real interactions during catalysis can often not be assessed precisely. In connection with this topic we would like to refer to hydrogenation catalysts developed by the groups of Jacobsen and Kagan, which contain a Rh^+ and a second Lewis-acidic center for additional positioning of a reactant.[17] These examples do not fit into the category of two-center catalysts as described above.

The catalytic systems and mechanisms described demonstrate the usefulness of two-center catalysis. Many, if not all of the examples were discovered empirically rather than rationally designed. In future it will be helpful to learn more about the principle of two-center catalysis and to consider it in the design of new catalytic systems. As a result the proposed classification will likely be enlarged and refined.

German version: *Angew. Chem.* **1996**, *108*, 2489–2492

Keywords: asymmetric syntheses · catalysis · chemzymes · synthetic methods · two-center catalysis

[1] In the literature terms like bimetallic catalysts, dinuclear catalysts, heterobimetallic complexes, and chemzyme are also used in connection with the term two-center catalysis.
[2] E. Jabri, M. B. Carr, R. P. Hausinger, P. A. Karplus, *Science* **1995**, *268*, 998–1004.
[3] S. J. Lippard, *Science* **1995**, *268*, 996–997; for further examples see: N. Sträter, W. N. Lipscomb, T. Klabunde, B. Krebs, *Angew. Chem.* **1996**, *108*, 2158–2191; *Angew. Chem. Int. Ed. Engl.* **1996**, *35*, 2024–2055.
[4] M. Kumar, D. Qiu, T. G. Spiro, S. W. Ragsdale, *Science* **1995**, *270*, 628–630.
[5] a) K. D. Karlin, *Science* **1993**, *261*, 701–708; b) N. N. Murthy, M. Mahroof-Tahir, K. D. Karlin, *J. Am. Chem. Soc.* **1993**, *115*, 10404–10405; c) M. W. Göbel, *Angew. Chem.* **1994**, *106*, 1201–1203; *Angew. Chem. Int. Ed. Engl.* **1994**, *33*, 1141.
[6] a) H. Sasai, T. Suzuki, S. Arai, T. Arai, M. Shibasaki, *J. Am. Chem. Soc.* **1992**, *114*, 4418–4420; b) H. Sasai, T. Suzuki, N. Ito, M. Shibasaki, *Tetrahedron Lett.* **1993**, *34*, 851–854; c) H. Sasai, N. Ito, T. Suzuki, M. Shibasaki, *ibid.* **1993**, *34*, 855–858; d) H. Sasai, T. Suzuki, N. Ito, S. Arai, M. Shibasaki, *ibid.* **1993**, *34*, 2657–2660; e) H. Sasai, T. Suzuki, N. Ito, K. Tanaka, T. Date, K. Okamura, M. Shibasaki, *J. Am. Chem. Soc.* **1993**, *115*, 10372–10373; f) H. Sasai, W.-S. Kim, T. Suzuki, M. Shibasaki, M. Mitsuda, J. Hasegawa, T. Ohashi, *Tetrahedron Lett.* **1994**, *35*, 6123–6126; g) H. Sasai, Y. M. A. Yamada, T. Suzuki, M. Shibasaki, *Tetrahedron* **1994**, *50*, 12313–12318; h) H. Sasai, T. Tokunaga, S. Watanabe, T. Suzuki, N. Ito, M. Shibasaki, *J. Org. Chem.* **1995**, *60*, 7388–7389; T. Arai, Y. M. A. Yamada, N. Yamamoto, H. Sasai, M. Shibasaki, *Chem. Eur. J.* **1996**, *2*, 1368.
[7] a) H. Sasai, T. Arai, M. Shibasaki, *J. Am. Chem. Soc.* **1994**, *116*, 1571–1572; b) H. Sasai, T. Arai, Y. Satow, K. N. Houk, M. Shibasaki, *ibid.* **1995**, *117*, 6194–6198.
[8] a) H. Sasai, S. Arai, Y. Tahara, M. Shibasaki, *J. Org. Chem.* **1995**, *60*, 6656–6657; b) T. Arai, M. Bougauchi, H. Sasai, M. Shibasaki, *ibid.* **1996**, *61*, 2926–2927.
[9] A. Takayoshi, H. Sasai, K.-I. Aoe, K. Okamura, T. Date, M. Shibasaki, *Angew. Chem.* **1996**, *108*, 103–105; *Angew. Chem. Int. Ed. Engl.* **1996**, *35*, 104.
[10] Review: P. Kafarski, B. Lejczak, *Phosphorus, Sulfur Silicon Relat. Elem.* **1991**, *63*, 193–215.
[11] a) R. Noyori, M. Suzuki, *Angew. Chem.* **1984**, *96*, 854–882; *Angew. Chem. Int. Ed. Engl.* **1984**, *23*, 847; b) M. Suzuki, A. Yanagisawa, R. Noyori, *J. Am. Chem. Soc.* **1985**, *107*, 3348–3349; c) *ibid.* **1988**, *110*, 4718–4726.
[12] a) E. J. Corey, R. K. Bakshi, S. Shibata, *J. Am. Chem. Soc.* **1987**, *109*, 5551–5553; b) E. J. Corey, R. K. Bakshi, S. Shibata, C.-P. Chen, V. K. Singh, *ibid.* **1987**, *109*, 7925–7926.
[13] Strictly speaking, also systems in which hydrogen or the heteroatom of a OH or NH_2 group functions as a participating center belong to this category; for examples of catalysts relying on this type of secondary ligand–substrate interactions see: M. Sawamura, Y. Ito, *Chem. Rev.* **1992**, *92*, 857–871.
[14] N. Oguni, T. Omi, Y. Yamamoto, A. Nakamura, *Chem. Lett.* **1983**, 841–842.
[15] a) R. Noyori, M. Kitamura, *Angew. Chem.* **1991**, *103*, 34–55; *Angew. Chem. Int. Ed. Engl.* **1991**, *30*, 49; b) M. Kitamura, S. Suga, M. Niwa, R. Noyori, *J. Am. Chem. Soc.* **1995**, *117*, 4832–4842.
[16] a) G. van Koten, *Pure Appl. Chem.* **1994**, *7*, 1455–1462; b) Q.-L. Zhou, A. Pfaltz, *Tetrahedron* **1994**, *50*, 4467–4478; c) Review: B. E. Rossiter, N. M. Swingle, *Chem. Rev.* **1992**, *92*, 771–806.
[17] a) A. Börner, J. Ward, K. Kortus, H. B. Kagan, *Tetrahedron: Asymmetry* **1993**, *4*, 2219–2228; b) L. B. Fields, E. N. Jacobsen, *ibid.* **1993**, *4*, 2229–2240.

 © VCH Verlagsgesellschaft mbH, D-69451 Weinheim, 1996 0570-0833/96/3520-2342 $ 15.00+.25/0

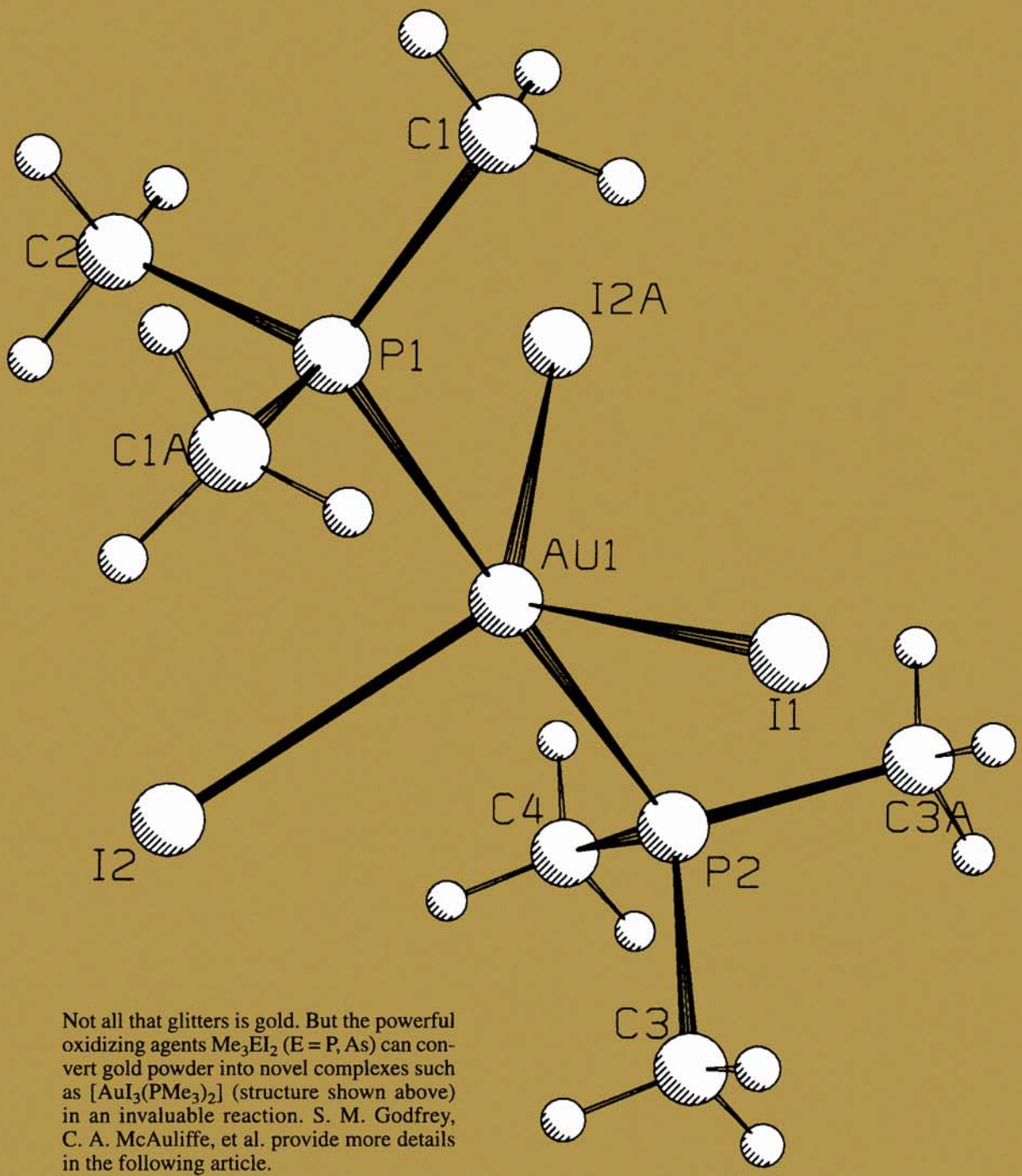

Not all that glitters is gold. But the powerful oxidizing agents Me_3EI_2 (E = P, As) can convert gold powder into novel complexes such as $[AuI_3(PMe_3)_2]$ (structure shown above) in an invaluable reaction. S. M. Godfrey, C. A. McAuliffe, et al. provide more details in the following article.

 © VCH Verlagsgesellschaft mbH, D-69451 Weinheim, 1996 0570-0833/96/3520-2343 $ 15.00+.25/0

The Oxidation of Gold Powder by Me_3EI_2 (E = P, As) under Ambient Conditions; Structures of $[AuI_3(PMe_3)_2]$, $[AuI_3(AsMe_3)]$, and $[(Me_3PO)_2H][AuI_2]$**

Stephen M. Godfrey*, Nicholas Ho,
Charles A. McAuliffe,* and Robin G. Pritchard

Historically, gold has always been considered as the most noble of all metals. It occurs naturally as the elemental metal and, unlike any other metal, is reluctant to form an oxide. Only one oxide of gold is known, Au_2O_3, and even this is unstable, decomposing to produce gold metal at moderately high temperatures (ca. 160 °C).[1] Consequently, to produce gold complexes it is necessary to solubilize the metal, usually by using rather severe reaction conditions, for example treatment with aqua regio and/or cyanide. Clearly, the development of a new reaction route starting with elemental gold to produce gold complexes under ambient conditions in a chemically inert solvent is highly desirable.

We are actively engaged in the development of certain R_3EX_2 compounds (E = P, As, Sb; $S_2 = Br_2$, I_2, IBr) as powerful oxidizing agents towards elemental metals and some zero-valent metal complexes. These compounds are capable of oxidizing crude nickel and cobalt metal powders directly to the +III oxidation state in a one-step reaction.[2-4] In addition to the surprising power of these species as oxidizing agents, their reaction with a variety of metal powders has resulted in the isolation of a number of metal complexes with unusual stoichiometries, for example $[CoI_8(PnBu_3)_3]$,[3] some which would not have been expected to exist according to the hard/soft acid/base theory, for example $[CoI_3(SbPh_3)_2]$.[5] Additionally, novel cationic species such as the linear $[Ph_3As\text{-}I\text{-}I\text{-}I\text{-}AsPh_3]^+$[6] and novel isomeric forms of known compounds, for instance the trigonal-bipyramidal $[MnI_2(PPhMe_2)]$,[2] are also available by this new synthetic route.

The chemistry of gold complexes containing tertiary phosphane ligands has been well studied and is well understood.[7-13] Two types of complex prevail, the linear gold(I) complexes $[R_3PAuX]$[9-13] and the square-planar gold(III) complexes $[R_3PAuX_3]$;[14-20] the latter are almost exclusively produced by the oxidation of a gold(I) complex, $[R_3PAuX]$, by dihalogen, X_2. The use of certain chelating agents can force the gold atom to adopt distorted trigonal-bipyramidal or, more commonly, square-pyramidal coordination geometry[21-25] due to the steric requirements of the ligand; however, no regular trigonal-bipyramidal complexes are known and, all gold(III) complexes known to date in which the ligands have no special steric requirements are square-planar.

In view of the demonstrated oxidizing power of our R_3EX_2 reagents and their versatility, we were intrigued to know if any of these species could oxidize the notoriously noble gold metal and, if this was possible, whether novel complexes could be produced. We thus treated trimethylarsinediiodine with gold metal powder according to Equation (a). The gold(III) complex

$$3\,Me_3AsI_2 + 2\,Au \xrightarrow[\text{ca. } 25\,^\circ C]{N_2,\ \text{ca. } 3\,d} 2[AuI_3(AsMe_3)] + Me_3As \qquad (a)$$

was obtained in quantitative yield; the other reaction product, Me_3As, was identified by ^1H NMR spectroscopy. Recrystallization of the dark green powder from diethyl ether at approximately 0 °C produced black crystals suitable for study by X-ray crystallography. The X-ray crystal structure of $[AuI_3(AsMe_3)]$[26] is shown in Figure 1. The gold center has the square-planar

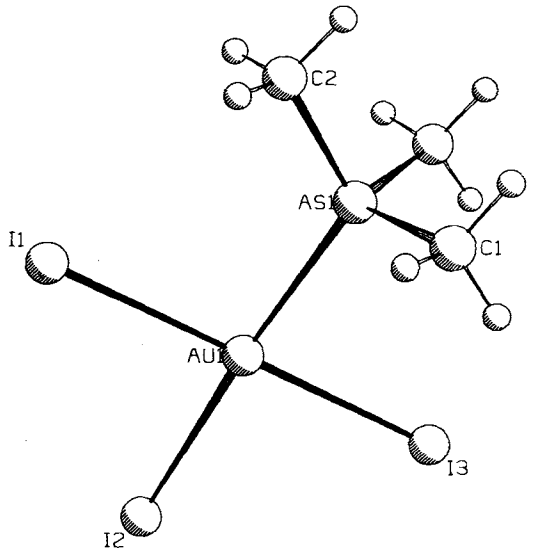

Fig. 1. X-ray crystal structure of $[AuI_3(AsMe_3)]$ (only one of the molecules in the unit cell is shown). Selected bond lengths [Å] and angles [°]: Au1-I1 2.594(7), Au1-I2 2.619(6), Au1-I3 2.651(7), Au2-I4 2.622(7), Au2-I5 2.621(7), Au2-I6 2.635(7), Au1-As1 2.41(1), Au2-As2 2.41(1); I1-Au1-I2 179.9(3), I1-A1-I3 90.0(2), I1-Au1-As1 86.4(3), I3-Au1-As1 176.3(3), I4-Au2-I5 179.8(2), I4-Au2-I6 90.7(2), I4-Au2-As2 92.7(3), I6-Au2-As2 176.6(3).

coordination geometry expected for a d^8 metal center. There are two nonequivalent molecules in the asymmetric unit. Additionally, the structure illustrates the *trans* effect; the iodo ligands that are *trans* to the trimethylarsino ligands are at an appreciably greater distance from the gold atom (2.651(7) and 2.635(7) Å) than the iodo ligands *trans* to another iodide (2.594(7), 2.619(6), 2.622(7) and 2.621(7) Å). Although this phenomenon is more pronounced in one of the molecules in the asymmetric unit than the other, the Au–As bonds for the two molecules (2.41(1) and 2.42(1) Å) are virtually identical.[26,27] These bond lengths are very similar to those found for the only other crystallographically characterized gold complexes containing an Au–As bond, $[AuI_2(diars)_2]I$ (diars = 1,2-phenylenebis(dimethylarsane)) which exhibits Au–As bonds of 2.43(3) and 2.46(2) Å.[28] The UV/Vis spectrum of $[AuI_3(AsMe_3)]$ in diethyl ether exhibits two main peaks at 355 and 621 nm, a profile similar to those of other square-planar gold(III) complexes previously investigated containing tertiary phosphane or amino donor ligands.[17]

In a second reaction Me_3PI_2 was allowed to react with gold metal powder according to Equation (b). The gold(III) complex

$$2\,Me_3PI_2 + Au \xrightarrow[\text{ca. } 25\,^\circ C]{N_2,\ \text{ca. } 3\,d} [AuI_3(PMe_3)_2] + {}^1/_2 I_2 \qquad (b)$$

was obtained in quantitative yield, and the other reaction product, I_2, was detected spectrophotometrically. Recrystallization of the dark blue powder at roughly 0 °C produced deep blue-black crystals suitable for study by X-ray crystallography; the crystal structure of $[AuI_3(PMe_3)_2]$[27] is shown in Figure 2. Remarkably, the gold center has trigonal-bipyramidal geome-

[*] Prof. Dr. C. A. McAuliffe, Dr. S. M. Godfrey, N. Ho, Dr. R. G. Pritchard
Department of Chemistry
University of Manchester Institute of Science and Technology
Manchester M60 1QD (UK)
Fax: Int. code + (161)228-1250

[**] This work has received financial support from the Engineering and Physical Sciences Research Council and Johnson Matthey.

 © VCH Verlagsgesellschaft mbH, D-69451 Weinheim, 1996 0570-0833/96/3520-2344 $ 15.00+.25/0

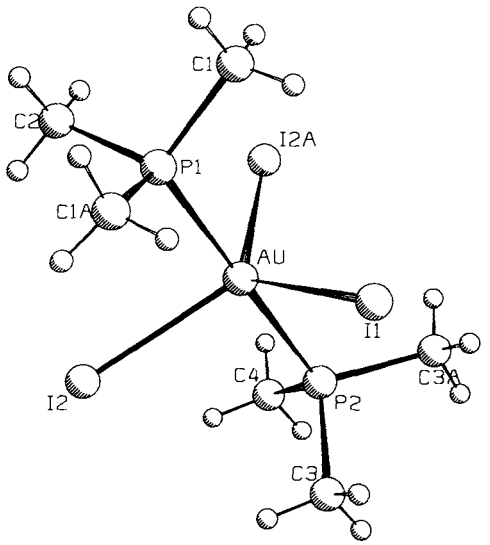

Fig. 2. X-ray crystal structure of $[AuI_3(PMe_3)_2]$. Selected bond lengths [Å] and angles [°]: Au-I1 1.709(3), Au-I2 2.761(2), Au-P1 2.333(9), Au-P2 2.347(8); I1-Au-I2 122.49(4), I1-Au-P1 89.6(2), I1-Au-P2 89.0(2), I2-Au-I2 115.01(9), I2-Au-P1 90.4(1), I2-Au-P2 90.3(1), P1-Au-P2 178.7(3).

try, although the gold(III) center has a d^8 configuration and a square-planar or square-pyramidal geometry would have been expected. This geometry is particularly surprising since there are no steric demands placed upon the gold(III) center by the ligands; in other words, the gold(III) atom is free to adopt the most stable coordination geometry. This, then, is the first trigonal-bipyramidal complex of gold(III) containing ligands that do not impose any steric demands on the metal center, and the first gold(III) complex that does not contain a chelating phosphane ligand but rather two tertiary phoshane ligands per metal center. The fact that gold halides have been treated with many tertiary phosphanes and no complex with this geometry has previously been observed indicates that our novel reaction of Me_3PI_2 with gold powder provides a new mechanistic pathway to gold complexes and thus offers the opportunity to synthesize complexes not accessible by the conventional reaction of gold halides with tertiary phosphanes.

These reactions not only indicate that even gold can be activated and oxidized by the Me_3EI_2 (E = P, As) agents, but also shows that distinctly different products form as a result of quite subtle changes in our reagents: Me_3AsI_2 yields square-planar $[AuI_3(AsMe_3)]$ and Me_3PI_2 yields trigonal-bipyramidal $[AuI_3(PMe_3)_2]$, complexes with both stoichiometric and geometric differences.

The UV/Vis spectrum of a $[AuI_3(PMe_3)_2]$ in diethyl ether exhibits two peaks at 379 and 572 nm, and is similar in profile to that of $[AuI_3(AsMe_3)]$. The $^{31}P\{H\}$NMR spectrum of $[AuI_3(PMe_3)_2]$ displays two signals at $\delta = -69.5$ and 30.1 of almost equal intensity, the former of which corresponds to the value expected for free trimethylphosphane. It therefore appears that in solution an equilibrium is set up between a four and five coordinate gold(III) complex [Eq. (c)].

$$[AuI_3(PMe_3)_2] \rightleftharpoons [AuI_3(PMe_3)] + PMe_3 \quad (c)$$

On a addition of a small quantity of water to a solution of $[AuI_3(PMe_3)_2]$ in diethyl ether, the deep blue solution turned almost colorless. After about seven days small colorless crystals had formed in the reaction vessel. A sample was removed and studied by single-crystal X-ray diffraction. From elemental analysis results the crystals appear to have the formula $[AuI_2(OPMe_3)_2]$, suggesting a gold(II) species; however, the X-ray crystal structure revealed the ionic gold(I) species $[(Me_3PO)_2H][AuI_2]$,[28] (Fig. 3). The reaction proceeds according to Equation (d). The other product from this reaction is assumed to be HI. Although this was not confirmed experimentally, evolution of a gas was observed when water was added to the diethyl ether solution of $[AuI_3(PMe_3)_2]$. Clearly the addition of water initiates reduction of the gold(III) center to form a gold(I) species accompanied by the oxidation of the PMe_3 ligands to produce $OPMe_3$. Since the interaction of a neutral oxygen donor ligand with a gold center is notoriously weak, the $OPMe_3$ ligand is released into solution. Protonation then occurs and the resulting cation, $[(Me_3PO)_2H]^+$, stabilizes the resultant gold-containing anion, $[AuI_2]^-$.

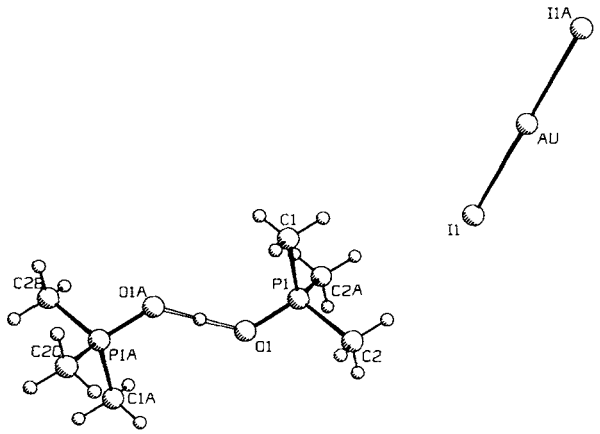

Fig. 3. X-ray crystal structure of $[(Me_3PO)_3H][AuI_2]$ (only one of the molecules in the unit cell is shown). Selected bond lengths [Å] and angles [°]: Au-I 2.616(2), P-O 1.49(2); I-Au-I 180.0(0), O-P-C(1) 111(1), O-P-C(2) 110.3(7).

$$[AuI_3(PMe_3)_2] + \text{excess } H_2O \longrightarrow [(Me_3PO)_2H][AuI_2] + HI \quad (d)$$

Experimental Procedure

Strictly anhydrous and anaerobic conditions (argon) were maintained throughout the reactions unless otherwise stated. $[AuI_3(AsMe_3)]$ and $[AuI_3(PMe_3)_2]$ were prepared by the reaction of coarse-grain gold powder (20–100 μm) and the appropriate Me_3EI_2 (E = P, As) compound. The synthesis of the Me_3EI_2 (E = P, As) compounds has been described elsewhere [29]. All reactions were performed in dry diethyl ether; reaction times were approximately 5 d at room temperature or 3 d under reflux at 60 °C in sealed tubes. The reaction of Me_3AsI_2 with gold afforded a dark green powder, which was recrystallized from diethyl ether to produce analytically pure $[AuI_3(AsMe_3)]$. Dark green – black crystals, m.p. >150 °C (decomp), correct elemental analysis (C, H, I). The UV/Vis spectrum of $[AuI_3(AsMe_3)]$ (2.71×10^{-4} M in diethyl ether) exhibits bands at $\lambda = 355$ and 621 nm. The intense color of the complex and high extinction coefficient, $\varepsilon_{max} = 9910\ dm^3 cm^{-1}$, is due to ligand–metal charge-transfer transition.

The reaction of Me_3PI_2 with gold yielded a dark blue powder, which was recrystallized from diethyl ether to produce analytically pure $[AuI_3(PMe_3)_2]$. Dark blue-black crystals, m.p. >125 (decomp), correct elemental analysis (C, H, I, P). The $^{31}P\{H\}$ NMR spectrum of $[AuI_3(PMe_3)_2]$ displays two peaks of almost equal intensity, one at $\delta = -69.5$ and the other at $\delta = 30.1$. By comparison with literature values, the former peak is assigned to free trimethylphosphane, indicating the compound dissociates in solution to form $[AuI_3(PMe_3)]$ and PMe_3. The latter peak is therefore assigned to the trimethylphosphane coordinated to the gold(III) center. The UV/Vis spectrum of $[AuI_3(PMe_3)_2]$ is similar in profile to that of $[AuI_3(AsMe_3)]$ and other square-planar gold(III) complexes, again indicating dissociation of one coordinated trimethylphosphane occurs in diethyl ether solution.

$[(Me_3PO)_2H][AuI_2]$ was prepared by the addition of a small quantity of water to a solution of $[AuI_3(PMe_3)_2]$ causing complete decolorization of the solution. After about seven days at 0 °C colorless crystals of $[(Me_3PO)_2H][AuI_2]$ formed, m.p. 185 °C, correct elemental analysis (C, H, I).

Received: February 23, 1996 [Z 8851 IE]
German version: *Angew. Chem.* **1996**, *108*, 2495–2498

Keywords: arsenic compounds · gold compounds · phosphorus compounds

[1] F. A. Cotton, G. Wilkinson, *Comprehensive Inorganic Chemistry*, 5th ed., Wiley, New York, **1988**.
[2] S. M. Godfrey, D. G. Kelly, A. G. Mackie, C. A. McAuliffe, R. G. Pritchard, S. M. Watson, *J. Chem. Soc. Chem. Commun.* **1991**, 1447.
[3] S. M. Godfrey, A. G. Mackie, C. A. McAuliffe, R. G. Pritchard, *Angew. Chem.* **1992**, *104*, 932; *Angew. Chem. Int. Ed. Engl.* **1992**, *32*, 919.
[4] N. Bricklebank, S. M. Godfrey, C. A. McAuliffe, R. G. Pritchard, *J. Chem. Soc. Dalton Trans.* **1995**, 2421.
[5] S. M. Godfrey, C. A. McAuliffe, R. G. Pritchard, *J. Chem. Soc. Chem. Commun.* **1994**, 45.
[6] S. M. Godfrey, H. P. Lane, C. A. McAuliffe, R. G. Pritchard, *J. Chem. Soc. Chem. Commun.* **1993**, 1190.
[7] P. L. Kuch, R. S. Tobias, *J. Organomet. Chem.* **1976**, *122*, 429.
[8] A. Laguna, M. Laguna, *J. Organomet. Chem.* **1990**, *394*, 743.
[9] A. D. Westland, *Can. J. Chem.* **1969**, *47*, 4135.
[10] N. W. Alcock, P. Moore, P. A. Lampe, K. F. Mok, *J. Chem. Soc. Dalton Trans.* **1982**, 207.
[11] P. A. Bates, J. M. Water, *Inorg. Chem. Acta* **1985**, *98*, 125.
[12] D. B. Dyson, R. V. Parish, C. A. McAuliffe, R. G. Pritchard, R. Fields, B. Beagley, *J. Chem. Soc. Dalton Trans.* **1989**, 907.
[13] G. A. Bowmaker, J. C. Dyason, P. C. Healy, L. M. Englehardt, C. Pakawatchai, A. H. White, *J. Chem. Soc. Dalton Trans.* **1987**, 1089.
[14] M. F. Perutz, O. Weisz, *J. Chem. Soc.* **1946**, 438.
[15] W. R. Mason, H. B. Grey, *Inorg. Chem.* **1968**, *7*, 55.
[16] G. Bandoli, D. A. Clemente, G. Marangoni, L. Cattalini, *J. Chem. Soc. Dalton Trans.* **1973**, 886.
[17] H. Brown, G. C. McKinlay, W. E. Smith, *Inorg. Chim. Acta* **1979**, *32*, 117.
[18] R. Uson, A. Laguna, H. Laguna, E. Fernandez, M. D. Villacampa, P. G. Jones, G. M. Sheldrick, *J. Chem. Soc. Dalton Trans.* **1983**, 1669.
[19] D. S. Eggleston, D. F. Chodosh, D. T. Hill, D. R. Girard, *Acta Crystallogr. Sect. C*, **1984**, *40*, 1357.
[20] R. J. Staples, T. Grant, J. P. Fackler, *Acta Crystallogr. Sect. C*, **1994**, *50*, 39.
[21] C. M. Harris, R. S. Nyholm, *J. Chem. Soc.* **1957**, 63.
[22] C. M. Harris, T. N. Lockyer, *J. Chem. Soc.* **1959**, 3083.
[23] L. F. Warren, M. A. Bennett, *Inorg. Chem.* **1976**, *15*, 3126.
[24] W. T. Robinson, E. Sinn, *J. Chem. Soc. Dalton Trans.* **1975**, 726.
[25] J. Vicente, M. C. Chicote, M. D. Bermudez, P. G. Jones, C. Fittschen, G. M. Sheldrick, *J. Chem. Soc. Dalton Trans.* **1986**, 2361.
[26] Crystal structure analysis of $[AuI_3(AsMe_3)]$: monoclinic, $P2_1/m$ (No. 11), $a = 10.089(4)$, $b = 7.576(3)$, $c = 15.016(6)$ Å, $\beta = 90.65(3)$, $V = 1148(1)$ Å^3, $Z = 4$, $R = 0.068$ $R_w = 0.050$ for 76 parameters and 759 observed reflections ($I > 3.00\sigma(I)$) collected at 296 K, $Mo_{K\alpha}$, $\mu = 235.64$ cm^{-1}, max. $2\theta = 47.1°$, $F(000) = 1192$ on a Siemens R3VS diffractometer absorption correction applied (max./min. transmission 1.19/0.82). The structure was solved by direct methods, all non-hydrogen atoms were refined anisotropically. The hydrogen atoms were included in fixed calculated positions with assigned isotropic temperature factors.
[27] Crystal structure analysis of $[AuI_3(PMe_3)_2]$: orthorhombic, *Pnma* (No. 62), $a = 10.488(4)$, $b = 11.122(b)$, $c = 14.279(3)$ Å, $V = 1666(2)$ Å^3, $Z = 4$, $R = 0.047$, $R_w = 0.052$ for 65 parameters and 817 observed reflections ($I > 3.00\ \sigma(I)$) collected at 296 K, $Mo_{K\alpha}$, $\mu = 144.68$ cm^{-1}, max. $2\theta = 49.9°$, $F(000) = 1288$ on a Rigaku R6S diffractometer, absorption correction applied (max./min. transmission 1.00/−0.13). The structure was solved by direct methods, all non-hydrogen atoms were refined anisotropically. The hydrogen atoms were included in fixed calculated positions with assigned isotropic temperature factors.
[28] Crystal structure analysis of $[(Me_3PO)_2H][AuI_2]$: monoclinic, $I2/m$ (No. 12), $a = 16.623(3)$, $b = 8.173(3)$, $c = 6.228(2)$ Å, $\beta = 89.81(3)°$, $V = 846.0(7)$ Å^3, $Z = 2$, $R = 0.037$, $R_w = 0.043$ for 38 parameters and 412 observed reflections ($I > 3.00\ \sigma(I)$) collected at 296 K, $Mo_{K\alpha}$, $\mu = 124.48$ cm^{-1}, max. $2\theta = 45.0°$, F(000) = 572 on a Rigaku R6S diffractometer, absorption corrction applied (max./min. transmission 0.75/−0.66). The structure was solved by direct methods, all non-hydrogen atoms were refined anisotropically. The hydrogen atoms were included in fixed calculated positions with assigned isotropic temperature factors. Crystallographic data (excluding structure factors) for the structures reported in this paper have been deposited with the Cambridge Crystallographic Data Centre as supplementary publication no. CCDC-179-108. Copies of the data can be obtained free of charge on application to The Director, CCDC, 12 Union Road, Cambridge CB21EZ (fax: Int. code + (1223)336-033; e-mail: teched@chemcrys.cam.ac.uk).
[29] N. Bricklebank, S. M. Godfrey, H. P. Lane, C. A. McAuliffe, R.G. Pritchard, J. M. Moreno, *J. Chem. Soc. Dalton Trans.* **1995**, 3873.

The Synthesis of Novel 6-Amido-6-Deoxy-L-Galactose Derivatives as Potent Sialyl Lewis^x Mimetics**

Michael W. Cappi, Wilna J. Moree, Lei Qiao, Thomas G. Marron, Gabriele Weitz-Schmidt, and Chi-Huey Wong*

Cell surface oligosaccharides are highly diversified in their structures and are associated with a variety of cell functions. Sialyl Lewis^x (SLe^x, Scheme 1) is found in the terminal fragment of certain glycoproteins and glycolipids as a ligand for several members of the selectin family, namely E-, L-, and P-selectin.[1] These selectins are adhesion receptors implicated in the initial interaction between leukocytes and vascular endothelium.[2] The binding of selectins to their carbohydrate ligands appears to be necessary for neutrophil extravasation and plays a major role in lymphocyte recirculation and platelet adhesion.

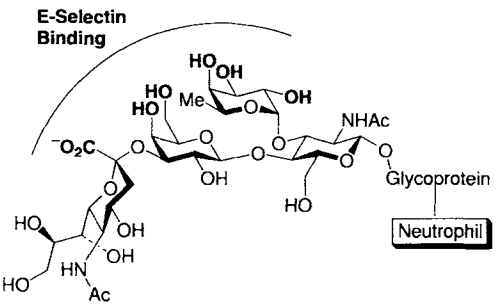

Scheme 1. Sialyl Lewis^x. The funtional groups necessary for binding are in bold.

Although the binding of SLe^x to the selectins under equilibrium conditions is weak, it is an effective anti-inflammatory agent in many acute disease models and is presently in second phase clinical trials.[3] Though the synthesis of SLe^x has recently been simplified by a chemo-enzymatic approach,[4] the high expense of its preparation and poor oral activity has resulted in many groups' searching for mimetics which are practical synthetically and inexpensive to produce. For the preparation of such mimetics a crystal structure of the receptor–ligand interaction would be advantageous. Unfortunately, because this connectivity is weak, no crystal structure of SLe^x bound to a selectin is available, although a crystal structure of free E-selectin has been reported.[5] Simpler working models must therefore be found, and the investigation of many structure–activity relationships has helped in the elucidation of the functional groups required for the SLe^x epitome binding to the selectins. The 2-, 3-, and 4-hydroxy groups of the fucose, the 4- and 6- hydroxy groups of the galactose, and the negative charge provided by the sialic acid in **1** proved to be crucial (bold atoms in Scheme 1).[6] With the aid of molecular mechanics calculations as well as analytical data, several groups have postulated the active-site structure of

[*] Prof. C.-H. Wong, Dr. M. W. Cappi, Dr. W. J. Moree, Dr. L. Qiao, Dr. T. G. Marron
Chemistry Department, The Scripps Research Institute
10666 North Torrey Pines Road
La Jolla, CA 92037 (USA)
Fax: Int. code + (619) 554-6731
Dr. G. Weitz-Schmidt
Preclinical Research, Sandoz Pharmaceuticals Ltd.
CH-4002 Basel (Switzerland)

[**] Financial support of this work was provided by the National Science Foundation (USA), Sandoz Pharmaceuticals Ltd., and NATO (fellowship for W. J. M.).

SLe^x (Scheme 1).[7] This active-site model has assisted the major effort of synthesizing SLe^x mimetics.[8] To date, several compounds show interesting in vitro activity equivalent to or better than that of SLe^x.

We have designed several SLe^x mimetics using the aforementioned structure–activity relationships for model construction. The majority of mimetics prepared to date contain the L-fucose moiety linked at the anomeric position to a suitable spacer unit.[8d, e] It was decided to replace the L-fucose unit with an L-galactose functionality to link a range of dihydroxy-α-amino acids (**3**–**7**) at the C6 position. The dihydroxy units would substitute the 4- and 6-hydroxy groups of galactose in SLe^x. Tethering a suitable alkyl side chain containing a terminal carboxylate would provide the required negative charge and afford molecules of either type **I** or **II** (Scheme 2).

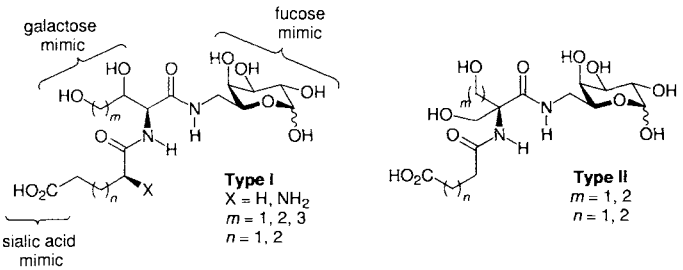

Scheme 2. Two types of designed glycopeptide mimics.

Galactose amine **2** serves as the core glycoside structure for all of the mimetics and is easily prepared in high yield from L-galactose (Table 1).[9] Amino acids **3**–**5** were synthesized from threonine aldolase with methodology developed in this laboratory and subsequently protected as their *N*-Boc derivatives.[10] Amino acids **6** and **7** were prepared in four steps from serine[11] and 1-hydroxy-4-benzyloxy-2-butanone,[12] respectively.

The key amide bond was efficiently formed with EDCI/HOBt to give the derivatives in high yields (Table 1). Deprotection of the Boc group allowed introduction of the carboxylate-bearing side chain, which would act as a surrogate for the sialic acid residue. Accordingly, aminoglycosides **8**–**12** were treated with a series of activated carboxylic acids to afford the protected mimetics in high yield (Table 2). Acidic hydrolysis of the acetonides followed by hydrogenolysis of the benzyl ethers provided the fully deprotected mimetics (**13**–**25**), which were purified by Biogel P2 chromatography with water as eluent. Compounds **13**–**25** were fully characterized by ^1H NMR spectroscopy and high-resolution mass spectrometry (Table 3).

The mimetics were assayed in a system which measured the binding of SLe^x glycoconjugate to immobilized recombinant E-selectin.[13] The IC_{50} values indicate that the activity is a function of two mutually exclusive factors, the amino acid used as the galactose mimic (**3**–**7**) and the type of carboxylate tether. Mimetics **13**–**15** showed poor activity suggesting that amino acid **3** is not a good replacement for the galactose residue. In almost all cases the length of the carboxylate tether proved to be critical, as seen for compounds **16**, **22**, and **24** in contrast to **17**, **23**, and **25**. Several of the mimetics were at least as active as SLe^x (**19**, **23**–**25**), and the activity of **25** was twice that of SLe^x.

Table 1. Coupling of galactose amine **2** with amino acids **3**–**7**.

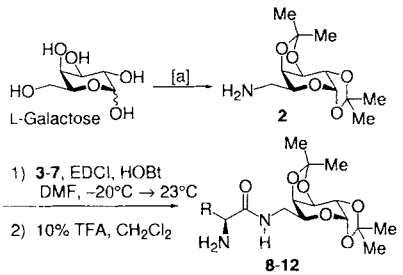

Amino acid		Product	Yield of **2** [%]
3	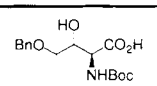	**8**	59
4	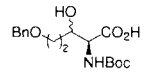	**9**	75
5	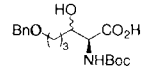	**10**	74
6	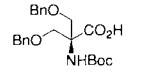	**11**	57
7	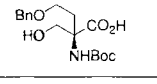	**12**	57

[a] a)$CuSO_4$, acetone, H_2SO_4, 88%; b) TsCl, pyridine, 90%; c) NaN_3, DMF, 115°, 91%; d) H_2 (35 psi), Pd/C, MeOH, 100%; Boc = *tert*-butoxycarbonyl; EDCI = *N*-ethyl-*N*′-(3-dimethylaminopropyl)carbodiimide; HOBt = hydroxybenzotriazole; Ts = $MeC_6H_4SO_2$.

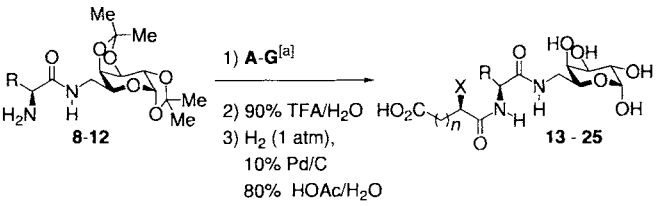

Table 2. Synthesis of glycopeptide mimics **13**–**25**.

Amine (P = Bn)	Coupling method [a]	R	*n*	X	Product (P = H)	Yield [%]	IC_{50} [mM]
8	A		1	H	**13**	52	10
8	B		2	H	**14**	50	10
8	C		1	NH_2	**15**	65	10
9	A		1	H	**16**	49	inactive [b]
9	B		2	H	**17**	56	4.2 [b]
9	C		1	NH_2	**18**	49	1 [b]
10	A		1	H	**19**	65	1 [c]
10	B		2	H	**20**	63	inactive [b]
10	C		1	NH_2	**21**	50	1.5
11	D		1	H	**22**	68	inactive
11	E		2	H	**23**	53	0.3
12	F		1	H	**24**	45	0.3 [b]
12	G		2	H	**25**	29	0.2 [b]

[a] Coupling methods: A) succinic anhydride, MeOH; B) glutaric anhydride, MeOH; C) EDCI, HOBt, DMF, *N*-Cbz-benzyloxyaspartic acid; D) $BnO_2C(CH_2)_2COCl$, CH_2Cl_2, Et_3N; E) $BnO_2C(CH_2)_3COCl$, CH_2Cl_2, Et_3N; F) EDCI, HOBt, DMF, $BnO_2C(CH_2)_2CO_2H$; G) EDCI, HOBt, DMF, $BNO_2C(CH_2)_3CO_2H$. [b] Actitivities were determined on the epimeric mixture at the amino acid centers. [c] The activity shown is of a single epimer at the 2° alcohol center which was separated from the diastereomeric mixture as the chiral champhanate derivative and subsequently hydrolyzed. The IC_{50} value for SLe^x is 0.5 mM. Cbz = benzyloxycarbonyl.

Received: April 12, 1996 [Z90261E]
German version: *Angew. Chem.* **1996**, *108*, 2501–2503

Keywords: glycopeptides · selectins · sialyl Lewis^x

Table 3. Spectroscopic data for compounds **13**, **16**, **19**, **22**, and **24**.

13: ^{1}H NMR (400 MHz, D_2O, 23 °C, TMS, β:α = 1:1.3): δ = 5.18 (d, J = 3.4 Hz; H1 α), 4.50 (d, J = 7.8 Hz; H1 β), 4.38–4.35 (m; H2′ $\alpha+\beta$), 4.05–4.02 (m; H5 α, H3′ α), 3.96–3.93 (m; H3′ β), 3.88 (br d, J = 3.4 Hz; H4 α), 3.81 (d, J = 3.1 Hz; H4 β), 3.80–3.77 (m; H3 α), 3.75 (dd, J = 11.5, 3.6 Hz; H2 α), 3.68–3.54 (m; H3 β, H5 β, C4′-H_2 $\alpha+\beta$), 3.57–3.49 (m; H2 β, C6-H_2 $\alpha+\beta$), 3.40–3.30 (m; C6-H_2 $\alpha+\beta$), 2.53 (m; C2″-H_2 $\alpha+\beta$, C3″-H_2 $\alpha+\beta$); HR-MS (− 80 eV): *m/z*: found 397.1446 ($M+H^+$), calcd 397.1458

16: ^{1}H NMR (400 MHz; D_2O, 23 °C, TMS, α/β mix): δ = 5.23 (d, J = 3.5 Hz; H1 α), 4.55 (dd, J = 7.9, 4.6 Hz; H1 β), 4.40–4.35 (m; H2′ $\alpha+\beta$), 4.30–4.27 (m; H3′ β), 4.11–4.05 (m; H5 α, H3′ α), 3.92 (br d, J = 2.8 Hz; H4 α), 3.86 (d, J = 3.4; H4 β), 3.83 (dd, J = 10.4, 3.2 Hz; H3 α), 3.77 (dd, J = 10.4, 3.7 Hz; H2 α), 3.76–3.68 (m; H5 β, C4′-H_2 $\alpha+\beta$), 3.62 (dd, J = 10.0, 3.4 Hz; H3 β), 3.56–3.34 (m; H2 β, C6-H_2 $\alpha+\beta$), 2.61–2.40 (m; C2″-H_2 $\alpha+\beta$, C3″-H_2 $\alpha+\beta$) 1.82–1.69 (m; C4′-H_2 $\alpha+\beta$); HR-MS (− 80 eV): *m/z*: found 433.1447 ($M+Na^+$), calcd 433.1434

19: ^{1}H NMR (400 MHz; D_2O, 23 °C, TMS): δ = 5.20 (d, J = 3.6 Hz; H1 α), 4.53–4.51 (m; H1 β), 4.35–4.33 (m; H2′ $\alpha+\beta$), 4.12–4.04 (m; H5 α, H3′ $\alpha+\beta$), 3.89 (br s; H4 α), 3.85–3.78 (br s; H3 α, H4 β), 3.77–3.57 (m; H2 α, H3 β, H5 β, C6′-H_2 $\alpha+\beta$), 3.51–3.33 (m; H2 β, C6-H_2 $\alpha+\beta$), 2.59–2.52 (m; C2″-H_2 $\alpha+\beta$, C3″-H_2 $\alpha+\beta$), 1.65–1.52 (m; C4′-H_2 $\alpha+\beta$, C5′-H_2 $\alpha+\beta$); HR-MS (− 80 eV): *m/z*: found 447.1607 ($M+Na^+$), calcd 447.1591

22: ^{1}H NMR (400 MHz; D_2O, 23 °C, TMS): δ = 5.20 (d, J = 3.5 Hz; H1 α), 4.52 (d, J = 7.8 Hz; H1 β), 4.06–4.03 (m; H5 α), 3.96–3.88 (m; H4 α, 2 × $CH_\gamma H_\beta$OH $\alpha+\beta$), 3.82–3.79 (m; H3 α, H4 β, 2 × $CH_\gamma H_\beta$OH $\alpha+\beta$), 3.77 (dd, J = 10.2, 3.6 Hz; H2 α), 3.66–3.63 (m; H5 β), 3.59 (dd, J = 9.9, 3.2 Hz; H3 β), 3.48–3.39 (m; H2 β, C6-H_2 $\alpha+\beta$), 3.36–3.29 (m; C6-H_2 $\alpha+\beta$), 2.52 (br s; C2″-H_2 $\alpha+\beta$, C3″-H_2 $\alpha+\beta$); MS (− 80 eV): *m/z*: found 419 ($M+Na^+$), calcd 419

24: ^{1}H NMR (400 MHz; D_2O, 23 °C, TMS): δ = 5.20 (d, J = 3.3 Hz; H1 α), 4.60–4.46 (m; H1 β, C4′-H_2 $\alpha+\beta$), 4.10–3.30 (m; H2 $\alpha+\beta$, H3 $\alpha+\beta$, H4 $\alpha+\beta$, H5 $\alpha+\beta$, C6-H_2 $\alpha+\beta$, CH_2OH $\alpha+\beta$), 2.69–2.50 (m; C2″-H_2 $\alpha+\beta$, C3″-H_2 $\alpha+\beta$), 2.19–1.98 (m; C3′-H_2 $\alpha+\beta$); HR-MS (− 80 eV): *m/z*: found 433.1448 ($M+Na^+$), calcd 433.1434

[1] a) P. J. Green, T. Tamatani, T. Watanabe, M. Miyasaka, A. Hasegawa, M. Kiso, C. T. Yuen, M. S. Stoll, T. Feizi, *Biochem. Biophys. Res. Commun.* **1992**, *188*, 244–251; b) M. L. Philips, E. Nudelman, F. C. A. Gaeta, M. Perez, A. K. Singhal, S. I. Hakomori, J. C. Paulson, *Science* **1990**, *250*, 1130–1132; c) G. Walz, A. Aruffo, W. Kolanus, M. Bevilacqua, B. Seed, *ibid.* **1990**, *250*, 1132–1135; d) J. B. Lowe, L. M. Stoolman, R. P. Nair, R. D. Larsen, T. L. Berhend, R. M. Marks, *Cell* **1990**, *63*, 475–484; e) C. R. Bertozzi, *Chemistry and Biology* **1995**, *2*, 703–708; f) L. A. Lasky, *Annu. Rev. Biochem.* **1995**, *64*, 113–139.

[2] E. Larsen, *Cell Adhesion*, 1st ed., CRC Press, Boca Raton, FL, **1995**, p. 203.

[3] a) T. Murohara, J. Margiotta, L. M. Phillips, J. C. Paulson, S. DeFrees, S. Zalipsky, L. S. S. Guo, A. M. Lefer, *Cardiovascular Research* **1995**, *30*, 965; b) M. Buerke, A. S. Weyrich, Z. Zheng, F. C. A. Gaeta, M. J. Forrest, A. M. Lefer, *J. Clin. Invest.* **1994**, 1140.

[4] Y. Ichikawa, Y.-C. Lin, D. P. Dumas, G.-J. Shen, E. Garcia-Junceda, M. A. Williams, R. Bayer, C. Ketcham, L. E. Walker, J. C. Paulson, C.-H. Wong, *J. Am. Chem. Soc.* **1992**, *114*, 9283–9298.

[5] B. J. Graves, R. L. Crowther, C. Chandran, J. M. Rumberger, S. Li, K.-S. Huang, D. H. Presky, P. C. Familletti, B. A. Wolitzky, D. K. Burns, *Nature* **1994**, *367*, 532–538.

[6] a) A. Giannis, *Angew. Chem.* **1994**, *106*, 188–191; *Angew. Chem. Int. Ed. Engl.* **1994**, *33*, 178–180; b) J. Y. Ramphal, Z.-L. Zheng, C. Perez, L. E. Walker, S. A. DeFrees, F. C. A. Gaeta, *J. Med. Chem.* **1994**, *37*, 3459–3463; b) B. K. Brandley, M. Kiso, S. Abbas, P. Nikrad, O. Srivasatava, C. Foxall, Y. Oda, A. Hasegawa, *Glycobiology* **1993**, *3*, 633–641; d) S. A. DeFrees, F. C. A. Gaeta, Y.-C. Lin, Y. Ichikawa, C.-H. Wong, *J. Am. Chem. Soc.* **1994**, *37*, 3459; e) C. T. Yuen, A. M. Lawson, W. Chai, M. Larkin, M. S. Stoll, A. C. Stuart, F. X. Sullivan, T. J. Ahern, T. Feizi, *Biochemistry* **1992**, *31*, 9126–9131.

[7] a) K. Scheffler, B. Ernst, A. Katopodis, J. L. Magnani, W. T. Wang, R. Weisemann, T. Peters, *Angew. Chem.* **1995**, *107*, 2034–2037; *Angew. Chem. Int. Ed. Engl.* **1995**, *34*, 1841–1844; b) Y. Ichikawa, Y.-C. Lin, D. P. Dumas, G.-J. Shen, E. Garcia-Junceda, M. A. Williams, R. Bayer, C. Ketcham, L. E. Walker, J. C. Paulson, C.-H. Wong, *J. Am. Chem. Soc.* **1992**, *114*, 9283–9298; c) G. E. Ball, R. A. O'Neill, J. E. Schultz, J. B. Lowe, J. B. W. Weston, J. O. Nagy, E. G. Brown, C. J. Hobbs, M. D. Bednarski, *ibid.* **1992**, *114*, 5449–5451.

[8] For representative examples of recently published SLe^x mimetics see: a) A. A. Birkbeck, S. V. Ley, J. C. Prodger, *Biorg. Med. Chem. Lett.* **1995**, *5*, 2637–2642; b) T. Uchiyama, V. P. Vassilev, T. Kajimoto, W. Wong, H. Huang, C.-C. Lin, C.-H. Wong, C.-H. *J. Am. Chem. Soc.* **1995**, *117*, 5395–5396; c) S. Hanessian, H. Prabhanjan, *Synlett* **1994**, 868–870; d) S.-H. Wu, M. Shimazaki, C.-C. Lin, L. Qiao, W. J. Moree, G. Weitz-Schmidt, C.-H. Wong, *Angew. Chem.* **1996**, *108*, 106–108; *Angew. Chem. Int. Ed. Engl.* **1996**, *35*, 88–90; e) T. P. Kogan, B. Dupre, K. M. Keller, I. L. Scott, H. Bui, R. V. Market, P. J. Beck, J. A. Voytus, B. M. Bevelle, D. Scott, *J. Med. Chem.* **1995**, *38*, 4976–4984; f) T. Eisele, A. Toepfer, G. Kretzschmar, R. R. Schmidt, *Tetrahedron Lett.* **1996**, *37*, 1389–1392; g) G. Thoma, F. Schwarzenback, R. O. Duthaler, *J. Org. Chem.* **1996**, *61*, 154; h) H. Ohmoto, K. Nakamura, T. Inoue, N. Kondo, Y. Inoue, K. Yoshimasa, H. Kondo, H. Ishida, M. Kiso, A. Hasagawa, *J. Med. Chem.* **1996**, *39*, 1339–1343; i) M. J. Bamford, M. Bird, P. M. Gore, D. S. Holmes, R. Priest, J. C. Prodger, V. Saez, *Bioorg. Med. Chem. Lett.* **1996**, *6*, 239–244; j) C. R. Bertozzi, *Chemistry and Biology* **1995**, *2*, 703–708; k) U. Sprengard, M. Schudok, W. Schmidt, G. Kretzschmar, H. Kunz, *Angew. Chem.* **1996**, *108*, 359–362; *Angew. Chem. Int. Ed. Engl.* **1996**, *35*, 321–324.

[9] J. A. May, A. C. Sartorelli, *J. Med. Chem.* **1979**, *22*, 971–976.

[10] V. P. Vassilev, T. Uchiyama, T. Kajimoto, C.-H. Wong, *Tetrahedron Lett.* **1995**, *36*, 4081–4084.

[11] a) T. T. Otani, M. Winitz, *Arch. Biochem. and Biophys.* **1960**, *90*, 254–259; b) Y. Nakamura, A. Ito, C.-G. Shin, *Bull. Chem. Soc. Jpn.* **1994**, *67*, 2151–2161.

[12] a) G. F. Hennion, F. P. Kupecki, *J. Org. Chem.* **1953**, *18*, 1601; b) G. Krüger in *Houben-Weyl: Methoden der Organischen Chemie, Band E5* (Ed.: J. Falbe), Düsseldorf, **1995**, p. 504.

[13] G. Weitz-Schmidt, D. Stokmaier, G. Scheel, N. E. Nifantev, A. B. Tuzikov, N. V. Bovin, *Anal. Biochem.* **1996**, *238*, 184–190.

A Practical Method for the Synthesis of *N*-Acetyl-D-lactosamine Derivatives by the Tandem Use of Galactose Oxidase and β-Galactosidase**

Teiji Kimura, Shuichi Takayama, Hongmei Huang, and Chi-Huey Wong*

As the understanding of the biological role of glycoconjugates increases,[1] so does the need for an inexpensive source of synthetic oligosaccharides in large quantities. *N*-Acetyl-D-lactosamine (Galβ1,4GlcNAc, LacNAc) and its derivatives are particularly useful for the study of biological recognition processes[2] and have been the object of much synthetic effort by means of standard chemical[3] and enzymatic methods.[4] Although syntheses by chemical methods are well known, the procedures often involve many steps and are complicated. The β-1,4-galactosyltransferase-catalyzed reaction coupled with in situ regeneration of UDP-galactose has been developed for the large-scale synthesis of LacNAc; this proceeds with high regioselectivity and yield.[5] However, the limited availability of the enzymes and their high cost and instability hamper their use.[6] The β-D-galactosidase from *Bacillus circulans* also forms Galβ-1,4-linkages by reverse hydrolysis or transglycosylation.[7] The advantages of the galactosidase-catalyzed reaction are low cost, high stability, and simple reaction conditions (there is no need for sugar nucleotides).[8] There are, however, some disadvantages in using galactosidase-catalyzed reactions. Because of the hydrolytic nature of the enzyme, the yields hitherto reported were low, and the desired product was difficult to isolate from the reaction mixture containing quite similar compounds.[7–9] We report here that the *p*-nitrophenyl glycoside of 6-oxo-D-galactose (the primary OH of galactose is oxidized to an aldehyde) can be used as a donor in the reaction catalyzed by β-galactosidase. Furthermore, the transglycosylation is kinetically favored over hydrolysis.

[*] Prof. Dr. C.-H. Wong, Dr. T. Kimura, Dipl.-Chem. S. Takayama, Dr. H. Huang
Chemistry Department, The Scripps Research Institute,
10550 North Torrey Pines Road, La Jolla, CA (USA)
Fax: Int. code + (619)784-2409

[**] Financial support of this work was provided by the National Institutes of Health (GM 44154). We thank Daiwa Kasei KK (Osaka, Japan) for providing us with β-galactosidase from *Bacillus circulans*.

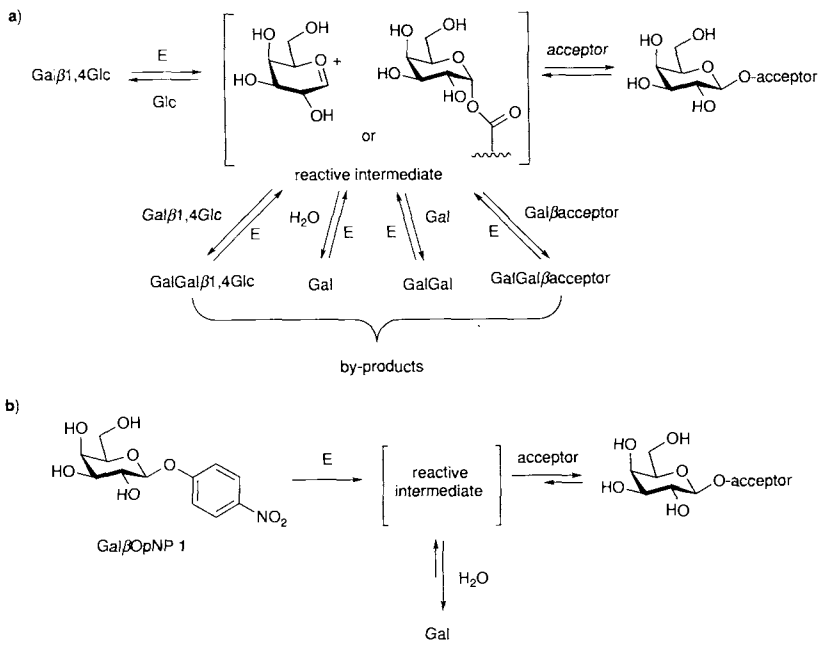

Scheme 1. β-Galactosidase-catalyzed transglycosylation and hydrolysis: a) substrate with poor leaving group (e.g. Galβ1,4Glc); b) substrate with good leaving group (e.g. **1**); E = β-galactosidase.

Scheme 1 shows the reactions catalyzed by β-galactosidase. As reported,[10] the use of a glycosyl donor substrate with a poor leaving group (such as lactose) often gave a complex mixture of products including mono, di, and trisaccharides. A substrate with a good leaving group (such as *p*-nitrophenyl galactoside) and an excess of glycosyl acceptor make the reaction irreversible and minimize secondary hydrolysis and further glycosylation of the transglycosyl product, the hydrolysis product, and the donor itself. To determine which step is kinetically controlled, the effect of acceptors on initial reaction rate, v_0, was investigated (Scheme 2, Table 1). In the case of *p*-nitrophenyl galactoside (**1**, GalβOpNP), the initial reaction rate, measured by released *p*-nitrophenol, did not increase with addition of acceptor (entries 1–3), although the transglycosylation yield increased from 14% to 30%. These results suggest that the rate-determining step is perhaps the formation of an [E–S] complex. The ratio of transglycosylation to hydrolysis mainly depends on the concentrations of acceptor and H_2O. Therefore, hydrolysis is the major pathway in aqueous solution. Addition of water soluble organic solvent would reduce water activity to some extent, but it often causes substrate and/or product inhibition and makes the enzyme unstable.[11] To shift the reaction in water toward transglycosylation, it is necessary to kinetically control the partitioning step in favor of the transglycosylation reaction. When compound **1** was oxidized to the 6-oxo-derivative **2**,[12] it was found to be a relatively weak substrate for β-galactosidase. The initial rate and transglycosylation yield, however, increased with amount of the acceptor **3** (entries 4–6). This indicates that the active species generated from **2** is less reactive with water than with the acceptor **3**.

Another problem in β-galactosidase-catalyzed reactions is that the product is also subject to enzymatic hydrolysis. The improved stability of 6′-oxo-LacNAc (**4**, $t_{1/2}$ = 31 h) relative to **2** ($t_{1/2}$ = 0.4 h) toward the β-galactosidase-catalyzed hydrolysis may also contribute to the high yield of the product.[13]

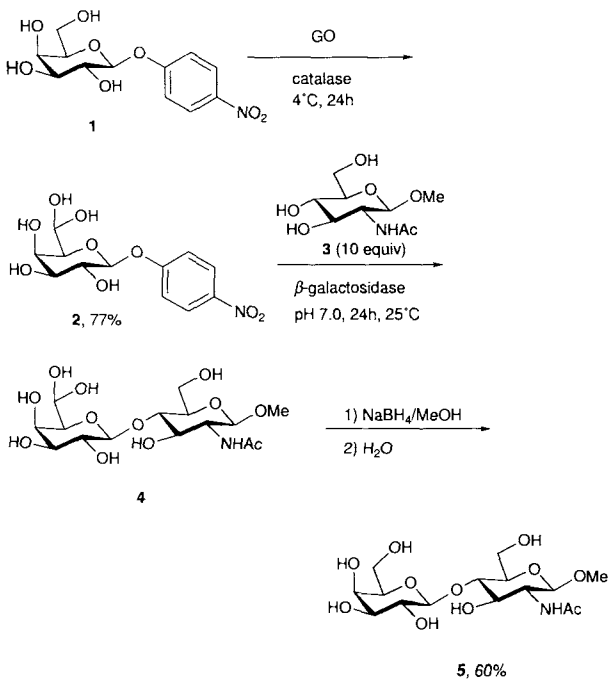

Scheme 2. Synthesis of *N*-acetyl-D-lactosamine with galactose oxidase (GO) and β-galactosidase from *B. circulans*.

Table 1. Comparison of β-galactosidase-catalyzed reactions with galactopyranose (GalβOpNP, **1**) and galactohexodialdose (6-oxo-GalβOpNP, **2**)

No.	Donor	*c*(Acceptor) [M]	Yield (LacNAc) [%] [a]	v_0 [mM min^{-1}] [b]
1	**1**	0	–	5.69 ± 0.11
2	**1**	0.05	14	4.68 ± 0.08
3	**1**	0.5	30	4.16 ± 0.23
4	**2**	0	–	0.074 ± 0.008
5	**2**	0.05	29 [c]	0.137 ± 0.006
6	**2**	0.5	60 [c]	0.393 ± 0.013

[a] The reaction mixture containing 0.05 M donor and various concentrations of methyl-*N*-acetyl-D-glucosamine in 0.05 M potassium phosphate buffer (pH 7.0) was gently stirred at room temperature in the presence of the enzyme (140 U mmol^{-1} of donor) for 24 h. [b] The mixture (containing the same components as described in [a]) was incubated with shaking for 5–10 min at room temperature. Absorbance was measured at 420 nm. [c] Methyl-β-*N*-acetyl-D-lactosamine (**5**) was obtained by reduction with $NaBH_4$ followed by product isolation as described in the text.

Although the transgalactosylation reaction of **2** proceeds smoothly with excellent regioselectivity and good yield under the reaction conditions, the presence of excess acceptor may complicate product purification. The aldehyde produced, however, may be reduced with $NaBH_4$ in nonaqueous solution to form a boron complex which decomposes to the desired alcohol upon addition of water. To test the feasibility of this approach, a mixture of **3** and **4** obtained from the enzymatic reaction was reduced with $NaBH_4$ in MeOH. Afterwards, the reaction mixture was separated by silica gel column chromatography. The galactoside **3** was eluted first with nonaqueous solvent ($CHCl_3$/MeOH 1/1) and recovered in 77%. Elution with aqueous solvent ($CHCl_3$/MeOH/H_2O 5/5/1) then provided **5** in 60% yield. Other regioisomers were not observed by NMR. The recovered

 © VCH Verlagsgesellschaft mbH, D-69451 Weinheim, 1996 0570-0833/96/3520-2349 $ 15.00+.25/0

compound **3** could be reused in the next cycle of the reaction without further purification. Furthermore, when the allyl, phenyl, and thiophenyl derivatives of **3** were used as acceptor, similar results were obtained.

In summary, a new method based on *Bacillus* galactosidase has been developed for the synthesis of β-galactosides using 6-oxo-GalβOpNP as donor. This method can be carried out in aqueous solution without organic solvent to give the transglycosylation product in high yield and regioselectivity.

Experimental Procedure

2: To a solution of **1** (306 mg, 1.02 mmol) in 50 mM potassium phosphate buffer (pH 7.0, 15 mL) was added galactose oxidase (135 U) and catalase (1 mg). The reaction mixture was gently stirred under an oxygen balloon for 24 h at 4 °C. After MeOH was added to terminate the reaction, the solvent was removed in vacuo. The residue was applied to a silica gel column ($CHCl_3$, then a 1:1 mixture of $CHCl_3$/MeOH) to obtain **2** (250 mg, 77%). ^1H NMR (500 MHz, D_2O): $\delta = 3.64$ (d, $J = 7.4$ Hz, 1H; H-5), 3.79 (dd, $J = 9.9$, 3.3 Hz, 1H; H-3), 3.88 (dd, $J = 9.9$, 7.7 Hz, 1H; H-2), 4.17 (d, $J = 3.3$ Hz, 1H; H-4), 5.13 (d, $J = 7.4$ Hz, 1H; H-6), 5.19 (d, $J = 7.7$ Hz, 1H; H-1), 7.26 (d, $J = 9.3$ Hz, 2H; ArH), 8.27 (d, $J = 9.3$ Hz, 2H; ArH).

To prepare **4** as an authentic sample, compound **5** was oxidized with galactose oxidase under the same conditions described for the synthesis of **2** except that $CuSO_4$ (0.5 mM) was added, and the product was purified by Biogel P-2.

4: ^1H NMR (500 MHz, D_2O): $\delta = 2.02$ (s, 3H; CH_3CO), 3.45 (d, $J = 7.5$ Hz, 1H; H-5'), 3.50 (s, 3H; OCH_3), 3.55 (dd, $J = 10.0$, 8.0 Hz, 1H; H-2), 3.57–3.63 (m, 1H; H-5), 3.66 (dd, $J = 10.0$, 3.5 Hz, 1H; H-3'), 3.67–3.74 (m, 3H; H-3, H-4, H-2'), 3.82 (dd, $J = 12.5$, 5.5 Hz, 1H; H-6), 3.98 (d, $J = 12.5$, 1.5 Hz, 1H; H-6), 4.07 (d, $J = 3.5$ Hz, 1H; H-4'), 4.45 (d, $J = 8.0$ Hz, 1H; H-1 or H-1'), 4.47 (d, $J = 8.0$ Hz, 1H; H-1 or H-1'), 5.12 (d, $J = 7.5$ Hz, 1H; H-6'). HR-MS: calcd for $C_{15}H_{25}NO_{11}Na$ ($M + Na^+$, aldehyde form) 418.1325, found 418.1310.

5: To a solution of **3** (181 mg, 770 μmol) and β-galactosidase (11 U) from *Baccilus circulans* in 50 mM potassium phosphate buffer (pH 7.0, 1.54 mL) was added **2** (24.4 mg, 77.0 μmol). The reaction mixture was gently stirred for 24 h at room temperature. After addition of MeOH (1 mL) to terminate the reaction, the solvent was removed in vacuo. The residue was dissolved in MeOH (5 mL), and $NaBH_4$ (29 mg) was added to the solution at 0 °C. After stirring for 1 h at 0 °C, the mixture was allowed to warm to room temperature within 10 h. The mixture was applied to a silica gel column and first eluted with $CHCl_3$/MeOH (1/1, 500 mL) to recover **3** (140.1 mg, 77% of starting amount). Subsequent elution with $CHCl_3$/MeOH/H_2O (5/5/1) provided **5** (18.2 mg, 60%).

Received: May 3, 1996 [Z9096IE]
German version: *Angew. Chem.* **1996**, *108*, 2503–2505

Keywords: oxidases · β-galactosidase · lactosamines

[1] a) J. B. Lowe, L. M. Stoolman, R. P. Nair, R. D. Larsen, T. L. Berhend, R. M. Marks, *Cell* **1990**, *63*, 475–484; b) T. Feizi, *Trends Biochem. Sci.* **1991**, *16*, 84–86.

[2] a) T. Feizi, J. C. Solomon, C.-T. Yuen, K. C. G. Jeng, L. G. Frigeri, D. K. Hsu, F.-T. Liu, *Biochemistry* **1994**, *33*, 6342–6349; b) F.-T. Liu, *Immunol. Today* **1993**, *14*, 486–490; c) C. P. Sparrow, H. Leffler, S. H. Barondes, *J. Biol. Chem.* **1987**, *262*, 7383–7390.

[3] a) K. Toshima, K. Tatsuta, *Chem. Rev.* **1993**, *93*, 1503–1531; b) R. R. Schmidt, *Angew. Chem.* **1986**, *98*, 213–236; *Angew. Chem. Int. Ed. Engl.* **1986**, *25*, 212–235; c) H. Paulsen, *ibid.* **1982**, *94*, 184–201 and **1982**, *21*, 155–173; d) P. Sinaÿ, *Pure Appl. Chem.* **1991**, *63*, 519–528; e) H. Paulsen, *Angew. Chem.* **1990**, *102*, 851–867; *Angew. Chem. Int. Ed. Engl.* **1990**, *29*, 823–839.

[4] a) C.-H. Wong, R. L. Halcomb, Y. Ichikawa, T. Kajimoto, *Angew. Chem.* **1995**, *107*, 453–474; *Angew. Chem. Int. Ed. Engl.* **1995**, *34*, 412–432; b) *ibid.* **1995**, *107*, 569–593 and **1995**, *34*, 521–546; c) E. J. Toone, E. S. Simon, M. D. Bednarski, G. M. Whitesides, *Tetrahedron* **1989**, *45*, 5365–5422.

[5] a) Y. Ichikawa, Y.-C. Lin, D. P. Dumas, G.-J. Shen, E. Garcia-Junceda, M. A. Williams, R. Bayer, C. Ketcham, L. E. Walker, J. C. Paulson, C.-H. Wong, *J. Am. Chem. Soc.* **1992**, *114*, 9283–9298; b) A. Zervosen, L. Elling, *ibid.* **1996**, *118*, 1836–1840.

[6] C. Augé, R. Fernandez-Fernandez, C. Gautheron, *Carbohydr. Res.* **1990**, *200*, 257–268.

[7] a) T. Usui, S. Kubota, H. Ohi, *Carbohydr. Res.* **1993**, *244*, 315–323; b) G. F. Herrmann, U. Kragl, C. Wandrey, *Angew. Chem.* **1993**, *105*, 1399–1400; *Angew. Chem. Int. Ed. Engl.* **1993**, *32*, 1342–1343; c) G. F. Herrmann, Y. Ichikawa, C. Wandrey, F. C. A. Gaeta, J. C. Paulson, C.-H. Wong, *Tetrahedron Lett.* **1993**, *34*, 3091–3094. For representative examples of other glycosidase-catalyzed syntheses see: K. G. I. Nilsson, *Trends Biotechnol.* **1988**, *6*, 256–264; D. H. G. Crout, D. A. MacManus, J.-M. Ricca, S. Singh, P. Critchley, W. T. Gibson, *Pure Appl. Chem.* **1992**, *64*, 1079–1084; J. Lehmann, E. Schröter, *Carbohydr. Res.* **1979**, *71*, 65–73; H.-J. Gais, A. Zeissler, P. Maidonis, *Tetrahedron Lett.* **1988**, *29*, 5743–5744; B. Sauerbrei, J. Thiem, *ibid.* **1992**, *33*, 201–204; S. Kobayashi, K. Kashiwa, T. Kawasaki, S.-I. Shoda, *J. Am. Chem. Soc.* **1991**, *113*, 3079–3084; R. López, A. Fernández-Mayoralas, *J. Org. Chem.* **1994**, *59*, 737–745; J.-M. Petit, F. Paquet, J.-M. Beau, *Tetrahedron Lett.* **1991**, *32*, 6125–6128.

[8] a) S. David, *Chemtracts-Org. Chem.* **1994**, *7*, 92–95. b) S. Takayama, M. Shimazaki, L. Qiao, C.-H. Wong, *Bioorg. Med. Chem. Lett.* **1996**, *6*, 1123–1126.

[9] K. Ajisaka, H. Fujimoto, M. Isomura, *Carbohydr. Res.* **1994**, *259*, 103–115.

[10] L. Hedbys, E. Johansson, K. Mosbach, P.-O. Larsson, *ibid.* **1989**, *186*, 217–223.

[11] A. P. G. Kieboom, *Recl. Trav. Chim. Pays-Bas* **1988**, *107*, 347–348.

[12] H. Bretting, G. Jacobs, *Biochim. Biophys. Acta* **1987**, *913*, 342–348.

[13] The half-lives of compounds **2** and **4** were determined from the pseudo first order kinetics of the β-galactosidase-catalyzed hydrolysis as follows. **2**: A 0.5 mL solution of potassium phosphate buffer (50 mM, pH 7.0) containing **2** (5 mM) and β-galactosidase (140 U per 1 mmol of **2**) was measured continuously in a plastic cell with a 1 cm light path at 420 nm against a control without enzyme. **4**: A 5 mM solution of **4** and the enzyme (140 U mmol^{-1}) in D_2O was placed in an NMR tube. The ratio between released **3** and remaining **4** was periodically determined by the integration of H-6 of **4** ($\delta = 3.98$) and H-6 of **3** ($\delta = 3.88$).

Chemoenzymatic Synthesis of a Sialylated Undecasaccharide–Asparagine Conjugate**

Carlo Unverzagt*

Dedicated to Professor Hans Paulsen on the occasion of his 75th birthday

Glycoproteins play an important role in organisms, and thus carbohydrates are involved in essential processes[1] directly or indirectly. Besides influencing proper folding and physical properties of proteins, oligosaccharides can also transfer biological information. Oligosaccharides are being discovered with increasing frequency as ligands in cellular recognition.[2] Adhesion phenomena mediated by the terminal tetrasaccharide sialyl Lewis^x[3] have stimulated great activity in the search for drugs against common diseases like rheumatoid arthritis and heart attack. The carbohydrate binding protein CD22[4] found on the surface of activated B lymphocytes recognizes the sequence α-*N*-acetylneuraminic acid-(2 → 6)-galactose present at the termini of asparagine-linked oligosaccharides (N-glycans). The following work presents the first synthesis of **1**, a fully glycosylated partial structure of glycoproteins. The key to the synthesis was the combination of chemical and enzymatic methods.

Many essential contributions on the chemical synthesis of N-glycans have been made by the groups of Ogawa[5] and Paulsen.[6] A milestone was the chemical synthesis of the entire carbohydrate moiety of **1**.[5a] The incorporation of these complex oligosaccharides into glycopeptides increases the demands on the protective groups employed in the peptide and in the sugar part, which may lead to severe complications in deprotection. To circumvent these difficulties, a novel concept was devel-

[*] Dr. C. Unverzagt
Institut für Organische Chemie und Biochemie
der Technischen Universität München
Lichtenbergstrasse 4, D-85748 Garching (Germany)
Fax: Int. code +(89) 2891-3210

[**] This work was supported by the Deutsche Forschungsgemeinschaft and by the Leonhard-Lorenz-Stiftung, and was presented at the Eighth European Carbohydrate Symposium 1995 in Seville (Spain). I would like to thank the Hoechst AG and Boehringer Mannheim for funding and Prof. Dr. H. Kessler for his generous support.

oped for the synthesis of N-glycans and their conjugates by using the synthetic strategies of both modern carbohydrate chemistry and the elegance of enzymatic glycosylation reactions.[8] The synthesis of the biantennary undecasaccharide–asparagine conjugate **1**, a fully glycosylated partial structure of human transferrin and ribonuclease, was accomplished for the first time by combining chemical and enzymatic methods and using the building blocks **2**–**6** (Scheme 1).

An efficient route to N-glycans developed previously relied on fragment couplings.[9] The key sequence of this strategy is a double regioselective glycosylation of the benzylidene-protected β-mannoside **3** at positions 3″ and 6″. Core trisaccharide **3** synthesized according to the β-mannosylation method of Kunz[10] was glycosylated at the equatorial 3″-OH function and not at the axial 2″-OH group. Elongation of trisaccharide **3** with the highly reactive disaccharide trichloroacetimidate **4**[9, 11, 12] gave the desired α-(1 → 3)-linked pentasaccharide **7** regio- and stereoselectively (Scheme 2). The yield of 84% is about 20% higher than that resulting from reaction with the analogous acetamido-substituted donor[9] introduced by Paulsen (62%). To exclude possible side reactions of the 2″-OH group at a later state, the pentasaccharide **7** was first acetylated (→ **8**) and the benzylidene acetal removed in aqueous acetic acid (→ **9**). Pentasaccharide **9** carries two OH groups (at positions 4″ and 6″) and reacted with donor **4** under dilute conditions to afford the α-(1 → 6)-linked heptasaccharide **10** regio- and stereoselectively. With a yield of 73% this reaction proceeded significantly better than the glycosylation of the corresponding acetamido-substituted pentasaccharide.[9] This procedure was used to prepare over five grams of heptasaccharide **10**. The advantage of phthalimido residues over acetamido groups can presumably be accounted for by the smaller amount of BF_3–OEt_2 needed for activation of trichloroacetimidates. This reduces the tendency of the imido ester in the donor molecule to rearrange to the unreactive trichloroacetamide.[14]

In the further conversion of the heptasaccharide **10** to the asparagine conjugate **13** the timing for connection to the amino acid and the sequence of deprotection had to be coordinated to

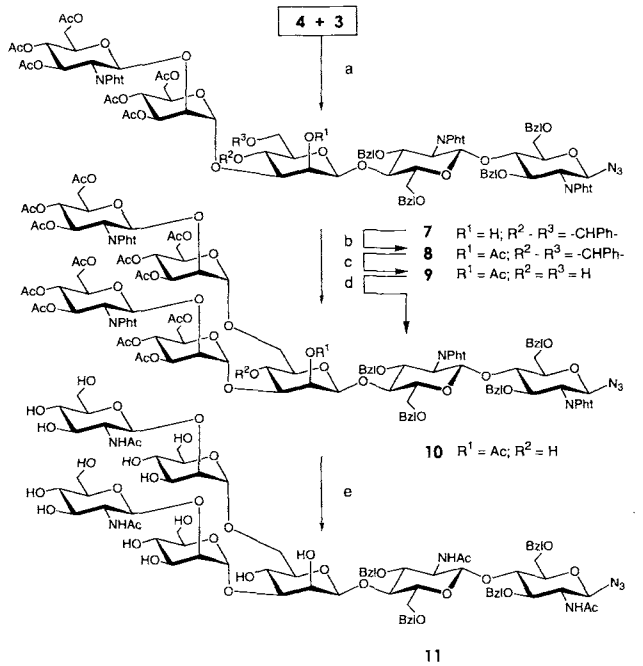

Scheme 2. BF_3–OEt_2, CH_2Cl_2 (84%); b) Ac_2O, pyridine (quant.); c) 80% AcOH, 80 °C (81%); d) **4**, BF_3–OEt_2, CH_2Cl_2 (73%); e) 1. *ethylenediamine*, *n*BuOH, 90 °C, 16 h; 2. Ac_2O, pyridine; 3. $MeNH_2$ (40%) in H_2O, (98% for steps 1–3).

accommodate the sensitive functional groups. The phthalimido groups required special attention. After the N-glycosidic linkage to asparagine was established, all attempts to remove the phthalimido residues failed. Therefore another tactic was applied. First, all acetates were removed and the phthalimido groups of **10** were replaced by acetamides. Since the four benzyl ethers of the resulting heptasaccharide **11** cannot be reduced in the presence of the anomeric azido function, the glycosylamine was generated at this point and coupled with the activated aspartic acid derivative **2**. The benzylic protective groups of the resulting heptasaccharide–asparagine conjugate **12** were removed in a single step by hydrogenolysis (Scheme 3).

The realization of this sequence required improved conditions for several reactions. Standard cleavage of the phthalimido groups of **10** with hydrazine hydrate in ethanol led to polar side products and the yields dropped to 50%. The side reactions are possibly caused by reduction of the anomeric azide by diimine,[15] which is generated from hydrazine in small amounts upon heating. When *N*-methyl hydrazine was used, the yields increased to about 70%. The best results were obtained with the conditions for dephthaloylation introduced by Hindsgaul.[16] Heating heptasaccharide **10** with ethylenediamine in *n*-butanol gave an intermediate tetraamino compound. After an acetylation–deacetylation sequence, the water-soluble heptasaccharide **11** was isolated in

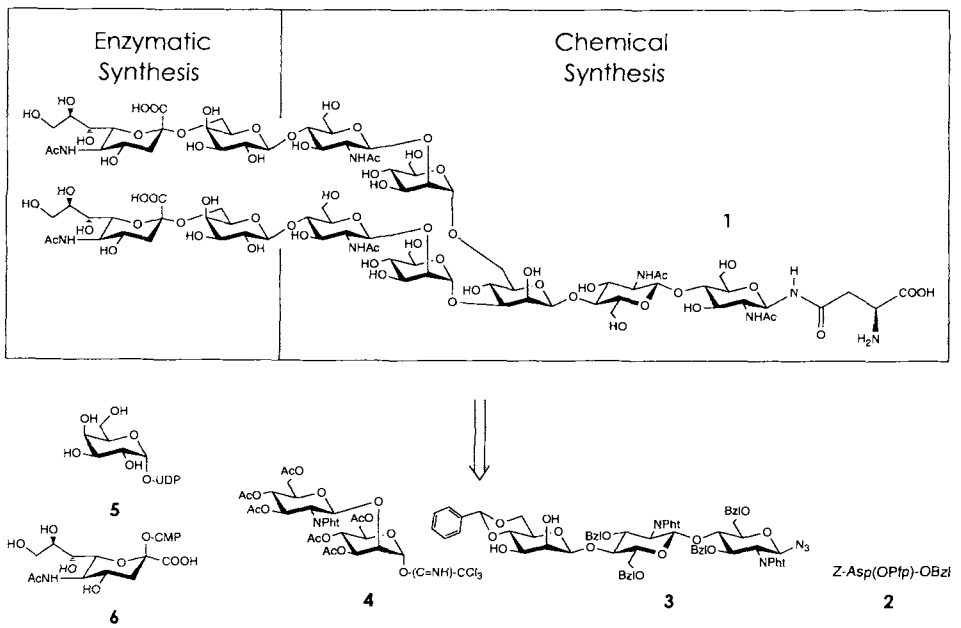

Scheme 1. The undecasaccharide–asparagine conjugate **1**, a partial structure of N-glycoproteins, was obtained by convergent chemoenzymatic synthesis using the building blocks **2**–**6**. Pht = phthaloyl, Pfp = pentafluorophenyl, CMP = cytidine-5′-monophosphate, UDP = uridine-5′-diphosphate.

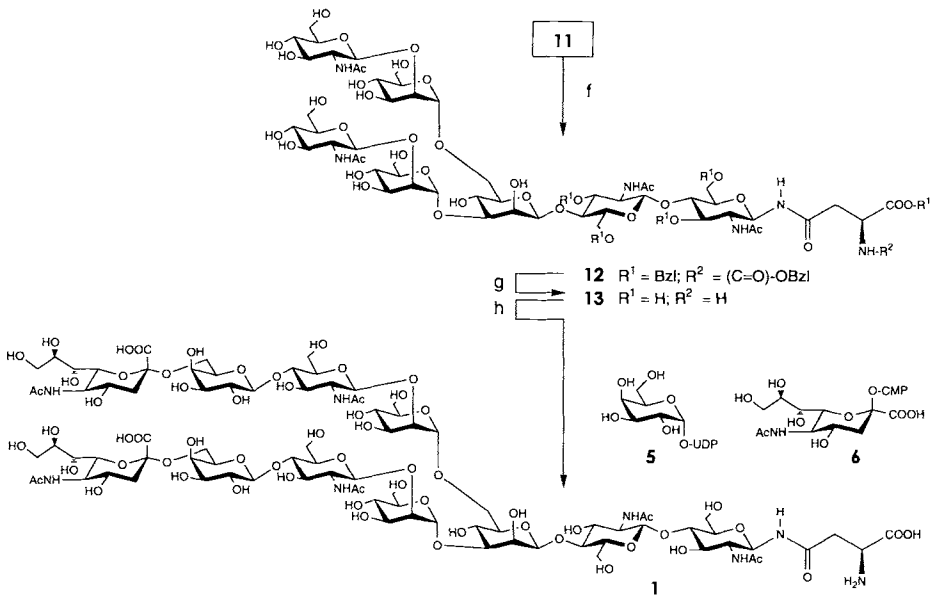

Scheme 3. f) 1. Propanedithiol, Et_3N, MeOH; 2. Z-Asp(OPfp)-OBzl, HOBt, *N*-methylpyrrolidone (NMP) (63%); g) Pd/H_2, MeOH, AcOH (95%); h) 1. UDP-Gal, galactosyl transferase, alkaline phosphatase; 2. CMP-*N*-acetylneuraminic acid (CMP-Neu5Ac), α-2,6-sialyl transferase, alkaline phosphatase (86%).

high yield (98%). This procedure proves to be very favorable for the deprotection of complex oligosaccharides containing azido groups. The selective reduction of the anomeric azide of **11** may be conducted by hydrogenolysis using Raney nickel or palladium on calcium carbonate. However, after acylation of the resulting glycosylamine with the pentafluorophenyl ester **2**, a mixture of the anomeric N-glycosides was obtained with an $\alpha:\beta$ ratio of 1:1. The proportion of the nonnatural α-glycoside exceeded 30% when the hydrogenation was conducted under basic conditions. Since glycosylamines anomerize rapidly in the presence of acids, it appears that in our case the noble metal catalyst accelerates the anomerization to the α-amine. Therefore we needed a reduction that proceeds under basic conditions without noble metals. These requirements were met by the reduction of the heptasaccharide azide **11** using excess propanedithiol in methanol–triethylamine.[19] After the reaction was terminated, the reagents were distilled off and the glycosylamine was coupled with **2**. The desired, β-configurated heptasaccharide–asparagine conjugate **12** was obtained in 63% yield after purification by HPLC. Glycosyl amino acid **12** is a chemically prepared building block useful for further conversion to **1** and for glycopeptide synthesis.[5c]

Prior to the the glycosyl transferase reactions the benzylic protective groups of **12** were removed by catalytic hydrogenation over palladium black. The deprotected heptasaccharide–asparagine conjugate **13** carries two terminal *N*-acetylglucosamine residues, which are known to be good substrates for galactosyl transferase (EC 2.4.1.22).[20] By using the alkaline phosphatase-enhanced glycosylation method,[21] two galactose residues were transferred onto **13** in one step. Alkaline phosphatase (EC 3.1.3.1) degraded the inhibitor uridine diphosphate formed during the reaction of UDP-galactose **5** with **13**. This increased the rate of reaction as well as the yield of the intermediate nonasaccharide–asparagine conjugate. Double sialylation was performed by subsequent incubation of the reaction mixture with α-(2 → 6)-sialyl transferase (EC 2.4.99.1), alkaline phosphatase, and the donor substrate CMP-*N*-acetylneuraminic acid. The enzymatic transfer of the four saccharide units was performed as a one-pot reaction and provided the undecasaccharide–asparagine conjugate **1** in 86% yield. Despite the preference[22] of both glycosyl transferases for the (1 → 3)-arm, the chosen reaction conditions led to nearly quantitative enzymatic glycosylation. Purification of the reaction mixture by size exclusion chromatography gave **1**, whose structure was confirmed by 500 MHz NMR spectroscopy,[23] comparison with reference spectra,[24] and electrospray mass spectrometry.[25] Thus the complex glycoconjugate **1**, which up to now could only be isolated from natural sources,[26] has been prepared by chemical synthesis for the first time.

The synthesis of *N*-glycans remains a challenging task that can be improved by combining the advantages of chemical and enzymatic methods. Currently, the incorporation of **1** into glycopeptides is being examined in the synthesis of fully glycosylated glycoprotein fragments.

Received: January 31, 1996 [Z8772IE]
German version: *Angew. Chem.* **1996**, *108*, 2507–2510

Keywords: carbohydrates · chemoenzymatic syntheses · glycoproteins · glycosides · polysaccharides

[1] a) A. Varki, *Glycobiology* **1993**, *3*, 97–130; b) R. A. Dwek, *Chem. Rev.* **1996**, *96*, 683–720.
[2] T. A. Springer, L. A. Lasky, *Nature* **1991**, *349*, 196–197.
[3] a) M. L. Phillips, E. Nudelman, F. C. A. Gaeta, M. Perez, A. K. Singhal, S.-I. Hakomori, J. C. Paulson, *Science*, **1990**, *250*, 1130–1132; b) G. Walz, A. Aruffo, W. Kolanus, M. Bevilaqua, B. Seed, *Science*, **1990**, *250*, 1132–1135; c) L. A. Lasky, *Science* **1992**, *258*, 964–969; d) A. Giannis, *Angew. Chem.* **1994**, *106*, 188–191; *Angew. Chem. Intl. Ed. Engl.* **1994**, *33*, 178–180.
[4] L. D. Powell, D. Sgroi, E. R. Sjoberg, I. Stamencovic, A. Varki, *J. Biol. Chem.* **1993**, *268*, 7019–7027.
[5] a) T. Ogawa, M. Sugimoto, T. Kitajma, K. K. Sadozai, T. Nukada, *Tetrahedron Lett.* **1986**, *27*, 5739–5742; b) Y. Nakahara, S. Shibayama, Y. Nakahara, T. Ogawa, *Carbohydr. Res.* **1996**, *280*, 67–84; c) I. Matsuo, Y. Nakahara, Y. Ito, T. Nukada, Y. Nakahara, T. Ogawa, *Bioorg. Med. Chem.* **1995**, *3*, 1455–1463.
[6] Review: H. Paulsen, *Angew. Chem.* **1990**, *102*, 851–857; *Angew. Chem. Intl. Ed. Engl.* **1990**, *29*, 823–839.
[7] H. G. Garg, K. von dem Bruch, H. Kunz in *Adv. Carbohydr. Chem. Biochem.* **1994**, *50*, 277–310.
[8] Review on enzymatic glycosylations: C.-H. Wong, R. L. Halcomb, Y. Ichikawa, T. Kajimoto, *Angew. Chem.* **1995**, *107*, 453–474, 569–593; *Angew. Chem. Int. Ed. Engl.* **1995**, *34*, 412–432, 521–546.
[9] C. Unverzagt, *Angew. Chem.* **1994**, *106*, 1170–1173; *Angew. Chem. Int. Ed. Engl.* **1994**, *33*, 1102–1104.
[10] a) H. Kunz, W. Günther, *Angew. Chem.* **1988**, *100*, 1118–1191; *Angew. Chem. Int. Ed. Engl.* **1988**, *27*, 1086–1087; b) W. Günther, H. Kunz, *Carbohydr. Res.* **1992**, *228*, 217–241.
[11] R. R. Schmidt, W. Kinzy in *Adv. Carbohydr. Chem. Biochem, Vol. 50* (Ed.: D. Horton), Academic Press, New York, **1994**, p. 21.
[12] Donor **4**[9] was obtained on a 20 g scale by the following reaction sequence: a) 1,3,4,6-tetra-*O*-acetyl-β-D-mannopyranose and 3,4,6-tri-*O*-acetyl-2-deoxy-2-phthalimido-β-D-glucopyranosyl-trichloroacetimidate, CH_2Cl_2, molecular sieves 4 Å, BF_3–Et_2O (59%); b) hydrazine acetate, DMF (85%); c) CCl_3CN, 1,8-diazabicyclo[5.4.0]undec-7-ene (DBU), CH_2Cl_2 (89%).
[13] H. Paulsen, B. Helpap, *Carbohydr. Res.* **1991**, *216*, 289–313.
[14] F. Cramer, N. Hennrich, *Chem. Ber.* **1961**, *94*, 976–989.
[15] S. Hünig, H. R. Müller, W. Thier, *Angew. Chem.* **1965**, *77*, 368–377; *Angew. Chem. Int. Ed. Engl.* **1965**, *4*, 271–280.
[16] O. Kanie, S. C. Crawley, M. M. Palcic, O. Hindsgaul, *Carbohydr. Res.* **1993**, *243*, 139–164.
[17] Preparation of **2**: M. Green, J. Bermann, *Tetrahedron Lett.* **1990**, *31*, 5851–5852.

 © VCH Verlagsgesellschaft mbH, D-69451 Weinheim, 1996 0570-0833/96/3520-2352 $ 15.00+.25/0

[18] Synthesis of the GlcNAc-β-Asn bond without use of noble metals: a) A. Y. Khorlin, S. E. Zurabayan, R. G. Macharadze, *Carbohydr. Res.* **1990**, *85*, 201–208; b) T. Inazu, K. Kobayashi *Synlett.* **1993**, 869–870; c) S. T. Cohen-Anisfield, P. T. Lansbury, Jr., *J. Am. Chem. Soc.* **1993**, *115*, 10531–10537.

[19] a) A. Bayley, D. N. Standring, J. R. Knowles, *Tetrahedron Lett.* **1978**, *19*, 3633–3634; b) According to this procedure an anthracene sulfonamide was cleaved with concomitant reduction of an azido group: J. Y. Roberge, X. Beebe, S. J. Danishefsy, *Science* **1995**, *269*, 202–204.

[20] a) L. J. Berliner, M. E. Davis, K. E. Ebner, T. A. Beyer, J. E. Bell, *Mol. Cell Biochem.* **1984**, *62*, 37–42; b) C. Augé, R. Fernandez-Fernandez, C. Gautheron, *Carbohydr. Res.* **1990**, *200*, 257–268; c) J. Lehmann, *Carbohydr. Res.* **1994**, *252*, 325–332.

[21] a) C. Unverzagt, H. Kunz, J. C. Paulson, *J. Am. Chem. Soc.* **1990**, *112*, 9308–9309; b) C. Unverzagt, S. Kelm, J. C. Paulson, *Carbohydr. Res.* **1994**, *251*, 285–301; c) We were informed that the influence of alkaline phosphatase in galactosylations was also examined by A. Redlitz (Diplomarbeit, Berlin, **1988**). d) Glycosyl transferases and nucleotide sugars were obtained from Sigma, alkaline phosphatase (calf intestine) from Boehringer Mannheim.

[22] Review: H. Schachter, *Biochem. Cell. Biol.* **1986**, *64*, 163–181.

[23] **1**: 5.6 mg yield (86% based on **13**); $[\alpha]_D^{23} = -9.1°$ (0.5, H_2O); ^1H NMR (500 MHz, D_2O): $\delta = 5.19$ (d, $J_{1,2} < 1.0$ Hz, 1H, H-1^A), 5.12 (d, $J_{1,2} = 9.7$ Hz, 1H, H-1^1), 5.01 (d, $J_{1,2} < 1.0$ Hz, 1H, H-1$^{A'}$), 4.83 (d, $J_{1,2} < 1.0$ Hz, 1H, H-1^3), 4.69–4.65 (m, 3H, H-1^2, H-1^5, H-1$^{5'}$), 4.505, 4.502 (2d, $J_{1,2} = 7.8$ Hz, 2H, H-1^6, H-1$^{6'}$), 4.31 (dd, $J_{2,3} = 1.9$ Hz, H-2^3), 4.25 (dd, $J_{2,3} = 1.9$ Hz, H-2^4), 4.17 (dd, $J_{2,3} = 1.9$ Hz, H-2$^{4'}$), 3.00 (dd, $J_{gem} = 17.2$ Hz, $J_{vic} = 4.2$ Hz, 1H, β-CHa-Asn), 2.92 (dd, $J_{vic} = 7.0$ Hz, 1H, β-CHb-Asn), 2.76–2.71 (m, 2H, H-3eq^N, H-3eq$^{N'}$), 2.14, 2.13, 2.09, 2.07, 2.06 (5s, 18H, NAc), 1.78 (t, $J_{gem} = 12.1$ Hz, 2H, H-3ax^N, H-3ax$^{N'}$). ^{13}C NMR (125 MHz, D_2O, [D_6] DMSO as internal standard; the chemical shifts were determined by an HMQC spectum): $\delta = 104.8$ C-1^6, C-1$^{6'}$, 102.6 C-1^2, 101.8 C-1^3, 100.7 C-1^4, 100.6 C-1^5, C-1$^{5'}$, 98.1 C-1$^{A'}$, 81.9 C-4^5, C-4$^{5'}$, 81.8 C-3^3, 80.9 C-4^2, 80.2 C-4^1, 79.4 C-1^1, 77.8 C-2^4, 77.6 C-2$^{4'}$, 77.5 C-5^3, 75.7 C-5^2, C-5^3, C-5^5, C-5$^{5'}$, 75.0 C-5^6, C-5$^{6'}$, 74.9 C-5^4, 74.1 C-5$^{4'}$, 74.0 C-3^1, 73.8 C-3^6, C-3$^{6'}$, C-3^N, C-3$^{N'}$, 73.3 C-3^2, C-3^5, C-3$^{5'}$, 73.0 C-8^N, C-8$^{N'}$, 72.0 C-2^6, C-2$^{6'}$, 71.4 C-2^3, 70.7 C-3^4, C-3$^{4'}$, 69.7 C-7^N, C-7$^{N'}$, 69.6 C-4^6, C-4$^{6'}$, 69.4 C-4^N, C-4$^{N'}$, 68.6 C-4^4, C-4$^{4'}$, 67.1 C-6^3, 67.0 C-4^3, 64.6 C-6^6, C-6$^{6'}$, 64.0 C-9^N, C-9$^{N'}$, 62.9 C-6^4, C-6$^{4'}$, 61.5 C-6^5, C-6$^{5'}$, 61.2 C-6^2, 61.1 C-6^1, 56.2 C-2^2, 55.9 C-2^5, C-2$^{5'}$, 54.9 C-2^1, 53.2 C-5^N, C-5$^{N'}$, 52.1 αC-Asn, 39.0 C-3^N, C-3$^{N'}$, 36.3 βC-Asn, 23.9, 23.8, 23.7 NAc.

[24] L. Dorland, J. Haverkamp, B. L. Schut, J. F. G. Vliegenthart, *FEBS Lett.* **1977**, *77*, 15–20.

[25] ESI-MS: (50% 0.01 M NH_4OAc, 50% acetonitrile): $C_{88}H_{144}N_8O_{64}$ M_r (calcd) = 2336.8; M_r (found) = 2337.8 ($M+1$).

[26] R. R. Townsend, E. Hilliker, Y.-T. Li, R. A. Laine, W. R. Bell, Y. C. Lee, *J. Biol. Chem.* **1982**, *257*, 9704–9710.

Aromatic Hydroxylation by H_2O_2 and O_2 Catalyzed by a μ-Oxo Diiron(III) Complex

Stéphane Ménage, Jean-Baptiste Galey, Georges Hussler, Michel Seité, and Marc Fontecave*

Recently a new class of enzymes, the diiron–carboxylato proteins, has emerged in which the active center contains two ferric ions linked by an oxo or hydroxo bridge and one or two carboxylato bridges of glutamate or aspartate residues.[1] Methane monooxygenase converts not only methane into methanol but reacts with a great variety of alkanes, alkenes, and aromatic compounds as well.[2] Ribonucleotide reductase oxidizes an endogeneous tyrosine to a tyrosyl radical, which initiates the conversion of ribonucleotide to deoxyribonucleotide.[3] The iron center of ribonucleotide reductase also has the potential to catalyze hydroxylation reactions as shown by the transformation of a tyrosine residue, brought into proximity of the active iron center by site-directed mutagenesis, into 3,4-dihydroxyphenylalanine (dopa).[4]

Many model compounds have been prepared but few are capable of displaying enzymatic activity such as hydroxylation of C–H bonds by molecular oxygen or hydrogen peroxide.[5, 6] Our approach here was to mimic quite closely the active center of methane monooxygenase as far as the carboxylato-rich environment of iron and the vicinity of a substrate site are concerned. An ethylenediamine tetraacetic acid (EDTA) derivative has been designed in which two carboxylato moities have been replaced by two phenyl groups which serve as substrates for the oxidation reaction.

Mixing a 1 mM solution of *N*,*N*′-bis-(3,4,5-trimethoxybenzyl)ethylenediamine *N*,*N*′-diacetic acid (ligand L)[7] with four equivalents of triethylamine in water/acetonitrile (1:1), one equivalent of $Fe(ClO_4)_3 \cdot 9H_2O$, and ten equivalents of sodium acetate led to the formation of the μ-oxo μ-acetato diferric complex $[Fe_2OL_2(CH_3CO_2)]^+$ (**1**). Its characterization in solution

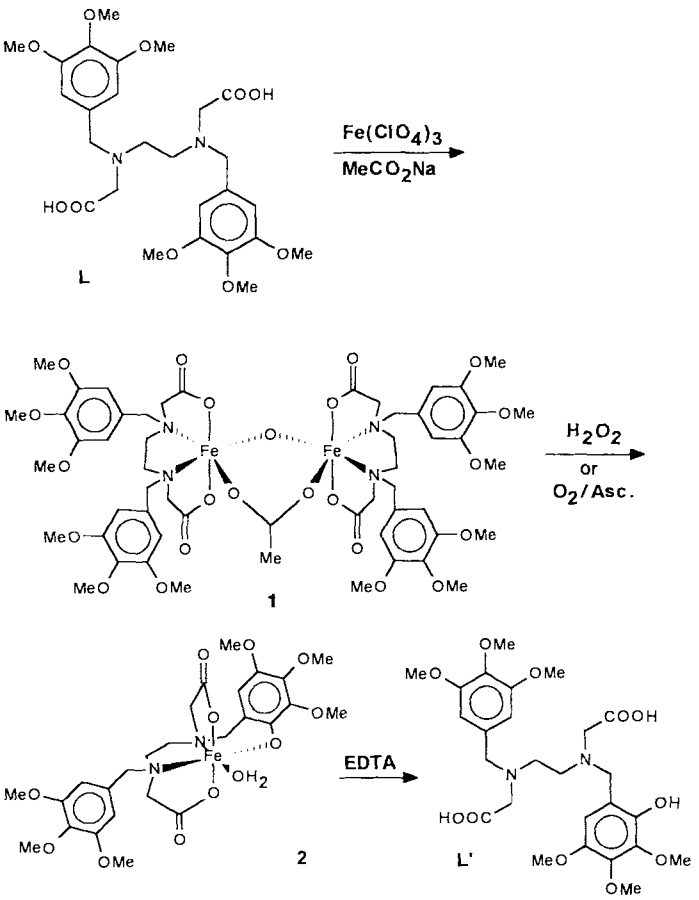

was based on its UV visible spectrum,[8] which is indeed typical of μ-oxo μ-carboxylato diferric complexes.[9] Its ESI-MS spectrum[10] displays one negative ion peak at m/z 1255.5 (100%) corresponding to the pseudo-molecular ion $[Fe_2OL_2(CH_3CO_2)]^-$.[11] Assignments were confirmed by a comparison to the calculated isotopic pattern (Fig. 1). The solution was found to be EPR silent suggesting that the ferric ions are antiferromagnetically coupled through the oxo bridge. The ^1H NMR (200 MHz, CD_3CN/D_2O) spectrum of **1** in solution displays few resonances. Of interest is the resonance at $\delta = 12.5$, which is attributed to the acetate methyl protons. Such a chemical shift

[*] Prof. M. Fontecave, Dr. S. Ménage
L. E. D. S. S., UMR 5616, Université J. Fourier
BP53X, F-38052 Grenoble, Cedex 09 (France)
Fax: Int. code +76514382
Dr. J.-B. Galey, Dr. G. Hussler, M. Seité
L'Oreal Research Center
1 avenue Eugène Schueller
F-93600 Aulnay sour bois (France)

 © VCH Verlagsgesellschaft mbH, D-69451 Weinheim, 1996 0570-0833/96/3520-2353 $ 15.00+.25/0

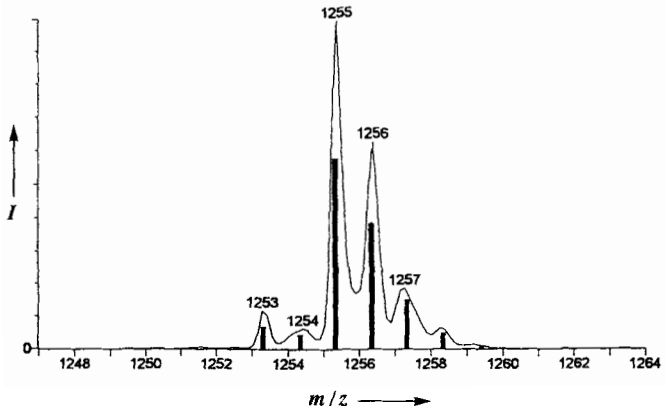

Fig. 1. Negative ionization electrospray mass spectrum of **1**. The calculated isotopic pattern for $C_{26}H_{36}O_{11}Fe$ is indicated by the bars.

indicates that the acetate is in a bridging coordination mode.[12] With a propionate as the bridging carboxylate group, the methylene protons resonated at $\delta = 11.3$ and the ring *m*-protons at $\delta = 9.03$ in the case of a benzoato bridge. All attempts to isolate and crystallize **1** were unsuccessful. However, based on the above data **1** is proposed to be a dinuclear ferric complex with one acetato and one oxo bridge. The coordination sphere for each iron is completed by two oxygen and two nitrogen atoms from the carboxylato and tertiary amino moieties of the ligand, respectively.

When three equivalents of hydrogen peroxide were added to a 1 mM solution of **1**, either in aqueous acetate buffer (pH 5.4) or acetonitrile/water (1:1), the solution turned deep blue as a result of the formation of a new chromophore with maximum absorption at 560 nm (Fig. 2). After saturation of the solution with NaCl, the new species **2** could be extracted with CH_2Cl_2. It was shown to be a monomeric ferric complex in which the ligand L is hydroxylated at position 2 of one of the phenyl groups. Monohydroxylation of L was assessed by ^1H and ^{13}C NMR spectroscopy after reduction of **2** with dithionite. The

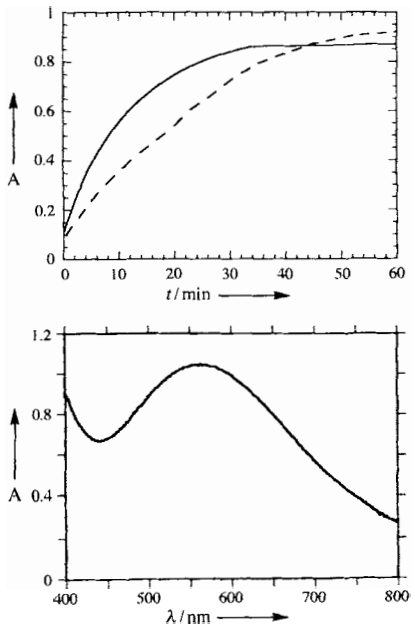

Fig. 2. Top: Absorbance at 560 nm versus time for the reaction of **1** [0.75 mM] with H_2O_2 (3 equiv, —) or O_2 (diffusing into the UV cell) and 15 equiv of ascorbate (– – –). Bottom: UV/Vis spectrum recorded at the end of the reaction.

positive mode ESI-MS analysis of **2** reveals only a signal at *m/z* 606 (90%) with the appropriate peak pattern for the pseudomolecular ion $[Fe(L') + H]^+$. No evidence was found for an ion corresponding to a binuclear species. After workup of the reaction mixture with excess EDTA to remove the metal ion, the modified ligand L′ was analyzed by HPLC/ESI-MS and confirmed to be *N*-(2-hydroxy-3,4,5-trimethoxybenzyl)-*N*′-(3,4,5-trimethoxybenzyl)ethylenediamine *N*,*N*′diacetic acid.[13] The yield of the oxidation reaction, based on the concentration of L, approached 80%. Attempts to crystallize the product were again unsuccessful due to its very high solubility in all solvents. The very intense transition at 560 nm in the visible region of the absorption spectrum of **2** can be attributed to a phenolato-to-iron charge transfer band ($\varepsilon = 1500\ M^{-1}cm^{-1}$).[14] The EPR spectrum of **2** displays a transition centered at $g = 4.3$ at 100 K for a mononuclear, hexacoordinated, high-spin iron(III) ion.[15] It is noteworthy that the EPR feature at $g = 4.3$ and the 560 nm absorption band simultaneously increased during the conversion of **1** into **2**. We thus propose that in **2** the iron(III) center is coordinated by two nitrogen atoms and four oxygen atoms (two from the carboxylato moities, one from the phenolate, and one from a water molecule).[16]

In the presence of acetate, L coordinates to iron to generate a dinuclear complex in which the ferric ions are doubly bridged by an oxo and an acetato group. The ligand L provides phenyl groups adjacent to the iron center as substrates for oxidation. Because of the well-established lability of acetato bridges,[17] reaction with H_2O_2 is possible and actually leads to aromatic hydroxylation. At the end of the reaction, the dinuclear unit is not recovered. Instead a mononuclear complex is obtained with the new phenolate moiety bound to iron. The ligand L is probably only monohydroxylated because the resulting iron–phenolato complex **2** is unable to bind and activate H_2O_2 as a consequence of the greatly decreased acidity of the ferric ion.

While alkylhydroperoxides, sodium hypochlorite, and *m*-chloroperbenzoic acid do not oxidize **1** under the conditions used with H_2O_2, monohydroxylation occurred in the absence of H_2O_2 but in the presence of molecular oxygen and excess ascorbate as a reductant (Fig. 2). The kinetics and yield of the reaction are comparable to those of the H_2O_2-dependent reaction. No reaction occurred in the absence of ascorbate. Treating **1** with ascorbate for half an hour under anaerobic conditions partially bleached the solution. Addition of O_2 then generated the 560 nm-absorbing complex **2**. This strongly indicates that ascorbate is involved in the formation of a ferrous complex which can bind and activate dioxygen. It is unlikely that the reaction depends on the formation of H_2O_2, since it is not affected by the addition of catalase.

To our knowledge, this is the first report of reductive activation of molecular oxygen resulting in aromatic hydroxylation which is promoted by a dinuclear ferric complex. This is a model for methane monooxygenase- or ribonucleotide reductase-dependent reactions. The hydroxylation of a tyrosine residue within a mutant of ribonucleotide reductase is here elegantly mimicked in that, as in the enzyme, the hydroxylated reaction product is bound to the iron center.[4] It must be noted that such chemistry is well established in the case of copper enzymes and their model compounds.[18]

Received: April 19, 1996 [Z9052IE]
German version: *Angew. Chem.* **1996**, *108*, 2535–2537

Keywords: complexes with oxygen ligands · enzyme models · iron compounds · oxidations

 © VCH Verlagsgesellschaft mbH, D-69451 Weinheim, 1996 0570-0833/96/3520-2354 $ 15.00+.25/0

[1] a) A. C. Rosenzweig, C. A. Frederick, S. J. Lippard, P. Nordlund, *Nature* **1993**, *366*, 537; b) P. Nordlund, H. Eklund, B.-M. Sjöberg, *ibid.* **1990**, *345*, 593; c) L. Que, Jr., A. E. True, *Prog. Inorg. Chem.* **1990**, *38*, 97; d) J. Sanders-Loehr in *Iron Carriers and Iron Proteins* (Ed.: T. M. Loehr), VCH, New York, **1989**, 375.

[2] J. Green, H. Dalton, *J. Biol. Chem.* **1989**, *264*, 17698.

[3] M. Fontecave, P. Nordlund, H. Eklund, P. Reichard, *Adv. Enzymol.* **1993**, *65*, 147.

[4] A. Åberg, M. Ormö, P. Nordlund, B.-M Sjöberg, *Biochemistry* **1993**, 9845.

[5] D. Kurtz, *Chem. Rev.* **1993**, 586.

[6] L. Que, Jr. in *Bioinorganic Catalysis* (Ed.: J. Reedjik), Dekker, **1993**.

[7] J. B. Galey, J. Dumats, S. Génard, O. Destrée, P. Pichaud, P. Catroux, L. Marrot, I. Beck, B. Fernandez, G. Barre, G. Hussler, M. Seité, M. Hocquaux, *Biochem. Pharmacol.* **1996**, *51*, 103.

[8] UV/Vis (CH_3CN/H_2O): λ_{max} (ε) = 640 (160), 495 (530), 435 (1250) 350 (shoulder), 325 nm (10000). These bands are attributed to oxo–Fe^{III} ligand-to-metal charge transitions.

[9] S. Ménage, L. Que, Jr., *New. J. Chem.* **1991**, 431.

[10] ESI-MS analysis has proven to be a powerful technique in characterizing iron and manganese polynuclear complexes: U. N. Andersen, C. J. Mackenzie, G. Bergesen, *Inorg. Chem.* **1995**, *34*, 1435.

[11] Two more positive mode peaks were present at *m/z* (%) 1257.3 (100) and 1279.2 (10) for $[Fe_2OL_2(CH_3CO_2)+2H]^+$ and $[Fe_2OL_2(CH_3CO_2)+H+Na]^+$, respectively, with the expected isotopic patterns.

[12] D. Kurtz, *J. Am. Chem. Soc.* **1989**, *111*, 6563.

[13] The blue solution was treated with 3 mM EDTA and heated at 40 °C for 40 min. HPLC analysis was performed on a Waters Pursil C18 120 column [7].

[14] A. B. P. Lever *Inorganic Electronic Spectroscopy*, Elsevier, New York, **1984**, 311.

[15] EPR titration were done at 100 K with $[Fe^{III}(L'')(H_2O)]$ as a reference.

[16] An analog of **2**, $[Fe^{III}(L'')(H_2O)]$ (L'' = *N*-(2-hydroxybenzyl)-*N'*-(benzyl)-ethylenediamine *N,N'*diacetic acid), which shows similar spectroscopic characteristics has been isolated as a powder. A high-spin ferric EPR signal was observed and a phenolato-to-Fe^{III} CT band was present at 520 nm (1500) in its electronic spectrum. Elemental analysis for $[Fe(L'')(H_2O)]\cdot 1.5\ H_2O$: calcd for $FeC_{20}H_{26}N_2O_{7.5}$ (M_r = 470.1): C 51.10, H 5.53, N 5.96, Fe 11.88; found: C 51.23, H 5.43, N 6.05, Fe 12.00.

[17] S. Ménage, J.- M. Vincent, C. Lambeaux, G. Chottard, A. Grand, M. Fontecave, *Inorg. Chem.* **1993**, *32*, 4766.

[18] a) S. Itoh, T. Kondo, M. Komatsu, Y. Ohshiro, C. Li, N. Kanehisa, Y. Kai, S. Fukuzumi, *J. Am. Chem. Soc.* **1995**, *117*, 4714, and references therein; b) M. S. Nasir, K. D Karlin, D. McGowty, J. Zubieta, *ibid.* **1991**, *113*, 698.

A New In_4 Cluster with Short In–In Bonds in Trigonal-Planar $In(InTrip_2)_3$**

Penelope J. Brothers,* Klaus Hübler, Ute Hübler, Bruce C. Noll, Marilyn M. Olmstead, and Philip P. Power*

Homocatenation is an important feature of the chemistry of Group 14 elements, but in Group 13 it appears widely only for the lightest element, boron. Nonetheless, the synthesis and structural characterization of metal–metal bonded organoelement compounds of the heavier Group 13 metals has undergone a very rapid development since the late 1980s, and new structural and bonding types continue to be reported frequently. The simplest of these are the dimetallanes, R_2M-MR_2 (M = Al, Ga, In, Tl; R = alkyl, aryl, silyl)[1–6] and their derivatives $[R_2M-MR_2]^-$ obtained by one-electron reduction.[7] Cluster compounds $(MR)_n$ exhibit tetrahedral ($[AlCp^*]_4$, $[MC(SiMe_3)_3]_4$, M = Ga, In), octahedral ($[AlrBu]_6^-$, $[InCp^*]_6$), or icosahedral ($[AliBu]_{12}^{2-}$) geometry.[1c, 8, 9] An Al_4 ring is found in $[Al_4Br_4(NEt_3)_4]$ whereas the cyclic trigallane dianion $[Ga(2,6\text{-}Mes_2C_6H_3)]_3^{2-}$ (Mes = 2,4,6-$Me_3C_6H_2$) is a cyclopropenium ion analog.[10, 11] Chlorogallium compounds $[Ga_4Cl_4\{Si(SiMe_3)_3\}_4]$ and $[Ga_5Cl_7(OEt_2)_5]$ consist of a Ga_4Cl_4 cage containing two Ga–Ga bonds[12] and a neopentane-like $GaGa_4$ skeleton,[13] respectively.

The tetraaryl dialane and digallane $Trip_2M-MTrip_2$ (Trip = 2,4,6-$iPr_3C_6H_2$) have been shown to be useful substrates for reduction by lithium metal to yield the one-electron π-bonded compounds $[Trip_2M\cdots MTrip_2]^{\cdot -}$ with an M–M π-bond order of 0.5.[7] We undertook the synthesis of the indium analog $Trip_2In-InTrip_2$ (**1**) to investigate its reduction by similar methods. Reaction of the tetrabromodiindane $[In_2Br_4(tmeda)_2]$[4] (tmeda = tetramethylethylenediamine) with TripMgBr at low temperature afforded **1** as large, bright orange crystals [Eq. (a)].

$$(tmeda)Br_2In-InBr_2(tmeda) \xrightarrow[Et_2O,\ -15°C]{TripMgBr} \underset{\mathbf{1}}{Trip_2In-InTrip_2} \qquad (a)$$

The compound is thermally and photochemically sensitive; above −10 °C decomposition results in the deposition of indium metal. The crystal structure of **1** (Fig. 1)[14] shows it to be a highly symmetrical compound, lying on a site of 222 symmetry in the unit cell. The In–In distance of 2.775(2) Å is comparable to that of the small number of related three-coordinate diindanes (Table 1). The angle between the normals to the C-In-C planes is 47.8° and each aryl ring is oriented at 63° with respect to this plane at the corresponding indium atom.

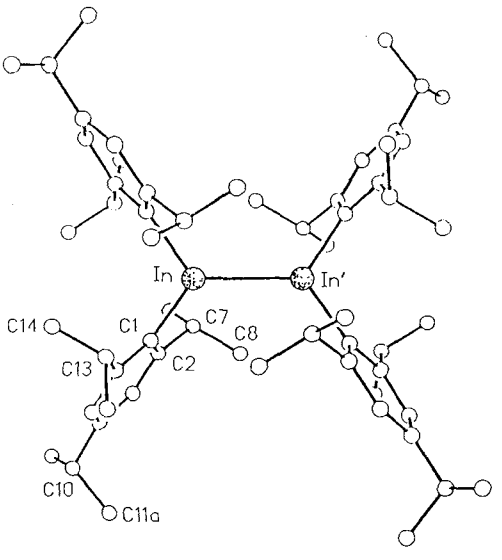

Fig. 1. Molecular structure of **1**. Selected bond lengths [Å] and angles [°]: In–In' 2.775(2), In–C1 2.184(7); In'-In-C1 121.6(2), C1-In-C1' 116.8(4).

[*] Dr P. J. Brothers, Dr K. Hübler, Dr U. Hübler
Department of Chemistry, University of Auckland
Private Bag 92019, Auckland (New Zealand)
Fax: Int. code +9 373 7422
email: p.brothers@auckland.ac.nz
Prof. P. P. Power, Dr B. C. Noll, Dr M. M. Olmstead
Department of Chemistry, University of California
Davis, CA 95616 (USA)

[**] This work was supported by the National Science Foundation. P. J. B. thanks the University of Auckland for granting sabbatical leave and K. H. thanks the Alexander von Humboldt Foundation (Lynen Fellowship).

 © VCH Verlagsgesellschaft mbH, D-69451 Weinheim, 1996 0570-0833/96/3520-2355 $ 15.00+.25/0

Table 1. Indium–indium bond lengths d(In–In) [Å] and oxidation states for organoindium complexes.

Compound	Ref.	Ox. state	d(In–In)
$In(InTrip_2)_3$	this work	1.5 [a]	2.696(2)
$\{2,4,6\text{-}(CF_3)_3C_6H_2\}_2InIn\{C_6H_2\text{-}2,4,6\text{-}(CF_3)_3\}_2$	[2]	2	2.744(2)
$(t\mathrm{BuN})_2\{MeSi(t\mathrm{Bu})N\}_2InIn\{N(t\mathrm{Bu})SiMe\}_2(Nt\mathrm{Bu})_2$	[3]	2	2.768(1)
$Trip_2InInTrip_2$	this work	2	2.775(2)
$\{(Me_3Si)_2CH\}_2InIn\{CH(SiMe_3)_2\}_2$	[4]	2	2.828(1)
$(t\mathrm{Bu}_3Si)_2InIn(Sit\mathrm{Bu}_3)_2$	[5]	2	2.9217(11)
$\{InC(SiMe_3)_3\}_4$[b]	[8]	1	3.002 [a], 3.09 [a]
$(PhCH_2C)_5InIn(CCH_2Ph)_5$	[19]	1	3.631 [a]
$(InCp^*)_6$	[9]	1	3.952 [a]
In–In (in the metal)	[18]	0	3.252, 3.377

[a] Average value. [b] Two independent determinations.

Compound **1** was reduced with lithium powder suspended in ether at −78 °C. The bright orange color rapidly darkened to give a deep red-brown solution [Eq. (b)]. Crystallization

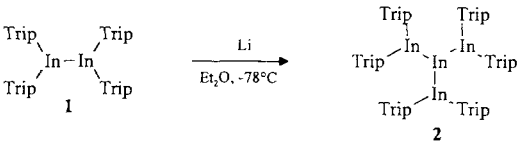

(b)

at −20 °C resulted in the new organoindium compound **2** in low yield. The identity of **2** was determined by X-ray crystallography,[15] which showed it to be a triindylindane with the formula $In(InTrip_2)_3$ (Fig. 2).[16] The compound consists of a central

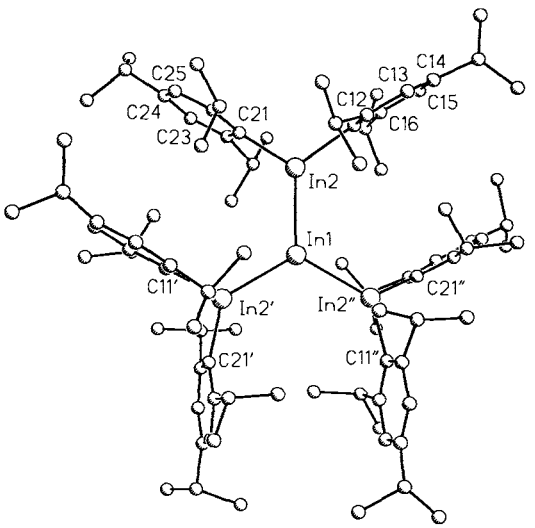

Fig. 2. Molecular structure of **2**. Selected bond lengths [Å] and angles [°]: In1–In2 2.696(2), In2–C11 2.25(2), In2–C21 2.19(2); In2-In1-In2' 120.0(1), In1-In2-C11 121.7(5), In1-In2-C21 123.0(6), C11-In2-C21 115.3(8).

indium atom bearing three $InTrip_2$ substituents, giving a trigonal-planar In_4 array with In-In-In angles of 120.0(1)° and In–In bond lengths of 2.696(2) Å. Since the molecule occupies a site of three-fold symmetry, there is just one unique $InTrip_2$ group. The C-In-C plane is tilted at an angle of 31.6° to the In_4 plane, and each aryl ring is oriented at about 77° to the C-In-C plane.

The reduction of **1** to give the new triindylindane **2** is a surprising result. When the aluminum and gallium analogs of **1** are reduced under the same conditions the only products isolated are the radical anions $[Trip_2M{\cdot\!\cdot}MTrip_2]^{\bullet-}$ (M = Al, Ga) with no change in composition of the molecules.[7] The formation of **2** (average In oxidation state +1.5) from **1** (oxidation state +2) does correspond to a formal reduction, but the overall stoichiometry is not clear due to the low yield of the isolated product and the presence of excess reducing agent. Other reduced In species may also be formed. The chemical sensitivity of **1**, which had been observed to produce small amounts of In metal upon decomposition, may also play a part in the reaction.

The trigonal $In(In)_3$ arrangement seen in the crystal structure of **2** is a geometry that is unprecedented for the heavier Group 13 elements. Catenated compounds (alkane analogs) with a σ-bonded metal–metal framework are well known for the neighboring element tin. They show chains containing up to six tin atoms, rings Sn_nR_{2n} with $n = 3$–9, branched polystannanes such as in the neopentane analog $Sn(SnMe_3)_4$, and other geometries like the propellane Sn_5Ar_6 and the cubane Sn_8Ar_8.[17] In contrast, metal–metal bonds connected by a σ-bonded framework in three-coordinate compounds of the heavier Group 13 elements have been limited to just two atoms in the dimetallanes $R_2M{-}MR_2$. Two further examples, $[Al_4Br_4(NEt_3)_4]$ containing an Al_4 ring[10] and the neopentane-like compound $[Ga_5Cl_7(OEt_2)_5]$,[13] exhibit coordination number four at the metal centers and are stabilized by NEt_3 or Et_2O donors. Al, Ga, or In compounds containing an M_4 cluster have hitherto existed in a tetrahedral arrangement with the stoichiometry M_4R_4, rather than the M_4R_6 formula existing in **2**.

Three-coordination at the metal center in **1** and its Al and Ga analogs can be attributed to the steric effect of the bulky Trip substituents. However, in **2** the central indium does not bear these bulky substituents and yet the three ether solvate molecules found in the unit cell are not coordinated to the unsaturated indium centers.

The In–In bond length in **2** (2.696(2) Å) is the shortest yet observed in a molecular indium compound and is significantly shorter than those in indium metal (3.252 and 3.377 Å,[18] Table 1). The diindane **1** and its analogs show In–In bonds ranging from 2.744(2) to 2.922(1) Å,[2–5] whereas those in the dimeric, tetrahedral, and octahedral cluster compounds $(InR)_n$ are longer than 3.0 Å.[8, 9, 19] The ternary oxide $In_{11}Mo_{40}O_{62}$, which contains linear In_5^{7+} and In_6^{8+} cations with In–In separations of 2.624–2.689 Å, is the only example exhibiting shorter In–In distances than **2**, but it is not a molecular species.[20] Since the valence electrons in **2** are fully accounted for in the $InIn_3$ σ-bonded framework, the bond shortening cannot be directly attributed to simple π-type multiple bonding and is most likely due to the lack of bulky organic substituents on the central In atom. Calculations are being undertaken to probe the bonding and properties of **2**.

Experimental Procedure

1: Under anaerobic and anhydrous conditions, $In_2Br_4(tmeda)_2$ (4.56 g, 5.83 mmol) was suspended in diethyl ether (30 mL) and cooled to −78 °C. TripMgBr (125 mL of a 0.16 M solution in diethyl ether, 20 mmol) was added dropwise through a cannula. The solution was stirred at −78 °C for 1 h and then warmed to −15 °C in an ice/salt bath, during which time the solution began to turn orange. Stirring was maintained at −15 °C for several hours. The orange solution was decanted through a cannula from the cream-colored residue, while the temperature was maintained below −10 °C. The ether was removed under reduced pressure, and the residue extracted three times with hexane (30 mL) at −10 °C. Reduction of the solvent volume to 50 mL and cooling to −20 °C resulted in large orange crystals of **1** (2.06 g, 34%). ^{1}H NMR (300 MHz, [D$_8$]toluene, −10 °C): 7.06 (s, 2H, ArH), 2.80 (sept, 1H, p-CH(CH$_3$)$_2$), 2.67 (sept, 2H, o-CH(CH$_3$)$_2$), 1.28 (d, 6H, p-CH(CH_3)$_2$), 1.25 (d, 12H, o-CH(CH_3)$_2$), ^3J (H,H) = 6.9 Hz. ^{13}C NMR (75 MHz, [D$_8$]-

toluene, −10 °C): 24.48 (*o*-CH(CH_3)$_2$), 25.01 (*o*-CH(CH_3)$_2$), 34.93 (*p*-CH(CH_3)$_2$), 41.16 (*p*-CH(CH_3)$_2$), 121.01 (*o*-C(Ar)), 148.87 (*ipso*-C(Ar)), 154.30 (*m*-C(Ar)), 160.85 (*p*-C(Ar)).

2: Compound **1** (2.09 g, 2.00 mmol) was dissolved in diethyl ether (30 mL) at −15 °C, the solution filtered onto lithium powder (0.06 g, 8 mmol) at −78 °C, and the resulting suspension stirred at this temperature. After 10 min the bright orange solution rapidly darkened to deep red-brown, and stirring was maintained for a further 3 h. The solution was filtered, concentrated under reduced pressure to 15 mL, and cooled at −20 °C to give dark red-brown crystals of **2** in about 5% yield.

Received: May 31, 1996 [Z9100IE]
German version: *Angew. Chemie.* **1996**, *108*, 2528–2530

Keywords: clusters · indium compounds · structure elucidation

[1] Reviews: a) M. J. Taylor, P. J. Brothers in *Chemistry of Aluminium, Gallium, Indium, and Thallium*, (Ed.: A. J. Downs), Blackie-Chapman-Hall, London, **1993**, Ch. 3; b) P. J. Brothers, P. P. Power, *Adv. Organomet. Chem.* **1996**, *39*, 1; c) W. Uhl, *Angew. Chem.* **1993**, *105*, 1449; *Angew. Chem. Int. Ed. Engl.* **1993**, *32*, 1386; d) C. Dohmeier, D. Loos, H. Schnöckel, *ibid.* **1996**, *108*, 141 and **1996**, *35*, 129.

[2] R. D. Schluter, A. H. Cowley, D. A. Atwood, R. A. Jones, M. R. Bond, C. J. Carrano, *J. Am. Chem. Soc.* **1993**, *115*, 2070.

[3] M. Veith, F. Goffing, S. Becker, V. Huch, *J. Organomet. Chem.* **1991**, *406*, 105.

[4] W. Uhl, M. Layh, W. Hiller, *J. Organomet. Chem.* **1989**, *368*, 139.

[5] N. Wiberg, K. Amelunxen, H. Nöth, M. Schmidt, H. Schwenk, *Angew. Chem.* **1996**, *108*, 110; *Angew. Chem. Int. Ed. Engl.* **1996**, *35*, 65.

[6] S. Henkel, K. W. Klinkhammer, W. Schwarz, *Angew. Chem.* **1994**, *106*, 721; *Angew. Chem. Int. Ed. Engl.* **1994**, *33*, 681.

[7] a) X. He, R. A. Bartlett, M. M. Olmstead, K. Ruhlandt-Senge, B. E. Sturgeon, P. P. Power, *Angew. Chem.* **1993**, *105*, 761; *Angew. Chem. Int. Ed. Engl.* **1993**, *32*, 717; b) R. J. Wehmschulte, K. Ruhlandt-Senge, M. M. Olmstead, H. Hope, B. E. Sturgeon, P. P. Power, *Inorg. Chem.* **1993**, *32*, 2983.

[8] a) W. Uhl, R. Graupner, M. Layh, U. Schütz, *J. Organomet. Chem.* **1995**, *493*, C1; b) R. D. Schluter, A. H. Cowley, D. A. Atwood, R. A. Jones, J. L. Atwood, *J. Coord. Chem.* **1993**, *30*, 25.

[9] O. T. Beachley, Jr., M. R. Churchill, J. C. Fettinger, J. C. Pazik, L. Victoriano, *J. Am. Chem. Soc.* **1986**, *108*, 4666.

[10] M. Mocker, C. Robl, H. Schnöckel, *Angew. Chem.* **1994**, *106*, 1860; *Angew. Chem. Int. Ed. Engl.* **1994**, *33*, 1754.

[11] X.-W. Li, W. T. Pennington, G. H. Robinson, *J. Am. Chem. Soc.* **1995**, *117*, 7578.

[12] G. Linti, W. Köstler, *Angew. Chem.* **1996**, *108*, 593; *Angew. Chem. Int. Ed. Engl.* **1996**, *35*, 550.

[13] D. Loos, H. Schnöckel, D. Fenske, *Angew. Chem.* **1993**, *105*, 1124; *Angew. Chem. Int. Ed. Engl.* **1993**, *32*, 1059.

[14] a) Crystal structure analysis of **1**: $C_{62}H_{92}In_2$: $M_r = 1067.0$, orthorhombic, space Group *Ccca*, $T = 130$ K, $a = 13.523(3)$, $b = 24.257(7)$, $c = 19.264(5)$ Å, $V = 6319(3)$ Å^3, $Z = 4$, $\rho_{calcd} = 1.122$ g cm^{-3}, $F(000) = 2248$, $\mu(Mo_{K\alpha}) = 0.762$ mm^{-1}. Suitable crystals (0.16 × 0.24 × 0.32 mm) were obtained by recrystallization from hexane. Siemens R3m/V diffractometer with $Mo_{K\alpha}$ radiation ($\lambda = 0.71069$ Å); ω scan. Of 3987 reflections with $0 \le 2\theta \le 55°$, 3637 were independent. The 2198 observed reflections ($F_o > 4\sigma(F_o)$) were used to refine 143 parameters. $R = 0.066$, $R_w = 0.079$, GOOF = 0.88. Minimal and maximal remaining electron densities: −0.99 and 1.52 e Å^{-3}. One of the isopropyl groups was disordered and modeled with two sets of methyl carbon atoms of 3 to 2 occupancy and restrained geometries but free thermal parameters. Anisotropic temperature factors were used for all other non-hydrogen atoms. Hydrogen atoms (except for the disordered methyl groups) were included in calculated positions or as part of riding groups. The refinement on F was carried out by full-matrix least squares techniques (SHELXTL Plus). An XABS absorption correction was applied ($0.83 < T < 0.90$). b) The structures were solved by Patterson methods (SHELXTL Plus). Crystallographic data (excluding structure factors) for the structures reported in this paper have been deposited with the Cambridge Crystallographic Data Centre as supplementary publication no. CCDC-179-88. Copies of the data can be obtained free of charge on application to the Director, CCDC, 12 Union Rd, GB-Cambridge CB2 1EZ, UK (fax: int. code +(1223)336-033; e-mail: teched@chemcrys.cam.ac.uk).)

[15] Crystal structure analysis of **2** × 3 Et_2O: $C_{102}H_{168}In_4O_3$: $M_r = 1901.73$, hexagonal, space group $R\bar{3}$, $T = 130$ K, $a = 17.804(1)$, $c = 28.806(4)$ Å, $V = 7907.7(13)$ Å^3, $Z = 3$, $\rho_{calcd} = 1.198$ g cm^{-3}, $F(000) = 3000$, $\mu(Cu_{K\alpha}) = 7.215$ mm^{-1}. Suitable crystals (0.6 × 0.3 × 0.2 mm) were obtained by recrystallization from diethyl ether. Siemens four-circle diffractometer P4 with $Cu_{K\alpha}$ radiation ($\lambda = 1.54178$ Å); 2θ-ω-scan. Of 2499 reflections with $3.3 \le \theta \le 49.9°$, 2019 were independent. The 1994 observed reflections were used to refine 286 parameters and 3 restraints. $wR2 = 0.158$, $R1 = 0.064$ (using 1225 reflections with $F_o > 4\sigma(F_o)$), GOF = 1.04. Minimal and maximal remaining electron densities: −0.27 and 0.43 e Å^{-3}. Anisotropic temperature factors were used for all non-hydrogen atoms except for the diethyl ether molecule. Hydrogen atoms were included in calculated positions or as part of rigid groups (CH_3). Refinement on F^2 was carried out by full-matrix least-squares techniques (SHELXL93); see also ref. [14b]. A Difabs absorption correction was applied ($0.747 < T < 1.000$).

[16] Three disordered molecules of diethyl ether per molecule of **2** are located in cavities between the indium molecules. The possibility that a disordered lithium cation might be associated with these donors is not supported by the color of the compound, which is typical of neutral organic derivatives and is similar to that of **1**. A lithium ion was not located in the crystal structure.

[17] L. R. Sita, *Adv. Organomet. Chem.* **1995**, *38*, 189.

[18] J. Donohue, *The Structures of the Elements*, Wiley, New York, **1974**, p. 244.

[19] H. Schumann, C. Janiak, F. Görlitz, J. Loebel, A. Dietrich, *J. Organomet. Chem.* **1989**, *363*, 243.

[20] H. Mattausch, A. Simon, E.-M. Peters, *Inorg. Chem.* **1986**, *25*, 3428.

Crystal Structures and Properties of Cyclic Polyenes Possessing Disulfide Units**

Toshio Shimizu, Kazuko Iwata, and Nobumasa Kamigata*

Cycloocta-1,5-diene has been the subject of considerable interest, in particular with respect to its conformational behavior[1] and role as ligand in organometallic complexes. Cycloocta-1,5-diene derivatives with heteroatom substituents at the sp^3-hybridized carbons are also of great interest in view of their conformation and reactivity. However, only a few monocyclic compounds are known. 3,4,7,8-Tetrakis(trifluoromethyl)-1,2,5,6-tetrathiacycloocta-3,7-diene[2] and the tetraselena derivative,[3] which have trifluoromethyl groups on the sp^2-hybridized carbons, are known but their chemical properties and reactivity have hardly been examined. We have successfully synthesized 1,2,5,6-tetrathiacycloocta-3,7-diene (**1**; trivial name: 1,2,5,6-tetrathiocin; see Scheme 1) and determined the crystal structure by X-ray analysis. It is very reactive in polar solvents and toward irradiation (even room light). The larger cyclic system **3** was also obtained and characterized by X-ray analysis.

Oxidation of a *cis*-disodium ethene-1,2-dithiolate with iodine/potassium iodide at −10 °C in a heterogeneous, dilute solution led to **1** in 14% yield (Scheme 1). Bicyclic trimer **2** (*meso*/*dl* = 5:2)[4] and tetramer **3** are also formed, although the monocyclic

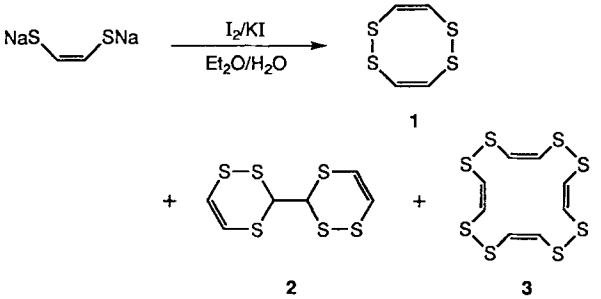

Scheme 1.

[*] Prof. Dr. N. Kamigata, Dr. T. Shimizu, K. Iwata
Department of Chemistry, Faculty of Science
Tokyo Metropolitan University
Minami-ohsawa, Hachioji, Tokyo 192-03 (Japan)
Fax: Int. code +(0426)77-2525
e-mail: kamigata-nobumasa@c.metro-u.ac.jp

[**] Presented in part at the 4th International Conference on Heteroatom Chemistry, Seoul, Korea, July 31, 1995.

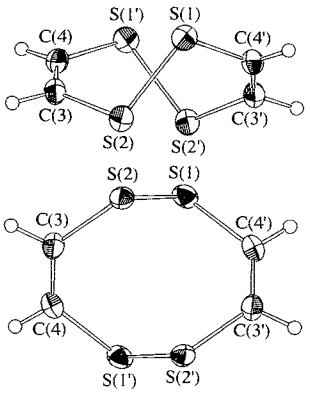

Fig. 1. ORTEP drawing of **1** with thermal ellipsoids at the 30% probability level. Selected interatomic distances [Å], bond angles [°], and torsional angles [°]: S(1)-S(2) 2.0574(8), S(2)-C(3) 1.752(3), C(3)-C(4) 1.329(3), C(4)-S(1') 1.747(3), S(1)-S(1') 3.431(1), S(2)-S(2') 3.336(1), S(1)-S(2') 3.530(1), C(4')-S(1)-S(2) 105.07(8), S(1)-S(2)-C(3) 104.55(8), S(2)-C(3)-C(4) 128.8(2), C(3)-C(4)-S(1') 129.2(2), S(2)-C(3)-C(4)-S(1') 2.5(4), C(4')-S(1)-S(2)-C(3) 108.8(1).

trimer expected for this reaction could not be detected. Based on ^{1}H NMR spectra, there is *cis* geometry at the olefin moieties in all of the products.

The structures of **1**[5] and **3**[6] were confirmed by X-ray crystallographic analysis (Figs. 1 and 2). The crystal structure of **1** shows a twist form (nearly D_2 symmetry) corresponding to the geometry calculated with a global minimum.[7] This is in contrast to the twist-boat form (C_2 symmetry) optimized as a global minimum for cycloocta-1,5-diene.[8] The bond lengths and angles of **1** are almost normal, and the dihedral angles around the olefin moieties yield strain-free geometries (2.5°). The dihedral angles around the sulfur–sulfur bonds (C-S-S-C; 109°) are slightly more extended than those of the most stable disulfide conformations (ca. 90°).[9, 10] The interesting point of the crystal structure of **1** is the nonbonding interatomic distances between sulfur atoms S(1)—S(1'), S(2)—S(2'), and S(1)—S(2') {S(1')-S(2)} are 3.43, 3.34, and 3.53 Å, respectively, and thus shorter than twice the van der Waals radius of a sulfur atom (3.70 Å). The tetramer **3** has a cage structure (approximately D_{2d} symmetry) possessing a cavity. The average distance from the center of the molecule to the sulfur atoms is 3.41 Å and that to carbon atoms is 2.53 Å. The torsional angles around the disulfide moieties (74°, average) are contracted relative to those of the most stable vertical geometry of disulfides, whereas those of **1** are extended. The cage structure of **3** indicates that it has the potential for becoming a new inclusion compound with two types of coordination sites (π-electrons of the olefins and lone pairs on the sulfur atoms).

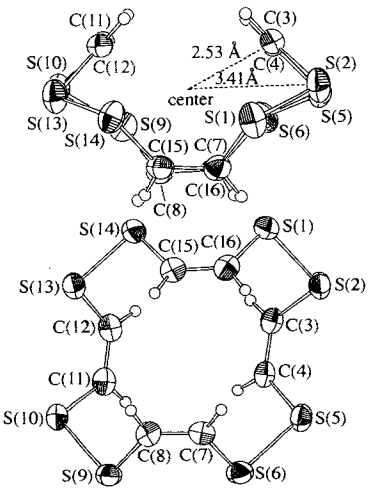

Fig. 2. ORTEP drawing of **3** with thermal ellipsoids at the 30% probability level. Selected interatomic distances [Å], bond angles [°], and torsional angles [°] as averages: S-S 2.05, S-C 1.75, C-C 1.32, S-S-C 100.4, S-C-C 123.3, C-S-S-C 73.6, S-C-C-S 0.7, S-S-C-C 133.9.

The UV spectrum of **1** shows an absorption maximum at 357 nm whereas the larger **3** has only one absorption maximum at lower wavelength (Fig. 3). The cyclic voltammograms of **1** and **3** display irreversible oxidation potentials at +150 and +50 mV, respectively, versus S. C. E. Furthermore, there are reduction potentials at −1.05 (shoulder) and −1.09 V (Fig. 4).

Tetrathiocin **1** is thermally stable: no decomposition was observed even in *p*-xylene at reflux after 3 h. Interestingly, compound **1** reacted in

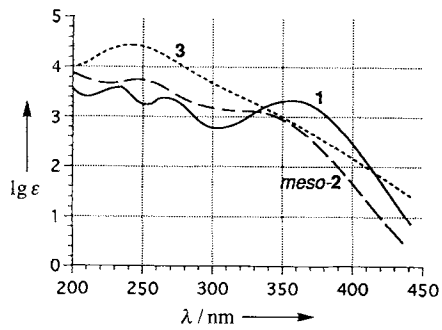

Fig. 3. UV spectra of **1**, *meso*-**2**, and **3** in cyclohexane.

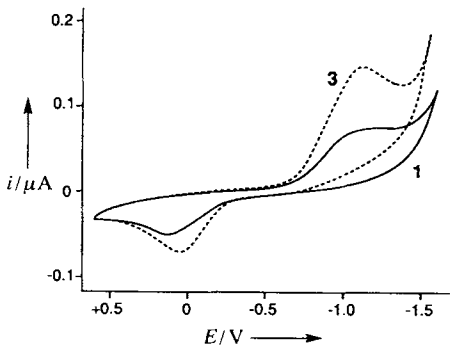

Fig. 4. Cyclic voltammograms of **1** (2.6 mM) and **3** (2.3 mM) in chloroform at 20 °C, nBu$_4$NBF$_4$ (250 mM) supporting electrolyte, glassy carbon working electrode, potential E vs. S. C. E.; scan rate, 100 mV s^{-1}.

acetonitrile/chloroform (4:1) solution even at room temperature to give the ring-expanded product **3** in moderate yield (76%) after 4.5 h, whereas no change was observed in *n*-hexane/chloroform (4:1) solution under similar conditions (Scheme 2). Compound **3** was also obtained from a methanol/chloroform solution (4:1) of **1**, although the yield was low (15%) and the main product was polymer (60%). The reaction in acetonitrile/chloroform solution is considered to proceed by a nucleophilic attack of acetonitrile on the sulfur atom in **1**.

Compound **1** is also unstable toward irradiation (even room light). When a benzene solution of **1** (1.2×10^{-3} M) was irradiated with a medium-pressure mercury lamp through a Pyrex filter, a rubberlike yellow polymer formed (>60%) together with the bicyclic compound **2** (7%; *meso*/*dl* = 3:1).[4] According to combustion analysis,[11] the polymer consisted of $(CHS)_n$ units; it was insoluble in both polar and nonpolar solvents. Irradiation of **1** in the presence of a large excess of 2,3-dimethylbutadiene hindered the formation of the polymer, and bicyclic product **4**[12] was obtained in 62% yield together with a small amount of **2** (Scheme 2). This indicates that the thioaldehyde **5**, generated

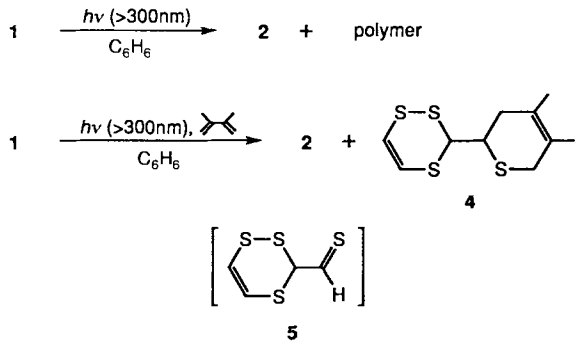

Scheme 2.

 © VCH Verlagsgesellschaft mbH, D-69451 Weinheim, 1996 0570-0833/96/3520-2358 $ 15.00+.25/0

by photochemical 1,3-rearrangement of **1**, is the reactive intermediate in the formation of the rubberlike polymer. Several mechanisms are plausible for the formation of **2**, which can be obtained by oxidation of ethene-1,2-dithiolate and the photochemical reaction of **1**, and are currently under investigation.

Experimental Procedure

Oxidation of *cis*-disodium ethene-1,2-dithiolate: an aqueous solution (150 mL) of *cis*-disodium ethene-1,2-dithiolate[13] (2.78 g, 20.4 mmol) and iodine (5.18 g, 20.4 mmol) in 20% aqueous potassium iodide (150 mL)[14] were added consecutively from two dropping funnels with vigorous stirring at $-10\,^{\circ}C$ under nitrogen to a heterogeneous solution of ether (300 mL) and water (250 mL) over 7 h. After additional stirring for 1 h, the products were extracted with ether and washed with 10% sodium thiosulfate solution and water. After chromatography on a short cellulose column (chloroform), purification was achieved by gel permeation chromatography (GPC).

1: 254 mg (14%); m. p. 97.5–98.5 °C (yellow prisms); ^{1}H NMR (400 MHz, $CDCl_3$) $\delta = 6.88$ (s); ^{13}C NMR (100 MHz, $CDCl_3$) $\delta = 127.6$; IR (KBr): $\tilde{\nu} = 3010$, 1515, 1170, 800, 650 cm^{-1}; UV (cyclohexane): λ (ε) = 357 (2.1×10^3), 265 (2.4×10^3), 235 (4.0×10^3) nm; EI MS: *m/z* 180 (M^+), 147, 116, 90, 57; elemental analysis for $C_4H_4S_4$ (calcd, found): C 26.64, 26.69; H 2.24, 2.24.

2: 9.6 mg (0.5%); a *meso*-isomer could be isolated from the diastereomeric mixture by recrystallization from chloroform. Spectral data for *meso*-**2**: m. p. 127.5–128.5 °C (yellow prisms); ^{1}H NMR (400 MHz, $CDCl_3$) $\delta = 6.77$ (d, 2H, J = 9.5 Hz), 6.62 (d, 2H, J = 9.5 Hz), 4.94 (s, 2H); ^{13}C NMR (100 MHz, $CDCl_3$) $\delta = 126.5$, 115.4, 56.1; IR (KBr): $\tilde{\nu} = 3030$, 3020, 2905, 1540, 1125, 810 cm^{-1}; UV (cyclohexane): λ (ε) = 325 (sh, 1.4×10^3), 247 (6.1×10^3) nm; EI MS: *m/z* 271 ($M^+ + 1$), 207, 180, 147, 135, 116, 90, 58; elemental analysis for $C_6H_6S_6$ (calcd, found): C 26.64, 27.14; H, 2.24, 2.36.

3: 32 mg (2%); m. p. 150 °C (decomp., yellow prisms); ^{1}H NMR (400 MHz, $CDCl_3$) $\delta = 6.48$ (s); ^{13}C NMR (100 MHz, $CDCl_3$) $\delta = 131.7$; IR (KBr): $\tilde{\nu} = 3025$, 1535, 1280, 1155, 910, 830, 730, 715 cm^{-1}; UV (cyclohexane): λ (ε) = 243 (2.8×10^4) nm; EI MS: *m/z* 360 (M^+), 270, 180, 147, 116, 90, 58; elemental analysis for $C_8H_8S_8$ (calcd, found): C, 26.64, 26.76; H, 2.24, 2.29.

Received: May 2, 1996 [Z 9087 IE]
German version: *Angew. Chem.* **1996**, *108*, 2505–2507

Keywords: cyclizations · polyenes · sulfur compounds · synthetic methods

[1] R. Pauncz, D. Ginsburg, *Tetrahedron* **1960**, *9*, 40; N. L. Allinger, J. T. Sprague, *J. Am. Chem. Soc.* **1972**, *94*, 5734; *Tetrahedron* **1975**, *31*, 21; O. Ermer, *J. Am. Chem. Soc.* **1976**, *98*, 3964; D. N. J. White, M. J. Bovill, *J. Chem. Soc., Perkin Trans. 1*, **1977**, 1610; W. R. Roth, O. Adamczak, R. Breuckmann, H.-W. Lennartz, R. Boese, *Chem. Ber.* **1991**, *124*, 2499.

[2] C. G. Krespan, B. C. McKusick, T. L. Cairns, *J. Am. Chem. Soc.* **1960**, *82*, 1515; C. G. Krespan, *J. Am. Chem. Soc.* **1961**, *83*, 3434; T. S. Cameron, R. C. Haddon, S. M. Mattar, S. Parsons, J. Passmore, A. P. Ramirez, *J. Chem. Soc., Dalton Trans.* **1992**, 1563.

[3] K. B. Borisenko, M. Broschag, I. Hargittai, T. M. Klapötke, D. Schröder, A. Schulz, H. Schwarz, I. C. Tornieporth-Oetting, P. S. White, *J. Chem. Soc., Dalton Trans.* **1994**, 2705.

[4] A *meso*-isomer of **2** could be isolated from the diastereomeric mixture by recrystallization. The structure of the *meso*-isomer was confirmed by X-ray crystallographic analysis; details will be reported later. The ratio of *meso*- and *dl*-isomers was determined by ^{1}H NMR spectroscopy in $CDCl_3$.

[5] Crystal structure analysis of **1** (yellow prisms from hexane): $C_4H_4S_4$, M_r = 180.34, crystal dimensions $0.45 \times 0.30 \times 0.15$ mm, $a = 8.092(2)$, $b = 11.254(3)$, $c = 7.674(2)$ Å, $V = 698.9(4)$ Å^3, $\rho_{calcd} = 1.71$ g cm^{-3}, $\mu = 11.99$ cm^{-1}, $Z = 4$, orthorhombic, space group *Pbcn* (No. 60), Mac Science MXC 18 diffractometer, $\lambda = 0.71069$ Å, $T = 296$ K, 1528 measured reflections, 1262 independent, $R = 0.042$, $Rw = 0.055$. Crystallographic data (excluding structure factors) for the structures reported in this paper have been deposited with the Cambridge Crystallographic Data Centre as supplementary publication no. CCDC-179-95. Copies of the data can be obtained free of charge on application to the Director, CCDC, 12 Union Rd, GB-Cambridge CB2 1EZ, UK (fax: int. code +(1223) 336-033; e-mail: teched@chemcrys.cam.ac.uk).

[6] Crystal structure analysis of **3** (yellow prisms from chloroform): formula $C_8H_8S_8$, $M_r = 360.68$, crystal dimensions $0.35 \times 0.30 \times 0.20$ mm, $a = 12.075(4)$, $b = 11.566(8)$, $c = 10.592(5)$ Å, $\beta = 95.12(3)^{\circ}$, $V = 1473(1)$ Å^3, $\rho_{calcd} = 1.62$ g cm^{-3}, $\mu = 11.38$ cm^{-1}, $Z = 4$, monoclinic, space group $P2_1/c$ (No. 14), Mac Science MXC 18 diffractometer, $\lambda = 0.71069$ Å, $T = 296$ K, 3843 measured reflections, 3368 independent, $R = 0.043$, $Rw = 0.041$.

[7] Among the three geometries (twist, chair, and half-chair) optimized for **1** at the local minima, the twist form was calculated to lie on the lowest potential level (MP2/D95*).

[8] T. Shimizu, K. Iwata, N. Kamigata, S. Ikuta, *J. Chem. Res. (S)* **1994**, 436.

[9] Ab initio MO calculations (MP2/D95*) on dimethyl disulfide provided a dihedral angle of 89.1° at the global minimum.

[10] A. Veillard, J. Demuynck, *Chem. Phys. Lett.* **1970**, *4*, 476; A. Rauk, *J. Am. Chem. Soc.* **1984**, *106*, 6517; R. Block, L. Jansen, *J. Chem. Phys.* **1985**, *82*, 3322; D. A. Dixon, D. Zeroka, J. J. Wendoloski, Z. R. Wasserman, *J. Phys. Chem.* **1985**, *89*, 5334.

[11] Combustion analysis for CHS (calcd, found): C 26.64, 27.54; H 2.24, 2.23.

[12] Ratio of diastereomeric isomers = 2:1. The major isomer could be separated from diastereomeric mixture of **4** by GPC: pale yellow liquid; ^{1}H NMR (400 MHz, $CDCl_3$) $\delta = 6.67$ (d, 1H, J = 9.8 Hz), 6.49 (d, 1H, J = 9.8 Hz), 4.57 (d, 1H, J = 8.3 Hz), 3.46–3.38 (m, 1H), 3.21 (d, 1H, J = 16.6 Hz), 3.02 (d, 1H, J = 16.6 Hz), 2.63–2.48 (m, 2H), 1.74 (s, 3H), 1.73 (s, 3H); ^{13}C NMR (100 MHz, $CDCl_3$) $\delta = 126.2$, 125.8, 123.4, 113.9, 56.9, 43.7, 36.1, 30.9, 20.3, 19.2; IR (neat): $\tilde{\nu} = 3020$, 2990, 2910, 2870, 2810, 1535, 1440, 1420, 1380, 1170, 805 cm^{-1}; EI MS: *m/z* = 262 (M^+), 198, 127, 103, 93; elemental analysis for $C_{10}H_{14}S_4$ (calcd, found): C 45.76, 46.07; H 5.38, 5.31.

[13] W. Schroth, J. Peschel, *Chimia* **1964**, *18*, 171.

[14] H. E. Wijers, H. Boelens, A. van der Gen, L. Brandsma, *Recl. Trav. Chim., Pays-Bas* **1969**, *88*, 519.

A Route to Pd^0 from Pd^{II} Metallacycles in Amination and Cross-Coupling Chemistry**

Janis Louie and John F. Hartwig*

Tri-*o*-tolylphosphane-bound palladium complexes, either isolated or generated in situ, have proven to be efficient catalysts for a wide range of coupling reactions including the Heck[1] and Suzuki[2] reactions. Amination of aryl halides has also recently been shown to be catalyzed by these palladium complexes.[3] Like the widely accepted mechanism for Heck and Suzuki reactions, the mechanism for aryl halide amination seems to involve an interconversion between Pd^0 and Pd^{II} species.[3b, d, 4] Our mechanistic and synthetic studies on such aminations led us to investigate whether the palladacycle **1** [Eq. (a)], recently reported

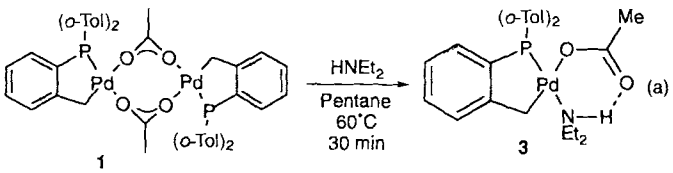

$[Pd\{P(o\text{-}Tol)_3\}_2]$ **2**

by Beller and Herrmann et al,[5] would operate by a mechanism different from that shown for the Pd^0 complex **2**, or whether **1** is a precursor to **2**.

[*] Prof. J. F. Hartwig, J. Louie
Department of Chemistry, Yale University
P. O. Box 208107, New Haven, CT 06520-8107 (USA)
Fax: Int. code +(203) 432-6144
e-mail: john.hartwig@yale.edu

[**] We would like to thank Susan de Gala for providing X-ray crystallography studies. We are grateful for support from the National Science Foundation NYI Award program, the Dreyfus Foundation for a New Faculty Award, Dupont for a Young Faculty Award, Union Carbide for an Innovative Recognition Award, and Yale University for a Junior Faculty Fellowship. J. F. H. is a fellow of the Alfred P. Sloan Foundation.

Our results delineate two different pathways for formation of Pd^0 complexes from **1**.[6] During the amination of aryl halides, formation and subsequent reaction of a palladium amide derived from the amine complex **3** gave the Pd^0 complex **2** by β-hydrogen elimination. During a cross-coupling reaction, **1** formed a Pd^0 complex containing the arylated P(*o*-Tol)$_3$ derivative P(*o*-Tol)$_2$(C$_6$H$_4$-*o*-CH$_2$Ph), which was formed by C–C bond-forming reductive elimination. As a result, the catalytic amination and some of the cross-coupling chemistry seen for **1** is strikingly similar to that of **2**.

Aryl halide palladium complexes with amine ligands catalyze the amination of aryl halides.[3b, d, 7] Metallacycle **1** was cleaved by secondary amines to form similar monometallic amine complexes such as the diethylamine complex **3** in Equation a. The ^{1}H NMR spectrum of **3** has broad signals at room temperature. These are resolved at $-80\,^\circ$C and show two singlets for the phosphane methyl groups along with two inequivalent sets of broad signals for amine ethyl groups. This indicates that the regions above and below the square plane are inequivalent, presumably due to a rigid and puckered metallacycle (vide infra). A broad singlet for the N–H proton is observed far downfield at $\delta = 9.24$. The amine N–H infrared vibration falls in the region of C–H vibrations. This assignment was confirmed by the synthesis of deuterated **3** and the observation of N–D stretching frequencies at 2238 cm^{-1} and 2163 cm^{-1}. The downfield ^{1}H NMR chemical shift and low infrared frequency corresponding to the amine N–H suggest the presence of a strong hydrogen bond, perhaps with the carbonyl oxygen.

An X-ray diffraction study was conducted on a single crystal of **3**, which was obtained by cooling a pentane solution from 60 °C to room temperature. All hydrogen atoms were located in successive difference maps and refined isotropically. The ORTEP drawing of **3**[8] shows that there is a hydrogen bond between the carbonyl oxygen and the amine proton (Fig. 1). The

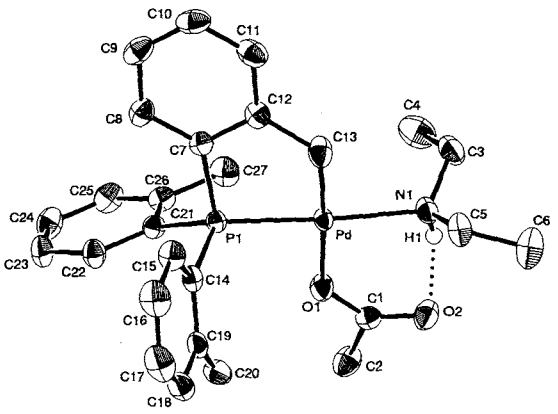

Fig. 1. Structure of **3** in the crystal. Selected bond lengths [Å] and angles [°]: O2-H1 2.10(2), Pd-P1 2.2452(5), Pd-O1 2.143(1), Pd-N1 2.150(2), Pd-C13 2.036(2), C1-O1 1.273(2), C1-O2 1.236(2), N1-H1 0.74(2); N1-H1-O2 163(2), C1-O2-H1 105.4(8), P1-Pd-O1 95.57(4), P1-Pd-C13 82.42(6), O1-Pd-N1 92.25(6), N1-Pd-C13 89.87(7), Pd-N1-H1 99(2), Pd-O1-C1 130.6(1), O1-C1-O2 126.2(2).

amine conformation, the C=O···H–N distance (2.15 Å), and the N1–H1–O2 bond angle (163°) are all characteristic of such a hydrogen bond.[8, 9] Moreover, the X-ray structure shows the ring pucker that was deduced from the ^{1}H NMR spectrum. The dihedral angle between the square plane, defined by N1-O1-P1-C13, and the metallacycle plane, defined by P1-C7-C12-C13, is 28.14°.

Formation of Pd^0, along with aryl amine products, has been shown to occur from amine-ligated aryl halide complexes upon addition of base to deprotonate the amine and generate a Pd^{II} amido species.[1e, 7] Amine complex **3** also reacts with base to generate Pd^0. Treatment of **3** with a slight excess of NaO*t*Bu in THF formed Pd^0 complex **2** in 48% yield, as determined by ^{31}P NMR spectroscopy. The yield of **2** was nearly quantitative based on the number of phosphanes that could be formed from **3**; an essentially quantitative yield of **2** based on palladium was obtained when the reaction was run in the presence of 3 equiv of P(*o*-Tol)$_3$.

Scheme 1 shows a rational mechanism for the formation of **2** from **3** in the presence of base. Deprotonation of the amine

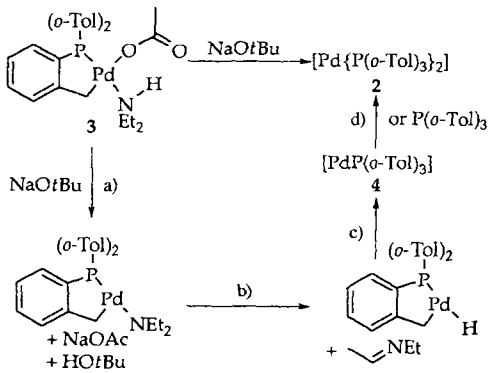

Scheme 1. Postulated mechanism for the synthesis of **2**: a) deprotonation, b) β-H elimination, c) reductive elimination, d) disproportionation.

proton would lead to the formation of a short-lived amido complex, along with NaOAc and HO*t*Bu. Rapid β-hydrogen elimination, the common reaction pathway followed by palladium amides with β-hydrogens, and subsequent reductive elimination with formation of a C–H bond would provide the palladium complex **4**, which contains a single, coordinated P(*o*-Tol)$_3$.[10] Dismutation between two of these highly unsaturated species would produce **2**, as well as an unligated Pd, in a total possible yield of 50% based on the starting palladacycle.

If the reactivity described above is relevant to amination reactions catalyzed by **1**, compound **3** must catalyze the amination of aryl halides in a fashion similar to **1** and **2**. Indeed, **3** catalyzes the reaction of aryl halides with amines in the presence of NaO*t*Bu base. The coupling of 4′-bromobenzophenone and *N*-methylaniline to form **5** with **1**, **2**, or **3** as catalyst was compared. Each catalyst gave yields between 81% and 85% (Table 1) and provided turnover numbers between 350–400 per Pd center for 0.1–0.2 mol% catalyst. Thus, metallacycles **1** and **3** clearly act as precursors to P(*o*-Tol)$_3$-ligated Pd^0 complexes in the amina-

Table 1. Reaction between 4′-bromobenzophenone and *N*-methylaniline.

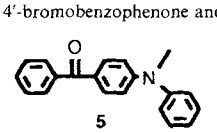

5

Catalyst	Yield [a] of **5** [%] [a]	TON [b] per mole cat.	TON [b] per Pd center
1	81.3	718	359
2	85.1	314	314
3	81.5	396	396

[a] Yields of isolated products. [b] Determined by ^{1}H NMR spectroscopy.

 © VCH Verlagsgesellschaft mbH, D-69451 Weinheim, 1996 0570-0833/96/3520-2360 $ 15.00+.25/0 Angew. Chem. Int. Ed. Engl. 1996, 35, No. 20

tion reactions. In order to evaluate whether the β-hydrogen elimination mechanism was necessary for activation of the catalyst, the amination of aryl bromides with diphenylamine was evaluated with **1** and **2**. Although **2** catalyzes such reactions in essentially quantitative yields, **1** was inert.

Palladacycle **1** effectively catalyzed Stille cross-coupling reactions. For example, a turnover number of 1650 was observed in the coupling of 4'-bromoacetophenone and Me_3SnPh catalyzed by 0.04 mol% catalyst **1**, as determined by ^{1}H NMR spectroscopy. An increase in catalyst concentration to 5 mol% led to complete conversion of aryl halide and a 96% yield of 4-$PhC_6H_4COCH_3$ (by ^{1}H NMR spectroscopy).

Since the reagents in these Stille reactions cannot produce ligands containing β-hydrogens, a pathway to generation of Pd^0 that is distinct from that in the amination chemistry would be required for a conventional mechanism involving Pd^0 and Pd^{II}. Palladacycle **1** and Me_3SnPh were heated to 70 °C in [D_6]benzene for 2.5 h to determine whether a Pd^0 complex formed. Monitoring of the reaction by NMR spectroscopy showed the conversion of the resonances for **1** into two new ^{31}P NMR resonances for complexed and free P(*o*-Tol)$_2$(C_6H_4-*o*-CH_2Ph) (**6**) at $\delta = -8.1$ (δ [Pd{P(*o*-Tol)$_3$}$_2$] = −6.7) and −29.9 (δ P(*o*-Tol)$_3$ = −29.1), respectively. From these reactions, the arylated *o*-tolyl phosphane **6** and P(*o*-Tol)$_3$ side product were isolated in a 5:1 ratio by column chromatography to give a total phosphane yield of 87%. As demonstrated by the two ^{31}P NMR resonances for the reaction mixture, both free and coordinated ligand **6** exist in the reaction, presumably along with unligated Pd^0 [Eq. (b)]. These results strongly suggest that Pd^0 complexes containing **5** and P(*o*-Tol)$_3$ are the active species in Stille couplings involving **1** and may be the active catalyst in Suzuki carbon–carbon bond-forming reactions.[11]

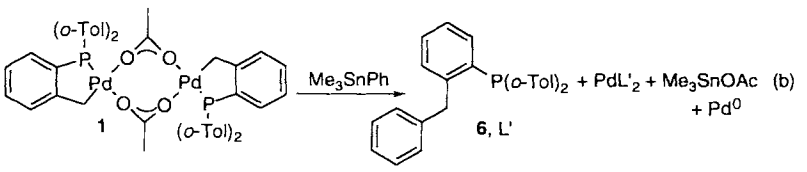

In summary, our data have shown that catalytically active Pd^0 complexes can be formed from **1** by two different routes: β-hydrogen elimination of a palladium amide or C–C bond-forming reductive elimination involving a palladium phenyl substituent. It is difficult to determine conclusively if these reactions occur in the catalytic chemistry of **1**. However, they would provide **1** with an entry into catalysis by Pd^0/Pd^{II} pathways and should be included in mechanistic considerations.

Experimental Procedure

3: Dimeric palladacycle **1** (145.0 mg, 0.155 mmol) was suspended in pentane (6 mL) under N_2. $HNEt_2$ (400 μL, 3.87 mmol) was added and the resulting mixture heated at 70 °C for 30 min. Slow cooling to room temperature produced analytically pure, air-stable, pale yellow crystals of **3** in 83.6% yield. Anal. calcd for $C_{27}H_{34}NPdO_2P$: C 59.84, H 6.32, N 2.58. Found: C 59.66, H 6.30, N 2.61; ^{31}P NMR (300 MHz, [D_8]toluene, 25 °C, H_3PO_4 standard): δ = 33.2 (s, 1P, PdP); ^{1}H NMR (300 MHz, [D_8]toluene, −80 °C, residual C_7H_8): δ = 9.24 (s, 1H, NH), 7.34–6.64 (broad m, 24H, aromatic CH), 3.16 (d, ^3J(H,H) = 14.2 Hz, 1H, $PdCH_2$), 3.06 (s, 3H, $PdC_6H_4CH_3$), 2.83 (s, 3H, $PdC_6H_4CH_3$), 2.65 (d, ^3J(H,H) = 14.9 Hz, 1H, $PdCH_2$), 2.37–2.18 (broad m, 4H, $2NCH_2$), 2.16 (s, 3H, $OCOCH_3$), 1.64 (t, ^3J(H,H) = 5.5 Hz, 3H, CH_2CH_3), 1.40 (t, ^3J(H,H) = 5.4 Hz, 3H, CH_2CH_3); ^{13}C NMR (300 MHz, [D_8]toluene, 25 °C, residual C_7H_8): δ = 179.0 (s, *C*O), 158.6 (d, ^1J(C,P) = 31.6 Hz, *P*C), 143.3 (d, ^2J(C,P) = 13.7 Hz, tolyl *C*CH_3), 137.4 (s, 2 overlapping tolyl *C*CH_3 signals), 135.2 (d, ^1J(C,P) = 53.8 Hz, 2*PC*), 132.7 (d, ^3J(C,P) = 5.5 Hz, *C*H), 132.2 (s, *C*H), 131.8 (d, ^2J(C,P) = 8.45 Hz, *C*H), 131.2 (d, ^3J(C,P) = 1.68 Hz, *C*H), 130.6 (broad s, *C*H), 128.0 (d, ^2J(C,P) = 21.0 Hz, *C*H), 125.8 (d, ^3J(C,P) = 7.3 Hz, *C*H), 125.7 (s, *C*H), 46.0 (broad s, *NCH*$_2$), 26.1 (s, *PdCH*$_2$), 25.6 (s, OC(O)*C*H$_3$), 22.6 (d, ^3J(C,P) = 10.5 Hz, 2*PC*$_6$H$_4$*C*H$_3$), 14.7 (s, 2*NCH*$_2$*C*H$_3$); IR (benzene): $\tilde{\nu}$ = 1581 cm^{-1} (C=O).

Catalytic aminations: In an inert atmosphere glove box, the palladium catalyst (0.036 mmol), P(*o*-Tol)$_3$ (0.12 mmol), 4'-bromobenzophenone (0.71 mmol), and NaO*t*Bu (1.1 mmol) were weighed into a screw-topped test tube equipped with a stir bar. Toluene (6 mL) was added, and the tube was sealed with a cap containing a Teflon septum. *N*-methylaniline (1.1 mmol) was syringed into the reaction mixture. The reaction was stirred at 80 °C for 5 h and cooled to room temperature. The product was isolated by adding brine, extracting the organic phases with ether, drying with $MgSO_4$, and removing the solvent. The product was purified by column chromatography (10:1 heptane/EtOAc).

Stille Couplings: In an inert atmosphere glove box, 4'-bromoacetophenone (0.34 or 0.042 mmol), Me_3SnPh (0.36 or 0.050 mmol), and 1,3,5-trimethoxybenzene (internal standard) were dissolved in C_6D_6 (0.6 mL). An initial ^{1}H NMR spectrum was taken. Palladacycle **1** (0.00013 or 0.0021 mmol, 0.04 mol% or 5.1 mol%) and P(*o*-Tol)$_3$ (0.00084 or 0.0072 mmol) were added to the mixture. The reaction with 0.04 mol% was heated at 120 °C overnight, while the reaction with 5.1 mol% was heated at 100 °C for 4 h. Afterwards, ^{1}H NMR spectra were obtained and compared to the initial spectra in order to determine the reaction yield and amount of remaining substrate.

Received: April 9, 1996 [Z 9002 IE]
German version: *Angew. Chem.* **1996**, *108*, 2531–2533

Keywords: aminations · catalysis · cross-coupling · palladium compounds

[1] a) V. N. Kalinin *Synthesis* **1992**, 413; b) R. F. Heck, *Acc. Chem. Rev.* **1979**, *12*, 146.
[2] W. J. Thompson, J. Gaudino, *J. Org. Chem.* **1984**, *49*, 5237.
[3] a) M. Kosugi, M. Kameyama, T. Migita, *Chem. Lett.* **1983**, 927; b) J. Louie, F. Paul, J. F. Hartwig, *Organometallics* **1996**, *15*, 2794; c) J. Louie, J. F. Hartwig, *Tetrahedron Lett.* **1995**, *36*, 3609; d) F. Paul, J. Patt, J. F. Hartwig, *J. Am. Chem. Soc.* **1994**, *116*, 5969; e) A. S. Guram, S. L. Buchwald, *ibid.* **1994**, *116*, 7901; f) A. S. Guram, R. A. Rennels, S. L. Buchwald, *Angew. Chem.* **1995**, *107*, 1456; *Angew. Chem. Int. Ed. Engl.* **1995**, *34*, 1348; g) J. P. Wolfe, S. L. Buchwald, *J. Org. Chem.* **1996**, *61*, 1133.
[4] a) N. Miyaura, A. Suzuki, *Chem. Rev.* **1995**, *95*, 2357; b) G. B. Smith, G. C. Dezeny, D. L. Hughes, A. O. King, T. R. Verhoeven, *J. Org. Chem.* **1994**, *59*, 8151.
[5] a) M. Beller, H. Fischer, W. A. Herrmann, K. Ofele, C. Brossmer, *Angew. Chem.* **1995**, *107*, 1992; *Angew. Chem. Int. Ed. Engl.* **1995**, *34*, 1848; b) W. A. Herrmann, C. Brossmer, K. Ofele, C.-P. Reisinger, T. Priermeier, M. Beller, H. Fischer, *ibid.* **1995**, *107*, 1989 and **1995**, *34*, 1844.
[6] The organic chemistry of palladacycles has been reviewed: A. D. Ryabov, *Synthesis* **1985**, 233.
[7] F. Paul, J. Patt, J. F. Hartwig, *Organometallics* **1995**, *14*, 3030.
[8] Crystal parameters: 0.19 × 0.27 × 0.48 mm, triclinic, $P\bar{1}$ (no. 2), a = 9.379(1), b = 11.287(1), c = 13.573(2) Å, α = 70.13(1), β = 83.68(1), γ = 69.239(9)°, V = 1263.6(7) Å^3, ρ_{calc} = 1.424 g cm^{-1}. Data collection: T = −82 °C, Mo$_{K\alpha}$ radiation, (λ = 0.71069 Å, μ = 8.08 cm^{-1}), ω-2θ technique to a $2\theta_{max}$ of 52.6°. The structure was solved by direct methods. The data were corrected for Lorentz and polarization effects, but no absorption correction was applied. The hydrogen atoms were located in successive difference maps and refined isotropically. Of the 5350 (5122 unique) reflections measured, 4889 that had $I > 3.00\sigma(I)$, along with 425 variable parameters, were used for a full-matrix least squares refinement. ($R = \Sigma||F_o| - |F_c||/\Sigma|F_o| = 0.023$, $R_w = [(\Sigma w(|F_o| - |F_c|)^2/\Sigma wF_o^2)]^{1/2} = 0.034$; min/max = −0.66 to 0.49 e$^-$ Å^{-3}). Crystallographic data (excluding structure factors) for the structure reported in this paper have been deposited with the Cambridge Crystallographic Data Centre as supplementary publication no. CCDC-179-85. Copies of the data can be obtained free of charge on application to the Director, CCDC, 12 Union Road, GB-Cambridge CB21EZ (UK) (Fax: Int. code + (1223) 336-033; e-mail: teched@chemcrys.cam.ac.uk).
[9] a) N. N. Lyalina, S. V. Dargina, A. N. Sobolev, T. M. Buslaeva, I. P. Romm, *Koord. Khim.* **1993**, *19*, 57; b) G. A. Jeffrey, W. Saenger, *Hydrogen Bonding in Biological Structures*; Springer, New York, **1991**.
[10] We have previously shown that intermediate **4** is consistent with kinetic data for oxidative addition of aryl halides to **2**: J. F. Hartwig, F. Paul, *J. Am. Chem. Soc.* **1995**, *117*, 5373.
[11] We have observed some formation of Suzuki coupling products with pure catalyst **1**, but have not enjoyed the same high turnover numbers observed by the authors of reference [5], despite observation of Suzuki products in high yields with **2**. Thus, our studies focus on Stille chemistry that gives high yields in our hands.

 © VCH Verlagsgesellschaft mbH, D-69451 Weinheim, 1996 0570-0833/96/3520-2361 $ 15.00+.25/0

Homogeneous Catalysts for Claus Chemistry: The Preparation and Structure of *cis*-$[(PPh_3)_2PtS_3O]$, a Catalytically Active Intermediate**

Alan Shaver,* Mohammad El-khateeb, and Anne-Marie Lebuis

The removal of sulfur from petroleum and natural gas may be the most important pollution abatement process in place today. Hydrodesulfurization (HDS)[1] of sulfur compounds gives hydrocarbons and the toxic gas H_2S, which is disposed of by the Claus process.[2] This reaction combines H_2S and SO_2, obtained by partial oxidation, over alumina at 300 °C, to give sulfur and

$$2H_2S + SO_2 \longrightarrow 3/8\,S_8 + 2H_2O$$

water with very high efficiencies. Many materials catalyze the reaction, which is also observed in water. Studies of the sequential adsorption and reactions of SO_2 and H_2S on alumina are, for the most part inconclusive.[3] While the details of the mechanism(s) of the Claus process are only partly understood, sulfur–sulfur bond formation and oxygen transfer must be involved—processes that have few precedents in homogeneous transition metal sulfur chemistry.

We are interested in Claus-like chemistry with soluble metal complexes and to that end have developed three conceptual models for the surface-catalyzed process and translated these into the appropriate reactions of homogeneous metal complexes. Model A depicts attack of H_2S on adsorbed SO_2, model B

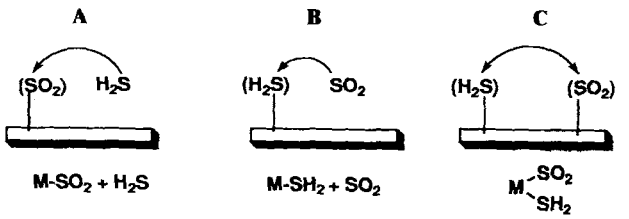

represents attack by SO_2 on adsorbed H_2S, and in C both gases are adsorbed before reaction. In this report we describe the reaction of *cis*-$[(PPh_3)_2Pt(SH)_2]$ (*cis*-**2**) with SO_2 (model B) to give $[(PPh_3)_2PtS_3O]$ (**1**) and water. This represents a step in the Claus reaction. Moreover, both the complexes **1** and **2** catalyze the Claus reaction, whereas *trans*-**2** does not.

Treatment of *cis*-**2**[4] in CH_2Cl_2 with one equivalent of SO_2 gave **1** in 82% yield [Eq. (a)]. H_2O was observed in the NMR spectrum of the reaction mixture in the correct relative ratio by

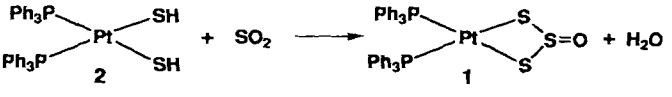

integration. The structure of **1** is shown in Figure 1.[5] The Pt-S1-S2-S3 ring is not planar: the dihedral angle between the plane formed by P1-P2-Pt-S1-S3 and the plane formed by S1-S2-S3 is 22.3°.[6]

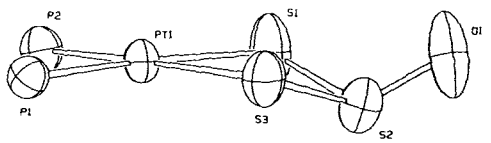

Fig. 1. ORTEP drawing of the structure of $[(PPh_3)_2Pt(S_3O)]\cdot CH_2Cl_2$ (**1**·CH_2Cl_2), excluding the phenyl rings of the PPh_3 ligands and the solvent atoms. Selected bond lengths [Å] and angles [°]: Pt–S1, 2.341(3); Pt–S3, 2.318(2); Pt–P1, 2.271(2); Pt–P2, 2.299(2); S1–S2, 2.042(2); S2–S3, 2.110(4); S2–O, 1.436(7); S1-Pt-S3, 80.73(9); P1-Pt-P2, 98.47(8); S1-Pt-P2, 88.37(8); S3-Pt-P1, 92.33(8); Pt-S1-S2, 91.3(1); S1-S2-S3, 93.2(2); Pt-S3-S2, 90.3(1).

Complex **1** reacts with H_2S at room temperature in THF to give the starting thiol complex *cis*-**2** which was identified in solution by NMR and also isolated. This regeneration prompted treatment of *cis*-**2** and of **1** with a 2:1 mixture of H_2S and SO_2. The reaction was conducted in dry CH_2Cl_2, in very dry flasks that had been previously treated with Me_2SiCl_2 (unsilylated glass catalyzes the reaction). The gases were added to the solution by syringe, and the molar ratio of the catalyst to SO_2 was 1:20. Sulfur, identified by thin layer chromatography, formed after 3 hours.[7] The yields of sulfur were high for complexes *cis*-**2**, **1**, and *cis*-$[(PPh_3)_2Pt(SCHMe_2)_2]$, whereas those for *cis*-$[(PPh_3)_2PtCl_2]$ were moderate and for *trans*-$[(PPh_3)_2Pt(SH)_2]$[8] negligible. The latter complex was recovered unchanged after treatment with pure SO_2. Addition of further aliquots of gases to solutions containing the active catalysts produced more sulfur. Peaks due to *cis*-**2** were found in the ^1H and ^{31}P NMR spectra of *cis*-$[(PPh_3)_2Pt(SCHMe_2)_2]$ upon treatment with H_2S. ^{31}P NMR spectra of the solid residues of the catalytic reactions identified the presence of the starting complex and also **1** in the cases of *cis*-**2** and *cis*-$[(PPh_3)_2Pt(SCHMe_2)_2]$; peaks due to Ph_3PS were also present.

Eller and Kubas[9] showed that treatment of $[(PPh_3)_2Pt(SPh)_2]$ with liquid SO_2 gave labile adducts of the type $[(PPh_3)_2Pt(S(SO_2)Ph)_2]$. We observed that the complexes $[(PPh_3)_2Pt(SR)_2]$, R = CMe_3, $CHMe_2$, and 4-C_6H_4Me, change color in CH_2Cl_2 from yellow to deep red upon treatment with SO_2. Addition of SO_2-saturated hexanes gave red-orange solids, which could only be characterized in solution because of facile loss of SO_2, which regenerates the thiolato complexes. These complexes are therefore formulated as bis(SO_2) adducts of the type $[(PPh_3)_2Pt(S(SO_2)R)_2]$.

Compound **1** is synthesized by a direct reaction between SO_2 and the thiolato complex **2**, which leads to sulfur–sulfur bond formation and oxygen transfer, thus mimicking a fundamental step in the Claus process.[10] The regeneration of the starting thiolato complex upon treatment of **1** with H_2S is consistent with the proposed catalytic cycle for the Claus reaction shown in Scheme 1. The first step is adduct formation between *cis*-**2** and SO_2, followed by insertion of SO_2 into the SH bond. Subsequent elimination of H_2O gives **1**, which reacts with H_2S to cleave the Pt–S bonds and regenerate *cis*-**2**. The other cleavage product is designated as "H_2S_3O" simply on the basis of the stoichiometry and was not detected. It is significant, however, that "H_2S_3O" is believed to be a key intermediate in the Claus process[11] and is expected to react rapidly with H_2S to give water and sulfur. These studies open a new chapter in the Claus process by introducing homogeneously catalyzed Claus chemistry.

(a)

[*] Prof. A. Shaver, Dr. M. El-khateeb, Dr. A.-M. Lebuis
Department of Chemistry, McGill University
801 Sherbrooke Street West
Montreal, Quebec H3A 2K6 (Canada)
Fax: Int. code +(514)398-3797
e-mail: shaver@omc.lan.mcgill.ca

[**] This work was supported by the Natural Sciences and Engineering Research Council of Canada and the Quebec Department of Education.

 © VCH Verlagsgesellschaft mbH, D-69451 Weinheim, 1996 0570-0833/96/3520-2362 $ 15.00+.25/0

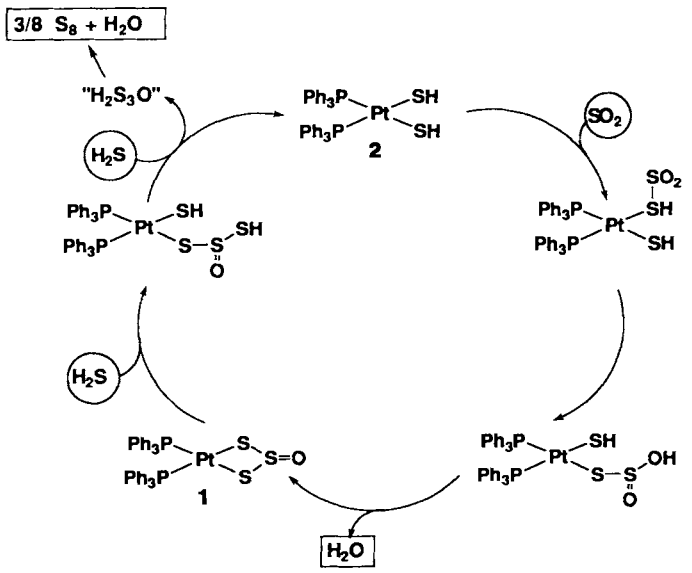

Scheme 1. Potential mechanism for Claus chemistry catalyzed by *cis*-$[(PPh_3)_2Pt(SH)_2]$.

Experimental Procedure

1: In a 100 mL Schlenk flask, *cis*-**2** (0.050 g, 0.064 mmol) in dichloromethane (5.0 mL) was treated with SO_2 gas for 30 minutes at room temperature and stirred thereafter for another 3 h. The volatiles were removed under vacuum, and the resulting yellow solid was recrystallized from in dichloromethane/hexanes. The yellow crystals were isolated by the removal of the mother liquor with a syringe (0.043 g, 82%). M.p. 262–263 °C. IR (Nujol): $\tilde{\nu}$(SO) = 1065(s) cm^{-1}. ^1H NMR ($CDCl_3$): 7.26 (m, PPh_3). ^{31}P NMR ($CDCl_3$): 18.5 (J(Pt,P) = 3200 Hz). Mass spectrum (FAB in NBA): *m/z* 832 [M^+], 784 [$M^+ - SO$], 752 [$M^+ - S_2O$], 720 [$M^+ - S_3O$]. C,H analysis calcd. for ($C_{36}H_{30}OP_2PtS_3 \cdot CH_2Cl_2$): 48.47% C, 3.52% H; found 47.98% C, 3.53% H.

Catalyzed reactions of H_2S with SO_2: H_2S was dried by passage through a column of P_2O_5, and SO_2 was purified by bubbling through concentrated sulfuric acid and then by passage through a column of P_2O_5. The Schlenk flasks (100 mL) were silylated by treatment of the flask with Me_2SiCl_2 (30 mL) for 12 h under a nitrogen atmosphere. Then the Me_2SiCl_2 was removed by syringe, and the flask dried under vacuum overnight. Sulfur produced from these reactions was identified by TLC (alumina) and mass spectroscopy.

The flask was charged with the solid catalyst (5.15×10^{-2} mmol), evacuated, filled with N_2 twice, and weighed. CH_2Cl_2 (20.0 mL) was added, and H_2S (2.06 mmol, 50.0 mL) was bubbled slowly (syringe) into the mixture, followed by the addition (by syringe) of SO_2 (1.03 mmol, 25.0 mL). The resulting solution was stirred at room temperature for 3 h, and then purged with nitrogen for 30 min. The volatiles were removed under vacuum, and the resulting solid was dried under vacuum for 4 days. The flask and its contents was weighed again to estimate the amount of sulfur formed.

Received: April 23, 1996 [Z9064IE]
German version: *Angew. Chem.* **1996**, *108*, 2510–2512

Keywords: catalysis · Claus process · complexes with sulfur ligands · platinum compounds · sulfur compounds

[1] a) C. M. Friend, J. T. Roberts, *Acc. Chem. Res.* **1988**, *21*, 994; b) R. J. Angelici, *ibid.* **1988**, *21*, 387.
[2] a) P. Grancher, *Hydrocarbon Process.* **1978**, *57*, 155; b) *ibid.* **1978**, *57*, 257.
[3] a) A. Datta, R. G. Cavel, T. W. Tower, Z. M. George, *J. Phys. Chem.* **1985**, *89*, 443; b) A. Datta, R. G. Cavell, *ibid.* 1985, *89*, 450; c) *ibid.* **1985**, *89*, 454; d) H. G. Karge, I. G. Dalla Lana, *ibid.* **1984**, *88*, 1958.
[4] A. Shaver, R. D. Lai, P. Bird, W. Wickramsasinghe, *Can. J. Chem.* **1985**, *63*, 2555.
[5] Crystal structure analysis of **1**·CH_2Cl_2: $C_{37}H_{32}O_1S_3Pt_1P_2Cl_2$, M_r = 916.78, yellow diamond-shaped crystal (0.27 × 0.15 × 0.10 mm). Triclinic $P\bar{1}$, a = 10.852(3), b = 13.411(3), c = 13.847(7) Å, α = 80.76(3), β = 86.56(4), γ = 68.01(2)°, V = 1844(1) Å^3, Z = 2, ρ_{calcd} = 1.651 gcm^{-3}, F(000) = 904, $\lambda(Mo_{K\alpha})$ = 0.71069 Å, μ = 42.7 cm^{-1}. Data collection: AFC6S diffractometer, graphite monochromator, 2 θ(max) = 50°, reflections measured: 12970, unique: 6485 (R_{int} = 0.067), observed 4265 ($I > 2.5\sigma I$). Data processing (TEXSAN): linear decay correction −0.6% and absorption (psi scans, transmission range from 0.81 to 1.00), solution by the Patterson method. The central sulfur atom of the PtS_3 ring is disordered over two sites S2 and S2a at 0.73 and 0.27 occupancies, respectively, corresponding to positions above and below the plane formed by PtS1S3. The position of the oxygen atom corresponding to the minor orientation (O_a) could not be resolved so the oxygen atom of the major orientation was assigned full occupancy. Distances given in the figure refer only to the major orientation. The carbon atom in the CH_2Cl_2 solvent is also disorded over two sites at 0.66 and 0.33 occupancies. All non-H atoms except S2a and the two solvent carbon atoms CS1 and CS2 were refined anisotropically, H-atoms were introduced in idealized positions. Final agreement factors: R = 0.040, Rw = 0.037 (418 parameters), S = 1.04. Crystallographic data (excluding structure factors) for the structure reported in this paper have been deposited with the Cambridge Crystallographic Data Centre as supplementary publication No. CCDC-179-94. Copies of the data can be obtained free of charge on application to the Director, CCDC, 12 Union Road, Cambridge CB2 1EZ, UK (fax: int. code +(1223)336-033; e-mail: teched@chemcrys.cam.ac.uk).
[6] For organic trithiolane oxides see: a) G. Derbesy, D. N. Harpp, *J. Org. Chem.* **1995**, *60*, 4468 and references therein; b) T. Ghosh, P. D. Bartlett, *J. Am. Chem. Soc.* **1988**, *110*, 7499; c) K. Steinle, M. Schmidt, *Z. Naturforsch. B.* **1973**, *28*, 686; d) *ibid.* **1972**, *27*, 83; e) R. Steudel, *ibid.* **1970**, *25*, 156.
[7] The yield (%) of sulfur in the presence of platinum complexes: control (8), *cis*-**2** (92), *cis*-**1** (93), *cis*-$[(PPh_3)_2Pt(SCHMe_2)_2]$ (98), *cis*-$[(PPh_3)_2PtCl_2]$ (50), *trans*-**2** (9). The control value is the average of three experiments. The catalyzed reactions proceed in the presence of anhydrous $MgSO_4$ ruling out autocatalysis by the water produced.
[8] H.-L. Boily, Ph.D. thesis, McGill University, **1995**.
[9] P. G. Eller, G. J. Kubas, *J. Am. Chem. Soc.* **1977**, *99*, 4346.
[10] For another metal-catalyzed reduction of SO_2 by a thiolato complex, see a) G. J. Kubas, R. R. Ryan, K. A. Kubat-Martin, *J. Am. Chem. Soc.* **1989**, *111*, 7823; b) G. J. Kubas, R. R. Ryan, *ibid.* **1985**, *107*, 6138.
[11] Y. Drozdova, R. Steudel, *Chem. Eur. J.* **1995**, *1*, 193.

Catalytic, Enantioselective Addition of Allylsilanes to Aldehydes: Generation of a Novel, Reactive Ti^{IV} Complex from TiF_4

Donald R. Gauthier, Jr., and Erick M. Carreira*

The stereoselective addition of allylmetal reagents to aldehydes is a powerful and important reaction for the preparation of homoallylic alcohols and has been extensively employed for the synthesis of stereochemically complex natural products.[1, 2] Recently, catalytic versions of this process that utilize Ti^{IV} complexes and allyl- or methallyltin reagents have been reported, which afford homoallylic alcohols with high enantioselectivities and yields.[3] However, additions involving the corresponding inexpensive, nontoxic allyltrimethylsilane to give protected homoallylic alcohols in useful yields and enantioselectivities have not been reported [Eq. (a)]. As a part of our interest in developing chiral complexes that function competently as catalysts in aldehyde additions, we have studied Ti^{IV} complexes prepared

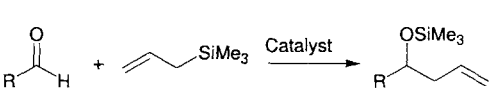

(a)

[*] Prof. E. M. Carreira, Dr. D. R. Gauthier, Jr.
Arnold and Mabel Beckman Laboratory for Chemical Synthesis
California Institute of Technology
Pasadena, CA 91125 (USA)
Fax: Int. code +(818)564-9297
e-mail: emc@starbase1.caltech.edu

[**] Financial support was provided by the Packard Foundation, National Science Foundation (USA), National Institutes of Health (USA), and generous funds from Upjohn, Pfizer, Merck, and Eli Lilly.

from TiF_4.[4-6] In this communication, we report catalytic, enantioselective additions of allyltrimethylsilane to aldehydes that give homoallylic alcohols in 60–94% *ee* and in 69–93% yield. The success of these reactions is attributed to the unique reactivity of the fluorotitanium complex prepared in acetonitrile from TiF_4 and (*R*)- or (*S*)-1,1′-bi-2-naphthol (-BINOL).

Allyltrialkylsilanes are known to be significantly less reactive nucleophiles than the corresponding stannanes. In comparison to allyltributyltin, the addition of allyltrimethylsilane to various electrophiles has been shown to be 10^3-10^4 times slower.[7] The use of allylsilanes in asymmetric, catalytic additions to aldehydes is precluded by the lack of suitably reactive Lewis acids capable of activating the carbonyl group of the aldehyde towards such additions.[2f] Thus, chiral catalysts that have been developed for aldol and allyltrialkyltin additions to aldehydes are not useful with the corresponding allyltrialkylsilanes. For example, the addition of allyltrimethylsilane to the reactive methyl glyoxylate in the presence of the chiral complex generated from (*S*)-BINOL and $TiBr_4$ has been reported to afford the adduct in only 40% yield and 30% *ee*.[8] Similarly, we have investigated reactions involving the complexes derived from BINOL and $Ti(OiPr)_xCl_{4-x}$ under a variety of different conditions without success.

We assumed that TiF_4-derived complexes would be sufficiently reactive and capable of mediating the addition of allyltrimethylsilane to aldehydes. This assumption follows from the increased electronegativity of fluorine (Pauling scale = 4)[9] in comparison with chlorine (Pauling scale = 3) and bromine (Pauling scale = 2.8). Additionally, the use of a complex bearing a strong Ti–F bond (D_0(Ti–F) = 140 kcal mol^{-1})[10] was an attractive feature. The development of a catalytic allylsilane addition to an aldehyde would necessitate that the allyltrimethylsilane and the resulting Me_3SiO-ethers be stable under the reaction conditions. In this regard, we proposed that the strong Ti–F bond would disfavor desilylation of the product with formation of Me_3SiF (D_0(Si–F) = 135 kcal mol^{-1}).

Polymeric TiF_4 is commercially available as an inexpensive solid, which is insoluble in common aprotic organic solvents (Et_2O, THF, CH_2Cl_2, C_6H_6) with the exception of acetonitrile. A solution of TiF_4 in CH_3CN may be prepared and can be stored at 23 °C for weeks without evident decomposition. Treatment of (*S*)-(−)-1,1′-bi-2-naphthol (20 mol%) with a solution of TiF_4 (10 mol%) in CH_3CN produces a deep red solution, which upon evaporation of solvent yields a red-brown solid. The reaction of a mixture of this solid in CH_2Cl_2 with allyltrimethylsilane and an aldehyde at 0 °C led to the corresponding Me_3Si-protected homoallylic alcohol product.[11] Analysis of the adducts was facilitated by treatment of the silyl ethers with Bu_4NF/THF to furnish homoallylic alcohols **3** [(Eq. (b), Table 1]. For the aldehydes screened, the enantiomeric purity of the products ranged from 60–94% *ee* and the yields from 69–93%.[12] For each of the deprotected adducts, preparation of the derived (*S*)-(−)- and (*R*)-(+)-α-methoxy-α-(trifluoromethyl)-phenylacetic acid (MTPA) esters allowed the extent of asymmetric induction to be assayed by gas chromatography.[13] The absolute configuration of the products was established unambiguously by correlation with the known enantiopure homoallylic alcohols,[2] or by preparation of and comparison to authentic products synthesized by using known methods.[14, 15] For the catalytic, enantioselective process described herein, α,α-disubstituted aldehydes are ideal substrates; they afford the corresponding substituted homoallylic alcohols in high enantiomeric excess (entries 1–4). The β,β-dimethyl-substituted

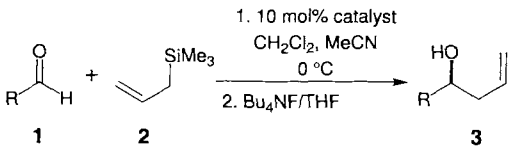

(b)

Table 1. Catalytic, enantioselective allyltrimethylsilane additions to aldehydes [a].

Entry	Aldehyde	*t* [h]	Yield [%]	*ee* [%]
1	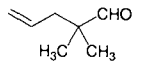	4	90	94
2	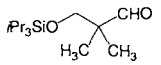	20	93	84
3	$(CH_3)_3CCHO$	4	91	94
4	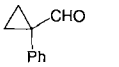	20	92	93
5	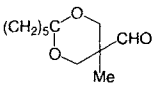	20	81 [b]	74
6	PhCHO	4	85	80
7	*c*-$C_6H_{11}CHO$	4	72	60
8	$PhCH_2CH_2CHO$	4	69	61 [c]

[a] The enantiomeric excess (*ee*) was determined by preparation of the derived (*S*)-(−)-α-methoxy-α-(trifluoromethyl)-phenylacetic acid (MTPA) ester and comparison to authentic material by analysis using gas chromatography on a J&W Cyclodex-B-column. [b] Based on 25% recovered aldehyde. [c] Determined by HPLC analysis of the free alcohol on a Chiracel OD column.

secondary alcohol is a common structural motif of many bioactive natural products such as the bryostatins,[16] elfamycins,[17] aplasmomycin,[18] boromycin,[19] and mycalamides.[20] In this regard, the adducts of entries 1 and 2 serve as useful starting materials for the asymmetric synthesis of such stereochemically complex compounds.

We have established that it is important to conduct the reaction in the presence of small amounts of acetonitrile. Thus, the catalyst prepared from (*S*)-(−)-1,1′-bi-2-naphthol and TiF_4 in CH_2Cl_2 affords the adduct of pivalaldehyde in 75% *ee* and only 10% yield. As for allylstannane and aldol additions, the process described herein exhibits a nonlinear relationship between the enantiomeric purity of the 1,1′-bi-2-naphthol and the observed optical purity of the resulting homoallylic alcohol. When the allylation is conducted with 50% *ee* (*S*)-(−)-BINOL and TiF_4 in CH_3CN/CH_2Cl_2, the adduct of pivalaldehyde is isolated in 82% *ee*.

^{1}H NMR spectroscopic investigations indicate that when allyltrimethylsilane (2 equiv) is added to a solution of (*S*)-(−)-1,1′-bi-2-naphthol (1 equiv) and TiF_4 (1 equiv) in CD_2Cl_2 in the presence of 3% CH_3CN (0 °C → 23 °C) clean formation of Me_3SiF and propene is observed. Subsequent addition of excess allylsilane only leads to the appearance of resonances corresponding to allyltrimethylsilane. Upon treatment of the reaction mixture with aldehyde, new signals are observed that can be assigned to the formation of product. These findings indicate that allyltrimethylsilane initially functions as a base by consuming two equivalents of HF to give propene and Me_3SiF during the catalyst preparation; moreover, in the absence of signals

 © VCH Verlagsgesellschaft mbH, D-69451 Weinheim, 1996 0570-0833/96/3520-2364 $ 15.00+.25/0

corresponding to an allyltitanium species,[21] the results indicate that transmetalation is not occurring and that the complex functions as a Lewis acid.

The new catalytic, enantioselective addition of allyltrimethylsilane to aldehydes described here is thus an alternative to methods that employ organotin reagents. The success of the reaction is attributed to the unique reactivity of a fluorotitanium complex prepared in acetonitrile from TiF_4 and (*R*)- or (*S*)-1,1′-bi-2-naphthol. The additions with allyltrimethylsilane are possible with the discovery that the TiF_4-derived catalyst is more reactive than the chloro-, bromo-, and alkoxytitanium complexes that have been previously employed. These results present new opportunities for the design and synthesis of well-defined chiral fluorotitanium complexes as catalysts in a variety of other important stereoselective processes. The study of such optically active complexes and their subsequent application are currently under investigation in our laboratory and will be reported in due course.

Experimental Procedure

To a solution of (*S*)-(−)-1,1′-bi-2-naphthol (57 mg, 0.20 mmol) in MeCN (0.5 mL) was added TiF_4 (0.20 mL, 0.10 mmol; 0.5 M solution in MeCN) to give a deep red solution that was stirred for 5 min prior to removing the solvent under reduced pressure. The residue was kept under reduced pressure (1 mm Hg) for 0.5 h and subsequently suspended in CH_2Cl_2 (0.5 mL), cooled to 0 °C, and treated dropwise with allyltrimethylsilane (0.24 mL, 1.5 mmol). After the mixture had been stirred at 0 °C for 1.5 h, the resulting red orange solution was treated with 2,2-dimethyl-4-pentenal (0.14 mL, 1.0 mmol). The reaction mixture was stirred at 0 °C for 4 h and then diluted with Et_2O/pentane (1:2; 10 mL). The mixture was filtered through a plug of silica and the filter cake washed with Et_2O/pentane (1:2; 50 mL). The filtrate was concentrated in vacuo to an oil, which was diluted with THF (2.0 mL). The resulting solution was treated with Bu_4NF (1.0 mL of a 1.0 M solution in THF), and stirred at 23 °C for 0.5 h. The reaction was quenched with Et_2O (50 mL) and washed with H_2O (20 mL). The ether extract was washed with saturated aqueous sodium chloride solution, dried over anhydrous Na_2SO_4, and concentrated in vacuo to give a colorless oil. Purification by chromatography on silica gel with Et_2O/pentane (1/10) afforded 138 mg (90%) of the product.

Received: July 1, 1996 [Z9272IE]
German version: *Angew. Chem.* **1996**, *108*, 2521–2523

Keywords: allylations · allylsilanes · asymmetric catalysis · synthetic methods · titanium compounds

[1] General reviews: a) J. A. Marshall, *Chem. Rev.* **1996**, *96*, 31; b) Y. Yamamoto, N. Asao, *ibid.* **1993**, *93*, 2207; c) W. R. Roush in *Comprehensive Organic Synthesis*, *Vol. 2* (Ed.: C. H. Heathcock), Pergamon, Oxford, **1990**, pp. 1–53; d) R. W. Hoffman, *Angew. Chem.* **1982**, *94*, 569; *Angew. Chem. Int. Ed. Engl.* **1982**, *21*, 555; e) W. R. Roush in *Applications of Allylboronates in the Synthesis of Carbohydrates and Polyhydroxylated Natural Products* (Eds.: D. Horton, L. D. Hawkins, G. J. McGarvey), *ACS Symp. Ser. 386*, American Chemical Society, Washington, DC, **1989**, pp. 242–277.

[2] a) A. Hafner, R. O. Duthaler, R. Marti, G. Rihs, P. Rothe-Streit, F. Schwarzenbach, *J. Am. Chem. Soc.* **1992**, *114*, 2321; b) J. A. Marshall, Y. Tang, *Synlett.* **1992**, 653; c) B. Schmidt, D. Seebach, *Angew. Chem.* **1991**, *103*, 100; *Angew. Chem. Int. Ed. Engl.* **1991**, *30*, 99; d) W. R. Roush, L. K. Hoong, M. A. Palmer, J. C. Park, *J. Org. Chem.* **1990**, *55*, 4109; e) H. C. Brown, U. S. Racherla, *ibid.* **1991**, *56*, 401; f) K. Furuta, M. Mouri, H. Yamamoto, *Synlett* **1991**, 561; g) E. J. Corey, C.-M. Yu, S. S. Kim, *J. Am. Chem. Soc.* **1989**, *111*, 5495; h) R. P. Short, S. Masamune, *ibid.* **1989**, *111*, 1892; i) M. T. Reetz, T. Zierke, *Chem. Ind.* **1988**, 663; j) R. W. Hoffman, T. Herold, *Chem. Ber.* **1981**, *114*, 375.

[3] a) G. E. Keck, K. H. Tarbet, L. S. Geraci, *J. Am. Chem. Soc.* **1993**, *115*, 8467; b) A. L. Costa, M. G. Piazza, E. Tagliavini, C. Trombini, A. Umani-Ronchi, *ibid.* **1993**, *115*, 7001; c) G. E. Keck, D. Krishnamurthy, M. C. Grier, *J. Org. Chem.* **1993**, *58*, 6543; d) J. W. Faller, D. W. Sams, X. Liu, *J. Am. Chem. Soc.* **1996**, *118*, 1217.

[4] For the use of fluorotitanium isopropoxides in the opening of epoxides, see: A. A. Nikitenko, B. M. Arshava, I. E. Mikerin, Y. E. Raifeld, *Tetrahedron Lett.* **1992**, *33*, 7087.

[5] For excellent, comprehensive reviews of Ti^{IV} complexes and their use in additions to aldehydes, see: a) R. O. Duthaler, A. Hafner, *Chem. Rev.* **1992**, *92*, 807; b) M. T. Reetz *Organotitanium Reagents in Organic Synthesis*, Springer, Berlin, **1986**.

[6] As part of some very elegant work on Ti-carbohydrate complexes in organic synthesis, Hafner and Duthaler have reported that the addition of the alkyltitanium reagent $CH_3Ti(OiPr)_3$ to aldehydes is catalyzed by CpTiF(TADDOLate), (TADDOL = αα′α′-tetraaryl-2,2-dimethyl-1,3-dioxolan-4,5-dimethanol): A. Hafner, R. O. Duthaler *Abstr. Pap. Seventh IUPAC Symposium on Organo-Metallic Chemistry Directed Towards Organic Synthesis (OMCOS-7)*, Kobe, Japan, 22.

[7] H. Mayr, M. Patz, *Angew. Chem.* **1994**, *106*, 990; *Angew. Chem. Int. Ed. Engl.* **1994**, *33*, 938.

[8] S. Aoki, K. Mikami, M. Terada, T. Nakai, *Tetrahedron* **1993**, *49*, 1783.

[9] L. Pauling, *The Nature of the Chemical Bond*. 3rd. ed., Cornell University Press, Ithaca, **1960**, p 93.

[10] For comparison : $D_o(Ti-Cl)(TiCl_4) = 103\ kcal\,mol^{-1}$, $D_o(Ti-Br)(TiBr_4) = 88\ kcal\,mol^{-1}$, J. E. Huheey, *Inorganic Chemistry: Principles of Structure and Reactivity*, 3rd ed.; Harper and Row, New York, **1983**, p 845.

[11] The silyl-protected adducts are the predominant product in all of the addition reactions. Small amounts of the free alcohol products could also be isolated albeit in 5–10% yields. The % *ee* value of the alcohol product was found to be equal to that of the silyl-protected adduct for each of the aldehydes examined.

[12] As an alternative experimental procedure, we have observed that a mixture of (*S*)-(−)-1,1′-bi-2-naphthol and TiF_4 in 3% CH_3CN/CH_2Cl_2 solution works well in the addition reaction and obviates the need to remove the bulk acetonitrile solvent.

[13] J. A. Dale, D. L. Dull, H. S. Mosher, *J. Org. Chem.* **1969**, *34*, 2543.

[14] H. C. Brown, P. K. Jadhav, *J. Am. Chem. Soc.* **1983**, *105*, 2092.

[15] W. R. Roush, L. Banfi, *J. Am. Chem. Soc.* **1988**, *110*, 3979.

[16] G. R. Pettit, *Pure Appl. Chem.* **1994**, *66*, 2271.

[17] H. Maehr, M. Leach, L. Yarmchuk, M. Mitrouic, *J. Antibiot.* **1979**, *32*, 361.

[18] T. Okazaki, T. Kitahara, Y. Okami, *J. Antibiot.* **1975**, *28*, 176.

[19] R. Hutter, W. Keller-Schierlein, F. Knusel, V. Prelog, G. C. Rodgers, P. Suter, G. Vogel, W. Voser, H. Zahner, *Helv. Chim. Acta* **1967**, *50*, 1533.

[20] N. B. Perry, J. W. Blunt, M. H. Munro, L. K. Pannell, *J. Am. Chem. Soc.* **1988**, *110*, 4850.

[21] For an extensive discussion of the structure and spectroscopy of a well-defined chiral allyltitanium complex, see: R. O. Duthaler, A Hafner, M. Riediker In *Organic Synthesis via Organometallics*, (Eds.: K. H. Dötz, R. W. Hoffman), Vieweg, Braunschweig, **1991**, p 285.

Structure of Silyl-Substituted Allenyl/Propargyllithium Reagents in Solution**

Hans J. Reich* and Johnathan E. Holladay

Theoretical studies of C_3H_3Li, which could fomally be either allenyl- or propargyllithium, have predicted a primarily allenyl structure.[1, 2] Experimentally, the question of structure has been addressed by X-Ray crystallography,[2, 3] IR spectroscopy,[1a, 4, 5] and ^{13}C NMR spectroscopy.[6a, b, 1a, 7] Both the central carbon (C_C, $\delta = 165-180$ for allenyl, $\delta = 90-100$ for propargyl) and the propargyl carbon (C_P) are very sensitive indicators of structure. Most reagents investigated have an allenyl structure; this includes compounds with alkyl groups at C_A (for example **1** and **2**, Scheme 1),[6a, b] which might destabilize the allenyl isomer. A few well-defined propargyllithium reagents are known in which C_P bears either a strained ring (**3**),[5, 6b] one or two carbanion stabilizing groups (PhS (**4**),[6b] PhSe,[6b] Ph[2, 7]), or a strong chelating group (carbamoyloxy).[6b, 8] We report results of an NMR study of silyl-substituted allenyl/propargyllithium reagents,[9] which provide insight into the thermodynamics, kinetics, and stereochemistry of the allenyl/propargyllithium interconversion, as well as the effect of lithium coordination on the electronic structure.

[*] Prof. Dr. H. J. Reich, Dr. J. E. Holladay
Department of Chemistry, University of Wisconsin
1101 University Avenue, Madison, WI 53711 (USA)
Fax: Int. code +(608)262-0381
e-mail: reich@chem.wisc.edu

[**] This work was supported by the U. S. National Science Foundation.

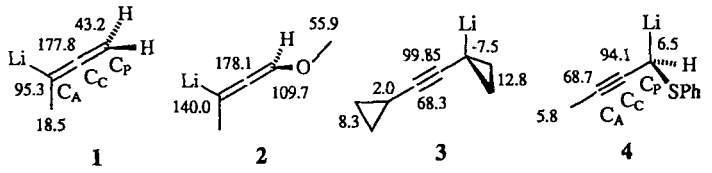

Scheme 1. ^{13}C chemical shifts of **1**–**4** in THF and Me_2O

The chemical shifts of the lithium reagent **6** (prepared by metalation of the propargylsilane **5**, Scheme 2) in THF are unambiguously allenic and essentially temperature-independent. Well-defined $^{13}C-^{7}Li$ coupling to C_A ($\delta = 77.5$, q (1:1:1:1), $J = 21$ Hz at $-152\,^{\circ}C$) and none to C_P is observed, indicating

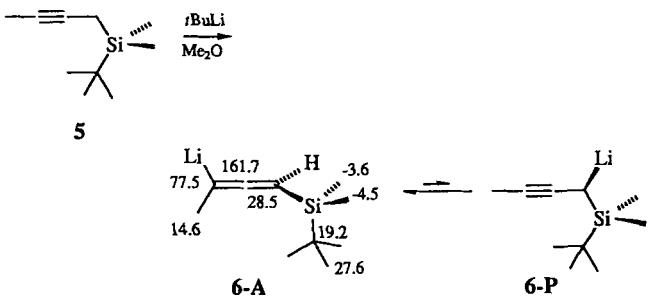

Scheme 2. Preparation and ^{13}C chemical shifts ($T = -152\,^{\circ}C$) of **6**-**A**.

the monomeric nature of the compound and localized bonding to lithium. At $-135\,^{\circ}C$ the maximum broadening for C_P is 2 Hz more than for C_A and C_C. Thus, J_{C-Li} for C_P is less than 0.6 Hz. Assuming that this value for a propargyl isomer is at least 15 Hz, there can be no more than 4% of **6**-**P** present. Values of 16 and 18 Hz have been measured for C_P $^{7}Li-^{13}C$ couplings in **4** and its selenium analog.[6b]

Because of the chiral allenyl group, the $SiMe_2$ group of **6** is diastereotopic at low temperature. The racemization of **6** can be detected by coalescence of the signals for the $SiMe_2$ group (coalescence temperature $-135\,^{\circ}C$, $\Delta G^{\ddagger}_{-142\,^{\circ}C} = 6.3$ kcal mol^{-1}). A remarkable feature of the racemization is that it is intramolecular;[10] the $Li-C_A$ coupling persists to more than $20\,^{\circ}C$ above the coalescence temperature ($\Delta\delta = 81$ Hz between the diastereotopic Me groups).[11] A barrier to inversion could also be estimated for **8** ($k = 400\ sec^{-1}$ at $-137\,^{\circ}C$, $\Delta G^{\ddagger} =$ 6.1 kcal mol^{-1}).

The ^{13}C NMR spectra of **8** (generated from **7**, Scheme 3), the phenyl analog of **6**, are less clear-cut. The strongly temperature-dependent chemical shift values are between those expected for allenyl and propargyl isomers, and the signals show poorly resolved Li–C coupling. The propargyl-like C_C shifts at low temperature move progressively towards allenyl values at higher temperatures. Since variations in chemical shifts of over 30 ppm (between -155 and $-35\,^{\circ}C$) are unlikely to arise from altered conformer populations or extent of solvation, substantial changes in structure or equilibrium composition must occur.

Figure 1 shows chemical shifts of C_C for a range of lithium reagents, from those that appear to be allenic (such as **1**) to those that are unambigously propargyllic (such as **4**). Compounds with intermediate δ values (**8**–**11**) must either consist of significant fractions of both allylic and propargyl isomers in rapid equilibrium on the NMR time scale or have a 1,3-lithium-bridged structure such as **12** in which the asymmetry of bridging is temperature-dependent. Such bridged structures have been

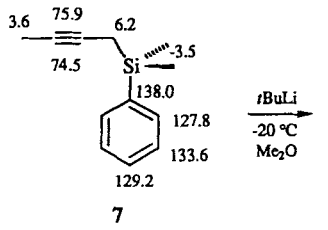

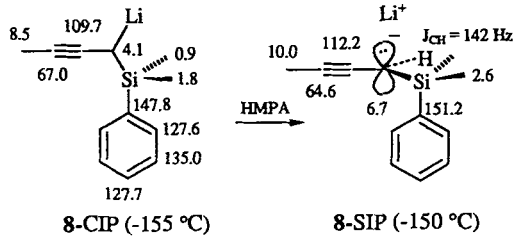

Scheme 3. Preparation and ^{13}C chemical shifts of **8** in Me_2O (CIP) and Me_2O-HMPA (SIP). See text for further details.

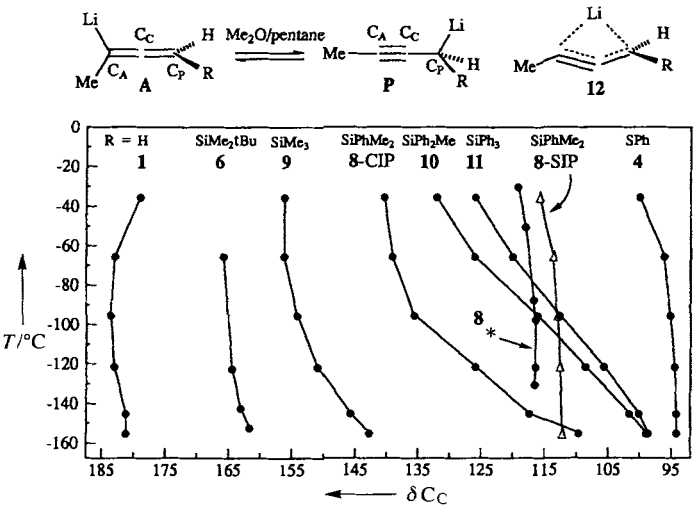

Fig. 1. Temperature dependence of the central carbon ^{13}C NMR chemical shifts of allenyl/propargyllithium reagents in THF/Me_2O (* = in 2,5-dimethyltetrahydrofuran).

predicted by calculations of unsolvated allenyllithium species, and there is evidence from HOESY experiments that dimeric 1-methoxyallenyllithium is partially bridged.[1a, 1b, 12] Since two species are detected by IR spectroscopy, we prefer an explanation involving tautomeric structures (although both could be unsymmetrically bridged). Absorptions at 1894 (strong) and 2179 (medium) cm^{-1} for **8** at $-78\,^{\circ}C$ indicate the presence of both allenyl and acetylenic structures.[1a, 4, 5] In contrast, the 2-pyridyl analog of **4** shows only an acetylenic stretch at 2164 cm^{-1}, whereas **1** shows an absorption at 1885 cm^{-1}. The ^{13}C chemical shifts of **1** and **4** are not significantly temperature-dependent; a static bridged structure such as **12** should not show the large changes in shift observed for **8**–**11**. If our interpretation of two tautomeric structures is correct, the propargyl isomer is enthalpically favored, whereas the allenyl isomer is entropically favored ($\Delta H^0 = 1.1 \pm 0.2$ kcal mol^{-1}, $\Delta S^0 = 6.1 \pm 1$ eu for **8**).[13] Solvation must play a key role in the structural changes, since the C_C chemical shifts of **8** in 2,5-dimethyltetrahydrofuran are only slightly temperature-dependent ($\delta = 119.2$ at $-30\,^{\circ}C$, 116.6 at $-130\,^{\circ}C$, Fig. 1).[14]

The temperature dependence and solvent effect suggest a difference in solvation between the allenyl and propargyl species.

 © VCH Verlagsgesellschaft mbH, D-69451 Weinheim, 1996 0570-0833/96/3520-2366 $ 15.00+.25/0

Perhaps the more highly directional, formally sp^2-hybridized carbanion orbital at the allenyl carbon C_A strengthens C–Li bonding and reduces the level of lithium solvation relative to that of the formally sp^3-hybridized propargyl carbanion carbon C_P. Higher temperatures would favor the isomer with the lower degree of solvation. Stronger C–Li covalency at C_A would also explain the tendency for more allenyl character in the contact ion pairs than in the solvent-separated ion pairs, as seen in most of the systems studied (see below).

When methyl groups on silicon are replaced by the more electron-withdrawing phenyl groups (compare **9** with **8**, **10**, and **11**), the fraction of propargyl isomer increases. This is consistent with the general observation that carbanion stabilizing groups (such as Ph, PhS, PhSe, or R_3Si) at the propargyl carbon favor the propargyl isomer. On the other hand, substitution of the methyl group on silicon by a *tert*-butyl group results in **6**, which has predominantly or exclusively allenyl character.

The identification of lithium reagents that are equilibrating mixtures of allenyl and propargyl isomers allowed an estimation of their rate of interconversion from D NMR line broadening. We chose the Me_3Si reagent **9** for more careful study, since it has nearly equal amounts of the two isomers at the lowest temperature investigated (Fig. 1). At $-150\,^{\circ}C$ in Me_2O/Et_2O/THF (5/2/1) the signal for C_C of **9** (estimated shifts of $\delta = 165$ and 98 in the two isomers) is 17 Hz wide. This gives a rate constant k greater than $10^5\ sec^{-1}$ and a free energy of activation $\Delta G^{\neq}$ smaller than 4 kcal mol^{-1} for interconversion of the isomers **9-A** and **9-P**. This low barrier to 1,3-lithium shift[15] has implications for the role of the isomeric lithium structures in the regioselectivity of reactions. Unless the rate of reaction for a lithium reagent with a substrate is greater than the rate of interconversion, the isomeric nature of the lithium reagent will not directly control the isomer produced (Curtin–Hammett principle). The rates of reaction for allenyl/propargyllithium reagents with typical substrates in THF are unknown. The very low barrier established here implies that the ratio of isomeric structures will directly determine regioselectivities for only the most rapid, if any, reactions of allenyl/propargyllithium reagents ($\Delta G^{\neq}_{-85\,^{\circ}C}$ for the reaction of *n*BuLi dimer and tetramer with benzaldehyde is about 9–10 kcal mol^{-1} [16]). The controlling feature will be the inherent reactivity of the individual isomers weighted by their concentrations. This conclusion is consistent with observations that a single allenyl/propargyllithium reagent can give dramatically different ratios of products with different electrophiles.[6c, 17]

HMPA titrations[6e] were carried out on most of the lithium reagents to establish the effect of lithium coordination on structure. Addition of HMPA to **8** first forms a mono-HMPA contact ion pair (CIP) followed by ion pair separation. Formation of the separated ion pair (SIP) is complete with four equivalents of HMPA. The chemical shifts are essentially temperature-independent (Fig. 1) and more propargyl- than allenyl-like. Although the C_C chemical shifts vary over 65 ppm (99 to 165 ppm) in the CIPs of **8** to **11**, the range for the SIPs is narrower (from $\delta = 106.9$ for $SiPh_3$ to $\delta = 118.7$ for $SiMe_2tBu$, $\delta(C_P)$ varies by only 2 ppm). The one-bond C–H coupling is significantly larger in the SIP (for example 146 Hz, for the $SiPh_3$ compound **11**) than in the CIP (128 Hz). Thus, there appears to be significant planarization of the carbanion carbon[6d] upon ion separation, but it is accompanied by surprisingly little change in the chemical shifts.

The significant changes in the ratio of propargyl to allenyl isomers that occur in compounds **8**–**11** can be principally ascribed to details of the interaction of the lithium cation and its associated solvent molecules with the anion. Changes in the inherent electronic structure of the carbanion play only a minor role.

Received: May 14, 1996 [Z9111IE]
German version: *Angew. Chem.* **1996**, *108*, 2498–2501

Keywords: allenes · NMR spectroscopy · propargylic compounds

[1] a) C. Lambert, P. v. R. Schleyer, E.-U. Würthwein, *J. Org. Chem.* **1993**, *58*, 6377; b) E. D. Jemmis, J. Chandrasekhar, P. v. R. Schleyer, *J. Am. Chem. Soc.* **1979**, *101*, 2848; c) W. K. Li, *Croat. Chem. Acta* **1988**, *61*, 833; J. K. Wilmshurst, C. E. Dykstra, *J. Am. Chem. Soc.* **1980**, *102*, 4668.

[2] P. Dem'yanov, G. Boche, M. Marsch, K. Harms, G. Fyodorova, V. Petrosyan, *Liebigs Ann.* **1995**, 457.

[3] Several X-ray crystal structures of dimeric allenyl/propargyllithium reagents have shown lithium coordination to both C_A and C_P [2]: a) P. v. R. Schleyer, *Pure and Appl. Chem.* **1984**, *56*, 151; b) W. N. Setzer, P. v. R. Schleyer, *Adv. Organomet. Chem.* **1985**, *24*, 353.

[4] a) W. Priester, R. West, T. L. Chwang, *J. Am. Chem. Soc.* **1976**, *98*, 8413; b) R. West, P. A. Carney, I. C. Mineo, *ibid.* **1965**, *87*, 3788; c) R. West, P. C. Jones, *ibid.* **1969**, *91*, 6156; d) J. Klein, J. Y. Becker, *J. Chem. Soc., Chem. Commun.* **1973**, 576; e) F. Jaffe, *J. Organomet. Chem.* **1970**, *23*, 53.

[5] G. Köbrich, D. Merkel, K. Imkampe, *Chem. Ber.* **1973**, *106*, 2017.

[6] a) H. J. Reich, I. L. Reich, K. E. Yelm, J. E. Holladay, D. Gschneidner, *J. Am. Chem. Soc.* **1993**, *115*, 6625; b) H. J. Reich, J. E. Holladay, *ibid.* **1995**, *117*, 8470; c) H. J. Reich, J. E. Holladay, J. D. Mason, W. H. Sikorski, *ibid.* **1995**, *117*, 12137; d) H. J. Reich, R. R. Dykstra, *ibid.* **1993**, *115*, 7041; H. J. Reich, R. R. Dykstra, *Angew. Chem.* **1993**, *105*, 1489; *Angew. Chem. Int. Ed. Engl.* **1993**, *32*, 1469; e) H. J. Reich, J. P. Borst, R. R. Dykstra, D. P. Green, *J. Am. Chem. Soc.* **1993**, *115*, 8728; f) H. J. Reich, K. J. Kulicke, *ibid.* **1995**, *117*, 6621.

[7] a) Allenyllithium: J. P C. M. van Dongen, H. W. D. van Dijkman, M. J. A. de Bie, *Rec. Trav. Chim. Pays Bas*, **1974**, *93*, 29; b) phenylallenes: P. I. Dem'yanov, I. M. Styrkov, D. P. Krut'ko, M. V. Vener, V. S. Petrosyan, *J. Organomet. Chem.* **1992**, *438*, 265.

[8] a) D. Hoppe, C. Riemenschneider, *Angew. Chem.* **1983**, *95*, 52; *Angew. Chem. Int. Ed. Engl.* **1983**, *22*, 54; b) D. Hoppe, C. Gonschorrek, *Tetrahedron. Lett.* **1987**, *28*, 785.

[9] Silyl-substituted allenyllithiums: a) E. J. Corey, C. Rücker, *Tetrahedron. Lett.* **1982**, *23*, 719; b) R. C. Hartley, S. Lamothe, T. H. Chan, *ibid.* **1993**, *34*, 1449.

[10] Several chelated lithium reagents have shown intramolecular racemization processes [6f]: G. Fraenkel, K. V. Martin, *J. Am. Chem. Soc.* **1995**, *117*, 10336.

[11] For other studies of allenyl/propargyllithium stereodynamics see [1, 5]: a) R. W. Hoffmann, J. Lanz, R. Metternich, G. Tarara, D. Hoppe, *Angew. Chem.* **1987**, *99*, 1196; *Angew. Chem, Int. Ed. Engl.* **1987**, *26*, 1145; b) D. Hoppe, C. Gonschorrek, *Tetrahedron. Lett.* **1987**, *28*, 785; c) E. M. G. A. van Kruchten, A. Haces, W. H. Okamura, *ibid.* **1983**, *24*, 3939; d) W. J. le Noble, D.-M. Chiou, Y. Okaya, *J. Am. Chem. Soc.* **1978**, *100*, 7743.

[12] a) π-Propargyl structures have been found in transition metal complexes: P. W. Blosser, J. C. Galucci, A. Wojcicki, *J. Am. Chem. Soc.* **1993**, *115*, 2994; b) these Cp_2Zr-propargyl compounds have $\delta(C_C)$ between 99 and 120: C. P. Casey, C. S. Yi, *ibid.* **1992**, *114*, 6597.

[13] The thermodynamic parameters were estimated by assigning $\delta(C_C) = 165$ for the allenyl (**8-A**) and 98 for the propargyl isomer (**8-P**). A principal source of uncertainty in the thermodynamic parameters is the estimation for the C_C-allenyl, which range from $\delta = 191.5$ for monomeric allenyllithium [6b,7a] to 162 for **6**.

[14] For an interesting example where increased solvation results in a more localized lithium coordination see: I. Hoppe, M. Marsch, K. Harms, G. Boche, D. Hoppe, *Angew. Chem.* **1995**, *107*, 2328; *Angew. Chem. Int. Ed. Engl.* **1995**, *34*, 2158.

[15] The 1,3-shift is probably intramolecular, since closely related compounds such as **6** retain C–Li coupling to much higher temperatures. The Li–C coupling was not well-resolved in **9**.

[16] Estimated from data presented in J. F. McGarrity, C. A. Ogle, Z. Brich, H.-R. Loosli, *J. Am. Chem. Soc.* **1985**, *107*, 1810.

[17] X. Creary, *J. Am. Chem. Soc.* **1977**, *99*, 7632.

 © VCH Verlagsgesellschaft mbH, D-69451 Weinheim, 1996 0570-0833/96/3520-2367 $ 15.00+.25/0

2,7,9-Trimethylenetricyclo[4.3.0.0^{3,8}]-non-4-ene**

Thilo Herb and Rolf Gleiter*

Among the many possible isomers of $C_{12}H_{12}$,[1] the family of tetraenes (**1**–**6**), in which a central tricyclic skeleton is surrounded by several 1,5-hexadiene units, is of particular interest. The double bonds can be either endocyclic or exocyclic. These attractive compounds not only offer a challenge for the synthetic chemist, but also invite studies of the interaction between the nonconjugated π-systems,[2] possible intramolecular rearrangements, and further intermolecular reactions.

There have been unsuccessful attempts to synthesize stellatetraene **1**[4] and **6**[5] (the systematic names of several compounds presented here are listed in Table 2). The latter is a potential precursor for the truncated tetrahedron **7**[6] and has, therefore, been the subject of several calculational studies. From our experience with the stellatriene **8**[7a] and its substitution products,[7b] it seems unlikely that **1** can be isolated at room temperature. However, the large increase in stability observed in going from **8** to the homologue twist-brendatriene **9**[8] suggests that species

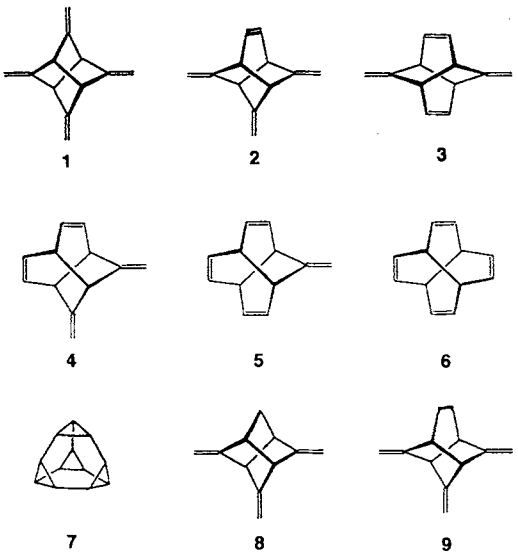

such as **2**–**6** should be stable enough to be isolated. Calculated strain energies for the tetraenes **1**–**6** support this idea (Table 1). In this paper we report the synthesis of **2**, the first member of the series of tricyclic $C_{12}H_{12}$ isomers.

The reaction sequence leading to **2** is summarized in Scheme 1. Our studies on the synthesis of the triene **9** suggested **13** as a key intermediate for the synthesis of **2**. Compound **13** has the proper functional groups to introduce the endocyclic double bond by cleavage of the acetal protecting group and to form simultaneously one further exocyclic double bond by the opening of the oxetane ring. The synthesis of **13** can be achieved by the Diels–Alder reaction of **10**[9] with acetylallene **11**[10]. The Paternò–Büchi reaction, first introduced by Sauers et al.[11] and Nakazaki et al.[12] proved useful for the construction of the pentacyclic system in **13**. Irradiation of **12** yielded **13**, and subsequent treatment with *n*-butyllithium provided **14** (30%) and **15** (36%), as anticipated. The former was transformed into the latter by repeated treatment with *n*BuLi. Compound **15** was oxidized under Swern conditions[13] to provide the ketone **16** in 70% yield (Scheme 1).

A final Wittig reaction gave the title compound, although the yield was very low (3%). This can be ascribed to two factors: the

Table 1. Calculated strain energies [kcal mol^{-1}] (MOLEK 9000) [3] of the tetraenes **1**–**6**.

	1	2	3	4	5	6
strain energy	77.6	65.2	53.6	57.7	51.2	52.6

Table 2. Systematic names of selected compounds.

1	2,4,6,8-tetramethylenetricyclo[3.3.0.0^{3,7}]octane
2	2,7,9-trimethylenetricyclo[4.3.0.0^{3,8}]non-4-ene
6	tricyclo[5.5.0.0^{4,10}]dodeca-2,5,8,11-tetraene
7	heptacyclo [5.5.0.0^{2,12}.0^{3,5}.0^{4,10}.0^{6,8}.0^{9,11}] dodecane
8	2,4,6-trimethylenetricyclo[3.3.0.0^{3,7}]octane
9	2,7,9-trimethylenetricyclo[4.3.0.0^{3,8}]nonane
10	7,9-dioxa-8-phenylbicyclo[4.3.0]nona-2,4-diene
12	*anti*-10-acetyl-11-methylene-4-phenyl-3,5-dioxatricyclo[5.2.2.0^{2,6}]undec-8-ene
13	1-methyl-11-methylene-7-phenyl-2,6,8-trioxapentacyclo-[8.2.1.0^{3,13}.0^{4,12}.0^{5,9}]tridecane
15	7,9-dimethylenetricyclo[4.3.0.0^{3,8}]non-4-en-2-ol
16	7,9-dimethylenetricyclo[4.3.0.0^{3,8}]non-4-en-2-one

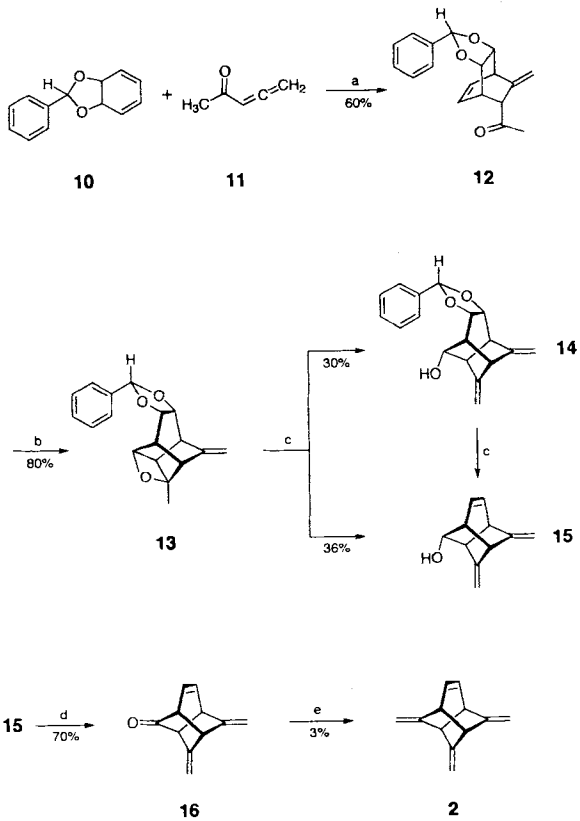

Scheme 1. a) C_6H_6, 60 °C; b) *hν* (282 nm), Et_2O; c) *n*BuLi, THF; d) $(COCl)_2$, DMSO, NEt_3, CH_2Cl_2, −60 °C; e) $[(C_6H_5)_3PCH_3]Br$, $NaNH_2$, THF, −20 °C.

[*] Prof. Dr. R. Gleiter, Dipl.-Chem. T. Herb
Organisch-chemisches Institut der Universität
Im Neuenheimer Feld 270, D-69120 Heidelberg (Germany)
Fax: Int. code +(6221) 54-4205

[**] We thank the Deutsche Forschungsgemeinschaft, the Fonds der Chemischen Industrie, and the BASF AG (Ludwigshafen) for financial support.

high volatility of **2** and the rearrangements of **2** and **16** at room temperature. Both compounds contain several 1,5-hexadiene units within a highly strained ring system, and it is likely that they undergo stepwise Cope rearrangements, as seen for **8**[7] and **9**.[8]

The yield of **2** in the last step of the synthesis can be increased by treating the ketone **16** with methyllithium to afford the tertiary alcohol **17** (Scheme 2). The structural assignment of **17** is

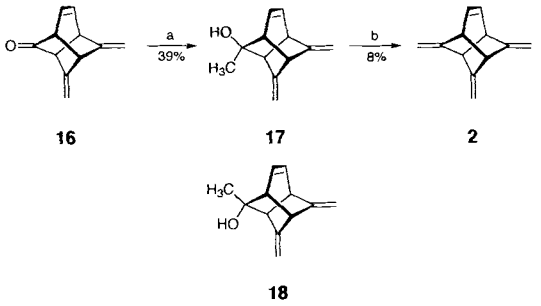

Scheme 2. a) MeLi, THF, −15 °C; b) $(COCl)_2$, DMSO, NEt_3, CH_2Cl_2, −60 °C.

based on H,H-NOESY experiments (Table 3). Comparison of the NMR data for **17** with values for similar tertiary alcohols containing such a tricyclic skeleton[7b, 14] supported the assignments for the hydroxyl and methyl groups. The epimeric alcohol **18** was not obtained by this reaction. The advantage of this protocol is the generation of a precursor (**17**) that is stable at room temperature. As shown in Scheme 2, **17** can be transformed under very mild conditions to the twist-brendatetraene **2**. This new dehydration procedure is based on the observation that the combination of $(COCl)_2$/DMSO/NEt_3, normally used for the oxidation of primary and secondary alcohols to aldehydes and ketones,[13] can be successfully applied for the elimination of water from tertiary alcohols with a β-hydrogen atom.[14] Our synthesis of **2**, one of the most strained members of the group of tricyclic tetraenes **1**–**6** (Table 1), indicates that it should also be possible to synthesize the less strained members of this series.

Table 3. Selected experimental data for **2**, **16**, and **17**.

2: Purification by silica gel column chromatography (elution with *n*-butane at −15 °C, colorless oil after removal of solvent at −15 °C; R_f(SiO_2, pentane, iodine) = 0.20; ^{1}H NMR (300 MHz, $CDCl_3$) [a]: δ = 3.00–3.03 (m, 2H, CH), 3.23–3.28 (m, 2H, CH), 4.45 (s, 2H, H_2C=), 4.46 (s, 2H, H_2C=) [b], 4.65 (s, 2H, H_2C=) [b], 6.27–6.31 (dd, $^3J_1$ = 4.6, $^3J_2$ = 3.5 Hz, 2H, HC=); ^{13}C NMR (50.32 MHz, $CDCl_3$) [c]: δ = 49.14 (d, 2C, CH), 55.25 (d, 2C, CH), 101.99 (t, 2C, H_2C=), 105.59 (t, H_2C=), 135.23 (d, 2C, HC=), 152.19 (s, 2C, C=), 154.10 (s, C=).

16: Purification by silica gel column chromatography, colorless oil; R_f(SiO_2, pentane/diethyl ether 1/1, iodine) = 0.50; ^{1}H NMR (300 MHz, $CDCl_3$) [a]: δ = 2.84–2.88 (m, 1H, CH), 3.25–3.35 (m, 3H, CH), 4.69 (s, 1H, H_2C=), 4.72 (s, 1H, H_2C=), 4.89 (s, 1H, H_2C=), 5.06 (s, 1H, H_2C=), 6.06–6.12 (m, 1H, HC=), 6.54–6.59 (m, 1H, HC=); ^{13}C NMR (50.32 MHz, $CDCl_3$) [c]: δ = 47.75 (d, CH), 48.56 (d, CH), 51.40 (d, CH), 55.28 (d, CH), 100.80 (t, H_2C=), 104.45 (t, H_2C=), 129.17 (d, HC=), 139.34 (d, HC=), 145.64 (s, C=), 151.48 (s, C=), 202.72 (s, C=O); IR (KBr): $\tilde{\nu}$ = 2990 (m), 1739 (vs, C=O), 1678 (s, C=C), 1663 (s, C=C), 1329 (m), 1065 (m), 911 (s), 886 (s, C=CH_2), 831 (s), 783 (m) cm^{-1}; UV/Vis (CH_2Cl_2): λ_{max} (lg ε) = 236 (3.55), 302 (2.68) nm; HRMS (EI, 70 eV): $C_{11}H_{10}O$, calcd 158.0732, found 158.0743.

17: Purification by silica gel column chromatography, colorless crystals, m.p. 32 °C; R_f (SiO_2, pentane/diethyl ether 1/1, iodine) = 0.43; ^{1}H NMR (200 MHz, CD_2Cl_2) [a]: δ = 1.34–1.35 (d, ^4J = 1.25 Hz, 3H, CH_3), 2.22–2.26 (m, 1H, CH), 2.45–2.47 (q, ^4J = 1.25 Hz, 1H, OH), 2.77–2.83 (m, 1H, CH), 2.86–2.91 (m, 1H, CH), 3.05–3.10 (t, ^3J = 5.4 Hz, 1H, CH), 4.28 (s, 1H, H_2C=), 4.29 (s, 1H, H_2C=), 4.65 (s, 2H, H_2C=), 5.94–6.01 (ddd, $^3J_1$ = 8.1, $^3J_2$ = 5.3, J_3 = 1.6 Hz, 1H, HC=), 6.81–6.89 (ddd, $^3J_1$ = 8.2, $^3J_2$ = 5.2, J_3 = 2.1 Hz, 1H, HC=); ^{13}C NMR (50.32 MHz, CD_2Cl_2) [c]: δ = 25.00 (q, CH_3), 29.96 (d, CH), 46.17 (d, CH), 49.91 (d, CH), 51.96 (d, CH), 76.61 (s, C-OH), 95.50 (t, =CH_2), 99.40 (t, =CH_2), 132.22 (d, =CH), 138.75 (d, =CH), 152.72 (s, C=CH_2), 156.93 (s, C=CH_2); MS (EI, 70 eV): *m/z* (%): 174 (6) [M^+], 159 (10) [$M^+ - CH_3$], 146 (13) [$C_{10}H_{10}O^+$], 145 (10), 141 (11), 132 (18), 131 (100) [$C_{10}H_{11}^+$], 129 (24), 128 (19), 117 (14), 116 (25), 115 (33) [$C_9H_7^+$], 92 (16), 91 (61) [$C_7H_7^+$], 77 (18), 65 (19), 51 (16); HRMS (EI, 70 eV): $C_{12}H_{14}O$, calcd 174.1045, found 174.1030.

[a] Assignment based on ^{1}H,^{1}H-COSY experiments. [b] The AB spectrum expected for the protons of the two radial exocyclic double bonds appears as a singlet. [c] Assigment based on DEPT experiments.

Received: May 23, 1996
Revised version: July 19, 1996 [Z9147IE]
German version: *Angew. Chem.* **1996**, *108*, 2546–2548

Keywords: cage compounds · hydrocarbons · Paternò-Büchi reactions · synthetic methods

[1] For valence isomers of [12]annulene see M. Banciu, C. Popa, A. T. Balaban, *Chem. Scr.* **1984**, *24*, 28–37.
[2] R. Gleiter, W. Schäfer, *Acc. Chem. Res.* **1990**, *23*, 369–375.
[3] MOLEK 9000 (P. Bischof) according to MMX; see J. J. Gajewski, K. E. Gilbert, Serena Software, Bloomington, IN, USA.
[4] H. Park, L. A. Paquette, *J. Org. Chem.* **1980**, *45*, 5378–5379.
[5] a) E. Vedejs, W. R. Wilber, R. Twieg, *ibid.* **1977**, *42*, 401–409; b) R. J. Brousseau, Ph.D. Thesis, Harvard University, **1977**.
[6] a) R. B. Woodward, R. Hoffmann, *The Conservation of Orbital Symmetry*, Verlag Chemie, Weinheim (Germany), **1970**; b) J. M. Schulman, R. L. Disch, M. L. Sabio, *J. Am Chem. Soc.* **1986**, *108*, 3258–3260; c) G. W. Schriver, D. J. Gerson, *ibid.* **1990**, *112*, 4723–4728.
[7] a) R. Gleiter, C. Sigwart, B. Kissler, *Angew. Chem.* **1989**, *101*, 1561–1563; *Angew. Chem. Int. Ed. Engl.* **1989**, *28*, 1525–1526; b) R. Gleiter, C. Sigwart, *J. Org. Chem.* **1994**, *59*, 1027–1038.
[8] R. Gleiter, T. Herb. O. Borzyk, I. Hyla-Kryspin, *Liebigs Ann.* **1995**, 357–364.
[9] a) N. C. Yang, M. J. Chen, P. Chen, K. T. Mak, *J. Am. Chem. Soc.* **1982**, *104*, 853–855; b) N. C. Yang, M. J. Chen. P. Chen, *ibid.* **1984**, *106*, 7310–7315.
[10] G. Buono, *Synthesis* **1981**, 872.
[11] a) R. R. Sauers, J. A. Whittle, *J. Org. Chem.* **1969**, *34*, 3579–3582; b) R. R. Sauers, W. Schinski, M. M. Mason, *Tetrahedron Lett.* **1969**, 79–82; c) R. R. Sauers, D. C. Lynch, *J. Org. Chem.* **1980**, *45*, 1286–1290, and references therein.
[12] a) M. Nakazaki, K. Naemura, S. Harita, *Bull. Chem. Soc. Jpn.* **1975**, *48*, 1907–1913; b) M. Nakazaki, K. Naemura, Y. Kondo, *J. Org. Chem.* **1976**, *41*, 1229–1233, and references therein.
[13] A. J. Mancuso, D. Swern, *Synthesis* **1981**, 165–185, and references therein.
[14] R. Gleiter, T. Herb, J. Hofmann, *Synlett.* in press.

Side-Arm Participation in a Four-Component Template Synthesis of a [30]Crown-10 Derivative**

Andreas Merz,* Oliver Schneider, and Laszlo Parkanyi

The cation template effect often facilitates the formation of medium-sized macrocyclic crown ethers by S_N2 cycloalkylation in high yield, without requiring high dilution conditions and regardless of whether α,ω-cyclizations or manifold ring-forming reactions of smaller building blocks are used.[1] Remarkable in this respect is the selective template-assisted formation of homologous [3*n*]crown-*n* ethers directly from oxirane.[2] In the preparation of large crowns, however, the template effect is less

[*] Prof. A. Merz, O. Schneider
Institut für Organische Chemie der Universität
D-93040 Regensburg (Germany)
Fax: Int. code + (941)943 4505
e-mail: andreas.merz@chemie.uni-regensburg.de
Dr. L. Parkanyi
Central Research Institute for Chemistry
Hungarian Academy of Sciences, H-1525 Budapest (Hungary)

[**] This work was supported by the Deutsche Forschungsgemeinschaft and the Fonds der Chemischen Industrie.

 © VCH Verlagsgesellschaft mbH, D-69451 Weinheim, 1996 0570-0833/96/3520-2369 $ 15.00+.25/0

efficient and difficult to predict.[3-5] In syntheses of [15]crown-5 derivatives from two components, for example of benzocrowns from catechols and tetraethyleneglycol disulfonates, smaller amounts of the "dimeric" [30]crown-10 homologues have occasionally been found.[6, 7] Here we report on the synthesis of the 30-membered crown ether ring **4** from the substituted benzoin **2** and tetraethyleneglycol dimesylate;[8] a reaction in which we had expected to form the bibracchial ("BIBLE"[9]) [15]crown-5 **3** (Scheme 1).

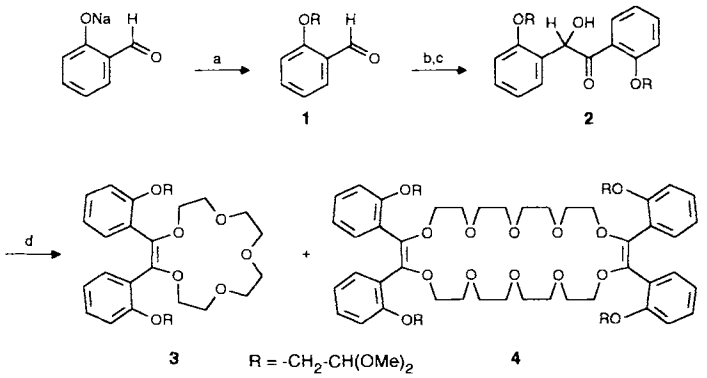

Scheme 1. Synthesis of the 30-membered crown ether **4**. a) $BrCH_2CH(OMe)_2$, DMF, 100 °C, 2d; b) $Me_3SiCN/ZnBr$; 1. LDA/THF, 2. 1 equiv **1**, 3. MeOH/cat. Bu_4NF/SiO_2; d) $MesOCH_2(CH_2OCH_2)_3CH_2OMes$, KOH powder, THF.

Compound **2** was prepared according to a protocol by Hünig et al.[10] Ring closure was achieved with tetraethyleneglycol dimesylate in THF; the intermediary orange enediolate of **2** was obtained with KOH as base (Scheme 1).[11] Addition of $NaClO_4$ in THF to the oily crude mixture, which was expected to contain the crown ether **3**, resulted in the formation of a crystalline precipitate in 35% yield. This surprisingly turned out to be the disodium complex **4**·2 $NaClO_4$, which was characterized by the $[M + Na^+]$ and $[M + 2Na^+ + ClO_4]$ ions in the FAB-MS spectrum. The free [30]crown-10 **4** was subsequently obtained from the complex. Both structures were confirmed by X-ray crystal structure analyses (Fig. 1).[12] The smaller ring **3**, which was not obtained in a pure form, was identified by mass spectrometry and detected by HPLC in 2–3% yield.

Evidently, the acetal side arms are responsible for the surprising and almost complete suppression of the formation of the smaller ring **3**. We propose the complex shown in Scheme 2 as the critical intermediate: following the first alkylation step the substituted phenyl group can rotate towards the podand-like complexed cation in such a way that the enolate structure is closed to give a quasi [18]crown-6 structure. In this way the nucleophilic center is blocked for direct ring closure and the outward oriented mesyloxyethyl group can be attacked by a second enediolate nucleophile. Based on this hypothesis the size of the template cation should have an influence on the outcome of the reaction. Indeed, when the base is NaOH the yield of **4** is only 30% as opposed to 50% with KOH (HPLC analysis).

A further effect of the acetal side arms is the peculiar conformational dynamics of **4**·2 $NaClO_4$. Above room temperature the ^1H NMR signals (400 MHz) of the crown ether methylene groups are broadened. The maximal broadening is observed at −20 °C, at which temperature all the remaining signals in the spectrum are also broadened. At −60 °C the broad singlet for the eight methoxy groups splits into two singlets of equal intensity, of which the upfield one splits again at −80 °C. At −90 °C only an enhanced resolution of the signals is observed. Remarkably, the signals for the aromatic protons now appear as two sets in a 3:1 ratio.

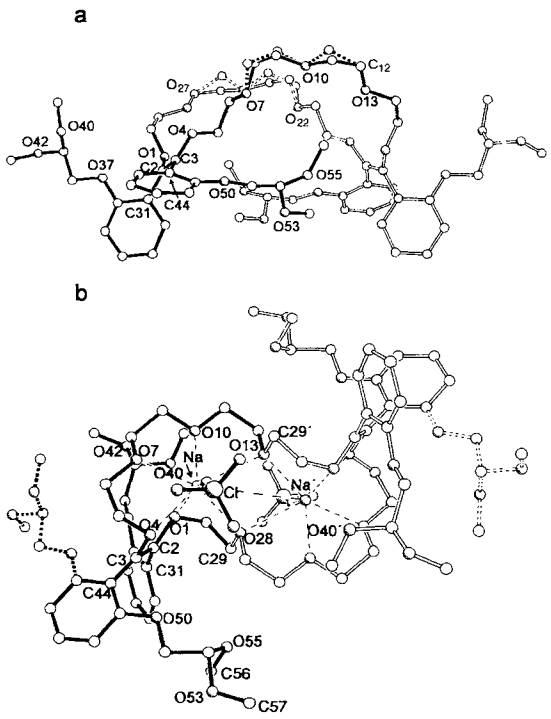

Fig. 1. Crystal structures of **4** and **4**·2 $NaClO_4$. The lightly printed parts are symmetry related to the bold ones by a C_2 axis (**4**) or an inversion center (**4**·$NaClO_4$), respectively. In the structure of **4** thermal disorder is indicated in the regions of O7 to C12 and O22 to C27. In the complex, thermal disorder exists with regard to the position of the acetal groups of the phenyl group at C3. Selected bond lengths [Å] and angles [°]: **4**: C2–C3 1.331(2), C3–O4 1.385(2), O1–C2 1.392; C2-C3-O4 123.6, C3-C2-O1 123.9, C3-C2-C31 122.9, C2- C3-C37 122.9, O1-C2-C31 113.5, O4-C3-C37 113.0. **4**·2 $NaClO_4$: Na–O1 2.430(4), Na–O4 2.508(5), Na–O7 2.413(5), Na–O10 2.392(5), Na–O13 2.736(5), Na–O(ClO_3) 2.263(3), O1–C2 1.427(2), C2–C3 1.338(2), C3–O4 1.426(2); C3-C2-O1 118.6(5), C3-C2-C31 123.9(4), O1-C2-C3 117.5(4), C2-C3-O4 116.8(5), O4-C3-C44 117.6(4), C3-C2-C31 125.6(4).

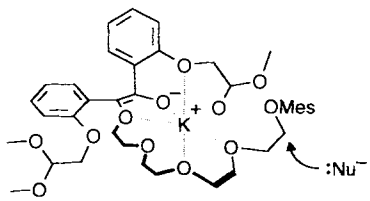

Scheme 2. Postulated reaction intermediate in the synthesis of **3** and **4**; $:Nu^-$ = enediolate of **2**.

Thus we conclude that there is a lariat interaction[9] between the acetal groups and the cations complexed in the crown ether ring. The unusual dynamic behavior above room temperature may result from an inter or intramolecular cation exchange. Apart from these conformational motions in the large crown ether ring, two important rotational processes at the periphery can be identified: the rotation of the aryl groups about the bond to the double bond and the rotation of the acetal groups about the CH_2–$CH(OCH_3)$ bond (Scheme 3).

Freezing of the rotation of the aryl groups would reduce the formal average symmetry of the crown ether from D_{2h} to C_i, as shown in Scheme 3. In this structure, two diagonal acetal groups (A and B) located above and below the crown ether plane get into a position for interaction with the nearest Na^+ ion. Freezing of the rotation of the acetal groups about the CH_2–$CH(OCH_3)$ bond will allow one of methoxy oxygen atoms in B to interact with a sodium ion, leading to the nonequivalence of

 © VCH Verlagsgesellschaft mbH, D-69451 Weinheim, 1996 0570-0833/96/3520-2370 $ 15.00+.25/0 Angew. Chem. Int. Ed. Engl. 1996, 35, No. 20

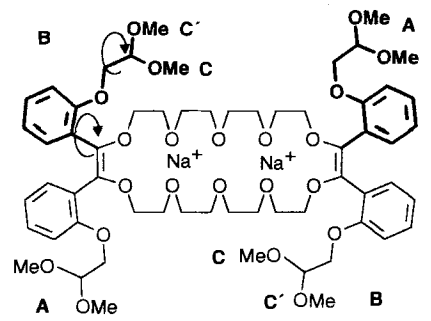

Scheme 3. Two important rotational processes that take place at the periphery of the crown ether ring.

the methoxy groups C and C'. The uncomplexed external methoxy groups (A) can still freely rotate. The free ligand **4** also shows signal broadening below $-20\,^{\circ}C$, but the dynamic effects are restricted to the crown ether CH_2CH_2 signals. The aromatic signals and the OCH_3 signals of the side arms remain sharp down to $-90\,^{\circ}C$.

Interestingly, the structure of $\mathbf{4}\cdot 2\,NaClO_4$ (Fig. 1b) closely resembles the low-temperature structure deduced from the low-temperature NMR spectrum, although, in the crystal, the distance of 5.32 Å between the sodium ions and the closest methoxy oxygen atoms (O40 and O40') of the side arms are much too long for a bonding interaction. The centrosymmetric 30-membered crown ether ring is separated by a step at the O13–C29' and O28–C29 bonds into two half-crowns, which are each occupied by a sodium cation. These Na^+ ions are located outside the average planes of the five oxygen atoms pointing towards the ClO_4^- ions, which are coordinating from different sides of the ring. The oxygen atoms O13 and O28 are shared by both sodium ions. Two diagonally opposite acetal groups (O40 and O40') are bent over the ring, whereas the other two point outward. As indicated in Figure 1b the peripheral side groups (O50 to C56) are thermally disordered, which may be considered as an explanation for the observed 3:1 splitting of the signals of the aromatic protons in the ^1H NMR spectrum of the complex at $-90\,^{\circ}C$.

The C_2 symmetric free ligand **4** has a concave shape with only *gauche*-type ethylenedioxy units. The resulting cavity is filled by the acetal side groups of two diagonally arranged aryl groups on the same side of the ring (Fig. 1a).

The structures of the crown ethers most closely related to **4** and $\mathbf{4}\cdot 2\,NaClO_4$, namely dibenzo[30]crown-10[13] and its disodium complex,[14] have been known for a long time. The crystal structure of the parent, unsubstituted [30]crown-10 was determined only recently;[15] the structures of **4** and $\mathbf{4}\cdot 2\,NaClO_4$ differ significantly from the latter, which is again attributed to the supramolecular interaction of the side arms.

Experimental Procedure

1: The sodium salt of salicylaldehyde [11] (35.0 g, 0.24 mol) and bromoacetaldehyde dimethyl acetal (40.0 g, 0.24 mol) were stirred in absolute DMF (400 mL) for 48 h at 70 °C. After addition of 2 N NaOH (150 mL) the mixture was extracted with ether and the extract was fractionally distilled (b.p. 140 °C, 4×10^2 bar). Yield 14.9 g (30%), slightly yellow oil. ^1H NMR (250 MHz, $cDCl_3$): $\delta = 3.48$ (s, 6H, OCH_3), 4.13 (d, 2H, $-CH_2-$, $J = 5.2$ Hz), 4.77 (t, 1H, -HC=), 6.99 (dd, 1H, H3), 7.05 (dt, 1H, H5), 7.54 (ddd, 1H, H4), 7.84 (dd, 1H, H6), 10.51 (s, 1H, CHO). Additional coupling contants $J_{3,4} = 8.4$ Hz, $J_{3,5} = 0.8$ Hz; $J_{4,5} = 7.6$ Hz, $J_{4,6} = 1.80$ Hz, $J_{5,6} = 7.8$ Hz.

2: The O-trimethylsilyl cyanohydrin of **1** (7.80 g, 25.0 mmol) was prepared and lithiated without further purification in THF with LDA according to the procedure given in reference [10]. At $-78\,^{\circ}C$ a solution of **1** (7.80 g, 25.0 mmol) in THF was added, and the mixture was allowed to warm up to room temperature, hydrolyzed (under nitrogen) with aqueous Na_2CO_3, and extracted with ether. After the solvent had been removed, an oil (11.0 g) was obtained that was dissolved in MeOH and stirred for 48 h over tetrabutylammonium fluoride on silica (Fluka Nr. 86876) at room temperature. Pure **2** was obtained by column chromatography (silica, hexane/ethyl acetate 1:1) as a colorless oil (8.01 g, 76%). ^1H NMR (250 MHz, $CDCl_3$): $\delta = 3.45, 3.46, 3.47, 3.50$ (4s, 12H, OCH_3); 3.90, 3.92, 4.00, 4.03 (4d, 4H, Ar-O-CH_2, $J = 5.2$ Hz), 4.59 (d, 1H, CHO*H*, $J = 6.6$ Hz), 4.65, 4.76 (2t, 2H, CHOMe), 6.05 (d, 1H, C*H*OH) 6.70–7.57 (m, 8H) (the signals of the side arm are split due to different site and diastereotopy).

4: Benzoin **2** (1.26 g, 3 mmol), tetraethylenglycol dimesylate (1.05 g, 3 mmol), and powdered KOH (1.70 g, 30 mmol) in absolute THF (20 mL) were heated to reflux and stirred under nitrogen for 24 h. After most of the solvent had been removed, the mixture was taken up in CH_2Cl_2 and washed with water. Removal of the solvent left a yellowish oil (1.14 g, 67%), which was dissolved in THF (8 mL) and treated with $NaClO_4$ (171 mg, 195 mmol) in THF (5 mL). The reaction mixture was layered with pentane and the complex $\mathbf{4}\cdot 2\,NaClO_4$ crystallized overnight. $\mathbf{4}\cdot 2\,NaClO_4$: 340 mg, 30%, m.p. 153–155 °C. ^1H NMR (400 MHz, $CDCl_3$): $\delta = 3.40$ (s, 24H, OCH_3), 3.75, 3.80, 3.96, 3.91 (m, 40H, four broad signals, crown ether-H + Ar-O-CH_2), 4.70 (t, 4H, CH-$(OMe)_2$), 6.75 (t, 4H, arom.-H5), 6.76 (d, 4H, arom.-H3), 7.07 (dd, arom.-H6), 7.18 (ddd, arom.-H4). For the isolation of the free ligand **4**, the complex was dissolved in CH_2Cl_2 and the salt was washed out with water. The oil obtained after removal of the solvent slowly crystallized on addition of ether: **4**: 153 mg, 56% (m.p. 84–86 °C), ^1H NMR (400 MHz, $CDCl_3$): $\delta = 3.29$ (s, 24H, OCH_3), 3.65–3.71 (m, 24H, inner crown ether-H), 3.95 (m, 8H, =C-OCH_2), 3.98 (d, 8H, Ar-O-CH_2), 4.77 (t, 4H, CH-$(OMe)_2$), 6.65 (dt, 4H, arom.-H5), 6.76 (dd, 4H, arom.-H3), 7.02 (dd, arom.-H6), 7.11 (ddd, 4H, arom.-H4).

Received: May 6, 1996
Revised version: July 5, 1996 [Z9099IE]
German version: *Angew. Chem.* **1996**, *108*, 2533–2535

Keywords: cyclizations · crown ethers · enolates · NMR spectroscopy · template synthesis

[1] B. Dietrich, P. Viout, J.-M. Lehn, *Macrocyclic Chemistry*, VCH, Weinheim, **1992**, pp. 108–112.
[2] J. J. Dale, K. Daasvatn, *J. Chem. Soc. Chem. Commun.* **1976**, 295–296.
[3] R. Chênevert, L. D'Astous, *J. Heterocycl. Chem.* **1986**, *23*, 1785–1787.
[4] A. Vitali, B. Masci, *Tetrahedron* **1989**, *45*, 2213–2222.
[5] H. W. Gibson, M. C. Bheda, P. Engen, Y. X. Shen, J. Sze, H. Zhang, M. D. Gibson, Y. Delaviz, S.-H. Lee, S. Liu, L. Wang, D. Nagkevar, J. Rancourt, L. T. Taylor, *J. Org. Chem.* **1994**, *59*, 2186–2196.
[6] C. J. Pedersen, *J. Am. Chem. Soc.* **1967**, *89*, 7017–7036.
[7] A. Merz, M. Rauschel, *Synthesis* **1993**, 797–802.
[8] A. Merz, *Angew. Chem.* **1977**, *89*, 484–485; *Angew. Chem. Int. Ed. Engl.* **1977**, *16*, 467–468.
[9] G. W. Gokel, J. E. Trafton, *Cation Binding by Macrocycles*, Marcel Dekker, New York, **1990**, pp. 253–310; F. R. Fronczek, R. D. Gandour, *ibid.* pp. 311–361.
[10] K, Deuchert, U. Hertenstein, S. Hünig, G. Wehner, *Chem. Ber.* **1979**, *112*, 2045–2061; S. Hünig, G. Wehner. *ibid.* **1979**, *112*, 2062–2067.
[11] A. Merz, A. Karl, T. Futterer, N. Stacherdinger, O. Schneider, J. Lex, E. Luboch, F. Biernat, *Liebigs Ann. Chem.* **1994**, 1199–1209.
[12] Crystal structure data: **4** and $\mathbf{4}\cdot 2\,NaClO_4$ had rather low scattering power even at liquid N_2 temperature (77 K). Intensity data for **4** were collected at this temperature. $\mathbf{4}\cdot 2\,NaClO_4$ showed a reversible and incomplete phase transformation on cooling, therefore data collection was performed at ambient temperature. The structures were determined with an Enraf Nonius Turbo CAD4 diffractometer with $Mo_{K\alpha}$, $\lambda = 0.71069$ Å, ω-2θ scan by using direct methods (SHELXS-86), refinement on F^2 (SHELXL-93); H atoms were calculated in idealized positions. **4**: $C_{60}H_{84}O_{22}$, $M_r = 1157.3$, crystal dimensions $0.30\times0.20\times0.15$ mm, monoclinic, $P2_1/c$, $a = 14.379(3)$, $b = 15.180(3)$, $c = 17.005(3)$ Å, $\beta = 90.95(3)^{\circ}$, $V = 3711.2(13)$ Å^3, $Z = 2$, $\rho_{calcd} = 1.255$ g cm^{-3}, $T = 128(2)$ K, $\mu = 0.178$ mm^{-1}; 4596 reflections, 4445 symmetry-independent reflections of which 4392 were observed ($I > 2\sigma(I)$), 482 parameters refined, $R1 = 0.093$, $wR2 = 0.231$, max/min residual electron density 0.739 and -0.613 e Å^{-3}. Note on the disorder: the carbon atoms in the middle portion of the crown ether (C8,9,11) split into two statistically filled positions. The C52,O53.... C56 moiety is rotationally disordered, but the disorder could not be completely resolved. $\mathbf{4}\cdot 2\,NaClO_4$: $C_{60}H_{84}O_{30}Cl_2Na_2$, $M_r = 1402.2$, crystal dimensions $0.21\times0.18\times0.15$ mm, monoclinic, $C2/c$, $a = 24.017(2)$, $b = 10.101(1)$, $c = 25.012(1)$ Å, $\beta = 91.98(1)^{\circ}$, $V = 6064.2(8)$ Å^3, $Z = 4$, $\rho_{calcd} = 1.268$ g cm^{-3}, $T = 128(2)$ K, $\mu = 0.096$ mm^{-1}. 13132 reflections, 6605 symmetry-independent reflections of which 5525 were observed ($I > 2\sigma(I)$), 466 parameters refined, $R1 = 0.053$, $wR2 = 0.162$, residual electron density 0.634 and -0.361 e Å^{-3}. Due to a low data to parameter ratio the structure could only be refined when bond length constraints were applied. These include the ClO_4 tetrahedron, rigid group refinement of the phenyl groups, and C–C and C–O bonds of the crown. Note on the disorder: The O50, C51... C56 moiety is disordered, it appears in both *ortho* positions with a statistical filling of 1:1. C54 lies close to the inversion center at 0.5, 0, 0.5 and therefore makes a bond

with itself through the inversion center, that is with another side chain in statistically filled positions. Crystallographic data (excluding structure factors) for the structure(s) reported in this paper have been deposited with the Cambridge Crystallographic Data Centre as supplementary publication no. CCDC-179-124. Copies of the data can be obtained free of charge on application to The Director, CCDC, 12 Union Road, Cambridge CB2 1EZ, UK (fax: Int. code +(1223) 336-033; e-mail: teched@chemcrys.cam.ac.uk).

[13] M. A. Bush, M. R. Truter, *J. Chem. Soc. Perkin Trans. II* **1972**, 345-350.

[14] J. D. Owen, M. R. Truter, *J. Chem. Soc. Dalton Trans.* **1979**, 1831-1835.

[15] M. C. Bheda, J. S. Merola, W. A. Woodward, V. J. Vaseduvan, H. W. Gibson, *J. Org. Chem.* **1994**, *59*, 1694-1702.

Unusual Enantiomeric Resolution Phenomenon Observed upon Recrystallization of a Racemic Compound**

Takanori Ushio, Rui Tamura,* Hiroki Takahashi, Nagao Azuma, and Keiji Yamamoto

Since its discovery by Pasteur[1] in 1848 and its modification as "preferential crystallization" by Gernez[2] in 1866, the enantiomeric resolution of a mixture of homochiral (+) and (−) crystals (racemic mixtures or conglomerates) has been one of the most frequently used methods for separating enantiomers. In contrast, enantiomeric resolution by recrystallization of heterochiral crystals composed of a regular packing of (+) and (−) molecules (racemic compounds) has been believed to be totally infeasible.[3-8] We have found a surprising exception: Simple recrystallization of certain racemic crystals of the antiallergenic agent (±)-[2-[4-(3-ethoxy-2-hydroxypropoxy)phenylcarbamoylethyl]dimethylsulfonium *p*-toluenesulfonate (±)-**ST**[9,10] led to a remarkable enantiomeric enrichment of up to 100% *ee* in the mother liquor. More astonishing is the fact that when the

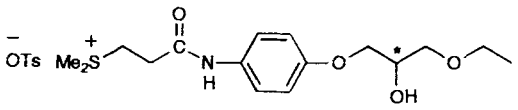

ST

slightly optically active crystals obtained by initial recrystallization of (±)-**ST** were recrystallized again without additional chiral influence, the resulting crystals displayed the opposite chirality and the **ST** remaining in the mother liquor was highly enriched with the enantiomer originally in excess. Therefore, simply collecting the mother liquors with the same chirality after each recrystallization led to efficient separation of enantiomers. Here we report this unusual enantiomeric resolution phenomenon and describe the unique properties of the **ST** crystals.

Crystallization of (±)-**ST** from a 25-fold supersaturated 2-propanol solution led to remarkable enantiomeric enrichment of up to 100% *ee* in the mother liquor (Fig. 1). As the crystallization proceeded, the enantiomeric purity of **ST** in solution gradually increased at 25 °C and could be improved further by lowering the temperature. As expected, large amounts of the deposited crystals contained the other enantiomer in small excess (Fig. 2). After more than 20 sets of recrystallizations, each conducted five times, using different samples of (±)-**ST** and various solvents, we have concluded that this enantiomeric resolution phenomenon is highly reproducible, and that the probability of obtaining one particular enantiomer in excess in the mother liquor after a number of recrystallizations of (±)-**ST** is 0.5 even if the same lot of (±)-**ST** is used. Typical examples of the time-course of the enantiomeric enrichment of the mother liquor observed during crystallization of (±)-**ST** are shown in Figure 1. More importantly, we found that when weakly optically active **ST** was recrystallized, the resulting crystals always displayed the opposite chirality (Fig. 2). This regular reversal of chirality in the deposited crystals accompanied by the enantiomeric enrichment of **ST** in the mother liquor was fully reproducible as long as optically active **ST** with less than 30% *ee* was employed. In one series of recrystallizations analogous to that described in Figure 2, weakly optically active **ST** originally en-

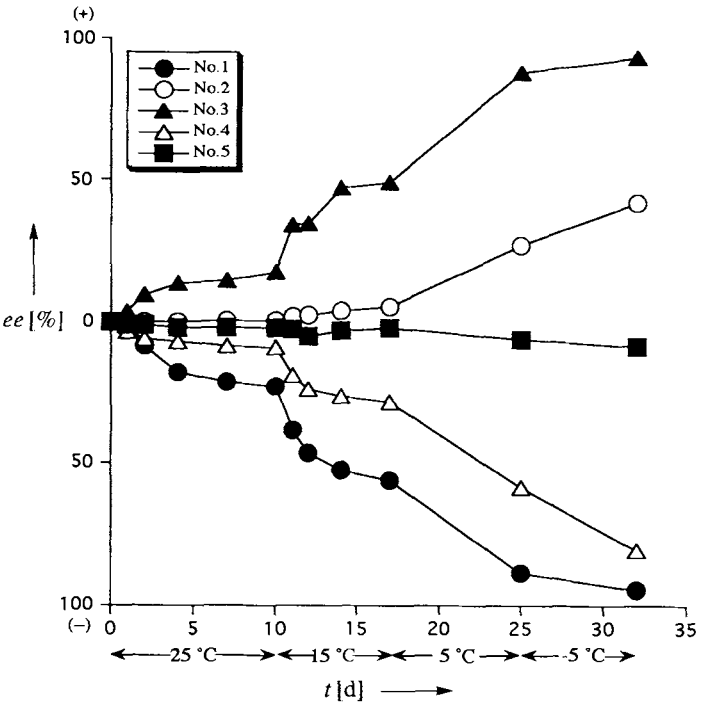

Fig. 1. Enantiomeric enrichment in aliquots of the mother liquor collected during crystallization of the same lot of (±)-**ST** carried out simultaneously in five different flasks (Nos. 1–5). The degree of enantiomeric enrichment differs each time, because it probably depends on how much and how fast the mixed crystals are deposited relative to crystals of the racemic compound. The enantiomeric excess (*ee*) [%] was determined by HPLC analysis using a chiral stationary phase (Daicel Chiralcel OD-H, hexane/EtOH/CF_3COOH/Et_2NH, 800:200:5:1). Conditions: **ST** (1.0 g) in 2-PrOH (4 mL) at 25 °C for 10 d, at 15 °C for 7 d, at 5 °C for 8 d, and at −5 °C for 7 d.

[*] Dr. R. Tamura, H. Takahashi
Laboratory of Organic Chemistry, Division of Material Science
Graduate School of Environmental Earth Science
Hokkaido University, Sapporo 060 (Japan)
Fax: Int. code +(11)757-5995
e-mail: tamura-r@kyoyo.high.hokudai.ac.jp
T. Ushio
Taiho Pharmaceutical Co., Ltd. (Japan)
Prof. N. Azuma
Department of Chemistry, Faculty of Science
Ehime University (Japan)
Prof. K. Yamamoto
Faculty of Pharmaceutical Sciences
Chiba University (Japan)

[**] This work was partly supported by a Grant-in-Aid for Scientific Research (Priority Area No. 07231222) from the Ministry of Education, Science, Sports and Culture of Japan.

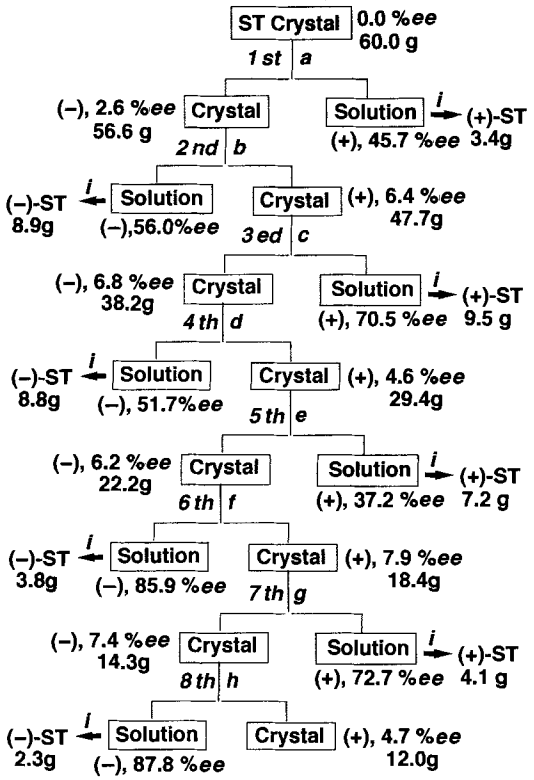

Fig. 2. Successive recrystallization of (±)-**ST** leading to the reversal of chirality in the resulting crystals and the enantiomeric enrichment in the mother liquors. The enantiomeric excess was determined by HPLC analysis. Crystallization conditions: *a*: mixed solvent system (120 mL EtOH, 60 mL iPr_2O 60 mL) at 5 °C for 18 h; *b*: EtOH (100 mL) at 5 °C for 18 h; *c*: EtOH (80 mL) at 5 °C for 3 d; *d*: EtOH (60 mL) at 5 °C for 3 d; *e*: EtOH (50 mL) at 5 °C for 15 h; *f*: mixed solvent of system (50 mL EtOH, 25 mL iPr_2O) at 5 °C for 18 h; *g*: EtOH (40 mL) at 5 °C for 2 d; h: mixed solvent system (30 mL EtOH, iPr_2O 30 mL) at 5 °C for 14 h; *i*: removal of the solvent by evaporation.

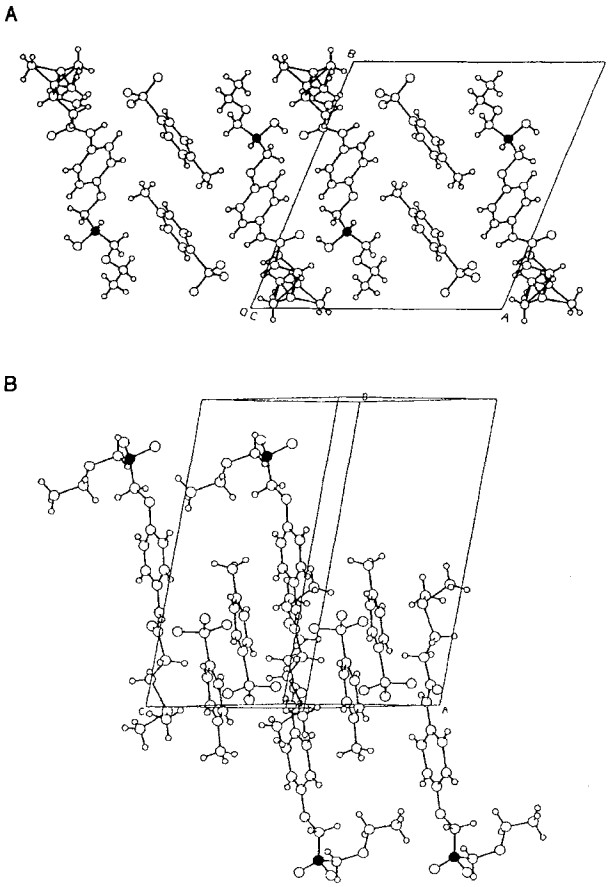

Fig. 3. Molecular and crystal structure of A) the racemic compound (±)-**ST** and B) a mixed crystal of the optical antipodes of **ST** (ca. 1% *ee*). Black circles represent the asymmetric carbon atoms. Orientational disorder was observed for the oxygen atoms in the mixed crystal; the occupancy factors were used to estimate the *ee* value.

riched in the (−) enantiomer (8.2% *ee*) was recrystallized successively from EtOH at 5 °C and then −30 °C four times in all. By simply collecting the mother liquors with the same chirality and recrystallizing the collected crystals after partial evaporation of the solvent, 4.45 g (41.1% based on the original amount of the enantiomer) and 2.96 g (32.2%) of highly optically active (+)- and (−)-**ST** crystals of 96–98% *ee*, respectively, were obtained.

In order to gain an insight into the mechanism of this unusual enantiomeric resolution phenomenon, we investigated the structure of the **ST** crystals. The X-ray crystallographic analysis of the single crystals of **ST** showed that the stable crystalline form of the racemate is a racemic compound (Fig. 3A),[11a] while the crystal of the pure enantiomer is chiral.[11b] Furthermore, it has been found that under the conditions of forced recrystallization **ST** was deposited as mixed crystals (solid solutions) of the optical antipodes with a wide range of enantiomeric purities. Namely, crystallization of **ST** with various enantiomeric purities (0 to 90% *ee*) in *i*PrOH at 25 °C by nucleation with the seed crystals of one pure enantiomer led to the deposition of the mixed crystals with the same chirality and enantiomeric purity as the original solution. The crystallographic parameters and molecular and crystal structures of these mixed crystals of various enantiomeric purities are almost identical with those of the crystals of the pure enantiomers, except that the C–OH bond is disordered in the mixed crystals (Fig. 3B).[11c] On the other hand, crystallization of (+)-enriched **ST** with low enantiomeric purity (less than 30% *ee*) in *i*PrOH by nucleation with seed crystals of the racemic compound (±)-**ST** resulted in the deposition of almost the racemic compound (somewhat (−)-rich) of less than 10% *ee* along with the enantiomeric enrichment of (+)-**ST** in the mother liquor, as confirmed by X-ray powder diffraction and HPLC analysis. In this case, as the enantiomeric purity of (+)-rich **ST** used for recrystallization increased (more than 50% *ee*), more mixed crystals were deposited with almost the same enantiomeric purity [(+)-rich] as the original solution together and fewer crystals of the racemic compound formed. From these results it was concluded that 1) the racemic form of **ST** exhibits polymorphism,[12] (in other words it forms crystals of the stable racemic compound and metastable mixed crystals (solid solutions) of 0% *ee*); 2) **ST** forms stable mixed crystals over a wide range of enantiomeric purities; and 3) mixed crystals with the same chirality and enantiomeric purity as the mother liquor and crystals with enantiomeric purities of less than 10% *ee* are liable to be deposited during recrystallization. Therefore, it is assumed that the melting point phase diagram of **ST** shows two eutectic temperatures around 10% *ee* resulting from the intersection of the phase diagrams of a racemic compound type and a mixed crystal type (Fig. 4).

Thus, it is apparent that the mechanism of this unusual enantiomeric resolution phenomenon of **ST** is quite different from that of the preferential crystallization of conglomerates, in which each deposited crystal is enantiomerically pure and the mother liquor is not as enantiomerically enriched.[1, 3] Another difference is the enantiomeric enrichment of the mother liquor resulting from the principal deposition of the racemic compound; in crystallization of nonracemates of ordinary racemic

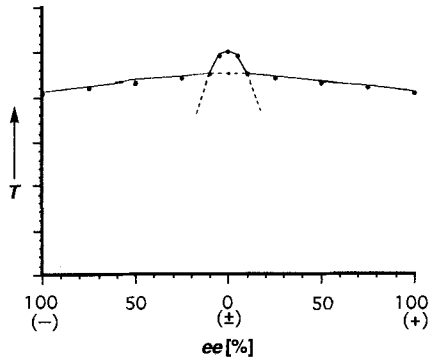

Fig. 4. Expected melting point phase diagram of **ST**; T = melting point (temperature of the end of fusion), *ee* = enantiomeric excess.

compounds the reversal of chirality in the deposited crystals never occurs. It should be emphasized that spontaneous isomerization of one enantiomer to the other one never occurred under our recrystallization conditions. Although the mechanism of the enantiomeric resolution phenomenon of **ST** is yet under investigation, it may be related to the unique polymorphism of the **ST** crystals described above. If this is true, this enantiomeric resolution phenomenon might be extended and become a powerful general method for the resolution of organic racemates showing similar polymorphism, by which both the racemic crystals and the mixed crystals are simultaneously produced.

Received: February 26, 1996
Revised version: May 28, 1996 [Z8863IE]
German version: *Angew. Chem.* **1996**, *108*, 2544–2546

Keywords: crystallization · enantiomeric resolution · mixed crystals · racemates

[1] L. Pasteur, *Ann. Chim. Phys.* **1848**, *24*, 442.
[2] M. Gernez, *C. R. Hebd. Seances Acad. Sci.* **1866**, *63*, 843.
[3] a) J. Jacques, A. Collet, S. H. Wilen, *Enantiomers, Racemates and Resolutions*, Wiley, New York, **1981**, p. 217; b) A. Collet, M.-J. Brienne, J. Jacques, *Chem. Rev.* **1980**, *80*, 215.
[4] P. Newman, *Optical Resolution Procedures for Chemical Compounds, Vol. 1–3*, Optical Resolution Information Center, New York, **1978**, **1981**, **1984**.
[5] F. Toda, *Top. Curr. Chem.* **1987**, *140*, 43.
[6] *Asymmetric Synthesis, Vol. 5* (Ed.: J. D. Morrison), Academic Press, Orlando, FL, USA, **1985**.
[7] K. Mori, Y. Funaki, *Tetrahedron* **1988**, *41*, 2369.
[8] *Chromatographic Chiral Separations* (Eds.: M. Zief, L. J. Crane), Marcel Dekker, New York, **1988**.
[9] A. Koda, Y. Yanagihara, N. Matsuura, *Agents Actions* **1991**, *34*, 369.
[10] T. Ushio, K. Yamamoto, *J. Chromatogr. A* **1994**, *684*, 235.
[11] X-ray data for a) the racemate: $P\bar{1}$, $Z = 2$, $a = 14.638(2)$, $b = 15.681(2)$, $c = 6.2281(6)$ Å, $\alpha = 100.32(1)$, $\beta = 99.781(9)$, $\gamma = 66.258(9)°$, $V = 1280(6)$ Å^3, $R = 0.052$, $Rw = 0.049$]; b) the (−) isomer: $P1$, $Z = 2$, $a = 10.762(3)$, $b = 15.615(2)$, $c = 8.223(2)$ Å, $\alpha = 100.41(2)$, $\beta = 108.50(2)$, $\gamma = 85.73(2)°$, $V = 1289(1)$ Å^3, $R = 0.043$, $Rw = 0.044$]; c) a mixed crystal of ca. 1% *ee*: $P1$, $Z = 2$, $a = 10.764(5)$, $b = 15.618(3)$, $c = 8.225(2)$ Å, $\alpha = 100.44(2)$, $\beta = 108.47(3)$, $\gamma = 85.62(3)°$, $V = 1289.6(8)$ Å^3, $R = 0.044$, $Rw = 0.042$. Crystallographic data (excluding structure factors) for the structures reported in this paper have been deposited with the Cambridge Crystallographic Data Centre as supplementary publication no. CCDC-179-107. Copies of the data can be obtained free of charge on application to The Director, CCDC, 12 Union Road, Cambridge CB2 1EZ, UK (Telefax: Int. code +(1223) 336-033; e-mail: teched@chemcrys.cam.ac.uk).
[12] Polymorphism between the crystals of the racemic compound crystal and racemic mixed crystals is quite rare, see ref. [3], p. 137. For polymorphyism between racemic compounds and conglomerates, see M. Leclercq, A. Collet, J. Jacques, *Tetrahedron* **1976**, *32*, 821; E. Eliel, S. H. Wilen, *Stereochemistry of Organic Compounds*, Wiley, New York, **1994**, p. 161.

Enantioselective Conjugate Addition of Dialkylzinc Reagents to Cyclic and Acyclic Enones Catalyzed by Chiral Copper Complexes of New Phosphorus Amidites**

André H. M. de Vries, Auke Meetsma, and Ben L. Feringa*

Conjugate addition reactions of organometallic reagents to enones are among the most widely used methods for carbon–carbon bond formation in organic synthesis.[1] A number of successful methods for stereoselective 1,4-addition based on chiral auxiliaries or stoichiometric organometallic reagents have been developed.[1, 2] Recently catalytic, enantioselective conjugate additions of organometallic reagent (RMgX, RLi, or R_2Zn) with chiral Cu^I, Ni^{II}, and Zn^{II} complexes have been demonstrated.[2, 3] All these catalysts, however, show enantioselectivity for only one specific type of enone.[3] For example, complexes prepared in situ from $[Ni(acac)_2]$ (acac = acetylacetonate) and chiral amino alcohols are enantioselective for the addition of Et_2Zn to acyclic enones, but for cyclic enones no enantioselectivity was found.[4] On the other hand chiral CuI complexes with sulfonylaryloxazoline ligands are only effective in 1,4-addition reactions of Grignard reagents to cyclic enones.[5] We now report chiral copper catalysts, capable of facilitating conjugate addition of readily available dialkylzinc reagents to cyclic and acyclic enones in high yields and with *ee* values up to 90%.

Since trivalent phosphorus compounds are known as ligands for stoichiometric conjugate organocopper additions,[6, 7] we examined the new chiral phosphorus amidite **1**, recently synthesized in our group from (*S*)-2,2′-binaphthol (**2**) and hexamethyl phosphoramide (HMPT),[8] as ligand in the CuI-catalyzed addition of Et_2Zn to cyclohexenone (**3a**) and chalcone (**5a**) [Eq. (a) and (b)].[9] Some remarkable results were observed: 1) Amidite **1** represents a new class of chiral ligands, which proved to be essential for this catalytic system. Within 3 h both substrates are converted into the 1,4-product exclusively (GC

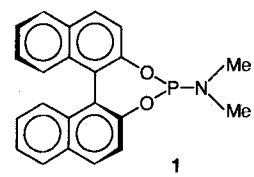

1

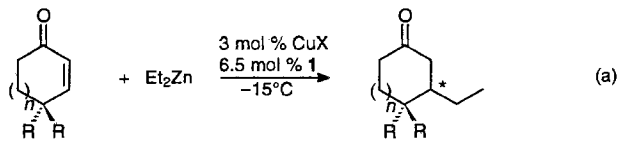

(a)

3a, $n = 1$, R = H
3b, $n = 2$, R = H
3c, $n = 1$, R = CH_3

4a-c

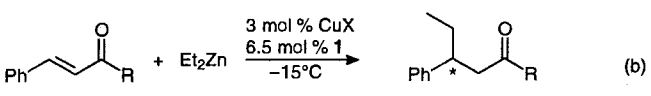

(b)

5a, R = Ph
5b, R = 4-$MeOC_6H_4$
5c, R = 2-Pyridyl

6a-c

[*] Prof. Dr. B. L. Feringa, A. H. M. de Vries, A. Meetsma
Department of Organic and Molecular Inorganic Chemistry
University of Groningen
Nijenborgh 4, NL-9747 AG Groningen (The Netherlands)
Fax: Int. code +(50)363-4296
e-mail: feringa@chem.rug.nl

[**] We thank Prof. Dr. P. Knochel, University of Marburg, for the opportunity given to A. H. M. de Vries to perform some experimental work in his laboratories, and Dr. R. Hulst, University of Groningen, for initial syntheses.

yields greater than 95%), whereas without the ligand the copper-catalyzed reaction is very slow and many side products were found. When a larger amount of **1** (50 mol%) was employed, the reaction proceeds only at room temperature and was far less selective. These observations provide potentially striking advantages for a successful asymmetric catalysis.[10] 2) For both substrates moderate enantioselectivities were found (**4a**, 35% (*S*) and **6a**, 47% (*R*)), which indicates that this chiral catalyst is not limited to one specific type of enone.

With this knowledge we set out to determine the structure of the complex of CuI and **1**. Crystallization from benzene provided white needles (**I**) suitable for X-ray analysis.[11] The molecular structure is shown in Figure 1.[12] Three chiral ligands are bound to the copper center creating a C_3-symmetrical complex. Examination of the structure showed that crucial positions for ligand modifications are the amine moiety and the 3,3'-positions of the binaphthyl part of the ligand.

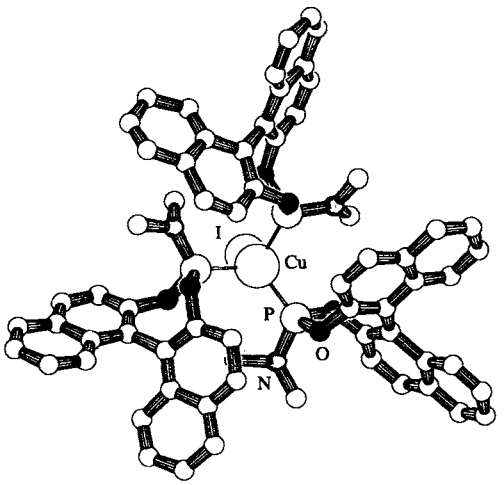

Fig. 1. Crystal structure of [CuI(**1**)] (**I**).

Therefore, starting from phosphoryl chloride (**7**),[13] several new phosphorus amidites **8**–**16** were prepared [Eq. (c)].[14] The

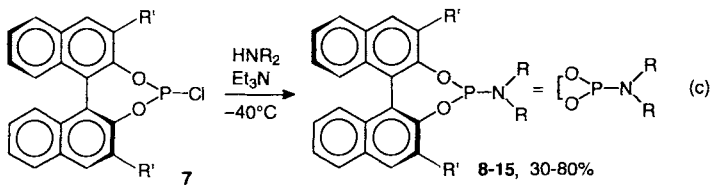

(c)

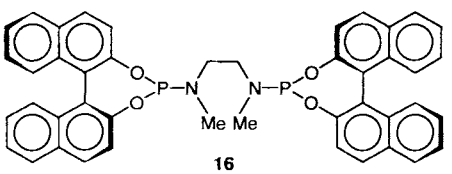

16

complexes generated in situ of these ligands and CuI gave unsatisfactory results, presumably due to low solubility. However, homogeneous catalyst solutions were obtained with CuOTf (Tf = CF_3SO_2), and the influence of the structural modifications in **8**–**15** on the enantiomeric excess of **4a** and **6a** could be determined (Table 1). For both products significant improvement in *ee* was observed when sterically demanding substituents were introduced on the ligand's nitrogen atom. The best results were obtained with the bis(*iso*-propyl)-substituted ligand **12**. Products **4a** and **6a** were isolated in high yields (>80%) and *ee* values of 60% and 83%, respectively. Ligands **13** and **14** (R' = CH_3) furnished the 1,4-products with comparable *ee* values. With ligand **15** (R' = Ph) lower enantioselectivities were found. Probably different clusters are formed with sterically demanding substituents on the 3- and 3'-position of the ligand creating less selective catalysts. In an effort to enhance the selectivity and realizing that Cu^{II} salts are used as catalyst for conjugate addition,[15] we investigated $Cu(OTf)_2$ together with **12** as chiral catalyst. Under the same conditions **4a** and **6a** were isolated with higher *ee* values (Table 2). The actual chiral catalyst is probably a Cu^{I} species, generated by in situ reduction of the Cu^{II} complex. The chiral copper complex of ligand **12** catalyzes the addition of Et_2Zn to various enones enantioselectively.

Table 1. Enantioselective CuOTf-catalyzed addition of Et_2Zn to **3a** and **5a** [a].

No.	Ligand		*ee* (**4a**) [%]	*ee* (**6a**) [%]
1	**8**	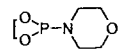	50	71
2	**9**	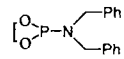	53	53
3	**10**	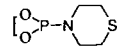	55	70
4	**11**	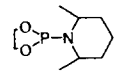	43	79
5	**12**	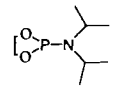	60	83
6	**13**, R = Me R' = Me	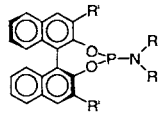	56	52
7	**14**, R = *i*Pr R' = Me		59	81
8	**15**, R = Me R' = Ph		35	<20

[a] Reaction conditions as in Equation (a). Yields of isolated products >80%. For *ee* determination see Experimental Procedure.

Table 2. Enantioselective conjugate addition of Et_2Zn to enones, catalyzed by $Cu(OTf)_2$/**12** [a].

No.	Enone	1,4-Adduct	Yield [%] [b]	*ee* [%] [c]
1	**3a**	**4a**	78 (68) [d]	63 (71) [d]
2	**3b**	**4b**	76	55
3	**3c**	**4c**	76	81
4	**5a**	**6a**	88	87
5 [e]	**5a**	**6a**	84	90
6	**5b**	**6b**	85	80

[a] Reaction conditions as in Eq. (a). [b] Yields of isolated products. [c] For *ee* determination see Experimental Procedure. [d] With $Cu(SbF_6)_2$ [16]. Yield of **4a**: 68%. [e] Temperature −50°C.

Cyclic and acyclic enones gave the corresponding 1,4-products in 55–90% *ee*. The best results were obtained for 4,4-dimethyl-2-cyclohexen-1-one (**3c**) and **5a**.

Mechanistic studies on the enantioselective catalyst are under way, and at present we emphasize the following observations. 1) With the catalyst derived from bidentate ligand **16** and copper salt (1:1) we achieve the same *ee* values as found for ligand **1**

(2:1), which indicates that during reaction two ligands are bound to the copper ion. The remaining sites in the tetrahedral coordination sphere of the copper ion are likely to be occupied by π-complexation of the enone's double bond,[17] and an ethyl fragment transfered from zinc.[18] 2) The pyridyl-substituted chalcone **5c** gave the corresponding 1,4-product in only 29% *ee*, presumably due to competitive binding of the copper catalyst to the enone's pyridine moiety.

Preliminary experiments showed that dioctylzinc, prepared directly from 1-octene by boron–zinc exchange,[19] can be used as well; it furnishes the 1,4-products with comparable *ee* values. This protocol can be extended to functionalized diorganozinc reagents. For instance, with the chiral catalyst derived from **12** and $Cu(OTf)_2$, 4-penten-1-yl acetate was added to **3a** with 56% *ee*. [Eq. (d)].

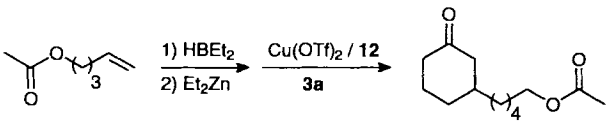

(d)

51%, 56% *ee*

In conclusion a new highly efficient catalyst for asymmetric conjugate addition of diorganozinc reagents to enones has been developed. Remarkable features are the excellent chemoselectivity to give nearly pure 1,4-products, the effective ligand acceleration by new phosphorus amidite ligands, the relatively high *ee* values for both cyclic and acyclic enones, the efficiency of a monodentate ligand in this asymmetric catalysis, and the fact that alkenes can be used as starting material.

Experimental Procedure

General procedure for ligands **8**–**16** (argon atmosphere): A warm solution (60 °C) of (*S*)-2,2′-binaphthol (**2**) (860 mg, 3 mmol) in toluene (25 mL) was added in 5 minutes to a cooled solution (− 60 °C) of PCl_3 (270 μL, 3 mmol), Et_3N (860 μL, 6 mmol), and toluene (5 mL). The reaction mixture was stirred for 2 h, warmed to room temperature, and filtered. The filtrate was treated with Et_3N (410 μL, 2.9 mmol) and 2.9 mmol of the appropriate secondary amine at −40 °C. After 16 h at room temperature, the reaction mixture was filtered, concentrated, and purified by chromatography (SiO_2, hexane:CH_2Cl_2 2:1) to give the pure amidite (yield 30–80%). (*S*)-**12**: $[\alpha]_D = +591$ ($c = 0.68$ in $CHCl_3$); ^{1}H NMR (200 MHz, $CDCl_3$): $\delta = 7.99$–7.89 (m, 4H), 7.55–7.22 (m, 8H), 3.42 (heptet, $J = 6.84$ Hz, 1H), 3.37 (heptet, $J = 6.84$ Hz, 1H), 1.24 (d, $J = 6.84$ Hz, 6H), 1.19 (d, $J = 6.84$ Hz, 6H); ^{13}C NMR ($CDCl_3$): $\delta = 150.2$, 150.1, 132.6, 131.2, 130.4, 130.0, 129.2, 128.2, 128.1, 127.0, 125.8, 125.7, 125.6, 124.5, 124.1, 122.4, 122.3, 44.6, 44.4, 24.3, 24.2; ^{31}P NMR ($CDCl_3$): $\delta = 151.7$.

Catalytic conjugate additions (argon atmosphere): A solution of $Cu(OTf)_2$ (10.9 mg, 0.030 mmol) and **12** (26.0 mg, 0.065 mmol) in toluene (3 mL) was stirred for 1 h. The colorless solution was cooled (− 20 °C) and enone (1-2 mmol) and 1.5 equivalent of dialkylzinc solution (1 M in toluene) were added. After 3 h at −15 °C the reaction mixture was poured into 25 mL of 1 N HCl and extracted with diethyl ether (2 × 25 mL). The combined organic layers were washed with brine (25 mL), dried ($MgSO_4$), filtered, and evaporated to give the crude 1,4-products. After purification by chromatography (SiO_2, hexane:diethyl ether 5:1) the *ee* values were determined. Cyclic substrates were derivatized with optically pure 1,2-diphenyl ethylene diamine and analyzed by ^{13}C NMR [20]. Acyclic substrates were studied by HPLC (Daicel OD or OJ column).

Received: April 9, 1996 [Z 9005 IE]
German version: *Angew. Chem.* **1996**, *108*, 2526–2528

Keywords: asymmetric syntheses · carbon–carbon coupling · copper compounds · phosphorus compounds · zinc compounds

[1] P. Perlmutter, *Conjugate Addition Reactions in Organic Synthesis*, Pergamon, Oxford, **1992**.
[2] B. E. Rossiter, N. M. Swingle, *Chem. Rev.* **1992**, *92*, 771.
[3] Recent review: B. L. Feringa, A. H. M. de Vries, in *Advances in Catalytic Processes, Vol 1* (Ed.: M. D. Doyle), JAI Press, Connecticut, **1995**, p. 151.
[4] a) K. Soai, T. Hayasaka, S. Ugajin, *J. Chem. Soc. Chem. Commun.* **1989**, 516; b) C. Bolm, M. Ewald, M. Felder, *Chem. Ber.* **1992**, *125*, 1205; c) A. H. M. de Vries, J. F. G. A. Jansen, B. L. Feringa, *Tetrahedron* **1994**, *50*, 4479.
[5] a) Q.-L. Zhou, A. Pfaltz, *Tetrahedron* **1994**, *50*, 4467. Other examples: b) G. M. Villacorta, C. P. Rao, S. J. Lippard, *J. Am. Chem. Soc.* **1988**, *110*, 3175; c) M. van Klaveren, F. Lambert, D. J. F. M. Eijkelkamp, D. M. Grove, G. van Koten, *Tetrahedron Lett.* **1994**, *35*, 6135; d) M. Spescha, G. Rihs *Helv. Chim. Acta* **1993**, *76*, 1219.
[6] a) G. H. Posner, *An Introduction to Synthesis using Organocopper Reagents*, Wiley, New York, **1980**; b) M. Suzuki, T. Suzuki, T. Kawagishi, Y. Morita, R. Noyori, *Isr. J. Chem.* **1984**, *24*, 118; c) A. Alexakis, S. Mutti, J. F. Normant, *J. Am. Chem. Soc.* **1991**, *113*, 6332.
[7] Recently enantioselective 1,4-addition of Grignard reagents to cyclic enones, catalyzed by a CuI complex containing a chiral, bidentate phoshane ligand, has been reported: M. Kanai, K. Tomioka, *Tetrahedron Lett.* **1995**, *36*, 4275.
[8] R. Hulst, N. K. de Vries, B. L. Feringa, *Tetrahedron: Asymmetry* **1994**, *5*, 699.
[9] Enantioselective CuI-catalyzed addition of Et_2Zn to **3a** has been reported (*ee* 32%); however, with **5a** no *ee* was found: A. Alexakis, J. Frutos, P. Mangeney, *Tetrahedron: Asymmetry* **1993**, *4*, 2427.
[10] For a discussion about ligand accelerated asymmetric catalysis, see D. J. Berrisford, C. Bolm, K. B. Sharpless, *Angew. Chem.* **1995**, *107*, 1159; *Angew. Chem. Int. Ed. Engl.* **1995**, *34*, 1059.
[11] Crystals of **I** efficiently catalyze the addition of Et_2Zn to **3a** (**4a**: yield 76%, *ee* 32%).
[12] Crystal structure data for **I** $[C_{66}H_{54}N_3O_6P_3CuI/(C_6H_6)_2]$: $T = 130$ K; space group $P2_12_12_1$, $a = 15.525(2)$, $b = 19.957(2)$, $c = 24.535(3)$ Å, $V = 7601.7(16)$ Å^3; $Z = 4$. The structure was solved by direct methods and refined to $R(F) = 0.120$, $Rw(F) = 0.131$. Crystallographic data (excluding structure factors) for the structure reported in this paper have been deposited with the Cambridge Crystallographic Data Centre as supplementary publication no. CCDC-179-114. Copies of the data can be obtained free of charge on application to The Director, CCDC, 12 Union Road, Cambridge CB2 1EZ UK (fax: int. code +(1223)336-033; e-mail: teched@chemcrys.cam.ac.uk).
[13] N. Greene, T. P. Kee, *Synth. Commun.* **1993**, *23*, 1651.
[14] All new ligands were remarkably stable to air and fully characterized. The corresponding 3,3′-substituted 2,2′-binaphthols were synthesized according to P. J. Cox, W. Wang, V. Snieckus, *Tetrahedron Lett.* **1992**, *33*, 2253.
[15] H. Sakata, Y. Aoki, I. Kuwajima, *Tetrahedron Lett.* **1990**, *31*, 1161.
[16] D. A. Evans, J. A. Murry, P. von Matt, R. D. Norcross, S. J. Miller, *Angew. Chem.* **1995**, *107*, 864; *Angew. Chem. Int. Ed. Engl.* **1995**, *34*, 798.
[17] a) C. Ullenius, B. Christenson, *Pure Appl. Chem.* **1988**, *60*, 57; b) N. Krause, R. Wagner, A. Gerold, *J. Am. Chem. Soc.* **1994**, *116*, 381.
[18] Transmetalation of organozinc compounds into the corresponding organocopper reagents is well established: P. Knochel, R. D. Singer, *Chem. Rev.* **1993**, *93*, 2117.
[19] F. Langer, A. Devasagayaraj, P.-Y. Chavant, P. Knochel, *Synlett*, **1994**, 410.
[20] A. Alexakis, J. C. Frutos, P. Mangeney, *Tetrahedron: Asymmetry* **1993**, *4*, 2431.

A Catalyst-Specific, Stereocontrolled Ring-Closing Metathesis**

Christoph M. Huwe, Janna Velder, and Siegfried Blechert*

Ring-closing olefin metatheses have been used increasingly for the synthesis of unsaturated carbo- and heterocycles.[1] To our knowledge, diastereoselective ring-closing metatheses have not been investigated to date.[2] We recently explored the synthesis of chiral, α-substituted heterocycles from amino acid derivatives,[3, 4] and used the chiral center for stereocontrolled secondary reactions of the double bond produced by the metathesis for the synthesis of natural products.[3]

Natural products or biologically active compounds such as various pheromones and glycosidase inhibitors contain α,α′-disubstituted pyrrolidine or piperidine units.[5, 6] To selectively ob-

[*] Prof. Dr. S. Blechert, Dipl.-Chem. C. M. Huwe, Dr. J. Velder
Institut für Organische Chemie der Technischen Universität Berlin
Strasse des 17. Juni 135, D-10623 Berlin (Germany)
Fax: Int. code +(30)314-23619
e-mail: sibl@wap0105.chem.tu-berlin.de

[**] This work was supported by the Fonds der Chemischen Industrie. We thank the state of Berlin for a doctoral fellowship (C. M. H.).

tain *syn*- or *anti*-α,α′-disubstituted compounds such as **2** and **3**, we were interested in ring-closing methatheses that use an existent chiral center to control the cyclization with a prochiral diene (Scheme 1). In these investigations we found that cyclization to give five-membered rings was highly catalyst-specific, and that the acyclic precursor **1** is thereby selectively converted into the *syn* or *anti* product.

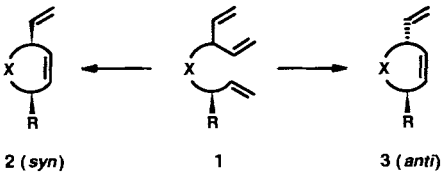

Scheme 1. Principle of the generation of a new stereocenter by ring-closing metathesis.

In general, this concept of performing a diastereoselective olefin metathesis requires that the olefins at the prochiral center do not react with each other and also that the primary attack of the catalyst occurs at the double bond of the chiral center. In the case of the ruthenium catalysts[7] (abbreviated [Ru], $[Cl_2(PCy_3)_2Ru{=}CHPh]$, Cy = cyclohexyl) reported by Grubbs et al. and the molybdenum catalysts[8] (abbreviated [Mo], $[PhMe_2CCH{=}Mo{=}N\{2,6\text{-}(iPr)_2C_6H_3\}\{OCMe(CF_3)_2\}_2]$) reported by Schrock et al. which we used, the metatheses can be significantly slowed down by steric effects.[1c] Thus, we attached an additional methyl group to the prochiral olefins and precluded the ring closure between these two double bonds by using a 1,4-diene. The trienes used in the metatheses were synthesized from the known Cbz-protected amino alcohols **4**[4] and **5**[9] (Scheme 2). The prochiral diallyl moiety was readily obtained by addition of propynylborane or -borate,[10] respectively, to the tetrolimine, followed by Birch reduction. In this way, **8** and **9** were obtained in 53% and 60% yield, respectively. Since ring-closing metatheses cannot be performed with the employed catalysts in the presence of basic amines, the trifluoroacetamides **10** and **12** as well as the 2-oxazolidinone **13** were prepared. The use of the heterocycle **13** could potentially lead to different stereochemical results in the cyclization. The O-deprotected compound **11** was not converted in the attempts at cyclization. All other ring closures could be carried out in good yields, by using either the ruthenium or molybdenum catalyst.[11] In the ruthenium-catalyzed cyclization to the six-membered rings **14** and **15**, no diastereomeric excess was observed by gas chromatography (see Scheme 2 and Table 1). In contrast, the best *syn*/*anti*-selectivity we could obtain in the molybdenum-catalyzed cyclization of **10** did not exceed a ratio of 26:74. Increasing the temperature by approximately 60 K resulted in only a moderate improvement in the selectivity, and no improvement was observed when the more rigid 2-oxazolidinone **13** was employed. Presumably due to the more pronounced steric interactions, the cyclization to give five-membered rings required significantly longer reaction times, while still showing incomplete conversion in some cases. The slower cyclization resulted, however, in a significant increase in selectivity (Scheme 3 and Table 1). In the best case, the ruthenium catalyst provided the *anti*-product **16** with a diastereomeric excess of 92%, whereas the molybdenum catalyst yielded the *syn*-product preferentially with 72% *de*. We believe that this catalyst-specificity is attributed to the different spatial arrangements of the respective ligands during the cyclization. Model investigations do not offer a clear explanation for, or enable one to predict, the observed selectivities. The

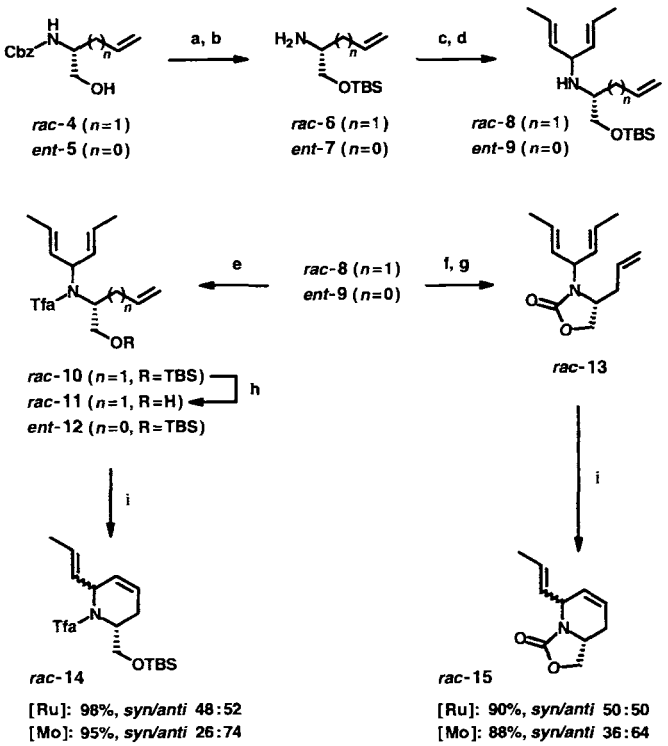

Scheme 2. Synthesis of the metathesis precursors **10**–**13**, six-membered ring metathesis experiments. a) TBSCl, imidazole, DMF, 11 h (room temperature) **4**: 88%, **5**: 96%; b) Na, liq. NH_3, *t*BuOH, 40 min, **4**: −60 °C, 83%, **5**: −40 °C, 77%; c) 1. $CH_3{-}C{\equiv}C{-}CHO$, CH_2Cl_2, molecular sieves 5 Å, 19 h, room temperature; 2. $Li{-}C{\equiv}C{-}CH_3$, $BF_3{\cdot}Et_2O$, 1 h, −78 °C, then 1.5 h, room temperature, **6**: 80%,7: 85%; d) Na, liq. NH_3, *t*BuOH, 1.5 h, −60 °C, **6**: 91%, **7**: 95%; e) $(CF_3CO)_2O$, pyridine, CH_2Cl_2, **8**: 20 min, −30 °C, 99%, **9**: 2 h, room temperature, 99%; f) $(CCl_3CO)_2O$, pyridine, CH_2Cl_2, 1.5 h, room temperature, 83%; g) Bu_4NF, THF, 2 h, room temperature, 65%; h) Bu_4NF, THF, 2 h, room temperature, 65%; i) see Table 1. Cbz = benzyloxycarbonyl, TBS = *tert*-butyldimethylsilyl, Tfa = trifluoroacetyl.

Table 1. Summary of the metathesis experiments.

Entry	Starting material	Product	Cat. (mol%)	Conditions [a]		*syn*/*anti* [b]	Yield [%]
1	*rac*-**10**	*rac*-**14**	[Ru] (5)	RT	20 h	48:52	97
2	*rac*-**10**	*rac*-**14**	[Ru] (5)	80 °C	1 h	48:52	98
3	*rac*-**10**	*rac*-**14**	[Mo] (10)	RT	22 h	34:66	92
4	*rac*-**10**	*rac*-**14**	[Mo] (10)	80 °C	20 h	26:74	95
5	*rac*-**13**	*rac*-**15**	[Ru] (5)	RT	2 h	50:50	90
6	*rac*-**13**	*rac*-**15**	[Mo] (5)	RT	1 d	36:64	88
7	*rac*-**13**	*rac*-**15**	[Mo] (5)	80 °C	12 h	40:60	95
8	*ent*-**12**	*ent*-**16**	[Ru] (10)	RT	2 d	4:96	88 [c]
9	*ent*-**12**	*ent*-**16**	[Ru] (10)	80 °C	4 d	8:92	98 [d]
10	*ent*-**12**	*ent*-**16**	[Mo] (5)	RT	1 d	84:16	92
11	*ent*-**12**	*ent*-**16**	[Mo] (10)	80 °C	3 d	86:14	97

[a] Solvent benzene. [b] Determined by GC. [c] Based on 25% conversion. [d] Based on 62% conversion.

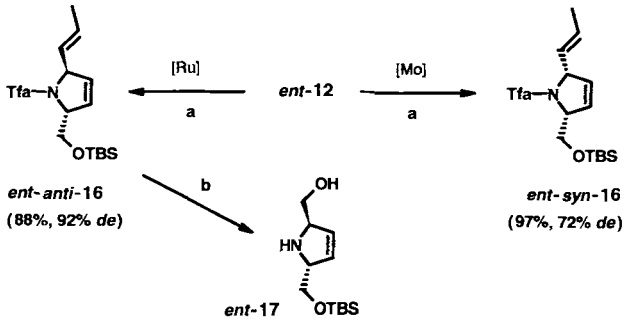

Scheme 3. Five-membered ring metathesis experiments. a) see Table 1; b) 1. O_3, CH_2Cl_2, −78 °C; 2. $LiAlH_4$, THF, RT, 18 h; 79%.

anti-**16** product can be used as an example to demonstrate the differentiation between the double bonds in the corresponding metathesis product. Careful ozonolysis of *anti*-**16** monitored by thin-layer chromatography, followed by reductive workup with lithium aluminum hydride, yielded 79% of the monoprotected aminodiol **17**, which offers a variety of possibilities for further elaboration.

Experimental Procedure

Typical procedure for the stereoselective ring-closing metathesis as exemplified by *ent-syn*-**16** (Table 1, entry 11): *ent*-**12** (50 mg, 0.13 mmol) was dissolved in anhydrous benzene (9.2 mL) under argon, [Mo] (4.9 μmol, 5 mol%) was then added, and the resulting mixture was stirred for 3 d at a bath temperature of 80 °C. The solvent was removed and the residue was purified by flash chromatography on silica gel by using *tert*-butyl methyl ether/petroleum ether (1:40) as eluent to afford 44 mg (97%) of the cyclization product (72% *de*, GC) as a yellow oil. Selected spectroscopic data: ^{1}H NMR (400 MHz, $CDCl_3$): two amide isomers, combined spectrum: $\delta = 0.05$ (s, 6H), 0.88 und 0.89 (s, 9H), 1.68 and 1.69 (dd, 3H, $J = 1.5, 6.5$ Hz), 3.82 (m, 1H), 3.87 (m, 1H), 4.76–4.97 (m, 2H), 5.11–5.45 and 5.59–5.95 (m, 4H). ^{13}C NMR (50 MHz, $CDCl_3$): two amide isomers, combined spectrum: $\delta = -5.5$ (CH_3), −5.4 (CH_3), 17.5 (CH_3), 17.7 (CH_3), 18.4 (C_q), 25.8 (CH_3), 25.9 (CH_3), 62.4 (CH_2), 67.0 (CH), 67.1 (CH), 68.2 (CH), 68.4 (CH), 126.7 (CH), 127.3 (CH), 128.1 (CH), 128.3 (CH), 129.2 (CH), 129.8 (CH), 130.0 (CH), 153.2 (C_q). HR-MS ($C_{15}H_{23}F_3NO_2Si$, $M^+ - CH_3$): calcd 334.1450, found 334.1450. IR (CCl_4): $1/\lambda = 1686$ cm^{-1}. Elemental analysis ($C_{16}H_{26}F_3NO_2Si$): calcd C 54.99 H 7.50 N 4.01, found C 55.09 H 7.50 N 4.24.

Received: May 15, 1996 [Z9120IE]
German version: *Angew. Chem.* **1996**, *108*, 2542–2544

Keywords: asymmetric syntheses · catalysis · heterocycles · metathesis

[1] a) H.-G. Schmalz, *Angew. Chem.* **1995**, *107*, 1981; *Angew. Chem. Int. Ed. Engl.* **1995**, *34*, 1833; b) U. Koert, *Nachr. Chem. Tech. Lab.* **1995**, *43*, 809; c) R. H. Grubbs, S. J. Miller, G. C. Fu, *Acc. Chem. Res.* **1995**, *28*, 446.
[2] Recently a report appeared on the ring-closing metathesis of a chiral molybdenum complex: O. Fujimura, R. H. Grubbs, *J. Am. Chem. Soc.* **1996**, *118*, 2499.
[3] C. M. Huwe, S. Blechert, *Tetrahedron Lett.* **1995**, *36*, 1621.
[4] C. M. Huwe, O. C. Kiehl, S. Blechert, *Synlett* **1996**, 65.
[5] See for example: J.-E. Bäckvall, H. E. Schink, Z. D. Renko, *J. Org. Chem.* **1990**, *55*, 826, and references therein.
[6] See for example: C.-H. Wong, L. Provencher, J. A. Porco, Jr., S.-H. Jung, Y.-F. Wang, L. Chen, R. Wang, D. H. Steensma, *J. Org. Chem.* **1995**, *60*, 1492, and references therein.
[7] P. Schwab, M. B. France, J. W. Ziller, R. H. Grubbs, *Angew. Chem.* **1995**, *107*, 2179; *Angew. Chem. Int. Ed. Engl.* **1995**, *34*, 2039.
[8] J. S. Murdzek, R. R. Schrock, *Organometallics* **1987**, *6*, 1373.
[9] a) B. M. Trost, R. C. Bunt, *Angew. Chem.* **1996**, *108*, 70; *Angew. Chem. Int. Ed. Engl.* **1996**, *35*, 99; b) Y. Ohfune, N. Kurokawa, *Tetrahedron Lett.* **1984**, *25*, 1071.
[10] M. Wada, Y. Sakurai, K. Akiba, *Tetrahedron Lett.* **1984**, *25*, 1083.
[11] The stereochemistry of the cyclization products was determined by NOE experiments. All products were fully characterized (^{1}H NMR, ^{13}C NMR, IR, HRMS and/or elemental analysis).

Reductive Carbon–Sulfur Bond Cleavage: A Simple Pathway to Nonstabilized (Lithiomethyl)amines**

Carsten Strohmann* and Bors Cajus Abele

(Lithiomethyl)amines are important building blocks in the synthesis of not only organic but also organoelement compounds.[1] Nonstabilized[2] α-heterocarbanions[3]—containing nitrogen or oxygen as the heteroatom—cannot ordinarily be synthesized by hydrogen–lithium or halogen–lithium exchange using either lithium bases or metallic lithium.[1] However, (lithiomethyl)amines[4] and (lithiomethyl)ethers[5] can usually be obtained by metal–lithium, typically tin–lithium, exchange. Reductive carbon–sulfur bond cleavage permits another pathway to (lithiomethyl)ethers;[6] in addition it circumvents the chromatographic separation necessary for stannylmethyl compounds.[5, 7]

During systematic investigations on the synthesis of 1,3-dimetalated compounds of general formula M–CR_2–El–CR_2–M (M = e.g. Li, MgBr; El = Group 14–16 element, when necessary containing substituents; R = H, alkyl, aryl),[8] we were also interested in the preparation of bis(lithiomethyl)amines.[9] There has only been one report[10] on the synthesis of nonstabilized, α-alkyl substituted, monometalated α-aminocarbanions using reductive C–S bond cleavage. The synthetic aspects of this reaction have not been further investigated. We report here on a simple pathway to nonstabilized mono(lithiomethyl)amines that are not substituted on the α-carbon atom by means of reductive C–S bond cleavage, as well as on the use of these synthetic building blocks in the construction of organic and organoelement compounds.

The required (phenylthiomethyl)amine starting materials can be synthesized in high yields from thiophenol, formaldehyde, and secondary amines[11] (Scheme 1). Treatment of the

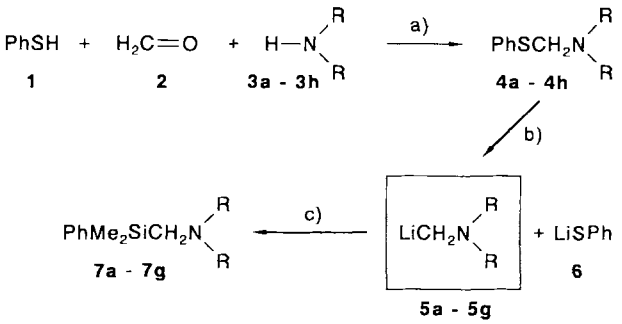

Scheme 1. Synthesis of (lithiomethyl)amines: a) $-H_2O$; b) $+2\,LiC_{10}H_8/-2\,C_{10}H_8$; c) $+2\,PhMe_2SiCl/-2\,LiCl$, $-PhMe_2SiSPh$. For NR_2 see Table 1.

(phenylthiomethyl)amines with a solution of lithium naphthalide ($LiC_{10}H_8$) in THF at −78 °C gives a red solution of the corresponding (lithiomethyl)amine. In order to prove that the

[*] Priv.-Doz. Dr. C. Strohmann, Dipl.-Chem. B. C. Abele
Institut für Anorganische Chemie der Universität
Im Stadtwald 6, D-66041 Saarbrücken (Germany)
Fax: Int. code +(681)302-3995
e-mail: c.strohmann@rz.uni-sb.de

[**] This work was supported by the Deutsche Forschungsgemeinschaft and the Fonds der Chemischen Industrie. B. C. A. would like to thank the Fonds der Chemischen Industrie for a doctoral fellowship. We thank Prof. Dr. M. Veith for his support.

(lithiomethyl)amine had been formed, the reaction solutions were treated with two equivalents[12] of chloro(dimethyl)-phenylsilane. The corresponding pure (aminomethyl)silanes **7a–f** were isolated in 67–80% yield (Table 1).

Table 1. Yields of **7a–7h**.

7	NR_2	Yield [%]	7	NR_2	Yield [%]
a	$N(C_2H_5)_2$	80	**e**	$NC_4H_8NCH_3$	68
b	NC_4H_8	72	**f**	$N(C_2H_4OCH_3)_2$	70
c	NC_5H_{10}	74	**g**	$N(i\text{-}C_3H_7)_2$	27
d	NC_4H_8O	67	**h**	$N(C_6H_5)_2$	0 [a]

[a] Isolation of the pure entrapped products of **5h** with $PhMe_2SiCl$ has not yet been successful. The trapping reaction with Bu_3SnCl gave diphenyl(tributylstannylmethyl)amine in 56% yield.

Sterically demanding amines such as diisopropyl(phenylthiomethyl)amine **4g** and diphenyl(phenylthiomethyl)amine **4h** show a somewhat different reaction behavior. Reaction of the (lithiomethyl)amines with the starting material lead to C–C bond formation so that the $LiC_{10}H_8$ was not completely consumed. When **4g** was treated with $LiC_{10}H_8$ followed by entrapment with $PhMe_2SiCl$, both **7g** and **8** were isolated (Scheme 2). The structure of further side products has not yet been clarified. Amine **4h** reacts in a similar manner.

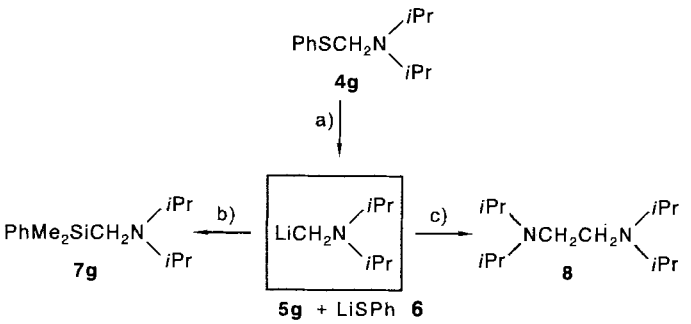

Scheme 2. a) $+2\ LiC_{10}H_8/-2\ C_{10}H_8$; b) $+2\ PhMe_2SiCl/-2$ LiCl, $-PhMe_2SiSPh$; c) $+$**4g**$/-2$ LiSPh.

In the reaction mixtures of the (lithiomethyl)amines obtained by reductive C–S bond cleavage, a further nucleophile, PhSLi **6**, which is not formed in the tin–lithium exchange reaction is generated. Nevertheless, **6** did not interfere with reactions with ketones, stannanes, and silanes, which furnished products in good yields (Scheme 3). Also stirring the (lithiomethyl)amines

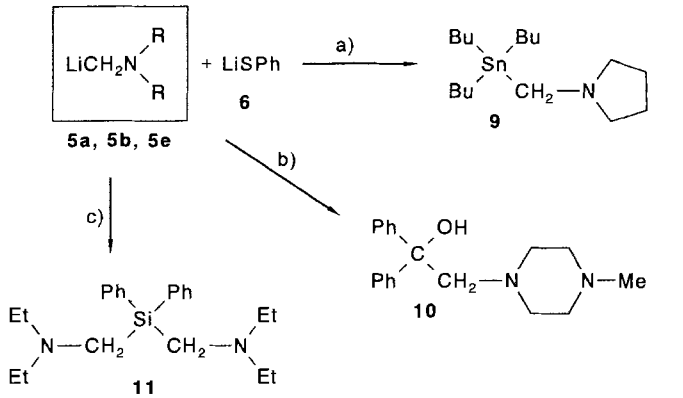

Scheme 3. Reactions of (lithiomethyl)amines: a) **5b** $+2\ Bu_3SnCl/-2$ LiCl, $-Bu_3SnSPh$; b) **5e** $+Ph_2CO$, $+2\ H_2O/-2$ LiOH, $-HSPh$; c) 2 **5a** $+Ph_2SiCl_2/-2$ LiCl, -2 LiSPh.

for 15 min at room temperature did not lead to a change in the product composition. Protonation of the metalated carbon atoms or carbenoid reactions[11b] (for example, the decomposition into lithium amides and methylene) was also not observed. We believe the synthesis of bis(aminomethyl)silanes such as **11** is particularly interesting (Table 2). As far as we know, the only representative of this class that has been reported so far is bis-(dimethylaminomethyl)dimethylsilane.[13]

Table 2. Selected spectroscopic data of the newly synthesized compounds.

7e: yield: 68%; b.p. 121 °C oven temperature/10^{-3} mbar; ^{1}H NMR (200.1 MHz, $CDCl_3$, 25 °C, TMS): $\delta = 0.28$ (s, ^2J(H,Si) = 6.6 Hz, 6H; $SiCH_3$), 2.10 (s, ^2J(H,Si) = 5.3 Hz, 2H; $SiCH_2N$), 2.18 (s, 3H; NCH_3), 2.30–2.35 (m, 8H; NCH_2CH_2N), 7.25–7.35, 7.45–7.55 (m, 5H; Ph); ^{13}C NMR (50.3 MHz, $CDCl_3$, 25 °C, $CDCl_3$): $\delta = -2.7$ (2 C, $SiCH_3$), 46.0 (NCH_3), 49.6 ($SiCH_2N$), 55.3, 56.9 (4 C, NCH_2CH_2N), 127.7 (2 C, *m*-Ph), 128.9 (*p*-Ph), 133.6 (*o*-Ph) 139.0 (*ipso*-Ph); ^{29}Si NMR (39.8 MHz, $CDCl_3$, 25 °C, TMS): $\delta = -7.0$; MS (EI, 70 eV): *m/z* (%) = 248 (5) [M^+], 233 (2) [$M^+ - CH_3$], 113 (100) [$CH_2NC_4H_8NCH_3^+$]; correct elemental analysis.

7f: yield: 70%; b.p. 128 °C oven temperature/10^{-3} mbar; ^{1}H NMR (200.1 MHz, $CDCl_3$, 25 °C, TMS): $\delta = 0.30$ (s, ^2J(H,Si) = 6.4 Hz, 6H; $SiCH_3$), 2.25 (s, 2H; $SiCH_2N$), 2.58 (t, ^3J(H,H) = 6.2 Hz, 4H; NCH_2C), 3.23 (s, 6H; OCH_3), 3.34 (t, ^3J(H,H) = 6.2 Hz, 4H; OCH_2C), 7.25–7.35, 7.45–7.50 (m, 5H; Ph); ^{13}C NMR (50.3 MHz, $CDCl_3$, 25 °C, $CDCl_3$): $\delta = -2.9$ (2 C, $SiCH_3$), 46.4 ($SiCH_2N$), 57.2 (2 C, NCH_2C), 58.7 (2 C, OCH_3), 71.0 (2 C, OCH_2C), 127.7 (2 C, *m*-Ph), 128.9 (*p*-Ph), 133.7 (2 C, *o*-Ph), 138.9 (*ipso*-Ph); ^{29}Si NMR (39.8 MHz, $CDCl_3$, 25 °C, TMS): $\delta = -6.6$; MS (EI, 70 eV): *m/z* (%) = 281 (4) [M^+], 236 (88) [$M^+ - CH_2OCH_3$], 204 (6) [$M^+ - C_6H_5$], 146 (50) [$CH_2N(C_2H_4OCH_3)_2]^+$, 102 (100); correct elemental analysis.

7g: yield: 27%; b.p. 95 °C oven temperature/10^{-3} mbar; ^{1}H NMR (200.1 MHz, $CDCl_3$, 25 °C, TMS): $\delta = 0.28$ (s, ^2J(H,Si) = 6.4 Hz, 6H; $SiCH_3$), 0.86 (d, ^3J(H,H) = 6.6 Hz, 12H; $NCCH_3$), 2.14 (s, 2H; $SiCH_2N$), 2.86 (sept, ^3J(H,H) = 6.6 Hz, 2H; $NCHC_2$), 7.20–7.30, 7.45–7.50 (m, 5H; Ph); ^{13}C NMR (50.3 MHz, $CDCl_3$, 25 °C, $CDCl_3$): $\delta = 2.8$ (2 C, $SiCH_3$), 20.3 (4 C, $NC(CH_3)_2$) 34.2 ($SiCH_2N$), 49.0 (2 C, $NCHC_2$), 127.6 (2 C, *m*-Ph), 128.7 (*p*-Ph), 133.7 (2 C, *o*-Ph), 140.0 (*ipso*-Ph); ^{29}Si NMR (39.8 MHz, $CDCl_3$, 25 °C, TMS): $\delta = -5.8$; MS (EI, 70 eV): *m/z* (%) = 249 (10) [M^+], 234 (10) [M^+-CH_3], 114 (100) $[CH_2N(C_3H_7)_2]^+$; correct elemental analysis.

11: yield: 45%; b.p. 185 °C oven temperature/10^{-3} mbar; ^{1}H NMR (200.1 MHz, $CDCl_3$, 25 °C, TMS): $\delta = 0.83$ (t, ^3J(H,H) = 7.0 Hz, 12H; $NCCH_3$), 2.33 (q, ^3J(H,H) = 7.0 Hz, 8H; NCH_2C), 2.51 (s, 4H; $SiCH_2N$), 7.25–7.35, 7.60–7.70 (m, 10H; Ph); ^{13}C NMR (50.3 MHz, $CDCl_3$, 25 °C, $CDCl_3$): $\delta = 11.4$ (4C, $NCCH_3$), 41.8 (2 C, $SiCH_2N$), 50.0 (4C, NCH_2C), 127.6 (2C, *m*-Ph), 129.1 (*p*-Ph), 135.4 (2 C, *o*-Ph), 136.5 (*ipso*-Ph); ^{29}Si NMR (39.8 MHz, $CDCl_3$, 25 °C, TMS): $\delta = -17.5$; MS (EI, 70 eV): *m/z* (%) = 354 (2) [M^+], 268 (53) [$M^+ - CH_2N(C_2H_5)_2$], 86 (100) $[CH_2N(C_2H_5)_2]^+$; correct elemental analysis.

14: yield: 55%; b.p. 150 °C oven temperature/1013 mbar; ^{1}H NMR (200.1 MHz, $CDCl_3$, 25 °C, TMS): $\delta = -0.02$ (s, ^2J(H,Si) = 6.4 Hz, 18H; $SiCH_3$), 1.83 (s, 4H; $SiCH_2N$), 2.33 (m, 8H; NCH_2CH_2N); ^{13}C NMR (50.3 MHz, $CDCl_3$, 25 °C, $CDCl_3$): $\delta = -1.1$ (6 C, $SiCH_3$), 50.8 (2 C, $SiCH_2N$), 57.3 (4 C, NCH_2CH_2N); ^{29}Si NMR (39.8 MHz, $CDCl_3$, 25 °C, TMS): $\delta = -1.6$; MS (EI, 70 eV): *m/z* (%) = 258 (20) [M^+], 243 (12) [$M^+ - CH_3$], 229 (2) [$M^+ - CH_3 - CH_2$], 185 (100) [$M^+ - SiCH_3$], 73 (32) $[SiCH_3]^+$; correct elemental analysis.

The synthesis of multimetalated systems is also possible using this reductive bond cleavage. The product of *N*,*N*-bis(lithiomethyl)piperazine **13** entrapped by Me_3SiCl was isolated in 55% yield (Scheme 4). The preparation of further multimetalated, nonstabilized (lithiomethyl)amines is currently under investigation.

Nonstabilized (lithiomethyl)amines can be obtained in high yields by reductive C–S bond cleavage in a two-step synthesis starting from the appropriate amines and starting materials, which are both easily obtainable and inexpensive. These (lithiomethyl)amines can be used as building blocks in further synthesis reactions. The advantages of this method over tin–lithium exchange include the shortening of the synthesis by one step (which utilizes relatively expensive alkyl tin compounds) and the circumvention of chromatographic purification of the

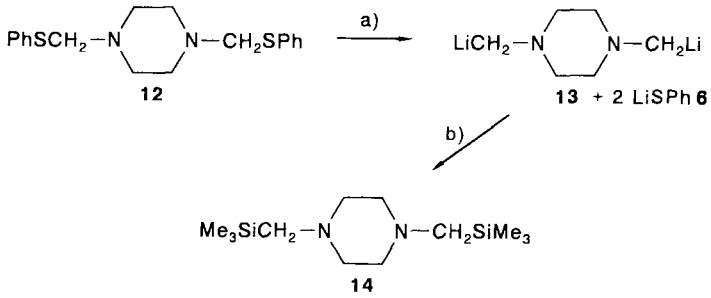

Scheme 4. Synthesis of *N,N'*-bis(trimethylsilylmethyl)piperazine: a) $+4\ LiC_{10}H_8/-4\ C_{10}H_8$; b) $4\ Me_3SiCl/-4\ LiCl, -2\ Me_3SiSPh$.

starting materials. On account of the simple pathway to (phenylthiomethyl)amines and the wide range of applications of the metalation reaction, reductive C–S bond cleavage could develop into an important method for the synthesis of compounds containing the $-CH_2NR_2$ structural unit.

Experimental Procedure

(Phenylthiomethyl)amines: The (phenylthiomethyl)amines were prepared by reported methods [11]. Amines **7a** [14], **7b** [15], **7c** [15], **7d** [11], **8** [16], **9** [7a], and **10** [7] have already been reported.

Preparation of the (lithiomethyl)amines and their reactions: To a freshly prepared solution of lithium naphthalide from lithium granules (694 mg, 100 mmol) and naphthalene (12.8 g, 100 mmol) in 150 mL THF at −78 °C was added (phenylthiomethyl)amine (50 mmol) in 50 mL THF precooled to the same temperature. After 10 min chloro(dimethyl)phenylsilane (**7a–7h**; 17.1 g, 100 mmol), dichlorodiphenylsilane (**11**; 12.7 g, 100 mmol), or chlorotrimethylsilane (**14**; 10.8 g, 100 mmol) was added. The mixture was warmed to room temperature and then subjected to an aqueous workup. After removal of the volatiles in vacuo, the residue was purified by Kugelrohr distillation.

Received: March 25, 1996
Revised version: July 17, 1996 [Z 8969 IE]
German version: *Angew. Chem.* **1996**, *108*, 2514–2516

Keywords: amines · lithium compounds · metalation · synthetic methods · transmetalation

[1] a) M. Braun, *Methoden Org. Chem. (Houben-Weyl) 4th ed.* **1952**, Vol. E19d, **1993**, pp. 853–1138; b) G. Boche, J. C. W. Lohrenz, A. Opel, *Lithium Chemistry* (Eds.: A.-M. Sapse, P. von R. Schleyer), Wiley, New York, **1995**, pp. 195–226.

[2] α-Heterocarbanions are regarded as stabilized if they carry stabilizing groups on the anionic C atom (e.g. π-systems) or dipole-stabilizing groups, for example acyl groups, on the heteroatom (cf. ref. [1a]).

[3] The term carbanion is used for strongly polar organometallic compounds, although it has been known for some time that they do not contain isolated carbanions either in solution or in the solid state. Cf. a) C. Lambert, P. von R. Schleyer, *Angew. Chem.* **1994**, *106*, 1187–1199; *Angew. Chem. Int. Ed. Engl.* **1994**, *33*, 1129–1141; b) *Methoden Org. Chem. (Houben-Weyl) 4th ed.* **1952–**, Vol. E19d, **1993**, pp. 1–106.

[4] a) D. Steinborn, F. Becke, R. Boese, *Inorg. Chem.* **1995**, *34*, 2625–2628; b) B. Elissondo, J.-B. Verlhac, J.-P. Quintard, M. Pereyre, *J. Organomet. Chem.* **1988**, *339*, 267–275; c) J.-P. Quintard, B. Elissondo, B. Jousseaume, *Synthesis* **1984**, 495–498; d) D. J. Peterson, *J. Organomet. Chem.* **1974**, *66*, 209–217; e) *J. Am. Chem. Soc.* **1971**, *93*, 4027–4031; f) *J. Organomet. Chem.* **1970**, *21*, P63–P64.

[5] a) R. Hoffmann, R. Brückner, *Angew. Chem.* **1992**, *104*, 646–648; *Angew. Chem. Int. Ed. Engl.* **1992**, *31*, 647–649; b) R. J. Lindermann, B. D. Griedel, *J. Org. Chem.* **1991**, *56*, 5491–5493; c) J. S. Sawyer, A. Kucerovy, T. L. McDonald, H. J. McGarvey, *J. Am. Chem. Soc.* **1988**, *110*, 842–853; d) J. A. Marshall, *Chem. Rev.* **1996**, *96*, 31–47.

[6] a) T. Cohen, M.-T. Lin, *J. Am. Chem. Soc.* **1984**, *106*, 1130–1131; b) T. Cohen, J. R. Matz, *ibid.* **1980**, *102*, 6900–6902; c) E. J. Verner, T. Cohen, *J. Org. Chem.* **1992**, *57*, 1072–1073; d) *J. Am. Chem. Soc.* **1992**, *114*, 375–377; e) S. D. Rychnovsky, D. J. Skalitzky, *J. Org. Chem.* **1992**, *57*, 4336–4339.

[7] a) A. R. Katritzky, H.-X. Chang, J. Wu, *Synthesis* **1994**, 907–908; b) W. H. Pearson, E. P. Stevens, *ibid.* **1994**, 904–906.

[8] a) C. Strohmann, *Angew. Chem.* **1996**, *108*, 600–601; *Angew. Chem. Int. Ed. Engl.* **1996**, *35*, 528–529; b) C. Strohmann, S. Lüdtke in *Organosilicon Chemistry II* (Eds.: N. Auner, J. Weis), VCH, Weinheim, **1996**, pp. 499–504.

[9] B. C. Abele, J. Frenzel, C. Strohmann, *3rd Int. Conf. Inorg. Chem.*, Brighton, **1995**, P58.

[10] T. Tsunoda, K. Fujiwara, Y. Yamamoto, S. Ito, *Tetrahedron Lett.* **1991**, *32*, 1975–1978.

[11] a) G. F. Grillot, H. R. Felton, B. R. Garrett, H. Greenberg, R. Green, R. Clementi, M. Moskowitz, *J. Am. Chem. Soc.* **1954**, *76*, 3969–3971; b) C. B. Pollard, D. E. Butler, *J. Org. Chem.* **1961**, *26*, 600–601.

[12] Treatment with one equivalent of chloro(dimethyl)phenylsilane gave somewhat diminished yields of **7a–7f**.

[13] a) R. D. Haugwitz, W. K. Anderson, J. Plowman, R. Kaslinal, D. M. Houston, V. L. Narayanan, *Appl. Organomet. Chem.* **1990**, *4*, 375–378; b) After this paper had been submitted, the synthesis of $LiCH_2N(Me)CH_2N(Me)CH_2Li$ by hydrogen–lithium exchange and its reactions with chlorosilanes was published: H. H. Karsch, *Chem. Ber.* **1996**, *129*, 483–484.

[14] K. A. Adrianov, V. M. Kopylov, A. I. Chernyshev, S. V. Andreeva, I. S. Shragin, *Zh. Obshch. Khim.* **1975**, *45*, 351–357.

[15] O. Wagner, P. Hencsei, J. Nagy, *Magy. Kem. Foly.* **1989**, *95*, 271–274.

[16] R. G. Shepherd, R. G. Wilkinson, *J. Med. Pharm. Chem.* **1962**, *5*, 823–835.

[17] H. E. Zaugg, R. J. Michaels, *J. Org. Chem.* **1968**, *33*, 2167–2169.

The Existence of Stable $Tm@C_{82}$ Isomers**

Uwe Kirbach and Lothar Dunsch*

Since the discovery of the fullerene synthesis by Krätschmer and Huffman[1] in 1990, the study of endohedral fullerenes is one of the main streams in current fullerene research[2] besides the growing field of chemical derivatization especially of C_{60}. The incorporation of metal atoms into the carbon cage results in an electron transfer from the metal atom to the carbon structure under the formation of a stable ion pair. Because of the steric hindrance by the surrounding fullerene the metal ion cannot leave the carbon cage nor react with other substances. The study of the electron transfer at such "caught" metal cations is a very new field in electrochemical research. Up till now the electron transfer to the carbon cage rather than the intramolecular transfer reactions is the main topic of these studies.

Our recent work concentrated on the preparation of several endohedral fullerenes containing different metals and their characterization by mass spectrometry, cyclic voltammetry, ex situ and in situ ESR, and UV/Vis spectroscopy.[3] New results were obtained by ex situ and in situ ESR spectroscopy on the composition of the fullerene soot extract, the differences in the redox behavior of empty and endohedral fullerenes, and the existence of different paramagnetic states at endohedral fullerenes. As metals, scandium, yttrium, lanthanum, and the rare earth metals cerium, praseodymium, samarium, holmium, thulium, and lutetium were used. In these studies the first successful mass spectrometric proof of the existence of endohedral thulium fullerene in the soot extract was reported.[3]

In this paper it will be demonstrated for the first time that three stable $Tm@C_{82}$ isomers exist, which can be isolated and structurally characterized. These isomers of an endohedral

[*] Dr. L. Dunsch, Dipl.-Chem. U. Kirbach
Institut für Festkörper- und Werkstofforschung Dresden
Institut für Festkörperforschung, Abt. Elektrochemie
Helmholtzstrasse 20, D-01069 Dresden (Germany)
Fax: Int. code +(351)465-9313
e-mail: dunsch@ifw-dresden.de

[**] This work was supported by a grant from the Sächsisches Ministerium für Wissenschaft und Kunst. We thank Heidi Zöller and Ulrike Feist for their experimental support and Dr. Anton Bartl for many helpful discussions. We are particularly grateful for the special contribution of Dr. Dieter Scheller, TU-Dresden (^{13}C NMR spectra).

fullerene may have a different arrangement of pentagons and hexagons in C_{82} (nine isomers according to Fowler and Manolopoulos[4]) as well as different positions of the metal inside the fullerene cage. The isomers formed in the presented procedure have different symmetry elements and belong to different point groups (Fig. 1). Although different $M@C_{82}$ isomers (M = Sc, Y, La) have been detected by ESR spectroscopy,[5, 6] only two

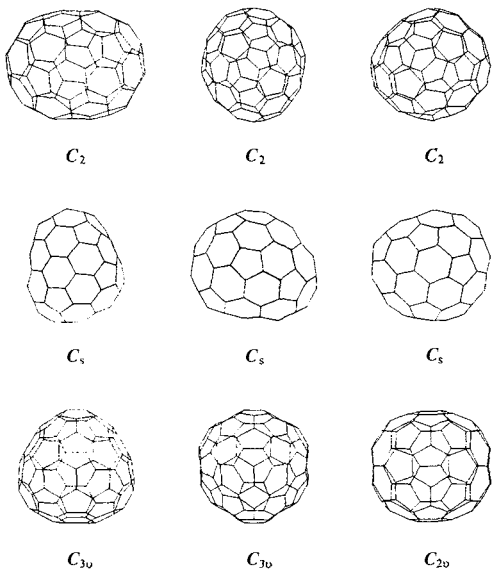

Fig. 1. The nine C_{82} isomers with isolated pentagons according to Fowler and Manolopoulos [4].

$La@C_{82}$ isomers were separated by chromatography.[7] These isomers differ markedly in their electronic properties and their stability in air. This type of isomerism is due to the positional isomerism of the lanthanum ion at the C_{82}, which can be interpreted as an endohedral or an exohedral structure.[8] In contrast the three isomers of the thulium endohedral fullerene have a similiar long-term stability but quite different electronic properties.

The fullerene soot produced by DC arc burning as well as the resulting soot extract had to be studied with high-resolution mass spectrometry as the differences in the mass of $Tm@^{12}C_x$ and $^{13}C^{12}C_{x+1}$ (x = 82, 84, 90, etc.) are very small. As already shown for the other well-known endohedral fullerenes the singly filled C_{82} was the most common structure. Furthermore the new structures $Tm@C_{84}$, $Tm@C_{90}$, $Tm@C_{92}$, $Tm@C_{94}$, $Tm@C_{96}$, $Tm_2@C_{80}$, and $Tm_2@C_{82}$ were found in addition to $Tm@C_{82}$.

By two-step HPLC separation of the soot extract with two different HPLC columns and special stationary phases, three fractions containing $Tm@C_{82}$ were obtained, all of which have the same parent mass peak at m/z 1153. This is the theoretical mass of the structure $Tm@C_{82}$. The analysis of the ^{13}C isotope peaks resulted in a ^{13}C abundance in C_{82} that was equivalent to the natural abundance.

The retention times of $Tm@C_{82}$ fullerenes in the HPLC chromatograms differ substantially from those of other endohedral fullerenes like $Sc@C_{82}$, $Y@C_{82}$, and $La@C_{82}$. The $Tm@C_{82}$ fullerenes are eluted shortly behind the peak for C_{84} in the first HPLC separation step, whereas $Sc@C_{82}$, $Y@C_{82}$, and $La@C_{82}$ appear at the beginning of the C_{88} fraction. This insignificant shift of the $Tm@C_{82}$ retention time relative to that of the empty C_{82} indicates a comparable interaction of thulium-containing fullerene with the stationary phase. The reason for this behavior is the lower electron density of the carbon cage of this endohedral fullerene. The two clearly visible peaks containing $Tm@C_{82}$ in the first separation step (Fig. 2a) split into three peaks **A**, **B**, and **C** containing the three different $Tm@C_{82}$ isomers in the second separation (Fig. 2b). The color of solutions of these isomers in toluene differs markedly even at similiar concentrations. Thus the solution of the isomers **A** is green, that of the isomers **B** yellowish brown, and that of isomers **C** brown-red. The solid samples of all three isomers do not differ and are black or black-brown microcrystalline powders.

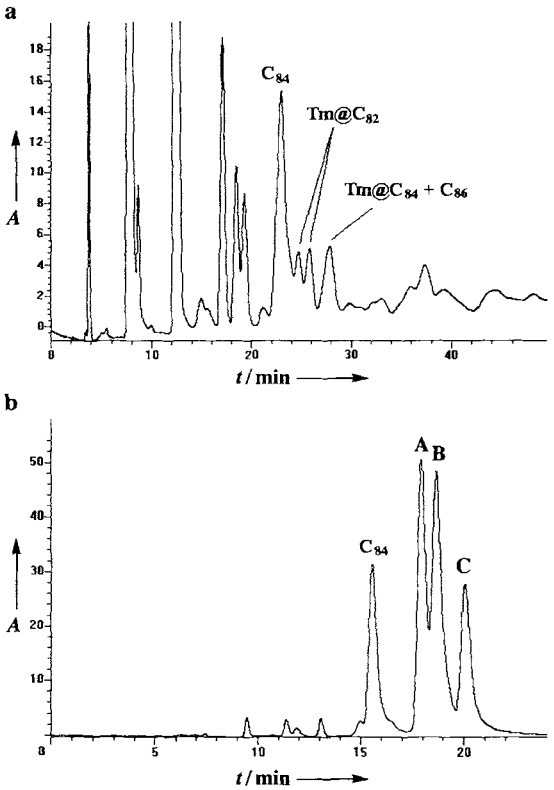

Fig. 2. a) Chromatogram of the preparative HPLC separation of $Tm@C_{82}$ soot extract (Cosmosil Buckyprep column, toluene as eluent, flow rate 10 mL min^{-1}). b) HPLC chromatogram of the preparative separation of a pre-separated thulium fullerene fraction (BuckyClutcher column, mixture of 70% toluene and 30% hexane as eluent, flow rate 2 mL min^{-1}, λ = 330 nm for both separations). For further details see Experimental Procedure. A = absorption in arbitrary units.

The existence of different $M@C_{82}$ isomers was already known and described,[5] but only one isomer seemed to have long-term stability. The concentration of the other isomers decreased rapidly during handling of the solutions in air, which pointed to exohedral fullerenes. By contrast the three $Tm@C_{82}$ isomers under study can be handled in air for several months without significant changes in their properties.

The electronic structure of these three isomers was further characterized by UV/Vis/NIR in toluene solutions, as well as by cyclic voltammetry in *o*-dichlorobenzene solutions. As expected from the different colors of the toluene solutions, the comparison of the UV/Vis/NIR spectra results in large differences especially in the visible absorption. The spectrum of isomer **A** consists of several relatively small absorption bands at 610, 660, 770, 1035, and 1200 nm. In contrast to the spectra of $La@C_{82}$, $Y@C_{82}$, $Ce@C_{82}$, $Pr@C_{82}$, and $Gd@C_{82}$,[9, 10, 11, 12] isomer **A** shows no absorptions between 1200 nm and 1700 nm. The situation changes for the isomer **B** and **C**. The number and intensity of the absorption bands are

 © VCH Verlagsgesellschaft mbH, D-69451 Weinheim, 1996 0570-0833/96/3520-2381 $ 15.00+.25/0

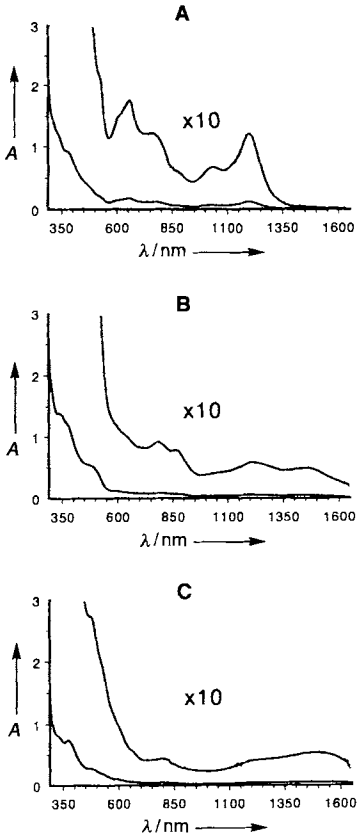

Fig. 3. UV/Vis/NIR spectra of the $Tm@C_{82}$ isomers **A**, **B**, and **C**; $c = 10^{-4}$ mol L^{-1} in toluene, room temperature, A = absorption in arbitrary units.

lower and they broaden. Furthermore new broad absorption bands appear at 1450 nm (**B**) and 1500 nm (**C**) (Fig. 3). Significant differences in the size and the number of the absorption bands are observed between the UV/Vis/NIR spectra of the $Tm@C_{82}$ isomers and the known spectra of $La@C_{82}$, $Y@C_{82}$, $Ce@C_{82}$, $Pr@C_{82}$, and $Gd@C_{82}$. These differences (for instance, several absorption bands at $\lambda < 1200$ nm for the isomer **A**) are due to a pronounced change in structural symmetry of the molecules. A higher symmetry is expected for isomer **A** than for isomers **B** and **C**, which can be explained by the C_{82} structures in Figure 1. The change of the solvent (toluene $\rightarrow CS_2$) causes a 10–15 nm bathochromic shift of the UV/Vis/NIR absorption bands. This confirms the assumption of $\pi-\pi^*$ transitions. Similiar shifts were already found for $La@C_{82}$.[9, 13]

The electron energy levels of the isomers ought to influence the electron transfer. This was tested by voltammetric measurements. The differences in the charge-transfer reactions of the three thulium-containing fullerene isomers parallel those of UV/Vis spectroscopy (Fig. 4). The change of the peak potentials of the two anodic peaks in the potential range between 0 and −350 mV is striking. At first these potentials are shifted to significantly more cathodic potentials than that of the reduction of $La@C_{82}$ and $Y@C_{82}$. Especially the isomer **A** gives peaks only at potentials more negative than −400 mV; that is, in the region where most endohedral fullerenes have two voltammetric peaks, no charge transfer occurs. The analysis of the peak currents led to the conclusion that both voltammetric peaks are attributable to one-electron transfers.

It was therefore appropriate to follow the electron transfer reactions by ESR spectroscopy too. In solution all the three isomers give no ESR signal in the magnetic field between 500 and 9000 G. Dimerization of the isomers, which could result in diamagnetic structures, was excluded by temperature-dependent measurements. The existence of an odd number of electrons at the C_{82} cage is thus less probable if splitting constants for thulium in fullerenes is assumed to be similiar to those in thulium salts. All the tests to produce a paramagnetic state by oxidation or reduction at a platinum electrode and to detect this state by in situ ESR spectroscopy failed. These results and the shift of the retention time $Tm@C_{82}$ relative to that of $La@C_{82}$ prompted us to assume the existence of the divalent $Tm^{2+}@C_{82}^{2-}$. First results of a study under progress on these isomers by ^{13}C NMR spectroscopy confirm this result. Thus the

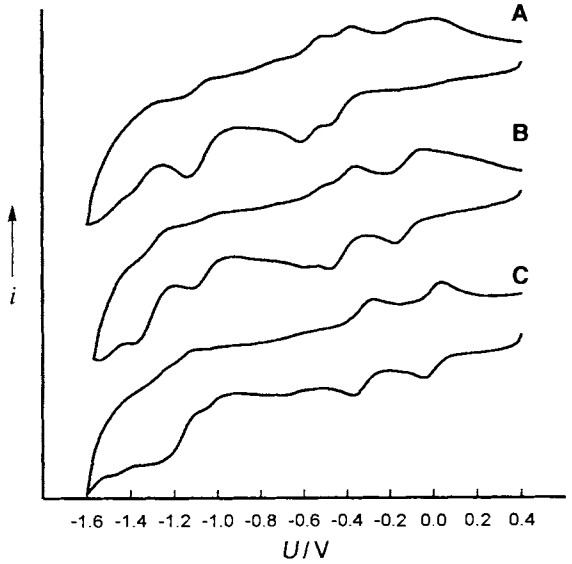

Fig. 4. Cyclic voltammograms of the three $Tm@C_{82}$ isomers **A**, **B**, and **C**; $c = 10^{-4}$ mol L^{-1} in *o*-dichlorobenzene, platinum electrode, scan rate = 100 mV s^{-1}, i = current, U = potential.

NMR spectra of $Tm@C_{82}$ isomers can be measured without any line broadening, which would seem to indicate the absence of an unpaired spin on the C_{82} cage (and consequently an even number of charges on the thulium ion). From energy considerations the +II state of the thulium is the most probable. Since the intensity of the NMR signals was very low despite a ^{13}C enrichment of 10%, 8000 accumulations per sample were required. The ^{13}C NMR measurements confirm the result that the isomer **A** has a higher symmetry than the other two isomers, as its signals were more intense and there were fewer of them. At first sight the number of lines points to a C_{3v} point group for isomer **A**. An assignment of the other isomers was impossible till now because of the low signal-to-noise ratio and the high number of lines, but C_2 or C_s symmetry is expected. The observed shift of the lines of the endohedral isomers relative to that of the empty C_{82} is due to the effect of thulium and/or its 4f magnetism. This effect is known and used in NMR shift reagents containing lanthanides.

The present study on endohedral fullerenes afforded the first preparation and separation of three stable $Tm@C_{82}$ isomers. The spectroscopic study of these new isomers shows remarkable differences between these thulium isomers that are not evident with the endohedral fullerenes of lanthanum, scandium, and yttrium. The electronic structure of the isomers is $Tm^{2+}@C_{82}^{2-}$. The isomerism is due to differences in the symmetry of the three carbon cages, as deduced from ^{13}C NMR measurements. The ^{13}C NMR spectroscopic studies will be continued to improve the resolution of the spectra in larger samples, and longer accumulation times will enable the unequivocal determination of the point groups of the $Tm@C_{82}$ isomers.

Experimental Procedure

The thulium-containing fullerenes were prepared by the arc burning method of Krätzschmer and Huffman [1]. Drilled graphite rods (Elektrokohle Lichtenberg AG, Spektralkohlestäbe TO-E, 6 × 200 mm) were filled with a mixture of thulium powder (Johnson Matthey GmbH/Alfa, 99.9%, smaller than 40 mesh) and graphite (Ringsdorf-Werke GmbH, Spektralkohlepulver RW-A). The thulium-to-carbon ratio used in the arc burning was 1:50. The current density of the arc was 175 A, and the helium pressure in the burning chamber 200 mbar. The resulting soot (4.5 to 5 g per burning) was extracted with CS_2 for 20 hours in a Soxhlet apparatus. The fullerene extract (300–350 mg) was dried and dissolved in *o*-xylene. The content of thulium-containing fullerenes was estimated by mass spectrometry

 © VCH Verlagsgesellschaft mbH, D-69451 Weinheim, 1996 0570-0833/96/3520-2382 $ 15.00+.25/0

to be a maximum of 0.8% of the total amount of fullerenes. The separation of the extract was done by a two-step HPLC method. In the first step a Cosmosil Buckyprep column (20 × 250 mm, Nacalai Tesque Inc.) with a nonpolar stationary phase ([2-(1-pyrenyl)propyl]silyl-silica gel) [14] was used in a preparative HPLC apparatus (M 305, Abimed-Gilson) with toluene as eluent to enrich the $Tm@C_{82}$ fraction (injection volume 5 mL, flow rate 10 mL min^{-1}). The resulting fraction was then separated into the three fractions of the $Tm@C_{82}$ isomers in an analytical HPLC apparatus HP1050 (Hewlett Packard) equipped with a semipreparative Buckyclutcher I column (10 × 250 mm, Regis Chemicals Corp.) filled with a polar stationary phase (Trident-Tri-DNP, flow rate 2 mL min^{-1}, mixture of toluene and hexane (70:30) as eluent).

The contamination of the fractions by empty fullerenes or other $Tm@C_{82}$ isomers was tested by a sector field mass spectrometer MAT 95 (Finnigan, Bremen) and by analytical HPLC after the second separation step. In the mass spectrometric study chemical ionization by methane was used, and the negative ions were detected. The endohedral fullerene content of all three $Tm@C_{82}$ fractions was higher than 97% as measured by mass spectrometry. The isomeric purity of the fullerene fractions determined by HPLC was greater than 90%.

The UV/Vis/NIR measurements were done in toluene with a UV-3101PC spectrometer (Shimadzu). UV/Vis/NIR data: Isomer **A**: λ = 375, 485 (w), 525 (w), 610, 660, 770, 880 (w), 1035, 1200 nm. Isomer **B**: λ = 330, 375, 485, 770, 860, 1200, 1450 nm. Isomer **C**: λ = 375, 485, 525, 800, 1200, 1500 nm. For the electrochemical measurements a potentiostat PAR 273 (EG & G, USA, software PARC M270, version 3.0) and a conventional voltammetric cell were used. The latter was installed in a glovebox to ensure inert conditions (solvent *o*-dichlorobenzene, supporting electrolyte $n-Bu_4NBF_4$; either platinum or glassy carbon working electrode, large platinum sheet counterelectrode, Ag/AgCl reference electrode in the same supporting electrolyte). The in situ ESR technique for electrochemical systems has already been described in detail [15]. The ^{13}C NMR study was done in saturated CS_2 solutions of the three $Tm@C_{82}$ isomers on samples with about 10% ^{13}C enrichment (Bruker spectrometer MSL 300 with external [D_6]acetone lock; number of accumulations: 7940 (isomer **A**), 7950 (isomer **B**), 8500 (isomer **C**); no relaxation reagent).

Received: February 12, 1996
Revised version: July 10, 1996 [Z 8806 IE]
German version: *Angew. Chem.* **1996**, *108*, 2518–2521

Keywords: electrochemistry · fullerenes · metallofullerenes · thulium compounds · UV/Vis spectroscopy

[1] W. Krätschmer, L. D. Lamb, K. Fostiropoulos, D. R. Huffman, *Nature* **1990**, *347*, 354–358.
[2] D. S. Bethune, R. D. Johnson, J. R. Salem, M. S. de Vries, C. S. Yannoni, *Nature* **1993**, *366*, 123.
[3] A. Bartl, L. Dunsch, J. Fröhner, U. Kirbach, *Chem. Phys. Letters* **1994**, *229*, 115–121.
[4] P. W. Fowler, D. E. Manolopoulos, *An Atlas of Fullerenes*, Clarendon Press, Oxford, **1995**.
[5] S. Suzuki, S. Kawata, H. Shiromaru, K. Yamauchi, K. Kikuchi, T. Kato, Y. Achiba, *J. Phys. Chem.* **1992**, *96*, 7159–7161.
[6] M. Hoinkins, C. S. Yannoni, D. S. Bethune, J. R. Salem, R. D. Johnson, M. S. Crowder, M. S. de Vries, *Chem. Phys. Letters* **1992**, *198*, 461–465.
[7] K. Yamamoto, H. Funasaka, T. Takahashi, T. Akasaka, T. Suzuki, Y. Maruyama, *J. Phys. Chem.* **1994**, *98*, 12831–12833.
[8] A. Bartl, L. Dunsch, U. Kirbach, *Appl. Magn. Reson.* **1996**, *10*, in press.
[9] K. Kikuchi, S. Suzuki, Y. Nakao, N. Nakahara, T. Wakabayashi, H. Shiromaru, K. Saito, I. Ikemoto, Y. Achiba, *Chem. Phys. Letters* **1993**, *216*, 67–71.
[10] K. Kikuchi, Y. Nakao, S. Suzuki, Y. Achiba, *J. Am. Chem. Soc.* **1994**, *116*, 9367–9368.
[11] R. H. Michel, D. Fuchs, R. D. Beck, M. M. Kappes in *Physics and Chemistry of Fullerenes and Derivatives* (Eds.: H. Kuzmany, J. Fink, M. Mehring, S. Roth), World Scientific, Singapore **1995**, p. 89–104.
[12] H. Shinohara, M. Kishida, T. Nakane, T. Kato, S. Bandow, X.-D. Wang, T. Hashizume, T. Sakurai, *Proc. Electrochem. Soc.* **1994**, *94–24*, 1361–1381.
[13] K. Yamamoto, H. Funasaka, T. Takahashi, T. Akasaka, *J. Phys. Chem.* **1994**, *98*, 2008–2011.
[14] R. E. Majors, *LC–GC International.* **1995**, *8*(5), 276.
[15] L. Dunsch, *Proc. Electrochem. Soc.* **1994**, *94–24*, 1068–1076.

Is Kekulene Really Superaromatic?**

Haijun Jiao and Paul von Ragué Schleyer*

Dedicated to Professor Heinz A. Staab on the occasion of his 70th birthday

The beautiful molecule kekulene (**1**), first synthesized by Diederich and Staab[1] in 1978, is truly a superbenzene aesthetically. The twelve annelated benzene rings comprising a closed cycle also offer the intriguing possibility of enhanced stabilization. But is kekulene really superaromatic in this sense? Even before its synthesis, the electronic structure of **1** was the subject of theoretical debate.[2] The nature of kekulene has remained controversial to the present day.[2–5]

However, unlike benzene, the two principle resonance structures of kekulene are not equivalent. The D_{6h} form **1a** has benzenoid character and can be depicted more clearly by employing the Robinson sextet "circle notation" (**1a'**), whereas its D_{3h} counterpart **1b** is annulenoid. Both the [18]annulene (**2**) inner and the [30]annulene outer moieties in **1b** follow the Hückel ($4n+2$) rule. However, a variety of evidence including X-ray structure, ^1H NMR shifts,[1] and the most recent theoretical treatments[2–5] are inconsistent with the annulenoid formulation **1b**.

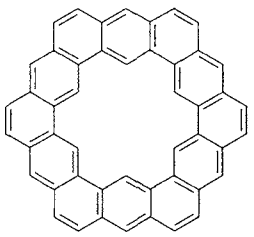

1a

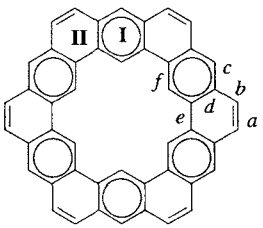

1a' (benzenoid, D_{6h})

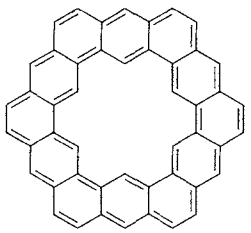

1b (annulenoid, D_{3h})

Nevertheless, the possible superaromaticity of kekulene has been disputed.[4, 5] Based on rather low-level ab initio calculations using an additive nodal increment method, Cioslowski et al.[4a] estimated the extra stabilization energy of kekulene to be 32.9 kcal mol^{-1} (HF/STO-3G) and 25.4 kcal mol^{-1} (HF/6-31G**) and discussed other evidence alleged to demonstrate the presence of superaromaticity in kekulene. This position was supported more simply based on the "hardness" concept.[4b]

[*] Prof. Dr. P. von R. Schleyer, Dr. H. Jiao
Computer-Chemie-Centrum
Institut für Organische Chemie der Universität Erlangen-Nürnberg
Henkestrasse 42, D-91054 Erlangen (Germany)
Fax: Int. code +(9131)859132
e-mail: pvrs@organik.uni-erlangen.de

[**] This work was supported by the Fonds der Chemischen Industrie, the Deutsche Forschungsgemeinschaft, the Volkswagen-Stiftung, and Convex Computer Corporation. We also thank Prof. J. Cioslowski for discussions.

Employing π-electron topological resonance energies, Aihara[5] reached the opposite conclusion: "Kekulene was found to be essentially non-super-aromatic with a small super-aromatic stabilization energy". Is **1a'**, with its semilocalized benzene rings, really the best representation of the bonding situation in kekulene?

We have used the Gaussian 94 program[6] to carry out ab initio and density functional theory evaluations of the superaromaticity of kekulene. Geometries were optimized first at the HF/3-21G level and then with the Becke3LYP/6-31G* functional, which includes dynamic electron correlation. Diamagnetic susceptibilities and diamagnetic susceptibility anisotropies (Becke3LYP/6-31G*) using the Continuous Set in Gauge Transformations (CSGT) method[7] and nucleus-independent chemical shifts (NICS, GIAO-SCF/3-21G)[8] were calculated with the Becke3LYP/6-31G* geometries. The computed energies, magnetic susceptibilities, and magnetic susceptibility anisotropies are summarized in Table 1.

Table 1. Computed total energies (in Hartree) for kekulene and reference molecules as well as CSGT magnetic susceptibilities (χ_{tot}, in ppm cgs) and anisotropies (χ_{anis}) at the Becke3LYP/6-31G*//Becke3LYP/6-31G* level.

Molecule	E (HF/3-21G)	E (Becke3LYP/6-31G*)	χ_{tot}	χ_{anis}
kekulene	−1821.55153	−1843.72103	−403.0	−769.7
anthracene	−533.00347	−539.53060	−114.7	−203.1
phenanthrene	−533.01572	−539.53875	−110.6	−190.5
naphthalene	−381.21581	−385.89279	−80.0	−135.0
1,2:7,8-dibenz-anthracene (**3**)	−836.60869	−846.82625	–	–
benzene	−229.41945	−232.24870	−46.1	−69.8
[18]annulene (**2**)	−688.06697 [a]	−696.64078 [b]	−320.8	−763.7

[a] At the HF/3-21G level, D_{6h} [18]annulene has one imaginary frequency (NIMAG = 1). [b] D_{6h} [18]annulene corresponds to an energy minimum at the Becke3LYP/6-31G* level.

Both HF- and Becke3LYP-optimized C–C bond lengths (Table 2) agree well with the values from the X-ray structure analysis.[1c] Comparison with the geometric parameters of

Table 2. Optimized bond lengths (in Å) calculated for kekulene compared with data from its X-ray structure analysis.

Bond [a]	HF/3-21G	HF/6-31G** [b]	Becke3LYP/6-31G*	RSA [c]
a	1.338	1.340	1.362	1.347–1.351
b	1.451	1.453	1.441	1.438–1.449
c	1.392	1.394	1.405	1.391–1.397
d	1.409	1.410	1.429	1.415–1.421
e	1.465	1.466	1.460	1.453–1.461
f	1.381	1.383	1.394	1.381–1.390

[a] The labeling system is shown in formula **1a'**. [b] Ref. [4a]. [c] Ref. [1c].

1,2:7,8-dibenzanthracene (**3**), anthracene, phenanthrene, and naphthalene (Scheme 1) confirms the description of kekulene as benzenoid (**1a**) rather than annulenoid (**1b**) but provides no evidence for superaromaticity. The alternations of the inner (0.066 Å) and outer (0.073 Å) C–C bond lengths in kekulene are larger than those (0.016 Å) in the parent [18]annulene (**2**) (Becke3LYP).

The aromatic stabilization energy (ASE) is a measure of cyclic electron delocalization in a molecule and thus of its aromaticity.[9–12] If kekulene were superaromatic, its ASE would exceed the sum of the values for its smaller benzenoid hydrocarbon

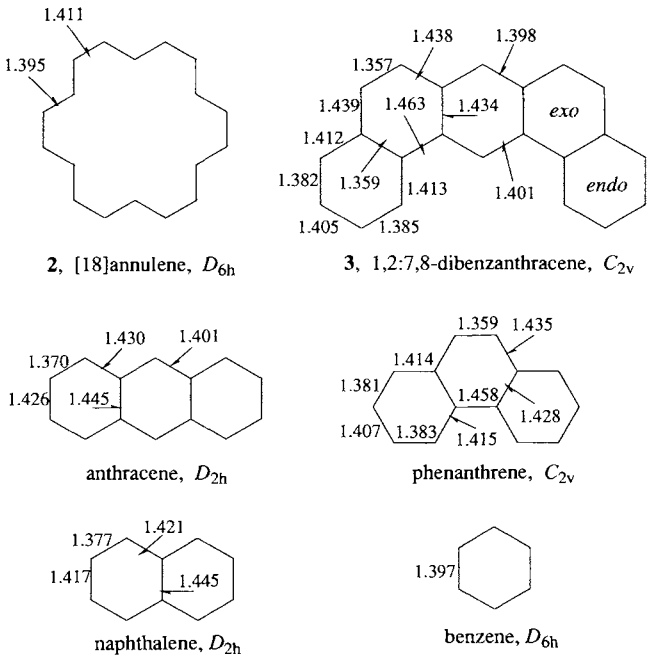

Scheme 1. Aromatic compounds used as references and their Becke3LYP/6-31G*-optimized bond lengths (in Å). Only the C–C bonds are shown.

components significantly. Since kekulene can be viewed as a set of cyclic angularly annelated benzenoid hydrocarbons, benzene, anthracene, phenanthrene, naphthalene, and 1,2:7,8-dibenzanthracene (**3**) have been employed as reference molecules. The extra aromatic stabilization energy can be evaluated simply by the homodesmic Equations (a)–(c).[12]

3[anthracene + phenanthrene − 2 benzene] = kekulene (a)

6[anthracene + phenanthrene − 2 naphthalene] = kekulene (b)

6[1,2:7,8-dibenzanthracene (**3**) − phenanthrene] = kekulene (c)

Based on Equation (a), the Becke3LYP/6-31G*-calculated extra ASE is only −3.3 kcal mol^{-1}, which is much smaller than the estimates made by Cioslowski et al.[4a] Their results were checked at the HF/3-21G level, which is also without dynamic electron correlation. Although the resulting extra ASE of −6.7 kcal mol^{-1} [Eq. (a)] is somewhat larger than the Becke3LYP value, it still is much smaller than Cioslowski's findings.[4a] Based on Equation (b), the extra ASE values are −11.6 kcal mol^{-1} (Becke3LYP/6-31G*) and −16.4 kcal mol^{-1} (HF/3-21G). With the more appropriate 1,2:7,8-dibenzanthracene (**3**) as reference molecule [Eq. (c)], the calculated extra ASE values, 2.5 kcal mol^{-1} (Becke3LYP/6-31G*) and 3.9 kcal mol^{-1} (HF/3-21G), are slightly positive but negligible. These small extra ASE values for such a large system agree with the Aihara's suggestion.[5b] We agree that the 48 π-electron kekulene does not have any appreciable extra stabilization energy and is a normal benzenoid rather than a superaromatic molecule. We thus support the conclusions that had been drawn from the original experimental work.[1b,c]

In addition to these geometric and energetic criteria, we also evaluated the magnetic criteria, specifically the diamagnetic susceptibility exaltation (Λ, ppm cgs), diamagnetic susceptibility anisotropy (χ_{anis}, ppm cgs), and the nucleus-independent chemical shifts (NICS) to characterize the superaromaticity of kekulene (Table 3). Λ, the only measurable property uniquely associated with aromaticity,[9,10,13] is defined as the difference

Table 3. GIAO-SCF NICS (ppm) and calculated magnetic susceptibility exaltations (Λ) for kekulene and reference molecules (Becke3LYP/6-31G* geometries).

Molecule	NICS (3-21G)	NICS (6-31+G* [a])	Λ [b]
kekulene			−227.8
center	+5.0	–	
ring **I**	−10.8	–	(−3.7) [c]
ring **II**	−4.3	–	(−11.2) [d]
benzene	−10.0	−9.7	−16.7
naphthalene	−10.0	−9.9	−36.5
cyclopentadienyl anion	−17.2	−14.3	−17.7
tropylium ion	−7.1	−7.6	−28.0
azulene			−36.8
five ring	−19.1	−19.7	
seven ring	−7.4	−7.0	
1,2:7,8-dibenzanthracene (**3**)			–
central ring	−11.6	–	
exo ring	−5.4	–	
endo ring	−10.1	–	
anthracene			−56.1
central ring	−12.9	−13.3	
outer ring	−8.6	−8.2	
phenanthrene			−52.0
central ring	−6.8	−6.5	
outer ring	−10.3	−10.2	
cyclobutadiene	+28.3	+27.6	+12.0
benzocyclobutadiene			+0.8
six ring	−3.7	−2.5	
four ring	+23.3	+22.5	
[18]annulene (**2**)	−13.4	–	−232.6

[a] From ref. [8]. [b] Calculated for the entire molecule based on an increment system (at the Becke3LYP-CSGT/6-31G* level). [c] Extra Λ evaluated with Equation (a). [d] Extra Λ evaluated with Equation (b).

between the bulk magnetic susceptibility (χ_M) of a compound and the susceptibility (χ'_M) estimated from an increment system for the same structure without cyclic delocalization ($\Lambda = \chi_M - \chi'_M$).[13] As expected from its aromatic nature and large ring size, kekulene has a large diamagnetic susceptibility exaltation ($\Lambda = -227.8$) and a large diamagnetic susceptibility anisotropy ($\chi_{anis} = -769.7$). Both of these values are close to those for [18]annulene (**2**) ($\Lambda = -232.6$ and $\chi_{anis} = -763.7$). However, if kekulene were superaromatic, both Λ and χ_{anis} would be significantly larger in magnitude than the sum of their values for the reference molecules, anthracene, phenanthrene, naphthalene, and benzene. The extra exaltation of the diamagnetic susceptibility and the extra anisotropy of kekulene can be obtained, like the evaluation of the extra ASE, by using the homodesmic Equations (a) and (b).[14] The negligibly small extra diamagnetic susceptibility exaltations of −3.7 [Eq. (a)] and −11.2 [Eq. (b)] (Table 3) further establish that kekulene is not superaromatic. In addition, the extra χ_{anis} enhancements of kekulene (−7.7 [Eq. (a)] and −28.1 [Eq. (b)]) are very small for a such large molecule.

NICS, a simple and efficient aromaticity probe,[8] is the negative of the absolute magnetic shielding constant, which can be computed easily, for example at ring centers (nonweighted mean of the heavy-atom coordinates of the ring perimeter), at the GIAO-SCF/6-31 + G* level with the Gaussian 94 program.[6] Negative NICS denote aromaticity (e.g. −9.7 for benzene) and positive NICS, antiaromaticity (e.g. 27.6 for cyclobutadiene). Nonaromatic molecules have negligible NICS (−2.2 for cyclohexane and −1.1 for adamantane). The NICS data agree with magnetic susceptibility exaltation (Λ) and serve as an additional criterion of aromaticity.[8] Furthermore, NICS has the advantage of being less dependent on ring size than the magnetic susceptibility exaltation, and can be used to analyze the ring effects of individual rings in polycyclic systems. For example, NICS for the five- (−19.7) and seven-membered (−7.0) rings of azulene resemble those of the cyclopentadienyl anion (−14.3) and the tropylium ion (−7.6). The six-ring aromaticity (−2.5) and four-ring antiaromaticity (22.5) of benzocyclobutadiene are less than the related values of benzene and cyclobutadiene (Table 3).[8]

NICS characterizes the aromaticity of individual rings in kekulene. The smaller 3-21G basis set was used, but as shown in Table 3, the 3-21G NICS values generally are very close to the 6-31 + G* results. If kekulene were superaromatic, the NICS values should be more negative than those of the reference molecules. However, this is not found. The GIAO-SCF/3-21G NICS in ring **I** of kekulene (−10.8) is less negative than that of the central ring in anthracene (−12.9) but close to the NICS of the phenanthrene outer rings (−10.3), naphthalene (−10.0), benzene (−10.0), and the central (−11.6) as well as *endo* rings (−10.1) in 1,2:7,8-dibenzanthracene (**3**). On the other hand, the NICS of the kekulene ring **II** (−4.3) is quite small in magnitude compared with the the values of the outer ring of anthracene (−8.3), the central ring of phenanthrene (−6.8), and with the *exo* rings in 1,2:7,8-dibenzanthracene (−5.4). The positive NICS (5.0) in the center of entire kekulene structure differs very significantly from the negative NICS (−13.4) in the [18]annulene (**3**) center, computed at the same level. These results agree with the ^{1}H NMR shifts for the inner hydrogens in [18]annulene (upfield shifted, $\delta = -3.0$)[15] and in kekulene (downfield shifted $\delta = 10.45$), which like NICS can be attributed to the local ring current effects of the individual rings.[1a] All these results establish kekulene to be a normal benzenoid hydrocarbon and not to be superaromatic.

The standard heat of formation (ΔH_f°) calculated at the Becke3LYP/6-31G* level for benzene (19.5 kcal mol^{-1}) on the basis of the homodesmic Equation (d) agrees with the experimental value of 19.7 ± 0.2 kcal mol^{-1}[16] (note that the zero-point vibrational energy and thermal corrections on ΔH_f° contribute only +0.2 kcal mol^{-1}).[17] Based on the experimental heat of formation[16] of anthracene (55.2 ± 0.5 kcal mol^{-1}), phenanthrene (49.6 ± 0.4 kcal mol^{-1}), naphthalene (35.9 ± 0.4 kcal mol^{-1}), and benzene, ΔH_f° for kekulene is evaluated to be 192.6 kcal mol^{-1} [Eq. (a)] and 186.0 kcal mol^{-1} [Eq. (b)]. These values are somewhat larger than Cioslowski's STO-3G estimate of 182.2 kcal mol^{-1}.

3[1,3-*trans*-butadiene −ethylene] = benzene (d)

In conclusion, the lack of significant equalization of the C–C bond lengths, the extra stabilization energy, the extra magnetic susceptibility exaltation and anisotropy, and the NICS values from the simpler benzenoid models show that kekulene is not superaromatic. The NICS of the individual rings and the fact that the bond length variations in ring **I** (0.035 Å) are smaller than those in ring **II** (0.098 Å) justify the Robinson depiction of kekulene **1a'** as the most realistic single representation of kekulene.

Received: March 20, 1996
Revised version: July 5, 1996 [Z8952IE]
German version: *Angew. Chem.* **1996**, *108*, 2548–2551

Keywords: ab initio calculations · aromaticity · kekulene · superaromaticity

[1] a) H. A. Staab, F. Diederich, *Angew. Chem.* **1978**, *90*, 383–385; *Angew. Chem. Int. Ed. Engl.* **1978**, *17*, 372–374; b) *Chem. Ber.* **1983**, *116*, 3487–3503, and references therein; c) H. A. Staab, F. Diederich, C. Krieger, D. Schweitzer, *ibid.* **1983**, *116*, 3504–3512.

[2] a) G. Ege, H. Fischer, *Tetrahedron* **1967**, *23*, 149–157; b) G. Ege, H. Vogler, *Theor. Chim. Acta* **1972**, *26*, 55–65; c) J. Aihara, *Bull. Chem. Soc. Jpn.* **1976**, *49*, 1429–1430.

[3] a) M. Randic, *Pure Appl. Chem.* **1983**, *55*, 347; b) H. Vogler, *J. Mol. Struct. (Theochem)* **1985**, *122*, 333–341; c) *Int. J. Quantum Chem.* **1986**, *30*, 97; d) P. M. Lahti, *J. Org. Chem.* **1988**, *53*, 4590–4593; e) N. L. Allinger, F. Li, L. Yan, J. C. Tai, *J. Comput. Chem.* **1990**, *11*, 868–895.

[4] a) J. Ciosłowski, P. B. O'Connor, E. D. Fleischmann, *J. Am. Chem. Soc.* **1991**, *113*, 1086–1089; b) Z. Zhou, *J. Phys. Org. Chem.* **1995**, *8*, 103–107.

[5] a) J. Aihara, *J. Am. Chem. Soc.* **1992**, *114*, 865–868; b) *J. Chem. Soc. Faraday Trans.* **1995**, *91*, 237–239.

[6] Gaussian 94, Revision B.2: M. J. Frisch, G. W. Trucks, H. B. Schlegel, P. M. W. Gill, B. G. Johnson, M. A. Robb, J. R. Cheeseman, T. Keith, G. A. Petersson, J. A. Montgomery, K. Raghavachari, M. A. Al-Laham, V. G. Zakrzewski, J. V. Ortiz, J. B. Foresman, J. Cioslowski, B. B. Stefanov, A. Nanayakkara, M. Challacombe, C. Y. Peng, P. Y. Ayala, W. Chen, M. W. Wong, J. L. Andres, E. S. Replogle, R. Gomperts, R. L. Martin, D. J. Fox, J. S. Binkley, D. J. Defrees, J. Baker, J. P. Stewart, M. Head-Gordon, C. Gonzalez, J. A. Pople, Gaussian Inc., Pittsburgh, PA, **1995**.

[7] a) T. A. Keith, R. F. Bader, *Chem. Phys. Lett.* **1992**, *194*, 1–8; b) R. F. Bader, T. A. Keith, *J. Chem. Phys.* **1993**, *99*, 3683–3693.

[8] P. von R. Schleyer, C. Maerker, A. Dransfeld, H. Jiao, N. J. R. van Eikema Hommes, *J. Am. Chem. Soc.* **1996**, *118*, 6137–6138.

[9] P. von R. Schleyer, H. Jiao, *Pure Appl. Chem.* **1996**, *68*, 209–218.

[10] a) P. von R. Schleyer, P. K. Freeman, H. Jiao, B. Goldfuß, *Angew. Chem.* **1995**, *107*, 332–335; *Angew. Chem. Int. Ed. Engl.* **1995**, *34*, 337–340; b) H. Jiao, P. von R. Schleyer in *AIP Conference Proceedings 330, E.C.C.C. 1, Computational Chemistry* (Eds.: F. Bernardi, J.-L. Rivail), American Institut of Physics, Woodbury, NY, **1995**, pp. 107–131.

[11] a) V. I. Minkin, M. N. Głukhovtsev, B. Y. Simkin, *Aromaticity and Antiaromaticity*, Wiley, New York, **1994**; b) P. J. Garrat, *Aromaticity*, Wiley, New York, **1986**.

[12] For a discussion of homodesmic equations, see: P. George, M. Trachtman, C. W. Bock, A. M. Bret, *J. Chem. Soc. Perkin Trans. 2*, **1976**, 1222–1227; For a more restricted subclass of homodesmic reactions, see: B. A. Hess, Jr., L. J. Schaad, *J. Am. Chem. Soc.* **1983**, *105*, 7500–7505.

[13] H. J. Dauben, Jr., J. D. Wilson, J. L. Laity, *Nonbenzenoid Aromaticity, Vol. II* (Ed.: J. P. Snyder), Academic Press, New York, **1971**, pp. 167–206, and references therein.

[14] H. Jiao, N. J. R. van Eikema Hommes, P. von R. Schleyer, A. de Meijere, *J. Org. Chem.* **1996**, *61*, 2826–2828.

[15] F. Sondheimer, *Acc. Chem. Res.* **1972**, *5*, 81–91.

[16] J. B. Pedley, R. D. Naylor, S. P. Kirby, *Thermochemical Data of Organic Compounds*, 2nd ed., Chapman and Hall, London, **1986**.

[17] R. L. Disch, J. M. Schulman, *Chem. Phys. Lett.* **1988**, *152*, 402–404.

Efficient Recognition of Chiral Carbamoyl-α-Hydroxyacids with a Cleft-Type Receptor**

Mercedes Martín, César Raposo, Marta Almaraz, Mercedes Crego, Cruz Caballero, Manuel Grande, and Joaquín R. Morán*

Efficient recognition of small, chiral organic molecules is still a challenge for organic chemists.[1] Recognition of α-substituted chiral carboxylic acids is difficult because the chiral centers of the guest and those of the host are usually far apart. This drawback, already pointed out by Rebek, Jr., et al.,[2] can be overcome in receptor **1** by making use of a suitable xanthone spacer,[3] which provides functional groups for forming additional hydrogen bonds with an α-functionalized carboxylic acid as the guest (Scheme 1).

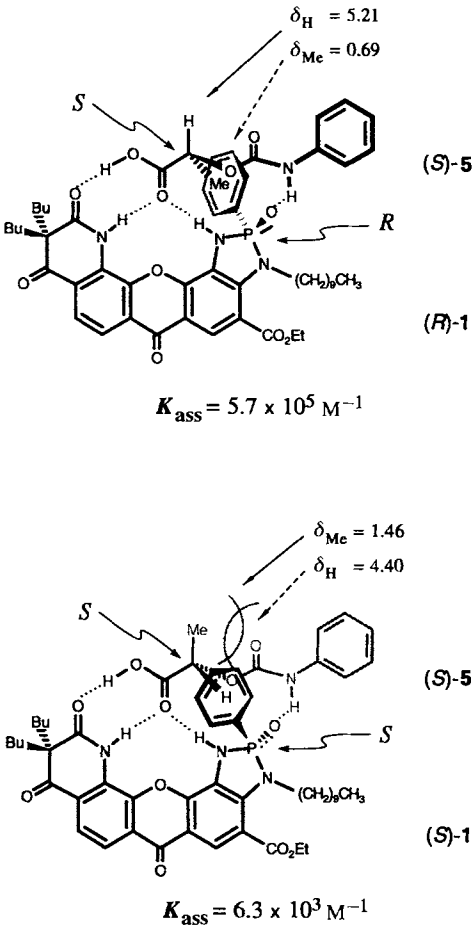

Scheme 1. Complexes formed by receptors (*R*)-**1** and (*S*)-**1** and the guest (*S*)-**5**.

Compound **1** was obtained as a racemic mixture from the known xanthone **2**[3] (Scheme 2). Carbamoyllactic acids should be good guests for this receptor (Scheme 1), and molecular models indicate that complexes of **1** and **5** should display chiral discrimination. When host and guest have different

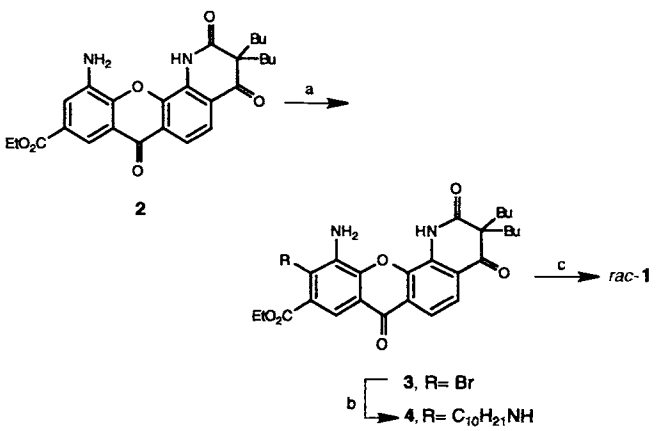

Scheme 2. Synthesis of *rac*-**1**. a) $Br_2/CHCl_3$, −20 °C (75%); b) $CH_3(CH_2)_9NH_2$, 170 °C (65%); c) $PhPOCl_2/PhBr$, 130 °C (90%).

[*] Prof. J. R. Morán, M. Martín, Dr. C. Raposo, M. Almaraz, Dr. M. Crego, Prof. C. Caballero, Prof. M. Grande
Departamento de Química Orgánica, Universidad de Salamanca
Plaza de la Merced 1–5, E-37008 Salamanca (Spain)
Fax: Int. code +(23)294574
e-mail: mgrande@gugu.usal.es

[**] We thank the Junta de Castilla y León for financial support (grant SA 73/94), Anna Lithgow for conducting the 400 MHz NMR titration experiments, and the MEC for a fellowship (C. R.).

configurations ((*R*,*S*) and (*S*,*R*) complexes), four linear hydrogen bonds can form without steric hindrance. In contrast, in the (*R*,*R*) and (*S*,*S*) complexes the methyl group of the lactic acid unit collides with the carbamate carbonyl group, thus weakening the fourth hydrogen bond between the carbamate NH group and the phosphoryl oxygen atom (Scheme 1, bottom).

Experimental data confirmed these predictions. When increasing amounts of (*S*)-**5** were added to a solution of *rac*-**1** in $CDCl_3$, ^1H NMR signals of receptor **1** were split as expected for the formation of two diastereomeric complexes.[4] Initial attempts to assess the relative stability of the two complexes by plotting the ^1H NMR shifts of the receptors against each other[5] indicated an association constant ratio greater than twenty. This result suggested that formation of the complex can be used to separate the enantiomers of the receptor.[6] Neither the host nor the guest are eluted separately by TLC on silica gel plates with CH_2Cl_2/Et_2O (99/1) as eluent. However, under these conditions using TLC plates impregnated with (*S*)-**5** (1% in Et_2O), the bright yellow enantiomeric receptors were easily separated (R_f((*R*)-**1**) = 0.8, R_f((*S*)-**1**) = 0.1). This large difference in R_f values can be explained because the complex is a closed structure in which all hydrogen bond donors are saturated, and it thus has a low affinity for silica gel. Host–guest association therefore offers a way in which the receptor can be eluted with solvents of low polarity. However, this mechanism is only very efficient in the case of the (*R*) host due to its large association constant with (*S*)-**5**; the less stable complex with the (*S*) host has only a slightly increased R_f.

Both preparative TLC and Pirkle-type column chromatography[7] on SiO_2 impregnated with (*S*)-**5** provide an easy way to isolate the complexes of the enantiomeric receptors **1**. Decomplexation was accomplished either by washing an ethereal solution of the complex with aqueous sodium carbonate, by conventional chromatography on SiO_2 with petroleum ether/EtOAc (1/1) as eluent, or by crystallization from methanol, in which the (*S*)-**5** remains in the solution. The receptors isolated are enantiomerically pure (m.p. 102–105 °C; (*R*)-**1**: $[\alpha]_D = -180$ ($c = 0.55$ in $CHCl_3$); (*S*)-**1**: $[\alpha]_D = +176$ ($c = 0.60$ in $CHCl_3$).

Owing to the presence of two independent aromatic chromophores in the receptor **1**, the absolute configurations could be confirmed by CD spectroscopy by applying the exciton chirality method.[8] The xanthone moiety (complex absorption bands at λ_{max} (ε) = 347 nm (ca. 10000; ^1L_b); 236, 252, 271 (ca. 21000, ^1L_a)) interacts with the phenylphosphonic group (absorption band at λ_{sh} = 235 nm) to give rise to bisignate bands with a split Cotton effect (Davidov splitting) around 280 and 240 nm (Fig. 1). The second is stronger because the absorption bands are more intense and closer to each other. In fact, the CD spectrum of the *dextro* host shows two bisignate bands at 296/265 nm ($\Delta\varepsilon = +13/-5$) and 246/228 nm ($\Delta E = +22/-20$; Fig. 1), which is in accord with a positive dihedral angle between the xanthone and the phenyl axis and corresponds to an (*S*) configuration at the chiral phosphorus atom (see insert in Fig. 1).

A strong anisotropic effect in the (*R*,*S*) complex also supports these assignments. The ^1H NMR signal of the methyl group in complexed (*S*)-**5** ($\delta = 0.69$) is shifted upfield by $\Delta\delta = 0.88$ relative to the analogous signal of the free guest ($\delta = 1.57$); this implies that the methyl group is fixed in the shielding cone of the phosphorus phenyl ring (Scheme 1). A similar shielding effect for the signal of the α-H of the lactic unit in the (*S*,*S*) complex ($\Delta\delta = 0.78$; shift from $\delta = 5.18$ to $\delta = 4.40$) suggests that the main difference in the geometry of the diastereomeric associates is the position of the hydrogen atom and the methyl group of the guest (Scheme 1).

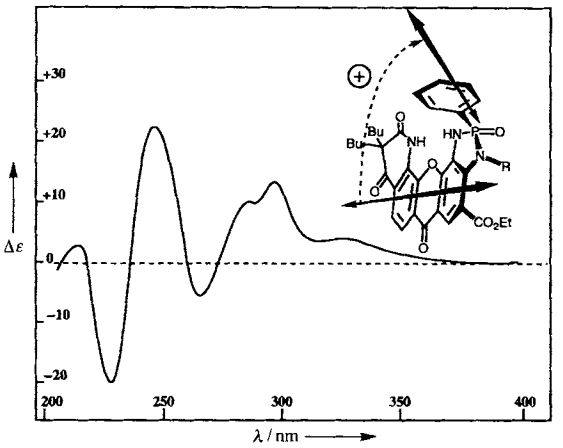

Fig. 1. CD spectrum of the receptor (*S*)-**1**.

Conventional NMR titration of these receptors with (*S*)-**5** is not an accurate method for quantifying the chiral discrimination. Only the association constant of the weak (*S*,*S*) complex ($K_{ass} = 6.3 \times 10^3\ M^{-1}$) lies in the range that can be measured with the NMR method,[9] whereas the strong (*R*,*S*) associate shows a value above $10^5\ M^{-1}$. Competitive titration, however, can be used to estimate this large association constant; a scale can be constructed (Table 1) which is similar to the reactivity scales developed by Huisgen.[10]

To apply this method, complexes with stabilities lying between those of the previously discussed diastereomeric associates are necessary. Competitive NMR titrations[11] were carried out with 10^{-2} M $CDCl_3$ solutions of both guests. Increasing amounts of a 5×10^{-2} M stock solution of optically pure host **1** were added until saturation was achieved. The proton shifts of the enantiomeric guests were plotted against each other, and the ratios of the association constants were calculated by making use of a Monte Carlo nonlinear curve-fitting method.

Guests **6**–**8** were tested (Table 1). The phenyl ring in (*S*)-carbamoylmandelic acid (*S*)-**6** slightly hinders complex formation

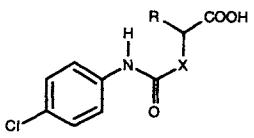

5, R = Me, X = O
6, R = Ph, X = O
7, R = Me, X = NH
8, R = Ph, X = NH

and a competitive titration provides an association constant that is 2.3 times less than that measured for (*S*)-**5**. However, this new complex is still too strong for a precise value to be obtained

Table 1. Association constants of the complexes between guests **5**–**8** and receptor **1** (in $CDCl_3$, 20 °C).

Host/guest complex [a]	K_{ass} [M^{-1}]	K_{ass} ratio
[(*R*)-**1**·(*S*)-**5**]	5.7×10^5 [b]	2.3
[(*R*)-**1**·(*S*)-**6**]	2.5×10^5 [b]	
[(*R*)-**1**·(*S*)-**7**]	6.4×10^4 [c, d]	3.9
[(*R*)-**1**·(*S*)-**8**]	5.8×10^4 [c, d]	
[(*R*)-**1**·(*R*)-**5**]	6.3×10^3 [d]	1.3 / 12 / 13 / 21
[(*R*)-**1**·(*R*)-**6**]	4.7×10^3 [d]	
[(*R*)-**1**·(*R*)-**7**]	3.1×10^3 [b]	

[a] Data for only one of the enantiomeric complexes is given. [b] From competition experiments. [c] Average from direct measurement and competition experiments. [d] Direct titration.

in direct NMR measurements. Steric interactions between the receptor phosphorus atom and the NH of amino acid derivatives lead to further reduction in complex stability. Urea derivatives of (*S*)-alanine and (*S*)-phenylglycine, (**7** and **8**, respectively), have association constants of $K_{ass} = 6.4 \times 10^4\ M^{-1}$ and $5.8 \times 10^4\ M^{-1}$, respectively. Due to its better association, the (*S*)-alanine derivative (*S*)-**7** was selected for competitive titration against (*S*)-**6** ($K_{ass}((S)\text{-}\mathbf{6})/K_{ass}((S)\text{-}\mathbf{7}) = 3.9$). The association constant of [(*R*)-**1**·(*R*)-**6**] could be readily measured by standard NMR titration ($K_{ass} = 4.7 \times 10^3\ M^{-1}$). Competitive titration between (*R*)-**6** and (*S*)-**7** afforded $K_{ass}((S)\text{-}\mathbf{7})/K_{ass}((R)\text{-}\mathbf{6}) = 13$, a ratio that, within the experimental error, confirms the previously measured value for the association constant of compound **7**.

From the above values the association constant for [(*R*)-**1**·(*S*)-**5**] was calculated to be $K_{ass} = 5.7 \times 10^5\ M^{-1}$ (Table 1). This indicates that the chiral recognition displayed by these complexes is the best in this series: $K_{ass}((R)\text{-}\mathbf{1})/K_{ass}((S)\text{-}\mathbf{1}) = 90$. With (*S*)-**6** this ratio is reduced to 53.

Received: May 2, 1996 [Z 9092 IE]
German version: Angew. Chem. 1996, *108*, 2512–2514

Keywords: enantiomeric resolution · hydroxyacids · molecular recognition · receptors

[1] a) J. Rebek, Jr., B. Askew, P. Ballester, A. Costero, *J. Am. Chem. Soc.* **1988**, *110*, 923; b) A. Galán, D. Andreu, A. M. Echavarren, P. Prados, J. de Mendoza, *ibid.* **1992**, *114*, 1511; c) A. Bochardt, W. C. Still, *ibid.* **1994**, *116*, 7467; d) V. Alcázar, F. Diederich, *Angew. Chem.* **1992**, *104*, 1503; *Angew. Chem. Int. Ed. Engl.* **1992**, *31*, 1521; e) K. Araki, K. Inada, S. Shinkai, *Angew. Chem.* **1996**, *108*, 92; *Angew. Chem. Int. Ed. Engl.* **1996**, *35*, 72; f) M. Crego, A. Partearroyo, C. Raposo, M. L. Mussons, J. L. López, V. Alcázar, J. R. Morán, *Tetrahedron Lett.* **1994**, *35*, 1435.

[2] B. C. Hamann, N. R. Branda, J. Rebek, Jr., *Tetrahedron Lett.* **1993**, *34*, 6837.

[3] M. Crego, C. Raposo, M. C. Caballero, E. García, J. G. Saez, J. R. Morán, *Tetrahedron Lett.* **1992**, *33*, 7437.

[4] V. Alcázar, L. Tomlinson, K. N. Houk, F. Diederich, *Tetrahedron Lett.* **1991**, *32*, 5309.

[5] K. A. Connors, *Binding Constants, The Measurement of Molecular Complex Stability*, Wiley, New York, **1987**.

[6] a) "Application of Biochemical Systems in Organic Chemistry": D. J. Cram in *Techniques of Chemistry Series, Vol. 10* (Eds.: J. B. Jones, C. S. Sih, D. Perlman.), Wiley, New York, **1976**, p. 815; b) H. Dugas, *Bioorganic Chemistry*, 2nd ed., Springer-Verlag, New York, **1989**; c) W. H. Pirkle, E. M. Doherty, *J. Am. Chem. Soc.* **1989**, *111*, 4113.

[7] W. H. Pirkle, J. Finn in *Asymmetric Synthesis, Vol. 1* (Ed.: J. D. Morrison), Academic Press, New York, **1985**, p. 87.

[8] K. Nakanishi, N. Berova, in *Circular Dichroism. Principles and Applications* (Eds.: K. Nakanishi, N. Berova, R. W. Woody) VCH, New York, **1994**, p. 361.

[9] C. S. Wilcox in *Frontiers in Supramolecular Organic Chemistry and Photochemistry* (Eds.: H.-J. Schneider, H. Durr), VCH, Weinheim, **1990**, p. 123.

[10] R. Huisgen, L. Xingya, *Tetrahedron Lett.* **1983**, *24*, 4185.

[11] The ratio of the association constants for the complexes formed in the competitive NMR titration was calculated according to Equation (a), where δ_f is the chemical shift of the free host, δ_c that of the complexed host, and δ that observed.

$$K_{ass,1}/K_{ass,2} = \frac{(\delta_1 - \delta_{f1})(\delta_{c2} - \delta_2)}{(\delta_2 - \delta_{f2})(\delta_{c1} - \delta_1)} \quad (a)$$

Enantioselective Synthesis of Vicinal Amino Alcohols by Oxa-Michael Addition of (−)-*N*-Formylnorephedrine to Nitroalkenes**

Dieter Enders,* Andreas Haertwig, Gerhard Raabe, and Jan Runsink

Enantiomerically pure 1,2-amino alcohols **A** are characteristic structural features of many natural products and drugs, and play an important role as chiral building blocks, auxiliaries, and ligands in transition metal catalyzed reactions.[1] They can be prepared from amino acids (for example, from the chiral pool), by resolution, or by asymmetric synthesis. Numerous diastereo- and enantioselective syntheses have been described that lead to vicinal amino alcohols for example by C–C[2] or C–N bond formation,[3] aminohydroxylation,[4] or indirectly by hydroboration of enamines.[5]

An alternative retrosynthetic analysis leads to a hydroxide synthon **B** and a β-amino cation synthon **C** by disconnection of the C–O bond. The oxa-Michael addition[6, 7] of a chiral synthetic hydroxide equivalent with a removable auxiliary, like (−)-(1*R*,2*S*)-*N*-formylnorephedrine ((*R*,*S*)-**2**), to (*E*)-nitroalkenes (**1**, as equivalents for **C**) should open a new enantioselective pathway to the title compounds **A**.

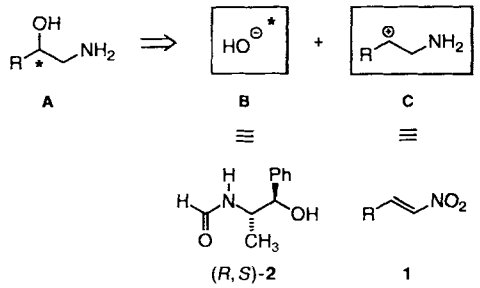

Interestingly, the oxa-analogous Michael addition was published in 1878 by F. Loydl in his work about the synthesis of malic acid from fumaric acid,[8] five years earlier than the discovery of the actual Michael reaction by Komnenos, Claisen, and Crismer. After further early work,[9] some groups tried later to find a diastereo- and enantioselective version of this reaction.[10] Some intermolecular oxa-Michael additions in which the chirality information is contained in the acceptor,[11] as well as several enzymatic variants[12] are already available. Diastereoselective intramolecular oxa-Michael addition is widely used in natural product synthesis.[13] To the best of our knowledge, the enantioselective intermolecular oxa-Michael addition with removable chirality information in the oxygen-containing nucleophile has not been reported. We have now succeeded in developing such an asymmetric oxa-Michael addition, by which vicinal amino alcohols are prepared with high asymmetric induction and in good yields by using an enantiomerically pure alcoholate.

[*] Prof. Dr. D. Enders, Dipl.-Chem. A. Haertwig, Dr. G. Raabe, Dr. J. Runsink
Institut für Organische Chemie der Technischen Hochschule
Professor-Pirlet-Strasse 1, D-52074 Aachen (Germany)
Fax: Int. code +(241)8888127
e-mail: enders@rwth-aachen.de

[**] This work was supported by the Deutsche Forschungsgemeinschaft (Leibniz Prize and Sonderforschungsbereich 380) and by the Fonds der Chemischen Industrie. We thank the companies Degussa AG, BASF AG, Bayer AG, and Hoechst AG for the donation of chemicals.

The alcoholate is obtained from (−)-(1*R*,2*S*)-*N*-formylnorephedrine ((*R*,*S*)-**2**)[14] by reaction with sodium hydride. It reacts highly diastereoselectively (*de*: 93 to ≥98%) at −78 °C with the (*E*)-nitroalkenes **1a–e** to give the nitro ethers **3a–e** in good yields (60–87%) (Table 1, Scheme 1). Virtually diastereomerically pure products (*de*: 96 to ≥98%) can be obtained for (*R*,*S*,*R*)-**3a–c** by using flash chromatography.

Table 1. Yields, diastereomeric excesses, and rotational values of the nitro ethers (*R*,*S*,*R*)-**3** obtained by asymmetric conjugated hydroxylation.

(*R*,*S*,*R*)-**3**	R	Yield [a] [%]	*de* [a, b] [%]	$[\alpha]_D^{24}$ (*c*, $CHCl_3$)
a	Me	60 (56)	94 (≥96)	−128.8 (1.1)
b	Et	75 (72)	93 (97)	−136.3 (1.1)
c	*i*Pr	87 (84)	96 (≥98)	−130.5 (1.0)
d	*t*Bu	67 [c]	≥98 [c]	−106.6 (1.5)
e	*c*Hex	85 [c]	94 [c]	−155.1 (1.1)

[a] Values in parentheses obtained after separation of the diastereomers by column chromatography (SiO_2, ether or ether/hexane 2/1 up to 1/1). [b] The *de* values are obtained by ^1H NMR spectroscopy (**3a**,**e** 300 MHz; **3b–d** 500 MHz). [c] After purification by column chromatography (SiO_2, ether/hexane 3:1), separation of the diastereomers **3e** was not possible.

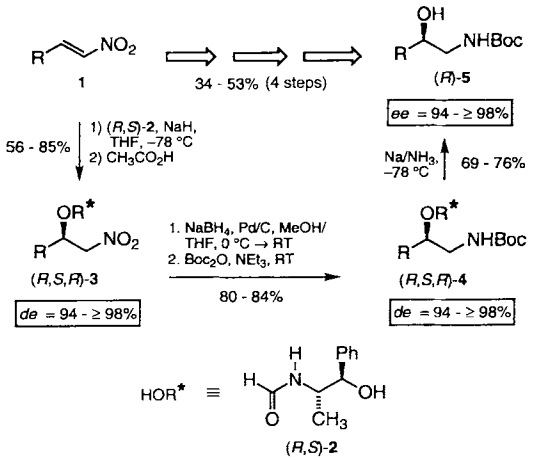

Scheme 1. Enantioselective synthesis of 1,2-amino alcohols **5**.

The preferred conformation in solution and hence the relative and absolute configuration of the newly formed stereogenic center can be determined by comparison of the ^1H NMR spectra of both diastereomers—NOE measurements, coupling constants, and ring current effects—to be (*R*) in the case of the major diastereomer and to be (*S*) for the minor diastereomer. These results were confirmed by the X-ray structure determination of (*R*,*S*,*R*)-**3b** (Fig. 1).[15]

The reduction of the nitro group to the amino function is carried out with sodium tetrahydridoborate and a Pd/C catalyst in methanol/THF (1:1); the hydroxylamine is the intermediate product.[18] The introduction of the Boc protecting group is carried out in the methanol-enriched solvent with di-*tert*-butyldicarbonate (Boc_2O) and triethylamine; the isolation of the free amine is unnecessary. The N-Boc-protected amino ethers **4a–e** are obtained after flash chromatography in good yields (80–84%).

The cleavage of the ethers with sodium in liquid ammonia at −78 °C leads to the protected amino alcohols **5a–e** without racemization and in good yields (69–75%).[19] The reaction must be stopped after 15 minutes to avoid loss of products by

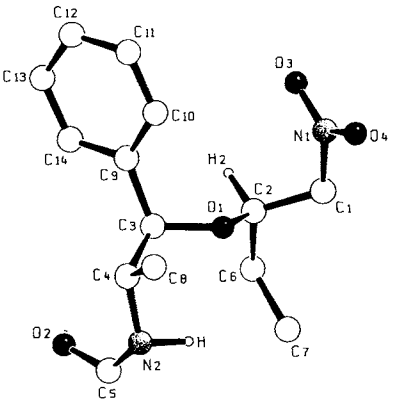

Fig. 1. Structure of the nitro ether (*R*,*S*,*R*)-**3b** in the crystal (Schakal plot) [17].

side reactions. The auxiliary is reduced to (*S*)-*N*-formylamphetamine during the ether cleavage and can be recovered. The overall yield of this procedure is 34–53% over four steps with high enantiomeric excesses (*ee*: 94 to ≥98%; Table 2).

Table 2. Yields, diastereomeric excesses, and rotational values of the *N*-Boc-protected amino alcohols **5**, and the yields of the *N*-Boc-protected amino ethers (*R*,*S*,*R*)-**4**.

(*R*)-**5**	R	Yield (**4**) [%]	Yield (**5**) [%]	*ee* [%]	$[\alpha]_D^{24}$ (*c*, $CHCl_3$)
a	Me	80	75	≥96 [a]	−23.2 (0.6)
b	Et	83	69	≥96 [a]	−16.2 (1.1)
c	*i*Pr	84	74	≥98 [b]	−19.4 (0.9)
d	*t*Bu	84	76	≥98 [b]	−28.8 (1.2)
e	*c*Hex	83	75	94 [c]	−19.4 (1.3)

[a] Determined by ^1H NMR spectroscopy with (−)-(*R*)-1-(9-anthryl)-2,2,2-trifluoroethanol as cosolvent. [b] Determined by GC analysis on a chiral stationary phase (heptakis(2,3,6-tri-*O*-methyl)-β-cyclodextrin/polysiloxane, 25 m × 0.25 mm) and by ^1H NMR spectroscopy with (−)-(*R*)-1-(9-anthryl)-2,2,2-trifluoroethanol as cosolvent. [c] Determined after conversion to the corresponding esters with MTPA (Mosher's reagent) by ^1H NMR spectroscopy [20].

In summary, the described asymmetric oxa-Michael addition under conjugate nucleophilic hydroxylation of (*E*)-nitroalkenes opens a new efficient entry to virtually enantiomerically pure vicinal amino alcohols. Since the chiral ephedra alkaloid norephedrine is readily available, it is possible to synthesize both enantiomers of vicinal amino alcohols and thus broadly applicable chiral building blocks.[21]

Experimental Procedure

(−)-(*R*,*S*,*R*)-**3a–e**: A solution of (−)-*N*-formylnorephedrine (215 mg, 1.2 mmol) in THF (15 mL) was added at room temperature to a suspension of sodium hydride (24 mg, 1 mmol) in THF (10 mL). This suspension was cooled to −78 °C and the (*E*)-nitroalkene **1a–e** (1 mmol) in THF (1 mL) was added (the reaction was monitored by TLC). The reaction was stopped after 24–96 h by quenching with glacial acetic acid and then allowed to warm up to room temperature. After aqueous work-up, extraction with ether (4 × 20 mL), washing with saturated $NaHCO_3$ (aq), and drying with Na_2SO_4, yellow, oily crude products were obtained that could be purified by flash chromatography (SiO_2, ether or ether/hexane 3/1 up to 1/1) to give colorless oils (*R*,*S*,*R*)-**3c**,**d** or solids (*R*,*S*,*R*)-**3a**,**b**,**e**.

(*R*,*S*,*R*)-**4a–e**: To a suspension of nitro ether **3** (1 mmol) and Pd/C (50 mg, 10%) in methanol/THF (1/1, 20 mL), $NaBH_4$ (151 mg, 4 mmol) was added at 0 °C. The reaction mixture was kept at this temperature for 2 h and then allowed to warm up to room temperature and stirred for 3 d. The Pd/C catalyst was removed by filtration over Celite and washed with methanol (30 mL). Boc_2O (218 mg, 1 mmol) and triethylamine (5 mL) were added to this solution (monitored by TLC). After 1–2 h, the solvent was removed and the residue was dissolved in CH_2Cl_2, washed with water and brine, and dried with Na_2SO_4. After removal of the solvent, the obtained

crude oils were purified by flash chromatography (SiO_2, ether/hexane 1/1 up to 1/3). (*R*)-**5a**–**e**: Sodium (58 mg, 2.5 mmol) was added to liquid ammonia (25 mL) at −78 °C. Then the *N*-Boc-protected amino ether **4a**–**e** (1 mmol) in THF (10 mL) was slowly added. After 15 min the reaction was stopped by addition of saturated NH_4Cl (aq) at −78 °C. After removal of the ammonia, the residue was dissolved in CH_2Cl_2 and dried with Na_2SO_4. The solvent was removed and the crude product purified by flash chromatography (SiO_2, ether/hexane 1/1 up to 2/1) affording the compounds **5** as colorless liquids (**5a**–**c**) or solids (**5d**,**e**). The (*S*)-*N*-formylamphetamine can also be isolated in yields of 70–75%.

Received: May 9, 1996
Revised version: July 8, 1996 [Z91081E]
German version: *Angew. Chem.* **1996**, *108*, 2540–2542

Keywords: amino alcohols · asymmetric syntheses · Michael additions · nitroalkenes · synthetic methods

[1] Reviews: a) R. Henning, *Nachr. Chem. Tech. Lab.* **1990**, *38*, 460-464; b) K. Tomioka, *Synthesis* **1990**, 541–549; c) R. Noyori, M. Kitamura, *Angew. Chem.* **1991**, *103*, 34–55; *Angew. Chem. Int. Ed. Engl.* **1991**, *30*, 49–69; d) Y. Ohfune, *Acc. Chem. Res.* **1992**, *25*, 360–366; e) A. Golebiowski, J. Jurczak, *Synlett* **1993**, 241–245; f) T. Kunieda, T. Ishizuka in *Studies in Natural Products Chemistry, Vol. 12* (Ed.: Atta-ur-Rahman), Elsevier, New York **1993**, pp. 411–444; g) D. J. Ager, I. Prakash, D. R. Schaad, *Chem. Rev.* **1996**, *96*, 835–875.

[2] a) H. Sasai, N. Itoh, T. Suzuki, M. Shibasaki, *Tetrahedron Lett.* **1993**, *34*, 855–858; b) H. Sasai, T. Suzuki, N. Itoh, S. Arai, M. Shibasaki, *ibid.* **1993**, *34*, 2657–2660; c) R. Chinchilla, C. Nájera, P. Sánchez-Agulló, *Tetrahedron: Asymmetry* **1994**, *5*, 1393–1402; d) N. Kise, N. Inakoshi, Y. Matsumura, *Tetrahedron Lett.* **1995**, *36*, 909–912; e) H. Sasai, T. Tokunaga, S. Watanabe, T. Suzuki, N. Itoh, M. Shibasaki, *J. Org. Chem.* **1995**, *60*, 7388–7389; f) R. E. Marti, J. Heinzer, D. Seebach, *Liebigs Ann.* **1995**, 1193–1215; g) D. Enders, U. Reinhold, *ibid.* **1996**, 11–26; h) *Angew. Chem.* **1995**, *107*, 1332–1334; *Angew. Chem. Int. Ed. Engl.* **1995**, *34*, 1219–1222; i) T. Wirth, *ibid* **1996**, *108*, 65–67 and **1996**, *35*, 61–63 and references therein.

[3] a) J. M. Klunder, S. Y. Ko, K. B. Sharpless, *J. Org. Chem.* **1986**, *51*, 3710–3712; b) M. Brunner, L. Mussmann, D. Vogt, *Synlett* **1993**, 893–894; c) C. E. Harris, G. B. Fischer, D. Beardsley, L. Lee, C. T. Goralski, L. W. Nicholson, B. Singaram, *J. Org. Chem.* **1994**, *59*, 7746–7751; d) H.-T. Chang, K. B. Sharpless, *Tetrahedron Lett.* **1996**, *37*, 3219–3222, e) J. L. Leighton, E. N. Jacobsen, *J. Org. Chem.* **1996**, *61*, 389–390. f) C. H. Senanayake, R. D. Larsen, L. M. DiMichele, J. Liu, P. H. Toma, R. G. Ball, T. R. Verhoeven, P. J. Reider, *Tetrahedron: Asymmetry* **1996**, *7*, 1501–1506.

[4] G. Li, H.-T. Chang, K. B. Sharpless, *Angew. Chem.* **1996**, *108*, 449-452; *Angew. Chem. Int. Ed. Engl.* **1996**, *35*, 451–454.

[5] a) C. T. Goralski, D. L. Hasha, L. W. Nicholson, D. Zakett, G. B. Fischer, B. Singaram, *Tetrahedron Lett.* **1994**, *35*, 3251–3254; b) G. B. Fischer, C. T. Goralski, L. W. Nicholson, D. L. Hasha, D. Zakett, B. Singaram, *J. Org. Chem.* **1995**, *60*, 2026–2034.

[6] Overview of oxa-Michael addition to nitroalkenes: V. V. Perealkin, E. S. Lipina, V. M. Berestovitskaya, D. A. Efremov, *Nitroalkenes*, Wiley, Chichester, **1994**, pp. 67–73 and references therein.

[7] a) J. R. Hwu, N. Wang, *J. Chem. Soc. Chem. Commun.* **1987**, 427–428; b) J. M. Aizpurua, M. Oiarbide, C. Palomo, *Tetrahedron Lett.* **1987**, *28*, 5361–5364; c) A. Kamimura, N. Ono, *ibid.* **1989**, *30*, 731–734; d) A. Kamimura, H. Sasatani, T. Hashimoto, T. Kawai, K. Hori, N. Ono, *J Org. Chem.* **1990**, *55*, 2437–2442; e) A. G. M. Barrett, S. A. Lebold, *ibid.* **1990**, *55*, 3853–3857; f) K. Hori, S. Higuchi, A. Kamimura, *ibid.* **1990**, *55*, 5900–5905; g) A. G. M. Barrett, P. D. Weipert, D. Dhanak, R. K. Husa, S. A. Lebold, *J. Am. Chem. Soc.* **1991**, *113*, 9820–9824; h) A. G. M. Barrett, *Chem. Soc. Rev.* **1991**, *20*, 95–127; i) J. L. Duffy, J. A. Kurth, M. J. Kurth, *Tetrahedron Lett.* **1993**, *34*, 1259–1260; j) N. Garg, N. Hossain, J. Chattopadhyaya, *Tetrahedron* **1994**, *50*, 5273–5278; k) A. G. M. Barrett, D. J. Rys, *J. Chem. Soc. Perkin Trans. 1* **1995**, 1009–1017.

[8] F. Loydl, *Justus Liebigs Ann. C* **1878**, *192*, 80–89.

[9] a) T. Purdie, *Ber. Dtsch. Chem. Ges.* **1881**, *14*, 2238; b) L. Claisen, L. Crismer, *Justus Liebigs Ann. C* **1883**, *218*, 129–144; c) C. Liebermann, *Ber. Dtsch. Chem. Ges.* **1893**, *26*, 1876–1879; d) C. F. Koelsch, *J. Am. Chem. Soc.* **1943**, *65*, 437–439.

[10] Overview of oxa-Michael addition: A. Berkessel, *Methods of Organic Chemistry (Houben-Weyl) 4th ed. 1952-, Vol. E21e* **1995**, pp. 4818–4856 and references therein.

[11] a) S. Thaisrivongs, D. Seebach, *J. Am. Chem. Soc.* **1983**, *105*, 7407–7413; b) J. Mulzer, M. Kappert, G. Huttner, I. Jibril, *Angew. Chem.* **1984**, *96*, 726–727; *Angew. Chem. Int. Ed. Engl.* **1984**, *23*, 704–705; c) A. Bernardi, S. Cardani, C. Scolastico, R. Villa, *Tetrahedron* **1990**, *46*, 1987–1998; d) S. Cardani, C. Scolastico, R. Villa, *ibid.* **1990**, *46*, 7283–7288; e) A. Dondoni, A. Marra, P. Merino, *J. Am. Chem. Soc.* **1994**, *116*, 3324–3336; f) T. Hosokawa, T. Yamanaka, M. Itotani, S.-I. Murahashi, *J. Org. Chem.* **1995**, *60*, 6159–6167.

[12] a) T. Kitazume, T. Ikeya, K. Murata, *J. Chem. Soc., Chem. Commun.* **1986**, 1331–1333; b) M. A. Findeis, G. M. Whitesides, *J. Org. Chem.* **1987**, *52*, 2838–2848.

[13] a) S. S. Ko, L. L. Klein, K.-P. Pfaff, Y. Kishi, *Tetrahedron Lett.* **1982**, *23*, 4415–4418; b) C. Iwata, K. Hattori, S. Uchida, T. Imanishi, *ibid.* **1984**, *25*, 2995–2998; c) B. D. Roth, W. H. Roark, *ibid.* **1988**, 29, 1255–1258; d) K. C. Nicolaou, C.-K. Hwang, M. E. Duggan, *J. Am. Chem. Soc.* **1989**, *111*, 6682–6690; e) V. S. Martin, M. T. Nuñez, M. A. Ramirez, M. A. Soler, *Tetrahedron Lett.* **1990**, *31*, 763–766; f) T. Mandai, M. Ueda, K. Kashiwagi, M. Kawada, J. Tsuji, *ibid.* **1993**, *34*, 111–114; g) J. M. Palazón, M. A. Soler, M. A. Ramirez, V. S. Martin, *ibid.* **1993**, *34*, 5467–5470; h) M. A. Soler, J. M. Palazón, V. S. Martin, *ibid.* **1993**, *34*, 5471–5474; i) D. A. Evans, J. A. Gauchet-Prunet, *J. Org. Chem.* **1993**, *58*, 2446–2453; j) S. D. Burke, K. W. Jung, J. R. Phillips, R. E. Perri, *Tetrahedron Lett.* **1994**, *35*, 703–706.

[14] The spectroscopic data of the auxiliary are identical with those found in the literature: a) I. A. Al-Meshal, M. Nasir, F. S. El-Feraly, *Phytochemistry* **1986**, *25*, 2241–2242; b) B. D. Berrang, A. H. Lewin, F. I. Carroll, *J. Org. Chem.* **1982**, *47*, 2643–2647; c) R. Vilvala, T. Haapanen, *Acta Pharm. Fenn.* **1980**, *89*, 253–257.

[15] Suitable crystals were obtained from ether/hexane mixtures at room temperature: monoclinic, space group $P2_1$ (no. 4), $a = 7.392(1)$, $b = 8.984(6)$, $c = 12.202(1)$ Å, $\beta = 106.728(6)°$; $V = 776.04$ Å^3, $Z = 2$, $M_{calc.} = 280.33$, $\rho = 1.200$ g cm^{-3}. Total number of electrons per unit cell is 300. The data were collected on an Enraf-Nonius CAD4-diffractometer, $Mo_{K\alpha}$ radiation (graphite-monochromator, $\lambda = 0.71069$ Å). The structure was solved by direct methods (GENSIN, GENTAN from XTAL3.2 [16]). The positions of the hydrogen atoms were calculated in ideal positions. 1576 observed reflections [$I > 2\sigma(I)$], 181 parameters refined, $R = 0.053$ ($Rw = 0.034$). Maximum residual electron density ± 0.3 e Å^{-3}. The configuration of C2 was obtained by using the known configuration of C3 and C4. Crystallographic data (excluding structure factors) for the structure(s) reported in this paper have been deposited with the Cambridge Crystallographic Data Centre as supplementary publication no. CCDC-179-91. Copies of the data can be obtained free of charge on application to The Director, CCDC, 12 Union Road, Cambridge CB2 1EZ, UK (fax: Int. code +(1223) 336-033; e-mail: teched@chemcrys.cam.ac.uk).

[16] S. R. Hall, H. D. Flack, J. M. Stewart *XTAL3.2 Reference Manual*, Universities of Western Australia, Geneva, and Maryland, Lamb, Perth **1992**.

[17] E. Keller, *Chem. Unserer Zeit* **1986**, *20*, 178–181.

[18] a) M. Petrini, R. Ballini, G. Rosini, *Synthesis* **1987**, 713–714; b) A. S. Kende, J. S. Mendoza, *Tetrahedron Lett.* **1991**, *32*, 1699–1702.

[19] L. F. Tietze, A. Dölle, K. Schiemann, *Angew. Chem.* **1992**, *104*, 1366–1367; *Angew. Chem. Int. Ed. Engl.* **1992**, *31*, 1372–1373.

[20] a) J. A. Dale, D. L. Dull, H. S. Mosher, *J. Org. Chem.* **1969**, *34*, 2543–2549; b) J. A. Dale, H. S. Mosher, *J. Am. Chem. Soc.* **1973**, *95*, 512–519.

[21] All new compounds gave appropriate spectroscopic data (IR, NMR, MS) and correct elemental analyses.

Thiolate Bridged Nickel–Iron Complexes Containing both Iron(0) and Iron(II) Carbonyls**

Chia-Huei Lai, Joseph H. Reibenspies, and Marcetta Y. Darensbourg*

The impressive synergism developed in the last decade between synthetic inorganic and biophysical chemists with regard to understanding the function and spectroscopic signature of nickel in [NiFe] hydrogenase has gained even more momentum by the report of a protein X-ray crystal structure in 1995.[1] Crystals isolated from *Desulfovibrio gigas* in a mixture of inactive (oxidized) and ready enzymatic states were investigated. The electron density around nickel was interpreted as a two-cysteine-bridged Ni–Fe bimetallic active site, which has a Ni–Fe distance of 2.7 Å and is removed by more than 6 Å from the closest Fe_4S_4 cluster in the electron

[*] Prof. Dr. M. Y. Darensbourg, C.-H. Lai, Dr. J. H. Reibenspies
Department of Chemistry, Texas A&M University
College Station, TX 77843-3255 (USA)
Fax: Int. code +(409) 845-0158
e-mail: marcetta@chemvx.tamu.edu

[**] Financial support from the National Science Foundation for this work (CHE 94-15901) and the X-ray diffractometer and crystallographic computing system CHE-8513273, as well as contributions from the R. A. Welch Foundation are gratefully acknowledged. We thank Professor Paul Lindahl for discussion and Jason Smee (TAMU) for his help with CACHe molecular modeling programs.

transport chain.[1] Two other cysteine sulfur atoms about nickel complete the pseudo-square-pyramidal coordination in which the basal position is partially occupied by an undetermined ligand forming a bridge to the iron. Additional intrigue arises from the remaining groups about the octahedral iron in the bimetallic site; they are not protein donors but rather exogenous ligands. These terminal ligands on iron were modeled as water in the initial resolution of the structure, but were later suggested to refine better as diatomics.[2, 3] In view of the results of other physical techniques whose interpretation does not require the presence of such a unique iron,[4, 5] the possibility that FeL_3 arises as an artifact introduced during the isolation or crystallization of the protein cannot be overlooked. On the other hand, the potential of diatomic ligands existing in the active site of the [NiFe] hydrogenase from *Chromatium vinosum* was demonstrated by infrared spectroscopic results from Woodruff et al. in 1994.[3]

While the controversy regarding this unexpected NiFe active site mandates additional structure determination of the enzyme isolated in pure states, increasing evidence suggests that bimetallic and heterobimetallic active sites in enzymes are *not* uncommon.[6] Hence, small molecule analogs are desired as evidence of what is *chemically possible*, either in nature's design or as artifacts, and as well-characterized prototypes for spectroscopic signatures.[7] In fact, there are few bimetallic NiFe complexes reported in the literature and, to our knowledge, no carbonyl derivatives.[8, 9] Herein we report results of the synthesis of such a target molecule in which both a reduced and an oxidized form of a NiFeCO complex were discovered. Since the role of redox chemistry in [NiFe] hydrogenase activity is pivotal, these complexes were deemed worthy of detailed examination.

The S-metalation of the N,N,S,S.-coordinated nickel (II) complex **1**[10] [see Eq. (a)] has produced a number of polynuclear complexes, which have been used to demonstrate the effect of S-charge neutralization on the accessibility of the Ni^{II}/Ni^{I} couple within the NiN_2S_2 coordination sphere.[11] The structure of the dimeric $[\{(\mathbf{1})FeCl_2\}_2]$ complex (Fig. 1)[8] shows a resemblance to the purported NiFe active site,[1] although the Ni–Fe distance of 3.1 Å is 0.4 Å longer than that in the [NiFe] hydrogenase structure. Furthermore, $[\{(\mathbf{1})FeCl_2\}_2]$ lacks a third ligand present in partial occupancy in the $[NiFe]H_2$-ase structure as a Ni–Fe bridge.[1] Since attempts to replace the chloride ligands with CO or thiolates were unsuccessful, the direct route to NiFe carbonyls shown below was developed.

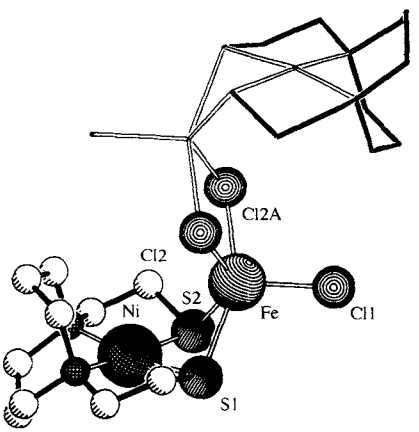

Fig. 1. PLUTON representation [21] of $[(\mathbf{1})FeCl_2]$ in the crystal [8]. Cl2 and Cl2A are bridging atoms to a second Ni–Fe unit.

On stirring a 2:1 mixture of **1** and $[Fe_2(CO)_9]$ in CH_3CN overnight at 22 °C, a moderately air-sensitive, red-brown solid precipitated [Eq. (a)]. After extraction with THF and concentration in vacuo, a crystalline compound analyzed[12] as $[(\mathbf{1})Fe(CO)_4]$ (**2**) was obtained in 70% yield by hexane diffusion into the THF solution. The $\tilde{\nu}_{CO}$ IR bands in the solution spectrum of **2**[13] are indicative of pseudo-C_{3v} symmetry about Fe [$2A_1 + E$ (split)], perturbed due to an asymmetric ligand in the axial position.[14a] Comparison with IR data of several $[LFe(CO)_4]$ complexes shows that the ligand in **1** is a σ-donor, similar to an anionic thiolate; lower $\tilde{\nu}_{CO}$ values than for ligation with thioethers or PPh_3 are observed.[13–15] This conclusion is supported by the observed CO lability of **2** which is similar to that of $[PhSFe(CO)_4]^-$.[14] For example, when THF solutions of **2** were exposed to ^{13}CO, changes in the IR spectra suggest a 50% incorporation of the labeled ligand within a few hours. The complicated spectrum indicative of multiple CO substitution reverted to the parent spectrum on removal of the ^{13}CO and replacement with a ^{12}CO atmosphere. In contrast to the CO lability, the metallothiolate ligand **1** is very slowly displaced ($t_{1/2}$ of days) from **2** by excess PPh_3 or CO at 22 °C.

The reaction of **2** and the single electron oxidant $NO(BF_4)$ in THF solution immediately led to a precipitate from which two compounds have been recovered and identified [Eq. (b)]. The red-black crystalline $[(\mathbf{1})_2Ni]^{2+}$ (10% yield of isolated product) is the result of thiolate sulfur oxidation to disulfide with loss of Ni^{2+} from one molecule of **1**. Free Ni^{2+} is known to nucleate two units of **1** rapidly and quantitatively.[16] The moderately air-sensitive, red-brown crystalline $[(\mathbf{1})_2Fe(CO)_2](BF_4)_2$ (**3**) arises from a two-electron oxidation at Fe^0 (yields ranged from 5% to 14%). These products were separated by fractional crystallization through diffusion of ether into CH_3CN solutions. Elemental analysis and $\tilde{\nu}_{CO}$ IR data[17] are consistent with the X-ray crystal structure of **3** (vide infra). In the presence of cobaltocene as reducing agent, carbon monoxide reacts with $[(\mathbf{1})_2Fe(CO)_2]^{2+}$ to re-form the Fe^0 complex **2** (eq. b); no reaction with CO occurs in the absence of a reductant.

The molecular structures of **2** and $[(\mathbf{1})_2Fe(CO)_2]^{2+}$ are shown in Figures 2 and 3, respectively.[18–21] The $Fe(CO)_4$ fragment of **2** is an almost regular trigonal bipyramid; square-planar **1** serves as a monodentate axial ligand. The $[(\mathbf{1})_2Fe(CO)_2]^{2+}$ complex is pseudo-octahedral with *cis* carbonyls and bidentate **1** thiolate ligands. The average Fe–S distance in $[(\mathbf{1})_2Fe(CO)_2]^{2+}$ is virtually the same as that of **2** and almost identical for that of $[PhSFe(CO)_4]^-$ (2.332(5) Å).[15] Consistent with earlier findings that Ni–S distances in **1** are fairly invariant with S-site modifications,[11] the two Ni–S distances of **2** are within the error limits indistinguishable from each other, from those of $[(\mathbf{1})_2Fe(CO)_2]^{2+}$, and from those of free **1** (2.16 Å).[10]

The most striking geometric variations in the structures of Ni–Fe heterometallics lie in the Ni···Fe distances. When compounds such as **1** and the similar Ni(dmpn)[22] (dmpn = *N,N'*-dimethyl-*N,N'*-bis(2-mercaptoethyl)-1,3-propanediamine) serv-

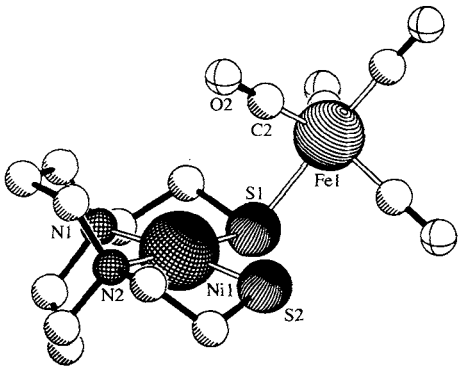

Fig. 2. Structure of **2** in the crystal. Selected distances [Å] and angles[°]: Ni···Fe 3.76(1), Ni-S1 2.172(4), Ni-S2 2.162(4), Ni-N1 1.996(1), Ni-N2 1.971(8), Fe-S1 2.332(4), Fe···S2 3.96(1), Fe-C1 1.77(2), Fe-C2 1.782(13), Fe-C3 1.754(13), Fe-C4 1.75(2), Fe-S1-Ni 113.37(14), S1-Fe-C4 175.4(4), S1-Fe-C2 89.3(4), S1-Ni-S2 90.3(2), S2-Ni-N(2) 90.8(3), N1-Ni-N2 89.7(4).

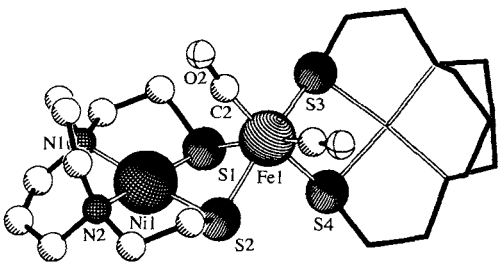

Fig. 3. Structure of the $[(1)_2Fe(CO)_2]^{2+}$ ion in the crystal. Selected distances [Å] and angles[°]: Ni1···Fe 3.088, Ni2···Fe 3.103, Ni1-S1 2.159(2), Ni1-S2 2.149(2), Ni1-N1 1.957(6), Ni1-N2 1.953(6), Fe-S1 2.345(2), Fe-S2 2.302(2), Fe-C1 1.769(8), Fe-C2 1.785(9), Fe-S1-Ni1 86.99(7), Fe-S2-Ni1 88.33(8), Fe-S3-Ni2 87.65(7), Fe-S4-Ni2 86.32(7), S1-Fe-S2 76.99(7), S2-Fe-C2 100.4(3), C1-Fe-C2 91.2(4), S1-Ni1-S2 84.39(7), S2-Ni1-N2 92.7(2), N1-Ni1-N2 89.5(2).

ing as *cis*-dithiolate, *bidentate* ligands to iron(II), this value lies in the range of 3.0–3.1 Å for the three known Ni–Fe^{II} compounds. For *monodentate* coordination of these same metallothiolates, Ni···Fe distances may vary substantially because of twisting of the planar NiS_2 unit away from the Fe center. In the case of **2** the large nonbonding Fe···S(2) distance of 3.961(4) Å correlates to a Ni–Fe distance of 3.76(1) Å and a Ni-S-Fe angle of 113°. For monodentate binding of the Ni(dmpn) ligand to Fe^{II} in $[\{(dmpn)Ni\}_3Fe^{II}]$, the analogous Ni···S (nonbonding) distance is 3.197(8) Å with a Ni–Fe distance of 3.269(4) Å and a Ni-S-Fe angle of 76.4°.[22]

While **1** is not ideal as a structural mimic of the three-dimensional nickel center in the Volbeda et al. crystal structure of [NiFe] hydrogenase,[1] the synthesis and structural results above are excellent examples of the facility with which **1** can capture iron carbonyl moieties and form robust heterometallic complexes. The isolated oxidation products of the reduced complex **2** indicate either sulfur- or iron-based but not nickel-based chemistry. Structural variations resulting from redox changes at iron do not affect the Ni–S distances, but rather incur dramatic changes in Ni-S-Fe angles and resultant Ni–Fe distances. These results are of importance for detailed X-ray absorption spectroscopic studies of *Thiocapsa roseopersicina*, which showed no change in NiK-edge spectra as the [NiFe] hydrogenase was taken through five oxidation levels. It was concluded that "No evidence to support a redox role for Ni in hydrogenase is found in the XAS data."[23] Although this conclusion is not universally accepted,[4, 5] it is supported by the "outer sphere" or non-Ni-based redox activity seen for the NiFe model complexes described above. Finally, it is within the realm of possibility that an Fe–CO moiety is present within metalloproteins that are related to CO_2 reduction chemistry in methanogenic bacteria, and demonstrations of biological Fe–CO binding are plentiful.[24, 25] Rather than completing a story or "raising more questions than it answers",[7] the Volbeda et al. crystal structure of [NiFe] hydrogenase[1] provides a focus and impetus for synthesizing interesting heterometallic complexes as structural and catalytic models.

Experimental Procedure

General procedures: Syntheses and isolation of the products was carried out under argon using standard Schlenk or glovebox techniques. Reagent grade solvents were purified according to published procedures and distilled under N_2.[11b] $[Fe_2(CO)_9]$ was purchased from Strem Chem. Co. and used as received. Infrared spectra were measured in solution cells (0.1 mm, NaCl) on an IBM IR/32 or a Mattson Galaxy 6021 instrument. Elemental analyses were carried out by Galbraith Laboratories, Knoxville, TN.

Received: April 24, 1996 [Z 9066 1E]
German version: *Angew. Chemie.* **1996**, *108*, 2551–2554

Keywords: hydrogenases · iron compounds · nickel compounds · sulfur compounds

[1] A. Volbeda, M.-H. Charon, C. Piras, E. C. Hatchikian, M. Frey, J. C. Fontecilla-Camps, *Nature* **1995**, *373*, 580–587.
[2] A. Volbeda, M.-H. Charon, C. Piras, E. C. Hatchikian, M. Frey, J. C. Fontecilla-Camps, *J. Inorg. Biochem.* **1995**, *59*, 637.
[3] A. K. Bagley, C. J. Van Garderen, M. Chen, E. C. Duin, S. P. J. Albracht, W. H. Woodruff, *Biochemistry* **1994**, *33*, 9229–9236.
[4] a) J. J. G. Moura, M. Teixeira, I. Moura, J. LeGall in *The Bioinorganic Chemistry of Nickel* (Ed.: J. R. Lancaster), VCH, New York, **1988**, Chapter 9, and references therein; b) M. A. Halcrow, G. Christou, *Chem. Rev.* **1994**, *94*, 2421–2481, and references therein; c) R. Cammack, D. S. Patil, E. C. Hatchikian, V. M. Fernández, *Biochimica et Biophysica Acta* **1987**, *912*, 98–109; d) V. M. Fernandez, E. C. Hatchikian, D. S. Patil, R. Cammack, *ibid.* **1986**, *883*, 145–154; e) B. H. Huynh, D. S. Patil, I. Moura, M. Teixeira, J. J. G. Moura, D. V. DerVartanian, M. H. Czechowski, B. C. Prickril, H. D. Peck, J. LeGall, *J. Biol. Chem.* **1987**, *262*, 795–800; f) M. Teixeira, I. Moura, A. V. Xavier, J. J. G. Moura, J. LeGall, D. V. DerVartanian, H. D. Peck, B.-H. Huynh, *ibid.* **1989**, *264*, 16435–16450.
[5] C. Bagyinka, J. P. Whitehead, M. J. Maroney, *J. Am. Chem. Soc.* **1993**, *115*, 3576–3585.
[6] a) S. Wang, M. H. Lee, R. P. Hausinger, P. A. Clark, D. E. Wilcox, R. A. Scott, *Inorg. Chem.* **1994**, *33*, 1589–1593; b) J. G. Dewitt, A. C. Rosenzweig, A. Salifoglou, B. Hedman, S. J. Lippard, K. O. Hodgson, *ibid.* **1995**, *34*, 2505–2515.
[7] M. A. Halcrow, *Angew. Chem.* **1995**, *107*, 1307–1310; *Angew. Chem. Int. Ed. Engl.* **1995**, *34*, 1193-1195.
[8] D. K. Mills, Y. M. Hsiao, P. J. Farmer, E. V. Atnip, J. H. Reibenspies, M. Y. Darensbourg, *J. Am. Chem. Soc.* **1991**, *113*, 1421–1423.
[9] G. J. Colpas, R. O. Day, M. J. Maroney, *Inorg. Chem.* **1992**, *31*, 5053–5055.
[10] D. K. Mills, J. H. Reibenspies, M. Y. Darensbourg, *Inorg. Chem.* **1990**, *29*, 4364–4366.
[11] a) P. J. Farmer, J. H. Reibenspies, P. A. Lindahl, M. Y. Darensbourg, *J. Am. Chem. Soc.* **1993**, *115*, 4665–4674; b) G. Musie, P. J. Farmer, T Tuntulani, J. H. Reibenspies, M. Y. Darensbourg, *Inorg. Chem.* **1996**, *35*, 2176–2183.
[12] Y.-M. Hsiao, *An Organometallic Approach to the Synthesis of Active Site Models for Nickel-Based Catalysts*, Ph.D. Dissertation, Texas A&M University, **1993**, p.125; elemental analysis for $C_{14}H_{20}O_4N_2S_2NiFe$ [calcd (found)]: C, 36.64 (36.24); H, 4.39 (4.04); N, 6.10 (6.12). UV/Vis (MeOH) solution at λ_{max} (ε, $cm^{-1}M^{-1}$) = 334 (7366), 534 (988) nm.
[13] IR of $[LFe(CO)_4]$ in solution, L = 1 (THF): $\tilde{\nu}_{CO}$ = 2030 (s), 1945(m), 1926(vs), 1907(vs) cm^{-1}; L = PPh_3 (hexane): 2052 (m), 1980 (m), 1947 (vs) cm^{-1} [14a]; L = MeSPh (hexane): 2057 (m), 1979 (s), 1956 (vs), 1946 (vs) cm^{-1} [15]; L = SPh^- (acetone): 2016 (m), 1910 (vs) cm^{-1} [15].
[14] a) D. J. Darensbourg, H. H. Nelson, C. L. Hyde, *Inorg. Chem.* **1974**, *13*, 2135–2145; b) D. J. Darensbourg, *Inorganica Chimica Acta* **1970**, *4*, 597–601.
[15] W.-F. Liaw, C. Kim, M. Y. Darensbourg, A. L. Rheingold, *J. Am. Chem. Soc.* **1989**, *111*, 3591–3597.
[16] P. J. Farmer, T. Solouki, D. K. Mills, T. Soma, D. H. Russell, J. H. Reibenspies, M. Y. Darensbourg, *J. Am. Chem. Soc.* **1992**, *114*, 4601–4605.
[17] Elemental analysis for $C_{24}H_{43}O_2N_3S_4B_2F_8Ni_2Fe$ [calcd (found)]: C, 31.72 (31.55); H, 4.77 (5.01); N, 7.71 (7.64). IR (CH_3CN): $\tilde{\nu}_{CO}$ = 2023 (vs), 1975(vs) cm^{-1}; UV/Vis (CH_3CN) λ_{max} (ε, $cm^{-1}M^{-1}$) = 352 (4022) and 466 (2232) nm.

 © VCH Verlagsgesellschaft mbH, D-69451 Weinheim, 1996 0570-0833/96/3520-2392 $ 15.00+.25/0

[18] X-ray diffraction data were collected at 23 °C on a Siemens R3m/V diffractometer with $Mo_{K\alpha}$ ($\lambda = 0.710731$ Å). Structures were solved by Direct Methods (SHELXS, SHELXTL-PLUS, Sheldrick, 1990 [19]); semi-empirical absorption corrections were applied. For [(1)Fe(CO)$_4$], site occupations of atoms C(5) and C(6) were refined to 56%; for C(5′) and C(6′), to 44% site occupation. A full report is given in Supplementary Information. [(1)Fe(CO)$_4$]: $a = 10.260(7)$, $b = 12.274(7)$, $c = 14.623(9)$ Å; orthorhombic, space group $P2_12_12_1$ (no. 19), $Z = 4$, $5.2° \leq 2\theta \leq 50.2°$, 3247 unique observed reflections, $R(F) = 0.07$, $wR(F^2) = 0.1857$. [(1)$_2$Fe(CO)$_2$](BF$_4$)$_2$: $a = 14.976(3)$, $b = 19.132(4)$, $c = 25.508(5)$ Å; $\beta = 94.63(3)°$, monoclinic, space group $C2/c$, $Z = 8$, $7° \leq 2\theta \leq 120°$, 5444 unique observed reflections, $R(F) = 0.061$ $wR(F^2) = 0.1601$. SHELXL-93, Sheldrick 1993 [20]. Crystallographic data (excluding structure factors) for the structures reported in this paper have been deposited with the Cambridge Crystallographic Data Centre as supplementrary publication no. CCDC-179-86. Copies of the data can be obtained free of charge on application to the Director, CCDC, 12 Union Road, Cambridge CB21EZ, UK (fax: Int. code +(1223) 336-033; e-mail: teched@chemcrys.cam.ac.uk).

[19] G. Sheldrick, SHELXS-86 Program for Crystal Structure Solution, Gottingen (Germany), **1986**.

[20] G. Sheldrick, SHELXL-93 Program for Crystal Structure Refinement, Gottingen (Germany), **1993**.

[21] A. L. Spek, PLUTON. Program for Molecular and Crystal Graphics. Vakgroep Algemene Chemie, University of Utrecht, Afdeling Kristal-En Structuurchemie, Padualaan 8, 3584 Ch Utrecht (NL), **1992**.

[22] See reference [9]. The [Ni(dmpn)$_3$Fe]$^{2+}$ complex contains both mono- and dithiolato bridges to pentacoordinate Fe^{II}; the former results in a Ni–Fe distance of 3.269(4) Å and ∢Ni-S-Fe of 89.4(2)°, while the Ni–Fe distances with dithiolato bridges are 2.976(4) and 3.123(3) Å with ∢Ni-S-Fe ranging from 76.4(2) to 84.1(2)°.

[23] C. Bagyinka, J. P. Whitehead, M. J. Maroney, *J. Am. Chem. Soc.* **1993**, *115*, 3576–3585.

[24] B. A. Averill, W. H. Orme-Johnson, *J. Am. Chem. Soc.* **1978**, *100*, 5234–5236.

[25] M. Kumar, D. Qiu, T. G. Spiro, S. W. Ragsdale, *Science* **1995**, *270*, 628–630.

Low-Temperature Complete Combustion of Methane over Mn-, Co-, and Fe-Stabilized ZrO_2**

Vasant R. Choudhary,* Balu S. Uphade, Suryakant G. Pataskar, and Alive Keshavaraja

The concentration of methane in the atmosphere is increasing continuously.[1] Since methane has a much larger greenhouse effect than carbon dioxide, the elimination of methane emission from natural gas engines and power plants as well as petroleum and petrochemical industries by complete combustion to carbon dioxide is a must. Methane is the most inert hydrocarbon and, hence, its oxidative destruction by complete combustion at low temperature (below 600 °C, for economic reasons) is rather difficult. Noble metal catalysts show high activity in the combustion of light hydrocarbons[2–4] and methane[5–10] at low temperature. However, the use of noble metal catalysts for methane emission control is limited because of their scarcity and high cost. Worldwide efforts are, therefore, being made to replace noble metal catalysts by mixed metal oxide catalysts based on perovskite oxides[11–18] of type ABO_3 (A = La or other rare earth metal with or without partial substitution by alkaline earth metals, B = transition metal such as Mn, Fe, Co, Ni). Here we show that Mn-, Co-, and Fe-stabilized ZrO_2 (cubic) catalysts display much higher methane combustion activity at low temperature than the perovskite oxide catalysts; the activity is somewhat comparable to that of the noble metal catalysts. Furthermore, incorporation of the transition metal in the ZrO_2 bulk structure not only stabilizes the metal oxide cubic (fluorite) modification but also drastically increases the reactivity of the lattice oxygens, which can be used for low-temperature complete combustion of methane (Fig. 1).

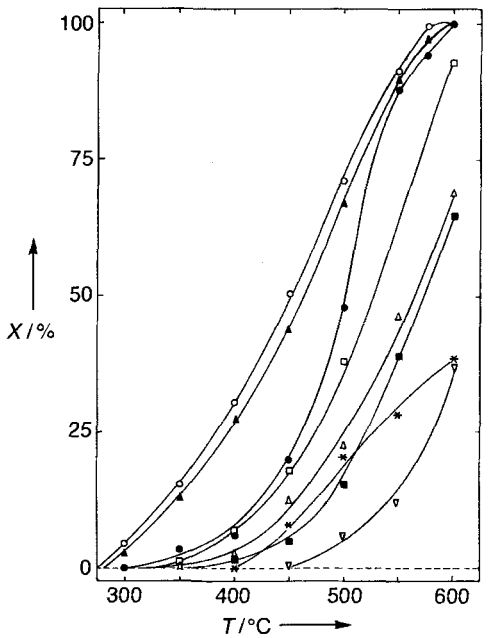

Fig. 1. Temperature dependence of the conversion of methane (X) in its complete combustion over Mn-stabilized ZrO_2 (○), Co-stabilized ZrO_2 (▲), Fe-stabilized ZrO_2 (●), Cr-stabilized ZrO_2 (□), Cu-stabilized ZrO_2 (△), Ni-stabilized ZrO_2 (■), Mn-impregnated ZrO_2 (*) and pure ZrO_2 (▽) [feed = 1 mol% CH_4 in air, gas hourly space velocity = 51 000 $cm^3 g^{-1} h^{-1}$].

The transition metals Mn, Co, Fe, Ni, Cu, and Cr are incorporated in 20 mol% concentration into the ZrO_2 bulk structure. The Mn-stabilized ZrO_2 shows the highest catalytic activity, which is much larger than that of the Mn-impregnated ZrO_2 with Mn/Zr ratio of 0.25; the latter is a mixture of MnO_2 and ZrO_2 (monoclinic). Mn-impregnated ZrO_2 with a lower Mn/Zr ratio (0.05) and pure MnO_2 (Mn/Zr = ∞) also show much lower methane combustion activity (methane conversion: 26.3 and 9.6%, respectively) at 500 °C. The Mn-stabilized ZrO_2 shows no sign of catalyst deactivation when used continuously for 50 h at 500 °C in the methane combustion process.

In the pulse reaction of pure methane over the Mn-stabilized ZrO_2 at 500 °C in the absence of free O_2, high conversion of methane to carbon dioxide is observed for the first pulse (Fig. 2, top). However, the conversion decreases with increasing pulse number and has a very low value after the 45th pulse. The initial high conversion is regained after the reoxidation of the deactivated catalyst by air (at 500 °C for 30 min). This clearly shows the involvement of the lattice oxygens of the catalyst in methane combustion and also confirms that a redox mechanism is operative in this catalytic process. The somewhat higher conversion observed for the initial few pulses after reoxidation may be due to chemisorbed oxygen on the catalyst and/or partial reduction of the virgin catalyst during storage before testing.

The Mn-stabilized ZrO_2, Mn-impregnated ZrO_2 (Mn/Zr = 0.25), and pure ZrO_2 catalysts were compared for reactivity of

[*] Dr. V. R. Choudhary, B. S. Uphade, S. G. Pataskar, A. Keshavaraja
Chemical Engineering Division National Chemical Laboratory,
Pune, 411 008 (India)
Fax : Int. code +(212)330233
e-mail: vrc@ncl.ernet.in

[**] B. S. Uphade and A. Keshavaraja are grateful to the Council of Scientific and Industrial Research, New Delhi, for the award of Senior Research Fellowships.

their lattice oxygen atoms in methane combustion by carrying out the methane pulse reaction (in the absence of free O_2) at different temperatures (Fig. 2, bottom). The conversion of methane over Mn-stabilized ZrO_2 is very high compared to that over the other two catalysts. This reveals that the reactivity of lattice oxygens in zirconia catalysts is drastically increased due to the Mn doping, which stabilizes the cubic phase as well. Our

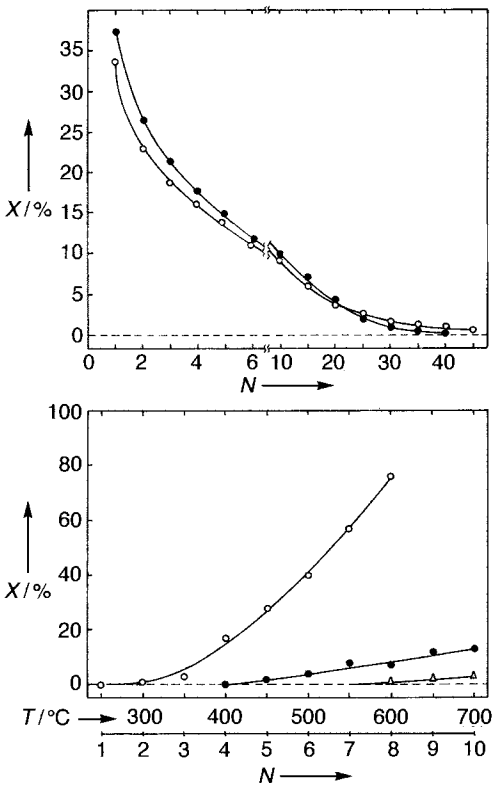

Fig. 2. Top: variation of methane conversion (X) with pulse number (N) in the pulse reaction of methane (in the absence of free O_2) at 500 °C over fresh Mn-stabilized ZrO_2 (○) and deactivated Mn-stabilized ZrO_2 after its reoxidation by air at 500 °C (●) [pulse: 0.2 cm^3 of pure methane, carrier gas: He (30 $cm^3 min^{-1}$), amount of catalyst: 0.1 g]. Bottom: temperature dependence of methane conversion (X) in the pulse reaction of methane (in the absence of free O_2) over Mn-stabilized ZrO_2 (○), Mn-impregnated ZrO_2 (●) and pure ZrO_2 (△) [amount of catalyst: 0.1 g, pulse: 0.2 cm^3 of pure methane, carrier gas: He (30 $cm^3 min^{-1}$)].

studies on the temperature-programmed reaction of pure methane (in the absence of free O_2) over the catalysts also indicate that the reactivity of lattice oxygens in all the transition metal stabilized ZrO_2 catalysts is much higher than that of pure ZrO_2 and is comparable to the observed methane combustion activity (in the presence of free O_2) shown by these catalysts. Thus, these observations reveal that the high catalytic activity in the methane combustion can be attributed to the high reactivity of the lattice oxygen atoms in the catalyst.

The methane combustion activity of the Mn-, Co-, and Fe-stabilized ZrO_2 catalysts was compared with that of the perovskite oxide catalysts (known to show high methane combustion activity) and noble metal catalysts for the same space velocity (Table 1). This clearly shows that the stabilized zirconia catalysts have much higher activity than the perovskite oxide catalysts; their activity is comparable to that of the noble metal catalysts. The stabilized ZrO_2 catalysts, particularly Mn- and Co-stabilized ZrO_2 catalysts, have a high potential for use as low-temperature combustion catalysts in methane emission control. Their high activity at low temperature is attributed to

Table 1. Comparison of Mn-, Co-, and Fe-stabilized ZrO_2 (cubic) catalysts with perovskite oxide and noble metal catalysts for complete combustion of methane (gas hourly space velocity = 51 000 $cm^3 g^{-1} h^{-1}$).

Catalyst	Surface area [$m^2 g^{-1}$]	T [°C] for 50% conversion	T [°C] for 90% conversion
$LaNiO_3$	4.5	793	>>800
$La_{0.7}Sr_{0.3}NiO_3$	3.5	620	740
$LaCoO_3$	2.4	633	750
$La_{0.7}Sr_{0.3}CoO_3$	2.2	637	753
$LaMnO_3$	3.2	693	793
$La_{0.7}Sr_{0.3}MnO_3$	5.9	670	760
$LaFeO_3$	6.8	617	713
$La_{0.7}Sr_{0.3}FeO_3$	5.3	610	712
$La_{0.7}Sr_{0.3}Co_{0.5}Fe_{0.5}O_3$	3.5	660	775
Pt/Al_2O_3 (1 wt.% Pt) [7]	–	545	650
Pd/Al_2O_3 (1 wt.% Pd) [7]	–	400	445
Fe-stabilized ZrO_2	102	503	557
Co-stabilized ZrO_2	98	464	550
Mn-stabilized ZrO_2	105	450	545

the high reactivity of their lattice oxygen atoms and to the high mobility of oxygen in the stabilized zirconia. This facilitates the redox process in catalytic methane combustion. In its cubic form the Mn-doped ZrO_2 is stable up to 700 °C.[19]

The enhancement of the reactivity of the lattice oxygens as a result of stabilization of zirconia by Mn or other transitional metals may be due to creation of crystal defects. This results in the formation of low-coordinated lattice oxygens and transition metal sites on the surface and increases the mobility of oxygen both on the surface and in the bulk catalyst.

Experimental Procedure

The Cr-, Mn-, Fe-, Co-, Ni,- and Cu-stabilized ZrO_2 (cubic) catalysts were prepared by mixing aqueous solutions of zirconyl nitrate and the appropriate transition metal nitrate (transition metal/Zr mole ratio = 0.25), coprecipitating the metal hydroxide from the solution with aqueous tetramethylammonium hydroxide (25%) under vigorous stirring at 30 °C and pH 8, washing with deionized water, drying the resulting precipitate at 110 °C for 2 h, and calcining it in air at 500 °C for 8 h and then at 600° C for 1 h. The stabilization of transition metal doped ZrO_2 catalysts in their cubic form was confirmed by comparing their d-spacing values [d = 2.96(vs), 2.56(m), 1.81(vs), 1.54(vs), 1.48(w), 1.28(w), 1.17(w) and 1.15(w)] obtained by X-ray diffraction (XRD). Stabilization of ZrO_2 in its cubic phase by doping with Mn [19], Fe [20, 21], and Co [22] has been reported earlier. The pure ZrO_2 catalyst was also prepared by the above procedure but without the addition of any transition metal compound. The Mn-impregnated ZrO_2 (Mn/Zr = 0.25 and 0.05) was prepared with ZrO_2 and $Mn(NO_3)_2$ by the incipient wetness method and calcining as above. For purposes of comparison, the perovskite oxide catalysts (Table 1) were prepared by coprecipitating the metal carbonate, decomposing it at 500 °C for 4 h, powdering and pelleting, and finally calcining in air at 900 °C for 6 h. The perovskite oxide structure of the catalysts was confirmed by XRD. The methane combustion activity of all the catalysts at different temperatures was measured at atmospheric pressure in a continuous, fixed bed, quartz microreactor (i.d. 10 mm) containing 0.1 g catalyst (22–30 mesh size) mixed uniformally with 0.4 g inert α-Al_2O_3 particles (22–30 mesh size). Methane in air (1 mol%) was fed at a space velocity (measured at 0 °C and 1 atm pressure) of 51 000 $cm^3 g^{-1} h^{-1}$. The reaction temperature was measured by a Chromel-Alumel thermocouple located in the catalyst bed. The products (after condensation of water from the product stream at 0 °C) were analyzed by an on-line GC with molecular sieve and Spherocarb columns. The pulse reaction of methane over the catalyst in the absence of free O_2 was carried out with He carrier gas in a quartz pulse microreactor connected to the GC described [23]. No formation of carbon monoxide (or partial oxidation of methane) was observed in any of the methane conversion reactions.

Received: February 5, 1996
Revised version: June 7, 1996 [Z 8788 IE]
German version: *Angew. Chem.* **1996**, 108, 2538–2540

Keywords: catalysis · oxidations · perovskite · zirconium compounds

[1] R. E. Dickinson, R. J. Cicerone, *Nature* **1986**, *319*, 109–115.
[2] R. B. Anderson, K. C. Stein, J. J. Freenan, L. J. E. Hofer, *Ind. Eng. Chem.* **1961**, *53*, 809–812.
[3] C. Cullis, D. Keene, D. L. Trimm, *J. Catal.* **1970**, *19*, 378–385.
[4] K. R. Thampi, J. Kiwi, M. Graztel, *Catal. Lett.* **1990**, *4*, 49–53.
[5] T. R. Baldwin, R. Burch, *Appl. Catal.* **1990**, *66*, 337–358.
[6] *ibid.* **1990**, *66*, 359–381.
[7] N. Mouaddib, C. Feumi-Jantou, E. Garbbowski, M. Primet, *Appl. Catal. A: General* **1992**, *87*, 129–144.
[8] Y. Mizushima, M. Hori, *ibid.* **1992**, *88*, 137–148.
[9] Y. Li, J. N. Armor, *Appl. Catal. B: Environment* **1994**, *3*, 275–282.
[10] T. Ishihara, H. Sumi, Y. Takita, *Chem. Lett.* **1994**, 1499–1502.
[11] L. G. Tejuca, J. L. G. Fierro, J. M. D. Tascon, *Adv. Catal.* **1989**, *36*, 237–328.
[12] T. Seiyama, *Catal. Rev. Sci. Eng.* **1992**, *34*, 281–300.
[13] H. Arai, T. Yamada, K. Eguchi, T. Seiyama, *Appl. Catal.* **1986**, *26*, 265–276.
[14] H. M. Zhang, Y. Teraoka, N. Yamazoe, *Catal. Today* **1989**, *6*, 155–162.
[15] J. G. McCarty, H. Wise, *ibid.* **1990**, *8*, 231–248.
[16] B. de Collongue, E. Garbowski, M. Primet, *J. Chem. Soc., Faraday Trans.* **1991**, *87*, 2493–2499.
[17] P. E. Marti, A. Baiker, *Catal. Lett.* **1994**, *26*, 71–84.
[18] P. E. Marti, M. Maciejewski, A. Baiker, *Appl. Catal. B: Environment* **1994**, *4*, 225–235.
[19] A. Keshavaraja, A. V. Ramaswamy, *J. Mater. Res.* **1994**, *9*, 837–840.
[20] S. Davison, R. Kershaw, K. Dwight, A. Wold, *J. Solid State Chem.* **1988**, *73*, 45–51.
[21] I. B. Inwang, F. Chyad, I. J. McColm, *J. Mater. Chem.* **1995**, *5*, 1209–1213.
[22] P. Wu, R. Kershaw, K. Dwight, A. Wold, *Mater. Res. Bull.* **1988**, *23*, 475–480.
[23] V. R. Choudhary, V. H. Rane, *J. Catal.* **1992**, *135*, 310–316.

New Course in the Search for Antitumor Agents: The Use of pH-Dependent Sources of Reactive Radicals**

Mark Vol'pin, Ilia Levitin,* and Sergei Osinsky

In our opinion, one of the most promising approaches to cancer therapy is making use of the microphysiological features of tumors that differentiate them from normal tissues. In particular, attempts to exploit the low pH values of malignant neoplasm seem attractive. This effect was thoroughly studied in the case of solid tumors.[1, 2] It is essential that their pH, which typically is 0.2–0.5 units lower than that of normal tissue, is selectively reduced by ≤ 2 units down to a value of roughly 5.5;[3, 4] this is possible first of all by glucose infusion. Hence the task consists in designing appropriate pH-dependent agents, either cytostatics that are activated under acidic conditions or pH-dependent modulators of known antitumor drugs or means.[5, 6] Several substances that generate conventional cytotoxic compounds on slight acidification have been suggested to suit this purpose. The development of this approach was reviewed by Tietze et al.[7, 8]

[*] Prof. I. Levitin, Prof. M. Vol'pin[+]
Institute of Organoelement Compounds
Russian Academy of Science
28, Vavilov Street, Moscow 117813 (Russia)
Fax: Int. code +(95)135-5085
e-mail: gbkeu@ineos.ac.ru
Prof. S. Osinsky
Institute of Experimental Pathology, Oncology, and Radiobiology
Kiev 252022 (Ukraine)
[+] Deceased

[**] We thank Dr. L. Bubnovskaya, Dr. I. Ganusevich, Dr. Yu. Istomin, Dr. E. Mironov, Dr. V. Roginsky, and M. Tsikalova for help, and Prof. R. Yakubovskaya for discussions. This work was partially supported by the Moscow City Administration, INTAS, and the Russian Foundation for Fundamental Research.

We propose a new line in the search for pH-dependent antitumor agents: the use of acid-sensitive sources of reactive radicals. This approach is based on the well-known ability of transient free radicals to damage biomolecules, in particular to cleave nucleic acids (see, for example, refs.[9, 10]). For this purpose, we have developed alkylcobalt(III) chelate complexes of type **1**, which contain tridentate Schiff bases as ligands, as a novel source of free radicals.[11] These complexes generate alkyl radicals at reduced pH under very mild conditions[12] [Eq. (a)]. Typically,

$$RCo^{III}\ldots \xrightarrow{H^+} R^{\bullet} + Co^{II}\ldots \qquad (a)$$

the plot of reaction rate versus decreasing pH displays an S-shaped curve between pH 8 and 4 at 0–50 °C. We have also observed that the decomposition of complex **2b**, the main compound used in the present work, is nearly three times faster at pH 6.5 than at pH 7.5 (aqueous phosphate buffers, 20 °C).

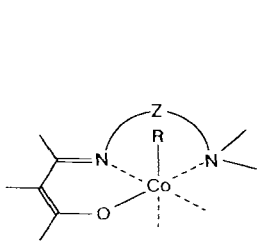

1

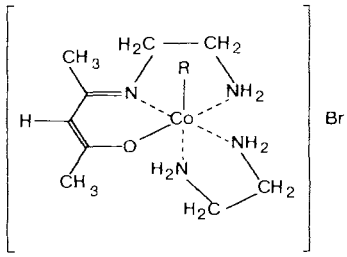

2a, R = Et; **2b**, R = *i*Pr

Furthermore, we have recently shown that alkyl radicals are not the only reactive species that may be generated by acid-induced homolytic decomposition of organocobalt complexes **1** in biological systems.[13] Although these complexes cause RNA cleavage at pH 5 under anaerobic atmosphere, this process is much more efficient in the presence of both dioxygen and ascorbic acid. Evidently, a cobalt(II) complex resulting from the homolytic decomposition of **1** catalyzes autooxidation of the biogenic reductant and generation of active oxygen species which are known[14] to cleave nucleic acids. Thus, an alkylcobalt complex with a tridentate Schiff base can serve as a source of both alkyl radicals and active oxygen species under mildly acidic conditions.

Obviously, one could expect that such sources of free radicals might selectively damage tumors since their pH is lower than that of healthy tissue. We confirmed the proposed antitumor activity of our pH-dependent sources of free radicals by examinations in vivo using several cancer models including Guerin carcinoma and sarcoma 45 in rats, and ascite L1210 leukemia and sarcoma 180 in mice. Tables 1–3 summarize some results obtained with the most thoroughly tested complex **2b**. Its direct anticancer action was noticeable in the case of ascite L1210 leukemia (Table 2, entries 1–4) and with Guerin carcinoma, provided the pH of the tumor cells was lowered (0.90 ± 0.10 units) by glucose infusion (Table 1, entries 1–3). Further, when **2b** was applied and the tumor was heated locally at 41 °C, the anticancer effect was greater than that obtained by heating alone at 43 °C (Table 1, entries 8 and 9). This result can be explained by the well-known decrease in pH when tumors are heated;[15] in our experiments the pH reduction in Guerin carcinoma was 0.30 ± 0.05 units. It is noteworthy that injection of **2b** did not substantially affect the pH decrease in tumors caused by glucose infusion or local heating.

It is particularly remarkable that complex **2b** substantially enhanced the effect of other anticancer therapeutics such as *cis*-diamminedichloroplatinum (cis-DDP; Table 1, entries 1,

Table 1. Antitumor and sensitizing activity of complex **2b** in rats bearing Guerin carcinoma [a–c].

Entry	Treatment [b]	TGD [days]	CR [%]	Cured rats [%]	Survival time [days]	ILS [%]
1	– (control)	–	0	0	15.8 ± 2.5	–
2	**2b**, 40 mg/kg	5.5 ± 1.0	0	0	19.5 ± 2.9	23
3	+ **2b**, 20 mg/kg glucose infusion	10.5 ± 1.0	40	35	22.5 ± 3.4	42
4	cis-DDP 3 mg/kg	23.0 ± 2.0	51	45	36.0 ± 2.5	128
5	cis-DDP 1.5 mg/kg	14.0 ± 2.5	32	25	27.7 ± 2.3	75
6	**2b**, 20 mg/kg + cis-DDP, 1.5 mg/kg	19.0 ± 2.0	47	40	32.7 ± 3.0	107
7	**2b**; 20 mg/kg + cis-DDP, 1.5 mg/kg + glucose infusion	25.0 ± 2.5	60	48	62.0 ± 5.7	292
8	local heating, 43 °C, 1 h	5.5 ± 1.0	0	0	19.6 ± 3.0	24
9	**2b**, 20 mg/kg + local heating, 41 °C, 1 h	10.0 ± 1.5	0	0	21.6 ± 2.5	37

[a] TGD (tumor growth delay): additional days needed for an treated tumor to reach a certain volume (relative to untreated controls); CR: complete regression of tumor; cured rats: number of rats that survived 120 days after complete regression; survival time: refers to uncured rats only; ILS: increase of life span of uncured rats (relative to that of untreated controls). [b] **2b** was injected intraperitoneally (i.p.) 90 min before start of glucose infusion and/or i.p. administration of cis-DDP, and 60 min before heating (microwave). Glucose was injected intravenously as a 20% solution at a rate of 80 mg/kg/min for 60 min. [c] All treatments were repeated after two days.

Table 2. Antitumor and chemosensitizing activity of complex **2b** in mice with ascite L1210 leukemia (entries 1–6) [a·b], and with sarcoma 180 (entries 7–10)[d].

Entry	Treatment	Cured rats [%]	Survival time [days]	ILS [%]	TGD [days]	CR [%]
1	– (control)	–	9.0 ± 0.2	–	–	–
2	**2b**, 50 mg/kg × 2	0	10.3 ± 0.4	14	–	–
3	**2b**, 100 mg/kg	0	10.5 ± 0.3	17	–	–
4	**2b**, 100 mg/kg × 3	0	14.5 ± 0.5	61	–	–
5	cis-DDP, 2.5 mg/kg × 2 [c]	25	13.5 ± 1.5	50	–	–
6	**2b**, 20 mg/kg + cis-DDP, 1.5 mg/kg × 2	28.5	13.3 ± 0.3	45	–	–
7	– (control)	0	11.0 ± 2.8	–	–	0
8	**2b**, 80 mg/kg	0	11.5 ± 0.7	0	0.5 ± 0.2	0
9	cis-DDP, 5 mg/kg	25	15.3 ± 2.7	40	3.0 ± 0.5	28
10	**2b**, 60 mg/kg + cis-DDP, 2.5 mg/kg	40	22.0 ± 1.0	100	6.0 ± 0.7	45

[a] See footnotes [a, b] in Table 1. [b] Treatment was repeated after two days. [c] Increase to three treatments was mostly fatal due to toxicosis. [d] See footnotes in Table 1.

4–7, and Table 2, entries 1, 5, 6, 7, 9, 10)) and high-energy radiation (Table 3). Owing to this chemo- and radiosensitizing activity of the complex, the dose (intensity) of the drug (radiation) can be reduced by a factor of 1.7 to 4 without change in therapeutic results. Similar, though somewhat weaker effects were observed with the slightly more acid-resistant complex **2a**.

Table 3. Radiosensitizing activity of complex **2b** in rats bearing sarcoma 45[a, b].

Entry	Treatment	CR [%]	Cured rats [%]	Survival time [days]	ILS [%]
1	– (control)	0	0	35.7 ± 2.3	–
2	10 Gy	10	10	54.7 ± 5.1	53
3	15 Gy	20	20	60.2 ± 6.4	69
4	20 Gy	40	20	74.0 ± 5.4	107
5	**2b**, 20 mg/kg + 10 Gy	30	30	64.4 ± 8.3	80

[a] See footnote [a] in Table 1. [b] Complex **2b** was injected i.p. 60 min before application of a single dose of X-ray (190 kV) radiation.

Early results of pharmacokinetic experiments indicate that starting isopropylcobalt chelate **2b**, despite its high lability, enters tumor at least partially intact. This fact also agrees with the suggested mechanism of anticancer action of our complexes.

On the basis of these results, we regard the use of pH-dependent sources of free radicals as a promising line in cancer therapy. Further examinations of antitumor and other biological activities of complexes **1** are in progress.

Received: February 20, 1996 [Z8842IE]
German version: *Angew. Chem.* **1996**, *108*, 2516–2518

Keywords: antitumor agents · cobalt compounds · radical formation

[1] J. L. Wike-Hooley, J. Haveman, H. S. Reinhold, *Radiother. Oncol.* **1984**, *2*, 243.
[2] I. F. Tannock, D. Rotin, *Cancer Res.* **1989**, *49*, 4373.
[3] M. von Ardenne, *Adv. Pharmacol.* **1972**, *10*, 339.
[4] S. Osinsky, L. Bubnovskaya, *Arch. Geschwulstforsch.* **1984**, *54*, 463.
[5] D. Rotin, P. Wan, S. Grinstein, I. Tannock, *Cancer Res.* **1987**, *47*, 1497.
[6] L. F. Tietze, M. Beller, R. Fisher, M. Lögers, E. Jähde, K.-H. Glüsenkamp, M. F. Rajewsky, *Angew. Chem.* **1990**, *102*, 812; *Angew. Chem. Int. Ed. Engl.* **1990**, *29*, 782.
[7] L. F. Tietze in *Molecular Aspects of Chemotherapy (Proc. Second Int. Symp. Mol. Aspects Chemother., Danzig (Polen) 1988* (Eds.: E. Borowski, D. Shugar)), Pergamon, Oxford, **1990**, p. 55–70.
[8] L. F. Tietze, A. Fischer-Beller, *Carbohydr. Res.* **1994**, *254*, 169.
[9] C. G. Riordan, P. Wei, *J. Am. Chem. Soc.* **1994**, *116*, 2189, and references therein.
[10] G. Pratviel, J. Bernadou, B. Meunier, *Angew. Chem.* **1995**, *107*, 819; *Angew. Chem. Int. Ed. Engl.* **1995**, *34*, 746.
[11] I. Ya. Levitin, M. V. Tsikalova, V. I. Bakhmutov, A. I. Yanovsky, Yu. T. Struchkov, M. E. Vol'pin, *J. Organomet. Chem.* **1987**, *330*, 161, and references therein
[12] I. Ya. Levitin, A. K. Yatsimirsky, M. E. Vol'pin, *Metalloorg. Khim.* **1990**, *3*, 865; *Organomet. Chem. USSR* **1990**, *3*, 442, and references therein.
[13] I. Ya. Levitin, V. M. Belkov, G. N. Novodarova, Z. A. Shabarova, M. E. Vol'pin, *Mendeleev Commun.* **1996**, 153.
[14] D. G. Knorre, O. S. Fedorova, E. I. Frolova, *Usp. Khim.* **1993**, *62*, 70.
[15] P. Vaupel, *Blood Flow, Oxygenation, Tissue pH Distribution, and Bioenergetic Status of Tumors*, Ernst Schering Res. Found., Berlin, **1994**, pp. 50–55.

Stereoselectivity in Reactions of 1,2-Dioxy-Substituted Radicals under Chelation Control: An Unexpected Result**

Michèle Gerster, Kurt Schenk, and Philippe Renaud*

Very recently we showed that 2-alkyl-1,2-dioxy-substituted radicals can react with substantial diastereoselectivities under chelation control.[1] For instance, treatment of the monoprotected diol **1** with trimethylaluminum,[2] followed by reaction with Bu_3SnD/azobisisobutyronitrile (AIBN) affords the *like* product *l*-**3** (Scheme 1). Presumably, the radical intermediate,

[*] Prof. P. Renaud, M. Gerster
Université de Fribourg, Institut de Chimie Organique
Pérolles, CH-1700 Fribourg (Switzerland)
Fax: Int. code +(37)29 97 39
e-mail: philippe.renaud@unifr.ch
Dr. K. Schenk
Université de Lausanne, Institut de Cristallographie
BSP, CH-1015 Lausanne (Switzerland)

[**] This work was supported by the Swiss National Science Foundation (Project CHiral2, grant no 2027-44'234.95). M. G. is very grateful to the Stipendienfonds der Chemischen Industrie Basel for financial support. We thank Ciba-Geigy (Marly, Switzerland) for the microanalysis.

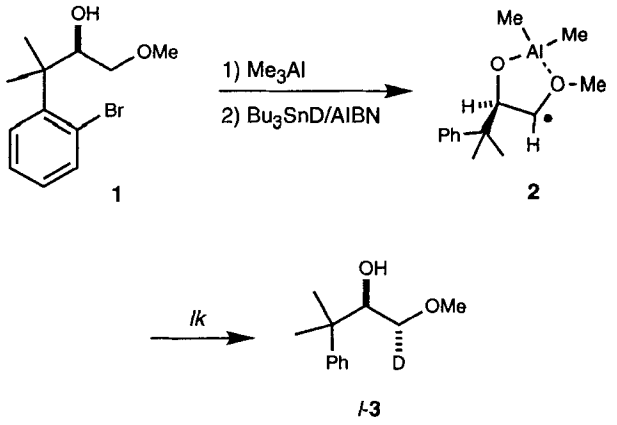

Scheme 1.

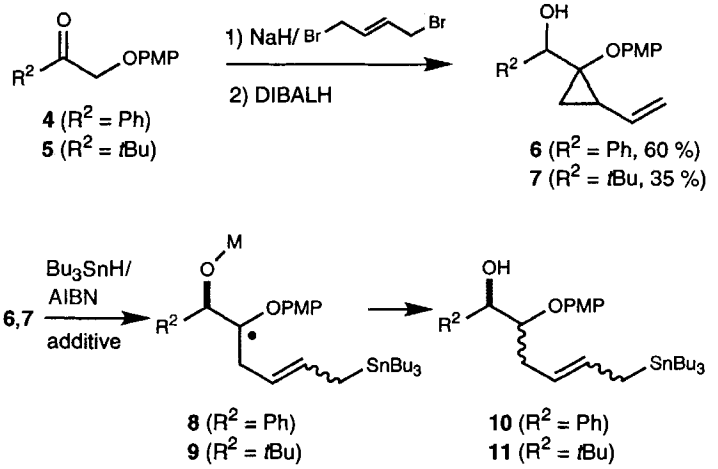

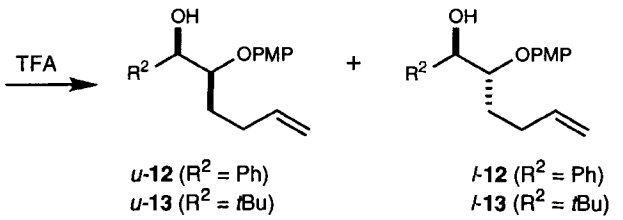

Scheme 2.

which is generated by a 1,5-shift, forms a chelate **2** and reacts with Bu_3SnD from the less hindered face, which is *anti* to the bulky vicinal $PhMe_2C$ group. This was the first example of the Cram chelation model in radical chemistry.[3-5]

We report herein that 1-alkoxy-1,2-dialkyl-2-hydroxy-substituted radicals of type **I** behave quite differently under chelation control and products with opposite configuration are formed. This is a rather rare example in which the model initially developed for ionic reactions (nucleophilic addition) is not applicable to analogous radical reactions. Our results confirm the importance of pyramidalization of the radical center in the ground and transition states.

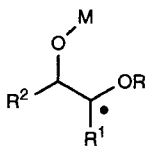

I: M = H, AlR_2 etc.
R^1, R^2 = alkyl

Type **I** radicals have been generated from vinylcyclopropanes by using the highly efficient ring-opening reaction of cyclopropylmethyl radicals.[6] The precursors **6** and **7** were prepared from (*p*-methoxyphenoxy (PMPO))methyl ketones **4** and **5**, respectively, by a one-pot double alkylation procedure,[7] followed by reduction with diisobutylaluminum hydride (DIBALH) (Scheme 2). Irradiation of the vinylcyclopropane **6** with a sun lamp in the presence of Bu_3SnH/AIBN in dichloromethane affords the acyclic monoprotected diol **10** via the intermediate radical **8** as a *u*/*l* 1.5:1 mixture of diastereoisomers (Table 1, entry 1). The diastereomeric ratio was determined after supression of the *E*/*Z* isomerism by protodestannylation of **10** to **12** with trifluoroacetic acid (TFA). Surprisingly, addition of 1.1 equivalents of Me_3Al does not influence the stereoselectivity (entry 2). However, based on our previous results,[1] we were convinced that under these reaction conditions the radical intermediate was chelating the metal atom as depicted in structure **8.1** (see below). The use of the bulky methylaluminum di(2,6-di-*tert*-butyl-4-methylphenoxide) (MAD) additive leads after treatment with TFA to preferential formation of *l*-**12** (entry 3).

The sterically more crowded radical **9** was investigated next. In the absence of additive, the conversion of **7** to **13** was not stereoselective (entry 4). However, when the aluminum alkoxide was prepared by preliminary treatment of **7** with 1.1 equivalents of Me_3Al, the reaction was highly stereoselective (*u*/*l* 1:>20, entry 5) with unexpected preferential formation of the *like* isomer. Other additives expected to favor chelation control such as MeMgCl (entry 6) and Et_2BH (entry 7) were found to be less efficient than Me_3Al. Use of MAD (entry 8) also gave, as in the case of **6**, preferentially the *like* isomer with a moderate selectivity. The relative configurations of *u*- and *l*-**12**,**13** were deduced by their conversion to *cis*- and *trans*-**14**,**15**, respectively, upon treatment with ammonium cerium(IV) nitrate (CAN) and by NOE measurements. The *like* configuration of the major isomer of **13** was confirmed by an X-ray structure analysis of its 3,5-dinitrobenzoate (3,5-DBN) ester **16** (Fig. 1).[8]

Table 1. Radical hydrostannylation of vinylcyclopropanes **6** and **7** in the presence of additives.

Entry	Starting material	Additive (equiv)	Product	Yield [%]	*u*/*l*
1	**6**	–	**10**	80	1.5:1
2	**6**	Me_3Al (1.1)	**10**	67	1.8:1
3	**6**	MAD (1.1)	**10**	43	1:1.6
4	**7**	–	**11**	87	1:1
5	**7**	Me_3Al (1.1)	**11**	77	1:>20
6	**7**	MeMgCl (1.1)	**11**	77	1:2.7
7	**7**	Et_2BH (1.1)	**11**	58	1:2.6
8	**7**	MAD (1.1)	**11**	51	1:3.2

In order to rationalize the results, we assume that the radicals generated after Me_3Al treatment of the free alcohols **6** and **7** are chelated aluminum alkoxides of type **8.1** and **9.1**, respectively.[9] This assumption is supported by the results we have obtained with radical **2**. This reacts preferentially with a *like* (*lk*) topicity; **8** reacts with low stereoselectivity, and **9** is reduced with a high *unlike* (*ul*) topicity.[10]

Hydrogen abstraction from the tin hydride is expected to occur via a pyramidalized transition state.[11] Even the ground-state conformation of alkoxy radicals is known to be pyramidal;[12] thus, the alkoxy-substituted radicals lie in the two conformations **A** and **B**. For radical **2**, the two conformations are easily accessible and reaction occurs preferentially from the less hindered face of **2B** (Curtin–Hammet principle). The radical **8.1**, in contrast, exists preferentially in conformation **8.1A**, thus

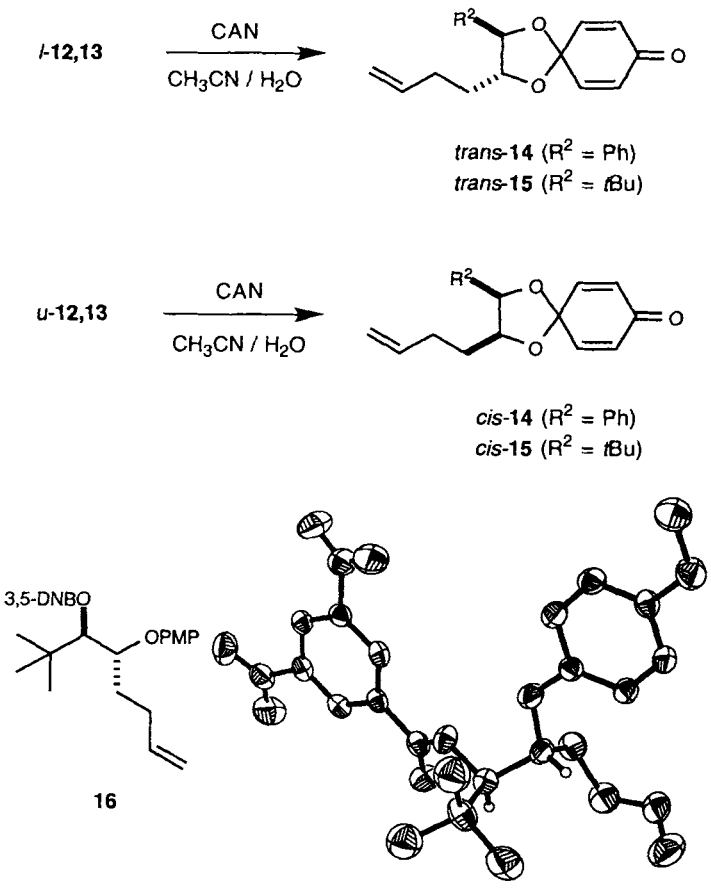

Fig. 1. Determination of the relative configurations of *u*- and *l*-**12,13**.

minimizing steric interactions between R^2 and R^1, but conformer **8.1B** is also accessible and presumably more reactive (less hindered). Therefore, both *lk* and *ul* topicities are observed Radical **9.1** exists exclusively in conformation **9.1A**, be-

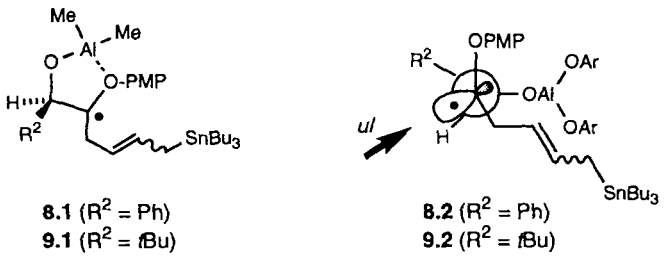

8.1 (R^2 = Ph)
9.1 (R^2 = *t*Bu)

8.2 (R^2 = Ph)
9.2 (R^2 = *t*Bu)

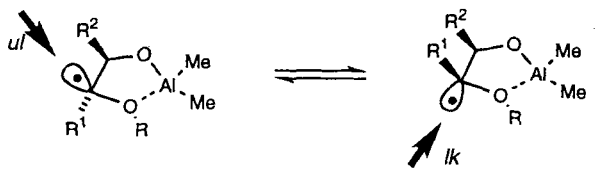

2A (R^1 = H, R^2 = C(Me)$_2$Ph) **2B**

8.1A (R^1 = $CH_2CH{=}CHCH_2SnBu_3$, R^2 = Ph) **8.1B**

9.1A (R^1 = $CH_2CH{=}CHCH_2SnBu_3$, R^2 = *t*Bu) **9.1B**

cause in **9.1B** a very large eclipsing interaction between the *tert*-butyl group and the alkyl R^1 group would be present. Pyramidalization of **9.1A** forces the reduction to occur from the most shielded face with *ul* topicity (*syn* to the *tert*-butyl group).[13] The low level of stereoselectivity observed when MAD is used as an additive (entries 3 and 8) can be explained by Felkin–Ahn type transition states **8.2** and **9.2**.

In conclusion, we have demonstrated that substitution at the C1 position of 1,2-dioxy-substituted radicals is of critical importance for the sense of the stereoselectivity during chelation-controlled reactions. To our knowledge, such an effect is not observed during nucleophilic addition to carbonyl compounds under chelation control.[14] The general phenomenon is caused by strong pyramidalization in the transition state and is expected to be important in several other types of systems with pyramidal radicals such as oxiranyl,[15] tetrahydrofuran-2-yl, and aziridinyl radicals.[16] Moreover, similar effects are also expected for any type of 1,2-disubstituted cycloalkyl radicals because of pyramidalization of the transition states, and their magnitude is currently under study in our laboratory.[17]

Experimental Procedure

Ring opening: **10,11**: To a solution of **6** or **7** (1.00 mmol) and AIBN (16 mg) in C_6H_6 (3.3 mL) was added under nitrogen the additive (1.10 mmol) followed by Bu_3SnH (380 mg, 1.30 mmol). The mixture was irradiated at 10 °C with a sun lamp (300 W). Further portions of AIBN (16 mg) were added every 8 h. After completion of the reaction (TLC monitoring), the solvent was evaporated and CH_2Cl_2 (15 mL) was added followed by $Na_2CO_3 \cdot 10\,H_2O$ (1.15 g) to hydrolyze the complex. The heterogeneous mixture was stirred for 1 h, filtered through Celite, and concentrated. The residue was purified by flash chromatography (FC).

Protodestannylation: **12,13**: TFA (1.30 mmol) was added to a solution of the stannane **10** or **11** (1.00 mmol) in chloroform (1.0 mL) under nitrogen. The mixture was stirred at room temperature for 1 h. After completion of the reaction, the organic layer was washed with H_2O and then $NaHCO_3$ solution, and dried over $MgSO_4$. After filtration and concentration, the residue was purified by FC. The ratio of diastereoisomers was deduced from ^{1}H NMR spectra.

Oxidation of the PMP ethers: **14,15**: $(NH_4)_2Ce(NO_3)_6$ (CAN) (3.00 mmol) was added in one portion to a solution of the PMP ether (1.00 mmol) in CH_3CN/H_2O (4/1) at 0 °C. The reaction mixture was stirred at 0 °C for 1 h, then poured into a mixture of EtOAc and brine. The organic layer was washed with saturated aqueous $NaHCO_3$, dried over $MgSO_4$, filtered, and concentrated. The residue was purified by FC.

2,2-dimethyl-4-(*p*-methoxyphenoxy)oct-7-en-3-ol **13**. Compound **7** (276 mg, 1.00 mmol) was converted to **11** (434 mg, 77%), which after FC (Et_2O/hexane 1/5) was obtained as a mixture of diastereoisomers that were directly submitted to protodestannylation. FC (Et_2O/hexane 1/3) of the crude material gave **13** (198 mg, 93%) as a mixture of diastereoisomers (*u*-**13**/*l*-**13**), which were separated by further chromatography.

u-**13**: ^{1}H NMR (360 MHz, $CDCl_3$): δ = 6.88–6.78 (m, 4 arom. H), 5.82 (dddd, J = 17.1, 10.2, 6.9, 6.3 Hz, $H_2C{=}CH$), 5.09–4.99 (m, $H_2C{=}CH$), 4.37–4.29 (m, CH–OAr), 3.78 (s, MeO), 3.27 (dd, J = 10.3, 0.9 Hz, HO–C*H*), 2.59 (d, J = 10.3 Hz, HO), 2.26–2.09 (m, $H_2C{=}CHCH_2$), 1.94 (ddd, J = 13.8, 8.5, 5.4 Hz, O–CH–C*H*H), 1.83–1.70 (m, O–CH–CH*H*), 0.95 (s, *t*Bu). ^{13}C NMR (50.3 MHz, $CDCl_3$): δ = 154.07 (s), 151.00 (s), 137.67 (d), 116.61 (d), 115.30 (t), 114.85 (d), 78.59 (d), 75.17 (d), 55.66 (q), 35.11 (s), 30.75 (t), 29.66 (t), 26.45 (q).

l-**13**: ^{1}H NMR (200 MHz, $CDCl_3$): δ = 6.84 (s, 4 arom. H), 5.97–5.70 (m, $H_2C{=}CH$), 5.10–4.92 (m, $H_2C{=}CH$), 4.30 (td, J = 6.5, 3.2 Hz, CH-OAr), 3.78 (s, MeO), 3.57 (t, J = 3.5 Hz, HO-C*H*), 2.46–2.07 (m, $H_2C{=}CH{-}CH_2$), 2.05–1.67 (m, O–CH–CH_2), 1.91 (d, J = 3.9 Hz, HO), 0.97 (s, *t*Bu). ^{13}C NMR (50.3 MHz, $CDCl_3$): δ = 154.14 (s), 151.88 (s), 138.53 (d), 117.56 (d), 115.01 (t), 114.83 (d), 79.24 (d), 78.97 (d), 55.72 (q), 34.22 (s), 29.74 (t), 29.16 (t), 26.90 (q). Mixture of diastereoisomers. Anal. calc. for $C_{17}H_{26}O_3$ (278.40): C 73.35, H 9.41; found: C 73.06, H 9.52.

trans-2-(But-3-en-1-yl)-3-*tert*-butyl-1,4-dioxaspiro[4,5]deca-6,9-dien-8-one (*trans*-**15**). Compound *l*-**13** (80 mg, 0.30 mmol) was converted to *trans*-**15** (60 mg, 80%), which after FC (Et_2O/hexane 1:3) was obtained as a pale yellow liquid. Starting from a mixture of *l*- and *u*-**13** a mixture of *trans*- and *cis*-**15** was prepared. The diastereoisomers were separated by chromatography.

trans-**15**: ^{1}H NMR (200 MHz, $CDCl_3$): δ = 6.72-6.53 (m, *H*C=CH–C=O, 2H), 6.22–6.04 (m, HC=C*H*–C=O, 2H), 5.82 (dddd, J = 17.2, 10.2, 7.0, 6.3 Hz, $H_2C{=}CH$), 5.13-4.92 (m, $H_2C{=}CH$), 4.01 (dt, J = 8.3, 3.2 Hz, O–*CH*–CH_2), 3.62 (d, J = 7.9 Hz, *t*Bu–*CH*), 2.45–2.06 (m, CH_2–CH–CH_2), 1.87–1.53 (m, O–CH–CH_2), 0.98 (s, *t*Bu). ^{13}C NMR (50.3 MHz, $CDCl_3$): δ = 185.36 (s), 144.77

 © VCH Verlagsgesellschaft mbH, D-69451 Weinheim, 1996 0570-0833/96/3520-2398 $ 15.00+.25/0

(d), 144.67 (d), 137.54 (d), 128.94 (d), 127.89 (d), 115.37 (t), 97.68 (s), 89.78 (d), 78.13 (d), 34.97 (t), 32.82 (t), 30.29 (s), 26.05 (q).

cis-**15**: ^{1}H NMR (360 MHz, $CDCl_3$): $\delta = 6.76$ (dd, $J = 10.2$, 2.9 Hz, *H*C=CH-C=O, 1H), 6.19 (dd, $J = 10.0$, 2.3 Hz, *H*C=CH-C=O, 1H), 6.13 (dd, $J = 10.2$, 2.2 Hz, HC=C*H*-C=O, 2H), 5.85 (dddd, $J = 17.2$, 10.2, 7.0, 6.3 Hz, H_2C=C*H*), 5.06 (dm, $J = 17.2$ Hz, *H*HC=CH), 5.02 (dm, $J = 10.2$ Hz, H*H*C=CH), 4.29–4.21 (m, O-C*H*-CH_3), 3.92 (d, $J = 5.3$ Hz, *t*Bu-C*H*), 2.36–2.28 (m, H_2C=CH-CH*H*), 2.17–2.05 (m, H_2C=CH-CH*H*), 1.76–1.65 (m, O-CH-CH_2), 1.06 (s, *t*Bu). ^{13}C NMR (50.3 MHz, $CDCl_3$): $\delta = 185.35$ (s), 145.71 (d), 143.49 (d), 137.63 (d), 129.52 (d), 127.84 (d), 115.40 (t), 96.73 (s), 86.81 (d), 79.19 (d), 32.71 (t), 31.21 (s), 30.12 (t), 26.99 (q). Mixture of diastereoisomers. Anal. calc. for $C_{16}H_{22}O_3$ (262.35): C 73.25, H 8.45; found: C 73.20, H 8.42.

Received: April 26, 1996 [Z9072IE]
German version: *Angew. Chem.* **1996**, *108*, 2523–2525

Keywords: asymmetric induction · chelate control · diols · hydrostannylations · radicals

[1] P. Renaud, M. Gerster, *J. Am. Chem. Soc.* **1995**, *117*, 6607–6608.
[2] Since the publication of our preliminary results [1], we have discovered that it is more convenient to use Me_3Al instead of Et_2AlCl/Na_2CO_3 to prepare the aluminum alkoxide.
[3] Reviews on the stereoselectivity of radical reactions: N. A. Porter, B. Giese, D. P. Curran, *Acc. Chem. Res.* **1991**, *24*, 296–304; W. Smadja, *Synlett* **1994**, 1–26; D. P. Curran, N. A. Porter, B. Giese, *Stereochemistry of Radical Reactions*, VCH, Weinheim, **1996**.
[4] For stereoselective reactions based on 1-oxy radicals, see: B. Giese, W. Damm, J. Dickhaut, F. Wetterich, S. Sun, D. P. Curran, *Tetrahedron Lett.* **1991**, *32*, 6097–6100; B. Giese, B. Carboni, T. Göbel, R. Muhn, F. Wetterich, *ibid.* **1992**, *33*, 2673–2676.
[5] For chelation control in radical reactions, see: Y. Guindon, J.-F. Lavallée, M. Llinas-Brunet, G. Horner, J. Rancourt, *J. Am. Chem. Soc.* **1991**, *113*, 9701–9702; Y. Guindon, B. Guérin, C. Chabot, N. Mackintosh, W. W. Ogilvie, *Synlett* **1995**, 449–451; H. Nagano, Y. Kuno, *J. Chem. Soc. Chem. Commun.* **1994**, 987–988; T. Toru, Y. Watanabe, M. Tsusaka, Y. Ueno, *J. Am. Chem. Soc.* **1993**, *115*, 10464–10465; M. Kito, T. Sakai, K. Yamada, F. Matsuda, H. Shiramana, *Synlett* **1993**, 158–162; T. Gillmann, *Tetrahedron Lett.* **1993**, *34*, 607–610; Y. Yamamoto, S. Onuki, M. Yumoto, N. Asao, *J. Am. Chem. Soc.* **1994**, *116*, 421–422; M. Kawatsura, F. Matsuda, H. Shirahama, *J. Org. Chem.* **1994**, *59*, 6900–6901; A. G. Molander, J. A. McKie, *ibid.* **1995**, *60*, 872–882; H. Urabe, K. Yamashita, K. Suzuki, K. Kobayashi, F. Sato, *ibid.* **1995**, *60*, 3576–3577; J. Hongliu, R. Radinov, N. A. Porter, *J. Am. Chem. Soc.* **1995**, *117*, 11029–11030; M. P. Sibi, C. J. Jasperse, J. Ji, *ibid.* **1995**, *117*, 10779–10780; H. Stadtmüller, P. Knochel, *Synlett* **1995**, 463–464. M. P. Sibi, J. Ji, *Angew. Chem.* **1996**, *108*, 198–200; *Angew. Chem. Int. Ed. Engl.* **1996**, *35*, 190–192.
[6] K. S. Feldman, H. M. Berven, P. H. Weinreb, *J. Am. Chem. Soc.* **1993**, *115*, 11364–11369.
[7] R. N. Saisic, R. Matovic, Z. Cekovic, *Gazz. Chim. Ital.* **1991**, *121*, 325–328.
[8] Crystallographic data (excluding structure factors) for the structure reported in this paper have been deposited with the Cambridge Crystallographic Data Centre as supplementary publication no. CCDC-179-89. Copies of the data can be obtained free of charge on application to The Director, CCDC, 12 Union Road, Cambridge CB2 1EZ, UK (fax: Int. code +(1223) 336-033; e-mail: teched(α chemcrys.cam.ac.uk).
[9] The preliminary ^{13}C NMR study supports the formation of a chelate. Details will be published in a forthcoming full paper.
[10] The reaction with *like*(*lk*) topicity affords the *unlike*(*u*) product and vice versa.
[11] J. E. Eksterowicz, K. N. Houk, *Tetrahedron Lett.* **1993**, *34*, 427–430; W. Damm, J. Dickhaut, F. Wetterich, B. Giese, *ibid.* **1993**, *34*, 431–434.
[12] R. D. McKelvey, T. Sugarawa, H. Iwamura, *Magn. Reson. Chem.* **1985**, *23*, 330–334; Y.-D. Wu, K. N. Houk, *J. Am. Chem. Soc.* **1992**, *114*, 1656–1661.
[13] Very recently it was found that the stereoselectivity of 1-amino-substituted cyclic radicals was strongly dependent of the nature of the R group attached at the radical center. An explanation based on pyramidalization of the reactive center in the transition state was proposed: D. Crich, S. Natarajan, *J. Org. Chem.* **1995**, *60*, 6237–6241.
[14] D. J. Cram, F. A. A. Elhafez, *J. Am. Chem. Soc.* **1952**, *74*, 5828–5835; D. J. Cram, K. R. Kopecky, *ibid.* **1959**, *81*, 2748–2755; D. J. Cram, D. R. Wilson, *ibid.* **1963**, *85*, 1245–1249; J. H. Stocker, P. Sidisunthorn, B. M. Benjamin, C. J. Collins, *ibid.* **1960**, *82*, 3913–3918; for a review, see: E. L. Eliel, S. H. Wilen, *Stereochemistry of Organic Compounds*, Wiley, New York, **1994**.
[15] Preliminary experiments have shown that the 2-*tert*-butyl-1-methyloxiranyl radical reacts preferentially with *ul* topicity that is *syn* to the *tert*-butyl group. For reaction with monosubstituted oxiranyl radicals, see: F. E. Ziegler, P. G. Harran, *Tetrahedron Lett.* **1993**, *34*, 4505–4508.
[16] *Syn* bromination of 2-substituted aziridinyl radicals has been reported: F. E. Ziegler, M. Belena, *J. Org. Chem.* **1994**, *59*, 7962–7967.
[17] For a recent result that may fit in this category, see: H. Urabe, K. Kobayashi, F. Sato, *J. Chem. Soc. Chem. Commun.* **1995**, 1043–1044. See also J. O. Metzger, K. Schwarzkopf, W. Saak, S. Pohl, *Chem. Ber.* **1994**, *127*, 1069–1073.

An Approach to Epothilones Based on Olefin Metathesis**

K. C. Nicolaou,* Yun He, Dionisios Vourloumis, Hans Vallberg, and Zhen Yang

Epothilones A and B (**1** and **2**, respectively; Scheme 1) represent a new class of natural products with interesting molecular architecture and considerable potential in medicine. Originally isolated by Höfle et al.[1] from myxobacteria *Sorangium cellulosum* strain 90, these compounds possess striking biological properties, for example potent antifungal activity[2] against oomyceten (*Plasmopara viticola*, *Phytopthora infestans*) both in vitro and in the greenhouse as well as cytotoxic activity against mouse fibroblasts [cell line L929, IC_{50} 2 mg mL^{-1} for epothilone B (**2**)]. Most importantly, the epothilones exhibit significant in vitro selectivity against breast and colon cell lines;[2, 3] they exert their cytotoxicity by the same mechanism as taxol,[4] namely by stabilization of microtubules. The latter observation made by Merck scientists, who also discovered the epothilones independently,[4] is both exciting and intriguing in view of taxol's success as an anticancer agent and the absence of any apparent structural similarity between taxol and epothilones. The structures of these compounds have recently been established by Höfle and his group[2] with spectroscopic

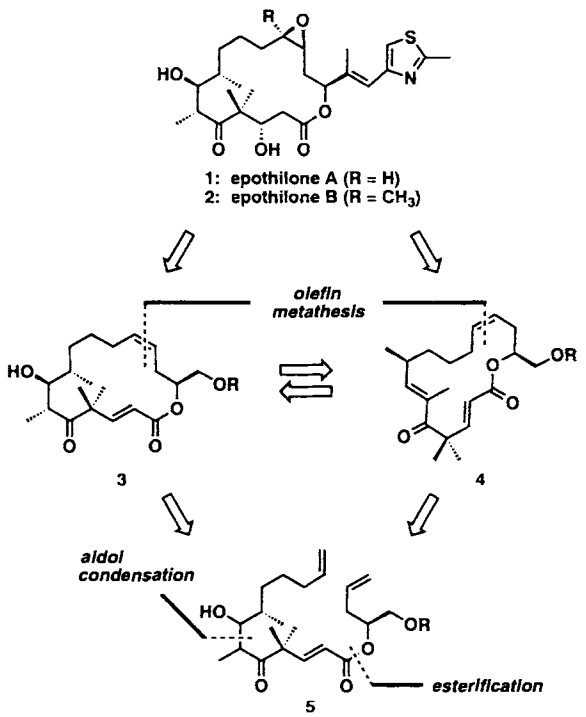

Scheme 1. Structures and retrosynthetic analysis of epothilones A (**1**) and B (**2**).

[*] Prof. Dr. K. C. Nicolaou, Y. He, Dr. D. Vourloumis, Dr. H. Vallberg, Dr. Z. Yang
Department of Chemistry and
The Skaggs Institute of Chemical Biology
The Scripps Research Institute
10550 N. Torrey Pines Road, La Jolla, CA 92037 (USA)
Fax: Int. code +(619)784-2469
and
Department of Chemistry and Biochemistry
University of California San Diego
9500 Gilman Drive, La Jolla, CA 92093 (USA)

[**] This work was financially supported by The Skaggs Institute of Chemical Biology and the National Institutes of Health (USA).

techniques and X-ray crystallographic analysis of epothilone B (**2**). In this communication we report a olefin metathesis based approach to the macrocyclic skeleton of the epothilones that may be used to construct not only the natural substances, but also a library of analogs for biological screening.

A plausible retrosynthetic strategy for epothilones is illustrated in Scheme 1. According to this metathesis-based approach, the epothilone structure is traced back to the 16-membered ring skeletons **3** or **4**, which lack, besides the side chain, a number of oxygen atoms. Further disconnection of **3** or **4** by a retro metathesis reaction reveals the open chain compound **5** as a potential precursor. Disassembly of **5** can easily be envisioned as indicated in Scheme 1, leading to three simple building blocks. Thus, though the exact sequence will have to await experimentation, the strategy evolved from this analysis will involve rapid assembly of **5**, ring closure by olefin metathesis,[5, 6] introduction of the required oxygen functions, and side chain attachment. Conformational effects of the 16-membered ring as well as neighboring group participation are expected to play important roles in setting the proper stereorelationships within the target molecules. Most importantly, the scheme is flexible enough to allow entry to all possible stereoisomers of the epothilones.

Since the stereochemical details of the epothilones A (**1**) and B (**2**) were at first unknown, we initially focused on a flexible sequence aimed at exploring a general strategy capable of delivering all possible stereoisomers and, eventually, an epothilone library of maximum diversity. To this end, the three requisite fragments **6**–**8** were synthesized as shown in Scheme 2. Construction of building block **6** involved oxidation of alcohol **9**[7] to the corresponding aldehyde, Wittig olefination, DIBAL-induced removal of the pivaloate groups, and sodium periodate cleavage of the resulting 1,2-diol (56% overall yield). Preparation of **7** proceeded smoothly from (*R*)-(+)-glycidol (**10**) through silyl ether formation, epoxide opening with the lithio derivative of dithiane, liberation of the aldehyde, and olefin formation (59% overall yield). Synthesis of **8** required selective phosphonate condensation with readily available ketoaldehyde **11**,[8] followed by acidic cleavage of the *tert*-butyl ester (87% overall yield, Scheme 2).

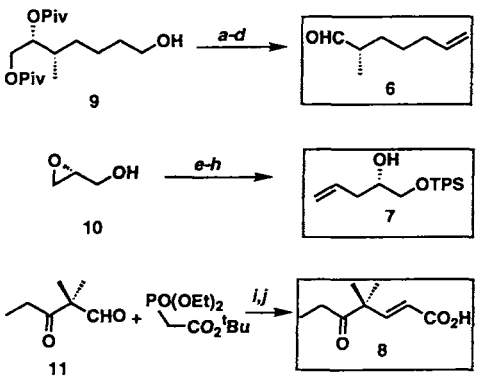

Scheme 2. Construction of the building blocks **6**–**8**. a) 3.0 equiv SO_3·Pyr, 5 equiv Et_3N, CH_2Cl_2:DMSO (4:1), 0 °C, 2 h, 88%; b) 1.5 equiv $Ph_3P{=}CH_2$, THF, 0 °C, 2 h, 94%; c) 2.4 equiv DIBAL, CH_2Cl_2, −78 → 25 °C, 20 h, 83%; d) 5.0 equiv $NaIO_4$, CH_2Cl_2:H_2O (4:1), 25 °C, 20 h, 81%; e) 1.1 equiv TPSCl, 1.2 equiv imidazole, CH_2Cl_2, 25 °C, 100%; f) 1.1 equiv 1,3-dithiane, 1.1 equiv *n*BuLi, THF, −30 → 25 °C, 84%; g) 1.1 equiv $Hg(ClO_4)_2$, 1.2 equiv $CaCO_3$, THF:H_2O (10:1), 12 h, 85%; h) 2.5 equiv $Ph_3P{=}CH_2$, THF, 0 °C, 1 h, 83%; 1.6 equiv NaH, THF, 0 → 25 °C, 1 h, 87%; j) CF_3COOH:CH_2Cl_2 (1:1), 25 °C, 0.5 h, 100%. TPS = $SiPh_2tBu$; Piv = $COtBu$.

The assembly of the epothilones skeleton from buidling blocks **6**–**8** is shown in Scheme 3. Coupling of **7** and **8** with dicyclohexylcarboiimide (DCC) led to **12** (99% yield) whose enolate, generated by the action of lithium diisopropylamide (LDA), reacted with aldehyde **6** to afford a mixture of diastereoisomers, **13** (29% yield) and **14** (60% yield). After chromatographic separation (silica, 20% ethyl acetate in hexanes), pure **13** was subjected to the Grubbs conditions for olefin metathesis with a $[RuCl_2(=CHPh)(PCy_3)_2]$ catalyst[5] (Cy = cyclohexyl) and furnished the 16-membered macrolide ring **15**[9] in 80% yield. Under similar conditions, diastereoisomer **14** led to cyclic system **16**[9] in 82% yield. The diastereomeric macrolide systems **17**[9] and **18**[9] were also synthesized in similar yields starting with the enantiomer of **10** and following the same sequence. The use of the enantiomer of **6** is expected to allow entry to yet another series of stereoisomers of the epothilone skeleton.

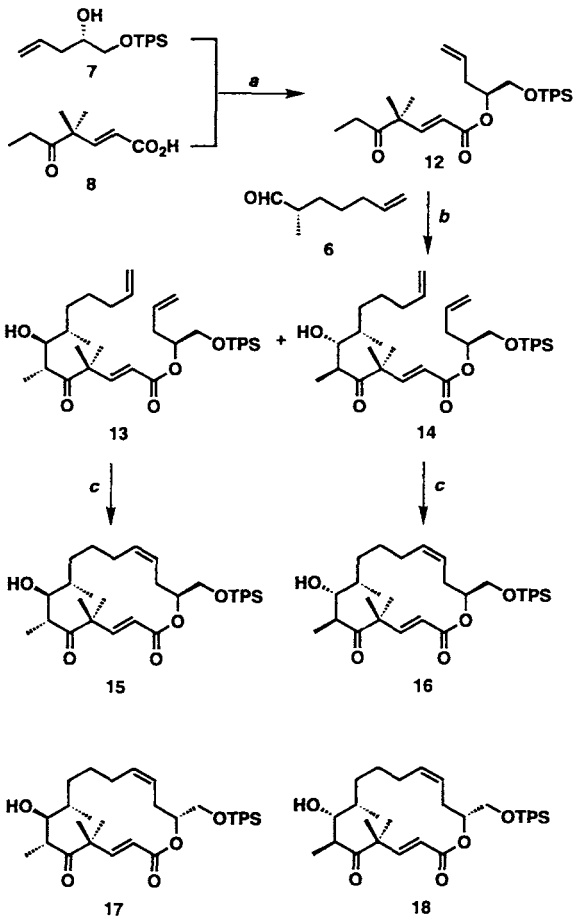

Scheme 3. Synthesis of the epothilone cyclic framework by olefin metathesis: a) 1.5 equiv DCC, 1.5 equiv 4-dimethylaminopyridine, toluene, 25 °C, 8 h, 99%; b) 1.2 equiv LDA, −78 °C, THF, 0.5 h; then **6** in THF, −78 °C, 0.5 h, **13** (29%), **14** (60%); c) substrate concentration: 0.006 M in CH_2Cl_2, 5–10 mol% $[RuCl_2(=CHPh)(PCy_3)_2]$, 25 °C, 4–12 h, 80–82%.

In conclusion, we have demonstrated the viability of a convergent and highly efficient approach to the epothilone cyclic framework through the olefin metathesis reaction. This strategy, and its many imaginable variants, pave the way for the total synthesis of both natural and designed members of this new class of compounds for biological investigations and possible therapeutic applications.[10]

Received: August 7, 1996 [Z9430IE]
German version: *Angew. Chem.* **1996**, *108*, 2554–2556

Keywords: cyclizations · epothilones · natural products · olefin metathesis · synthetic methods

[1] a) G. Höfle, N. Bedorf, K. Gerth, H. Reichenbach, DE-4138042, **1993** [*Chem. Abstr.* **1993**, *120*, 52841]; b) K. Gerth, N. Bedorf, G Höfle, H. Irschik, H. Reichenbach, *J. Antibiot.* **1996**, *49*, 560–563.

[2] G. Höfle, N. Bedorf, H. Steinmetz, D. Schomburg, K. Gerth, H. Reichenbach, *Angew. Chem.* **1996**, *108*, 1671–1673; *Angew. Chem. Int. Ed. Engl.* **1996**, *35*, 1567–1569.

[3] M. R. Grever, S. A. Schepartz, B. A. Chabner, *Semin. Oncol.* **1992**, *19*, 622–638.

[4] D. M. Bollag, P. A. McQueney, J. Zhu, O. Hensens, L. Koupal, J. Liesch, M. Goetz, E. Lazarides, C. M. Woods, *Cancer Res.* **1995**, *55*, 2325–2333.

[5] For the development of the olefin metathesis as a ring forming reaction, see a) W. J. Zuercher, M. Hashimoto, R. H. Grubbs, *J. Am. Chem. Soc.* **1996**, *118*, 6634–6640; b) P. Schwab, R. H. Grubbs, J. W. Ziller, *ibid.* **1996**, *118*, 100–110; c) R. H. Grubbs, S. J. Miller, G. C. Fu, *Acc. Chem. Res.* **1995**, *28*, 446–452, and references therein.

[6] Applications of the olefin metathesis reaction in medium and large ring synthesis, see a) A. Fürstner, K. Langemann, *J. Org. Chem.* **1996**, *61*, 3942–3943; b) S. F. Martin, H.-J. Chen, A. K. Courtney, Y. Liao, M. Pätzel, M. N. Ramser, A. S. Wagman, *Tetrahedron* **1996**, *52*, 7251–7264; c) T. D. Clark, M. R. Ghadiri, *J. Am. Chem. Soc.* **1995**, *117*, 12364–12365; d) A. F. Houri, Z. Xu, D. A. Cogan, A. H. Hoveyda, *ibid.* **1995**, *117*, 2943–2944; e) B. C. Borer, S. Deerenberg, H. Bieräugel, U. K. Pandit, *Tetrahedron Lett.* **1994**, *35*, 3191–3194.

[7] Compound **9** was synthesized from geraniol by standard chemistry: D. F. Taber, K. K. You, *J. Am. Chem. Soc.* **1995**, *117*, 5757–5762, and references therein. Both enantiomers of **6** may also be reached by asymmetric synthesis with chiral auxiliaries.

[8] Ketoaldehyde **11** was prepared from propionyl chloride according to a published procedure: T. Inukai, R. Yoshizawa, *J. Org. Chem.* **1967**, *32*, 404–407.

[9] Selected physical properties of compounds: **15**: $R_f = 0.29$ (silica, 20% ethyl acetate in hexanes); IR (film): $\tilde{\nu}_{max} = 3522$ (br, OH), 1718 (C(O)O), 1698 (COC), 1646 (CH=CHCO); ^{1}H NMR (400 MHz, $CDCl_3$): $\delta = 7.67-7.35$ (m, 10H, $SiPh_2$), 7.07 (d, 1H, $J = 16.0$ Hz, $=CHCOO$), 5.85 (d, 1H, $J = 16.0$ Hz, $(CH_3)_2CH=$), 5.29 (m, 2H, $CH=CHCH_2$), 5.23 (m, 1H, $COOCH$), 3.76 (dd, 1H, $J_1 = 6.3$ Hz, $J_2 = 10.6$ Hz, CH_2OSi), 3.69 (dd, 1H, $J_1 = 5.2$ Hz, $J_2 = 10.6$ Hz, CH_2OSi), 3.26 (d, 1H, $J = 9.1$ Hz, $CH(OH)$), 3.13 (q, 1H, $J = 7.0$ Hz, $(CH_3)CHCO$), 2.87 (s, 1H, $CHOH$), 2.47 (m, 1H, $CH_2CH=CHCH_2$), 2.30 (m, 1H, $CH_2CH=CHCH_2$), 2.09 (m, 1H, $CH_2CH=CHCH_2$), 1.96 (m, 1H, $CH_2CH=CHCH_2$), 1.50 (m, 2H, $CH(CH_3)CH_2CH_2$), 1.37 (m, 1H, $CH(CH_3)CH_2CH_2$), 1.35 (m, 2H, $CH(CH_3)CH_2CH_2$), 1.33 (s, 3H, $C(CH_3)_2$), 1.24 (s, 3H, $C(CH_3)_2$), 1.04 (s, 9H, $C(CH_3)_3$), 1.02 (d, 3H, $J = 6.9$ Hz, $CH(CH_3)CO$), 0.96 (d, 3H, $J = 6.6$ Hz, $CH(OH)CH(CH_3)$); HRMS for $C_{36}H_{50}O_5SiCs$ ($M + Cs^+$): calcd 723.2482, found 723.2506. **16**: $R_f = 0.20$ (silica, 20% ethyl acetate in hexanes); IR (film): $\tilde{\nu}_{max} = 3520$ (br, OH), 1711 (C(O)O), 1705 (COC), 1646 (CH=CHCO); ^{1}H NMR (400 MHz, $CDCl_3$): $\delta = 7.68-7.35$ (m, 10H, $SiPh_2$), 6.78 (d, 1H, $J = 15.8$ Hz, $=CHCOO$), 5,98 (d, 1H, $J = 15.8$ Hz, $(CH_3)_2CH=$), 5.40 (m, 2H, $CH=CHCH_2$), 5.20 (m, 1H, $COOCH$), 3.75 (dd, 1H, $J_1 = 6.0$ Hz, $J_2 = 10.7$ Hz, CH_2OSi), 3.68 (dd, 1H, $J_1 = 5.8$ Hz, $J_2 = 10.7$ Hz, CH_2OSi), 3.57 (m, 1H, $CH(OH)$), 3.05 (m, 2H, $(CH_3)CHCO$, $CH(OH)$), 2.42 (m, 1H, $CH_2CH=CHCH_2$), 2.21 (m, 1H, $CH_2CH=CHCH_2$), 2.08 (m, 1H, $CH_2CH=CHCH_2$), 1.98 (m, 1H, $CH_2CH=CHCH_2$), 1.44 (m, 2H, $CH(CH_3)CH_2CH_2$), 1.36 (s, 3H, $C(CH_3)_2$), 1.25 (m, 1H, $CH(CH_3)CH_2CH_2$), 1.20 (s, 3H, $C(CH_3)_2$), 1.15 (m, 2H, $CH(CH_3)CH_2CH_2$), 1.04 (s, 9H, $C(CH_3)_3$), 1.02 (d, 3H, $J = 6.9$ Hz, $CH(CH_3)CO$), 0.90 (d, 3H, $J = 6.5$ Hz, $CH(OH)CH(CH_3)$); HRMS for $C_{36}H_{50}O_5SiCs$ ($M + Cs^+$): calcd 723.2482, found 723.2508. **17**: $R_f = 0.34$ (silica, 20% ethyl acetate in hexanes); IR (film): $\nu_{max} = 3524$ (broad, OH), 1722 (-C(O)-O), 1699 (COC), 1648 (CH=CHCO); ^{1}H NMR (400 MHz, $CDCl_3$): $\delta = 7.67-7.35$ (m, 10H, $SiPh_2$), 6.90 (d, 1H, $J = 15.8$ Hz, $=CHCOO$), 5.98 (d, 1H, $J = 15.8$ Hz, $(CH_3)_2CH=$), 5.35 (m, 2H, $CH=CHCH_2$), 5.20 (m, 1H, $COOCH$), 3.73 (dd, 1H, $J_1 = 5.7$ Hz, $J_2 = 10.7$ Hz, CH_2OSi), 3.69 (dd, 1H, $J_1 = 5.8$ Hz, $J_2 = 10.7$ Hz, CH_2OSi), 3.14 (q, 1H, $J = 6.9$ Hz, $(CH_3)CHCO$), 3.10 (d, 1H, $J = 9.6$ Hz, $CHOH$), 2.96 (s, 1H, (OH)), 2.42 (m, 1H, $CH_2CH=CHCH_2$), 2.27 (m, 1H, $CH_2CH=CHCH_2$), 2.14 (m, 1H, $CH_2CH=CHCH_2$), 1.97 (m, 1H, $CH_2CH=CHCH_2$), 1.44 (m, 2H, $CH(CH_3)CH_2CH_2$), 1.19 (m, 1H, $CH(CH_3)CH_2CH_2$), 1.15 (m, 2H, $CH(CH_3)CH_2CH_2$), 1.33 (s, 3H, $C(CH_3)_2$), 1.22 (s, 3H, $C(CH_3)_2$), 1.04 (s, 9H, $C(CH_3)_3$), 1.02 (d, 3H, $J = 6.9$ Hz, $CH(CH_3)CO$), 0.96 (d, 3H, $J = 6.5$ Hz, $CH(OH)CH(CH_3)$); HRMS calcd for $C_{36}H_{50}O_5SiCs$ ($M + Cs^+$): 723.2482, found: 723.2508. **18**: $R_f = 0.18$ (silica, 20% ethyl acetate in hexanes); IR (film): $\nu_{max} = 3523$ (broad, OH), 1719 (C(O)O), 1699 (COC), 1646 (CH=CHCO); ^{1}H NMR (400 MHz, $CDCl_3$): $\delta = 7.68-7.32$ (m, 10H, $SiPh_2$), 7.01 (1H, $J = 16.0$ Hz, $=CHCOO$), 5.83 (d, 1H, $J = 16.0$ Hz, $(CH_3)_2CH=$), 5.33 (m, 2H, $CH=CHCH_2$), 5.22 (m, 1H, $COOCH$), 3.73 (dd, 1H, $J_1 = 5.5$ Hz, $J_2 = 11.4$ Hz, $-CH_2OSi$), 3.69 (dd, 1H, $J_1 = 4.3$ Hz, $J_2 = 11.4$ Hz, CH_2OSi), 3.57 (m, 1H, $CHOH$), 3.04 (m, 2H, $(CH_3)CHCO$, $CH(OH)$), 2.42 (m, 1H, $CH_2CH=CHCH_2$), 2.27 (m, 1H, $CH_2CH=CHCH_2$), 2.14 (m, 1H, $CH_2CH=CHCH_2$), 1.97 (m, 1H, $CH_2CH=CHCH_2$), 1.44 (m, 2H, $CH(CH_3)CH_2CH_2$), 1.19 (m, 1H, $CH(CH_3)CH_2CH_2$), 1.15 (m, 2H, $CH(CH_3)CH_2CH_2$), 1.33 (s, 3H, $C(CH_3)_2$), 1.22 (s, 3H, $C(CH_3)_2$), 1.04 (s, 9H, $C(CH_3)_3$), 1.02 (d, 3H, $J = 6.9$ Hz, $-CH(CH_3)CO$), 0.96 (d, 3H, $J = 6.5$ Hz, $CH(OH)CH(CH_3)$); HRMS calcd for $C_{36}H_{50}O_5SiCs$ ($M + Cs^+$): 723.2482, found: 723.2506.

[10] All new compounds exhibited satisfactory spectral and analytical and/or exact mass data. Yields refer to chromatographically and spectroscopically homogeneous materials.

Biotechnology Now—From Theory to Scale-Up

Downstream Processing of Natural Products. A Practical Handbook. Edited by *M. S. Verrall.* Wiley, Chichester, 1996. 354 pp., hardcover £ 65.00.—ISBN 0-471-96326-7

It is becoming increasingly difficult, even for those working in the field, to keep abreast with the latest developments in the methodology of natural products research, as the various specialist areas demand an ever greater degree of detailed knowledge.

This book is concerned with the production, isolation, and characterization of secondary metabolites and proteins from natural sources obtained by fermentation processes, so as to yield new active agents and lead structures for the pharmaceutical industry. In addition to a familiarity with the basic principles, such work requires specialist knowledge in the areas of microbiology, process technology, biochemistry, and physical and organic chemistry.

The various processing stages leading from the fermentation brew to the purified active agent are nowadays usually carried out as a team effort, whether in industry or in university research groups. The researchers involved rely greatly on many kinds of external support by specialist firms, which supply equipment, materials, and techniques of continually improving performance.

This book brings together a number of specialists from academic and industrial research laboratories to report on the current state of research in the downstream processing of natural products. Although certain aspects, in particular the isolation and breeding of the producing organisms, and the determination of the molecular structure of the end-product, receive little attention here, all the stages between these are treated in detail. Thus, "downstream processing" here means essentially the production, work-up, and isolation of pure secondary metabolites and proteins from biological sources.

The editor, M. S. Verrall, is a natural products expert with the British pharmaceutical company Smith-Kline-Beecham. In the first article he begins by reviewing the historical development of research on biologically active natural products and their importance as active agents and lead structures for the pharmaceutical industry, then discusses the common features and differences of the various isolation strategies, e.g. as applied to plants or to microorganisms, and for the isolation of secondary metabolites as compared with that of polypeptides. He also discusses likely future developments and technological advances (such as the increased use of molecular-biological methods for the production of secondary metabolites), thus setting the scene for the chapters that follow. These deal with the state of the art in the production, work-up, and purification of natural products with biological activity.

In addition to the editor's colleagues, the list of authors consists mainly of researchers from leading British universities, and practitioners and experts from industrial companies, both large and small. Accordingly, there are several chapters on routine technical processes such as freeze-drying, centrifuging, cell breakdown, concentration of the required product by solvent extraction or solid phase extraction, and the usual methods of fermentation analysis and process control. The individual authors discuss these topics from different points of view, while avoiding too much overlapping of subject matter.

Methods for isolating biologically active agents are covered especially thoroughly, with separate chapters describing a wide variety of available techniques. As well as detailed treatments of ion exchange chromatography, affinity chromatography, and HPLC, these chapters also discuss some innovative and less well known methods, such as radial flow chromatography and the use of supercritical liquids and liquid membranes in extraction and chromatography. Other topics covered include, for example, the properties and applications of DIAION adsorption resins for nonionic solid phase extraction (in a chapter by H. Tayakanaki et al., of the Mitsubishi research team that developed these resins), and an account by A. Thompson of the many different ways by which proteins can be modified to make their isolation easier. Although the book has a practical bias, as intended, the physical-chemical fundamentals are also covered, and the most important mathematical formulas are included where they are necessary for a basic understanding. There are also plenty of illustrations, which are well coordinated with the text. Separate chapters explain the detailed theoretical background to topics such as the integration of processes in biotechnology, the scale-up from the laboratory to industrial production, and good manufacturing practice as an important prerequisite for licencing and quality control. For the reader who needs more information on a particular topic there is a comprehensive and up-to-date list of references at the end of each chapter.

Anyone engaged in work in this field knows from reading recent literature on, for example, new biologically active natural products, that such publications usually place the main emphasis on the end-products of the evaluation process, whereas the methodology used in their discovery is given less prominence. This is probably because it is considered unnecessary to repeat descriptions of commonly used standard methods in successive publications. To complement this results-orientated type of literature, which is already plentifully available, the authors of this book have set out to provide a reference source on downstream processing methodology, and have succeeded well in that purpose. The subject matter is presented in a clearly understandable form, helped by the excellent standard of production and the numerous illustrations.

This work is an important and valuable contribution to the literature in this important area of biotechnology, not least because all the articles are thoroughly up-

This section contains book reviews and a list of new books received by the editor. Book reviews are written by invitation from the editor. Suggestions for books to be reviewed and for book reviewers are welcome. Publishers should send brochures or (better) books to the editorial office: Redaktion Angewandte Chemie, Postfach 101161, D-69451 Weinheim, Germany. The editor reserves the right of selecting which books will be reviewed. Uninvited books not chosen for review will not be returned.

to-date. It can therefore be recommended for everyone involved in the production and isolation of secondary metabolites and proteins from biological sources.

Marc Stadler, Klaus Frobel
Bayer AG, Pharma Forschungszentrum
Wuppertal (Germany)

Carbohydrate Building Blocks. By *M. Bols*. Wiley, Chichester, 1996. 182 pp., hardcover £ 40.00.—ISBN 0-471-13339-6

In 1983 there appeared a book which has since become a classic work in its field: *Total Synthesis of Natural Products. The Chiron Approach*, by Stephen Hanessian. It made many chemists aware for the first time of the importance of carbohydrates as chiral building blocks for synthesizing natural products and active agents. Although that book covered the "master strategies" in the script of carbohydrates-based synthesis, it did not include details of the "opening moves". The book by M. Bols reviewed here fills that gap admirably.

Carbohydrate Building Blocks is not a textbook of carbohydrates chemistry. Instead it aims to give the reader guidelines for learning to use this group of natural products, by describing the most important and well-proven synthetic pathways that afford access to a wide variety of chiral building blocks, starting from a collection of 26 relatively cheap carbohydrates. Most of the synthetic procedures consist of three or four stages, although a few have as many as seven or eight.

The first chapter familiarizes the reader with the most important starting materials and their origins. Current trends in the choice of starting materials for synthesizing various well-known stereosequences are shown by listing quantitative data on how frequently the different sugars have been used.

The next ten chapters, which occupy about a third of the book, contain a very condensed survey of commonly used transformations in carbohydrate chemistry. The topics include acetalizations, various other important protecting group strategies, oxidations and reductions, eliminations, and skeletal rearrangements induced by acids or bases. The author includes important rules and other information intended specifically to help the chemist who is less familiar with carbohydrates. Thus, for example, data are provided on the relative reactivities of the different hydroxy groups in aldoses, ketoses, anhydro-sugars, and sugar lactones, in reactions with electrophiles or in substitution reactions.

The real core of the book is the 120-page appendix. This consists of a catalog describing 691 (!) chiral building blocks derived from carbohydrates, together with several shorter subject indexes. In the catalog, which makes no claim to be exhaustive, each structure is accompanied by a CA number, a literature reference, the sugar used as the starting material, and the number of stages in the synthesis. The list of building blocks is arranged in eleven sections which correspond to Chapters 1-11 of the book, thus forming a close connection between the two parts. Each of these sections is completed by a bibliography. However, that is not all. To help the reader wishing to plan a retrosynthesis, there follows an important additional resource, namely a stereochemical index containing 98 stereochemical sequences with up to seven stereogenic centers, shown in open-chain form. These include not only the oxygen-substituted chiral centers that one expects to find, but also others with different heteroatoms as substituents, and in particular those with carbon branching. Alongside these centers are listed the corresponding building blocks from the catalog that have the specified chain-length and absolute configuration. If the user also wants to know about all the partially oxygen-blocked, carbocyclic, and carbon-branched structures included in the catalog, this information is provided by the last three indexes in the appendix, which are structured along the same lines as the stereochemical index. These various indexes together equip the reader with a range of tools for finding a required building block.

The book contains a wealth of densely-packed information. However, in the first part a somewhat more detailed treatment, especially in Chapters 3 (partially blocked sugars) and 7 (unsaturated sugars), would have improved the book still further. Also a few of the structures contain errors (e.g., **8.23** on p. 56, **7.22** on p. 28, and Scheme 3.8), and it would have been useful to include overall yields in the details of all the building blocks.

This book will be especially useful to everyone who wishes to carry out syntheses using carbohydrates as enantiomeric starting materials with a known absolute configuration. The clear and easily understandable layout makes the subject readily accessible to the reader, and it is to be hoped that the book will overcome the inhibitions of many organic chemists towards working with this class of compounds. If it had been available ten years ago, this reviewer would have been spared a good deal of laborious effort.

Andreas Kirschning
Institut für Organische Chemie
der Technischen Universität Clausthal
(Germany)

Methods in Molecular Biology. Vol. 59, Protein Purification Protocols. Edited by *S. Doonan*. Humana Press, Totowa, NJ, 1996. 405 pp., loose-leaf $ 64.50.—ISBN 0-89603-336-8

This book edited by Shawn Doonan contains 36 chapters written by 33 different authors. In the first chapter the editor himself sets out some general strategies for the purification of proteins, then the following few chapters describe methods for extracting proteins from various animal and plant tissues and from bacteria and fungi. Next some articles on subcellular fractionation are followed by chapters of a more general kind on topics such as concentration and ultrafiltration. A large part of the book is devoted to various column chromatograpy procedures, then further chapters deal with the purification of membrane proteins and the use of detergents. The last part of the book contains contributions on the lyophilization and storage of proteins and on methods for electroelution from gels and electroblotting. The editor himself concludes with a chapter on practical aspects of column chromatography.

The list of the contents and the cover (in ring-binder form) lead one to expect here a handbook that belongs in every laboratory, but unfortunately the text does not live up to that promise. The separation into Methods and Notes within the individual chapters makes the book troublesome to read, and one can easily lose sight of the theme through frequent turning back and forth. It also becomes apparent that the bulkiness of the book is partly due to the fact that different authors cover the same points in their notes, for example when repeating advice about the correct use of a centrifuge and the care of rotors. It would certainly have served the newcomer better to include an introductory chapter on centrifugation, to which all the others could then refer, and would also have saved paper. Cross-references to other chapters are rare, so it is not surprising that Doonan himself, in his chapter on fractional precipitation using ammonium sulfate, again devotes nearly two pages to dialysis, despite the fact that he has already contributed a chapter on this topic.

 © VCH Verlagsgesellschaft mbH, D-69451 Weinheim, 1996 0570-0833/96/3520-2404 $ 15.00+.25/0

In the first of the chapters on column chromatography, the reader who expects to learn something about ion exchange will be disappointed. The authors of this chapter, Sheehan and Fitzgerald, limit their discussion mainly to the preparation of a DE-cellulose exchange medium, and do not refer to more recent materials. There is no mention of variables such as column dimensions, capacities, gradients, etc., which are so important when planning purification strategies. These are only discussed in the final chapter, which again illustrates the book's lack of a systematic structure. However, notwithstanding these criticisms, the collection includes some very useful contributions, such as the chapters introducing the reader to the extraction of proteins from different types of tissues. Another chapter worth mentioning here is that by Bill Neville on reverse phase chromatography of proteins. The three chapters by Kay Ohlendieck on the extraction and purification of membrane proteins and the removal of detergents also certainly belong among the better examples, although it might have been better to combine these topics in a single chapter. However, the selected chapters mentioned here are again unnecessarily extended by including detailed descriptions of enzyme assay methods. The detailed description of the isolation of eggs from the sea-urchin and of the preparation of artificial sea-water is of limited interest to a broad readership, and a different example would have been more appropriate here. It would have been useful to include an article on the use of Triton X 114 for the separation of peripheral and integral membrane proteins.

The reader who hopes to find new materials or methods in this book will be disappointed. In many cases the information given is one-sided, as in the chapter on isoelectric focussing by Reiner Westermeier. This author is constrained by his admiration for a wellknown Swedish instrument manufacturer, and consequently fails to mention alternative methods of isoelectric focussing such as the Bio-Rad Rotofor cell or the high-resolution free-flow method (Octopus, Dr. Weber). The editor too is quite open about including an advertisement for the above-mentioned firm, and the last chapter even includes price information about some of the products. Here, though, the competitors are at least mentioned by name.

Finally there is the question of which readership this book is intended for. In my view it seems unsuitable for newcomers to the field, especially with regard to column chromatography. Although it contains sufficient information for these readers, they would need to hunt through the various chapters to bring it together, which is a difficult task without cross-references. The book also appears not to have been intended as a reference source for experienced protein chemists, as it does not cover new techniques and materials. This group is in any case already well served by the standard works cited in many of the chapters, such as *Methods in Enzymology*, or by the compact and informative handbooks in the *Practical Approach* series.

Sabine Wolf
Institut für Biochemie
der Technischen Hochschule Darmstadt
Darmstadt (Germany)

Sensors. Vol. 8. Micro- and Nanosensor Technology/Trends in Sensor Markets. Edited by *H. Meixner* and *R. Jones*. (Series: Sensors. A Comprehensive Survey. Series editors: *W. Göpel, J. Hesse* and *J. N. Zemel*. VCH Verlagsgesellschaft, Weinheim/VCH Publishers, New York, 1995. 565 pp., hardcover DM 410.00.—ISBN 3-527-26774-3

The final volume of this well-known work of reference has at last appeared. The publishers' original plans were revised so that the series could be extended to take into account the most recent changes in sensors research.

In the last few years research in this field has undergone some fundamental changes of direction. The main causes for this were the rapid growth of knowledge in three-dimensional microprocessing techniques (micromachining of silicon, and the LIGA technique), major advances in experimental methods for studying physical processes on the nanometer scale (STM, AFM, near-field spectroscopy), and the ability to synthesize nanostructured materials of various functionalities. This brought on the one hand new possibilities for system integration (microsystem techniques), and on the other hand the ability to control objects with dimensions in the nanometer range (nanotechnology). Also researchers in this field have become more keenly aware of needs in the market for sensors. In the new climate with regard to investment in research and development one sees a definite trend for companies to treat high-tech know-how as an essential prerequisite for strengthening their market position.

This volume is divided into two parts: Chapters 1–11 covering micro- and nanotechnologies, and Chapters 12–18 covering the markets for sensors.

Chapter 1 is a general introduction to the topics covered in this volume. Chapter 2 contains an overview of the three main types of microsystem technologies, namely the "beside-IC" type (hybrid design), "in-IC" (integrated design), and "above-IC" (design as a multilayer structure). This includes descriptions of some of the technological solutions that have resulted, such as pressure sensors and acceleration sensors (examples of "beside-IC" technology), and an electromagnetic actuator (an example of an "in-IC" design). The technologies are considered from two standpoints: firstly the needs of the market, and secondly the essential factors that contribute to the successful development of innovative microsystems.

Chapter 3 describes the design and production of microsystems within the area of integrated technologies, i.e., using only industrial IC methods, with or without additional IC-compatible production stages that are specific to the sensor concerned. In particular the chapter describes CMOS sensors for measuring humidity, magnetic fields, and electric fields.

Chapter 4 deals with the production of microsystems using the LIGA technique and several other technologies that do not belong to conventional microelectronics. The examples chosen to illustrate the LIGA method include microspectrometers and acceleration sensors. Other examples are a micropump manufactured by thermoplastic compression molding and an electrochemical microanalytical system. From this article it becomes clear that there is a distinction between microsystem technologies and microelectronic technologies. Production methods that can be used to make miniaturized sensors and control devices belong to microsystem technology.

The subject matter of Chapter 5 overlaps to some extent with the chapter on mass-sensitive detectors that appeared in Volume 2. In the present chapter the main emphasis is on the design of SAW structures, and the use of these in security passes for controlling access by a non-contact interrogator.

Chapter 6 discusses problems arising in the manufacture of miniaturized gas sensors for use at high temperatures, and possible ways of overcoming these. There is a particularly high demand for such sensors in the automobile industry. The main difficulty is that existing sensors have too short a useful life. The chapter describes attempts to overcome this problem by the use of new materials and by improving the mode of operation of such sensors. Chap-

ters 7 and 8 review the latest developments in the area of integrated optics and fiber-optic sensors.

The following three chapters are devoted to the basic concepts in the fields of nanostructured materials (Ch. 9), nanotechnologies (Ch. 11), and molecular electronics (Ch. 10). Chapter 9 emphasizes the innovative possibilities arising from the latest developments in nanostructured materials. However, the subject is treated too briefly here, covering only a few aspects of the synthesis of the materials and the production of thin films. There are no examples of applications of such materials in sensors. In Chapter 10 special attention is given to the importance of understanding the molecular and atomic processes for developing high-performance chemical sensors. Some prime examples are gas sensors based on inorganic films in which charge transfer occurs by a variety of mechanisms, other types of gas sensors depending on host–guest interactions, and the principles of function and recognition in biosensors using enzymes, antibodies, and cellular membranes. There is also a short description of the principles of molecular electronics and bioelectronics, and the use of pattern-recognition algorithms in chemical sensor technology. Chapter 11 presents a rather speculative subject-nanosensors. According to the definition given here for an nanosensor, it must have one of the following properties at nanoscale: sensitivity, surface area at which the interaction occurs or characteristic dimensions. The examples described are displacement sensors working in the nanometer and picometer ranges, force-measuring sensors based on the STM principle, optical near-field nanosensors, and Hall effect nanosensors. Apart from the optical sensors all these structures are produced by micromachining of silicon.

The purpose of the second part of this volume is to disseminate reliable information about the market for sensors. The analysis of the market for innovative sensors and microsystems is arranged under the following six key areas: aerospace industry (Ch. 13); industrial process control (Ch. 14); medical and clinical applications (Ch. 15); environment (Ch. 16); automobile industry (Ch. 17); production engineering and quality control (Ch. 18). The authors of this report describe basic requirements for measurements, and technical and commercial limitations that are specific to each of the fields discussed. They also give information about the size of the market and the commercial significance of already existing products, the requirements for new types of products in the area of sensors, and potential new markets.

The book as a whole is set out in a clear and systematic style, and has a comprehensive index. It can be recommended for all scientists and technologists who are looking for a systematic overview of the current state of sensor and microsystem technology, despite the risk that a book dealing with such a rapidly developing area of research may quickly become outdated. University and technical college students of sensor and microsystem technologies should also have access to this work, at least through a library.

Alexandre Choulga
Institut für Chemo- und Biosensorik e. V.
Münster (Germany)

Metal Complexes in Aqueous Solution. By *A. E. Martell* and *R. D. Hancock*. (Series: Modern Inorganic Chemistry. Series editor: *J. P. Fackler, Jr.*). Plenum, New York, 1996. 253 pp., hardcover $ 59.00.—ISBN 0-306-45248-0

The two authors of this book have been engaged in research in coordination chemistry for many years and have contributed greatly to the subject. They have done much detailed work on the determination of thermodynamic quantities for metal complexes and the interpretation of such data in relation to steric and electronic effects in metal–ligand interactions. These studies form the subject of the book reviewed here.

An introduction, which includes a brief historical survey and a concise summary of the most important physicochemical quantities relating to metal ions, is followed by three chapters in which the thermodynamic aspects of metal–ligand interactions are discussed in detail. Taking a representative selection of monodentate ligands as illustrative examples, the authors describe the essential characteristics of complex formation, first in the gas phase then in aqueous solution. The increased stability with multidentate ligands (chelate effect) and with macrocycles (macrocyclic effect) is explained by conformational considerations based on molecular mechanics calculations. In particular, the authors show that some commonly accepted ideas, such as the explanation of the chelate effect purely in terms of entropy, or the assumption that the selectivity of macrocyclic ligands can be predicted from the diameter of the molecular cavity, are incorrect or at least oversimplified. The second part of the book presents some topical examples from biology and medicine, such as chelate therapy, contrast agents for magnetic resonance imaging, and radiopharmaceutical applications. The authors give a survey of the various ligands that are currently used, and present some ideas for the design of new tailored ligands. The book ends with a short description of experimental methods for determining stability constants. Each chapter contains a detailed list of references to original publications, although with a definite emphasis on the authors' own work.

In view of the great importance of metal complexes in present-day medicine, biology, and environmental chemistry, the appearance of an authoritative work on the subject by two recognized experts is very welcome. Nevertheless, the wide-embracing title of the book leads one to expect more than the authors have included here. For example, reversible electron transfer processes play an important role in the chemistry of transition metal complexes (e.g., one need only think about the respiratory chain), and yet there is nothing at all here on redox reactions (with regard, for example, to the question of how the ligand shell affects the redox potential). Again, there is no discussion of hydrolytic polymerisation. One very important reaction pattern exhibited by metal complexes is the formation of polynuclear aggregates with oxo or hydroxo bridging, and should at least have been given a mention (for example, in the summary of possible types of reactions on pp. 221–222). The kinetics of ligand substitution are touched on only briefly in the introduction, and the authors do not take the opportunity to go into more detail later. One searches in vain for important keywords such as "*trans* effect" and "base catalysis". The discussion of experimental methods concentrates mainly on potentiometric techniques [including passages in Sections 7.4 to 7.7 that are mostly taken word-for-word from the book *Determination and Use of Stability Constants*, by A. E. Martell and R. J. Motekaitis (VCH Verlagsgesellschaft, 1988)]. Other methods such as NMR and ESR are mentioned briefly but are not explained in more detail.

Most of the (inevitable) printing errors are of a kind that do not interfere significantly with one's understanding. However, there are some regrettable mistakes, for example in the legend and labeling of Figure 2.19. In Sections 5.5 to 5.9 there are problems with the numbering system used for the ligands, as the numbers in the text do not agree with those in the graphics. Water ligands should be denoted by

 © VCH Verlagsgesellschaft mbH, D-69451 Weinheim, 1996 0570-0833/96/3520-2406 $ 15.00+.25/0

"aqua" rather than "aquo" according to IUPAC recommendations. The text as a whole could have been written somewhat more concisely. The frequent repetitions detract from the clarity of the book; for example, Tables 5.1 and 6.4 are identical. Equation 6.1, which reads: $\log K_1(\text{multidentate}) = \log \beta_n(\text{unidentate}) + (n-1)\log 55.5$ corresponds to Equation 3.1, which is identical except that there "multidentate" is replaced by "polydentate". Figures 3.16 and 6.10 show the same linear plot of $\log K(\text{DFO})$ against $\log K(OH^-)$ (relationship between the free energies), except that different values are given for Pu^{4+}! On the other hand, some of the explanations given in the introductory chapter (Ch. 1) are a little too brief. For example, in Figure 1.5 the various metal centers are classified into "hard", "soft", and "borderline" types (Pearson's HSAB principle). Here Fe and Cu are classed as "borderline", Ag as "soft", and Ga as "hard", without any indication of oxidation states. Although these assignments are appropriate for Fe^{II}, Cu^{II}, Ag^{I}, and Ga^{III}, the same is not true for Fe^{III}, Cu^{I}, Ag^{II}, and Ga^{I}.

To sum up, this book can be recommended for advanced undergraduate students, as well as for researchers working in the areas of coordination chemistry, aquatic chemistry, medicinal chemistry, and bioinorganic chemistry. It will give them a better understanding of the selectivity of metal complexing agents and provide valuable insights for the design of new tailored chelate ligands. However, the discussions are confined to thermodynamic aspects of mononuclear complexes (treated from an unconventional and also rather one-sided point of view). In this respect the book does not fully live up to its title.

Kaspar Hegetschweiler
Institut für Anorganische Chemie
der Universität des Saarlandes
Saarbrücken (Germany)

Stereochemistry of Coordination Compounds. By *A. von Zelewsky*. Wiley, Chichester, 1996. 254 pp., paperback £ 24.95.—ISBN 0-471-95599-X

This book on the stereochemistry of coordination compounds goes well beyond the basic information typically found in textbooks of inorganic chemistry, and even covers recent developments in the chemistry of complexes, such as helicates, complexes of macropolycycles, and siderophores. The emphasis is on "topographical stereochemistry", an aspect that deals with the type and number of stereoisomers and their symmetry properties. The book is essentially concerned with "classical" complexes, so that organometallic compounds and clusters are not treated, for good reasons that are explained on page 9. The literature references provided (over 500) give the reader access to the original papers to study topics in greater depth.

In the introduction (Ch. 1) the author mentions the important contributions of Alfred Werner, whose coordination theory, formulated towards the end of the 19th century, was based mainly on stereochemical considerations. The clarity of this chapter could have been improved by separating the many figures and inserts more obviously from the running text, since the reader might easily lose the thread of the discussion in a few places.

Chapter 2 contains a critical discussion of the experimental methods used for investigating the stereochemical structures of coordination compounds. Chapter 3 then gives a brief survey of the most important types of coordination geometry for complexes of main-group and transition metals. Unfortunately Table 3.1 (p. 31) contains several blunders: for example, the commonest coordination geometry for Cu^{II} is the square-pyramidal, not the tetrahedral.

Chapter 4 deals with some basic concepts of topographical stereochemistry, beginning with general considerations regarding the symmetry and isomerism of metal complexes, and continuing with a classification of ligand types. In deciding which stereochemical nomenclature to use, the author opts for a sensible compromise. In general he follows the IUPAC rules for the nomenclature of inorganic compounds, but in the interests of clarity he occasionally departs from these in some details and adopts alternative principles. Thus, the introduction of several different reference systems for describing the chirality of metal complexes (pp. 67–70) seems entirely appropriate. On the other hand, it takes a little while to get used to some of the unconventional symbols introduced on pages 40-46, such as $A = A$ for planar chelate ligands and $A \approx A$ for nonplanar ones.

Chapter 5 treats the stereochemistry of mononuclear coordination compounds, illustrated by many examples. Here, if not earlier, the discussion of stereoisomeric octahedral chelate complexes (pp. 119-128) reveals one of the main strengths of the book, in that the discussions are supported by a wealth of informative examples. Even complex macrocyclic and macropolycyclic ligands and siderophore complexes are included. Here, however, I feel I must make a correction (p. 148): the first flexible polyazamacrocycle was synthesized as early as 1937 by Alphen, well before the work of Curtis in 1960. The figures in all the chapters have been prepared with much care, and I noticed scarcely any errors [although Fig. 5.73(i) on p. 159 is incorrect].

In Chapter 6 the reader is introduced to the more complex multinuclear systems, beginning with compounds having simple bridging ligands such as hydroxide, halide, or bipyrimidyl. In supramolecular coordination compounds such as the helicates and Sauvage's molecular chains and loops, the stereochemistry is of central importance.

Finally, Chapter 7 deals with stereochemical processes in the reactions of coordination compounds. Due to the complexity of this subject, only selected aspects could be covered. Here the main emphasis is on isomerizations and substitutions at the metal atom. Other topics, such as reactions of coordinated ligands and enantioselective catalysis, are treated only briefly.

To summarize, the book *Stereochemistry of Coordination Compounds* is an excellent and clearly set out reference source for chemists working on metal complexes, with a wealth of examples and many figures. The reader should be able to quickly extract information on a wide range of problems in static stereochemistry. Furthermore, the book is well written from a teaching standpoint and should be suitable for use by advanced students, although the subject matter is quite specialized for these readers.

Roland Krämer
Anorganisch-chemisches Institut
der Universität Münster (Germany)

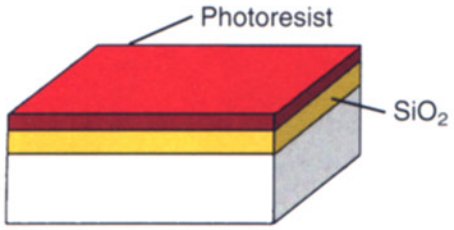

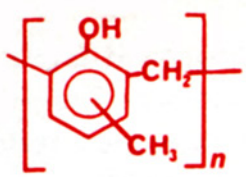

Novolak

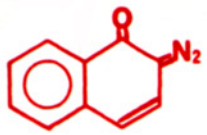

DNC

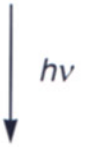

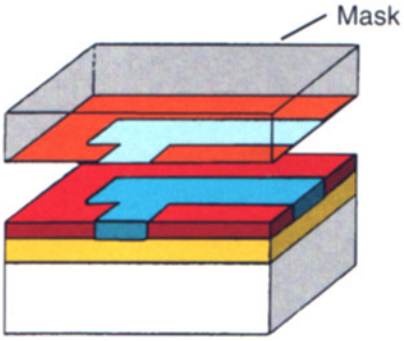

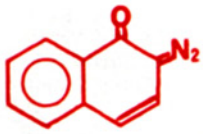

DNC

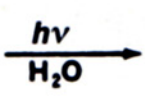

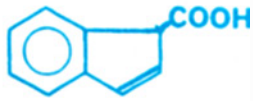

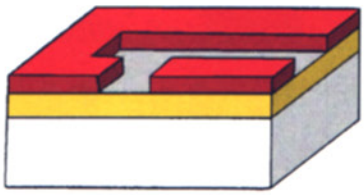

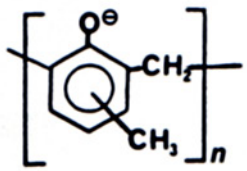

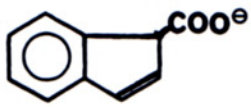

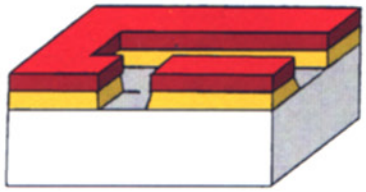

$$SiO_2 + 4\,HF \rightarrow SiF_4 + 2H_2O$$

Some of the fundamental steps of microlithography (coating, irradiation, development of the film with base, removal of the SiO_2 layer) and on the right the chemical processes involved.

Novolak-Diazoquinone Resists: The Imaging Systems of the Computer Chip

Arnost Reiser,* Hsiao-Yi Shih, Tung-Feng Yeh, and Jian-Ping Huang

This year some twenty billion integrated circuits will be produced worldwide. Almost all (98%) of them will be made with a photosensitive varnish, the photo resist, that allows the transfer of a fine line-pattern from an original transparency onto a silicon wafer. This photoresist has two components: one is a novolak resin, a low molecular weight phenol–formaldehyde condensation polymer; the other is a diazonaphthoquinone derivative (DNQ), which is the photoactive part of the system. Novolak–diazoquinone resists have played a crucial role in the microminiaturization of electronics. They are photographic materials of extremely high resolution, able to define features as small as 0.25 μm. Although they are now an indispensible ingredient of modern computer technology, until quite recently their molecular mechanism was not understood. We report here on work at Polytechnic University in New York aimed at solving the mystery of these important and intriguing systems. The solution, in so far as it has revealed itself to us, is rather unique and quite unexpected.

Keywords: diazonaphthoquinones · microlithography · novolak resists · percolation theory · photographic materials

1. Introduction

1.1. Initial Observations and Explanations

In the early 1940s, Oskar Süs, a leading organic chemist at Kalle in Wiesbaden, noticed that coatings of pure novolak dissolved in aqueous alkali within minutes, whereas similar coatings containing diazoquinone derivatives took an hour or more to dissolve. However, when these coatings were exposed to sunlight, they dissolved even faster than pure novolak films. It seemed that diazoquinones inhibited the dissolution of novolak, but lost their inhibiting power on exposure to light. Süs realized the potential of his observation and designed a lithographic printing plate that functioned like a film positive: irradiated and unexposed areas could be distinguished by a large differential in dissolution rate.[1] On the same principle, Süs formulated a light-sensitive varnish ("Kopierlack"),[2] which is now termed a lithographic resist.

The use of resists in the building of semiconductor devices is illustrated in Figure 1. The top of a silicon wafer carrying a layer of SiO_2 (glass) is coated with a thin resist film. The dry film is exposed to UV light through a transparency (the mask) that defines the desired pattern. The exposed film is immersed in a solution of base (the developer) long enough to remove the resist from the irradiated areas. The film is washed and dried to form a template that protects the covered areas of the wafer, but allows chemical action to take place in those areas that were uncovered by exposure and development. Thus, the SiO_2 layer may be removed image by image, and subsequently various dopants introduced in small, well-defined regions of the silicon substrate.

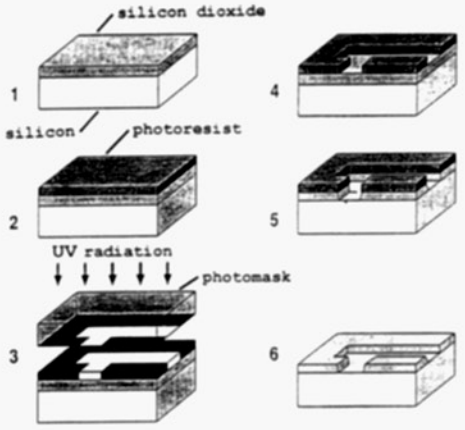

Fig. 1. The basic steps of microlithography: 1) oxidation of the silicon wafer, 2) coating with resist, 3) irradiation through a patterned mask, 4) development of the exposed film in aqueous base, 5) etching away the SiO_2 layer, 6) system ready for localized chemical action. (Reproduced with permission from "Electronic and Photonic Applications of Polymers" in *Adv. Chem. Ser.* **1988**, *218*, 5.)

Novolak–diazoquinone resists have taken the semiconductor device industry almost from its inception to the present state,

[*] Prof. Dr. A. Reiser, Dr. H.-Y. Shih
Institute of Imaging Sciences
Polytechnic University, Six Metrotech Center
Brooklyn, NY 11201 (USA)
Fax: Int. code +(718) 260-3136
e-mail: areiser@duke.poly.edu
Dr. T.-F. Yeh
Polaroid Graphics Imaging, Waltham, MA 02154.
Dr. J.-P. Huang
Lord Corporation, Cary, NC 27511

from integrated circuits with a few hundred transistors to the 16-megabit chip.[3] They have become a crucial part of modern technology. Yet in spite of this, their molecular mechanism was not understood until quite recently.

When Süs first tried to rationalize the behavior of these materials, he tested a series of diazoquinones and found that, to a varying degree, all worked as "photoactive component" in novolak resins. He surmised that image discrimination in the resists was based on a common photoreaction of diazoquinones, and he investigated their photochemistry. On irradiation with a mercury lamp (Scheme 1), diazonaphthoquinone (**1**) loses a molecule of nitrogen and, in the presence of small quantities of water, is transformed into indene carboxylic acid (**2**).[4]

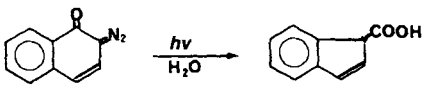

1 2

Scheme 1. Photolysis of diazonaphthoquinone (**1**).

Acid **2** is soluble in alkali in contrast to DNQ, and at the time that seemed an adequate explanation for the observed behavior. Of course, the photochemistry of diazoquinone does not address dissolution inhibition in the unexposed films, nor can it account quantitatively for the behavior of exposed resists. In fact, dissolution inhibition in novolak is a unique phenomenon. Just how unusual it is can be appreciated by comparison with the effect of additives on the dissolution of common polymers. For example, the addition of 10 percent of an insoluble component to a polymethacrylate may change the dissolution rate of the polymer in acetone by 10 to 20 percent;[5] however, 10 percent of a diazonapthoquinone (DNQ) slows down the dissolution of novolak in aqueous base by more than 2000%. Several interpretations of this phenomenon have recently been proposed,[6-11] but none seems completely convincing. In this paper we present a model of novolak dissolution and dissolution inhibition based on the concepts of percolation theory.[12]

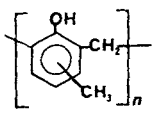

3

1.2. Novolak Dissolution and the Penetration Zone

Novolak (**3**) is a low molecular weight phenol–formaldehyde condensation polymer. The dissolution of novolak in aqueous base predicates the deprotonation of the phenolic hydroxyl groups of the polymer Ⓟ to phenolates [reaction (a)].[6] In

$$Ⓟ\,OH + OH^- \rightleftharpoons Ⓟ O^- + H_2O \qquad (a)$$

that process, base is used and a molecule of water is formed. When a novolak film is immersed in aqueous base (the developer), the base penetrates the resin matrix and a thin layer of phenolate is formed at the interface between the resin film and the developer solution. This layer is a new phase, the penetration zone. Figure 2 is a schematic representation of the zone; the

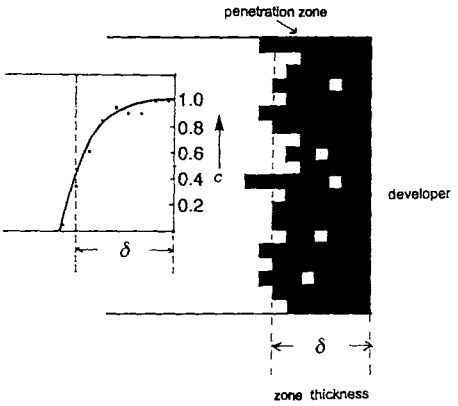

Fig. 2. The penetration zone formed at the interface of the matrix with the developer solution. The black squares represent phenolate ion sites; the white squares are phenolic OH units. The inset shows the concentration profile of phenolate ions in the zone.

phenolate ions are indicated by black squares. As soon as a sufficient number of OH groups has been ionized, the polymer chains at the back of the penetration zone become soluble in water; they disentangle and float off into the aqueous developer. When the rate of transfer of ionized novolak chains at the interface with the developer balances the rate of formation of phenolate at the front of the zone, a stationary dissolution regime is established. Without changing its thickness or its composition, the zone moves forward at a constant speed, which is identical with the dissolution rate (loss of thickness) of the novolak film.[13]

Since the deprotonation reaction is very fast, the rate of travel of the zone depends entirely on the rate at which base is supplied to the reaction site at the interface of the penetration zone with the virgin matrix. Thus, the rate of dissolution is controlled by the rate of base diffusion through the penetration zone. Arcus,

Arnost Reiser is Distinguished Research Professor and Director of the Institute of Imaging Sciences at Polytechnic University in Brooklyn, New York. Prior to that he was head of the Photochemistry Laboratory of Kodak Limited in England, where he became closely associated with the early development of photoresists. He has published extensively on polymer photochemistry and imaging, and he is the author of the book "Photoreactive Polymers: the Science and Technology of Resists", Wiley, New York, 1989. He holds the Henderson Medal of the Royal Photographic Society and was awarded a D. Sc. by the National Council for Academic Awards of Great Britain. He is a Fellow of the Society of Imaging Science and Technology.

who discovered the penetration zone and demonstrated its physical existence as a separate phase, sensed that the zone acted as a kind of control membrane,[14] and that various agents, including light, influence the permeability of this membrane to produce the unusual dissolution behavior of the system.

Since it comprises almost entirely phenolate/counterion pairs, the zone is a solid polyelectrolyte of exceptionally high ionic strength (total ionic strength as high as 10 M). The electrostatic forces between the polymer-bound phenolate anions and the countercations give it a high degree of cohesion, which has an unexpected consequence: at room temperature, the penetration zone of most resins is in a rigid glassy state. This can be demonstrated by monitoring the dissolution of resin films over an appropriate temperature range.[15] Figure 3 shows the Arrhenius plot for the dissolution of a typical novolak resin at room temperature in a 0.20 N solution of KOH. The plot has two branches separated by a discontinuity. The temperature at the discontinuity is the glass transition temperature T_g' of the zone. For the resin referred to in Figure 3 the glass transition temperature T_g' of the zone is 30 °C. In contrast, the glass transition temperature T_g of the bulk of the resin film is about 120 °C.

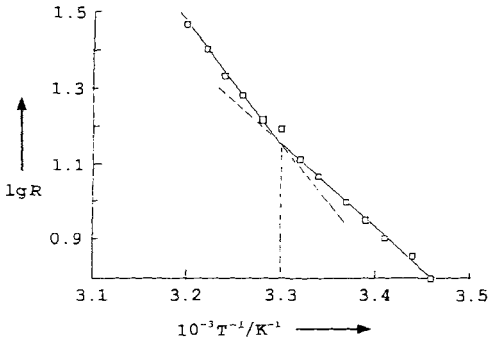

Fig. 3. Arrhenius plot of $\lg R$ vs. $1/T$ for a novolak resin dissolving in 0.2 N KOH. The discontinuity of the plot corresponds to the glass transition temperature T_g' of the penetration zone (30 °C).

Some insight into the significance of the glass transition in these systems can be gained from the activation energies calculated for the two branches of the Arrhenius plot. The activation energy of dissolution E is 4.3 kcal mol^{-1} below T_g', and 8.6 kcal mol^{-1} above T_g'. It is unusual that a higher activation energy is associated with a higher diffusion rate. The reason for this behavior is a profound change in the mechanism of base diffusion. Below the glass transition, the hydrophilic sites (OH groups and phenolate ions) are fixed in their locations, and the distribution of open bonds (that is, bonds passable by the diffusant; see Section 2) in the percolation field is independent of time. Under these conditions the activation energy corresponds to the average energy barrier between adjacent sites that form open bonds. Above the glass transition, the hydrophilic sites in the penetration zone become mobile, and site diffusion becomes the rate-determining process. The activation energy of dissolution is now associated with the movement of sites. Below T_g' the diffusant percolates in a field of stationary sites, above T_g' the sites are mobile and cooperate in the diffusional transport.

The interface of the zone with the resin matrix is a fractal surface[16, 17] (Fig. 2). The fractal nature of the interface produces a concentration profile of phenolate ions in the zone that is matched by a corresponding concentration profile of base established during the dissolution process. The form of this profile, schematically shown in the inset of Figure 2, is responsible for the nonlinear dependence of the dissolution rate on the base concentration of the developer.[18] Details on this aspect of the system can be found in references [13] and [18].

The dissolution rate R (in cm s^{-1}) is linked to the diffusional flux F of base through the zone (in mol L^{-1} cm^{-1} s^{-1}) by the mean base concentration c (in mol L^{-1}) in the zone [Fig. 4, Eq. (1)].[18] Applying Fick's law to this situation and

$$F = Rc \qquad (1)$$

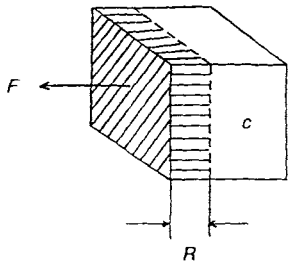

Fig. 4. Diffusional flux F of base per unit area (in mol cm^{-2} s^{-1}) of the penetration zone in a developer of base concentration c (in mol cm^{-3}). R is the rate of travel of the membrane in the direction of the concentration gradient (in cm s^{-1}).

ignoring the precise shape of the concentration profile in the penetration zone, one may in a first approximation replace the average concentration gradient $\left(\frac{dc}{dx}\right)$ in the zone by the ratio of the base concentration in the developer (c_0) to the thickness δ of the penetration zone [Eq. (2)]. This leads to a relation between

$$F = -D\frac{dc}{dx} = -D\frac{c_0}{\delta} \qquad (2)$$

the dissolution rate and the mean diffusion coefficient D of base in the penetration zone [Eq. (3)]. By inserting reasonable values

$$R = 2\frac{D}{\delta} \qquad (3)$$

for the dissolution rate ($R = 200$ A s^{-1}) and for the thickness of the penetration zone ($\delta = 100$ Å) one obtains a mean diffusion coefficient of base in the zone of approximately 10^{-12} cm^2 s^{-1}.[13]

This value is rather low compared with the diffusion coefficients of small solvent molecules in common polymers (10^{-6} to 10^{-8} cm^2 s^{-1}), but it is not unrealistic; Barker and Thomas measured the mobilities of alkali ions in cellulose films and found diffusion coefficients of the order of 10^{-18} cm^2 s^{-1}.[19]

There is a fundamental difference between the diffusion of solvent into common polymers and the diffusion of base into novolak films. The key to understanding this difference is the recognition that novolak and other phenolic resins are amphiphilic materials that contain hydrophilic as well as hydrophobic moieties. A novolak film may thus be regarded as a hydrophobic solid in which hydrophilic sites (the OH groups of the phenols) are embedded. Base ions are attracted to the hydrophilic sites and repelled by the hydrophobic regions. As a result, they migrate into the solid by transferring from one hydrophilic site to the next.[12] This mode of progression is a typical percolation process, and if our view is correct, the diffusion of base into amphiphilic solids will be governed by the rules of percolation theory.

2. Percolation Theory

Percolation theory describes the progression of a particle through a system of cells, some of which are occupied and others empty.[20-22] Figure 5 is a schematic representation of a two-dimensional square percolation field where the occupied cells are indicated by open circles. The mobile particle is allowed to reside in occupied cells, and it may transfer from one occupied cell to its occupied neighbor, but it cannot enter an unoccupied cell. As a result its movement is circumscribed by the size of the cluster of occupied cells in which it happens to find itself. The state of the percolation field is characterized by a percolation parameter p, which is simply the fraction of occupied cells. The higher the percolation parameter p, the larger the average size of the cell clusters. At some stage the cluster becomes "infinite", that is, it extends across the whole percolation field. At that point continuous diffusion throughout the system sets in. The critical p value at which this occurs is called the percolation threshold, p_c.

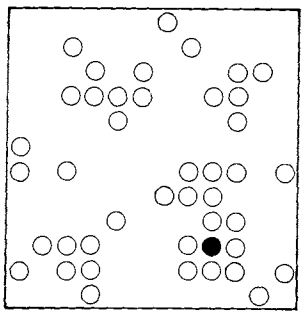

Fig. 5. Two-dimensional square percolation field in which only the occupied cells are marked by open circles. The filled circle represents the mobile particle.

It is a fundamental thesis of percolation theory that the macroscopic properties of the system are functions of the difference $(p - p_c)$. For diffusion in three dimensions this function takes the form of a quadratic scaling law [expression (4)].

$$D \sim (p - p_c)^2 \tag{4}$$

To apply the concepts of percolation theory to novolak we identify the occupied cells as those which contain either a phenol group or a phenolate ion. Both have the main attributes of a percolation site (an occupied cell): they attract, or tolerate, the (ionic) diffusant. The situation may be represented in terms of potential energy surfaces. In a hydrophobic continuum the OH group is characterized by the potential energy surface of a dipole interacting with an ion. Figure 6 shows a cross-section through the potential energy surfaces of two adjacent potassium phenolate sites (dipole moment μ = 3.0 Debye); part of the potential energy surface of a phenol site (μ = 1.5 debye) is also indicated. The potential energies were calculated based on electrostatic considerations and a Lennard-Jones potential.[23] The elementary event of base diffusion is the transfer of an ion from one potential energy trough to the next. In that transfer step the diffusant must overcome the energy barrier E_b at the intersection of the potential energy surfaces of the two adjacent sites. The probability of transfer is given by a Boltzmann factor $\exp(-E_b/RT)$, and we shall assume that above a certain critical energy barrier the transfer probability between two sites is so small that it may be neglected, while for all energy barriers below that critical value transfer will be certain. This crude device allows us to fit the dissolution problem into the established formalism of percolation theory in which a transition is either allowed or forbidden.

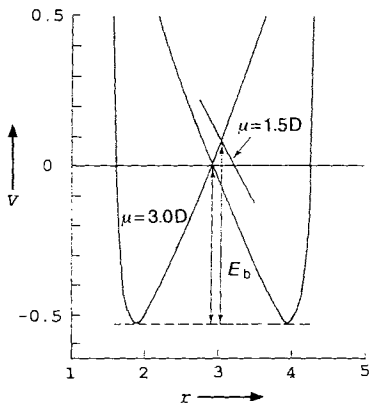

Fig. 6. Intersection of the potential energy hypersurfaces of two adjacent phenolate sites (dipole moments μ = 3.0 Debye) at a separation of about 6 Å. Part of the potential energy curve of a phenol site (dipole moment μ = 1.5 Debye) is also indicated. V: energy in eV; r: radius in Å; E_b: the energy barrier.

Figure 5 represents a site percolation field, but percolative diffusion is, in fact, a bond percolation process,[20, 21] a bond being the link between two adjacent sites. In a bond percolation field the diffusant migrates along an unbroken sequence of open bonds. The energy barrier between two sites decides whether a bond is open (that is, passable by the diffusant) or closed, and that energy barrier depends in the first place on the spatial separation of the two sites. The relationship between site separation and the energy barrier between sites can be illustrated by measuring the activation energy of dissolution in resin films in which the average site separation varies. In Figure 7 we have plotted the experimentally determined activation energy of dissolution as a function of the average intersite distance for a series of polyvinylphenol resins in which the average intersite distance had been modulated by partial methylation of the OH groups of the resin.[12]

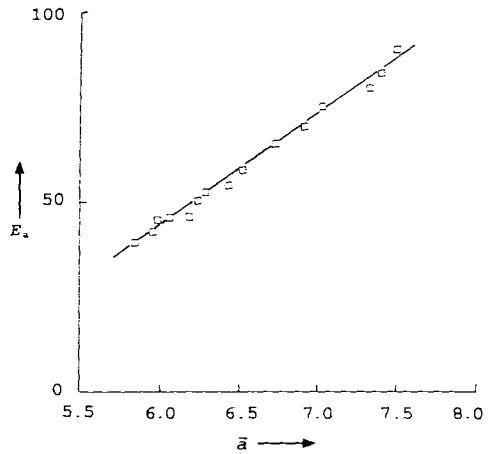

Fig. 7. Activation energies E_a (in kJ mol^{-1}) of dissolution for partially methylated poly(vinylphenol) resins, plotted as a function of the average intersite distance $\bar{a}$ (in Å).

The view that percolative diffusion in amphiphilic solids is a bond percolation process is supported by a variety of observations, and also by the experimentally found value of the percolation threshold (p_c = 0.20), which is very near the theoretical percolation threshold for a cubic bond-percolation system.[15] The theoretical threshold for bond percolation in a simple cubic lattice is 0.25, and in a body-centered cubic lattice it is 0.18. (The corresponding values for a site percolation field are significantly higher: 0.312 and 0.245).[21]

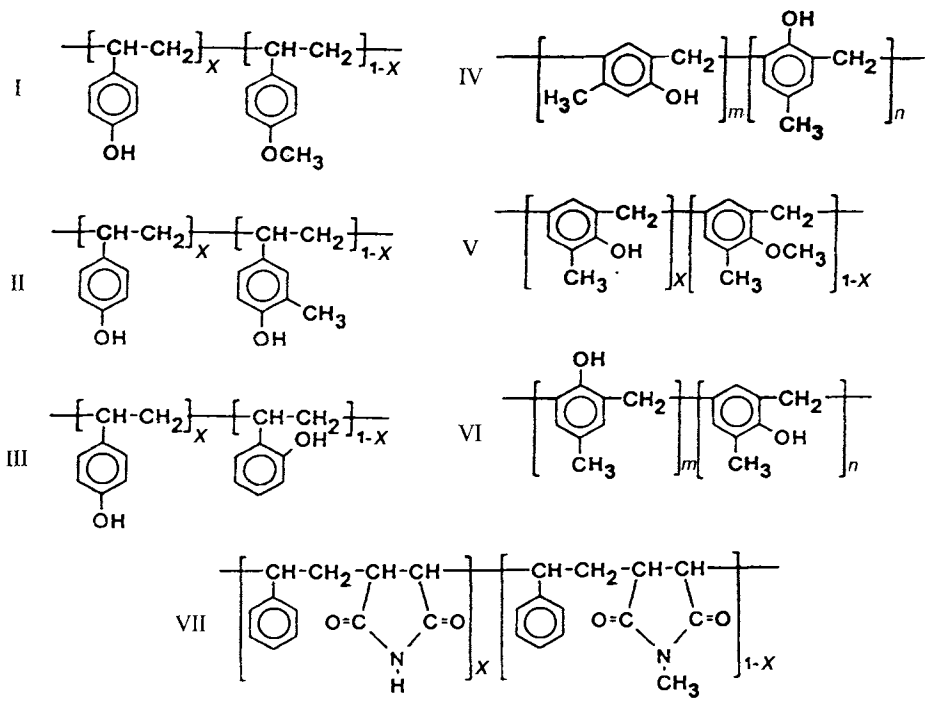

Scheme 2. Amphiphilic resins: I) partially methylated poly(4-hydroxystyrene) resins [1, 5]; II) copolymers of 4-hydroxystyrene and 3-methyl-4-hydroxystyrene [9]; III) copolymers of 4-hydroxystyrene and 2-hydroxystyrene [10]; IV) novolak resins made from mixtures of *m*-cresol and *p*-cresol [11]; V) partially methylated *o*-cresol novolak resins; VI) partially methylated novolak resins made from equimolar quantities of *o*-cresol and *p*-cresol; VII) partially methylated alternating copolymers of styrene and maleimide.

2.1. A Percolation Model of Novolak Dissolution

We tested the bond percolation model of novolak dissolution by fitting the experimentally determined dissolution rates with the scaling law (5). The percolation parameter p in a phenolic

$$R \sim (p - p_c)^2 \tag{5}$$

resin is proportional to the concentration of OH groups. We selected seven amphiphilic resins (Scheme 2)[1,5] and changed their percolation parameter either by successively methylating some of their OH groups (I, V to VII), or by changing the accessibility of OH groups through steric hindrance (II to IV). Resins I to III are polyvinylphenols, IV to VI are novolak resins, and VII is an alternating copolymer of styrene and maleimide. By modifying the base resins we produced 52 amphiphilic resins with different values of p. Each resin was characterized by its fraction (x) of unaltered OH groups, and it was assumed that the unaltered base resin ($x = 1$) of each series had a percolation parameter of unity ($p = 1$). The logarithm of the dissolution rate ($\lg R$) was then plotted against $\lg(p - p_c)$. An appropriate value for the percolation threshold of all our resins was found to be $p_c = 0.20$.

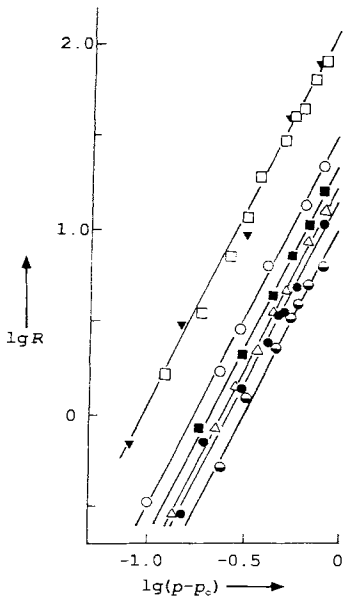

Fig. 8. Plot of $\lg R$ against $\lg(p - p_c)$ for seven series of amphiphilic resins (see Scheme 2). □ resin I, △ resin II, ■ resin III, ▼ resin IV, ○ resin V, ● resin VI, ◒ resin VII.

The results of these experiments are shown in Figure 8: the data points lie on straight lines that have a slope of 2, as demanded by the quadratic scaling law of Equation (5). Figure 8 also indicates that the dissolution behavior of these systems can be generalized. By translating the correlation lines to the left, they can be brought into superposition with the correlation line of the fastest dissolving resins, the polyvinylphenols I. In that case the experimental points fall on a single line, represented by a dimensionless scaling law [Eq. (6), where R° is the dissolution rate of the reference

$$\lg \frac{R}{R^\circ} = 2 \lg \frac{p - p_c}{1 - p_c} = f(p) \tag{6}$$

resin (unmethylated polyvinylphenol)]. The reference resin is assigned a percolation parameter of unity ($p = 1$); all other resins, including the base resins of other series, have lower values of p. In Figure 9 the dimensionless dissolution rate log R/R°

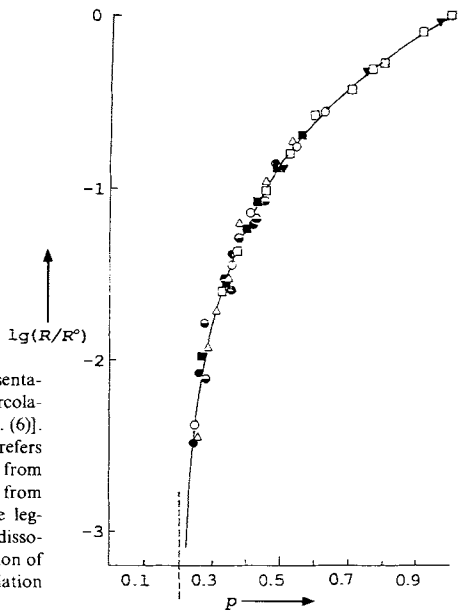

Fig. 9. Dimensionless presentation of the scaling law of percolative dissolution [Eq. (6)]. Each experimental point refers to an amphiphilic resin from one of the seven groups from Scheme 2. For symbols, see legend of Figure 8. R = rate of dissolution, R° = rate of dissolution of reference resin, p = percolation parameter.

is presented as a function of the percolation parameter p. The experimental points of all 52 resins fit the theoretical curve of the scaling law rather well.[15]

The generalized scaling law can also be used to define the percolation parameter p by an inversion of Equation 6 [Eq. (7)].

$$(p - p_c) = (1 - p_c)\sqrt{\frac{R}{R^\circ}} \tag{7}$$

This expression links the percolation parameter p directly to the dissolution rate R, rather than to the concentration of hydrophilic sites, and that is appropriate for a bond percolation process.

2.2. Dissolution Inhibition

After novolak dissolution was recognized to be a percolation process, it seemed a foregone conclusion that dissolution inhibitors function by blocking some of the hydrophilic sites (OH groups). To test this idea quantitatively we needed a measure of inhibition. In his study of the kinetics of resist dissolution Meyerhofer had found that a plot of the logarithm of the dissolution rate against the inhibitor concentration is linear over a significant concentration range (Fig. 10).[24] We used the slope

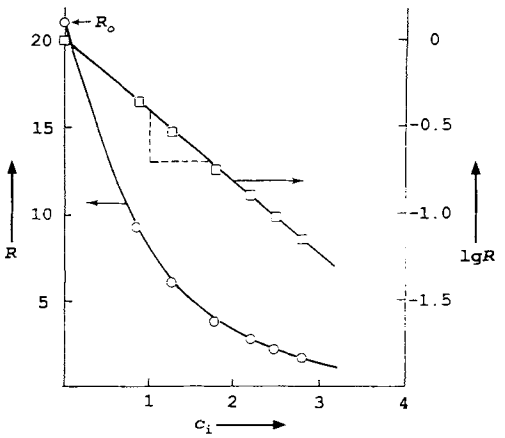

Fig. 10. Meyerhofer plot of the logarithm of dissolution rate ($\lg R$) vs. the concentration of inhibitor (c_i in wt%) in novolak films that contain a monofunctional diazonaphthoquinone inhibitor (DNQ). In addition the dependence of R (in $\mu m\,min^{-1}$) on c_i is shown.

of the Meyerhofer plot as a concentration-independent measure of the strength of the inhibition effect, and termed it the inhibition factor f_{ij} of inhibitor i in resin j [Eq. (8)]. If the inhibitor

$$f_{ij} = -\frac{d\lg R}{dc_i} \tag{8}$$

acts by changing the concentration of available hydrophilic sites, it must also change the percolation parameter of the system. The change in $\lg R$ is given by Equation (6). Accordingly, the inhibition factor f_{ij} is linked at the level of differentials to the slope of Equation (6) at the dissolution rate of the uninhibited resin. The differential at the right hand side of Equation (9) can be expanded, and on using the relation between dissolution rate and percolation parameter [Eq. (7)] it can be rewritten as Equation (10), where e is the base of the natural logarithm.

$$f_{ij} = -\frac{d\lg R}{dc_i} = \alpha\frac{d\lg R}{dp} \tag{9}$$

$$f_{ij} = \alpha_i \frac{2\lg e}{1 - p_c}\sqrt{\frac{R^\circ}{R}} \tag{10}$$

Equation 10 is a significant result. It establishes a relation between two seemingly unrelated, but directly measurable quantities: the inhibition factor of an inhibitor/resin pair and the dissolution rate of the pure, uninhibited resin. We have tested Equation 10 by plotting values of f_{ij} against the reciprocal square root of the dissolution rate ($R^{-1/2}$) of the uninhibited resins.[25] We used a standard monofunctional diazonaphthoquinone (DNQ) inhibitor (the *tert*-butyl ester of 2-diazonaphthoquinone-5-sulfonic acid) in three different types of resins: groups I and II are polyvinylphenol derivatives; group III contains partly methylated novolak resins. The results in Figure 11 show that straight lines are obtained for every group of resins, in agreement with Equation (10), but that the plots consist of two branches. The discontinuity is associated with the glass transition of the penetration zone.

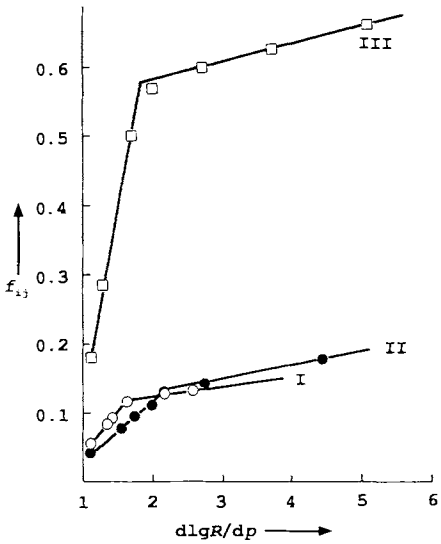

Fig. 11. Inhibition factor f_{ij} of a standard monofunctional DNQ inhibitor as a function of $d\lg R/dp$ for three series of phenolic resins: I) partially methylated poly(4-hydroxystyrenes); II) copolymers of 4-hydroxystyrene and 3-methyl-4-hydroxystyrene; III) partially methylated samples of a single novolak resin [15].

To prove this point we have determined T_g' for all the methylated novolak resins of group III by measuring the temperature dependence of their dissolution rates (Fig. 12).[25] The glass transition temperatures of the resins that give the discontinuities for group III observed in the f_{ij} plot of Figure 11 ($T_g' = 20\,^\circ C$) coincide with the temperature at which the inhibition factors were measured. As will be shown later, inhibition depends on the existence of phenolate clusters in the penetration zone. The glass transition T_g' marks the onset of site motion in the zone; above T_g' the phenolate clusters are no longer stable, and the inhibition effect does not grow any more with the slope of the scaling law function [Eq. (9)].

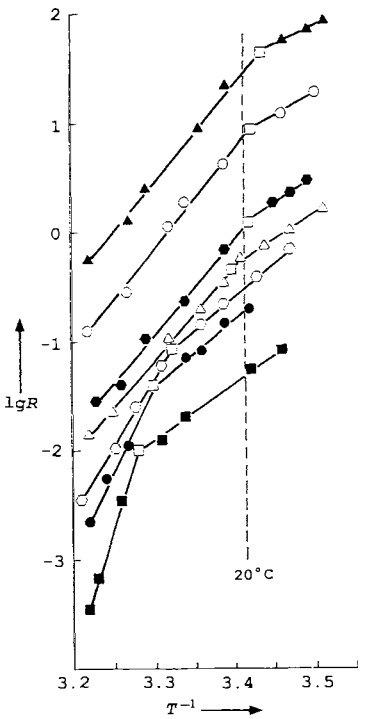

Fig. 12. Temperature dependence of the dissolution rate R (Arrhenius plot) of a group of partially methylated novolak resins (group III of Fig. 11). □: glass transition temperature T_g'.

The slope of the plots in Figure 11 depends not only on the type of resin used, but also on the structure of the inhibitor. We have investigated nine aromatic ketones (inhibitors) in six partially methylated novolak resins that have different image points (Fig. 9) and slopes on the scaling law curve. All the resins had T_g' well above room temperature, so that the inhibition factors of the additives were measured in the glassy state of the penetration zone. In Figure 13 we have plotted the inhibition factors of inhibitors **4**–**11** against the reciprocal of the dissolution rate of the methylated novolak resins according to Equation (10). The experimental points for all inhibitors lie again on straight lines.[25]

The slopes of the correlation lines in Figure 13 are characterized by a proportionality constant α_i. This has the dimension of a molar volume and may be interpreted as that volume in the resin matrix that is made unavailable to percolation by the presence of one mole of inhibitor. Assuming that the least effective inhibitor, benzophenone (not shown in Fig. 13), blocks a single OH group of the resin, the ratio α_i/α_B (where α_B refers to benzophenone) measures the number of OH groups (hydrophilic sites) that a particular inhibitor would have to disable in order to produce the observed inhibition effect. Values of these "blocking numbers" (α_i/α_B) are listed in Table 1 together with the inhibition factors of the aromatic ketones.[26] According to this analysis, one molecule of the standard diazonaphthoquinone inhibitor blocks 7 OH groups, and one molecule of α-naphthoflavone eliminates some 16 phenolic sites. Clearly, inhibitors must be able to affect more than one phenolic OH to account for the inhibition effect routinely encountered in commercial resists.

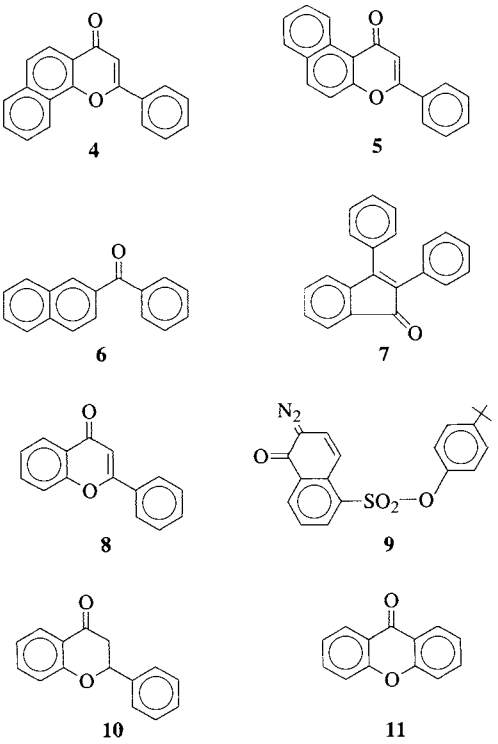

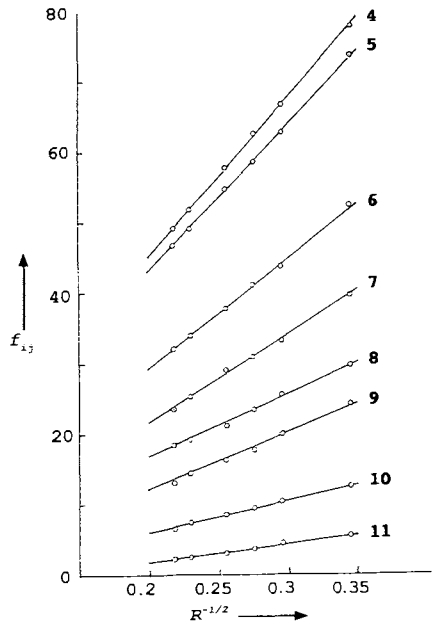

Fig. 13. Inhibition factors f_{ij} of eight additives incorporated into partially methylated novolak resins (group III of Fig. 11), plotted against $R^{-1/2}$ [25].

Table 1. Numbers of sites blocked by selected inhibitors normalized against benzophenone (given as the site blocking numbers α_i/α_B).

Inhibitor	f_{ij} [a]	M_i[b]	α_i/α_B
Benzophenone	0.55	182	1
Xanthone	2.26	196	2.13
Flavanone	6.80	223	3.78
DNQ	13.1	396	6.79
Flavone	18.3	221	7.65
2,3-Diphenylindenone	23.6	282	9.73
β-Naphthoflavone	46.6	271	16.4
α-Naphthoflavone	49.1	271	16.6

[a] f_{ij} is the inhibition factor of inhibitor i in resin j. [b] M_i is the molecular mass of the inhibitor.

Earlier, to explain this phenomenon Honda et al. had proposed the formation of a supramolecular complex in which a single inhibitor molecule could block up to 18 OH groups in a calixarene-like configuration. They termed this the "octopus pot" model.[27] The idea of supramolecular structures was also supported by Dammel and others.[28] Although the octopus pot

would explain the large inhibition factors of common diazoquinones (and such structures may be formed in special cases), it is unlikely that they arise in the typical novolak resins of practical microlithography. The most serious difficulty here is the requirement of multiple hydrogen bonding by a single center, when it is known that hydrogen bonds saturate and are formed only between single donor–acceptor pairs. We have now proposed an alternative mechanism that allows inhibitors to influence more than one phenolic OH group. It is based on the inductive polarization of hydrogen bonds.

2.3. Phenolic Clusters

Hydroxyl groups can function simultaneously as hydrogen donors and hydrogen acceptors. As a result water forms extended networks in ionic solutions, and phenols congregate in hydrogen-bonded strings or clusters. The driving force here is the autopolarization of the OH groups in hydrogen bonds. When an OH group is involved as the hydrogen donor in a hydrogen bond, the partial negative charge on its oxygen atom increases, and that oxygen becomes a stronger hydrogen acceptor than the oxygen of a free, uninvolved OH group (Scheme 3). Phenolic dimers are therefore more desirable partners for an OH group than monomeric phenols. Hydrogen bonding in phenolic solutions does not stop at the dimer, but immediately forms larger aggregates, the phenol clusters. This is illustrated by a plot of the absorbance of the IR band of free *p*-cresol (3614 cm^{-1}) as a function of the phenol concentration in solution (Fig. 14).[29] The dramatic deviations from Lambert–Beer's law at concentrations above 0.1 M indicate the formation of phenolic aggregates.

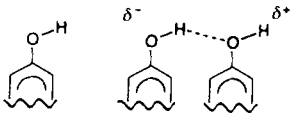

Scheme 3. Hydroxyl groups in hydrogen bonds.

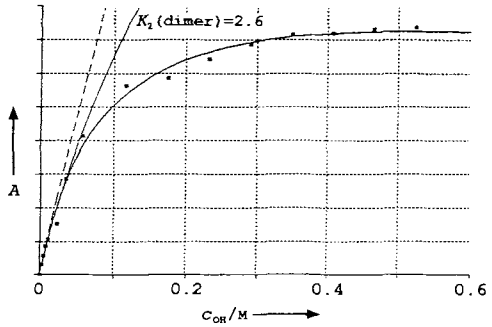

Fig. 14. Absorbance A (arbitrary units) of the OH stretching vibration at 3614 cm^{-1} in the IR spectrum of *p*-cresol as a function of the cresol concentration in CCl_4.

When a strong H-acceptor such as a diazoquinone or another aromatic ketone is introduced into a phenolic system, the inductive polarization effect is greatly intensified. The inhibitor forms a strong hydrogen bond with the nearest OH group, and in so doing polarizes the oxygen atom of its partner, making it a stronger hydrogen acceptor that can in turn attract other hydrogen donors (Scheme 4). In this way the stronger inductive effect of the inhibitor propagates some distance into the neighborhood and leads to the formation of larger and more tightly bound phenolic clusters. It is these clusters that are at the root of the inhibition effect.

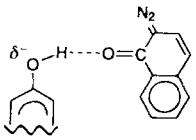

Scheme 4. Hydrogen bonds between phenolic groups and DNQ inhibitor.

The consequences of the inductive polarization of hydrogen bonds can be demonstrated by simple bulk experiments.[28] For example, addition of strong hydrogen acceptors to novolak solutions produces a significant increase in solution viscosity (Fig. 15) caused by the polarization of OH groups adjacent to those that are directly linked to the hydrogen acceptor (inhibitor). Figure 15 shows viscosity increases in two novolak solutions to which three aromatic ketones of differing acceptor strength had been added. Similar effects were observed when the bulk glass transition temperature of dry novolak films containing strong hydrogen acceptors was measured.[26]

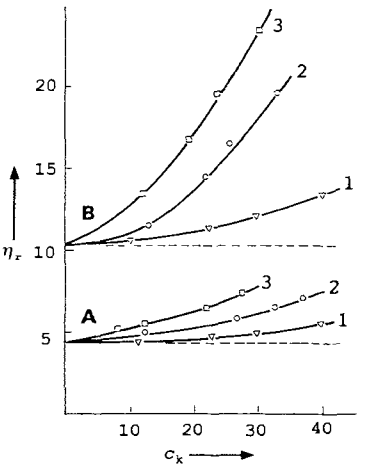

Fig. 15. The effect of the concentration c_k (in wt%) of three aromatic ketones (1: flavanone; 2: flavone; 3: α-naphthoflavone) on the viscosity η_r of two novolak solutions (A: 18.4% novolak in *iso*-amylacetate; B: 24.2% novolak in *iso*-amylacetate) at 20 °C.

How do phenolic clusters affect the dissolution rate? They concentrate some of the hydrophilic sites in small regions, depleting the surroundings of percolation sites. This creates large regions of low site density where the overall connectivity of the open bond network is reduced. Thus, the base diffusion rate is lowered and by implication also the dissolution rate. The effect may be illustrated by a simple simulation experiment.[26] Figure 16 shows a two-dimensional percolation field of a hundred cells where each cell is subdivided into nine compartments (not shown in Figure 16). One hundred sites are

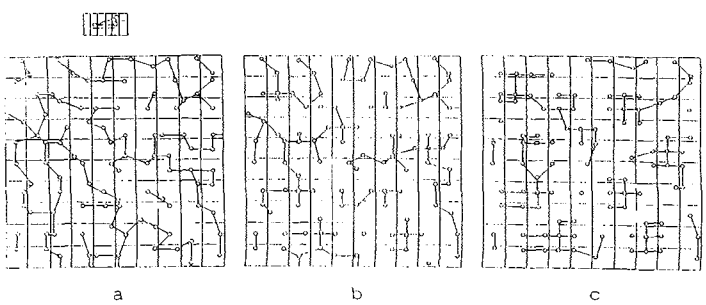

Fig. 16. Simulation experiment to illustrate the effect of clustered OH groups on the dissolution rate. The two-dimensional square percolation field represents 100 cells. One hundred sites are distributed over the 100 cells. a) The position of the sites within the cells are random. b) Ten sites (the attractors) are allowed to attract four sites each in neighboring cells, thus forming 10 four-membered clusters. c) The same attractors are allowed to attract 7 neigboring sites. For details, see text.

placed into the field, so that each cell contains one site, but the position of the sites in the compartments within the cells is random (Figure 16a). We choose a critical intersite distance (indicated in the small diagram on top of Fig. 16a), which is the separation of two neighboring sites that still constitute an open bond. We now form a network by connecting all open bonds. In the case of Figure 16a this network contains 71 sites and links opposite sides of the field, in which macroscopic diffusion is now possible. We now introduce the inhibitor by selecting ten random sites as "attractors" and allow each of these sites to attract four sites from neighboring cells. The attracted sites will move from their original compartments to the compartment nearest to the attractor site, while still remaining in their own cells (Fig. 16b). By again connecting the open bonds we find that the infinite network in this case contains only 56 sites. The connectivity of the system has clearly decreased, and diffusion will slow down since the number of opportunities for migration along open bonds has declined. Continuing in that fashion we let the same attractors as before draw to themselves up to seven sites (Fig. 16c). In this case the bond network is no longer infinite, and macroscopic diffusion ceases. We conclude that in a bond percolation field the site connectivity decreases when site clusters are formed and the fraction of sites per cluster increases.

2.4. Phenolate Ion Clusters

At this point we need to remind ourselves that the dissolution rate of novolak films is controlled by the diffusion of base through the penetration zone. If cluster formation is the controlling factor in regulating diffusion, site clusters must exist in the penetration zone. We have seen that the percolation sites in the zone are not phenolic OH groups but phenolate ions, and these are no longer connected to each other by hydrogen bonds. If the phenol clusters of the coating solution survive as phenolate clusters into the penetration zone, they do so by virtue of the glassy state of the zone.[30]

We have shown earlier that the glass transition temperature T_g' of the zone lies above the temperature of development for all useful resins.[15] Adding inhibitors to novolak increases the glass transition temperature of the zone.[26] For example, with 2% of α-naphthoflavone, T_g' increases from 30° to 43 °C for a group III resin. This increase indicates stronger cohesion in the zone. In the concentrated solid polyelectrolyte of the penetration zone, the electrostatic cohesive forces are proportional to the local charge density, which is increased at the location of the clusters. The increase in T_g' is proportional to the inhibition factor of the additive (Fig. 17); both depend on the cluster-forming capability of the inhibitor.

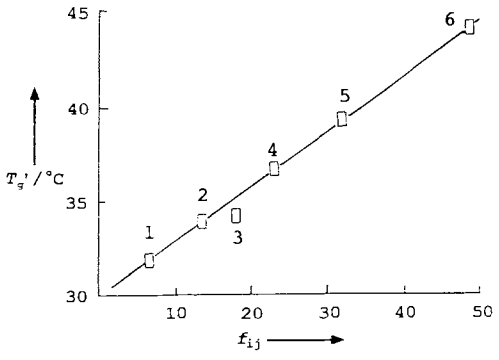

Fig. 17. The glass transition temperature T_g' of the penetration zone as a function of the inhibition factor f_{ij} of six inhibitors (1: flavanone; 2: DNQ; 3: flavone; 4: 2,3-diphenylindenone; 5: benzoylnaphthalene; 6: α-naphthoflavone).

3. The Dissolution of Exposed Resist Films

After these preliminaries we can consider the behavior of exposed resist films. When a resist film is exposed to light or UV radiation, the dissolution rate increases from a value far below that of pure novolak to a value somewhat higher than that of novolak. It is this change that makes it possible to differentiate between exposed and unexposed areas in practical applications. The situation is represented by the Meyerhofer plot in Figure 18, which depicts the dissolution rate of unexposed and exposed novolak films containing increasing quantities of a monofunctional DNQ inhibitor.[24, 30] What happens during exposure that brings about this dramatic change in behavior?

On exposure DNQ (**1**) is changed to indene carboxylic acid (**2**). That is converted into carboxylate ions in the penetration zone, where it augments the number of hydrophilic sites. However, this modest increase in the concentration of percolation sites cannot account for the large change in dissolution rate. We can demonstrate this by eliminating indene carboxylic acid from the exposed resist. Because carboxylic acids are thermally not very stable, indene carboxylic acid is decarboxylated in about one hour at 70 °C. We exposed a series of films with increasing DNQ content and kept the fully exposed films at 70 °C for two hours. When the dissolution rate of the films was measured in the usual way, all films dissolved at the same rate, irrespective of their original DNQ content, and that rate was similar to the dissolution rate of pure novolak (Fig. 18b). The small lowering of the dissolution rate relative to that of novolak is probably caused by a mild densification effect.[30]

If dissolution inhibition is caused by cluster formation, the results of these experiments must mean that exposure has, in

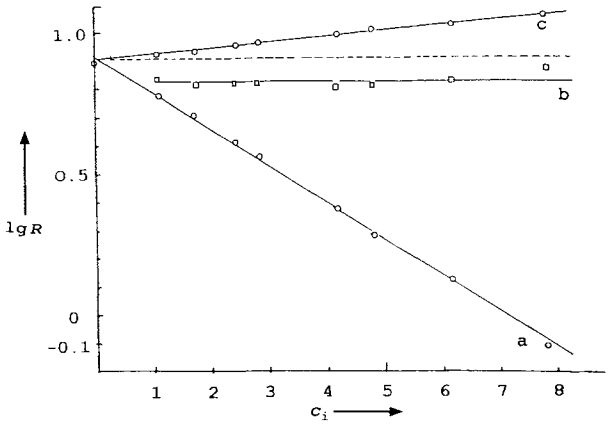

Fig. 18. Meyerhofer plot of the effect of inhibitor concentration c_i on the logarithm of dissolution rate (lg R) before (a) and after exposure to UV light (c). The experimental points indicated by squares (b) refer to films that were exposed to completion and then heated to 70 °C for two hours to decarboxylate the indene carboxylic acid produced on exposure.

some way, dispersed the clusters and returned the system to the percolation state of novolak. It also means that the dissolution promotion effect invariably observed in exposed resists (the increase of the dissolution rate above that of pure novolak) is caused by the indene carboxylate ions which contribute their share to the overall concentration of hydrophilic sites. However, by what mechanism are the phenolic clusters dispersed on irradiation?

3.1. The Thermal Effect of DNQ Photolysis

It is known from the classical work of Süs that the conversion of DNQ **1** into acid **2** has three stages:[4] The first step is the photoreaction of diazoquinone, which releases molecular nitrogen and leads to the formation of a carbene (Scheme 5). The carbene then undergoes a Wolff rearrangement to form a ketene,[31] which is finally hydrated to give the carboxylic acid **2**.

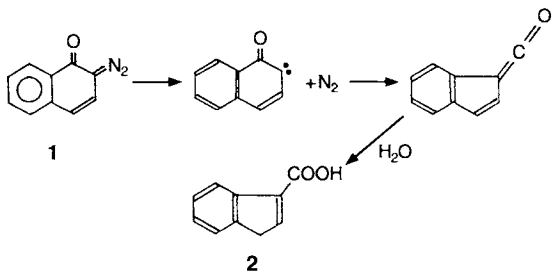

Scheme 5. Mechanism of the transformation of DNQ (**1**) into indene carboxylic acid (**2**).

The Wolff rearrangement is not only fast, but also highly exothermic. A lower bound to the enthalpy change associated with the rearrangement of the carbene to a ketene can be estimated from bond energies and heats of atomization.[32] From these data the molar heat of reaction of the Wolff rearrangement is found to be not less than $\Delta H^{\circ}_{298} = -66\ \mathrm{kcal\,mol^{-1}}$, which corresponds to a molecular heat of reaction of $\Delta h^{\circ}_{298} = -11 \times 10^{-20}\ \mathrm{cal\,molecule^{-1}}$.

Δh° is the heat released by a single molecule of DNQ into its immediate surroundings. Let us assume that the reacting molecule is located within a cluster of ten phenolic units that occupy a volume of about $2000\ \text{Å}^3$ and represent a mass of 2000×10^{-24} g. The specific heat of the polymer is about $0.25\ \mathrm{cal\,K^{-1}}$, and therefore the heat capacity of the cluster is $c = 500 \times 10^{-24}\ \mathrm{cal\,K^{-1}}$. If the molecular heat of reaction ($q = 11 \times 10^{-20}$ cal) is released "instantaneously" into the cluster, the temperature of the cluster will increase by $\Delta T = \frac{q}{c} = \frac{11 \times 10^{-20}}{500 \times 10^{-24}} = 220\,^{\circ}\mathrm{C}$. The rate of release of heat from the Wolff rearrangement exceeds the flow of heat out of the cluster by several orders of magnitude;[30] consequently, the event has the character of an adiabatic transaction. The photoreaction and the subsequent Wolff rearrangement inject a powerful heat pulse into the cluster, and the resulting temperature spike releases the backbones of the polymer chains in the neighborhood. The phenolic clusters disperse, being no longer held together by the inductive polarization effect of the inhibitor. We believe that this is the mechanism by which phenolic clusters are eliminated from the system at the moment of exposure. This happens before development and before the penetration zone is formed.

3.2. The Effect of Indene Carboxylate in the Penetration Zone

Films that have been exposed, but not post-baked, dissolve faster than films of pure novolak. The upper trace of Figure 18 shows the dissolution promotion effect, which is absent in post-exposure baked films. The promotion effect is associated with the emergence of newly generated carboxylate ions which function as additional percolation sites. Figure 19 compares the promotion effect of indene carboxylic acid to that of 3-hydroxybenzophenone and 4-hydroxybenzophenone. Since these effects are of the same order, we conclude that dissolution promotion can be accounted for by the additional percolation sites that carboxylate ions introduce into the penetration zone.

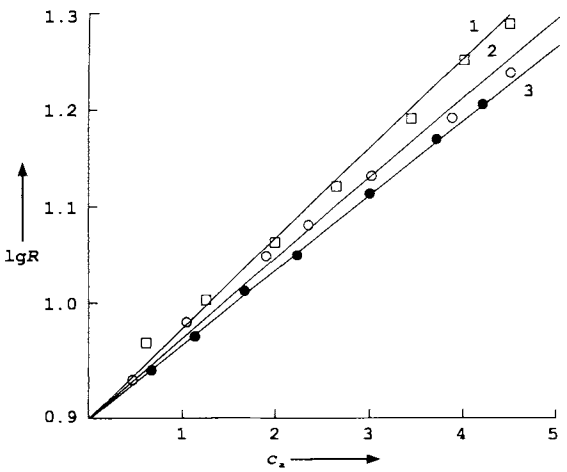

Fig. 19. Comparison of the dissolution promotion effect of 4-hydroxybenzophenone (1), 3-hydroxybenzophenone (2), and indene carboxylic acid produced in situ by exposure of the corresponding DNQ (3). The logarithm of the dissolution rate ($\lg R$) is plotted against the concentration c_a in mol%.

The presence of carboxylate has yet another effect on the penetration zone: it lowers its cohesion. We can substantiate this by determining the effect of (exposed) inhibitor on the glass transition temperature of the exposed films. Figure 20 refers to films containing 6.2% of the standard monofunctional DNQ inhibitor. It shows Arrhenius plots for the dissolution of films in 0.2N KOH before and after exposure. From the break in the traces we find that the glass transition temperature of the zone is 43 °C before exposure and 16 °C after exposure. In the exposed films the glass transition is well below the temperature of development.

The lowering of T_g in the exposed films indicates a loss of cohesion in the penetration zone. The lower cohesion is the result of the appearance of a new electrolyte, indene carboxylate. This is analogous to the behavior of aqueous solutions of

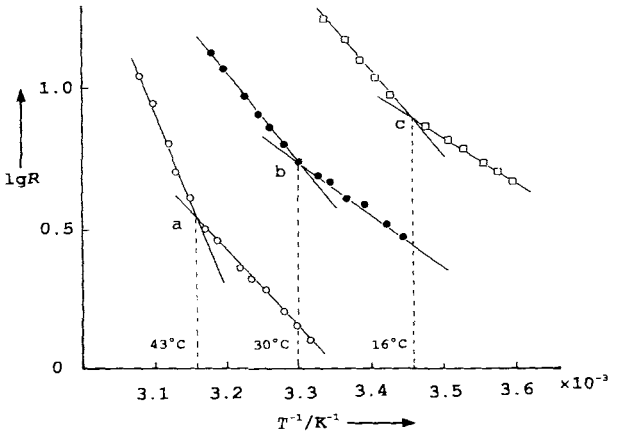

Fig. 20. Determination of the glass transition temperature T_g' of a resist containing 6.2% DNQ before (a) and after (c) exposure, as well as after irradiation and decarboxylation of the indene carboxylic acid at 70 °C (b).

polyelectrolytes, where the introduction of salt lowers the viscosity. We can demonstrate a similar effect directly in the penetration zone by adding various salts to the developer base and monitoring T_g'. For example, on addition of KCl to a 0.24 N KOH developer, the decrease in T_g' is directly proportional to the KCl concentration (Fig. 21a). The added electrolyte intercalates itself between the phenolate ions and the K^+ counterions. The intercalated ion pairs interrupt the lines of force and thereby lower the strength of the electrostatic field. If this interpretation is correct, larger anions should have a greater effect on T_g': in Figure 21b T_g' of films dissolving in 0.24 N KOH to which 0.06 N of various potassium salts was added is plotted against the size of the size of the additive ion. The effect of the added salt on T_g' does increase linearly with the ionic radius of the salt anion.

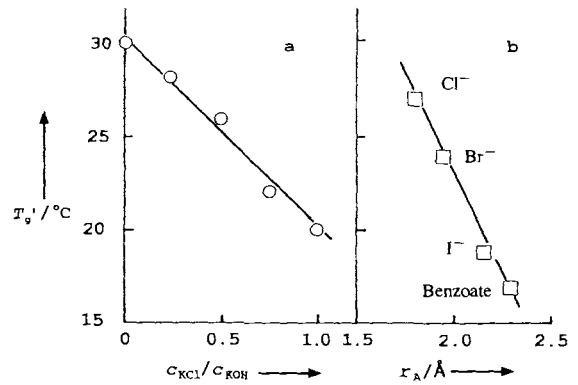

Fig. 21. The effect of concentration and size of additives in the developer solution on T_g'. a) Depression of T_g' on successive addition of KCl to a 0.20 N KOH base solution; b) depression of T_g' of a resist developing in 0.24 N KOH as a function of the radius r_A of the anion of four potassium salts (concentration 0.06 N).

4. Conclusions and Outlook

The dissolution of novolak films is controlled by the diffusion of base through the penetration zone. We have found that the transport of base through the zone can be modulated not only by changing the overall density of hydrophilic sites (for example by gradual methylation of OH groups), but also by altering their spatial distribution (that is, by site clustering). Phenolic clusters are formed in the coating solution used to make resist films by an inductive polarization effect of the diazoquinone function. They are perpetuated in the solid matrix and persist as phenolate clusters in the penetration zone by virtue of the rigid glassy state of the zone. Hydrophilic site clusters modulate the diffusive flux by an effect germane to a percolation process: they lower the connectivity of the bond percolation field and with it the diffusion coefficient of base. This is the mechanism by which diazoquinones inhibit novolak dissolution.

On exposure to light, diazonaphthoquinones produce carbenes, which subsequently undergo a highly exothermic secondary reaction, the Wolff rearrangement. This injects a heat pulse into the center of the phenolic cluster and causes a temperature spike that is intense enough to release the polymer backbones in the vicinity of the reacting DNQ. The clusters, which are no longer inductively polarized, disperse at the high temperature. Moreover, the newly created indene carboxylate ions in the penetration zone provide additional percolation sites for the base, and that is reflected in an increase of the dissolution rate of exposed resist films above that of pure novolak.

The percolation model of novolak dissolution offers an outline of the functional mechanism of novolak resists. It has begun to find acceptance in the R & D groups of industry. Several aspects of the system still await clarification, such as the effect of resin structure on photographic performance, the function of dissolution accelerators, and the surprisingly large effect of resin molecular weight on the rate of dissolution. These topics are presently under investigation at the Institute of Imaging Sciences at Polytechnic University.

Finally, the percolation approach is not limited to novolak–diazoquinone resists. Oertel et al.[33] have used it to describe the dissolution behavior of X-ray resists. In general, the method can be used effectively on any system based on dissolution inhibition, including, for example, the *t*BOC-protected polyvinylphenols introduced by Fréchet, Ito, and Willson,[34] and other systems with chemical amplification.[35]

We are grateful to the National Science Foundation, to the Office of Naval Research, to the Semiconductor Research Corporation, to IBM, to Hoechst Celanese Corporation, and to OCG Microelectronic Materials for financial support. Ralph Dammel from Hoechst Celanese Corporation has been a frequent and inspiring conversation partner for us, and we have greatly benefited from discussions with H.-J. Merrem (Hoechst Celanese), with R. J. Hurditch, K. Honda, and their colleagues (OCG), with C. Szmanda (Shipley Company), with Grant Willson (University of Texas at Austin), with A. Kessel (University of Kazan, Russia), and with T. K. Kwei and A. Izmailov (Polytechnic University).

Received: November 21, 1995 [A 141 IE]
German version: *Angew. Chem.* **1996**, *108*, 2609–2620

[1] Kalle AG, DBP. 879205, **1949**.
[2] Azoplate Corp., US-Pat. 2766118, **1956**; US-A 3046122, **1962**.
[3] R. R. Dammel, *Diazonaphthoquinone-based Resists*, SPIE Press, Tutorial Text No. 11, Bellingham, WA **1993**.
[4] O. Süs, *Justus Liebigs Ann. Chem.* **1944**, *556*, 65; *ibid.* **1947**, *557*(2), 237; O. Süs, J. Munder, H. Stephan, *Angew. Chem.* **1962**, *74*, 985.
[5] K. Ueberreiter, F. Asmussen, *J. Polym. Sci.* **1962**, *57*, 187.
[6] W. D. Hinsberg, M. L. Guttierez, *SPIE Annu. Tech. Symp. Proc. 15th* **1984**, *469*, 57.

[7] M. K. Templeton, C. R. Szmanda, A. Zampini, *SPIE Annu. Tech. Symp. Proc. 15th* **1987**, *771*, 136.
[8] C. M. Garza, C. R. Szmanda, R. L. Fischer, *SPIE Annu. Tech. Symp. Proc. 15th* **1988**, *920*, 321.
[9] M. Hanabata, Y. Uetani, A. Furuta, *SPIE Annu. Tech. Symp. Proc. 15th* **1988**, *925*, 340.
[10] M. Koshiba, M. Murata, M. Matsui, *SPIE Annu. Tech. Symp. Proc. 15th* **1988**, *929*, 364.
[11] M. Murata, M. Koshiba, Y. Harita, *SPIE Annu. Tech. Symp. Proc. 15th* **1989**, *1086*, 48.
[12] T. F. Yeh, H. S. Shih, A. Reiser, *Macromolecules* **1992**, *25*, 5345.
[13] J. P. Huang, T. K. Kwei, A. Reiser, *Macromolecules* **1989**, *22*, 4106.
[14] R. A. Arcus, *SPIE Annu. Tech. Symp. Proc. 15th* **1986**, *631*, 124.
[15] T. F. Yeh, A. Reiser, R. R. Dammel, G. Pawlowski, H. Roeschert, *Macromolecules* **1993**, *26*, 3862.
[16] B. Sapoval, M. Rosso, J. F. Gouyet, *J. Phys. Lett.* **1985**, *46*, L149.
[17] M. Rosso, J. F. Gouyet, B. Sapoval, *Phys. Rev. Lett.* **1986**, *57*, 3195.
[18] T. F. Yeh, H. Y. Shih, A. Reiser, M. A. Toukhy, B. T. Beauchemin, *J. Vac. Sci Technol. B* **1992**, *10*, 715.
[19] R. E. Barker, C. R. Thomas, *J. Appl. Phys.* **1964**, *35*, 87.
[20] J. M. Ziman, *Models of Disorder, The Theoretical Physicsl of Homogeneously Disordered Systems*, Cambridge University Press, Cambridge, UK, **1979**, Chap. 2.
[21] D. Stauffer, A. Ahorony, *Introduction to Percolation Theory*, Taylor & Francis, London, **1985**.
[22] G. Rimmet, *Percolation*, Springer, New York, **1989**.
[23] R. S. Berry, S. A. Rice, J. Ross, *Physical Chemistry*, Wiley, New York, **1980**, p. 407.
[24] D. Meyerhofer, *IEEE Trans. Electron Devices* **1980**, *ED-27*, 921.
[25] H. Y. Shih, A. Reiser, R. R. Dammel, H. J. Merrem, G. Pawlowski, *Macromolecules* **1994**, *27*, 3330.
[26] H. Y. Shih, A. Reiser, *Macromolecules* **1995**, *28*, 5595.
[27] K. Honda, B. T. Beauchemin, R. J. Hurditch, A. J. Blakeney, Y. Kawaba, T. Kokubo, *Proc. SPIE* **1990**, *1262*, 493.
[28] R. R. Dammel, M. Khadim, *Proc SPIE* **1993**, *1925*, 205.
[29] C. C. Lin, T. F. Yeh, A. Reiser, K. Honda, B. T. Beauchemin, Jr., *J. Photopolym. Sci. Technol.* **1993**, *6*, 147.
[30] H. Y. Shih, A. Reiser, *Macromolecules* **1996**, *29*, in press.
[31] L. Wolff, *Justus Liebigs Ann. Chem.* **1902**, *325*, 129; *ibid.* **1912**, *394*, 23.
[32] *Handbook of Chemistry and Physics*, 51st ed, McGraw-Hill, New York, **1970–71**, *F-158-165*.
[33] H. K. Oertel, M. Weiss, R. Dammel, J. Theis, *Microcircuit Engl.* **1990**, 267; H. Oertel, M. Weiss, J. Chlebek, H. L. Huber, R. Dammel, C. R. Lindley, J. Lingnau, J. Theis, *SPIE Annu. Tech. Symp. Proc. 15th* **1989**, *1086*, 283.
[34] J. M. J. Fréchet, E. Eichler, H. Ito, C. G. Willson, *Polymer* **1983**, *24*, 995.

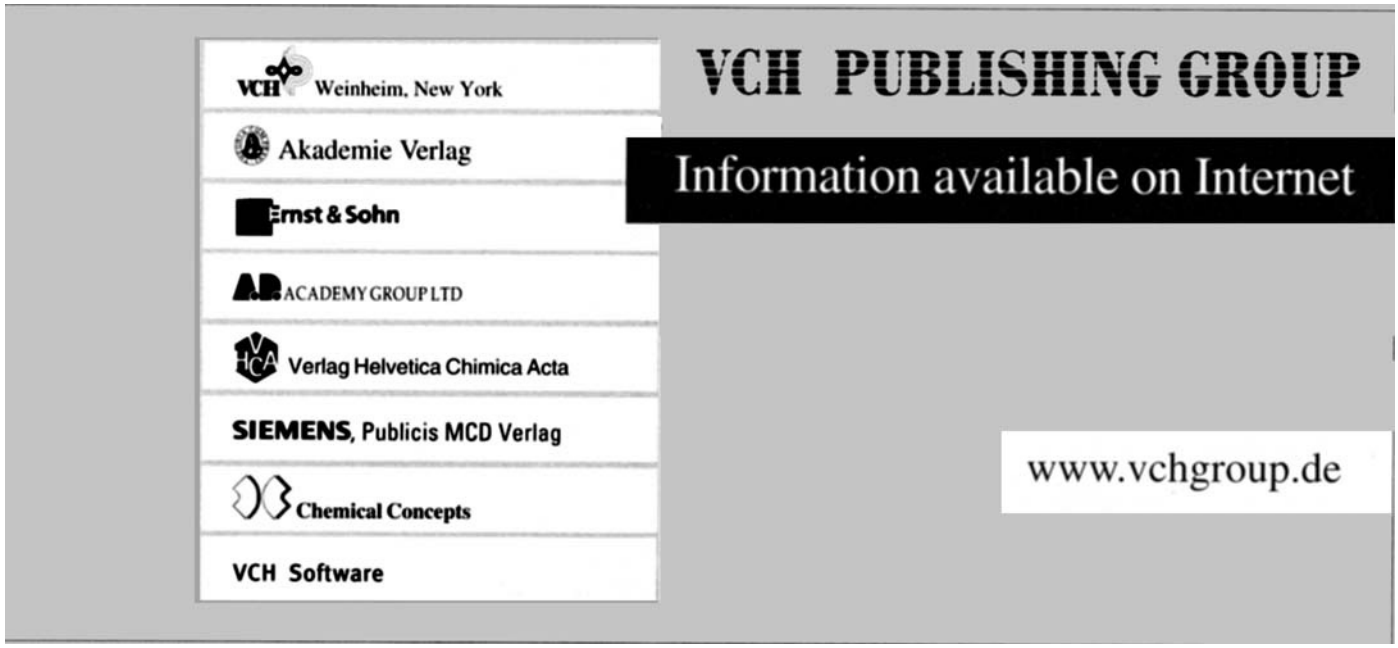

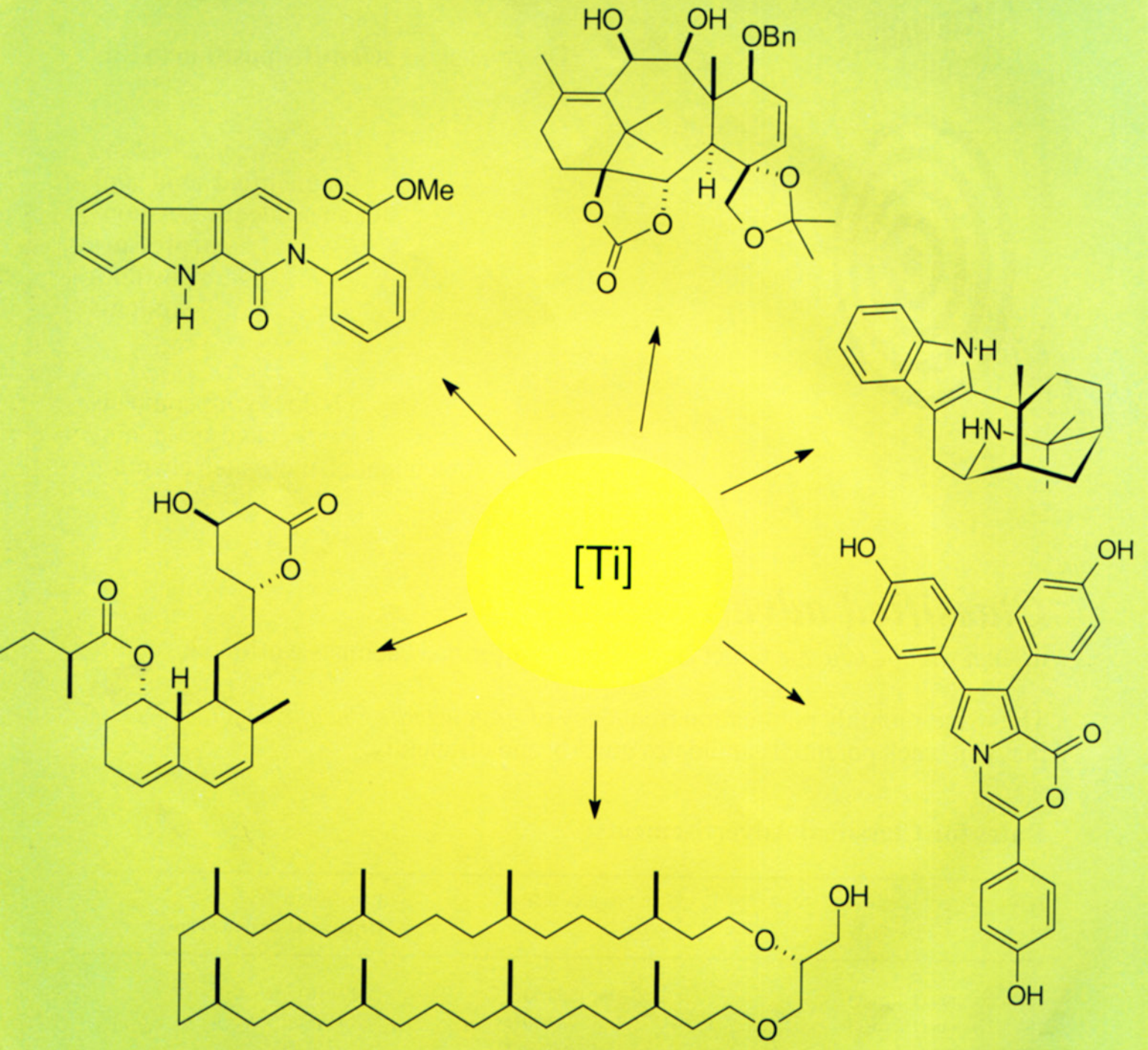

Annelations, macrocyclizations, pinacol couplings, and heterocycle syntheses are all possible with low-valent titanium.

New Developments in the Chemistry of Low-Valent Titanium

Alois Fürstner* and Borislav Bogdanović*

Dedicated to Professor Henri B. Kagan on the occasion of his 65th birthday

Among the applications of low-valent titanium in organic synthesis, the reductive coupling of carbonyl compounds to produce alkenes (the McMurry reaction) is particularly prominent. Discovered at the beginning of the 1970s, it has been developed and tested repeatedly, for example in numerous syntheses of natural products. This alkene synthesis has become a standard reaction in the repertoire of preparative chemists. However, the possibilities of low-valent titanium are by no means limited to this process: the last few years have brought some spectacular applications of the conventional McMurry reaction (for example the synthesis of taxol) along with a considerable extension of the scope of reductive carbonyl couplings. Thus, diverse heterocycles are now accessible following novel and efficient pathways based on intramolecular cross-coupling of functional groups—some of which were hitherto considered to be inert to titanium. The use of this method for the synthesis of indole and pyrrole alkaloids illustrates the new possibilities. At the same time, considerably simplified methods for conducting McMurry-type reactions have been developed. Examples include the particularly convenient "instant" method, the first ketone–amide coupling reactions requiring only catalytic amounts of titanium salts, and the first application of commercially available titanium powder as a coupling agent. Last but not least, the detailed investigation of diverse classical McMurry reagents has afforded a deeper understanding of the nature and mode of action of low-valent titanium. Revision of some of the current conceptions of the process of reductive carbonyl coupling is thus indispensable.

Keywords: alkenes · carbonyl compounds · heterocycles · McMurry reactions · titanium compounds

1. Introduction

The broad interest in low-valent titanium species as reagents only arose in the 1960s after Vol'pin and Shur[1] as well as van Tamelen et al.[2] recognized that these species could fix molecular nitrogen under mild conditions. Van Tamelen's group also succeeded in the reductive dimerization of alcohols to give hydrocarbons.[2f] Shortly afterwards, the research teams of Mukaiyama, Tyrlik, and McMurry independently described at about the same time the reductive coupling of aldehydes or ketones with the help of low-valent titanium to give alkenes (Scheme 1).[3–6] By lowering the temperature, it is possible to stop the reaction at the stage of the intermediate pinacol.

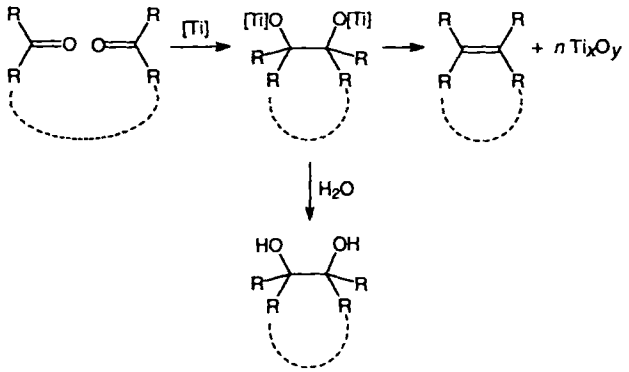

Scheme 1. Principle of the McMurry reaction. [Ti] = low-valent titanium.

Generally referred to as McMurry reactions after one of the discoverers, these reductive C–C couplings quickly acquired great importance in preparative organic chemistry. They have served as key steps in numerous syntheses of natural products, as well as in the preparation of sterically hindered alkenes of theoretical interest. The strong template effect of low-valent titanium deserves particular consideration: the yields of cycloalkenes obtained from intramolecular McMurry couplings are largely independent of the size of the ring formed, thus opening an efficient access to medium-sized and large rings. These applications of low-valent titanium have been summarized in several excellent reviews.[7, 8] Therefore, this account concentrates on the discussion of new developments in this field.

[*] Priv.-Doz. Dr. A. Fürstner, Prof. Dr. B. Bogdanović
Max-Planck-Institut für Kohlenforschung
Kaiser-Wilhelm-Platz 1, D-45470 Mülheim an der Ruhr (Germany)
Fax: Int. code +(208) 306-2980

One of these advances concerns functional groups previously considered to be hardly reactive or even inert, for example esters, amides, urethanes, and ureas; they have been found to undergo intramolecular cross-coupling with aldehydes and ketones quite smoothly. This permits the synthesis of new types of products such as aromatic heterocycles[9–18] by reductive carbonyl coupling reactions and thus opens new entries for alkaloid synthesis and pharmaceutical research. Parallel to this increase in structural diversity, considerable methodological advances have also been made: the development of a particularly easy to perform "instant" method[17] and a catalytic variation thereof,[18] as well as the first application of commercially available titanium powder as a McMurry reagent.[18]

Furthermore, there have been new insights into the inorganic aspects of the McMurry reaction, in other words the nature and mode of action of the titanium species involved, which had aroused little interest until recently.[19] Thus, a more specific conception of the classical McMurry reagent generated from $TiCl_3$ and $LiAlH_4$[20] as well as of low-valent titanium species from $TiCl_x$ ($x = 3, 4$) and Mg[21] could be developed. Likewise, the reaction mechanism of carbonyl couplings using $TiCl_3/LiAlH_4$ and $TiCl_3/Zn(Cu)$ combinations[22] as well as $TiCl_2 \cdot 2LiCl$[22, 23] were more or less elucidated. The knowledge gained from this not only necessitates a revision of the ideas to date, but also confirmed our previous conjecture that titanium halides in solution are not reduced to metallic titanium by common reducing agents, but, depending on the method of preparation, are present as low-valent titanium species having different structures and modes of action.[24]

2. Newer Applications of Low-Valent Titanium in Organic Synthesis

2.1. Conventional McMurry Couplings: Natural Products and their Analogs

Ever since it was discovered, the McMurry reaction has served as a key step in numerous syntheses of natural products. In particular, the variety of ring systems of differing sizes found in the terpene series offers an ideal field in which to prove the advantages of intramolecular carbonyl couplings.[25] While sparcely functionalized target molecules were initially chosen, knowledge gained on the compatibility of diverse functional groups with low-valent titanium[7, 8] has led to the synthesis of more highly substituted compounds. The natural products presented in Figure 1 give an idea of the current state of the art.

(Poly)oxygenated compounds are a particular challenge because of the pronounced affinity of low-valent titanium for oxygen. A striking example of this is Clive's total synthesis of (+)-compactin (**8**, R = H, Scheme 2) and (+)-mevinolin (**9**, R = Me). Thus, the annelation of the A-ring in **12**, an advanced intermediate in this synthesis, was successful after careful optimization of the reaction conditions.[29, 30] This cyclization could only be made reproducible and high-yielding by using titanium–graphite,[24, 31] produced from $TiCl_3$ and two equivalents of C_8K.

In the same context the rather sparse reports describing cyclizations of two out of three carbonyl groups on a substrate, in which the third carbonyl group is unaffected, deserve particular mention. This semicompatibility of unprotected carbonyls towards activated titanium is documented by early syntheses of

Alois Fürstner was born in 1962 in Bruck/Mur (Austria) and studied chemistry at the Technical University in Graz (Austria), where he earned his doctorate in 1987 under the direction of Prof. H. Weidmann. After postdoctoral research with Prof. W. Oppolzer at the University of Geneva (Switzerland), he completed his "habilitation" in organic chemistry at the Technical University in Graz in 1992. Since 1993 he has been the head of a research group at the Max-Planck-Institut für Kohlenforschung in Mülheim an der Ruhr (Germany). He was a guest professor at the Université Claude Bernard - Lyon I in Villeurbanne (France) in 1994, and received a fellowship from the Fonds der Chemischen Industrie. His research interests include the development of new methods for organic synthesis with organometallic reagents and their application in natural product chemistry, the development and characterization of supported reagents, and homogeneous catalysis.

A. Fürstner

B. Bogdanović

Borislav Bogdanović studied chemistry at the University of Belgrade and received his PhD in 1962 at the Technische Hochschule in Aachen (Germany) under the direction of Prof. G. Wilke. He has been at the Max-Planck-Institut für Kohlenforschung in Mülheim an der Ruhr (Germany) since 1960 and currently heads a catalysis research group. Since his "habilitation" in 1974 he has taught at the University of Bochum, and was a guest professor at the Universities of Pisa, Paris-Sud, Toulouse, and Lyon. He was awarded the Ruhrpreis für Kunst and Wissenschaft der Stadt Mülheim an der Ruhr and the German–French Research Prize of the Alexander von Humboldt Foundation. His research interests in the area of organometallic chemistry and catalysis currently focus on "inorganic Grignard reagents" and on the use of metal hydrides in energy storage.

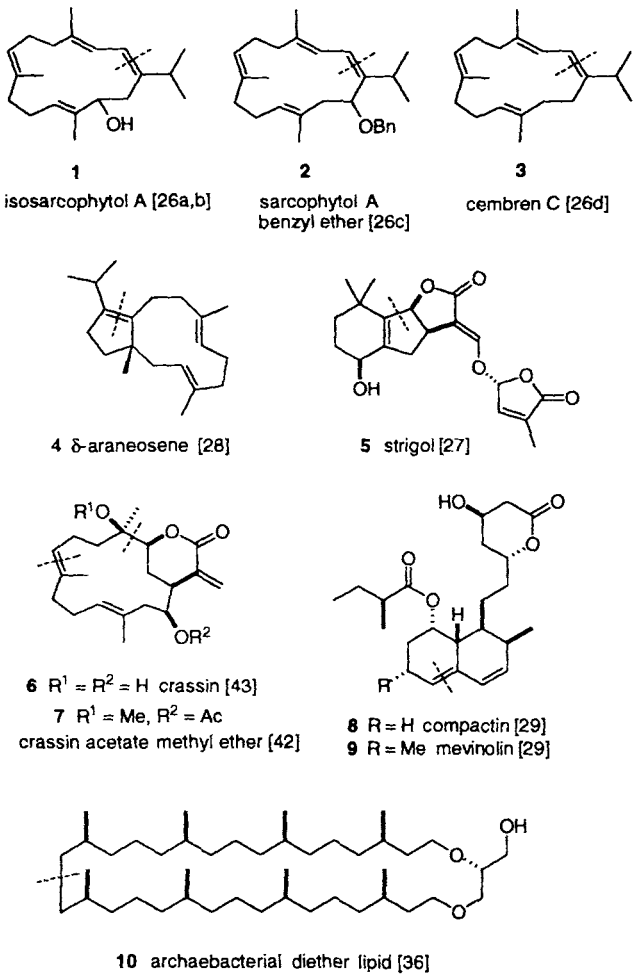

Fig. 1. Natural products prepared with McMurry reactions. See also refs. [26–29, 36, 42, 43].

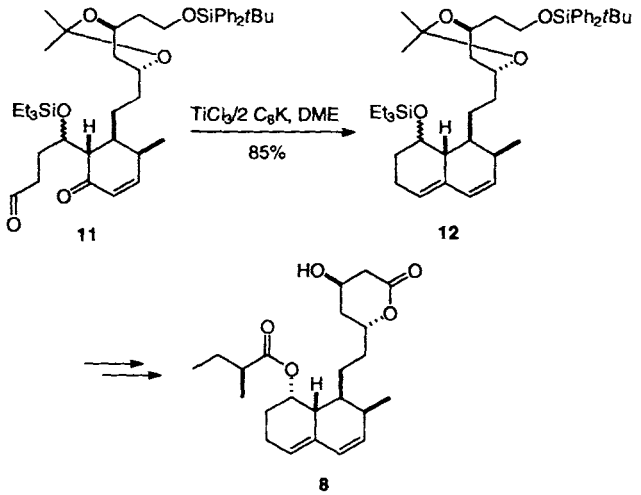

Scheme 2. Clive's synthesis of (+)-compactin (**8**).

(±)-estrone methyl ether (**14**)[32] and (+)-9(11)dehydroestrone methyl ether (**15**),[33] an efficient access to isokhusimone (**16**),[34], and an elegant preparation of the tetracyclic diterpene kempene-2 (**13**).[35]. Reference should also be made to the reductive cyclization, discussed in Section 3.4, of a diketoamide to give the simple alkaloid salvadoricine (**17**). Here the amide group, which was long considered to be inert, reacts smoothly, whilst one of the two keto groups remains unchanged.[10]

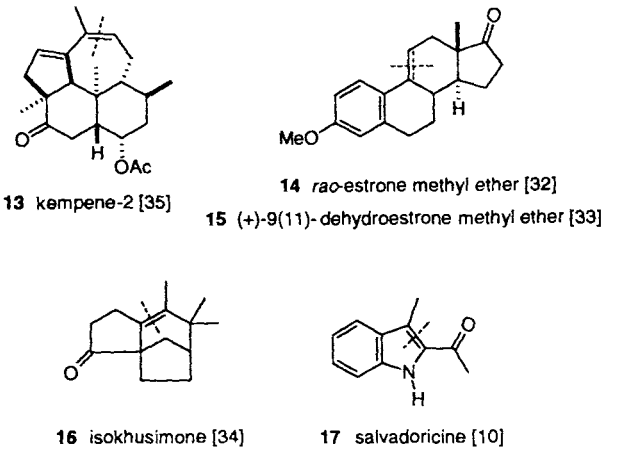

The record for the largest ring generated by the McMurry reaction in a natural product is currently held by the 36-membered diether lipid **10**, isolated from the cell membrane of archaebacteria.[36, 37]

One of the most outstanding achievements in preparative organic chemistry in the last few years is, without a doubt, the total synthesis of taxol, which was successfully carried out by three teams.[38, 39] Taxol is a promising anticancer drug and already in clinical use. During the construction of the taxane skeleton, and following the work of Kende et al.,[40] the titanium-mediated cyclization of the eight-membered B-ring formed a key step of Nicolaou's synthesis[39] of this structurally exceptionally demanding target molecule. Starting from the conformationally preorganized dialdehyde **18** and using $[TiCl_3(dme)_{1.5}]/Zn$-(Cu), the desired pinacol **19** was obtained with a 23–25% yield along with three side products (Scheme 3). In spite of the

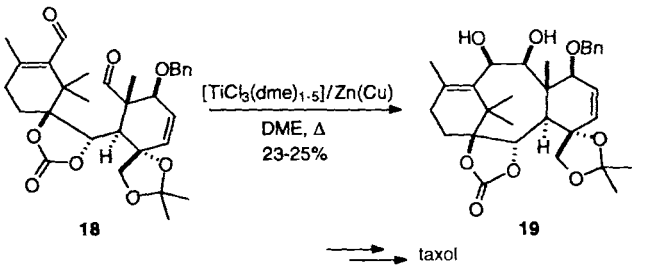

Scheme 3. Key step in Nicolaou's synthesis of taxol.

comparatively low yield, this application is a milestone in the chemistry of low-valent titanium. Similar titanium-mediated pinacol couplings were also used in the synthesis of numerous taxol analogs.[41]

The comparison of two syntheses of crassin (**6**), a diterpenoid cembranoid with antibiotic and carcinostatic activity, is instructive. Dauben's approach is based on the formation of the trisubstituted C7–C8 double bond of the macrocycle.[42] Thus, ketoaldehyde **20** is treated with low-valent titanium ($TiCl_3/Zn$-(Cu)), and the resulting compound **21** ($E:Z = 4:3$) subsequently converted into **7** in a few routine steps (Scheme 4). In contrast

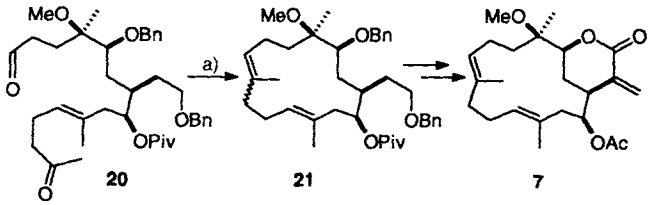

Scheme 4. Key step in Dauben's synthesis of crassin acetate methyl ether (7). a) $TiCl_3$, Zn(Cu), DME reflux, $E:Z = 4:3$, 65%.

to this, McMurry's crassin synthesis is based on an intramolecular pinacol reaction with formation of the C3–C4 diol unit of the 14-membered ring system.[43] However, the main product **23** of the cyclization of **22** proved to be an isomer of the desired diol **25**, so that a correction of the configuration on both chiral centers was necessary to complete the synthesis. This was cleverly achieved via epoxide **24** (Scheme 5).

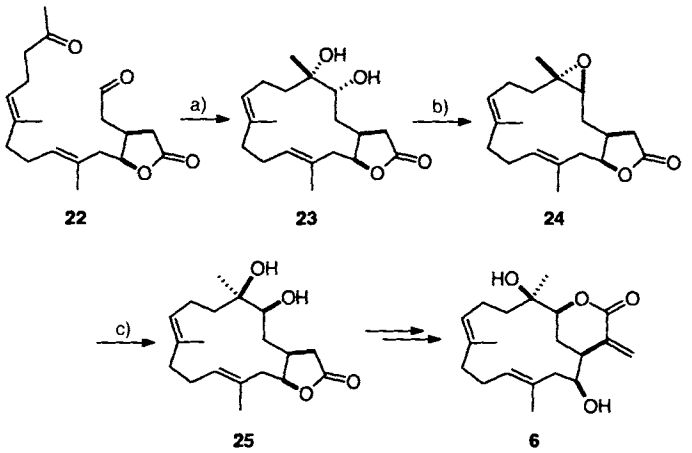

Scheme 5. McMurry's synthesis of crassin (**6**). a) $[TiCl_3(dme)_{1.5}]$, Zn(Cu), DME, room temperature, 20% (+ isomers, 30%); b) i. MsCl, pyridine; ii. benzyltrimethylammonium hydroxide, benzene, 68%; c) H_2O, $HClO_4$, THF, 77%.

Furthermore, McMurry recognized the close relationship between crassin (**6**) and isolobophytolide (**28**):[43] whilst the precursor **22** required for the crassin synthesis has a *cis*-annelated butyrolactone structure, the analogous *trans*-annelated compound **26** undergoes an intramolecular pinacol reaction to give an advanced intermediate for the synthesis of **28** (Scheme 6). Again, all four stereoisomers are obtained. Additionally, a titanium-mediated ketone–lactone cyclization was observed as a side reaction (see Section 3.3). Even so, these syntheses prove that

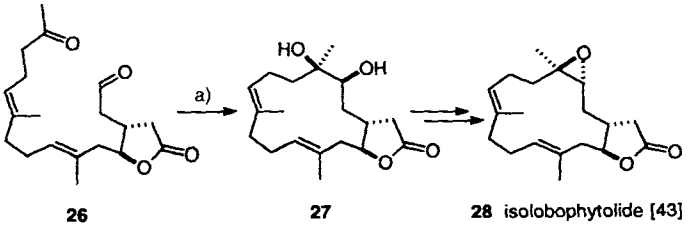

Scheme 6. McMurry's synthesis of isolobophytolide (**28**) by intramolecular pinacol coupling. a) $[TiCl_3(dme)_{1.5}]$, Zn(Cu), DME, room temperature, 21% (+ isomeric diols, 37%).

(poly)oxygenated substrates can undergo selective, titanium-mediated carbonyl coupling.

The difficulties arising in titanium-mediated pinacol formation can clearly been seen in these examples and are substantiated by some further applications. In spite of intensive efforts, the stereochemistry of a cyclic 1,2-diol formed by a reductive carbonyl coupling cannot be predicted with any certainty,[44] much less controlled. This is illustrated by the synthesis of periplanone C (**31**); the key step is the synthesis of the ten-membered ring diol **30**, which is produced in good yields but with low stereoselectivity (Scheme 7).[45] Another case is that of the pina-

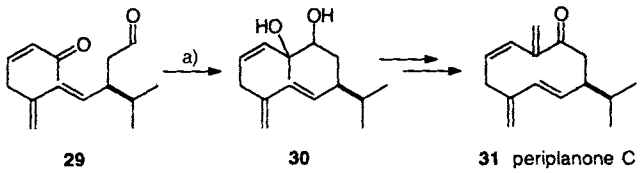

Scheme 7. Synthesis of periplanone C (**31**). a) $[TiCl_3(dme)_{1.5}]$, Zn(Cu), DME, room temperature, 60% (mixture of the four diastereomeric diols).

colization of N-protected aminoaldehydes to C_2-symmetrical diols, which are of interest as potential inhibitors of HIV protease. Again, the diastereoselectivity attained by the titanium-based method makes it inferior to the pinacol method developed by Pedersen et al., which employs $[V_2Cl_3(thf)_6]_2[Zn_2Cl_6]$ as a reagent.[46, 47]

Numerous applications of the McMurry reaction were reported in the preparation of nonnatural porphyrin derivatives. The pioneering work of the research team working with Vogel,[48] which culminated in the preparation of porphycene (**32**), corrphycene (**33**), and numerous "expanded" porphyrin analogs such as **35**, triggered many closely related syntheses. For example, porphyrin analogs were obtained in which one or several of the pyrrole units were replaced by other heterocyclic rings (furans, thiophenes, etc.) and/or were extended by an additional heteroarene ring system (e.g. **34**, **36**).[49] These compounds are used in the study of the aromaticity of expanded annulenes, and some are employed in the photodynamic therapy of tumors.

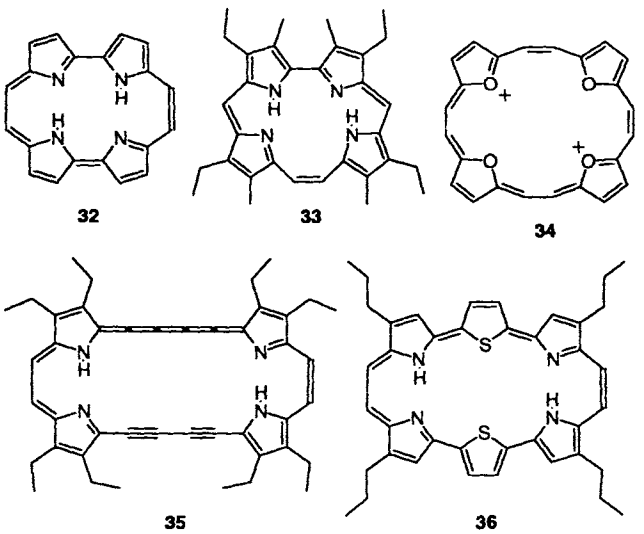

Scheme 8 gives as an example the synthesis of porphycene. The approach is based on a double (cross)coupling of suitable 1,ω-dials containing two or more heterocyclic units. Since only the (Z) isomer of the alkene formed after the first coupling can lead to ring closure, such tandem cyclizations are not usually very high-yielding.

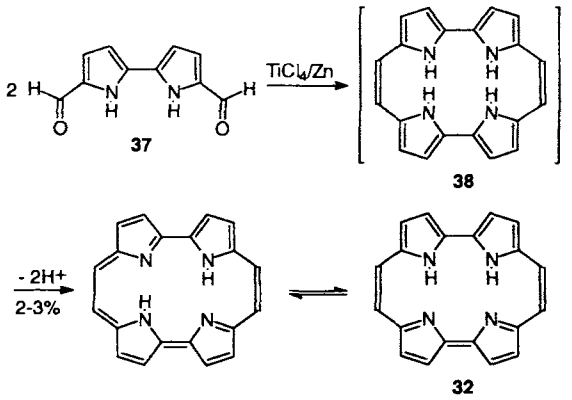

Scheme 8. Vogel's synthesis of porphycene (**32**).

2.2. Conventional McMurry Couplings: Nonnatural Products

Titanium-mediated carbonyl coupling reactions are particularly suitable for the synthesis of strained alkenes because of the high driving force resulting from the formation of titanium oxides as the inorganic by-products. Although the preparation of the long-awaited tetra-*tert*-butylethene was not successful even with the McMurry reaction, it was possible to obtain numerous theoretically interesting olefins that were inaccessible or very difficult to prepare by other means.[7, 8]

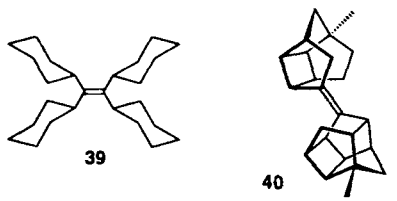

A recent example is the preparation of tetracyclohexylethylene (**39**),[50] in which the rotational barrier of the cyclohexyl groups is as high as 18.7 kcal mol^{-1}. The "cage-functionalized" alkene **40** was also obtained,[51] whilst the dimerization of **41** to the "tied-back" tetra-*tert*-butylethylene derivative **42** failed, and obviously marks the limits of this method (Scheme 9).[52] It has been estimated that products with a strain energy of $\leq$19 kcal mol^{-1} can be accessed by a McMurry coupling.[8]

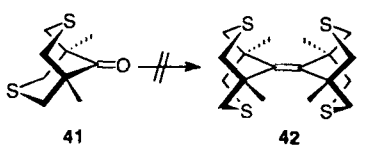

Scheme 9.

Several symmetrical alkenes were prepared in order to investigate their specific physicochemical properties. These include rod-shaped distellenes **43** (interaction of nonconjugated double bonds),[53] (E)-configurated enediynes **44** (propargyl stabilization energy),[54] triene **46**, and pentaene **47** (kinetic and thermodynamic parameters of the *anti–syn* isomerization),[55] as well as the bifluorenylidene derivative **45** with axial chirality, which was obtained from the corresponding ketone as a mixture of (E) and (Z) isomers.[56] From the thermodynamic point of view, only the (E) alkene was expected from dimerizations of 5-formylporphyrins such as **48** (Scheme 10); however, the (Z)-configurated product **49** was also produced in substantial proportions—in some cases even as the main product.[57] This points to the preorganization of the substrate by strong $\pi-\pi$ stacking interactions preceeding the C–C coupling step.

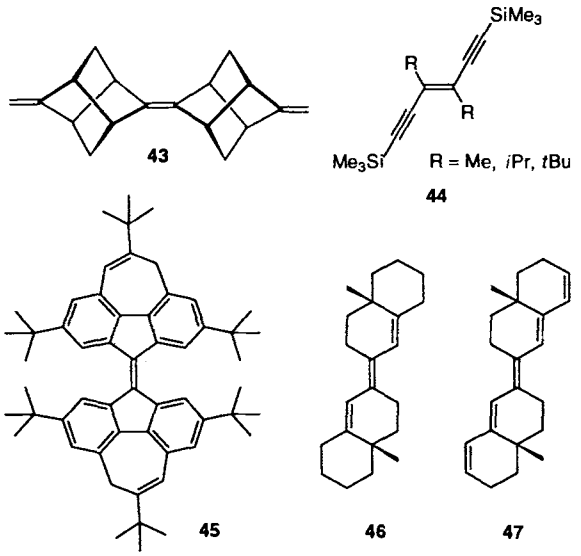

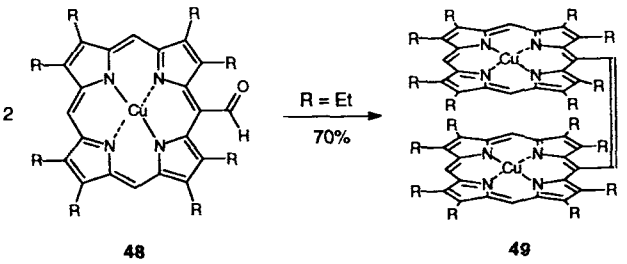

Scheme 10. Synthesis of **49**.

The McMurry reaction has also been used for the preparation or functionalization of organometallic compounds. For example, the acylated cyclopentadienyl derivatives **50** and **53** reacted to give the ethene-bridged *ansa*-titanocene complex **52**[58] and the binuclear cyclopentadienyltricarbonylmanganese complexes **54** and **55**,[59] respectively (Scheme 11). Diferrocenyl-

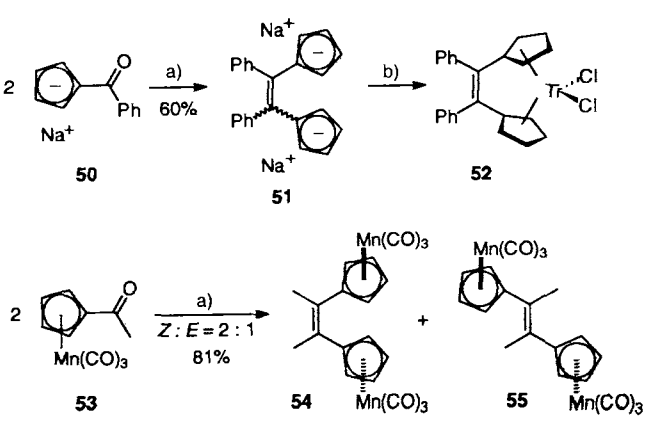

Scheme 11. Synthesis of **52**, **54**, and **55**. a) Ti-graphite; b) $TiCl_4$, 25%.

ketone can be dimerized under McMurry coupling conditions to give tetraferrocenylethene, a molecule with a strongly twisted propellerlike shape.[60] For further applications with π-complexed substrates see ref. [61].

Some products that form in a series of intramolecular carbonyl-coupling reactions are also worth mentioning. The studies of bicyclic carbocations containing a three-center two-electron C–H–C bond (Scheme 12) are particularly noteworthy.

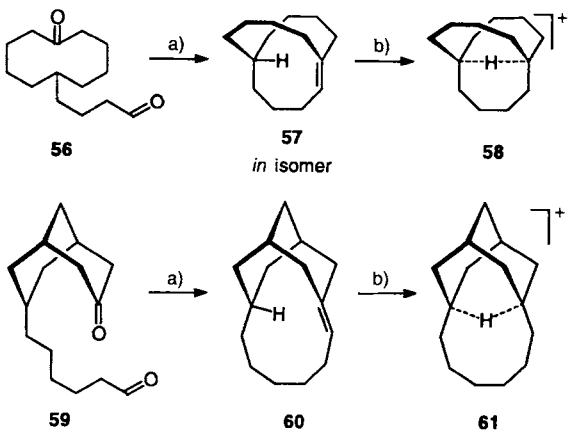

Scheme 12. Synthesis of **58** and **61**. a) $TiCl_3$, Zn(Cu), DME; b) H^+.

These were obtained by the McMurry coupling of suitable ketoaldehyde precursors such as **56** to give bridgehead alkenes of type **57**, which were then protonated.[62] It is remarkable that the bicyclic alkene **57** is only found as the *in* isomer, whilst the formation of the corresponding *out* isomer was not observed. Similar work by Sorensen et al. deals with the dependence of the "nonclassical" carbocation character of **61** on the chain-length of the alkyl bridge.[63]

The preparation of diverse cyclophanes such as **63** (Scheme 13)[64–66] and related crown ether bridged stilbene

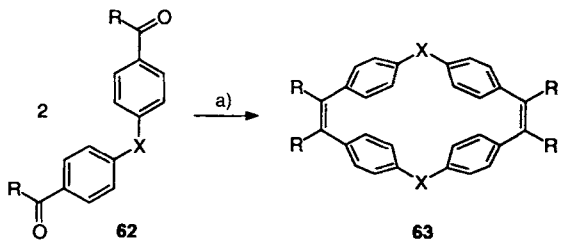

Scheme 13. Synthesis of **63**. X = O, CH_2; R = H, CH_3, Ph; a) $TiCl_4$, Zn(Cu), DME, 72 h, high dilution.

derivatives (**65**) (Scheme 14)[66–68] are representative examples of macrocycle syntheses. Since the latter are photochemically switchable, but only the (*Z*) isomer can be complexed to suitable cations, they constitute a chemical device for binary information storage. Unfortunately, they were not sufficiently stable for practical purposes. Comparison of the efficiency of different low-valent titanium species in the preparation of such "crownophanes" led to a better understanding of the template effect exerted by this metal.[68] The existence of this effect had been surmised for some time, but had hardly been probed experimentally. In some cases the preorganization of the substrate by

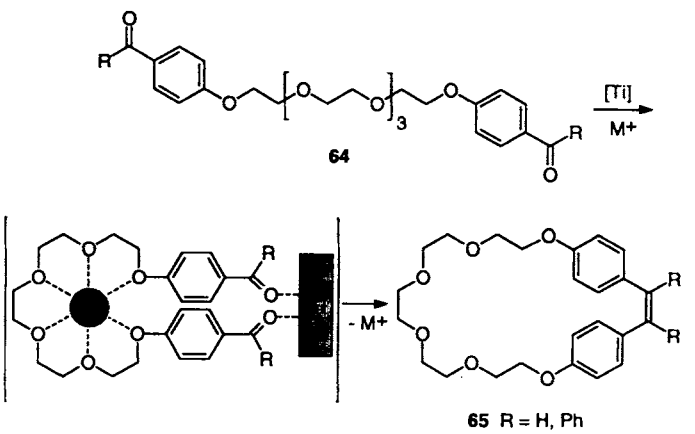

Scheme 14. Synthesis of **65**. [Ti] = low-valent titanium.

the low-valent titanium is apparently so strong that macrocycles with up to 36 members can be formed in excellent yields even without recourse to high dilution.[18, 66, 68]

A series of transannular carbonyl coupling reactions has been described (Scheme 15). These include the "tying-off" of higher

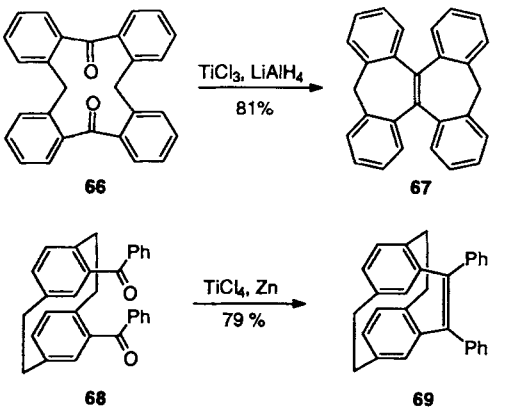

Scheme 15. Transannular carbonyl couplings.

orthocyclophane derivatives such as **66** to give **67**.[69] The reductive cyclization of diketone **68** to provide the triply bridged cyclophane **69** was successful despite considerable steric hindrance.[70] Highly strained calix[4]arene derivatives of fixed conformation could be produced from suitable diformyl precursors.[71] Even the preparation of the doubly bridged derivative **71** was successful (Scheme 16). Here it was found that the par-

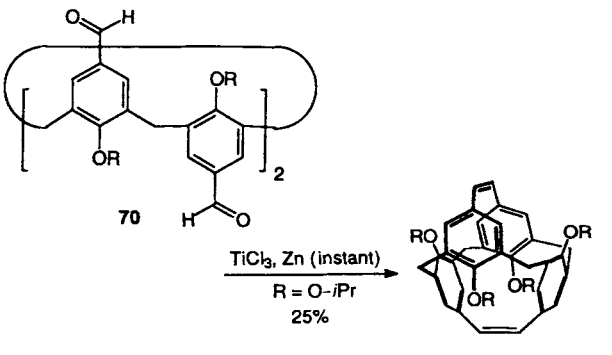

Scheme 16. Synthesis of **71**.

ticularly convenient "instant" method (see Section 3.4.1)[117] developed for the reductive synthesis of indoles is also suitable for conventional McMurry reactions.

2.3. Conventional McMurry Couplings: Polymer Syntheses

Syntheses of polyvinylene derivatives or polypinacols from dicarbonyl compounds and low-valent titanium have been described in recent years. Such polymerizations are successful with substrates that are stiff enough to prevent competing intramolecular reactions. Thus, the reactions of terephthalaldehyde and 2,5-diformylfuran at 0 °C led to the corresponding polypinacols **72** and **73** (M_n = 2850 and 5540, respectively).[72] The formation of poly(1,4-phenylene-vinylene) **74** and poly(2,5-difurylene-vinylene) **75** (X = O, R = H) at reflux temperature is

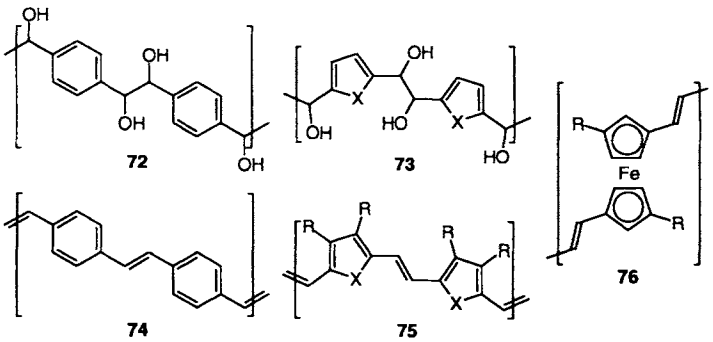

impaired by the poor solubility: the mole masses achieved are low because the product precipitates prematurely out of the reaction solution.[72] This situation can be improved by attaching solubilizing side chains to the monomers. Thus, in the case of poly(3,4-dibutoxy-2,5-thienylene-vinylene) **75** (X = S, R = OBu), M_n lies at 35000,[73] and for poly(3,3'-ferrocenylene-vinylene) **76** carrying appropriate alkyl groups, M_n is still at 10000.[74]

Another possible use of the McMurry reaction in polymer chemistry lies in the synthesis of new monomers with interesting properties. For example, the symmetrical, bridged 1,2-dithienylethene **77** was prepared, which on electrochemical polymerization gave a material with a low band gap E_g and good electrochemically reversible redox behavior.[75] Compound **78** can be obtained by intramolecular McMurry coupling

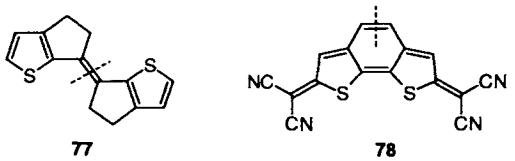

and subsequent oxidation with bromine. If it is pressed together with a typical organic electron donor such as tetrathiafulvalene, the charge-transfer complexes formed exhibit favorable electrical conducting properties.[76]

3. New Types of Substrates and Further Developments of the Method

3.1. Dimerization of Imines and Iminium Salts

In close analogy to the pinacol reaction of carbonyl compounds, the reductive coupling of aldimines to give *vic*-diamines can be successfully carried out by means of low-valent titanium species (Scheme 17).[77,78] The reaction runs particularly smoothly with imines of aromatic aldehydes (R^1 = aryl) and is compatible with a series of functional groups.

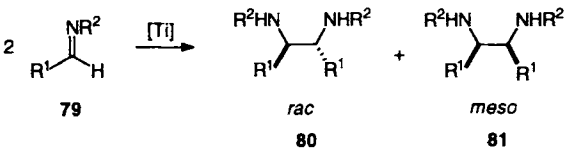

Scheme 17. Synthesis of **80** and **81**. [Ti] = low-valent titanium.

The reaction of an aldehyde with a lithium amide produces a semi-aminal salt in situ. Treatment with $TiCl_4$ liberates an iminium ion; subsequent addition of low-valent titanium followed by aqueous workup furnishes the corresponding *vic*-diamine.[78] This aminative reductive C–C coupling, which can be carried out as a one-pot reaction, permits numerous structural variations of both the aldehyde and the amine components (Scheme 18).

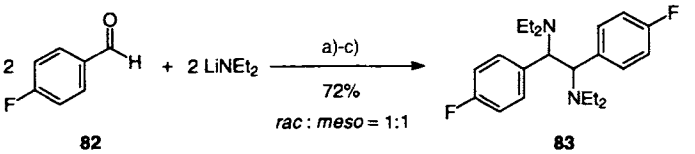

Scheme 18. Aminative reductive coupling following Seebach's method: a) $TiCl_4$; b) low-valent titanium from $TiCl_4$/Mg; c) H_3O^+.

The *vic*-diamines are usually produced as a mixture of the *meso* and *rac* forms. The latter can be removed and then separated into the optical antipodes by fractional crystallization. The enantiomerically pure diamines thus obtained have great importance in syntheses as chelate ligands for asymmetric catalysis and also as chiral auxiliaries. Reductive coupling of imines can also be carried out with reducing agents other than titanium, some of which afford more favorable *rac*:*meso* ratios.[79]

3.2. Acyl Silanes

In many respects the chemical behavior of acyl silanes mimics that of sterically hindered ketones. In spite of this close relationship, McMurry reactions of acyl silanes were unknown, except for one example of a rather inefficient intramolecular cross-coupling of an acyl silane with an aldehyde.[80] Only recently, however, it was demonstrated that aromatic acyl silanes **84** are suitable substrates for inter- and intramolecular alkene synthe-

ses.[81] The best yields of the 1,2-disilylated stilbene derivative **85** were obtained with low-valent titanium on an inorganic support (Al_2O_3, TiO_2, or NaCl)[66] (Scheme 19). Furthermore, from the observed substituent effects, it is clear that the critical step in this reaction is the deoxygenation of the C-silylated pinacol intermediates. A Brook rearrangement may interfere, which leads to silyl enol ethers of type **86** as the result of a silatropic migration.[81] Analogous McMurry reactions with aliphatic acyl silanes, however, have not succeeded to date.

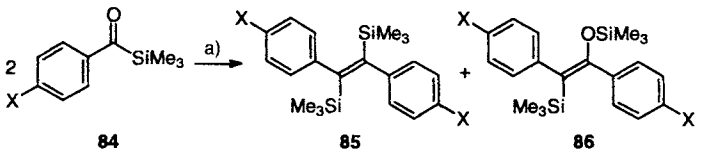

84 **85** **86**

Scheme 19. Reductive coupling of aroyl silanes. a) [Ti] on Al_2O_3 (prepared from $TiCl_3 + 2Na/Al_2O_3$). X = H: 67% + 10%; X = Br: 33% + 43% (hydrolysis product of the silyl enol ether); X = OMe: 56% + 6% (hydrolysis product of the silyl enol ether).

3.3. Ketone–Ester Cyclizations

As early as 1983 McMurry et al. reported an important extension to the range of substrates for titanium-mediated cyclizations. They showed that keto esters can be coupled by low-valent titanium to give enol ethers and subsequent acidic workup of the reaction mixture provides the corresponding cyclanones (Scheme 20, type I).[82] Formally this reaction is one of the rare

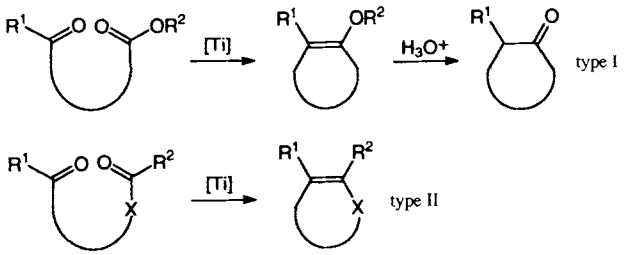

Scheme 20. Intramolecular cross-coupling reactions; see text for details. [Ti] = low-valent titanium.

examples of an intramolecular alkylidenation of an ester and is therefore particularly attractive.[83] However, success depends greatly on the careful optimization of the reaction conditions. The best results were obtained with a low-valent titanium species prepared from $TiCl_3/LiAlH_4$, which was modified by the addition of triethylamine. Titanium–graphite is also a suitable reagent.[31] In contrast to conventional couplings of diketones and dialdehydes, the formation of medium-sized rings by means of this ketone–ester cyclization gave somewhat reduced yields.[82] A strong influence is also exerted by the chain length and the steric demands of R^2.[9a]

However, this attractive process has found few applications in the synthesis of natural products. Examples include the formation of the nine-membered ring of isocaryophyllene (**88**),[84] ring closure of the C-ring of capnellene (**90**),[85] and the recent syntheses of cembrene (**92**) and acoragermacrone (**93**), which

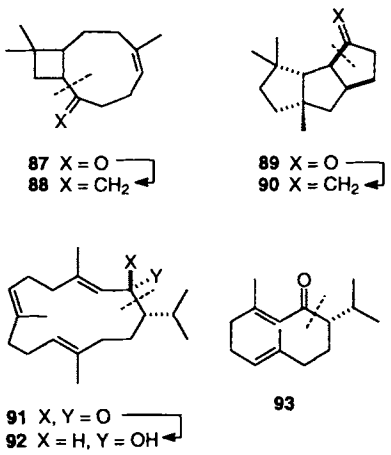

are both based on the cross-coupling of an α,β-unsaturated ester with a ketone.[86] The condensation of a cyclic anhydride with a neighboring aldehyde function is closely related (Scheme 21).[87]

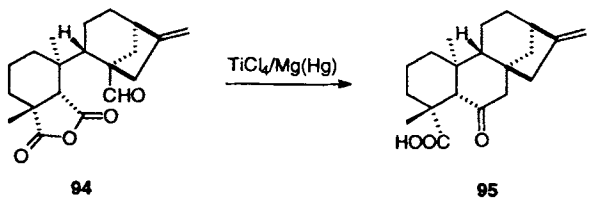

94 **95**

Scheme 21. Synthesis of **95**.

A conceptual advancement is marked by the intramolecular alkylidenations of type II (Scheme 20, X = O). With this reaction aromatic heterocycles such as furans and benzo[*b*]furans can be obtained from simple precursors (Scheme 22).[9, 88] Originally titanium–graphite was used as the coupling agent, but in the meantime the considerably more convenient "instant" method has been used successfully.[17]

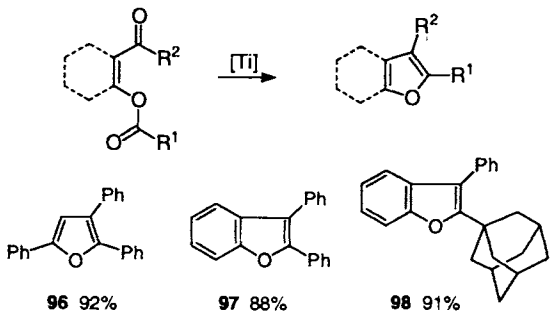

96 92% **97** 88% **98** 91%

Scheme 22. [Ti] = low-valent titanium.

3.4. Titanium-Mediated Synthesis of Pyrroles and Indoles

Although amides were considered to be inert towards low-valent titanium,[7a] intramolecular type II alkylidenation of acylamidocarbonyl compounds (Scheme 20, X = NH, NR) has proved to be a remarkably efficient entry to substituted pyrrole

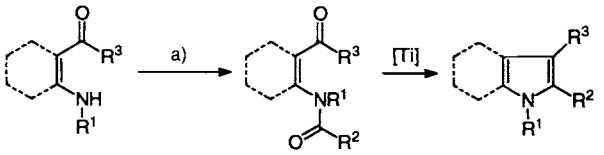

Scheme 23. Reductive indole and pyrrole synthesis by intramolecular ketone–amide coupling: R^1 = H, alkyl, aryl, tosyl; R^2 = H, alkyl, aryl, heteroaryl, OR, NR_2; R^3 = alkyl, aryl, heteroaryl, (H). a) Acylation. [Ti] = low-valent titanium.

and indole derivatives.[9–18] This new heteroarene synthesis (Scheme 23), employing an intramolecular cross-coupling of two functional groups of greatly differing redox potentials, displays the following profile.

1) The reaction proved to be very flexible with regard to the substitution pattern in the enamine region of the product formed. Because all types of amides undergo reductive cyclization smoothly,[9, 17] the acylation of a parent aminocarbonyl compound with different carboxylic acid derivatives and subsequent coupling of the oxoamides thus obtained, ensures easy variation of the R^2 group (Scheme 23). Therefore, this procedure is particularly attractive, for example, in pharmaceutical chemistry for elucidating structure–activity profiles. Such variations can also be carried out as a combinatorial step.[89] Some of the products synthesized and their yields are listed in Figure 2.

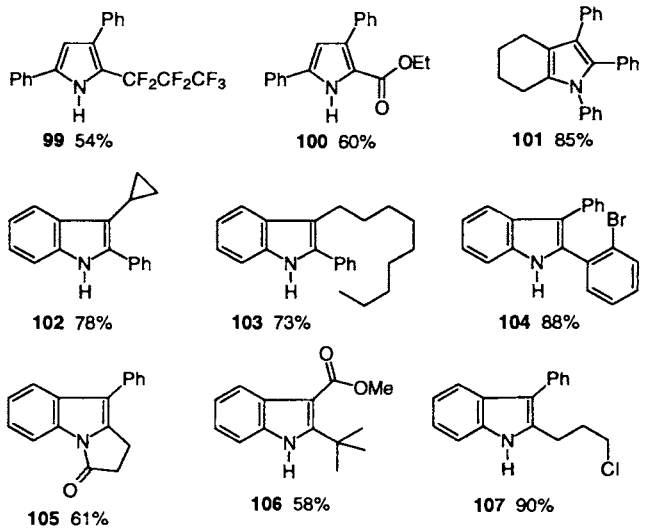

Fig. 2. Selected pyrrole and indole derivatives prepared by the McMurry reaction and their yields.

2) In contrast to many classical methods such as Fischer's indole synthesis, the substitution pattern of the product is defined unequivocally and formation of regioisomers is excluded.
3) In spite of the high reducing capacity of low-valent titanium, the method is compatible with an array of potentially reducible and/or acid-labile functional groups. Table 1 gives an overview.[9–18]
4) Preexisting stereocenters in the substrates are not racemized under the reaction conditions (Scheme 24).[17]

Table 1. Titanium-mediated heterocyclic syntheses: compatibility of functional groups.

Compatible	Semicompatible	Incompatible
alkene	acetal	acyloin
alkyl chloride	alkyne	nitro
amide (distal)	aryl iodide	
amine	carboxylic acid	
aryl bromide	dithioacetal	
aryl chloride	ketone (distal)	
aryl fluoride		
cyclopropyl		
ester (distal)		
ether		
heterocycles (benzofuran, furan, pyridine, thiazole, etc.)		
nitrile		
sulfonamide		
trifluoromethyl		

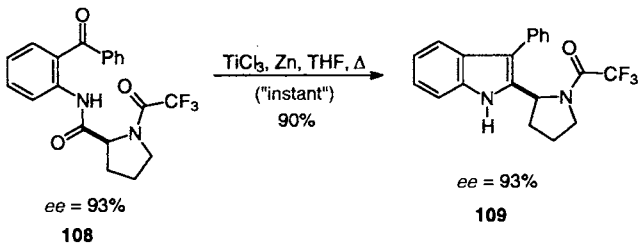

Scheme 24. Synthesis of **109**.

5) This method is also suitable for the preparation of sterically encumbered products, as illustrated by the formation of the indole derivatives **110**–**112**.[17] The 2,2-di-*tert*-butyl-3-indolinone formed as a side product (15%) during the preparation of 2,3-di-*tert*-butyl-1-methylindole **112** provides some insight into the reaction mechanism.

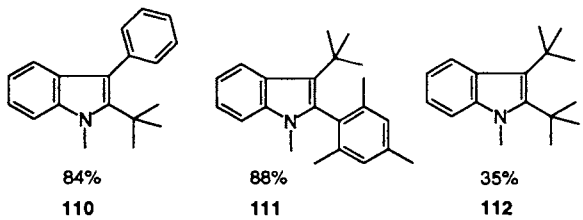

6) The reaction is probably triggered by a two-electron reduction of the carbonyl group, whereas no electrons are transferred to the amide function. The titanium-complexed "carbonyl dianion" thus formed (side-on complexation of the carbonyl group) acts as a nucleophile and attacks the neighboring amide with formation of the C–C bond. Subsequent deoxygenation of the resulting titanium diolate leads to the aromatic heterocycle.[17] This mechanism is in accord with the selectivity observed and is also supported by the results of electrochemical studies. As demonstrated by the data summarized in Section 4.1, comparable nucleophilic "dianionic" intermediates may play a more prominent role in conventional McMurry reactions than previously thought.

7) A particularly striking feature of this cyclization is its marked chemo- and regioselectivity. The formation of the indole or pyrrole ring by the coupling of a carbonyl group to a neighboring amide is highly preferred over other titanium-mediated reactions of polyfunctional substrates. However, distal amide, ester, and even keto groups are inert to [Ti]. Examples of this include the regioselective and non-racemizing cyclization of the N-trifluoroacetylated proline derivative **108** (Scheme 24),[17] as well as the preparation of **115**,[10, 17] a precursor of the drug diazepam by regioselective ketone–amide coupling (Scheme 25). In the latter case the ketone–ester cyclization, which is a possible side reaction, is not observed. This preference for indole formation is particularly apparent in the cyclization of the pyruvic acid amide **113** to salvadoricine (**17**):[10] here the ketone–amide cyclization is even superior to the conceivable McMurry coupling of the two keto groups (Scheme 25). The evident driving force of titanium-mediated formation of indoles is also responsible for the selective ketone–amide cyclizations of polyfunctional precursors, for example, in the syntheses of the alkaloids secofascaplysin (**157**)[13] and lukianol A (**165**)[15] (see Section 3.4.4).

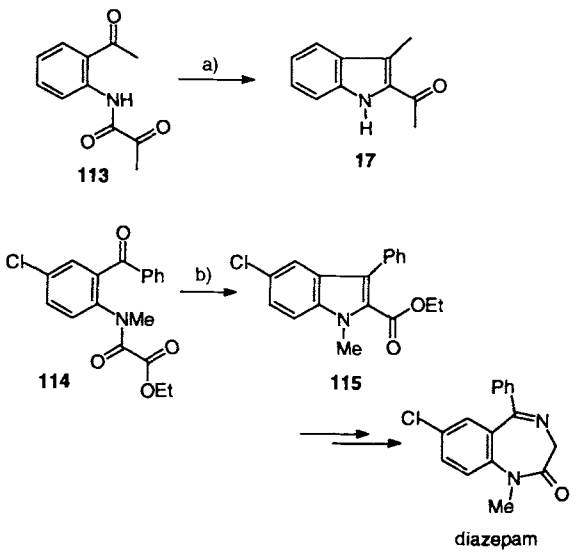

Scheme 25. Regioselective ketone–amide coupling. a) Ti–graphite, DME, reflux, 0.5 h, 60%; b) Ti–graphite, DME, reflux, 1 h, 94%

8) This distinct selectivity accounts for polycyclization reactions with formation of oligoheteroarene structures of exactly defined length and substitution pattern such as **117** (Scheme 26).[14]
9) Because of the great driving force of titanium-mediated formation of indoles, there is no need to run the reactions under high dilution.[9, 14, 17, 18] As a rule, they proceed with good yields even at concentrations of 0.1 M for the individual substrates.
10) It is particularly significant that different titanium species with formal oxidation states of 0, +I, and +II are able to induce the cross-coupling.[17] Therefore, the reaction conditions can be simplified and/or adapted to the requirements of the given substrate.

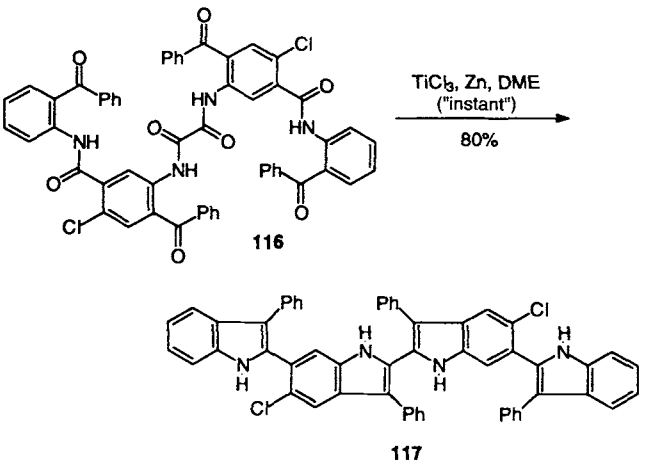

Scheme 26. Selective polycyclization in the synthesis of **117**.

Ketone–amide couplings of this type were originally carried out with titanium–graphite[31] as the reagent, which is obtained by reducing $TiCl_3$ with three equivalents of potassium–graphite laminate C_8K (thus, formally a Ti^0 species). In C_8K the 4s electrons of potassium are delocalized in the conducting band of graphite: the reduction of a metal salt can therefore take place at any site on the large surface of the laminate, thus ensuring a high level of dispersion and excellent reactivity of the resulting particles.[24, 91] Since these particles are adsorbed on the surface of the graphite, they are also protected against premature aggregation.[92] This metal activation procedure has also been highly successful in numerous other cases.

Clive et al. reported, however, that during a total synthesis of compactin (see Section 2.1) the formally monovalent titanium species formed by the reduction of $TiCl_3$ with only two equivalents of C_8K gave higher yields and more reproducible results.[29, 30] An extensive comparative study of titanium-mediated indole synthesis employing these two modifications of Ti–graphite confirmed Clive's observation, and therefore the use of the reagent prepared from $TiCl_3/2\,C_8K$ is strongly recommended.[17]

Since "Ti^0" is evidently neither essential nor necessarily the best choice, many other "low-valent" titanium samples were subsequently examined as coupling agents on a test reaction. Although they differ in their efficiency, all of the investigated titanium species with formal valencies of zero, one, or two were able to couple 2-benzamidobenzophenone (**118**) to give 2,3-diphenylindole (**119**) (Table 2).[17] This was a clear experimental confirmation of our previous assemption that different "McMurry reagents" can exist and be active.[24]

3.4.1. The "Instant" Method

With very few exceptions, McMurry reactions are carried out in two consecutive steps.[7, 8] First, $TiCl_x$ ($x = 3, 4$) is reduced to the active species by means of an appropriate reducing agent, and only then the substrate is added. Because the active species was assumed to be metallic titanium, aggressive reducing agents such as K, C_8K, Na, Li, $LiAlH_4$ etc. were often chosen; since they are incompatible with a carbonyl compound, such a two-step sequence is mandatory.

Table 2. Reductive cyclization of **118** to give 2,3-diphenylindole **119**: screening of different low-valent titanium reagents.

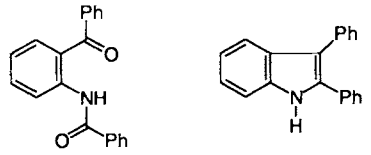

118 **119**

Reagent	Formal oxidation state	Yield [%] [a]	Reagent	Formal oxidation state	Yield [%] [a]
$TiCl_3 + 3C_8K$	0	90	$[Ti(biphenyl)_2]$	0	70
$TiCl_3 + 2C_8K$	+I	90	$[TiHCl \cdot (thf)_{0.5}]$	+II	85
$TiCl_4 + 4K[BEt_3H]$	0	67 [b]	$[Cp_2Ti(PMe_3)_2]$	+II	79
Ti cluster [c]	0	45 [b]	$[TiH_2 \cdot (thf)_2(MgCl_2)]_n$	+II	69
$[Ti(toluene)_2]$	0	75			

[a] Yield of isolated product unless otherwise stated. [b] Yield determined by GC. [c] Cluster produced by electrochemical means.

Based on the insight that carbonyl coupling reactions are by no means restricted to metallic titanium, it was possible to devise a new and significantly simplified procedure (Scheme 27). Thus, $TiCl_x$ is added to the respective substrate and reduced

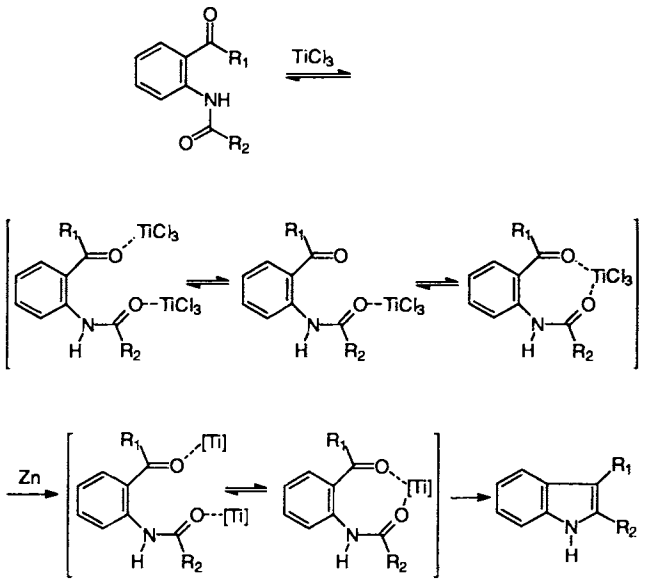

Scheme 27. Reductive carbonyl coupling by the "instant" method.

to some "low-valent" titanium species within the complex formed in situ by action of a mild reducing agent such as zinc dust or iron powder. This procedure known as the "instant" method[17] combines several advantages.

1) Reagent and substrate are preorganized: the active species [Ti] is produced regioselectively at the reaction site.
2) Both steps of the carbonyl coupling process—the preparation of the active species and its subsequent reaction—are combined into a single synthetic operation. By avoiding any hazardous reducing agent, coupling reactions according to the "instant" protocol are simple to perform and easy to scale up.[90]
3) The reactions are distinguished by a high tolerance towards functional groups. The only limitations are found with acid-labile derivatives.
4) "Instant" couplings can even be carried out in nonethereal solvents such as ethyl acetate, acetonitrile, and DMF.

This method has proved to be particularly successful for the reductive synthesis of heterocycles. However, it can also be employed for conventional inter- and intramolecular McMurry couplings of (di)aldehydes and (di)ketones.[17] This was recently confirmed by its application to the formation of calix[4]arenes of fixed conformation (see Section 2.2).[71a]

Zinc had already been used as a reducing agent for $TiCl_x$ before the "instant" method was developed.[3, 93, 94] The conceptional difference and methodological advance lies in the deliberate avoidance of any prereduction of the titanium species.[17] This is not only fully justified in view of the preparative results obtained but also by the insight gained into the nature of low-valent titanium, which is summarized in Section 4.4. According to this work, zinc is capable of reducing $TiCl_3$ to "low-valent" titanium ($TiCl_2$) only if the redox potential of the latter has been sufficiently lowered by coordination to a carbonyl compound![22] Thus, when zinc is used as the reducing agent, a two-step procedure is futile.

3.4.2. Titanium-Catalyzed Carbonyl Coupling Reactions

The driving force of Ti-induced carbonyl coupling stems from the formation of titanium oxides as the inorganic by-products of the reaction. In the presence of reducible substrates, however, these oxides are much too stable to be reduced back to the active low-valent titanium [Ti]. As a consequence, all reactions to date have had to be carried out with at least stoichiometric amounts of titanium; in practice a (huge) excess is mandatory.[7, 8]

The "instant" method enables the generation of activated titanium [Ti] from $TiCl_x$ in the presence of the substrate. If the initial inorganic product, titanium oxychloride, can be reconverted into $TiCl_x$ in situ, then a catalytic cycle may emerge (Scheme 28).[18] The required metathetic ligand exchange may

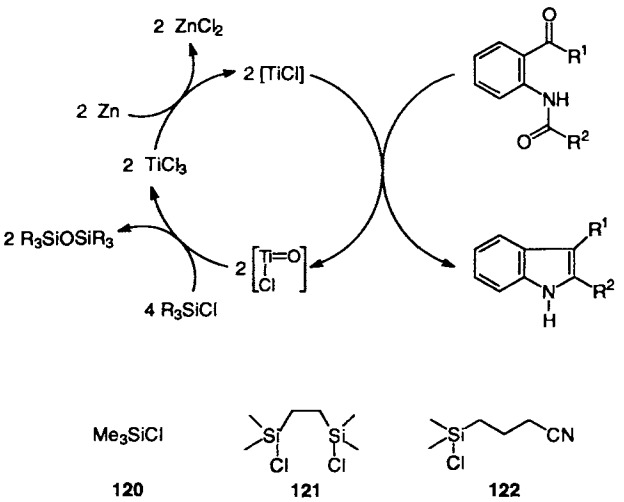

120 **121** **122**

Scheme 28. Titanium-catalyzed indole synthesis. The catalytic cycle shown is only a formal representation of the reaction mechanism. The nature of the low-valent species involved was not investigated more closely; however, the results summarized in Section 4.4 suggest the intermediate formation of $TiCl_2$ as the active species from $TiCl_3/Zn$.

be achieved by addition of chlorosilanes as oxophilic additives. As can be seen from Table 3, a few mole% of $TiCl_3$ is in fact sufficient to couple oxoamides smoothly to yield the corresponding indoles, provided that the reactions are carried out under "instant" condititons in the presence of chlorosilanes.

Table 3. Selected titanium-catalyzed indole syntheses.

R^1	R^2	R^3	$TiCl_3$ [mol %]	Chlorosilane	Yield [%] [a]
H	Ph	Ph	10	**120**	80
H	Ph	Ph	5	**120**	71
H	Ph	Ph	2	**121**	85
H	CF_3	Ph	10	**120**	88
H	$CF_2CF_2CF_3$	Ph	11	**120**	73
H	$(CH_2)_{14}CH_3$	Ph	10	**120**	77
H	Ph	CH_3	8	**122**	82
CH_3	Ph	$(CH_2)_3CH_3$	8	**122**	67
H	*N*-trifluoroacetyl-2-pyrrolidinyl	Ph	17	**120**	67

[a] Yield of isolated product.

Control experiments proved that these transformations are indeed titanium-catalyzed.[18] Without the addition of $TiCl_3$ the substrates do react, but the desired indole is formed in only minor amounts. The quantity of $TiCl_3$ required for good yields depends on the specific chlorosilane chosen. When trimethylsilyl chloride (TMSCl, **120**) is used, 5–10 mol% of $TiCl_3$ is necessary, whereas with $ClMe_2SiCH_2CH_2SiMe_2Cl$ (**121**) as the additive 1–2 mol% of $TiCl_3$ suffices. Most likely the entropically favored intramolecular formation of siloxane is responsible for the higher turnover number in this case.

The preparation of indole derivatives with an alkyl group at C3 requires special care in the choice of the additive. Because the starting oxoamides are less likely to cyclize, the noncatalytic decomposition of the substrate competes with Ti-catalyzed carbonyl coupling. However, the latter reaction can be sufficiently accelerated by the use of $ClMe_2Si(CH_2)_3CN$ (**122**). This commercially available additive combines an affinity towards titanium, stemming from its nitrile group, with the oxophilicity of a chlorosilane. Thus, the critical transfer of oxygen from titanium to silicon is intramolecular, which favors the regeneration of $TiCl_x$ and hence the catalytic cycle.[18] The use of **122** as an additive for the catalytic method affords 3-alkylated indole derivatives in good yields (Table 3).

The insight gained in this "titanium case study"—that reactions involving early transition metals in low oxidation states can be rendered catalytic simply by the addition of chlorosilanes—nicely applies to other processes as well. Following this basic idea, Ti-catalyzed fixation of nitrogen[95] as well as Nozaki–Hiyama reactions catalytic in $CrCl_2$[96] have been successfully carried out.

3.4.3. *Commercially Available Titanium Powder as a McMurry Reagent*

The extreme passivation of commercially available titanium caused by a surface oxide layer ruled it out as a reagent for carbonyl coupling.[97] Due to this extraordinary resistance metallic titanium has gained great importance as an industrial material, but does not play any role as a chemical.

During investigations of the catalytic procedure we discerned that chlorosilanes do react with titanium oxides. This suggested a reevaluation of titanium powder as a reagent. Indeed, numerous carbonyl coupling reactions were accomplished with a combination of titanium powder (100–325 mesh) and TMSCl in good yields.[18] In spite of long reaction times, this procedure is attractive as it gives high yields and good selectivity, and is particularly simple to perform. Because only titanium compounds of no toxicological concern are involved and other metal cations are avoided, this method should be suitable for the synthesis of pharmaceutically relevant products.

It is now possible to use titanium powder/TMSCl for the reductive coupling of aromatic as well as α,β-unsaturated carbonyl compounds. The reagent exerts a pronounced template effect, which manifests itself, for example, in good yields in macrocyclizations even without slow addition of the substrate. The newly developed heterocycle syntheses based on reductive ketone–ester and ketone–amide cyclizations are also possible with Ti/TMSCl. A few representative examples are given in Table 4.[18] If catalytic amounts of $[Ti(OiPr)_4]$ or $[ClTi(OiPr)_3]$ are added, the generally long reaction times can be distinctly shortened. Unfortunately, this combination of reagents has not

Table 4. Selected carbonyl coupling reactions using commercially available titanium powder as the reagent.

Substrate	Product (yield [%])
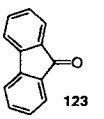 **123**	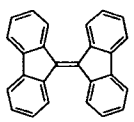 **124** (94)
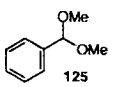 **125**	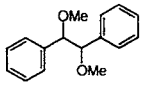 **126** (88)
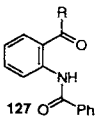 **127**	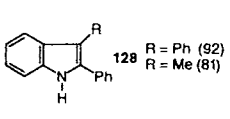 **128** R = Ph (92), R = Me (81)
retinal (**129**)	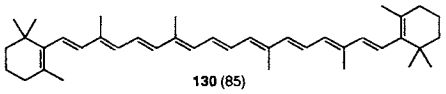 **130** (85)
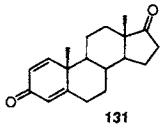 **131**	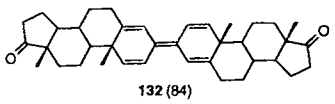 **132** (84)
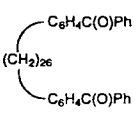 **133**	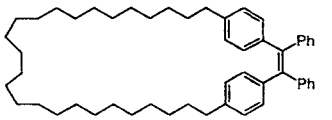 **134** (90)

yet been successful with aliphatic aldehydes or ketones. This sharply defined profile makes chemo- and regioselective coupling reactions possible: androsta-1,4-dien-3,17-dione (**131**) is dimerized exclusively at the enone site, whilst the unprotected aliphatic keto group is not affected by the reaction.[18]

^{29}Si NMR investigations indicate that the chlorosilane not only leads to the degradation of the passivating surface layer of titanium powder, but that the observed activation is a more complex (redox) process.[18] This was confirmed by investigations with electron microscopy, which clearly show morphological changes of the titanium powder caused by the chlorosilanes.[98]

3.4.4. Titanium-Mediated Heterocycle Syntheses: Applications to Natural Products and Biologically Active Compounds

The selectivity of titanium-mediated heterocycle syntheses (see Section 3.4) is a prerequisite for application of this procedure to natural products and biologically active compounds. For example, the reaction of pyruvic acid amide **113** led to salvadoricine (**17**) (Scheme 25).[10] In this particular case the preference of the ketone–amide cyclization over the conceivable ketone–ketone coupling clearly contrasts with all the earlier findings[7, 8] in reactions employing low-valent titanium, and points to the pronounced driving force of reductive heteroarene formation. In light of this result, the selective ketone–amide coupling of the polyfunctional substrate **114** to give indole **115**, a known precursor of diazapam, is not surprising. Originally carried out with Ti–graphite,[10] this cyclization can also be accomplished with the "instant" method on a multigram scale.[17, 90]

Another successful application of the "instant" procedure is the transannular coupling of **135** to afford (+)-aristoteline (**136**) (Scheme 29).[17] Because the product is strongly coordinated

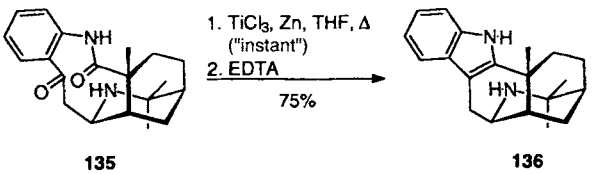

Scheme 29. Synthesis of (+)-aristoteline (**136**).

through its basic nitrogen function to the Lewis-acidic titanium salt, the crude reaction mixture must be worked up by extraction with aqueous ethylenediaminetetraacetate (EDTA).

The synthesis of camalexin (**141**), a representative example of 3-(2-thiazolyl)-substituted indole alkaloids, is particularly simple (Scheme 30).[12] This phytoalexin from *Camelina sativa* is accessible in four steps with an overall yield of 50%. Acylation of the commercially available 2-trimethylsilylthiazole (**137**) with 2-nitrobenzoyl chloride affords ketone **138**, hydrogenation of the nitro group gives amine **139**, N-formylation yields **140**, and finally coupling under "instant" conditions furnishes the desired natural product. If acylation reagents other than formic acid are used, the same sequence leads to analogs of camalexin, which differ from the natural product in the substituents at C2.

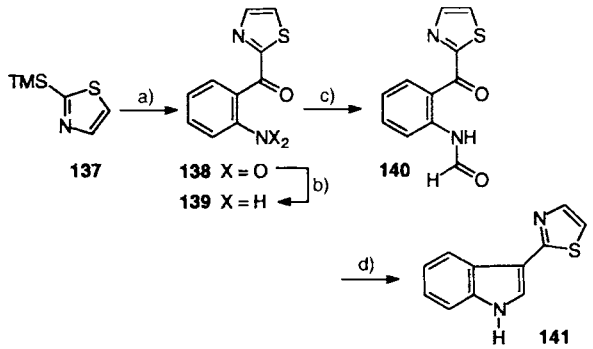

Scheme 30. Synthesis of camalexin (**141**). a) 2-nitrobenzoyl chloride, CH_2Cl_2, 83%; b) H_2 (1 atm, Pd/C (5%), EtOAc, 98%; c) HCOOH/Ac_2O, 87%; d) i. $TiCl_3$ (5 equiv), Zn dust (5 equiv), DME, reflux; ii. EDTA disodium salt, H_2O, 71%.

Ti-mediated indole formation led to two flexible entries to the class of indolo[2,3-*a*]quinolizine alkaloids.[12, 13] Recently, the interest in this group of natural products greatly increased after they were discovered to be physiologically active due to intercalation into DNA .

Our first synthesis[12] starts from 2-iodoaniline (**144**), which is converted into ketone **146** in two steps (Scheme 31). For the synthesis of indolopyridocoline **142**, the parent compound of this class of natural products, the amino group is acylated with pyridine-2-carboxylic acid chloride (**147**, R = H) and the resulting ketoamide **148** (R = H) subsequently coupled by using Ti–graphite to give the indole **149** (R = H). Cleavage of the methyl ether by BBr_3 leads to spontaneous cyclization of the C-ring, which can be aromatized with 2,3-dichloro-5,6-dicyano-1,4-benzoquinone (DDQ) (**150** → **142**, R = H). The individual representatives of this alkaloid family differ essentially in the

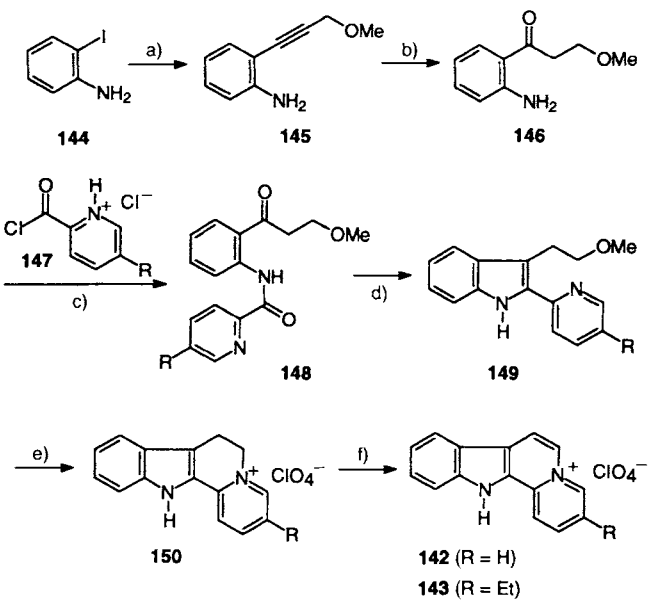

Scheme 31. Syntheses of the perchlorate salts of 6,7-dihydroflavopereirine (**150**, R = Et), indolopyridocoline (**142**), and flavopereirine (**143**). a) Propargyl methyl ether (2 equiv), $PdCl_2$ (10 mol%), CuI (10 mol%), PPh_3 (20 mol%), NEt_3, room temperature, 16 h, 96%; b) $HgSO_4$ (10 mol%), MeOH/H_2O, 48 h, reflux, 53%; c) **147**, CH_2Cl_2, pyridine, DMAP cat., 89% (R = H), 85% (R = Me); d) Ti–graphite ($TiCl_3$:C_8K = 1:2), THF, reflux, 2.5–4.5 h, 62% (R = H), 52% (R = Me); e) i. BBr_3, CH_2Cl_2, −78 °C (1 h) → −15 °C (5 h); ii. HCl, $CHCl_3$; iii. $NaClO_4$, H_2O, 79% (R = H), 67% (R = Me); f) i. DDQ, HOAc, reflux; ii. NaOH, $CHCl_3$; iii. $NaClO_4$, H_2O, 74% (**142**), 78% (**143**).

substitution pattern of the D-ring. Therefore, they can be obtained analogously by acylation of **146** with an appropriately substituted pyridine-2-carboxylic acid chloride derivative. This is demonstrated by the syntheses of 6,7-dihydroflavopereirine (**150**, R = Et) and flavopereirine (**143**, R = Et),[12] and highlights once again the flexibility of the titanium-based method with regard to the substituent at C2 of the newly formed indole derivative (cf. Section 3.4).

Alternatively, compound **151**, which is easily accessible from 2-nitroacetophenone, can be used as starting material for the synthesis of indolo[2,3-*a*]quinolizine alkaloids (Scheme 32).[13] In this case the aromatic C-ring of the desired product is formed during the hydrolysis of the acetal once the indole unit has been generated.

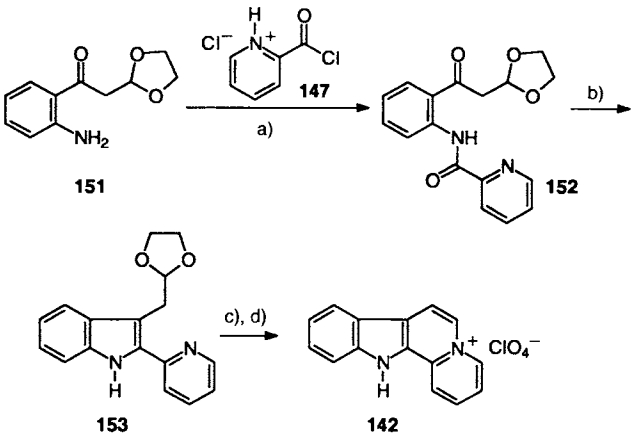

Scheme 32. Alternative synthesis of indolopyridocoline **142**. a) CH_2Cl_2, pyridine, DMAP cat., 0 °C → room temperature, 4 h, 89%; b) i. Ti–graphite ($TiCl_3$:C_8K = 1:2), THF, reflux, 6.5 h; ii. EDTA disodium salt, H_2O, 57%; c) HCl, THF, reflux, 8 h; d) i. Ac_2O, reflux; ii. $NaClO_4$, H_2O, 77% (for steps c) and d)).

Extracts from marine sponges of the genus *Fascaplysinopsis* have attracted attention because of their antimicrobial, cytotoxic, and antiviral activity. These properties stem from alkaloids of novel structure such as secofascaplycin (**157**). Building block **151**, already utilized in the preparation of indolopyridocoline, is a good starting material for a total synthesis of this particular natural product as well (Scheme 33). N-acylation with acyl chloride **154** (readily obtained from anthranilic acid methyl ester and oxalyl chloride) gave good yields of the polyfunctional compound **155**. Although this substrate bears five different carbonyl functions, it underwent a chemo- and regioselective coupling of the ketone with the proximate amide to produce indole **156** on treatment with Ti–graphite. The other potentially reducible groups (distal amide, ester, acetal) were not attacked.[13] Hydrolytic workup of the crude reaction mixture gave the desired alkaloid in 60% yield.

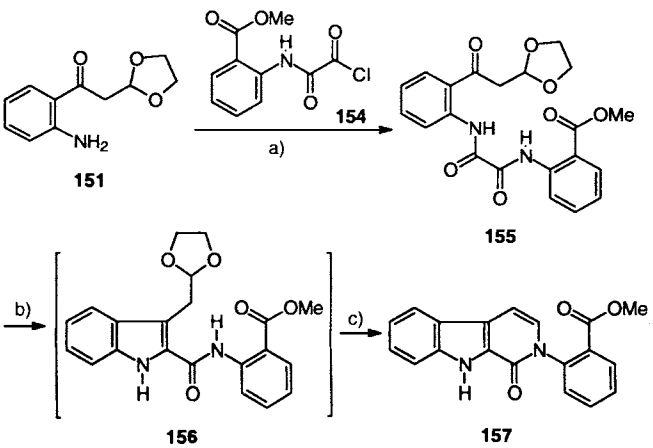

Scheme 33. Synthesis of secofascaplysin (**157**). a) CH_2Cl_2, pyridine, 20 h, 66%; b) Ti–graphite ($TiCl_3$:C_8K = 1:2), THF, 0 °C (21 h) → reflux (5 h); c) aq. HCl (5%), THF, 60 °C, 5 h, 60% (over both steps).

In the last three syntheses Ti–graphite ($TiCl_3/2C_8K$) was used as the coupling reagent.[17, 31] The aldol substructures of the individual substrates render them sensitive towards Lewis acids such as $TiCl_3$; for this reason the "instant" method is unsuitable. The same is true for the first total syntheses of the pyrrole alkaloids lukianol A (**165**) and lamellarin dimethyl ether **163** (Scheme 34). These natural products have not yet been well investigated. Although they obviously share similar structural features, these metabolites are produced by unrelated marine organisms. They have been synthesized starting from 4,4′-dimethoxychalcone, which can be converted to isoxazole **159** in two steps. Reductive cleavage of the N–O bond and acylation of the resulting ketoamine **160** with methyl oxalyl

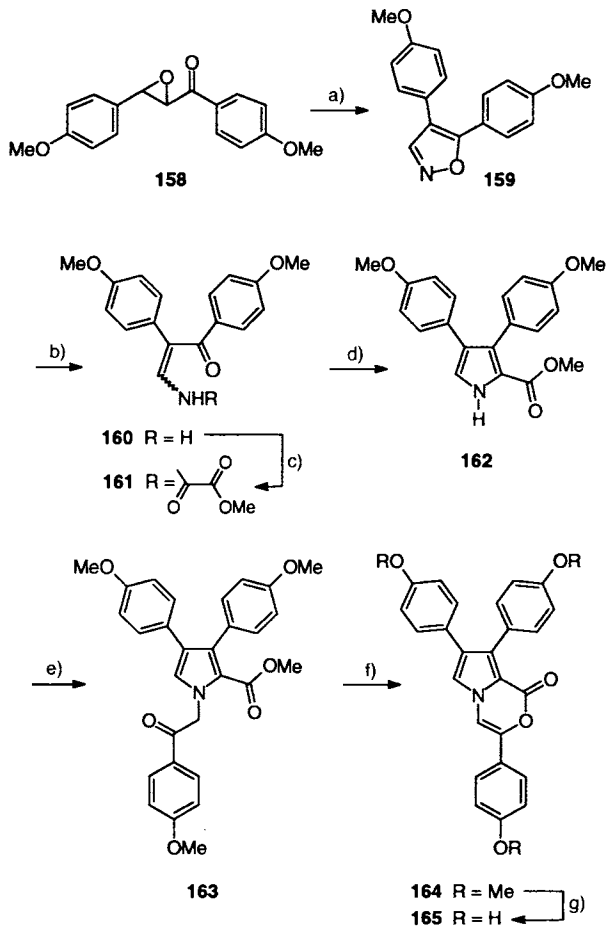

Scheme 34. Synthesis of two pyrrole alkaloids: a) i. $BF_3 \cdot Et_2O$, Et_2O, reflux; ii. $NH_2OH \cdot HCl$, pyridine, EtOH, reflux, 67% (over both steps); b) H_2 (1 atm), Pd/C (5%), THF, 94%, *Z*:*E* = 1:1; c) ClOCCOOMe, pyridine, THF, 73%, *Z*:*E* = 2.5:1; d) Ti–graphite ($TiCl_3$:C_8K = 1:2), DME, reflux, 52%; e) *p*-MeO-$C_6H_4COCH_2Br$, K_2CO_3, acetone, reflux, 91%; f) i. KO*t*Bu, H_2O, Et_2O, 0 °C → room temperature; ii. Ac_2O, NaOAc, reflux, 59% (over both steps); g) BBr_3, CH_2Cl_2, −78 °C → room temperature, 99%.

chloride gives the acid-labile ketoamide **161**, which, when treated with Ti–graphite regioselectively cyclizes to give pyrrole **162**. N-Benzylation and subsequent manipulation of the protecting groups gives good yields of both lamellarin dimethyl ether (**163**) and the corresponding enol lactone lukianol A (**165**).[115]

Alongside these applications to natural products, the advantages of Ti–mediated heterocycle synthesis could also be demonstrated in the preparation of pharmacologically active compounds. For example, the indole derivative zindoxifene (**167**), which is active against estrogen-dependent tumors, was obtained in a few steps from 2-amino-5-methoxyacetophenone.[111] Once again, because of the flexibility of this method, several new analogs (e.g. **168**, **169**) of this anticancer agent are easily accessible for investigating structure–activity relationships. The indole-2-carboxylic acid derivative **170**, recently reported as an antagonist of the endothelin receptor, was also readily accessed by Ti-mediated ketone–amide coupling and, if necessary, the structure can be varied.[113] In this case, the coupling was performed by the particularly convenient "instant" method on a multigram scale.

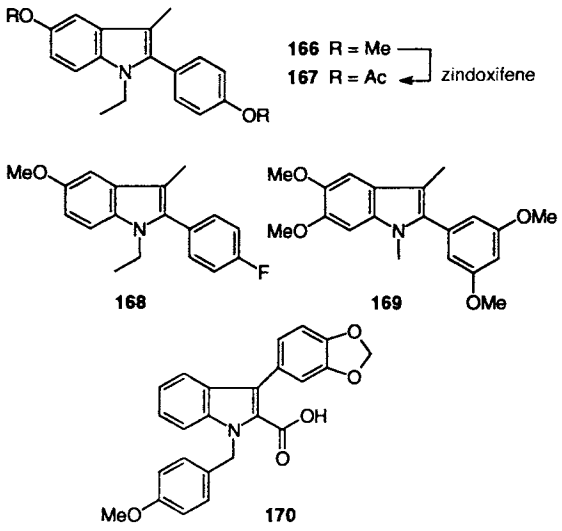

4. Recent Results on the Structure of Low-Valent Titanium Reagents and on the Reaction Mechanism of the McMurry and Related Reactions

Since the discovery of the McMurry reaction[3–5] various reducing agents and methods have been used to prepare low-valent titanium reagents. The first reductive couplings of ketones and aldehydes to furnish alkenes employed Mg[4] or Zn[3] in THF to reduce titanium tri- or tetrachloride; in the former case $[TiCl_3(thf)_3]$ was "prereduced" with Mg before addition of the carbonyl compound; in the latter case $TiCl_4$ was treated with Zn powder in the presence of the carbonyl substrate. The reagent introduced by McMurry et al.[5] prepared from $TiCl_3$ and 0.5 equivalents of $LiAlH_4$ found extensive application in such reactions[99] (cf. Section 4.1.1). According to Corey et al.,[103] the combination $TiCl_4$/Mg-amalgam, as well as the discrete hexamethylbenzene–Ti^{II} π-complex **171** are favorable reagents for the coupling of aldehydes and ketones to give pinacols.[104]

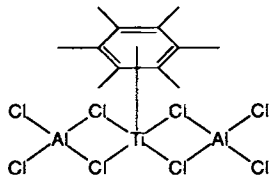

171

In the 1970s the search for improvements in the effectivity and reproducibility of McMurry reactions brought the successive introduction of K,[105] Li,[106] Zn in the presence of pyridine,[94] and the Zn–Cu couple[93b] (referred to hereafter as Zn(Cu)) in THF or DME as reducing agents for $TiCl_3$ and $TiCl_4$. Tkatchenko et al.[107] demonstrated the use of the discrete Ti^0 complex bis(benzene)titanium for McMurry coupling reactions as well as for deoxygenations of unsaturated alcohols to afford alkenes (see also Table 2). The low-valent titanium species prepared from $TiCl_3$ and C_8K proved to be an excellent reagent for inter- and intramolecular coupling of aldehydes and ketones[29–31] and permitted the syntheses of furans, pyrroles, and indoles (described in Sections 3.3 and 3.4). The most efficient reagent, which is currently recommended[8] for all types of reductive coupling, is the $[TiCl_3(dme)_{1.5}]$/Zn(Cu)/DME system perfected by McMurry et al.[93a] The processes by which reductive coupling of aldehydes and ketones produce alkenes were studied by Barteau et al.[108] by temperature-programmed desorption on the surface of single crystals of TiO_2 which had been reduced by bombardment with Ar^+ ions. There is only one result as yet on the suitability of a Ti^0 colloid prepared by Bönnemann et al.[109] from $TiCl_4$ and $K[BEt_3H]$ as a coupling reagent (see Table 2).[17] The more recent developments in the methodology are discussed in Sections 3.4.1–3.4.3 and 4.1–4.4 of this review. In contrast to the widespread application of low-valent titanium reagents in organic syntheses, there have been relatively few in-depth investigations in the past on their nature and mode of action; these are summarized below.

In studies of N_2 fixation (cf. Section 1) with the $TiCl_3$/Mg/THF system, Yamamoto et al.[110] were able to isolate a complex of composition $[TiNMg_2Cl_2(thf)]$ (**172**). On hydrolysis it produced ammonia (Scheme 35). In the absence of nitrogen 2.5 moles of Mg per mole of $TiCl_3$ are consumed in the reduction of $TiCl_3$ with Mg in THF. However, the resulting THF solution proved to be inactive for N_2 fixation.[110]

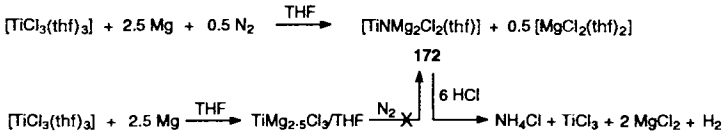

Scheme 35.

According to Sobota et al.[111] reduction of $TiCl_4$ with Mg in THF leads to a black complex $[TiMg_2Cl_2(thf)]_{2x}$ (**173**, Scheme 36). On the basis of the chemical properties and diamagnetism, a dimeric (or oligomeric) structure with direct Ti–Mg bonds was proposed for **173**.[112]

Investigations on the nature of the low-valent titanium species obtained by the reduction of $TiCl_3$ or $TiCl_4$ with Li, K, Mg,

$$2\,TiCl_4 + 6\,Mg \xrightarrow{THF} [TiMg_2Cl_2(thf)]_{2x} + [2\,MgCl_2(thf)]$$

173 ($x \geq 1$)

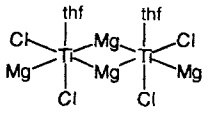

173

Scheme 36. Preparation and postulated structure of **173**.

and $LiAlH_4$ in refluxing THF were carried out by Geise et al.[113] in the early 1980s. The highest yields in the McMurry coupling of benzophenone or cyclohexanone were obtained when $TiCl_3$ was prereduced in molar ratios of 1:3.2 (Li, K), 1:1.7 (Mg), and 1:0.5 ($LiAlH_4$). In qualitative ESR investigations of the reduction process it was observed that the ESR signals of Ti^{III} centers disappeared after the reduction had ended. On the basis of the amount of reducing agent consumed in the reduction, and on the results of ESR and other studies, the active titanium species was suggested to consist of aggregates of metallic titanium particles adsorbed on an inorganic support (KCl, $MgCl_2$, etc.). The titanium particles formed by reaction with the various reducing agents would differ in their surface-bound ligands—H, Cl, or THF. This and the results of earlier work[93b] led to the supposition that the active titanium species in the McMurry reaction—regardless of the method of preparation—are finely divided Ti^0 particles, which differ only in the corn size, specific surface area, and morphology.[7a] The mechanism of the McMurry reaction is generally believed to be C–C coupling by dimerization of ketyl radicals, which are bound to the surface of the titanium particles, to give a pinacolate, followed by stepwise cleavage of the C–O bonds to produce the alkene and surface-oxidized titanium particles.[7a, 44]

However, in contrast to this hitherto[8] widespread[7c, d, 114] idea, there have been numerous indications for a considerable length of time [31a, b, 94, 103] that $TiCl_4$ and $TiCl_3$ in solution are not reduced to metallic titanium by common reducing agents, and that the presence of zero-valent titanium is not a prerequisite for the McMurry reaction.[108]

In the following we present a summary of more recent investigations on the structure and mode of operation of common as well as some new low-valent titanium reagents. As it turns out, reduction of $TiCl_3$ with $LiAlH_4$ (or MgH_2), Mg, and Zn(Cu) (in this case only in the presence of the carbonyl substrate) in THF or DME afford, as surmised,[24] not metallic titanium particles, but rather low-valent titanium complexes with differing structure and reactivity.

4.1. Chlorohydridotitanium $[HTiCl(thf)_{\approx 0.5}]_x$ as the Active Component of the McMurry Reagent

4.1.1. Characterization of $[HTiCl(thf)_{\approx 0.5}]_x$ and a New Formulation of the McMurry Reaction

Magnesium hydride prepared catalytically as a solid[115] or in solution [116] (in the following referred to as MgH_2^* (**174**) and MgH_2' (**175**), respectively) can be employed in both forms as a reagent for the preparation of intermetallic compounds and their hydrides in a highly reactive form.[19] $[TiCl_3(thf)_3]$ reacts with both active forms of magnesium hydride in THF at room temperature with liberation of hydrogen.[20] On close examination of the H_2 evolution it was found that as the $MgH_2'/TiCl_3$ ratio increases, the amount of H_2 increases at first and then remains constant at 0.5 H_2/Ti from a 1:1 molar ratio onwards. This result gave the first indication that under the applied conditions Ti^{III} is reduced only to (formally) Ti^{II}.

In the reaction with a 1:1 molar ratio of MgH_2^* or MgH_2' to $TiCl_3$, a highly pyrophoric black solid precipitates out of the THF solution. It is amorphous to X-rays and proved to be the new chlorohydridotitanium complex $[HTiCl(thf)_{\approx 0.5}]$ (**177**, Scheme 37); the deuterated compound **D-177** can be prepared

$$[TiCl_3(thf)_3] + MgH_2^*\ (MgH_2') \longrightarrow [HTiCl(thf)_{\sim 0.5}]\downarrow + 0.5\,H_2\uparrow + MgCl_2$$

174 (**175**) **177** (70-75%)

$$[TiCl_3(thf)_3] + MgD_2^* \longrightarrow [DTiCl(thf)_{\sim 0.5}]\downarrow + 0.5\,D_2\uparrow + MgCl_2$$

176 **D-177**

Scheme 37. Synthesis of **177** and **D-177**.

in an analogous manner. Deuterolysis of **177** gives HD and D_2 (along with a little H_2) as well as Ti^{III} salts. Hydrolysis of **D-177** gives HD, H_2, and Ti^{III} salts. Iodolysis of **177** (**D-177**) gives 0.5 moles of H_2 (D_2) per mole of titanium (Scheme 38). This proves the presence of hydrogen bound as a hydride in **177**.

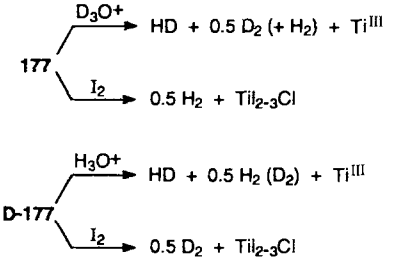

Scheme 38. Reactions of **177** and **D-177**.

The preparation of the McMurry reagent was repeated and it was found that **177** was the reaction product in this case too. The reduction of $TiCl_3$ with 0.5 equivalents of $LiAlH_4$ in THF produced H_2 (0.5 mole of H_2 per mole of Ti) and on addition of pentane to the reaction mixture a black, X-ray amorphous powder could be isolated in 46% yield. The IR spectrum and the composition of this powder agreed with that of **177**. As demonstrated below, **177** is a fully active reagent for the McMurry reaction. The formation of the McMurry reagent can therefore be formulated according to Equation (a).

$$[TiCl_3(thf)_3] + 0.5\,LiAlH_4 \longrightarrow \mathbf{177} + 0.5\,H_2\uparrow + 0.5\,LiCl + 0.5\,AlCl_3 \quad (a)$$

The surroundings of the titanium center in **177** was investigated with X-ray absorption spectroscopy (EXAFS).[117]

A comparison of the EXAFS spectrum of **177** with that of titanium foil rules out the possibility that **177** consists of titanium particles or nanoparticles.[113] Results of the EXAFS analysis reveal that the local environment of the titanium center in **177** consists of oxygen (0.4 atoms at 2.13 Å), chlorine (1.5 atoms at 2.44 Å), and titanium atoms at two different distances (1.3 and 1.9 atoms at 3.10 and 4.04 Å, respectively). Possible structural models compatible with the EXAFS results are represented in Figure 3.[120]

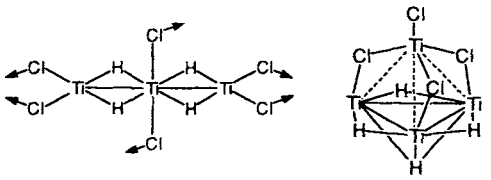

Fig. 3. Possible structures of **177** (without THF molecules).

The complexes **177** and **D-177** proved to be active reagents for the reductive coupling of benzophenone to afford tetraphenylethene (**178a**) as well as of acetophenone to furnish 2,3-diphenyl-2-butene (**178b**) (Scheme 39).[118] In the course of the reaction 0.5 moles of H_2 (or D_2) are liberated per mole of titanium. Titanium(III) oxychloride was found to be the inorganic end product. The complete course of the McMurry reaction with **177** or **D-177** can therefore be described along the lines of Scheme 39.

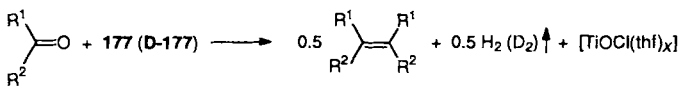

Scheme 39.

When carried out under standard conditions, the reductive coupling of carbonyl compounds with **177** gave the same alkenes with comparable yields as those obtained with the McMurry reagent.[113a, 119] Additionally, **177** can be isolated from the $TiCl_3/0.5\,LiAlH_4$/THF reaction mixture [Eq. (a)]. Therefore, it can be considered as proved that **177**, and not finely divided metallic titanium,[113] is the active species of the McMurry reagent.

To obtain the most complete insight into the reaction process, the McMurry and related reactions were each started at low temperatures and, during the course of the reaction, the temperature was gradually increased to the boiling point of the solvent. At the same time samples were removed and quickly hydrolyzed, and the organic intermediates and end products identified and quantified by GC analysis. The reaction profile of the McMurry reaction of acetophenone with **177** as the reagent (Scheme 39) is given in Figure 4. The pinacolate forms even at low temperatures but is converted into the alkene only at higher temperatures. The appearance of 2,3-diphenyl-2-butanol (**181**, Scheme 40) as a side product of the reaction gives an experimental indication for the stepwise (radical)[7a] elimination of TiOCl from pinacolate **180**.

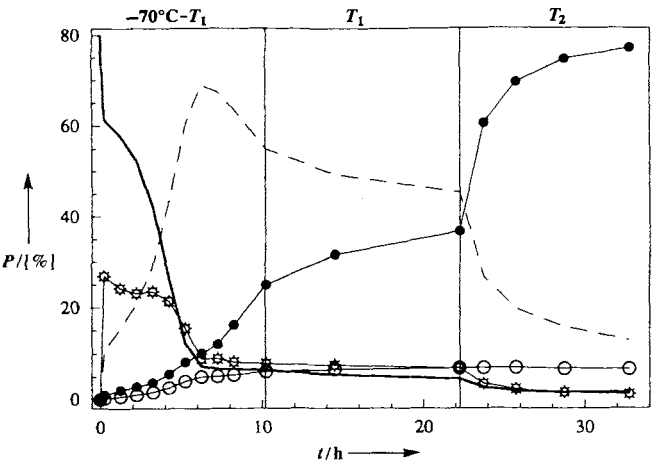

Fig. 4. The progression of the coupling reaction of acetophenone with [HTiCl(thf)$_{\le 0.5}$] (**177**) as a reagent (molar ratio 1:1) in THF; the samples were hydrolyzed with H_2O; (—) acetophenone, (●) 2,3-diphenyl-2-butene (**178b**), (✡) 1-phenylethanol (**179a**), (– – –) 2,3-diphenyl-2,3-butandiol (**180b**); (○) 2,3-diphenyl-2-butanol (**181**). T_1 = room temperature; T_2 = reflux temperature; P = product distribution.

It is of particular interest that, at the beginning of the reaction, a possible precursor of the pinacolate could be intercepted, which on hydrolysis gives 1-phenylethanol (**179a**). The amount

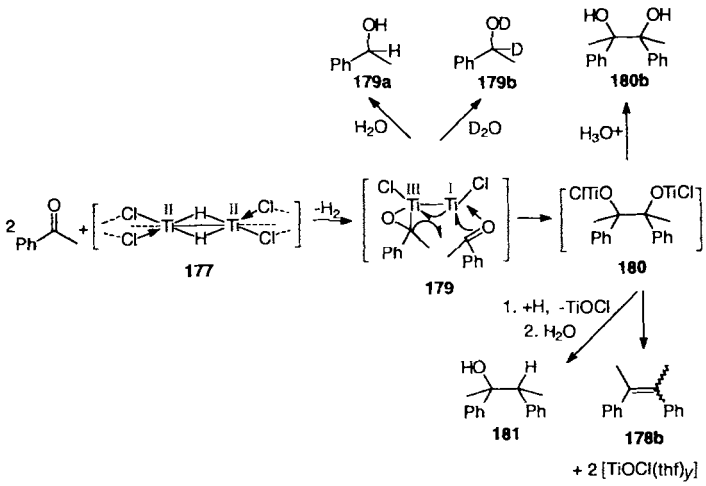

Scheme 40. Reaction of acetophenone with **177**.

of the hydrolysis product **179a** (Fig. 4) was 20–25% at the beginning and decreased to zero as the reaction proceeded. Therefore, **179a** appears to be the hydrolysis product of the postulated[9a, 12, 16, 17, 93b, 106] "ketone dianion" intermediate (**179**) of the McMurry reaction. This hypothesis was supported by a deuterolysis experiment at low temperature. Here a 23% yield of 1-phenylethanol was produced with 98% deuterium incorporation in the 1-position (**179b**). The results thus point to a "ketone dianion" as the precursor of the titanium pinacolate **180**. The existence of "dianions" of aromatic ketones is substantiated by the X-ray structural analyses of dilithium benzophenone[120] and ytterbium benzophenone.[121] In both cases the carbonyl group is bound side-on to the metal center. Zr and Hf

complexes with carbonyl compounds coordinated side-on are also known; they occur as intermediates in C–C coupling reactions.[122]

The likely appearance of the side-on coordination of acetophenone to titanium (left side of **179**, Scheme 40) as a precursor of the pinacolate in the McMurry reaction favors a nucleophilic reaction mechanism rather than a radical path for the C–C coupling step of aromatic ketones.[123] According to this mechanism, and on the basis of the structural model proposed for **177**,[20] the C–C coupling step can be envisaged to occur by the following sequence on the surface of the insoluble $[HTiCl(thf) \approx 0.5]_x$ particle (**177**, Scheme 40): After the hydride ligand in **177** has been expelled by the ketone (evolution of H_2 already starts at low temperatures![20]), the ketone coordinates side-on at the vacated coordination site of the metal. Subsequent C–C coupling to produce pinacolate **180** proceeds by nucleophilic attack of the reduced, side-on coordinated ketone at the carbonyl group of a nonreduced ketone molecule (**179**), which is coordinated to a neighboring Ti atom. Alternatively, the "ketone dianion" could nucleophilically attack a free ketone molecule (not shown in Scheme 40).

4.1.2. *Carbenoid Reactions of* $[HTiCl(thf)_{\approx 0.5}]$

Further similarities in the reaction behavior of **177** and the McMurry reagent are evident from conversions of geminal dichloro compounds. The formation of 7,7-dichloronorcarane (**183**) from cyclohexene and carbon tetrachloride, and of tetraphenylethene (**178a**) from dichlorodiphenylmethane, promoted by the McMurry reagent, was reported by Mukaiyama et al.[125] and Olah et al., respectively.[126] The analogous reactions with **177** lead to the same products in comparable yields (Schemes 41 and 42). At the onset of the reactions roughly

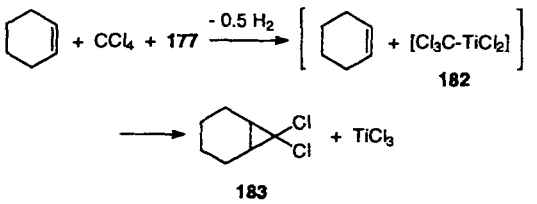

Scheme 41. Synthesis of **183**.

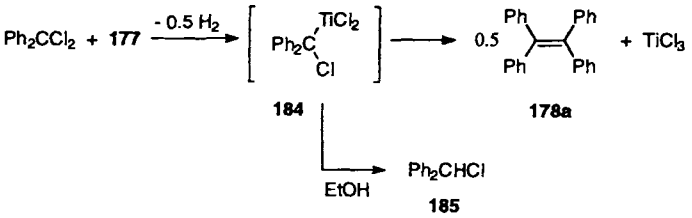

Scheme 42. Synthesis of **185** and **178a**.

0.5 moles of H_2 per mole of **177** evolved[124] and $TiCl_3$ is the inorganic end product. Therefore, the reactive intermediates can be postulated as titanium-based carbenoids[127,128] **182** and **184**, respectively. In the reaction presented in Scheme 42, intermediate **184** could be trapped with ethanol to give chlorodiphenylmethane (**185**) (Fig. 5). Thus, intermediate **184** could clearly be demonstrated as the precursor to alkene **178a**.[124]

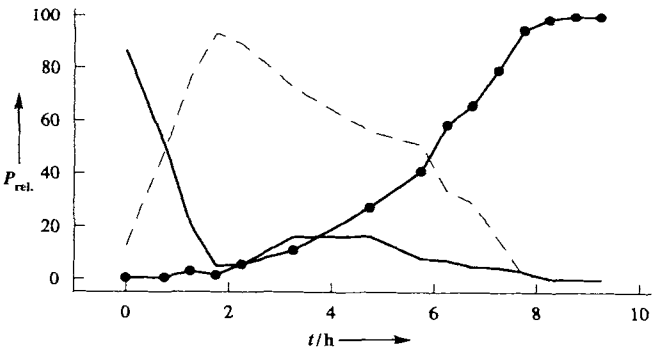

Fig. 5. The progression of the coupling reaction of dichlorodiphenylmethane with $[HTiCl(thf)_{\approx 0.5}]$ (**177**) as a reagent (molar ratio 1:1) in THF; the samples were quenched with EtOH; (—) dichlorodiphenylmethane, (•) tetraphenylethene (**178a**), (– – –) diphenylchloromethane (**185**). P_{rel} = relative product distribution.

The conversions of benzal chloride into (*E*)-stilbene (**186**, 97%, Scheme 43) and of benzotrichloride into 1,2-dichlorostilbene (**187**, 81%) in the presence of **177** both probably

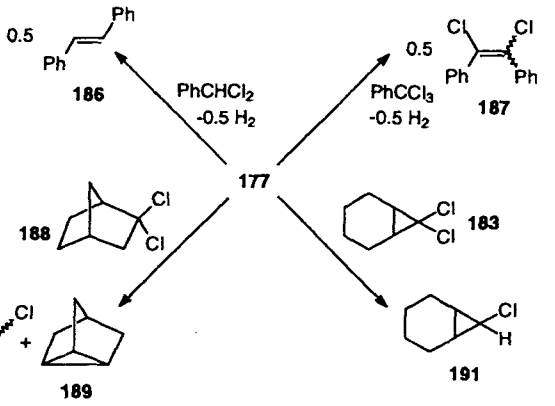

Scheme 43.

proceed via titanium-based carbenoid intermediates as well. In the reaction of 2,2-dichloronorbornane (**188**) with **177** a rearrangement typical for carbenes, producing nortricyclane (**189**) (in a mixture with 2-chloronorbornane **190**), was observed. In contrast, 7,7-dichloronorcarane (**183**) on reaction with **177** only gave the monodehalogenated product 7-chloronorcarane (**191**).

The products diphenylacetylene, stilbene, and 1,2-diphenylethane (total yield ca. 25%) from the reaction of 1,1-dichloro-2,2-diphenylethene (**192**) with **177** (Scheme 44) proved

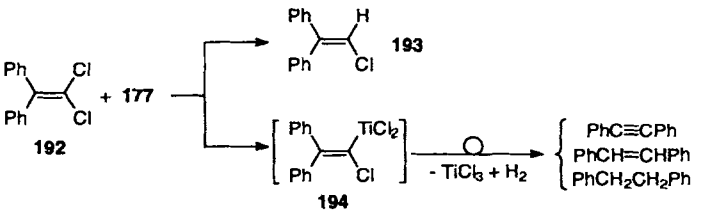

Scheme 44. Fritsch–Buttenberg–Wiechell rearrangement of carbenoid intermediate **194**.

that a Fritsch–Buttenberg–Wiechell rearrangement,[127] a characteristic reaction of carbenoids (**194**), had taken place. However, the main product of the reaction (ca. 75%) was 1-chloro-2,2-diphenylethene (**193**).[124]

4.2. $[TiH_2 \cdot (MgCl_2 \cdot 2thf)_{0.2-0.3}]$: A New, Highly Reactive Titanium Dihydride

If the reaction of $TiCl_3$ with MgH_2*[115] in THF is carried out with a 1:1.5 molar ratio instead of in a 1:1 molar ratio (Section 4.1), then a solid of composition $[TiH_2 \cdot (MgCl_2 \cdot 2thf)_{0.2-0.3}]$ (**195**, Scheme 45) is isolated in 77% yield. This

$$[TiCl_3(thf)_3] + 1.5\ MgH_2^* \xrightarrow[-0.5\ H_2]{THF} \underset{\mathbf{195}}{[TiH_2 \cdot (MgCl_2 \cdot 2thf)_{0.2\text{-}0.3}]\downarrow} + 1.2\text{-}1.3\ MgCl_2$$

Scheme 45. Synthesis of **195**.

solid is black, highly pyrophoric and amorphous to X-rays. Deuterolysis of **195** produces 2.5 moles of a mixture of HD, D_2, and a little H_2 per mole of titanium, with an H/D ratio of 2/3; iodolysis of **195** produces 1.0 mole of H_2 per mole of titanium (Scheme 46). Consequently, **195** is a titanium(II) dihydride. Since **195** is produced with a relatively constant proportion of 0.2–0.3 moles of $MgCl_2$ per mole of Ti, which can barely be reduced by washing with THF, it must be assumed that $MgCl_2$ and $MgCl_2 \cdot 2thf$ are chemically bound in **195**.[129]

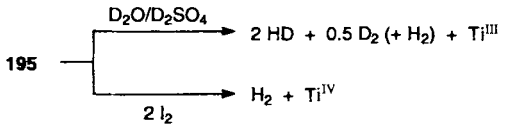

Scheme 46. Reactions of **195**.

The properties of the new titanium dihydride strongly deviate from those of the inorganic solid TiH_2 known to date.[130] In contrast to TiH_2, **195** has a certain—if only slight—solubility in THF ($\approx 0.015\ mol\,L^{-1}$ at 20 °C), which is probably due to the solubilizing action of $MgCl_2 \cdot 2thf$. **195** is much less thermally stable than TiH_2.[130] In boiling THF, 1,4-dioxane, toluene, or tetramethylethylendiamine **195** loses hydrogen quantitatively within a few hours. The dehydrogenation products are finely divided titanium and $MgCl_2$ or a $MgCl_2$–donor adduct. Solid **195** must be handled with care as it is highly pyrophoric and decomposes *explosively* (!) at temperatures above 90 °C. The strongly exothermic decomposition of solid **195** is probably due to the reaction of the low-valent titanium with the bound THF.[129]

Preliminary investigations[129] indicate that **195** is suitable as a reagent for deoxygenation or dehalogenation of organic compounds. Thus, the use of **195** in a McMurry reaction with acetophenone or benzophenone produces the corresponding alkenes, whilst diisopropyl ketone, cyclohexanone, and 3,3,5,5-tetramethylcyclohexanone are reduced to the corresponding secondary alcohols, and benzaldehyde is reduced to toluene. 1,2-Diols and epoxides are deoxygenated by **195**, in some cases with quite high yields. Furthermore, it is worth mentioning that **195** reduces *n*-hexanol to *n*-hexane, cyclohexanol to cyclohexane, and 1,6-hexanediol and 1,8-octanediol to mixtures of *n*-alkanes and monoalcohols. However, these reactions have proceeded with only modest conversions of 40–50% so far.

1,2-Dichloro-, 1-chloro-2-hydroxy-, and 1,2-dibromocyclohexane could be dehalogenated in the presence of **195** to give cyclohexene in high yields. It was interesting to observe that in some cases the use of **195** caused the regioselective coupling of allyl halides to afford 1,5-dienes. Thus, (*E*)-crotyl chloride (**196**), cinnamyl bromide (**197**), and geranyl chloride (**198**) could be dimerized in this way to give the corresponding 1,5-dienes with total yields of 85–98% and with α–α'/α–γ' selectivities of 95/5 and 97/3 (Scheme 47).[131] Highly regio- and stereoselective reductive couplings of allyl halides to 1,5-dienes have been made possible recently by use of activated barium.[132]

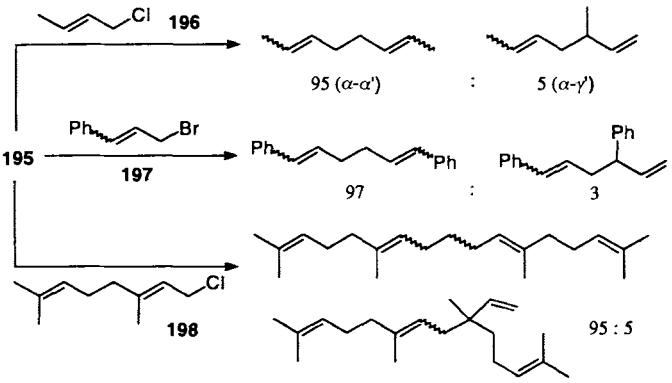

Scheme 47. Coupling of allyl halides **196**–**198**.

4.3. Low-Valent Titanium Complexes from Titanium Halides and Magnesium in THF: $[Ti(MgCl)_2(thf)_x]$ as an Inorganic Grignard Compound

As discussed at the beginning of Section 4, the reaction of titanium chlorides with magnesium in THF was intensively investigated in the past, in particular with respect to the preparation of catalysts and reagents for the McMurry reaction,[113], N_2 fixation,[110], H_2 fixation, and other reactions.[111, 112] According to our investigations,[21] the reduction of α-$TiCl_3$ (or $TiCl_4$) with excess magnesium in THF at room temperature proceeds in two steps (Fig. 6 and Scheme 48). In the first, relatively fast step of the reaction, 1.5 moles of magnesium per mole of titanium are consumed, so that the Mg:Ti ratio in solution increases to a value of 1.5 (in the case of $TiCl_4$ to 2.0) (Fig. 6). During protolysis of the black solution (Scheme 48) 1.5 moles of H_2 per mole of titanium as well as Ti^{III} are produced. This indicates that titanium is present in the reaction mixture in the formal oxidation state 0. If the reaction is carried out up to this step in THF saturated with $MgCl_2$, then 0.5 moles of $MgCl_2$ per mole of titanium crystallize out of the supersaturated solution. This indicates that 0.5 moles of free $MgCl_2$ per mole of titanium are produced in the reaction. Therefore, the first step of the reaction furnishes 0.5 moles of $MgCl_2$ and 1 mole of the bimetallic complex $[TiMgCl_2(thf)_x]$ (**199**, Scheme 48)[19, 21, 133].

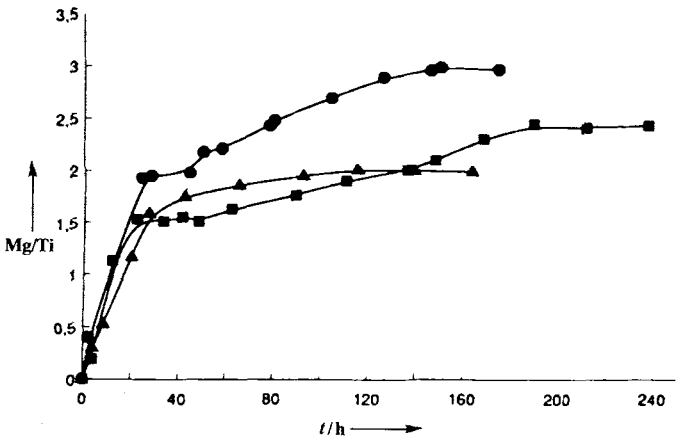

Fig. 6. The increase of the Mg/Ti ratio in solution during the reaction of α-$TiCl_3$ (■), $TiCl_4$ (●), and $[TiCl_2(tmeda)_2]$ (▲) with magnesium turnings (Mg/Ti molar ratio ≈ 10:1) in THF at room temperature.

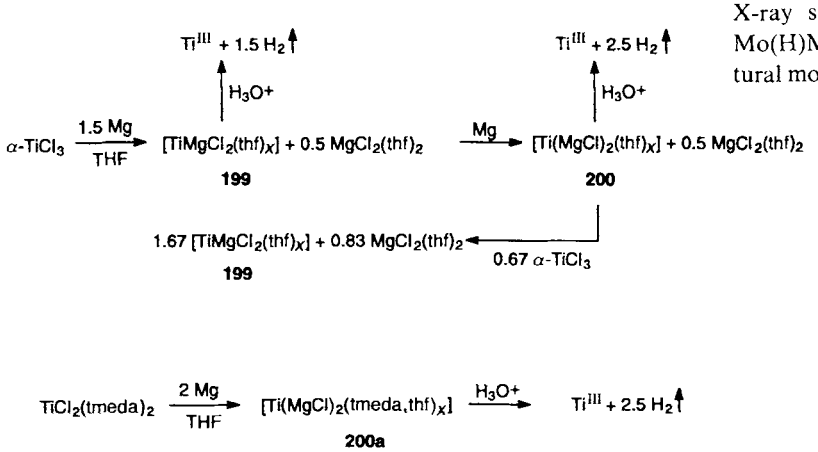

Scheme 48.

In the second, considerably slower step of the reaction, a further mole of magnesium per mole of titanium is consumed (Fig. 6). The existence of the more strongly reduced complex $[Ti(MgCl)_2(thf)_x]$ (**200**) is supported by hydrolysis, which produces 2.5 moles of H_2 per mole of titanium and Ti^{III} (Scheme 48). This corresponds to a formal oxidation state of −II for titanium in **200**. As the reaction with $TiCl_3$ proves, the reduction of **199** to give **200** is reversible. The consumption of a total of 2.5 moles of magnesium per mole of titanium in the reaction of $TiCl_3$ with Mg, and the formation of a complex with the Ti:Mg:Cl ratio of 1:2:2 from $TiCl_4$ and Mg (Scheme 48) confirm the earlier results of Yamamoto et al.[110] (Scheme 35) and Sobota et al. (Scheme 36).[111, 112]

The complex system **200a** with a Ti:Mg:Cl ratio of 1:2:2 is also accessible from $[TiCl_2(tmeda)_2]$[134] and Mg in THF, although no $MgCl_2$ is produced as a side product in this case. Accordingly, the plateau of the Mg/Ti ratio (Fig. 6) is reached after the consumption of 2.0 moles of magnesium per mole of titanium, and hydrolysis produces once again 2.5 moles of H_2 per mole of titanium (Scheme 48). Complexes **199**, **200**, and **200a** can be obtained after removal of the solvents as black, X-ray amorphous powders with variable THF or TMEDA content.

The structure of complex **200** in the solid state and in solution was investigated by EXAFS methods[117] (titanium K-edge). Complex **200** was found to have the shortest Ti–Mg distance (2.72 Å) yet observed. When compared to the corresponding distances in other transition metal/magnesium complexes[135–137] determined by X-ray crystal structure analysis, this distance was found to correspond to a covalent Ti–Mg bond. Evaluation of the EXAFS spectrum reveals that the local environment around the Ti center in **200** consists of 1.4(4) oxygen atoms (2.03 Å), 5(2) carbon atoms (3.02 Å), 2.2(4) magnesium atoms (2.72 Å), and 3.6(7) chlorine atoms (4.05 Å). The results of the EXAFS analysis indicate that there are two THF ligands and two Mg atoms bound to chlorine atoms in the coordination sphere of the titanium center in **200**. On the basis of the EXAFS data, the simplest structural model for **200** is that of a dimer, in which two titanium units are joined by bridging chlorine atoms (Fig. 7a). A comparable dimeric structure containing bridging halogens was previously determined by Green et al.[135] by X-ray structure analysis of the crystalline complex $[\{Cp_2Mo(H)MgBr(OEt_2)MgBr(C_6H_{11})\}_2]$ (**201**, Fig. 7b). The structural model of **200**, based on EXAFS analysis, comparison with **201**, and chemical reactivity (vide supra), differs from the structure originally proposed (**173**),[112] among other features, by the absence of direct Ti–Cl bonds.

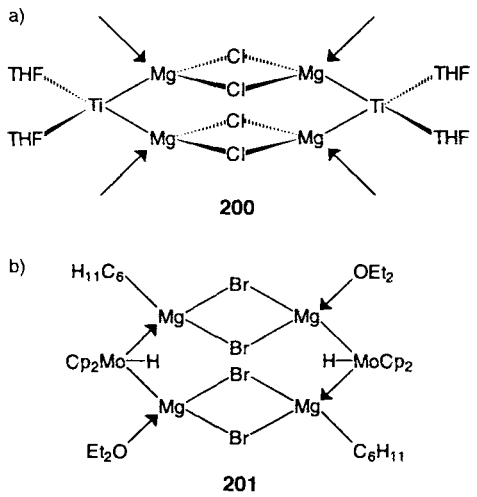

Fig. 7. a) Proposed structural model for $[Ti(MgCl)_2(thf)_x]$ (**200**) based on the results of chemical and spectroscopic studies. b) X-ray crystal structure of the inorganic Grignard complex $[\{Cp_2Mo(H)MgBr(OEt_2)MgBr(C_6H_{11})\}_2]$ (**201**)[135].

The molybdenum complex **201**[135] as well as Felkin's[136] iron complex [CpFe(diphos)MgBr(thf)$_2$] (diphos = 1,2-diphenylphosphinoethane) (**202**) were discovered 20 years ago and have been described as inorganic analogs of a Grignard compound or "inorganic Grignard compounds".

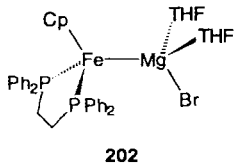

202

Complex **200**, as well as some other purely inorganic complexes recently described by us[133] with the general formula $[\{M(MgCl)_n(thf)_x\}_p]$ (M = Ni, Fe, Pd, Pt, Ru, Rh, Ir; $n = 1, 2, 3$), can also be described as inorganic Grignard analogs. The $[\{M(MgCl)_n(thf)_x\}_p]$ complexes are suitable as inorganic

Grignard reagents for the wet-chemical synthesis of highly active, nanocrystalline metals, intermetallic compounds, and alloys.[19, 133] For example, **200** reacts with $FeCl_2$ in THF to yield a finely divided, highly active powder, which according to its Mössbauer spectrum consists of a mixture of the intermetallic phases TiFe and $TiFe_2$ in a ratio of roughly 2:1; elemental iron could not be detected in the samples. The formation of the two intermetallic compounds can be described by the equations in Scheme 49, whereby the soluble Ti^0 complex **199** is formed as a side product in the reaction yielding $TiFe_2$.[133]

$$[Ti(MgCl)_2(thf)_x] + FeCl_2 \longrightarrow TiFe\downarrow + 2\,MgCl_2$$
200

$$2\,\mathbf{200} + 2\,FeCl_2 \longrightarrow TiFe_2\downarrow + [TiMgCl_2(thf)_x] + 3\,MgCl_2$$
199

Scheme 49.

It was interesting to investigate the behavior of the soluble Ti complexes **199** and **200** as reagents for carbonyl coupling. From the profile of the reaction of acetophenone with complex **200** (molar ratio 1.1:1; Fig. 8) it can be seen that only a few percent of the expected 2,3-diphenyl-2-butene is produced because the reaction stops at the pinacol stage. The reaction of acetophenone with the Ti^0 complex **199** follows an almost identical course. Additionally, the distribution of the reaction products changes insignificantly if the molar ratio **199** or **200** to acetophenone is varied between 2:1 and 1:2.

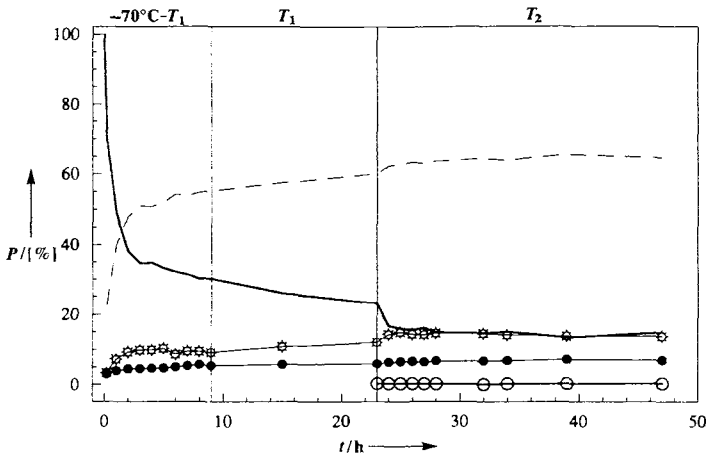

Fig. 8. The progression of the coupling reaction of acetophenone with $[Ti(MgCl)_2(thf)_x]$ (**200**) as a reagent (molar ratio 1.1:1) in THF; the samples were hydrolyzed with H_2O; (—) acetophenone, (· · ·) 2,3-diphenyl-2,3-butanediol (**180b**), (✡) 1-phenylethanol (**179a**), (●) 2,3-diphenyl-2-butene (**178b**), (○) 2,3-diphenyl-2-butanol (**181**). T_1 = room temperature; T_2 = reflux temperature; P = product distribution.

A possible explanation for this unexpected behavior in the reaction of **200** (and of **199**) with acetophenone might be that it is not the titanium pinacolate but the magnesium pinacolate (**203**, Scheme 50) which is formed. It is known that it is not possible to cleave magnesium oxides from magnesium pinacolates to form alkenes.

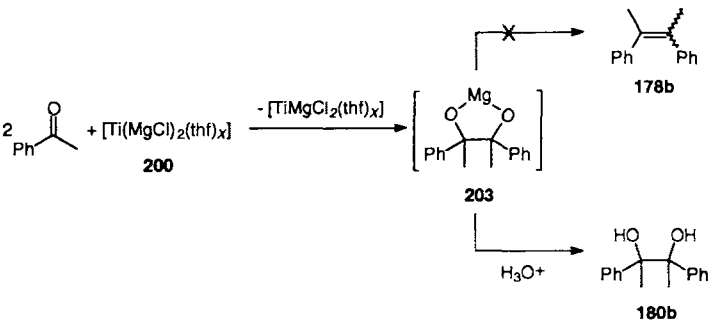

Scheme 50.

Nevertheless, it turned out that the McMurry coupling of acetophenone to give alkenes using the system $TiCl_3$/Mg/THF can proceed in high yields. Instead of prereducing $TiCl_3$ with Mg in refluxing THF as previously reported[113a] or at room temperature to give the soluble complexes **199** and **200** (Scheme 48), $TiCl_3$ was treated with Mg powder in the presence of acetophenone, according to the "instant" method[17] (Section 3.4.1). As shown in Figure 9, alkene **178b** was produced

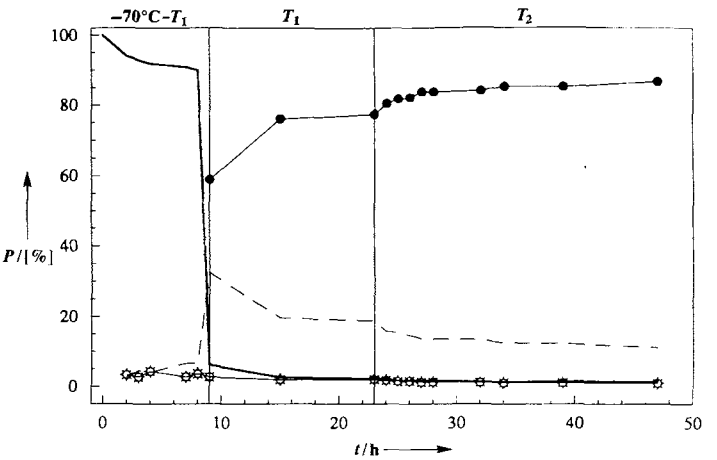

Fig. 9. The progression of the coupling reaction of acetophenone in the $TiCl_3$/Mg system under "instant" conditions (molar ratio 1:1.1:4.4) in THF; the samples were hydrolyzed with H_2O; (—) acetophenone, (· · ·) 2,3-diphenyl-2,3-butandiol (**180b**), (●) 2,3-diphenyl-2-butene (**178b**), (✡) 1-phenylethanol (**179a**). T_1 = room temperature; T_2 = reflux temperature; P = product distribution.

via the intermediate pinacolate even at room temperature. The yield of **178b** increases to over 80% at reflux temperature (Scheme 51).[138]

A comparison of Figures 8 and 9 shows that the reductive coupling of acetophenone under otherwise identical conditions can lead to different products depending on the method used: prereduction gave pinacol **180b** and the "instant" method alkene **178b**. In the experiment with the "instant" method (Scheme 51) it is conceivable that Ti^I and/or Ti^{II} species are involved (cf. Sections 4.1 and 4.4 and refs. [103, 104]).[139]

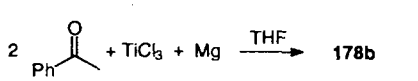

Scheme 51.

4.4. Comparison of $[TiCl_3(dme)_{1.5}]/Zn(Cu)$ and $TiCl_2 \cdot LiCl$ as Coupling Reagents in the McMurry Reaction

According to the procedure described in 1989 by McMurry et al.[93a] for the McMurry reaction, the $[TiCl_3(dme)_{1.5}]$ complex in boiling DME is prereduced by the Zn(Cu) couple; the resulting active titanium suspension is subsequently treated at reflux temperature with the carbonyl substrate to produce the alkene. It has been proposed[7a, 8] that the active species is finely divided metallic titanium in this case as well.

As an alternative to the prereduction of titanium halides with zinc, the "instant" method[17] (cf. Section 3.4.1) was recently suggested, particularly for titanium-induced pyrrole and indole syntheses.[9–18] The prereduction step is deliberately omitted and a solution of $TiCl_3$ in DME is treated directly with zinc powder in the presence of the carbonyl substrate. One of the reasons for the excellent results of the synthesis of indoles by this method is thought to be that the reduction of Ti^{III} occurs within the $TiCl_3$–substrate complex, which was detected by IR spectroscopy (cf. Scheme 27).

4.4.1. Attempted Reduction of $[TiCl_3(dme)_{1.5}]$ with Zn in DME

In order to explain the mode of action of the $[TiCl_3(dme)_{1.5}]$/Zn and Zn(Cu) reagents (which are now of considerable preparative importance) the attempt was made to discover the nature of the active species produced in this system by the prereduction method. Mixtures of $[TiCl_3(dme)_{1.5}]$ with Zn(Cu), with Zn(Cu) in the presence of pyridine, and with active zinc (Zn*)[140] were refluxed in DME for 20 hours. The solids and filtrates were separated and then tested for their activity in the McMurry coupling of acetophenone to give 2,3-diphenyl-2-butene (**178b**). All three isolated solids were found to be completely active as coupling reagents, whilst only the filtrate obtained from the experiment with Zn* exhibited slight activity.[141] Surprisingly, combined TEM-EDX analyses (*T*ransmission *E*lectron *M*icroscopy/*E*nergy *D*ispersive *X*-ray analysis), powder X-ray analyses, and IR spectra of the isolated solids only showed mixtures of the starting materials; in other words, there was no indication for the formation of low-valent titanium species! Therefore, refluxing the $[TiCl_3(dme)_{1.5}]/Zn(Cu)$ mixture for several hours before adding the carbonyl substrate is totally unnecessary in the McMurry coupling affording pinacols or alkenes.[22, 124]

As the experiments described in the following section prove, the reduction of $TiCl_3$ by Zn only takes place in the presence of (coordinated) acetophenone; that is, the McMurry reaction in this system proceeds along the lines of the "instant" method anyway.[17]

4.4.2. Stoichiometry and Reaction Mechanism of the McMurry Coupling of Acetophenone with the $[TiCl_3(dme)_{1.5}]/Zn(Cu)$ Reagent in DME

The formation of a donor–acceptor complex between acetophenone and $TiCl_3$ in DME is proved by the shift of the carbonyl stretching frequency from 1680 cm^{-1} for free acetophenone to 1620 cm^{-1} for the solid acetophenone–$TiCl_3$ adduct (**204**, Scheme 52). Since the reduction of $TiCl_3$ by Zn(Cu) takes place only in the presence of acetophenone, it can be assumed that the reduction potential of the $TiCl_3$–acetophenone system is lower than that of $TiCl_3$. Therefore the reaction begins with the reduction of a $TiCl_3$–acetophenone complex by Zn(Cu) (Scheme 52). This hypothesis is supported by findings (vide supra) that the McMurry reaction of acetophenone succeeds even with metals such as Fe or Sn as the reductant for $TiCl_3$, metals whose standard potentials are considerably lower than that of Zn.

The reaction profile of the McMurry reaction of acetophenone with the $[TiCl_3(dme)_{1.5}]/Zn(Cu)$ system is shown in Figure 10 for the temperature range from −60 °C to the boiling point of DME. An obvious feature of the reaction between 0 °C and room temperature is that the reaction stops at the pinacol step. The pinacol is converted quantitatively into 2,3-diphenyl-2-butene (**178b**) only when the reaction mixture is refluxed for several hours. This situation permitted the elucidation of the stoichiometry of the two reaction steps.

For this purpose $[TiCl_3(dme)_{1.5}]$, acetophenone, and Zn(Cu) (molar ratio 1:1:2.3) in DME were stirred in the temperature

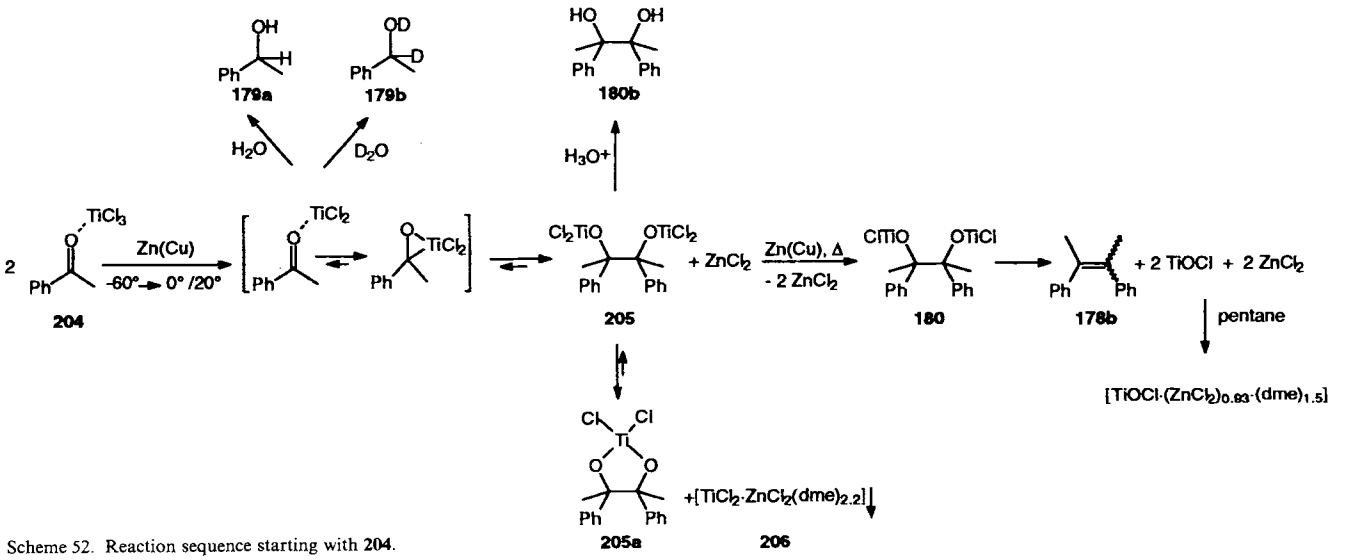

Scheme 52. Reaction sequence starting with **204**.

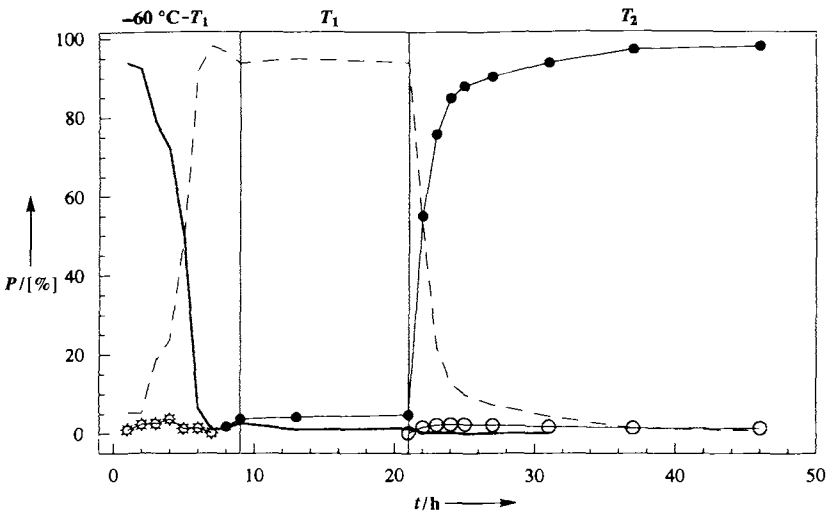

Fig. 10. The progression of the coupling reaction of acetophenone with $[TiCl_3(dme)_{1.5}]$/Zn(Cu) (molar ratio 1:4:16) in DME; the samples were hydrolyzed with H_2O; (—) acetophenone, (– – –) 2,3-diphenyl-2,3-butandiol (**180b**), (●) 2,3-diphenyl-2-butene (**178b**), (✡) 1-phenylethanol (**179a**), (○) 2,3-diphenyl-2-butanol (**181**). T_1 = room temperature; T_2 = reflux temperature; P = product distribution.

range from −50 to 0 °C. The reaction solution was subsequently separated from the unreacted Zn(Cu) and the precipitated $[TiCl_2 \cdot ZnCl_2(dme)_{2.2}]$ (**206**, Scheme 52). If the solution was left to stand at 0 °C, then further violet **206** precipitated whilst the complex **205a** and a little $ZnCl_2$ remained in solution. The low solubility of complex **206** appears to favor the disproportionation of the initially formed titanium pinacolate **205** to the Ti^{IV} and Ti^{II} complexes **205a** and **206** (Scheme 52). Based on the amount of complexes **205a** and **206** formed, it can be concluded that the composition of the reaction mixture in the pinacolate step corresponds to **205** + $ZnCl_2$, and that the disproportionation (**205** → **205a** + **206**) is virtually complete. Furthermore, these results show that the reaction up to the pinacolate stage consumes one mole of Zn(Cu) per mole of **205**. This represents a formal temporary reduction of Ti^{III} to Ti^{II} (Scheme 52), because Ti^{III} is present once again in pinacolate **205**. In another experiment, acetophenone, $[TiCl_3(dme)_{1.5}]$, and Zn(Cu) (molar ratio 1:1:1) in DME were refluxed for 48 h (Table 5, entry 3), which resulted in an 84% yield of alkene **178b** and complete consumption of Zn(Cu). After addition of pentane to the reaction solution, a solid precipitated with the composition $[TiOCl \cdot (ZnCl_2)_{0.9}(dme)_{1.5}]$ (Scheme 52). The total consumption of approximately two moles of Zn(Cu) per mole of **178b** and the composition of the inorganic end product of the reaction (TiOCl) indicate that the conversion of the pinacolate into the alkene requires a further mole of Zn(Cu) per mole of **178b**. The overall reaction of acetophenone with the $[TiCl_3(dme)_{1.5}]$/Zn(Cu) system is shown in Scheme 53.

The course of the reaction (Schemes 52 and 53) is supported by experiments in which the molar ratio acetophenone:$[TiCl_3(dme)_{1.5}]$:Zn(Cu) was varied (Table 5). If the molar ratio 1:0.5:0.5 (entry 1) is employed, then a high yield of the pinacol (93.8%) is obtained but an alkene yield of at best ≈50% can be reached. If a molar ratio of 1:1:1 or higher is used (entries 2–6), then excellent yields of the alkene are obtained in every case; this is in agreement with Scheme 53. However, if the amounts of the titanium and zinc reagents used are increased, then the conversion of the pinacolate into alkene accelerates. A large excess of the reagents (entry 6) is not necessarily required since a yield of 95% alkene after 16.5 h is already attained with a 1:2:2 ratio (entry 5). It is interesting here that when the starting materials are in a 1:2:2 molar ratio, high yields of alkene **178b** (90–92%) can also be achieved with Fe or Sn powders as the reducing agent.[22, 124]

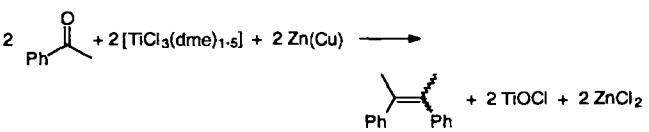

Scheme 53. **178b**

4.4.3. *McMurry Coupling of Acetophenone with the $TiCl_2 \cdot LiCl$ Reagent*

Further support of the course of reaction displayed in Schemes 52 and 53 was provided by comparative experiments in which the $TiCl_2 \cdot LiCl$ reagent proposed by Eisch et al.[23] was used for the McMurry coupling of acetophenone (Table 6). The reaction profile of the 1:1 reaction (Fig. 11) shows that a high

Table 5. Reductive coupling of acetophenone (AC) with the $[TiCl_3(dme)_{1.5}]$/Zn(Cu) reagent in DME; influence of the reaction temperature and variation of the molar ratio of the starting materials on the product distribution.

Entry	AC:$[TiCl_3(dme)_{1.5}]$:Zn(Cu)	T [°C]	t [h]	Yield [%] [b] AC	**180b**	**178b**
1	1:0.5:0.5	0	1.5	3.8	93.8	2.3
		[a]	16.6	9.4	38.4	36.8
			161.5	5.2	7.9	46.9
2	1:1:1	0	1.5	1.0	94.5	3.6
		[a]	16.6	0.5	19.6	76.5
		[a]	161.5	0	3.7	93.5
3	1:1:1	[a]	48			84 [c]
4	1:2:1	0	1.5	2.2	96.2	1.6
		[a]	16.6	0	3.3	93.7
		[a]	161.5	0	1.7	93.9
5	1:2:2	0	1.5	0.7	97.5	1.9
		[a]	16.6	0	3.3	94.9
		[a]	40.5	0	1.6	97.0
6	1:4:16	−60 → 0	7	1.0	98.0	0
		[a]	46	0	0.7	98.0

[a] Reflux. [b] After hydrolysis. [c] Yield of isolated product.

Table 6. Reductive coupling of acetophenone using the $TiCl_2 \cdot LiCl$ reagent in DME; influence of the reaction temperature and variation of the molar ratio of the starting materials on the product distribution.

Entry	AC:$TiCl_2 \cdot LiCl$	T [°C]	t [h]	Yield [%] [b] AC	**180b**	**178b**
1	1:1	−70 → 20	9	4.1	91.4	1.1 [c]
		20	15			
		[a]	93	28.5	16.2	46.0 [c]
2	1:2	20	0.5			
		[a]	48			90 [d]
3	1:4	[a]	48			91 [d]

[a] Reflux. [b] After hydrolysis. [c] See Fig. 11. [d] Yield of isolated product.

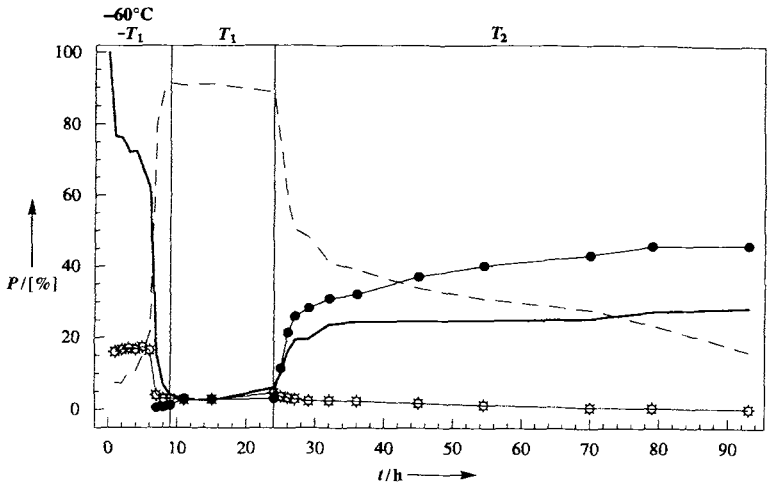

Fig. 11. The progression of the coupling reaction of acetophenone with the $TiCl_2 \cdot LiCl$ reagent (molar ratio 1:1) in DME; the samples were hydrolyzed with H_2O; (—) acetophenone, (- - -) 2,3-diphenyl-2,3-butandiol (**180b**), (●) 2,3-diphenyl-2-butene (**178b**), (✡) 1-phenylethanol (**179a**). T_1 = room temperature; T_2 = reflux temperature; P = product distribution.

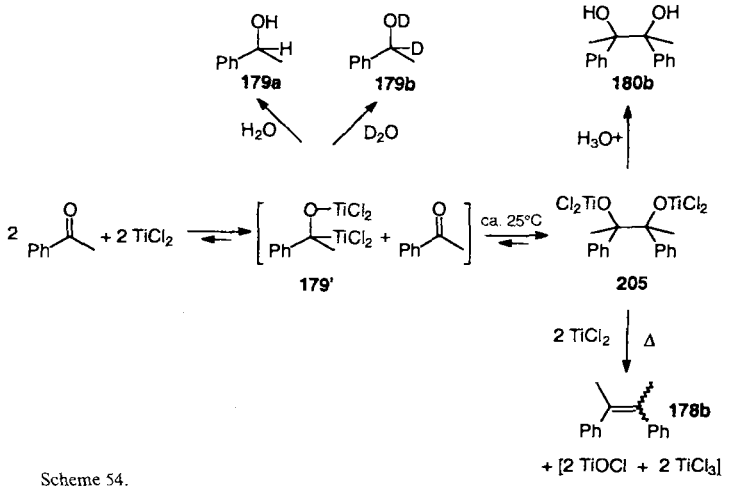

Scheme 54.

yield (91.4%) of pinacolate (**205**, Scheme 54) is produced at room temperature. When the mixture is heated at refluxed (Table 6 and Fig. 11) in the absence of a further amount of $TiCl_2$, then the maximum yield of alkene is 46%. The formation of the alkene **178b** (Fig. 11) is accompanied by a partial regeneration of acetophenone; this indicates that the formation of the pinacolate is reversible.[142] The partial reversal of pinacolate formation probably liberates the required amount of $TiCl_2$ for the conversion of the remaining pinacolate into the alkene (Scheme 54). This implies that $TiCl_2$ can only act as a one-electron reducing agent for the formation of alkene from the pinacolate. In agreement with this, when acetophenone:$TiCl_2 \cdot LiCl$ is used in a 1:2 or 1:4 molar ratio (Table 6), high yields of alkene are achieved in both cases.

Once again the intermediate appearance of the hydrolysis product 1-phenylethanol (**179a**, Scheme 54) at the beginning of the reaction is interesting (Fig. 11). In this case too (cf. Fig. 4, Section 4.1.1) a deuterolysis experiment yielded a quantitatively deuterated 1-deutero-1-phenylethanol (**179b**, Scheme 54). Therefore, the side-on coordinated acetophenone–$TiCl_2$ complex **179'** (Scheme 54) could be either a formal Ti^{IV} (as in Scheme 52) or a Ti^{III} complex.

4.5. Final Remarks and Outlook

The results summarized above on the stoichiometry and course of the reductive coupling reaction of acetophenone using different types of low-valent titanium reagents permits new, refined insights into the mechanism of the McMurry and related reactions. If complex **177** is used as a reagent, then the titanium center is oxidized during the reaction from formally Ti^{II} (in **177** and in pinacolate **180**) to Ti^{III} (in **179** and TiOCl). On account of the homolytic dissociation of the hydride ligand, an additional electron is available for the reaction. Therefore, complex **177** behaves as a (strong) two-electron reductant and a 1:1 molar ratio of ketone to **177** is sufficient to produce alkenes in high yields. In contrast, $TiCl_2$ acts as a one-electron reductant in the formation of the alkene ($\approx$50% yield of alkene for a 1:1 molar ratio of the reactants), whereby Ti^{II} is oxidized to Ti^{III} during the reaction (Scheme 54). The results obtained from the coupling reaction with the $[TiCl_3(dme)_{1.5}]/Zn(Cu)$ system (Scheme 52) indicate quite clearly that each of the two reaction steps involves a one-electron reduction of Ti^{III} by Zn. Therefore, there are short-lived Ti^{II} intermediates taking part in the reaction. The reduction of Ti^{III} to Ti^{II} with weak reducing agents such as Zn, Fe, and Sn is only possible in the presence of the (complexed) carbonyl substrate.

As these investigations demonstrate, the low-valent titanium complexes $[HTiCl(thf)_{\approx 0.5}]$,[20] $[TiH_2 \cdot (MgCl_2 \cdot 2thf)_{0.2-0.3}]$,[129] $[TiMgCl_2(thf)_x]$, $[Ti(MgCl)_2(thf)_x]$,[21] and $[TiCl_2 \cdot LiCl]$[22,23] have specific reactivities. In future, the use of such defined low-valent titanium complexes instead of the reagents produced in situ may lead to improved reproducibility and yields. Additionally, it is possible, for example by varying the ligands of the Ti^{II} complexes or by the choice of the reducing agent, of directly influencing the course of the reaction and thus increasing the selectivity. New impetus for preparative chemistry can be expected from the reactions of the reactive intermediates, for example the proposed ketone–titanium chloride complexes **179** and **179'** and the carbenoids such as **182** and **184**, with reaction partners other than those used to date.

We would like to thank our co-workers listed in the references for their valuable contributions resulting from their personal initiative and excellent teamwork. One of us (B. B.) thanks Prof. J. Rozière and Dr. D. J. Jones, University of Montpellier, France, for the EXAFS investigations. We thank the Volkswagen-Stiftung and the Fonds der Chemischen Industrie for financial support.

Received: March 29, 1996 [A 161 IE]
German version: *Angew. Chem.* **1996**, *108*, 2582–2609
Translated by Gillian Scheibelein, Offenburg (Germany)

[1] a) M. E. Vol'pin, V. B. Shur, *Nature* **1966**, *209*, 1236; b) M. E. Vol'pin, V. B. Shur, R. V. Kudryavtsev, L. A. Prodayko, *Chem. Commun.* **1968**, 1038; c) Y. G. Borodko, I. N. Ivleva, L. M. Kachapina, E. F. Kvashina, A. K. Shilova, A. E. Shilov, *ibid.* **1973**, 169; d) M. E. Vol'pin, *Pure Appl. Chem.* **1972**, *30*, 607; e) See also: H. H. Brintzinger, *J. Am. Chem. Soc.* **1966**, *88*, 4305, 4307.

[2] a) E. E. van Tamelen, G. Boche, S. W. Ela, R. B. Fechter, *J. Am. Chem. Soc.* **1967**, *89*, 5707; b) E. E. van Tamelen, G. Boche, R. Greeley, *ibid.* **1968**, *90*, 1677; c) E. E. van Tamelen, R. B. Fechter, S. W. Schneller, G. Boche, R. H. Greeley, B. Åkermark, *ibid.* **1969**, *91*, 1551; d) E. E. van Tamelen, H. Rudler,

ibid. **1970**, *92*, 5253; e) E. E. van Tamelen, *Acc. Chem. Res.* **1970**, *3*, 361; f) E. E. van Tamelen, B. Åkermark, K. B. Sharpless, *J. Am. Chem. Soc.* **1969**, *91*, 1552.

[3] T. Mukaiyama, T. Sato, J. Hanna, *Chem. Lett.* **1973**, 1041.

[4] S. Tyrlik, I. Wolochowicz, *Bull. Soc. Chim. Fr.* **1973**, 2147.

[5] J. E. McMurry, M. P. Fleming, *J. Am. Chem. Soc.* **1974**, *96*, 4708.

[6] Titanium-induced syntheses of olefins from carbonyl compounds were previously known. For example, tetraphenylethene was obtained in good yields during the attempt to swap the metal ions between sodium benzophenone ketyl radical and $TiCl_4$. However, these observations did not have any impact on the development of preparative chemistry. a) E. Blanck, *Justus Liebigs Ann. Chem.* **1969**, *724*, 56; b) W. Hieber, R. E. Nitzschmann, *Z. Naturforsch. B* **1963**, *18*, 413.

[7] a) J. E. McMurry, *Chem. Rev.* **1989**, *89*, 1513; b) D. Lenoir, *Synthesis* **1989**, 883; c) G. M. Robertson in *Comprehensive Organic Synthesis, Vol. 3* (Eds.: B. M. Trost, I. Fleming, G. Pattenden), Pergamon, Oxford, **1991**, p. 563; d) R. G. Dushin in *Comprehensive Organometallic Chemistry II, Vol. 12* (Ed.: L. S. Hegedus). Pergamon, Oxford, **1995**, p. 1071; e) C. Betschart, D. Seebach, *Chimia* **1989**, *43*, 39; f) J. E. McMurry, *Acc. Chem. Res.* **1983**, *16*, 405; g) P. C. Auderset, T. C. C. Gartenmann, E. R. F. Gesing, *Kontakte (Darmstadt)*, **1985**, 14; h) Y. Dang, H. J. Geise, *Janssen Chim. Acta* **1988**, *6*, 3; *ibid.* **1989**, *7*, 3; i) P. Welzel, *Nachr. Chem. Techn. Lab.* **1983**, *31*, 814; j) B. König, *J. Prakt. Chem.* **1995**, *337*, 250. Reviews on other applications of low-valent titanium: j) J. E. McMurry, *Acc. Chem. Res.* **1974**, *7*, 281; k) T. L. Ho, *Synthesis* **1979**, 1; l) H. N. C. Wong, *Acc. Chem. Res.* **1989**, *22*, 145; m) Y. Dang, H. J. Geise, *J. Organomet. Chem.* **1991**, *405*, 1; n) Review on the use of Cp_2Ti^{II}: S. L. Buchwald, R. B. Nielsen, *Chem. Rev.* **1988**, *88*, 1047.

[8] a) T. Lectka in ref. [8b], p. 85; b) *Active Metals. Preparation, Characterization, Applications* (Ed.: A. Fürstner), VCH, Weinheim, **1996**.

[9] a) A. Fürstner, D. N. Jumbam, *Tetrahedron* **1992**, *48*, 5991; b) A. Fürstner, D. N. Jumbam, H. Weidmann, *Tetrahedron Lett.* **1991**, 6695.

[10] A. Fürstner, D. N. Jumbam, *J. Chem. Soc. Chem. Commun.* **1993**, 211.

[11] A. Fürstner, D. N. Jumbam, G. Seidel, *Chem. Ber.* **1994**, 1125.

[12] A. Fürstner, A. Ernst, *Tetrahedron* **1995**, *51*, 773.

[13] A. Fürstner, A. Ernst, H. Krause, A. Ptock, *Tetrahedron* **1996**, *52*, 7329.

[14] A. Fürstner, A. Ptock, H. Weintritt, R. Goddard, C. Krüger, *Angew. Chem.* **1995**, *107*, 725; *Angew. Chem. Int. Ed. Engl.* **1995**, *34*, 678.

[15] A. Fürstner, H. Weintritt, A. Hupperts, *J. Org. Chem.* **1995**, *60*, 6637.

[16] A. Fürstner, D. N. Jumbam, N. Shi, *Z. Naturforsch. B* **1995**, *50*, 326.

[17] A. Fürstner, A. Hupperts, A. Ptock, E. Janssen, *J. Org. Chem.* **1994**, *59*, 5215.

[18] A. Fürstner, A. Hupperts, *J. Am. Chem. Soc.* **1995**, *117*, 4468.

[19] Short review: L. E. Aleandri, B. Bogdanović in ref. [8b], p. 299.

[20] L. E. Aleandri, S. Becke, B. Bogdanović, D. J. Jones, J. Rozière, *J. Organomet. Chem.* **1994**, *472*, 97.

[21] L. E. Aleandri, B. Bogdanović, A. Gaidies, D. J. Jones, S. Liao, A. Michalowicz, J. Rozière, A. Schott, *J. Organomet. Chem.* **1993**, *459*, 87.

[22] B. Bogdanović, A. Bolte, *J. Organomet. Chem.* **1995**, *502*, 109.

[23] J. J. Eisch, X. Shi, J. Lasota, *Z. Naturforsch. B* **1995**, *50*, 342.

[24] A. Fürstner, *Angew. Chem.* **1993**, *105*, 171; *Angew. Chem. Int. Ed. Engl.* **1993**, *32*, 164.

[25] Review: J. E. McMurry, R. G. Dushin, *Stud. Nat. Prod. Chem.* **1991**, *8*, 15.

[26] a) Y. Li, W. Li, Y. Li, *Tetrahedron Lett.* **1992**, 1225; b) *J. Chem. Soc. Perkin Trans. 1* **1993**, 2953; c) W. Li, J. Mao, Y. Li, Y. Li, *Org. Prep. Proc. Int.* **1994**, *26*, 445; d) Y. Li, W. Li, Y. Li, *Synth. Commun.* **1994**, *24*, 721; e) W. Li, Y. Li, Y. Li, *ibid.* **1992**, *22*, 817.

[27] U. Berlage, J. Schmidt, U. Peters, P. Welzel, *Tetrahedron Lett.* **1987**, 3091.

[28] L. Jenny, H.-J. Borschberg, *Helv. Chim. Acta* **1995**, *78*, 715.

[29] D. L. J. Clive, K. S. K. Murthy, A. G. H. Wee, J. S. Prasad, G. V. J. da Silva, M. Majewski, P. C. Anderson, C. F. Evans, R. D. Haugen, L. D. Heerze, J. R. Barrie, *J. Am. Chem. Soc.* **1990**, *112*, 3018.

[30] a) D. L. J. Clive, K. S. K. Murthy, C. Zhang, W. D. Hayward, S. Daigneault, *J. Chem. Soc. Chem. Commun.* **1990**, *509*; b) D. L. J. Clive, C. Zhang, K. S. K. Murthy, W. D. Hayward, S. Daigneault, *J. Org. Chem.* **1991**, *56*, 6447.

[31] Titanium–graphite combinations: a) A. Fürstner, H. Weidmann, *Synthesis* **1987**, 1071; b) A. Fürstner, R. Csuk, C. Rohrer, H. Weidmann, *J. Chem. Soc. Perkin Trans. 1* **1988**, 1729; c) G. P. Boldrini, D. Savoia, E. Tagliavini, C. Trombini, A. Umani-Ronchi, *J. Organomet. Chem.* **1985**, *280*, 307; d) See also: M. A. Araya, F. A. Cotton, J. H. Matonic, C. A. Murillo, *Inorg. Chem.* **1995**, *34*, 5424.

[32] F. E. Ziegler, H. Lim, *J. Org. Chem.* **1982**, *47*, 5229.

[33] K. Mikami, K. Takahashi, T. Nakai, T. Uchimaru, *J. Am. Chem. Soc.* **1994**, *116*, 10948.

[34] Y. J. Wu, D. J. Burnell, *Tetrahedron Lett.* **1988**, 4369.

[35] W. G. Dauben, I. Farkas, D. P. Bridon, C. P. Chuang, K. E. Henegar, *J. Am. Chem. Soc.* **1991**, *113*, 5883.

[36] a) T. Eguchi, T. Terachi, K. Kakinuma, *J. Chem. Soc. Chem. Commun.* **1994**, 137; b) T. Eguchi, T. Terachi, K. Kakinuma, *Tetrahedron Lett.* **1993**, 2175.

[37] For the synthesis of a 36-membered ring in a nonnatural product see refs. [18, 66].

[38] a) Review: K. C. Nicolaou, R. K. Guy, *Angew. Chem.* **1995**, *107*, 2247; *Angew. Chem. Int. Ed. Engl.* **1995**, *34*, 2079; b) R. A. Holton, C. Somoza, H. B. Kim, F. Liang, R. J. Biediger, P. D. Boatman, M. Shindo, C. C. Smith, S. Kim, H. Nadizadeh, Y. Suzuki, C. Tao, P. Vu, S. Tang, P. Zhang, K. K. Murthi, L. N. Gentile, J. H. Liu, *J. Am. Chem. Soc.* **1994**, *116*, 1597, 1599; c) J. J. Masters, J. T. Link, L. B. Snyder, W. B. Young, S. J. Danishefsky, *Angew. Chem.* **1995**, *107*, 1886; *Angew. Chem. Int. Ed. Engl.* **1995**, *34*, 1723.

[39] a) K. C. Nicolaou, Z. Yang, J. J. Liu, H. Ueno, P. G. Nantermet, R. K. Guy, C. F. Claiborne, J. Renauld, E. A. Couladouros, K. Paulvannan, E. J. Sorensen, *Nature*, **1994**, *367*, 630; b) K. C. Nicolaou, Z. Yang, J. J. Liu, P. G. Nantermet, C. F. Claiborne, J. Renauld, R. K. Guy, K. Shibayama, *J. Am. Chem. Soc.* **1995**, *117*, 645; c) K. C. Nicolaou, J. J. Liu, Z. Yang, H. Ueno, E. J. Sorensen, C. F. Claiborne, R. K. Guy, C. K. Hwang, M. Nakada, P. G. Nantermet, *ibid.* **1995**, *117*, 634.

[40] A. S. Kende, S. Johnson, P. Sanfilippo, J. C. Hodges, L. N. Jungheim, *J. Am. Chem. Soc.* **1986**, *108*, 3513.

[41] a) K. C. Nicolaou, Z. Yang, E. J. Sorensen, M. Nakada, *J. Chem. Soc. Chem. Commun.* **1993**, 1024; b) K. C. Nicolaou, C. F. Claiborne, P. G. Nantermet, E. A. Couladouros, E. J. Sorensen, *J. Am. Chem. Soc.* **1994**, *116*, 1591; c) C. S. Swindell, W. Fan, P. G. Klimko, *Tetrahedron Lett.* **1994**, 4959; d) C. S. Swindell, W. Fan, *J. Org. Chem.* **1996**, *61*, 1109; e) C. S. Swindell, M. C. Chander, J. M. Heerding, P. G. Klimko, L. T. Rahman, J. V. Raman, H. Venkataraman, *ibid.* **1996**, *61*, 1101.

[42] W. G. Dauben, T. Z. Wang, R. W. Stephens, *Tetrahedron Lett.* **1990**, 2393.

[43] J. E. McMurry, R. G. Dushin, *J. Am. Chem. Soc.* **1990**, *112*, 6942.

[44] For model calculations, see: J. E. McMurry, N. O. Siemers, *Tetrahedron Lett.* **1993**, 7891.

[45] J. E. McMurry, N. O. Siemers, *Tetrahedron Lett.* **1994**, 4505.

[46] Titanium-mediated formation of pinacols from amino aldehyde derivatives: a) D. J. Kempf, D. W. Norbeck, L. M. Codavoci, X. C. Wang, W. E. Kohlbrenner, N. E. Wideburg, D. A. Paul, M. F. Knigge, S. Vasavanonda, A. Craig-Kennard, A. Saldivar, W. Rosenbrook, J. J. Clement, J. J. Plattner, J. Erikson, *J. Med. Chem.* **1990**, *33*, 2687; b) D. J. Kempf, T. J. Sowin, E. M. Doherty, S. M. Hannick, L. M. Codavoci, R. F. Henry, B. E. Green, S. G. Spanton, D. W. Norbeck, *J. Org. Chem.* **1992**, *57*, 5692. Für V^{2+} als Pinacolbildner siehe: c) J. H. Freudenberger, A. W. Konradi, S. F. Pedersen, *J. Am. Chem. Soc.* **1989**, *111*, 8014; V^{2+}-mediated formation of pinacols from amino aldehyde derivatives: d) A. W. Konradi, S. F. Pedersen, *J. Org. Chem.* **1992**, *57*, 28; e) B. Kammermeier, G. Beck, D. Jacobi, H. Jendralla, *Angew. Chem.* **1994**, *106*, 719; *Angew. Chem. Int. Ed. Engl.* **1994**, *33*, 685; f) B. Kammermeier, G. Beck, W. Holla, D. Jacobi, B. Napierski, H. Jendralla, *Chem. Eur. J.* **1996**, *2*, 307; g) M. T. Reetz, N. Griebenow, *Liebigs Ann.* **1996**, 335.

[47] For further examples of mixtures of stereoisomeric diols in titanium-mediated formation of pinacols, see: a) N. Kato, H. Kataoka, S. Ohbuchi, S. Tanaka, H. Takeshita, *J. Chem. Soc. Chem. Commun.* **1988**, 354; b) N. Kato, X. Wu, H. Nishikawa, K. Nakanishi, T. Takeshita, *J. Chem. Soc. Perkin Trans. 1* **1994**, 1047.

[48] a) E. Vogel, M. Köcher, H. Schmickler, J. Lex, *Angew. Chem.* **1986**, *98*, 262; *Angew. Chem. Int. Ed. Engl.* **1986**, *25*, 257; b) E. Vogel, P. Koch, X. L. Hou, J. Lex, M. Lausmann, M. Kisters, M. A. Aukauloo, P. Richard, R. Guilard, *ibid.* **1993**, *105*, 1670 and **1993**, *32*, 1600; c) J. L. Sessler, E. A. Brucker, S. J. Weghorn, M. Kisters, M. Schäfer, J. Lex, E. Vogel, *ibid.* **1994**, *106*, 2402 and **1994**, *33*, 2308; d) D. O. Martire, N. Jux, P. F. Aramendia, R. M. Negri, J. Lex, S. E. Braslavsky, K. Schaffner, E. Vogel, *J. Am. Chem. Soc.* **1992**, *114*, 9969; e) R. Guilard, M. A. Aukauloo, C. Tardieux, E. Vogel, *Synthesis* **1995**, 1480.

[49] a) G. Märkl, H. Sauer, P. Kreitmeier, T. Burgemeister, F. Kastner, G. Adolin, H. Nöth, K. Polborn, *Angew. Chem.* **1994**, *106*, 1211; *Angew. Chem. Int. Ed. Engl.* **1994**, *33*, 1151; b) Z. Hu, C. Scordilis-Kelley, M. P. Cava, *Tetrahedron Lett.* **1993**, 1879; c) F. Ellinger, A. Gieren, T. Hübner, J. Lex, F. Lucchesini, A. Merz, R. Neidlein, J. Salbeck, *Monatsh. Chem.* **1993**, *124*, 931; d) G. DeMunno, F. Lucchesini, R. Neidlein, *Tetrahedron* **1993**, *49*, 6863; e) D. C. Miller, M. R. Johnson, J. A. Ibers, *J. Org. Chem.* **1994**, *59*, 2877; f) T. Kawase, H. R. Darabi, R. Uchimiya, M. Oda, *Chem. Lett.* **1995**, 499; g) Z. Hu, J. L. Atwood, M. P. Cava, *J. Org. Chem.* **1994**, *59*, 8071, and references therein.

[50] I. Columbus, S. E. Biali, *J. Org. Chem.* **1994**, *59*, 3402.

[51] A. P. Marchand, A. Zope, F. Zaragoza, S. G. Bott, H. L. Ammon, Z. Du, *Tetrahedron* **1994**, *50*, 1687.

[52] P. R. Brooks, R. Bishop, D. C. Craig, M. L. Scudder, J. A. Counter, *J. Org. Chem.* **1993**, *58*, 5900.

[53] R. Gleiter, O. Borzyk, *Angew. Chem.* **1995**, *107*, 1094; *Angew. Chem. Int. Ed. Engl.* **1995**, *34*, 1001.

[54] W. R. Roth, H. Hopf, C. Horn, *Chem. Ber.* **1994**, 1781.

[55] W. von E. Doering, Y. Q. Shi, D. C. Zhao, *J. Am. Chem. Soc.* **1992**, *114*, 10763.

[56] U. Grieser, K. Hafner, *Tetrahedron Lett.* **1994**, 7759.

[57] a) M. O. Senge, K. R. Gerzevske, M. G. H. Vicente, T. P. Forsyth, K. M. Smith, *Angew. Chem.* **1993**, *105*, 745; *Angew. Chem. Int. Ed. Engl.* **1993**, *32*, 750; b) M. G. H. Vicente, K. M. Smith, *J. Org. Chem.* **1991**, *56*, 4407; c) L. Jaquinod, D. J. Nurco, C. J. Medforth, R. K. Pandey, T. P. Forsyth, M. M. Olmstead, K. M. Smith, *Angew. Chem.* **1996**, *108*, 1085; *Angew. Chem. Int. Ed. Engl.* **1996**, *35*, 1013.

[58] P. Burger, H. H. Brintzinger, *J. Organomet. Chem.* **1991**, *407*, 207.
[59] S. Pitter, G. Huttner, O. Walter, L. Zsolnai, *J. Organomet. Chem.* **1993**, *454*, 183.
[60] a) B. Bildstein, P. Denifl, K. Wurst, M. André, M. Baumgarten, J. Friedrich, E. Ellmerer-Müller, *Organometallics* **1995**, *14*, 4334; b) Alternative synthesis: D. Schütte, T. Oeser, H. Irngartinger, M. Wiessler, *Tetrahedron Lett.* **1995**, 5163.
[61] J. Besançon, J. Szymoniak, C. Moise, *J. Organomet. Chem.* **1992**, *426*, 325.
[62] a) J. E. McMurry, T. Lectka, *J. Am. Chem. Soc.* **1993**, *115*, 10167; b) *ibid.* **1990**, *112*, 869; c) J. E. McMurry, T. Lectka, C. N. Hodge, *ibid.* **1989**, *111*, 8867; d) *ibid.* **1984**, *106*, 6450; e) J. E. McMurry, T. Lectka, *Acc. Chem. Res.* **1992**, *25*, 47.
[63] T. S. Sorensen, S. M. Whitworth, *J. Am. Chem. Soc.* **1990**, *112*, 8135.
[64] a) H. P. Michels, M. Nieger, F. Vögtle, *Chem. Ber.* **1994**, 1167; b) F. Vögtle, C. Thilgen, *Angew. Chem.* **1990**, *102*, 1176; *Angew. Chem. Int. Ed. Engl.* **1990**, *29*, 1162.
[65] a) H. F. Grützmacher, A. Mehdizadeh, A. Mülverstedt, *Chem. Ber.* **1994**, 1163; b) H. F. Grützmacher, G. Nolte, *ibid.* **1994**, 1157; c) H. F. Grützmacher, E. Neumann, *ibid.* **1993**, 1495; d) H. F. Grützmacher, E. Neumann, F. Ebmeyer, K. Albrecht, P. Schelenz, *ibid.* **1989**, 2291.
[66] A. Fürstner, G. Seidel, *Synthesis* **1995**, 63.
[67] a) A. Merz, A. Karl, T. Futterer, N. Stacherdinger, O. Schneider, J. Lex, E. Luboch, J. F. Biernat, *Liebigs Ann.* **1994**, 1199; b) J. Tirado-Rives, M. A. Oliver, F. R. Fronczek, R. D. Gandour, *J. Org. Chem.* **1984**, *49*, 1627.
[68] A. Fürstner, G. Seidel, C. Kopiske, C. Krüger, R. Mynott, *Liebigs Ann.* **1996**, 655.
[69] a) W. Y. Lee, C. H. Park, Y. D. Kim, *J. Org. Chem.* **1992**, *57*, 4074; b) W. Y. Lee, C. H. Park, H. J. Kim, S. Kim, *ibid.* **1994**, *59*, 878.
[70] H. Hopf, C. Mlynek, *J. Org. Chem.* **1990**, *55*, 1361.
[71] a) P. Lhotak, S. Shinkai, *Tetrahedron Lett.* **1996**, 645; b) A. Arduini, S. Fanni, A. Pochini, A. R. Sicuri, R. Ungaro, *Tetrahedron* **1995**, *51*, 7951.
[72] a) A. W. Cooke, K. B. Wagener, *Macromolecules* **1991**, *24*, 1404; b) *Synth. Met.* **1989**, *29*, E525.
[73] a) S. Iwatsuki, M. Kubo, Y. Itoh, *Chem. Lett.* **1993**, 1085; b) M. Rehahn, A. D. Schlüter, *Macromol. Chem. Rapid Commun.* **1990**, *11*, 375; c) W. J. Feast, I. S. Millichamp, *Polym. Commun.* **1983**, 102; d) R. Bayer, O. Nuyken, *Kautsch. Gummi Kunstst.* **1996**, *49*, 28.
[74] T. Itoh, H. Saitoh, S. Iwatsuki, *J. Polym. Sci Part A Polym. Chem.* **1995**, *33*, 1589.
[75] J. Roncalli, C. Thobie-Gautier, E. H. Elandaloussi, P. Frère, *J. Chem. Soc. Chem. Commun.* **1994**, 2249.
[76] S. Yoshida, M. Fujii, Y. Aso, T. Otsubo, F. Ogura, *J. Org. Chem.* **1994**, *59*, 3077.
[77] a) P. Mangeney, T. Tejero, A. Alexakis, F. Grosjean, J. Normant, *Synthesis* **1988**, 255; b) P. Mangeney, F. Grosjean, A. Alexakis, J. F. Normant, *Tetrahedron Lett.* **1988**, 2675.
[78] a) C. Betschart, D. Seebach, *Helv. Chim. Acta* **1987**, *70*, 2215; b) C. Betschart, B. Schmidt, D. Seebach, *ibid.* **1988**, *71*, 1999.
[79] a) R. Imwinkelried, D. Seebach, *Helv. Chim. Acta* **1984**, *67*, 1496; b) E. J. Enholm, D. C. Forbes, D. P. Holub, *Synth. Commun.* **1990**, *20*, 981; c) T. Imamoto, S. Nishimura, *Chem. Lett.* **1990**, 1141; d) K. Takaki, Y. Tsubaki, S. Tanaka, F. Beppu, Y. Fujiwara, *ibid.* **1990**, 203; e) H. Tanaka, H. Dhimane, H. Fujita, Y. Ikemoto, S. Torii, *Tetrahedron Lett.* **1988**, 3811; f) N. Kise, H. Oike, E. Okazami, M. Yashimoto, *J. Org. Chem.* **1995**, *60*, 3980; g) M. Shimizu, T. Iida, T. Fujisawa, *Chem. Lett.* **1995**, 609; g) A. Alexakis, I. Aujard, T. Kanger, P. Mangeney, *Org. Synth.*, in print. We thank Prof. Alexakis for providing us with this manuscript prior to publication. h) S. V. Pansare, M. G. Malusare, *Tetrahedron Lett.* **1996**, 2859.
[80] Cited in ref. [7a, 8] as unpublished results.
[81] A. Fürstner, G. Seidel, B. Gabor, C. Kopiske, C. Krüger, R. Mynott, *Tetrahedron* **1995**, *51*, 8875.
[82] J. E. McMurry, D. D. Miller, *J. Am. Chem. Soc.* **1983**, *105*, 1660.
[83] For other methods of the alkylidenation of esters see for example: a) K. A. Brown-Wensley, S. L. Buchwald, L. Cannizzo, L. Clawson, S. Ho, D. Meinhardt, J. R. Stille, D. Straus, R. H. Grubbs, *Pure Appl. Chem.* **1983**, *55*, 1733; b) S. H. Pine, *Org. React.* **1993**, *43*, 1; c) J. R. Stille in *Comprehensive Organometallic Chemistry II, Vol. 12* (Ed.: L. S. Hegedus), Pergamon, Oxford, **1995**, p. 577; d) K. Takai, T. Kakiuchi, Y. Kataoka, K. Utimoto, *J. Org. Chem.* **1994**, *59*, 2668, and references therein.
[84] J. E. McMurry, D. D. Miller, *Tetrahedron Lett.* **1983**, 1885.
[85] M. Iyoda, T. Kushida, S. Kitami, M. Oda, *J. Chem. Soc. Chem. Commun.* **1987**, 1607.
[86] a) W. Li, Y. Li, Y. Li, *Chem. Lett.* **1994**, 741; b) *Synthesis* **1994**, 678; c) *ibid.* **1994**, 267.
[87] C. A. Davis, J. R. Hanson, F. G. Tellado, *J. Chem. Res. Synop.* **1989**, 226.
[88] A. Banerji, S. K. Nayak, *J. Chem. Soc. Chem. Commun.* **1990**, 150.
[89] A. Fürstner, A. Ernst, unpublished results.
[90] A. Fürstner, G. Seidel, A. Hupperts, *Org. Synth.*, submitted.
[91] A. Fürstner in ref. [8b], p. 381.
[92] F. Hofer in ref. [8b], p. 427.
[93] a) J. E. McMurry, T. Lectka, J. G. Rico, *J. Org. Chem.* **1989**, *54*, 3748; b) J. E. McMurry, M. P. Fleming, K. L. Kees, L. R. Krepski, *ibid.* **1978**, *43*, 3255.
[94] D. Lenoir, *Synthesis* **1977**, 553.
[95] a) M. Hori, M. Mori, *J. Org. Chem.* **1995**, *60*, 1480; b) M. Mori, M. Kawaguchi, M. Hori, S. I. Hamaoka, *Heterocycles* **1994**, *39*, 729; c) M. Kawaguchi, S. I. Hamaoka, M. Mori, *Tetrahedron Lett.* **1993**, 6907.
[96] A. Fürstner, N. Shi, *J. Am. Chem. Soc.* **1996**, *118*, 2533.
[97] Early attempts to use commercially available titanium powder for reductive couplings were unsuccessful [93b].
[98] A. Fürstner, B. Tesche, unpublished results.
[99] The McMurry reagent was used for a number of other valuable synthetic applications including the deoxygenation of arene-1,4-endoxides to give arenes [7b,100], of 2-ene-1,4-diols to yield conjugated dienes [101], and of sulfones to afford sulfides [102].
[100] a) P. Müller, J.-P. Schaller, *Helv. Chim. Acta.* **1989**, *72*, 1608; b) Y. Tobe, H. Ishii, S. Saiki, K. Kakiuchi, K. Naemura, *J. Am. Chem. Soc.* **1993**, *115*, 11604; c) C. Valdés, U. P. Spitz, S. W. Kubik, J. Rebek, Jr., *Angew. Chem.* **1995**, *107*, 2031; *Angew. Chem. Int. Ed. Engl.* **1995**, *34*, 1885.
[101] a) H. M. Waborsky, H. H. Wüst, *J. Am. Chem. Soc.* **1982**, *104*, 5807; b) G. Solladié, A. Girardin, G. Lang *J. Org. Chem.* **1989**, *54*, 2620; c) G. Solladié, V. Berl, *Tetrahedron Lett.* **1992**, 3477; d) G. Solladié, G. B. Stone, A. Rubro, *ibid.* **1993**, 1803; e) G. Solladié, G. B. Stone, C. Hamdouchi, *ibid.* **1993**, 1807.
[102] E. Akgün, K. Mahmood, C. A. Mathis, *J. Chem. Soc. Chem. Commun.* **1994**, 761.
[103] E. J. Corey, R. L. Danheiser, S. Chandrasekaran, *J. Org. Chem.* **1976**, *41*, 260.
[104] High yields of alkenes can also be obtained from aldehydes and ketones by using the $TiCl_4$–Mg amalgam reagent without prereduction in refluxing THF: A. R. Carroll, W. C. Taylor, *Aust. J. Chem.* **1990**, *43*, 1439.
[105] J. E. McMurry, M. P. Fleming, *J. Org. Chem.* **1976**, *41*, 896.
[106] J. E. McMurry, L. R. Krepski, *J. Org. Chem.* **1976**, *41*, 3229.
[107] H. Ledon, I. Tkatchenko, D. Young, *Tetrahedron Lett.* **1979**, 173.
[108] a) H. Idriss, K. G. Pierce, M. A. Barteau, *J. Am. Chem. Soc.* **1991**, *113*, 715; b) K. G. Pierce, M. A. Barteau, *J. Org. Chem.* **1995**, *60*, 2405, and references therein.
[109] H. Bönnemann, B. Korall, *Angew. Chem.* **1992**, *104*, 1506; *Angew. Chem. Int. Ed. Engl.* **1992**, *31*, 1490.
[110] A. Yamamoto, S. Go, M. Ookawa, M. Takahashi, S. Ikeda, T. Keii, *Bull. Chem. Soc. Jpn.* **1972**, *45*, 3110.
[111] a) B. Jezowska-Trzebiatowska, P. Sobota, *J. Organomet. Chem.* **1974**, *76*, 43; b) P. Sobota, B. Jezowska-Trzebiatowska, J. Wroblewski, *Bull. Acad. Pol. Sci. Ser. Sci. Chim.* **1980**, *28*, 679.
[112] P. Sobota, B. Jezowska-Trzebiatowska, *Coord. Chem. Rev.* **1978**, *26*, 71.
[113] a) R. Dams, M. Malinowski, I. Westdorp, H. J. Geise, *J. Org. Chem.* **1982**, *47*, 248; b) R. Dams, M. Malinowski, H. J. Geise, *Transition Met. Chem. (London)* **1982**, *7*, 37; c) *Bull. Soc. Chim. Belg.* **1981**, *90*, 1141.
[114] See for example: F. A. Carey, R. J. Sundberg, *Organische Chemie*, VCH, Weinheim, **1995**, p. 1007.
[115] a) B. Bogdanović, S. Liao, M. Schwickardi, P. Sikorsky, B. Spliethoff, *Angew. Chem.* **1980**, *92*, 845; *Angew. Chem. Int. Ed. Engl.* **1980**, *19*, 818; b) B. Bogdanović, G. Koppetsch, M. Schwickardi in *Organometallic Syntheses, Vol. 4* (Eds.: R. B. King, J. J. Eisch), Elsevier, Amsterdam, **1988**, p. 404; c) B. Bogdanović, P. Bons, S. Konstantinović, M. Schwickardi, U. Westeppe, *Chem. Ber.* **1993**, *126*, 1371; d) B. Bogdanović, G. Koppetsch, S. Liao, K. Schlichte, M. Schwickardi, P. Sikorsky, B. Spliethoff, U. Westeppe in ref. [115e], p. 41; e) *Synthetic Methods of Organometallic and Inorganic Chemistry, Vol. 1* (Ed.: W. A. Herrmann), Thieme, Stuttgart, **1996**.
[116] a) B. Bogdanović, P. Bons, M. Schwickardi, K. Seevogel, *Chem. Ber.* **1991**, *124*, 1041; b) B. Bogdanović, P. Bons, M. Schwickardi in ref. [115e], p. 43.
[117] H. Bertagnolli, T. S. Ertel, *Angew. Chem.* **1994**, *106*, 15; *Angew. Chem. Int. Ed. Engl.* **1994**, *33*, 45.
[118] **177** was used successfully as a reagent for the cyclization of aromatic acylamidocarbonyl compounds to give indoles (cf. Table 2) [17] and from ketoesters to enol ethers (F. Schmidt, R. Lett, *Journees de Chimie Organique*, Palaiseau, France, **1995**, p. A-313).
[119] F. A. Bottino, P. Finocchiaro, E. Libertini, A. Reale, A. Recca, *J. Chem. Soc. Perkin Trans. 2* **1982**, 77.
[120] B. Bogdanović, C. Krüger, B. Wermeckes, *Angew. Chem.* **1980**, *92*, 844; *Angew. Chem. Int. Ed. Engl.* **1980**, *19*, 817.
[121] a) Z. Hou, H. Yamazaki, K. Kobayashi, Y. Fujiwara, H. Taniguchi, *J. Chem. Soc. Chem. Commun.* **1992** 722; b) *Organometallics* **1992**, *11*, 2711.
[122] a) D. M. Roddick, J. E. Bercaw, *Chem. Ber.* **1989** *122*, 1579; b) P. Hofman, P. Stauffert, M. Frede, K. Tatsumi, *ibid.* **1989**, *122*, 1559; c) G. Erker, U. Dorf, P. Czisch, J. L. Petersen, *Organometallics* **1986**, *5*, 668, and references therein.
[123] For a discussion of the mechanism of the C–C coupling step in the McMurry reaction and other arguments in favor of a nucleophilic reaction mechanism, see refs. [9a,17].
[124] A. Bolte, Dissertation, Universität Bochum, **1995**.
[125] T. Mukaiyama, M. Shiono, K. Watanabe, M. Onaka, *Chem. Lett.* **1975**, 711; see also M. Mitani, Y. Kobayashi, *Bull. Chem. Soc. Jpn.* **1994**, *67*, 284.
[126] G. A. Olah, G. K. Surya Prakash, *Synthesis* **1976**, 607.

[127] a) G. Boche, M. Marsch, A. Müller, K. Harms, *Angew. Chem.* **1993**, *105*, 1081; *Angew. Chem. Int. Ed. Engl.* **1993**, *32*, 1279; b) A. Maercker, *ibid.* **1993**, *105*, 1072 and **1993**, *32*, 1023.
[128] H. C. Stiasny, R. W. Hoffmann, *Chem. Eur. J.* **1995**, *1*, 619.
[129] a) B. Becker, B. Bogdanović, *Z. Naturforsch. B* **1995**, *50*, 476; b) B. Becker, Dissertation, Universität Bochum, **1995**.
[130] a) G. Brendell, *Ullmanns Encykl. Tech. Chem. 4. Aufl. 1972–1984* **1977**, *13*, 129; b) *Kirk-Othmer Encycl. Chem. Technol. 3rd. ed. 1978–1984* **1980**, *12*, 777.
[131] In other examplex the $\alpha-\alpha'/\alpha-\gamma'$ selectivity was lower.
[132] Review: A. Yanagisawa, H. Yamamoto in ref. [8], p. 61.
[133] L. E. Aleandri, B. Bogdanović, P. Bons, C. Dürr, A. Gaidies, T. Hartwig, S. C. Huckett, M. Lagarden, U. Wilczok, R. A. Brand, *Chem. Mater.* **1995**, *7*, 1153.
[134] J. J. H. Edema, R. Duchateau, S. Gambarotta, R. Hynes, E. Gabe, *Inorg. Chem.* **1991**, *30*, 154.
[135] a) M. L. H. Green, G. A. Moser, I. Packer, F. Petit, R. A. Forder, K. Prout, *J. Chem. Soc. Chem. Commun.* **1974**, 839; b) K. Prout, R. A. Forder, *Acta Crystallogr. Sect. B* **1975**, *1331*, 852; c) S. G. Davies, M. L. H. Green, K. Prout, A. Coda, V. Tazzoli, *J. Chem. Soc. Chem. Commun.* **1977**, 135.
[136] a) H. Felkin, P. J. Knowles, B. Meunier, A. Mitschler, L. Ricard, R. Weiss, *J. Chem. Soc. Chem. Commun.* **1974**, 44; b) H. Felkin, P. J. Knowles, B. Meunier, *J. Organomet. Chem.* **1978**, *146*, 151.
[137] K. Jonas, G. Koepe, C. Krüger, *Angew. Chem.* **1986**, *98*, 901; *Angew. Chem. Int. Ed. Engl.* **1986**, *25*, 923.
[138] J. Rieke-Zapp, Diplomarbeit, Universität Bonn, **1995**.
[139] According to preliminary results, this also holds for the experiments described in ref. [113a], in which $TiCl_3$ was prereduced at reflux with Mg: B. Bogdanović, J. Rieke-Zapp, unpublished results..
[140] Prepared from $ZnCl_2$ and magnesium anthracene·3THF in a molar ratio of 1:1; a) H. Bönnemann, B. Bogdanović, R. Brinkmann, B. Spliethoff, D. W. He, *J. Organomet. Chem.* **1993**, *451*, 23; b) B. Bogdanović, K. Schlichte, unpublished results.
[141] The weak coupling activity of the filtrate observed in this case is due to the dissolved $[TiCl_3(dme)_{1.5}]$ combined with the very finely divided, nonfilterable Zn* particles[22].
[142] a) R. S. P Coutts, P. Wailes, R. L. Martin, *J. Organomet. Chem.* **1973**, *50*, 145; b) J. E. McMurry, W. Choy, *J. Org. Chem.* **1978**, *43*, 1800; c) B. P. Mundy, R. Srinivasa, Y. Kim, T. Dolph, R. J. Warnet, *ibid.* **1982**, *47*, 1657; d) B. P. Mundy, D. R. Bruss, Y. Kim, R. D. Larsen, R. J. Warnet *Tetrahedron Lett.* **1985**, *26*, 3927.

Time is money...

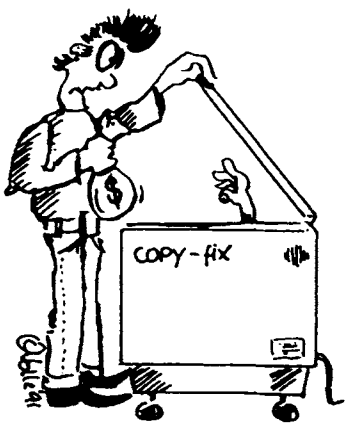

Save both by starting a personal subscription to *Angewandte Chemie* (now with *Chemistry - A European Journal*). At 9¢ per page you can't go wrong. With your own private copy you can read the "hot" articles before they cool, and waste less time in front of the copier.

Order now!
An order form can be found on the last page of this issue.

Electron Transfer and Chemical Reactions—Stepwise or Concerted? *On the Competition between Nucleophilic Substitution and Electron Transfer* **

Bernd Speiser*

Dedicated to Professor Michael Hanack on the occasion of his 65th birthday

Reaction mechanisms are important concepts for our comprehension of chemical transformations: mechanisms allow not only a pictorial description of reactions but also their classification into some fundamental types. Sometimes, however, it is asked whether our list of mechanisms is sufficient to explain experimental data, whether explanations of a particular mechanism are correct, and how we can distinguish between similar pathways.

Recently, it has been asked whether the nucleophilic substitution of a leaving group X^- by a nucleophile Nu^- can proceed by mechanisms other than the well-known[1] S_N1 [two elementary steps, Eq. (1)] and S_N2 variants [one elementary step, Eq. (2)]. In particular, electron transfer (ET) reactions[2] have

$$R\text{-}X \longrightarrow R^+ + X^- \xrightarrow{Nu^-} R\text{-}Nu + X^- \quad (1)$$

$$Nu^- + R\text{-}X \longrightarrow [Nu\cdots R\cdots X]^- \longrightarrow R\text{-}Nu + X^- \quad (2)$$

been proposed, in which Nu^- acts as a single electron donor. This is in contrast with the classical characterization of Nu^- as an electron pair donor.

In many instances when the electron transfer is separated from the subsequent step (monomolecular cleavage of the bond to the leaving group) by a substrate radical anion intermediate (outer sphere ET, definition in ref. [3]), an $S_{RN}1$ chain reaction [Eq. (3)] has been found[4, 5] (initiation by photo- or electrochemical means, by a chemical reducing agent, or "thermally" by Nu^- itself; termination reactions not included here).

$$\begin{aligned}
&\text{Initiation:} && R\text{-}X + e^- \longrightarrow R\text{-}X^{\bullet -}\\
&\text{Propagation:} && R\text{-}X^{\bullet -} \longrightarrow R^\bullet + X^-\\
& && Nu^- + R^\bullet \longrightarrow R\text{-}Nu^{\bullet -}\\
& && R\text{-}Nu^{\bullet -} + R\text{-}X \longrightarrow R\text{-}Nu + R\text{-}X^{\bullet -}\\
&\text{Overall reaction:} && Nu^- + R\text{-}X \longrightarrow R\text{-}Nu + X^-
\end{aligned} \quad (3)$$

An inner sphere process (definition in ref. [3]) with ET, bond breaking, and bond formation occurring in a single step corresponds to the classical S_N2 mechanism [Eq. (2)]. In a hypothetical third variant (dissociative outer sphere ET[5] [Eqs. (4) and (5)]), ET and cleavage of the R–X bond occur concertedly,

$$Nu^{\bullet -} + R\text{-}X \longrightarrow Nu + R^\bullet + X^-;\ R^\bullet + Nu^{\bullet -} \longrightarrow R\text{-}Nu^- \quad (4)$$

$$Nu^- + R\text{-}X \longrightarrow Nu^\bullet + R^\bullet + X^- \longrightarrow R\text{-}Nu + X^- \quad (5)$$

while product (bond) formation constitutes a second elementary step. In contrast to the S_N2 case, the nucleophile does not bind to the reaction center in the transition state: with regards to Nu^-, both (4) and (5) are outer sphere reactions.

The question of alternatives to the classical view of S_N reactions is thus intimately linked to the theory of ET (Marcus theory)[6] and its extension to dissociative ET[7] by Savéant.[8] Both Marcus's and Savéant's theories apply to ET reactions between an electron donor and an electron acceptor as well as to electrochemical reactions between a donor or acceptor and an electrode. In the latter case, cyclic voltammetry can be used to determine the free energy of activation $\Delta G^\ddagger$ for the electron transfer.[7, 9–12] Important experimental features are peak broadening in the voltammograms, quantitatively expressed by the half-peak width $E_p - E_{p/2}$ and the peak shift with the scan rate v, $dE_p/d\log v$ (for a definition of the peak parameters, see Fig. 1). Theoretical predictions have been tested experimentally

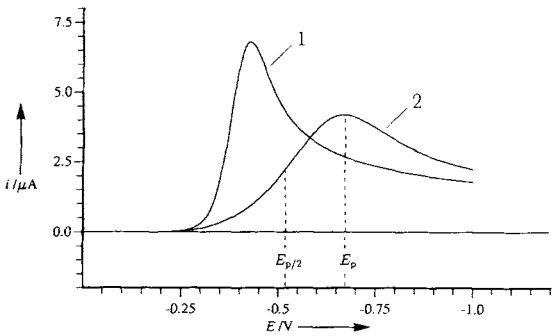

Fig. 1. Cyclic voltammetric peaks for a reversible diffusion-controlled process (curve 1) and for a quasi-reversible process controlled by diffusion and ET (curve 2). E_p: peak potential; $E_{p/2}$: potential at which the current reaches half its peak value; both potentials are shown here for curve 2; $E_p - E_{p/2}$: half-peak width; simulated voltammograms with $E^0 = -0.4$ V, concentration $c = 10^{-4}$ M, electroactive area $A = 0.08\ cm^2$, diffusion coefficient $D = 10^{-5}\ cm^2 s^{-1}$, $v = 1.0\ V s^{-1}$; additional parameters for curve 2: transfer coefficient $\alpha = 0.3$, rate constant of the heterogeneous ET $k_s = 10^{-3}\ cm\,s^{-1}$.

[*] Priv.-Doz. Dr. B. Speiser
Institut für Organische Chemie der Universität
Auf der Morgenstelle 18, D-72076 Tübingen (Germany)
Fax: Int. code +(7071)29-6205.
e-mail: bs@echem3.orgchemie.chemie.uni-tuebingen.de

[**] *I thank the Deutsche Forschungsgemeinschaft for a Heisenberg fellowship, J.-M. Savéant, Paris, and H. Lund, Aarhus, for kindly supplying me with pre- and reprints, and U. Bee for technical help in preparing Figure 2.*

and confirmed for several electrochemical cleavage reactions [e.g. Scheme 1, a)–c)].

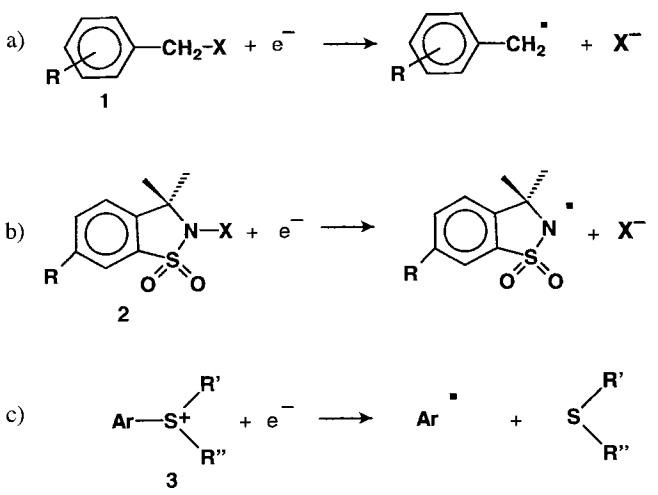

Scheme 1. Reductive cleavage of benzyl halides **1**, *N*-halosultams **2**, and sulfonium cations **3**.

Several factors have been identified that control the transition between a stepwise sequence [Eq. (6)] and a concerted reaction [Eq. (7)] (Fig. 2). For the reduction of benzyl halides **1**, *N*-halo-

$$R{-}X + e^- \longrightarrow R{-}X^{\bullet -} \longrightarrow R^\bullet + X^- \quad (6)$$

$$R{-}X + e^- \longrightarrow R^\bullet + X^- \quad (7)$$

sultams **2**, and sulfonium cations **3**, the energy of the π^* LUMO, which accomodates the incoming electron, and the bond dissociation energy of the R–X bond are most important (Figs. 2b and 2c). Thus, nitro-substituted benzyl halides **1** (R = NO_2; X = Cl, Br) with a low-lying π^* LUMO react according to Equation (6), since reduction to the radical anion proceeds easily (not very negative formal potential $E^0_{RX/RX^{\bullet -}}$). Cyano- or unsubstituted benzyl halides (R = CN, H; X = Cl, Br) with a higher energy π^* LUMO, on the other hand, undergo concerted cleavage according to Equation (7).[10] Although characterized by LUMO energies similar to those found for the benzyl halides, sultams **2** (R = NO_2; X = Br, Cl) react concertedly [Eq. (7)][10] since the N–X bond is weaker than its C–X counterpart. Only the fluorosultam (R = NO_2; X = F), which has a high N–F bond dissociation energy, returns to stepwise cleavage [Eq. (6)]. Analogous results were found for the reductive cleavage reactions of alkyl halides (weaker C–X bond: concerted) and aryl halides (stronger C–X bond: stepwise).[7]

In the reduction of aryldialkyl sulfonium cations **3**[11] the mechanism for two compounds (R′ = CH_3, R″ = $CH_2{-}C_6H_5$, Ar = phenyl or naphthyl) changes when the cyclic voltammetric scan rate is increased: for small v the data agree with a concerted, for large v with a stepwise mechanism. This difference is related to the v-dependent peak shift in the voltammograms. With smaller v (slower timescale) the peaks move to less negative potentials E in agreement with the fact that the ET is kinetically controlled. If the reaction proceeds at more positive E, however, the energy of $RX + e^-$ and thus the thermodynamic driving force[8] of the reaction decreases. This leads to a concerted reaction (Fig. 2d). An increased driving force is expected for an ET induced by pulse radiolysis. Indeed, the reaction of 3-cyanobenzyl bromide in water is stepwise under such conditions, while its electrochemical reduction in CH_3CN is concerted.[11]

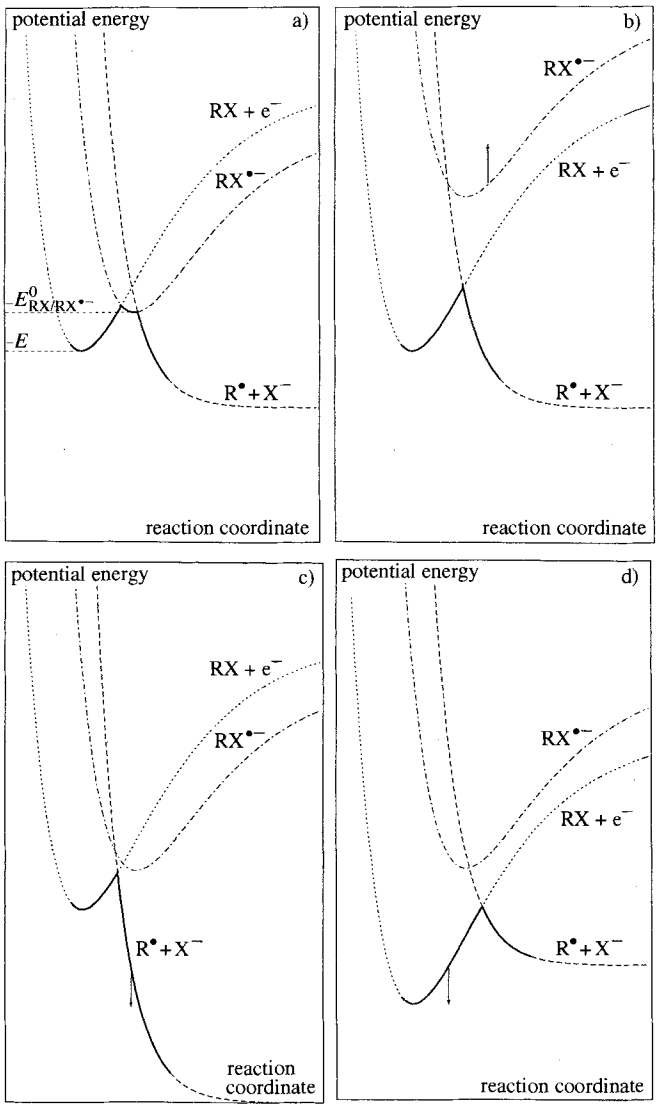

Fig. 2. Influences on an ET reaction with coupled bond cleavage; potential energies of substrate R–X (---), its reduction products $R{-}X^{\bullet -}$ (– · – · –), and the cleavage products $R^\bullet + X^-$ (– – –) given as function of the reaction coordinate (simplified: distance R–X); the energetically favored pathway for the reaction (energy profile) follows the thick line. The arrows indicate changes of the potential curve relative to situation a) (stepwise mechanism, two transition states, outer sphere ET); b) increase of $R{-}X^{\bullet -}$ LUMO energy, more negative $E^0_{RX/RX^{\bullet -}}$; c) decrease of dissociation energy, weaker R–X bond; d) decrease of driving force, more positive electrode potential E. All three variations lead to the concerted pathway (one transition state, outer sphere dissociative ET).

Solvent effects could also play a role. Consequently, the influence of different solvents on the reductive cleavage of CF_3Cl has been estimated by ab initio calculations.[13] Polar solvents were found to favor the concerted reaction, and the minimum for $CF_3Cl^{\bullet -}$ on the potential energy surface for "gas-phase" calculations disappears.

Can we apply these electrochemical results to homogeneous reactions? The cathode as an electron source is then replaced by a one-electron donor $D^{\bullet -}$. During the ET according to Equations (8) (stepwise, outer sphere) and (9) (concerted, outer

$$D^{\bullet -} + R\text{–}X \longrightarrow D + R\text{–}X^{\bullet -} \longrightarrow D + R^{\bullet} + X^{-} \quad (8)$$

$$D^{\bullet -} + R\text{–}X \longrightarrow D + R^{\bullet} + X^{-} \quad (9)$$

sphere dissociative) $D^{\bullet -}$ does not bind to the reaction center. Examples of donor molecules are anion radicals of aromatic hydrocarbons and heteroarenes. These species are persistent in DMF, and their reactions with acceptors have been well characterized.[14] Experimentally, the reactions are followed again by cyclic voltammetry,[15] but studies with rotating disk electrodes and ultramicroelectrodes have also been conducted.[16] The radical anion $D^{\bullet -}$ is formed at the electrode and reacts with R–X according to Equation (8) or (9)[17] to regenerate the neutral donor. The redox couple $D/D^{\bullet -}$ serves as the mediator in an indirect electrolysis.[18]

Lund's group has tested extensive series of substrates such as alkyl and aryl halides, activated olefins, CO_2, and anhydrides.[14] The driving force of the reaction and hence its rate is affected by the reduction potential of the donor. Stepwise [Eq. (8)] and concerted pathways [Eq. (9)] are observed as before for direct ET at an electrode.[7]

The transition to the S_N2 reaction is reached if $D^{\bullet -}$ and R interact. Then $D^{\bullet -}$ corresponds to a nucleophile and is bound to RX in the transition state. The outer sphere ET becomes an inner sphere process, and formation and cleavage of the two bonds occur simultaneously. The dissociative outer sphere and S_N2 variants are expected to differ in their stereochemical results, their activation entropy ΔS^{+}, and their activation enthalpy ΔH^{+}. A S_N2 reaction [Eq. (2)] at a carbon atom proceeds with inversion of configuration (Walden inversion).[19] The nucleophile attacks the reaction center as an electron pair donor from the side opposite to the leaving group for electronic and steric reasons. The resulting transition state has strict requirements for the relative alignment of Nu, R, and X, which explains the observed high activation entropy (for example $\Delta S^{+} = -67.3\ J\,K^{-1}\,mol^{-1}$ for the reaction between *n*-butyl bromide and anthracene radical anion).[20] Since the nucleophile and the reaction center form a bonding interaction, ΔH^{+} is relatively small ($37.4\ kJ\,mol^{-1}$ for the example mentioned[20]).

Nevertheless, in a series of bimolecular nucleophilic substitutions at least partial racemization has been observed (Scheme 2),[14, 21] a fact that can be explained easily by formation of an intermediate radical R$^{\bullet}$ through dissociative ET (for further examples, see ref. [5]). In these cases, the nucleophile does not have to attack along the C–X axis. Rather, the bond cleavage may proceed through action of the nucleophile as one-electron donor without directional preference. This results in a smaller absolute value of ΔS^{+} (for example $-36\ J\,K^{-1}\,mol^{-1}$ for the reaction of bornyl bromide with anthracene radical anion).[14] The intermediate R$^{\bullet}$ reacts with a second molecule $Nu^{\bullet -}$ and forms the product anion [Eq. (4)], which is subsequently protonated.[22] If the nucleophile itself does not have radical character, the product is formed directly according to Equation (5).

The influence on ΔG^{+} is usually determined by the "kinetic advantage" technique.[14, 23] The rate constants k_{ET} for ET reactions of the substrate with donors having various redox potentials and thus different driving forces are compared to the rate constants k_{SUB} for the substitution reaction. If the value of k_{SUB} is within the range expected for an ET reaction with the particular driving force, an ET pathway like that in Equation (9) is assumed. For an S_N2 reaction with a stabilizing interaction in the transition state, k_{SUB} has appreciably higher values. The latter effect is found for sterically less demanding alkyl halides, while in the case of isobornyl bromide $k_{ET}/k_{SUB} \approx 1$.

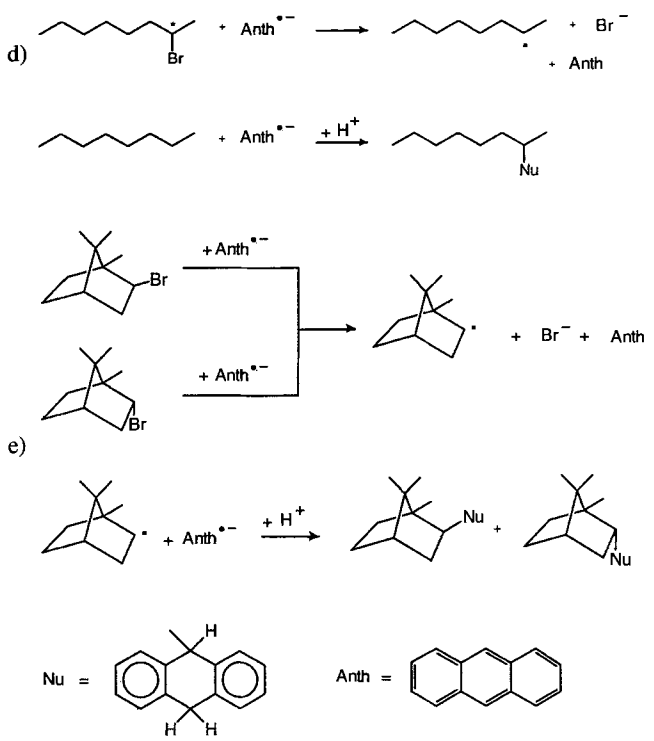

Scheme 2. Examples of bimolecular nucleophilic substitutions that proceed with (partial) racemization; d) 92% racemization, e) 1:1 ratio of isomers independent of the bromide employed.

The following picture emerges from these considerations and experiments: If the reaction center can be approached by the nucleophile easily from the back side, the concerted S_N2 pathway is energetically advantageous. A sterically hindered reaction center, however, may still form products by a less direction-specific reaction which is favored by ΔS^{+}.

The question whether the ET and the S_N2 reactions have to be described by two separate transition states is still controversial.[2, 5, 14] Alternatively, a spectrum of reaction pathways through a single transition state with a variable proportion of ET could exist whose extremes correspond to the two mechanisms.[14] Put in another way:[24, 25] is there an activated complex different from the S_N2 transition state that leads to a substitution and where the reaction is initiated by dissociative outer sphere ET?

Lund and co-workers argue in favor of a spectrum of mechanisms.[14, 16, 26] Since the logarithm of the rate constant depends linearly on the driving force, a change of the transition state is unlikely. Other results (D = anthracene, R–X = methyl halides;[27] D = 1,4-naphthalenedicarbonitrile, R–X = benzyl bromide[28]) also point to a competition between mechanisms; in the latter example it is controlled by the solvent (CH_3CN vs. DMF).

Sastry and Shaik tried to locate the transition states for S_N2 and ET reactions on the calculated potential energy surface of the reaction between $CH_2{=}O^{\bullet -}$ and CH_3Cl. They found, how-

ever, only inner sphere variants with bonding of the donor.[25] Similarly, for the reaction between $CHY{=}O^{\bullet -}$ and CH_3X (Y = H, CH_3, CN; X = Cl, Br, I) only one transition state could be characterized, from which either inner sphere ET or substitution may occur depending on X and Y[29] (spectrum of mechanisms).

In a most recent manuscript, Savéant and co-workers,[30] on the other hand, used ab initio calculations to identify two transition states (S_N2, ET) for the reaction of $CH_2{=}CH_2^{\bullet -}$ with CH_3F and three transition states (S_N2 at the O atom and at the C atom of the formaldehyde radical anion, ET) for the reactions of $CH_2{=}O^{\bullet -}$ with CH_3F or CH_3Cl. The relative energies and entropies closely correspond to those expected from the discussion above.

Calculations for more complex systems may contribute further to the understanding of the S_N2 reaction; however, more sophisticated experiments are needed for the final verdict. Already in 1987, Eberson predicted that the alternatives to the classical S_N reaction "in all likelihood ... will create vigorous discussion in parts of the scientific community, and agreement about their mechanism will be slow to come to."[31] Almost ten years later the question has not yet been fully resolved. Despite current criticism,[2, 25] the outer sphere dissociative ET must be regarded as a supplementary pathway for S_N2-like substitutions,[2, 25] just as the $S_{RN}1$ mechanism is discussed for monomolecular reactions. Even textbook reaction mechanisms are not immune to changes.

German version: *Angew. Chem.* **1996**, *108*, 2623–2626

Keywords: cyclic voltammetry · electron transfer · nucleophilic substitutions · reaction mechanisms

Marcus computes the standard free energy of activation $\Delta G_0^{\ddagger}$ of an ET reaction as the sum of an inner (λ_i) and an outer (λ_o) reorganization energy [Eq. (10)] [6]. These energies result from changes in bond angles and lengths, and reorientation of solvent molecules, respectively. Saveant [7] substitutes the harmonic oscillator parabola by a Morse curve for the case of an ET with concerted bond cleavage. This results in Equation (11), where D corresponds to the dissociation energy of the cleaved bond. In both cases the activation energy $\Delta G^{\ddagger}$ shows a quadratic dependence on the driving force of the reaction, $-\Delta G^0$, according to Equation (12) [32] (+ for forward, − for reverse reaction; work terms for the formation of precursor and successor complexes are neglected [32]). The standard value $\Delta G_0^{\ddagger}$ follows for $\Delta G^0 = 0$.

$$\Delta G_0^{\ddagger} = \frac{\lambda_i + \lambda_o}{4} \tag{10}$$

$$\Delta G_0^{\ddagger} = \frac{D + \lambda_i + \lambda_o}{4} \tag{11}$$

$$\Delta G^{\ddagger} = \Delta G_0^{\ddagger}\left(1 \pm \frac{\Delta G^0}{4\Delta G_0^{\ddagger}}\right)^2 \tag{12}$$

[1] F. A. Carey, R. J. Sundberg, *Advanced Organic Chemistry. Part A: Structure and Mechanism*, Plenum Press, New York, **1990**, p. 257.

[2] L. Eberson, *Electron Transfer Reactions in Organic Chemistry*, Springer, Berlin, **1987**.

[3] In an outer sphere electron transfer either no bonds are formed or cleaved on the timescale of the experiment or this happens in an elementary step separate from the ET [5, 23]. The inner sphere case, on the other hand, describes an elementary step corresponding to an ET with a concerted change in bonding.

[4] E. C. Ashby, *Acc. Chem. Res.* **1988**, *21*, 414–421.

[5] J.-M. Savéant, *Adv. Phys. Org. Chem.* **1990**, *26*, 1–130.

[6] R. A. Marcus, *Angew. Chem.* **1993**, *105*, 1161–1172; *Angew. Chem. Int. Ed. Engl.* **1993**, *32*, 1111–1121.

[7] J.-M. Savéant, *Adv. Electron Transfer Chem.* **1994**, *4*, 53–116.

[8] Based on the assumption of harmonic oscillators for substrates and products (potential energy as a function of bond length represented by a parabola)

[9] J.-M. Savéant, *J. Am. Chem. Soc.* **1992**, *114*, 10595–10602.

[10] C. P. Andrieux, E. Differding, M. Robert, J.-M. Savéant, *J. Am. Chem. Soc.* **1993**, *115*, 6592–6599.

[11] C. P. Andrieux, M. Robert, F. D. Saeva, J. M. Savéant, *J. Am. Chem. Soc.* **1994**, *116*, 7864–7871.

[12] C. P. Andrieux, A. Le Gorande, J.-M. Savéant, *J. Am. Chem. Soc.* **1992**, *114*, 6892–6904.

[13] J. Bertran, I. Gallardo, M. Moreno, J.-M. Savéant, *J. Am. Chem. Soc.* **1992**, *114*, 9576–9583.

[14] H. Lund, K. Daasbjerg, T. Lund, S. U. Pedersen, *Acc. Chem. Res.* **1995**, *28*, 313–319.

[15] C. P. Andrieux, J. M. Savéant, in *Investigations of Rates and Mechanisms of Reactions, Vol. 6, 4/E, Part 2* (Ed.: C. F. Bernasconi), Wiley **1986**, pp. 305–390.

[16] K. Daasbjerg, S. U. Pedersen, H. Lund, *Acta Chem. Scand.* **1991**, *45*, 424–430.

[17] If the equilibrium $D^{\bullet -} + RX \rightleftharpoons D + RX^{\bullet -}$ (controlled by the potentials $E^0_{D/D^{\bullet -}}$ and $E^0_{RX/RX^{\bullet -}}$) is not shifted to the side of the products, the irreversible cleavage to give $R^{\bullet}$ and X^- still drives the reaction.

[18] E. Steckhan, *Angew. Chem.* **1986**, *98*, 681–699; *Angew. Chem. Int. Ed. Engl.* **1986**, *25*, 683–701.

[19] T. H. Lowry, K. S. Richardson, *Mechanism and Theory in Organic Chemistry*, Harper & Row, New York, **1987**, p. 331.

[20] C. P. Andrieux, G. Delgado, J.-M. Savéant, K. B. Su, *J. Electroanal. Chem.* **1993**, *348*, 141–154.

[21] É. Hebert, J.-P. Mazaleyrat, Z. Welvart, L. Nadjo, J.-M. Savéant, *Nouv. J. Chim.* **1985**, *9*, 75–81.

[22] Radicals $R^{\bullet}$ are susceptible to further reduction to form anions in a competing reaction [14].

[23] D. Lexa, J.-M. Savéant, K.-B. Su, D.-L. Wang, *J. Am. Chem. Soc.* **1988**, *110*, 7617–7625.

[24] Ref. [2], p. 191.

[25] G. N. Sastry, S. Shaik, *J. Am. Chem. Soc.* **1995**, *117*, 3290–3291.

[26] K. Daasbjerg, H. Lund, *Acta Chem. Scand.* **1996**, *50*, 299–302.

[27] K. Daasbjerg, T. B. Christensen, *Acta Chem. Scand.* **1995**, *49*, 128–132.

[28] Y. Huang, D. D. M. Wayner, *J. Am. Chem. Soc.* **1994**, *116*, 2157–2158.

[29] G. N. Sastry, D. Danovich, S. Shaik, *Angew. Chem.* **1996**, *108*, 1208–1211; *Angew. Chem. Int. Ed. Engl.* **1996**, *35*, 1098–1100.

[30] J. Bertran, I. Gallardo, M. Moreno, J.-M. Savéant, *J. Am. Chem. Soc.*, in press.

[31] Ref. [2], p. 202.

[32] J.-M. Savéant, *J. Am. Chem. Soc.* **1987**, *109*, 6788–6795.

 © VCH Verlagsgesellschaft mbH, D-69451 Weinheim, 1996 0570-0833/96/3521-2474 $ 15.00+.25/0

Late Transition Metal Complexes: Catalysts for a New Generation of Organic Polymers

Adnan S. Abu-Surrah and Bernhard Rieger*

Since the pioneering by Karl Ziegler and Giulio Natta in the the early 1950s on the polymerization of simple olefins,[1] there has been intense interest in the application of early transition metal catalysts for the selective polymerization of inexpensive olefins. Current studies on metallocene-based catalysts have far-reaching implications for the development of new poly(α-olefin) materials as well as for an understanding of basic reaction mechanisms responsible for the growth of polymer chains at a catalyst center and for the control of polymer microstructures and molecular weights.[2] However, due to the sensitivity of early transition metal complexes to electron-donating functional groups, this catalyst generation allows only the use of a limited number of polar monomers bearing sterically hindered functionalities.[3] Thus, copolymers of readily available polar monomers with ethene are exclusively produced by radical routes in high-pressure processes.[4]

The corresponding α-olefin copolymers are not accessible by these techniques; related structures have been achieved by applying grafting reactions of acrylates on an isotactic polypropene backbone. Controlled copolymerization of ethene and propene with polar olefins such as readily available acrylates, their derivatives, and vinyl ethers is still a long-standing goal in polyolefin engineering, since copolymers of this type might endow a new generation of materials with remarkably high adhesive, dyeing, and moisture adsorption properties.

The first successes in this direction were recently achieved by using rare earth transition metal compounds. Lanthanide complexes were used to prepare block copolymers comprising a polyethene and a polar polyacrylate or polyester moiety. In this reaction, ethene is first polymerized by a samarocene complex. The second block is then introduced by a consecutive group-transfer polymerization of methyl methacrylate or by ring-opening polymerization of a lactone[5] (Scheme 1).

It was established in the 1970s that alkyl complexes of late transition metals such as iron and cobalt could also be applied for the insertion polymerization of acrylic acid derivatives.[6] Yamamoto et al. used diethylbis(bipyridine)iron(II) and related cobalt complexes for the homopolymerization of acrylonitrile. The observed low monomer conversion is probably due to a labile coordination of the bipyridine ligands, which leads to a facile deactivation of the catalyst by β-H-migration and reductive elimination of the growing polymer chain.[7] In 1995 Brookhart et al. reported that certain Pd^{II} and Ni^{II} catalysts can convert ethene and α-olefins to high molecular weight polymers at low pressure.[8] These late transition metal compounds are either monocationic alkyl complexes of the type $[(N\cap N)M(CH_3)(solvent)][B(Ar_f)_4]$ or methyl aluminoxane (MAO)-activated nickel(II) dibromide complexes bearing a bidentate imine ligand[9] with a sterically demanding substitution pattern (Scheme 2).

The counteranion $[\{3,5\text{-}(CF_3)_2C_6H_3\}_4B]^-$ increases the solubility of these catalyst systems, and the bulky substituents on the aryl groups of the diimine ligands block an associative olefin exchange, thus effectively retarding chain transfer processes. Both aspects are important prerequisites that make such palladium(II) complexes the first transition metal catalyst systems capable of copolymerizing ethene or propene with readily avail-

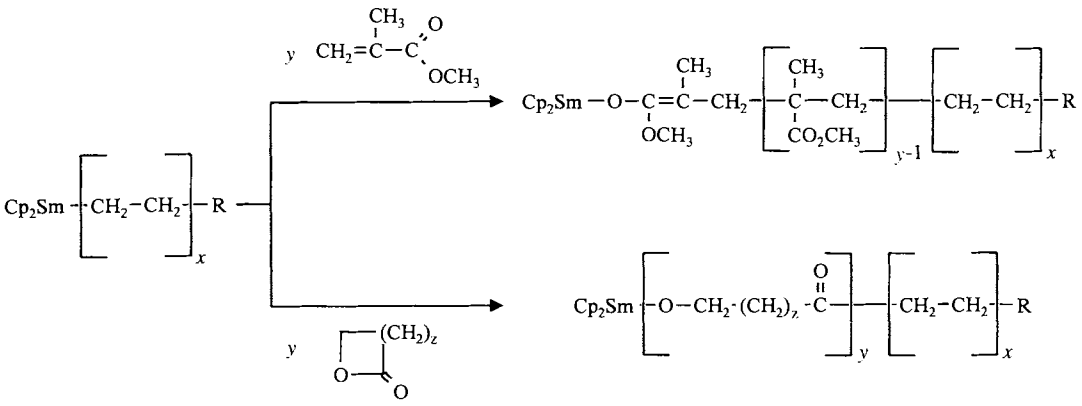

Scheme 1. Synthesis of AB block copolymers with samarocene catalysts. R = polymer chain.

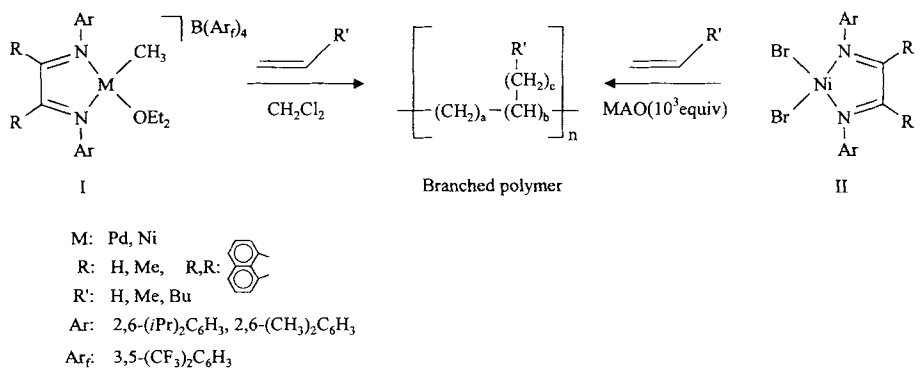

Scheme 2. Olefin polymerization with sterically hindered Ni^{II} and Pd^{II} catalysts.

[*] Prof. Dr. B. Rieger, A. S. Abu-Surrah
Abteilung Makromolekulare Chemie der Universität
D-89069 Ulm (Germany)
Fax: Int. code +(731)502-2883

 © VCH Verlagsgesellschaft mbH, D-69451 Weinheim, 1996 0570-0833/96/3521-2475 $ 15.00+.25/0

able acrylic monomers to give high molecular weight copolymers[10, 11] (Scheme 3). The diethyl ether adducts **I** (Scheme 2) or the more stable chelate complexes **III** (Scheme 3), which

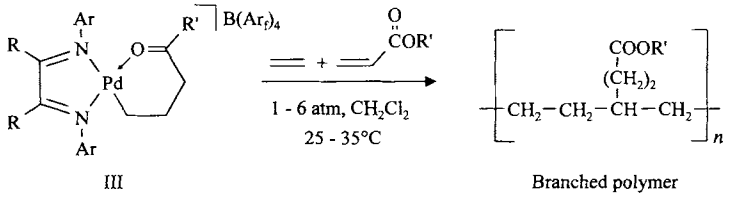

III

Branched polymer

R' = Me, *t*Bu, $CH_2(CF_2)_6CF_3$

Scheme 3. Synthesis of long-chain-branched copolymer structures of ethene and acrylates by insertion polymerization at catalytically active Pd^{II} centers. R and Ar_f see Scheme 2.

were prepared from the corresponding monoalkyl complex $[(N\cap N)Pd(CH_3)Cl)]$, acrylate monomer, and $NaB(Ar_f)_4$, are suitable precursors of the catalytically active species in the copolymerization reactions. The resulting ethene copolymers are amorphous, highly branched materials, in which the ester groups are predominantly located at the end of the branches.

Similar Pd^{II} catalysts (**IV**, Scheme 4) bearing enantiomerically pure, C_2-symmetric bis(dihydrooxazole) ligands have also been

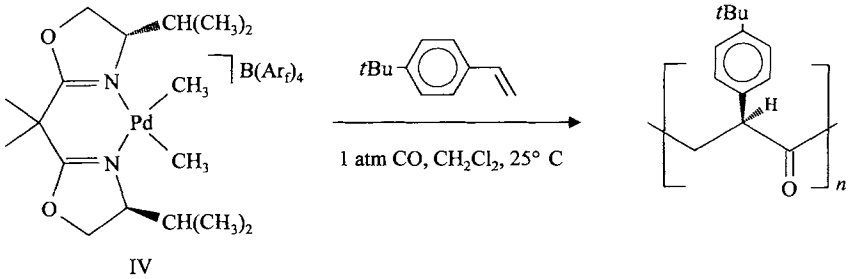

IV

Scheme 4. Synthesis of isotactic, optically active polyketones with chiral bis(dihydrooxazole)palladium(II) catalysts. Ar_f see Scheme 2.

applied by Brookhart et al. for asymmetric polymerization reactions.[12] Optically active, isotactic polyketones are formed by an alternating insertion of bulky olefins (e. g. 4-*tert*-butylstyrene) and carbon monoxide.

Comparable alternating polymers comprising more simple olefins are accessible by using palladium(II) phosphane complexes. Sen et al.[13] and Takaya et al.[14] obtained highly isotactic, optically active alternating propene/carbon monoxide copolymers by using Pd^{II} complexes of (*R*)-Me-DUPHOS (**V**) or the asymmetric ligand (*R*,*S*)-BINAPHOS (**VI**)[15] (Scheme 5). These polyketones are a new and versatile class of polymers, whose property profiles range from crystalline thermoplastics[16] to high molecular weight elastomers.[17] In contrast to regio- and stereoregular poly(α-olefins), which possess a mirror plane perpendicular to the main chain, the polyketones are chiral polymers that can show optical activity when enantiomerically pure catalysts are applied. Only time will tell whether the formation of complexes with other chiral polymers, such as

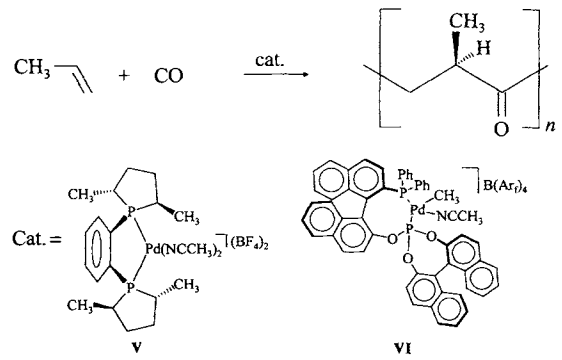

V VI

Scheme 5. Alternating enantioselective copolymerization of propene with carbon monoxide. Ar_f see Scheme 2.

polylactides, will open a route to compounds with new material properties.[18]

German version: *Angew. Chem.* **1996**, *108*, 2627–2629

Keywords: catalysis · copolymerizations · polyketones · polymerizations · polyolefins

[1] a) K. Ziegler, E. Holzkamp, H. Breil, H. Martin, *Angew. Chem.* **1955**, *67*, 541; b) K. Ziegler, *Angew. Chem.* **1964**, 76, 545; c) G. Natta, *Angew. Chem.* **1956**, *68*, 393; *ibid.* **1964**, *76*, 553; d) see also *Applied Homogeneous Catalysis with Organometallic Compounds* (Eds.: B. Cornils, W. A. Herrmann), VCH, Weinheim, **1996**.

[2] H. H. Brintzinger, D. Fischer, R. Mülhaupt, B. Rieger, R. M. Waymouth, *Angew. Chem.* **1995**, *107*, 1255; *Angew. Chem. Int. Ed. Engl.* **1995**, *34*, 1143 and references therein.

[3] R. Kesti, G. W. Coates, R. M. Waymouth, *J. Am. Chem. Soc.* **1992**, *114*, 9679.

[4] a) K. W. Doak in *Encyclopedia of Polymer Science and Engineering, Vol. 6* (Ed.: H. F. Mark), Wiley, New York, **1986**, p. 386.

[5] a) H. Yasuda, H. Yamamoto, K. Yokota, S. Miyake, A. Nakamura, *J. Am. Chem. Soc.* **1992**, *114*, 4908; b) H. Yasuda, N. Furo, H. Yamamoto, A. Nakamura, S. Miyake, N. Kibino, *Macromolecules* **1992**, *25*, 5115; c) H. Yasuda, H. Yamamoto, M. Yamashita, K. Yokota, A. Nakamura, S. Miyake, Y. Kai, N. Tanehisa, *ibid.* **1993**, *26*, 7134.

[6] A. Yamamoto, T. Shimizu, S. Ikeda, *Makromol. Chem.* **1970**, *136*, 297.

[7] a) A. Yamamoto, *J. Am. Chem. Soc.* **1967**, *89*, 5989; b) A. Yamamoto, K. Morifuji, S. Ikeda, T. Saito, Y. Uchida, A. Misono, *J. Am. Chem. Soc.* **1968**, *90*, 1878; c) T. Yamamoto, A. Yamamoto, S. Ikeda, *Bull. Chem. Soc.* **1972**, 1104; d) T. Yamamoto, A. Yamamoto, S. Ikeda, *Polym. Lett.* **1971**, *9*, 281; e) T. Yamamoto, A. Yamamoto, S. Ikeda, Polym. Lett. **1972**, *10*, 835; f) W. Lau, J. C. Huffman, J. K. Kochi, *Organometallics*, **1982**, *1*, 155.

[8] L. K. Johnson, C. M. Killian, M. Brookhart, *J. Am. Chem. Soc.* **1995**, *117*, 6414.

[9] a) M. H. Normant, *C. R. Acad. Sci. Paris Ser. C* **1969**, *268*, 1811; b) G. Van Koten, K. Vrieze, *Adv. Organomet. Chem.* **1982**, *21*, 151; c) R. van Asselt, E. E. C. G. Gielens, R. E. Rülke, K. Vrieze, C. J. Elsevier, *J. Am. Chem. Soc.* **1994**, *116*, 977; d) J. H. Groen, C. J. Elsevier, K. Vrieze, W. J. J. Smeets, A. L. Spek, *Organometallics* **1996**, *15*, 3445.

[10] L. K. Johnson, S. Mecking, M. Brookhart, *J. Am. Chem. Soc.* **1996**, *118*, 267.

[11] a) Drent et al. described a Pd^{II}-catalyzed copolymerization of ethene and methyl methacrylate to give low molecular weight products: E. Drent, D. H. L. Pello, W. W. Jager, *Eur. Pat. Appl.* **1994**, 589527. b) Klabunde et al. reported on copolymerization experiments of ethene with polar monomers. All trials with methyl methacrylate or vinyl acetate failed. Only comonomers with at least two CH_2 spacers between the vinyl group and the functional group led to copolymer products: U. Klabunde, S. D. Ittel, *J. Mol. Catal.* **1987**, *41*, 123. c) Norbornene derivatives containing ester groups are polymerized by (allyl)palladium(II) complexes: A. Reinmuth, J. P. Mathew, J. Melia, W. Risse, *Macromol. Chem. Rapid Commun.* **1996**, *17*, 173.

[12] a) M. Brookhart, M. I. Wagner, *J. Am. Chem. Soc.* **1994**, *116*, 3641; b) M. Brookhart, J. M. DeSimone, J. C. Barborak, F. C. Rix, S. Tahiliani, M. I.

Wagner, D. Elder, *Polym. Prepr. Am. Chem. Soc. Div. Polym. Chem.* **1994**, *35(2)*, 530.
[13] Z. Jiang, A. Sen, *J. Am. Chem. Soc.* **1995**, *117*, 4455.
[14] K. Nozaki, N. Sato, H. Takaya, *J. Am. Chem. Soc.* **1995**, *117*, 9911.
[15] Me-DUPHOS: (−)-1,2-Bis[(2*R*,5*R*)-2,5-dimethyl-1-phospholanyl]benzene; (*R*,*S*)-BINAPHOS: (*R*)-2-(diphenylphosphino)-1,1′-binaphth-2′-yl-(*S*)-1,1′-binaphthalene-2,2′-diyl phosphite.
[16] a) E. Drent, J. A. M. Van Broekhoven, M. J. Doyle, *J. Organomet. Chem.* **1991**, *417*, 235; b) E. Drent, P. H. M. Budzelaar, *Chem. Rev.* **1996**, *96*, 663; c) E. Drent, J. A. M. van Broekhoven, P. H. M. Budzelaar, *Recl. Trav. Chim. Pays-Bas* **1996**, *115*, 263.
[17] a) A. S. Abu-Surrah, R. Wursche, B. Rieger, G. Eckert, W. Pechhold, *Macromolecules* **1996**, *29*, 4806; b) B. Rieger, A. S. Abu-Surrah, Ch. Horn, R. Spahl, H.-J. Müller, *DE Pat. Appl.* **1996**, 19610358.4; c) A. S. Abu-Surrah, G. Eckert, W. Pechhold, W. Wilke, B. Rieger, *Makromol. Chem. Rapid Commun.* **1996**, *17*, 559.
[18] a) D. Brizzolara, H.-J. Cantow, K. Diederichs, E. Keller, A. J. Domb, *Macromolecules* **1996**, *29*, 191.

Deposition of Data from X-ray Structure Analyses

In order to make life easier for authors and referees the Cambridge Crystallographic Data Centre (CCDC) and the Fachinformationszentrum Karlsruhe (FIZ) have unified their procedures for the deposition of data from single-crystal X-ray structure analyses.

From now on prior to submitting your manuscripts please deposit the data for your compound(s) **electronically** at the appropriate data bank, that is, at the CCDC for organic and organometallic compounds and at the FIZ for inorganic compounds. Both data banks will be pleased to provide help (see our *Notice to Authors* in the first issue of this year). In general, you will receive a depository number from the data bank within one working day after electronic deposition; please include this number with the appropriate standard text (see our *Notice to Authors*) in your manuscript. This will enable the referees to retrieve the structure data quickly and efficiently if they need this information to reach their decision.

This is now the uniform procedure for manuscripts submitted to the journals *Angewandte Chemie, Chemische Berichte, Chemistry—A European Journal*, and *Liebigs Annalen*.

Chiral Recognition of (*R*)-(−)-1,7-Dioxaspiro-[5.5]undecane by Hexakis(2,3,6-tri-*O*-methyl)-α-cyclodextrin**

Konstantina Yannakopoulou, Dimitris Mentzafos, Irene M. Mavridis,* and Konstantina Dandika

The principles underlying the mechanism of chiral recognition, a process essential in all living systems, have been approached in studies with various model host–guest systems. Cyclodextrins (CDs), one class of chiral hosts,[1] were recognized early on as capable of binding guests with chiral discrimination,[1b,c] and this selective binding is the basis for enantiomeric resolution by chiral gas and liquid chromatography.[2] Enantiomeric species can also be differentiated in solution by NMR spectroscopy after addition of cyclodextrins and formation of diastereomeric inclusion complexes.[2e,3] Moreover, enrichment in one of the enantiomers during crystallization of CD inclusion complexes of racemic guests has been observed by X-ray crystallography.[4] Although these findings document the propensity of CDs for chiral discrimination, reliable predictive rules have not been set forth so far. Armstrong's model[5] adequately explains the observed enantioselectivity in some cases[6] but not in others.[4c,7]

We have investigated the enantioselective complexation of 1,7-dioxaspiro[5.5]undecane (**1**), the primary constituent of the sex pheromone of the female olive fly *Bactrocera oleae* and other *Bactrocera* species, by CDs.[8] Natural **1** isolated from the

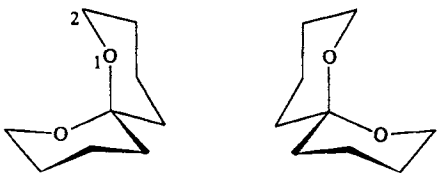

(*R*)-(−)-1 (*S*)-(+)-1

glands of the insect has been identified as the racemic mixture, and synthetic (±)-**1**[9] has the same biological activity as the natural extract. Further entomological studies, however, have suggested that the individual enantiomers may affect the behavior of male and female insects differently.[10] Several multistep enantioselective syntheses of (*R*)-(−)-**1** and the (*S*)-(+)-**1**, have established the absolute configuration of the pure enantiomers.[11] We report here on the totally selective separation of (*R*)-**1** from its (*S*) enantiomer through simple complexation with hexakis-(2,3,6-tri-*O*-methyl)-α-cyclodextrin (TMαCD), as determined by X-ray crystallography[12] and NMR spectroscopy.

A complex precipitated from an aqueous solution containing equimolar amounts of TMαCD and (±)-**1**. The precipitate was redissolved in water and stirred vigorously with *n*-pentane (TMαCD was recovered from the aqueous phase). The organic layer afforded a colorless liquid; its ^1H and ^{13}C NMR spectra are identical to those of **1**, and its optical rotation ($[\alpha]_D^{21} = -115$ ($c = 0.172$ in *n*-pentane)) is close to the literature value[11b] for (*R*)-**1** ($[\alpha]_D^{21} = -121$ ($c = 1.84$ in *n*-pentane)).[13] Additional confirmation of this remarkable resolution was obtained by chiral GC using a capillary column[14] coated with heptakis-(2,3,6-tri-*O*-methyl)-βCD (TMβCD). The chromatogram of the racemate showed two peaks but that of the extracted spiroacetal showed only one. This liquid was also examined by ^{13}C NMR spectroscopy in D_2O in the presence of two equivalents of αCD as a chiral solvating agent.[15a] Only one signal was detected for C2 (presumably due to (*R*)-**1**) at an excellent signal-to-noise ratio, indicating complete enantioselectivity, whereas the racemate displayed two distinct signals for C2 (Fig. 1). A ^{13}C NMR

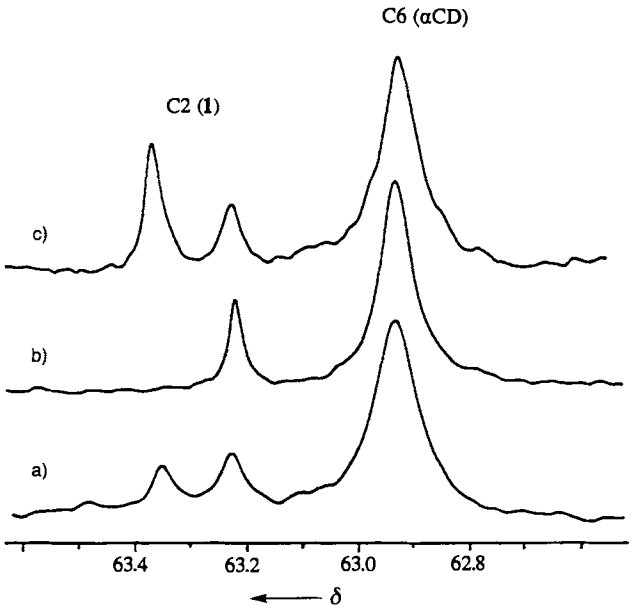

Fig. 1. Section of the ^{13}C NMR spectrum of 1,7-dioxaspiro[5.5]undecane (**1**) in D_2O in the presence of a twofold excess of αCD at 298 K (routine experiment, relaxation delay = 1 s). a) (±)-**1**, b) (*R*)-**1** only, c) **1** enriched in the (*S*) enantiomer.

titration study of (±)-**1** with TMαCD in aqueous solution showed that the exchange of the guest between free and complexed states was fast on the NMR timescale. In an inverse gated decoupling experiment the racemic guest gave rise to two ^{13}C NMR signals of the same intensity for C2.[16] Thus, the preferential binding of (*R*)-**1** by TMαCD could not be detected owing to the conditions of fast exchange for the guest, according to which the initial enantiomeric ratio (of the racemate) is detected. The chemical shift difference of the C2 signals in the racemate in the presence of αCD was much greater than in the presence of TMαCD.

The TMαCD/(*R*)-**1** complex is stable in aqueous solution; even after several days no racemization was evident by additional peaks in its ^{13}C NMR spectrum. This complex can be prepared in high yields exceeding the theoretically possible 50% owing to conversion of (*S*)-**1** to (*R*)-**1**. Gradual increase of the concentration of each reactant in the aqueous solution, from 20 mM to 80 mM led to increased yields of the (*R*)-**1** complex. The maximum yield of 77% was obtained at a concentration of 80 mM after 48 h at ambient temperature. Clearly, in aqueous solution the two enantiomers of **1** equilibrate, presumably via an open form, but only (*R*)-**1** is isolated from the precipitate. To exclude the possibility that the enantioselectivity of TMαCD

[*] Dr. I. M. Mavridis, Dr. K. Yannakopoulou, K. Dandika
Institute of Physical Chemistry
National Center for Scientific Research "Demokritos"
Aghia Paraskevi 15310, Athens (Greece)
Fax: Int. code +(1)6511766
e-mail: mavridi@cyclades.nrcps.ariadne-t.gr
Assoc. Prof. D. Mentzafos
Physics Laboratory
Agricultural University of Athens (Greece)

[**] This research was supported by the EU (VALUE CTT 472, K. Y., I. M. M., K. D).

towards (*R*)-**1** results from the differential solubility of the diastereomeric complexes TMαCD/(*R*)-**1** and TMαCD/(*S*)-**1**, we measured the binding constants $K_{(R)}$ and $K_{(S)}$. We prepared a TMβCD/(±)-**1** complex enriched in (*S*)-**1**. The ^{13}C NMR spectrum of its extract indicated that it contained at least 80% of the (*S*) enantiomer. However, in the presence of one equivalent of TMαCD in D_2O the guest racemized within a few days without formation of a precipitate. Its NMR spectrum was then similar to that of (±)-**1**, thus indicating that the (*R*) enantiomer is much more stable than its antipode. The approximate binding constant[15b] of (*R*)-**1** (6800 M^{-1}) is greater than that of the (*S*)-enriched-**1** (4000 M^{-1}); however, the latter value is only indicative since the sample was not enantiomerically pure. Therefore, (*R*)-**1** is very stable in the presence of TMαCD, whereas (*S*)-**1** converts to its enantiomer, which forms a much more stable complex. These experiments were carried out in clear solutions to eliminate solubility effects. The remarkably enantioselective binding found in aqueous solution results in the complete separation of (*R*)-**1** by precipitation as its complex with TMαCD.

The crystal structure of the precipitate[12] shows that only (*R*)-**1** guest exists in the complex. Attempts to refine the structure with complexed (*S*)-**1** alone or with a mixture of complexed (*R*)- and (*S*)-**1** failed. The complex is situated on a twofold axis. (*R*)-**1** is located at the secondary side of TMαCD and exhibits statistical disorder in the crystal. Only two of the primary methoxy groups (C63–O63 and the corresponding symmetry equivalent) of TMαCD are directed towards the exterior of the cavity; the rest are directed towards the interior, thus blocking the primary entrance (Fig. 2). As a result, the

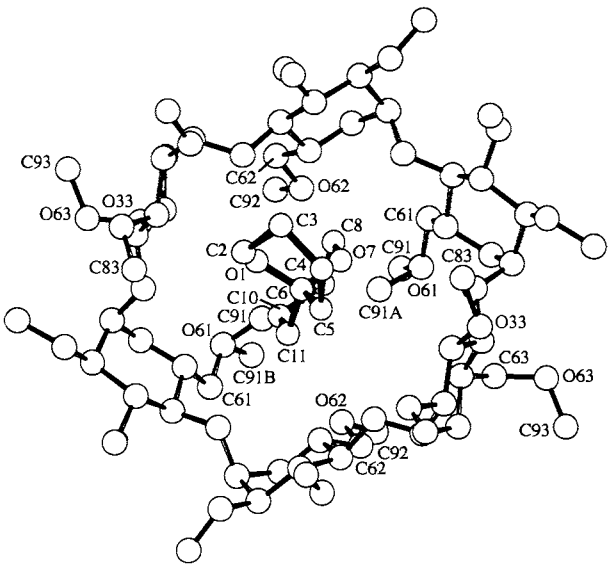

Fig. 2. ORTEP diagram of the TMαCD/(*R*)-**1** complex as viewed from the secondary side of the cyclodextrin. Note the methoxy groups O61–C91 and O62–C92 extending into the cavity on the primary side and the O33–C83 methoxy group (and its symmetry equivalent) pointing inside the cavity and interacting with O1 and O7 of the guest.

free space left to the guest, if we take into account the van der Waals radii of the host, is small (Fig. 3), and (*R*)-**1** enters the cavity only partly. The thermal parameters of the guest atoms are of the same order of magnitude as those of the host, a rather rare feature for CD complexes, implying a tight fit of the guest. Indeed, the TMαCD geometry is distorted in order to better accommodate the guest (induced fit).[17] The six glucosidic oxygen atoms form a distorted hexagon (Fig. 2), and the tilting of the glucose units with respect to the molecular axis is very uneven. These features combined with the orientation of the methoxy groups result in numerous van der Waals contacts between the guest atoms (except for the central C6) and atoms of the methoxy groups of either the host molecule or neighboring CDs; these distances range from 3.29 to 4.04 Å. The shortest distances are between the O1 and O7 atoms of (*R*)-**1** and the methoxy group C83 and its symmetry equivalent (3.29 and 3.31, respectively, Fig. 3); C–H···O interactions where O is an ether oxygen are involved. It is worth noting that most of the other contacts also involve the same kind of interactions, which are quite common in solid-state structures of carbohydrates.[18] Chiral recognition of (*S*)-**1** by a modified αCD has been attributed previously[4c] to the asymmetry imposed by the unusual substitution of the host. In the present case it is shown that a symmetrically substituted βCD is sufficiently flexible to undergo conformational changes to better accommodate the same guest. The time-averaged structure proposed for the complex TMαCD/**1** in solution[15b] from NMR studies resembles the solid-state structure in that only one ring of the guest is included.

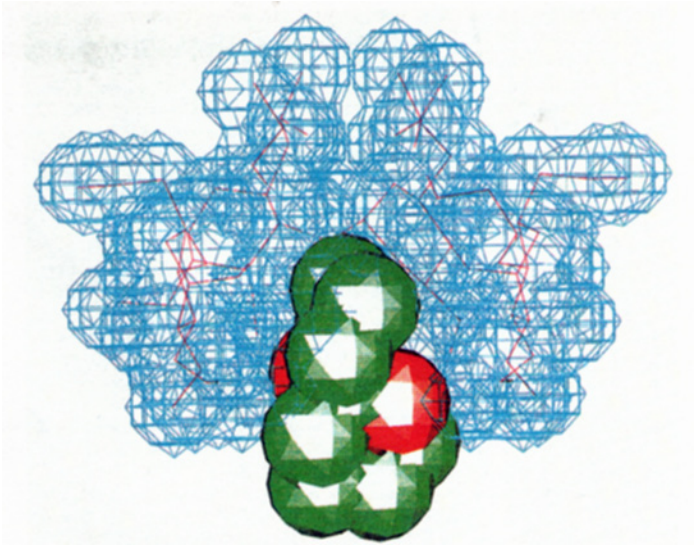

Fig. 3. Side view of the inclusion complex TMαCD/(*R*)-**1**. Van der Waals surfaces computed for the host show the free space left for the guest (CPK model, radius 1.5 Å; O1, O7 in red). The front atoms of the host have been removed for clarity [19].

In conclusion, we have observed that the inclusion of (*S*)-**1** in TMαCD is completely enantioselective in solution and in the solid state. The main requirement for chiral recognition as indicated by the crystal structure is the tight fit of host and guest achieved without the aid of conventional hydrogen bonds. In addition, (*R*)-**1** can be separated from its enantiomer in high yields and on a large scale by means of recyclable materials (TMαCD) and simple laboratory techniques. Furthermore, TMαCD can be used to store (*R*)-**1** and prevent its racemization.

Received. May 6, 1996 [Z 9101 IE]
German version: *Angew. Chem.* **1996**, *108*, 2632–2634

Keywords: chiral recognition · crystallization · cyclodextrins · enantiomeric resolution · inclusion compounds

 © VCH Verlagsgesellschaft mbH, D-69451 Weinheim, 1996 0570-0833/96/3521-2481 $ 15.00+.25/0

[1] a) W. Saenger, *Angew. Chem.* **1980**, *92*, 343–359; *Angew. Chem. Int. Ed. Engl.* **1980**, *19*, 344–362; b) F. Cramer, *Angew. Chem.* **1952**, **64**, 136; c) J. Knabe, N. S. Agarwal, *Dtsch. Apoth. Ztg.* **1973**, *113*, 1449–1453.

[2] a) V. Schurig, H. -P. Nowotny, *Angew. Chem.* **1990**, *102*, 969; *Angew. Chem. Int. Ed. Engl.* **1990**, *29*, 939–956; b) S. Li, W. C. Purdy, *Chem. Rev.* **1992**, *92*, 1457–1470; c) W. A. König in *New Trends in Cyclodextrins and Derivatives* (Ed.: D. Duchêne), Editions de Santé, **1991**, Chapter 16, pp. 551–594; d) M. L. Hilton, D. W. Armstrong, *ibid*, Chapter 15, pp. 515–549; e) J. E. H. Köhler, M. Hohla, M. Richters, W. A. König, *Angew. Chem.* **1992**, *104*, 362; *Angew. Chem. Int. Ed. Engl.* **1992**, *31*, 319–320.

[3] a) A. F. Casey, A. D. Mercer, *Magn. Reson. Chem.* **1988**, *26*, 765–774; b) A. Botsi, K. Yannakopoulou, E. Hadjoudis, B. Perly, *J. Chem. Soc. Chem. Commun.* **1993**, 1085–1086; c) J. Klein, H. Hartenstein, D. Sicker, *Magn. Reson. Chem.* **1994**, *32*, 727–731.

[4] a) K. Harata, K. Uekama, M. Otagiri, F. Hirayama, *J. Incl. Phenom.* **1984**, *2*, 583–594; b) J. A. Hamilton, L. Chen, *J. Am. Chem. Soc.* **1988**, *110*, 5833–5841; c) N. Rysanek, G. Le Bas, F. Villain, G. Tsoucaris, *Acta Crystallogr. Sect. C* **1992**, *48*, 1466–1471.

[5] a) D. W. Armstrong, T. J. Ward, R. D. Armstrong, T. E. Beesley, *Science* **1986**, *232*, 1132–1135; b) J. I. Seeman, H. V. Secor, D. W. Armstrong, K. D. Timmons, T. J. Ward, *Anal. Chem.* **1988**, *60*, 2120–2127.

[6] a) K. B. Lipkowitz, S. Raghothama, J. Yang, *J. Am. Chem. Soc.* **1992**, *114*, 1554–1562; b) M. V. Rekharsky, R. N. Goldberg, F. P. Schwarz, Y B. Tewari, P. D. Ross, Y. Yamashoji, Y. Inoue, *ibid.* **1995**, *117*, 8830–8840.

[7] a) K. Kano, K. Yoshiyasu, S. Hashimoto, *J. Chem. Soc. Chem. Commun.* **1989**, 1278–1279; b) K. Kano, M. Tashumi, S. Hashimoto, *J. Org. Chem.* **1991**, *56*, 6579–6586.

[8] a) B. E. Mazomenos, G. E. Haniotakis, *J. Chem. Ecol.* **1985**, *11*, 397–405; b) M. T. Fletcher, W. Kitching, *Chem. Rev.* **1995**, *95*, 789–828, and references therein.

[9] F. Perron, K. F. Alibizati, *Chem. Rev.* **1989**, *89*, 1617–1661.

[10] G. Haniotakis, W. Francke, K. Mori, H. Redlich, V. Schurig, *J. Chem. Ecol.* **1986**, *12*, 1559–1568.

[11] a) H. Redlich, W. Francke, *Angew. Chem.* **1984**, *906*, 56; *Angew. Chem. Int. Ed. Engl.* **1984**, *23*, 519–520; b) K. Mori, H. Watanabe, K. Yanagi, M. Minobe, *Tetrahedron* **1985**, *41*, 3663–3672; c) M. T. Fletcher, M. F. Jacobs, W. Kitching, S. Krohn, R. A. I. Drew, G. E. Haniotakis, W. Francke, *J. Chem. Soc. Chem. Commun.* **1992**, 1457–1459.

[12] Crystal data: $C_{27}H_{48}O_{15}\cdot(C_9H_{16}O_2)_{0.5}\cdot(H_2O)_3$, $M_r = 728.82$, space group $C222_1$, $a = 24.0021(17)$, $b = 14.8120(13)$, $c = 21.7916(18)$ Å; $V = 7747$ Å^3, $Z = 8$, $\rho_{calc} = 1.277$ g cm^{-3}, $R = 0.0828$ for 1540 unique observed reflections with $F_0 \geq 4.0\sigma(F_0)$. Full description of the structure will be published elsewhere (manuscript in preparation).

[13] The small deviation in the optical rotation from the literature value is due to the presence of traces of TMαCD ($[\alpha]_D^{21} = 140$) in (*R*)-**1**, which could not be easily removed.

[14] Column type: Rt-βDEX$_m$ (30 m, 0.32 i.d.), Restek Corporation; 70 C isothermal run, He carrier gas; Retention times: $t_R(S) = 19.33$ s, $t_R(R) = 19.74$ s, resolution 0.6; we thank A. Ortiz, Dr. V. Roussis, and Dr. V. Mazomenos for the GC analysis.

[15] a) A. Botsi, Ph.D. Thesis, University of Athens, **1994**; b) A. Botsi, K. Yannakopoulou, B. Perly, E. Hadjoudis, *J. Org. Chem.* **1995**, *60*, 4017–4023.

[16] This quantitative ^{13}C NMR experiment (inverse gated decoupling, INVGATE) was carried out with a delay time of 10 s (T_1 measurements of (±)-**1** in aqueous solution suggested a maximum relaxation time of 1.45 s for the protonated carbon atoms) on a Bruker AC 250 MHz NMR spectrometer at 298 K.

[17] K. Harata, *J. Chem. Soc. Perkin 2* **1990**, 799–804.

[18] T. Steiner, W. Saenger, *J. Am. Chem. Soc.* **1992**, *114*, 10146–10154.

[19] Molecular modeling program "0", T. A. Jones, M. Kjelgaad, Version 5.9, **1993**.

A Ferrimagnetic Manganese Oxide with a Layered Perovskite Structure: $YBaMn_2O_5$**

Jon P. Chapman, J. Paul Attfield,* Michele Molgg, Chris M. Friend, and Tim P. Beales

There is renewed interest in perovskite-type $Ln_{1-x}A_xMnO_3$ phases (Ln = trivalent lanthanide; A = Ca, Sr, or Ba), following the discovery of giant negative magnetoresistances (GMR) at the transition between their conducting ferromagnetic and insulating paramagnetic states.[1] GMR has been found in both thin film[2] and sintered polycrystalline samples[3] with $x \approx 0.3$, and anisotropic GMR phenomena have recently been reported in layered Ruddlesden–Popper type perovskites $(Ln,A)_{n+1}Mn_nO_{3n+1}$ for $n = 2$.[4] Similar effects have also been observed in the oxygen-deficient cubic pyrochlore $Tl_2Mn_2O_{7-\delta}$.[5]

The chemical features common to these materials are a highly connected Mn-O-Mn network, with a three-dimensional or multilayered structure, and a mean Mn oxidation state between +3 and +4, that is hole-doped Mn^{III}. The hole-doping suppresses the long-range cooperative Jahn–Teller distortion found in the parent Mn^{III} structure and gives rise to the ferromagnetic conducting phase at low temperatures through a "double exchange" mechanism.[6] This shows some similarities to the hole-doping of layered Cu^{II} oxide perovskites which enables superconductivity to occur.[7] The structural similarities between these two groups of materials suggests that new Mn analogues of the high-temperature superconducting Cu oxides may be prepared. There are also chemical analogies, for example, Cu^{II} forms many oxocarbonates with Ba or Sr, such as $(Ba,Sr)_2CuO_2CO_3$,[8] and a Mn^{III} oxocarbonate, $Sr_5Mn_4O_{10}CO_3$, has recently been reported.[9] We have attempted to prepare a Mn analogue of $YBa_2Cu_3O_{7-\delta}$, in which Y^{III}/Ba^{II} cation ordering gives rise to oxygen vacancy ordering and hence anisotropic electronic properties.[10] This has resulted in the discovery of the new phase $YBaMn_2O_5$.

Attempts to prepare triple perovskite "$YBa_2Mn_3O_{9-x}$" phases by sintering mixtures of $BaMnO_{3-\delta}$ and $YMnO_3$ at 900–1100 °C under a variety of atmospheres were unsuccessful. However, a new perovskite-related phase was observed in samples treated under reducing conditions, for example at 1000 °C under argon containing less than 1 ppm O_2, and this has been identified as $YBaMn_2O_5$. This double perovskite phase is difficult to prepare in a pure form and long reaction times, in excess of a week, are required at 1000 °C under a controlled oxygen atmosphere. We have found syntheses in sealed, evacuated, silica glass tubes to be the most reliable (see Experimental Procedure).

The Rietveld-fitted X-ray powder diffraction pattern of $YBaMn_2O_5$ is shown in Figure 1 and the refined parameters and

[*] Dr. J. P. Attfield, J. P. Chapman
IRC in Superconductivity, University of Cambridge
Madingley Road, Cambridge CB3 0HE (UK)
and
Department of Chemistry, Lensfield Road
University of Cambridge, Cambridge CB2 1EW (UK)
Fax: Int. code +(1223) 336362
e-mail: jpa14@cam.ac.uk

Dr. M. Molgg, Dr. C. M. Friend, Dr. T. P. Beales
BICC Cables Ltd., Superconductivity Group
Hedgeley Road, Hebburn, Tyne & Wear NE31 1XR (UK)

[**] We thank A. Tyler (IRC), Dr. G. Wltschek (IRC) and Dr. L. Le Lay (BICC) for assistance with measurements. J. P. C. thanks BICC Cables Ltd. and the UK Engineering and Physical Sciences Research Council for a CASE studentship. This work was funded by BICC Cables Ltd. and the European Union under contract BRE2-CT93-3035.

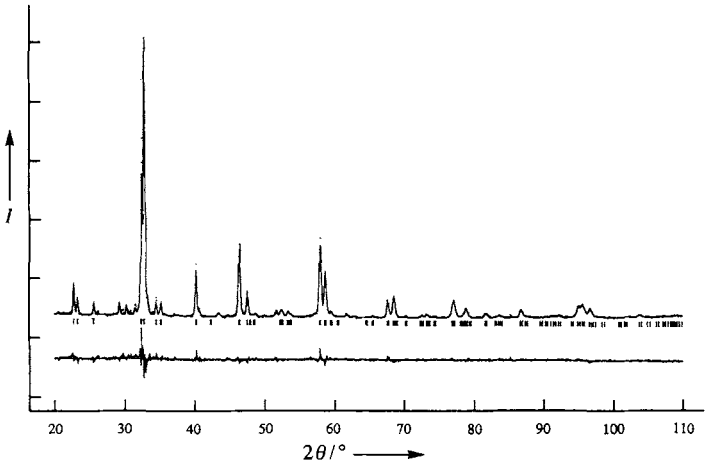

Fig. 1. Observed (points), calculated (full line), and difference powder X-ray diffraction profiles with the reflection positions of $YBaMn_2O_5$ marked.

Table 1. Atomic parameters and calculated distances [Å] and angles [°] for $YBaMn_2O_5$ [a].

Atom	Position	x	y	z	U_{iso} [Å^2]
Ba	1*d*	0.5000	0.5000	0.5000	0.0056(9)
Y	1*c*	0.5000	0.5000	0.0000	0.012(1)
Mn	2*g*	0.0000	0.0000	0.2385(7)	0.0081(7)
O1	4*i*	0.5000	0.0000	0.1868(8)	0.021(2)
O2	1*b*	0.0000	0.0000	0.5000	0.021
Distances					
Ba–O1	× 8	3.098(5)	Mn–O1	× 4	2.000(2)
Ba–O2	× 4	2.7722(1)	Mn–O2	× 1	2.004(5)
Y–O1	× 8	2.427(4)	Mn···Mn	× 1	3.654(10)
Angles					
O1-Mn-O1	× 4	87.8(1)	Mn-O1-Mn	× 1	157.1(5)
O1-Mn-O1	× 2	157.1(5)	Mn-O2-Mn	× 1	180
O1-Mn-O2	× 4	101.4(2)			

[a] The unit cell is tetragonal, space group $P4/mmm$, with $a = 3.9204(1)$ and $c = 7.6614(3)$ Å.

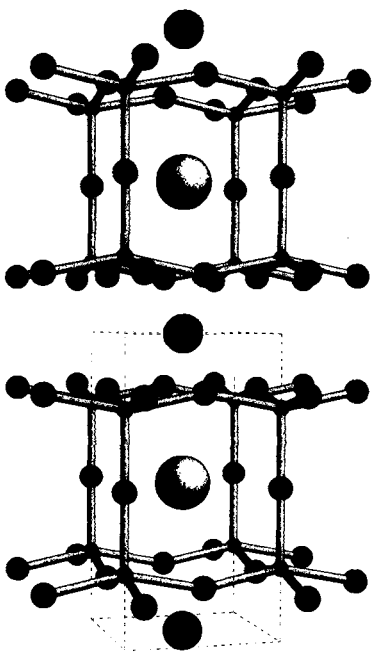

Fig. 2. Crystal structure and unit cell of $YBaMn_2O_5$. The Mn–O bonds are drawn. The black unbonded atoms are Y atoms, the white unbonded ones are Ba atoms.

distances and angles are presented in Table 1. The structure (Fig. 2) shows that a layered arrangement has been formed due to the presence of oxygen vacancies in the yttrium plane, reducing the yttrium coordination number to 8, while barium occupies a typical 12-coordinate perovskite site. The manganese–oxygen network consists of double layers of identical MnO_5 square pyramids linked through all their apices, and the basal and apical Mn–O distances are almost equal. The $YBaMn_2O_5$ structure is derived from the $YBa_2Cu_3O_7$ arrangement by removal of the chains of CuO_4 square planes between the two sheets of CuO_5 square pyramids. This structure type is not found in the Y-Ba-Cu-O system, but is adopted by $YBaCuFeO_{5+\delta}$[11] and by $YBaCo_2O_{5+x}$ $(0 < x < 0.5)$.[12]

The oxygen stoichiometry of $YBaMn_2O_5$ is confirmed by thermogravimetric reduction in H_2/N_2 (see Experimental Procedure). In air or oxygen, $YBaMn_2O_5$ decomposes irreversibly into $YMnO_3$ and $BaMnO_{3-\delta}$ above 220 °C. Attempts to intercalate additional oxygen into the yttrium plane to give $YBaMn_2O_{5+x}$ compositions analogous to those of the above isostructural materials were unsuccessful. For example, after heating the sample in air at 200 °C for 6 h, both the unit cell parameters determined by Rietveld analysis and the magnetic ordering temperature measured by alternating current (AC) susceptometry were unchanged.

Both direct current (DC) and AC susceptibility measurements show a magnetic ordering transition at 167 K. A ferromagnetically ordered component is clearly revealed by the peak in the imaginary susceptibility (Fig. 3) and by the observation of hysteresis loops at 10 K (Fig. 4) and 130 K, but not at 250 K. However, the saturated moment obtained from both the DC susceptibility and hysteresis measurements is only about 0.5 μ_B per $YBaMn_2O_5$ formula unit, compared to the total moment of about 9 μ_B that would result from a ferromagnetically ordered

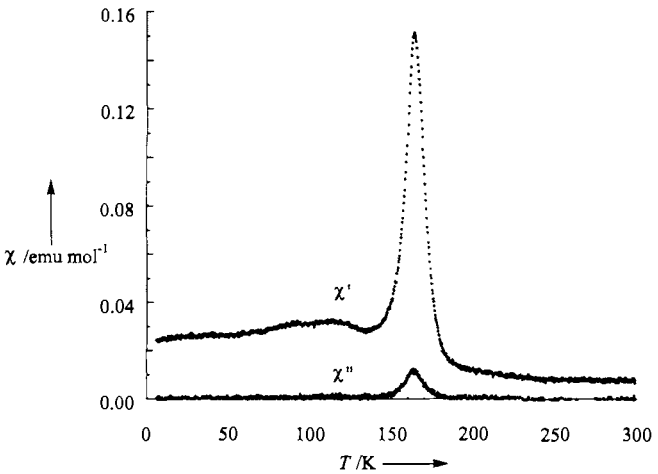

Fig. 3. Real (χ') and imaginary (χ'') components of the AC magnetic susceptibility of $YBaMn_2O_5$.

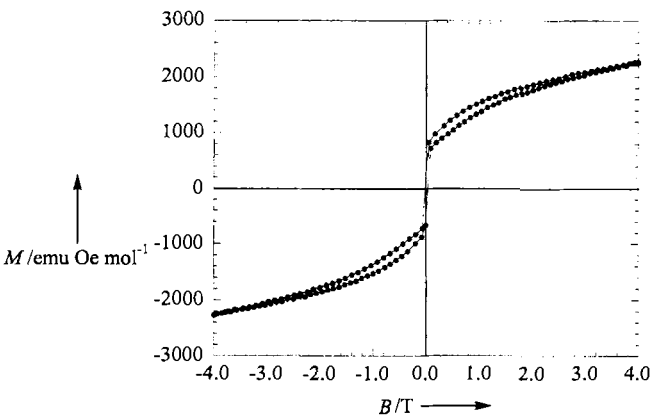

Fig. 4. Magnetization hysteresis loop for $YBaMn_2O_5$ at 10 K.

 © VCH Verlagsgesellschaft mbH, D-69451 Weinheim, 1996 0570-0833/96/3521-2483 $ 15.00+.25/0

array of $S = 5/2$ Mn^{II} and $S = 2$ Mn^{III} spins. Hence, the overall order is ferrimagnetic, with a small ferromagnetic component due to the inexact cancellation of antiferromagnetically ordered sublattices.

The ferrimagnetic order in $YBaMn_2O_5$ is consistent with ordering of the Mn^{II} and Mn^{III} valences, as the high electrical resistivity shows that the d-electrons are localized below at least 300 K. Valence ordering in perovskite-related structures results in an alternation of valence states (a commensurate charge density wave), as is found in the perovskite $Ba_2Bi^{III}Bi^{V}O_6$.[13] This will give rise to the arrangement shown in Figure 5 for

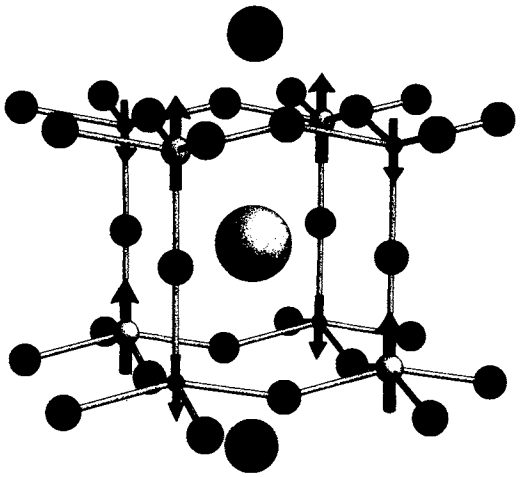

Fig. 5. Proposed valence and magnetic ordering model for $YBaMn_2O_5$ showing an alternation of Mn^{II} (large, lightly shaded spheres) with $S = 5/2$ spins (up) and Mn^{III} (small, filled spheres) with $S = 2$ spins (down). The other atoms are labeled as in Figure 2.

$YBaMn_2O_5$, in which each Mn^{II} ion is linked through Mn-O-Mn bridges to five Mn^{III} ions, and vice versa. These near-linear Mn^{II}-O-Mn^{III} linkages will give rise to antiferromagnetic interactions between the cation spins, due to both σ and π superexchange, hence in the magnetically ordered state all the $S = 5/2$ Mn^{II} spins will be antiparallel to the $S = 2$ Mn^{III} spins. This results in a net spin of 1/2 per $YBaMn_2O_5$ formula unit, ideally giving a saturated moment of 1 μ_B. This is consistent with the small observed value of about 0.5 μ_B allowing for moment reduction due to Mn–O covalency.[14] If extended over long distances, the proposed valence ordering will give rise to a $\sqrt{2}a \times \sqrt{2}a \times c$ superstructure which is not observed in the present X-ray data, and powder neutron diffraction will be needed to detect this and confirm the ordered magnetic arrangement.

In conclusion, we have prepared a new, layered perovskite $YBaMn_2O_5$. This phase appears only to be stable with an oxygen content close to the stoichiometric value, at which the mean Mn oxidation state is +2.5. This is an unusually low oxidation state for Mn in a perovskite oxide, as values between +3 and +4 are normally found, and so opens up the possibility of preparing electron-doped phases (relative to Mn^{III}) with conducting and magnetic properties similar to those of the hole-doped phases. In $YBaMn_2O_5$, the exact +2.5 oxidation state leads to Mn^{II}/Mn^{III} valence ordering and insulating electronic behavior below 300 K, which results in a ferrimagnetic state with a small resultant moment below the ordering transition at 167 K.

Experimental Procedure

An almost phase pure sample of $YBaMn_2O_5$ (2 g) was synthesized from an equimolar mixture of $YMnO_3$, BaO, and MnO. $YMnO_3$ was prepared by heating Y_2O_3 and $MnCO_3$ in air at 1350 °C. BaO and MnO were produced by decomposing BaO_2 and $MnCO_3$ under flowing H_2/N_2 at 900 °C. All the reactants were found to be phase pure by powder X-ray diffraction. The reaction mixture was ground, pelleted, sealed in an evacuated silica glass tube, and heated for four days at 1000 °C. This treatment was repeated three times.

Thermogravimetric reduction of $YBaMn_2O_5$ (51.8 mg) under a $0.05H_2 + 0.95N_2$ mixture (flow rate 58 $cm^3 min^{-1}$, heating rate 2 °C min^{-1}) showed a single-step reduction starting at 400 °C. X-ray analysis showed the product to be a mixture of Ba^{II}, Y^{III}, and Mn^{II} oxides. The 1.9% mass loss for this process corresponds to that calculated for 5.0 oxygen atoms per formula unit. Oxidation of $YBaMn_2O_5$ under flowing O_2 resulted in a single weight uptake between 220 and 400 °C to give $YMnO_3$ and $BaMnO_{3-\delta}$. The observed 3.0% weight change is less than the theoretical value for this reaction (3.8%) which may be due to a significant oxygen deficiency (δ) in the latter phase.

X-ray powder diffraction data were recorded for $2\Theta = 20$–$110°$ on a Philips PW1710 diffractometer using $Cu_{K\alpha}$ radiation, counting for 15 s per 0.02° step. Rietveld analysis [15] using the GSAS package [16] enabled the structural model to be refined, and the contributions from traces of secondary phases ($YMnO_3$ and MnO) to the profile were also fitted (Fig. 1). The refined model for $YBaMn_2O_5$ (Table 1 and Fig. 2) gave residuals $R_{WP} = 0.047$, $R_P = 0.033$, and $R_F = 0.073$. No significant Y/Ba cross-substitution or Mn deficiency was found by X-ray refinement, confirming the cation stoichiometry.

Magnetic measurements between 4 and 300 K were performed on a Quantum Design DC SQUID magnetometer and AC susceptometer. The DC magnetization was measured in a field of 2.0 T and the AC measurement used a field of 0.1 mT at a frequency of 105 Hz. DC hysteresis loops were recorded at 10, 130, and 250 K, while the applied field was swept continuously at 10 mTs^{-1}. The resistivity of a sintered pellet of $YBaMn_2O_5$ was found to be greater than 10^5 Ωcm between 30 and 300 K.

Received: June 3, 1996 [Z9185IE]
German version: *Angew. Chem.* **1996**, *108*, 2634–2637

Keywords: magnetic properties · manganese compounds structure elucidation · superconductors · yttrium compounds

[1] G. H. Jonker, J. H. Van Santen, *Physica*, **1950**, *16*, 337–349.
[2] R. von Helmholt, J. Wecker, B. Holzapfel, L. Schultz, K. Samwer, *Phys. Rev. Lett.* **1993**, *71*, 2331-2333.
[3] B. Raveau, A. Maignan, V. Caignaert, *J. Solid State Chem.* **1995**, *117*, 424–426.
[4] Y. Moritomo, A. Asamitsu, H. Kuwahara, Y. Tokura, *Nature* **1996**, *380*, 141–144.
[5] Y. Shimakawa, Y. Kubo, T. Manako, *Nature* **1996**, *379*, 53–55.
[6] C. Zener, *Phys. Rev. 1951*, **82**, 403–405.
[7] J. B. Torrance, A. Bezinge, A. I. Nazzal, T. C. Huang, S. S. Parkin, D. T. Keane, S. L. LaPlaca, P. A. Horn, G. A. Held, *Phys. Rev. B* **1989**, *40*, 8872–8877.
[8] K. Kinoshita, T. Yamada, *Nature* **1992**, *357*, 313–315.
[9] V. Caignaert, B. Domenges, B. Raveau, *J. Solid State Chem.* **1995**, *120*, 279–289.
[10] W. I. F. David, W. T. A. Harrison, J. M. F. Gunn, O. Moze, A. K. Soper, P. Day, J. D. Jorgensen, D. G. Hinks, M. A. Beno, L. Soderholm, D. W. Capone II, I. K. Schuller, C. U. Segre, K. Zhang, J. D. Grace, *Nature* **1987**, *327*, 310–312.
[11] L. Er Rakho, C. Michel, P. Lacorre, B. Raveau, *J. Solid State Chem.* **1988**, *73*, 531–535.
[12] W. Zhou, *Chem. Mater.* **1994**, *6*, 441–447.
[13] D. E. Cox, A. W. Sleight, *Acta Crystallogr. Sect. B* **1979**, *35*, 1–8.
[14] B. C. Tofield, *The Study of Covalency by Magnetic Neutron Scattering*, Springer, Heidelberg, **1975**.
[15] H. M. Rietveld, *J. Appl. Crystallogr.* **1969**, *2*, 65-71.
[16] A. C. Larson, R. B. Von Dreele, Los Alamos Laboratory Rep. No. LA-UR-86-748, **1987**.

 © VCH Verlagsgesellschaft mbH, D-69451 Weinheim, 1996 0570-0833/96/3521-2484 $ 15.00+.25/0

Space-Separated 1,10-Phenanthroline, 4,5-Diazafluorene, or 3,6-Di(2-pyridyl)pyridazine Units as Ligands in Diruthenium Complexes: Preliminary Studies of Metal–Metal Interactions**

Ronald N. Warrener,* Aurélio B. B. Ferreira, Austin C. Schultz, Douglas N. Butler, F. Richard Keene,* and Laurence S. Kelso

There has been much activity in the field of intramolecular energy transfer and electron transfer in large molecular assemblies, and the next advances will clearly require sophisticated molecular design. Where metal complexes are involved as the light-harvesting chromophore[1] the design and construction of ligands becomes an important component. Studies on intramolecular electron transfer have been reported in which metal complexes have been tethered to redox-active chromophores, but almost all of these systems contain flexible linkages.[2] Elegant syntheses have been reported recently for fully conjugated diad systems incorporating the 1,10-phenanthroline moiety as the bidentate ligand,[3] and we have described the first molecular rack (molrac) in which two units of the same ligand are spatially separated.[4] We report here on the preparation of a new set of rigid bis(bidentate ligand) structures in which the individual bidentate ligands (1,10-phenanthroline, 4,5-diazafluorene, or 3,6-di(2-pyridyl)pyridazine) are fused to an alicyclic framework.

The versatile spacers in molracs permit the development of bridging ligands in which the ligating groups are placed at a set distance and relative orientation in space. These compounds should allow assessment of the factors controlling intramolecular energy- and electron-transfer processes in polymetallic species, as well as lead to new reagents for the study of self-assembly processes.[5] Rigid alicyclic frameworks have been used in molrac systems since they have proven their worth in diad and triad systems devoid of metal centers[6] and are available in an increasing range of shapes and sizes.[4, 7–10]

The typical olefinic spacers in the molracs have norbornene or cyclobutene diester end groups (or mixtures thereof), and these offer different dienophilic character. When the cycloaddition reagents **3**, **2**, and **1** (Scheme 1) are used to deliver the specific ligand center, it is possible to introduce 3,6-di(2-pyridyl)-pyridazine,[9] 1,10-phenanthroline,[4] and 4,5-diazafluorene groups, respectively,[10] to the norbornene end, and 1,10-phenanthroline and 4,5-diazafluorene functionalization to the cyclobutene diester end of molracs. Given that these bidentate ligands can be attached in homo or hetero pairs as shown herein, and that the 4,5-diazafluorene is linked orthogonally to the plane of the spacer whereas the other two ligands are fused in a coplanar fashion, numerous ligand and geometric variants are available by this procedure.

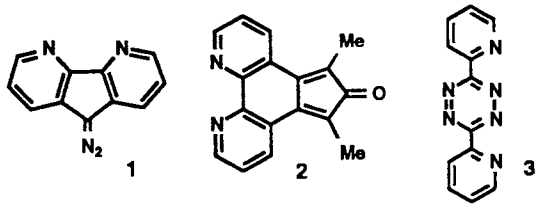

Scheme 1. Ligand-delivery agents used in this study.

For the production of molrac systems containing two diazafluorene (DAF) ligands, 9-diazo-4,5-diazafluorene (DADAF) **1** was employed as the delivery agent for 4,5-diazafluorene. Reaction of the known bis(cyclobutene) **4**[11] with excess **1** (Scheme 2) produced a regiomeric pair of pyrazolines of type **5**, which were not separated but thermally deazotized to form the bisligand **6** (63% yield) (bisligand = a molrac having two ligand groups).[12] The ^{1}H NMR resonances[13] of the bisligand **6** are entirely in keeping with the assigned structure. This reaction is general and more extended spacer bis-DAF ligands have been produced in our laboratory.[14]

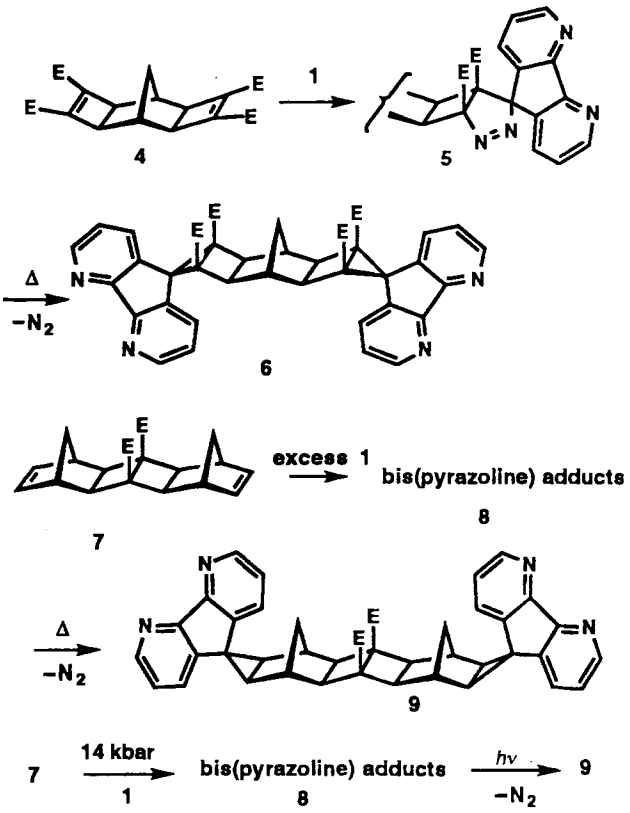

Scheme 2. Synthesis of molracs **6** and **9** in which the ligand units are coplanar with and orthogonal to the central spacer, respectively.

[*] Prof. Dr. R. N. Warrener, A. C. Schultz
Centre for Molecular Architecture, Central Queensland University Rockhampton, Queensland, 4702 (Australia)
Fax: Int. code +(79)309917
e-mail: r.warrener@cqu.edu.au
Dr. F. R. Keene, L. S. Kelso
Department of Chemistry and Chemical Engineering
School of Molecular Sciences
James Cook University of North Queensland
Townsville, Queensland 4811 (Australia)
Fax: Int. code +(77)814600
e-mail: richard.keene@jcu.edu.au
Dr. A. B. B. Ferreira
Departamento de Química, ICE
Universidade Federal Rural do Rio de Janeiro (Brazil)
Dr. D. N. Butler
Department of Chemistry, York University
North York (Canada)

[**] This work was funded by the Australian Research Council (ARC Senior Research Fellowhip to R. N. W. (1992–1996), grants to R. N. W. and F. R. K.) and Central Queensland University. Dr. G. A. Heath and co-workers (Australian National University) are thanked for their assistance in undertaking spectroelectrochemical studies on the dinuclear species. D. N. B thanks the Centre for Molecular Architecture, Central Queensland University for the award of a Senior Visiting Fellowship (1995).

 © VCH Verlagsgesellschaft mbH, D-69451 Weinheim, 1996 0570-0833/96/3521-2485 $ 15.00+.25/0

Addition of DADAF **1** to the norbornene π-bonds of bis(olefin) **7**[9] (Scheme 2) was sluggish and required prolonged heating (toluene, reflux, 60 h). Addition of DADAF **1** (fourfold excess) in three portions to **7**, over a period of 60 h, afforded **9** in 68% yield. Alternatively, **9** could be produced by photochemical deazotization of the bis(pyrazolines) **8**, themselves generated under high-pressure conditions (14 kbar, room temperature, CH_2Cl_2 from **7** and **1**.

While an X-ray structure of a mono-DAF-substituted molrac has been reported,[10] the bisligand described herein has only been obtained as microcrystals unsuitable for single-crystal structure analysis. Since the results of molecular modeling (SPARTAN, AM1) are in good agreement with the X-ray derived parameters in molrac systems, computational techniques (AM1) can be used to obtain structural parameters such as separation distances and shapes.

Cyclopentadienone **2**[4] was used as the delivery agent for the 1,10-phenanthroline ligand; it served as a standard electron-demand diene in Diels–Alder reactions with olefins in the order of reactivity cyclobutene-1,2-diesters > benzonorbornenes > nor-bornenes.[4] Diels–Alder addition of **2** to bis(cyclobutene) **4** occurred stereospecifically to produce first the monoadduct **10** and then the bisadduct **11** (Scheme 3). The C_s symmetry of **11**

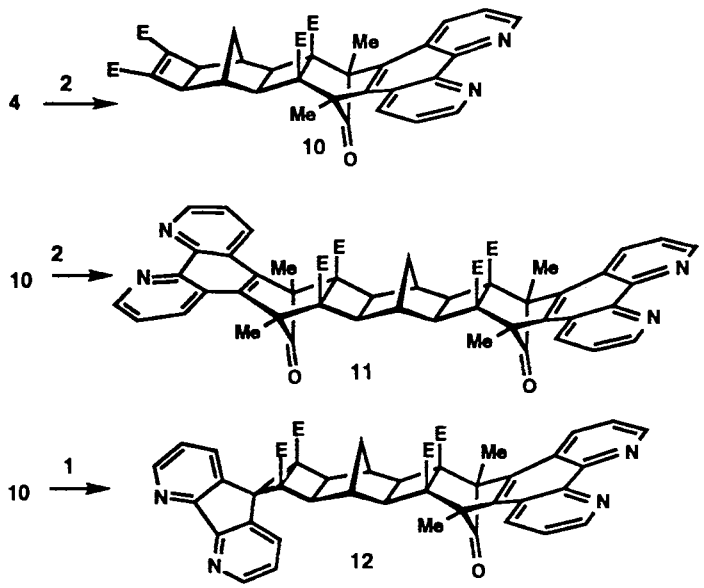

Scheme 3. Reaction of cyclopentadienone **2** with diene **4** produces the monoadduct **10**; reaction with more **4** provides the bisligand **11**. Reaction of **10** with DADAF **1** yields the mixed bisligand **12**.

was supported by its ^1H and ^{13}C NMR spectra and the assigned stereochemistry by the upfield position of the ester methyl proton resonances ($\delta = 3.14$). Separate reaction of **10** with DADAF **1** to form **12** led to the first of the mixed ligand systems. The two ligands bear an orthogonal relationship to one another, which is reflected in the ^1H NMR shifts of the two sets of methyl ester resonances; the phenanthroline ligand shields the proximate ester groups ($\delta = 3.16$), whereas the diazafluorene ring lying orthogonal deshields the other set ($\delta = 3.60$).

Reaction of Smith's diene[15] with 3,6-di(2-pyridyl)-*s*-tetrazine/DDQ (DDQ = 2,3-dichloro-5,6-dicyanobenzoquinone) according to our reported procedure[9] occurred preferentially at the norbornene π-center to produce the fused dpp molrac **13** (Scheme 4). Treatment of **13** with **1** gives the mixed bisligand **14**,

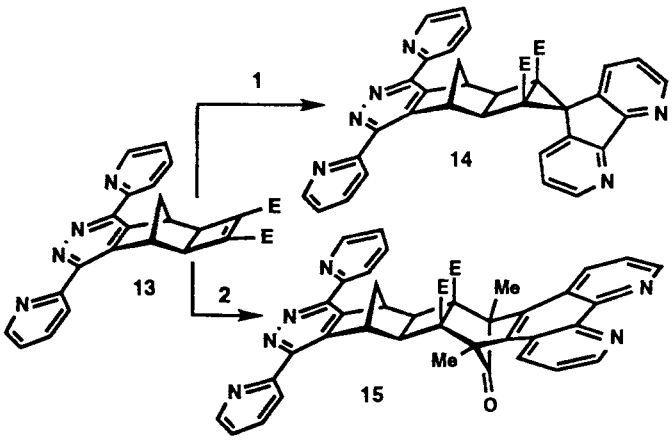

Scheme 4. Synthesis of mixed bisligands in which the two ligand units are orthogonal (**14**) and roughly parallel to each other (**15**).

where the two ligands again have an orthogonal relationship. The alternative reaction of **13** with DAPC **2** produced the bisligand **15** in which the two ligands are now parallel.

In conclusion, the versatile ligand-delivery agents **1** (for 4,5-diazafluorene), **2** (for 1,10-phenanthroline), and **3** (for 3,6-di-(2-pyridyl)pyridazine) can be attached to bis(olefins) to produce an array of doubly(bidentate ligand) molracs of varied size and geometry through simple cycloaddition reactions.

The bridged diruthenium species $[\{Ru(bpy)_2\}_2(\mu\text{-BL})]^{4+}$ (BL = **6**, **9**, **11**; bpy = 2,2′-bipyridine) were synthesized by reaction of the respective ligands with excess $[Ru(bpy)_2(CF_3SO_3)_2]$ in chloroform/2-methoxyethanol mixtures under microwave conditions.[16, 17] In all three cases, electrochemical studies

Table 1. Selected physical data for representative compounds.

6: M.p. >340 °C (decomp); yield 63%; ^1H NMR (300 MHz, $CDCl_3$): $\delta = 8.86$ (dd, $J = 1.2$, 4.8 Hz, 2H), 8.73 (dd, $J = 1.4$, 4.8 Hz, 2H), 8.01 (dd, $J = 1.2$, 8.1 Hz, 2H), 7.87 (dd, $J = 1.4$, 8.1 Hz, 2H), 7.41 (dd, $J = 4.8$, 8.1 Hz, 2H), 7.24 (dd, $J = 4.8$, 8.1 Hz, 2H), 3.63 (s, 12H), 3.09 (s, 4H), 2.93 (s, 2H), 2.65 (s, 2H); ^{13}C NMR (75 MHz, $CDCl_3$): $\delta = 165.6$, 160.1, 157.2, 150.2, 150.0, 136.6, 134.9, 133.5, 131.9, 122.5, 122.3, 52.2, 46.5, 44.6, 42.2, 38.9, 38.7.

9: M.p. >340 °C (decomp); yield 68%; ^1H NMR (300 MHz, $CDCl_3$): $\delta = 8.66$ (br. d, $J = 4.7$ Hz, 4H), 7.98 (dd, $J = 1.2$, 8.3 Hz, 2H), 7.15–7.35 (m, 6H), 3.78 (s, 6H), 2.86 (s, 4H), 2.73 (s, 4H), 2.14 (br. s, 4H), 1.95 (s, 4H).

10: M.p. 290 °C (decomp); yield 14%; ^1H NMR (300 MHz, $CDCl_3$): $\delta = 9.20$ (dd, $J = 4.2$, 1.5 Hz, 2H), 8.54 (dd, $J = 8.5$, 1.5 Hz, 2H), 7.65 (dd, $J = 8.4$, 4.3 Hz, 2H), 3.81 (s, 6H), 3.16 (s, 6H), 2.69 (s, 2H), 2.65 (s, 2H), 2.15 (s, 2H), 2.07 (s, 6H), 1.85 (d, $J = 12.6$ Hz, 1H), 1.40 (d, $J = 12.6$ Hz, 1H).

11: M.p. 315 °C (decomp); yield 68%; ^1H NMR (300 MHz, $CDCl_3$): $\delta = 9.21$ (dd, $J = 4.2$, 1.5 Hz, 4H), 8.54 (dd, $J = 8.5$, 1.6 Hz, 4H), 7.65 (dd, $J = 8.4$, 4.2 Hz, 4H), 3.14 (s, 12H), 3.01 (s, 2H), 2.10 (s, 4H), 2.09 (s, 12H), 1.96 (s, 2H).

12: M.p. 281 °C (decomp); yield 44%; ^1H NMR (300 MHz, $CDCl_3$): $\delta = 9.23$ (dd, $J = 4.2$, 1.5 Hz, 2H), 8.85 (dd, $J = 4.8$, 1.0 Hz, 1H), 8.71 (dd, $J = 4.7$, 1.3 Hz, 1H), 8.54 (dd, $J = 8.5$, 1.6 Hz, 2H), 8.03 (br. d, $J = 7.3$ Hz, 1H), 7.84 (dd, $J = 8.1$, 1.3 Hz, 1H), 7.68 (dd, $J = 8.4$, 4.3 Hz, 2H), 7.43 (dd, $J = 8.0$, 4.8 Hz, 1H), 7.21 (dd, $J = 8.1$, 4.8 Hz, 1H), 3.60 (s, 6H), 3.16 (s, 2H), 2.87 (s, 2H), 2.85 (s, 2H), 2.73 (d, $J = 12.8$ Hz, 1H), 2.31 (s, 2H), 2.12 (d, $J = 12.8$ Hz, 1H), 2.10 (s, 6H).

14: M.p. 262–263 °C (decomp); yield 51%; ^1H NMR (300 MHz, $CDCl_3$): $\delta = 8.65$–8.75 (m, 4H), 8.63 (br. d, $J = 7.8$ Hz, 2H), 7.95 (dd, $J = 1.4$, 8.1 Hz, 1H) 7.87 (ddd, $J = 1.8$, 7.8, 7.8 Hz, 2H), 7.59 (dd, $J = 1.0$, 8.1 Hz, 1H), 7.33 (ddd, $J = 1.1$, 4.8, 7.8 Hz, 2H), 7.24 (dd, $J = 4.8$, 8.1 Hz, 1H), 7.06 (dd, $J = 4.8$, 8.1 Hz, 1H), 4.70 (s, 2H), 3.70 (s, 6H), 3.03 (d, $J = 10.8$ Hz, 1H), 3.23 (s, 2H), 1.93 (d, $J = 10.8$ Hz, 1H); EI-MS: m/z (%): 606 (M^+, 3.1), 334 (38), 272 (86), 243 (22), 95 (25).

15: M.p. 301 °C (decomp); yield 85%; ^1H NMR (300 MHz, $CDCl_3$): $\delta = 9.22$ (dd, $J = 4.2$, 1.6 Hz, 2H), 8.80 (ddd, $J = 4.8$, 1.8, 0.9 Hz, 2H), 8.64–8.60 (m, 4H), 7.92 (ddd, $J = 7.8$, 7.8, 1.8 Hz, 2H), 7.67 (dd, $J = 8.5$, 4.3 Hz, 2H), 7.40 (ddd, $J = 7.5$, 4.8, 1.1 Hz, 2H), 4.83 (s, 2H), 3.24 (s, 6H), 2.51 (s, 2H), 2.27 (d, $J = 11.3$ Hz, 1H), 2.11 (s, 6H), 1.73 (d, $J = 11.3$ Hz, 1H).

 © VCH Verlagsgesellschaft mbH, D-69451 Weinheim, 1996 0570-0833/96/3521-2486 $ 15.00+.25/0

(cyclic voltammetry and differential pulse voltammetry) indicated a single oxidation (n = two electrons, by coulometry). Similarly, careful spectroelectrochemical studies at $-32\,^{\circ}C$ in acetonitrile solution provided no evidence for the transient accumulation of a Ru^{II},Ru^{III} state. Accordingly, the Ru^{II},Ru^{III} form of these complexes appears to be thermodynamically disfavored with respect to disproportionation.

These results indicate a weak interaction between the metal centers and are consistent with results reported recently for a complex in which the bridging ligand is composed of two diazofluorene units linked by an adamantane spacer.[18] As noted previously,[18, 19] such weak interactions do not preclude the existence of rapid intercomponent energy or electron transfer, and photophysical studies are in progress on Ru/Ru, Ru/Os, and Os/Os analogues of the complexes described here to assess the consequences of spatial separation on such processes.

Received: April 29, 1996 [Z 9078 1E]
German version: *Angew. Chem.* **1996**, *108*, 2651–2653

Keywords: cycloadditions · cyclopentadienones · Diels–Alder reactions · ruthenium compounds

[1] A. Juris, S. Barigelletti, S. Campagna, V. Balzani, P. Belser, A. von Zelewsky, *Coord. Chem. Rev.* **1988**, *84*, 85.

[2] a) J.-P. Sauvage, J.-P. Collin, J.-C. Chambron, S. Guillerez, C. Coudret, V. Balzani, F. Barigelletti, L. Decola, L. Flamigni, *Chem. Rev.* **1994**, *94*, 993; b) K. S. Schanze, K. Sauer, *J. Am. Chem. Soc.* **1988**, *110*, 1180; c) L. F. Cooley, S. L. Larson, C. M. Elliott, D. F. Kelley, *J. Phys. Chem.* **1991**, *95*, 10694; d) C. K. Ryu, R. Wang, R. H. Schmehl, S. Ferrere, M. Ludwikow, J. W. Merkert, C. E. L. Headford, C. M. Elliott, *J. Am. Chem. Soc.* **1992**, *114*, 430; e) S. L. Mecklenburg, B. M. Peek, J. R. Schoonover, D. G. McCafferty, C. G. Wall, B. W. Erickson, T. J. Meyer, *ibid.* **1993**, *115*, 5479; f) K. A. Opperman, S. L. Mecklenburg, T. J. Meyer, *Inorg. Chem.* **1994**, *33*, 5295.

[3] J. Bolger, A. Gourdon, E. Ishow, J.-P.-Launay, *J. Chem. Soc. Chem. Commun.* **1995**, 1799; M. J. Crossley, P. L. Burn, S. J. Langford, J. K. Prashar, *ibid.* **1995**, 1921.

[4] R. N. Warrener, M. A. Houghton, A. C. Schultz, F. R. Keene, L. S. Kelso, R. Dash, D. N. Butler, *Chem. Commun.* **1996**, 1151.

[5] M.-T. Youinou, N. Rahmouni, J. Fischer, J. A. Osborn, *Angew. Chem.* **1992**, *104*, 771; *Angew. Chem. Int. Ed. Engl.* **1992**, *31*, 733; P. N. W. Baxter, J.-M. Lehn, J. Fischer, M.-T. Youinou, *ibid.* **1994**, *106*, 2432 and **1994**, *33*, 2284.

[6] J. M. Lawson, D. C. Craig, A. M. Oliver, M. N. Paddon-Row, *Tetrahedron* **1995**, *51*, 3841; K. Kumar, R. J. Tepper, Y. Zeng, M. B. Zimmt, *J. Org. Chem.* **1995**, *60*, 4051, and references therein.

[7] a) R. N. Warrener, S. Wang, L. Maksimovic, P. M. Tepperman, D. N. Butler, *Tetrahedron Lett.* **1995**, *36*, 6141; b) R. N. Warrener, G. M. Elsey, M. A. Houghton, *J. Chem. Soc. Chem. Commun.* **1995**, 1417; c) R. N. Warrener, G. Abbenante, R. G. Solomon, R. A. Russell, *Tetrahedron Lett.* **1994**, *35*, 7639; d) R. N. Warrener, L. Maksimovic, G. M. Elsey, D. N. Butler, *J. Chem. Soc. Chem. Commun.* **1994**, 1831; e) R. N. Warrener, G. Abbenante, C. H. L. Kennard, *J. Am. Chem. Soc.* **1994**, *116*, 3645; f) R. N. Warrener, I. G. Pitt, E. E. Nunn, *Tetrahedron Lett.* **1994**, *35*, 621; g) R. N. Warrener, *Chem. Aust.* **1992**, *59*, 578; h) R. N. Warrener, P. Groundwater, I. G. Pitt, D. N. Butler, R. A. Russell, *Tetrahedron Lett.* **1991**, *32*, 1885; i) R. N. Russell, *Tetrahedron Lett.* **1991**, *32*, 1885; i) R. N. Warrener, D. A. Evans, R. A. Russell, *ibid.* **1984**, *25*, 4833; j) D. N. Butler, P. M. Tepperman, R. A. Gau, R. N. Warrener, W. H. Watson, R. P. Kashyap, *ibid.* **1995**, *36*, 6145.

[8] R. N. Warrener, I. G. Pitt, D. N. Butler, *J. Chem. Soc. Chem. Commun.* **1983**, 1340.

[9] a) R. N. Warrener, G. M. Elsey, I. V. Sankar, D. N. Butler, P. Pekos, C. H. L. Kennard, *Tetrahedron Lett.* **1994**, *35*, 6745; b) D. N. Butler, R. A. Gau, P. M. Tepperman, R. N. Warrener, *ibid.* **1996**, *37*, 2825.

[10] R. N. Warrener, A. B. B. Ferreira, E. R. T. Tiekink, *Tetrahedron Lett.* **1996**, *37*, 2161.

[11] T. Mitsudo, K. Kokurya, T. Shinsugi, Y. Nakagawa, Y. Watanabe, Y. Takegami, *J. Org. Chem.* **1979**, *44*, 4492.

[12] The monoadduct can be isolated when less DADAF is employed and added in one portion.

[13] All new compounds were characterized by spectroscopic techniques (^1H NMR, ^{13}C NMR, IR) and the molecular formula established by microanalysis or mass spectrometry (see Table 1).

[14] A. B. B. Ferreira, R. N. Warrener, unpublished results.

[15] C. D. Smith, *J. Am. Chem. Soc.* **1966**, *88*, 4273.

[16] M. J. Ridd, D. J. Gakowski, G. E. Sneddon, F. R. Keene, *J. Chem. Soc. Dalton Trans.* **1992**, 1949.

[17] $[\{Ru(bpy)_2\}_2(\mu\text{-}\mathbf{6})](PF_6)_4$: yield 82%; λ_{max} (metal–ligand charge transfer, MLCT) = 448 nm ($\varepsilon = 25300\ mol^{-1}dm^3cm^{-1}$), CH_3CN solution; $E_{1/2}$ (Ru^{III}/Ru^{II}) = +1.04 V (vs. Ag/Ag^+, 0.1 M $[(C_4H_9)_4N]ClO_4$ in CH_3CN, Pt working electrode). $[\{Ru(bpy)_2\}_2(\mu\text{-}\mathbf{9})](PF_6)_4$: yield 88%; λ_{max} (MLCT) = 448 nm ($\varepsilon = 26100\ mol^{-1}dm^3cm^{-1}$), CH_3CN solution; $E_{1/2}$ (Ru^{III}/Ru^{II}) = +0.97 V (vs. Ag/Ag^+, 0.1 M $[(C_4H_9)_4N]ClO_4$ in CH_3CN, Pt working electrode). $[\{Ru(bpy)_2\}_2(\mu\text{-}\mathbf{11})](PF_6)_4$: yield 92%; λ_{max} (MLCT) = 450 nm ($\varepsilon = 31400\ mol^{-1}dm^3cm^{-1}$), CH_3CN solution; $E_{1/2}$ (Ru^{III}/Ru^{II}) = +1.06 V (vs. Ag/Ag^+, 0.1 M $[(C_4H_9)_4N]ClO_4$ in CH_3CN, Pt working electrode).

[18] L. De Cola, V. Balzani, F. Barigelletti, L. Flamigni, P. Belser, S. Bernhard, *Recl. Trav. Chim. Pays-Bas* **1995**, *114*, 534.

[19] V. Balzani, F. Scandola, *Supramolecular Photochemistry*, Ellis Horwood, Chichester, **1991**.

Highly Diastereoselective Synthesis and Epoxidation of Chiral 1,2-Dihydronaphthalenes**

Torsten Linker,* Karl Peters, Eva-Maria Peters, and Frank Rebien

Epoxidations are one of the most important methods for the formation of carbon–oxygen bonds.[1] Catalytic enantioselective processes, which have been studied particularly intensively, were first developed for allylic alcohols[2] and have been extended to unfunctionalized olefins in the last few years.[3] The diastereoselective epoxidation of chiral alkenes is also very important with regard to the directing effect of various functional groups.[4] Although epoxidations of monocyclic alkenes have attracted the most attention,[5] the analogous reactions of chiral 1,2-dihydronaphthalenes have not been investigated in detail.[6] This is surprising, since achiral dihydronaphthalenes and structurally related chromenes are prime substrates for asymmetric epoxidations.[3] We were interested in the synthesis and epoxidation of chiral 1,2-dihydronaphthalenes in the context of the synthesis of podophyllotoxin analogues.[7]

Oxazolines (dihydrooxazoles) **2**, which are easily accessible starting from 2-naphthoic acid (**1**), have proven themselves to be good precursors for 1,2-dihydronaphthalenes[8] (Scheme 1). The nucleophilic addition of phenyllithium occurs with high regioselectivity at the 1-position and the trapping of the azaenolate intermediate with trifluoroacetic acid (TFA) gives the salt *rac*-**3** in good yield. The use of TFA has been shown to be especially important here, since with other proton sources isomerization to 1,4-dihydronaphthalenes occurs. The exclusive formation of the *trans* product is due to rapid and complete epimerization at the 2-position and is in accordance with additions to 1-naphthyloxazolines.[8b] To examine the influence of different substituents on the stereoselectivity of the epoxidations, the salt *rac*-**3** was transformed into the derivatives *rac*-**4** (Scheme 1).

The oxidations were first performed with *m*-chloroperbenzoic acid (MCPBA), which smoothly led to the epoxides *rac*-**5** (Scheme 2; Table 1, entries 1–3). The yields could be improved

[*] Dr. T. Linker, Dipl.-Chem. F. Rebien
Institut für Organische Chemie der Universität
Am Hubland, D-97074 Würzburg (Germany)
Fax: Int. code +(931)888-4606
e-mail: linker@chemie.uni-wuerzburg.de
Dr. K. Peters, E.-M. Peters
Max-Planck-Institut für Festkörperforschung, Stuttgart (Germany)

[**] This work was generously supported by the Deutsche Forschungsgemeinschaft (Li 556/2-1, Li 556/3-1) and the Universitätsbund Würzburg. We thank Prof. W. Adam for his continuous encouragement.

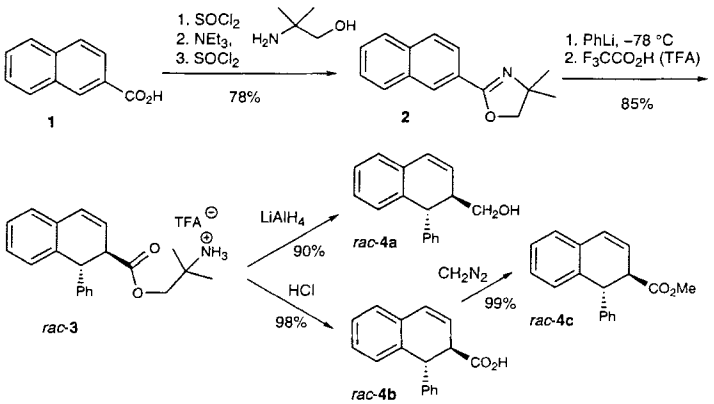

Scheme 1. Synthesis of the chiral 1,2-dihydronaphthalenes *rac*-**4**.

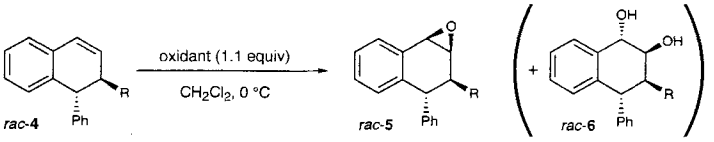

Scheme 2. Oxidation of *rac*-**4** with MCPBA and with DMD.

Table 1. Epoxidation of 1,2-dihydronaphthalenes *rac*-**4**.

Entry	Substrate	R	Oxidant	*ds* [a]	Yield [b] *rac*-**5**	Yield [b] *rac*-**6**
1	*rac*-**4a**	CH_2OH	MCPBA	>95	89	–
2	*rac*-**4b**	CO_2H	MCPBA	>95	82 [c]	–
3	*rac*-**4c**	CO_2Me	MCPBA	>95	94	–
4	*rac*-**4c**	CO_2Me	DMD	>95	–	76
5	*rac*-**4a**	CH_2OH	DMD	>95	94	–
6	*rac*-**4b**	CO_2H	DMD	>95	89 [c]	–
7	*rac*-**4c**	CO_2Me	DMD	>95	98	–
8	*rac*-**4c**	CO_2Me	DMD [d]	>95	26	67

[a] Diastereoselectivities (*ds*, in %) determined from ^1H NMR spectra (250 MHz) of the crude product. [b] Yields (in %) of isolated product after crystallization or column chromatography. [c] Isolated as the ester after reaction with diazomethane. [d] Water and perchloric acid added.

by using dimethyldioxirane (DMD) as oxidant, which allows epoxidations to be conducted under milder conditions.[9] The surprising formation of the diol *rac*-**6c** in the reaction of the ester *rac*-**4c** (entry 4) is due to acid-catalyzed opening of the epoxide in the presence of traces of water. By using dimethyldioxirane (DMD), which was synthesized under anhydrous conditions,[9c] the desired epoxides *rac*-**5** could be successfully prepared in excellent yields (entries 5–7). The postulated acid-catalyzed epoxide opening was supported by a control experiment in the presence of water (entry 8).

Interestingly, only one diastereomer was formed in all reactions, regardless of the oxidant and the substituents R. The assignment of the relative configurations of the epoxides *rac*-**5** was not possible from the NMR data; however, the signals of 1-H to 4-H of the ring-opened product *rac*-**6c** had a characteristic coupling pattern, which confirmed the assigned configuration. The structure of epoxide *rac*-**5c** was assigned unequivocally by X-ray structure analysis.[10]

The oxidant attacks *cis* to the substituents R in all reactions. However, a *syn*-directing effect of the hydroxy groups,[4, 5a, b] which has often been observed previously, can be excluded for the 1,2-dihydronaphthalenes investigated, since the homoallylic alcohol *rac*-**4a** and the ester *rac*-**4c** show the same stereoselectivity. Rather, it is the phenyl group that controls the reaction, irrespective of the substituents R. From this point of view, the observed selectivities are surprisingly high, since sterically controlled epoxidations previously reported proceed with only moderate diastereomeric excesses.[5c, d, 6b] Apparently, the preferred conformation of 1,2-dihydronaphthalenes[11] is responsible for the high stereoselectivities. In AM1 calculations[12] we found that in the most favorable rotamer of *rac*-**4** the phenyl group is orthogonal to the plane of the dihydronaphthalene. Consequently the steric requirements of this substituent is particularly large and the bottom face of the dihydronaphthalene is effectively shielded (Scheme 3). The high-field shift of 8-H, which is due to the induced magnetic field of the phenyl group, is also in accordance with these calculations.

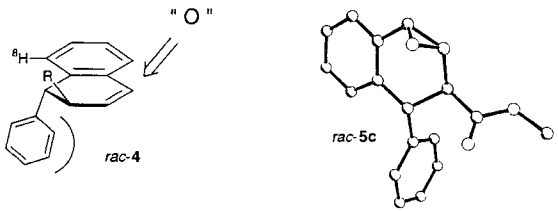

Scheme 3. Preferred conformation of the 1,2-dihydronaphthalenes *rac*-**4** and crystal structure of *rac*-**5c**.

In summary, the reaction sequence Meyers oxazoline synthesis, nucleophilic addition of phenyllithium, and epoxidation, starting from 2-naphthoic acid (**1**), gives easy access to the diastereomerically pure epoxides *rac*-**5**. The selectivities of the reactions are strongly controlled by the steric requirements of the phenyl group, whereas polar substituents have no influence on the epoxidations. As 1,2-dihydronaphthalenes can be prepared enantioselectively,[8] this new epoxidation protocol may find application in the synthesis of optically active podophyllotoxin analogues.

Experimental Procedure

Oxazoline **2** [8b] (22.53 g, 100 mmol) was dissolved in anhydrous THF (180 mL) under argon at −40 °C. To this was added dropwise a solution of PhLi in hexane/diethyl ether 7/3 (2.06 M, 60 mL, 124 mmol). The reaction mixture was stirred for 3 h at this temperature, then a mixture of TFA (30 mL, 389 mmol) and THF (20 mL) was added. After 10 min the reaction mixture was poured into a saturated ammonium chloride solution (200 mL) and extracted with diethyl ether (3 × 80 mL). The combined organic phases were dried over Na_2SO_4 and crystallized at 0 °C, directly yielding the salt *rac*-**3** (29.6 g, 68%; m.p. 155–156 °C). Upon concentration of the mother liquor a further crop of the product was obtained (7.4 g, 17%). Under argon atmosphere a solution of *rac*-**3** (13.06 g, 30 mmol) in 3 N HCl (200 mL) was heated at reflux for 7.5 h, cooled, and then extracted with ethyl acetate (4 × 50 mL). The combined organic phases were dried over Na_2SO_4 and then concentrated under vacuum. Filtration through a short column of silica gel (hexane/ethyl acetate 6/4) yielded the acid *rac*-**4b** in the form of white crystals (7.35 g, 98%; m.p. 121–122 °C). To a solution of *rac*-**4b** (2.5 g, 10 mmol) in dichloromethane (50 mL) at 0 °C was added a solution of diazomethane in diethyl ether until the yellow color persisted. After 12 h at 20 °C the solution was concentrated and filtered over a short column of silica gel (hexane/ethyl acetate 8/2) to yield the ester *rac*-**4c** (2.62 g, 99%). Anal. calcd. for $C_{18}H_{16}O_2$: C 81.79, H 6.10; found: C 81.47, H 5.97; ^1H NMR (200 MHz, $CDCl_3$): δ = 3.63 (s, 3H, OMe), 3.70 (ddd, J = 8.6, 4.3, 2.1 Hz, 1H, 2-H), 4.64 (d, J = 8.6 Hz, 1H, 1-H), 5.94 (dd, J = 9.6, 4.3 Hz, 1H, 3-H), 6.66 (dd, J = 9.6, 2.1 Hz, 1H, 4-H), 6.89 (d, J = 7.2 Hz, 1H, 8-H), 7.12–7.32 (m, 8H, aromat. H); ^{13}C NMR (50 MHz, $CDCl_3$): δ = 45.8, 48.5, (2d, C-1, C-2), 52.1 (q, CO_2Me), 123.6, 126.5, 126.8, 127.0, 128.0, 128.3, 128.5, 128.6, 129.1 (9d, C-3, C-4, C-5, C-6, C-7, C-8, C-Ph), 132.4, 136.2, 142.8 (3s, C-9, C-10, C-Ph), 173.6 (s, CO_2Me).

The ester *rac*-**4c** (2.12 g, 8.02 mmol) was dissolved in anhydrous dichloromethane (120 mL). A solution of DMD [9c] in acetone (0.06 M,150 mL, 1.1 equiv) was added dropwise to this solution at 0 °C over 30 min. After 2 h at 0 °C the reaction mixture was concentrated directly on a rotary evaporator. Crystallization from diethyl ether gave the epoxide *rac*-**5c** as white needles (2.2 g, 98%; m.p. 97–98 °C). Anal. calcd. for $C_{18}H_{16}O_3$: C 77.12, H 5.75; found: C 76.86, H 5.63; ^1H NMR

(200 MHz, $CDCl_3$): δ = 3.20 (dd, J = 12.0, 0.8 Hz, 1H, 3-H), 3.61 (s, 3H, OMe), 3.96 (dd, J = 4.3, 0.8 Hz, 1H, 2-H), 4.06 (d, J = 4.3 Hz, 1H, 1-H), 4.33 (d, J = 12.0 Hz, 1H, 4-H), 6.56 (dd, J = 7.4, 1.0 Hz, 1H, 5-H), 7.12–7.49 (m, 8H, aromat. H); ^{13}C NMR (50 MHz, $CDCl_3$): δ = 43.1, 48.1, (2 d, C-3, C-4), 52.2 (q, CO_2Me), 53.0, 55.6 (2 d, C-1, C-2), 126.5, 127.3, 128.4, 128.7, 128.8, 129.7, 129.8 (7 d, C-5, C-6, C-7, C-8, C-Ph), 131.4, 139.1, 140.1 (3 s, C-9, C-10, C-Ph), 172.7 (s, CO_2Me).

Received: June 7, 1996 [Z 9196 IE]
German version: *Angew. Chem.* **1996**, *108*, 2662–2664

Keywords: asymmetric syntheses · dihydrooxazoles · epoxidations · naphthalene derivatives · synthetic methods

[1] Reviews: a) G. Berti, *Top. Stereochem.* **1973**, *7*, 93–251; b) H. Mimoun, *Angew. Chem.* **1982**, *94*, 750–766; *Angew. Chem. Int. Ed. Engl.* **1982**, *21*, 734–750; c) A. S. Rao, S. K. Paknikar, J. G. Kirtane, *Tetrahedron* **1983**, *39*, 2323–2367; d) V. Schurig, F. Betschinger, *Chem. Rev.* **1992**, *92*, 873–888; e) P. Besse, H. Veschambre, *Tetrahedron* **1994**, *50*, 8885–8927; f) S. Pedragosa-Moreau, A. Archelas, R. Furstoss, *Bull. Soc. Chim. Fr.* **1995**, *132*, 769–800.

[2] a) T. Katsuki, K. B. Sharpless, *J. Am. Chem. Soc.* **1980**, *102*, 5974–5976; b) R. A. Johnson, K. B. Sharpless in *Comprehensive Organic Synthesis, Vol. 7* (Eds.: B. M. Trost, I. Fleming, S. V. Ley), Pergamon, New York, **1991**, p. 389–436; c) R. A. Johnson, K. B. Sharpless in *Catalytic Asymmetric Synthesis* (Ed.: I. Ojima), VCH, Weinheim, **1993**, pp. 103–158.

[3] a) W. Zhang, J. L. Loebach, S. R. Wilson, E. N. Jacobsen, *J. Am. Chem. Soc.* **1990**, *112*, 2801–2803; b) R. Irie, K. Noda, Y. Ito, N. Matsumoto, T. Katsuki, *Tetrahedron Lett.* **1990**, *31*, 7345–7348; c) E. N. Jacobsen in *Catalytic Asymmetric Synthesis* (Ed.: I. Ojima), VCH, Weinheim, **1993**, pp. 159–202; d) T. Katsuki, *Coord. Chem. Rev.* **1995**, *140*, 189–214.

[4] Review: A. H. Hoveyda, D. A. Evans, G. C. Fu, *Chem. Rev.* **1993**, *93*, 1307–1370.

[5] a) W. Adam, A. K. Smerz, *Tetrahedron* **1995**, *51*, 13039–13044; b) R. J. Linderman, R. J. Claassen, II, F. Viviani, *Tetrahedron Lett.* **1995**, *36*, 6611–6614; c) R. W. Murray, M. Singh, B. L. Williams, H. M. Moncrieff, *J. Org. Chem.* **1996**, *61*, 1830–1841; d) E. Vedejs, W. H. Dent, III, J. T. Kendall, P. A. Oliver, *J. Am. Chem. Soc.* **1996**, *118*, 3556–3567.

[6] A few exceptions: a) R. W. Irvine, R. A. Russell, R. N. Warrener, *Tetrahedron Lett.* **1985**, *26*, 6117–6120; b) M. J. Martinelli, B. C. Peterson, V. V. Khau, D. R. Hutchison, M. R. Leanna, J. E. Audia, J. J. Droste, Y.-D. Wu, K. N. Houk, *J. Org. Chem.* **1994**, *59*, 2204–2210; c) F. Orsini, F. Pelizzoni, *Tetrahedron: Asymmetry* **1996**, *7*, 1033–1040.

[7] Review: R. S. Ward, *Synthesis* **1992**, 719–730.

[8] a) M. Reumann, A. I. Meyers, *Tetrahedron* **1985**, *41*, 837–860; b) A. I. Meyers, K. A. Lutomski, D. Laucher, *ibid.* **1988**, *44*, 3107–3118; c) G. T. Gant, A. I. Meyers, *ibid.* **1994**, *50*, 2297–2360.

[9] a) W. Adam, R. Curci, J. O. Edwards, *Acc. Chem. Res.* **1989**, *22*, 205–211; b) R. W. Murray, *Chem. Rev.* **1989**, *89*, 1187–1201; c) W. Adam, L. Hadjiarapoglou, J. Bialas, *Chem. Ber.* **1991**, *124*, 2377; d) R. Curci, A. Dinoi, M. F. Rubino, *Pure Appl. Chem.* **1995**, *67*, 811–822.

[10] Crystal data for *rac*-**5c**: $C_{18}H_{16}O_3$, Siemens P4 diffractometer, monoclinic, $P2_1/n$, a = 1615.4(7), b = 548.4(3), c = 1646.3(6) pm, β = 96.16(2)°, $V = 1450(1) \times 10^6$ pm^3, $\rho_{calcd} = 1.284$ g cm^{-3}, $2\theta_{max} = 55°$, $Z = 4$, $Mo_{K\alpha}$ radiation, λ = 71.073 pm, ω-scan, $\mu = 0.09$ mm^{-1}, T = 293 K, structure solved by direct methods, 3351 measured reflections, 2945 unique reflections, of which 1792 had $F > 3\sigma(F)$, F_0/parameter ratio = 9.43, $R = 0.066$, $R_w = 0.065$, refined versus $|F|$. Residual electron density of the difference-Fourier map: max = 0.22, min = −0.35 e Å^{-3}. Program: SHELXTL-PLUS. Further details of the X-ray structure investigation may be obtained from the Fachinformationszentrum Karlsruhe, D-76344 Eggenstein-Leopoldshafen (Germany), under the depository number CSD-405437.

[11] P. W. Rabideau, A. Sygula, *The Conformational Analysis of Cyclohexenes, Cyclohexadienes, and Related Hydroaromatic Compounds*, VCH, Weinheim, **1989**, pp. 77–81.

[12] G. Rauhut, J. Chandrasekhar, A. Alex, T. Steinke, T. Clark, VAMP 5.0, Universität Erlangen, **1993**.

Catalytic Activation of C–H Bonds in Aromatic Hydrocarbons, Ethene, and Methane by the Naphthalene/Sodium System in Tetrahydrofuran**

Siegbert Rummel,* Margarita A. Ilatovskaya, Evgeny I. Mysov, Vladimir S. Lenenko, Helmuth Langguth, and Vladimir B. Shur

Radical anions formed from naphthalene and alkali metals are classical objects of chemical research, frequently used because they can efficiently transfer electrons to organic and inorganic substrates. They have achieved particular importance as catalysts for the polymerization of 1,3-dienes and some monoenes, in which "living" polymers are formed.

One of the characteristic reactions of the radical anion adducts of alkali metal ions with naphthalene and other aromatic hydrocarbons is the rapid and reversible electron transfer between the anionic species and the hydrocarbon [Eq. (a)]. Analogous elec-

$$ArH^{\bullet -} + ArH \rightleftharpoons ArH + ArH^{\bullet -} \quad (a)$$

tron transfer processes can also take place between the radical anions themselves [Eq. (b)]. Although there are already numer-

$$2\ ArH^{\bullet -} \rightleftharpoons ArH + ArH^{2-} \quad (b)$$

ous publications on electron transfer of this type,[1] to the best of our knowledge no one has hitherto investigated the reversible hydrogen transfer reactions between C–H bonds of hydrocarbons in these and similar systems. To clarify this question we chose the naphthalene/sodium system, which is formed by addition of sodium to an equimolar mixture of [D_0]naphthalene and [D_8]naphthalene in [D_0]THF, and investigated whether hydrogen isotope exchange takes place between the naphthalene rings.

The experiments were carried out under argon with careful exclusion of air and moisture. The molar ratio of sodium to naphthalene was 0.5:1, 1:1, and 2:1. In the last case some of the sodium remained undissolved because of the excess employed. After removal of the solvent by distillation in vacuum at 20 °C we analyzed the sublimed naphthalene by mass spectrometry.[2, 3] In addition to the H/D exchange in naphthalene we investigated whether analogous isotope exchange processes take place with other hydrocarbons, for example, with benzene, toluene, ethene, and methane.[3]

In our earlier work we had found[4, 5] that adducts of active carbon with metallic potassium, and also graphite–potassium lamellar compounds, are able to activate C–H bonds in various hydrocarbons and to catalyze the hydrogen isotope exchange at room temperature. Herein we report that analogous H/D exchange reactions take place in the naphthalene/sodium system in THF.

In a typical experiment, metallic sodium and [D_0]THF were added under argon to a 1:1 mixture of [D_0]naphthalene and

[*] Dr. habil. S. Rummel, Dr. H. Langguth
Institut für Oberflächenmodifizierung e. V.
Permoserstrasse 15, D-04303 Leipzig (Germany)
Fax: Int. code +(341)235-2584
e-mail: rummel@serveri.rz.uni-leipzig.de
Dr. M. A. Ilatovskaya, Dr. E. I. Mysov, Dr. V. S. Lenenko, Prof. Dr. V. B. Shur
A. N. Nesmayanov Institute of Organo-Element Compounds of the Russian Academy of Sciences
Vavilov Street 28, 117813 Moscow (Russia)

[**] This work was supported by the Bundesministerium für Forschung und Technologie (BMFT), Bonn.

 © VCH Verlagsgesellschaft mbH, D-69451 Weinheim, 1996 0570-0833/96/3521-2489 $ 15.00+.25/0

$[D_8]$naphthalene (mole ratio Na:naphthalene = 2:1, $c_0(C_{10}H_8 + C_{10}D_8) = 2$ M). The resulting dark-green solution of naphthalene–sodium was then stirred at room temperature. Mass spectroscopic analysis of the naphthalene obtained showed that redistribution of hydrogen isotopes between the naphthalene rings had taken place. After 7 h the isolated naphthalene had the following isotopic composition: $[D_0] = 22.9\%$, $[D_1] = 16.0\%$, $[D_2] = 7.1\%$, $[D_3] = 4.4\%$, $[D_4] = 6.3\%$, $[D_5] = 11.2\%$, $[D_6] = 14.5\%$, $[D_7] = 12.3\%$, and $[D_8] = 5.3\%$. At the same time, the total D-content (f_D) of the naphthalene had decreased—apparently as a result of isotope exchange with the undeuterated THF—from 50.8 to 42.5 atom%. The formation of deuterated naphthalene ($[D_0] = 9.8\%$, $[D_1] = 24.5\%$, $[D_2] = 29.9\%$, $[D_3] = 21.7\%$, $[D_4] = 10.1\%$, $[D_5] = 3.2\%$, $[D_6] = 0.7\%$, $[D_7] = 0.1\%$, $f_D = 26.3$ atom%, 22 °C, 3.5 h) from $[D_0]$naphthalene and sodium in $[D_8]$THF (99.9 atom%) supports this assumption. A reduction in the ratio Na:naphthalene from 2:1 to 1:1 or 0.5:1 led to a reduction in the rate of the isotope exchange in our test system.

A remarkable feature of the isotope exchange observed here is the strong dependence on the type of reagent used. For example, if sodium is replaced with potassium or lithium, no isotope exchange occurs. The same result is observed on the addition of [15]crown-5 and also by using dimethoxyethane (DME) in place of THF. On the other hand, one can significantly increase the rate of the H/D exchange in this system if alkanes or cycloalkanes, for example, cyclohexane, are added to the THF. By increasing the amount of cyclohexane in the mixture the rate of isotope exchange passes through a maximum, which lies at a THF/cyclohexane volume ratio of about 1:1, as shown clearly in Figure 1. If the isotope exchange is carried out in this solvent

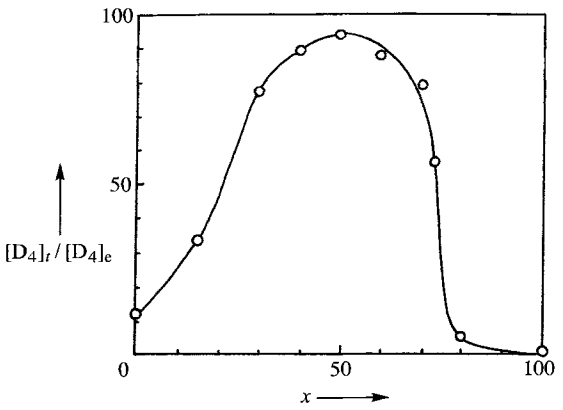

Fig. 1. Influence of the volume ratio x of cyclohexane in $[D_0]$THF on the rate of the H/D exchange in the system $[D_0]$naphthalene + $[D_8]$naphthalene + Na, given as the ratio $[D_4]_t/[D_4]_e$ in percent (22 °C, 3.5 h; mole ratio Na:naphthalene = 2:1; isotope composition of the initial naphthalene: $[D_0] = 48.6\%$, $[D_7] = 1.6\%$, $[D_8] = 49.8\%$, $f_D = 51.3$ atom%; initial naphthalene concentration = 2 M). $[D_4]_t$ = content of $[D_4]$naphthalene at time t, $[D_4]_e$ = content of $[D_4]$naphthalene in deuterated naphthalene after reaching the statistical isotope equilibrium.

mixture (Fig. 2, curve 1), a mixture of $[D_0]$naphthalene and $[D_8]$naphthalene leads, after only 3.5 h at room temperature, to that mixture of isotopomers ($[D_0] = 2.7\%$, $[D_1] = 10.7\%$, $[D_2] = 21.3\%$, $[D_3] = 25.9\%$, $[D_4] = 21.3\%$, $[D_5] = 12.4\%$, $[D_6] = 4.6\%$, $[D_7] = 1.1\%$, $f_D = 39.2$ atom%) that nearly corresponds to the statistical isotope equilibrium.[6] Under otherwise identical conditions, but without cyclohexane (Fig. 2, curve 2), only 11.6% of the statistical isotope equilibrium (based on $[D_4]$naphthalene) is reached. An even more pronounced accelerating effect of cyclohexane on the H/D exchange is observed when the reaction is carried out with a mole ratio of Na:naphthalene of 1:1 or 0.5:1 ($c_0(C_{10}H_8 + C_{10}D_8) = 2$ M).

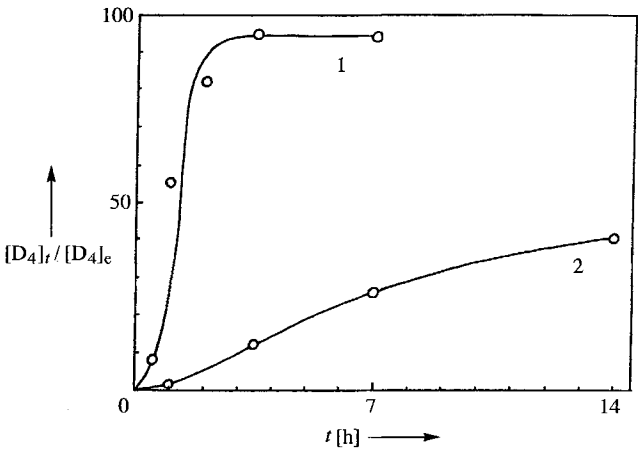

Fig. 2. Time-dependence of the H/D exchange in the system $[D_0]$naphthalene + $[D_8]$naphthalene + Na in cyclohexane/$[D_0]$THF 1/1 (curve 1) and in pure $[D_0]$THF (curve 2) (22 °C, Na:naphthalene = 2:1, initial naphthalene concentration = 2 M).

Further experiments showed that the sodium/naphthalene system in THF is not only able to activate the C–H bonds in naphthalene but also in a series of other hydrocarbons. For example, if one adds $[D_6]$benzene and metallic sodium to $[D_0]$naphthalene ($c_0 = 1.47$ M) in $[D_0]$THF (mole ratio $C_{10}H_8$:Na:$C_6D_6 \approx 1:2:2$), an efficient hydrogen isotope exchange takes place between C_6D_6 and the naphthalene–sodium even at room temperature. After 3.5 h the deuterium content in the naphthalene (obtained from the naphthalene–sodium) had increased from zero to 21.5 atom% (isotope composition: $[D_0] = 15.6\%$, $[D_1] = 30.8\%$, $[D_2] = 29.2\%$, $[D_3] = 16.6\%$, $[D_4] = 6.3\%$, $[D_5] = 1.5\%$) and that in benzene had decreased from 99.2 to 77.1 atom% (isotope composition: $[D_0] = 0.2\%$, $[D_1] = 0.8\%$, $[D_2] = 3.0\%$, $[D_3] = 10.6\%$, $[D_4] = 25.9\%$, $[D_5] = 36.5\%$, $[D_6] = 23.0\%$). In addition to benzene and naphthalene, THF is also involved in the isotope exchange, which was demonstrated by an experiment involving $[D_8]$THF and a mixture of $[D_0]$naphthalene and $[D_0]$benzene. Reduction in the ratio of sodium to naphthalene leads in this system, too, to a decrease in the rate of the isotope exchange.

Analogous isotope exchange processes in the naphthalene/sodium system can also be observed with toluene and ethene. In the case of toluene the exchange involves both the hydrogen atoms of the ring and of the methyl group. Finally, it could be shown that even methane can be drawn into the isotope exchange with this system, albeit with a lower rate. The experiments with ethene and methane were carried out in sealed glass ampoules ($V \approx 10$ mL) at an initial gas pressure of 600 Torr. Under these conditions a mixture of deuterated ethene ($[D_1] = 12.0\%$, $[D_2] = 22.9\%$, $[D_3] = 37.6\%$, $[D_4] = 27.5\%$) with a D-content of about 70.2 atom% was obtained after only 0.5 h with $[D_0]$ethene, $[D_8]$naphthalene (1.5 mmol, $c_0 = 2$ M, 99.9 atom% D), and sodium in $[D_8]$THF at room temperature (Na:$C_{10}D_8$ = 2:1); after 1.5 h the deuterium enrichment in the ethene was 89.6 atom% ($[D_1] = 0.8\%$, $[D_2] = 5.3\%$, $[D_3] = 28.6\%$, $[D_4] = 65.2\%$). The reaction of $[D_0]$methane with the $[D_8]$naphthalene/sodium system in $[D_8]$THF (3 mmol of $C_{10}D_8$, $c_0(C_{10}D_8) = 2$ M, Na:$C_{10}D_8$ = 2:1) gave a mixture of $[D_1]$methane (14.7%), $[D_2]$methane (0.8%), and $[D_3]$methane

 © VCH Verlagsgesellschaft mbH, D-69451 Weinheim, 1996 0570-0833/96/3521-2490 $ 15.00+.25/0

(0.1%) after 70 h at 22 °C. The addition of dodecane to the [D_8]THF (in a volume ratio of 1:1) increased the rate of isotope exchange with methane: after 70 h under otherwise identical conditions we obtained 20.2% [D_1]methane, 1.6% [D_2]methane, and 0.1% [D_3]methane—in contrast there was no deuterium enrichment in the dodecane.

An interpretation of our results using "simple" exchange mechanisms presents considerable difficulties. This is particularly the case for those mechanisms that involve a reversible $H^{\bullet}(D^{\bullet})$ or $H^{+}(D^{+})$ abstraction from the hydrocarbon by naphthalene–sodium with formation of the corresponding free radicals or carbanions. The first of these two mechanisms appears to be unlikely from a thermodynamic point of view, as the abstraction of a hydrogen atom from a hydrocarbon would lead to a much less stable radical (Ph$^{\bullet}$, Me$^{\bullet}$, etc.) than the radical anion of naphthalene. In addition, on the basis of this mechanism it is not easy to understand why cyclohexane and dodecane, in contrast to methane, are not involved in the H/D exchange, because it is well-known that the rate of $H^{\bullet}$ abstraction from alkanes and cycloalkanes by radicals decreases in the order *tert*-CH > *sec*-CH > *prim*-CH > methane.[7]

Attempts to interpret the experimental data by means of the proton abstraction mechanism also present serious difficulties. In particular, it is not clear whether naphthalene–sodium is at all capable of removing protons from such weak CH acids as, for example, methane at room temperature. Another difficulty in this case lies in explaining the accelerating effect of cyclohexane and the excess sodium present on the H/D exchange.[8]

However, there is a mechanistic interpretation—although also hypothetical—that satisfactorily describes the experimental observations. This is based on the assumption that atomic sodium, which can aggregate to form sodium clusters Na_n,[9] is formed in the naphthalene(ArH)/sodium system in THF by the reactions (c)–(e). These clusters are stabilized by the formation

$$Na_{met.} + ArH^{\bullet-}Na^{-} \rightleftharpoons Na^{+}ArH^{\bullet-} + Na_{at.} \quad (c)$$

$$ArH^{\bullet-}Na^{+} + ArH^{\bullet-}Na^{+} \rightleftharpoons ArH + Na^{+}ArH^{\bullet-} + Na_{at.} \quad (d)$$

$$ArH^{\bullet-}Na^{+} \rightleftharpoons ArH + Na_{at.} \quad (e)$$

of surface complexes with naphthalene. We now assume that activation of the hydrocarbon C–H bonds takes place on the surface of these sodium clusters, the result of which is an observable H/D exchange.

With sodium/naphthalene ratios of 0.5:1 and 1:1 atomic sodium could be formed by reactions (d) and (e). In addition, the conditions required for reaction (c) could be satisfied in the presence of excess metallic sodium: the resulting higher content of sodium clusters would cause the observed increase in rate of the H/D exchange.

Addition of nonpolar solvents such as alkanes and cycloalkanes to THF shift the equilibria (d) and (e), by a reduction in the solvation of the sodium cations, apparently in the direction of formation of atomic sodium. Thus, it can be explained why the addition of certain amounts of cyclohexane to the naphthalene/sodium system in THF initially led to an acceleration of the H/D exchange. If the amount of added hydrocarbon becomes too large, however, the system is deactivated by destruction of the naphthalene–sodium with formation of naphthalene and metallic sodium.[10] As a result, the rate of H/D exchange passes through a maximum with increasing content of cyclohexane in the mixture.

The H/D exchange itself takes place apparently by reversible cleavage of the hydrocarbon C–H bonds with formation of surface groups Na_{surf}–Ar, Na_{surf}–H, Na_{surf}–R, and Na_{surf}–D, where Ar is naphthyl and R is either naphthyl or another hydrocarbon group that undergoes exchange with naphthalene. A requirement for this mechanism to be valid for the isotope exchange appears to be direct contact of the sodium atoms on the surface with the naphthalene or other hydrocarbon molecules. This means that the intermediate complexes formed from the hydrocarbon molecules and the sodium atoms must have the character of contact ion pairs and not that of solvent-separated ion pairs. Presumably, this is the reason why the systems naphthalene/lithium in THF, naphthalene/potassium in THF, naphthalene/sodium in THF in the presence of [15]crown-5 and naphthalene/sodium in DME show no isotope exchange, in contrast to the naphthalene/sodium system in THF. In this connection, according to literature data[1, 11, 12] only contact ion pairs are present in naphthalene/sodium in THF at room temperature, whereas naphthalene/lithium and naphthalene/potassium in THF, and naphthalene/sodium in DME, form solvent-separated ion pairs.

Received: February 27, 1996 [Z 8872 IE]
German version: *Angew. Chem.* **1996**, *108*, 2678–2681

Keywords: C–H activation · H/D exchange · naphthalene–sodium

[1] See, for example, M. Szwarc, *Carbanions, Living Polymers and Electron Transfer Processes*, Wiley-Interscience, New York, **1968**.
[2] With sodium/naphthalene ratios 1:1 and 2:1 naphthalene is formed as a result of a partial decomposition of naphthalene–sodium during the removal of THF.
[3] The mass spectroscopic investigations were carried out on VG 7070 E and Trio 1000 (Fison) equipment. Ionization energies: 17.5 eV for naphthalene, benzene, methane, and ethene, 8 eV for toluene.
[4] S. M. Yunusow, M. A. Ilatovskaya, S. Rummel, M. Herrmann, E. I. Mysov, M. Wahren, V. B. Shur, M. E. Vol'pin, *Izv. Akad. Nauk SSSR Ser. Khim.* **1989**, 1214.
[5] M. A. Ilatovskaya, S. Rummel, Yu. V. Isaev, S. M. Yunusov, N. D. Lenenko, M. Herrmann, M. Wahren, Yu. N. Novikov, V. B. Shur, *Izv. Akad. Nauk SSSR Ser. Khim.* **1991**, 1935.
[6] Under these conditions cyclohexane is not involved in the H/D exchange.
[7] D. C. Nonhebel, J. C. Walton, *Free-Radical Chemistry. Structure and Mechanism*, University Press, Cambridge, **1974**.
[8] It is improbable that the naphthalene dianion could play the part of the active species in the H/D exchange, because the dianion is not formed in the naphthalene/sodium system in THF, even in the presence of excess sodium [12].
[9] For reports on the experimental detection of alkali metal clusters in the gas phase and in solid, inert gas matrices, and for quantum-chemical calculations of such cluster, see, for example, *Metal Clusters* (Ed.: M. Moskovitz), Wiley-Interscience, New York, **1986**; B. Mile, P. D. Sillman, A. R. Yacob, J. A. Howard, *J. Chem. Soc. Dalton Trans.* **1996**, 653–665; P. Fantucci, P. Balzarini, *J. Mol. Catal.* **1978**, *4*, 337–348; J. Flad, H. Stoll, H. Preuss, *J. Chem. Phys.* **1979**, *71*, 3042–3052.
[10] For the decomposition of naphthalene–sodium in ethers into naphthalene and metallic sodium on strong dilution with hydrocarbon solvents, see N. D. Scott, J. F. Walker, V. L. Hansley, *J. Am. Chem. Soc.* **1936**, *58*, 2442 and Ref. [1].
[11] N. M. Atherton, S. I. Weissman, *J. Am. Chem. Soc.* **1961**, *83*, 1330.
[12] J. Smid, *J. Am. Chem. Soc.* **1965**, *87*, 655.

 © VCH Verlagsgesellschaft mbH, D-69451 Weinheim, 1996 0570-0833/96/3521-2491 $ 15.00+.25/0

Complexes Containing Phosphorus and Arsenic as Terminal Ligands**

Manfred Scheer,* Jan Müller, and Marco Häser

Alkali metal bis(trimethylsilyl)phosphanides react with different halogenophosphorus compounds to form multiple P–P bonds.[1] The alkali metal phosphanide serves as a reagent for metalation of silylphosphorus functionalities with the elimination of $P(SiMe_3)_3$ and as a source for the central phosphorus atom in the resulting tri- and isotetraphosphanes. Our interests have focused on the extension of the above concept by the use of transition metal halides and the heavier homologues $[E(SiMe_3)_2]^-$ (E = As, Sb, Bi).[2] The paramagnetic W^{IV} halogenide $[(N_3N)WCl]$[3] **1b** $[(N_3N) = N(CH_2CH_2NSiMe_3)_3]$ serves as an ideal starting material in both respects. With this species and the corresponding molybdenum compound **1a**,[4] Schrock et al. were able to synthesize the first examples of compounds containing a metal–phosphorus triple bond (**2**) [Eq. (a)] that were structurally characterized.[5] At the same time Cummins et al. reported the synthesis of a complex containing a Mo–P triple bond by using $[Mo(NAr'R)_3]$ (Ar' = 3,5-$C_6H_3Me_2$, R = $C(CD_3)_2CH_3$) and white phosphorus as starting materials.[6]

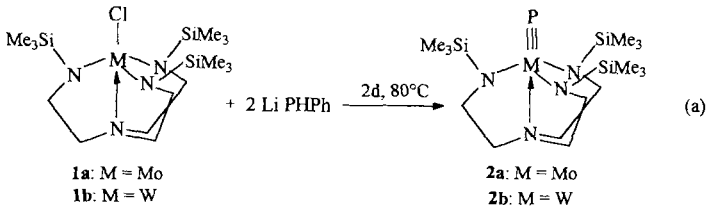

(a)

The $^{183}W,^{31}P$ coupling constant of **2b** (138 Hz) differs significantly from the coupling constants determined for the stabilized phosphido complexes **3a,b** (**3a**: 536 Hz, **3b**: 554 Hz), which we synthesized according to the methathesis reaction given in Equation (b).[7] Limited amounts of **3**, as well as alkylidyne complexes, react under cycloaddition with the phosphaalkyne to form four-membered ring derivatives. A subsequent 1,3-O*t*Bu shift yielded the corresponding phosphaalkoxy-substituted compounds **4** and **5**. Due to decomposition of the alkoxides on the column material, chromatographic separation of the reaction mixture has not been possible, nor have we been able to obtain single crystals of **3** suitable for structural analysis. It has been possible, however, to enrich solutions of **3** by fractional crystallization.

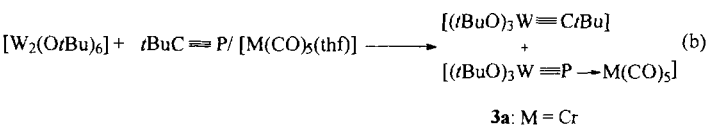

(b)

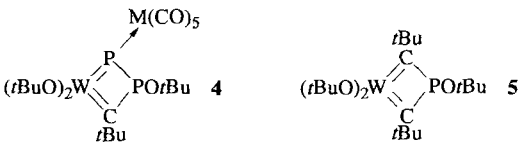

In an effort to find an explanation for the different $^{183}W,^{31}P$ coupling constants, we decided to synthesize **2b**, starting with lithium bis(trimethylsilyl)phosphanide and subsequent complexation with $[W(CO)_5(thf)]$. Furthermore, it should be possible to use bis(trimethylsilyl)pnictides $[E(SiMe_3)_2]^-$ (E = As, Sb, Bi) to synthesize complexes containing the heavier homologues of phosphorus.[8]

The reaction of **1b** with $[P(SiMe_3)_2]^-$ at 80 °C for two days afforded the phosphido complex **2b** in 65% yield [Eq. (c)]. To prepare the corresponding arsenido complex **6** temperatures of 110 °C are needed. Whereas Schrock et al. observed and isolated the phosphanido complex $[(N_3N)W-PPh(H)]$ as an intermediate in reaction (a), no corresponding Me_3Si-substituted phosphanido derivative could be detected by monitoring reaction (c) by ^{31}P NMR spectroscopy.[9] Instead, with growing amounts of **2b** an increase in the amount of $P(SiMe_3)_3$ is detected. Evidently, the rate-determining step of reaction (c) is the formation of the phosphanido complex $[(N_3N)W-P(SiMe_3)_2]$, which is subsequently metalated by a second equivalent of $LiP(SiMe_3)_2$ with the elimination of $P(SiMe_3)_3$, forming the phosphido complex **2b**, presumably, by the metal-catalyzed elimination of $LiSiMe_3$. These conclusions are in accordance with our results on the reaction pathway of multiple P–P bond formation[1] as well as with findings by Schrock et al., who emphasize the need for a base (LiPPhH or LiR) in the transformation of phosphanido to phosphido complexes **2** by the elimination of LiPh.[10]

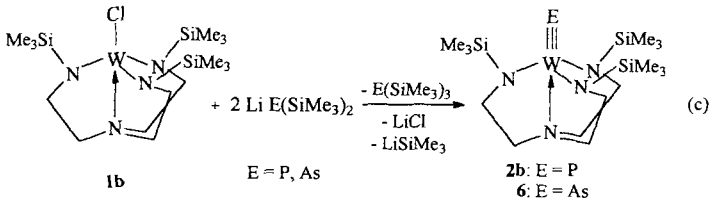

(c)

The phosphido complex **2b** first reacts with $[M(CO)_5(thf)]$ (M = Cr, W) to form complexes **7**, although a second substitution in the *trans*-position is preferred, leading to the $M(CO)_4$ complexes **8**, which can be isolated in 68 to 74% yield [Eq. (d)].[11] Complexes **6** and **8** are yellow and red crystalline materials, respectively, which are moderately soluble in *n*-hexane, although well soluble in toluene and THF. These compounds were completely characterized by spectroscopic methods.[12] The mass spectrum of **6** reveals the molecular peak, whereas for **8** the peak of the $[(N_3N)W\equiv P\rightarrow M]^+$ fragment is the highest one observed. In the range of CO vibrations, IR spectra show a strong band at 1912 (**8a**) and 1896 cm^{-1} (**8b**), respectively, corresponding to local D_{4h} symmetry of the $M(CO)_4$ unit. A discussion of the W≡E vibrations in the Raman spectra of **2a** and **6**, can be found in a publication by Schrock et al.,[13] who synthesized **6** and the corresponding Mo derivative by reaction (a) starting with LiAsPhH.

The crystal structure analyses of **1b** and **6** (Fig. 1)[14] confirm their isostructural relationships with **2b**. All compounds exhibit

[*] Prof. Dr. M. Scheer, Dipl.-Chem. J. Müller
Institut für Anorganische Chemie der Universität
D-76128 Karlsruhe (Germany)
Fax: Int. code +(721)661921
e-mail: mascheer@achibm6.chemie.uni-karlsruhe.de
Priv.-Doz. Dr. M. Häser
Institut für Physikalische Chemie der Universität
D-76128 Karlsruhe (Germany)
Fax: Int. code +(721)6084856
e-mail: marco@tchibm3.chemie.uni-karlsruhe.de

[**] This work was supported by the Fonds der Chemischen Industrie and the Deutsche Forschungsgemeinschaft. We thank Prof. Dr. R. Ahlrichs for valuable comments and his coworkers K. Eichkorn and F. Weigend for unpublished basis sets.

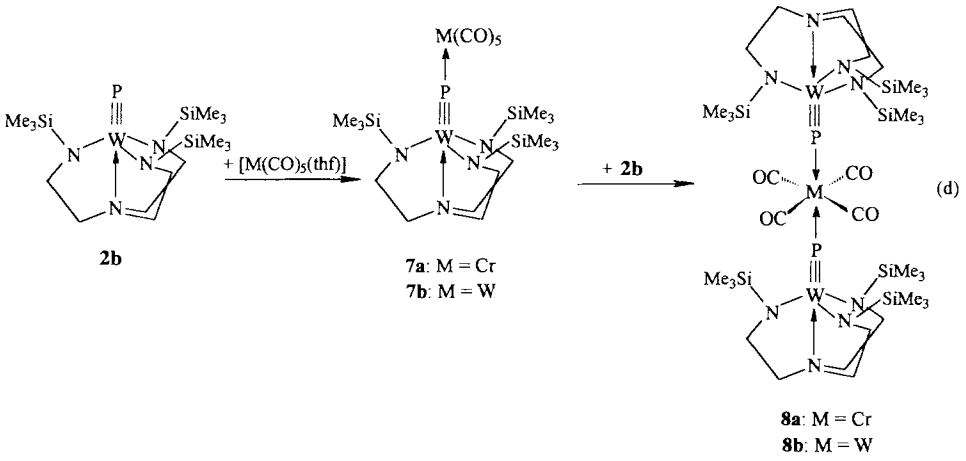

2b

7a: M = Cr
7b: M = W

8a: M = Cr
8b: M = W

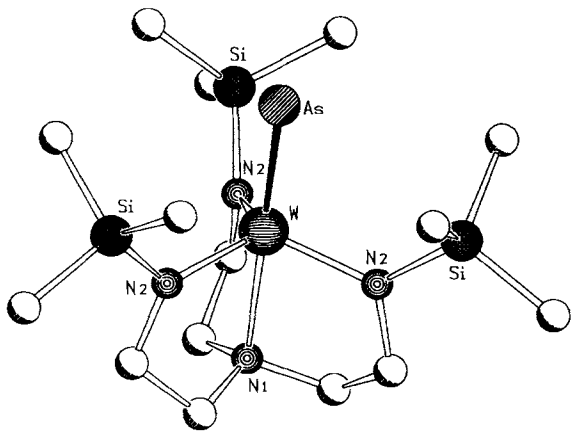

Fig. 1. Molecular structure of **6** (without H atoms).

a linear N_{ax}-W-E axis with a distorted trigonal-bipyramidal geometry at the central W atom. The W–As distance in **6** is 2.290(1) Å and is therefore 13 pm longer than the analogous W–P distance in **2b** (2.16 Å). The corresponding Mo–As bond length is reported to be 2.25 Å.[10] The distortion of the trigonal bipyramid is most pronounced for the As derivative **6** (E-W-N2 angle in Table 1 and 2) and lessens for the phosphido complex **2b** and still further for the chloro derivative **1b**. Whereas the W–N2 distances are almost not influenced by the substituent E, the extent of intramolecular N1 → W coordination is strongly dependent on it. In accordance with the higher electronegativity, this distance in the chloro-substituted compound **1b** (2.182(6) Å) is shorter than that in the As derivative **6** (2.336(6) Å), which is almost identical to the distance found for the phosphido complex **2b**.

Complex **8b** (Fig. 2)[14] exhibits a linear N_{ax}-W-P-W-P-W-N_{ax} axis. The W1 atoms are coordinated in a trigonal-bipyramidal fashion, the W2 atom resides in an octahedral environment. In comparison with **2b** the coordination of the phosphido ligands at the W^0 center causes a lengthening of the W–P triple bond by 4 pm to 2.202(2) Å (Table 1 and 2). The mean W2–P distance is 2.460 Å and is therefore shorter than that observed in $[(CO)_5W(PMe_3)]$[15] (2.516 Å), although it is within the same region as that in *trans*-$[(CO)_4W(PR_3)_2]$ (2.458 Å).[16] π Back donation of the central W^0 atom to the phosphido ligand weakens the triple bond.

Table 1. Comparison of selected experimental and calculated bond lengths [Å] and angles [°] of complexes **1b**, **2b**, **6**, and related compounds (see Fig. 1 for atom labeling).

Compd	W–E	W–N1$_{ax}$	W–N2$_{eq}$	E-W-N2	N2-W-N2	N1-W-N2
1b (expt)	2.399(2)	2.182(6)	1.985(11)	98.89(11)	117.66(6)	81.11(11)
1b (calcd)	2.434	2.434	2.028	99.8	117.2	80.3
[(N_3N)W≡N] (calcd)	1.724	2.524	2.021	102.9	115.2	77.1
2b (expt)[5]	2.162(4)	2.34(1)	1.975(6)	101.9(2)	115.8(11)	78.1(2)
2b (calcd)	2.181	2.527	2.019	103.5	114.7	76.5
6 (expt)	2.2903(11)	2.336(6)	1.989(4)	102.15(11)	115.69(8)	77.85(11)
6 (calcd)	2.290	2.521	2.020	103.6	114.7	76.4
[(N_3N)W≡Sb] (calcd)	2.514	2.530	2.020	104.0	114.4	76.0
[(N_3N)W≡P–BH_3] (calcd)[a]	2.175	2.391	2.025	102.1	115.7	77.9

[a] The P · B distance is 1.943 Å.

Table 2. Comparison of selected experimental and calculated bond lengths [Å] and angles [°] of complexes **7b** and **8b** (see Fig. 2 for atom labeling).

Compd	W1–E	W1–N_{ax}	W1-N_{eq}	P–W2	E-W1-N_{eq}	N_{eq}-W1-N_{eq}	N_{ax}-W1-N_{eq}
7b (calcd)	2.198	2.457	N1: 2.020 N2: 2.022 N3: 2.024	2.568	N1: 102.7 N2: 103.5 N3: 103.8	N1, N2: 114.3 N1, N3: 114.9 N2, N3: 115.4	N1: 76.8 N2: 76.6 N3: 76.8
8b (expt)	2.202(2)	2.290(6)	N1: 1.985(7) N2: 1.997(8) N3: 2.001(8)	2.459(2) 2.460(2)	N1: 101.7(2) N2: 102.1(2) N3: 102.8(2)	N1, N2: 115.9(4) N1, N3: 114.5(3) N2, N3: 116.6(4)	N1: 78.2(3) N2: 77.5(3) N3: 77.6(3)
8b (calcd)	2.205	2.457	N1: 2.024 N2: 2.028 N3: 2.031	2.501	N1: 102.7 N2: 103.3 N3: 103.9	N1, N2: 114.1 N1, N3: 114.4 N2, N3: 116.1	N1: 76.8 N2: 76.5 N3: 77.8

 © VCH Verlagsgesellschaft mbH, D-69451 Weinheim, 1996 0570-0833/96/3521-2493 $ 15.00+.25/0

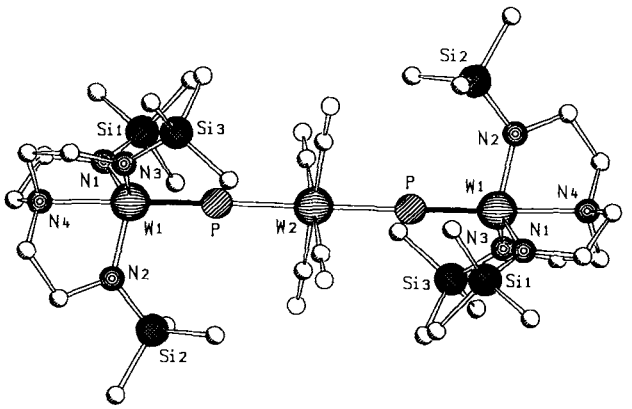

Fig. 2. Molecular structure of **8b** (without H atoms).

The comparison of the ^{31}P NMR data[12] of **2b**, **7**, and **8** indicates that the additional coordination of a metal center by the phosphido substituent leads to a high-field shift and to a considerable increase in the $^1J(^{183}W,^{31}P)$ values.[12] Thus, ^{31}P NMR chemical shifts and the $^1J(^{183}W,^{31}P)$ values in **3** (**3a**: $\delta = 595.4$, $J = 535.8$ Hz; **3b**: $\delta = 544.6$, $J = 554$, 163 Hz) are within the range of those found for complexes **7** and **8**.

The following points were investigated by theoretical methods: 1) For which ligands E is reaction (c) thermodynamically favored? 2) Why does **2b** react with $[M(CO)_5(thf)]$ to afford **8** instead of **7**? 3) Which ligating properties does **2b** have? 4) What causes the considerable change in the $^1J(^{183}W,^{31}P)$ value on linear coordination of tungsten complexes with terminal phosphido ligands to Lewis acids? In order to discuss these points, equilibrium structures of all compounds in question were calculated by applying the B-P86/SVP density functional approximation (see Tables 1 and 2).[17] There is good agreement between the calculated and experimentally observed structural parameters, with exception that the distance between W and the axial nitrogen atom is calculated to be 0.17–0.25 Å longer (the corresponding bond is rather weak).[18]

Electronic energies, calculated with the B-P86/SVP approximation, show reaction (c) to be slightly exothermic (exception: E = N; cf. Table 3). These calculated reaction energies are

Table 3. Calculated reaction energies (without correction of zero point vibrations) of reaction (c) in kJ mol^{-1} as a function of the terminal ligands E.

E	Method B-P86/SVP	B3-LYP/SVP
N	+61	+104
P	−14	+26
As	−30	+13
Sb	−25	+19

based upon the assumption that all lithium compounds appear in a partially aggregated state: $LiE(SiMe_3)_2$ as a dimer with D_2 symmetry,[19] LiCl as a tetramer,[20] and $LiSiMe_3$ as a hexamer.[21] Interactions with the solvent (toluene) and with donor compounds ($E(SiMe_3)_3$, THF) that are present in low concentration are ignored.[22] Reaction (c) is supposed to be favored by entropy due to an increase in the number of particles.

Reaction energies were also determined by the B3-LYP/SVP density functional approximation[23] at fixed B-P86/SVP equilibrium geometries (Table 3). This yields reaction energies that are shifted by $+42 \pm 2$ kJ mol^{-1} into the endothermic region. The reason for this systematic difference is the different spin multiplicity of starting materials and products: compound **1b** exhibits a triplet spin state. A more accurate calculation of the spin coupling energies for molecules of this size is currently not feasible. Nevertheless, the following conclusions can be drawn: A) Reaction (c) is equally favored from a thermodynamic point of view for E = P, As, or Sb, but not for E = N. This is surprising since compounds containing nitrido ligands have been known for a long time. The probable explanation lies in the high stability of the amide $LiN(SiMe_3)_2$, which would be a starting material in reaction (c). B) Reaction (c) is most exothermic when E = As. C) From a purely thermodynamic point of view, since reaction (c) had been carried out successfully for E = P, it should work for E = Sb as well.

To establish why **2b** and $[W(CO)_5(thf)]$ form **7b** only as an intermediate, which then preferentially yields **8b**, reaction energies for the reactions **2b** + $[W(CO)_5(thf)]$ → **7b** + THF, and **2b** + **7b** → **8b** + CO were calculated. In the B-P86/SVP (B3-LYP/SVP) approximation these reaction energies are −51 (−40) kJ mol^{-1}, and +66 (+58) kJ mol^{-1}, respectively. Evidently, CO is a more strongly binding ligand than **2b**. The apparent contradiction with experimental findings can be resolved if the reaction $[W(CO)_5(thf)] + CO \rightarrow [W(CO)_6] + THF$ is taken into account. With the formation of $[W(CO)_6]$ acting as a driving force,[24] the overall reaction **2b** + **7b** + $[W(CO)_5(thf)]$ → **8b** + $[W(CO)_6]$ + THF has a reaction energy of −19 (−14) kJ mol^{-1}. Further reaction of **8b** with elimination of CO is not feasible for steric reasons.

The characteristics of bonding in **2b** and in the other complexes were investigated by PESHO analysis[25] (PESHO = *p*air of *e*lectron *s*haring *h*ybrid *o*rbitals).[26] The W≡P bond in **2b** largely consists of one d_σ–p_σ bond and two d_π–p_π bonds (Table 4, Fig. 3); there are only small contributions from the 6s

Table 4. Bonding in **2b** and its complexes characterized by PESHOs. For further explanations about the information given in the Table see reference [25]. The η_h values associated with the radii R_A, R_B are recorded in columns 5–8.

Compound	*A*	*B*	*h*	R_A, R_B [pm] 60	80	100	120	[a]
2b	W	P	1	0.09	0.24	0.46	0.72	d_σ–p_σ[b]
			2	0.07	0.20	0.37	0.54	d_π–p_π[b]
			3	0.07	0.20	0.37	0.54	d_π–p_π[b]
			4	0.02	0.04	0.07	0.12	[c]
$[(N_3N)WP–BH_3]$	W	P	1	0.09	0.22	0.40	0.67	d_σ–p_σ[b]
			2	0.07	0.20	0.37	0.54	d_π–p_π
			3	0.07	0.20	0.37	0.54	d_π–p_π
	P	B[d]	1	0.11	0.30	0.55	0.84	σ
			2	0.02	0.06	0.11	0.20	π[e]
			3	0.02	0.06	0.11	0.20	π
8b	W1	P	1	0.08	0.21	0.39	0.62	d_σ–p_σ
			2	0.07	0.19	0.36	0.52	d_σ–p_σ
			3	0.07	0.19	0.35	0.51	d_π–p_π
	P	W2	1	0.06	0.16	0.28	0.44	p_σ–d_σ
			2	0.02	0.06	0.12	0.19	p_π–d_π[f]
			3	0.02	0.06	0.12	0.18	p_π–d_π

[a] Dominant electron sharing mechanism. [b] See Figure 3. [c] The fourth PESHO with its significantly smaller shared electron number η_h signals that electron sharing between W and P is qualitatively described by a triple bond (as opposed to a "quadruple bond"). [d] $\eta_h(A,R_A;B,R_B)$ for A = P and B = B cannot be directly compared to $\eta_h(A,R_A;B,R_B)$ for A = P and B = W2, because typical valence radii of W and B are different (PESHO analysis does not rely on empirical data). [e] Electron sharing between P and B in $[(N_3N)WP \rightarrow BH_3]$ is dominantly of σ type; π contributions are smaller by a factor of 5. [f] σ and π contributions to electron sharing between P and W2 in **8b** differ by a factor of 2.5. A comparison of radial electron densities $\rho_P(r,l,m)$ (not shown) reveals that s and p_σ densities at phosphorus in **2b** are larger than in **8b**, while the reverse holds for p_π densities. This may be interpreted as σ donation and π acceptance of **2b** in **8b**.

 © VCH Verlagsgesellschaft mbH, D-69451 Weinheim, 1996 0570-0833/96/3521-2494 $ 15.00+.25/0

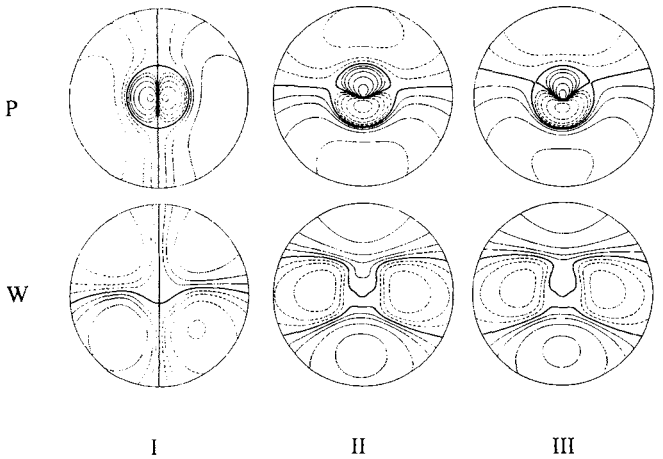

Fig. 3. PESHOs $|A,R_A;\tilde{h}\rangle$ and $|B,R_B;\tilde{h}\rangle$ with A = W and B = P; $R_A = R_B$ = 100 pm (radii of the circles drawn) for compounds **2b** (I: $h = 2$; II: $h = 1$) and $[(N_3N)W{\equiv}P\ \ BH_3]$ (III: $h = 1$). The amplitudes of the PESHOs were multiplied by η_h (cf. Table 4) and subsequently plotted as contour lines. Bold lines correspond to nodal lines (zero amplitude); other contour lines represent amplitudes of ± 0.02, ± 0.04, ± 0.08, etc (in $a_0^{-3/2}$). The centers of the circular frames are occupied by the corresponding nuclei (not drawn), their vertical distances are to scale. Since an effective core potential has been used at W, its valence orbitals exhibit few if any inner nodes. Otherwise, I corresponds to a typical p_π–d_π bond between P and W. Comparison of II and III shows the increasing contribution from the phosphorus 3s orbital to the p_σ–d_σ bond upon coordination to BH_3.

orbital of tungsten and the 3s orbital of phosphorus to the $d_\sigma - p_\sigma$ bond (Fig. 3). Coordination of **2b** to an σ acceptor, for example BH_3, leads to formation of a weak σ bond between P and B (Table 4), with simultaneous *shortening* of the W≡P bond (cf. calculated values in Tables 1 and 2). This effect can be explained by increased participation of the 3s orbital of phosphorus in covalent interactions with its partners (Fig. 3). The energy of the reaction $[(N_3N)WP] + H_3B(thf) \rightarrow [(N_3N)WP{-}BH_3] + THF$ is calculated to be $-22\ (-2)$ kJ mol^{-1} by using the B-P86/SVP approximation (B3-LYP/SVP approximation). Accordingly, a possible borane adduct of **2b** would be much less stable than the complex with $[W(CO)_5]$, which compares with our experimental observations. This can probably be explained by the π acceptor ability of ligand **2b**, which is shown, for example, by PESHO analysis of **8b** (Table 4). Since the W≡P-π bond is thereby weakened, the W≡P distance in **8b** is 2.4 pm (calculated) or 4.0 pm (observed) greater than in **2b**. Thus, the phosphido complex **2b** is characterized by similar, but less pronounced, ligating properties than CO.

The increase of the $^{183}W,^{31}P$ coupling constant upon linear coordination of **2b** to a σ acceptor may be rationalized by the stronger phosphorus 3s orbital involvement in W≡P bonding upon complex formation (Fermi contact term).

Experimental Procedure

2b, **6**: **1b** (103 mg, 0.18 mmol) and $LiE(SiMe_3)_2 \cdot 2THF$ (0.37 mmol) (E = P [27], As [28]) in toluene (10 mL) were stirred for 48 h at 80 and 110 °C, respectively. The deep red suspension was reduced to dryness in vacuum and the residue was extracted twice with hexane (40 mL). The solvent was removed in vacuum until the onset of crystallization. Compounds **2b** and **6** crystallized at −20 °C as yellow-orange cubes. The compounds could be recrystallized from Et_2O (**2b**: 67 mg, 65%; **6**: 53 mg, 48%).

8: To a solution of **2b** (104 mg, 0.18 mmol) dissolved in toluene (10 mL), $[M(CO)_5(thf)]$ (M = Cr, W) (9 mL of a 0.02 M solution in THF), prepared by irradiating $M(CO)_6$ in a UV-apparatus, was added and stirred for 60 h at ambient temperature. The solvent was removed in vacuum until crystals began to form. At −20 °C **8a** (81 mg, 68%), **8b** (96 mg, 74%), respectively, crystallized as red rhombuses from deep red solutions.

Received: June 18, 1996 [Z 9238 IE]
German version: *Angew. Chem.* **1996**, *108*, 2637–2641

Keywords: arsenido complexes · complexes with elements of group 15 · phosphido complexes · tungsten compounds

[1] M. Scheer, S. Gremler, E. Herrmann, U. Grünhagen, M. Dargatz, E. Kleinpeter, *Z. Anorg. Allg. Chem.* **1991**, *600*, 203–210; M. Scheer, F. Uhlig, T. T. Nam, M. Dargatz, H.-D. Schädler, E. Herrmann, *ibid.* **1990**, *585*, 177–188; M. Scheer, S. Gremler, E. Herrmann, P. G. Jones, *J. Organomet. Chem.* **1991**, *414*, 337–349; M. Scheer, S. Gremler, *Z. Anorg. Allg. Chem.* **1993**, *619*, 471–475.

[2] K. Schuster, Diplomarbeit, Universität Halle-Wittenberg, **1991**; M. Scheer, K. Schuster, J. Müller, E. Matern, unpublished results.

[3] K.-Y. Shih, K. Totland, S. W. Seidel, R. R. Schrock, *J. Am. Chem. Soc.* **1994**, *116*, 12103.

[4] Z. Duan, J. G. Verkade, *Inorg. Chem.* **1995**, *34*, 1576–1578.

[5] N. Zanetti, R. R. Schrock, W. M. Davis, *Angew. Chem.* **1995**, *107*, 2184–2186; *Angew. Chem. Int. Ed. Engl.* **1995**, *34*, 2044–2046.

[6] C. E. Laplaza, W. M. Davis, C. C. Cummins, *Angew. Chem.* **1995**, *107*, 2181–2183; *Angew. Chem. Int. Ed. Engl.* **1995**, *34*, 2042–2043.

[7] M. Scheer, K. Schuster, T. A. Budzichowski, M. H. Chisholm, W. E. Streib, *J. Chem. Soc. Chem. Commun.* **1995**, 1671–1672.

[8] Highlight: M. Scheer, *Angew. Chem.* **1995**, *107*, 2151–2153; *Angew. Chem. Int. Ed. Engl.* **1995**, *34*, 1997–1999; some of the results were presented in a lecture: M. Scheer, lecture at the 211th ACS Meeting, New Orleans **1996**, see INOR 222 in the book of abstracts.

[9] In a sealed NMR tube, reaction (c) was monitored for 48 h by ^{31}P NMR spectroscopy in [D$_8$]toluene starting at ambient temperature and heating to 60 and 80 °C. Measurements were taken every 2 h in the beginning, later every 8 h. Small amounts of **2b** and $P(SiMe_3)_3$ could already be detected after 2 h. The increase in the amount of **2b** formed is accompanied by a decrease in the amount of $LiP(SiMe_3)_2$ and an increase in that of $P(SiMe_3)_3$. The trace amounts of $HP(SiMe_3)_2$, evidently caused by hydrolysis at the inner wall of the tube, remain constant.

[10] R. R. Schrock, lecture at the 211th ACS Meeting, New Orleans **1996**, see INOR 517 in book of abstracts.

[11] The reaction was monitored by ^{31}P NMR spectroscopy between −40 °C and ambient temperature. Intensities of the products showed that the complexes **7** are only intermediates; complexes **8** are formed as the main products with an increase in temperature and time. After 48 h **8** is formed quantitatively.

[12] IR (CH_2Cl_2): **8a**: 1912 (s); **8b**: 1896 (s) cm^{-1}; ^1H NMR (250.133 MHz, C_6D_6, 298 K, TMS) **6**: δ = 3.54 (t, 6H, CH_2), 1.55 (t, 6H, CH_2) 0.79 (s, 27H, CH_3); **8b**: δ = 3.14 (t, 6H, CH_2), 1.60 (t, 6H, CH_2) 0.64 (s); ^{13}C NMR (62.896 MHz, toluene-[D$_8$]THF, 298 K). **6**: δ = 55.3 (s, CH_2), 52.3 (s, CH_2), 6.9 (s, CH_3); $^{31}P\{^1H\}$ NMR (101.256 MHz, C_6D_6, 298 K, 85% H_3PO_4 ext.); **2b**: δ = 1077.6, $^1J(^{183}W,^{31}P)$ = 136 Hz; **7a**: δ = 708.1, $^1J(^{183}W,^{31}P)$ = 442, **7b**: δ = 662.6, $^1J(^{183}W,^{31}P)$ = 450, 135; **8a**: δ = 728.1, $^1J(^{183}W,^{31}P)$ = 413 Hz; **8b**: δ = 679.8, $^1J(^{183}W,^{31}P)$ = 426, 151; EI-MS (70 eV; 100 °C) **6**: *m/z* (%): 618 (16) [M^+], 603 (100) [$M^+ - CH_3$]; **8a** (140 °C): *m/z* (%): 611 (6) [$(N_3N)W{\equiv}P \rightarrow Cr]^+$, 574 (7) [$(N_3N)W{\equiv}P]^+$, 559 (8) [$(N_3N)W{\equiv}P\text{-}CH_3]^+$; **8b** (130 °C): *m/z* (%): 758 (6) [$(N_3N)W{\equiv}P \rightarrow W]^+$, 574 (4) [$(N_3N)W{\equiv}P]^+$, 559 (6) [$(N_3N)W{\equiv}P - CH_3]^+$.

[13] R. R. Schrock, personal communication; J. A. Johnson-Carr, N. Zanetti, R. R. Schrock, M. D. Hopkins, *J. Am. Chem. Soc.*, in press.

[14] Crystal data and details of refinement: data were collected on a Stoe IPDS diffractometer using $Mo_{K\alpha}$ (λ = 0.71069 Å) radiation, T = 200(1) K, no absorption corrections were performed; the structures were solved by direct methods, method of least-squares refinement, all non-hydrogen atoms were refined anisotropically. Hydrogen atoms were fixed in calculated positions and were refined isotropically. **1b**: $C_{15}H_{39}ClN_4Si_3W$, M_r = 579.07, crystal dimensions 0.30 × 0.30 × 0.18 mm^3, cubic, space group $Pa\bar{3}$ (no. 205); a = 17.220(2) Å, Z = 8, V = 5106.2(10) Å^3, ρ_{calcd} = 1.507 Mg m^{-3}, $\mu(Mo_{K\alpha})$ = 47.76 cm^{-1}, 1687 independent reflections ($2\theta_{max}$ = 52°), 1494 observed with $F_0 \geq 4\sigma(F_0)$; 76 parameters, R_1 = 0.0340, wR_2 = 0.0958; **6**: $C_{15}H_{39}AsN_4Si_3W$, M_r = 618.54, crystal dimensions 0.38 × 0.38 × 0.15 mm^3, cubic, space group $Pa\bar{3}$ (no. 205); a = 17.255(2) Å, Z = 8, V = 5137.4(10) Å^3, ρ_{calcd} = 1.599 Mg m^{-3}, $\mu(Mo_{K\alpha})$ = 59.21 cm^{-1}, 2080 independent reflections ($2\theta_{max}$ = 56°), 1785 observed with $F_0 \geq 4\sigma(F_0)$; 76 parameters, R_1 = 0.0402, wR_2 = 0.1063; **8b**: $C_{34}H_{78}O_4P_2Si_6N_8W_3 \times 2C_7H_8$, M_r = 1629.34, crystal dimensions 0.2 × 0.08 × 0.08 mm^3, monoclinic, space group $P2(1)/n$ (no. 14); a = 11.587(2), b = 16.700(3), c = 16.971(3) Å, β = 97.21(3)°, Z = 2, V = 3258(1) Å^3, ρ_{calcd} = 1.661 Mg m^{-3}, $\mu(Mo_{K\alpha})$ = 54.87 cm^{-1}, 6088 independent reflections ($2\theta_{max}$ = 52°), 4939 observed with $F_0 \geq 4\sigma(F_0)$; 294 parameters, R_1 = 0.0487, wR_2 = 0.1278. All calculations were performed by using the SHELXS-86 [29], SHELXL-93 [29] and Schakal-92 programs. Further details of the crystal structure investigations may be obtained from the Fachinformationszentrum Karlsruhe, D-76344, Eggenstein-Leopoldshafen, on quoting the depository numbers CSD-405518, CSD-405519, and CSD-405520.

[15] F. A. Cotton, D. J. Darensbourg, B. W. S. Kolthammer, *Inorg. Chem.* **1981**, *20*, 4440–4442.

[16] E. Fluck, P. Kuhn, A. Müller, H. Bögge, *Z. Anorg. Allg. Chem.* **1988**, *567*, 13–22.

 © VCH Verlagsgesellschaft mbH, D-69451 Weinheim, 1996 0570-0833/96/3521-2495 $ 15.00+.25/0

[17] Structure optimizations were performed by using the TURBOMOLE set of programs with the RI-*J* approximation (K. Eichkorn, O. Treutler, H. Öhm, M. Häser, R. Ahlrichs, *Chem. Phys. Lett.* **1995**, *242*, 652–660). For definition of the B-P86 density functional see A. D. Becke, *Phys. Rev. A* **1988**, *38*, 3098; J. P. Perdew, *Phys. Rev. B* **1986**, *33*, 8822; *ibid.*, **1986**, *34*, 7046. The acronym SVP refers to TURBOMOLE split valence basis sets, augmented by a shell of polarization functions, cf. A. Schäfer, H. Horn, R. Ahlrichs, *J. Chem. Phys.* **1992**, *97*, 2571. Quasi-relativistic pseudopotentials were used for the elements W and Sb (D. Andrae, U. Häussermann, M. Dolg, H. Stoll, H. Preuss, *Theor. Chim. Acta* **1990**, *77*, 123; A. Bergner, M. Dolg, W. Küchle, H. Stoll, H. Preuss, *Mol. Phys.* **1993**, *80*, 1431). The corresponding SVP basis sets optimized for W and Sb by F. Weigend, K. Eichkorn and R. Ahlrichs are unpublished.

[18] Results are not improved upon switching to the MP2/SVP approximation ($SiMe_3$ in **2b** replaced by Me).

[19] D_2-symmetric $(LiE(SiMe_3)_2)_2$ corresponds to the crystal structures of $[LiP(SiMe_3)_2(thf)]_2$ (cf. G. Becker, H.-M. Hartmann, W. Schwarz, *Z. Anorg. Allg. Chem.* **1989**, *577*, 9–22) and $[LiAs(SiMe_3)_2(dme)]_2$ (cf. G. Becker, C. Witthauer, *Z. Anorg. Allg. Chem.* **1982**, *492*, 28–36). The analogous antimony compound prefers a slightly different mode of aggregation (cf. G. Becker, A. Münch, C. Witthauer, *Z. Anorg. Allg. Chem.* **1982**, *492*, 15–27).

[20] In the experiment, LiCl is formed as a solid in reaction (c).

[21] The difference in energy between the hexamer and the tetramer was calculated to be 4.5 kJ per mol of $LiSiMe_3$ (B-P86/SVP). The crystal structure of the hexamer is known: T. F. Schaaf, W. Butler, M. D. Glick, J. P. Oliver, *J. Am. Chem. Soc.* **1974**, *96*, 7593–7594; W. H. Ilsley, T. F. Schaaf, M. D. Glick, J. P. Oliver, *ibid.* **1980**, *102*, 3769–3774.

[22] Calculated reaction energies will be correct as long as solvation and aggregation of the lithium compounds are considered in a similar approximation for the starting materials and for the products. Relative reaction energies amongst pnictido ligands E are supposed to be very reliable, since they are not influenced by errors associated with lithium aggregation.

[23] For a concise definition of the B3-LYP density functional see C. W. Bauschlicher, H. Partridge, *Chem. Phys. Lett.* **1994**, *231*, 277. The calculations were performed by using the TURBOMOLE set of programs (R. Ahlrichs, M. Bär, M. Häser, H. Horn, C. Kölmel, *Chem. Phys. Lett.* **1989**, *162*, 165; O. Treutler, R. Ahlrichs, *J. Chem. Phys.* **1995**, *102*, 346).

[24] M. Scheer, C. Troitzsch, P. G. Jones, *Angew. Chem.* **1992**, *104*, 1395–1397; *Angew. Chem. Int. Ed. Engl.* **1992**, *31*, 1377–1379; M. Scheer, U. Becker, *Phosphorus, Sulfur, Silicon*, **1994**, *93–94*, 391–392; M. Scheer, C. Troitzsch, L. Hilfert, M. Dargatz, E. Kleinpeter, P. G. Jones, J. Sieler, *Chem. Ber.* **1995**, *128*, 251–257; M. Scheer, U. Becker, J. C. Huffman, M. H. Chisholm, *J. Organomet. Chem.* **1993**, *461*, C1–C3.

[25] M. Häser, *J. Am. Chem. Soc.* **1996**, *118*, 7311–7325. A PESHO is a pair of atomic hybrid orbitals $|A,R_A;\tilde{h}\rangle$ and $|B,R_B;\tilde{h}\rangle$; here "atomic" means $|A,R_A;\tilde{h}\rangle$ and $|B,R_B;\tilde{h}\rangle$ are contained within spherical neighborhoods of the nuclei A and B, respectively, with radii given by R_A and R_B, respectively; the PESHOs are obtained by requiring the closest description of electronic delocalization between the atomic neighborhoods of A and B (thus approximating the oneelectron density operator) for any pre-set number of PESHOs ($h=1,2,3,\ldots$). Each PESHO ($|A,R_A;\tilde{h}\rangle$, $|B,R_B;\tilde{h}\rangle$) is characterized by a number $0\leq\eta_h(A,R_A;B,R_B)\leq 2$ of electrons shared between $|A,R_A;\tilde{h}\rangle$ and $|B,R_B;\tilde{h}\rangle$. The number of PESHOs with values $\eta_h(A,R_A;B,R_B)$ significantly different from zero relates to the number of covalent bonds between A and B, while η_h itself refers to the extent of the corresponding electron sharing phenomenon. Entries in Table 4 are values of $\eta_h(A,R_A;B,R_B)$ for $R_A=R_B=60$, 80, 100, and 120 pm.

[26] The analysis of bonding was based on Kohn–Sham orbitals from the B-P86/SVP calculations. Conclusions regarding electronic delocalization remain valid only in as far as electronic correlations are of minor importance.

[27] F. Uhlig, S. Gremler, M. Dargatz, M. Scheer, E. Herrmann, *Z. Anorg. Allg. Chem.* **1991**, *606*, 105–108.

[28] G. Becker, G. Gutekunst, H.-J. Wessely, *Z. Anorg. Allg. Chem.* **1980**, *462*, 113–129.

[29] G. M. Sheldrick, *SHELXS*-86, Universität Göttingen, **1986**; *SHELXL*-93, Universität Göttingen, **1993**.

Self-Assembling Covalently Linked Supramolecular Arrays of Defined Structure: The Remarkable Redox Reactivity of 15-*meso*-Substituted 5-Oxyporphyrins**

Richard G. Khoury, Laurent Jaquinod, Daniel J. Nurco, Ravindra K. Pandey, Mathias O. Senge, and Kevin M. Smith*

The synthesis and chemistry of organized supramolecular assemblies have received considerable attention recently, particularly with regard to self-assembly of macromolecules to give supramolecular arrays possessing, or potentially possessing, biological or other catalytic activity.[1, 2] It is hoped that such biofunctional assemblies might show unique biomimetic function, demonstrate molecular discrimination enabling unique catalytic activity, or act as selective transport agents. In the present paper we show that, based on their redox properties, certain carefully designed oxyporphyrins (oxophlorins) can be induced to reversibly self-assemble, by way of covalent carbon–carbon bonds, to give supramolecular assemblies with defined structures.

Iron complexes of oxophlorins **1** have been postulated as intermediates in the catabolism of heme leading to bile pigments.[3] Oxophlorins are porphyrinoids that have a *meso* carbonyl group, and exist in the keto form **1** rather than in the enol form **2** in neutral solution.[4] In acidic solution or in the presence

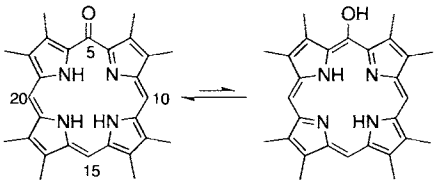

1 **2**

of divalent metals, the enol structure predominates, but with trivalent metal ions such as iron(III), either the keto or enol form can predominate, depending upon pH.[4] Based on the known radical chemistry of metallooxophlorins (due to their low oxidation potentials)[5] and the tendency of the radicals to dimerize to give unique structures,[6] we chose to synthesize a number of *meso*-substituted oxophlorins and then investigate their chemical oxidation to provide regio- and stereochemically pure oligomers. All known radical dimerizations of 5-oxophlorins[5, 6] involve the 15-position, and thus the largest oligomer that can be obtained is a dimer. In order to investigate access to oligomers (and therefore supramolecular assemblies), we targeted 15-substituted 5-oxophlorins in the hope that radical oligomerization reactions of these substrates would take place

[*] Prof. Dr. K. M. Smith, R. G. Khoury, Dr. L. Jaquinod, D. J. Nurco, Dr. R. K. Pandey,[+] Dr. M. O. Senge[++]
Department of Chemistry, University of California
Davis, CA 95616-5295 (USA)
Fax: Int. code +(916) 752-8995
e-mail: smith@chem.ucdavis.edu

[+] Permanent address: Department of Radiation Biology
Roswell Park Cancer Institute, Buffalo, NY 14263 (USA)

[++] Permanent address: Institut für Organische Chemie (WE02)
Freie Universität Berlin, Takustrasse 3, D-14195 Berlin (Germany)

[**] This work was supported by the National Science Foundation (CHE-93-05577), by the National Institutes of Health (HL-22252), and by the Deutsche Forschungsgemeinschaft and the Fonds der Chemischen Industrie.

 © VCH Verlagsgesellschaft mbH, D-69451 Weinheim, 1996 0570-0833/96/3521-2496 $ 15.00+.25/0

at both the 10- and 20-positions. Moreover, the electronic nature of the substituent at C-15 should enable facile control over the oxidation potential of the oxophlorin, and therefore over the ease of formation of the supramolecular assembly.

Several approaches have been developed for the synthesis of oxophlorins;[7, 8] we selected the MacDonald-type 2+2 condensation of 1,9-diformyldipyrroketones and dipyrromethane-1,9-dicarboxylic acids,[8] because this approach would enable us to readily prepare a series of 15-substituted 5-oxophlorins. Condensation of a 1,9-diformyldipyrroketone with a 5-ethyldipyrromethane-1,9-dicarboxylic acid[9] predominantly afforded the 15-ethyl-5-isooxophlorin **3**, which existed as the iso tautomer rather than the expected oxophlorin form **4** owing to steric congestion between the substituents at positions 13, 15, and 17.[8b] However, another product was isolated more recently in smaller amounts from this reaction, and is identified as 10,10′-bis-(15-ethyl-10*H*-5-oxophlorin). This compound exists in the isomeric forms **5** and **6**, each of which demonstrate that 15-substituted-5-oxophlorins do indeed dimerize at the 10,10′-positions. Stereoisomers **5** and **6** are stable as a solid

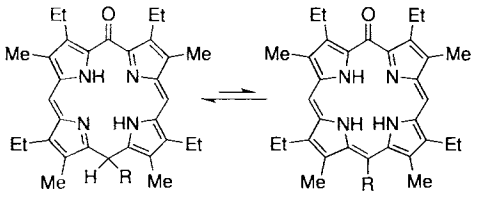

3, R = Et

4, R = Et
7, R = C_6H_5
10, R = C_6F_5

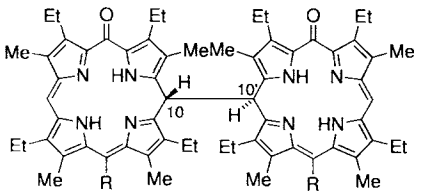

5, R = Et
8, R = C_6H_5
11, R = C_6F_5

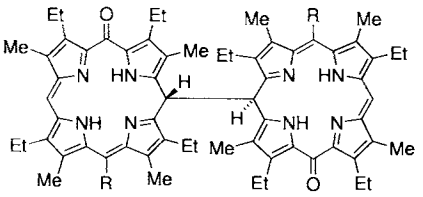

6, R = Et
9, R = C_6H_5
12, R = C_6F_5

and in solution, and are separable. The molecular structure of **5** was confirmed by X-ray crystallography (Fig. 1).[10a, c] Molecules of **5** pack in a crystalline lattice with alternating columns of stacked dimers and ordered molecules of cyclohexane (not shown).

The 15-phenyl-5-oxophlorin **7** was synthesized by using the same conditions as those in the attempted preparation of **4**; under the acidic conditions, both the mono- and dications of the oxophlorin **7** were observed spectrophotometrically. Basic workup of this reaction product, followed by exposure to air in

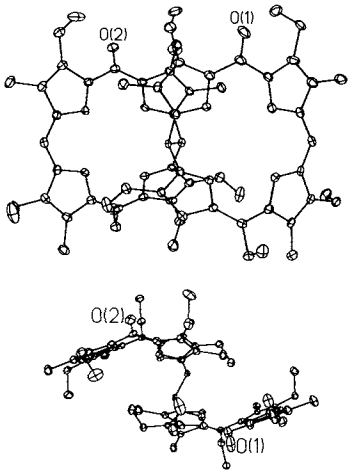

Fig. 1. Molecular structure of isooxophlorin dimer **5** (35% probability thermal ellipsoids) in the crystal. The lower portion shows an edge-on view of the same dimer. Hydrogen atoms have been omitted for clarity.

CH_2Cl_2 and daylight (which accelerates the dimerization) afforded, in 89% yield, the novel isooxophlorin dimer as a mixture of regioisomers **8** and **9**. Figure 2 shows the UV/Vis spectrum ($CHCl_3$). The ^1H NMR spectrum (in $CDCl_3$) indicates

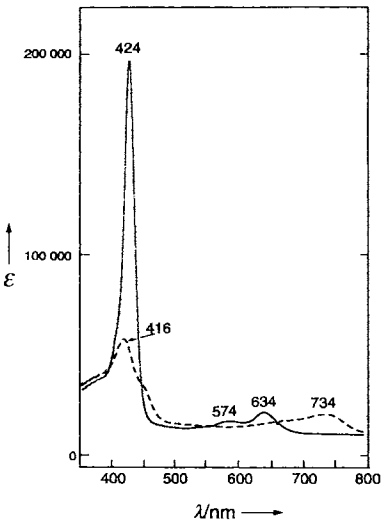

Fig. 2. UV/Vis spectra ($CHCl_3$) isooxophlorin dimer **8/9** (– · –) and the salt of diprotonated **7** (—).

interrupted conjugation and features signals for exchangeable NH protons at $\delta = 13.46$, 13.27, 13.25, and 13.18 (each 2H); the 10-H protons give rise to signals at $\delta = 5.35$ and 5.30 (each 2H, two isomers). Dimerization of 15-phenyl-5-oxophlorins required a longer period of time than that of the 15-ethyl analogue, confirming that the 15-*meso* substituent plays a role in moderating the oxidation potential of the oxophlorin macrocycle. Synthesis of 15-pentafluorophenyl-5-oxophlorin **10** and further treatment as described above resulted in even a slower rate of dimerization; treatment with an oxidizing agent such as $[K_3Fe(CN)_6]$ resulted in complete dimerization to give the mixture of regioisomers **11** and **12** in 20 minutes.

Having established the oxidative dimerization of the 15-substituted 5-oxophlorins, we next attempted to synthesize an oxophlorin supramolecular array. 5-Oxophlorin dimer **13** was prepared by condensing diformyldipyrroketone **14** with a symmetrical bis(dipyrromethane) **15**.[12] Oxidative dimerization of **13** afforded a 93% yield of the macromolecule **16** consisting of four

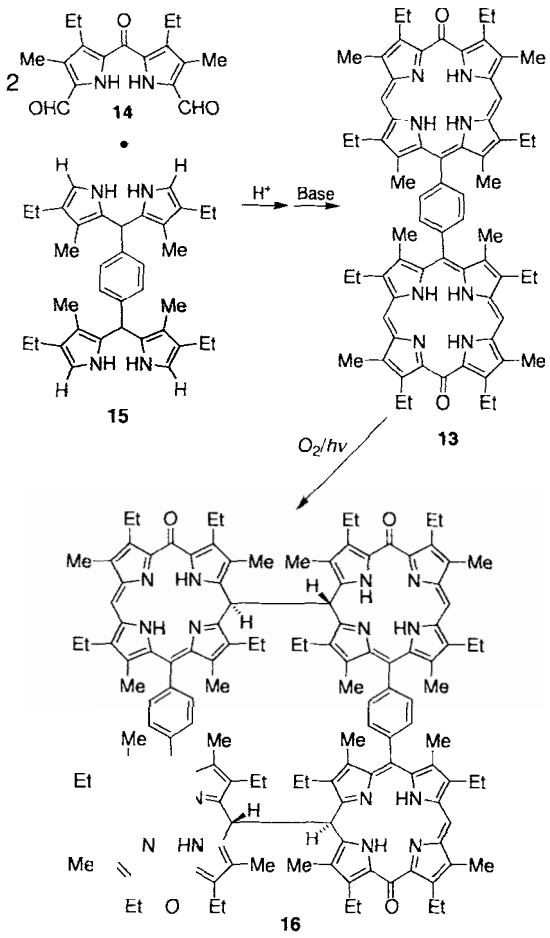

isooxophlorin-type subunits connected in a stereochemically unique fashion. The UV/Vis spectrum of **16** resembles that shown in Figure 2A, but the major bands are blue-shifted (λ_{max} = 378, 654 nm). The ^{1}H NMR spectrum (in $CDCl_3$) of **16** again demonstrates interrupted conjugation in the macrocycle, with signals for exchangeable NH groups at δ = 13.20 and 12.85 (each 4H), as well as the 10-H signal at δ = 5.41 (4H). The molecular structure of **16** was confirmed by X-ray crystallography (Fig. 3).[10b,c] The molecule has an overall helical structure

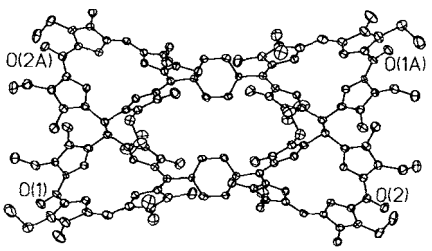

Fig. 3. Molecular structure of isooxophlorin tetramer **16** in the crystal (35% probability thermal ellipsoids). Hydrogen atoms have been omitted for clarity.

with disordered molecules of *n*-hexane fitting into the groove of the helix (not shown).

The radical dimerizations to afford the regioisomeric pairs **8**/**9**, **11**/**12**, and tetramer **16** are reversible, and involve the extremely facile reduction of oxophlorin radicals;[5] treatment with acid serves to regenerate the protonated oxophlorins (see Fig. 2), which can be quantitatively transformed back into the dimers or tetramer as already described above. ^{1}H NMR signals for the internal NH groups are shifted downfield $\Delta\delta$ = 15 upon dimerization of **4**, **7**, **10**, and **13** (indicating a disruption in the porphyrin-type ring current) and are exchangeable with D_2O/Et_3N. The protons at the 10-positions give rise to ^{1}H NMR signals around δ = 5.30 and the ^{13}C NMR signal of C-10 occurs at about δ = 40.0.

The structural features of **16** are unique. We consider compound **16** to be a remarkable example of a robust, self-assembled supramolecular array having a defined structure composed of versatile chromophores linked by covalent bonds. Studies of metal-binding and other chemical characteristics of a series of compounds such as **16** will be reported in due course. Most other synthetic supramolecular arrays of which we are aware are either irreversibly linked through covalent bonds or are only tenuously associated by way of relatively weak dative or hydrogen bonding interactions.

Received: June 4, 1996
Revised version: July 29, 1996 [Z9193IE]
German version: *Angew. Chem.* **1996**, *108*, 2657–2660

Keywords: dimerizations · porphyrinoids · redox reactions · self-assembly · supramolecular chemistry

[1] See for example a) D. E. Robertson, R. S. Farid, C. C. Moser, J. L. Urbauer, S. E. Mulholland, R. Pidikiti, J. D. Lear, A. J. Wand, W. F. DeGrado, P. L. Dutton, *Nature (London)* **1994**, *368*, 425; b) S. Anderson, H. L. Anderson, A. Bashall, M. McPartlin, J. K. M. Sanders, *Angew. Chem.* **1995**, *107*, 1196; *Angew. Chem. Int. Ed. Engl.* **1995**, *34*, 1096; D. W. J. McCallien, J. K. M. Sanders, *J. Am. Chem. Soc.* **1995**, *117*, 6611; c) K. M. Smith, L. A. Kehres, J. Fajer, *J. Am. Chem. Soc.* **1983**, *105*, 1387; d) H. Tamiaki, T. Miyatake, R. Tanikaga, A. R. Holzwarth, K. Schaffner, *Angew. Chem.* **1996**, *108*, 810; *Angew. Chem. Int. Ed. Engl.* **1996**, *35*, 772.

[2] See for example *Supramolecular Assemblies—New Developments in Biofunctional Chemistry* (Ed.: Y. Murakami), Mita Press, Tokyo, **1990**; J.-M. Lehn, *Supramolecular Chemistry*, VCH, Weinheim, **1995**; H. Kurreck, M. Huber, *Angew. Chem.* **1995**, *107*, 929; *Angew. Chem. Int. Ed. Engl.* **1995**, *34*, 849.

[3] P. O'Carra in *Porphyrins and Metalloporphyrins* (Ed.: K. M. Smith), Elsevier, Amsterdam, **1975**, pp. 123–150, and references therein.

[4] A. H. Jackson, G. W. Kenner, K. M. Smith, *J. Chem. Soc. C* **1968**, 302.

[5] J.-H. Fuhrhop, S. Besecke, J. Subramanian, *J. Chem. Soc. Chem. Commun.* **1973**, 1.

[6] See for example J.-H. Fuhrhop, S. Besecke, J. Subramanian, C. Mengersen, D. Riesner, D. Mauzerall, *J. Am. Chem. Soc.* **1975**, *97*, 7141; J.-H. Fuhrhop, E. Baumgartner, H. Bauer, *ibid.* **1981**, *103*, 5854; A. L. Balch, B. C. Noll, S. L. Phillips, S. M. Reid, E. P. Zovinka, *Inorg. Chem.* **1993**, *32*, 4730.

[7] See for example K. M. Smith in *Porphyrins and Metalloporphyrins* (Ed.: K. M. Smith), Elsevier, Amsterdam, **1975**, p. 36, 40–41, 630, and references therein; R. Bonnett, M. J. Dimsdale, G. F. Stephenson, *J. Chem. Soc. C* **1969**, 564; G. H. Barnett, M. F. Hudson, S. W. McCombie, K. M. Smith, *J. Chem. Soc. Perkin Trans. 1* **1973**, 691.

[8] a) P. S. Clezy, A. J. Liepa, G. A. Smythe, *Aust. J. Chem.* **1970**, *23*, 603, 589; b) R. G. Khoury, L. Jaquinod, D. J. Nurco, K. M. Smith, *Chem. Commun.* **1996**, 1143.

[9] D. A. Lee, J. M. Brisson, K. M. Smith, *Heterocycles* **1995**, *40*, 131.

[10] Crystallographic details: a) **5**: A crystal with dimensions 0.56 × 0.16 × 0.10 mm crystallized in the monoclinic space group $P2_1/n$; a = 14.893(3), b = 18.165(4), c = 25.214(5) Å, β = 92.92(3)°, V = 6812.2(24) Å^3, Z = 4. Of 9980 reflections measured 9206 were unique (R_{int} = 0.0218, T_{min} = 0.86, T_{max} = 0.90, μ = 0.527 mm^{-1}, ρ_{calc} = 1.140 g cm^{-3}). $R1$ = 0.069, $wR2$ = 0.209 (822 parameters). b) **16**: A crystal with dimensions 0.56 × 0.30 × 0.20 mm crystallized in the monoclinic space group $C2/c$; a = 36.106(5), b = 17.4906(15), c = 29.190(5) Å, β = 123.501(9)°, V = 15371.5(35) Å^3, Z = 4. Of 10891 reflections measured 10035 were unique (R_{int} = 0.0215, T_{min} = 0.81, T_{max} = 0.98, μ = 0.811 mm^{-1}, ρ_{calc} = 1.063 g cm^{-3}). $R1$ = 0.086, $wR2$ = 0.278 (988 parameters). c) Data for **16** were collected at 130(2) K on a Siemens P4 diffractometer with a rotating anode [$\lambda(Cu_{K\alpha})$ = 1.54178 Å] in $\theta/2\theta$ scan mode to $2\theta_{max}$ = 112°. Data for **5** were collected at 130(2) K on a Syntex $P2_1$ diffractometer [$\lambda(Cu_{K\alpha})$ = 1.54178 Å] in $\theta/2\theta$ scan mode to $2\theta_{max}$ = 114°. The structures were solved by direct methods and refined (based on F^2 using all independent data) by full matrix least squares methods (Siemens SHELXTL V. 5.03). R values are reported for $R1$ (based on observed data, $I > 2\sigma$) and $wR2$ (based on all data). Non-hydrogen atoms were refined with anisotropic thermal parameters. Hydrogens were placed in calculated positions refined with a riding model using isotropic thermal parameters. The crystal structure of **16** exhibited disorder in

a small portion of the tetramer and in the solvate *n*-hexane. The datasets were corrected for absorption [11]. Crystallographic data (excluding structure factors) for the structures reported in this paper have been deposited with the Cambridge Crystallographic Data Centre as supplementary publication no. CCDC-179-101. Copies of the data can be obtained free of charge on application to The Director, CCDC, 12 Union Road, Cambridge, CB2 1EZ, UK (fax: Int. code +(1223)336033; e-mail: teched@chemcrys.cam.ac.uk).

[11] S. R. Parkin, B. Moezzi, H. Hope, *J. Appl. Crystallogr.* **1995**, *28*, 53.

[12] a) J. L. Sessler, M. R. Johnson, S. F. Creager, J. C. Fettinger, J. A. Ibers, *J. Am. Chem. Soc.* **1990**, *112*, 9310; b) R. K. Pandey, T. P. Forsyth, K. R. Gerzevske, J. J. Lin, K. M. Smith, *Tetrahedron Lett.* **1992**, *33*, 5315; c) R. Paolesse, R. K. Pandey, T. P. Forsyth, L. Jaquinod, K. R. Gerzevske, D. J. Nurco, M. O. Senge, S. Liccocia, T. Boschi, K. M. Smith, *J. Am. Chem. Soc.* **1996**, *118*, 3869.

Synthesis, Structure, and Vibrational Spectra of Al_3BC_3, a Carbidecarboborate of Aluminum with Linear $(C{=}B{=}C)^{5-}$ Anions**

Harald Hillebrecht* and Falko D. Meyer

Dedicated to Professor Hans Georg von Schnering on the occasion of his 65th birthday

Compounds of the Al/B/C system are of great importance for the development of light, nonoxidic ceramics because of their high chemical and thermal stability,[1] which has led to a great number of recent publications and patents in this field.[2] While boron-rich compounds such as $B_{51}Al_2C_8$ ("AlB_{10}",[3]) and $B_{48}Al_3C_2$ ("diamond-like boron", "β-AlB_{12}" [4]) have been known for a long time, an aluminum-rich phase $Al_4B_xC_4$ with variable boron content ($x = 1-3$) was first reported in 1964.[5] Later the composition $Al_8B_4C_7$ was proposed without data on a crystal structure of the compound.[6] A detailed characterization was thus desirable, because this phase plays an important role in the investigation of hard materials ("cermets") based on boron carbide "B_4C" and aluminum.[7] The structure analysis of single crystals, which were obtained from the synthesis in molten aluminum, showed[8] that the correct composition is Al_3BC_3, that is a carbidecarboborate of aluminum.[9] Vibrational spectra confirm that the linear CBC group in Al_3BC_3 can be formulated as a complex anion $(C{=}B{=}C)^{5-}$ and thus represents the 16-electron system isoelectronic to CO_2 with the highest negative charge.

Single crystals of Al_3BC_3 in the form of hexagonal light yellowish transparent platelets were prepared from the elements at 1500 °C (see Experimental Procedure). The light yellow color is attributed to a weak and very broad absorption band at 380 nm in the UV/Vis spectrum. Single crystals of Al_3BC_3 are not sensitive to hydrolysis, and are stable in air up to about 600 °C. With the exception of HF and HNO_3 they are not attacked by dilute acids and bases at room temperature.

In the structure of Al_3BC_3 (Fig. 1), Al_5C trigonal bipyramids are linked by common corners of the basal plane to give layers of the composition Al_3C ($=CAl_2Al_{3/3}$), similar to Al_4C_3.[10] The most striking structural feature of the compound is located between these layers, namely isolated linear CBC groups with a B–C distance of 1.44 Å.

[*] Dr. H. Hillebrecht, Dipl.-Chem. F. D. Meyer
Institut für Anorganische und Analytische Chemie
and
Freiburger Materialforschungszentrum FMF
Albertstrasse 21, D-79104 Freiburg (Germany)
Fax: Int. code +(761)203-6012

[**] We thank Prof. Dr. G. Thiele (Freiburg) for the generous support of our work.

These CBC units are parallel to each other and connect the Al_3C layers. Hitherto, comparable linear CBC groups were only found for Sc_2BC_2.[11] In the latter, the B–C distance (1.48 Å) is longer than in Al_3BC_3, possibly as a result of the metallic properties of Sc_2BC_2.

If the crystal structure is described based on the coordination polyhedra of the C atoms, corner-shared double tetrahedra Al_3CBCAl_3 in a staggered orientation with the boron atom as common corner connect the Al_3C layers of CAl_5 bipyramids through the terminal Al atoms, which are thus also tetrahedrally coordinated (Al–C: 2.00–2.06 Å). As a result of the formation of the superstructure,[8] the equatorial Al atoms (shaded in Fig. 1) are coordinated as slightly distorted tetrahedra with Al–C distances of 1.98 Å (3×) and 2.23 Å. In contrast to some of the conclusions drawn by Matkovich et al.,[5] the boron content does not vary. Therefore, Al_3BC_3 is the only stoichiometric ternary compound of the Al/B/C system.

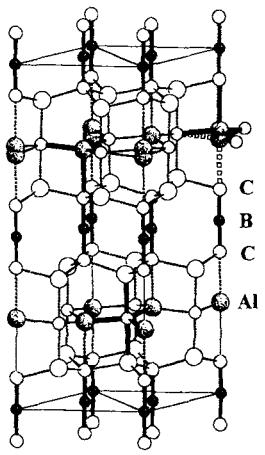

Fig. 1. Crystal structure of Al_3BC_3 with Al_3C layers and CBC groups. The Al atoms of the distorted AlC_5 trigonal bipyramids are shaded.

The structural similarity of Al_3BC_3 to Al_4C_3 and Al_5C_3N is a good reason for an ionic formulation as $(Al^{3+})_3(C^{4-})$-$(CBC)^{5-}$. According to this the CBC group can be interpreted as an anion $(C{=}B{=}C)^{5-}$ with 16 valence electrons. The analogy to CO_2 is confirmed by the vibrational spectra (Fig. 2). The

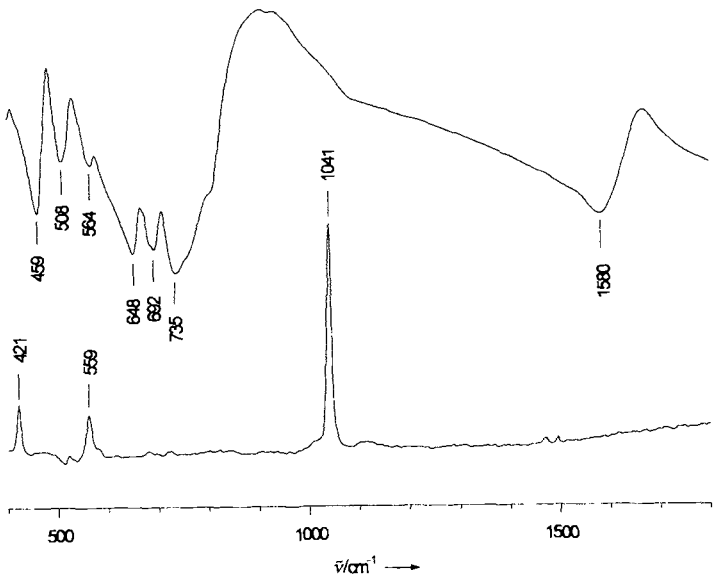

Fig. 2. FT-IR (top) and FT-Raman spectrum (bottom) of Al_3BC_3 (Bruker IFS66v, KBr and PE pellets, respectively).

predicted spectrum of a linear group YXY with $D_{\infty h}$ symmetry consists of three bands (symmetric stretching mode ν_s, Raman active; antisymmetric stretching mode ν_{as}, IR active; doubly degenerate bending mode δ, IR active). The strong band at 1041 cm^{-1} in the Raman spectrum of Al_3BC_3 can be assigned to the ν_s mode of the CBC group. The bands at 421 cm^{-1} and 560 cm^{-1} can be interpreted as Al–C stretching modes.[12] IR

 © VCH Verlagsgesellschaft mbH, D-69451 Weinheim, 1996 0570-0833/96/3521-2499 $ 15.00+.25/0

active modes at 1580 cm^{-1} (ν_{as}) and 735 cm^{-1} (δ) complete the vibrational spectrum of the CBC group. The calculation of the three force constants led to values of $f = 6.59\ N cm^{-1}$ (stretching force constant), $f' = 1.05\ N cm^{-1}$ (interaction force constant), and $f_d = 0.60\ N cm^{-1}$ (bending force constant). The quite high value of f_d results from the interaction between the C atoms of the CBC group and the surrounding Al atoms. As shown for the anion $(N{=}B{=}N)^{3-}$ f_d rises with the charge/radius ratio of the countercation.[13] Because of the broad signals and the low ^{10}B content (20%), the isotope splitting expected for the IR active modes is not observed.

According to Pauling[18] a bond order of 1.6 is calculated on the basis of the B–C distance. This is in good agreement with a value of 1.7 calculated from the force constant f according to the method of Siebert.[19] As expected the formal double bond is weakened significantly by the high negative charge. The effective charge of the CBC group is difficult to estimate because of the covalency of the Al–C bonds and will be investigated in more detail in the course of calculations. The comparison of bond lengths and force constants of anions with 16 valence electrons and boron as central atom shows (Table 1) that the results for the CBC group fit excellently in this series.

Table 1. Distances and force constants of 16-electron systems.

	$(OBO)^-$	$(NBN)^{3-}$	$(CBN)^{4-}$	$(CBC)^{5-}$
d[Å]	1.25	1.34	1.44/1.38	1.44
f[$N cm^{-1}$]	10.1	8.0	5.0/8.0	6.6
ref.	[13, 14]	[13, 15]	[16, 17]	this work

In summary, we have characterized the anion $(C{=}B{=}C)^{5-}$ for the first time by vibrational spectroscopy and by a structure analysis of Al_3BC_3. In terms of the maximum negative charge, the series of linear systems isoelectronic to CO_2 appears to be completed with $(C{=}B{=}C)^{5-}$. With respect to the ionic description, Al_3BC_3 can be regarded as the first carbidecarboborate.

Experimental Procedure

Single crystals of Al_3BC_3 were prepared from the elements. In an atmosphere of Ar the precursors (molar ratio Al/B/C = 40:2:3) were heated in a corundum crucible to 1500 °C, followed by slow cooling at a rate of 10 $K h^{-1}$ to 600 °C and then to room temperature by turning off the heat. Excess Al was removed with dilute aqueous HCl. By-products (AlB_2, Al_4C_3) were separated under the microscope.

Received: May 29, 1996 [Z9164IE]
German version: *Angew. Chem.* **1996**, *108*, 2655–2657

Keywords: aluminum carbidecarboborate · boron compounds · carboborates · structure elucidation

[1] R. Riedel, *Adv. Mater.* **1994**, *6*, 549–560.
[2] a) A. I. Kharlamov, T. I. Duda, V. V. Fomenko, *AIP Conf. Proc.* **1991**, *231*, 512–514; b) R. J. Oscroft, P. H. A. Roebuck, D. P. Thompson, *Br. Ceram. Trans. J.* **1995**, *94*, 25–27; c) J. I. Jeong, B. M. Lim, J. H. Moon, J. H. Hong, J. S. Kang, Y. P. Lee, *J. Vac. Sci. Technol. A* **1994**, *12*, 873–877.
[3] a) J. A. Kohn, G. Katz, A. A. Giardini, *Z. Kristallogr.* **1958**, *111*, 53–60; b) G. Will, *J. Am. Chem. Soc.* **1963**, *85*, 2335–2337; c) A. J. Perrotta, W. D. Townes, J. A. Potenza, *Acta Crystallogr. Sect. B* **1969**, *25*, 1223–1228.
[4] a) F. Wöhler, H. S. Claire Deville, *Justus Liebigs Ann. Chem.* **1857**, *101*, 75; b) H. Biltz, *Ber. Dtsch. Chem. Ges.* **1910**, *43*, 297.
[5] V. I. Matkovich, J. Economy, R. F. Giese, *J. Am. Chem. Soc.* **1964**, *86*, 2337–2340.
[6] Z. Inoue, H. Tanaka, Y. Inomata, *J. Mater. Sci.* **1980**, *15*, 3036–3040.
[7] A. J. Pyzik (Dow Chemical), US-A 5298468 A, **1994** [*Chem. Abstr.* **1994**, *121*, 40639]; R. J. Hoffman, C. S. Hart (Dow Chemical), US-A 5021368 A, **1991** [*Chem. Abstr.* **1991**, *115*, 237630].
[8] Structure analysis: No structure model could be developed on the basis of the unit cell as determined by film methods (a = 5.90 Å, c = 15.9 Å). However, a structure model was found for the subcell with a' = 3.405 Å ($= a/\sqrt{3}$), constituted by the reflections of high intensity (space group $P6_3/mmc$, $wR_2(I) = 0.048$, $R_1(F) = 0.020$, 122 reflections, 14 parameters). In this structure one Al atom is coordinated in a trigonal bipyramidal way [Al–C: 1.97 Å (3×), 2.53 Å (2×)]. As well known for similar structures (Al_4C_3, Al_5C_3N, ..) the Al atom is not located in the plane of the triangle, but moved to one of the tops of the bipyramid, thus forming a distorted tetrahedron. In the subcell this shift can be simulated by a disorder of Al in the z direction ($wR_2(I) = 0.030$, $R_1(F) = 0.013$). On the basis of this structure model a number of superstructure models were developed with tetrahedral coordination of Al. A satisfactory refinement was possible in the space group $P\bar{3}c1$ [dimensions of the crystal: 0.7 × 0.7 × 0.03 mm, M_r = 383.34, a = 5.900(2), c = 15.900(2) Å, V = 479.0(2) Å^3, space group $P\bar{3}c1$ (no. 165), Z = 6, ρ = 2.66 gcm^{-3}, CAD4 (Nonius), $Mo_{K\alpha}$ radiation, graphite monochromator, $\omega/2\theta$ scan, $2° < \theta < 32.5°$ ($\pm h$, $\pm k$, l), no absorption correction, structure solution: SHELXS86, refinement: SHELX93, 584 independent reflections (439 with $I > 2\sigma(I)$), 36 parameters, $wR_2(I) = 0.057$, $R_1(F) = 0.023$]. Four of the six trigonal bipyramidally coordinated Al atoms are located on a fourfold position (4d) in an ordered way, while the two remaining Al atoms occupy half of a fourfold position (4c). In that way a partial resolution of the disorder is possible. The symmetry reduction to space group $P3c1$ and the assumption of twinning (inversion twins, merohedral twins) led to unsatisfactory refinements. The complete separation of all Al atoms according to a 1:1 pattern is impossible on the basis of this unit cell if a trigonal space group is assumed. However, more complex patterns of ordering with orthorhombic or monoclinic symmetry and/or enlarged unit cells can be developed, but on the basis of the present data a satisfactory refinement seems to be impossible. The refinement in $P\bar{3}c1$ should be seen as a good approximation to the real structure. Further details of the crystal structure investigation may be obtained from the Fachinformationszentrum Karlsruhe, D-76344 Eggenstein-Leopoldshafen (Germany), on quoting the depository number CSD-380116.
[9] Single crystals were analyzed by WDX (wavelength dispersive X-ray). No foreign elements heavier than boron were detected. Quantitative analysis gave the values: Al: calc. 42,8%, obs. 42,5%; B: calc. 14,3%, obs. 10,2%; C: calc. 42,8%, obs. 47,3%. The deviations for B and C are attributed to technical problems associated with the higher uncertainties for light elements.
[10] M. von Stackelberg, E. Schnorrenberg, *Z. Phys. Chem.* **1934**, *27*, 37–46.
[11] J.-F. Halet, J.-Y. Saillard, J. Bauer, *J. Less-Common Met.* **1990**, *158*, 239–245.
[12] J. Weidlein, U. Müller, K. Dehnicke, *Schwingungsfrequenzen I*, Thieme, Stuttgart, **1981**.
[13] M. Somer, *Z. Naturforsch. B* **1991**, *46*, 1664–1668.
[14] P. Pyykkö, Y. Zhao, *J. Phys. Chem.* **1990**, *94*, 7753–7760.
[15] H. Yamane, S. Kikkawa, M. Koizumi, *J. Solid State Chem.* **1987**, *71*, 1–13.
[16] H.-J. Meyer, *Z. Anorg. Allg. Chem.* **1991**, *594*, 113–120.
[17] M. Somer, Max-Planck-Institut, Stuttgart, personal communication.
[18] L. Pauling, *The Nature of the Chemical Bond*, Cornell University Press, Ithaca, New York, **1960**.
[19] See J. Weidlein, U. Müller, K. Dehnicke, *Schwingungsspektroskopie*, Thieme, Stuttgart, **1988**.

Asymmetric Cyclization of α-Silyl Esters to Give Functionalized Hydrindanones**

Dieter Schinzer,* Thorsten Blume, and Peter G. Jones

Intramolecular additions of α-silyl esters to carbonyl groups, also known as intramolecular Peterson olefinations,[1] are rarely observed.[2, 3] In general, the starting materials for these reactions must be carefully selected so that the base does not remove one of the acidic protons adjacent to the carbonyl group. These competing deprotonations limit the utility of the Peterson olefination for cyclization reactions. We here report on the first

[*] Prof. Dr. D. Schinzer, Dipl.-Chem. T. Blume
Institut für Organische Chemie der Technischen Universität
Hagenring 30, D-38106 Braunschweig (Germany)
Fax: Int. code +(531)391-5386
e-mail: d.schinzer@tu-bs.de
Prof. Dr. P. G. Jones
Institut für Analytische und Anorganische Chemie
der Technischen Universität Braunschweig

[**] This work was supported by the Fonds der Chemischen Industrie (doctoral stipend for T. B.). We thank the Schering AG for their financial support and donation of chemicals.

desilylations of alicyclic tricarbonyl compounds in which ester enolates are selectively formed and react further to yield functionalized hydrindanones (**5**, **6**) by means of a crossed, intramolecular aldol reaction. The cyclization products of these transformations are extremely important building blocks for the synthesis of steroids (for example the Hajos–Wiechert ketone).[4]

The required starting materials can be prepared readily in simple syntheses. The reaction of α-silyl ester **1** with **2**[5] afforded diketal **3**, which was hydrolyzed in the presence of amberlyst 15 to yield diketone **4** (Scheme 1, Table 1).[6] When **4a**

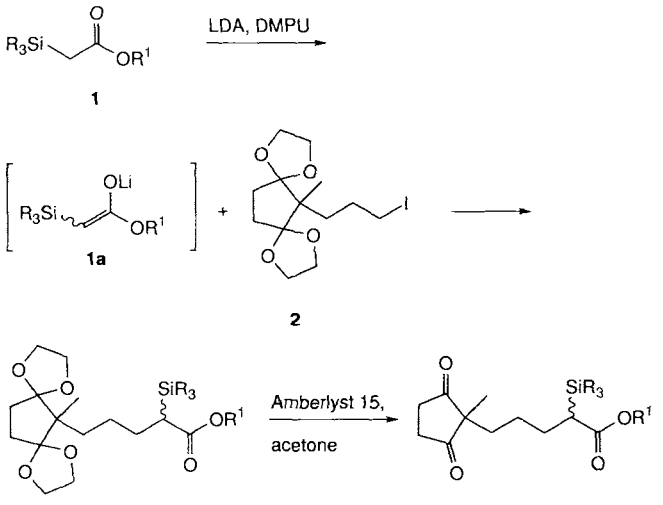

Scheme 1. Synthesis of **4**. R^1 = Me, *t*Bu, (−)-menthyl, (−)-, (+)-phenylmenthyl; SiR_3 = $SiMe_3$, $SiPh_2Me$.

Table 1. Yields of the syntheses of **3** and **4** and of the cyclization giving *rac*-**5** and *rac*-**6**.

	Starting compound				Yield [%]	
	SiR_3	R^1	**3**	**4**	*rac*-**5**	*rac*-**6**
1a	$SiMe_3$	Me	70	77	41	64
1b	$SiPh_2Me$	*t*Bu	73	62	40	68
1c	$SiPh_2Me$	(−)-menthyl	59	62		
1d	$SiMe_3$	(−)-phenylmenthyl	72	71		
1e	$SiMe_3$	(+)-phenylmenthyl	69	71		

(R^1 = Me; SiR_3 = $SiMe_3$) was treated with one equivalent of tetra-*n*-butylammonium fluoride (TBAF) at −78 °C, the functionalized hydrindanones *rac*-**5** and *rac*-**6** were exclusively

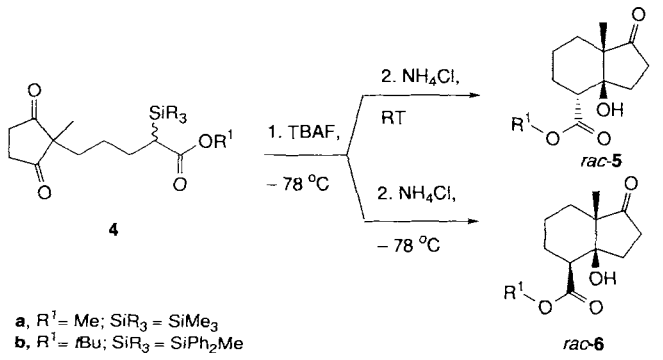

a, R^1 = Me; SiR_3 = $SiMe_3$
b, R^1 = *t*Bu; SiR_3 = $SiPh_2Me$

formed depending on the workup conditions (hydrolysis at −78 °C and at room temperature (RT), respectively) (Table 1; the relative configurations were determined by COSY and NOE NMR experiments). When less than one equivalent of TBAF was used, the reaction did not go to completion, implying that this reaction corresponds to a desilylation/aldol sequence.[7] The transformation with lithium diisopropylamide did not yield any cyclization product. When potassium *tert*-butoxide was used, however, *rac*-**5** was isolated in 23% yield.

The corresponding reaction of the *tert*-butyl ester **4b** (R^1 = *t*Bu; SiR_3 = $SiPh_2Me$) proceeds in a different way. Depending on the workup conditions (hydrolysis at −78 °C or at RT), treatment of **4b** with TBAF resulted in the formation of the expected hydrindanones *rac*-**5** and *rac*-**6** (R^1 = *t*Bu), respectively. In contrast, however, the transformation of **4b** with potassium *tert*-butoxide surprisingly led to the medium-sized ring **7** (R^1 = *t*Bu) in 40% yield.[6] In this case, the nine-membered ring β-oxo ester, which exists exclusively in the enol form, is presumably formed by a retro-aldol reaction[8] following the cyclization step.

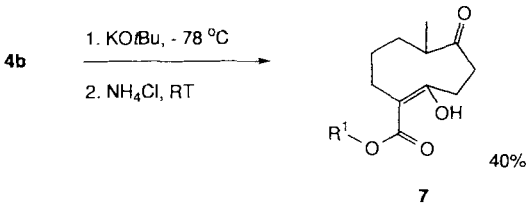

Since substrates **4** contain a prochiral center with diastereotopic groups, they can potentially be exploited in asymmetric syntheses. To explore this possibility, we prepared the optically active esters **4c–e** (R^1 = (−)-menthyl, (−)- and (+)-phenylmenthyl, respectively). For the synthesis of **4c**, commercially available (−)-menthyl acetate was first C-silylated with diphenylmethylsilyl chloride as described in the literature;[9] the trimethylsilyl derivatives were prepared according to the silyl ketene acetal method.[10] The resulting α-silyl ester was then alkylated with the diacetal iodide **2**, and the acetal groups were subsequently cleaved to form an inseparable 60:40 mixture of diasteromers (**4c** (R^1 = (−)-menthyl, SiR_3 = $SiPh_2Me$)).

Treatment of **4c** with TBAF in THF at −78 °C afforded the all-*cis* compounds (*S*,*S*,*S*)-**6A** and (*R*,*R*,*R*)-**6B** as an inseparable mixture of diastereomers in a total yield of 61% and a ratio of 35:65.[6]

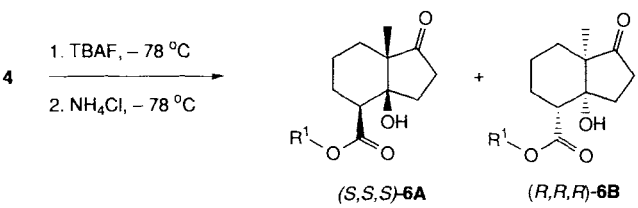

The transition from (−)-menthol to (−)-phenylmenthol as a chiral auxiliary generally results in enhanced stereochemical discrimination.[11] Hence we synthesized the phenylmenthyl esters **4d** and **4e** (R^1 = (−)- and (+)-phenylmenthyl, respectively, SiR_3 = $SiMe_3$) to investigate their cyclization behavior. Compound **4d** reacted with TBAF in THF at −78 °C to form the cyclization products (*S*,*S*,*S*)-**6A** and (*R*,*R*,*R*)-**6B** (R^1 = (−)-phenylmenthyl) in a somewhat improved diastereomeric ratio relative to that resulting from the corresponding menthyl ester (Table 2). An additional preparative advantage is that the

 © VCH Verlagsgesellschaft mbH, D-69451 Weinheim, 1996 0570-0833/96/3521-2501 $ 15.00+.25/0

Table 2. Desilylation of **4** ($SiR_3 = SiMe_3$).

R^1	Reaction conditions	T [°C]	**6A**:**6B**	Yield [%] **6A**	**6B**
(−)-phenylmenthyl	TBAF, THF	− 78	31:69	26	58
(−)-phenylmenthyl	TBAF, THF, HMPT [a]	− 78	34:66	25	49
(−)-phenylmenthyl	TBAF, THF	−105	28:72	23	60
(−)-phenylmenthyl	CsF, DMF/THF	− 70	31:69	13	29
(+)-phenylmenthyl	TBAF, THF	− 78	71:29	55	22

[a] Hexamethylphosphoric triamide.

diastereomers (*S,S,S*)-**6A** and (*R,R,R*)-**6B** (R^1 = (−)-phenylmenthyl) can be separated easily by flash chromatography. The transformation with the (+)-phenylmenthyl ester **4e** yielded the (*S,S,S*)-phenylmenthyl ester **6A** as the major product. The absolute configurations of (*S,S,S*)-**6A** and (*R,R,R*)-**6B** (R^1 = (−)-phenylmenthyl) were confirmed by X-ray crystallography.[12]

Compounds such as **6A** and **6B** are interesting synthetic C–D ring intermediates for the biologically active cardiac glycosides.[13] In order to obtain the equally important *trans*-annulated C–D building blocks necessary for the synthesis of vitamin D_3,[14] the tertiary OH group must be eliminated. The transformation of (*S,S,S*)-**6A** in pyridine (Py) and thionyl chloride affords exclusively the β,γ-unsaturated compound (*S,S*)-**8**, which can then be hydrogenated to furnish the desired *trans*-hydrindanone.[5]

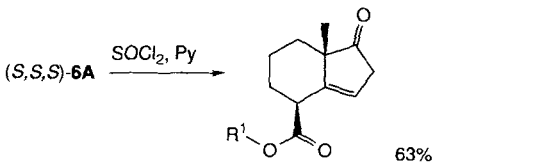

(*S,S*)-**8**, R^1 = (+)-phenylmenthyl

Experimental Procedure

A solution of TBAF in THF (1.1 M, 0.289 mmol, 0.26 mL) was stirred in anhydrous THF (2 mL) for 20 min at room temperature with activated molecular sieves to bind any residual water in the TBAF solution. The resulting anhydrous TBAF solution was then added dropwise to a solution of diketone **4d** (120 mg, 0.241 mmol) in THF (3 mL) cooled to −105 °C. The solution was stirred for 20 min at −105 °C and subsequently hydrolyzed with NH_4Cl. The mixture was extracted twice with diethyl ether, the combined organic layers were washed with NaCl solution and dried over $MgSO_4$, and the solvent was removed. Purification by flash chromatography with pentane/ether (5/1) yielded 62 mg of (*R,R,R*)-**6B** (R^1 = (−)-phenylmenthyl; 60%) and 24 mg of (*S,S,S*)-**6A** (R^1 = (−)-phenylmenthyl; 23%).

(*R,R,R*)-**6B** (R^1 = (−)-phenylmenthyl): colorless crystals: m.p. 96 °C; $[\alpha]_D^{20}$ = −13.37 (c = 0.8 in $CHCl_3$); ^{1}H-NMR (600 MHz): δ = 0.85 (m, 1H, C-14), 0.86 (d, ^3J = 6.5 Hz, 3H, C-27), 0.92 (m, 1H, C-17), 0.98 (s, 3H, C-10), 1.02 (m, 1H, C-7), 1.09 (m, 1H, C-15), 1.19 (s, 3H, C-19 or C-20), 1.24 (m, 1H, C-8), 1.28 (s, 3H, C-19 or C-20), 1.39 (m, 1H, C-6), 1.40 (m, 1H, C-7), 1.46 (m, 1H, C-16), 1.51 (m, 1H, C-6), 1.57 (dd, ^3J = 10.7, 3.3 Hz, 1H, C-5), 1.62 (m, 1H, C-14), 1.64 (m, 1H, C-15), 1.72 (m, 1H, C-8), 1.84 (m, 1H, C-17), 1.89 (ddd, ^2J = 12.9, ^3J = 9.4, 3.5 Hz, 1H, C-3), 2.03 (m, 2H, C-3/13), 2.15 (ddd, ^2J = 19.3, ^3J = 9.4, 9.1 Hz, 1H, C-2), 2.49 (ddd, ^2J = 19.3, ^3J = 10.3, 3.5 Hz, 1H, C-2), 4.79 (ddd, ^3J = 10.7, 10.7, 4.3 Hz, 1H, C-12), 4.83 (s, 1H, OH), 7.12 (m, 1H, Ar), 7.24 (m, 4H, Ar); ^{13}C NMR (100 MHz): 18.5 (q, C-10), 21.7 (q, C-27), 21.8 (t, C-7), 25.1 (q, C-19 or C-20), 25.2 (t, C-6), 26.5 (t, C-15), 27.8 (q, C-19 or C-20), 29.11 (t, C-8), 31.2 (d, C-16), 31.3 (t, C-3), 34.2 (t, C-2), 34.4 (t, C-14), 39.6 (s, C-18), 41.2 (t, C-17), 47.2 (d, C-5), 49.8 (d, C-13), 53.6 (s, C-9), 75.4 (d, C-12), 76.9 (s, C-4), 125.2 (3 × d, Ar), 127.9 (2 × d, Ar), 151.3 (s, C-21), 175.4 (s, C-11), 218 (s, C-1); MS (EI): *m/z* (%): 426 (M^+, 2), 408 (2), 307 (5), 214 (10), 167 (10), 119 (100), 105 (31), 91 (30); IR: $\tilde{\nu}$ = 3451 (m), 2957 (m), 2927 (m), 1742 (s), 1698 (s), 1428 (m), 1213 (m), 1120 (m), 865 (m), 700 cm^{-1}(s); UV: λ_{max} = 194 nm; elemental analysis (%): calcd ($C_{27}H_{38}O_4$): C 76.02, H 8.98; found: C 76.01, H 9.06.

Received: May 30, 1996 [Z9175IE]
German version: *Angew. Chem.* **1996**, *108*, 2669–2671

Keywords: aldol reactions · enolates · hydrindanones · silyl esters

[1] D. J. Ager, *Org. React. NY* **1990**, *38*, 1.
[2] Y. Kita, J. Sekihashi, Y. Hayashi, Y.-Z. Da, M. Yamamoto, S. Akai, *J. Org. Chem.* **1990**, *55*, 1108.
[3] G. Bartolini, M. Bosko, R. Dalpozzo, P. E. Todeso, *J. Chem. Soc. Chem. Commun.* **1988**, 807.
[4] U. Eder, G. Sauer, R. Wiechert, *Angew. Chem.* **1971**, *83*, 492; *Angew. Chem. Int. Ed. Engl.* **1971**, *10*, 496; Z. G. Hajos, D. R. Parrish, *J. Org. Chem.* **1974**, *39*, 1615.
[5] T. Mandai, Y. Kaihara, J. Tsuji, *J. Org. Chem.* **1994**, *59*, 5847.
[6] All new compounds were fully characterized by standard methods.
[7] L. Birkhofer, A. Ritter, *Angew. Chem.* **1965**, *77*, 414.
[8] M. S. Newman, J. H. Manhart, *J. Org. Chem.* **1961**, *26*, 2113.
[9] G. L. Larson, V. C. Maldonado, L. M. Fuentes, L. E. Torres, *J. Org. Chem.* **1988**, *53*, 633.
[10] K. Maruoka, H. Banno, H. Yamamoto, *Synlett* **1991**, 253.
[11] E. J. Corey, H. E. Ensley, *J. Am. Chem. Soc.* **1975**, 97, 6908.
[12] Crystal structure data for (*S,S,S*)-**6A** (R^1 = (−)-phenylmenthyl): $C_{27}H_{38}O_4$, monoclinic, space group $P2_1$, a = 863.91(10), b = 1311.3(2), c = 1072.90(10) pm; β = 94.194(8)°, V = 1.2122 nm^3, Z = 2, μ = 0.08 mm^{-1}, T = −100 °C. Colorless prism (0.85 × 0.45 × 0.4 mm), Siemens R3 diffractometer, 5781 reflections with $2\theta_{max}$ = 55° ($Mo_{K\alpha}$ radiation), of which 2895 were independent. The structure was solved by direct methods and refined anisotropically against F^2 (SHELXL-93 program system, G. M. Sheldrick, Universität Göttingen); H atoms were refined with a riding model with rigid methyl groups; the absolute configuration of the phenylmenthyl substituent is known; $wR(F^2)$ = 0.087, with conventional $R(F)$ = 0.034, 285 parameters and 292 restraints (for the components of the displacement factors); S = 1.00; max. $\Delta\rho$ = 141 e nm^{-3}. Crystal structure data for (*R,R,R*)-**6B** (R^1 = (−)-phenylmenthyl): $C_{27}H_{38}O_4$, orthorhombic, space group $P2_12_12_1$, a = 709.47(12), b = 1299.2(2), c = 2632.2(4) pm, V = 2.4263 nm^3, Z = 4, μ = 0.08 mm^{-1}, T = −130 °C. Colorless prism (0.8 × 0.35 × 0.2 mm), Stoe-STADI-4 diffractometer, 3412 intensities with $2\theta_{max}$ = 55°, of which 3375 were independent. Structure elucidation and refinement as for (*S,S,S*)-**6A**; $wR(F^2)$ = 0.141, $R(F)$ = 0.056, 285 parameters and 291 restraints; S = 1.08; max. $\Delta\rho$ = 200 e nm^{-3}. Crystallographic data (excluding structure factors) for the structures reported in this paper have been deposited with the Cambridge Crystallographic Data Centre as supplementary publication no. CCDC-179-102. Copies of the data can be obtained free of charge on application to The Director, CCDC, 12 Union Road, Cambridge CB2 1EZ, UK (fax: Int. code +(1223)336-033; e-mail: teched@chemcrys.cam.ac.uk).
[13] J. A. Bristol, D. B. Evans, *Annu. Rep. Med. Chem.* **1981**, *16*, 93.
[14] G.-D. Zhu, W. H. Okamura, *Chem. Rev.* **1995**, *95*, 1877.

Model Calculations on the Stereoselectivity of the Triplet Photoreaction of 1,2-Dimethyltrimethylene

Marcus Böckmann and Martin Klessinger*

In a nonadiabatic photoreaction, excitation from the ground state (S_0) into the lowest singlet state (S_1) or triplet state (T_1) brings about geometrical changes followed by return from S_1 to S_0 by a conical intersection or from T_1 to S_0 by intersystem crossing (ISC), and thermal equilibration in the ground state.[1] Although the structures of the products and the efficiencies of their formation depend on the nature of the motions in the excited state, on the geometry of return to the S_0 state, and the final steepest descent motion on the S_0 surface, the geometry of return is of a paramount importance in solution reactions. For a nonadiabatic singlet reaction, this is the conical intersection, which from a mechanistic point of view plays a similar role as the transition state in a thermal reaction.[2] In triplet photoreac-

[*] Prof. Dr. M. Klessinger, Dr. M. Böckmann
Organisch-chemisches Institut der Universität
Corrensstrasse 40, D-48149 Münster (Germany)
Fax: Int. code +(251)839772,
e-mail: klessim@uni-muenster.de

 © VCH Verlagsgesellschaft mbH, D-69451 Weinheim, 1996 0570-0833/96/3521-2502 $ 15.00+.25/0

tions the geometries most favorable for ISC may be considered to be of similar relevance.[3]

Thus, the knowledge of the "reactive structure", that is the transition structure of a thermal reaction, the structure of the conical intersection accessible on the excited state potential energy surface (PES) of a singlet photoreaction, or the geometries favorable for ISC in a triplet photoreaction, is decisive for the discussion and prediction of the stereochemical outcome of the reaction. Triplet stereoselectivity has recently been exploited mainly in synthetic applications of the Paternò–Büchi reaction.[4]

Herein we present a general procedure for determining the reactive structure and discussing the stereoselectivity of triplet photoreactions. The ring-closure reaction of 1,2-dimethyltrimethylene (DMTM) will be used as an example to show that on the basis of the PES of the ground state S_0 and the lowest triplet state T_1 in combination with SOC surfaces, where the spin-orbit coupling value SOC rather than the energy E is plotted as a function of the reaction coordinates, it is possible to locate the regions of large SOC and small singlet–triplet separation E_{ST} that are most favorable for ISC.[5] All calculations are based on recently developed methods to treat SOC within the framework of the semiempirical configuration interaction (CI) approach.[6]

Computational results for unsubstituted trimethylene (TM) have been reported,[6, 7] and the structural dependence of SOC has been discussed previously[6, 7a, b] and rationalized on the basis of the two-electron two-orbital model and symmetry considerations.[8] It was shown that conrotatory ($\beta = \alpha$) and disrotatory ($\beta = 180° - \alpha$) motions of the terminal methylene groups yield similar results. On the basis of a combined analysis of PES and SOC surfaces, ISC and the ring-closure reaction could be discussed: the minimum energy valley of the triplet PES that corresponds to nearly free rotation of the radical centers is unfavorable for ISC since the S_0 state lies energetically above the T_1 state. However, in the region of large SOC, in which the terminal methylene groups are rotated by $\alpha > 45°$ toward a face-to-face arrangement (Scheme 1), decreasing the C-C-C valence

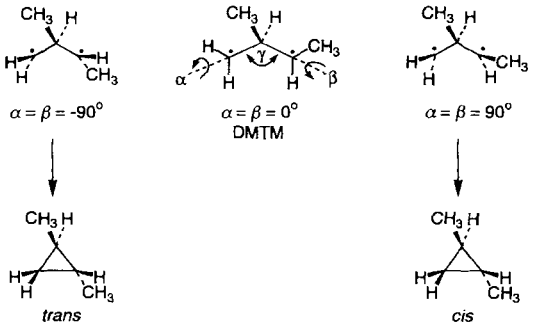

Scheme 1. Definition of the rotational angles α and β, and of the bond angle γ. $\alpha = \beta = 0$ corresponds to a side-to-side arrangement of the radical centers, and $|\alpha| = |\beta| = 90°$ to a face-to-face arrangement.

angle γ to a value of 105° raises the energy only slightly (1–2 kcal mol^{-1}) and leads to singlet–triplet degeneracy ($E_{ST} = 0$) and therefore to geometries very favorable to ISC.[6]

In DMTM there are two different modes of conrotatory motion ($\beta = \alpha$) of the radical centers, leading to stereoisomeric cyclization products: rotation by positive ($\alpha > 0$) and negative ($\alpha < 0$) values of the rotational angle yields *cis*- and *trans*-dimethylcyclopropane, respectively (see Scheme 1). S_0 and T_1 PES together with SOC surfaces are shown for both modes of rotation in Figure 1.[9] From a comparison of these results with

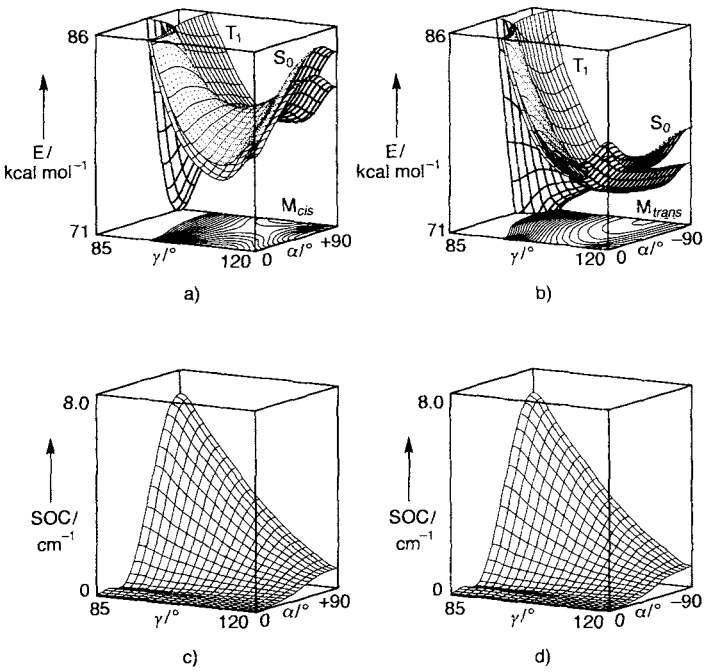

Fig. 1. The ring-closure reaction of 1,2-dimethyltrimethylene. Lowest singlet and triplet PES for conrotatory motion of the radical centers toward a) the *syn* ($\alpha > 0°$) and b) the *anti* conformation ($\alpha < 0°$), as well as SOC surfaces c) for $\alpha > 0°$ and d) for $\alpha < 0°$.

those of TM[6] it is evident that to a first approximation the methyl substituents do not at all affect the SOC values, while steric effects appreciably change the appearance of the valley on the T_1 PES. For the *syn* mode of rotation a barrier of approximately 3.4 kcal mol^{-1} is found to separate the local minimum M_{cis} at $\alpha = 90°$ from the planar structure ($\alpha = 0°$) that is 1.0 kcal mol^{-1} lower in energy than the barrier. For the *anti* mode of rotation, however, the valley descends practically without a barrier toward the minimum M_{trans} at $\alpha = -90°$, 5.0 kcal mol^{-1} lower in energy than M_{cis}. Some data for selected geometries including the singlet–triplet intersection line ($E_{ST} = 0$), are collected in Table 1. By decreasing the bond angle γ, geometries are accessible both from M_{cis} and M_{trans} at which S_0 and T_1 are degenerate ($E_{ST} = 0$) and SOC is appreciable (SOC > 2 cm^{-1}); the necessary energies are less than 1 kcal mol^{-1}. For rotational angles $|\alpha| < 45°$, however, much larger energies (> 10 kcal mol^{-1}) are required and geometries with SOC < 1 cm^{-1} are reached.

Table 1. 1,2-Dimethyltrimethylene. State energies and SOC values for selected geometries from MNDOC-CI calculations [a].

Geometry [γ, α] [b]		Energy [kcal mol^{-1}] ^3E [c]	E_{ST} [d]	SOC [cm^{-1}]
[111, −90]	M_{trans}	0	1.5	1.778
[112, 0]		2.6	1.1	0.002
[109, 60]	B	6.0	1.0	1.090
[110, 90]	M_{cis}	5.0	1.3	1.912
[105, 90]		5.4	0	2.631
[105, 75]		5.8	0	2.315
[103, 60]		6.6	0	1.613
[96, 45]		0.6	0	0.923
[106, −90]		0.6	0	2.612
[105, −75]		0.7	0	2.316
[103, −60]		1.5	0	1.627
[96, −45]		6.8	0	0.930

[a] Singlet open-shell 3-3′ CI. [b] $\beta = \alpha$. [c] Relative to $\Delta H_f(^3M_{trans}) = 73.4$ kcal mol^{-1}. [d] $E_{ST} = {}^1E - {}^3E$.

 © VCH Verlagsgesellschaft mbH, D-69451 Weinheim, 1996 0570-0833/96/3521-2503 $ 15.00+.25/0

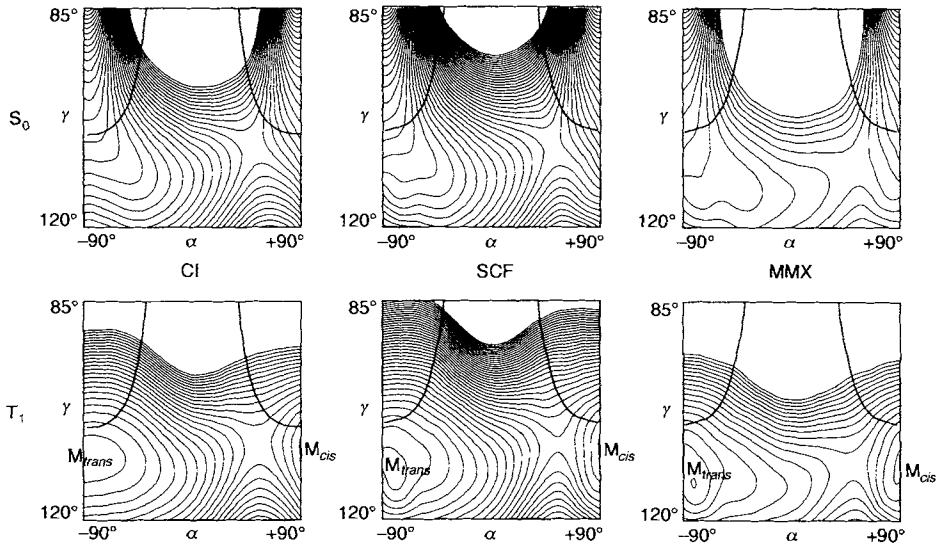

Fig. 2. Contour diagrams of the S_0 and T_1 PES for the ring-closure reaction of 1,2-dimethyltrimethylene, as calculated by the CI approach and estimated by SCF and force-field (MMX) methods. Triplet–singlet intersection $E_{ST} = 0$ is indicated by heavy lines.

From these results, it can be concluded that, as in the unsubstituted TM, the reactive structure of optimal ISC is characterized by a face-to-face orientation of the radical centers and a C-C-C angle γ slightly smaller than for the triplet minima. As the singlet PES drops steeply toward the cyclopropane minimum for small values of γ, the triplet reaction yields preferably cyclic products. The conditions for optimal ISC are similar for both minima M_{cis} and M_{trans}; therefore, the stereochemical differentiation between *cis*- and *trans*-substituted products is due, in this special case, to the energy difference of the two minima M_{cis} and M_{trans}. This explains the experimental observation that the triplet-sensitized photoreaction of *cis*- as well as *trans*-3,4-dimethyl-1-pyrazoline yields preferably *trans*-1,2-dimethylcyclopropane, and negligible amounts of acyclic products, in contrast to the singlet photoreaction, which occurs preferably with retention of the configuration and yields appreciable amounts of acyclic products.[10]

Thus, the reactive structure of the triplet photoreaction of trimethylene that corresponds to optimal ISC is hardly affected by methyl substitution, and the product ratio reflects the energy difference between M_{cis} and M_{trans} on the T_1 surface. Since this energy difference is due mainly to steric effects, it should be possible to estimate it on the basis of simple models. For this purpose we calculated the difference PES E(DMTM) − E(TM) for DMTM and the unsubstituted TM by SCF-MO as well as by force-field methods[11] and added this difference to the PES of the unsubstituted TM.[6] The resulting contour diagrams together with the singlet–triplet intersection line ($E_{ST} = 0$) are shown in Figure 2 for the T_1 as well as the S_0 state. For comparison, results of the complete CI calculations are also given. The rotational angle is varied from $\alpha = -90°$ to $\alpha = 90°$, thus including the *syn* and *anti* motions that are shown separately in Figure 1 (cf. the contour diagrams of the triplet PES given at the bottom of Figure 1). It is quite apparent that both methods describe the main features of steric effects on the PES quite correctly; the SCF results slightly overestimate and the force-field results slightly underestimate the nuclear repulsions at small values of the C-C-C angle .

In summary, the combined analysis of PES and SOC surfaces is very well suited for determining the reactive geometries that are most favorable for ISC. The knowledge of these geometries together with the T_1 excited-state PES then allows for a detailed elucidation of the mechanism of a triplet photoreaction and a rationalization of the stereoselectivity. Since purely steric substituents like methyl groups do not affect the SOC values, it is possible to evaluate the structural dependence of SOC for the unsubstituted system only, and to use simple models to estimate steric effects on the PES. In the case of DMTM different reactive geometries leading to *cis*- and *trans*-1,2-dimethylcyclopropane may be reached from the minima M_{cis} and M_{trans}, and the necessary energies are less than 1 kcal mol^{-1}. Thus, stereodifferentiation is due to energetic behavior of the T_1 PES. Since this is, to our knowledge, the first triplet photoreaction for which the mechanism has been elucidated in detail, future investigations have to show whether this is a general feature of stereodifferentiation in triplet reactions.

Received: May 20, 1996 [Z9129IE]
German version: *Angew. Chem.* **1996**, *108*, 2681–2683

Keywords: photochemistry · theoretical chemistry · trimethylene

[1] M. Klessinger, J. Michl, *Excited States and Photochemistry of Organic Molecules*, VCH, New York, **1995**.
[2] M. Olivucci, F. Bernardi, S. Ottani, M. Robb, *J. Am. Chem. Soc.* **1994**, *116*, 2034.
[3] M. Klessinger, M. Böckmann, J. Mählmann, *J. Inf. Rec. Mats.* **1994**, *21*, 549.
[4] a) H. Buschmann, H.-D. Scharf, N. Hoffmann, M. Plath, J. Runsink, *J. Am. Chem. Soc.* **1989**, *111*, 5367; b) A. G. Griesbeck, H. Mauder, S. Stadtmüller, *Acc. Chem. Res.* **1994**, *27* 70; c) T. Bach, *Liebigs Ann.* **1995**, 855; *Angew. Chem.* **1996**, *108*, 976; *Angew. Chem. Int. Ed. Engl.* **1996**, *35*, 884.
[5] S. P. McGlynn, T. Azumi, M. Kinoshita, *Molecular Spectroscopy of the Triplet State*, Prentic Hall, Englewood Cliffs, NJ, **1969**.
[6] M. Böckmann, M. Klessinger, *J. Phys. Chem.* **1996**, *100*, 10570.
[7] a) T. R. Furlani, H. F. King, *J. Chem. Phys.* **1985**, *82*, 5577; b) L. Carlacci, C. Doubleday Jr., T. R. Furlani, H. King, J. M. McIver Jr., *J. Am. Chem. Soc.* **1987**, *109*, 5323; c) H. E. Zimmerman, A. G. Kutateladze, *ibid.* **1996**, *118*, 249.
[8] J. Michl, *J. Am. Chem. Soc.* **1996**, *118*, 3568.
[9] Geometry taken from ref. [6] with idealized methyl groups; radical centers were rotated by α in steps of 15°, while the C-C-C γ angle was varied in steps of 5°. The CI wavefunctions include all configuration state functions (CFS) within an 3-3′ active space. For further details see Ref. [6].
[10] R. Moore, A. Mishra, R. J. Crawford, *Cand. J. Chem.* **1968**, *46*, 3305.
[11] MMX force field of PCMODEL V 5.0, Serena Software, Bloomington, IN, **1993**.

 © VCH Verlagsgesellschaft mbH, D-69451 Weinheim, 1996 0570-0833/96/3521-2504 $ 15.00+.25/0

Proof of a Reversible, Pairwise Hydrogen Transfer during the Homogeneously Rhodium(I)-Catalyzed Hydrogenation of α,β-Unsaturated Carbonic Acid Derivatives with In Situ NMR Spectroscopy and Parahydrogen**

Andreas Harthun, Rüdiger Selke,* and Joachim Bargon*

In recent years hydrogenations with para-enriched hydrogen (p-H_2) in combination with in situ NMR spectroscopy have been successfully applied to elucidate mechanistic aspects of homogeneously catalyzed hydrogenations.[1] Contrary to the usual Boltzmann distribution, hydrogenation with p-H_2 leads to a selective population of nuclear spin levels, which generates enhanced (up to 10^5) ("polarization") signals in emission and absorption in the ^{1}H NMR spectra of the hydrogenated products. This leads to a high sensitivity for registering these products in low concentration. A prerequisite for detecting polarization signals is a pairwise transfer of both p-H_2 atoms to the product.[2] This polarization phenomenon is known by the acronyms PASADENA (*P*arahydrogen *A*nd *S*ynthesis *A*llows *D*ramatically *E*nhanced *N*uclear *A*lignment)/ALTADENA (*A*diabatic *L*ongitudinal *T*ransport *A*fter *D*issociation *E*ngenders *N*et *A*lignment)[3] and PHIP (*P*arahydrogen *I*nduced *P*olarization).[4]

For the first time, we have used the PHIP method to detect polarization not only in the products but also in the reactant employed, which indicates a *reversible* hydrogenation reaction. For this purpose we investigated the hydrogenation of substituted alkenes with an α- and/or β-carbonyl function by using the cationic rhodium(I) precatalyst **1**.[5] The question of whether the hydrogenation proceeds reversibly or not usually cannot be decided when normal hydrogen is used for the hydrogenation, because the regenerated reactant cannot be distinguished from the original substrate. Deuteration experiments can give indications whether the reaction is reversible or not, but they are not conclusive for a *concerted* reaction, that is, a *pairwise* exchange mechanism. Therefore, it remains uncertain in which step the exchange of the olefinic protons occurs.

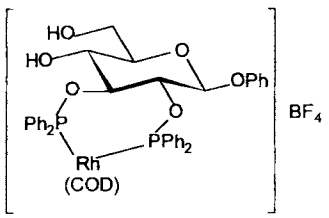

1

The hydrogenation of methyl acrylate **2a** with p-H_2 was investigated as an example for a pairwise exchange of the geminal protons in the olefinic starting material. From the beginning of the hydrogenation, polarization signals are detected in the reactant, which are superimposed by usual reactant NMR signals, however. Nevertheless, the observed polarization pattern reveals the formation of regenerated reactant, which must result from a pairwise p-H_2 transfer into the *geminal* positions of the double bond (Fig. 1).

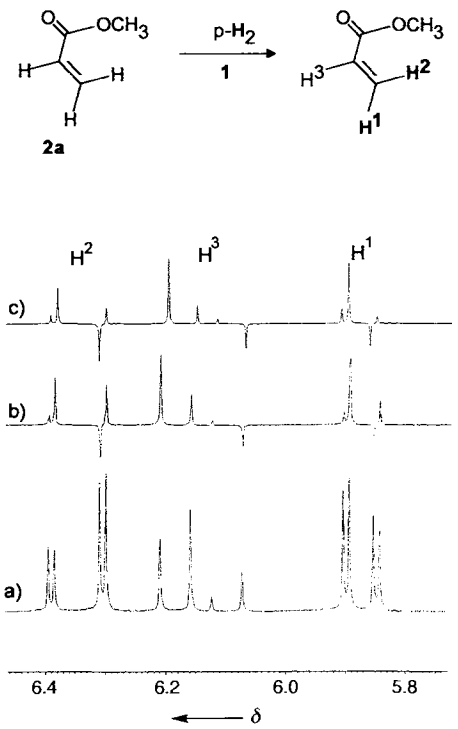

Fig. 1. The olefinic region of the ^{1}H NMR spectra (δ = 5.7–6.5) of the hydrogenation of methyl acrylate **2a** with **1**: a) spectrum of the starting material; b) spectrum after starting the hydrogenation with p-H_2. The polarization of the regenerated reactant ($R_{pol.}$) is identified by characteristic emission signals; c) simulation of spectrum b), considering normal reactant signals R ($R_{pol.}$: R = 3:1).

In contrast to the reaction of **2a**, at the beginning of the hydrogenation of itaconic acid **2b** only rather weak polarization signals in the resonances of the geminal protons of **2b**—resembling somewhat a "phase shift"—are observed besides huge polarization signals of the saturated hydrogenation product methyl succinic acid. The intensity of this signal changes during the reaction until it becomes a significant polarization signal. Figure 2 illustrates a comparison of simulated spectra[6] with the experimental spectrum. The observed time-dependent change of the signal phase is a result of a superimposition of normal reactant signals and reactant signals that are generated by polarization transfer due to a reversible pairwise proton exchange.

The superimposition of normal reactant signals with freshly generated polarization signals can be suppressed if deuterated [D_3]methyl acrylate (98%) **2c** is used as the substrate. As an example, Figure 3 shows the experimental spectrum of the olefinic protons of [D_8]methyl methacrylate (96%) **2d** after hydrogenation with p-H_2 compared with appropriate simulations.

When using itaconic acid anhydride **2e** as the substrate, this reactant is not hydrogenated itself. Nevertheless, polarization signals are observed that can be attributed to itaconic acid **2b**. Apparently, some part of the anhydride gets converted to the acid during the reaction. Therefore, polarization signals of the acid are readily detected, and are not superimposed by normal signals of **2b**, because of the low acid concentration at the beginning of the hydrogenation reaction.

To confirm the pairwise proton exchange, deuteration experiments were conducted. The substrate **2a** also becomes deuterat-

[*] Prof. Dr. J. Bargon, Dipl.-Chem. A. Harthun
Institut für Theoretische und Physikalische Chemie der Universität
Wegelerstrasse 12, D-53115 Bonn (Germany)
Fax: Int. code +(228)-732551
e-mail: bargon@rs1.thch.uni-bonn.de
Prof. Dr. R. Selke
Max-Planck-Gesellschaft
Arbeitsgruppe "Asymmetrische Katalyse" an der Universität Rostock
Buchbinderstrasse 5-6, D-18055 Rostock (Germany)
Fax: Int. code +(381)46693-24

[**] This work was financially supported by the Volkswagenstiftung, the Bundesministerium für Bildung, Wissenschaft, Forschung und Technologie (BMFT), the Deutsche Forschungsgemeinschaft (SFB 334: Wechselwirkungen in Molekülen), and the Fonds der Chemischen Industrie.

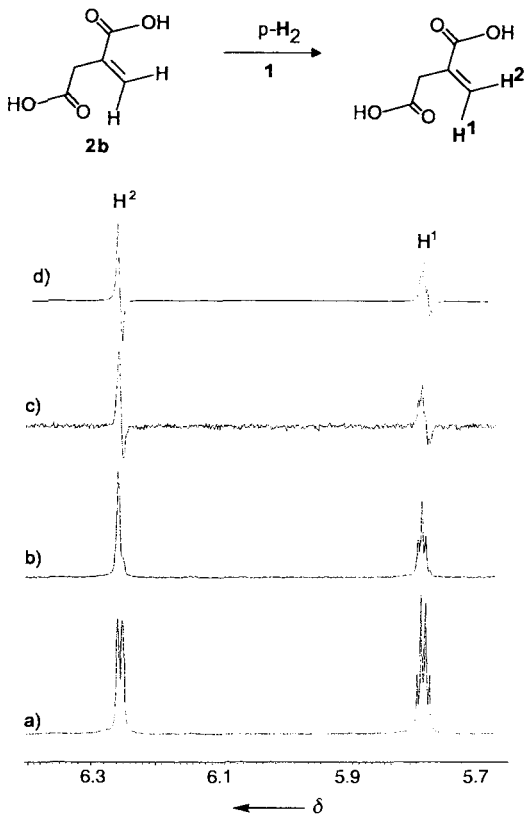

Fig. 2. The olefinic region of the ^{1}H NMR spectra (δ = 5.65–6.4) of the hydrogenation of itaconic acid **2b** with **1**: a) spectrum of the starting material; b) spectrum after starting the hydrogenation with p-H_2; c) spectrum at the end of the hydrogenation reaction with p-H_2; d) simulation of spectrum c), considering normal reactant signals R ($R_{pol.}$: R = 4:1).

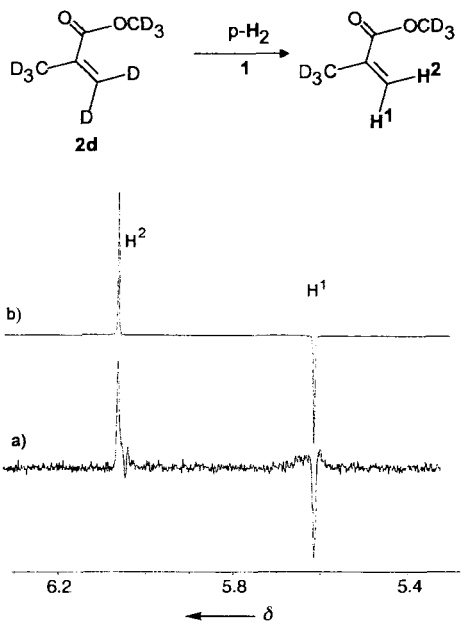

Fig. 3. The olefinic region of the ^{1}H NMR spectra (δ = 5.3–6.3) of the hydrogenation (p-H_2) of [D_6]methyl methacrylate (96%) **2d** with **1**: a) spectrum of the hydrogenation of **2d**; b) simulation. The simulation considers the coupling of the exchanged geminal protons to the nonexchanged deuterium atoms.

ed in the geminal positions by H/D exchange, as is evident from the ^{2}H NMR spectrum, which confirms the result of the former hydrogenation experiment that used p-H_2. The ^{2}H NMR spectrum of **2b** also demonstrates that both olefinic protons in starting material are exchanged by H/D exchange. Moreover, the ^{1}H NMR spectrum recorded after the deuteration of **2b** reveals that the monodeuterated H/D exchange product is formed likewise. The proton signals of the monodeuterated substrate **2b** are slightly shifted to higher field, because of an isotope effect,[7] and are, therefore, easily identified. The results of these and of analogous hydrogenation and deuteration experiments are summarized in Table 1.

Table 1. Hydrogenation of alkenes **2** with an α- and/or β-carbonyl function with **1** (+ = detected, − = not detected, o = experiment not performed).

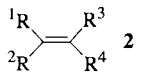

Compd.	R^1	R^2	R^3	R^4	p-H_2 Polarization (pairwise) ^{1}H NMR	D_2 H/D-exchange (mono) ^{1}H NMR	D_2 ^{2}H{^{1}H} NMR
2a	H	H	CO_2CH_3	H	+	−	+
2b	H	H	CO_2H	CH_2CO_2H	+	+	+
2c	D	D	CO_2CH_3	D	+	o	o
2d	D	D	CO_2CD_3	CD_3	+	o	o
2f[b]	H	H	CO_2CH_3	CH_3	−	−	+
2g	H	H	$CH_2CO_2CH_3$	CO_2CH_3	+	+	+
2h	H	H	$NHCOCH_3$	CO_2CH_3	−	−	−

[a] The detected polarization signals are proof for a pairwise proton exchange mechanism. In favorable cases, mono H/D exchange is detected in ^{1}H NMR spectra due to a shift of the nonexchanged protons (isotope shift); in the ^{2}H NMR spectra the broad resonances of the partially exchanged olefinic deuterium atoms do not reveal whether a mono- or bisdeuterated substrate is generated. [b] Itaconic acid anhydride **2e** is not listed in Table 1 since this substrate is not hydrogenated itself.

A generalized hydrogenation mechanism depicted in Figure 4, considers an individual mono H/D exchange as well as a pairwise H/D exchange of the geminal substrate protons. Formation of the catalyst–substrate complex **A** and of the alkylhydrido complex **B** is assumed to be reversible. Reversibility of the hydrogenation reaction as suggested here has so far not been proposed[11,12] for either dimethyl itaconate **2g** or for the N-acetamidoacrylic acid derivatives, which are structurally related[8] (compare Table 1 **2h**). ^{1}H NMR measurements conducted at low temperature have been used previously to demonstrate that the substrate **2g** changes the coordination side of the olefin from *Re* to *Si* and vice versa in a catalyst–substrate complex **A**. The process is favorable due to an intramolecular equilibrium reaction that leads to the formation of diastereomeric catalyst–substrate complexes.[9] The result confirms that during a "major–minor isomerization"[9,10] a reversible intramolecular coordination of the olefin to the catalyst is favored over an intermolecular isomerization, without leaving the catalyst's sphere of coordination. At present we cannot yet decide whether the pairwise proton exchange in the geminal position of olefinic reactants really follows the intramolecular mechanism depicted in Figure 4. Conclusive proof of our theses has to await a detailed analysis and characterization of the intermediates of the exchange reaction.

Experimental Procedure

All substrates were purchased and used without further purification: **2a,b,e–h** (Aldrich), **2c,d** (Promochem).

Deuteration experiments: The NMR tube (Wilmad WPS500) was filled with acetone (1 mL) (Aldrich) (degassed with argon for 5 min), substrate **2a,g** (ca. 40 μL) (and 20 mg **2b**, respectively), **1** (5 mg), and about 3 bar D_2, and was shaken for 1 min. The reacting solution was then investigated immediately by ^{2}H NMR and ^{2}H{^{1}H} NMR spectroscopy.

Hydrogenation experiments (p-H_2): Parahydrogen was enriched to about 50% at 77 K and taken successively out of a U-shaped flow-through cell filled with activated charcoal [11]. The NMR tube was filled with [D_6]acetone (1 mL) (Promochem),

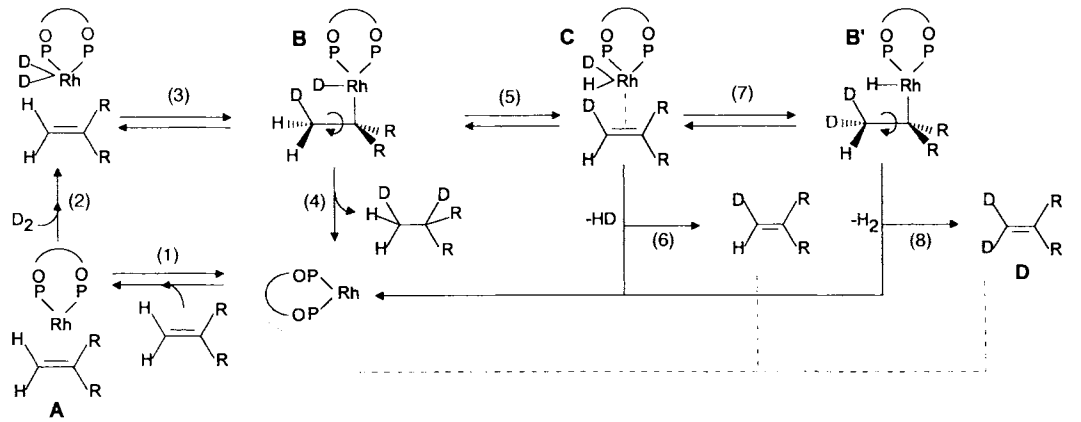

Fig. 4. Proposed mechanism for the deuteration of terminal alkenes by the rhodium(I) bis(phosphinite) complex **1** as a precatalyst. The mechanism explains both the partial deuteration of the saturated product and a mono- and pairwise H/D exchange in the geminal olefinic protons. The coordination of the solvent molecules and substrate is generally not depicted. The formation (1) of the catalyst–substrate complex **A** is considered to be reversible [8]. The intermediately generated complex **B** (2,3) reacts either to give the 1,2-deuterated product (4) or reversibly (5) to give **C**. The *side-on*-bound monodeuterated alkene is either set free from **C** (6), or it generates the complex **B'** in a reversible reaction (7). The statistically generated bisdeuterated alkene can be eliminated from **B'** by a reversible reaction step (8). If D_2 is substituted by p-H_2, the bisdeuterated substrate **D** is generated, which contains two parahydrogen atoms. These display nuclear spin polarization, which indicates that a pair correlation is maintained in spite of the two-step exchange process.

different amounts of substrate, namely **2f,g** (20 μL), **2a,c,d** (40 μL), **2b,e,h** (5 mg), **1** (5 mg), and about 3 bar p-H_2, and was shaken for about 10 s and transferred into the NMR spectrometer. After this procedure a ^{1}H NMR spectrum was recorded directly by using a 45° pulse [2]. ^{1}H NMR (200 MHz, [D$_6$]acetone, 25 °C): **2a**: δ = 3.71 (s, 3H; CH_3), 5.87 (dd, ^3J(H,H) = 10.27, ^2J(H,H) = 2.06 Hz, 1H; =C*H*H), 6.14 (dd, ^3J(H,H) = 17.15, ^3J(H,H) = 10.27 Hz, 1H; =CH-), 6.35 (dd, ^3J(H,H) = 17.15, ^2J(H,H) = 2.06 Hz, 1H; =CH*H*).

2b: δ = 3.33 (d, ^4J(H,H) = 1.16 Hz, 2H; CH_2), 5.75 (dt, ^2J(H,H) = 1.6, ^4J(H,H) = 1.16 Hz, 1H; =C*H*H), 6.23 (d, ^2J(H,H) = 1.6 Hz, 1H; =CH*H*).

Simulation parameters of the geminally hydrogenated (p-H_2) reactants of **2d**: **2d'**: δ = 5.61 (dd, ^2J(H,H) = 1.62, ^4J(H,D) = 0.25 Hz, 1H; =C*H*H), 6.04 (dd, ^2J(H,H) = 1.62, ^4J(H,D) = 0.16 Hz, 1H, =CH*H*), **D** (dd, ^4J(D,H) = 0.25 Hz, ^4J(D,H) = 0.16 Hz, 3D; CD_3).

Received: May 28, 1996 [Z 9155 IE]
German version: *Angew. Chem.* **1996**, *108*, 2666–2669

Keywords: deuteration · NMR spectroscopy · parahydrogen · reaction mechanisms

[1] A. Thomas, M. Haake, F.-W. Grevels, J. Bargon, *Angew. Chem.* **1994**, *106*, 820–822; *Angew. Chem. Int. Ed. Engl.* **1994**, *33*, 755–757; A. Harthun, K. Woelk, A. Weigt, J. Bargon, *Tetrahedron* **1995**, *51*, 11199–11206, and references therein.
[2] C. R. Bowers, D. P. Weitekamp, *Phys. Rev. Lett.* **1986**, *57*, 2645–2648, and references therein.
[3] C. R. Bowers, D. P. Weitekamp, *J. Am. Chem. Soc.* **1987**, *109*, 5541–5542.
[4] R. U. Kirss; T. C. Eisenschmidt, R. Eisenberg, *J. Am. Chem. Soc.* **1988**, *110*, 8564–8566.
[5] R. Selke, *J. Organomet. Chem.* **1989**, *370*, 241–248.
[6] The simulations were performed by using the computer program PHIP + + developed by T. Greve, Bonn.
[7] H. Günther, *NMR-Spektroskopie*, 3rd ed., Thieme, Stuttgart, **1992**, 438.
[8] W. Leitner, J. M. Brown, H. Brunner, *J. Am. Chem. Soc.* **1993**, *115*, 152–159, and references therein.
[9] R. Kadyrov, T. Freier, D. Heller, M. Michalik, R. Selke, *J. Chem. Soc. Chem. Commun.* **1995**, 1745–1746.
[10] J. A. Ramsden, T. D. W. Claridge, J. M. Brown, *J. Chem. Soc. Chem. Commun.* **1995**, 2469–2471.
[11] J. Kandels, K. Woelk, J. Bargon, *Z. Phys. Chem.* **1993**, *180*, 65–93.
[12] After this study had been completed and these results submitted, we became aware of a concept similar to ours D. J. Hardick, I. S. Blagbrough, and B. V. L. Potter (*J. Am. Chem. Soc.* **1996**, *118*, 5897–5903), which postulates reversibility of the hydrogenation step as well. However, their results do not prove that the hydrogen transfer occurs pairwise.

Lithium Arsanylalanates as Arsenide Sources: A Simple Route to the Zintl Anion As_7^{3-} and the Synthesis of a Tetraarsatetrasilacubane**

Matthias Driess,* Klaus Merz, Hans Pritzkow, and Rudolf Janoschek

Dedicated to Professor Walter Siebert on the occasion of his 60th birthday

Multiple phosphanyl-substituted and arsanyl-substituted element hydrides of groups 13 and 14, $E_n(XH_2)_m$ (E = B, Al, Ga, In, Si, Ge, Sn; X = P, As), are of importance as potential starting materials for the preparation of optoelectronic layers (doping, organometallic chemical vapor epitaxy (OMCVE) methods).[1] We have therefore been concerned with the synthesis of multiple arsanyl-substituted silanes, germanes, and stannanes such as $RE(AsH_2)_3$ and $E_2(AsH_2)_6$ (E = Si, Ge, Sn; R = alkyl, aryl), which can be prepared by mild arsanylation of the corresponding element halides. In order to be in a position to carry out multiple arsanylations, in analogy to the successful oligophosphanylation of chlorosilanes, chlorogermanes, and chlorostannanes that works with the nucleophilic and at the same time only slightly basic $[LiAl(PH_2)_4]$,[2] we first focused our attention on the existence of lithium arsanylalanates **1**.

We report here on the thermolabile lithium tetraarsanylalanate **1a**, which is only stable in solution, and on the related compounds **1b** and **1c**, which in comparison to $[LiAsH_2(dme)]$ (dme = 1,2-dimethoxyethane) surprisingly lead to the Zintl an-

[*] Priv.-Doz. Dr. M. Driess, Dr. K. Merz, Dr. H. Pritzkow
Anorganisch-chemisches Institut der Universität
Im Neuenheimer Feld 270, D-69120 Heidelberg (Germany)
Fax: Int. code +(6221)544197
e-mail: dp0@ix.urz.uni-heidelberg.de
Prof. Dr. R. Janoschek
Institut für Theoretische Chemie der Universität
Mozartgasse 14, A-8010 Graz (Austria)

[**] This work was supported by the Deutsche Forschungsgemeinschaft (Schwerpunktprogramm "Polyeder"), the Fonds der Chemischen Industrie, and by the Land Baden-Württemberg (Landesforschungsschwerpunkt "Von Molekülen zu Stoffen: Neue Materialien"). We thank Messer-Griessheim GmbH and Wacker-Chemie GmbH for the donation of chemicals.

 © VCH Verlagsgesellschaft mbH, D-69451 Weinheim, 1996 0570-0833/96/3521-2507 $ 15.00+.25/0

ion As_7^{3-} on thermal decomposition. In addition, we describe the first tetraarsatetrasilacubane, which was obtained by the reaction of **1a** with (2,4,6-triisopropylphenyl)trichlorosilane.

The alanate **1a**[3] was best prepared by introduction of AsH_3 into a solution of $[LiAlH_4]$ **2** in DME; the course of the reaction was monitored by ^{27}Al NMR spectroscopy. Once the reaction had gone to completion and **1a** had been formed in quantitative

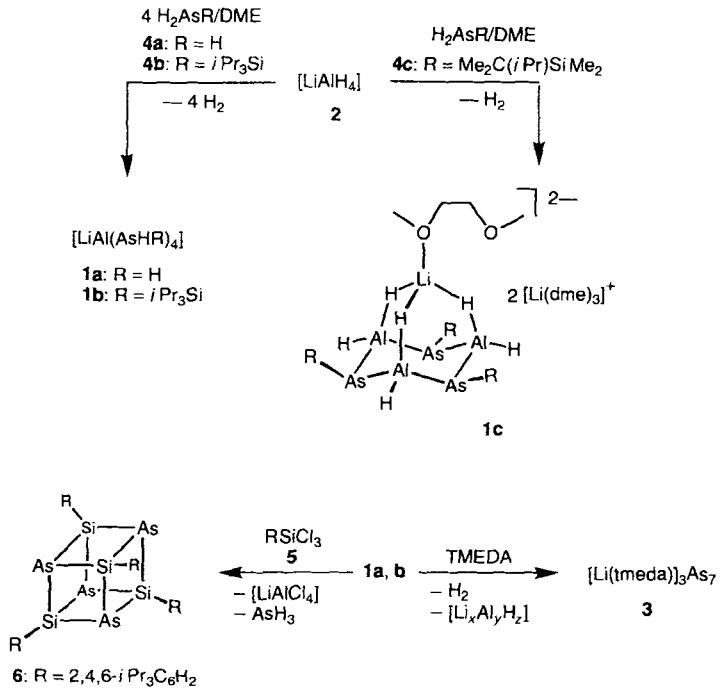

yield, a singlet was observed in the ^{27}Al NMR spectrum of the solution at $\delta = 150.4$. The protolysis produced the expected amount of AsH_3 as the sole gaseous product. Compound **1a** is admittedly only moderately stable even in solution and decomposed immediately on removal of the solvent to form AsH_3, H_2, and a brown insoluble solid that could not be identified. We have now found that the decomposition of **1a** in solution at 25 °C over a period of 3–4 days leads to the formation of the Zintl ion As_7^{3-} in high yield, H_2, and as yet hitherto unknown (polymeric?) lithium alanates. The formation of As_7^{3-} was confirmed by the isolation and characterization[4] of the structure of its TMEDA-solvated trilithium salt **3** (TMEDA = *N,N'*-tetramethylethylenediamine), which was formed on addition of TMEDA to the reaction solution and was isolated by fractional crystallization in 85 % yield in the form of orange needles. This was the first time that a solvate of Li_3As_7 had been characterized crystallographically (Fig. 1), whereas related silylated, germylated, and stannylated molecular As_7 derivatives were already known.[5] The salt **3** is isotypic with the phosphorus analogue.[6] The four-coordinate Li centers bridge each of the otherwise two-coordinate As atoms. The three different As-As distances *a*–*c* reflect the same electronic relationships as in the phosphorus analogue.[6]

The formation of As_7^{3-} does not only occur on decomposition of **1a**, however, but somewhat surprisingly also takes place on reaction of solutions of lithium tetrakis(silylarsanyl)alanate **1b** with TMEDA; in this case, **3** is also formed in 73 % yield. The alanate **1b** is formed quantitatively (^{27}Al NMR spectroscopy) on reaction of **2** with four molar equivalents of the primary arsane **4b** and is, like **1a**, in spite of, or perhaps even because of, its bulky silyl groups, only stable in solution and

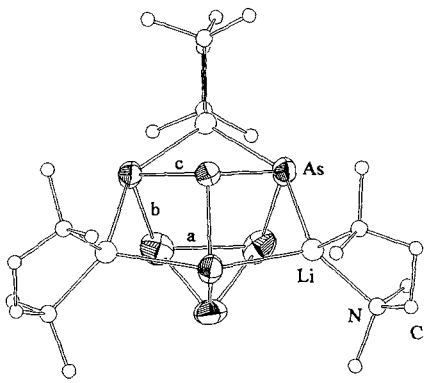

Fig. 1. Molecular structure of **3** in the crystal. Selected average distances [Å]: Li–As 2.63(2), a = 2.487(2), b = 2.372(2), c = 2.427(2).

decomposes slowly at room temperature. The mechanism of the Si–As bond cleavage and the fate of the silyl groups at the As atoms have not yet been clarified. The chelation of the Li cation by TMEDA apparently increases the reactivity of the alanate ion to such an extent that a "self-destruction" of the $AlAs_4$ framework sets in. The intrinsically weak Al–As bond is probably also responsible for the formation of the thermodynamically more favorable As_7 framework, because other decomposition reactions occur with analogous lithium phosphanylalanates in which the phosphorus analogue of **3** is not formed.[7]

In addition to this we also obtained the first lithium arsanylalanate stable in the solid state; the unusual aggregate **1c** is formed in 81 % yield by the reaction of **2** with one molar equivalent of the primary arsane **4c** in DME at 25 °C. The crystal structure analysis [4] of the colorless crystals showed that a ion-triple is present, consisting of two $[Li(dme)_3]^+$ ions and one cyclotriarsatrialanate with alternating Al and As atoms coordinating to a DME-solvated lithium cation (Li1) through three Al–H bonds in a tripodal fashion; consequently, a dianionic heteroadamantane-like framework is present (Fig. 2). Whereas donor stabilization of Li^+ by hydridic H atoms has also been observed in other molecular lithium alanates,[8] the coordinative surroundings of the Li1 center shows additional characteristics: The hydridic H atoms are evidently better (harder) donors than the As atoms, and the DME molecule functions rather surpris-

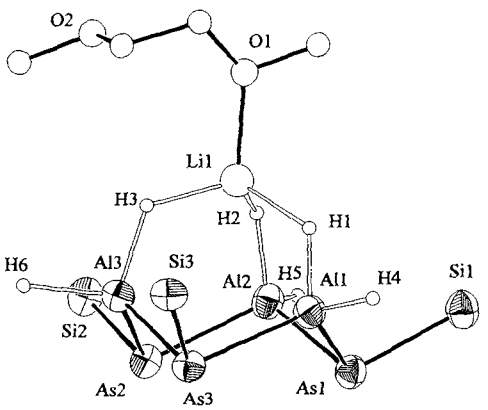

Fig. 2. Molecular structure of the dianion of **1c** in the crystal. The organo groups on the silicon atoms are omitted for clarity. Selected distances [Å] and angles [°]: As–Al 2.472(3) (average), As–Si 2.333(3) (average), Al1-H1 1.59(7), Al1–H4 1.54(6), Al2–H2 1.78(7), Al2–H5 1.70(7), Al3–H3 1.56(7), Al3–H6 1.59(7), Li1–H1 1.90(7), Li1–H2 1.65(6), Li1–H3 1.85(7), Li1–O1 2.01(2); Al-As-Al 95.04(9) (average), As-Al-As 105.03(10); sums of bond angles: As1 295.5(1), As2 297.2(1), As3 293.8(1).

 © VCH Verlagsgesellschaft mbH, D-69451 Weinheim, 1996 0570-0833/96/3521-2508 $ 15.00+.25/0

ingly as a monodentate ligand. In contrast, the Li2 and Li3 centers are octahedrally coordinated. The Li1–H distances lie between 1.65–1.90(7) Å, that is they are the same as the values that were determined for related complexes.[8] The As–Si distances of 2.327–2.341(3) Å are not unusual. The bulky silyl groups are arranged equatorially. The Al–As distances in the chair-shaped Al_3As_3 framework lie between 2.457–2.485(3) Å and are thus only slightly longer than in a trialuminatriarsacyclohexane with λ^3,σ^3-coordinate Al and As atoms (2.43 Å).[9] The alanate **1c** does not exhibit the same thermal behavior as **1a** and **1b** because of its different Al, As framework; the As_7^{3-} ion is neither formed by heating nor by reaction with TMEDA. The $Li1(HAl)_3$ arrangement in the complex dianion of **1c** is apparently not retained in organic solvents at 20 °C. Instead, a rapid exchange of the [Li(dme)] units takes place, since only one sharp singlet can be found in the ^{7}Li NMR spectrum at $\delta = -3.0$. Low-temperature NMR investigations in solution and CP/MAS solid-state NMR studies are not yet complete and will be reported in due course.

In spite of its lability, initial results show that **1a** is a valuable synthetic building block for the construction of novel polyarsenic compounds with elements of group 14. The reaction of **1a** with the bulky trichlorosilane **5**, for example, led to the first tetraarsatetrasilacubane $(AsSiIs)_4$ **6** (Is = 2,4,6-iPr$_3$C$_6$H$_2$), which was obtained in 36 % yield in the form of bright yellow crystals. The mechanism of formation is not yet known. It is highly probable, however, that **6**—analogous to the $(PSitBu)_4$ cubane—is formed in a number of steps from polycyclic precursors.[10] Its structure was determined by single-crystal X-ray analysis (Fig. 3).[4] The As_4Si_4 framework is strongly distorted

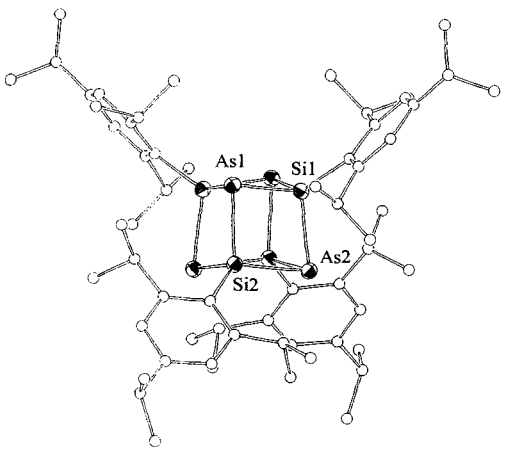

Fig. 3. Molecular structure of **6** in the crystal. Selected distances [Å] and angles [°]: As1–Si1 2.400(3), As1–Si1a 2.408(3), As1–Si2 2.411(3), As2–Si2a 2.398(3), As2–Si1 2.409(3), As2–Si2 2.409(3), Si–C(ipso) 1.896(8), 1.890(8); Si1-As1-Si1a 80.20(1), Si1-As1-Si2 79.01(8), Si1a-As1-Si2 78.60(8), Si2a-As2-Si1 78.83(8), Si2a-As2-Si2 80.1(1), Si1-As2-Si2 78.87(8), As1-Si1-As1a 98.43(10), As1-Si1-As2 100.42(9), As1a-Si1-As2 100.46(8), As2a-Si2-As2 98.54(9), As2a-Si2-As1 100.69(9), As2-Si2-As1 100.11(9).

in comparison to the recently synthesized As_4C_4 cubane $(AsCtBu)_4$,[11] so that its topography can be most simply described as an overlap of a Si_4 and an As_4 tetrahedron (C_2 point symmetry). The As–Si distances of 2.398–2.409(3) Å are almost identical with those in less strained As_2Si_2 cyclobutanes.[12] The endocyclic angles at the Si (98.4–100.5(1)°) and at the As atom (78.8–80.2°) reflect very similar bonding relationships to those in the $(PSitBu)_4$ cubane with a partial negative charge on the pnictogen, whereas in the carbon analogues positively polarized pnictogen atoms with strong n/σ interactions are present.[13] The geometry optimization of $(AsSiMe)_4$ (**6***), carried out by using the density functional method according to Becke (B3LYP/6-31G*),[14] resulted in T_d point symmetry with slightly longer As–Si distances (2.429 Å) than in **6**, and almost identical endocyclic angles at the Si (100.6°) and at the As atom (78.3°). Moreover, the ^{29}Si NMR chemical shift of **6*** ($\delta = -35.8$) was calculated at the GIAO/6-311 + + G(2d,2p) level;[14] in spite of the aryl group at the Si atom it is very similar to the experimental value of **6** ($\delta = -30.4$).

Experimental Procedure

1a: A moderate gas stream of **4a** (approx. 1–3 gas bubbles per second) was fed into a solution of **2** (7.4 g, 195 mmol) in DME (150 mL) at 25 °C for about 6 h. A clear yellow solution was formed, from which DME-solvated Li_3As_7 precipitated as a yellow solid after about 12 h. The end point of the reaction was determined by ^{27}Al NMR spectroscopy ($\delta = 150.4$); the ^{7}Li NMR spectrum then showed one singlet at $\delta = -2.7$.

1b: **2** (1 mmol, 0.7 mL of a 1.4 M solution in DME) was added to a solution of **4b** (0.96 g, 4.1 mmol) in DME (10 mL) at 25 °C. The reaction mixture was stirred for 24 h whereupon a clear orange-yellow solution was formed. The end point of the reaction was determined by ^{27}Al NMR spectroscopy ($\delta = 145$); the ^{7}Li NMR spectrum then showed a singlet at $\delta = -3.4$.

1c: **2** (3.6 mmol, 2.6 mL of a 1.4 M solution in DME) was added to a solution of **4c** (0.8 g, 3.6 mmol) in DME (10 mL) at 25 °C. The reaction mixture was heated under reflux for 2 h and the solvent removed under reduced pressure to leave approximately 5 mL of the solution. The product crystallized at 25 °C in the form of colorless columns. ^{27}Al NMR ([D$_8$]THF): $\delta = 132.3$ (s); ^{7}Li NMR ([D$_8$]THF): $\delta = -3.0$ (s); ^{29}Si NMR ([D$_8$]THF): $\delta = 13.6$ (s); ^{1}H NMR ([D$_8$]THF): $\delta = 1.0$ (br. m, 36H, $Me_2C(CHMe_2)$), 2.3 (m, 3H, J(H,H) ≈ 6.8 Hz, $Me_2C(CHMe_2)$), 3.17 (s, 42H, DME), 3.25 (s, 28H, DME), 4.2 (br., $h_{1/2}$ = 60 Hz, 6H, Al-H).

3: a) TMEDA (1 g, 8.6 mmol) was added to **1a** (10 mL of a 1.3 M solution in DME) at 25 °C. After 12 h **3** crystallized in the form of orange needles. Yield: 2.1 g (2.3 mmol, 81 % with respect to TMEDA); ^{7}Li NMR (THF): $\delta = -2.0$ (s). b) TMEDA (1 g, 8.6 mmol) was added to a solution of **1b** (7.2 g, 7.5 mmol) in DME ((25 mL). Compound **3** crystallized after 48 h. Yield: 1.9 g (2.1 mmol, 73 % with respect to TMEDA).

6: A solution of **5** (0.6 g, 1.8 mmol) in DME (10 mL) was treated with freshly prepared **1a** (1.4 mmol, 0.93 mL of a 1.3 M solution in DME) under continuous stirring at 25 °C. The dark red reaction solution was stirred for a further 3 h. Solvent was removed under reduced pressure to leave approximately 5 mL of the solution. The salts were then precipitated by addition of n-pentane (5 mL) and filtered off. TMEDA (0.5 mL) was added to the clear, dark green filtrate. The product crystallized in the form of light yellow cubes after a period of 96 h. Yield: 0.2 g (0.16 mmol, 36 %). ^{1}H NMR (C_6D_6): $\delta = 1.24$ (br. m, 72H, $CHMe_2$), 3.0 (m, 4H, p-$CHMe_2$), 4.2 (br., 8H, o-$CHMe_2$), 7.29 (s, 8H, arom. H); ^{29}Si-NMR (C_6D_6): $\delta = -30.4$ (s); MS (EI, 70 eV): m/z (%): 1224 (M^+, 100), 993 ($(M - SiIs)^+$, 6), 687 ($(M - (IsSi)_2As)^+$, 21), 231 ($(SiIs)^+$, 56).

Received: May 30, 1996 [Z9169IE]
German version: *Angew. Chem.* **1996**, *106*, 2688–2691

Keywords: aluminum compounds · arsenic compounds · heterocubanes · lithium compounds · silanes · Zintl anions

[1] a) M. L. Hitchman, K. F. Jensen in *Chemical Vapor Deposition—An Overview in Chemical Vapor Deposition-Principles and Applications* (Eds.: M. L. Hitchman, K. F. Jensen), Academic Press, San Diego, **1993**; b) M. L. Hitchman, K. F. Jensen in ref. [1a], p. 22; c) "Organometallic Vapor Phase Epitaxy of III-V Materials": R. L. Moon, Y.-M. Houng in ref. [1a], p. 245.

[2] A. D. Norman, D. C. Wingeleth, *Inorg. Chem.* **1970**, *9*, 98; A. D. Norman, *ibid.* **1970**, *9*, 870; M. Baudler, G. Scholz, W. Oehlert, *Z. Naturforsch. B* **1989**, *44*, 627; M. Baudler, G. Scholz, *Chem. Ber.* **1990**, *123*, 1261; M. Driess, G. Huttner, N. Knopf, H. Pritzkow, L. Zsolnai, *Angew. Chem.* **1995**, *107*, 354; *Angew. Chem. Int. Ed. Engl.* **1995**, *34*, 316; on the oligophosphanylation of germanes and stannanes: M. Driess, H. Pritzkow, unpublished results

[3] Solutions of **1a** in diglyme have already been used in the synthesis of primary monosilyl- and monogermylarsanes. However, neither the preparation and characterization nor the characteristic thermal lability of **1a** were described: J. W. Anderson, J. E. Drake, *J. Chem. Soc. A* **1970**, 3131, and references therein.

[4] Crystal structure analyses: **3**: orthorhombic, space group $P2_12_12_1$, a = 11.409(6), b = 16.137(8), c = 19.555(10) Å, V = 3600(3) Å^3, Z = 4, 5214 independent reflections ($Mo_{K\alpha}$ radiation, ω scans, $2\theta_{max} = 50°$). As and N atoms refined anisotropically, Li and C atoms refined isotropically, and H atoms inserted in calculated positions, $R1 = 0.044$ (observed reflections), $wR2 = 0.094$ (*all reflections*) [14]. *Two of the three TMEDA molecules are disordered.* **1c**: orthorhombic, space group $P2_12_12_1$, a = 14.756(7), b = 21.535(11), c = 25.346(13) Å, V = 8054(7) Å^3, Z = 4, 8633 independent reflections ($Mo_{K\alpha}$

 © VCH Verlagsgesellschaft mbH, D-69451 Weinheim, 1996 0570-0833/96/3521-2509 $ 15.00+.25/0

radiation, ω scans, $2\theta_{max} = 52°$), Li and H atoms at Al refined isotropically, all other atoms refined anisotropically, $R1 = 0.058$ (observed reflections), $wR2 = 0.113$ (all reflections) [15]. **6**: monoclinic, space group $P2/c$, $a = 14.144(7)$, $b = 9.544(5)$, $c = 27.537(14)$ Å, $\beta = 92.07(4)°$, $V = 3715(3)$ Å^3, $Z = 4$, 5428 independent reflections ($Mo_{K\alpha}$ radiation, ω scans, $2\theta_{max} = 48°$), all non-hydrogen atoms refined anisotropically, $R1 = 0.065$ (4203 observed reflections), $wR2 = 0.236$ (all reflections) [15]. The cell also contains other atoms (6–8 in the asymmetric unit) that probably belong to disordered solvent molecules (hexane), but which cannot be unequivocally assigned. Crystallographic data (excluding structure factors) for the structures reported in this paper have been deposited with the Cambridge Crystallographic Data Centre as supplementary publication no. CCDC-179-96. Copies of the data can be obtained free of charge on application to The Director, CCDC, 12 Union Road, Cambridge CB2 1EZ, UK (fax: Int. code +(1223) 336-033; e-mail: teched@chemcrys.cam.ac.uk).

[5] W. Hönle, J. Wolf, H. G. von Schnering, *Z. Naturforsch. B* **1988**, *43*, 219.

[6] W. Hönle, H. G. von Schnering, A. Schmidpeter, G. Burget, *Angew. Chem.* **1984**, *96*, 796; *Angew. Chem. Int. Ed. Engl.* **1984**, *23*, 817.

[7] M. Driess, M. Reisgys, K. Merz, H. Pritzkow, unpublished results.

[8] Overview: R. Snaith, D. S. Wright, *Complexes of Inorganic Lithium Salts in Lithium Chemistry—A Theoretical and Experimental Overview* (Eds.: A.-M. Sapse, P. von Ragué Schleyer), Wiley, New York, **1995**, p. 269, and references therein.

[9] P. J. Brothers, P. P. Power, *Adv. Organomet. Chem.* **1996**, *39*, 30.

[10] M. Baudler, G. Scholz, K.-F. Tebbe, M. Fehér, *Angew. Chem.* **1989**, *101*, 352; *Angew. Chem. Int. Ed. Engl.* **1989**, *28*, 339.

[11] P. B. Hitchcock, J. A. Johnson, J. F. Nixon, *Angew. Chem.* **1993**, *105*, 86; *Angew. Chem. Int. Ed. Engl.* **1993**, *32*, 103.

[12] M. Driess, R. Janoschek, H. Pritzkow, *Angew. Chem.* **1992**, *104*, 449; *Angew. Chem. Int. Ed. Engl.* **1992**, *31*, 460.

[13] T. Wettling, J. Schneider, O. Wagner, C. G. Kreiter, M. Regitz, *Angew. Chem.* **1989**, *101*, 1035; *Angew. Chem. Int. Ed. Engl.* **1989**, *28*, 1013; R. Gleiter, K.-H. Pfeifer, M. Baudler, G. Scholz, T. Wettling, M. Regitz, *Chem. Ber.* **1990**, *123*, 757.

[14] GAUSSIAN 94, Revision B.3., M. J. Frisch, G. W. Trucks, H. B. Schlegel, P. M. W. Gill, B. G. Johnson, M. A. Robb, J. R. Cheeseman, T. Keith, G. A. Petersson, J. A. Montgomery, K. Raghavachari, M. A. Al-Laham, V. G. Zakrzewski, J. V. Ortiz, J. B. Foresman, C. Y. Peng, P. Y. Ayala, W. Chen, M. W. Wong, J. L. Andres, E. S. Replogle, R. Gomperts, R. L. Martin, D. J. Fox, J. S. Binkley, D. J. Defrees, J. Baker, J. P. Stewart, M. Head-Gordon, C. Gonzalez, J. A. Pople, Gaussian Inc., Pittsburgh, PA, **1995**.

[15] a) G. M. Sheldrick, SHELXS86, Universität Göttingen, **1986**; b) G. M. Sheldrick, SHELXL93, Universität Göttingen, **1993**.

Orthogonal Glycosylation Strategy for Rapid Assembly of Oligosaccharides on a Polymer Support**

Yukishige Ito,* Osamu Kanie, and Tomoya Ogawa

Solid-phase synthesis has been demonstrated to be extremely valuable for routine preparations of oligopeptides and oligonucleotides, and is attracting renewed attention in connection with combinatorial chemistry.[1] Recently, the synthesis of oligosaccharides on polymer supports has also attracted interest and several intriguing approaches have been reported.[2–5] We report here on a novel strategy for the synthesis of oligosaccharides on polymer supports based on the concept of orthogonal glycosylation,[6] which enables the ready preparation of oligosaccharides.

For the synthesis of oligosaccharides on polymer supports two approaches can be considered with respect to the direction of chain elongation: from the reducing end to the non-reducing end (Approach A), and from the non-reducing end to the reducing end (Approach B). Approach A is generally considered to be more advantageous because when both the polymer-supported aglycon and the glycosyl donor are reactive enough to ensure that all glycosylations go to completion, a nearly homogeneous product can be obtained. Approach B is less straightforward in principle because all by-products accumulate on the polymer phase together with desired O-glycoside, which complicates the isolation of the correctly assembled oligosaccharide, and after each glycosylation the the anomeric position at the reducing end must be transformed into a leaving group.

In addressing the problems inherent to Approach B, our attention has turned to the application of the orthogonal glycosylation strategy to chemistry on polymer supports (Scheme 1).

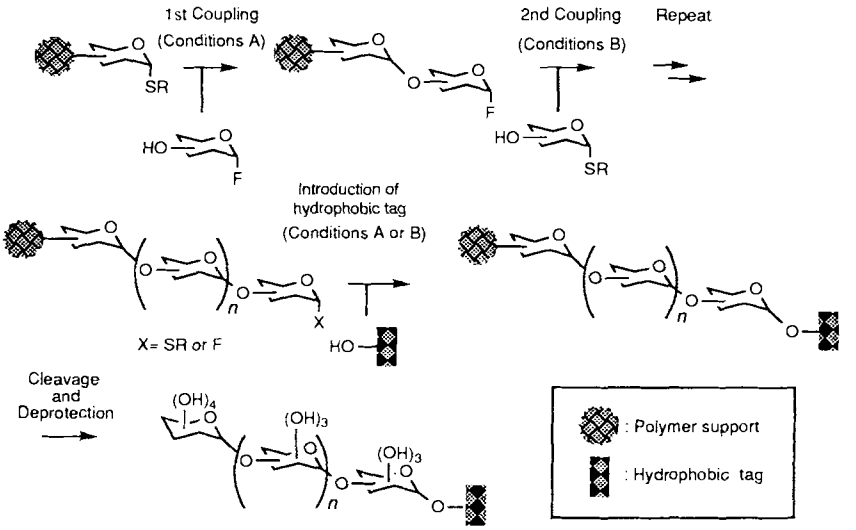

Scheme 1. Oligosaccharide synthesis on solid supports based on an orthogonal glycosylation strategy.

Thioglycoside and glycosyl fluoride were used in combination, because these were demonstrated to be a competent set of orthogonal glycosyl donors.[6] To avoid potential difficulties in isolating the final product, a hydrophobic aglycon was to be incorporated as a tag at the anomeric position of the reducing end after the oligosaccharide had been assembled. The target oligosaccharide can thus be distinguished from all other polymer-supported products, since it should be the only tag-carrying molecule. Therefore, the product should be isolable in a single step, irrespective of the number of glycosylation steps, by using reversed-phase silica gel chromatography.[7]

To test this hypothesis, the first attempt was made with polyethylene glycol (PEG) as a "soluble" polymer,[3] and the trimannoside portion (i.e. **13**) of high mannose type glycoprotein oligosaccharides[8] was chosen as a target (Scheme 2). In this instance, the 2-(trimethylsilyl)ethyl (SE) group was used as a hydrophobic tag.[9]

The synthesis started with the ester **1**, which was prepared from the chloride **2**[10] via **3**, **5**, and **6**. Saponification yielded

[*] Dr. Y. Ito, Dr. O. Kanie, Prof. Dr. T. Ogawa[+]
The Institute of Physical and Chemical Research (RIKEN)
2-1 Hirosawa, Wako-shi, Saitama 351-01 (Japan)
Fax: Int. code +(48)462-4680
e-mail: yukito@postman.riken.go.jp.

[+] Alternative address:
Graduate School of Agriculture and Life Science
University of Tokyo, Yayoi, Bunkyo-ku, Tokyo 113 (Japan)

[**] This work was supported in part by a Grant-in-Aid for Scientific Research from the Ministry of Education, Science, and Culture and also by the Special Coordination Funds of the Science and Technology Agency of the Japanese Government. We thank Ms. M. Yoshida and her staff for elemental analyses, and Ms. A. Takahashi for technical assistance.

 © VCH Verlagsgesellschaft mbH, D-69451 Weinheim, 1996 0570-0833/96/3521-2510 $ 15.00+.25/0

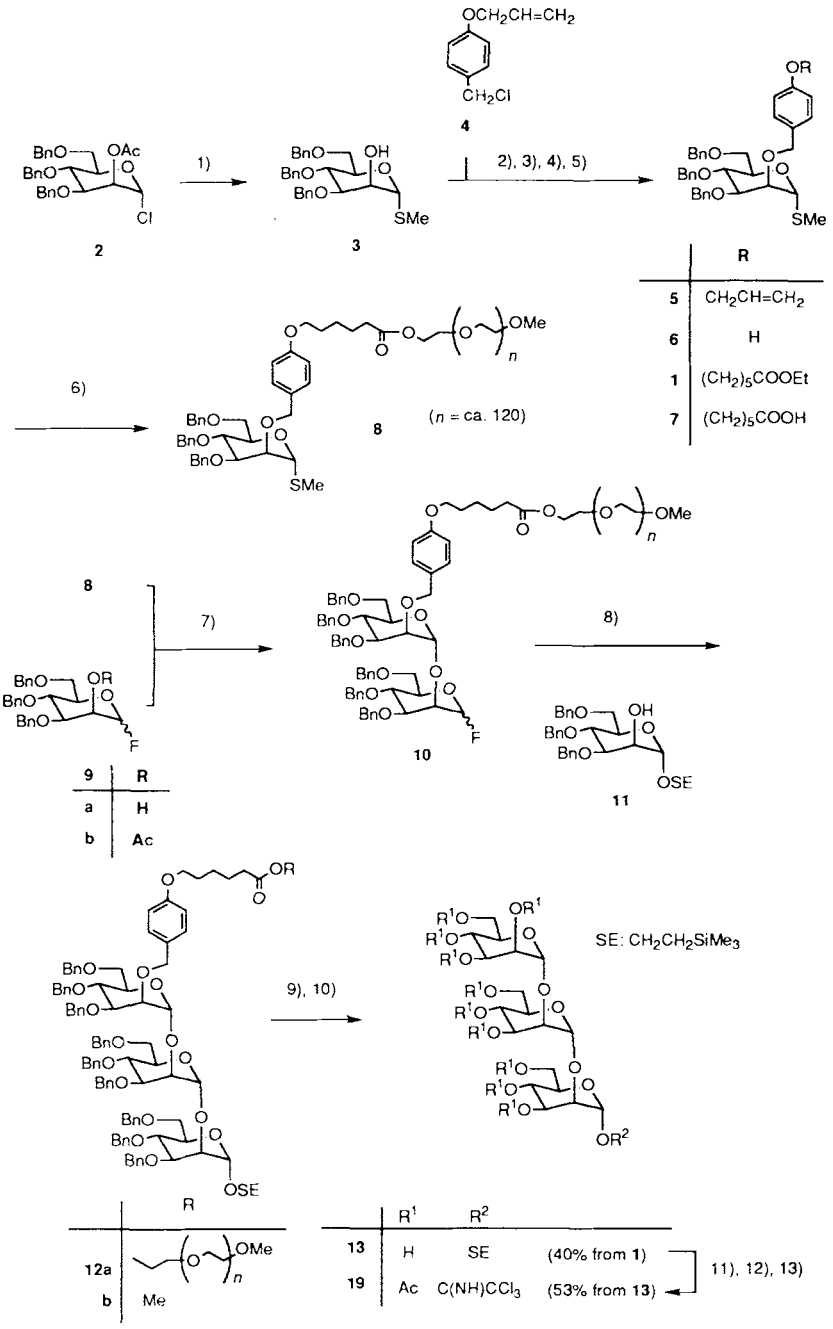

Scheme 2. Synthesis of trimannoside **13**. 1) MeSSMe, *n*BuLi/THF, 87%; 2) **4**, NaH/DMF, 100%; 3) $[(Ph_3P)_4Pd]$, $NaBH_4$/THF, 96%; 4) $Br(CH_2)_5CO_2Et$, Cs_2CO_3/DMF, 91%; 5) aq. NaOH/THF–EtOH, quantitative; 6) $EtO_2C-N=N-CO_2Et$, Ph_3P, PEG monomethyl ether/THF–CH_2Cl_2, 95%; 7) $MeOSO_2CF_3$, MeSSMe, molecular sieves 4Å/CH_2Cl_2, room temperature, 89%; 8) **11**, $[Cp_2HfCl_2]$, $AgOSO_2CF_3$, molecular sieves 4Å/CH_2Cl_2, 0 °C to room temperature, 99%; 9) NaOMe/MeOH; 10) H_2, $Pd(OH)_2$/MeOH–ethyl acetate; 11) Ac_2O, 4-dimethylaminopyridine (4-DMAP)/pyridine; 12) CF_3COOH/CH_2Cl_2; 13) CCl_3CN, 1,8-diazabicyclo[5.4.0]undec-7-ene (DBU)/CH_2Cl_2, then chromatographic purification.

carboxylic acid **7**, which was coupled with PEG monomethyl ether (Aldrich, average molecular mass 5000) to afford the thiomannoside–polymer conjugate **8**.[11] The first coupling with the fluoride **9a**[12] was performed in the presence of $MeOSO_2CF_3$[13] and MeSSMe in CH_2Cl_2 to furnish the disaccharide–PEG conjugate **10** in 89% yield.[11,14] In the second coupling the reducing end of the diasaccharide was linked to the 2-(trimethylsilyl)ethyl (SE) glycoside **11**,[15] in which the SE group served as a hydrophobic aglycon. The reaction was performed under Suzuki conditions ($[Cp_2HfCl_2]$/$AgOSO_2CF_3$/CH_2Cl_2)[16] to afford the trisaccharide–PEG **12a**.[11] After the trisaccharide sequence had been completed, PEG was cleaved off under basic conditions, and the crude trisaccharide **12b** was hydrogenated over $Pd(OH)_2$. The resulting mixture was then passed through a short column of C_{18} reversed-phase silica gel (Senshu Kagaku, Tokyo), which was first eluted with water to remove all by-products. Subsequent elution with 50% MeOH gave the desired trisaccharide **13**[17,18] in 40% overall yield from **1**.

Disaccharide–PEG **10** was also converted into the tetrasaccharide **18**, which corresponds to the partially protected form of the common carbohydrate structure of the glycosyl phosphatidyl inositol (GPI) anchor (Scheme 3).[19] Thus, disaccharide **14** was synthesized from the monosaccharide derivatives **15** and **16**, and then coupled with **10** in the presence of $[Cp_2HfCl_2]$/$AgOSO_2CF_3$ in benzene.[20] The resultant tetrasaccharide–PEG conjugate **17**[11] was subjected to catalytic hydrogenation. In this case, due to its *p*-methoxyphenyl and phthalimide groups, the product is hydrophobic enough to be retained on a C_{18} column. Thus, reversed-phase chromatographic separation, in a similar manner as that described for **13**, gave tetrasaccharide **18**[17,21] in 42% yield based on **10**.

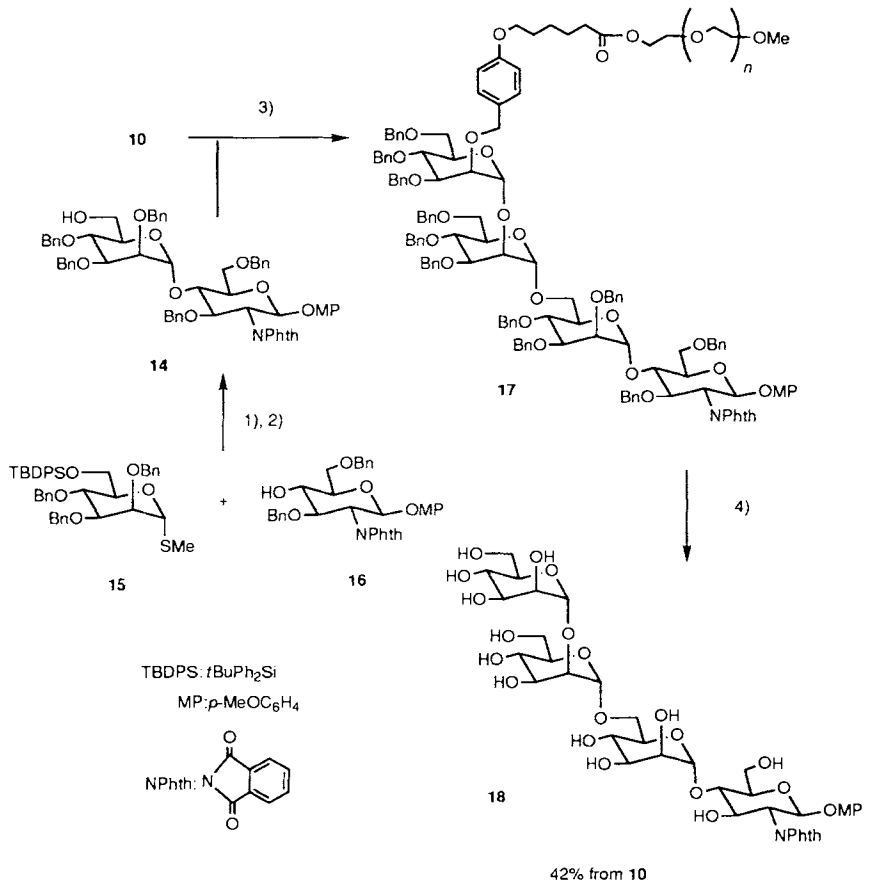

Scheme 3. Synthesis of tetrasaccharide **18**. 1) $MeOSO_2CF_3$, MeSSMe, molecular sieves 4Å/$ClCH_2CH_2Cl$, room temperature, 80%; 2) $(nBu)_4NF$, acetic acid/THF, 93%; 3) $[Cp_2HfCl_2]$, $AgOSO_2CF_3$, molecular sieves 4Å/benzene, room temperature, 86%; 4) H_2, $Pd(OH)_2$/MeOH.

The strategy reported here, featuring a novel combination of chemistry on polymer supports and orthogonal glycosylation, results in the construction of oligosaccharides by a minimum number of operations. It should also be noted that the anomeric positions of **13** and **18** are masked by protecting groups that are selectively cleavable.[22] For example, the trisaccharide **13** was easily transformed into the trichloroacetimidate **19**,[17, 23] which should be a valuable synthetic building block for mannose-rich glycans (Scheme 2).

Received May 21, 1996 [Z9141IE]
German version: *Angew. Chem.* **1996**, *108*, 2691–2693

Keywords: glycoproteins · glycosylations · oligosaccharides · solid-phase syntheses

[1] L. A. Thompson, J. A. Ellman, *Chem. Rev.* **1996**, *96*, 555–600.
[2] L. Yan, C. M. Taylor, R. Goodnow, Jr., D. Kahne, *J. Am. Chem. Soc.* **1994**, *116*, 6953–6954.
[3] S. P. Douglas, D. Whitfield, J. J. Krepinsky, *J. Am. Chem. Soc.* **1991**, *113*, 5095–5097; *ibid.* **1995**, *117*, 2116–2117.
[4] M. Schuster, P. Wang, J. C. Paulson, C.-H. Wong, *J. Am. Chem. Soc.* **1994**, *116*, 1135–1136.
[5] S. J. Danishefsky, K. F. McClure, J. T. Randolph, R. B. Ruggeri, *Science*, **1993**, *260*, 1307–1309; J. T. Randolph, K. F. McClure, S. J. Danishefsky, *J. Am. Chem. Soc.* **1995**, *117*, 5712–5719.
[6] O. Kanie, Y. Ito, T. Ogawa, *J. Am. Chem. Soc.* **1994**, *116*, 12073–12074.
[7] M. M. Palcic, L. D. Heeze, M. Pierce, O. Hindsgaul, *Glycoconjugate J.* **1988**, *5*, 49–63.
[8] A. Kobata, *Acc. Chem. Res.* **1993**, *26*, 319–324.
[9] For the use of an SE group in an SE glycoside as a hydrophobic aglycon in chemoenzymatic synthesis of ganglioside, see Y. Ito, J. C. Paulson, *J. Am. Chem. Soc.* **1993**, *115*, 1603–1604. A more hydrophobic aglycon similar to SE was reported recently: P. Stangier, M. M. Palcic, D. R. Bundle, *Carbohydr. Res.* **1995**, *267*, 153–159.
[10] For preparation of **2**, see T. Ogawa, K. Katano, K. Sasajima, M. Matsui, *Tetrahedron*, **1981**, *37*, 2779–2786. *p*-Allyloxybenzyl chloride (**4**) was prepared from *p*-hydroxybenzaldehyde (1. allyl bromide, K_2CO_3/acetone; 2. $LiAlH_4$/ether; 3. $SOCl_2$, DMF/CH_2Cl_2).
[11] All PEG-supported products were isolated by precipitation from *tert*-butyl methyl ether as described [3]. Yields were calculated based on mass balances and do not necessarily reflect the purity.
[12] Y. Ito, T. Ogawa, *Angew. Chem.* **1994**, *106*, 1843–1845; *Angew. Chem. Int. Ed. Engl.* **1994**, *33*, 1765–1767.
[13] H. Lönn, *J. Carbohydr. Chem.* **1987**, *6*, 301–306.
[14] The corresponding stereoisomer was not evident in spectra recorded with a 270 MHz ^1H NMR spectrometer.
[15] Prepared from fluoride **9b** (1. $Me_3SiCH_2CH_2OH$, $[Cp_2HfCl_2]$, $AgOSO_2CF_3/CH_2Cl_2$; 2. NaOMe/MeOH).
[16] K. Suzuki, K, H. Maeta, T. Matsumoto, *Tetrahedron Lett.* **1989**, *30*, 4853–4856.
[17] ^1H (270 MHz) and ^{13}C (68.4 MHz) NMR data: **13**: δ_H (D_2O, 50 °C) = 5.25 (d, J = 2 Hz, H-1^2), 5.06 (s, H-1^3), 5.03 (d, J = 2 Hz, H-1^1), 4.09 and 4.05 (dd, J = 3, 2 Hz, H-2^1, H-2^2), 0.95 (m, CH_2SiMe_3), 0.02 ($SiMe_3$); δ_C (D_2O, 50 °C) = 103.68, 102.19, and 98.97 (anomeric carbons), 80.57 and 80.03 (C-2^1 and C-2^2), 18.47 (CH_2SiMe_3), −0.89 ($SiMe_3$); **18**: δ_H (D_2O, 70 °C) = 5.70 (d, J = 8.6 Hz, H-1^1), 5.28 (d, J = 1.7 Hz, H-1^2), 5.13 (d, J = 1 Hz, H-1^4), 5.06 (d, J = 1.7 Hz, H-1^3); δ_C (D_2O, 50 °C) = 103.64, 103.14, 99.88, and 98.83 (anomeric carbons); **19**: δ_H ($CDCl_3$) = 8.76 (NH), 6.43 (d, J = 2.3 Hz, H-1^1), 5.20 (d, J = 2.3 Hz, H-1^3), 4.97 (d, J = 2.0 Hz, H-1^2).
[18] This material was a 3.5:1 mixture of α and β anomers with respect to the Man^2 residue. Isomers can be separated by eluting the C_{18} column with linear gradient of H_2O to H_2O/MeOH (1/1).
[19] M. J. McConville, M. A. J. Ferguson, *Biochem. J.* **1993**, *294*, 305–324.
[20] K. Suzuki, H. Maeta, T. Suzuki, T. Matsumoto, *Tetrahedron Lett.* **1989**, *30*, 6879–6882.
[21] A 8:1 mixture of α and β anomers with respect to the Man^2 was obtained. The reaction proceeded in a nearly stereorandom manner in CH_2Cl_2 (α:β = 1.2:1).
[22] K. Jansson, S. Ahlfors, T. Freid, J. Kihlberg, G. Magnusson, *J. Org. Chem.* **1988**, *53*, 5629–5647; T. Fukuyama, A. A. Laird, L. M. Hotchkiss, *Tetrahedron Lett.* **1985**, *26*, 6291–6292.
[23] For a recent review of trichloroacetimidate method, see R. R. Schmidt, W. Kinzy, *Adv. Carbohydr. Chem. Biochem.* **1994**, *50*, 21–123.

 © VCH Verlagsgesellschaft mbH, D-69451 Weinheim, 1996 0570-0833/96/3521-2512 $ 15.00+.25/0

Silaethene $H_2C{=}SiH_2$: Millimeter Wave Spectrum and Ab Initio Calculations**

Stephane Bailleux, Marcel Bogey,* Jürgen Breidung, Hans Bürger,* Radek Fajgar, Yuyan Liu, Josef Pola, Michael Senzlober, and Walter Thiel*

While silaethenes $CR^1R^2{=}SiR^3R^4$ that are kinetically stabilized by bulky ligands R^1-R^4 are well documented, the parent molecule $CH_2{=}SiH_2$ (silene, silaethene, **1**) still awaits unambiguous characterization in the gas phase, although convincing evidence for its formation as a transient has been deduced from trapping experiments.[1] Moreover, IR and UV spectra of products isolated in an Ar matrix at 10 K and generated by vacuum flash pyrolysis of 5,6-bis(trifluoromethyl)-2-silabicyclo[2.2.2]-octa-5,7-diene (SBO) at 650 °C and 1.4×10^{-5} mbar were attributed to **1**, and this conclusion was supported by ab initio calculations of the vibrational wavenumbers and by deuteration experiments.[2] Furthermore, the first band observed and predicted at 8.95 eV in the He(I) photoelectron (PE) spectrum of **1** produced from SBO under similar conditions showed vibrational fine structure that was consistent with the expected vibrational energy pattern.[3]

Photochemical generation of **1** both from silacyclobutane (SCB) and 1,3-disilacyclobutane (DSB) has been achieved by using pulsed ArF (193 nm) and TEA CO_2 lasers (10P(20) line) at low flux.[4] Since the CO_2-laser-induced decomposition of SCB and DSB is a promising technique for low-temperature chemical vapor deposition of amorphous SiC,[5] there is great interest in the nature of the transients involved. Spectroscopic techniques are most suited to provide answers to this question. Microwave and millimeter wave (mmw) spectroscopy combine sensitivity and specificity, and their potential to detect short-lived silicon-containing transients has been recently demonstrated for H_2Si_2[6] and H_2SiO.[7] More importantly these techniques provide accurate information on molecular parameters for which predictions may be obtained from ab initio calculations. Furthermore, decay processes can be monitored, and decomposition products identified.

We have guided our mmw spectroscopic search for **1** by predictions derived from ab initio calculations. Although ab initio calculations at different levels have been previously performed,[8] we needed optimized ground state rotational constants to predict transitions as reliably as possible.

[*] Dr. M. Bogey, S. Bailleux, Dr. Y. Liu
Laboratoire de Spectroscopie Hertzienne, Associé au CNRS
Université des Sciences et Technologies de Lille
F-59655 Villeneuve d'Ascq Cedex (France)
Fax: Int. code +20434084
e-mail: marcel@lsh.univ-lille1.fr

Prof. Dr. H. Bürger, Dipl.-Chem. M. Senzlober
Anorganische Chemie, FB 9 der Universität-Gesamthochschule
D-42097 Wuppertal (Germany)
Fax: Int. code +(202)439 2901
e-mail: buerger1@wrcs3.urz.uni-wuppertal.de

Prof. Dr. W. Thiel, Dr. J. Breidung
Organisch-chemisches Institut der Universität Zürich
CH-8057 Zürich (Switzerland)
Fax: Int. code +(1)361 9895
e-mail: thiel@oci.unizh.ch

Dr. R. Fajgar, Dr. J. Pola
Institute of Chemical Process Fundamentals, Academy of Sciences, 16502 Prague 6 (Czech Republic)

[**] We thank the Deutsche Forschungsgemeinschaft, the Centre National de la Recherche Scientifique (GDR "PCMGI"), the German/French PROCOPE program, the Volkswagen-Stiftung, and the Schweizerischer Nationalfonds for financial support. Y. L. thanks the European Union for a Human Capital and Mobility postdoctoral fellowship.

The molecular geometry of **1** was optimized within the constraints of C_{2v} point group symmetry at the Hartree–Fock self-consistent field (SCF) level of theory[9] and at the correlated levels of second-order Møller–Plesset perturbation theory (MP2),[10] coupled cluster theory with single and double excitations (CCSD),[11] and CCSD augmented by a perturbational estimate of the contributions from triple excitations (CCSD(T)).[12] The geometry optimizations were performed with analytical gradients as implemented in the GRADSCF,[13] GAUSSIAN 92,[14] and ACES II[15] program systems. All quantum-chemical calculations were performed by employing a valence triple-zeta plus double polarization plus f functions basis set (TZ2Pf): Si: (12s9p)/[6s5p] basis[16] with two sets of d and one set of f polarization functions;[17] C: (10s6p)/[5s3p] basis[18] with two sets of d and one set of f polarization functions;[19] H: (5s)/[3s] basis (scale factor 1.2)[18] with two sets of p and one set of d polarization functions.[19] Spherical harmonics were used in the correlated calculations, whereas SCF wavefunctions were represented by cartesian Gaussian-type orbitals. All electrons were correlated in the MP2, CCSD, and CCSD(T) treatments. At the theoretical equilibrium geometries the harmonic force fields were evaluated either analytically (SCF, MP2)[13, 14] or numerically from analytical energy gradients (CCSD, CCSD(T)).[15] Anharmonic normal coordinate force fields were determined (SCF, MP2) by using a finite difference procedure.[20] Spectroscopic constants that are listed in Table 1 were then derived by established methods.[21]

Table 1. Molecular constants of **1** (A reduction, I' representation).

Parameter [a]	ab initio, $^{12}CH_2{}^{28}SiH_2$				experimental [b]
	SCF	MP2	CCSD	CCSD(T)	$^{12}CH_2{}^{28}SiH_2$
r_e (CSi)	1.6922	1.7085	1.7084	1.7167	
r_e (CH)	1.0739	1.0777	1.0781	1.0799	
r_e (SiH)	1.4684	1.4680	1.4713	1.4728	
α_e (HCH)	115.37	116.33	115.76	115.93	
α_e (HSiH)	113.97	114.73	114.71	115.01	
A_e	107153	105943	105862	105300	
B_e	14992	14779	14761	14643	
C_e	13152	12970	12954	12855	
A_0	106554	105200	105119 [c]	104557 [c]	104716.60(18)
B_0	14944	14719	14700 [c]	14583 [c]	14786.7020(12)
C_0	13082	12890	12875 [c]	12776 [c]	12936.2854(12)
Δ_J	10.87	11.84	11.71	12.02	12.6395(11)
Δ_{JK}	141.58	156.05	157.56	160.50	160.8581(94)
Δ_K	1650.95	1714.89	1740.08	1737.68	1908(70)
δ_J	1.46	1.58	1.57	1.60	1.7336(10)
δ_K	107.41	117.44	118.31	119.99	128.91(44)
Φ_{KJ}					$-0.741(67)\times10^{-3}$
Φ_K					7.04(15)
μ_e	1.114	0.867 [d]		0.810 [d]	0.700 [d]

[a] Equilibrium bond lengths r_e [Å] and angles α_e [°]; equilibrium (A_e, B_e, C_e) and ground state rotational constants (A_0, B_0, C_0) [MHz], quartic (Δ,δ), and sextic centrifugal distortion constants Φ [kHz]; electric dipole moment μ_e [D]. [b] One standard deviation in parentheses. [c] Derived from MP2 ground state corrections. [d] Obtained as energy derivatives by means of finite field calculations.

The mmw spectrometer used has been described in detail.[6, 7] The mmw irradiation was obtained by harmonic generation from phase-locked Varian klystrons using Schottky barrier diodes mounted in a commercial multiplier. In the highest frequency range (340–473 GHz), two phase-locked carcinotrons (backward wave oscillators) were used. The detection of the signal was achieved with a helium-cooled InSb detector. Source modulation at 40 kHz and lock-in detection at twice this frequency were used, inducing a second derivative line shape.

 © VCH Verlagsgesellschaft mbH, D-69451 Weinheim, 1996 0570-0833/96/3521-2513 $ 15.00+.25/0

Frequency scanning, data acquisition, signal processing, and frequency measurement were controlled by uisng a microcomputer; the estimated errors were less than 50 kHz.

The measurement cell consisted of a 1 m long pyrex tube connected at one end to the pump and at the other end to a cross-shaped glass vessel (50 cm long and 10 cm internal diameter), into the side-arm of which a small oven was introduced. This comprised a quartz tube (2 cm long, 0.8 cm internal diameter) heated by a tungsten coil. The cross-shaped part of the cell was cooled by flowing liquid nitrogen through a rubber tube around it. This system allowed production of the reactive species directly in the cell. Argon served as a buffer and carrier gas and was flowed together with SBO through the oven heated to 600 °C. The best experimental conditions were $p(\mathrm{SBO}) = 7\times10^{-3}$ mbar and $p(\mathrm{Ar}) = 1.5\times10^{-2}$ mbar.

We have also generated a spectrum of **1**, which is half as intense, by pyrolysis of SCB at about 1000 °C, but at higher partial pressure. Very weak signals could also be obtained from DSB, but this required even higher temperatures and pressure. In both cases, lines of CH_3SiH_3 were observed with significant intensity.

Photolytic generation of **1** from SBO was studied by using an ArF excimer laser. Although the efficiency of the photolysis was poor, the pulsed emission of the laser allowed the measurement of the lifetime of **1** in the gas phase at room temperature by recording the decay of the $7_{1,6}\leftarrow6_{1,5}$ rotational line.[22] A least squares adjustment of this experimental signal to an exponential decay led to a $1/e$ lifetime of 30 ± 2 ms.

Since the dipole moment of **1** lies along the C_2 symmetry axis, which is the axis of the least moment of inertia, the rotational spectrum should display the characteristic *a*-type pattern of a slightly asymmetric prolate top, $\kappa = -0.9597$. Owing to the two pairs of identical hydrogen nuclei, the relative intensities of the rotational lines were determined by employing nuclear spin statistical weights; that is, 10 for the K_aK_c = oo and oe and 6 for the ee and eo rotational levels.

According to the rotational and centrifugal distortion constants calculated by ab initio methods (Table 1), for the three levels of theory MP2, CCSD, and CCSD(T), the $K_a = 0$, $J = 7\leftarrow6$ line was predicted to lie at 191575, 191508, and 190012 MHz, respectively. Starting a frequency scan at 190 GHz, lines corresponding to an *a*-type pattern with the right relative intensities were observed; the $K_a = 0$ component lies at 192484 MHz. A first least squares fit of the K_a components of the $J = 7\leftarrow6$ series allowed a more precise prediction of the other transitions. Repeating this procedure eventually led to the measurement of 139 rotational lines corresponding to $6\geq J\geq16$ and $K_a\geq11$ in the 180–473 GHz frequency range. These frequencies were fitted to Watson's A-reduced Hamiltonian in I^r representation[23] with a standard deviation of 16.9 kHz. The residuals were well below 50 kHz, the estimated accuracy of the measurements. Two experimentally unresolved K_a doublets, $J = 7\leftarrow6$, $K_a = 4$, and $J = 13\leftarrow12$, $K_a = 5$, were not taken into consideration in the fit. The adjusted rotational and centrifugal distortion constants are given in Table 1 and can be compared with the values calculated by ab initio methods. The two sextic parameters Φ_{KJ} and Φ_K can only be considered as fitting terms.

The CCSD(T)/TZ2Pf results should generally be the most reliable because they represent the highest theoretical level applied. By comparing analogous theoretical and experimental results for $H_2C{=}S$, it is found that the CCSD(T) calculations overestimate the C=S bond length by 0.009 Å, while the MP2 and CCSD values are virtually identical with the experimental results. The same applies to **1**, for which the theoretical B_o/C_o values are only 0.46/0.36 and 0.59/0.47% higher than the experimental ones at the MP2 and CCSD levels, respectively.[24] The quartic centrifugal distortion parameters are in close agreement with the theoretical predictions.

The excellent agreement between experiment and theory enables us to ascertain that we have observed the rotational spectrum of $H_2C{=}SiH_2$. This is the first high-resolution spectroscopic identification of this compound, and additional confirmation was provided by the observation of lines belonging to the ^{29}Si isotopomer in natural abundance and other isotopomers from isotopically labeled precursors. Work directed towards the determination of an experimental structure is in progress. The observed nuclear spin statistics confirm the assumed C_{2v} symmetry of **1**, and the small size of the inertial defect, $\Delta = 0.0627$ u Å^2, proves the planarity of the molecule.

By comparing the present experiment with previous fruitless attempts, started in 1981 by M. Bogey in collaboration with H. P. Reisenauer, G. Maier, and M. Winnewisser, it seems that three experimental modifications have led to its success: the shortening of the oven, the use of Ar as a carrier gas, and the cooling of the cell. We are convinced that each of the two latter modifications are indispensable since only when these conditions were applied was the observed spectrum very clean and the strongest observed lines belonged only to **1** and CH_3SiH_3. Thus present results explain the failure of the previous attempts in mmw spectroscopy and confirm observations made by Rosmus et al.[3] when studying the photoelectron spectrum.

Received: May 20, 1996 [Z 9133 IE]
German version: *Angew. Chem.* **1996**, *108*, 2683–2685

Keywords: ab initio calculations · millimeterwave spectroscopy · silicon compounds · structure elucidation

[1] G. Raabe, J. Michl, *Chem. Rev.* **1985**, *85*, 419–509.
[2] G. Maier, G. Mihm, H. P. Reisenauer, *Chem. Ber.* **1984**, *117*, 2351–2368.
[3] P. Rosmus, H. Bock, B. Solouki, G. Maier, G. Mihm, *Angew. Chem.* **1981**, *93*, 616–618; *Angew. Chem. Int. Ed. Engl.* **1981**, *20*, 598–599.
[4] S. Dhanya, K. Awadhesh, R. K. Vatsa, R. D. Saini, J. P. Mittal, J. Pola, *J. Chem. Soc. Faraday Trans.* **1996**, *92*, 179–183.
[5] Z. Bastl, H. Bürger, R. Fajgar, D. Pokorná, J. Pola, M. Senzlober, J. Šubrt, M. Urbanová, *Appl. Organomet. Chem.* **1996**, *10*, 83–99.
[6] Dibridged: a) M. Bogey, H. Bolvin, C. Demuynck, J. L. Destombes, *Phys. Rev. Lett.* **1991**, *66*, 413–416; monobridged: b) M. Cordonnier, M. Bogey, C. Demuynck, J. L. Destombes, *J. Chem. Phys.* **1992**, *97*, 7984–7989.
[7] S. Bailleux, M. Bogey, C. Demuynck, J. L. Destombes, A. Walters, *J. Chem. Phys.* **1994**, *101*, 2729–2733.
[8] a) R. S. Grev, G. E. Scuseria, A. C. Scheiner, H. F. Schaefer, III, M. S. Gordon, *J. Am. Chem. Soc.* **1988**, *110*, 7337–7339; b) M. E. Colvin, J. Kobayashi, J. Bicerano, H. F. Schaefer, III., *J. Chem. Phys.* **1986**, *85*, 4563–4566.
[9] C. C. J. Roothaan, *Rev. Mod. Phys.* **1951**, *23*, 69–89.
[10] C. Møller, M. S. Plesset, *Phys. Rev.* **1934**, *46*, 618–622.
[11] G. D. Purvis, III, R. J. Bartlett, *J. Chem. Phys.* **1982**, *76*, 1910–1918.
[12] K. Raghavachari, G. W. Trucks J. A. Pople, M. Head-Gordon, *Chem. Phys. Lett.* **1989**, *157*, 479–483.
[13] A. Komornicki, GRADSCF: An ab Initio Gradient Program System, Version 9.5, Polyatomics Research Institute, Mountain View, CA, **1988**.
[14] M. J. Frisch, G. W. Trucks, H. B. Schlegel, P. M. W. Gill, B. G. Johnson, M. W. Wong, J. B. Foresman, M. A. Robb, M. Head-Gordon, E. S. Replogle, R. Gomperts, J. L. Andres, K. Raghavachari, J. S. Binkley, C. Gonzalez, R. L. Martin, D. J. Fox, D. J. Defrees, J. Baker, J. J. P. Stewart, J. A. Pople, GAUSSIAN 92/DFT, Revision G2; Gaussian, Pittsburgh, PA, **1993**.
[15] J. F. Stanton, J. Gauss, J. D. Watts, W. J. Lauderdale, R. J. Bartlett, *Int. J. Quantum Chem. Quantum Chem. Symp.* **1992**, *26*, 879–894.
[16] A. D. McLean, G. S. Chandler, *J. Chem. Phys.* **1980**, *72*, 5639–5648.
[17] D. E. Woon, T. H. Dunning, Jr., *J. Chem. Phys.* **1993**, *98*, 1358–1371.
[18] T. H. Dunning, Jr., *J. Chem. Phys.* **1971**, *55*, 716–723.
[19] T. H. Dunning, Jr., *J. Chem. Phys.* **1989**, *90*, 1007–1023.
[20] W. Schneider, W. Thiel, *Chem. Phys. Lett.*, **1989**, *157*, 367–373.

 © VCH Verlagsgesellschaft mbH, D-69451 Weinheim, 1996 0570-0833/96/3521-2514 $ 15.00+.25/0

[21] a) E. B. Wilson, Jr., J. C. Decius, P. C. Cross, *Molecular Vibrations*, McGraw-Hill, New York, **1955**; b) S. Califano, *Vibrational States*, Wiley, New York, **1976**; c) D. A. Clabo, Jr., W. D. Allen, R. B. Remington, Y. Yamaguchi, H. F. Schaefer, III., *Chem. Phys.* **1988**, *123*, 187–239; d) I. M. Mills in *Molecular Spectroscopy: Modern Research, Vol. 1* (Eds.: K. Narahari Rao, C. W. Mathews), Academic Press, New York, **1972**, pp. 115–140.

[22] H. Kanamori, J. E. Butler, K. Kawaguchi, C. Yamada, E. Hirota, *J. Chem. Phys.* **1985**, *83*, 611–615.

[23] J. K. G. Watson in *Vibrational Spectra and Structure, Vol. 6.* (Ed.: J. R. Durig), Elsevier, Amsterdam, **1977**, pp. 2–89.

[24] Comparison may be made with a distance, r_0 (Si=C) 1.692 Å, obtained by a three parameter fit to the three experimental ground state rotational constants of $(CH_3)_2Si{=}CH_2$ (H. S. Gutowsky, J. Chen, P. J. Hajduk, J. D. Keen, C. Chuang, T. Emilsson, *J. Am. Chem. Soc.* **1991**, *113*, 4747–4751).

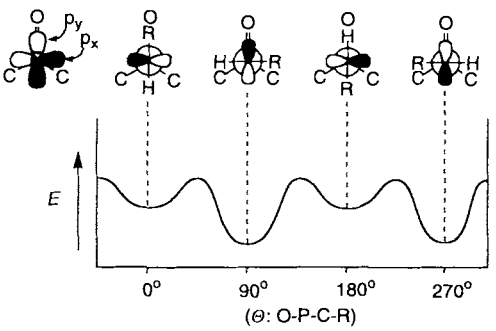

Fig. 1. Energy profile of conformation for P-stabilized anions.

Solution and Solid-State Structure of a Lithiated Phosphane Oxide**

Scott E. Denmark,* Kevin A. Swiss, and Scott R. Wilson

The report by L. Horner et al. in 1959 on the use of lithiated phosphane oxides to carry out carbonyl olefination further ensured a lasting legacy for organophosphorus reagents in organic synthesis.[1] Beyond the already established Wittig[2] and Wadsworth–Emmons[3] reactions, the Horner–Wittig process allowed interception of the critical intermediate in the olefination, and therefrom, mechanistic insight and practical value. Given the importance of these reagents in modern synthesis,[4] it is remarkable that the solution and solid-state structures of lithiated phosphane oxides have not been established.[5, 6]

Our interest in lithiated phosphane oxides derives from our general program on the design, development, and application of chiral, phosphorus-based anionic reagents.[7] We have extensively investigated these features in phosphonamide and thiophosphonamide anions,[8] and have recently disclosed the solution and X-ray structures of lithio phosphonamides $Li^+\mathbf{1}^-$ (Li(**1** – H), that is the lithium salt of **1** generated by the reaction with, for example, *n*BuLi)[8a] and $Li^+\mathbf{3}^-$[8b] and lithio thiophosphonamides $Li^+\mathbf{2}^-$[8c] and $Li^+\mathbf{4}^-$.[8e] The benzylic anions have

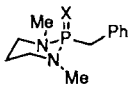

X = O: **1**
X = S: **2**

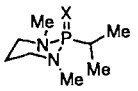

X = O: **3**
X = S: **4**

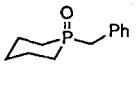

5

strikingly similar characteristics: 1) no C–Li contact, 2) antiparallel alignment of the benzylic moiety to the P=X bond ($\theta = 180°$, see Fig. 1), and 3) a planar anionic carbon atom. An important difference between phosphonamide and thiophosphonamide anions is that the rotational barrier about the C–P bond is approximately 3.1 kcal mol^{-1} larger in $Li^+\mathbf{4}^-$[8c] than in $Li^+\mathbf{3}^-$.[8c, e, 9]

[*] Prof. Dr. S. E. Denmark, Dr. K. A. Swiss, Dr. S. R. Wilson
Department of Chemistry
University of Illinois
Urbana, IL 61801 (USA)
Fax: Int. code +(217)333-3984
e-mail: denmark@aries.scs.uiuc.edu

[**] We are grateful to the National Institutes of Health (GM 45532) for generous support of this research. We thank Dr. Vera Mainz for NMR technical assistance.

To provide support for our understanding of the electronic contributions to anion conformation and energetics, we chose to examine a phosphane oxide anion. We proposed that the origin of the conformational ground state preference is the splitting of the $2e_x$ and $2e_y$ acceptor orbitals on phosphorus (Fig. 1).[8d, 9] In phosphonamides the $2e_x$ orbital is the better acceptor orbital (constructed from P–N σ^* orbitals) thus leading to a parallel anion. If this were true, replacement of the nitrogen atoms in $Li^+\mathbf{1}^-$ or $Li^+\mathbf{2}^-$ with less electronegative carbon atoms would attenuate the acceptor properties of the $2e_x$ orbital, leading to a preference for an orthogonal-like anion ($\theta = 90°$, Fig. 1) on the basis of a more effective $2e_y$ acceptor orbital.

For this study, the *P*-benzylphosphorinane-1-oxide **5** was selected due to its structural similarity to **1** and **2**. Moreover, the benzyl group would vouchsafe the selective generation of a single anionic species. Since lithiated phosphane oxide anions have not previously been spectroscopically characterized, $Li^+\mathbf{5}^-$ was compared with $Li^+\mathbf{1}^-$ and $Li^+\mathbf{2}^-$ (Table 1).[10] Several features immediately distinguished $Li^+\mathbf{5}^-$ from the phosphonamides. First, the ^{31}P NMR shifts for **5** and $Li^+\mathbf{5}^-$ were found to be very similar. This contrasts remarkably to $Li^+\mathbf{1}^-$ and $Li^+\mathbf{2}^-$, which are shifted strongly downfield and upfield, respectively, in their ^{31}P NMR spectra. Presumably the polarization of the P=O bond and the increase of anionic charge on C6 cancel each other out. The position of the ^{13}C NMR resonance of the benzylic carbon atom C6 was found to be more strongly shifted downfield in $Li^+\mathbf{5}^-$ than in **5**. These attributes clearly suggest a carbanion devoid of a lithium contact. The large change in chemical shift is indicative of a stronger delocalization of the phenyl ring in $Li^+\mathbf{5}^-$ than in the other anions[11]. The differences in the coupling constants $\Delta\ ^1J_{CP}$ and $\Delta\ ^1J_{CH}$, which are indicators of hybridization, also increased in magnitude upon lithiation of **5**, indicating an increase in s-character of the carbanionic carbon atom. All of these features signal the presence of an sp^2-hybridized carbanion. Finally, a

Table 1. Selected NMR data for $Li^+\mathbf{1}^-$, $Li^+\mathbf{2}^-$, and $Li^+\mathbf{5}^-$ [a].

Compd.	$\Delta\delta\ ^{31}P$	$\Delta\delta\ ^{13}C$ C6	$\Delta\ ^1J_{CP}$ [b]	$\Delta\ ^1J_{CH}$ [c]	$\delta\ ^7Li$ [d]	^6Li signal, $^2J_{LiP}$ [e]	$^2J_{HP}$ [f]
$Li^+\mathbf{5}^-$	0.0	9.8	85.3	24.6	−0.26	t, 0.8	24.8
$Li^+\mathbf{2}^-$	−13.5	6.5	90.0	25.8	−0.06	s	25.9
$Li^+\mathbf{1}^-$	18.4	4.6	105.7	21.3	−0.45	t, 1.2	13.7

[a] Δ-Values correspond to the difference in chemical shift or a coupling constant [Hz] in the anion and in the neutral compound; negative numbers are upfield shifts. [b] ^{13}C NMR (125 MHz), −5 °C; [D_8]THF. [c] ^{13}C NMR (100.6 MHz), HET2DJ, 2 °C; [D_8]THF. [d] ^7Li (116 MHz), [D_8]THF (LiCl, D_2O external reference). [e] −105 °C, [D_8]THF. [f] ^1H (500 MHz), −105 °C, [D_8]THF.

 © VCH Verlagsgesellschaft mbH, D-69451 Weinheim, 1996 0570-0833/96/3521-2515 $ 15.00+.25/0

triplet was found in the ^{6}Li NMR spectrum, which indicates a static, dimeric anion similar to the phosphonamide $Li^+\mathbf{1}^-$ but with a slightly smaller ^{6}Li–P coupling constant.

Determination of the P–C6 rotational barrier and the conformation of the benzyl group in solution for $Li^+\mathbf{5}^-$ was very difficult. The ground state conformations are expected to be degenerate and have C_1 symmetry ($\theta = 90°/270°$, Fig. 1). ^{1}H and ^{13}C NMR spectroscopic examination of the resonances of the backbone (H_2C1, H_2C5) of $Li^+\mathbf{5}^-$ showed no broadening at temperatures as low as $-100\,°C$.

Insight into the preferred ground state conformation is available from analysis of the $^2J_{HP}$ coupling constant (P-C6-H). This parameter has been shown experimentally[12] and by theory[13] to be sensitive to conformations around the P–C bond. We and others have found that a $^2J_{HP}$ coupling of more than 20 Hz is indicative of a conformation with an O-P-C-H dihedral angle of 0–60°, while a small $^2J_{HP}$ coupling (<9 Hz) indicates a dihedral angle of approximately 120–180° (Fig. 1).[14] Remarkably, the $^2J_{HP}$ coupling constants for $Li^+\mathbf{5}^-$ and $Li^+\mathbf{2}^-$ are similar (Table 1). This data is indicative of a solution conformation biased in the ±-synclinal range.

Crystallization of $Li^+\mathbf{5}^-$ in THF afforded twinned crystals, but fortunately a suitable crystal was found.[15] Like the phosphonamides, $Li^+\mathbf{5}^-$ crystallizes as a C_2-symmetric dimer with each lithium bound to both P=O groups and solvated by two THF molecules; the anionic carbon atom C6 resides in a nearly planar environment (Fig. 2). The planarity of the carbon environment is judged by the following criteria: 1) the sum of the angles around C6 is 358.9°, 2) the distance of C6 above the P1-H6-C7 plane (δ) is 0.08 Å, and 3) the angle (γ) between the C6–P1 vector and the C6-H6-C7 plane is 10.4°.[16]

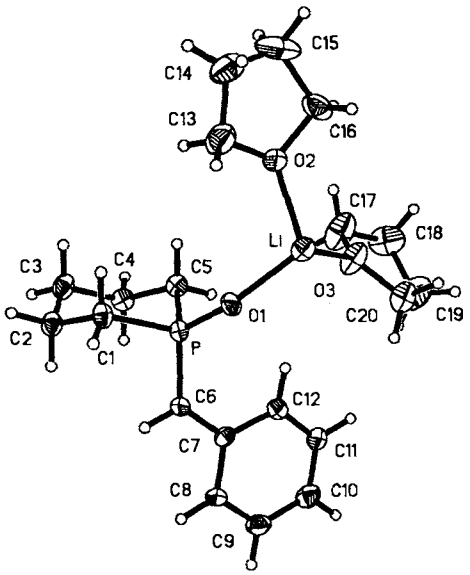

Fig. 2. ORTEP plot of the structure of $[Li^+\mathbf{5}^-\cdot 2THF]_2$; monomeric unit shown for clarity (35% thermal ellipsoids). Selected bond lengths [Å] and angles [°]: P–O1, 1.522(4), P–C1, 1.806(5), P–C5 1.806(5), P–C6 1.690(5), Li–O1 1.918(10); O1-P-C1 111.2(2), O1-P-C5 106.9(1), O1-P-C6 118.2(2), P-O1-Li 142.7(3), P-C6-C7 127.5(4).

The most significant differences between $Li^+\mathbf{5}^-$ and the other compounds are concerned with the conformations of the ring and the benzyl group. In all of the anions studied to date, the chalcogen attached to the phosphorus atom occupies an axial position, thus placing the carbanionic moiety equatorially. In $Li^+\mathbf{5}^-$ the benzyl group is disposed axially in the phosphorinane ring. Moreover, in all of the anions studied previously, the benzyl (or isopropyl) group is oriented in an antiparallel fashion with respect to the P=X group. In $Li^+\mathbf{5}^-$ the benzyl group adopts a *gauche* conformation. The O1-P-C6-C7 and P-C6-C7-C12 dihedral angles were determined to be $-65.1(6)°$ and 6.4(8)°, respectively, from the X-ray structure analysis.

In $Li^+\mathbf{1}^-$ the idealized anomeric stabilization of nitrogen- and carbon-bearing pairs of electrons leads to the familiar "pinwheel" conformation of methyl and benzyl groups.[8e, 9] This can best be accommodated in a chair conformation with the P=O group axially oriented. Replacement of the nitrogen atoms in $Li^+\mathbf{1}^-$ with carbon atoms, as in $Li^+\mathbf{5}^-$, has a dramatic effect on the electronic structure of the phosphanyl carbanion. Now, there is no electronic advantage to orient the P=O group in an axial position. The primary hyperconjugative-type stabilization arises from $n \rightarrow \sigma^*_{PO}$ donation which is best accommodated in a perfectly orthogonal conformation ($\theta = 90°$, Fig. 1). However, it appears that avoidance of nonbonding interactions between the *ortho* hydrogen atoms of the benzene ring and the equatorial hydrogen atoms on C1 and C5 adjusts the torsional angle. The lack of electronic significance to this nonideal conformation is supported by the identical P–C1 and P–C5 bond lengths.[17]

Of the four benzylic P-stabilized anions that we have crystallographically characterized, $Li^+\mathbf{5}^-$ is the most pyramidalized and in this regard approximates $Li^+\mathbf{3}^-$. This behavior most certainly arises from the less effective stabilization afforded by the phosphanyl moiety and the lower symmetry environment around the phosphorus atom. Future studies will address the rotational barrier and the ground state conformation of related anions in solution.

Experimental Procedure

5 [17]: A solution of sodium bis(2-methoxyethoxy)aluminum hydride (Red-Al, 70%, 3.4 M in toluene, 30 mL, 102 mmol, 2.08 equiv) in THF (30 mL) was added dropwise to a refluxing solution of diethyl benzylphosphonate (11.12 g, 49 mmol, 1.0 equiv) in THF (250 mL) over 1 h. The mixture was heated to reflux for 1 h further and then 1,5-dibromopentane (7.2 mL, 53 mmol, 1.04 equiv) was added at once and the mixture was heated to reflux for 16 h. The suspension was cooled in an ice bath and water (7 mL) was added dropwise. The mixture was filtered through a Celite pad and the filtrate was concentrated in vacuo to give a viscous oil that was purified by column chromatography (SiO_2) with EtOAc (1 L) 10% *i*PrOH/EtOAc (500 mL), 20% *i*PrOH/EtOAc (500 mL), and finally 50% *i*PrOH/EtOAc (1 L) to give 4.395 g (46%) of **5** as a white solid. Two recrystallizations from hot toluene (5 mL g^{-1}) gave 2.16 g (22%) of analytically pure **5**. M.p. 143–145 °C (toluene); $R_f = 0.28$ (3/7, *i*PrOH/EtOAc); ^{1}H NMR (500 MHz, $CDCl_3$, 25 °C): $\delta = 7.28$ (m, 5H, HC8–12), 3.16 (d, $^2J_{HP} = 13.9$, 2H, H_2C6), 2.04 (m, 2H, $H_{ax}2,4$), 1.72 (m, 6H, $H_{eq}2,4$, $H_2C1,5$), 1.52 (m 2H, H_2C3); ^{13}C NMR (125.8 MHz, $CDCl_3$, 25 °C): $\delta = 131.61$ (d, $^2J_{CP} = 7.7$, C7), 129.24 (d, $J_{CP} = 4.6$, C8,12 or C9,11), 128.50 (d, $J_{CP} = 2.3$, C9,11 or C8,12), 126.54 (d, $^5J_{CP} = 2.3$, C10), 35.46 (d, $^1J_{CP} = 60.3$, C6), 26.39 (d, $^1J_{CP} = 62.5$, C1,5), 26.07 (d, $^3J_{CP} = 6.9$, C3), 22.41 (d, $^2J_{CP} = 5.4$, C2,4); ^{31}P NMR (121.7 MHz, $CDCl_3$, 25 °C): $\delta = 39.32$; IR (KBr) $\tilde{\nu}$: [cm^{-1}] = 3080, 2946, 2934, 2926, 1600, 1493, 1161 (P=O); MS (EI, 70 eV) *m/z* (%): 209 (14) [$M^+ + 1$], 208 (94) [M^+], 207 (27) [$M^+ - H$], 91 (100); elemental analysis $C_{12}H_{17}OP$ (208.24) calcd. C, 69.21; H, 8.23; P, 14.87; found: C, 69.23; H, 8.26; P, 14.82.

In situ preparation of $Li^+\mathbf{5}^-$: A 10-mm NMR tube was charged with **5** (56.6 mg, 0.291 mmol) and [D_8]THF (2.5 mL). The sample was cooled to −60 °C and *n*-butyllithium (10 M, 29 µL, 0.29 mmol, 1.0 equiv) was added (monitored by ^{31}P NMR spectroscopy) to give a 0.11 M solution.

Received: May 22, 1996 [Z9145IE]
German version: *Angew. Chem.* **1996**, *108*, 2686–2688

Keywords: carbanions · lithium compounds · phosphorus compounds · structure elucidation

[1] a) L. Horner, H. Hoffmann, H. G. Wippel, G. Klahre, *Chem. Ber.* **1959**, *92*, 2499; b) L. Horner, H. Hoffmann, W. Klink, H. Ervel, V. G. Toscano, *ibid.* **1962**, *95*, 581; for reviews see: c) B. J. Walker in *Organophosphorus Reagents in Organic Synthesis*, (Ed. J. I. G. Cadogan), Academic Press, London, **1979**, Chapter 3; d) B. E. Maryanoff, A. B. Reitz, *Chem. Rev.* **1989**, *89*, 863.

[2] E. Vedejs, M. Petersen, *Top. Stereochem.* **1994**, *21*, 1.

[3] W. S. Wadsworth, *Organic React.* **1977**, *25*, 73.

[4] a) S. E. Kelly in *Comprehensive Organic Synthesis, Additions to C–X π Bonds, Part 1, Vol. 1* (Ed.: S. L. Schreiber), Pergamon, Oxford, **1991**, Chapter 3.1; b) J. Clayden, S. Warren, *Angew. Chem.* **1996**, *108*, 261–291; *Angew. Chem. Int. Ed. Engl.* **1996**, *35*, 241–270.

[5] For studies on structure-stabilized phosphane oxide anions see: a) T. Bottin-Strzalko, G. Etemad-Moghadam, J. Seyden-Penne, M.- J. Pouet, M.-P. Simonnin, *Nouv. J. Chim.* **1983**, *7*, 155; b) T. Strzalko, J. Seyden-Penne, I. Froment, J. Corset, M.-P. Simonnin, *Can. J. Chem.* **1988**, *66*, 391; c) J. Seyden-Penne, *Bull. Soc. Chim. Fr.* **1988**, 238.

[6] There is a considerable corpus of literature on the use of mono-, bis-, and tris(diphenylphosphanyl)methane and various combinations of sulfur analogs as ligands for Ni^{II}, Pt^{II}, Pt^{IV}, Hg^{II}, Ag^{II}, Au^{I}, Au^{III}, Rh^{I}, Ir^{I}, Pb^{IV}, W^{I}, Al^{III}. All of the derivatives of diphenylphosphanylmethane (except the tungesten structure) are C-metalated and have no relevance to Horner–Wittig chemistry.

[7] S. E. Denmark, C.-T. Chen, R. A Read, *Adv. Carbanion Chem.*, in preparation.

[8] a) S. E. Denmark, R. L. Dorow, *J. Am. Chem. Soc.* **1990**, *112*, 864; b) S. E. Denmark, P. C. Miller, *ibid.* **1991**, *113*, 1468; c) S. E. Denmark, K. A. Swiss, S. R. Wilson, *ibid.* **1993**, *115*, 3826; d) S. E. Denmark, K. A. Swiss, *ibid.* **1993**, *115*, 12195; e) M. Kranz, S. E. Denmark, K. A. Swiss, S. R. Wilson, *J. Org. Chem.*, in press; f) for a phosphonate-stabilized anion see: W. Zarges, M. Marsch, K. Harns, F. Haller, G. Frenking, G. Boche, *Chem. Ber.* **1991**, *124*, 861.

[9] a) S. E. Denmark, C. J. Cramer, P. M. Miller, R. L. Dorow, K. A. Swiss, S. R. Wilson, *J. Am. Chem. Soc.* **1994**, *116*, 2437; b) M. Kranz, S. E. Denmark, *J. Org. Chem.* **1995**, *60*, 5867.

[10] Spectra were recorded on a General Electric GN-500 (^1H 500.10 MHz, ^7Li 194.35 MHz, ^{13}C 125.75 MHz, and ^6Li 73.59 MHz), on a General Electric GN-300 (^7Li 116.79 MHz and ^{31}P 121.65 MHz), and on a Varian U-400 (^{13}C 100.58 MHz and ^1H 399.95 MHz, HET2DJ only). Temperature calibration for all probes was done by the methanol method of A. L. Van Geet, *Anal. Chem.* **1968**, *40*, 2227. Temperatures below −100 °C were extrapolated from the methanol curve.

[11] S. Brandamante, G. A. Pagani, *J. Chem. Soc. Perkin Trans. 2* **1986**, 1035 and 1047.

[12] a) A. Bond, M. Breen, S. C. Pearson, *J. Chem. Soc.(B)* **1968**, 929; b) W. R. Purdum, K. D. Berlin, *J. Org. Chem.* **1974**, *39*, 2904; c) D. M. Washecheck, D. van der Helm, W. R. Purdum, K. D. Berlin, *J. Org. Chem.* **1974**, *39*, 3305; d) O. Awerbouch, Y. Kashman, *Tetrahedron* **1975**, *31*, 33; e) M. Rotem, Y. Kashman, *Tetrahedron Lett.* **1978**, 63; f) A. Fitzgerald, J. A Campbell, G. D. Smith, C. N. Caughlan, S. E. Cremer, *J. Org. Chem.* **1978**, *43*, 3513; g) H. Yamamoto, K. Yamamoto, H. Kawamoto, S. Inokawa, M.-A. Armour, T. T. Nakashima, *ibid.* **1982**, *47*, 191.

[13] a) Y. Y. Samitov, R. K. Saphyullin, R. M. Aminova, N. D. Chuvylkin, G. M. Zhidomirov, *Phosphorus* **1975**, *5*, 151; b) Y. Y. Samitov, *J. Org. Chem. USSR (Engl. Trans.)* **1983**, *52*, 1967.

[14] W. G. Bentrude, W. N. Setzer, In *Phosphorus-31 NMR Spectroscopy in Stereochemical Analysis*, (Eds.: J. G. Verkade, L. D. Quin), VCH, Deerfield Beach, **1987**, pp 380–382.

[15] X-ray crystal structure analysis of $Li^+\mathbf{5}^-$: A suitable crystal of $Li^+\mathbf{5}^-$ was obtained from THF solution at −20 °C: formula $C_{40}H_{68}Li_2O_6P_2$, $M_r = 720.81$, crystal dimensions $0.4 \times 0.5 \times 0.5$ mm, $a = 10.531(3)$, $b = 19.504(6)$, $c = 10.656(3)$ Å, $\beta = 112.98(2)°$, $V = 2015(21)$ Å^3, $\rho_{calcd} = 1.181$ g cm^{-3}, $\mu = 1.45$ cm^{-1}. Empirical absorption correction, $Z = 2$, monoclinic space group $P2_1/c$ (no. 14), Enraf-Nonius CAD-4 k-axis diffractometer with $Mo_{K\alpha}$ radiation, $T = 198$ K, 3564 measured reflections ($\pm h, -k, +l$) $2\theta_{max} = 48.0°$, 3148 independent and 1621 observed reflections [$I > 2.58\sigma I$], $R = 0.061$, $wR = 0.051$, programs used: SHELXS-76, SHELXS-86. Crystallographic data (excluding structure factors) for the structure reported in this paper have been deposited with the Cambridge Crystallographic Data Centre as supplementary publication no. CCDC-179-100. Copies of the data can be obtained free of charge on application to The Director, CCDC, 12 Union Road, Cambridge CB2 1EZ, UK (fax: Int. code +(1223) 336-033; e-mail: teched@chemcrys.cam.ac.uk).

[16] For explanation of planarity criteria see ref. [8b]. Note: for an idealized sp^2 anion $d = 0.00$ Å, $\gamma = 0.0°$.

[17] Adapted from the preparation of 1-phenylphosphorinane-1-oxide from R. B. Wetzel, G. L. Kenyon, *J. Am. Chem. Soc.* **1972**, *94*, 1774 and R. B. Wetzel, G. L. Kenyon, *J. Org. Chem.* **1974**, *39*, 1531.

A Novel Strategy towards the Total Synthesis of Cyclopeptide Alkaloids

Jieping Zhu,* Taoues Laïb, Jacqueline Chastanet, and René Beugelmans

Since the first structural determination of pandamine (**1**) by Goutarel and Païs in 1963,[1] the family of cyclopeptide alkaloids has grown rapidly and now encompasses over 200 compounds. These 13-, 14-, and 15-membered macrocycles typically contain a para- or metacyclophane unit with a characteristic aryl–alkyl ether linkage.[2] The widespread occurence of these compounds in nature makes them an important class of natural products. However, little is known about their biological and pharmacological properties due to their limited availability.[3] The development of a practical synthetic method is therefore of utmost importance.

The total synthesis of cyclopeptide alkaloids has been investigated by a number of research groups, notably those of Schmidt,[4a] Rapoport,[4b] Joullié,[4c] and Lipshutz.[4d] The main difficulty is the construction of the obviously strained macrocycles. As shown in Scheme 1, various strategies based upon

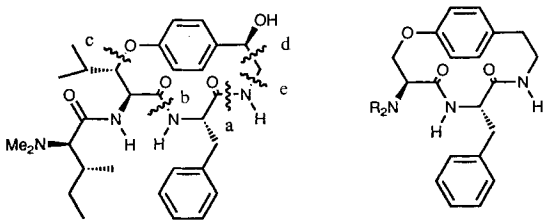

Pandamine **1**

2a R = allyl
2b R = Bn

Scheme 1.

macrolactamization (disconnections a and b), intramolecular Michael addition (disconnection c), intramolecular aldol condensation (disconnection d), and very recently, intramolecular amide alkylation (disconnection e)[4d] have been studied.[2] Until now, only macrolactamization has been fruitful; this strategy culminated in the total syntheses of three natural products[5] by means of an efficient activating method developed by Schmidt et al.[6]

Because of the synthetic challenges posed by this family of natural products, we were interested in an approach based upon the hitherto unknown ring-forming process in which formation of aryl–alkyl ether bond is the crucial step (disconnection f, Scheme 2). The realization of this intramolecular S_NAr-based[7] strategy illustrated by the synthesis of 14-membered macrocycle **2** is the subject of the present communication.

Synthesis of the linear peptide **11** is shown in Scheme 3. Coupling of 2-(3′-nitro-4′-fluoro)phenylethylamine (**8**), prepared in five steps from 4-fluorobenzaldehyde,[7b] with *N*-Boc-Phe afforded dipeptide **9**. Deprotection under mild acidic conditions (HCl/MeCN) followed by reaction with *N*-Boc-Ser(TBS)OH (TBS = *tert*-butyldimethylsilyl) gave the tripeptide **10** in 68% overall yield. Selective removal of the silyl ether (CsF, DMF) furnished compound **11**, which was ready for cyclization studies.

[*] Dr. J. Zhu, T. Laïb, J. Chastanet, R. Beugelmans
Institut de Chimie des Substances Naturelles, CNRS
F-91198 Gif-sur-Yvette (France)
Fax: Int. code +(1)69077247
e-mail: zhu@icsn.cnrs-gif.fr

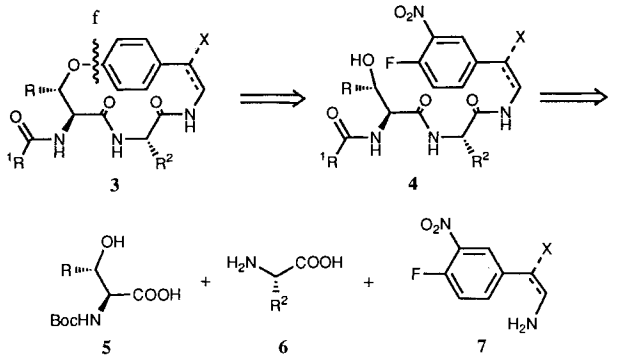

Scheme 2.

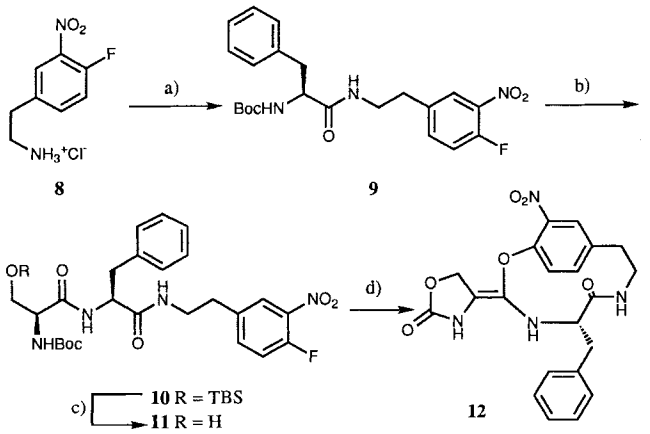

Scheme 3. a) Et_3N, *N*-Boc-Phe (Boc = *tert*-butoxycarbonyl), 1-ethyl-3-(3-dimethylaminopropyl)carbodiimide (EDC), 1-hydroxy-1*H*-benzotriazole (HOBt), 85%; b) 1) HCl/MeCN; 2) Et_3N, *N*-Boc-Ser(TBS)OH (TBS = *tert*-butyldimethylsilyl), EDC, HOBt, 68%; c) CsF, DMF, 86%; d) TBAF, THF, 48%.

Extensive efforts to effect ring closure of **11**, including variations in solvent (THF, DMF, DMSO), base (NaH, potassium hexamethyldisilazanide (KHDMS), K_2CO_3, and CsF), temperature, and concentration, were unsuccessful. Surprisingly, when a THF solution of **10** or **11** was treated with tetrabutylammonium fluoride (TBAF) in the presence of molecular sieves, the unstable compound **12** was obtained as the only isolable product in 48% yield. The structure of **12** was tentatively assigned as that shown in Scheme 3 from detailed spectroscopic studies, and a possible reaction path is proposed in Scheme 4 to explain its formation. Owing to the proximity between the hydroxyl group and the N-carbamate function in **11**, oxazolidinone **13** formed readily at the expense of the desired macrocyclization. Participation of the amide oxygen in an S_NAr reaction gave then the 12-membered macrocycle **14**, which tautomerized into the observed product **12**. Supporting this mechanism, compound **13**, obtained after brief treatment of **11** with TBAF, cyclized under identical conditions to afford **12** in similar yield.

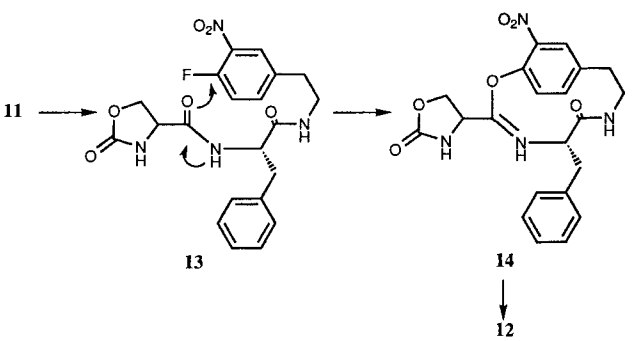

Scheme 4.

To avoid oxazolidinone formation, the protecting group of amine needs to be carefully reconsidered. We reasoned that the N-bisalkylated derivative meet our requirements. As shown in Scheme 5, simultaneous deprotection of the N-carbamate and O-silyl ether with HCl/MeCN gave amino alcohol **15** without event. Selective N-bisallylation or N-bisbenzylation in the presence of the primary hydroxyl function was best realized with $NaHCO_3$[8] in a mixed solvent system (DMSO/THF = 1/4) to afford **16** and **17** in 78% yield. Under these conditions, neither O- nor amide alkylation were observed.

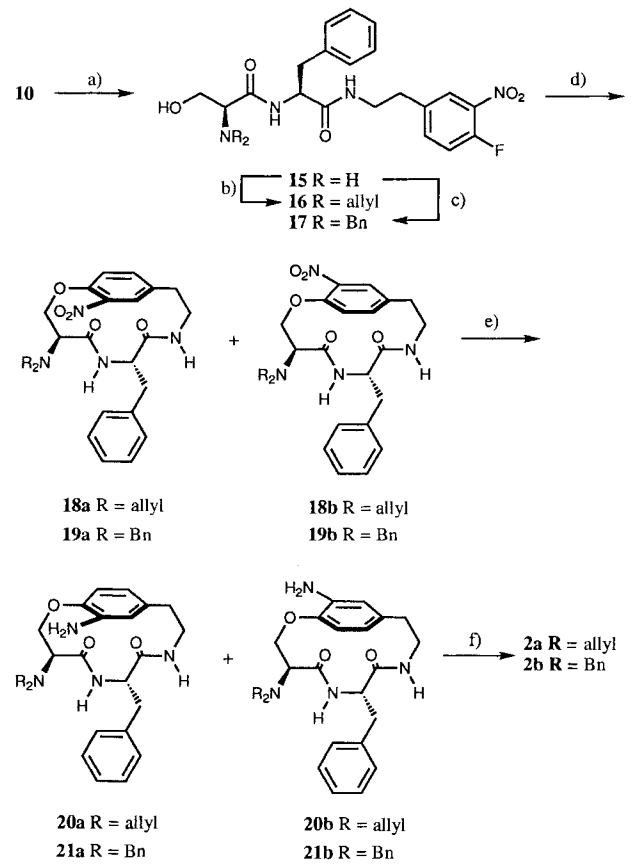

Scheme 5. a) HCl/MeCN, 93%; b) THF/DMSO (4/1), allyl bromide, $NaHCO_3$, 80 °C, 82%; c) THF/DMSO (4/1), BnBr, $NaHCO_3$, 80 °C, 78%; d) TBAF, DMF, molecular sieves, room temperature, 4 h, 60–75%; e) $NaBH_4$, elemental sulfur, THF, reflux, 81%; f) 1) *t*BuONO, $BF_3 \cdot Et_2O$, CH_2Cl_2, −15 °C; 2) $FeSO_4$, DMF, room temperature, 45–55%.

When a DMF solution of **16** (0.01 M) was treated with TBAF in the presence of molecular sieves at room temperature, a mixture of the two cyclized monomers **18a** and **18b** was isolated in 70% overall yield. Interestingly, similar treatment of compound **17** afforded the two separable products **19a** (32%) and **19b** (48%), which were identified as atropisomers based on spectroscopic studies; the assignment was confirmed by subsequent chemical transformation. The presence of a single nitro substituent on the aromatic ring *ortho* to the aryl–alkyl linkage is sufficient to hinder free rotation of that bond creating thus a plane of chirality.[9] A control experiment showed that

compounds **19a** and **19b** do not equilibrate under the cyclization conditions, indicating therefore that the product distribution is kinetically controlled. The lack of atropdiastereoselectivity is of no consequence as the plane of chirality will be destroyed on removal of nitro group at the final stage of the synthesis. This ring-forming process is noteworthy in that high-dilution techniques[10] were not needed and possible side reactions such as β-elimination, transacylation, and dimerization were not observed. THF could also be used as solvent though the reaction time was significantly prolonged. The easy formation of the 14-membered macrocycles **18a,b** and **19a,b** is rather spectacular considering the obvious strain in this ring system and the fact that only very few methods are available. Intramolecular recognition leading to the preorganized, reactive conformation of the linear precursor may be responsible for such facile cyclization.[11]

The nitro group was removed in a two-step sequence. Reduction of mixture of **18a** and **18b** with sulfurated $NaBH_4$[12] in THF gave the corresponding amino compounds, and two atropisomers were separable at this stage by flash chromatography. Diazotization of **20a** and **20b** under Doyle's conditions[13] followed by $FeSO_4$-mediated reduction of the crude diazonium salts[14] gave the desired cyclophane **2a**[15] (R = allyl) in 53% nonoptimized yield. The same sequence applied to **19a** and **19b** gave the amino compounds **21a** and **21b,** and then the target compound **2b** (R = Bn) in 47% yield.

In conclusion, we have developed a new synthetic strategy for the synthesis of 14-membered cyclopeptide alkaloids. This report, to the best of our knowledge, gives the first examples of S_NAr-based macrocyclization with formation of an aryl–alkyl ether bond.[16] Application of this methodology to the synthesis of natural cyclopeptide alkaloids will be reported in due course.

Received: May 23, 1996 [Z91491E]
German version: *Angew. Chem.* **1996**, *108*, 2664–2666

Keywords: alkaloids · atropisomerism · cyclizations · macrocycles · peptides

[1] M. Païs, F.-X. Jarreau, X. Lusinchi, R. Goutarel, *Ann. Chim. (Paris)* **1966**, 83–105.

[2] For reviews, see: a) U. Schmidt, A. Lieberknecht, E. Haslinger, in *The Alkaloids, Vol. 26* (Ed.: A. Brossi), Academic Press, New York, **1985**, pp. 299–326; b) M. M. Joullié, R. Nutt, in *Alkaloids: Chemical and Biological Perspectives, Vol. 3* (Ed.: S. W. Pelletier), Wiley, New York, **1985**, pp. 113–168.

[3] K. Kawai, Y. Nozawa, Y. Ogihara, *Experientia* **1977**, *33*, 1454.

[4] a) U. Schmidt, A. Lieberknecht, H. Grisser, J. Häusler, *Angew. Chem.* **1981**, *93*, 272; *Angew. Chem. Int. Ed. Engl.* **1981**, *20*, 281–282; b) J. C. Lagarias, R. A. Houghten, H. Rapoport, *J. Am. Chem. Soc.* **1978**, *100*, 8202–8209; c) R. J. Heffner, M. M. Joullié, *Tetrahedron Lett.* **1989**, *30*, 7021–7024; d) B. H. Lipshutz, B. E. Huff, K. E. McCarthy, T. A. Miller, S. M. J. Mukarram, T. J. Siahaan, W. D. Vaccaro, H. Webb, A. M. Facilk, *J. Am. Chem. Soc.* **1990**, *112*, 7032–7041.

[5] a) U. Schmidt, M. Zäh, A. Lieberknecht, *J. Chem. Soc. Chem. Commun.* **1991**, 1002–1004; b) R. J. Heffner, J. Jiang, M. M. Joullié, *J. Am. Chem. Soc.* **1992**, *114*, 10181–10189; c) B. H. Han, Y. C. Kim, M. K. Park, J. H. Park, H. J. Go, H. O. Yang, D. Y. Suh, Y. H. Kang, *Heterocycles* **1995**, *41*, 1909–1914.

[6] U. Schmidt, A. Lieberknecht, H. Griesser, J. Talbiersky, *J. Org. Chem.* **1982**, *47*, 3261–3264.

[7] The formation of biaryl ethers with concomitant formation of macrocycles based on the intramolecular S_NAr reaction is well-documented. Synthesis of 16-membered macrocycles: a) R. Beugelmans, J. Zhu, N. Husson, M. Bois-Choussy, G. P. Singh, *J. Chem. Soc. Chem. Commun.* **1994**, 439–440; b) R. Beugelmans, G. P. Singh, M. Bois-Choussy, J. Chastanet, J. Zhu, *J. Org. Chem.* **1994**, *59*, 5535–5542; c) M. Bois-Choussy, R. Beugelmans, J. P. Bouillon, J. Zhu, *Tetrahedron Lett.* **1995**, *36*, 4781–4784; d) J. Zhu, J. P. Bouillon, G. P. Singh, J. Chastanet, R. Beugelmans, *ibid.* **1995**, *36*, 7081–7084; e) A. V. R. Rao, K. L. Reddy, A. S. Rao, *ibid.* **1994**, *35*, 8465–8468; f) A. V. R. Rao, K. L. Reddy, A. S. Rao, T. V. S. Vittal, M. M. Reddy, P. L. Pathi, *ibid.* **1996**, *37*, 3023–3026; g) D. L. Boger, R. M. Borzilleri, S. Nukui, *Biorg. Med. Chem. Lett.* **1995**, *5*, 3091–3096; h) D. A. Evans, P. S. Watson, *Tetrahedron Lett.* **1996**, *37*, 3251–3254; i) A. J. Pearson, G. Bignan, P. Zhang, M. Chelliah, *J. Org. Chem.* **1996**, *61*, 3940–3941. Synthesis of 14-membered macrocycles: j) R. Beugelmans, S. Bourdet, J. Zhu, *Tetrahedron Lett.* **1995**, *36*, 1279–1282; k) J. Zhu, R. Beugelmans, S. Bourdet, J. Chastanet, G. Roussi, *J. Org. Chem.* **1995**, *60*, 6389–6396; l) R. Beugelmans, A. Bigot, J. Zhu, *ibid.* **1996**, *61*, 771–774; m) R. Beugelmans, L. Neuville, M. Bois-Choussy, J. Zhu, *Tetrahedron Lett.* **1995**, *36*, 8787–8790; n) D. L. Boger, R. M. Borzilleri, *Bioorg. Med. Chem. Lett.* **1995**, *5*, 1187–1190; o) D. L. Boger, J. Zhou, R. M. Borzilleri, S. Nukui, *Biorg. Med. Chem. Lett.* **1996**, *6*, 1089–1092; p) D. L. Boger, J. Zhou, *J. Org. Chem.* **1996**, *61*, 3938–3939. Synthesis of 17-membered macrocycles: q) R. Beugelmans, A. Bigot, J. Zhu, *Tetrahedron Lett.* **1994**, *35*, 7391–7394; r) J. W. Janetka, D. H. Rich, *J. Am. Chem. Soc.* **1995**, *117*, 10585–10586; In their synthesis of a 16-membered vancomycin model, Hamilton et al. employed an intermolecular S_NAr reaction for the construction of biaryl ether bond: s) N. Pant, A. D. Hamilton, *ibid.* **1988**, *110*, 2002–2003; t) M. J. Mann, N. Pant, A. D. Hamilton, *J. Chem. Soc. Chem. Commun.* **1986**,158–160.

[8] S. Lemaire-Audoire, M. Savignac, C. Dupuis, J. P. Genêt, *Bull. Soc. Chim. Fr.* **1995**, *132*, 1157–1166.

[9] E. L. Eliel, S. H. Willen, *Stereochemistry of Organic Compounds*, Wiley, New York, **1994**, p. 1119.

[10] A small quantity of dimer was isolated when the concentration of the reaction was higher than 0.01 M.

[11] To gain information regarding the conformations of the cyclization precursor in solution, we have carried out computational simulation [Macromodel, Batchmin version 3.5a, OPLS force field (W. L. Jorgensen, J. Tirado-Rivers, *J. Am. Chem. Soc.* **1988**, *110*, 1657–1666), water set]. The lowest energy conformer observed for **17** has a bent orientation in which an edge-to-face arrangement of aromatic rings is evident. The two reactive sites (HO and C_ε) are thus separated by only 4.67 Å, resulting in a low activation energy and favorable entropy for cyclization.

[12] J. M. Lalancette, A. Frêche, J. R. Brindle, M. Laliberté, *Synthesis* **1972**, 526–532.

[13] M. P. Doyle, W. J. Bryker, *J. Org. Chem.* **1979**, *44*, 1572–1574.

[14] F. W. Wassmundt, W. F. Kiesman, *J. Org. Chem.* **1995**, *60*, 1713–1719.

[15] Physical data of **2a**: $[\alpha]_D = -18.4$ ($c = 0.3$ in $CHCl_3$); ^1H NMR (400 MHz, $CDCl_3$, TMS): $\delta = 2.43$ (ddd, $J = 6.5, 11.9, 13.8$ Hz, 1H), 2.67 (dd, $J = 7.5, 14.7$ Hz, 2H), 2.73 (dd, $J = 7.2, 13.6$ Hz, 1H), 2.86 (dd, $J = 8.3, 13.6$ Hz, 1H), 2.91–3.03 (m, 3H), 3.09 (dd, $J = 1.4, 8.1$ Hz, 1H), 3.14 (tdd, $J = 1.9, 4.5, 14.7$ Hz, 2H), 4.10 (dd, $J = 1.4, 11.6$ Hz, 1H), 4.21 (dt, $J = 7.7, 8.5$ Hz, 1H), 4.86 (d, $J = 10.5$ Hz, 1H), 4.95 (dd, $J = 8.1, 11.6$ Hz, 1H), 5.10–5.17 (m, 4H), 5.37 (d, $J = 9.1$ Hz, 1H), 5.69 (dddd, $J = 4.5, 7.5, 10.2, 17.4$ Hz, 2H), 6.81 (dd, $J = 2.7, 8.3$ Hz, 1H), 6.84 (dd, $J = 2.3, 8.4$ Hz, 1H), 6.94 (dd, $J = 2.7, 8.3$ Hz, 1H), 7.04 (dd, $J = 2.3, 8.4$ Hz, 1H), 7.1–7.3 (m, 5H); ^{13}C NMR (50 MHz, $CDCl_3$): $\delta = 34.6, 39.5, 39.7, 53.9, 54.6, 64.2, 71.2, 117.4, 117.7, 121.1, 126.9, 128.6, 129.3, 129.6, 131.5, 136.4, 136.8, 156.1, 169.0, 170.5$; IR ($CHCl_3$): $\tilde{\nu} = 3634, 3437, 3121, 2973, 1666, 1602, 1511, 1497, 1447, 1384, 1321, 1258\ cm^{-1}$; MS (CI): m/z (%) 490 ($M^+ + 57$, 5), 434 ($M^+ + 1$, 100).

[16] Synthesis of a seven-membered ring by means of an intramolecular S_NAr reaction has been reported: a) K. A. Parker, C. A. Coburn, *J. Org. Chem.* **1991**, *56*, 4600–4601; *ibid.* **1992**, *57*, 97–100; b) G. A. Kraus, P. Liu, *Tetrahedron Lett.* **1995**, *36*, 7595–7598; c) W. H. Miller, T. W. Ku, F. E. Ali, W. E. Bondinell, R. R. Calvo, L. D. Davis, K. F. Erhard, L. B. Hall, W. F. Huffman, R. M. Keenan, C. Kwon, K. A. Newlander, S. T. Ross, J. M. Samanen, D. T. Takata, C. K. Yuan, *ibid.* **1995**, *36*, 9433–9436.

 © VCH Verlagsgesellschaft mbH, D-69451 Weinheim, 1996 0570-0833/96/3521-2519 $ 15.00+.25/0

A Unique Ni^{II} Complex with Three Different Azido Bridges: Magneto-Structural Correlations in the First Triply Alternating $S = 1$ Chain**

Joan Ribas,* Montserrat Monfort, Immaculada Resino, Xavier Solans, Pierre Rabu, Fabrice Maingot, and Marc Drillon

The μ-azido bridging ligand is undoubtedly one of the most versatile for the creation of new materials with different magnetic properties. This ligand also allows the study of magneto-structural correlations in discrete complexes as well as in polymeric one- (1D), two- (2D), and three-dimensional (3D) complexes. There are two main coordination modes for azido bridging ligands: end-to-end (or μ-1,3) (EE) and end-on (or μ-1,1) (EO) (Fig. 1). The EO mode leads to ferromagnetic coupling and the EE mode to antiferromagnetic. This variation in magnetic behavior appears to be generally valid for metal ions like Ni^{II},[1-7] Cu^{II},[8] Mn^{II},[9] Mn^{III},[10] Co^{II},[11] and Fe^{II}.[12]

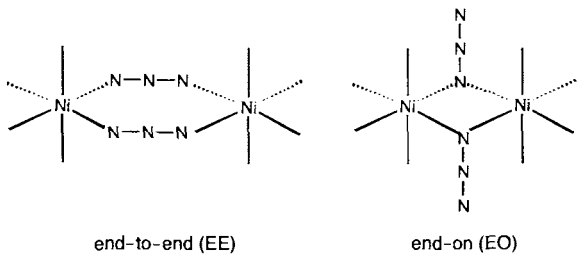

Fig. 1. Schematic representation of the two coordination modes of the μ-azido bridging ligand (see text for effects on the magnetic properties).

Recently we synthesized and fully characterized new Ni^{II} compounds that exhibited the two kinds of coordination mode: 1) a new two-dimensional molecular magnet[5] of empirical formula $[Ni\{H_2NCH_2CH(CH_3)_2CH_2NH_2\}(\mu\text{-}N_3)_2]$, 2) a unique triply EO- and singly EE-bridged alternating chain of empirical formula $[Ni(tmen)(\mu\text{-}N_3)_2]$ (tmen = *N,N,N',N'*-tetramethylethylenediamine),[6] and 3) two alternating EO and EE chains: $[Ni(N,N\text{-dmen})(\mu\text{-}N_3)_2]$ and $[Ni(aep)(\mu\text{-}N_3)_2]$ (dmen = *N,N*-dimethylethylenediamine; aep = 2-aminoethylpyridine).[7]

Here we report on the synthesis and characterization of $[Ni(N,N'\text{-dmen})(\mu\text{-}N_3)_2]$ (*N,N'*-dmen = *N,N'*-dimethylethylenediamine), an unprecedented and unexpected complex. According to the X-ray structure analysis[13] the molecular structure consists of Ni^{II} centers alternatively linked by three double EO entities (two of them crystallographically equivalent) and one double EE entity (Fig. 2). Each Ni^{II} ion completes its distorted octahedral coordination by binding to one bidentate *N,N'*-dmen ligand. The Ni–Ni distances are 3.27 Å and 3.35 Å for the EO part and 5.25 Å for the EE part. These values lie in the range for all known $[Ni(\mu\text{-}N_3)_2Ni]$ units with two μ-azido bridging ligands.[2,4] The Ni–N distances of between 2.11 and

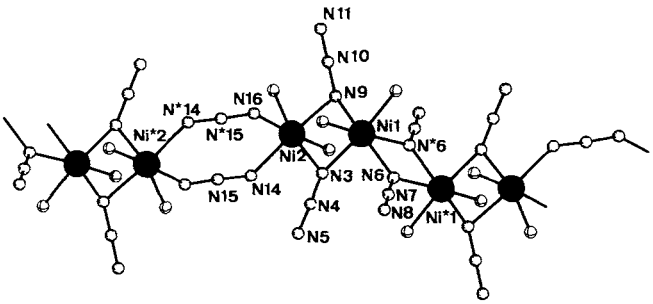

Fig. 2. Molecular structure of $[Ni(N,N'\text{-dmen})(\mu\text{-}N_3)_2]$. The C atoms of the *N,N'*-dmen rings have been omitted for clarity. In the Ni1-N6-Ni1*-N6* part there is an inversion center as in the Ni2-N15-Ni2*-N15* part. Selected bond lengths [Å] and angles [°] (standard deviation in parentheses): Ni1–N3 2.111(3), Ni1–N6* 2.123(3), Ni1–N9 2.121(3), Ni1–N6 2.161(3), Ni2–N3 2.145(3), Ni2–N9 2.114(3), Ni2–N14 2.118(4), Ni2–N16 2.099(4), Ni1–Ni1* 3.350(2), Ni1–Ni2 3.272(4), Ni2–Ni2* 5.247(3); N3-Ni1-N9 79.18(13), N9-Ni2-N3 78.56(12), Ni1-N3-Ni2 100.50(14), Ni2-N9-Ni1 101.19(14), Ni1*-N6-Ni1 102.88(14), N6*-Ni1-N6 77.12(14), N16-Ni2-N14 91.58(14), N15-N14-Ni2 132.9(3), N15-N16-Ni2 130.9(3).

2.14 Å also lie in the expected range. The most important structural features are the $Ni(\mu\text{-}N_3)_2Ni$ angles, which are directly related to the magnetic coupling. The angles in the two crystallographically independent EO modes are 100.5, 101.2, and 102.9°, and thus also lie in the range of all known $Ni(\mu_{1,1}\text{-}N_3)_2Ni$ (between 100.6 and 104.9°).[4] In the EE fragment the N-N-Ni angles are 130.9 and 132.9°, and thus lie in the middle of the range of known values (between 120.0 and 139.0°).[2] The $Ni(\mu_{1,3}\text{-}N_3)_2Ni$ dihedral angle δ is 8.4° (Fig. 3).

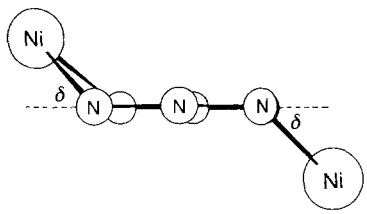

Fig. 3. Schematic representation for the $Ni(\mu_{1,3}\text{-}N_3)_2Ni$ dihedral angle δ (see text for its importance in magnetic coupling).

The temperature dependence of the molar magnetic susceptibility is illustrated in Figure 4. The χ_M value increases with de-

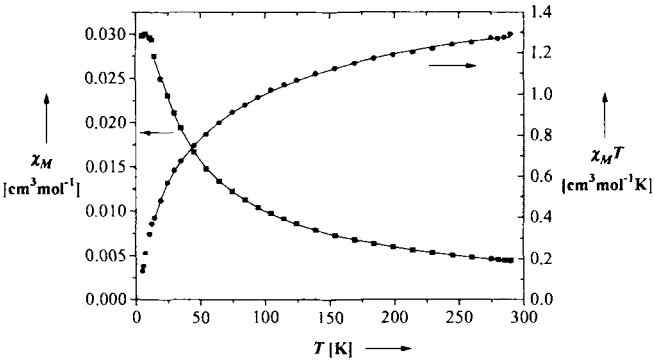

Fig. 4. Plots of χ_M and $\chi_M T$ versus T for $[Ni(N,N'\text{-dmen})(\mu\text{-}N_3)_2]$. Solid lines correspond to the best theoretical fitting.

creasing temperature, reaching a maximum near 15 K, and then slightly decreases down to 4 K. The variation of the product $\chi_M T$, from 1.3 $cm^3 mol^{-1}$ K at 290 K down to zero at very low temperature, clearly indicates the predominance of antiferromagnetic interactions. To explain these data we considered a stacking of quasi-isolated Ni^{II} chains with nearest-neighbor interactions. From the structural features, three exchange interac-

[*] Prof. J. Ribas, Dr. M. Monfort, I. Resino, Prof. X. Solans
Departament de Química Inorgànica
Universitat de Barcelona
Diagonal, 647, E-08028 Barcelona (Spain)
Fax: Int. code +(3)4907725
e-mail: jribas@kripto.qui.ub.es
Dr. P. Rabu, F. Maingot, Dr. M. Drillon
IPCMS UMR46 (CNRS-UCP-EHICS)
Groupe des Matériaux Inorganiques, Strasbourg (France)

[**] This work was supported by the Spanish Dirección General de Investigación Científica y Técnica (project PB93-0772).

tions may be assumed, namely J_1 and J_2 for the EO mode and J_3 for the EE mode. Based on previous findings with azido-bridged dimeric units, J_1 and J_2 are expected to be ferromagnetic couplings and J_3 an antiferromagnetic coupling.[1-5] The Heisenberg spin Hamiltonian may be formulated as Equation (a). The S_i values stand for the spin operator ($S = 1$), D is the

$$\boldsymbol{H} = -\sum_{i=0}^{N-1}[J_1(S_{4i}S_{4i+1} + S_{4i+2}S_{4i+3}) + J_2S_{4i+1}S_{4i+2} + J_3S_{4i+3}S_{4i+4}] - D\sum_{i=0}^{4N-1}S_i^{z2} - g\mu_B H\sum_{i=0}^{4N-1}S_i^z \quad \text{(a)}$$

zero-field splitting for Ni^{II}, H the applied field, and g the Landé factor. For simplification, it is assumed that D and g are identical for all the sites. There is no mathematical expression to evaluate the susceptibility of such a complicated alternating $S = 1$ system. Thus, the usual numerical procedure was used,[14] based on the extrapolation of results computed for rings of $4N$ spins. The resolution of the Hamiltonian operator requires the diagonalization of matrices of the dimensions $3^{4N} \times 3^{4N}$, which rapidly becomes intractable when N increases. However, a significant reduction of the computational work is achieved by introducing the spin space symmetries of the $4N$-site closed chain.[15] In the present case the calculations were performed up to $N = 2$ (eight spins), which gave a satisfactory description of the magnetic behavior in an acceptable amount of computer time.[16] The experimental data have been analyzed in the range 20 K – 300 K by using the above model of eight spins, and by adjusting the J_i and D parameters and the g factor. A first attempt, in which no distortion ($D = 0$) and $g = 2.2$ (as mean value for octahedral Ni^{II}[17]) were assumed, was not entirely satisfactory. In particular, the shape of the $\chi_M T = f(T)$ curve is not well reproduced. Thus, by varying all the parameters, the best agreement between theory and experiment (Fig. 4) is obtained with $J_1 = 20\ cm^{-1}$, $J_2 = 37\ cm^{-1}$, $J_3 = -120\ cm^{-1}$, $D = 6\ cm^{-1}$, and $g = 2.39$. The estimated errors are 10% for J_i and D, and 1% for g. These values for the interaction are similar to those obtained previously with fixed D and g, except for J_3 which is somewhat higher but of the same order of magnitude. The number of parameters (five) could mitigate their significance. Note, however, that the examination of the correlation matrix does not reveal very strong correlations between the refined J_i. In fact, the most important source of error is the limited number of spins considered in the model. It remains that these values agree very well with those predicted according to the structural features. Indeed, our previous study[2] on dinuclear Ni^{II} complexes with EE coordination shows that the antiferromagnetic coupling is highest for a $Ni(\mu_{1,3}\text{-}N_3)_2Ni$ dihedral angle of 0° (Fig. 3). The lower the angle, the higher the coupling. In the present case, this angle is low and the Ni–N distance is short (2.11 Å); thus J_3 (antiferromagnetic interaction) must be high. In fact, assuming that the refined value is correct ($J = -120\ cm^{-1}$), it would be the highest one reported so far for this kind of structure. The behavior of the $Ni(\mu_{1,1}\text{-}N_3)_2Ni$ core is more difficult to predict. Very recently Christou et al.[1g] attempted to correlate the $Ni(\mu_{1,1}\text{-}N_3)Ni$ angles with J values, but the correlation appeared not to be very pronounced. We can only note that all experimental J values for $Ni(\mu_{1,1}\text{-}N_3)Ni$ angles between 86.2 and 104.9° lie in the range of $15-40\ cm^{-1}$. For similar Cu^{II} complexes Kahn et al. explained the ferromagnetic behavior by way of the accidental orthogonality[18] concept and with ab initio calculations on model systems,[19] which led to the development of the theory of spin polarization. Accidental orthogonality occurs for angles close to 100°;[18] the Ni-N-Ni angles in all the Ni^{II} systems reported lie close to this value. Consequently, it is not surprising that all the Ni centers in these complexes are ferromagnetically coupled.

In conclusion the present complex is a further example in which changing the nonbridging ligand (*N,N'*-dmen instead of *N,N*-dmen[6]) has a dramatic effect on the μ-azido bonding mode. In terms of the magnetic behavior, it is the first time that an alternating ferro–antiferromagnetic $S = 1$ chain has been studied and its magnetic behavior analyzed. The J values obtained here agree well with the reported data for simpler polynuclear Ni^{II} complexes.

Experimental Procedure

A solution of *N,N'*-dmen (0.176 g, 2 mmol) in MeCN (10 mL) was added dropwise to a stirred aqueous solution (20 mL) of $Ni(NO_3)_2 \cdot 6H_2O$ (0.58 g; 2 mmol). This solution was filtered and NaN_3 (0.26 g, 4 mmol) dissolved in water (10 mL) was added slowly. The clear dark green solution was filtered to remove impurities and left to stand undisturbed at room temperature. One week later, X-ray quality green single crystals were obtained, which were filtered, washed with cold water, and air dried. Yield: 65%. The analysis for the bulk material was consistent with the formula proposed.

Received: April 15, 1996
Revised version: July 17, 1996 [Z9040IE]
German version: *Angew. Chem.* **1996**, *108*, 2671–2673

Keywords: azides · complexes with nitrogen ligands · magnetic properties · nickel compounds

[1] a) F. Wagner, M. T. Mocella, M. J. D'Aniello, A. H. J. Wang, E. K. Barefield, *J. Am. Chem. Soc.* **1974**, *96*, 2625; b) C. G. Pierpont, D. N. Hendrickson, D. M. Duggan, F. Wagner, E. K. Barfield, *Inorg. Chem.* **1975**, *14*, 604; c) P. Chaudhuri, M. Guttmann, D. Ventur, K. Wieghardt, B. Nuber, J. Weiss, *J. Chem. Soc. Chem. Commun.* **1985**, 1618; d) M. I. Arriortua, R. Cortés, L. Lezama, T. Rojo, X. Solans, M. Font-Bardía, *Inorg. Chim. Acta* **1990**, *174*, 263; e) R. Cortés, J. I. Ruiz de Larramendi, L. Lezama, T. Rojo, K. Urtiaga, M. I. Arriortua, *J. Chem. Soc. Dalton Trans.* **1992**, 2723; f) P. D. Beer, M. G. B. Drew, P. B. Lesson, K. Lyssenko, M. I. Ogden, *J. Chem. Soc. Chem. Commun.* **1995**, 929; g) M. A. Halcrow, J. S. Sun, J. C. Huffman, G. Christou, *Inorg. Chem.* **1995**, *34*, 4167.

[2] J. Ribas, M. Monfort, C. Diaz, C. Bastos, X. Solans, *Inorg. Chem.* **1993**, *32*, 3557.

[3] a) R. Vicente, A. Escuer, J. Ribas, X. Solans, *Inorg. Chem.* **1992**, *31*, 1726; b) A. Escuer, R. Vicente, J. Ribas, M. S. El Fallah, X. Solans, *ibid.* **1993**, *32*, 1013; c) A. Escuer, R. Vicente, J. Ribas, M. S. El Fallah, X. Solans, M. Font-Bardía, *ibid.* **1993**, *32*, 3727; d) A. Escuer, R. Vicente, J. Ribas, M. S. El Fallah, X. Solans, M. Font-Bardia, *ibid.* **1994**, *33*, 1842; e) J. Ribas, M. Monfort, C. Diaz, C. Bastos, C. Mer, X. Solans, *ibid.* **1995**, *34*, 4986; f) A. Escuer, R. Vicente, M. S. El Fallah, J. Ribas, X. Solans, M. Font-Bardía, *J. Chem. Soc. Dalton Trans.* **1993**, 2975.

[4] a) R. Vicente, A. Escuer, J. Ribas, M. S. El Fallah, X. Solans, M. Font-Bardía, *Inorg. Chem.* **1993**, *32*, 1920; b) A. Escuer, R. Vicente, J. Ribas, X. Solans, *ibid.* **1995**, *34*, 1793; c) J. Ribas, M. Monfort, C. Diaz, C. Bastos, X. Solans, *ibid.* **1994**, *33*, 484; d) J. Ribas, M. Monfort, R. Costa, X. Solans, *ibid.* **1993**, *32*, 695.

[5] a) M. Monfort, J. Ribas, X. Solans, *J. Chem. Soc. Chem. Commun.* **1993**, 350; b) J. Ribas, M. Monfort, X. Solans, M. Drillon, *Inorg. Chem.* **1994**, *33*, 742.

[6] J. Ribas, M. Monfort, B. K. Ghosh, X. Solans, *Angew. Chem.* **1994**, *106*, 2177; *Angew. Chem. Int. Ed. Engl.* **1994**, *33*, 2087.

[7] J. Ribas, M. Monfort, B. K. Ghosh, X. Solans, M. Font-Bardia, *J. Chem. Soc. Chem. Commun.* **1995**, 2375.

[8] a) J. P. Costes, F. Dahan, J. Ruiz, J. P. Laurent, *Inorg. Chim. Acta* **1995**, *239*, 53 and references therein; b) G. A. Albada, M. T. Lakin, N. Veldman, A. L. Spek, J. Reedijk, *Inorg. Chem.* **1995**, *34*, 4910.

[9] a) R. Cortés, J. L. Pizarro, L. Lezama, M. I. Arriortua, T. Rojo, *Inorg. Chem.* **1994**, *33*, 2697; b) R. Cortés, L. Lezama, J. L. Pizarro, M. I. Arriortua, X. Solans, T. Rojo, *Angew. Chem.* **1994**, *106*, 2520; *Angew. Chem. Int. Ed. Engl.* **1994**, *33*, 2488.

[10] B. R. Stults, R. S. Marianell, V. W. Day, *Inorg. Chem.* **1975**, *14*, 722; b) A. K. Gregson, N. T. Moxon, *ibid.* **1982**, *21*, 586.

[11] A. Bencini, C. A. Ghilardi, S. Midollini, A. Orlandini, *Inorg. Chem.* **1989**, *28*, 1958.

[12] K. Pohl, K. Wieghardt, B. Nuber, J. Weiss, *J. Chem. Soc. Dalton Trans.* **1987**, 187.

[13] X-ray structure analyses: Enraf-Nonius CAD4 diffractometer; $Mo_{K\alpha}$, 0.71069 Å, graphite monochromator, $\omega/2\theta$ scan, 293 K. Lorentz-polarization but no absorption corrections. Solution and refinement: standard Patterson methods with SHELXS computer program and refined with SHELXS93 computer program. The position of all hydrogen atoms was computed and refined with an overall isotropic temperature factor, using a riding model. $C_{16}H_{48}N_{32}Ni_4$ ($M_r = 923.7$); triclinic, space group $P\bar{1}$, $a = 9.888(2)$, $b = 10.113(2)$, $c = 10.955(2)$ Å, $\alpha = 116.05(2)$, $\beta = 92.83(2)$, $\gamma = 103.79(2)°$, $V =$

940.8(3) Å^3, $Z=1$, $\rho_{calcd}=1.630\,g\,cm^{-3}$, $\mu=2.032\,mm^{-1}$, crystal size $0.20\times0.20\times0.40$ mm, $F(000)=480.0$; 5531 unique reflections and 5468 assumed as observed with $I>2\sigma(I)$, 268 parameters, $R(F_o)=0.0461$, $R_w|F_o|^2=0.1025$ and $S=0.966$. Crystallographic data (excluding structure factors) for the structure reported in this paper have been deposited with the Cambridge Crystallographic Data Centre as supplementary publication no. CCDC-179-97. Copies of the data can be obtained free of charge on application to The Director, CCDC, 12 Union Road, Cambridge CB2 1EZ, UK (fax: Int. code +(1223) 336-033; e-mail: teched@chemcrys.cam.ac.uk).

[14] M. Drillon, R. Georges, *J. Chem. Soc. Farad. Trans.* **1974**, *75*, 810; b) M. Drillon, R. Georges, *Phys. Rev. B* **1981**, *24*, 1278.

[15] a) M. Drillon, J. C. Granduzzio, R. Georges, *Phys. Rev. Lett. A* **1983**, 96, 41; b) M. Drillon, E. Coronado, R. Georges, J. C. Granduzzio, J. Curely, *Phys. Rev. B* **1989**, *40*, 10992.

[16] The fit was carried out by using the MINUIT function minimization program of the CERN program library (v.92.1), CERN, Geneva, Switzerland; the C98 vectorial computer of IDRIS, Orsay, France, was used for the fitting procedure involving up to 1107×1107 matrices.

[17] R. L. Carlin, *Magnetochemistry*, Springer, Berlin, **1986**, p. 67.

[18] J. Commarmond, P. Plumeré, J. M. Lehn, Y. Agnus, R. Louis, R. Weiss, O. Kahn, I. Morgenstern-Badarau, *J. Am. Chem. Soc.* **1982**, *104*, 6330.

[19] M. F. Charlot, O. Kahn, M. Chaillet, C. Larrieu, *J. Am. Chem. Soc.* **1986**, *108*, 2574.

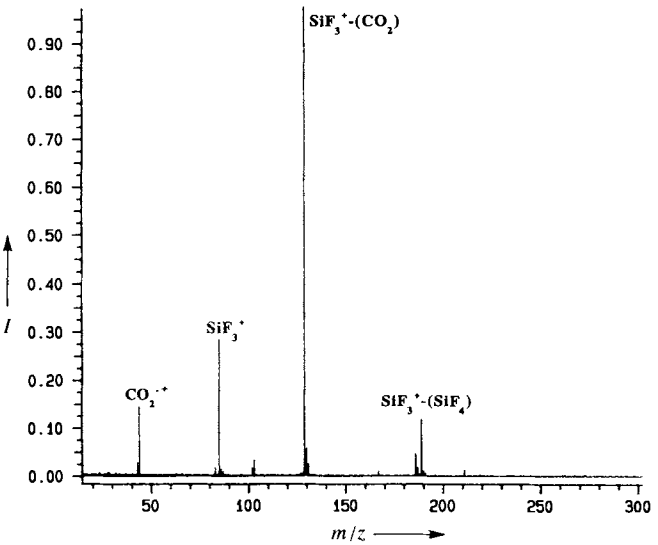

Fig. 1. Mass spectrum (70 eV) of a CO_2/SiF_4 gaseous mixture (P approximately 1.5×10^{-4} mbar; approximate ratio 2/1). I = relative intensity.

Activation of Carbon Dioxide by Coordination with Cations in the Gas Phase: SiF_3^+-Mediated Coupling of CO_2 and Aromatic C–H Bonds**

Patrizio Cecchi, Maria Elisa Crestoni, Felice Grandinetti,* and Vittorio Vinciguerra

Activation of carbon dioxide and its conversion into useful products still remains a fascinating challenge facing chemists.[1] Considerable progress has been made recently, but additional, intense effort is required "to put together the pieces of the mosaic".[2] Gas-phase ion chemistry can substantially contribute to investigations on fundamental aspects of CO_2 activation[3] and, in addition, may provide suggestions for novel synthetic procedures. Thus, the recently reported[4] Ta^+-mediated coupling of CH_4 and CO_2 in the gas phase has to be regarded with respect to the catalytic formation of acetic acid.

Fixation of CO_2 at active centers of biomolecules, solid catalysts, or transition metal complexes is considered a key elementary step of most natural and synthetic sequences that use carbon dioxide as a C_1 building block.[1] This concept could be convincingly demonstrated if carbonylation or carboxylation products were unambiguously observed arising from an intact CO_2 ligated to a cation in the gas phase; this model reaction would be even more interesting if it amounted to functionalization by CO_2 of unreactive hydrogen or hydrocarbons. In studies with this perspective, Schwarz and Schwarz recently isolated an Fe^+-(CO_2) complex and probed its reactivity toward H_2 and CH_4.[5a] A slow ligand exchange of carbon dioxide for methane was observed, but no evidence was found for the generation of CH_3CO_2H by activation of CO_2/CH_4. They rationalized this in terms of the low bond dissociation energy (BDE) of Fe^+ and CO_2 (experimental BDE: 9 ± 2 kcal mol^{-1}).[5b]

As a continuation of our interest in the gas-phase chemistry of fluorinated inorganic cations,[6] we report here on the coupled activation of CO_2 and aromatic C–H bonds mediated by SiF_3^+ in the gas phase and occurring under the conditions of Fourier transform ion cyclotron resonance (FT-ICR) spectrometry.[7]

Only few complexes of CO_2 with cations in the gas phase have yet been reported.[3f-g, 8] Figure 1 shows a typical mass spectrum from the ionization of a mixture of CO_2 and SiF_4 introduced into the external source of the FT-ICR. Besides the signals arising from the ionization of CO_2 and SiF_4, including SiF_3^+-(SiF_4) at $m/z=189$, we draw attention to the abundant ions detected at $m/z=129$, which are unambiguously assigned as $SiF_3CO_2^+$ by exact mass measurements. The observation of SiF_3^+ exclusively in the corresponding CID spectrum (CID = collision-induced dissociation) is consistent with an SiF_3^+-(CO_2) adduct, but does not help in assigning its detailed connectivity. However, in line with the high oxophilicity of silicon, we found that the oxygen-coordinated isomer shown in Figure 2 is by far the most stable among several conceivable SiF_3^+-(CO_2) adducts investigated at the MP2/6-311G**//HF/6-311G** level of theory. The computed Si–O2 distance of 1.770 Å suggests a significant interaction between SiF_3^+ and CO_2. Consistently, we arrived at an experimental BDE of SiF_3^+ and CO_2 as large as 58 ± 12 kcal mol^{-1}

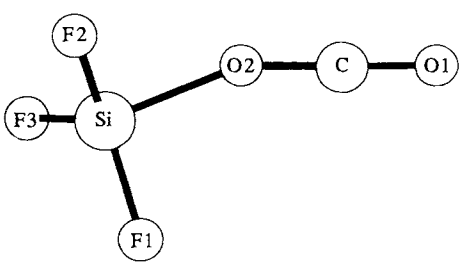

Fig. 2. HF/6-311G** optimized parameters (symmetry is C_s): C–O1 1.100, C–O2 1.179, Si–O2 1.770, Si–F1 1.531, Si–F2 1.527 Å, O1-C-O2 178.5, C-O2-Si 156.3, F1-Si-O2 101.8, F2-Si-O2 102.1, F2-Si-O2-F1 119.7°.

[*] Prof. F. Grandinetti, Dr. P. Cecchi, Dr. V. Vinciguerra
Dipartimento di Scienze Ambientali
Università della Tuscia
Via S. C. De Lellis, I-01100 Viterbo (Italy)
Fax: Int. code +(761)35-7179
Dr. M. E. Crestoni
Università di Roma La Sapienza (Italy)

[**] This work was supported by the Italian Ministero dell' Università e della Ricerca Scientifica e Tecnologica (MURST) and the Consiglio Nazionale delle Ricerche (CNR).

from the observation of the ligand-displacement reactions (1) and (2) and the BDEs of SiF_3^+ and HF and H_2O (46 and

$$F_3Si{-}FH^+ + CO_2 \longrightarrow SiF_3^+{-}(CO_2) + HF \quad (1)$$

$$SiF_3^+{-}(CO_2) + H_2O \longrightarrow F_3Si{-}OH_2^+ + CO_2 \quad (2)$$

70 kcal mol^{-1}, respectively).[9, 10] As an aside, we determined the enthalpy of formation of $SiF_3^+{-}(CO_2)$ to be -181 ± 12 kcal mol^{-1}. Detailed investigation of the conceivable ion–molecule reactions leading to $SiF_3^+{-}(CO_2)$ threw light on the ligand displacement reaction (3), which was unambiguously

$$SiF_3^+{-}(SiF_4) + CO_2 \longrightarrow SiF_3^+{-}(CO_2) + SiF_4 \quad (3)$$

detected by reacting thermalized $SiF_3^+{-}(SiF_4)$ from the external source of the FT-ICR with CO_2 in the resonance cell. The efficiency of reaction (3) is evaluated as 0.44 from the ratio of the experimental rate constant $k_3 = 2.8 \times 10^{-10}$ cm^3 molecule^{-1} s^{-1} and the collision rate constant $k_3(\mathrm{ADO}) = 6.38 \times 10^{-10}$ cm^3 molecule^{-1} s^{-1}, calculated from the average dipole orientation (ADO) theory.[11]

The $SiF_3^+{-}(CO_2)$ ions isolated from the external source and allowed to react with nucleophiles introduced in the resonance cell of the FT-ICR are unreactive toward H_2, CH_4, and other saturated hydrocarbons, and are only able to undergo ligand displacement with C_2H_2, C_2H_4, and C_3H_6. However, treatment of $SiF_3^+{-}(CO_2)$ with benzene gave reactions (4a) and (4b) in the indicated proportions.

$$SiF_3^+{-}(CO_2) + C_6H_6 \xrightarrow{0.75} C_6H_5{-}CO^+ + SiF_3OH \quad (4a)$$

$$SiF_3^+{-}(CO_2) + C_6H_6 \xrightarrow{0.25} SiF_3^+{-}(C_6H_6) + CO_2 \quad (4b)$$

Typical intensity–time curves of the observed ions are shown in Figure 3. From the overall rate constant k_4 (8.8×10^{-10} cm^3 molecule^{-1} s^{-1}) we determine k_{4a} and k_{4b} to be 6.6×10^{-10} and 2.2×10^{-10} cm^3 molecule^{-1} s^{-1}, respectively. In addition, using the collision rate constant of $SiF_3^+{-}(CO_2)$ with C_6H_6 ($k_4(\mathrm{ADO}) = 1.1 \times 10^{-9}$ cm^3 molecule^{-1} s^{-1}) we evaluate the efficiency of reaction (4a) as $k_{4a}/k_4(\mathrm{ADO}) = 0.6$. The CID spectrum of the $C_7H_5O^+$ ions from (4a) ($C_7H_5O^+$ 34%, $C_6H_5^+$ 100%, $C_4H_3^+$ 27%) was indistinguishable from the CID spectrum of the $C_6H_5{-}CO^+$ ions of the model obtained from the ionization of $C_6H_5{-}CO{-}OCH_3$; however, the FT-ICR experiments do not provide direct structural information on the

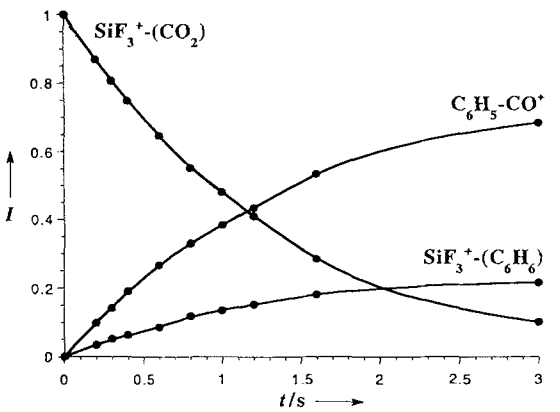

Fig. 3. Dependence of the relative intensities (I) on time of the ions observed when thermalized $SiF_3^+{-}(CO_2)$ is allowed to react with C_6H_6 ($P = 3.4 \times 10^{-8}$ mbar).

obtained neutral(s). Thus, we can only infer the formation of SiF_3OH and calculate $\Delta H°(4a)$ (-31 ± 12 kcal mol^{-1}).[12]

The carbonylation reaction (4a) provides unambiguous evidence for the activation of carbon dioxide by coordination to a gaseous cation. In addition, combining (3) with (4a) yields the net reaction equation (5), which describes the *coupled* activation

$$SiF_3^+{-}(SiF_4) + CO_2 + C_6H_6 \longrightarrow C_6H_5{-}CO^+ + SiF_3OH + SiF_4 \quad (5)$$

of CO_2 and aromatic C–H bonds. Indeed, a high intensity of $C_6H_5{-}CO^+$ is detected when thermalized $SiF_3^+{-}(SiF_4)$ from the external source of the FT-ICR is subjected to reaction with CO_2/C_6H_6 mixtures in the resonance cell (typical ratio 3/1, P approximately 5×10^{-8} mbar). Reaction (5) commences with the ligand-exchange (3), which converts the unreactive carbon dioxide into an electrophile that undergoes efficient carbonylation (4a). Since the $SiF_3^+{-}(C_6H_5{-}CO_2H)$ intermediate conceivably involved in this reaction is excited by the exothermicity of its formation process and lacks thermal stabilization in the low-pressure domain of the FT-ICR cell (P about 10^{-8} mbar), it undergoes fast elimination of SiF_3OH to give $C_6H_5{-}CO^+$ as the only product ion. The actual observation of an $SiF_3^+{-}(C_6H_5{-}CO_2H)$ adduct in the higher pressure domain of the FT-ICR external source (P about 10^{-4} mbar) supports this proposal (Fig. 4). The observation of $C_6H_5{-}CO^+$ exclusively in the CID

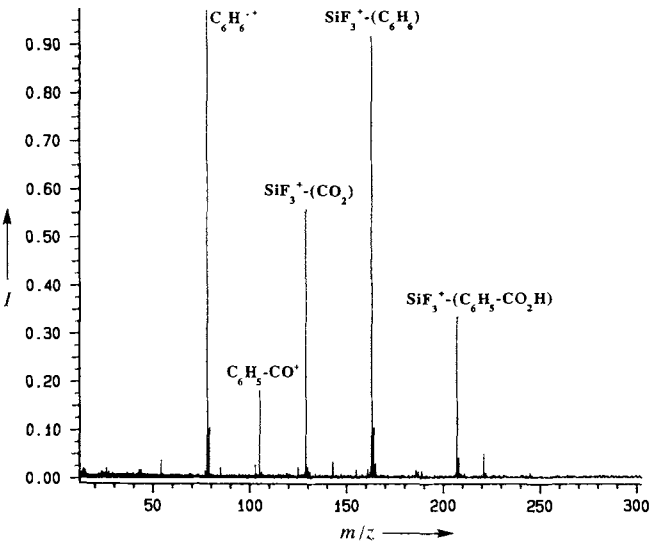

Fig. 4. Mass spectrum (70 eV) of a $CO_2/SiF_4/C_6H_6$ gaseous mixture (P about 1.7×10^{-4} mbar; approximate ratio 7/3/1).

spectrum of the $SiF_3C_7H_6O_2^+$ ions suggests the formation of an adduct between $C_6H_5{-}CO_2H$ and SiF_3^+ rather than a terbody complex ($SiF_3^+/CO_2/C_6H_6$), which we would expect to lose intact C_6H_6 and/or CO_2. In addition, we obtained a CID spectrum indistinguishable from that of the $SiF_3C_7H_6O_2^+$ ions generated in the external source of the FT-ICR from the ionization of a mixture of $C_6H_5{-}CO_2H$ and SiF_4 and reasonably regarded as a model for $SiF_3^+{-}(C_6H_5{-}CO_2H)$.

Mass spectra of ionized $CO_2/SiF_4/C_6H_5X$ mixtures (X = CH_3, F, Cl) were quite similar to that reported in Figure 4; we invariably detected the formation of $XC_6H_4{-}CO^+$ from the reaction of $SiF_3^+{-}(CO_2)$ from the external source of the FT-ICR with C_6H_5X introduced in the resonance cell. Thus, coordination of CO_2 to SiF_3^+ makes accessible the reactions (6), which

$$CO_2 + C_6H_5{-}X \longrightarrow X{-}C_6H_4{-}CO_2H \quad (6)$$

 © VCH Verlagsgesellschaft mbH, D-69451 Weinheim, 1996 0570-0833/96/3521-2523 $ 15.00+.25/0

are endothermic in the gas phase by several kcal mol^{-1} ($\Delta H°(6) = 3.9$ kcal mol^{-1}, X = H; 3.0 kcal mol^{-1}, X = CH_3; 4.9 kcal mol^{-1}, X = F). Besides providing unambiguous evidence for CO_2 activation by a coordination mechanism, this finding demonstrates the possibility of promoting endothermic reactions involving carbon dioxide by taking advantage of the larger interaction energy with the reaction products of a cation ligated to CO_2 in the gas phase.

Experimental Procedure

All experiments were performed on a Bruker Spectrospin Apex 47e FT-ICR spectrometer equipped with an external ion source [13]. To investigate the reactivity of selected ions produced in the external source, the ions were transferred to the resonance cell, trapped in the field of a superconducting magnet (4.7 T), isolated with single-shot and broad-band-ejection techniques [14], thermalized by unreactive collisions with argon pulsed into the cell with peak values of ca. 10^{-6} mbar, and reisolated. The pseudo-first-order rate constants were derived from the logarithmic decay of the precursor-ion intensity with time, corrected for reactions with background impurities, and converted into absolute rate constants by dividing by the number density of the neutral molecules in the ICR cell. To this end, the pressure readings from the ion gauge were first calibrated against the rate constants of suitable ion–molecule reactions and subsequently corrected for the different sensitivities toward the neutral molecules [15]. The estimated error in the absolute rates is about ±30%. All the neutral species were introduced into the cell at corrected pressures ranging from 2×10^{-8} to 8×10^{-8} mbar. The reported ligand-exchange reactions were confirmed by treating thermalized ions from the external source with the neutral species in the cell. The CID [16] experiments were performed by colliding isolated ions with argon, pulsed into the cell with peak values of about 1×10^{-6} mbar. Exact mass measurements were performed by operating the instrument in the high-resolution mode.

Standard ab initio calculations were performed with a RISC/6000 version of the Gaussian 94 set of programs [17].

Received: April 16, 1996
Revised version: June 4, 1996 [Z 9045 IE]
German version: *Angew. Chem.* **1996**, *108*, 2674–2676

Keywords: benzene activation · carbon dioxide activation · mass spectrometry · silicon compounds

[1] Selected monographs: a) M. Aresta, G. Forti, *Carbon Dioxide as a Source of Carbon, Biochemical and Chemical Uses (NATO ASI Ser. Ser. C)* **1987**, *206*; b) A. Behr, *Carbon Dioxide Activation by Metal Complexes*, VCH, Weinheim, **1988**; c) M. Aresta, J. V. Schloss, *Enzymatic and Model Carboxylation and Reduction Reactions for Carbon Dioxide Utilization (NATO ASI Ser. Ser. C)* **1990**, 314; d) B. P. Sullivan, K. Krist, H. E. Guard, *Electrochemical and Electrocatalytic Reactions of Carbon Dioxide*, Elsevier, Lausanne, **1993**.

[2] W. Leitner, *Angew. Chem.* **1995**, *107*, 2391; *Angew. Chem. Int. Ed. Engl.* **1995**, *34*, 2207.

[3] See, for example, a) T. B. McMahon, C. J. Northcott, *Can. J. Chem.* **1978**, *56*, 1069; b) P. B. Armentrout, J. L. Beauchamp, *Chem. Phys.* **1980**, *50*, 27; c) M. M. Kappes, R. H. Staley, *J. Phys. Chem.* **1981**, *85*, 942; d) S. Dheandhanoo, B. K. Chatterjee, R. Johnsen, *J. Chem. Phys.* **1985**, *83*, 3327; e) D. J. Hajdasz, Y. Ho, R. R. Squires, *J. Am. Chem. Soc.* **1994**, *116*, 10751; f) R. L. Asher, D. Bellert, T. Buthelezi, P. J. Brucat, *Chem. Phys. Lett.* **1994**, *227*, 623; g) R. L. Asher, D. Bellert, T. Buthelezi, G. Weerasekeera, P. J. Brucat, *ibid.* **1994**, *228*, 390.

[4] R. Wesendrup, H. Schwarz, *Angew. Chem.* **1995**, *107*, 2176; *Angew. Chem. Int. Ed. Engl.* **1995**, *34*, 2033.

[5] a) J. Schwarz, H. Schwarz, *Organometallics* **1994**, *13*, 1518; b) J. Schwarz, C. Heinemann, H. Schwarz, *J. Phys. Chem.* **1995**, *99*, 11405.

[6] a) F. Grandinetti, G. Occhiucci, O. Ursini, G. de Petris, M. Speranza, *Int. J. Mass Spectrom. Ion Processes* **1993**, *124*, 21; b) F. Cacace, F. Grandinetti, F. Pepi, *Angew. Chem.* **1994**, *106*, 104; *Angew. Chem. Int. Ed. Engl.* **1994**, *33*, 123; c) F. Cacace, F. Grandinetti, F. Pepi, *Inorg. Chem.* **1995**, *34*, 1325; d) R. Cipollini, F. Grandinetti, *J. Chem. Soc. Chem. Commun.* **1995**, 773.

[7] *FT-ICR/MS: Analytical Applications of Fourier Transform Ion Cyclotron Resonance Mass Spectrometry* (Ed.: B. Asamoto), VCH, Weinheim, **1991**.

[8] D. Smith, B. J. McIntosh, N. G. Adams, *J. Chem. Phys.* **1989**, *90*, 6213; b) D. E. Lessen, R. L. Asher, P. J. Brucat, *ibid.* **1991**, *95*, 1414; c) I. K. Gregor, R. C. Gregor, *Rapid Commun. Mass Spectrom.* **1992**, 6, 221; d) C. S. Yeh, K. F. Willey, D. L. Robbins, J. S. Pilgrim, M. A. Duncan, *J. Chem. Phys.* **1993**, *98*, 1867.

[9] Unless stated otherwise, all thermochemical data are taken from *Gas-Phase Ion and Neutral Thermochemistry*: S. G. Lias, J. E. Bartmess, J. F. Liebman, J. L. Holmes, R. D. Levin, W. G. Mallard, *J. Phys. Chem. Ref. Data Suppl.* **1988**, *17*, 66.

[10] The BDE of SiF_3^+ and HF was obtained from the enthalpy of formation of SiF_3^+ (−28.7 kcal mol^{-1}) reported in E. R. Fisher, B. L. Kickel, P. B. Armentrout, *J. Phys. Chem.* **1993**, *97*, 10204. The enthalpy of formation of SiF_3–OH_2^+ (−156.3 kcal mol^{-1}) was obtained by combining the tabulated proton affinity of SiF_3OH with its enthalpy of formation (−360 kcal mol^{-1}) taken from R. Damrauer, R. Simon, M. Krempp, *J. Am. Chem. Soc.* **1991**, *113*, 4431.

[11] T. Su, M. T. Bowers, *Int. J. Mass Spectrom. Ion Phys.* **1973**, *12*, 347.

[12] However, assuming alternative neutrals, the reaction would result significantly endothermic and should not be observed to any appreciable extent under our FT-ICR conditions (e.g. using the estimated enthalpy of formation of F_2SiO, −231 ± 6 kcal mol^{-1}, reported in: J. W. Larson, T. B. McMahon, *Inorg. Chem.* **1987**, *26*, 4018, $\Delta H°(4a) = 33 \pm 18$ kcal mol^{-1} if formation of F_2SiO and HF is assumed).

[13] P. Kofel, M. Allemann, H. P. Kellerhals, K. P. Wanczek, *Int. J. Mass Spectrom. Ion Processes* **1985**, *65*, 97.

[14] L. J. de Köning, R. H. Fokkens, F. A. Pinkse, N. M. N. Nibbering, *Int. J. Mass Spectrom. Ion Processes* **1987**, *77*, 95.

[15] J. E. Bartmess, R. M. Georgiadis, *Vacuum* **1983**, *33*, 149.

[16] R. C. Burnier, R. B. Cody, B. S. Freiser, *Anal. Chem.* **1982**, *54*, 96.

[17] Gaussian 94 (Revision C.2), M. J. Frish, G. W. Trucks, H. B. Schlegel, P. M. W. Gill, B. G. Johnson, M. A. Robb, J. R. Cheeseman, T. A. Keith, G. A. Petersson, J. A. Montgomery, K. Raghavachari, M. A. Al-Laham, V. G. Zakrzewski, J. V. Ortiz, J. B. Foresman, J. Cioslowski, B. B. Stefanov, A. Nanayakkara, M. Challacombe, C. Y. Peng, P. Y. Ayala, W. Chen, M. W. Wong, J. L. Andres, E. S. Replogle, R. Gomperts, R. L. Martin, D. J. Fox, J. S. Binkley, D. J. Defrees, J. Baker, J. P. Stewart, M. Head-Gordon, C. Gonzalez, and J. A. Pople, Gaussian, Inc., Pittsburgh PA, 1995.

Fast Atom Bombardment Mass Spectrometry for Characterizing Cationic Chelated Species**

Jeffery A. Whiteford, Elliot M. Rachlin,* and Peter J. Stang*

Dedicated to Professor Michael Hanack on the occasion of his 65th birthday

Supramolecular chemistry encompasses several areas of interest including organic macrocycles with covalent bonds, hydrogen-bonded species, and aggregates derived through metal coordination.[1–4] Moreover, self-assembly resulting in macrocycles has become a driving force in all of these areas.[4–11] Determining the structures and relative molecular masses of the self-assembled aggregates and macrocycles are major challenges in this field. Commonly employed techniques such as X-ray crystallography, vapor-phase osmometry (VPO), and gel permeation chromatography (GPC) all have limitations and shortcomings,[12, 13] which are particularly acute in the analysis of aggregates and macrocycles arising from metal coordination.[4–10] 1) X-ray quality single crystals are often difficult to obtain because of the considerable void space in these systems. Furthermore, removal of the crystals from the mother liquor generally results in rapid solvent loss and collapse to amorphous material.[8] Even when the single crystal survives, extensive solvent occlusion can cause disorder and consequent poor structure resolution (large *R*-value). 2) Molecular masses determined by VPO generally deviate substantially from those calculated, and error values tend to increase with increasing molecular mass.[13]

[*] Prof. Dr. P. J. Stang, J. A. Whiteford, Dr. E. M. Rachlin
Department of Chemistry, University of Utah
Salt Lake City, UT 84112 (USA)
Fax: Int. code +(801) 581-8433

[**] The authors thank Jun Fan for preparing squares **9** and **10** and Bogdan Olenyuk for preparing squares **14** and **15**. Financial support by the National Science Foundation (CHE-9529093, CHE-9002690) and the University of Utah Institutional Funds Committee is gratefully acknowledged.

 © VCH Verlagsgesellschaft mbH, D-69451 Weinheim, 1996 0570-0833/96/3521-2524 $ 15.00+.25/0

3) GPC works well for large biomolecules such as proteins and nucleic acids, as well as neutral linear polymers. For the latter, acceptable molecular weight distributions are obtainable by this technique.[14] Unfortunately, few coordination complexes, metal-based aggregates, or macrocycles survive GPC conditions, and GPC is usually best at molecular weights exceeding 10000.

Recently, electrospray (ES), fast atom bombardment (FAB), and matrix assisted laser desorption time of flight (MALDI-TOF) mass spectrometry have proven useful for the characterization of organic and inorganic supramolecular species formed in solution.[12, 15, 16] To date, several types of macrocycles have been distinguished by MS such as palladium catenanes with dative bonds,[17] covalently bound rapamycin,[18] and self-assembled hydrogen-bonded organic species.[12, 13] ES mass spectrometry has been used to characterize unique chains of interlocking oligoalkyne macrocycles and porphyrins linked through the coordination of copper(I) ions by 1,10-phenanthroline subunits.[19] The stability of the complex in the matrix and within the mass spectrometer typically determine the feasibility of mass spectral characterization.

Tetranuclear, transition metal based complexes termed "molecular squares" are some of the newest members of the family of supramolecular macrocycles.[4, 7, 8] Although MS data is reported for a rhenium–palladium-based square [10] and an all-silicon-based square,[15] mass spectral data for platinum–palladium, platinum–iodine, and palladium–iodine squares have not been reported. ESMS has been particularly useful in the characterization of organometallic species[20] and found advantageous for the observation of proteins and copper coordination compounds with higher molecular masses and charge states.[21] However, molecular squares have exhibited limited stability under commonly employed MS methods such as ESMS in both protic and aprotic solvents. This is probably due to the lability of the metal–ligand coordination bonds in the macrocycle. Although charge state resolution was possible by ESMS, isotopic resolution was not feasible on the triple quadrupole mass spectrometer used which had a limited m/z range. However, isotopic resolution was achieved with an ESIFTICR system (electrospray ionization Fourier transform ion cyclotron resonance), which verified the charges of the fragments observed.

Typically, molecular squares such as **4** and **5** containing only coordination bonds (Scheme 1) fragment by successive loss of each chelated metal corner and loss of the bipyridine units. Molecular squares containing σ-bonded ligands (Schemes 2–4) tend to fragment into the σ-bonded monomeric organometallic component and the previously dative-bonded metal chelate corners. Although use of ESMS has been unsuccessful to date for the characterization of molecular squares in solution, ongoing development will likely render this technique fruitful for the observation of self-assembled molecular squares.

We now report a Fast Atom Bombardment Mass Spectrometry (FABMS) method for the characterization of chelated cationic tetranuclear species formed by self-assembly in solution. Important data obtained by this method are the isotopic abundance patterns for species **4**, **5**, **9**, **10**, **14**, **15**, **17**, and **18**. The charge of each fragment or assembly is typically identified by the separation of the major peak of the fragment from the smaller peaks in the observed isotopic distribution. For example, for a doubly charged ion this separation is 0.5 m/z units, while for a singly charged ion it is 1.0 m/z units. Therefore optimal resolution is needed for the identification of each fragment. Sufficient resolution was obtained using the method we describe herein (see Experimental Procedure).

The M − OTf peak (m/z = 4097.0) and the peak corresponding to the corner fragment (m/z = 607.0) were observed for the coordination-bonded square **4**, which was formed from **1** and **2**, (Scheme 1, Table 1). Similarly, the M − OTf peak (m/z = 3743.2) and the peak for the corner fragment (m/z = 518.0) were

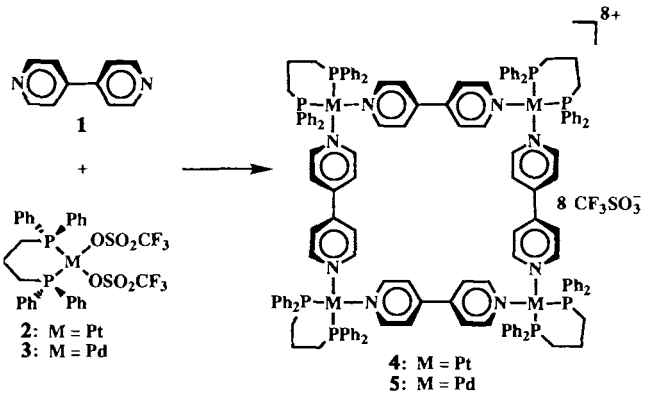

Scheme 1. Synthesis of Pt_4 and Pd_4 squares, in which the corners result from metal–ligand coordination.

Table 1. Fragment ions identified in the FAB mass spectra of compounds **4**–**6**, **9**, **10**, and **14**–**18**[a].

Cmpd.	m/z	Observed fragment	Composition	Calculated base peak
4	4097.0	**4** − OTf	$C_{155}H_{136}P_8N_8F_{21}S_7O_{21}Pt_4$	4097.4
4	607.0	**2** − 2OTf	$C_{27}H_{26}P_2Pt$	607.1
5	3740.0	**5** − OTf	$C_{155}H_{136}P_8N_8F_{21}S_7O_{21}Pd_4$	3743.2
5	518.0	**3** − 2OTf	$C_{27}H_{26}P_2Pd$	518.1
6	435.1	**6** − OTf	$C_{22}H_{16}I_2N_2$	435.0
9	2937.8	**9** − OTf	$C_{117}H_{88}P_8N_4F_{15}S_5O_{15}Pd_2I_2Fe_2$	2936.8
9	1393.8	**9** − 2OTf	$C_{116}H_{88}P_4N_4F_{12}S_4O_{12}Pd_2I_2Fe_2$	1393.6
9	660.2	**7** − 2OTf	$C_{34}H_{28}P_2PdFe$	660.0
9	435.1	**6** − OTf	$C_{22}H_{16}I_2N_2$	435.0
10	3115.4	**10** − OTf	$C_{117}H_{88}P_4N_4F_{15}S_5O_{15}Pt_2I_2Fe_2$	3114.0
10	435.1	**6** − OTf	$C_{22}H_{16}I_2N_2$	435.0
14	2770.0	**14** − OTf	$C_{113}H_{80}P_4N_4F_{15}S_5O_{15}I_2Pd_2$	2768.9
14	728.7	**11** − 2OTf	$C_{44}H_{32}P_2Pd$	728.1
14	255.0	**13** − OTf	$C_{10}H_8I$	255.0
15	1397.8	**15** − 2OTf	$C_{112}H_{80}P_4N_4F_{12}S_4O_{12}I_2Pt_2$	1398.0
15	817.7	**12** − 2OTf	$C_{44}H_{32}P_2Pt$	817.2
15	255.2	**13** − OTf	$C_{10}H_8I$	255.0
16	812.2	**16** + H	$C_{41}H_{35}P_2N_2Pt$	812.2
17	1569.3	**17** − 2OTf	$C_{138}H_{120}P_8N_4F_6S_2O_6Pt_4$	1569.1
17	812.2	**16** + H	$C_{41}H_{35}P_2N_2Pt$	812.2
18	812.2	**16** + H	$C_{41}H_{35}P_2N_2Pt$	812.2

[a] OTf = trifluoromethanesulfonate.

observed for the coordination-bonded square **5**, accessible analogously from **1** and **3**. The isotopic distribution patterns for squares **4** and **5** both indicate a charge of 1+ (peak separation of 1.0 m/z units).

The fragmentation pattern for square **9**, which arises from **6** and **7** (Scheme 2), includes a M − OTf peak (m/z = 2937.8), which is in agreement with the calculated value (Table 1). Importantly, comparison of the calculated and experimental isotopic distribution for the M − OTf fragment of **9** are in excellent agreement and in accord with the expected m/z separation of 1 m/z units. The M − 2OTf peak was also observed for **9** (m/z = 1393.8). Further fragmentation of **9** resulted in the iodonium monomer **6** − OTf fragment (m/z = 435.1) as well as the ferrocenediyl corner fragment (m/z = 660.2), which are also in agreement with the calculated isotopic distribution patterns and

 © VCH Verlagsgesellschaft mbH, D-69451 Weinheim, 1996 0570-0833/96/3521-2525 $ 15.00+.25/0

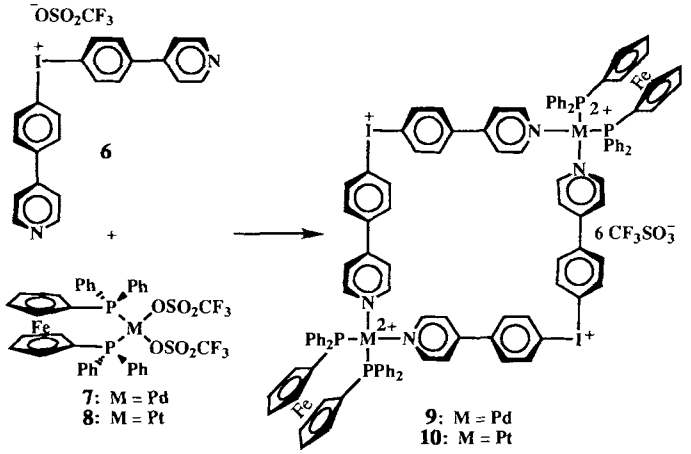

Scheme 2. Synthesis of Pt_2I_2 and Pd_2I_2 squares, in which two corners result from covalent bonds.

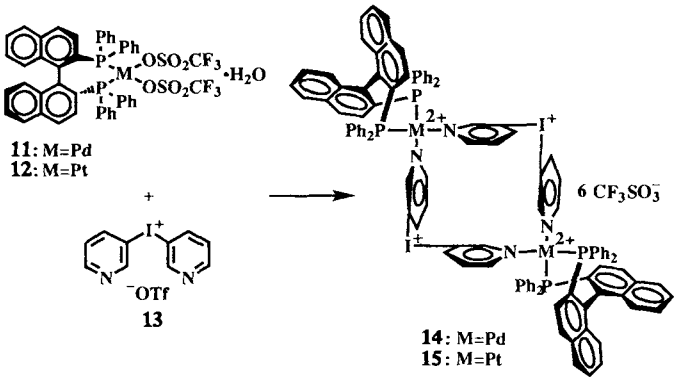

Scheme 3. Synthesis of **14** and **15**.

m/z values (Table 1). The M − OTf peak at m/z = 3115.4 was observed as well when square **10**, prepared from **6** and **8**, was subjected to FABMS conditions, and each of the isotope peaks were separated by 1 m/z units, as expected, indicating that this macrocyclic fragment has a charge of 1+ . Further evidence for this specific species was established by close correlation of the calculated isotopic distribution pattern with the experimental pattern (Fig. 1). The charge distribution, isotopic abundance pattern, and the m/z value for the base peak provide direct evidence for the existence of this specific species (**10** − OTf) in solution. Each macrocycle displayed different stability characteristics under FABMS conditions. Although peaks corresponding to M − 2OTf peak and the monomeric corner fragment **7** − 2OTf were observed for **9**, analogous signals were not observed for **10**; however, the iodonium monomer **6** − OTf peak was observed for both **9** and **10** (m/z = 435.1).

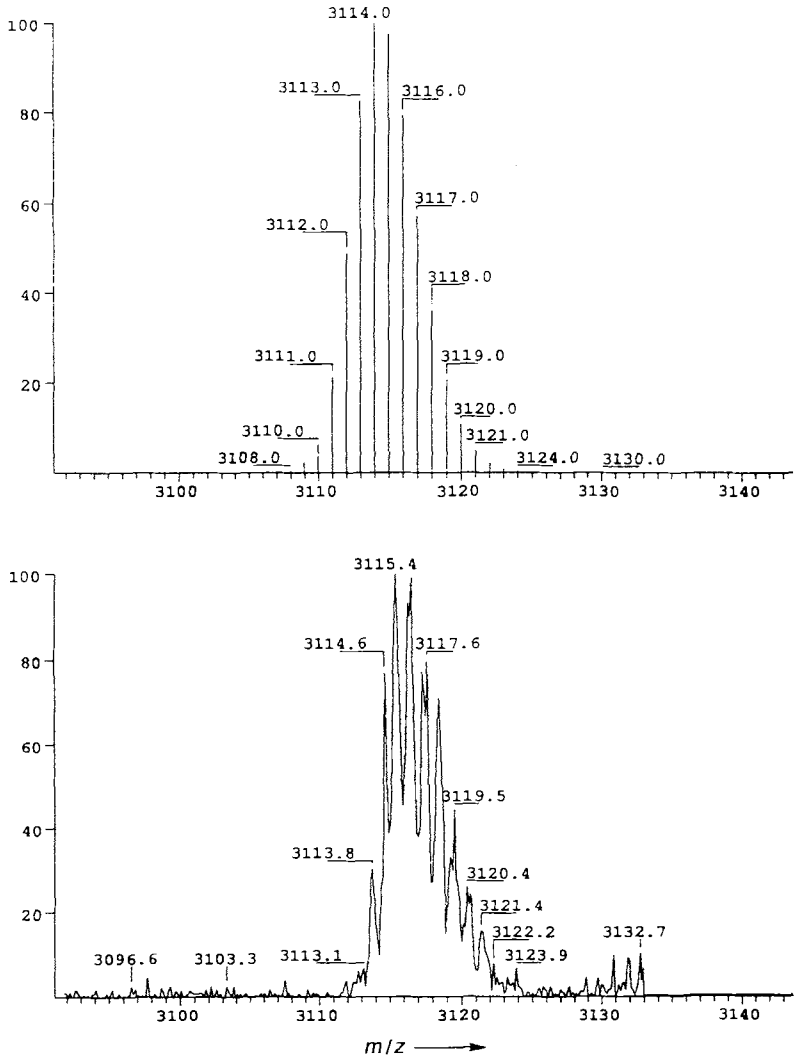

Fig. 1. Calculated (top) and observed (bottom) isotopic distribution patterns of the M − OTf peak for **10**.

Square **14**, the product of **11** and **13** (Scheme 3), exhibited the M − OTf peak at m/z = 2770 with an isotopic distribution pattern that is in close agreement with that calculated (Fig. 2). Although a peak was observed with the correct molecular weight for the M − 2OTf species, close inspection of the isotopic distribution revealed that it corresponded to a charge of 1+ and not 2+ , indicating that square **14** simply fragmented into two equal halves. In contrast, subjection of square **15**, which was prepared from **12** and **13**, to the same FABMS conditions resulted in the M − 2OTf peak (1397.8), but not the M−OTf peak, with a separation of 0.5 m/z units between the peaks of the isotopic pattern although **15** has about the same stability as **14** in the matrix. Further fragmentation of squares **14** and **15** resulted in the the respective palladium and platinum binapthalene phosphane chelated corners (728.7 and 817.7) and iodonium monomer fragments (255.0 and 255.2; Table 1).

The M − 2OTf peak (m/z = 1569.3) was observed for the all transition metal based square **17**, formed from the bisalkynyl complex **16** and **2** (Scheme 4), but the M − OTf peak was not evident. This may be attributed to the difference in stability of **4**, **5**, **9**, **10**, and **14** in solution compared to that of **17**. Although the hybrid iodonium/transition metal squares **9** and **10** are stable for several days in solution, square **17** decomposes within 12 h in the matrix. The 2+ charge was indicated for **17** by the peak separation of 0.5 m/z

 © VCH Verlagsgesellschaft mbH, D-69451 Weinheim, 1996 0570-0833/96/3521-2526 $ 15.00+.25/0

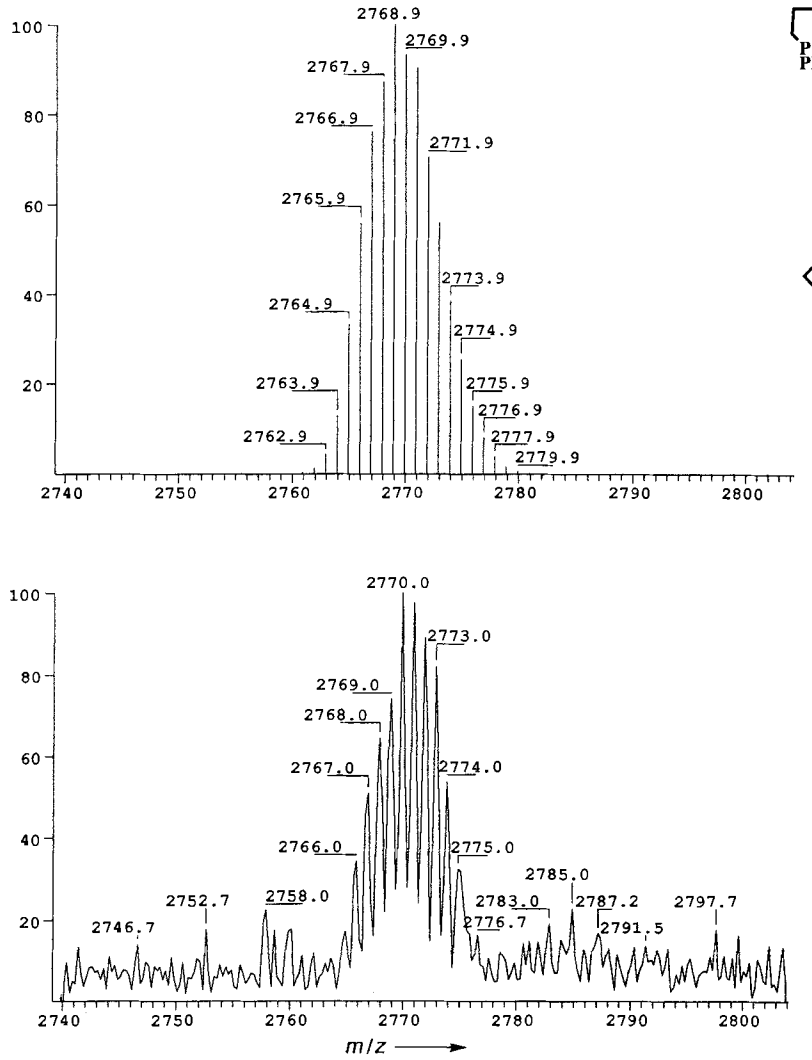

Fig. 2. Calculated (top) and observed (bottom) isotopic distribution patterns of the $M - OTf$ peak for **14**.

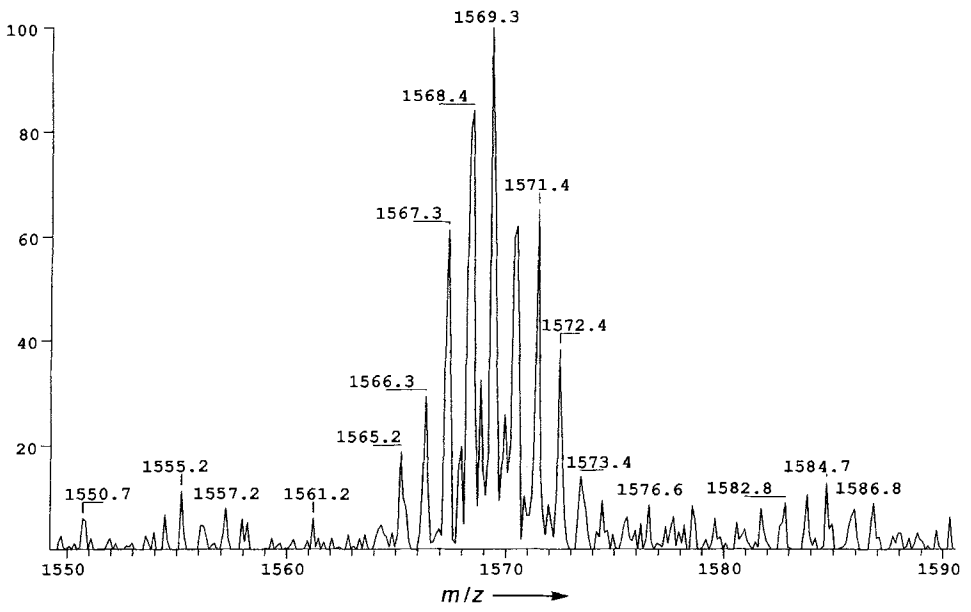

Fig. 3. Observed isotopic distribution pattern of the $M - 2OTf$ peak for **17** (charge 2+).

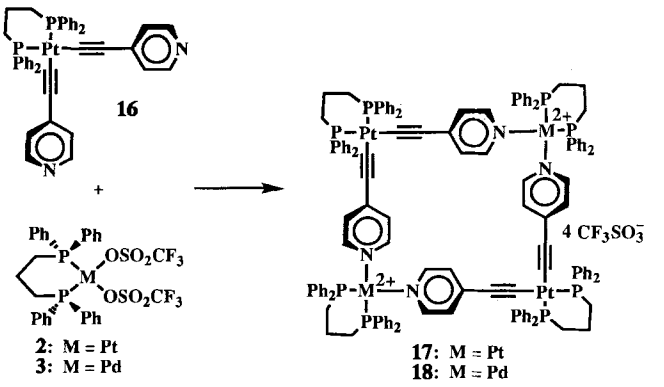

Scheme 4. Synthesis of the squares **17** and **18**, in which the corners result from metal–carbon σ bonds.

units in the isotopic distribution pattern (Fig. 3). As expected, when the least stable square **18** was subjected to the same FABMS parameters as squares **4**, **5**, **9**, **10**, **14**, **15**, and **17**, a peak corresponding to the protonated form of the platinum monomer fragment **16** ($m/z = 812.2$) was observed as the major species.

Monomers **6** and **16** were also studied in matrices similar to those used with the corresponding squares and observed by FABMS. In analogy with the square, the derived isotopic pattern and m/z value for monomer **6** were calculated and are in agreement with the observed spectrum. The $M - OTf$ peak was observed for **6** ($m/z = 435.1$) as well as a peak corresponding to loss of a 4-(4-pyridyl)phenyl substituent ($m/z = 282.1$) and a peak for this fragment alone ($m/z = 154.2$). Monomer **16** gave similar results, yielding the expected $M + H$ peak ($m/z = 812.2$) typically seen with this technique for a neutral chelated species that can be protonated (on the pyridine moiety). Also observed for **16** were the loss of each of the (4-pyridyl)ethynyl ligands ($m/z = 709.2$ and 607.3, respectively, Fig. 4). Finally, the calculated and the experimental isotopic distribution patterns for **16** are in full agreement (Fig. 5, Table 1).

In conclusion, self-assembled macrocyclic cationic chelated species in solution were characterized by FABMS along with monomeric charged and neutral chelated species. The observed fragmentation data and isotopic abundance patterns are in excellent agreement with calculated values and confirm the existence of these tetrameric macrocyclic species. As these examples illustrate, FABMS is a powerful technique for determining reliable molecular masses and for obtaining structural information on coordinated metal species. Particularly impressive is the applicability of this technique to self-assembled macrocycles based upon metal–ligand coordination. Hence, we think that the FABMS technique may be widely employed to characterize a broad range of coordinated

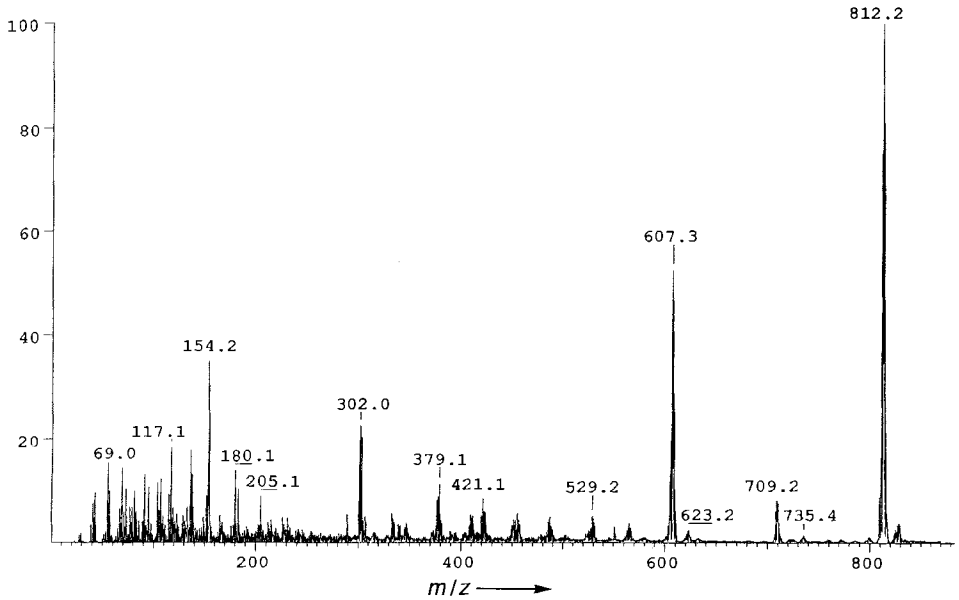

Fig. 4. FAB mass spectrum of the neutral chelated monomer **16**.

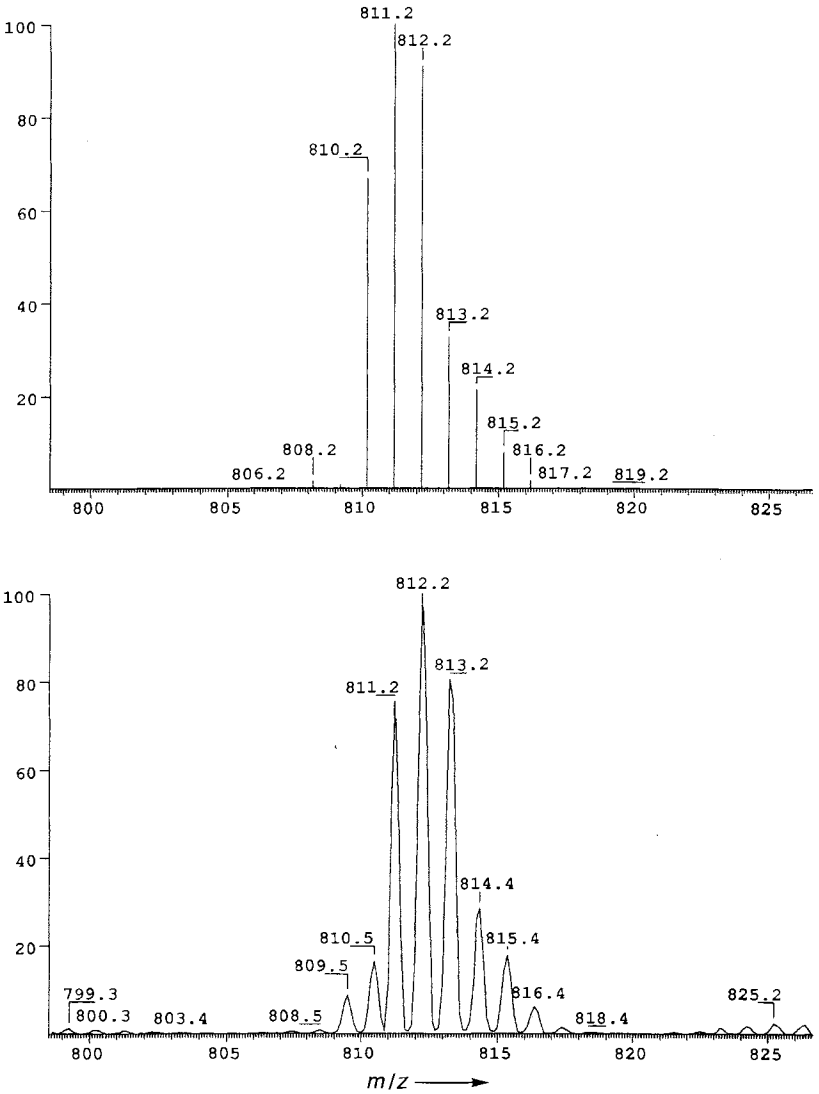

Fig. 5. Calculated (top) and observed (bottom) isotopic distribution patterns for the M and $M+H$ peaks of **16**.

transition metal species including discrete supramolecular assemblies particularly in the molecular mass range of 300–5000. A particularly valuable aspect of this method is that it provides molecular mass and structural information in solution where most aggregates self-assemble under equilibrium conditions.

Experimental Procedure

Mass spectra were obtained with a Finnigan MAT 95 mass spectrometer under positive-ion fast atom bombardment (FAB) conditions using a CsI gun at 20 keV. 3-Nitrobenzyl alcohol was used as a matrix in dichloromethane, acetone, or dimethylsulfoxide as solvent; polypropylene glycol and CsI were used as calibration references. Each sample was dissolved in the appropriate solvent and mixed with the matrix on a standard Finnigan FAB probe. For optimal performance a thin film of matrix and sample on the target surface should form. Bombardment of the sample on the target surface by the CsI gun must result in an even introduction of all components of the mixture into the mass analyzer. To accomplish this, the solvent, substrate, and matrix used must form a homogeneous solution. Matrix systems that are not compatible with each other and form heterogeneous mixtures are easily recognized by erratic peak generation [22]. A reference spectrum of a standard aqueous solution of CsI was obtained by scanning from $m/z = 50$ to $m/z = 4500$. The mass spectrometer was then calibrated with the CsI spectrum. After slit adjustment to obtain a resolution of $m/z > 4500$ using the calibration mixture (entrance slit approximately 165–200, exit slit approximately 165–190) followed by standard tuning, a mass range of $m/z = 1000$ to $m/z = 4500$ was scanned to locate calibration peaks near the expected mass-to-charge range of each respective square. (The range was varied according to the molecular mass of the compound analyzed to scan for species larger than the target molecule to rule out pentamers, hexamers, etc.). Next, the mass range was increased to scan from $m/z = 50$ to $m/z = 4500$. Molecular squares **4**, **5**, **17**, and **18** were dissolved in dichloromethane (0.01 M), while **9**, **10**, **14**, and **15** were dissolved in acetone (0.01 M). Next, 3-nitrobenzylalcohol (0.5 μL) was used as a matrix and mixed with 1 μL of each of the standard solutions of the squares. The mass range of $m/z = 1000$ to $m/z = 4500$ was then scanned to obtain the $M - OTf$ peak and isotopic distribution. The range was then expanded again from $m/z = 50$ to $m/z = 4500$ to obtain the complete fragmentation pattern of each respective square. Then the scan range was changed to focus on the $M - 2OTf$ and/or the $M - OTf$ region from $m/z = 1000$ to $m/z = 4500$. Next, the scan range was changed to include only the $M - OTf$ peak from $m/z = 2700$ to $m/z = 4500$. Upon observation of the $M - OTf$ peak, 10–15 scans were compiled and averaged. The isotopic abundance pattern for each respective fragment peak obtained was calculated and compared to the experimental isotopic distribution. Next, the calibration standard was subjected to the same FABMS ionization conditions as the sample and the instrument calibration was verified. The mass spectral data of the squares was then compared to that of the standard and corrected according to software protocol. Extrapolation from the spectrum of the standard resulted in m/z values consistent with the predicted masses within error limits.

Monomer **6** was dissolved in dimethylsulfoxide (0.01 M); **16** was dissolved in dichloromethane (0.01 M). Next, 3-nitrobenzylalcohol (0.5 μL) was used as a matrix and mixed with 1 μL of each of the respective standard monomer solutions. The mass range of $m/z = 20$ to $m/z = 1000$ was used for obtaining spectra for monomers **6** and **16**.

Received: May 3, 1996 [Z9095IE]
German version: *Angew. Chem.* **1996**, *108*, 2643–2648

 © VCH Verlagsgesellschaft mbH, D-69451 Weinheim, 1996 0570-0833/96/3521-2528 $ 15.00+.25/0

Keywords: chelates · complexes with nitrogen ligands · iodine compounds · mass spectrometry · supramolecular chemistry

[1] Reviews: a) J.-M. Lehn, *Supramolecular Chemistry, Concepts and Perspectives*, VCH, Weinheim, **1995**; b) *Supramolecular Chemistry* (Eds.: V. Balzani, L. Decola), Kluwer, Dordrecht, **1992**.

[2] V. Katta, S. K. Chowdhury, B. T. Chait, *J. Am. Chem. Soc.* **1990**, *112*, 5348.

[3] G. R. Newkome, C. N. Moorefield, J. M. Keith, G. R. Baker, G. H. Escamilla, *Angew. Chem.* **1994**, *106*, 701; *Angew. Chem. Int. Ed. Engl.* **1994**, *33*, 666.

[4] a) P. J. Stang, D. H. Cao, S. Saito, A. M. Arif, *J. Am. Chem. Soc.* **1995**, *117*, 6273; b) P. J. Stang, D. H. Cao, *ibid.* **1994**, *116*, 4981; c) P. J. Stang, J. A. Whiteford, *Organometallics* **1994**, *13*, 3776.

[5] M. Fujita, Y. J. Kwon, S. Washizu, K. Ogura, *J. Am. Chem. Soc.* **1994**, *116*, 1151; M. Fujita, S. Nagao, M. Iida, K. Ogata, K. Ogura, *ibid.* **1993**, *115*, 1574; M. Fujita, J. Yazaki, K. Ogura, *ibid.* **1990**, *112*, 5645.

[6] a) H. Rauter, E. C. Hillgeris, A. Erxleben, B. Lippert, *J. Am. Chem. Soc.* **1994**, *116*, 616; b) C. M. Drain, J.-M. Lehn, *J. Chem. Soc. Chem. Commun.* **1994**, 2313.

[7] a) P. J. Stang, V. V. Zhdankin, *J. Am. Chem. Soc.* **1993**, *115*, 9808; b) A. I. Boldyrev, V. V. Zhdankin, J. Simons, P. J. Stang, *ibid.* **1992**, *114*, 10569.

[8] a) P. J. Stang, K. Chen, A. M. Arif, *J. Am. Chem. Soc.* **1995**, *117*, 8793; b) P. J. Stang, K. Chen, *ibid.* **1995**, *117*, 1667.

[9] P. M. Stricklen, E. J. Volcko, J. G. Verkade, *J. Am. Chem. Soc.* **1983**, *105*, 2494.

[10] R. V. Slone, D. I. Yoon, R. M. Calhoun, J. T. Hupp, *J. Am. Chem. Soc.* **1995**, *117*, 11813.

[11] Reviews: *Monographs in Supramolecular Chemistry 1 and 2* (Ed.: J. F. Stoddart), Royal Society of Chemistry, Cambridge, **1989** and **1991**; *Host-Guest Complex Chemistry/Macrocycles* (Eds: F. Vögtle, E. Weber), Springer, Berlin, **1985**; *Inclusion Phenomena and Molecular Recognition* (Ed.: J. L. Atwood), Plenum, New York, **1990**; "Molecular Inclusion and Molecular Recognition—Clathrates II": E. Weber, *Top. Curr. Chem.* **1987**, *149*.

[12] K. C. Russell, E. Leize, A. Van Dorsselaer, J.-M. Lehn, *Angew. Chem.* **1995**, *107*, 244; *Angew. Chem. Int. Ed. Engl.* **1995**, *34*, 209.

[13] X. Cheng, Q. Gao, R. D. Smith, E. E. Simanek, M. Mammen, G. M. Whitesides, *J. Org. Chem.* **1996**, *61*, 2204.

[14] a) "Steric Exclusion Liquid Chromatography of Polymers": J. Janca, *Chromatogr. Sci. Ser.* **1984**, *25*, 87); b) "Detection and Data Analysis in Size Exclusion Chromatography": H. G. Barth, *ACS Symp. Ser.* **1987**, *352*, 31–41.

[15] J. H. Small, D. J. McCord, J. Greaves, K. J. Shea, *J. Am. Chem. Soc.* **1995**, *117*, 11588.

[16] E. Leize, A. Van Dorsselaer, R. Krämer, J.-M. Lehn, *J. Chem. Soc. Chem. Commun.* **1993**, 990.

[17] M. Fujita, F. Ibukuro, H. Hagihara, K. Ogura, *Nature* **1994**, *367*, 720.

[18] Y.-T. Li, Y.-L. Hsien, J. D. Henion, T. D. Ocain, G. A. Schiehser, B. Ganem, *J. Am. Chem. Soc.* **1994**, *116*, 7487.

[19] F. Bitsch, C. O. Dietrich-Buchecker, A.-K. Khémiss, J.-P. Sauvage, A. Van Dorsselaer, *J. Am. Chem. Soc.* **1991**, *113*, 4023.

[20] R. Colton, A. D'Agostino, J. C. Traeger, *Mass Spectrom. Rev.* **1995**, *14*, 79.

[21] M. Przybylski, M. O. Glocker, *Angew. Chem.* **1996**, *108*, 879; *Angew. Chem. Int. Ed. Engl.* **1996**, *35*, 806.

[22] *Continuous-Flow Fast Atom Bombardment Mass Spectrometry* (Ed.: R. M. Caprioli), Wiley, West Sussex, **1990**, pp. 1–9.

Selective Photocyclization of Glycine in Dipeptides**

Caroline Wyss, Rohit Batra, Christian Lehmann, Stefan Sauer, and Bernd Giese*

Recently we showed that the substituted glycine **1** undergoes a stereoselective photocyclization and yields proline derivative **3**.[1] Biradical **2** is the intermediate that cyclizes via conformer **4**. In this conformation the steric repulsion between the phenyl group and the attached chiral auxiliary **5** is minimized (Ts = *p*-toluenesulfonyl).

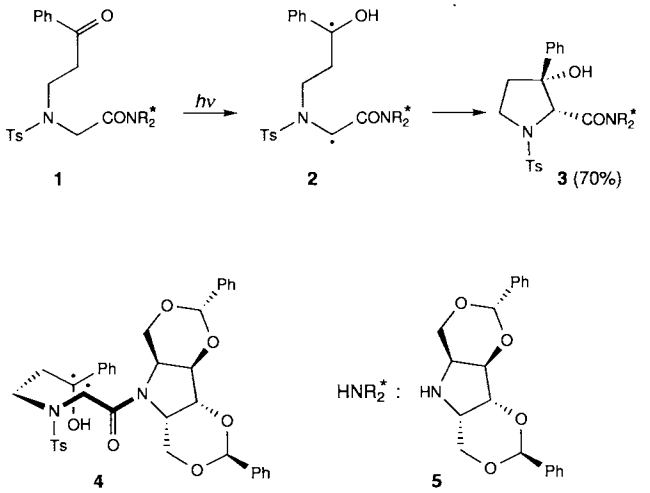

We have now observed that stereoselective photocyclization can also be carried out with dipeptides in which the asymmetric induction is caused by a constituent α-amino acid (substrate control). The dipeptides were synthesized in a Michael addition (**6** + **7** → **8**) and subsequent peptide coupling (**8** → **9**) (Z = benzyloxycarbonyl; CMC = *N*-cyclohexyl-*N'*-(2-morpholinoethyl)carbodiimide-methyl-*p*-toluenesulfonate). Photolysis of dipeptides **9a–d** produces δ-lactams **11a–d** and **12a–d** in about 70% yield.[2] Crystal structure analysis and NMR spectroscopy proved the structures of the δ-lactams.[3]

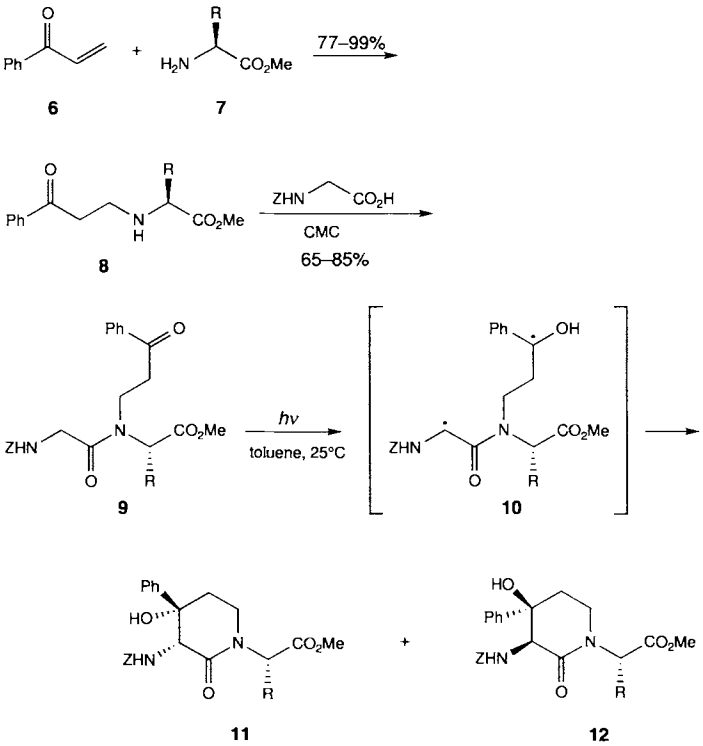

a, R = H	35%	35%
b, R = CH_3	48%	22%
c, R = $CH(CH_3)_2$	59%	8%
d, R = $CH_2C_6H_5$	63%	8%

[*] Prof. B. Giese, Dr. C. Wyss, Dipl.-Chem. R. Batra, Dr. C. Lehmann, Dipl.-Chem. S. Sauer
Institut für Organische Chemie der Universität
St.-Johanns-Ring 19, CH-4056 Basel (Switzerland)
Fax: Int. code +(61)267-1105

[**] This work was supported by grants from the Schweizerische Nationalfonds zur Förderung der wissenschaftlichen Forschung and by the Bundesamt für Bildung und Wissenschaft. We thank Prof. M. Zehnder and M. Neuburger for crystal structure analyses. C. W. thanks the Stipendienfonds der Basler Chemischen Industrie for a grant. We would like to thank Hoffmann-La Roche for providing us with the force field program MOLOC.

The high regioselectivity[4] of the formation of the six-membered ring, which proceeds via the 1,6-diradical **10**, is surprising. Ab initio calculations[5] of the isomeric radicals **13** and **15** offer a possible explanation. These radicals are generated by hydrogen abstraction from the tertiary amide **14**, which is a model of dipeptide **9**. The steric repulsion between the methyl group of the tertiary amide and the ester oxygen causes the ester group to twist out of the plane of the amide group. But hydrogen abstraction adjacent to the ester group (**14** → **15**) fixes the ester group in the plane of the amid function. The resulting steric interaction between the N-methyl group and the ester oxygen makes radical **15** 4.6 kcal mol^{-1} higher in energy than the isomeric radical **13**. The more stable radical **13** corresponds to biradical **10**, which yields the δ-lactams **11** and **12**.

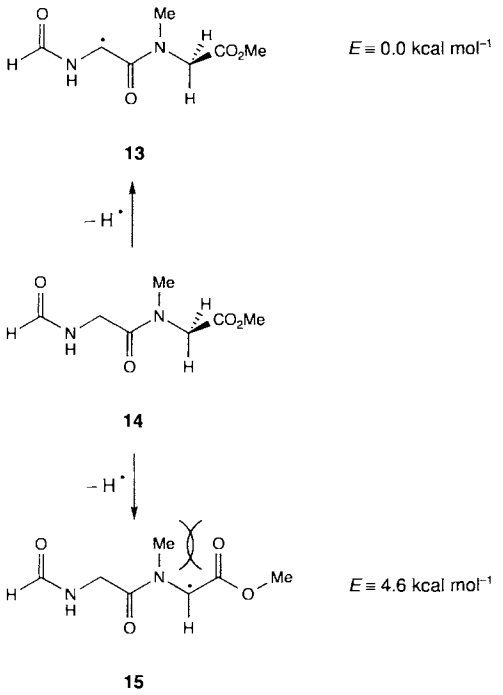

Presumably, the regioselectivity is not only governed by the stability of the radicals but also by the conformations of the substrates. Force field calculations[6] with the substituted dipeptide **16** suggest that in the preferred conformation the distance between the carbonyl function of the phenyl ketone in **9** and the ε-methylene group is considerably shorter (366 pm) than that to the δ-methylene group (517 pm; Fig. 1).

In toluene only *cis* isomers of the δ-lactams are formed. In this configuration hydrogen bonds can exist between the OH and NHZ substituents, and the phenyl group remains in an equatorial position. In contrast, hydrogen bonds between the heterosubstituents in *trans* isomers is only possible when the phenyl group is in an axial position.[7, 8] According to this interpretation,[9] reduced stereoselectivity should be expected for reactions conducted in solvents that break intramolecular hydrogen bonding. Indeed, the *cis*:*trans* stereoselectivity decreased from >20:1 in toluene to 2.7:1 in acetone, 2.4:1 in diethyl ether, and 1.7:1 in methanol (25 °C).

The asymmetric induction caused by the stereogenic centers in valine and phenylalanine is also very surprising. Crystal structures and MOLOC calculations[8] indicate that the amino acids in **11** and **12** adopt the preferred conformations **A** and **B** in which 1,3-allylic strain is minimized. In the main products **11c,d**

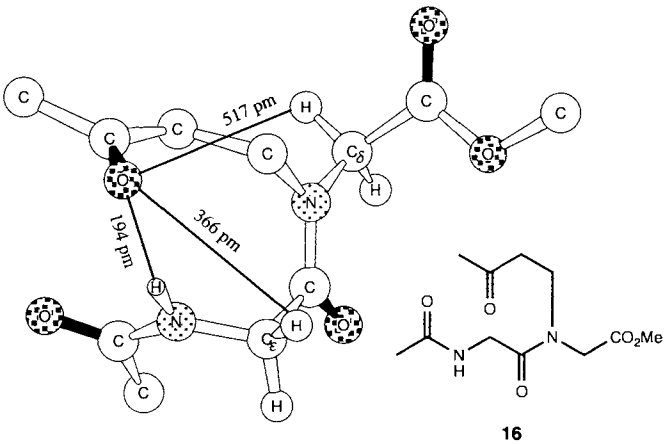

16

Fig. 1. Structure of the dipeptide **16** according to force field calculations.

and **A**, respectively, the amide and ester groups are on opposite sides of the lactam ring and the dipole moments (AM1 calculations) are 1.0 and 1.4 Debye smaller than that of **B**. The negligible asymmetric induction of the cyclization with alanine (**9b** → **11b** + **12b**) is reflected in the dipole moments of **A** and **B**, which are comparable.[9]

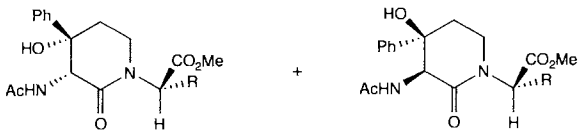

A **B**

R = CH_3	5.4 D	5.5 D
R = $CH(CH_3)_2$	4.0 D	5.4 D
R = $CH_2C_6H_5$	3.8 D	4.8 D

Reaction products **11** and **12** are important peptidomimetics, which are conformationally restricted because of the δ-lactam structure.[10] Until now dipeptides of this type had been synthesized by functionalization and subsequent cyclization of the side chains of amino acids.[11] Our photochemical method opens a short, flexible route. In preliminary experiments γ-lactams such as **18** have been synthesized by photolysis of benzoylmethyl peptide **17**.[12]

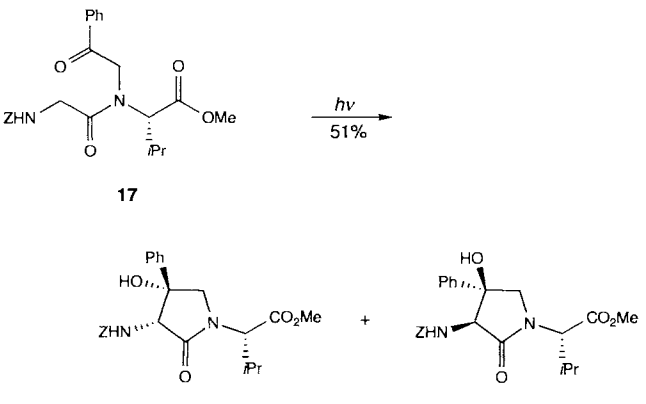

17

18a **18b**

10 : 1

Received: June 3, 1996 [Z9182IE]
German version: *Angew. Chem.* **1996**, *108*, 2660–2662

Keywords: asymmetric syntheses · diradicals · peptide mimetics · photocyclizations

[1] P. Wessig, P. Wettstein, B. Giese, M. Neuburger, M. Zehnder, *Helv. Chim. Acta* **1994**, *77*, 829. For the synthesis of the L-proline derivative, see B. Giese, S. N. Müller, C. Wyss, H. Steiner, *Tetrahedron: Asymmetry* **1996**, *7*, 1261.

[2] A degassed solution (100–200 mL toluene) was cooled to 20–25 °C, and 100–500 mg of **9**, **16**, or **18** was added. The solution was irradiated with a 150 W Hg high-pressure lamp (Heraeus TQ 150) for 1.5–2.5 h. The products were separated by chromatography. All new compounds were characterized by spectroscopy and elemental analysis.

[3] The configurations of **11d** (*p*-nitrobenzenesulfonyl instead of the Z protecting group) and the *trans* isomers of the glycine-substituted δ-lactams **11a** and **12a** (Boc instead of the Z protecting group) were determined by X-ray structure analysis. Crystallographic data (excluding structure factors) for the structures reported in this paper have been deposited with the Cambridge Crystallographic Data Centre as supplementary publication no. CCDC-179-103. Copies of the data can be obtained free of charge on application to The Director, CCDC, 12 Union Road, Cambridge CB21EZ, UK (fax: Int. code +(1223)336-033; e-mail: teched@chemcrys.cam.ac.uk). The ^{13}C NMR signals of C-4 and C-5 in the δ-lactam rings in **11b–d** are $\Delta\delta = 0.3-1.3$ ppm upfield of those of **12b–d**.

[4] The regioselectivity of the dipeptide cyclization is 8:1 for **9a** and greater than 20:1 for **9b–d** (25 °C).

[5] The calculations were carried out at the PMP2/6-31G*//UHF/3-21G* level of theory: Gaussian 94, Revision B.2: M. J. Frisch, G. W. Trucks, H. B. Schlegel, P. M. W. Gill, B. G. Johnson, M. A. Robb, J. R. Cheeseman, T. Keith, G. A. Petersson, J. A. Montgomery, K. Raghavachari, M. A. Al-Laham, V. G. Zakrzewski, J. V. Ortiz, J. B. Foresman, J. Cioslowski, B. B. Stefanov, A. Nanayakkara, M. Challacombe, C. Y. Peng, P. Y. Ayala, W. Chen, M. W. Wong, J. L. Andres, E. S. Replogle, R. Gomperts, R. L. Martin, D. J. Fox, J. S. Binkley, D. J. Defrees, J. Baker, J. P. Stewart, M. Head-Gordon, C. Gonzalez, J. A. Pople, Gaussian Inc., Pittsburgh, PA, **1995**. A similar explanation was used to discuss the preferred hydrogen abstraction from glycine in intermolecular reactions with peptides: C. J. Easton, in *Advances in Detailed Reaction Mechanism, Vol. 1*, (Ed.: J. M. Coxon), Jai, Greenwich **1991**, p. 83.

[6] The calculations were performed with MacroModel 4.5 and with the Amber* force field: D. Q. McDonald, W. C. Still, *Tetrahedron Lett.* **1992**, *33*, 7743.

[7] Calculations with the force field program MOLOC [8] show that the *cis* isomer is favored by at least 1 kcal mol^{-1} over both a) a hydrogen-bonded *trans* isomer with an axial phenyl group at the δ-lactam ring and b) a *trans* isomer with an equatorial phenyl group without hydrogen bonding.

[8] Force field program MOLOC: K. Müller, H. J. Ammann, D. M. Doran, P. R. Gerber, K. Gubernator, G. Schrepfer, *Bull. Soc. Chim. Belg.* **1988**, *97*, 655. Kraftfeld: P. R. Gerber, K. Müller, *J. Comput. Aided Mol. Design* **1995**, *9*, 251. Peptide force field: a) P. R. Gerber, *Biopolymers* **1992**, *32*, 1003; b) in *Computer Simulation of Biomolecular Systems, Vol. 2* (Eds.: W. F. van Gunsteren, P. K. Weiner, A. J. Wilkinson), ESCOM, Leiden, **1993**, p. 213. Conformational analysis: a) P. R. Gerber, K. Gubernator, K. Müller, *Helv. Chim. Acta* **1988**, *71*, 1429; b) P. R. Gerber in *Computer Simulation of Biomolecular Systems* (Eds.: W. F. van Gunsteren, P. K. Weiner), ESCOM, Leiden, **1989**, p. 183. Structure superposition: P. R. Gerber, K. Müller, *Acta Crystallogr. Sect. A* **1987**, *43*, 426.

[9] This interpretation is based on the steric arrangement of the substituents in the product and therefore its importance should not be overestimated. For the triplet–singlet transition the radical centers of the biradical have to come close to each other. Possibly the singlet biradical cyclizes directly to give the product. Therefore the steric and polar effects of the products may already play an important part in the transition state. For further discussion see a) A. G. Griesbeck, H. Mauder, S. Stadtmüller, *Acc. Chem. Res.* **1994**, *27*, 70; b) I. V. Khudyakov, Y. A. Serebrennikov, N. J. Turro, *Chem. Rev.* **1993**, *93*, 537; c) P. J. Wagner, *Acc. Chem. Res.* **1983**, *16*, 461.

[10] Reviews: a) R. M. J. Liskamp, *Recl. Trav. Chim. Pays-Bas* **1994**, *113*, 1; b) G. Hölzemann, *Kontakte (Darmstadt)* **1991**, 3.

[11] a) H. Yanagisawa, S. Ishihara, A. Ando, T. Kanazaki, S. Miyamoto, H. Koike, Y. Iijima, K. Oizumi, Y. Matsushita, T. Hata, *J. Med. Chem.* **1988**, *31*, 1430; b) E. Thorsett, E. E. Harris, S. D. Aster, J. P. Snyder, J. P. Springer, J. Hirshfeld, E. W. Tristram, A. A. Patchett, E. H. Ulm, T. C. Vassil, *ibid.* **1986**, *29*, 251; c) R. M. Freidinger, D. Schwenk Perlow, D. F. Veber, *J. Org. Chem.* **1982**, *47*, 104.

[12] Compound **17** was synthesized from valine benzyl ester and benzoyl methyl bromide and coupled with a Z-protected glycine. The structures of **18a** and **18b** were assigned by NMR spectroscopy. NOE experiments proved the *cis* configuration, and the quaternary C-4 signal of the γ-lactams shows the same relative shifts as that of the δ-lactams.

Models of Oxovanadium(IV)–Protein Interactions: The First Oxovanadium(IV) Complexes with Dipeptides**

Anastasios J. Tasiopoulos, Antonis T. Vlahos, Anastasios D. Keramidas, Themistoklis A. Kabanos,* Yiannis G. Deligiannakis, Catherine P. Raptopoulou, and Aris Terzis

Vanadium is a trace element that produces significant physiological effects; for example, vanadate inhibits ion transport ATP-ases,[1] phosphotyrosine phosphatase[2] etc. Arguably, the most important physiological effect is the stimulation of glucose uptake and glucose metabolism, that is, the insulin-like properties of both vanadate[3] and oxovanadium(IV) species.[4] The efficacy and relative lack of toxicity of oxovanadium(IV) derivatives in animal models of diabetes makes them a potential oral therapy in human diabetes in general, and in those forms of the disease that are resistant to insulin in particular. The mode of action of oxovanadium(IV) species is still not understood. Cornman[5] and co-workers have suggested that a possible mechanism of $V^{IV}O^{2+}$ action is the inhibition of protein tyrosine phosphatases (PTPases) by binding thiolate sulfur to $V^{IV}O^{2+}$. In addition, Saper[6] and co-workers have recently reported an X-ray crystal structure of *Yersinia* PTPase with $V^{V}O_4^{3-}$, where there is a covalent bond between vanadium and the sulfur of the 403-cysteine residue. The elucidation of the mode and the site of $V^{IV}O^{2+}$ action could provide valuable insight into the mechanism of insulin action as well as in the design of more potent oral insulin substitutes.

In order to understand the function of VO^{2+} species in diabetes and in various biological processes in general, it is first necessary to develop its coordination chemistry[7] with biologically relevant ligands such as peptides and in particular sulfhydryl-containing peptides in light of Cornman's[5] observation and Saper's crystallographic characterization of $V^{V}O_4^{3-}$ with *Yersinia* PTPase mentioned above. To date, several complexes of oxovanadium(IV)[8–10] have been prepared and structurally characterized, but only with aromatic amides. Herein we report the synthesis and structural and physicochemical characterization of the first oxovanadium(IV)–dipeptide complex with the sulfhydryl-containing dipeptide *N*-(2-mercaptopropionyl)glycine (H_3mpg), as well as the first synthesis of VO^{2+} with the dipeptides glycylglycine (glygly) and glycylalanine (glyala).

Sequential addition of one equivalent of 1,10-phenanthroline (phen) and of an acetonitrile solution containing one equivalent of H_3mpg and five equivalents of triethylamine to a solution of $[VOCl_2(CH_3CN)_2]$ in acetonitrile yields the complex **1**. The reaction was carried out at −15 °C. At this point two features are worth noting: 1) the ease with which $V^{IV}O^{2+}$ promotes amide

$Et_3NH[VO(mpg)(phen)]$ **1**

[*] Dr. T. A. Kabanos, A. J. Tasiopoulos, A. T. Vlahos, Dr. A. D. Keramidas
Department of Chemistry, Section of Inorganic and Analytical Chemistry
University of Ioannina, 45110 Ioannina (Greece)
Fax: Int. code +(651)44831
Dr. Y. G. Deligiannakis
Section de Bioénergétique, URA CNRS 1290
Département de Biologie
Cellulaire et Moleculaire, CEA Saclay, 91191 Gif-sur-Yvette (France)
Dr. C. P. Raptopoulou, Prof. A. Terzis
NRPCS Demokritos, Institute of Material Science
Attikis (Greece)

[**] This work was supported by the Greek General Secretariat of Research and Technology.

 © VCH Verlagsgesellschaft mbH, D-69451 Weinheim, 1996 0570-0833/96/3521-2531 $ 15.00+.25/0

hydrogen ionization, in marked contrast to almost all other cases with aromatic amides[8-10] where the ionization of hydrogen in the presence of $V^{IV}O^{2+}$ takes place under reflux with the use of strong bases, and 2) the deprotonation of amide nitrogen at room temperature as revealed by solution studies (water) of vanadium(v) with dipeptides.[11, 12] Figure 1 shows a perspective view[13] of the anion of **1**. The vanadium atom in the anion

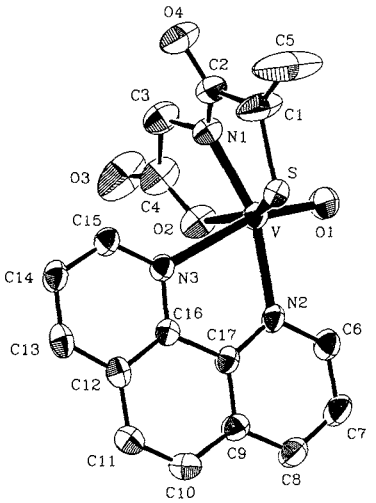

Fig. 1. Structure of the anion of **1** (ORTEP drawing with 30% probability ellipsoids) giving atomic numbering. For clarity, hydrogen atoms are omitted. Selected interatomic distances [Å] and angles [°]: V–O1 1.602(3), V–O2 2.014(4), V–N1 1.997(4), V–N2 2.173(4), V–N3 2.343(4), V–S 2.3820(14); O1-V-N1 108.9(2), O1-V-O2 100.4(2), N1-V-O2 79.9(2), O1-V-N2 90.3(2), N1-V-N2 160.2(2), O2-V-N2 92.15(14), O1-V-N3 162.0(2), N1-V-N3 88.8(2), O2-V-N3 78.73(14), N2-V-N3 71.81(12), O1-V-S 101.8(2), N1-V-S 81.74(12), O2-V-S 154.81(11), N2-V-S 99.46(10), N3-V-S 83.75(9).

of **1** has a severely distorted octahedral geometry. It is bonded to a tridentate mpg^{3-} ligand at the sulfur atom, the deprotonated N_{amide} atom N1, and one of the $O_{carboxylato}$ atoms O2, as well as an oxo group O1 and two phenanthroline nitrogens N2 and N3. The $V-N_{amide}$ bond length [1.997(4) A] is very close (almost indentical) to the reported mean $V-N_{amide}$ value[10] [1.999(12) Å] for various vanadium–aromatic amide structures and is slightly shorter (approximately 0.03 Å) than the $V-N_{amide}$ bond distance of the only other vanadium(v)–peptide[14] complex studied structurally, $Et_4N[VO(O_2)(glygly)]\cdot 1.58\,H_2O$ [$V-N_{amide}$ = 2.032(5) Å]. The V–S distance [2.3820(14) Å] is consistent with values found in other oxovanadium(IV) complexes,[10, 15] but is substantially longer (about 0.14 Å) than the V–S bond length [mean ($V-S_{thiolato}$ = 2.246(3) Å] of the recently reported first oxovanadium(v)–thiolate complex, $[VO(SCH_2CH_2)_3N]$;[16] this is unexpected[17] as the V^VO^{3+} is considered a "hard acid", the sulfur a "soft" base, and the $V^{IV}O^{2+}$ a "softer" acid than V^VO^{3+}.

Complexes **2** and **3** were prepared in a fashion similar to that used for complex **1**, but at room temperature and with methanol

$[V^{IV}O(glygly)(phen)]\cdot 2CH_3OH$ **2**

$[V^{IV}O(glyala)(phen)]\cdot CH_3OH$ **3**

as solvent. The elemental analyses[18] for complexes **2** and **3** are in accord with the formulas given above. The $A_{x,y}$ and $g_{x,y}$ values of continuous wave (cw) EPR data for the complexes **2** and **3** (Table 1) can be compared with those previously reported for various oxovanadium(IV) complexes.[19, 20] According to this correlation the $A_{x,y}$ and $g_{x,y}$ values estimated for **2** and **3** (Table 1) are intermediate between those for oxovanadium(IV)

Table 1. EPR parameters [a] for the complexes **1**–**3**.

Complex	g_z	$g_{x,y}$	A [$cm^{-1} \times 10^{-4}$] $A_{x,y}$	A_z	$A_{z,amide}$
1	1.956	1.987	52.1	151.1	35
2	1.951	1.984	54.8	158.9	36
3	1.951	1.984	54.9	159.0	36

[a] Errors: g values ±0.003; hyperfine coupling constants $\pm 0.7 \times 10^{-4}\,cm^{-1}$.

complexes with equatorial ligands of the types $V^{IV}O(N_2O_2)$ and $VO(N_4)$. This, in combination with the additivity for A_z, is conistent with the binding of $V^{IV}O^{2+}$ to three nitrogens and one oxygen. Strong support for this comes from ^{14}N Electron Spin Echo Envelope Modulation (ESEEM) experiments, which indicate that $V^{IV}O^{2+}$ binds to amine, amide, as well as one phenanthroline nitrogen atoms. From the cw EPR, ESEEM, and IR data it is concluded that the dipeptides glycylglycine and glycylalanine are bonded to $V^{IV}O^{2+}$ center through the amine nitrogen, the deprotonated amide nitrogen, and one of the carboxylato oxygens.

The redox properties of **1** in acetonitrile have been studied by cyclic voltammetric and polarographic techniques. The complex displays a reversible one-electron redox process [Eq. (a); $E_{1/2}$

$$[V^{IV}O(mpg)(phen)]^- + e^- \longrightarrow [V^{III}O(mpg)(phen)]^{2-}\ E_{1/2} = -1.42\,V \quad (a)$$

versus normal hydrogen electrode]. The electronic absorption spectrum of **1** in acetonitrile (λ[nm], $\varepsilon[M^{-1}cm^{-1}]$) consists of five bands and a shoulder: 532 (970), 356 (1550), 288 sh (9000), 269 (22900), 225 (31500), 200 (35000). The intense absorptions in the visible region of the spectrum are assigned as $S \rightarrow V^{IV}$ charge transfer transitions. Continuous wave EPR spectra for the complexes **1**, **2**, and **3** were recorded at 40 K in C_2H_5OH. The calculated values[20] for $A_{z,amide}$ (35×10^{-4}, 36×10^{-4}, and $36 \times 10^{-4}\,cm^{-1}$ for the complexes **1**, **2**, and **3**, respectively) are slightly higher than the average $A_{z,amide}$ value [$34 \times 10^{-4}\,cm^{-1}$] reported by Corman[9] and co-workers for oxovanadium(IV) center with various aromatic amides.

Experimental Procedure

All syntheses were carried out under an inert atmosphere (argon) and with dry and deoxygenated solvents distilled just prior to use.

1: To a stirred acetonitrile (10 mL) solution of $VOCl_2\cdot 2CH_3CN$ (0.300 g, 1.36 mmol) at −15 °C was added in one portion solid 1,10-phenanthroline (0.246 g, 1.36 mmol). The color immediately changed from blue to green and a green solid precipitated. The mixture was stirred for 15 min before a solution (5 mL in acetonitrile) containing H_3mpg (0.222 g, 1.36 mmol) and triethylamine (0.690 g, 6.82 mmol) was added to it. A series of color changes ensued, followed by the formation of a deep purple solution and of a purple precipitate. The solution was stirred for 6 h, and the solid was collected by filtration, washed with diethyl ether, and dried to yield 0.523 g of **1** (75%). Elemental analysis: $C_{23}H_{30}N_4O_4SV$ (509.52), calcd C 54.22, H 5.93, N 11.00, S 6.29, V 10.00; found C 54.15, H 5.90, N 10.85, S 6.15, V 10.01; IR (KBr disk) $\tilde{\nu}$(V=O) = 938 cm^{-1}.

Received: April 23, 1996 [Z9051IE]
German version: *Angew. Chem.* **1996**, *108*, 2676–2678

Keywords: EPR spectroscopy · peptides · solid-state structures · vanadium compounds

[1] B. R. Nechay, *Annu. Rev. Pharmacol. Toxicol.* **1984**, *24*, 501.
[2] G. Swarup, K. V. Speeg, S. Cohen, D. L. Garbers, *J. Biol. Chem.* **1982**, *257*, 7298.
[3] A. Green, *Biochem. J.* **1986**, *238*, 663.
[4] P. Caravan, L. Gelmini, N. Glover, G. G. Herring, H. Li, J. H. McNeil, S. J. Rettig, I. A. Setyawati, E. Shuter, Y. Sun, A. S. Tracey, V. G. Yuen, C. Orvig, *J. Am. Chem. Soc.* **1995**, *117*, 12759, and references therein.

 © VCH Verlagsgesellschaft mbH, D-69451 Weinheim, 1996 0570-0833/96/3521-2532 $ 15.00+.25/0

[5] C. R. Cornman, E. P. Zovinka, M. H. Meixner, *Inorg. Chem.* **1995**, *34*, 5099.
[6] J. M. Denu, D. L. Lohse, J. V. Vijayalakshmi, M. Saper, J. E. Dixon, *Proc. Natl. Acad. Sci. USA* **1996**, 93, 2493.
[7] D. Rehder in *Metal Ions in Biological Systems, Vol. 31* (Eds.: H. Sigel, A. Sigel), Marcel Dekker, New York, **1995**, p. 1.
[8] A. S. Borovik, T. M. Dewey, K. N. Raymond, *Inog. Chem.* **1993**, *32*, 413.
[9] C. R. Cornman, E. P. Zovinka, Y. D. Boyajian, K. M. Geiser-Bush, P. D. Boyle, P. Singh, *Inorg. Chem.* **1995**, *34*, 4213.
[10] A. D. Keramidas, A. B. Papaioannou, A. Vlahos, T. A. Kabanos, G. Bonas, A. Makriyannis, C. P. Raptopoulou, A. Terzis, *Inorg. Chem.* **1996**, *35*, 357, and references therein.
[11] K. Elvingson, M. Fritzsche, D. Rehder, L. Petterson, *Acta Chem. Scand.* **1994**, *48*, 878.
[12] D. C. Crans, H. Holst, A. D. Keramidas, D. Rehder, *Inorg. Chem.* **1995**, *34*, 2524.
[13] Crystal data for $\mathbf{1}\cdot CH_3OH$: $C_{24}H_{34}N_4O_5SV$ $\{Et_3NH[VO(mpg)(phen)]\cdot CH_3OH\}$; $M_r = 541.56$; monoclinic; space group $P2_1/a$; $a = 14.828(2)$, $b = 11.513(1)$, $c = 16.637(2)$ Å, $\beta = 112.735(4)^\circ$, $V = 2619.5(5)$ Å^3, $Z = 4$, $\rho_{calcd} = 1.373$ g cm^{-3}; $\mu = 4.25$ mm^{-1}; max. absorption correction factor 1.60; $2\theta_{max} = 115.24^\circ$; $Cu_{K\alpha}$ radiation; $T = 298$ K; $\theta - 2\theta$ scan; reflections collected/unique/used, 3767/3579 ($R_{int} = 0.0219$)/3577; parameters refined, 352; $R1/wR2$ [2794 reflections with $I > 2\sigma I$], 0.0576/0.1579; $GOF = 1.029$; $[\Delta/\sigma]_{max} = 0.003$; $[\Delta\rho]_{max}/[\Delta\rho]_{min}$ 0.373/ − 0.308 e Å^{-3}; structure solution and refinement with the programs SHELXS-86 and SHELXL-93; H atoms of 1,10-phenanthroline were located by difference maps and refined isotropically, the rest were introduced at calculated positions as riding on bonded atoms; all non-H atoms refined anisotropically (except atoms of the solvent methanol which refined isotropically with occupancy fixed at 10.5. Crystallographic data (excluding structure factors) for the structure reported in this paper have been deposited with the Cambridge Crystallographic Data Centre as supplementary publication no. CCDC-179-98. Copies of the data can be obtained free of charge on application to The Director, CCDC, 12 Union Road, Cambridge CB2 1EZ, UK (fax: int. code +(1223) 336-033; e-mail: teched(@chemcrys.cam.ac.uk).
[14] F. W. B. Einstein, R. J. Batchelor, S. J. Angus-Dunne, A. S. Tracey, *Inorg. Chem.* **1996**, *35*, 1680.
[15] H. Sakurai, Z. Taira, N. Sakai, *Inorg. Chim. Acta* **1988**, *151*, 85; W. Tsagkalidis, D. Rodewald, D. Rehder, V. Vergopulos, *ibid.* **1994**, *219*, 213; J. G. Reynolds, S. C. Sendlinger, A. M. Marray, J. C. Huffman, G. Christou, *Inorg. Chem.* **1995**, *34*, 5745.
[16] K. N. Nanda, E. Sinn, A. W. Addison, *Inorg. Chem.* **1996**, *35*, 1.
[17] R. G. Pearson, *J. Chem. Ed.* **1968**, *45*, 581.
[18] Elemental analysis for $\mathbf{2}\cdot 2CH_3OH$: $C_{18}H_{22}N_4O_6V$ (441.33) calcd C 48.99, H 5.02, N 12.70, V 11.54; found C 48.70, H 4.89, N 12.85, V 11.44; yield 63%; $\tilde{\nu}$(V=O) = 962 cm^{-1}. Elemental analysis for $\mathbf{3}\cdot CH_3OH$: $C_{18}H_{20}N_4O_5V$ (423.32) calcd C 51.07, H 4.76, N 13.25, V 12.03; found C 51.01, H 4.75, N 13.20, V 12.24; yield 70%; $\tilde{\nu}$(V=O) 950 cm^{-1}.
[19] W. H. Holyk, M. Sc. Thesis, University of New Hampshire, **1979**.
[20] The calculated $A_{z,amide}$ values were derived from the relation $A_{z,total} = \sum n_i A_{z,i}/4$, where i denotes the different types of equatorial ligand donor groups ($i = 1-4$), n_i is the number of equatorial ligands of type i and $A_{z,i}$ is the measured coupling constant (from model studies) when all four equatorial ligand donor groups are of type i. See N. D. Chasteen in *Biological Magnetic Resonance, Vol. 3* (Eds.: L. J. Berliner, J. Reuben), Plenum, New York, **1981**, p. 53.

Spontaneous Magnetization in a Sulfur–Nitrogen Radical at 36 K

Arthur J. Banister, Neil Bricklebank, Ian Lavender, Jeremy M. Rawson,* Christopher I. Gregory, Brian K. Tanner, William Clegg, Mark R. J. Elsegood, and Fernando Palacio

There has been considerable interest in the magnetic behavior of organic free radicals,[1, 2] and particularly in the development of materials that exhibit spontaneous magnetic order or ferromagnetism. The number of radicals of this type are few and have been based exclusively on NO radicals[3–5], with magnetic ordering temperatures of a few Kelvin. We now report a new phase of the sulfur–nitrogen dithiadiazolyl radical *p*-NC·C_6F_4·CNSSN$^\bullet$ (**1**), which exhibits weak ferromagnetism at the unprecedentedly high temperature of 36 K. It is the first main-group radical to exhibit spontaneous magnetization above liquid helium temperature.

Radical **1** is a member of a large class of dithiadiazolyl radicals,[6] which are particularly suitable for study as potential "organic metals".[7] Most dithiadiazolyl radicals are diamagnetic, associating to form dimers in the solid state[6] through an out-of-plane, spin-paired interaction between sulfur atoms. This dimerization energy is small and has been estimated at about 35 kJ mol^{-1}.[8] In order to prepare dithiadiazolyl radicals with unusual magnetic properties we must first overcome this dimerization process. This has been achieved in **1** by carefully chosen substituents, in which 1) in-plane cyano–sulfur interactions compete with the out-of-plane dimerization process and 2) fluorine–fluorine repulsions between molecules assist the break-up of the dimeric structure. The synthesis of **1** has been described previously.[9] It can be prepared as either of two polymorphs, the formation of which is dependent upon sublimation conditions. We recently reported[9] the structure and magnetic properties of the α-phase (**1**α) obtained by very rapid sublimation (120 °C, 10^{-2} Torr) of crude **1**. Phase **1**α is paramagnetic at room temperature, and has an effective magnetic moment of 1.60 μ_B, slightly less than that expected for unpaired $S = \frac{1}{2}$ spins. It exhibits Curie–Weiss behavior ($\theta = -25$ K) down to low temperature, at which point long-range magnetic order sets in with a Néel temperature of 8 K.[9] The X-ray crystal structure of this phase consists of chains of monomeric radical units packed in a head-to-tail manner.[9]

The β-phase of **1** (**1**β) forms as long, plastically deformable needles by slow sublimation of **1** (100 °C, 10^{-2} Torr). The structure[10] consists of discrete monomeric dithiadiazolyl radicals. In **1**β the twist-angle between heterocyclic and aryl rings is more prominent than in **1**α: the twist angles about the C–C bond are 58° and 32° in **1**β and **1**α, respectively. The structures

[*] Dr. A. J. Banister, Dr. N. Bricklebank, Dr. I. Lavender, Dr. J. M. Rawson[+]
Department of Chemistry, University of Durham, (UK)
Dr. C. I. Gregory, Prof. B. K. Tanner
Department of Physics, University of Durham (UK)
Prof. W. Clegg, Dr. M. R. J. Elsegood
Department of Chemistry, University of Newcastle (UK)
Prof. F. Palacio
Instituto de Ciencia de Materiales de Aragon
CSIC-Universidad de Zaragoza (Spain)
[+] Present address: Dr. J. M. Rawson
Department of Chemistry, University of Cambridge
Lensfield Road, Cambridge CB2 1EW (UK)
Fax: Int. code +(1223)336362

[**] This work has been supported by the SERC, the Royal Society, and the CICYT (Grant No. MAT92-896 and MAT 94-043). We thank Dr. C. M. Grant (University of Edinburgh) for additional magnetic measurements.

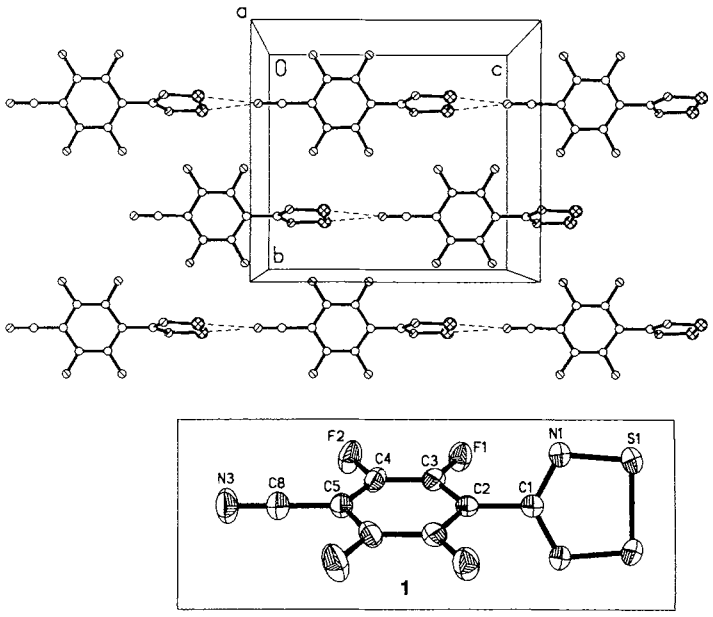

Fig. 1. Molecular packing of **1β**, illustrating the parallel alignment of radical chains. Inset: atom labeling and 50% probability ellipsoids.

of both **1α** and **1β** consist of infinite chains of monomeric radicals (Fig. 1) held together in a head-to-tail arrangement through strong CN···S interactions between neighboring radical units. The intermolecular CN···S distances in **1β** are slightly shorter and more symmetrical than those in **1α**, ($d_{N\cdots S}$: **1β** 2.986 Å, **1α** 3.068 Å and 3.105 Å). The key structural difference between the two phases is that the chains of **1β** are all aligned in the same direction, whereas chains of **1α** are arranged antiparallel to one another, and molecules in neighboring chains are related through an inversion center. This has important magnetic implications, which will be discussed later. There are no short range S···S or S···N interactions between the radical chains of **1β**, although a number of close S···F and CN···F contacts are observed.

Reports of "organic" materials exhibiting ferromagnet-like behavior have often been controversial[11] (especially with weakly ferromagnetic samples) and have been linked to contamination of the sample with small quantities of ferromagnetic impurity.[11] Our own magnetic measurements have been recorded on three different instruments[12] at different institutions, each examining separate samples of material. Crystalline samples (typically 40–150 mg) were prepared by vacuum sublimation, and reproducible sets of data were recorded on multiple samples from the same batch of material and from different batches. A total of 12 independent samples have been examined on these machines. This reliability, coupled with results from atomic absorption spectroscopy, which indicate that Fe, Co, and Ni concentrations are below the level of detection, and the absence of frequency dependence of the alternating current susceptibility vs. T curves in the range from 1 to 1000 Hz makes the likelihood of persistently small quantities of ferromagnetic impurity extremely unlikely.

At room temperature, the effective magnetic moment of 1.55 μ_B is somewhat less than the spin-only value of 1.73 μ_B expected for noninteracting spins and is comparable to that observed for the α-phase (1.60 μ_B). Extrapolation of the inverse susceptibility plot above 120 K produces a Weiss constant ($\theta = -102$ K) indicative of a strongly antiferromagnetically coupled regime and noticeably larger than that observed for the α-phase. As the temperature decreases, the susceptibility rises to a broad maximum centered at 60 K, below which it decreases, indicative of the existence of short-range antiferromagnetic interactions. This behavior can be modeled with a modified Bonner–Fischer equation[13] for a one-dimensional chain, with an intra-chain exchange term, $J = -83$ K (Fig. 2). However, interchain interactions are not negligible.

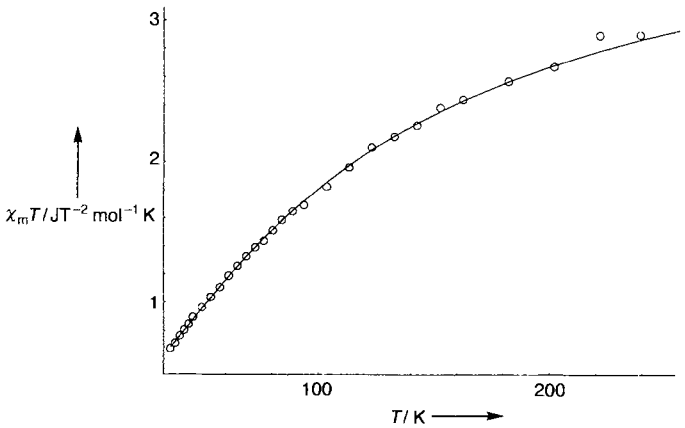

Fig. 2. Plot of $\chi_m T$ against T for **1β** in the region between 40 and 240 K. Solid line: best-fit curve according to Fischer for a classical linear chain.

The variation of magnetic susceptibility as a function of both temperature and applied magnetic field is shown in Figure 3, which highlights the discontinuity in the gradient of magnet-

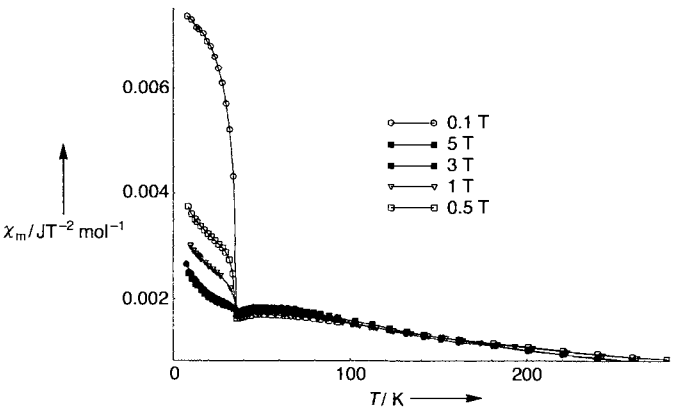

Fig. 3. Variation of molar magnetic susceptibility χ_m of **1β** as a function of temperature and applied magnetic field.

ization with temperature at 36 K. Below this temperature the susceptibility is field-dependent, indicative of the onset of long-range magnetic order. Although the measured differential susceptibility is constant, a residual field-independent magnetization is observed. This residual magnetization is strongly temperature-dependent, falling to zero at 36 K and saturating as T approaches zero (Fig. 4). At 1.8 K, low-field magnetization measurements show clear evidence of hysteresis (Fig. 5). The value of the spontaneous magnetization extrapolated to $T = 0$ K, $M_s(0)$, is $(1.5 \pm 0.1) \times 10^{-3}$ μ_B, significantly lower than that anticipated for a purely ferromagnetic material.

The phase-change from a low-dimensional antiferromagnetically coupled material to a weakly ferromagnetic state can be explained in terms of a spin-canting mechanism in which canting of the antiferromagnetically aligned spins on each sublattice

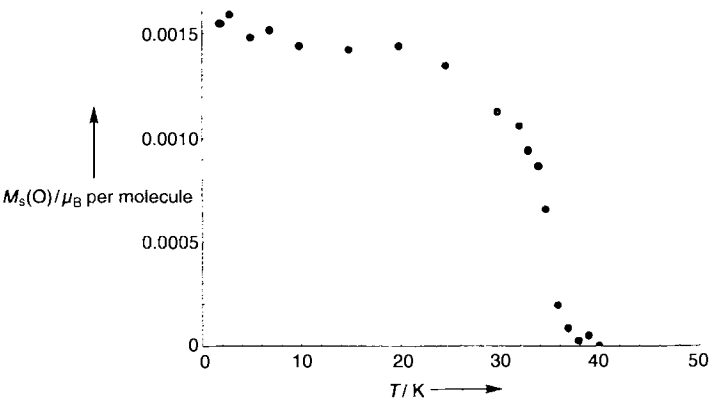

Fig. 4 Spontaneous magnetization M_s of **1β** extrapolated to zero field as a function of temperature.

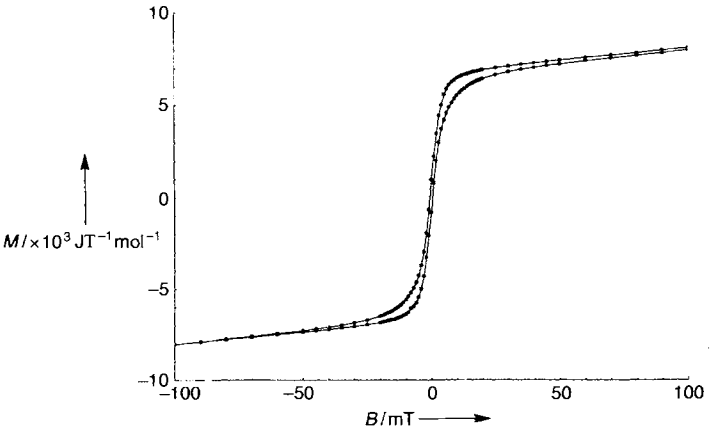

Fig. 5. Hysteresis loop exhibited by **1β** at 1.8 K.

leads to a small spontaneous magnetization, which saturates in a small field. Using the value of the spontaneous magnetization M_s we can estimate a canting angle of about $(0.085 \pm 0.005)°$. Spin-canting is known to be favored in low-dimensional systems[13] and results from antiferromagnetic alignment of spins on two sublattices that are equivalent in number but not exactly antiparallel. The sublattices are canted in the absence of a magnetic field provided that the total symmetry is unchanged, and this leads to a net magnetization. Spin-canting cannot be observed in compounds whose spins are related through an inversion center (for example **1α**, space group $P\bar{1}$) but can be achieved in **1β**. Canting may arise through a Dzyaloshinsky–Moriya interaction,[13] which minimizes the coupling energy when the two spins are perpendicular to one another. This is proportional to $\Delta g/g$, which is found to be 0.005 ± 0.001 from e.p.r. measurements. The isotropic g-tensor for S/N radicals of this type is typically about 2.01, whilst for organic radicals the g-value is normally very close to the free-electron value, and the term $\Delta g/g$ tends to zero.

We have shown that **1β** would appear to constitute the first example of an open-shell molecule that exhibits a spontaneous magnetization above liquid helium temperature and may also possibly be the first example of an "organic" radical to exhibit spin-canting. We are now investigating the nature of the exchange interactions leading to both the strong antiferromagnetic coupling above the ordering temperature and those giving rise to canting of the sublattices.

Received: May 6, 1996 [Z9102IE]
German version: *Angew. Chem.* **1996**, *108*, 2648–2650

Keywords: magnetic properties · nitrogen compounds · radicals · sulfur compounds

[1] D. A. Dougherty, in *Research Frontiers in Magnetochemistry* (Ed.: C. J. O'Connor), World Scientific, Singapore **1993**; P. Day, *Nature* **1993**, *363*, 113.
[2] J. S. Miller, A. J. Epstein, *Chem. Eng. News* **1995**, *73*, Oct. 2, 30; M. Kinoshita, *Jap. J. Appl. Phys.* **1994**, *33*, 5718.
[3] H. Tamura, Y. Nakazawa, D. Shiomi, K. Nozawa, Y. Hosokoshi, M. Ishikawa, M. Takahashi, M. Kinoshita, *Chem. Phys. Lett.* **1991**, *186*, 401.
[4] P.-M. Allemand, K. C. Khemani, A. Koch, F. Wudl, H. Kolczer, S. Donovan, G. Gruner, J. D. Thompson, *Science* **1991**, *253*, 301.
[5] R. Chiarelli, M. A. Novak, A. Rassat, J. L. Tholence, *Nature* **1993**, *363*, 147.
[6] J. M. Rawson, A. J. Banister, I. Lavender, *Adv. Heterocycl. Chem.* **1995**, *62*, 137.
[7] A. W. Cordes, R. C. Haddon, R. T. Oakley in *The Chemistry of Inorganic Ring Systems* (Ed.: R. Steudel) **1995**, Elsevier, Amsterdam; A. W. Cordes, R. C. Haddon, R. T. Oakley, *Adv. Mater.* **1994**, *6*, 798.
[8] S. A. Fairhurst, K. M. Johnson, L. H. Sutcliffe, K. F. Preston, A. J. Banister, Z. V. Hauptman, J. Passmore, *J. Chem. Soc. Dalton Trans.* **1986**, 1465.
[9] A. J. Banister, N. Bricklebank, W. Clegg, M. R. J. Elsegood, C. I. Gregory, I. Lavender, J. M. Rawson, B. K. Tanner, *J. Chem. Soc. Chem. Commun.* **1995**, 679.
[10] **1β**: $C_8F_4N_3S_2$, $M_r = 278.23$, orhorhombic, *Fdd2*, $a = 15.105(3)$, $b = 10.828(2)$, $c = 11.933(3)$ Å, $V = 1951.7(8)$ Å^3, $Z = 8$ (molecule lies on a two-fold rotation axis), $\rho_{calcd} = 1.894$ g cm^{-3}, $\mu = 0.582$ mm^{-1} ($Mo_{K\alpha}$ radiation, $\lambda = 0.71073$ Å), $F(000) = 1096$, $T = 160$ K. Of 1403 reflections measured on a Stoe-Siemens diffractometer and corrected semiempirically for absorption (transmission 0.650–0.789), 865 were unique data ($2\theta < 50°$, $R_{int} = 0.0248$). The structure was solved by direct methods and refined by full-matrix methods on F^2 values for all reflections [14] with anisotropic displacement parameters and statistical weights to give $wR2 = \{\sum[w(F_o^2 - F_c^2)^2]/\sum[w(F_o^2)^2]\}^{\frac{1}{2}} = 0.0784$; conventional $R = 0.0315$ for F values of all reflections, goodness of fit $S = 1.057$ on F^2 for all reflections and 80 refined parameters; largest residual electron density $0.22/-0.16$ e Å^{-3}; the refined enantiopole parameter of $-0.11(10)$ indicates the correct absolute structure [15]. Crystallographic data (excluding structure factors) for the structure reported in this paper have been deposited with the Cambridge Crystallographic Data Centre as supplementary publication no. CCDC-179-93. Copies of the data can be obtained free of charge on application to The Director, CCDC, 12 Union Road, Cambridge CB2 1EZ, UK (fax: Int. code +(1223) 336-033; e-mail: teched@chemcrys.cam.ac.uk).
[11] J. S. Miller, *Adv. Mater.* **1992**, *4*, 435.
[12] Static magnetization measurements were performed on an Oxford Instruments Maglab Faraday Balance (University of Durham): A typical sample of material (50–150 mg) was cooled to 4.2 K in zero magnetic field, and data were recorded at increasing temperature in applied fields of 0.1, 0.5, 1.0, 3.0, and 5.0 T. Further measurements were made on Quantum Design SQUID magnetometers (University of Zaragoza and University of Edinburgh) between 1.8 and 300 K. Alternating current susceptibility measurements were made on a SQUID magnetometer equiped with an a.c. susceptibility attachment (Zaragoza). In another set of experiments isothermal magnetization curves were measured as a function of the magnetic field.
[13] R. L. Carlin, *Magnetochemistry*, Springer, Berlin, **1989**. Note: Although the Bonner–Fischer equation reproduced the experimental data reported here, the magnitude of zJ_{inter}/J_{intra} [of the order of 0.1] indicates that **1β** is not a good one-dimensional system. We have used two independent approaches to calculate this ratio, and a full analysis will be included in a future paper.
[14] G. M. Sheldrick, SHELXTL Manual, Siemens Analytical X-ray Instruments Inc., Madison, WI, USA **1990**; G. M. Sheldrick, SHELXL-93, program for crystal structure refinement, University of Göttingen **1993**.
[15] H. D. Flack, *Acta. Crystallogr. Sect. A.* **1983**, *39*, 876.

Decakis(dichloromethyl)-1,12-dicarba-*closo*-dodecaborane(12): Camouflage of an Icosahedral Carborane by Using Bulky Functional Substituents**

Wei Jiang, Carolyn B. Knobler, and M. Frederick Hawthorne*

Dedicated to Professor Walter Siebert on the occasion of his 60th birthday

The icosahedral carboranes constitute a class of structurally unique molecules with properties common to both organic and polyhedral borane chemistry. Their exceptional thermal and chemical stabilities and their ability to hold substituents in rigid three-dimensional spatial orientations has made their derivatives desirable synthetic targets for modular chemistry.[1] In contrast to the well-developed chemistry of the CH vertices of the carboranes,[2] substitution reactions that occur at BH vertices tend to be less straightforward and of limited utility due to a lack of regiospecific control. Thus, electrophilic substitution reactions at BH vertices typically lead to mixtures of products.[3] Under robust conditions, however, substitution of all available BH vertices may occur to give a single final product.[4] Thus, we have developed a synthetic procedure that leads to a class of 1,12-dicarba-*closo*-dodecaborane derivatives (*para*-carborane derivatives), which are methylated at all boron vertices and which also may have none, one, or both of the two CH vertices similarly substituted.[5] Molecules of this class are structural hybrids composed of an icosahedral carborane substructure covered by an external sheath of hydrocarbon. Consequently, the general reactivity of these molecules should resemble that of aliphatic hydrocarbons, although the steric constraints placed upon the alkyl groups present in these species would be expected to control reactivity in a manner not exhibited by simple alkanes. Functionalization of the full array of alkyl groups on the icosahedral framework will generate an outer sphere of molecular camouflage composed of reactive organic groups of great importance to the further elaboration of carborane chemistry. Depending upon the specific substituent groups introduced, such compounds should be accessible for modular syntheses and serve as precursors for other derivatives, as well. We here report an entry into this chemistry. Beginning with decamethyl-1,12-dicarba-*closo*-dodecaborane(12) (**1**), we have synthesized a derivative in which all the methyl groups at the boron centers are halogenated under radical-inducing conditions to afford decakis(dichloromethyl)-1,12-dicarba-*closo*-dodecaborane(12) (**2**), which has been structurally characterized by X-ray diffraction studies (see Fig. 1).

Chlorination of compound **1** (Scheme 1) in solution in carbon tetrachloride by reacting **1** with chlorine under UV light for eight hours at room temperature afforded **2** in 88% yield. In the ^{1}H NMR spectrum of **2**, only two peaks were observed in a 1:5 integrated ratio. The signal at $\delta = 2.95$ was assigned to the H atoms attached to the C atoms of the icosahedral framework, while the dichloromethyl groups attached to the B atoms gave rise to a resonance at $\delta = 1.55$, which may be compared to the resonances of the methyl groups at the boron atoms in **1** ($\delta = 0.05$[5]). Similarly, in the ^{13}C{^{1}H} NMR spectrum of **2**, only resonances arising from a single type of CH vertex and a single type of dichloromethyl group were observed. A single, relatively broad signal in the ^{11}B NMR spectrum with no BH coupling further confirmed the structure of **2**. Mass spectral analysis was consistent with a decamethyl *para*-carborane in which twenty hydrogen atoms had been replaced with chlorine.

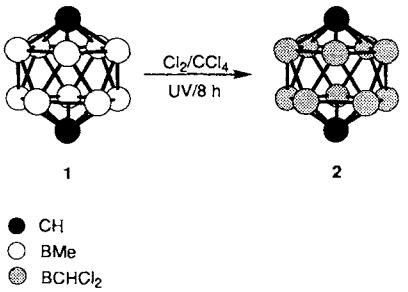

Scheme 1. Chlorination of **1**.

Reaction of **1** with chlorine under these conditions is relatively rapid. Control experiments based upon EI mass spectra indicated that within thirty minutes the chlorination of **1** had reached 80% completion. Species **2** exhibited reduced solubility in typical organic solvents compared to **1**; it was only moderately soluble in carbon tetrachloride.

The radical-induced halogenation of methyl groups attached to aromatic rings is a well-known organic procedure. Chlorination of methylated aromatic compounds can be carried out in the presence of halogenation reagents such as *N*-chlorosuccinimide in a controlled way. However, this synthetic methodology has not previously been explored with B-methyl groups attached to a carborane cage, since halogenation of the BH vertices normally present is a facile competing reaction.[7] In this study of the halogenation reactions of **1**, such reactions are not a problem since all of the hydrogen atoms originally attached to boron atoms in *para*-carborane have been replaced by methyl groups. Interestingly, even in the presence of a large excess of halogenation reagent and under rather robust photochemical conditions, great selectivity is exhibited in the degree of halogenation of the methyl groups. Chlorination of **1** affords only dichlorination at each methyl carbon atom, whereas bromination under a variety of conditions has, as yet, been unsuccessful. Substitution of a chlorine atom, however, activates the methyl carbon atom towards attack by a second chlorine atom and, under normal circumstances, a third reaction of this sort will occur. Clearly, steric constraints which arise on the crowded surface of the carborane restrict this process to the formation of dichloromethyl groups.

The synthesis of a mono(chloromethyl) derivative of **1** was attempted by using a photochemical reaction which employed only 1.3 equivalents of *N*-chlorosuccinimide. Analysis of the product mixture by GC-MS revealed that both a monochlorinated and a single dichlorinated product were formed, together with unconverted starting material. This result suggests that the chloromethyl group first formed is more susceptible to radical attack than are any of the nine remaining methyl groups, since otherwise, several isomeric bis(chloromethyl) derivatives of **1** would have been observed. We speculate that the perfluoro derivative of **1** may be an accessible compound exhibiting enhanced acidity of the carborane CH vertices coupled with steric protection at these sites by surrounding CF_3 groups.

A structural study was carried out on compound **2**, and an ORTEP representation of the structure is shown in Figure 1.[8] In the solid state the dichloromethyl groups attached to the

[*] Prof. M. F. Hawthorne, Dr. W. Jiang, Dr. C. B. Knobler
Department of Chemistry and Biochemistry
University of California, Los Angeles
Los Angeles, CA 90095
Fax: Int. code +(310) 825-5490
e-mail: mfh@chem.ucla.edu

[**] Camouflaged Icosahedral Carboranes: Part 2. This work was supported by the National Science Foundation (Grant CHE 9314037). Part 1: ref. [5].

 © VCH Verlagsgesellschaft mbH, D-69451 Weinheim, 1996 0570-0833/96/3521-2536 $ 15.00+.25/0

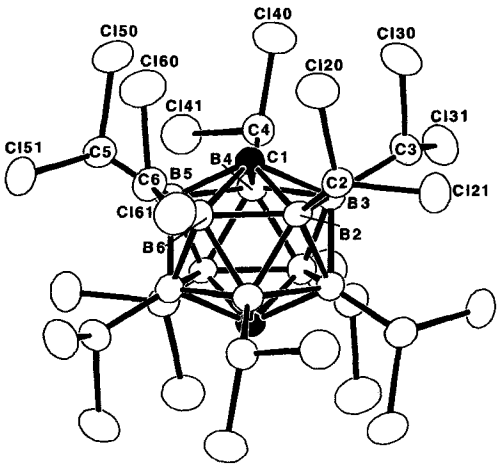

Fig. 1. The structure of **2** (ORTEP representation). Hydrogen atoms are omitted for clarity. The molecule has a crystallographically imposed center of symmetry. Selected bond lengths [Å]: C1–B2 1.735(7), C2–B2 1.613(7), B2–B3 1.824(7), C2–Cl20 1.779(5), C2–Cl21 1.797(5).

boron centers adopt a highly symmetrical arrangement with each group having an "equatorial" chlorine atom and an "axial" chlorine atom. Thus, each of the carborane CH vertices is surrounded by a ring of five axial chlorine atoms, providing very effective steric shielding; the remaining ten chlorine atoms form two coplanar belts around the icosahedron. This arrangement minimizes steric repulsions between the large chlorine atoms.

The C1–C1 distance in **2** is fairly short [3.080(7) Å] compared to most *para*-carborane derivatives,[9] but longer than the corresponding distances found in other decakis-substituted derivatives. We have posited a sterically induced "roll-over" effect on the orbitals responsible for cluster bonding in decakis-substituted *para*-carborane derivatives,[5, 9] leading to a displacement of the substituents on the boron vertices towards the relatively unhindered CH vertices, accompanied by a shortening of the C–C crosscage distance. This effect is not particularly pronounced in **2**, possibly due to the crowding around the CH vertices by the axial chlorine atoms, but there is a significant, if small, displacement of the boron substituents towards the C1–C1 axis. The average angle defined by a carbon vertex, the midpoint of the C1–C1 axis, and the carbon atom of a dichloromethyl group is 61.9(2)°, whereas the value of the average carbon vertex-midpoint-boron vertex angle is 63.7(2)° in **2**.

The successful radical chlorination of **1** leading to **2** represents an important elaboration of this unique icosahedral cluster. The new species reported here should undergo transformations to form an unprecedented class of carborane-supported multifunctionalized compounds. The juxtaposition of organic-type reactivity onto cluster rigidity and the sheer density of functional groups is expected to lead to novel properties including an increase in molecular dimensions. Exploratory reactivity studies with these molecules is currently under active investigation.

Experimental Procedure

Standard Schlenk line techniques were employed for all manipulations. Carbon tetrachloride was freshly distilled from calcium hydride under nitrogen prior to use and degassed by three freeze-pump-thaw cycles. All reactions were carried out under a N_2 atmosphere. Photolysis reactions were carried out using a Hanovia high-pressure mercury vapor lamp.

2: Compound **1** (0.10 g, 0.35 mmol) was dissolved in carbon tetrachloride (25 mL) in a tube-type quartz photoreactor equipped with a gas bubbler connected to a chlorine gas cylinder. The solution was photolyzed at room temperature for 8 h. Solvent was removed in vacuo, and the crude product was extracted with hexane. After filtration, the solid was recrystallized from a solvent mixture of carbon tetrachloride and hexane to afford **2** as a white solid (0.30 g, 88%). 290 °C (decomp) (sealed capillary); ^{1}H NMR ($CDCl_3$): δ = 2.95 (s, 2H, CH), 1.55 (br s, 10H, BCH-Cl_2); $^{13}C\{^1H\}$ NMR ($CDCl_3$ in CCl_4): δ = 73.2 (CH), d = 4.6 (vbr, $BCHCl_2$); ^{11}B NMR (Et_2O): δ = −7.2 (10B, $BCHCl_2$); MS (EI) for $C_{12}B_{10}H_{12}Cl_{20}$ (*m/z*): calcd. 973.3, found 973.2 (M^+).

Received: May 17, 1996 [Z 9128 IE]
German version: *Angew. Chem.* **1996**, *108*, 2653–2655

Keywords: carboranes · chlorinations · radical reactions

[1] a) V. I. Bregadze, *Chem. Rev.* **1992**, *92*, 209–223; b) V. V. Grushin, V. I. Bregadze, V. N. Kalinin, *J. Organomet. Chem. Lib.* **1988**, *20*, 1–68, and references therein.

[2] R. N. Grimes, *Carboranes*, Academic Press, New York, **1970**, pp. 54–180, and references therein.

[3] J. Plešek, Z. Plzák, J. Stuchlík, S. Heřmánek, *Coll. Czech. Chem. Commun.* **1981**, *46*, 1748–1763.

[4] R. R. Srivastava, D. S. Wilbur, Abstracts of Papers, 208th National Meeting of the American Chemical Society, American Chemical Society, Washington D. C., **1994**, p. 208.

[5] W. Jiang, C. B. Knobler, M. D. Mortimer, M. F. Hawthorne, *Angew. Chem.* **1995**, *107*, 1470–1473; *Angew. Chem. Int. Ed. Engl.* **1995**, *34*, 1332–1334.

[6] a) A. D. N. Vaz, G. Schoellmann, *J. Org. Chem.* **1984**, *49*, 1286; b) R. S. Neale, R. G. Schepers, M. R. Walsh, *ibid.* **1964**, *29*, 3390; c) K. Ohkata, Y. Ohyama, K. Akiba, *Heterocycles* **1994**, *37*, 859.

[7] L. I. Zakharkin, V. I. Stanko, A. I. Klimova, *Izv. Akad. Nauk SSSR Ser. Khim.* **1964**, 771.

[8] Crystallographic data for **2**·2(C_7H_8): $C_{26}B_{10}H_{28}Cl_{20}$, M_r = 1157.8, monoclinic, space group $P2_1/c$, a = 10.589(7), b = 10.626(7), c = 19.662(13) Å, β = 92.68(2)°, V = 2210 Å^3, Z = 2, ρ_{calcd} = 1.74 g cm^{-3}, T = 25 °C, μ = 12.7 cm^{-1}. Data were collected on a Huber diffractometer constructed by Prof. C. E. Strouse of this department, by using $Mo_{K\alpha}$ radiation (λ = 0.7107 Å) to a maximum 2θ = 60°, giving 6444 unique reflections, of which 3098 reflections with $I > 3\sigma(I)$ were retained for structure analysis. The data were corrected for Lorentz and polarization effects and for secondary extinction and absorption. The Cl atoms were located by using direct methods (SHELX86). The crystal contains two molecules of toluene per carborane molecule. All non-hydrogen atoms were refined anisotropically. All solvent hydrogen atoms were placed in calculated positions, C–H = 1.0 Å. The benzene ring of the toluene molecule has been treated as a rigid group, angle = 120°, C–C = 1.395 Å. All other H atoms were located and were included but parameters were not refined. The final discrepancy index was R = 0.049, R_w = 0.062. The largest peak on a final difference electron density map was 0.57 e Å^{-3}. Crystallographic data (excluding structure factors) for the structure reported in this paper have been deposited with the Cambridge Crystallographic Data Centre as supplementary publication no. CCDC-179-104. Copies of the data can be obtained free of charge on application to The Director, CCDC, 12 Union Road, Cambridge CB2 1EZ, UK (fax: Int. code +(1223) 336-033; e-mail: teched@chemcrys.cam.ac.uk).

[9] W. Jiang, C. B. Knobler, C. E. Curtis, M. D. Mortimer, M. F. Hawthorne, *Inorg. Chem.* **1995**, *34*, 3491.

Large Sulfur–Nitrogen Heterocycles: Preparation of the Sulfur Imides S_nNH (n = 8, 9, 11) and Structures of S_8NH and S_9NH**

Ralf Steudel,* Klaus Bergemann, Jürgen Buschmann, and Peter Luger

A considerable number of sulfur homocycles S_n has been prepared as pure materials (n = 6–13, 15, 18, 20) and most of these have been characterized by X-ray crystal structure analyses.[2]

[*] Prof. Dr. R. Steudel, Dr. K. Bergemann
Institut für Anorganische und Analytische Chemie
der Technischen Universität, Sekr. C 2
Strasse des 17. Juni 135, D-10623 Berlin (Germany)
Fax: Int. code +(30)31 42 65 19
e-mail: steudel@wap0204.chem.tu-berlin.de
Prof. Dr. P. Luger, Dr. J. Buschmann
Institut für Kristallographie der Freien Universität
Takustrasse 6, D-14195 Berlin (Germany)

[**] Sulfur Compounds, Part 196. This work has been supported by the Deutsche Forschungsgemeinschaft and the Fonds der Chemischen Industrie. Part 195: see ref. [1].

In addition, the structures of several compounds with S_nC frameworks are known (with $n = 2, 5-8, 11$).[3] In contrast, of the conceivable compounds with an S_nN framework, only that with $n = 7$ is known to date. Heptasulfur imide S_7NH like S_8 forms a crown-shaped ring,[4] of which quite a number of organic derivatives S_7NR have been prepared.[5] The fact that neither S_5NH, S_6NH, nor $S_{11}NH$ have been prepared or identified in reaction mixtures was probably attributable to the lack of a suitable synthetic route and to the assumption that S_nN rings with more or less than eight members could not exist in the presence of basic nitrogen atoms, since ammonia and amines catalyze the conversion of S_6, S_7, and S_{12} to S_8. Here we report on the preparation of the novel sulfur imides S_8NH, S_9NH, and $S_{11}NH$ utilizing the recently discovered titanocene complex $[Cp_2Ti(\mu\text{-}S_2)(\mu\text{-}S_5)NH]$ **1** ($Cp = \eta^5\text{-}C_5H_5$), which is accessible from $[Cp_2Ti(CO)_2]$ and S_7NH,[6] and which may gain a similar importance in sulfur–nitrogen chemistry as $[Cp_2TiS_5]$ has for the chemistry of elemental sulfur. The two chlorosulfanes SCl_2 and S_2Cl_2 react with **1** at 20 °C in dichloromethane to give octa- and nonasulfur imide [Eq. (a)].

$$[Cp_2TiS_7NH] + S_nCl_2 \longrightarrow S_{7+n}NH + [Cp_2TiCl_2] \quad (a)$$
$$n = 1, 2$$

For the synthesis of undecasulfur imide $S_{11}NH$, complex **1** was treated with $S_6(CN)_2$, which reacts as $S_4(SCN)_2$ [Eq. (b)].[7]

$$[Cp_2TiS_7NH] + S_4(SCN)_2 \longrightarrow S_{11}NH + [Cp_2Ti(NCS)_2] \quad (b)$$

In the by-product $[Cp_2Ti(NCS)_2]$, the pseudo-halide ligands coordinate the metal through the nitrogen atom, as was shown by comparison of the color of the compound and the IR spectrum with those of an authentic sample.[8] The three new sulfur imides form pale yellow crystalline solids that are well soluble in carbon disulfide but less so in *n*-hexane. At −22 °C in the dark they can be stored for weeks without decomposition; at 25 °C in diffuse daylight, S_8NH decomposes after about one week, S_9NH after about four days, but $S_{11}NH$ only after several weeks. Decomposition products are S_7NH and S_8. Rapid decomposition occurs at the melting points of each of the compounds (S_8NH: 85 °C, S_9NH: 84–90 °C, $S_{11}NH$: 117 °C). The three imides have been characterized by correct elemental analyses, HPLC analyses, as well as IR, Raman, and mass spectra. The vibrational spectra are highly characteristic and quite different from those of S_7NH,[9] allowing the identification of these S_nNH species (Table 1). The range 400–525 cm^{-1} is particularly informative since it contains the SS stretching and the SNH out-of-plane bending (γ) vibration. The different number of S–S bonds and the geometry-dependent coupling between γ(SNH) and the symmetric SS stretching modes results in marked differences in the spectra of the cyclic sulfur imides. The EI mass spectra of all species exhibit a signal for the molecular ion, either with high (S_8NH) or low relative intensity (S_9NH, $S_{11}NH$). In addition, only fragments of types $S_n^{\cdot+}$, $S_nNH^{\cdot+}$, and S_nN^+ were observed.

On chromatography by reversed-phase HPLC[10] the three new compounds behave like members of a homologous series: the logarithms of the capacity factors k' ($k' = t_R - t_o/t_o$) linearly depend on the number n of sulfur atoms in the molecule.[11] This relationship allows the retention time of the still unknown molecule $S_{10}NH$ to be calculated by interpolation. In fact, the reaction solutions obtained according to Equations (a) and (b) showed a peak at the retention time of $S_{10}NH$. This observation indicates that the imides S_nNH form a similar homologous series as the homocycles S_n. Only one HPLC signal was observed for the pure substances S_nNH.

Octasulfur imide S_8NH was obtained as needlelike, pale yellow single crystals from a solution in $CS_2/CHCl_3$. An X-ray structural analysis[12] carried out at −85 °C revealed asymmetric molecules (C_1 symmetry), the conformation of which is similar to that of homocyclic nonasulfur (Fig. 1). The motif of S_8NH (the signs of torsional angles within the ring) is $++--++-+-$, which is identical to the motif of S_9.[7] The values of the torsional angles range from 70.0 to 114.6°. Since complex **1** shows the same conformation of the TiS_7N ring it can be concluded that the structures of these nine-membered

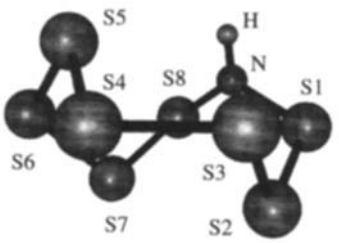

Fig. 1. Structure of S_8NH in the crystal. Selected bond lengths [pm], valence and torsion angles [°]: S1–S2 206.5(3), S2–S3 206.7(2), S3–S4 205.5(2), S4–S5 206.6(2), S5–S6 206.5(2), S6–S7 204.6(2), S7–S8 204.5(2), S8–N 170.4(5), N–S1 172.0(5); N-S1-S2 108.8(2), S1-S2-S3 104.1(1), S2-S3-S4 106.71(8), S3-S4-S5 105.43(9), S4-S5-S6 107.4(1), S5-S6-S7 107.21(7), S6-S7-S8 106.5(1), S7-S8-N 106.2(2), S8-N-S1 121.9(3), N-S1-S2-S3 −72.6(2), S1-S2-S3-S4 110.6(1), S2-S3-S4-S5 −80.1(1), S3-S4-S5-S6 114.61(9), S4-S5-S6-S7 −68.0(1), S5-S6-S7-S8 −68.5(1), S6-S7-S8-N 77.6(2), S7-S8-N-S1 74.5(3), S8-N-S1-S2 −75.1(3).

Table 1. IR and Raman spectra of the crystalline sulfur imides S_nNH ($n = 7-9, 11$) in the range 400–3500 cm^{-1}. Relative intensities based on the strongest line in the full spectra (Raman: 15–3500 cm^{-1}) in parentheses [a].

S_7NH [9]		S_8NH		S_9NH		$S_{11}NH$		Assignment
IR	Ra	IR	Ra	IR	Ra	IR	Ra	according to [9]
3270(m)	3258(m)	3258(m)	3259(7)	3272(m)	3274(2)	3305(w)	3307(1)	υ(NH)
1274(vw)		1302(w)	1302(2)			1270(vw)	1270(1)	δ(SNH)
816(vs)		797(vs)	795(1)	834(vs)	839(1)	797(vs)	792(1)	υ_{as}(SN)
694(w)		729(w)	730(4)	692(w)	700(1)			υ_s(SN)
522(w)		521(vs)	519(1)					
500(m)	496(m)		480(6)	485(m)	483(40)			
	473(s)	468(vw)	470(100)	476(m)	475(8)	467(sh)	470(sh)	υ (SS) partly
456(s)	456(m)	460(w)	462(8)	463(vw)	461(30)	461(m)	461(100)	coupled
			450(54)	449(m)	447(7)		450(40)	with
	433(m)	442(m)	443(10)	426(m)	428(24)	434(m)	435(12)	γ(SNH)
427(s)	424(w)	427(vw)	427(19)			422(m)		
			413(21)					

[a] IR: KBr discs. Sample temperatures: 25 °C, ν stretching, δ bending, γ out-of-plane bending mode.

 © VCH Verlagsgesellschaft mbH, D-69451 Weinheim, 1996 0570-0833/96/3521-2538 $ 15.00+.25/0

rings are not dominated by intermolecular interactions. The S–S and S–N internuclear distances in S_8NH lie in the expected range, the position of the hydrogen atom has been calculated.

Nonasulfur imide S_9NH crystallized from a $CS_2/CHCl_3$ mixture as transparent, pale yellow prismatic single crystals, which were subjected to an X-ray structural analysis at $-150\,^{\circ}C$.[12] The structure consists of ten-membered heterocycles, between which there are only van der Waals intermolecular interactions and no hydrogen bonds. The molecules occupy sites of C_S symmetry. Surprisingly, the conformation of the ten-membered ring is different from that of S_{10} (symmetry D_2)[15] and characterized by the following motif: $+-+-+-+--+$. In this respect S_9NH resembles the S_8 molecule (motif $+-+-+-+-$); it can be derived from the latter by insertion of the SN(H) unit.

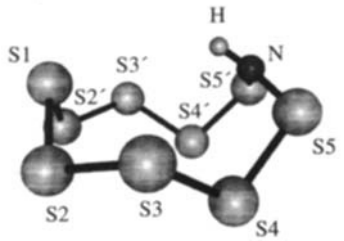

Fig. 2. Structure of S_9NH in the crystal. Selected bond lengths [pm], valence and torsion angles [°]: S1–S2 207.4(3), S2–S3 204.2(3), S3–S4 206.6(3), S4–S5 205.2(3), S5–N 167.1(5), N–H 85(13); S2′-S1-S2 103.2(2), S1-S2-S3 109.8(1), S2-S3-S4 107.3(1), S3-S4-S5 103.2(1), S4-S5-N 109.3(3), S5-N-S5′ 124.0(6), S5-N-H 116(2), S2′-S1-S2-S3 120.9(1), S1-S2-S3-S4 −86.1(1), S2-S3-S4-S5 119.1(1), S3-S4-S5-N −81.1(3), S4-S5-N-S5′ −85.0(6).

As a result the torsion angles τ at the bonds S1–S2, S1′–S2′, S3–S4, and S3′–S4′ increase from 99° in S_8 to $120\pm1°$ in S_9NH, while the remaining torsion angles decrease to values of 81–86°. Nevertheless, the S–S and S–N bond lengths are normal and comparable to those of S_7NH.[4] As in other sulfur imides[4, 5] and their derivatives[5, 6] the coordination of the nitrogen atom in S_9NH is almost planar: the sum of the angles S-N-S, S-N-H, and S′-N-H is 356.8°. Consequently the nitrogen atom is not very basic.[16]

The similarity of the spectra shows that $S_{11}NH$ must also be a cyclic molecule (Table 1). As is the case with S_{12}, $S_{11}NH$ is thermally more stable than S_8NH and S_9NH. This allows the conclusion that it should be possible to prepare even more sulfur-rich imides in analogy to S_{13}, S_{15}, S_{18}, and S_{20}. The chemistry of cyclic sulfur–nitrogen compounds has so far been dominated by small rings. The syntheses according to Equations (a) and (b)—with a variety of reagents—open the access to a new area of SN chemistry.

Experimental Procedure

S_8NH: SCl_2 (0.44 mmol, 2.8 mL of a 0.157 M solution in CH_2Cl_2) was added dropwise to a solution of **1** (198 mg, 0.47 mmol) in dichloromethane (200 mL) and stirred at 20 °C. After 30 min the solvent was removed in a vacuum, the residue was dissolved in a little carbon disulfide, and the solution stored for 2 h at −22 °C. The precipitate of $[Cp_2TiCl_2]$ was filtered off. The filtrate was stirred with a little silica gel for a short time to remove residual $[Cp_2TiCl_2]$ and after filtration the volume was reduced by 50%. *n*-Hexane was added until a permanent turbidity appeared and the mixture was cooled to −22 °C to afford S_8NH, which after recrystallization from a $CS_2/CHCl_3$ (1:1) mixture was collected in 33% yield (41 mg) based on SCl_2.

S_9NH: In analogy to the preparation of S_8NH by using **1** (350 mg, 0.84 mmol), S_2Cl_2 (0.06 mL, 0.75 mmol), and CH_2Cl_2 (370 mL). Yield: 123 mg (54% based on S_2Cl_2).

$S_{11}NH$: In analogy to the preparation of S_8NH by using **1** (372 mg, 0.9 mmol), $S_6(CN)_2$ (197 mg, 0.8 mmol), and CH_2Cl_2 (390 mL). Yield: 90.5 mg (31% based on $S_6(CN)_2$). For further details see ref. [17].

Received: May 31, 1996
Revised version: July 11, 1996 [Z 9179 IE]
German version: *Angew. Chem.* **1996**, *108*, 2641–2643

Keywords: nitrogen compounds · structure elucidation · sulfur compounds

[1] R. Steudel, *Chem. Unserer Zeit*, **1996**, *30*, 226.
[2] R. Steudel, *Top. Curr. Chem.* **1982**, *102*, 149; R. Laitinen, P. Pekonen, R. J. Suontamo, *Coord. Chem. Rev.* **1994**, *130*, 1.
[3] CS_{11} ring: R. Steudel, V. Münchow, J. Pickardt, *Z. Anorg. Allg. Chem.* **1996**, *622*, 1594; CS_8 ring: N. Takeda, N. Tokitoh, T. Imakubo, M. Goto, R. Okazaki, *Bull. Soc. Chem. Japan* **1995**, *68*, 2757; CS_7 ring: W. Lutz, T. Pilling, G. Rihs, H. R. Wasepe, T. Winkler, *Tetrahedron Lett.* **1990**, *31*, 5457; CS_6 and CS_5 ring: F. Fehér, J. Lex, *Z. Anorg. Allg. Chem.* **1976**, *423*, 103; F. Fehér, K.-H. Linke, *Z. Naturforsch. B* **1969**, *24*, 1485; CS_2 ring: A. Ishii, T. Akasaka, T. Maruta, J. Nakayama, M. Hoshino, M. Shiro, *Angew. Chem.* **1994**, *106*, 829; *Angew. Chem. Int. Ed. Engl.* **1994**, *33*, 777.
[4] H.-J. Hecht, R. Reinhardt, R. Steudel, H. Bradaczek, *Z. Anorg. Allg. Chem.* **1976**, *426*, 43.
[5] H. G. Heal, *The Inorganic Heterocyclic Chemistry of Sulfur, Nitrogen and Phosphorus*, Academic Press, London **1980**; T. Chivers in *The Chemistry of Inorganic Homo- and Heterocycles, Vol. 2*, (Eds.: I. Haiduc, D. B. Sowerby), Academic Press, **1987**, p. 793.
[6] K. Bergemann, M. Kustos, P. Krüger, R. Steudel, *Angew. Chem.* **1995**, *107*, 1481; *Angew. Chem. Int. Ed. Engl.* **1995**, *34*, 1330.
[7] R. Steudel, K. Bergemann, J. Buschmann, P. Luger, *Inorg. Chem.* **1996**, *35*, 2184.
[8] I. Jibril, S. T. Abu-Orabi, S. A. Klaib, L. Zsolnai, G. Huttner, *J. Organomet. Chem.* **1994**, *467*, 189.
[9] R. Steudel, *J. Phys. Chem.* **1977**, *81*, 343.
[10] On the HPLC analysis of sulfur–nitrogen heterocycles see R. Steudel, D. Rosenbauer, *J. Chromatogr.* **1981**, *216*, 399.
[11] Stationary phase: octadecylsilane (C_{18}), eluent: methanol, flow-rate 2 mL min^{-1}, detection: absorbance at 254 nm, dead time t_o determined by injection of methanol/water mixture (80/20 v/v).
[12] Crystal structure data for S_8NH: $M_r = 271.50$ orthorhombic, space group $Pca2_1$ (no. 29), $Z = 4$, $a = 1273.4(4)$, $b = 806.4(3)$, $c = 841.4(2)$ pm, $V = 864.0(5) \times 10^6$ pm^3, $\rho_{calcd} = 2.087$ $g\,cm^{-3}$ (−85 °C), $Mo_{K\alpha}$, $\lambda = 71.068$ pm, $\mu = 19.80$ cm^{-1}. With a Siemens four-circle diffractometer with N_2 gas cooling device 2461 reflections (1345 independent; 1158 with $F_o > 4\sigma(F_o)$) were collected at $T = -85(2)$ °C in the range $2\theta = 5.1$–$60.1°$ (ω-2θ scan). The structure was solved by direct methods (SIR92 [13]) and refined to $R = 0.0452$ for 1158 observed reflections (SHELXL93 [14]). Crystal structure data for S_9NH: $M_r = 303.56$, orthorhombic, space group *Pbnm* (no. 62), $Z = 4$, $a = 518.7(1)$, $b = 1325.0(1)$, $c = 1428.7(2)$ pm, $V = 981.9(8) \times 10^6$ pm^3, $\rho_{calcd} = 2.053$ $g\,cm^{-3}$ (−150 °C), $Mo_{K\alpha}$, $\lambda = 71.068$ pm, $\mu = 19.59$ cm^{-1}. With a Siemens four-circle diffractometer with N_2 gas cooling device 1978 reflections (629 independent with $F_o > 4\sigma(F_o)$) were collected at $T = -150(2)$ °C in the range $2\theta = 5.7$–$55.1°$ (ω-2θ scan). The structure was solved by direct methods (SIR92 [13]) and refined to $R = 0.0571$ for 629 observed reflections (SHELXL93 [14]). Further details of the crystal structure investigations may be obtained from the Fachinformationszentrum Karlsruhe, D-76344 Eggenstein-Leopoldshafen, on quoting the depository numbers CSD-405497 (S_8NH) and CSD-405274 (S_9NH).
[13] A. Altomare, G. Cascarano, C. Giacovazzo, A. Guagliardi, M. C. Burla, G. Polidori, M. Camalli, *J. Appl. Crystallogr.* **1994**, *27*, 435.
[14] G. M. Sheldrick, SHELXL93, program for refinement of crystal structures, Universität Göttingen, Germany **1993**.
[15] Motif of S_{10}: $+-++-+-++-$; see R. Steudel, J. Steidel, R. Reinhardt, *Z. Naturforsch. B* **1983**, *38*, 1548.
[16] The cyclic sulfur imides of type S_nNH may also be treated as derivatives of the cyclosulfanes S_{n+1} (sulfur homocycles). According to the substitution nomenclature S_9NH, for instance, may then be termed azacyclodecasulfane.
[17] For further details see: K. Bergemann, Dissertation, Technische Universität Berlin **1996**.

 © VCH Verlagsgesellschaft mbH, D-69451 Weinheim, 1996 0570-0833/96/3521-2539 $ 15.00+.25/0

No Longer a Laboratory Curiosity

Metallomesogens. Synthesis, Properties, and Applications. Edited by *J. L. Serrano*. VCH Verlagsgesellschaft, Weinheim/VCH Publishers, New York, 1996. 498 pp., hardcover DM 298.00.—ISBN 3-527-29296-9

Over a hundred years have passed since the discovery of the first liquid crystals by F. Reinitzer in 1888, yet the chemistry of mesogens has lost none of its attraction and fascination. In particular it was the close collaboration between synthetic chemists and materials scientists that led to a renaissance in liquid crystals, with the result that much of modern everyday life is scarcely imaginable without these materials. Metallomesogens are a relatively new offshoot of conventional liquid crystals. The chemistry of metal-containing liquid crystals, at first just a laboratory curiosity attracting little attention, has developed almost explosively within the last ten years. There now exists an enormous wealth of research results in this field, and its collection together in book form was long overdue. Although there have been several important review articles in the last few years, in many cases these have only treated selected aspects. It can already be said at the outset that the book edited by J. L. Serrano fills this gap admirably. His name is a guarantee of the soundness of the work, since he and the other authors have for many years been actively engaged in the synthesis of paramagnetic and ferroelectric metallomesogens as one of their main interests.

The book contains four sections giving clear and thorough treatments of the following aspects: the various characteristic structural features of metallomesogens (Part A, Chapters 2-5), synthetic aspects (Part B, Chapters 6 and 7), physical methods of characterization (Part C, Chapters 8 and 9), and physical properties and applications (Part D, Chapters 10 and 11). It all adds up to an excellent collection of articles covering all modern aspects of this field.

In Chapter 1 the editor, J. L. Serrano, gives a short introduction to thermotropic and lyotropic mesophases, with special reference to metallomesogens, thus easing the way for the novice approaching the subject for the first time. The brief account of the history describes the contribution of F. Reinitzer, but should also have mentioned O. Lehmann and G. Friedel. Chapter 2 (T. Sierra), on lyotropic metallomesogens, is the first comprehensive overview of this topic, which has hitherto been rather neglected in the literature. Chapters 3 and 4 (J. L. Serrano, T. Sierra, J. Barberá) are concerned with the well-known classes of the calamitic and discotic low molecular mass metallomesogens, which are treated very thoroughly and comprehensively, with over 300 literature references. These chapters include clear tables which list details for each example discussed, including the general formula types and the melting behavior of the complexes for different metal ions and chain lengths. Each subsection is followed by a short summary recapitulating the characteristic features of that class of substances. Chapter 5 (L. Oriol) contains a detailed account of the new and fascinating topic of metallomesogenic polymers, emphasizing the great potential of such macromolecules for materials science.

In Chapters 6 and 7 (Part B) M. Marcos and L. Oriol deal with the synthetic aspects of the chemistry of metallomesogens. Their separate treatment of this topic is thorough and competent, but it would perhaps have been better to combine this part with Chapters 3-5, thereby avoiding some repetition of textual content and literature citations. Also, the inclusion of a few carefully chosen laboratory procedures for synthesizing some typical ligands and metallomesogens of different classes would have better justified the title "Design and Synthesis ".

Part C is devoted to physical methods for determining the structures of mesogenic phases, with treatments of X-ray diffraction in Chapter 8 (J. Barberá) and EPR spectroscopy in Chapter 9 (P. J. Alonso). However, there is not a word here about the "classical" methods such as optical polarization microscopy and thermal analysis (DSC). Although these are of a routine nature, they should at least have been mentioned, especially bearing in mind the needs of readers entering this field for the first time.

The last two chapters (Chs. 10 and 11, Part D) are concerned with the materials science properties of metallomesogens and with applications. The lucid survey by M. B. Ros covers a wide variety of properties and conveys a good impression of the many-faceted nature of this class of substances. On the other hand, P. J. Alonso adopts a rather too specialized approach in Chapter 11, concentrating only on the magnetic properties.

As stated at the beginning of this review, J. L. Serrano and his team of authors have produced a very important contribution to the literature on liquid crystals. The book provides an up-to-date treatment of the subject, very clearly presented (apart from a few minor cosmetic shortcomings, such as inconsistencies in the style of the figures, and some structural formulas that are upside-down), and with comprehensive coverage of the primary literature. However, the potential readership is relatively small, not least because of the high price. The book can be recommended unreservedly for chemists already active in this field and for those seeking a good introduction into it.

Wolfgang Weigand
Institut für Anorganische Chemie
der Universität München
Munich (Germany)

Fundamentals of Chemical Kinetics. By *S. R. Logan*. Longman, Harlow, 1996. 264 pp., paperback £ 19.99.—ISBN 0-582-25185-0

S. R. Logan has set out to provide students of chemistry and related disciplines with a textbook which, at an affordable

This section contains book reviews and a list of new books received by the editor. Book reviews are written by invitation from the editor. Suggestions for books to be reviewed and for book reviewers are welcome. Publishers should send brochures or (better) books to the editorial office: Redaktion Angewandte Chemie, Postfach 101161, D-69451 Weinheim, Germany. The editor reserves the right of selecting which books will be reviewed. Uninvited books not chosen for review will not be returned.

price, covers all the essential aspects of the study of chemical reactions as they progress towards an equilibrium state. The author's aim is is to teach the fundamental concepts rather than to treat the subject in minute detail. This has resulted in a book that will be useful not only for physical chemists but also for organic and inorganic chemists, whose work nowadays includes an increasing amount of kinetic studies. Logan's book covers reactions in the gas phase, in solutions, and at solid catalyst surfaces. Solid state kinetics has rightly been excluded, as it is outside the scope of a book of this kind. Each of the twelve chapters, except for the last one, ends with a set of exercise problems that are intended to give deeper insights into what has been learned. The data for the examples are mostly taken from the chemical literature, thereby linking the discussion to real situations.

In Chapter 1 the author explains the empirical framework of chemical kinetics. After introducing the concept of the reaction rate he formulates a general rate equation and uses this to explain the idea of the order of a reaction. The rate equations for different reaction orders are integrated, and methods for determining the reaction order are described. Lastly, the temperature dependence of rate constants is discussed on the basis of the Arrhenius equation. Regrettably, this chapter contains several annoying errors. Thus, a minus sign is missing from Equation (1.11), the definition of the reaction rate. The treatment of signs is again rather haphazard in the integration of the rate equation for a first-order reaction [Equations (1.14) and (1.15)]. In the integration of the rate equation for a second-order reaction (first-order in each of the two educts) the author merely refers the student to "simple algebra" instead of explicitly setting out the breakdown into partial fractions. Here he fails to completely live up to his assurance on the back cover of the book, which states that the mathematics involved will be carefully explained for students with limited capabilities in that direction. The omission of units in the calculation of the activation energy from the gradient of an Arrhenius plot (p. 19) is also questionable from a teaching standpoint.

Chapter 2 is concerned with practical aspects of planning and carrying out kinetic experiments. After discussing certain minimal requirements (such as temperature control, rapid mixing of the reactants, and a clearly defined reaction path) the author describes different methods for monitoring the progress of reactions in solutions: the "clock method", polarimetry, spectrophotometry, electrical conductivity measurements, and dilatometry. For gas phase reactions the conventional method of measuring the total pressure is described, and also the possibility of using mass spectrometry is discussed. A description of modern stopped-flow techniques is followed by warnings about the risks of errors being introduced when determining rate constants, arising for example from incorrect weighting in a linear regression analysis.

Chapter 3 deals with a number of simple types of reaction mechanisms, such as sequential reactions, the formation of intermediate complexes, parallel reactions, and opposing reactions, and discusses the kinetic behavior resulting from these. The important distinction between the molecularity and the order of a reaction is clearly explained. The author also introduces the stationarity principle that is often used in analyzing the subsequent stages. Chapter 4 discusses theoretical treatments of bimolecular reactions (collision theory, transition state theory, the theory of diffusion-controlled reactions in solutions).

Chapter 5 is concerned with the interpretation of measurements on bimolecular reactions in solutions, including the Marcus theory for electron transfer reactions. After treating unimolecular gas phase reactions in Chapter 6, the author devotes Chapter 7 to chain reactions. Chapters 9 and 10 then deal with the important subject of catalysis, including such interesting aspects as oscillatory reactions and enzyme kinetics. The last three chapters are devoted respectively to studies of fast reactions using modern relaxation techniques, the reaction kinetics of photochemically excited molecules, and studies of elementary reactions in crossed molecular beams.

The book is completed by two short appendices, brief answers to the exercise problems, a keyword index, and an index of reactions mentioned in the text. Despite the minor shortcomings in Chapter 1 as already mentioned, this is a valuable book in which the author has succeeded in conveying an impression of a very broad range of aspects of chemical kinetics in the gas and solution phases and on solid catalysts. It provides the reader with a comprehensive overview encompassing both the history of chemical kinetics and the latest developments in the field.

In view of the reasonable price, *Fundamentals of Chemical Kinetics* can be recommended unreservedly for readers seeking a broad introductory insight into the subject.

Dirk Wilmer
Institut für Physikalische Chemie
der Universität Münster (Germany)

Stereochemistry of Radical Reactions. By *D. P. Curran, N. A. Porter and B. Giese*. VCH Verlagsgesellschaft, Weinheim, 1995. 280 pp., hardcover DM 148.00.—ISBN 3-527-29372-8

Until a decade ago, a researcher contemplating how to construct a carbon-carbon bond stereoselectively would not have considered radical reactions as a method of choice. This is partly because radical reactions with high stereoselectivity were an anomaly rather than the norm. In the past ten years, however, one can scarcely open a new issue of a journal without seeing some work on stereoselective radical reactions. It is timely that three leading experts in organic free radical chemistry, Professors Curran, Porter, and Giese, have now written an outstanding monograph on stereoselective radical reactions.

The monograph is divided into six chapters. In Chapter 1 the reader is introduced to the basic concepts required for successful execution of a radical reaction and to the general principles of stereoselectivity in ionic as well as radical reactions. A brief discussion of the different methods for generating radicals is followed by a liberal citation of key reviews and leading articles at the end of the chapter. The next four chapters discuss different aspects of stereoselective radical reactions. The reactions are classified according to substrate or chiral auxiliary control of stereoselectivity. Chapter 2, a major portion of the monograph, focuses on stereocontrol in radical cyclizations. The reactions in this chapter are further classified on the basis of ring size. Although this is not intended to be an exhaustive treatment, the important factors responsible for stereoselectivity in cyclizations are described in a very authoritative and concise manner. A short section on stereoselectivity of cyclizations under group transfer conditions is also included. The third chapter deals with aspects of substrate controlled diastereoselectivity in cyclic systems. The focus of this chapter is again on control of stereochemistry in radical reactions of five- and six-membered rings, systems which are generally more selective. Chapter 4 discusses issues of stereocontrol in radical reactions of acyclic systems. The models used for explaining stereoselectivity in acyclic systems undergoing ionic reactions are extended to radical processes and are nicely illustrated. Chapter 5 takes the reader through chiral auxiliary mediated diastereoselective reactions. This portion of the monograph, reflecting the strengths of the three authors, is well written and

 © VCH Verlagsgesellschaft mbH, D-69451 Weinheim, 1996 0570-0833/96/3521-2542 $ 15.00+.25/0

gives a detailed account of the present state of knowledge of diastereoselective radical reactions. The monograph ends with a short chapter on stereoselectivity occurring during radical combinations, radical rearrangements, and formation of alkenes from radical intermediates. The information in this monograph gives guidelines which should ensure that a scientist embarking on a stereoselective radical reaction has enough control over its design and will be able to predict its outcome with reasonable confidence.

Overall, this is a very well written, easy to read, and timely work on the stereochemistry of radical reactions. It is well referenced and the citations are current up to the beginning of 1995. The index at the end is more than adequate. This is a "must buy" book for libraries and practitioners of organic free radical chemistry, or for scientists who wish to venture into the fascinating field of stereoselective organic free radical reactions. The monograph will be an excellent "recommended text" for a graduate course on stereochemistry or free radical chemistry.

Mukund P. Sibi
North Dakota State University
Fargo, ND (USA)

Free Radicals in Organic Chemistry. By *J. Fossy, D. Lefort* and *J. Sorba*. Wiley, New York, 1995. 307 pp., paperback $ 39.80.—ISBN 0-471-95496-9

Development of new synthetic organic methodology using free radical intermediates continues to advance at a rapid rate. Although there are excellent monographs and review articles on organic free radical chemistry, there are no good textbooks. With such an active and important branch of organic chemistry, if one is required to teach an upper level undergraduate or beginning graduate level class on organic free radical chemistry, one is at a loss to find an appropriate textbook. The book by Fossy, Lefort, and Sorba fills this void to a certain extent. They have written a good book on organic free radical chemistry.

The book is divided into four parts. Part 1 contains eight chapters. This part of the book introduces the reader to the fundamental aspects of free radical chemistry. A brief chapter on the detection and characterization of free radicals by electron paramagnetic resonance (EPR) and chemically induced dynamic nuclear polarization (CIDNP) starts the text. The next six chapters discuss the issues of radical structure, stability, reactivity, mechanisms, and kinetics. Carbon as well as heteroatom radicals are covered as part of the discussion. Although each chapter is quite short, enough details including tables are included. Aspects of radical reactions are the main thrust of the second part of the book. Chapter 9 describes different methods for generating radicals. The important low-temperature radical initiation method using triethylborane-oxygen is absent from this discussion. Different aspects of radical-radical and radical-molecule reactions are detailed in the next three chapters. Radical substitution, addition, and fragmentation reactions are analyzed, including aspects of their regio- and stereochemical outcome. Radical cyclizations and rearrangements are discussed in some detail in Chapter 13. Aromatic homolytic substitutions and reactivity of radical cations and anions are discussed in Chapters 14 and 15 respectively. A short chapter on free radicals in biochemistry is included as Chapter 16. This section of the text ends with a discussion of different methods used to determine whether or not a particular reaction proceeds through a radical intermediate. Part 3 of the book treats synthetic aspects of organic free radical chemistry. These include: functionalization of non-activated carbon-hydrogen bonds leading to halogenation and hydroxylation, functional group interconversion, addition to multiple bonds, cyclization, aromatic substitution, and coupling reactions. This section ends with a brief discussion on the industrial application of free radical methods. Part 4 of the book provides references and a set of tables containing important thermochemical and kinetic data for a variety of reactions.

This book is an ambitious project. The authors attempt to cover all aspects of organic free radical chemistry, but sometimes these are treated only in a cursory manner. The tables at the end are very useful and the index is adequate. The book could have been strengthened by a better and more up-to-date reference section. Overall, this is a valuable addition to any library and to the bookshelves of practitioners of free radical chemistry. With supplementary information from the teacher, the book could serve as a text for upper level undergraduate or beginning graduate level courses on organic free radical chemistry.

Mukund P. Sibi
North Dakota State University
Fargo, ND (USA)

 © *VCH Verlagsgesellschaft mbH, D-69451 Weinheim, 1996* *0570-0833/96/3521-2543 $ 15.00+.25/0*

The enantioselective protonation of prochiral *Z*- and *E*-enolates (top right and bottom left, respectively) by protonation with a chiral proton donor…

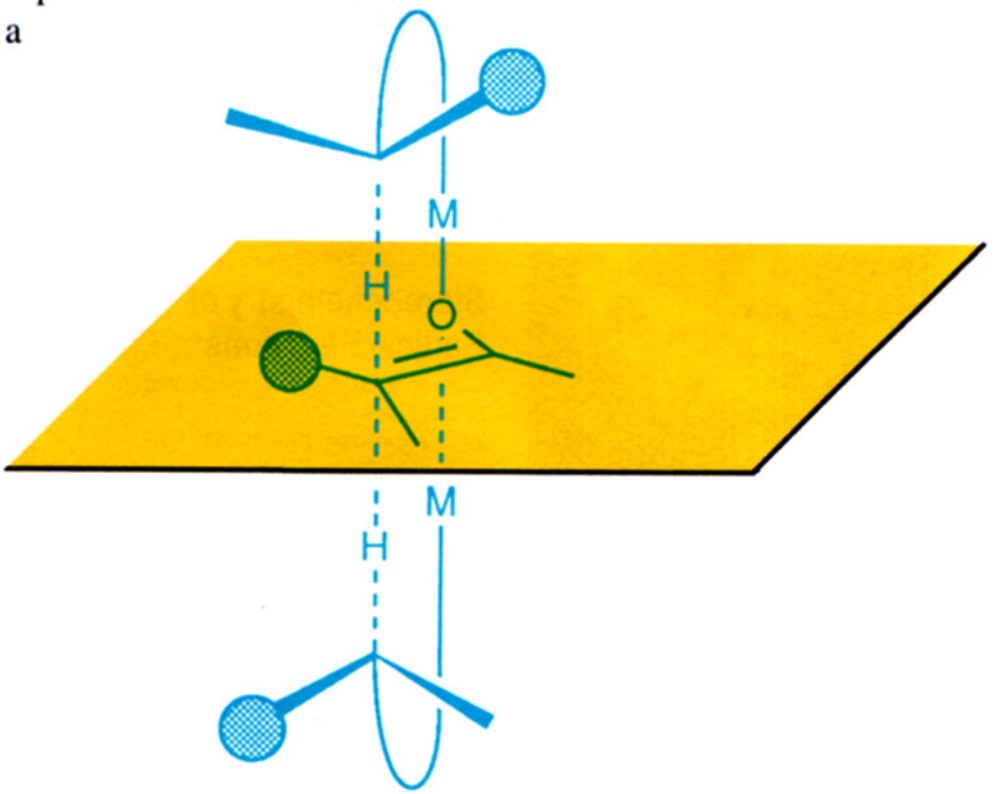

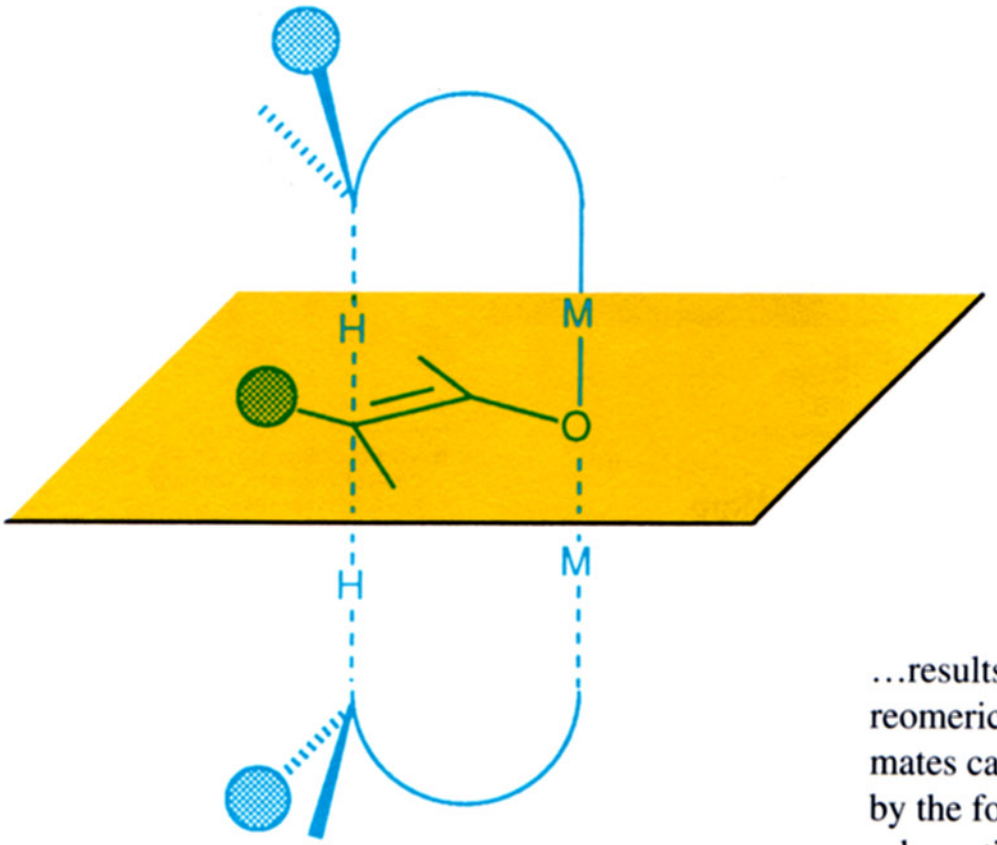

…results in a total of four diastereomeric transition states. Racemates can thus be "deracemized" by the formation of enolates. This schematic representation indicates that *Z*- and *E*-enolates react with different enantiofacial selectivities.

Enantioselective Protonation of Enolates and Enols

Charles Fehr*

In memory of Wolfgang Oppolzer

Enantioselective protonation, until recently a largely overlooked reaction, has, in the last five years, developed into a field of intense research activity. The progress achieved parallels or complements that obtained in the understanding of enolate structures and reactivities. The conceptual simplicity and attractiveness of enantioselective protonation results from the fact that after reaction, the chiral proton donor is regenerated in its original protonated form by an extractive workup. Enantioselective protonation has been applied to the synthesis of amino acids, antiinflammatory agents (2-arylpropanoic acids), and fragrance compounds such as (*S*)-α-damascone, for which its industrial feasibility has been demonstrated.

Keywords: asymmetric syntheses · enols · lithium compounds · protonations

1. Introduction

Conceptually, enantioselective protonation is extremely simple. Because a prochiral enolate has two enantiotopic faces, the transfer of a proton from a chiral, nonracemic proton source to the enolate will be kinetically favored either from the top or bottom face, thus affording the carbonyl compound enriched with either the (*R*) or (*S*) enantiomer (Scheme 1).[1] The importance of enolates as intermediates in synthesis, the recent advances achieved in the regio- and stereoselective generation of enolates with the desired counterion, and the increased knowledge of their structure and reactivity[2] make their protonation a very attractive method for obtaining enantiomerically pure carbonyl compounds. Indeed, the enolate, obtained either by deprotonation of the parent carbonyl compound or directly from a synthetic operation such as nucleophilic addition to a ketene[3] or an enone,[4] is "quenched" with the chiral proton donor to afford the enantiomerically enriched carbonyl compound. On addition of water, the chiral reagent is reprotonated and recovered by simple extraction!

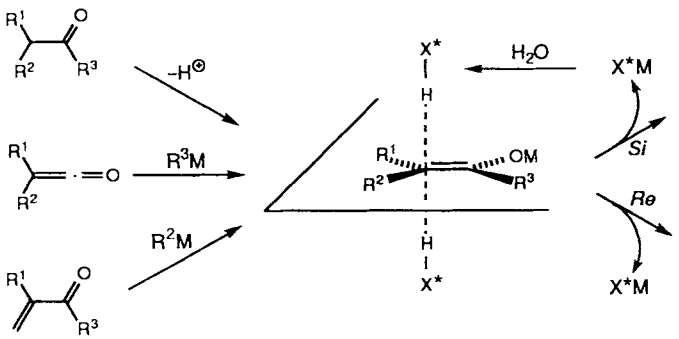

Scheme 1. Enolate generation and enantioselective protonation.

Enantioselective protonation can also be performed on enols. In this case (M = H; Scheme 1) the chiral reagent (X*H or $X^{*\ominus}$) is not consumed. Therefore, in principle, these tautomerizations require only catalytic amounts of the chiral reagent. Still another possible variant is the protonation of a complex formed between the enolate and the chiral ligand with an achiral proton source.[5] These three reaction types are closely interrelated, and because of possible reversible proton exchange reactions between the various reaction partners, it is often difficult to unambiguously differentiate between them.

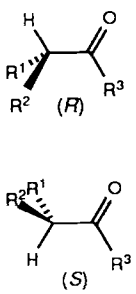

2. What Has Refrained Chemists from Exploring Enantioselective Protonations?

In spite of the potential synthetic power of enantioselective protonation, this subject has not attracted great interest until recently.[6] This is probably due to the following reasons:

- Proton exchange reactions between electronegative atoms are considered to be among the most rapid, often diffusion-controlled reactions,[7] and thus it is difficult to discriminate efficiently between two diastereomeric transition states. There-

[*] Dr. C. Fehr
Firmenich SA, Corporate Research Division
P. O. Box 239, CH-1211 Geneva 8 (Switzerland)
Fax: Int. code +(22)780-3436
e-mail: charles.fehr@firmenich.ch

fore, the chiral reagent should be only weakly acidic. In addition, O-protonation of enolates leads reversibly to enols, which may be transformed into ketones without enantiofacial discrimination, or may act as an undesired proton source for C-protonation. The risk can be minimized by using an excess of a chiral proton source and by applying reaction conditions that allow complete C-protonation (for example appropriate temperature range).

- Enantioselective protonations are kinetically controlled reactions. Under thermodynamic control racemic products are obtained. To prevent concomitant or subsequent racemization in the polar protic medium the choice of a chiral proton donor of appropriate acidity is essential and short reaction times enhance the chances of success. Evidently, this does not apply to bulky systems, where racemization is difficult. Quenching the reaction mixture with Me_3SiCl prior to hydrolysis is often recommended for following the progress of the reaction (see Sections 3 and 4).
- *E*- and *Z*-enolates exhibit different enantiofacial selectivities, because the two diastereomeric transition states for the protonation of the *E*-enolate are different from those for the *Z*-enolate. This is schematically represented with a chelate model (Scheme 2), in which both the enolate O and C(2) atoms are involved in the transition state. Accordingly, the four possible transition state structures are diastereomeric, as evidenced by the relative positioning of the substitutents. It is thus important to minimize the amount of that enolate isomer which leads to lower, possibly reversed asymmetric induction.
- The preferred trajectory for the C-protonation of enolates is a vertical approach of the "proton" to the plane defined by the enolate π-system, with a preferential colinear arrangement between donor atom, proton, and acceptor atom (Scheme 1). More precise information concerning transition state structures is, however, still lacking. As will be discussed in Section 3, solvation, aggregation, and complexation phenomena also often dramatically influence the outcome of the reaction. Efficient chiral proton donors or chiral ligands generally have electron-rich groups capable of undergoing chelation (see Section 3.2).
- The first synthetically useful example of enolate protonation that afforded a maximum enantiomeric excess of 70 % was reported in 1978 by L. Duhamel and J.-C. Plaquevent.[8] Prior to this study only scattered publications had appeared, describing for the most part only very weak inductions.[9] This early period was reviewed in detail by Duhamel et al. in 1984.[6a]

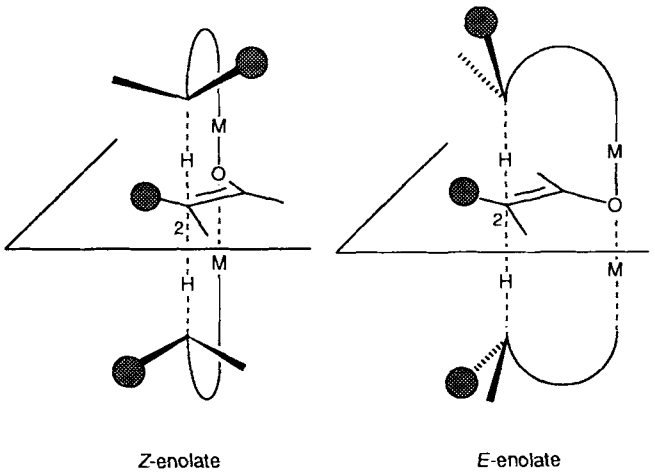

Scheme 2. Two diastereomeric enolates: four diastereomeric transition states. The gray circles represent the largest substituents.

In recent years, intense research activity has concentrated on the general scope of enantioselective protonation. Due to the vast structural diversity of chiral reagents investigated, it seems judicious to subdivide the following section, after a presentation of Duhamel's work, into substrate structural classes.

3. Enantioselective Protonation of Enolates

3.1. The Pioneering Work of the Duhamel Group

The first in-depth study on the "deracemization" of amino acid derivatives by enantioselective protonation of the corresponding anions was carried out by L. Duhamel and J.-C. Plaquevent,[8] who proposed the commercially available (*R*,*R*)-di-*O*,*O*′-pivaloyltartaric acid ((−)-**2a**) to be the chiral reagent of choice. Thus, deprotonation of racemic methyl *N*-benzylidenephenylglycinate ((±)-**1a**) with lithium diisopropylamide (LDA) and protonation of the resulting enolate with excess (−)-**2a** gives (*S*)-**1a** with 50 % *ee* (Scheme 3; Table 1, entry 1).

The size of the acyl group of the chiral acid is very critical, as replacement of the *tert*-butyl groups by methyl or triethylmethyl groups almost completely destroys the enantiofacial selectivity of the chiral reagent (Table 1, entries 2 and 3). A wide range of

Charles Fehr, born in Zürich, Switzerland, in 1946, studied chemistry at the ETH in Zürich. He completed his doctoral thesis in 1974 under the direction of Dr. Theodor Petrzilka for work conducted in the group of Prof. Albert Eschenmoser. From 1974 to 1977 he conducted postdoctoral research at the University of Geneva with Prof. Wolfgang Oppolzer and at the Johns Hopkins University, Baltimore, with Prof. Gary H. Posner. In 1978 he joined the Corporate Research Division of Firmenich SA and in 1990 he received the Ruzicka Prize.

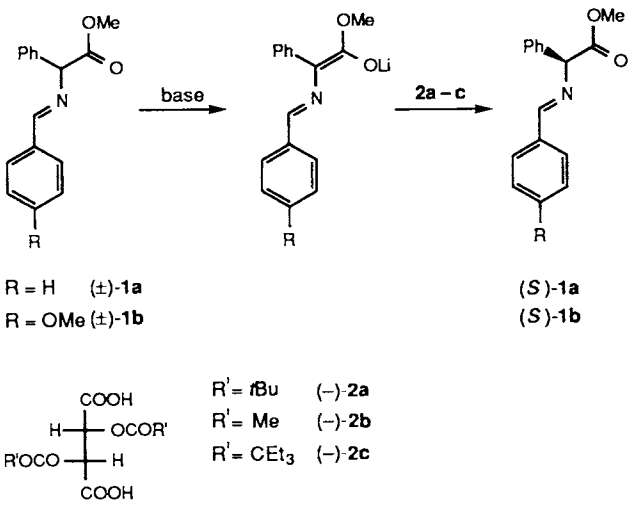

Scheme 3. Deracemization of amino acid derivatives.

Table 1. Deracemization of amino acid derivatives.

Entry	Substrate	Base	T[°C]	H-Donor	Product	*ee* [%]	Yield [%]
1	(±)-**1a**	LDA	−70	(−)-**2a**	(*S*)-**1a**	50	85
2	(±)-**1a**	LDA	−70	(−)-**2b**	(*S*)-**1a**	3	
3	(±)-**1a**	LDA	−70	(−)-**2c**	(*S*)-**1a**	5	
4	(±)-**1b**	LDA	−70	(−)-**2a**	(*S*)-**1b**	57	70
5	(±)-**1b**	LDA	−105	(−)-**2a**	(*S*)-**1b**	70	95
6	(±)-**1a**	$LiNEt_2$	−70	(−)-**2a**	(*S*)-**1a**	28	
7	(±)-**1a**	LTMP [a]	−70	(−)-**2a**	(*S*)-**1a**	22	
8	(±)-**1a**	[b]	−70	(−)-**2a**	(*S*)-**1a**	70	
9	(±)-**1a**	[b]	−70	(+)-**2a**	(*R*)-**1a**	5	
10	(±)-**1a**	[b]	−70	(±)-**2a**	(*S*)-**1a**	39	
11	(±)-**1a**	[b]	−70	*meso*-**2a**	(*S*)-**1a**	24	

[a] LTMP = Lithium 2,2,6,6-tetramethylpiperidide. [b] (*R*)-LiN(Et)CH(Me)Ph.

aldimino esters was investigated and shown to afford selectivities of 24–70% *ee*.[8, 10, 11] Aldimino groups possessing electron-donating groups have a beneficial effect, whilst lowering the temperature increases both the yield and the enantioselectivity (entries 4 and 5).

The French group has also demonstrated the crucial role that the secondary amine, which is liberated after metalation, plays in the proton transfer. Whereas the combination LDA/(−)-**2a** affords (*S*)-**1** with 50% *ee* (entry 1), a much weaker induction results when the deprotonation is performed with $LiNEt_2$ or with lithium 2,2,6,6-tetramethylpiperidide (LTMP) (entries 6 and 7). It is therefore not surprising that the combination of (−)-**2a** with a chiral amine leads to a substantially improved selectivity of 70% *ee* (entry 8). In line with this example of double stereodifferentiation, the mismatched pair (entry 9) produces almost racemic product, and protonation with either racemic (±)-**2a** (entry 10) or achiral *meso*-**2a** (entry 11) also gives significant induction.[10, 12] The same results are obtained by deprotonation of the ester with lithium bis(trimethylsilyl)-amide (LHMDS) and subsequent addition of the appropriate amine.[13] Apparently, the disilazane does not form a strong complex with the enolate and therefore does not actively participate in the protonation.[14, 15] It is not yet established whether the importance of amine ligands rests exclusively on the formation of an enolate–amine complex[16] or whether an ammonium tartrate formed in situ acts as a proton transfer agent.

The deracemization of a variety of α-amino acid derivatives with (−)-**2a** as the chiral proton donor predictably afforded the (*S*)-esters as the major enantiomers (34–70% *ee*).[11] A model based on minimal steric interactions between (−)-**2a** and the enolate–amine complex was proposed.[10] However, the deconjugation–protonation sequence shown in Scheme 4 led to the

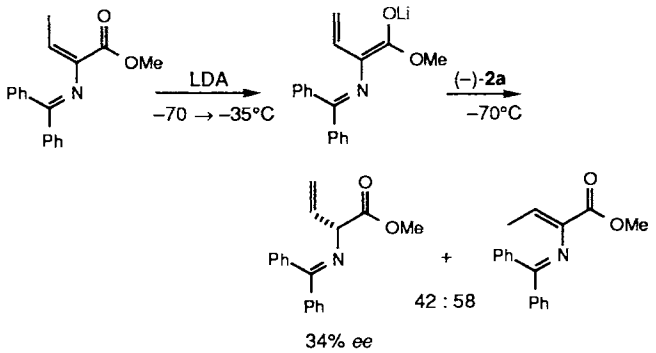

Scheme 4. Formation of a vinylglycine ester by deconjugation and enantioselective protonation.

(*R*)-vinylglycine ester (34% *ee*).[11, 17] This reversal of the sense of induction can be rationalized by the altered configuration of the ester enolate.

Finally, (*R*,*R*)-di-*O*,*O*'-pivaloyltartaric acid ((−)-**2a**) was also successfully used for the preparation of (*S*)-benzoin with 80% *ee* (see Section 5).[18]

3.2. Protonation of Open-Chain Ketone Enolates

In our laboratory, enantioselective protonation of open-chain enolates is under development and has been applied to the synthesis of fragrance compounds of high enantiomeric purity[19] (for example **3**-MgCl → (*S*)-α-damascone ((*S*)-**4**), Scheme 5).[20, 21] In contrast to the amino- and hydroxyl-substituted enolates discussed above, ketone enolate **3**-MgCl has no internal chelation sites. Thus, both its formation and protonation were anticipated to be more difficult to achieve in a stereocontrolled manner.

In the search for an efficient chiral protonating agent we were guided by the following criteria.[6b, 20] Ideally, the chiral reagent should be only weakly acidic to allow better discrimination between transition states. It should also contain electron-rich groups capable of coordinating or chelating, which may enhance conformational rigidity in the transition state. Optimally, the transferred proton should be located near the stereogenic center (within the "chiral environment"). Finally, to be synthetically useful, the protonating agent should be readily accessible in both enantiomeric forms and be easily recuperable. These criteria are satisfied with the ephedrine derivatives (+)-**6** and (−)-**6**, and (+)-**7**-H and (−)-**7**-H (Scheme 5). In imidazolidinone **6** an NH bond is confined in a rigid cyclic system, and **7**-H (and the corresponding alkoxide) can attain conformational rigidity through chelation. It should be added that (+)-**6** and (−)-**6** are commercially available (Merck), and that both enantiomers of **7**-H are readily accessible by treatment of enantiomerically pure ephedrine with acetone under conditions of catalytic hydrogenation.[22]

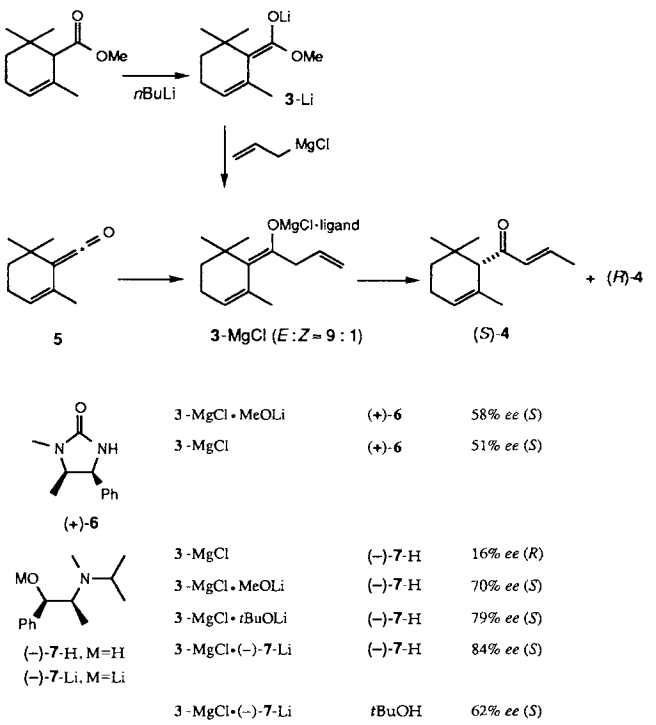

Scheme 5. Generation of a ketone enolate by C–C bond formation and enantioselective protonation of a Mg-enolate with or without a Li-alkoxide ligand. Proton sources: (+)-**6**, (−)-7-H, and *t*BuOH.

For the synthesis of (*S*)-α-damascone ((*S*)-**4**),[20, 21] the required enolate cannot be generated by deprotonation of the parent ketone because of preferential deprotonation in the side chain. However, the enolate **3**-MgCl is directly produced as a 9:1 mixture of *E*- and *Z*-isomers by C–C bond formation through a Grignard reaction with either the ester enolate[23, 24] or the ketene **5** (Scheme 5).[25] It should be emphasized that this reaction of the ester enolate also produces one equivalent of lithium alkoxide, which can profoundly alter the subsequent protonation step. Addition to ketenes generally takes place from the least hindered side, affording with good selectivity the enolate in which the oxygen atom is oriented towards the larger group.[3] When the required ketenes are stable and readily accessible, they are the best precursors to alkoxide-free enolates, which can be complexed subsequently.

The protonations performed on enolates **3**-MgCl and **3**-MgCl·MeOLi revealed that modification of the ligand sphere of the enolate only slightly influenced proton delivery from urea (+)-**6**, affording consistent enantiofacial discriminations ranging between 50 and 60% *ee*. A transition state model in which the enolate complexes the carbonyl group of (+)-**6** was proposed to rationalize the observed absolute configuration.[6b] In sharp contrast, protonation with (−)-*N*-isopropylephedrine ((−)-7-H) proved to be highly sensitive to the exact nature of the enolate: whereas alkoxide-free enolate afforded (*R*)-α-damascone as the major enantiomer (16% *ee*), the LiOMe-complexed Mg-enolate (prepared from either the methyl ester or the ketene) gave (*S*)-**4** with 70% *ee*.[26] LiO*t*Bu proved to be a superior ligand (79% *ee*), and the best results were obtained with the chiral Li-alkoxide (−)-**7**-Li (84% *ee*).[27] If the formation of a chiral complex between Mg-enolate and Li-alkoxide is a prerequisite for high enantioselectivity,[28] then protonation of a chiral complex with an achiral proton source should also lead to asymmetric induction. Indeed, protonation of the same chiral enolate complex with *t*BuOH affords (*S*)-**4** with 62% *ee*. In view of the complexity of the described reaction (see Section 8) and the lack of structural information about the complexes involved we consider it premature to propose a transition state model.

During further investigations it was found that protonation of the ligand-free, *E*-enriched enolate **3**-Li ($E:Z \gg 98:2$)[29] with (−)-7-H afforded (*S*)-**4** with excellent enantioselectivity (95% *ee*; Scheme 6).[30] Likewise, protonation of *E*-rich enolate **9** ($E:Z = 97:3$), obtained from the reaction of *n*BuLi with ketene **5**, produced ketone (*S*)-**10** with 96% *ee*. For the first time, a marked difference in the the protonation rates of *E*- and *Z*-enolates was noticed and exploited to further improve the enantioselectivity. Thus, when enolate **9** ($E:Z = 97:3$) was treated with 0.95 equivalents of (−)-7-H and the unreacted enolate was quenched as an enol silyl ether ($E:Z \approx 1:1$), ketone (*S*)-**10** was generated with an enantiomeric ratio of >99:1.[31] We have recently succeeded in generating the *Z*-enolate (*Z*)-**9**, which displays the same enantiofacial preference on protonation with (−)-7-H but with a dramatically decreased enantiofacial discrimination of 40% *ee* (Scheme 7).[32] This result convincingly illustrates the statement made in Section 2 (Scheme 2): For transition state considerations, the *global* enolate structure

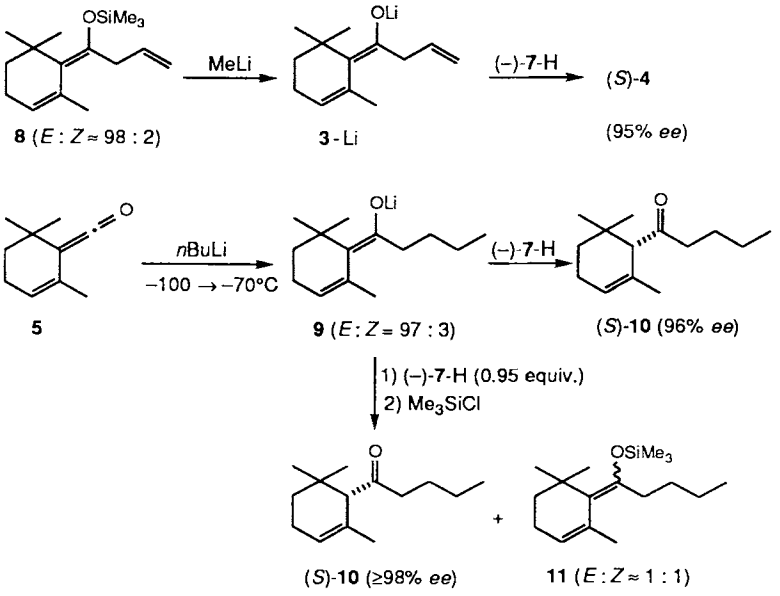

Scheme 6. Enantioselective protonation of Li-enolates.

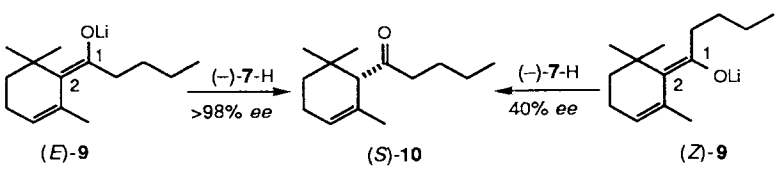

Scheme 7. Dependence of enantiofacial discrimination on enolate configuration.

has to be taken into account, and thus the relative positioning of all four substituents of the enolate double bond.[33]

Enantioselective protonation was also used as the key step in the synthesis of (*S*)-γ-damascone (Scheme 8). The synthetic

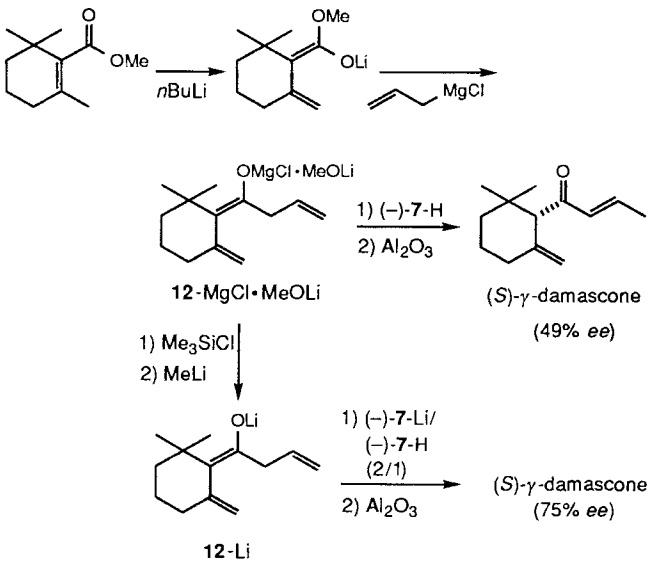

Scheme 8. Synthesis of (*S*)-γ-damascone by enantioselective protonation.

route for racemic γ-damascone proceeds via the prochiral *E*-enolate **12**-MgCl·MeOLi.[34] Its protonation with (−)-**7**-H, followed by alumina-catalyzed isomerization of one double bond, produces (*S*)-γ-damascone with a 3:1 ratio of enantiomers. Interestingly, protonation of the Li-enolate **12**-Li by addition to (−)-**7**-H proceeds with low enantioselectivity in the early stages of the reaction (roughly 35% *ee* after addition of 50%) and with increased selectivity towards the end of addition (final value 49% *ee*). Thus, the production of chiral Li-alkoxide during the process increases the selectivity of the proton transfer. An optimum *ee* value of 75% is obtained by addition of the Li-enolate to a 2:1 mixture of Li-alkoxide (−)-**7**-Li and amino alcohol (−)-**7**-H.[35] The complexity of this reaction is further demonstrated by the nonlinear relationship between enantiomeric purity of chiral reagent and reaction product (100% *ee* (reagent) → 75% *ee* (product); 50% *ee* (reagent) → 50% *ee* (product)).

Enantioselective protonation using (−)-**7**-H or its enantiomer is not restricted to damascone-like enolates. In a recent enantioselective synthesis of the more relevant enantiomer of the important tetralin musk odorant (±)-**14**[36] the required chiral building block was prepared in 90% *ee* by chelation-controlled deprotonation of enone **13** and enantioselective protonation of the *Z*-enolate (Scheme 9).[37]

The SmI_2-mediated allylation of ketenes with allyl iodide and hexamethylphorphoric triamide (HMPA) in THF,[38] believed to proceed via an allylsamarium species, has been demonstrated by Takeuchi and co-workers to afford diastereoselectively Sm-enolates, which can be then protonated enantioselectively.[39] The most efficient chiral proton donor proved to be the C_2-symmetric diol **15**; methoxy alcohol **16** gave slightly inferior results (Table 2). Both reagents are prepared from (*S*)-mandelic acid.

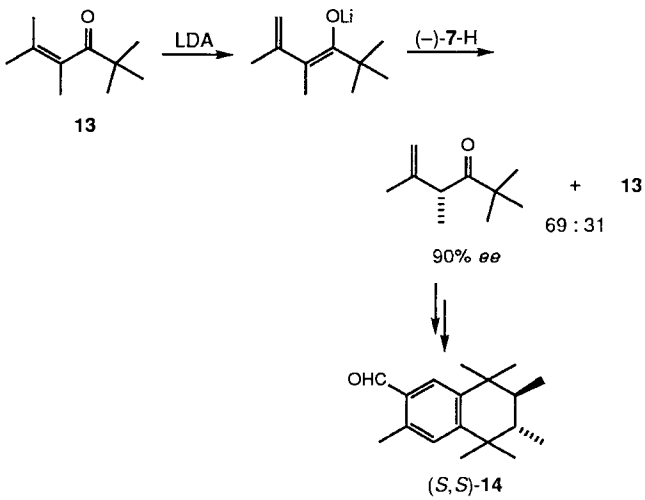

Scheme 9. Synthesis of a musk odorant by enantioselective protonation.

Table 2. Enantioselective protonation of Sm-enolates.

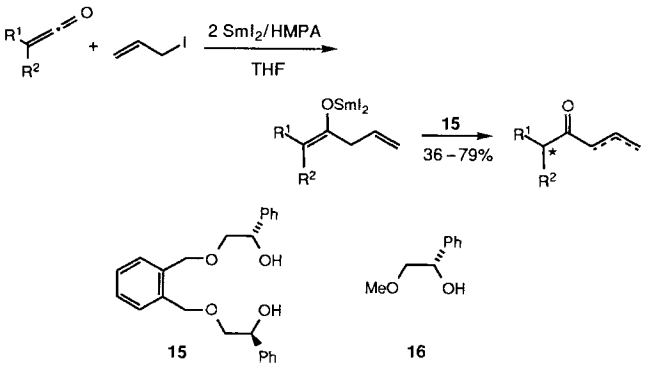

Entry	R^1	R^2	*de* [%]	*ee* [%]
1	Ph	Et	85 (*Z*)	84 (75 [a]) (*R*)
2	Ph	Me	92 (*Z*)	91 (*R*)
3	$PhCMe_2$	Me	>98 (*Z*)	97 (*R*)
4	nBuCMe$_2$	Me	>98 (*Z*)	91 (*R*)
5	p-ClC_6H_4	iPr	75 (*E*)	85 (*S*)
6	$PhCH_2$	Et	29 (*E*)	29 (*S*)
7	$PhCH_2$	iPr	72 (*Z*) [b]	68 (*R*) [b]
8	2,6-$Cl_2C_6H_3$	Me	64 (*E*)	62 (*R*)
9	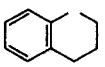		>98 (*Z*)	48 (*R*)

[a] With **16** as proton source. [b] The assignment reported in ref. [39b] ((*E*) and (*S*)) is probably incorrect (according to IUPAC priority rules).

The enolate configurations reflect, with one exception (entry 8), preferential nucleophilic attack of the allylsamarium species from the least hindered side. The striking similarity between enolate *de* values and ketone *ee* values led the authors to speculate that with pure *Z*-enolates selectivities approaching 100% *ee* would result, and analogously, the corresponding pure *E*-enolates would undergo protonation with high, but opposite enantiofacial selectivity. If this were the case, the chiral recognition would be solely accomplished by the $OSmI_2$ and allyl substituents, regardless of R^1 and R^2.[33] Until the authors confirm their hypothesis by separate protonation of *E*- and *Z*-isomeric enolates, an alternative explanation seems more likely. High selectivity in the enolate-forming step could be due to the

strong steric (and electronic) control exercised by the structurally different R^1 and R^2 groups, and these substituents would also allow better enantiofacial discrimination in the protonation step.[40] The same methodology was also applied to benzylation/protonation, affording benzyl ketones in lower yield but with satisfactory enantioselectivity (Scheme 10).[39a]

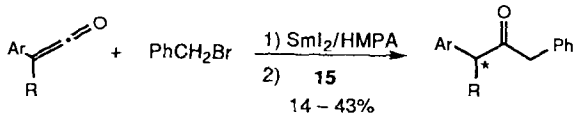

Ar, R: Ph, Me	88% *ee* (*R*)
Ar, R: Ph, Et	90% *ee* (*R*)
Ar, R: *p*-Cl-Ph, *i*Pr	61% *ee* (*S*)

Scheme 10. Benzyl ketones prepared by enantioselective protonation of Sm-enolates.

Takeuchi's tetradentate reagent is very promising, as it proved efficient with structurally diverse enolates. However, this ketone synthesis appears to be limited to allylic and benzylic systems, the reaction requires two equivalents of SmI_2, and its success critically depends on the correct relative proportions of the chiral reagent, SmI_2, and HMPA. Finally, the same group reported the generation of (*R*)-benzoin (91% *ee*) by protonation of the corresponding Sm-enediolate with quinidine.[41] Presumably, these protonations are governed by complexation of the tetradentate diol **15** with the highly oxophilic and coordinatively unsaturated Sm-enolates.

3.3. Protonation of Cyclic Ketone Enolates

Based on the criteria that had led to the design of urea **6** and amino alcohol **7** as chiral proton donors,[20] Rebek et al. prepared the chiral lactam **18**, starting from Kemp's triacid (**17**) (Section 3.4).[42] Similarily, Yamamoto et al. have elaborated the chiral imide-2-oxazoline system **19** to serve as a proton

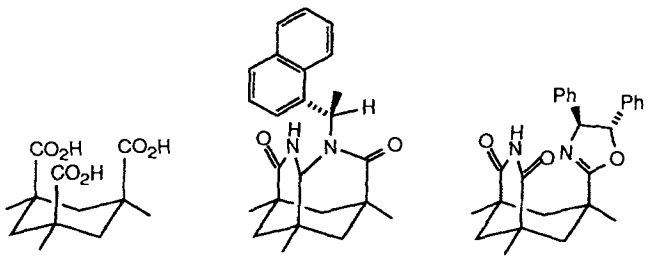

17 **18** **19**

source.[43] Imide **19** and its enantiomer can be prepared from **17** and (1*R*,2*S*)-2-amino-1,2-diphenylethanol and its enantiomer, respectively, in four efficient steps. Imide **19** has been used to protonate structurally simple cyclic enolates (Scheme 11) with high enantioselectivity.

The low-temperature protonation ($\leqq -78\,^\circ C$) of a structurally related cyclic enolate, generated (together with LiO*t*Bu!) from the reaction of the corresponding enol acetate with MeLi, has been studied by three Japanese groups (Scheme 12).

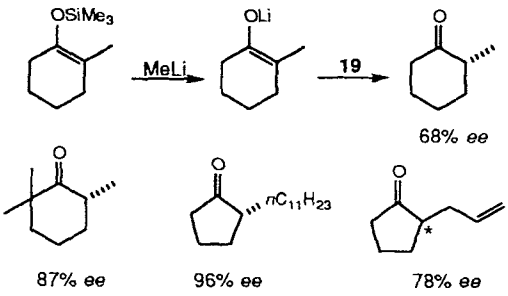

Scheme 11. Cycloalkanones prepared by enantioselective protonation with imide **19**.

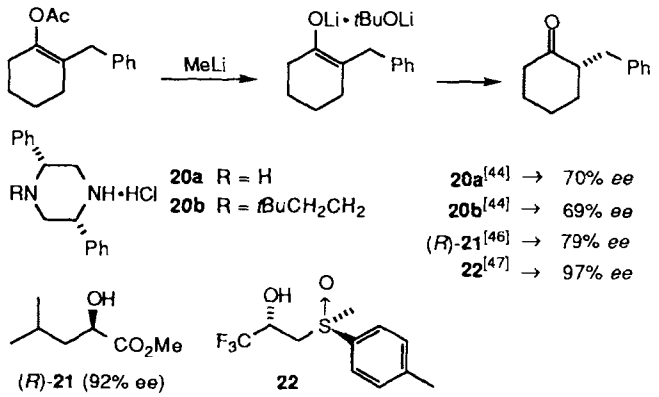

Scheme 12. (*S*)-2-Benzylcyclohexanone prepared by enantioselective protonation with **20a**, **20b**, (*R*)-**21**, and **22** as proton donors.

Fuji et al.[44] used various salts of chiral piperazine derivatives as proton donors. A maximum selectivity of 70% *ee* was obtained for the reaction of (*S*)-2-benzylcyclohexanone with **20a** in Et_2O/CH_2Cl_2 at $-90\,^\circ C$. Replacement of one amine proton by an alkyl group (as in **20b**) still led to significant inductions (32–69% *ee*), but dialkylated piperazines were totally ineffective. The enantiofacial differentiation showed a strong dependence on the nature of the ammonium salt, the solvent, and the temperature. For unspecified reasons, protonations could be effected with only 0.6 equivalents of the ammonium salt.[45]

Matsumoto and Ohta[46] found that quite high enantioselectivities were achieved for the same substrate when the enolate was protonated at $-100\,^\circ C$ with an excess of an α-hydroxy ester, ideally (*R*)-**21**. The enantiomeric hydroxy ester (*S*)-**21** of higher enantiomeric purity (96% *ee*) was used in related systems (Scheme 13).

Most recently, Kosugi et al.[47] reported that 2-sulfinyl alcohol **22** (Scheme 12) is a powerful chiral protonating agent. The

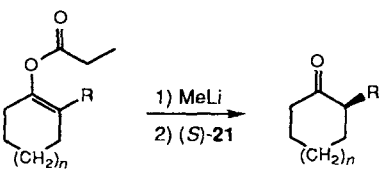

n = 0,	R = CH_2Ph	34% *ee*
n = 1,	R = CH_2Ph	82% *ee*
n = 1,	R = Me	57% *ee*
n = 1,	R = Allyl	72% *ee*

Scheme 13. Cycloalkanones prepared by enantioselective protonation with (*S*)-**21** as the proton donor.

excellent enantiofacial discrimination is most likely due to the ability of the hydroxy sulfoxide to coordinate to the lithium enolate. Presumably, electronic effects also influence the enantiofacial selection.

3.4. Protonation of Enolate/Chiral Amine Complexes

The pioneering work on the protonation of an enolate/chiral amine complex by Duhamel et al.[10, 12, 13] using an achiral proton donor (→ 24% *ee*) was discussed in Section 3.1. Inspired by these results, Hogeveen and Zwart[48] deprotonated the racemic ketone (±)-**23** (Scheme 14) with four equivalents

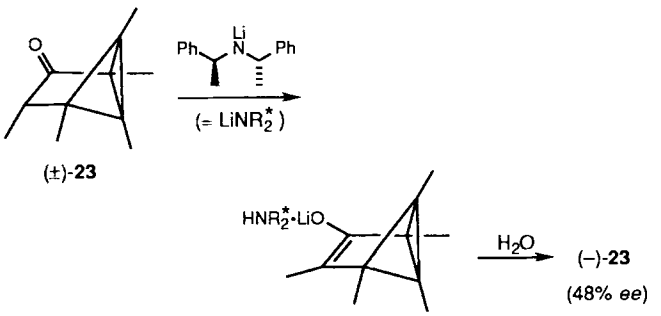

Scheme 14. Protonation (with H_2O) of a complex composed of a lithium enolate and a chiral amine.

of lithium (*S*,*S*)-bis(1-phenylethyl)amide between −90 and −75 °C and quenched the enolate/chiral amine complex with water. Ketone (−)-**23** of unknown absolute configuration was obtained with 48% *ee*. Unfortunately, it was not verified whether the deprotonation had been complete (for example by silylation), and therefore the observed induction could also be the result of enantioselective deprotonation by kinetic resolution.[49]

Yasukata and Koga[50] reported on the very efficient protonation of a complex formed between an achiral lithium enolate, a chiral secondary amine, and LiBr with AcOH (Scheme 15). Tetralone (*S*)-**26** was thus obtained with 91% *ee*. Interestingly, enantioselective methylation of the analogous *nor*-methyl complex, using excess MeI under almost identical conditions, also furnished (*S*)-**26** with 87% *ee*.[51] Thus, protonation occurs from the *Re* face and alkylation from the *Si* face of the lithium enolate. Perhaps the amine shields one enolate face, and alkylation occurs from the opposite side,[52] whereas the protonation takes place within the framework of the complex. Such an explanation would be compatible with Vedejs's discovery that an enantioselective "internal proton return" from a complexed chiral amine to the enolate can be achieved by addition of a Lewis acid.[53]

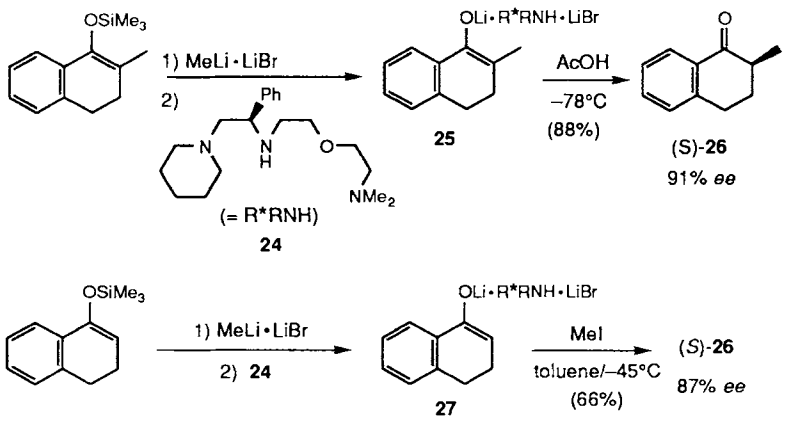

Scheme 15. Comparison of enantioselective protonation and enantioselective alkylation of an enolate/chiral amine complex.

3.5. Protonation of Amide, Ester, and Thioester Enolates

The enantioselective protonation of amide enolates has been investigated by the Vedejs group.[53, 54] Deprotonation of the racemic naproxen amide (±)-**28** with two equivalents of *s*BuLi afforded a yellow enolate, which was shown by silylation to consist of a 14:1 mixture of *E*- and *Z*-isomers. Treatment of this solution with two equivalents of triamine **29b** generated the wine-red complex **30** (a 1:1:1 complex of enolate, amine, and lithium amide; Scheme 16). Protonation of this complex with

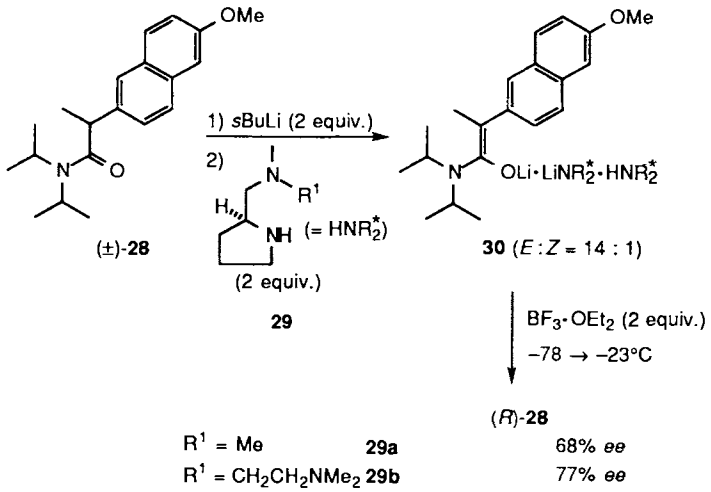

Scheme 16. Enantioselective protonation of a complex composed of an amide enolate and a chiral amine by BF_3-induced internal proton return.

protic acids gave (*R*)-**28** with at best 6% *ee* (CF_3CO_2H). However, in the presence of $BF_3 \cdot OEt_2$, the NH acidity of the amine ligand is increased, and the proton is transferred within "a specific, highly chirotopic environment" to produce amide (*R*)-**28** with 77% *ee* (internal proton return).[53] Treatment of the *ligand-free* enolate with a 1:1 mixture of **29b** and $BF_3 \cdot OEt_2$ leads to only weak induction (25% *ee*), thus further demonstrating the importance of proper complexation. Nevertheless, the exact nature of the actual proton donor remains to be determined. Moderate success was achieved in applications to other 2-arylpropionamides (50–60% *ee*).

More recently, Vedejs et al.[54] have achieved very high enantioselectivities by external protonation of lithium enolates of β,γ-unsaturated amides with commercially available *N*-methylaniline **31**. Using the same amide (±)-**28** as before, and an excess of *s*BuLi (1.75 equiv) to ensure complete

deprotonation, the resulting enolate was protonated by addition of diamine **31** (2 equiv), which delivered its proton while the reaction mixture warmed from −78 to 0 °C, to yield (*R*)-**28** (Scheme 17). Although there is no prior complexation step, a

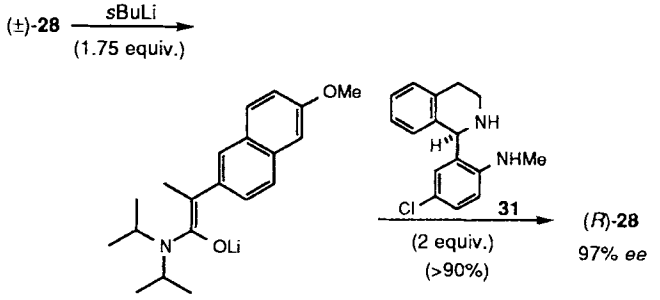

Scheme 17. External, enantioselective protonation of an amide enolate.

precomplexation of the enolate with lithiated aniline may be envisaged, due to the excess *s*BuLi.

Since the pK_a of the aniline is lower than that of amide **28** by only two to three orders of magnitude, the effective acidities of proton donor and acceptor are well-matched. However, if the pK_a values are too similar, incomplete proton transfer would result and the risk of product racemization would be augmented. Reversible deprotonation was indeed observed with the slightly more acidic amide **32**. Whereas the usual protonation of

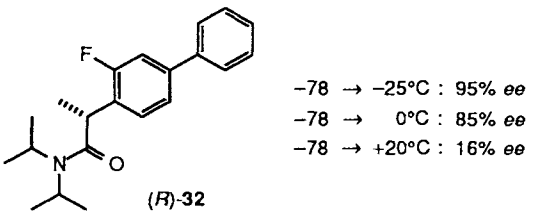

the corresponding enolate between −78 and −25 °C and subsequent addition of aqueous NH_4Cl solution afforded (*R*)-**32** with 95% *ee*, quenching of the reaction mixture at 0 or 20 °C led to diminished *ee* values of 85 and 16%, respectively.

The enantioselective protonation with aniline **31** was successfully extended to various amide dienolates (Scheme 18). With the exception of the β-unbranched enolate ($R^1 = H$), all examples gave consistently high *ee* values (95–97%). In two cases, competing γ-protonation also gave rise to significant amounts of the α,β-unsaturated isomers.

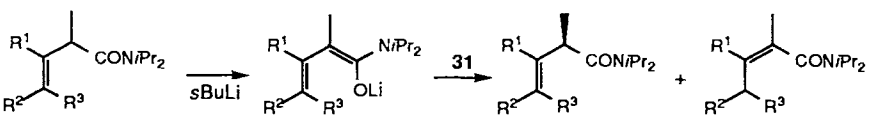

$R^1, R^2 = (CH_2)_4$; $R^3 = H$	97% *ee*	(>90%)	
$R^1, R^2 = (CH_2)_3$; $R^3 = H$	95% *ee*	(18%)	(66%)
$R^1, R^2 = CH_3$; $R^3 = H$	97% *ee*	(>90%)	
$R^1, R^3 = CH_3$, $R^2 = H$	95% *ee*	(60%)	(30%)
$R^1 = H$; $R^2, R^3 = CH_3$	53% *ee*	(>90%)	

Scheme 18. Enantioselective protonation of amide dienolates.

Hünig et al.[14, 55] have extensively studied the enantioselective protonation of cyclic ester enolates of type **34** derived from mandelic acid (Scheme 19). Of the multitude of proton donors tested, the most efficient bifunctional reagents (45–54% *ee*) are listed.[14a, b]

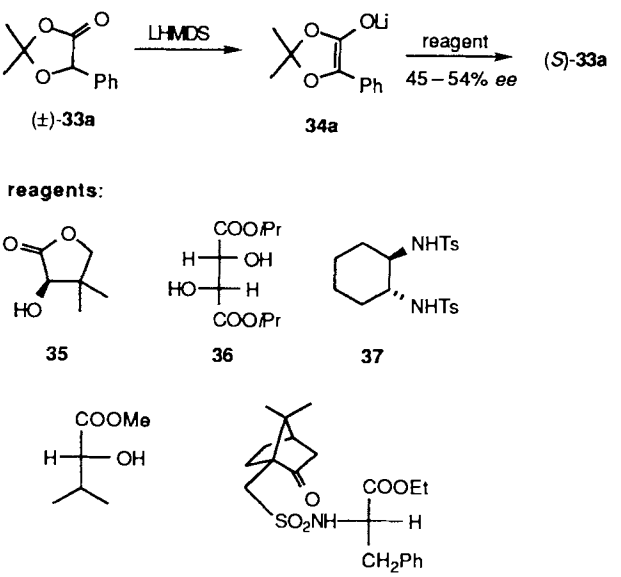

Scheme 19. Enantioselective protonation of a dioxolanone enolate.

Protonation of the oxathiolanone enolate **38** revealed a strong dependence on the precise reaction conditions; oxathiolanone (*S*)-**39** was obtained with a maximum *ee* value of 77%. Interestingly, a very pronounced solvent effect was observed when enolate **38** was protonated with (*R*)-pantolactone (**35**): the highest selectivity (72% *ee*) was achieved in Et_2O/THF (9/1) (Scheme 20)![14c]

With tartrate **36** as the chiral proton source, a dramatic salt effect was noticed: the *ee* of (*S*)-**39** increases from 39% (no LiCl) to 77% in the presence of excess LiCl, but only when the LiCl is already present during the deprotonation of (±)-**39** with LHMDS.[14c] The generation of an ate complex with two equivalents of $Ti(OiPr)_4$ is also beneficial, as shown by the protonation of **38** with diamine **37**. However, other Lewis acids led to decreased enantioselectivities and sodium or potassium enol-

38	(*S*)-**39**
35, THF	44% *ee*
35, Et_2O/THF, 9/1	72% *ee*
35, Et_2O	27% *ee*
36, THF	39% *ee*
36, THF, LiCl (2 equiv.)	67% *ee*
36, THF, LiCl (5 equiv.)	77% *ee*
37, THF	40% *ee*
37, THF, $Ti(OiPr)_4$ (2 equiv.)	67% *ee*

Scheme 20. Enantioselective protonation of an oxathiolanone enolate.

ates of **33a** proved unsuitable for enantioselective protonation ($\leq 3\%$ *ee* with **35**).[14c]

Hünig's study shows that an understanding of the underlying chemistry is extremely difficult and that it is still premature to establish any guidelines for the protonation of enolates **34a** and **38**.[56] Indeed, all described effects are only strongly pronounced in conjunction with specific chiral reagents. Likewise, structually related lactone enolates such as **I** and **II** show totally unpredictable enantiofacial selectivities.[14d]

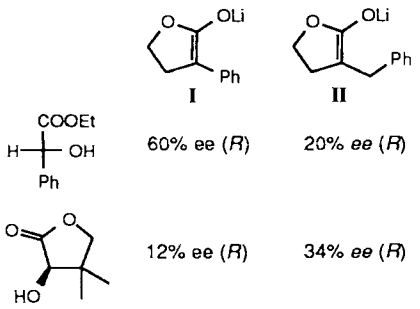

Surprisingly, the protonation of the lithium endates is insensitive to the presence or absence of secondary amines, although deuterium incorporation strongly depends on the nature of the amine present (see Section 8).[14a, c]

The noncovalent interactions between substrate and reagents can lead, via highly varied aggregates, to a multitude of diastereomeric transition states, which account for the generally modest protonation selectivities. For this reason Hünig's group has extended its study to the stereoselective protonation of a monomeric, chiral boron enolate, in which the chiral ligands are covalently bound to boron.[55] This enolate was prepared by treatment of the lithium enolate **38** with (−)-*B*-chlorodiisopinocampheylborane (**40**) (Scheme 21).

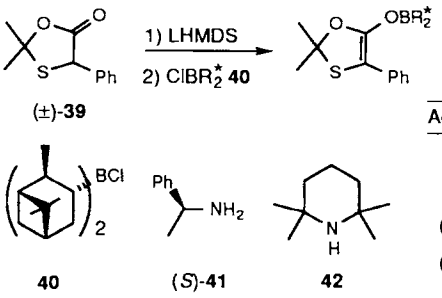

Additive	HX	*ee*	Config.
–	AcOH	54	(*R*)
–	TFA	32	(*S*)
(*S*)-**41**	AcOH	43	(*R*)
(*R*)-**41**	AcOH	2	(*R*)
42	AcOH	76	(*R*)
42	TFA	39	(*S*)

Scheme 21. Protonation of a chiral boron enolate.

Whereas protonation of the boron enolate with AcOH at −70 °C leads to an enrichment of (*R*)-**39** (54% *ee*), protonation with the less nucleophilic trifluoroacetic acid (TFA) favors the formation of the (*S*) enantiomer (32% *ee*). It is assumed that the binding of the AcOH carbonyl group by the boron atom allows the proton to be transferred internally in an eight-membered, cyclic transition state. In contrast, TFA predominantly delivers its proton without prior complexation from the opposite face of the enolate. The outcome of the protonation is strongly influenced by the presence of excess primary or secondary amines. For instance, in conjunction with AcOH, the enantiomeric 1-phenylethylamines (**41**) produce a complete selectivity change (43% *ee* (*R*) with (*S*)-**41**, 2% *ee* with (*R*)-**41**). The best result (76% *ee* (*R*)) was obtained with piperidine **42**, and the combination **42**/TFA furnished (*S*)-**39** with 39% *ee*. These results demonstrate that the amines are incorporated into the transition state. Whether a rapidly formed ammonium species is the effective proton donor was not discussed, and protonation with a preformed ammonium carboxylate was not tested.

Rebek and co-workers[42] reasoned that higher selectivities should be achieved in the protonation **34a** → **33a** (Scheme 22)

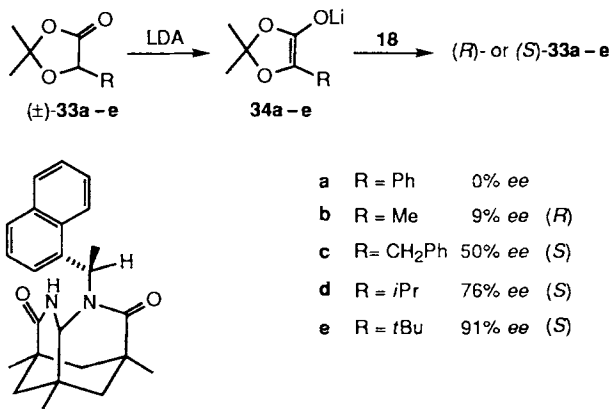

a	R = Ph	0% *ee*	
b	R = Me	9% *ee*	(*R*)
c	R= CH_2Ph	50% *ee*	(*S*)
d	R = *i*Pr	76% *ee*	(*S*)
e	R = *t*Bu	91% *ee*	(*S*)

18

Scheme 22. Enantioselective protonation of dioxolanone enolates with **18**.

with a chiral reagent, in which the proton is "buried within an asymmetric environment". For this purpose, they prepared chiral lactam **18**, in which the NH group is shielded by a naphthyl group, as evident in the ^{1}H NMR spectrum. Protonation of **34a**, initially reported to be highly enantioselective,[57] led to irreproducible results which were subsequently withdrawn. Apparently, **18** is not acidic enough to protonate the weakly basic enolate **34a**. However, the alkyl-substituted enolates **34b–e** were successfully protonated with selectivities ranging between 9 and 91% *ee* (Scheme 22), depending on the size of the R substituent. A chelated eight-membered ring transition structure in which the larger R group preferentially remains outside the cavity was proposed to rationalize the observed absolute configurations.

In our laboratory, the enantioselective protonation of ketone enolates (Section 3.2.) was extended to ester and thioester enolates derived from α-cyclogeranates, whose enantiomers are pivotal, versatile building blocks for the synthesis of fragrances and pharmaceuticals (Scheme 23).[58] When the racemic methyl es-

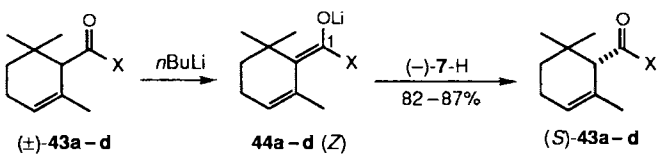

a	X = OMe	36% *ee*
b	X = OPh	77% *ee*
c	X = SPh	99% *ee*
d	X = S-2-Naphth	99% *ee*

Scheme 23. Enantioselective protonation of α-cyclogeranates and α-thiocyclogeranates. 2-Naphth = 2-naphthyl.

ter **43a** was deprotonated with *n*BuLi at −78 °C and the resulting enolate **44a** (*Z*:*E* = 19:1) protonated with (−)-*N*-isopropylephedrine ((−)-7-H) at low temperature (−100 → −10 °C), ester (*S*)-**43a** was produced with a selectivity of only 36% *ee*. This marked difference to the protonation of related ketone enolates (>90% *ee*) led us to assume that the low enantiofacial differentiation was due to insufficient structural differentiation of the substituents at C(1) of the enolate (OLi vs. OMe) and an overly rapid protonation of **44a** due to the high pK_a of **43a**. In line with our expectations, protonation of the phenyl ester enolate is more selective (77% *ee*), and the thioester enolates **44c** and **44d** afford the respective (*S*)-thioesters with an unprecedented enantioselectivity of >200:1. Likewise, protonation with the enantiomeric amino alcohol (+)-7-H affords (*R*)-**43c** with 99% *ee*.[58]

It should be added that esters **43b–d** were deprotonated at −100 °C because the corresponding enolates (≥98% *Z*) are unstable, decomposing above −80 °C to give ketene **5** and LiSPh. The reverse reaction, the enantioselective thiol addition to **5** in the presence of stoichiometric or catalytic amounts of (−)-7-H,[59] is discussed in Section 4.

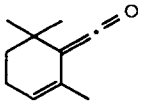

5

In view of the importance of γ-cyclogeranates **47** in the perfume industry and as synthetic intermediates, we also applied enantioselective protonation to the enolates **46a** and **46b** (Scheme 24).[35] Here, deprotonation of the β-cyclogeranates **45a** and **45b** with *n*BuLi or LDA generates, in a highly selective manner, the *E*-enolates, and the use of the dextrorotatory amino alcohol (+)-7-H provides (*S*)-**47a** and (*S*)-**47b**. As observed with the α-cyclogeranate series (Scheme 23), methyl ester enolate **46a** is a much poorer substrate for protonation (50% *ee*) than the thioester enolate **46b** (94–97% *ee*). Although neither the amine nor excess LDA affect the enantioselectivity, they influence the regioselectivity of protonation (**47a,b**:**45a,b**). The same protocol was also applied to enolate **49** of undetermined configuration to afford thioester (*R*)-**50** with 55% *ee* (Scheme 25).[60]

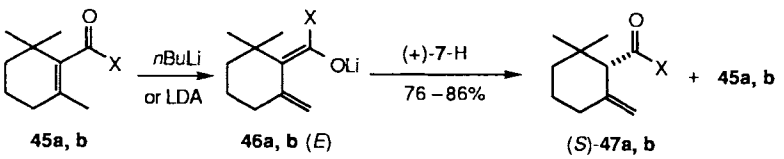

45a, b **46a, b** (*E*) (*S*)-**47a, b**

a	X = OMe	LDA (3 equiv.)	(+)-7-H (3.3 equiv.)	50% *ee*;	33 : 67
b	X = SPh	*n*BuLi (2 equiv.)	(+)-7-H (2.7 equiv.)	96% *ee*;	43 : 57
b	X = SPh	LDA (3 equiv.)	(+)-7-H (4 equiv.)	96–97% *ee*;	55 : 45
b	X = SPh	LDA (1.5 equiv.)	(+)-7-H (2 equiv.)	94% *ee*;	55 : 45

Scheme 24. Enantioselective protonation of γ-cyclogeranates and γ-thiocyclogeranates.

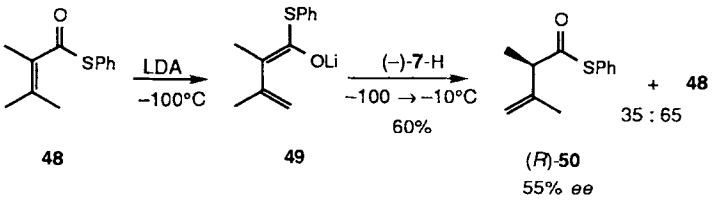

48 **49** (*R*)-**50** 55% *ee*

Scheme 25. Enantioselective protonation of a thioester enolate.

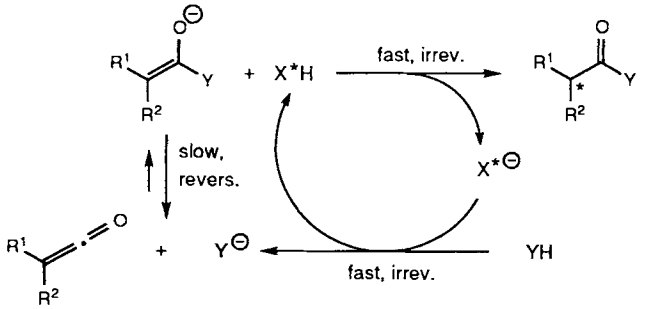

Scheme 26. Principle of catalytic enantioselective protonation involving transient enolates.

One attractive strategy for rendering a stoichiometric process catalytic without altering the reagent/enolate molar ratio consists of slowly generating the enolate (for example by addition of $Y^{\ominus}$ to a ketene, Scheme 26) under conditions that allow rapid, irreversible protonation of the transient species. The rate of regeneration of the catalyst, and thus of the enolate, can be adjusted by the delivery of the external protonating agent YH. Obviously, for such a scheme to be feasible, the proton exchange between YH and $X^{*\ominus}$ must be fast and complete, and $Y^{\ominus}$ must be more nucleophilic than the chiral reagent. Because the added species YH may also act as an undesired proton source for the enolate, its concentration in the reaction medium should be kept as low as possible.[61]

This concept has been realized in our laboratory for the synthesis of thioester (*S*)-**43c** by addition of thiophenol to ketene **5** in the presence of (−)-7- Li (Scheme 27).[59] As discussed in Section 3.5, thioester (*S*)-**43** is obtained with 99% *ee* by protonation of enolate **44c** at −100 °C, using (−)-7-H as the chiral proton donor (Scheme 27, top line). At temperatures above −80 °C the enolate eliminates PhSLi to give ketene **5**. In order to favor the addition reaction, the presence of a protic species is necessary. Thus, slow addition of equimolar amounts of (−)-7-H to a solution of ketene **5** and PhSLi in THF at −55 °C afforded (*S*)-**43c** with 95% *ee*.

For the extension of this reaction to a catalytic process, the continually added thiol serves as both nucleophile and proton source in the presence of catalytic amounts of (−)-7-Li. The rate of introduction of PhSH has to be kept low (addition over 3–4 h at −27 °C) to prevent accumulation ([PhSH] ≤ [(−)-7-Li]) and to minimize the risk of enolate protonation by PhSH. As shown in Scheme 27, very high enantioselectivities have been achieved with as little as 2–5 mol% (−)-7-Li. Of the other thiols tested, 4-chlorothiophenol, which is more acidic than PhSH, proved the most efficient (97% *ee* with 1 equiv (−)-7-Li;

4. Catalytic Enantioselective Protonation of Enolates

4.1. Processes Involving Transient Enolates

Up to this point we have considered preformed enolates, which have been submitted to at least equimolar amounts of a chiral proton donor X*H according to Scheme 26 (top line).

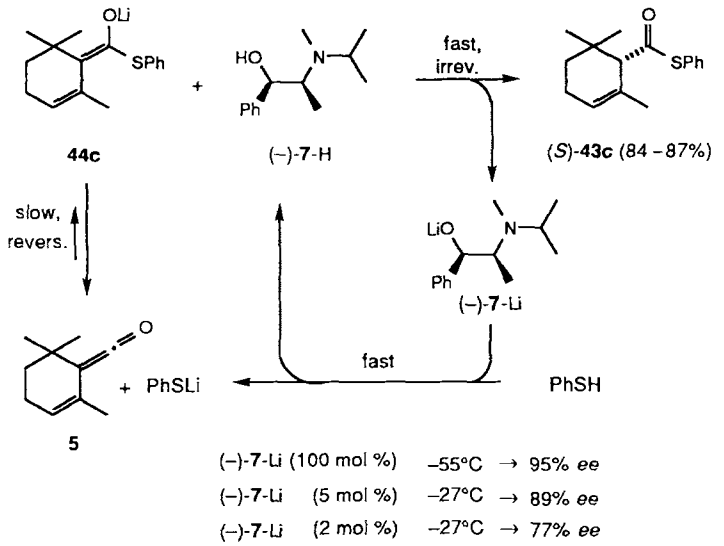

Scheme 27. Catalytic enantioselective addition–protonation of a thiophenol to a ketene.

90% *ee* with 0.05 equiv (−)-7-Li), whereas aliphatic thiols and alcohols were inefficient (10–40% *ee*).

It should be added that the presence of free thiol in the reaction medium has a deleterious effect. A reaction solution containing ketene **5**, thiophenol, and 20 mol% (−)-7-Li afforded racemic thioester **43c**! However, this restriction does not apply to the related enantioselective additions of alcohols to ketenes, which were studied by Pracejus et al.[62] as early as the 1960s, in which the alcohol (MeOH, EtOH) serves as solvent (Scheme 28).

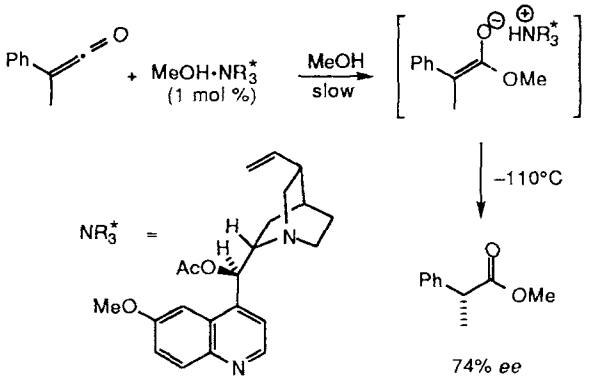

Scheme 28. Catalytic enantioselective addition–protonation of methanol to a ketene.

They found that the nucleophilic species in the low-temperature reaction (< −50 °C) consists of a 1:1 aggregate of the alcohol and the chiral tertiary amine; the uncatalyzed addition was negligible. A slow, rate-determining addition step is followed by a fast, selectivity-determining proton transfer from the postulated ammonium ion to the enolate. Among the hundreds of experiments performed with the most diverse amine catalysts under different reaction conditions, the most successful case in terms of asymmetric induction (74% *ee*) is shown in Scheme 28. In his work, Pracejus put special emphasis on the temperature dependence of the stereoselectivity. Thus, in the above example, a reaction temperature of −70 °C (instead of −110 °C) leads to almost racemic ester (< 5% *ee*). The complexity of the reaction is due to the existence of rapidly interconverting conformers leading to competing transition states, which undergo proton transfers at different rates. This and related work have been extensively reviewed by Scharf and co-workers[63] in their article on the isoinversion principle[64] and will not be discussed further here.

Pracejus et al.[65] have also extended their work on reaction sequences consisting of a thiol Michael addition and enantioselective protonation in the presence of a catalytic amount of a chiral amine. A prerequisite for achieving significant inductions (20–54% *ee*) is the use of a *β*-*N*,*N*-dialkylamino alcohol. The addition of phenylmethanethiol to methyl 2-phthalimidoacrylate with 5 mol% quinidine as catalyst furnishes the (*R*)-cysteine ester with 54% *ee* (Scheme 29). Recently, the closely related quinidine-catalyzed addition of thiophenol to 2-phenylacrylates has also been reported (45–51% *ee*).[66]

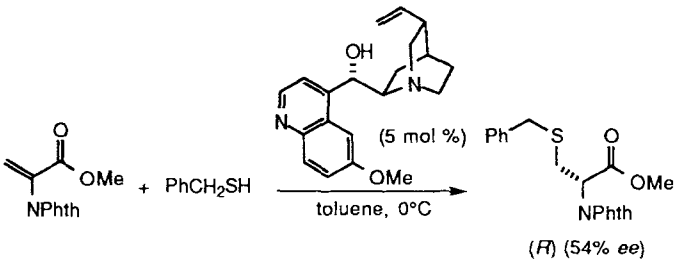

Scheme 29. Catalytic enantioselective sequence: Michael addition followed by protonation. Nphth = phthalimido.

4.2. Preformed Enolates

In catalytic, enantioselective protonations of preformed enolates, the concentration of the enolate exceeds that of the chiral catalyst. Formally, an external, achiral proton donor ZH selectively reprotonates $X^{*\ominus}$ (Scheme 30), whilst the enolate is unaffected.[67]

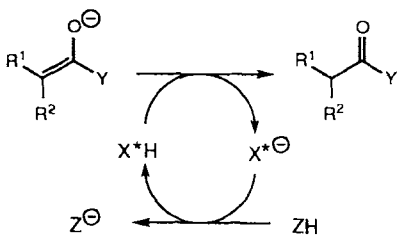

Scheme 30. Formal reaction scheme for the catalytic enantioselective protonation of preformed enolates.

The first reported enolate protonation using catalytic amounts of a chiral reagent is a special case, because the most acidic proton of the product ketone (*S*)-**48** (at C(2)) serves to protonate (−)-7-Li or, more likely, the mixed aggregate **3**-Li,(−)-7-Li (Scheme 31).[30] Whereas protonation of enolate **3**-Li with an equimolar quantity of amino alcohol (−)-7-H affords ketone (*S*)-**48** with 95% *ee*, as little as 0.3 equivalents of (−)-7-H also suffice for highly enantioselective protonation. The α-damascone isomer (*S*)-**48** and subsequently (*S*)-**4** are produced efficiently with 93% *ee* and 86% yield.[68] This autocatalytic cycle is based on subtle kinetic differences in the proton transfer reactions between chiral reagents, enolate, and non-inducing proton donor.[69] When the quantity of (−)-7-H

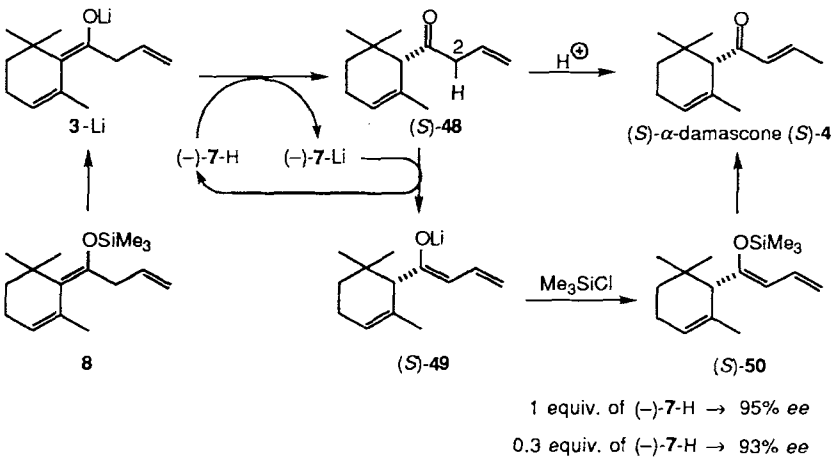

Scheme 31. "Autocatalytic" enantioselective protonation of 3-Li.

is reduced to less than about 0.2 equivalents, the reaction rate and selectivity are significantly decreased.

This case is, of course, very particular, because the product ketone (*S*)-**48** is rapidly and exclusively deprotonated at C(2). An analogous autocatalytic reaction is not possible with enolate **9**, as the acidity of the C(2) protons of (*S*)-**10** is substantially weaker. To circumvent this problem, phenyl-2-propanone has been successfully used as an external, achiral proton donor (Scheme 32).[70] Thus, protonation of **9** (*E*:*Z* = 97:3), readily

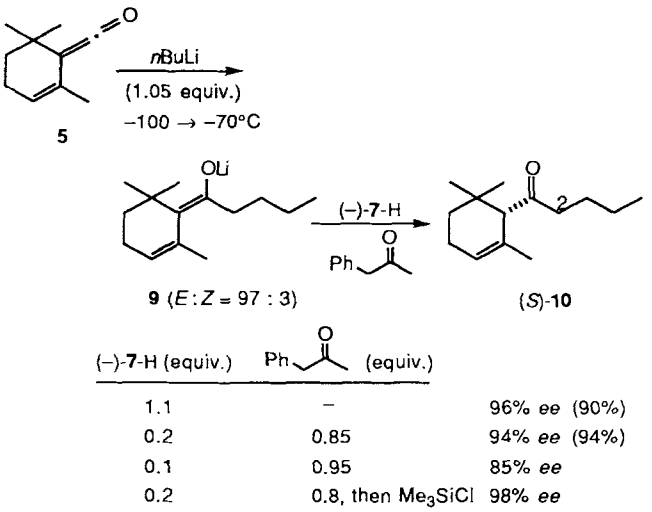

(−)-7-H (equiv.)	Ph (equiv.)	
1.1	–	96% *ee* (90%)
0.2	0.85	94% *ee* (94%)
0.1	0.95	85% *ee*
0.2	0.8, then Me_3SiCl	98% *ee*

Scheme 32. Catalytic enantioselective protonation of **9**.

obtained from ketene **5** and *n*BuLi, with equimolar amounts of (−)-7-H affords the butyl ketone (*S*)-**10** with 96% *ee*, and the catalytic enantioselective protonation with 0.2 equivalents of (−)-7-H, followed by the addition of 0.85 equivalents of phenyl-2-propanone furnishes (*S*)-**10** also with high enantioselectivity (94% *ee*). With 0.1 equivalents of (−)-7-H the selectivity decreases to 85% *ee*.

We have succeeded in further improving the attained selectivity by exploiting the observed rate difference between protonation of (*E*)-**9** and (*Z*)-**9** (Section 3.2.). When slightly less than one equivalent of the proton donor (0.2 equiv (−)-7-H, 0.8 equiv phenyl-2-propanone) for a total amount of 1.05 equiv *n*BuLi are used, and the reaction mixture is quenched with Me_3SiCl, (*S*)-**10** is obtained with 98% *ee*![31] Under these conditions, only (*E*)-**9**, which allows a better enantiofacial discrimination, is protonated (see also Section 3.2.). Interestingly, this experiment also revealed that deprotonation of phenyl-2-propanone is kinetically controlled, as the (*Z*)-silyl enol ether was formed exclusively.

In contrast to the simplified reaction in Scheme 30, which implies a rapid proton transfer between ZH and $X^{*\ominus}$, the proton exchanges between (−)-7-Li and phenyl-2-propanone are slow, incomplete (in other words reversible), and unselective (mixture of *E*- and *Z*-enolates). However, protonation of enolate (*E*)-**9** by phenyl-2-propanone is rapid, irreversible, and selective, affording the (*Z*)-silyl ether (*Z*)-**51** after silylation (Scheme 33). Therefore, phenyl-2-propanone certainly furnishes

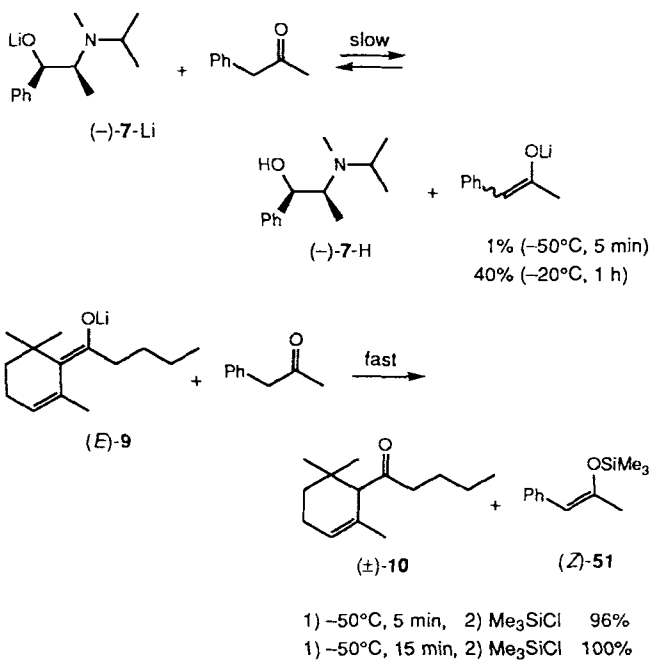

Scheme 33. Proton exchange reactions between phenyl-2-propanone and (−)-7-Li and (*E*)-**9**.

its proton directly to enolate (*E*)-**9** or to a chiral enolate complex formed from (*E*)-**9** and (−)-7-Li.[71] The catalytic conditions were also extended to the preparation of thioesters of high enantiomeric purity (Scheme 34).[35]

Very recently, Yamamoto et al.[72] have reported that enolate **52** can be enantioselectively protonated at −78 °C by sequential addition of (*S*,*S*)-imide **19** (0.1 equiv) and succinimide (1 equiv) (Scheme 35). The selectivity (83% *ee*) approaches that obtained with stoichiometric quantities of **19** (87% *ee*, see Section 3.3.). With phenol **54**, as little as 0.01 equivalents of chiral imide **19** were required to achieve 81% *ee*. The reaction is believed to follow the general mechanism shown in Scheme 30.[73]

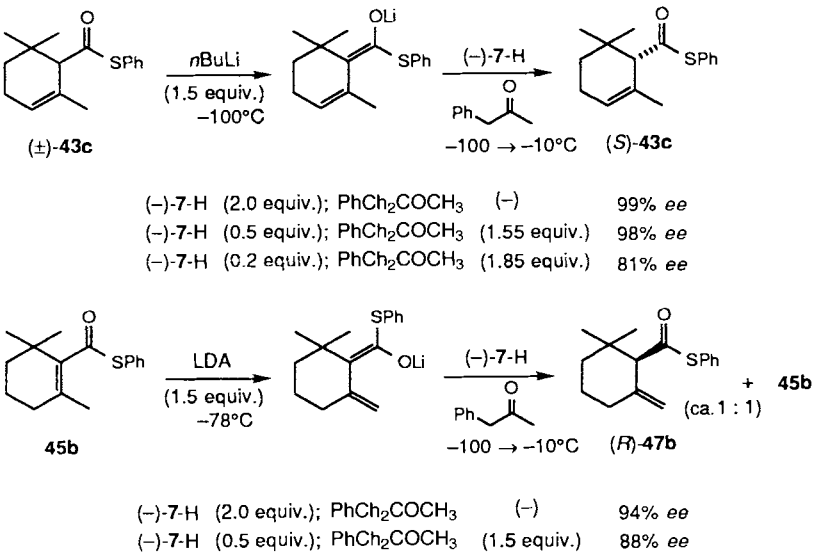

Scheme 34. Enantioselective protonation of thioester enolates with substoichiometric amounts of (−)-7-H.

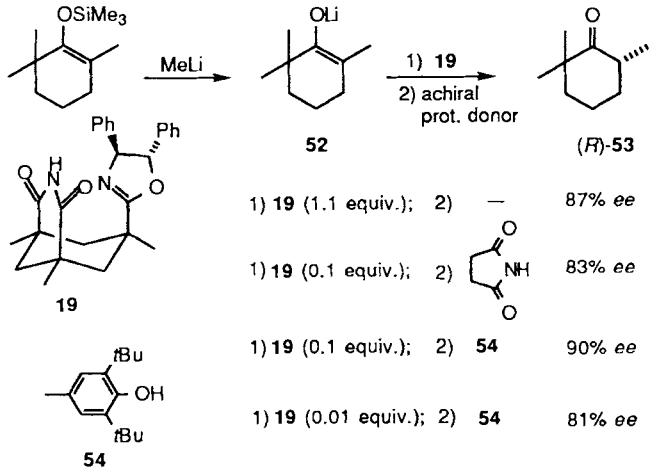

Scheme 35. Enantioselective protonation with catalytic amounts of **19**.

5. Enantioselective Tautomerization of Enols

In this section the reactions proceeding via enol intermediates are reviewed. Since enols and enolates are often rapidly interconverting, enol tautomerizations are closely related to the previously discussed enolate protonations.

As a borderline case, Duhamel's protonation of enediolate **56** has to be cited (Scheme 36).[18] In the presence of (*R*,*R*)-di-*O*,*O'*-pivaloyltartaric acid ((−)-**2a**) at −70 °C, enediol **57** is rapidly formed. Its tautomerization, however, is much slower, and quenching of the reaction mixture after less than 1 h affords essentially benzil (**58**), which is formed by autoxidation of enediol **57** during workup. In contrast, when the reaction is allowed to continue for 15 h, (*S*)-benzoin ((*S*)-**55**) is obtained in high yield (80%) with 80% *ee*. As **57** is certainly in equilibrium with its monoanion **59**, we suggest **59** as the reactive intermediate. The fact that large excesses of chiral diacid (−)-**2a** are deleterious to the process may also be rationalized by an unfavorable shift of the equilibrium between **57** and **59**.

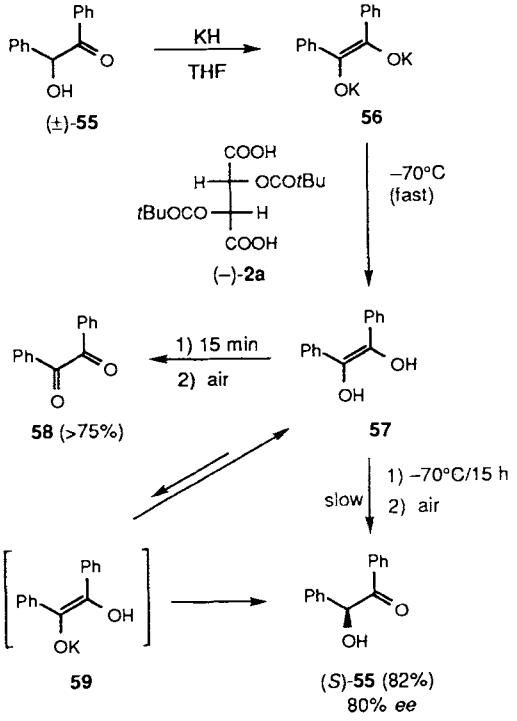

Scheme 36. Enantioselective tautomerization of an enediol.

The most important contribution to the enantioselective protonation of dienols is attributed to Pete and co-workers. In a series of publications[74] they have demonstrated that α,β-unsaturated esters and lactones can be enantioselectively deconjugated by irradiation at 254 nm in the presence of a chiral catalyst (Scheme 37). This reaction involves an intramolecular γ-hydrogen abstraction of the allylic hydrogen from the singlet excited state (**B** → **C**; Norrish type II).[75] The transient dienol species **C**, which is in equilibrium with ester **B** (thermal 1,5 H-shift), then undergoes a base-catalyzed tautomerization. With catalytic amounts (0.1–0.15 equiv) of chiral β-amino alcohols, this rate-determining, irreversible C-protonation affords enantiomerically enriched esters with fair to excellent *ee* values (Scheme 38). Essential to this photodeconjugation is that the dienol is maintained at a low steady-state concentration ([**C**] < [X*H]) and that the reaction product **D** is more inert than **A** to the photochemical conditions. For good results,

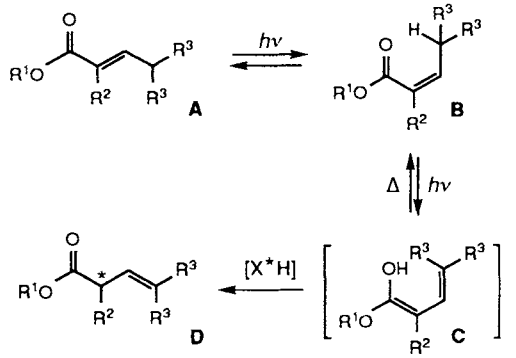

Scheme 37. Enantioselective photodeconjugation of an α,β-unsaturated ester.

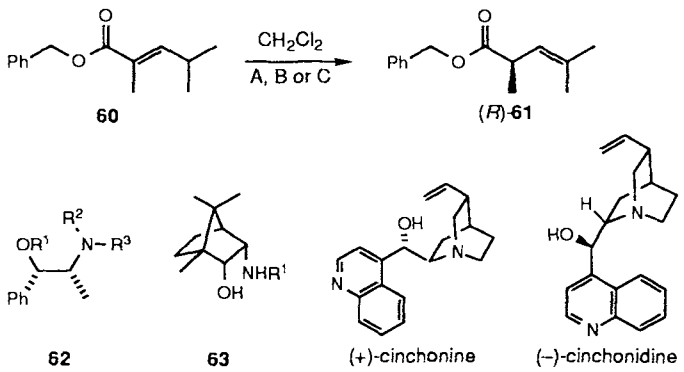

Catalyst	R^1	R^2	R^3	Method	*ee* [%]	Yield [%]
62a	H	Me	H	A	31	78
62b	H	Me	Me	A	6	80
62c	Me	Me	H	A	7	70
62d	H	*i*Pr	H	C	**70**	65
62e	H	$CHEt_2$	H	A	62	47
62f	H	$CHiPr_2$	H	C	8	56
62g	H	*t*Bu	H	C	5	68
63a	Me			B	<5	61
63b	*i*Pr			B	**89**	76
63c	CH_2Ph			B	**81**	75
(+)-cinchonine				C	41 (*S*)	40
(−)-cinchonidine				A	37 (*R*)	66

Scheme 38. Structural requirements of the chiral catalyst in the enantioselective photodeconjugation of ester **60**. A: 0.1 equiv catalyst, −78 °C; B: 0.15 equiv catalyst, −55 °C; C: 0.1 equiv catalyst, −40 °C (or −50 °C).

rigorously moisture-free, apolar solvents such as *n*-heptane and CH_2Cl_2 had to be used, and the optimal temperature was determined to be approximately −55 °C.[74a, 76]

Amino alcohols that have a secondary NH group were found to be more efficient inductors. The size of the N-alkyl substituents is extremely critical; **62d**, **63b**, and **63c** (R^2 = *i*Pr, $PhCH_2$) gave the best results (70–91 % *ee*). Either decreasing or increasing the size of the amine substituent led to diminished enantioselectivities. (+)-Cinchonine and (−)-cinchonidine gave modest, opposite inductions. With bornane **63b**, various other esters of type **A** have been deconjugated with 43–77 % *ee*. In general, better results were obtained with γ-disubstituted esters.[74c]

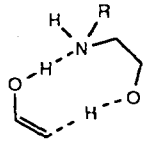

E

Pète et al. propose that the enantioselective protonation of the dienol proceeds by the formation of a complex of type **E**.[74] The hydrogen bonding between the enolic proton and the nitrogen atom increases the electron density on C(2) and allows a more or less concerted proton transfer via a nine-membered cyclic transition state. An alternative reaction course involving the intermediacy of an enolate/ammonium ion pair was considered unlikely in view of the analogous phenol/tertiary amine complexes in apolar solvents, in which the OH bond is not cleaved.

These enantioselective tautomerizations are not restricted to dienols. Aryl enols **66** and **67** have been generated by Norrish type *II* photoeliminations from **64** and **65** in acetonitrile ($\lambda > 290$ nm) and tautomerized in the presence of β-amino alcohols (Scheme 39).[77] Enol **66** was shown to be stable under the irradiation conditions ($\lambda = 337$ nm) in the absence of amino alcohol catalysts, but it tautomerized in the dark with as little as 1 mol % (−)-ephedrine (**62a**) (**68**: 45 % *ee*). One disadvantage of this interesting method is that prolonged irradiation times lead,

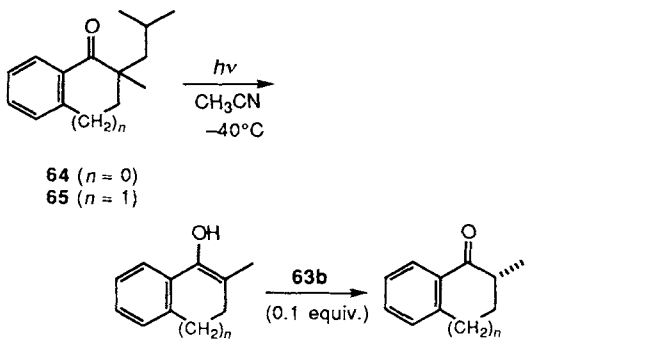

Scheme 39. Enantioselective tautomerization of aryl enols.

through Norrish type I fission, to competing cleavage reactions and product racemization.

Alternatively, enols **66** and **67** have also been generated by Pd-catalyzed cleavage reactions of appropriate precursors (Scheme 40) and ketonized in the presence of chiral β-amino alcohols (max. 64 % *ee*).[78] The intermediacy of enol species remains, however, speculative, and the possibility of the C-protonation of a Pd-enolate cannot be excluded. Also worthy of mention are a related enol tautomerization catalyzed by [Rh-(*S*)-BINAP]$^{\oplus}$ (BINAP = 2,2′-bis(diphenylphosphanyl)-1,1′-binaphthyl) affording 2-phenylpropanol with 18 % *ee*,[79] and a Cu^{I}-alkoxide-catalyzed decarboxylation of methylphenylmalonates (max. 36 % *ee*).[80]

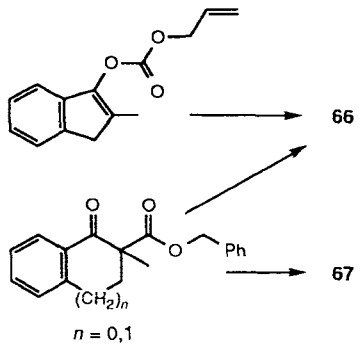

Scheme 40. Pd-catalyzed generation of enols.

6. Enantioselective Protonation of Enol Ethers, Ketene Acetals, and Enol Esters

6.1. $SnCl_4$-Complexed Binaphthol as a New Chiral Proton Donor

Yamamoto et al.[81] have found that the complex between (*R*)-binaphthol and $SnCl_4$, (*R*)-**69**, generated in situ is highly effective for the enantioselective protonation of 2-aryl enol ethers but less suitable for the protonation of 2-alkyl enol ethers (Scheme 41). This reaction was also successfully applied to ketene bis(trialkylsilyl) acetals, affording 2-aryl esters with 60–95 % *ee* (Scheme 42). Ketene acetals with different substituents R^2 and R^3 usually exist as mixtures of (*E*) and (*Z*) isomers and undergo protonation with lower induction. The authors propose a transition state model based on minimum steric interactions, which accounts for the fact that the highest enantiofacial discriminations are observed with small R^1 groups (methyl). In one case it was ascertained that the protonation did not occur via a tin enolate, but the question of a concerted or

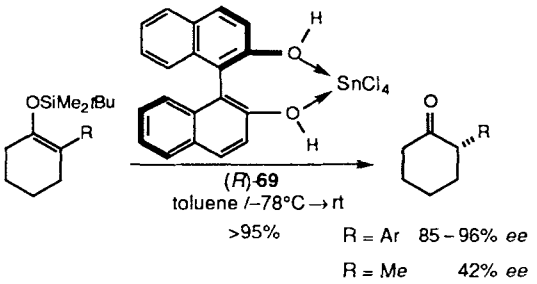

Scheme 41. Enantioselective protonation of enol ethers. rt = room temperature.

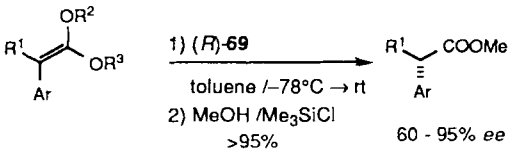

Scheme 42. Enantioselective protonation of ketene acetals. rt = room temperature.

stepwise[82] mechanism was not clarified.[83] It should also be noted that in this process the chiral reagent is transformed into the monosilylated binaphthol derivative.

6.2. A Polymer-Supported Chiral Proton Donor

The enantioselective protonation of ketene acetal **70** (see also Section 3.5) has been achieved with excellent enantioselectivity (94% *ee*) when the proton donor (*R*)-mandelic acid (**71**) was bound to a polymeric resin (→**72**, Scheme 43).[84] Most intrigu-

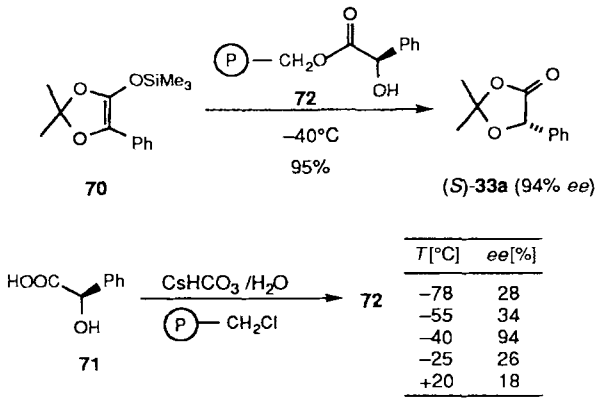

T[°C]	ee[%]
–78	28
–55	34
–40	94
–25	26
+20	18

Scheme 43. Enantioselective protonation of a ketene acetal using a polymer-supported chiral proton donor. (P) $-CH_2Cl$ = Merrifield resin.

ingly, this protonation is highly temperature dependent: when the temperature deviates only slightly from −40 °C, a surprisingly large decrease in enantioselectivity results. In application of the isoinversion principle[63, 64] Verducci et al. attribute these changes to a two-step mechanism involving the preliminary formation of rapidly interconverting diastereomeric complexes. However, it can be verified readily that the selectivity of 94% *ee* obtained at −40 °C does not fit the Eyring plot.[76] Therefore, these results cannot be explained solely by a change in dominance of enthalpy and entropy in the partial steps.

In a previous investigation the same group found that protonation of **70** with (*R*)-pantolactone (**35**) and with (*R*)-methyl mandelate with or without $ZnCl_2$ or LiCl additives at −78 °C led to (*S*)-**33a** with generally low selectivities (13–50% *ee*).[85] In conclusion, the polymer-supported chiral reagent leads to a substantially improved asymmetric induction and offers the advantage of simple recovery of the reagent by filtration without loss of activity.

6.3. Enzyme-Mediated Hydrolysis of Enol Esters

Enzymatic ester hydrolyses are known to generally proceed by acylation of the enzyme, followed by hydrolysis of the acylated species. When this hydrolysis method is applied to prochiral enol esters, concomitant acyl group cleavage and C-protonation of the liberated enols by the enzyme is expected to give enantiomerically enriched products. With this reasoning, Ohta et al.[86] have thoroughly investigated the hydrolysis of a series of α-substituted cycloalkanone enol esters. After extensive screening, the yeast *Pichia farinosa* IAM 4682 was found to be the most efficient in terms of reactivity and selectivity. Generally, when the reaction was performed with a large excess of *Pichia farinosa*, high *ee* values were obtained with a variety of substrates (Scheme 44). For example, 78 mg of enol acetate

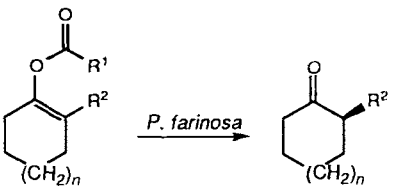

n	R^1	R^2	ee[%]	Yield[%]
1	Me	Me	90	79
1	Et	Me	92	78
1	Ph	Me	71	71
1	Et	Pr	86	78
1	Et	All	78	57
1	Et	CH_2Ph	84	75
3	Me	Me	67	71
5	Et	Me	89	83
7	Me	Me	95 (*R*)	67
7	Ph	Me	96 (*R*)	59
10	Me	Me	<2	38
10	Ph	Me	11	25

Scheme 44. Enzyme-mediated enantioselective hydrolysis of enol esters. The yeast strain *P. farinosa* is used in large excess. For enol esters with $n = 7$ the induction is opposite to that with other ring sizes although the configuration is the same.

(Scheme 44; $n = 1$, $R^1 = R^2 = Me$) and 14 g of grown, centrifuged cells in phosphate buffer (pH 6.5) at 30 °C furnished (*S*)-2-methylcyclohexanone with 90% *ee*. Reducing the weight of the cells to 2.7 g slowed down the reaction rate and favored nonspecific reactions catalyzed by other enzymes of the cell (41% *ee*). The possibility of racemization due to prolonged reaction times at 30 °C (24 h instead of 3 h) should also be taken into consideration.

The large amount of yeast cells necessary for this process and the severe emulsion problems encountered during the extraction prompted the Japanese group to develop a procedure that would be more amenable to large-scale preparations.[87] As hydrolysis with immobilized cells resulted in only very poor conversions, a new system ("interface bioreactor") was tested, in

which the microorganism was grown on a hydrophilic polysaccharide layer (agar plate). For the desired hydrolysis a solution of the substrate enol ester in an apolar solvent was added, and the reaction proceeded at the interface between the entrapped cells and solvent. In this way, the microorganisms are protected against toxic compounds, the freshly grown cells can be used directly in organic solvents, and the recovery of the product is greatly facilitated. Thus, with 50 mL of isooctane as the solvent, 500 mg of enol ester ($n = 1$, $R^1 = Et$, $R^2 = CH_2Ph$) was hydrolyzed with 21 g of wet cells (on a surface of 638 cm^2) to afford, after 24 h at 25 °C, (*R*)-2-benzylcyclohexanone in 66% yield with 84–87% *ee*.

6.4. Antibody-Catalyzed Protonation of Enol Ethers

Whereas active enzymes are found by screening, catalytic antibodies (or abzymes) are raised against rationally designed antigens (haptens) that mimic the transition state of the planned reaction.[88] The first encouraging result—the enantioselective protonation of an enol ester affording (*R*)-2-methylcyclohexanone with 42% *ee*—was achieved by an antibody elicited against a hapten possessing a phosphonate moiety.[89] For the acid-catalyzed protonation of enol ethers **73**, **74**, and **76**, the scientists at the Scripps Research Institute selected cationic haptens such as **78** and structurally related ammonium species,[90] with the assumption that the antibodies generated would contain a carboxylate group in the combining site for reasons of electrostatic complementarity. This functional group may either stabilize the transition state or assist the desired C-protonation. In view of the similarity between the hapten and the pyramidalized transition state for the proton transfer, a good binding affinity of the activated substrate to the antibody was expected (Scheme 45).

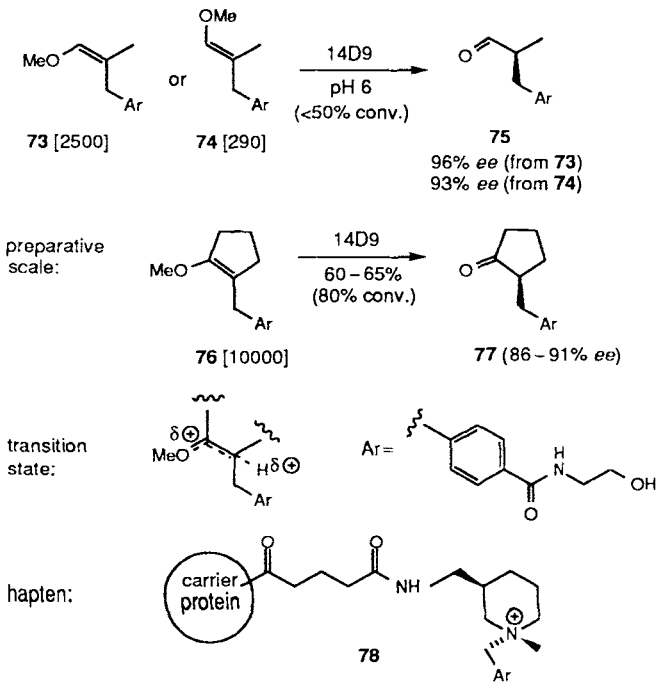

Scheme 45. Antibody-catalyzed enantioselective protonation of enol ethers. The rate enhancements k_{cat}/k_{uncat} are given in square brackets.

Indeed, monoclonal antibody 14D9 (from 23 antibodies raised against **78**) showed excellent activity for both rate enhancement and enantioselectivity in the hydrolysis of **73** ($k_{cat}/k_{uncat} = 2500$; 96% *ee*) and to a lesser degree **74** ($k_{cat}/k_{uncat} = 290$; 93% *ee*).[90a] Interestingly, the *E*- and *Z*-enol ethers afford the same enantiomer. The reaction was performed in a cyanide buffer (pH 6) at 25 °C for several days (< 50% conversion). Under these conditions the formed aldehyde **75** is protected from racemization by conversion into the corresponding cyanohydrin diastereomers. However, an estimated loss in enantiomeric purity of approximately 1.5% *ee* (hydrolysis of **73**) and about 5% *ee* (hydrolysis of **74**) is attributed to the noncatalyzed background reaction.

The same abzyme hydrolyzes **76** with a rate enhancement (k_{cat}/k_{uncat}) of 10^4.[90b] When a catalytic amount of antibody 14D9 (400 mg, ca. 2.7 μmol; ca. 0.15 mol%) is used, hydrolysis of **76** (500 mg, 1.83 mmol) proceeds to 80% conversion in 5 h giving ketone **77** with 89–91% *ee*. After separation of the low molecular weight compounds **76** and **77** by dialysis, **77** is obtained after recrystallization in 60–65% yield (86% *ee*), and the antibody is recycled with roughly 5% loss of activity. The background reaction is considered to have eroded the *ee* by about 10%. If larger amounts of abzyme had been used, it could have been proved that the antibody-catalyzed hydrolysis is indeed 100% enantioselective.

Very recently,[91] a rate acceleration of 65 000 and an enantiofacial discrimination greater than 200:1 was measured for the 14D9-catalyzed hydrolysis of *Z*-enol ether **79** (Scheme 46). In

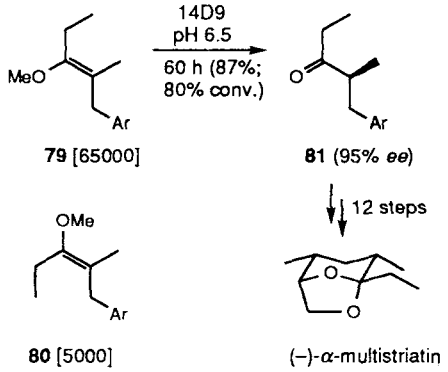

Scheme 46. Antibody-catalyzed enantioselective protonation of an enol ether. The rate enhancements k_{cat}/k_{uncat} are given in square brackets.

analogy to the reaction of *Z*- and *E*-enol ethers **73** and **74**, catalysis is much more effective with **79** than with **80** ($k_{cat}/k_{uncat} = 5000$). On a preparative scale, with 180 mg of **79** and 0.23 mol% partially purified 14D9, **81** was isolated after 80% conversion in 87% yield and with 95% *ee*. Ketone **81** was used as a chiral building block for the synthesis of the insect aggregation pheromone (–)-α-multistriatin.

Based on recent mechanistic investigations, Reymond, Lerner, et al.[92] arrived at the conclusion that the assumed carboxylate function in the antibody active site is not within binding distance of the transient tetragonal carbon undergoing protonation, but it more likely interacts with the electron-deficient carbon bearing the methoxy group. Indeed, hydrolysis of both **76** and the regioisomeric enol ether **82** is significantly catalyzed by

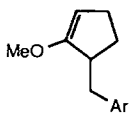

82

14D9. Therefore, the initially proposed structural similarity between the hapten and the transition state does not fully account for the observed effect.[92a] From inhibition experiments of the hydrolysis of **73** in the presence of hapten analogs, the orientation of the enol ether at the transition state relative to the hapten was deduced, and the importance of hydrophobic binding interactions between enol ether substituents and the antibody for pyramidalization of the proton-accepting carbon atom was recognized.[92b]

7. Enantioselective Protonation of a Phosphane Oxide Carbanion

Recently, Vedejs and Garcia-Rivas[93] were able to deracemize phosphane oxide **83** by enantioselective protonation of the corresponding carbanion **84** (Scheme 47), thus confirming that benzylic carbanions stabilized by a P=O substituent are either planar or invert rapidly.

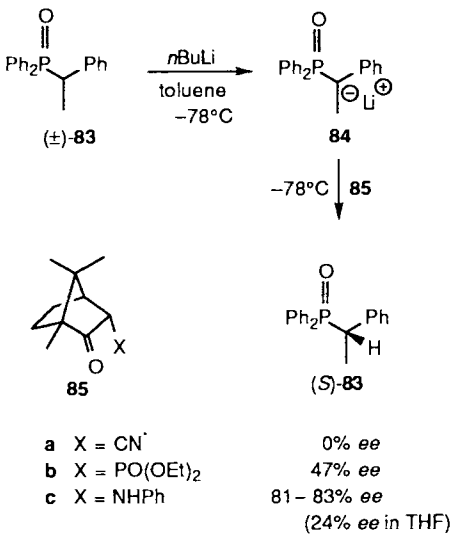

Scheme 47. Enantioselective protonation of a phosphane oxide carbanion.

For the protonation of carbanion **84**, the camphor-derived chiral proton donors **85b** and **85c** gave satisfactory enantiofacial discriminations of 47 and 81–83% *ee*, respectively. Interestingly, the chiral di- and triamines **29a** and **29b**, which efficiently promote enolate protonation (see Section 3.5), were ineffective for anion **84** (0–29% *ee*). In this reaction, where the least acidic camphor derivative **85c** gives the highest induction, the formation of transient mixed-aggregate species of defined but unknown structure appears to be crucial.[94] With the strongly coordinating solvent THF, the reaction course is markedly changed and a selectivity of only 24% *ee* results.

8. Summary and Outlook

In recent years enantioselective protonation has become a field of intense research, and numerous procedures have been developed allowing direct and efficient access to carbonyl compounds of high enantiomeric purity. The importance of this "young" reaction is now being confirmed by a growing number of applications in the syntheses of antiinflammatory agents,[53,54,66] pheromones[87,92] and fragrances.[19] However, currently, no generally applicable reagent is known and each chiral proton donor is only specific for a particular type of substrate under well-defined reaction conditions.

The complexity of enolate protonation stems from the fact that the reaction partners are not simple monomolecular entities, but a multitude of interconvertible aggregates of differing reactivity. During protonation the changing composition of the reaction mixture further complicates the process. The effects of amines and lithium salts,[5] the crucial role of solvent,[14c] and the nonlinearity between chiral induction and the enantiomeric composition of the reagent[35] are typical phenomena of changes in the supramolecular structure of the reaction species.

The participation of amines and lithium amides was first demonstrated by Duhamel's group[10,12,13] (see Section 3.1), who showed that the enantiofacial selectivity of protonation is strongly dependent on the chiral or achiral lithium amide employed. Protonation of an enolate/chiral amine complex[5] with an achiral proton source also afforded enantiomerically enriched product.[10,12,48]

Hünig et al.[14a,c] demonstrated that amines interact or interfere during protonation, as incomplete deuteration was observed when (±)-**33a** was deprotonated with LDA and the enolate/$HN(iPr)_2$ complex was submitted to deuteration with [D]**36** (Scheme 48). However, the amine has no effect on the

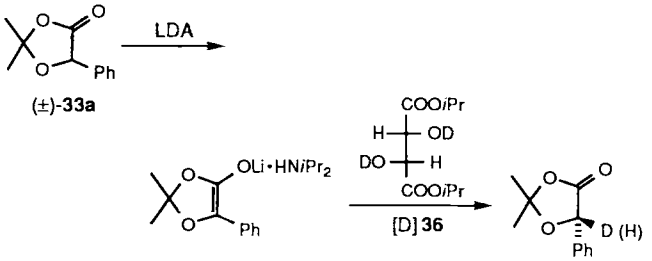

[D]**36**: 55% *ee*
([D] : [H] = 41 : 59)
36: 45% *ee*

Scheme 48. D/H-scrambling in the enantioselective deuteration of an enolate/secondary amine complex.

enantioselectivity and does not necessarily participate in the transition state. Complete deuteration and a selectivity of 57% *ee* could be attained by substituting LDA for LHMDS in the deprotonation step. The absence of an amine effect during deuteration in the presence of the less basic HMDS was already noticed by Duhamel et al.[13] Likewise, we have observed that the site selectivity for protonation of dienolates is improved in the presence of LDA and $HN(iPr)_2$, although the amine has little effect on the enantioselectivity (see Schemes 10,[37] 25,[35] and 26[60]).[95]

In contrast, the groups of Vedejs[53] and Koga[50] demonstrated that chiral amine ligands can efficiently control the enantiofacial proton delivery to the enolate. The "internal proton return"[53] from the 1:1:1 complex **30**, which consists of an

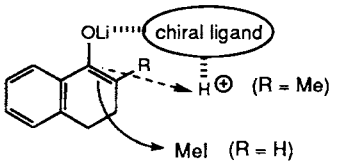

25 R = Me
27 R = H

enolate, a chiral amine, and a chiral lithium amide, back to the enolate has been achieved by increasing the acidity of the NH group with $BF_3 \cdot OEt_2$ (see Section 3.5). A very impressive example of "external" protonation of a complex composed of an enolate, a tetradentate chiral amine, and LiBr with AcOH was recently reported by Yasukata and Koga.[50] Interestingly, protonation of the chiral enolate complex **25** and methylation of the chiral enolate complex **27** take place with opposite enantiotopicity, thus giving the *same* product (see Section 3.3). In view of Vedejs's results, it may be assumed that the proton is transferred internally from the chiral ligand to one enolate face, whereas the methylation of a structurally and conformationally related complex proceeds from the opposite face.[52, 96]

The presence of LiBr in toluene is essential for the success of the aforementioned reaction. Added lithium halides, lithium alkoxides, and lithium amides are known to profoundly affect enolate aggregation and to favor deaggregation of enolate tetramers **F** and dimers **G**, leading to monomeric, mixed aggregates **H** (Scheme 49).[2a, 97, 98] In addition, oligomeric cyclic enolate structures are disfavored for sterically hindered systems.[97a]

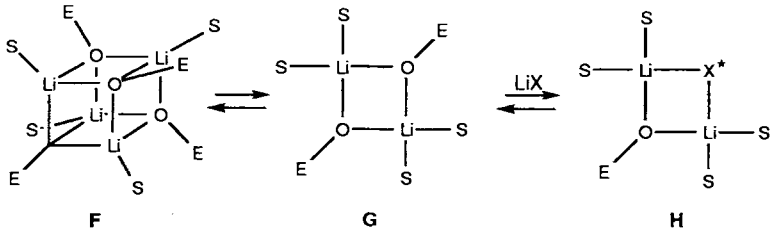

F **G** **H**

Scheme 49. Structures of enolate aggregates. E = enolate, S = solvent, X = ligand (halide, $RO^{\ominus}$, $R_2N^{\ominus}$).

It therefore seems reasonable to assume that efficient enantioselective protonation reactions proceed by the formation of monomeric enolate complexes of type **I**, **J**, or **K** (X* = bi- (or poly-) dentate chiral ligand, X = achiral ligand), which are followed immediately by irreversible C-protonation.[6b, 99] In these complexes the chiral information necessary for the subsequent irreversible proton transfer is still intact. Some support in favor of the intermediacy of hybride enol/enolate structures (for example **87** in Scheme 50) was obtained from the enantioselective ketonization of isolated enol **86** in the presence of chiral lithium alkoxide (−)-7-Li, which afforded the same (*S*)-ketone **48** as that obtained by enolate protonation. The lower *ee* value (60%) is presumably due to concurrent nonenantioface-discriminating protonation.[100] Complex **87**, which is probably further aggregated with chiral or achiral ligands, may ultimately transfer the proton with the participation of the N atom, via a nine-membered ring transition state, in which a more or less colinear arrangement is attained for N–H–C.

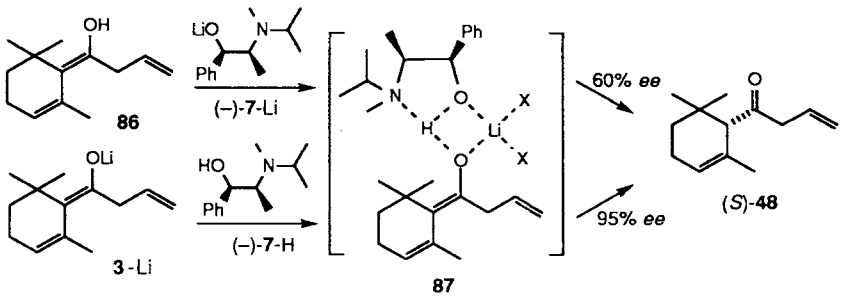

Scheme 50. Comparison of enol and enolate protonation.

In view of the related deprotonations of ketones, often involving two lithium amide molecules in an optimal eight-membered cyclic transition structure,[97a, c] an analogous general model for enolate protonations can be formulated by inspection of the more highly aggregated structures **J** and **K**: Formal disconnection of the inner bond in the ladder structures **J** and **K** would lead to complex **L**,[101] which then would undergo C-protonation via the eight-membered ring transition state **M**.

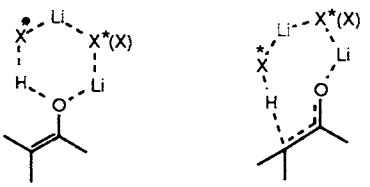

L **M**

At least two examples can be cited in which protonation indicates the participation of two or more chiral reagent molecules, namely Vedejs's internal protonations of 1:1:1 complexes **30** consisting of an enolate, a chiral amine, and a chiral lithium amide[53] (Scheme 51, see Section 3.5), and the protonation of enolate **12**-Li with a 1:2 mixture of the amino alcohol (−)-7-H and the corresponding lithium alkoxide (−)-7-Li[35] (see Section 3.2). The outcome of this reaction is not significantly changed when the enolate is first complexed with the lithium alkoxide and then protonated by the amino alcohol. Nevertheless, it is essential that (−)-7-Li is present at the beginning of the protonation. Consistent with these facts, a nonlinear relationship between the enantiomeric purity of the chiral reagent and the enantiomeric excess of the reaction product was found. Possibly (−)-7-Li not only affects the structure of the interacting species but also lowers its acidity.[102]

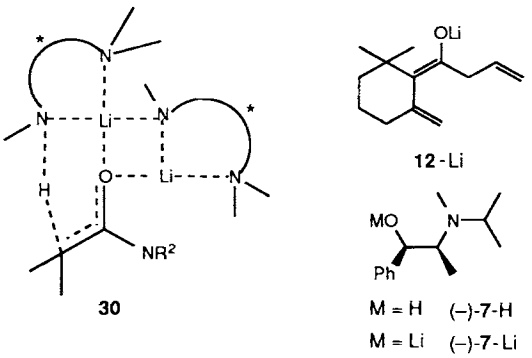

Scheme 51. Representation of complex **30** and structural formulas of the chiral compounds **12**-Li, (–)-7-H, and (–)-7-Li.

In analogy to the tetrameric structure **88** (simplified representation) of crystalline lithium ephedrate,[103] it is tempting to speculate on analogous 3:1 mixed aggregates **N** for enolate protonations promoted by amino alcohols. In solution and in the presence of a proton donor, a multitude of partially disconnected species such as **O** would be expected to be in equilibrium with each other.

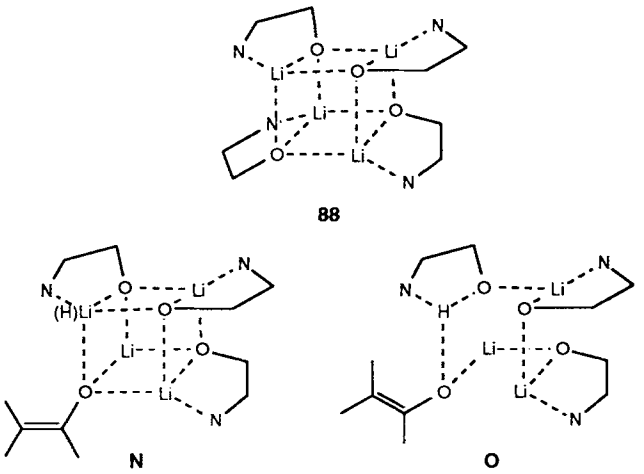

88

N **O**

Recent stability evaluations of eight-membered ring aggregates[97] as well as fascinating X-ray structures of "partially deprotonated" mixed aggregates (with Li- and H-binding),[104] give some credibility to the above mechanistic considerations and also highlight the complexity of proton transfer reactions. Certainly the application of new spectroscopic and computational methods will lead to a better understanding of the dynamic behavior of interacting aggregates and open the door to the development of tailor-made reagents and catalysts in the area of enolate protonation.

After this review had been written two relevant articles appeared: the efficient enantioselective protonation of Mg-enolates of 2-alkyltetralones with 1,1′-binaphthalene-8,8′-diol-derived carbamates has been reported[105] and a review article on enantio- and diastereoselective protonation has been published.[106]

I would like to thank my colleagues, in particular Dr. R. L. Snowden, Dr. B. Winter, Dr. V. Rautenstrauch, and Dr. B. Maurer, for valuable suggestions and critical proofreading of the manuscript.

Received: November 21, 1995 [A140IE]
German version: *Angew. Chem.* **1996**, *108*, 2726–2748

[1] In the special cases of enolates or dienolates with C_s symmetry, protonation can also be viewed as an enantiotopic group differentiation. For an example of enantioselective protonation of a dicarboxylate with C_s symmetry, see K. Fuji, M. Node, S. Terada, M. Murata, H. Nagasawa, *J. Am. Chem. Soc.* **1985**, *107*, 6404.

[2] Leading references: a) D. Seebach, *Angew. Chem.* **1988**, *100*, 1685; *Angew. Chem. Int. Ed. Engl.* **1988**, *27*, 1624; E. Juaristi, A. K. Beck, J. Hansen, T. Matt, T. Mukhopadhyay, M. Simson, D. Seebach, *Synthesis*, **1993**, 1271; D. Seebach, *Proc. Robert A. Welch Found. Conf. Chem. Res.* **1984**, *27*, 93–145; b) H. C. Brown, R. K. Dhar, K. Ganesan, B. Singaram, *J. Org. Chem.* **1992**, *57*, 2716; I. Paterson, *Pure Appl. Chem.* **1992**, *64*, 1821; C. H. Heathcock, *Aldrichimica Acta* **1990**, *23*, 99; D. A. Evans, *Asymmetric Synthesis, Vol. 3*, (Ed.: J. D. Morrison), Academic Press, Orlando, **1984**, 1; R. M. Pollack, *Tetrahedron* **1989**, *45*, 4913.

[3] T. T. Tidwell, *Ketenes*, Wiley, New York, **1995**; *Acc. Chem. Res.* **1990**, *23*, 273; H. R. Seikaly, T. T. Tidwell, *Tetrahedron* **1986**, *42*, 2587.

[4] B. H. Lipshutz, S. Sengupta, *Org. React.* **1992**, *41*, 135; M. P. Cooke, Jr., *J. Org. Chem.* **1986**, *51*, 1637.

[5] Chiral amine ligands: P. J. Cox, N. S. Simpkins, *Tetrahedron: Asymmetry* **1991**, *2*, 1.

[6] Reviews: a) L. Duhamel, P. Duhamel, J.-C. Launay, J.-C. Plaquevent, *Bull. Soc. Chim. Fr.* **1984**, II-421; b) C. Fehr, *Chimia* **1991**, *45*, 253; c) H. Waldmann, *Nachr. Chem. Tech. Lab.* **1991**, *39*, 413.

[7] R. Stewart, *The Proton: Applications to Organic Chemistry* (Ed.: H. H. Wasserman), Academic Press, Orlando, **1985**; H. E. Zimmerman, *Acc. Chem. Res.* **1987**, *20*, 263; J. R. Keeffe, A. J. Kresge, *The Chemistry of Enols* (Eds.: S. Patai, Z. Rappoport), Wiley, Chichester, **1990**, p. 399; B. Capon, *The Chemistry of Enones* (Eds.: S. Patai, Z. Rappoport), Wiley, Chichester, **1989**, p. 1063.

[8] L. Duhamel, J.-C. Plaquevent, *J. Am. Chem. Soc.* **1978**, *100*, 7415.

[9] T. Kinoshita, T. Miwa, *J. Chem. Soc. Chem. Commun.* **1974**, 181.

[10] L. Duhamel, J.-C. Plaquevent, *Bull. Soc. Chim. Fr.* **1982**, II-75.

[11] L. Duhamel, P. Duhamel, S. Fouquay, J. J. Eddine, O. Peschard, J.-C. Plaquevent, A. Ravard, R. Solliard, J.-Y. Valnot, H. Vincens, *Tetrahedron* **1988**, *44*, 5495.

[12] L. Duhamel, J.-C. Plaquevent, *Tetrahedron Lett.* **1980**, *21*, 2521.

[13] L. Duhamel, S. Fouquay, J.-C. Plaquevent, *Tetrahedron Lett.* **1986**, *27*, 4975.

[14] a) U. Gerlach, S. Hünig, *Angew. Chem.* **1987**, *99*, 1323; *Angew. Chem. Int. Ed. Engl.* **1987**, *26*, 1283; b) U. Gerlach, T. Haubenreich, S. Hünig, *Chem. Ber.* **1994**, *127*, 1969; c) *ibid.* **1994**, *127*, 1981; d) U. Gerlach, T. Haubenreich, S. Hünig, N. Klaunzer, *ibid.* **1994**, 1989.

[15] E. M. Arnett, F. J. Fisher, M. A. Nichols, A. A. Ribeiro, *J. Am. Chem. Soc.* **1990**, *112*, 801.

[16] T. Laube, J. D. Dunitz, D. Seebach, *Helv. Chim. Acta* **1985**, *68*, 1373.

[17] (*S*)-Vinylglycine has been found to occur in mushrooms and plays a role in the enzymatic transformation of homoserine into threonine and α-oxobutyrate: G. Dardenne, J. Casimir, M. Marlier, P. O. Larsen, *Phytochem.* **1974**, *13*, 1897.

[18] L. Duhamel, J.-C. Launay, *Tetrahedron Lett.* **1983**, *24*, 4209.

[19] C. Fehr, *Chirality in Industry II* (Eds.: A. N. Collins, G. N. Sheldrake, J. Crosby), Wiley, Chichester, **1997**, p. 335.

[20] C. Fehr, J. Galindo, *J. Am. Chem. Soc.* **1988**, *110*, 6909; C. Fehr, J. Galindo (Firmenich), EP326869 **1988** [*Chem. Abstr.* **1990**, *112*, 98909g].

[21] (*S*)-**4**, whose odor is reminiscent of rose petals, is by far the more precious and powerful fragrance[20].

[22] R. J. Adamski, S. Numajiri, US 3860651 **1969** [*Chem. Abstr.* **1975**, *82*, 170330t].

[23] a) C. Fehr, J. Galindo, *J. Org. Chem.* **1988**, *53*, 1828; b) R. Häner, T. Laube, D. Seebach, *J. Am. Chem. Soc.* **1985**, *107*, 5396.

[24] The electrophilic nature of ester enolates may be due to charge delocalization. It is also possible that loss of LiOMe allows the Grignard reaction to proceed via a ketene[23b] or ketenoid species.

[25] F. Naef, R. Decorzant, *Tetrahedron* **1986**, *42*, 3245.

[26] Protonation with (*R,R*)-di-*O,O'*-pivaloyltartaric acid[8] or with (*R*)-pantolactone[14] provides (*S*)-**4** with 8 and 25% *ee*, respectively.

[27] Likewise, use of the enantiomeric reagent (+)-7-H affords (*R*)-**4** with 84% *ee*. The enantiofacial discrimination with pure *E*-enolate is expected to be even higher. This synthetic scheme can be used to prepare (*S*)-α-damascone ((*S*)-**4**) with excellent enantiomeric purity (99% *ee* after recrystallization) and in an improved yield of 55% starting from ketene **5**: C. Fehr, O. Guntern, *Helv. Chim. Acta* **1992**, *75*, 1023.

[28] The analogous Li-enolate/Li-alkoxide complex shows lower enantiofacial discrimination (65% *ee*), and the MgCl-enolate/MgCl-alkoxide complex is ineffective (10% *ee*).

[29] Addition of allyl-Li to ketene **5** gives a mixture of *E*-and *Z*-enolates (**3**-Li, $E:Z = 2:1$).

[30] C. Fehr, J. Galindo, *Angew. Chem.* **1994**, *106*, 1967; *Angew. Chem. Int. Ed. Engl.* **1994**, *33*, 1888.

[31] C. Fehr, J. Galindo, presented at the New Swiss Chemical Society (Berne, Switzerland, October 21, 1994).

[32] C. Fehr, J. Galindo, unpublished results.
[33] If *E*- and *Z*-enolates would give rise to equally high, but opposite induction, the enantiofacial selectivity would be determined entirely by the substituents at C(1) of the enolate, since the substituents at C(2) are nondiscriminating (see Scheme 7). See also L. Duhamel, P. Duhamel, *C. R. Acad. Sci. II* **1995**, *320*, 689.
[34] C. Fehr, J. Galindo, *J. Org. Chem.* **1988**, *53*, 1828.
[35] C. Fehr, J. Galindo, *Helv. Chim. Acta* **1995**, *78*, 539.
[36] C. Fehr, J. Galindo, R. Haubrichs, R. Perret, *Helv. Chim. Acta* **1989**, *72*, 1537.
[37] C. Fehr, F. Delay, P.-A. Blanc, N. Chaptal-Gradoz (Firmenich), EP Appl. 664286 **1994** [*Chem. Abstr.* **1995**, *123*, 169378g].
[38] D. P. Curran, M. J. Totleben, *J. Am. Chem. Soc.* **1992**, *114*, 6050.
[39] a) S. Takeuchi, N. Miyoshi, Y. Ohgo, *Chem. Lett.* **1992**, 551; b) S. Takeuchi, A. Ohira, N. Miyoshi, H. Mashio, Y. Ohgo, *Tetrahedron: Asymmetry* **1994**, *5*, 1763.
[40] The importance of the substituents R^1 and R^2 is acknowledged in one example (Table 2, entry 9), in which only a fair enantioselectivity (48% *ee*) is measured from the protonation of a pure *Z*-enolate. In this case it appears that the rigid planar phenyl group is not sterically demanding enough in the direction orthogonal to the enolate plane.
[41] S. Takeuchi, N. Miyoshi, K. Hirata, H. Hayashida, Y. Ohgo, *Bull. Chem. Soc. Jpn.* **1992**,*65*, 2001.
[42] D. Potin, K. Williams, J. Rebek, Jr., *Angew. Chem.* **1990**, *102*, 1485; *Angew. Chem. Int. Ed. Engl.* **1990**, *29*, 1420.
[43] A. Yanagisawa, T. Kuribayashi, T. Kikuchi, H. Yamamoto, *Angew. Chem.* **1994**, *106*, 129; *Angew. Chem. Int. Ed. Engl.* **1994**, *33*, 107.
[44] K. Fuji, K. Tanaka, H. Miyamoto, *Tetrahedron: Asymmetry* **1993**, *4*, 247.
[45] It is possible that the piperazine forms a complex with unreacted enolate. Protonation of this complex during the hydrolytic workup may also occur enantioselectively.
[46] K. Matsumoto, H. Ohta, *Tetrahedron Lett.* **1991**, *32*, 4729.
[47] H. Kosugi, K. Hoshino, H. Uda, *Phosphorous, Sulfur Silicon Relat.* Elem. **1994**, *95–96*, 401.
[48] H. Hogeveen, L. Zwart, *Tetrahedron Lett.* **1982**, *23*, 105.
[49] In this case silylation would have permitted the recovery of highly enantioenriched (−)-**23**.
[50] T. Yasukata, K. Koga, *Tetrahedron: Asymmetry* **1993**, *4*, 35.
[51] M. Murakata, M. Nakajima, K. Koga, *J. Chem. Soc. Chem. Commun.* **1990**, 1657.
[52] For analogous diastereoface-selective alkylations see K. A. Durkin, D. Liotta, *J. Am. Chem. Soc.* **1990**, *112*, 8162; L. A. Castonguay, J. W. Guiles, A. K. Rappé, A. I. Meyers, *J. Org. Chem.* **1992**, *57*, 3819.
[53] a) E. Vedejs, N. Lee, *J. Am. Chem. Soc.* **1991**, *113*, 5483; *ibid.* **1995**, *117*, 891.
[54] E. Vedejs, N. Lee, S. T. Sakata, *J. Am. Chem. Soc.* **1994**, *116*, 2175.
[55] T. Haubenreich, S. Hünig, H.-J. Schulz, *Angew. Chem.* **1993**, *105*, 443; *Angew. Chem. Int. Ed. Engl.* **1993**, *32*, 398.
[56] Protonation of **34a** with (*R*,*R*)-di-*O*,*O'*-pivaloyltartaric acid[8] afforded (*R*)-**33a** with 5% *ee*; protonation of **38** with ephedrine derivatives[20] gave fair enantioselectivities (20–36% ee).
[57] J. Rebek, Jr., *Chemtracts Org. Chem.* **1989**, *2*, 337; *Angew. Chem.* **1990**, *102*, 206; *Angew. Chem. Int. Ed. Engl.* **1990**, *29*, 245.
[58] a) C. Fehr, I. Stempf, J. Galindo, *Angew. Chem.* **1993**, *105*, 1091; *Angew. Chem. Int. Ed. Engl.* **1993**, *32*, 1042; b) J. A. Marshall, *Chemtracts Org. Chem.* **1994**, *7*, 38.
[59] C. Fehr, I. Stempf, J. Galindo, *Angew. Chem.* **1993**, *105*, 1093; *Angew. Chem. Int. Ed. Engl.* **1993**, *32*, 1044; ref. [58b].
[60] C. Fehr, N. Chaptal-Gradoz, unpublished results. The absolute configuration of the aromatic musk odorant (*S*,*S*)-**14** was determined by chemical correlation with (*R*)-**50**.
[61] Alternatively, $Y^{\ominus}$ can also be preformed. On addition of an external proton donor ZH, unreactive $Z^{\ominus}$ would be formed.
[62] H. Pracejus, *Liebigs Ann. Chem.* **1960**, *634*, 9; H. Pracejus, G. Kohl, *ibid.* **1969**, *722*,1; A. Tille, H. Pracejus, *Chem. Ber.* **1967**, *100*, 196.
[63] H. Buschmann, H.-D. Scharf, N. Hoffmann, P. Esser, *Angew. Chem.* **1991**, *103*, 480; *Angew. Chem. Int. Ed. Engl.* **1991**, *30*, 477.
[64] According to the isoinversion principle, the temperature-dependent enantioselectivity is due to changes in the entropy and enthalpy activation parameters of the two selectivity-determining steps.
[65] H. Pracejus, F.-W. Wilcke, K. Hanemann, *J. Prakt. Chem.* **1977**, *319*, 219.
[66] A. Kumar, R. V. Salunkhe, R. A. Rane, S. Y. Dike, *J. Chem. Soc. Chem. Commun.* **1991**, 485.
[67] This reaction type may also proceed by O-protonation either by X*H or ZH, followed by enantioselective tautomerization of the enol or by protonation of an enolate/chiral ligand complex (see Section 8).
[68] The formation of enolate **49** was proved by isolation of the corresponding silyl enol ether **50**. Under acidic conditions both **48** and **50** are converted into (*S*)-α-damascone ((*S*)-**4**).
[69] (*S*)-**48** does not protonate **3**-Li enantioselectively in the absence of (−)-**7**-H.
[70] Various CH-, OH-, and SH-acidic compounds (β-ketoesters, phenols, thiophenol, carboxylic acids, and *rac*-**48**), all of which are more acidic than (*S*)-**10** by several orders of magnitude, were tested and shown to be effective.
[71] See ref. [67]. As the catalytic enantioselective reaction (Scheme 32) is even more rapid (2 min at −50 °C), protonation of an enolate/chiral ligand complex seems more probable.
[72] A. Yanagisawa, T. Kikuchi, T. Watanabe, T. Kuribayashi, H. Yamamoto, *Synlett* **1995**, 372.
[73] The small but significant gain in enantioselectivity under catalytic conditions (0.1 equiv **19** in the presence of **54** rather than 1 equiv **19**) reflects a more complex scenario, in which **54** (or its anion) is involved in the transition state. It would be interesting to verify that this difference is not due to a modified workup procedure (which includes treatment with Me_3SiCl).
[74] a) J. Muzart, F. Hénin, J.-P. Pète, A. M'Boungou-M'Passi, *Tetrahedron: Asymmetry* **1993**, *4*, 2531; b) O. Piva, R. Mortezaei, F. Henin, J. Muzart, J.-P. Pète, *J. Am. Chem. Soc.* **1990**, *112*, 9263; c) O. Piva, J.-P. Pète, *Tetrahedron Lett.* **1990**, *31*, 5157; d) J.-P. Pète, F. Henin, R. Mortezaei, J. Muzart, O. Piva, *Pure Appl. Chem.* **1986**, *58*, 1257, and references therein.
[75] R. M. Duhaime, D. A. Lombardo, I. A. Skinner, A. C. Weedon, *J. Org. Chem.* **1985**, *50*, 873.
[76] In application of the isoinversion principle [63, 64], the inversion temperature can be determined from the two linear regions of the Eyring diagram ($\log[R]/[S] \sim 1/T$).
[77] F. Henin, J. Muzart, J.-P. Pète, A. M'Boungou-M'Passi, H. Rau, *Angew. Chem.* **1991**, *103*, 460; *Angew. Chem. Int. Ed. Engl.* **1991**, *30*, 416; F. Hénin, A. M'Boungou-M'Passi, J. Muzart, J.-P. Pète, *Tetrahedron* **1994**, *50*, 2849.
[78] F. Hénin, J. Muzart, *Tetrahedron: Asymmetry* **1992**, *3*, 1161; S. J. Aboulhoda, F. Hénin, J. Muzart, C. Thorey, W. Behnen, J. Martens, T. Mehler, *ibid.* **1994**, *5*, 1321; S. J. Aboulhoda, S. Létinois, J. Wilken, I. Reiners, F. Hénin, J. Martens, J. Muzart, *ibid.* **1995**, *6*, 1865.
[79] S. H. Bergens, B. Bosnich, *J. Am. Chem. Soc.* **1991**, *113*, 958.
[80] O. Toussaint, P. Capdevielle, M. Maumy, *Tetrahedron Lett.* **1987**, *28*, 539; H. Brunner, M. Kurzwart, *Monats. Chem.* **1992**, *123*, 121.
[81] K. Ishihara, M. Kaneeda, H. Yamamoto, *J. Am. Chem. Soc.* **1994**, *116*, 11179.
[82] M. H. Novice, H. R. Seikaly, A. D. Seiz, T. T. Tidwell, *J. Am. Chem. Soc.* **1980**, *102*, 5835.
[83] A rate-determining C-protonation that precedes fast desilylation would be anticipated based on a mechanistic study on acid-catalyzed hydrolysis of *tert*-butyldimethyl silyl enol ethers[82].
[84] F. Cavelier, S. Gomez, R. Jacquier, J. Verducci, *Tetrahedron Lett.* **1994**, *35*, 2891.
[85] F. Cavelier, S. Gomez, R. Jacquier, J. Verducci, *Tetrahedron: Asymmetry* **1993**, *4*, 2501.
[86] K. Matsumoto, S. Tsutsumi, T. Ihori, H. Ohta, *J. Am. Chem. Soc.* **1990**, *112*, 9614.
[87] O. Katoh, T. Sugai, H. Ohta, *Tetrahedron: Asymmetry* **1994**, *5*, 1935.
[88] Reviews: P. G. Schultz, *Angew. Chem.* **1989**, *101*, 1336; *Angew. Chem. Int. Ed. Engl.* **1989**, *28*, 1283; R. A. Lerner, P. G. Benkovic, P. G. Schultz, *Science* **1991**, 252, 659; P. G. Schultz, R. A. Lerner, *Acc. Chem. Res.* **1993**, *26*, 391; G. M. Blackburn, P. Wentworth, *Chem. Ind. (London)* **1994**, 338.
[89] I. Fujii, R. A. Lerner, K. D. Janda, *J. Am. Chem. Soc.* **1991**, *113*, 8528.
[90] a) J.-L. Reymond, K. D. Janda, R. A. Lerner, *J. Am. Chem. Soc.* **1992**, *114*, 2257; b) J.-L. Reymond, J.-L. Reber, R. A. Lerner, *Angew. Chem.* **1994**, *106*, 485; *Angew. Chem. Int. Ed. Engl.* **1994**, *33*, 475.
[91] S. C. Sinha, E. Keinan, *J. Am. Chem. Soc.* **1995**, *117*, 3653.
[92] a) J.-L. Reymond, G. K. Jahangiri, C. Stoudt, R. A. Lerner, *J. Am. Chem. Soc.* **1993**, *115*, 3909; b) G. K. Jahangiri, J.-L. Reymond, *ibid.* **1994**, *116*, 11264.
[93] E. Vedejs, J. A. Garcia-Rivas, *J. Org. Chem.* **1994**, *59*, 6517.
[94] Whereas **85a** and **85b** are carbon acids, **85c** is believed to transfer the aniline NH proton.
[95] Possibly, γ-protonation involves a [1,5] H-shift of the s-*cis* dienol. In the presence of amines, the enol/enolate equilibrium is shifted towards the enolate, thus suppressing γ-protonation.
[96] For the alternative possibility of an *anti* protonation of an enol or enolate (*anti*-S_E2' reaction), see V. R. Bodepudi, W. J. Le Noble, *J. Org. Chem.* **1994**, *59*, 3265.
[97] a) F. E. Romesberg, D. B. Collum, *J. Am. Chem. Soc.* **1994**, *116*, 9187; b) F. E. Romesberg, D. B. Collum, *ibid.* **1994**, *116*, 9198; c) F. E. Romesberg, D. B. Collum, *ibid.* **1995**, *117*, 2166, and references therein.
[98] P. Caubère, *Chem. Rev.* **1993**, *93*, 2317.
[99] For the importance of monomeric enolates as reactive species, see A. Abbotto, A. Streitwieser, *J. Am. Chem. Soc.* **1995**, *117*, 6358; F. Abu-Hasanayn, M. Stratakis, A. Streitwieser, *J. Org. Chem.* **1995**, *60*, 4688; for enantioselective hydroxylations of monomeric enolate species, see R. D. Bach, J. L. Andrés, F. A. Davis, *J. Org. Chem.* **1992**, *57*, 613; Y. Wei, R. Bakthavatchalam, X.-M. Jin, C. K. Murphy, F. A. Davis, *Tetrahedron Lett.* **1993**, *34*, 3715.
[100] C. Fehr, J. Galindo, unpublished results.
[101] Recently, the stability of ladder structures for lithium enolate/lithium amide mixed aggregates in solution was questioned, and six- or eight-membered ring

structures (obtained by formal removal of the inner "rungs") were favored [97a]. For disassembly of lithium amide ladder structures by insertion of THF molecules, see W. Clegg, L. Horsburgh, F. M. Mackenzie, R. E. Mulvey, *J. Chem. Soc. Chem. Commun.* **1995**, 2011.

[102] The comparison of pK_a values is often problematic, as these values are determined under conditions that differ from those prevailing in enolate protonations; see E. M. Arnett, K. D. Moe, *J. Am. Chem. Soc.* **1991**, *113*, 7288. It should also be stressed that proton donors that are seemingly too weak can protonate an enolate under kinetically controlled conditions to completion, if deprotonation of the resulting carbonyl compound is prohibited.

[103] M. A. Nichols, A. T. McPhail, E. M. Arnett, *J. Am. Chem. Soc.* **1991**, *113*, 6222.

[104] C. Lambert, F. Hampel, P. von R. Schleyer, *Angew. Chem.* **1992**, *104*, 1242; *Angew. Chem. Int. Ed. Engl.* **1992**, *31*, 1209; C. Lambert, P. von R. Schleyer, U. Pieper, D. Stalke, *ibid.* **1992**, *104*, 78; and **1992**, *31*, 77; M. C. Etter, G. Ranawake, *J. Am. Chem. Soc.* **1992**, *114*, 4430.

[105] K. Fuji, T. Kawabata, A. Kuroda, *J. Org. Chem.* **1995**, *60*, 1914.

[106] S. Hünig, *Houben-Weyl, Methods of Organic Chemistry, Vol. E21d* (Eds.: G. Helmchen, R. W. Hoffmann, J. Mulzer, E. Schaumann), Thieme, Stuttgart, **1995**, 3851.

EVENTS

GDCh

Fachgruppe Medizinische Chemie
International Symposium

How Rational Can Drug Design Be?

Frankfurt am Main/Germany, February 7, 1997

A Report about Novel Combinations of Rational Design and Screening Techniques
H. Kessler, München/D

Rational Drug Design: The Holy Grail
J. G. Topliss, Michigan/USA

The Discovery and Optimization of Potent Non-Peptidic Matrix-Metalloprotease Inhibitors
H. Kluender, West Haven/USA

Current Issues in De Novo Design
C. W. Murray, Macclesfield/GB

3D-QSAR: What Can We Learn from the Obtained Correlations?
G. Klebe, Marburg/D

Design of Pharmacokinetic Properties
D. A. Smith, Sandwich/GB

Molecular Pharmacological and Modelling Approaches in the Design of Agonists and Antagonists of G-Protein-Coupled Receptors
M. A. Cascieri, Rahway/USA

Structure-Based Drug Design: Which Information Can Really Be Obtained from Structures?
H. Kogler, Frankfurt am Main/D

Design of New Peptide Mimetics of both Continous and Non-Continous Peptide, Epitopes and their Pharmacological Profiles
D. C. Horwell, Cambridge/GB

Indirect Drug Design: Fact or Fantasy? A Case Study with Squalene Cyclase Inhibitors
P. Müller, Biberach/D

Further Information

GESELLSCHAFT DEUTSCHER CHEMIKER
Abteilung Tagungen, Postfach 90 04 40, D-60444 Frankfurt am Main, Germany

Phone	+49 (69) 7917-366	E-Mail	tg@gdch.de
Fax	+49 (69) 7917-475	GDCh-Homepage	http://www.gdch.de

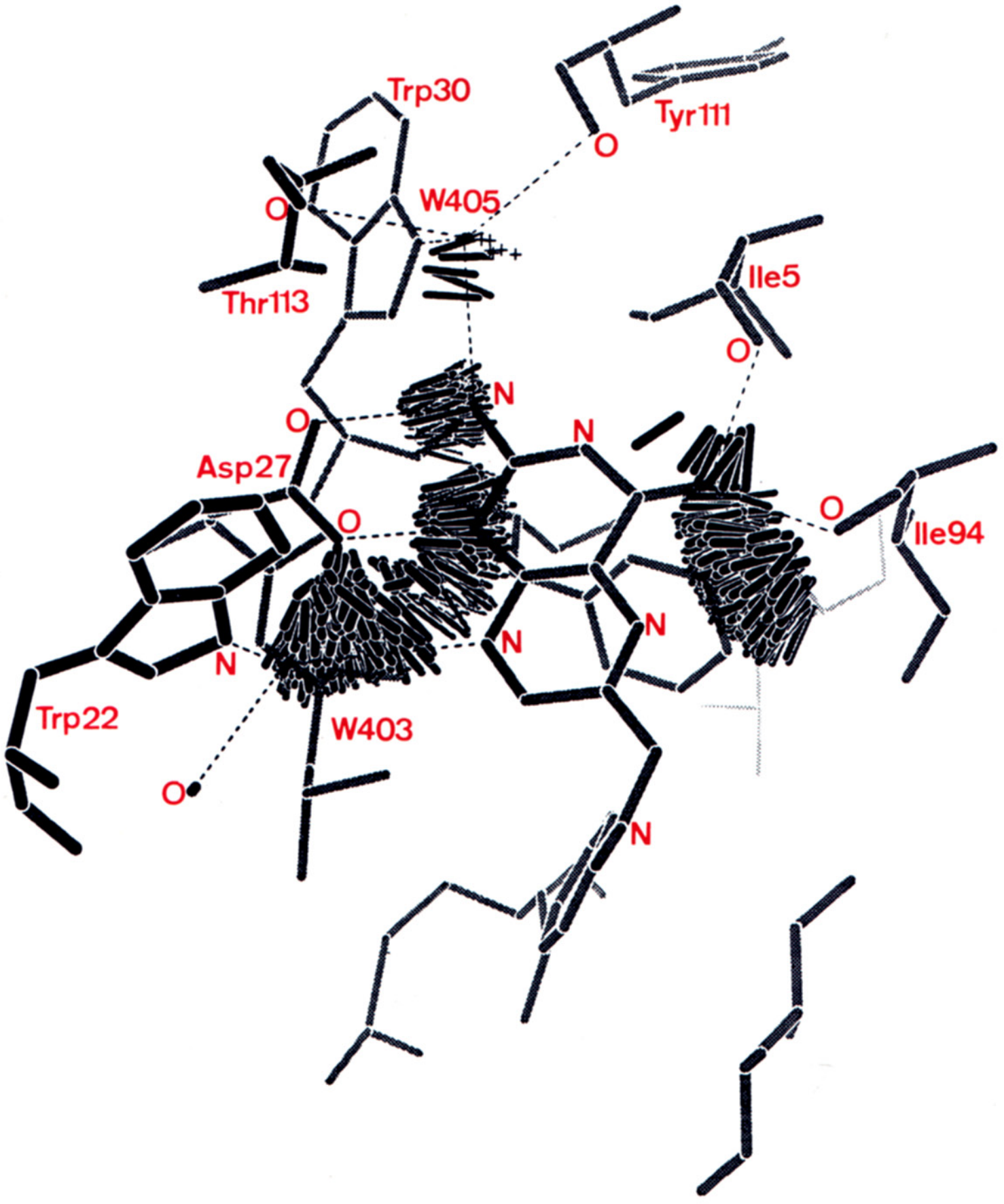

The spatial orientations of hydrogen-bonding contacts, which were derived from the crystal structures of small molecules (mass of rods), fit excellently with the orientation of methotrexate in the binding pocket of the dihydrofolate reductase from *Escherichia coli*.

What Can We Learn from Molecular Recognition in Protein–Ligand Complexes for the Design of New Drugs?

Hans-Joachim Böhm* and Gerhard Klebe*

The understanding of noncovalent interactions in protein–ligand complexes is essential in modern biochemistry and should contribute toward the discovery of new drugs. In the present review, we summarize recent work aimed at a better understanding of the physical nature of molecular recognition in protein–ligand complexes and also at the development and application of new computational tools that exploit our current knowledge on structural and energetic aspects of protein–ligand interactions in the design of novel ligands. These approaches are based on the exponentially growing amount of information about the geometry of protein structures and the properties of small organic molecules exposed to a structured molecular environment. The various contributions that determine the binding affinity of ligands toward a particular receptor are discussed. Their putative binding site conformations are analyzed, and some predictions are attempted. The similarity of ligands is examined with respect to their recognition properties. This information is used to understand and propose binding modes. In addition, an overview of the existing methods for the design and selection of novel protein ligands is given.

Keywords: computer chemistry · drug design · molecular recognition · protein–ligand complexes

1. Introduction

Molecular recognition in protein–ligand complexes is responsible for the selective binding of a low molecular weight ligand to a specific protein.[1] In biological systems, the protein–ligand interactions serve a particular purpose, for example an enzymatic transformation, substance transportation, or signal transduction. They are usually noncovalent in nature. The experimentally determined binding constants K_i are typically in the range of 10^{-2} to 10^{-12} M, which corresponds to a negative free energy of binding of 10–80 kJ mol^{-1} in aqueous solution.[2]

Compounds that interact specifically with a particular protein of pharmacological interest can be useful in the treatment of various diseases. In particular, enzymes that regulate biochemical reactions are important targets in contemporary medicinal chemistry. Two representative examples should be mentioned: 1) The enzyme inhibitor trimethoprim (**1**), which inhibits the bacterial dihydrofolate reductase, has proven its potency in the treatment of bacterial infections for quite some time.[3] 2) Recently dorzolamide (**2**) has been approved as a drug against glaucoma.[4] This inhibitor of carbonic anhydrase is the first compound introduced into the market for which the methods of structure-based drug design contributed significantly to its discovery. Besides enzymes, another important class of protein targets are receptors such as G-protein-coupled receptors.[5]

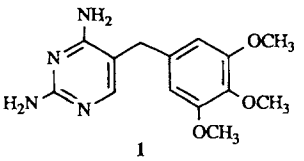

1

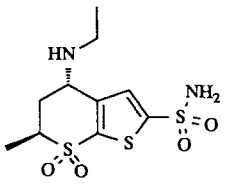

2

Our current knowledge about the structures of protein–ligand complexes is derived mostly from globular proteins. Although a few membrane proteins have been studied by X-ray crystallography,[6–13] no high-resolution structure of a pharmacologically relevant, membrane-bound receptor is yet available. Therefore we restrict our discussion to data from small-molecule ligands bound to globular proteins, especially enzymes. However, we are confident that data from these systems are also applicable to membrane-bound receptor proteins.

An understanding of the principles of molecular recognition in protein–ligand complexes is important for structure-based ligand design. If the three-dimensional (3D) structure of a given protein is known, this information can be directly exploited in

[*] Dr. H.-J. Böhm[+], Prof. Dr. G. Klebe[++]
BASF AG, D-67056 Ludwigshafen (Germany)

[+] New address:
Hoffmann-La Roche AG, Pharma Research – New Technologies
CH-4002 Basel (Switzerland)
Fax: Int. code +(61)6881075
e-mail: Hans-Joachim.Boehm@Roche.com

[++] New address:
Institut für pharmazeutische Chemie der Universität
Marbacher Weg 6, D-35032 Marburg (Germany)
Fax: Int. code +(6421)288994
e-mail: klebe@mailer.uni-marburg.de

 © VCH Verlagsgesellschaft mbH, D-69451 Weinheim, 1996 0570-0833/96/3522-2589 $ 15.00+.25/0

the design process. Progress in the isolation and crystallization of pure proteins and the subsequent structure determination either by multidimensional NMR spectroscopy[14–17] or by X-ray crystallography[18,19] has led to an exponential increase in the number of solved protein structures. The August 1995 release from the Brookhaven Protein Database contains more than 4000 entries.[20] Furthermore, our knowledge on the structures of small organic molecules and their interactions with a structured molecular environment is based on the steadily increasing supply of crystal structures stored in the Cambridge Crystallographic Database (>140000 entries),[21–23] and the results obtained from high-level ab initio calculations.[24]

As a consequence, structure-based design and discovery of protein ligands has emerged as a new tool in medicinal chemistry.[25] In particular, the knowledge of the three-dimensional structure of a protein can be used to derive new protein ligands with improved binding properties (Table 1).[26–42] In most examples, a tailored optimization of a known lead structure has been achieved but in some cases the 3D structures have been used to design novel ligands "de novo". This new approach in drug discovery calls for the development of new software tools. Algorithms and methods along these lines have emerged in the literature. They are concerned with the following questions:

- What is the binding affinity of a novel ligand toward a particular receptor?
- What are the likely conformations of a ligand at the binding site?
- What are the similarities of different ligands in terms of their recognition capabilities?
- Where and in which orientation will a ligand bind to the active site?
- What strategies are available to select and rank new protein ligands?

Structure-based ligand design is an iterative approach. First of all, the crystal structure or a model derived from the crystal structure of a closely related homologue of the target protein, preferably complexed with a ligand, is required. This complex acts as the starting point for identifying the binding mode and conformation of a ligand under investigation as well as the essential aspects that determine its binding affinity. This knowledge is then used to create new ideas about how to improve an existing ligand or how to develop new alternative bonding skeletons. Computational methods supplemented by molecular graphics are applied to assist this step of hypotheses generation. At this stage, discussions with synthetic organic chemists take place to eliminate unfeasible proposals for synthesis. Then, the newly proposed compounds have to be synthesized or purchased and tested. Subsequently, their binding properties are determined by biochemical, crystallographic, and spectroscopic methods. By carefully analyzing the obtained results, the next cycle of ligand design is started. The important advantage of this approach is clearly the information provided by every new 3D structure of a protein–ligand complex. They reveal the binding

Table 1. Examples of structure-based design of enzyme inhibitors.

Enzyme	Therapeutic goal	Ref.
dihydrofolate reductase	antibacterial agent	[28]
thrombin	anticoagulant agent	[36,42]
elastase	treatment of emphysema	[40,50,51]
neuramidase	antiviral agent	[35]
thymidylate synthase	anticancer agent	[27,30]
purine nucleoside phosphorylase	anticancer agent	[33]
HIV protease	anti-AIDS agent	[27,29,34]
phospholipase A_2	antiinflammatory agent	[32,38]
trypanosomal GAPDH	antiparasitic agent	[26,41]
glycogen phosphorylase	treatment of diabetis	[58]
carbonic anhydrase	treatment of glaucoma	[4,27,31]

Hans-Joachim Böhm, born in 1956 in Frankfurt am Main, studied chemistry in Karlsruhe, where he received his doctorate in theoretical chemistry under the supervision of Reinhart Ahlrichs in 1984. During work on his thesis, he spent one year as a DAAD fellow at the Department of Physical Chemistry at the University of Cambridge, where he worked with Ian McDonald and Paul Madden. In 1993 he habilitated in theoretical chemistry at the Universität Karlsruhe. From 1985 to 1987 he worked in the central research laboratory of Siemens AG in München, and subsequently from 1988 to 1996 at the Hauptlaboratorium of BASF AG in Ludwigshafen, where he was responsible for the development and application of new methods for structure-based drug design. In April 1996, he joined Hoffmann-La Roche in Basel.

H.-J. Böhm

G. Klebe

Gerhard Klebe, born in 1954 in Frankfurt am Main, studied chemistry at the university there, and received his doctorate in physical chemistry in 1982. As a fellow of the Studienstiftung he spent a year in Grenoble at the CNRS and ILL at the Crystallographic Institute of Erwin F. Bertaut. After post-doctorate periods in crystallography with Hartmut Fuess (Frankfurt) and Hans-Beat Bürgi (Bern, Switzerland), he joined the Hauptlaboratorium of BASF AG in 1984. In 1992 he habilitated in pharmaceutical and structural chemistry at the Universität Heidelberg. In the summer of 1995 he received a call to a chair in pharmaceutical chemistry at the Universität Marburg, and he took up the position in the winter semester 1996/97. His main field of interest is the determination and correlation of crystal structures, and the development and application of methods for structure-based drug design.

modes of the ligands. If a proposed ligand does not show the expected affinity, the analysis often gives an explanation for this finding. This can then provide new insights on how to improve the ligand.

Besides lead optimization this approach also offers a new route to create completely novel lead structures. Based on the structural features of a particular binding site, de novo design strategies propose novel molecular frameworks as putative ligands. The suggestions are based on extensive database searches or on the docking and assembly of smaller molecular portions into larger drug-size molecules.

Despite the above-mentioned advances in experimental methods, we still face a situation that for many of the pharmacologically relevant proteins no 3D structures to atomic resolution are available. What can structure-based ligand design contribute in the absence of an experimental structure? A comparative analysis of known ligands can provide some ideas about the essential prerequisites for receptor binding. Such similarity analyses of existing ligands with respect to their recognition properties can stimulate the discovery of novel molecules with deviating bonding skeletons. However, most crucial are reliable estimates about possible binding geometries within a set of ligands. This information can be derived from either pharmacophore hypotheses or systematic ligand rigidizations. Methods applied to handle these problems have to be developed and subsequently validated by using the growing knowledge base of structurally characterized protein–ligand complexes.

In the present review, we summarize some of the recent experimental results that shed some light on the physical nature of protein–ligand interactions. We do not attempt to review all recent work on the nature of these interactions but instead focus on structural aspects that provide a better understanding and description of the relationship between 3D structures and binding properties. Our own recent studies have focussed on the question of how the vast and rapidly growing knowledge base on the 3D structures of protein–ligand complexes and small organic molecules can be exploited in the development of computational procedures to predict binding affinities, molecular conformation, and binding modes. These different approaches are used for the design of novel protein ligands. Nevertheless, we will show in this contribution that ligand design still requires a substantial amount of basic research and thus is far from being a pure engineering technique.

2. Experimental Data Used To Correlate Structure with Binding Properties

Herein, we evaluate structural and binding data from different sources. Before we start to draw conclusions from these data, we would like to summarize some aspects concerning their accuracy. Binding site geometries are obtained from protein–ligand complexes, mainly determined by protein crystallography. Structures from these experiments are not resolved to atomic resolution; however, they are the only reliable source to learn about the protein–ligand interface. The average errors in atomic positions depend on the diffraction powers of the protein crystals. For a resolution of about 2.4 Å it has been estimated to about 0.4 Å in space[43–46] (as a general rule of thumb, the positional error amounts to approximately 1/6 of the resolution). Owing to improvements in the crystal growth techniques and the equipment used for diffraction experiments, the resolution of structure determinations has steadily increased over recent years. If a resolution of 1.5–1.8 Å is achieved and full occupancy of the binding pocket by the ligand is detected, the electron density is well defined and the molecules can be docked without ambiguities. However, in the range beyond 2.0–3.0 Å, or in the case of partial occupancy, the assignment becomes more difficult. Usually, small molecules are modeled into the trace of the electron density during structure determination.[47] The setting of the initial ligand conformation is the most crucial step in this procedure. Starting with some arbitrary conformation using standard bond lengths and angles of the ligand, subsequent rotations are manually performed about the various rotatable bonds of the ligand in order to optimize its fit to the electron density. Finally, the entire protein–ligand complex is refined to minimize the difference between observed and calculated structure factors. Due to an unsatisfactory observation-to-parameter ratio in protein structure determination, the manually adjusted conformation of the ligand is often kept rigid during refinement. At best, some degrees of torsional freedom are allowed to vary according to the applied force field and the structure–factor constraints.[48] However, these force fields are usually tailored toward protein structures, and their accuracy for normal organic molecules is difficult to assess. These limitations are of minor importance if data from crystals that diffract to high resolution are used, but become more serious with decreasing resolution, disorder, or partial occupancy.

For the statistical analyses of conformational preferences and interaction geometries, data from crystal structures of small molecules are used. Generally, these data are resolved to atomic resolution with low positional errors. The positions of hydrogen atoms are less precisely defined than those of heavier atoms by X-ray diffraction. However, the accuracy of structural data of small molecules can be influenced, for example, by crystal defects, inappropriate data collection and reduction, space group uncertainties, or disorder phenomena. Data are retrieved from the Cambridge Crystallographic Database[21–23] by using a predefined query structure. In some cases the matching of a chemical connectivity onto crystal coordinates is not unambigious. Thus, a small number of inadequate examples might still be contained in the data sets collected for the statistical evaluation as undetected noise.

The experimental binding data can be used to derive models for predictions of the affinities. Difficulties arise if binding data from different laboratories obtained on different proteins are compared. Variations in the experimental conditions (e.g., temperature, salt concentration) can have an impact on the data. For instance, several measurements have been published on the same protein–ligand complex, however, a variation of up to a factor of five[49] has been reported. This finding stands as a caveat and poses a limit to any theoretical description.

3. Noncovalent Interactions in Protein–Ligand Complexes

Low molecular weight ligands can interact with macromolecular receptors through both covalent and noncovalent interactions. Examples of ligands that form covalent bonds with the

target protein are trifluoromethyl ketone inhibitors of elastase,[50, 51] β-lactam antibiotics, aspirin, and other nonsteroidal antiinflammatory drugs.[52] However, in the present discussion, we shall exclude such examples and consider only noncovalently interacting ligands. The major contributions to noncovalent protein–ligand interactions are shown in Figure 1, in which the

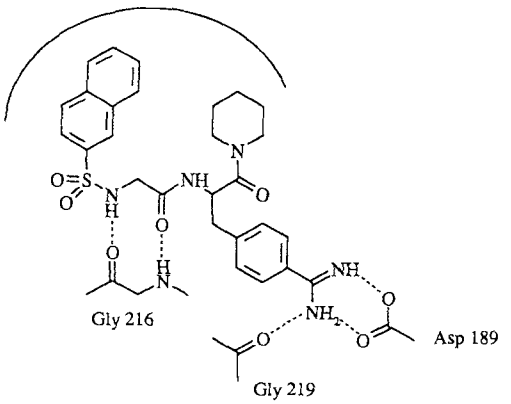

Fig. 1. Interactions between the serine protease thrombin and the thrombin inhibitor NAPAP, as observed in the X-ray crystal structure of the complex solved by Brandstedter et al. [53]. The arc denotes the lipophilic binding site.

thrombin–NAPAP complex[53] is used as an example. Usually, several hydrogen bonds are formed between the protein and the ligand.[54] In addition, oppositely charged functional groups of the protein and the ligand are paired. Furthermore, lipophilic groups of the ligand are found in hydrophobic pockets formed by side chains of the hydrophobic amino acids. The binding constant K_i and the related free binding enthalpy ΔG ($\Delta G = -RT\ln K_i$) have been determined for a large number of protein–ligand complexes. The binding constant K_i is routinely measured in numerous laboratories.

The knowledge-base from these data immediately leads to the following questions: 1) How does the binding constant relate to structural properties of a complex? 2) What are the important properties that allow a protein to bind a ligand tightly and selectively? 3) What makes a cleft in a protein structure a ligand binding site? Our current understanding of protein–ligand interactions is still far from being sufficient to fully answer these questions. The most important prerequisite appears to be good steric and electronic complementarity between protein and ligand. However, due to desolvation effects this criterion alone is not sufficient to fully describe tight binding of ligands.

3.1. Hydrogen Bonds

We have analyzed a set of 80 diverse protein–ligand complexes for which both the 3D structure and the binding constant are known. In Figure 2 the binding constants K_i are plotted against the number of hydrogen bonds formed between proteins and their ligands. Although the binding affinities roughly increase by one order of magnitude per hydrogen bond, it is evident that there is a very broad scatter of the data. Several protein–ligand complexes exhibit strong binding in the nanomolar range with no hydrogen bonds (e.g., the complex between the retinol binding protein and retinol[55]) or very few hydrogen bonds (e.g. that

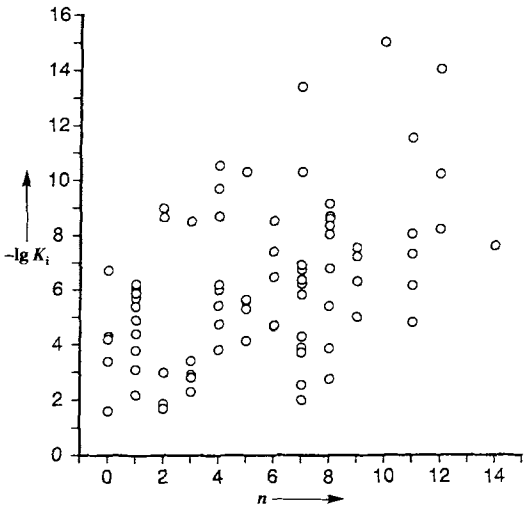

Fig. 2. The contribution from hydrogen bonds to the binding affinity of protein ligands. The logarithm of the binding constant K_i is plotted as a function of the number n of hydrogen bonds between the protein and the ligand (data were extracted from 80 structures of protein–ligand complexes determined by crystallography).

between an antibody and a steroid,[56] as well as that between an antibody and fluorescein [57]). The binding of these ligands arises from nonpolar interactions. Furthermore, some ligands form many hydrogen bonds with the protein but exhibit only very weak binding (e.g. glycogen phophorylase–glucose,[58] hemagglutinin–sialic acid,[59] gluthathion S transferase–gluthathion complexes[60]). Interestingly, these ligands are all characterized by the absence of significant lipophilic groups.

On the other hand, our current knowledge indicates that unpaired buried polar groups at the protein–ligand interface are strongly adverse to binding. A recent statistical analysis of high-resolution protein structures showed that in proteins less than 2% of the polar atoms are buried without forming a hydrogen bond.[61] There is a strong tendency to saturate polar groups in hydrogen bonds. Therefore, in the ligand design process one has to ensure that the polar functional groups either of the protein or the ligand will find suitable counterparts if they become buried upon ligand binding.

In addition to hydrogen bonding, there are other important polar interactions in protein–ligand complexes such as coordinative bonds with metal ions. For example, hydroxamic acids and thiols bind strongly to the zinc ion in the active site of metalloproteases.[62] This interaction is the most important contribution to binding in many metalloprotease-inhibitor complexes.

3.2. The Role of Solvent in Polar Protein–Ligand Interactions

The contribution of a hydrogen bond depends on its microscopic environment in the protein–ligand complex and can vary drastically. Desolvation effects can completely compensate for the intermolecular hydrogen bond so that the net contribution to binding is close to zero. On the other hand, large contributions to the binding affinity seem to arise from those hydroxy groups that constitute an essential structural element of a tran-

sition state analog in enzyme inhibitors.[63] As demonstrated by Matthews et al. for lysozyme mutants, the effect of buried and solvent-accessible salt bridges on protein stability differs considerably.[64]

An instructive example underlining the importance of desolvation effects was reported by Bartlett et al. for the binding of inhibitors containing phosphonamides, phosphonates, and phosphinates to thermolysin.[65] The measured binding constants are summarized in Table 2. The interactions between

Table 2. Binding constants K_i [μM] for inhibitors of thermolysin containing a phosphonamide (X = NH), phosphonate (X = O) or phosphinate (X = CH_2).

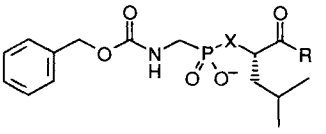

R	X = NH	O	CH_2
OH	0.76	660	1.4
Gly-OH	0.27	230	0.3
Phe-OH	0.08	53	0.07
Ala-OH	0.02	13	0.02
Leu-OH	0.01	9	0.01

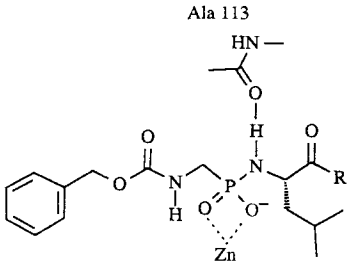

Scheme 1. Interactions between the phosphonamide group of the thermolysin inhibitor ZG^{P}LR and thermolysin.

the phosphonamide moiety and thermolysin are shown in Scheme 1. The PO_2 group interacts with the zinc atom, and the NH group forms a hydrogen bond with the backbone carbonyl group of Ala113. The replacement of this NH group by a CH_2 group does not affect the binding affinity. These results can be understood by comparing the number of hydrogen bonds formed between the inhibitor and the protein or the solvent. The NH group of the phosphonamide forms a hydrogen bond with the protein. It also forms a hydrogen bond with a water molecule in solution. Therefore, ligand binding maintains the total number of hydrogen bonds. On the other hand, the CH_2 group is unable to form a hydrogen bond with thermolysin or with a water molecule in solution. Therefore, the hydrogen bond inventory is also balanced for the CH_2 group. In contrast, the analogous phosphonates exhibit a 1000-fold reduced binding affinity to thermolysin (see Table 2). This poor binding is a result of the repulsive electrostatic interaction between the oxygen atom of the ligand and the C=O group of Ala113, which both bear a negative partial charge. The oxygen derivative lacks a hydrogen bond, which is presumably present in solution. The X-ray structure analysis of the phosphonate revealed that this inhibitor does indeed bind to thermolysin in the same way as the phosphonamide.[66] Interestingly, the relative binding affinities of these three classes of inhibitors were correctly computed by Bash et al.[67] and Merz and Kollman[68] by using a thermodynamic perturbation method implemented with molecular dynamics simulation (see also Section 3.7).

Tight binding can be achieved if the total number of hydrogen bonds increases upon ligand binding. We believe that the complex avidin–biotin[69] achieves tight binding partly through a large number of hydrogen bonds that water molecules cannot form to the same extent at the binding site. The X-ray structures of both the complexed and uncomplexed protein have been determined. The binding site of the uncomplexed protein contains four water molecules, according to the X-ray structure. If we assume that this figure underestimates the actual number of water molecules in the binding site because mobile water molecules cannot be detected in the crystal structure, and employ a molecular mechanics calculation to fill the binding site with water molecules, we end up with nine to ten water molecules [Böhm, unpublished results]. These water molecules still form fewer hydrogen bonds with avidin than biotin.

One of the keys to a better understanding of protein–ligand interactions is the role of water. All direct protein–ligand interactions compete with interactions to water molecules. Both the ligand and the protein are solvated before complex formation. They lose part of their solvation shell upon binding, a process that involves various enthalpic and entropic contributions.[70–73] Hydrogen bonds are broken and new ones are formed. Furthermore, the solvent structure is reorganized at the protein–ligand interface. Water has the unique ability to form an extensive network of hydrogen bonds.[54] The hydrogen bond between two water molecules in the gas phase is strong: the dimerization enthalpy is roughly $-20\ kJ\,mol^{-1}$.[74, 75] Therefore, if the binding of a ligand simply replaces tightly bound water molecules and does not yield additional interactions, its binding affinity will be small. On the other hand, the replacement of loosely bound water molecules contributes to binding because both entropic (release of water molecules into bulk solvent) and enthalpic factors (favorable interactions with other water molecules) favor the replacement by the ligand. Unfortunately, detailed investigations of the role of water molecules in protein–ligand interactions have underlined a fairly complex picture.[76] For example, results from recent calorimetric studies suggest that in certain cases solvent reorganization provides more than 25% of the observed enthalpy of binding.[77] An upper limit of $28\ J\,mol^{-1}\,K^{-1}$ for the entropy gain from the release of a water molecule into bulk solvent was given by Dunitz[78] based on thermodynamic arguments.

Interestingly, several small molecules containing functional groups, which are frequently involved in protein–ligand interactions, do not associate in water. For example, acetic acid does not form a stable complex with guanidine in water.[79] Similarly, simple amides do not associate in water.[80] Apparently, the direct interaction between the small molecules is not strong enough to override the factors favoring the dissociation such as interactions with solvent molecules. As further discussed by Williams and others,[70–73] there is also an entropic penalty for complex formation, which may overcompensate favorable interactions.

3.3. Lipophilic Interactions

A plot of the binding constants K_i against the lipophilic contact surfaces using the same 80 protein–ligand complexes as for the hydrogen-bond statistics (see Fig. 2) is given in Figure 3.

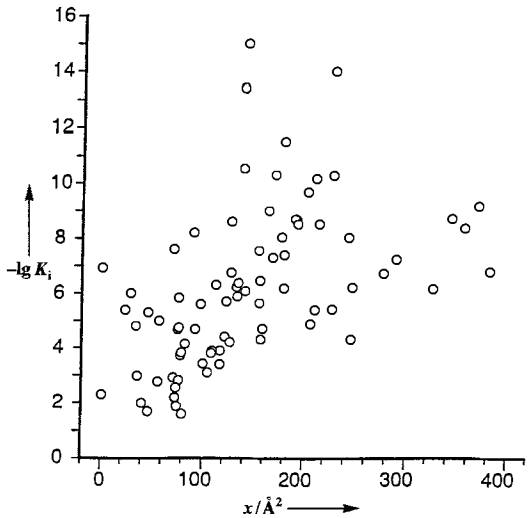

Fig. 3. The contribution from lipophilic contacts to the binding affinity of protein ligands. The logarithm of the binding constant K_i is plotted as a function of the lipophilic contact surface x between the protein and the ligand (data were extracted from 80 structures of protein–ligand complexes determined by crystallography).

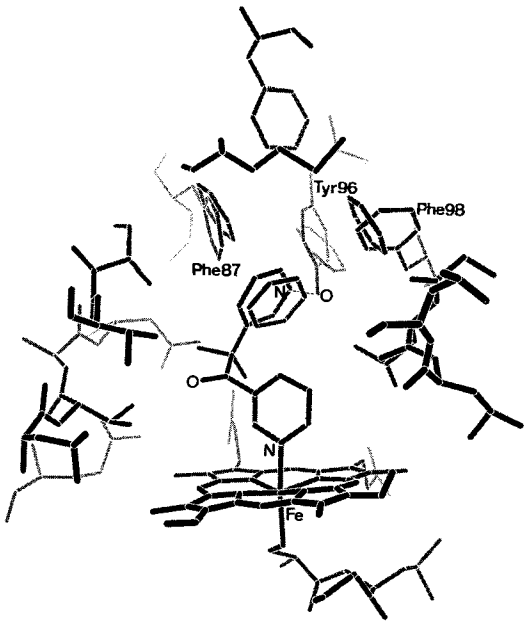

Fig. 4. Structure of the metyrapone–cytochrome $P450_{CAM}$ complex determined by crystallography, superimposed with a section from the crystal packing of benzene. Four phenyl moieties fall close to the aromatic groups of the ligand, Phe87, Tyr96, and Phe98.

There is a correlation between the binding affinity and the lipophilic contact surface, but the spread of data is again large. Retinol is an example of a ligand that binds to the protein (retinol-binding protein) solely by lipophilic interactions.[54] The X-ray structure analysis of this complex shows no hydrogen bonds between the protein and the ligand. The binding constant K_i is 190 nM, corresponding to a free energy of binding of $-38\ kJ\,mol^{-1}$. The total molecular surface of retinol, as determined by a grid-based program,[81] amounts to 326 $Å^2$ of which 295 $Å^2$ (90%) become buried upon binding. On the other hand, ligands such as SO_4^{2-} have no lipophilic contact surface, but are tighly bound to an appropriate receptor (e.g. SO_4^{2-} binds to the sulfate binding protein with $K_i = 100$ nM[82]). The generally accepted view is that lipophilic interactions are mainly due to the replacement and release of ordered water molecules and are therefore entropy-driven.[83, 84] The entropic gain arises because the water molecules are no longer positionally confined. There are also enthalpic contributions to lipophilic interactions. Water molecules occupying lipophilic binding sites are unable to form hydrogen bonds with the protein. If they are released they can form hydrogen bonds with other water molecules. In addition, there is a favorable interaction between the lipophilic groups in contact (mainly dispersion interactions).

Recently the role of specific interactions between aromatic rings has attracted increasing attention.[85] A statistical analysis of the interaction between phenyl rings in proteins reveals a preference for contact geometries that lead to electrostatically favorable quadrupole–quadrupole interactions.[86] In addition, data from the binding of aromatic guest molecules to cyclophanes in water suggest that the binding is enthalpy-driven.[87] We observed a striking similarity between the noncovalent contact patterns of aromatic rings found in the crystal packing of benzene and in several protein–ligand or aromatic host–guest complexes.[88] An example is shown in Figure 4. Furthermore, due to their large polarizability, aromatic side chains can also interact with the positive charge of a quarternary ammonium group. This type of interaction is found for example in the complex of acetylcholinesterase with acetylcholine.[89] It also contributes significantly to the binding in host–guest complexes.[90] On the other hand, results obtained from many different protein–ligand complexes indicate that a phenyl group occupying a lipophilic binding site can be replaced by a cyclohexyl group without loss of binding affinity.[91] In addition, recent results on the effect of aromatic interactions on conformational preferences appear to contradict the notion of a dominant role of this type of interaction.[92]

3.4. Additivity of Protein–Ligand Interactions

An important aspect of protein–ligand interactions is the additivity of group contributions. Data from protein mutants yield estimates of $-5 \pm 2.5\ kJ\,mol^{-1}$ for the contribution from individual hydrogen bonds to the binding affinity.[93, 94] Similar values have been obtained for the contribution of an intramolecular hydrogen bond to protein stability.[95–97] The consistency of values derived from different proteins suggests some degree of additivity in the hydrogen-bonding interactions. In a recent analysis of thermolysin-inhibitor complexes, Bohacek and McMartin[98] observed a linear relationship between the binding constant and the number of hydrogen bonds and lipophilic contacts. Similar observations have been reported by Schneider and coworkers for the binding of host–guest complexes.[99] The concept of pairwise additivity of noncovalent interactions in protein–ligand complexes is also supported by the success of simple empirical approaches,[2, 81, 100–102] which assume this additivity.

Similar to polar interactions, the additivity of apolar interactions has been the subject of several investigations. For lipophilic interactions, the free enthalpy of binding is proportional to the lipophilic surface buried from solvent.[103–105] Contributions to ΔG for lipophilic surfaces that are removed

from the aqueous solution and get buried upon binding, range from 80[106-108] to 200 J mol^{-1} Å^{-2}).[109] On the other hand, the binding of some inhibitors to carboxypeptidase-A offers a striking example for nonadditive effects. The replacement of the C-terminal alanine by phenylalanine in the inhibitor ZFA^{P}(O)A increases its lipophilic surface. As a consequence, the binding affinity is enhanced by more than a factor of 50000.[110] The replacement of the second alanine residue by valine also increases the lipophilic surface and increases binding affinity by an additional factor of 100. ZFV^{P}(O)F binds to carboxypeptidase-A with $K_i = 10-27$ fM. The first strong affinity enhancing replacement (Ala → Phe) results in a perfect filling of a lipophilic pocket, which was unoccupied in the complex with the Ala derivative. The second less enhancing replacement (Ala → Val) has two effects. First, the larger side chain of Val results in an increased intermolecular lipophilic contact with the protein. Second, there is also a larger intramolecular lipophilic contact in the protein-bound conformation of the Val derivative than in that of the Ala peptide. The second effect stabilizes the bound conformation in solution, resulting in a preorganization of the ligand. This phenomenon of minimization of the lipophilic surface in aqueous solution was termed "hydrophobic collapse" by Wiley and Rich.[111] Similar behavior is observed for the thrombin inhibitor D-Phe-Pro-boro-Arg (where "boro" of boro-Arg indicates that the carbonyl group of the amino acid residue is replaced by $B(OH)_2$).[112] The intramolecular contact between the side chains of the amino acids D-Phe and Pro stabilizes the receptor-bound conformation. NMR studies reveal a conformation for this molecule in water that is very similar to the receptor-bound one. The authors estimate that the preorganization of the ligand increases the binding affinity by a factor of 10. Other examples of preorganized protein ligands have been reported.[113] Improved binding due to preorganization is clearly a nonadditive phenomenon.

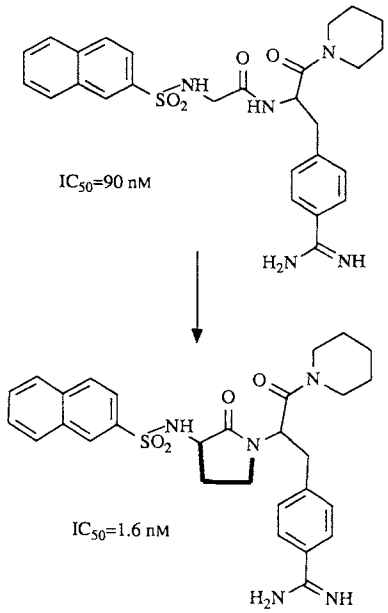

Scheme 2. The introduction of a lactam (highlighted as thick bonds) into the known thrombin inhibitor NAPAP (top) reduces the flexibility and improves the binding affinity by a factor of 60.

3.5. The Role of Ligand Flexibility and Mobility

The flexibility of the ligand is another important factor in determining the strength of protein–ligand interactions. In this section we discuss energetic aspects (structural aspects are described in Section 4). If a flexible and a rigid ligand form the same pattern of hydrogen bonds and lipophilic interactions with the protein, the rigid ligand will exhibit much stronger binding. A central tenet in structure-based ligand design is that the binding affinity of a flexible ligand will be improved if its conformational motion can be restricted to that of the bound state.[114] Several studies have been reported on the design of constrained inhibitors that are found to bind much more tightly than the unconstrained structure.[36, 37, 115] The consequence of conformational rigidization is illustrated in a study by Mack et al. on inhibitors of thrombin.[36] The X-ray structure of thrombin complexed with the inhibitor NAPAP was used to design novel inhibitors with improved binding properties. The 3D structure suggested the introduction of a lactam ring as shown in Scheme 2. The conformational immobilization by the additional ring reduces the number of rotatable bonds in the inhibitor. The binding affinity of the new inhibitor to thrombin is 60 times higher than NAPAP.

Experimental data indicate that in several cases the ligand still has considerable mobility when bound to the protein. An interesting example is the binding of camphane, adamantane, and thiocamphor to cytochrome $P450_{CAM}$.[116] These ligands do not form hydrogen bonds to the enzyme and can freely rotate in the binding site. As a result of the residual mobility they are hydroxylated without clear stereoselectivity. In a recent molecular dynamics simulation of this system, a good correlation between the calculated statistical probability of the various ligand orientations in the active site with the experimentally observed hydroxylation rates was observed.[117]

Crystallographic and thermodynamic studies, performed in parallel by Weber et al.,[118] demonstrate that the water displacement from the ligand binding site, and the retention of considerable ligand flexibility in the bound state contribute favorably to entropy changes upon ligand binding. In a series of streptavidin ligands, the ligand exhibiting the highest binding affinity appears to have a larger residual mobility than the other compounds.[118] Similar results have also been obtained for the binding of small guest molecules to α-, β-, and γ-cyclodextrins in water.[119]

3.6. Enthalpic and Entropic Contributions to Protein–Ligand Interactions

In summary it appears that the physical nature of ligand binding is more complicated than has been assumed by many workers in the field. Figure 5 summarizes various effects that determine the binding affinity. The ligand and the protein binding site are fully solvated before binding; the polar groups form hydrogen bonds with the solvent. The ligand is usually flexible with several rotatable bonds and can, in principle, adopt a potentially large number of low energy conformations (see Section 4). The protein is also flexible and its conformation in the unbound state can be significantly different from that in the protein–ligand complex. Upon binding to the protein, the lig-

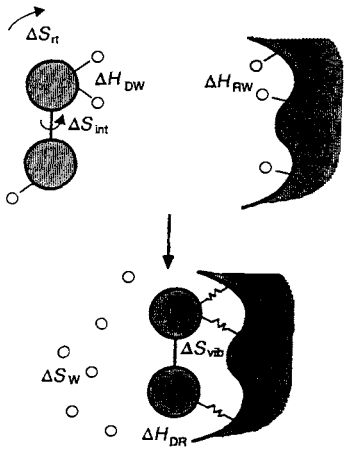

Fig. 5. Factors that influence the strength of protein–ligand interactions. In the uncomplexed state (top), the protein receptor (R) and drug ligand (D) both interact with water molecules (small circles, ΔH_{DW}, ΔH_{RW}). On complexation, an enthalpic contribution ΔH_{DR} arises from direct protein–ligand interactions. In the unbound state the ligand has an overall rotational and translational entropy ΔS_{rt} and an internal entropy ΔS_{int} owing to conformational degrees of freedom. Upon binding, both terms change; they are (partially) compensated by an increase in entropy due the liberation of bound water from the surface and from the binding site of the protein and the ligand (ΔS_W). In addition, new low-frequency vibrational modes associated with the noncovalent protein–ligand interactions contribute to this value (sketch adapted from Andrews et. al [2]).

and loses part of its solvation shell and replaces the water molecules that occupy the binding site. This process involves the breaking of several hydrogen bonds with water molecules. The ligand is then able to form favorable direct interactions with the protein. As a consequence of binding, the ligand and also the protein may change their conformation and also lose some internal flexibility. Due to steric restrictions of the binding site, certain parts of the conformational space of the ligand are no longer accessible.

ΔG has an enthalpic and an entropic component ($\Delta G = \Delta H - T\Delta S$). Both individual contributions to binding can be obtained, for example, from microcalorimetric measurements.[120] Unfortunately, these important experimental studies on the enthalpic and entropic contributions to ligand binding are still sparse. Nevertheless, the available data[121–124] suggest a number of conclusions. First, and most important, all studies show that there is no correlation between the binding enthalpy ΔH and the free binding enthalpy ΔG. For a given protein, different ligands can bind by enthalpy- or entropy-driven mechanisms. For example, the binding of biotin to streptavidin is enthalpy-driven, whereas the binding of azobenzene ligands to the same protein is entropy-driven.[125] If ΔH is plotted against ΔS for a set of related protein ligands, frequently a straight line is obtained. This enthalpy–entropy compensation has been explained by a solvent reorganization effect.[126]

The experimental determination of ΔH and ΔS sometimes yields surprising results. For example, Connelly et al.[94] studied the thermodynamics of hydrogen bond formation in the complex of FK506 or rapamycin with FK506-binding protein. Binding to the wild type and to the mutant Tyr82 → Phe was studied. From X-ray studies, it is known that the side chain of Tyr82 forms a hydrogen bond with the ligand. If Tyr82 is replaced by Phe, one hydrogen bond between the protein and the ligand is lost. As expected, the ligand binding affinity is slightly reduced by the replacement of Tyr with Phe. The free enthalpy difference is $4 \pm 1.5\ kJ\,mol^{-1}$. Somewhat unexpectedly, however, this destabilization is attributed to an entropy loss. In other words, the formation of this particular hydrogen bond is enthalpically unfavorable but entropically favorable. The entropy gain appears to be mainly due to the replacement of two water molecules.

In order to understand and be able to make predictions about ligand binding, a partition of the free energy of binding into individual, physically interpretable terms is desirable; however, these attempts are not without problems. In an early quantitative analysis of drug–receptor interactions by Andrews et al.,[2] it was assumed that a bound ligand loses its translational and rotational degrees of freedom (both rigid body rotation and internal rotations) completely. Rather high contributions adverse to binding ($\Delta G_{trans.,rot} = +48\ kJ\,mol^{-1}$, $\Delta G_{rot.,bond} = +5.6\ kJ\,mol^{-1}$) have been reported. As a consequence of this assumption, the analysis of binding data yielded large contributions for the individual functional groups to binding. Several studies by Williams and coworkers[127] have highlighted the difficulty in separating these contributions. One important conclusion from their work is that ligand binding leads to a loss in entropy that is significantly smaller than estimated earlier by Page.[70] Apparently, a significant residual vibrational motion remains for the bound ligands. Recently Murphy et al.[128] showed that the calculation of the translational entropy loss using the Sackur–Tetrode equation produces largely overestimated values. They argue that the volume available for the movement of a ligand in solution and in a complex are similar. They conclude that the cratic entropy (contribution arising from the mixing of solute and solvent molecules) provides the best estimate for the loss of translational entropy.

3.7. The Role of Computational Methods in Predicting Ligand Binding Affinities

The observation that both ΔH and ΔS contribute significantly to ligand binding has important consequences for the theoretical description of protein–ligand interactions. A popular approach for investigating the energetics of protein–ligand interactions is to perform a molecular mechanics force field optimization and then to analyze the interaction energies of the optimized structure. Several groups have tried to correlate experimentally determined binding affinities with protein–ligand interaction energies obtained from a force field calculation. For one set of HIV-protease inhibitors,[129] and for an ensemble of thrombin inhibitors,[130] a good correlation was observed. However, this approach will only be successful if the entropic contributions to the binding are similar for different ligands; although, this is not generally the case. Therefore, interaction energies obtained from molecular mechanics calculations should in general not be expected to correlate with measured free energies of binding.

In principle, relative free enthalpies of binding can be calculated, for example, from free energy perturbation (FEP) or thermodynamic integration (TI) methods.[131] Some impressive results have been obtained by using these techniques.[132, 133] The FEP and TI calculations have provided valuable insights into

the physical nature of specific protein–ligand interactions. For example, the relative binding affinities in a series of thermolysin inhibitors[67, 68] and HIV-protease inhibitors[132] were correctly predicted. The advantage of these methods is the rigorous treatment of basically all effects in protein–ligand interactions, including solvent effects and conformational changes. In practice, however, the methods suffer from convergence problems and therefore require very long simulation times. Furthermore, the calculations are still based on several approximations such as the use of a force field. In addition, at present the approaches are only capable of predicting differences in binding affinities between closely related ligands. Therefore, it appears quite difficult to accurately predict binding energies of protein–ligand complexes, even if the 3D structure of the complex is known. The rigorous modeling of such interactions is still a considerable challenge.[134] In view of the current limitations with the FEP and the TI approach, a number of different approaches have been evaluated for predicting binding affinities. Recently Warshel et al.[135] have shown that the semimacroscopic version of the Protein Dipoles Langevin Dipoles method (PDLD/S) can provide a good estimate for ΔG in a reasonable amount of computer time on current workstations.

In view of the importance of interactions with the solvent, a substantial amount of work has been invested into the development of methods for calculating solvation energies, in particular free energies of solvation.[136] Empirical[137, 138] and quantum mechanical methods[139, 140] have been used to calculate solvation energies of small organic molecules.

3.7.1. Scoring Functions for Protein–Ligand Complexes

The prediction of the binding affinity of a ligand is currently the most challenging problem in computer-aided ligand design. We have tested a simple empirical scoring function for predicting binding affinities for a protein–ligand complex with a known 3D structure.[81] The purpose of the scoring function is to prioritize the hits obtained from a computer program for de novo design or from a search of 3D structures in a database (see also Section 5). The noncovalent protein–ligand interactions are assumed to be additive. The function takes into account hydrogen bonds, ionic interactions, the lipophilic protein–ligand contact surface, and the number of rotatable bonds in the ligand, and is formulated according to Equation (a).

$$\Delta G_{\text{binding}} = \Delta G_0 + \Delta G_{\text{hb}} \sum_{\text{H-bonds}} f(\Delta R,\Delta\alpha) + \delta G_{\text{ionic}} \sum_{\text{ionic int.}} f(\Delta R,\Delta\alpha) + \Delta G_{\text{lipo}} |A_{\text{lipo}}| + \Delta G_{\text{rot}} \text{NROT} \quad \text{(a)}$$

$f(\Delta R,\Delta\alpha)$ is a penalty function that accounts for large deviations of the hydrogen bonds from ideal geometries.[81] It tolerates small deviations of up to 0.2 Å and 30° from the ideal geometry that are often due to positional uncertainties in the X-ray structures. ΔG_0 is a contribution to the binding energy that does not directly depend on any specific interactions with the protein, but is associated with the overall loss of translational and rotational entropy of the ligand on binding. ΔG_{hb} describes the contribution from an ideal hydrogen bond. ΔG_{ionic} is the contribution from an unperturbed ionic interaction. ΔG_{lipo} is the contribution from lipophilic interactions, and is assumed to be proportional to the lipophilic contact surface A_{lipo} between the protein and the ligand. The final parameter ΔG_{rot} describes the loss of binding energy due to the immobilization of internal degrees of freedom in the ligand. NROT is the number of rotatable bonds.

The data set used for the calibration of the function consisted of 45 protein–ligand complexes. For this set, the energy function reproduced the binding constants (ranging from 2.5×10^{-2} M to 4×10^{-14} M, corresponding to binding energies between -9 and -76 kJ mol^{-1}) with a standard deviation of 7.9 kJ mol^{-1} corresponding to 1.4 orders of magnitude in binding affinity. The individual contributions to protein–ligand binding obtained from the scoring function are: for an unperturbed uncharged hydrogen bond (ΔG_{hb}): -4.7 kJ mol^{-1}, an ideal ionic interaction (ΔG_{ionic}): -8.3 kJ mol^{-1}, lipophilic contact (ΔG_{lipo}): -0.17 kJ mol^{-1} Å^2, one rotatable bond in the ligand (ΔG_{rot}): $+1.4$ kJ mol^{-1}. The constant contribution (ΔG_0) obtained from the calibration is $+5.4$ kJ mol^{-1} (adverse to binding). The present approach is fast: For a given protein it allows the scoring of 10 small ligands per second on a current single-processor UNIX workstation.

We are currently investigating an improved scoring function. This function contains three additional new terms. The first new term (ΔG_{aro}) accounts for specific interactions between aromatic rings. The replacement of water molecules that form hydrogen bonds with the protein ($\Delta G_{\text{H-bonded water}}$) and the replacement of those water molecules that do not form a hydrogen bond ($\Delta G_{\text{not H-bonded water}}$) are considered as different contributions. In addition, the terms ΔG_{hb} and ΔG_{ionic} are now modulated by a new factor to discriminate between buried interactions and solvent-accessible interactions. The new scoring function is currently based on 80 protein–ligand complexes. It is applicable to a broader range of protein–ligand complexes [Böhm, unpublished results].

4. Molecular Conformation at the Binding Site

The binding of a small-molecule ligand to a protein requires shape and property complementarity. In the course of binding they have to adapt to each other in order to achieve a successful recognition process. The small-molecule ligand, which is usually the more flexible partner with several rotatable bonds, can adopt a large variety of different low-energy conformations. Hopefully one of these corresponds to the receptor-bound situation. An appropriate handling of conformational flexibility is essential for the prediction of ligand binding and binding affinities.

4.1. Methods for Generating Multiple Conformers

A variety of computational search techniques have been developed to generate a large number of multiple conformers for a given drug-size molecule (< 500 D).[141–143] These methods generate low-energy conformers that correspond to local minima on a particular energy surface. The efficiency and reliability of these methods is usually assessed by the following criteria: 1) Is the global minimum found? 2) How many

local minima are detected within a particular energy range above the global minimum. Mostly, in this context the ligand is considered alone, not just for the sake of simplification to keep the problem computationally tractable, but often because no information about the protein binding site is available. Therefore, the important question arises whether ligands adopt conformations at the protein binding site that correspond to local energy minima also exhibited in the isolated state. One can imagine that a local environment is capable of modifying conformational properties, and therefore an appropriate definition of system boundaries becomes essential. In the consideration of ligand–receptor interactions, the system should include, at least, the ligand, the protein, and the neighboring solvent molecules or a membrane environment. With respect to these considerations, is a limitation to local minima of the ligand itself justified and can we expect any relevant conclusions?

The best approach to address this latter question is to start with experimental data on protein–ligand complexes, determined, for example, by protein crystallography.[20] We have to remember that protein structures are resolved to a limited resolution. Ligand conformations are fitted into the trace of the electron density. Recently the need for caution in setting initial ligand conformations for protein structure determination has been indicated by a series of structure determinations of glucose-type ligands with glycogen phosphorylase.[144] As found in related complexes of this enzyme, the glucose derivative **3** (a rather weakly binding inhibitor, K_i = 37 mM) was fitted to the difference Fourier electron density with the usual, energetically most favored chair conformation of a pyranose ring. Since only an unsatisfactory fit was obtained (data to 2.3 Å), the molecular structure of the ligand was investigated in parallel by X-ray crystallography.[145] Surprisingly, a skew-boat conformation was observed. The unexpected ring conformation in this derivative also gave a much better fit to the electron density in the protein structure. In the development of nonpeptidic seven-membered cyclic ureas as HIV-protease inhibitors, crystallography of small molecules has been used to confirm unusual conformational preferences observed at the protein binding site.[29]

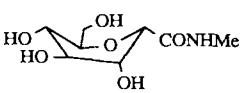

3

4.1.1. Conformational Libraries Derived from Crystal Structures

The above-mentioned examples might suggest that the crystal structure of a ligand is a good starting point to collect information about the receptor-bound conformation. In several cases, such as the nonpolar ligand retinol, the adopted conformation at the binding site is indeed very similar to that found in the corresponding crystal structure of the ligand.[146] However, the inspection of a larger data set of ligands shows that the reliance on just the crystal structures of the ligand itself is not, in most cases, an infallible and reliable indicator of a biologically active conformation.[147, 148] Perhaps, this correspondence is to some extent given for rather nonpolar and rigid ligands in which the environment is composed of many isotropically distributed atom/atom potential contributions. In such cases, the adopted conformation is mainly determined by intramolecular forces, and no significant perturbations arise from strong directional interactions with the crystal or active-site environment. Presumably, this assumption is also valid for hydrophobic portions of a ligand skeleton.

Which conclusions can be drawn for polar ligands? Let us consider citric acid as an example. In small-molecule crystal structures it has been found to adopt a number of distinct conformations.[146] Therefore, it appears difficult to predict a correct receptor-bound conformation for this molecule, for example at the binding site of the enzyme citrate synthase. Fortunately, its geometry has been determined in the complex with this enzyme. The torsion angles in this structure are similar to those found in several small-molecule crystal structures. But, instead of using individual structures to suggest a single possible conformation, we rather analyze them in terms of conformational preferences adopted in various molecular and crystal environments. This approach provides important information also relevant for conformations adopted in the structured environment of a protein binding site. Through exhausive searches of the Cambridge Crystallographic Data Base[21–23] we have retrieved conformational libraries for torsional fragments. These libraries can be used in a conformational analysis to generate biologically relevant conformations.[146, 149]

To illustrate the key aspects of this approach, some results are given. A data set of 80 ligands observed in crystallographically determined protein structures has been analyzed for frequently occurring torsion angle fragments. The considered examples show rotatable bonds between two sp^3 or an sp^2 and an sp^3 center. The angular distribution in these torsional fragments is shown in Figure 6. For comparison, univariate statistics on equivalent fragments observed in small-molecule crystal structures were also compiled.[141] Apparently, comparable distributions are obtained. The angular ranges outlined by the higher populated small-molecule data coincide convincingly with those obtained from protein complexes. These findings underline the relevance of torsional libraries as guidelines for the prediction of putative binding-site geometries.

4.1.2. Comparison of Conformational Preferences in Crystal Packing and in the Environment of a Binding Site

The inhibitor trimethoprim (**1**) has been cocrystallized with dihydrofolate reductase (DHFR) from two different species (*Escherichia coli* and chicken liver).[150] Surprisingly, it adopts distinctly different conformations at the binding sites of both proteins. In the chicken liver enzyme, a butterfly-like conformation is observed (torsion angles between the bridging atom and the two phenyl rings: $\tau_1/\tau_2 = -85°/102°$), whereas in the bacterial enzyme, the aromatic rings are oriented nearly perpendicular to each other ("twisted" conformation, $\tau_1/\tau_2 = 177°/76°$). The skeleton of trimethoprim resembles that of a diphenylmethane fragment. A statistical analysis of the torsion angles in crystalline diphenylmethane derivatives[151, 152] reveals both receptor-bound conformations to be also populated in low-molecular weight structures. In these, the twisted conformation is more frequently adopted than the butterfly-like one, suggesting that the latter is higher in energy. Interestingly, the inhibitor shows higher affinity for the bacterial enzyme, and the lower

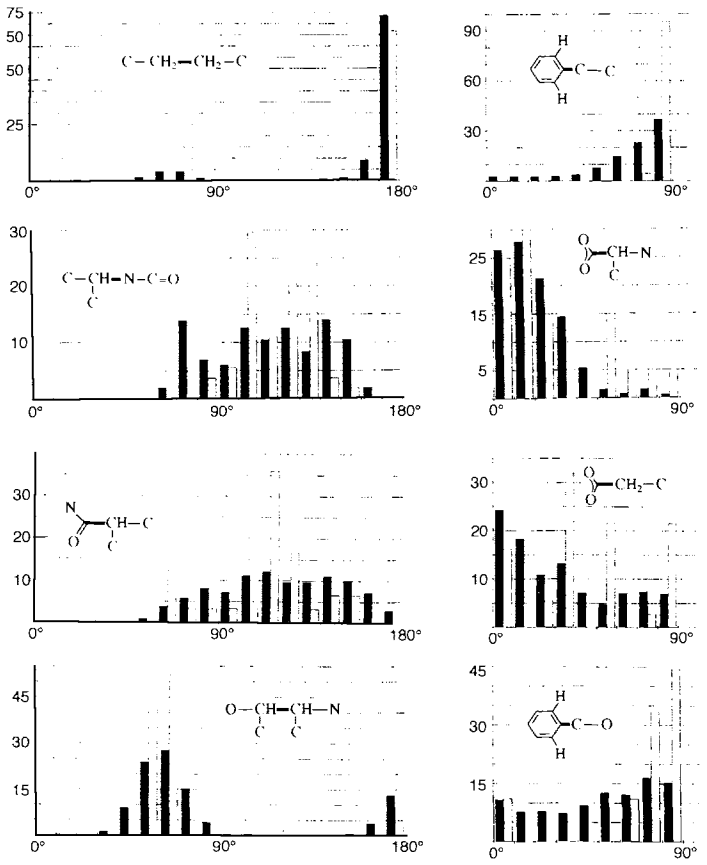

Fig. 6. Histographical distribution of torsion angles found in frequently occurring fragments (see formulae) in small organic molecules (solid columns) and ligands bound to proteins (open columns). Data are taken from crystal structures either of small molecules or protein–ligand complexes. Each distribution (y axis) is given as a percentage of the total number of structures considered in each case.

energy of the twisted conformation may be partially responsible for the greater binding affinity.

In order to analyze the correspondences in conformational properties in more detail, we have considered a ligand for which enough data are available to perform statistics both on protein and small-molecule crystal data. Adenosine and guanosine monophosphate fragments **4** are frequently found in proteins as part of cofactors. In parallel, they have often been studied in small-molecule crystal structures.[141, 146] Two distinct conformations of the ribose ring (C(2′)- and C(3′)-*endo*[153, 154]) cover the major part of structural variances either in protein or small-molecule structures. The remaining variance can be ascribed to the torsion angles in the phosphate side-chain and to the purine moiety. A reasonable agreement is found between small-molecule and protein data for the two angles next to the phosphate group (C-C-O-P about 180°, C-O-P-O about ±60°, 180°) and to the purine base (broad distribution between 0 and 90°). Data from protein structures are less sharply clustered, a result that may be due to their limited accuracy. The side-chain angle adjacent to the ribose ring shows remarkable differences between protein and small-molecule structures. In the low-molecular weight compounds, the O-C-C-O fragment mostly occurs in a *g*-conformation, whereas for the protein environment frequently g^+ and g^-, and a considerable number of examples with *trans* geometry are observed. In agreement with this observation, the distance between phosphorus and the purine moiety is found to be about 6.5 Å in most small-molecule structures. In the protein cases, this distance covers the entire range between 6 and 9 Å with a pronounced cluster of values at 8.8 Å. In their crystal structures, the molecules preferentially adopt a compact folded conformation, whereas in the protein environment both geometries, a compact and an extended one, are observed. The preference for the folded conformation of the nucleotides in the small-molecule structures is also observed in solution. In most crystalline examples, it results from a stabilization through a cation or a bridging water molecule that mediates an interaction between the phosphate group and a basic nitrogen atom of the purine moiety. The extended conformation, more frequently found in proteins, is supposedly observed because a long and polar molecule can expose its polar groups better and thus binds more efficiently to the surface of a globular protein. This fact indicates that special conditions in the different environments can bias the statistics.

For polar molecules, which are embedded into a network of strongly directional interactions, such as hydrogen bonds, the environment has a strong impact on the adopted conformation. As a consequence, in some protein structures ligands are observed in arrangements that appear to correspond to "high-energy" conformations, "high" with respect to the conformation adopted in the isolated state. For example, in the enzyme creatinase, the natural substrate creatine **5** or a related inhibitor carbamoyl sarcosine **6** occur with a twisted guanidinium or carbamoyl moiety.[155, 156] This moiety forms strong charge-assisted hydrogen bonds. For the isolated molecule one would expect a planar geometry of the unsaturated π-system. Nevertheless, by using small-molecule crystal data as a reference, possible perturbations in a structured environment toward twisted geometries are indicated. In these latter structures the guanidinium group forms strong charge-assisted hydrogen bonds similar to those in creatine in the enzyme. Quantum chemical studies show that the energy difference between twisted and planar geometry is dramatically reduced in a polar environment with hydrogen bonds.[157, 158] These polarizing interactions result in a redistribution of the electron density in the molecule. Accordingly, the barrier to rotation is substantially reduced. Experimental evidence for the pronounced redistribution of the molecular electron density on going from the isolated state to a structured molecular environment originates from precise diffraction data, which determines the charge density distribution in crystals.[159]

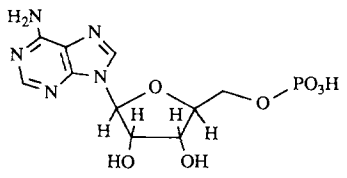

4

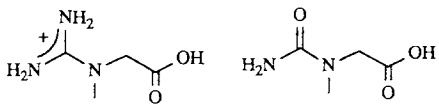

5 **6**

Peptidic inhibitors of carboxypeptidase A such as **7** bind a *cis*-oriented peptide bond in a terminal carbamate moiety.[160]

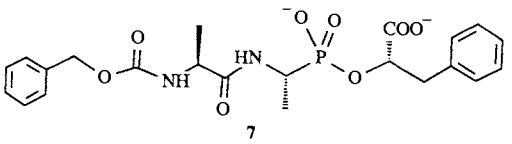

7

Apart from proline residues, *cis* conformation is rarely observed in noncyclic peptides.[161] A statistical evaluation of small-molecule crystal data shows a clear preference for *trans* peptide bonds in carbamates; however, a remarkable number of *cis*-oriented structures occur. Closer inspection of their molecular structures does not provide a simple "intramolecular rationale" for the observed preference. In contrast, the ester bond in the carbamates occurs nearly exclusively in a *trans* conformation.

4.1.3. Intramolecular Hydrogen Bonds in Receptor-Bound Conformations

The importance of environmental effects on molecular conformations is particularly apparent if the formation of possible intramolecular hydrogen bonds is considered. Geometry optimizations performed on isolated molecules capable of forming hydrogen bonds will result in local minima showing intramolecular hydrogen bonds. For example, a conformational analysis on citric acid, performed in vacuum, only generates low-energy conformers with intramolecular hydrogen bonds.[146] However, at the binding site of citrate synthase, solely intermolecular hydrogen bonds with the protein are observed. The presence of intramolecular hydrogen bonds at the binding site appears to be very rare. Usually all groups capable of forming hydrogen bonds are involved in intermolecular interactions with the protein. For example, in the crystal structure and in nonpolar solvents the undecapeptide cyclosporin A (**8**) forms four intramolecular hydrogen bonds that organize the molecule in a β-sheet geometry.[162, 163] At the binding site of cyclophillin, this intramolecularly organized fold is completely disrupted:[164] Virtually all groups intramolecularly satisfied by hydrogen bonds are turned inside-out. The ligand now forms solely intermolecular hydrogen bonds with the protein. NMR studies performed on polar derivatives of cyclosporin in water show a conformation related to the one adopted at the binding site.[165]

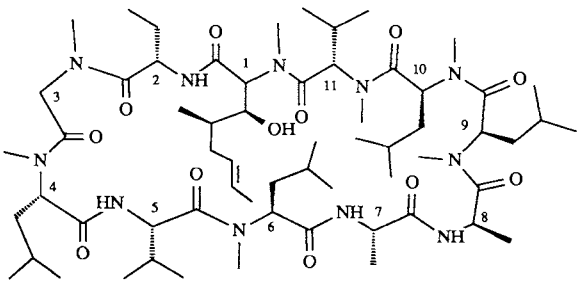

Cyclosporin A **8**

Nevertheless, a few examples with intramolecular hydrogen bonds at the binding site are known. For instance, phosphoramidon (**9**), a potent inhibitor of the endopeptidase thermolysin,[166] binds to the enzyme with one intramolecular hydrogen bond. This bond is formed between the carboxy terminus of the inhibitor and the C2-hydroxyl group of the rhamnose moiety. It may serve two purposes: on the one hand, it helps to immobilize the inhibitor in a conformation optimal for binding, and, on the other, it binds its free carboxy terminus, which is not appropriately satisfied through contacts to the enzyme, in a hydrogen bond. A free negatively charged carboxylate function is not assumed to occur at this position in the natural thermolysin substrate (polypeptide chain). Thus, not surprisingly, the enzyme does not provide, for example, a specific bidentate recognition site for this carboxylate. Another example is the receptor-bound conformation of the peptidic inhibitor H-142 (**10**) of endothiapepsin.[167] This ligand contains a reduced H_2C-NH_2 isoster for the scissile peptide bond. Overall, it adopts an extended conformation, forming an antiparallel pleated sheet with the active-site residues of the enzyme. The putative transition-state isoster at P1–P1′ is in close juxtaposition with the two catalytic carboxy groups of Asp32 and Asp215. The observed binding geometry can be interpreted to mean that the amino acid group, which is protonated under physiological conditions, interacts through one of its NH protons with the two carboxylate groups, similar to the OH group in the transition state-like statine residues. The remaining NH hydrogen bond donor is involved in an intramolecular γ-turn-type hydrogen bond with the neighboring carbonyl group. Such a second hydrogen-bond donor group does not occur during the peptide cleavage reaction. Accordingly, no specific recognition site is provided by the enzyme for this additional acceptor group. Supposedly, intramolecular hydrogen bonds are only observed at the binding site if an unbalanced ratio of hydrogen-bond donors and acceptors is present between ligand and receptor, and if this bond assists in immobilizing the ligand precisely in the required receptor-bound conformation.

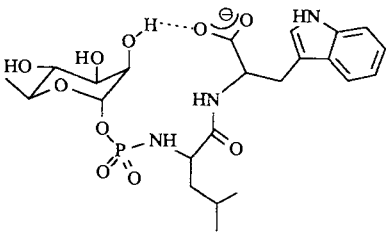

9

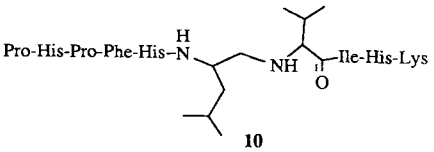

10

4.2. Toward a Fast Method for Generating Biologically Relevant Conformations

In the previous section, we analyzed the conformational properties of low-molecular weight ligands in their receptor-bound states. We concluded that the structured environment

present at the protein binding site imposes substantial influences on the geometry of a ligand. Accordingly, a crystal structure of a ligand itself or any local minima identified for the isolated state are of little or no relevance for the situation in a protein. However, we also noticed that conformational preferences observed for torsional fragments in the structured environment of a small-molecule crystal are in accordance with those observed in protein binding pockets. Any computational method that deals with the prediction of binding site geometries without explicitly taking the protein environment into account has to consider implicitly the presence or possible influences of a structured molecular environment in terms of appropriate "selection rules".

To demonstrate that the described libraries of torsion angles possess some potential for predicting putative binding site geometries of ligands, we have incorporated this information into a computer algorithm.[149] In the program MIMUMBA, a ligand is analyzed by assigning rotatable bonds. The ligand is split into rigid fragments or flexible ring portions. For the latter, low-energy conformations are taken from a library of predefined ring templates that have been obtained from crystal data. A relative energy scaling has been assigned to the various templates. Any conformational multiplicity due to pseudorotation or inversion of each elementary ring is considered.[168]

Dihedral angles for rotatable bonds in the open-chain portions are selected according to the conformational preferences of torsional fragments as retrieved from small-molecule crystal structures.[149] The various angles stored for the different fragments are ranked in terms of their relative energy. Similar to the study of cyclic ring portions, the program builds the entire molecule from the individual fragments by using preferably those open-chain torsion angles that are more frequently found in crystal structures. While merging all fragments in their various conformations, the individual energy contributions are added, and again an energy "penalty" is assigned if fragments overlap. In a subsequent geometry optimization, performed in torsion angle space, the program removes steric overlaps. In this step, only van der Waals and torsion angle potentials are considered. The latter potentials are derived from the statistically observed torsion angle distributions. They guarantee that during the minimization step the individual torsion angles are maintained as close as possible to the most frequently occurring values in experimental structures.[149] The method is fast: for each generated conformer 1–2 s are required on a single-processor UNIX workstation.

To check how well minimum structures obtained by this approach correspond to conformations of ligands bound to proteins, the crystallographically observed geometries of 63 ligands (containing 3–45 rotatable bonds) have been minimized into the next local minimum by using the force-field in MIMUMBA.[141] Visual inspection of these structures shows that the experimental and minimized structures closely resemble each other. On average, a root mean square deviation for all atoms of 0.07 Å per rotatable bond (that is 0.7 Å for 10 rotatable bonds) has been obtained between crystallographically observed and minimized structures.

A closer inspection of the examples with the largest deviations shows that in the experimental structures nonbonded interatomic contacts below 1.5 Å are present. These obviously unreasonable geometries built into the electron density must drift away during a minimization procedure that considers van der Waals interactions. One example (PDB code: 1HRI) is an antiviral compound (**11**) that binds to human rhinovirus (HRV14). In the

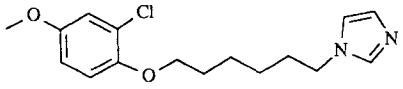

11

refined protein structure it is given with an eclipsed conformation along an aliphatic carbon chain and a rather unlikely torsion angle at an *ortho*-substituted phenoxy fragment (the methylene group at the oxygen atom bends toward a chlorine atom located at the *ortho* position).[169] The minimized structure drifts away from its experimental reference. Nevertheless, another local minimum can be found that avoids unreasonably short contacts and unlikely torsion angles that should fit equally well into the trace of the electron density (Fig. 7). For a subset

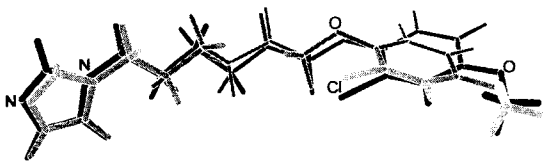

Fig. 7. Conformation of an antiviral compound (**11**) as modeled into the electron density in protein structure determination (gray), and an alternative conformation that avoids an unfavorable torsion angle in the *ortho*-substituted phenoxy fragment (black). The latter structure should fit equally well into the trace of the electron density.

of 23 ligands showing up to 15 rotatable bonds, multiple conformers (between 6 and 150) have been generated to assess the relevance of the conformers generated by MIMUMBA. On average, a deviation of 0.1 Å per rotatable bond has been obtained for those of the computed conformers that approximate experimentally observed geometries most closely. A random superposition of the generated conformers, in which only the centers of mass are placed in equal positions, reveals a mean root mean square deviation of about 0.3 Å per rotatable bond.[141]

4.3. Molecular Recognition Properties of Molecules and Their Mutual Similarity

In drug discovery, lead compounds are modified in a well-planned manner to enhance their affinities and to improve their selectivities. Receptor binding is a molecular recognition process dependent on the properties of both partners. They determine the mutual interactions of the different functional groups in the ligands with the amino acid residues of the protein. They define the relative orientations of the ligands in the binding pocket ("binding mode"). Assuming unchanged properties of a given receptor, can we correlate the binding modes observed for a set of ligands with the differences in their recognition capabilities? If such a relationship can be established it can be used to compare molecules and to predict their binding modes.

Appropriate steric and electronic complementarities of the ligand and the binding pocket are prerequisites for successful recognition between a ligand and its receptor. Shape and electronic properties are determined by the electron density distri-

bution, which also defines the hydrogen-bond donor and acceptor properties, the hydrophobicity, and the polarizability. All these features define the recognition capabilities of ligands. They can be used to compare molecules and to measure their similarity. However, since such similarities are always measured with respect to the binding properties toward a particular receptor (therefore relative to some reference) they will never be defined in absolute terms. However, the basic assumption is that similar molecules will bind to a receptor in a similar way. Is this assumption justified?

4.3.1. Binding Modes Observed for Different Ligands in the Same Protein

Again, structures of experimentally determined protein–ligand complexes can be used to address this question. In the last few years, several structure determinations have become available, in which a particular protein has been crystallized together with a series of different ligands. For many of these complexes the structure determinations revealed that ligands with related bonding skeletons also occupy similar regions in the binding pocket (e.g. α-lytic protease,[170] endothiapepsin,[171] renin,[172] HIV-protease[173–175]). For example, the structures of thrombin with four different inhibitors have been reported to deviate by not more than 1 Å for any of the residues. Several rearrangements on the order of 0.5–1.0 Å are observed, which can be clearly explained in terms of the protein adapting to a particular inhibitor.[176] HIV protease-inhibitor complexes have been determined in five different crystal forms. Independent of the crystal form and nature of a particular inhibitor, the enzyme structure is well conserved; the root mean square deviations lie in the range of 0.7 Å. This structural conservation also extends to the active site.[177] These series suggest that molecules with common or related skeletons show similar binding modes. However, a substantial number of examples is available that indicate a more complex and less clear-cut relationship. In the following we shall describe some of these examples to highlight the problems involved.

The inhibitor methotrexate (MTX, **12**) and the natural substrate dihydrofolate (DHF, ionic form of folic acid **13**) are both recognized by dihydrofolate reductase (DHFR).[150, 178] Considering the heterocyclic portion only, one might be tempted to directly compare the molecules in terms of an atom-by-atom correspondence (Fig. 8). If we match the hydrogen-bonding capabilities of the two molecules (pK_a considerations suggest MTX to be protonated at N1[178]) and neglect the underlying molecular skeleton, we find that the protein environment experiences quite different hydrogen-bonding patterns in this orientation (Fig. 8 top). Flipping the heterocycle in **13** about the bond to the side chain reveals an orientation, in which both moieties are no longer in optimal space-filling correspondence. However, in this conformation the hydrogen-bonding pattern now shows much better correspondence (Fig. 8, bottom). Crystallographic data on the binding modes are available for both ligands.[178, 179] They show that considerations based on simi-

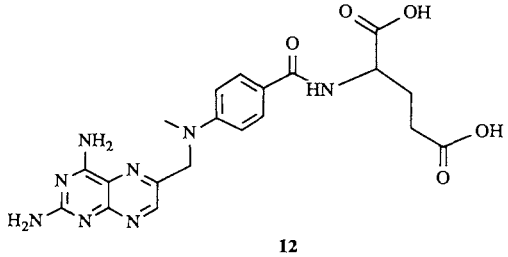

12

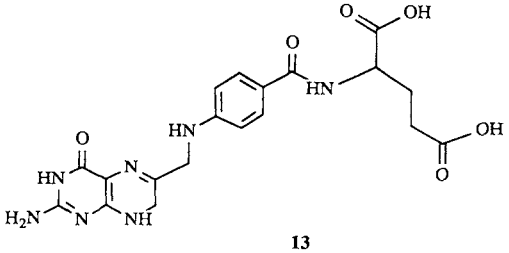

13

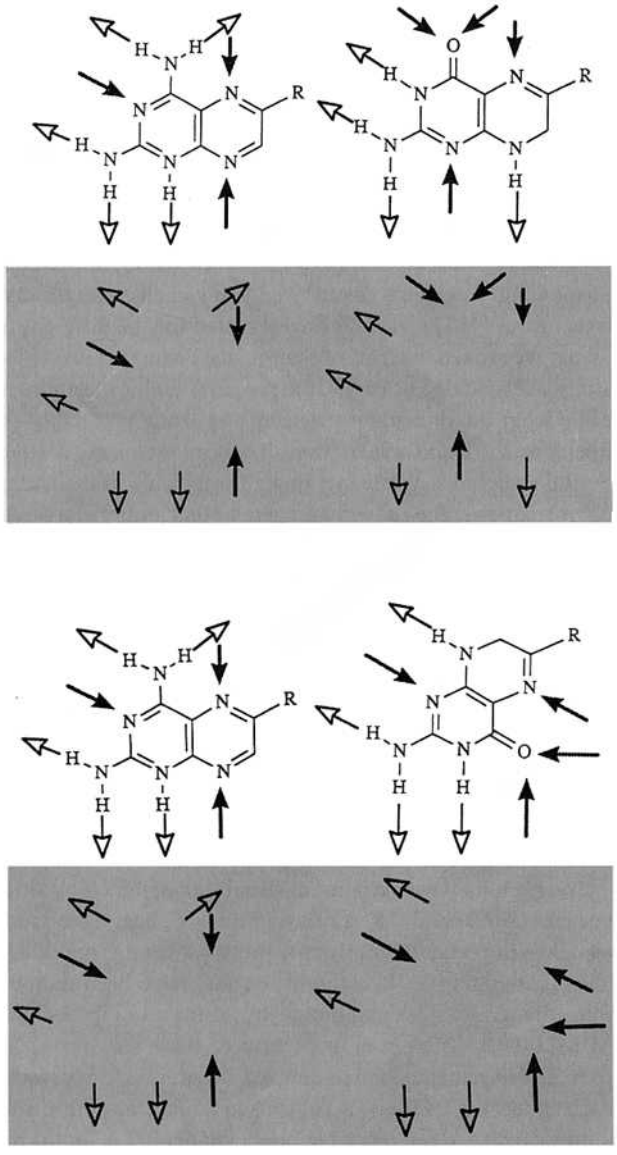

Fig. 8. Comparison of the heterocyclic building blocks in the two ligands methotrexate (**12**) and dihydrofolate (ionized form of **13**). In a direct atom-by-atom superimposition of the two ligands (top), very little similarity in the hydrogen-bonding patterns is achieved (the arrows pointing toward the ligand correspond to hydrogen-bond acceptor properties, those pointing away to donor properties). Changing the conformation of **13** by flipping the heterocycle about 180° (bottom) results in a mutual orientation that shows convincing similarity in the hydrogen-bonding patterns.

larities in the hydrogen-bonding properties lead to the correct binding modes.[178] A comparison of the electrostatic properties leads to similar conclusions.

Rather surprising binding modes are observed for two antiviral compounds (**14**, **15**), which possess very similar bonding

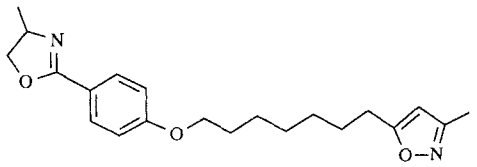

14

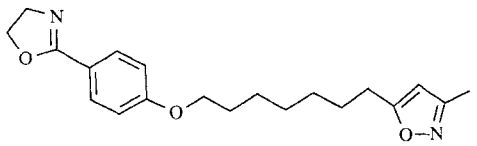

15

skeletons. They bind with reverse orientation into a canyon on the surface of human rhinovirus.[180] Approximate mirror symmetry is apparent when their volume requirements and electrostatic fields are taken into consideration.[181] Figure 9 shows the similar shape of the electrostatic potential (isocontour planes at different levels) for both ligands in the ("regular" vs. "reverse") orientation observed at the protein binding site.

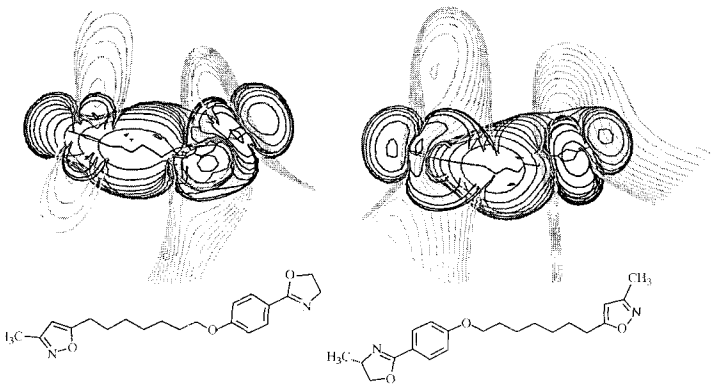

Fig. 9. Two structurally related antiviral compounds (**14**,**15**) in their binding orientations, as determined by X-ray crystallography. The electrostatic potentials calculated from AM1 charges (gray/light gray/black: $4.14/0/-4.14\,kJ\,mol^{-1}$) are displayed by isocontour surfaces. At first glance, the potentials for both molecules possess an approximately mirror symmetrical pattern with respect to the long molecule axis. This observation is a possible explanation why the two molecules in the binding site are observed with "reverse" orientation.

Another example of two ligands with very similar bonding skeletons but exhibiting binding geometries that deviate from a simple atom-by-atom matching are *N*-(3-phenylpropionyl)-phenylalanine (**16**) and *N*-benzyloxycarbonyl)phenylalanine (**17**). Both inhibit the zinc protease thermolysin.[182] They are composed of two hydrophobic terminal groups and a central polar part capable of forming hydrogen bonds or coordinating the zinc center. According to the geometry determined by crystallography, the terminal phenyl groups of both compounds occupy two hydrophobic pockets in a comparable manner. Compound **17** coordinates to zinc through its carboxy group, whereas **16** orients its carbonyl group toward the metal ion (Fig. 10). The opposing residues Ala113 and Arg203 provide two additional binding sites. In **17** the central amide function forms hydrogen bonds to both residues; however, that to Arg203 is mediated through a water molecule. In **16** the carboxy groups interact directly with Arg203, and a hydrogen bond is formed to Ala113.

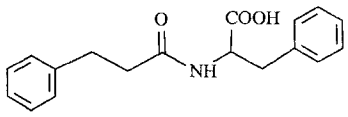

16

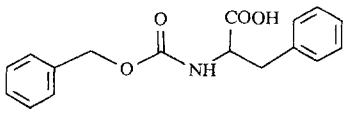

17

4.3.2. Similar, Alternative, and Multiple Binding Modes

To describe the orientation of different ligands in the binding pocket of a protein, expressions like "similar", "alternative", and "multiple" binding mode are used in literature. In our opinion, the application of these expressions is somewhat confusing and requires a proper definition. Related molecules with similar recognition properties (see above) that interact with the same functional groups of the protein thereby covering a largely analogous contact surface exhibit "similar" binding modes (e.g. MTX **12** and DHF **13**). If different amino acid residues are involved in the binding, or distinct functional groups of the ligands are engaged in the ligand/protein interface, "alternative" binding modes are detected (e.g. in thrombin,[42, 183] in thyroid binding protein,[184] in elastase,[185, 186] and in P450 camphor[187]). Even minor modifications with respect to the topology of the underlying bonding skeleton can substantially modify the conformational and accordingly the recognition

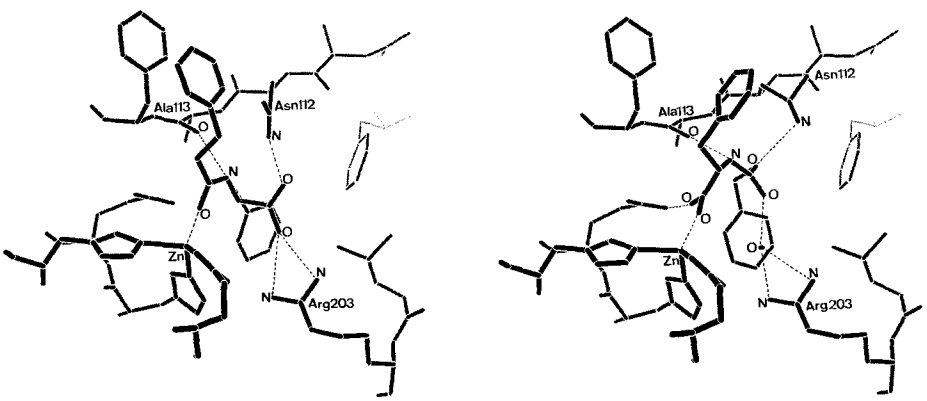

Fig. 10. Alternative binding modes as observed crystallographically for the two thermolysin inhibitors **16** (left) and **17** (right), which differ in their bonding skeleton by only one atom. In **17** the central amide bond forms hydrogen bonds to Ala113 and, mediated through a water molecule, to Arg203, and its carboxy group coordinates to the zinc ion. However, **16** coordinates the metal ion through its amide carbonyl group, and the carboxy group is directly hydrogen bonded to Arg203. In addition, a hydrogen bond is formed with Asn112 and through the amide nitrogen atom to Ala113.

properties. At present, our understanding of the similarity of flexible molecules is not thorough enough to uniquely relate changes in these properties with changes in the bonding topology.

In our opinion, the expression "multiple" binding mode should only be used in cases where more than one orientation of the same ligand in the binding pocket has been detected experimentally. An association with small-molecule crystal structures should be given where positional disorder is a well-known phenomenon. However, only in very rare cases the actual nature of the disorder in crystal packing has been elucidated. It can result either from a random disorder (from unit cell to unit cell) or from a domain-wise disorder of regularly packed mosaic blocks. The first and presumably rather rare case indicates that a particular molecular portion can be recognized by its environment in two or more ("multiple") orientations. It is likely that also in proteins "multiple" binding modes with respect to the features determining recognition are more the exception than the rule. Soaking experiments with trypsin crystals in an almost saturated solution of *p*-guanidiniobenzoate have revealed multiple binding modes.[188] Two disordered orientations have been fitted to the electron density (1.8 Å resolution) in the specificity pocket, one with the usual bidentate hydrogen bonding interaction between the guanidinium group and Asp 189. A third position is found near His 57 with the guanidinium group pointing toward Cys 58 and Lys 60. In all cases, the carboxylate of the inhibitor is close to the γ-O atom of Ser 195. Multiple binding modes have also been observed for chymotrypsin,[189] HIV protease [190] or *para*-hydroxybenzoate hydroxylase.[191] Some care is, however, required in the assignment of multiple binding modes. Such situations can result in ligand disorder or partial occupancy. Accordingly, a less clearly defined electron density has to be interpreted.

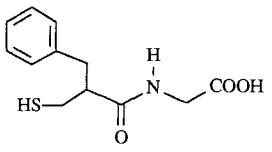

18

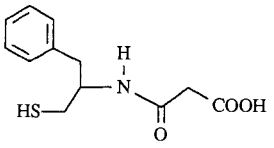

19

Molecules with structurally different bonding topologies can interact similarly with a protein (similar binding mode). The inhibitors thiorphan (**18**) and retrothiorphan (**19**) both inhibit the metalloprotease thermolysin,[192] and both molecules bind with the same functional groups to the same residues of the protein. A similar "reverse" recognition of a peptide group has been observed in lysozyme for α- and β-*N*-acetylglucosamide (**20**).[193] The *N*-acetyl side chain of both compounds that exhibits enantiomeric configuration at atom C2 is equivalently recognized by Ala 107 and Asn 59 (Fig. 11). The recognition properties of both forms are so strongly modified that different regions of the binding pocket are occupied (alternative binding mode): The

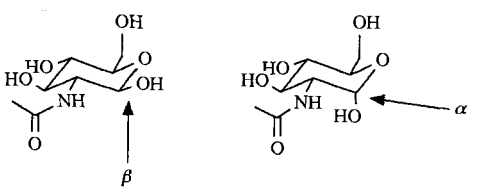

20

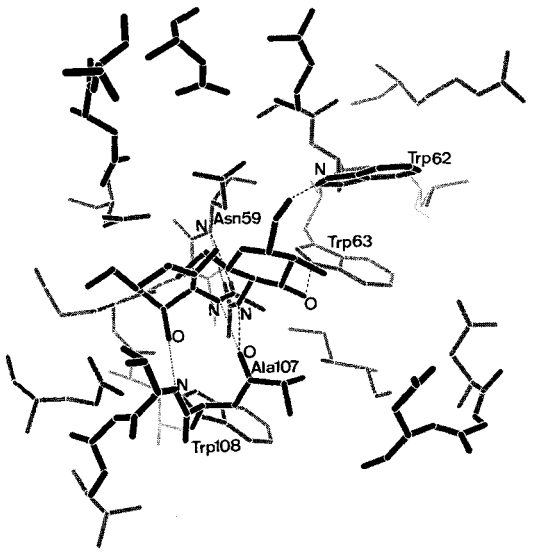

Fig. 11. Binding geometry of α- and β-**20** to lysozyme as determined by X-ray crystallography. Both ligands are shown superimposed in the same figure. The β-form orients to the right and is hydrogen-bonded (dashed lines) to Trp 62 and Trp 63. The amide group of the ligand interacts with the carbonyl oxygen atom of Ala 107 and the backbone NH group of Asn 59. The α-form orients to the left and forms the same interactions through its amide group to lysozyme (dotted lines). In addition, it forms a hydrogen bond to the backbone NH group of Trp 108.

α-form is engaged in a hydrogen bond to Trp 108, whereas the β-isomer interacts with Trp 62 and Trp 63. Lysozyme provides a rather extended binding pocket that can accommodate molecules much larger than **20**. In the lysozyme complex with tri-*N*-acetylchitotriose $(GlcNAC)_3$, the first sugar moiety binds similarly to the pyranose moiety in the β-form,[194] and the region occupied by the α-isomer is filled by five water molecules. Owing to the chirality of protein structures, different binding modes for enantiomers appear not very surprising. However, also the opposite has been observed. For instance, the affinities of the two enantiomeric sulfonamides (**21**) for human carbonic anhydrase[195] differ by a factor of 100. Protein crystallography revealed that both ligands occupy similar regions in the binding pocket (similar binding modes).

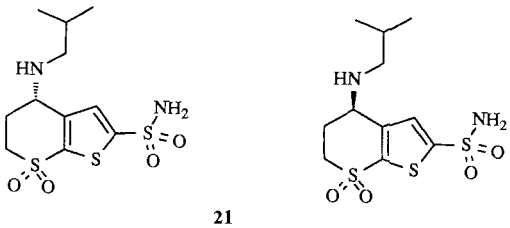

21

4.3.3. *Ligand-Induced Fit at the Binding Site*

So far we have considered only the properties of the ligand, and have assumed the protein to be rigid. However, ligand binding is a recognition process between two flexible molecules. Accordingly, the binding of a ligand can also induce spatial rearrangements in the protein. In a number of cases the protein structures have been determined with and without bound ligand. These studies give some indication about possible conformational changes upon ligand binding. Proteins such as trypsin[196] have fairly rigid binding sites. In other cases, parts

of the protein (e.g. a loop) move as a consequence of the ligand binding.[171, 172, 197] Fortunately, these changes appear to be quite similar for a set of different ligands (e.g. conserved orientation of the amino acid residue in thrombin,[176] HIV-protease,[177] thermolysin,[198] renin,[172] and endothiapepsin[170]). The structure of uninhibited renin shows two independent molecules in the asymmetric unit of a cubic crystal form.[172] Both adopt different conformations due to different crystal contacts. They can be characterized as an "open" and "closed" form and differ by a rigid-body rotation of the C- toward the N-terminal domain around an axis near the active site. Interestingly, the "closed" form is conformationally much more similar to the structure of an inhibited renin complex determined from tetragonal crystals. The conformational changes induced by crystal contacts are very similar to those resulting from ligand binding. For the structurally related endothiapepsin, inspection of 15 protein–ligand complexes reveals two forms of the enzyme.[171] However, no clear correlation with the type of inhibitor or the crystal contacts is evident. Presumably many of the conformational changes observed upon ligand binding can be related to functional rigid-body transitions of the protein. Pronounced changes in the active site have been reported between apo- and complexed form, for example, for HRV-14.[180]

An instructive example highlighting the importance of such induced-fit effects is provided by the binding of guanine to the active site of purine nucleoside phosphorylase.[199] This ligand forms hydrogen bonds through N7 and the oxygen atom at C6 to the side chain amide group of Asn 243 (Scheme 3). A simple and formally isosteric replacement of N by C at the 9-position implies an exchange of a hydrogen-bond acceptor by a donor at the 7-position. Surprisingly, 9-deazaguanine shows an even higher affinity, adopting a binding geometry very similar to that of guanine. The reason for this is that the adjacent Asn residue swings over and presents, instead of its NH_2 group, one of its NH protons and the C=O group to the ligand. This induced fit can hardly be predicted without determining protein–ligand structures.

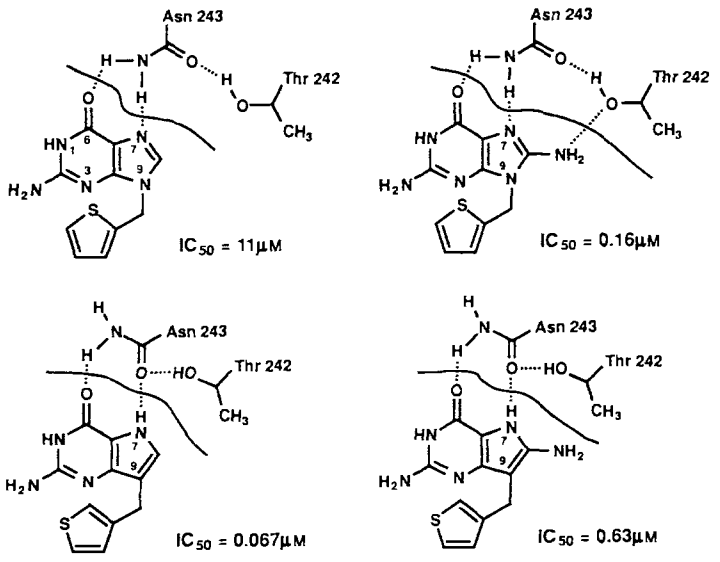

Scheme 3. Binding modes of four different ligands in purine nucleoside phosphorylase. The replacement of N by C at the 9-position of the guanine moiety results in an unexpected induced fit: In the 7-position a hydrogen-bond acceptor changes to a donor, and the Asn 243 side chain swings by and presents instead of its NH_2 group its NH and C=O groups to the ligands. This induced fit explains why only in the aza-analogue (top) an additional NH_2 group at the 8-position improves affinity. In the deaza derivative (bottom) an unfavorable steric repulsion occurs between the NH_2 group and the methyl group of the adjacent threonine.

4.3.4. Binding Modes in Different Species and at Different pH Conditions

Binding geometries can also differ between enzymes from different species. As already mentioned, trimethoprim (**1**) binds to chicken liver dihydrofolate reductase (DHFR) with a butterfly-type conformation, whereas in the bacterial enzyme from *E. coli* a twisted conformation is found.[150] This example may serve as a caveat for using data observed in one protein to describe the conditions in binding modes to others (e.g. modeled homologues).

The binding modes of molecules in the active site of a protein depend on the protonation state of the amino acid residues involved. A simple case that illustrates this influence is the pH-dependent binding of carbonate to creatinase.[156] Two crystal forms of the enzyme, each of which have a carbonate ion and a water molecule in the active site, have been grown under different pH conditions (5.4, 7.4) and structurally characterized. The guest molecules occupy different positions in the two structures, thus indicating pH-dependent binding modes. At low pH values, the recognition site for the anion, presumably present as bicarbonate, is formed by two protonated Glu residues. The water molecule mediates a hydrogen-bond network to the opposing Arg residues. At high pH values, the anion (again assumed to be a bicarbonate) binds in a reverse orientation. It now faces two Arg residues, while the water molecule bridges to the two Glu residues.

This observation also has consequences for the design of enzyme ligands possessing tailored recognition properties. Phosphastatine analogs have been reported to be potent inhibitors of the aspartyl protease pepsin, but they are relatively weak inhibitors of renin, another aspartyl protease. The difference may be attributed, at least in part, to the different pH optima at which the two enzymes function. Pepsin is a digestive protease that operates in a strongly acidic medium, whereas renin operates under neutral conditions. For the latter, it has to be assumed that the hydroxy group at phosphorus is largely deprotonated and therefore not suited to bind to the aspartates in the active site of renin.[200]

4.4. Automatic Alignment of Molecules in the Binding Pocket by Comparing Their Recognition Capabilities

The experimentally observed examples, discussed in the last section, indicate a rather complex relationship between the bonding skeletons of ligands, their binding modes, and their recognition properties. Nevertheless, let us return to our initial question and examine to what extent we can describe and predict binding modes by comparing recognition properties. When attempting to define a spatial difference or similarity measure among ligands, we have to remember that binding properties are defined with respect to a particular receptor. Measures of similarity are therefore defined relative to some reference.

Computational approaches that are applied to handle this problem can suggest alternatives for docking novel ligands into the binding site of a protein.[181] In the absence of a detailed structure of a receptor such methods can be used to superimpose ligands. The resulting alignment is a prerequisite for a comparative molecular field analysis (CoMFA).[201] This method can be used to quantify differences between ligands that are responsible for the variations of their binding affinities. Several approaches have been described for the computation of such alignments.[202-209] We have extended the procedure SEAL, originally described by Kearsley and Smith,[209] to allow a simultaneous consideration of steric, electrostatic, hydrophobic, and hydrogen-bonding properties.[141, 210] To quantify the similarity of two molecules, their shape is approximated by a set of spatial Gaussian-type functions centered at the atomic positions. For each molecule these functions are then associated with a vector of physicochemical properties derived from atom-based descriptors. To compute the similarity of two molecules in space, the scalar product of the vectors corresponding to the two molecules and weighted by the overlap of the associated Gaussian functions is evaluated. The obtained quantity is used to maximize spatial similarity. Starting from random orientations, it is subsequently optimized by minimizing the mutual distances between molecular portions having similar physicochemical properties. This method does not require predefined pairs of matching centers in the molecular framework. Accordingly, also strongly deviating bonding skeletons can be compared and aligned.

This alignment function has been applied to a data set of 184 ligand pairs binding to the same protein.[141] Their actual binding modes and accordingly their relative structural alignments are known from protein crystallography. Across this reference set, the observed alignments could be reproduced in one third of the cases with a root mean square deviation below 0.7 Å; 51% below 1 Å, and nearly 90% below 2 Å. Considering the inherent accuracy limits of about 0.7 Å for such a superposition of two experimentally determined protein–ligand complexes, the observed agreements are rather convincing.[210] The alignment function exhibits several minima. Thus, the approach generates several alignments, each with a particular similarity scoring. In two thirds of the test cases, the solution with the highest similarity scoring also approximates the experimentally observed alignment. In 91% of the investigated cases, the experimental observations are covered by the best and second best solutions. The different solutions suggest alternative binding modes. For example, the "reverse" binding mode of the two antiviral compounds **14** and **15** with very similar bonding skeletons (see Fig. 9) are proposed since the best solution corresponds to the "regular" superposition. However, the second best solution, ranked only 4% less in similarity, approximates correctly the experimentally observed binding mode.

The alignment function incorporated into the described approach considers steric, electrostatic, hydrophobic, and hydrogen-bond donor and acceptor properties. Strictly speaking, these properties are not independent, they highlight different aspects responsible for molecular recognition. A closer inspection of their contributions to the similarity scorings calculated from 184 test examples provides the opportunity to estimate their relative importance. Interestingly, in all cases, steric similarity achieves the greatest importance, contributing between 30 and 85% to the total similarity scoring. This finding underlines the importance of a similar spatial occupancy in a binding pocket as a prerequisite for successful binding.

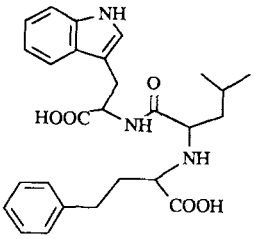

22

One example should be given, however, where the approach fails to perform satisfactorily. The two thermolysin inhibitors **16**[182] and **22**[211] are superimposed with a residual root mean square deviation of 0.54 Å. Similarly, the reaction product Val-Trp of the proteinase cleavage reaction can be superimposed onto **22** with a root mean square deviation of 1.03 Å (Fig. 12). Val-Trp and **16** are both smaller in size than **22** and their superpositions with **22** involve different parts of the molecule. However, if a comparative alignment of **16** and Val-Trp is calculated, steric overlap is optimized among both inhibitors. Thus, no correspondence with the observed situation is achieved. This example clearly indicates the limitation of approaches that consider the 3D structures of ligands only. It also serves as a warning not to use the superimposition of molecules as a prerequisite for 3D QSAR analyses without additional considerations.

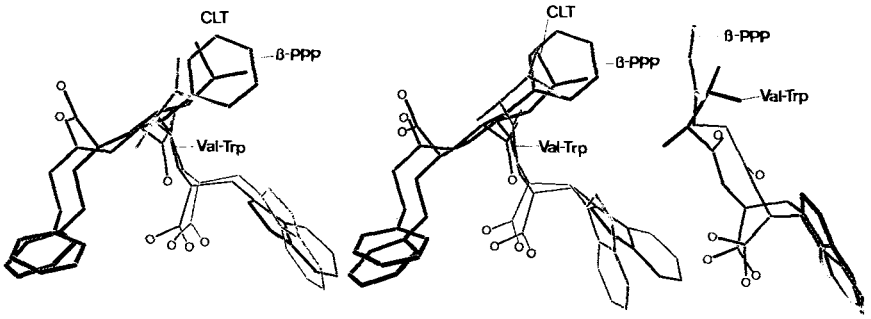

Fig. 12. Observed and computed structural alignment of thermolysin inhibitors. In the center the mutual alignment of CLT **22** (black), β-PPP **16** (dark gray), and Val-Trp (light gray) are shown, as determined by X-ray crystallography. On the left, the computed alignment is given using CLT (black) as a reference. The residual root mean square deviation to the experimental arrangement is 0.54 Å, and for Val-Trp 1.03 Å. On the right, the alignment of β-PPP (gray) with Val-Trp (black) as a reference is shown. An arrangement, like that found in thermolysin, which cannot be achieved since the steric overlap at the protein binding site is rather small (cf. center).

In the computational approach described so far, molecular flexibility has not yet been incorporated. To account for flexibility during the superposition process, the above-mentioned similarity condition has been introduced as additional term into the potential function used in MIMUMBA.[210] Since the approach performs only a local optimization, an initial orientation and start conformation are required. To circumvent this important limitation, multiple conformations, generated by a conformational search with MIMUMBA, are subjected to mutual alignments. Subsequently, those of the pairwise aligned conformers that receive the highest similarity scores are subjected to local

conformational relaxations with simultaneous similarity maximizations. This combined approach has been applied to thrombin and thermolysin inhibitors. Conformers are generated and selected that approximate experimentally observed geometries and orientation.[210]

5. Current Computational Methods for Lead Discovery

The 3D structures of proteins and protein–ligand complexes can be used to identify the essential interactions in these structures and to search for additional binding sites not used by previously known ligands. Possible binding sites may be positions where hydrogen bonds can be formed with the enzyme, or hydrophobic pockets in the enzyme structure which can be occupied by lipophilic groups. A number of computational tools have recently been described to select putative ligands and to predict their interactions with the protein. In general, these novel tools for ligand design can be divided into the following major categories:[212]

1) Analysis of the protein structure
2) Ligand docking and 3D database searching
3) De novo ligand design
4) Assessment of the ligand binding affinity
5) Analysis of the electronic and conformational properties of the ligand

We briefly summarize the current status of these methods. Basically, to find new ligands one can either search 3D databases of known small molecules, or one can attempt a de novo design. The latter approach tries to construct a new molecule completely or in part from scratch. The possible approaches are sketched in Figure 13.

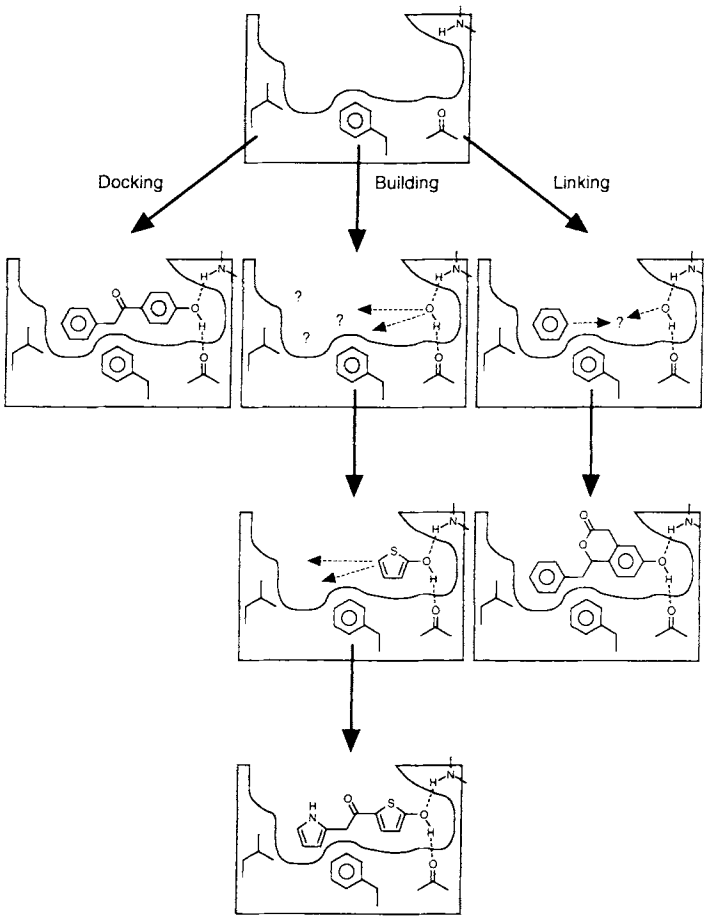

Fig. 13. Strategies for discovering new lead structures by ligand docking (see also Section 5.3.1). A complete ligand, for example taken from a database, can be docked into the binding site (left). The de novo design of new ligands can be performed either by positioning a seed which is further extended by additional building blocks (center) or by the simultaneous placement of several fragments that are connected by suitable linking groups (right). The sketch was adapted from Verlinde and Hol [26].

5.1. Analysis of the Protein Structure

The first step in the search for a new ligand is the analysis of the 3D structure of the target protein. The surface of the protein can be displayed together with certain properties such as the lipophilicity[213, 214] or the electrostatic potential.[215] Computational methods have been described that can detect clefts or cavities in the protein.[216–218] Other approaches are available for predicting favorable binding sites for probes or small molecules such as a water molecule or a carbonyl group.[219–221] One of the most frequently used approaches is to calculate interaction energies with different probes on a grid spanning the binding site. Such grids can be displayed and then subsequently be used as a valuable guide in the design of new ligands.

Probably the most widely used technique for the computational analysis of protein–ligand interactions is molecular mechanics. Recently new force fields have been developed[222–225] that provide an improved description of noncovalent and covalent interactions in these complexes. Simple molecular mechanics geometry optimizations can be useful in addressing the problem of steric and electronic complementarity between the protein and the ligand.

The program MCSS developed by Miranker and Karplus[226] combines the analysis of the protein binding site with a placement of small functional groups in an energetically favorable orientation. MCSS uses a molecular mechanics force field for the placement of small ligands.

We have adopted a different approach to the analysis of the protein binding site focussing on the geometric aspects of protein–ligand interactions.[227] Information on typical interaction patterns between functional groups of a ligand and amino acids of a protein can be obtained from a statistical analysis of intermolecular contact geometries found between various functional groups in the crystal packings of organic molecules. Composite pictures of these interaction geometries can be used to elucidate orientational preferences. As an example, the composite picture of hydrogen-bonding partners that interact as donors or acceptors with a phenolic oxygen are shown in Figure 14. The observed clusters in space are representative of preferred interactions with the tyrosine side chain. To justify that these composite crystal-field environments indeed serve as reliable guides in the prediction of binding site geometries, we have mapped them onto the amino acids pointing into the binding site of a protein. In Figure 15, the crystallographically determined binding geometry of methotrexate (**12**) in dihydrofolate reductase is shown together with the distribution around the functional groups that interact with the in-

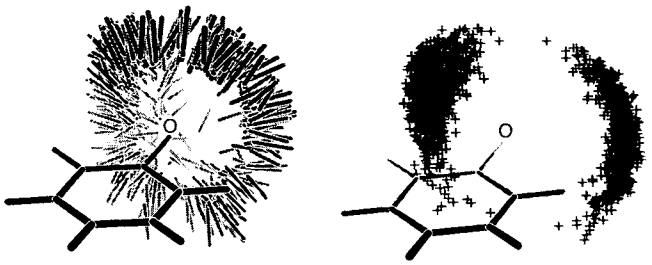

Fig. 14. Composite picture of the contact geometries used to map out possible spatial orientations of interactions between a phenolic oxygen atom and hydrogen-bond donors (left) or acceptors (right). Data were retrieved from crystal structure analyses of small molecules. The coordinates of the probe functional group together with those of the contacting atoms (NH, OH or N, O) were extracted. A common orientation of all considered examples was achieved by a least-squares superposition of the atoms of the phenyl rings. The hydrogen atoms directly bound to the phenol oxygen have been omitted for clarity.

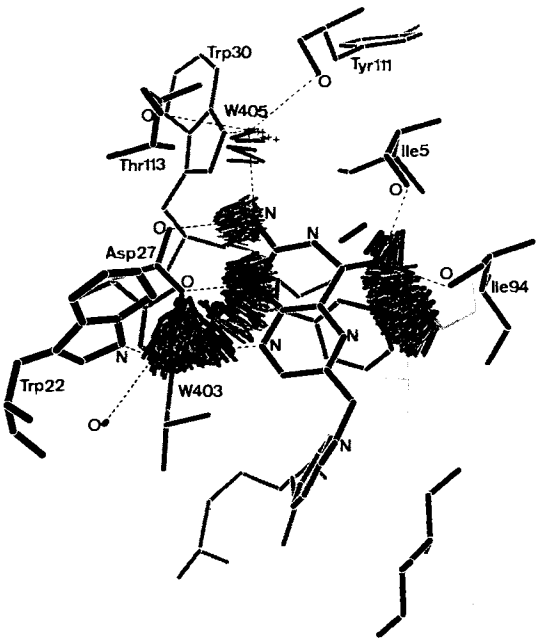

Fig. 15. Section through the binding pocket of the dihydrofolate reductase from *E. coli* with the ligand **12**. View perpendicular to the pteridine moiety, hydrogen bonds as dashed lines. The water molecules 403 and 405 mediate hydrogen bonds from the protein to the ligand. Matched onto the amino residues oriented towards the binding site are the appropriate distributions from the crystal structures. After contact atoms that penetrate into atoms of the protein have been rejected, the indicated positions remain as putative binding sites about the carboxylate group of Asp27, the backbone carbonyl group of Ile5, Ile94, and Tyr111, the side-chain oxygen atom of Thr113 (NH, OH bond vectors), and the indole NH group of Trp30 (N, O atom positions).

hibitor. The positions of the ligand atoms coincide with regions that are frequently occupied by similar partners in organic crystal structures. A similar picture was found for several other protein–ligand complexes.[227] The information contained in these composite crystal-field environments has been translated into rules that serve as guidelines for the automatic docking of small molecules into the active site of proteins (see Section 5.3).

A very important property of proteins is their flexibility. The most widely used computational technique to obtain information about protein flexibility is molecular dynamics (MD) simulation. Several reviews have summarized the potential of this method.[228, 229] Significant progress has recently been obtained in the methodology of molecular dynamics simulations.[230–232] Together with the developments in computer hardware, these advances now enable us to perform longer and more accurate MD simulations. Indeed, several impressive calculations have been reported that provide new insights into the nature of protein flexibility.[233, 234]

5.2. Database Searching

The most direct way to find a new ligand with a computer is to search a database containing 3D structures.[235–237] The pioneering program in this field is DOCK developed by Kuntz and coworkers (see Fig. 13, left).[238] DOCK is used to search a 3D database for possible ligands based on shape complementarity between protein and ligand. Recently the ability to account for electronic complementarity by means of a molecular mechanics force field was also incorporated into the program.[239, 240] A number of successful applications of DOCK have been reported.[241–243] Other computer programs for searching 3D databases have been described:[244, 245] CLIX[244] uses the GRID force field[219, 220] in the docking of putative ligands; the program FLOG developed by Miller et al.[245] accounts for ligand flexibility by including up to 25 conformers of each structure in the database; the program LUDI described in the following section can also be used for searching 3D databases.[246]

5.3. De Novo Ligand Design

A number of computer programs have recently been described that attempt to design new ligands for a given protein structure automatically.[247–270] Several reviews have been published on this topic.[247, 248] Most programs try to assemble novel molecules from pieces. These pieces are either atoms[249–252] or larger, chemically reasonable fragments.[253–255, 269, 270] Both approaches have advantages and disadvantages. The use of single atoms as building blocks can generate the largest possible diversity of chemical structures. However, a large structural diversity can also be obtained with a fragment-based approach by using a large variety of different fragments. A potential advantage of the fragment-based approach is the synthetic accessibility of the generated structures. The use of fragments offers the advantage that chemical knowledge can be built into the fragment connection step. For example, amino acids can be used as building blocks to construct peptides.[253] The extension to other simple chemical reactions such as the formation of an ether is straightforward. In contrast, this control of synthetic accessibility is difficult to achieve for atom-by-atom build-up programs. Therefore, the latter approach requires that the synthetic accessibility is checked at the very end of the design cycle. This is a much more complex task than to check whether the formation of a particular bond is synthetically feasible.

Two major strategies exist for fragment-based de novo ligand design. The first possibility is to place several fragments independently (or take them from a known ligand structure) and then to search for suitable templates that connect these fragments into one molecule (see Fig. 13, right). The advantage of

this approach is that the individual fragments are placed without any bond constraints and are likely to be at their optimal positions. Furthermore, this strategy has the desired tendency to generate rigid structures. A possible disadvantage is that it may be difficult to find appropriate templates that connect the fragments in a stereochemically and synthetically reasonable way. The alternative is to start with a seed fragment in a certain region of the binding site, and then to append additional fragments in a stepwise build-up procedure (Fig. 13, center). An advantage of this approach is that chemical knowledge can be easily incorporated into the linking step. Therefore, synthetically accessible structures are more likely to be obtained by this approach. However, it tends to generate more flexible structures. Furthermore Rotstein and Murcko[255] have pointed out that the build-up procedure can run into difficulties if a large gap between two separated regions of the binding pocket has to be bridged without the possibility of forming extensive specific interactions with the protein in the gap region.

The most important challenge both in de novo design and 3D database searching is currently the development of new methods to prioritize the large number of diverse putative protein ligands resulting from such calculations. Available computational procedures based on a molecular dynamics simulation are too time-consuming to score more than 10–100 ligand structures. Therefore, a fast and reliable ranking of the candidate structures is required. A possible approach is to use a two-step procedure. First, a fast and simple empirical scoring function is used to prioritize the hits. Then the top scoring structures are analyzed more rigorously by using more accurate and computationally demanding approaches. Several simple scoring functions have been proposed,[2, 81, 100–102, 253] among them the one we described in Section 3.7.

5.3.1. The Computer Program LUDI

LUDI is a fragment-based de novo design program that can be used both for searching 3D databases and for the automatic construction of novel ligands either through building (step-by-step build-up) or linking (placement of individual fragments and subsequent connection, see Fig. 13).[269, 270] The program positions molecules or adds new substituents to a given lead in clefts of a protein such that hydrogen bonds can be formed and hydrophobic pockets are filled with lipophilic groups. Like other programs for ligand design, LUDI basically requires the following information: 1) the 3D structure of the target protein, 2) 3D structures of putative ligands or fragments for docking or constructing novel molecules, and 3) information about possible favorable interactions between the protein and the ligand.

The program first calculates "interaction sites", which are discrete positions and vectors in space suitable for forming hydrogen bonds or for filling a hydrophobic pocket. These interaction sites are derived from composite crystal-field environments as described in Section 5.1.[227] In the next step molecular fragments are fitted onto these sites. The fragments are taken from a library containing 1100 diverse small molecules. Larger fragment libraries can also be searched, as compiled from the "Available Chemicals Directory" (ACD)[271] or the Cambridge Structural Database (CSD).[21–23] Then LUDI can be used in the "link-mode", in which the placed fragments are connected by bridge fragments to form a single molecule. Alternatively, LUDI can append new fragments onto an already positioned fragment or lead compound. Finally, the obtained structures are scored by using the function described in Section 3.7. The concept of LUDI is summarized in Figure 16.

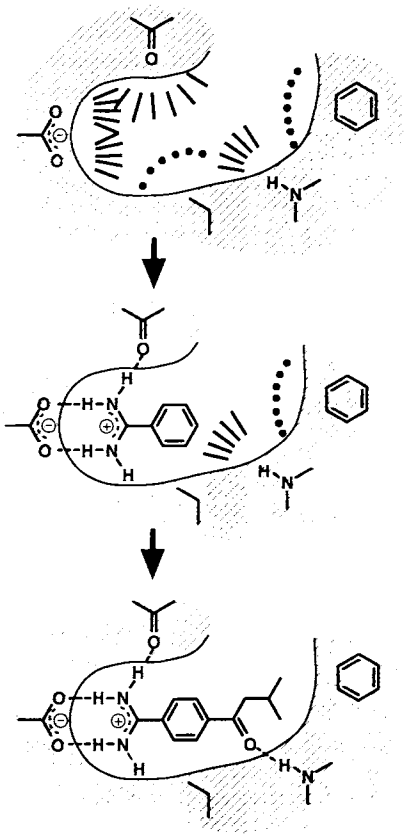

Fig. 16. Basic steps in de novo ligand design using the program LUDI. First the interaction sites are generated according to a rule-based approach (top). Then small fragments are fitted onto the interaction sites (center). Finally, positioned fragments are linked together or extended by additional substituents (bottom).

An important aspect of LUDI is its ability to tolerate small uncertainties in the experimentally determined protein structures. Any positioning of fragments is completely based on geometric operations. We have decided to refrain from using force-field calculations either in the positioning or the ligand scoring step. The latter methods would be computationally rather demanding. Futhermore, the uncertainties in protein geometry can give rise to unreasonably large contributions to the protein–ligand interaction energy if calculated by a force field. The resulting values can only be interpreted if a full geometry optimization including all degrees of freedom is performed. Instead, we decided to use the fast and error-tolerant empirical scoring function in LUDI described in Section 3.7.[81]

In a validation study, we successfully applied LUDI to the design of inhibitors of dihydrofolate reductase and HIV-protease.[270] Pisabarro et al.[38] used the program in the successful design of a novel inhibitor of human synovial fluid phospholipase A_2 with enhanced binding affinity. Recently Babine et al.[39] used LUDI to design **23** as a novel ligand for FKBP-12.

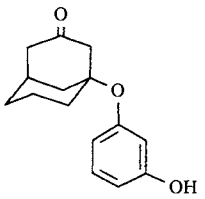

23

Subsequently, compound **23** was synthesized and found to be a strongly binding ligand of FKBP-12 (K_i = 12 μM). In another application,[246] a subset of about 30000 small molecules (< 40 atoms, 0–2 rotatable bonds) from the fine chemicals directory (FCD[271]) was used to suggest possible novel ligands for trypsin, HIV-protease, purine nucleoside phosphorylase, and streptavidin. The 3D ligand structures were generated with the program CONCORD[272] (more recently, we also employed the program CORINA[273] for the generation of the 3D structures). For the specificity pocket of the enzyme trypsin, the calculation took two hours on a Silicon Graphics Indigo R4000 workstation and retrieved 153 compounds. The hits obtained with the highest score are *para*-methylbenzamidine and benzamidine. Both compounds are indeed found experimentally to bind trypsin with micromolar binding affinities.[274, 275]

One of the strengths of LUDI is its ability to find small polar ligands for tight polar binding sites as present, for example, in trypsin. Our current experience indicates that for such proteins the program can retrieve interesting small molecules that form multiple hydrogen bonds with the protein. LUDI is now widely used in the pharmaceutical industry.[276]

6. Outlook and Future Developments

During the last five years we have witnessed dramatic improvements in computational tools for structure-based ligand design. New computer programs for conformational analysis, ligand docking, structural alignment, and de novo ligand design have been described. The first examples for a successful design of protein ligands are emerging.[29–42] The motivation for further developments of these methods is the intellectual challenge of understanding the nature of protein–ligand interactions, but also the need to speed-up the drug discovery process. As this driving force gets even stronger, the development of advanced methods for structure-based ligand design becomes more and more important.

Despite the remarkable recent progress, the current computational methods for lead discovery still face a number of limitations. Most important is the availability of the 3D structure of the target protein. Substantial efforts are still necessary to develop techniques to make these systems accessible to structure determination. In the optimal case, their 3D structures are determined together with a series of different ligands. In the absence of such data, it may be possible to construct a model of the target protein from the known structure of a closely related homologue. Otherwise design methods have to rely on comparisons of ligands only. It should be noted that in such cases the comparison has to refer to the spatial distribution of the physicochemical properties. However, as the level of information on the structural aspects of the protein–ligand system decreases, the results from design methods get less and less conclusive and reliable.

Design methods consider ligands and their putative interactions with the target. Other important factors are not taken into account, such as transport properties, metabolic stability, good oral availability, low toxicity, sufficient half life, and minor addictive potential. These factors also determine whether a ligand can be applied as a drug. Furthermore, the current de novo design programs hardly address the problem of the synthetic accessibility of the suggested structures. Finally, current methods for the prediction of binding affinities need to be improved.

In cases where the protein structure is available, most current docking and de novo design methods treat the protein as rigid. In reality, however, ligand-induced fit is observed and has to be considered. Nevertheless, since similar changes of the protein have been observed with several related ligands, the 3D structure of a complex appears to be a good starting point for de novo design. The consideration of molecular flexibility of the ligand, especially for species with more than five rotatable bonds, still represents a considerable challenge. This property has to be efficiently incorporated into methods for comparing molecules and ligand docking.

Computational methods are only one aspect in the strategy for drug research and development. In the last few years experimental high throughput screening methods have been established based on molecular test systems. In favorable cases, several thousand compounds can be tested in an assay per day. This has stimulated the development of new methods to synthesize large libraries of diverse molecules. Combinatorial chemistry[277–279] offers great promise in the discovery of new lead structures. In our opinion, the computer-based methods nicely complement such screening approaches. Hits from these searches often display rather diverse structures. Molecular comparison methods have to elucidate common features that are likely to be responsible for receptor binding. Once lead structures have been discovered, either through experimental or computer screening methods, molecular modeling and X-ray crystallography come into play to assist efficient optimization of lead structures.

At present, we are starting to understand some important phenomena and underlying principles that determine molecular recognition in protein–ligand complexes. Computational approaches based on empirical knowledge provide powerful tools to support the finding and optimization of new lead structures. It can be expected that with the growing experimental data on structures and thermodynamics of protein–ligand complexes the range of applicability of these approaches will be further extended.

We are very grateful to our colleagues Wolfgang Höffken, Hugo Kubinyi, Thomas Mietzner, and Nigel Walker for numerous stimulating discussions. Some of our own work described in the article was funded by the BMBF projects RELIWE and ÄBAV. The offered financial support is gratefully acknowledged.

Received: July 26, 1995 [A 125 IE]
German version: *Angew. Chem.* **1996**, *108*, 2750–2778

[1] J. M. Lehn, *Angew. Chem.* **1988**, *100*, 91–116; *Angew. Chem. Int. Ed. Engl.* **1988**, *27*, 89–112.
[2] P. R. Andrews, D. J. Craik, J. L. Martin, *J. Med. Chem.* **1984**, *27*, 1648–1657.
[3] a) B. Roth, E. A. Falco, G. H. Hitchings, S. R. M. Bushby, *J. Med. Pharm. Chem.* **1962**, *5*, 1103–1123; b) D. A. Matthews, J. T. Bolin, J. M. Burridge, D. J. Filman, K. W. Volz, B. T. Kaufmann, C. R. Beddell, J. N. Champness, D. K. Stammers, J. Kraut, *J. Biol. Chem.* **1985**, *260*, 381–391.
[4] *Drugs, News Perspect.* **1995**, *8*, 237.

[5] a) S. Trumpp-Kallmeyer, J. Hoflack, A. Bruinvels, M. Hibert, *J. Med. Chem.* **1992**, *35*, 3448–3462; b) J. Findley, E. Eliopoulos, *TIPS* **1992**, *11*, 492–499; c) C. Humblet, T. Mirzadegan, *Annu. Rep. Med. Chem.* **1992**, *27*, 291–300; d) P. Cronet, C. Sander, G. Vriend, *Protein Eng.* **1993**, *6*, 59–64; e) M. Kontoyianni, T. P. Lybrand, *Med. Chem. Res.* **1993**, *3*, 407–418.

[6] J. Deisenhofer, O. Epp, K. Miki, R. Huber, H. Michel, *J. Mol. Biol.* **1984**, *180*, 385–398; *Nature* **1985**, *318*, 618–624.

[7] See also: J. Deisenhofer, H. Michel, *Angew. Chem.* **1989**, *101*, 872–892; *Angew. Chem. Int. Ed. Engl.* **1989**, *28*, 829–847; R. Huber, *ibid.* **1989**, 101, 849-871 and **1989**, *28*, 848–869.

[8] A. Kreusch, G. E. Schultz, *J. Mol. Biol.* **1994**, *243*, 891–905.

[9] M. S. Weiss, U. Abele, J. Weckesser, W. Welte, E. Schiltz, G. E. Schulz, *Science* **1991**, *254*, 1627–1630.

[10] R. Henderson, J. M. Baldwin, T. A. Ceska, F. Zemlin, E. Beckmann, K. H. Downing, *J. Mol. Biol.* **1990**, *213*, 899–929.

[11] W. Kühlbrandt, D. N. Wang, Y. Fujiyoshi, *Nature* **1994**, *367*, 614–621.

[12] D. Picot, P. J. Loll, M. Garavito, *Nature* **1994**, *367*, 243–249.

[13] a) N. Unwin, *J. Mol. Biol.* **1993**, *229*, 1101–1124; b) *Nature* **1995**, *373*, 37–43.

[14] H. Oschkinat, T. Müller, T. Dieckmann, *Angew. Chem.* **1994**, *106*, 284–300; *Angew. Chem. Int. Ed. Engl.* **1994**, *33*, 277–293.

[15] S. W. Fesik, *J. Med. Chem.* **1991**, *34*, 2937–2945.

[16] E. R. P. Zuiderweg, S. R. van Doren, A. V. Kurochkin, R. R. Neubig, A. Majumdar, *Perspect. Drug Discovery Des.* **1993**, *1*, 391–417.

[17] a) M. Billeter, *Q. Rev. Biophys.* **1992**, *25*, 325; b) K. Wüthrich, *Acta Crystallogr. Sect. D* **1995**, *51*, 249–270.

[18] B. Cudney, S. Patel, K. Weisgraber, V. Newhouse, *Acta Crystallogr. Sect. D* **1994**, *50*, 414–423.

[19] J. Jancarik, S. H. Kim, *J. Appl. Crystallogr.* **1991**, *24*, 409–411.

[20] F. C. Bernstein, T. F. Koetzle, G. J. B. Williams, E. F. Meyer, Jr., M. D. Brice, J. R. Rodgers, O. Kennard, T. Shimanouchi, T. Tasumi, *J. Mol. Biol.* **1977**, *112*, 535–542.

[21] F. H. Allen, O. Kennard, R. Taylor, *Acc. Chem. Res.* **1983**, *16*, 146–153.

[22] F. H. Allen, S. Bellard, M. D. Brice, B. A. Cartwright, A. Doubleday, H. Higgs, T. Hummelink-Peters, O. Kennard, W. D. S. Motherwell, J. R. Rodgers, D. G. Watson, *Acta Crystallogr. Sect. B* **1979**, *35*, 2331–2339.

[23] F. H. Allen, J. E. Davies, J. J. Galloy, O. Johnson, O. Kennard, C. F. Macrae, E. M. Mitchell, G. F. Mitchell, J. M. Smith, D. G. Watson, *J. Chem. Inf. Comput. Sci.* **1991**, *31*, 187–204.

[24] W. J. Hehre, L. Radom, P. von R. Schleyer, J. A. Pople, *Ab initio molecular orbital theory*, Wiley, New York, **1986.**

[25] a) W. G. J. Hol, *Angew. Chem.* **1986**, *98*, 765–777; *Angew. Chem. Int. Ed. Engl.* **1986**, *25*, 767–778; b) M. D. Walkinshaw, *Med. Res. Rev.* **1992**, *12*, 317–372; c) M. A. Navia, M. A. Murcko, *Curr. Opin. Struct. Biol.* **1992**, *2*, 202–210; d) H.-J. Böhm, G. Klebe, H. Kubinyi, *Wirkstoffdesign*, Spektrum Akademischer Verlag, Heidelberg, **1996**.

[26] C. L. M. J. Verlinde, W. G. J. Hol, *Structure* **1994**, *2*, 577–587.

[27] J. Greer, J. W. Erickson, J. J. Baldwin, M. D. Varney, *J. Med. Chem.* **1994**, *37*, 1035–1054.

[28] L. F. Kuyper, B. Roth, D. P. Baccanari, R. Ferone, C. R. Bedell, J. N. Champness, D. K. Stammers, J. G. Dann, F. E. Norrington, D. J. Baker, P. J. Goodford, *J. Med. Chem.* **1982**, *25*, 1120–1122.

[29] P. Y. S. Lam, P. K. Jadhav, C. J. Eyermann, C. N. Hodge, Y. Ru, L. T. Bacheler, J. L. Meek, M. L. Otto, M. M. Rayner, Y. N. Wong, C. H. Chang, P. C. Weber, D. A. Jackson, T. R. Sharpe, S. Erickson-Viitanen, *Science* **1994**, *263*, 380–384.

[30] a) K. Appelt, R. J. Bacquet, C. A. Bartlett, C. L. J. Booth, S. T. Freer, M. A. M. Fuhry, M. R. Gehring, S. M. Herrmann, E. F. Howland, C. A. Janson, T. R. Jones, C. C. Kan, V. Kathardekar, K. K. Lewis, G. P. Marzoni, D. A. Matthews, C. Mohre, E. W. Moomaw, C. A. Morse, S. J. Oatley, R. C. Ogden, M. R. Reddy, S. H. Reich, W. S. Schoettlin, W. W. Smith, M. D. Varney, J. E. Villafranca, R. W. Ward, S. Webber, S. E. Webber, K. M. Welsh, J. White, *J. Med. Chem.* **1991**, *34*, 1925–1934; b) S. H. Reich, M. A. M. Fuhry, D. Nguyen, M. J. Pino, K. M. Welsh, S. Webber, C. A. Janson, S. R. Jordan, D. A. Matthews, W. W. Smith, C. A. Bartlett, C. L. J. Booth, S. M. Herrmann, E. F. Howland, C. A. Morse, R. W. Ward, J. White, *ibid.* **1992**, *35*, 847–858; c) M. D. Varney, G. P. Marzoni, C. L. Palmer, J. G. Deal, S. Webber, K. M. Welsh, R. J. Bacquet, C. A. Bartlett, C. A. Morse, C. L. J. Booth, S. M. Herrmann, E. F. Howland, R. W. Ward, J. White, *ibid.* **1992**, *35*, 663–676; d) M. D. Varney, C. L. Palmer, J. G. Deal, S. Webber, K. M. Welsh, C. A. Bartlett, C. A. Morse, W. W. Smith, C. A. Janson, *ibid.* **1995**, *38*, 1892–1903.

[31] J. J. Baldwin, G. S. Ponticello, P. S. Anderson, M. E. Christy, M. A. Murcko, W. C. Randall, H. Schwam, M. F. Sugrue, J. P. Springer, P. Gautheron, J. Grove, P. Mallorga, M. P. Viader, B. M. McKeever, M. A. Navia, *J. Med. Chem.* **1989**, *32*, 2510–2513.

[32] a) W. C. Ripka, W. J. Sipio, J. M. Blaney, *Lect. Heterocycl. Chem.* **1987**, *9*, 95–104; b) R. W. Schevitz, N. J. Bach, D. G. Carlson, N. Y. Chirgadze, D. K. Clawson, R. D. Dillard, S. E. Draheim, L. W. Hartley, N. D. Jones, E. D. Mihelich, J. L. Olkowski, D. W. Snyder, C. Sommers, J. P. Wery, *Nature Struct. Biol.* **1995**, *2*, 458–465.

[33] S. E. Ealick, Y. S. Babu, C. E. Bugg, M. D. Erion, W. C. Guida, J. A. Montgomery, J. A. Secrist, *Proc. Natl. Acad. Sci. USA* **1991**, *88*, 11540–11544.

[34] a) W. J. Thompson, P. Fitzgerald, M. K. Holloway, E. A. Emini, P. L. Darke, B. M. McKeever, W. A. Schleif, J. C. Quintero, J. A. Zugay, T. J. Tucker, J. E. Schwering, C. F. Homnick, J. Nunberg, J. P. Springer, J. R. Huff, *J. Med. Chem.* **1992**, *35*, 1685–1701; b) E. E. Kim, C. T. Baker, M. D. Dwyer, M. A. Murcko, B. G. Rao, R. D. Tung, M. A. Navia, *J. Am. Chem. Soc.* **1995**, *117*, 1181–1182.

[35] M. von Itzstein, W. Y. Wu, G. B. Kok, M. S. Pegg, J. C. Dyason, B. Jin, T. V. Phan, M. L. Smythe, H. F. White, S. W. Oliver, P. M. Colman, J. N. Varghese, D. M. Ryan, J. M. Woods, R. C. Bethell, V. J. Hotham, J. M. Cameron, C. R. Penn, *Nature* **1993**, *363*, 418–423.

[36] H. Mack, T. Pfeiffer, W. Hornberger, H. J. Böhm, H. W. Höffken, *J. Enzyme Inhib.* **1995**, *9*, 73–86.

[37] B. P. Morgan, D. R. Holland, B. W. Matthews, P. A. Bartlett, *J. Am. Chem. Soc.* **1994**, *116*, 3251–3260.

[38] M. T. Pisabarro, A. R. Ortiz, A. Palomar, F. Cabre, L. Garcia, R. C. Wade, F. Gago, D. Mauleon, G. Carganico, *J. Med. Chem.* **1994**, *37*, 337–341.

[39] R. E. Babine, T. M. Bleckman, C. R. Kissinger, R. Showalter, L. A. Pelletier, C. Lewis, K. Tucker, E. Moomaw, H. E. Parge, J. E. Villafranca, *Bioorg. Med. Chem. Lett.* **1995**, *5*, 1719–1724.

[40] a) C. A. Vale, J. R. Damewood, G. B. Steelman, C. Bryant, B. Gomes, J. Williams, *J. Med. Chem.* **1995**, *38*, 86–97; b) C. A. Vale, P. R. Bernstein, C. Bryant, C. Ceccarelli, J. R. Damewood, R. Earley, S. W. Feeney, B. Gomes, B. J. Kosmider, G. B. Steelman, R. M. Thoms, E. P. Vacek, J. C. Williams, D. J. Wolanin, S. Woolson, *ibid.* **1995**, *38*, 98–108.

[41] C. L. M. J. Verlinde, M. Callens, S. van Calenbergh, A. van Aerschot, P. Herdewijn, V. Hannaert, P. A. M. Michels, F. R. Opperdos, W. G. J. Hol, *J. Med. Chem.* **1994**, *37*, 3605–3613.

[42] K. Hilpert, J. Ackermann, D. W. Banner, A. Gast, K. Gubernator, P. Hadvary, L. Labler, K. Müller, G. Schmid, T. B. Tschopp, H. van de Waterbeemd, *J. Med. Chem.* **1994**, *37*, 3889–3901.

[43] J. L. Chambers, R. M. Stroud, *Acta Crystallogr. Sect. B* **1979**, *35*, 1861–1874.

[44] P. Dauber-Osguthorpe, V. A. Roberts, D. J. Osguthorpe, J. Wolff, M. Genest, A. T. Hagler, *Proteins* **1988**, *4*, 31–47.

[45] A. Wlodawer, J. Nachman, G. L. Gilliland, W. Gallagher, C. J. Woodward, *J. Mol. Biol.* **1987**, *198*, 469–480.

[46] A. A. Kossiakoff, M. Randal, J. Guenot, C. Eigenbrot, *Proteins* **1992**, *14*, 65–74.

[47] T. A. Jones, J. Y. Zou, S. W. Cowan, M. Kjeldgaard, *Acta Crystallogr. Sect. A* **1991**, *47*, 110–119.

[48] A. T. Brünger, A. Krukowski, *Acta Crystallogr. Sect. A* **1990**, *46*, 585–593.

[49] a) H. Zollner, *Handbook of Enzyme Inhibitors*, VCH, Weinheim, **1993**; b) J. Erickson, D. J. Neidhart, J. VanDrie, D. J. Kempf, X. C. Wang, D. W. Norbeck, J. J. Plattner, J. W. Rittenhouse, M. Turon, N. Wideburg, W. E. Kohlbrenner, R. Simmer, R. Helfrich, D. A. Paul, M. Knigge, *Science* **1990**, *249*, 527–533; c) B. R. Baker, E. H. Erickson, *J. Med. Chem.* **1967**, *10*, 1123–1128; d) I. V. Kurinov, R. W. Harrison, *Struct. Biol.* **1994**, *1*, 735–743; e) R. Kikumoto, Y. Tamao, K. Ohkubo, T. Tezuka, S. Tonomura, H. Hara, K. Ninomiya, A. Hijikata, S. Okamoto, *Biochemistry* **1994**, *23*, 85–90; f) C. Taparelli, R. Metternich, C. Erhardt, N. S. Cook, *Trends Pharmacol. Sci.* **1993**, *14*, 366–376.

[50] J. R. Damewood, P. D. Edwards, S. Feeney, B. C. Gomes, G. B. Steelman, P. A. Tuthill, J. C. Williams, P. Warner, S. A. Woolson, D. J. Wolanin, C. A. Veale, *J. Med. Chem.* **1994**, *37*, 3303–3312.

[51] P. R. Bernstein, D. Andisik, P. K. Bradley, C. B. Bryant, C. Ceccarelli, J. R. Damewood, R. Earley, P. D. Edwards, S. Feeney, B. C. Gomes, B. J. Kosmider, G. B. Steelman, R. M. Thomas, E. P. Vacek, C. A. Veale, J. C. Williams, D. J. Wolanin, S. A. Woolson, *J. Med. Chem.* **1994**, *37*, 3313–3326.

[52] R. B. Silverman, *The organic chemistry of drug design and drug action*, Academic Press, San Diego, **1992**; *Medizinische Chemie*, VCH, Weinheim, **1994.**

[53] H. Brandstetter, D. Turk, H. W. Höffken, D. Grosse, P. D. Martin, B. F. P. Edwards, W. Bode, *J. Mol. Biol.* **1992**, *226*, 1085–1099.

[54] G. A. Jeffrey, W. Saenger, *Hydrogen bonding in biological structures*, Springer, Berlin, **1991.**

[55] S. W. Cowan, M. E. Newcomer, T. A. Jones, *Proteins* **1990**, *8*, 44–61.

[56] J. H. Arevalo, E. A. Stura, M. J. Taussig, I. A. Wilson, *J. Mol. Biol.* **1993**, *231*, 103–118.

[57] J. N. Herron, X. He, M. L. Mason, E. W. Voss, A. B. Edmundson, *Proteins* **1989**, *5*, 271–280.

[58] K. A. Watson, E. P. Mitchell, L. N. Johnson, J. C. Son, C. J. F. Bichard, M. G. Orchard, G. W. J. Fleet, N. G. Oikonomakos, D. D. Leonidas, M. Kontou, A. Papageorgiou, *Biochemistry* **1994**, *33*, 5745–5758.

[59] N. K. Sauter, M. D. Bednarski, B. A. Wurzburg, J. E. Hanson, G. M. Whitesides, J. J. Skehel, D. C. Wiley, *Biochemistry* **1989**, *28*, 8388–8396.

[60] W. Janes, G. E. Schulz, *J. Biol. Chem.* **1990**, *265*, 10443–10445.

[61] I. K. McDonald, J. M. Thornton, *J. Mol. Biol.* **1994**, *238*, 777–793.

[62] J. C. Powers, J. W. Harper in *Proteinase Inhibitors* (Eds.: A. J. Barrett, G. Salvesen), Elsevier, New York, **1986**, 244–253.

[63] R. Wolfenden, W. M. Kati, *Acc. Chem. Res.* **1991**, *24*, 209–215.

[64] S. Dao-pin, H. Nicholson, W. A. Baase, X. J. Zhang, J. A. Wozniak, B. W. Matthews, *Protein Conformation* (Ciba Foundation Symposium 161), Wiley, Chichester, **1991**, p. 52.
[65] B. P. Morgan, J. M. Scholtz, M. D. Ballinger, I. D. Zipkin, P. A. Bartlett, *J. Am. Chem. Soc.* **1991**, *113*, 297–307.
[66] D. H. Tronrud, H. M. Holden, B. W. Matthews, *Science* **1987**, *235*, 571–574.
[67] P. A. Bash, U. C. Singh, F. K. Brown, R. Langridge, P. A. Kollman, *Science* **1987**, *235*, 574–576.
[68] K. M. Merz, P. A. Kollman, *J. Am. Chem. Soc.* **1989**, *111*, 5649–5658.
[69] O. Livnah, E. A. Bayer, M. Wilchek, J. L. Sussman, *Proc. Natl. Acad. Sci. USA*, **1993**, *90*, 5076–5080.
[70] M. I. Page, *Angew. Chem.* **1977**, *89*, 456–467; *Angew. Chem. Int. Ed. Engl.* **1977**, *16*, 449–459.
[71] W. P. Jencks, *Proc. Natl. Acad. Sci. USA* **1981**, *78*, 4046–4050.
[72] M. S. Searle, D. H. Williams, *J. Am. Chem. Soc.* **1992**, *114*, 10690–10697.
[73] M. S. Searle, D. H. Williams, U. Gerhard, *J. Am. Chem. Soc.* **1992**, *114*, 10697–10704.
[74] G. Chalasinski, M. M. Szczesniak, *Chem. Rev.* **1994**, *94*, 1723–1765.
[75] K. S. Kim, B. J. Mhin, U. S. Choi, K. Lee, *J. Chem. Phys.* **1992**, *97*, 6649–6662.
[76] V. W. Blokzijl, J. B. F. N. Engberts, *Angew. Chem.* **1993**, *105*, 1610–1648; *Angew. Chem. Int. Ed. Engl.* **1993**, *32*, 1545–1579.
[77] M. C. Chervenak, E. J. Toone, *J. Am. Chem. Soc.* **1994**, *116*, 10533–10539.
[78] J. D. Dunitz, *Science* **1994**, *264*, 670.
[79] B. Spriggs, P. Haake, *Bioorg. Chem.* **1977**, *6*, 181–190.
[80] S. E. Krikorian, *J. Phys. Chem.* **1982**, *86*, 1875–1881.
[81] H. J. Böhm, *J. Comput. Aided Mol. Des.* **1994**, *8*, 243–256.
[82] B. L. Jacobson, J. J. He, P. S. Vermesch, D. D. Lemon, F. A. Quiocho, *J. Biol. Chem.* **1991**, *266*, 5220–5225.
[83] C. Tanford, *The Hydrophobic Effect*, 2nd ed, Wiley, New York, **1980**.
[84] A. Ben-Naim, *Hydrophobic Interactions*, Plenum, New York, **1980**.
[85] a) S. K. Burley, G. A. Petsko, *Science* **1985**, *229*, 23–28; b) C. A. Hunter, J. Singh, J. M. Thornton, *J. Mol. Biol.* **1991**, *218*, 837–846.
[86] C. A. Hunter, *Chem. Soc. Rev.* **1994**, 101–109.
[87] D. B. Smithrud, T. B. Wyman, F. Diederich, *J. Am. Chem. Soc.* **1991**, *113*, 5420–5426.
[88] G. Klebe, F. Diederich, *Philos. Trans. R. Soc. London A* **1993**, *345*, 37–48.
[89] J. L. Sussman, M. Harel, F. Frolow, C. Oefner, A. Goldman, L. Toker, I. Silman, *Science* **1991**, *253*, 872–879.
[90] D. A. Dougherty, D. A. Staufer, *Science* **1990**, *250*, 1558–1560.
[91] a) R. T. Shuman, R. B. Rothenberger, C. S. Campbell, G. F. Smith, D. S. Gifford-Moore, P. D. Gesellchen, *J. Med. Chem.* **1993**, *36*, 314–319; b) N. Balasubramanian, D. R. St. Laurent, M. E. Federici, N. A. Meanwell, J. J. Wright, W. A. Schumacher, S. M. Seiler, *ibid.* **1993**, *36*, 300–303; c) C. Hutchins, J. Greer, *Crit. Rev. Biochem. Mol. Biol.* **1991**, *26*, 77–127.
[92] S. Paliwal, S. Geib, C. S. Wilcox, *J. Am. Chem. Soc.* **1994**, *116*, 4497–4498.
[93] a) A. R. Fersht, J. P. Shi, J. Knill-Jones, D. M. Lowe, A. J. Wilkinson, D. M. Blow, P. Brick, P. Carter, M. M. Y. Waye, G. Winter, *Nature* **1985**, *314*, 235–238; b) J. S. Thorson, E. Chapman, P. G. Schultz, *J. Am. Chem. Soc.* **1995**, *117*, 9361–9362.
[94] P. R. Connelly, R. A. Aldape, F. J. Bruzzese, S. P. Chambers, M. J. Fitzgibbon, M. A. Fleming, S. Itoh, D. J. Livingston, M. A. Navia, J. A. Thomson, K. P. Wilson, *Proc. Natl. Acad. Sci. USA* **1994**, *91*, 1964–1968.
[95] B. A. Shirley, P. Stanssens, U. Hahn, C. N. Pace, *Biochemistry* **1992**, *31*, 725–732.
[96] Y. W. Chen, A. R. Fersht, K. Henrick, *J. Mol. Biol.* **1993**, *234*, 1158–1170.
[97] S. K. Jandu, S. Ray, L. Brooks, R. J. Leatherbarrow, *Biochemistry* **1990**, *29*, 6264–6269.
[98] R. S. Bohacek, C. McMartin, *J. Med. Chem.* **1992**, *35*, 1671–1684.
[99] H. J. Schneider, T. Schiestel, P. Zimmermann, *J. Am. Chem. Soc.* **1992**, *114*, 7698–7703.
[100] S. Vajda, Z. Weng, R. Rosenfeld, C. DeLisi, *Biochemistry* **1994**, *33*, 13977–13988.
[101] S. Krystek, T. Stouch, J. Novotny, *J. Mol. Biol.* **1993**, *234*, 661–679.
[102] N. Horton, M. Lewis, *Protein Sci.* **1992**, *1*, 169–181.
[103] C. N. Pace, *J. Mol. Biol.* **1992**, *226*, 29–35.
[104] a) J. L. Cohen, K. A. Connors, *J. Pharm. Sci.* **1970**, *59*, 1271; b) J. Gao, S. Qiao, G. M. Whitesides, *J. Med. Chem.* **1995**, *38*, 2292–2301.
[105] M. Matsumura, W. J. Becktel, B. W. Matthews, *Nature* **1988**, *334*, 406–410.
[106] F. M. Richards, *Annu. Rev. Biophys. Bioeng.* **1977**, *6*, 151–176.
[107] C. Chothia, *Nature* **1975**, *254*, 304–308.
[108] M. Matsumura, W. J. Becktel, B. W. Matthews, *Nature* **1988**, *334*, 406–410.
[109] K. A. Sharp, A. Nicholls, R. Friedman, B. Honig, *Biochemistry* **1991**, *30*, 9686–9697.
[110] A. P. Kaplan, P. A. Bartlett, *Biochemistry* **1991**, *30*, 8165–8170.
[111] R. A. Wiley, D. H. Rich, *Med. Res. Rev.* **1993**, *13*, 327–384.
[112] M. S. L. Lim, E. R. Johnston, C. A. Kettner, *J. Med. Chem.* **1993**, *36*, 1831–1838.
[113] H. Sakamoto, Y. Shimohigashi, T. Ogawa, K. Sakamoto, M. Ohno, *Bull. Chem. Soc. Jpn.* **1991**, *64*, 2519–2523.
[114] a) W. P. Jencks, *Adv. Enzymol.* **1975**, *43*, 219–410; b) A. Fersht, *Enzyme Structure and Mechanism*, 2nd ed, Freeman, New York, 1995.
[115] a) T. W. Ku, F. E. Ali, L. S. Barton, J. W. Bean, W. E. Bondinell, J. L. Burgess, J. F. Callahan, R. R. Calvo, L. Chen, D. S. Eggleston, J. G. Gleason, W. F. Huffman, S. M. Hwang, D. Jakas, C. B. Karash, R. M. Keenan, K. D. Kopple, W. M. Miller, K. A. Newlander, A. Nichols, M. F. Parker, C. E. Peishoff, J. M. Samanen, I. Uzinskas, J. W. Venslavsky, *J. Am. Chem. Soc.* **1993**, *115*, 8861–8862; b) P. R. Bovy, F. S. Tjoeng, J. G. Rico, T. E. Rogers, R. J. Lindmark, J. A. Zablocki, R. B. Garland, D. E. McMackins, H. Dayringer, M. V. Toth, M. E. Zupec, S. Rao, S. G. Panzer-Knodle, N. S. Nicholson, A. Salyers, B. B. Taite, M. Herin, M. Miyano, L. P. Feigen, S. P. Adams, *Bioorg. Med. Chem.* **1994**, *2*, 881–895; c) D. G. Alberg, S. L. Schreiber, *Science* **1993**, *262*, 248–250.
[116] R. Raag, T. L. Poulos, *Biochemistry* **1991**, *30*, 2674–2684.
[117] M. D. Paulsen, R. L. Ornstein, *J. Comput. Aided Mol. Des.* **1992**, *6*, 449–460.
[118] P. C. Weber, M. W. Pantoliano, D. M. Simons, F. R. Salemme, *J. Am. Chem. Soc.* **1994**, *116*, 2717–2724.
[119] Y. Inoue, T. Hakushi, Y. Liu, L. H. Tong, B. J. Shen, D. S. Jin, *J. Am. Chem. Soc.* **1993**, *115*, 475–481.
[120] T. Wieseman, S. Wiliston, J. Brandts, L. Lin, *Analyt. Biochem.* **1989**, *179*, 131–137.
[121] R. Hitzemann, *Trends Pharmacol. Sci.* **1988**, *9*, 408–411.
[122] R. Hitzemann, M. Murphy, J. Currell, *Eur. J. Pharmacol.* **1985**, *108*, 171–177.
[123] G. A. Weiland, G. P. Minnemann, P. B. Molinoff, *Mol. Pharmacol.* **1980**, *18*, 341–347.
[124] a) D. E. Epps, J. Cheney, H. Schostarez, T. K. Sawyer, M. Prairie, W. C. Krueger, F. Mandel, *J. Med. Chem.* **1990**, *33*, 2080–2086; b) B. C. Braden, W. Dall'Asqua, E. Eisenstein, B. A. Fields, F. A. Goldbaum, E. L. Malchiodi, R. A. Mariuzza, F. P. Schwartz, X. Ysern, R. J. Poljak, *Pharm. Acta. Helv.* **1995**, *69*, 225–230.
[125] P. C. Weber, J. J. Wendoloski, M. W. Panoliano, F. R. Salemme, *J. Am. Chem. Soc.* **1992**, *114*, 3197–3200.
[126] E. Grunewald, C. Steel, *J. Am. Chem. Soc.* **1995**, *117*, 5687–5692.
[127] D. H. Williams, M. S. Searle, J. P. Mackay, U. Gerhard, R. A. Maplestone, *Proc. Natl. Acad. Sci. USA* **1993**, *90*, 1172–1178.
[128] K. P. Murphy, D. Xie, K. S. Thompson, L. M. Amzel, E. Freire, *Proteins Struct. Funct. Genet.* **1994**, *18*, 63–67.
[129] M. K. Holloway, J. M. Wai, T. A. Halgren, *J. Med. Chem.* **1995**, *38*, 305–317.
[130] P. D. J. Grootenhuis, P. J. M. Van Galen, *Acta Crystallogr. Sect. D* **1995**, *51*, 560–566.
[131] W. F. van Gunsteren, P. K. Weiner, *Computer simulations of biomolecular systems*, Escom, Leiden, **1989**.
[132] a) M. R. Reddy, V. N. Viswanadhan, J. N. Weinstein, *Proc. Natl. Acad. Sci. USA* **1991**, *88*, 10287–10291; b) B. G. Rao, R. F. Tilton, U. C. Singh, *J. Am. Chem. Soc.* **1992**, *114*, 4447–4452.
[133] a) C. F. Wong, J. A. McCammon, *J. Am. Chem. Soc.* **1986**, *108*, 3830–3832; b) L. M. Hansen, P. A. Kollman, *J. Comput. Chem.* **1990**, 11, 994–1002; c) K. M. Merz, M. A. Murcko, P. A. Kollman, *J. Am. Chem. Soc.* **1991**, *113*, 4484–4490; d) J. J. McDonald, C. L. Brooks III, *ibid.* **1991**, *113*, 2295–2301; e) S. Miyamoto, P. A. Kollman, *Proteins* **1993**, *16*, 226–245; f) *Proc. Natl. Acad. Sci. USA* **1993**, *90*, 8402–8406.
[134] a) P. A. Kollman, *Chem. Rev.* **1993**, *93*, 2395–2417; b) *Curr. Opin. Struct. Biol.* **1994**, *4*, 240–245.
[135] A. Warshel, H. Tao, M. Fothergill, Z. T. Chu, *Isr. J. Chem.* **1994**, *34*, 263–256.
[136] B. Honig, A. Nicholls, *Science* **1995**, *268*, 1144–1149.
[137] Y. K. Kang, K. D. Gibson, G. Nemethy, H. A. Scheraga, *J. Phys. Chem.* **1988**, *92*, 4739–4742.
[138] R. L. Williams, J. Vila, G. Perrot, H. A. Scheraga, *Proteins* **1992**, *14*, 110–119.
[139] C. J. Cramer, D. G. Truhlar, *J. Am. Chem. Soc.* **1991**, *113*, 8305–8311.
[140] C. J. Cramer, D. G. Truhlar, *J. Comput. Aided Mol. Des.* **1992**, *6*, 629–666.
[141] G. Klebe, *Perspect. Drug Des. Develop.* **1995**, *3*, 85–105.
[142] M. Saunders, *J. Comput. Chem.* **1991**, *12*, 645–663.
[143] M. Saunders, K. N. Houk, Y. D. Wu, W. C. Still, M. Lipton, G. Chang, W. C. Guida, *J. Am. Chem. Soc.* **1990**, *112*, 1419–1427.
[144] K. A. Watson, E. P. Mitchell, L. N. Johnson, J. C. Son, C. J. F. Bichard, M. G. Orchard, G. W. J. Fleet, N. G. Oikonomakos, D. D. Leonidas, M. Kontou, A. Papageorgioui, *Biochemistry* **1994**, *33*, 5745–5758.
[145] K. A. Watson, E. P. Mitchell, L. N. Johnson, J. C. Son, C. J. F. Bichard, G. W. J. Fleet, P. Ford, D. J. Watkin, N. G. Oikonomakos, *J. Chem. Soc. Chem. Commun.* **1993**, 654–656.
[146] G. Klebe in *Structure Correlation* (Eds.: H. B. Bürgi, J. D. Dunitz), VCH, Weinheim, **1994**, Chapter 13, p. 543–603.
[147] E. M. Ricketts, J. Bradshaw, M. Hann, F. Hayes, N. Tanna, D. M. Ricketts, *J. Chem. Inf. Comput. Sci.* **1993**, *33*, 905–925.
[148] M. C. Nicklaus, S. Wang, J. S. Driscoll, G. W. A. Milne, *Bioorg. Med. Chem.*, in press.
[149] G. Klebe, T. Mietzner, *J. Comput. Mol. Aided Des.* **1994**, *8*, 583–606.
[150] D. A. Matthews, J. T. Bolin, J. M. Burridge, D. J. Filman, K. W. Volz, J. Kraut, *J. Biol. Chem.* **1985**, *260*, 392–399.
[151] G. Klebe, *Struct. Chem.* **1990**, *1*, 597–616.
[152] G. Klebe, *J. Mol. Struct. Theochem* **1994**, *308*, 53–89.

[153] M. Sundaralingam, *Ann. N. Y. Acad. Sci.* **1975**, 255.
[154] W. Saenger, *Angew. Chem.* **1973**, *85*, 680–690; *Angew. Chem. Int. Ed. Engl.* **1973**, *12*, 591–601.
[155] H. W. Hoeffken, S. H. Knof, P. A. Bartlett, R. Huber, H. Moellering, G. Schumacher, *J. Mol. Biol.* **1988**, *204*, 417–433.
[156] M. Coll, S. H. Knof, Y. Ohga, A. Messerschmidt, R. Huber, H. Moellering, L. Rüssmann, G. Schumacher, *J. Mol. Biol.* **1990**, *214*, 597–610.
[157] G. Klebe in *The Application of Charge Density to Chemistry and Drug Design* (Ed.: G. A. Jeffrey), Plenum, **1990**, p. 287.
[158] M. Häser, R. Ahlrichs, *J. Comput. Chem.* **1989**, *10*, 104–111.
[159] M. A. Spackman, *Chem. Rev.* **1992**, *92*, 1769–1797.
[160] H. Kim, W. N. Lipscomb, *Biochemistry* **1991**, *30*, 8171–8180.
[161] T. Ashida, Y. Tsunogae, I. Tanaka, T. Yamane, *Acta Crystallogr. Sect. B* **1987**, *43*, 212–218.
[162] H. R. Loosli, H. Kessler, H. Oschkinat, H. P. Weber, T. J. Petcher, A. Widmer, *Helv. Chim. Acta* **1985**, *68*, 682–704.
[163] H. Kessler, M. Köck, T. Wein, M. Gehrke, *Helv. Chim. Acta* **1990**, *73*, 1818–1832.
[164] C. Weber, G. Wider, B. von Freyberg, R. Traber, W. Braun, A. Widmer, K. Wüthrich, *Biochemistry* **1991**, *30*, 6563–6574.
[165] S. W. Fesik, Vortrag auf dem 206th Am. Chem. Soc. Natl. Meeting, Chicago, **1993**.
[166] L. H. Weaver, W. R. Kester, B. W. Matthews, *J. Mol. Biol.* **1977**, *114*, 119–132.
[167] S. I. Foundling, J. Cooper, F. E. Watson, A. Cleasby, L. H. Pearl, B. L. Sibanda, A. Hemmings, S. P. Wood, T. L. Blundell, M. J. Valler, C. G. Norey, J. Kay, J. Boger, B. M. Dunn, B. J. Leckie, D. M. Jones, B. Atrash, A. Hallett, M. Szelke, *Nature* **1987**, *327*, 349–352.
[168] P. J. DeClerq, J. Hoflack, S. Cauwbergh, QCPE Program No. QCMP079.
[169] A. Zhang, R. G. Nanni, T. Li, G. F. Arnold, D. A. Oren, A. Jacobo-Molina, R. L. Williams, G. Kamer, D. A. Rubenstein, Y. Li, E. Rozhon, S. Cox, P. Buontempo, J. O. Connell, J. Schwartz, G. Miller, B. Bauer, R. Versace, P. Pinto, A. Ganguly, V. Girijavallabhan, E. Arnold, *J. Mol. Biol.* **1993**, *230*, 857–867.
[170] R. Bone, D. Frank, C. Kettner, D. A. Agrad, *Biochemistry* **1987**, *26*, 7609–7614.
[171] A. Sali, B. Veerapandian, J. B. Cooper, D. S. Moss, T. Hofmann, T. L. Blundell, *Proteins: Struct. Funct. Genet.* **1992**, *12*, 158–170.
[172] J. Rahuel, J. P. Priestle, M. G. Grütter, *J. Struct. Biol.* **1991**, *107*, 227–236.
[173] M. Clare, *Perspect. Drug Discovery Des.* **1993**, *1*, 49–68.
[174] S. C. Pettit, S. F. Michael, R. Swanstrom, *Perspect. Drug Discovery Des.* **1993**, *1*, 69–83.
[175] M. L. Moore, G. B. Dreyer, *Perspect. Drug Discovery Des.* **1993**, *1*, 85–108.
[176] D. W. Banner, P. Hadvary, *J. Biol. Chem.* **1991**, *166*, 20085–20093.
[177] K. Appelt, *Perspect. Drug Discovery Des.* **1993**, *1*, 23–48.
[178] J. T. Bolin, D. J. Filman, D. A. Matthews, R. C. Hamlin, J. Kraut, *J. Biol. Chem.* **1982**, *257*, 13650–13662.
[179] C. Bystroff, S. J. Oatley, J. Kraut, *Biochemistry* **1987**, *26*, 3263–3277.
[180] J. Badger, I. Minor, M. J. Kremer, M. A. Oliveira, T. J. Smith, J. P. Griffith, D. M. A. Guerin, S. Krishaswamy, M. Luo, M. G. Rossmann, M. A. McKinlay, G. T. D. Diana, F. J. Dutko, M. Fancher, R. R. Rueckert, B. A. Heinz, *Proc Natl. Acad. Sci. USA* **1988**, *85*, 3304–3308.
[181] G. Klebe in *3D QSAR in Drug Design* (Ed.: H. Kubinyi), Escom, Leiden, **1993**, p. 173–199.
[182] W. R. Kester, B. W. Matthews, *Biochemistry* **1977**, *16*, 2506–2516.
[183] D. Banner, J. Ackermann, A. Gast, K. Gubernator, P. Hadvary, K. Hilpert, L. Labler, K. Müller, G. Schmid, T. Tschopp, H. van den Waterbeemd, B. Wirz in *Perspectives in Medical Chemistry* (Eds.: B. Testa, E. Kyburz, W. Fuhrer, R. Giger), Helvetica Chimica Acta & VCH, Basel, **1993**, p. 27–43.
[184] A. Wojtczak, J. Luft, V. Cody, *J. Biol. Chem.* **1992**, *267*, 353–357.
[185] C. Mattos, D. Ringe in *3D QSAR in Drug Design* (Ed.: H. Kubinyi), Escom, Leiden, **1993**, p. 226–254.
[186] C. Mattos, B. Rasmussen, X. Ding, G. A. Petsko, D. Ringe, *Struct. Biol.* **1994**, *1*, 55–58.
[187] T. L. Poulos, A. J. Howard, *Biochemistry* **1987**, *26*, 8165–8174.
[188] O. Matsumoto, T. Taga, M. Matsushima, T. Higashi, K. Machida, *Chem. Pharm. Bull.* **1990**, *38*, 2253–2255.
[189] E. F. Meyer, R. Radhakrishnan, G. J. M. Cole, L. G. Presta, *J. Mol. Biol.* **1986**, *189*, 533–539.
[190] E. Rutenber, E. B. Fauman, R. J. Keenan, S. Fong, P. S. Furth, P. R. Ortiz de Montellano, E. Meng, I. D. Kuntz, D. L. DeChamp, R. Salto, J. R. Rose, C. S. Craik, R. M. Stroud, *J. Biol. Chem.* **1993**, *268*, 15343–15346.
[191] D. L. Gatti, B. A. Palfey, M. S. Lah, B. Entsch, V. Massey, D. P. Ballou, M. L. Ludwig, *Science* **1994**, *266*, 110–114.
[192] S. L. Roderick, M. C. Fournie-Zaluski, B. P. Roques, B. W. Matthews, *Biochemistry* **1989**, *28*, 1493–1497.
[193] T. Imoto, L. N. Johnson, A. C. T. North, D. C. Phillips, J. A. Rupley in *The Enzymes, Vol. VII* (Ed.: P. D. Boyer), 3rd ed, Academic Press, New York, **1972**, p. 665–868.
[194] J. C. Cheetham, P. J. Artymuik, D. C. Phillips, *J. Mol. Biol.* **1992**, *224*, 613–628.
[195] J. J. Baldwin, G. S. Ponticello, P. S. Anderson, M. E. Christy, M. A. Murcko, W. C. Randall, H. Schwam, M. F. Sugrue, J. P. Springer, P. Gautheron, J. Grove, P. Mallorga, M. P. Viader, B. M. McKeever, M. A. Navia, *J. Med. Chem.* **1989**, *32*, 2510–2513.
[196] M. Marquart, J. Walter, J. Deisenhofer, W. Bode, R. Huber, *Acta Crystallogr. Sect. B* **1983**, *39*, 480–490.
[197] R. K. Wierenga, M. E. M. Noble, R. C. Davenport, *J. Mol. Biol.* **1992**, *224*, 1115–1126.
[198] B. W. Matthews, *Acc. Chem. Res.* **1988**, *21*, 333–340.
[199] J. A. Montgomery, S. Niwas, J. D. Rose, J. A. Secrist III, Y. S. Babu, C. E. Bugg, M. D. Erion, W. C. Guida, S. E. Ealick, *J. Med. Chem.* **1993**, *36*, 55–69.
[200] M. C. Allen, W. Fuhrer, B. Tuck, R. Wade, J. M. Wood, *J. Med. Chem.* **1989**, *32*, 1652–1661.
[201] R. D. Cramer III, D. E. Patterson, J. D. Bunce, *J. Am. Chem. Soc.* **1988**, *110*, 5959–5967.
[202] Y. Kato, A. Itai, Y. Iitaka, *Tetrahedron* **1987**, *43*, 5229–5236.
[203] Y. Kato, A. Inoue, M. Yamada, N. Tomioka, A. Itai, *J. Comput. Aided Mol. Des.* **1992**, *6*, 475–486.
[204] R. B. Herrmann, D. K. Herron, *J. Comput. Aided Mol. Des.* **1991**, *5*, 511–524.
[205] M. Manaut, F. Sanz, J. Jose, M. Milesi, *J. Comput. Aided Mol. Des.* **1991**, *5*, 371–380.
[206] A. C. Good, E. E. Hodgkin, W. G. Richards, *J. Chem. Inf. Comput. Sci.* **1992**, *32*, 188–191.
[207] P. M. Dean, P. L. Chau, *J. Mol. Graph.* **1987**, *5*, 152–164.
[208] P. M. Dean, P. Callow, P. L. Chau, *J. Mol. Graph.* **1988**, *6*, 28–34.
[209] S. K. Kearsley, G. M. Smith, *Tetrahedron Comput. Methodol.* **1990**, *3*, 615–633.
[210] G. Klebe, T. Mietzner, F. Weber, *J. Comput. Aided Mol. Des.* **1994**, *8*, 751–778.
[211] A. F. Monzingo, B. W. Matthews, *Biochemistry* **1984**, *23*, 5724–5729.
[212] N. C. Cohen, J. M. Blaney, C. Humblet, P. Gund, D. C. Barry, *J. Med. Chem.* **1990**, *33*, 883–894.
[213] F. C. Wireko, G. E. Kellogg, D. J. Abraham, *J. Med. Chem.* **1991**, *34*, 758–767.
[214] G. E. Kellog, G. S. Joshi, D. J. Abraham, *Med. Chem. Res.* **1992**, *1*, 444–453.
[215] A. Nicholls, K. A. Sharp, B. H. Honig, *Proteins* **1991**, *11*, 281–296.
[216] M. L. Connolly, *Biopolymers* **1992**, *32*, 1215–1236.
[217] R. A. Lewis, *J. Comput. Aided Mol. Des.* **1989**, *3*, 133–147.
[218] G. J. Kleywegt, T. A. Jones, *Acta Crystallogr. Sect. D* **1994**, *50*, 178–185.
[219] P. J. Goodford, *J. Med. Chem.* **1985**, *28*, 849–857.
[220] D. N. A. Boobbyer, P. J. Goodford, P. M. McWhinnie, R. C. Wade, *J. Med. Chem.* **1989**, *32*, 1083–1094.
[221] N. Tomioka, A. Itai, *J. Comput. Aided Mol. Des.* **1994**, *8*, 347–366.
[222] W. L. Jorgensen, J. Tirado-Rives, *J. Am. Chem. Soc.* **1988**, *110*, 1657–1666.
[223] W. D. Cornell, P. Cieplak, C. I. Bayly, I. R. Gould, K. M. Merz, D. M. Ferguson, D. C. Spellmeyer, T. Fox, J. W. Caldwell, P. A. Kollman, *J. Am. Chem. Soc.* **1995**, *117*, 5179–5197.
[224] J. R. Maple, M. J. Hwang, T. P. Stockfisch, U. Dinur, M. Waldman, C. Ewig, A. T. Hagler, *J. Comput. Chem.* **1994**, *15*, 162–182.
[225] T. Halgren, *J. Am. Chem. Soc.* **1992**, *114*, 7827–7843.
[226] A. Miranker, M. Karplus, *Proteins: Struct. Funct. Genet.* **1991**, *11*, 29–34.
[227] G. Klebe, *J. Mol. Biol.* **1994**, *237*, 212–235.
[228] C. L. Brooks, M. Karplus, B. M. Pettitt, *Proteins: a theoretical perspective of dynamics, structure and thermodynamics*, Wiley, New York, **1988**.
[229] J. A. McCammon, S. C. Harvey, *Dynamics of proteins and nucleic acids*, Cambridge University Press, Cambridge, **1987**.
[230] H. Q. Ding, N. Karasawa, W. A. Goddard III, *J. Chem. Phys.* **1992**, *97*, 4309–4315.
[231] J. A. Board, J. W. Causey, J. F. Leathrum, A. Windemuth, K. Schulten, *Chem. Phys. Lett.* **1992**, *198*, 89–94.
[232] J. A. Braatz, *J. Biomol. Struct. Dyn.* **1992**, *9*, 935.
[233] I. Chandrasekhar, G. M. Clore, A. Szabo, A. M. Gronenborn, B. R. Brooks, *J. Mol. Biol.* **1992**, *226*, 239–250.
[234] K. Lim, J. N. Herron, *Biochemistry* **1995**, *34*, 6962–6974.
[235] Y. C. Martin, *J. Med. Chem.* **1992**, *35*, 2145–2154.
[236] J. M. Blaney, J. S. Dixon, *Perspect. Drug Discovery Des.* **1993**, *1*, 301–319.
[237] I. D. Kuntz, E. C. Meng, B. K. Shoichet, *Acc. Chem. Res.* **1994**, *27*, 117–123.
[238] R. L. DesJarlais, R. P. Sheridan, G. L. Seibel, J. S. Dixon, I. D. Kuntz, R. Venkataraghavan, *J. Med. Chem.* **1988**, *31*, 722–729.
[239] E. C. Meng, B. K. Shoichet, I. D. Kuntz, *J. Comput. Chem.* **1992**, *13*, 505–524.
[240] E. C. Meng, D. A. Gschwend, J. M. Blaney, I. D. Kuntz, *Proteins* **1993**, *17*, 266–278.
[241] I. D. Kuntz, *Science* **1992**, *257*, 1078–1082.
[242] B. K. Shoichet, R. M. Stroud, D. V. Santi, I. D. Kuntz, K. M. Perry, *Science* **1993**, *259*, 1445–1450.
[243] Z. Li, X. Chen, E. Davidson, O. Zwang, C. Mendis, C. S. Ring, W. R. Roush, G. Fegley, R. Li, P. J. Rosenthal, G. K. Lee, G. L. Kenyon, I. D. Kuntz, F. E. Cohen, *Chem. Biol.* **1994**, *1*, 31–37.

[244] M. C. Lawrence, P. C. Davis, *Proteins* **1992**, *12*, 31–41.
[245] M. D. Miller, S. K. Kearsley, D. J. Underwood, R. P. Sheridan, *J. Comput. Aided Mol. Des.* **1994**, *8*, 153–174.
[246] H. J. Böhm, *J. Comput. Aided Mol. Des.* **1994**, *8*, 623–632.
[247] R. A. Lewis, A. R. Leach, *J. Comput. Aided Mol. Des.* **1994**, *8*, 467–475.
[248] H. J. Böhm in *3D-QSAR in drug design* (Ed.: H. Kubinyi), Escom, Leiden, **1993**, p. 386–405.
[249] Y. Nishibata, A. Itai, *Tetrahedron* **1991**, *47*, 8985–8990.
[250] Y. Nishibata, A. Itai, *J. Med. Chem.* **1993**, *36*, 2921–2928.
[251] R. S. Bohacek, C. McMartin, *J. Am. Chem. Soc.* **1994**, *116*, 5560–5571.
[252] D. K. Gehlhaar, K. E. Moerder, D. Zichi, C. J. Sherman, R. C. Ogden, S. T. Freer, *J. Med. Chem.* **1995**, *38*, 466–472.
[253] J. B. Moon, W. J. Howe, *Proteins* **1991**, *11*, 314–328.
[254] V. Tschinke, N. C. Cohen, *J. Med. Chem.* **1993**, *36*, 3863–3870.
[255] S. H. Rotstein, M. A. Murcko, *J. Med. Chem.* **1993**, *36*, 1700–1710.
[256] M. B. Eisen, D. C. Wiley, M. Karplus, R. E. Hubbard, *Proteins* **1994**, *19*, 199–221.
[257] A. Caflish, A. Miranker, M. Karplus, *J. Med. Chem.* **1993**, *36*, 2142–2167.
[258] R. A. Lewis, D. C. Roe, C. Huang, T. E. Ferrin, R. Langridge, I. D. Kuntz, *J. Mol. Graphics* **1992**, *10*, 66–78.
[259] V. J. Gillet, A. P. Johnson, P. Mata, S. Sike, *Tetrahedron Comput. Methodol.* **1990**, *3*, 681–696.
[260] V. Gillet, P. Johnson, P. Mata, S. Sike, P. Williams, *J. Comput. Aided Mol. Des.* **1993**, *7*, 127–153.
[261] P. Mata, V. J. Gillet, P. Johnson, J. Lampreia, G. J. Myatt, S. Sike, A. L. Stebbings, *J. Chem. Inf. Comput. Sci.* **1995**, *35*, 479–493.
[262] S. H. Rotstein, M. A. Murcko, *J. Comput. Aided Mol. Des.* **1993**, *7*, 23–43.
[263] P. A. Bartlett, G. T. Shea, S. J. Telfer, S. Waterman in *Molecular Recognition: Chemical and Biological Problems* (Ed.: S. M. Roberts), Royal Society London, **1989**, p. 182–196.
[264] D. A. Pearlman, M. A. Murcko, *J. Comput. Chem.* **1993**, *14*, 1184–1193.
[265] R. A. Lewis, P. M. Dean, *Proc. R. Soc. London B* **1989**, *236*, 125–140.
[266] R. A. Lewis, P. M. Dean, *Proc. R. Soc. London B* **1989**, *236*, 141–162.
[267] P. L. Chau, P. M. Dean, *J. Comput. Aided Mol. Des.* **1992**, *6*, 385–396.
[268] J. VanDrie, D. Weininger, Y. C. Martin, *J. Comput. Aided Mol. Des.* **1989**, *3*, 225–251.
[269] H. J. Böhm, *J. Comput. Aided Mol. Des.* **1992**, *6*, 61–78.
[270] H. J. Böhm, *J. Comput. Aided Mol. Des.* **1992**, *6*, 593–606.
[271] The *Fine Chemicals Directory* (FCD) and the *Available Chemicals Directory* (ACD) are distributed by Molecular Design, San Leandro, 2132 Farallon Drive, CA 94577, USA.
[272] Program CONCORD, distributed by Tripos Ass., 1699 S. Hanley Rd., St. Louis, MO 63144, USA.
[273] J. Sadowski, C. Rudolph, J. Gasteiger, *Tetrahedron Comput. Methodol.* **1990**, *3*, 537–547.
[274] M. Mares-Guia, E. Shaw, *J. Biol. Chem.* **1965**, *240*, 1579–1585.
[275] M. Recanatini, T. Klein, C. Z. Yang, J. McClarin, R. Langridge, C. Hansch, *Mol. Pharmacol.* **1986**, *29*, 436–446.
[276] LUDI is available from BIOSYM Technologies, 9685 Scranton Road, San Diego, CA 92121–2777, USA.
[277] M. A. Gallop, R. W. Barett, W. J. Dower, S. P. A. Fodor E. M. Gordon, *J. Med. Chem.* **1994**, *37*, 1233–1248, 1385–1401.
[278] R. N. Zuckermann, E. J. Martin, D. C. Spellmeyer, G. B. Stauber, K. R. Shoemaker, J. M. Kerr, G. M. Figliozzi, D. A. Goff, M. A. Siani, R. J. Simon, S. C. Banville, E. G. Brown, L. Wang, L. S. Richter, W. H. Moos, *J. Med. Chem.* **1994**, *37*, 2678–2685.
[279] G. Jung, A. G. Beck-Sickinger, *Angew. Chem.* **1992**, *104*, 375–391; *Angew. Chem. Int. Ed. Engl.* **1992**, *34*, 367–383; T. Carell, E. A. Wintner, J. Rebek, Jr., *ibid.* **1994**, *106*, 2159–2162, 2162–2165 and **1994**, *33*, 2059–2061, 2061–2064; J. K. Chen, S. L. Schreiber, *ibid.* **1995**, *107*, 1041–1058 and. **1995**, *34*, 953–969.

EVENTS

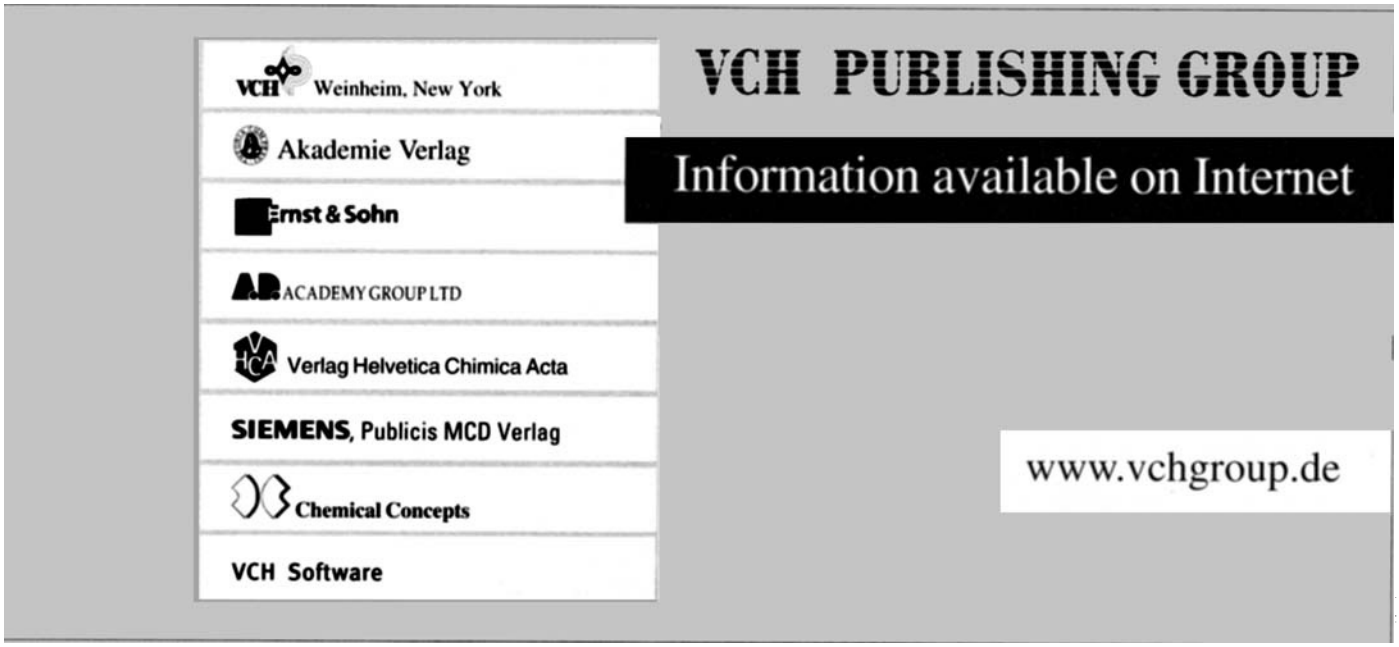

Defluorination of Perfluoroalkanes and Chlorofluorocarbons**

Graham C. Saunders*

The great strength of the carbon–fluorine bond has been the basis for much technological progress. Inert polyfluoro- and perfluorocarbons have found many industrial and domestic applications because of their low toxicity and noninflammability coupled with their high thermal stability and good thermodynamic properties. Chlorofluorocarbons (CFCs), however, pose a severe environmental problem because of their large contribution to ozone depletion, due to the release of chlorine radicals under UV photolysis in the stratosphere, and their contribution to global warming. Effective disposal of existing stockpiles of CFCs is thus extremely desirable but, because of the chemical inertness of the C–F bond, represents a significant challenge.

The chemical activaion of C–F bonds has attracted much attention, and recent research, driven partly by academic interest in the properties of these strong bonds and partly by the development of new, biologically active organofluorine compounds, has yielded exciting results. The cleavage of strong and apparently inert C–F bonds, which has always been a considerable challenge to the synthetic chemist, is being achieved in an increasing number of systems. Although aryl C–F bonds are stronger than alkyl C–F bonds, greater success has been achieved in activating the former. It has been known for some time that aryl C–F bonds are susceptible to nucleophilic attack, especially as the degree of fluorination increases,[1] and can be activated by transition metal and lanthanide complexes.[2] Indeed, recently Aizenberg and Milstein[3] and Kiplinger and Richmond[4] have described catalytic processes for the hydrogenolysis of perfluoroarenes using $[RhH(PMe_3)_4]$ and $[(\eta^5\text{-}C_5H_5)_2ZrCl_2]$ respectively. In contrast, the activation of the C–F bonds of perfluoroalkanes had only been achieved under extreme conditions. For example, in the elemental analysis of organofluorine compounds the substrate is treated with either alkali metal cations, peroxides, or oxygen at elevated temperatures, typically above 600 °C,[5] and formerly hexafluorobenzene was manufactured industrially by the defluorination of perfluorocyclohexane with iron at 450–500 °C.[6] A small number of highly reactive organometallic complexes have also been reported to activate alkyl C–F bonds. For example, $[(\eta^5\text{-}C_5H_4Me)_3(UCMe_3)]$ reacts with dodecafluorocyclohexane to give undecafluorocyclohexane.[7]

As tertiary C–F bonds possess low-lying σ^* orbitals that may readily accept electrons under certain conditions,[8] one possible approach to activating C–F bonds involves electron transfer from a reducing agent to the fluorocarbon moiety. This occurs in the reactions between fluorocarbons and strong reducing agents such as alkali metals and organic radical anions.[5, 9] These reactions are usually unselective and lead to complete defluorination of the fluorocarbon. The sodium benzophenone radical anion, however, has been reported by Pez et al. to selectively defluorinate perfluorocycloalkanes to give perfluoroarenes at ambient temperature (Scheme 1).[10] Single-electron

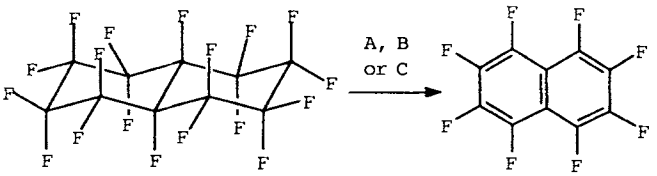

Scheme 1. A) $10\,Na^+[Ph_2CO]^-$, THF, room temperature, 1.5 h, $-10\,NaF$, $-10\,Ph_2CO$, 61%; B) $10[(C_5H_5)_2Co]$, $10\,LiO_3SCF_3$, Et_2O, room temperature, 12 h, $-10[(C_5H_5)_2Co]^+$, $[O_3SCF_3]^-$, $-10\,LiF$, 53%; C) $[(C_5H_5)_2TiF_2]$ (cat.), Al/$HgCl_2$, THF, room temperature, 130 h, 40%.

transfer processes have also been postulated in a number of reactions involving transition metal and lanthanide complexes,[3, 11] and ESR evidence supports this mechanism in the reaction between *trans*-$[Pt(H)_2\{P(cyclo\text{-}C_6H_{11})_3\}_2]$ and pentafluorobenzonitrile.[12]

Richmond et al. reported that cobaltocene and perfluorodecalin react readily at ambient temperature to yield cobaltocenium fluoride, which is a potent source of "naked" fluoride ions.[13] Presumably the reaction proceeds by single-electron transfer from the cobaltocene to the fluorocarbon. The fate of the perfluorodecalin was not determined, but when the reaction was carried out with cobaltocene and perfluorodecalin in a 10:1 ratio and in the presence of LiO_3SCF_3, the lithium cation of which acts as a fluoride-abstracting agent, perfluoronaphthalene was obtained in 53% yield (Scheme 1). Subsequently, Kiplinger and Richmond have developed a catalytic system for the synthesis of perfluoroarenes from perfluorocycloalkanes. The process uses $[(\eta^5\text{-}C_5H_5)_2TiF_2]$ or $[(\eta^5\text{-}C_5H_5)_2ZrCl_2]$ as catalyst and aluminum as terminal reducing agent;[14] 6.2 mmol of perfluorodecalin in the presence of an

[*] Dr. G. C. Saunders
University of Leicester
Leicester LE1 7RH (UK)
Fax: Int. code +(116) 2523789
e-mail: gs14@leicester.ac.uk

[**] The author thanks Prof. J. H. Holloway and Dr. E. G. Hope for many fruitful discussions and acknowledges BNFL Fluorochemicals Ltd. for financial support.

excess of aluminum (87 mmol), $HgCl_2$ (0.19 mmol), and 0.026 mmol of $[(\eta^5\text{-}C_5H_5)_2TiF_2]$ in THF at ambient temperature produced 3.2 mmol of octafluoronaphthalene after 130 h; this conversion corresponds to 12 turnovers (Scheme 1). Other perfluorocycloalkanes were also defluorinated to afford perfluoroarenes under similar conditions. Richmond suggests that the organometallic complex in these systems acts as an "electron shuttle", transferring electrons from aluminum to the fluorinated substrate. Richmond's system leads exclusively to aromatic products.

Crabtree et al. have used similar methods to defluorinate perfluoroalkanes to yield perfluoroalkenes. They reported that the mercury-photosensitized reduction of perfluoroalkanes by ammonia yields perfluoroimines and perfluoronitriles, and proposed that the reactions proceed via perfluoroalkene intermediates.[15] Further development of this reaction led to a catalytic process for the defluorination of perfluoroalkanes to give perfluoroalkenes (Scheme 2).[16] Decamethylferrocene was used as

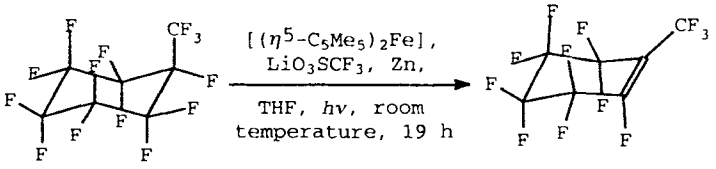

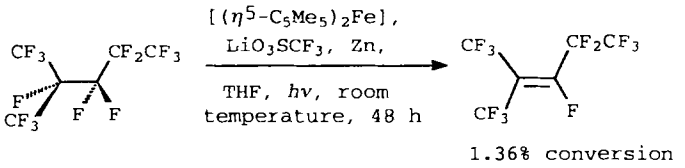

Scheme 2.

a one-electron reducing agent which, under irradiation from a medium-pressure Hg lamp, activated alkyl C–F bonds by photoinduced charge transfer. THF was found to favor this process and was therefore the preferred solvent. The resulting decamethylferrocenium ion was reduced by zinc to complete the cycle. As in Richmond's cobaltocene system the fluoride ions were abstracted by the lithium cations of LiO_3SCF_3. Conversions, however, were low even after lengthy periods. Perfluoromethylcyclohex-1-ene was obtained from perfluoromethylcyclohexane (11.43 mmol) in 11.9% conversion after 19 h of irradiation in the presence of $[(\eta^5\text{-}C_5Me_5)_2Fe]$ (0.30 mmol) and LiO_3SCF_3 (8.33 mmol), and perfluoro-2-methylpent-2-ene was produced from perfluoro-2-methylpentane in 1.36% conversion (40 turnovers) after 40 h under similar conditions. Attempts to increase the conversion resulted in byproducts. Unlike Richmond's system, however, defluorination of perfluorocycloalkanes to yield perfluoroarenes was not observed.

The catalytic selective defluorination of compounds that have usually been considered as inert has thus been realized. The selectivity and convenience of these methods, which require easily handled reagents and mild conditions, represent a major advance in the chemistry of the C–F bond. If further elaboration can increase the conversions, these methods may become powerful weapons in the armory of the synthetic organofluorine chemist.

Crabtree has further utilized reducing agents in the activation of C–F bonds to develop a convenient thermal process for the destruction of chlorofluorocarbons.[17] Passage of chlorofluorocarbon vapor through a bed of powdered sodium oxalate at 270 °C and at a rate of 4 mL min^{-1} resulted in the mineralization of the substrate with the formation of NaF, NaCl, and C, and evolution of CO_2, as shown for CF_2Cl_2 in Scheme 3. The

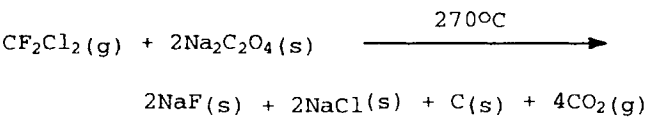

Scheme 3.

oxalate dianion acts as a two-electron reducing agent, which obviates the problems associated with radicals formed in single-electron transfer reactions. The sodium ions act as halide-abstracting agents. Evidence for an electron transfer process is provided by the observation that perhalocarbons react, but partially hydrogenated species such as $ClCH_2CH_2Cl$, which are poorer electron acceptors, do not.

For certain CFCs such as ClF_2CCF_2Cl only a single pass through the sodium oxalate bed was required, and no more than three passes were ever required. Complete mineralization was achieved, and the reactions showed no tendency to give uncontrollable exotherms. As sodium oxalate is an inexpensive, noncorrosive reagent, and the solid products are easily handled, this reaction is an efficient, convenient, and relatively cheap method for the destruction of CFCs.

The oxalate dianion can also be used to defluorinate perfluorocycloalkanes to produce perfluoroarenes. Passage of the perfluoroalkane vapor in nitrogen through sodium oxalate at 230 °C at rate of 200 mL min^{-1} gave the perfluoroarene in yields exceeding 40% after a single pass. Perfluoromethylcyclohexane was defluorinated to produce perfluorotoluene in 70% yield after several passes (Scheme 4). For perfluorodecalin a mixture

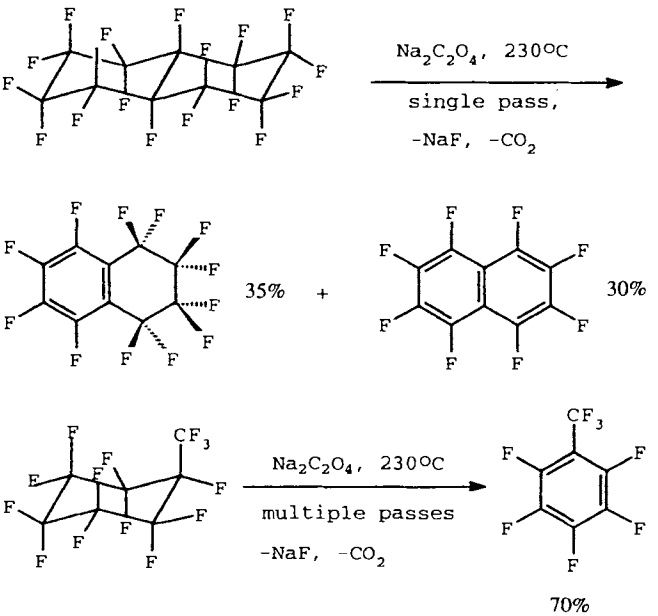

Scheme 4.

of perfluoronaphthalene and perfluorotetralene was obtained. The cation has a significant effect on these reactions. At 200 °C potassium oxalate defluorinates perfluoromethylcyclohexane to give perfluorotoluene in 72% yield, whereas sodium oxalate and lithium oxalate gave no reaction. At 230 °C, however, the yields of perfluorotoluene were 70 and 50%, respectively.

In summary, Richmond et al. and Crabtree et al. have developed convenient, catalytic processes for the cleavage of alkyl C–F bonds under mild conditions. Furthermore, Crabtree et al. have detailed a convenient and inexpensive method for the destruction of CFCs that has significant environmental benefits. This work highlights the special properties of C–F bonds and, together with the research cited here, begins to provide a rationale for the activation of these bonds. The prospect of further developments promises an exciting future for the synthetic organofluorine chemist.

German version: *Angew. Chem.* **1996**, *108*, 2783–2785

Keywords: chlorine compounds · defluorination · electron transfer · fluorine compounds

[1] B. E. Smart in *Chemistry of Organic Fluorine Compounds II* (Eds.: M. Hudlicky, A. E. Pavlath), Washington, **1995**, pp. 979–1010.

[2] a) J. L. Kiplinger, T. G. Richmond, C. E. Osterberg, *Chem. Rev.* **1994**, *94*, 373–431; b) M. J. Atherton, J. Fawcett, E. G. Hope, J. H. Holloway, A. Karaçar, D. R. Russell, G. C. Saunders, *J. Chem. Soc. Chem. Commun.* **1995**, 191–192; c) M. L. H. Green, J. Haggitt, C. P. Mehnert, *ibid.* **1995**, 1853–1854; d) M. Crespo, X. Solans, M. Font-Bardía, *Organometallics* **1995**, *14*, 355–364; e) R. M. Cedar, J. Granell, G. Muller, M. Font-Bardía, X. Solans, *ibid.* **1995**, *14*, 5544–5551; f) M. Ballhorn, M. G. Partridge, R. N. Perutz, M. K. Whittlesey, *Chem. Commun.* **1996**, 961–962.

[3] M. Aizenberg, D. Milstein, *J. Am. Chem. Soc.* **1996**, *117*, 8674–8675.

[4] J. L. Kiplinger, T. G. Richmond, *J. Chem. Soc. Chem. Commun.* **1996**, 1115–1116.

[5] R. Perry in *Fluorine – The First Hundred Years* (Eds.: R. E. Banks, D. W. A. Sharp, J. C. Tatlow), Elsevier, New York, **1986**, pp. 293–295.

[6] B. Gething, C. R. Patrick, J. C. Tatlow, R. E. Banks, A. K. Barbour, A. E. Tipping, *Nature* **1959**, *183*, 588.

[7] M. Weydert, R. Andersen, R. G. Bergman, *J. Am. Chem. Soc.* **1993**, *115*, 8837–8838.

[8] P. Kebarle, S. Chowdhury, *Chem. Rev.* **1987**, *87*, 513–534.

[9] a) J. F. Miller, H. Hunt, E. T. McBee, *Anal. Chem.* **1947**, *19*, 148–149; b) P. Johncock, W. K. R. Musgrave, A. Wiper, *Analyst* **1959**, 245–247; c) L. Kavan, F. P. Dousek, *J. Fluor. Chem.* **1988**, *41*, 383–391; d) D. D. MacNicol, C. D. Robertson, *Nature (London)* **1988**, *332*, 59.

[10] J. A. Marsella, A. G. Gilicinski, A. M. Coughlin, G. P. Pez, *J. Org. Chem.* **1992**, *57*, 2856–2860.

[11] a) G. B. Deacon, P. I. MacKinnon, T. D. Tuong, *Aust. J. Chem.* **1983**, *36*, 43–53; b) R. G. Finke, S. R. Keenan, D. A. Schiraldi, P. L. Watson, *Organometallics* **1986**, *5*, 598–601; c) R. G. Finke, S. R. Keenan, D. A. Schiraldi, P. L. Watson, *ibid.* **1987**, *6*, 1356–1358; d) M. J. Burk, D. L. Staley, W. Tumas, *J. Chem. Soc. Chem. Commun.* **1990**, 809–810; e) O. Blum, F. Frolow, D. Milstein, *ibid.* **1991**, 258–259.

[12] S. Hintermann, P. S. Pregosin, H. Rüegger, H. C. Clark, *J. Organomet. Chem.* **1992**, *435*, 225–234.

[13] B. K. Bennett, R. G. Harrison, T. G. Richmond, *J. Am. Chem. Soc.* **1994**, *116*, 11165–11166.

[14] J. L. Kiplinger, T. G. Richmond, *J. Am. Chem. Soc.* **1996**, *118*, 1805–1806.

[15] J. Burdenuic, W. Chupka, R. H. Crabtree, *J. Am. Chem. Soc.* **1995**, *117*, 10119–10120.

[16] J. Burdenuic, R. H. Crabtree, *J. Am. Chem. Soc.* **1996**, *118*, 2525–2526.

[17] J. Burdenuic, R. H. Crabtree, *Science* **1996**, *271*, 340–341.

 © *VCH Verlagsgesellschaft mbH, D-69451 Weinheim, 1996* *0570-0833/96/3522-2617 $ 15.00+.25/0*

Ylidic Four-Membered Rings with Four π-Electrons—Another Exciting Chapter in Phosphorus Chemistry

Lothar Weber*

The synthesis of stable four-membered ring compounds containing four π-electrons (**A**–**E**) remains a challenge for chemists even though the quest for stable cyclobutadienes ended successfully.[1] In 1968 the first unsupported cyclobutadiene **1** was reported, and its existence was ascribed to the push–pull effect of the two ethyl ester and the two diethylamino substituents.[2] Tetra-*tert*-butylcyclobutadiene (**2**) has to be regarded as a highlight in the field of cyclobutadiene chemistry. It was obtained quantitatively from the thermolysis of tetra-*tert*-butyltetrahedrane (**3**) at 130 °C, and, in contrast to mono-, di-, and tri-*tert*-butylcyclobutadiene, does not dimerize. The thermally induced ring-opening of **3** to yield **2** is reversed upon irradiating the cyclobutadiene derivative. The surprising stability of the tetrahedrane was attributed to the "corset effect" displayed by four bulky substituents, which resulted in a reduction of the steric hindrance.[1]

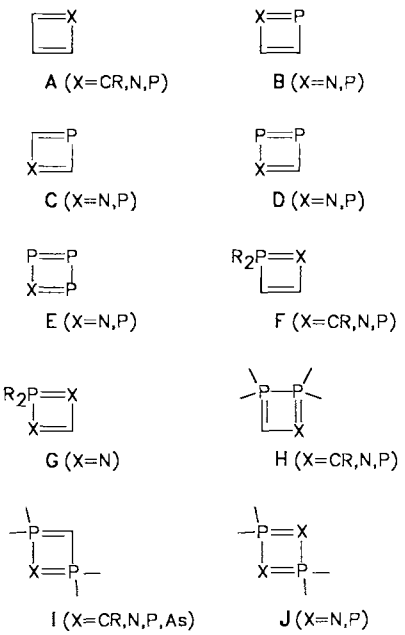

The interest in heterocyclobutadienes was stimulated by the preparation of tris(dimethylamino)azete (**4**)[3a] and its kinetically stabilized analogue $(t\mathrm{BuC})_3\mathrm{N}$.[3b] Calculations previously indicated that a nitrogen atom has a stabilizing effect on the cyclodiene system (decrease of the negative resonance energy).[3c] In contrast, λ^3-phosphetes (type **A**, X = P) have only been identified as η^4 ligands in transition metal complexes such as $[\mathrm{Co}(\eta^5\text{-}\mathrm{C_5H_5})\{\eta^4\text{-}t\mathrm{Bu(Me_3Si)_2C_3P}\}]$[4] and $[\mathrm{Rh}(\eta^5\text{-}\mathrm{C_5H_5})\{\eta^4\text{-}\mathrm{RPh_2C_3P}\}]$ (R = *t*Bu, N*i*Pr(SiMe$_3$)).[5] Unsupported diphosphetes of types **B** and **C** (X = P) are extremely reactive species, which spontaneously oligomerize to give tricyclic compounds such as **5**[6, 7] and **6**,[6] or the tetraphosphacubanes **7** (R = *t*Bu, $\mathrm{CMe_2Et}$, 1-adamantyl),[8] respectively.

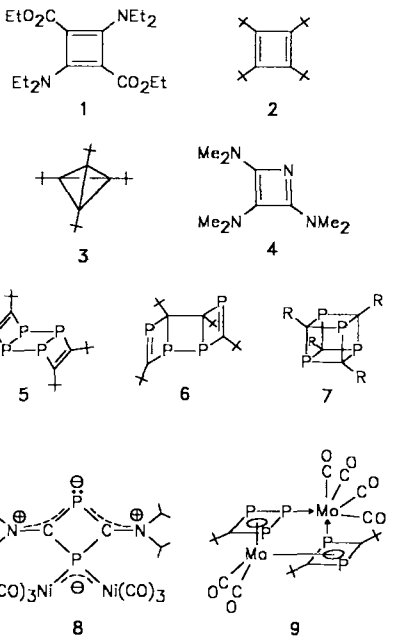

η^4-Diphosphete ligands are usually generated by metal-assisted dimerization of phosphaalkynes in the coordination sphere of transition metal complexes.[9] The 1,3-diphosphabutadiene ligand $(i\mathrm{Pr_2NCP})_2$ in complex **8** is stabilized by σ-coordination to two $[\mathrm{Ni(CO)_3}]$ fragments.[10] Compound **9** is the only $\eta^4{:}\eta^1$-triphosphete complex known to date.[11] *cyclo*-$\mathrm{P_4}$, which is isomeric to white phosphorus, only exists as a ligand in coordination compounds such as $[\mathrm{Ta}\{(1,3\text{-}t\mathrm{Bu})_2\mathrm{C_5H_3}\}(\mathrm{CO})_2\{\eta^4\text{-}\mathrm{P_4}\}]$[12] and $[\mathrm{W(CO)_4}\{(\mathrm{CO})_5\mathrm{WP}\}_4]$.[13, 14]

In addition to ring strain, negative resonance energy ("antiaromaticity") accounts for the instability of cyclobutadienes, azetes, and phosphetes. As we now know, the exchange of a single CH group by a $\mathrm{R_2P}$ function efficiently suppresses the conjugation of the four π-electrons, allowing the preparation of significantly more stable systems of the type **F**. Two nitrogen atoms in the α positions of the λ^5-phosphorus are also tolerated in the four-membered ring (type **G**).

Whereas, monocyclic λ^5-phosphetes are still elusive compounds and are postulated as intermediates in the reaction of $(i\mathrm{Pr_2N})_2\mathrm{P(Cl)}{=}\mathrm{C(H)SiMe_3}$ with dimethyl acetylenedicarboxylate, the benzo- and naphtho-λ^5-phosphetes **10a,b** are synthesized from suitable P-chlorophosphorus ylides and $\mathrm{AlCl_3}$.[15] 1,2λ^5-Azaphosphetes **F** (X = N) are accessible by two different routes. The [2 + 4]cycloaddition of azidobis(diisopropylamino)phosphane with dimethyl acetylenedicarboxylate yields a 1,2,3,4λ^5-triazaphosphinine derivative, which is smoothly converted into **11** in boiling toluene by elimination of dinitro-

[*] Prof. Dr. L. Weber
Fakultät für Chemie der Universität
Universitätsstrasse 25, D-33615 Bielefeld (Germany)
Fax: Int. code + (521)106-6146

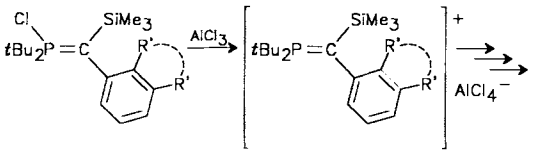

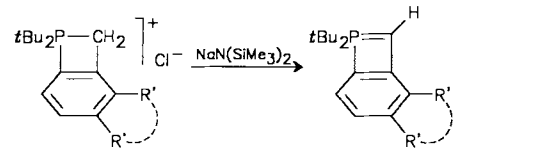

10a,b

a R' = H; b R'–R' = CH=CH–CH=CH

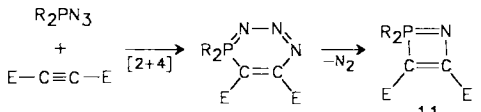

11

R = iPr$_2$N; E = CO$_2$Me

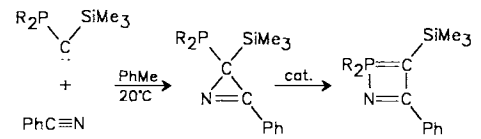

12 13

R = (c-C$_6$H$_{11}$)$_2$N; cat. = [(p-cymene)RuCl$_2$]

gen.[16] A catalytic amount of $PdCl_2$ induces the ring contraction even at room temperature.[16c]

The ring expansion of 2H-azirine **12** to **13** is achieved by catalysis with [(p-cymene)RuCl$_2$].[17] The array of four-membered heterocycles with four π-electrons is enriched by the 1λ^5,2λ^3-diphosphete **15**, which is obtained as a yellow oil during the codimerization of tBuC≡P with the in situ photochemically generated λ^5-phosphaalkyne (phosphinocarbene) **14**. The reaction of bromophenyldiazirine with (iPr$_2$N)$_2$PSnMe$_3$ gives the crystalline, colorless 1,3,2λ^5-diazaphosphete **17** by ring expansion of the transient N-phosphinodiazirine **16**.[19]

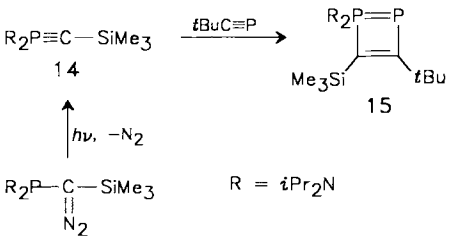

14 15

R = iPr$_2$N

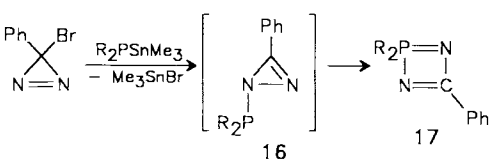

16 17

R = iPr$_2$N

Diphosphetes with two λ^5-phosphorus centers can be expected as 1λ^5,2λ^5 or 1λ^5,3λ^5 isomers (**H** and **I**), but only examples of type **I** are known. 1λ^5,3λ^5-diphosphetes (type **I**, X = CR) are among the longest known four-membered rings with four π-electrons. Treatment of $CH_3PF_2(NMe_2)_2$ with two equivalents of n-butyllithium affords compound **18**,[20a] and this procedure is also useful for the preparation of C-substituted diphosphetes.[20b] Reactive λ^5-phosphaalkynes are assumed as intermediates in this process. More recently λ^5-phosphaalkynes were generated by thermolysis or photolysis of phosphinodiazoalkanes, and by using sufficient kinetic stabilization through bulky substituents at the P≡C unit they could be isolated. However, without such protection λ^5-phosphaalkynes dimerize to give 1λ^5,3λ^5-diphosphetes such as **19**.[21]

The photochemical synthesis of 1,2λ^5,4λ^5,6λ^5-azatriphosphinines from phosphinodiazomethanes $R_2PC(N_2)SiMe_3$ involve transient 1,2λ^5,4λ^5-azadiphosphetes (type **I**, X = N), which presumably result from the [2 + 2]cycloaddition between transient λ^5-phosphaalkynes $R_2P{\equiv}CSiMe_3$ and nitrilo-λ^5-phosphanes $R_2P{\equiv}N$.[21c]

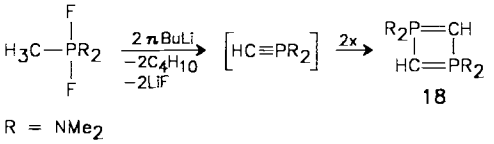

18

R = NMe$_2$

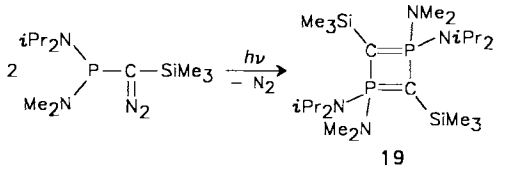

19

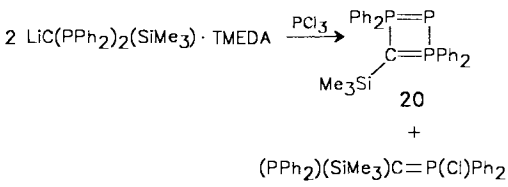

20

+

(PPh$_2$)(SiMe$_3$)C=P(Cl)Ph$_2$

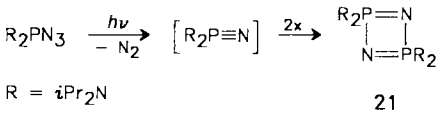

21

The reaction of PCl_3 with Li[C(PPh$_2$)$_2$(SiMe$_3$)] gave the first triphosphete **20** (type **I**, X = P), which was isolated in the form of colorless crystals. The ylide Ph$_2$P(Cl) = C(PPh$_2$)(SiMe$_3$) is obtained in this reaction as a by-product.[22] The analogous 1,2λ^5,4λ^5-arsadiphosphete was obtained when $AsCl_3$ was used instead of PCl_3.[22] An alternative synthetic approach to compound **20** is based on the treatment of the lithium diphosphinomethanide with white phosphorus.[22] The course of the reaction with PCl_3 is sensitive to the nature of the substituents and the solvent. For example, diphosphetes have not been obtained from reactions of Li[C(PMe$_2$)$_2$(SiMe$_3$)] with PCl_3[23] or $AsCl_3$.[24]

A few 1,3,2λ^5,4λ^5-diazadiphosphetes **21** (cyclodiphosphazenes) of type **J** (X = N) are dimerization products of transient nitrilo-

λ^5-phosphanes, which result from the photolysis or thermolysis of suitably functionalized azidophosphanes.[25] The first $1\lambda^5,3\lambda^5,2\lambda^3,4\lambda^3$-tetraphosphete (**22**; type **J**, X = P), which occurs as the central building block in a dispiro compound, may formally be related to a series of $1\lambda^5,3\lambda^5$-diphosphetes and 1,3,2-$\lambda^5,4\lambda^5$-diazadiphosphetes. Compound **22** is produced by the reduction of the respective bis(amino)chlorophosphane with lithium metal.[26]

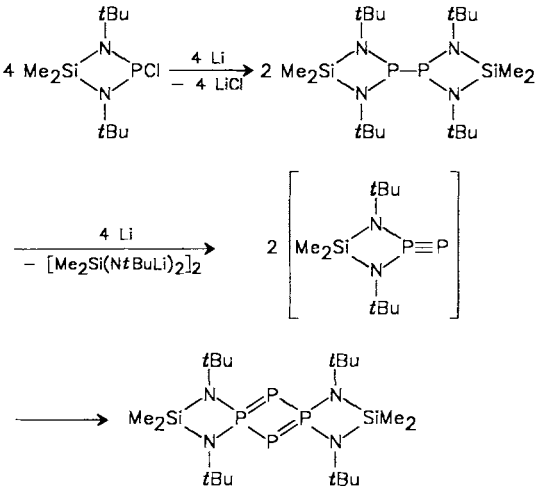

22

According to calculations and the X-ray crystal structure analysis the bonding in the planar four-membered rings **F-J** is best described as zwitterionic (ylidic); the P–X bond lengths range between those of single and double bonds. Therefore, the comparison with phosphorus ylides, phosphazenes,[27] phosphinidene phosphoranes,[28] and triphosphenium systems is particularly pertinent (Scheme 1).

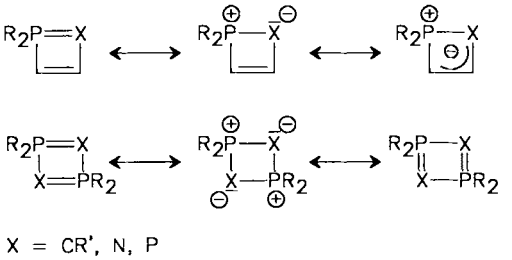

Scheme 1. Bonding in the planar four-membered rings of the type **F**–**J**.

The rich chemistry of these new four-membered ring compounds is particularly interesting and innovative. The ring expansion processes, oxidative additions with retention of the ring skeleton, substitution reactions, and complex formation all merit attention, and the synthetic potential is illustrated here with a few examples. The sole product observed in the reaction of diphosphete **18** with *t*BuC≡P is the $1\lambda^5,3\lambda^5,5\lambda^3$-triphosphabenzene **23**.[30] Treatment of **11** with piperidine at ambient temperature gives rise to the rapid formation of the five-membered heterocycle **24**.[16c] The two-coordinate phosphorus atom of the $1\lambda^5,2\lambda^3$-diphosphete **15** reacts with elemental selenium (one or two equivalents) or with tetrachloro-*o*-benzoquinone (TCBQ; two equivalents) to afford the heterocycles **25**–**27**,[31] respectively. Remarkably, the P–P bond remains intact during these oxidations.

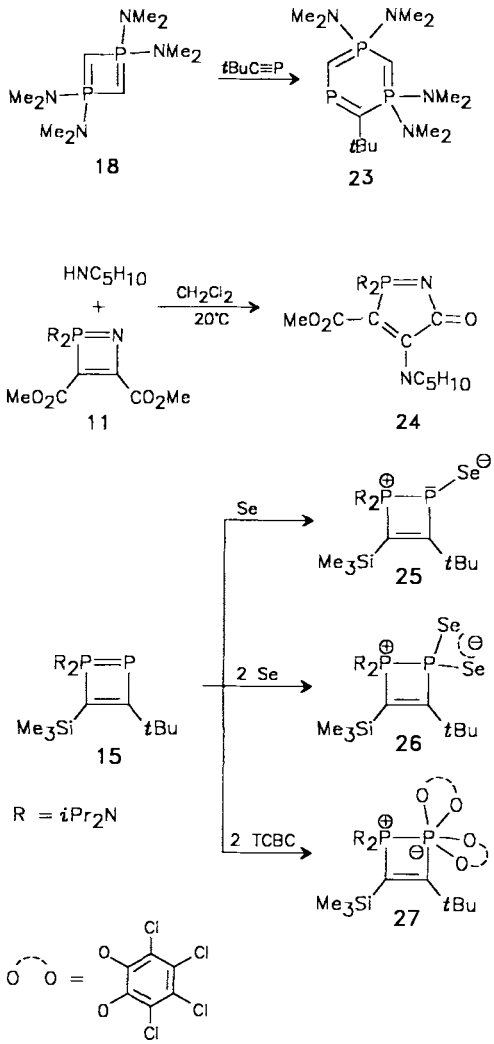

Particularly noteworthy is the reaction of the triphosphete **20** with $Ph_2(Cl)P{=}C(PPh_2)(SiMe_3)$, in which chloride abstraction of the ylidic precursor leads to the formation of the spirocyclic 10e cation **28** with an unprecedented pseudo trigonal bipyramidal PP_4 skeleton.[22] The cation of **28** is an additional member in the family of isoelectronic element(II) compounds of the general composition $E[C(PR_2)_2(SiMe_3)]_2$ (E = Si, Ge, Sn, Pb).[32]

The coordination chemistry of these new ring compounds is also unusual. A representative example is the conversion of diphosphete **18** into the phosphonium acetylide complex **29** and the acylylide complex **30** by exposure to $[Fe(CO)_5]$.[33]

The chemistry of small unsaturated phosphorus heterocycles has been developed in parallel to the chemistry of low-coordinate phosphorus compounds. While the "antiaromatic" four-membered rings with λ^3,σ^2-phosphorus centers remain elusive and undergo spontaneous oligomerization, or in special cases may be intercepted as ligands in transition metal complexes, doubly unsaturated four-membered rings with λ^5,σ^4-phosphorus centers are "non-antiaromatic" zwitterionic isolable com-

 © VCH Verlagsgesellschaft mbH, D-69451 Weinheim, 1996 0570-0833/96/3522-2620 $ 15.00+.25/0

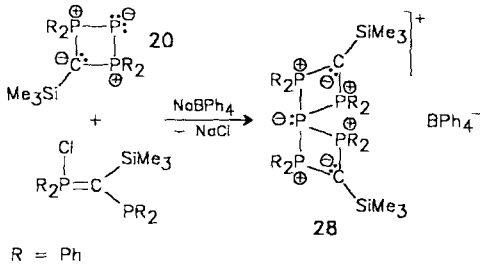

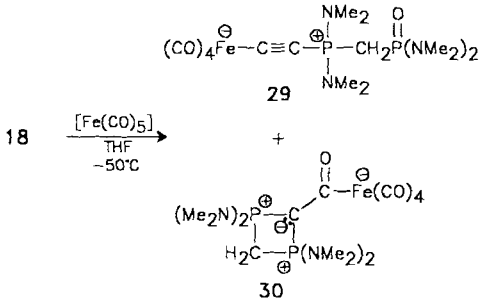

pounds. They are employed as key compounds in the synthesis of a number of novel heterocycles and polycycles that exhibit unusual bonding situations. Besides the four-membered rings discussed, the chemistry of five-membered phosphorus heterocycles still has a number of surprises in store, as emphasized by the synthesis of an unprecedented "aromatic" 1,2,3,4-diazadiphosphole from $Li[CH(SiMe_3)N_2]$ and white phosphorus.[34]

German version: *Angew. Chem.* **1996**, *108*, 2779–2782

Keywords: heterocycles · phosphorus compounds

[1] Review: G. Maier, *Angew. Chem.* **1988**, *100*, 317–341; *Angew. Chem. Int. Ed. Engl.* **1988**, *27*, 309–322.
[2] R. Gompper, G. Seybold, *Angew. Chem.* **1968**, *80*, 804–806; *Angew. Chem. Int. Ed. Engl.* **1968**, *7*, 824–826.
[3] a) G. Seybold, U. Jersak, R. Gompper, *Angew. Chem.* **1973**, *85*, 918–920; *Angew. Chem. Int. Ed. Engl.* **1973**, *12*, 847–849; b) U. J. Vogelbacher, M. Regitz, R. Mynott, *ibid.* **1986**, *98*, 835–836, and **1986**, *25*, 842–843; c) M. J. S. Dewar, N. Trinajstil, *Theor. Chim. Acta.* **1970**, *17*, 235–238.
[4] P. Binger, R. Milczarek, R. Mynott, M. Regitz, *J. Organomet. Chem.* **1987**, 323, C35–C38.
[5] P. Binger, J. Haas, A. T. Herrmann, F. Langshauser, C. Krüger, *Angew. Chem.* **1991**, *103*, 316–318; *Angew. Chem. Int. Ed. Engl.* **1991**, *30*, 310–312.
[6] B. Geissler, S. Barth, U. Bergsträsser, M. Slany, J. Durkin, P. B. Hitchcock, M. Hofmann, P. Binger, J. F. Nixon, P. von R. Schleyer, M. Regitz, *Angew. Chem.* **1995**, *107*, 485–488; *Angew. Chem. Int. Ed. Engl.* **1995**, *34*, 484–487.
[7] P. Binger, G. Glaser, S. Albus, C. Krüger, *Chem. Ber.* **1995**, *128*, 1261–1265.
[8] T. Wettling, B. Geissler, R. Schneider, S. Barth, P. Binger, M. Regitz, *Angew. Chem.* **1992**, *104*, 761–762; *Angew. Chem. Int. Ed. Engl.* **1992**, *31*, 758–759.
[9] Recent reviews: J. F. Nixon, *Coord. Chem. Rev.* **1995**, *145*, 201–258; P. Binger in *Multiple Bonds and Low Coordination in Phosphorus Chemistry* (Eds.: M. Regitz, O. J. Scherer), Thieme, Stuttgart, **1990**, 90–111.
[10] J. Grobe, D. Le Van, M. Hegemann, B. Krebs, M. Läge, *Angew. Chem.* **1992**, *104*, 94–96; *Angew. Chem. Int. Ed. Engl.* **1992**, *31*, 95–96.
[11] J. Haas, Diploma Thesis, Universität Bonn, **1988**; cited in J. Haas, PhD Thesis, Universität Kaiserslautern, **1990**, p. 13.
[12] O. J. Scherer, R. Winter, G. Wolmershäuser, *Z. Anorg. Allg. Chem.* **1993**, *619*, 827–835.
[13] M. Scheer, E. Herrmann, J. Sieler, M. Oehme, *Angew. Chem.* **1991**, *103*, 1023–1025; *Angew. Chem. Int. Ed. Engl.* **1991**, *30*, 969–971.
[14] M. E. Barr, S. K. Smith, B. Spencer, L. F. Dahl, *Organometallics*, **1991**, *10*, 3983–3991.
[15] U. Heim, H. Pritzkow, U. Fleischer, H. Grützmacher, M. Sanchez, R. Réau, G. Bertrand, *Chem. Eur. J.* **1996**, *2*, 68–74.
[16] a) J. Tejeda, R. Réau, F. Dahan, G. Bertrand, *J. Am. Chem. Soc.* **1993**, *115*, 7880–7881; b) K. Bieger, J. Tejeda, R. Réau, F. Dahan, G. Bertrand, *ibid* **1994**, *116*, 8087–8094; c) K. Bieger, G. Bouhadir, R. Réau, F. Dahan, G. Bertrand, *ibid* **1996**, *118*, 1038–1044.
[17] G. Alcaraz, U. Wecker, A. Baceiredo, F. Dahan, G. Bertrand, *Angew. Chem.* **1995**, *107*, 1358–1359; *Angew. Chem. Int. Ed. Engl.* **1995**, *34*, 1246–1248.
[18] R. Armbrust, M. Sanchez, R. Réau, U. Bergsträsser, M. Regitz, G. Bertrand, *J. Am. Chem. Soc.* **1995**, *117*, 10785–10786.
[19] G. Alcaraz, A. Baceiredo, M. Nieger, G. Bertrand, *J. Am. Chem. Soc.* **1994**, *116*, 2159–2160.
[20] a) J. Stava, E. Fluck, H. Riffel, *Z. Naturforsch B* **1985**, *40*, 1258–1263; b) B. Neumüller, E. Fluck, *Phosphorus Sulfur Relat. Elem.* **1986**, *29*, 23–29.
[21] a) G. R. Gillette, A. Baceiredo, G. Bertrand, *Angew. Chem.* **1990**, *102*, 1486–1488; *Angew. Chem. Int. Ed. Engl.* **1990**, *29*, 1429–1431; b) G. Bertrand, R. Reed, *Coord. Chem. Rev.* **1994**, *137*, 323–355; c) cited as personal communication by M. Regitz in ref. [21b].
[22] H. H. Karsch, E. Witt, F. E. Hahn, *Angew. Chem.* **1996**, *108*, 2380–2382; *Angew. Chem. Int. Ed. Engl.* **1996**, *35*, 2242–2244.
[23] H. H. Karsch, E. Witt, A. Schneider, E. Herdtweck, M. Heckel, *Angew. Chem.* **1995**, *107*, 628–631; *Angew. Chem. Int. Ed. Engl.* **1995**, *34*, 557–560.
[24] H. H. Karsch, A. Schier, *J. Chem. Soc. Chem. Commun.* **1994**, 2703–2704.
[25] a) A. Baceiredo, G. Bertrand, J.-P. Majoral, G. Sicard, J. Jaud, J. Galy, *J. Am. Chem. Soc.* **1984**, *106*, 6088-6089; b) A. Baceiredo, G. Bertrand, J.-P. Majoral, F. El Anba, G. Manuel, *ibid.* **1985**, *107*, 3945.
[26] W. Frank, V. Petry, E. Gerwalin, G. J. Reiss, *Angew. Chem.* **1996**, *108*, 1616–1618; *Angew. Chem. Int. Ed. Engl.* **1996**, *35*, 1512–1514.
[27] A. W. Johnson, *Ylides and Imines of Phosphorus*, Wiley, Chichester, **1993**.
[28] F. Zurmühlen, M. Regitz, *New J. Chem.* **1989**, *13*, 335–340.
[29] A. Schmidpeter, S. Lochschmidt, W. S. Sheldrick, *Angew. Chem.* **1985**, *97*, 214–215; *Angew. Chem. Int. Ed. Engl.* **1985**, *24*, 226–227.
[30] E. Fluck, G. Becker, B. Neumüller, R. Knebl, G. Heckmann, H. Riffel, *Angew. Chem.* **1986**, *98*, 1018–1019; *Angew. Chem. Int. Ed. Engl.* **1986**, *25*, 1002–1003.
[31] M. Sanchez, R. Réau, F. Dahan, M. Regitz, G. Bertrand, *Angew. Chem.* **1996**, *108*, 2386–2388; *Angew. Chem. Int. Ed. Engl.* **1996**, *35*, 2228–2230.
[32] a) E = Si: H. H. Karsch, U. Keller, S. Gamper, G. Müller, *Angew. Chem.* **1990**, *102*, 297–298; *Angew. Chem. Int. Ed. Engl.* **1990**, *29*, 295–296; b) E = Ge: H. H. Karsch, B. Deubelly, G. Hanika, J. Riede, G. Müller, *J. Organomet. Chem.* **1988**, *344*, 153–161; c) E = Sn: H. H. Karsch, A. Appelt, G. Müller, *Angew. Chem.* **1985**, *97*, 404–406; *Angew. Chem. Int. Ed. Engl.* **1985**, *24*, 402–404; d) E = Pb: A. L. Balch, D. E. Oram, *Inorg. Chem.* **1987**, *26*, 1906–1912.
[33] F. Rosche, G. Heckmann, E. Fluck, F. Weller, *Z. Anorg. Allg. Chem.* **1996**, *622*, 974–980.
[34] C. Charrier, N. Maigrot, L. Ricard, P. Le Floch, F. Mathey, *Angew. Chem.* **1996**, *108*, 2282–2283; *Angew. Chem. Int. Ed. Engl.* **1996**, *35*, 2133–2134.

Within a week, hexagonal-prismatic seed crystals (below left) grow into dumbbell-shaped aggregates, which close to form fluorapatite spheres.

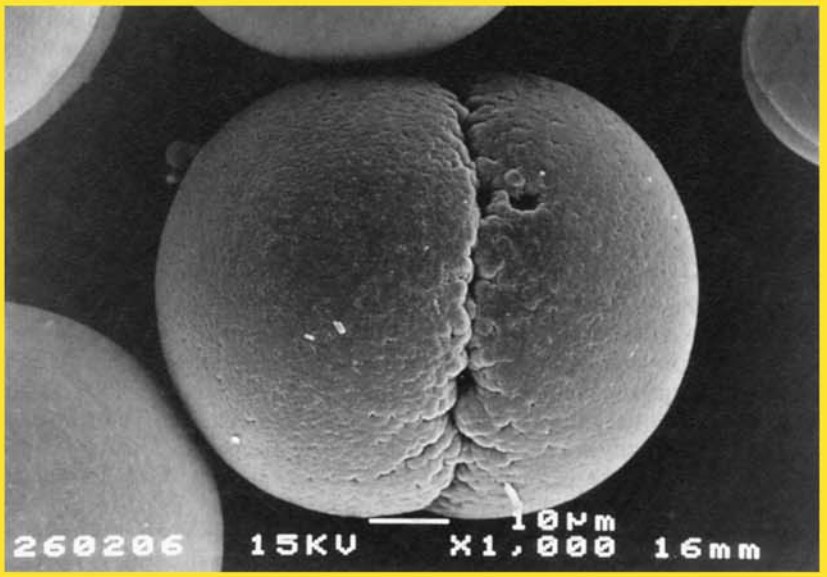

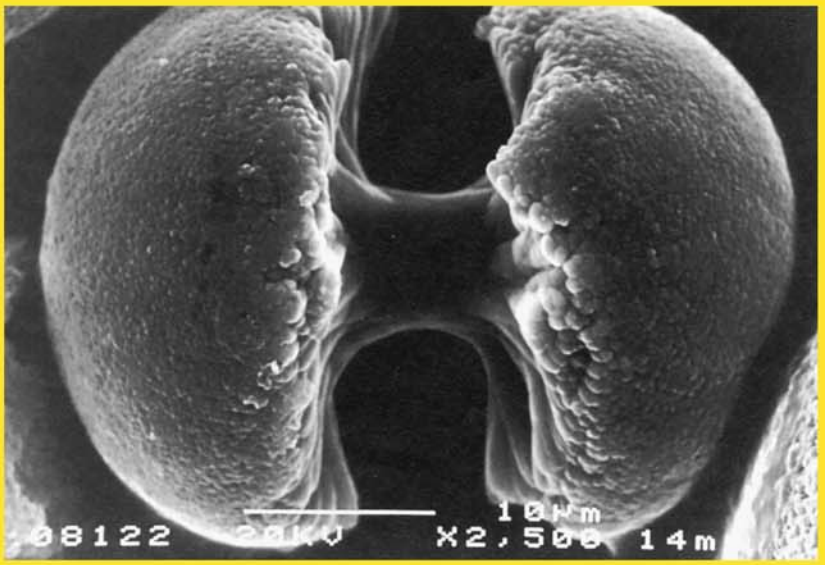

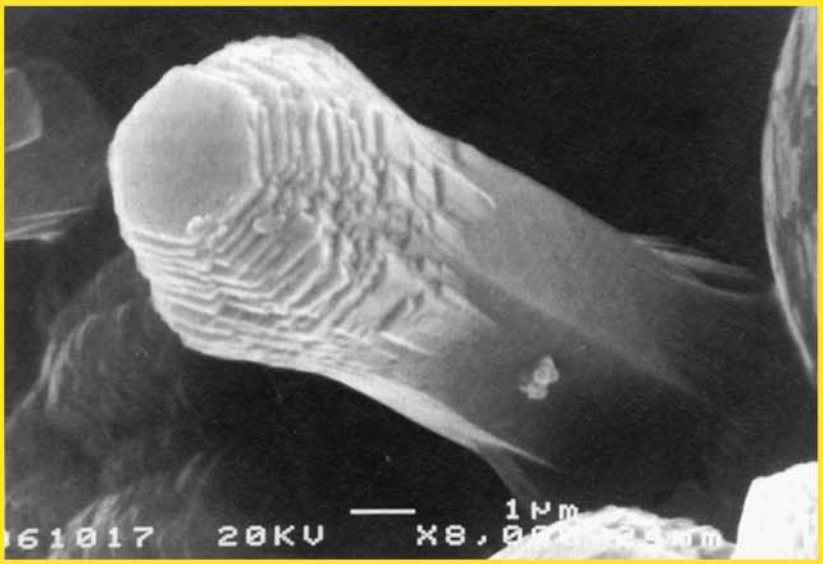

More about the biomimetic crystallization is reported by R. Kniep and S. Busch on the following pages.

 © VCH Verlagsgesellschaft mbH, D,-69451 Weinheim, 1996 0570-0833/96/3522-2623 $ 15.00 + .25/0

Biomimetic Growth and Self-Assembly of Fluorapatite Aggregates by Diffusion into Denatured Collagen Matrices**

Rüdiger Kniep* and Susanne Busch

Nature produces inorganic solids with fascinating outer shapes well suited to their function. The mechanisms of formation of these biogenic solids involve the combination of organic and inorganic components. Organic matrices control the mass transfer, define the location and number of nucleation centers, determine the orientation of the (crystal) growth, and/or act as templates for the final morphology of the inorganic solids.

In our studies on mimicking the processes involved in bone or tooth formation,[1] we have investigated the biomimetic growth of fluorapatite in gelatin matrices. A simple (static) diffusion cell was employed, like that known, in principle, for solid-state reactions[2] and that already used in more complex form in dynamic collagen systems.[3] The experimental conditions[4] were chosen such that at constant temperature (25 °C) solutions of calcium and of phosphate/fluoride diffuse into a gelatin plug from opposite ends (the so-called double diffusion technique[5]). In the course of the diffusion, discrete crystallization zones form, which are denoted as Liesegang bands in analogy to the classical work of Liesegang (Liesegang rings).[6] The time-dependent growth of the fluorapatite aggregates can be particularly well monitored in the middle band on the phosphate side; the largest aggregates were also obtained in this band. The crystallization products in all stages of development correspond to the fluorine-rich boundary region of the solid solution series hydroxyapatite/fluorapatite (Fig. 1).[7, 8]

Although the gelatin[4] used here as the organic matrix is of rather poorly defined structure,[9, 10] it is responsible for a specific function in the control of the growth of the fluorapatite aggregates. The use of other organic matrices (e.g., polysaccharides, agar, and carragenan) under otherwise identical experimental conditions[4] leads to fundamentally different morphologies of the fluorapatite (irregular intergrowth of short hexagonal prisms or xenomorphic precipitates). When gelatin is used as the organic matrix, "anisotropic" spheres are formed as the end product, the centers of which contain an elongated hexagonal-prismatic seed crystal.

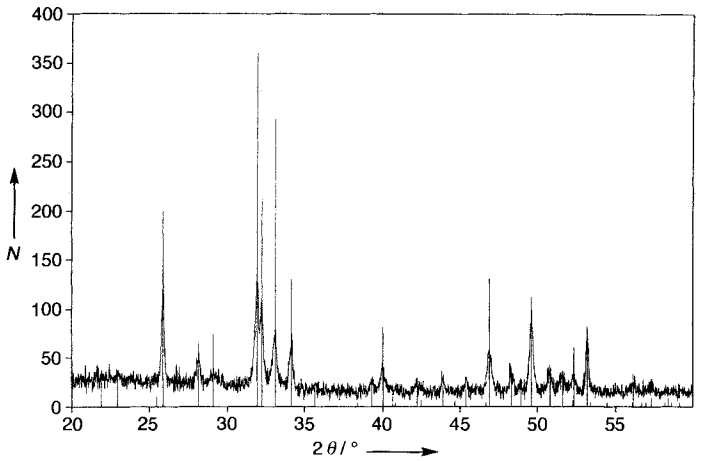

Fig. 1. X-ray powder diagram ($Cu_{K\alpha 1}$ radiation) of a sphere fraction and calculated diagram of fluorapatite ($P6_3/m$; $a = 936.6(3)$, $c = 688.3(3)$ pm) [8]. Refined lattice constants of the sphere fraction: $a = 937.6(3)$, $c = 688.6(2)$ pm (hydroxyapatite [7]: $a = 942.4(4)$, $c = 687.9(4)$ pm). Remarkably, the diffraction peaks of the sphere fraction are comparatively sharp for biomimetic apatite, the X-ray diagram indicates a single phase, and the background is relatively low (small amounts of X-ray amorphous components). N = count rate.

For unchanged morphology of the aggregates, the rates of diffusion of the solutions and of formation of the Liesegang bands, and hence the rate of growth of the fluorapatite are determined by the initial pH of the gelatin. Thus, in a gelatin plug that has not been acidified (pH 5.5, length 3 cm), apatite spheres with diameters of 100 μm are first observed after six weeks in the middle Liesegang band on the phosphate side. If the pH of the gelatin is adjusted to 2.5–3.5, apatite spheres with a diameter of 100 μm are formed after only two weeks. The growth of the fluorapatite spheres begins with elongated hexagonal-prismatic seed crystals, which reach a critical length of 5–10 μm. The progressive stages of the self-assembled growth of the needlelike seed crystals to give spherical aggregates are shown in Figure 2, and require approximately one week. First, oriented upgrowths occur on the prism faces at both ends of the seed crystal simultaneously and roughly symmetrically (mirror symmetry perpendicular to the prism axis), leading to the formation of dumbbell-shaped aggregates. The orientation of these upgrowths does not necessarily indicate the existence of strict crystallographic relations; nevertheless, the maximum angle of divergence (between the prism axes of the growing crystals and the prism axis of the seed crystal) appears to be fixed at approximately 45°. The dumbbell region is extended through further growing generations according to the principles of self-similarity;[11] however, the "bar" of the dumbbell (seed crystal) initially remains visible. This situation can be simulated in a two-dimensional form which mirrors reality very well in a simplified way, as shown in Figure 3.[12] Starting from a needlelike seed crystal, in the first generation similar needlelike crystals are formed at both ends, which have a maximum angle of 45° to the long axis of the seed crystal. The length of the crystals of each successive generation is shorter than the length of the crystals of the preceding generation by a factor of about 0.68 (estimated mean value from scanning electron microscope (SEM) images, error = ca. ±10%). Each "new" end of a crystal generation leads to self-similar multiplication. The result is illustrated in Figure 3, which shows the simulation of five successive self-similar crystal generations at each end of the seed crystal. The fact that the crystals interpenetrate in the simulation is certainly not realistic, but this has no great effect on the morphology of the aggregate. It is more important that the bar of the dumbbell (the seed crystal) remains visible in this growth state and correspondingly in the simulation, that the surface curvature of the dumbbell in the direction of the seed crystal is already indicative of the "closing" of the aggregate, and that the extent of the aggregate, growing from the two ends of the seed crystal, increases by a factor of approximately 2 relative to the length of the seed crystal. The further development of the aggregate—going from the dumbbell to a sphere—can again be seen in Figure 2. Figure 4 shows the SEM image of the surface of a just completed (notched) surface of a sphere. This reveals that also in this last generation needlelike crystals are formed. Their prism cross section is only about 0.05 μm, which means that the closed aggregate has a very large surface area.

The (notched) spheres formed in the gelatin matrix continue their growth by adding radial shells of material and forming almost perfect spheres. This is a second (probably more conven-

[*] Prof. Dr. R. Kniep, Dipl.-Ing. S. Busch
Eduard-Zintl-Institut der Technischen Hochschule
Hochschulstrasse 10, D-64289 Darmstadt (Germany)
Fax: Int. code +(6151)166029

[**] This work was supported by the Fonds der Chemischen Industrie.

 © VCH Verlagsgesellschaft mbH, D-69451 Weinheim, 1996 0570-0833/96/3522-2624 $ 15.00+.25/0

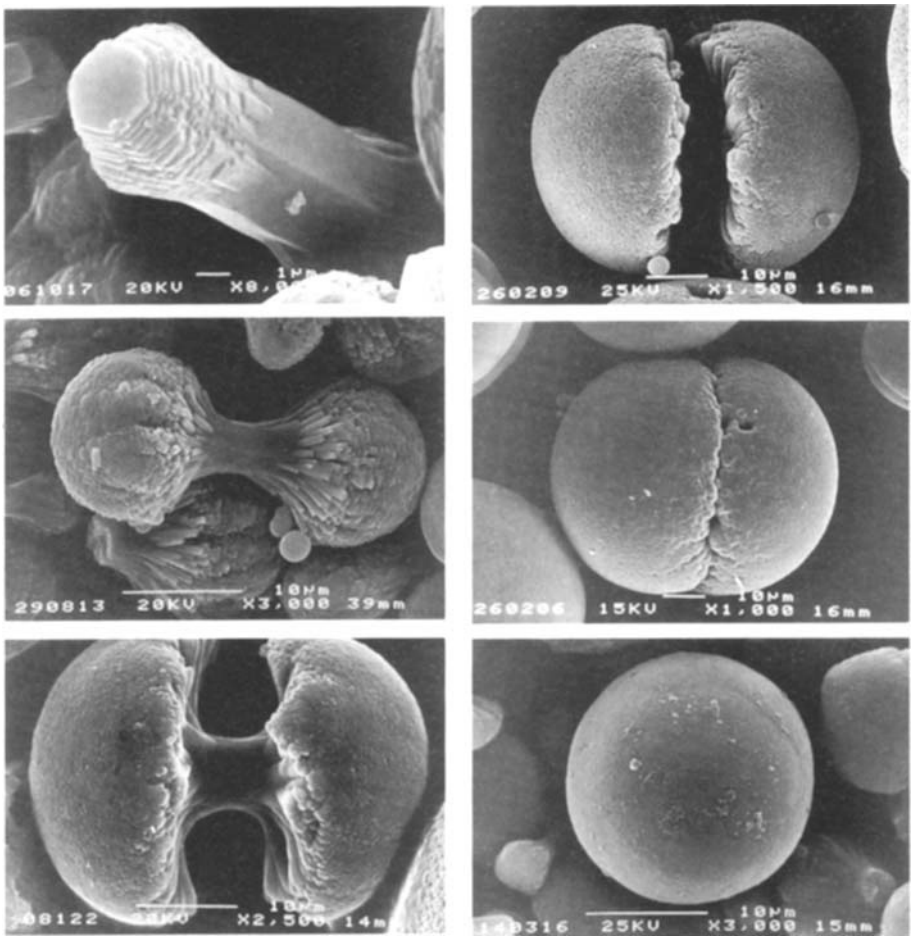

Fig. 2. SEM images of progressive stages of the self-assembled (hierarchical) growth of the fluorapatite aggregates: from the elongated hexagonal-prismatic seed (top left) through dumbbell shapes to the sphere (bottom right).

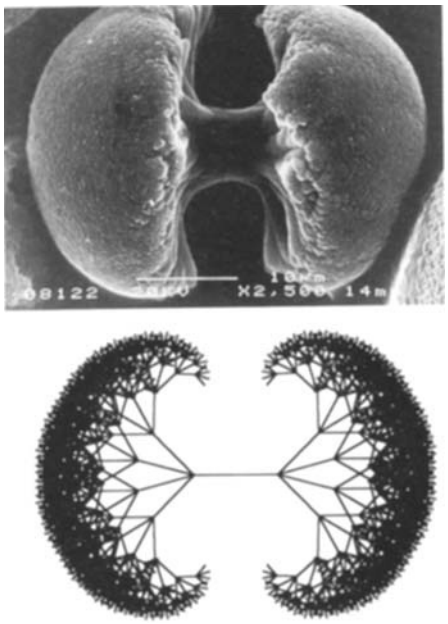

Fig. 3. SEM image of a dumbbell-shaped fluorapatite aggregate (top). Two-dimensional simulation [12] of self-similar branching in five successive generations (bottom). The simulation shows branching (splitting) into only four crystals (with divergence angles of 30°) of the new generation, which is a simplified representation. In fact, orders of branching are higher (see also Fig. 2), and are, in principle, only limited by the maximum angle of divergence (ca. $\pm 45°$) formed by the long axis of the new crystals and the long axis of the preceding seed crystal. The factor of shortening of preceding generations is discussed in the text.

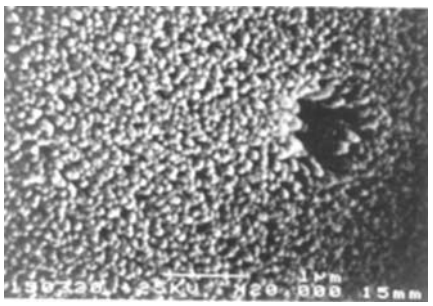

Fig. 4. SEM image of the surface of a just closed sphere aggregate. In accordance with the self-similar branching patterns [12] described in the text and shown in Figure 3, the dumbbell-shaped aggregates close to give notched spheres after the tenth generation.

tionally spherolitic) growth mechanism, which will not be described further here. After about four weeks, sphere diameters of up to 400 μm are found. Our observations indicate that the important limiting factor in the growth of the spheres is the gelatin matrix, which, under the given experimental conditions, is stable for only about six weeks.

The self-assembled hierarchical growth of the fluorapatite aggregates shows immediate parallels to the topological branching criteria of the macromolecular starburst dendrimers.[13] However, the dimensionality—and thus the information transfer—in the aggregates described here extends to the macroscopic range.

In accordance with their microcrystalline structure, the spherical aggregates are opalescent. A fraction of spheres with diameters of up to 300 μm is shown in Figure 5. On a flat support, the

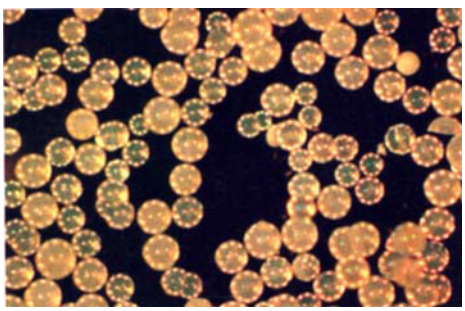

Fig. 5. Optical micrograph of a fluorapatite sphere fraction. The long edge of the figure corresponds to about 4 mm.

spheres orient themselves preferentially to form chains (electrostatic effects), and can be lifted out in the form of "strings of beads" by using the point of a needle. Thermoanalytical investigations (thermogravimetry (TG) and differential thermal analysis (DTA)) on spherical aggregates dried at room temperature were carried out at temperatures up to a maximum of 1000 °C (heating rate 4 °C min^{-1}; atmosphere: air).[14] The X-ray powder diagram of the sample after thermal treatment is identical to

the diagram shown in Figure 1 except that the profiles of the diffraction peaks are sharper (refined lattice constants: $a = 937.4(1)$ pm, $c = 688.7(1)$ pm). The mass loss (total ca. 6.5%) takes place in two stages: stage 1 (80–200 °C) 1.5 wt%, and stage 2 (200–860 °C) 5 wt%. In accord with DTA experiments on human dentine,[15] the second stage is associated with an exothermic reaction (pyrolysis of the protein fibers).

Figure 6 shows the interference image of a just closed fluorapatite aggregate with a diameter of 125 μm, which was obtained with an optical microscope with cross polarizers, as viewed along the optical axis of the hexagonal central seed. The

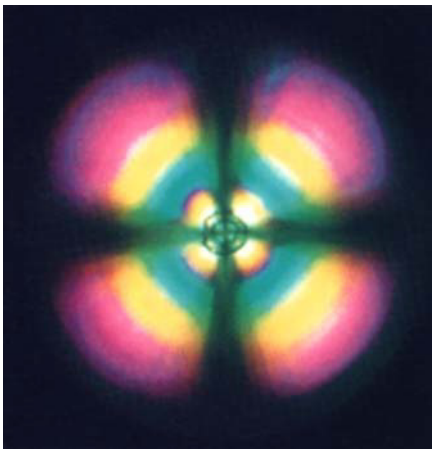

Fig. 6. Image from a polarization microscope (cross polarizers) of a just closed fluorapatite aggregate of diameter 125 μm. Viewed along the hexagonal-prismatic seed.

hexagonal cross section of the seed crystal can be seen in the center, its diameter increases approximately twofold during the course of the growth of the spherical aggregate. The interference pattern of the total aggregate is characterized by the "Brewster polarization cross" and the polarization colors within the cross segments (increasing thickness of the spheres from the surface to their centers, and variable inclination between the optical axes of the individual crystallites and the incident polarized light).

We conclude by mentioning some possible interpretations of the growth phenomenon described, although detailed investigations have either not been started or are not yet complete.[12, 16, 17] There are two basic possibilities, which, individually or taken together, could be responsible for the self-assembled control of the aggregate growth:

1) The aggregates correspond to organized composite systems in which the growth of generations is controlled by an epitaxially linked composite of fluorapatite and the organic component.
2) The individual crystallites or composite units contain a permanent dipole, so that intrinsic electrical lines of force take over control of the growth of the aggregates. The polarity of collagen, the piezoelectric properties of calcified bone tissue,[18] and the structural peculiarity of the apatite family, fluctuating between centrosymmetric and acentric distribution of the X species (X = F, Cl, OH),[19] support these ideas, also bearing in mind the extremely mild biomimetic growth conditions, which should favor a high degree of order of the atomic arrangements, and the fact that partial exchange of F^- by OH^- causes an asymmetric displacement of the two species from their normal positions.[20]

In summary, a wide interdisciplinary area is emerging, which encompasses chemistry, physics, materials science, and medicine.

Received: April 29, 1996 [Z 9077 IE]
German version: *Angew. Chem.* **1996**, *108*, 2787–2791

Keywords: apatite · biomineralization · fluorine compounds · gelatin · solids

[1] L. T. Kuhn, D. J. Fink, A. H. Heuer in *Biomimetic Materials Chemistry* (Ed.: S. Mann), VCH, New York, **1996**.
[2] H. Schmalzried, T. Frick, *Ber. Bunsenges. Phys. Chem.* **1995**, *99*, 914.
[3] A. L. Boskey, *J. Phys. Chem.* **1989**, *93*, 1628.
[4] *Experimental Procedure*: Pig skin gelatin (5.5 g, 300 Bloom, Aldrich) was placed in water (50 mL), acidified with glutamic acid or 2 N HCl to pH 2.5–3.5, and then heated with stirring for a few minutes in a water bath. The central tube of the diffusion cell (length 3 cm, diameter 2.5 cm, closed at one end) was filled with the hot gelatin and left at room temperature for 24 h in a vertical position until gelation occurred. The L-shaped tubes (vertical section: 18 cm, horizontal section: 6 cm, standard ground joints) were then attached to the central gelatin tube, filled with the aqueous solutions (0.133 M $CaCl_2$ or 0.08 M Na_2HPO_4/0.027 M KF), and closed with ground glass stoppers. Both solutions were previously adjusted to the physiological pH of 7.4 with α,α,α-tris(hydroxymethyl)methylamine/HCl. The diffusion experiments were carried out at 25 °C (thermostat). At the end of the experiment, the gelatin plug was pressed out of the central tube and cut into sections corresponding to the Liesegang bands. To isolate the solids, these sections were washed several times with hot water and centrifuged.
[5] K. T. Wilke, J. Bohm, *Kristallzüchtung*, Harri Deutsch, Frankfurt/Main, **1988**.
[6] R. E. Liesegang, *Z. Phys. Chem.* **1914**, *88*, 1.
[7] K. Sudarsanan, R. A. Young, *Acta Crystallogr. Sect. B* **1978**, *34*, 1401.
[8] P. E. Mackie, R. A. Young, *J. Appl. Crystallogr.* **1973**, *6*, 26.
[9] *The Science and Technology of Gelatin* (Eds.: A. G. Ward, A. Courts), Academic Press, London, **1977**.
[10] W. Babel, *Chem. Unserer Zeit*, **1996**, *30*, 86.
[11] B. B. Mandelbrot, *Die fraktale Geometrie der Natur*, Birkhäuser, Basel, **1991**.
[12] "Selbstähnliche Verzweigungen" und "Simulation von elektrischen Feldlinien im Bereich selbstorganisierter polarer Aggregate": H. Dolhaine, unpublished.
[13] D. A. Tomalia, A. M. Naylor, W. A. Goddard III, *Angew. Chem.* **1990**, *102*, 119; *Angew. Chem. Int. Ed. Engl.* **1990**, *29*, 138.
[14] Liberation of the constitutional water from hydroxyapatite above 1250 °C: P. W. Arnold, *Trans. Faraday. Soc.* **1950**, *46*, 1061.
[15] M. Okazaki, J. Takahashi, H. Kimura, *J. Osaka Univ. Dent. Sch.* **1989**, *29*, 1989.
[16] "Kristallfeldberechnungen an Apatiten", J. Brickmann, S. Hauptmann, unpublished .
[17] "Messung von permanenten Dipolen an kleinen Aggregaten", F. Laeri, unpublished.
[18] S. Mann in *Inorganic Materials*, (Eds.: D. W. Bruce, D. O'Hare), Wiley, Chichester, **1992**.
[19] M. Bauer, W. E. Klee, *Z. Kristallogr.* **1993**, *206*, 15.
[20] M. Braun, C. Jana, *Chem. Phys. Lett.* **1995**, *245*, 19.

Prototypical Reagent for the Synthesis of Substituted Hydrazines**

Uno Mäeorg, Leif Grehn, and Ulf Ragnarsson*

Dedicated to Professor Ivar Ugi on the occasion of his 65th birthday

Substituted hydrazines are valuable precursors of heterocycles and components of many pharmaceuticals, agrochemicals, and dyestuffs. Direct alkylation of hydrazine normally gives rise to mixtures of mono-, di-, and trisubstituted products in which all the groups are located at the same nitrogen atoms.[1] This often makes purification troublesome. Although many

[*] Dr. U. Ragnarsson, Dr. U. Mäeorg, Dr. L. Grehn
Department of Biochemistry
University of Uppsala, Biomedical Center
P.O. Box 576, S-75123 Uppsala (Sweden)
Fax: Int code +18552139
e-mail: urbki@bmc.uu.se

[**] We thank the Swedish Natural Science Research Council, the National Agency for Higher Education, the National Board for Industrial and Technical Development, and Astra Draco AB for their generous support of our programs.

other methods to prepare mono- and dialkylated hydrazines have been developed,[1] a simple, general procedure is still lacking. This is the background to the present work in which the triprotected hydrazine **4** has been developed and investigated.

The idea of alkylating acylated hydrazines is not new,[1] but only little work has been done using modern techniques.[2] Młotkowska and Zwierzak, however, made simple alkylhydrazines in two steps by alkylating diphenylphosphinic hydrazide with bromides under phase-transfer catalysis (PTC) in boiling benzene, followed by deprotection with boiling HCl.[3a] A similar approach was later used with the triprotected derivative acetone *N*-(diethoxyphosphoryl)hydrazone.[3b] When an additional acetylation step was included, selective alkylation of the second nitrogen was possible with the first reagent, resulting, after removal of both protecting groups, in *N,N'*-dialkyl derivatives.[3c] We realized that triacylated derivatives like **4** might possibly undergo alkylations similar to those of the two hydrazine reagents mentioned. Besides, in **4** and its derivatives, one of the Boc groups of the imidodicarbonate function should be particularly labile to acid[4] and thus, after deprotection, allow selective alkylation on the other nitrogen.

We have earlier expanded the scope of Boc protection of amino functions.[5] In this context we designed an efficient synthesis of $HNBoc_2$,[5c,e] which was used to prepare amines including ^{15}N-labeled derivatives. Now we have produced reagent **4** from Z-hydrazine **1**, liberated from the hydrochloride,[6] and treated it with Boc_2O in the presence of 4-(dimethylamino)pyridine (DMAP).[7] The best results are obtained when this reaction is allowed to take place in two consecutive steps, in other words, with formation of **2** before DMAP is added (Scheme 1).

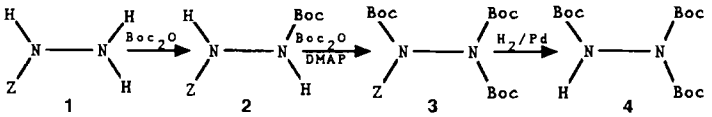

Scheme 1. Synthesis of **4**. Boc = *tert*-butoxycarbonyl, Z = benzyloxycarbonyl.

Crude **3** was obtained as an oil which, after catalytic hydrogenolysis, directly furnished crystalline **4** in an overall yield of 82%. Compound **4** is stable on storage. Moreover, it undergoes rapid alkylation with several reagents under various PTC conditions in benzene at room temperature to give **5**. Although the reaction conditions have not yet been optimized, the six examples in Table 1 indicate that compound **4** reacts satisfactorily.

Compound **5** was treated with small quantities of trifluoroacetic acid[4] to cleave the imidodicarbonate function, giving rise to **6** (Table 1). Thus, also in hydrazines of type **5** one of the Boc groups on the bisprotected nitrogen is indeed selectively cleavable as postulated.

A second alkylation has so far been undertaken only in two cases under experimental conditions similar to those used in the case of **4** (Table 1). In products **7c** and **7d**, however, the Boc groups cannot be cleaved selectively, so both compounds were treated with 4 M HCl/dioxane to give **8c** (96%) and **8d** (87%), respectively, as hydrochlorides. The former was diacetylated as previously described[9] to give **9c** (R^3 = Ac). Upon treatment with a suitable reducing agent, compounds of this type should give rise to tetraalkylhydrazines.

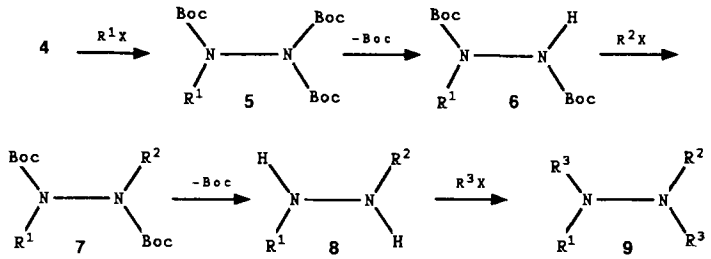

Our experiments with the prototypical reagent **4** led us to conclude that an analogous reagent having two Boc functions and one additional protecting group orthogonal to Boc, should provide hydrazine derivatives with four nonidentical substituents in a similar fashion. Furthermore, a similar strategy might be useful also for the derivatization of diamines.

Table 1. Synthesis of hydrazines **5**–**7** [8].

	R^1	**5**		**6**		R^2	**7**	
		Yield [%]	M.p. [°C]	Yield [%]	M.p. [°C]		Yield [%]	M.p. [°C]
a	Me	97	[a]	–	–			
b	n-C_6H_{13}	94	[a]	–	–			
c	Bzl	81–100	58–59	89	102–103	Me	96	[a]
d	p-$NO_2C_6H_4CH_2$	98	68–70	74	108.5–110	2,4-$(NO_2)_2C_6H_3$	91	66–68
e	2,4-$(NO_2)_2C_6H_3$	86–90	143–144	95	134–135			
f	dansyl [b]	61	144.5–145.5	–	–			

[a] Exists as an oil. [b] dansyl = 5-(dimethylamino)naphthalene-1-sulfonyl.

Experimental Procedure

4: To molten Boc_2O (43.3 g, 200 mmol) hydrazine **1** (10.0 g, 60.2 mmol) was added in one portion under vigorous stirring. After 15 min of violent gas evolution when the reaction was deemed complete by TLC, a solution of DMAP (183 mg, 1.5 mmol) in CH_3CN (6 mL) was added over 10 min with rapid stirring. After another 15 min, when gas evolution had subsided, the reaction was complete (TLC). The reaction mixture was concentrated, the residue dissolved in diethyl ether, and the solution extracted with citric acid, $NaHCO_3$, and brine, and then dried ($MgSO_4$). Removal of volatiles afforded **3** as a colorless oil in nearly quantitative yield. ^1H NMR (270 MHz, $CDCl_3$): δ = 1.42 (s, 18H, $NBoc_2$), 1.49 (s, 9H, NHBoc), 5.26 (s, 2H, CH_2Ph), 7.30–7.41 (br.m, 5H, Ph). Compound **3**, dissolved in CH_3OH (500 mL), was hydrogenolyzed over Pd/C (5%/carbon, 1.2 g) for 3 h. When TLC indicated complete reaction, the catalyst was filtered off (Celite). The solvent was removed to give a solid, which was recrystallized from light petroleum ether to afford pure **4** as white crystals; yield: 16.3 g (82% from **1**); m.p. 104.5–105.5 °C; pure by TLC. ^1H NMR (270 MHz, $CDCl_3$, 20 °C, TMS): δ = 1.48/1.51 (2 signals, together 27H, Boc), 6.47/6.18 (2 br. signals, together 1H, NH); correct C,H,N analysis.

Received: June 20, 1996 [Z 9246 IE]
German version: *Angew. Chem.* **1996**, *108*, 2802–2803

Keywords: alkylations · hydrazines · phase transfer catalysis · protecting groups

[1] Review: U. Jensen-Korte, *Methoden Org. Chem. (Houben-Weyl) 4th ed. 1952–1990*, Vol. 16a, pp. 421–529.
[2] T. W. Greene, P. G. M. Wuts, *Protective Groups in Organic Synthesis*, 2nd ed., Wiley, New York, **1991**, Chapter 7.
[3] a) B. Młotkowska, A. Zwierzak, *Tetrahedron Lett.* **1978**, 4731–4734; b) S. Zawadzki, K. Osowska-Pacewicka, A. Zwierzak, *Synthesis* **1987**, 485–487; c) M. Kluba, A. Zwierzak, *ibid.* **1981**, 537–539.
[4] R. D. Connell, T. Rein, B. Åkermark, P. Helquist, *J. Org. Chem.* **1988**, *53*, 3845–3849.
[5] a) L. Grehn, U. Ragnarsson, *Angew. Chem.* **1984**, *96*, 291–292; *Angew. Chem. Int. Ed. Engl.* **1984**, *23*, 296–301; b) *ibid.* **1985**, *97*, 519–520 and **1985**, *24*, 510–511; c) *Synthesis* **1987**, 275–276; d) *Coll. Czech. Chem. Commun.* **1988**, *53*, 2778–2786; e) F. Degerbeck, L. Grehn, U. Ragnarsson, *Acta Chem. Scand.* **1993**, *47*, 896–898.
[6] E. Wünsch, *Chem. Ber.* **1965**, *98*, 797–802.
[7] a) G. Höfle, W. Steglich, H. Vorbrüggen, *Angew. Chem.* **1978**, *90*, 602–615; *Angew. Chem. Int. Ed. Engl.* **1978**, *17*, 569–582; b) D. L. Flynn, R. E. Zelle, P. A. Grieco, *J. Org. Chem.* **1983**, *48*, 2424–2426.
[8] All solid products **5**–**7** for which melting points are listed gave satisfactory C,H,N analyses. All compounds gave interpretable ^1H NMR spectra, in many cases indicating the presence of two or more conformers.
[9] T. Curtius, *J. Prakt. Chem.* **1900**, *62*, 83–126.

 © VCH Verlagsgesellschaft mbH, D-69451 Weinheim, 1996 0570-0833/96/3522-2627 $ 15.00+.25/0

Catalytic Antibodies as Probes of Evolution: Modeling of a Primordial Glycosidase**

Doron Shabat, Subhash C. Sinha,* Jean-Louis Reymond,* and Ehud Keinan*

Enzymes achieve remarkable catalytic efficiency by several effects operating in concert. This is the result of evolution and natural selection over eons. One might wonder how primordial enzymes became catalytically active in the first place. To answer such a question it is important to know which of the effects operating in a modern enzyme is capable of triggering catalysis independently of the others. Catalytic antibodies,[1] which are designed by the experimenter, offer a unique opportunity to study such issues and to examine experimentally various hypotheses about primordial enzymes. It is much easier to dissect the individual parameters of catalysis in catalytic antibodies than in highly evolved enzymes in which all these parameters operate together. Indeed, Schultz et al.'s fundamental structural studies provide much insight into the evolution of catalytic capabilities in proteins.[2]

Along these lines and owing to the importance of carbohydrates in the early stages of evolution, the emergence of glycosidase activity is of particular interest. Herein we report on an antibody-catalyzed hydrolysis of unactivated cyclic ketals, a reaction that is closely related to the cleavage of the glycosidic bond.[3] These catalytic antibodies may therefore be considered as mechanistic analogs of the glycosidase enzymes. We show here that general acid catalysis and/or strain effects, which are of central importance in the activity of modern glycosidases,[4] have only minor significance in these catalytic antibodies. Conversely, simple charge complementarity proves to be the major factor in determining their catalytic activity.

Hydrolysis of ketal **I** involves protonation at one of the oxygen atoms, followed by heterolysis of a C–O bond to generate the intermediate ion **IV** and ultimately the carbonyl compound **V** (Scheme 1). In the case of ketals and acetals with an activated

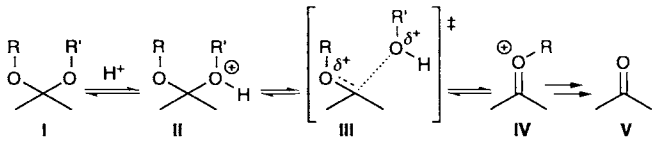

Scheme 1. General mechanism of ketal hydrolysis under acidic conditions.

leaving group (e.g. R′ = aryl), the first step is the rate-limiting one, and their hydrolysis can be catalyzed by weak acids (general acid catalysis).[5, 6] In contrast, with unactivated ketals (e.g. R′ = alkyl)[7] the O-protonated species **II** is a relatively stable intermediate formed in a preequilibrium. In such cases cleavage of the C–O bond (via transition state **III**) is the rate-limiting step. Therefore, the hydrolysis of unactivated ketals or acetals is not catalyzed by weak acids and depends only on the pH (specific acid catalysis). This reactivity pattern, which also applies for the hydrolysis of glycosidic bonds, poses a particular challenge for the design of a biocatalyst since the presence of a weak acid alone is not sufficient to promote the reaction.

Dioxolane **1**[8] is hydrolyzed in aqueous acidic medium to give ketone **2** and ethylene glycol. Although the hydrolysis rate is pH-dependent, it is totally indifferent to the buffer type and concentration. The observed inverse solvent isotope effect ($k_H/k_D = 0.4$) confirms that the reaction is specific acid catalyzed; the rate-limiting cleavage of the C–O bond of the protonated intermediate **II** leads to the intermediate **IV**. This step involves expansion of the protonated dioxolane ring, during which the positive charge moves from the leaving oxygen atom to the remaining one. We reasoned that the piperidinium ion **3** would be an accurate analog of transition state **VI** (Scheme 2). The positively charged nitrogen center in **3** mimics the emerging ion **IV**, and the six-membered piperidinium ring mimics the expanded five-membered ring of **VI**.

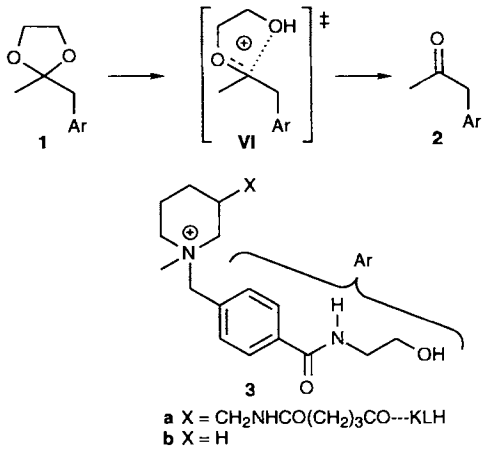

Scheme 2. Transition state **VI** and transition state analog **3** for the hydrolysis of ketal **1** to ketone **2**. KLH = Keyhole Limpet H aemocyanin (carrier protein).

A series of 46 monoclonal antibodies directed against **3a**[6a] were assayed for catalysis of the hydrolysis of **1**. Two of them, antibody 14D9 and antibody 20B11,[9] catalyzed the reaction. In both cases catalysis followed Michaelis–Menten kinetics (Fig. 1) and was totally inhibited by the hapten (**3b**), indicating that the catalytic reactions take place in the combining sites of these antibodies.[10]

In most of the glycosidase enzymes, shape complementarity to the transition state plays a key role in catalysis by inducing productive strain in the substrate.[11] We attempted to obtain similar, shape-selective recognition of the inflated dioxolane ring in the transition state **VI** by using a six-membered ring transition state analog in eliciting the antibodies. To appreciate the effect of this shape complementarity on catalysis by our antibodies we studied the six- and seven-membered ring ketal analogs of substrate **1**: dioxane **4** and dioxepane **5**.

Both antibody 14D9 and antibody 20B11 catalyzed hydrolysis of dioxane **4**. However, in comparison to the hydrolysis of **1**, catalytic efficiency was reduced, in terms of both rate enhancement (k_{cat}/k_{uncat} is decreased 2.6-fold with 14D9 and 8.2-fold

[*] Dr. S. C. Sinha, Dr. J.-L. Reymond, Prof. E. Keinan
Department of Molecular Biology and
the Skaggs Institute for Chemical Biology
The Scripps Research Institute
10550 N. Torrey Pines Road, La Jolla, CA 92037 (USA)
Fax: Int. code +(619) 784-7313
Prof. E. Keinan, D. Shabat
Department of Chemistry, Technion - Israel Institute of Technology
Technion City, Haifa 32000 (Israel)

[**] J.-L. R. thanks the U. S. National Institutes of Health (GM 49736) for funding. E. K. thanks the US–Israel Binational Science Foundation and PharMore Biotechnologies Ltd. for financial support.

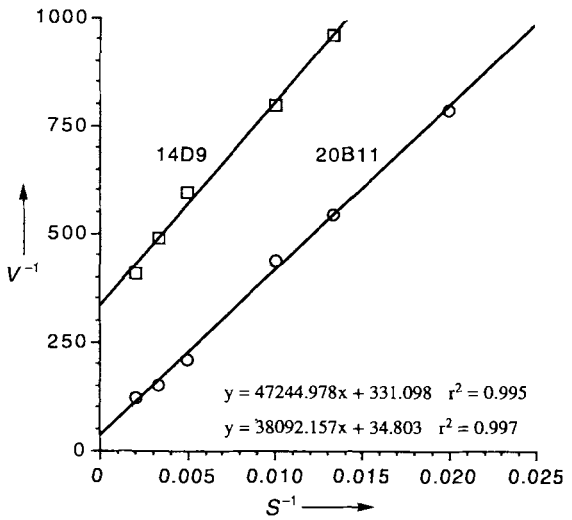

Fig. 1. Lineweaver–Burk plot of antibody-catalyzed hydrolysis of ketal **1** with antibodies 14D9 (squares) and 20B11 (circles). For the reaction conditions see ref. [10]. V = hydrolysis velocity ($\mu M\,h^{-1}$), S = substrate concentration (μM).

with 20B11) and transition state binding (K_{TS} is increased 4.5-fold with 14D9 and 2.9-fold with 20B11) (Table 1). This trend continued further with the seven-membered substrate **5** with a further decrease in k_{cat}/k_{uncat} and increase in K_{TS} relative to the hydrolysis of **1** (k_{cat}/k_{uncat} is decreased 28-fold with 14D9 and 12-fold with 20B11 and K_{TS} is increased 6- and 3.8-fold, respectively).

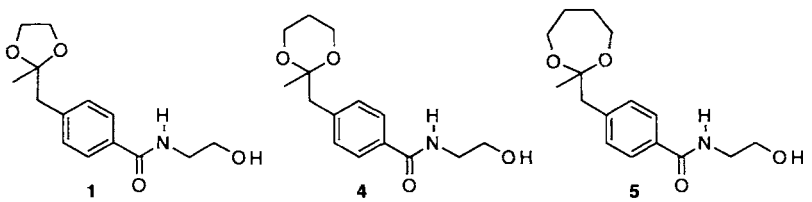

Table 1. Kinetic data for antibody-catalyzed hydrolysis of ketals **1**, **4**, and **5** (K_m and K_{TS} in μM).

Antibody	1 K_m	1 k_{cat}/k_{uncat}	1 K_{TS}	4 K_m	4 k_{cat}/k_{uncat}	4 K_{TS}	5 K_m	5 k_{cat}/k_{uncat}	5 K_{TS}
14D9	143	113	1.3	250	43	5.8	30	4	7.8
20B11	1095	870	1.3	403	106	3.8	376	76	5.0

Antibody 14D9 was chosen for further studies because it showed a more distinct shape discrimination in catalysis. The shape complementarity between this antibody and the piperidinium ring was estimated by measuring competitive inhibitions with hapten homologs having larger rings. For convenient kinetic analysis with this series of inhibitors their binding efficiency was uniformly reduced by changing the 2-hydroxyethylamide side chain to a carboxylate functionality.[12] Antibody 14D9 bound pyrrolidinium **6** (K_i = 2.5 μM)[12] less tightly than piperidinium **7** (K_i = 0.9 μM)[12] and showed almost no discrimination between **7** and its two higher homologs, azepinium **8** (K_i = 0.6 μM) and the ion **9** (K_i = 1.0 μM).[13]

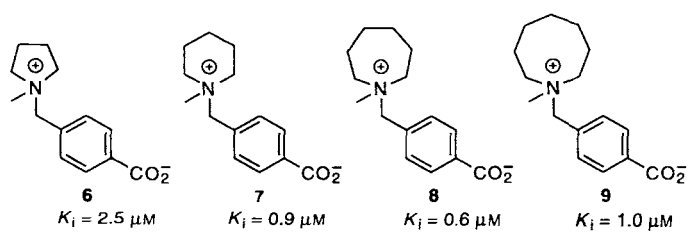

The active site of antibody 14D9 has been shown previously to possess an ionizable functionality, presumably an aspartate or glutamate side chain, capable of general acid–base catalysis.[14] The solvent kinetic isotope effect in the 14D9-catalyzed hydrolysis of **1** showed that the reaction is specific acid catalyzed (k_{catH}/k_{catD} = 0.4), with no direct participation of this protein side chain as a general acid. In this case the antibody side chain might act as an electrostatic point charge that stabilizes the transition state.[15] Substrate **4** (K_m = 250 μM), which can be considered as a neutral analog of the hapten, was bound by antibody 14D9 approximately 10^4-fold less tightly than the hapten **3b** ($K_i \approx 10^{-8}$ M). In fact the actual transition states for hydrolysis of **1**, **4**, and **5**, whose affinities are given by K_{TS}, are bound approximately 10^2 times tighter than the substrates themselves. These effects on transition state and hapten binding are much stronger than those seen by modulating molecular shapes and indicate that catalysis of ketal hydrolysis with antibody 14D9 depends primarily on electrostatic complementarity. This is also consistent with the observation that dimethyl ketal **10** (k_{cat}/k_{uncat} = 70, K_m = 70 μM) and its homolog **11** (k_{cat}/k_{uncat} = 430, K_m = 230 μM)[16] are also substrates of antibody 14D9.[17] The substrate's shape probably plays only a limited role in enabling the formation of a catalytically productive complex with the antibody.

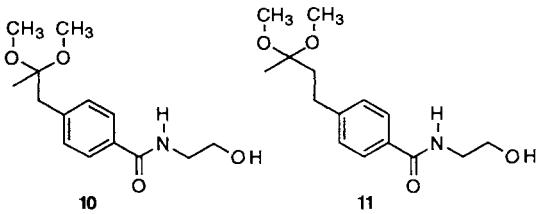

We have shown here that antibodies catalyzing the hydrolysis of unactivated ketals can be achieved by a very simple design. We have presented evidence that the observed catalysis is triggered by electrostatic complementarity of the antibody binding site to the transition state, and that the effect of shape complementarity on catalysis is relatively limited. Since the hydrolysis of unactivated ketals is mechanistically closely related to the cleavage of glycosidic bonds, this study provides experimental support for the hypothesis that glycosidases would have first appeared as "electrostatic" catalysts. Shape complementarity and general acid catalysis, which dominate the catalytic effect in modern glycosidase,[3] would only have emerged in the later course of evolution.

Received: June 20, 1996 [Z9247IE]
German version: *Angew. Chem.* **1996**, *108*, 2800–2802

Keywords: catalytic antibodies · enzyme models · ketals

[1] P. G. Schultz, R. A. Lerner, *Science* **1995**, *269*, 1835.
[2] P. A. Patten, N. S. Gray, P. L. Yang, C. B. Marks, G. J. Wedemayer, J. J. Boniface, R. C. Stevens, P. G. Schultz, *Science* **1996**, *271*, 1086.
[3] a) A. J. Kirby, *CRC Crit. Rev. Biochem.* **1987**, *22*, 283; b) M. L. Sinnott, *Chem. Rev.* **1990**, *90*, 1171; c) P. Deslongchamps, *Stereoelectronic Effects in Organic Chemistry (Organic Chemistry Series, Vol. 1* (Ed.: J. E. Baldwin)), Pergamon, Oxford, **1989**.
[4] A commonly accepted argument to explain this catalysis is the existence of strain. Binding by the enzyme induces strain in the glycoside substrate to a point where it becomes sensitive to catalysis by carboxylic acids. See [3].

 © VCH Verlagsgesellschaft mbH, D-69451 Weinheim, 1996 0570-0833/96/3522-2629 $ 15.00+.25/0

[5] a) T. H. Fife, S. H. Jaffe, R. Natarajan, *J. Am. Chem. Soc.* **1991**, *113*, 7646; b) T. H. Fife, E. Anderson, *ibid.* **1971**, *93*, 6610.
[6] a) J.-L. Reymond, K. D. Janda, R. A. Lerner, *Angew. Chem.* **1991**, *103*, 1690; *Angew. Chem. Int. Ed. Engl.* **1991**, *30*, 1711; b) J. Yu, L. C. Hsieh, L. Kochersperger, S. Yonkovich, J. S. Stephans, M. A. Gallop, P. G. Schultz, *ibid.* **1994**, *106*, 327 bzw. **1994**, *33*, 339.
[7] E. Anderson, T. H. Fife, *J. Am. Chem. Soc.* **1969**, *91*, 7163.
[8] All ketals were prepared from methyl (4-bromomethyl)benzoate in a four-step sequence: Cross-coupling with divinyl cuprate [prepared from vinylmagnesium bromide (2 equiv) and cuprous iodide (1 equiv) in THF at $-30\,^{\circ}C$] afforded methyl (4-allyl)benzoate. Wacker oxidation at room temperature with $PdCl_2$ (0.1 equiv) and $CuCl_2$ (1.5 equiv) in DMF/H_2O (2/1) afforded (4-methoxycarbonyl)phenylacetone, which was ketalized in benzene at reflux in the presence of the appropriate diol (ethylene glycol, 1,3-dihydroxypropane, 1,4-dihydroxybutane) and catalytic amounts of *p*-toluenesulfonic acid. Dimethyl ketal **10** was obtained by treating the corresponding ketone with trimethylorthoformate and methanol in the presence of *p*-toluenesulfonic acid. Finally, the methyl ester was converted to the 2-hydroxyethylamide by heating it in 2-aminoethanol (100 °C, 2 h).
[9] A. Koch, J.-L. Reymond, R. A. Lerner, *J. Am. Chem. Soc.* **1994**, *116*, 803.
[10] All reactions were carried out at 24 °C with 5 μM antibody and 50–2000 μM substrate in 1,3-bis[tris(hydroxymethyl)methylamino]propane-buffered saline solution (50 mM buffer, 50 mM NaCl, pH 6.0). The progress of the reaction was monitored by HPLC (Hitachi L-6200A; $\lambda = 254$ nm; C18-RP column (25 cm × 2.2 mm, 5 μm)), eluting with 20% acetonitrile in water (retention times in minutes: **2**: 5.2, **1**: 9.83, **4**: 9.95, **5**: 23.06).
[11] a) B. Ganem, G. Papandreou, *J. Am. Chem. Soc.* **1991**, *113*, 8984; b) H. Suga, N. Tanimoto, A. J. Sinskey, S. Masamune, *ibid.* **1994**, *116*, 11197.
[12] G. K. Jahangiri, J.-L. Reymond, *J. Am. Chem. Soc.* **1994**, *116*, 11264.
[13] Compounds **8** and **9** were prepared by alkylation of hexamethylene imine and heptamethylene imine, respectively, with methyl (4-bromomethyl) benzoate, followed by quaternization with iodomethane and saponification with aqueous NaOH. The products were purified by preparative RP-HPLC (water/acetonitrile gradient) and obtained as trifluoroacetate salts (colorless solids). Competitive inhibition constants of **8** and **9** were measured following the procedure described for **6** and **7** [12].
[14] a) J.-L. Reymond, G. K. Jahangiri, C. Stoudt, R. A. Lerner, *J. Am. Chem. Soc.* **1993**, *115*, 3909; b) S. C. Sinha, E. Keinan, J.-L. Reymond, *ibid.* **1993**, *115*, 4893; c) D. Shabat, H. Itzaky, J.-L. Reymond, E. Keinan, *Nature* **1995**, *374*, 143.
[15] Antibody 14D9 has been cloned and its sequence shows five aspartate or glutamate residues in the CDR regions. J.-L. Reymond, C. F. Barbas, unpublished results.
[16] S. C. Sinha, E. Keinan, J.-L. Reymond, *Proc. Natl. Acad. Sci. USA* **1993**, *90*, 11910.
[17] Hydrolysis of **10** was carried out at 24 °C, pH 7.4, and that of **11** at 0 °C, pH 7.55; both were conducted in 50 mM phosphate/100 mM NaCl).

Synthesis and Structure of $CoB_2P_3O_{12}(OH)\cdot C_2H_{10}N_2$: The First Metal Borophosphate with an Open Framework Structure**

Slavi C. Sevov*

The most notable trend in the field of molecular sieve synthesis in the past few years is the profound expansion of the variety of studied systems and the rapidly growing number of acronyms associated with them. In addition to the conventional zeolites there are AlPOs (Al-P-O systems), SAPOs (Si-Al-P-O systems), GaPOs (Ga-P-O systems), MeAPOs (metal-Al-P-O systems), Ga-As-O systems, Al-As-O systems, etc. Virtually all combinations of the mixed oxides of the heavier analogs of the boron and nitrogen groups have been explored. With this in mind it is quite surprising that molecular sieves in the B-P-O or Me-B-P-O systems have not yet been synthesized. This is even more surprising considering that BPO_4 itself is a catalyst used industrially for many reactions including hydration, dehydration, alkylation, and oligomerization,[1] and extensive research efforts have been devoted to finding ways to increase its surface-to-volume ratio.[2] Furthermore, incorporation of boron in zeolites and molecular sieves has been a goal pursued for quite some time, since even small amounts of boron have been shown to improve enormously the properties of the host.[3] With a few exceptions, however,[4] such boron incorporation has been possible only on a very small scale, usually less than one percent.[3a, 5] Reported here is the first member of a new class of molecular sieves, namely metal borophosphates (BPOs) with open framework structures in which boron is an integral part of the framework.

The title compound (designated BPO-1) was made hydrothermally from H_3BO_3, H_3PO_4, $[Co(en)_3Cl_3]$ (en = ethylenediamine), and $BF_3\cdot CH_3CH_2NH_2$. Although fluorine is not incorporated in the compound (see Experimental Procedure), boron trifluoride apparently plays an important role in the synthesis since attempts to make the compound without it or with other fluoride sources were unsuccessful. The role of fluorides in the formation of novel framework structures has been well documented, although it is not quite clear what exactly that role might be.[6]

The structure of BPO-1 was determined by single-crystal X-ray diffraction (see Experimental Procedure). The atomic coordinates and some selected bond lengths are listed in Tables 1 and 2, respectively. The structure of the deep purple BPO-1 can be best described as an open framework with one-dimensional channels along the *b* direction of the orthorhombic unit cell (Fig. 1). The framework is built of corner-sharing CoO_6 octahedra and BO_4 and PO_4 tetrahedra. All but two oxygen atoms are shared by two polyhedra. The two exceptions are O13, which is shared by three polyhedra (one CoO_6 octahedron and two BO_4 tetrahedra), and O12, which belongs to only one polyhedron (PO_4 tetrahedron) and is a part of an OH group. No two

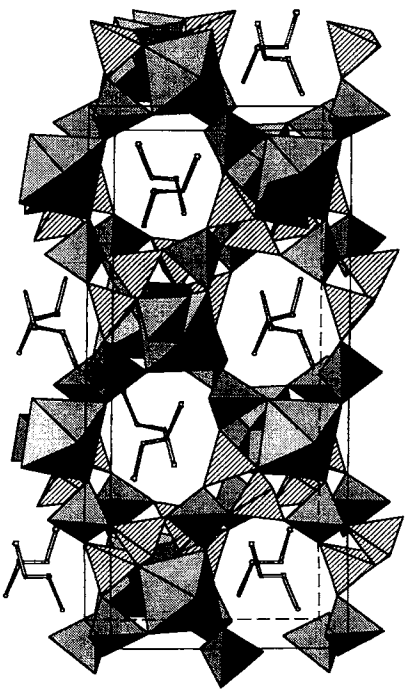

Fig. 1. View of BPO-1 nearly along the *b* axis; the *c*-axis is vertical and the unit cell is outlined. The striped tetrahedra are BO_4 units and the rest are PO_4 units. The octahedra correspond to CoO_6. The ethylenediamine molecules are shown without the hydrogen atoms.

[*] Prof. S. C. Sevov
Department of Chemistry and Biochemistry
University of Notre Dame
Notre Dame, IN 46556 (USA)
Fax: Int. code +(219)631-6652
e-mail: ssevov@nd.edu

[**] I thank Dr. A. G. Lappin for his suggestions and Dr. M. Shang for his help with X-ray data collection.

Table 1. Atomic coordinates and isotropic displacement parameters for the non-hydrogen atoms in BPO-1.

Atom	x	y	z	U_{eq} [Å^2] [a]
Co	0.1784(1)	0.1887(1)	0.4052(1)	0.007(1)
P1	0.4739(1)	0.2225(1)	0.4772(1)	0.008(1)
P2	−0.1002(1)	0.6718(1)	0.2473(1)	0.009(1)
P3	0.2807(1)	0.4343(1)	0.3663(1)	0.007(1)
B1	0.4577(4)	0.2635(3)	0.3475(2)	0.008(1)
B2	0.1427(4)	0.5909(3)	0.2948(2)	0.007(1)
O1	−0.1414(3)	−0.0239(2)	0.5990(1)	0.012(1)
O2	0.3231(3)	0.1794(2)	0.4779(1)	0.014(1)
O3	−0.0050(3)	−0.1960(2)	0.5300(1)	0.013(1)
O4	0.1980(3)	0.3594(2)	0.4103(1)	0.014(1)
O5	0.3847(3)	0.3636(2)	0.3255(1)	0.011(1)
O6	−0.0830(3)	0.7533(2)	0.3035(1)	0.013(1)
O7	0.5036(3)	−0.0767(2)	0.7386(1)	0.009(1)
O8	0.1765(3)	0.4811(2)	0.3155(2)	0.018(1)
O9	0.5714(3)	0.2789(2)	0.6832(1)	0.014(1)
O10	0.5119(3)	0.2813(2)	0.4126(1)	0.012(1)
O11	−0.2519(3)	0.6262(2)	0.2546(1)	0.014(1)
O12	0.5803(3)	0.1244(2)	0.4813(2)	0.019(1)
O13	0.3666(3)	0.1688(2)	0.3455(1)	0.007(1)
C1	0.3273(4)	0.0904(4)	0.6198(2)	0.023(1)
C2	0.2141(4)	0.0020(4)	0.6147(2)	0.018(1)
N1	0.1532(4)	0.0029(3)	0.5493(2)	0.019(1)
N2	0.3634(4)	0.1142(3)	0.6866(2)	0.020(1)

[a] U_{eq} is defined as one-third of the trace of the orthogonalized U_{ij} tensor.

Table 2. Selected bond lengths [Å] for BPO-1.

Co-O1	2.049(3)	P2-O6	1.549(3)	B1-O10	1.467(5)
Co-O2	2.037(3)	P2-O7	1.544(2)	B1-O13	1.439(4)
Co-O4	2.100(3)	P2-O9	1.491(3)	B2-O7	1.486(4)
Co-O3	2.114(3)	P2-O11	1.532(3)	B2-O8	1.447(5)
Co-O9	2.137(3)	P3-O1	1.503(3)	B2-O11	1.491(4)
Co-O13	2.170(3)	P3-O4	1.511(3)	B2-O13	1.427(4)
P1-O2	1.506(3)	P3-O5	1.556(2)	C1-C2	1.517(6)
P1-O3	1.515(3)	P3-O8	1.550(3)	C1-N2	1.465(5)
P1-O10	1.569(3)	B1-O5	1.476(4)	C2-N1	1.478(5)
P1-O12	1.562(3)	B1-O6	1.494(4)		

Table 3. Crystallographic data for BPO-1.

empirical formula	$CoB_2P_3O_{12}(OH)\cdot C_2H_{10}N_2$
formula weight	889.18
crystal appearance	bar-shaped, transparent, deep purple
space group, Z	*Pbca* (No. 61), 4
unit cell dimensions	$a = 9.3501(5)$, $b = 12.2426(9)$, $c = 20.880(2)$ Å
volume	2390.1(3) Å^3
ρ_{calcd}	2.471 g cm^{-3}
$\mu(Mo_{K\alpha})$	19.23 cm^{-1}
transmission range	0.8536–0.9993
reflections collected	4051
independent reflections	2098 ($\bar{R} = 0.02$)
parameters	217
final R-values ($I \geq 2\sigma_I$)	$R_1 = 0.0442$[a], $wR_2 = 0.1133$[b]
final R-values (all data)	$R_1 = 0.0478$[a], $wR_2 = 0.1211$[b]
goodness of fit	1.124[c]
extinction coefficient	$3(4) \times 10^{-4}$
residual electron density	+1.2/−0.8 e Å^{-3} (1.35 and 1.19 Å from Co, respectively)

[a] $R = \Sigma||F_o| - |F_c||/\Sigma|F_o|$. [b] $wR_2 = [\Sigma[w(F_o^2 - F_c^2)^2/\Sigma[w(F_o^2)^2]]]^{1/2}$. [c] goof $= \Sigma[[w(F_o^2 - F_c^2)^2]/(n-p)]^{1/2}$; $w = 1/[\sigma^2 F_o^2 + (0.0875P)^2 + 4.7318P]$, $P = (F_o^2 + 2F_c^2)/3$.

PO_4 tetrahedra are bonded to each other but the two BO_4 tetrahedra share a corner, O13, the same three-coordinate oxygen atom that is also part of the CoO_6 octahedron. The P–O, Co–O, and B–O distances are within the expected ranges.

The channels in the structure are formed from eight polyhedra sharing corners in the following sequence: -PO_4-CoO_6-PO_4-BO_4-PO_4-BO_4-PO_4-CoO_4-. The channels are not exactly straight and round but rather wavelike and oblong (Fig. 1). The short axis of the opening is about 5.2 Å, and the long one is about 7.6 Å (O–O distances). The channels are occupied by the ethylenediamine molecules, which are positioned nearly perpendicular to the direction of the channel and with their N–N axis along the long axis of the ellipse. The two C–N distances and the C–C distance (1.465(5), 1.478(5), and 1.517(6) Å, respectively) are in the normal range. The molecules are well locked in their positions by hydrogen bonds to oxygen atoms lining the channel (Fig. 2), and no disorder was observed at the C, N, and

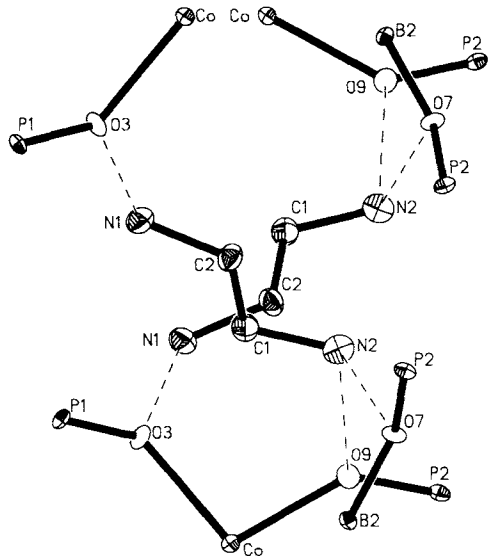

Fig. 2. An ORTEP drawing (thermal ellipsoids at 50% probability) of one ethylenediamine molecule (without the hydrogen atoms) and its hydrogen bonds (broken lines) to oxygen atoms lining the channel.

H positions. One of the hydrogen atoms at N1 is involved in hydrogen bonding ($d_{N1-O3} = 2.878(5)$ Å, $d_{H-O3} = 2.05$ Å, $\alpha_{N1-H-O3} = 168.4°$), while two of the hydrogens at N2 form hydrogen bonds ($d_{N2-O7} = 2.892(4)$ Å, $d_{H-O7} = 2.06$ Å, $\alpha_{N2-H-O7} = 171.1°$; $d_{N2-O9} = 2.802(5)$ Å, $d_{H-O9} = 1.91$ Å, $\alpha_{N2-H-O9} = 167.5°$).

The oxygen atom of the OH group, O12, is also hydrogen bonded. It is only 2.525(4) Å from O4 ($d_{H-O4} = 1.83$ Å, $\alpha_{O12-H-O4} = 170.3°$). The OH group is also positioned in the channel but is between the ethylenediamine molecules and not hydrogen bonded to them.

Upon heating under vacuum the compound is stable up to roughly 500 °C, above which it becomes amorphous. This structural change is most likely due to decomposition of the ethylenediamine dication followed by a collapse of the framework. The amorphous mass was further heated at 950 °C for a few hours. After cooling to room temperature it was put back in an autoclave, water was added, and the autoclave was heated for four days at 180 °C. The product of this reaction (without an organic template) is the known cobalt (hydrogen)phosphate $Co_7P_6O_{20}(OH)_4$,[7] which is composed of well-packed CoO_6 octahedra and PO_4 tetrahedra.

In conclusion, it is possible to synthesize molecular sieve type compounds with networks constructed from BO_4 and PO_4 tetrahedra (and CoO_6 octahedra) similarly to the way the AlPOs are built. It is very likely that the organic template can be removed from similar compounds and that the channels can then be used for appropriate catalytic reactions. The presence of boron at relatively high concentrations should improve the catalytic properties of such catalysts.

Experimental Procedure

Synthesis: BPO-1 was synthesized hydrothermally (heated at 180 °C for five days followed by oven cooling) in Teflon-lined stainless steel autoclaves from a mixture of $[Co(en)_3Cl_3]\cdot 2H_2O$, H_3BO_3, H_3PO_4 (85%), $BF_3\cdot CH_3CH_2NH_2$ (all from Aldrich), and water in the molar ratio of 0.25:1:1:1:45. Bar-shaped as well as large spheres (3–5 mm diameter) of wedge-shaped, deep purple crystals were recovered and washed with water. Both types of crystals were of the same compound (nearly 100% yield with respect to Co). Chemical analysis confirmed the amounts of ethylenediamine (M-H-W Laboratories: C 5.07, H 2.52, N 6.30%; theoretical: C 5.40, H 2.49, N 6.30%) and the absence of fluorine (Galbraith Laboratories: F 0.27%; theoretical if one atom of oxygen is replaced by fluorine: F 4.2%) in the compound.

Structure Determination: A few bar-shaped crystals of BPO-1 were cut into smaller pieces and then checked for singularity by oscillation film technique. One of the crystals ($0.4 \times 0.3 \times 0.2$ mm) was additionally studied by taking Weissenberg photographs of the zeroth and first layers. These revealed an *mmm* Laue class, the possible space groups, and the approximate unit cell dimensions. Two octants of data up to $2\theta = 50°$ were collected at 21 °C with monochromated $Mo_{K\alpha}$ radiation on a CAD4 single-crystal diffractometer with ω-2θ scans. (Some additional details of the data collection and refinement are listed in Table 3.) Corrections for Lorentz and polarization effects and for absorption (SDP package, Enraf-Nonius, 1985) with the aid of the average of five ψ-scans collected at different θ angles gave a data set that was consistent with only one space group, *Pbca*. Subsequent structure solution and refinement were performed with the aid of the SHELXTL program package. Application of direct methods revealed the Co and P positions and most of the oxygen sites. Successive least-square cycles and difference Fourier syntheses provided the positions of the remaining non-hydrogen atoms. One oxygen atom, O12, was one-coordinate, which suggested that it was part of an OH group. Additionally, ten more hydrogen atoms were needed for the ethylenediamine dication. Eleven peaks from the subsequent difference Fourier synthesis were at distances around O, C, and N appropriate for hydrogen atoms. These were assigned as such. Refinement of the hydrogen atoms (without constraints) with isotropic thermal parameters, refinement of the non-hydrogen atoms with anisotropic thermal parameters, and application of a secondary extinction coefficient gave final residuals of R and wR of 0.044 and 0.113, respectively (as defined in Table 1). Further details of the crystal structure investigation may be obtained from the Fachinformationszentrum Karlsruhe, D-76344 Eggenstein-Leopoldshafen (Germany) on quoting the depository number CSD-405370.

Received: June 17, 1996 [Z9237IE]
German version: *Angew. Chem.* **1996**, *108*, 2814–2816

Keywords: boron compounds · cobalt compounds · microporosity · molecular sieves

[1] R. Tartarelli, M. Giorgini, A. Lucchesi, G. Stoppato, F. Moreli, *J. Catal.* **1970**, *17*, 41; J. Haber, U. Szybalska, *Faraday Discuss. Chem. Soc.* **1981**, *72*, 263; J. B. Moffat, *Catal. Rev. Sci. Eng.* **1978**, *18*, 199; S. S. Jewur, J. B. Moffat, *J. Catal.* **1979**, *57*, 167; J. B. Moffat, A. Schmidtmeyer, *Appl. Catal.* **1986**, *28*, 161; F. Nozaki, I. Kimura, *Bull. Chem. Soc. Jpn.* **1977**, *50*, 614; T. Sodesawa, I. Kimura, F. Nozaki, *ibid.* **1979**, *52*, 2431; J. Morrey, J. M. Marinas, J. V. Sinisterra, *React. Kinet. Catal. Lett.* **1982**, *22*, 175; A. Tada, H. Suzuka, Y. Imizu, *Chem. Lett.* **1987**, 423.

[2] S. Sato, M. Hasegawa, T. Sodesawa, F. Nozaki, *Bull. Chem. Soc. Jpn.* **1991**, *64*, 516; C. Keary, J. B. Moffat, *J. Colloid. Interface Sci.* **1992**, *154*, 8; H. L. Goltz, J. B. Moffat, *J. Catal.* **1971**, *22*, 85.

[3] a) B. Andersen, C. T. O'Connor, M. Kojima in *Zeolites: Facts, Figures, Future* (Eds.: P. A. Jacobs, R. A. van Santen), Elsevier, Amsterdam, **1989**, p. 1193; S. I. Woo, J. K. Lee, S. B. Hong, Y. K. Park, Y. S. Uh, *ibid.*, p. 1095; G. Coudurier, A. Auroux, J. C. Vedrine, R. D. Farlee, L. Abrams, R. D. Shannon, *J. Catal.* **1987**, *108*, 1; C. T. W. Chu, C. D. Chang, *J. Phys. Chem.* **1985**, *89*, 1569; G. Coudurier, J. C. Vedrine, *Pure Appl. Chem.* **1986**, *58*, 1389; P. J. O'Malley, J. Dwyer, *J. Chem. Soc. Chem. Commun.* **1987**, 72; *Chem. Phys. Lett.* **1988**, *143*, 97; b) S. I. Zones, L. T. Yuen, Y. Nakagawa, R. A. van Nordstrand, S. D. Toto in *Proc. 9th Intl. Zeolite Conference* (Eds.: R. von Ballmoos et al.), Butterworth-Heinemann, Montreal, **1993**, p. 163.

[4] W. T. A. Harrison, T. E. Gier, G. D. Stucky, *Angew. Chem.* **1993**, *105*, 788; *Angew. Chem. Int. Ed. Engl.* **1993**, *32*, 724.

[5] Q. Shilun, P. Wenqin, Y. Shangqing in *Zeolites: Facts, Figures, Future* (Eds.: P. A. Jacobs, R. A. van Santen), Elsevier, Amsterdam, **1989**, p. 133; B. L. Meyers, S. R. Ely, N. A. Kutz, J. A. Kaduk, *J. Catal.* **1985**, *91*, 352.

[6] J. L. Guth, H. Kessler, P. Caullet, J. Hazm, A. Merrouche, J. Patarin in *Proc. 9th Intl. Zeolite Conference* (Eds.: R. von Ballmoos et al.), Butterworth-Heinemann, Montreal, **1993**, p. 215; J. Dwyer, J. Zhao, D. Rawlence, *ibid.*, p. 155.

[7] P. Lightfoot, A. K. Cheetham, *Acta Crystallogr. Sect. C* **1988**, *44*, 1331.

Synthesis and Properties of PNA/DNA Chimeras**

Eugen Uhlmann,* David W. Will, Gerhard Breipohl, Dietrich Langner, and Antonina Ryte

Synthetic oligonucleotides play a central role in a multitude of molecular biology techniques.[1–3] They are, for example, routinely used as linkers, primers, and gene probes. More recently their potential use as antisense or antigene oligonucleotides has attracted increasing interest.[4–7] To develop the desired biological activity in vivo, oligonucleotides must be stable against the nucleases found in serum and in cells. They must also be capable of entering the cell in order to bind sequence-specifically to their intracellular target sequence. From the huge variety of modifications carried out on oligonucleotides,[4, 8] the nonionic oligonucleotide analogues[9] are of particular interest. Besides their increased stability toward nucleases they can also be expected to have a higher binding affinity to their target nucleic acid because of the lack of charge–repulsion effects. One of the most remarkable of the nonionic oligonucleotide analogues are the polyamide nucleic acids (PNAs), since these bind to complementary DNA and RNA with a higher affinity than natural oligonucleotides.[10–13]

PNAs are nucleic acid mimetics in which the entire sugar–phosphate backbone is replaced by *N*-(2-aminoethyl)glycine units. Although the recognition of complementary nucleic acid sequences by PNAs obeys the Watson–Crick base-pairing rules, the orientation of the strands is ambiguous. This means that PNAs can form both parallel and antiparallel duplexes,[13] in contrast to the purely antiparallel strand orientation in natural nucleic acids. As well as their tendency to self-aggregate, a further hurdle to their application as antisense oligomers is their extremely low, or nonexistent cellular uptake.[12] Here we report on a method for the fully automated synthesis of PNA/DNA chimeras (Fig. 1) that contain all four natural nucleobases. We have found that these PNA/DNA chimeras bind to their complementary DNA and RNA exclusively in the antiparallel orientation. The negative charge on the DNA part of the chimeras reduces their tendency to self-aggregation and thus improves their solubility.

Ideally the synthesis of PNA/DNA chimeras of any desired sequence (5′-DNA-PNA-pseudo-3′; pseudo-5′-PNA-DNA-3′) should be carried out "online" on an automated synthesizer with commercially available DNA monomers. The synthesis of PNA/DNA chimeras has been reported previously; however, in those reports the DNA part of the chimeras was composed entirely of acid-stable pyrimidine nucleotides.[14–16] In one case the use of specially protected DNA monomers was necessary.[14] The binding affinities of the PNA–DNA chimeras[14] and the DNA–(HomoPNA) chimeras[15] were reported to be lower than the corresponding DNA sequences. Recently we reported on the synthesis of pure PNAs with a new type of PNA monomer,[17] in which the acid-labile monomethoxytrityl (Mmt) group is employed for temporary protection of the amino function of the aminoethylglycine and the exocyclic amino functions of the nucleobases are protected with base-

[*] Dr. E. Uhlmann, Dr. D. W. Will, Dr. G. Breipohl, D. Langner, Dr. A. Ryte
Hoechst AG, Zentrale Pharma Forschung G 838
D-65926 Frankfurt am Main (Germany)
Fax: Int. code + (69) 305-89713
e-mail: uhlmann@msmrd.frankfurt.hoechst-ag.d400.de

[**] We thank Silvia Hein, Lothar Hornung, Norbert Laub, Michael Reiter, Gerd Schluckebier, and Sabine Schülke for their expert technical assistance, and Dr. A. Schäfer and Dr. W. Fehlhaber for the measurement of the mass spectra.

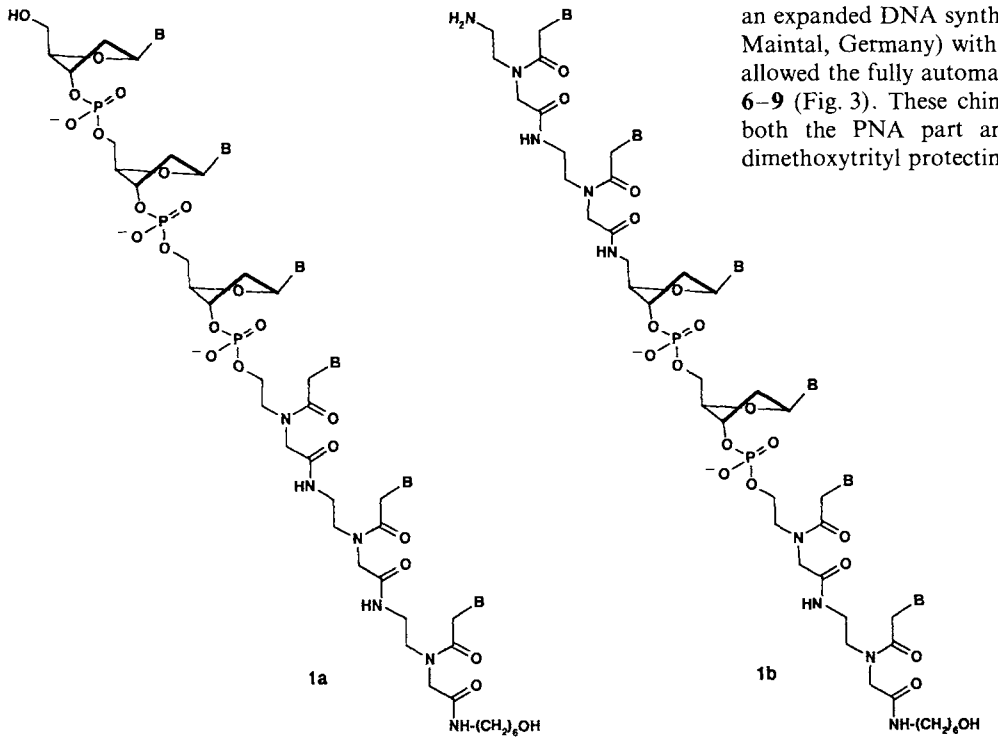

Fig. 1. Structural formula of DNA–PNA chimera **1a** and PNA–DNA–PNA chimera **1b**. In chimera **1a** the DNA part forms the 5′ terminus of the oligomer. B = nucleobase residue.

labile acyl protecting groups. This orthogonal protecting-group strategy was designed to be fully compatible with the phosphoramidite DNA synthesis method of Caruthers.[18]

For the synthesis of DNA–PNA chimera **1a**, which is composed of a DNA 5′-terminus and a PNA (pseudo) 3′-terminus, the PNA part is synthesized first on CPG (controlled pore glass) solid support from PNA monomers **2a–d** (Fig. 2), as described previously.[17] One of the linker monomers **3a–d**, which are derivatives of *N*-(2-hydroxyethyl)glycine, is then coupled to the amino terminus. This allows the synthesis of the DNA part by reaction with the nucleoside phosphoramidites **4a–d**. The use of an expanded DNA synthesizer (Eppendorf–Biotronik GmbH, Maintal, Germany) with ten positions for monomer solutions allowed the fully automatic synthesis of DNA–PNA chimeras **6–9** (Fig. 3). These chimeras contain all four nucleobases in both the PNA part and the DNA part. The 5′-terminal dimethoxytrityl protecting group is cleaved on the synthesizer, and the chimera is treated with aqueous ammonia solution to cleave it from the solid support and to remove the base-labile phosphate- and amino-protecting groups. Since a base-labile 6-aminohexylsuccinate linker is employed[17] the resulting DNA–PNA chimeras are obtained as C-terminal hydroxyhexylamides. DNA–PNA chimeras **6–9** are highly water-soluble and can be analyzed and purified by polyacrylamide gel electrophoresis or by ion-exchange HPLC. For the synthesis of PNA–DNA–PNA chimera **10** the DNA–PNA part is synthesized as described for **6–9**. A 5′-*N*-monomethoxytrityl-5′-amino-2′,5′-dideoxynucleoside-3′-*O*-phosphoramidite (**5a–d**) is then coupled to the free 5′-hydroxyl function and serves as a linker to the 5′-terminal PNA part of the chimera (Fig. 1, structure **1b**). After detritylation with trichloroacetic acid the 5′-terminal PNA part is synthesized as described above. All of the new PNA/DNA chimeras **6–11** were characterized by electrospray mass spectrometry.

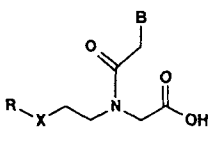

2a-d
3a-d

	X	R
2	NH	Mmt
3	O	Dmt

B: **a**: T, **b**: 4-*N*-anisoyl-C, **c**: 6-*N*-anisoyl-A, **d**: 2-*N*-isobutyryl-G

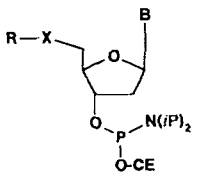

4a-d
5a-d

	X	R
4	O	Dmt
5	NH	Mmt

B: **a**: T, **b**: 4-*N*-benzoyl-C, **c**: 6-*N*-benzoyl-A, **d**: 2-*N*-isobutyryl-G

Fig. 2. Structure of PNA monomers (**2a–d**), DNA monomers (**4a–d**), PNA → DNA linkers (**3a–d**), and DNA → PNA linkers (**5a–d**).

	PNA/DNA chimera	Proportion of PNA
6	5′-ACATCAtggtcg-h	50%
7	5′-ATGacggaata-h	72%
8	5′-GGGACCAtggcagcc-h	53%
9	5′-CGCGAAttcgcg-h	50%
10	(5′)Ac-ctcttcTTTTtcttctc-h	76%
11	5′-TTTTTTZttttttt-h	50%

Complementary sequences and refernce sequences:

12	5′-ACATCATGGTCG-3′,	**21**	5′-CGTCCATGATGT-3′
13	(5′)-acatcatggtcg-h	**22**	5′-TATTCCGTCAT-3′
14	5′-ACATCATGGTCG-3′	**23**	5′-GGCTGCCATGGTCCC-3′
15	5′-CGACCATGATGT-3′	**24**	5′-TTTTTTTTTTTT-3′
16	5′-TGTAGTACCAGC-3′	**25**	5′-GAGAAG-3′
17	5′-r(CGACCATGATGT)-3′	**26**	5′-CTCTTCTTTTTCTTCTC-3′
18	5′-r(TGTAGTACCAGC)-3′	**27**	5′-GGGACCATGGCAGCC-3′
19	5′-CGACCATGTTGT-3′	**28**	5′-ATGACGGAATA-3′
20	5′-CGACCTTGATGT-3′	**29**	5′-CGCGAATTCGCG

h = HN-$(CH_2)_6$-OH Ac = CH_3-CO Z = O-$(CH_2)_3$CO

n =

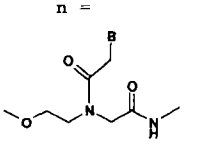

N =

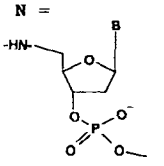

N =

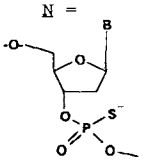

Fig. 3. Sequences of the oligomers described in the text. Nucleotide units are written in upper case, PNA units in lower case.

 © VCH Verlagsgesellschaft mbH, D-69451 Weinheim, 1996 0570-0833/96/3522-2633 $ 15.00+.25/0

The binding affinity of the DNA–PNA chimeras to their complementary nucleic acid sequences was investigated by measuring the melting temperatures T_m of the duplexes. Figure 4 compares the UV-melting curves of the chimeric (DNA–PNA)·DNA duplex **6·15** (Fig. 4A) with those of the

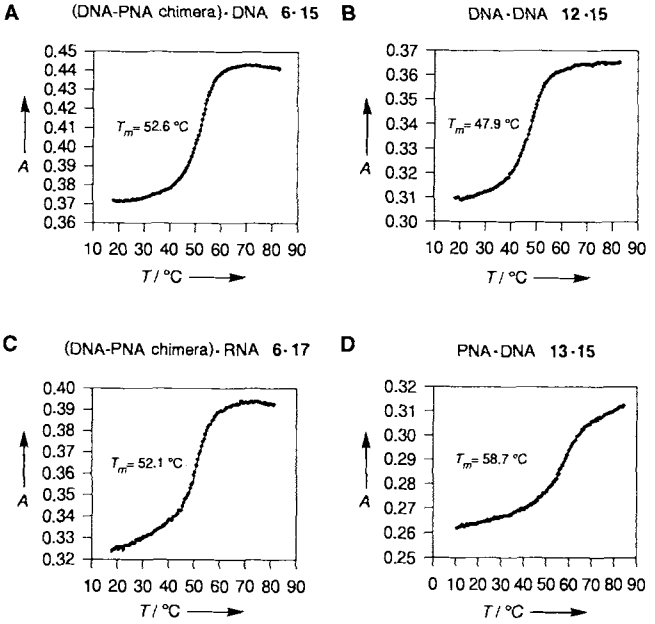

Fig. 4. Comparison of the UV-melting curves of the duplex formed by DNA–PNA chimera **6** and the complementary DNA **15** (A) and RNA **17** (C) sequences with those of the duplexes formed by DNA **12** (B) and pure PNA **13** (D) with the complementary DNA **15**.

DNA·DNA duplex **12·15** (Fig. 4B) and the PNA·DNA duplex **13·15** (Fig. 4D). The PNA·DNA duplex is the most stable (T_m = 59 °C). However, the (DNA–PNA)·DNA duplex (T_m = 53 °C) also has a considerably higher stability than the natural DNA·DNA duplex (T_m = 48 °C). The pure PNA **13** binds with **15** in the antiparallel orientation (T_m = 59 °C) and with **16** in the parallel orientation (T_m = 48 °C), whereas the analogous DNA–PNA chimera **6** binds only to the antiparallel oligonucleotide **15**, but no binding to the parallel oligonucleotide **16** is detected at room temperature (Table 1). The T_m values of the various oligomers against their complementary RNA sequences were also measured (Table 1, Fig. 4C). This is the most relevant model for the use of DNA–PNA chimeras as mRNA-targeting antisense oligomers. Again oligomer **6**, which is composed of 50% PNA, has a significantly higher antiparallel duplex stability than the pure DNA analogue (ΔT_m = 8 K). Although the pure PNA has a higher binding affinity than either the chimera or the oligonucleotide, it also binds to the parallel complementary sequence.

Oligonucleotide phosphorothioates are the most thoroughly investigated and widely used oligonucleotide analogues in biological systems. We compared the binding affinities of the DNA–PNA chimera **6** with the analogous phosphodiester–phosphorothioate chimera **14** in which the PNA is replaced by phosphorothioate-linked DNA (S-DNA). Interestingly, the DNA–PNA chimera **6** forms a duplex with complementary RNA **17** that melts 10 K higher than the DNA–(S-DNA) chimera **14**. The binding affinity is largely dependent upon the ratio of PNA to DNA in the chimera. Thus undecamer **7**, in which 72% of the sequence is composed of PNA, melts 14 K higher than the corresponding DNA analogue **28** (Table 2). In chimera **8** the DNA part contains phosphorothioate linkages but still binds better to the complementary DNA sequence than the corresponding oligonucleotide **27**.

Table 1. Comparison of the T_m values [a] of the oligomers **6** and **12–14** when hybridized to their complementary parallel and antiparallel DNA or RNA sequences.

	Sequence		Orientation of the duplex	T_m [°C] against DNA	T_m [°C] against RNA
15/17	3'-TGT AGT ACC AGC-5'	DNA/RNA [b]			
6	5'-ACA TCA **t**gg tcg-h	DNA-PNA	ap [c]	52.6	52.1
12	5'-ACA TCA TGG TCG-3'	DNA	ap	47.9	44.5
13	(5')aca tca tgg tcg-h	PNA	ap	58.7	62.3
14	5'-ACA TCA TGG TCG	DNA-(S-DNA)	ap	43.4	41.7
16/18	5'-TGT AGT ACC AGC-3'	DNA/RNA [b]			
6	5'-ACA TCA **t**gg tcg-h	DNA-PNA	p [d]	<25	<25
13	(5')aca tca tgg tcg-h	PNA	p	47.6	43.5

[a] The T_m values were measured under physiologically relevant conditions (140 mM KCl, 10 mM NaH_2PO_4, 0.1 mM Na-EDTA pH 7.4) by cooling from 85 °C to 15 °C at 0.5 K min^{-1} and measuring the UV absorbance at 260 nm. [b] For RNA: T = U. [c] ap = antiparallel duplex; [d] p = parallel duplex.

Table 2. Comparison of the T_m values of PNA/DNA chimeras **7–10** in duplexes with the corresponding DNA oligomers **26–29**.

Chimera · DNA	T_m [°C]	DNA · DNA	T_m [°C]
7 · 22	53.5	**28 · 22**	39.9
8 · 23	68.4	**27 · 23**	64.6
9 · 9 [a]	67.5	**29 · 29**	54.5
10 · 25 [b]	64.6	**26 · 25**	27.3

[a] Forms a chimera·chimera duplex:
5'-CGCGAA**t**tcgcg-3'
3'-gcgct**t**AAGCGC-5'
[b] Measured at pH 5, forms a triple helix:
5'-ctcttc-**TT**
3'-GAGAAG T
(3')-ctcttc-**t**T

The self-complementary DNA–PNA chimera **9**, which forms a duplex **9·9** in which all PNA bases are opposite DNA bases, has a T_m value 13 K higher than the analogous DNA duplex **29·29**. The PNA–DNA–PNA chimera **10** is designed so that the C-terminal PNA part (pseudo 3' end) forms a Watson–Crick duplex with complementary hexamer **25**. The DNA part acts as a loop to allow the N-terminal PNA part (pseudo 5' end) to fold back and form Hoogsteen base-pairs under acidic conditions. The resulting triplex has a remarkably high T_m (65 °C) for a hexamer complex. The corresponding DNA analogue melts at 27 °C.

To investigate the specificity of the base-pairing in the PNA and DNA parts of the PNA/DNA chimeras, the melting temperatures of duplexes formed by DNA–PNA chimera **6**, DNA oligonucleotide **12**, and PNA oligomer **13** with complementary DNA sequences each containing one base mismatch in three different positions were determined. One of the mismatches was positioned in the DNA part, one in the PNA part, and one directly at the DNA → PNA crossover.

As can be seen in Figure 5, the destabilising effect of a PNA–DNA mismatch is approximately the same as that of a DNA–DNA mismatch at the same position. It should be emphasized that a base mismatch at the DNA → PNA crossover also results in a clear reduction of the T_m. This strongly suggests that the nucleobase at the crossover is also involved in cooperative binding to the complementary nucleic acid. However, since the ΔT_m

12 (6, 13)	5'-A C A T C A T G G T C G-3'
15	3'-T G T A G T A C C A G C-5'
19	3'-T G T ***T*** G T A C C A G C-5'
20	3'-T G T A G T ***T*** C C ***A*** G C-5'
21	3'-T G T A G T ***A*** C C ***T*** G C-5'

Sequence		19	20	21	
6	PNA-DNA	10.1	6.8	11.0	
12	DNA	10.3	7.3	9.3	ΔT_m
13	PNA	10.2	7.5	10.5	

Fig. 5. Comparison of the difference in the T_m value (ΔT_m [K]) between the duplex formed by DNA-PNA chimera **6**, DNA **12**, or PNA **13** with the complementary DNA **15** and the corresponding duplexes formed with the complementary DNA strands that contain base mismatches (A → T) in three different positions (**19**-**21**).

is smaller than that for the pure PNA or DNA oligomers there might be a minor disturbance in the duplex structure at the site of the crossover. It is also possible to use simple linkers that are not involved in base-pairing, such as the γ-hydroxybutyric acid linker in sequence **11**.

The use of PNA/DNA chimeras as antisense or antigene oligomers requires that they are capable of entering cells. The uptake of DNA-PNA chimera **11** by Vero cells was determined by labeling the oligomer at the 5′ end with ^{35}S-γ-ATP and incubating the cells with the radiolabeled oligomer. Figure 6 shows that cellular uptake of the DNA-PNA chimera, measured as cell-associated oligomer,[19] is almost identical to that of the analogous oligonucleotide **24** at both 1 μM and 10 μM extracellular concentration.

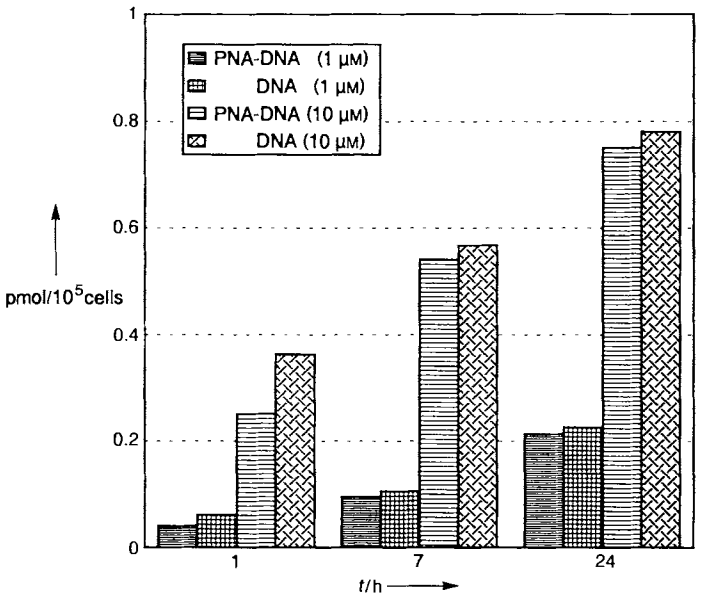

Fig. 6. Comparison of the cellular uptake of the DNA-PNA chimera **11** labeled at the 5′ end with ^{35}S-γ-ATP with that of the analogously labeled DNA oligomer **24** at 37 °C in Vero cells.

Preliminary experiments in cell culture have shown that DNA-PNA chimeras used as antisense oligomers are capable of inhibiting the expression of specific target genes, even when only 30% of the oligomer is composed of DNA. The fact that PNA/DNA chimeras activate cellular RNase H, which cleaves the RNA strand of a DNA·RNA duplex, may well be of importance in this respect. Pure PNAs do not activate RNase H. The biological activity of RNase H inducing oligonucleotide analogues is generally superior to that of those which do not activate this enzyme.[4, 5]

We have developed a generally applicable method for the automated synthesis of DNA/PNA chimeras. This method is fully compatible with standard DNA synthesis methods and requires no additional deprotection steps at the end of oligomer synthesis. The binding affinity of DNA-PNA chimeras is higher than that of the comparable DNA-phosphorothioate chimeras or natural oligonucleotides. Unlike pure PNAs, the DNA-PNA chimeras investigated bind only in the antiparallel orientation to their complementary nucleic acids under physiological conditions. The DNA-PNA chimeras in which the PNA part was attached to the 3′ end of the DNA part are especially stable against degradation by 3′-exonucleases, which are the major type of oligonucleotide-degrading enzymes found in serum. DNA-PNA chimeras are taken up by cells to a similar extent as oligonucleotides, are largely nuclease-resistant, and have an excellent binding affinity to complementary RNA. They thus fulfill the basic requirements for antisense oligomers to be biologically active.

Received: July 15, 1996 [Z9333IE]
German version: *Angew. Chem.* **1996**, *108*, 2793-2797

Keywords: antisense oligonucleotides · helices · nucleic acids

[1] J. Engels, B. Sprunkel, E. Uhlmann in *Biotechnology, Vol. 2* (Ed.: A. Pühler) VCH, Weinheim **1993**, p. 317.
[2] U. Englisch, D. H. Gauss, *Angew. Chem.* **1991**, *103*, 629-46; *Angew. Chem. Int. Ed. Engl.* **1991**, *30*, 613-630.
[3] E. Uhlmann in *Proceedings of the 6th European Congress on Biotechnology, ECB6*, (Eds.: L. Alberghina, L. Frontali, P. Sensi), Elsevier, Amsterdam, **1994**, p. 667.
[4] E. Uhlmann, A. Peyman, *Chem. Rev.* **1990**, *90*, 543-84.
[5] E. Uhlmann, A. Peyman in *Molecular Biology and Biotechnology* (Ed.: R. A. Meyers), VCH, Weinheim **1995**, p. 38.
[6] N. T. Thuong, C. Helene, *Angew. Chem.* **1993**, *105*, 697-723; *Angew. Chem. Int. Ed. Engl.* **1993**, *32*, 666-690.
[7] H. Schreier, *Pharm. Acta Helv.* **1994**, *68*, 145-159.
[8] S. T. Crooke, B. Lebleu, *Antisense Research and Applications*, CRC Press, Boca Raton, **1993**.
[9] E. Uhlmann, A. Peyman in *Methods in Molecular Biology, Vol 20* (Ed.: S. Agrawal), Humana Press, New Jersey, Totowa, **1993**, p. 355.
[10] P. E Nielsen, M. Egholm, R. H. Berg, O. Buchardt, *Science* **1991**, *254*, 1497-1500.
[11] C. Meier, J. Engels, *Angew. Chem.* **1992**, *104*, 1039-1041; *Angew. Chem. Int. Ed. Engl.* **1992**, *31*, 1008-1010.
[12] P. E. Nielsen, M. Egholm, O. Buchardt, *Bioconjugate Chem.* **1994**, *5*, 3-7; W. M. Pardridge, R. J. Boado, Y.-S. Kang, *Proc. Natl. Acad. Sci. USA* **1995**, *92*, 5592-5596; J. C. Norton, M. A. Piatyszek, W. E. Wright, J. W. Shay, D. R. Corey, *Nature Biotechnol.* **1996**, *14*, 615-619; B. Hyrup, P. E. Nielsen, *Bioorg. Med. Chem.* **1996**, *4*, 5-23.
[13] P. Wittung, P. E. Nielsen, O. Burchardt, M. Egholm, B. Norden, *Nature* **1994**, *368*, 561-563.
[14] F. Bergmann, W. Bannwarth, S. Tam, *Tetrahedron Lett.* **1995**, *36*, 6823-6826.
[15] K. H. Petersen, D. K. Jensen, M. Egholm, P. E. Nielsen, O. Buchardt, *Bioorg. Med. Chem. Lett.* **1995**, *5*, 1119-1124.
[16] A. C. van der Laan, N. J. Meeuwenoord, E. Khyl-Yeheskiely, R. S. Oosting, R. Brands, J. H. van Boom, *Rec. Trav. Chim. Pays-Bas* **1995**, *114*, 295-297; D. A. Stetsenko, E. N. Lubyako, V. K. Potapov, T. L. Azhikina, E. D. Sverdlov, *Tetrahedron Lett.* **1996**, *37*, 3571-3574.
[17] D. W. Will, G. Breipohl, D. Langner, J. Knolle, E. Uhlmann, *Tetrahedron* **1995**, *51*, 12069-12082.
[18] M. D. Matteucci, M. H. Caruthers, *J. Am. Chem. Soc.* **1981**, *103*, 3185-3191.
[19] The total cell uptake was determined according to A. Peyman, A. Ryte, M. Helsberg, G. Kretzschmar, M. Mag, E. Uhlmann, *Nucleosides Nucleotides* **1995**, *14*, 1077-1081.

 © VCH Verlagsgesellschaft mbH, D-69451 Weinheim, 1996 0570-0833/96/3522-2635 $ 15.00+.25/0

Phosphonic Ester Nucleic Acids (PHONAs): Oligonucleotide Analogues with an Achiral Phosphonic Acid Ester Backbone

Anusch Peyman,* Eugen Uhlmann, Konrad Wagner, Sascha Augustin, Gerhard Breipohl, David W. Will, Andrea Schäfer, and Holger Wallmeier

Oligonucleotides have become increasingly important as potential therapeutics and diagnostic tools.[1, 2] When used as antisense oligonucleotides they are not only required to recognize their specific mRNA target, but also to be taken up by cells and to be nuclease-resistant.[1, 2] A plethora of modified oligonucleotide analogues with improved properties has been synthesized.[1] These modifications range from simple modifications of the phosphodiester bridge, such as phosphorothioates, to total replacement of the phosphate group,[1, 3] or even to replacement of the complete sugar–phosphate backbone, such as the "morpholino-nucleoside oligomers"[4] or the polyamide nucleic acids (PNAs).[5]

Due to their excellent binding properties the PNAs (Scheme 1) are the most interesting of the oligonucleotide analogues. Structurally PNAs consist of oligomers of *N*-(2-aminoethyl)glycine to which the nucleobases are attached by carboxymethylene units. PNAs are synthesized by condensation

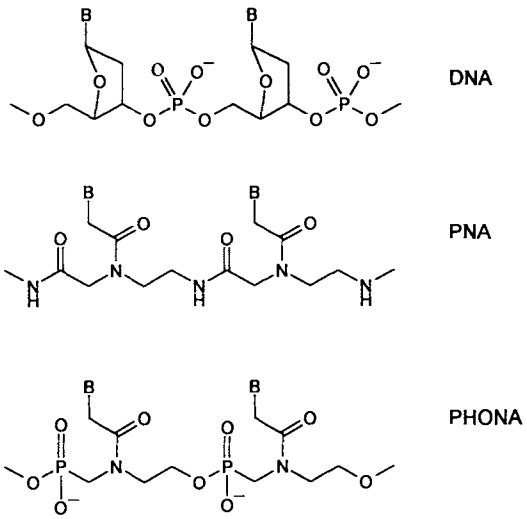

Scheme 1. Structural elements of DNA, PNA, and PHONA.

of appropriately protected monomers using peptide synthesis methodology.[5–7] As well as forming duplexes with complementary DNA, PNAs can also form extraordinarily stable $(PNA)_2$–DNA triple helices. The biggest obstacles to the use of PNAs as therapeutics are their poor water-solubility, their tendency to self-aggregate, and their insufficient cellular uptake.[5, 8]

The aim of the work described here was to synthesize a new PNA analogue with an achiral and negatively charged backbone to which the nucleobases are attached through carboxymethylene linkers. In order to maintain the strong binding to complementary nucleic acids the new structure was designed to be isosteric with PNAs, and the introduction of negative charges in the backbone should lead to improved solubility characteristics. A scaffold that fulfills the described requirements is the carboxymethylene nucleobase derivatized, *N*-(2-hydroxyethyl)aminomethylphosphonic acid ester (Scheme 1, *phos*phonic ester *n*ucleic *a*cid = PHONA). Here we describe the synthesis of a PHONA nonamer and its DNA-binding properties. Thymine was chosen as the nucleobase, as it requires no additional protecting groups.

The synthesis of the nonamer was carried out by block condensation in solution by the phosphotriester method that has been used successfully for DNA synthesis.[9] The choice of protecting groups is critical for successful oligomer synthesis. For the monomers **1a–c** the orthogonal protecting group combination of 4-methoxyphenyldiphenylmethyl (Mmt) for the hydroxyl function and 2-(4-nitrophenyl)ethyl group (NPE)[10] for the phosphonic acid was chosen (Scheme 2). Removal of the Mmt

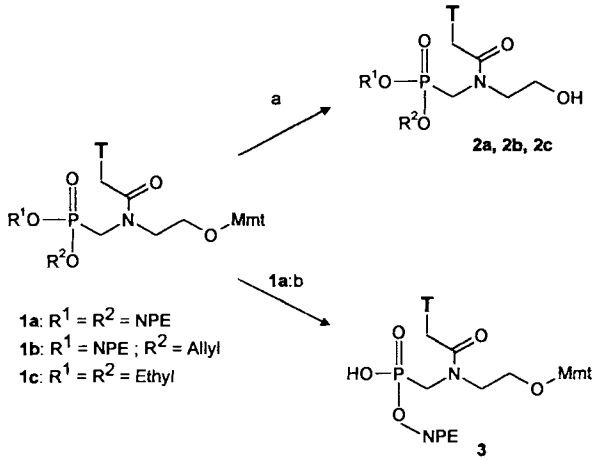

Scheme 2. Synthesis of monomers **2** and **3** from **1**. T: thymine; Mmt: 4-methoxyphenyldiphenylmethyl; NPE: 2-(4-nitrophenyl)ethyl; a) 80% AcOH, RT, 4 h, 80%; b) 0.1 M DBU, pyridine (py), 4 h, 90%.

group of compounds **1a–c** with acetic acid gave compounds **2a–c** with free hydroxyl functions. Selective cleavage of one of the two NPE phosphonic acid protecting groups of **1a** by β-elimination with 0.1 M DBU gave monomer **3**. The synthetic route to monomers **1** is shown in Scheme 3. The backbone scaffold **6** is synthesized by addition of a phosphite to the trimeric Schiff base **5**. The coupling of the carboxymethylene nucleobase is carried out analogously to PNA monomer synthesis.[6] To activate the PHONA trimer selectively during block condensation it was necessary to synthesize monomer **1b**, which contains additional orthogonal protection[11] of the phosphonic ester. The allyl phosphonic ester protection was introduced by condensation of **3** with allyl alcohol and 3-nitro-1-(*p*-toluenesulfonyl)-1*H*-1,2,4-triazole (TSNT) in pyridine.[1, 9]

The trimers **8** were synthesized by stepwise condensation of **2** with **3** (Scheme 4), again with TSNT in pyridine. The yield of isolated product was 70–90%. The allyl group of **8b** could be removed under neutral conditions with Pd^0, without loss of the Mmt or NPE groups,[11] to give the phosphonic acid monoester **9**.

The synthesis of PHONA nonamer **12** is carried out by consecutive condensation of trimer **8c** with two trimers **9** (Scheme 5). The Mmt group is removed by treatment with 80% acetic acid, and finally the NPE protecting groups are removed

[*] Dr. A. Peyman, Dr. E. Uhlmann, K. Wagner, S. Augustin, Dr. G. Breipohl, Dr. D. W. Will, Dr. A. Schäfer, Dr. H. Wallmeier
Hoechst AG, Central Pharma Research G838
D-65926 Frankfurt (Germany)
Fax: Int. code +(69)331399

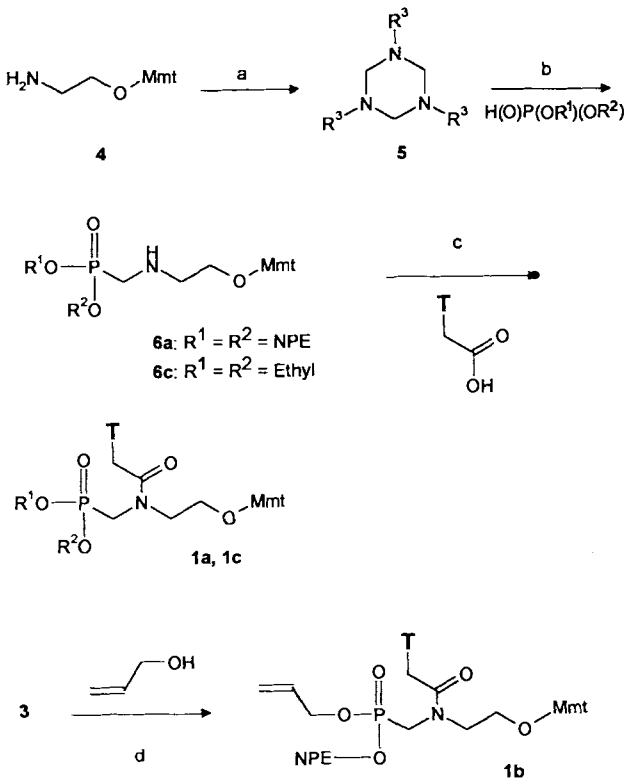

Scheme 3. Synthesis of monomers **1**; R^3: CH_2CH_2O–Mmt. a) CH_2O, MeOH, RT, 4 h, 55%; b) 100 °C, 30 min, 60%; c) thymin-1-yl acetic acid [6], hydroxybenzotriazole, *N*-ethylmorpholine, diisopropylcarbodiimide, DMF; RT, 16 h, 90%; d) 3-nitro-1-(*p*-toluenesulfonyl)-1*H*-1,2,4-triazole (TSNT), py, 95%.

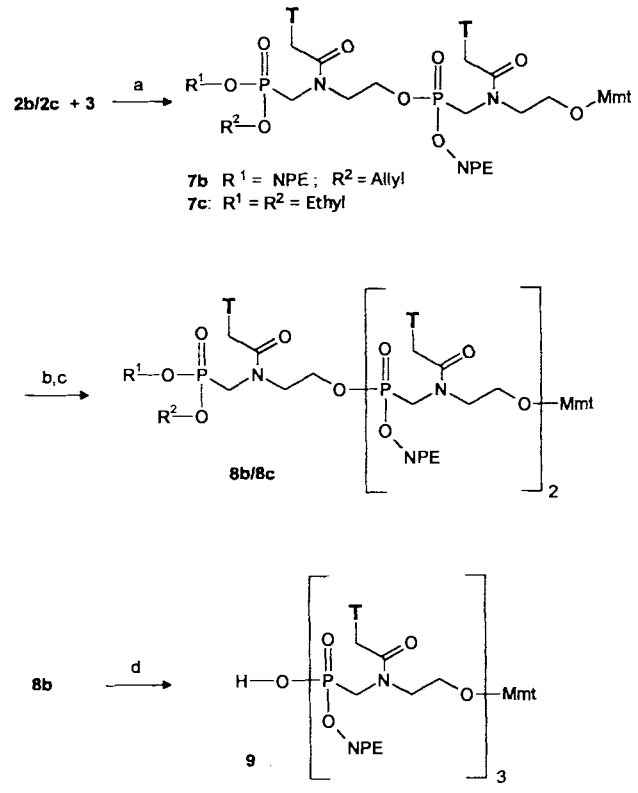

Scheme 4. Synthesis of trimer **9**; a) TSNT, py, 95%; b) 80% AcOH, RT, 4 h, 80%; c) **3a**, TSNT, py, 70%; d) Tetrakis(triphenylphosphano)palladium(0), triphenylphosphane, diethylammonium hydrogencarbonate, CH_2Cl_2, 15 °C, 30 min, 57%.

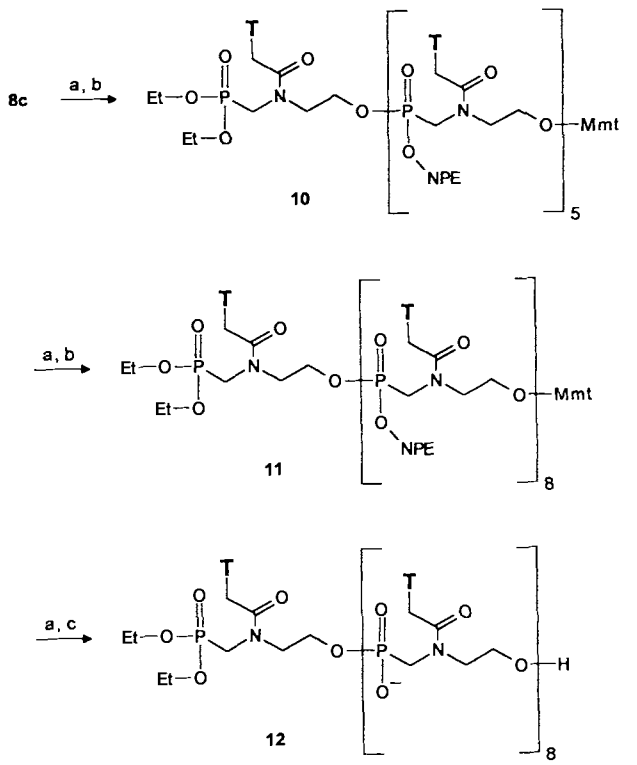

Scheme 5. Block synthesis of a PHONA nonamer (**12**) from three trimers. a) 80% AcOH, RT, 4 h, 80%; b) **9**, TSNT, py, 70%; c) 0.5 M DBU, py, 24 h, RT, 80%.

by treatment with 0.5 M DBU in pyridine. As expected the PHONA **12** is highly water-soluble and shows no tendency to self-aggregate. The purity and identity of **12** were confirmed by HPLC and mass spectrometry [ES^- (*m/z*): calcd 2803; found 2802 $(M-H)^-$].

The ability of the new oligomer to form stable hybrids with complementary DNA was investigated by UV-melting and gel-shift experiments and by mass spectrometry. Figure 1 shows the

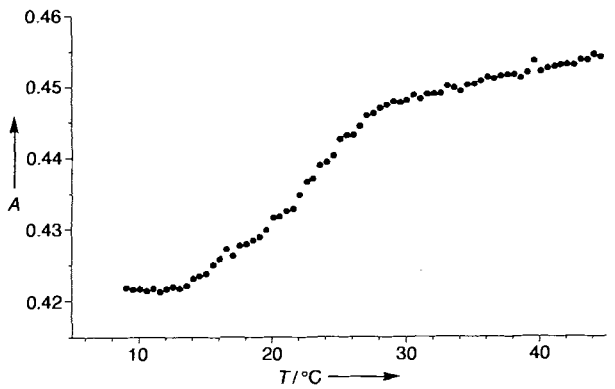

Fig. 1. UV-melting curve (λ = 260 nm) of the hybrid between **12** and $d(A_9)$: 0.15 OD **12** and 0.15 OD $d(A_9)$ in 0.7 mL buffer (1 M NaCl, 20 mM $MgCl_2$, 10 mM HEPES [= 2-(4-(hydroxyethyl)piperazin-1-yl)ethanesulfonic acid], pH 7.5); heating rate: 1 K min^{-1}; T_m of the duplex: 21 °C.

UV-melting curve of **12** with $d(A_9)$ (1:1) in 1 M NaCl at pH 7.5. A clear transition can be seen with a melting temperature T_m of approximately 21 °C. For comparison, the T_m of the corresponding DNA–DNA hybrid from $d(T_9)$ and $d(A_9)$ is 22 °C. No transition was observed on heating **12** alone. A 2:1 mixture

of **12** and $d(A_9)$ gave an identical UV-melting curve, which suggests that the stoichiometry of the hybrid is 1:1. On cooling, a clear transition was not observed, probably due to the hysteresis commonly observed for some PNA sequences.

The hybridization of **12** with $d(A_9)$ was also demonstrated in a gel-shift experiment. PHONA **12** and $d(A_9)$ were loaded on a nondenaturing polyacrylamide gel (20%, 50 mM tris(hydroxymethyl)aminomethaneborate, pH 8.0, 2 mM EDTA, 10 mM $MgCl_2$) either alone or mixed in the ratios 1:1, 1:2, 1:5, or 1:10. The gel mobility of the components was then determined at 10 °C, which is below the hybrid melting temperature. The results are shown in Figure 2: $d(A_9)$ runs faster than **12**; in the

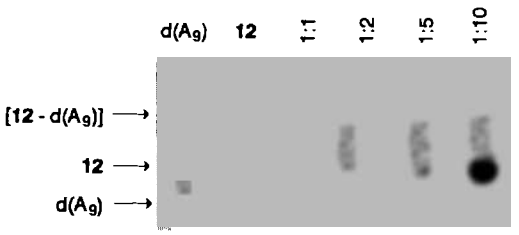

Fig. 2. Gel-shift experiment showing formation of a hybrid between $d(A_9)$ and **12**. The gel mobilities of $d(A_9)$ and **12** alone, and mixed in the ratios 1:1, 1:2, 1:5, and 1:10 (0.1 OD $d(A_9)$ and 0.1, 0.2, 0.5, and 1.0 OD **12**), were determined on a 20% nondenaturing polyacrylamide gel. (Buffer: 50 mM tris(hydroxymethyl)aminomethaneborate, pH 8.0, 2 mM EDTA, 10 mM $MgCl_2$, 10 °C).

1:1 mixture both components are difficult to see, but a slower-running band corresponding to a complex between the two components appears. In the 1:2 mixture the $d(A_9)$ band can no longer be seen, but the complex band is much stronger. The same is also true for the 1:5 and 1:10 mixtures, where the excess of **12** can clearly be seen. The results of the gel-shift experiment strongly suggest that a 1:1 PHONA–DNA hybrid is formed, since in similar experiments[12] duplex formation results in the formation of one new band, whereas triple helix formation gives two new bands, corresponding to the duplex and the triplex. It should be noted, however, that in the case of homopyrimidine PNAs, the initial PNA–DNA duplex is almost undetectable, as it immediately binds to a second PNA strand to form a $(PNA)_2$–DNA triple helix. This process, although unlikely, may also occur for PHONAs.

The **12**–$d(A_9)$ hybrid as well as the $d(T_9)$–$d(A_9)$ hybrid are also detectable by negative-ion electrospray mass spectrometry.[13] A mass of 5559.8 (calcd: 5559.9) was found for the nonameric PHONA–DNA duplex. The corresponding DNA–DNA duplex $d(T_9)$–$d(A_9)$ had a mass of 5431.4 (calcd: 5432.7). Evidence for triple helix formation was not found in this experiment.

We have described the synthesis of a new class of DNA analogues based on an achiral (2-hydroxyethyl)aminomethylphosphonic acid ester backbone. These compounds have promising binding properties to complementary DNA, and excellent water-solubility. Other important properties such as nuclease stability require further investigation. We are now extending our work to the synthesis of PHONAs with mixed base sequences.

Received: July 15, 1996 [Z9334IE]
German version: *Angew. Chem.* **1996**, *108*, 2797–2800

Keywords: antisense oligonucleotides · helices · nucleic acids

[1] E. Uhlmann, A. Peyman, *Chem. Rev.* **1990**, *90*, 543–584; *Antisense Research and Applications* (Eds.: S. T. Crooke, B. Lebleu), CRC Press, Boca Raton, FL, **1993**; *Antisense Oligonucleotides–Chemical Modifications*, E. Uhlmann, A. Peyman in *Encyclopedia of Molecular Biology and Biotechnology* (Ed.: E. Meyer), VCH, New York, **1995**; A. De Mesmaker, R. Häner, P. Martin, H. E. Moser, *Acc. Chem. Res.* **1995**, *28*, 366–374.

[2] U. Englisch, D. Gauss, *Angew. Chem.* **1991**, *103*, 629–646; *Angew. Chem. Int. Ed. Engl.* **1991**, *30*, 613–630; S. Beck, H. Köster, *Anal. Chem.* **1990**, *62*, 2258; F. C. Tenover, *Clin. Microbiol. Rev.* **1988**, *1*, 82–101.

[3] E. Uhlmann, A. Peyman in *Methods in Molecular Biology, Vol 20: Protocols for Oligonucleotides and Analogs* (Ed.: S. Agrawal), Humana Press, New Jersey, Totowa, Chapter 16, **1993**, pp. 355–389; P. E. Nielsen, *Annu. Rev. Biophys. Biomol. Struct.* **1995**, *24*, 167–183; A. De Mesmaker, K.-H. Altmann, A. Waldner, S. Wendeborn, *Curr. Opin. Struct. Biol.* **1995**, *5*, 343–355.

[4] E. P. Stirchak, J. E. Summerton, D. D. Weller, *Nucleic Acids Res. Future Dev. Proc. Symp.* **1989**, *17*, 6129–6141.

[5] B. Hyrup, P. E. Nielsen, *Bioorg. Med. Chem.* **1996**, *4*, 5–23.

[6] K. L. Dueholm, M. Egholm, C. Behrens, L. Christensen, H. F. Hansen, T. Vulpius, K. H. Petersen, R. H. Berg, P. E. Nielsen, O. Buchardt, *J. Org. Chem.* **1994**, *59*, 5767–5773.

[7] D. W. Will, G. Breipohl, D. Langner, J. Knolle, E. Uhlmann, *Tetrahedron* **1995**, *44*, 12069–12082; G. Breipohl, J. Knolle, D. Langner, G. O'Malley, E. Uhlmann, *Bioorg. Med. Chem. Let.* **1996**, *6*, 665–670.

[8] J. C. Hanvey, N. J. Peffer, J. E. Bisi, S. A. Thomson, R. Cadilla, J. A. Josey, D. J. Ricca, F. Hassman, M. A. Bonham, K. G. Au, S. G. Carter, D. A. Bruckenstein, A. L. Boyd, S. A. Noble, L. E. Babiss, *Science* **1992**, *258*, 1481–1485.

[9] C. B. Reese, *Tetrahedron* **1978**, *34*, 3143–3179.

[10] E. Uhlmann, W. Pfleiderer, *Helv. Chim. Acta* **1981**, *64*, 1688–1703.

[11] H. Kunz, C. Unverzagt, *Angew. Chem.* **1984**, *96*, 426–427; *Angew. Chem. Int. Ed. Engl.* **1984**, *23*, 436–437; Y. Hayakawa, M. Hirose, R. Noyori, *J. Org. Chem.* **1993**, *58*, 5551–5555.

[12] R. G. Shea, P. Ng, N. Bischofberger, *Nucleic Acid Res. Future Dev. Proc. Symp.* **1990**, *18*, 4859–4866; T. L. Trapane, R. I. Hogrefe, M. A. Reynolds, L.-S. Kan, P. O. P. Ts'O, *Biochemistry* **1996**, *35*, 5495–5508.

[13] B. Ganem, Y.-T. Li, J. D. Henion, *Tetrahedron Lett.* **1993**, *34*, 1445–1448.

Are the Most Stable Fused Heterobicycles the Most Aromatic?**

Govindan Subramanian, Paul von Ragué Schleyer,* and Haijun Jiao

The quantitative relationships among the magnetic, energetic, and geometric criteria of aromaticity have been demonstrated recently for a wide ranging set of five-membered heterocycles.[1] However, we emphasize here that these three criteria also can deviate strongly[2] when other influences are important. This is shown by our theoretical investigations on the positional isomers of furanofuran (**1a–d**), thienothiophene (**2a–d**), benzofuran (**3a,b**), and benzothiophene (**4a,b**). According to the topological charge stabilization rule,[3] the best placement of electronegative heteroatoms is at the positions with the greatest charge in the isovalence-electronic and isostructural hydrocarbons, for example, the pentalene dianion (**I**) and indenyl anion (**II**, Scheme 1). Such placements can give lower energies, but lead to less symmetrical geometries and decreased aromaticity.

Thus, the stability orders of the furanofuran (**1a** > **1b** > **1c** > **1d**) and thienothiophene positional isomers (**2a** > **2b** > **2c** > **2d**) based on the topological rule[3] are verified by our Becke3LYP/6-311+G** relative energies (Table 1 and Fig. 1).[5] Similarly, the relative energies of benzofuran (**3a,b**)

[*] Prof. P. von R. Schleyer, Dr. G. Subramanian, Dr. H. Jiao
Computer-Chemie-Centrum
Institut für Organische Chemie
Universität Erlangen-Nürnberg
Henkestrasse 42, D-91054 Erlangen (Germany)
Fax: Int. code +(9131)85-9132
e-mail: pvrs@organik.uni-erlangen.de

[**] Support from the Fonds der Chemischen Industrie, the Deutsche Forschungsgemeinschaft, the Volkswagen-Stiftung, and the Convex Computer Corporation is acknowledged with appreciation. G. S. thanks the Alexander-von-Humboldt Stiftung for a postdoctoral fellowship. We also thank Dr. M. Hofmann (Erlangen) and Prof. A. R. Katritzky (Gainesville, FL, USA) for helpful discussions.

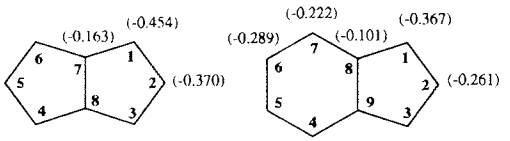

$C_8H_6^{2-}$ **I**, D_{2h} $C_9H_7^-$ **II**, C_{2v}

Scheme 1. The hydrocarbon analogues **I** and **II** of the fused heterobicycles studied in this work. The charges calculated according to a natural population analysis [4] are given in parentheses.

and benzothiophene (**4a,b**) isomers follow the charge density pattern of the indenyl anion (**II**).

While no experimental or theoretical study is available for **1a–d**, various early π-electron treatments have been used to assess the aromaticity in **2–4**. Dewar and Trinajstic's[6] resonance energy (DRE) evaluation of the thienothiophene (**2a–d**) and the benzothiophene isomers (**4a,b**) (Table 1), suggested that **2d** is a very unstable antiaromatic compound. Further, they predicted that the thiophene ring in **4b** should destroy the aromaticity of the benzene moiety, whereas both the rings in **4a** should retain their aromaticity.[6] Earlier, Gimarc[3] showed that the qualitative stability ordering of the isomers of **2–4** follows the same trend as the Hess–Schaad resonance energies (HSRE),[7] the topological resonance energies (TRE) of Gutman et al.,[8] and DRE.[6] Hess et al.[7] concluded that the furan

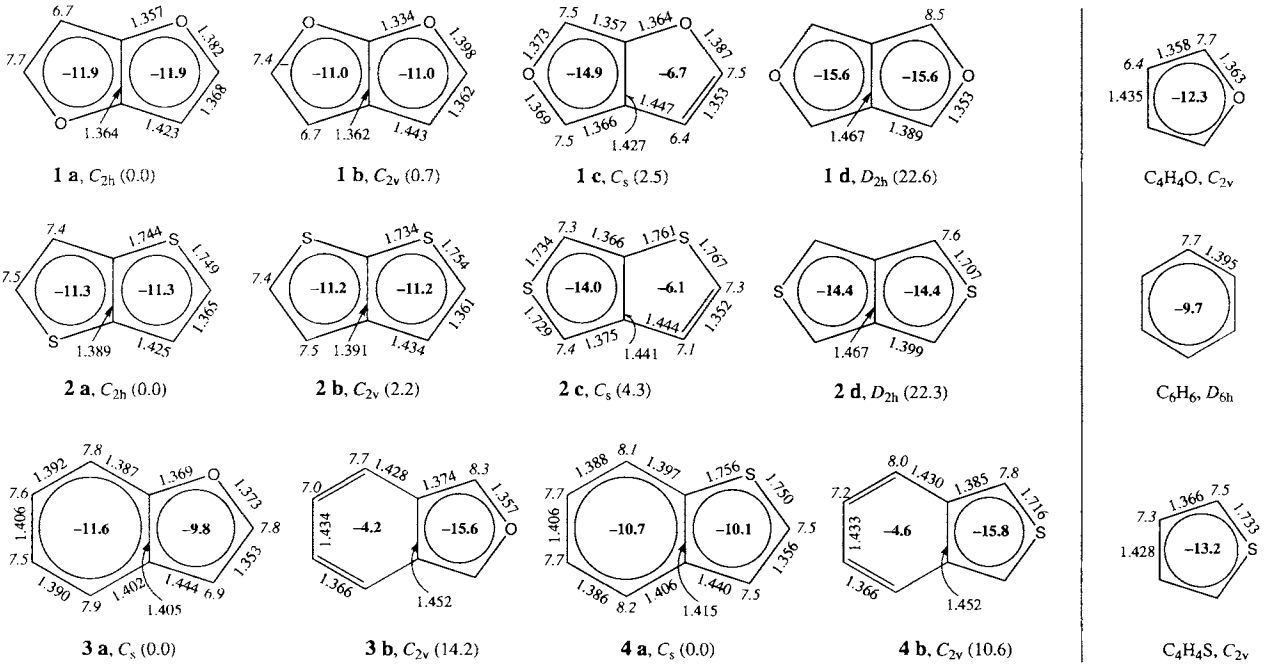

Fig. 1. Relative energies [kcal mol^{-1}] at the Becke3LYP/6-311+G**//Becke3-LYP/6-311+G** level (in parentheses), bond lengths [Å] at the Becke3LYP/6-311+G** level, computed ^{1}H NMR chemical shifts at the GIAO-HF/6-31+G*//Becke3LYP/6-311+G** level (in italics), and NICS values computed in the geometrical centers of individual rings at the GIAO-HF/6-31+G* level (in boldface) for **1–4** and for the reference monocycles furan, benzene, and thiophene (right-hand column).

Table 1. Various criteria and indices of aromaticity for the fused heterobicycles **1–4** and for their component monocyclic parts.

Molecule	ΔE[a]	χ[b]	χ_{anis}[c]	DRE[d]	HSRE[e]	TRE[f]	η[g]	$\Delta\chi$[h]	χ_r[i]	BAI[j]	ΣNICS[k]
furan		−37.9		4.3	0.042	0.042	0.650			41.8	−12.3
thiophene		−50.5		6.5	0.192	0.198	0.796			56.4	−13.2
benzene		−51.3		22.6	0.390	0.276	1.000			100.0	−9.7
I		−73.6	−98.5			0.460				94.0	−24.2
II		−82.3	−115.9			0.400				84.7	−25.6
1a	0.0	−57.4	−59.6					3.6	0.76	41.4	−23.8
1b	0.7	−57.7	−56.3					3.3	0.76	39.4	−22.0
1c	2.5	−56.1	−53.0					4.9	0.74	37.7	−21.6
1d	22.6	−61.0	−84.1					0.0	0.80	53.9	−31.2
2a	0.0	−81.9	−77.2	11.3	0.240	0.310	0.644	6.5	0.81	52.9	−22.6
2b	2.2	−80.7	−75.3	10.5	0.220	0.310	0.778	7.7	0.80	52.7	−22.4
2c	4.3	−79.7	−67.4	5.9	0.150	0.260	0.564	8.7	0.79	48.5	−20.1
2d	22.3	−88.4	−97.3	−33.9		0.040	0.292	0.0	0.88	75.3	−28.8
3a	0.0	−72.6	−97.6		0.360	0.270	0.676	0.0	0.81	57.0	−21.4
3b	14.2	−67.6	−87.0		0.020	0.110	0.324	5.0	0.76	58.2	−19.8
4a	0.0	−83.3	−104.9	24.8	0.440	0.350	0.695	0.0	0.82	62.6	−20.8
4b	10.6	−82.3	−100.5	9.3	0.250	0.290	0.448	1.0	0.81	69.4	−20.4

[a] Relative energies of isomers [kcal mol^{-1}] (Becke3LYP/6-311+G**+ZPE (Becke3LYP/6-311+G**; all structures are minima)). [b] Magnetic susceptibilities [ppm cgs] at CSGT-HF/6-31+G*//Becke3LYP/6-311+G**. [c] Anisotropy of the magnetic susceptibility [ppm cgs] at CSGT-HF/6-31+G*//B3LYP/6-311+G**. [d] In kcal mol^{-1}, taken from ref. [6]. [e] In units of β, taken from ref. [7]. [f] In units of β, taken from ref. [8]. [g] In units of $-\beta$, taken from ref. [9]. [h] Relative magnetic susceptibilities [ppm cgs]. [i] $\chi_r = (\chi_{bicycle}/\sum\chi_{monocycle})$. [j] Calculated with Becke3LYP/6-311+G** optimized geometries. [k] At GIAO-HF/6-31+G*//Becke3LYP/6-311+G**. NICS is the negative of the magnetic shieldings that can be computed easily, for example at the ring centers.

ring in **3a** is not aromatic, because the total resonance energy of **3a** (0.356 β) was close to that of benzene (0.39 β). Similarly, **2d** and **3b** were claimed to be nonaromatic, since their resonance energies were very low (Table 1).[7, 8] Recently, Zhou and Parr[9] justified the use of absolute hardness (η) as an indicator of aromaticity by correlations with TRE and HSRE (Table 1). However, the reliability of the semiempirical DREs, HSREs, and TREs have never been verified. For example, in contradiction to the conclusion deduced from the HSRE,[7] Warrener[10] concluded from the experimental ^{1}H NMR chemical shifts that **3b** possesses a strong diamagnetic ring current, typical for 10π-electron, planar Hückel arenes. Similarly, Bird's Aromaticity Index (BAI),[11] evaluated from the bond lengths, indicates that **2d** is more aromatic than **2a**,[12] in disagreement with DRE,[6] TRE,[8] and η.[9]

We have reevaluated the BAIs[13] (Table 1) using Becke3LYP/6-311+G** geometries throughout (Fig. 1). In agreement with Bird's earlier findings concerning **2d**,[12] **1d** and **2d** have the largest BAIs, followed by **1a** > **1b** > **1c** and **2a** > **2b** > **2c**. Similarly, the aromaticity of **3b** is greater than that of **3a**[2b, 11] and **4b** is more aromatic than **4a**. Thus, according to the geometric criterion the least stable positional isomers, **1d**, **2d**, **3b**, and **4b**, should be the most aromatic.

Anisotropies and exaltations of the magnetic susceptibility, as well as abnormal ^{1}H NMR chemical shifts, are effective aromaticity criteria in a wide range of molecules.[14–17] The computed ^{1}H NMR chemical shifts (GIAO-HF/6-31+G*//Becke3LYP/6-311+G**)[18] of the various positional isomers (**1**–**4**, Fig. 1) correspond closely to the ^{1}H NMR data for furan, thiophene, and benzene. This strongly suggests that all these bicyclic systems retain significant aromaticity.

The relative aromaticities of **1**–**4**, characterized by comparing their magnetic susceptibilities ($\Delta\chi$) and anisotropies (χ_{anis}), computed at CSGT-HF/6-31+G*,[19] show the least stable forms, **1d** and **2d**, to be the most strongly aromatic (Table 1), in striking contrast to the earlier conclusions on **2d** based on DRE,[6] TRE,[8] and η.[9] However, the relative energies (ΔE) and $\Delta\chi$ of **2a**–**c**, **3a** vs. **3b**, and **4a** vs. **4b** agree roughly with DRE, HSRE, and TRE, but not with BAI for the benzo-fused molecules (Table 1).

The most stable positional isomers (e.g., **1a**, **2a**) need not have the largest aromatic or resonance stabilization. Thermodynamic stability is influenced by strain and many other effects besides aromaticity. Aromaticity is best associated with cyclic electron delocalization and can be revealed most directly by the magnetic criteria.[1, 15–17] The aromaticity ratio (χ_r) of **1**–**4**, based on $\sum\chi$(monocycles) is given in Table 1. The substantial χ_r values of **1**–**4**, varying between 0.74 (**1c**) to 0.88 (**2d**), demonstrate that both rings in **1**–**4** contribute to the aromaticity. This contradicts many of the earlier conclusions on the aromaticity of **2d**, **3a**, **3b**, and **4a**, **4b** (Table 1).[6–9]

Resonance energies and magnetic susceptibilities are measures of the overall aromaticity of a polycycle, but do not provide information about the individual rings. However, the two annelated rings in **1**–**4**, unless related by symmetry, do not contribute to the overall aromaticity to the same extent. Further, the resonance energies of polycyclic aromatics are not the sum of the component rings.[20] Our new magnetic criterion, NICS (Nucleus Independent Chemical Shift),[1c, 17] provides an effective and simple way to assess the aromaticity of individual rings in the polycyclic systems (Fig. 1).

The five-membered rings of **1d**, **2d**, **3b**, and **4b**, and the six-membered rings of **3a** and **4a** have larger NICS values (greater aromaticity) than the corresponding monocycles. As indicated by the schematic representation in Figure 1, one of the rings of **1c**, **2c**, **3b**, and **4b** is weakly aromatic (NICS is less than half that of the corresponding monocycles), whereas the second ring in each case has a somewhat enhanced NICS value. Furthermore, the sum of the NICS values of the two rings along the **1a**–**c** and the **2a**–**c** series (Table 1) are less than twice the NICS values of furan and of thiophene, respectively. The NICS trends of the positional isomers agree qualitatively with the magnetic susceptibility data ($\Delta\chi$ and χ_r, as well as χ_{anis}) and with BAI (except for the benzo-fused isomers), and contradict many of the earlier conclusions based on, for instance, π-electron treatments.[6–9]

In conclusion, we have demonstrated that there need not be any direct relationship between the thermodynamic stability of heterobicyclic isomers and their aromaticity. The aromatic character in **1**–**4** is delineated by the ^{1}H NMR chemical shifts, the relative magnetic susceptibilities ($\Delta\chi$ and χ_r) and anisotropies (χ_{anis}), the NICS values and, less uniformly, by the geometric parameters (BAI). Our results quantify the rule of topological charge stabilization,[3] but refute many other earlier conclusions, for example, that **2d** is "antiaromatic" and the furan ring in **3a** is "not aromatic".[6–9] Hence, the reliability of DRE, TRE, HSRE, and the hardness concept as aromaticity indices in such fused bicyclics is questioned strongly. In contrast, the NICS criterion appears to function well as a general and quantitative measure for delineating the aromaticity of individual rings in polycyclic frameworks.

Received: July 5, 1996 [Z 9300 IE]
German version: *Angew. Chem.* **1996**, *108*, 2824–2827

Keywords: ab initio calculations · aromaticity · condensed rings · heterobicycles

[1] a) P. von R. Schleyer, P. K. Freeman, H. Jiao, B. Goldfuss, *Angew. Chem.* **1995**, *107*, 332–335; *Angew. Chem. Int. Ed. Engl.* **1995**, *34*, 337–340; b) H. Jiao, P. von R. Schleyer in *AIP Conference Proceedings 330, E. C. C. C. 1, Computational Chemistry* (Eds.: F. Bernardi, J.-L. Rivail), American Institute of Physics, Woodbury, NY, **1995**, pp. 107–131 and refs. [16, 17]; c) P. von R. Schleyer, C. Maerker, A. Dransfeld, H. Jiao, N. J. R. van Eikema Hommes, *J. Am. Chem. Soc.* **1996**, *118*, 6317–6318.

[2] a) A. R. Katritzky, P. Barczynski, G. Musumarra, D. Pisano, M. Szafran, *J. Am. Chem. Soc.* **1989**, *111*, 7–15; b) A. R. Katritzky, V. Feygelman, G. Musumarra, P. Barczynski, M. Szafran, *J. Prakt. Chem.* **1990**, *332*, 870–884.

[3] B. M. Gimarc, *J. Am. Chem. Soc.* **1983**, *105*, 1979–1984.

[4] a) A. E. Reed, F. Weinhold, *Chem. Rev.* **1988**, *88*, 899–926; b) A. E. Reed, P. von R. Schleyer, *J. Am. Chem. Soc.* **1990**, *112*, 1434–1445.

[5] a) Gaussian 94: M. J. Frisch, G. W. Trucks, H. B. Schlegel, P. M. W. Gill, B. G. Johnson, M. A. Robb, J. R. Cheeseman, T. Keith, J. A. Petersson, J. A. Montgomery, K. Raghavachari, M. A. Al-Laham, V. G. Zakrzewski, J. Y. Ortiz, J. B. Foresman, J. Cioslowski, B. B. Stefanov, A. Nanayakkara, M. Challacombe, C. Y. Peng, P. Y. Ayala, W. Chen, M. W. Wong, J. L. Andres, E. S. Replogle, R. Gomperts, R. L. Martin, D. J. Fox, J. S. Binkley, D. J. DeFrees, J. Baker, J. J. P. Stewart, M. Head-Gordon, C. Gonzalez, J. A. Pople, Gaussian Inc., Pittsburgh, PA, **1995**; b) W. Hehre, L. Radom, P. von R. Schleyer, J. A. Pople, *Ab Initio Molecular Orbital Theory*, Wiley, New York, **1986**; c) J. B. Foresman, Æ. Frisch, *Exploring Chemistry with Electronic Structure Methods: A Guide to using Gaussian*, Gaussian Inc., Pittsburgh, PA, **1993**.

[6] M. J. S. Dewar, N. J. Trinajstic, *J. Am. Chem. Soc.* **1970**, *92*, 1453–1459.

[7] B. A. Hess, Jr., L. J. Schaad, C. W. Holyoke, Jr., *Tetrahedron* **1972**, *28*, 3657–3667, *ibid.* **1975**, *31*, 295–298.

[8] I. Gutman, M. Milun, N. Trinajstic, *J. Am. Chem. Soc.* **1977**, *99*, 1692–1704.

[9] Z. Zhou, R. G. Parr, *J. Am. Chem. Soc.* **1989**, *111*, 7371–7379.

[10] R. N. Warrener, *J. Am. Chem. Soc.* **1971**, *93*, 2346–2348.

[11] C. W. Bird, *Tetrahedron* **1985**, *41*, 1409–1414; *ibid.* **1986**, *42*, 89–92; *ibid.* **1992**, *48*, 335–340.

[12] C. W. Bird, *Tetrahedron* **1987**, *43*, 4725–4730.

[13] Definition of BAI: BAI = $100(1 - V/V_k)$, where V_k is chosen to be 35.0 [11, 12] and $V = 100/\tilde{N}[(\sum(N_n - \tilde{N})^2/n]^{0.5}$. $\tilde{N}$ is the arithmetic mean n of the various ring bond orders N_n. A bond order N is calculated from the corresponding bond length R from the equation $N = a/R^2 - b$, where a and b are constants [11].

[14] V. I. Minkin, M. N. Glukhovtsev, B. Y. Simkin, *Aromaticity and Antiaromaticity*, Wiley-Interscience, New York, **1994**, and references therein.

[15] a) J. A. Elvidge, L. M. Jackman, *J. Chem. Soc.* **1961**, 859–866; b) H. J. Dauben, Jr., J. D. Wilson, J. L. Laity in *Non-Benzenoid Aromatics, Vol. 2* (Ed.: J. P. Snyder), Academic Press, New York, **1971**; c) U. Fleischer, W. Kutzelnigg, P. Lazzeretti, V. Mühlenkamp, *J. Am. Chem. Soc.* **1994**, *116*, 5298–5306.
[16] a) P. von R. Schleyer, H. Jiao, *Pure Appl. Chem.* **1996**, *68*, 209–218; b) H. Jiao, N. J. R. van Eikema Hommes, P. von R. Schleyer, A. de Meijere, *J. Org. Chem.* **1996**, *61*, 2826–2828.
[17] H. Jiao, P. von R. Schleyer, *Angew. Chem.* **1996**, *108*, 2548–2551; *Angew. Chem. Int. Ed. Engl.* **1996**, *35*, 2383–2386.
[18] K. Wolinski, J. F. Hinton, P. Pulay, *J. Am. Chem. Soc.* **1990**, *112*, 8251–8260.
[19] a) T. A. Keith, R. F. W. Bader, *Chem. Phys. Lett.* **1992**, *194*, 1–8; b) R. F. W. Bader, T. A. Keith, *J. Chem. Phys.* **1993**, *99*, 3683–3693.
a) E. Clar, *Polycyclic Hydrocarbons*, Academic Press, New Yorl
T. M. Krygowski, M. Cyranski, *Tetrahedron* **1996**, *52*, 1713–1722.

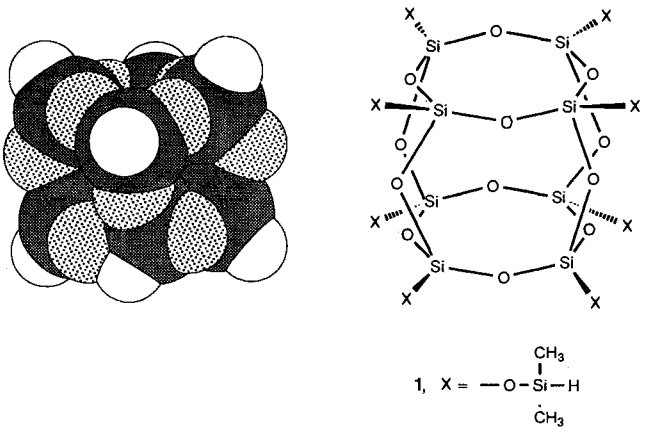

Fig. 1. The structure of octasilsesquioxane **1** (right) and the space-filling model of the minimum energy (at 0 K in the gas phase) conformation of the cubic unit (left, X = H).

Liquid-Crystalline, Substituted Octakis-(dimethylsiloxy)octasilsesquioxanes: Oligomeric Supermolecular Materials with Defined Topology**

Georg H. Mehl* and John W. Goodby

Oligomeric liquid-crystalline materials, which form a distinct class of supramolecular mesogens, have become interesting subjects of research in recent years, because they combine properties of low molar mass liquid crystals, for example low viscosity and fast response to external stimuli, with those of polymers, for example mechanical stability and robustness. However, the physical properties of oligomeric liquid crystals have been found to depend strongly on the degree of polymerization and dispersity. Consequently, greater interest is now being paid to well-defined, discrete molecular systems comprising simple dimers, trimers, tetramers...to dendrimers.

The possibility of synthesizing oligomeric liquid crystals with defined topological, configurational, and conformational features has, until now, centered mainly on the use of small cyclic or tetrahedral systems as the central core units.[1, 2, 3–5] Thus, the concept of utilizing a cuboid silsesquioxane as the core unit in a mesogenic material (Fig. 1) provides a novel approach to oligomeric liquid crystals of defined structure. This core unit can be used as a basic building block for the creation of interesting classes of monodispersed materials with defined topologies, which are essentially supermolecules that reside structurally between simple dimers or trimers and complex dendrimers.[6]

Conveniently, families of cuboid liquid crystals can be prepared by a convergent synthetic route that combines an octa-substituted variant of the core with an appropriately substituted olefinic mesogenic unit. The octa-substituted core was obtained by the reaction of tetramethylammonium silicate with dimethylchlorosilane,[7a–c] which yielded compound **1** (Fig. 1). 4′-ω-Alkenyl-4-cyanobiphenyls were prepared according to published methods and employed as the mesogenic substrates in preparation of the cubic oligomers (Fig. 2).[5]

Initial coupling experiments between the core unit and the mesogenic substrates, with dicyclopentadienylplatinum and Speier's catalyst (H_2PtCl_6) as the catalysts, led to incomplete

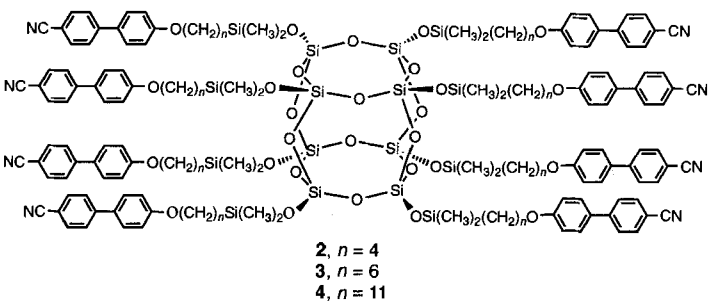

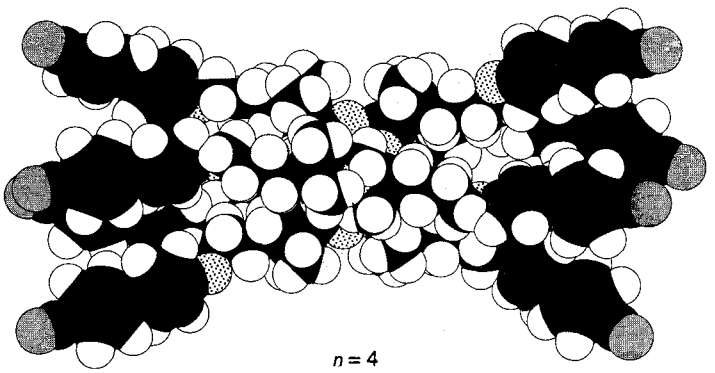

Fig. 2. Structure of the liquid-crystalline materials **2** to **4**, the space-filling model of compound **2** demonstrating the alignment of the mesogenic side chains.

substitution of the hydrogen atoms at the peripheral Si–H groups of the core. The targeted products were obtained, however, by hydrosylations in toluene at room temperature with Karstedt's catalyst.[8] These reactions gave complete substitution of the eight Si–H groups. The replacement of these groups was monitored by the disappearance of the Si–H bands in the IR spectra at 2142 cm^{-1} and by the disappearance of the peak at $\delta = 4.7$ in the ^1H NMR spectrum. The absence of peaks in the vicinity of $\delta = 2.0$ in the ^1H NMR spectra was indicative (within experimental error) of complete α-addition of the hydridosilicones to the vinyl groups. The addition of a small amount of triphenylphosphane was used in these reactions to convert the catalyst into a less reactive platinum–triphenylphosphane complex. This technique allowed for a controlled termination of the reaction. Furthermore, upon precipitation into methanol the platinum–triphenylphosphine complex remained in solution, which allowed for the easy isolation of products. Consequently,

[**] We thank the EPSRC and the DRA (Malvern) for their financial support and Dr. I. M. Saez for helpful discussions on the chemistry of organometallic materials. We acknowledge Dr. D. Ewing and Mrs. B. Worthington for spectroscopic analyses.

the final products were not colored by platinum residues. The monodispersities of the products were confirmed by GPC analysis with polystyrene standards. The single peaks were calculated to have M_w/M_n values of 1.00 to 1.01 for each material. The occurrence of a signal at $\delta = -108.8$ in the ^{29}Si NMR spectra indicated that the silicon atoms bound to four oxygen atoms were totally substituted and in a symmetrical environment. The singlet with a chemical shift at $\delta = 12.34$ is typical for the dimethylalkylsiloxy group. These results were matched by high resolution ^1H NMR spectra, which is not usually the case for oligomeric materials.

Calorimetric studies reveal that the final products **2**–**4** exhibit liquid crystal phases. The values for the transition temperatures, and the associated enthalpies and entropies for the second heating cycles of each compound are listed in Table 1. Thermal polarized light transmission microscopy reveals the formation of a

Table 1. The transition temperatures [°C] and enthalpic data (ΔH [$J g^{-1}$], ΔC_p [$J g^{-1} K^{-1}$]) obtained for compounds **2** to **4**. S_1, S_2, S_3 are smectic or soft crystalline phases.

Cmpd	Spacer length	T_g [°C] {ΔC_p [$J g^{-1} K^{-1}$]}	Transitions [°C] {ΔH [$J g^{-1} K^{-1}$]}	$\Delta S_{mol}/R$
2	4	11.0 {0.22}	S_A 93.9 {4.31} Iso	4.35
3	6	3.0 {0.32}	S_1 22.5 {0.19} S_A 116.5 {5.40} Iso	5.50
4	11	−7.5 {0.28}	Cr 34.4 {10.2} S_2 54.6 {0.77} S_3 64.5 {1.20} S_A 128.5 {8.66} Iso	9.68

focal-conic defect texture, with hyperbolic and elliptical lines of optical discontinuity, as each material is cooled from the amorphous liquid into the liquid-crystalline state. These observations classify the high-temperature, liquid-crystalline phase of each material as smectic A. Mechanical shearing of the specimens in the microscope shows that the high-temperature mesophase flows easily and has a relatively low viscosity. In addition, the short time required to form focal-conic defect textures on cooling from the isotropic liquid indicates that the compounds have properties more in keeping with low molar mass materials than polymers.

Increasing the number of methylene units in the spacer chain between the biphenyl moiety and the core units from four to eleven carbon atoms results in an increase of the isotropization temperature from 93.9 to 128.5 °C. In addition, the size of the enthalpy peak also increases with increasing spacer length, which suggests that the molecules are more ordered within the liquid-crystalline phase. This conjecture is supported by the increase in the calculated reduced molar entropy ($\Delta S_{mol}/R$), from 4.35 to 9.68, as the series is ascended. Moreover, the injection of a higher ordered smectic phase close to the glass transition in compound **3**, and the occurrence of two soft crystalline phases and a crystalline phase in **4** indicates a strong increase in ordering of the molecules with increasing spacer length. On a molecular level this can be explained by the increasing separation of the mesogenic cyanobiphenyl groups from the core. Stronger intramolecular interactions between the mesogenic groups are favored as the spacer length is increased (Fig. 2), thereby enhancing the mesomorphic properties as the series is ascended.

Materials **2** and **3** exhibit glass transition transitions in the region of 11.0 and 3.0 °C, for which the values of the specific heats (0.22 and 0.32 $J g^{-1} K^{-1}$, respectively) were found to be similar. The decrease of the value of the glass transition temperature with increasing spacer length is attributed to the plastifying effect of the aliphatic spacers. This is supported by the fact that the glass transition temperature for compound **4** is the lowest of all at −7.5 °C.

The high-temperature liquid-crystalline phase of each material showed an X-ray diffraction pattern that was obtained from fiber samples recorded in Lindemann tubes and found to be typical of the smectic A phase.[5] The X-ray spacings found are listed in Table 2. Compound **4**, as well as the other final products, showed a diffuse, wide angle halo at 4.5 Å typical for the

Table 2. The *d* spacings [Å] determined by X-ray diffraction for compounds **2** to **4**.

Cmpd	Spacer length	T [°C]	*d* [Å]			
2	4	25.0	4.5	11.3	–	32.2
3	6	25.0	4.5	12.0	17.6 [a]	35.4 [a]
4	11	75.0	4.5	13.2	21.6	43.1
4	11	85.0	4.5	13.2	21.4	42.8
4	11	100.0	4.5	13.2	21.3	42.8
4	11	110.0	4.5	13.2	21.0	42.1
4	11	120.0	4.5	13.2	21.0	42.1
4	11	125.0	4.5	13.2	21.0	42.1

[a] Reflections are very weak.

lateral distance between mesogenic units and a diffuse reflection at 13.2 Å, which was attributed to the periodicity of the arrangement of the silicone cores.[1, 2, 5] At 125.0 °C pointlike small-angle reflections at 42.1 and 21.0 Å corresponding to the values for the first- and second-order reflections of the smectic layers were observed. The small increase in the lattice dimensions at lower temperatures was attributed to a decrease in the disordering of the structures of the molecules as the molecules themselves become more ordered within the layers as the temperature falls. Materials **2** and **3** exhibit similar behavior; however, a decrease in the lattice dimensions was found to occur with shortening of the spacer unit. Additionally the layer reflections become very weak for **3**, and for **2** the second order reflection is lost altogether. The structures of the crystal or soft crystalline phases S_1, S_2, and S_3 occurring for compounds **3** and **4** will be the subject of a seperate report.

These results are consistent with a structure in which the silicone cores are located in the central regions of the layers and the terminal cyanobiphenyl groups overlap somewhat.[5, 9] This classifies the high-temperature smectic phase as an S_{Ad} phase.

The isotropization temperatures of the materials were lower than those of comparable linear siloxanes bearing mesogenic side-chains of similar structure.[10] Materials with analogous tetrahedral or cyclic siloxane cores are found to have similar isotropization temperatures and higher glass transition temperatures, but to exhibit less rich polymorphism.[5, 1, 9, 11] Thus the results obtained for the octasilsesquioxanes are intermediate between those of linear polymers and the smaller tetramers and cyclic systems. This outcome is not too surprising, since, in principle, octasilsesquioxanes can be viewed as twinned tetrahedrons or doubled four-membered cyclic rings.

Experimental Procedure

The equipment and techniques used to evaluate material structures and purities, and to determine mesophase behavior have been described elsewhere [5].

1: Tetramethylammonium silicate (4.7 g, 0.05 mol) was added as a 10% aqueous solution to a solution of heptane (100 mL), dimethylformamide (200 mL), and chlorodimethylsilane (100 mL) that had been previously stirred for 20 min. The weakly exothermic reaction was then cooled slowly to 4 °C, and 1 L of water at 4 °C was added slowly. The organic phase was separated from the aqueous phase and

 © VCH Verlagsgesellschaft mbH, D-69451 Weinheim, 1996 0570-0833/96/3522-2642 $ 15.00+.25/0

washed with water until acid free. The organic solution was concentrated by evaporation under reduced pressure, and the resulting mixture was cooled to 4 °C to facilitate the precipitation of **1** as a white solid, which was isolated after purification by recrystallization from acetone. Yield 1.48 g (73.8%). Spectroscopic data: IR (KBr): $\tilde{\nu}$ = 2960 (C–H), 2142 (Si–H); ^{1}H NMR (270 MHz, $CDCl_3$, TMS): δ = 4.7 (s, 1H, SiH), 0.2 (s, 6H, $SiCH_3$), ^{29}Si NMR (53.5 MHz, $CDCl_3$, TMS): δ = 0.5 ($HSiCH_3$), –108.8 ($Si(O)_4$).

2: A solution of toluene (20 mL), 4-cyano-4′-(5-hexenyloxy)biphenyl) (0.55 g, 1.58 mmol), and 10 μL of a 3.0–3.5% solution of Karstedt's catalyst dissolved in xylene was prepared. The solution was gently aerated for 20 s, and then a solution of **1** (0.1 g, 0.098 mmol) in dry toluene (10 mL) was added dropwise at room temperature over a period of 1 h. A few minutes after the addition was complete, no Si–H band (2142 cm^{-1}) could be detected in the IR spectrum. A spatula tip of triphenylphosphane was added to convert the catalyst into the less reactive triphenylphosphane complex, and the solution was concentrated under reduced pressure. The oligomeric material was isolated by precipitation in methanol. The product was separated by filtration and purified by repetitive precipitation from methanol until no monomer could be detected by chromatographic methods. Recrystallization from pentane/dichloromethane yielded 0.31 g of **2** (85% yield). Spectroscopic data: IR (KBr): $\tilde{\nu}$ = 3020 (Ar–H), 2940 (C–H), 2220 (C≡N), 1600 (Ar), 860 (C–H) cm^{-1}; ^{1}H NMR (270 MHz, $CDCl_3$, TMS): δ = 7.65 (m, 4H, ArH), 7.52 (m, 2H, ArH), 6.95 (m, 2H, ArH), 3.93 (t, 2H, $ArOCH_2$), 1.75 (m, 2H, OCH_2CH_2), 1.45 (m, 6H, $CH_2CH_2CH_2$), 0.62 (t, 2H, t, CH_2Si), 0.14 (s, 6H, CH_3Si); ^{13}C NMR (67.8 MHz, $CDCl_3$): δ = 0.01 (CH_3Si), 18.14 (CH_2Si), 23.49, 26.31, 24.78, 33.75, ($CH_2CH_2CH_2$), 110.82 (aryl C4′, CCN), 115.19 (aryl C3, C5), 126.89, 128.48 (aryl C2, C6, C2′, C6′), 131.56 (aryl C1), 132.49 (aryl C3′, C5′), 144.71 (aryl C1′), 160.11 (aryl C4, OC), 118.87 (CN); ^{29}Si NMR (53.5 MHz, $CDCl_3$, TMS): δ = 12.34 ($SiCH_3$), –108.8 ($Si(O)_4$).

Received: April 22, 1996 [Z 9060 IE]
German version: *Angew. Chem.* **1996**, *108*, 2791–2793

Keywords: liquid crystals · mesophases · silicon compounds

[1] F.-H. Kreuzer, D. Andrejewski, W. Haas, N. Häberle, G. Riepl, P. Spes, *Mol. Cryst. Liq. Cryst.* **1991**, *199*, 345, and references therein; R. D. C. Richards, W. D. Hawthorne, J. S. Hill, M. S. White, D. Lacey, J. A. Semlyn, G. W. Gray, T. C. Kendrick, *J. Chem. Soc. Chem. Commun.* **1990**, 95.

[2] T. J. Bunning, H. E. Klei, E. T. Samulski, R. L. Crane, R. J. Linville, *Liq. Cryst.* **1991**, *10*, 445; B. Hahn, V. Percec, *Mol. Cryst. Liq. Cryst.* **1988**, *157*, 125; M. Schellhorn, G. Lattermann, *Liq. Cryst.* **1994**, *17*, 529.

[3] R. Eidenschink, F.-H. Kreuzer, W. H. de Jeu, *Liq. Cryst.* **1990**, *8*, 879.

[4] A. Sellinger, R. M. Laine, V. Chu, C. Viney, *J. Polym. Sci. Part A Polym. Chem.* **1994**, *32*, 3069, and references therein.

[5] G. H. Mehl, J. W. Goodby, *Chem. Ber.* **1996**, *129*, 521, and references therein.

[6] F. H. Kreuzer, R. Maurer, P. Spes, *Makromol. Chem. Makromol. Symp.* **1991**, *50*, 215, and references therein.

[7] a) D. Hoebbel, W. Wieker, *Z. Anorg. Allg. Chem.* **1971**, *384*, 43; D. Hoebbel, G. Garz-, G. Engelhardt, E. Lippma, M. Alla, *ibid.* **1980**, *465*, 15; D. Hoebbel, I. Pitsch, W. Hiller, S. Schelm (Akademie der Wissenschaften der DDR), EP 0348705, **1990** [Chem. Abstr. **1990**, *113*, 125354b]; b) R. Weidner, N. Zeller, B. Deubzer, V. Frey (Wacker Chemie), EP 0367222, **1990**, [Chem. Abstr. **1990**, *113*, 116465m]; c) M. Moran, C. M. Casado, I. Cuadrodo, J. Losada, *Organometallics* **1993**, *12*, 4327.

[8] B. D. Karstedt (General Electrics), US-Pat. (US-PS 3.814.730), **1974** [Chem. Abstr. **1974**, *80*, 16134j].

[9] B. J. Ostrovskij, *Liq. Cryst.* **1993**, *14*, 131.

[10] V. Percec, C. Pugh in *Side Chain Liquid Crystals* (Ed.: C. B. McArdle), Blackie, London, **1989**.

[11] H. Coles, E. A. Corsellis, *Mol. Cryst. Liq. Cryst.* **1995**, 261, 71; M. Ibn-Elhaj, A. Skoulios, D. Gouillon, J. Newton, P. Hodge, H. J. Coles, *Liq. Cryst.* **1995**, *19*, 373.

Oligo-THF Peptides: Synthesis, Membrane Insertion, and Studies of Ion Channel Activity**

Holger Wagner, Klaus Harms, Ulrich Koert,* Sabine Meder, and Günther Boheim*

The physiological importance and pharmacological relevance of membrane-bound ion channels have led to intensive studies on this class of compounds.[1, 2] Although the function of biological ion channels has been thoroughly examined, their structure is not well understood.[3] Artificial ion channels[4–6] with a predictable active conformation may be important for understanding their biological counterparts. We have reported on 2,5-*trans*-linked oligo(tetrahydrofurans) as potential building blocks for a polyether helix with ion channel activity.[7a, 7b] However, the THF-pentamer **1** was too short to span a membrane bilayer. To achieve longer oligo(tetrahydrofurans)[7c] at a reasonable synthetic expense we turned to oligo-THF peptides of the type **3**–**6**.

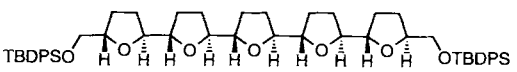

1

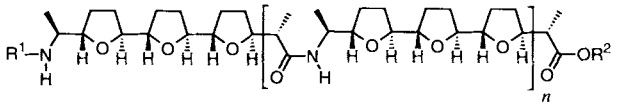

2a n = 0, R^1 = BOC, R^2 = H
2b n = 0, R^1 = BOC, R^2 = Bn
2c n = 0, R^1 = H, R^2 = Bn
3 n = 1, R^1 = BOC, R^2 = Bn
4 n = 3, R^1 = BOC, R^2 = Bn
5 n = 5, R^1 = BOC, R^2 = Bn
6a n = 9, R^1 = BOC, R^2 = Bn
6b n = 9, R^1 = H • CF_3COOH, R^2 = Bn
6c n = 9, R^1 = H • CF_3COOH, R^2 = H

The starting point for the synthesis of ter(tetrahydrofuranyl) amino acid **2a** was *N*-tosyl-L-alanine (**7**) (Scheme 1). Addition of the lithium salt of **7** to 3-butenylmagnesium bromide gave ketone **8**. Subsequent reduction with L-selectride (stereoselectivity 85:15) and separation of the major epimer by recrystallization led to the desired alcohol **9** in 80% yield.[8] After epoxidation of the terminal double bond in **9** and intramolecular 5-*exo* opening

[*] Prof. Dr. U. Koert,[+] Dr. H. Wagner, Dr. K. Harms
Fachbereich Chemie der Universität
Hans-Meerwein-Strasse, D-35032 Marburg (Germany)
Fax: Int. code +(6421)288917
Prof. Dr. G. Boheim, Dr. S. Meder
Lehrstuhl für Zellphysiologie
Arbeitsgruppe Biophysikalische Chemie von Membranen
der Universität, D-44780 Bochum (Germany)
Fax: Int. code +(234)7094-129
[+] New address:
Institut für Chemie der Humboldt Universität zu Berlin
Fachinstitut für Organische und Bioorganische Chemie
Hessische Strasse 1–2, D-10115 Berlin (Germany)
Fax: Int. +(30)2093-7266

[**] This work was supported by the Deutsche Forschungsgemeinschaft (SFB 260 and Graduiertenkolleg Metallorganische Chemie), the Fonds der Chemischen Industrie, the Pinguin-Stiftung, and Degussa AG.

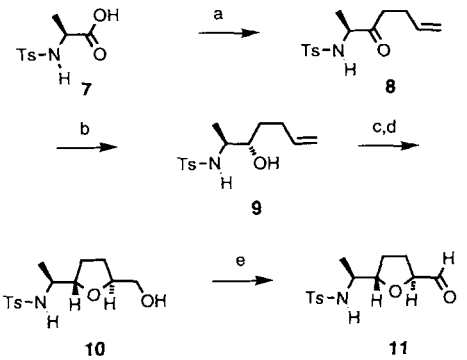

Scheme 1. Synthesis of the mono-THF aldehyde **11**; Ts = tosyl. a) 1. 1.5 equiv *n*BuLi, Et_2O, −78 °C → 50 °C, 1 h, 2. 3 equiv $BrMg(CH_2)_2CH{=}CH_2$, 0 °C, 15 h, (50%); b) 2 equiv L-selectride, THF, −95 °C, 1 h, (82%); c) 2 equiv *m*CPBA, CH_2Cl_2, room temperature (rt), 6 h; d) cat. TsOH, CH_2Cl_2, rt, 2 h, (45% **10** + 45% *cis* epimer); e) $(COCl)_2$, DMSO, Et_3N, CH_2Cl_2, (85%).

of the epoxide, the *trans*-THF alcohol **10** was obtained in 45% yield.[9] A Swern oxidation converted alcohol **10** into the mono-THF aldehyde **11**.

For the synthesis of sulfone **20**, aldehyde **12**[10] was transformed into alcohol **13** by the chelate-controlled addition of allyltrimethylsilane (Scheme 2).[11] A few standard steps converted alcohol **13** into the bromide **17**. The reaction of **17** with the dilithium salt of 3-butyn-1-ol gave alkyne **18**. After an *E*-selective reduction of alkyne **18** to afford alkene **19** and conversion of the primary hydroxyl group into an arylsulfone, the desired building block **20** was obtained.

In the coupling step the lithiated sulfone prepared from **20** was allowed to react with aldehyde **11** at −78 °C (Scheme 3).

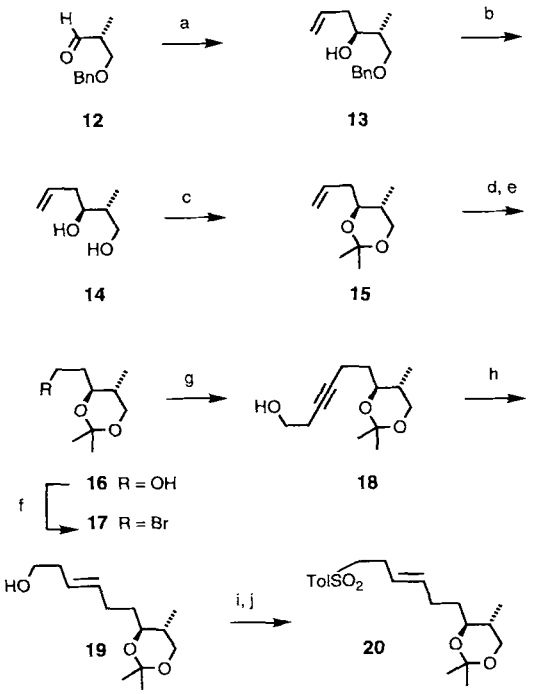

Scheme 2. Synthesis of sulfone **20**; Tol = *p*-tolyl. a) 1 equiv $SnCl_4$, 1.1 equiv allyltrimethylsilane, CH_2Cl_2, −78 °C, 0.5 h, (87%); b) 2.4 equiv Na, NH_3/THF 2.5:1, −40 °C, 1 h (98%); c) 2 equiv 2,2-dimethoxypropane, cat. TsOH, CH_2Cl_2, 4 h, rt (95%); d) 1. O_3, −78 °C, CH_2Cl_2, 2. 2 equiv PPh_3, −78 °C → rt; e) 5.4 equiv $NaBH_4$, MeOH, 12 h, 0 °C → rt (75%, 2 steps); f) 1. 2 equiv TsCl, pyridine, 2. 2 equiv LiBr, THF, 4 h, 50 °C (88%, 2 steps); g) 2.3 equiv 3-butyn-1-ol, 4.8 equiv $LiNH_2$, NH_3/DMSO 2.5/1, 7 h, −40 °C → 0 °C (82%); h) 8 equiv Na, NH_3/THF 2/1, 4 h, −35 °C, (89%); i) 1. 3 equiv TsCl, pyridine, 2. 4 equiv LiBr, THF, 2.5 h, 50 °C (88%, 2 steps); j) 3.5 equiv sodium *p*-toluenesulfinate dihydrate, PEG-400, 3 h, 130 °C, (90%).

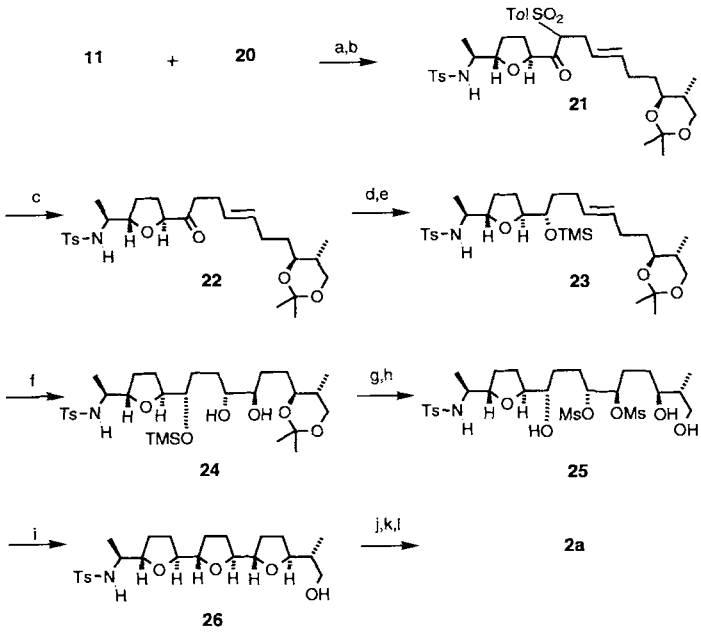

Scheme 3. Synthesis of the ter-THF amino acid **2a**; Ts = tosyl, Tol = *p*-tolyl, TMS = trimethylsilyl, Ms = methanesulfonyl, BOC = *tert*-butyloxycarbonyl. a) **20**, 0.9 equiv *n*BuLi, THF, −50 °C, 1 h, then 0.3 equiv **11**, −78 °C → −30 °C, 4 h (78%); b) 1.2 equiv periodinane, 10 equiv pyridine, CH_2Cl_2, rt, 4 h (96%); c) Al/Hg, THF/*n*PrOH/H_2O 40/10/1, 3 h, 40 °C (80%); d) 2 equiv L-Selectride, THF, −95 °C → −60 °C, 3 h (99%, 2 steps); e) 5 equiv TMSCl, 10 equiv imidazole, CH_2Cl_2, 0 °C, 3 h (91%); f) 1 equiv AD-mix-*β*, *t*BuOH/H_2O 1/1, 0 °C → rt, 12 h (89%, 85:15); g) 8 equiv MsCl, 16 equiv Et_3N, CH_2Cl_2, −40 °C → −20 °C, 1 h (99%); h) HOAc/H_2O 10/1, 12 h, rt; i) 10 equiv NaH, cat. DMSO, THF, 40 °C, 3 h (86%, 2 steps); j) 1. 4.7 equiv Na, NH_3/THF 1/1, −40 °C, 15 min, 2. 2 equiv. $(BOC)_2O$, NaOH, THF/H_2O 10/1, 3 h, rt, (75%, 2 steps); k) 1. $(COCl)_2$, DMSO, Et_3N, CH_2Cl_2, 2. 6.5 equiv $KMnO_4$, *t*BuOH/5% NaH_2PO_4 3/1, 30 min, 86%, 2 steps); l) 1.5 equiv *O*-benzyl-*N*,*N*'-diisopropylisourea, CH_2Cl_2, 3 d, rt (61%).

The resulting alcohol could be oxidized to oxosulfone **21** by the Dess–Martin[12] procedure. After reductive desulfonation the stereochemically pure ketone **22** was obtained. Stereoselective reduction of the carbonyl group in **22** and subsequent protection of the resulting hydroxyl group as a TMS ether yielded alkene **23**. The two THF units still missing were installed simultaneously by a Sharpless dihydroxylation (**23** → **24**) followed by a multiple Williamson reaction[13] (**25** → **26**). In preparation for the peptide synthesis the tosyl protecting group in **26** was exchanged for the BOC group. In the last step of the synthesis of the BOC-protected ter-THF amino acid **2a** the primary hydroxyl group was oxidized to provide the corresponding carboxylic acid.

With the ter-THF amino acid **2a** in hand, oligo-THF peptides of type **3**–**6** were readily accessible. By employing standard peptide protecting group techniques[14] and pentafluorophenyldiphenyl phosphinate[15] as coupling reagent the two ter-THF building blocks **2a** and **2c** were linked to the dipeptide **3** in 78% yield (Table 1). Two dipeptide building blocks were coupled to provide tetrapeptide **4** in 71% yield. Reaction of a dipeptide with a tetrapeptide afforded the hexapeptide **5** in 70% yield. Finally the coupling of a hexapeptide with a tetrapeptide gave decapeptide **6a** in 42% yield.[16]

To span the lipophilic part of a lipid bilayer a functional ion channel must be at least 3 nm long. For instance, gramicidin A, a naturally occurring peptide with a *β*-helical secondary structure, forms an ion channel active structure 3 nm in length in membranes.[17] Inspection of molecular models of oligo-THF peptides indicate that a decapeptide of the type **6a** with a helical arrangement and five turns may have the required minimum length (Fig. 1).

 © VCH Verlagsgesellschaft mbH, D-69451 Weinheim, 1996 0570-0833/96/3522-2644 $ 15.00+.25/0

Table 1. Selected analytical and spectroscopic data for compounds **2b** and **3**.

2b: colorless oil; $[\alpha]_D^{20} = -10$ ($c = 3.12$ in $CHCl_3$); ^1H NMR [a]: $\delta = 1.05$ (d, $J = 6.3$ Hz, 6H), 1.36 (s, 9H), 1.45–1.96 (m, 12H), 2.51–2.63 (m, 1H), 3.51–3.64 (m, 1H), 3.69–3.91 (m, 5H), 4.09 (dt, $J = 5.7$, 8.2 Hz, 1H), 4.74 (br. s, 1H), 5.03–5.11 (m, 2H), 7.22–7.32 (m, 5H); ^{13}C NMR [b]: $\delta = 13.0$, 19.3, 28.0, 28.2, 28.4, 28.9, 29.4, 45.1, 48.8, 66.0, 78.9, 80.7, 81.6, 81.7, 82.1, 128.0, 128.1, 128.5, 136.3, 156.0, 174.7.

3: colorless oil; $[\alpha]_D^{20} = -20$ ($c = 1.06$ in $CHCl_3$); ^1H NMR [a]: $\delta = 1.10$ (d, $J = 7.0$ Hz, 3H), 1.11 (d, $J = 7.0$ Hz, 3H), 1.16 (d, $J = 6.8$ Hz, 3H), 1.17 (d, $J = 6.8$ Hz, 3H), 1.42 (s, 9H), 1.50–2.06 (m, 24H), 2.20–2.35 (m, 1H), 2.55–2.70 (m, 1H), 3.64 (br. s, 1H), 3.82–3.95 (m, 10H), 3.95–4.02 (m, 1H), 4.04–4.09 (m, 1H), 4.12–4.20 (m, 1H); 4.79 (bs, 1H), 5.10 (d, $J = 12.3$ Hz, 1H), 5.14 (d, $J = 12.3$ Hz, 1H), 6.24 (d, $J = 9.1$ Hz, 1H), 7.30–7.35 (m, 5H); ^{13}C NMR [b]: $\delta = 12.9$, 14.4, 19.1, 19.2, 28.4, 27.9, 28.0, 28.1, 28.2, 28.6, 28.8, 29.3, 30.2, 45.0, 46.4, 46.5, 48.6, 66.0, 78.9, 80.7, 81.6, 81.9, 82.0, 82.1, 127.9, 128.0, 128.4, 136.2, 156.0, 174.2, 174.7; correct HRMS.

[a] 300 MHz ($CDCl_3$), 20 °C; [b] 75 MHz ($CDCl_3$), 20C.

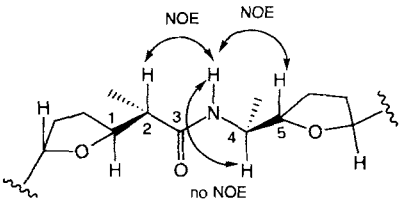

Fig. 2. Prefered conformation of the oligo-THF dipeptide **2b** in the area of the amide bond, as deduced from NOESY spectra.

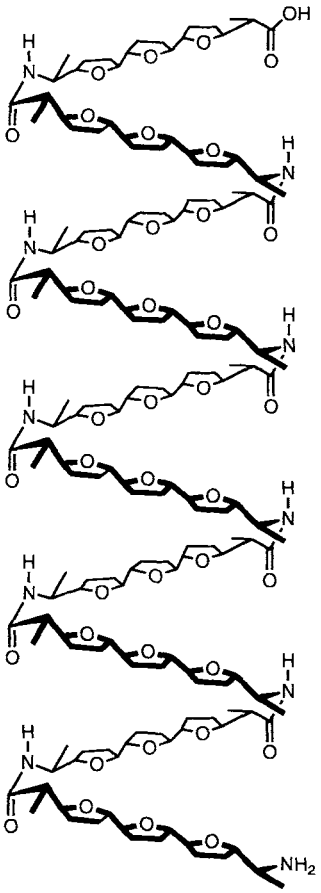

Fig. 1. Schematic illustration of an oligo-THF peptide helix.

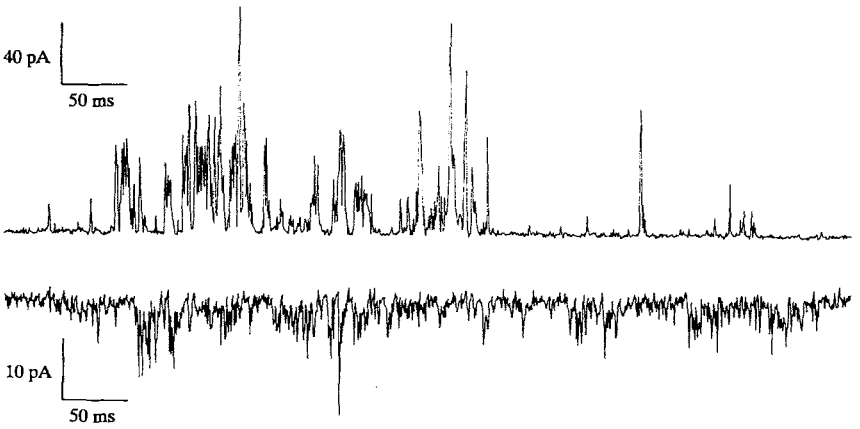

Fig. 3. Changes in the conductance of planar lipid bilayers after addition of the oligo-THF peptide **6b** (top: +50 mV; bottom: −50 mV). The experimental conditions are described in ref. [18].

The stereogenic centers bearing methyl groups and adjacent to the carbonyl and amino groups serve to stabilize the helical structure in the area of the peptide bond. To examine the influence of these stereogenic centers on the conformation of the oligo-THF peptide chain NMR studies in $CDCl_3$ were carried out. Owing to its polarity, $CDCl_3$ is a good model for the lipophilic part of the membrane. Figure 2 summarizes the results of NOE studies on dipeptide **2b**. A NOESY crosspeak between the NH signal of the peptide bond and the H-2 signal is in accord with the expected *anti* conformation of the peptide bond and the torsions angle C1-C2-C3-N. No NOE interaction was evident between NH and H-4, but there was one between NH and H-5. This indicates the conformation indicated at C3-N-C4-C5.

We examined the following three oligo-THF peptide derivatives in terms of their propensity to modify membranes and increase conductance: the N- und C-protected decapeptide **6a**, the N-deprotected compound **6b**, and the completely deprotected compound **6c**. The conductance measurements were carried out with planar lipid bilayers.[18] The increase in conductance of the membrane caused by additional transport of potassium ions was examined. The oligo-THF peptide **6b** was inserted into the membrane with an applied a membrane voltage (+ 50 mV). This led to rapid changes in conductance on the order of milliseconds, which could not be resolved as a series of discrete single events (frequency limit 3 kHz, Fig. 3, top). The observed current peaks of varying intensity (up to 100 pA) are indicative of a membrane-spanning, porelike structure rather than a carrier mechanism.[19] However, the possibility of short-lived permeation structures, which could arise as a result of disturbances in the lipid structure due to the insertion of oligo-THF peptides into the membrane, may not be excluded.

When the polarity of the membrane voltage was changed to −50 mV, smaller current peaks were detected (Fig. 3, bottom). The asymmetric insertion and transport characteristics displayed by compound **6b** are similar to the properties of defensines,[20] naturally occuring peptidic pore formers.

In contrast to **6b**, the N-protected oligo-THF peptide **6a** showed voltage-symmetric increases in conductance. However, at the same membrane voltage, current peaks could already been observed at lower peptide concentrations. Even at lower concentrations of the completely deprotected oligo-THF peptide **6c** ($> 10^{-6}$ g mL^{-1}) no changes in membrane conductance could be detected. Probably the high solubility of **6c** in water prevents insertion into the membrane. This shows that variation of an end group that is small in relation to the whole molecule may have remarkable effects on the properties of such compounds.

This work opens an efficient approach towards enantiomerically pure oligo-THF amino acids and oligo-THF peptides. The decapeptides **6a** and **6b** show conductance-increasing properties and are possible lead structures for future artificial ion channels. Variations in the length of the molecule and the end groups are conceivable for optimization of this lead structure.

Received: April 12, 1996
Revised version: July 17, 1996 [Z90181E]
German version: *Angew. Chem.* **1996**, *108*, 2836–2839

 © VCH Verlagsgesellschaft mbH, D-69451 Weinheim, 1996 0570-0833/96/3522-2645 $ 15.00+.25/0

Keywords: ion channels · membrane · oligomers · polyethers · synthetic methods

[1] a) B. Hille, *Ionic Channels of Excitable Membranes*, 2rd, Sinauer Associates, Sunderland, **1992**; b) R. B. Gennis, *Biomembranes, Molecular Structure and Function*, Springer, New York, **1989**, p. 270.

[2] a) J. J. Tabcharani, J. M. Rommens, Y.-X. Hou, X.-B. Chang, L.-C. Tsui, J. R. Riordan, J. W. Hanrahan, *Nature* **1993**, *366*, 79; b) M. J. Welsh, *ibid.* **1995**, *376*, 640.

[3] Function: B. Rudy, L. E. Iverson in *Methods in Enzymology, Vol. 207* (Eds.: J. N. Abelson, M. I. Simon), Academic Press, New York, **1992**; structure: a) H. Luecke, B. T. Chang, W. S. Mailliard, D. D. Schlaepfer, H. T. Haigler, *Nature* **1995**, *378*, 512; b) N. Unwin, *ibid.* **1995**, *373*, 37.

[4] Ion channels with polyether structure: a) N. Voyer, M. Robitaille, *J. Am. Chem. Soc.* **1995**, *117*, 6559; b) G. G. Cross, T. M. Fyles, T. D. James, M. Zojaji, *Synlett* **1993**, 449; c) M. J. Pregel, L. Jullien, J.-M. Lehn, *Angew. Chem.* **1992**, *104*, 1695; *Angew. Chem. Int. Ed. Engl.* **1992**, *31*, 1637; d) A. Nakano, Q. Xie, J. V. Mallen, L. Echegoyen, G. W. Gokel, *J. Am. Chem. Soc.* **1990**, *112*, 1287; e) U. F. Kragton, M. F. Roks, R. J. M. Nolte, *J. Chem. Soc. Chem. Commun.* **1985**, 1275; J.-H. Fuhrhop, U. Liman, H. H. David, *Angew. Chem.* **1985**, *97*, 337; *Angew. Chem. Int. Ed. Engl.* **1985**, *24*, 339.

[5] Ion channels with peptide structure: a) G. A. Woolley, A. S. I. Jaikaran, Z. Zhang, S. Peng, *J. Am. Chem. Soc.* **1995**, *117*, 4448; b) M. R. Ghadiri, J. R. Granja, L. K. Buehler, *Nature* **1994**, *369*, 301; c) K. S. Akerfeldt, J. D. Lear, Z. R. Wasserman, L. A. Chung, W. F. DeGrado, *Acc. Chem. Res.* **1993**, *26*, 191; d) Y. Kobuke, K. Ueda, M. Sokabe, *J. Am. Chem. Soc.* **1992**, *114*, 7618; e) F. M. Menger, D. S. Davis, R. A. Persichetti, J. J. Lee, *ibid.* **1990**, *112*, 2451; f) M. Montal, M. S. Montal, J. M. Tomich, *Proc. Natl. Acad. Sci. USA* **1990**, *87*, 6929; g) C. J. Stankovic, S. H. Heinemann, J. M. Defino, F. Sigworth, S. L. Schreiber, *Science* **1989**, *244*, 813; h) G. Menestrina, K. P. Voges, G. Jung, G. Boheim, *J. Membr. Biol.* **1986**, *93*, 111.

[6] Further ion channels: a) D. Seebach, A. Brunner, H.-M. Bürger, R. N. Reusch, L. L. Bramble, *Helv. Chim. Acta* **1996**, *79*, 507; b) Y. Tanaka, Y. Kobuke, M. Sobake, *Angew. Chem.* **1995**, *107*, 717; *Angew. Chem. Int. Ed. Engl.* **1995**, *34*, 693; b) J. H. Fuhrhop, U. Liman, V. Koesling, *J. Am. Chem. Soc.* **1988**, *110*, 6840; c) I. Tabushi, Y. Kuroda, K. Yokota, *Tetrahedron Lett.* **1982**, *23*, 4601; d) review on functionalized membranes: J.-H. Fuhrhop, J. Köning in *Membranes and Molecular Assemblies: The Synkinetic Approach* (Eds.: J. F. Stoddart), Monographs in Supramolecular Chemistry No. 5, R. Soc. Chem., Cambridge, **1994**.

[7] a) U. Koert, M. Stein, K. Harms, *Angew. Chem.* **1994**, *106*, 1238; *Angew. Chem. Int. Ed. Engl.* **1994**, *33*, 1180; b) U. Koert, M. Stein, H. Wagner, *Liebigs Ann.* **1995**, 1415; c) sugar amino acids: E. G. v. Roedern, H. Kessler, *Angew. Chem.* **1994**, *106*, 684; *Angew. Chem. Int. Ed. Engl.* **1994**, *33*, 687.

[8] R. C. Roemmele, H. Rapaport, *J. Org. Chem.* **1989**, *54*, 1866.

[9] The relative configuration of **10** was established unequivocally by X-ray crystallography: K. Harms, H. Wagner, U. Koert, *Z. Kristallogr.*, submitted.

[10] G. E. Keck, D. E. Abbott, *Tetrahedron Lett.* **1984**, *25*, 1883.

[11] C. H. Heathcock, S.-I. Kiyooka, T. A. Blumenkopf, *J. Org. Chem.* **1984**, *49*, 4214.

[12] D. B. Dess, J. C. Martin, *J. Org. Chem.* **1983**, *48*, 4156.

[13] a) H. Wagner, U. Koert, *Angew. Chem.* **1994**, *106*, 1939; *Angew. Chem. Int. Ed. Engl.* **1994**, *33*, 1873; b) U. Koert, *Synthesis* **1995**, 115.

[14] BOC was used as the N-terminal protecting group (cleavage with CF_3COOH, CH_2Cl_2); a benzyl ester was used as the C-terminal protecting group (cleavage with H_2, Pd/C, MeOH).

[15] J. Dudash Jr., J. Jiang, S. L. Mayer, M. M. Joullie, *Synth. Commun.* **1993**, *23*, 349.

[16] The oligo-THF peptides were characterized by NMR spectroscopy and electrospray mass spectroscopy (**6a**: calcd $M_r = 3302$; found $M_r = 3302$; see Table 1).

[17] D. W. Urry, T. C. Trapane, K. U. Prasad, *Science* **1983**, *221*, 1064.

[18] Planar lipid bilayer membranes were prepared by the method of Mueller and Rudin; membrane surface: 3×10^{-4} cm^2; lipid: 2-oleylglycero-1-palmitoyl-3-phosphatidylethanolamine (90:10 weight.%) in *n*-decane 12 mg mL^{-1}; electrolyte: 1 M KCl, 10 mM Hepes, pH 7.2; the decapeptide **6b** was added to the *cis* compartment with a final concentration of 1.5×10^{-7} g mL^{-1}; temperature: 20 °C. Membrane potential: +50 and −50 mV. The voltage refers to the potential of the *cis* compartment, the *trans* compartment is virtual earth connected. The current direction is from *cis* to *trans*; for further experimental details see T. Rink, H. Bartel, G. Jung, W. Bannwarth, G. Boheim, *Eur. Biophys. J.* **1994**, *23*, 155.

[19] W. Hanke, C. Methfessel, H.-U. Wilmsen, E. Katz, G. Jung, G. Boheim, *Biochim. Biophys. Acta* **1983**, *727*, 108.

[20] P. Nicolas, A. Mor, *Annu. Rev. Microbiol.* **1995**, *49*, 277.

The Novel, $[n\text{-}B_{20}H_{18}]^{2-}$-Induced Nucleophilic Ring Opening of Tetrahydrofuran by Alkoxide Anions**

Fangbiao Li, Kenneth Shelly, Robert R. Kane, Carolyn B. Knobler, and M. Frederick Hawthorne*

Boron neutron capture therapy (BNCT) is a binary cancer treatment that requires the selective deposition of a significant amount of the ^{10}B isotope within cancer cells.[1] Various derivatives of the polyhedral borate anion $[n\text{-}B_{20}H_{18}]^{2-}$ (**1**)[***] have been synthesized in order to investigate the effects of charge, substituent, and structure upon the tumor retention of these anionic borate species.[2, 3] We have recently described the reaction of ethoxide ion with **1** in diethyl ether solution to produce the $[ae\text{-}B_{20}H_{17}OCH_2CH_3]^{4-}$ ion (**2**, Scheme 1).[3] This species was subsequently oxidized to produce an unusual oxygen and hydrogen doubly-bridged polyhedral borate, the $[\mu\text{-}B_{20}H_{17}OCH_2CH_3]^{2-}$ ion (**3**, Scheme 1).[3]

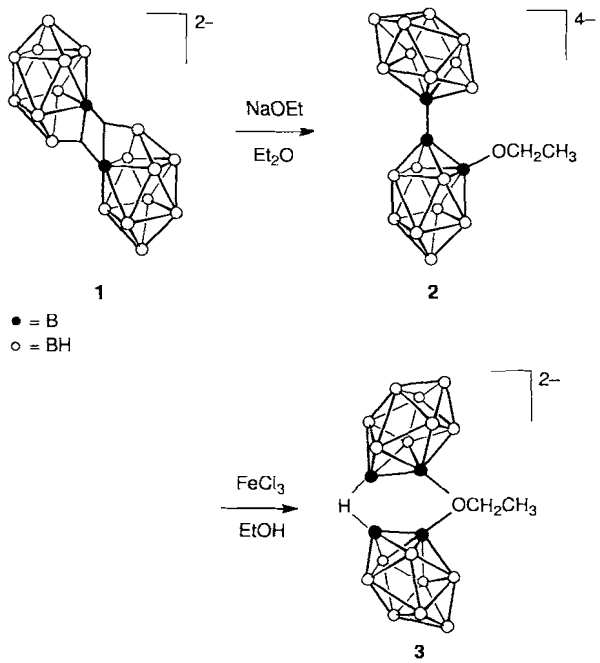

Scheme 1. Synthesis of **2** and **3**

Recent studies of the reaction of alkoxide ions (RO^-) with **1** in tetrahydrofuran (THF) did not result in the expected $[ae\text{-}B_{20}H_{17}OR]^{4-}$ ions. Instead, the products obtained were the ions **4** ($[ae\text{-}B_{20}H_{17}O(CH_2)_4OR]^{4-}$: **4a**, R = methyl; **4b**, R = isopentyl) shown in Scheme 2. These species contain a substituent comprising a terminal alkoxyl group attached to a bu-

[*] Prof. M. F. Hawthorne, F. Li, Dr. K. Shelly, Dr. C. B. Knobler
Department of Chemistry and Biochemistry
University of California at Los Angeles
Los Angeles, California 90095-1569 (USA)
Fax: Int. code +(310)825-5490
e-mail: mfh@chem.ucla.edu
Dr. R. R. Kane
Baylor University, Waco, Texas

[**] This work was supported by the U. S. Department of Energy (DE-FG02-95ER61975).

[***] The following prefixes are used as isomer designations: *n* normal isomer of $[B_{20}H_{18}]^{2-}$, *ae* and *a*^{2} apical-equatorial and apical-apical isomers of $[B_{20}H_{18}]^{4-}$ derivatives.

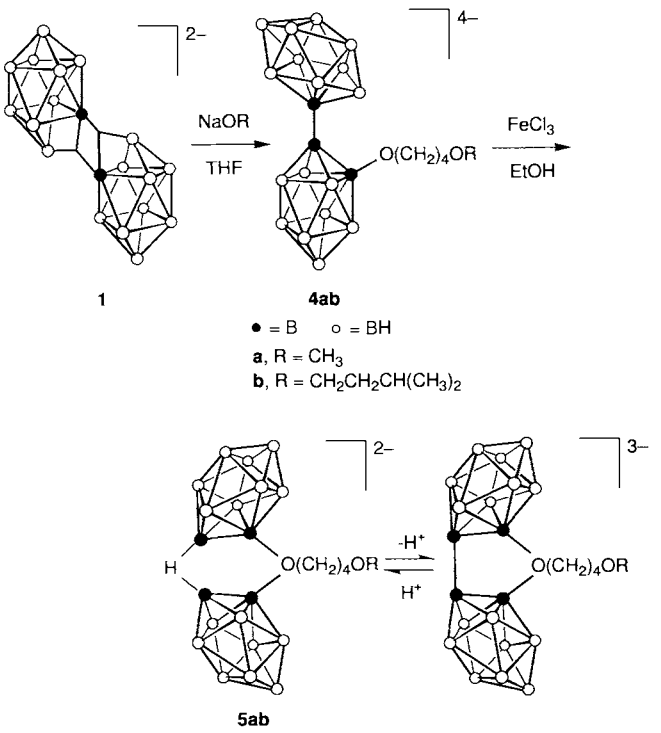

Scheme 2. Synthesis of **4a,b** and **5a,b**.

toxide group that is bonded to the polyhedral borate substrate. This substituent originates from the $[n\text{-}B_{20}H_{18}]^{2-}$ promoted nucleophilic ring opening of a THF solvent molecule by the alkoxide nucleophile.

The subsequent oxidation of **4** produced the oxygen- and hydrogen-bridged polyhedral borates **5** (Scheme 2). We report here the synthesis, crystal stucture, and reactions of **5**.

The addition of $(Et_3NH)_2$**[1]**[4] to a stirred suspension of NaOR (prepared in situ from NaH and ROH) in dry THF resulted in the formation of Na_4**[4]** (**4a** R = methyl, **4b** R = isopentyl) in high yield (Scheme 2). The anion was isolated as its tetramethylammonium salt. Aqueous solutions of **4** are stable only under basic conditions. In neutral aqueous media, $[ae\text{-}B_{20}H_{17}O(CH_2)_4OR]^{4-}$ slowly isomerizes to $[a^2\text{-}B_{20}H_{17}O\text{-}(CH_2)_4OR]^{4-}$; in strongly acidic solutions (1 N HCl), **4** decomposes to form $[B_{10}H_{10}]^{2-}$ and other unidentified products.

The oxidation of **4** at room temperature by Fe^{3+} in anhydrous ethanol produced the ions **5**, isolated in approximately 70% yields as the corresponding tetramethylammonium salts (Scheme 2). The products were characterized by electrospray ionization mass spectroscopy (ESI-MS) and multinuclear (^1H, ^{13}C, and ^{11}B) NMR spectroscopy. The structure of $(Me_4N)_2$-**[5b]** was determined by single crystal X-ray diffraction studies (Fig. 1).[5] The polyhedral borane anion consists of two intact decaborate cages joined together by one oxygen atom and one hydrogen atom. The bonding distances within the two decaborate cages are normal and similar to those found in other structures derived from $[B_{10}H_{10}]^{2-}$. As a consequence of the bridging atoms between the two borane cages a six-membered BHBBOB ring is formed, which is essentially planar. This configuration has been observed previously in the structure of the polyhedral borate anion $[\mu\text{-}B_{20}H_{17}OH]^{2-}$ (**6**).[3] The carbon atom (C2) also lies in the plane of the six-membered ring, and the three-coordinate oxygen atom of **5b** exhibits trigonal-planar geometry. The sum of the three bond angles about the oxonium center of **5b** is 359.4° (which may be compared to the value of

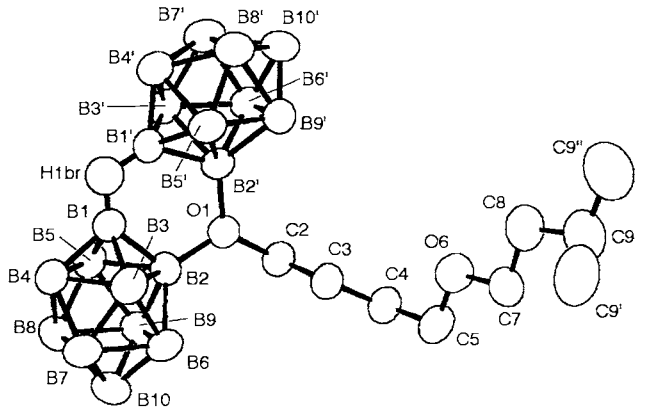

Fig. 1. ORTEP representation of **5b** depicting the atom numbering scheme. For clarity, the terminal B–H hydrogen atoms have been omitted. Selected bond lengths [Å] and angles [°] (estimated standard deviations in parentheses): O1–B2 = 1.500(6), O1–B2′ = 1.499(6), B1–B2 = 1.651(7), B1′–B2′ = 1.652(7), B1–B1′ = 1.895(7), B1–H1br = 1.23(5), B1′–H1br = 1.16(5), O1 C2 = 1.469(5); B2-O1-B2′ = 113.5(3), O1-B2-B1 = 112.5(4), B1′-B2′-O1 = 112.6(4), B1-H1br-B1′ = 112(4), B2′-O1-C2 = 122.9(3), B2-O1-C2 = 123.0(3).

353.7° observed in **6**).[3] This planar geometry of tricoordinate oxygen atom has been observed previously in several other structurally characterized species containing oxygen atoms bound to polyhedral boranes and carboranes.[6]

A significant feature of the structure of **5b** is the presence of an $-O(CH_2)_4-$ group inserted between the polyhedral borate and the isopentoxide nucleophile. The resulting $-O(CH_2)_4OR$ substituent arises from the nucleophilic attack of an alkoxide ion on, and the subsequent ring opening of, a THF solvent molecule (Scheme 3). The product of this reaction (**4**) may then be oxidized to produce **5**.

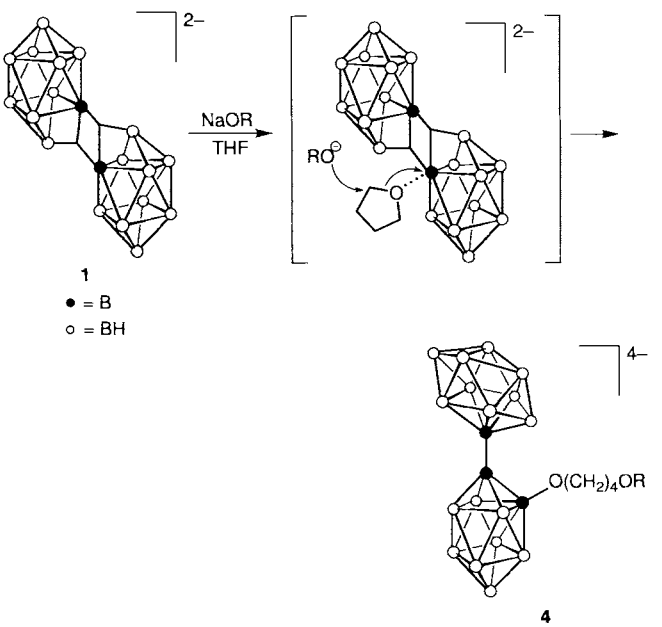

Scheme 3. Postulated mechanism for the synthesis of **4**.

The nucleophilc ring opening of THF induced by metal cations or neutral Lewis acids has been reported previously,[7] but similar reactions promoted by anions are unknown. To our knowledge, the electrophilic $[n\text{-}B_{20}H_{18}]^{2-}$ ion is the only anion capable of providing the requisite Lewis acidity to produce this

type of reactivity. No evidence for the formation of a discrete thf·**1** complex was discerned; the ^{11}B NMR of **1** remained essentially unchanged when dissolved in THF, H_2O, CH_3CN, or CH_2Cl_2. However, it may be reasonably assumed that the solvation of $[n\text{-}B_{20}H_{18}]^{2-}$ by THF places a solvent molecule close to the electrophilic boron atoms of **1** as shown in Scheme 3. When the alkoxide nucleophile approaches the borate ion, it is apparently unable to penetrate this solvation shell to reach the reactive boron site before it attacks an α-carbon atom of THF. The resulting nucleophilic ring opening is promoted by incipient bond formation between the THF oxygen atom and an electrophilic boron atom of **1**. No evidence was found for the formation of the simple alkoxide derivative $[ae\text{-}B_{20}H_{17}OR]^{4-}$ in THF; this product may be obtained by performing the reaction in diethyl ether.[3]

The hydrolysis of **5** in H_2O at 100 °C produced **6** (Scheme 4) in approximately 75% yield. The anion **6** was previously reported to arise from the hydrolysis of **3**[3] and is a useful precursor for the production of derivatives with a variety of other oxygen-bound substituents through O-alkylation.[3]

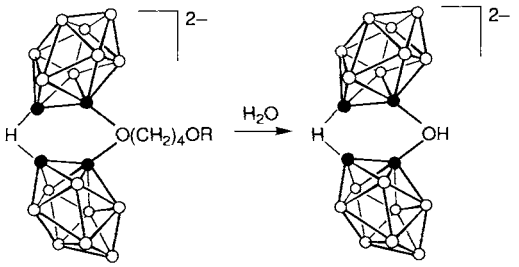

5ab **6**

• = B ○ = BH

a, R = CH_3

b, R = $CH_2CH_2CH(CH_3)_2$

Scheme 4. Hydrolysis of **5a,b**.

The bridging hydrogen atom of **5** is weakly acidic and can be titrated by aqueous base (Scheme 2). This deprotonation results in the formation of the corresponding $[\mu\text{-}B_{20}H_{16}O(CH_2)_4OR]^{3-}$ ion, which can be easily distinguished from **5** in the ^{11}B NMR spectrum. The pK_a of this bridging hydrogen was estimated to be 6.3,[8] which is comparable to the acidity of $[a^2\text{-}B_{20}H_{19}]^{3-}$ ($pK_a = 7.3$),[9] a hydrogen-bridged species that does not contain the bridging oxygen atom of **5**.

The unusual THF ring opening and insertion reaction induced by the $[n\text{-}B_{20}H_{18}]^{2-}$ ion provides an efficient means for the synthesis for oxygen-substituted derivatives of this polyhedral borane anion containing a variety of ether functionalities. We are currently extending these investigations to other cyclic ethers and nucleophiles.

Experimental Procedure

$(Me_4N)_4$**[4a]**: Dry $(Et_3NH)_2$**[1]** (2.00 g, 4.57 mmol) was added to a stirred suspension prepared from NaH (500 mg, 20.8 mmol) and methanol (500 μL, 12.4 mmol) in 125 mL THF. Hydrogen gas was evolved, and the mixture was stirred at room temperature for 3 h. Crude Na_4**[4a]** was obtained by removal of the solvent in vacuo. The crude product was dissolved in 100 mL of absolute ethanol. The addition of excess tetramethylammonium hydroxide in ethanol resulted in a white precipitate of $(Me_4N)_4$**[4a]**. The precipitate was separated by filtration, washed with absolute ethanol (3 × 30 mL) and dried in vacuo to yield 2.54 g of $(Me_4N)_4$**[4a]** (4.01 mmol, 88%). $^{11}B\{^1H\}$ NMR (160 MHz, H_2O): $\delta = 7.9$ (2B, B–B), 2.9 (1B, apical B–H), 2.6 (2B, B–O and apical B–H), −9.4 (1B, apical B–H), −24.3, −25.6, −29.2, −33.6 (total 14B, equatorial B–H); ^1H NMR (400 MHz, D_2O): $\delta = 3.35$ (t, $J = 7.0$ Hz, 2H), 3.27 (t, $J = 7.1$ Hz, 2H), 3.22 (s, 3H), 1.36 (m, 2H), 1.28 (m, 2H); ^{13}C NMR (100 MHz, D_2O): $\delta = 72.79$, 70.11, 57.62, 27.46, 25.27; ESI-MS (*m/z*): 169.2 $\{(H)_2(B_{20}H_{17}O(CH_2)_4OCH_3)\}^{2-}$, 339.2 $\{(H)_3(B_{20}H_{17}O(CH_2)_4OCH_3)\}^-$, 412.5 $\{(Me_4N)(H)_2(B_{20}H_{17}OC_4H_8OCH_3)\}^-$.

4b: $(Me_4N)_4$**[4b]** was prepared as described above for $(Me_4N)_4$**[4a]** except for the use of isopentyl alcohol (1.00 mL, 9.18 mmol) instead of methanol. Yield: 2.84 g (4.11 mmol, 90%). $^{11}B\{^1H\}$ NMR (160 MHz, H_2O): $\delta = 7.5$ (2B, B–B), 3.5 (1B, apical B–H), −2.1 (2B, B–O and apical B–H), −8.0 (1B, apical B–H), 24.35, 25.45, 28.72, 30.68, 32.61 (total 14B, equatorial B–H); ^1H NMR (400 MHz, D_2O): $\delta = 3.29$ (t, $J = 7.0$ Hz, 2H), 3.26 (t, $J = 7.0$ Hz, 2H), 3.14 (t, $J = 7.0$ Hz, 2H), 1.93 (m, 2H), 1.53 (m, 1H), 1.33 (m, 2H), 1.15 (m, 2H), 0.83 (d, $J = 7.0$ Hz, 6H); ^{13}C NMR (100 MHz, D_2O): $\delta = 69.39$, 65.46, 55.42, 38.33, 24.92, 24.90, 21.99, 17.83. ESI-MS(*m/z*): 196.8 $\{(H)_2(B_{20}H_{17}O(CH_2)_4OCH_2CH_2CH(CH_3)_2)\}^{2-}$, 395.8 $\{(H)_3(B_{20}H_{17}O(CH_2)_4OCH_2CH_2CH(CH_3)_2)\}^-$, 468.8 $\{(Me_4N)(H)_2(B_{20}H_{17}O(CH_2)_4OCH_2CH_2CH(CH_3)_2)\}^-$.

5a: A suspension of Na_4**[4a]** in THF was prepared from $(Et_3NH)_2$**[1]** (2.00 g, 4.57 mmol) as described above. After removal of the THF solvent in vacuo, the residue was dissolved in 50 mL of absolute ethanol. A solution of anhydrous $FeCl_3$ (2.30 g, 14.2 mmol) dissolved in absolute ethanol (100 mL) was added, and the mixture was stirred at room temperature for 4 h. The solution was filtered, and the ethanol was removed from the filtrate in vacuo. The residue was dissolved in 50 mL of H_2O, cooled to 0 °C, and $(Me_4N)_2$**[5a]** was precipitated by the addition of aqueous Me_4NCl. The precipitate was removed by filtration, and the resulting solid was dissolved in 50 mL of CH_3CN/H_2O (1/1) and passed through a column of cation exchange resin (Bio-Rad AG 50W-X2, sodium form) to produce a solution of Na_2**[5a]**. The product was again precipitated by the addition of Me_4NCl and removed by filtration to afford a white powder. Recrystallization from CH_3CN/C_2H_5OH yielded $(Me_4N)_2$**[5a]** (1.52 g, 3.13 mmol, 69%). $^{11}B\{^1H\}$NMR (160 MHz, H_2O): $\delta = 14.0$ (2B, B–B), 6.2 (2B, apical B–H), −8.8 (2B, B–O–B), −20.7, −26.8, −29.5 (total 14B, equatorial B–H); ESI-MS (*m/z*): 165.7 $\{B_{20}H_{17}O(CH_2)_4OCH_3\}^{2-}$, 336.1 $\{(H)(B_{20}H_{17}O(CH_2)_4OCH_3)\}^-$, 410.5 $\{(Me_4N)(B_{20}H_{17}O(CH_2)_4OCH_3)\}^-$. The compound was dissolved in CH_3CN/H_2O (1/1) and ion-exchanged to produce a solution of Na_2**[5a]**. ^1H NMR (400 MHz, D_2O): $\delta = 2.76$ (t, $J = 7.0$ Hz, 2H); 2.70 (m, 3H), 0.70 (m, 2H), 0.62 (m, 2H); ^{13}C NMR (100 MHz, D_2O): $\delta = 82.81$, 71.32, 57.51, 23.54, 23.38.

5b: $(Me_4N)_2$**[5b]** was prepared from Na_4**[4b]** as described above for the transformation of **4a** to **5a**. Yield: 1.75 g, 3.23 mmol, 71%. $^{11}B\{^1H\}$ NMR (160 MHz, H_2O): $\delta = 14.7$ (2B, B–B), 7.0 (2B, apical B–H), −8.4 (2B, B–O–B), −19.85, −20.50, −26.22, −28.89 (total 14B, equatorial B–H); ESI-MS (*m/z*): 195.8 $\{B_{20}H_{17}O(CH_2)_4OCH_2CH_2CH(CH_3)_2\}^{2-}$, 466.2 $\{(Me_4N)(B_{20}H_{17}O(CH_2)_4OCH_2CH_2CH(CH_3)\}^-$. The compound was dissolved in CH_3CN/H_2O (1/1) and ion-exchanged to produce a solution of Na_2**[5a]**. ^1H NMR (400 MHz, CD_3CN): $\delta = 2.90$ (t, $J = 7.0$ Hz, 2H), 2.81 (t, $J = 7.0$ Hz, 2H), 2.73 (t, $J = 7.0$ Hz, 2H), 1.07 (m, 1H), 0.87(m, 2H), 0.78 (m, 2H), 0.67 (m, 2H), 0.33 (d, $J = 6.6$ Hz, 6H); ^{13}C NMR (100 MHz, D_2O): $\delta = 82.76$, 69.33, 68.90, 37.21, 24.29, 23.81, 23.62, 22.00.

6: Solid $(Me_4N)_2$**[5a]** (1.00 g, 2.06 mmol) was placed in 50 mL H_2O. The solid dissolved upon heating, and the mixture was heated at reflux for 24 h. The solution was cooled to 0 °C to produce a white precipitate. The precipitate was separated by filtration and dried in vacuo. Recrystallization from CH_3CN/C_2H_5OH yielded $(Me_4N)_2$**[6]** (610 mg, 77%). The product was identified by its $^{11}B\{^1H\}$ NMR and ESI-MS.[3] The hydrolysis of $(Me_4N)_2$**[5b]** also produced $(Me_4N)_2$**[6]** in 74% yield.

Received: July 9, 1996 [Z9315IE]
German version: *Angew. Chem.* **1996**, *108*, 2811–2813

Keywords: boron compounds · cluster compounds · nucleophilic ring opening

[1] M. F. Hawthorne, *Angew. Chem.* **1993**, *105*, 997–1033; *Angew. Chem. Int. Ed. Engl.* **1993**, *32*, 950–984.

[2] D. A. Feakes, K. Shelly, C. B. Knobler, M. F. Hawthorne, *Proc. Natl. Acad. Sci. USA* **1994**, *91*, 3029–3033; K. Shelly, D. A. Feakes, M. F. Hawthorne, T. A. Krisch, W. F. Bauer, *ibid.* **1992**, *89*, 9039–9043.

[3] F. Li, K. Shelly, R. R. Kane, C. B. Knobler, M. F. Hawthorne, *J. Am. Chem. Soc.* **1996**, *118*, 6506–6507.

[4] M. F. Hawthorne, R. L. Pilling, P. F. Stokely, *J. Am. Chem. Soc.* **1965**, *87*, 1893–1899; B. L. Chamberland, E. L. Muetterties, *Inorg. Chem.* **1964**, *3*, 1450–1456.

[5] Crystal structure analysis of $(Me_4N)_2$**[5b]** (colorless crystals from ethanol/acetonitrile): $B_{20}C_{17}H_{60}N_2O_2$, $M_r = 540.9$; crystal dimensions: 0.25 × 0.3 × 0.48 mm; Syntex $P\bar{1}$ diffractometer, $Cu_{K\alpha}$ radiation, $\lambda = 1.5418$ Å, 298 K; θ–2θ scan mode to $2\theta_{max} = 115$ °C; unit cell parameters were determined from 29 accurately centered reflections (17.7 °C < 2θ < 36.2 °C): monoclinic, space group $P2_1/c$, $a = 11.714(3)$, $b = 19.951(6)$, $c = 15.972(5)$ Å, $\beta = 98.883(8)$ °C, $V = 3688$ Å^3, $Z = 4$, $\rho_{calcd} = 0.97$ g cm^{-3}, $\mu = 3.4$ cm^{-1}. Of the 4410 unique reflections measured ($+h, +k, \pm l$), 2846 were considered observed ($I > 2\sigma(I)$), and the structure was solved by direct methods; 474 refined parameters, maximum residual electron density 0.39 e Å^{-3}, least-squares refinement against $|F^2|$;

$R = 0.086$ for the observed reflections, $R_w = 0.276$ for all 4410 reflections. All reflections were used in the refinement; all programs used are contained in the UCLA Crystal Structure Package; data were corrected for Lorentz and polarization effects and for secondary extinction but not for absorption. Programs used in this work include locally modified versions of the following programs: CARESS (Broach, Coppens, Becker and Blessing, peak profile analysis, Lorentz and polarization corrections); ORFLS (Busing, Martin and Levy, structure factor calculation and full-matrix least-squares refinement), SHELX76, SHELX86, SHELXL93 (Sheldrick, crystal structure packages), and ORTEP (Johnson). With the exception of the nitrogen atoms of the cations, all non-hydrogen atoms were refined with nonisotropic parameters; with the exception of the B-H-B hydrogen atom, hydrogen atoms were included in calculated positions; position parameters for the bridging hydrogen atom were allowed to vary. Hydrogen atoms were assigned isotropic displacement values based approximately on the value for the attached atom. Crystallographic data (excluding structure factors) for the structure reported in this paper have been deposited with the Cambridge Crystallographic Data Centre as supplementary publication no. CCDC-179-116. Copies of the data can be obtained free of charge on application to The Director, CCDC, 12 Union Road, Cambridge CB2 1EZ, UK (fax: int. code +(1223)336-033; e-mail: teched@chemcrys.cam.ac.uk).

[6] T. Peymann, E. Lork, D. Gabel, *Inorg. Chem.* **1996**, *35*, 1355–1360; D. F. Mullica, E. L. Sappenfield, F. G. A. Stone, S. F. Woollam, *Organometallics* **1994**, 13, 157–166; Z. Wang, E. Sinn, R. N. Grimes, *ibid.* **1985**, *24*, 834–839.

[7] W. J. Evans, T. A. Ulibarri, L. R. Chamberlain, J. W. Ziler, D. Alvarez, *Organometallics* **1990**, *9*, 2124–2130; M. E. Woodhouse, F. D. Lewis, T. J. Marks, *J. Am. Chem. Soc.* **1982**, *104*, 5586–5594; S. Penczek, P. Kubisa, K. Matyjaszewski, *Adv. Polym. Sci.* **1980**, *37*, 1–144.

[8] The pK_a of the bridging hydrogen was estimated from the pH at half-neutralization of an aqueous titration of Na_2[**5a**] and Na_2[**5b**].

[9] R. Watson-Clark, C. B. Knobler, M. F. Hawthorne, *Inorg. Chem.* **1996**, *35*, 2963–2966.

Towards Synthetic Adrenaline Receptors—Strong Binding of Amino Alcohols by Bisphosphonates**

Thomas Schrader*

Research on the mechanism of action of the adrenergic receptor family has received much attention during the past decade,[1] notably because many pharmaceuticals act as agonists or antagonists for the β-adrenergic receptor, for example the well-known β-blockers.[2] Scheme 1 summarizes the present understanding of neurotransmitter binding.[3] The ammonium functionality is recognized through electrostatic and hydrogen bond interactions with an aspartate carboxylate group; simultaneously the NH_3^+ protons are in close contact with three electron-rich aromatic residues, resulting in π–cation stabilization. The aliphatic and catechol hydroxyls are each hydrogen-bonded to a serine OH group, while the aromatic ring is buried in a deep cleft flanked by two phenylalanine aromatic rings that are involved in double π-stacking. We recently embarked on a program for the development of synthetic receptors for adrenaline derivatives that focuses on imitation of the natural receptor–ligand interactions. This led to the design of simple benzylic bisphosphonates that should be able to act as strong chelating agents for the alkylammonium group (Scheme 2). The great advantage of the phosphonate over a carboxylate group stems from the fact that at pH 7 phosphonates are fully dissociated due to their much lower pK_a values (1.8 vs. 4.8).[4] The phosphonic acid methyl ester can be easily replaced by more sophisticated alcohol moieties for lateral and possibly chiral recognition of the substrate. Force-field calculations show that when an alkylammonium ion approaches the *p*-xylylene bisphosphonate, not only strong electrostatic attractions result, but also an almost ideal array of short linear hydrogen bonds can be formed (Fig. 1).[5] In addition, the ammonium protons lie exactly 3.5 Å above the aromatic ring, a distance that is ideal for π–cation interactions.[6]

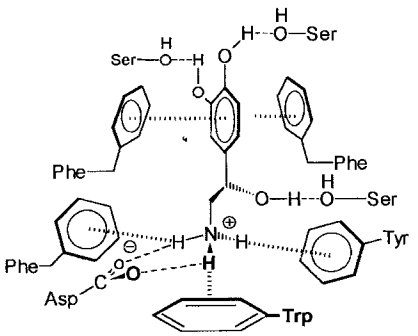

Scheme 1. Noncovalent interactions between noradrenaline and the β-adrenergic receptor.

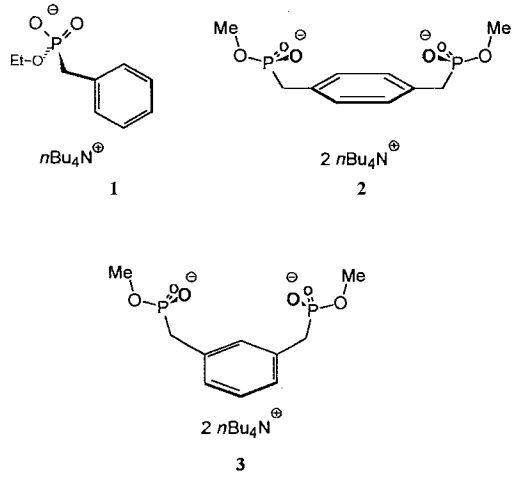

Scheme 2. Phosphonate receptors.

In both the ^1H and ^{31}P NMR spectra of equimolar mixtures of aliphatic primary ammonium chlorides with phosphonate receptors **2** and **3** large complexation-induced shifts (CIS) of host and guest signals can be observed.[7]

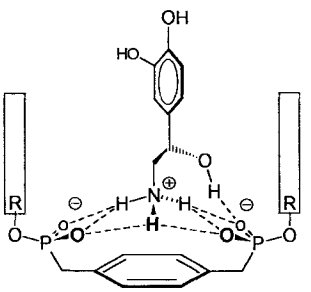

Fig. 1. Complex of *p*-xylylene bisphosphonates with noradrenaline according to force-field calculations [5].

We performed NMR titrations of benzylammonium chloride with phosphonate receptors **1**–**3** in [D_6]DMSO. We measured the CIS of the α-methylene protons and analyzed the binding curves by nonlinear regression methods.[8] The calculated association constants are summarized in Table 1. The 14-fold differ-

[*] Dr. T. Schrader
Institut für Organische Chemie und Makromolekulare Chemie der Universität
Universitätsstrasse 1, D-40225 Düsseldorf (Germany)
Fax: Int. code +(211)8114788
e-mail: schrat@iris-oc2.oc2.uni-duesseldorf.de

[**] I thank Prof. H.-J. Schneider, Saarbrücken, for his program to evaluate 1:1 complexes.

Table 1. Association constants $K_{1:1}$ [a] from NMR titrations in DMSO at 20 °C.

Receptor	Benzylamine 10^3 [M^{-1}]	(±)-**4** 10^3 [M^{-1}]
1	0.2	-
2	2.8	15.5
3	7.4	55.0

[a] Because of the strongly hygroscopic character of both titration partners the [D_6]DMSO solution contained about 0.1% of water. Errors in K_a are estimated at ±10–40%.

ence in K_a values between the mono- and *p*-diphosphonates **1** and **2** indicates strongly that the chelate effect results in double electrostatic attraction for the alkylammonium ion. Unfortunately the signal for the *p*-xylylene aromatic protons remains unchanged, so that a π–cation interaction seems doubtful. Force-field calculations suggest that in going from *para* to *meta* substitution (i.e. from **2** to **3**), the PO $\cdots HN^+$ distance decreases slightly in favor of both electrostatic interactions and hydrogen bonding.[5]

Job's method of continuous variations confirms the postulated 1:1 stoichiometry of the complex.[9] Maxima in the range of $x = 0.5-0.55$ are observed for signals of both the guest and the host.

When 2-hydroxy-2-phenylethylamine hydrochloride (**4**, a model for the amino alcohol moiety in adrenaline derivatives, Scheme 3) is employed, its K_a value is significantly greater than that of benzylamine, reaching 55000 M^{-1} for **3** (Table 1). We examined other biologically important 1,2-amino alcohols (Scheme 3) and compared them to the respective amines (Table 2). We obtained the following results:

a) Binding to the bisphosphonate receptor **3** is three to nine times stronger for all amino alcohols except for the serine

Table 2. Association constants $K_{1:1}$ [a] from NMR titrations with **3** in DMSO at 20 °C.

Amine	$K_{1:1} \times 10^3$ [M^{-1}]	Amino alcohol	$K_{1:1} \times 10^3$ [M^{-1}]
benzylamine	7	(*L*)-serine methyl ester **6**	7
(L)-alanine methyl ester	10	serinol **7**	16
2-phenylethylamine	12	(±)- **4**	55
N-benzyl-*N*-methylamine	19	α-D-glucosamine **8**	59
		(1*S*,2*R*)-norephedrine **5**	62
		(*R*)-propranolol **9**	66
		(±)-adrenaline **10**	16

[a] Because of the strongly hygroscopic character of both titration partners the [D_6]DMSO solution contained about 0.1% of water. Errors in K_a are estimated at ±20–40%.

derivatives **6** and **7**. Only the latter, however, are able to form an intramolecular hydrogen bond, giving a six-membered ring that has to be broken before hydrogen bonding to the phosphonate can occur (Scheme 3).

b) Further structural information based on the NMR experiments confirms the strong hydroxyl binding: In the free glucosamine **8** only the signals of OH-1 and OH-3, which are adjacent to the ammonium functionality, shift during the titration. In propranolol **9** the diastereotopic ammonium and methylene protons immediately become magnetically nonequivalent on addition of phosphonate because the OH group is conformationally locked.

c) The binding constant for adrenaline **10** seems to contradict the general trend; however, the ^1H NMR spectrum shows large shifts of the signals of the catechol OH groups on addition of

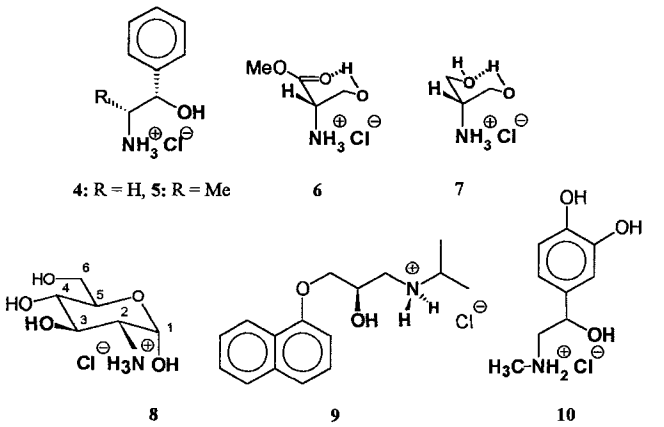

Scheme 3. Amino alcohols for the NMR titrations.

phosphonate, so that its evaluation has to take into account a second superimposed equilibrium. We therefore assume that adrenaline also binds to the bisphosphonate **3** as strongly as the other amino alcohols.

These results suggest that we have indeed found a basic structural motif for a receptor of 1,2-amino alcohols. Very few synthetic receptors are known that selectively bind to this biologically and pharmaceutically important structure. Reetz created a host for amines *and* alcohols, but only in nonpolar dichloromethane;[10a] Gellman's P=O/S=O "bowls" are also restricted to organic solvents.[10b] For complexations that strongly rely on hydrogen bonds our binding constants of around 60000 in a competitive solvent such as DMSO are remarkably high. The binding constant for **3** with **4** in methanol is still 620 M^{-1} (glucosamine 490 M^{-1}) and even in water weak binding can be observed (Fig. 2).

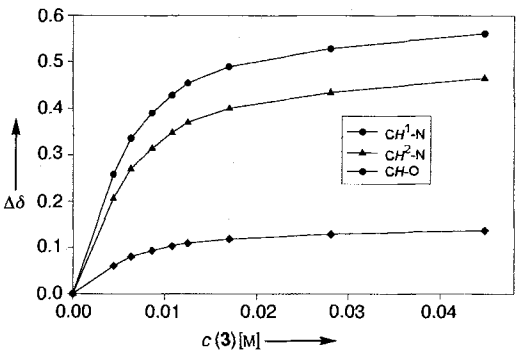

Fig. 2. Dependance of the change in chemical shift of three CH signals of 2-hydroxy-2-phenylethylamine **4** (c = 8 mM) on the concentration of bisphosphonate **3** in [D_4]methanol at 20 °C.

To realize biomimetic recognition of the aromatic ring by π-stacking interactions we are at present examining bisaryl esters of **2**. Macrocycles should provide preorientation and possibly embed the guest in an aromatic groove similar to the natural receptor.

Received: June 13, 1996 [Z9231IE]
German version: *Angew. Chem.* **1996**, *108*, 2816–2818

Keywords: adrenergic receptors · amino alcohols · molecular recognition · supramolecular chemistry

[1] C. D. Strader, T. M. Fong, M. R. Tota, D. Underwood, *Annu. Rev. Biochem.* **1994**, *63*, 101–132.
[2] C. R. Craig, R. E. Stitzel, *Modern Pharmacology*, Little, Brown & Co, Boston, **1990**.
[3] S. Trumpp-Kallmeyer, J. Hoflack, A. Bruinvels, M. Hibert, *J. Med. Chem.* **1992**, *35*, 3448–3462.
[4] A bisphosphonate and a tetraphosphate have recently been used for strong glucoside binding in acetonitrile: a) G. Das, A. D. Hamilton, *J. Am. Chem. Soc.* **1994**, *116*, 11139–11140; b) S. Anderson, U. Neidlein, V. Gramlich, F. Diederich, *Angew. Chem.* **1995**, *107*, 1722–1725; *Angew. Chem. Int. Ed. Engl.* **1995**, *34*, 1596–1600.
[5] Molecular modeling program: CERIUS² from *Molecular Simulations*; force-field program: *Dreiding* 2.21.
[6] D. A. Dougherty, *Science* **1996**, *271*, 163–167.
[7] No self-association of the simple phosphonates **1**–**3** could be detected by simple dilution experiments.
[8] C. S. Wilcox in *Frontiers in Supramolecular Chemistry and Photochemistry* (Eds.: H.-J. Schneider, H. Dürr), VCH, Weinheim, **1991**, p. 123.
[9] M. T. Blanda, J. H. Horner, M. Newcomb, *J. Org. Chem.* **1989**, *54*, 4626.
[10] a) M. T. Reetz, C. M. Niemeyer, K. Harms, *Angew. Chem.* **1991**, *103*, 1517–1519; *Angew. Chem. Int. Ed. Engl.* **1991**, *30*, 1474; b) P. B. Savage, S. H. Gellman, *J. Am. Chem. Soc.* **1993**, *115*, 10448–10449.

$K_7HW_5O_{19}\cdot 10H_2O$—A Novel Isopolyoxotungstate(VI)**

Joachim Fuchs, Rosemarie Palm, and Hans Hartl*

On acidification of an aqueous tungstate solution, addition (expansion of the tetrahedral to the octahedral coordination of W) and condensation reactions occur, leading to the formation of polymolecular isopolytungstate ions,[1] of which nine types are known. Which structure type is formed depends primarily on the degree of acidification of the tungstate solution, that is on the molar ratio of protons to monotungstate ions.[2] In addition the age of the solution and the total concentration (no aggregation occurs in highly dilute solutions) plays a role.[3] Investigations on how the pH value influences aqueous tungstate solutions are difficult to perform due in part to the very slow establishment of equilibrium and are often hard to interpret. Therefore, one is still dependent on being able to carry out crystal structure investigations on isolable compounds to be in a position, for example, through ^1H, ^{183}W, and ^{17}O NMR spectroscopic studies,[4, 5] to draw conclusions on the state of the solution. Unlike for polymolybdates[6] the influence of the inorganic counterion present in the tungstate solutions has hitherto been studied very little. We have ascertained that the influence of the cation can be very large, at least in solids, which crystallize from the solutions.[7] There are also clear indications that the nature of the cation has a strong influence on the reaction pathways in solution. Thus, ^{183}W NMR spectroscopic investigations in the presence of Li^+ indicate that cations influence the protonation of polyoxometalates (by blocking the positions of oxygen atoms) and thereby also the condensation processes in different ways.[5]

Recently we reported the synthesis and structure of the sodium hexatungstate $Na_5H_3W_6O_{22}\cdot 18H_2O$ **1**.[8] Our attempts to prepare the corresponding potassium salt by an analogous method in which potassium monotungstate K_2WO_4 was used instead of sodium monotungstate $Na_2WO_4\cdot 2H_2O$, however, resulted in no potassium hexatungstate(VI). Crystals were obtained from the solution after about a year whose vibrational spectra resembled those of the sodium hexatungstate, but showed several distinct differences. (Fig. 1). IR spectra are particularly suitable for identifying polyoxoanions. Whereas the different types of anion show a characteristic IR spectrum in the fingerprint region (roughly between 1000 and 300 cm^{-1}) that is almost unaffected by the participating cations, Raman spectra were strongly influenced by the different cations and amounts of water present.

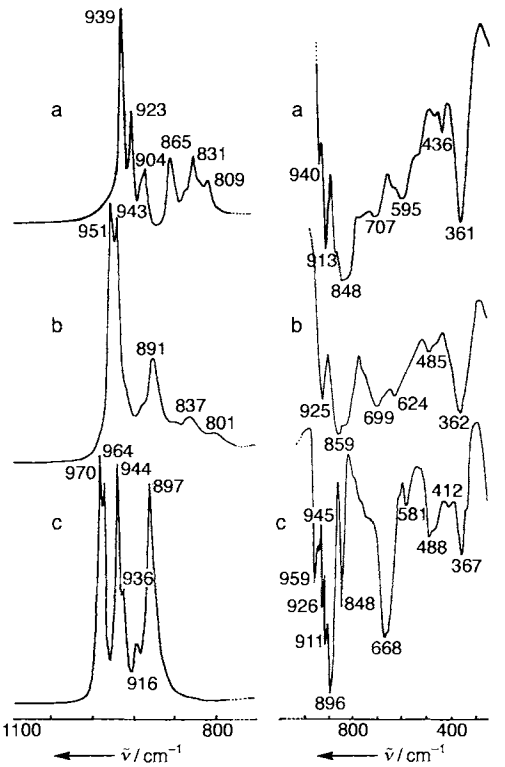

Fig. 1. IR and Raman spectra of a) $Na_5H_3W_6O_{22}\cdot 18H_2O$ **1**, b) $K_7HW_5O_{19}\cdot 10H_2O$ **2**, and c) $Na_6W_7O_{24}\cdot 18H_2O$ (in the region for the W–O vibrational bands). Left: Raman, right: IR spectrum.

According to X-ray structure analysis[9] the potassium pentatungstate $K_7HW_5O_{19}\cdot 10H_2O$ **2** surprisingly existed with a hitherto unknown polytungstate ion. This anion has one of the three structures[10] possible for blocklike W_5O_{19} frameworks, and is a fragment of the hexatungstate ion $[H_3W_6O_{22}]^{5-}$ and thus also of the heptatungstate ion $[W_7O_{24}]^{6-}$[11] (Fig. 2). It consists of five WO_6 octahedra, two of which have free faces, thus each face contains three neighboring terminal oxygen

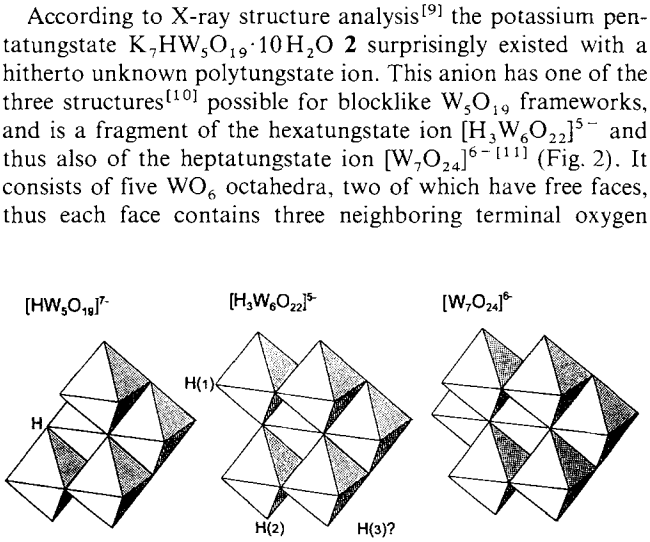

Fig. 2. Polyhedral representation of the structures of $[HW_5O_{19}]^{7-}$, $[H_3W_6O_{22}]^{5-}$, and $[W_7O_{24}]^{6-}$.

[*] Prof. Dr. H. Hartl, Prof. Dr. J. Fuchs, R. Palm
Institut für Anorganische und Analytische Chemie der Freien Universität
Fabeckstrasse 34/36, D-14195 Berlin (Germany)
Fax: Int. code +(30)8382424

[**] This work was supported by the Fonds der Chemischen Industrie.

atoms. Two octahedra have a free edge with two terminal oxygen atoms, one octahedron has only one free corner. Of the seven potassium ions, five are coordinated to both oxygen atoms of the polyanion and to water molecules. They all have a bridging function and form a link from one polyanion to five neighboring polyanions. The coordination numbers range between 6 and 8. The two remaining potassium ions are only coordinated by water molecules. Thus, tetranuclear K^+/H_2O clusters consisting of square antiprisms $[K(H_2O)_8]^+$ and monocapped octahedra $[K(H_2O)_7]^+$ are formed; these are bridged alternately through common square faces and edges (Fig. 3, right).

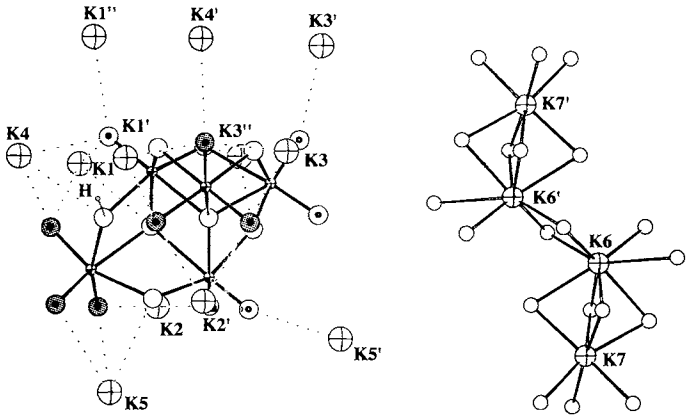

Fig. 3. Ball-and-stick representation of the anion $[HW_5O_{19}]^{7-}$ (with the K^+ coordination by K1 to K5; left) and the K^+/H_2O polyhedra of K6 and K7 (right), small spheres: W; medium: O; large: K, gray: terminal O of the *fac*-$[WO_3]$ grouping, spheres with cross: terminal O. W–O and K–O bond lengths [Å]: $W-O_{terminal}$ 1.71–1.79 (av 1.75), $W-\mu_2$-O 1.78–2.34 (av 2.02), $W-\mu_3$-O 1.93–2.31 (av 2.14), $W-\mu_4$-O 2.14–2.26 (av 2.20), K–O 2.63–3.12 (av 2.89), $K-OH_2$ 2.66–3.30 (av 2.92), average standard deviation ±0.02 Å.

Through a comparison of the systems with Na^+ and K^+ ions, it was clear that the influence of the cation is of greater significance than the degree of acidification of the tungstate solution. The hexatungstate **1** and the pentatungstate **2** were not obtained from acidic, but from alkaline solution (pH about 9).

The hexatungstate ion requires a H^+/WO_4^{2-} ratio of 7/6 = 1.167 [Eq. (a)]; thus, like the heptatungstate ion it formally

$$6WO_4^{2-} + 7H^+ \longrightarrow [W_6O_{19}(OH)_3]^{5-} + 2H_2O \quad (a)$$

belongs to the group of paratungstates. For the pentatungstate ion a lower H^+/WO_4^{2-} ratio of 3/5 = 0.60 [Eq. (b)] can be calculated; and in fact the solution was much less acidified than would be necessary according to the reaction equation (degree of acidification of the 2 M tungstate solution: 0.29; in the preparation of **1** with a H^+/WO_4^{2-} ratio of 1.167, the real degree of acidification of the tungstate solution was only 0.15).

$$5WO_4^{2-} + 3H^+ \longrightarrow [W_5O_{18}(OH)]^{7-} + H_2O \quad (b)$$

In light of the structure of **2**, a general assumption, which was previously also shared by us, needs to be corrected: WO_6 octahedra with three or more terminal oxygen atoms should generally not occur (Lipscomb rule[12]) in polyoxotungstates(VI). They should only be stable when at least one of the three terminal oxygen atoms of the face is protonated. Compound **2** contains two free faces (Fig. 2) and only one OH group, and according to calculations of the valence sums, the proton is not located at one terminal oxygen atom but at the bridging oxygen atom marked in Figure 2. Without the proton, this oxygen atom has a bonding valence sum[13] of only 1.0, whereas all other oxygen atoms of the anion have valence sums greater than 1.65.

The occurrence of free octahedra faces has been explained previously[1, 14] by the fact that at higher pH values no diprotonated monometalate ions participate in the condensation reactions (no possibility for the formation of closed structures). The two WO_6 octahedra present in the anion of **2**, each having three terminal oxo groups, in the crystal are coordinated and thereby stabilized partly by K^+ (Fig. 3, left) and by hydrogen bonding of water of crystallization. In solution such terminal *fac*-$[MO_3]$ groups (M = Mo, W) are very unstable and reactive;[15, 16] the number of neighboring terminal oxo groups is reduced by addition and condensation reactions. Although with the methods currently available it cannot be proved experimentally that the penta- and hexatungstate ions are precursors of the anion $[W_7O_{24}]^{6-}$ (Fig. 2), this appears plausible (cf. ref. [1,14]). The reason why the anions of the polytungstates **1** and **2** could not be proven analogously to $[W_7O_{24}]^{6-}$ by Raman or ^{17}O and ^{183}W NMR spectroscopic measurements[4, 5] in solution, seems to be that the anions of **1** and **2** immediately react further to give the more stable, more highly condensed heptatungstate ion, and thus exist in such low concentrations that they cannot be detected experimentally. The $[W_7O_{24}]^{6-}$ ion found in solution and in the solid state has no free octahedra faces with *fac*-$[WO_3]$ groups.

Experimental Procedure

K_2WO_4 (11.2 g, 0.0343 mol) was stirred with $WO_3 \cdot H_2O$ (1.25 g, 0.005 mol; degree of acidification (formal ratio H^+/WO_4^{2-} = 0.2) in water (12.5 mL) (tungstate concentration of the solution: about 2 mol L^{-1}) in a closed Cautex vessel at 20 °C with exclusion of CO_2. The initially yellow suspension lost color and turned almost white and was filtered. From the mother liquor, which had completely dried up after about a year, air-stable single crystals of **2** were obtained together with two other compounds (main product $K_{10}H_2W_{12}O_{42} \cdot 10H_20$ **3**).

Compound **2** could be obtained in slightly larger quantities in (almost) pure form if, at intervals of about one month, the crystals of **3** were centrifuged off from the mother liquor three times. After seeding the solution with single crystals of **2** followed by careful addition of acetone, **2** was formed in a finely crystalline form, as has been confirmed by IR spectroscopy. The yield in both cases was very low.

Received: June 10, 1996 [Z9222IE]
German version: *Angew. Chem.* **1996**, *108*, 2820–2822

Keywords: polyion aggregates · polyoxometalates · synthetic methods · tungsten compounds

[1] K. H. Tytko, O. Glemser, *Adv. Inorg. Chem. Radiochem.* **1976**, *19*, 239–315.
[2] M. T. Pope, *Heteropoly and Isopoly Oxometallates*, Springer, Berlin, **1983**, p. 19.
[3] In tungstate(VI) solutions very slow equilibrium reactions take place, which in unfavorable cases result in very long crystallization times and low yields. See for example: V. Hubert, H. Hartl, *Z. Naturforsch. B* **1996**, *51*, 969–974.
[4] R. I. Maksimovskaya, K. G. Burtseva, *Polyhedron* **1985**, *4*, 1559–1562.
[5] J. J. Hastings, O. W. Howarth, *J. Chem. Soc. Dalton Trans.* **1992**, 209–215.
[6] *Gmelin Handbook of Inorganic Chemistry*, 8th ed., *Molybdenum Suppl., Vol. B3a*, **1987**, S. 339; *Vol. B3b*, **1989**, p. 19–22, 227–229.
[7] A. Chrissafidou, J. Fuchs, H. Hartl, R. Palm, *Z. Naturforsch. B* **1995**, *50*, 217–222; H. Hartl, V. Hubert, *Acta Crystallogr. Sect. C* **1996**, *52*, 755–757; V. Hubert, Diessertation FU Berlin, **1994**.
[8] H. Hartl, R. Palm, J. Fuchs, *Angew. Chem.* **1993**, *105*, 1545–1547; *Angew. Chem. Int. Ed. Engl.* **1993**, *32*, 1492–1494.
[9] Crystal structure analysis of **2**: colorless crystals, $K_7HW_5O_{19} \cdot 10H_2O$, M_r = 1678.01; triclinic, space group $P\bar{1}$, a = 8.938(5), b = 10.972(4), c = 15.892(10) Å, α = 101.05(4), β = 101.87(5), γ = 98.42(4)°, Z = 2, V = 1468.6 Å, ρ = 3.66 g cm^{-3}, μ = 21.3 mm^{-1}; Stoe four-circle diffractometer, $Mo_{K\alpha}$ graphite monochromator, ω scanning, T = 293 K, 5401 measured reflections in the range $3 \le 2\theta \le 50°$, 5057 independent reflections, 3569 reflections with intensities greater than $2\sigma(I)$; structure solution with direct methods

(SHELXS-86) and difference Fourier techniques (XTAL 3.0), 370 refined parameters (W, K, and O atoms anisotropic, no H atoms), absorption correction (DIFABS), isotropic extinction correction, uniform weights, final R values: $R_F = 0.046$ [$I > 2\sigma(I)$] and $R_F = 0.087$ (all reflections). Further details of the crystal structure investigation may be obtained from the Fachinformationszentrum Karlsruhe, D-76344 Eggenstein Leopoldshafen (Germany), on quoting the depository number CSD-405326.

[10] K. H. Tytko, O. Glemser, *Z. Naturforsch. B* **1971**, *26*, 659–678.

[11] J. Fuchs, E. P. Flindt, *Z. Naturforsch. B* **1979**, *34*, 1393–1404; K. G. Burtseva, T. S. Chernaya, M. I. Sirota, *Sov. Phys. Dokl. (Engl. Transl.)* **1978**, *23*, 784–787.

[12] W. N. Lipscomb, *Inorg. Chem.* **1965**, *4*, 132–134.

[13] I. D. Brown, K. K. Wu, *Acta Crystallogr. Sect. B* **1975**, *32*, 1957–1959.

[14] K. H. Tytko, *Chem. Scr.* **1983**, *22*, 201–208.

[15] L. Ma, S. Liu, J. Zubieta, *Inorg. Chem.* **1989**, *28*, 175–177.

[16] A. Müller, E. Krickemeyer, S. Dillinger, J. Meyer, H. Bögge, A. Stammler, *Angew. Chem.* **1996**, *108*, 183–185; *Angew. Chem. Int. Ed. Engl.* **1996**, *35*, 171–173.

Dimeric Triaryltelluronium Arenetellurolates: New Metastable Tetramers of Diaryltellurium**

Jörg Jeske, Wolf-Walther du Mont,* and Peter G. Jones

Dedicated to Professor Max Herberhold on the occasion of his 60th birthday

Water and its homologous dihydrogen chalcogenides H_2E (E = S, Se, Te) dissociate to only a very limited extent. Neither their ionic dimers $H_3E^+EH^-$ nor organic derivatives $R_3E^+ER^-$ have been isolated in a pure state. Water dimers are typically formed by O–H···O hydrogen bonds. However, in the case of sulfur, selenium, and tellurium, metastable "dimers" R_3EER might exist as ion pairs or as molecular compounds with covalent chalcogen–chalcogen bonds. The "dimer" of SF_2 (S_2F_4) is indeed the mixed-valent molecule $F_3S–SF$ with a covalent $S^{III}–S^{I}$ bond.[1] Thus the existence and structures of the hypothetical nonclassical dimeric or oligomeric relatives of diorganotellurides R_2Te are of considerable interest, especially since it was recognized that contributions from packing of cations and anions are most important for the structures of nonclassical polytellurides implying expanded valence shells.[2–4] Possible features of "nonclassical diaryltellurium" compounds could be ionic telluronium tellurolate interactions ($R_3Te^+TeR^-$) and covalent tellurium(IV)–tellurium(II) bonds ($R_3Te–TeR$, perhaps similar to Böttcher's $CsTe_4$).[2] Cooperative charge-transfer-like interactions between tellurium atoms would also be possible. Such interactions are typical for intermolecular contacts in elemental iodine,[5] diorganic ditellurides,[6] and tetraalkyl distibanes,[6–8] and for homonuclear cation–anion contacts in iodophosphonium iodides.[9] These homonuclear interactions (n → σ* overlap) imply hypervalency of the acceptor atoms.

Oxonium salts $R_3O^+BF_4^-$ are known to alkylate alcoholates very efficiently. Accordingly triphenyltelluronium salts in THF solution transfer quantitatively one of their phenyl groups to tellurolates under mild conditions [Eq. (a)]. This phenyl transfer

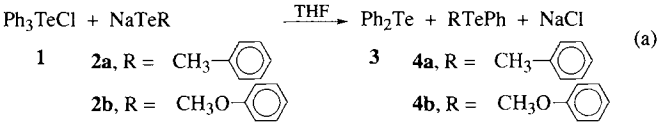

(a)

Scheme 1.

can be inhibited by adding triphenyltelluronium chloride (**1**) dissolved in methanol to an ethanolic solution of the sodium tellurolates **2a,b** at low temperatures. At temperatures below −30 °C orange powders of Ph_3TeTeR (**5**: **5a**, R = *p*-$CH_3C_6H_4N$; **5b**, R = *p*-$CH_3OC_6H_4N$) precipitated immediately from the alcoholic solutions. These reactions can be controlled to yield single crystals of the metastable **5** suitable for X-ray structure determinations. The by-product, sodium chloride, remains in solution [Eq. (b)].

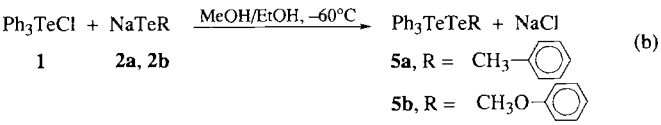

(b)

Scheme 2.

The orange crystals of **5a** and **5b** are stable below −18 °C. At room temperature they decompose gradually, furnishing oily mixtures of diaryltellurides (Ph_2Te **3**, PhTeR **4a**: R = *p*-$CH_3C_6H_4N$; **4b**: R = *p*-$CH_3OC_6H_4N$), which accelerate this decomposition. Among the products are minor amounts of diorganic ditellurides (**6a,b**) and biphenyl (detected by EI mass spectra). Telluronium tellurolates **5** are insoluble in ethanol, THF, toluene, and hexane, but slightly soluble in cold methanol. However, in solution decomposition takes place even at low temperature (−18 °C). Therefore all attempts failed to dissolve **5** for the purpose of recrystallization or for recording NMR spectra. Mass spectra always show peaks and fragments of decomposition products [Eq. (c)].

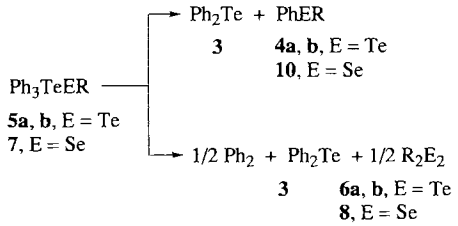

Scheme 3.

From the class of chalcogenotelluranes or telluronium chalcogenolates (R_3TeER', E = O, S, Se, Te; R = alkyl or aryl) only the (monomeric) phenoxide compound **9a** (that is, E = O) and two derivatives have been structurally characterized.[10] A nitro function *para* to the phenoxide leads to longer Te–O bonds (**9a**: 2.294, **9b**: 2.461 Å). The 2,4,6-trichlorophenoxide derivative **9c** is a dimer with inversion symmetry. Te–O distances within the dimer lie between 2.762 and 2.787 Å.[10] The first arylthio derivatives (E = S) have been postulated as inter-

[*] Prof. Dr. W.-W. du Mont, Dipl.-Chem. J. Jeske, Prof. Dr. P. G. Jones
Institut für Anorganische und Analytische Chemie
der Technischen Universität
Postfach 3329, D-38023 Braunschweig (Germany)
Fax: Int. code + (531) 391-5387
e-mail: dumont@mac1.anchem.nat.tu-bs.de

[**] Properties of Chalcogen–Chalcogen Bonds, Part 21. This work is supported by Deutsche Forschungsgemeinschaft and Fonds der Chemischen Industrie. Part 20: H. U. Meyer, T. Severengiz, W.-W. du Mont, *Bull. Soc. Chim. Fr.* **1993**, *130*, 691–694.

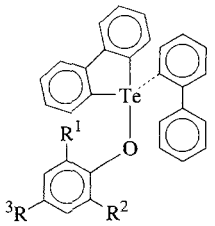

9a, $R^1 = R^2 = R^3 = H$
9b, $R^1 = R^2 = H$, $R^3 = NO_2$
9c, $R^1 = R^2 = R^3 = Cl$ (as Te_2O_2 dimer)

mediates in the thermal decomposition of telluronium carboxylates;[11] they decompose above 0 °C, especially in solution.[12]

X-ray single-crystal structure analyses of the solids **5a** and **5b**[13] show cyclic units of the composition R_8Te_4 containing tellurium–tellurium interactions. These units can be (formally) regarded as tetramers of diaryltellurium compounds. The nearly planar Te_4 rings contain alternate triphenyltelluronium and aryltellurolate units (Fig. 1). The tellurium–tellurium contacts

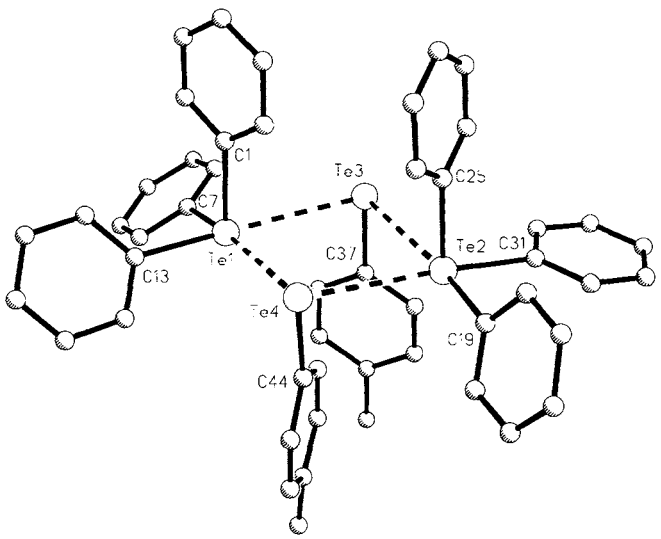

Fig. 1. Crystal structure of **5a**. Selected bond lengths [Å] and angles [°]: Te1 ··· Te3 3.5259(13), Te1 ··· Te4 3.3796(13), Te2 ··· Te3 3.3233(13), Te2 ··· Te4 3.5958(13); Te3-Te1-Te4 87.52(3), Te3-Te2-Te4 87.24(3), Te1-Te3-Te2 93.51(3), Te1-Te4-Te2 91.32(3).

(Te ··· Te: **5a** 3.3233(13), 3.5958(13), 3.3796(13), 3.5259(13); **5b** 3.481(2), 3.441(2), 3.396(2), 3.447(2) Å) within the four-membered ring system are substantially longer than covalent Te–Te single bonds[5] and than the distances between hypervalent and divalent tellurium atoms within solid $CsTe_4$.[2] However, Te–Te contacts in **5a,b** are significantly shorter than the sum of the van der Waals radii (4.40 Å). On average they are slightly shorter than the shortest intermolecular Te–Te distances between diorganic ditellurides or the distances between tellurium chains in elemental tellurium (3.50 Å).[4, 5] Corresponding *intermolecular* Se–Se interactions in elemental gray selenium are only slightly shorter (3.44 Å);[5] but covalent Se–Se bonds are about 0.40 Å shorter than Te–Te bonds. Therefore the question arises whether a mixed tellurium–selenium compound Ph_3TeSeR would exhibit nearly the same chalcogen–chalcogen distances as its analogues **5a,b** or whether the Se–Te distances would be significantly shorter.

Triphenyltelluronium 4-methylphenylselenolate (**7**) was isolated analogously to **5a** after treating triphenyltelluronium chloride with sodium 4-methylphenylselenolate. The structure of the metastable yellow–orange crystals was also determined by X-ray diffraction at −130 °C. The selenolate **7** appears to be slightly more stable than tellurolate **5a**; after thermal decomposition more diaryldiselenide and biphenyl is formed than with **5a** [Eq. (c), detected by EI-mass spectra and ^{77}Se-NMR, ratio of diarylselenide to diaryldiselenide approximately 2:1]. Solid **7** reveals the same essentially planar, four-membered ring of chalcogen atoms as in **5a,b** (Fig. 2); the average Te–Se distance (3.151–3.339 Å) is about 0.20 Å shorter than the average Te–Te distance of compounds **5a,b**.

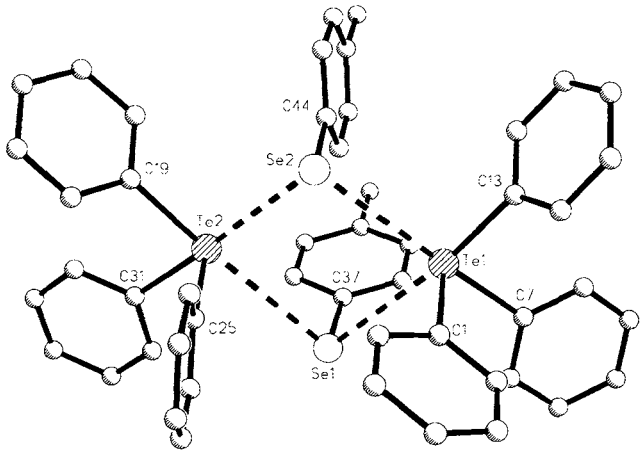

Fig. 2. Crystal structure of **7**. Selected bond lengths [Å] and angles [°]: Te1 ··· Se1 3.3081(8), Te1 ··· Se2 3.2768(9), Te2 ··· Se1 3.1507(8), Te2 ··· Se2 3.3388(8); Se1-Te1-Se2 86.382(14), Se1-Te2-Se2 87.924(14), Te1-Se1-Te2 94.129(14), Te1-Se2-Te2 91.272(14).

Including the bridging chalcogen anions, the acceptor tellurium atoms of the triphenyltelluronium cations of **5a,b** and **7** achieve the coordination number 5 (12-Te-5).[14] The coordination geometry is (3+2)-distorted, pseudo-tetragonal-monopyramidal. The coordination geometry of the donating chalcogen atoms is trigonal-pyramidal (8-Te-3, 8-Se-3). Thus the solid state structures of **5a,b** and **7** are in accordance with the valence shell electron pair repulsion (VSEPR) theory. The Te–C bonds and angles of the triphenyltelluronium fragments are scarcely distorted by cation–anion interactions.[15] Stable monomeric 2,2′-biphenylylene-2-biphenyltellurium phenoxide (10-Te-4) **9a** has a pseudo-trigonal-bipyramidal-coordinated tellurium center. The apical Te–C bond of the chelating biphenyl moiety opposite the phenoxide group is considerably longer than the equatorial Te–C bonds (2.103, 2.122 Å).[10] Dimeric **9c** contains two Te–C bonds *trans* to bridging oxygen atoms. Only one of these—the Te–C bond involving the 2-biphenyl substituent—is significantly elongated (2.159 Å). The gradual elongation of Te–O bonds in the sequence of tellurium phenoxides **9a–c** reflects the gradual change from predominantly hypervalent covalent bonds (**9a**) to a more onium-salt-like structure (**9c**).[10]

Our finding that the Te–Te and Te–Se contacts in **5a,b** and **7** are about 0.65–0.70 Å longer than the corresponding covalent bonds of Te^{II} or Se^{II} indicates that the contribution from covalence of the Te–Te and Te–Se interactions is only slight relative to that of the Te–O bond of **9a**.

Calculations (EHT, PM3) based on models of **5a,b** and **7** with appropriate symmetry give no indication of explicit bonding contributions from orbital overlap within Te_4 or Te_2Se_2 ring systems.[16] The compounds can be best described as pairs of ion pairs. The existence of the solid compounds **5a,b**, which are metastable with respect to the diaryltellurides **3** and **4**, as well as of color (**1** and **2** are colorless) and of a geometry in accordance with VSEPR indicates the importance of cooperative tellurium–tellurium interactions in the solids.

 © VCH Verlagsgesellschaft mbH, D-69451 Weinheim, 1996 0570-0833/96/3522-2654 $ 15.00+.25/0

Experimental Procedure

5a,b; 7: To a solution of 1.0 mmol sodium aryltellurolate or -selenolate (freshly prepared from diaryditellurium and -diselenium, respectively, and sodium borohydride in 20 mL of ethanol) was added triphenyltelluronium chloride (0.39 g, 1.0 mmol) in methanol (20 mL) at -60 °C. Immediately a microcrystalline product precipitated. After filtration at -60 °C and washing with ethanol it was dried in vacuo. Crystals suitable for X-ray diffraction were obtained by diffusion of the dissolved starting materials at -30 °C. **5a** (triphenyltelluronium 4-methylphenyltellurolate): Yield 0.51 g (89%). Elemental analysis of $C_{25}H_{22}Te_2$: calcd C 51.98, H 3.84; found C 52.75, H 4.00. **5b** (triphenyltelluronium 4-methoxyphenyltellurolate): Yield 0.47 g (80%). Elemental analysis of $C_{25}H_{22}OTe_2$: calcd C 50.58, H 3.74; found C 50.48, H 3.75. **7** (triphenyltelluronium 4-methylphenyl selenolate): Yield 0.35 g (67%). Elemental analysis of $C_{25}H_{22}SeTe$: calcd C 56.76, H 4.19; found C 56.03, H 3.96.

Received: March 21, 1996
Revised version: June 14, 1996 [Z 8955 IE]
German version: *Angew. Chem.* **1996**, *108*, 2822–2824

Keywords: cations · chalcogen compounds · tellurium compounds

[1] F. Seel, *Adv. Inorg. Chem. Radiochem.* **1974**, *16*, 297.
[2] P. Böttcher, U. Kretschmann, *Z. Anorg. Allg. Chem.* **1985**, *523*, 145.
[3] P. Böttcher, *Angew. Chem.* **1988**, *100*, 781; *Angew. Chem. Int. Ed. Engl.* **1988**, *27*, 759.
[4] M. G. Kanatzidis, *Angew. Chem.* **1995**, *107*, 2281–2283; *Angew. Chem. Int. Ed. Engl.* **1995**, *34*, 2109–2111.
[5] A. F. Wells, *Structural Inorganic Chemistry*, 5th ed., Clarendon Press, Oxford, **1984**.
[6] G. Becker, O. Mundt in *Unkonventionelle Wechselwirkungen in der Chemie metallischer Elemente*, (Ed.: B. Krebs), VCH, Weinheim, **1992**, pp. 199–217.
[7] H. J. Breunig, S. Gülec in *Unkonventionelle Wechselwirkungen in der Chemie metallischer Elemente*, (Ed.: B. Krebs), VCH, Weinheim, **1992**, pp. 218–230.
[8] A. J. Ashe, *Adv. Organomet. Chem.* **1990**, *30*, 77.
[9] W.-W. du Mont in *Unkonventionelle Wechselwirkungen in der Chemie metallischer Elemente*, (Ed.: B. Krebs), VCH, Weinheim, **1992**, pp. 231–244.
[10] S. Sato, N. Kondo, N. Furukawa, *Organometallics* **1994**, *13*, 3393–3395; S. Sato, N. Kondo, N. Furukawa, *ibid.* **1995**, *14*, 5393–5398.
[11] M. Wieber, E. Schmidt, *Z. Anorg. Allg. Chem.* **1988**, *556*, 189–193.
[12] M. Wieber, S. Rohse, *Z. Anorg. Allg. Chem.* **1991**, *592*, 202–206.
[13] Structure determinations: **5a**: $C_{50}H_{44}Te_4$, $M_r = 1155.25$; triclinic, space group $P\bar{1}$: $a = 12.390(4)$, $b = 13.955(4)$, $c = 14.221(4)$ Å, $\alpha = 93.28(2)$, $\beta = 99.96(2)$, $\gamma = 114.25(2)$ °; $V = 2185.5(11)$ Å^3; $Z = 2$; $\rho_{calcd} = 1.756$ Mg m^{-3}; $\lambda = 0.71073$ pm. $T = 173$ K; the crystal ($0.60 \times 0.42 \times 0.06$ mm) was mounted in inert oil. The intensities were measured to 2θ 50° using $Mo_{K\alpha}$ radiation on a Siemens R3 diffractometer. Of 7755 reflections, 7383 were unique ($R_{int} = 0.0181$) and used for all calculations (programm SHELXL-93). After absorption correction (psi-scans), the structure was solved by direct methods and refined anisotropically on F^2. The final *wR2* was 0.0959 with conventional *R*(*F*) 0.0359, 489 parameters, and 468 restraints; max. $\Delta\rho$ 1262 e nm^{-3}. **5b**: $C_{50}H_{44}O_2Te_4$, $M_r = 1187.25$; triclinic, space group $P\bar{1}$: $a = 12.344(5)$, $b = 13.503(6)$, $c = 15.262(6)$ Å, $\alpha = 93.51(4)$, $\beta = 98.99(4)$, $\gamma = 115.30(4)$°; $V = 2248.2(16)$ Å^3; $Z = 2$; $\rho_{calcd} = 1.754$ Mg m^{-3}, $\lambda = 0.71073$ pm, $T = 173$ K; $0.80 \times 0.54 \times 0.03$ mm, 2θ range 6–55°, absorption correction (SHELXA), 8818 data, 8817 unique; structure solved and refined as above, *wR2* = 0.1803, *R1* = 0.0542, 507 parameters, and 474 restraints; max. $\Delta\rho$ 1496 e nm^{-3}. **7**: $C_{50}H_{44}Sc_2Te_2$, $M_r = 1057.97$; triclinic, space group $P\bar{1}$: $a = 12.108(3)$, $b = 13.968(3)$, $c = 14.169(3)$ Å, $\alpha = 93.751(10)$, $\beta = 100.64(1)$, $\gamma = 114.04(1)$°; $V = 2124.2(8)$ Å^3; $Z = 2$; $\rho_{calcd} = 1.654$ Mg m^{-3}, $\lambda = 0.71073$ pm, $T = 143$ K; $0.50 \times 0.50 \times 0.35$ mm, 2θ range 6–50°, absorption correction (psi-scans), 7969 data, 7589 unique, STOE Stadi-4 diffractometer; structure solved by using non-hydrogen atom coordinates of **5a**, refinement as above, *wR2* = 0.0763, *R1* = 0.0267, 489 parameters and 468 restraints; max. $\Delta\rho$ 948 e nm^{-3}. Because of similar cell dimensions and atomic positions these crystal structures can be treated as isostructural. Crystallographic data (excluding structure factors) for the structures reported in this paper have been deposited with the Cambridge Crystallographic Data Centre as supplementary publication no. CCDC-179-113. Copies of the data can be obtained free of charge on application to The Director, CCDC, 12 Union Road, Cambridge CB2 1EZ, UK (fax: int. code +(1223)336-033; e-mail: teched@chemcrys.cam.ac.uk).
[14] (12-Te-5) means that 12 valence electrons surround the central atom Te, which has 5 substituents: C. W. Perkins, J. C. Martin, A. J. Arduengo III, W. Lau, A. Alegria, J. K. Kochi, *J. Am. Chem. Soc.* **1980**, *102*, 7753.
[15] I. Haiduc, R. B. King, M. G. Newton, *Chem. Rev.* **1994**, *94*, 301–326.
[16] C. Janiak, unpublished results.

Coelenterands: A New Class of Metal-Encapsulating Ligands

Chris M. Hartshorn and Peter J. Steel*

Heterocyclic tripodal ligands have long been used in coordination and organometallic chemistry,[1] most notably the anionic tripyrazolylborates (scorpionates),[2, 3] and their neutral carbon analogues, the tripyrazolylmethanes.[4] A separate area of chemistry that has received much attention is the study of π-arene complexes of transition metals. Benzene forms stable organometallic complexes with many metals, for example, $[Ru(\eta^6\text{-}C_6H_6)_2]^{2+}$,[5] but half-sandwich complexes of ruthenium (e.g., $[Ru(\eta^6\text{-}C_6H_6)L_3]^{2+}$; L = monodentate ligand) are less well studied.[5, 6] In this paper we bring together for the first time these two important areas of chemistry and introduce a new class of ligands, the coelenterands.[7] The structures of these molecules is such that a coordinated metal is simultaneously involved in η^6-bonding to the benzene ring and tripodal coordination to suitably placed heterocycles.

We are currently engaged in the synthesis and study of an extensive range of compounds (represented by the generalized structure **1**) that comprise a benzene (or other arene) ring to

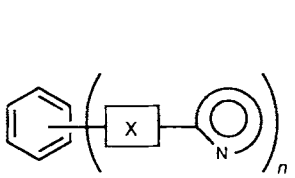

1

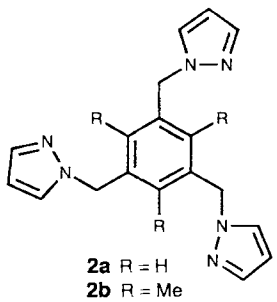

2a R = H
2b R = Me

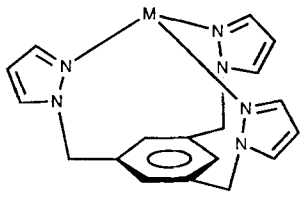

3

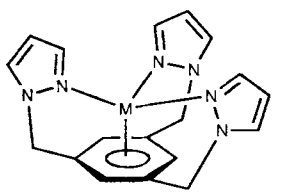

4

which are appended multiple heterocyclic rings connected through a variety of spacer groups. These polyheteroaryl-substituted arenes exhibit a variety of modes of coordination to different transition metals.[8] We recently reported[9] the syntheses of a number of poly(pyrazol-1-ylmethyl)benzenes including the 1,3,5-tri(pyrazol-1-ylmethyl)benzenes (**2a,b**), and speculated that such compounds might act as tripodal chelating ligands, as in **3**, or even encapsulate a metal with additional coordination to the benzene ring, as in **4**. We now report the successful realization of this second mode of coordination.

Reaction of **2b**, readily available in two steps from mesitylene,[9] with $[Ru(dmso)_4Cl_2]$ in ethanol/water at reflux

[*] Dr. P. J. Steel, C. M. Hartshorn
Department of Chemistry
University of Canterbury, Christchurch (New Zealand)
Fax: Int. code +(3)3642110
e-mail: p.steel@chem.canterbury.ac.nz

gave a product that was isolated in 42% yield as the hexafluorophosphate salt (Scheme 1). X-ray quality crystals of **5** proved very elusive; of the several counterions tried, only the tetrachlorozincate anion furnished single crystals.[10]

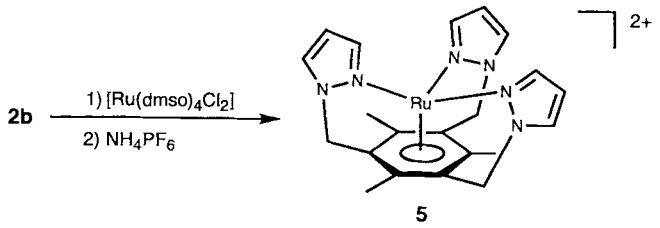

5

Scheme 1. Preparation of **5**.

Figure 1 shows a perspective view of the structure of cation **5**.[11,12] This clearly shows that the ligand encapsulates the ruthenium atom, with joint chelation by the three pyrazole nitrogens and π-coordination by the benzene ring, in this 18-electron species. The cation has approximate C_{3v} symmetry; the coordination about the ruthenium atom is distorted octahedral. The benzene ring is measurably distorted towards a chair conformation: the pyrazolylmethyl-substituted carbons are displaced towards the ruthenium atom (mean deviation from the plane 0.029 Å). Whereas the three methyl substituents lie in the plane of the benzene ring (maximum deviation from the plane 0.069 Å), the three attached methylene carbons are severely displaced from this plane (mean deviation 0.470 Å), an indication of significant pyramidalization of the aromatic carbons. By necessity, the the structure has an eclipsed, rather than staggered, piano-stool-type arrangement.

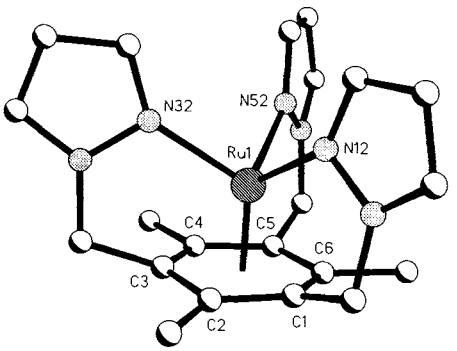

Fig. 1. Perspective view and atom labeling of the X-ray crystal structure of the cation **5**. Selected bond lengths [Å] and angles [°]: Ru1–N12 2.107(8), Ru1–N32 2.091(8), Ru1–N52 2.094(8), Ru1–C1 2.103(9), Ru1–C2 2.186(9), Ru1–C3 2.096(9), Ru1–C4 2.156(9), Ru1–C5 2.083(9), Ru1–C6 2.149(9); N12-Ru1-N32 96.7(3), N12-Ru1-N52 94.5(3), N32-Ru1-N52 92.6(3).

A search of the Cambridge Crystallographic Data Base for [Ru(η^6-arene)] structures with three additional nitrogens coordinated to the ruthenium disclosed five related structures, with $B(pz)_4^-$,[13] $(pzH)_2pz$,[14] $(PhNH^-)_3$,[15] $(MeCN)_3$,[16] and $pyCH_2N(Me)CH_2CH_2py$[6] (where pz = pyrazole and py = pyridine) as additional ligands. The structures of two *p*-cymeneruthenium complexes of a tripyrazolylborate and a tripyrazolylmethane have also recently been reported.[17] In none of these literature structures is any of the nitrogen atoms linked to the benzene ring. The most significant difference between these structures and that of **5** is in the distance of the ruthenium atom from the arene ring; in **5** the ruthenium lies 1.579 Å from the centroid of the benzene ring, whereas in the previously reported structures the corresponding distances are significantly longer, lying in the range 1.67–1.70 Å. This indicates a strong metal–arene interaction in **5**, which is undoubtedly reinforced by multiple chelate effects. In the published structures[6,13–17] the N-Ru-N angles are generally acute, whereas in the case of **5** the internal attachments to the benzene rings result in these angles being obtuse (92.6–96.7°).

According to the similarity of the spectroscopic and electrochemical[18] properties of **5** to those of Ru(η^6-arene) complexes with additional nitrogen donors, this structure is maintained in solution.[6,14,17,19] In particular, the large upfield shifts (about 30 ppm) of the arene carbons in the ^{13}C NMR spectrum clearly establish their coordination to the ruthenium atom.

Having demonstrated the ability of these ligands to encapsulate a ruthenium atom, we are currently studying their complexation of other metal ions. We are also synthesizing other coelenterands with different heterocyclic rings and different spacer groups. For example, we have prepared the new, less symmetrical ligand **6**, with a 2-pyridoxy group, from 2,4,6-trimethylphenol by a reaction sequence involving heteroarylation,[8] double bromomethylation,[20] and phase-transfer-catalyzed alkylation[21] with pyrazole (Scheme 2). This new coelenterand also reacts with $[Ru(dmso)_4Cl_2]$ to form a complex analogous to that of **5**.

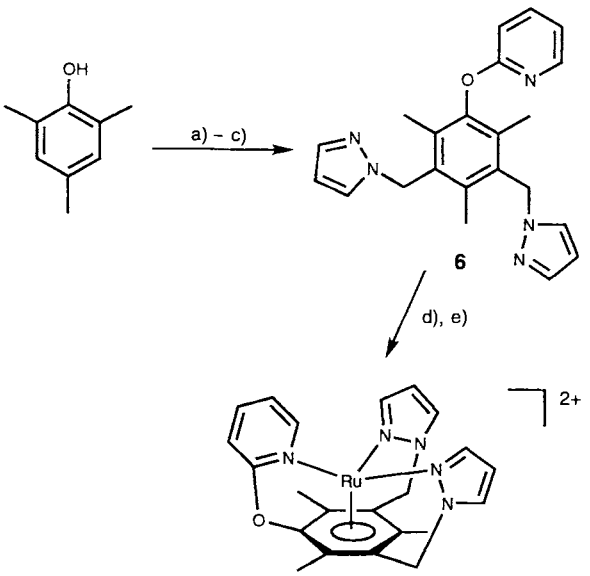

Scheme 2. Preparation and complexation of **6**. a) 2-Bromopyridine/K_2CO_3/Δ; b) CH_2O/HBr; c) pyrazole/NaOH/NBu_4OH; d) $[Ru(dmso)_4Cl_2]$; e) NH_4PF_6

In conclusion, we here describe the formation of novel organometallic compounds derived from a new class of ligands, the coelenterands, which encapsulate metal ions with simultaneous η^6-arene coordination and tripodal chelation from within the same ligand.

Experimental Procedure

5: An equimolar mixture of **2b** and $[Ru(dmso)_4Cl_2]$ was heated at reflux in ethanol/water (3/1) for 12 h. The ethanol was removed under reduced pressure to give the chloride salt of **5**. High-resolution MS: calcd for $[C_{21}H_{24}N_6{}^{35}Cl^{102}Ru]^+$ 497.0795, found 497.0801. This was dissolved in water and filtered. Ammonium hexafluorophosphate was added to the filtrate to give a pale yellow/green precipitate of **5** as the PF_6 salt in 42% overall yield. M.p. >250 °C (decomp). UV/Vis (CH_3CN):

 © VCH Verlagsgesellschaft mbH, D-69451 Weinheim, 1996 0570-0833/96/3522-2656 $ 15.00+.25/0

λ [nm] (ε [$M^{-1}cm^{-1}$]) = 222 (11200), 344 (625). ^{1}H NMR (300 MHz, CD_3CN): δ = 2.19 (s, 9H), 5.48 (s, 6H), 6.70 (t, 3H), 7.69 (d, 3H), 8.12 (d, 3H). ^{13}C NMR (75 MHz, CD_3CN): δ = 13.0 (CH_3), 51.6 (CH_2), 100.6 (C2,4,6), 109.2 (C1,3,5), 109.6 (C4'), 135.1 (C5'), 140.7 (C3'). Alternatively, zinc chloride (2 equiv) and hydrochloric acid were added to the above filtrate, which, over a period of weeks, furnished yellow crystals of the $ZnCl_4^{2-}$ salt of **5**, which were suitable for single crystal X-ray structure analysis. C,H,N anal. calcd. for $C_{21}H_{24}N_6RuZnCl_4 \cdot 2H_2O$: C 35.79, H 4.00, N 11.92; found: C 35.60, H 3.91, N 11.83.

6: a) 2,4,6-Trimethylphenol (2 equiv), 2-bromopyridine (1 equiv) and potassium carbonate (1 equiv) were heated, with stirring, at 220–230 °C for 8 hours. The resulting mixture was extracted repeatedly with diethyl ether, and the extracts combined and washed with aqueous sodium hydroxide. Removal of the solvent under reduced pressure yielded 2,4,6-trimethyl(2-pyridoxy)benzene in 62% yield. b) A mixture of 2,4,6-trimethyl(2-pyridoxy)benzene (1 equiv), paraformaldehyde (4 equiv), and 40% hydrobromic acid was heated at reflux in acetic acid for 14 days; additional hydrobromic acid was added to the reaction mixture every second day. The resulting solution was poured into water, and the solid filtered and recrystallized from petroleum ether to give 3,5-bis(bromomethyl)-2,4,6-trimethyl(2-pyridoxy)benzene in 29% yield. M.p. = 160–161 °C. C,H,N anal. calcd. for $C_{16}H_{17}Br_2NO$: C 48.15, H 4.29, N 3.51; found: C 48.57, H 4.28, N 3.44. ^{1}H NMR (300 MHz, $CDCl_3$): δ = 2.18 (s, 6H), 2.47 (s, 3H), 4.59 (s, 4H), 6.90 (d, 1H), 6.95 (t, 1H), 7.69 (t, 1H), 8.11 (d, 1H). ^{13}C NMR (75 MHz, $CDCl_3$): δ = 12.79, 14.92, 29.71, 109.96, 117.84, 131.73, 133.52, 134.26, 139.56, 147.75, 148.53, 162.95. c) A mixture of 3,5-bis(bromomethyl)-2,4,6-trimethyl(2-pyridoxy)benzene (1 equiv) pyrazole (2 equiv) and tetrabutylammonium hydroxide was heated at reflux in benzene/aqueous sodium hydroxide for 18 hours. The benzene layer was then separated, dried (sodium sulfate), and concentrated under reduced pressure to give a crude product, which was recrystallized from petroleum ether to give the pyridoxybenzene **6** as a colorless solid in 58% yield. M.p. = 127 °C. C,H,N anal. calcd. for $C_{22}H_{23}N_5O$: C 70.76, H 6.21, N 18.75; found: C 70.51, H 6.05, N 18.66. ^{1}H NMR (300 MHz, $CDCl_3$): δ = 2.15 (s, 6H), 2.27 (s, 3H), 5.43 (s, 4H), 6.20 (t, 2H), 6.94 (d, 1H), 6.95 (t, 1H), 7.09 (d, 2H), 7.53 (d, 2H), 7.70 (t, 1H), 8.10 (d, 1H). ^{13}C NMR (75 MHz, $CDCl_3$): δ = 13.24, 15.58, 50.42, 105.33, 110.07, 117.86, 127.85, 131.36, 132.52, 135.55, 139.22, 139.53, 147.67, 148.88, 162.88.

Received: April 19, 1996 [Z 9053 IE]
German version: *Angew. Chem.* **1996**, *108*, 2818–2820

Keywords: arenes · chelate ligands · ruthenium compounds

[1] A. Shaver in *Comprehensive Coordination Chemistry, Vol. 2* (Eds.: G. Wilkinson, R. D. Gillard, J. A. McCleverty), Pergamon, Oxford, **1987**, p. 245.
[2] S. Trofimenko, *Prog. Inorg. Chem.* **1986**, *34*, 115–210; *Chem. Rev.* **1993**, *93*, 943–980; G. Parkin, *Adv. Inorg. Chem.* **1995**, *42*, 291–393; N. Kitajima, W. B. Tolman, *Prog. Inorg. Chem.* **1995**, *43*, 419–531.
[3] S. Trofimenko, *J. Am. Chem. Soc.* **1967**, *89*, 3170–3177, 6288–6294.
[4] P. K. Byers, A. J. Canty, R. T. Honeyman, *Adv. Organomet. Chem.* **1992**, *34*, 1–65; T. Astley, J. M. Gulbis, M. A. Hitchman, E. R. T. Tiekink, *J. Chem. Soc. Dalton Trans.* **1995**, 509–515; D. L. Reger, J. E. Collins, R. Layland, R. D. Adams, *Inorg. Chem.* **1996**, *35*, 1372–1376, and references therein.
[5] M. A. Bennett, M. I. Bruce, T. W. Matheson in *Comprehensive Organometallic Chemistry, Vol. 4* (Eds.: G. Wilkinson, F. G. A. Stone, E. W. Abel), Pergamon, Oxford, **1982**, p. 691; M. A. Bennett in *Comprehensive Organometallic Chemistry II, Vol. 7* (Eds.: E. W. Abel, F. G. A. Stone, G. Wilkinson), Pergamon, Oxford, **1995**, p. 549.
[6] Z. Shirin, R. Mukherjee, J. F. Richardson, R. M. Buchanan, *J. Chem. Soc. Dalton Trans.* **1994**, 465–469, and references therein.
[7] We propose the name coelenterand for this type of ligand and coelenterate for its metal complex, after the animal phylum Cœlenterata, from the Greek for "hollow stomach". We thank Dr. J. A. Gerrard for suggesting this name.
[8] C. M. Hartshorn, P. J. Steel, *Inorg. Chem.*, in press.
[9] C. M. Hartshorn, P. J. Steel, *Aust. J. Chem.* **1995**, *48*, 1587–1599.
[10] We thank Prof. D. A. House for this useful suggestion.
[11] Crystal structure analysis of $C_{21}H_{24}N_6Ru \cdot ZnCl_4 \cdot 3H_2O$: M_r = 722.75, triclinic, space group $P\bar{1}$, a = 10.330(2), b = 11.557(3), c = 12.835(3) Å, α = 114.86(2), β = 102.61(2), γ = 93.59(2)°, V = 1336.0(5) Å^3, $F(000)$ = 728, ρ_{calcd} (Z = 2) = 1.797 g cm^{-1}, μ = 1.90 mm^{-1}, approximate crystal dimensions 0.40 × 0.29 × 0.06 mm, $2\theta_{max}$ = 50°, radiation $Mo_{K\alpha}$ (λ = 0.71073 Å), ω scans, T = −85 C, 4303 measured data, 4078 unique data, Lp corrections, no absorption correction, Patterson/Fourier (SHELXS), full-matrix least-squares refinement on F^2 with all data (SHELXL93), 338 parameters, H atoms in calculated positions, conformational orientation of methyl hydrogens deduced from circular Fourier syntheses, residual electron density < 1.6 e Å^{-3}, GOF = 0.92, wR(all data) = 0.156, conventional R value [2571 data with $I > 2\sigma(I)$] = 0.061. Crystallographic data (excluding structure factors) for the structure reported in this paper have been deposited with the Cambridge Crystallographic Data Centre as supplementary publication no. CCDC-179-115. Copies of the data can be obtained free of charge on application to the Director, CCDC, 12 Union Road, Cambridge CB2 1EZ, UK (fax: int. code +(1223) 336-033; e-mail: teched@chemcrys.cam.ac.uk).
[12] The structure is held together by a complex network of hydrogen bonds between the tetrachlorozincate anion and three water solvate molecules, one of which is disordered over two sites.
[13] R. J. Restivo, G. Ferguson, D. J. O'Sullivan, F. J. Lalor, *Inorg. Chem.* **1975**, *14*, 3046–3052.
[14] D. Carmona, J. Ferrer, L. A. Oro, M. C. Apreda, C. Foces-Foces, F. H. Cano, J. Elguero, M. L. Jimeno, *J. Chem. Soc. Dalton Trans.* **1990**, 1463–1476.
[15] G. C. Martin, G. J. Palenik, J. M. Boncella, *Inorg. Chem.* **1990**, *29*, 2027–2030.
[16] W. Luginbühl, P. Zbinden, P. A. Pittet, T. Armbruster, H.-B. Bürgi, A. E. Merbach, A. Ludi, *Inorg. Chem.* **1991**, *30*, 2350–2355.
[17] S. Bhambri, D. A Tocher, *Polyhedron* **1996**, *15*, 2763–70.
[18] In acetonitrile **5** showed only a series of irreversible reductions starting at −0.91 V (vs. SCE) and no observable oxidation process within the solvent limits. Ru(η^6-benzene) complexes with tridentate nitrogen ligands behave similarly [6]. We thank Dr. A. J. Downard for these measurements.
[19] M. Stebler-Rothlisberger, A. Ludi, *Polyhedron* **1986**, *5*, 1217–1221.
[20] A. W. van der Made, R. H. van der Made, *J. Org. Chem.* **1993**, *58*, 1262–1263.
[21] A. J. Downard, G. E. Honey, P. J. Steel, *Inorg. Chem.* **1991**, *30*, 3733–3737, and references therein.

Molecular Redox-Switches by Ligand Exchange**

Christophe Canevet, Jacqueline Libman, and Abraham Shanzer*

The increasing interest in molecule-based technologies[1] is stimulating extensive research on the synthesis of task-oriented molecules such as molecular wires,[2, 3] diodes,[4, 5] light converters,[6] and switches.[7–14] Recently, several molecular switches have been introduced that respond to external triggers such as photons, protons, and electrons. Examples include photochromic materials that undergo reversible, light-induced cyclizations,[11] rotaxanes in which macrocyclic structures shuttle between two stations on a rodlike molecule,[12] catenates in which redox processes of a guest ion promote swinging motions of two rings relative to each other,[13] and triple-stranded helices that undergo electron-induced translocation of an iron atom between neighboring cavities.[14] Here we introduce a novel redox-switch that interconverts between two distinct states by ligand exchange. At the heart of this switch is a molecule that possesses two sets of ion-binding groups: one set of "hard" and one set of "soft" ligating groups. The two sets are anchored on a calix[4]arene ring[15] in an alternating fashion, such that they can form either a "hard" or a "soft" ion-binding cavity; one cavity is formed at the exclusion of the other. Calix[4]arene was selected as the anchor since it directs both sets of ion-binding groups to the same face of the ring and allows either set to converge by means of a rocking motion. When loaded with Fe^{III}, the "hard" binding groups, hydroxamates, converge to embrace the "hard" metal ion, while the soft groups diverge. Upon reduction, the ligand rearranges to engulf Fe^{II} with its "soft"

[*] Prof. A. Shanzer, C. Canevet, Dr. J. Libman
Weizmann Institute of Science
Department of Organic Chemistry
Rehovot 76100 (Israel)
Fax: Int. code +8934-4142
e-mail: coshanzr@weizmann.weizmann.ac.il

[**] This work was financially supported by the Israel Academy of Sciences and Humanities and by the Minerva Foundation. We thank Dr. S. J. Harris, Dublin University, Ireland, for sharing his knowledge of calix[4]arene chemistry. The French–Israeli l'Arc-en-ciel Program is acknowledged.

bipyridyl groups (Fig. 1), while the "hard" groups diverge. Subsequent oxidation reverses this process. The distinctly different spectroscopic characteristics of this switch in its two states enables ready monitoring of the switching process in real time, as it turns from orange into pink upon reduction.

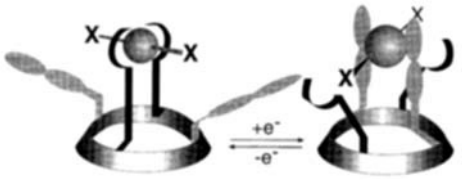

Fig. 1. Schematic representation of the redox-switch.

The mixed-ligand binders **3** and **5** and the reference binders **1**, **2**, and **4** were prepared from calix[4]arene by a series of steps shown in Figure 2. The structures of the compounds were established by ^{1}H NMR, FT IR and, FAB MS, and their cone conformations were confirmed by the large chemical shift difference of the anchors' methylene bridges[15] ($\Delta\delta$(Ar-CH_AH_B-Ar) = 0.88, 0.96, 0.72, 1.02, and 1.10, for ligands **1**, **2**, **3**, **4**, and **5**, respectively).

Addition of $FeCl_3$ to a buffered solution of the mixed-ligand binder **3** resulted in the formation of the bishydroxamate complex Fe^{III}-**3**, as indicated by its UV/Vis spectrum (λ_{max} (ε) = 464 nm (1900)).[16] Subsequent addition of ascorbic acid caused the appearance of new, bathochromically displaced maxima (λ_{max} (ε) = 494 (3000), 526 nm (3000)), characteristic for the Fe^{II}–bipyridyl complex Fe^{II}-**3**.[17] Addition of ammonium persulfate reversed this process (Fig. 3). The identity of the reduced form of the switch, Fe^{II}-**3**, was confirmed by comparison with the same complex prepared directly by reaction of **3** with $FeCl_2$ under argon. Independent characterization of each state of the switch was achieved by FAB MS, which confirmed the presence of 1:1 calixarene:iron complexes without contamination of higher oligomers (see *Experimental Procedure*). Moreover, the stability of binder **3** to the reduction and oxidation procedures applied was demonstrated by thin layer chromatography.

These redox processes are most likely to occur intramolecularly, as the half life of the reduction processes was found to be shorter ($t_{1/2}$ = 30 min) than that for the complexation of solvated Fe^{II} ions to the mixed-ligand binder **3** under the same conditions ($t_{1/2}$ > 2 h).[18] Considering the coordinative requirements of iron, it is plausible that each set of ligating groups on the calixarene binds the guest ion in a cisoid, square-planar arrangement, which is completed by two buffer molecules to form an octahedral coordination environment (Fig. 1). The redox processes of the guest ions are consequently accompanied by a rearrangement in which the two sets of ligating chains exchange positions.

The closely related calix[4]arene binder **5**, in which the bipyridyl residues had been attached to the 6-positions rather than 5-positions, failed to form uniquely defined Fe^{III}–hydroxamate and Fe^{II}–bipyridyl complexes. Binder **5** yielded mixed-ligand complexes as indicated by the UV/Vis spectra of Fe^{III}-**5** and Fe^{II}-**5**, and therefore failed to function as switch. The different behaviors of **5** and **3** can readily be rationalized by molecular models. In **5** the two sets of ligands lie in the same imaginary plane above the calixarene ring and may therefore bind the guest ions simultaneously. In switch **3** the two sets of ligands lie in different planes, prohibiting simultaneous coordination.

Because this switch is amphiphilic it is eminently suited for incorporation into air/water or lipid/water interfaces.[19]

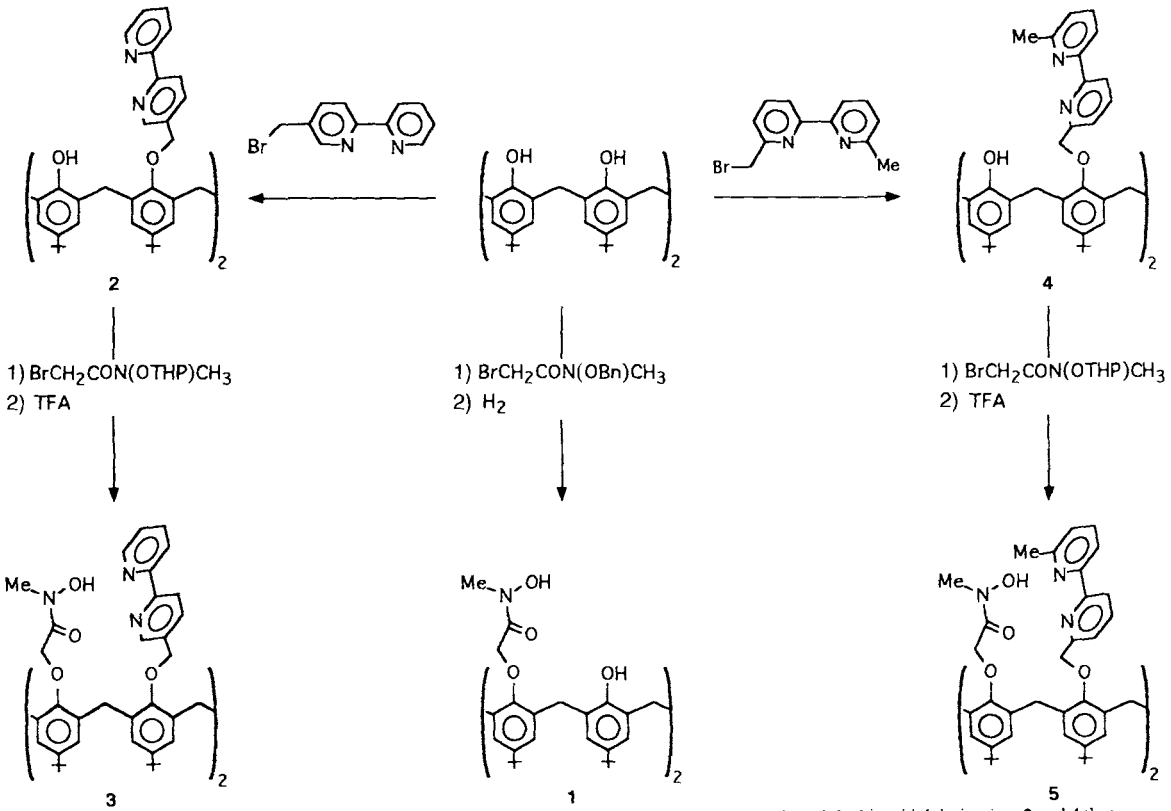

Fig. 2. Synthetic scheme for the preparation of the mixed-ligand binders **3** and **5**, the hydroxamate **1**, and the bipyridyl derivatives **2** and **4** that serve as reference compounds. THP = tetrahydropyran, TFA = trifluoroacetic acid.

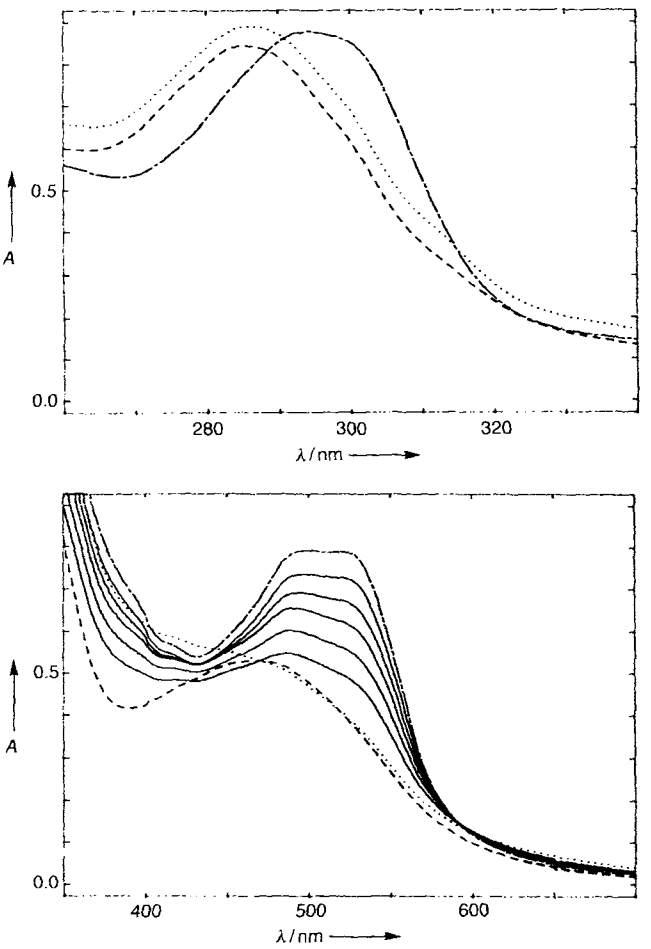

Fig. 3. UV (top) and Vis (bottom) absorption spectra of Fe^{III}-**3** (– – – –) and Fe^{II}-**3** (- · · · -) (0.27 mM); Changes in the Vis spectrum (bottom) of Fe^{III}-**3** after treatment with ascorbic acid at several time intervals (——), and final Vis (bottom) and UV (top) spectra after subsequent treatment with ammonium persulfate (....).

These options are under current consideration as is the possibility of disrupting the orientation of organized assemblies by the pronounced conformational changes of these switches.

Experimental Procedure

1: To a solution of tetra-*tert*-butylcalix[4]arene [15] (0.25 g, 0.38 mmol) in anhydrous DMSO (10 mL) was added $BrCH_2CON(OBn)Me$ (0.40 g, 1.5 mmol) and anhydrous potassium carbonate (0.25 g, 1.8 mmol). The reaction mixture was stirred for 2 d at ambient temperature and poured into 10% aq. HCl (40 mL). The precipitate was removed by filtration and washed twice with water. Chromatographic purification provided protected **1**, which was hydrogenated at atmospheric pressure in the presence of Pd/C to yield **1** (0.15 g, 40%). M.p. 208–213 °C; ^{1}H NMR (400 MHz, $CDCl_3$, 25 °C, TMS): $\delta = 7.03$ and 6.93 (each s, each 4H, ArH), 4.82 (s, 4H, CH_2), 4.26 and 3.38 (each d, each 4H, Ar-CH_AH_B-Ar, $\Delta\delta = 0.88$, $J_{A,B} = 13$ Hz), 3.40 (s, 6H, CH_3), 1.25 and 1.06 (each s, each 18H, *t*Bu); IR ($CDCl_3$): $\tilde{\nu} = 1657\ cm^{-1}$ (C=O); FAB MS: *m/z*: 845.4 $[(M + Na)^+]$.

2: To a solution of tetra-*tert*-butylcalix[4]arene [15] (0.50 g, 0.77 mmol) in anhydrous DMF (20 mL) was added *5-bromomethyl-2,2'-bipyridine* [20] (1.0 g, 4.0 mmol) and anhydrous potassium carbonate (0.50 g, 3.6 mmol). The reaction mixture was stirred for 20 h at 70 °C, cooled, and poured into water (100 mL). The precipitate was collected by filtration. Chromatography provided pure **2** (0.24 g, 30%). M.p. 161–163 °C; ^{1}H NMR (400 MHz, $CDCl_3$, 25 °C, TMS): $\delta = 8.88$, 8.60, 8.47, 8.39, 8.18, 7.71, 7.27–7.13 (d, md, dd, td, dd, dt, and m, respectively, each 2H, pyH), 7.13 (s, 2H, OH), 7.05 and 6.81 (each s, each 4H, ArH), 5.18 (s, 4H, CH_2), 4.24 and 3.28 (each d, each 4H, Ar-CH_AH_B-Ar, $\Delta\delta = 0.96$, $J_{A,B} = 13$ Hz), 1.29 and 0.96 (each s, each 18H, *t*Bu); FAB-MS: *m/z*: 985.7 $[(M + H)^+]$.

3: Bisbipyridine **2** (0.21 g, 0.21 mmol) in anhydrous THF (20 mL) was treated with $BrCH_2CON(OTHP)Me$ (0.84 g, 3.3 mmol), potassium iodide (0.31 g, 1.9 mmol), and sodium hydride (37 mg, 1.2 mmol), and heated at reflux overnight. The product was filtered and chromatographed to provide 70 mg (25% yield) of protected tetra-substituted calix[4]arene. Deprotection by treatment with trifluoroacetic acid, neutralization with diethylaminomethyl polystyrene, and chromatographic purification yielded switch **3** in 20% yield. M.p. 213–215 °C; ^{1}H NMR (400 MHz, $CDCl_3$, 25 °C, TMS): $\delta = 8.68$, 8.65, 8.26, 8.12, 7.91, 7.79, 7.41 (d, s, d, d, t, d, and m, respectively, each 2H, pyH), 7.05 and 6.97 (each s, each 4H, ArH), 5.22 and 4.49 (each s, each 4H, CH_2), 3.83 and 3.11 (each d, each 4H, Ar-CH_AH_B-Ar, $\Delta\delta = 0.72$, $J_{A,B} = 12$ Hz), 3.73 (s, 6H, CH_2), 1.14 and 1.07 (each s, each 18H, *t*Bu); IR ($CDCl_3$): $\tilde{\nu} = 1653\ cm^{-1}$ (C=O); FAB-MS: *m/z*: 1181.7 $[(M + Na)^+]$.

4: In a procedure analogous to that used for **2**, tetra-*tert*-butylcalix[4]arene [15] (0.20 g, 0.31 mmol) was treated with 6-bromomethyl-6'-methyl-2,2'-bipyridine [21] (0.43 g, 1.6 mmol) and anhydrous potassium carbonate (0.20 g, 1.4 mmol) in anhydrous DMF (10 mL) to yield **4** (0.17 g, 55% yield). M.p. 108–110 °C; ^{1}H NMR (400 MHz, $CDCl_3$, 25 °C, TMS): $\delta = 8.34$, 8.20, 7.73–7.62, 7.15 (d, t, m, d, 2H, 4H, 4H, 2H, respectively, pyH), 7.34 (s, 2H, OH), 7.08 and 6.82 (each s, each 4H, ArH), 5.26 (s, 4H, CH_2), 4.37 and 3.35 (each d, each 4H, Ar-CH_AH_B-Ar, $\Delta\delta = 1.02$, $J_{A,B} = 13$ Hz), 2.65 (s, 6H, CH_3), 1.30 and 0.95 (each s, each 18H, *t*Bu); FAB-MS: *m/z*: 1013.5 $[(M + H)^+]$.

5: In a procedure analogous to that used for **3**, calixarene **4** (0.35 g, 0.35 mmol) was treated with $BrCH_2CON(OTHP)Me$ (1.25 g, 5.0 mmol), potassium iodide (0.50 g, 3.0 mmol), and sodium hydride (60 mg, 2.0 mmol), in anhydrous THF (25 mL) to provide 200 mg (45% yield) of the protected product. Deprotection by treatment with TFA yielded binder **5** in 40% yield. M.p. > 300 °C; ^{1}H NMR (400 MHz, $CDCl_3$, 25 °C, TMS): $\delta = 8.19$, 7.90, 7.74, 7.67, 7.56, and 7.17 (d, t, d, t, d, and d, respectively, each 2H, pyH), 7.03 and 6.94 (each s, each 4H, ArH), 5.15 and 4.45 (each s, each 4H, CH_2), 4.17 and 3.07 (each d, each 4H, Ar-CH_AH_B-Ar, $\Delta\delta = 1.10$, $J_{A,B} = 12$ Hz), 3.57 and 2.59 (each s, each 6H, CH_3), 1.15 and 1.04 (each s, each 18H, *t*Bu); IR ($CDCl_3$): $\tilde{\nu} = 1654\ cm^{-1}$ (C=O); FAB-MS: *m/z*: 1209.6 $[(M + Na)^+]$.

Fe^{III}-**3**: 1.0 mL of a solution of **3** (1.2 mM in CF_3CH_2OH) was diluted with 1.0 mL of CH_3OH, and 1.2 mL of a solution of $FeCl_3$ (0.90 mM in CH_3OH) and 0.80 mL of 2-(*N*-morpholino)ethanesulfonic acid (MES) (0.10 M in H_2O) were added. The pH was adjusted to 6.2 with NaOH (1.0 N in H_2O). FAB-MS: *m/z*: 1213.4 $[(M + Fe^{III} - 2H^+)]$.

Fe^{II}-**3**: A procedure analogous to that used for Fe^{III}-**3** was applied, except a solution of $FeCl_2$ was used and the experiments were conducted under argon.

Redox reactions: 3.0 mL of a solution of Fe^{III}-**3** (as prepared above) was treated with 30 μL of a solution of ascorbic acid (0.20 M in H_2O) and the reduction process was monitored at regular time intervals by recording the Vis spectra. The reduced solution was subjected to FAB-MS: *m/z*: 1215.2 $[(M + Fe^{II})]$; *m/z*: 1237.1 $[(M + Fe^{II} + Na^+)]$. 2.0 mL of the resulting mixture was then oxidized by treatment with 26 μL of a solution of ammonium persulfate (0.40 M in H_2O) at 70 °C for 5 min. Oxidation was indicated by the conversion of the pink color of the mixture to the original orange color, and by its UV/Vis spectra.

Received: April 19, 1996
Revised version: July 26, 1996 [Z 9057 IE]
German version: *Angew. Chem.* **1996**, *108*, 2842–2845

Keywords: calixarenes · iron compounds · molecular switches · redox reactions

[1] F. L. Carter, *Molecular Electronic Devices II*, Dekker, New York, **1987**.
[2] M. D. Ward, *Chem. Soc. Rev.* **1995**, 121–133.
[3] V. Grosshenny, A. Harriman, R. Ziessel, *Angew. Chem.* **1995**, *107*, 1211–1214; *Angew. Chem. Int. Ed. Engl.* **1995**, *34*, 1100–1102.
[4] A. Aviram, M. A. Ratner, *Chem. Phys. Lett.* **1974**, *29*, 277–283.
[5] A. S. Martin, J. R. Sambles, G. J. Ashwell, *Phys. Rev. Lett.* **1993**, *70*, 218–221.
[6] B. Alpha, V. Balzani, J.-M. Lehn, S. Perathoner, N. Sabbatini, *Angew. Chem.* **1987**, *99*, 1310–1311; *Angew. Chem. Int. Ed. Engl.* **1987**, *26*, 1266–1268.
[7] M. R. Wasielewski, M. P. O'Neill, D. Gosztola, M. P. Niemczyk, W. A. Svec, *Pure Appl. Chem.* **1992**, *64*, 1319–1325.
[8] L. Fabbrizzi, A. Poggi, *Chem. Soc. Rev.* **1995**, *24*, 197–202.
[9] R. A. Bissell, A. P. de Silva, H. Q. N. Gunaratne, P. L. M. Lynch, G. E. M. Maguire, K. R. A. S. Sandanayake, *Chem. Soc. Rev.* **1992**, *21*, 187–195.
[10] P. Gütlich, A. Hauser, H. Spiering, *Angew. Chem.* **1994**, *106*, 2109–2141; *Angew. Chem. Int. Ed. Engl.* **1994**, *33*, 2024–2054.
[11] S. L. Gilat, S. H. Kawai, J.-M. Lehn, *J. Chem. Soc. Chem. Comm.* **1993**, 1439–1442.
[12] R. A. Bissell, E. Cordova, A. E. Kaifer, J. F. Stoddart, *Nature* **1994**, *369*, 133–137.
[13] A. Livoreil, C. O. Dietrich-Buchecker, J.-P. Sauvage, *J. Am. Chem. Soc.* **1994**, *116*, 9399–9400.
[14] L. Zelikovitch, J. Libman, A. Shanzer, *Nature* **1995**, *374*, 790–792.
[15] C. D. Gutsche in *Calixarenes, Monographs in Supramolecular Chemistry* (Ed.: J. F. Stoddart), The Royal Society of Chemistry, Cambridge, **1989**.
[16] The observed spectral data are indicative of an Fe^{III}-3-bishydroxamate complex: M. Birus, Z. Bradic, N. Kujundzic, M. Prjbanic, P. C. Wilkins, R. G. Wilkins, *Inorg. Chem.* **1985**, *24*, 3980–3983.
[17] The observed spectral data are indicative of an Fe^{II}-3-bipyridine complex, since the *tris(bipyridyl)iron(II) complex* derived from the same bipyridyl chromophore exhibits significantly larger extinction coefficients ($\varepsilon \approx 5000$).

[18] Comparative intermolecular redox experiments with **1** and **2** could not be performed because of the preference of **1** to form Fe^{III}-trishydroxamate (λ_{max} = 428 nm) rather than-bishydroxamate complexes and the tendency of these complexes to precipitate under analogous reaction conditions.
[19] Y. Ishikawa, T. Kunitake, T. Matsuda, T. Otsuka, S. Shinkai, *J. Chem. Soc. Chem. Commun.* **1989**, 736–738.
[20] 5-Bromomethyl-2,2′-bipyridine was prepared by bromination of 5-methyl-2,2′-bipyridine with *N*-bromosuccinimide (NBS), and 5-methyl-2,2′-bipyridine was prepared according to a procedure provided by Prof. A. von Zelewsky (University of Fribourg, Switzerland).
[21] 6-Bromomethyl-6′-methyl-2,2′-bipyridine was prepared by bromination of 6,6′ dimethyl-2,2′-bipyridine with NBS, and 6,6′-dimethyl-2,2′-bipyridine was prepared according to a procedure provided by Prof. J.-M. Lehn (Université Louis Pasteur, France).

Hexaaryltellurium, the First Neutral Compounds Comprising Hexaarylated Elements**

Mao Minoura, Takao Sagami, Kin-ya Akiba,* Claudia Modrakowski, Allexander Sudau, Konrad Seppelt,* and Stephan Wallenhauer

The rich diversity and practical utility of organotellurium chemistry[1] continues to attract widespread interest, for instance in organic synthesis[2] and in the chemistry of low-[3] and hypervalent[4] compounds. Although considerable attention has been paid to the hypervalency of some tetraaryltellurium derivatives ($TeAr_4$) over the past forty years,[5, 6] a hexaaryltellurium ($TeAr_6$), with tellurium in its highest oxidation state, has not been reported.[7] Only three examples of neutral peralkylated hexavalent compounds[8] ($W(CH_3)_6$,[9, 10] $Re(CH_3)_6$,[10, 11] and $Te(CH_3)_6$[12, 13]) have been published. Here we report the synthesis and structure of the first neutral hexaarylated compounds, namely, $TeAr_6$ (Ar = C_6H_4-4-CF_3: **1a**; Ar = C_6H_5: **1b**), which are thermally extraordinarily stable (up to 300 °C).

First we succeeded in preparing **1a** (13.5% yield based on tellurium) by a one-pot reaction of LiC_6H_4-4-CF_3 (ArLi) and $TeCl_4$ in the molar ratio 4:1, $TeAr_2$ (**2a**, 28.1%) was also formed. The reaction of a stoichiometric quantity (6:1) or excess of ArLi with $TeCl_4$ did not produce **1a**.

The reaction sequence is obviously multistep (Scheme 1) and has not been studied in detail. However, the key step seems to involve a disproportionation reaction between $TeAr_4$ (**3**) and Cl_2TeAr_2 (**4**), which are formed in situ, to afford Cl_2TeAr_4 (**5**) and $TeAr_2$ (**2**). $TeAr_6$ (**1a**) is most likely formed by the succeeding reaction of **5** with ArLi during warming of the reaction mixture to room temperature. Unfortunately, $Te(C_6H_5)_6$ (**1b**) was obtained only in low yield (ca. 0.5%) in the above-mentioned one-pot process. We could, however, prepare **1b** by reaction of $F_2Te(C_6H_5)_4$ (**6**) with phenyllithium (PhLi). Following our experience with **1a**, we successfully treated **6** with PhLi at room temperature[14] for several hours (**1b**, 7.1%). Difluoride

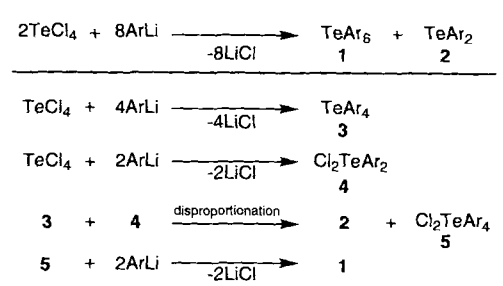

Scheme 1. Probable course of the synthesis of **1**.

6 was prepared as described in Ref. [7a] from XeF_2 and $Te(C_6H_5)_4$,[5a] and the *cis*-configuration was established by a single crystal structure determination.[15]

Compounds **1a** and **1b** are both thermally extremely stable, colorless solids and are not light sensitive, unlike tetraorganotellurium compounds.[5, 6] Crystals of **1a** and **1b** were obtained from chloroform. Molecular structures of both $TeAr_6$ were determined by X-ray crystallographic analysis (Figs. 1 and 2).[16]

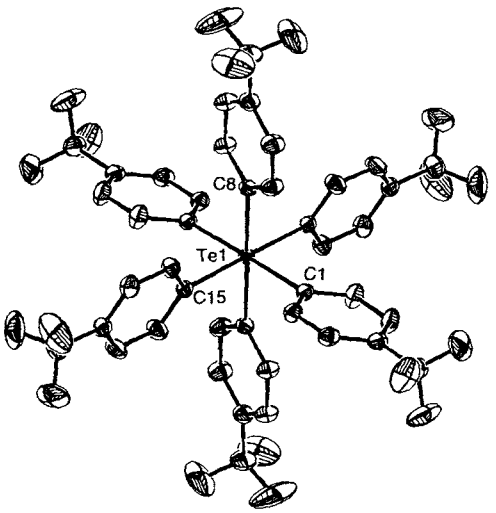

Fig. 1. ORTEP drawing of the structure of **1a** (thermal ellipsoids represent 50% probability). Selected bond lengths [Å] and bond angles [°]: Te1–C1 2.229(4), Te1–C8 2.240(2), Te1–C15 2.226(4); C1–Te1–C8 88.9(1), C1–Te1–C15 91.4(2), C8–Te1–C15 88.8(1).

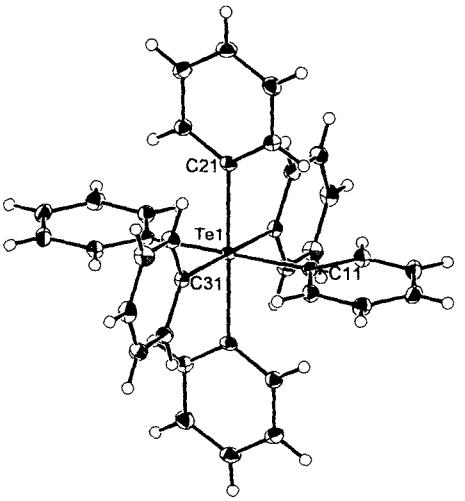

Fig. 2. ORTEP drawing of the structure of **1b** (thermal ellipsoids represent 50% probability). Selected bond lengths [Å] and bond angles [°]: Te1–C11 2.228(1), Te1–C21 2.228(1), Te1–C31 2.227(1); C11–Te1–C21 90.63(5), C11–Te1–C31 90.33(5), C21–Te1–C31 90.34(5).

[*] Prof. Dr. K.-y. Akiba, Dr. M. Minoura, T. Sagami
Department of Chemistry, Faculty of Science, Hiroshima University
1-3-1 Kagamiyama, Higashi-Hiroshima 739 (Japan)
Fax: Int. code +(824)24-0723
e-mail: akiba@sci.hiroshima-u.ac.jp
Prof. Dr. K. Seppelt, C. Modrakowski, A. Sudau, Dr. S. Wallenhauer
Institut fuer Anorganische und Analytische Chemie der
Freien Universität
D-14195 Berlin (Germany)
Fax: Int. code +(30)838-2424
e-mail: seppelt@chemie.fu-berlin.de

[**] Financial support from the Ministry of Education, Science, Culture, and Sports, Japan, the Deutsche Forschungsgemeinschaft, and the Fonds der Chemischen Industrie is gratefully acknowledged.

The octahedral tellurium environment is very regular. The six Te–C bond lengths in each molecule are very similar [**1a** 2.226(4)–2.240(2), **1b** 2.227(1)–2.228(1) Å] and a little longer than average Te^{II}–Caryl bonds (2.116 Å),[17] but comparable to the average (2.21 Å) of axial (2.29 Å) and equatorial (2.13 Å) bond lengths of tetraphenyltellurium.[5g] The planes of adjacent phenyl groups are nearly perpendicular, and *trans*-phenyl groups are coplanar. These molecules have approximate T_h symmetry, which is not common in chemistry.[18] This peculiar symmetry seems to be favorable with regard to interligand repulsion.

The ^{125}Te NMR spectra of **1a** ($\delta = 467$) and **1b** ($\delta = 493$) exhibit upfield resonances relative to $Te(C_6H_5)_4$ ($\delta = 509$) and the corresponding diaryltellurides ($\delta = 727$ and 685). This upfield shift upon increasing the valency state of the Te center in $Te(C_6H_5)_n$ ($n = 2$, 4, 6) contrasts with the irregular trend for $Te(CH_3)_n$.[12a] In the ^{13}C NMR of **1a** the *ipso* carbons resonate at $\delta = 152.1$, and the coupling constant $^1J_{C,Te}$ is 42 Hz. The resonance signal is shifted significantly downfield, and the coupling constant is very much smaller than those of $TeAr_2$ (**2**, $\delta = 119.9$, 288 Hz) and other organotellurium compounds.[19] Further investigation of physical and chemical properties of **1** and the applicability of the one-pot synthesis for other hexaorganotellurium are currently in progress.

Experimental Procedure

1a. A solution of LiC_6H_4-4-CF_3 was prepared from BrC_6H_4-4-CF_3 (4.95 g, 22.0 mmol) in ether (30 mL) and *n*BuLi (1.63 M solution in hexane, 13.5 mL, 22.0 mmol) at −78 °C. The mixture was warmed to room temperature and stirred for 1 h. At −78 °C a suspension of $TeCl_4$ (1.35 g 5.00 mmol) in ether (30 mL) cooled to −78 °C was added through a Teflon tube within 30 min. After stirring for 1.5 h, warming to room temperature, and further stirring for another 3 h, the solvent was removed under reduced pressure. The residue was washed with hexane and water, and dried to afford **1a** (685 mg, 0.686 mmol; 13.7% based on tellurium) after recrystallization from dichloromethane. Chromatographic separation and distillation of hexane-soluble products gave **2a**, Ar = C_6H_4-4-CF_3 (586 mg, 28.1%). **1a**: colorless crystals, m.p. 328–330 °C (decomp.). ^{1}H NMR (400 MHz, $CDCl_3$): δ = 7.12 (d, J = 8.3 Hz), 7.55 (d, J = 8.3 Hz); ^{19}F NMR (376 MHz, $CDCl_3$) $\delta = -63.1$; ^{13}C NMR (100 MHz, $CDCl_3$): δ = 123.7 (q, ^1J(C,F) = 272 Hz), 125.8 (d), 131.9 (q, ^2J(C,F) = 33 Hz), 133.5 (d), 152.1 (s); ^{13}C NMR (100 MHz, [D$_8$] THF): δ = 126.1 (q, ^1J(C,F) = 273 Hz), 125.8 (d), 133.4 (q, ^2J(C,F) = 33 Hz), 136.0 (s), 154.7 (s, ^1J(C,Te) = 42 Hz); ^{125}Te NMR (126 MHz, [D$_8$]THF, Me_2Te): δ = 467.3; IR (KBr) 3075 (w), 2356 (w), 1926 (w), 1598 (m), 1390 (m), 1326 (s), 1274 (m), 1032 (s), 1008 (m), 957 (m), 846 (w), 825 (s), 773 (s), 631 (w), 595 (m), 498 (m), 408 (m) cm^{-1}; Raman (solid, Ar ion laser) 1600 (m), 1560 (w), 1490 (w), 1395 (w), 1330 (m), 1205 (w), 1080 (m), 1040 (m), 1025 (w), 998 (w), 835 (m), 780 (s), 730 (w), 650 (s), 595 (w), 500 (w), 395 (m), 345 (m), 240 (m), 140 (vs) cm^{-1}. C, H analysis: ($C_{42}H_{24}F_{18}Te$, 998.22): calcd. C 50.54, H 2.42; found C 50.83, H 2.32.

1b: To a suspension of **6** (2.50 g, 5.27 mmol) in ether (30 mL) was added a 1.8 M solution of PhLi in cyclohexane/ether (6.45 mL, 11.6 mmol) at −78 °C. Stirring at room temperature for 1 day, filtration of the colorless residue, washing with hexane and water, and drying afforded **1b** (220 mg, 7.1%). **1b**: colorless crystals, m.p. 312 °C (decomp.). ^{1}H NMR (400 MHz, $CDCl_3$) δ = 7.04 (d), 7.15 (t), 7.29 (d). ^{13}C NMR (100 MHz, $CDCl_3$) δ = 128.1 (d), 128.3 (d), 133.6 (d), 150.1 (s). ^{125}Te NMR (126 MHz, CD_2Cl_2, Me_2Te): δ = 493.0; IR (KBr) 3049 (m), 1569 (m), 1476 (m), 1428 (s), 1187 (m), 1058 (s), 997 (m), 743 (s), 693 (s), 641 (w), 473 (s), 279 (s) cm^{-1}; Raman (solid, Ar ion laser) 1572 (m), 1478 (w), 1434 (w), 1335 (w), 1189 (w), 1125 (m), 1051 (w), 1016 (m), 1003 (s), 914 (w), 646 (w), 638 (m), 616 (w), 211 (w), 183 (m), 78 (vs) cm^{-1}. MS (70 eV, EI): *m/z* (%) 591 (0.41) [M^+], 515 (16) [$Te(C_6H_5)_5^+$], 361 (94) [$Te(C_6H_5)_3^+$], 154 (100) [$(C_6H_5)_2^+$].

6: $Te(C_6H_5)_4$ (12.3 g, 28.3 mmol) in CH_3CN (85 mL) was treated with XeF_2 (4.78 g, 28.3 mmol) at −45 °C. The colorless solid was filtered off at room temperature. Recrystallization from $CHCl_3$ afforded *cis*-$F_2Te(C_6H_5)_4$ (**6**, 11.6 g, 86.7%); m.p. 187 °C (decomp.). ^{1}H NMR (400 MHz, $CDCl_3$) δ = 7.18 (t), 7.24 (t), 7.32 (t), 7.40 (d), 7.49 (d). ^{13}C NMR (100 MHz, $CDCl_3$) δ = 128.0 (d), 128.5 (d), 129.4 (d), 130.3 (d), 131.4 (d), 132.4 (d), 139.0 (s), 148.1 (s). ^{19}F NMR (376 MHz, $CDCl_3$) $\delta = -30.98$ (^1J(^{19}F,^{125}Te) = 2049 Hz, ^1J(^{19}F,^{123}Te) = 1698 Hz.). ^{125}Te NMR (126 MHz, $CDCl_3$, Me_2Te): δ = 650.8 (^1J(^{19}F,^{125}Te) = 2049 Hz).

Received: May 28, 1996 [Z 9159IE]
German version: *Angew. Chem.* **1996**, *108*, 2827–2829

Keywords: hypervalent compounds · structure elucidation · tellurium compounds

[1] K. Y. Irgolic in *Houben-Weyl, Methoden Org. Chem. Vol. E12b* (Ed.: D. Klamann), Thieme, Stuttgart, **1990**; I. D. Sadekov, A. A. Maksimenko, V. I. Minkin, *Sulfur Reports* **1990**, *9*, 359–398.

[2] N. Petragnani, *Tellurium in Organic Synthesis*, Academic Press, New York, **1994**.

[3] M. Minoura, T. Kawashima, R. Okazaki, *J. Am. Chem. Soc.* **1993**, *115*, 7019–7020; M. Minoura, T. Kawashima, N. Tokitoh, R. Okazaki, *J. Chem. Soc. Chem. Commun.* **1996**, 123–124; D. Rabinovich, G. Parkin, *Inorg. Chem.* **1995**, *34*, 6341–6361; T. Chivers, *J. Chem. Soc. Dalton Trans.* **1996**, 1185–1194, and references therein.

[4] J. I. Musher, *Ann. N. Y. Acad. Sci.* **1972**, *192*, 52–59; D. Hellwinkel, *ibid.* **1972**, 158–166; J. Bergman, L. Engman, L. Sidén in *The Chemistry of Organic Selenium and Tellurium Compounds, Vol. 1* (Ed.: S. Patai, Z. Rappoport), Wiley, New York, **1986**, pp 517–558; M. R. Detty, M. B. O'Regan in *Tellurium-Containing Heterocycles* (Ed.: E. C. Taylor), Wiley, New York, **1994**, pp 425–490.

[5] a) G. Wittig, H. Fritz, *Liebigs Ann. Chem.* **1952**, *577*, 39–43; b) D. Hellwinkel, G. Fahrbach, *Tetrahedron Lett.* **1965**, *23*, 1823–1827; c) D. Hellwinkel, G. Fahrbach, *Liebigs Ann. Chem.* **1968**, *712*, 1–20; d) D. Hellwinkel, G. Fahrbach, *Chem. Ber.* **1968**, *101*, 574–584; e) D. H. R. Barton, S. A. Glover, S. V. Ley, *J. Chem. Soc. Chem. Commun.* **1977**, 266–267; f) S. A. Glover, *J. Chem. Soc. Perkin Trans. 1* **1980**, 1338–1344; g) C. S. Smith, J.-S. Lee, D. D. Titus, R. F. Ziolo, *Organometallics* **1982**, *1*, 350–354; h) C. H. W. Jones, R. D. Sharma, *J. Organomet. Chem.* **1987**, *332*, 115–121; i) S. Ogawa, S. Sato, N. Furukawa, *Tetrahedron Lett.* **1992**, *33*, 7925–7928; j) S. Ogawa, Y. Matsunaga, S. Sato, T. Erata, N. Furukawa, *ibid.* **1992**, *33*, 93–96; k) S. Sato, N. Kondo, N. Furukawa, *Organometallics* **1994**, *13*, 3393–3395; l) S. Sato, N. Furukawa, *Tetrahedron Lett.* **1995**, *36*, 2803–2806.

[6] Recently tetraalkyltellurium compounds have been reported. D. Naumann, B. Willkes, *J. Fluorine Chem.* **1985**, *27*, 115–117; R. W. J. Gedridge, D. C. Harris, K. T. Higa, R. A. Nissan, *Organometallics* **1989**, *8*, 2817–2820; R. W. J. Gedridge, K. T. Higa, R. A. Nissan, *ibid.* **1991**, *10*, 286–291; A. J. Blake, C. R. Pulham, T. M. Greene, A. J. Downs, A. Haaland, H. P. Verne, H. V. Volden, C. J. Marsden, B. A. Smart, *J. Am. Chem. Soc.* **1994**, *116*, 6043–6044.

[7] a) K. Alam, A. F. Janzen, *J. Fluorine Chem.* **1985**, *27*, 467–469; b) S. Secco, K. Alam, B. J. Blackburn, A. F. Janzen, *Inorg. Chem.* **1986**, *25*, 2125–2129; c) A. F. Janzen, K. Alam, M. Jang, B. J. Blackburn, A. S. Secco, *Can. J. Chem.* **1988**, *66*, 1308–1312.

[8] Some anionic hexaarylpnictogen compounds have been described. a) G. Wittig, K. Clauss, *Liebigs Ann. Chem.* **1952**, *577*, 26–39; b) D. Hellwinkel, G. Kilthau, *ibid.* **1967**, *705*, 66–75; c) D. Hellwinkel, U. Bach, *ibid.* **1968**, *720*, 198–200; d) S. Wallenhauer, D. Leopold, K. Seppelt, *Inorg. Chem.* **1993**, *32*, 3948–3951.

[9] A. J. Shortland, G. Wilkinson, *J. Chem. Soc. Dalton Trans.* **1973**, 872–876; A. Haaland, A. Hammel, K. Rypdal, H. V. Volden, *J. Am. Chem. Soc.* **1990**, *112*, 4547–4549.

[10] V. Pfennig, K. Seppelt, *Science* **1996**, *271*, 626–628.

[11] K. Mertis, G. Wilkinson, *J. Chem. Soc. Dalton Trans.* **1976**, 1488–1492.

[12] a) L. Ahmed, J. A. Morrison, *J. Am. Chem. Soc.* **1990**, *112*, 7411–7413; b) A. Haaland, H. P. Verne, H. V. Volden, J. A. Morrison, *J. Am. Chem. Soc.* **1995**, *117*, 7554–7555.

[13] For theoretical studies of hexamethylchalcogens, see J. E. Fowler, T. P. Hamilton, H. F. Schaefer III, *J. Am. Chem. Soc.* **1993**, *115*, 4155–4158; J. E. Fowler, H. F. Schaefer III, K. N. Raymond, *Inorg. Chem.* **1996**, *35*, 279–281.

[14] The attempted reaction of F_2TePh_4 with PhLi at low temperatures was unsuccessful.

[15] Crystal structure of **6**: triclinic, space group $P\bar{1}$, $Z = 4$, $a = 9.865(2)$, $b = 11.435(1)$, $c = 17.743(2)$ Å, $\alpha = 81.483(6)$, $\beta = 78.37(1)$, $\gamma = 86.29(1)°$. Av. bond lengths [Å]: Te–F 1.971 ± 0.003, Te–C (*anti* to F) 2.152 ± 0.002, Te-C (*trans* Ph groups) 2.141 ± 0.003; bond angles [°]: F-Te-F 89.09, C-Te-C (anti to F), 97.80, C-Te-C (*trans* Ph groups) 163.37.

[16] Crystallographic data for **1a**: $C_{42}H_{24}F_{18}Te$, $M_r = 998.2$, triclinic, space group $P\bar{1}$, $a = 9.210(2)$, $b = 11.200(2)$, $c = 11.245(2)$ Å, $\alpha = 96.05(1)$, $\beta = 114.18(1)$, $\gamma = 105.72(1)°$, $V = 987.2(3)$ Å^3, $Z = 1$, $\rho_{calcd} = 1.68$ g cm^{-3}, $T = 25$ °C, $\mu = 7.78$ cm^{-1}, $F(000) = 490$. Crystal dimensions = 0.40 × 0.30 × 0.15 mm^3. The intensity data ($2\theta = 3–55°$) were collected on a Mac-Science-MXC3 diffractometer with graphite-monochromated $Mo_{K\alpha}$ radiation ($\lambda = 0.71073$ Å); a ψ scan absorption correction was applied. The structure was solved by direct methods. Non-hydrogen atoms were refined anisotropically. The final cycle of full-matrix, least-squares refinement was based on 4462 observed reflections [$I > 3.00\,\sigma(I)$] and 319 variable parameters with $R(R_w) = 0.040(0.046)$, GOF = 2.87; residual electron density (e Å^{-3}): min = −0.81, max = 0.98. Crystallographic data for **1b** · $2CHCl_3$: $C_{38}H_{32}Cl_6Te$, $M_r = 828.3$, triclinic, space group $P\bar{1}$, $a = 8.325(1)$, $b = 10.797(1)$, $c = 11.009(1)$ Å, $\alpha = 60.47(1)$, $\beta = 82.47(1)$, $\gamma = 88.00(1)°$; $V = 853.0(2)$ Å^3; $Z = 1$, $\rho_{calcd} = 1.61$ g cm^{-3}, $T = -143$ °C. Crystal dimensions = 0.40 × 0.10 × 0.10 mm^3. A suitable crystal was mounted on the tip of a glass capillary and intensity data ($2\theta = 6–60°$) were collected on an ENRAF-Nonius CAD4 diffractometer at 130 K with graphite-monochromated $Mo_{K\alpha}$ radiation ($\lambda = 0.71063$ Å); a Ψ scan absorption correction was applied. The structure was solved by direct methods. Non-hydrogen atoms were refined anisotropically. The final cycle of full-matrix, least-squares refinement was based on 4963 observed reflections [$I > 2.00\,\sigma(I)$]

 © VCH Verlagsgesellschaft mbH, D-69451 Weinheim, 1996 0570-0833/96/3522-2661 $ 15.00+.25/0

and 254 variable parameters with $R(R_w) = 0.021\ (0.054)$. GOF = 1.09; residual electron density (e Å^{-3}): min = −0.88, max = 0.56. Crystallographic data (excluding structure factors) for the structures reported in this paper have been deposited with the Cambridge Crystallographic Data Centre as supplementary publication no. CCDC-179-111. Copies of the data can be obtained free of charge on application to The Director, CCDC, 12 Union Road, Cambridge CB2 1EZ UK (fax: int. code +(1223)336-033; e-mail: teched@chemcrys.cam.ac.uk).

[17] F. H. Allen, O. Kennard, D. G. Watson, L. B. Brammer, G. A. Orpen, R. Taylor, *J. Chem. Soc. Perkin Trans. 2* **1987**, S1–S19.

[18] Other examples of T_h symmetry species: $[Co(NO_2)_6]^{3-}$: M. Driel, H. J. Verweel, *Z. Kristallogr.* **1936**, *A 95*, 308–314; I. Nakagawa, T. Shimanouchi, *Spectrochim. Acta* **1966**, *22*, 1707–1728; $C_{60}[Pt(PEt_3)_2]_6$: P. J. Fagan, J. C. Calabrese, B. Malone, *J. Am. Chem. Soc.* **1991**, *113*, 9408–9409. $[Bi(C_6H_5)_6]^-$: Ref. [8d].

[19] E. G. Hope, T. Kemmitt, L. William, *Organometallics* **1988**, *7*, 78–83.

Inversion of Optically Active Dihydropyridines by Oxidation and Electroreduction**

Alexander Straub* and Axel Goehrt

Dihydropyridines (DHPs) **1** play an important role as calcium channel ligands in cardiovascular therapy.[1] The pharmacological activity of asymmetrically substituted DHPs depends on the configuration of the stereogenic C4 carbon atom, which determines whether the compound acts as a calcium antagonist or as an calcium agonist.[1c] A stereoselective route to this class of compounds is therefore extremely important. As most of the enantioselective synthetic methods known to date are not generally applicable,[1c] optically active compounds are usually obtained by resolution of racemates via diastereomeric derivatives. This methodology, however, provides 50% of the undesired enantiomer, which cannot be used further. For this reason, we sought to develop a strategy for the conversion of the wrong enantiomer into the desired one.

Although DHPs can be oxidized to pyridines by numerous methods,[2, 3] the stereochemical course of these oxidations has not been investigated to date. However, appropriately substituted 4-arylpyridines obtained by such methods are suitable intermediates for an optical inversion process, since they store the chiral information of the DHPs in the form of atropisomers. The subsequent reduction of the 4-arylpyridine to the DHP should then proceed with stereochemical induction. From the various methods known for the reduction of pyridines[2–6] we selected the electrochemical cathodic reduction.[5, 6] Since it is a heterogenous reaction, this method appears to be most suitable for a stereocontrolled process[7, 8] and it displays the highest efficiency in terms of atom economy. We herein describe the stereochemical course of the oxidation and reduction reactions of 4-aryl-DHPs and -pyridines.

DHPs **1** exist as two rotamers (Scheme 1), which are referred to as the synperiplanar (*sp*) and antiperiplanar (*ap*) rotamers.

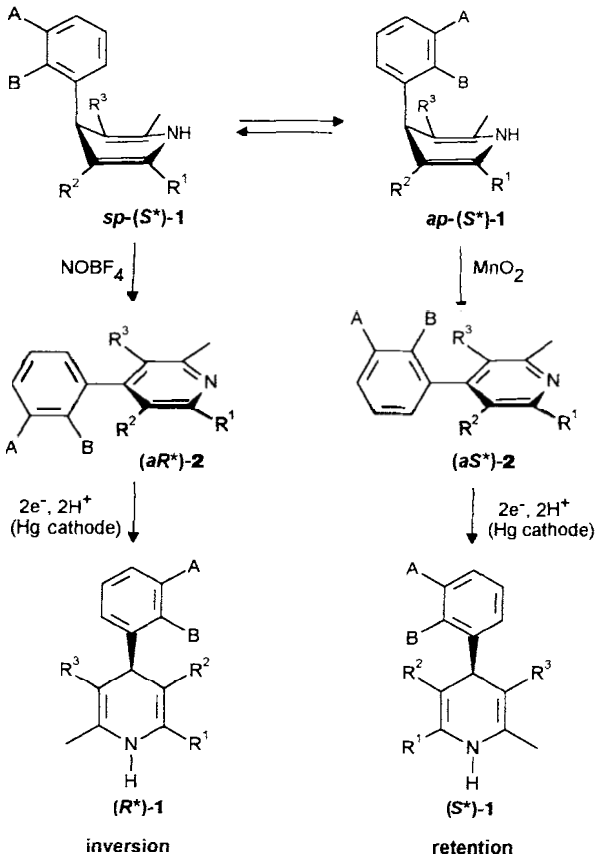

Scheme 1

The *sp* rotamer is the predominant conformer in the solid and solution state,[9] and has been confirmed by X-ray analysis to be present in several of the examples we will discuss here. We assumed, therefore, that when the *sp* form of DHP (−)-(*S*)-**1e**, the absolute configuration of which has been determined for the well-crystallizing derivative (−)-(*S*)-**1g** (*sp* rotamer),[24] is oxidized with manganese dioxide, the atropisomer (*aR*)-**2e** should result (Table 1). In **2e** the *ortho* aryl substituent blocks

Table 1. Compounds investigated

1, 2	A	B	R^1	R^2	R^3
a [10]	CN	Cl	Me	$CO_2(CH_2)_2OMe$	CO_2iPr
b [11]	H	Me	$-CH_2OCO-$		CO_2iPr
c	H	CH_2CH_2Ph	$-CH_2OCO-$		CO_2Et
d [11]	H	SCH_2Ph	$-CH_2OCO-$		CO_2Et
e [11]	H	SCH_2CH_2Ph	$-CH_2OCO-$		CO_2Et
f [12]	$-COCH=C(Ph)-S-$		$-CH_2OCO-$		CO_2Et
g	H	SCH_2CH_2Ph	$-CH_2OCO-$		COOH

one side of the molecule such that an electrochemical reduction should proceed preferentially from the opposite side, thus providing the inverted (*R*)-DHP enantiomer. Interestingly, the oxidation with manganese dioxide afforded with high enantioselectivity the unexpected atropisomer (+)-(*aS*)-**2e**, the absolute configuration of which was determined by X-ray crystallography.[24] This indicates that the oxidation with manganese dioxide occurs with the thermodynamically less stable *ap* form. Thus the accessibility of the H4 atom seems to be crucial for the kinetics of the oxidation. Prompted by this observation, we used

[*] Dr. A. Straub
Bayer AG, PH-R-CF Chemisch-Wissenschaftliches Laboratorium
Pharma-Forschungszentrum, D-42096 Wuppertal (Germany)
Fax: Int. code +(202)364061
e-mail: debayeak@ibmmail.com
Dr. A. Goehrt
Bayer AG, Zentrale Forschung (Abteilung Strukturforschung)
D-51368 Leverkusen (Germany)

[**] We thank Dr. R. Grosser for the enantiomeric resolution, Dr. V. Muschalek for the enantiomer analysis, and Dipl.-Ing. H. Geeven for technical support.

(−)-(*S*)-**1d** to investigate the influence of various oxidizing agents (including those functioning by single-electron transfer and hydride-type mechanisms) on the atropisomer ratio of **2d** (Table 2). We observed that the atropisomer ratio resulting from the oxidation with concentrated nitric acid was opposite to that resulting from the oxidation with manganese dioxide. Since this advantageous ratio was not obtained in reactions using either dilute nitric acid or nitrogen oxide formed in situ, the nitronium ion present in the strongly acidic solution is presumably responsible for the selectivity of the oxidation. This assumption was supported by the use of nitronium and nitrosonium tetrafluoroborate (Table 2). When $NOBF_4$ was employed, the *sp*-DHP rotamer of (*S*)-**1e** was selectively oxidized to form the desired atropisomer (*aR*)-**2e** (Table 3). This high selectivity, which is opposite to that of the manganese dioxide oxidation, can be explained by the electrophilic character of the nitrosonium ion, which leads to a different oxidation mechanism than that of the manganese dioxide oxidation.[19, 22] It is conceivable that the atropisomer ratios obtained with $NOBF_4$ might reflect the *sp* fraction present in the equilibrium of DHP rotamers.[9a, h]

Table 2. Oxidation of (−)-(*S*)-**1d** to **2d** with various oxidizing agents and the resulting atropisomer and enantiomeric ratios (in %).

Oxidant	Atropisomer ratio (−)-**2d**:(+)-**2d**	*ee*
$K_3[Fe(CN)_6]$/K_2CO_3 [14]	2.0:98.0	96.0
MnO_2 [13]	3.0:97.0	94.0
methylacridinium iodide [15]	6.1:93.9	87.8
$KMnO_4$/montmorillonite in CH_2Cl_2/H_2O [16]	9.0:91.0	83.0
chloranil [17]	23.0:77.0	54.0
$KMnO_4$/montmorillonite in benzene [16]	25.9:74.1	48.0
iodosobenzene diacetate in CH_3CN	28.6:71.4	42.8
cerium(IV) ammonium nitrate [18]	39.5:70.5	31.0
HNO_3 (dilute)	35.0:65.0	30.0
$NaNO_2$/glacial acetic acid [19]	45.0:55.0	10.0
$Cu(NO_3)_2$ montmorillonite in $CHCl_3$ [20]	59.0:41.0	18.0
Pt anode [21]	76.2:23.8	52.4
HNO_3 (65%)/$CHCl_3$	94.3:5.7	88.6
NO_2BF_4 in CH_3CN	95.0:5.0	90.0
$NOBF_4$ in CH_3CN [22]	97.2:2.8	94.4

Table 3. Atropisomer ratios of pyridines **2** after oxidation of **1** with MnO_2 and $NOBF_4$, and enantiomeric ratios of dihydropyridines **1** upon electroreduction of **2**. (*R** and *S** refer to relative configurations.)

1	*S**:*R** [b]	Oxidant	Atropisomer ratio (**2**) [b]	*S**:*R** (**1**) [a, b]
a	100:0	MnO_2	98.0:2.0	61.0:39.0 (*R*:*S*)
	0:100	$NOBF_4$	46.3:53.7	
b	100:0	MnO_2	16.0:84.0	46.0:54.0
	0:100	$NOBF_4$	20.8:79.2	47.0:53.0
c	99.7:0.3	$NOBF_4$	22.4:77.6	35.0:65.0
	99.7:0.3	MnO_2	95.7:4.3	80.4:19.6
d	100:0	MnO_2	3.0:97.0	90.3:9.7 (*S*:*R*)
	97.3:2.7	$NOBF_4$	96.0:4.0	4.6:95.4
	0:100	$NOBF_4$	2.3:97.7	
e	98.7:1.3	MnO_2	1.3:98.7 (*aR*:*aS*)	
	98.7:1.3	$NOBF_4$	98.0:2.0	
	0:100	MnO_2	98.8:1.2	16.3:83.7 (*S*:*R*)
	0:100	$NOBF_4$	2.9:97.1	89.5:10.5
f	100:0	MnO_2 at 0 °C	0.5:99.5 (*aR*:*aS*)	not chemoselective (*S*:*R*)
	100:0	MnO_2 at 200 °C	6.0:94.0	

[a] After electroreduction of **2**. [b] The first number in the ratio refers to the proportion of the enantiomer eluting first from the chiral HPLC column (all numbers in %); the absolute configurations determined by crystallography are given in parentheses.

In order to obtain the inverted DHP from the atropisomeric pyridine derivative, **2** was reduced at a mercury cathode in a divided electrolytic cell. The voltammetric measurement showed a half-wave potential between −1.6 and −1.7 V. The transfer of the hydrogen atom to the pyridine ring proceeds from the sterically less hindered side (Table 3). The expected pronounced dependency of the selectivity on the steric demand of the aryl *ortho* substituent can be readily seen: with the benzylthio substituent (**1d**) good selectivities for both oxidation and reduction were obtained, whereas the methyl substituent (**1b**) resulted in only average selectivity for the oxidation and very low selectivity for the electrochemical reduction.

This is the first report on both inversion and racemization of optically active dihydropyridines. Due to the importance of DHPs as biologically active compounds, future investigations will focus on alternative oxidation methods as well as various substituent effects.

Experimental Procedure

Enantiomeric ratios were determined by HPLC primarily with the chiral phase Chiralcel OD-H (5 μm particle size; mobile phase: 85% *n*-heptane and 15% of a mixture of 1% water and 2% trifluoroacetic acid in ethanol). The free racemic DHP-carboxylic acids such as **1g**, which were resolved into both enantiomers by preparative chiral chromatography[23], were converted into the chiral esters **1** by reaction with ethyl iodide in DMF in the presence of cesium fluoride.

Oxidation of (−)-**1d** with manganese dioxide to yield (+)-**2d** : (−)-**1d** (3.3 mmol, $[\alpha]_D^{20} = -45.1$, $c = 0.93$ in DMSO) was dissolved in chloroform (150 mL), manganese dioxide (5.73 g, Merck-Schuchardt, precipitated, activated, reagent grade) was added, and the resulting mixture was sonicated. Vacuum filtration and removal of the solvent afforded (+)-**2d** (89% yield, $[\alpha]_D^{20} = +51.35$, $c = 0.56$ in $CHCl_3$).

Oxidation of (−)-**1d** with nitrosonium tetrafluoroborate to yield (−)-**2d** : To a solution of (−)-**1d** (9.5 mmol) in acetonitrile (200 mL) was added a solution of nitrosonium tetrafluoroborate (10.3 mmol) in acetonitrile (200 mL). After 4 h the solution was concentrated in vacuum, and the residue was dissolved in toluene/ethyl acetate and stirred overnight with an aqueous solution of sodium hydrogen carbonate. The organic layer was concentrated to dryness and the residue subjected to chromatography on silica gel. The yield of (−)-**2d** was 80%, ($[\alpha]_D^{20} = -48.72$, $c = 0.77$ in $CHCl_3$).

Cathodic reduction of (−)-**2d** to yield (+)-**1d**: A divided electrolytic cell equipped with a glass frit diaphragm, a mercury pool cathode, Pt anode, and Ag/AgCl reference electrode was employed. The cathode compartment contained a solution of (−)-**2d** (0.72 mmol) and tetraethylammonium tetrafluoroborate (1.1 g) in methanol (50 mL), and the anode compartment contained the same solution without the starting material. The solution was electrolyzed under argon between 10 and 20 mA (−1.6 to −2 V) until the starting material could no longer be detected by thin layer chromatography. The cathodic solution was removed and concentrated to a small volume, water was added, and the precipitate of **1** was removed by filtration. Chromatography on silica gel afforded (+)-**1d** in 83% yield ($[\alpha]_D^{20} = +46.8$, $c = 1.0$ in DMSO). The mercury used in the electrolysis was washed with methanol and reused.

Received: July 16, 1996 [Z8970IE]
German version: *Angew. Chem.* **1996**, *108*, 2832–2834

Keywords: atropisomerism · configuration inversion · electrochemistry · pyridine derivatives · synthetic methods

[1] a) F. Bossert, H. Meyer, E. Wehinger, *Angew. Chem.* **1981**, *93*, 755; *Angew. Chem. Int. Ed. Engl.* **1981**, *20*, 762; b) D. J. Triggle, D. A. Langs, R. A. Janis, *Med. Res. Rev.* **1989**, *9*, 123; c) S. Goldmann, J. Stoltefuss, *Angew. Chem.* **1991**, *103*, 1587; *Angew. Chem. Int. Ed. Engl.* **1991**, *30*, 1559.
[2] a) U. Eisner, J. Kuthan, *Chem. Rev.* **1972**, *72*, 1; b) A. Sausins, G. Duburs, *Heterocycles* **1988**, *27*, 291.
[3] D. M. Stout, A. I. Meyers, *Chem. Rev.* **1982**, *82*, 223.
[4] Kyoto Pharm. Ind. KK, JP 312299, **1991**.
[5] J. E. Toomey, *Adv. Heterocycl. Chem.* **1984**, *37*, 167.
[6] a) G. Abou-Elenien, J. Rieser, N. Ismail, K. Wallenfels, *Z. Naturforsch. B* **1981**, *36*, 386; b) E. Schmidt, Dissertation, Technische Universität Braunschweig, **1990**; c) J. E. O'Reilly, P. J. Elving, *J. Am. Chem. Soc.* **1972**, *94*, 7941; d) J.

Nadra, H. Giradinovitch, M. Devand, *J. Chem. Res. (S)*, **1983**, 192; e) V. Kadis, G. Duburs, J. Stradins, J. Uldrikis, *Khim. Geterosikl. Soedin.* **1978**, 641 [*Chem. Abstr.* **1978**, *89*, 107457u]; f) J. N. Burnett, A. L. Underwood, *J. Org. Chem.* **1965**, *30*, 1154.

[7] T. Nonaka in *Organic Electrochemistry* (Eds.: H. Lund, M. M. Baizer), Marcel Dekker, New York, **1991**, pp. 1131–1195.

[8] E. Wehinger, *Abstracts der 5th Intern. Conf. Org. Synthesis*, Freiburg, **1984**, p. 122.

[9] a) G. Rovnyak, N. Andersen, J. Gougoutas, A. Hedberg, S. D. Kimball, M. Malley, S. Moreland, M. Porubcan, A. Pudzianowski, *J. Med. Chem.* **1988**, *31*, 936; b) S. Goldmann, W. Geiger, *Angew. Chem.* **1984**, *96*, 302; *Angew. Chem. Int. Ed. Engl.* **1984**, *23*, 301; c) U. Rose, *Chem. Ztg.* **1989**, *113*, 85; d) H.-D. Höltje, S. Marrer, *J. Comput. Aided Mol. Des.* **1987**, *1*, 23; e) G. Rovnyak, N. Andersen, J. Gougoutas, A. Hedberg, S. D. Kimball, M. Malley, S. Moreland, M. Porubcan, A. Pudzianowski, *J. Med. Chem.* **1991**, *34*, 2521; f) D. A. Langs, P. D. Strong, D. J. Triggle, *J. Comput. Aided Mol. Des.* **1990**, *4*, 215; g) R. Fossheim, *Acta Chem. Scand. B* **1987**, *41*, 581; h) R. B. Palmer, N. H. Andersen, *Tetrahedron* **1996**, *52*, 9665.

[10] H. Meier, W. Hartwig, B. Junge, R. Schohe-Loop, Z. Gao, B. Schmidt, M. de Jong, T. Schuurman (Bayer AG), EP 657430, **1995** [*Chem. Abstr.* **1995**, *123*, 83217].

[11] G. Franckowiak, H. Böshagen, F. Bossert, S. Goldmann, H. Meyer, E. Wehinger, J. Stoltefuss, M. Schramm, G. Thomas, R. Towart (Bayer AG), DE 3130041, **1981** [*Chem. Abstr.* **1983**, *98*, 198038].

[12] S. Goldmann, F. Bossert, M. Schramm, G. Thomas, R. Gross (Bayer AG), DE 3311003, **1983** [*Chem. Abstr.* **1985**, *102*, 45915].

[13] J. J. Vanden Eynde, F. Delfosse, A. Mayence, Y. Van Haverbeke, *Tetrahedron* **1995**, *51*, 6511.

[14] M. E. Brewster, J. J. Kaminski, Z. Gabanyi, K. Czako, A. Simay, N. Bodor, *Tetrahedron* **1989**, *45*, 4395, and references therein.

[15] D. D. Tanner, A. Kharrat, *J. Org. Chem.* **1988**, *53*, 1646.

[16] J. J. Vanden Eynde, R. D'Orazio, Y. Van Haverbeke, *Tetrahedron* **1994**, *50*, 2479.

[17] S. H. Rosenberg, H. Rapoport, *J. Org. Chem.* **1984**, *49*, 56.

[18] J. R. Pfister, *Synthesis* **1990**, 689.

[19] B. Loev, K. M. Snader, *J. Org. Chem.* **1965**, *30*, 1914.

[20] M. Balogh, I. Hermecz, Z. Meszaros, P. Laszlo, *Helv. Chim. Acta* **1984**, *67*, 2270.

[21] K. Ueno, T. Umeda, *Chem. Pharm. Bull.* **1992**, *40*, 1376.

[22] T.-L. Ho, G. A. Olah, *J. Org. Chem.* **1977**, *42*, 3097.

[23] U. Schwartz, R. Grosser, K. E. Piejko, B. Bömer, D. Arlt (Bayer AG), DE 3532356, **1987**.

[24] Crystallographic data (excluding structure factors) for (−)-(*S*)-**1g** and (+)-(*aS*)-**2e** have been deposited with the Cambridge Crystallographic Data Centre as supplementary publication no. CCDC-179-117. Copies of the data can be obtained free of charge on application to The Director, CCDC, 12 Union Road, GB-Cambridge CB2 1EZ, UK (fax: Int. code +(1223)336-033; e-mail: teched@chemcrys.cam.ac.uk).

Cyclic [6]- and [8]Paraphenylacetylenes**

Takeshi Kawase, Hossein R. Darabi, and Masaji Oda*

The π-orbitals of carbocyclic conjugated systems (annulenes) are oriented usually vertical to the plane of the ring. Besides this type of cyclic conjugation, another type is topologically possible in which the π-orbitals are aligned horizontally on a rigid surface and form a belt-shaped conjugated system. Since the recent discovery of fullerenes[1] and carbon nanotubes,[2] fully conjugated systems with a curved surface have received much attention.[3] In this context, the attempted syntheses of belt-shaped compounds having a conjugated π-system, for example [*n*]cyclocarbons,[4] cyclacene,[5] cyclic oligoparaphenylene,[6] and others,[7] have been reported. These molecules are of interest not only from the synthetic and theoretical points of view but also as host molecules having a rigid cavity lined with a conjugated π-system. Another class of belt-shaped molecules with a conjugated π-system are the cyclic oligomers of phenylacetylene linked at the *para* position, namely [2$_n$]paracyclophane-*n*-yne (**1**, cyclic [*n*]paraphenylacetylene, [*n*]CPPA)[8]. One of these compounds, [6]CPPA **1b**, is a structural isomer of kekulene **2**[9] and both have D_{6h} symmetry. We report here on the syntheses of **1b** and [8]CPPA **1c**, which are the first isolable, belt-shaped compounds with a conjugated π-system.

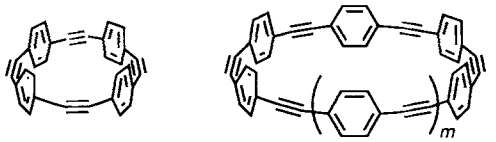

1a (*n* = 4)

1b (*n* = 6) (*n* = *m* + 5)
1c (*n* = 8)

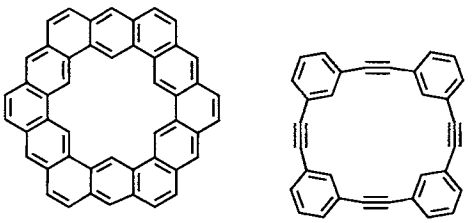

2 **3**

We have recently described the synthesis of [2$_4$]metacyclophanetetrayne **3**, a structural isomer of [4]CPPA **1a**, through bromination–dehydrobromination of the precursor tetraenes.[10] In view of the successful formation and fair stability of **3** under basic conditions despite sizable strain, we expected that **1**, which has a more favorable ring size, could be synthesized similarly. In analogy to kekulene, the high symmetry of the CPPA should disperse the strain energy over the molecule and reduce its kinetic instability.

The reaction of a mixture of [2$_6$]paracyclophanehexaene **4b** and [2$_8$]paracyclophaneoctaene **4c** (ca. 4:1), which was obtained from the McMurry coupling of 4,4′-diformyl-(*Z*)-stilbene in about 20% yield (together with [2$_4$]paracyclophanetetraenes in 30–40% yield),[11] with bromine (10 equiv, $CHCl_3$, room temperature) and subsequent treatment of the crude bromide mixture with *t*BuOK (16 equiv, room temperature) in diethyl ether afforded a mixture of **1b** and **1c** (4:1) in 85% yield (Scheme 1). The CPPA mixture (45% yield) also resulted when

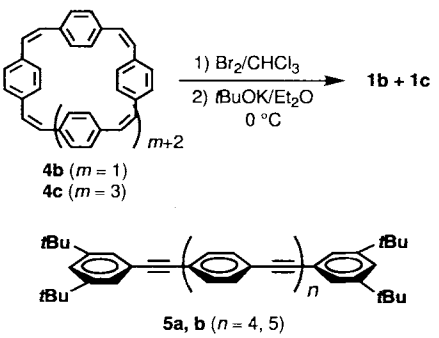

Scheme 1.

[*] Prof. Dr. M. Oda, H. R. Darabi, Dr. T. Kawase,
Department of Chemistry
Graduate School of Science, Osaka University
Toyonaka, Osaka 560 (Japan)
Fax: Int. code +(6)850-5387

[**] This work was supported by Grants-in-Aid for Scientific Research (08454201 and 08640683) from the Ministry of Education, Science and Culture (Japan).

furan was used as the solvent, but reactions in THF and DME gave complex mixtures.

The CPPAs were separated by gel permeation chromatography[12] to afford **1b** and **1c** as fine yellow needles. Both compounds, in particular **1b**, are sensitive to oxygen both in solution and in the solid state but are fairly stable under inert gas. Upon heating under air, **1b** explosively decomposed at about 80 °C producing a brown polymeric material, but in a degassed sealed glass capillary tube it did not decompose until about 240 °C. The less strained **1c** decomposed at about 120 °C under air. Notably, **1b** and **1c** are fairly soluble in organic solvents, whereas acyclic oligomers **5**[13] having *tert*-butyl groups were poorly soluble at the stage of hexamer **5b**.

The structures of **1b** and **1c** were deduced from their spectral data (Table 1).[14] Both compounds show only one singlet in the

Table 1. Physical and spectral data of **1b**, **1c**, **5a**, **5b**, **6**, and 7.

1b: MS (FAB): $m/z = 600$ (M^+); ^{1}H NMR (270 MHz, $CDCl_3$): $\delta = 7.35$ (s); ^{13}C NMR (67.8 MHz, $CDCl_3$): $\delta = 97.65, 123.93, 130.87$; UV/Vis (cyclohexane): λ_{max} [nm] ($\log \varepsilon$) = 252 (4.55), 330 sh (4.85), 350 (5.09), 400 sh (3.95); Raman (KBr): $\tilde{\nu} = 2203.4\ cm^{-1}$ (C≡C).

1c: MS (FAB): $m/z = 800$ (M^+); ^{1}H NMR (270 MHz, $CDCl_3$): $\delta = 7.40$ (s); ^{13}C NMR (67.8 MHz, $CDCl_3$): $\delta = 94.95, 123.67, 131.21$; UV/Vis (cyclohexane): λ_{max} [nm] ($\lg \varepsilon$) = 245 (4.55), 335 sh (4.85), 356 (4.91), 390 sh (4.40); Raman (KBr): $\tilde{\nu} = 2204.5\ cm^{-1}$ (C≡C).

5a: M.p. 290–291 °C; MS (FAB): $m/z = 803$ ($M^+ + H$); ^{1}H NMR (270 MHz, $CDCl_3$): $\delta = 1.34$ (s, 36H), 7.39 (t, $J = 1.5$ Hz, 2H), 7.42 (d, $J = 1.5$ Hz, 4H), 7.52 (br. s, 16H); ^{13}C NMR (67.8 MHz, $CDCl_3$): d = 31.34, 34.83, 87.85, 90.80, 91.07, 91.23, 92.69, 121.96, 122.55, 123.00, 123.70, 125.89, 126.56, 128.32, 129.15, 131.54, 131.57, 131.99, 150.94); UV/Vis (cyclohexane): λ_{max} [nm] ($\log \varepsilon$) = 351 (4.91), 360 (4.87), 384 sh (4.70).

5b: M.p. 309–310 °C; MS (FAB): $m/z = 903$ ($M^+ + H$); ^{1}H NMR (270 MHz, $CDCl_3$): $\delta = 1.34$ (s, 36H), 7.39 (t, $J = 1.5$ Hz, 2H), 7.42 (d, $J = 1.5$ Hz, 4H), 7.52 (br. s, 20H); UV/Vis (cyclohexane): λ_{max} [nm] ($\log \varepsilon$) = 345 sh (5.00), 358 (5.05), 388 sh (4.75) [a].

6 (ca. 1:1 mixture of regioisomers): MS (FAB): $m/z = 548$ (M^+); ^{1}H NMR (270 MHz, $CDCl_3$): $\delta = 1.40$ (s, 18H), 6.34 (br. s, 2H), 6.73 (br. d, $J = 8.6$ Hz, 2H), 6.94 (d, $J = 8.6$ Hz, 1H), 6.95 (d, $J = 8.6$ Hz, 1H), 7.08 (d, $J = 8.6$ Hz, 1H), 7.09 (d, $J = 8.6$ Hz, 1H), 7.13 (d, $J = 8.6$ Hz, 1H), 7.14 (d, $J = 8.6$ Hz, 1H); ^{13}C NMR (67.8 MHz, $CDCl_3$): sp carbon atoms: $\delta = 93.32, 93.82, 93.86, 94.39$.

7 (ca. 1:1 mixture of stereoisomers): ^{1}H NMR (270 MHz, $CDCl_3$): $\delta = 4.11$ (br. s, 4H), 6.34 (br. s, 4H), 6.73 (d, $J = 7.9$ Hz, 4H), 6.94 (d, $J = 8.6$ Hz, 4H), 7.1–7.2 (m, 8H).

[a] Owing to the poor solubility of this compound, proof of the sp carbon atoms could not be obtained.

^{1}H NMR spectrum and a set of three signals in the ^{13}C NMR spectrum in accord with their D_{6h} and D_{8h} symmetry, respectively. While the chemical shifts of the ^{1}H and ^{13}C signals arising from the benzene rings of **1b** and **1c** are comparable to those of the acyclic oligomers **5a** and **5b**, the signals of the acetylenic carbons are observed at considerably lower field than those of **5a** and **5b**; this reflects the appreciable strain in the triple bonds due to bending. In particular, the chemical shift of the sp carbon in **1b** ($\delta = 97.65$) is considerably lower than that of **3** ($\delta = 92.20$) and even lower than that of 1,5-cyclooctadiyne ($\delta = 95.8$[15]). The Raman frequencies of the triple bonds ($\tilde{\nu} = 2203.4\ cm^{-1}$ for **1b** and $2204.5\ cm^{-1}$ for **1c**) are comparable to that of **3** ($\tilde{\nu} = 2202.0\ cm^{-1}$).

The UV/Vis spectra of **1b**, **1c**, **5a**, and **5b** show similar absorption maxima, except for the relative decrease in the intensity of the shoulder absorptions at the longest wavelength band at about 390 nm (the smaller the cycle the weaker the intensity). In contrast, the fluorescence spectra differ appreciably in the emission wavelengths and quantum yields (Fig. 1 and Table 2). The fluorescence quantum yields of the CPPAs are considerably

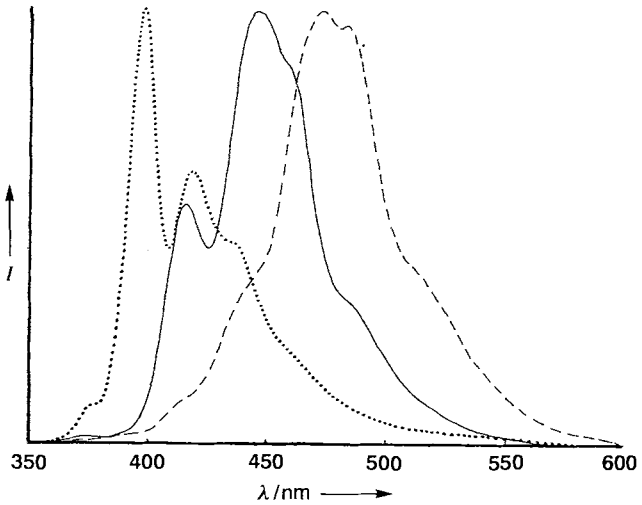

Fig. 1. Fluorescence spectra of **1b** (broken line), **1c** (solid line), and **5b** (dotted line) in cyclohexane.

Table 2. Data from the emission spectra of **1b**, **1c**, **5a**, and **5b** [a].

Cmpd.	Emission maxima [nm]	Stokes shift [nm]	Quantum yield [b]
1b	471, 483	121	0.27
1c	416, 447	91	0.15
5a	394, 416	65 [c]	0.84
5b	398, 418	60 [c]	0.74

[a] In cyclohexane, $\lambda_{excitation} = 375$ nm. [b] Ref. [16]. [c] Difference between the middle of the absorption and emission because of appreciable change of the spectral shape.

smaller than those of the acyclic oligomers, and the Stokes shift becomes larger as the ring decreases in size.[16] This observation suggests greater geometrical changes between the ground state and excited state in CPPAs of smaller ring size.

The analogous synthesis of [4]CPPA **1a** from **4a** was unsuccessful, affording a mixture of *tert*-butanol adducts **6**[17] in 30–40% yield. Dehydrobromination in furan, on the other hand, yielded a stereoisomeric mixture of furan adducts **7** (36%),[18] which were aromatized and deoxygenated with $TiCl_4$/Zn to yield the known dibenzodiyne **8**.[17] For the formation of **7** we

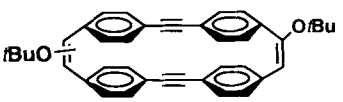

6

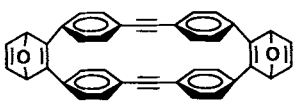

7

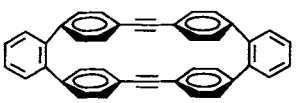

8

currently prefer the stepwise elimination–addition sequence rather than the intermediacy of **1a** from an energetic point of view. Thus, [4]CPPA **1a** seems too strained to be formed by the present approach.

Received: June 11, 1996 [Z9218IE]
German version: *Angew. Chem.* **1996**, *108*, 2803–2805

Keywords: cycloalkynes · cyclophanes · hydrocarbons · strained rings

[1] H. W. Kroto, J. R. Heath, S. C. O'Brien, R. F. Curl, R. E. Smalley, *Nature* **1985**, *318*, 162–163; W. Krätschmer, L. D. Lamb, K. Fostiropoulos, D. R. Huffman, *ibid.* **1990**, *347*, 354–358; H. W. Kroto, *Angew. Chem.* **1992**, *104*, 113–252; *Angew. Chem. Int. Ed. Engl.* **1992**, *31*, 111–129.
[2] S. Iijima, *Nature* **1991**, *354*, 56–58; S. Iijima, T. Ichihashi, Y. Ando, *ibid.* **1992**, *356*, 776–778.
[3] R. Faust, *Angew. Chem.* **1995**, *107*, 1559–1562; *Angew. Chem. Int. Ed. Engl.* **1995**, *34*, 1429–1432; L. T. Scott, *Pure Appl. Chem.* **1996**, *68*, 291–300 and references therein.
[4] F. Diederich, Y. Rubin, C. B. Knobler, R. L. Whetten, K. E. Schriver, K. N. Houk, Y. Li, *Science* **1989**, *245*, 1088–1090; Y. Rubin, C. B. Knobler, F. Diederich, *J. Am. Chem. Soc.* **1990**, *112*, 1607–1617; Y. Tobe, T. Fujii, H. Matsumoto, K. Naemura, Y. Achiba, T. Wakabayashi, *ibid.* **1996**, *118*, 2758–2759.
[5] P. R. Ashton, N. S. Isaacs, F. H. Kohnke, A. M. Z. Slawin, C. Spencer, J. F. Stoddart, D. J. Williams, *Angew. Chem.* **1988**, *100*, 981–983; *Angew. Chem. Int. Ed. Engl.* **1988**, *27*, 966–969; R. J. Graham, L. A. Paquette, *J. Org. Chem.* **1995**, *60*, 5770–5777; R. M. Cory, C. L. McPhail, A. J. Dikmans, J. J. Vittal, *Tetrahedron Lett.* **1996**, *37*, 1983–1986; R. M. Cory, C. L. McPhail, *ibid.* **1996**, *37*, 1987–1990.
[6] R. Fiederich, M. Nieger, F. Vögtle, *Chem. Ber.* **1993**, *126*, 1723–1732.
[7] F. Vögtle, A. Schröder, D. Karbach, *Angew. Chem.* **1991**, *103*, 582–584; *Angew. Chem. Int. Ed. Engl.* **1991**, *30*, 575–577; A. Schröder, D. Karbach, R. Günther, F. Vögtle, *Chem. Ber.* **1992**, *125*, 1881–1887; W. Josten, D. Karbach, M. Nieger, F. Vögtle, K. Hägele, M. Svoboda, M. Przybylski, *ibid.* **1994**, *127*, 767–777; W. Josten, S. Neumann, F. Vögtle, M. Nieger, K. Hägele, M. Przybylski, F. Beer, K. Müllen, *ibid.* **1994**, *127*, 2089–2096.
[8] For brevity we refer to **1** as [*n*]CPPA.
[9] F. Diederich, H. A. Staab, *Angew. Chem.* **1978**, *90*, 383–385; *Angew. Chem. Int. Ed. Engl.* **1978**, *17*, 372–374; H. A. Staab, F. Diederich, *Chem. Ber.* **1983**, *116*, 3487–3503.
[10] T. Kawase, N. Ueda, H. R. Darabi, M. Oda, *Angew. Chem.* **1996**, *108*, 1658–1660; *Angew. Chem. Int. Ed. Engl.* **1996**, *35*, 1558–1560.
[11] H. R. Darabi, T. Kawase, M. Oda, *Tetrahedron Lett.* **1995**, *36*, 9525–9526.
[12] JAIGEL-1H (JAI Co Ltd.) column was used and eluted with THF or $CHCl_3$.
[13] Compounds **5a** and **5b** were also prepared by bromination–dehydrobromination of the corresponding oligo-paraphenylenevinylenes [19] because the reported data of known oligoparaphenylacetylenes were not informative enough for comparison. See S. Misumi, *Bull. Chem. Soc. Jpn.* **1961**, *34*, 1827–1832; J. S. Schumm, D. L. Pearson, J. M. Tour, *Angew. Chem.* **1994**, *106*, 1445–1448; *Angew. Chem. Int. Ed. Engl.* **1994**, *33*, 1360–1363.
[14] Attempts to obtain single crystals of **1b** and **1c** suitable for X-ray analysis have been unsuccessful.
[15] E. Kloster-Jensen, J. Wirz, *Angew. Chem.* **1973**, *85*, 723; *Angew. Chem. Int. Ed. Engl.* **1973**, *12*, 671.
[16] The quantum yields were estimated by using 9,10-diphenylanthracene (Φ = 0.90) as a standard. See D. F. Eaton, *Pure Appl. Chem.* **1988**, *60*, 1107–1114.
[17] C. W. Chan, H. N. C. Wong, *J. Am. Chem. Soc.* **1988**, *110*, 462–469.
[18] J. Heinze, J. Mortensen, K. Müllen, R. Schenk, *J. Chem. Soc. Chem. Commun.* **1987**, 701–703.

Designed Synthesis of $[TiSe_2]_m[NbSe_2]_n$ Superlattices from Modulated Reactants**

Myungkeun Noh and David C. Johnson*

Artificially structured materials—new materials with planned spatial variations in composition on length scales as short as 5–10 Å—have received considerable attention because of their unique properties. The ability to produce nanostructured materials has already led to many advances in technology associated with semiconductors (for example, higher device speeds,[1] solid-state lasers, and "band-gap engineering" of materials[2]) and also to fundamentally new physical phenomena such as the quantized Hall effect[3] and the fractional quantized Hall effect.[4] The ability to control the length scale of the artificial structure of materials containing metals has also lead to interesting physical phenomena of technological importance such as giant magnetoresistance.

The methods used to produce these artificially structured materials are dominated by the need to prepare the samples at low temperatures, where interdiffusion of the constituents is low. At thermal equilibrium these materials would either be uniform solid solutions or phase-separated with much larger domain sizes. The compositional modulation in these new materials is kinetically stable, because the bulk diffusion process in solids near room temperature is so slow.

Common synthesis techniques include sequential evaporation or sputtering on to a heated substrate, molecular beam epitaxy (MBE), chemical vapor deposition (CVD), and liquid phase epitaxy. In these techniques the deposition and substrate conditions are carefully controlled such that epitaxial growth of the sample occurs layer by layer. In MBE growth of a binary compound, the deposition rate of the less volatile element is used to control the growth rate, while the deposition rate of the more volatile element is typically much higher to prevent vacancy formation. The substrate temperature controls desorption rates and lateral mobility of the constituent atoms. In situ probes are used to optimize the layer by layer growth of the growing crystal. The reward for determining the optimal growth conditions is the ability to prepare high-purity epitaxial materials with atomically smooth interfaces and designed compositional profiles.[5]

The above approaches to artificially structured materials become more difficult as systems become more complicated. In ternary systems, for example, finding suitable growth conditions can be a difficult process. If the ternary system contains more than one volatile element, it is often difficult to find substrate temperatures where all three elements are mobile but the volatile elements still have sufficient concentrations on the growing surface. If two elements are involatile, the difficulty then becomes controlling the relative deposition rates accurately enough in addition to finding temperatures where all elements have compatible surface mobilities. The development of alternative synthetic approaches to artificially structured materials containing interleaved binary and ternary compounds continues to be a significant challenge.

In this regard, an interesting series of experiments regarding the high quality epitaxial growth of metal silicides were reported in the early 1980s. In these studies, silicides were formed by the room-temperature deposition of metals on silicon followed by high-temperature anneals. The best results were obtained with nickel depositions, in part due to the small lattice mismatch between $NiSi_2$ and silicon. A sequence of nonepitaxial nickel silicides were initially formed before the final growth of $NiSi_2$, which was found to be epitaxial with respect to the silicon substrate. The growth rate for the formation of the silicides is determined by the rate of diffusion of silicon through the silicide. Consequently, growth temperatures near 800 °C are required in this system to achieve reasonable growth rates.[6] Subsequent research showed that much lower growth temperatures and higher quality epitaxial structures could be obtained if the nickel deposition thickness was less than 20 Å.[7]

In an extension of these results, we recently demonstrated that we could use the kinetics of solid-state reactions to prepare materials with controlled nanoscale structure.[8] In this approach to artificially structured materials, we prepare interwoven layers of the elements within a superlattice reactant. Subsequent annealing at low temperatures results in interfacial nucleation and growth of the constituent heterostructure com-

[*] Prof. D. C. Johnson, M. Noh
Department of Chemistry
University of Oregon, Eugene, OR 97403 (USA)
Fax: Int. code +(541)346-3422
e-mail: davej@oregon.uoregon.edu

[**] This work was supported by the Office of Naval Research (N0014-93-1-0205). Acknowledgment is also made to the Petroleum Research Fund, administered by the American Chemical Society, and the National Science Foundation (DMR-9308854 and DMR-9510562) for partial support of this research.

pounds, which kinetically traps the desired superlattice structure. Low- and high-angle diffraction studies permitted us to follow the evolution of the initial superlattice reactant into the final, crystalline superlattice product. The information from these studies enabled us to propose a model or mechanism for this transformation. Our hope was that this model would permit us to extend our initial results easily and allow us to prepare structurally related products. Conceptually, this approach parallels that of molecular chemists in the development of a working model for a reaction mechanism, which is subsequently used to aid design of reactants that will react to form structurally related products in kinetically controlled reactions.

We chose for this investigation artificially structured superlattices containing the compounds $NbSe_2$ and $TiSe_2$ for several reasons. First, the binary constituents independently have interesting physical properties, and we wanted to study the interplay of these properties as a function of the length scale of the artificial nanostructure. $NbSe_2$ is metallic with a charge density wave transition that varies with polytype, as well as being a 7 K superconductor, and $TiSe_2$ is either a metal with a low density of states or a semimetal, depending upon stoichiometry. Second, previous studies in our laboratory revealed that modulated reactants of either metal with selenium-rich overall composition result in the initial formation of the diselenide at the interfaces. Finally, the van der Waals epitaxy studies by Koma et al. on similar dichalcogenides[9, 10] and the work described above on silicides provided additional reasons to expect the formation of high-quality artificially structured superlattices containing the compounds $NbSe_2$ and $TiSe_2$.

This paper uses our previously proposed mechanism to design superlattice reactants and guide the kinetic trapping of desired heterostructured products.[8] A series of superlattice reactants with the overall structure shown in Figure 1 were prepared with niobium and titanium layers of varying thicknesses and number to yield several series of compounds with superlattice periods corresponding to $[TiSe_2]_m[NbSe_2]_6$ ($m = 1$, 2, 3, 6, and 9), $[TiSe_2]_m[NbSe_2]_9$ ($m = 1$, 3, 6, 9, and 12), $[TiSe_2]_m[NbSe_2]_{12}$ ($m = 3$, 6, 9, and 12), and $[TiSe_2]_m[NbSe_2]_{15}$ ($m = 6$, 9, 12, and 15). These samples were made in a custom-built ultra-high vacuum chamber with element sources independently controlled and monitored with quartz crystal microbalances. Above each of the sources are computer-controlled shutters to allow precise control of elemental layer thicknesses.[11] The elements were sequentially deposited in layers as shown schematically in Figure 1. Through calibration samples, the composition of each niobium–selenium and titanium–selenium block was adjusted to be that of the desired dichalcogenide compounds. The total amount of each component was also calibrated and adjusted to be the desired integral multiple of the known crystallographic unit cells, so that there would be no elemental reactants left in the superlattice after extended annealing. Table 1 summarizes the layer thicknesses used to prepare the initial reactants, the expected and measured repeat layer thickness of the initial reactant as well as the measured and calculated lattice parameters of the crystalline superlattice products.

Table 1. Layer thicknesses d [Å] and lattice parameters c [Å] of selected titanium–niobium–selenides [a]

Compound	d_{Ti} [b]	d_{Se} [c]	d_{Nb} [d]	d_{Se} [e]	$\sum d$ [f]	d_W [g]	$c_{exp.}$ [h]	c_{calcd} [i]
$[TiSe_2]_3[NbSe_2]_{12}$	1×4.07	1×15.52	4×3.93	4×16.39	(100.87)	100.09(56)	94.23(96)	94.72
$[TiSe_2]_6[NbSe_2]_{12}$	2×4.07	2×15.52	4×3.93	4×16.39	(120.46)	119.98(93)	112.1(17)	112.87
$[TiSe_2]_9[NbSe_2]_{12}$	3×4.07	3×15.52	4×3.93	4×16.39	(140.05)	138.8(10)	130.2(20)	131.03
$[TiSe_2]_{12}[NbSe_2]_{12}$	4×4.07	4×15.52	4×3.93	4×16.39	(159.64)	154.6(30)	148.1(34)	149.18
$[TiSe_2]_6[NbSe_2]_{15}$	2×4.07	2×15.52	5×3.93	5×16.39	(140.78)	138.3(11)	131.2(23)	132.01
$[TiSe_2]_9[NbSe_2]_{15}$	3×4.07	3×15.52	5×3.93	5×16.39	(160.37)	158.19(49)	149.2(29)	150.17
$[TiSe_2]_{12}[NbSe_2]_{15}$	4×4.07	4×15.52	5×3.93	5×16.39	(179.96)	177.6(10)	166.9(27)	168.32
$[TiSe_2]_{15}[NbSe_2]_{15}$	5×4.07	5×15.52	5×3.93	5×16.39	(199.55)	188.6(40)	185.6(33)	186.48
$[TiSe_2]_1[NbSe_2]_9$	1×1.36	1×5.17	3×3.93	3×16.39	(67.49)	65.69(39)	63.35(35)	63.47
$[TiSe_2]_3[NbSe_2]_9$	1×4.07	1×15.52	3×3.93	3×16.39	(80.55)	78.42(15)	75.16(92)	75.58
$[TiSe_2]_6[NbSe_2]_9$	2×4.07	2×15.52	3×3.93	3×16.39	(100.14)	98.36(42)	93.2(15)	93.73
$[TiSe_2]_9[NbSe_2]_9$	3×4.07	3×15.52	3×3.93	3×16.39	(119.73)	120.62(74)	110.9(17)	111.89
$[TiSe_2]_{12}[NbSe_2]_9$	4×4.07	4×15.52	3×3.93	3×16.39	(139.32)	136.48(28)	129.1(27)	130.04
$[TiSe_2]_1[NbSe_2]_6$	1×1.36	1×5.17	2×3.93	2×16.39	(47.17)	47.10(11)	44.09(22)	44.33
$[TiSe_2]_2[NbSe_2]_6$	1×2.71	1×10.35	2×3.93	2×16.39	(53.70)	53.39(13)	50.23(31)	50.38
$[TiSe_2]_3[NbSe_2]_6$	1×4.07	1×15.52	2×3.93	2×16.39	(60.23)	59.40(16)	56.15(40)	56.44
$[TiSe_2]_6[NbSe_2]_6$	2×4.07	2×15.52	2×3.93	2×16.39	(79.82)	78.89(31)	74.16(85)	74.59
$[TiSe_2]_9[NbSe_2]_6$	3×4.07	3×15.52	2×3.93	2×16.39	(99.41)	95.07(11)	92.4(11)	92.75

[a] The factor in front of the layer thickness indicates the number of times a layer was deposited. [b] Intended thickness of the titanium layer. [c] Intended thickness of the selenium layer. [d] Intended thickness of the niobium layer. [e] Intended thickness of the selenium layer. [f] Thickness of the total layer. [g] Measured thickness of the repeat unit after deposition. [h] Calculated lattice parameter c of the superlattice of the product, based on the lattice parameters of the binary constituents. [i] Calculated lattice parameter c of the superlattice of the reactant.

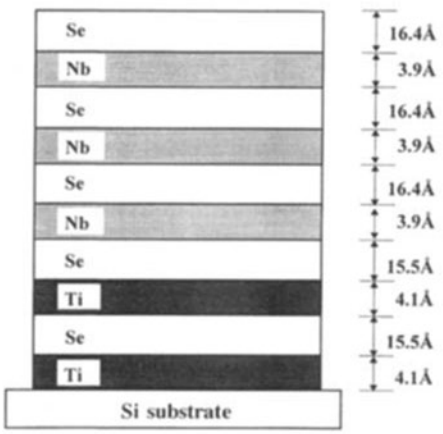

The structure and compositional modulation of the as deposited reactants was determined by low-angle X-ray diffraction. The low-angle diffraction of the as-deposited reactants (Fig. 2) contained Bragg diffraction maxima from the compositional modulation as well as subsidiary maxima resulting from interference from the front and back of the film and incomplete destructive interference from the modulated structure of the initial reactants. The modulation period of the reactants varied as expected given the thicknesses of the deposited elements in the repeating unit.

Following deposition, the superlattice reactants were removed from the deposition system and annealed in a nitrogen atmosphere. The annealing conditions were based on previous results, which showed that low-temperature annealing resulted in the nucleation and growth of the dichalcogenide components along the reacting metal–selenium interfaces.[8] We observed a decrease in the repeat layer thickness during the annealing, presumably due to the elimination of vacancies formed during deposition (see Fig. 2). The reactants evolved into crystalline su-

 © VCH Verlagsgesellschaft mbH, D-69451 Weinheim, 1996 0570-0833/96/3522-2667 $ 15.00+.25/0

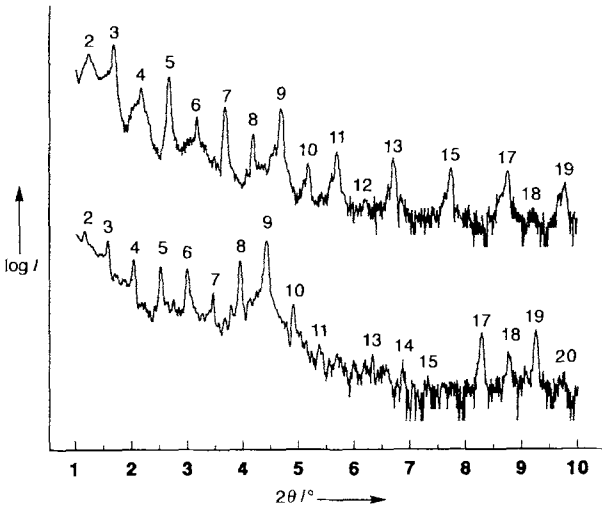

Fig. 2. Low-angle diffraction data collected for a superlattice reactant in which elemental layers of appropriate thickness were deposited to yield twelve $TiSe_2$ layers and fifteen $NbSe_2$ layers in the unit cell. The bottom diffraction scan was collected for the as-deposited reactant, whereas the upper diffraction scan was collected after annealing to form the crystalline superlattice. Note the shift in positions as a result of the contraction of the unit cell on annealing. The numbers above the diffraction maxima refer to the index of the Bragg diffraction maxima.

perlattices containing many well resolved diffraction maxima as shown in Figures 3 and 4. The diffraction patterns qualitatively resemble those expected for the intended structures; they consist

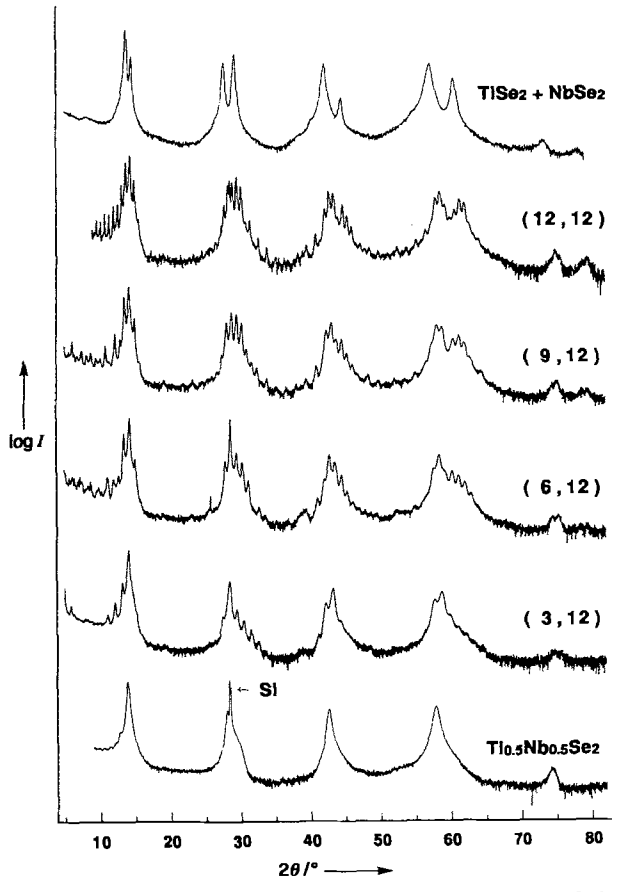

Fig. 3. Diffraction data collected for members of the series $[TiSe_2]_m[NbSe_2]_{12}$. The diffraction patterns of the homogenous alloy $NbTiSe_4$ (bottom diffraction pattern) and 3/12, 6/12, 9/12, and 12/12 $TiSe_2/NbSe_2$ units as the unit cell of the superlattice, and a mixture of the binary compounds (top diffraction pattern) are shown offset for clarity.

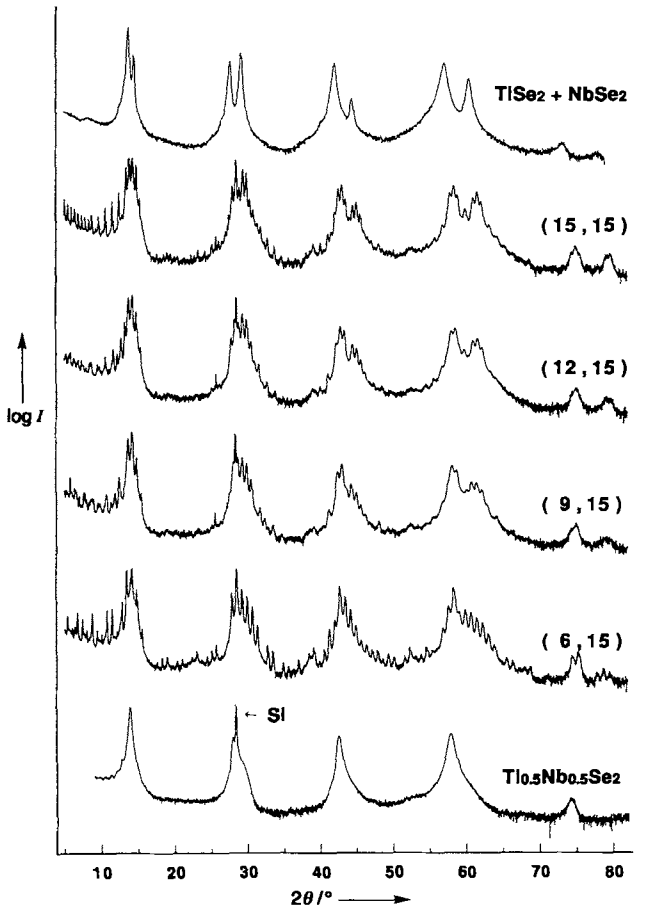

Fig. 4. Diffraction data collected for members of the series $[TiSe_2]_m[NbSe_2]_{15}$. The diffraction patterns of the homogenous alloy $NbTiSe_4$ (bottom diffraction pattern), and 6/15, 9/15, 12/15, and 15/15 $TiSe_2/NbSe_2$ units as the unit cell of the superlattice, and a mixture of the binary compounds (top diffraction pattern) are shown offset for clarity.

of the convolution of the supercell diffraction and the bulk dichalcogenide diffraction. The maxima in the diffraction patterns can be indexed as 00*l* reflections resulting in *c*-axis lattice parameters consistent with the desired number of $NbSe_2$ and $TiSe_2$ layers in the repeating unit of the superlattice sample as summarized in Figure 5. The lines fitted through each set of samples shown in Figure 5 contain information on the average *c*-axis lattice parameter of the $TiSe_2$ layers in the superlattices (the slopes) as well as the average *c*-axis lattice parameter of the $NbSe_2$ layers (the intercepts). From the calculated slopes of these four linear fits, the average $TiSe_2$ *c*-axis lattice parameter is 6.005 ± 0.028 Å, which is very close to the value observed in the binary compound $TiSe_2$ (6.008 Å).[12] The average $NbSe_2$ lattice parameter calculated from the intercepts of these lines is 6.349 ± 0.016 Å, which is close to the range of values reported for the different polytypes of the binary compound $NbSe_2$ (6.27–6.31 Å).[13] For a more quantitative evaluation of the structures, the observed diffraction intensities were compared with simulated diffraction patterns based on the interfacial structure determined previously for a $[TiSe_2]_6[NbSe_2]_6$ superlattice.[8] The similarity of the diffraction intensities between the data and the simulations suggests that the composition gradient at the $TiSe_2$–$NbSe_2$ interface is confined to a single mixed dichalcogenide layer. The agreement between the lattice parameters of the binary compounds and the layer thicknesses observed in the superlattice, as well as the high quality of the 00*l* diffraction patterns, highlights the well-formed structure that

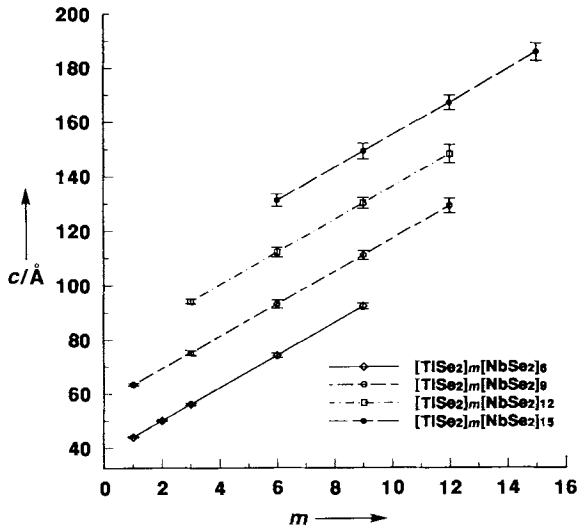

Fig. 5. A plot of the refined c-axis lattice parameters for the superlattices versus the desired number of $TiSe_2$ units m, the unit cell of the superlattice. The linear relationship between these parameters highlights the ability of this approach to design the structure of the desired final product through control of the initial reactant.

develops along the c axis as the superlattice structures are kinetically trapped.

This synthetic advance sets the stage for the synthesis of materials with unexpected bonding and mechanical and electrical properties that can be systematically examined as a function of heterostructure length scales. Other phenomena, such as phase transformations and interface-related processes in thin-film and layered alloys, may also be profoundly different in these heterostructured materials from those which are now well-known in the bulk alloy or composite systems. In addition, a transition from composite behavior to that of a new compound should occur as the length scale of the compositional modulation decreases; the length scale of the transition would depend upon the property being monitored. This new synthesis approach provides new opportunities to probe for these effects by enabling the preparation of superlattice materials for which epitaxial growth conditions have yet to be determined. This ability to synthesize new "designed" layer structures from superlattice reactants also implies the potential design of physical and chemical properties.

Received: June 24, 1996 [Z9258IE]
German version: *Angew. Chem.* **1996**, *108*, 2805–2809

Keywords: nanostructures · niobium compounds · selenium compounds · titanium compounds

[1] N. Sano, H. Kato, S. Chiko, *Solid State Commun.* **1984**, *49*, 123.
[2] F. Capasso, *Physica B* **1985**, *129*, 92.
[3] K. von Klitzing, G. Dorda, M. Pepper, *Phys. Rev. Lett.* **1980**, *45*, 494.
[4] D. C. Tsui, H. L. Stormer, A. C. Gossard, *Phys. Rev. Lett.* **1982**, *48*, 1559.
[5] A. Cho in *Key Papers in Applied Physics, Vol. 1* (Eds.: P. S. Peercy, J. M. Poate), AIP Press, New York, **1994**, p. 569; K. Ploog, *Angew. Chem.* **1988**, *100*, 611; *Angew. Chem. Int. Ed. Engl.* **1988**, *27*, 593.
[6] K. C. R. Chiu, J. M. Poate, L. C. Feldman, C. J. Doherty, *Appl. Phys. Lett.* **1980**, *36*, 544.
[7] R. T. Tung, J. M. Gibson, J. M. Poate, *Phys. Rev. Lett.* **1983**, *50*, 429.
[8] M. Noh, J. Thiel, D. C. Johnson, *Science* **1995**, *270*, 1181.
[9] A. Koma, K. Yoshimura, *Surf. Sci.* **1986**, *174*, 556.
[10] A. Koma, K. Saiki, Y. Sato, *Appl. Surf. Sci.* **1989**, *41/42*, 451.
[11] L. Fister, X. M. Li, T. Novet, J. McConnell, D. C. Johnson, *J. Vac. Sci. Technol. A* **1993**, *11*, 3014.
[12] C. Riekel, *J. Solid State Chem.* **1976**, *17*, 389.
[13] P. Villars, L. D. Calvert, *Pearson's Handbook of Crystallographic Data for Intermetallic Phases, Vol. 4*, 2nd ed., ASM International, Materials Park, OH, USA, **1991**.

Ring-Expanding Metathesis of Tetradehydroanthracene—Synthesis and Structure of a Tubelike, Fully Conjugated Hydrocarbon**

Stefan Kammermeier, Peter G. Jones, and Rainer Herges*

In principle, tubelike molecules[1] can be synthesized in three ways (Scheme 1). Firstly, rings can be stacked, as was successful with cyclodextrins,[2] cyclopeptides,[3] and cyclic hydrocarbons,[4] and which is probably how "nanotubes" are formed in

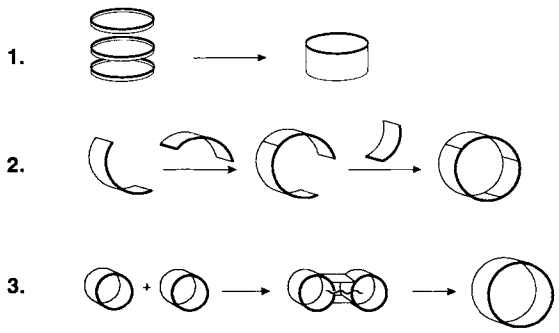

Scheme 1. Three approaches for the construction of tube-shaped molecules.

a direct-current electric arc[5] and during chemical vapor deposition of carbon-containing gases.[6] Secondly, prefabricated convex parts can be assembled (see for example the synthesis of 12[collarene] by Stoddart et al.[7] and of the ribbon-shaped cyclophanes by Vögtle and co-workers[8])[9]. We pursued a third approach based on a ring-expanding metathesis reaction,[10] which is analogous to the formation of a large bubble by the combination of two small ones.

Tetradehydrodianthracene (TDDA)[11] **1** was used as the starting material because its structure is well-suited for the synthesis of a tubelike molecule and because its extremely high strain energy provides the driving force for a metathesis reaction; the metathesis is therefore directed towards ring expansion. In earlier studies we investigated the general reactivity of TDDA towards electrophiles,[12] nucleophiles,[13] and Diels–Alder partners.[14] Photochemically induced metathesis reactions with ethene, propene, cyclic alkenes, and even with benzene have already been performed.[15] The attempted dimerizing metathesis, however, was achieved only after numerous variations of the reaction conditions finally by photolysis of a suspension of TDDA in benzene with a high-pressure mercury lamp in a quartz apparatus (Scheme 2).

In homogeneous solution in benzene only very small amounts of the dimerization product were obtained. The main product is the known metathesis product with the solvent.[15] In other solvents like toluene and hexane transfer of hydrogen and ring opening to bianthryl is predominant. Apparently a suspension of the reactant in benzene is essential for dimerization of **1**.

An X-ray analysis of TDDA **1**[16] was performed to test the hypothesis of a solid-phase mechanism (Fig. 1). In the crystal

[*] Prof. Dr. R. Herges, Dipl.-Chem. S. Kammermeier
Institut für Organische Chemie der Technischen Universität
Hagenring 30, D-38106 Braunschweig (Germany)
Fax: Int. code +(531)391-5388
e-mail: r.herges@tu-bs.de
Prof. Dr. P. G. Jones
Institut für Anorganische und Analytische Chemie
der Technischen Universität Braunschweig (Germany)

[**] This work was supported by the Deutsche Forschungsgemeinschaft and by the Fonds der Chemischen Industrie (scholarship for S. K.).

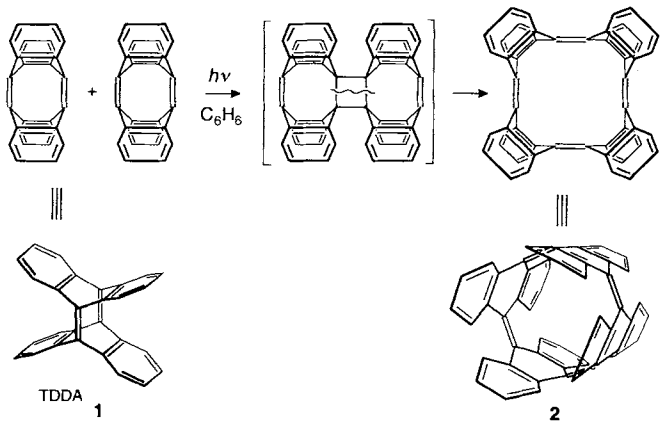

Scheme 2. Dimerizing metathesis of TDDA.

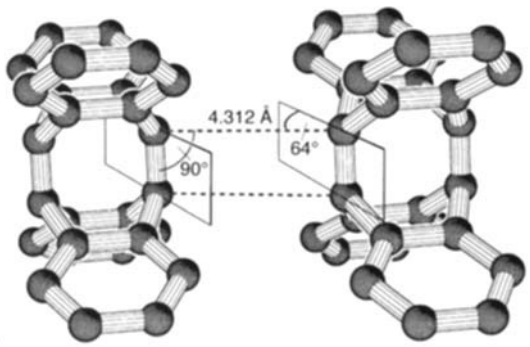

Fig. 1. X-ray crystal structure of TDDA **1**.

the double bonds are oriented in a favorable arrangement for a [2 + 2]cycloaddition. Both π-planes[17] are parallel and form an angle of 64° with the two cyclobutane C–C bonds made during the cycloaddition. The distance between bridgehead atoms in neighboring molecules of **1** is 4.31 Å and in the upper range of distances suitable for cycloaddition[18] (Fig. 1).

One observation does not support the solid-phase reaction of **1**: irradiation of solid TDDA in an argon atmosphere does not lead to an observable reaction. This, however, could be due to the very strong UV absorption of the product in the range of the π–π* transition of TDDA (282 nm), and thus the crystal surface could be "passivated" towards further reaction in the interior. In suspension in benzene the surface of the dimer would be continuously dissolved and removed. Additionally benzene probably acts as a singlet sensitizer. The π–π* transition of TDDA is symmetry forbidden ($\varepsilon_{max} = 1270$). Since the photolysis is performed in a quartz apparatus, excitation of benzene followed by energy transfer to TDDA is likely. A triplet reaction can be excluded because the addition of triplet sensitizers such as acetone and benzophenone leads almost exclusively to the formation of anthracene.

The ^{1}H NMR spectrum with two signals and the ^{13}C NMR spectrum with only four signals indicates that the metathesis product **2**, at least on time average, should have a very high (D_{4h}) symmetry. Besides the M^+ peak at m/z 704 there is only one additional peak in the mass spectrum at half the molecular weight at m/z 352. Most probably this does not arise from a fragment but from the aromatic dication of **1**. The final proof of structure was provided by a crystal structure analysis. Unfortunately the crystals of **2** contain large amounts of disordered THF, which prevented sufficient refinement of the structure ($R(F) = 0.14$). The connectivity of the atoms and the high symmetry of D_{4h}, however, can be determined unequivocally (Fig. 2).[19]

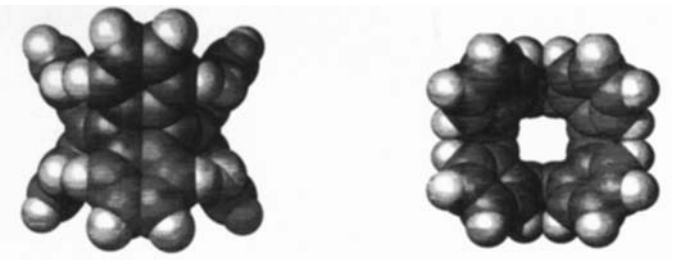

Fig. 2. Van der Waals surface of **2** (D_{4h}) based on the data from an X-ray structure analysis.

The "picotube"[20] **2** consisting of four anthracene units has an approximate tubular structure with a diameter of 5.4 Å and a length of 8.2 Å (Fig. 2). All C=C bonds are conjugated and the 16 e perimeter is antiaromatic. To our knowledge **2** is the first conventionally synthesized and completely conjugated belt- or tubelike hydrocarbon besides the nano- and buckytubes, which are formed by vaporization of carbon. Unlike typical aromatic compounds, which have a perfect or a at most slightly curved π-plane, the π-plane of **2** is tubular.

In contrast to the crystal structure, semiempirical calculations of **2** indicate that it has only time-averaged D_{4h} symmetry. The lowest energy conformation is a D_{2d} structure, which is formed by a 20° twist of the quinoid double bonds (Fig. 3). Lowering the symmetry, however, provides a gain in energy of only 6.5 kcal mol^{-1} (AM1 calculations). The two possible D_{2d} structures should interconvert very rapidly at room temperature. Freezing of the conformational motion could not be observed at temperatures down to −70 °C.

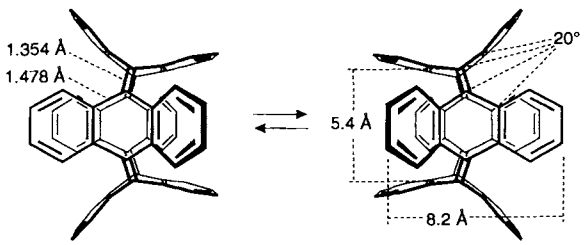

Fig. 3. AM1-calculated conformational movement of **2**.

Picotube **2** is extraordinarily stable and unreactive. Neither melting nor decomposition were observed at temperatures up to 450 °C. **2** also is completely inert towards *m*-chloroperbenzoic acid and bromine at room temperature. The cylindrical cavity and the π-orbitals pointing towards the interior suggest that **2** could be used as a π-spherand.[21] Experiments with silver(I) salts provide preliminary evidence.[19] Poorly soluble **2** suspended in THF can be dissolved by addition of silver(I) triflate. The FAB mass spectrum of the residue after removal of the solvent shows peaks at m/z 811 and 813, which correspond to the mass of 1:1 complexes of **2** with $^{107}Ag^+$ and $^{109}Ag^+$, respectively. The ^{13}C NMR spectrum, however, does not exhibit a low-field shift or a carbon–silver coupling. Apparently there is a fast equilibrium at room temperature in which the solvent-separated reaction partners are predominant.

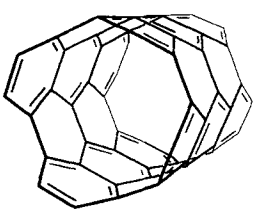

3

Intramolecular cyclization–dehydrogenation of **2** would lead to the buckytube **3** with a length of three and a perimeter of eight benzene rings. Experiments aimed at this target are underway.

 © VCH Verlagsgesellschaft mbH, D-69451 Weinheim, 1996 0570-0833/96/3522-2670 $ 15.00+.25/0

Experimental Procedure

1: M.p. 388 °C; ^{1}H NMR (400 MHz, $CDCl_3$): $\delta = 7.15$ (m, 8H), 6.89 (m, 8H); ^{13}C NMR (100.6 MHz, $CDCl_3$): $\delta = 152.2$ (C=C), 147.0 (C_q), 125.8 (CH, arom.), 124.1 (CH, arom.); IR (KBr, cm^{-1}): $\tilde{\nu} = 3064$ m, 3037 sh, 1566 m, 1449 s, 747 s, 614 s; UV/Vis (CH_2Cl_2): λ_{max} (ε) = 233 (10700), 270 (2500), 282 (1270) nm; MS (70 eV): *m/z* (%): 352 (100) [M^+]; C,H-analysis ($C_{28}H_{16}$): calc. C 95.42, H 4.58; found C 95.31, H 4.51.

2: Tetradehydrodianthracene **1** (60 mg, 0.170 mmol) was suspended in 10 mL of benzene in a quartz tube and irradiated from the exterior for 10 h with a high-pressure mercury lamp (150 W). The solvent was removed in vacuo and the residue purified by chromatography with hexane/dichloromethane over silica gel. After crystallization from toluene, **2** was obtained as a colorless solid. Yield: 19 mg (32%). M.p. >450 °C; ^{1}H NMR (400 MHz, $CDCl_3/CS_2$): $\delta = 7.83$ (dd, $J = 3.3$, 5.7 Hz, 16H, H-2), 7.00 (dd, $J = 3.3$, 5.7 Hz, 16H, H-1); ^{13}C NMR (100.6 MHz, $CDCl_3/CS_2$): $\delta = 138.90$ (C_q, C-3), 134.55 (C_q, C-4), 129.07 (CH, C-2), 124.94 (CH, C-1); IR (KBr, cm^{-1}): $\tilde{\nu} = 3126$, 3058, 3023 (m, C-H, arom.), 1632 (w, C=C), 1447 (s, C=C, arom.), 1089 (m), 764 (s, C-H, arom.), 750 (s, C-H, arom.), 632 (s); UV/Vis (CH_2Cl_2): λ_{max} (ε) = 231 (21000), 257 (27000), 300 (15000) nm; MS (70 V): *m/z* (%): 704 (100) [M^+], 352 (15) [M^{2+}]; high-resolution MS: calc. for $C_{56}H_{32}$: 704.2504, found: 704.2502.

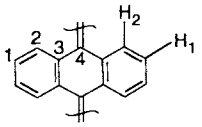

Received: May 28, 1996 [Z9154IE]
German version: *Angew. Chem.* **1996**, *108*, 2834–2836

Keywords: aromaticity · cycloadditions · hydrocarbons · metatheses

[1] For a recent survey of beltlike and tubelike molecules see: A. Schröder, H.-B. Mekelburger, F. Vögtle, *Top. Curr. Chem.* **1994**, *172*, 180–200.
[2] For a recent review see: a) A. Harada, *Farumashia* **1995**, *31*, 1263–1267; P. R. Ashton, C. L. Brown, S. Menzer, S. A. Nepogodiev, J. F. Stoddart, D. J. Williams, *Chem. Eur. J.* **1996**, *2*, 580–591.
[3] a) M. R. Ghadiri, K. Kobayashi, J. R. Granja, R. K. Chada, D. E. McRee, *Angew. Chem.* **1995**, *107*, 76–78; *Angew. Chem. Int. Ed. Engl.* **1995**, *34*, 93–95; b) M. R. Ghadiri, *Adv. Mater.* **1995**, *7*, 675–677; c) M. Engels, D. Bushford, M. R. Ghadiri, *J. Am. Chem. Soc.* **1995**, *117*, 9151–9158.
[4] H. Meier, K. Müller, *Angew. Chem.* **1995**, *107*, 1598–1600; *Angew. Chem. Int. Ed. Engl.* **1995**, *34*, 1437–1439.
[5] a) S. Iijima, *Nature* **1991**, *354*, 56–58; b) S. Iijima, T. Ichihashi, Y. Ando, *Nature* **1992**, *356*, 776–778; c) For recent review see R. S. Ruoff, *Nature* **1994**, *372*, 731–732.
[6] K. Hernadi, A. Fonseca, J. B. Nagy, D. Bernaerts, J. Riga, A. Lucas, *Synth. Met.* **1996**, *77*, 31–43.
[7] a) F. H. Kohnke, A. M. Z. Slawin, J. F. Stoddart, D. J. Williams, *Angew. Chem.* **1987**, *99*, 941–943; *Angew. Chem. Int. Ed. Engl.* **1987**, *26*, 892–894; b) P. R. Ashton, N. S. Isaacs, F. H. Kohnke, A. M. Z. Slawin, C. M. Spencer, J. F. Stoddart, D. J. Williams, *ibid.* **1988**, *100*, 981–983, and **1988**, *27*, 966–968.
[8] W. Josten, S. Neumann, F. Vögtle, M. Nieger, K. Hägele, M. Przybylski, F. Beer, K. Müllen, *Chem. Ber.* **1994**, *127*, 2089–2096.
[9] For further examples see ref. [1].
[10] a) G. Schröder, J. F. M. Oth, *Tetrahedron Lett.* **1966**, 4083–4088; reviews: b) G. Mehta, *J. Chem. Educ.* **1982**, *59*, 313–316; c) G. Kaupp, *Houben Weyl, Methoden der organischen Chemie, Photochemie 1*, Thieme, **1975**, 298–299.
[11] R. L. Viavattene, F. D. Greene, L. D. Cheung, R. Majeste, L. M. Trefonas, *J. Am. Chem. Soc.* **1974**, *96*, 4342–4343.
[12] R. Herges, H. Neumann, *Liebigs Ann.* **1995**, 1283–1289.
[13] R. Herges, H. Neumann, F. Hampel, *Angew. Chem.* **1994**, *106*, 1024–1026; *Angew. Chem. Int. Ed. Engl.* **1994**, *33*, 993–995.
[14] R. Herges, S. Kammermeier, H. Neumann, F. Hampel, *Liebigs Ann.* **1996**, 1795–1800.
[15] S. Kammermeier, R. Herges, *Angew. Chem.* **1996**, *108*, 470–472; *Angew. Chem. Int. Ed. Engl.* **1996**, *35*, 417–419.
[16] See also ref. [11]. Crystal data: triclinic, $P\bar{1}$, $a = 6.5047(8)$, $b = 8.1019(8)$, $c = 9.0281(8)$ Å, $\alpha = 85.131(8)$, $\beta = 73.351(8)$, $\gamma = 72.232(8)°$, $V = 434.09$ Å^3, $Z = 1$, $\lambda(Mo_{K\alpha}) = 0.71073$ Å, $T = -100$ °C. 2001 Independent reflections were measured on a Siemens four-circle diffractometer up to $2\theta = 55°$. The structure was solved with direct methods and anisotropically refined on F^2 (H-atoms riding; program SHELXL-93, G. M. Sheldrick, Universität Göttingen). The final R value $wR(F^2)$ was 0.097, with conventional $R(F) = 0.037$: max. $\Delta\rho$ 0.25 e Å^{-3}, S 1.06. The crystallographic data (excluding structure factors) for the structure reported in this paper have been deposited with the Cambridge Crystallographic Data Centre as supplementary publication no. CCDC-179-99. Copies of the data can be obtained free of charge on application to The Director, CCDC, 12 Union Road, Cambridge CB2 1EZ, UK (fax: Int. code +(1223)336-033; e-mail: teched(@chemcrys.cam.ac.uk).
[17] The π-planes are defined by the four substituents of the bridgehead double bonds.
[18] a) V. Ramamurthy, K. Venkatesan, *Chem. Rev.* **1987**, 433–481; b) M. D. Cohen, G. M. J. Schmidt, *J. Chem. Soc.* **1964**, 1996, 2000, 2014; c) K. Gnanaguru, N. Ramasubbu, K. Venkatesan, V. Ramamurthy, *J. Photochem.* **1984**, *27*, 355.
[19] Note added in proof (25.09.96): In the meantime we have obtained a crystal structure analysis of a 2:1 complex of silver triflate with **2** which unequivocally confirms the D_{4h} structure of **2**.
[20] "Picotube" in analogy to the larger and also fully conjugated nanotubes.
[21] a) J. L. Pierre, P. Baret, P. Chautemps, M. Armant, *J. Am. Chem. Soc.* **1981**, *103*, 2986–2988; b) C. Cohen-Addad, P. Baret, P. Chautemps, J.-L. Pierre, *Acta Crystallogr. Sect. C.* **1983**, *39*, 1346–1349; c) H. C. Kang, A. W. Hanson, B. Eaton, V. Boeckelheide, *J. Am. Chem. Soc.* **1985**, *107*, 1979–1985; d) T. Probst, O. Steigelmann, J. Riede, H. Schmidbaur, *Angew. Chem.* **1990**, *102*, 1471–1473; *Angew. Chem. Int. Ed. Engl.* **1990**, *29*, 1397–1399; e) F. Inokuchi, Y. Miyahara, T. Inazu, S. Shinkai, *ibid.* **1995**, *107*, 1459–1461 and **1995**, *34*, 1364–1366; f) J. Gross, G. Harder, F. Vögtle, H. Stephan, K. Gloe, *ibid.* **1995**, *107*, 523–526 and **1995**, *34*, 481–484; g) J. E. McMurry, G. J. Haley, J. R. Matz, J. C. Clardy, J. Mitchell, *J. Am. Chem. Soc.* **1986**, *108*, 515–516.

Samarium Diiodide Mediated Coupling of Glycosyl Phosphates with Carbon Radical or Anion Acceptors—Synthesis of C-Glycosides**

Shang-Cheng Hung and Chi-Huey Wong*

C-Glycosides, which have conformations similar to those of the parent O-linked structures,[1] have been used as stable carbohydrate mimetics for the study of carbohydrate recognition in biological systems.[2–7] C-Glycosides are often prepared through the coupling of anomeric carbocations, radicals, carbanions, and carbenes.[8] Recently, Sinaÿ et al.[9] and Beau et al.[10] reported that glycosylsamarium(III) derivatives, generated from glycosyl chlorides or sulfones, undergo a Barbier-type reaction with carbonyl compounds to form C-glycosides. The reactions were considered to proceed through two consecutive one-electron reductions to form a glycosyl anion intermediate. Dilithiated D-glucopyranosyl derivatives have been developed by Kessler and his co-workers.[11] The use of a phosphate group as an acceptor in the initial electron transfer mediated by SmI_2/THF has already been described for α-cyanophosphates[12] and allylic phosphates.[13] Here, we report a relatively simple method for the synthesis of C-glycosides under very mild conditions by the umpolung coupling of pyranosyl or furanosyl phosphates with a carbon radical or anion acceptor in the presence of samarium diiodide (Scheme 1).

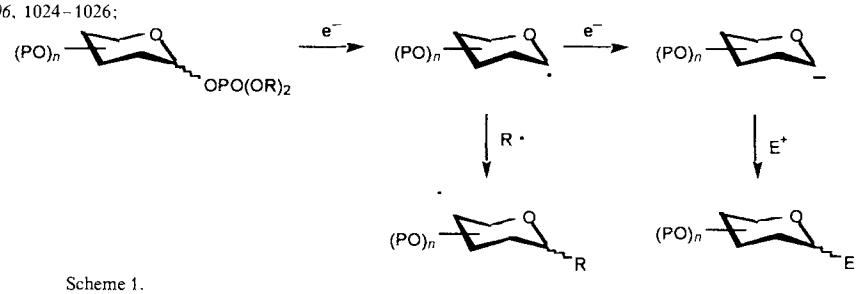

Scheme 1.

[*] Prof. Dr. C.-H. Wong, Dr. S.-C. Hung
Department of Chemistry, The Scripps Research Institute
10550 North Torrey Pines Road, La Jolla, CA 92037 (USA)
Fax: Int. code +(619)784-2409

[**] We thank Dr. Kap-Sun Yeung and Chun-Chen Lin for supplying some starting materials.

In a representative study, a solution of glycosyl dibenzylphosphate **1a**[14] or a glycosyl diphenylphosphate (**1b**, **7**, **9**, or **12**[15,16]) in tetrahydrofuran was mixed with an electrophilic acceptor in the presence of samarium diiodide[17] (Table 1). In the absence of electrophiles, the reaction of D-mannopyranosyl dibenzylphosphate **1a** with SmI_2 gave the 1-deoxymannose derivative **2** and 3,4,6-tri-*O*-benzyl-D-glucal (*β*-elimination product) in 72 and 11% yields, respectively. The yield of the coupling was improved to 85% (6% elimination) on addition of *tert*-amyl alcohol as a proton source. When cyclopentanone, acetone, and isobutyraldehyde were used as electrophiles, only the α-anomeric products **3**, **4**, and **5** were isolated, respectively, in yields of 81, 74, and 68% after purification by silica gel column chromatography. Compound **5** was found to consist of a 12/1 mixture of epimers at the newly generated stereogenic center as determined by ^1H NMR analysis. When diphenylphosphate **1b** was used as a substrate, similar results were obtained. Reaction with dry carbon dioxide gas at room temperature afforded the carboxylic acid **6** in 56% yield. The configuration of **3**–**6** was deduced from the $J_{H1,H2}$ coupling constant and further confirmed by the observation of a nuclear Overhauser effect in the 2D ROESY spectra between H1 and H6.[10a] When the glucosyl phosphate **7** was allowed to react with acetone, only the *β*-isomer **8** was isolated (52%), as indicated by the coupling constant ($J_{H1,H2}$ = 9.2 Hz); the other main by-product was 3,4,6-tri-*O*-benzyl glucal (28%). In the furanoside system, when diphenylphosphate **9** (*β*/α = 1.9/1) and *tert*-amyl alcohol were treated with a solution of samarium diiodide in tetrahydrofuran, the 1-deoxy sugar **10** and the *β*-elimination product were isolated in 76 and 18% yield, respectively. When cyclopentanone was used as an electrophile, a 1/3.6 α/*β* mixture of the C-glycoside **11** was isolated in 77% yield. When 2,3:5,6-di-*O*-isopropylidene-D-mannofuranosyl phosphate **12** was used as a substrate, however, only the α-isomers **14**–**16** were isolated in good yields and no *β*-elimination was observed. The configuration of **14**–**16** at the anomeric center was verified by the NOE effect between H2 and the protons of the cyclopentyl group, the dimethyl group, and the new stereogenic center, respectively. It appears that the high 1,2-*trans*-diastereoselectivity observed in both the furanoside and the pyranoside systems is mainly controlled by steric effects.

Application of this method to the preparation of a 1,6-C-linked disaccharide via anionic intermediates is shown in Scheme 2. Aldehyde **19**[18], which was obtained from **17** via **18**, was used as the acceptor for formation of the 1,6-C-linked disaccharide **20**[19] (Table 2; 22/1 mixture of epimers at the newly formed stereogenic center) in 73% yield after purification by silica gel column chromatography.

With regard to the mechanism of the C-glycosylation, the reduction of glycosyl phosphates with samarium diiodide is believed to proceed through two consecutive one-electron processes. A similar mechanism was proposed for the reaction of glycosyl sulfones[9b,10a] and chlorides.[9a] After the generation of the glycosyl anion, addition to a carbonyl compound and *syn*-elimination compete with each other. As suggested by Beau et al.,[10a] unproductive

Table 1. SmI_2-mediated umpolung coupling of glycosyl phosphates with various electrophiles [a].

Glycosyl phosphate	Electrophile	Product	Yield
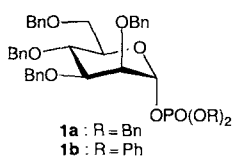 **1a**: R = Bn **1b**: R = Ph		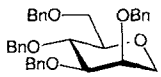	R = Bn, 72%
			2 R = Bn, 85% R = Ph, 83%
		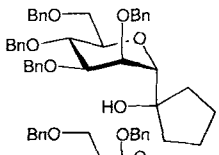	**3** R = Bn, 81% R = Ph, 85%
		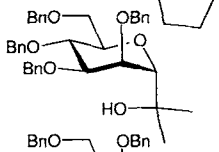	**4** R = Bn, 72% R = Ph, 74%
		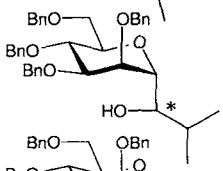	**5** R = Bn, 68% (11.7/1)[b] R = Ph, 65% (10.2/1)[b]
	CO_2	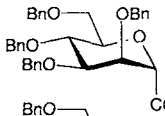	**6** R = Ph, 56%
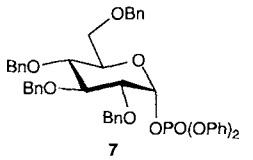 **7**		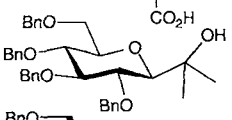	**8** 52%
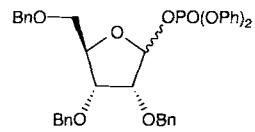 **9** (*β*/α = 1.9/1)		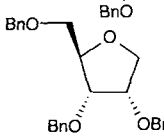	**10** 76%
		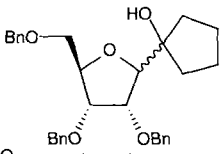	**11** 77% (*β*/α = 3.6/1)
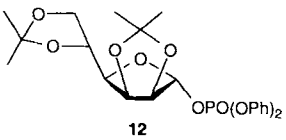 **12**		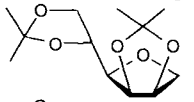	**13** 89%
		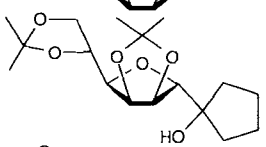	**14** 91%
		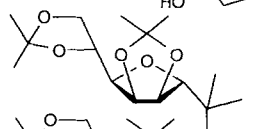	**15** 85%
	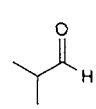	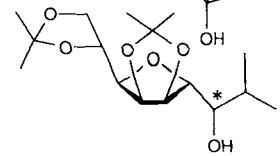	**16** 77% (2.5/1)[b]

[a] All reactions perhaps proceed through a glycosyl anion intermediate. [b] Ratio of epimers at the newly formed stereogenic center.

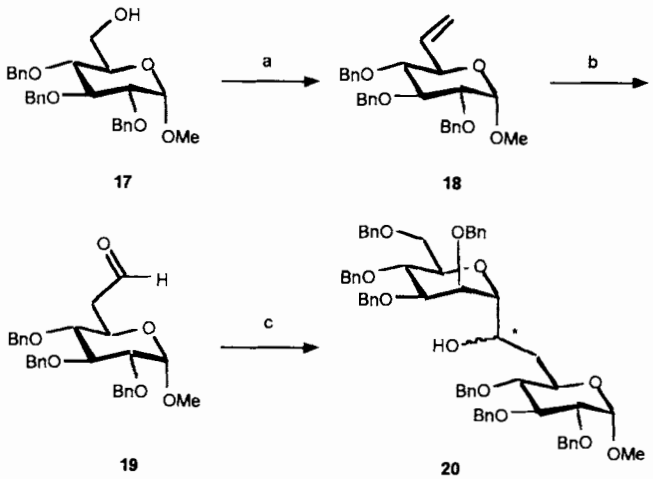

Scheme 2. a) 1. DMSO, $(COCl)_2$, Et_3N, CH_2Cl_2, $-78\,^{\circ}C$, 93%; 2. Ph_3PCH_3Cl, *n*BuLi, THF, $-78 \rightarrow 25\,^{\circ}C$, 55%; b) 1. BH_3/DMS, THF, 25 °C; 30% H_2O_2, 2 N NaOH, 0 °C, 79%; 2. DMSO, $(COCl)_2$, Et_3N, CH_2Cl_2, $-78\,^{\circ}C$, 90%; c) **1b**, SmI_2, THF, 25 °C, 73%, 91% *de*.

syn-elimination might occur when the C1–Sm and C2–O bonds are *syn-coplanar* (with possible coordination). In the reaction with 2,3:5,6-di-*O*-isopropylidene-D-mannofuranosyl phosphate, high diastereoselectivity was observed and no elimination was detected, perhaps due to the lack of coordination between samarium(III) and the oxygen atom at C2.

In another reaction (Scheme 3), compound **23** (obtained from **21** via **22**), when treated with SmI_2 at 25 °C, underwent a *5-exo-trig* cyclization to give adduct **24**[9b] (ca. 1/1 mixture of epimers) in 63% yield. This reaction is believed to proceed through a glycosyl radical intermediate because the reaction occurs under very mild conditions.

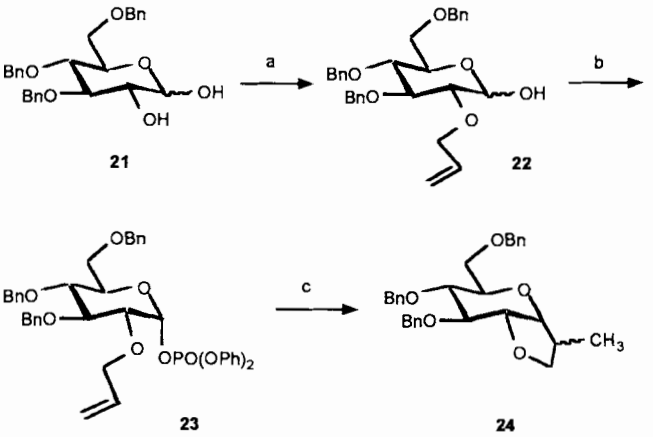

Scheme 3. a) 1. NaH, $H_2C{=}CHCH_2Br$, DMF, 60 °C, 88%; 2. 2 N H_2SO_4, HOAc, 90 °C, 74%; b) *n*BuLi, $(PhO)_2POCl$, THF, $-78\,^{\circ}C$, 82%; c) 0.1 N SmI_2, THF, 25 °C, 63%.

We have described a new effective method for the synthesis of C-linked glycosides. Work is in progress to apply this method to the synthesis of bioactive C-glycosides.

Experimental Procedure

General procedure for the preparation of C-glycosides: Glycosyl dibenzylphosphate **1a** [14] or a glycosyl diphenylphosphate (**1b**, 7, **9**, or **12**) [15, 16] (0.1 mmol) in degassed tetrahydrofuran (0.4 mL) was mixed with an electrophilic acceptor (0.15 mmol of a carbonyl compound or *tert*-amyl alcohol) and a solution of 0.1 N samarium diiodide [17] in tetrahydrofuran (3 mL, 0.3 mmol) at 25 °C under argon. After the deep blue reaction solution turned yellow (approximately 15–30 min), it was quenched by addition of a saturated aqueous ammonium chloride solution (3 mL) and extracted with ethyl acetate (3 × 5 mL). The combined organic layers were washed with brine, dried with anhydrous magnesium sulfate, filtered, and concentrated to dryness. The residue was purified by column chromatography on silica gel to obtain the product (Table 1).

Table 2. Selected physical data for **3**, **6**, **8**, **11β**, **14**, **20** [a].

3: ^1H NMR (400 MHz, $CDCl_3$): $\delta = 7.33-7.23$ (m, 20H, Ar-*H*), 4.58–4.44 (m, 8H, -OC*H*$_2$Ph), 4.16 (ddd, $J = 7.4, 6.0, 2.2$ Hz, 1H, H-5), 3.97 (dd, $J = 8.0, 2.9$ Hz, 1H, H-2), 3.91 (dd, $J = 4.6, 2.9$ Hz, 1H, H-3), 3.83 (dd, $J = 10.1, 7.4$ Hz, 1H, H-6), 3.80 (d, $J = 8.0$ Hz, 1H, H-1), 3.71 (dd, $J = 4.6, 2.2$ Hz, 1H, H-4), 3.67 (dd, $J = 10.1, 6.0$ Hz, 1H, H-6), 2.85 (s, 1H, -O*H*), 1.85–1.75 (m, 4H, Cp-*H*), 1.60–1.54 (m, 4H, Cp-*H*); ^{13}C NMR (100 MHz, $CDCl_3$): $\delta = 138.24, 138.15, 137.71, 128.42, 128.37, 128.34, 127.91, 127.78, 127.66, 127.58, 83.79, 75.73, 75.40, 74.78, 74.68, 73.56, 73.17, 72.64, 71.97, 71.16, 68.33, 37.31, 36.31, 24.40, 23.72$; HRMS (FAB, Cs^+): calcd for $C_{39}H_{44}O_6Cs$ 741.2192, found 741.2160.

6: ^1H NMR (400 MHz, $CDCl_3$): $\delta = 7.38-7.12$ (m, 20H), 4.84 (d, $J = 10.6$ Hz, 1H), 4.73–4.62 (m, 4H), 4.58–4.51 (m, 3H), 4.48 (d, $J = 10.6$ Hz, 1H), 4.29 (t, $J = 2.6$ Hz, 1H), 3.96–3.91 (m, 2H), 3.75–3.68 (m, 2H), 3.60 (dd, $J = 8.4, 2.8$ Hz, 1H); ^{13}C NMR (100 MHz, $CDCl_3$): $\delta = 182.08, 137.90, 137.66, 128.41, 128.34, 128.00, 127.97, 127.92, 127.78, 127.70, 127.62, 80.56, 76.08, 75.06, 73.98, 73.97, 73.84, 73.30, 72.16, 71.86, 69.25$; HRMS (FAB, Cs^+): calcd for $C_{35}H_{36}O_7Cs$ 701.1515, found 701.1535.

8: ^1H NMR (400 MHz, $CDCl_3$): $\delta = 7.34-7.09$ (m, 20H), 5.05 (d, $J = 10.8$ Hz, 1H), 4.98 (d, $J = 11.1$ Hz, 1H), 4.86 (d, $J = 11.1$ Hz, 1H), 4.82 (d, $J = 10.8$ Hz, 1H), 4.70 (d, $J = 10.8$ Hz, 1H), 4.63 (d, $J = 10.8$ Hz, 1H), 4.60 (d, $J = 12.2$ Hz, 1H), 4.55 (d, $J = 12.2$ Hz, 1H), 3.80 (t, $J = 8.9$ Hz, 1H), 3.71 (br. d, $J = 3.2$ Hz, 2H), 3.66 (t, $J = 8.9$ Hz, 1H), 3.65 (t, $J = 9.1$ Hz, 1H), 3.57 (s, 1H), 3.46 (dt, $J = 9.2, 3.2$ Hz, 1H), 3.17 (d, $J = 9.2$ Hz, 1H), 1.25 (s, 3H), 1.24 (s, 3H); ^{13}C NMR (100 MHz, $CDCl_3$): $\delta = 138.27, 138.23, 137.97, 137.35, 128.58, 128.48, 128.44, 128.36, 127.99, 127.93, 127.89, 127.81, 127.66, 127.63, 127.59, 127.54, 127.47, 87.85, 83.10, 79.59, 79.21, 78.76, 75.43, 74.96, 74.61, 73.29, 72.02, 68.87, 26.74, 25.49$; HRMS (ES, H^+): calcd for $C_{37}H_{43}O_6$ 583.3059, found 583.3065.

11β: ^1H NMR (400 MHz, $CDCl_3$): $\delta = 7.35-7.27$ (m, 15H, Ar-*H*), 4.96 (d, $J = 10.7$ Hz, 1H, -OC*H*$_2$Ph), 4.64 (d, $J = 11.7$ Hz, 1H, -OC*H*$_2$Ph), 4.62 (d, $J = 12.1$ Hz, 1H, -OC*H*$_2$Ph), 4.60 (d, $J = 11.7$ Hz, 1H, -OC*H*$_2$Ph), 4.52 (d, $J = 10.7$ Hz, 1H, -OC*H*$_2$Ph), 4.50 (d, $J = 12.1$ Hz, 1H, -OC*H*$_2$Ph), 4.32 (dt, $J = 8.0, 2.9$ Hz, 1H, H-4), 4.29–4.22 (m, 2H, H-2, H-3), 3.81 (dd, $J = 11.0, 2.9$ Hz, 1H, H-5), 3.77 (s, 1H, H-1), 3.60 (dd, $J = 11.0, 2.9$ Hz, 1H, H-5), 1.78–1.47 (m, 8H, Cp-*H*), 1.25 (s, 1H, -O*H*); ^{13}C NMR (100 MHz, $CDCl_3$): $\delta = 138.30, 137.65, 137.31, 128.50, 128.46, 128.31, 128.19, 128.04, 127.93, 127.78, 127.67, 127.56, 84.01, 82.40, 79.99, 79.81, 79.39, 74.05, 73.42, 73.06, 69.13, 38.35, 37.97, 24.27, 24.13$; HRMS (FAB, Cs^+): calcd for $C_{31}H_{36}O_5Cs$ 621.1617, found 621.1638.

14: ^1H NMR (400 MHz, $CDCl_3$): $\delta = 4.85$ (dd, $J = 6.1, 2.1$ Hz, 1H, H-2), 4.83 (dd, $J = 6.1, 3.7$ Hz, 1H, H-3), 4.36 (ddd, $J = 7.4, 6.1, 4.8$ Hz, 1H, H-5), 4.18 (dd, $J = 7.4, 3.7$ Hz, 1H, H-4), 4.11 (dd, $J = 8.6, 6.1$ Hz, 1H, H-6), 4.07 (dd, $J = 8.6, 4.8$ Hz, 1H, H-6), 3.84 (d, $J = 2.1$ Hz, 1H, H-1), 1.83–1.78 (m, 4H, Cp-*H*), 1.69–1.63 (m, 4H, Cp-*H*), 1.52 (s, 3H, -C*H*$_3$), 1.45 (s, 3H, -C*H*$_3$), 1.38 (s, 3H, -C*H*$_3$), 1.37 (s, 3H, -C*H*$_3$); ^{13}C NMR (100 MHz, $CDCl_3$): $\delta = 112.80, 109.07, 90.66, 84.32, 82.76, 82.65, 81.59, 74.08, 66.70, 38.44, 36.37, 26.88, 26.55, 25.23, 24.82, 24.05, 23.92$; HRMS (FAB, H^+): calcd for $C_{17}H_{29}O_6$ 329.1964, found 329.1975.

20: ^1H NMR (400 MHz, $CDCl_3$): $\delta = 7.34-7.24$ (m, 35H), 4.95 (d, $J = 10.8$ Hz, 1H), 4.90–4.73 (m, 3H), 4.66–4.25 (m, 11H), 4.15–4.08 (m, 2H), 3.98–3.89 (m, 2H), 3.85 (dd, $J = 4.8, 3.2$ Hz, 1H), 3.83–3.69 (m, 5H), 3.49 (dd, $J = 9.7, 3.6$ Hz, 1H), 3.30 (s, 3H), 3.24 (t, $J = 9.3$ Hz, 1H), 2.81 (d, $J = 5.1$ Hz, 1H), 2.01 (dt, $J = 14.2, 3.2$ Hz, 1H), 1.81 (dt, $J = 14.2, 8.9$ Hz, 1H); ^{13}C NMR (100 MHz, $CDCl_3$): $\delta = 138.65, 138.41, 138.28, 138.21, 138.12, 138.07, 128.45, 128.36, 128.32, 128.29, 128.09, 127.95, 127.88, 127.75, 127.61, 127.59, 127.54, 127.47, 97.95, 81.97, 81.80, 79.85, 77.20, 75.72, 75.61, 75.07, 74.72, 74.48, 73.39, 73.14, 72.98, 72.88, 72.48, 72.29, 71.84, 69.78, 68.76, 68.50, 55.39, 35.05$; HRMS (FAB, Cs^+): calcd for $C_{63}H_{68}O_{11}Cs$ 1133.3816, found 1133.3860.

[a] Cp = cyclopentyl.

Received: June 14, 1996 [Z92321E]
German version: *Angew. Chem.* **1996**, *108*, 2829–2832

Keywords: carbon–carbon coupling · C-glycosides · radicals · samarium compounds · synthetic methods

[1] a) A. Wei, K. M. Boy, Y. Kishi, *J. Am. Chem. Soc.* **1995**, *117*, 9432; b) A. Wei, A. Haudrechy, C. Audin, H.-S. Jun, N. Haudrechy-Bretel, Y. Kishi, *J. Org. Chem.* **1995**, *60*, 2160; c) D. J. O'Leary, Y. Kishi, *ibid.* **1994**, *59*, 6629; d) A. Wei, Y. Kishi, *ibid.* **1994**, *59*, 88; e) D. J. O'Leary, Y. Kishi, *ibid.* **1993**, *58*, 304; f) J.-F. Espinosa, M. Martin-Pastor, J. L. Asensio, H. Dietrich, M. Martin-Lomas, R. R. Schmidt, J. Jimenez-Barbero, *Tetrahedron Lett.* **1995**, *36*, 6329.

[2] C. Barbaud, M. Bols, I. Lundt, M. R. Sierks, *Tetrahedron* **1995**, *51*, 9063.

[3] a) W. Spevak, J. O. Nagy, D. H. Charych, M. E. Schaefer, J. H. Gilbert, M. D. Bednarski, *J. Am. Chem. Soc.* **1993**, *115*, 1146; b) J. O. Naggy, P. Wang, J. H. Gilbert, M. E. Schaefer, T. G. Hill, M. R. Callstrom, M. D. Bednarski, *J. Med. Chem.* **1992**, *35*, 4501; c) C. R. Bertozzi, D. G. Cook, W. R. Kobertz, F. Gonzalez-Scarano, M. D. Bednarski, *J. Am. Chem. Soc.* **1992**, *114*, 10639; d) C. R. Bertozzi, M. D. Bednarski, *ibid.* **1992**, *114*, 5543; e) C. R. Bertozzi, P. D. Hoeprich, M. D. Bednarski, *J. Org. Chem.* **1992**, *57*, 6092; f) C. R. Bertozzi, M. D. Bednarski, *Carbohydr. Res.* **1992**, *223*, 243.

[4] a) H. Kessler, V. Wittmann, M. Kock, M. Kottenhahn, *Angew. Chem.* **1992**, *104*, 874; *Angew. Chem. Int. Ed. Engl.* **1992**, *31*, 902; b) R. R. Schmidt, H. Dietrich, *ibid.* **1991**, *103*, 1348 and **1991**, *30*, 1328; c) J. N. BeMiller, M. P. Yadar, V. N. Kalabokis, R. W. Myers, *Carbohydr. Res.* **1990**, *200*, 111.

[5] a) X. Wang, P. H. Gross, *J. Org. Chem.* **1995**, *60*, 1201; b) J. M. Tronchet, M. Balkadjian, G. Zosimo-Landolfo, F. Barbalat-Rey, P. Lichtle, A. Ricca, I. Komaromi, G. Bernardinelli, M. Geoffroy, *J. Carbohydr. Chem.* **1995**, *14*, 17.

[6] a) K. J. Kaur, O. Hindsgaul, *Carbohydr. Res.* **1992**, *226*, 219; b) K. N. Drew, P. H. Gross, *Tetrahedron* **1991**, *47*, 6113.

[7] a) U. Hacksell, G. D. Daves, Jr., *Prog. Med. Chem.* **1985**, *22*, 1; b) K. M. Valant-Vetschera, *Bot. Rev.* **1985**, *51*, 1; c) P. Tan, C.-Y. Hou, Y.-L. Liu, L.-J. Lin, G.-A. Cordell, *J. Org. Chem.* **1991**, *56*, 7130.

[8] a) M. H. D. Postema, *C-Glycoside Synthesis*, CRC Press, **1995**; b) P. C. Tang, D. E. Levy, *Chemistry of C-Glycosides*, Elsevier, **1995**; c) G. Casiraghi, F. Zanardi, G. Rassu, P. Spanu, *Chem. Rev.* **1995**, *95*, 1677; d) C. Jaramillo, S. Knapp, *Synthesis* **1994**, 1; e) M. H. D. Postema, *Tetrahedron* **1992**, *48*, 8545; f) J. Herscovici, K. Antonakis, *Studies in Natural Products Chemistry, Vol. 10* (Ed.: Atta-ur-Rahman), Elsevier, Amsterdam, **1992**, p. 337.

[9] a) P. D. Pouilly, A. Chenede, J.-M. Mallet, P. Sinaÿ, *Bull. Soc. Chim. Fr.* **1993**, *130*, 256; b) *Tetrahedron Lett.* **1992**, *33*, 8065; c) P. D. Pouilly, B. Vauzeilles, J.-M. Mallet, P. Sinaÿ, *C. R. Acad. Sci. Ser. 2* **1991**, *313*, 1391; d) P. Sinaÿ, *Phosphorus Sulfur Silicon Relat. Elem.* **1994**, *95–96*, 89.

[10] a) D. Mazeas, T. Skrydstrup, J.-M. Beau, *Angew. Chem.* **1995**, *107*, 990; *Angew. Chem. Int. Ed. Engl.* **1995**, *34*, 909; b) D. Mazeas, T. Skrydstrup, O. Doumeix, J.-M. Beau, *ibid.* **1994**, *106*, 1457 and **1994**, *33*, 1383.

[11] a) O. Frey, M. Hoffmann, H. Kessler, *Angew. Chem.* **1995**, *107*, 2194; *Angew. Chem. Int. Ed. Engl.* **1995**, *34*, 2026; b) O. Frey, M. Hoffmann, V. Wittmann, H. Kessler, *Helv. Chim. Acta* **1994**, *77*, 2060; c) V. Wittmann, H. Kessler, *Angew. Chem.* **1993**, *105*, 1138; *Angew. Chem. Int. Ed. Engl.* **1993**, *32*, 1091.

[12] R. Yoneda, S. Harusawa, T. Kurihara, *Tetrahedron Lett.* **1989**, *30*, 3681.

[13] S. Araki, M. Hatano, H. Ito, Y. Butsugan, *J. Organomet. Chem.* **1987**, *333*, 329.

[14] a) H. Kondo, Y. Ichikawa, C.-H. Wong, *J. Am. Chem. Soc.* **1992**, *114*, 8748; b) M. M. Sim, H. Kondo, C.-H. Wong, *ibid.* **1993**, *115*, 2260; c) H. Kondo, S. Aoki, Y. Ichikawa, R. L. Halcomb, H. Ritzen, C.-H. Wong, *J. Org. Chem.* **1994**, *59*, 864.

[15] S.-I. Hashimoto, T. Honda, S. Ikegami, *J. Chem. Soc. Chem. Commun.* **1989**, 685.

[16] D. L. Boger, T. Honda, *J. Am. Chem. Soc.* **1994**, *116*, 5647.

[17] Reviews: a) G. A. Molander, C. R. Harris, *Chem. Rev.* **1996**, *96*, 307; b) T. Imamoto, *Lanthanides in Organic Synthesis*, Academic Press, **1994**; c) G. A. Molander in *Organic Reactions, Vol. 46* (Ed.: L. A. Paquette), Wiley, **1994**, p. 211; d) D. P. Curran, T. L. Fevig, C. P. Jasperse, M. L. Totleben, *Synlett* **1992**, 943; e) J. L. Namy, J. Collin, C. Bied, H. B. Kagan, *ibid.* **1992**, 733; f) G. A. Molander, *Chem. Rev.* **1992**, *92*, 29.

[18] D. Rouzaud, P. Sinaÿ, *J. Chem. Soc. Chem. Commun.* **1983**, 1353.

Prodrugs of the Cytostatic CC-1065 That Can Be Activated in a Tumor-Selective Manner**

Lutz F. Tietze,* Robert Hannemann, Wilm Buhr, Michael Lögers, Pia Menningen, Monika Lieb, Dorothea Starck, Thomas Grote, Angela Döring, and Ingrid Schuberth

The limited therapeutic spectrum of available cytostatics is a problem in modern cancer therapy. Serious side effects can arise, which are dose-limiting and often lead to a discontinuation of the treatment.[1] One promising approach to selective cancer therapy makes use of the genetic and phenotypic differences between malignant and normal cells.[2] In studies in vitro and in vivo we have discovered that the increased glycolysis rate observed in hyperglycemic cancer cells and the drop in pH associated with it[3] can be used to selectively release a cytostatic drug within a malignant tumor from an acid-labile, nontoxic prodrug.[4] Here we describe the synthesis of novel glycosidic prodrugs of the highly cytotoxic antibiotic CC-1065 (**1**), which can be cleaved by enzymatic hydrolysis with glycohydrolases. The cytostatic can be selectively released in the tumor by conjugates of glycohydrolases and monoclonal antibodies which bind to tumour-associated antigens on the surface of malignant cells.

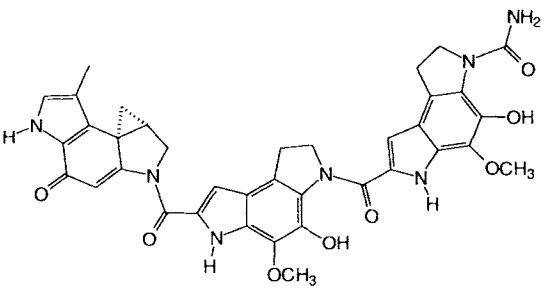

1

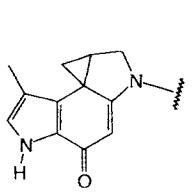

2

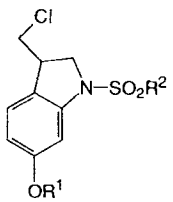

3: $R^1 = H$, $R^2 = CH_3$
4: $R^1 = CH_2Ph$, $R^2 = Ph$

The cytostatic used, seco-CI[6] **3**, is the simplified *seco* form of the pharmacophoric group **2** of the antibiotic CC-1065 (**1**). This compound was first isolated from *Streptomyces zelensis* in 1978

[*] Prof. Dr. L. F. Tietze, Dr. R. Hannemann, Dr. W. Buhr, Dr. M. Lögers, Dipl.-Chem. P. Menningen, Dipl.-Chem. M. Lieb, Dr. D. Starck, Dr. T. Grote, A. Döring, Dr. I. Schuberth
Institut für Organische Chemie der Universität
Tammanstrasse 2, D-37077 Göttingen (Germany)
Fax: Int. code +(551)39-9476

[**] This work was supported by the Deutsche Forschungsgemeinschaft (SFB 416) and by the Fonds der Chemischen Industrie. T. G., M. Lö., P. M., and D. S. thank the Fonds for doctoral scholarships.

and is one of the most effective cytostatics known.[7] Our studies have demonstrated that the cytotoxicity of compounds such as **4**, which are etherified at the phenol hydroxyl group, is significantly less than that of **3**. We therefore prepared the seco-CI-galactoside **11** and the seco-CI-glucoside **12a**, and tested their cytotoxicity with and without added glycohydrolases.

Iodobenzene **5**, which can be prepared in a few steps from the commercially available 4-methoxy-3-nitroaniline, was converted into the indoline derivative **7** by a Heck reaction and subsequent hydroboration (Scheme 1). After protecting group

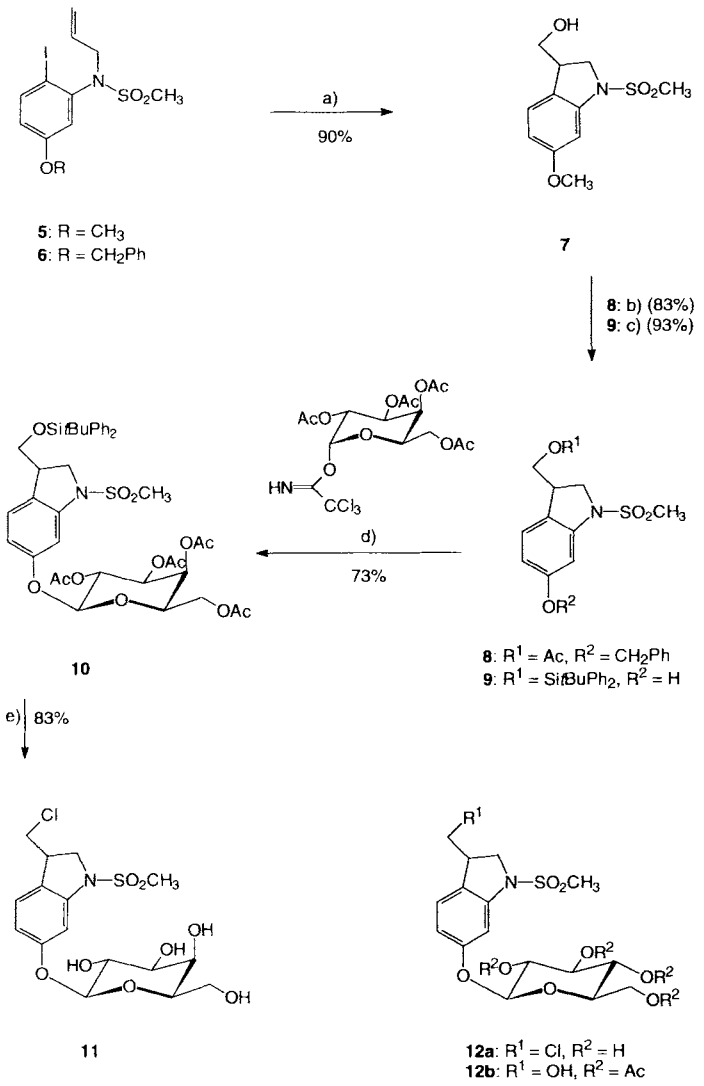

Scheme 1. Synthesis of the seco-CI-glycosides **11** and **12a**. a) 1. $Pd(OAc)_2$, Ag_2CO_3, PPh_3, DMF, 3 h, 25 °C; 2. $BH_3 \cdot SMe_2$, THF, 3 h, 0 °C; 3. NaOH, H_2O_2, H_2O, 50 °C; b) 1. Ac_2O, NaOAc; 2. BBr_3, CH_2Cl_2, 24 h, −15 °C; 3. $PhCH_2Br$, K_2CO_3, acetone, DMF, 20 h, 25 °C; c) 1. K_2CO_3, MeOH, 30 min, 25 °C; 2. $tBuPh_2SiCl$, NEt_3, DMAP, 24 h, 25 °C; 3. Pd/C, H_2 (3 bar), ethyl acetate, 16 h, 25 °C; d) $BF_3 \cdot Et_2O$, 4 Å molecular sieves, CH_2Cl_2, 2 h, −10 °C; e) 1. TBAF/SiO_2, 20 h, 0 °C; 2. PPh_3, CCl_4, 5 h, 50 °C; 3. K_2CO_3, MeOH, 10 min, 25 °C.

manipulations, the phenol derivative **9** was obtained in 70% yield, which was then used for glycosidations. The series of protecting group exchanges on the hydroxyl groups was necessary because substrate **5** is available simply and in very good yields, whereas the benzyloxy derivative **6** gave only moderate yields in the Heck reaction.

For the glycosidation we tested the Koenigs–Knorr reaction,[8] the reaction with tetraacetyltrimethylsilylglycosides in the presence of trimethylsilyltriflate, and the reaction with tetraacetylglycosyltrichloroacetimidates according to Schmidt;[10] the latter gave the best results. Reaction of **9** with tetraacetyl-α-D-galactosyltrichloroacetimidate in the presence of boron trifluoride etherate gave a 73% yield of the β-D-galactoside, with high selectivity (α-galactoside < 3%). Cleavage of the silyl protecting group with tetrabutylammonium fluoride (TBAF) on silica gel, conversion of the hydroxymethyl group into a chloromethyl group according to Appel,[11] and cleavage of the acetyl groups by solvolysis with methanol and potassium carbonate afforded the desired prodrug **11**.[12] The β-D-glucoside **12a** was synthesized from **9** in a similar manner, in 52% overall yield.

Since racemic **9** was used in the synthesis of **11** and **12a**, the glycosidation reaction led to a 1:1 mixture of two diastereomers in each case. For the glucoside, these could be separated by column chromatography over silica at the stage of **12b**. By solvolysis of the acetyl groups and enzymatic cleavage of the diastereomers of **12b**, both enantiomers of **9** can be isolated and subsequently used for the synthesis of the seco-CI-glycosides. However, here the biological studies were carried out with the diastereomeric mixtures of **11** and **12a**.

In toxicity tests[13] with **3**, **4**, **11**, and **12a** on human bronchial carcinoma cells of line A 549[14] we found that **4** displays almost no cytotoxicity, whereas **3** is considerably cytotoxic, with an ED_{50} value of 1.8 μM (Fig. 1). Analysis of the glycosides **11** and

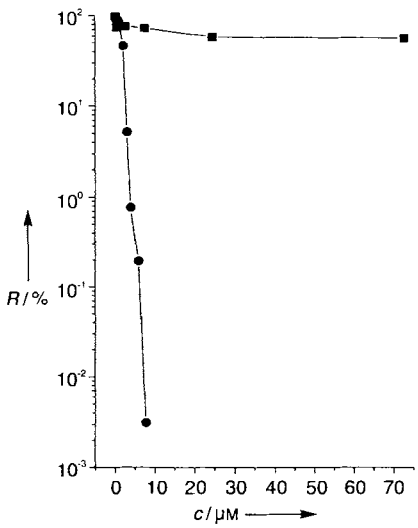

Fig. 1. In vitro cytotoxicity of compounds **3** (●) and **4** (■) on human bronchial carcinoma cells of line A 549 after 24 hours of incubation. The relative clone formation rates R of the cell population were determined by comparing the ability to form colonies in the absence or presence of **3** and **4**, respectively; R = relative clone forming rate, c = concentration.

12a gave unexpected results. Although the phenolic hydroxyl group is blocked, these compounds significantly inhibited cell proliferation in the usual incubation medium. The media were checked for possible glycohydrolase activities[15] caused by the addition of fetal calf serum (FCS) or of serum substitute (Basal Medium Supplement, BMS). Indeed, the FCS medium showed a β-D-galactosidase activity of 0.73 mU mL^{-1} and a β-D-glucosidase activity of 1.00 mU mL^{-1}, whereas the BMS medium gave values of 0.03 mU mL^{-1} and 0.05 mU mL^{-1} respectively. However, with DMEM (Dulbecco's modified Eagle's Medium) without addition of FCS or BMS, neither galactosidase nor glucosidase activities were detected (Fig. 2). Control experi-

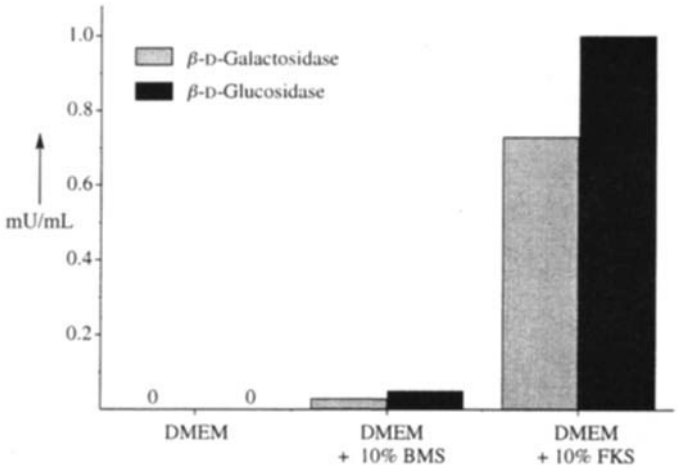

Fig. 2. β-D-galactosidase and β-D-glucosidase activities in various media.

ments showed that cell growth was not impaired if FCS or BMS was removed from the medium during the 24 h exposure to **11** or **12a**, and resupplemented afterwards.

As expected, proliferation was not significantly inhibited by **11** or **12a** in nonsupplemented DMEM, whereas the toxic effect of the prodrug in other media could be correlated with the respective enzyme activities (Fig. 3). In DMEM enriched with BMS, an ED_{50} value of 62 μM was observed for the seco-CI-galactoside **11**, and an ED_{50} value of 14 μM for the seco-CI-glucoside **12a**. This indicates that either the concentration or the activity of the β-D-glucosidase is higher than that of the β-D-galactosidase in the medium. With DMEM (10% FCS added), an ED_{50} value of 3.6 μM was measured for **11**. A similar toxic effect on the tumor cells (ED_{50} = 3.3 μM) is also apparent if 0.2 U mL^{-1} β-D-galactosidase is added with the seco-CI-galactoside **11** in the DMEM incubation medium, since in both cases **11** is rapidly cleaved to release **3**.

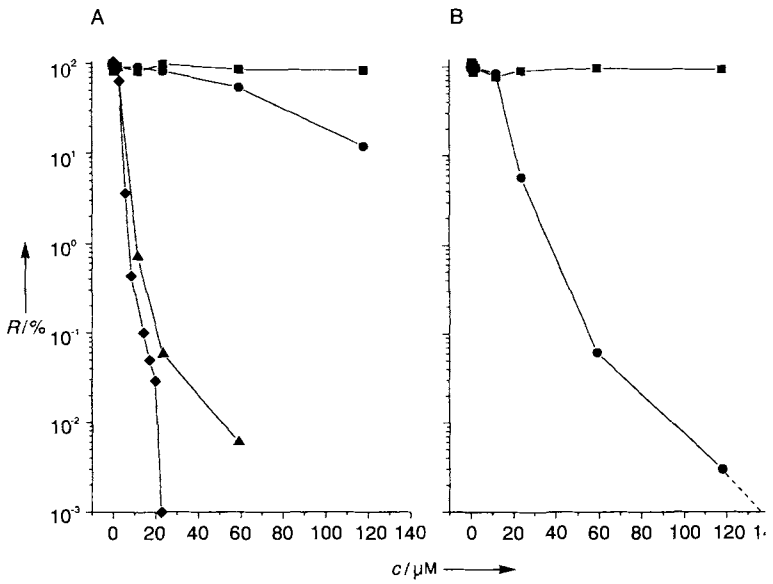

Fig. 3. In vitro cytotoxicity of **11** (A) and **12a** (B) on the cell line A 549 in various media during 24 hours of incubation with the toxin: DMEM (■), DMEM +10% BMS (●), DMEM +10% FCS (▲), DMEM +0.2 U mL^{-1} β-galactosidase (◆); R = relative clone forming rate, c = concentration.

The investigations have shown that the highly cytotoxic seco-CI derivative **3** of the antibiotic CC-1065 (**1**) can be converted into a nontoxic prodrug by O-glycosidation, which after enzymatic cleavage of the glycosidic bond regains its cytotoxicity. In vivo experiments with the prodrugs using conjugates of glycohydrolases and monoclonal antibodies are the subject of our ongoing studies.

Experimental Procedure

Adherent cells of a human tumor cell line were sown in triplicate in 6 multiwell plates at concentrations of 10^2, 10^3, 10^4, and 10^5 cells per cavity, and were incubated with freshly prepared solutions of the compound to be tested at various concentrations. DMSO was used as solubilizing agent (final concentration 0.2%). After 24 h of exposure, the test substance was removed and the cells were treated with fresh medium. After 12 d of cultivation at 37 °C and 7.5% CO_2 in air, the medium was removed; the clones were dried, stained with Löffler's methylene blue, and counted macroscopically. The relative clone forming rate was determined according to the following formula: relative clone forming rate [%] = (number of clones counted after exposure)/(number of clones counted in the control) × 100.

Cells for the toxicity tests were cultivated at 37 °C and 7.5% CO_2 in air in DMEM (Biochrom) supplemented with 4 mM L-glutamine (Gibco), 44 mM $NaHCO_3$ (Biochrom), and 10% fetal calf serum (FCS; heat-inactivated for 30 min at 56 °C, Gibco). During exposure of the cells to the test substances various incubation media were used. The base medium DMEM contained either (a) 4 mM L-glutamine and 44 mM $NaHCO_3$, (b) additional 10% BMS (Biochrom), (c) additional 10% FCS, or (d) additional 0.2 U mL^{-1} β-D-galactosidase (G 5635 Sigma).

Received: May 20, 1996 [Z 9134 IE]
German version: *Angew. Chem.* **1996**, *108*, 2840–2842

Keywords: antitumor agents · enzymes · β-galactosidase · β-glucosidase · Heck reactions

[1] a) P. Erbar, *Onkologie: Einführung in die Pathophysiologie, Klinik und Therapie maligner Tumoren*, Schattauer, **1994**; b) D. M. Prescott, A. S. Flexer, *Krebs-Fehlsteuerung von Zellen – Ursachen und Konsequenzen*, Spektrum der Wissenschaft, Heidelberg **1990**; c) V. Schirrmacher, *Krebs-Tumoren, Zellen, Gene*, Spektrum der Wissenschaft, Heidelberg, **1987**.

[2] a) L. F. Tietze in *Molecular Aspects of Chemotherapy*, (Eds.: E. Borowski, D. Shugar), Pergamon, **1990**, pp. 55–70; b) L. F. Tietze, *Nachr. Chem. Tech. Lab.* **1988**, *36*, 728–737.

[3] I. F. Tannock, D. Rotin, *Cancer Res.* **1989**, *49*, 4373–4384.

[4] a) L. F. Tietze, A. Fischer-Beller, *Carbohydr. Res.* **1994**, *254*, 169–182; b) L. F. Tietze, M. Beller, R. Fischer, M. Lögers, E. Jähde, K. H. Glüsenkamp, M. F. Rajewsky, *Angew. Chem.* **1990**, *102*, 812–813; *Angew. Chem. Int. Ed. Engl.* **1990**, *29*, 782–783; c) L. F. Tietze, M. Neumann, T. Möllers, R. Fischer, K. H. Glüsenkamp, M. F. Rajewsky, E. Jähde, *Cancer Res.* **1989**, *49*, 4179–4184; d) L. F. Tietze, R. Fischer, H. J. Guder, A. Goerlach, M. Neumann, T. Krach, *Carbohydr. Res.* **1987**, *164*, 177–194.

[5] L. N. Jungheim, T. A. Shepherd, *Chem. Rev.* **1994**, *94*, 1552–1566.

[6] a) L. F. Tietze, W. Buhr, *Angew. Chem.* **1995**, *107*, 1485–1487; *Angew. Chem. Int. Ed. Engl.* **1995**, *34*, 1366–1368; b) L. F. Tietze, T. Grote, *J. Org. Chem.* **1994**, *59*, 192–196; c) T. Sakamoto, Y. Kondo, M. Uchiyama, H. Yamanaka, *J. Chem. Soc. Perkin Trans. 1* **1993**, 1941–1942; d) L. F. Tietze, T. Grote, *Chem. Ber.* **1993**, *126*, 2733–2737; e) S. L. Buchwald, *J. Org. Chem.* **1992**, *57*, 6380–6382; f) D. L. Boger, T. Ishizaki, H. Zarrinmayeh, S. A. Munk, P. A. Kitos, O. Suntornwat, *J. Am. Chem. Soc.* **1990**, *112*, 8961–8971; g) R. Baird, S. Winstein, *ibid.* **1963**, *85*, 567–578; D. L. Boger, D. S. Johnson, *Angew. Chem.* **1996**, *108*, 1542–1580; *Angew. Chem. Int. Ed. Engl.* **1996**, *35*, 1438–1474.

[7] a) V. L. Reynolds, J. P. McGroven, L. H. Hurley, *J. Antibiot.* **1986**, *39*, 319–334; b) J. P. McGroven, G. L. Clarke, E. A. Pratt, T. F. DeKoning, *ibid.* **1984**, *37*, 63–70; c) L. J. Hanka, A. Dietz, S. A. Gerpheide, S. L. Kuentzel, D. G. Martin, *ibid.* **1978**, *31*, 1211–1217.

[8] a) G. J. Boons, *Tetrahedron* **1996**, *52*, 1095–1121; b) K. Toshima, K. Tatsuta, *Chem. Rev.* **1993**, 1503–1531; c) H. Paulsen, *Angew. Chem.* **1982**, *94*, 184–201; *Angew. Chem. Int. Ed. Engl.* **1982**, *21*, 155–172.

[9] L. F. Tietze, R. Fischer, H. J. Guder, *Tetrahedron Lett.* **1982**, *23*, 4661–4664.

[10] R. R. Schmidt, *Angew. Chem.* **1986**, *98*, 213–236; *Angew. Chem. Int. Ed. Engl.* **1986**, *25*, 212–235.

[11] J. Hooz, S. S. H. Giliani, *Can. J. Chem.* **1968**, *46*, 86–87.

 © VCH Verlagsgesellschaft mbH, D-69451 Weinheim, 1996 0570-0833/96/3522-2676 $ 15.00+.25/0

[12] **11**: ^{1}H NMR (300 MHz, CD_3OD): $\delta = 2.96$ (s, 3H, SO_2CH_3), 3.34 (s, 4H, OH), 3.56 (dd, $J = 10.0$, 7.5 Hz, 1H, 2-H_a), 3.64–3.96 (m, 9H, 3-CH_a, 3-CH_b, 3-H, 2′-H, 3′-H, 4′-H, 5′-H, 6′-H_a, 6′-H_b), 4.12 (m, 1H, 2-H_b), 4.84 (d, $J = 7.5$ Hz, 1H, 1′-H), 6.82 (dd, $J = 9.0$, 3.0 Hz, 1H, 5-H), 7.16 (d, $J = 3.0$ Hz, 1H, 7-H), 7.25 (d, $J = 9.0$ Hz, 1H, 4-H); ^{13}C NMR (125 MHz, C_6D_6), $\delta = 34.71$ (C-3), 43.20 (C3-*C*), 47.73 (SO_2CH_3), 55.68 (C-2), 62.27 (C-6′, 70.12, 72.21, 74.87, 76.92 (C-2′, C-3′, C-4′, C-5′), 102.9 (C-1′), 103.9 (C-5), 112.8 (C-7), 126.3 (C-3a), 126.9 (C-4), 144.8 (C-7a), 160.1 (C-6).

[13] The in vitro cytotoxicity tests were carried out in the cell culture laboratory of the Institut für Organische Chemie using a clone formation rate assay.

[14] Cell line A 549 (ATCC CCL 185) was kindly provided by the Institut für Zellbiologie, Universität Essen.

[15] Measurements of β-D-galactosidase activities were made colorimetrically in citrate buffer at 405 nm with *p*-nitrophenyl β-D-galactopyranoside; β-D-glucosidase activities were measured with *p*-nitrophenyl β-D-glucopyranoside.

$[(enH_2)_{0.5}][Zr_2(PO_4)_2(HPO_4)F]\cdot H_2O$: A Unique Zirconium Fluoride Phosphate with a Cavity Structure**

Erhard Kemnitz,* Martin Wloka, Sergej Trojanov, and Anja Stiewe

The discovery of microporous aluminophosphates ($AlPO_4$-*n*) by Wilson et al.[1] has spurred great interest in this class of compounds. The substitution of aluminum in the lattice by gallium has led to a series of new phases[2] including several aluminophosphate analogs.[3–5] A key achievement in this field reported by Guth et al.[6] is the development of a new synthetic procedure conducted in the presence of fluoride ions, in which the fluoride is incorporated into the open framework of the structure. The best example of one of the new compounds obtained by this route is cloverit,[7] which contains three-dimensional, 20-membered ring channels, in which the fluoride ion is located at the center of a double, four-membered cage. Likewise, a series of gallium phosphates has been synthesized hydrothermally by Férey et al.[8–12] by using fluoride as a mineralizer and several amines of varying chain lengths as templates. The compounds were structurally characterized and dubbed ULM phases after the authors' location (Université Le Mans). Some isotypic 3D structures analogous to the $AlPO_4$-*n* phases were also found with similar cavities and channels.[13]

The synthesis of transition metal coordinated microporous materials with defined pore structures is of particular interest, owing to their potential as catalysts. Compounds such as vanadium phosphate containing elliptic cavities,[14] microporous cobalt phosphates,[15] and microporous heteropolyoxometalates with Dawson anions[16] have already been synthesized. Clearfield[17] has synthesized and characterized multilayered zirconium phosphates. Xu et al.[18] have recently reported the synthesis of a new zirconium phosphate of composition **1**, the structure of which has now been reported.[19] However, since **1** has a double-stranded chain structure without cavities, and considering its hydrogen bonding system, it can also in fact be described as layered.

$(enH_2)_{1.5}[Zr(HPO_4)(PO_4)F_2]$ **1**

[*] Prof. Dr. E. Kemnitz, Dipl.-Chem. M. Wloka, Dr. S. Trojanov, Dipl.-Chem. A. Stiewe
Institut für Chemie der Humboldt-Universität
Hessische Strasse 1–2, D-10115 Berlin (Germany)
Fax: Int. code +(30)284-68277

[**] This work was supported by the Deutsche Forschungsgemeinschaft, by the Volkswagenstiftung, and by the Fonds der Chemischen Industrie. en = ethylenediamine.

We report here on the synthesis and characterization of the new zirconium fluoride phosphate **2** containing a microporous

$[(enH_2)_{0.5}][Zr_2(PO_4)_2(HPO_4)F]\cdot H_2O$ **2**

3D structure, which we refer to as $ZrPO_4$-1 because of its similarity to the $AlPO_4$-*n* phases.

Well-formed crystals of compound **2** were prepared by hydrothermal synthesis starting from zirconyl chloride, ethylenediamine, hydrogen fluoride, and phosphoric acid.[20] The composition of **2** was deduced by single-crystal X-ray structure determination[21] and confirmed by chemical analysis. The crystal structure determination reveals that the incorporated fluorine does not participate in fluorophosphate bonding, but rather is directly bonded to zirconium, leading to the formation of what might be the first example of a zirconium phosphate with channels in the structure.

Both of the crystallographically independent Zr atoms are octahedrally coordinated, either as ZrO_6 or as ZrO_5F (Fig. 1). Each of the coordinating oxygen atoms belong to different PO_4

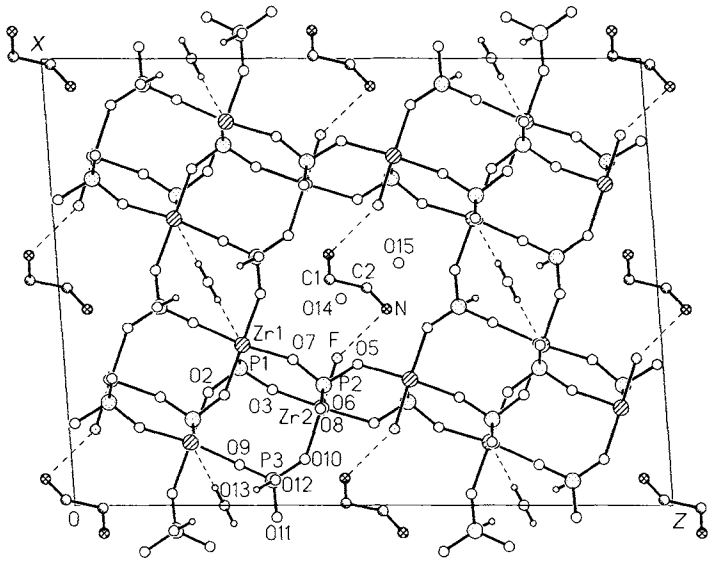

Fig. 1. Projection of the crystal structure of **2** along the crystallographic *b* axis with atom labels (O1 and O4 are not shown below Zr1). The ZrO_6 and ZrO_5F octahedra shown are linked by PO_4 and $PO_3(OH)$ tetrahedra, respectively. Half of the water molecules are situated in the smaller cavities and half are in the larger channels together with protonated ethylenediamine (O14 and O15 are shown only once).

tetrahedra. In contrast to these bridging oxygen atoms, the fluorine atom is terminally bound. Both types of octahedra are slightly distorted with Zr–O distances ranging from 2.022 to 2.101 Å. The terminal Zr–F bond with a bond length of 1.988 Å is only 0.01 to 0.03 Å shorter than that in compound **1** (1.998–2.016 Å).[17] The octahedra are linked by three crystallographically distinct PO_4 and $PO_3(OH)$ tetrahedra. The P–O distances in the PO_4 tetrahedra range from 1.513 to 1.542 Å, similar to the values given for compound **1**. As was expected, the P–OH bond (P3–O12 1.568 Å) is about 0.04 Å longer than the average P–O bond. As is already known from many other examples of SO_4 and $SO_3(OH)$ tetrahedra[22], the P–O bonds of the PO_4 tetrahedra are longer (1.527–1.542 Å) than that of the $PO_3(OH)$ tetrahedra (1.513–1.523 Å). The reduced fluorine content in **2** (0.5 F atoms per Zr atom) results in a lower charge distribution in the anionic region of the structure and therefore the degree of aggregation is higher than that of **1** (2 F atoms per Zr atom). This

finding should encourage further investigation and synthesis of additional examples of this class of compound.

The polyhedra representation in Figure 2 clearly shows the three-dimensional linkage of the structure. The bridging O atoms in the [010] direction are O1 and O4 from the P1 tetrahedra and O6 and O8 from the P2 tetrahedra. The protonated

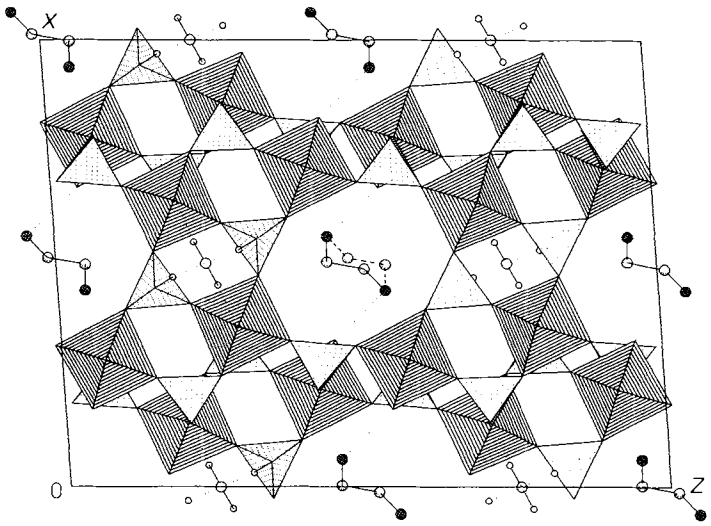

Fig. 2. Projection of the crystal structure of compound **2** in a polyhedra presentation. The enH_2 ions are disordered around the inversion center (the second position is shown only at one site). Half of the water molecules (those at the position of the disordered enH_2 ions) are not shown.

ethylenediamine molecules and half of the water molecules are situated in the channels of the framework. The size of the channels in the [010] direction is limited by eight-membered rings (two ZrO_6 and two ZrO_5F octahedra, alternating with two PO_4 and two $PO_3(OH)$ tetrahedra). The width of the channels varies slightly with the height and depends on the interatomic distances F···F′ (6.11 Å) and O12···O12′ (7.91 Å) at the level of the enH_2 ions and by the distances O5···O(10) (5.63 Å) and O7···O11′ (7.14 Å) at the level of the eight-membered rings.

The situation is slightly complicated because the enH_2 ions are statistically disordered. Consequently, the water molecules at this position appear disordered as well (occupancy for two O atoms 0.25). This disordering phenomena made it impossible to determine the positions of the hydrogen atoms on the amine nitrogen. The same situation arises with the water molecules incorporated on alternating free amine sites; their hydrogen atoms could not be directly determined. However, the measureable N···F and O···O distances and angles are indicative of hydrogen bonds.

The other half of the water molecules are located in the small cavities of the framework and have four hydrogen bonds, two O13–H13···O4 and two O12–H12···O13. Thus water is bound in two different cavities in the structure. Surprisingly, simultaneous DTA/TG measurements[23] exhibit a nonstructured continuous TG curve, with a mass decrease of 3.6%, which corresponds to the loss of one mole of water. This dehydration occurs completely at temperatures above 140 °C. The inorganic framework is unaffected; the powder diffraction pattern recorded for the dehydrated sample showed no changes. At room temperature the sample rehydrates completely after a few hours of contact with air ($\Delta m = +3.6\%$). First attempts at removing all of the ethylenediamine template from the channels failed when acids or bases were utilized. As would be expected, thermal degradation of the amine proceeds by a more complex mechanism and is the focus of current investigation. Preliminary sorption experiments[24] with pure, dehydrated, and partially amine-free samples of compound **2** using nitrogen as a sorbant do not give any evidence for channel accessibility. Further investigations should focus not only on the microporosity and catalytic potential of compound **2**, but also on the influence of other amines on the framework structure. Nevertheless, the first successful preparation of a zirconium phosphate fluoride having a cavity structure may provide a preparative route to novel compounds, which may be of interest, for example, as heterogeneous catalysts.

Received: June 4, 1996 [Z9189IE]
German version: *Angew. Chem.* **1996**, *108*, 2809–2811

Keywords: hydrothermal syntheses · microporosity · zirconium compounds

[1] S. T. Wilson, B. M. Lok, C. A. Messina, T. R. Cannan, E. M. Flanigen, *J. Am. Chem. Soc.* **1982**, *104*, 1146–1147.
[2] J. L. Guth, H. Kessler, R. Wey, *Stud. Surf. Sci. Catal.* **1991**, *60*, 63–64.
[3] J. B. Parise, *J. Chem. Soc. Chem. Commun.* **1985**, 606–607.
[4] J. B. Parise, *Inorg. Chem.* **1985**, *24*, 4312–4316.
[5] J. B. Parise, *Acta Crystallogr. Sect. C* **1986**, *42*, 144–147.
[6] J. L. Guth, H. Kessler, R. Wey, *Stud. Surf. Sci. Catal.* **1986**, *28*, 121–127.
[7] M. Estermann, L. B. McCusker, C. Baerlocher, A. Merrouche H. Kessler, *Nature* **1991**, *352*, 320–323.
[8] T. Loiseau, G. Fèrey, *J. Chem. Soc. Chem. Commun.* **1992**, 1197–1198.
[9] T. Loiseau, G. Fèrey, *J. Solid State Chem.* **1994**, *111*, 416–421.
[10] D. Riou, G. Fèrey, *J. Solid State Chem.* **1994**, *111*, 422–426.
[11] M. Cavallec, D. Riou, G. Fèrey, *J. Solid State Chem.* **1994**, *112*, 441–447.
[12] M. Cavallec, D. Riou, G. Fèrey, *Eur. J. Solid State Inorg. Chem.* **1994**, *31*, 583–594.
[13] T. Loiseau, D. Riou, M. Licheron, G. Fèrey, *J. Solid State Chem.* **1994**, *111*, 397.
[14] V. Soghomonian, Q. Chen, R. C. Haushalter, J. Zubieta, *Angew. Chem.* **1993**, *105*, 601–603; *Angew. Chem. Int. Ed. Engl.* **1993**, *32*, 610–612.
[15] J. Chen, R. H. Jones, S. Natarajan, M. B. Hursthouse, J. M. Thomas, *Angew. Chem.* **1994**, *106*, 667–668; *Angew. Chem. Int. Ed. Engl.* **1994**, *33*, 639–640.
[16] M. Hölscher, U. Englert, B. Zibrowius, W. F. Hölderich, *Angew. Chem.* **1994**, *106*, 2552–2554; *Angew. Chem. Int. Ed. Engl.* **1994**, *33*, 2491–2493.
[17] A. Clearfield, *Comments Inorg. Chem.* **1990**, *10*, 89–128.
[18] Y. Zhao, T. Tian, J. Xu, R. Xu, Gaodeng Xuexiao Huaxue Xuebao **1995**, *16*, 179–180.
[19] M. B. Hursthouse, K. M. A. Malik, J. M. Thomas, J. Chen, J. Xu, T. Song, R. Xu, *Rus. Chem. Bul.* **1994**, *43*, 1787–1791.
[20] A mixture of $ZrOCl_2 \cdot 8H_2O$, ethylene diamine monohydrate, phosphoric acid, hydrogen fluoride, and water in a molar ratio of 1:1:5:2:50 was heated at 180 °C for six days in a PTFE-lined autoclave (filled volume 80%). The solid product was removed by filtration, washed with distilled water and alcohol, and dried at room temperature to yield well-formed crystals of **2**.
[21] Crystal structure analysis of **2**: Four-circle diffractometer STADI-4 (STOE & Cie.) with a graphite monochromator; $Mo_{K\alpha}$ radiation; $\lambda = 0.71073$ Å; $\theta/2\theta$-scan method; 293 K; crystal system: monoclinic; space group: $C2/c$; cell dimensions: $a = 17.277(3)$, $b = 6.620(1)$, $c = 23.104(5)$ Å; $\beta = 94.21(3)°$, $Z = 8$; $V = 2635.4(8)$ Å^3; $\rho_{calcd} = 2.704$ g cm^{-3}; $2\theta_{max} = 55°$; reflections (measured/independent): 3017/2962, of these 2786 with $I > 2\sigma(I)$; $\mu = 2.03$ mm^{-1}; crystal dimensions: $0.3 \times 0.2 \times 0.2$ mm^3, absorption correction with Psi-scan; structure solution with direct methods (SHELXS-86 [25]), refined by a full-matrix leastsquares method against F^2 with SHELXL-93 [26], 222 parameters; hydrogen atoms isotropic, all the others anisotropic; $wR_2 = 0.1152$, $R_1 = 0.0401$. Further details of the crystal structure investigation may be obtained from the Fachinformationszentrum Karlsruhe, D-76344 Eggenstein-Leopoldshafen (Germany), on quoting the depository number CSD-405566.
[22] E. Kemnitz, C. Werner, S. I. Trojanov, *Eur. J. Solid State Inorg. Chem.* **1996**, *33*, 563–596.
[23] Simultaneous thermal analysis: Netzsch STA 429 (mini-sample carrier system with thermocouples Pt/PtRh10, α-Al_2O_3 as reference, Pt crucible, dry air 100 mL min^{-1}, heating rate 5 K min^{-1}, sample mass 5–15 mg.
[24] Sorption measurements: surface area and porosity system ASAP 2000 (Micromeritics), sorption gas N_2, temperature 77 K.
[25] G. M. Sheldrick, SHELXS-86, Program for solution of crystal structures from diffraction data, Universität Göttingen, **1986**.
[26] G. M. Sheldrick, SHELX-93, program for refinement of crystal structures from diffraction data, Universität Göttingen, **1993**.

 © VCH Verlagsgesellschaft mbH, D-69451 Weinheim, 1996 0570-0833/96/3522-2678 $ 15.00+.25/0

NMR—A Tool for all Disciplines

Encyclopedia of Nuclear Magnetic Resonance. Editors-in-chief: *D. M. Grant* and *R. K. Harris*. Wiley, Chichester, 1996. 5323 pp., hardcover £ 2250.00.—ISBN 0-471-93871-8

The publication of this hefty work, consisting of eight volumes in large-page format, weighing about 23 kg and occupying 0.4 m of shelf space, coincides with the golden jubilee of the discovery of nuclear magnetic resonance in 1945/1946. Volume 1 ("Historical Perspectives", 728 pages of text, ISBN 0-471-95839-5) is also available separately at the price of £ 125.00 (an offer well worth considering – see below); apart from this exception, the eight volumes can only be bought as a set. The publishers, Wiley, have been active for some time in the area of encyclopedias covering aspects of chemistry, produced in a similar style and organized along the same lines as this one, such as the *Encyclopedia of Inorganic Chemistry* previously reviewed in this journal (*Angew. Chem.* **1996**, *108*, 1333; *Angew. Chem. Int. Ed. Engl.* **1996**, *35*, 1738). Editors-in-chief of the *Encyclopedia of Nuclear Magnetic Resonance* ("ENMR") are two well recognized experts, David M. Grant (University of Utah, USA) and Robin K. Harris (University of Durham, UK), who have been active in the NMR field since the late 1950s. They have classified the contents into six topic groups and appointed a specialist as section editor for each group: E. D. Becker (National Institutes of Health, USA) for the volume "Historical Perspectives", J. W. Emsley (University of Southampton, UK) for the topics "Inorganic Applications", "Polymer and Liquid Crystalline Solutions", "Quadrupolar Nuclei", and "One- and Multidimensional Spectroscopy of Solutions", B. C. Gerstein (Iowa State University, USA) for "Physics Applications", "Solid Methods", and "Solid-State Applications", S. I. Chan (California Institute of Technology, USA) for "Biological Applications", T. C. Farrar (University of Wisconsin, USA) for "Instrumentation", "Organic Applications", "Relaxation Topics", and "Theory", and I. R. Young (Hammersmith Hospital, UK) for "Biomedical Applications" and "Imaging Principles and Applications". From these section titles it can be seen that in this encyclopedia "nuclear magnetic resonance" means much more than NMR spectroscopy and its use in chemistry. It includes aspects such as imaging, NMR microscopy, in-vivo spectroscopy, data processing, and alongside chemistry such diverse fields of application as biology (e.g., plant physiology), medicine (e.g., clinical applications), physics, materials science, geology (oil exploration), and agriculture. The topics named above have been covered in about 520 separate articles contributed by nearly 630 specialists. The articles vary greatly in length, from two to thirty pages. The level of treatment also varies, which is not necessarily a disadvantage since the users of the work will also differ widely in their expectations. Moreover, the level of treatment must also be partly determined by the nature of the topic. It would not be appropriate to discuss individual contributions in this review, as there are so many that only a small selection could be mentioned, which would be unfair to the rest of the authors.

Because of the alphabetical arrangement the articles belonging to a given section do not appear together, but are distributed through the different volumes. However, the preface is repeated in each of the volumes 2 to 8, and includes a seven-page list of the titles of all the articles in the complete work. This list is set out under sections and subsections, so that one can see at a glance the connections between articles on related subjects. Each volume also contains a complete alphabetical list of all the articles. Furthermore, the individual articles consistently provide cross-references to related articles. Volume 8 contains a comprehensive 205-page keyword index, a list of authors (33 pp.), and a glossary of medical terms and those relating to imaging (11 pp.), which is very useful for users unfamiliar with these fields. Where else would such a user learn, for example, that MRV stands for magnetic resonance venography, or that US means not the United States but ultrasonography? The list of authors and the topics that they cover is also repeated, in a corrected version, as a separate supplement. Thus it can be seen that much effort has been devoted to making it as easy as possible for the reader to find the required information.

Volume 1 is a delightful treat which I read with much pleasure. It describes the development of NMR, from its beginnings in the hands of a small number of physicists to its emergence as a fully-fledged area of research, subsequently maturing to become a practical method with applications in a remarkably wide variety of scientific disciplines. The volume begins with a very interesting and detailed contribution entitled "The Development of NMR", by E. D. Becker, C. L. Fisk, and C. L. Khetrapal (158 pp., 1099 literature references). The article includes reprints of the two short communications (*Phys. Rev.*, **1946**) by the groups led by Purcell and Bloch, which eventually led to the shared award of the Nobel Prize for physics in 1952. This is followed by a collection of short articles in which more than 200 authors describe the development of NMR and their roles in it, often from very personal viewpoints. These contributions contain much anecdotal material which, because it would be unsuitable for separate publication, might otherwise have been lost forever. The list of authors includes many pioneers from the early days of NMR, as well as other scientists whose names have only come to prominence in recent times. These personal recollections make fascinating reading. Short biographical notes about the authors are attached to all these essays, and also to the more specialized articles in Volumes 2–8.

Thanks to the combined efforts of the editors and of the many authors, ENMR is a very impressive work. It will be of special value to users who are in the pro-

This section contains book reviews and a list of new books received by the editor. Book reviews are written by invitation from the editor. Suggestions for books to be reviewed and for book reviewers are welcome. Publishers should send brochures or (better) books to the editorial office: Redaktion Angewandte Chemie, Postfach 101161, D-69451 Weinheim, Germany. The editor reserves the right of selecting which books will be reviewed. Uninvited books not chosen for review will not be returned.

cess of getting to grips with a new area in the broad field of nuclear magnetic resonance, and to those wishing to look beyond the boundaries of their own, usually fairly narrow, specialist area. The price of this highly desirable work is likely to put it beyond the means of most private individuals, other than true fanatics. However, libraries whose budgets are not yet exhausted, despite present-day cuts in funding, are strongly recommended to buy it. All readers interested in nuclear magnetic resonance would certainly appreciate having access to this reference source. Finally, a suggestion for the publishers: might not a CD-ROM version tempt private individuals to buy the work, if the saving in production cost were passed on to the potential buyer? Admittedly though, for this reviewer at least, the prospect of browsing via the monitor screen seems less attractive. By contrast, the idea of retiring to the sofa with Volume 1 of ENMR is most inviting.

Ludger Ernst
NMR-Laboratorium der Chemischen Institute
der Technischen Universität Braunschweig
Braunschweig (Germany)

Industrial Organic Chemicals. By *H. A. Wittcoff* and *B. G. Reuben*. Wiley, New York, 1996. 531 pp., hardcover £ 60.00.—ISBN 0-471-54036-6

This book is a completely revised and enlarged version of *Industrial Organic Chemicals in Perspective*, by the same authors, originally published in 1980. It aims to provide a wide range of users, from students to industrial chemists, with a survey of the technologies and products of industrial organic chemistry.

The contents are arranged in a clear and systematic structure. The preface gives an overview of the chapters that follow, and a summary of available monographs, encyclopedias, and the most important industrially-orientated journals and on-line data banks that contain relevant information. Each chapter also has a useful and often quite extensive section headed "Notes and References", which lists publications for further reading, recent review articles, key patents, and sources of information on related topics, and even includes occasional anecdotes relating to the history of the petrochemical industry. Often, however, only the cryptic comment "see note" in the main text tells the reader that there is a reference to a source of further information, and one is left to search for the relevant item.

Chapter 1 (33 pp.) discusses the importance of the chemical industry in the context of the overall economic environment, and describes modern developments such as economies of scale, problems of overcapacity, market saturation, research and development costs, and effects of legislation. Here one becomes aware of one of the book's limitations, which also applies to the later chapters, in that the main emphasis is on the USA chemical industry. Developments in Western Europe and Japan only appear occasionally and, for example, the discussion of political influences makes no mention of European legislation on chemicals.

Chapter 2 contains a very clear description of the production of basic petrochemicals by the distillation of crude oil and the subsequent refining processes.

Chapters 3–11 then deal in turn with these basic chemicals and their associated downstream chemistry, from ethylene through aromatics to alkanes. The various derivatization processes and routes to end-products are described systematically, with special attention to polymer production. Thus the reader is provided with a good insight into the entire materials flow of the industry. For example, one can follow the series of processes leading from ethylene via ethylene oxide and ethanolamine to quaternary ammonium compounds. As one is taken along the route to the end-product the amount of industrial background information diminishes, so that often the later stages are described only by reaction schemes with a few general comments about the process. However, one should not be surprised at this, because otherwise the book would have expanded well beyond its planned size. The authors also give examples of the uses of the end-products, so as to give an impression of the range of potential applications. However, the reader will sometimes find it difficult to gain a true picture of the importance of the markets, as the information given is usually only of a general nature.

As a consequence of the decision to include a very wide range of undoubtedly interesting topics, the main industrial processes are not treated in such depth as one finds in other standard works. The reader from an industrial background may have hoped to find more detailed factual information, going beyond an introductory treatment. Also, data such as annual tonnages are not always presented in a convenient form for easy reference, and one has to search laboriously through the text.

Chapters 12–14 deal with the chemistry of coal, natural oils, fats, and carbohydrates. The chapter on oils and fats gives only an incomplete picture of the industrial processes based on these increasingly important feedstocks. Some important processes, such as physical refining, are not mentioned at all, whereas much space is devoted to less important raw materials and reactions, and some outdated areas of application are described. In the section on fatty alcohols the authors seem to be unaware that a process for manufacturing unsaturated fatty alcohols based on a "new catalyst" has already been in commercial use for several decades. Even if the authors consider that the annual tonnages are trivial in the context of petrochemicals, the reader has the right to expect that a little more care is taken after the decision to devote a whole chapter to these products Chapters 15 and 16, which complete the book, deal with polymer production and catalysis.

On the whole the book provides a good overview of the industrially important aspects of organic chemistry and polymer chemistry, giving concise and informative descriptions of the most important chemicals and polymers, and relegating reactions of little industrial importance to the background. However, it should be regarded more as a textbook of applied organic synthesis than a detailed description of industrial practice.

Horst Eierdanz
Henkel KGaA
Düsseldorf (Germany)

Asymmetric Synthesis. By *G. Procter*. Oxford University Press, Oxford, 1996. 237 pp., paperback £ 19.50.—ISBN 0-19-855725-6

Enantioselective Reactions in Organic Chemistry. By *O. Červinka*. Ellis Horwood, London, 1995. 194 pp., hardcover $ 119.95.—ISBN 0-13-276239-0

We have here two further additions to the considerable family of books on the subject of stereoselective synthesis. As will be seen below, these are widely different in all respects apart from their similarity in length. Procter's book originated from a lecture course and is intended for students. As the title indicates, the emphasis is on synthesis. The book is concerned with various methods for preparing chiral non-racemic compounds, and describes important applications to the synthesis of natural products and active agents. The author has deliberately kept "stereochemical jargon" to a minimum. Thus, instead of the usual lengthy introduction explaining all the terms employed in stereochemistry, the explanations are limited to the expressions actually used in the book, and are given

 © VCH Verlagsgesellschaft mbH, D-69451 Weinheim, 1996 0570-0833/96/3522-2680 $ 15.00+.25/0

where they first appear. All the topics are treated clearly and systematically.

The subject matter is arranged according to reaction types. Each chapter is self-contained and includes a bibliography. Chapter 1 is devoted to diastereoselective and enantioselective addition reactions of carbonyl compounds, and Chapter 2 describes reactions of chiral enolates with electrophiles. The following chapters deal in turn with asymmetric aldol reactions, additions to carbon–carbon double bonds, reductions and oxidations, rearrangement reactions, and enzymatic hydrolyses and esterifications.

All the important concepts of stereochemistry are covered, beginning with the Cram and Felkin–Ahn models, then ranging from the Zimmermann–Traxler transition state through "chiral amplification", enolate geometry, CBS reduction, DIOP, BINAP, BINAL-H, alpineborane, RAMP, SAMP, the Claisen and Wittig rearrangements, etc., to the Sharpless epoxidation and dihydroxylation reactions. The author discusses the preparation and the various applications of chiral auxiliaries based on the oxazoline, oxazolidinone, sultam, and η^5-CpFe(PPh$_3$)(CO) structures. Organometallic reagents discussed include allylboranes, allylstannanes, allylsilanes, organozinc compounds, and boron, tin, and titanium enolates.

This first edition contains many mistakes such as incorrect structural formulas or printing errors, but most are harmless and of a kind that will be immediately obvious to the reader who is able to follow the discussion. As examples, on page 32 the formulas shown for (+)- and (−)-α-pinene are identical, on page 35 the relative configuration is given as *trans* instead of *anti*, on page 116 compounds 6.40 and 6.39 have become interchanged in the text, and on page 212 the double bond has been omitted from a molecule that is undergoing hydrogenation. I found no errors more serious than these.

There are a few instances where important reactions relevant to the topic under discussion have been omitted. For example, the treatment of asymmetric cyclopropanation reactions fails to mention the well-established chiral rhodium catalysts described by Doyle, Davies, and Pfaltz. As many of the chiral auxiliaries appear in more than one chapter, I suggest that the second edition of the book should include an appendix summarizing the different applications of each of the auxiliaries. Also it would be desirable to break down some of the chapters into sections so that changes of topic would be more clearly evident. This applies especially to Chapters 5, 6, and 7, each of which is a giant block of nearly fifty pages without subdivisions, the three together occupying over half the book. The subject index, containing about 500 entries, is satisfactory, and there are about 400 literature references extending up to 1993.

The book covers the core aspects of modern asymmetric synthesis and can therefore be emphatically recommended for students and other newcomers to the subject, especially in view of its affordable price.

The book by Červinka is orientated more towards the fundamental principles of chirality and enantioselective reactions, with synthetic applications relegated to a secondary role.

There are 18 chapters on topics such as racemate cleavage, enantioselective reactions, strategies for asymmetric synthesis, synthesis of enantiomeric compounds, asymmetric reactions using transition metal catalysts, asymmetric reactions using chiral auxiliaries, enantiomerically pure building blocks, and enzyme-catalyzed reactions. This range of topics looks excellent at first glance, but on closer examination it turns out that almost half the chapters (Chs. 1, 2, 6, 9, 11, 13, and 14) consist of only one or two pages each. Often these merely refer the reader to review articles. If this were an appropriate way of treating the subject, the author might as well have replaced the whole book by similar references! Chapters 8 and 18 contain only literature references (see below).

The work as a whole has the appearance of a classification of the field of stereochemistry into subject areas, amplified here and there by motley collections of information. For example, enantioselective cyclopropanation reactions appear in the section on double bond isomerizations using transition metal complexes (p. 95), and the reaction of an allylborane with an aldehyde is described in the chapter on hydroboranation reactions (p. 104). Where topics are treated more thoroughly the main thread of the discussion tends to get lost. Often one finds that relatively unimportant matters are covered in great detail, whereas more important ones are only mentioned briefly or even neglected entirely. Thus, in the discussion of chiral ligands for transition metal catalyzed reactions, DIPAMP and DIOP are buried within a mass of information about numerous exotic ligands (pp. 69–83), and in describing the use of Diels–Alder reactions (pp. 108 ff) there is no mention of the possible formation of regioisomers.

Reading the book is made more difficult by the circumlocutory style and a tendency towards abstract and woolly language. For example, it would be difficult to make sense of the description of kinetic racemate cleavage on page 55 if one did not already know what this was all about. The translation from Czech into English may be responsible for these problems, but whether that is the case is immaterial to the reader.

The difficulties also extend into the formula diagrams. Almost all the equations lack important information such as yields and reaction conditions, and equilibrium arrows are sometimes omitted (e.g., on p. 88). The problems are further aggravated by the Roman numerals used to identify compounds. For example, it is not particularly easy to distinguish at a glance between compounds CXXXVII and CXXXVIII. In general the quality of the figures and formulas is not very good. The more disturbing examples include Figure 12 (p. 34), which at first glance looks as though a dozen graphics have been accidentally superimposed, Scheme 3 (p. 14), which could hardly be described as self-explanatory, and Figure 1 (p. 167), which shows a "diamond lattice" that could have been the work of Escher. Also many molecular structures are shown wrongly: examples are the Darvon alcohol on page 55, the nonsensical stereochemical structure of compound II shown on page 70, the chiral compounds with C_s symmetry shown in Scheme 2 on page 72, the geminal dimethyl groups that are claimed on page 87 to appear with 96% *ee*, the peracid with only two oxygen atoms on page 98, and a pentavalent carbon atom on page 94. There are occasional examples of incorrect terminology, as on page 18 where "homochiral" and "enantiomerically pure" are treated as synonymous. On page 71 there is a mention of "diphosphines with a chiral group connecting two chiral phosphorus atoms"; in fact there are no such compounds in the book, but in any case a phosphorus atom, although it may be a chiral center, is not itself chiral.

The subject index is rather scanty, containing only about 260 entries. Chapter 8 consists solely of 205 references (up to the year 1990) for Chapters 1–7, and Chapter 18 similarly consists of 416 references (up to 1994) for Chapters 9–17.

This book is only suitable for the reader who already has a good grasp of stereochemistry, and who might discover in it a few facts that he or she has not previously known. The contents of the book does not justify its cost relative to other works on this subject.

A. Stephen K. Hashmi
Institut für Organische Chemie
der Universität Frankfurt am Main
Frankfurt am Main (Germany)

 © VCH Verlagsgesellschaft mbH, D-69451 Weinheim, 1996 0570-0833/96/3522-2681 $ 15.00+.25/0

Organometallics in Synthesis – A Manual. Edited by *M. Schlosser*. Wiley, Chichester, 1994. 603 pp., hardcover £ 60.00.—ISBN 0-471-93637-5

Two of the most interesting publications of recent years in the field of organometallic chemistry are the second edition of *Comprehensive Organometallic Chemistry* and the book under review here, *Organometallics in Synthesis,* edited by Manfred Schlosser. The difference between the two books could hardly be greater: on the one hand a 14-volume "encyclopedia" of organometallic chemistry with many thousands of pages, on the other hand a manual covering the most important recent developments in the field in just over 600 pages. Schlosser's book is intended mainly for the newcomer to the area, who has scarcely any knowledge of the basic principles and working techniques. The approach is rather similar to that of *Best Synthetic Methods,* first providing the reader with an understanding of the fundamental reaction mechanisms, then following this up with practical advice, rules of thumb, and, most importantly, carefully chosen laboratory recipes, so as to enable the novice to successfully synthesize organic compounds using organometallic reagents. The choice of examples has necessarily been restricted to what are described in the preface as the "most popular metals and methods".

To achieve this goal the editor has assembled a team of well qualified authors, whose names are inseparably associated with this field of study. In Chapter 1 (166 pp.) M. Schlosser describes the use of organometallic compounds of the alkali metals in synthetic applications. This is followed by a short chapter (28 pp.) in which the industrial chemists F. Totter and P. Rittmeyer discuss the handling and industrial applications of organolithium compounds. Chapters 3 and 4 (88 and 100 pp. respectively) provide detailed treatments of the synthetic applications of titanium compounds (by M. T. Reetz) and organocopper reagents (B. H. Lipshutz). Chapter 5, by L. S. Hegedus (77 pp.), is devoted to palladium-catalyzed reactions, and this is followed by three shorter chapters, dealing with organoboron chemistry (Ch. 6, 48 pp., by K. Smith), organoaluminum compounds (Ch. 7, 25 pp., H. Yamamoto), and organotin chemistry (Ch. 8, 44 pp., H. Nozaki). The book is completed by a detailed subject index and a very useful formula index, which enables one to compare different organometallic species. All the chapters have comprehensive bibliographies, which in some cases cover publications up to very recent dates. The visual quality of the book is excellent: a consistent typeface has been used throughout, and the structural formulas have been very carefully drawn.

Does "Schlosser" achieve its declared aim of helping the novice to overcome the psychological and practical barriers to getting started in organometallic chemistry? Well, to begin with, it comes as no surprise that in a multiauthor work of this kind the contributions vary considerably in both length and quality. I liked especially the chapters on titanium, copper, and boron compounds and their reactions, not least because they contain a wealth of practical advice and laboratory recipes (in the chapters by Lipshutz and Smith the procedures have been blended into the text in a very successful way). All three chapters cover not only "classical" applications in chemo-, regio-, and stereoselective reactions but also many important recent developments. Examples of these include the use of chiral organotitanium catalysts for enantioselective additions and cycloadditions, and the preparation of organocopper reagents with complex structures by transmetallation from organozinc, organoaluminum, and organozirconium compounds. However, in the copper chapter on page 199 an error with possibly serious consequences has crept in: only one half of the quantity of methyllithium needed for the preparation of the cuprate is shown, so that instead of Me_2CuLi one would obtain methylcopper, which is unstable in its pure form and could decompose explosively during the subsequent removal of the solvent!

The chapter on the industrial applications of organolithium compounds does not, of course, contain laboratory recipes, but there is much useful advice concerning the stability and handling of these reagents. On the other hand, the rest of the chapters are, in my view, not quite so good as those just mentioned. In particular, Schlosser seems to have given way to the temptation to devote a disproportionate amount of space to his own field of research, as the chapter on organic compounds of alkali metals contains many details and anecdotes of a marginal kind that are unlikely to be very useful to the intended readers. In contrast, the chapters on palladium-catalyzed reactions and organoaluminum and organozinc compounds contain little in the way of practical advice; these are more like abbreviated monographs, and the few laboratory recipes that have been grafted on sit uneasily in these chapters. It is also doubtful whether the claim to cover the "most popular metals and methods" is fully justified. With a better organization of the contents it would certainly have been possible to include some more metals, for example by covering organozinc reagents, which are important in stereoselective synthesis (e.g., the work of Noyori et al.), and are also compatible with a wide variety of functional groups (as shown by Rieke and Knochel). However, the preface promises that there will eventually be a second, enlarged edition covering these topics.

Notwithstanding these criticisms, I was left with a very good impression of "Schlosser", and one hopes that the weaknesses will be remedied in a new edition in due course. No chemist seriously interested in synthetic applications of organometallic reagents can afford to be without this book.

Norbert Krause
Institut für Organische Chemie
und Biochemie
der Universität Bonn
Bonn (Germany)

Crystallographic Methods and Protocols. (Series: Methods in Molecular Biology. Vol. 56). Edited by *C. Jones, B. Mulloy* and *M. R. Sanderson*. Humana Press, Clifton, NJ, 1996. 394 pp., loose-leaf edition $ 69.50.—ISBN 0-896-03259-0

This publication is intended as a "recipe book" for protein crystallographers. It gives information about practical laboratory procedures that cannot be found in ordinary textbooks. Cryocrystallographic methods, which are becoming ever more important, are described in practical detail, as also is the installation and operation of different types of commonly used area detectors. The book gives details of computer programs for processing X-ray diffraction data and determining and refining protein crystal structures. The use of such programs is explained clearly and in sufficient detail to enable even the novice to succeed in getting results. The information provided here is normally only available in the dedicated handbooks supplied with the relevant hardware and software, and it should also be helpful in choosing and buying equipment. The book describes strategies for determining the positions of heavy atoms, which are needed for phase determination, and gives protocols for refining a structure once it has been solved. All these working procedures ("recipes") are described clearly and in detail, so that the reader with a back-

 © VCH Verlagsgesellschaft mbH, D-69451 Weinheim, 1996 0570-0833/96/3522-2682 $ 15.00+.25/0

ground in molecular biology or biochemistry and an interest in structural biology can quickly master the methods. The final part of the book describes methods for crystallizing oligonucleotides, protein–DNA complexes, viruses, and membrane proteins.

The contents are clearly arranged, and all the chapters have been written by internationally recognized experts. In the first chapter ("Introduction"), the fundamentals of protein crystallography are briefly explained. Next, in "Overexpression, Isolation and Crystallization of Proteins", the production of proteins in prokaryontic and eukaryontic overexpression systems and their isolation and purification are described, followed by strategies for obtaining suitable crystals by "screening" and improving the process by seeding. Under the heading "Preliminary Characterization of Crystals", the subject of crystal symmetries is introduced, followed by the "mounting" of crystals in capillaries and the shock-freezing process used in cryocrystallography. The recording and evaluation of precession patterns to yield information on space groups and cell constants is then described. The chapter "Modern Methods for Rapid X-Ray Diffraction Data Collection from Crystals of Macromolecules" introduces the area detectors that are now generally used, and gives a clear and detailed description of their manner of operation and the processing and reduction of the data. Here the subject of cryocrystallography is again addressed. The next chapter has the title "Use of Multiple Wavelength Anomalous Diffraction (MAD) Measurements in ab initio Phase Determination for Macromolecular Structures". An introduction to the theory of anomalous dispersion leads into an account of how data recorded at different wavelengths using a synchrotron source are analyzed to determine phase angles. The chapter on "Structure Determination Using Isomorphous Replacement" describes the preparation of heavy-atom derivatives, the use of Patterson methods to determine the positions of the introduced atoms, and the final refinement of these positional data. Various criteria used in the calculations are discussed, such as the "figure of merit", the Cullis *R*-factor, and the "lack of closure error", as also is the use of Patterson difference and Fourier difference methods. In "Molecular Replacement Using Known Structural Data" the reader is introduced to these methods, which are becoming increasingly important as a result of the continuing growth of protein data banks. The various programs of importance for rotation and translation methods are clearly described and their use is illustrated by examples of practical applications. Next is a chapter on "Density Modification in X-Ray Crystallography", describing the very effective methods based on this principle which can improve the initial electron density distribution, thus facilitating comparison with model predictions. The chapter "Refinement of Protein and Nucleic Acids Structures" discusses the most recently developed programs whereby the refinement can be carried out more effectively, describes their applications, and sets out protocols. Methods are also described whereby models are first constructed manually and subsequently improved; these can be used alternately in conjunction with refinement procedures. The chapter ends by discussing quality criteria that can be applied to a structure model, such as the *R*-factor and the free *R*-factor. The latter topics are treated in greater depth in "Recent Developments for Crystallographic Refinement of Macromolecules", where the methods are described in detail, as also is the use of "simulated annealing".

The next four chapters are devoted to methods for preparing crystals and determining the structures of oligonucleotides, protein–DNA complexes, viruses, and membrane proteins. These chapters form a very useful extension to the crystallization protocols for proteins that were described at the beginning of the book. I regard the tables listing the oligonucleotides, protein–DNA complexes, and viruses that have so far been crystallized, together with the protocols used to achieve the crystallization, as a valuable and important resource. The particular problems that arise in the crystallization, data collection, data processing, and structure determination for molecules of this type are discussed. Special attention is given to the difficulties caused by noncrystallographic symmetry and phase broadening in analyzing the structures of viruses. The final chapter is mainly concerned with the two-dimensional crystallization of membrane proteins; in addition there is a discussion of methods for growing three-dimensional crystals, with references to the relevant literature so that the interested reader can pursue this aspect in more detail. However, a list of the commonly used detergents would have been a useful addition.

This book fills a gap in the literature on protein crystallography, as the main emphasis here is on the practical matter of protocols for analyzing protein crystal structures rather than on the theoretical fundamentals. It can be recommended not only for biochemists and molecular biologists who wish to learn and apply the methods of protein crystallography, but also for experienced protein crystallographers, who will find in it a very good overview of the subject and many useful ideas and tips in relation to their work. Accordingly, I have just ordered three copies of the book for my research group.

Wolfram Saenger
Institut für Kristallographie
der Freien Universität Berlin
Berlin (Germany)

 © *VCH Verlagsgesellschaft mbH, D-69451 Weinheim, 1996* *0570-0833/96/3522-2683 $ 15.00+.25/0*

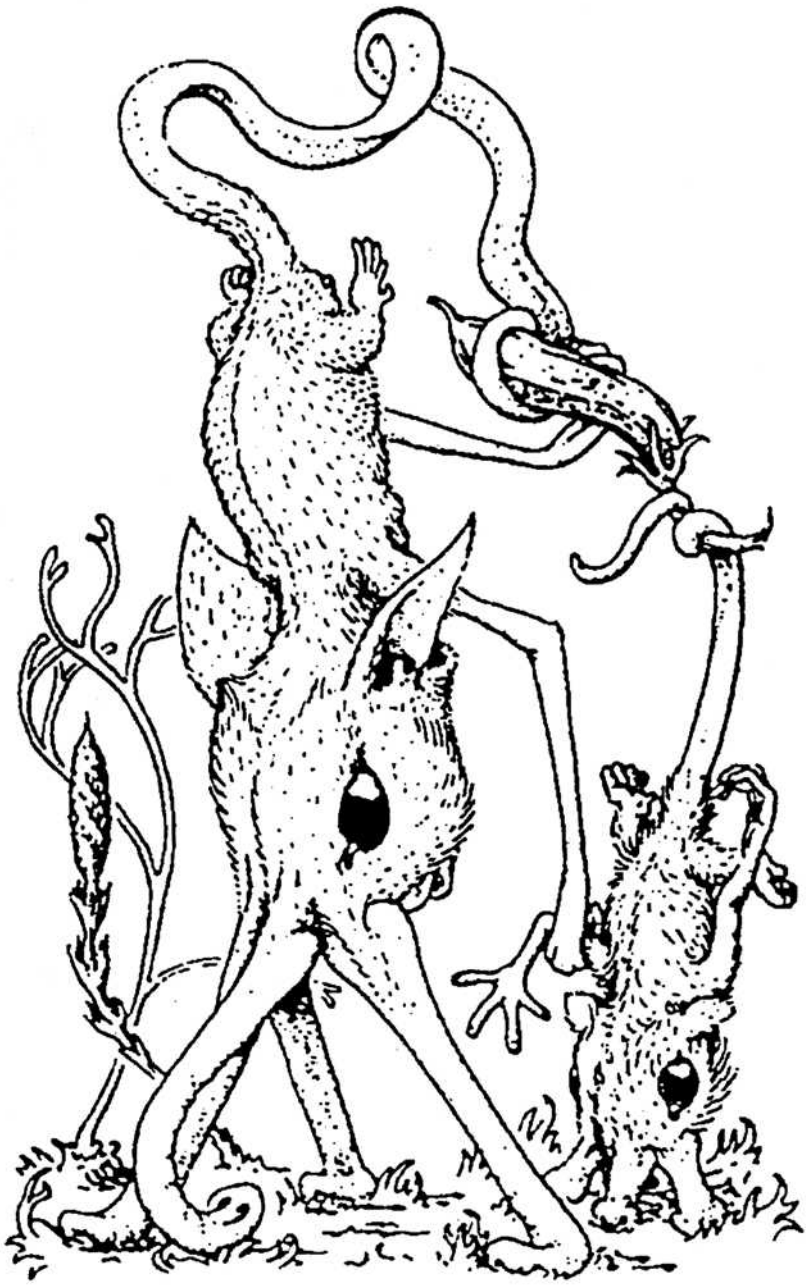

In the same manner that the Nasobem, Stümpke's mythical creature, teaches his child the peculiar way of life of the species *Nasobema lyricum*, the work of Seebach et al. on the self-regeneration of stereocenters has been governed by a fanciful idea. On the way, many tricks have been learned and much knowledge gained. Finally, they have come back down to earth and find themselves once again in the unimaginative world of enantiomer separation for the synthesis of enantiomerically pure compounds.

Self-Regeneration of Stereocenters (SRS)—Applications, Limitations, and Abandonment of a Synthetic Principle

Dieter Seebach,* Andrea R. Sting, and Matthias Hoffmann

Dedicated to our much-admired teacher and mentor, Professor Dr. Vladimir Prelog, on the occasion of his 90th birthday

In order to replace a substituent at a single stereogenic center of a chiral molecule without racemization, a temporary center of chirality is first generated diastereoselectively, the original tetragonal center is then trigonalized by removal of a substituent, a new ligand is introduced, again diastereoselectively, and finally, the temporary center is removed. By means of these four steps (the "Self-Regeneration of Stereocenters", SRS), 2- and 3-amino-, hydroxy-, and sulfanylcarboxylic acids have been successfully alkylated with formation of tertiary carbon centers and without the use of a chiral auxiliary. Use of this methodology has allowed the potential of these inexpensive chiral building blocks to be expanded considerably. This article aims to demonstrate (using, in part, examples from natural product syntheses) that chiral heterocyclic acetals with enamine, enol ether, enolate, dienolate, enoate, radical, and acyliminium functionalities and also those that are potential reactants for Michael additions and pericyclic processes (for example, electron-rich and electron-poor dienophiles and dienes) are now easily accessible, more often than not, in both enantiomeric forms. Stereogenic nitrogen atoms of aziridines, boron atoms of cyclic or linear systems, and stereogenic planes of π-complexes can also be used as the temporary chirality element in other approaches to the realization of the SRS principle. Enantiomerically pure derivatives of, for example, glycine, hydroxy- and sulfanylacetic acid, 3-aminopropanoic acid, and 3-oxocarboxylic acids can be prepared by resolution of racemic mixtures via diastereoisomeric salts or by chromatography on a chiral column. Hence, the extensive reactivity of compounds developed to test the SRS principle and, above all, the outstanding stereoselectivities of the reactions can be put to good use even when no suitable chiral precursor is available—even though this amounts to an abandonment of the principle! The readily available 2-*tert*-butyl-1,3-imidazolidin-3-one, -oxazolidin-5-one, -dioxin-3-one, and -hydropyrimidinone (all of which contain a single stereogenic center at the acetal C atom) can thus be used in the preparation of a vast range of 2-amino- and 3-hydroxycarboxylic acids, and no chiral auxiliary has to be removed or regenerated during these procedures. (One example is the synthesis of 4-fluoro-MeBmt, a derivative of the C_9 amino acid found in cyclosporin.) In the final chapter we will discuss the most useful findings gained from investigations into both the self-regeneration of stereocenters and the use of chiral acetals in the synthesis of enantiomerically pure compounds (EPC synthesis): the formation and characteristics of complexes obtained from Li-enolates and other Li compounds with secondary amines; the application of α-alkoxy and α-amino-Li-alkoxides as in situ bases and sources of aldehydes in C–C bond forming reactions with unstable enolates or nitronates; the significance of $A^{1,3}$ effects on the stereochemical course of nucleophilic, radical, and electrophilic reactions of *N*-acylated heterocycles and homo- or heterocyclic carboxylic ester enolates; and the effects of the amide protecting group on the reactivity of neighboring centers and on the stereoselectivity of the reactions at those centers. At the end of this article we have included an appendix containing tables, which are intended to summarize all the examples known in as complete a fashion as possible.

Keywords: asymmetric syntheses · chiral synthetic building blocks · enolates · lithium compounds

1. Introduction and Definition of the Problem

Was nicht sein kann,
das nicht sein darf![**]

It is a fundamental part of every basic lecture course in organic chemistry that a reaction at a trigonal center bearing three different substituents in an achiral molecule results, if neither

[*] Prof. Dr. D. Seebach, Dr. A. R. Sting, Dipl.-Chem. M. Hoffmann
Laboratorium für Organische Chemie
der Eidgenössischen Technischen Hochschule
ETH-Zentrum, Universitätstrasse 16, CH-8092 Zürich (Switzerland)
Fax.: Int. code +(1)632-1144
e-mail: seebach@org.chem.ethz.ch

[**] "Surely the impossible is just not possible."

the other reactants nor the surroundings are chiral, in the formation of a racemic product containing one center of chirality. The consequence of this is that a substitution that proceeds in either a homolytic or heterolytic manner at a solitary stereogenic center of a molecule yields enantiomeric products in a 1:1 ratio and hence, a racemic mixture is formed (Scheme 1a). If the trigonal center in the intermediate is cationic or part of a π-system, it will have a trigonal-planar geometry and if it is radical or anionic in nature, it may have a trigonal-pyramidal geometry but will be capable of rapid inversion, particularly in noncyclic systems.

There are, of course, exceptions that can be of practical significance. These include the S_Ni substitution of OH by Cl using thionyl chloride (Scheme 1b),[1] which proceeds with retention of configuration, and the cationic cyclization of linalol *p*-nitrobenzoate to terpineol (Scheme 1c).[2] Stereoselective reactions proceeding via carbanionic intermediates are also known. For example, the D/H exchange with retention of configuration shown in Scheme 1d,[3] which is really of rather academic interest, and the decarboxylation, with retention, of an intermediate used in the preparation of the anaesthetic Desfluran[4] (Scheme 1e). Once it had been appreciated that within so-called carbanion chemistry, there is also a cation, more often than not a metal ion, which can be sufficiently strongly bound[5] to allow the formation of configurationally stable organometallic derivatives[6–8] such as those shown in Scheme 1f, a whole new branch of stereoselective synthesis developed.[9–14]

Even in enolate chemistry there are exceptions to the rules formulated above (see the examples in Scheme 2). Although the sole center of chirality in the starting material is removed, enantiomerically pure or enantiomerically enriched products may result. This can be attributed to the formation of aggregates of achiral enolates with chiral components in the reaction mixture (Scheme 2a)[15] or also to sufficiently conformationally stable enolate intermediates which possess axes of chirality (Scheme 2b–e).[16–20] The cation also plays a decisive role in the reactions of enolates. Owing to the successful creation of a variety of alternatives, today practically any type of imaginable reactivity or selectivity of these nucleophiles, which are of central importance in organic synthesis, can be achieved. Possibilities include the participation of aggregates ("supramolecular" structures) of Li-, Na-, K- and Mg-enolates[21–25] and their complexes with salts,[26, 27] amides,[28] and amines,[21–24, 29, 30] the reduction of the coordination sphere of the participating metal

A. R. Sting D. Seebach M. Hoffmann

Andrea Rolf Sting was born in Samedan, Canton Graubünden (Switzerland) in 1963. After an apprenticeship and then a further three years working in the chemistry laboratories of Ciba-Geigy in Basel (Dyes and Chemicals Division), he studied from 1986 to 1989 at the "Ingenieurschule Beider Basel" (IBB) in Muttenz (Canton Basel-Land), where he earned the title Dipl.-Chem. HTL. Subsequently, he moved to the ETH in Zürich to continue his chemistry studies (Diploma 1992). In the spring of 1993 he began working in the group of Prof. D. Seebach and completed his Ph.D. thesis on the synthesis of 4-fluoro-MeBmt in the spring of 1996. He is now working in the Division of Crop Protection of Ciba-Geigy in Basel.

Dieter Seebach was born in Karlsruhe (Germany) in 1937. He studied chemistry at the University of Karlsruhe and completed his Ph.D. thesis on small rings and peroxides under the supervision of Prof. R. Criegee in 1964. After a two-year stay at Harvard University as postdoctoral co-worker (with Prof. E. J. Corey) and lecturer, he returned to Karlsruhe and, in 1969, completed his "habilitation" on the topic of S- and Se-stabilized carbanion and carbene derivatives. In 1971 he moved to the University of Giessen as a full professor and then in 1977 to the Eidgenössische Technische Hochschule (Swiss Federal Institute of Technology) in Zürich. He has been a visiting professor at the Universities of Wisconsin–Madison, Strasbourg, Munich (TU), and Kaiserslautern and also at Caltech (Pasadena) and the Max Planck Institute in Mülheim. A main emphasis of his research is the development of new synthetic methods; in the last decade the subject discussed here and the Ti-TADDOLates have been major interests. His work also involves mechanistic studies and determination of structures. More recent research topics include chiral dendrimers, the short-chain oligomers of 3-hydroxybutanoic acid, the bioploymer PHB, and backbone-modified peptides.

Matthias Hoffmann was born in Zürich (Switzerland) in 1969. He completed his Diploma studies in chemistry at the ETH in Zürich in 1993 with research conducted in the group of Prof. D. Seebach. Later that year, he began working on his Ph.D. thesis in the same area. His research focuses on the development of methods for the preparation of enantiomerically pure, non-proteinogenic amino acids.

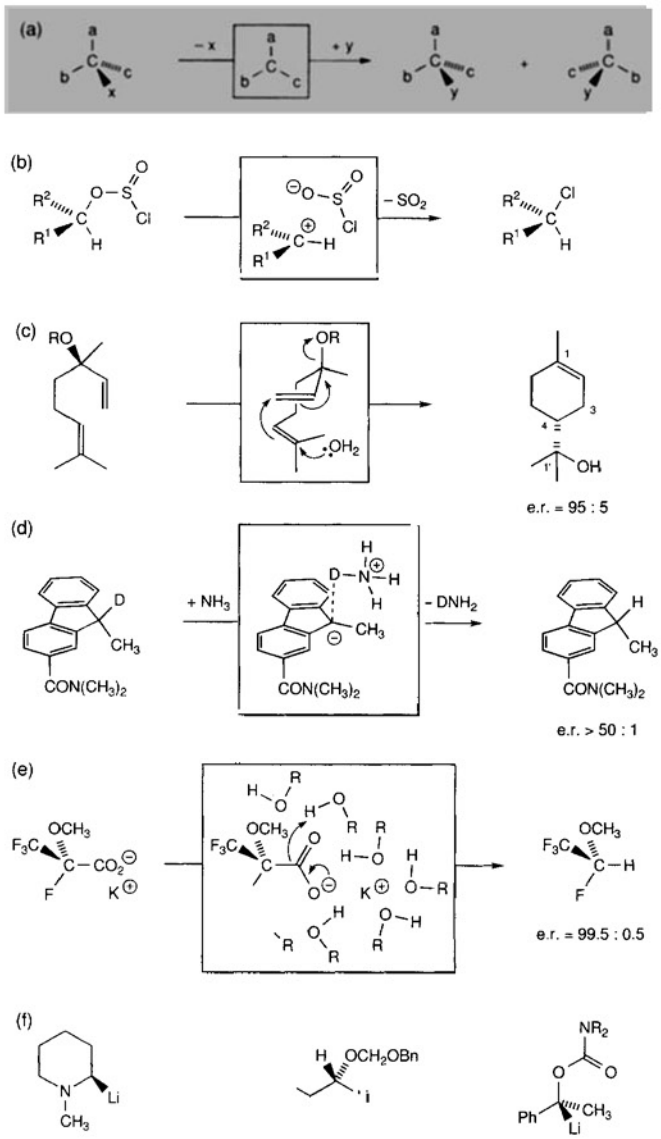

Scheme 1. Dissociative reactions at stereogenic centers (a–e) and chiral organolithium compounds (f). In this article, the enantiomeric purity of compounds will be given exclusively in the form of enantiomer ratios (e.r.), which are typically determined by NMR, GC, or HPLC analysis. a) Racemization during dissociative substitution at a stereogenic center proceeding via a trigonal intermediate. b) OH/Cl substitution using thionyl chloride with retention of configuration [1]. c) The highly stereoselective cyclization of linalol to terpineol. The use of appropriately labeled derivatives has shown that the carbon atoms C4, C3 (H/D), and C1′ (CH_3/CD_3) are present in only one configuration in the product [2]. d) D/H exchange, with retention, in a fluorene derivative using ammonia as the base; the ratio of the rate of isotope exchange (k_e) to the rate of racemization (k_r) is greater than 50:1 [3]. e) Decarboxylation, with retention of configuration, of (*R*)-2,3,3,3-tetrafluoro-2-methoxypropanoate to give (*R*)-1,1,1,2-tetrafluoro-2-methoxyethane [4]. f) Configurationally stable organolithium compounds described by Gawley et al. [6], Still et al. [7], and Hoppe et al. [8].

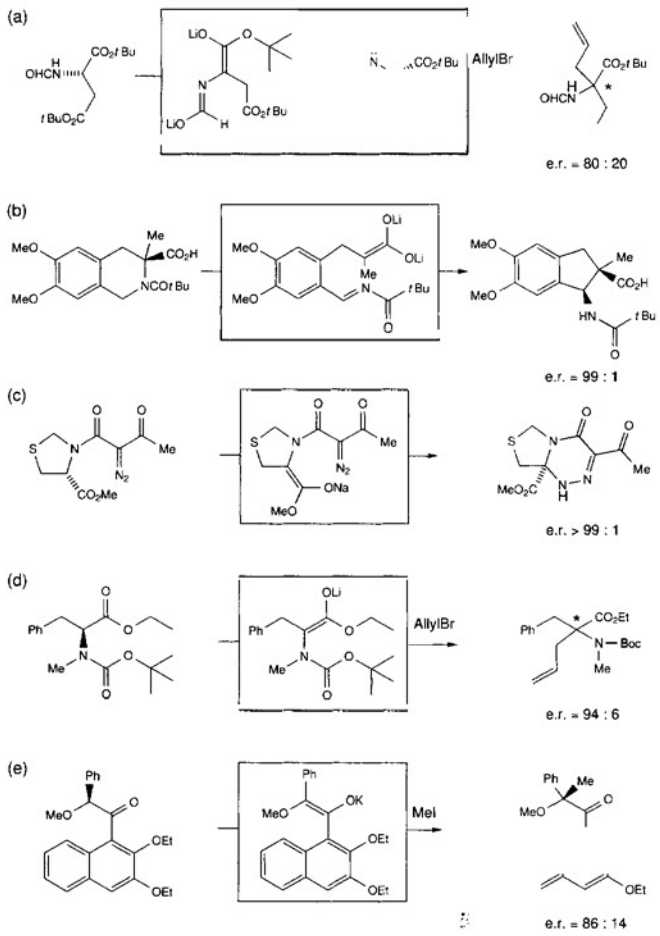

Scheme 2. Some reactions of enantiomerically pure esters and a ketone, which have only one center of chirality in the α-carbonyl position, giving enantiomerically pure or enriched products via the appropriate enolate. a) Enantioselective reaction of an achiral enolate in the presence of a chiral enolate [15]. b) Tetrahydroisoquinoline/aminoindane ring contraction without loss of enantiomeric purity, presumably via an imino-enediolate [16]. Strictly speaking, this is the nitrogen analog of the Wittig rearrangement, with retention of configuration at the migrating C atom (cf. the Stevens, Sommelet, and Hauser rearrangements [17]). c) Stereoselective intramolecular trapping of an enolate by a diazooxoketo group with retention [18]. d) Preparation of an α,α-disubstituted *N*-methylamino acid derivative without the aid of a chiral auxiliary and without a temporary stereogenic center [19]. e) H/Me exchange with inversion of configuration of a 1-naphthylketone (via an axially chiral intermediate?) [20].

center in boron enolates[31] and its enlargement in titanium enolates,[32–34] the activation of the reaction partners with a variety of Lewis acids,[34] and the generation of enolates by the use of metal-free bases such as F^- in Bu_4NF[35] and phosphazenes,[36–38] from silyl enol ethers,[39] or by direct deprotonation.

Within the framework of our work over many years devoted to the incorporation of inexpensive, simple, chiral, naturally occurring compounds (the "pool of chiral building blocks"[40]) into complex target molecules, we wondered whether it would be possible to develop some sort of "trick" for producing enolates of α-amino or α-hydroxy acids such that subsequent reactions with electrophiles yield nonracemic products. This led us to a simple yet broadly applicable synthetic principle[41–43] that we call the "Self-Regeneration of Stereocenters" (SRS).[44–48]

Wenn zwei das Gleiche tun,
ist es noch lange nicht Dasselbe.[*]

The principle is extremely simple (Scheme 3): The chiral starting material possessing two functional groups but one (and only

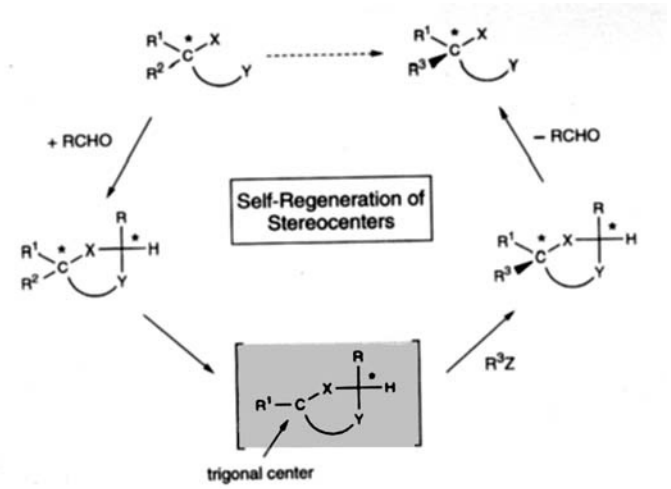

Scheme 3. The principle of the self-regeneration of a stereogenic entity illustrated with the example of a chirality center. In fact, the replacement of one of the four substituents at a single stereogenic center of the starting material requires four steps and is achieved without formation of a racemic product. The auxiliary is an achiral aldehyde.

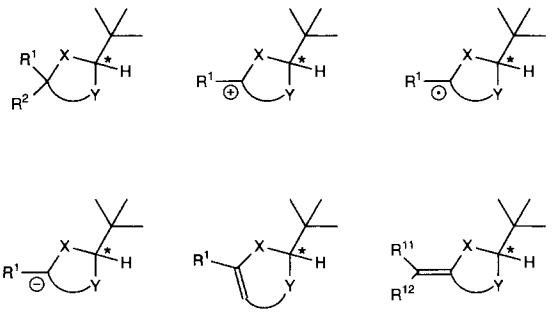

Scheme 4. Chiral species with cationic, radical, and anionic trigonal centers and also those with a π-system, all of which can act as the intermediate in the self-regeneration of a stereocenter (see Scheme 3).

one) stereogenic center is allowed to react with an aldehyde to form an acetal, with preference for one isomer. Annihilation of the original stereogenic center and concomitant formation of a trigonal center yields an intermediate, which, due to the stereogenic center of the acetal, is chiral. Subsequent reaction at the trigonal center proceeds diastereoselectively under the influence of this temporary stereogenic center, and finally, cleavage of the acetal unit leads to a product in which one of the substituents at the stereogenic center of the starting material has been replaced by a new one. The reaction sequence proceeds by dissociative, enantioselective substitution at a center of chirality and without the need for a chiral auxiliary—hence, the name "Self-Regeneration". Of course, an auxiliary is necessary—the aldehyde, which is introduced at the acetalization step and is then regenerated by hydrolysis.

Naturally, an unsymmetrical ketone[49–52] or some other achiral compound can be used in place of the aldehyde such that reaction with the precursor occurs diastereoselectively, and hence, the stereogenic center of the precursor can be destroyed with no cause for concern. The temporary center of chirality can also be replaced by an alternative, but again temporary, element of chirality (axis or plane[53–56], see Section 6).

An illustration of the breadth of possible applications of the SRS principle is given in Scheme 4. It shows suitable reactive intermediates or derivatives, in which the original stereocenter is destroyed by removal of one of the ligands (R^2). Cationic (electrophilic), radical, or anionic (nucleophilic) reactivity can be generated, and endocyclic or exocyclic π-systems can be formed in which one or more trigonal centers with diastereotopic faces are present. In Scheme 4, a *tert*-butyl group is shown as the substituent at the acetal temporary stereogenic center. In our own work in this area, we prefer to use pivalaldehyde as the acetalization reagent for a number of reasons: a) the bulky *t*Bu group results in particularly high diastereoselectivity in the acetalization step (Scheme 3); b) the yields of acetalization are generally good (indeed, they are practically quantitative when the new transition metal catalysts[52] developed by Venanzi et al.[57] are employed); c) the *t*Bu group also leads to high diastereoselectivities in subsequent reactions at the trigonal center; d) the *t*Bu group is completely unreactive (in contrast to the Ph group introduced by the use of benzaldehyde) and enol derivatives cannot be formed; e) since the NMR signal of the

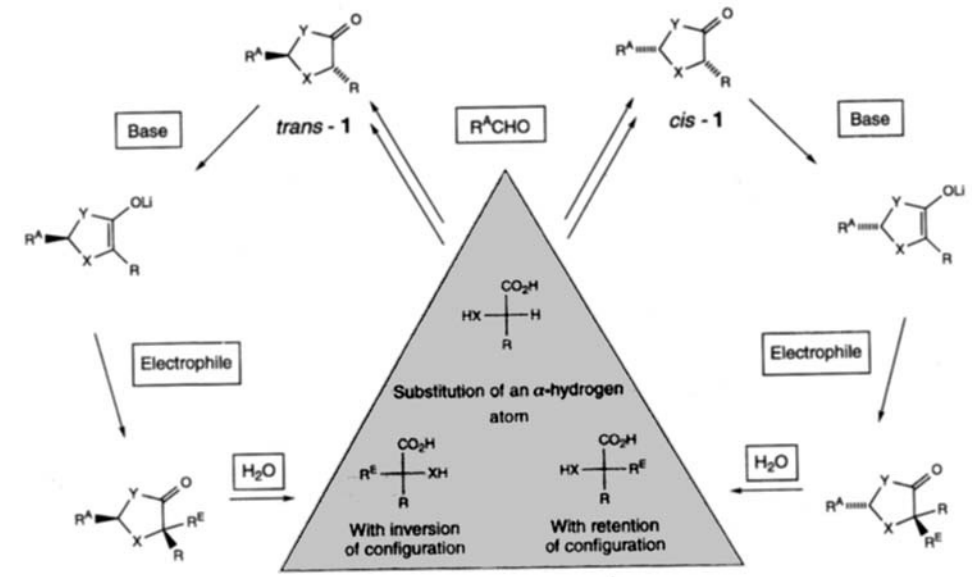

Scheme 5. α-Alkylation of an α-amino, α-hydroxy-, or α-sulfanylcarboxylic acid without racemization. Depending on whether a *cis*-substituted heterocycle **1** (when Y = NH, NCH_3, O) or the other isomer *trans*-**1** (when X = NH, Y = NCH_3) is formed, heterochiral enolates are formed in the deprotonation step, and subsequent diastereoselective alkylation leads to the enantiomerically pure products resulting from electrophilic substitution of the α-carbonyl proton. The letter A in R^A on the aldehyde reagent and at the acetal temporary stereogenic center stands for auxiliary. R^E represents the group in the product introduced by way of the electrophile. Specific examples can be found in Table A in the appendix. Short review articles on imidazolidinones [75] and oxazolidinones [66] derived from amino acids and dioxolanones [67] derived from α-hydroxycarboxylic acids have been published in the *Encyclopedia of Reagents for Organic Synthesis* (see also the reviews in refs. [48, 68]).

*t*Bu group is one sharp singlet, it does not overlap with signals in large areas of the spectrum, and it can also serve as a useful reference in NMR analysis of the crude product; f) pivalaldehyde is available on a large scale (it is obtained as a side-product during the hydroformylation of isobutylene[58] and is also used in the synthesis of fragrances[59]); g) as pivalaldehyde has a low boiling point (74 °C), it can be readily removed after the last step of the reaction sequence shown in Scheme 3, the hydrolysis.[60]

3. Chiral Heterocyclic Enolates of 2-Amino-, 2-Hydroxy-, and 2-Sulfanylcarboxylic Acids

It's the exception that proves the rule!

The twenty proteinogenic amino acids and the related α-hydroxy acids (which are formed by diazotization of the amino acids in aqueous media with retention of configuration), as well as other naturally occurring members of this class of compounds—for example lactic acid, glyceric acid, malic acid, and mandelic acid—provide us with vast reserves of chiral building blocks. By applying the SRS principle these compounds can be alkylated at the stereogenic center to yield products containing a tertiary C atom.[61]

In the acetalization (the first step of the reaction sequence), the *cis*-substituted oxazolidinone, dioxolanone, or thioxolanone usually results from the thermodynamically controlled reaction of the carboxylic acid derivatives listed above.[62] The *cis*-substituted product is also formed in the case of the imidazolidinone derivative,[63, 64] which is obtained from an amino acid amide, and this is the precursor of a particularly reactive Li-enolate. Under kinetic control the reaction leads to the *trans*-imidazolidinone. Hence, acetals derived from (*S*)-amino-, -hydroxy-, and -sulfanylcarboxylic acids can be produced with (*R*) and/or (*S*) configuration at the acetal center. Subsequent formation of the Li-enolate, reaction with an electrophile, and finally cleavage of the acetal results in a wide variety of α-branched, α-heterosubstituted carboxylic acids (see Scheme 5[65-68] and Table A in the appendix, which contains numerous references.[47, 48])

The *cis*-heterocycle **1** is formed with a selectivity that is usually over 90%, and clearly the enantiomeric purity of the intended substitution product cannot exceed the diastereoisomeric purity of the cyclic acetal. It is, therefore, usually necessary to purify these acetals by recrystallization or chromatography.[69] Detailed procedures are available for the preparation of the imidazolidinones (**1**, X = NCOPh, Y = NMe)[63] and oxazolidinones (**1**, X = NCOPh, Y = O)[70, 71] from alanine, phenylalanine, valine, and methionine.[71, 72] The synthesis of the dioxolanone (**1**, X = Y = O, R^A = *t*Bu, R = Me) from lactic acid and pivalaldehyde has also been described.[46, 47] (This compound is obtained with a *cis*/*trans* ratio of 96:4 after crystallization.) Finally, the acid-catalyzed acetalization of malic acid, which yields a dioxolanylacetic acid and not a dioxanone carboxylic acid, has been published.[47, 73, 74]

The Li-enolates of the imidazolidinones have the greatest stability and tolerate reactions with electrophiles at temperatures above 0 °C, whereas enolates of the dioxolanones[46, 47, 75-79] can only be handled at low temperatures. The most successful method for formation of the enolates relies on the use of lithium diisopropylamide (LDA) or hexamethyldisilazanide (LHMDS). All the common electrophiles such as H^+, D^+, alkyl, allyl, and benzyl halides, α-haloesters and amides, aldehydes, ketones, α,β-unsaturated carbonyl compounds, and nitroolefins together with the more unusual ones such as tricarbonyl(benzene)-

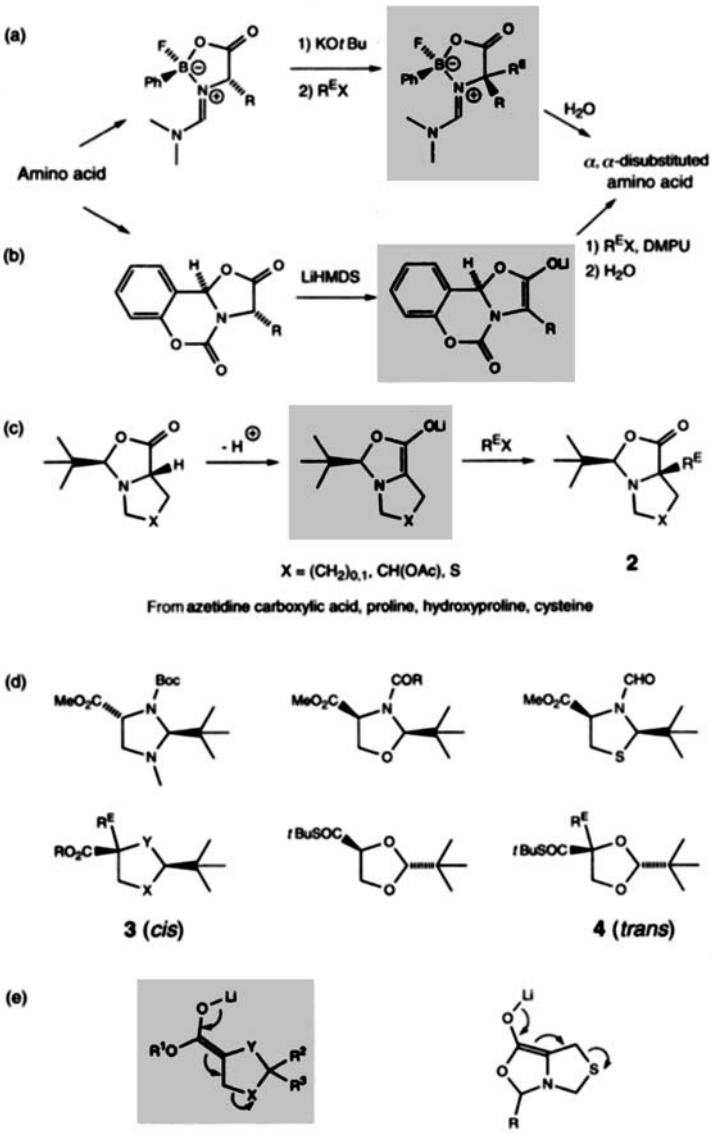

Scheme 6. Further α-alkylations of amino acids following the SRS principle. a) A boraoxazolidinone [84] is alkylated via its K-enolate, and the boron atom serves as the stereogenic center. (This has been applied to phenylalanine, phenylglycine, and valine, which were allowed to react with methyl and propyl iodide, and allyl and benzyl bromide.) b) The amino acids alanine, phenylalanine, and leucine have been methylated and allylated via a tricyclic compound (derived from salicylaldehyde) [85]. c) Alkylation of a cyclic amino acid via a bicyclic enolate [43, 45, 86-89]; enolization of the cysteine derivative (X = S) without β-elimination (see e)) is successful only when a special trick is used (see Section 9) [89, 90]; with *O*-acetyl-hydroxyproline (X = CHOAc), the acetate group is also enolized [87, 88]. d) Branching of 2,3-diaminopropanoic acid [99], serine [93, 100, 101], cysteine [103-109], and glyceric acid [93, 102] via the geminal-disubstituted intermediates **3** and **4**; the Li-enolate intermediate (see e)) with an exocyclic double bond is fairly stable despite the (endocyclic) β-leaving group [93, 102-109]; as can be seen in the case of the cysteine derivative, the stability is very sensitive to the nature of the *N*-acyl group. Only the enolate formed from the formyl derivative is stable enough to undergo alkylation [93, 105-109] (see also Scheme 33 in Section 9). Further examples are given in Scheme 7 and in Tables B and C in the appendix. LiHMDS = lithium hexamethyldisilazanide, DMPU = *N*,*N*′-dimethyl-*N*,*N*′-propyleneurea, Boc = *tert*-butoxycarbonyl.

chromium have been employed (see the R^E groups in Table A of the appendix and the accompanying references). The reactions proceed with high selectivity at the face of the enolate double bond[80] opposite to that shielded by the *tert*-butyl substituent on the acetal center. Furthermore, the products are usually highly crystalline or are easily purified by chromatography, such that a single diastereoisomer may be subjected to the final hydrolysis step. As the stereogenic center in the final product (the α-heterosubstituted α,α-disubstituted carboxylic acid) is stable, rather drastic conditions may be used for the hydrolysis of the heterocycles in the last step of the SRS sequence of Scheme 5.[64, 81–83]

α-Substituents have also been introduced to simple amino acids via other heterocyclic derivatives and their enolates. In the particularly clever "trick" outlined in Scheme 6a the temporary stereogenic center is a boron atom, and, of course, hydrolysis after the alkylation can be achieved under very mild conditions in this case.[84] Salicylaldehyde has also been employed as an achiral auxiliary for the SRS alkylation of amino acids (see Scheme 6b).[85] Cyclic amino acids such as azetidine carboxylic acid,[86] proline,[43, 45] hydroxyproline,[87, 88] and the cysteine derivative 4-thiaproline[89, 90] may be alkylated via bicyclic enolates, which react with a wide variety of electrophiles at the *exo* face exclusively (see **2** in Scheme 6c and Table B in the appendix).[91–98]

The heterocycles derived from 2,3-diamino-,[99] 2-amino-3-hydroxy-,[93, 100, 101] and 2,3-dihydroxycarboxylic acids[93, 102] (Scheme 6d) are of particular interest. *cis*/*trans* Mixtures are formed during acetalization and the diastereoisomeric purity is highly dependent upon reaction conditions (thermodynamic control for acid catalysis,[62, 93, 101–109] kinetic control for Rh^{3+} catalysis[52, 57]), upon the substitution of the ring, and upon the nature of the heteroatoms in the ring. Both the oxazolidine[93, 100, 101] and the thiazolidinecarboxylic esters[103–109] are normally formed as 1:1 *cis*/*trans* mixtures. However, the subsequent *N*-acylation results in the formation of only the *cis* derivative.[62, 93, 100, 101, 103–110] The enolates of the N,N-, N,O- and N,S-heterocycles are alkylated from the side opposite to that shielded by the *tert*-butyl group to give the products *cis*-**3** (Scheme 6d[100, 104–109]). The reactivity of the glyceric acid derivative is somewhat different: the *tert*-butylthiol ester cyclizes preferentially (5:1) to give the *trans* product, and subsequent alkylation occurs *cis* to the *t*Bu group (→ **4**).[93, 102] The enolates of the heterocyclic carboxylic esters have a range of stabilities with regard to β-elimination (Scheme 6e left), which should, in fact, be stereoelectronically unfavorable.[111] In spite of this problem, very high yields of the required product can be obtained under suitable reaction conditions. Examples with references can be found in Table C of the appendix and in Schemes 7 and 8, in which structures of some amino acids and natural products are shown that have been prepared using the intermediates shown in Schemes 5 and 6c,d,e or by different applications of the SRS principle.[112–131]

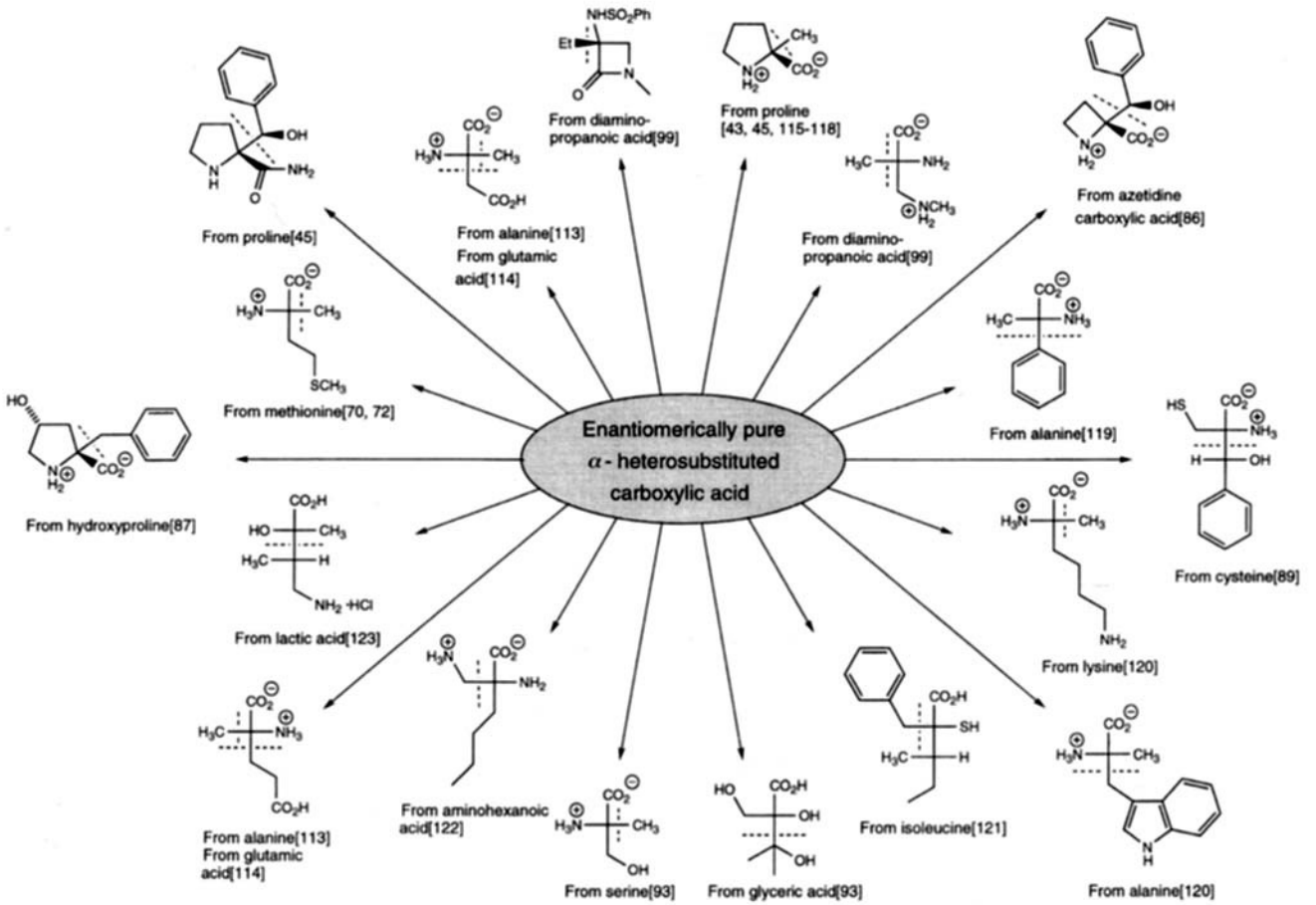

Scheme 7. Selected examples of α,α-disubstituted α-heterocarboxylic acids prepared following the SRS principle described in Schemes 5 and 6. TBDMS = *tert*-butyldimethylsilyl.

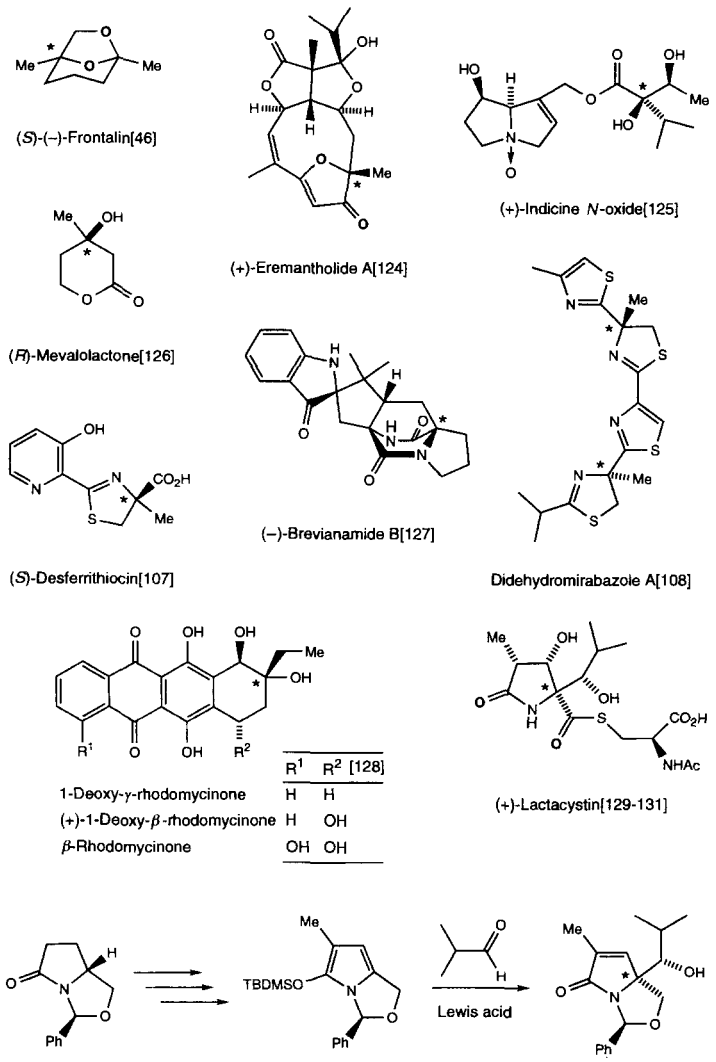

Scheme 8. At least one step in the syntheses of the natural products shown here follows the principle of self-regeneration of stereocenters; the tertiary carbon atoms formed in this way are marked by an asterisk. (*S*)-(−)-Frontalin was obtained by alkylation of the enolate of *cis*-**1** (X = Y = O, R^A = *t*Bu, R = Me, Scheme 5, derived from lactic acid) with 1-iodo-4,4-dimethoxypentane, reduction with lithium aluminium hydride, and interchange of acetals. The key step in the synthesis of (+)-eremantholide A was the reaction of the same lactic acid enolate with 2,3-dibromopropene; the final product was obtained after many more steps. In the alkaloid (+)-indicine *N*-oxide the carboxylic acid unit in the ester side chain was prepared by hydroxyalkylation of *cis*-**1** (X = Y = O, R^A = *t*Bu, R = *i*Pr) with acetaldehyde in 43% yield. (*R*)-Mevalolactone was prepared from both lactic acid (via *cis*-**1** (X = Y = O, R^A = *t*Bu, R = Me)) and malic acid (**1**, X = Y = O, R^A = *t*Bu, R = CH_2CO_2*t*Bu) following the SRS principle. The important point about this synthesis is that labels (^{13}C, ^2H, ^3H) can be introduced at numerous positions to produce derivatives suitable for biosynthetic investigations. Proline was the starting point for an elegant total synthesis of brevianamide B. The synthesis proceeded via compound **2** (R^E = allyl), which was prepared by the reaction of the bicyclic compound shown in Scheme 6c (X = CH_2) with allyl bromide. The mirabazoles are a group of alkaloids that all contain an α-methylcysteine functionality. Dehydromirabazole A was synthesized from the methyl ester of α-methylcysteine, which was obtained from the appropriate heterocycle of type *cis*-**3** (Y = NCHO, X = S, R = Me, R^E = Me, Scheme 6). α-Methylcysteine was employed in the same way in the synthesis of (*S*)-desferrithiocin. The synthesis of rhodomycinone began with enantiomerically pure (*S*)-aminobutanoic acid, which was converted into the hydroxy acid by diazotization. Subsequent reaction of the enolate of **1** (X = Y = O, R^A = *t*Bu, R = Et, Scheme 5) with allyl bromide proceeded in the normal manner. Reduction of the carbonyl functionality with DIBAH, acetal interchange, and ozonolysis led to the 1,4-dialdehyde, which was suitably protected such that a Marschalk reaction with the appropriately substituted anthrahydroquinones could then be carried out. This resulted in the formation of the rhodomycinones. The total synthesis of (+)-lactacystin was achieved by three different routes; two [129, 130] followed the SRS principle and the third used the strategy described in ref. [92]. The synthesis carried out by E. J. Corey and co-workers [129] began with the oxazolidine derived from serine, which was hydroxyalkylated with isobutyraldehyde to yield a product of type *cis*-**3** (X = O, Y = BnN, R = Me, R^E = $Me_2CHCH(OH)$, Scheme 6); J. E. Baldwin and co-workers described an extremely sophisticated application of the SRS principle. Pyroglutamic acid was allowed to react with benzaldehyde and then reduced to the bicyclic compound, shown in the last line. A series of subsequent steps led to the silyloxypyrrole shown, which reacted stereoselectively with isobutyraldehyde in the following key step.

4. Using the SRS Principle in the Preparation and Reactions of α,β-Unsaturated, α- and/or β-Heterosubstituted Carboxylic Acid Derivatives (Dienolates, Radicals, Michael Acceptors, and Components for Cycloadditions)

Ich habe nicht mehr Glück als Sie, aber ich probiere mehr als Sie![*]

Adolf von Baeyer

Cyclic acetals with endo- or exocyclic C–C double bonds must be prepared in order to introduce new substituents at the position β or γ to a carbonyl group of a chiral, heterosubstituted carboxylic acid, as was described in the previous scheme for the α-position. This can be achieved in a number of ways (Scheme 9). Firstly, the familiar five-membered cyclic acetal is prepared diastereoselectively from an aldehyde R^ACHO and the α- or α,β-amino-, -hydroxy-, or -sulfanylcarboxylic acids. Subsequently, the resulting dioxolanones, oxazolidinones, and imidazolidinones can be, for example, brominated by means of a radical process. Such brominations display a surprisingly high preference for the CH-position adjacent to the carbonyl group (captodative radical stabilization[132]) over the acetal center (this has a bulky R^A substituent, *t*Bu, and is therefore sterically hindered).[133–136] Diastereoselectivity was observed early on in brominations that proceed via an α-carbonyl radical intermediate[133] (see Section 9.3) rather than via an enolate (Schemes 5 and 6). Elimination of HBr then leads to acetals **5**, which have an exocyclic double bond (Path a in Scheme 9). In the simplest case (R=H), these are chiral non-racemic derivatives of α-hydroxy- or α-aminoacrylic acid, in other words, of pyruvic acid! An alternative method (Path b in Scheme 9) begins with a carboxylic acid bearing functional groups in the α- and β-positions. After the necessary functional group manipulations, a five-membered cyclic acetal with a leaving group in the exocyclic position β to the carbonyl group is obtained and hence, the alkylidene derivative **5** can now be readily prepared.[137–139] Furthermore, the oxazoline and thiazoline carboxylic esters **6**, heterocycles with conjugated endocyclic C–C double bonds, can be prepared from the appropriate acetals of serine, threonine,[140] and cysteine[103, 104] (Schemes 6d and 9c). Finally, perhydropyrimidinones[62, 141–149] and dioxanones[150–162] can be prepared diastereoselectively from β-amino- and β-hydroxycarboxylic acids, respectively, by a variety of

[*] "I am not luckier than you, I simply try harder!"

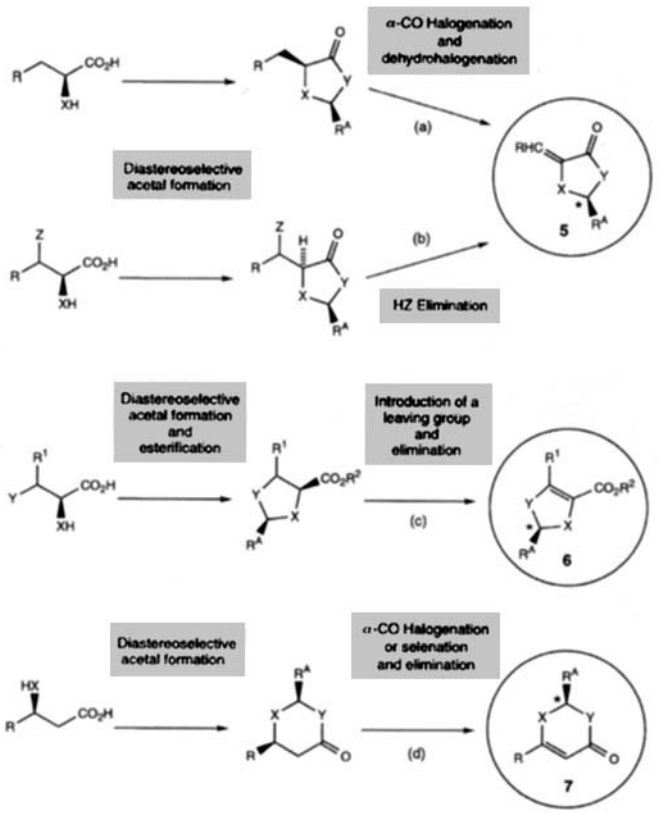

Scheme 9. Preparation of chiral α,β-unsaturated carbonyl compounds from amino-, hydroxy-, and sulfanylcarboxylic acids with destruction of the original stereogenic center in the position α or β to the carbonyl group. (For specific examples, see Scheme 10; for further reactions, see Schemes 11–14. See the text for a discussion of pathways (a)–(d). Tables D1–D4 in the appendix give examples of the applications of these heterocycles.)

methods. Subsequent formal dehydrogenation leads to the heterocyclic α,β-unsaturated carbonyl compounds **7** (Scheme 9d), which are, in fact, chiral, nonracemic acetals of, for example, acetoacetic acid and other β-ketocarboxylic acids.

The formulas of several five- and six-membered cyclic heterocycles with α,β-unsaturated carbonyl functionality, together with the appropriate precursors and literature references are given in Schemes 10a and b.[163–166] An α-sulfinylacrylate and a 2-propenylsulfoxide are depicted in Scheme 10c; here, the stereogenic center of a sulfoxide, rather than that of an acetal, is utilized to preserve the chirality of the Michael acceptor.[167, 168] These readily prepared α,β-unsaturated carbonyl compounds can be used as chiral building blocks in a variety of processes: the Michael addition of nucleophiles (such as cuprates or Cu^I-doped Grignard reagents), the addition of radicals, in cycloadditions (photochemical [2+2] cycloadditions, Diels–Alder reactions), and catalytic *cis*-hydrogenations or deuterations. Reactions with electrophiles are also possible (via the dienolates shown in Scheme 11), and in this way new substituents can be introduced at the position α or γ to the carbonyl group (see the examples in Schemes 11a–c). An assortment of products, which may be prepared by various types of additions at the C–C double bond of the heterocyclic acceptors discussed above, is shown in Scheme 12.[169–176] Structures derived from

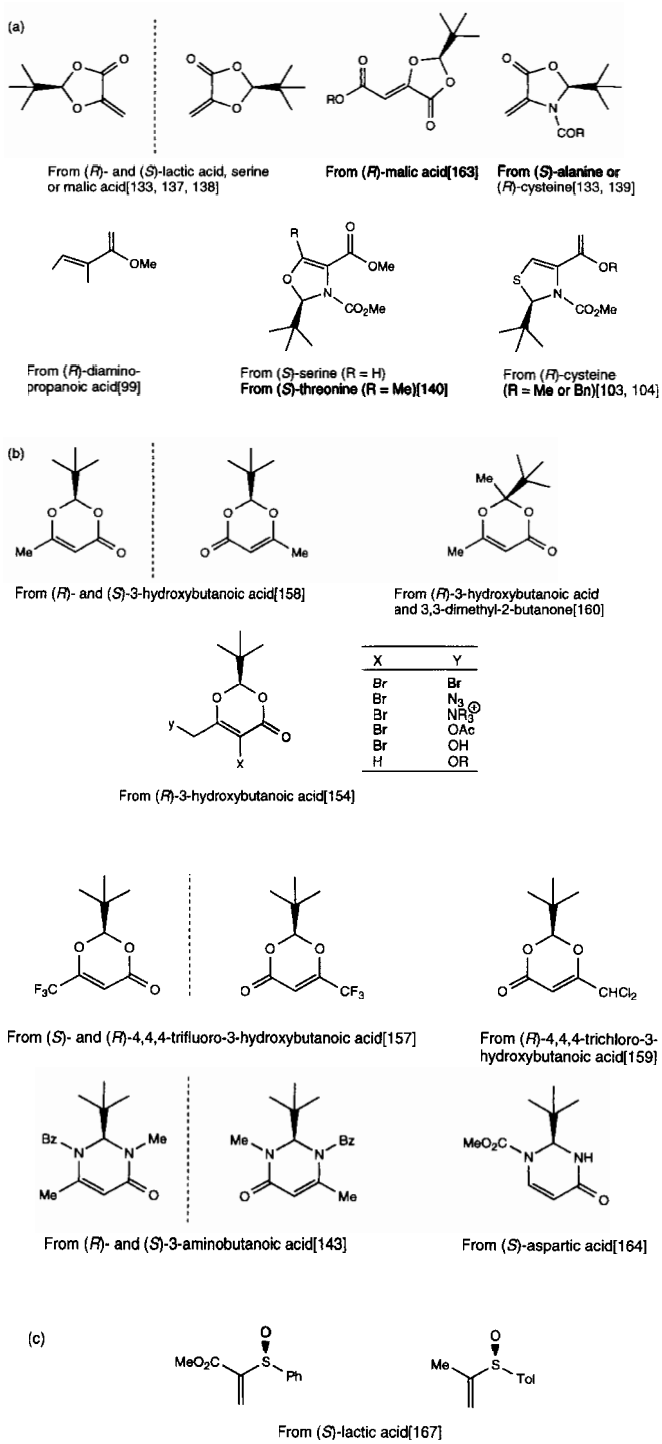

Scheme 10. Chiral products of formal dehydrogenation derived from lactic acid, malic acid, 3-hydroxybutanoic acid, and the amino acids alanine, serine, threonine, cysteine, aspartic acid, and 3-aminobutanoic acid. a) Five-membered ring heterocycles from α- and α,β-disubstituted carboxylic acids. b) Six-membered ring heterocycles from β-hydroxy and β-amino acids. c) Chiral, noncyclic sulfoxides from lactic acid. Subsequent products are depicted in Schemes 11–14 and in Tables D1–D4 in the appendix. For short review articles with information on methylene derivatives of dioxolanones [67], oxazolidinones [66], oxazolidine dicarboxylates [165], and dioxinones [166] see the *Encyclopedia of Reagents for Organic Synthesis*. Bz = COC_6H_5, Tol = $C_6H_4CH_3$.

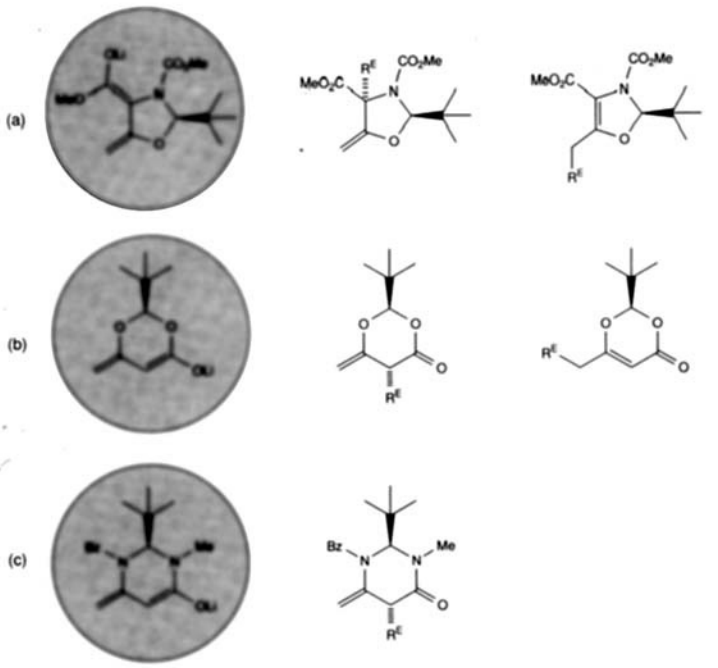

Scheme 11. Chiral Li-dienolates derived from threonine (a), 3-hydroxybutanoic acid (b), and 3-aminobutanoic acid (c) together with products resulting from their reactions with electrophiles. Specific examples are given in Schemes 12 and 13.

3-hydroxybutanoic acid[151, 177] and constructed via the previously mentioned dioxinones **7** (Schemes 9d, 10b, and 11b) are depicted in Scheme 13.[178–180] Finally, Tables D1–D4 in the appendix document, in as complete a fashion as possible, previous applications of the SRS principle to reactions of α,β-unsaturated carbonyl compounds. It is not always immediately clear that self-regeneration is involved in these processes; the two examples shown in Scheme 14 should demonstrate this point. In the first case, a hydrogen atom at the C3 position of serine is replaced by a butyl group in a diastereoselective fashion,[140] and apparently nothing has happened at the original stereogenic center of serine. However, upon closer examination of the reaction sequence, it becomes clear that substitution at the C2 position has also occurred: The H atom is initially replaced with bromine by reaction with *N*-bromosuccinimide (NBS); the trigonal center of the enolate, which is generated by cuprate addition, is then diastereoselectively protonated such that a "new" hydrogen atom occupies the 2-position of the chain-extended serine derivative! Similarly in the second reaction sequence shown in Scheme 14 (part of a synthesis of soraphen[181]), the stereogenic center (indicated by an asterisk) of the hydroxy acid starting material appears to be present in an unchanged form in the product. In reality, however, this reaction sequence relies on the use of a temporary trigonal center at every C atom: Func-

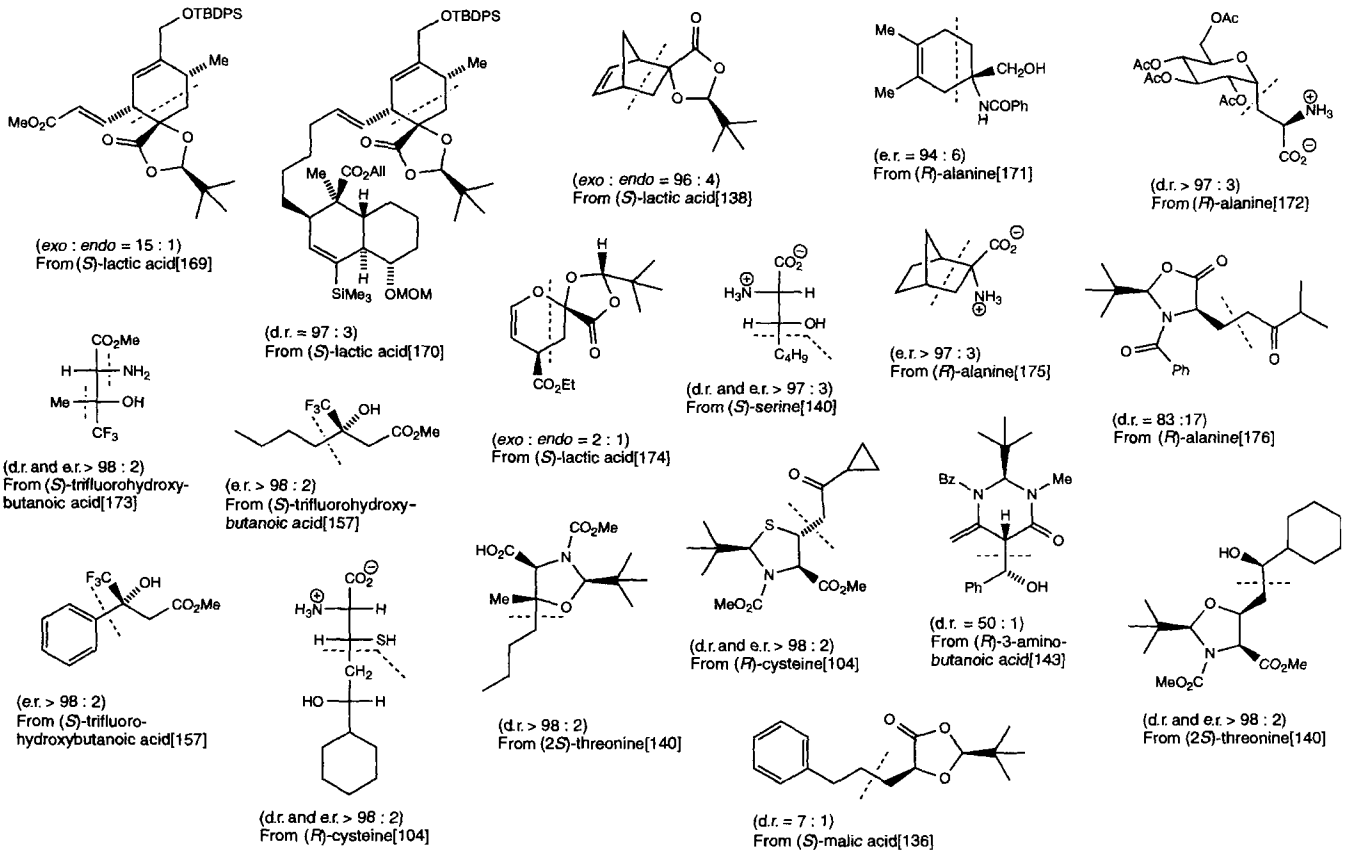

Scheme 12. Selected examples of products prepared via the unsaturated heterocycles shown in Schemes 9–11. Dashed lines are used to mark the newly formed bonds, which result from Michael additions, radical additions, Diels–Alder reactions, and reactions of enolates and dienolates with electrophiles; further examples are given in Schemes 13 and 14 and also in Tables D1–D4 in the appendix. Complete details can be found in the literature references. TBDPS = *tert*-butyldiphenylsilyl, All = allyl, MOM = methoxymethyl.

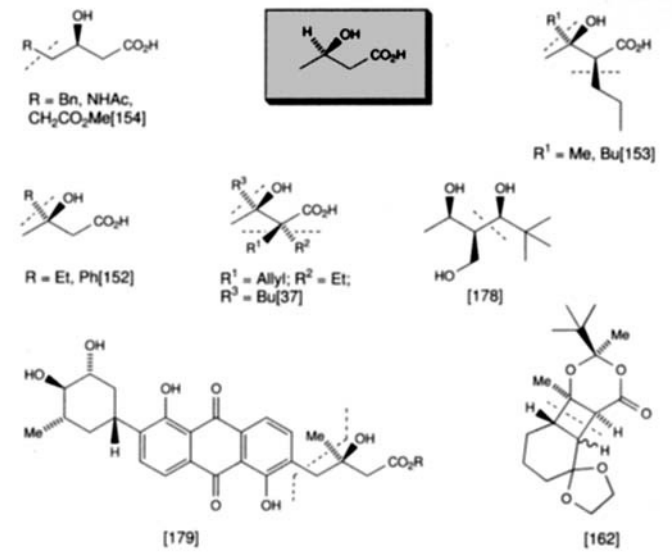

Scheme 13. Products prepared from (*R*)-3-hydroxybutanoic acid in which the preparation involves the temporary destruction of the original stereogenic center; see the dioxinone derivatives in Schemes 9d, 10b, 11b, 14b and in Tables D3 and D4 of the appendix. Of course, the methods used here are not only applicable to both enantiomers of hydroxybutanoic acid but are also generally applicable to 3-hydroxycarboxylic acids (for example, see ref. [180]).

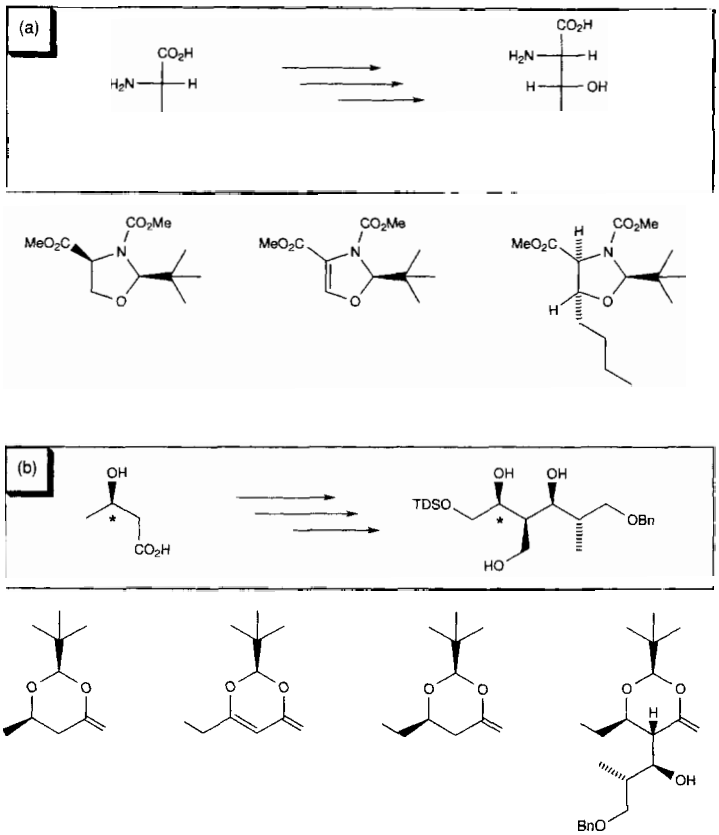

Scheme 14. Reactions of serine (a) [140] and (*R*)-3-hydroxybutanoic acid (b) [181] with substitution of the hydrogen atom in the position β or γ to the carbonyl functionality by C_4H_9 or RO groups. The formulas of the most important intermediates are shown. The original stereogenic center is temporarily destroyed in order to achieve the necessary reactivity at the 3- or 4-position of the carbon skeleton. In both products, an H atom (at C2 of serine and at C3 of hydroxybutanoic acid) is stereoselectively replaced (with retention!) by a new one; this could have been proved by deuterolysis in case (a) and by the use of D_2 in case (b).

tionalization of the terminal CH_3 group of the hydroxybutanoic acid is only possible via the dioxinone derivative, and the hydrogen atom at the C atom marked by the asterisk is derived from the H_2 used in a catalytic hydrogenation step!

5. SRS via Acyliminium Ions and the Resulting Products

Umpolung doubles the possibilities.

In the previous two sections we have shown that new substituents can be introduced, without racemization, at the 2- or 3-position of carboxylic acids by means of enolate and enoate chemistry with the aid of electrophilic and nucleophilic reagents. The crucial intermediates derived from serine for the preparation of modified 2-amino-3-hydroxycarboxylic acids are depicted in Scheme 15. In all of the previous examples, it has been a hydrogen atom that has been replaced by a new substituent.

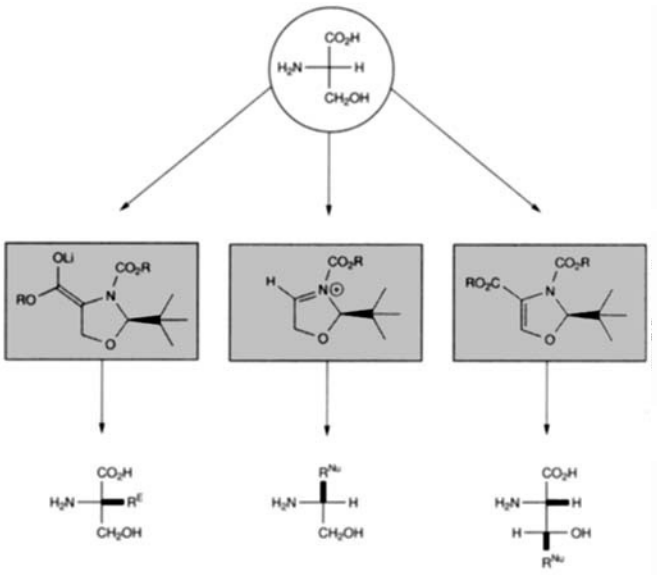

Scheme 15. Stereoselective replacement of H atoms and of the CO_2H group of serine by new substituents following the SRS principle. Bonds marked in bold are those resulting from this transformation and do not break the convention used for the depiction of Fischer projections (see center and right). The alkylation yielding the α,α-disubstituted amino acid (left) and the modification resulting in chain extension at the C atom in β-position (right) are also possible with simple amino acids such as alanine (Schemes 5, 9a, 10a), whereas the decarboxylation (center) [182] is not.

However, in the case of the trifunctional amino acids such as serine, threonine, cysteine, and aspartic acid the SRS principle can be applied to replace the carboxyl functionality with other groups. For example, in the case of aspartic acid, the reaction sequence proceeds via the dihydropyrimidinone[145–149] (shown in Scheme 10b), and for serine, the acyliminium ion[182] (shown in the center of Scheme 15) is involved. As can be seen, the carboxyl group is replaced by a new substituent R^{Nu}, which is introduced by the use of a nucleophilic reagent (umpolung of the nucleophilic reactivity of the Li-enolate to produce electrophilic reactivity at the former C2 of the acid). Interestingly, these reactions often proceed in a far superior fashion when an *i*Pr rather than the usual *t*Bu substituent is present at the tempo-

rary stereogenic center, and generally the new substituent enters *cis* to the substituent at the acetal C atom![183]

The key step in the removal of the carboxyl group from the derivatives of serine, threonine, and cysteine is the electrolytic anodic oxidation of the carboxylic acid. Faraday[184] and Kolbe[185] demonstrated that simple carboxylic acids are coupled under these conditions ($2\,RCO_2H \rightarrow R-R + 2CO_2 + H_2$), and Hofer and Moest[186] showed that oxidative decarboxylation occurs with carboxylic acids when R is a cation-stabilizing substituent ($RCO_2H + R'OH \rightarrow ROR' + CO_2 + H_2$). The reaction of the amino acids mentioned occurs as shown at the top of Scheme 16. In contrast to most other electrolysis procedures,

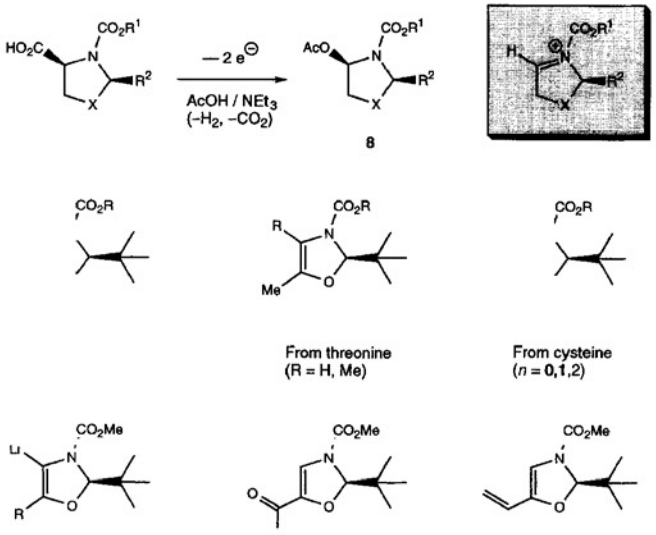

Scheme 16. Electrolysis of the oxazolidine and thiazolidine carboxylic acids (e.g. **8**) derived from L-amino acids, elimination of HOAc to yield the oxazoline and thiazoline derivatives (e.g. **9**), and electrophilic substitution at the C–C double bond by means of lithiation or by direct Vilsmeier formylation (subsequent Wittig olefination produces the electron-rich diene **10**) [101, 103, 140, 182, 190]. A short review article about **9** has been published in the *Encyclopedia of Reagents for Organic Synthesis* [165].

this decarboxylation is a simple, easily conducted reaction. The electrodes need not be separated by diaphragms and the addition of a supporting electrolyte is also not required. A solution of the oxazolidine[101] or oxidothiazolidine carboxylic acid[103] in a protic solvent such as acetic acid (this is much less susceptible to decarboxylation!) or methanol is mixed with triethylamine (formation of the supporting electrolyte, $RCO_2^- Et_3NH^+$) and then electrolyzed in an undivided cell until the gas evolution ceases and the conductivity falls due to complete consumption of the carboxylate. This reaction can be carried out at high concentrations of the carboxylic acid on a multigram scale and results in excellent yields of the decarboxylated product (**8**, X = O, R^1 = Me, R^2 = *t*Bu, ca. 90% yield for the decarboxylation step, ca. 55% yield from serine over four steps;[101] the 2-isopropyl derivative can be prepared analogously). Here again, the *cis*-acetoxyoxazolidine is produced, which results from attack of the acyliminium salt (shown in the box in Scheme 16) at the apparently more sterically hindered face.[183] Lewis acid assisted nucleophilic substitution of the AcO group of the useful, readily available, enantiomerically pure derivatives **8**[140, 187–194] can be performed, and once again, this proceeds via the acyliminium ion. Products obtained from the reaction with bis(trimethylsilyl)acetylene or from the Michaelis–Arbuzov reaction (triphenylphosphite/$TiCl_4$) (yields of 80 and 95%, respectively; diastereoselectivities of 90 and 80%, respectively) are shown at the top of Scheme 17.[182, 195]

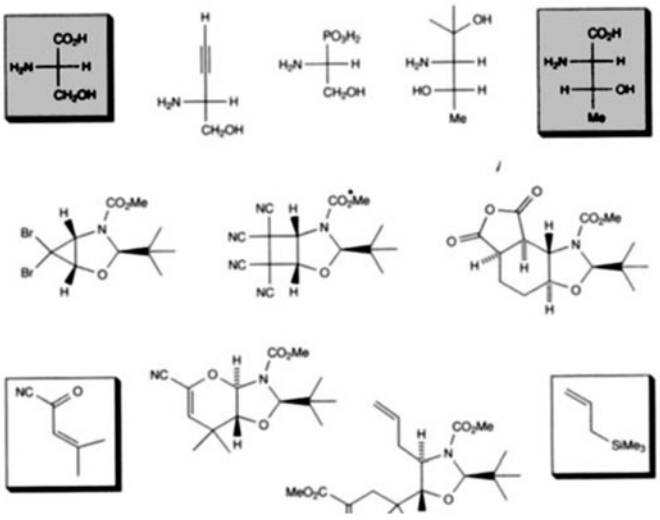

Scheme 17. Top: An acetylenic amino alcohol and a phosphoserine derived from heterocycle **8** [182, 195], which is shown in Scheme 16 and derived from serine; an amino diol prepared by addition of the Li threonine derivative from Scheme 16 to acetone, hydrogenation of the double bond, and hydrolysis [140]. Middle: Compounds resulting from addition of dibromocarbene, tetracyanoethylene, and an acyl cyanide to heterocycle **9**; a product with four neighboring stereogenic centers (two of which are derived from serine) results from hydrogenation of the Diels–Alder adduct of maleic anhydride and diene **10** [192]. Bottom: The addition of the α,β-unsaturated acyl cyanide to **9** apparently proceeds via a zwitterion (enolate/acyl iminium ion) and results in the formation of a *trans*-fused bicyclic compound. The allylation of this compound (allylsilane/$TiCl_4$, Sakurai method) proceeds *cis* to the *tert*-butyl group with formation of a 6-amino-5-hydroxy-4,4-dimethyl-2-oxonon-8-ene carboxylic acid derivative (the two C atoms derived from serine in the C_9 chain are both stereogenic centers).

Nucleophilic substitution of the electrolysis products **8**, derived from serine, threonine, and cysteine, gives these intermediates a wide-ranging potential in synthesis. Elimination of acetic acid yields the heterocycles shown in the center of Scheme 16, which have highly reactive C–C double bonds. The oxazoline **9** contains the structural features of both an enol ether and an *N*-acyl-enamine.[101, 140, 182, 190, 192] The hydrogen atoms at the double bond of **9** can be substituted by means of an *N*-acyl-directed metalation (next to the N atom) and by the use of a Friedel–Crafts type reaction (next to the O atom). Here, once again, the stability of the acyliminium ion is responsible for the regioselectivity of the kinetically controlled reaction with electrophiles[140, 192, 196] (see the formyl- and vinyloxazoline carboxylic acid ester **10** in Scheme 16 and the bicyclic and tricyclic species in Scheme 17, resulting from cycloaddition reactions). The relative configuration of the products, which are frequently formed with complete diastereoselectivity, was assigned by chemical correlation or NMR spectroscopy. All products are enantiomerically pure and all are also available in the enantiomeric form by the use of D- instead of L-serine, -threonine, or -cysteine.

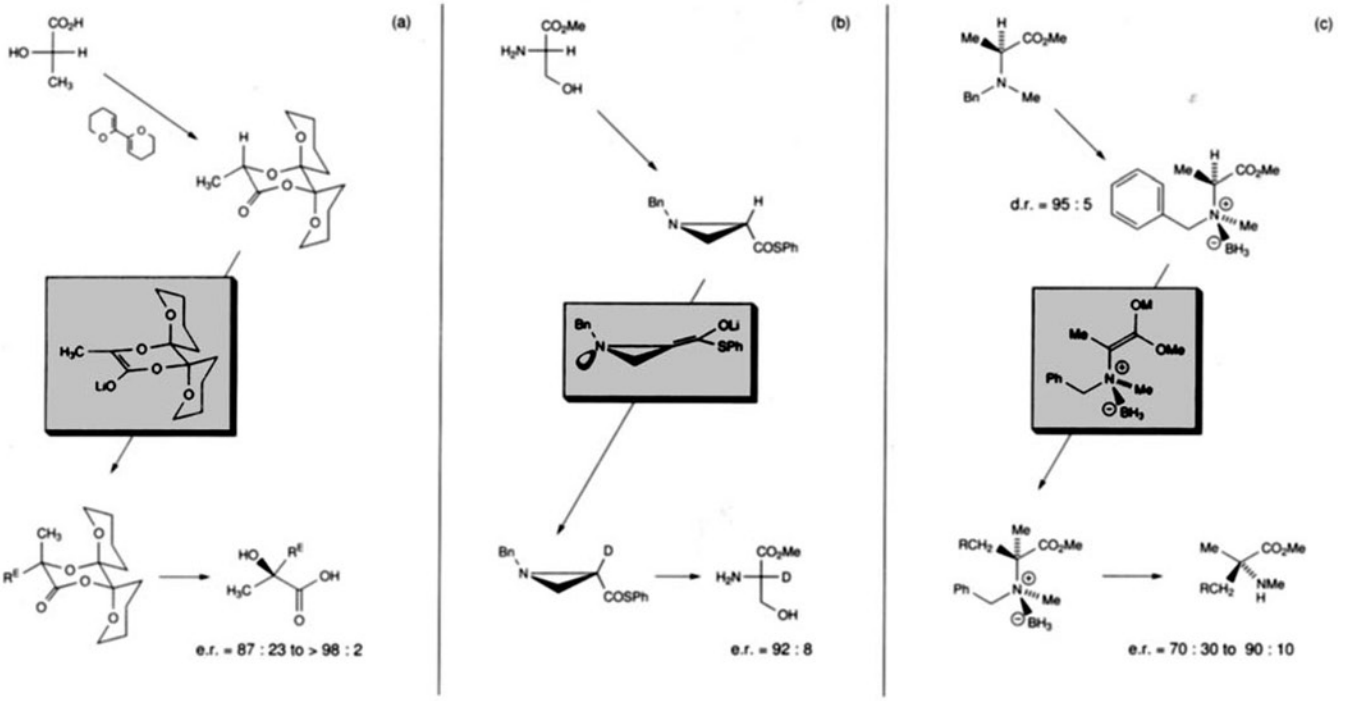

Scheme 18. Three applications of the SRS principle in which the temporary stereogenic center is a) a spiroacetal C atom [205], b) an aziridine nitrogen atom [208], and c) a nitrogen atom of a boron–amine adduct $R^1R^2R^3N^+BH_3^-$ [211].

6. Other "Tricks" for the Self-Regeneration of Stereocenters

Phantasie ist wichtiger als Wissen.[*]

Albert Einstein

Once a synthetic principle has been understood, only the chemist's imagination sets the limits! In recent years numerous reactions have been described that intentionally or unintentionally make use of the self-regeneration of stereocenters.[197, 198] We describe only a few here.

In Scheme 18a the key step[205] is the diastereoselective formation of a dispirodiacetal from 1,1′-bis(dihydropyran) and lactic acid, a procedure that is useful in a variety of other transformations.[199–204] In Scheme 18b the configurationally stable stereogenic center at the nitrogen atom of an aziridine facilitates the introduction of new substituents at the 2-position of serine[206] via enolates of the aziridine carboxylic ester.[207–209] Scheme 18c depicts a highly refined, and yet conceptually simple α-allylation of an amino acid derivative: After diastereoselective formation of a Lewis acid/Lewis base complex from BH_3 and *N*-benzyl-*N*-methylalanine methyl ester, an enolate is formed, which is chiral owing to the stereogenic center at the nitrogen atom. This intermediate reacts diastereoselectively with alkyl halides such that removal of BH_3 and debenzylation leads to α,α-disubstituted *N*-methylamino acids with enantiomer ratios of up to 9:1.[210, 211]

Obviously, not only stereogenic centers but also stereogenic axes and planes are able to self-regenerate. Hence, it is also clear that not only temporary stereogenic centers but also every other chirality element (axis, plane, helix) can be employed in self-regeneration. The application of chirality planes within transition metal complexes is well-documented. The principle is described in Scheme 19 (cf. Scheme 3) and some specific examples are given in Scheme 20.[212–217] As can be seen, the single stereogenic center of the starting material is destroyed in the process. Simultaneously, a plane of chirality is formed[218] or preserved. The metal center, together with its

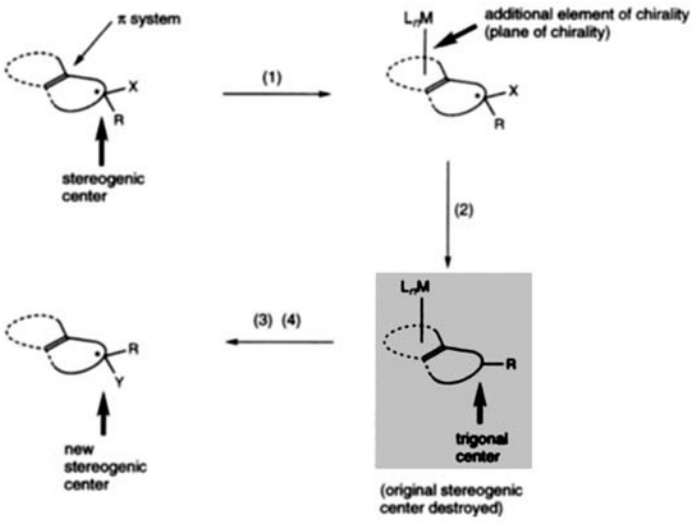

Scheme 19. Self-regeneration of stereocenters with the assistance of transition metal π-complexes. An enantiomerically pure compound with only one stereogenic center is complexed diastereoselectively (1). The configurationally stable plane of chirality ensures that the subsequent destruction of the stereogenic center results in the formation of a nonracemic intermediate (2). Hence the next reaction (3) proceeds diastereoselectively and the destruction of the π-complex (4) results in the formation of an enantiomerically pure or enriched compound [212–217] (cf. Scheme 3).

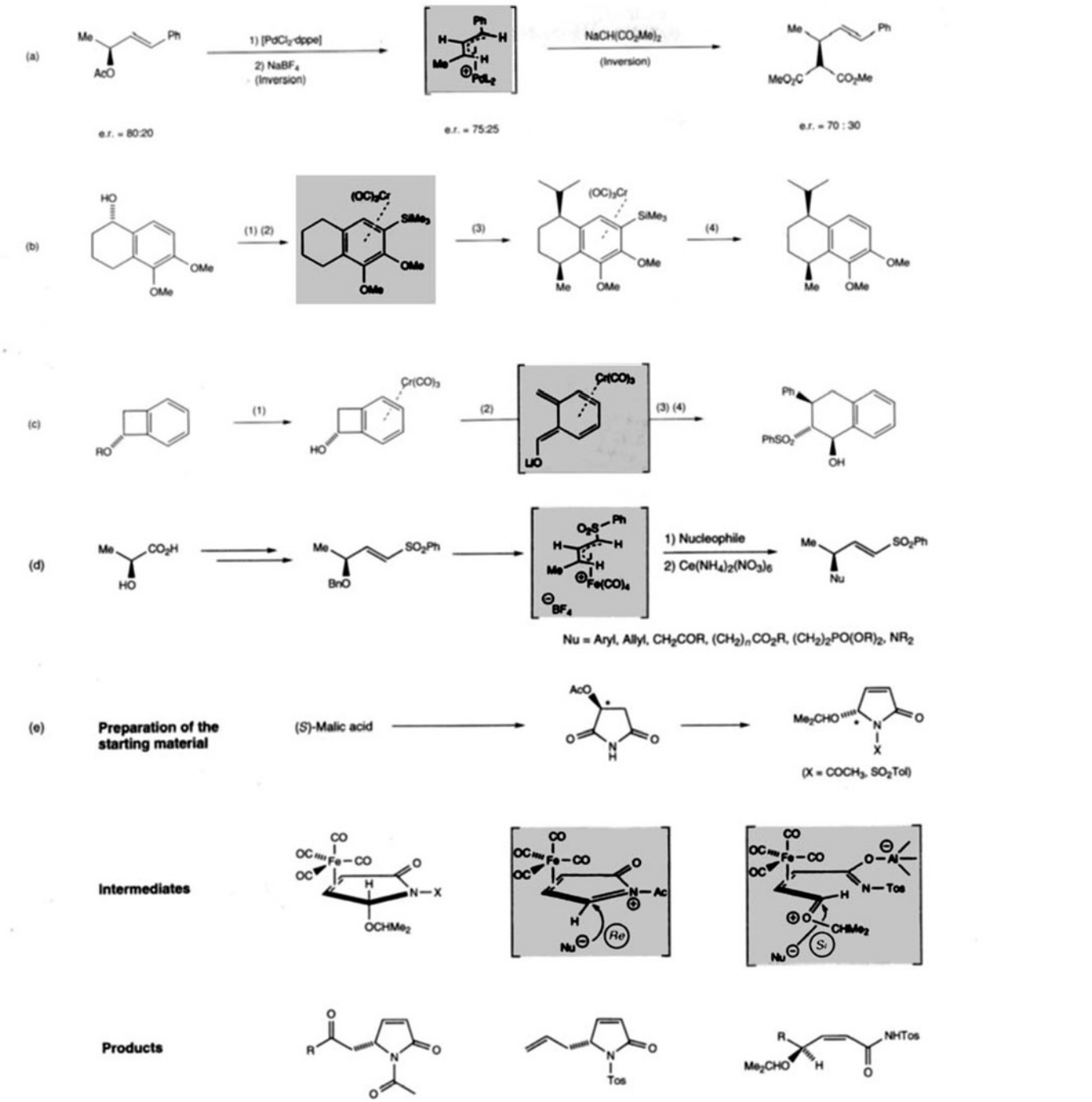

Scheme 20. SRS processes via π-complexes with planes of chirality. Steps (1)–(4) in (b) and (c) correspond to steps (1)–(4) in Scheme 19. a) Nucleophilic substitution, with two inversions of configuration, at the allylic position via a stoichiometrically or catalytically generated Pd–π-allyl complex [213] (dppe = ethane-1,2-diylbis(diphenylphosphane)). b) Substitution of an OH by an *i*Pr group with inversion. The intermediate is a benzene–chromium(tricarbonyl) complex, which is Me_3Si-protected in the position on the benzene ring *ortho* to the methoxy group. This complex is first lithiated and methylated next to the methoxy group, and then an isopropyl group is introduced at the second benzylic position in an analogous fashion. The sequence shown is part of the total synthesis of the sesquiterpene *cis*-7,8-dihydroxy-11,12-dehydrocalamenene [214]. c) Diels–Alder reaction of an *ortho*-quinodimethane with ω-phenylsulfonylstyrene. The starting alcohol is produced by enzymatic kinetic resolution. The lithium alkoxide of the benzene–chromium(tricarbonyl) complex ring opens to the planar-chiral quinodimethane at approximately −30 °C [215]. d) Reaction of one of the π-allyl(carbonyl)iron complexes, available by transformation of lactic acid, with nucleophiles. This reaction was used in the synthesis of simple natural products such as pheremones and terpenes [216a]; analogous reactions are also possible with the complex derived from benzyloxy-2-pentenoic acid [216b]. e) Substitutions via cationic tetracarbonyliron complexes, in which the organic ligand is formally a derivative of maleic aldehyde but actually derived from malic acid [216c] (cf. the substitution reactions of **8**, Schemes 16 and 17). Similar reactions have been carried out with the tricarbonyliron complexes of 2-alkoxy-4-vinyl-2,5-dihydrofurans [217].

ligands, acts as a temporary substituent and hence, influences the stereochemical course of subsequent reaction(s) and the formation of new centers of chirality. Once the metal complex has been destroyed, the organic ligand is released in an enantiomerically pure or enriched form. The result of this reaction sequence is that a new substituent is introduced stereoselectively at the original stereogenic center. Since this is achieved without the aid of a chiral auxiliary, this sequence can also be considered to follow the general concept of the self-regeneration of stereocenters.

7. What Can Be Done When No Suitable Precursor for the Self-Regeneration of a Stereocenter Is Available?

Nothing is worse than harping on principles!

The heterocyclic products described in Sections 3–5 (Li-enolates, Michael acceptors, radical intermediates, acyliminium salts) display high reactivity, and their reactions usually proceed with outstanding diastereoselectivity. Availability, reactivity, and stereoselectivity are the marks of quality of synthetically useful compounds. For this reason we aimed to make such enantiomerically pure dioxolanones, oxazolidinones, imidazolidinones, perhydropyrimidinones, and dioxinones readily available, even when no suitable, inexpensive chiral precursors were available. The solution to this problem is illustrated with examples from the synthesis of α-amino acids.[219, 220] As was shown in Section 3, amino acids can be substituted at the α-position by applying the principles of SRS. This approach provides relatively easy access only to compounds in which one of the substituents at the stereogenic center is derived from one of the 20 proteinogenic amino acids. It is, however, impossible to produce an amino acid with a single, "unnatural" side chain in the α-position by this method. Clearly what is needed is a chiral glycine derivative with an oxazolidine or imidazolidine structure. Reaction of this compound either once or twice with appropriate electrophiles and subsequent hydrolysis would lead to the desired amino acid. There are three ways to prepare a glycine derivative of this type, and we wish to denote them as the *laborious*, the *fashionable*, and the *classical* approach.

If you want to strictly follow the SRS principle then you have to use the laborious approach[221] (see Scheme 21 top). Serine is O-benzyl-protected and the imidazolidinone is formed by the usual methods (Scheme 5). This is then debenzylated, oxidized to an aminomalonic acid derivative,[222, 223] and then decarboxylated. A chiral, nonracemic glycine derivative results owing to the acetal center, and it can be alkylated via the Li-enolate in the usual manner.[71, 224]

Today, the most commonly used method (the fashionable approach) for the synthesis of enantiomerically pure compounds (EPC synthesis)[225] on a laboratory scale relies on covalently bound chiral auxiliaries which force the reaction to proceed in a diastereoselective fashion. In the extremely successful approach based on chiral auxiliaries, a readily available, enantiomerically pure compound is attached to the achiral compound that is to be modified enantioselectively in the overall process. The reaction is then carried out with as high a diastereoselectivity as possible and finally, the chiral auxiliary is cleaved. On a laboratory scale, the chiral auxiliary is commonly sacrificed, but in industrial applications, the auxiliary, which is used in a stoichiometric amount, must be recovered for further reactions.[226] Evans's method employing an oxazolidin-2-one, which is usually derived from an amino acid, with an appropriate substituent in the 4-position is perhaps the archetype of this form of EPC synthesis.[31, 227] There are numerous examples of compounds derived from glycine and a chiral auxiliary; Scheme 22 shows the different types together

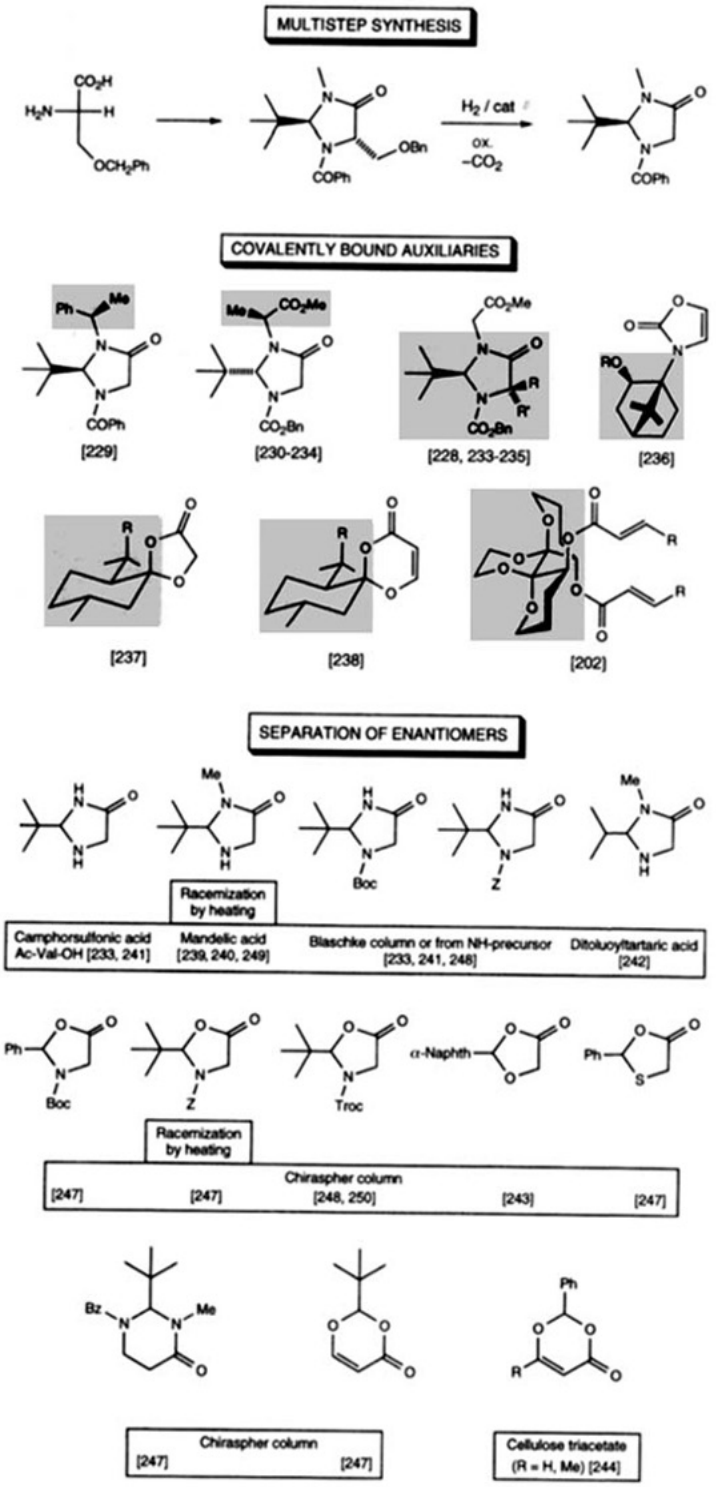

Scheme 21. Three possible routes to chiral acetals of achiral amino- and hydroxycarboxylic acids (glycine, glycolic acid, thioglycolic acid, formyl- and acetoacetic acid, 3-aminopropanoic acid). *Multistep syntheses* that "uphold" the SRS principle [71, 221–224]; the *auxiliary approach* via covalently bound auxiliaries (see text for further references; the auxiliary component is highlighted in each case). The *separation of enantiomers* via diastereoisomeric salts or by preparative chromatography on a chiral solid support. Short review articles on imidazolidinones [65], oxazolidinones [66], dioxolanones [67], and dioxinones [166] can be found in the *Encyclopedia of Reagents for Organic Synthesis*. α-Naphth = α-naphthyl, Bn = $CH_2C_6H_5$, Bz = COC_6H_5, Boc = CO_2tBu, Z = CO_2Bn, Troc = $CO_2CH_2CCl_3$.

with the names of their creators and references.[228] Some of the chiral imidazolidinone-containing derivatives of glycine are shown in Scheme 21, which also contains references to the use of the chiral auxiliary approach in the reactions of oxazolines (cf.

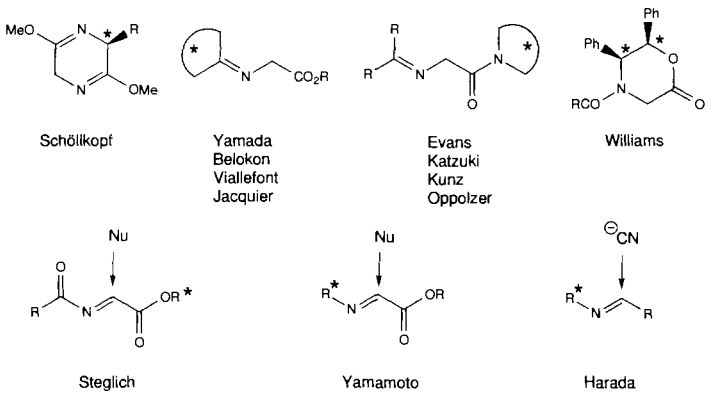

Scheme 22. Some glycine, dehydroglycine, and imine derivatives that have been used (or proposed for application) in the auxiliary approach to *C–C bond formation* in amino acid synthesis. Due to the wide variety of different systems and the large number of research groups working in this field, the names of only a few of the authors are listed here. For further information, see Williams's book [219] and the recent review articles [220, 228]. The method developed by Williams is in some respects very similar to the "Separation of Enantiomers" method outlined in Scheme 21 as the 2-amino-1,2-diphenylethanol used is obtained by resolution of a racemic mixture. However, in the latter case the stereogenic center is actually eliminated at the end (→aldehyde), whereas here the auxiliary, which initially also had to be prepared, is destroyed by hydrogenolysis (→1,2-diphenylethane!).

9 in Scheme 16), dioxolanones (glycolic acid, cf. Scheme 5), dioxinones (cf. **7** in Scheme 9 and Schemes 10b, 11b, 13, 14) and the dispiro-THP derivative (cf. Scheme 18a).[229–238]

The third, so-called *classical* approach is the route we have chosen to adopt: either the resolution of a racemic mixture through diastereoisomeric salts or, the more recently developed approach, the separation of enantiomers by preparative HPLC on a chiral column. The structures of the heterocyclic acetals separated in this way are shown at the bottom of Scheme 21.[239–250] The following advantages rapidly became clear:

1) Large quantities of both enantiomers are readily available. Hundreds of grams, even several kilograms, of 2-*tert*-butyl-3-methyl-1,3-imidazolidin-4-one (BMI) can, for example, be prepared by crystallization of the mandelate salt.[240, 249, 251] The chromatographic separation of enantiomers (for example, benzyloxycarbonyl (Z) protected 2-*tert*-butyl-oxazolidin-5-one on a 100 × 400 mm Chiraspher column) is possible on a multigram scale.[246, 247]
2) The enantiomer that is not required for a particular synthetic target can be easily recycled by thermally induced racemization (BMI,[240] oxazolidinone[246]).
3) Since the enantiomerically pure cyclic acetals are obtained by resolution (Scheme 21 bottom), an auxilary does not have to be recovered. The aldehyde (ArCHO, *i*PrCHO, *t*BuCHO) formed during the hydrolysis step is cheap and can be discarded. In this case, the chiral auxiliary is the carboxylic acid or chromatography column used for the separation of the enantiomers. This is done at a very early stage of the overall process and of course, further use of this type of auxiliary ("recycling") is not a problem.
4) The reactivity of the heterocyclic glycine enolates and other intermediates is outstanding; the *t*Bu group is the source of the high diastereoselectivity.
5) The majority of the products are not only solid but also have a high tendency to crystallize. If necessary, the major product can be further purified by recrystallization in most cases.
6) Those heterocycles that are not derived from glycine (the dioxolanones, thioxolanones, perhydropyrimidinones, and dioxinones, see Scheme 21 bottom) can also be separated on chiral columns.[243, 244, 247]

8. The Synthesis of Amino Acids via Chiral, Glycine-Derived Imidazolidinones and Oxazolidinones—Even Better than the SRS Principle

Le mieux est l'ennemi du bien.[*]

Voltaire

In this section, we aim to demonstrate the wide variety of possibilities now open to us by using the glycine derivatives produced by the resolution of a racemic mixture as an example. Only the 2-*tert*-butyl-*N*-acyl-1,3-imidazolidinones and -oxazolidinones will be considered because they have proved to be particularly useful and their chemistry has been investigated in the most depth.[252]

The heterocycles described by the general formula **11** in Scheme 23 can be either mono- or dialkylated (a). The yield of

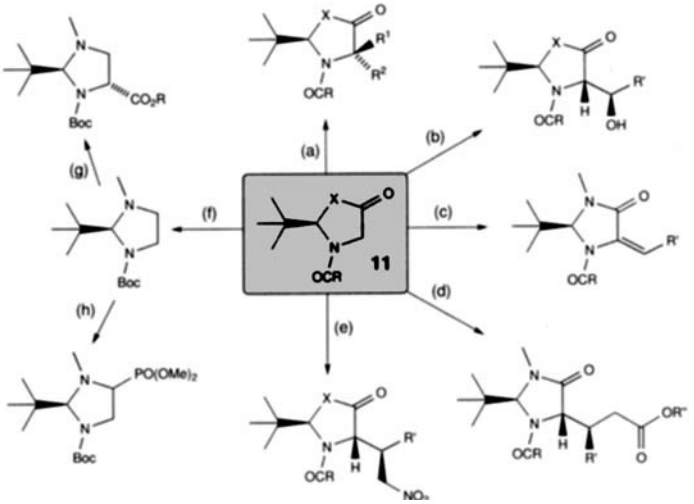

Scheme 23. Reactions (a)–(h) of acyl-*tert*-butyloxazolidinones **11** (X = O) and acyl-*tert*-butylmethylimidazolidinones **11** (X = NMe) to give a variety of amino acid derivatives. See text for references; short review articles can be found in refs. [65, 66]; specific examples are shown in Schemes 24 and 25 and also in Table E (appendix). Compound **11** (X = NMe, RCO = Boc) is also known as Boc-BMI and oxazolidinone **11** (X = O, RCO = Z) is also known as Z-BOX.

the first alkylation[81, 240] is usually so high with a wide variety of alkyl halides that the second alkylation can be carried out immediately in situ.[82, 83] The order of addition of the two different electrophiles determines the absolute configuration of the α-branched amino acid isolated at the end of the procedure. Good procedures[83] now exist for the hydrolysis of imidazolidinones with even the bulkiest substituents (derived from Boc-BMI, **11**, X = NMe, R = *t*BuO). This method has also been applied frequently for the synthesis of radiolabeled amino acids (examples in Table E in the appendix). The aldol addition (b) of

[*] "The best is the enemy of the good."

oxazolidinone **11**, X = O, R = BnO (Z-BOX),[245, 246] to aldehydes proceeds with high diastereoselectivity. If the aldehyde is chiral, the relative topicity is almost always determined by the enolate component.[71, 245, 250] (See the notes on the mechanism in Section 9.3, Scheme 29 and Table F.) Aldol condensations (c) are best brought about by a Wittig–Horner olefination using Boc-BMI. The imidazolidinone is brominated with NBS, the bromide is then converted by the Michaelis–Arbuzow procedure into a phosphonic ester ($PO(OMe)_2$ *cis* to *t*Bu), and this is condensed with an aldehyde to yield the (*E*)-alkylidene derivative.[134] These compounds are superb Michael acceptors and the addition of cuprates followed by aqueous workup yields pure derivatives of β-branched α-amino acids with almost complete diastereoselectivity (R″ and H add to the exocyclic double bond in a *cis* fashion from the face opposite to that occupied by the *t*Bu group).[253] Michael additions of enolates derived from **11** to enoates[254] and enones (d)[255] and to nitroolefins (e)[240] proceed selectively with respect to both of the newly formed stereogenic centers. Finally, the oxygen atom on the ring of Boc-BMI can be smoothly removed with $LiBH_4$ (Scheme 23 (f)) and the resulting chiral 1,2-diaminoethane derivative can be alkoxycarbonylated (g) or phosphonylated (h). This methodology provides α-branched α,β-diaminopropanoic[99, 256] and -ethanephosphonic acids,[257] respectively, in enantiomerically pure form. Selected examples of such amino acids are shown in Scheme 24,[258, 259] and Table E in the appendix contains a complete list. The synthesis of (*S*,*S*,*S*)-2-amino-4-fluoro-3-hydroxy-*N*,4-dimethyl-(*E*)-6-octenoic acid (MeBmt) is outlined in Scheme 25.[250] This synthesis follows a route very similar to that used for the preparation of the parent compound MeBmt,[245] the unique amino acid found in the immunosuppressant cyclosporin. The preparation of MeBmt once again underlines the peculiar effects of a fluorine substituent on the properties and reactivities of organic compounds.[260, 261]

All of the advantages of the glycine derivative **11** have been emphasized, but the conditions necessary for the hydrolysis of

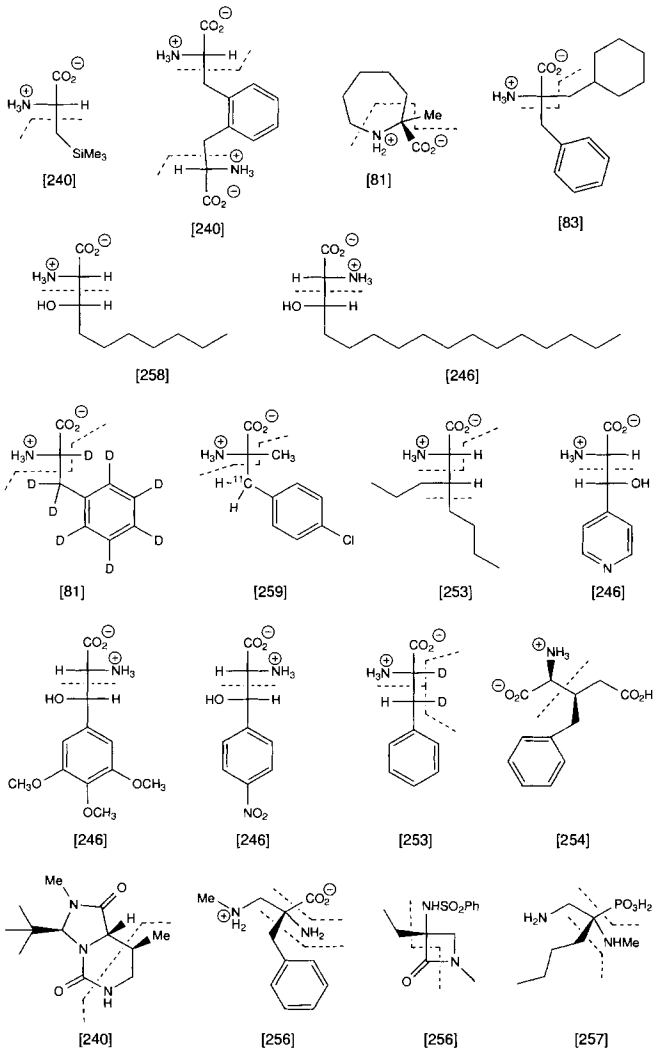

Scheme 24. Amino, diamino, and aminohydroxy acids derived from Boc-BMI and Z-BOX (**11**, X = NMe, RCO = Boc and X = O, RCO = Z, respectively, Scheme 23). The C–H, C–D, C–N, C–C, and C–P bonds resulting from connections to the skeleton of building block **11** are marked with dashed lines. These components were introduced by enolate protonation, deuterolysis, and alkylation, by aldol additions (to give (*S*)- or (*R*)-threonines or allothreonines), by aldol condensations and Michael additions, by catalytic hydrogenation of C–C double bonds, and by carboxylation and phosphonylation. See also Table E in the appendix, where many further examples can be found.

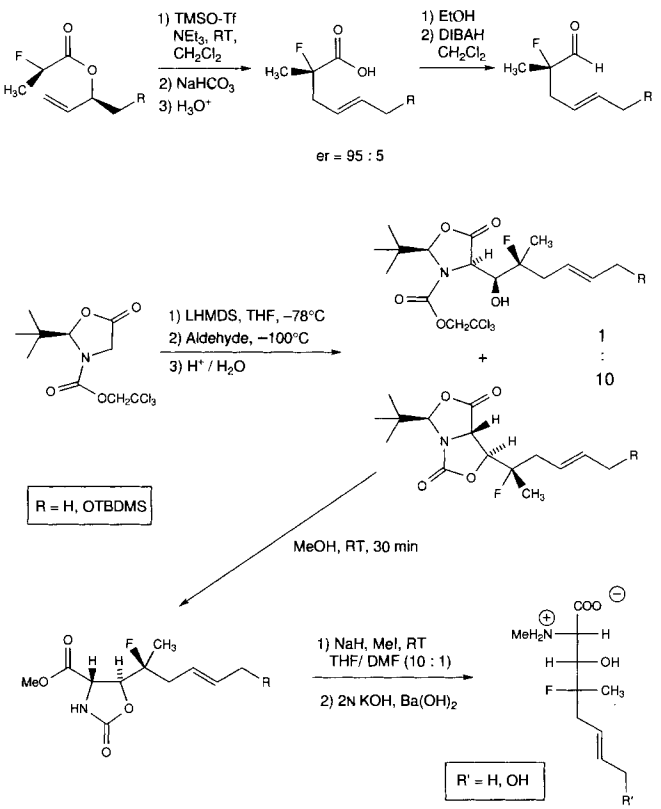

Scheme 25. Synthesis of fluorinated analogs of MeBmt (formula bottom right, R′ = H and H in place of F), the unique amino acid in cyclosporin. A modified Ireland–Claisen rearrangement of the 2-fluoropropanoic acid allyl esters shown led to the appropriate (2*S*,4*E*)-2-fluoro-2-methylhex-4-enoic acid (R = H, OTBDMS) with enantiomer ratios of 95:5 (yields 45–52%). Esterification and subsequent reduction yielded the aldehydes (formula top right), which were allowed to react with the enantiomerically pure (*R*)-oxazolidinone Troc-BOX to give the products shown (65%). Methanolysis of the bicyclic major product, followed by methylation at nitrogen, yielded the *trans*-substituted cyclic carbamates. Finally, these carbamates were converted to the free, 4-fluoro-substituted amino acids under the mildest possible conditions (danger of epoxide formation via the intermediate alkoxide with loss of F^-) [250].

the amino acid precursors prepared from Boc-BMI still leave a lot to be desired. As the last step is the cleavage of an *N*-alkylcarboxylic acid amide, the highly acidic conditions required are not surprising. These conditions range (according to the substituent in the α-position) from 0.75 N HCl/acidic ion-exchange resin/reflux,[240] to 4 N HCl/dioxane/H_2O/80 °C, to 6 N HCl/10% MeOH/reflux,[83] to conc. HCl/100 °C[83] and finally up to 6 N HCl/180 °C/sealed tube.[64, 81, 262] A solution to this problem has now been found with the imidazolines **12** shown in Scheme 26. 2-*tert*-Butylimidazolidin-4-one, which is unsubstituted at both nitrogen atoms and available by the resolution of a racemic mixture with camphor sulfonic acid and *N*-acetylvaline, can be converted into the methoxyimidazoline **12** by protection of the amine nitrogen with either a Boc or Z group and then O-methylation with Meerwein's salt. The enolate—or to be more precise, enaminate—is an extremely reactive nucleophile particularly when the nitrogen is Boc-protected. Here too, the yields of alkylation are so high that a second alkylation can be carried out immediately in situ. The stereoselectivity of both steps is outstanding, and the 5-monosubstituted products can be hydrolyzed with 0.1 N aqueous trifluoroacetic acid at 4 °C; hydrolysis of the 5,5-disubstituted products requires 4 N trifluoroacetic acid in water at room temperature.[233, 241] It is, therefore, now possible to produce amino acids with highly acid-sensitive side chains (see the lower section of Scheme 26) by this procedure.

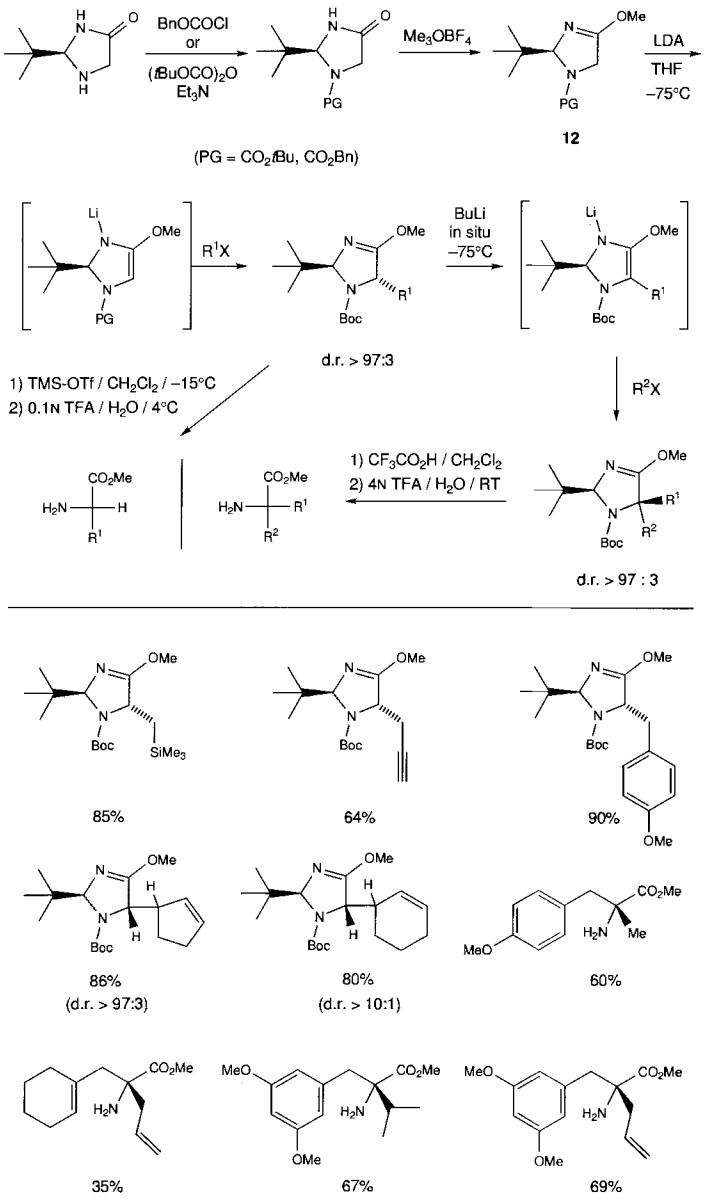

Scheme 26. 1-Boc- and 1-Z-2-*tert*-butyl-3-methoxy-Δ^3-imidazoline **12** (PG = Boc and Z, respectively) as chiral, nonracemic, glycine-derived, synthetic building blocks [233, 241]. Reactions with alkyl halides proceed with high selectivity; the use of an excess of the racemic allylation reagents bromocyclopentene and -hexene results in an efficient kinetic resolution (as in the reaction of Boc-BMI-enolate with 1-bromo-1-phenylethane [240, 254]); the absolute configuration at the cycloalkenyl C atom is not yet known. The quoted diastereoisomer ratio, d.r. > 97:3, means that the second isomer is not detectable in the high-field NMR spectrum of the crude product. The yields listed below the imidazolines refer to the alkylation step and those below the amino acids refer to the hydrolysis step. Addition of the deprotonated iminoester Li-**12** to the aldehyde does not result, after hydrolysis, in threonine (as observed with the enolate of heterocycle **11**) but gives allothreonine derivatives instead. LDA = lithium diisopropylamide, TFA = trifluoroacetic acid.

The reactions of the glycine derivatives, which are prepared by resolution of racemic mixtures, proceed so well that these synthetic building blocks are now preferred even for the synthesis of α,α-disubstituted amino acids derived from natural amino acids, in other words when the side chain is "proteinogenic" and the principles of SRS could also be applied.

9. What Have We Learned?

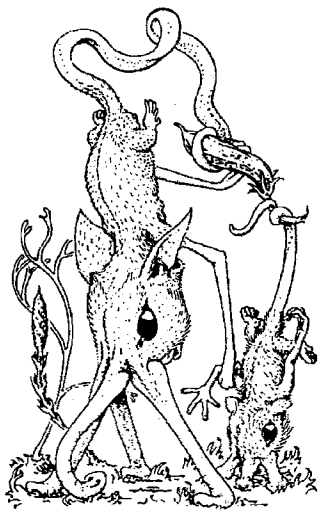

"Nasobem with Child" (from H. Stümpke, *Bau und Leben der Rhinogradentia*, Copyright© Gustav Fischer, Stuttgart, **1961**).

There is no disgrace in not knowing, but there is in not wanting to learn.

Socrates

There have been a few record-breaking cases of stereoselectivity resulting from long-range effects (with up to six atoms between the "inducing" and the newly formed stereogenic center!)[263–266] and spectacular effects of fluorine substitution (reversal of the regio- and stereochemical course of the reaction on replacement of a CH_3 group by CF_3 in a reactant).[267] In the past we have somewhat cautiously speculated (sometimes only in footnotes) about the causes of these observations. They have, however, led us to become interested in the nucleophilic, radical, and electrophilic reactivity of the heterocycles prepared in stud-

ies of the SRS principle, and this in turn has led to some insights into the reactivity that are of general importance and not simply confined to this area. These topics will be discussed in the following sections.

9.1. The Effect of Secondary Amines

We first stumbled upon this effect while studying the reactions of the lithium enolates of oxazolidinones and imidazolidinones, and it is now clear that this effect is particularly marked for polylithiated derivatives.[29, 45, 114, 268] One example is the reaction of the enolate derived from glutamic acid[269] (Scheme 27). The enolate-carboxylate forms a complex with the diisopropylamine that results from the enolate formation. (The structure of such a complex has been determined by X-ray crystallography.[29]) Subsequent reaction of the complex with electrophiles results in the recovery of up to 50% of the starting material. It

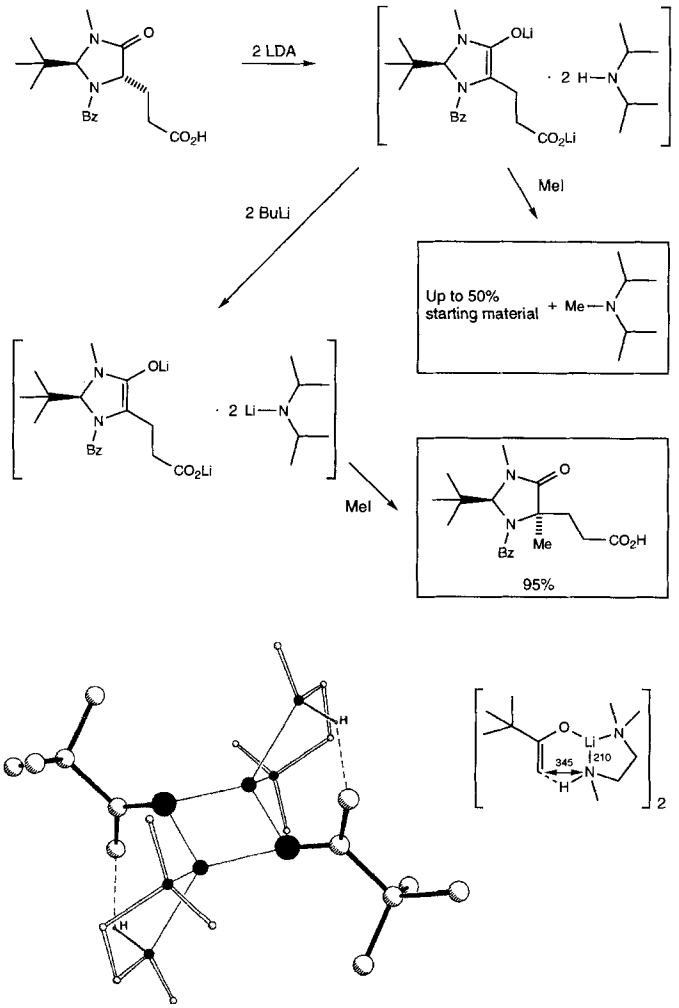

Scheme 27. The effect of secondary amines on the reactivity of Li-enolates and other Li derivatives. In a complex formed between an enolate and an amine, the nucleophilicity of the amine is enhanced, and hence, in the ensuing reaction with electrophiles, it acts as a proton source! Similarly, the reactivity of the Li-enolate·Li-amide complex is very different from that of the enolate alone [269]. The structure shown is that of a complex between the Li-enolate of pinacolone and *N,N,N*-trimethylethylenediamine, which contains a hydrogen bond between the NH hydrogen atom and the enolate C atom [29]. (The numbers on the formula in the bottom right-hand corner are the interatomic distances in pm.)

was proved that the proton of the amine was actually donated back to the enolate (apparently contrary to the relative pK_a values of a lactam and an amine!) and that the amine was N-methylated under these conditions, although, in the absence of the Li-enolate, it would not normally react. Irreversible removal of the NH proton with BuLi leads to the formation of a new complex between the Li-enolate and the Li-amide, and subsequent alkylation now proceeds in excellent yield.[269] Today it is now commonplace to attempt to improve poor results of reactions between lithiated compounds, generated with LDA and an electrophile, by adding BuLi prior to the electrophile; it often, but not always, helps.[270]

9.2. LiX Adducts with Aromatic Aldehydes—In Situ Sources of Bases and Electrophiles

During attempts to α-alkylate cysteine via a bicyclic acetal in an analogous fashion to the proline derivative, it became clear to us that the (expected?)[271] β-elimination interferes in any reaction with LDA under all the conditions tested.[45] However, when a complex of an aromatic aldehyde and LDA[272] or lithium *tert*-butoxide is employed, the aldol products shown in Scheme 28 are formed in good yield.[48, 89] Transformations of

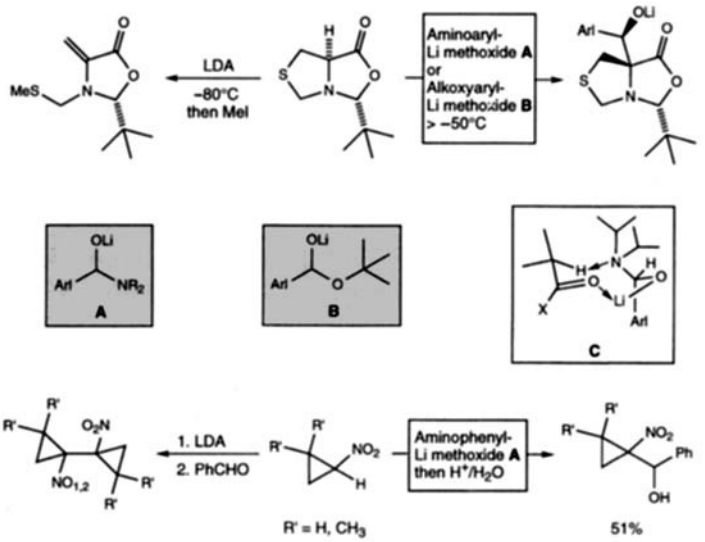

Scheme 28. In situ generation and trapping of unstable enolates [48, 89] and nitronates [273, 274] with aromatic aldehydes with the assistance of the aldehyde adducts **A** [272] and **B** (lithiated hemi-aminal and lithiated hemi-acetal [89], respectively); the Li derivative **A** is usually used for the orthometalation of aromatic aldehydes [272]. In light of the instability of the enolates formed from the bicyclic compound shown, we conclude that this does not result from reaction of the free $LiNR_2$, which exists in equilibrium with **A**, but that deprotonation, generation of the aldehyde, and aldol or nitroaldol addition result in a "collision complex" (see for example **C** and the accompanying caveat in the text). Arl = aryl.

other unstable anionic derivatives such as those derived from nitrocyclopropane[273] are possible when functionalized, lithiated hemi-aminals or hemi-acetals are used as both base and electrophile.[274] Fully realizing the complexity of the reactions of lithiated compounds[5, 21–29] and hence with all due caution, we have proposed a mechanistic model for this process.[275]

9.3. *cis* Selectivity Here, There, and Everywhere—The Power of the $A^{1,3}$ Effect

An observant reader of Sections 3 through 8 and the accompanying schemes can hardly have failed to notice that numerous, at first sight surprising, stereochemical outcomes of reactions have been presented; these could all be collected together loosely under the heading "the *cis* effect" and they are summarized in Scheme 29. Except for a few examples from the early publications, we have interpreted[276] and summarized these results in more recent articles.[62, 196, 254]

First of all, it must be stressed that the level of stereoselectivity found in the alkylations and hydroxyalkylations of our heteromonocyclic enolates has still not been achieved with the carbocyclic analogs.[277] For example, the reactions of the Li-enolates of 4- and 3-*tert*-butylcyclohexanone with CH_3I proceed with diastereoselectivities of 55:45 and 80:20, respectively.[278] The addition of the Li-enolate of cyclohexanone to PhCHO proceeds with a maximum diastereoselectivity of 92:8,[279] whereas the equivalent reactions of the five- and six-membered ring enolates of dioxolanones, dioxanones, oxazolidinones, imidazolidinones, thioxolanones, and perhydropyrimidinones with alkyl halides, aldehydes, and Michael acceptors are so highly selective that the second diastereoisomer cannot normally be seen in the high-field NMR spectrum of the crude product. The same is true for Michael additions to alkylidene derivatives (for example, that from Boc-BMI[253] or from dioxanones[153, 280]).

Together with these questions of the degree of stereoselectivity, the direction of selectivity has also always surprised us, in other words, both the type and manner of the influence on the relative topicity of the reaction process of certain substituents on the heterocycle. Scheme 29 summarizes reactions in which an

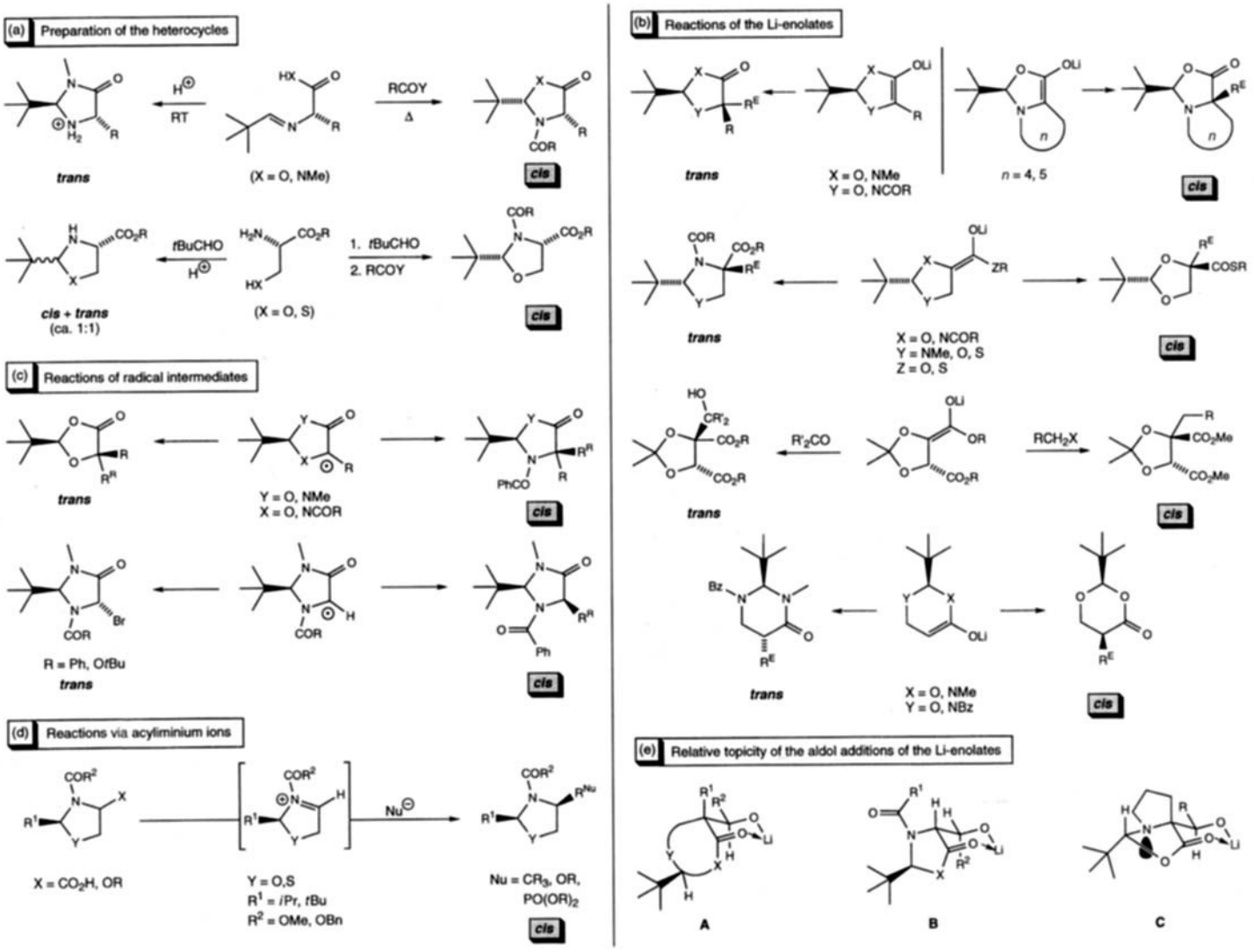

Scheme 29. Examples of reactions which, during the SRS process, result in substitution *cis* to the original substituent on the heterocycles (see Sections 3–5 for references). a) *cis*-Disubstituted five-membered ring heterocycles that are more stable than the *trans* isomers. b) Reactions of Li-enolates of the five- and six-membered ring N,N-, N,O-, N,S-, and O,O-acetals that often lead preferentially to the *cis* products; the geometry of the exocyclic enolate double bond is unknown and is drawn arbitrarily here. c) Dichotomy of reactions of captodative-substituted radical centers in *cis*- and *trans*-selective processes. The assignment of the configuration of the bromo derivative is somewhat uncertain [135]. d) Known reactions of 1,3-oxazolidines and -thiazolidines via acyliminium ions that proceed with a strong preference for the *cis* product. e) Three Zimmerman–Traxler diagrams [291] **A**, **B**, and **C** for the interpretation of aldol additions of heterocyclic enolates to aldehydes. For a compilation of the topicities observed in additions of the five- and six-membered ring heterocyclic enolates discussed here to aldehydes, enones, enoates, and nitroolefins, see Table F in the appendix. For the definition of the "*cis* effect", see the text and Schemes 30–32.

apparently small change in the structure of the reactant results in the reversal of the stereochemical course of the reaction. As has already been mentioned, the point most worthy of note is perhaps that these reactions so often occur with *cis* selectivity. In these cases, either the *cis* product is thermodynamically more stable than the *trans* isomer or, when the reaction proceeds under kinetic control, the trigonal enolate, radical, or acyliminium center of the reactant reacts preferentially from the side that features the substituent (usually a *t*Bu group) at the acetal center. In this fashion, the cyclization with concomitant acylation of a Schiff base derived from an amino acid or amide yields the *cis*-oxazolidines, -oxazolidinones, or -imidazolidinones either predominantly or exclusively (Scheme 29a).[281,282] The example shown in Scheme 29b (top right) is the *cis* attack on a bicyclic enolate[283] leading to the thermodynamically more stable product (*cis* fusion of four and five-membered rings, with substituents in the *exo* position!). The *cis*-selective reaction of dioxolanone enolates with exocyclic double bonds[284] and the reversal of this preference on moving from alkylation to hydroxyalkylation of a tartrate derivative are particularly interesting.[92–94,285] When a dioxanone enolate is replaced with a perhydropyrimidinone enolate, the poor *cis* selectivity is transformed into an excellent *trans* preference (66% vs. 97% *ds*,[141,286] Scheme 29b bottom). This increase in selectivity is typical of the differences observed in reactions of all O-substituted heterocycles relative to those of an N-heterocycle with an N-acyl exocyclic group (cf. the ester enolate of dioxolane and the *N*-acyloxazolidine and thiazolidine carboxylic acids[287]). The stereochemical course of radical reactions is also very dependent upon the heteroatoms in the ring. Such reactions occur with preferential *cis* attack at an *N*-acyl derivative and *trans* attack at a dioxolanone, and the result also appears to be dependent upon the reaction partner (R_3SnH vs. NBS, see Scheme 29c[288–290]). Nucleophilic substitution next to the nitrogen atom of the *N*-acyloxazolidine and -thiazolidine (Scheme 29d) occurring via acyliminium ions (with the assistance of a Lewis acid) virtually always provides the *cis*-substituted compound as the major product (see Section 5 and the references cited therein). Finally, examination of the six-membered ring chair model[291] for the Li-enolate aldol addition of *N*-acylimidazolidinones and -oxazolidinones shows a preference for the R group of RCHO to adopt an axial position, that is, *cis* to the heterocyclic ring (Scheme 23b and **B** in Scheme 29e; Table F[254]).

Closer examination of X-ray crystal structures (either those carried out by us to determine the configuration of our products[62,143,157,229,255,292,293] or by others, which were retrieved from the Cambridge Database) proved to be crucial in the interpretation of the observed *cis* effects. It is well known that five-membered rings ("natural" angle 108°) with trigonal, sp^2 centers ("natural" angle 120°) are strained and that pyramidalization leads to a reduction in this strain.[294] However, the crystal structures made us realize the enormous effect of the 1,3-allyl ($A^{1,3}$) strain[295–297] of amide and carbamate groups. The substituent at the acetal C atom of 1,3-dioxolanones, 1,3-dioxanones, 1,3-dioxinones, and even of 1,3-oxazolidinones and 1,3-imidazolidinones not having *N*-acyl substituents adopts an equatorial or quasi-equatorial position (**A**, **C**, **E** in Scheme 30). In contrast, in the *N*-acyl derivatives, these substituents are usually found in a quasi-axial position on five-membered rings and in fully axial positions on the hydropyrimidones (see **B** and **D** in Scheme 30). The amide nitrogen in the five-membered ring is indeed considerably pyramidalized ($\Delta \leq 0.43$ Å,[298] indicative of a nearly sp^3 amine nitrogen). However, in the majority of cases, the amide group is hardly twisted at all. Obviously much less resonance energy is lost if the nitrogen of the amide group is pyramidalized rather than the R_2N-CO bond rotated.[299] The resulting substructures of the *N*-acyl heterocycles then appear, if viewed from the carbonyl C atom, like structure **F** in Scheme 30. If possible, the O=C–R unit adopts a position to a greater (five-membered ring) or lesser (six-membered ring) extent[300] below the plane formed by the C,N,C ring atoms; the substituents at the neighboring C atoms are above the plane. Some particularly impressive examples are shown in Scheme 31.[301]

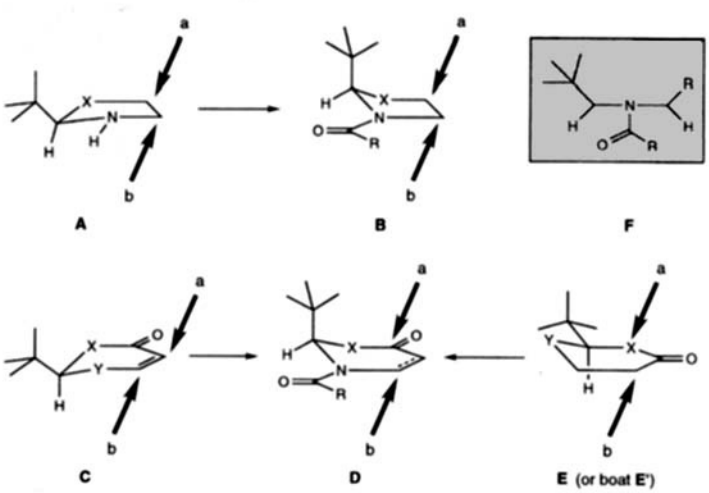

Scheme 30. A compilation of schematic diagrams of the typical structures of acylated (**B**, **D**) and nonacylated heterocycles (**A**, also when NH = O, **C** and **E**) such as dioxolanones, imidazolidinones, oxazolidinones, dioxanones, dioxinones, and hydropyrimidinones, which have been used in reactions employing the SRS principle (see also Scheme 29). Between 1991 and 1995 the Cambridge Structural Database listed 55 structures of such molecules (CSD codes given below), an additional 8 structures have been published in ref. [143], and a further 14 older structures are shown and discussed in ref. [62]. **F** is the most commonly found arrangement with a pyramidalized amide nitrogen (to minimize the angle strain) and with the neighboring centers pointing in the opposite direction so as to minimize the $A^{1,3}$ strain. Six of the structures referred to belong to Type **A** (HEBSEM, KOYXIF, LERLEZ, VURBEP, VURBIT, YADSEB), 18 to Type **B** (HEVTIL, JILROL, JILRUR, JODMEU10, JOPWUG, JOPXER, LAFWEU, LAFWIY, LAXWEM, LAXXIR, PATCAO, PEFLOB, PEVWUI, PEXFED, PIWFIK, SOSDEJ, TAPSOS, VOBYUG), 2 to Type **C** (HEJNAL, KOHKEX), 8 to Type **D** (JOPYUI, JOPZAP, JOPZET, JOPZIX, JOPZOD, SUCJEF, SUCJIJ, SUMNIX), 8 further Type **D** structures are described in [143], 16 belong to Type **E** (*sofa* conformers) (JOPYAO, JOPYES, JOPYIW, JOPYOC, LEDXAT, LEDXEX, LESJEY, LESJIC, LESJOI, LESJUO, PEKTII, SOSFIP, WEBXAC, WEBXEG, WEBXIK, WEBXUW) and 5 to Type **E'** (*boat* conformers) (PALFEN, PIPJAZ, PIPJED, PIPJIH, PIPJON). The majority of the structures were determined by the groups of A. L. J. Beckwith, S. G. Pyne, D. Seebach, and F. J. Urban; the literature citations not given here can be retrieved from the CSD files.

This structural information explains the higher thermodynamic stability of the *cis*-substituted *N*-acyl five-membered ring heterocycles (Scheme 29a) and also the many differences in the reactivity of heterocycles with or without exocyclic *N*-acyl groups (Scheme 29b,c,e[302]). However, another type of $A^{1,3}$ strain (Scheme 32) is responsible for the *cis* selectivity of several enolate and radical reactions (cf. Scheme 29b,c). It is known that an exocyclic CH_2R group at an enolate double

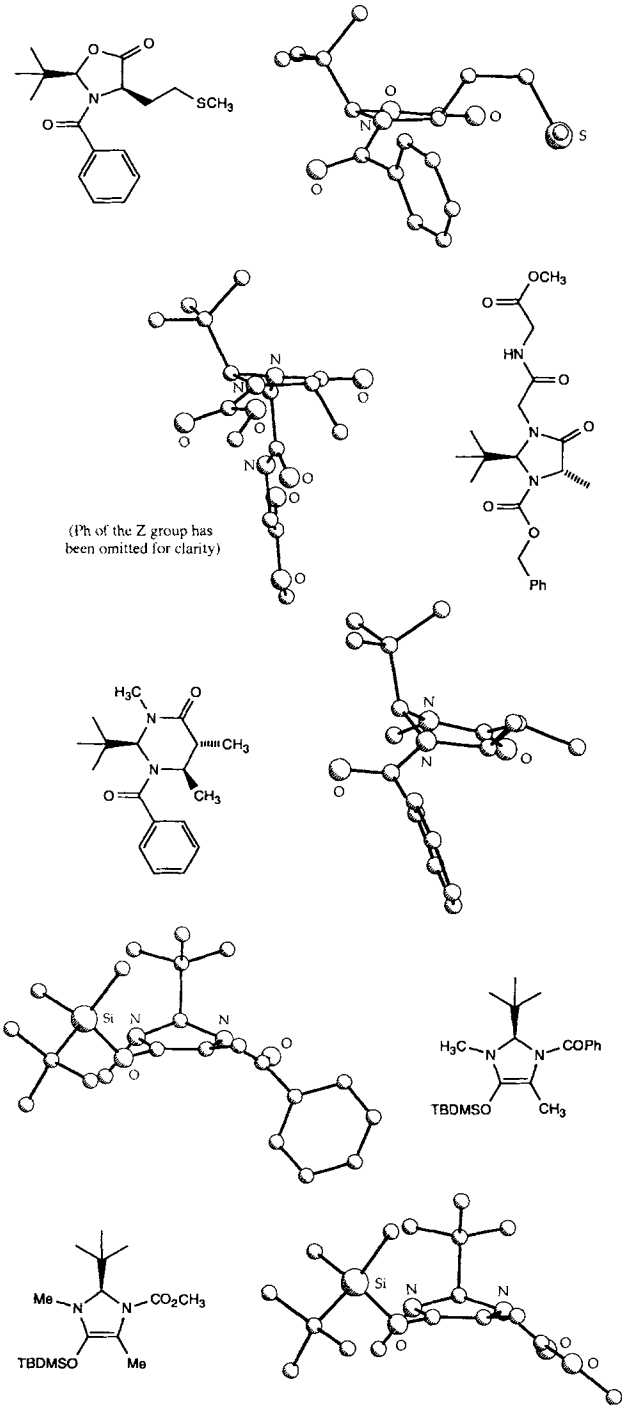

Scheme 31. Typical crystal structures of derivatives of *N*-acylimidazoline [301], -imidazolidine [234], -oxazolidine [62], and -perhydropyrimidine [62,143]. The plane of the benzene ring of the *N*-benzoyl group in the structures shown here, and in almost all those of this type known, is practically perpendicular to the carbonyl plane. The degree of pyramidalization Δ [298] at the methyl-substituted ring C atom of the methyl carbamate and of the benzamide silyl enol ether is 0.07 and 0.11 Å, respectively. In most of the structures the carbonyl oxygen of the *N*-acyl group is in a *cisoid* arrangement with the acetal center; exceptions are found in structures of compounds in which there is a bulky substituent on the α-carbonyl carbon. For details of further structures of this type and the corresponding referenees, see Scheme 30.

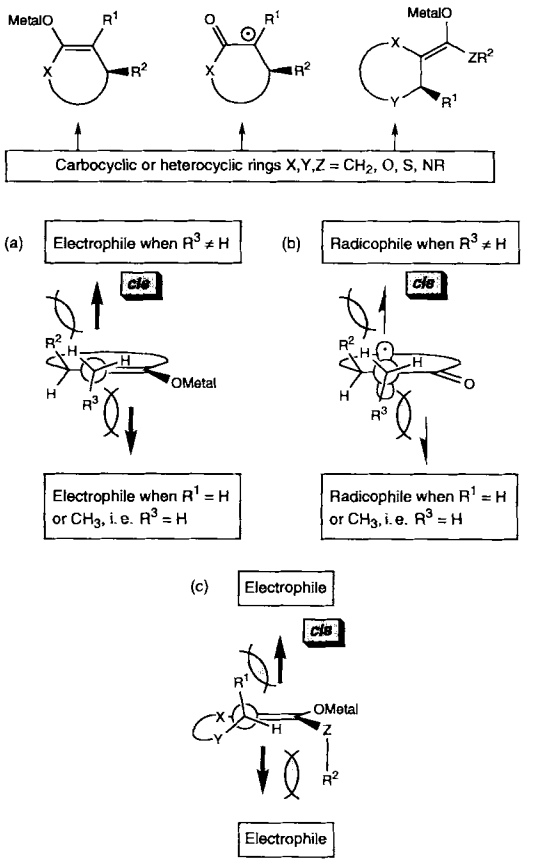

Scheme 32. Reactions of enolates and α-carbonyl radicals. When R^1 is H or CH_3 in those systems with an endocyclic double bond, reaction occurs from below (*trans* to R^2). When $R^1 = CH_2R^3$, the R^3 group is positioned beneath the plane due to $A^{1,3}$ strain and hence, the lower face is shielded to a greater extent than the top face is by R^2 (see a) and b)). An analogous effect is likely to be responsible for the *cis* selectivity observed with certain ester enolates containing exocyclic double bonds (c). References are given in the text.

bond can lead to a reversal of the topicity of attack at the double bond due to the "allylic" endocyclic substituent (Scheme 32a). This has been observed for both carbocyclic (cyclopentanones[303]) and heterocyclic enolates (lactones,[304] dioxanones[37,153,280]) with endocyclic double bonds. Equally, in a whole range of examples of reactions of carboxylic ester and thioester Li-enolates with carbocycles[98] and heterocycles[93–95,102,285] electrophilic attack at the exocyclic enolate double bond occurs *cis* to a substituent in the ring (Scheme 29b, 32[305,306]). This can also be explained by some form of the $A^{1,3}$ effect: the RO or RS group of the ester enolate shields the "lower face" of the enolate plane and the allylic substituent on the neighboring stereogenic center shields the "upper face". (Furthermore, in the case of the heterocyclic carboxylic ester enolates, a chelate effect might be involved.[306]) Whether or not attack occurs from the side *cis* to R^1 at the trigonal center is dependent upon whether the transition state of the electrophilic attack at the enolate double bond is early or late and also upon the relative sizes of the R^1 and R^2 groups (Scheme 32c). The movement of the RZ group out of the plane of the ester enolate has been confirmed by X-ray crystal structure analysis,[209,307–312] and the relationship between *cis* selectivity and size of the RO group has been noticed previously.[95]

Incidentally, $A^{1,3}$ effects of this type in reactions of α-carbonyl radicals, in which the radical center in the ring bears a RCH_2 substituent and is adjacent to a stereogenic center in the ring (Scheme 32b[290]), were first noticed in 1977.[313]

The *cis* selectivity of reactions that proceed via acyliminium ions (Scheme 29d) can be traced back to, amongst other things, the barrier to rotation of the RCO–N bond, which is much lower for cations than for amides (by roughly one-third), and hence the $A^{1,3}$ effect no longer dominates the course of the reaction.[62, 183, 196]

9.4. Protecting Groups Are Not Just Passive Spectators!

Numerous examples have confirmed one observation: a protecting group can have differing influences on the course of a reaction at a neighboring functional group—it is certainly not simply a spectator. For example, the diastereoselectivity of reactions of the Li-enolate of *N*-acyl-2-*tert*-butyl-1,3-oxazolidine-5-ones is extremely dependent upon the nature of the acyl group (Scheme 33[314]). It can be seen from the structures of enol

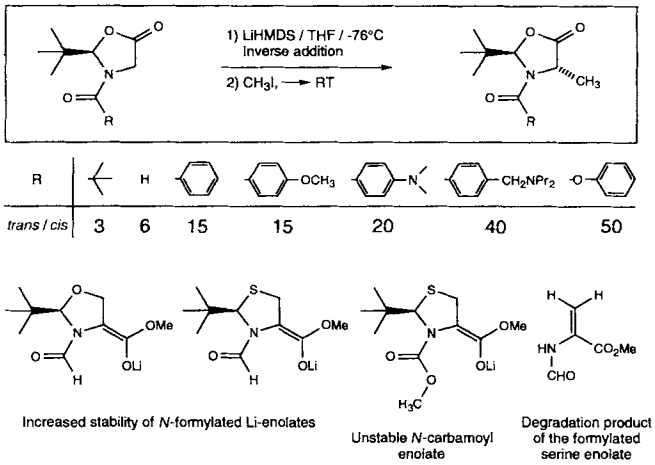

Scheme 33. The influence of "protecting" groups on the course of the reaction. Top: The diastereoselectivity of methylation of a range of N-protected 2-*tert*-butyl-1,3-oxazolidin-5-ones varies from 3:1 to 50:1. Bottom: The stability of enolates of 2-*tert*-butyl-1,3-oxazolidine and -thiazolidine carboxylic esters is highly dependent on the nature of the *N*-acyl group. The reaction of the aldehyde $CH_3CH{=}CHCH_2CF(CH_3)CHO$, shown in Scheme 25, with a variety of Li-enolates of *N*-acylated 2-*tert*-butyl-1,3-oxazolidin-5-ones is a further example of the influence of *N*-acyl groups on enolate reactions of these types of heterocycles: Use of allyloxy-, benzyloxy-, and phenyloxycarbonyl-substituted oxazolidinones did not lead to the required products; the use of the trichloroethoxycarbonyl protecting group led to the first success. As in all the examples shown in this article, the geometry of the enolate double bond is not known and is drawn arbitrarily. For details about the *cisoid* arrangement of the carbonyl oxygen atom of the *N*-acyl group and the acetal center, see also the legend of Scheme 31; to date, the conformation of the *N*-formyl group has not been determined.

derivatives of such heterocycles (Scheme 31 bottom[315]) that the substituent at the carbonyl C atom of the acyl group could formally be in contact with the atoms and groups involved in the transition sate of an S_N2 reaction. This also applies to the acyl groups of the oxazolidine and thiazolidine carboxylic esters (Scheme 33 bottom): The *N*-formyl derivative is more stable than the carbamoyl analog possibly because the formyl-substituted enolate has less $A^{1,3}$ strain than the carbamoyl derivative[316] and not only because the formyl group is more electron-withdrawing.

10. Concluding Remarks

The principle of the self-regeneration of stereocenters has led not only to the increase in the synthetic potential of readily available, chiral synthetic building blocks such as naturally occurring amino acids, but also to the development of simple, synthetic, heterocyclic starting materials which are available by resolution of racemic mixtures. There is very little risk involved in predicting that the SRS principle will find many more applications and that the chiral acetals, which are now also commercially available in large quantities, will be employed more and more frequently in EPC synthesis.

The enthusiastic work of many graduate students and postdoctoral co-workers over the last 15 years has led to the results of our group described in this article. D. S. expresses his deepest thanks to them all; their names are given in the list of references. The following people are due special thanks: Reto Naef[317] *for his crucial contributions during the conception of the SRS principle and also Robert Fitzi,*[318] *Stefan Müller, Urs Gysel,*[319] *and Joachim Kinkel*[320] *for solving the problems related to the resolution of racemic mixtures of glycine acetals. We thank the following companies for their generous donations of chemicals: BASF AG (Ludwigshafen, Germany; pivalaldehyde), Degussa AG (Hanau, Germany; amino acids and Boc-BMI), Zeneca Bio Products (Billingham, UK; PHB and BIOPOL). We are very grateful to Sandoz Pharma AG (Basel, Switzerland) for their generous financial support of our research group over so many years. S. Sigrist and M. Graedel are thanked for their considerable help during the preparation of this manuscript. Finally, we also acknowledge Privatdozent Dr. Volker Gramlich, the organizer of the crystallography laboratory courses at ETH-Zürich, where so many of the crystal structures were solved; his work has had so much significance, in so many different ways, on the work from our laboratories described here.*

Received: March 7, 1996 [A153IE]
German version: *Angew. Chem.* **1996**, *108*, 2880–2921
Translated by Dr. Jennifer L. Matthews, Zürich (Switzerland)

Appendix

The following abbreviations are used in the tables: All = $H_2C{=}CHCH_2$; Alloc = $H_2C{=}CHCH_2OCO$; Bn = $PhCH_2$; Boc = *t*BuOCO; Bz = PhCO; MOM = CH_3OCH_2; TBS = TBDMS = *tert*-butyldimethylsilyl; TBDPS = *tert*-butyldiphenylsilyl; Z = $PhCH_2OCO$.

Table A. Examples of the α-alkylation of a variety of amino-, hydroxy-, and sulfanylcarboxylic acids according to Scheme 5. In many cases the heterocyclic alkylation products were not hydrolyzed to give the corresponding α-,α-disubstituted, α-heterosubstituted carboxylic acids. Some examples of carboxylic acid derivatives prepared in this manner and some applications in natural product synthesis are shown in Scheme 7 and 8.

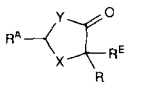

R	R^A	X	Y	R^E
Alanine				
Me	*t*Bu	NBz	NMe	Et [64], Bn [64], 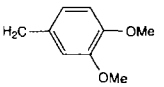 [64], CH_2(Boc-Indolyl) [120], $CH(Me)CH_2NO_2$ [123]
Me	Ph	NBoc	NMe	*i*Pr [321]
Me	*t*Bu	NBz	O	Allyl [322], Ph [119], Bn [70], CH_2(Boc-Indolyl) [120]
Me	Ph	NBz	O	Et [323], CH_2CO_2Et [113]
Me	Ph	NZ	O	H [324,325], Bn [324,325], CH_2CO_2tBu [326], $(CH_2)_2CO_2tBu$ [326], $(CH_2)_4N(Boc)_2$ [326]
Me	2,4-$Cl_2C_6H_3$	NZ	O	Bn [324,325]
Me		$NCOtBu$	O	Bn [327]
Valine				
*i*Pr	*t*Bu	NBz	NMe	D [64], Me [64], Et [64], Allyl [64]
*i*Pr	*t*Bu	NBz	O	Me [70], Bn [70]
*i*Pr	Ph	NBz	O	CH_2CO_2Et [113]
*i*Pr	*t*Bu	NAlloc	O	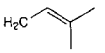 [328]
*i*Pr	Ph	NZ	O	Me [329]
Leucine				
*i*Bu	*t*Bu	NAlloc	O	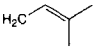 [328]
*i*Bu	Ph	NZ	O	Et [329]
Isoleucine				
$CH(Me)CH_2Me$	Ph	NZ	O	Me [329]
Methionine				
$(CH_2)_2SMe$	*t*Bu	NBz	NMe	D [223], Me [64,223], Et [64,223], *i*Pr [223], CHMe(OH) [71]
$(CH_2)_2SMe$	*t*Bu	NH	NMe	$C(Me)_2OBz$ [71], CHPhOBz [71]
$(CH_2)_2SMe$	*t*Bu	NBz	O	Me [70,72], CH_2CN [330], CH_2(Boc-Indolyl) [120], CHMe(OH) [71], 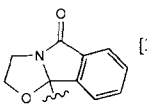 [330]
$(CH_2)_2SMe$	Ph	NBz	O	CH_2CO_2Et [113]
Phenylalanine				
Bn	*t*Bu	NBz	O	Me [70], CHPh(OH) [70]
Bn	Ph	NBz	O	CH_2CO_2Et [113]
Bn	Ph	NZ	O	Me [324,325], CH_2COR (R = Cl, OH, $OCHPh_2$) [331], $(CH_2)_2OH$ [332], $CH_2COC(CO_2Et)=PPh_3$ [331]
Bn	2,4-$Cl_2C_6H_3$	NZ	O	D [324,325], Me [324,325]
Bn	*t*Bu	NAlloc	O	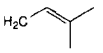 [328]
Aspartic acid				
CH_2CO_2H	*t*Bu	NBz	NMe	D [114], Me [114], Bn [114]
Glutamic acid				
$(CH_2)_2CO_2H$	*t*Bu	NBz	NMe	D [114], Me [114], Bn [114]
Lysine				
$(CH_2)_4NHZ$	*t*Bu	NBz	NMe	Me [120], Bn [120], CHMe(OH) [120], CHPh(OH) [120]
$(CH_2)_4NHBoc$	*t*Bu	NBz	O	Me [120]
$(CH_2)_4NHZ$	Ph	NZ	O	*i*Pr [329]
Ornithine				
$(CH_2)_3NHZ$	*t*Bu	NBz	NMe	Me [120]
$(CH_2)_3NHZ$	Ph	NZ	O	Et [329]
Vinylglycine				
$CH=CH_2$	*t*Bu	NBz	NMe	D [223], Me [223], Et [223], Allyl [223], Bn [223], $CMe_2(OH)$ [71], CHMe(OH) [71]

Table A. (continued)

R	R^A	X	Y	R^E
2-Aminohexanoic acid				
Bu	Ph	NBz	O	CH_2NPhthaloyl [122]
Tyrosine				
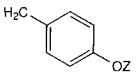	Ph	NZ	O	Me [329]
DOPA				
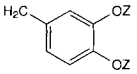	Ph	NZ	O	Me [329]
Tryptophan				
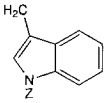	Ph	NZ	O	Et [329]
Lactic acid				
Me	*t*Bu	O	O	Et [43,47], Pr [47], Bu [42,47], Heptyl [47], Allyl [42,43,47,126,333], Bn [43,47], $CH_2CBr{=}CH_2$ [124], CH_2CONMe_2 [47], $(CH_2)_3C(OMe)_2Me$ [46], $CMe_2(OH)$ [43,47], $C(CH_2)_4(OH)$ [43,47], $CPh_2(OH)$ [43,47], CPh(OH)Me [43,47], CHMe(OH) [43,47], CHEt(OH) [47], CH*t*Bu(OH) [43,47], $CH(OH)CH_2{=}CHPh$ [47], CHPh(OH) [43,47], $(CH_2)_2NO_2$ [123], $CH(Me)CH_2NO_2$ [123], $CH(Et)CH_2NO_2$ [123], $CH(CH_2Br)CH_2NO_2$ [123], $CH(Ph)CH_2NO_2$ [123], 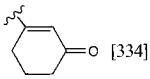 [334], [47], [334], 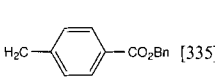 [335], 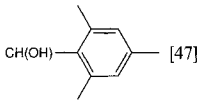 [47]
3-Chlorolactic acid				
CH_2Cl	*t*Bu	O	O	(R = H, Me) [336]
3-(2,5-Dimethoxy)phenyllactic acid				
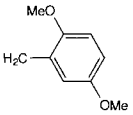	*t*Bu	O	O	CH_2COR (R = Cl, OH) [337]
3,3,3-Trifluorolactic acid				
CF_3	*t*Bu	O	O	Me [250]
2-Hydroxybutanoic acid				
Et	*t*Bu	O	O	Allyl [128]
2-Hydroxy-3-methylbutanoic acid				
*i*Pr	*t*Bu	O	O	CHMe(OH) [125, 338]
Malic acid				
CH_2CO_2H	*t*Bu	O	O	Me [47], CD_3 [126], Allyl [47], $CH(Me)CH_2NO_2$ [123], Bn [47], 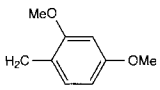 [337]
Mandelic acid				
Ph	*t*Bu	O	O	D [339], Me [42], Pr [42,43,47], CH_2Cl [336], Allyl [42], $CH(Me)CH_2NO_2$ [123]
Ph	*i*Pr	O	O	Me [42]
Ph	Me	O	O	D [339]
Ph	Et	O	O	D [339]
Ph	Me	O	NMe	D [339]
Ph	Ph	O	NMe	D [339]
3-Methylphenylglycolic acid				
3-MePh	*t*Bu	O	O	CH_2Cl [336]
3-Phenyllactic acid				
Bn	*t*Bu	O	O	Me [47], Et [47], Pr [47], Allyl [47]

Table A. (continued)

R	R^A	X	Y	R^E
Thiolactic acid				
Me	*t*Bu	S	O	Et [121], Allyl [47, 121], Bn [121], $CMe_2(OH)$ [121], CHPh(OH) [121], CHMe(OH) [121], $CMe(CH{=}CH_2)(OH)$ [121], $(CH_2)_2COMe$ [121]
4-Methyl-2-sulfanylpentanoic acid				
*i*Bu	*t*Bu	S	O	Me [121], Bn [121]
(3*S*)-3-Methyl-2-sulfanylpentanoic acid				
$CH(Me)CH_2Me$	*t*Bu	S	O	Me [121], Bn [121]
Thiomandelic acid				
Ph	*t*Bu	S	O	Me [121], Bn [121]
3-Phenylthiolactic acid				
Bn	*t*Bu	S	O	Me [121]

Table B. Examples of α-alkylations of bicyclic derivatives of azetidine carboxylic acids, proline, hydroxyproline, and cysteine, shown in Scheme 6, to give products of type **2**. These reactions proceed with retention of configuration.

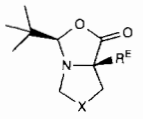

2

X	R^E
Azetidinecarboxylic acid	
–	D [86], CHMe(OH) [86], [86], 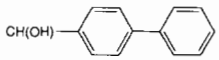 [86], 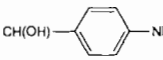 [86], 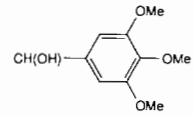 [86], 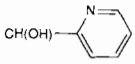 [86], 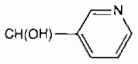 [86], 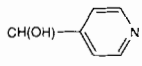 [86]
Proline	
CH_2	D [45], Me [45, 117, 118], Allyl [43, 45, 118, 127], Ph [45], PhS [45], Bn [45, 118], CH_2NMe_2 [45], CH_2CO_2Me [45], CH_2CONMe_2 [45], CHMe(OH) [45], $CHtBu(OH)$ [45], $CMe_2(OH)$ [45], $CMe(OH)CH_2CO_2Me$ [45], Ac [45], Bz [45], CO_2Me [45], 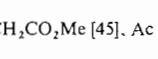 [340], [45], 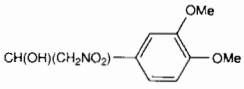 [45], 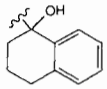 [45], 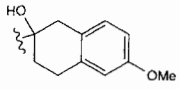 [45], 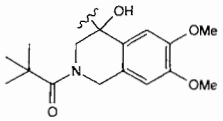 [45], [45], 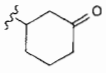 [45], 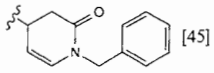 [45]
Hydroxyproline	
CHOAc	D [87], Me [87], Allyl [87], Bn [87], CHMe(OH) [87], [87]
Cysteine	
S	[89], [89], [89], 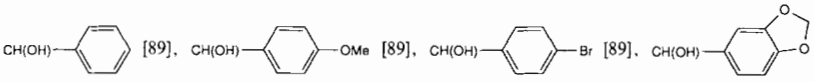 [89], [89], [89], [89], 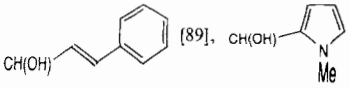 [89], [89]

Table C. Examples of the imidazolidine, oxazolidine, and thiazolidine derivatives **3**, depicted in Scheme 6d, which were obtained by alkylation of enolates having exocyclic double bonds (Scheme 6e, left). It should be noted that, in the case of cysteine, a satisfactory yield can only be obtained when the nitrogen atom in the ring is protected by a formyl group (in addition, see refs. [104–109], the discussion in ref. [111], Scheme 33 bottom).

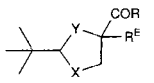

3

X	Y	R	R^E
Serine			
O	NCHO	OMe	D [93], Me [93], Et [93], Allyl [93], Bn [93], $CMe_2(OH)$ [93], Bz [93], C_9H_{19} [330], $C_{15}H_{31}$ [330], $CH_2CH{=}CH(CH_2)_{12}Me$ [330], $CO(CH_2)_{16}Me$ [341], 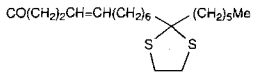 [341]
O	NCHO	OBn	C_9H_{19} [330]
O	NBn	OMe	CH*i*Pr(OH) [129]
Glyceric acid			
O	O	S*t*Bu	D [93], Allyl [93], Bn [93], $CMe_2(OH)$ [93], CHMe(OH) [93], CHPh(OH) [93], CH(CH=CHPh)(OH) [93], CMePh(OH) [93]
Cysteine			
S	NCHO	OMe	Me [105–109], Et [106], Bn [106], Allyl [106], CH_2CO_2Me [106]
2,3-Diaminopropanoic acid [342]			
NMe	NBoc	OMe	D [99], Me [99], Et [99], *i*Pr [99], Bu [99], Allyl [99], Bu [99], SPh [99], SePh [99], OH [99], $CHRCH_2COCPh_3$ (R = Me, Ph) [255]

Table D1. Products of Michael and radical additions to derivative **5**, which has an exocyclic double bond. The preparation of **5** is outlined in Scheme 9a,b; a few of these products are shown at the top of Scheme 10a. R^2 denotes the newly introduced substituent. Some selected examples of products of this type can also be found in Scheme 12.

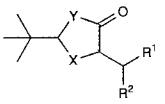

X	Y	R^1	R^2
NBoc	NMe	H	Me [253], Bu [253]
NBoc	NMe	Me	Me [253], Et [253], Bu [253], Ph [253]
NBoc	NMe	Me	Et [253], Bu [253], Ph [253]
NBoc	NMe	Pr	Bu [253]
NCOPh	O	H	Me [139,172], Pr [172], *t*Bu [139,172], CH_2OMe [172], CH_2CO_2Me [172], $C(Me)_2NO_2$ [343], $(CF_2)_3CF_3$ [172], Bn [139], Adamantyl [172], Tetra-*O*-acetylglucosyl [172], *c*-C_6H_{11} [172], 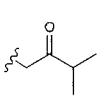 [176], [176], [176]
NCOPh	NMe	H	*c*-C_6H_{11} [139]
NCOMe	O	H	*c*-C_6H_{11} [172]
NCOBn	O	H	*c*-C_6H_{11} [172]
NCO(1-Naphthyl)	O	H	*c*-C_6H_{11} [172]
NCOOMe	O	H	*c*-C_6H_{11} [172]
NCOOPh	O	H	*c*-C_6H_{11} [172]
NCOOBn	O	H	*c*-C_6H_{11} [172]
O	O	CO_2Et	Me [344], Et [344], Bu [344], *t*Bu [344], *c*-C_6H_{11} [344]
O	O	H	Bn [136], $(CH_2)_2Ph$ [136], *c*-C_6H_{11} [136]

Table D2. Products of Michael addition to derivative **6**, which has an endocyclic double bond. The preparation of **6** is outlined in Scheme 9c; a few of these products are shown at the bottom of Scheme 10a. Some selected examples of products prepared in this manner can be found in Schemes 12 and 14a (see also Scheme 15).

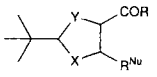

X	Y	R	R^{Nu}
NMe	NBoc	OMe	Bu [99]
NMe	NBoc	Ph	Ph [99]
O	NCO_2Me	OMe	Bu [140]
S	NCO_2Me	OMe	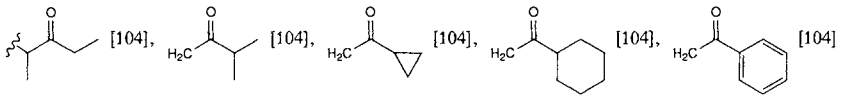 [104], [104], [104], [104], [104]
S	NCO_2Bn	OMe	Bu [104]

Table D3. Products of Michael addition to derivative **7**, which has an endocyclic double bond. The preparation of **7** is outlined in Scheme 9d; a few of these products are shown in Scheme 10b. Some examples of products shown here can be found in Schemes 12, 13, and 14b.

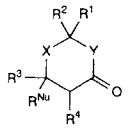

X	Y	R^1	R^2	R^3	R^4	R^{Nu}
NAc	NMe	H	*t*Bu	H	H	Bu [147]
O	O	H	*t*Bu	CF_3	H	Me [157], CD_3 [157], Et [157], Pr [157], *i*Pr [157], Bu [157], *t*Bu [157], $CH_2CH{=}CH_2$ [157], Ph [157], Bn [157]
O	O	H	*t*Bu	Me	H	Me [152], CD_3 [152], Et [152], Pr [152], Bu [152], Oct [152], Ph [152], $CH_2CH{=}CH_2$ [152]
O	O	H	*t*Bu	Me	Me	Me [153], Bu [153], Ph [153]
O	O	H	*t*Bu	Me	Et	Me [153], Bu [153], Ph [153]
O	O	H	*t*Bu	Me	Pr	Me [153], Bu [153]
O	O	H	*t*Bu	Me	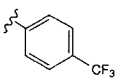	Me [153]
O	O	H	*t*Bu	Et	H	Me [152]
O	O	H	*t*Bu	$CH_2OTBDMS$	H	Bu [152]
O	O	H	*t*Bu	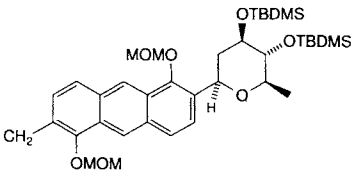	H	Me [179]
O	O	Me	*t*Bu	Me	H	Et [161, 162], Bu [161, 162]
O	O	H	Ph	H	H	Pr [244], Dec [244]
O	O	H	Ph	Me	H	Bu [244], Ph [244]

Table D4. Structural formulas of products of cycloaddition reactions (Diels–Alder reactions, [2 + 2] cycloadditions) of compounds **5–7** (Scheme 9). See also Schemes 10, 12, and 13.

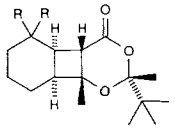

(R = H; R,R = OCH_2CH_2O)
[161, 162]

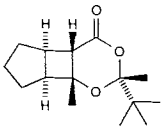

[161, 162]

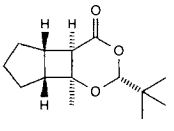

[161, 162]

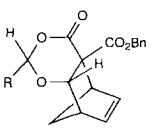

(R = *t*Bu, C_6H_{11})
[345]

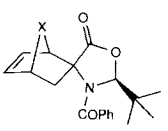

(x = CH_2, $(CH_2)_2$)
[175]

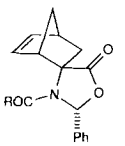

(R = Me, Ph)
[171]

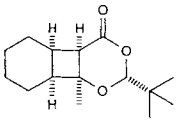

[161, 162]

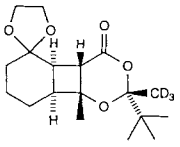

[162]

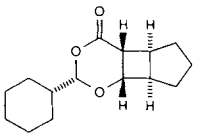

[345]

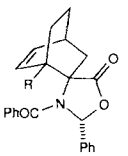

(R = H, OMe, OTMS) [171]

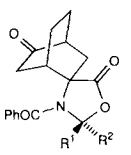

R^1 R^2 [171]
H Ph
Ph H

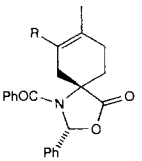

(R = H, Me)
[171]

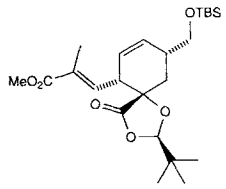

[347]

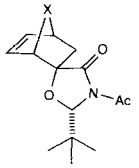

(X = CH_2, $(CH_2)_2$)
[137]

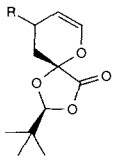

(R = H, CO_2Et)
[174]

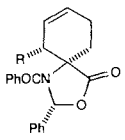

(R = Me, OMe)
[171]

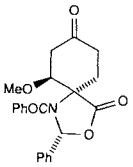

[171]

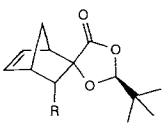

(R = H [346], CO_2Et [163])

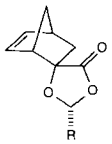

(R = *t*Bu, C_6H_{11})
[173, 138]

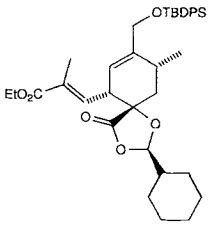

[348]

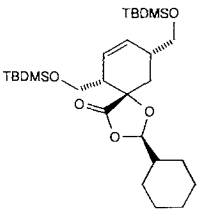

[137]

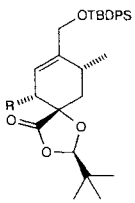

(R = $CH{=}CHCO_2Me$, $CH{=}CH(CH_2)_5OTBDMS$)
[169]

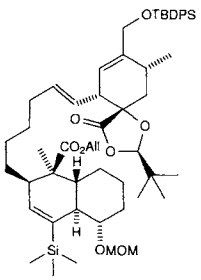

[170]

Table E. Some products obtained by the reaction of enolates of Boc-BMI, Z-BOX, and other similar heterocyclic acetals of type **11** (Schemes 21, 23, 25, and 33). In most cases, products with R^1 or R^2 + H were prepared by carrying out a second alkylation of the monoalkylated product in situ, without isolation of the intermediate product (see Scheme 26 and text). A few of these compounds are also shown in Scheme 24.

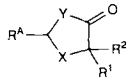

R^A	X	Y	R^1	R^2
*t*Bu	NBoc	NMe	Allyl [240], Br [134], Bn [81], CH_2CN [240], CH_2CO_2Me [81], $CHMe(OH)$ [258], $CHEt(OH)$ [258], $CH(OH)(C_7H_{15})$ [258], $CH(Me)Ph$ [240], $CH(Me)CH_2NO_2$ [240], $(CH_2)_2Ph$ [240], $CH_2CH{=}CHMe$ [240], $CH_2C(CO_2Me){=}CH_2$ [240], $(CH_2)_3Cl$ [240], $(CH_2)_4Cl$ [240], $(CH_2)_5Cl$ [81], $(CH_2)_2{}^{11}CN$ [349], $(CH_2)_3{}^{11}CN$ [349], $(CH_2)_2CO_2tBu$ [254], $CH(Me)CH_2CO_2Me$ [254], $CH(Me)CH_2CO_2Et$ [254], $CHRCH_2COCPh_3$ (R = Me, Ph) [255], [240], 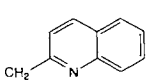 [350], 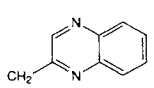 [350],	H

Table E. (continued)

R^A	X	Y	R^1	R^2
*t*Bu	NBoc	NMe	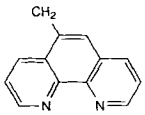 [350], 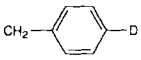 [81], 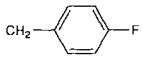 [81], 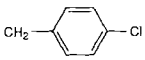 [81,351], 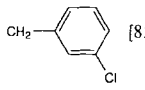 [81], 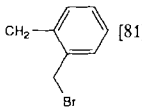 [81], 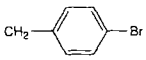 [81,240], 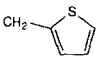 [81], 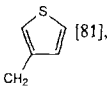 [81], 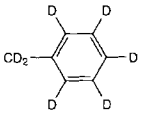 [81], 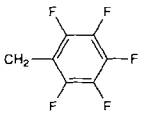 [81,240], 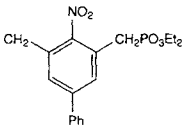 [352], 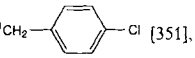 [351], 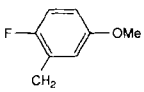 [353], 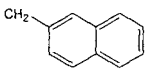 [81], 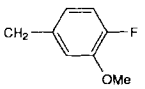 [353], 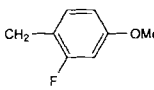 [353], 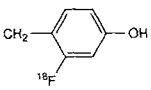 [354], 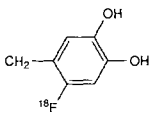 [355], 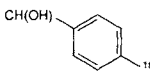 [356], 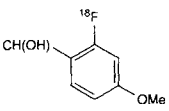 [356], 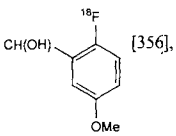 [356], 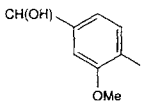 [356], 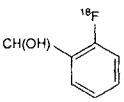 [356], 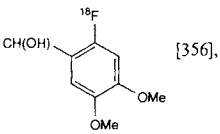 [356], 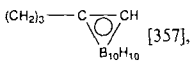 [357], 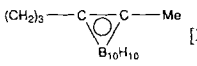 [357], 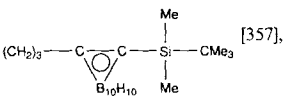 [357], 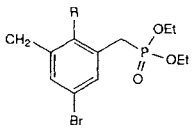 (R = H, OAc) [352], 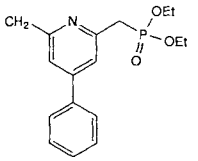 [352], 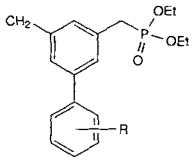 (R = H, 4-F, 4-Ph, 3-NHAc) [242], 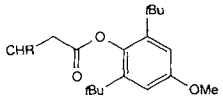 (R = Me, Et, *i*Pr, Ph, Bn) [254]	H
*t*Bu	NMe	NBoc	Me [99]	H
*i*Pr	NBoc	NMe	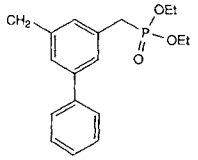 [242]	H

Table E. (continued)

R^A	X	Y	R^1	R^2
*t*Bu [358]	NBz	NMe	Me [71,224], *i*Pr [71,224], Bu [71,224], Allyl [359], $(CH_2)_2OH$ [240], $(CH_2)_3Br$ [360], $(CH_2)_3PO(OH)_2$ [361], Bn [71,224], 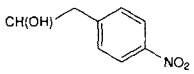 [362]	H
*t*Bu	NZ	NMe	Me [71], *i*Pr [240], CH_2CO_2Me [240], CH_2CO_2Et [240], CH_2SiMe_3 [240], CHPh(OH) [71]	H
*t*Bu	NZ	NCH_2CO_2Et	Allyl [234], [234], 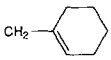 [234], [234], 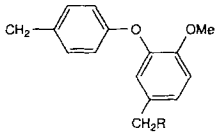 (R = Br, OH, OTBDPS) [234]	H
*t*Bu	NZ	NCH_2CO_2Et	Me [230,232], Et [230,232]	H
*t*Bu	NZ	$NCH(Me)CO_2Me$	Me [230,232]	H
*t*Bu	NZ	NCH_2CO-Gly-OMe	Me [234], Bn [234], 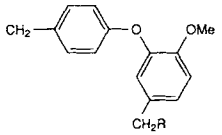 (R = Br, OH, OTBDPS) [234], 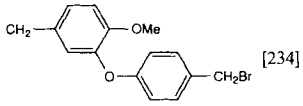 [234]	H
*t*Bu	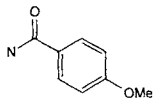	NMe	Me [71]	H
*i*Pr	NBz	NMe	Me [71]	H
*i*Pr	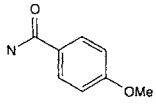	NMe	Me [71]	H
*i*Pr	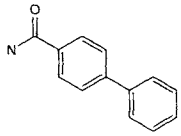	NMe	Me [71]	H
*t*Bu	NCHO	O	Me [82]	H
*t*Bu	NCO*t*Bu	O	Me [82]	H
*t*Bu	NBz	O	Me [82], Bu [82], Bn [82]	H
*t*Bu	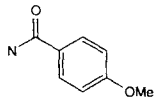	O	Me [82]	H
*t*Bu	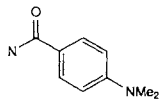	O	Me [82], Et [82], Allyl [82], Bn [82]	H
*t*Bu	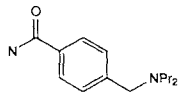	O	Me [82], Et [82]	H
*t*Bu	NCO_2Ph	O	Me [82], Allyl [82], Bn [82]	H
*t*Bu	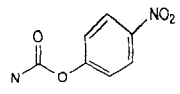	O	Me [82]	H
Ph	NBoc	O	Me [247], 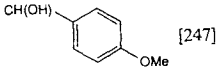 [247]	H

R^	X	Y	R¹	R²
*t*Bu [363]	NZ	O	CH(OH)Et [246], CH(OH)*i*Pr [246], CH(OH)Ph [246], 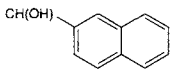 [246], 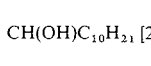 [246], 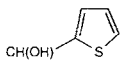 [246], 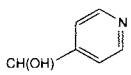 [246], 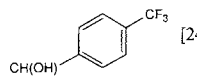 [246], 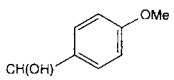 [246], 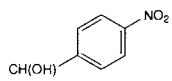 [246], 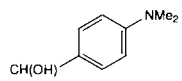 [246], 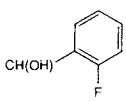 [246], 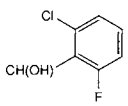 [246], 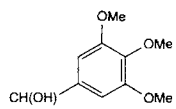 [246]	H
*t*Bu	NBoc	NMe	Me [81], Et [81], CH_2*i*Pr [81], Bn [81], $CD_2C_6D_5$ [81]	D
*t*Bu	NBoc	NMe	Me	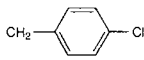 [351], 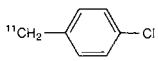 [259, 351], 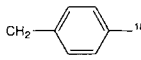 [356], 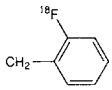 [356], 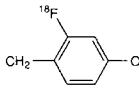 [356], 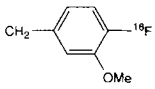 [356], 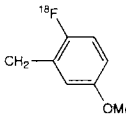 [356], 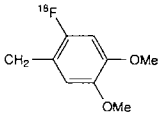 [356]
*t*Bu	NBoc	NMe	Et	Allyl [240]
*t*Bu	NBoc	NMe	Et [81]	$(CH_2)_2Cl$
*t*Bu	NBoc	NMe	Me [81], Et [81]	$(CH_2)_4Cl$
*t*Bu	NBoc	NMe	Me [81]	$(CH_2)_5Cl$
*t*Bu	NBoc	NMe	Me	Et [82], 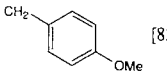 [82]
*t*Bu	NBoc	NMe	Bn	*i*Pr [82], 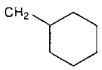 [82]
*t*Bu	NBoc	NMe	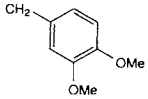	Et [82], *i*Pr [82], Bn [82], 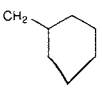 [82]

Table E. (continued)

R^A	X	Y	R^1	
*t*Bu	NBz	O	Me	Et [82], 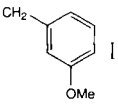
				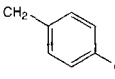
*t*Bu	NBz	O	Bn	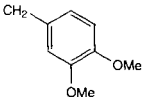
*t*Bu	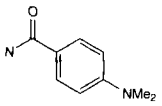	O	Me	Allyl [82]
*t*Bu	NCO_2Ph	O	Me	Et [82], Bn [82], Allyl [82

Table F. Stereochemical course of the aldol addition of cyclic enolates **a**–**o** to aldehydes **u**, and the Michael addition to α,β-unsaturated carbonyl compounds **v** and nitroolefins **w** [364]. The primary adducts are presented as Newman projections and as Zimmerman–Traxler diagrams on the right side of the table. The substituent R^4 is always equatorial in case **A** and axial in case **B** for the adducts shown in the chair conformation (see the discussion in the text and Scheme 29e).

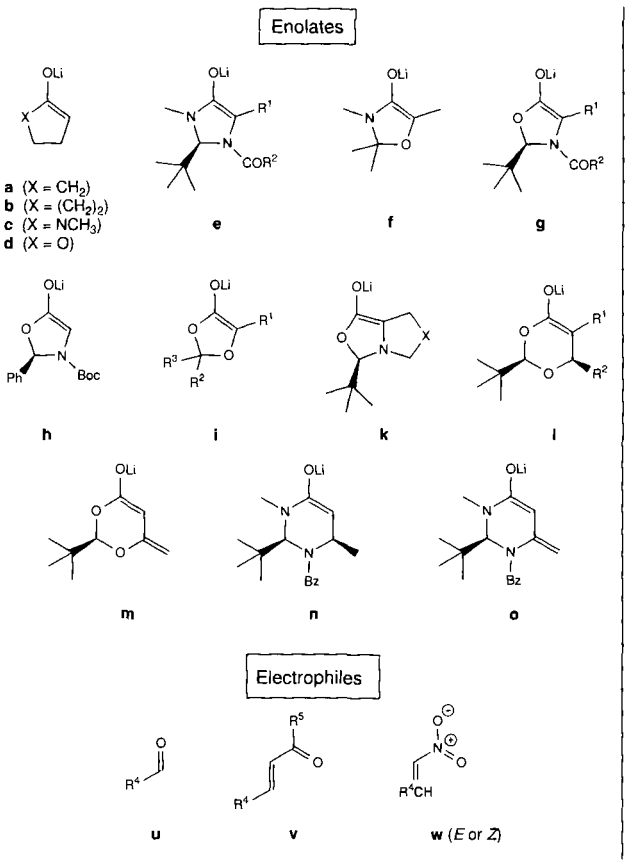

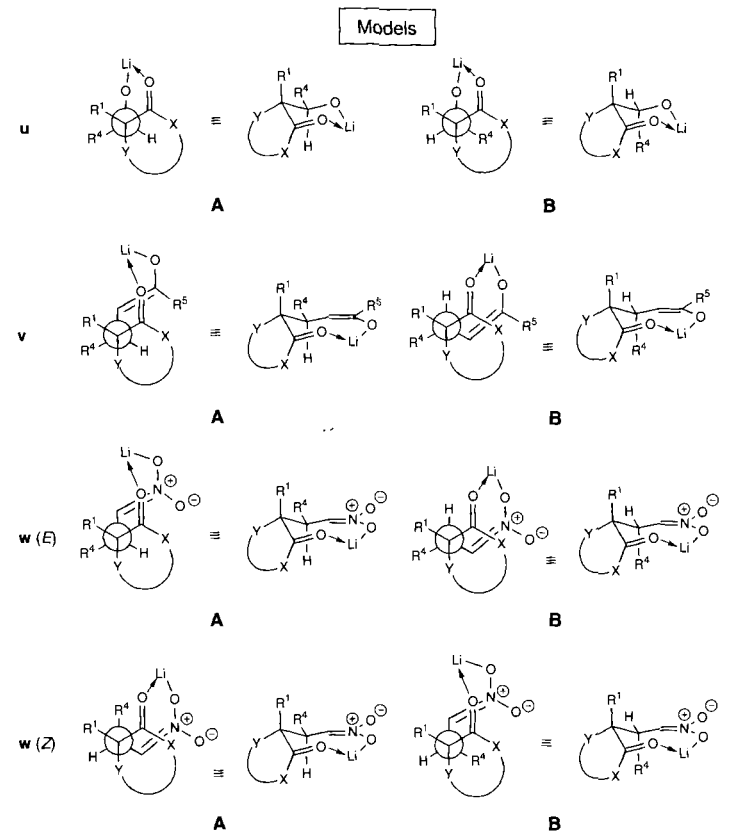

Enolate R^1	R^2	R^3	X		Electrophile R^4	R^5	Config.	Model	Selectivity [a]	Ref.
a				**u**	Aryl			**A**	+ +	[22, 39, 366, 367]
a				**w**	Me		(*E*)	**A**	+ +	[368]
a				**w**	Me		(*Z*)	**B**	+ +	[368]
b				**u**	Aryl			**A**	+ + +	[22, 39, 366, 367]
b				**w**	Me		(*E*)	**A**	+ +	[368]
b				**w**	Me		(*Z*)	**B**	+ +	[368]

Table F. (continued)

	Enolate				Electrophile					
	R^1	R^2	R^3	X	R^4	R^5	Config.	Model	Selectivity [a]	Ref.
c				**v**	Me	Aryl		**B**	+ to + + +	[369]
c				**v**	Alkyl	Alkyl		**B**	+ +	[369]
d				**u**	Aryl			**A**	+	[370]
e	H	Ph		**u**	Alkyl			**B**	+ + +	[71]
e	H	Ph		**u**	Aryl			**B**	+ + +	[71]
e	$(CH_2)_2SMe$	Ph		**u**	Alkyl			**B**	+ + +	[71]
e	$(CH_2)_2SMe$	Ph		**u**	Aryl			**B**	+ + +	[71]
e	H	O*t*Bu		**u**	Alkyl			**B**	+ to + + +	[134, 258]
e	H	O*t*Bu		**v**	Alkyl	OAlkyl		**A**	+ +	[254]
e	H	O*t*Bu		**v**	Alkyl, Aryl	OAryl		**A**	+ + +	[254]
e	H	O*t*Bu		**w**	Me		(*E*)	**B**	+ +	[240, 318]
f				**u**	Aryl			**A**	+	[302]
g	$(CH_2)_2SMe$	Ph		**u**	Me			**B**	+ + +	[71]
g	H	OBn		**u**	Alkyl, Aryl			**B**	+ + +	[246]
h				**u**	Aryl			**B**	+ + +	[247]
i	Me	H	H	**u**	Alkyl, Aryl			**A**	+	[302]
i	Me	Me	Me	**u**	Alkyl, Aryl			**A**	+	[302]
i	Me	*t*Bu	H	**u**	Alkyl			**B**	+ to + +	[43, 47]
i	Me	*t*Bu	H	**u**	Aryl			**B**	+ to + + +	[43, 47]
i	Me	*t*Bu	H	**w**	Me		(*E*)	**A**	+ + +	[123]
i	Me	*t*Bu	H	**w**	Me		(*E*)	**A**	+	[123]
i	Ph	*t*Bu	H	**w**	Me		(*E*)	**A**	+ + +	[123]
i	CH_2CO_2Li	*t*Bu	H	**w**	Me		(*E*)	**A**	+ +	[123]
k				–	Me			**A**	+ + +	[45]
k				–	Aryl			**A**	+ +	[86]
k				CH_2	Alkyl, Aryl			**A**	+ + +	[86]
k				S	Aryl			**A**	+ + +	[89]
l	H	Me		**u**	Alkyl			**A**	+ to + +	[178, 280]
l	H	Me		**u**	Aryl			**A**	+ +	[280]
l	H	CF_3		**u**	Alkyl			**A**	+ + +	[293]
m				**u**	Alkyl			**A**	+ + +	[264, 265]
n				**u**	Alkyl, Aryl			**A**	+	[143]
o				**u**	Me			**B**	+	[143]
o				**u**	Aryl			**B**	+ + +	[143]

[a] + : < 60% *ds*; + + : 60–80% *ds*; + + + : > 80% *ds*.

[1] C. K. Ingold, *Structure and Mechanism in Organic Chemistry*, Cornell University Press, Ithaca, London, **1969**; P. R. Schreiner, P. von R. Schleyer, R. K. Hill, *J. Org. Chem.* **1994**, *59*, 1849–1854.

[2] S. E. Godtfredsen, J. P. Obrecht, D. Arigoni, *Chimia* **1977**, *31*, 62–63; S. E. Godtfredsen, Dissertation No. 6243, ETH, Zürich, **1978**.

[3] D. J. Cram, *Fundamentals of Carbanion Chemistry*, Academic Press, New York, London, **1965**, pp. 85–135; Inversion of configuration (i.e. racemization without loss of deuterium in a protic medium) has been observed in similar systems when other bases are used. Cram has suggested that the term "conducted tour mechanism" be used to describe such reactions.

[4] Initially, Ramig et al. suggested that the decarboxylation described proceeds with inversion of configuration: L. A. Rozov, K. Ramig, *Tetrahedron Lett.* **1994**, *35*, 4501–4504; K. Ramig, L. Brockunier, P. W. Rafalko, L. A. Rozov, *Angew. Chem.* **1995**, *107*, 254–255; *Angew. Chem. Int. Ed. Engl.* **1995**, *34*, 222–223. However, Schurig et al. have recently shown that this occurs with retention and not with inversion of configuration: V. Schurig, M. Juza, B. S. Green, J. Horakh, A. Simon, *Angew. Chem.* **1996**, *108*, 1814–1816; *Angew. Chem. Int. Ed. Engl.* **1996**, *35*, 1660–1682. A mechanistic discussion on stereoselective decarboxylation, C–C bond cleavage, and proton transfers of this type can be found in Cram's classic textbook [3].

[5] M. Schlosser, *Struktur und Reaktivität polarer Organometalle*, Springer, Berlin, **1973**; "Are Polar Organometallic Compounds "Carbanions"? The Gegenion Effect on Structure and Energies of Alkali-Metal Compounds": C. Lambert, P. von R. Schleyer, *Angew. Chem.* **1994**, *106*, 1187–1199; *Angew. Chem. Int. Ed. Engl.* **1994**, *33*, 1129–1140.

[6] R. E. Gawley, Q. Zhang, *Tetrahedron* **1994**, *50*, 6077–6088.

[7] W. C. Still, C. Sreekumar, *J. Am. Chem. Soc.* **1980**, *102*, 1201–1202.

[8] "The Homoaldol Reaction, or How to Overcome Problems of Regio- and Stereoselectivity": D. Hoppe, *Angew. Chem.* **1984**, *96*, 930–946; *Angew. Chem. Int. Ed. Engl.* **1984**, *23*, 932–948; A. Carstens, D. Hoppe, *Tetrahedron* **1994**, *50*, 6097–6108.

[9] An excellent summary of new work in this area can be found in "Mechanistic Aspects of Polar Organometallic Chemistry": *Tetrahedron* **1994**, *50*, 5845–6128. For some work from our group, see refs. [10–12].

[10] D. Seebach, W. Wykypiel, W. Lubosch, H.-O. Kalinowski, *Helv. Chim. Acta* **1978**, *61*, 3100–3102.

[11] D. Seebach, J. Hansen, P. Seiler, J. M. Gromek, *J. Organomet. Chem.* **1985**, *285*, 1–13.

[12] I. M. P. Huber, D. Seebach, *Helv. Chim. Acta* **1987**, *70*, 1944–1954.

[13] For example, the diastereoselective formation of such organometallic derivatives has been demonstrated with Li-dithianes such as **I** ("Umpolung of the Reactivity of Carbonyl Compounds Through Sulfur-Containing Reagents": B.-T. Gröbel, D. Seebach, *Synthesis* **1977**, 357–402; A. G. Abatjoglou, E. L. Eliel, L. F. Kuyper, *J. Am. Chem. Soc.* **1977**, *99*, 8262–8269; R. Amstutz, D. Seebach, P. Seiler, B. Schweizer, J. D. Dunitz, *Angew. Chem.* **1980**, *92*, 59–60; *Angew. Chem. Int. Ed. Engl.* **1980**, *19*, 53–54; R. Amstutz, J. D. Dunitz, D. Seebach, *Angew. Chem.* **1981**, *93*, 487–488; *Angew. Chem. Int. Ed. Engl.* **1981**, *20*, 465–466; "Synthetic Uses of the 1,3-Dithiane Grouping from 1977 to 1988": P. C. Bulman Page, M. B. van Niel, J. C. Prodger, *Tetrahedron* **1989**, *45*, 7643–7677; A. Dondoni, *Advances in the Use of Synthons in Organic Chemistry, Vol. 1*, JAI Press, London, **1993**, pp. 1–49; "2-Lithio-1,3-dithianes": M. Kolb in *Encyclopedia of Reagents for Organic Synthesis, Vol. 5* (Ed.: L. A. Paquette), Wiley, Chichester, **1995**, pp. 2983–2989) and with lithiated dioxanes such as **II**–**IV** (A. I. Meyers, A. L. Campbell, A. G. Abatjoglou, E. L. Eliel, *Tetrahedron Lett.* **1979**, *43*, 4159–4162; D. R. Cheshire in *Comprehensive Organic Synthesis. Selectivity, Strategy, and Efficiency in Modern Organic Chemistry, Vol. 3* (Eds.: B. M. Trost, I. Fleming), Pergamon, Oxford, **1991**, pp. 193–205; S. D. Rychnovsky, K. Plzak, D. Pickering, *Tetrahedron Lett.* **1994**, *35*, 6799–6802).

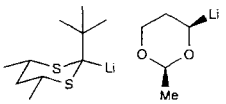

I II III

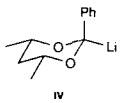

IV

[14] Claude Wintner's definition of retention/inversion is used here: C. E. Wintner, *J. Chem. Educ.* **1987**, *64*, 587–590.

[15] D. Seebach, D. Wasmuth, *Angew. Chem.* **1981**, *93*, 1007–1008; *Angew. Chem. Int. Ed. Engl.* **1981**, *20*, 971. We believe that an aggregate of the achiral enolate and the chiral enolate (shown in Scheme 2a) may be responsible for the observed effect: D. Wasmuth, Dissertation No. 7033, ETH, Zürich, **1982**.

[16] T. Gees, W. B. Schweizer, D. Seebach, *Helv. Chim. Acta* **1993**, *76*, 2640–2653.

[17] Books about named reactions: H. Krauch, W. Kunz, *Reaktionen der Organischen Chemie*, 5th ed. revised and extended by W. Kunz and E. Nonnenmacher, Hüthig, Heidelberg, **1976**; "Organic Name Reactions": *The Merck Index*, 10th ed. (M. Windholz), Merck & Co., Rahway (USA), **1983**, pp. ONR 1–ONR 100; W. Uhl, A. Kyriatsoulis, *Namen- und Schlagwortreaktionen in der Organischen Chemie*, Vieweg, Braunschweig, **1984**; T. Laue, A. Plagens in *Namen- und Schlagwort-Reaktionen der Organischen Chemie*, (Eds.: C. Elschenbroich, F. Hensel, H. Hopf), Teubner, Stuttgart, **1994**; A. Hassner, C. Stumer in *Organic Syntheses Based on Name Reactions and Unnamed Reactions*, Pergamon, New York, **1994**.

[18] B. Beagley, M. J. Betts, R. G. Pritchard, A. Schofield, R. J. Stoodley, S. Vohra, *J. Chem. Soc. Chem. Commun.* **1991**, 924–925.

[19] T. Kawabata, T. Wirth, K. Yahiro, H. Suzuki, K. Fuji, *J. Am. Chem. Soc.* **1994**, *116*, 10809–10810.

[20] "Memory of Chirality": T. Kawabata, K. Fuji, *J. Synth. Org. Chem. Jpn.* **1994**, *52*, 589–595. Some further examples of reactions of this type are mentioned in this article.

[21] "Crystal Structures and Stereoselective Reactions of Organic Lithium Derivatives": D. Seebach, *Proceedings of The Robert A. Welch Foundation Conferences on Chemical Research. XXVII Stereospecificity in Chemistry and Biochemistry*, Houston, TX, **1984**, pp. 93–145.

[22] "Structure and Reactivity of Lithium Enolates. From Pinacolone to Selective C-Alkylations of Peptides. Difficulties and Opportunities Afforded by Complex Structures": D. Seebach, *Angew. Chem.* **1988**, *100*, 1685–1715; *Angew. Chem. Int. Ed. Engl.* **1988**, *27*, 1624–1654.

[23] "Enantioselective Aldol and Michael Additions of Achiral Enolates in the Presence of Chiral Lithium Amides and Amines": E. Juaristi, A. K. Beck, J. Hansen, T. Matt, T. Mukhopadhyay, M. Simson, D. Seebach, *Synthesis* **1993**, 1271–1290.

[24] "The Structures of Lithium Compounds of Sulfones, Sulfoximides, Sulfoxides, Thioethers and 1,3-Dithianes, Nitriles, Nitro Compounds and Hydrazones": G. Boche, *Angew. Chem.* **1989**, *101*, 286–306; *Angew. Chem. Int. Ed. Engl.* **1989**, *28*, 277–297; "Carbanions of Alkali and Alkaline Earth Cations: (i) Synthesis and Structural Characterization": P. G. Williard in *Comprehensive Organic Synthesis. Selectivity, Strategy and Efficiency in Modern Organic Chemistry, Vol. 1* (Eds.: B. M. Trost, I. Fleming), Pergamon, Oxford, **1991**, pp. 1–47.

[25] "Structures of Lithium Enolates and Phenolates in Solution": L. M. Jackman, J. Bortiatynski in *Advances in Carbanion Chemistry, Vol. 1* (Ed.: V. Snieckus), JAI Press, Greenwich, **1992**, pp. 45–87.

[26] "How We Stumbled Into Peptide Chemistry": D. Seebach, *Aldrichimica Acta* **1992**, *25*, 59–66.

[27] "Some Effects of Lithium Salts, of Strong Bases, and of the Cosolvent DMPU in Peptide Chemistry, and Elsewhere": D. Seebach, A. K. Beck, A. Studer in *Modern Synthetic Methods, Vol. 7* (Eds.: B. Ernst, C. Leumann), Verlag Helvetica Chimica Acta/VCH, Basel/Weinheim, **1995**, pp. 1–178.

[28] "Solution Structures of Lithium Dialkylamides and Related *N*-Lithiated Species: Results from ^{6}Li–^{15}N Double Labeling Experiments": D. B. Collum, *Acc. Chem. Res.* **1993**, *26*, 227–234.

[29] T. Laube, J. D. Dunitz, D. Seebach, *Helv. Chim. Acta* **1985**, *68*, 1373–1393.

[30] E. Vedejs, N. Lee, *J. Am. Chem. Soc.* **1995**, *117*, 891–900.

[31] The pioneering work of Heathcock, Masamune, and Evans is discussed in the following review articles: "Stereoselective Aldol Reactions with α-Unsubstituted Chiral Enolates": M. Braun, *Angew. Chem.* **1987**, *99*, 24–37; *Angew. Chem. Int. Ed. Engl.* **1987**, *26*, 24–37; "Recent Developments in Stereoselective Aldol Reactions": M. Braun in *Advances in Carbanion Chemistry, Vol. 1* (Ed.: V. Snieckus), JAI Press, Greenwich, **1992**, pp. 177–247. See also the ref. [227].

[32] "Titanium and Zirconium Derivatives in Organic Synthesis. A Review with Procedures": D. Seebach, B. Weidmann, L. Widler in *Modern Synthetic Methods, Vol. 3* (Ed.: R. Scheffold), Salle + Sauerländer, Aarau, and Wiley, New York, **1983**, pp. 217–353.

[33] M. T. Reetz, *Organotitanium Reagents in Organic Synthesis*, Springer, Berlin, **1986**.

[34] M. Nerz-Stormes, E. R. Thornton, *J. Org. Chem.* **1991**, *56*, 2489–2498; M. A. Walker, C. H. Heathcock, *J. Org. Chem.* **1991**, *56*, 5747–5750; D. A. Evans, D. L. Rieger, M. T. Bilodeau, F. Urpi, *J. Am. Chem. Soc.* **1991**, *113*, 1047–1049.

[35] I. Kuwajima, E. Nakamura, *J. Am. Chem. Soc.* **1975**, *97*, 3257–3258.

[36] "Starke ungeladene Stickstoffbasen": R. Schwesinger, *Nachr. Chem. Tech. Lab.* **1990**, *38*, 1214–1226; R. Schwesinger, J. Willaredt, H. Schlemper, M. Keller, D. Schmitt, H. Fritz, *Chem. Ber.* **1994**, *127*, 2435–2454.

[37] T. Pietzonka, D. Seebach, *Chem. Ber.* **1991**, *124*, 1837–1843.

[38] T. Pietzonka, D. Seebach, *Angew. Chem.* **1992**, *104*, 1543–1545; *Angew. Chem. Int. Ed. Engl.* **1992**, *31*, 1481–1482; *ibid.* **1993**, *105*, 741–742 and **1993**, *32*, 716–717; D. Seebach, O. Bezençon, B. Jaun, T. Pietzonka, J. L. Matthews, F. N. M. Kühnle, W. B. Schweizer, *Helv. Chim. Acta* **1996**, *79*, 588–608.

[39] "The Directed Aldol Reaction": T. Mukaiyama in *Organic Reactions, Vol. 28* (Ed.: W. G. Dauben), Wiley, New York, **1982**, pp. 203–331.

[40] "Enantiomerenreine Naturstoffe und Pharmaka aus billigen Vorläufern (Chiral Pool). – Zur Frage der chiral ökonomischen und ökologischen Totalsynthese": D. Seebach, H.-O. Kalinowski, *Nachr. Chem. Techn.* **1976**, *24*, 415–418.

[41] One of the first applications of this principle was independently published by G. Fráter [42] and by us [43].

[42] G. Fráter, U. Müller, W. Günther, *Tetrahedron Lett.* **1981**, *22*, 4221–4224.

[43] D. Seebach, R. Naef, *Helv. Chim. Acta* **1981**, *64*, 2704–2708.

[44] Initially, we used the term "self-reproduction of chirality" or "of stereogenic centers" [45–48]. Our colleague Vladimir Prelog has, however, convinced us that the term "self-reproduction" should be reserved only for living organisms.

[45] D. Seebach, M. Boes, R. Naef, W. B. Schweizer, *J. Am. Chem. Soc.* **1983**, *105*, 5390–5398.

[46] R. Naef, D. Seebach, *Liebigs Ann. Chem.* **1983**, 1930–1936.

[47] "α-Alkylation of α-Heterosubstituted Carboxylic Acids without Racemization. EPC-Syntheses of Tertiary Alcohols and Thiols": D. Seebach, R. Naef, G. Calderari, *Tetrahedron* **1984**, *40*, 1313–1324.

[48] "EPC Syntheses with C,C Bond Formation via Acetals and Enamines": D. Seebach, R. Imwinkelried, T. Weber in *Modern Synthetic Methods, Vol. 4* (Ed.: R. Scheffold), Springer, Berlin, **1986**, pp. 125–259.

[49] Many people call such a ketone prochiral. Vladimir Prelog, who could be described as our "stereochemical conscience", always points out that this definition is absurd, because it gives no clear structural definition (see also Scheme 5 in ref. [48]). Hence, for example, the imine **V** is prochiral as far as the addition of a nucleophilic alkylation reagent such as a Grignard reagent is concerned, but it is not prochiral with respect to reduction or hydrogenation. For the correct use and definition of the term "prochirality center" and other stereochemical terms, see the glossaries in: E. L. Eliel, S. H. Wilen, L. N. Mander, *Stereochemistry of Organic Compounds*, Wiley, New York, **1994**; "Nomenclature and Vocabulary of Organic Stereochemistry": G. Helmchen in *Methods of Organic Chemistry, Vol. E21a* (Eds.: G. Helmchen, R. W. Hoffmann, J. Mulzer, E. Schaumann), Thieme, Stuttgart, **1995**, pp. 1–74; "Principles of Asymmetric Synthesis": R. E. Gawley, J. Aubé in *Tetrahedron Organic Chemistry Series, Vol. 12* (Eds.: J. E. Baldwin, P. D. Magnus), Pergamon, Oxford, **1996**.

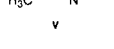

V

[50] 2,2-Disubstituted 1,3-dioxolanones have been prepared from lactic acid, mandelic acid, and alkyl aryl and other unsymmetrical ketones by using acid catalysis [51] or Ru catalysis [52]. However, reactions of the resulting enolates tend to occur, albeit not unexpectedly, in a not particularly stereoselective fashion [51]. On the other hand, the diastereoselectivity of Michael additions to dioxinones remains high even when the acetal center is substituted by both a *t*Bu and a Me group or when the six-membered ring derived from menthone is the substituent on the acetal center. See the work of Lange et al. [160–162] and of Kaneko et al. [238] and ref. [302].

[51] A. Greiner, J.-Y. Ortholand, *Tetrahedron Lett.* **1992**, *33*, 1897–1900; J.-Y. Ortholand, N. Vicart, A. Greiner, *J. Org. Chem.* **1995**, *60*, 1880–1884.

[52] M. Neveux, B. Seiller, F. Hagedorn, C. Bruneau, P. H. Dixneuf, *J. Organomet. Chem.* **1993**, *451*, 133–138.

[53] "Specification of Molecular Chirality": R. S. Cahn, C. Ingold, V. Prelog, *Angew. Chem.* **1966**, *78*, 413–447; *Angew. Chem. Int. Ed. Engl.* **1966**, *5*, 385–415.

[54] "Basic Principles of the CIP-System and Proposals for a Revision": V. Prelog, G. Helmchen, *Angew. Chem.* **1982**, *94*, 614–631; *Angew. Chem. Int. Ed. Engl.* **1982**, *21*, 567–583.

[55] "The Unambiguous Specification of the Steric Course of Asymmetric Syntheses": D. Seebach, V. Prelog, *Angew. Chem.* **1982**, *94*, 696–702; *Angew. Chem. Int. Ed. Engl.* **1982**, *21*, 654–660.

[56] See Schemes 2c–e and the refs. [212–218].

[57] F. Gorla, L. M. Venanzi, *Helv. Chim. Acta* **1990**, *73*, 690–697; D. Seebach, T. Sommerfeld, Q. Jiang, L. M. Venanzi, *ibid.* **1994**, *77*, 1313–1330; see also Chapter II.4.2 in ref. [27].

[58] BASF kindly donated large quantities of pivalaldehyde to us over many years. We thank them for their generosity.

[59] Shell Chemicals is a source of large quantities of pivalaldehyde.

[60] It is highly likely that transformations previously described in the literature have followed the principles of self-regeneration of stereocenters; however, we know of no example where this synthetic principle was recognized, explicitly formulated, and systematically used before our own work.

[61] For more recent work on the stereoselective formation of tertiary centers, see also: S. V. Frye, E. L. Eliel, *J. Am. Chem. Soc.* **1988**, *110*, 484–489; T. Harder, T. Löhl, M. Bolte, K. Wagner, D. Hoppe, *Tetrahedron Lett.* **1994**, *35*, 7365–7368; B. Weber, D. Seebach, *Angew. Chem.* **1992**, *104*, 96–97; *Angew. Chem. Int. Ed. Engl.* **1992**, *31*, 84–86; B. Weber, D. Seebach, *Tetrahedron* **1994**, *50*, 6117–6128, and references cited therein. An article written by S. F. Martin deals with the particularly difficult problem of the stereoselective formation of quaternary centers: "Methodology for the Construction of Quaternary Carbon Centers": S. F. Martin, *Tetrahedron* **1980**, *36*, 419–460.

[62] "Structure and Reactivity of Five- and Six-Ring N,N-, N,O-, and O,O-Acetals: A Lesson in Allylic 1,3-Strain ($A^{1,3}$ Strain)": D. Seebach, B. Lamatsch, R. Amstutz, A. K. Beck, M. Dobler, M. Egli, R. Fitzi, M. Gautschi, B. Herradon, P. C. Hidber, J. J. Irwin, R. Locher, M. Maestro, T. Maetzke, A. Mourino, E. Pfammatter, D. A. Plattner, C. Schickli, W. B. Schweizer, P. Seiler, G. Stucky, W. Petter, J. Escalante, E. Juaristi, D. Quintana, C. Miravitlles, E. Molins, *Helv. Chim. Acta* **1992**, *75*, 913–934, and references therein.

[63] R. Naef, D. Seebach, *Helv. Chim. Acta* **1985**, *68*, 135–143.

[64] D. Seebach, J. D. Aebi, R. Naef, T. Weber, *Helv. Chim. Acta* **1985**, *68*, 144–154.

[65] "(2*R*,5*S*)- and (2*S*,5*S*)-1-Benzoyl-2-*t*-butyl-3,5-dimethyl-1,3-imidazolidin-4-one": A. Studer, D. Seebach in *Encyclopedia of Reagents for Organic Synthesis, Vol. 1* (Ed.: L. A. Paquette), Wiley, Chichester, **1995**, pp. 306–308.

[66] "(2*S*,4*S*)-3-Benzoyl-2-*t*-butyl-4-methyl-1,3-oxazolidin-5-one": A. R. Sting, D. Seebach in *Encyclopedia of Reagents for Organic Synthesis, Vol. 1* (Ed.: L. A. Paquette), Wiley, Chichester, **1995**, pp. 308–309.

[67] "(*R*,*R*)- and (*S*,*S*)-2-*t*-Butyl-5-methyl-1,3-dioxolan-4-one": A. R. Sting, D. Seebach in *Encyclopedia of Reagents for Organic Synthesis, Vol. 2* (Ed.: L. A. Paquette), Wiley, Chichester, **1995**, pp. 931–933.

[68] "Chirale Cyclische Acetale in der Synthese": H.-J. Altenbach, *Nachr. Chem. Tech. Lab.* **1988**, *36*, 1212–1217; J. Mulzer, H.-J. Altenbach, M. Braun, K. Krohn, H.-U. Reissig, *Organic Synthesis Highlights*, VCH, Weinheim, **1991**, pp. 19–24.

[69] The acid-catalyzed cyclization of the appropriate alanine derivative to give imidazolidinone **1** (R^A = *t*Bu, R = Me, X = Y = NH) results in a 1:1 mixture of the *cis* and *trans* products. As the *cis* isomer can be *tert*-butoxycarbonylated at N1 under mild conditions while the *trans* isomer remains unprotected, they can be easily separated: see Section 7 and ref. [235].

[70] D. Seebach, A. Fadel, *Helv. Chim. Acta* **1985**, *68*, 1243–1250.

[71] D. Seebach, E. Juaristi, D. D. Miller, C. Schickli, T. Weber, *Helv. Chim. Acta* **1987**, *70*, 237–261.

[72] A. K. Beck, D. Seebach, *Chimia* **1988**, *42*, 142–144.

[73] D. Seebach, P. Renaud, *Helv. Chim. Acta* **1985**, *68*, 2342–2349.

[74] D. Seebach, M. A. Maestro, M. Sefkow, A. Neidlein, F. Sternfeld, G. Adam, T. Sommerfeld, *Helv. Chim. Acta* **1991**, *74*, 2112–2118; D. Seebach, M. A. Maestro, M. Sefkow, G. Adam, S. Hintermann, A. Neidlein, *Liebigs Ann. Chem.* **1994**, 701–717.

[75] For the preparations and reactions of dioxolanones derived from chiral α-hydroxy acids and acetaldehyde, isobutyraldehyde, benzaldehyde, cyclohexanecarboxaldehyde, acetone, 2-hexanone, acetophenone, or pivalophenone, see refs. [51, 52, 76–79].

[76] H. Moorlag, R. M. Kellogg, M. Kloosterman, B. Kaptein, J. Kamphuis, H. E. Shoemaker, *J. Org. Chem.* **1990**, *55*, 5878–5881.

[77] A. Greiner, J.-Y. Ortholand, *Tetrahedron Lett.* **1990**, *31*, 2135–2138.

[78] N. Chapel, A. Greiner, J.-Y. Ortholand, *Tetrahedron Lett.* **1991**, *32*, 1441–1442.

[79] N. Vicart, J.-Y. Ortholand, G. Y. Emeric, A. Greiner, *Tetrahedron Lett.* **1994**, *35*, 3917–3918.

[80] The selectivity with regard to the configuration of the newly formed stereogenic center at the 1′-position (addition to aldehydes and Michael acceptors) is generally low. For highly diastereoselective reactions of chiral, glycine-derived enolates with concomitant formation of two new stereogenic centers, see Section 9.3 and Scheme 29e.

[81] D. Seebach, E. Dziadulewicz, L. Behrendt, S. Cantoreggi, R. Fitzi, *Liebigs Ann. Chem.* **1989**, 1215–1232.

[82] D. Seebach, T. Gees, F. Schuler, *Liebigs Ann. Chem.* **1993**, 785–799; Erratum: *ibid.* **1994**, 529.

[83] A. Studer, D. Seebach, *Liebigs Ann. Chem.* **1995**, 217–222.

[84] E. Vedejs, S. C. Fields, M. R. Schrimpf, *J. Am. Chem. Soc.* **1993**, *115*, 11612–11613; E. Vedejs, S. C. Fields, S. Lin, M. R. Schrimpf, *J. Org. Chem.* **1995**, *60*, 3028–3034.

[85] T. M. Zydowsky, E. de Lara, S. G. Spanton, *J. Org. Chem.* **1990**, *55*, 5437–5439.

[86] D. Seebach, T. Vettiger, H.-M. Müller, D. A. Plattner, W. Petter, *Liebigs Ann. Chem.* **1990**, 687–695.

[87] T. Weber, D. Seebach, *Helv. Chim. Acta* **1985**, *68*, 155–161.

[88] The use of the SRS principle is not necessary in the case of hydroxyproline as this amino acid contains a second stereogenic center.

[89] D. Seebach, T. Weber, *Tetrahedron Lett.* **1983**, *24*, 3315–3318; D. Seebach, T. Weber, *Helv. Chim. Acta* **1984**, *67*, 1650–1661.

[90] See also the discussion in Sections 9.2 and 9.4, and Schemes 28 and 33, which relate to this particularly problematic case.

[91] It has recently been reported that when the bicyclic compound **VI**, which is prepared from pyroglutamic acid and pivalaldehyde, is deprotonated with LHMDS, it is not the amide enolate (deprotonation at the CH_2 group α to the carbonyl) but the ester enolate **VII** (new sp^2 center at the bridgehead position between two five rings!) that is formed. This results in a route to the α,α-disubstituted α-amino acid derivatives **VIII**. D. K. Dikshit, A. Maheshwari, S. K. Panday, *Tetrahedron Letters* **1995**, *36*, 6131–6134.

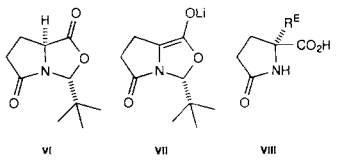

[92] Amino-, hydroxy-, and dihydroxycarboxylic acids with a temporary stereogenic center (for example, threonine, dihydroxybutanoic acid, and tartaric acid) may also be α-alkylated via the appropriate heterocycles. In these cases, the generation of a temporary stereogenic center is not necessary and the reaction sequence cannot be described as an example of the SRS principle. For the formation of products of type **XII** from reactions of threonine-derived enolates of type **IX**, see ref. [93] and D. Seebach, J. D. Aebi, *Tetrahedron Lett.* **1983**, *24*, 3311–3314; G. Fronza, C. Fuganti, G. Pedrocchi-Fantoni, *J. Carbohydr. Chem.* **1989**, *8*, 85–101; G. Fronza, A. Mele, G. Pedrocchi-Fantoni, D. Pizzi, S. Servi, *J. Org. Chem.* **1990**, *55*, 6216–6219; see also ref. [131]. For the formation of products of type **XIII** and **XIV** from reactions of dioxolanone carboxylic ester enolates such as **X** and **XI** and for related reactions of cyclopentane carboxylic ester enolates, which interestingly may proceed *cis* to the neighboring substituent at the stereogenic center, see refs. [62, 93–98]. The enolate **XI** has a relatively high tendency to decompose by β-elimination (see the discussion in the text and the legends of Scheme 6 and Schemes 29b and 32c, and also the review in ref. [36]).

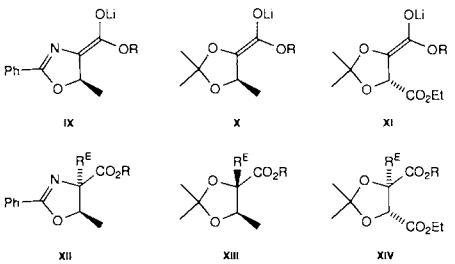

[93] D. Seebach, J. D. Aebi, M. Gander-Coquoz, R. Naef, *Helv. Chim. Acta* **1987**, *70*, 1194–1216.

[94] R. Naef, D. Seebach, *Angew. Chem.* **1981**, *93*, 1113–1113; *Angew. Chem. Int. Ed. Engl.* **1981**, *20*, 1030–1031.

[95] W. Ladner, *Chem. Ber.* **1983**, *116*, 3413–3426.

[96] K. Ditrich, R. W. Hoffmann, *Liebigs Ann. Chem.* **1990**, 15–21.

[97] R. Stürmer, *Liebigs Ann. Chem.* **1991**, 311–313.

[98] H. Kigoshi, Y. Imamura, K. Yoshikawa, H. Niwa, K. Yamada, *Tetrahedron Lett.* **1991**, *32*, 4541–4544.

[99] E. Pfammatter, D. Seebach, *Liebigs Ann. Chem.* **1991**, 1323–1336.

[100] D. Seebach, J. D. Aebi, *Tetrahedron Lett.* **1984**, *25*, 2545–2548.

[101] D. Seebach, G. Stucky, P. Renaud, *Chimia* **1988**, *42*, 176–178.

[102] D. Seebach, M. Coquoz, *Chimia* **1985**, *39*, 20–22.

[103] D. Seebach, A. Jeanguenat, J. Schmidt, T. Maetzke, *Chimia* **1989**, *43*, 314–317.

[104] A. Jeanguenat, D. Seebach, *J. Chem. Soc. Perkin Trans. 1* **1991**, 2291–2298.

[105] G. Pattenden, S. M. Thom, *J. Chem. Soc. Perkin Trans. 1* **1993**, 1629–1636.

[106] G. Pattenden, S. M. Thom, M. F. Jones, *Tetrahedron* **1993**, *49*, 2131–2138.

[107] G. C. Mulqueen, G. Pattenden, D. A. Whiting, *Tetrahedron* **1993**, *49*, 5359–5364.

[108] R. J. Boyce, G. C. Mulqueen, G. Pattenden, *Tetrahedron Lett.* **1994**, *35*, 5705–5708.

[109] R. J. Boyce, G. Pattenden, *Synlett* **1994**, 587–588.

[110] R. Parthasarathy, B. Paul, W. Korytnyk, *J. Am. Chem. Soc.* **1976**, *98*, 6634–6643; P. N. Confalone, G. Pizzolato, E. G. Baggiolini, D. Lollar, M. R. Uskokovic, *ibid.* **1977**, *99*, 7020–7026; L. Szilágyi, Z. Györgydeák, *ibid.* **1979**, *101*, 427–432; Z. Györgydeák, M. Kajtár-Peredy, J. Kajtár, M. Kajtár, *Liebigs Ann. Chem.* **1987**, 927–934; E. Poetsch, M. Casutt, *Chimia* **1987**, *41*, 148–150; Z. Györgydeák, J. Kajtár, M. Kajtár, M. Kajtár-Peredy, *Liebigs Ann. Chem.* **1990**, 281–286.

[111] The eliminations depicted in Scheme 6e cannot proceed along the optimal trajectory (Bürgi–Dunitz rules) and, to use a different terminology, are "Baldwin-forbidden retro-5-*endo*-*trig* processes": a) J. E. Baldwin, *J. Chem. Soc. Chem. Commun.* **1976**, 734–736; b) J. E. Baldwin, J. Cutting, W. Dupont, L. I. Kruse, L. Silberman, R. C. Thomas, *ibid.* **1976**, 736–738; c) J. E. Baldwin, R. C. Thomas, L. I. Kruse, L. Silberman, *J. Org. Chem.* **1977**, *42*, 3846–3852; d) J. E. Baldwin, L. I. Kruse, *J. Chem. Soc. Chem. Commun.* **1977**, 233–235; e) J. D. Dunitz, *X-Ray Analysis and the Structure of Organic Molecules*, Cornell University Press, Ithaca, **1979**; f) "Stereoelectronic Effects in Organic Chemistry": P. Deslongchamps, *Organic Chemistry Series, Vol. 1* (Ed.: J. E. Baldwin), Pergamon, Oxford, **1983**; g) A. J. Kirby, *The Anomeric Effect and Related Stereoelectronic Effects at Oxygen*, Springer, Berlin, **1983**; h) "From Crystal Statics to Chemical Dynamics": H.-B. Bürgi, J. D. Dunitz, *Acc. Chem. Res.* **1983**, *16*, 153–161; i) *J. Am. Chem. Soc.* **1987**, *109*, 2924–2926; j) *Acta Crystallogr. Sect. B* **1988**, *44*, 445–448; k) H.-B. Bürgi, K. C. Dubler-Steudle, *J. Am. Chem. Soc.* **1988**, *110*, 4953–4957; *ibid.* **1988**, *110*, 7291–7299; l) H.-B. Bürgi, J. D. Dunitz, *Structure Correlation, Vol. 1 + 2*, VCH, Weinheim, **1994**; m) J. D. Dunitz, *X-Ray Analysis and the Structure of Organic Molecules*, Verlag Helvetica Chimica Acta, Basel, **1995**.

[112] In the base-initiated cyclization of derivatives of type **XV** ($R^1 = CO_2Et$; R^2 = H, Me, Ph) attack occurs *trans* to the *t*Bu group (→ **XVI**) as expected. Altering the substituents in **XV** (R^1 = H, R^2 = CN; R^1 = Ph, R^2 = H) results in the formation of products of type **XVII** ($R^3 = NH_2$ or OH); this must be due to formation of the *trans* isomer of **XV** by epimerization at C4 before the cyclization step. M. D. Andrews, A. Brewster, M. G. Moloney, *Tetrahedron: Asymmetry* **1994**, *5*, 1477–1478.

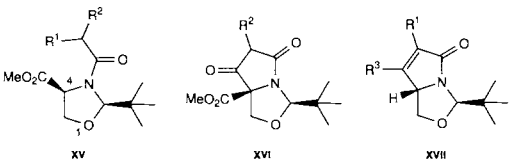

[113] A. Fadel, J. Salaün, *Tetrahedron Lett.* **1987**, *28*, 2243–2246.

[114] J. D. Aebi, D. Seebach, *Helv. Chim. Acta* **1985**, *68*, 1507–1518.

[115] S. Thaisrivongs, D. T. Pals, J. A. Lawson, S. R. Turner, D. W. Harris, *J. Med. Chem.* **1987**, *30*, 536–541.

[116] M. G. Hinds, J. H. Welsh, D. M. Brennand, J. Fisher, M. J. Glennie, N. G. J. Richards, D. L. Turner, J. A. Robinson, *J. Med. Chem.* **1991**, *34*, 1777–1789.

[117] A. K. Beck, S. Blank, K. Job, D. Seebach, T. Sommerfeld, *Organic Syntheses* **1995**, *72*, 62–73.

[118] M. J. Genin, P. W. Baures, R. L. Johnson, *Tetrahedron Lett.* **1994**, *35*, 4967–4968.

[119] M. Chaari, A. Jenhi, J.-P. Lavergne, P. Viallefont, *J. Organomet. Chem.* **1991**, *401*, C10–C13.

[120] M. Gander-Coquoz, D. Seebach, *Helv. Chim. Acta* **1988**, *71*, 224–236.

[121] B. Strijtveen, R. M. Kellogg, *Tetrahedron* **1987**, *43*, 5039–5054.

[122] R. C. F. Jones, A. K. Crockett, D. C. Rees, I. H. Gilbert, *Tetrahedron: Asymmetry* **1994**, *5*, 1661–1664.

[123] G. Calderari, D. Seebach, *Helv. Chim. Acta* **1985**, *68*, 1592–1604.

[124] R. K. Boeckman, Jr., S. K. Yoon, D. K. Heckendorn, *J. Am. Chem. Soc.* **1991**, *113*, 9682–9684.

[125] T. Ogawa, H. Niwa, K. Yamada, *Tetrahedron* **1993**, *49*, 1571–1578.

[126] K. Krohn, A. Meyer, *Liebigs Ann. Chem.* **1994**, 167–174.

[127] R. M. Williams, T. Glinka, E. Kwast, *J. Am. Chem. Soc.* **1988**, *110*, 5927–5929.

[128] K. Krohn, I. Hamann, *Liebigs Ann. Chem.* **1988**, 949–953.

[129] E. J. Corey, G. A. Reichard, *J. Am. Chem. Soc.* **1992**, *114*, 10677–10678.

[130] H. Uno, J. E. Baldwin, A. T. Russell, *J. Am. Chem. Soc.* **1994**, *116*, 2139–2140.

[131] T. Sunazuka, T. Nagamitsu, K. Matsuzaki, H. Tanaka, S. Omura, A. B. Smith III, *J. Am. Chem. Soc.* **1993**, *115*, 5302–5302.

[132] "Capto-dative Substituent Effects in Synthesis with Radicals and Radicophiles": H. G. Viehe, R. Merényi, L. Stella, Z. Janousek, *Angew. Chem.* **1979**, *91*, 982–997; *Angew. Chem. Int. Ed. Engl.* **1979**, *18*, 917–932.

[133] J. Zimmermann, D. Seebach, *Helv. Chim. Acta* **1987**, *70*, 1104–1114.

[134] C. P. Schickli, D. Seebach, *Liebigs Ann. Chem.* **1991**, 655–668.

[135] "Centenary Lecture. The Pursuit of Selectivity in Radical Reactions": A. L. J. Beckwith, *Chem. Soc. Rev.* **1993**, 143–151.

[136] A. L. J. Beckwith, C. L. L. Chai, *Tetrahedron* **1993**, *49*, 7871–7882.

[137] W. R. Roush, A. P. Essenfeld, J. S. Warmus, B. B. Brown, *Tetrahedron Lett.* **1989**, *30*, 7305–7308.

[138] W. R. Roush, B. B. Brown, *J. Org. Chem.* **1992**, *57*, 3380–3387.

[139] A. L. J. Beckwith, C. L. L. Chai, *J. Chem. Soc. Chem. Commun.* **1990**, 1087–1088; see also ref. [175].

[140] G. Stucky, D. Seebach, *Chem. Ber.* **1989**, *122*, 2365–2375.

[141] E. Juaristi, D. Quintana, B. Lamatsch, D. Seebach, *J. Org. Chem.* **1991**, *56*, 2553–2557.

[142] E. Juaristi, J. Escalante, B. Lamatsch, D. Seebach, *J. Org. Chem.* **1992**, *57*, 2396–2398.

[143] P. Murer, B. Rheiner, E. Juaristi, D. Seebach, *Heterocycles* **1994**, *39*, 319–344.

[144] P. M. Hardy, D. J. Samworth, *J. Chem. Soc. Perkin Trans. 1* **1977**, 1954–1960.

[145] J. P. Konopelski, K. S. Chu, G. R. Negrete, *J. Org. Chem.* **1991**, *56*, 1355–1357.

[146] G. R. Negrete, J. P. Konopelski, *Tetrahedron: Asymmetry* **1991**, *2*, 105–108.

[147] K. S. Chu, G. R. Negrete, J. P. Konopelski, F. J. Lakner, N.-T. Woo, M. M. Olmstead, *J. Am. Chem. Soc.* **1992**, *114*, 1800–1812.

[148] K. S. Chu, J. P. Konopelski, *Tetrahedron* **1993**, *49*, 9183–9190.

[149] "Enantioselective Synthesis of α-Substituted and α,β-Disubstituted β-Amino Acids via Chiral Derivatives of 3-Aminopropionic Acid": E. Juaristi, D. Seebach in *Enantioselective Synthesis of β-Amino Acids*, (Ed.: E. Juaristi), VCH, Weinheim, in press.

[150] D. Seebach, J. Zimmermann, *Helv. Chim. Acta* **1986**, *69*, 1147–1152; M. Bruncko, D. Crich, *J. Org. Chem.* **1994**, *59*, 7921–7923.

[151] "Biological-Chemical Preparation of 3-Hydroxycarboxylic Acids and Their Use in EPC-Syntheses": D. Seebach, S. Roggo, J. Zimmermann in *Workshop Conferences Hoechst, Vol. 17: Stereochemistry of Organic and Bioorganic Transformations* (Eds.: W. Bartmann, K. B. Sharpless), VCH, Weinheim, **1987**, pp. 85–126.

[152] D. Seebach, J. Zimmermann, U. Gysel, R. Ziegler, T.-K. Ha, *J. Am. Chem. Soc.* **1988**, *110*, 4763–4772.

[153] W. Amberg, D. Seebach, *Chem. Ber.* **1990**, *123*, 2429–2438.

[154] Y. Noda, D. Seebach, *Helv. Chim. Acta* **1987**, *70*, 2137–2145.

[155] A. K. Beck, M. Gautschi, D. Seebach, *Chimia* **1990**, *44*, 291–295.

[156] M. Gautschi, D. Seebach, *Angew. Chem.* **1992**, *104*, 1061–1062; *Angew. Chem. Int. Ed. Engl.* **1992**, *31*, 1083–1085.

[157] M. Gautschi, W. B. Schweizer, D. Seebach, *Chem. Ber.* **1994**, *127*, 565–579.

[158] D. Seebach, U. Gysel, K. Job, A. K. Beck, *Synthesis* **1992**, 39–40.

[159] A. K. Beck, A. Brunner, V. Montanari, D. Seebach, *Chimia* **1991**, *45*, 379–382.

[160] G. L. Lange, M. G. Organ, M. R. Roche, *J. Org. Chem.* **1992**, *57*, 6000–6002.

[161] G. L. Lange, M. G. Organ, *Tetrahedron Lett.* **1993**, *34*, 1425–1428.

[162] M. G. Organ, R. J. Froese, J. D. Goddard, N. J. Taylor, G. L. Lange, *J. Am. Chem. Soc.* **1994**, *116*, 3312–3323.

[163] G. Kneer, J. Mattay, G. Raabe, C. Krüger, J. Lauterwein, *Synthesis* **1990**, 599–603.

[164] "Synthesis of Enantiomerically Pure β-Amino Acids from 2-*t*-Butyl-1-carbomethoxy-2,3-dihydro-4(1*H*)-pyrimidinone: (*R*)-3-Amino-3-(*p*-methoxyphenyl)propionic Acid": F. J. Lakner, K. S. Chu, G. R. Negrete, J. P. Konopelski in *Organic Syntheses, Vol. 73* (Ed.: R. K. Boeckman, Jr.), Wiley, New York, **1995**, pp. 201–214.

[165] "(*R*)-Methyl 2-*t*-Butyl-3(2*H*)-oxazolecarboxylate": J. Podlech, D. Seebach in *Encyclopedia of Reagents for Organic Synthesis, Vol. 5* (Ed.: L. A. Paquette), Wiley, Chichester, **1995**, pp. 3452–3453.

[166] "(*R*)-2-*t*-Butyl-6-methyl-4*H*-1,3-dioxin-4-one": A. K. Beck, D. Seebach in *Encyclopedia of Reagents for Organic Synthesis, Vol. 2* (Ed.: L. A. Paquette), Wiley, Chichester, **1995**, pp. 929–931.

[167] R. Breitschuh, D. Seebach, *Synthesis* **1992**, 1170–1178.

[168] In a similar fashion, a thiolactic acid derivative **XVIII** may be alkylated (→ **XIX**) at the α-carbonyl carbon and due to the presence of a sulfoxide center, a nonracemic product results. R. Breitschuh, Dissertation. No. 9654, ETH, Zürich, **1992**.

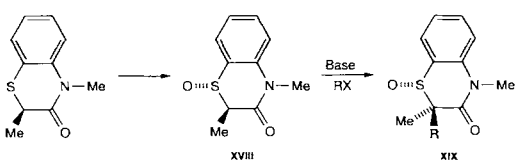

[169] W. R. Roush, R. J. Sciotti, *Tetrahedron Lett.* **1992**, *33*, 4691–4694.
[170] W. R. Roush, R. J. Sciotti, *J. Am. Chem. Soc.* **1994**, *116*, 6457–6458.
[171] S. G. Pyne, J. Safaei-G, D. C. R. Hockless, B. W. Skelton, A. N. Sobolev, A. H. White, *Tetrahedron* **1994**, *50*, 941–956.
[172] J. R. Axon, A. L. J. Beckwith, *J. Chem. Soc. Chem. Commun.* **1995**, 549–550.
[173] A. R. Sting, D. Seebach, *Tetrahedron* **1996**, *52*, 279–290.
[174] J. Mattay, G. Kneer, J. Mertes, *Synlett* **1990**, 145–147.
[175] S. G. Pyne, B. Dikic, P. A. Gordon, B. W. Skelton, A. H. White, *J. Chem. Soc. Chem. Commun.* **1991**, 1505–1506; *Aust. J. Chem.* **1993**, *46*, 73–93.
[176] S. G. Pyne, A. Javidan, B. W. Skelton, A. H. White, *Tetrahedron* **1995**, *51*, 5157–5168.
[177] "Biopolymers and -oligomers of (*R*)-3-Hydroxyalkanoic Acids—Contributions of Synthetic Organic Chemists": D. Seebach, A. Brunner, B. M. Bachmann, T. Hoffmann, F. N. M. Kühnle, U. D. Lengweiler in *Ernst Schering Research Foundation Lecture, Vol. 28* (Eds.: Information and Standards Medical Scientific Publications, R. A. Henry, A. Schlemmer), Ernst Schering Research Foundation, Berlin, **1995**.
[178] a) D. Seebach, J.-M. Lapierre, W. Jaworek, P. Seiler, *Helv. Chim. Acta* **1993**, *76*, 459–475; b) J.-M. Lapierre, K. Skobridis, D. Seebach, *ibid.* **1993**, *76*, 2419–2432; c) D. Seebach, J.-M. Lapierre, G. Greiveldinger, K. Skobridis, *ibid.* **1994**, *77*, 1673–1688; d) D. Seebach, J.-M. Lapierre, K. Skobridis, G. Greiveldinger, *Angew. Chem.* **1994**, *106*, 457–458; *Angew. Chem. Int. Ed. Engl.* **1994**, *33*, 440–442; e) P. Murer, D. Seebach, *ibid.* **1995**, *107*, 2297–2300 and **1995**, *34*, 2116–2119.
[179] M. A. Tius, X. Gu, J. Gomez-Galeno, *J. Am. Chem. Soc.* **1990**, *112*, 8188–8189.
[180] D. Seebach, B. Herradón, *Tetrahedron Lett.* **1987**, *28*, 3791–3794; B. Herradón, D. Seebach, *Helv. Chim. Acta* **1989**, *72*, 690–714.
[181] S. Hintermann, D. Seebach, presently unpublished results; S. Hintermann, Dissertation, ETH, Zürich.
[182] P. Renaud, D. Seebach, *Angew. Chem.* **1986**, *98*, 836–838; *Angew. Chem. Int. Ed. Engl.* **1986**, *25*, 843–844.
[183] We have speculated in great detail about the possible reasons for the behavior of acyliminium intermediates, which differs completely from that of their enolate and enoate counterparts [62]. See also refs. [187, 192, 194, 196]; G. Stucky, Dissertation No. 8904, ETH, Zürich, **1989**; I. Collado, J. Ezquerra, C. Pedregal, *J. Org. Chem.* **1995**, *60*, 5011–5015.
[184] M. Faraday, *Pogg. Ann. Phys. Chem.* **1834**, *33*, 433–451.
[185] H. Kolbe, *Justus Liebigs Ann. Chem.* **1849**, *69*, 257–294.
[186] H. Hofer, M. Moest, *Justus Liebigs Ann. Chem.* **1902**, *323*, 284–323.
[187] For further applications of electrolytic decarboxylation of 2-*N*-acylaminocarboxylic acids and subsequent reactions, see refs. [103, 140, 188–194]. For a review article about the chemistry of acyliminium ions that do not proceed with an electrochemical key step, see "Additions to *N*-Acyliminium Ions": H. Hiemstra, W. N. Speckamp in *Comprehensive Organic Synthesis, Vol. 2* (Eds.: B. M. Trost, I. Fleming), Pergamon, Oxford, **1991**, pp. 1047–1082. This topic has been documented in detail in Section II.4. of ref. [27] (and refs. [253–273] cited therein).
[188] P. Renaud, D. Seebach, *Synthesis* **1986**, 424–426.
[189] P. Renaud, D. Seebach, *Helv. Chim. Acta* **1986**, *69*, 1704–1710.
[190] D. Seebach, G. Stucky, *Angew. Chem.* **1988**, *100*, 1398–1404; *Angew. Chem. Int. Ed. Engl.* **1988**, *27*, 1351–1353.
[191] D. Seebach, R. Charczuk, C. Gerber, P. Renaud, H. Berner, H. Schneider, *Helv. Chim. Acta* **1989**, *72*, 401–425.
[192] D. Seebach, G. Stucky, E. Pfammatter, *Chem. Ber.* **1989**, *122*, 2377–2389.
[193] "Elektrochemische Oxydation von Carbonsäuren zur Synthese enantiomerenreiner Verbindungen": G. Stucky, *GIT Fachz. Lab.* **1988**, *5*, 535–540.
[194] F. Beck, *Elektroorganische Chemie. Grundlagen und Anwendungen*, VCH, Weinheim, **1974**; T. Shono, *Electroorganic Chemistry as a New Tool in Organic Synthesis*, Springer, Berlin, **1984**; S. Torii, *Electroorganic Syntheses. Methods and Applications. Part 1: Oxidations*, Kodansha/VCH, Tokyo/Weinheim, **1985**; E. Steckhan, *Electrochemistry III. Topics in Current Chemistry, Vol. 148*, Springer, Berlin, **1988**; A. J. Fry, *Synthetic Organic Electrochemistry*, 2nd ed., Wiley, New York, **1989**; H. Lund, M. M. Baizer, *Organic Electrochemistry. An Introduction and a Guide*, 3rd ed., Marcel Dekker, New York, **1991**; T. Shono, *Electroorganic Synthesis*, Academic Press, London, **1991**.
[195] P. Renaud, Dissertation No. 8155, ETH, Zürich, **1986**.
[196] B. Lamatsch, D. Seebach, T.-K. Ha, *Helv. Chim. Acta* **1992**, *75*, 1095–1110.
[197] Together with "memory of chirality", which was referred to in ref. [20], other newfangled expressions such as "asymmetric memory technology", "asymmetric memory concept", "chiral memory", "chiral relay system", and "disposable chirality center" have appeared in the literature in recent years in relation to the SRS principle (A. S. Anslow, L. M. Harwood, H. Phillips, D. Watkin, *Tetrahedron: Asymmetry* **1991**, *2*, 169–172, and refs. [84, 217]).
[198] In a true case of self-regeneration with concomitant generation of another stereogenic center, which clearly cannot have been conceived as a synthetic procedure, a stereoselective 1,5-hydride shift (**XX** → **XXI**) is followed by a diastereoselective ring closure (**XXI** → **XXII**), whereby substitution at the original stereogenic center occurs with retention (W. H. N. Nijhuis, W. Verboom, D. N. Reinhoudt, *J. Am. Chem. Soc.* **1987**, *109*, 3136–3138).

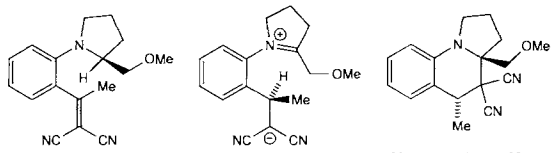

XX **XXI** **XXII**

[199] P. J. Edwards, D. A. Entwistle, C. Genicot, K. S. Kim, S. V. Ley, *Tetrahedron Lett.* **1994**, *35*, 7443–7446.
[200] B. C. B. Bezuidenhoudt, G. H. Castle, S. V. Ley, *Tetrahedron Lett.* **1994**, *35*, 7447–7450.
[201] B. C. B. Bezuidenhoudt, G. H. Castle, J. V. Geden, S. V. Ley, *Tetrahedron Lett.* **1994**, *35*, 7451–7454.
[202] G. H. Castle, S. V. Ley, *Tetrahedron Lett.* **1994**, *35*, 7455–7458.
[203] C. Genicot, S. V. Ley, *Synthesis* **1994**, 1275–1277.
[204] P. J. Edwards, D. A. Entwistle, C. Genicot, S. V. Ley, G. Visentin, *Tetrahedron: Asymmetry* **1994**, *5*, 2609–2632.
[205] G.-J. Boons, R. Downham, K. S. Kim, S. V. Ley, M. Woods, *Tetrahedron* **1994**, *50*, 7157–7176.
[206] Compare this with the modifications of serine via oxazolidine dicarboxylic acid derivatives shown in Schemes 6d, 7, 9, 10a, 11a, 12, 14a, 15 and in Table C in the appendix.
[207] D. Seebach, R. Häner, *Chemistry Lett. Jpn.* **1987**, 49–52.
[208] R. Häner, B. Olano, D. Seebach, *Helv. Chim. Acta* **1987**, *70*, 1676–1693.
[209] The crystal structure analysis of the Li-enolate of a cyclopropanoic acid thiol ester confirms the presence of a completely planar trigonal center in the three-membered ring: E. Hahn, T. Maetzke, D. A. Plattner, D. Seebach, *Chem. Ber.* **1990**, *123*, 2059–2064.
[210] V. Ferey, T. Le Gall, C. Mioskowski, *J. Chem. Soc. Chem. Commun.* **1995**, 487–489.
[211] V. Ferey, L. Toupet, T. Le Gall, C. Mioskowski, *Angew. Chem.* **1996**, *108*, 475–477; *Angew. Chem. Int. Ed. Engl.* **1996**, 430–432.
[212] Reviews about chiral, nonracemic transition metal complexes: "Some Uses of Metal Carbonyl Complexes in Organic Synthesis": M. Franck-Neumann in *Organometallics in Organic Synthesis*, (Eds.: A. de Meijere, H. tom Dieck), Springer, Berlin, **1987**, pp. 247–264; H.-J. Knölker, *Synlett* **1992**, 371–387.
[213] T. Hayashi, M. Konishi, M. Kumada, *J. Chem. Soc. Chem. Commun.* **1984**, 107–108; U. Leutenegger, G. Umbricht, C. Fahrni, P. von Matt, A. Pfaltz, *Tetrahedron* **1992**, *48*, 2143–2156.
[214] H.-G. Schmalz, B. Millies, J. W. Bats, G. Dürner, *Angew. Chem.* **1992**, *104*, 640–643; *Angew. Chem. Int. Ed. Engl.* **1992**, *31*, 631–633; H.-G. Schmalz, J. Hollander, M. Arnold, G. Dürner, *Tetrahedron Lett.* **1993**, *34*, 6259–6262; H.-G. Schmalz, M. Arnold, J. Hollander, J. W. Bats, *Angew. Chem.* **1994**, *106*, 77–79; *Angew. Chem. Int. Ed. Engl.* **1994**, *33*, 109–111.
[215] E. P. Kündig, J. Leresche, *Tetrahedron* **1993**, *49*, 5599–5615.
[216] a) D. Enders, M. Finkam, *Liebigs Ann. Chem.* **1993**, 551–555; D. Enders, B. Jandeleit, G. Raabe, *Angew. Chem.* **1994**, *106*, 2033–2035; *Angew. Chem. Int. Ed. Engl.* **1994**, *33*, 1949–1951; D. Enders, B. Jandeleit, *Synthesis* **1994**, 1327–1330; *Liebigs Ann. Chem.* **1995**, 1173–1176; D. Enders, B. Jandeleit, O. F. Prokopenko, *Tetrahedron* **1995**, *51*, 6273–6284; D. Enders, S. von Berg, B. Jandeleit, *Synlett* **1996**, 18–20; b) D. Enders, M. Finkam, *Synlett* **1993**, 401–403; c) W.-J. Koot, H. Hiemstra, W. N. Speckamp, *J. Chem. Soc. Chem. Commun.* **1993**, 156–158; J. C. P. Hopman, H. Hiemstra, W. N. Speckamp, *J. Chem. Soc. Chem. Commun.* **1995**, 617–618; "*N*-Acyliminium Methods in Natural Product Chemistry": W. N. Speckamp, *Merck Swiss Lectureship '94*, lecture arranged by the Chemischen Gesellschaft Zürich, University of Zürich, July 7, 1994.
[217] H.-G. Schmalz, E. Hessler, J. W. Bats, G. Dürner, *Tetrahedron Lett.* **1994**, *35*, 4543–4546; E. Hessler, H.-G. Schmalz, G. Dürner, *ibid.* **1994**, *35*, 4547–4550.
[218] The decision as to whether we should include the usually catalytic process of the allylation of nucleophiles via Pd-π-allyl complexes such as that shown in Scheme 20a in this discussion was not an easy one. On no account would we wish to cram an S_N2 reaction that proceeds with inversion of configuration at a single stereogenic center of an enantiomerically pure substrate into the corset of the SRS principle!
[219] R. M. Williams, *Synthesis of Optically Active α-Amino Acids*, Pergamon, Oxford, **1989**.
[220] "Recent Developments in the Stereoselective Synthesis of α-Amino Acids": R. O. Duthaler, *Tetrahedron* **1994**, *50*, 1539–1650.
[221] If one considers the necessary steps, the chiral cyclic acetals shown in Schemes 10 and 16, which are derivatives of achiral carboxylic acids and are prepared by decarboxylation (aspartic acid → dihydropyrimidinone; serine, threonine, cysteine → imidazoline, oxazoline, thiazoline), are perhaps already results of overextending the SRS principle (laborious), despite their unique reactivity!
[222] The glycine derivative shown in Scheme 21 (top right) may also be prepared from methionine by formation of the imidazolidinone, elimination via a vinylglycine derivative, oxidative cleavage, and finally decarboxylation [223].

[223] T. Weber, R. Aeschimann, T. Maetzke, D. Seebach, *Helv. Chim. Acta* **1986**, *69*, 1365–1377.

[224] D. Seebach, D. D. Miller, S. Müller, T. Weber, *Helv. Chim. Acta* **1985**, *68*, 949–952. In the overall process, amino acids prepared by alkylation of the imidazolidinone shown in Scheme 21 (top) are the result of the replacement of the serine CH_2OH group by another substituent following the SRS principle.

[225] "Syntheses of Enantiomerically Pure Compounds (EPC-Syntheses).—Tartaric Acid, an Ideal Source of Chiral Building Blocks for Syntheses?": D. Seebach, E. Hungerbühler in *Modern Synthetic Methods, Vol. 2* (Ed.: R. Scheffold), Salle + Sauerländer, Frankfurt/Aarau, **1980**, pp. 91–171.

[226] The separation of the product may also cause difficulties: for example, in Schöllkopf's synthesis of amino acids via bislactim ethers derived from diketopiperazines, the final step requires the separation of two amino acid esters (for a reference, see Scheme 22).

[227] a) "Stereoselective Aldol Condensations": D. A. Evans, J. V. Nelson, T. R. Taber in *Topics in Stereochemistry, Vol. 13* (Eds.: N. L. Allinger, E. L. Eliel, S. H. Wilen), Wiley, New York, **1982**, pp. 1–115; b) "Stereoselective Alkylation Reactions of Chiral Metal Enolates": D. A. Evans in *Asymmetric Synthesis, Vol. 3* (Ed.: J. D. Morrison), Academic Press, Orlando, **1984**, pp. 1–110; c) "The Aldol Addition Reaction": C. H. Heathcock in *Asymmetric Synthesis, Vol. 3* (Ed.: J. D. Morrison), Academic Press, Orlando, **1984**, pp. 111–212; d) J. R. Gage, D. A. Evans in *Organic Syntheses, Vol. 68* (Ed.: J. D. White), Wiley, New York, **1990**, pp. 77–82; J. R. Gage, D. A. Evans in *Organic Syntheses, Vol. 68* (Ed.: J. D. White), Wiley, New York, **1990**, pp. 83–91; e) "Modern Enolate Chemistry: Regio- and Stereoselective Formation of Enolates and the Consequence of Enolate Configuration on Subsequent Reactions": C. H. Heathcock in *Modern Synthetic Methods, Vol. 6* (Ed.: R. Scheffold), Verlag Helvetica Chimica Acta/VCH, Basel/Weinheim, **1992**, pp. 1–102; f) see also ref. [31]. New books that collate many examples of the auxiliary approach include: g) J. Seyden-Penne, *Chiral Auxiliaries and Ligands in Asymmetric Synthesis*, Wiley, New York, **1995**; h) D. J. Ager, M. B. East, *Asymmetric Synthetic Methodology*, CRC Press, Boca Raton, **1996**.

[228] For articles dealing with the application of amino acid derivatives as auxiliaries in organic synthesis, see: "Construction of Chiral Molecules Using Amino Acids": G. M. Coppola, H. F. Schuster in *Asymmetric Synthesis*, Wiley, New York, **1987**; "Synthesis and Use of Enantiomerically Pure *t*-Leucine": A. S. Bommarius, M. Schwarm, K. Stingl, M. Kottenhahn, K. Huthmacher, K. Drauz, *Tetrahedron: Asymmetry* **1995**, *6*, 2851–2888; "Amino Acids and their Derivatives as Stoichiometric Auxiliaries in Asymmetric Synthesis": A. Studer, *Synthesis* **1996**, 793–815.

[229] E. Juaristi, B. Rizo, V. Natal, J. Escalante, I. Regla, *Tetrahedron: Asymmetry* **1991**, *2*, 821–826; E. Juaristi, J. L. Anzorena, A. Boog, D. Madrigal, D. Seebach, E. V. García-Baez, O. García-Barradas, B. Gordillo, A. Kramer, I. Steiner, S. Zürcher, *J. Org. Chem.* **1995**, *60*, 6408–6415.

[230] R. Polt, D. Seebach, *Helv. Chim. Acta* **1987**, *70*, 1930–1936.

[231] M. Egli, R. Polt, D. Seebach, *Chimia* **1989**, *43*, 4–5.

[232] R. Polt, D. Seebach, *J. Am. Chem. Soc.* **1989**, *111*, 2622–2632.

[233] S. Blank, D. Seebach, *Angew. Chem.* **1993**, *105*, 1780–1781; *Angew. Chem. Int. Ed. Engl.* **1993**, *32*, 1765–1766.

[234] O. Bezençon, Dissertation No. 11350, ETH, Zürich, **1995**; O. Bezençon, D. Seebach, *Liebigs Ann. Chem.* **1996**, 1259–1276.

[235] A. Studer, T. Hintermann, D. Seebach, *Helv. Chim. Acta* **1995**, *78*, 1185–1206.

[236] T. Ishizuka, S. Ishibuchi, T. Kunieda, *Tetrahedron Lett.* **1989**, *30*, 3449–3452; *Tetrahedron* **1993**, *49*, 1841–1852.

[237] W. H. Pearson, M.-C. Cheng, *J. Org. Chem.* **1987**, *52*, 1353–1355. A camphor derivative of thioglycolic acid has been used in an aminoalkylation: S.-Y. Po, B.-J. Uang, *Tetrahedron: Asymmetry* **1994**, *5*, 1869–1872.

[238] C. Kaneko, M. Sato, J. Sakaki, Y. Abe, *J. Heterocycl. Chem.* **1990**, *27*, 25–30; "Chiral 1,3-Dioxin-4-ones and Related Compounds as Versatile Intermediates for EPC Synthesis": C. Kaneko in *Organic Synthesis in Japan. Past, Present, and Future*, (Ed.: R. Noyori), Tokyo Kagaku Dozin Co. Ltd., Tokyo, **1992**, pp. 175–183; M. Sato, M. Murakami, C. Kaneko, *Tetrahedron* **1993**, *49*, 8529–8540. For an excellent discussion of the stereochemical course of additions to dioxinones, see M. Sato, M. Murakami, S. Sunami, C. Kaneko, T. Furuya, H. Kurihara, *J. Am. Chem. Soc.* **1995**, *117*, 4279–4287.

[239] R. Fitzi, D. Seebach, *Angew. Chem.* **1986**, *98*, 363–364; *Angew. Chem. Int. Ed. Engl.* **1986**, *25*, 345–346; *ibid.* **1986**, *98*, 842 and **1986**, *25*, 766.

[240] R. Fitzi, D. Seebach, *Tetrahedron* **1988**, *44*, 5277–5292.

[241] M. Hoffmann, presently unpublished results; Dissertation, ETH, Zürich.

[242] W. Müller, D. A. Lowe, H. Neijt, S. Urwyler, P. L. Herrling, D. Blaser, D. Seebach, *Helv. Chim. Acta* **1992**, *75*, 855–864.

[243] D. Seebach, S. G. Müller, U. Gysel, J. Zimmermann, *Helv. Chim. Acta* **1988**, *71*, 1303–1318.

[244] D. Seebach, U. Gysel, J. N. Kinkel, *Chimia* **1991**, *45*, 114–117.

[245] D. Blaser, S. Y. Ko, D. Seebach, *J. Org. Chem.* **1991**, *56*, 6230–6233.

[246] D. Blaser, D. Seebach, *Liebigs Ann. Chem.* **1991**, 1067–1078.

[247] J. N. Kinkel, U. Gysel, D. Blaser, D. Seebach, *Helv. Chim. Acta* **1991**, *74*, 1622–1635.

[248] D. Seebach, A. R. Sting, M. Hoffmann, J. N. Kinkel, M. Schulte, E. Küsters, unpublished results.

[249] "Optically Active 1-Acyl-3-alkyl-2-*t*butyl-4-imidazolidinone Production From Racemic 3-Alkyl-2-*t*butyl-4-imidazolidinone by Optical Resolution and Acylation": D. Seebach, R. Fitzi (Degussa AG), DE-B 3604591, **1987**; "Preparation of Optically Active 1,3-Imidazolidin-4-ones as Intermediates for Optically Active Amino Acids": D. Seebach, K. Drauz, M. Kottenhahn, H. Lotter, M. Schwarm (Degussa AG), DE-B 4137186, **1991**; DE-B 4137663, **1991** [*Chem. Abstr.* **1993**, *119*, 180781].

[250] A. R. Sting, Dissertation No. 11669, ETH, Zürich, **1996**; A. R. Sting, D. Seebach, unpublished results.

[251] Boc-BMI, Bz-BMI, and Z-BMI are commercially available in both enantiomeric forms from the following companies: Aldrich Chemical Company, Fluka Chemie AG, Interchim s. a. (France), E. Merck (Germany), Senn Chemicals AG (Switzerland), Wako Chemicals (USA).

[252] There are many examples in the literature of other applications of the chiral acetals shown at the bottom of Scheme 21. Two examples are briefly described here: 1) Formation of ylide **XXIII** by reaction of BMI with formaldehyde and subsequent treatment with, for example, *N*-phenylmalonic acid imide results in the tricyclic compound **XXIV**, which contains three new stereocenters (J.-F. Peyronel, S. Grisoni, B. Carboni, T. Courgeon, R. Carrié, *Tetrahedron* **1994**, *50*, 189–198). 2) Michael addition to a methyl phenyl dioxinone (→ **XXV**) with subsequent hydrogenolysis of one of the benzylic C–O bonds results in the formation of *O*-benzyl-protected 3-hydroxy-3-methylheptanoic acid **XXVI** [244].

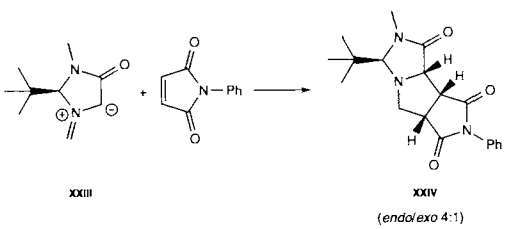

XXIII XXIV (*endo*/*exo* 4:1) XXV XXVI

[253] D. Seebach, H. M. Bürger, C. P. Schickli, *Liebigs Ann. Chem.* **1991**, 669–684.

[254] K. Suzuki, D. Seebach, *Liebigs Ann. Chem.* **1992**, 51–61.

[255] D. Seebach, E. Pfammatter, V. Gramlich, T. Bremi, F. Kühnle, S. Portmann, I. Tironi, *Liebigs Ann. Chem.* **1992**, 1145–1151.

[256] D. Seebach, A. Studer, E. Pfammatter, H. Widmer, *Helv. Chim. Acta* **1994**, *77*, 2035–2050.

[257] A. Studer, D. Seebach, *Heterocycles* **1995**, *40*, 357–378.

[258] S. Blank, D. Seebach, *Liebigs Ann. Chem.* **1993**, 889–896.

[259] M. J. Al-Darwich, C. Lemaire, G. Delfiore, D. Comar, *J. Labelled Compds. Radiopharm.* **1994**, *35*, 108–110.

[260] For example, see the discussion about "flustrates" in Section 2.2 of ref. [261].

[261] D. Seebach, *Angew. Chem.* **1990**, *102*, 1363–1409; *Angew. Chem. Int. Ed. Engl.* **1990**, *29*, 1320–1367.

[262] Only the use of a special trick allows the formation of the free α-branched amino acids that bear two bulky substituents [83]. Interestingly, drastic conditions are required for the hydrolysis of the 5,5-disubstituted *N*-benzoyl oxazolidinones with bulky substituents; the final step in which the benzoyl amide is cleaved requires: HOAc/conc. HCl (2/1), reflux [82], cf. ref. [83] and D. Obrecht, C. Spiegler, P. Schönholzer, K. Müller, H. Heimgartner, F. Stierli, *Helv. Chim. Acta* **1992**, *75*, 1666–1696; D. Obrecht, U. Bohdal, R. Ruffieux, K. Müller, *ibid.* **1994**, *77*, 1423–1429.

[263] For example, the addition of a cuprate to an alkylidene-Boc-BMI derivative is completely selective (rel. topicity 1,4-*lk*) by NMR analysis, even though three bonds and three trigonal centers separate the inducing and newly formed stereogenic centers (**XXVII** → **XXVIII**) [134, 253]. It is even more surprising that the reaction of the dienylidene **XXIX** with dibutylcuprate leads to a single product **XXX** (to date of unknown configuration), although five bonds separate the stereogenic acetal center and the site of substitution in the substrate (see ref. [253] and footnote [27] therein). Stereogenic centers positioned in a 1,5-fashion result from the 1,2- or 1,4-addition of the dienolate **XXXI** of 2-*tert*-butyl-6-methyl-1,3-dioxin-4-one, at the 5- and 1′-position, to an aliphatic aldehyde (→ **XXXII**) or enal (→ **XXXIII**), respectively [264, 265].

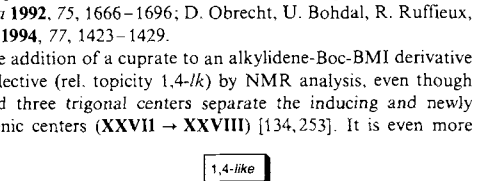

XXVII XXVIII

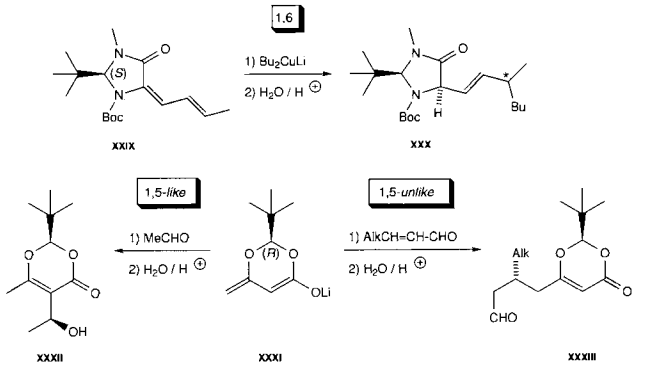

[264] D. Seebach, U. Misslitz, P. Uhlmann, *Angew. Chem.* **1989**, *101*, 484–485; *Angew. Chem. Int. Ed. Engl.* **1989**, *28*, 472–473.
[265] D. Seebach, U. Misslitz, P. Uhlmann, *Chem. Ber.* **1991**, *124*, 1845–1852.
[266] For examples of 1,5-, 1,6-, and 1,7-induction see M. Nógrádi, *Stereoselective Synthesis—A Practical Approach*, 2nd ed., VCH, Weinheim, **1995**.
[267] Reactions of 4-methyl and 4-trifluoromethyldioxinones with Cu-doped benzyl Grignard reagents (to give **XXXIV** and **XXXV**, respectively) under identical conditions. In the first case, the standard *trans* addition (of the benzylic C atom) occurs, but the second example shows a *cis* addition (of the *para* C atom) with concomitant formation of the quinoid system [156, 157]! We have previously called F-containing reactants "flustrates" [261].

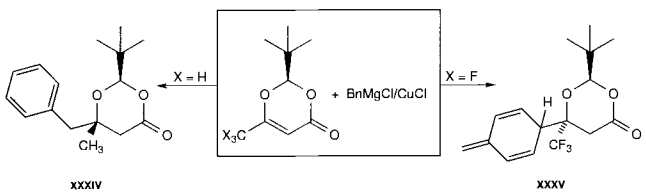

[268] As is evident from the discussion in ref. [29], it has been accepted for many years (work of Creger and Pfeffer) that deuterolysis of an enolate produced by the use of LDA is not a reliable method for determining the degree of enolate formation.
[269] For a review article dealing with the themes [Li-enolate·HNR_2] and [Li-enolate·$LiNR_2$], see refs. [21–23, 26–28, 48] and K. Rück, *Angew. Chem.* **1995**, *107*, 475–477; *Angew. Chem. Int. Ed. Engl.* **1995**, *34*, 433–435.
[270] One further equivalent of Li-amide is produced, such that the desired product of the reaction with electrophiles is now at the mercy of this strong base!
[271] The stereoelectronic barrier, already discussed in Section 3, which protects the corresponding enolate from facile β-elimination, is nowhere near as high when the leaving group is RS^- in place of RO^-. When the rules for cyclization (the reverse of this elimination) were initially proposed, Baldwin explicitly stated that these are only valid for cases in which no elements of the second or a higher period are involved (see also Scheme 6 and ref. [111a]).
[272] "The Synthetic Utility of α-Amino-Alkoxides": D. L. Comins, *Synlett* **1992**, 615–625.
[273] Y. Kai, P. Knochel, S. Kwiatkowski, J. D. Dunitz, J. F. M. Oth, D. Seebach, *Helv. Chim. Acta* **1982**, *65*, 137–161.
[274] P. E. O'Bannon, W. P. Dailey, *J. Am. Chem. Soc.* **1989**, *111*, 9244–9245.
[275] Such adducts of RXLi and carbonyl groups appear to be involved in other reactions of Li-enolates and possibly play a much larger role than previously thought [272]. They could, for example, be responsible for the 2:1 reactions of aldehydes with Li-enolates and also possibly for the known stabilization of Li-aldolates against elimination to give α,β-unsaturated carbonyl compounds (see **XXXVI** → **XXXVII** and **XXXVIII** → **XXXIX** → **XL** [293]).

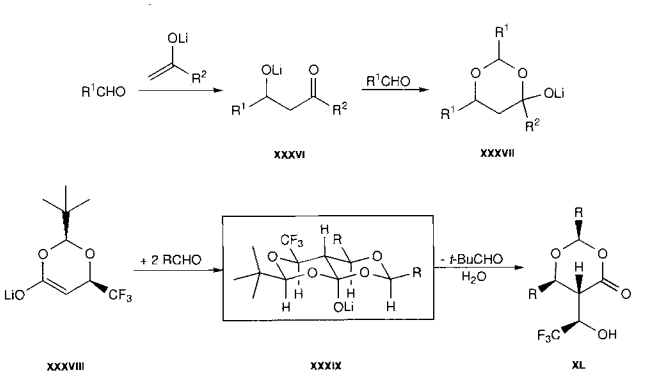

[276] For the first attempts at explaining a few of the observed effects, see ref. [48].
[277] See ref. [227b].
[278] H. O. House, B. A. Tefertiller, H. D. Olmstead, *J. Org. Chem.* **1968**, *33*, 935–942.
[279] See footnotes [41–45] in ref. [23] and the general discussion in ref. [254].
[280] W. Amberg, D. Seebach, *Angew. Chem.* **1988**, *100*, 1786–1787; *Angew. Chem. Int. Ed. Engl.* **1988**, *27*, 1718–1719; *Chem. Ber.* **1990**, *123*, 2413–2428; *ibid.* **1990**, *123*, 2439–2444.
[281] See Section 3 and Schemes 5 and 6 for references to the literature.
[282] The alternative course of the cyclization reaction when transition metal acetalization catalysts are used has already been pointed out in Section 3 [57].
[283] See the bicyclic azetidine carboxylic acid, proline, thiaproline, hydroxyproline, and pyroglutamic acid derivatives in Section 3, Schemes 6 and 28, Table C in the appendix and ref. [91].
[284] See Section 3 and ref. [92] for references to the literature.
[285] D. A. Evans, J. C. Barrow, J. L. Leighton, A. J. Robichaud, M. Sefkow, *J. Am. Chem. Soc.* **1994**, *116*, 12111–12112.
[286] J. Zimmermann, D. Seebach, T.-K. Ha, *Helv. Chim. Acta* **1988**, *71*, 1143–1155.
[287] For example, compare the benzylation of the dioxolane carboxylic *tert*-butylthioester (d.r. = 80:20, *cis* [93, 102]) with that of the *N*-formyloxazolidinecarboxylic acid methyl ester (d.r. = 98.5:1.5, *trans* [93, 100]) and also with the methylation of *N*-formylthiazolidinecarboxylic acid methyl ester (d.r. > 98:2, *trans* [106]). See the equations in the second line of Scheme 29b, Section 3, and Table B.
[288] See our work on NCS reactions [133, 134].
[289] Reactions at radical centers of the heterocycle with formation of C–C and C–H bonds have been studied by Beckwith et al. [135]. Furthermore, see the radical reactions of methylenedioxanones performed by B. Giese et al. (discussion and references in [290]).
[290] For a comprehensive review article, see D. P. Curran, N. A. Porter, B. Giese, *Stereochemistry of Radical Reactions—Concepts, Guidelines, and Synthetic Applications*, VCH, Weinheim, **1996**.
[291] H. E. Zimmerman, M. D. Traxler, *J. Am. Chem. Soc.* **1957**, *79*, 1920–1923.
[292] See ref. [178a].
[293] J.-M. Lapierre, M. Gautschi, G. Greiveldinger, D. Seebach, *Chem. Ber.* **1993**, *126*, 2739–2746.
[294] It was not to be expected that the larger stability of the 1,3-*cis*-substituted five-membered ring heterocycle would be due to the diequatorial arrangement of the substituents in an envelope conformation (the *cis*/*trans* energy difference of 1,3-dimethylcyclopentane is 0.2 kcal mol^{-1}!). See: J. Dale, *Stereochemie und Konformationsanalyse*, 1st ed., VCH, Weinheim, **1978**.
[295] F. Johnson, *Chem. Rev.* **1968**, *68*, 375–413.
[296] R. W. Hoffmann, *Chem. Rev.* **1989**, *89*, 1841–1860.
[297] J. L. Broeker, R. W. Hoffmann, K. N. Houk, *J. Am. Chem. Soc.* **1991**, *113*, 5006–5017.
[298] Here, we use Dunitz's definition for pyramidalization (Δ) of trigonal centers: K. L. Brown, L. Damm, J. D. Dunitz, A. Eschenmoser, R. Hobi, C. Kratky, *Helv. Chim. Acta* **1978**, *61*, 3108–3135.
[299] The value of almost 20 kcal mol^{-1} of the partial amide C=N bond corresponds to practically a third of that of the C=C bond.
[300] For example, see the data in Table 1 of both refs. [62] and [178a] and also Table 4 of ref. [143].
[301] D. Seebach, T. Maetzke, W. Petter, B. Klötzer, D. A. Plattner, *J. Am. Chem. Soc.* **1991**, *113*, 1781–1786.
[302] Hence, the reversal of topicity from a weakly *unlike* to a strongly *like* preference during the aldol addition reaction of a trigonal center of a dioxolanone, *N*-acyloxazolidinone, or *N*-acylimidazolidinone Li-enolate to an aldehyde might be attributed to the close proximity of R^1 and H (in comparison with R^1 and R^2) (see structure **B** in Scheme 29e). See the general discussion in ref. [254] and the collection of data in Table F. Aldol additions of dioxolanones: ref. [47] and C. H. Heathcock, M. C. Pirrung, S. D. Young, J. P. Hagen, E. T. Jarvi, U. Badertscher, H.-P. Märki, S. H. Montgomery, *J. Am. Chem. Soc.* **1984**, *106*, 8161–8174; of oxazolidinones: [71, 246, 250]; of imidazolidinones: [71, 134, 258]. The higher proportion of *ul*-combination seen in the transition from aliphatic to aromatic aldehydes in the aldol addition of dioxanone-enolates [153, 178, 265, 293] may be due to a π–π interaction (see **XLI** und **XLII**).

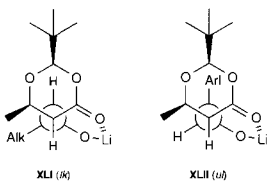

[303] A. J. Birch, G. S. R. Subba Rao, *Aust. J. Chem.* **1970**, *23*, 547–552.
[304] T. Takahashi, M. Nisar, K. Shimizu, J. Tsuji, *Tetrahedron Lett.* **1986**, *27*, 5103–5104; K. Tomioka, K. Yasuda, H. Kawasaki, K. Koga, *Tetrahedron Lett.* **1986**, *27*, 3247–3250; K. Tomioka, H. Kawasaki, K. Yasuda, K. Koga, *J. Am. Chem. Soc.* **1988**, *110*, 3597–3601.
[305] Following a suggestion of B. Trost during a discussion with R. W. Hoffmann, the rather unfortunate expression "contrasteric" has been used in the literature for this effect [95, 98].

[306] In previous publications [93, 102], we have suggested that the *cis* selectivity could be due to the bicyclic nature of the dioxolane carboxylic ester enolate, which is attacked by the electrophile at the *exo* face, that is, *cis* to the existing substituent (see **XLIII** and compare the reactions of the bicyclic enolates derived from proline, hydroxyproline, thiaproline, azetidine carboxylic acid, and pyroglutamic acid, Section 3 and Table B). The chelate structure of the Li-enolate of α-RO-substituted carbonyl compounds has been established by NMR analysis of the corresponding silyl enol ether [31, 227].

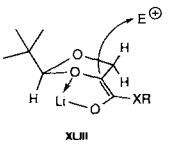

XLIII

[307] D. Seebach, R. Amstutz, T. Laube, W. B. Schweizer, J. D. Dunitz, *J. Am. Chem. Soc.* **1985**, *107*, 5403–5409.
[308] R. E. Babston, V. Lynch, C. S. Wilcox, *Tetrahedron Lett.* **1989**, *30*, 447–450.
[309] Like the parent esters [312], chelated enolates such as those from β-ketoesters [310] or from α-dialkylaminoesters [311] adopt a planar arrangement.
[310] C. Cambillau, G. Bram, J. Corset, C. Riche, *Canad. J. Chem.* **1982**, *60*, 2554–2565.
[311] J. T. B. H. Jastrzebski, G. van Koten, W. F. van De Mieroop, *Inorg. Chim. Acta* **1988**, *142*, 169–171.
[312] W. B. Schweizer, J. D. Dunitz, *Helv. Chim. Acta* **1982**, *65*, 1547–1554.
[313] B. Giese, J. Meixner, *Tetrahedron Lett.* **1977**, *32*, 2783–2784.
[314] See the examples in ref. [82], and references therein.
[315] See also Fig. 7 in ref. [301].
[316] Compare with the X-ray crystal structure analysis of an alkylidene-Boc-BMI-derivative in ref. [62] and the legend of Scheme 31.
[317] R. Naef, Dissertation No. 7442, ETH, Zürich, **1983**.
[318] R. Fitzi, Dissertation No. 8654, ETH, Zürich, **1988**.
[319] S. G. Müller, Dissertation No. 8616, ETH, Zürich, **1988**; U. Gysel, Dissertation No. 9473, ETH, Zürich, **1991**.
[320] *Forschung Chromatographie*, E. Merck, Darmstadt (Germany).
[321] "Electrochemical Formation and Transformation of Chiral Heterocycles as Key Intermediates in Stereoselective Reactions": E. Steckhahn, P. Brungs, A. Zietlow, A. Stahl, B. Lewall, G. Kardassis, A. Papadopoulos in *Modern Methodology in Organic Synthesis* (Ed.: T. Shono), Kodansha/VCH, Tokyo/Weinheim, **1992**, pp. 323–337.
[322] A. Frauer, M. Mehlführer, K. Thirring, H. Berner, *J. Org. Chem.* **1994**, *59*, 4215–4222.
[323] K. Nebel, M. Mutter, *Tetrahedron* **1988**, *44*, 4793–4796.
[324] S. Karady, J. S. Amato, L. M. Weinstock, *Tetrahedron Lett.* **1984**, *25*, 4337–4340.
[325] M. A. Walker, C. H. Heathcock, *J. Org. Chem.* **1992**, *57*, 5566–5568.
[326] E. Altmann, K. Nebel, M. Mutter, *Helv. Chim. Acta* **1991**, *74*, 800–806.
[327] F. Alonso, S. G. Davies, *Tetrahedron: Asymmetry* **1995**, *6*, 353–356.
[328] A. B. Smith III, R. C. Holcomb, M. C. Guzman, T. P. Keenan, P. A. Sprengeler, R. Hirschmann, *Tetrahedron Lett.* **1993**, *34*, 63–66.
[329] "Process for Preparation of α-Alkyl Amino Acids": J. S. Amato, L. M. Weinstock, S. Karady (Merck & Co.), US-A 4508921, **1985**.
[330] N. P. Singh, A. Giannis, E. Henk, T. Kolter, K. Sandhoff, R. R. Schmidt, *J. Carbohydr. Chem.* **1990**, *9*, 543–559.
[331] A. D. Abell, J. M. Taylor, *J. Org. Chem.* **1993**, *58*, 14–15.
[332] H. Cheng, P. Keitz, J. B. Jones, *J. Org. Chem.* **1994**, *59*, 7671–7676.
[333] K. Krohn, U. Müller, *Tetrahedron* **1986**, *42*, 6635–6644.
[334] T. Fukuyama, Y. Kanda, *J. Synth. Org. Chem. Jpn.* **1994**, *52*, 888–899.
[335] G. Scherowsky, M. Sefkow, *Mol. Cryst. Liq. Cryst.* **1991**, *202*, 207–216.
[336] T. Früh, G. M. R. Tombo, *Synlett* **1994**, 727–728.
[337] K. Krohn, H. Rieger, *Liebigs Ann. Chem.* **1987**, 515–520.
[338] H. Niwa, T. Ogawa, K. Yamada, *Tetrahedron Lett.* **1989**, *30*, 4985–4986.
[339] S. Hünig, Y. Keita, K. Peters, H.-G. von Schnering, *Chem. Ber.* **1994**, *127*, 1495–1500.
[340] N. Isono, M. Mori, *J. Org. Chem.* **1995**, *60*, 115–119.

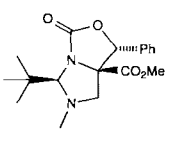

XLIV

[341] T. Fujita, N. Hamamichi, T. Matsuzaki, Y. Kitao, M. Kiuchi, M. Node, R. Hirose, *Tetrahedron Lett.* **1995**, *36*, 8599–8602.
[342] When benzaldehyde is used as the electrophile, the bicyclic product **XLIV** is formed [99].
[343] M. J. Crossley, C. W. Tansey, *Aust. J. Chem.* **1992**, *45*, 479–481.
[344] G. Kneer, J. Mattay, A. Heidbreder, G. Raabe, B. Krebs, M. Läge, *J. Prakt. Chem.* **1995**, *337*, 113–124.
[345] M. Sato, Y. Abe, C. Kaneko, *J. Chem. Soc. Perkin Trans. 1* **1990**, 1779–1783.
[346] J. Mattay, J. Mertes, G. Maas, *Chem. Ber.* **1989**, *122*, 327–330.
[347] W. R. Roush, K. Koyama, *Tetrahedron Lett.* **1992**, *33*, 6227–6230.
[348] W. R. Roush, B. B. Brown, *Tetrahedron Lett.* **1989**, *30*, 7309–7312.
[349] "Synthesis of ^{11}C-Labelled Acidic and Basic L- and D-Amino Acids": K. Hörnfeldt, K.-J. Fasth, B. Långström in *Synthesis and Applications of Isotopically Labelled Compounds 1994* (Eds.: J. Allen, R. Voges), Wiley, Chichester, **1995**, pp. 367–370.
[350] G. Y. Krippner, M. H. Harding, *Tetrahedron: Asymmetry* **1994**, *5*, 1793–1804.
[351] A. Plenevaux, M. J. Al-Darwich, C. Lemaire, G. Delfiore, D. Comar, *Appl. Radiat. Isot.* **1994**, *45*, 361–369.
[352] W. Müller, P. Kipfer, D. A. Lowe, S. Urwyler, *Helv. Chim. Acta* **1995**, *78*, 2026–2035.
[353] M. Monclus, C. Masson, A. Luxen, *J. Fluorine Chem.* **1995**, *70*, 39–43.
[354] C. Lemaire, A. Plenevaux, P. Damhaut, M. Guillaume, L. Christiaens, D. Comar, *J. Labelled Compd. Radiopharm.* **1993**, *32*, 139–140.
[355] C. Lemaire, A. Plenevaux, R. Cantineau, L. Christiaens, M. Guillaume, D. Comar, *Appl. Radiat. Isot.* **1993**, *44*, 737–744.
[356] P. Damhaut, C. Lemaire, A. Plenevaux, L. Christiaens, D. Comar, *J. Labelled Compds. Radiopharm.* **1994**, *35*, 178–180.
[357] S. Sjöberg, M. F. Hawthorne, S. Wilmouth, P. Lindström, *Chem. Eur. J.* **1995**, *1*, 430–435.
[358] Hydroxyalkylation with acetone yields the following **XLV** [71]. In the reaction with aldehydes, if the reaction mixture is allowed to warm to room temperature before workup, the rearranged product **XLVI** is formed as virtually the only product [71].

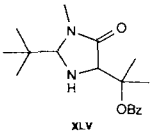

XLV

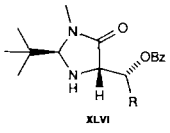

XLVI

R = Me, CF_3, *i*Pr, Ph, $CH(Me)CH_2CH{=}CHMe$,

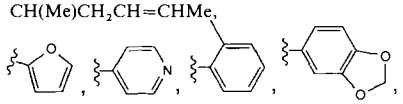

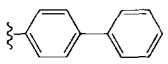

[359] M. Mehlführer, H. Berner, K. Thirring, *J. Chem. Soc. Chem. Commun.* **1994**, 1291–1291.
[360] Y. Song, D. Niederer, P. M. Lane-Bell, L. K. P. Lam, S. Crawley, M. M. Palcic, M. A. Pickard, D. L. Pruess, J. C. Vederas, *J. Org. Chem.* **1994**, *59*, 5784–5793.
[361] O. García-Barradas, E. Juaristi, *Tetrahedron* **1995**, *51*, 3423–3434.
[362] C. Lowe, Y. Pu, J. C. Vederas, *J. Org. Chem.* **1992**, *57*, 10–11.
[363] A portion of the aldol product cyclizes with formation of the carbamate **XLVII**.

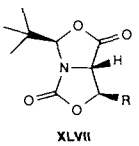

XLVII

R = Et [246], *i*Pr [246], *t*Bu [246],

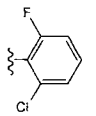

[246],

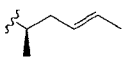

[245],

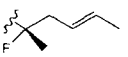

[250],

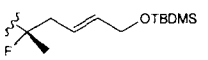

[250].

[364] The reversal of relative topicity between the addition of **XLVII** to a "normal" aliphatic and an aromatic aldehyde [233, 241] would be consistent with a chair (→ **XLIX**) or with a boat-type transition state (→ L) (in the case of a 3-benzyloxyaldehyde, the topicity is once again reversed [365]).

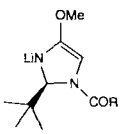

XLVIII

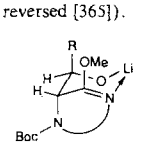

XLIX

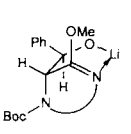

L

[365] K. Matsuda, unpublished results (1995).
[366] See refs. [39, 227c].
[367] R. Amstutz, Dissertation No. 7210, ETH, Zürich, **1982**; J. Hansen, Dissertation No. 7863, ETH, Zürich, **1985**.
[368] R. Häner, T. Laube, D. Seebach, *Chimia* **1984**, *38*, 255–257.
[369] D. A. Oare, M. A. Henderson, M. A. Sanner, C. H. Heathcock, *J. Org. Chem.* **1990**, *55*, 132–157.
[370] D. A. Widdowson, G. H. Wiebecke, D. J. Williams, *Tetrahedron Lett.* **1982**, *23*, 4285–4288.

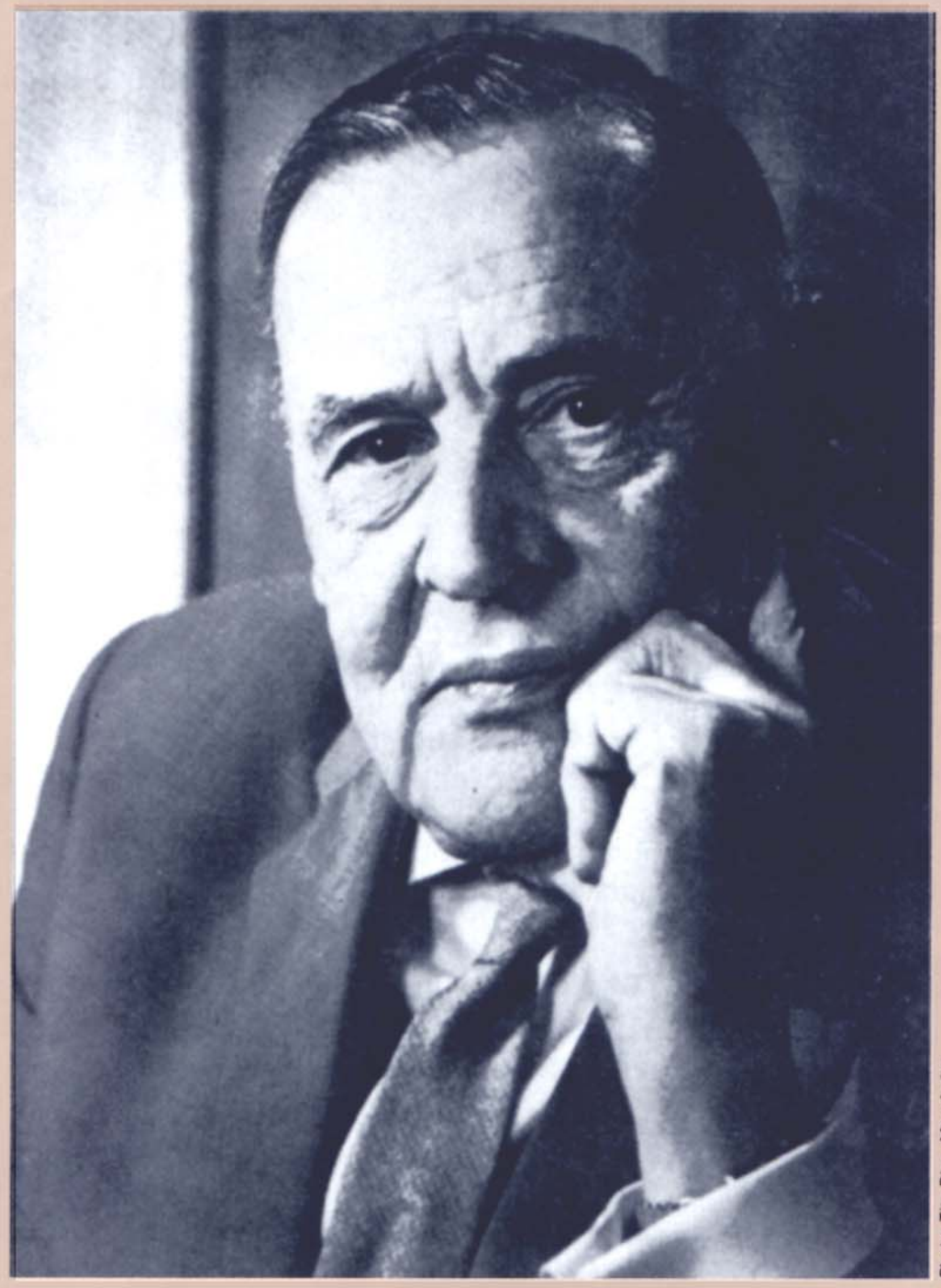

Photo: Tita Binz, Mannheim

Erich Hückel

A scientist caught between two stools: physicists found his work too nonphysical, and chemists didn't listen to him because he was a physicist.

Erich Hückel, Pioneer of Organic Quantum Chemistry: Reflections on Theory and Experiment

Jerome A. Berson*

In the period between 1930 and 1937, Erich Hückel, a theoretical physicist, made profound contributions to organic chemistry in his quantum mechanical descriptions of unsaturated and conjugated compounds. A brief account of his academic career is followed by simplified expositions, from the point of view of an organic chemist, of the highly approximate theoretical methods he used. Of special significance in the case of cyclic molecules of the class C_nH_n is the concept of filled shells when the number of π electrons is $(4N+2)$ $(N = 0, 1, 2, \ldots)$. Examinations of key applications of Hückel's ideas reveal how they eventually motivated the exploration of new fields in organic synthesis and organic reaction mechanism. Another significant (but until recently, virtually ignored) contribution by Hückel was the recognition that atomic connectivity is a strong determinant of spin multiplicity in non-Kekulé molecules. This idea provides, in principle, a basis for predicting violations of Hund's rule, as recent computational and experimental developments confirm. The interaction of experiment with different styles of quantum theory, and the impact of this relationship on the development of chemistry, are briefly considered. Speculations are given on why Hückel's work exerted so little influence on organic chemistry for decades before its importance finally began to be recognized.

Keywords: aromaticity · history of chemistry · Hückel, Erich · pericyclic reactions

1. Introduction

Erich Hückel's position as one of the early leaders in the development of quantum chemistry now is secure. Every modern chemist uses ideas that sprang from his work. Yet certain causes, undoubtedly connected but still not entirely clear, marked his career with bitter frustration, delayed the recognition that he deserved, and not incidentally, retarded the development of organic chemistry by muffling the impact of his contributions.

To trace the intellectual origins of his work is a challenge to the historian of science. How did a man trained as a theoretical physicist have the insight to choose problems of such significance to organic chemistry? Where did he find the daring self-confidence to make the gross (but ultimately successful) approximations of Hückel molecular orbital theory? What circumstances delayed the incorporation of his ideas into the everyday working knowledge of organic chemists?

[*] Prof. J. A. Berson
Department of Chemistry, Yale University
225 Prospect Street, New Haven, CT 06520-8107 (USA)
Fax: Int. code +(203)432-6144
e-mail: berson%kekule@biomed.med.yale.edu.

2. Biographical Sketch[1–3]

This is the centennial year of Erich Hückel, who was born on August 9, 1896, the second of three sons of Marie and Armand Hückel. The intellectual development of the three boys was strongly influenced by their father, a physician with an interest in pure science. In the family line were several scientific notables, including the distinguished botanist Josef Gärtner (1732–1791). Erich Hückel enriched this heritage in 1921, when he married Anne Zsigmondy, the daughter of Professor Richard Zsigmondy of Göttingen, a renowned colloid chemist (Nobel Prize in Chemistry, 1925). The marriage endured until Hückel's death in 1980. Erich Hückel's brothers, Rudi (1899–1949) and Walter (1895–1973), followed in the family tradition. Rudi became a physician, but died prematurely. Walter achieved prominence as a professor of organic chemistry and a prolific author of significant research contributions and influential textbooks.[4]

Erich Hückel was trained as a physicist. His thesis for the D. Phil. at Göttingen (1921) under the supervision of Peter Debye was an experimental study of the scattering of X-rays. Afterward, he served briefly as an assistant to the mathematician David Hilbert at Göttingen but then rejoined Debye, who had moved to the Eidgenössische Technische Hochschule in Zürich. Hückel stayed in Zürich until 1927. Two years on a Rockefeller

 © VCH Verlagsgesellschaft mbH, D-69451 Weinheim, 1996 0570-0833/96/3523-2751 $ 15.00+.25/0

Foundation scholarship, which he spent with Donnan in London and with Bohr in Copenhagen, were followed by two more years on a Deutsche Notgemeinschaft scholarship in Leipzig with Heisenberg and Hund. It was in Leipzig in 1930 that Hückel finished the first of his landmark papers on organic quantum chemistry.

Note that nine years after the D. Phil, Hückel still had no permanent job. In effect, his situation was like that of all too many of today's postdoctoral researchers, who float in semi-employed limbo. Through Debye's intervention, a *dozentur* of sorts was arranged for him at the Technische Hochschule in Stuttgart during the period 1930–1937. However, this was not a regularly budgeted position, and even Hückel's salary was insecure. In his book published in 1975,[1] Hückel relates that his wife often referred to this time as "seven years of disgrace".

Finally, in 1937 came a call to Marburg as Extraordinary Professor (Associate Professor) of Theoretical Physics. Except for a brief period immediately following the war, Hückel held this position until it was upgraded to that of Ordinary (Full) Professor in 1961, a year before his formal retirement. It was a mean career, blighted by marginalization and outright humiliation, and in some ways incommensurate with the magnitude of his contributions to science. As we shall see, some of his difficulties in gaining recognition arguably were self-inflicted, but others were not. More research would be needed to unravel all the causes, but there is little doubt that that the personal frustrations of Hückel's career mirrored the decades-long delay in general acceptance of the significance of his work.

3. Hückel's Early Contributions to Fundamental Physical Chemistry: The Debye–Hückel Theory of Electrolytic Solutions

As an assistant in Zürich, Hückel collaborated on the famous Debye–Hückel theory of strong electrolytes (1923),[5] which is described authoritatively elsewhere.[2, 6, 7] The details of the theory need not detain us here, but even an amateur comes away after reading these accounts with an appreciation of two major characteristics of Hückel's later independent work, particularly in the field of organic quantum chemistry: first the identification of the significant questions for which no satisfactory answers were yet available, and second the design of a theory based upon bold simplifying assumptions, which although perhaps not rigorously justifiable at the time, nevertheless showed the way to plausible explanations of known facts and to testable predictions. What is really operating here in this early phase of Hückel's career is a particular style of theory in which the goal is not a perfect, unshakable construct that will last for eternity, but rather a more pragmatic procedure, which might be described with the motto: *let's see if this works, and if it does, let's keep using it until it shows deficiencies.* Of course, this is the way many theoreticians often operate, whether or not they admit as much.

It is true, as has been said,[2] that we don't know for sure whether Debye or Hückel was the dominant partner in designing the approach to their joint problem, but this issue is almost beside the point here. One way or another, Hückel learned (or invented, or re-invented) this style in the work on the theory of electrolytes. It was to be a hallmark of his later independent research.

4. The Nature of the Double Bond

4.1. Origins of Hückel's Interest in Organic Chemistry

In searching for a pattern of influence on Hückel's famous 1930 papers[8] "Zur Quantentheorie der Doppelbindung," we note that he acknowledges the stimulus given by Bohr, in whose institute in Copenhagen he began the work in the summer of 1929. The first paper was finished in Leipzig at the end of the year. Hückel's autobiography[1] implies that Bohr's role consisted largely of identifying chemistry as a field to which the new quantum ideas might be fruitfully applied. There is no indication that Bohr made specific suggestions as to the areas of chemistry that might be interesting to examine.

Where then did Hückel get the idea to work on unsaturated and aromatic compounds? One might imagine that this much insight into the details of so foreign a discipline would have been unusual for a theoretical physicist of the time. It is conceivable that as a student or subsequently in preparation for his theoretical work, he may have acquired enough knowledge of chemistry, especially of organic chemistry, to generate the required motivation, but he makes no mention of special study. One can hardly avoid the conjecture that Walter Hückel's encyclopedic knowledge of the subject offered a far more accessible source. According to Erich Hückel's acknowledgment in the 1930 paper, Edward Teller was especially helpful on quantum mechanical questions and Walter Hückel on chemical matters. Our understanding of the human factors that condition the interaction of theory and experiment would be greatly enhanced if we knew

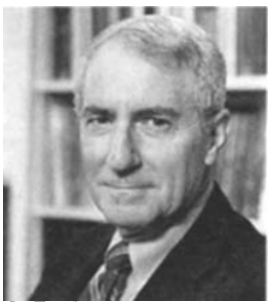

Jerome A. Berson was born in Sanford, Florida in 1924. He received the degree of B. S. in chemistry from the City College of New York in 1944. After service in the Army of the United States (1944–1946, China-Burma-India Theater), he returned to the study of chemistry at Columbia University, where he received MA (1947) and PhD (1949) degrees, working with W. von E. Doering. Following a postdoctoral year (1949–1950) at Harvard University with R. B. Woodward, Berson held faculty positions successively at the University of Southern California (1950–1963) and the University of Wisconsin (1963–1969). Since 1969, he has been on the faculty of Yale University, where he is now Sterling Professor Emeritus of Chemistry.

more about Walter's role. Although Erich's autobiography and other writings so far available to me are quite nonspecific about just what Walter provided, it is my (as yet undocumented) working hypothesis that Walter served as more than a mere source of factual information. It seems likely that his professional immersion in the culture of organic chemistry made it natural for him to point out to Erich several profound unsolved problems of the structure and reactions of organic compounds which one could hope to illuminate with the new quantum theory. In other words, Walter was in a position to perform a crucial service to Erich: he could ask the right questions. Whether he did so remains to be established.

4.2. Restricted Rotation of Double Bonds

In his first paper on organic quantum chemistry, Erich Hückel undertook to solve an intimidatingly deep problem, which is concisely stated in his own words:[8]

> "The chemist, especially the organic chemist, tends to link more to the concept of valence than merely the valence of the atoms. He would like to ascribe to the valence lines between bonded atoms a definite real existence, in which, especially in the chemistry of carbon, not only the number of valence bonds, but also their direction in space should have significance... In this work the generality of this question will not be treated; rather only a special case will be examined, which makes a contribution to this question. This case concerns what chemists call the 'restricted rotation of double bonds'".

The persistence of stereochemical configuration about C=C and C=N bonds had long been known and had been rationalized by the postulate of restricted rotation in such compounds. J. H. van't Hoff[9] had provided a classical (that is a prequantum theoretical) "explanation." The carbon–carbon double bond was imagined to be made up by contact of two tetrahedrally disposed valences of each atom (Fig. 1). This would result in the

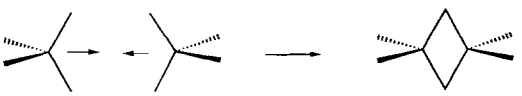

Fig. 1. Junction of two sets of tetrahedral carbon valences to produce a double bond, in the manner of van't Hoff [9]. The bonds lie outside the C–C direction; the remaining four valences lie pairwise above and below the plane of the paper.

stereochemistry shown, with the four remaining valences lying in the same plane as the carbon atoms. The structure would be resistant to rotation of the carbon atoms with respect to each other about the line joining them, because such twisting would diminish the contact of the valences. Of course, this proposal begged the question that Hückel was concerned with: what is the physical nature of these valences?

Soon after the first[8] of Hückel's papers on the double bond appeared, Pauling[10a] and Slater[11] independently were to develop a quantum mechanical description of ethylene which was very close in spirit to van't Hoff's representation. They visualized the two carbon–carbon bonds as *equivalent entities* made up by overlap of sp^3 hybrid orbitals whose axes lay on either side of the actual C–C internuclear line. As part of a general theory of directed valence, these same sp^3 hybrid orbitals had been postulated to account for the tetrahedral orientation of the bonds of tetravalent carbon atom.

Several textbook authors have wrongly ascribed to Pauling the concept of trigonal (sp^2) hybridization of the doubly bonded carbon atoms in ethylene (see below). Pauling's example of this hybridization was graphite, not ethylene. In fact, he remained strongly opposed to the concept that the two ethylene C–C bonds were different, an unavoidable consequence of trigonal hybridization. The H–C=C angle in a trigonally hybridized alkene is predicted to be 120°, but Pauling's *The Nature of the Chemical Bond* (1961 edition[10a]), which cites a number of experimental determinations near 125°17′, stoutly defends the tetrahedral model, which predicts the latter value (half the difference between 360° and the tetrahedral angle H-C-H angle 109°26′). It is probably fair to say that in the current era of ab initio theory, a decision between these two approaches, which are after all only models, has become moot.[10b]

Curiously, one often sees, in implied or direct form, similar misattributions of the trigonal hybridization concept to Hückel. It is true that the essence of Hückel's model is that the two C–C bonds are *nonequivalent*, one σ and one π bond, a basic distinction from the tetrahedral model favored by Pauling. However, Hückel's ethylene model in the first instance did not arise from hybridization considerations and did not require trigonal hybridization. In fact, the $\sigma-\pi$ ethylene model originated in the quantum theoretical treatment of a seemingly very different molecule, molecular oxygen, O_2. How Hückel's new plant sprang from such unlikely soil makes a long story, but the lessons to be learned about the genesis of ideas justify an abbreviated version. The hybridization question is discussed in more detail in Section 4.4.

4.3. From Dioxygen to Formaldehyde to Ethylene

In 1929 the year just preceding the appearance of Hückel's paper, Lennard-Jones[12] had made a molecular orbital analysis of the electronic structure of dioxygen in its ground state, which he represented as having the following occupation pattern: $(1s)^2(1s)^2(2s)^2(2s)^2(2p_+)^2(2p_-)^2(2p\sigma)^2\{2p\pi_+, 2p\pi_-\}$ As Hückel points out,[8] this notation differs from the "united atom" MO formalism of Hund and Mulliken, which is more familiar now, and which had been developed for diatomic molecules. Lennard-Jones's notation is more suitable for showing the electronic states that are being generated during dissociation of the "united atom."

The results are shown in Figure 2.[13] Note that the interaction of the two filled 2s atomic orbitals gives rise to no net bonding in this approximation, which (with apologies) limits the discussion to the molecular orbitals (MOs) derived from the atomic 2p orbitals and alters Lennard-Jones's presentation to a "united atom" form. An oxygen atom in its ground state has four electrons in the three mutually perpendicular p atomic orbitals (AOs). When two such atoms are brought into bonding distance, the six AOs give rise to six MOs. Two of the MOs, a strongly bonding ($\sigma 2p$) and a strongly antibonding ($\sigma^* 2p$) pair,

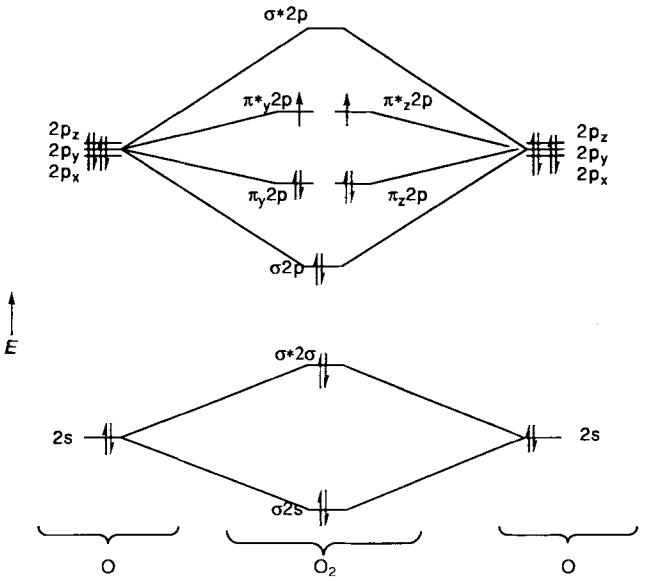

Fig. 2. Formation of O_2 molecular orbitals from oxygen atomic orbitals. The occupation pattern and spin state are derived by application of Hund's highest multiplicity rule. The energies are shown schematically (adapted ref. [13] with permission of Oxford University Press).

result from mixing of the two original p orbitals that lie along the internuclear line. The remaining four atomic p orbitals mix to form two degenerate π MOs and two degenerate π* MOs. The nodal planes of the π MOs are a mutually perpendicular (arbitrarily chosen) pair containing the two atomic nuclei, and the π* MOs each have the same pair of nodal planes in addition to a perpendicular nodal plane bisecting the internuclear O–O line. The total of eight electrons (originally from p orbitals) now must be fed into this set of MOs. Two each, with opposed spins, go into the bonding σ and the two bonding π MOs. Although formally the remaining two electrons can go into the pair of π* orbitals in any of several occupancy and spin configurations, Lennard-Jones assumed that, in energy, "that state is held to be lowest which has the greatest multiplicity, as is the case in atoms". Here, this would be a triplet state, in which the last two electrons each occupy one of the degenerate π_y^* and π_z^* orbitals and their spin vectors are parallel. The nominal overall bond order is two, since although there are three bonds, one of them can be considered to be formally cancelled by an antibond.

By this explanation of the experimentally known fact that dioxygen is paramagnetic in its ground state, Lennard-Jones's analysis provided a brilliant early triumph for the quantum theory. Apparently, Hund's first rule,[14, 15] which originally had been promulgated for atoms, also applies to certain molecules. Dioxygen is a case in which the rule might be expected to apply strictly, because of the symmetry-enforced degeneracy of the π* orbitals (see below).

Nevertheless, this insight was not the major focus of Hückel's interest in Lennard-Jones's paper. In fact, the triplet nature of dioxygen might well have bemused a lesser intellect, and a connection between the intriguing special case of dioxygen and the less spectacular but far more general problem of ethylene might never have become clear. What attracted Hückel was the idea that there can be *two kinds* of oxygen–oxygen bonds, σ and π.

The next step toward the description of doubly bonded carbon was an ingenious *gedanken* experiment. Hückel imagined the conversion of one of the oxygen nuclei of dioxygen to carbon by the extraction of two protons, which then were bound to the resulting carbon nucleus to give formaldehyde. If we today were following this protocol, we probably would make formaldehyde analogously to the construction of dioxygen shown in Figure 2, with the exception that one of the oxygen atoms would be replaced by an sp^2-hybridized fragment CH_2, and the units would be brought together so that all four atoms were in a common plane. Again, one of the carbon 2p orbitals could form a σ bond by overlapping a 2p orbital of the oxygen, and the other carbon 2p orbital would form a π bond with the oxygen p orbital. However, Hückel declined to make the assumption of coplanarity at the start, and argued his way through alternative geometries before rejecting them in favor of the planar one. Also, in 1930, it was not obvious what should be the ordering of the energies of the MOs resulting from the procedure. Hückel again presented arguments that favored the ordering we accept today.

The details, though interesting, are too lengthy to give here, but one major point is worth emphasizing. In both arguments, Hückel resorted to experimental data to make his decisions. With regard to the multiplicity question, it was clear that because of the need to bind the substituent hydrogens to the carbon atom in formaldehyde, the π* MOs would not be each singly occupied, and the degeneracy that causes a triplet ground state in dioxygen would not exist in formaldehyde. Nevertheless, it was (then) a difficult computational problem to decide whether the multiplicity of the ground state of formaldehyde should be a singlet π or a triplet π–π*. Hückel's basis for rejecting the triplet was analogical: although no experimental information on the magnetic properties of formaldehyde was available, it was known that acetaldehyde was diamagnetic and hence a singlet.

Similarly, with regard to the molecular geometry, Hückel pointed out that a nonplanar monosubstituted formaldehyde, for example, acetaldehyde, would be pyramidal, with three nonequivalent substituents, and hence one would predict the existence of optical isomers. No such isomers were known. It is heartening to realize that Hückel, a pioneer of theory, was in the latter case not too proud to use the organic chemist's traditional (but nonrigorous) argument of isomer numbers! We have no evidence that Walter Hückel provided this insight to his brother, but it is easy to imagine his doing so.

Formaldehyde-to-ethylene then required only a repetition of the oxygen-to-CH_2 *gedanken* step. Again, the presence of the substituent hydrogens is the key structural feature that favors a singlet ground state. Hückel had now achieved his first objective, a quantum mechanical description of the double bond that would explain restricted rotation. In his model, the C=C double bond is made up of a σ and a π bond. The σ bond is axially symmetric about the internuclear C–C line, but the π bond is not. Rotation of one of the CH_2 groups out of the plane of the other is resisted because to continue this process to 90° would require breaking a π bond. Hückel did not provide a quantitative estimate of the strength of this bond, but it must be substantial to account for the thermal stability of olefinic *cis–trans* isomers. He emphasized the deep structural difference between this model and that of van't Hoff, in which both of the C–C bonds are equivalent.

4.4. Hybridization in Double Bonds

It will be clear that a bit of mystery still lingers over Hückel's picture of ethylene at this point: What is the nature of the C–H bonds? Hückel never clarified this but left it to others. In 1931 and 1932, the years immediately following Hückel's first paper on ethylene, the concept of quantum mechanical hybridization was introduced as the basis of a theory of directed bonding. As we have seen, this idea played an important role in the development of the Pauling–Slater equivalent-bond model of ethylene. In 1933 Mulliken[16] suggested trigonal hybridization of the carbon valences in ethylene, and in 1934 Penney[17] made a more extensive comparison of this model with two alternatives, the so-called "right angle" model and the van't Hoff-like Pauling–Slater tetrahedral model.

In the right angle model (Fig. 3), Penney imagined the C–H bonds to be pure 2pσ bonds, and the double bond joining the two carbons to be made up of one (s,s) and one (σ,σ) bond.

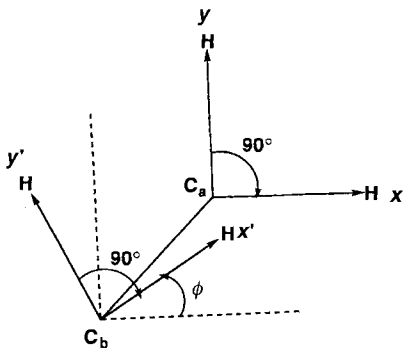

Fig. 3. Penney's right angle model (ultimately rejected in favor of the σ–π model) for ethylene.

The vicinal hydrogen interactions are neglected, and the C–C bonds, although not equivalent, are both axially symmetrical about the C–C direction, so that the energy of the configuration does not depend on the the angle ϕ through which one carbon is rotated with respect to the other. As Penney recognized, this model predicts free rotation about the C=C bond, and therefore cannot account for one of the characteristic properties of alkenes.

Penney compared the tetrahedral model and the trigonal model by means of a valence bond calculation and concluded that the trigonal model was energetically preferred. Although the sp^3 hybrid orbitals of the tetrahedral model have more extension along the orbital axis than the sp^2 orbitals of the trigonal model, the sp^3 orbitals are necessarily canted outward from the internuclear C–C line and hence overlap poorly. He subsequently proposed trigonally hybridized carbon as the building block of the σ framework of the benzene ring.

Eventually these suggestions became widely adopted for discussions of doubly bonded carbon. In part, this acceptance must have been furthered by later group theoretical arguments by Kimball,[18] but one may speculate that it also was based on the simple conceptual continuity of the hybridization picture (sp^3 for methane, sp^2 for ethylene, sp for acetylene), which made the idea pedagogically attractive. Actually a more hard-eyed evaluation of the quantitative merits of Penney's calculations might have been appropriate. One certainly should have been concerned about Penney's conclusion that the energy needed to rotate one CH_2 plane in sp^2 hybridized ethylene by 90° with respect to the other was "quite small, probably about 1/2 volt," (about 11.5 kcal mol^{-1}). If a similar value were required in substituted ethylenes, stable *cis–trans* isomerism could not have been observed at room temperature. In other words, were one to take the calculation at face value, the same argument used to reject the right angle model logically would have required rejection of the trigonal model.

5. The Benzene Problem

It might be surmised that Hückel proceeded from ethylene to conjugated chain compounds such as allyl, butadiene, pentadienyl, hexatriene, etc., and then to benzene, and other cyclopolyenes, in the systematic manner that we teach Hückel molecular orbital (HMO) theory to students today. Actually, this is not the sequence that occurred. Hückel eventually considered unsaturated chains as a class,[19] but in the breakthrough paper in 1931,[20] his target was benzene itself.

The paper was Hückel's *Habilitationsschrift* for attaining the *venia legendi* (right to teach) in theoretical physics at the Technische Hochschule Stuttgart. A massive document of 84 printed pages, it gave two descriptions of benzene and other conjugated cyclopolyenes: the "first method," which eventually came to be the valence bond (VB) theory, and the "second method," now called the molecular orbital (MO) theory. Hückel gave reasons for preferring the MO procedure, and although some of these might not be very convincing today, he persisted in this choice thereafter. Both the first method and the second method assumed that the unique properties of cyclic conjugated systems could be attributed approximately to the π electrons without explicit consideration of their interaction with the σ electrons.

5.1. Hückel's First Method and Classical Valence Bond Theory

The valence bond method, which Hückel had rejected, was taken up soon after by Pauling and others,[10, 21–25] who simplified the mathematical procedures and gave reasons for preferring the VB to the MO method. Again, with regard to the problem of cyclic conjugated molecules, their reasons seem insufficient today, but these workers held unwaveringly to their choice in later years. This "classical" VB method, and Pauling's pedagogical packaging of its major results in the form of the "theory of resonance," dominated theoretical chemistry for 25 years after 1930. The reasons for this, further examined below, were not necessarily that the theory was "correct" in any absolute sense, but rather that Pauling, with consummate knowledge of the whole field of chemistry, convincingly showed how a broad range of chemical phenomena, especially in small molecules, could be explained by some kind of quantum ideas[10a] and thereby established a faithful and largely uncritical following. As it happened, however, the classical VB method, in the truncated form of it he used, was to prove theoretically inadequate when applied to the problem of aromaticity.

It is true that with the emergence of high-speed digital computers, as is described elsewhere,[14, 26, 27] the MO method, in increasingly sophisticated manifestations, gradually became the major basis for the explosive computational development of electronic structure theory. However, one should not conclude that VB theory is without adherents today. On the contrary, many investigators have contributed developments of advanced VB methods and successful applications to significant problems, including as we shall see, the reconciliation of the VB and MO theories of aromaticity.[28, 29]

The most characteristic feature of the valence bond method is that it considers the combining atoms as a whole.[30] The formation of a molecule is thought of as arising from the bringing together of complete atoms, which are then allowed to interact. In this it differs from the MO method, in which only the nuclei (or nuclei + electron inner shells) are first brought into position, and afterwards the valence electrons are allotted to polycentric molecular orbitals. Clearly the VB method corresponds more closely with the conventional chemical picture, which probably accounts for its widespread acceptance in the form presented by Pauling.

Hückel's first method, the early form of VB theory, was derived from Heitler–London[31] theory for the formation of molecular hydrogen from two hydrogen atoms. It starts with each atom in a specified quantum state and then introduces exchange. The exchange procedure, which takes into account the indistinguishability of the two electrons 1 and 2 in the form of the exchange integral $\langle \Psi_A(1)\Psi_B(2)|\mathscr{H}|\Psi_B(1)\Psi_A(2)\rangle$, has major significance in the VB method. For example, the binding energy of hydrogen calculated without exchange is only 5.5 kcal mol^{-1} but when exchange is included in the wave function, the binding energy rises to 69 kcal mol^{-1}, a substantial fraction of the experimental value of 104 kcal mol^{-1}.[30]

By application of group theoretical procedures, Heisenberg[32] used this exchange method to explain ferromagnetism. Slater[32] then developed a useful determinantal method which made possible the treatment of interaction among a large number of atoms without group theory and applied it to electrons in metallic lattices. This method was further applied by Bloch[33] in place of the Heisenberg group theoretical method for the theory of ferromagnetism. Hückel used the Bloch formalism directly in his first method.

As described by Hückel,[34] the treatment of a conjugated molecule (such as benzene) by the classical VB method begins by assigning to each carbon atom a π electron which is in a given state with the positional eigenfunction $\phi_a(r_{ia})$, where the suffixes indicate the ith electron in the atom a. The total positional eigenfunction, taking coupling of the π electrons into account, is written as a linear combination of the products $\phi_1(r_{i1}) \ldots \phi_6(r_{i6})$. Starting from this, the Heitler–London perturbation method is worked out to the first approximation. Spin is taken into account, and only the linear combinations that conform to the Pauli principle are considered.

In the Pauling modification of VB theory,[21] one selects from these linear combinations those which correspond to the smallest value of the total spin (in this case $S = 0$), and chooses from these the ones that are linearly independent. These functions which belong to the value $S = 0$ can be associated with models of the valency pattern of the π electrons in which the atoms are joined in pairs by single bonds, one and only one bond radiating from each atom in such a way that the bonds do not cross one another. Pauling called the schemes of valencies corresponding to the functions "canonical structures." One then formulates and solves the secular perturbations corresponding to these functions, restricting the coupling to that between adjacent atoms.

Wheland[22] gives a simple example of the application of this method to the case of cyclobutadiene. The canonical structures are **A** and **B**. One designates the eigenvalue of the energy as W, the 2p function on the ith carbon atom as Ψ_i, the coulomb integral $\langle \Psi_1\Psi_2\Psi_3\Psi_4|\mathscr{H}|\Psi_1\Psi_2\Psi_3\Psi_4\rangle$ as Q, and the single exchange integral between adjacent carbons, for example, $\langle \Psi_1\Psi_2\Psi_3\Psi_4|\mathscr{H}|\Psi_2\Psi_1\Psi_3\Psi_4\rangle$ as α'. All single interchange integrals of the energy between nonadjacent atoms, all multiple interchange integrals, and all interchange integrals of unity are neglected. The Slater valence-bond eigenfunction may be expressed as secular equation (a).

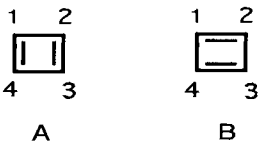

$$\begin{vmatrix} Q+\alpha'-W & (1/2)Q+2\alpha'-(1/2)W \\ (1/2)Q+2\alpha'-(1/2)W & Q+\alpha'-W \end{vmatrix} = 0 \qquad \text{(a)}$$

This has the solutions $W = Q + 2\alpha'$ and $W = Q - 2\alpha'$, of which the former represents the ground state since the exchange integral α' is presumably negative. The resonance energy is obtained by subtracting from this a quantity $Q + \alpha'$, the energy of one of the two canonical structures: $Q + 2\alpha' - (Q + \alpha') = \alpha'$.

In the case of benzene, there are five canonical structures with corresponding canonical functions: **C** and **D** correspond to the Kekulé forms, **E**, **F**, and **G** to the Dewar forms. Other structures,

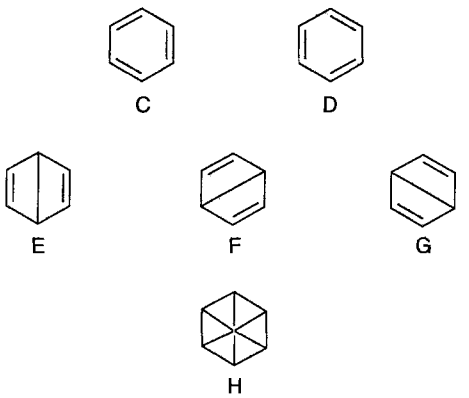

such as for example **H**, that of Claus, can be expressed as linear combinations of the canonical functions [Eq. (b)].

$$\phi_H = \phi_C + \phi_D - [\phi_E + \phi_F + \phi_G] \qquad \text{(b)}$$

Following a procedure similar to that used for cyclobutadiene, the coupling energy for benzene is $6Q + 2.6055\alpha'$, and the molecular eigenfunction is given by Equation (c).

$$\phi_{benzene} = 0.62435\,(\phi_C + \phi_D) + 0.27101\,(\phi_E + \phi_F + \phi_G) \qquad \text{(c)}$$

In the sense of the approximation, the ground state thus may be considered to result from the superposition of the two Kekulé and the three Dewar forms.

One might be concerned about the approximation which limits the exchanges to pairwise nearest neighbors. Clearly there are many more permutations that could be included. Wheland[22] himself states:

"This assumption is an extremely drastic one and no rigorous justification for it can be given. The integrals we ignore are probably, to be sure, rather smaller in magnitude than the other ones which we retain. There are, however, an enormous number of the former integrals, and, even though some of them are positive and some are negative, we can have no assurance that their net effect is negligible. We shall, nevertheless, make the assumption because, without it, our calculation would become impracticably complicated, and because, with it, surprisingly satisfactory results can be obtained."

As we shall see, the neglect of some of these other permutations has serious consequences for the description of cyclic conjugated systems.

Although the classical VB procedure came to be called[22] the Heitler–London–Slater–Pauling (HLSP) method, Slater in fact preferred to put some distance between himself and Pauling in applications of the method. Thus, in a discussion[35] at the International Conference of Physics in 1934, Slater remarked that he was in "entire agreement" with Hückel and Hund that the MO method is superior to the Heitler–London method for computing interatomic forces, and that "the calculations of Pauling, for instance, seem to make quite unwarranted use of the theory." Slater gave no further details, but it seems a reasonable conjecture that he was expressing misgivings over the truncation.

5.2. Hückel's Second Method and Molecular Orbital Theory

This procedure, subsequently called[22] the Hund–Mulliken–Hückel (HMH) method, had as an immediate intellectual precursor another study[36] by Bloch on the quantum mechanics of electrons in crystal lattices. Bloch, at that time in Leipzig, was actively developing the theory of metals in order to understand such phenomena as conduction and magnetism. Subsequently, of course, he became famous for providing some of the theoretical foundations for the field of nuclear magnetic resonance.

Bloch approached the problem of the electronic interactions in a many-electron system by considering the properties of a single electron in a spatial force field perturbed by the atomic nuclei and the statistical charge distribution of the remaining electrons. The idea is very similar to the Hartree–Fock method for treating many-electron atoms. In Bloch's sinewy words, "the force field has the same periodicity as the crystal lattice itself," and "we are thus dealing with plain de Broglie waves which are modulated in rhythm with the lattice."

The procedure Hückel used[20] was to set up such a lattice for benzene, calculate the MOs (wave functions) and energy levels in terms of the parameters α and β (defined below) by solving the Schrödinger equation, and construct the electronic configuration by *aufbau*, in accord with the Pauli principle and in analogy to the practice of Hund, Mulliken, and Lennard-Jones for diatomic molecules. Hückel's benzene lattice was a regular hexagonal array of carbon $2p_z$ orbitals. As every chemistry student now knows, the results can be expressed as shown in Figure 4,

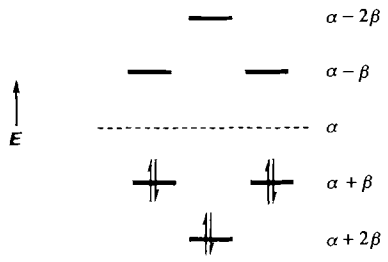

Fig. 4. Energy levels of benzene and occupation pattern in the ground state as calculated by Hückel's second method. The parameters α and β are defined in the text.

where α is the energy of an electron in an unperturbed carbon 2p orbital, and β is the stabilization energy (relative to α) experienced by an electron when two such units interact at a defined distance.

Hückel generalized this result to other conjugated systems with n centers, both to rings of other sizes and to chains.[19, 20, 34, 37] The energy levels can be expressed in the famous Hückel Equations (d), $j = 1, 2, 3, \ldots n$, and (e), $k = 0, \pm 1, \pm 2, \ldots m$, where $m = (n-1)/2$ for n odd and $m = n/2$ for n even.

$$\text{Chains } C_nH_{n+2}\text{: } E = \alpha + 2\beta\cos[j\pi/(n+1)] \quad \text{(d)}$$

$$\text{Rings } C_nH_n\text{: } E = \alpha + 2\beta\cos[2k\pi/n] \quad \text{(e)}$$

Among the messages that these equations convey are that the energy levels for the chains are unique, whereas some of those for the rings are doubly degenerate, that is, the eigenvalues sometimes occur in pairs of equivalent energy. As Hückel pointed out,[37] these degeneracies are a direct consequence of the cyclic nature of the electron circulation in the ring compounds. The physical reason is that in the energy states that have a finite angular momentum associated with the electronic motion, the circulation is *directional* in either a clockwise or a counterclockwise sense. The eigenfunctions corresponding to these states are not identical, even though the energies are, so *two* MOs must exist at that energy. An equally important point is that for n even or odd the lowest eigenvalues of the ring compounds are unique, and for n even, the highest also are unique. These are nonintuitive results that come out of the solution of the Schrödinger equation and that mark this approach as fundamentally different from the old (Bohr) quantum theory. Whereas in the old theory, for example, the lowest atomic s states still had angular momentum $h/2\pi$, in the new theory the s states now have zero angular momentum. Similarly, in the unique states of benzene, the angular momentum is zero, and consequently, the "sense" of the electronic circulation becomes meaningless.

This difference between rings and chains will be familiar to students of elementary quantum mechanics,[38–41] where a favorite pedagogical exercise is the calculation of the eigenvalues of the "one-dimensional" Schrödinger equation. An electron is

imagined to be constrained to move along a line or in a circle under zero potential. The solutions for the linear case are unique; those for the circular case have the lowest energy level unique but all the rest pairwise degenerate.

Hückel[19, 20, 34, 37] emphasized that the MO method, in producing such energy level patterns, led to the idea of closed electron shells analogous to those of the noble gas closed shells in atoms. Particularly significant for the n even conjugated rings was the case of six electrons in benzene, which had been recognized for some time as a feature leading to aromatic properties. Since the Pauli principle allows each orbital to accommodate two electrons of opposite spin, filling the first three orbitals (first two energy levels) of the benzene set 1, 2, 2, 1 in this way would give a stable configuration. On the other hand, four electrons in cyclobutadiene would not give a closed shell, since only the lowest level of the 1, 2, 1 set could be filled. The next higher level could accommodate four electrons but only would have two available. Moreover, in the case of ions derived from odd-membered rings, where all levels above the lowest are degenerate, a closed shell configuration again is reached with six electrons, as in the cyclopentadienide ion, but not with eight, as in the cycloheptatrienide ion or with four as in the cyclopentadienylium ion.

This rule, subsequently stated by others in the abbreviated form $(4N+2)$ $(N = 0,1,2...)$, namely that aromaticity should be associated with monocyclic π electron systems containing $2, 6, 10...$ electrons, was in accord with the known facts of organic chemistry at the time. In addition, predictions now could be made about the existence and properties of unknown but easily imaginable new structures. Although the rule does not apply strictly to polycyclic compounds such as naphthalene or biphenyl, Hückel showed by explicit MO calculations[37] that these systems too should be considered aromatic, as might have been expected. There are limitations to the rule, but much computational research in recent years confirms the essential fact that Hückel's broad classification of aromatic and antiaromatic character survives at higher levels of MO theory and is not just an artifact of the approximations used in the early treatment.[42]

Significantly, the classical VB method did not produce these results. For example, it predicted that cyclobutadiene should have the highest resonance energy per electron of any of the even cyclic polyenes, and it gave no reason to expect that cyclopentadiene should be a much stronger acid than cycloheptatriene. These failures of classical VB theory were among the reasons that Hückel in 1931 turned away from it as a basis for understanding aromaticity. More than half a century later, the opinion persists[43] that classical VB theory is "decisively unsuccessful"[44] for this purpose.

Nevertheless, one feels intuitively that a higher level of VB theory should be capable of reproducing the Hückel rule. After all, both the MO and the VB approaches are approximations of the complete solution of the Schrödinger equation. At successively higher degrees of approximation, the two methods should converge to give equivalent results. In fact, such convergence can be shown analytically for a simple molecule such as H_2 and is expected generally, however complicated the molecule may be.[45] It comes as no real surprise, therefore, that eventually methods for deriving the Hückel rule by VB theory should emerge.[44, 46, 47] The key insight in solving this problem is the crucial necessity to include *cyclic* permutations of the π electrons in the exchange procedure. Just such exchange integrals were among those omitted in the classical VB method. An experimentalist senses a gratifying propriety in this result.

6. A Chilly Reception from the Experimentalists

Hückel's pioneering papers on the molecular orbital theory of unsaturated and aromatic compounds appeared in the period 1930–1931, but they seemed to make little impact on the community of chemists for many years after. In their biographical memoir on Hückel, Hartmann and Longuet-Higgins[3] ascribe the general neglect of his results to the national culture of German science:

> "... physicists in that country in any case were not ready to accept investigations about more complicated chemical bond phenomena as a typical contribution of a physicist. Still more difficult was his (Hückel's) relationship to the chemists. Before World War II, especially in the Anglo-Saxon countries, chemical physics and within that field quantum chemistry also was accepted by both physicists and chemists as an interesting new field of science. Chemists in Germany, on the other hand maintained that chemistry is what chemists do. They did not do quantum chemistry and therefore this kind of science did not belong to chemistry."

It may well be true that German chemists of that period or even later resisted quantum ideas. Although Rolf Huisgen reports[48] that he was teaching Hückel's results (but not the details of how the calculations were done) as early as 1949, this undoubtedly was exceptional. Even Walter Hückel makes only cursory reference in his textbook[49] to the contribution his brother had made to the problem of the aromatic sextet.

However, I regret to say that crediting a more receptive attitude to "Anglo-Saxon" chemists, especially the experimental organic chemists, pays them a higher compliment than most of them deserve. Again, there were scattered exceptions. For example, Ingold[50] in Britain and Hammett[51] in the United States clearly were aware of the importance of Hückel's work. Elsewhere in these countries, however, even though the problem of aromaticity was prominent in the minds of chemists, and much experimental effort was devoted to it, whatever theoretical reasoning experimentalists brought to bear on such issues in their research or teaching depended almost entirely on resonance theory.[52] Noller's review of 1950,[53] ostensibly an exposition of molecular orbital theory prepared for the edification of organic chemistry teachers, does not cite a single reference to Hückel. Most elementary and even advanced textbooks of those years make no mention whatever of Hückel's ideas. One of the most influential books in the field, the second edition (1943) of the multi-authored *Organic Chemistry – An Advanced Treatise*, edited by Gilman, contains a substantial chapter by Fieser on aromatic compounds.[54] The question of aromaticity is presented only from a historical perspective, and for a theoretical rationale, Fieser defers entirely to Pauling, who contributes a chapter on theory in the same work,[23] using the already well-known resonance method. Although Pauling mentions the Hückel theory there, he declines to discuss it further on the grounds that the

resonance approach "is the more closely related to the usual concepts of chemistry". Not surprisingly, Pauling's omissions of scholarly exposition and comparison here and elsewhere infuriated Hückel.[1]

It is true that there was a flurry of theoretical activity, especially in Britain, following up further implications of some of Hückel's ideas. This included work[55] by, among others, Coulson on mobile bond orders, Coulson and Rushbrooke on alternant π-conjugated systems, Longuet-Higgins on non-Kekulé-molecules, and Dewar on a range of chemical properties deducible from perturbational MO considerations. These papers, written in the elegant lapidary style familiar to mathematicians, and often published outside the conventional chemical journals, were important, but they were either unknown or largely unintelligible to many organic chemists.

Similarly, a key two-part paper[56a] by Mulliken and an important early textbook by the Pullmans,[56b] both in French, influenced a few young theoretically able workers such as Simonetta, and through him, Heilbronner,[57] but their immediate impact on the thinking of most organic chemists was not great.

Having lived through that period, I can attest that the attitude of many American organic chemists toward MO theory was uninformed and indifferent, if not hostile. Few of them would have taken the trouble to slog through Hückel's highly technical papers, which bristled with equations and matrices, and which, with one obscurely placed exception,[34] were not available in English. The charismatic Pauling had provided them with a theory which at some level required no mathematics and could be applied by using familiar bond structures. Most of them were content with that.

7. Experimental Tests of the MO Description of Conjugated Cyclic Compounds

If organic chemists were to a large extent unaware of the Hückel rule, how could there have been deliberate tests to explore its scope? In fact, a number of molecules synthesized or discovered in nature after Hückel's papers in the early 1930s eventually turned out to be relevant test species, even though the authors originally had some other motivation for studying them. In this inadvertent process, we see again the familiar paradoxical sequence encountered so frequently in science: "Here's the answer, what's the question?"

Early examples of this come from the chemistry of the azulenes (Scheme 1), a fascinating group of blue or violet substances, several of which, including the parent compound, are found in nature as such or are formed by chemical transformation of hydroazulenic sesquiterpenoid precursors.[58-60]

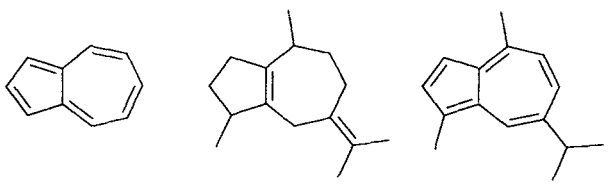

Scheme 1. Structural formulae of azulene (left) and its derivatives guaiene (center) and guaiazulene (right).

The substantial variety of natural and synthetic azulenes available from the work of Plattner[58] and others[59] was augmented by the powerful new Ziegler-Hafner synthesis,[61] which made azulenes accessible in a small number of steps without the difficult final dehydrogenation previously employed. A rich store of facts embodying the chemical and physical properties of these substances now called for theoretical rationalization, which, as has been instructively summarized by Heilbronner,[60] Hückel MO theory ultimately provided.

This theme of answers anticipating questions lies at the heart of one of the inspiring stories of organic chemistry, the discovery of the troponoids.[62] Space does not permit a full recounting here, but a brief outline may suffice to make the relevant point. In 1926 the Japanese chemist Tetsuo Nozoe settled in Formosa (now Taiwan), where he was to live and work for the next 22 years. During the period between 1944 and 1947, he and his co-workers had deduced the structure of hinokitiol (Scheme 2),

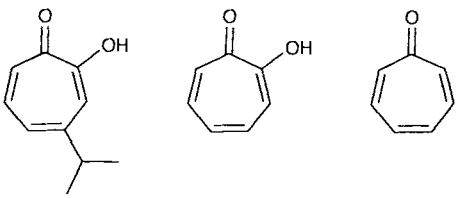

Scheme 2. Structural formulae of hinokitiol (β-thujaplicin, left), tropolone (center), tropone (right).

an isopropyltropolone, but because of disruptions caused by the war and the remoteness of his location, he was not aware of related activity elsewhere,[62] nor did others know of his work on this subject, most of which was not published in readily accessible journals until 1950.

Nozoe[62] recounts his attempts to explain by the theory of resonance the peculiar aromatic properties of hinokitiol and of tropolone itself, which he subsequently synthesized. His first exposure to this form of quantum theory came in 1942/43, when copies of the 1940 edition of Pauling's *Nature of the Chemical Bond* became available in Formosa. However, although one could write resonance structures, this gave no real enlightenment on the aromaticity of tropolone, and the matter remained somewhat mysterious to him until 1951. In that year, simultaneously published papers by Dauben and Ringold[63a] and by Doering and Detert[63b] described the first syntheses of tropone. Both papers called attention to the electronic structure of this ketone and emphasized the presence of a potential aromatic sextet. The Doering paper, giving an explicit reference to Hückel's 1937 summary[37] of π electron theory, pointed out that the sextet was but one of a general class of stable configurations characterized by having $(4N + 2)$ π electrons. (To my knowledge, this was the first time that Hückel's rule was stated in this succinct form). Nozoe reports[62] that at that time, he had not heard of such a rule, but it was immediately obvious to him that tropolone's aromaticity must be derived from the same source.

Forerunners of numerous contributions by many authors that followed,[64] the two tropone papers[63] clearly were examples of directed rather than serendipitous tests of π electron

theory. Nevertheless, the most persuasive pieces of evidence leading to the acceptance of Hückel's ideas seem to have been the subsequent syntheses of tropylium[65] and cyclopropenylium[66] ions, which were specifically mentioned in the citation to Hückel's Otto Hahn Prize in 1965 (see below).

8. Orbital Symmetry—The Extension of Cyclic π-Electron MO Theory to Transition States of Pericyclic Reactions[67–69]

Pericyclic reactions, as the name implies, are those "in which all first-order changes in bonding relationships take place in concert on a closed curve".[69] It would be natural to conjecture that Hückel MO methods, which had been successful in rationalizing the behavior of *ground state* conjugated cyclic molecules, also might give a fruitful account of the *transition states* of pericyclic reactions. The idea of applying π-electron theory to reactions with cyclic transition states probably was first put forth by M. G. Evans in 1939.[70] He treated the six-electron transition state of the Diels–Alder reaction as an analog of benzene (Scheme 3) and actually wrote down a secular determi-

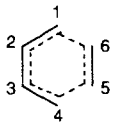

Scheme 3. The transition state of the Diels–Alder reaction between butadiene (centers 1–4) and ethylene (centers 5 and 6) as benzene analogs.

nant for it differing from that of benzene only in the 1,6 and 4,5 bond integrals. In his words:

> "very qualitatively we may say that whereas in the initial state the mobile electrons are those characteristic of an ethylene and a butadiene structure in the transition state they simulate the behaviour in a benzene structure."

This is a definite insight, quite remarkable for its time. However, it is questionable to maintain, as some have, that Evans was thus formulating a "rule" of aromatic transition states. Such a rule requires not only that one assert that aromatic transition states are more favorable, but also that one have a procedure for recognizing which transition states are aromatic. Without such a procedure, a "rule" of aromatic transition states verges on a tautology. Evans undoubtedly recognized this, and in fact, he attempted to provide a procedure. Unfortunately, his suggestions did not solve the problem. Apparently as a result of an improper conflation of MO and classical VB resonance ideas, Evans had only an uncertain grasp of the concept of aromaticity and especially of antiaromaticity. In this way, he was led to a formulation that stressed the *total number* of reactive electrons:

> "... there are qualitative rules which follow. The energy levels of the mobile electrons lie lower in cyclical structures than in straight chain compounds with the same number of centres available. The energy levels of the mobile electrons are lower the greater the number of available centres. These rules imply that the lowering of the activation energy due to the resonance effect will be greater in cyclisation reactions than in chain formation and that the resonance energy in the transition state will increase with the increasing degree of conjugation of the reacting molecules."

These rules must be carefully distinguished from the orbital symmetry rules. The overarching lesson taught by orbital symmetry and related theories is that favorable ("allowed") pericyclic transition states *in a given geometry* can be recognized according to whether the number of reactive electrons is $4N$ or $4N + 2$. In disrotatory electrocyclic reactions and *supra–supra* cycloadditions, for example, this number is $4N + 2$, whereas in conrotatory electrocyclic reactions and *supra–antara* cycloadditions it is $4N$. The predictions thus alternate accordingly. Violation of these requirements results in a "forbidden" reaction.

A literal application of the Evans rule favoring more highly conjugated reactants would predict, for example, that resonance stabilization in the cyclooctatetraene-like transition state of the hypothetical *supra–supra* [4+4] dimerization of butadiene should be greater than that in the benzene-like transition state of the *supra–supra* [4+2] association of butadiene and ethylene. But we now recognize the *supra–supra* [4+4] transition state as *antiaromatic* and therefore orbital symmetry forbidden.

Moreover, stereochemistry and electron count are inseparably entwined in orbital symmetry theory. Because Evans had no experimental examples of reactions whose stereochemistry would be favorable with $4N$ electrons, he could not have incorporated them into his thinking except by imagining them, which he did not do. Nothing in his paper gives any indication that he anticipated the idea that is central to orbital symmetry, that of allowed versus forbidden (aromatic vs. antiaromatic) transition states dependent on orbital phasing. To the contrary, continuation along the direction he started would have ended in a theoretical cul-de-sac. Therefore, Evans's contribution was at most a collateral, rather than a lineal, antecedent in the development of orbital symmetry theory.

On the other hand, the intimate relationship of orbital symmetry and the Hückel "magic numbers" is obvious. Quite analogously to our previous discussion of ground state molecules, it is precisely because of the *cyclic* nature of pericyclic reactions that one expects them to be more properly described by Hückel MO methods than by classical VB theory. The major extension needed for the application of Hückel theory to transition states was the expansion of the original Hückel $(4N + 2)$ magic numbers, derived for conventional cyclic conjugated π-electron systems with no forced orbital phase inversions, to another arrangement with a forced phase inversion, for which the magic number is $4N$.

9. Violations of Hund's Rule in Biradicals

As we have seen, Lennard-Jones[12] applied to molecules (for example, O_2, B_2) the generalization that later came to be known as Hund's first rule. This governs the prediction of the spin multiplicity in cases where two electrons occupy degenerate orbitals: "that state is held to be lowest which has the greatest

multiplicity."[12-15] Some theoreticians choose to interpret Hund's rule as applicable only when the orbitals in question are exactly degenerate, which except for rare accidental cases, would limit the rule to molecules like O_2, in which the degeneracy is symmetry-enforced. Other theoreticians apply the rule even when the degeneracy is only approximate.

Longuet-Higgins[55] invoked the approximate form (without so identifying it) in a seminal 1950 paper, which is perhaps the most influential theoretical writing on π-conjugated biradicals in the period between 1930 and 1970. He showed that, at the Hückel MO theoretical level, non-Kekulé molecules such as trimethylenemethane (TMM), *meta*-quinodimethane (MQDM), and tetramethyleneethane (TME), each have a de-

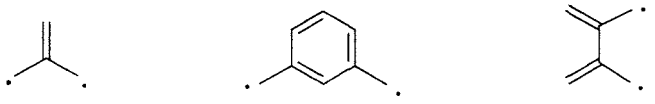

generate pair of nonbonding (NB) MOs occupied by only two electrons, and predicted for each of these molecules a triplet ground state. The symmetry point group of TMM (D_{3h}) contains E representations, but those of MQDM (C_{2v}) and TME (D_{2h}) do not. Thus, in the latter two cases, the NBMO degeneracies are not symmetry-enforced, and the energies are expected to split apart at higher levels of theory.

Longuet-Higgins cited no precedent for his predictions of spin multiplicities in organic biradicals, and apparently there had been only one prior such case in the literature: In 1936, Hund himself[71] had predicted a triplet ground state for one of the Schlenk-Brauns hydrocarbons studied by Müller et al. (Scheme 4).[72] This molecule too has degenerate NBMOs at the Hückel level of theory and would have fit easily into the Longuet-Higgins scheme.

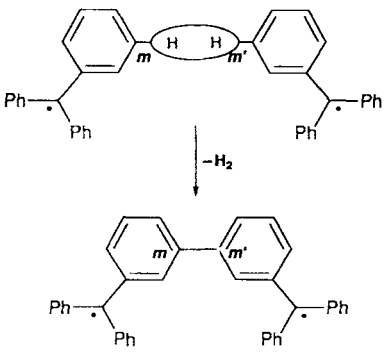

Scheme 4. Formal synthesis of the *m,m'*-Schlenk-Brauns hydrocarbon.

However, Hund's prediction was immediately challenged by Hückel,[73] who pointed out reasons why the rule of highest multiplicity was of dubious validity in the case of the Schlenk-Brauns compound. Hückel's argument developed from his recognition that the Schlenk-Brauns structure could be derived (conceptually) by a union of two triphenylmethyl radicals at the *m* and *m'* positions. In the NBMO of triphenylmethyl, the *m* positions of the phenyl rings are *nodes*, that is, they have π-electron coefficients of zero at this level of approximation. In these circumstances, the exchange energy between the two halves of the Schlenk-Brauns molecule is close to zero. Since it is essentially just the exchange energy that accounts for the separation between the triplet and the lowest singlet,[14, 15] these two states will be almost degenerate. Note that the argument has nothing directly to do with the fact that the NBMO degeneracy in the Schlenk-Brauns hydrocarbon is accidental and will be lifted at higher levels of theory. Instead, in MO terminology, it really is a recognition of the spatial separability of the NBMOs, a property later to be called "disjoint" by Borden and Davidson[74a] (see below). Hückel's main conclusion was that the ground state is not predictable at this level of theory, contrary to the previous assumption of Hund's rule.

The Schlenk-Brauns hydrocarbon, one of the few biradicals known in 1936, after all was an esoteric species. One might then think of Hückel's argument as pertaining to a highly specialized compound of little interest to those outside the small field of biradicals. Indeed the paper stimulated little or no interest. In my view, however, it had significance far beyond the specific compound, because it showed that the magnetic properties of molecules cannot be treated by imagining that the exchange interaction of two electrons in the field of the nuclei and the remaining electrons will always favor the triplet. On the contrary, such a problem must take into account the *connectivity* of the atoms. This is a profoundly *chemical* point of view, which emphasizes something familiar to every chemist: molecular structure determines molecular properties.

A simple extension of Hückel's argument reveals that of the three biradicals TMM, MQDM, and TME, the latter has the same connectivity feature as the Schlenk-Brauns compound: it can be made by a union of two radicals (allyl in this case) at NBMO nodal positions. Applying Hückel's argument, we can see that TME should not have been classified by Hund's rule.

Because of Longuet-Higgins' (deservedly) high reputation in the field of theory, his unqualified use of Hund's rule in this case had the effect of steering experimentalists along the same oversimplified line of thinking. Also, the absence of a citation to Hückel's 1936 work contributed to decades of obscurity for that paper. One does not disparage the seminal significance of the work of Borden and Davidson[74a] and of Ovchinnikov[74b] by noting that they rediscovered the essence of Hückel's connectivity argument after a lapse of forty years. As might be expected after such a passage of time, these papers went far beyond Hückel's original rather qualitative discussion.[73] They brought to bear the full power of modern electronic structure theory to derive, by both MO (Borden and Davidson) and VB (Ovchinnikov) methods, the idea that when the π-electron system of a biradical has the Hückel type of NBMO node-to-node connectivity, only a small energy gap separates the multiplet states.[75] Ironically, at the time of their publications, these workers also were unaware of Hückel's paper!

Recent experimental and computational confirmations that Hund's rule is violated in properly constituted disjoint π-conjugated biradicals are reviewed elsewhere.[76]

10. Honors

Formal recognitions of Hückel's work were sparse until late in his career. Three notable distinctions were: in 1965, the Otto Hahn Prize, jointly awarded by the German Chemical Society and the German Physical Society; in 1966, nearly 30 years after his departure, an honorary degree from the Technische Hochschule in Stuttgart; and in 1977, election as a Foreign Member of the Royal Society.

11. Reflections on Hückel's Career

Hückel's entire contribution to organic quantum chemistry amounted to 17 papers, a list that includes several summaries and reviews. After 1937, when he was only 41 years old, his original contributions to this field virtually stopped. (If Hückel were working now, subject to our dubious emphasis on "productivity", that publication record would put his grant applications in grave jeopardy). As a member of the Marburg physics department, he unsuccessfully tried to initiate work on the theory of the nucleus, but apparently did not bestir himself to seek professional contact with chemists such as, for example, the talented and creative Hans Meerwein, then professor of organic chemistry at Marburg. One cannot put all the blame for the missed collaborative opportunities on Hückel, however. For example, in the period around 1950, Meerwein tried to persuade one of his graduate students to undertake the preparation of the cycloheptatrienide ion,[77] apparently unaware that a few yards away in the physics department lived a man who twenty years before had predicted the properties of this very species.

The history of the field of organic quantum chemistry after 1937 shows that there was much more to be done. What can explain Hückel's withdrawal? Some have the opinion that he became discouraged when he failed to develop any further ideas in the field comparable in significance to his early work. This may be true, but, of course, it merely pushes the problem one step deeper: Why did he run out of ideas?

Although there are shadowed aspects of Hückel's life that may hide some clues, I think we already know enough to make a few plausible speculations. Hückel[1] blamed the experiences of the war, the political atmosphere of the Third Reich, and a succession of illnesses for the exhaustion of his energies. The recollection of several colleagues who knew him tend to confirm this diagnosis, but there is also agreement that his was a difficult and even paradoxical personality—shy yet sardonically witty, hypochondriacal, petulant, pessimistic, depressed, ultimately lethargic and withdrawn from academic contact with colleagues and students. Reasons why these characteristics came to dominate Hückel's psyche remain to be elucidated.

A glimpse of Hückel's quirky character comes through in the story of his absence from the Hahn Prize ceremony, which was held in Bonn in September 1965, simultaneously with a symposium celebrating the 100th anniversary of Kekulé's benzene formula. In his letter[78] to Richard Kuhn, president of the German Chemical Society, Hückel pleads that, "the state of my health does not permit me to receive this honor in person", but from his autobiography[1] we get a significantly different excuse: "I was on vacation and dreaded first the trip and then the pompous style in which the Kekulé symposium was planned. In November the medal was presented to me in a small ceremony, which went very harmoniously and was more to my taste than a big display."

Hückel's personality traits surely contributed to his inability to persuade others of the significance of his scientific work.[1, 77, 79] This would have required a level of showmanship above his capacities. The dull, pedagogically ineffective lectures for which Hückel was known,[79] for example, did little to enhance his impact.

Particularly damaging was his confrontation with Pauling. As we have seen, Pauling's classical VB theory, although successful in other applications, really did not provide a good account of conjugation and aromaticity, yet his ideas dominated the field for decades. Here was a clear case of the power of persuasion. Pauling's personal magnetism, expository skill, and intellectual breadth were dazzling. Few organic chemists really knew the theoretical basis of Pauling's ideas on aromatic molecules, but he made it easy for them to apply his theory, such as it was. One can only guess what the history of this field might have been had Hückel just made an effort to reach his potential constituency in chemistry, for example by casting his equations in the form of the simple mnemonic diagram put forward twenty years later by Frost and Musulin,[80] or even by making use of the catchy $(4N+2)$ slogan. These steps would have gone far to popularize his results and make them more intelligible.

12. Summary and Outlook

In the introduction to his landmark paper on partial valence, Johannes Thiele[81] gives his view of the role of theory in nurturing a fruitful relationship with experiment:

> "The opinions about unsaturated compounds that I shall develop in the following may appear quite rash to many. However, if one holds fast to the idea that a theory actually is nothing other than a point of view which permits known facts to be surveyed in a unified way and new facts to be predicted, a point of view whose value and significance naturally can change with the progress of scientific knowledge, then it seems to me that my opinions satisfy both of these requirements."

Certainly, the development of modern electronic structure theory, from the early approaches by Hückel and his followers to the powerful methods of today, illustrates this view. Because the original Hückel MO method was a very approximate form of a theory that others later took to a much higher level, one senses now a certain amused condescension from some adepts, who view it as a quaint relic. One must ask, however, whether any other theoretical advance ultimately has done more to enlighten the thinking of organic chemists than Hückel's brief, bright flare of cognition, regrettably quenched too soon. Words suitable to his legacy are found in Eliot's terse homage to pioneers:[82]

> "Someone said: 'The dead writers are remote from us because we *know* so much more than they did.' Precisely, and they are that which we know."

Many colleagues have provided relevant advice and documentation. Several have submitted to recorded personal interviews. I am greatly indebted to P. D. Bartlett, A. D. Buckingham, J. Fruton, K. Hafner, M. Hanack, E. Heilbronner, P. C. Hiberty, E. F. Hilinski, R. Hoffmann, H. Hopf, R. Huisgen, F. Hund, T. Komm, W. Lüttke, T. Nozoe, A. Streitwieser, H. Tietz, H. A. Turner, E. Vogel, W. Walcher, E. Wasserman, and K. B. Wiberg. B. Z. Berson and staff members of the Yale University Library Department of Manuscripts and Archives provided bibliographic help.

Received: April 12, 1996 [A163IE]
German version: *Angew. Chem.* **1996**, *108*, 2922–2937

[1] E. Hückel, *Ein Gelehrtenleben. Ernst und Satire*, Verlag Chemie, Weinheim, **1975**.
[2] H. Hartmann, H. C. Longuet-Higgins, *Biographical Memoirs of Fellows of the Royal Society*, **1982**, *28*, 153.
[3] R. G. Parr, *Int. J. Quantum Chem. Symp.* **1977**, 25 gives a theoretician's view of some of the topics covered here.
[4] A biographical sketch of Walter Hückel is given by: R. Neidlein, M. Hanack, *Chem. Ber.* **1980**, *113*, I.
[5] P. Debye, E. Hückel, *Phys. Z.* **1923**, *24*, 185, 305.
[6] H. C. Longuet-Higgins, M. E. Fisher, *Biogr. Mem. Natl. Acad. Sci.* **1991**, *60*, 183 (Memoir of Lars Onsager).
[7] L. Onsager, *Les Prix Nobel en 1968*, Stockholm, Norstedt and Söner, **1969**, p. 169; *Science*, **1969**, *166*, 1359.
[8] E. Hückel, *Z. Phys.* **1930**, *60*, 423; *Z. Elektrochem. Angew. Phys. Chem.* **1930**, *36*, 641.
[9] J. H. van't Hoff, *The Arrangement of Atoms in Space*, 2nd ed. Longmans, Green, London, **1898**.
[10] a) L. Pauling, *J. Am. Chem. Soc.* **1931**, *53*, 1367, 3225; *Nature of the Chemical Bond*, Cornell University Press, Ithaca, NY, 2nd ed. **1940**, Chapter III; 3rd ed. **1961**; b) For further discussion of this point, see K. B. Wiberg, *Acc. Chem. Res.* **1996**, *29*, 229.
[11] J. C. Slater, *Phys. Rev.* **1931**, *37*, 481; *ibid.* **1931**, *38*, 1109.
[12] J. E. Lennard-Jones, *Trans. Faraday Soc.* **1929**, *25*, 668.
[13] Adapted from C. A. Coulson, *Valence*, Oxford University Press, London, **1952**, p. 100.
[14] For a review, references, and conceptual discussion, see a) W. Kutzelnigg, *Angew. Chem.* **1996**, *108*, 629; *Angew. Chem. Int. Ed. Engl.* **1996**, *35*, 573 - 586; b) W. Kutzelnigg, J. D. Morgan III, *Z. Phys. D Mol. Clusters* **1996**, *36*, 197.
[15] See also J. A. Berson, in *The Chemistry of Quinonoid Compounds, Vol. II*, (Eds.: S. Patai, Z. Rappoport), Wiley, New York, **1988**, Chapter 10, and references therein.
[16] R. S. Mulliken, *Phys. Rev.* **1933**, *43*, 279.
[17] a) W. G. Penney, *Proc. R. Soc. London A* **1934**, *144*, 166; b) *ibid.* **1934**, *146*, 223. For an account of Penney's later career as a leader of Britain's nuclear bomb program, see Lord Sherfield, *Biogr. Mem. Fellows R. Soc.* **1994**, *39*, 283. Penney served on the target committee for the bombing of Hiroshima and Nagasaki: R. Rhodes, *The Making of the Atomic Bomb*, Simon and Schuster, New York, **1986**, pp. 522, 626, 628, 677–678.
[18] G. E. Kimball, *J. Chem. Phys.* **1940**, *8*, 188.
[19] E. Hückel, *Z. Phys.* **1932**, *76*, 628.
[20] E. Hückel, *Z. Phys.* **1931**, *70*, 204.
[21] L. Pauling, *J. Chem. Phys.* **1933**, *1*, 280; L. Pauling, G. W. Wheland, *ibid.* **1933**, *1*, 362; L. Pauling, J. Sherman, *ibid.* **1933**, *1*, 679.
[22] G. W. Wheland, *J. Chem. Phys.* **1934**, *2*, 474.
[23] L. Pauling in *Organic Chemistry – An Advanced Treatise Vol. II*, (Ed.: H. Gilman) 2nd ed., Wiley, New York, **1943**, Chapter 26.
[24] G. W. Wheland, *The Theory of Resonance and Its Application to Organic Chemistry*, Wiley, New York, **1944**.
[25] G. W. Wheland, *Resonance in Organic Chemistry*, Wiley, New York, **1955**, p. 632.
[26] R. S. Mulliken, *Annu. Rev. Phys. Chem.* **1978**, *29*, 1, and references therein.
[27] W. J. Hehre, L. Radom, P. von R. Schleyer, J. A. Pople, *Ab Initio Molecular Orbital Theory*, Wiley, New York, **1986**.
[28] P. C. Hiberty, G. Ohanessian, S. Shaik, J.-P. Flament, *Pure Appl. Chem.* **1993**, *65*, 35; S. Shaik, P. C. Hiberty, *Adv. Quant. Chem.* **1995**, *26*, 99, and references therein.
[29] W. Goddard, III, L. B. Harding, *Annu. Rev. Phys. Chem.* **1978**, *29*, 363.
[30] C. A. Coulson, *Valence*, Oxford, **1952**, p. 109 ff.
[31] W. Heitler, F. London, *Z. Phys.* **1927**, *44*, 455.
[32] W. Heisenberg, *Z. Phys.* **1928**, *49*, 619; J. C. Slater, *Phys. Rev.* **1929**, *34*, 1293; cf. J. C. Slater, *Introduction to Chemical Physics*, McGraw-Hill, New York, **1939**, p. 367 ff.
[33] F. Bloch, *Z. Phys.* **1930**, *61*, 206.
[34] E. Hückel, *Pap. and Discuss. Int. Conf. Phys. Vol. II*, The Physical Society, London, **1935**, p. 9.
[35] J. C. Slater, *Pap. and Discuss. Int. Conf. Phys. Vol. II*, The Physical Society, London, **1935**, p. 53.
[36] F. Bloch, *Z. Phys.* **1928**, *52*, 555.
[37] E. Hückel, *Z. Elektrochem. Angew. Physik. Chem.* **1937**, *42*, 752, 827. Reissued as an off-print: "*Grundzüge der Theorie ungesättigter und aromatischer Verbindungen*", Verlag Chemie, Berlin, **1938**.
[38] E. Heilbronner in ref. [64c], p. 179.
[39] A. Streitwieser, Jr. *Molecular Orbital Theory for Organic Chemists*, Wiley, New York, 1961, p. 5.
[40] K. B. Wiberg, *Physical Organic Chemistry*, Wiley, New York, 1964, p. 9.
[41] J. P. Lowe, *Quantum Chemistry*, Academic Press, New York, 1978,
[42] V. I. Minkin, M. N. Glukhovtsev, B. Ya. Simkin *Aromaticity and Antiaromaticity*, Wiley, New York, **1994**, p. 116 ff.
[43] H. M. McConnell, *Science*, **1996**, *271*, 603.
[44] S. Kuwajima, *J. Am. Chem. Soc.* **1984**, *106*, 6496.
[45] C. A. Coulson, *Valence*, Oxford, **1952**, p. 147 ff; H. C. Longuet-Higgins, *Proc. Phys. Soc.* **1948**, *60*, 270.
[46] D. Maynau, J.-P. Malrieu, *J. Am. Chem. Soc.* **1982**, *104*, 3029.
[47] J. J. C. Mulder, L. J. Oosterhoff, *Chem. Commun.* **1970**, 305, 307.
[48] R. Huisgen, tape-recorded interview with J. A. Berson, New Haven, October 29, **1995**.
[49] W. Hückel, *Theoretical Principles of Organic Chemistry, Vol. I*, Elsevier, New York, **1958**, (English translation of *Theoretische Grundlagen der Organischen Chemie*, Verlag Chemie, Weinheim, 7th ed.).
[50] C. K. Ingold, *Structure and Mechanism in Organic Chemistry*, Cornell University Press, Ithaca, NY, **1953**, p. 185.
[51] L. P. Hammett, *Physical OrganicChemistry*, McGraw-Hill, New York, **1940**, p. 16 ff.
[52] Personal notes by J. A. Berson on lectures in Advanced Organic Chemistry, a course given by W. von E. Doering, Columbia University, 1946–1947.
[53] C. R. Noller, *J. Chem. Educ.* **1950**, *27*, 504.
[54] L. F. Fieser in *Organic Chemistry – An Advanced Treatise Vol. I*, (Ed.: H. Gilman), 2nd ed., Wiley, New York, **1943**, Chapter 3; see also L. F. Fieser, M. Fieser, *Advanced Organic Chemistry*, Reinhold, New York, **1961**, p. 618.
[55] a) C. A. Coulson, *Proc. R. Soc. A* **1939**, *169*, 414; b) C. A. Coulson, G. S. Rushbrooke, *Proc. Cambridge Philos. Soc.* **1940**, *36*, 193; c) H. C. Longuet-Higgins, *J. Chem. Phys.* **1950**, *18*, 265; d) M. J. S. Dewar, *J. Am. Chem. Soc.* **1952**, *74*, 3345, 3357.
[56] a) R. S. Mulliken, *J. Chim. Phys. Phys. Chim. Biol.* **1949**, *46*, 497, 675; b) B. Pullman, A. Pullman, *Les Théories Electroniques de la Chimie Organique*, Masson & Cie, Paris, **1952**.
[57] E. Heilbronner, tape-recorded interview with J. A. Berson, Herrliberg, Switzerland, March 30, 1996. Heilbronner reports that in a conversation in 1950–51, Pauling remarked that only two people had ever read the Mulliken paper: Mulliken and the poor guy who had to translate it into French.
[58] A. S. Pfau, P. A. Plattner, *Helv. Chim. Acta*, **1936**, *19*, 858; P. A. Plattner, *Angew. Chem.* **1942**, *55*, 131, 154.
[59] Review: W. Keller-Schierlein, E. Heilbronner in ref. [64c], Chapter VI.
[60] E. Heilbronner in ref. [64c], Chapter V.
[61] K. Hafner, *Angew. Chem.* **1958**, *70*, 419; K. Ziegler, K. Hafner, *ibid.* **1955**, *67*, 301.
[62] T. Nozoe, *Seventy Years in Organic Chemistry*, American Chemical Society, (Ed.: J. I. Seeman), Washington, DC, **1991**; T. Nozoe, interview with J. A. Berson, Tokyo, May 18, 1995; T. Nozoe to J. A. Berson, personal letter, June 6, 1995. Review: T. Nozoe in ref. [64c] p. 339.
[63] a) H. J. Dauben, H. Ringold, *J. Am. Chem. Soc.* **1951**, *73*, 876; b) W. von E. Doering, F. L. Detert, *ibid.* **1951**, *73*, 876.
[64] See among others: a) *Theoretical Organic Chemistry. Proceedings and Discussions of the Kekulé Symposium*, Butterworths Scientific Publications, London, **1959**; b) *Aromaticity, an International Symposium*, The Chemical Society Special Publication No. 21, London, **1967**; c) *Non-benzenoid Aromatic Compounds*, (Ed.: D. Ginsburg), Interscience, New York, **1959**; d) P. J. Garratt, *Aromaticity*, Wiley, New York, **1986**.
[65] W. von E. Doering, L. H. Knox, *J. Am. Chem. Soc.* **1954**, *76*, 3203.
[66] R. Breslow, H. Höver, H. W. Chang, *J. Am. Chem. Soc.* **1962**, *84*, 3168, and references therein.
[67] R. B. Woodward, R. Hoffmann, *The Conservation of Orbital Symmetry*, Verlag Chemie, Weinheim and Academic Press, New York, **1970**, and references therein.
[68] K. Fukui, *Acc. Chem. Res.* **1971**, *4*, 57; H. E. Zimmerman, *ibid.* **1972**, *5*, 393; M. J. S. Dewar, *Angew. Chem.* **1971**, *83*, 859; *Angew. Chem. Int. Ed. Engl.* **1971**, *10*, 761; an important insight undergirding the latter two papers is given by E. Heilbronner, *Tetrahedron Lett.* **1964**, 1923.
[69] Further references: ref. [67], p. 169.
[70] M. G. Evans, *Trans. Faraday Soc.* **1939**, *35*, 824. For a much closer early approach to modern orbital symmetry ideas, see Ya. K. Syrkin, *Bull. Acad. Sci. USSR, Div. Chem. Sci.* **1959**, 218; *Izv. Akad. Nauk SSSR, Arm. Khim. Nauki*, **1959**, 238; Ya. K. Syrkin, I. I. Moiseev, *Uspekhi Khim.* **1958**, *27*, 1321.

[71] F. Hund, personal communication to E. Müller, as cited by Müller and Bunge in ref.[72].
[72] E. Müller, I. Müller-Rudloff, *Justus Liebigs Ann. Chem.* **1936**, *517*, 134; E. Müller, W. Bunge, *Ber. Dtsch. Chem. Ges.* **1936**, *69*, 2168.
[73] E. Hückel, *Z. Phys. Chem. Abt. B*, **1936**, *34*, 339.
[74] a) W. T. Borden, E. R. Davidson, *J. Am. Chem. Soc.* **1977**, *99*, 4587; b) A. A. Ovchinnikov, *Theor. Chem. Acta*, **1977**, *47*, 497.
[75] Similar arguments led to the idea that square planar cyclobutadiene (not formally a non-Kekulé molecule) also might violate Hund's rule: W. T. Borden, *J. Am. Chem. Soc.* **1975**, *97*, 5968. H. Kollmar, V. Staemmler, *ibid.* **1977**, *99*, 3586.
[76] J. H. Reynolds, J. A. Berson, K. K. Kumashiro, J. C. Duchamp, K. W. Zilm, J. C. Scaiano, A. B. Berinstain, A. Rubello, P. Vogel, *J. Am. Chem. Soc.* **1993**, *115*, 8073; W. T. Borden, H. Iwamura, J. A. Berson, *Acc. Chem. Res.*, **1994**, *27*, 109, and references therein; P. G. Wenthold, D. A. Hrovat, W. T. Borden, W. C. Lineberger, *Science* **1996**, *272*, 1456.
[77] K. Hafner, tape-recorded interview with J. A. Berson, Darmstadt, April 3, 1996.
[78] Undated letter of E. Hückel to R. Kuhn, reproduced in the *Program of the Kekulé Celebration*, Bonn, 1965.
[79] H. Tietz, "Einige persönliche Worte zu Erich Hückel," unpublished text of a celebratory colloquium, presented in Marburg, November 14, 1980; W. Walcher, letter to J. A. Berson, March 6, 1996.
[80] A. A. Frost, B. Musulin, *J. Chem. Phys.* **1953**, *21*, 572.
[81] J. Thiele, *Justus Liebigs Ann. Chem.* **1899**, *306*, 87. I thank Prof. R. Huisgen for this citation, which appears epigraphically in his own doctoral dissertation.
[82] "Tradition and the Individual Talent", T. S. Eliot in *The Sacred Wood*, Methuen, London, p. 52.

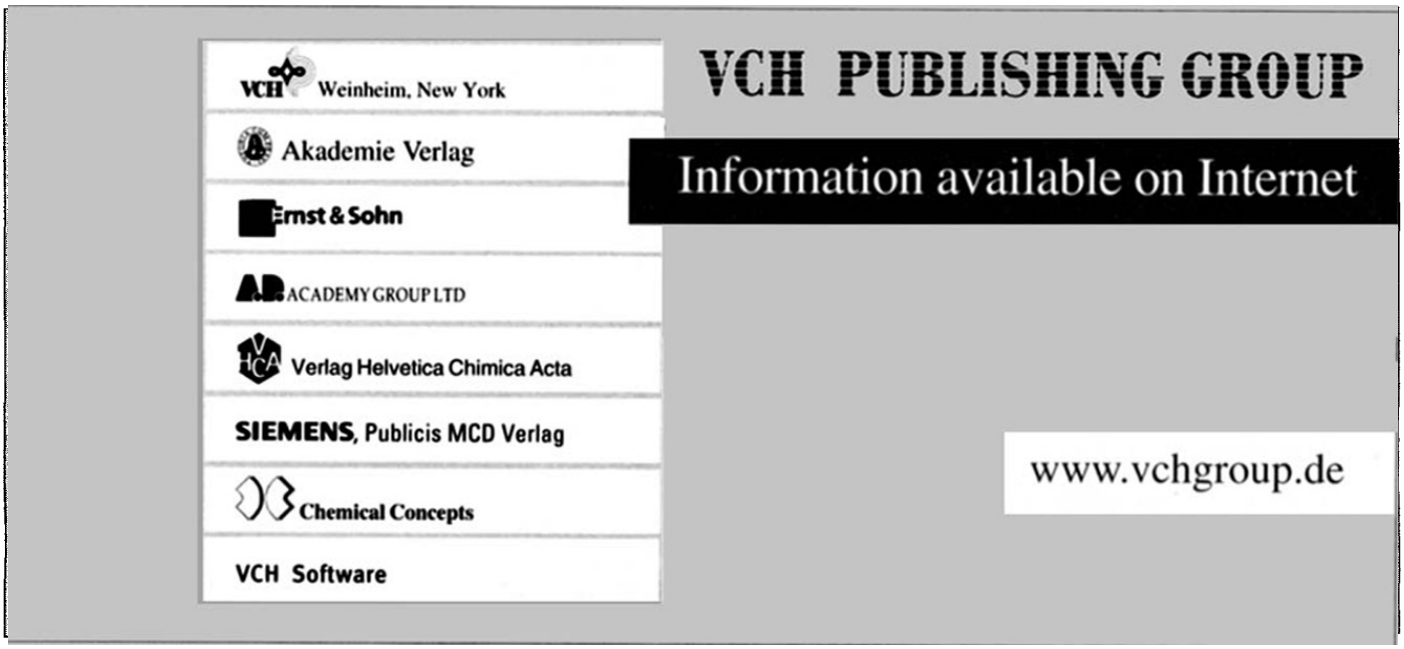

New Carbocations—From Physical Organic Chemistry to Biochemistry**

Thomas Laube*

Carbocations are an important class of reactive intermediates in organic chemistry along with radicals, carbanions, and carbenes. The 1994 Nobel Prize in Chemistry was awarded to George A. Olah, the pioneer in the area of physical chemical investigations of carbocations, for the development of methods for the preparation of stable solutions of carbocations and their NMR spectroscopic investigation. In this highlight, four interesting new publications are discussed, which illustrate intriguing aspects of modern carbocation chemistry. Carbocations are not only important in physical organic chemistry, but also in crystal engineering, organometallic chemistry, and biochemistry.

Head et al.[1] have prepared the first carbotetracation **2** from the tetraalcohol **1**. The tetracation **2**, in which the positive charges have a tetrahedral arrangement, shows four and seven signals in temperature-independent ^1H and ^{13}C NMR spectra, respectively, between -80 and $-40\,^\circ C$. The positive charge in **2** is more delocalized into the phenyl rings and less into the adamantane cage than in the dication **3**.[2] This is explained by the stronger repulsion of the four positive charges in **2**. Polycations like **2** are very interesting because of possible applications in the design and synthesis of stable salts. The tetrahedral arrangement of the charged groups in **2** could be used in "crystal engineering"[3] for the formation of three-dimensional networks with suitable bidentate donor ligands. The tetracation could also be used as an initiator in cationic polymerizations that should lead to dendrimeric and hyperbranched polymers.

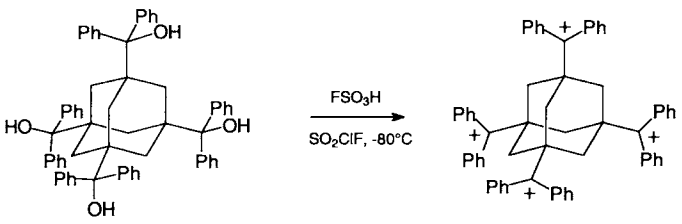

1 **2**

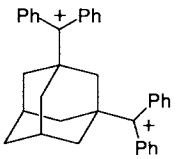

3

Winstein et al.,[4] Saunders et al.,[5] Olah et al.,[6] and other groups demonstrated the bishomoaromatic character of the norbornadienyl cation (**4**) by solvolytic methods and by NMR spectroscopy. Bremer et al.[7] confirmed these results by high-level ab initio calculations, and the structure of a substituted 7-norbornenyl cation[8] was determined by X-ray diffraction. Recently Evans et al.[9] found that the reaction of tris(pentamethylcyclopentadienyl)samarium (**5**) with carbon monoxide gives the unexpected product **6**, which they characterized by

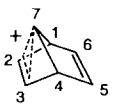

4

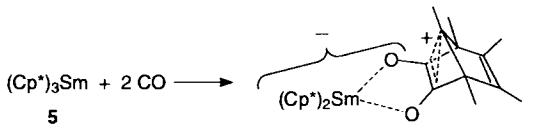

5 **6**

NMR spectroscopy and a crystal structure analysis. The two incorporated CO molecules form a new ligand with one (formally anionic) Cp* ligand—a 2,3-dioxygen-substituted norbornadienyl cation. In this fragment of **6** (atom numbering analogous to that in cation **4**), the short C2–C7 and C3–C7 distances (1.876(4) Å) and the elongated C2–C3 double bond (1.426(4) Å) can be rationalized by invoking bishomoaromatic stabilization involving C2, C3, and C7 centers. The cationic center C7 interacts only with the C2–C3 bond but not with the C5–C6 bond (1.328(5) Å). The structure of the cation fragment in **6** agrees relatively well with that of the substituted 7-norbornenyl cation;[8] the synthesis of **6** provides additional evidence for the facile formation of substituted bishomoaromatic carbocations.

Bicyclobutonium ions, rapidly equilibrating nonclassical cations generated from cyclopropylmethyl or cyclobutyl compounds, are among the conceptually most difficult nonclassical carbocations.[10] Only one static cyclopropylmethyl cation, **7**, had been observed previously.[11] Olah et al. now describe the preparation of a new, substituted bicyclobutonium ion, the triaxane-2-methyl cation (**9**), starting from the alcohol **8**.[12] Between -100 and $-40\,^\circ C$, seven signals with unchanged chemi-

[*] Priv.-Doz. Dr. T. Laube
Zeunerstrasse 1, CH-8037 Zürich (Switzerland)
Fax: Int. code +(1)272-4924
e-mail: cplus@wawona.vmsmail.ethz.ch

[**] This article was written during a ten and a half month stay at the Loker Hydrocarbon Research Institute, University of Southern California. I thank Prof. G. A. Olah and Prof. R. Bau, Los Angeles, for their support.

cal shifts are observed in the ^{13}C NMR spectrum of **9**. This result is in accord with a static cation (point group C_s) as well as with a rapidly equilibrating mixture of less symmetric cations. The authors have computed the structures and the NMR chemical shifts of all possible cations by ab initio methods. For the ions with the lowest energy, the bicyclobutonium ion **9a** and its enantiomer **9b** (both point group C_1), the experimental and the computed chemical shifts are in good agreement if one assumes a rapid equilibrium between **9a** and **9b**. The involvement of

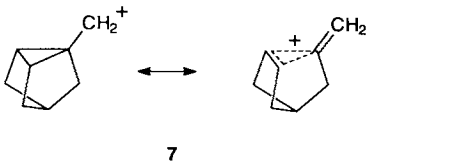

7

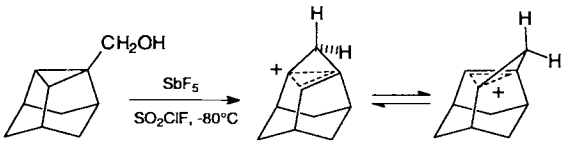

8 **9a** **9b**

higher energy cations need not to be considered despite the flat potential energy surface of such systems. An analogous result was obtained for a related dication, the ditriaxane-2,10-dimethyl dication, which contains two bicyclobutonium moieties. Comparison of these results with the properties of **7** seem to indicate that subtle changes in cyclopropylmethyl cations can lead to different structures.

The occurrence of a carbocation intermediate having a pentacoordinate carbon atom is also the subject of a recent paper of Berkessel and Thauer,[13] in which the possible mechanism of the reversible, stereospecific hydrogen transfer by a metal-free enzyme to a substituted amidinium ion **13** is discussed (see Scheme 1, the italicized H atom is not involved). A new mechanism is proposed for the enzymatic reaction, since the hydrogenase that catalyzes the reaction **10** $\rightleftharpoons$ **13** does not contain a metal atom that could activate H_2. It is suggested that in the enzyme the amidinium ion is activated by N-protonation such that it binds a H_2 molecule with a three-center, two-electron bond at C14a (**12**). Nearly 30 years ago, Olah et al.[14,15] and Hogeveen et al.[16,17] showed that analogous reactions of saturated hydrocarbons (or of aliphatic carbocations in the reverse direction) occur in superacidic media, and they discussed pentacoordinate carbocations as intermediates. Very recently Olah proposed this type of activation in enzymatic systems.[18] Thus it seems reasonable and justified to dub the hydrogenase involved in the reaction mentioned above an "Olah enzyme".[19]

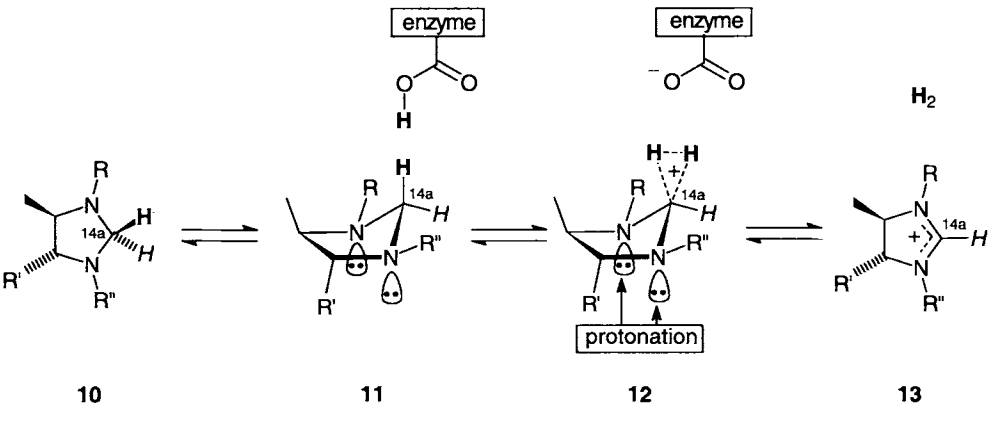

10 **11** **12** **13**

Scheme 1.

German version: *Angew. Chem.* **1996**, *108*, 2939–2940

Keywords: carbocations · enzyme mechanisms · reaction mechanisms

[1] N. J. Head, G. K. S. Prakash, A. Bashir-Hashemi, G. A. Olah, *J. Am. Chem. Soc.* **1995**, *117*, 12005–12006.
[2] M. D. Heagy, Q. Wang, G. A. Olah, G. K. S. Prakash, *J. Org. Chem.* **1995**, *60*, 7351–7354.
[3] G. R. Desiraju, *Crystal Engineering: The Design of Organic Solids*, Elsevier, Amsterdam, **1989**; see also: *Angew. Chem.* **1995**, *107*, 2541; *Angew. Chem. Int. Ed. Engl.* **1995**, *34*, 2328.
[4] S. Winstein, M. Shatavsky, C. Norton, R. B. Woodward, *J. Am. Chem. Soc.* **1955**, *77*, 4183–4184.
[5] P. R. Story, M. Saunders, *J. Am. Chem. Soc.* **1962**, *84*, 4876–4882.
[6] G. A. Olah, G. Liang, *J. Am. Chem. Soc.* **1975**, *97*, 6803–6806.
[7] M. Bremer, K. Schötz, P. von R. Schleyer, U. Fleischer, M. Schindler, W. Kutzelnigg, W. Koch, P. Pulay, *Angew. Chem.* **1989**, *101*, 1063–1065; *Angew. Chem. Int. Ed. Engl.* **1989**, *28*, 1042.
[8] T. Laube, *J. Am. Chem. Soc.* **1989**, *111*, 9224–9232.
[9] W. J. Evans, K. J. Forrestal, J. W. Ziller, *J. Am. Chem. Soc.* **1995**, *117*, 12635–12636.
[10] G. A. Olah, P. V. Reddy, G. K. S. Prakash in *The Chemistry of the Cyclopropyl Group, Vol. 2* (Ed.: Z. Rappoport), Wiley, Chichester, **1995**, pp. 813–859.
[11] L. R. Schmitz, T. S. Sorensen, *J. Am. Chem. Soc.* **1982**, *104*, 2600–2604.
[12] G. A. Olah, H. A. Buchholz, G. K. S. Prakash, G. Rasul, J. J. Sosnowski, R. K. Murray Jr., M. A. Kusnetsov, S. Liang, A. de Meijere, *Angew. Chem.* **1996**, *108*, 1623–1626; *Angew. Chem. Int. Ed. Engl.* **1996**, *35*, 1499–1501.
[13] A. Berkessel, R. K. Thauer, *Angew. Chem.* **1995**, *107*, 2418–2421; *Angew. Chem. Int. Ed. Engl.* **1995**, *34*, 2247–2250.
[14] G. A. Olah, N. Hartz, G. Rasul, G. K. S. Prakash, *J. Am. Chem. Soc.* **1995**, *117*, 1336–1343.
[15] G. A. Olah, G. Klopman, R. H. Schlosberg, *J. Am. Chem. Soc.* **1969**, *91*, 3261–3268.
[16] H. Hogeveen, C. J. Gaasbeek, *Recl. Trav. Chim. Pays-Bas* **1968**, *87*, 319–320.
[17] A. F. Bickel, C. J. Gaasbeek, H. Hogeveen, J. M. Oeldrick, J. C. Platteeuw, *J. Chem. Soc. Chem. Commun.* **1967**, 634–635.
[18] G. A. Olah, *Angew. Chem.* **1993**, *105*, 805; *Angew. Chem. Int. Ed. Engl.* **1993**, *32*, 767–788.
[19] L. Jaenicke, *Chem. Unserer Zeit* **1995**, *29*, 276–277.

 © VCH Verlagsgesellschaft mbH, D-69451 Weinheim, 1996 0570-0833/96/3523-2766 $ 15.00+.25/0

The β Turn as a Selectivity Switch: βI or βII′? That Is the Question**

Gerhard Müller*

The discovery of low molecular weight compounds capable of selectively modulating the functions of enzymes or receptors is a central topic in medicinal chemistry. Once a lead compound is identified it is developed further into a potential drug candidate by a repetitive procedure comprising the synthesis and biological characterization of successive generations of analogs. In this context medicinal chemists constantly seek new molecular templates patentable for a particular pharmaceutical indication, which facilitate the controlled spatial orientation of interacting groups and thus enable the chemist to exercise steric control over the construction of a potential pharmacophore.

Nature apparently utilizes a generic set of presentation scaffolds, since the demand of biochemical processes on molecular recognition is extremely high. The biological activity of endogenous peptide hormones is often encoded in exposed loop regions, in which two to four amino acid residues, essential for the activity, adopt β turn conformations.[1] These β turns have been employed as structural scaffolds in the design of biologically active oligopeptides, for which the research area of antiadhesive Arg-Gly-Asp (RGD in the one-letter notation; a universal cell recognition sequence[2]) mimetics turned out to be an excellent example.[3] Using modified RGD peptide analogs and non-peptide RGD mimics it has been attempted to selectively address the endogenous targets, which are members of the integrin receptor family.[4] Interaction with the platelet-associated $\alpha_{IIb}\beta_3$ integrin inhibits thrombus formation, whilst the tumor cell associated $\alpha_v\beta_3$ integrin appears to influence the adhesion properties of metastatic cells. RGD mimics are therefore promising candidates not only for the development of antithrombotics, but also as inhibitors of formation of new blood vessels (angiogenesis), necessary for tumor growth, which qualifies them as potential antimetastatic drugs.[3, 4] In addition, the implications of integrins in the pathogenic mechanisms of osteoporosis is about to emerge, which may have a significant biomedical potential.[5]

These therapeutically promising perspectives motivated several research groups at the beginning of the 1990s to study cyclic RGD peptides[3] with the aim of deducing the biologically active, in other words receptor-complementary, conformation by determining their three-dimensional structures.[6] Not only highly active, but also receptor-selective adhesion antagonists emerged from the systematic study of β turns as presentation modules.[3, 7] In this context, researchers from the American pharmaceutical company DuPont Merck recently reported on the structure determination of some RGD peptides (**1a–c**, Fig. 1), which show pronounced $\alpha_v\beta_3$-integrin selectivity.[8]

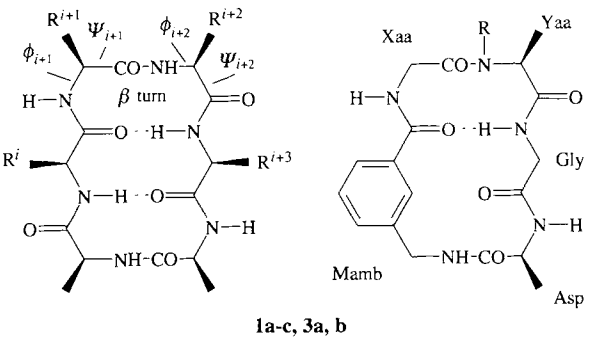

1a-c, 3a, b

Fig. 1. Comparison of a cyclic hexapeptide comprising two β turns (left) with the basic structure of the cyclic peptides **1a–c** and **3a,b** (right). Yaa: L-Arg.

These compounds resulted from a systematic investigation of structure–activity relationships on cyclic RGD peptide analogs at DuPont Merck,[9] all of which were rationally designed based on the experimentally determined three-dimensional structure of the disulfide-bridged pentapeptide *cyclo*-(1,5)-[Ac-Cys-(NMe)Arg-Gly-Asp-Pen-NH_2] (Pen: penicillamine, β,β'-dimethylcysteine) **2** (SK & F 106760) from the company Smith Kline Beecham.[10] The primary aim of these studies at that time was to develop active antithrombotics, selective $\alpha_{IIb}\beta_3$-integrin binding RGD mimetics, which, at DuPont Merck, resulted in the compound DMP 728 (**3a**) as a candidate for clinical development.[11]

The main conclusion of the work presented by the DuPont Merck group[8] refers to the exchange of the dipeptide units D-Abu-(NMe)Arg (in **3a**, D-Abu: D-2-aminobutanoic acid) and D-Ala-(NMe)Arg (in **3b**) for L-Xxx-Arg (Xxx = Ala, Pro in **1a** and **1c**, respectively), which transforms a $\alpha_{IIb}\beta_3$-selective peptide into a $\alpha_v\beta_3$-selective compound (Table 1). This in itself did not

Table 1. Comparison of the biological activity of the DuPont Merck peptide discussed here against tumor cell associated ($\alpha_v\beta_3$) and platelet-associated ($\alpha_{IIb}\beta_3$) integrins. Yaa = L-Arg.

Cmpd.	Xaa	R	$IC_{50}(\alpha_v\beta_3)$ [nM]	$IC_{50}(\alpha_{IIb}\beta_3)$ [nM]	β Turn type
1a	L-Ala	H	20	18000	I
1b	Aib	H	36	9000	I
1c	L-Pro	H	13	45000	I
3a	D-Abu	CH_3	500	2	II′
3b	D-Ala	CH_3	500	8	II′

seem particularly noteworthy, since on the one hand the structure of an active $\alpha_v\beta_3$-selective cyclic pentapeptide (*cyclo*-[-Arg-Gly-Asp-D-Phe-Val-] **4**) was already published in 1991 by Kessler et al.,[3a, 12] and on the other hand many orally active non-peptide $\alpha_{IIb}\beta_3$-antagonists have entered phase III of clinical development.[3e] However, if the results described by Bach et

[*] Dr. G. Müller
Bayer AG, MD-IM-FA, Geb. Q18
D-51368 Leverkusen (Germany)
Fax: Int. code + (214) 30-50351
e-mail: debay829@ibmmail.com

[**] The author would like to thank William F. DeGrado and Alvin C. Bach for supplying the structural coordinates of some of the peptides described in this contribution.

al.[8] are correlated with the experimentally determined three-dimensional structures of the peptides mentioned above, the conformation–activity data are extremely interesting and deserve a detailed discussion.

The structure of peptides **1a–c**, **3a**, and **3b** closely resembles the main structural features of the generic template of a cyclic hexapeptide composed of two β turn modules[7] (Fig. 1). Since the *meta*-aminomethylbenzoic acid (Mamb) moiety in **1a–c**, **3a**, and **3b** lacks a hydrogen bond donor functionality at the C2 atom of the benzene ring, only a single hydrogen bond is formed between Gly-NH and Mamb-CO, while the cyclic hexapeptide displays two hydrogen bonds. This single hydrogen bond stabilizes a β turn with residues L-Ala (**1a**), L-Pro (**1c**), D-Abu (**3a**), and D-Ala (**3b**) at the $i+1$ position and L-Arg (**1a**, **1c**) and L-(NMe)Arg (**3a**, **3b**) at the $i+2$ position. The most striking structural difference between the $\alpha_{IIb}\beta_3$-selective DMP 728 (**3**) and the $\alpha_v\beta_3$-selective peptides **1a–c** refers to the type of the β turn. Whilst all L-Xaa^{i+1}-L-Arg^{i+2} peptides form type I β turns, the sequences D-Abu^{i+1}-L-(NMe)Arg^{i+2} in **3a** and D-Ala^{i+1}-L-(NMe)Arg^{i+2} in **3b** adopt β turns of type II′. Apart from the opposite orientation of the hydrogen bonds relative to the peptide ring plane, the turns of types βI and βII′ differ in the relative spatial orientation of the ingoing and outgoing peptide strands (Fig. 2).

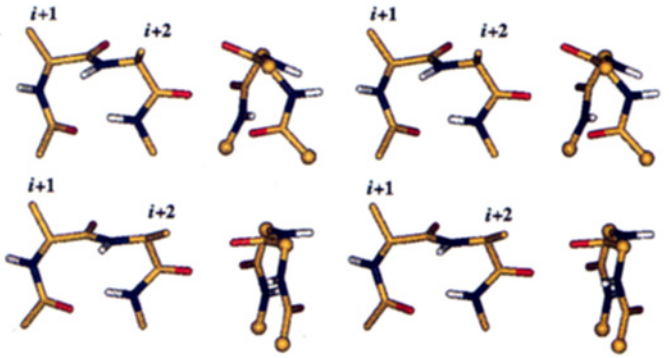

Fig. 2. Stereoview of a βI (top) and a βII′ turn (bottom). For clarity only heavy atoms and the amide hydrogen atoms of the model compounds Ac-L-Ala- L-Ala-$NHCH_3$ (top) and Ac-D-Ala-L-Ala-$NHCH_3$ (bottom) are shown. A front view of the turns is shown on the left; a Newman-type projection is depicted on the right. The four consecutive C^α atoms of the β turn forming a pseudo-dihedral angle are shown as small spheres.

In the βI turn the pseudo-dihedral angle spanned by the four consecutive C^α atoms of the amino acids in turn positions i to $i+3$ is 49° (assuming ideal values for the backbone torsions[11]) and results in an approximate synclinal (+ sc, *gauche*) orientation. In contrast, the βII′ turn displays a synperiplanar (− sp, *eclipsed*) conformation (− 3° assuming ideal values for the backbone torsions[11]) (Fig. 2). This difference in the type of the β turn has profound influence on the relative vectoral orientation of the Arg and Asp side chains and thus on the discriminating selectivity profile of the peptides. These amino acid side chains, constituting the potential pharmacophore, are found in a pseudo-diaxial arrangement in peptides **1a–c**, whereas the βII′ turn enables a diequatorial alignment in peptides **3a** and **3b** (Fig. 3).

The authors succeeded in correlating receptor selectivity with vectoral orientation of the Arg and Asp side chains[8]. The

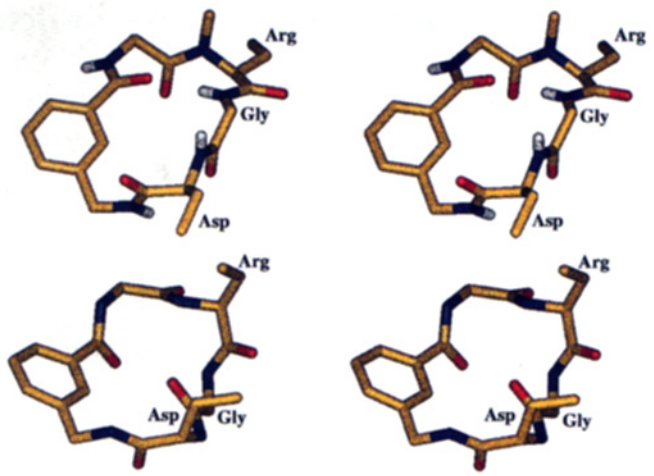

Fig. 3. Comparison of the three-dimensional structure of **3a** (top) with **1c** (bottom), which are shown as stereoviews. For clarity only the backbone atoms and the C^β and C^γ atoms of the Arg and Asp side chains are shown. The structure of **3a** is available from the Cambridge Crystal Structure Data Base (code: HAJRAP).

change in β turn type from βII′ to βI leads to an inverted selectivity profile of the described peptides. This discovery is in accord with the structural characteristics of the $\alpha_v\beta_3$-selective prototype peptide **4** mentioned above.[3a, 8, 12, 13] The superimposed structures of the RGD sequences of **4** and **1c** depicted in Figure 4 display an unexpected correspondence, although the crucial recognition sequence in **1c** "extends" along the longitudinal edge of the generic hexapeptide template structure (see Fig. 1), whilst in **4**, it adopts an extremely tight γ turn conformation.[12]

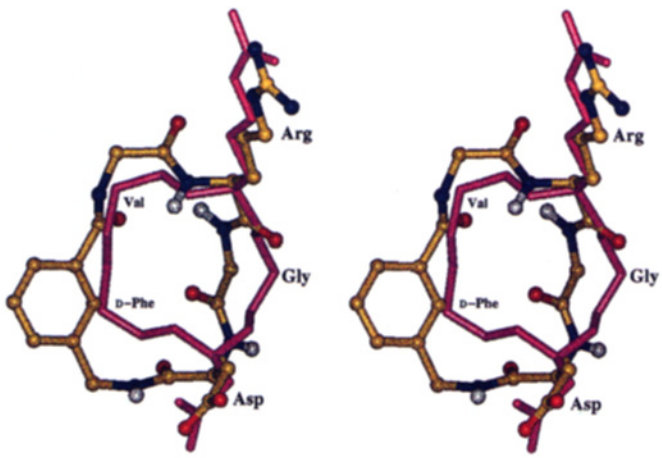

Fig. 4. Stereoview of the superimposed structures of **1c** and **4** (magenta). The C^α and C^β atoms of the Arg and Asp side chains served as reference atoms for superposition. Apart from the backbone atoms of **4** only the side chains of Arg and Asp are depicted.

The βI turn of, for example, **1c** enables an approximate synperiplanar orientation of two side chains at the $i+2$ and $i+4$ positions, which is apparently essential for $\alpha_v\beta_3$-complementarity. This particular arrangement can additionally only be achieved by incorporation of the RGD tripeptide into a regular γ turn, thereby occupying the turn positions i, $i+1$, and $i+2$, as shown by **4**. This stuctural analogy worked out by Bach et al. has led to a new peptide design principle, namely the Mamb-Pro element of **1c** can be utilized as a "structural clamp" in cyclic

 © VCH Verlagsgesellschaft mbH, D-69451 Weinheim, 1996 0570-0833/96/3523-2768 $ 15.00+.25/0

pentapeptides of the type *cyclo*-[-Mamb-Pro-Xaa-Yaa-Zaa-], thereby inducing a γ turn compatible conformation for the Xaa-Yaa-Zaa tripeptide.

These results have not only further refined the existing pharmacophore models for $\alpha_v\beta_3$-integrin binding, which can be employed as search profiles for mining structure databases in attempt to discover lead structures of $\alpha_v\beta_3$-selective RGD mimics, but have also increased awareness of the importance of controlled variation of the β turn type for spatial fine-tuning of potential pharmacophore groups. For the "peptide designers" among medicinal chemists the work described here and other findings have evolved into guidelines for the sterically controlled orientation of functional groups. It has been shown several times that β turns can be induced in cyclic peptides at specific positions by incorporation of turn-favoring elements such as proline, glycine, D-amino acids, and α,α'-dialkylated amino acids into the sequence.[6, 7] The DuPont Merck work[8, 9, 11] further underlines the importance of the steric control over the β turn architecture and the effect on receptor selectivity, exemplified with a biomedical application of significant importance.

The entire potential of β turns as structural templates is just becoming apparent, owing to numerous projects in current pharmaceutical research aimed at developing peptide receptor agonists and antagonists,[14] for which the members of the G-protein coupled receptor family are mentioned as representative examples.[16] In this context, the structural aspects discussed here almost take on the characteristics of a model applicable to related research projects dealing with structure-based drug design. For further development of therapeutics it would be desirable to turn to non-peptide β turn mimetics,[16] which would not only enable control of the turn type formed, but would also allow for optional functionalization of the turn mimetic, so that any underlying di-, tri-, or tetrapeptide sequence could be mimicked. This is, without doubt, a tremendous challenge for synthetic organic chemists motivated by structural chemistry, but it would also address an aspect of pharmaceutical research neglected so far.

In conclusion, the research area of antiadhesive RGD mimetics provides an excellent example of the complementarity of rational structure-based drug design and screening efforts for the discovery of new leads. In the near future, both approaches will certainly lead to non-peptidic $\alpha_v\beta_3$-selective RGD mimetics.

German version: *Angew. Chem.* **1996**, *108*, 2441–2443

Keywords: β turns · conformations · integrins · peptides · receptors

[1] a) J. S. Richardson, *Adv. Protein Chem.* **1981**, *34*, 167–339; b) G. D. Rose, L. M. Gierasch, J. A. Smith, *Adv. Protein Chem.* **1985**, *37*, 1–109.

[2] a) M. D. Pierschbacher, E. Ruoslahti, *Nature* **1984**, *309*, 30–33; b) E. Ruoslahti, M. D. Pierschbacher, *Science* **1987**, *238*, 491–497; c) S. E. D'Souza, M. H. Ginsberg, E. F. Plow, *Trends Biochem. Sci.* **1991**, *16*, 246–250.

[3] a) M. Aumailley, M. Gurrath, G. Müller, J. Calvete, R. Timpl, H. Kessler, *FEBS Lett.* **1991**, *291*, 50–54; b) N. S. Cook, G. Kottrisch, H.-G. Zerwes, *Drugs Future* **1994**, *19*, 135–159; c) T. Weller, L. Alig, M. Hürzeler-Müller, W. C. Kouns, B. Steiner, *ibid.* **1994**, *19*, 461–476; d) V. Austel, F. Himmelsbach, T. Müller, *ibid.* **1994**, *19*, 757–764; e) I. Ojima, S. Chakravarty, Q. Dong, *Bioorg. Med. Chem.* **1995**, *3*, 337–360; f) P. Raddatz, J. Gante, *Exp. Opin. Ther. Patents* **1995**, *5*, 1163–1183; g) R. Hirschmann, P. A. Sprengeler, T. Kawasaki, J. W. Laehy, C. Shakespeare, A. B. Smith III, *J. Am. Chem. Soc.* **1992**, *114*, 9699–9701; h) J. W. Bean, K. D. Kopple, C. E. Peishoff, *ibid.* **1992**, *114*, 5328–5334.

[4] a) R. A. Brown, C. D. McFarland, *Curr. Opin. Ther. Patents* **1993**, 1117–1140; b) D. Cox, T. Aoki, J. Seki, Y. Motoyama, K. Yoshida, *Med. Res. Rev.* **1994**, *14*, 195–228; c) P. C. Brooks, A. M. P. Montgomery, M. Rosenfeld, R. A. Reisfeld, T. Hu, G. Klier, D. A. Cheresh, *Cell* **1994**, *79*, 1157–1164.

[5] P. G. Robey, *Annu. Rep. Med. Chem.* **1993**, *28*, 227–236.

[6] a) H. Kessler, *Angew. Chem.* **1982**, *94*, 509–520; *Angew. Chem. Int. Ed. Engl.* **1982**, *21*, 512–523; b) V. Hruby, *Life Sci.* **1982**, *31*, 189–199.

[7] a) M. Gurrath, G. Müller, H. Kessler, M. Aumailley, R. Timpl, *Eur. J. Biochem.* **1992**, *210*, 911–921; b) G. Müller, M. Gurrath, H. Kessler, *J. Comput. Aided Mol. Design* **1994**, *8*, 709–730; c) H. Kessler, R. Gratias, G. Hessler, M. Gurrath, G. Müller, *Pure Appl. Chem.* **1996**, *68*, 1201-1205.

[8] A. C. Bach II, J. R. Espina, S. A. Jackson, P. F. W. Stouten, J. L. Duke, S. A. Mousa, W. F. DeGrado, *J. Am. Chem. Soc.* **1996**, *118*, 293–294.

[9] a) A. C. Bach II, C. J. Eyermann, J. D. Gross, M. J. Bower, R. L. Harlow, P. C. Weber, W. F. DeGrado, *J. Am. Chem. Soc.* **1994**, *116*, 3207–3219; b) S. A. Jackson, W. F. DeGrado, A. Dwivedi, A. Parthasarathy, A. Highley, J. Krywko, A. Rockwell, J. Markwalder, R. Wexler, S. A. Mousa, R. L. Harlow, *ibid.* **1994**, *116*, 3220–3230.

[10] J. Samanen, F. Ali, T. Romoff, R. Calvo, E. Sorenson, J. Vasko, B. Storer, D. Berry, D. Bennett, M. Strohsacker, D. Powers, J. Stadel, A. Nichols, *J. Med. Chem.* **1991**, *34*, 3114–3125.

[11] a) S. A. Mousa, J. M. Bozarth, M. S. Forsythe, W. Lorelli, S. A. Jackson, N. Ramachandran, W. F. DeGrado, *Cardiology* **1993**, *83*, 374–382; b) S. A. Mousa, S. Flint, W. Lorelli, S. Hassell, J. M. Bozarth, W. F. DeGrado, T. M. Reilly, *Thromb. Res.* **1994**, *76*, 109–119; c) S. A. Mousa, J. M. Bozarth, M. S. Forsythe, S. A. Jackson, A. Leamy, M. M. Diemer, R. P. Kapil, R. M. Knabb, M. C. Mayo, S. K. Pierce, *Circulation* **1994**, *89*, 3–12; d) W. E. Rote, J. H. Davis, S. A. Mousa, T. M. Reilly, B. R. Luccesi, *J. Cardiovasc. Pharmacol.* **1994**, *23*, 681–689.

[12] G. Müller, M. Gurrath, H. Kessler, R. Timpl, *Angew Chem.* **1992**, *104*, 341–343; *Angew. Chem. Int. Ed. Engl.* **1992**, *31*, 326–328.

[13] a) M. Pfaff, K. Tangemann, B. Müller, M. Gurrath, G. Müller, H. Kessler, R. Timpl, J. Engel, *J. Biol. Chem.* **1994**, *269*, 20233–20238; b) E. Noiri, J. Gailit, D. Sheth, H. Magazine, M. Gurrath, G. Müller, H. Kessler, M. S. Goligorsky, *Kidney Int.* **1994**, *46*, 1050–1058.

[14] a) R. Hirschmann *Angew. Chem.* **1991**, *103*, 1305–1330; *Angew. Chem. Int. Ed. Engl.* **1991**, *30*, 1278–1301; b) A. E. P. Adang, P. H. H. Hermkens, J. T. M. Linders, H. C. J. Ottenheijm, C. J. van Staveren, *Recl. Trav. Chim. Pays-Bas* **1994**, *113*, 63–78.

[15] T. P. Iismaa, T. J. Biden, J. Shine, *G protein-coupled Receptors*, Springer, **1995**.

[16] a) G. Hölzemann, *Kontakte (Darmstadt)* **1991**, 3–12, b) G. Hölzemann, *ibid.* **1991**, 55–63; c) A. Giannis, T. Kolter, *Angew. Chem.* **1993**, *105*, 1303–1326; *Angew. Chem. Int. Ed. Engl.* **1993**, *32*, 1244–1267.

 © *VCH Verlagsgesellschaft mbH, D-69451 Weinheim, 1996* *0570-0833/96/3523-2769 $ 15.00+.25/0*

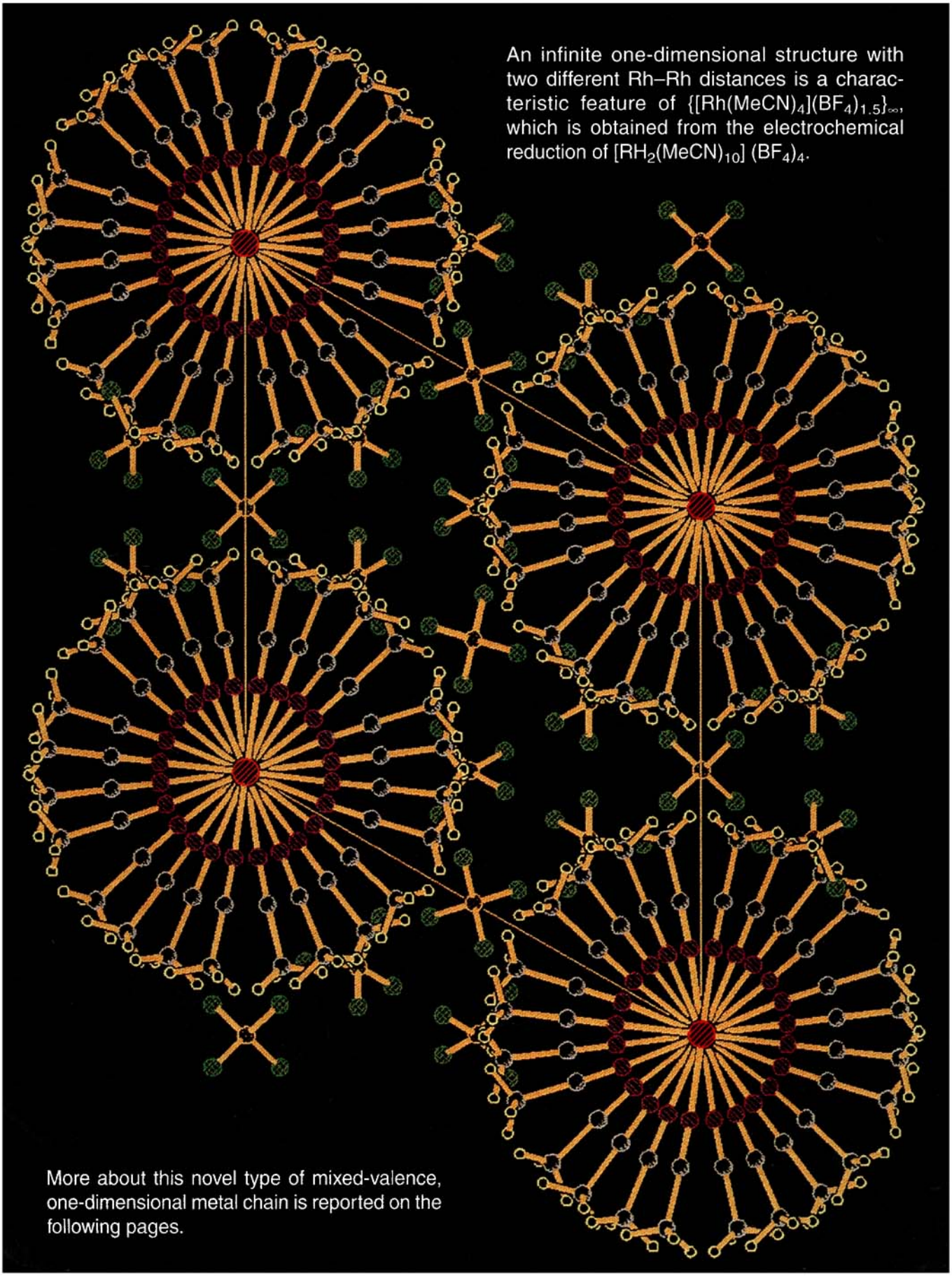

 © VCH Verlagsgesellschaft mbH, D,-69451 Weinheim, 1996 0570-0833/96/10823-2771 $ 15.00 + .25/0

Unprecedented Conversion of a Compound with Metal–Metal Bonding into a Solvated Molecular Wire**

Gary M. Finniss, Enric Canadell, Charles Campana, and Kim R. Dunbar*

One-dimensional (1D) compounds have intrigued chemists and physicists for decades.[1, 2] A primary reason for this fascination is the theoretical prediction advanced by Little over thirty years ago that 1D conductors may exhibit high-temperature superconductivity.[3] The largest class of 1D inorganic compounds are square-planar d^8 complexes that form columnar stacks in the solid-state.[4] The closed-shell systems are poor conductors, but oxidative doping to give a mixed-valence state leads to the onset of metallic behavior as exemplified by the partially oxidized tetracyanoplatinates (POTCPs) often referred to as Krogmann salts.[4a, c, d] Mononuclear Rh^I compounds also form oligomers at high concentrations in solution and in the solid state, but oxidation of these compounds yields "dimerized" compounds with metal–metal bonding or mononuclear Rh^{II} radicals if bulky ligands are employed.[5a, b, 6] Although less common, mixed-valence Rh^I/Rh^{II} species have been documented,[7] but these are also dinuclear with the exception of several well-characterized examples.[8a–c]

It is evident from the tremendous body of available data that the formation of discrete "dimers" with metal–metal (M–M) bonding (the extreme case of Peierls distortion) is a dominant theme in transition metal chemistry.[5] This situation aroused our curiosity as to the role of the ligands on the tendency for unbridged dinuclear compounds to crystallize without intermolecular metal–metal interactions. One reason for the scarcity of infinite M–M bonded chains may be the fact that the typical ligands used in coordination compounds, such as carboxylates, halides, and phosphanes, do not facilitate the direct approach of metal atoms along the axial direction. In support of this theory are the reports by Peng et al., that planar diimine ligands stabilize short oligomers that exhibit both metal–metal and ligand–ligand interactions.[8a] We reasoned that, given the proper ligand set, it may be possible to induce a dinuclear complex to actually "polymerize" into an infinite metal–metal bonded array. The unbridged compounds $[M_2(MeCN)_8]^{4+}$ and $[M_2(MeCN)_{10}]^{4+}$ with quadruple (M = Mo, Tc), triple (M = Re), and single (M = Rh) bonds were chosen for this investigation because these molecules possess only small, linear MeCN ligands whose steric effects are minimal. Our objective was to oxidize or reduce these diamagnetic molecules by one electron and to elucidate the solid-state structures of the resulting radical species. Herein we report the synthesis, X-ray crystal structure analysis, and band structure calculations of a novel solvated molecular wire prepared from a discrete metal-metal bonded precursor.

$[Rh_2(MeCN)_{10}](BF_4)_4$ exhibits an irreversible redox process at −0.05 V versus Ag/AgCl that corresponds to a one-electron reduction.[9, 10] Bulk electrolysis performed at −0.20 V versus Ag/AgCl in $(Bu_4N)BF_4$/MeCN immediately yields a gray-green microcrystalline solid that exhibits a solid-state EPR spectrum with axial symmetry.[11] Dissolution of this material in pure MeCN without supporting electrolyte yields an orange solution whose electronic properties resemble those of a mixture of the original $(Rh^{II})_2$ species (λ_{max} = 468 nm) and a Rh^I compound (λ_{max} = 414 nm).[10, 12] Slow galvanostatic reduction of $[Rh_2(MeCN)_{10}](BF_4)_4$ at low currents produces single crystals of **1** at the Pt cathode in about 30% yield over a period of three weeks.[13]

The novel material $\{[Rh(MeCN)_4](BF_4)_{1.5}\}_\infty$ (**1**) crystallizes in the acentric space group $P6_222$ which does not impose symmetry on adjacent Rh–Rh distances. As a consequence, there are two different Rh–Rh interactions in the chain: 2.8442(8) and 2.9277(8) Å. An ORTEP representation of the portion of the chain contained in each unit cell, namely "$[Rh_6(MeCN)_{24}]^{9+}$", is depicted in Figure 1. The charge of 9 + for the Rh_6 segment was

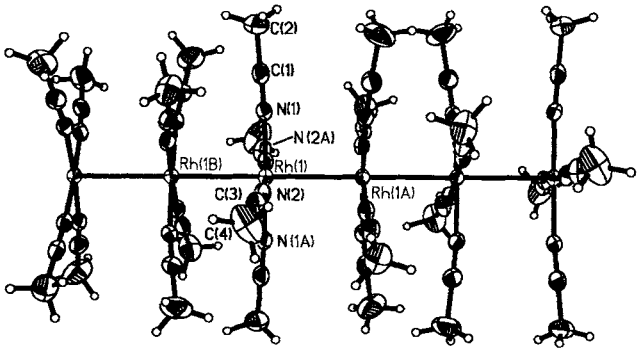

Fig. 1. ORTEP representation of a $[Rh_6(MeCN)_{24}]^{9+}$ segment of **1** with selected distances [Å] and angles [°]: Rh(1)–Rh(1A) 2.9277(8), Rh(1)–Rh(1B) 2.8442(8), Rh(1)–N(1) 1.991(4), Rh(1)–N(2) 1.985(4); N(1)-Rh(1)-N(2) 91.2(2), N(1)-Rh(1)-N(2A) 88.7(2), N(1)-Rh(1)-N(1A) 176.9(2), N(2)-Rh(1)-N(2A) 177.8(2), N(1)-Rh(1)-Rh(1A) 88.91(11), N(1)-Rh(1)-Rh(1B) 91.09(11), N(2)-Rh(1)-Rh(1A) 88.44(11), N(2)-Rh(1)-Rh(1B) 91.56(11).

deduced from the number of independent BF_4^- ions, which is precisely nine from refinement of the occupancies. These results are convincing evidence for the description of the material as being composed of Rh atoms in an average oxidation state of + 1.5.

A salient feature of the chain geometry is the orientation of the $Rh(MeCN)_4$ planes with respect to each other. Dinuclear complexes with a single M–M bond, including the parent molecule $[Rh_2(MeCN)_{10}]^{4+}$ ($\bar{\chi}$ = 44.8[2]°), typically adopt torsion angles of 45°. In **1** the MeCN ligands on Rh(1) and Rh(1B) that define the shorter Rh–Rh distance are twisted by 44.8°, whereas the ligands on Rh(1) and Rh(1A) adopt a torsion angle of 15.3°. These angles add up to 60° which allows for the presence of a 6_2 screw axis along the direction of the chain. As a result of subtle, but evidently real, steric effects brought about by the small differences in torsion angles, the MeCN ligands actually bend slightly away (ca. 1°) from the longer Rh–Rh interactions (2.9277(8) Å) and towards the shorter Rh–Rh contact (2.8442(8) Å) as can be seen in the space-filling representation of a portion of the chain (Fig. 2). A packing diagram of **1** in the crystal along the *c* axis is provided in Figure 3.

The calculated band structure of **1** (Fig. 4) reveals that the bands appear as six folded sub-bands, which is attributed to the

[*] Prof. K. R. Dunbar, G. M. Finniss
Department of Chemistry
Michigan State University
East Lansing, MI 48824 (USA)
Fax: Int. code +(517)353-1793
e-mail: dunbar@cemvax.cem.msu.edu
Dr. E. Canadell
Institut de Ciència de Materials de Barcelona (CSIC)
Campus de la UAB, E-08193 Bellaterra (Spain)
Dr. C. Campana
Siemens Industrial Automation
Madison, WI (USA)

[**] This research was supported by the National Science Foundation. We are grateful to Patrick Batail at the Université de Nantes for his guidance on electrocrystallization and for encouraging us to proceed with this work.

Fig. 2. Space-filling diagram of the segment $[Rh_6(MeCN)_{24}]^{9+}$.

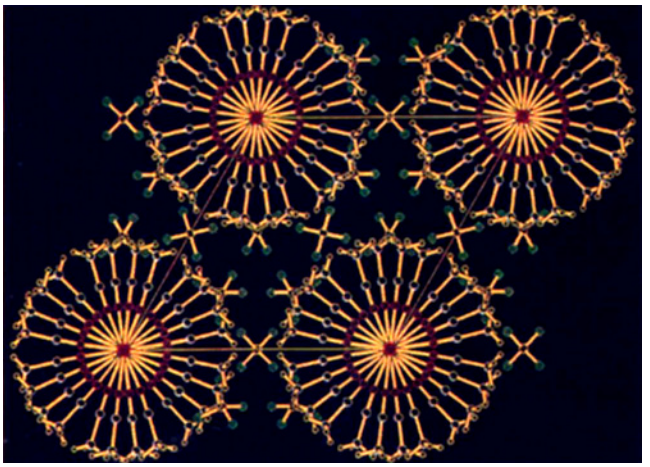

Fig. 3. Packing diagram of the unit cell along the *c* axis. Atom color shadings are: red (Rh), purple (N), grey (C), green (F), yellow (H).

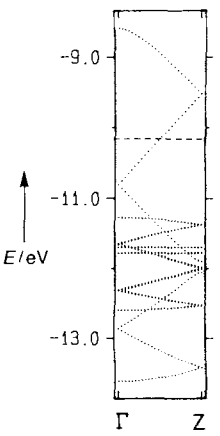

Fig. 4. Calculated band structure for the $[Rh_6(MeCN)_{24}]^{9+}$ chain. The dotted line denotes the Fermi level calculated by assuming double occupancy of the levels.

fact that the unit cell contents are $[\{Rh(MeCN)_4\}_6]^{9+}$.[14] Essentially, there is a dispersive d_{z^2} band, which in the lower part of the diagram overlaps with a series of flatter bands that originate mainly from xy,xz, and yz orbitals of the square-planar Rh units. As a consequence of the "dimerization" there is a gap between the third and fourth sub-bands (i.e. the middle of the z^2 band), but there are no gaps between the other sub-bands. Assuming that a double occupancy of the levels occurs, the stoichiometry dictates that the second sub-band from the top should be half-filled. Consequently, if the metallic state of this material can be stabilized, for example by applying pressure, the material is expected to undergo a metal-to-insulator Peierls type distortion like every 1D metal, which would double the size of the unit cell. It should be noted that the total width of the entire z^2 band is quite large. In fact the dispersion of the upper group of three sub-bands, which are partially filled, is as large as the z^2 band of potassium tetracyanoplatinate (KCP).[15] The preliminary charge transport data obtained by D. Jerome et al.[16] suggest that the appropriate electronic description of the chain is that of a series of $[\{Rh(MeCN)_4\}_2]^{3+}$ dimers with two electrons in the bonding combination (Ψ^+) of the two z^2 orbitals of the dimer and one electron in the antibonding combination (Ψ^-). The results of the calculation, however, indicate that these Y^- levels interact quite strongly along the chain so that it is not unreasonable to predict that a metallic state for the chain could be stabilized. If so, it would be interesting to observe the influence of the methyl groups in the possible Peierls distortion. Because of the interlocking of the groups on adjacent monomers, the methyl groups could provide an important elastic energy cost for the distortion. Thus, a systematic replacement of these methyl groups would be very interesting. Such tailoring would also be worthwhile in terms of the possibility for obtaining materials with different numbers of anions.

$\{[Rh(MeCN)_4](BF_4)_{1.5}\}_\infty$ (**1**) is novel in several respects. It is the first mixed-valence 1D compound of rhodium and is the only example of an infinite metal–metal bonded chain synthesized from a dinuclear precursor. Furthermore, the ligands are neutral donors which leads to a cationic charge on the chains, as opposed to the tetracyanoplatinates which are anionic. Most importantly, the new material provides a rare opportunity to apply the theories of one-dimensionality to a metal chain that differs considerably from the partially oxidized cyanoplatinate systems. Owing to the potential for tailoring the ligands, which is not possible for cyanide-based systems, one can envision the use of nitriles with much longer or bulkier aliphatic substituents. Such alterations will serve to increase the insulating organic "sheath" around the central core of metal atoms in the chain and may allow for the onset of liquid crystallinity if, for example, *n*-octyl groups were employed. The effects of these chemical modifications on the structures and transport properties will be extremely valuable for the understanding of this novel class of mixed-valence materials.

Experimental Procedure

Solutions of $[Rh_2(CH_3CN)_{10}](BF_4)_4$ (0.030 g, 0.031 mmol) and $[(nC_4H_9)_4N]BF_4$ (0.103 g, 0.311 mmol) in MeCN were loaded into a fritted two-compartment cell. Pt electrodes were inserted and a current of 2.0 μA was applied. After three weeks, bronze needles were harvested from the cathode (ca. 0.007 g, 28.3%). A large-scale preparation with 200 mg of precursor leads to bulk quantities of the material.

Received: May 17, 1996 [Z9127IE]
German version: *Angew. Chem.* **1996**, *108*, 2946–2948

Keywords: mixed-valent compounds · molecular wires · rhodium compounds

[1] a) T. J. Marks, *Ann. N. Y. Acad. Sci*, **1978**, *313*, 594; b) I. D. Brown, W. R. Daters, R. J. Gillespie in *Extended Linear Chain Compounds, Vol.3* (Ed.: J. S. Miller), Plenum, New York, **1982**, p. 1.

[2] a) P. Delhaes, S. Flandrois, J. Amiell, G. Keryer, E. Toreilles, J. M. Fabre, L. Giral, C. S. Jacobsen, K. Bechgaard, *Ann. N. Y. Acad. Sci.* **1978**, *313*, 467; b) J. R. Ferraro, J. M. Williams, *Introduction to Synthetic Electrical Conductors*, Academic Press, Orlando, FL, USA, **1987**, p. 8.

[3] W. A. Little, *Phys. Rev. A* **1964**, *134*, 1416.

[4] a) K. Krogmann, *Angew. Chem.* **1969**, *81*, 10; *Angew. Chem. Int. Ed. Engl.* **1969**, *8*, 35; b) A. L. Balch in *Extended Linear Chain Compounds, Vol. 1* (Ed.: J. S. Miller), Plenum, New York, **1982**, 1; c) A. H. Reis, Jr, in *Extended Linear Chain Compounds, Vol. 1* (Ed. J. S. Miller), Plenum, New York, **1982**, p. 157; d) J. M. Williams, A. J. Schultz in *Molecular Metals*, (Ed.: W. E. Hatfield), Plenum Press, New York, **1979**, p. 337–368; e) J. R. Ferraro, J. M. Williams, *Introduction to Synthetic Electrical Conductors*, Academic Press, Orlando, FL, USA, **1987**, p. 139.

[5] a) T. R. Felthouse *Prog. Inorg. Chem*, **1982**, *29*, 73; b) F. A. Cotton, R. A. Walton, *Multiple Bonds Between Metal Atoms*, 2nd ed., Clarendon Press, Oxford, New York, **1993**, p. 431; c) A theoretical study on quadruply bonded Mo_2 compounds concluded that direct M–M axial interactions are energetical-

 © VCH Verlagsgesellschaft mbH, D-69451 Weinheim, 1996 0570-0833/96/3523-2773 $ 15.00+.25/0

ly accessible: E. Canadell, R. Poilblanc, D. de Montauzon, E. C. de Felicio, *New J. Chem.* **1991**, 15, 623; d) M. H. Chisholm, *Pure & Appl. Chem.* **1991**, *63*, 665.
[6] a) K. R. Dunbar, S. C. Haefner, *J. Am. Chem. Soc.* **1991**, *113*, 9540; b) K. R. Dunbar, *Comments Inorg. Chem.* **1992**, *13*, 313–357; c) K. K. Pandey, *Coord. Chem. Rev.* **1992**, *121*, 1; d) D. G. DeWitt, *ibid.* **1996**, *147*, 209.
[7] a) J. L. Bear, L.-M. Liu, K. M. Kadish, *J. Am. Chem. Soc.* **1985**, *107*, 7195; b) P. Piriano, G. Bruno, S. L. Schiavo, F. Laschi, P. Zanello *Inorg. Chem.* **1987**, *26*, 2205.
[8] a) S.-S. Chern, G.-H. Lee, S.-M. Peng, *J. Chem. Soc. Chem. Commun.* **1994**, 1645; b) K. R. Mann, M. J. DiPierro, T. P. Gill, *J. Am. Chem. Soc.* **1980**, *102*, 3965; c) I. S. Sigal, K. R. Mann, H. B. Gray, *ibid.* **1980**, *102*, 7252.
[9] a) K. R. Dunbar, *J. Am. Chem. Soc.* **1988**, *110*, 8247. b) K. R. Dunbar, L. E. Pence, *Inorg. Synth.* **1992**, *29*, 182.
[10] L. E. Pence, PhD Thesis, Michigan State University, **1992**.
[11] The g tensors and linewidths vary slightly for different samples. A representative EPR spectrum gives $g_{\perp} = 2.26$, $g_{\parallel} = 2.02$ (solid-state at 77 K).
[12] C. A. James, D. E. Morris, S. K. Doorn, C. A. Arrington, K. R. Dunbar, G. M. Finnis, L. E. Pence, W. H. Woodruff, *Inorg. Chim. Acta.* **1996**, *242*, 91.
[13] Crystal data for **1** at -100 ± 2 °C: $RhF_6N_4C_8B_{1.5}H_{12}$, $0.32 \times 0.04 \times 0.04$ mm^3, hexagonal, $P6_222$, $a = b = 12.1121(5)$, $c = 17.3157(10)$ Å, $V = 2199.9(2)$ Å^3, $Z = 6$, $\rho_{calcd} = 1.800$ g cm^{-3}, $Mo_{K\alpha}$ radiation ($\lambda = 0.71073$ Å), $\mu = 1.22$ mm^{-1}. Data were collected on a Siemens CCD Smart system in the range $4 < 2\theta < 54°$. 11859 measured reflections, 1625 unique, 1276 with $F_o^2 4\sigma(F_o^2)$ were used to refine 98 parameters to $R(wR) = 0.0479\,(0.0786)$, GOF $= 1.185$; F^2 refinement in SHELXTL 5.0. A ψ scan absorption correction gave min. and max. transmission factors of 0.79 and 0.91. The highest peak in the final difference map $= 0.527$ e Å^{-3}. Crystallographic data (excluding structure factors) for the structure reported in this paper have been deposited with the Cambridge Crystallographic Data Centre as supplementary publication no. CCDC-179-110. Copies of the data can be obtained free of charge on application to The Director, CCDC, 12 Union Road, Cambridge CB2 1EZ, UK (fax: Int. code +(1223) 336-033; e-mail: teched@chemcrys.cam.ac.uk).
[14] a) The tight binding band structure calculations used an extended Hückel-type Hamiltonian: R. Hoffmann, *J. Chem. Phys.* **1963**, *39*, 1397. b) A modified Wolfsberg–Helmholz formula was used to evaluate the nondiagonal H_{ij} values: J. Ammeter, H.-B. Bürgi, J. Thibeault, R. Hoffmann, *J. Am. Chem. Soc.* **1978**, *100*, 3686. c) The exponents and parameters used were taken from R. H. Summerville, R. Hoffmann, *J. Am. Chem. Soc.* **1976**, *98*, 7240.
[15] M.-H. Whangbo, R. Hoffmann, *J. Am. Chem. Soc.* **1978**, *100*, 6093.
[16] Preliminary data support a localized system as a result of strong electron correlation effects in one dimension. Application of pressure (ca. 25 kbar) is expected to restore metallic character (room temperature conductivity = 2 S cm^{-1}): P. Batail, K. R. Dunbar, G. Finniss, D. Jerome, J. P. Pouget, unpublished results.

E/*Z* Isomerization in Crystals—Phase Rebuilding on Photolysis with Long-Wavelength Radiation**

Gerd Kaupp* and Michael Haak

In the crystal lattice of organic compounds the molecules have only very small freedom of movement, because they are as closely packed as possible. Therefore, the few known *E*/*Z* isomerizations that involve internal rotations of about 180° for unsaturated compounds containing large substituents are difficult to understand according to topochemical concepts.[1] The principle of phase rebuilding[2] should be more suitable, as it considers the far-reaching, anisotropic, molecular migrations with lattice-controlled formation of characteristic features on the surface, as was shown for cycloadditions and other reaction types.[2] Irradiation with wavelengths that correspond to the absorption tail of the crystals ("tail irradiation")[3] leads to a deeper penetration of the light into the crystal and to concomitant formation of features on the surfaces that are anchored deeper in the crystal, and therefore stable. This was demonstrated for the [4+4] photodimerization of 9-chloroanthracene (which according to earlier views conformed to the topochemical principle),[4] and implies that on tail irradiation the mechanism does not change.[5]

We now report on the space-intensive *E*/*Z* photoisomerization of **1** to form **2** on excitation with radiation of very long wavelength, on atomic force microscopy (AFM) imaged surface features, and on the X-ray crystallographic characterization[6] of **1**. The phase rebuilding on *E*/*Z* isomerization in the crystal is crystallographically explicable without resorting to "electronically excited phantom dimers".[7, 8] The few known *E*/*Z* isomerizations in organic crystals are collated in ref. [2]. Only with unselective irradiation ($\lambda > 300$ nm) does the photodimerization follow after the reaction of **1** to form **2**.[2, 4, 9] Figure 1 contrasts the diffuse reflectance spectra of crystals of **1** and **2** with the much shorter wavelength absorptions in solution. The $\lg(k/s)$ curves of the Kubelka–Munk function (k = absorption coefficient, s = scattering coefficient) formally correspond to absorption spectra.[10] They show that the forming crystal **2**, unlike **1**, no longer absorbs at 365 nm (bandpass 6.4 nm).

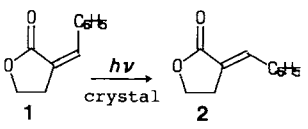

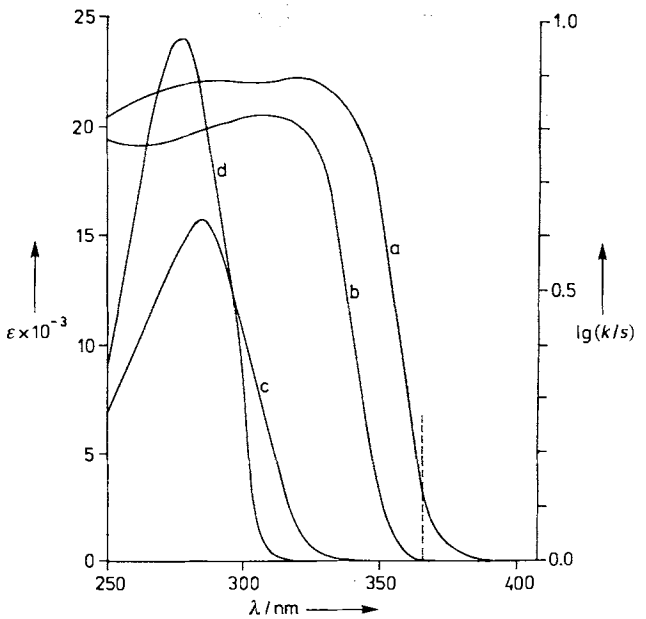

Fig. 1. Comparison of the diffuse reflectance spectra of **1** and **2** (a and b, respectively; $\lg(k/s)$) and the absorption spectra in acetonitrile (c and d, respectively; ε).

Figure 2 shows the effect of long-wavelength radiation (365 nm) on the initially only slightly rough ($R_{ms} = 0.42$ nm) (010) face of **1** (Fig. 2a). After five minutes the form of the irregularities on the surface changes, though without significant increase in roughness. Only after 10 min irradiation are craters observed (1.5–2 μm wide and 10–20 nm deep, angle of slope 1–3°; Fig. 2b) with upcast edges that are better formed than is shown in ref. [2,4] because they are anchored deeper in the

[*] Prof. Dr. G. Kaupp, Dipl.-Ing. M. Haak
FB9 – Organische Chemie I – der Universität
Postfach 2503, D-26111 Oldenburg (Germany)
Fax: Int. code +(441)798-3409
e-mail: kaupp@kaupp.chemie.uni-oldenburg.de

[**] This work was supported by the Fonds der Chemischen Industrie. We thank Prof. Dr. R. Boese, Essen, for performing the X-ray structure analysis and for releasing the data for publication.

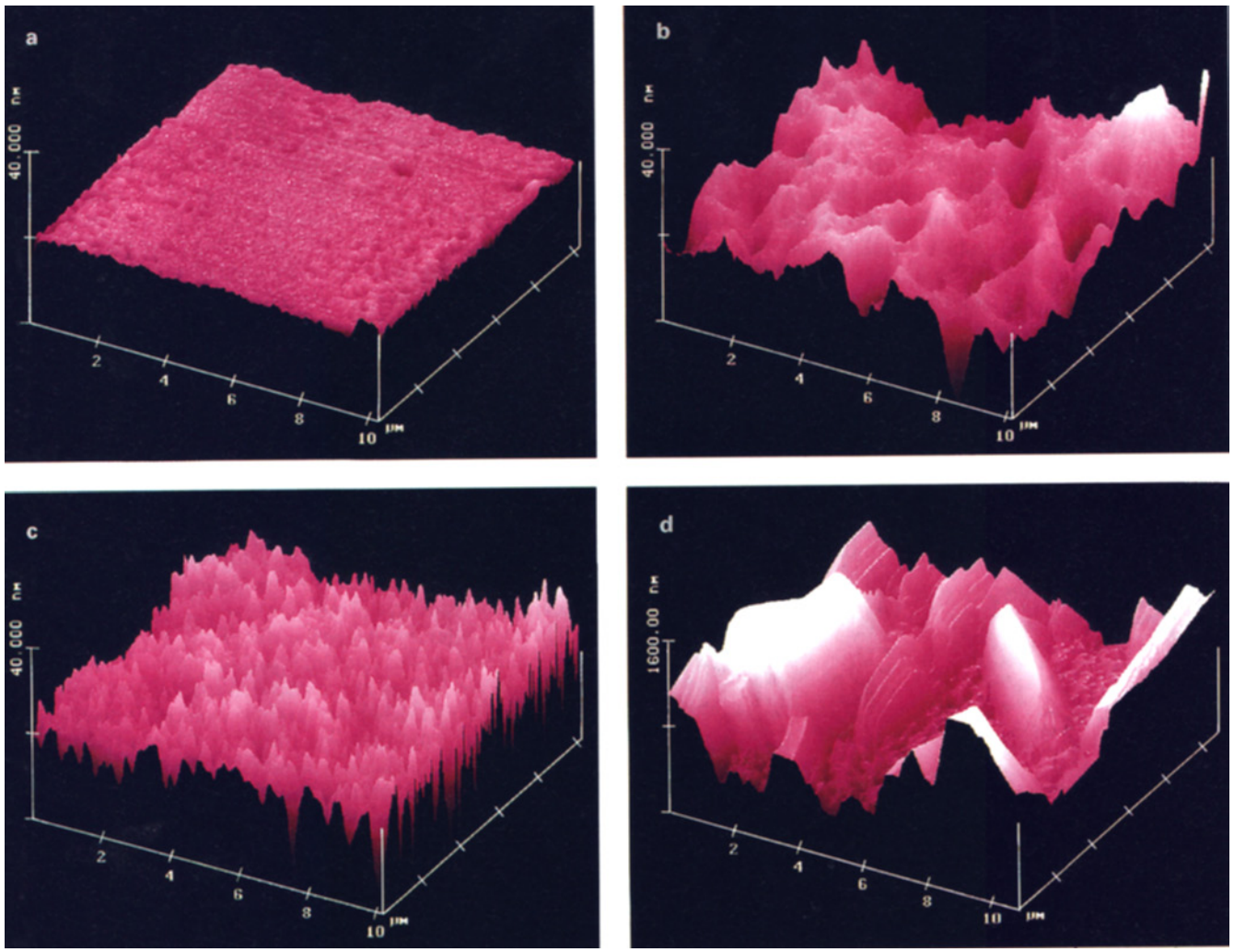

Fig. 2. Contact-AFM surfaces of **1** (crystallized from ether/*n*-hexane) on (010): a) starting surface; b) after 10 min irradiation (365 nm, 6.0 mWcm^{-2}, bandpass 6.4 nm); c) after 15 min irradiation; d) after 60 min irradiation, *z* axis magnified 40 times relative to Figs. a–c. The direction of imaging is always from left to right in the *x* direction. The crystallographic *c* axis of **1** is parallel to the *y* axis.

crystal and because here the complications of a reverse reaction are absent.[11] On further irradiation (15 min) the craters grow together, and many more are formed (typical diameter now 300–500 nm but with the same depth, Fig. 2c). Continued stepwise irradiation (20 min, 25 min) leads to further decrease in the size of the craters (approximately halving the diameter); some, nevertheless, double in depth. Only after 30 min irradiation (and suddenly) large, angular crystalline protrusions form, predominantly oriented along the *c* axis (parallel to (100)) of the original crystal, just as was found under preparative conditions.[2, 4] Figure 2d shows the result (with 40-fold magnification of the *z* axis) after 60 min irradiation. The steep, angular crystallites are as high as 1.5 µm, and the orientation of only very few deviate from the direction of the *c* axis.

Whereas crater formation is attributed to the phase rebuilding stage (little product in the lattice of the starting material), the deep-seated changes in the second stage are seen as phase transformation (little starting material in the product lattice).[12] The two-stage process of the lattice changes can also be observed on the (001) face of **1**. Short broad-band irradiation creates volcanoes and craters ("egg trays") with preferred direction along the *b* axis. The cleavage plane (100) coincides with this direction.[4] Long-wavelength radiation (365 nm, 6 mWcm^{-2}; not depicted) provides no striking improvement in the features of the phase rebuilding. Just as here, the µm-high, final crystallites of the phase transformation are aligned parallel to the *b* axis but are narrower on (001) than on (010): Interestingly, they are no longer deeply anchored in the base, but can break off and turn out of the preferred alignment. It is repeatedly observed that a µm-high crystallite changes its orientation relative to all other crystallites between two successive AFM measurements. In general these large crystallites parallel to the front face (100) grow epitactically around the whole crystal, despite the preceding phase rebuilding.

We wish to emphasize that the phase transformation to form the 1.5 µm-high crystallites also proceeds without any (nano)-liquid phase; characteristic instabilities in the contact-AFM images would otherwise result.[2, 4, 13] The lowest eutectic temperature of 67 °C lies distinctly above the photolysis temperature.[14]

For successful *E*/*Z* photoisomerization, each crystal layer must have a phase rebuilding mechanism available. This can be derived from or founded in the packing diagrams from the X-ray structure data.[6] Molecule **1** has the normal screw geometry: its double bond is twisted by 4.6° and the phenyl group

 © VCH Verlagsgesellschaft mbH, D-69451 Weinheim, 1996 0570-0833/96/3523-2775 $ 15.00+.25/0

turned by 35.6°. The other bond lengths and angles lie within the normal range. Molecules of **1** arrange in a monoclinic crystal lattice ($P2_1/c$) with complicated packing: bands of molecules with the same alignment lie at angles of 77° to one another; the bands have alternating alignments. The formation of the (less convincing) "phantom dimers"[7, 8] is not possible. Figure 3 depicts a model of a stereoview onto the (001) face. The central molecule with the highlighted double bond (violet) shows how after irradiation the $Z \rightarrow E$ isomerization proceeds by internal rotation. If the remaining lattice is held rigid, the phenyl group (in Fig. 3a) can rotate by up to 45° (counterclockwise) and the lactone moiety by −45° (clockwise), without excessive van der Waals hindrance (modeling in 5° steps with the program SCHAKAL indicates that the approach is never below 76% of the standard radii). Figure 3b shows this rotational state as a model of the transition state. The central molecule in the fixed lattice can make way to the left to allow the rotation to continue to planar **2** (a total of 184.6°). In the process, the phenyl group is also turned in by −35.6° (Fig. 3c).

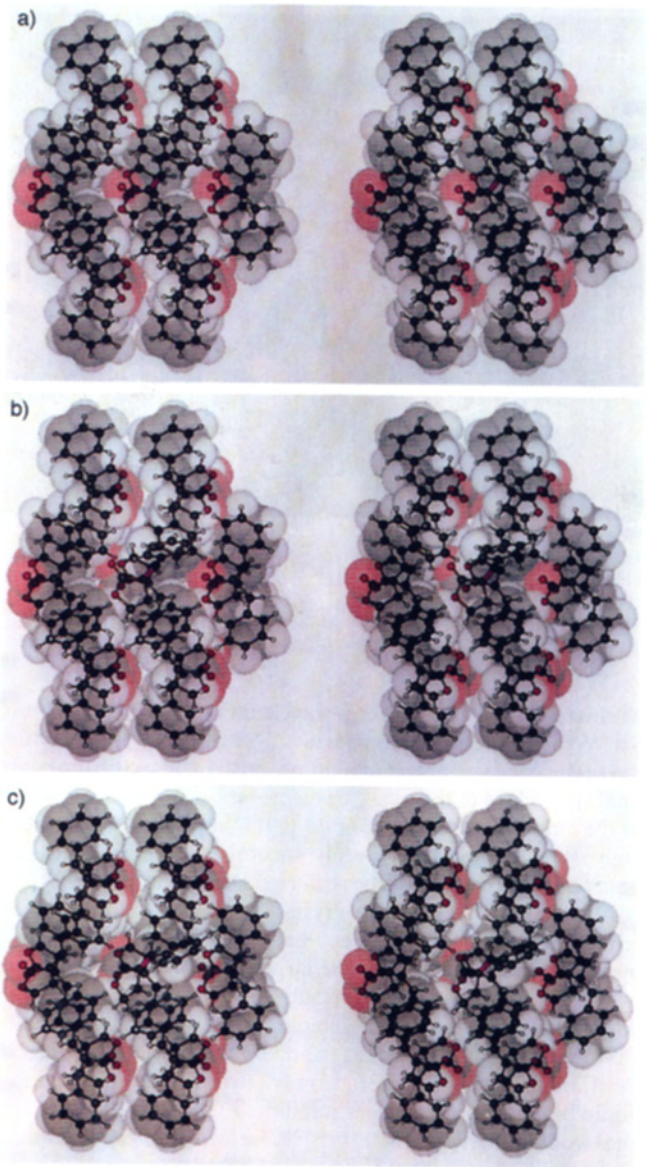

Fig. 3. Stereoscopic representation of the packing of **1** on (001) ((010) face on top) and modeling of the partial rotations for isomerization of the central molecule with highlighted double bond for fixed lattice and without relaxation by molecular migration. a) Prior to isomerization, b) model of the transition state with rotation of the CHPh moiety by 45° and the lactone moiety by −45°, c) after completed isomerization.

After their formation, the molecules of **2** must arrange themselves in a supramolecular way as foreign molecules within the fundamental lattice. They can find access into the corrugated planes perpendicular to the illustrated plane between the lattice molecules and initiate the long-range molecular transport for up to 50 nm. On (010) this leads to shallow craters with ridges, whereas on (001) the features align along the cleavage plane direction (aligned volcanoes and craters;[4] not depicted). Thus, the availability of the required phase rebuilding mechanism for **1** becomes evident. The crystal lattice of **1** does not simply change continuously into that of **2** ($P2_1/n$).[15] Rather the lattice of **2** (phase transformation) forms on both surfaces discontinuously after the phase rebuilding with molecular migration, but only when the product concentration is so high that the old lattice is no longer energetically viable. Interestingly, it is equally discontinuous when the reaction zone is generated with more pronounced absorption gradients ($\lambda > 300$ nm)[2] or with 365 nm light[16] that penetrates deeper into the crystal. In both cases the influence of the original lattice is still present, as is verified by the edges that are predominantly parallel to the original (100) cleavage plane.

The molecular mechanism deduced for **1** from AFM and X-ray diffraction measurements exploits supramolecular cooperative effects. This is not an isolated case. A supramolecular phase rebuilding mechanism was also deduced from X-ray diffraction data[8] for the isomerization of 1,2-bis(1-naphthyl)-ethene,[2] and the same can be expected for the other examples.[2] Complications through transitions from nontopotactic to topotactic courses of reaction need not be anticipated in any of these cases. A reviewer suggested attempting a single-crystal to single-crystal transformation for **1** through irradiation with a very low intensity (over months) very close to the equilibrium conditions for the crystal transformations. Such experiments with daylight filtered through Pyrex filters (see Fig. 1) in an inert atmosphere have been initiated.

E/*Z* isomerizations in the crystal have unusually large spatial requirements and therefore are particularly impressive examples of the new understanding of organic solid-state reactions, which imparts fundamental significance to the model systems for all kinds of crystal reactions that have larger or smaller space demands and in the face of previous reservations stimulates their execution and practical evaluation.

Received: April 23, 1995
Revised: August 6, 1995 [Z9065IE]
German version: *Angew. Chem.* **1996**, *108*, 2948–2951

Keywords: atomic force microscopy · isomerizations · phase transitions · solid-state reactions

[1] M. D. Cohen, G. M. J. Schmidt, F. I. Sonntag, *J. Chem. Soc.* **1964**, 2000; G. M. J. Schmidt, *ibid.* **1964**, 2014.

[2] G. Kaupp, *Adv. Photochem.* **1995**, *19*, 119; in *Comprehensive Supramolecular Chemistry, Vol. 8* (Eds.: J. E. D. Davies, J. A. Ripmeester), Elsevier, Oxford, **1996**, p. 381.

[3] V. Enkelmann, G. Wegner, K. Novak, K. B. Wagener, *J. Am. Chem. Soc.* **1993**, *115*, 10390; *Mol. Cryst. Liq. Cryst.* **1994**, *240*, 121.

[4] G. Kaupp, J. Schmeyers, M. Haak, T. Marquardt, A. Herrmann, *Mol. Cryst. Liq. Cryst.* **1996**, *276*, 315.

[5] We could not repeat the contrary data on the [2+2] photodimerization of α-cinnamic acid [3]: G. Kaupp, M. Haak, lecture at the Incom'96, Düsseldorf, March 26, 1996; this will be reported in detail soon.

[6] $P2_1/c$; $a = 6.241$, $b = 12.303$, $c = 12.113$ Å, $\beta = 95.75°$, $Z = 4$, $V = 934$ Å^3, $\rho_{calcd} = 1.239$ g cm^{-3}, 1659 measured reflections, of which 1324 were observed with $F > 4.0\sigma(F)$, $R = 0.0428$, $R_w = 0.0719$. Crystallographic data (excluding structure factors) for the structure reported in this paper have been deposited with the Cambridge Crystallographic Data Centre as supplementary publica-

tion no. CCDC-179-119. Copies of the data can be obtained free of charge on application to The Director, CCDC, 12 Union Road, Cambridge CB2 1EZ, UK (fax: int. code +(1223)336-033; e-mail: teched@chemcrys.cam.ac.uk).
[7] J. Bregman, K. Osaki, G. M. J. Schmidt, F. I. Sonntag, *J. Chem. Soc.* **1964**, 2021.
[8] S. M. Aldoshin, M. V. Alfimov, L. O. Atovmyan, U. F. Kaminsky, V. F. Razumov, A. G. Rachinsky, *Mol. Cryst. Liq. Cryst.* **1984**, *108*, 1.
[9] G. Kaupp, E. Jostkleigrewe, H. J. Herrmann, *Angew. Chem.* **1982**, *94*, 457; *Angew. Chem. Int. Ed. Engl.* **1982**, *21*, 435.
[10] H. G. Voelz, *Angew. Chem.* **1975**, *87*, 721; *Angew. Chem. Int. Ed. Engl.* **1975**, *14*, 688; U. Hezel, *ibid.* **1973**, *85*, 334 and **1973**, *12*, 298.
[11] As long as product molecules of **2** are not yet aligned in their own crystal lattice, but in the rebuilt lattice of **1**, short-wavelength excitation can cause a photochemical reverse reaction. Only crystalline **2** photodimerizes exclusively to form the cyclobutane derivative [9].
[12] The lack of absorption of light at $\lambda = 365$ nm by the crystalline product **2** prevents the formation of its [2+2]-dimer. Irradiation of **1** (4 h) with light from a 150 W Hanau Hg high-pressure lamp passed through a Wertheimer UVW-55 bandpass filter (isolation of the 365 nm light with 2.8% contribution from 334 nm light (% transmission <1 at 315 nm and at 410 nm)) in a powder cuvette leads to a considerable shift of the diffuse reflectance spectrum to curve b in Figure 1, whereas the broad-band irradiation ($\lambda > 300$ nm) of crystalline **2** produces a decrease in the long-wavelength absorption and an increase in a band of the photodimer [9] at 266 nm.
[13] G. Kaupp, *GIT Fachz. Lab.* **1993**, *37*, 284, 581, and references therein (English translation in WWW under http://kaupp@kaupp.chemie.uni-oldenburg.de); *Angew. Chem.* **1992**, *104*, 606, 609; *Angew. Chem. Int. Ed. Engl.* **1992**, *31*, 592, 595; G. Kaupp, J. Schmeyers, *ibid.* **1993**, *105*, 1656 and **1993**, *32*, 1587.
[14] The compounds **1** and **2** melt at 92.8 and 118.2 °C, respectively. Their enthalpies of melting according to differential scanning calorimetry (DSC, 40–150 °C, 20 K per min) are $\Delta H_{fu} = 19.6$ and 25.4 kJ mol^{-1}. After solidification of **1** another phase with m.p. 73.4 °C and $\Delta H_{fu} = 18.7$ kJ mol^{-1} appears without chemical change (according to ^{1}H NMR analysis). The state diagram of **1**/**2** is complicated: between the eutectics at 67 and 114 °C there are several other endothermic peaks in DSC irrespective of the mixing ratio (particularly pronounced at 80 and 101 °C), which cannot yet be reliably interpreted. Microscopy of copulverized samples of **1** and **2** indicate that liquid phases can be excluded.
[15] S. K. Kearsley, G. R. Desiraju, *Proc. R. Soc. A* **1985**, *397*, 157.
[16] The 90% light penetration depth derived with the Lambert–Beer law for $\varepsilon_{max} \approx 15000$ L mol^{-1} cm^{-1}, $d = 1.239$ g cm^{-3} from Figure 1 at approximately diagonal position of the chromophore is less than 100 double layers at 302, 313, and 334 nm, and 370 double layers at 365 nm.

Designed Restructuring of Iodine with Microporous SiO_2**

Gernot Wirnsberger, Harald P. Fritzer, Alois Popitsch, Gianpietro van de Goor, and Peter Behrens*

Tailor-made host systems with designed topologies and adapted surface properties are an important prerequisite for supramolecular inorganic host–guest chemistry.[1] Herein, we show how the interactions between iodine molecules can be controlled by the topotactical insertion into selected, crystalline porous materials which assume a structure-directing role for the arrangement of the guest species.

[*] Prof. Dr. P. Behrens, Dr. G. van de Goor
Institut für Anorganische Chemie der Universität
Meiserstrasse 1, D-80333 München (Germany)
Fax: Int. code +(89)5902-578
e-mail: pbe@anorg.chemie.uni-muenchen.de
Dipl.-Ing. G. Wirnsberger, Prof. Dr. H. P. Fritzer,
Institut für Physikalische und Theoretische Chemie
Technische Universität
A-8010 Graz (Austria)
Dr. A. Popitsch
Institut für Anorganische Chemie
Karl-Franzens-Universität
A-8010 Graz (Austria)

[**] Part of this work was supported by the Deutsche Forschungemeinschaft (Be 1664/1-2) and the Fonds der Chemischen Industrie. We thank Andreas M. Schneider for assistance with the preparation of the figures.

The pore systems of zeolites, which are accessible to many ions and molecules, can not only be used in technical applications as catalysis and sorption, but also offer the opportunity for a rich host–guest chemistry. Inorganic clusters with special electronic[2] or magnetic[3] properties can be stabilized inside the well-defined and uniform cavities of aluminosilicate zeolites. However, the use of zeolites as host matrices bears an inherent problem: As the framework is composed of $[AlO_{4/2}]^-$ and $[SiO_{4/2}]$ tetrahedra, it carries a negative charge that must be balanced by the inserted species themselves or by guest cations that are present in addition. Therefore, the properties of the guest components will always be influenced by ionic interactions with the host matrix or with the charge-compensating guest cations.

In our attempts[4] at the restructuring of guest components by porous solids, we have used porosils[5] rather than zeolites as host components. The structures of porosils resemble those of zeolites; however, their frameworks are composed of $[SiO_{4/2}]$ tetrahedra only, which are interlinked through their vertices; thus, the composition of a porosil framework is neutral SiO_2. Porosils are prepared under mild solvothermal conditions; organic molecules, which are necessary to form a desired porosil structure, become occluded in the cavities of the crystallizing SiO_2 framework.[6] The organic molecules can be removed oxidatively by calcination (treatment at high temperature), leaving behind a (thermodynamically metastable)[7] microporous SiO_2 modification, whose empty void system can now be filled. In the case of host–guest compounds with a porosil as the host component and with neutral guest species, the interactions are restricted to weak van der Waals type forces. The void structure of the host framework thus determines the geometrical arrangement of the guest species and consequently also limits the electronic interactions between them. Insertion compounds of iodine serve as an especially impressive example of this concept, as changes in the electronic properties of the guest arrangement can be monitored directly by changes in color.

We have used porosils with zero-, one-, two-, and three-dimensional pore systems as host compounds: decadodecasil 3R (DDR[8]), silica-ZSM-22 (TON), silica-ferrierite (FER), and silicalite-1 (MFI). Their cavities or channel systems are shown in Figure 1. Since the diameters of the pores of these host

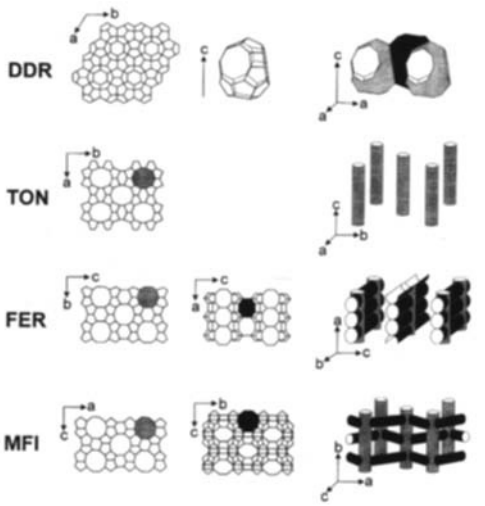

Fig. 1. Structures of the host systems (oxygen atoms are omitted): For DDR, a view of the layers consisting of pentagon dodecahedra is given on the left. In an ABCABC stacking of these layers, cages (center) are formed which are typical for this structure. Each cage is surrounded by three other cages arranged at angles of 120° to each other (right). For the other porosils, views along the channels (left and center) and schematic views of the channel systems (right) are given.

 © VCH Verlagsgesellschaft mbH, D-69451 Weinheim, 1996 0570-0833/96/3523-2777 $ 15.00+.25/0

Fig. 2. Colors of the iodine–porosil composites compared to that of solid iodine. From top to bottom: iodine in DDR, iodine in TON, iodine in FER, iodine in MFI, and solid iodine.

systems are similar, they are suitable for investigating the influence of the different dimensionalities on the interactions between the iodine molecules. Figure 2 shows the colors of the iodine–porosil composites that were prepared by the insertion of iodine into these hosts. Iodine in DDR is violet, similar to the color of gaseous iodine, indicating that the iodine molecules are in a vapor-phase-like state. In contrast, the iodine in the TON host, in which the unidimensional channel system permits interactions between the iodine molecules in one dimension, is violet to dark blue, similar to the color observed for iodine–starch compounds. Iodine inserted into the two-dimensional channel system of FER exhibits a color between that of iodine in DDR and TON. Interactions between iodine molecules in three dimensions, which are, however, regularly interrupted by the MFI silica framework, result in a red–brown color resembling that of liquid iodine.

These visual impressions can be quantified by UV/Vis spectroscopy. The absorptions in the visible region, which are responsible for the colors, vary in a characteristic fashion (Fig. 3).

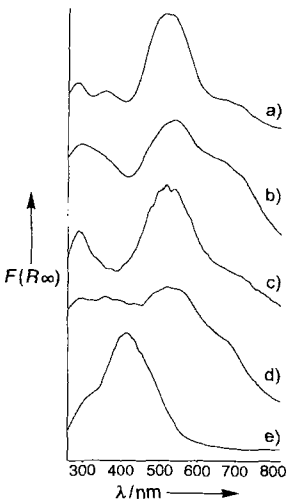

Fig. 3. UV/Vis spectra (converted to Kubelka–Munk functions $F(R_\infty)$) of the iodine–porosil composites and of solid iodine: a) iodine in DDR, b) iodine in TON, c) iodine in FER, d) iodine in MFI, and e) solid iodine.

The spectrum of iodine in DDR exhibits a relatively strong band at 518 nm and one of weaker intensity at 688 nm. The positions of these bands coincide with those observed for gaseous iodine, and are atrributed to the B←X transition (518 nm) and the A←X transition (688 nm).[10] The notion that iodine in DDR is in fact in a vapor-phase-like state is also supported by the composition of the compound,[11a] which fits for a structure in which each cage of the DDR host structure is occupied by one iodine molecule and thus the iodine molecules can be regarded as isolated from each other.[11b]

In contrast to the cage structure of DDR, the one-dimensional channels of TON permit interactions between the iodine molecules along the channel axis. The transition from isolated molecules to molecules that are part of an infinite chain (in the limiting case) should manifest itself by a shift of the absorption bands to higher wavelengths.[12] In fact, a 22 nm shift of the B←X transition to 540 nm was observed for the iodine in TON. In addition, the spectrum contains a broad shoulder in the region of the A←X transition, which is responsible for the dark blue hue of this compound. Thus, the changes in the electronic structure caused by the chainlike aggregation of the iodine molecules (which in turn is caused by the templating action of the TON framework) are not only evident from a shift of the absorption band maxima, but also from changes in the intensities and thus the transition probabilities.

A further enhancement of the interaction between the iodine molecules might be expected for the insertion compound of FER, which possesses a two-dimensional channel structure. However, the electronic spectrum shows that in this case the geometric restrictions by the host are too strong to allow the formation of a two-dimensional layered structure (which would be regularly pierced by SiO_2). The double maximum in the strongest absorption band indicates the presence of two different iodine species, one of which is in a vapor-phase-like state (maximum at 519 nm). For the second maximum at 537 nm, we observe a shift to higher wavelengths, similar to that observed for iodine in TON.

The MFI-based insertion compound reveals most clearly the tendency of the iodine molecules to use the available volume for maximizing their interactions. It possesses the highest concentration of iodine[13] and its UV/Vis spectrum shows enhanced intensity in the region between 400 and 260 nm in which liquid iodine also has its strongest absorptions.[14]

The Raman spectra in Figure 4 confirm and supplement the picture gained from the UV/Vis spectra. The band for iodine encaged in the DDR host structure occurs at 208 cm^{-1}, similar to that of gaseous iodine (213 cm^{-1}), which again supports the idea of a vapor-phase-like state of the inserted iodine. For the iodine molecules restructured to a chainlike arrangement by the TON framework, the iodine–iodine vibration shifts to 199 cm^{-1}. We attribute this shift to the presence of intermolecular iodine–iodine interactions, which cause a weakening of the intramolecular iodine–iodine bond, resulting in a decrease of its force constant. However, a comparison with the spectrum of solid iodine[15] (Fig. 4e) shows that the extent of these interactions is much weaker than in bulk iodine. The splitting of the B←X transition in the UV/Vis spectra indicated the presence of two different iodine species for the iodine in FER; the Raman spectrum confirms this presumption. We ascribe the weak band at 210 cm^{-1} to isolated iodine molecules, and the stronger band at 196 cm^{-1} to a chainlike arrangement of iodine molecules. Evidently, the apertures of the ten-ring channels are just large enough to allow for interactions between the iodine molecules (band at 196 cm^{-1}), whereas the iodine molecules in the eight-ring channels remain isolated like those in iodine–DDR. For the insertion compound of MFI we observe a band at 202 cm^{-1}, which we attribute again to a chainlike arrangement of iodine molecules. In addition, this signal exhibits a shoulder at 188 cm^{-1}; this has to be ascribed to iodine molecules that are allowed to exert even stronger interactions. The only regions that permit such interactions are the spherical voids at the intersections of the channel systems. On the one hand, each of these voids (9 Å diameter) can accommodate several iodine molecules, on the other, the molecules inside them are able to interact with those molecules that reside in the channels through the ten-ring channels. It is

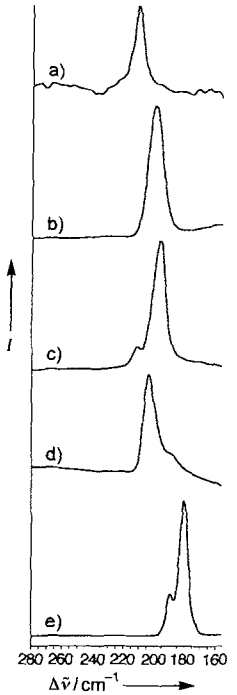

Fig. 4. Raman spectra of the iodine–porosil composites and of solid iodine: a) iodine in DDR, b) iodine in TON, c) iodine in FER, d) iodine in MFI, and e) solid iodine; I in arbitrary units.

 © VCH Verlagsgesellschaft mbH, D-69451 Weinheim, 1996 0570-0833/96/3523-2778 $ 15.00+.25/0

noteworthy that broad bands in the range from 175 to 185 cm^{-1} in Raman experiments on liquid iodine have been attributed to the presence of $(I_2)_n$ molecular clusters.[16]

Our investigations on iodine insertion compounds prepared by topotactical reactions show that by restricting the geometrical arrangement of the iodine molecules, the electronic properties of the guest species can be engineered.

Experimental Procedure

Syntheses of the porosils TON, FER, and MFI were performed according to the literature [17]. A new procedure was developed for DDR: A mixture of hydrofluoric acid, water, ammonium fluoride, 1-aminoadamantane, and SiO_2 (Cab-osil M-5, Fluka) in the molar ratio 0.15:20:1:0.15:1 was maintained at 433 K for 21 days in a Teflon-lined autoclave. After the mixture had been cooled to room temperature, the crystalline product was filtered off, freed from amorphous gel residues by treatment with 2M NaOH, and washed neutral with H_2O. The organic molecules occluded inside the porosils were removed by calcination in air. For that purpose, the porosils are heated to the final calcination temperature (DDR, TON, FER: 1123 K, MFI: 923 K) over two days, kept at this temperature for another two days and then cooled to room temperature within one day. Insertion of iodine was performed in the vapor phase at 433 K in Teflon-lined autoclaves. After a reaction time of four days, iodine–porosil compounds were obtained, from which iodine desorbed above 313 K. At room temperature, they are stable for several weeks.

UV/Vis spectra in diffuse reflection were obtained on a Beckmann spectrometer model DK-2A. Quartz powder was used as a reference and for dilution of the samples. Raman spectra were recorded with an FT-Raman apparatus (Nicolet FT-Raman 910); the 1064 nm line of a Nd:YAG laser was used for excitation. For each measurement 200 scans were accumulated; the laser power was 200 mW for the insertion compounds, and 20 mW for bulk iodine.

Received: June 3, 1996 [Z9184 IE]
German version: *Angew. Chem.* **1996**, *108*, 2951–2953

Keywords: iodine compounds · host–guest chemistry · silicon compounds · zeolite analogues

[1] A. Müller, H. Reuter, S. Dillinger, *Angew. Chem.* **1995**, *107*, 2505–2539; *Angew. Chem. Int. Ed. Engl.* **1995**, 34, 2328–2361.

[2] G. D. Stucky, *Prog. Inorg. Chem.* **1992**, *40*, 99–178; G. A. Ozin, A. Kuperman, A. Stein, *Angew. Chem.* **1989**, *101*, 373–390; *Angew. Chem. Int. Ed. Engl.* **1989**, 28, 359–376; G. A. Ozin, *Adv. Mater.* **1992**, *4*, 612–649; G. A. Ozin, S. Özkar, *ibid.* **1992**, *4*, 11–22; G. A. Ozin, *ibid.* **1994**, *6*, 71–76; N. Herron, *J. Inclusion Phenom. Mol. Recognit. Chem.* **1995**, *21*, 283–298; P. Behrens, G. D. Stucky, in *Comprehensive Supramolecular Chemistry, Vol. 7* (Eds.: G. Alberti, T. Bein), Pergamon, Oxford, pp. 721–772.

[3] P. P. Edwards, L. J. Woodall, P. A. Anderson, A. R. Armstrong, M. Slaski, *Chem. Soc. Rev.* **1993**, 305–312; V. I. Srdanov, N. P. Blake, D. Markgraber, H. Metiu, G. D. Stucky, *Stud. Surf. Sci. Catal.* **1994**, *85*, 115–144.

[4] G. van de Goor, Thesis, University of Konstanz, **1995**; P. Behrens, G. van de Goor, M. Wark, A. Trnoska, A. Popitsch, *J. Mol. Struct.* **1995**, *348*, 85–90.

[5] For the classification and nomenclature of dense and microporous silicate modifications see: F. Liebau, H., Gies, R. P. Gunawardane, B. Marler, *Zeolites* **1986**, *6*, 373–377.

[6] M. E. Davis, R. F. Lobo, *Chem. Mater.* **1992**, *4*, 756–768.

[7] I. Petrovic, A. Navrotsky, M. E. Davis, S. I. Zones, *Chem. Mater.* **1993**, *5*, 1805–1813; A. Navrotsky, I. Petrovic, Y. Hu, C.-Y. Chen, M. E. Davis, *Micropor. Mater.* **1995**, *4*, 95–98; N. J. Henson, A. K. Cheetham, J. D. Gale, *Chem. Mater.* **1994**, *6*, 1647–1650.

[8] These abbreviations conform to the guidelines for the nomenclature of zeolites and zeolite-type materials proposed by the International Zeolite Association. See: W. M. Meier, D. H. Olson, C. Baerlocher, *Atlas of Zeolite Structure Types*, 4th ed., Butterworth-Heinemann, London, **1996**; W. M. Meier, D. H. Olson, C. Baerlocher, *Zeolites* **1996**, *17*.

[9] It should be noted that, in spite of the similarities between iodine–starch and iodine–cyclodextrin inclusion compounds on the one hand and the iodine insertion compound of TON on the other, the iodine species are chemically different: In TON, the iodine chains are made up of neutral iodine molecules, whereas the iodine chains in iodine–starch compounds and its derivatives always exhibit a negative charge: R. C. Teitelbaum, S. L. Ruby, T. J. Marks, *J. Am. Chem. Soc.* **1980**, *102*, 3322–3328; W. Saenger, *Naturwissenschaften* **1984**, *71*, 31–36.

[10] An extensive description of these transitions and of the term scheme of gaseous iodine can be found in: R. S. Mulliken, *J. Chem. Phys.* **1971**, *55*, 288–309, and references therein.

[11] a) From thermogravimetry (Mettler TA 2, heating rate: 10 K min^{-1}, reference: Al_2O_3, crucible material: Al_2O_3, atmosphere: Ar, flux rate: 5 L h^{-1}) the following compositions result: DDR: $120SiO_2:6.0I_2$, TON: $24SiO_2:1.2I_2$, FER: $36SiO_2:3.2I_2$, MFI: $96SiO_2:11.5I_2$. b) The free volume of the cages is 350 $Å^3$, and thus, there is sufficient space to accommodate more than one I_2 molecule per cage. Modeling studies in our group have shown, however, that the inclusion of a second molecule per cage is disfavored energetically over single occupation. The shortest intermolecular iodine–iodine distance from the modeling studies is about 5.5 Å, clearly larger than the value of twice the van der Waals radius of iodine (4.3 Å). A. M. Schneider, P. Behrens, unpublished results.

[12] J. K. Burdett, *Prog. Solid State Chem.* **1984**, *15*, 173–255.

[13] In order to compare the iodine concentrations in the different porosils, we have normalized them to molecules per 1000 $Å^3$. The following values were obtained: DDR: 0.886, TON: 0.989, FER: 1.63, MFI: 2.15.

[14] M. Yao, N. Nakamura, H. Endo, *Z. Phys. Chem.* **1988**, *157*, 569–573.

[15] B. V. Shanabrook, J. S. Lannin, *Solid State Commun.* **1981**, *38*, 49–52.

[16] R. J. Magaña, J. S. Lannin, *Phys. Rev. B* **1985**, *32*, 3819–3823.

[17] J.-L. Guth, H. Kessler, J. M. Higel, J. M. Lamblin, J. Patarin, A. Seive, J. M. Chezeau, R. Wey, *ACS Symp. Ser.* **1989**, *398*, 176–195; A. Kuperman, S. Nadimi, S. Oliver, G. A. Ozin, J. M. Garces, M. M. Olken, *Nature* **1993**, *365*, 239–242; J. Patarin, M. Soulard, H. Kessler, J.-L. Guth, J. Baron, *Zeolites* **1989**, *9*, 397–404.

A Noninterpenetrated Molecular Ladder with Hydrophobic Cavities**

Pierre Losier and Michael J. Zaworotko*

Crystal engineering of supramolecular architectures sustained by coordinate covalent bonds[1, 2] or hydrogen bonds[3] represents a rapidly expanding field that offers potential for rational development of new classes of functional solids. It is now established that the architectures of coordination polymers can be reliably predicted, since previously known metal coordination environments are propagated into one- (1D), two- (2D), and three-dimensional (3D) motifs with rigid multitopic organic "spacer" ligands. Recent examples include diamondoid,[4] honeycomb,[5] grid,[1, 2, 6] ladder,[7] brick wall,[7] and octahedral[8] frameworks from tetrahedral, trigonal, and octahedral metal templates (e.g. Zn^{II}, Cd^{II}, Ag^{I}, Cu^{I}, Scheme 1). Unfortunately, if the void created in this way is more than 50% of the crystal by volume, it is almost always reduced by interpenetration or self-inclusion.[1, 4–7] We report herein what is to our knowledge the first example of a noninterpenetrated molecular ladder:[7] $[Co(NO_3)_2(4,4'\text{-bpy})_{1.5}]_\infty$ (1) (4,4'-bpy = 4,4'-bipyridine), an open framework infinite ladder that clathrates small organic guests despite possessing a cavity that is large enough to self-include.[6]

In principle, the formation of molecular square grids[1, 2, 4] or molecular ladders/brick walls[7] depends on the metal-to-ligand ratio (1:2 or 1:1.5, respectively). We therefore anticipated that reaction of $[Co(NO_3)_2]\cdot 6H_2O$ with three molar equivalents of 4,4'-bpy would afford a square grid polymeric motif.[9] However, when the reaction was conducted with 1.5 or 3 molar

[*] Prof. Dr. M. J. Zaworotko, Dr. P. Losier
Department of Chemistry, Saint Mary's University
Halifax, Nova Scotia, B3H 3C3 (Canada)
Fax: Int. code +(902) 496 8106
e-mail: mike.zaworotko@stmarys.ca

[**] This work was supported by the NSERC (Canada) and the Environmental Science and Technology Alliance of Canada.

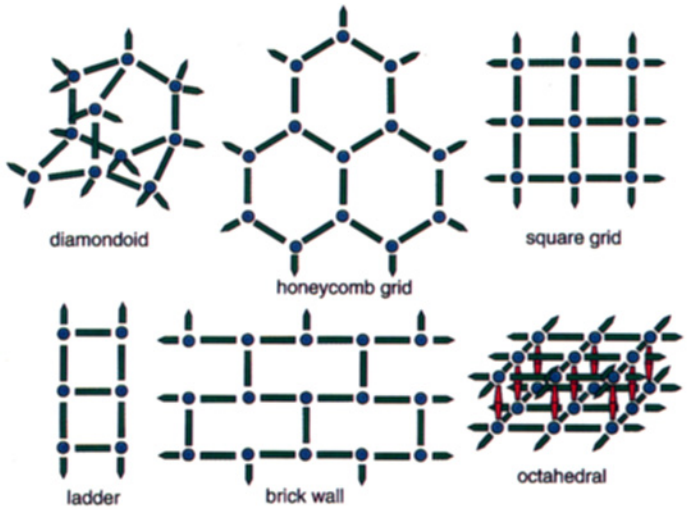

Scheme 1. Examples of coordination polymer frameworks formed from metal ions and linear ditopic ligands.

equivalents of 4,4′-bpy in MeOH/MeCN or MeOH/$CHCl_3$ mixtures, the MeCN and $CHCl_3$ solvates of **1**, **1a** and **1b**, respectively, were isolated.[10] The X-ray crystal structures of **1a** and **1b** reveal that **1** adopts an infinite molecular ladder motif that

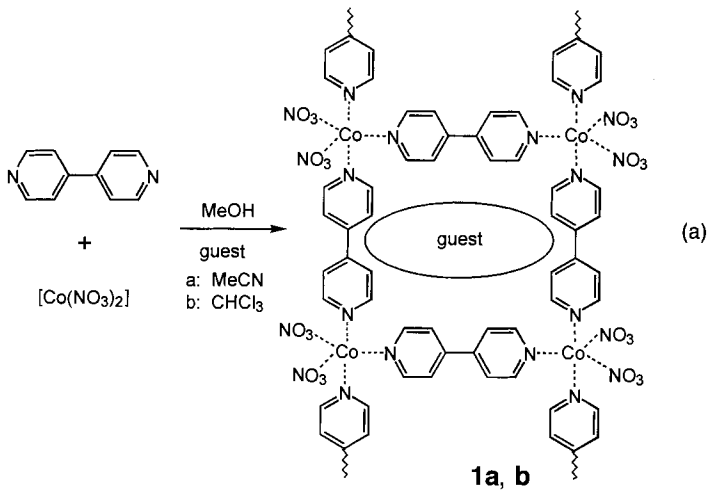

(a)

can be regarded as a manifestation of self-assembly of "T-shaped" units (Fig. 1).[11] The 4,4′-bpy ligands coordinate to Co^{II} ions and form the "side rails" and "rungs" of a ladder that extends along the *a* and *b* axes for **1a** and **1b**, respectively. The remaining coordination sites at the metal are occupied by two bidentate nitrate ions.[12]

Compound **1** possesses large square hydrophobic cavities with dimensions of 11.4 × 11.4 Å enclosed by the 4,4′-bpy ligands. In **1a** a disordered MeCN solvent molecule sits at the center of the square void,[13] whereas in **1b** there are two crystallographically independent molecules of $CHCl_3$ per metal atom. Each square cavity is effectively sandwiched by four chloroform molecules, two above and two below (Fig. 2). One chlorine atom from each chloroform molecule is directed towards the inside of the cavity through weak Cl···H-C interactions (3.68 and 3.77 Å).[14] Hydrogen bonding is also apparent between the chloroform molecules and the terminal oxygen atom of nitrates on neighboring ladders (O···H-C 3.50 and 3.23 Å). Schemes 2

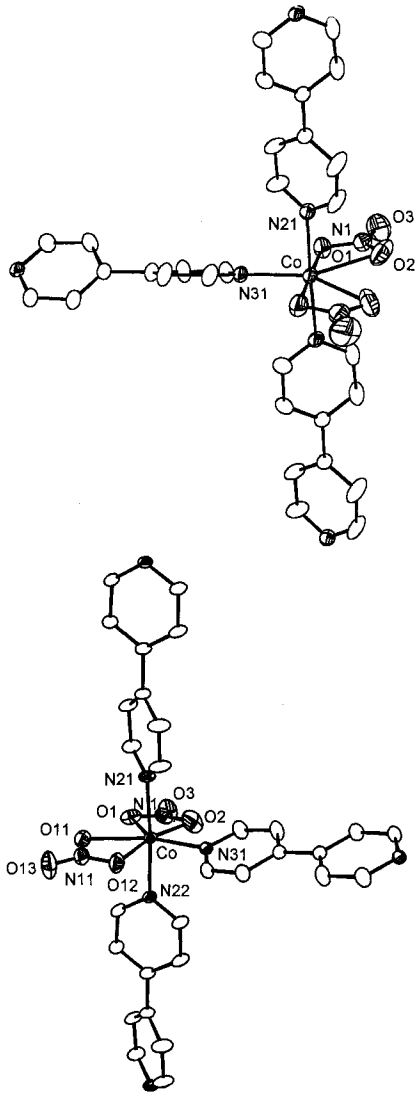

Fig. 1. ORTEP views of the structures of **1a** (top) and **1b** (bottom), showing the metal coordination environment. The Co–N bonds are comparable in both structures (av 2.15 and 2.14 Å, respectively) [12] and the "rungs" are orthogonal to the "rails" in **1a** but slightly distorted ($\measuredangle$ = 82.6°) in **1b**. The nitrate ions in **1b** are almost symmetrically bound to the metal (Co–O 2.207(4), 2.228(3), 2.226(4), and 2.322(5) Å); however, in **1a** they approach a unidentate coordination (Co–O 2.127(4) and 2.436(5) Å).

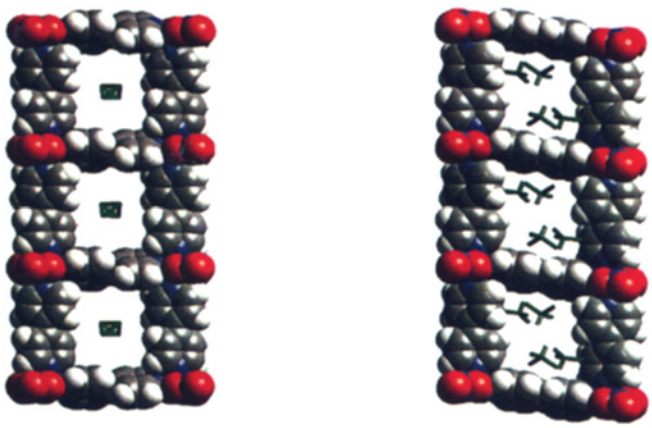

Fig. 2. Space-filling views of molecular ladders **1a** (left) and **1b** (right). Enclathrated solvent molecules are shown in green in stick form. In **1a** the enclathrated MeCN molecules are disordered, therefore only the region of occupancy is shown.

 © VCH Verlagsgesellschaft mbH, D-69451 Weinheim, 1996 0570-0833/96/3523-2780 $ 15.00+.25/0

Scheme 2. A schematic representation of the crystal packing in **1a**. The arrow denotes the direction of the channels.

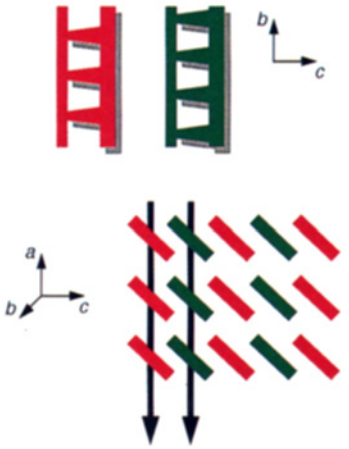

Scheme 3. A schematic representation of the crystal packing in **1b**. The arrow denotes the direction of the channels.

and 3 illustrate the crystal packing of the ladders. In **1a** two infinite ladders are juxtaposed in the *ac* plane and are offset by half a "step" along *a*. These sheets subsequently stack along *b* in a close-packed stairlike manner (interplanar separation: 5.2 Å) and are offset by a quarter of a "step" along *a*. Such packing yields oblique solvent-filled microchannels that criss-cross. In **1b** the ladders stack sideways along *c* in a "bookshelf" fashion with a spacing of 10.6 Å and, as in **1a**, adjacent ladders are offset by half a "step" along *b*. The superposition of these layers along *a* results in a much larger interplanar separation of 11.3 Å due to the presence of the solvent molecules. Microchannels extending along the *a* axis are also formed and have columns of chloroform molecules running through their cavities.

The design of square- or box-shaped macrocycles self-assembled from square-planar metal centers and 4,4′-bpy has attracted much attention in the context of molecular recognition of guests by tailored hosts.[1 5] Compound **1** is effectively a one-dimensional polymer of macrocyclic squares that exhibit a clear preference for hydrophobic guests (i.e. arenes,[9] $CHCl_3$, and MeCN over MeOH and H_2O). This study illustrates the importance of solvent medium upon anion coordination, interpenetration, and which polymeric motif is generated.[9, 11] However, it remains to be seen if this new class of polymeric structure can reversibly adsorb guest molecules, an issue we are currently addressing.

Experimental Procedure

1a: A solution of $[Co(NO_3)_2]\cdot 6H_2O$ (0.29 g, 1.0 mmol) in MeOH (20 mL) was added to a solution of 4,4′-bpy (0.23 g, 1.5 mmol) in MeCN (20 mL). After the solution was left to stand at room temperature for 3 h, red crystals of **1a** were obtained (yield: 0.17 g, 0.39 mmol, 39%). IR (KBr diffuse reflectance): $\tilde{\nu}$ [cm^{-1}] = 3053, 2510, 2447, 2252 (C≡N), 1609, 1535, 1490, 1415, 1325, 1297, 1221, 1074, 1025, 1010, 858, 812, 736. Crystals exposed to the atmosphere appear stable for hours but eventually become opaque. TGA analysis reveals the following: gradual 5% weight loss from 60–200 °C and stability to 240 °C; 17% weight loss from 240–280 °C; 58% weight loss from 280–320 °C. This data suggests loss of 0.75 moles of MeCN, conversion of $[Co(NO_3)_2]$ to Co_3O_4, NO_2, and O_2, and loss of 4,4′-bipyridine, respectively. The remaining 18% would correspond to Co_3O_4.

1b: A solution of $[Co(NO_3)_2]\cdot 6H_2O$ (0.29 g, 1.0 mmol) in MeOH (20 mL) was added to a solution of 4,4′-bpy (0.29 g, 1.5 mmol) in $CHCl_3$. Deep red crystals of **1b** were collected (yield: 0.33 g, 0.50 mmol, 50%) after the mixture was left to stand at room temperature for 12 h. IR (KBr diffuse reflectance): $\tilde{\nu}$ [cm^{-1}] = 3050, 2509, 2446, 1608, 1535, 1492, 1414, 1326, 1295, 1221, 1074, 1025, 1010, 859, 812, 754 (C–Cl). Crystals exposed to the atmosphere become opaque within hours. TGA analysis reveals the following: gradual 36% weight loss from 60–180 °C and stability to 240 °C; 12% weight loss from 240–280 °C; 40% weight loss from 280–320 °C. This data suggests loss of 2 moles of $CHCl_3$, conversion of $Co(NO_3)_2$ to Co_3O_4, NO_2, and O_2, and loss of 4,4′-bipyridine, respectively. The remaining 12% would correspond to Co_3O_4.

Received: June 5, 1996
Revised version: August 13, 1996 [Z9195IE]
German version: *Angew. Chem.* **1996**, *108*, 2957–2960

Keywords: cobalt compounds · crystal engineering · molecular ladders · molecular recognition

[1] R. Robson, B. F. Abrahams, S. R. Batten, R. W. Gable, B. F. Hoskins, J. Liu, *Supramolecular Architecture*, ACS, Washington, DC, **1992**, chapter 19.
[2] M. Fujita, Y. J. Kwon, S. Washizu, K. Ogura *J. Am. Chem. Soc.* **1994**, *116*, 1151.
[3] C. B. Aakeroy, K. R. Seddon, *Chem. Soc. Rev.* **1993**, 397; G. R. Desiraju, *Crystal Engineering. The Design of Organic Solids*, Elsevier, Amsterdam, **1989**; *Angew. Chem.* **1995**, *107*, 2541; *Angew. Chem. Int. Ed. Engl.* **1995**, *35*, 2311; M. C. Etter, *Acc. Chem. Res.* **1990**, *23*, 120.
[4] L. R. MacGillivray, S. Subramanian, M. J. Zaworotko, *J. Chem. Soc. Chem. Commun.* **1994**, 1325; M. J. Zaworotko, *Chem. Soc. Rev.* **1994**, 283.
[5] G. B. Gardner, D. Venkataraman, J. S. Moore, S. Lee, *Nature* **1995**, *374*, 792.
[6] R. W. Gable, B. F. Hoskins, R. Robson, *J. Chem. Soc. Chem. Commun.* **1990**, 1677.
[7] To our knowledge, the only other example of an infinite molecular ladder is $[Cd(NO_3)_2(C_{17}H_{16}N_2)_{1.5}]$ which crystallizes in space group $P2_1/n$ with $Z = 4$ and two interpenetrated networks: M. Fujita, Y. J. Kwon, O. Sasaki, K. Yamaguchi, K. Ogura, *J. Am. Chem. Soc.* **1995**, *117*, 7287. A related structure that can be regarded as a flexible discrete ladder has also been reported: T. M. Garrett, U. Koert, J.-M. Lehn, A. Rigault, D. Meyer, J. Fischer, *J. Chem. Soc. Chem. Commun.* **1990**, 557.
[8] S. Subramanian, M. J. Zaworotko, *Angew. Chem.* **1995**, *107*, 2295; *Angew. Chem. Int. Ed. Engl.* **1995**, *34*, 2127.
[9] Square grid polymers based upon $[Co(NO_3)_2(4,4'\text{-bpy})_2]$ are afforded if this reaction is effected in the presence of aromatic solvents such as benzene, xylenes, and chlorobenzenes. Up to five moles of arene per mole of metal are present and the reaction appears to be independent of the stoichiometry of the system: C. Hogg, P. Losier, K. N. Power, M. J. Zaworotko, R. D. Rogers, unpublished results.
[10] Structure analysis of **1a**: 0.2 × 0.3 × 0.4 mm, red rectangular crystal, orthorhombic, *Fddd*, $a = 11.3681(12)$, $b = 20.767(3)$, $c = 34.585(4)$ Å, $Z = 16$, $V = 8164.8(17)$ Å^3, $\rho_{calcd} = 1.534$ M gm^{-3}, $\mu = 0.88$ mm^{-1}, min./max. transmission = 0.873/0.980, $2.0 < 2\theta < 49.8$. Structure analysis of **1b**: 0.2 × 0.5 × 0.4 mm, red rectangular crystal, triclinic, $P\bar{1}$, $a = 11.2902(9)$, $b = 11.3776(10)$, $c = 11.8358(13)$ Å, $Z = 2$, $V = 1302.52(21)$ Å^3, $\rho_{calcd} = 1.673$ M gm^{-3}, $\mu = 1.32$ mm^{-1}, min./max. transmission = 0.790/0.999, $2.0 > 2\theta > 49.9$. Data were collected on an Enraf-Nonius CAD-4 diffractometer with $Mo_{K\alpha}$ radiation ($\lambda = 0.70930$ Å) using the ω scan mode at 290 K. Structures were solved by direct methods using the NRCVAX system. Non-hydrogen atoms of the coordination polymer were refined with anisotropic thermal parameters. The solvent molecules in **1a** were observed to be disordered in a manner that could not be readily resolved. These solvent atoms were therefore treated as carbon atoms and refined with fixed isotropic thermal parameters and variable site occupancy. Values of $R = 0.047$ and $R_w = 0.053$ were obtained for 1027 out of 1795 reflections with $I > 3.0\sigma(I)$ and 135 parameters. For **1b**, values of $R = 0.055$ and $R_w = 0.055$ were obtained for 3535 out of 4585 reflections with $I > 3.0\sigma(I)$ and 343 parameters. Hydrogen atoms of the 4,4′-bpy moieties were placed in calculated positions with d(C–H) = 1.00 Å. Residual electron density (min./max., e Å^{-3}): −0.980/0.420 and −0.590/0.750 for **1a** and **1b**, respectively. Crystallographic data (excluding structure factors) for the structures reported in this paper have been deposited with the Cambridge Crystallographic Data Centre as supplementary publication no. CCDC-179-126. Copies of the data can be obtained free of charge on application to The Director, CCDC, 12 Union Road, Cambridge CB2 1EZ, UK (fax: Int. code +(1223) 336-033; e-mail: teched@chemcrys.cam.ac.uk).
[11] Alternate motifs are possible for assembly of "T-shape" moieties: F. Robinson, M. J. Zaworotko, *J. Chem. Soc. Chem. Commun.* **1995**, 2413; O. M. Yaghi, H. Li, *J. Am. Chem. Soc.* **1996**, *118*, 295. Indeed, when CS_2 is employed as a solvent, **1** crystallizes as an alternate motif which can be best described as a bilayer: P. Losier, K. N. Power, M. J. Zaworotko, unpublished results.

 © VCH Verlagsgesellschaft mbH, D-69451 Weinheim, 1996 0570-0833/96/3523-2781 $ 15.00+.25/0

[12] A. F. Cameron, D. W. Taylor, R. H. Nuttall, *J. Chem. Soc. Dalton Trans* **1972**, 1603.
[13] The presence of acetonitrile is supported by IR spectroscopy. The band at $\nu = 2252\ cm^{-1}$ is assigned to a C≡N stretch: K. Nakamoto, *Infrared Spectra of Inorganic and Coordination Compounds*, 2nd ed., Wiley, New York, **1970**, p. 186.
[14] J. A. R. P. Sarma, G. R. Desiraju, *Acc. Chem. Res.* **1986**, *19*, 222.
[15] C. A. Hunter, *Angew. Chem.* **1995**, *107*, 1181; *Angew. Chem. Int. Ed. Engl.* **1995**, *34*, 1079; M. Fujita, J. Yazaki, K. Ogura, *J. Am. Chem. Soc.* **1990**, *112*, 5645; P. J. Stang, D. H. Cao, *ibid.* **1994**, *116*, 4981; R. V. Slone, D. I. Yoon, R. M. Calhoun, J. T. Hupp, *ibid.* **1995**, *117*, 11813; P. J. Stang, B. Olenyuk, *Angew. Chem.* **1996**, *108*, 798; *Angew. Chem. Int. Ed. Engl.* **1996**, *35*, 732.

Anion Binding: Self-Assembly of Polypyrrolic Macrocycles**

Jonathan L. Sessler,* Andrei Andrievsky, Philip A. Gale, and Vincent Lynch

In memory of Professor Emanuel Gil-Av

The self-assembly of complementary fragments occurs throughout Nature and plays an essential role in the construction of such biological "superstructures" as nucleic acids (for example their duplexes and complexes with peptides), multicomponent enzymes, cell membranes, and viral capsids.[1] The structural information required for facile self-assembly is preprogrammed in the topography and functionality of the building block surfaces. These small subunits bind together reversibly through multiple weak noncovalent interactions. This minimalistic yet effective approach to molecular architecture has challenged supramolecular chemists to design systems capable of recognition, self-assembly, replication, and transport.[2, 3] However, it has not been until recently, that the first abiotic self-assembling supramolecular aggregates were reported.[2–15]

Most notably, many of the structural motifs discovered were employed for production of the "functioning structures" such as interlocked molecules[4] (capable of switching, information storage, and electron transfer), noncovalent dimers (capable of encapsulation[5] and binding[6] of small molecules), molecules capable of self-replication,[7] noncovalent dendrimers,[8] helices, racks, ladders, and grids,[3a] nanotube-forming cyclic peptides,[9] molecular zippers,[10] oligonucleotide-based supramolecular assemblies,[11] monolayers, multilayers, and vesicles,[12] ordered solid-state structures,[3a–e, 13] and self-assembled photoactive aggregates.[14] Noncovalent forces used to generate these arrays include hydrogen bonding, metal–ligand coordination, π-π stacking, and hydrophobic interactions. On the other hand, there are but few self-assembled supramolecular systems that are predicated on anion chelation.[15] These include chiral bicyclic guanidinium dimers and tetramers that assemble into a double helix around sulfate templates,[15a] copper(II)–arginine complexes that form chiral double-helical structures with aromatic dicarboxylates,[15b] self-assembling diamidopyridinium phosphates,[15c] and dianionic and dicationic moieties that form self-assembled infinite rods.[15d] In all cases, the resulting complexes contain a minimum of two different components, one of which is an anion.

It occurred to us that the anion binding properties of expanded porphyrins such as sapphyrins (e.g. **1**)[16] could be effectively employed for the self-assembly of novel supramolecular species. In particular, we speculated that the previously synthesized zwitterionic sapphyrins **1a** and **1c**,[16d] which contain anionic carboxylate groups attached to a protonated sapphyrin core,[17] but which are precluded from "biting their own tails," due to the length of the carboxylate-sapphyrin spacer, should self-assemble readily. This assumption was made on the basis of our previous finding that sapphyrins, when protonated, effectively chelate carboxylate ions through a combination of hydrogen bonding and electrostatic attractions involving the pyrrolic hydrogens and the ligated oxyanion.[16b, c] Herein we report that this is indeed the case in the gas phase, in solution, and in the solid state. Taking this methodology a step further, and exploiting our recent discovery that calix[4]pyrroles (a class of molecules known for over a century[18]) are capable of anion chelation through multiple hydrogen bonds,[19] we have synthesized a new calix[4]pyrrole with a carboxylate pendant arm, and found that these purely anionic species also self-assemble. In contrast to the previously reported anionic systems capable of self-assembly,[15] the sapphyrin- and calix[4]pyrrole-based carboxylate building blocks of this report are self-complementary, and thus, no other extra components are required for self-assembly.

Calix[4]pyrrole monoacid **2a** was synthesized by the acid-catalyzed condensation of methyl 4-acetylbutyrate and cyclohexanone with pyrrole. This produced the monomethyl ester **2b** in 12% yield (after chromatographic purification). Subsequent hydrolysis of **2b** (sodium hydroxide ethanol/water solution at reflux; see Experimental Procedure) afforded the monoacid **2a**, which was immediately converted to its tetrabutylammonium or trimethylammonium salts (see Experimental Procedure).

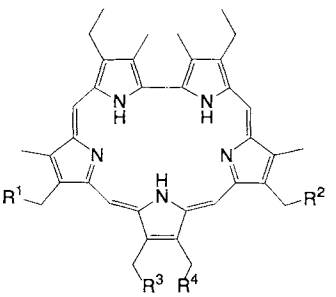

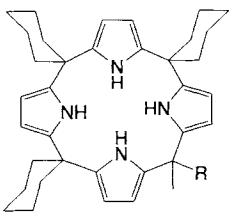

1a: $R^1 = R^2 = CH_3$; $R^3 = H$; $R^4 = CH_2CO_2H$
1b: $R^1 = R^2 = CH_3$; $R^3 = H$; $R^4 = CH_2CO_2CH_3$
1c: $R^1 = R^2 = CH_2CO_2H$; $R^3 = R^4 = CH_3$
1d: $R^1 = R^2 = CH_2CO_2CH_3$; $R^3 = R^4 = CH_3$

2a: $R = (CH_2)_3CO_2H$
2b: $R = (CH_2)_3CO_2CH_3$

Initial evidence for self-assembly in the gas phase came from low- and high-resolution fast atom bombardment (FAB) mass spectrometry. Intense peaks for the dimer (but not trimer or tetramer) at double the molecular weight were observed for the carboxylates **1a**, **1c**, and **2a** (Fig. 1). Such peaks, however, were not seen with "control" methyl esters **1b**, **1d**, and **2b**. This indicates that the presence of unprotected carboxylate groups in the molecule is essential for self-assembly, and rules out formation of dimers due to simple van der Waals or hydrophobic attractions between the macrocycles. In addition, and in support of the

[*] Prof. J. L. Sessler, A. Andrievsky, Dr. P. A. Gale, V. Lynch
Department of Chemistry and Biochemistry
The University of Texas at Austin
Austin, TX 78712 (USA)
Fax: Int. code + (512) 471-7550
e-mail: sessler@mail.utexas.edu

[**] This research was supported by the National Institutes of Health (grant AI 33577) and National Science Foundation (grant CHE 9122161). P. A. G. wishes to thank the Fulbright Commission for a post-doctoral research scholarship.

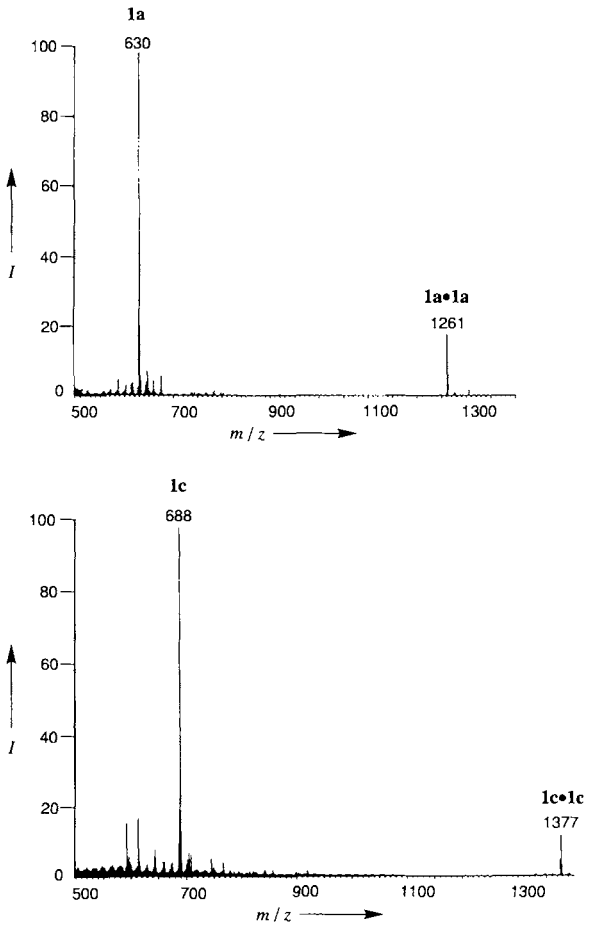

Fig. 1. FAB mass spectra of sapphyrin carboxylates.

versatility of the zwitterionic and anionic self-assembly of sapphyrin and calix[4]pyrrole carboxylates, all possible supramolecular heterodimers were detected by mass spectrometry when two different species (i.e. **1a**, **1c**, and **2a**) were mixed in a ratio of approximately 1:1 prior to FAB MS analysis (Table 1).

Table 1. Molecular masses of selected homo- and heterodimers.

Dimer	**1a**·**1a** [a]	**1c**·**1c** [a]	**2a**·**2a** [b]	**1a**·**1c** [a]	**1a**·**2a** [b]	**1c**·**2a** [a]
M(found)	1260.7595	1376.7737	1239.8087	1318.7679	1249.7775	1308.7961
M(calculated)	1260.7616	1376.7726	1239.8102	1318.7671	1249.7820	1308.7953

[a] Positive ion FAB mass spectrometry. [b] Negative ion FAB mass spectrometry.

As a further test of the proposed self-assembly process, experiments were carried out in the presence of fluoride ion. Since protonated sapphyrins have a significantly higher affinity for fluoride ion than other anions,[16e] it was expected that the addition of fluoride ion would inhibit sapphyrin dimer formation in the gas phase. This proved to be the case. When tetrabutylammonium fluoride was added to the samples of sapphyrin mono- and/or dicarboxylates, the peaks in the mass spectra ascribed to the dimer species disappeared completely. In the case of **2a**, addition of tetrabutylammonium fluoride decreased the intensity of the dimer ion peak but did not eliminate it completely.

X-ray quality crystals of sapphyrin carboxylate **1c** were obtained by slow diffusion of ether into a solution of **1c** in dichloromethane/methanol (3/1).[20] The structure analysis revealed that the appended macrocycle forms a supramolecular dimer in the solid state (Fig. 2a). A carboxylate "hook" from one molecule of **1c** is chelated to the pyrrole core of the second macrocycle. Simultaneously, this second macrocycle shares its carboxylate "tail" with the first sapphyrin subunit. A trifluoroacetate ion is coordinated to each of unchelated faces in the dimer and prevents these sites from being involved in further binding. Perhaps as a result of this, the second carboxylic acid is not bound to a sapphyrin core, but is coordinated to a methanol molecule. The macrocycles of the dimer are related by a crystallographic inversion center at 1/2, 1/2, 0. The separation between the root mean square (RMS) planes of the nitrogen atoms in this structure is 3.39(1) Å.

X-ray quality crystals of the tetrabutylammonium salt of calix[4]pyrrole carboxylate **2a** were obtained by slow evaporation of a solution of **2a** in dichloromethane in the presence of excess tetrabutylammonium fluoride trihydrate.[21] The resulting crystal structure confirmed that this anionic calix[4]pyrrole also self-assembles into dimers in the solid state. In this instance, in analogy to the sapphyrin case, the carboxylate moiety is hydrogen-bonded to the pyrrole array of an adjacent calix[4]pyrrole (Fig. 2b). Now, however, the separation between the RMS planes of the nitrogen atoms in each macrocycle is 7.41(1) Å. The calix[4]pyrrole **2a** adopts a cone conformation in the dimer, as is observed in the anion complexes of related systems.[19]

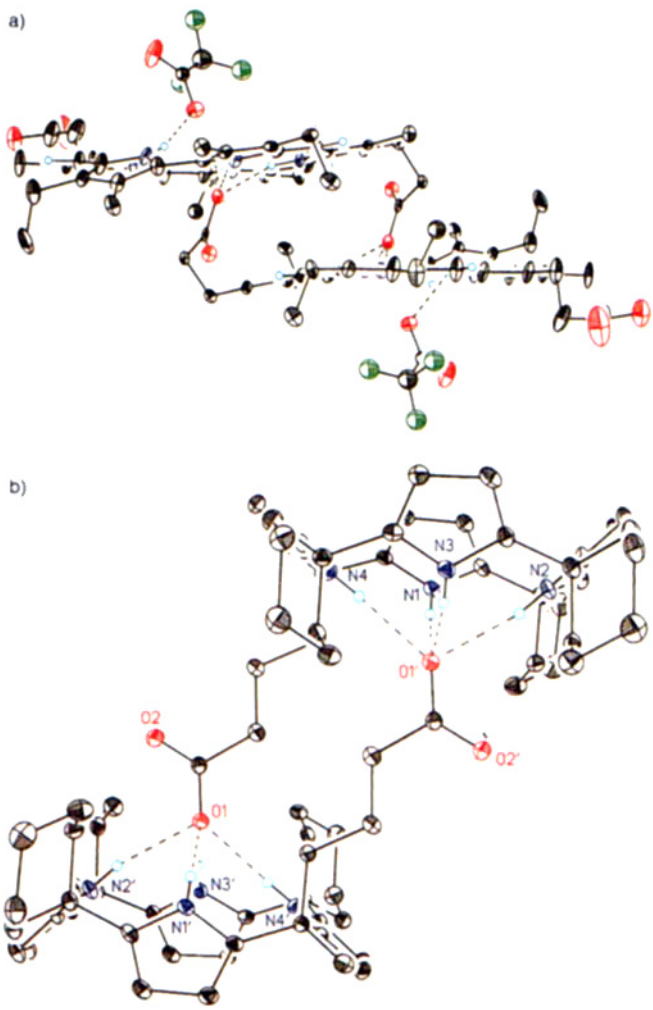

Fig. 2. Side view of the supramolecular sapphyrin dimer **1c**·**1c** (a) and of the noncovalent calix[4]pyrrole dimer **2a**·**2a** (b) in the solid state (thermal ellipsoids are scaled to the 30% probability level). C: black, H: light blue, N: blue, O: red, F: green.

 © *VCH Verlagsgesellschaft mbH, D-69451 Weinheim, 1996* *0570-0833/96/3523-2783 $ 15.00+.25/0*

The ^{1}H NMR spectra of sapphyrin monocarboxylate **1a** in [D_4]methanol or $CDCl_3$, and dicarboxylate **1c** in a [D_4]-methanol/$CDCl_3$ (2/1) mixture[22] showed strong line broadening, which is consistent with self-aggregation of these species.[23] Dilution experiments performed over a concentration range of 50 to 5 mM in these solvents showed little change in the spectra, which is taken as an indication that the putative aggregates prevail over the monomers at these concentrations even in these highly polar solvent mixtures.

In order to determine the stoichiometry of aggregation, vapor pressure osmometry (VPO) measurements were carried out in 1,2-dichloroethane using compound **1a**. The average molecular weight of the species in solution determined by this method ($M = 1281\ g\,mol^{-1}$; calculated 1261 $g\,mol^{-1}$) corresponds to that of the dimer. In contrast, these same VPO measurements carried out under identical conditions with the control sapphyrin methyl ester **1b** confirmed its monomeric state in solution ($M = 690\ g\,mol^{-1}$ calculated 643 $g\,mol^{-1}$).

Fluoride inhibition of sapphyrin dimerization was also studied by ^{1}H NMR spectroscopy. This was done by adding aliquots of tetrabutylammonium fluoride trihydrate solution (up to 3 equiv) to stock solutions of the sapphyrin carboxylates **1a** and **1c**, and recording the resulting changes in the proton NMR spectra. Generally, upon addition of fluoride ion, the spectra became well-resolved and all sapphyrin proton signals were seen to shift. The signals of the ethylene protons of the linker between the sapphyrin macrocycle and its carboxylate pendant arm were found to be particularly diagnostic. These, undergo downfield shifts on addition of fluoride ion (**1a**: $\delta = 1.67$ and 1.07 for $CH_2CH_2CO_2^-$ and $CH_2CH_2CO_2^-$, respectively).[24, 25] These signals are the ones most affected by the ring current of the "partner" aromatic sapphyrin macrocycle, and are thus the most indicative of dimer break-up. This is because in solution, as in the solid state, the dimers are probably held together in an offset manner. Such a binding arrangement would force the protons of the ethylene "arm" to resonate at higher field. When fluoride ion is added in sufficient quantities (generally less than 2 equiv), it binds to the sapphyrin cavity and displaces the carboxylates. This breaks the dimers and reestablishes the "normal" lower field chemical shift for the ethylene proton signals (Fig. 3).

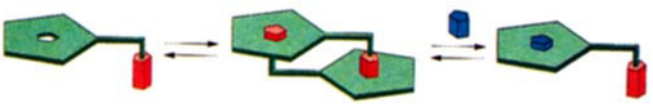

Fig. 3. Schematic representation of the sapphyrin **1a**, dimerization, and fluoride ion inhibition thereof. Green blocks: sapphyrin **1a**; red blocks: carboxylate appendages of **1a**; blue block: fluoride ion.

Unfortunately, the low solubility of the trimethylammonium salt of **2a** in organic solvents precluded a quantitative ^{1}H NMR analysis of this system. However, a ROESY NMR spectrum of of a suspension of this salt in CD_2Cl_2 provides evidence for association of the calix[4]pyrrole anions in solution. For instance, two resonances are observed between $\delta = 7.0$ and 7.5. These are typical shifts for NH protons in other noncomplexed calix[4]pyrroles[19] and are thus assigned to the signals of NH protons in the calix[4]pyrrole monomer. In addition, a broad resonance is observed at about $\delta = 11$, which is ascribed to an exchange peak involving the NH protons bound to the carboxylate portion of complementary, paired calix[4]pyrrole. Upon addition of [D_4]methanol, the resonance at $\delta = 11$ vanishes as would be expected upon break-up of the calix[4]pyrrole aggregates. From these experiments it is thus inferred that, as was true for sapphyrins **1a** and **1c**, conditions can be found under which dimerization is precluded.

In conclusion, anion-binding interactions may be used as a means of effecting the spontaneous self-assembly of appropriately designed supramolecular ensembles. This is important because it shows yet one more way in which a simple to control recognition motif (in this case sapphyrin- or calix[4]pyrrole-based anion binding) may be used to "program in" information that encodes for the self-controlled construction of higher order structures that, in turn, display considerable molecular complexity.

Experimental Procedure

2b: Methyl 4-acetylbutyrate (0.80 g, 5.6 mmol), cyclohexanone (0.55 g, 5.6 mmol), and pyrrole (0.75 g, 11.2 mmol) were dissolved in methanol (50 mL), and the mixture cooled to 0 °C. Methanesulfonic acid (0.5 mL) was added dropwise over the course of five minutes, and the mixture stirred at 0 °C for 1 h and then at room temperature overnight. The solvent was removed in vacuo. FAB mass spectra showed the presence of mono-, di-, tri-, and tetrafunctionalized material in the crude reaction mixture. Chromatographic purification (silica gel, dichloromethane) yielded **2b** as a white foamy solid (211 mg, 0.33 mmol, 12%). ^{1}H NMR (250 MHz, $CDCl_3$): $\delta = 7.07$ (br. m, 4H, NH), 5.88 (m, 8H, pyrrole CH), 3.63 (s, 3H, OCH_3), 2.22 (t, $J = 7.2$ Hz, 2H, CH_2), 1.93 (br., 14H, $6CH_2$(cyclohexyl), + CH_2(hook)), 1.56–1.35 (br., 23H, CH_2(hook) + $9CH_2$(cyclohexyl) + CCH_3). The term hook refers to the propionic acid side chain. ^{13}C NMR (62.9 MHz, $CDCl_3$): $\delta = 173.8$, 137.2, 136.5, 136.3, 130.7, 103.6, 103.5, 103.2, 53.4, 51.4, 39.7, 39.5, 39.4, 38.5, 37.5, 37.2, 36.9, 36.8, 34.0, 26.1, 25.9, 22.8, 22.7, 19.9. CI MS: *m/z*: 635 (MH^+); HRMS: calculated for $C_{41}H_{54}N_4O_2$: *m/z*: 634.4247; found: 634.4236; elemental analysis: calculated for $C_{41}H_{54}N_4O_2$: C 77.56, H 8.57, N 8.82; found: C 77.41, H 8.50, N 8.84.

2a: Methyl ester **2b** (211 mg, 0.33 mmol) in ethanol (20 mL) was heated to reflux. Aqueous sodium hydroxide (20 mL, 2.0 M) was then added and the mixture stirred at reflux for 4 h. The solution was allowed to cool and ethanol removed in vacuo. After acidification with perchloric acid (70%), the product was extracted with dichloromethane (50 mL). The organic layer was then washed with water (100 mL) and dried over $MgSO_4$. Removal of the solvent afforded **2a** as a white foamy solid (187 mg, 0.30 mmol, 91%). ^{1}H NMR (250 MHz, $CDCl_3$): $\delta = 7.02$ (br. m, 4H, NH), 5.89 (m, 8H, pyrrole CH), 2.26 (t, 2H, CH_2), 1.91 (br. m, 14H, $6CH_2$(cyclohexyl) + CH_2(hook)), 1.44 (br. m, 24H, $9CH_2$(cyclohexyl) + CH_2-(hook) + CCH_3 + $0.5H_2O$). The term hook refers to the propionic acid side chain. ^{13}C NMR (62.9 MHz, $CDCl_3$): $\delta = 179.4$, 137.3, 136.6, 136.2, 103.7, 103.6, 103.5, 103.2, 53.4, 39.7, 39.4, 39.3, 38.5, 37.4, 37.2, 36.9, 36.8, 33.8, 26.0, 25.9, 22.7, 22.6, 19.5. FAB MS: *m/z*: 620 (MH^+). HRMS: calculated for $C_{40}H_{52}N_4O_2$: *m/z*: 620.4090; found 620.4073; elemental analysis: calculated for $C_{40}H_{52}N_4O_2$: C 77.38, H 8.44, N 9.02; found: C 76.78, H 8.42, N 8.92.

The tetrabutylammonium salt of **2a** was precipitated in quantitative yield from a solution of **2a** in diethyl ether by the addition of tetrabutylammonium hydroxide (2.0 equiv). It was then washed with ether and water followed by drying in vacuo. Elemental analysis: calculated for $C_{56}H_{87}N_5O_2 \cdot H_2O$: C 76.40, H 10.19, N 7.96; found: C 76.58, H 10.04, N 7.95.

The trimethylammonium salt of **2a** was obtained by passing trimethylamine gas through a methanolic solution of **2a** at −10 °C. The salt precipitated in quantitative yield and was then dried in vacuo. Elemental analysis: calculated for $C_{43}H_{62}N_5O_2 \cdot 1/3(H_2O)$: C 75.18, H 9.18, N 10.19; found: C 75.00, H 8.97, N 10.10.

Received: June 17, 1996 [Z9234IE]
German version: *Angew. Chem.* **1996**, *108*, 2954–2957

Keywords: anion binding · calixarenes · sapphyrin · self-assembly

[1] For examples of self-assembly in biological systems, see: a) D. Voet, J. G. Voet, *Biochemistry*, 2nd ed., Wiley, New York, **1995**; b) C. Branden, J. Tooze, *Introduction to Protein Structure*, Garland, New York, **1991**; c) A. Fersht, *Enzyme Structure and Mechanism*, 2nd ed., Freeman, New York, **1985**.

[2] a) For an excellent collection of reviews on self-assembling systems, see ref. [2b], *Vol. 9 (Templating, Self-assembly, and Self-organization)*; b) *Comprehensive Supramolecular Chemistry* (Eds.: J. L. Atwood, J. E. D. Davies, D. D. Macnicol, F. Vögtle), Elsevier, Exeter, **1996**.

[3] For reviews, see: a) J.-M. Lehn, *Supramolecular Chemistry*, VCH, Weinheim, **1995**; b) D. S. Lawrence, T. Jiang, M. Levett, *Chem. Rev.* **1995**, *95*, 2229–2260; c) D. Philp, J. F. Stoddart, *Angew. Chem.* **1996**, *108*, 1242–1286; *Angew. Chem. Int. Ed. Engl.* **1996**, *35*, 1154–1196; d) F. Vögtle, *Supramolecular Chemistry*,

Wiley, Chichester, **1991**; e) G. M. Whitesides, E. E. Simanek, J. P. Mathias, C. T. Seto, D. N. Chin, M. Mammen, D. M. Gordon, *Acc. Chem. Res.* **1995**, *28*, 37–44; f) J. S. Lindsey, *New J. Chem.* **1991**, *15*, 153–180; g) J. Rebek, Jr. *Angew. Chem.* **1990**, *102*, 261–272; *Angew. Chem. Int. Ed. Engl.* **1990**, *29*, 245–255; h) C. A. Hunter, *ibid.* **1995**, *107*, 1181–1183 and **1995**, *34*, 1079–1081.

[4] For reviews, see: a) D. A. Amabilino, J. F. Stoddart, *Chem. Rev.* **1995**, *95*, 2725–2828; b) J.-C. Chambron, C. Dietrich-Buchecker, J.-P. Sauvage, in ref. [2a], pp. 43–84.

[5] a) R. M. Grotzfeld, N. Branda, J. Rebek, Jr., *Science*, **1996**, *271*, 487–489, and references therein; b) R. S. Meissner, J. Rebek, Jr., J. de Mendoza, *Science* **1995**, *270*, 1485–1488; c) B. C. Hamann, K. D. Shimizu, J. Rebek, Jr. *Angew. Chem.* **1996**, *108*, 1425–1427; *Angew. Chem. Int. Ed. Engl.* **1996**, *35*, 1326–1329; d) D. J. Cram, J. M. Cram, *Container Molecules and their Guests*, Royal Society of Chemistry, Cambridge, **1994**.

[6] a) C. A. Hunter, L. D. Sarson, *Angew. Chem.* **1994**, *106*, 2424–2426; *Angew. Chem. Int. Ed. Engl.* **1994**, *33*, 2313–2316; b) M. S. Goodman, A. D. Hamilton, J. Weiss, *J. Am. Chem. Soc.* **1995**, *117*, 8447–8455.

[7] a) E. A. Wintner, B. Tsao, J. Rebek, Jr. *J. Org. Chem.* **1995**, *60*, 7997–8001, and references therein; b) D. N. Reinhoudt, D. M. Rudkevich, F. de Jong, *J. Am. Chem. Soc.* **1996**, *118*, 6880–6889, and references therein; c) D. Sievers, G. von Kiedrowski, *Nature* **1994**, *369*, 221–224, and references therein; d) D. H. Lee, J. R. Gravija, J. A. Martinez, K. Severin, H. R. Ghadiri, *Nature* **1966**, *382*, 525–528.

[8] S. C. Zimmerman, F. Zeng, D. E. C. Reichert, S. V. Kolotuchin, *Science* **1996**, *271*, 1095–1098.

[9] a) J. D. Hartgerink, J. R. Granja, R. A. Milligan, M. R. Ghadiri, *J. Am. Chem. Soc.* **1996**, *118*, 43–50; b) M. R. Ghadiri, J. R. Granja, L. K. Buehler, *Nature* **1994**, *369*, 301–304.

[10] A. P. Bisson, F. J. Carver, C. A. Hunter, J. P. Waltho, *J. Am. Chem. Soc.* **1994**, *116*, 10292–10293.

[11] a) C. Giovannangeli, J.-S. Sun, C. Hélène in ref. [2b], *Vol. 4*, pp. 177–192; b) Y. Ohya, H. Noro, M. Komatsu, T. Ouchi, *Chem. Lett.* **1996**, 447–448.

[12] a) A. Ulman, *An Introduction to Ultrathin Organic Films: From Langmuir-Blodgett to Self-Assembly*, Academic Press, San Diego, **1991**; b) J. Lahiri, G. D. Fate, S. B. Ungashe, J. T. Groves, *J. Am. Chem. Soc.* **1996**, *118*, 2347–2358; c) F. Arias, L. A. Godinez, S. R. Wilson, A. E. Kaifer, L. Echegoyen, *ibid.* **1996**, *118*, 6086–6087.

[13] a) J. C. MacDonald, G. M. Whitesides, *Chem. Rev.* **1994**, *94*, 2383–2420; b) C. B. Aakeröy, K. R. Seddon, *Chem. Soc. Rev.* **1993**, *22*, 397–407; c) special issue "*Molecular Engineering and Structure Design*", *Isr. J. Chem.* **1985**, *25*; d) see also ref. [2b], *Vol. 6* (*Solid-state Supramolecular Chemistry: Crystal Engineering*), and *Vol. 7* (*Solid-state Supramolecular Chemistry: Two- and Three-dimensional Inorganic Networks*).

[14] a) H. Tamiaki, T. Miyatake, R. Tanikaga, A. R. Holzwarth, K. Schaffner, *Angew. Chem.* **1996**, *108*, 810–812; *Angew. Chem. Int. Ed. Engl.* **1996**, *35*, 772–774; b) J. L. Sessler, B. Wang, S. L. Springs, C. T. Brown in ref. [2b], *Vol. 4*, pp. 311–336; c) V. Balzani, F. Scandola, *Supramolecular Photochemistry*, Ellis Horwood, New York, **1991**.

[15] For examples of self-assembly involving anion chelation, see: a) J. Sánchez-Quesada, C. Seel, P. Prados, J. de Mendoza, I. Dalcol, E. Giralt, *J. Am. Chem. Soc.* **1996**, *118*, 277-278; b) N. Ohata, H. Masuda, O. Yamauchi, *Angew. Chem.* **1996**, *108*, 570–572; *Angew. Chem. Int. Ed. Engl.* **1996**, *35*, 531–532; c) S. J. Geib, S. C. Hirst, C. Vicent, A. D. Hamilton, *J. Chem. Soc. Chem. Commun.* **1991**, 1283–1285; d) M. W. Hosseini, R. Ruppert, P. Schaeffer, A. De Cian, N. Kyritsakas, J. Fischer, *ibid.* **1994**, 2135–2136.

[16] a) J. L. Sessler, A. K. Burrell, *Top. Curr. Chem.* **1991**, *161*, 177–273; b) V. Král, A. Andrievsky, J. L. Sessler, *J. Am. Chem. Soc.* **1995**, *117*, 2953–2954; c) V. Král, S. L. Springs, J. L. Sessler, *ibid.* **1995**, *117*, 8881–8882; d) V. Král, J. L. Sessler, H. Furuta, *ibid.* **1992**, *114*, 8704–8705; e) M. Shionoya, H. Furuta, V. Lynch, A. Harriman, J. L. Sessler, *ibid.* **1992**, *114*, 5714–5722.

[17] Due to its size and basicity, the pentapyrrolic core of sapphyrin is monoprotonated at neutral pH [16].

[18] A. Baeyer, *Ber. Dtsch. Chem. Ges.* **1886**, *19*, 2184–2185.

[19] P. A. Gale, J. L. Sessler, V. Král, V. Lynch *J. Am. Chem. Soc.* **1996**, *118*, 5140–5141.

[20] a) Crystallographic data for $(C_{42}H_{50}N_5O_4^+)(CF_3CO_2^-)\cdot CH_3OH$. Dark green needles, triclinic, $P\bar{1}$, $Z = 2$, $a = 10.635(2)$, $b = 12.514(3)$, $c = 16.307(4)$ Å, $\alpha = 82.88(2)$, $\beta = 77.98(2)$, $\gamma = 85.54(2)°$, $V = 2103.3(9)$ Å^3, $\rho_{calcd} = 1.32$ g cm^{-3}, $F(000) = 884$. A total of 6565 reflections were measured, 5490 unique ($R_{int} = 0.152$) on a Siemens P3 diffractometer using graphite-monochromatized $Mo_{K\alpha}$ radiation ($\lambda = 0.71073$ Å). The structure was refined on F^2 to an $R_w = 0.250$, with a conventional $R = 0.131$ (1567 reflections with $F_o > 4[\sigma(F_o)]$), and a goodness of fit = 1.192 for 523 refined parameters. Geometry of the hydrogen-bonding interaction (distances [Å], angles [°]): N1–H1N···O1a, N···O 2.827(13), H···O 1.959(13), N–H···O 161.7(12); N2–H2N···O1a, N···O 2.901(14), H···O 2.235(14)), N–H···O 130.5(12); N3–H3N···O42 (related by $1-x$, $1-y$, $-z$), N···O 2.763(13), H···O 1.944(13), N–H···O 150.5(12); N4–H4N···O42 (related by $1-x$, $1-y$, $-z$), N···O 2.816(13), H···O 1.945(13), N–H···O 160.4(12); N5–H5N···O42 (related by $1-x$, $1-y$, $-z$), N···O 2.810(14), H···O 1.957(14), N H···O 157.7(11). b) Crystallographic data (excluding structure factors) for the structures reported in this paper have been deposited with the Cambridge Crystallographic Data Centre as supplementary publication no. CCDC-179-112. Copies of the data can be obtained free of charge on application to The Director, CCDC, 12 Union Road, Cambridge CB2 1EZ, UK (fax: Int. code +(1223) 336-033; e-mail: teched@chemcrys.cam.ac.uk).

[21] Crystallographic data for $(C_{40}H_{51}N_4O_2^-)(C_{16}H_{36}N^+)\cdot 2CH_2Cl_2$. Colorless needles were grown from CH_2Cl_2, triclinic, $P\bar{1}$, $Z = 2$, $a = 12.682(2)$, $b = 13.127(2)$, $c = 17.871(2)$ Å, $\alpha = 99.913(9)$, $\beta = 90.527(9)$, $\gamma = 98.49(1)°$, $V = 2896.7(6)$ Å^3, $\rho_{calcd} = 1.18$ g cm^{-3}, $F(000) = 1116$. A total of 11364 reflections were measured, 10078 unique ($R_{int} = 0.044$) on a Siemens P4 diffractometer using graphite-monochromatized $Mo_{K\alpha}$ radiation ($\lambda = 0.71073$ Å). The structure was refined on F^2 to an $R_w = 0.220$, with a conventional $R = 0.084$, with a goodness of fit = 1.031 for 661 refined parameters. Geometry of the hydrogen-bonding interaction (distances [Å], angles [°]): N1–H1N···O1 (related by $1-x$, $1-y$, $1-z$), N···O 2.975(5), H···O 2.19(4), N-H···O 162(4); N2–H2N···O1, N···O 2.980(5), H···O 2.18(5), N–H···O 167(4); N3–H3N···O1, N···O 2.950(5), H···O 2.14(4), N–H···O 163(4); N4–H4N···O1, N···O 2.916(5), H···O 2.09(4), N-H···O 176(4) [20b].

[22] The sapphyrin bisacid **1c** is insoluble in either pure chloroform (or dichloromethane) or methanol, but is soluble in mixtures of these solvents.

[23] The signals of the ^{1}H NMR spectra of sapphyrin methyl esters **1b** and **1d** are, on the other hand, well resolved in these solvents.

[24] These same linker ethylene signals in sapphyrin bisacid **1c** were broadened to such an extent that their initial shifts could not be determined accurately.

[25] The proton chemical shifts of the linker ethylene group in the control methyl ester **1b**, recorded under conditions analogous to those of the fluoride titration, were found to remain almost unchanged.

In Situ Observation of Transient Reaction Phenomena Occurring on Zeolite Catalysts with the Aid of Positron Emission Profiling

Rutger A. van Santen,* B. G. Anderson, R. H. Cunningham, A. V. G. Mangnus, Dr. L. J. van IJzendoorn, and M. J. A. de Voigt

Zeolites are widely used in the petroleum refining industry as solid acid catalysts to convert hydrocarbons into gasoline products of high octane number by isomerization or by cracking reactions.[1] Stable operation at mild reaction conditions is made possible by the addition of noble metals to acidic zeolites. For example, after addition of platinum to the zeolite H-mordenite *n*-hexane isomerizes to its structural isomers at 240 °C rather than at 400 °C.[2] The state of the platinum in the working catalyst and the distribution profiles of the reactive surface intermediates are strongly dependent on pretreatment and reaction conditions. Thus in situ measurement is necessary.

Positron emission tomography (PET) is a noninvasive, in situ, radiochemical imaging technique used in nuclear medicine to monitor biomedical functions.[3, 4] This technique has recently been applied to systems in engineering research by Bridgwater et al.[5, 6] to study mechanical mixing within a powder mixer. In addition we have shown that this technique can be used to provide information on the concentration distributions of reactants and products as a function of time and position along the reactor bed during the CO oxidation under steady-state conditions.[7, 8] This information is essential for the development of kinetic models describing the rates of elementary reaction steps.

[*] Prof. Dr. R. A. van Santen, Dr. B. G. Anderson, Dr. R. H. Cunningham
Department of Chemical Engineering and Chemistry
Schuit Institute of Catalysis
Eindhoven University of Technology
P. O. Box 513, 5600 MB Eindhoven (The Netherlands)
Fax: Int. code +(40)245-5054
e-mail: tgtaba@chem.tue.NL
Ir. A. V. G. Mangnus, Dr. L. J. van IJzendoorn, Prof. Dr. M. J. A. de Voigt
Department of Technical Physics
Schuit Institute of Catalysis (The Netherlands)

We have since developed a new detection system for positron emission profiling (PEP), which is a one-dimensional analogue to PET. This study is the first to measure in situ reaction profiles under transient conditions.

Due to the short half-life of ^{11}C (20.3 min) the positron-emitting molecules must be produced on-site with a cyclotron in combination with chemical processing. We have developed a unique route for on-line synthesis of $^{11}CH_3C_nH_{2n+1}$ $(3 \geq n \leq 6)$[10, 11] based on our method for the homologation of olefins by ^{11}CO.[12] An optimized vanadium-promoted Ru/SiO_2 system is used to adsorb ^{11}CO and 1-pentene. Secondly, the mixture of hydrocarbons formed by hydrogenative desorption at 110 °C is separated by a technique of freezing, flash heating, and gas chromatography. Finally, a pulse that contains approximately 2×10^{-6} moles of nonlabeled *n*-hexane and 1 MBq of *n*-$^{11}CH_3C_5H_{11}$ (about 10^{-15} mol) can be injected into the feed stream of the zeolite-containing, solid-bed reactor positioned in a newly developed PEP detection system.

The PEP system is based on two banks of nine detection elements. Each element consists of a specially shaped and polished $Bi_4Ge_3O_{12}$ scintillation crystal and a slit-shaped photomultiplier. The system is optimized for imaging in one dimension; the detector thus has a faster sampling time (0.5 s) and a higher sensitivity than state-of-the-art research PET cameras whilst maintaining a resolution of 2.7 mm.[9] Reactor bed lengths varying between 4 and 50 cm can be handled.

Figure 1a shows the PEP image obtained after a pulse of labeled *n*-hexane was injected into a feed stream of *n*-hexane/hydrogen flowing through a bed of Pt/H-mordenite. The catalytic reactor was operating under steady-state conditions at 230 °C,

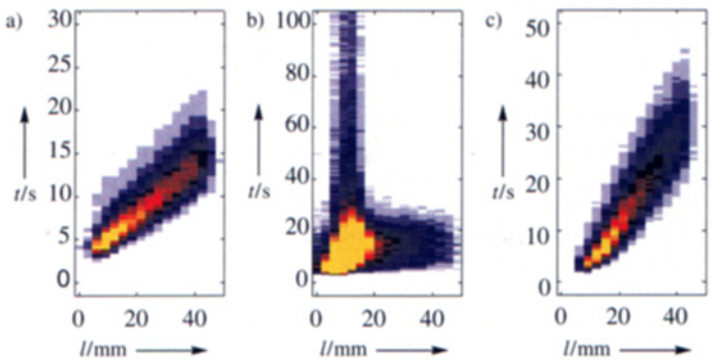

Fig. 1. Positron emission profiling (PEP) images of *n*-$^{11}CH_3C_5H_{11}$ pulse experiments on a Pt/H-mordenite catalyst bed (l = position along the catalyst bed, t = residence time). The color scale indicates the concentration of the ^{11}C label: the brighter the color, the higher the concentration. Labeled samples were injected into the feed streams (1 atm; 150 NmL min^{-1} total flow rate). a) The reactor was operating under steady-state conditions at 230 °C with a feed mixture of *n*-hexane/H_2 (1/28 mol). b) [^{11}C]-*n*-hexane pulse in hydrogen over the catalyst with freshly reduced Pt at 230 °C. c) [^{11}C]-*n*-hexane pulse in hydrogen over the catalyst, which was previously used in the hydroisomerization reaction at 230 °C.

which converts 19% of hexane into structural isomers. Since these isomers have similar adsorption/desorption and diffusion properties on H-mordenite to *n*-hexane, the pulse continues through the reactor in a manner similar to that of *n*-hexane on the zeolite alone.[13]

A very different behavior is observed if the platinum metal is freshly reduced. After reduction by H_2 at 400 °C, the temperature was lowered to 230 °C, and a pulse of labeled *n*-hexane was then injected into a hydrogen stream. The pulse adsorbs strongly near the beginning of the reactor bed and reacts rapidly (Fig. 1b). Some of the radio-labeled species exit the reactor very quickly (the near horizontal band), and some remain on the catalyst surface. Analysis of the radio-labeled reaction products by trapping and subsequent GC separation with NaI scintillation detection revealed light alkanes between C_1 and C_4.

When one uses a Pt/H-mordenite catalyst that was first used in the steady-state hydroisomerization of *n*-hexane at 230 °C, very different results were obtained. The reaction was interrupted by stopping the hexane feed, and after 5 minutes the labeled *n*-hexane was again injected into the hydrogen stream (see Fig. 1c). In contrast to the profile shown in Figure 1b, an image similar to that shown in Figure 1a was obtained. (The difference in the observed retention times between (a) and (c) is due to differences in the number of adsorption sites available[13]). Analysis of the trapped products revealed only C_6 hydrocarbons.

Apparently, the undesirable metal cracking reactions that occur on freshly reduced platinum are suppressed by "preconditioning" the surface of the platinum metal by the hydroisomerization reaction. As concluded from Figure 1b this "preconditioning" involves the deposition of a carbonaceous overlayer that prevents cracking of the hexane. As we will see from the experiments reported in Figure 2, the only function of the "preconditioned" platinum surface is to dehydrogenate hexane to hexene or to hydrogenate olefins. This result is consistent with the conclusions of others who work on model transition metal catalysts: hydrogenation and dehydrogenation reactions occur on a surface covered by a carbonaceous overlayer.[14–16] The effect of the carbonaceous overlayer may be to restrict the surface ensemble size available to the cracking reaction; the hydrogenation and dehydrogenation reactions are less structure-sensitive.[17]

The hydroisomerization reaction must be carried out in the presence of hydrogen in order to avoid loss of activity through "deactivation". The following type of experiments illustrate the details of deactivation of the acid sites. Steady-state hydroisomerization of *n*-hexane over Pt/H-mordenite at 240 °C is interrupted by replacing the feed with flowing helium. After 5 minutes labeled *n*-hexane is injected into the helium stream (Fig. 2a). A rapid reaction near the beginning of the reactor bed forms products that remain strongly adsorbed. Only a small portion of the pulse passes through the bed. Radio-GC analysis of this fraction revealed mainly unchanged C_6 hydrocarbons with small amounts of C_1 and C_2 hydrocarbons. All of the labeled products remaining on the surface could be removed if

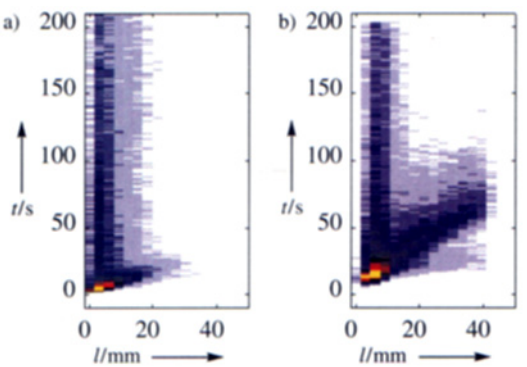

Fig. 2. PEP images of separate *n*-$^{11}CH_3C_5H_{11}$ pulse experiments on a Pt/H-mordenite catalyst. The hydroisomerization reaction under steady-state conditions was interrupted 5 min prior to injection by switching to a flow of hydrogen. Injection was then made into a stream of helium (75 NmL min^{-1}) at 240 °C. a) The majority of *n*-hexane is dehydrogenated to hexene on the Pt surface, and the hexene isomers remain strongly adsorbed to acidic sites in the absence of hydrogen. b) Conditions similar to those for (a) but at injection made at 230 °C.

 © VCH Verlagsgesellschaft mbH, D-69451 Weinheim, 1996 0570-0833/96/3523-2786 $ 15.00+.25/0

the temperature was increased to 400 °C in a stream of hydrogen. Analysis of this fraction revealed mainly C_6 hydrocarbons with small amounts of C_7, C_8, C_1, and C_2 species. This shows that *n*-hexane is rapidly dehydrogenated by platinum, and the resulting hexene molecules are adsorbed on the acid sites of the zeolite. In the absence of hydrogen they can not be rehydrogenated and therefore remain adsorbed, poisoning the sites for subsequent reaction. Dimerization or further oligomerization reactions do not occur to a great extent, since no large fraction of higher and lower hydrocarbons was found. The PEP image shown in Figure 2b was obtained when the above reaction was repeated at 230 °C. Comparison with Figure 2a reveals that a greater portion of the hexane pulse passes unchanged through the bed; the lower reaction rate is due to the lower reaction temperature.

These experiments under transient conditions provide the first direct demonstration of the so-called bifunctional reaction mechanism[18, 19] proposed for alkane hydroisomerization. The platinum promoter acts as an alkane dehydrogenation and an alkene hydrogenation catalyst. The zeolitic protons protonate the alkanes, which then, as predicted by theory,[20, 21] remain strongly adsorbed (enthalpy of protonation $\approx 180 \pm 20\ kJ\,mol^{-1}$).

The protonated alkenes isomerize. From steady-state experiments we deduced an activation energy of isomerization to isohexane of approximately $135 \pm 20\ kJ\,mol^{-1}$.[22] The protonated, isomerized intermediate remains strongly adsorbed. Further reaction only proceeds in the presence of gaseous hydrogen. Desorbing alkenes then will be hydrogenated by platinum to form the product alkanes. This is consistent with previous studies, which showed that the reaction has a positive order in hydrogen partial pressure in the absence of platinum.[23]

In summary a technique has been developed that enables the analysis of reactant concentration profiles as a function of time. Radiochemical PEP measurements with a great variety of alkanes extensively used in practice are now possible under a wide range of practical reaction conditions. Here we have demonstrated the use of the technique to probe the elementary reaction steps in the hydroisomerization of hexane.

Received: June 28, 1996 [Z 9271 IE]
German version: *Angew. Chem.* **1996**, *108*, 2964–2966

Keywords: heterogeneous catalysis · hydroisomerisations · radiolabeling · reaction mechanisms · zeolites

[1] I. E. Maxwell, W. H. J. Stork, *Stud. Surf. Sci. Catal.* **1991**, *58*, 571.
[2] H. W. Kouwenhoven, *Molecular Sieves (ACS Adv. Chem. Ser.* **1973**, *121*), p. 529.
[3] M. E. Phelps, J. C. Mazziotta, H. R. Schelbert, *Positron Imaging Computed Tomography and Autoradiography*, Raven Press, New York, **1986**.
[4] S. Webb, *The Physics of Medical Imaging*, Medical Science Series, Adam Hilger, Bristol, **1988**.
[5] J. Bridgwater, C. J. Broadbent, D. J. Parker, *Chem. Eng. Res. Des.* **1993**, *71*, 675.
[6] C. J. Broadbent, J. Bridgwater, D. J. Parker, *Chem. Eng. J.* **1995**, *56*, 119.
[7] G. Jonkers, K. A. Vonkeman, S. W. A. van der Wal, R. A. van Santen, *Nature* **1992**, *355*, 63.
[8] K. A. Vonkeman, G. Jonkers, R. A. van Santen, *Stud. Surf. Sci. Catal.* **1991**, *71*, 239.
[9] A. V. G. Mangnus, L. J. van IJzendoorn, J. J. M. de Goeij, R. H. Cunningham, R. A. van Santen, M. J. A. de Voigt, *Nucl. Instrument. Meth. Phys. Res. Sect. B* **1995**, *99*, 649.
[10] R. H. Cunningham, R. A. van Santen, J. van Grondelle, A. V. G. Mangnus, L. J. van IJzendoorn, *J. Chem. Soc. Chem. Commun.* **1994**, 1231.
[11] R. H. Cunningham, A. V. G. Mangnus, J. van Grondelle, R. A. van Santen, *Catal. Today* **1994**, *21*, 431.
[12] T. Koerts, P. A. Leclercq, R. A. van Santen, *J. Am. Chem. Soc.* **1992**, *114*, 7272.
[13] R. A. van Santen, B. G. Anderson, R. H. Cunningham, J. van Grondelle, L. J. van IJzendoorn, A. V. G. Mangnus, *Stud. Surf. Sci. Catal.* **1996**, *101*, 791.
[14] S. M. Davis, F. Zaera, G. A. Somorjai, *J. Catal.* **1982**, *77*, 439.
[15] S. Thomson, G. Webb, *J. Chem. Soc. Chem. Commun.* **1976**, 526.
[16] P. S. Cremer, G. A. Somorjai, *J. Chem. Soc. Faraday Trans.* **1995**, *94*, 3671.
[17] W. M. H. Sachtler, R. A. van Santen, *Adv. Catal.* **1977**, *26*, 69.
[18] P. B. Weisz, *Adv. Catal.* **1962**, *13*, 137.
[19] M. L. Coonradt, W. E. Garwood, *Ind. Eng. Chem. Prod. Res. Dev.* **1964**, *3*, 38.
[20] I. N. Senchenya, V. B. Kazansky, *Catal. Lett.* **1991**, *81*, 317.
[21] P. Viruela-Martin, C. M. Zicovich-Wilson, A. Corma, *J. Phys. Chem.* **1993**, *97*, 13713.
[22] A. van de Runstraat, P. J. Stobbelaar, J. van Grondelle, B. G. Anderson, L. J. van IJzendoorn, R. A. van Santen, *Stud. Surf. Sci. Catal.* **1996**, in press.
[23] A. Corma, J. Meusingen, *J. Catal.* **1995**, *152*, 189.

The Titanium(IV)-Catalyzed Epoxidation of Alkenes by *tert*-Alkyl Hydroperoxides**

Richard D. Oldroyd, John Meurig Thomas,* Thomas Maschmeyer, Philip A. MacFaul, Darren W. Snelgrove, Keith U. Ingold,* and Danial D. M. Wayner

Ever since it was reported that titanosilicalites, such as TS-1 synthesized by the company Enichem,[1] could catalytically and selectively oxidize certain organic compounds in the presence of H_2O_2 (for example, phenol to hydroquinone[2] and propene to propene oxide[3]), there has been considerable interest in other low-temperature selective oxidations with various kinds of Ti^{IV}-containing siliceous microporous catalysts.[4] Corma et al. have demonstrated the catalytic merit of using larger pore microporous materials,[5] such as Ti^{IV}-containing β-zeolite, and the commercially available *tert*-butyl hydroperoxide (TBHP) as a sacrificial oxidant.

Interest in Ti^{IV}-catalyzed epoxidations of alkenes has recently intensified, because Ti^{IV}-containing mesoporous MCM41 silicas with their larger pore apertures (typically 30 Å) are capable of oxidizing relatively bulky reactants.[6, 7] Two distinct kinds of Ti^{IV}-modified MCM41 epoxidation catalysts have been described. The first (Ti→MCM41) accommodates the titanium ions (identified along with distances between Ti and the O atoms attached to silicon by X-ray absorption spectroscopy)[6] within the walls of the mesoporous silica. The second (Ti↑MCM41) has the tetracoordinated Ti^{IV} ions grafted onto the inner surfaces of the mesoporous host and is formed from a titanocene dichloride precursor as recently described by Maschmeyer et al.[8, 9] The Ti→MCM41 reported here (Si:Ti ratio of 1:0.058) was synthesized from $Ti(OiPr)_4$, which was incorporated into the MCM41 synthesis gel, according to the procedure of Rey et al.[10] The Ti↑MCM41 used in this study had a Si:Ti ratio of 1:0.041.

Sheldon and co-workers have concluded that alkyl hydroperoxide catalyzed epoxidation of olefins occurs by a heterolytic mechanism in the presence of TiO_2–SiO_2 mixed-oxide cata-

[*] Prof. J. M. Thomas, Dr. R. D. Oldroyd, Dr. T. Maschmeyer
Davy-Faraday Research Laboratory
The Royal Institution of Great Britain
21 Albemarle Street, London W1X4BS (UK)
Fax: Int. code +(171)629 3569
Dr. K. U. Ingold, Dr. P. A. MacFaul, D. W. Snelgrove, Dr. D. D. M. Wayner
Steacie Institute for Molecular Sciences
National Research Council of Canada
100 Sussex Drive, Ottawa, Ontario K1A 0R6 (Canada)

[**] This work was supported by a ROPA award and rolling grant from the EPSRC (UK), and by a fellowship from the NRC (Canada).

lysts.[11] In this communication we show that this is also the case for our two catalyst systems, and, in addition, we answer the following questions:

1. Is 2-methyl-1-phenyl-2-propyl hydroperoxide (MPPH) an effective epoxidizing agent with our two catalysts?
2. Can MPPH be used as a reliable probe for free-radical mechanisms in other metal-catalyzed hydrocarbon oxidations utilizing *tert*-alkyl hydroperoxides as oxidizing agents ?
3. By how much does the reported[8] improved efficiency of epoxidation using a Ti^{IV} ion protruding from the silica surface (Fig. 1a) surpass that of buried Ti^{IV} ions (Fig. 1b)?

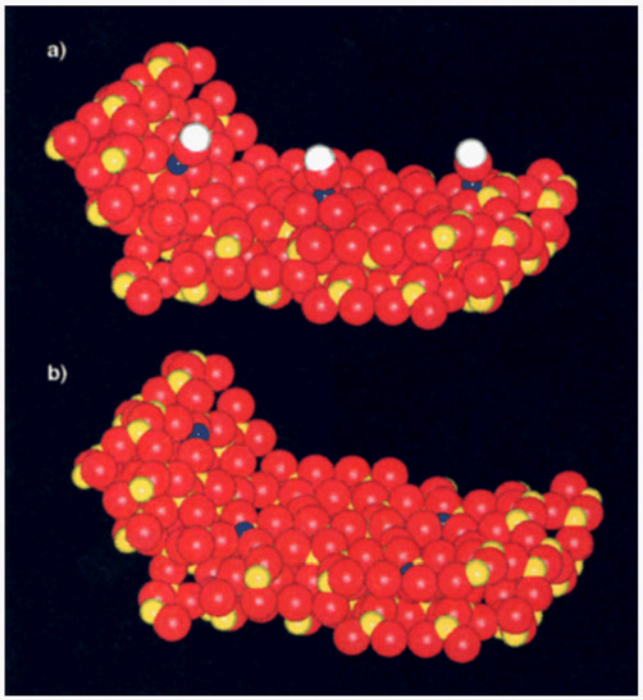

Fig. 1. Environment of the titanium ions in the two modified MCM41 catalysts. Blue = Ti, yellow = Si, red = O, white = H. a) Surface-grafted Ti↑MCM41 and b) framework-embedded Ti→MCM41. (Surface silanol groups have been omitted for clarity).

The importance of MPPH is that homolytic cleavage of its peroxidic O–O bond yields an alkoxyl radical (MPPO), which undergoes an extremely rapid β-scission ($k_1 \approx 2 \times 10^8\ s^{-1}$) [Eq. (a)].[12] The very short lifetime of the MPPO radical

$$\underset{\text{MPPH}}{PhH_2CMe_2OOH} \longrightarrow \underset{\text{MPPO}}{PhCH_2CMe_2O^{\bullet}} \xrightarrow{k_1} PhCH_2^{\bullet} + Me_2CO \qquad \text{(a)}$$

precludes reaction with any substrate at concentrations smaller than or equal to 1 M, even when the alkoxyl radical and substrate reaction is diffusion-controlled.

Some of us have recently used MPPH as a mechanistic probe in some iron(III)-catalyzed cycloalkane oxidations.[12–14] Previously[15, 16] *tert*-butyl hydroperoxide (TBHP) was employed as the oxidant, and cycloalkane oxidation products were formed. However, when TBHP was replaced by MPPH, no cycloalkane oxidation products were evident, the main products were instead benzyl alcohol, benzaldehyde, and bibenzyl, all of which clearly arise from the benzyl radical formed by β-scission of MPPO. The difference between TBHP and MPPH is most simply explained by the very much slower β-scission of the *tert*-butoxyl radical,[14] which has a sufficiently long lifetime for it to abstract a hydrogen atom from the cycloalkane. Despite the simplicity of this explanation, both explicit[17] and implicit[18] arguments have been made that MPPH is not a competent substitute for TBHP in iron(III)-catalyzed oxidations of cycloalkanes[17] and epoxidations of cycloalkenes.[18] Instead, nonradical mechanisms that involve TBHP coordination to the Fe^{III} centers are favored with subsequent heterolytic cleavage of the O–O bond to yield a high-valent iron–oxo intermediate (formally Fe^{V}=O) which inserts its oxygen atom into C–H and C=C bonds. Therefore, we decided to extend our studies of cyclohexene epoxidation by using our heterogeneous Ti^{IV} catalysts with both TBHP and MPPH in order to see whether MPPH is a competent replacement for TBHP in what is probably[11] a nonradical oxidation.

The first six entries in Table 1 show that epoxide is the major product with both TBHP and MPPH at room temperature; no products are formed in the absence of hydroperoxide. This convincingly proves that *tert*-alkyl hydroperoxides convert cyclohexene into cyclohexene oxide by a nonradical mechanism in the presence of both Ti↑MCM41 and Ti→MCM41. Moreover, MPPH is revealed to be an extremely effective oxidant, surpassing TBHP in this regard.[19] This is the first time, to our knowledge, that MPPH has been shown to be capable of oxidizing a hydrocarbon substrate. A third conclusion is that, as an epoxidation catalyst, Ti↑MCM41 is over ten times as active per Ti^{IV} ion as Ti→MCM41.[20]

If radicals had been involved in these Ti^{IV}-catalyzed oxidations, we would expect to obtain very little cyclohexene oxide relative to the yields of cyclohexenol, cyclohexenone, and *tert*-alkyl cyclohexenyl peroxide (see Scheme 1) and, with MPPH, products derived from benzyl radicals would be formed. These products were indeed produced when reactions were initiated by UV irradiation of the reactants in the absence of catalyst (see entries 10–12 in Table 1).

Table 1. Cyclohexene epoxidation at 25 °C in acetonitrile. Two numbers indicate the results from duplicate experiments.

No.	Catalyst	Oxidant	Cyclohexene oxide [%] [a]	Other products [%] [b]	Selectivity w.r.t. the epoxide [%] [c]	Turnover frequency [h^{-1}] [d]
1	Ti↑MCM41	TBHP	13.5, 12.4	0.7, 0.2	95.2, 98.7	16.4, 15.3
2	Ti↑MCM41	MPPH	36.3, 23.5	0.3, 0.4	99.2, 99.0	37.3, 28.9
3	Ti↑MCM41	air	0.0	0.0	0.0	0.0
4	Ti→MCM41	TBHP	1.8, 1.5	0.1, 0.1	94.4, 94.7	1.5, 1.3
5	Ti→MCM41	MPPH	3.3, 3.2	0.5, 1.8	88.3, 73.6	2.5, 2.7
6	Ti→MCM41	air	0.0	0.0	0.0	0.0
7	MCM41	TBHP	0.0	0.7 [e]	0.0	
8	MCM41	MPPH	0.0	0.0	0.0	
9	MCM41	air	0.0	0.0	0.0	
10	UV light	TBHP	0.3	9.6 [f]	2.5	
11	UV light	MPPH	0.1	28.6 [g]	0.3	–
12	UV light	air	0.0	0.0	0.0	
13	Ti↑MCM41	TBHP [h]	0.1	0.1	ca. 50	<0.1
14	Ti↑MCM41	MPPH [h]	0.0	0.0	0.0	0.0

[a] Percentages given are based on the amount of cyclohexene converted into cyclohexene oxide. [b] Other products derived from cyclohexene and in the case of MPPH reactions from benzyl radicals. [c] Based on cyclohexene-derived products. [d] Number of moles of epoxide produced per mole Ti^{IV} per hour. [e] Only cyclohexenol detected. [f] Cyclohexenol (6.6%), cyclohexenone (1.0%), and *tert*-butyl cyclohexenyl peroxide (1.9%). [g] Cyclohexenol (11.3%), benzyl alcohol (7.5%), and bibenzyl (9.8%). [h] The catalyst was pretreated with the indicated hydroperoxide.

 © VCH Verlagsgesellschaft mbH, D-69451 Weinheim, 1996 0570-0833/96/3523-2788 $ 15.00+.25/0

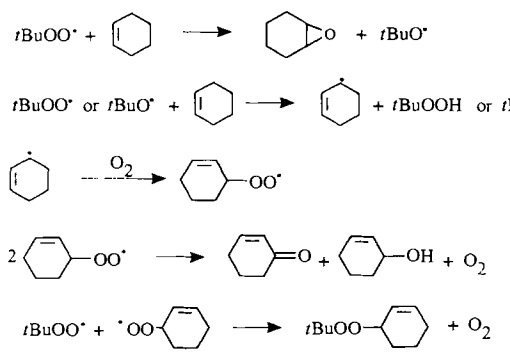

Scheme 1. Potential reactions between cyclohexene and TBHP under free-radical conditions.

The oxidation of *cis*-stilbene with *tert*-butyl peroxyl radicals, generated by the thermal decomposition of di-*tert*-butyl hyponitrite in the presence of TBHP [Eq. (b)], yields benzaldehyde and

$$t\mathrm{BuO{-}N{=}N{-}O}t\mathrm{Bu} \xrightarrow{\Delta} \mathrm{N_2} + 2\ t\mathrm{BuO}^{\bullet} \xrightarrow{2\ t\mathrm{BuOOH}} 2\ t\mathrm{BuOH} + 2\ t\mathrm{BuOO}^{\bullet} \quad \text{(b)}$$

trans-stilbene oxide in approximately equal amounts, together with a small quantity of *trans*-stilbene. However, reaction of *cis*-stilbene with TBHP or MPPH, in the presence of our two Ti^{IV} catalysts, gave *cis*-stilbene oxide as the only oxidation product (Table 2). (Low levels of *trans*-stilbene were also identified, which probably arose from photo- or acid-catalyzed isomerization on the mildly acidic surface of the support.) The formation of *cis*-stilbene oxide as the sole oxidation product provides further evidence in favor of a nonradical epoxidation mechanism.[21]

Table 2. *cis*-Stilbene epoxidation at 25 °C in acetonitrile. Two numbers indicate the results from duplicate experiments.

No.	Catalyst	Oxidant	*cis*-Stilbene oxide [%] [a]	*trans*-Stilbene [%] [a]	Selectivity w.r.t. the epoxide [%] [b]	Turnover frequency [h^{-1}] [c]
1	Ti↑MCM41	TBHP	5.4, 4.1	1.6, 1.2	77.3, 77.6	3.7, 2.4
2	Ti↑MCM41	MPPH	16.0, 17.9	0.7, 1.0	95.7, 94.9	9.7, 11.7
3	Ti↑MCM41	air	0.0	0.0	0.0	0.0
4	Ti→MCM41	TBHP	0.3, 0.4	1.8, 2.1	14.2, 17.1	0.1, 0.1
5	Ti→MCM41	MPPH	3.5, 1.9	0.9, 0.4	80.6, 84.5	1.0, 0.5
6	Ti→MCM41	air	<0.02	0.0	–	–
7	MCM41	TBHP	0.0	3.2	0.0	–
8	MCM41	MPPH	0.0	0.0	0.0	–

[a] Percentages given are based on the amount of *cis*-stilbene converted into the listed products. [b] Based on stilbene-derived products. [c] Moles of epoxide produced per mole Ti^{IV} per hour.

Pretreatment of Ti↑MCM41 with either neat TBHP or an acetonitrile solution of MPPH caused the initially white catalyst to turn yellow. This color was retained even after filtration and thorough washing with acetonitrile. Mixing the yellow, washed catalyst with cyclohexene gave little or no cyclohexene oxide (entries 13 and 14 in Table 1). If all the Ti centers managed to coordinate peroxide and if each of these reacted with one molecule of cyclohexene, approximately 2% conversion into epoxide should have been observed. Similar results have been previously obtained for a homogeneous titanium–porphyrin catalyst pretreated with TBHP in a similar fashion.[22] The obvious conclusion is that the yellow titanium–peroxo complex (presumably containing η^2-coordinated peroxide, based on a recent crystal structure of a model complex)[23] is not the oxygen atom transfer agent. This implicates a coordination of cyclohexene to the titanium center (as opposed to its merely reacting with coordinated peroxide from outside the coordination sphere). Further studies are in progress in order to gain greater insight into the nature of the active intermediate.

Since there are literature precedents for alkane oxidations catalyzed by titanium silicalites,[4b, 24] we assumed that cyclooctane would be oxidized by *tert*-alkyl hydroperoxides in the presence of Ti↑MCM41. However, with TBHP, no reaction took place at room temperature. Significant oxidation was only achieved when the temperature was increased to 70 °C with the formation of radical-derived products, namely, cyclooctanol, cyclooctanone, *tert*-butyl cyclooctyl peroxide, and cyclooctene oxide (the last presumably formed by catalytic oxidation of cyclooctene created during the reaction by cyclooctyl radical–radical disproportionation. The reaction with MPPH at the same temperature gave mainly benzyl alcohol.

In summary, we conclude that "surface-grafted" Ti↑MCM41 catalysts are substantially more active than "framework-embedded" Ti→MCM41 materials in terms of activity per titanium center. We have also demonstrated that MPPH is a better alkene epoxidizing agent than TBHP in the presence of these Ti^{IV}-modified MCM41 catalysts. It is clear that epoxidation proceeds by nonradical chemistry, and results indicate that the alkene and the peroxide must both be coordinated to the titanium centers for reaction to occur. MPPH is inactive as a cycloalkane oxidizing agent, which demonstrates that a radical mechanism is in operation. It is now abundantly evident that, whenever MPPH and TBHP give different hydrocarbon oxidation products in the presence of metal catalysts, there are compelling reasons to presume that both hydroperoxides are involved in free-radical and not in radical-free chemistry.

Experimental Procedure

Catalysts were prepared by published methods [8,10]. MPPH was synthesized by a slightly modified literature procedure [25]. TBHP and acetonitrile were distilled prior to use to remove water. Cyclohexene and *cis*-stilbene were purified to remove 2,6-di-*tert*-butyl-4-methylphenol (BHT) in the former and *trans*-stilbene in the latter. All experiments were performed under argon in degassed solutions, unless no hydroperoxide was used (these were carried out in air). At the end of all catalytic reactions, PPh_3 (1.5 g) was added to destroy any unchanged hydroperoxide. Products were analyzed by GC and GC-MS with either dibromobenzene or hexadecane as internal standards.

Cyclohexene oxidation: catalyst (75 mg) was added to cyclohexene (0.5 mL, 4.9 mmol), hydroperoxide (5 mmol), and acetonitrile (8 mL). The reaction was stopped after one hour.

cis-Stilbene oxidation: Ti↑MCM41 (40 mg) or Ti→MCM41 (65 mg) was added to *cis*-stilbene (0.5 mL, 2.7 mmol), hydroperoxide (3.1 mmol), and acetonitrile (5.2 mL). These reactions were carried out in a foil-covered reaction flask (to keep out light) for two hours.

Cyclooctane oxidation: Experiments were performed over 5 h at 70 °C, cyclooctane (0.67 mL, 5.0 mmol), peroxide (5.0 mmol), and acetonitrile (15 mL) in the presence of Ti↑MCM41 catalyst (75 mg).

Reactions with UV light: The solutions were made as above in quartz tubes, but no catalyst was added. They were then subjected to UV light for the specified time.

Hydroperoxide pretreatment of Ti↑MCM41: Ti↑MCM41 (150 mg) was stirred in either neat TBHP or an acetonitrile solution of MPPH for 3 h. The yellow material formed was filtered off, washed with acetonitrile (200 mL), and subsequently stirred in cyclohexene (0.5 mL) and acetonitrile (8 mL) overnight before analysis.

Di-*tert*-butyl hyponitrite and *cis*-stilbene: A mixture of hyponitrite (5.2 mg), TBHP (0.11 mL), glacial acetic acid (0.3 mL), pyridine (3 mL), and *cis*-stilbene (0.096 mL) were sealed in a vessel and kept at 37 °C in the dark for 72 h.

Received: July 16, 1996 [Z9337IE]
German version: *Angew. Chem.* **1996**, *108*, 2966–2969

Keywords: alkyl hydroperoxides · epoxidations · heterogeneous catalysis · titanosilicalite

[1] M. Tanamasso, B. Notari (Enichem), US-A 4410501, **1983** [*Chem. Abstr.* **1981**, *95*, 206272].

[2] M. Keshavaraja, V. Ramaswamy, H. S. Soni, A. V. Ramaswamy, P. Ratnasamy, *J. Catal.* **1995**, *157*, 501–511.

[3] M. G. Clerici, G. Belussi, U. Romano, *J. Catal.* **1991**, *129*, 159–167.

[4] a) B. Notari, *Stud. Surf. Sci. Catal.* **1988**, *37*, 413–425; b) T. Tatsumi, M. Nakamura, S. Negishi, H. Tominaga, *J. Chem. Soc. Chem. Commun.* **1990**, 476-477; c) D. R. C. Huybrechts, L. Debruycker, P. A. Jacobs, *Nature* **1990**, 345, 240–242; d) J. M. Thomas, *Philos. Trans. R. Soc. London A* **1990**, *333*, 173; e) M. S. Rigutto, R. Deruiter, J. P. M. Niederer, H. van Bekkum, *Stud. Surf. Sci. Catal. A–C* **1994**, *84*, 2245–2251; f) B. Notari, *Adv. Catal.* **1996**, *41*, 253–334.

[5] a) T. Blasco, A. Corma, M. T. Navarro, J. Perez-Pariente, *J. Catal.* **1995**, *156*, 65–74; b) M. A. Camblor, M. Constantini, A. Corma, L. Gilbert, P. Esteve, A. Martínez, S. Valencia, *Chem. Commun.* **1996**, 1339–1340; c) T. Blasco, M. A. Camblore, A. Corma, J. Perez-Pariente, *J. Am. Chem. Soc.* **1993**, *115*, 11806–11813; d) R. Hutter, D. C. M. Dutoit, T. Mallat, M. Schneider, A. Baiker, *J. Chem. Soc. Chem. Commun.* **1995**, 163–164.

[6] G. Sankar, F. Rey, J. M. Thomas, G. N. Greaves, A. Corma, B. R. Dobson, *J. Chem. Soc. Chem. Commun.* **1994**, 2279–2280.

[7] a) J. M. Thomas, *Nature* **1994**, *368*, 289–290; b) J. M. Thomas, G. N. Greaves, *Science* **1994**, *265*, 1675–1676; c) P. T. Tanev, M. Chibwe, T. J. Pinnnavaia, *Nature* **1994**, *368*, 321–323.

[8] T. Maschmeyer, F. Rey, G. Sankar, J. M. Thomas, *Nature* **1995**, *378*, 159–162.

[9] T. Maschmeyer, J. M. Thomas, A. F. Masters, *NATO ASI Conference*, Lucca, Italy **1995**.

[10] F. Rey, G. Sankar, T. Maschmeyer, J. M. Thomas, R. G. Bell, G. N. Greaves, *Top. Catal.* **1996**, *3*, 121–134.

[11] a) R. A. Sheldon, J. A. van Doorn, *J. Catal.* **1973**, *31*, 427–437; b) R. A. Sheldon, J. A. van Doorn, C. W. A. Schram, A. J. de Jong, *ibid.* **1973**, *31*, 438–443; c) R. A. Sheldon, *J. Mol. Catal.* **1980**, *7*, 107–126.

[12] I. W. C. E. Arends, K. U. Ingold, D. D. M. Wayner, *J. Am. Chem. Soc.* **1995**, *117*, 4710–4711.

[13] D. W. Snelgrove, P. A. MacFaul, K. U. Ingold, D. D. M. Wayner, *Tetrahedron Lett.* **1996**, *37*, 823–826.

[14] a) I. W. C. E. Arends, P. A. MacFaul, D. W. Snelgrove, D. D. M. Wayner, K. U. Ingold, *NATO ASI Conference*, Bardolino, Italy **1996**; b) P. A. MacFaul, I. W. C. E. Arends, K. U. Ingold, D. D. M. Wayner, *J. Chem. Soc. Perkin Trans. 2*, in press.

[15] a) R. A. Leising, R. E. Norman, L. Que, Jr., *Inorg. Chem.* **1990**, *29*, 2553–2555; b) R. A. Leising, Y. Zang, L. Que, Jr., *J. Am. Chem. Soc.* **1991**, *113*, 8555–8557; c) T. Kojima, R. A. Leising, S. Yan, L. Que, Jr., *ibid.* **1993**, *115*, 11328–11335; d) R. A. Leising, J. Kim, M. A. Perez, L. Que, Jr., *ibid.* **1993**, *115*, 9525–9530.

[16] D. H. R. Barton, W. Chavasiri, *Tetrahedron* **1994**, *50*, 19–30.

[17] J. Kim, R. G. Harrison, C. Kim, L. Que, Jr., *J. Am. Chem. Soc.* **1996**, *118*, 4373–4379.

[18] T. G. Traylor, C. Kim, J. L. Richards, F. Xu, C. L. Perrin, *J. Am. Chem. Soc.* **1995**, *117*, 3468–3474.

[19] The fate of MPPH after oxidation was determined by treating it with a 30-fold molar excess of cyclohexene in the presence of Ti↑MCM41 for 16 h. Analysis by GC (without quenching the reaction with PPh_3) revealed that the only major MPPH-derived product was the alcohol MPPOH, which was present in roughly similar amounts to the cyclohexene oxide produced (MPPOH:epoxide ≈1.2:1). This effectively demonstrates that MPPH does not form MPPO radicals, and hence epoxidation does not occur by peroxyl addition to the olefinic double bond followed by loss of the alkoxyl radical (see Scheme 1).

[20] Some very recent work by A. Corma et al, yet to be published, demonstrates that the maximum catalytic activity as a function of titanium loading for Ti→MCM41 is different from that for Ti↑MCM41. Therefore, in a "worst case scenario", we could possibly be comparing the most catalytically efficient loading for Ti↑MCM41 with a poorly efficient loading for Ti→MCM41.

[21] Under the same conditions *trans*-stilbene was not oxidized to *trans*-stilbene oxide. Since the pore dimensions of the catalyst are large enough to allow free passage of both *cis*- and *trans*-stilbene molecules throughout its structure, the lack of oxidation implies that steric effects may be important around the Ti^{IV} centers.

[22] H. J. Ledon, F. Varescon, *Inorg. Chem.* **1994**, *23*, 2735–2737.

[23] G. Boche, K. Möbus, K. Harms, M. Marsch, *J. Am. Chem. Soc.* **1996**, *118*, 2770–2771.

[24] a) C. B. Khouw, C. B. Dartt, J. A. Labinger, M. E. Davies, *J. Catal.* **1994**, *149*, 195–205; b) E. V. Spinacé, H. O. Pastore, U. Schuchardt, *ibid.* **1995**, *157*, 631–635.

[25] A. G. Davies, R. V. Foster, A. M. White, *J. Chem. Soc.* **1953**, 1541–1547.

Amide Backbones with Conformationally Restricted Furanose Rings: Highly Improved Affinity of the Modified Oligonucleotides for Their RNA Complements**

Alain De Mesmaeker,* Catherine Lesueur, Marc-Olivier Bévière, Adrian Waldner, Valérie Fritsch, and Romain M. Wolf

The replacement of phosphodiester bonds in natural 2′-deoxyoligonucleotides by amide bonds was recently described[1] for their application to the antisense strategy.[2] Among the five structural amide isomers we incorporated into oligonucleotides, compounds with modification 2 (Fig. 1) contributed to a slight increase in the thermodynamic stability of the duplexes formed with complementary RNA strands. Moreover, oligonucleotides with alternating phosphodiester and amide linkages showed a largely increased resistance towards endo- and exonucleases.

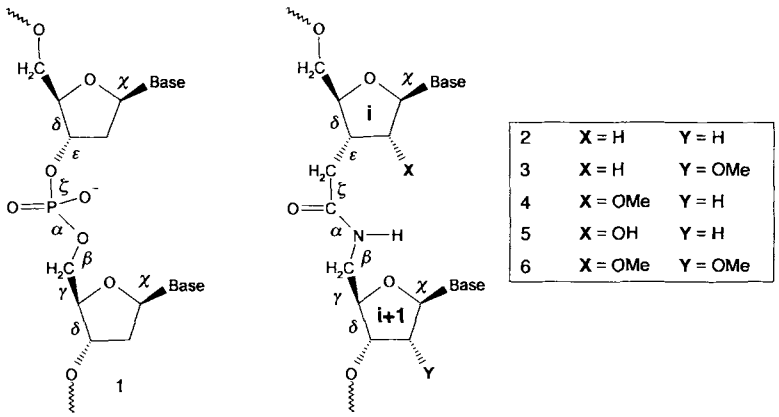

Fig. 1. Structure of a dimer in a natural DNA strand (left) and of modified dimers 2–6 (right). Torsion angles in the modified structure are defined as in natural nucleic acids (IUPAC-IUB, Joint Commission on Biochemical Nomenclature, *Eur. J. Biochem.* **1983**, *131*, 9). In modified strands where the modified residues alternate with wild-type monomers, there are two distinct types of residues: residue i, in which the modified backbone portion is attached to C3′, and residue i + 1, in which the modified linkage is attached at C5′.

The charge reduction might have a positive effect on their penetration into cells.[3] In light of the very promising properties of compounds with modification 2, we investigated further structural changes of this prototype in an effort to improve the affinity of the corresponding oligonucleotides for their RNA complements. Although many parameters may influence the potential activity of an oligonucleotide as antisense agent under physiological conditions,[2, 4] it is essential that the structural modifications introduced in this strand contribute substantially to an increase in affinity for an RNA target. We describe here the syntheses of dimers with the amide modifications 3–6, which carry additional 2′-substituents in their furanosyl residues, and the incorporation of these dimers into oligonucleotides (Fig. 1). The highly increased thermodynamic stability (a measure of which is the melting temperature T_m) of the du-

[*] Dr. A. De Mesmaeker, Dr. C. Lesueur, Dr. M.-O. Bévière, Dr. A. Waldner, Dr. V. Fritsch, Dr. R. M. Wolf
Central Research Laboratories, Ciba-Geigy
CH-4002 Basel (Switzerland)
Fax: Int code +(61) 697 82 52

[**] We thank Dr. U. Pieles and Dr. D. Hüsken for the synthesis and the purification of the oligonucleotides.

plexes formed between the oligonucleotides containing the modifications 3 and 6 and an RNA complement are presented together with a molecular modeling study.

Our NMR[5] and molecular mechanics studies[6] on RNA·DNA duplexes with DNA strands modified with 2 have shown that the furanose bearing the modified backbone portion at the C3′ end (i residue in Fig. 1) tends to adopt a conformation closer to C3′-*endo* than the sugar with the amide-modified portion attached at C5′ (i + 1 residue in Fig. 1). The latter was found to behave like the deoxyribose in an unmodified RNA·DNA duplex; that is, it oscillates between the C2′-*endo* and C3′-*endo* conformations.[7]

We postulated that an increase in the thermodynamic stability of the duplex might be achieved if both sugar moieties could be forced into the C3′-*endo* puckering conformation.[8] A 2′-O-alkyl substituent in a ribonucleoside having a phosphodiester or a phoshorothioate backbone favors the C3′-*endo* conformation of the five-membered ring[9] and increases the melting temperature T_m of the duplexes with an RNA complement.[10] However, the effect of a 2′-O-alkyl substituent on the sugar residues of a modified backbone is very difficult to predict. Depending on the preferred conformation adopted by a modified backbone, the effects of the puckering of the upper and lower sugar moieties will be different. Our molecular modeling and NMR data suggested that oligonucleotides containing modification 3 would display a better affinity than those containing the prototype 2 for a complementary RNA strand. In contrast, a 2′-O-alkyl substituent on the upper sugar moiety (as in modification 4) should not substantially influence the stability of the duplex because this residue already tends more to a C3′-*endo* conformation in the parent backbone 2. The combination of 2′-O-alkyl substituents on both sugar residues (as in modification 6) would thus lead to a thermal stability of the duplex that is similar or slightly better than that for modification 3. As described below, our hypotheses were fully validated by our experiments.

Modifications 3–6 were introduced into oligonucleotides as dimers containing a 5′-DMT group (DMT = dimethoxytrityl) and a phosphoramidite at the 3′-end. The required amines **3** and **4** were synthesized starting from 2′-OMe thymidine **1** (Scheme 1). The primary iodide was obtained in high yield by treatment of **1** with iodine and triphenylphosphane in pyridine.[11] After substitution with sodium azide and protection of the 3′-hydroxylic function with tBuPh$_2$SiCl, the intermediate **2** was obtained. The transformation of thymidine to the *N*-methylpyrrolidino-protected 5-methyl cytidine was realized in a high overall yield.[12] As in the case of the preparation of the dimer with the modification 2, the amine **4** was used without purification for the formation of the amide dimer.[13]

Initially we attempted the synthesis of the carboxylic acid derivative **10** (Scheme 2) by addition of the 3′-centered radical to allyltributyltin, followed by oxidative cleavage of the C–C double bond. This process is

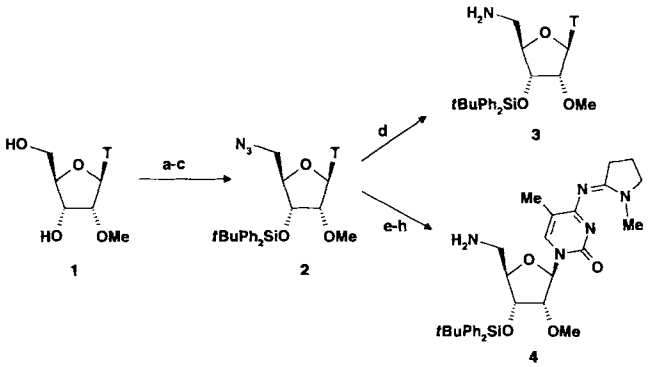

Scheme 1. a) 1.3 equiv I_2, 1.3 equiv PPh_3, Py, RT, 5 h (90%); b) 3 equiv NaN_3, DMF, 60 °C, 24 h (89%); c) 1.3 equiv tBuPh$_2$SiCl, 1.1 equiv (4-dimethylamino)pyridine (DMAP), 2 equiv imidazole, DMF, RT, 24 h (87%); d) 2 equiv $SnCl_2 \cdot 2H_2O$, MeOH, RT, 20 h (72%); e) 1.5 equiv p-$ClC_6H_4OPOCl_2$, 3 equiv 1*H*-1,2,4-triazole, Py, 50 °C, 20 h; f) NH_3 (aq.) (25%), dioxane, RT, 17 h (84%); g) 1.6 equiv *N*-methylpyrrolidinone dimethylacetal, THF/Py (1/1), RT, 20 h; h) 3 equiv $SnCl_2 \cdot 2H_2O$, MeOH, RT, 2 h (93%).

very efficient in the case of the 2′-deoxy derivatives.[1] In contrast, the radical addition reaction between allyltributyltin and the 3′-thionocarbonate derived from **1** (having a 2′-OMe substituent) furnished the β-3′-allyl derivative as the major product rather than the desired α-3′-allyl derivative. These difficulties could be circumvented by using the anhydro derivative **5**[14] (Scheme 2).

The radical addition of **6** to allyltributyltin was highly stereoselective because all the substituents were on the β face. Only the 3′-allyl derivative **7** was detected by ^{1}H NMR spectroscopy (500 MHz) of the crude reaction mixture. The anhydro ring was hydrolyzed, and the resulting thymine base was protected by treatment with BOMCl and DBU. The 2′-hydroxylic function was inverted by a Mitsunobu reaction with chloroacetic acid.[15] After removal of the chloroacetate residue with NaOMe, the resulting alcohol was methylated. Cleavage of the BOM-protective group was realized after dihydroxylation of the C–C double

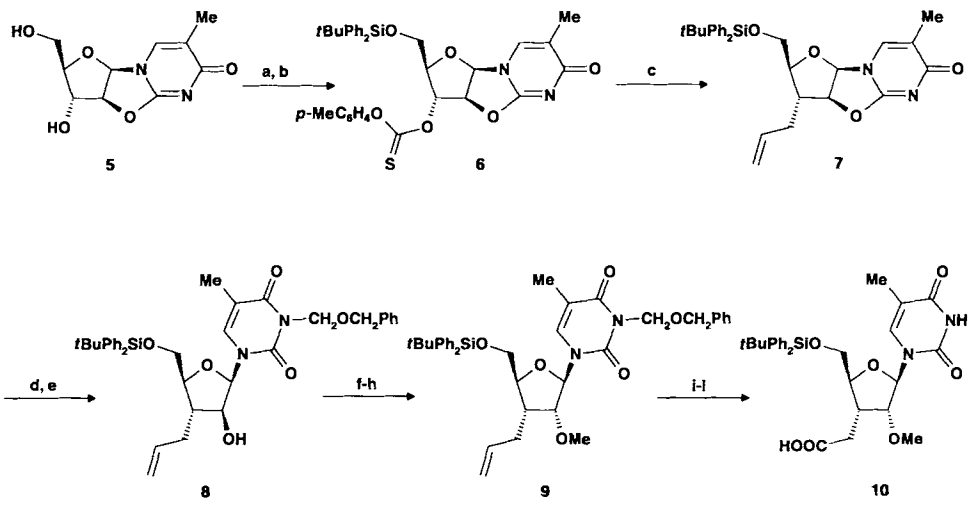

Scheme 2. a) 1.1 equiv tBuPh$_2$SiCl, 2 equiv imidazole, DMF, RT, 18 h (72%); b) 4 equiv p-MeC_6H_4OCSCl, 4 equiv NEt_3, 2 equiv DMAP, 10 equiv Py, CH_2Cl_2, RT, 40 h (82%); c) 5 equiv allyltributyltinn, 0.7 equiv α,α'-azobisisobutyronitrile (AIBN), benzene, 20 h under reflux (79%); d) 2 equiv NaOH (2 N), THF/H_2O (2/1), RT, 5 h (90%); e) 1.2 equiv benzyloxymethyl chloride (BOMCl), 1.2 equiv 1,8-diazabicyclo[5.4.0]undec-7-ene (DBU), MeCN, RT, 18 h (92%); f) 2.5 equiv PPh_3, 2.5 equiv diisopropylazodicarboxylate, 3 equiv $ClCH_2COOH$, toluene, RT, 50 h (83%); g) 0.3 equiv MeONa, MeOH, RT, 1 h (92%); h) 1.5 equiv NaH, 1.5 equiv MeI, THF, RT, 17 h (94%); i) 0.05 equiv OsO_4, 1.1 equiv *N*-methylmorpholine-*N*-oxide, acetone/H_2O (4/1), RT, 18 h (61%); j) H_2 (1 atm), Pd/C (10%), MeOH, RT, 18 h (83%); k) 1.1 equiv $NaIO_4$, dioxane/H_2O (3/1), RT, 18 h (81%); l) 6 equiv $NaClO_2$, 4 equiv 2-methyl-2-butene, 4 equiv $NaH_2PO_4 \cdot H_2O$, tBuOH/H_2O (5/3), RT, 30 min (92%).

bond in **9** with OsO_4. The desired carboxylic acid **10** was obtained by treatment with $NaIO_4$ and oxidation of the resulting aldehyde with $NaClO_2$. The coupling of the carboxylic acid **10** with the amines **3** or **4** was realized in high yield (Scheme 3, Table 1). The dimers were activated for the solid-phase synthesis of the corresponding oligonucleotides.[16]

Table 1. Yields of the synthesis steps a–d starting from the monomers **3**, **4**, **12**, and **13** via the dimers **14**–**18** (cf. Scheme 3; MeC* = 5-methyl-*N*-methylpyrrolidone).

	Monomer	Dimer		Yield [%]			
				a	b	c	d
3	T, Y = OMe	X = H, Y = OMe	T*T	79	95	78	71
4	MeC*, Y = OMe	X = H, Y = OMe	T*MeC*	70	80	80	79
12	T, Y = H	X = OMe, Y = H	T*T	80	91	81	74
13	MeC*, Y = H	X = OMe, Y = OMe	T*T	75	91	88	84
		X = OMe, Y = OMe	T*MeC*	80	70	74	83

For the synthesis of compounds with the modification 5, which carry a 2′-OH group on the upper sugar moiety, we developed a new strategy that relies on the stereoselective glycosylation of a primarily formed dimer that already contains a thymine residue on the lower sugar moiety (Scheme 4). The carboxylic acid **25**[17] was coupled in very good yield to the amine **12**.[1b] The selective removal of the 1,2-isopropylidene group in **26** with thiophenol in the presence of CF_3COOH afforded the β-thioglycoside in 51% yield. The stereoselective introduction of the second thymine base on the 2′-acetoxy derivative, obtained by acetylation (Ac_2O, Py, RT), was performed by glycosylation of the anomeric phenylsulfoxide **27**.[18] The selective oxidation of the thiophenyl derivative to the sulfoxide **27** was achieved at low temperature with purified *m*CPBA; this avoids the formation of the sulfone, which does not undergo the desired glycosylation reaction. The introduction of the upper thymine residue of **28** was performed in good yield (65%) without epimerization of the lower one and without interference (cyclization) of the amide bond of the backbone (Scheme 4). The corresponding phosphoramidite **29** was obtained after exchange of protective groups.

The melting temperature T_m of the duplexes formed between the modified oligonucleotides and their RNA and DNA complements are summarized in Table 2.[19] The T_m values obtained for the duplexes that contain the oligonucleotides with the modifications 3–6 are compared to the those for oligonucleotides of the parent modification 2 and the wild type 1.[1b, 13] A 2′-OMe substituent on the lower sugar unit of the amides (modifications 3 and 6) has a dramatic effect on the T_m value of the duplexes with RNA (sequence A): the additional 2′-OMe substituent in modification 3 increases the melting temperature by +1.7 °C compared to the value for modification 2. When the modification 3 was introduced in an alternating mode with phosphodiester linkages in sequence C, the T_m value increased by +2.5 °C per modification 3 with respect to the value for the wild type (sequence C). It is noteworthy that the increase of the melting

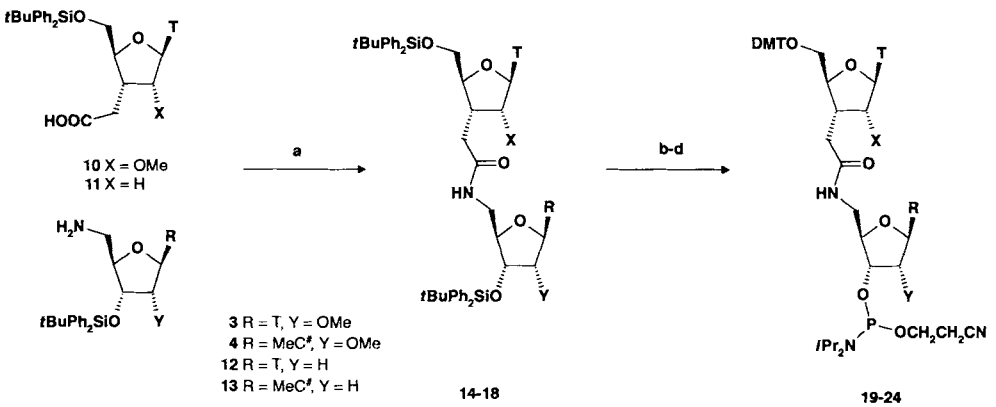

Scheme 3. a) 1.1 equiv NEt_3, 1.1 equiv *O*-(1*H*-benzotriazol-1-yl)-*N*,*N*,*N*′,*N*′-tetramethyluronium tetrafluoroborate, 0.5 equiv *N*-hydroxybenzotriazole, MeCN/THF (1/1), RT, 1 h; 1 equiv of the 5′-amino derivative, 1.5 equiv NEt_3, RT, 12 h; b) 2.2 equiv nBu_4NF, THF, RT, 9 h; c) 1.5 equiv dimethyloxytrityl chloride (DMTCl), Py, RT, 24 h; d) 2.2 equiv $(iPr_2N)_2POCH_2CH_2CN$, 2.2 equiv diisopropylammonium tetrazolide, CH_2Cl_2, RT, 24 h.

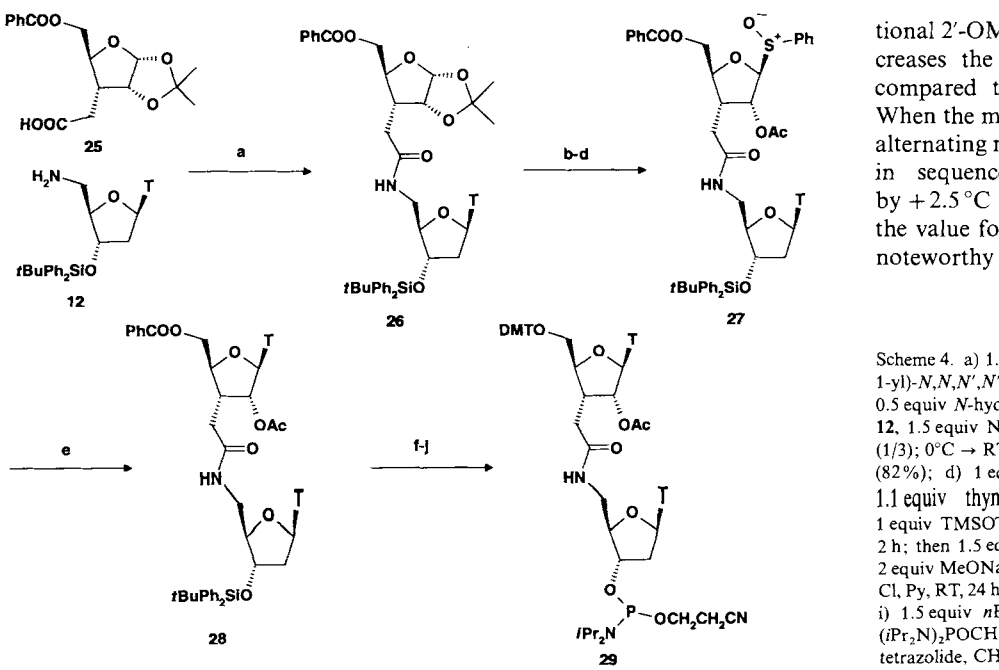

Scheme 4. a) 1.1 equiv NEt_3, 1.1 equiv *O*-(1*H*-benzotriazol-1-yl)-*N*,*N*,*N*′,*N*′-tetramethyluronium tetrafluoroborate, 0.5 equiv *N*-hydroxybenzotriazole, MeCN, RT, 1 h; 1 equiv **12**, 1.5 equiv NEt_3, RT, 12 h (89%); b) $PhSH/CF_3COOH$ (1/3); 0°C → RT, 7 h (51%); c) 15 equiv Ac_2O, Py, RT, 20 h (82%); d) 1 equiv *m*CPBA, CH_2Cl_2, −78 °C (96%); e) 1.1 equiv thymine, 2.2 equiv bistrimethylsilylacetamide, 1 equiv TMSOTf (Tf = triflate), 1,2-dichloroethane, 90 °C, 2 h; then 1.5 equiv $BF_3 \cdot OEt_2$, $CHCl_3$, RT, 18 h (65%); f) 2 equiv MeONa, MeOH, RT, 3 h (78%); g) 2.4 equiv DMTCl, Py, RT, 24 h (76%); h) 5 equiv Ac_2O, Py, RT, 20 h (48%); i) 1.5 equiv nBu_4NF, THF, RT, 3 h (94%); j) 2.3 equiv $(iPr_2N)_2POCH_2CH_2CN$, 2.2 equiv diisopropylammonium tetrazolide, CH_2Cl_2, RT, 24 h (92%).

 © VCH Verlagsgesellschaft mbH, D-69451 Weinheim, 1996 0570-0833/96/3523-2792 $ 15.00+.25/0

Table 2. Melting temperatures T_m [°C] of the wild type duplex 1 and differences between the melting temperatures ΔT_m [K] of duplexes that contain [5′ → 3′] oligonucleotides with modifications 2–5 and that of the wild type duplex [a].

Sequence	Oligonucleotide	Modification:	1	2	3	4	5	6
			T_m			ΔT_m [b]		
A	TTTT*TCTCTCTCTCT		51.6	+0.4	+2.1	0	−1.2	+2.6
B	T*TT*TT*CT*CT*CT*CT*CT		51.6	+0.6				
C	T*TT*TT*MeCT*MeCT*MeCT*MeCT*MeCT		56.9		+2.5			
D	GCGT*TT*TT*TT*TT*TGCG		50.2	−0.3	+2.0	+0.8		+3.0
E	TTTT*TCTCTCTCTCT		42.3	−1.7	−2.2			
F	GCGT*TT*TT*TT*TT*TGCG		54.1	−1.5	+0.1	−1.5		+0.6

[a] A–D with RNA complement, E–F with DNA complement. [b] $\Delta T_m = [T_m$(modified oligonucleotide) $- T_m$ (wild-type)$]/$(number of modified dinucleosides)

temperature gained with the additional 2′-OMe substituent in the case of the amide backbone 3 is greater than that observed for the natural phosphodiester backbone. Indeed, the T_m value that is reached with the 2′-OMe substituent on thymidine and 5-methylcytosine residues in sequence C is only +1.0 °C per modification higher than that of the corresponding natural 2′-deoxyribofuranosides.[20]

A 2′-OMe group on the upper sugar unit had a much less pronounced effect than the one on the lower sugar unit (modifications 4 and 3, respectively). The upper sugar adopted a conformation closer to the C3′-*endo* conformation in the parent amide modification 2. Therefore, the additional 2′-OMe group in modification 4 does not significantly change the puckering scheme of the ribofuranose ring. However, when a 2′-OH group is present, this can form an intramolecular hydrogen bond with the amide backbone. This would result in a conformational change of the backbone. The negative impact of the 2′-OH substituent in the upper sugar in modification 5 was confirmed experimentally ($\Delta T_m = -1.2$ °C). The substitution of both sugar residues with 2′-OMe groups (modification 6; sequences A and D) increased the T_m value by +2.6 and +3.0 °C, respectively, with respect to the value for the wild type.

Interestingly, the amide modifications 2, 3, 4, and 6 have a much less favorable effect on the thermodynamic stability of the duplexes formed with a DNA complement (sequences E, F) than with the RNA complement.

Molecular mechanics and dynamics studies have been carried out with the AMBER[21] force field as incorporated in the DISCOVER 2.9.5. software from BIOSYM Technologies, San Diego, USA. The conformational analysis was performed on octamer duplexes r[GA_6G]·d[CTTT*TTTC] with one modified dimer T*T in the middle of the DNA strand; molecular dynamics studies were carried out on alternatingly modified 14mer RNA·DNA duplex structures r[$G(A)_{12}G$]·d[$CT(T*T)_5TC$], by using the settings for amide modifications.[1, 6]

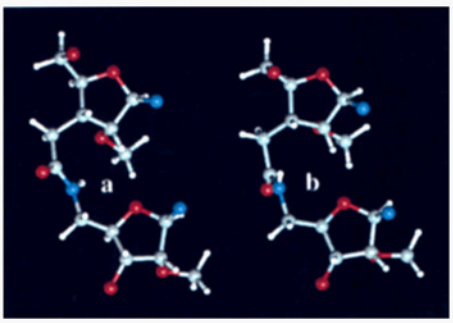

Fig. 2. Lowest energy conformations of modification 6 (modified dimer cut out of the DNA strand of the RNA·DNA octamer duplex). Conformation **b** is 0.5 kcal mol^{-1} higher in energy than conformation **a** (when the energies of the entire octamer hybrid duplex are compared) and differs mainly in torsion angles β(i) and ζ(i + 1) (see Fig. 1 for definitions).

Irrespective of the various modifications at C2′, the conformational analysis generally confirms the results found for the corresponding amide-modified backbone without further substituents at C2′. The two lowest energy conformations of the modifications 3–6 resemble **a** (lowest energy level) and **b** (second lowest energy level), as shown for modification 6 in Figure 2. Like for the parent structure 2, the conformation **b** is generally 0.5 to 1.5 kcal mol^{-1} higher in energy than conformation **a** (energy based on entire octamer duplex). The conformation **a** corresponds to $(\alpha, \beta, \gamma) \approx (t, t, t)$, a geometry sometimes observed in A-form DNA duplexes as a variant of the standard (g^-, t, g^+) backbone conformation of DNA.[22]

Molecular dynamics (MD) trajectories have been recorded for all modifications; the low-energy conformations were used as starting structures. Generally, standard Watson–Crick base pairing is conserved over the entire MD trajectories. However, some notable differences with respect to the unsubstituted amide modification 2 are observed. The introduction of an oxygen atom at C2′ of the furanose limits the sugar puckering to the C3′-*endo* puckering range; the phase angle of pseudorotation P[23] is around 18° (Fig. 3). Thus, the i + 1 residues in modifications 3 and 6 clearly behave differently from those in the unsubstituted modification 2. The effect of introducing an oxygen at the C2′ of the i residue is less pronounced, since even in modification 2, this sugar tends more to A-type puckering (average value for P is 86° for conformation **a** and 48° for conformation **b**).[6]

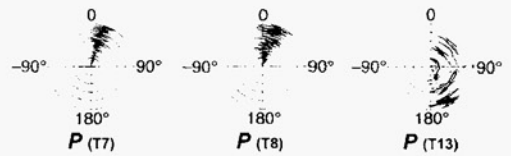

Fig. 3. Phase angle of pseudorotation P [23] of the bases T7, T8, and T13 in the DNA strand (modification 6) of a RNA·DNA 14mer duplex. The values are given in the form of polar coordinates with P as phase, and time as radial coordinate; circles represent intervals of 20 picoseconds. The sugars in T7 (i residue) and T8 (i + 1 residue) remain in the C3′-*endo* conformation, whereas the unmodified deoxyribose of T13 oscillates between the C3′-*endo* and C2′-*endo* conformations.

The average MD structure of the RNA·DNA duplex r[$G(A)_{12}G$]·d[$CT(T*T)_5TC$] (T*T: dimer with modification 6) is depicted in Figure 4. The ribbons symbolize the backbone, whose position was determined by instantaneous MD pictures recorded at intervals of 10 picoseconds. Qualitatively, this modified hybrid duplex behaves definitely more conservative during the molecular dynamics simulations than the corresponding wild-type duplex; this is mainly ascribed to the constrained C3′-*endo* puckering of the furanoses in the modified DNA strand. The modifications introduced in the DNA strand do not affect the RNA strand.[7]

In conclusion, we have designed and incorporated amide modifications into oligonucleotides that substantially increase their affinity for an RNA target compared to the wild type and

 © VCH Verlagsgesellschaft mbH, D-69451 Weinheim, 1996 0570-0833/96/3523-2793 $ 15.00+.25/0

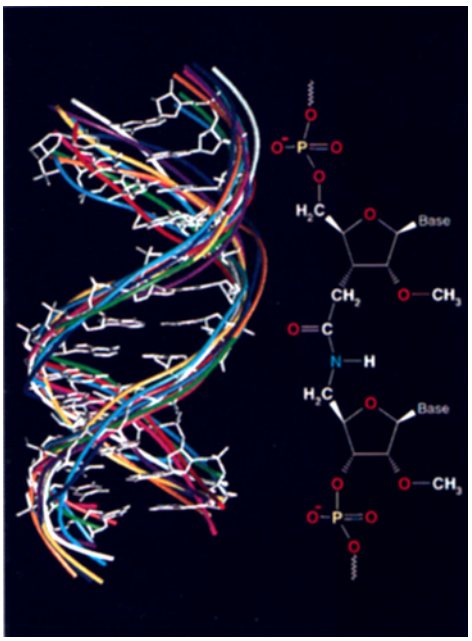

Fig. 4. Hybrid duplex RNA·DNA with an alternatingly modified DNA strand d[CT(T*T)$_5$TC]; T*T: dimer with the modification 6, X = Y = OMe (see Fig. 1). The structure corresponds to the molecular dynamics average structure (hydrogens are not shown). The ribbons pass through the backbones of momentary molecular dynamics structures spaced by 10 picoseconds.

to the parent modification 2. The introduction of a 2′-OMe group on the lower sugar moiety in the amide modifications 3 and 6 increased the T_m value of the duplexes with RNA by 2.0–3.0 °C. The second 2′-OMe substituent on the upper sugar moiety in modification 6 has also a positive effect on the thermodynamic stability of the duplex with an RNA complement, although less pronounced. The very large increase in T_m observed for modifications 3 and 6 results from the compatibility of the preferred conformations adopted by the amide backbone with the C3′-*endo* puckering of both furanose rings. These modifications are very promising for their application in the antisense strategy, in particular because of the increased stability of the corresponding oligonucleotides towards nucleases.

Received: June 21, 1996 [Z9251IE]
German version: *Angew. Chem.* **1996**, *108*, 2960–2964

Keywords: amides · antisense oligonucleotides · deoxysugars · molecular modeling · nucleic acids

[1] a) J. Lebreton, A. De Mesmaeker, A. Waldner, V. Fritsch, R. M. Wolf, S. M. Freier, *Tetrahedron Lett.* **1993**, *34*, 6383; b) A. De Mesmaeker, A. Waldner, J. Lebreton, P. Hoffmann, V. Fritsch, R. M. Wolf, S. M. Freier, *Angew. Chem.* **1994**, *106*, 237; *Angew. Chem. Int. Ed. Engl.* **1994**, *33*, 226; c) I. Idziak, G. Just, M. J. Damha, P. A. Giannaris, *Tetrahedron Lett.* **1993**, *34*, 5417; d) S. Wendeborn, R. M. Wolf, A. De Mesmaeker, *ibid.* **1995**, *36*, 6879; e) G. Stork, C. Zhang, S. Gryaznov, R. Schultz, *ibid.* **1995**, *36*, 6387; f) L. De Napoli, A. Iadonisi, D. Montesarchio, M. Varra, G. Piccialli, *Bioorg. Med. Chem. Lett.* **1995**, *5*, 1647; g) M. J. Robins, S. Sarker, M. Xie, W. Zhang, M. A. Peterson, *Tetrahedron Lett.* **1996**, *37*, 3921.

[2] a) E. Uhlmann, A. Peyman, *Chem. Rev.* **1990**, *90*, 543; b) S. T. Crooke, *Annu. Rev. Pharmacol. Toxicol.* **1993**, *32*, 329; c) A. De Mesmaeker, R. Haener, P. Martin, H. E. Moser, *Acc. Chem. Res.* **1995**, *28*, 366; d) A. De Mesmaeker, K.-H. Altmann, A. Waldner, S. Wendeborn, *Curr. Opin. Struct. Biol.* **1995**, *5*, 343.

[3] See for example a) Y. Shoji, S. Akhtar, A. Periasamy, B. Herman, R. L. Juliano, *Nucleic Acids Res.* **1991**, *19*, 5543; b) R. Fathi, Q. Huang, G. Coppola, W. Delaney, R. Teasdale, A. M. Krieg, A. F. Cook, *ibid.* **1994**, *22*, 5416.

[4] C. Moulds, J. G. Lewis, B. C. Froehler, D. Grant, T. Huang, J. F. Milligan, M. D. Matteucci, R. W. Wagner, *Biochemistry* **1995**, *34*, 5044.

[5] M. J. J. Blommers, U. Pieles, A. De Mesmaeker, *Nucleic Acids Res.* **1994**, *22*, 4187.

[6] V. Fritsch, A. De Mesmaeker, A. Waldner, J. Lebreton, M. J. J. Blommers, R. M. Wolf, *Bioorg. Med. Chem.* **1995**, *3*, 321.

[7] V. Fritsch, R. M. Wolf, *J. Biomol. Struct. Dyn.* **1994**, *11*, 1161, and references therein.

[8] For examples of backbone modifications with 2′-substituted furanosides see: a) X. Cao, M. D. Matteucci, *Bioorg. Med. Chem. Lett.* **1994**, *4*, 807; b) B. Meng, S. H. Kawai, D. Wang, G. Just, P. A. Giannaris, M. J. Damha, *Angew. Chem.* **1993**, *105*, 733; *Angew. Chem. Int. Ed. Engl.* **1993**, *32*, 729; c) E. R. Kandimalla, J. Temsamani, S. Agrawal, *Nucleosides Nucleotides* **1995**, *14*, 1031.

[9] W. Guschlbauer, K. Jankowski, *Nucleic Acids Res.* **1980**, *8*, 1421.

[10] H. Inoue, Y. Hayase, A. Imura, S. Iwai, K. Miura, E. Ohtsuka, *Nucleic Acids Res.* **1987**, *15*, 6131; b) E. A. Lesnik, C. J. Guinosso, A. M. Kawasaki, H. Sasmor, M. Zounes, L. L. Cummins, D. J. Ecker, P. D. Cook, S. M. Freier, *Biochemistry* **1993**, *32*, 7832.

[11] J. Huang, E. B. McElroy, T. S. Widlanski, *J. Org. Chem.* **1994**, *59*, 3520.

[12] L. J. McBride, R. Kierzek, S. L. Beaucage, M. H. Caruthers, *J. Am. Chem. Soc.* **1986**, *108*, 2040.

[13] J. Lebreton, A. Waldner, C. Lesueur, A. De Mesmaeker, *Synlett* **1994**, 137.

[14] R. F. Schinazi, M. S. Chen, W. H. Prusoff, *J. Med. Chem.* **1979**, *22*, 1273.

[15] M. Saïah, M. Bessodes, K. Antonakis, *Tetrahedron Lett.* **1992**, *33*, 4317.

[16] The oligonucleotides were prepared on an ABI 390 DNA synthesizer by using standard phosphoramidite chemistry according to M. J. Gait, *Oligonucleotide Synthesis: A Practical Approach*, IRL, Oxford **1984**, but with prolonged coupling times (10 min). DMT oligonucleotides were purified by reversed-phase HPLC (column: Nucleosil RPC$_{18}$, 10μm, 10 × 250 mm; eluent A: 50 mM triethylammonium acetate (TEAA), pH 7.0; eluent B: 50 mM TEAA, pH 7.0 in 70% acetonitrile; elution with gradient from A:B = 85:15 to 55:45 in 45 min). After purification by HPLC the oligonucleotides were checked by capillary gel electrophoresis (concentration: 35 μg oligonucleotide per mL; injection: 2 kV; separation; 9 kV; capillary: effective length 30 cm, internal diameter 100 μm, polyacrylamide 10% T; buffer: 100 mM H_3PO_4, 100 mM 2-amino-2-hydroxymethyl-1,3-propanediol (Tris), 2 mM ethylenediaminetetraacetate (EDTA), 7 M urea, pH 8.8). The molecular weight of each oligonucleotide was checked by mass spectrometry (MALDI-TOF: U. Pieles, W. Zürcher, M. Schär, H. Moser, *Nucleic Acids Res.* **1993**, *21*, 3191). The oligonucleotide was desorbed from a matrix of 2,4,6-trihydroxyacetophenone (detection of negatively charged ions) with diammonium hydrogen citrate as additive (25 mM final concentration).

[17] J. S. Pudlo, L. B. Townsend, *Tetrahedron Lett.* **1990**, *31*, 3101.

[18] L. Chanteloup, J. M. Beau, *Tetrahedron Lett.* **1992**, *33*, 5347.

[19] The thermal denaturation of DNA/RNA hybrids was performed at 260 nm with a Gilford Response II spectrophotometer (Ciba-Corning Diagnostics, Oberlin, OH, USA) or a Varian Cary 3 UV/Vis spectrophotometer. The extinction versus temperature profiles were measured for each strand (4 μM) in 10 mM phosphate (pH 7.0, Na^+ salts) with 100 mM total [Na^+] (supplemented as NaCl) and 0.1 mM EDTA. T_m values were obtained from fitting the extinction versus temperature curves to a two-state model with linear slope baselines (S. M. Freier, D. D. Albergo, D. H. Turner, *Biopolymers*, **1983**, *22*, 1107). All values are averages from at least three experiments. The absolute error of the T_m values is ±0.5 °C.

[20] P. Martin, *Helv. Chim. Acta* **1995**, *78*, 486.

[21] S. J. Weiner, P. A. Kollman, D. T. Nguyen, D. A. Case, *J. Comput. Chem.* **1986**, *7*, 230.

[22] a) C. A. Frederick, G. J. Quigley, M.-K. Teng, M. Coll, G. A. van der Marel, J. H. van Boom, A. Rich, A. H.-J. Wang, *Eur. J. Biochem.* **1989**, *181*, 295; b) B. Ramakrishnan, M. Sundaralingam, *Biochemistry* **1993**, *32*, 11458; c) *J. Mol. Biol.* **1993**, *231*, 43.

[23] S. T. Rao, E. Westhof, M. Sundaralingam, *Acta Crystallogr. Sect. A* **1981**, *37*, 421.

 © VCH Verlagsgesellschaft mbH, D-69451 Weinheim, 1996 0570-0833/96/3523-2794 $ 15.00+.25/0

Synthesis and Enzymatic Degradation of Dendrimers from (*R*)-3-Hydroxybutanoic Acid and Trimesic Acid**

Dieter Seebach,* Guido F. Herrmann, Urs D. Lengweiler, Beat M. Bachmann, and Walter Amrein

Dendrimers are attracting growing interest for use in stereoselective synthesis,[1] as a new type of material,[2] and in biological studies, for example as DNA carriers.[3] We now report on the first synthesis of monodisperse, enzymatically degradable, polyanionic dendrimers from (*R*)-3-hydroxybutanoic acid (HB)[4] and trimesic acid.

The convergent synthesis starts with the previously described[4] benzyl esters **1a** and **1b** of the dimer and the tetramer of HB, respectively, which were used as elongation units. For the assembly of the dendritic core and the branching units we employed the commercially available trimesic acid trichloride **3** and the TBDPS-protected 5-hydroxymethyl-1,3-benzenedicarboxylic acid dichloride **4**,[5] which can be easily obtained from the corresponding trimethyl trimesate. Acylation of the HB-oligomers **1** with **3** gave the core structures **5**, and debenzylation yielded the tricarboxylic acids **6**. Branching unit **7** was obtained by acylation of **1** with **4**. The branches **10** for the dendrimers of the second generation were synthesized starting from the silylated ester **7**, followed by debenzylation (→ **8**), then activation (→ **9**),[5] and subsequent acylation of the desilylated derivative of **7** with the acid chloride **9**. The coupling of **6** with the desilylated branches **7** and **10** finally gave the dendrimers of the first (green circle in formula **11**/**12**) and of the second generation (**11**), respectively. The selective hydrogenolysis of the terminal benzyl groups of the dendrimers was achieved by catalytic transfer hydrogenation[6] and gave the polyanionic dendrimers of the first and second generation (**12a**). The dendritic compounds were obtained in 150 mg (**11b**) to 450 mg (**11a**) quantities as viscous oils that were soluble in CH_2Cl_2. All compounds were fully characterized (optical rotation, IR, ^1H and ^{13}C NMR spectroscopy, MS, elemental analysis; see experimental part a); Figure 1 shows five MALDI-MS molecular peaks and proves the identity and the monodispersity of the corresponding compounds.

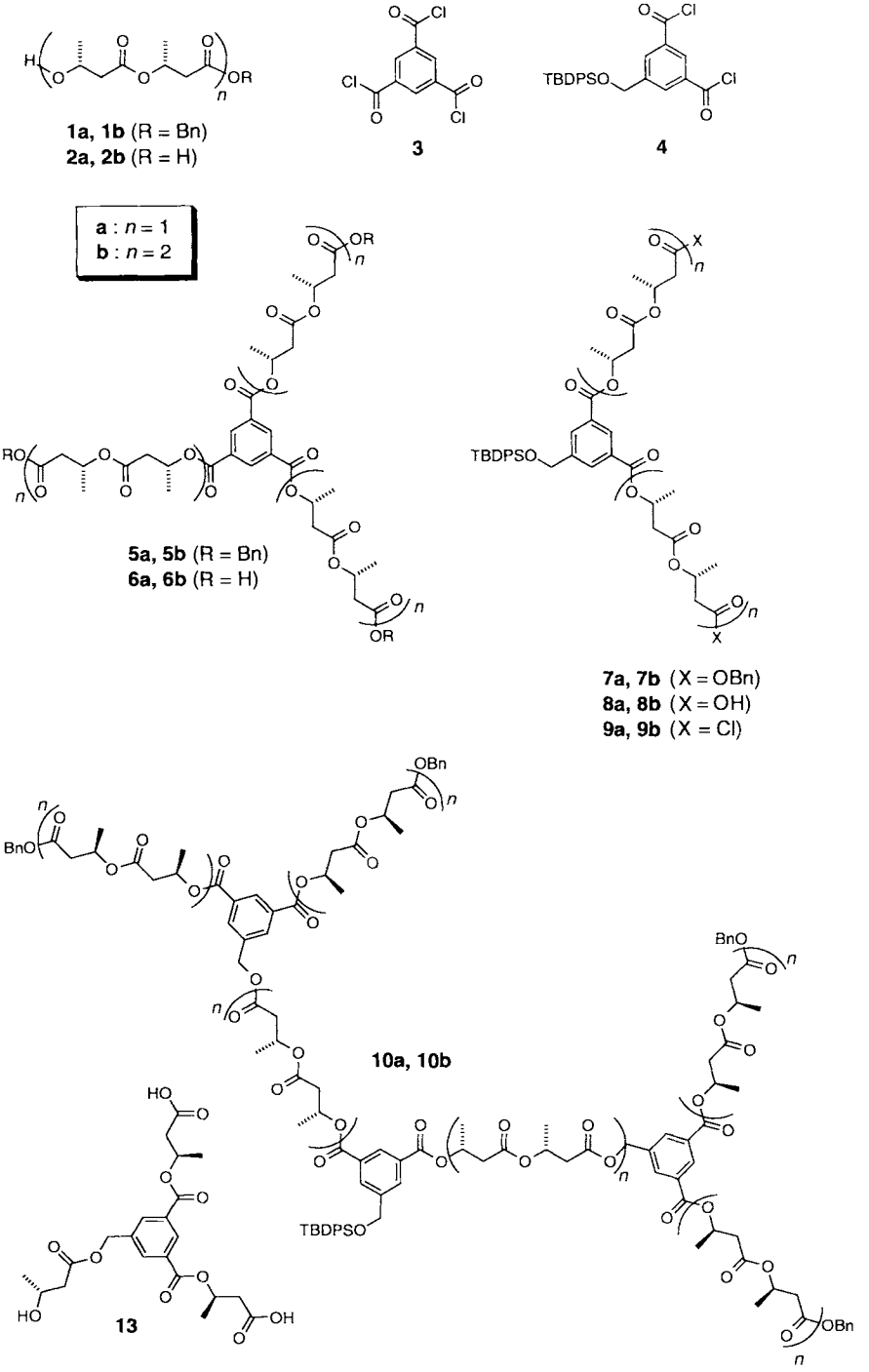

To study the biodegradability[7] of the dendrimers, we tested their stability in the presence of various hydrolases. Figure 2 depicts the degradation of three dendritic compounds **6a**, **6b**, and **11b** with a PHB-depolymerase.[8] The linear tetrameric HB **2b** was used as the standard substrate for the depolymerase. The protected dendrimers with dimeric HB-elongation units were not degraded by the depolymerase, whereas the free acids were moderately good substrates for this enzyme.[9] This observation is surprising as the simple dimeric HB **2a** is not a substrate for the depolymerase. ^1H NMR spectroscopic investigations of the degradation products of the deprotected, first-generation dendrimer with dimeric HB-elongation units (green circle in formula **11**/**12**) revealed free HB, the triester of 1,3,5-benzenetricarboxylic acid with HB, and also compound **13**.[10] The enzymatic hydrolysis of the deprotected, first-generation dendrimer, which has dimeric HB-elongation units, was followed by ti-

[*] Prof. Dr. D. Seebach, Dr. G. F. Herrmann, Dr. U. D. Lengweiler, dipl.-phil. II B. M. Bachmann, Dr. W. Amrein
Laboratorium für Organische Chemie
der Eidgenössischen Technischen Hochschule
ETH Zentrum, Universitätstrasse 16, CH-8092 Zürich (Schweiz)
Fax: Int. code +(1)632-1144
e-mail: seebach(@ org.chem.ethz.ch

[**] G. F. H. wishes to thank the Deutsche Forschungsgemeinschaft for financial support. This paper contains parts of the dissertation of U. D. L. (Dissertation No. 11405, ETH Zürich, 1995) and parts of the projected dissertation of B. M. B. We thank Metabolix Inc., Cambridge, MA for the generous donation of transformed *E. coli*, Prof. Dr. Robert W. Lenz (University of Massachusetts, Amherst) for helping us with the isolation of the PHB-depolymerase, and Monica G. Fritz (ETH) for compound **1b**.

 © VCH Verlagsgesellschaft mbH, D-69451 Weinheim, 1996 0570-0833/96/3523-2795 $ 15.00+.25/0

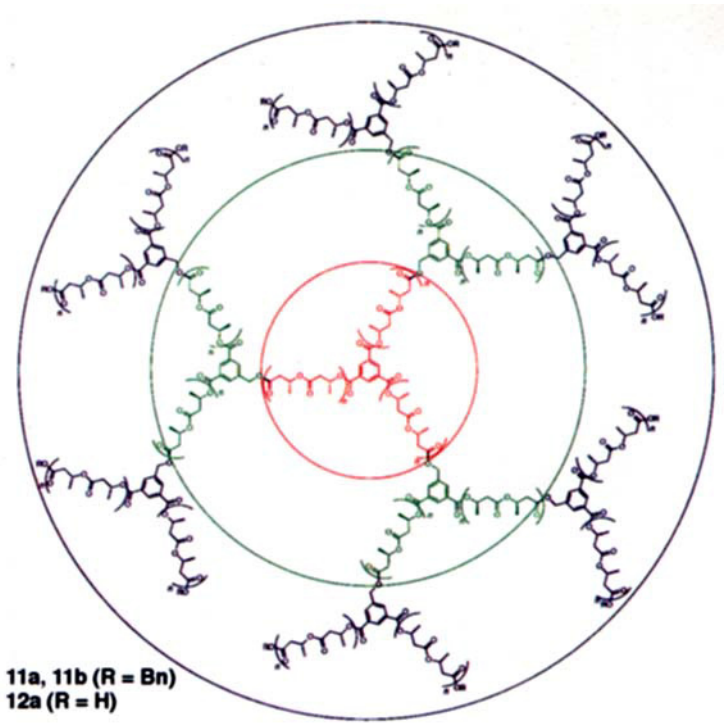

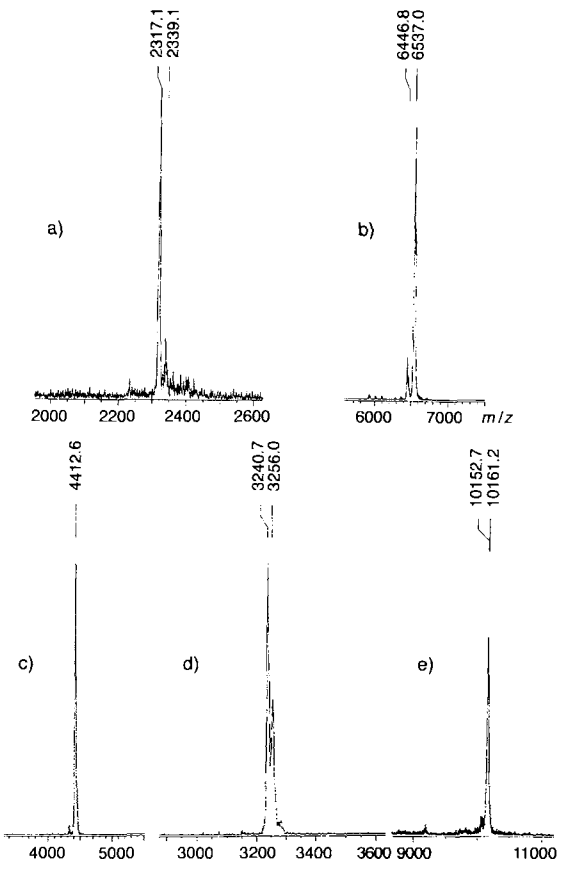

Fig. 1. Characterization of the dendrimers and the building blocks by mass spectrometry (MALDI-MS): a) first generation with dimeric HB-elongation units and free acid groups ($C_{108}H_{132}O_{54}$, 2294.2 g mol^{-1}, 2317 $[M+Na]^+$); b) second generation with dimeric HB-elongation units and R = Bn (**11a**: $C_{342}H_{384}O_{126}$, 6510.7 g mol^{-1}, 6537 $[M+Na]^+$); c) first generation with tetrameric HB-elongation units and protected acid groups ($C_{222}H_{282}O_{90}$, 4390.6 g mol^{-1}, 4412 $[M+Na]^+$); d) protected branch of the second generation with tetrameric HB-elongation units (**10b**: $C_{167}H_{206}O_{61}$, 3217.5 g mol^{-1}, 3240 $[M+Na]^+$, 3256 $[M+K]^+$); e) second generation with tetrameric HB-elongation units and R = Bn (**11b**: $C_{510}H_{640}O_{210}$, 10130.5 g mol^{-1}, 10153 $[M+Na]^+$).

tristatic experiments over 24 hours. More than five equivalents of base were consumed, which corresponds to a conversion of more than 55%. Like **2b**, all dendrimers with tetrameric HB-elongation units are good substrates for the depolymerase (Fig. 2). Zero-order kinetics is observed for the first de-

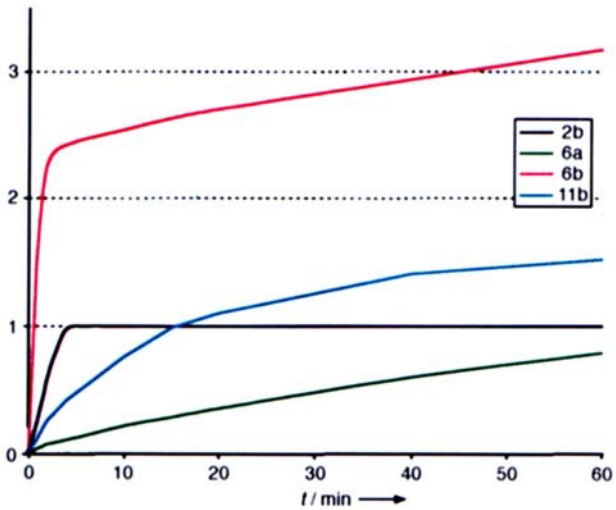

Fig. 2. Enzymatic degradation of the tetrameric HB **2b**, the core unit **6**, and the second-generation dendrimer **11b** with the PHB-depolymerase (0.25 mg mL^{-1} substrate in H_2O, 4.25 U mL^{-1} depolymerase from *Alcaligenes faecalis* [8], pH = 7.5, 30 °C). x = "acid equivalents" formed, in arbitrary units.

gradation step. The reaction is about one hundred times faster than the degradation of dendrimers with dimeric HB-elongation units. In the second degradation step (also zero order), the kinetics is comparable with that of dendrimers with dimeric HB-elongation units. Furthermore, the dendritic compounds were degraded by an esterase, a lipase, and a protease.[11]

In conclusion, we have described the first examples of biodegradable[7] dendrimers, which may have applications in materials science (for example, for the construction of defined nanocavities[2h]) that are similar to those for chemically degradable dendritic and hyperbranched organosilicon compounds.[12] Furthermore, they could possibly be used as drug carriers.[3]

Experimental Procedure

a) Analytical data of two selected compounds [13]:

11a (6510.7 g mol^{-1}): 48% yield (450 mg of material purified on 75 g silica gel, eluent CH_2Cl_2/Et_2O 4/1) for the coupling of **6a** and 3 equiv. desilylated **10a**). $[\alpha]_D = -32.9$ ($c = 1.275$, CH_2Cl_2); IR ($CHCl_3$, cm^{-1}): $\tilde{\nu}$ = 3035 w, 2986 w, 1735 vs, 1607 w, 1498 w, 1455 m, 1383 m, 1303 s, 1248 s, 1135 s, 1101 m, 1057 s, 973 w; ^{1}H NMR (500 MHz, $CDCl_3$): δ = 8.75 (s, 3H, arene H), 8.53 (t, J = 1.57 Hz, 9H, arene H), 8.15 (d, J = 1.58 Hz, 6H, arene H), 8.14 (d, J = 1.60 Hz, 12H, arene H), 7.34–7.27 (m, 60H, arene H), 5.55–5.44 (m, 21H, HC), 5.34–5.26 (m, 21H, HC), 5.18–5.10 (m, 18H, H_2C), 5.09–5.05 (m, 24H, H_2C), 2.88–2.50 (m, 84H, H_2C), 1.44–1.38 (m, 63H, H_3C), 1.25–1.21 (m, 63H, H_3C); ^{13}C NMR (125 MHz, $CDCl_3$): δ = 169.83, 169.69, 169.09, 169.00, 164.44, 136.75, 135.67, 133.21, 131.21, 130.35, 128.54, 128.30, 128.28, 68.89, 68.63, 68.57, 67.69, 67.56, 67.52, 66.41, 65.22, 40.98, 40.91, 40.62, 40.36, 19.83, 19.78; MALDI-MS (see Fig. 1b): 6537.0 $[M+3H+Na]^+$; Analysis calcd for $C_{342}H_{384}O_{126}$: C 63.06, H 5.99; found: C 62.99, H 6.20.

10b (3217.48 g mol^{-1}): 69% yield (900 mg of material purified on 80 g silica gel, eluent CH_2Cl_2/Et_2O 8/1) for the coupling of **9b** and 2 equiv. desilylated **7b**). $[\alpha]_D = -16.03$ ($c = 1.135$, CH_2Cl_2); IR ($CHCl_3$, cm^{-1}): $\tilde{\nu}$ = 3032 m, 2986 m, 2936 m, 2878 w, 1736 vs, 1607 w, 1497 w, 1456 s, 1383 s, 1302 s, 1177 m, 1134 s, 1101 m, 1056 s, 976 m; ^{1}H NMR (400 MHz, $CDCl_3$): δ = 8.54 (t, J = 1.63 Hz, 2H, arene H), 8.48 (s, 1H, arene H), 8.17 (s, 2H, arene H), 8.15 (d, J = 1.59 Hz, 4H,

 © VCH Verlagsgesellschaft mbH, D-69451 Weinheim, 1996 0570-0833/96/3523-2796 $ 15.00+.25/0

arene H), 7.67–7.65 (d, J = 7.02 Hz, 4H, arene H), 7.42–7.30 (m, 26H, arene H), 5.54–5.49 (m, 6H, HC), 5.30–5.18 (m, 18H, HC), 5.17 (d, J = 3.13 Hz, 4H, H_2C), 5.10 (s, 8H, H_2C), 4.82 (s, 2H, H_2C), 2.81–2.35 (m, 48H, H_2C), 1.42 (d, J = 6.31 Hz, 9H, H_3C), 1.41 (d, J = 6.26 Hz, 9H, H_3C), 1.28–1.20 (m, 54H, H_3C), 1.11 (s, 9H, $(H_3C)_3C$); ^{13}C NMR (100 MHz, $CDCl_3$): 169.88, 169.71, 169.14, 169.11, 169.07, 164.46, 136.76, 135.69, 135.51, 133.24, 131.22, 130.39, 129.86, 128.57, 128.31, 127.80, 68.61, 68.29, 67.66, 67.63, 67.56, 67.49, 66.44, 65.23, 40.96, 40.75, 40.64, 40.39, 26.81, 19.89, 19.78, 19.75, 19.69; MALDI-MS (see Fig. 1d): 3256.0 $[M + K]^+$; 3240.7 $[M + Na]^+$; Analysis calcd for $C_{167}H_{206}O_{61}Si$: C 61.73, H 6.39; found: C 61.80, H 6.39.

b) Determination of the biodegradability: The substrate (1.0 mg) was dissolved or suspended in 4 mL H_2O. The pH was adjusted to 7.5 after which the hydrolase was added. The pH was kept constant throughout the addition of 5 mM NaOH at 30 °C, and the consumption of base was recorded (1 U = 1 μmol acid formed per min^{-1}). Enzymes used for the experiments: 35 mg of a PHB-depolymerase [8] (from *Alcaligenes faecalis*, 486 U mg^{-1} [14]), 1 mg of an esterase (from pig liver, 220 U mg^{-1} [14]), 1 mg of a lipase (from *Pseudomonas fluorescens*, 42 U mg^{-1} [14]) and 1.25 mg of a protease (trypsin, from bovine pancreas).

Received: July 25, 1996 [Z9377IE]
German version: *Angew. Chem.* **1996**, *108*, 2969–2972

Keywords: biodegradability · chirality · dendrimers · enzymes

[1] P. Murer, D. Seebach, *Angew. Chem.* **1995**, *107*, 2297; *Angew. Chem. Int. Ed. Engl.* **1995**, *34*, 1995.

[2] a) J. Issberner, R. Moors, F. Vögtle, *Angew. Chem.* **1994**, *106*, 2507; *Angew. Chem. Int. Ed. Engl.* **1994**, *33*, 2413; b) G. R. Newkome, *Advances in Dendritic Macromolecules, Vols. 1 and 2*, Jai, Greenwich, **1994**, **1995**; c) J.-J. Lee, W. T. Ford, *Macromolecules* **1994**, *27*, 4632; d) R. G. Duan, L. L. Miller, D. A. Tomalia, *J. Am. Chem. Soc.* **1995**, *117*, 10783; e) P. G. H. M. Muijselaav, H. A. Claessens, C. A. Cramers, J. F. G. A. Jansen, E. W. Meijer, E. M. M. de Brabander-va den Berg, S. van de Wal, *J. High Resol. Chromatogr.* **1995**, *18*, 121; f) V. Percec, P. Chu, G. Ungar, J. Zhou, *J. Am. Chem. Soc.* **1995**, *117*, 11441; g) D. Bradley, *Science* **1995**, *270*, 1924; h) J. M. Tour, *Chem. Rev.* **1996**, *96*, 537; i) G. R. Newkome, C. N. Moorefield, F. Vögtle, *Dendritic Molecules: Concepts, Syntheses, Perspectives*, VCH, Weinheim, **1996**.

[3] a) O. Boussif, F. Lezoualc'h, M. A. Zanta, M. D. Mergny, D. Scherman, B. Demeneix, J.-P. Behr, *Proc. Natl. Acad. Sci. USA* **1995**, *92*, 7297; b) J. F. Kukowska-Latallo, A. U. Bielinska, J. Johnson, R. Spindler, D. A. Tomalia, J. R. Baker, Jr., *Proc. Natl. Acad. Sci. USA* **1996**, *93*, 4897.

[4] a) H.-M. Müller, D. Seebach, *Angew. Chem.* **1993**, *105*, 483; *Angew. Chem. Int. Ed. Engl.* **1993**, *32*, 477; b) U. D. Lengweiler, M. G. Fritz, D. Seebach, *Helv. Chim. Acta* **1996**, *79*, 670.

[5] Compound **4** was synthesized by reduction of trimethyl 1,3,5-benzenetricarboxylate with lithium aluminum hydride, chromatographic separation of the singly and doubly reduced compounds, followed by silylation of the hydroxyl group and saponification of the ester group, and subsequent conversion to the acid chloride with $(COCl)_2$ (this reagent was also used for the synthesis of **9** and for the activiation of the tricarboxylic acid **6** for the coupling with desilylated **7**/**10**).

[6] The hydrogenolysis was carried out in DMF with Pd/C as catalyst and 1,4-cyclohexadiene as hydrogen source; a) A. M. Felix, E. P. Heimer, T.-J. Lambros, C. Tzougraki, J. Meienhofer, *J. Org. Chem.* **1978**, *43*, 4194; b) J. S. Bajwa, *Tetrahedron Lett.* **1992**, *33*, 2299; c) G. M. Anantharamaiah, K. Sivanandaiah, *J. Chem. Soc. Perkin Trans. 1* **1977**, 490.

[7] a) A. L. Iordanskii, T. E. Rudakova, G. E. Zaikov, *Interaction of Polymers in Bioactive and Corrosive Media*, VSP BV, Utrecht, The Netherlands, **1994**; b) E. Wintermantel, S.-W. Ha, *Biokompatible Werkstoffe und Bauweisen*, 1st ed., Springer, Berlin, Heidelberg, New York, **1996**. The authors define polymers as biodegradable, if the degradation follows at least one of the following mechanisms: 1. disintegration of the polymer, 2. nonspecific hydrolysis, 3. enzymatic degradation, 4. dissociation of polymer–polymer complexes.

[8] Isolation and purification of PHB-depolymerase from *A. faecalis*, of which the gene was overproduced in *E. coli*, was carried out as described in T. Saito, K. Suzuki, J. Yamamoto, T. Fukui, K. Miwa, K. Tomita, S. Nakanishi, S. Odani, J.-I. Suzuki, K. Ishikawa, *J. Bacteriol.* **1989**, *171*, 184.

[9] v_{max}^{app} [U mg^{-1}]: **2a**: 0; **2b**: 24.5; **5a**: 0; **5b**: 1.9/0.32; **6a**: 0.5; **6b**: 38.6/0.24; protected, first-generation dendrimer with dimeric HB-elongation units: 0; deprotected, first-generation dendrimer with dimeric HB-elongation units: 0.32; protected, first-generation dendrimer with tetrameric HB-elongation units: 0.84/<0.1; deprotected, first-generation dendrimer with tetrameric HB-elongation units (two-stage kinetics): 25.7/0.18; **11a**: 0; **11b**: <0.1; **12a**: 0.24 (all values are given for the PHB-depolymerase).

[10] The signals of 9 of a total of 18 HB-methine protons in the intact, deprotected, first-generation dendrimer with dimeric HB-elongation units (green circle in formula **11**/**12**; see Fig. 1a; ^1H NMR (500 MHz, $CDCl_3$): 5.19–5.38 (m, 9H, HC)) shifted in a characteristic manner after enzymatic degradation for 72 h (^1H NMR (300 MHz, CD_3OD): 4.23–4.18 (m, 3H, HC); 4.08–4.02 (m, 6H, HC)). The integral of the last signal and its chemical shift correspond to the expected 6 equivalents of free HB.

[11] Deprotected, first-generation dendrimer with dimeric HB-elongation unit: v_{max}^{app} [U mg^{-1}]: 0.3 (PHB-Depolymerase), 10^{-3} (esterase), 10^{-3} (lipase), 0.4 (trypsin); for further details about the enzymes employed, see [8] and experimental part (b).

[12] a) A. M. Muzafarov, M. Golly, M. Müller, *Macromol.* **1995**, *28*, 8444; b) A. M. Muzafarow, A. Rebrov, O. B. Gorbacevich, M. Golly, H. Gankema, M. Müller, *Macromol. Symp.* **1996**, *102*, 35.

[13] The optical rotations of the dendrimers do not exhibit any significant dependence upon their generation or the number of HB-molecules in the elongation units, see experimental part (a).

[14] The activities [U] refer to the standard substrate of the corresponding enzyme.

Synthesis and a Preliminary DNA Binding Study of Hybrids of the Carbohydrate Domain of Calicheamicin γ_1^I and the Aglycone of Daunorubicin: Calichearubicins A and B**

Kristopher M. Depew, Steven M. Zeman, Serge H. Boyer, Derek J. Denhart, Norihiro Ikemoto, Samuel J. Danishefsky,* and Donald M. Crothers

Many important medicinal agents of natural origin contain a sugar or sugarlike moiety. From a chemical standpoint, such agents can be dissected into aglycone and carbohydrate domains. In most instances, both components in themselves are totally lacking in useful biological activity.[1] Traditionally, considerations about the mechanism of action of the drug have been directed to the aglycone, with the carbohydrate viewed as a necessary appendage for biotransport or for other factors related to drug availability.

While the nature of interplay of the aglycone and carbohydrate components in various drugs presumably varies from case to case, it is now apparent that in some important instances the carbohydrate domain may play a critical role in drug receptor recognition. One example of such a critical role for the carbohydrate sector in receptor contact is that of the enediyne antibiotics[2] such as calicheamicin γ_1^I (**1**)[3] (Fig. 1). Work from our laboratories,[4] as well as from Nicolaou et al.[5] and others[6–8] has established that contacts between the pentacyclic carbohydrate region and the minor groove of DNA provide much of the remarkable sequence selectivity of calicheamicin γ_1^I. Similarly, such interactions also foster the molecular contacts between esperimicin A_1 and its target DNA.[9] Though the aglycones such as calicheamicinone (**2**) retain cytotoxicity and some double-strand cleaving ability, sequence selectivity requires the existence of the carbohydrate domain.[4c] Indeed, moderate sequence selectivity can be realized through co-incubation of non-

[*] Prof. S. J. Danishefsky,[a–c] K. M. Depew,[b] S. M. Zeman,[a] S. H. Boyer,[a] D. J. Denhart,[b] N. Ikemoto,[c] Prof. D. M. Crothers
[a] Department of Chemistry, Yale University
225 Prospect Street, New Haven, CT, 06511 (USA)
Fax: Int. code +(212) 772–8691
[b] Department of Chemistry, Columbia University
Havemeyer Hall, New York, NY 10027 (USA)
[c] Laboratory for Bioorganic Chemistry
The Sloan-Kettering Institute for Cancer Research
1275 York Avenue, New York, NY 10021 (USA)

[**] This research was supported by the National Institutes of Health (Grant nos. CA 28824 and HL 28549). Predoctoral fellowships are gratefully acknowledged by K. M. D. (Lilly), S. H. B. (Kent) and D. J. D. (NSERC/Canada). We thank Dr. John Decatur for help with 2D-NMR analyses and Vinka Parmakovich and Barbara Sporer for mass spectral data.

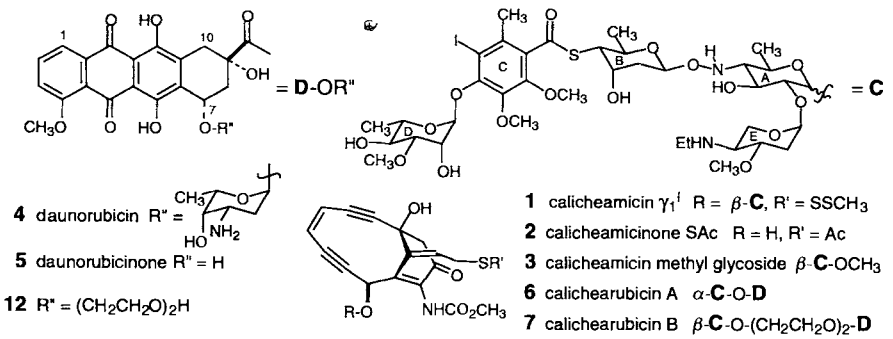

Fig. 1. Anthracycline and calicheamicin antibiotics and the calichearubicins.

linked carbohydrate (**3**) and aglycone moieties, further underscoring the role of the complex carbohydrate network at the level of molecular recognition.[4a]

Another family of drugs bearing a carbohydrate unit is the anthracyclines, exemplified by daunorubicin (**4**).[10] One function of these compounds involves intercalation of the aglycone, a tetracyclic anthraquinone moiety, between DNA base pairs. The aglycones alone (for example daunorubicinone (**5**)) are inactive both as drugs and as intercalating agents.[10a] The role of the carbohydrate domain in facilitating molecular reaction to the DNA "receptor" appears to be confined to a relatively nonspecific salt bridge type of contact to the phosphate backbone.[11] Unlike the enediyne drugs, daunorubicin does not exhibit appreciable sequence selectivity in its intercalation.[10d, 10g]

From this perspective, we wondered about the possibility of a hybrid entity containing both the daunorubicinone aglycone **5** and calicheamicin sugar domains. We term these constructs "calichearubicins".[12] Here we describe the synthesis and preliminary evaluation of calichearubicins A and B (**6** and **7**, respectively). The former is the product of the direct glycosylation of **5** with the carbohydrate domain of calicheamicin γ_1^I; in **7** a bis(ethylene)glycol spacer is inserted between these domains.

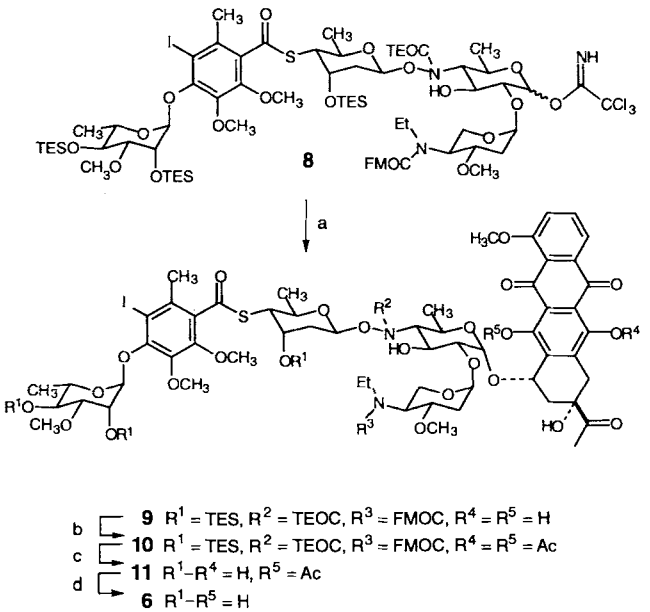

Scheme 1. Synthesis of calichearubicin A (**6**). a) **5**, AgOTf, 4Å molecular sieves, CH_2Cl_2 (α:β = 5:1, 45%); b) Ac_2O/py (2/5), 0°C, 10 min (89%); c) TBAF, THF, −5°C (92%); d) 3 equiv 0.1 N LiOH, THF (0.0015 M dilution), 12 h (44%). FMOC = 9-fluorenylmethoxycarbonyl, py = pyridine, TBAF = tetrabutylammonium fluoride, TEOC = trimethylsilylethoxycarbonyl, TES = triethylsilyl, Tf = trifluoromethanesulfonate.

The synthesis of such compounds posed no small challenge. In the end, it was accomplished by relying heavily on chemistry we had previously developed for both families of drugs. We exploited our synthesis[13] of the Schmidt[14] type of glycosyl donor, trichloroacetimidate **8** (Scheme 1). Here the glycosyl donor version of the calicheamicin γ_1^I carbohydrate is delivered at the correct oxidation level and appropriately substituted, and ideally all blocking groups would be cleaved upon brief exposure to fluoride ions. In practice, coupling[13] of **5** with **8** by employing AgOTF afforded a 5:1 ratio of **9** and its β anomer (not shown). However, the anthracycline proved to be unstable to the fluoridolysis conditions[15] needed to discharge the protecting groups from the construct. Interestingly, the anthracyclinone sector is apparently more vulnerable than the enediyne core of **1** toward tetrabutylammonium fluoride, which had served us so well in our total synthesis of calicheamicin γ_1^I.

Fortunately, our work in the anthracycline area helped to chart a response to this serious and unexpected problem. Earlier, we had demonstrated[16] that acetylation of the phenolic hydroxyl groups of daunorubicin (**4**) facilitates a major stabilizing effect toward reductively induced quinone methide formation. With this analogy in mind, compound **9** was acetylated to afford **10**. Treatment of **10** with fluoride ion led to the discharge of all of the blocking groups in the carbohydrate sector as well as the C11 acetyl group, resulting in the formation of **11**. Apparently, when even one acetyl protecting group is maintained at C6, the hybrid is stable to fluoridolysis. In the last step, calichearubicin A (**6**) was obtained by treatment of **11** with 0.1 N lithium hydroxide.

In a similar way, compound **12**[17] was coupled with **8** to give rise to a mixture of **13** and its α anomer (α:β ratio = 5:1; only the β isomer is shown in Scheme 2) in 30% yield. Preliminary molecular modeling and minimization based on structural information available from NMR solution spectra[8] of **1** bound to a d(TCCT)·d(AGGA) sequence, in conjunction with the crystal structure[11] of **4** intercalated between a pyrimidine/purine step within a DNA oligomer, had suggested that a five-

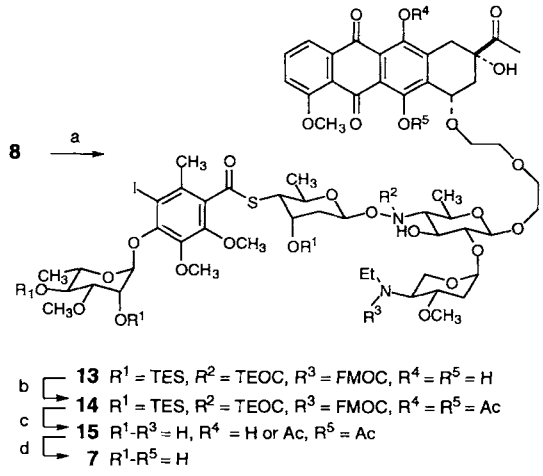

Scheme 2. Synthesis of calichearubicin B (**7**). a) **12**, $BF_3 \cdot OEt_2$, 4Å molecular sieves, CH_2Cl_2, −78C (β:α = 5:1, 35%); b) Ac_2O/py (2/5), 0°C, 10 min (79%); c) TBAF, THF, −5°C (90%); d) 5 equiv 0.1 N LiOH, THF (0.0015 M dilution), 6 h (35%).

 © VCH Verlagsgesellschaft mbH, D-69451 Weinheim, 1996 0570-0833/96/3523-2798 $ 15.00+.25/0

atom spacer with a β-glycosidic linkage would be required for concurrent intercalation and contact with the minor groove. Fortunately, through the use of $BF_3 \cdot OEt_2$,[18] anomers **13** were obtained in a 4:1 β:α ratio in 35% yield. After acetylation, the anomers were separated to give **14**, which was processed as before to afford calichearubicin B (**7**).

The interactions of **6** and **7** with double-stranded DNA (dsDNA) were studied spectrophotometrically. The dsDNA·**4** complex served as a valuable spectroscopic standard.[10] Upon intercalating dsDNA, **4** exhibits a bathochromic shift of 29 nm[19] from the maximum wavelength of its nonintercalated form at 479 nm (Table 1).[19, 20] Because **6** and **7** bear the same chromophoric element as **4**, it was presumed that comparison of absorbance profiles upon addition of DNA to these hybrids might suggest whether **6** and **7**, like **4**, intercalate dsDNA.

In contrast to the natural drug **4**, the synthetic construct **6** is not appreciably red-shifted beyond experimental error on addition of DNA (see Table 1). At least by this measure, hybrid **6** would seem to be incapable of intercalating dsDNA under these conditions.[21] By sharp contrast, hybrid **7** is red-shifted to virtually the same extent as the natural drug **4**. Thus, the ethoxyethyl tether in the linked structure **7** disposes its anthracycline domain to strong intercalation.

Table 1. Absorption maxima und shifts of free and DNA-associated anthracyclines (pbp = pairs of base pairs) [21].

Drug	λ_{max}(drug)	λ_{max}(DNA(pbp)/drug) [a]	$\Delta\lambda_{max}$
4	479	508	+29
6	483	484.5	+1.5
7	482	508	+26

[a] [DNA(pbp)]:[drug] = 1:5.

Of particular interest was the question whether the carbohydrate domain confers any sequence preference to the anthracycline. To answer this question, $Fe^{II} \cdot MPE$[22] footprinting analyses (MPE = methidium propyl EDTA) were performed on the 155 base pair [^{32}P-3′-end-labeled] *Sph*I/*Sgr*AI fragment of pBR322. This fragment contains several sites for which calicheamicin γ_1^I has shown specificity,[6a, 7] as well as ample random DNA sequences to evaluate new affinities. The results for **4**, **6**, and **7** are shown in Figure 2. At a concentration of 100 μM, **7** demonstrated specificity in binding, but this specificity manifested itself as areas of enhanced $Fe^{II} \cdot MPE$ cleavage rather than as sites protected against cleavage, which are characteristic of standard footprinting analyses. This phenomenon had been previously observed in $Fe^{II} \cdot MPE$ studies with carbohydrate **3** alone, and was postulated to be the result of widening of the minor groove[4a] or local helical unwinding. While the cleavage enhancements caused by **7** do not occur at areas known to display calicheamicin γ_1^I preference, Figure 2 shows that this hypersensitivity correlates with the 3′ side of other homopyrimidine/homopurine tracts, namely d(CTTC)·d(GAAG) and d(TTTC)·d(GAAA). A model encompassing concurrent intercalation contacts and carbohydrate–DNA contacts in the minor groove is proposed in Figure 3. Each of these hypersensitive sites contains a pyrimidine/purine motif, for which **4** had demonstrated moderate selectivity.[10f, 10h] High concentrations of **4** (Fig. 2, lane 12) led to a general washing out of all bands, suggesting surface blockage of the $Fe^{II} \cdot MPE$ cleavage by nonspecific binding to DNA phosphates.

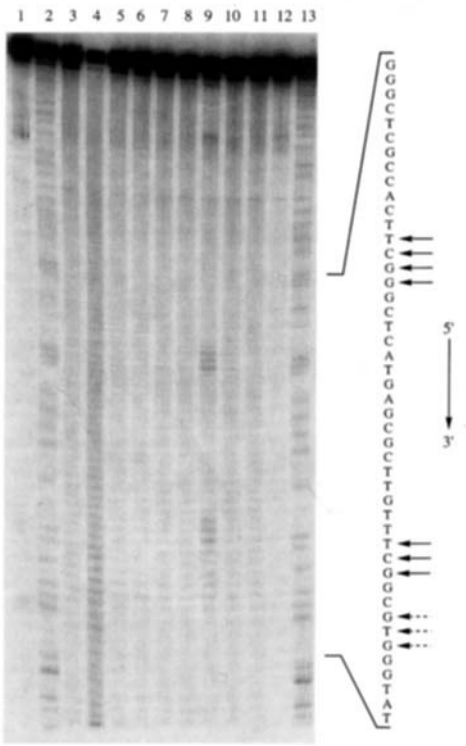

Fig. 2. $Fe^{II} \cdot MPE$ enhancement of DNA cleavage elicited by **7**: Autoradiogram scan of 12% denaturing polyacrylamide gel (8 M urea, 90 mM Tris-HCl, 90 mM boric acid, 3 mM EDTA) showing the binding of the drug to a region of the 155 bp *Sph*I/*Sgr*AI restriction fragment of pBR322. (Plasmid DNA was linearized with *Sph*I, ^{32}P-labeled on the 3′ end, and further restricted with *Sgr*AI.) The gel- and electroelution-purified fragment was preincubated in a (10 μL) solution containing Tris-HCl (10 mM, pH 7.6), NaCl (25 mM) and sonicated calf thymus DNA (1 mM in nucleotides) at 25 °C. After 25 min dithiothreitol (30 mM) and freshly prepared $Fe^{II} \cdot MPE$ (5 μM) were added to the solutions (concentrations of 2.5 mM and 0.4 μM, respectively), and the reaction mixture (now 12 μL total volume) was incubated an additional 15 min at 10 °C. The DNA in each reaction was precipitated by addition of ethanol and resolved by gel electrophoresis. The gel was dried at 80 °C; an autoradiogram was prepared (exposure time: 5 d, Fuji X-ray film) and then photographed. Lane 1: untreated labeled DNA fragment; lanes 2 and 13: Maxam-Gilbert A + G sequencing ladder; lane 3: $Fe^{II} \cdot MPE$-treated fragment containing no drug (control); lanes 4–6: labeled DNA fragment and 1, 10, and 100 μM **6**, respectively; lanes 7–9: labeled DNA fragment and 1, 10, and 100 μM **7**, respectively; lanes 10–12: labeled DNA fragment and 1, 10, and 100 μM **4**, respectively. The region of the sequence containing the enhancement sites discussed in the text is shown at the right with solid and dashed arrows respectively, indicating the stronger and weaker sites of cleavage enhancement elicited by **7**.

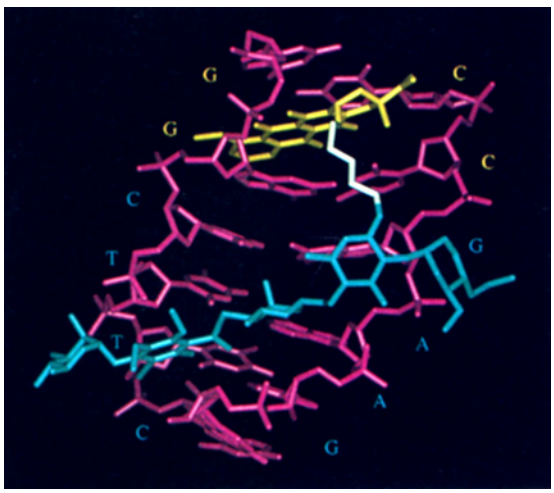

Fig. 3. A model of a possible drug–DNA complex containing calichearubicin B (**7**) and d(CCGAAG)·d(CTTCGG) (*magenta*). The minor groove binding carbohydrate domain [8] (cyan) and the intercalation domain [11d] (yellow) are tethered by an ethoxyethyl linker (white).

 © VCH Verlagsgesellschaft mbH, D-69451 Weinheim, 1996 0570-0833/96/3523-2799 $ 15.00+.25/0

It seems, then, that our synthetically derived hybrid **7** combines elements of the unique specificities exhibited by each of its parent component domains.

Having accomplished this demonstration, we will work on melding components of other drug–carbohydrate domains. Clearly, molecular modeling can be a valuable asset in identifying promising constructs.

Experimental Procedure

Calichearubicin A (**6**): Argon was bubbled through a THF solution (2.7 mL, 0.0015 M) of **11** (5.6 mg, 0.0040 mmol) for 20 min. Three equivalents of 0.1 N LiOH solution (argon saturated, 0.12 mL) was added and the solution was stirred for 12 h at ambient temperature; the color of the solution changed from bright yellow to deep blue. When an aliquot of the solution spotted red on TLC, the reaction was poured into saturated NH_4Cl solution and extracted with EtOAc. The organic layer was separated, washed with brine, dried over Na_2SO_4, filtered, concentrated, and chromatographed on a preparative TLC plate ($10 \times 20\ cm^2 \times 0.25$ mm, $CHCl_3$/MeOH (9/1)) to yield 2.4 mg (44%) of **6** as an orange-red amorphous solid; $R_f = 0.32$ (9/1 $CHCl_3$/MeOH); $[\alpha]_D^{25} = +16$ ($c = 0.275$ in $CHCl_3$); ^1H NMR (500 MHz, $CDCl_3$): Dau = daunorubicinone portion; A, B, C, D, and E (in parentheses) refer to the individual rings of the carbohydrate (see Fig. 1). The numbering of the protons refers to the hydrogens of the aglycone (see Fig. 1): $\delta = 14.18$ (s, 1H, C6-OH (Dau)), 13.41 (br. s, 1H, C11-OH (Dau)), 8.07 (d, $J = 7.7$ Hz, 1H, H1 (Dau)), 7.82 (t, $J = 8.1$ Hz, 1H, H2 (Dau)), 7.40 (d, $J = 8.5$ Hz, 1H, H3 (Dau)), 6.68 (br. s, 1H, NH-O), 5.72 (s, 1H, H1 (D)), 5.61 (br. s, 1H, H7 (Dau)), 5.25 (d, $J = 4$ Hz, 1H, H1 (A)), 5.19 (br. s, 1H, H1 (E)), 5.08 (d, $J = 7$ Hz, 1H, H1 (B)), 4.64 (m, 1H, H5 (A)), 4.50 (br. s, 1H, H2 (D)), 4.30 (t, $J = 10$ Hz, 1H, H3 (A)), 4.21 (m, 1H, H5 (D)), 4.10 (m, 1H, H5 (B)), 4.08 (s, 3H, OCH_3 (Dau)), 3.95 (br. s, 1H, H3 (B)), 3.84 (s, 6H, $2 \times OCH_3$ (C)), 3.83 (m, 1H, H3 (D)), 3.73 (dd, $J = 9.4$, 7.7 Hz, 1H, H2 (A)), 3.65 (pseudo-t, $J = 9.8$ Hz, 2H, H4 (B), H4, D)), 3.58 (s, 3H, OCH_3 (D)), 3.38 (s, 3H, OCH_3 (Dau)) (E)), 3.38 (d, $J = 18$ Hz, 1H, H10b (Dau)), 3.13 (d, $J = 18$ Hz, 1H, H10a (Dau)), 3.00–2.80 (br. s, 3H, NH, $NHCH_2CH_3$), 2.64 (d, $J = 18.5$ Hz, 1H, 8b (Dau)), 2.45 (s, 3H, $C(O)CH_3$ (Dau)), 2.31 (s, 3H, CH_3 (C)), 2.31 (m, 1H, H4 (A)), 2.17 (m, 1H, $H2_{eq}$ (E)), 1.98 (dd, $J = 14.0$, 4.0 Hz, 1H, H8a (Dau)), 1.71 (m, 1H, $H2_{ax}$ (E)), 1.59 (br. d, $J = 9$ Hz, 1H, $H2_{eq}$ (B)), 1.46 (m, 1H, $H2_{ax}$ (B)), 1.46 (d, $J = 6.2$ Hz, 3H, H6 (A)), 1.39 (d, $J = 6.2$ Hz, 3H, H6 (B)), 1.31 (d, $J = 6.2$ Hz, 3H, H6 (D)), 1.25 (br. s, 3H, $NHCH_2CH_3$); four protons H3, H4, $H5_{ax}$, and $H5_{eq}$ (of ring E) were unassignable; selective ROESY on H1 (A) enhanced H2 (A), H4 (A), H7 (Dau)); IR ($CHCl_3$): $\tilde{\nu} = 3686$, 3608, 3500, 3029, 2960, 2931, 1715, 1671, 1602, 1587, 1455, 1416, 1381, 1283, 1234, 1072, 1038, 989, 910 cm^{-1}; HRMS (FAB): *m/z*: 1343.3511; $[M+H]^+$; calcd for $C_{58}H_{76}IN_2O_{24}S$: 1343.3550.

Calichearubicin B (**7**): The same procedure was used as that for **6** except that five equivalents of 0.1 N LiOH solution were used and the reaction mixture was stirred for 6 h to give, after workup and chromatography, **7** as an orange-red amorphous solid in 35% yield: $R_f = 0.20$ ($CHCl_3$/MeOH (9/1)); $[\alpha]_D^{22} = +23$ ($c = 0.2$ in $CHCl_3$); ^1H NMR (500 MHz, $CDCl_3$): $\delta = 13.93$ (s, 1H, C6-OH (Dau)), 13.29 (s, 1H, C11-OH (Dau)), 7.94 (dd, $J = 7.7$, 1.0 Hz, 1H, H1 (Dau)), 7.71 (pseudo-t, $J = 8.1$ Hz, 1H, H2 (Dau)), 7.35 (d, $J = 7.8$ Hz, 1H, H3 (Dau)), 6.36–6.30 (br. s, 1H, NH-O), 5.73 (d, $J = 1.4$ Hz, 1H, H1 (D)), 5.30 (br. s, 1H, H1 (E)), 5.04 (m, 2H, H7, H1 (B)), 4.77 (d, $J = 1.4$ Hz, 1H, H2 (D)), 4.34 (d, $J = 7.8$ Hz, 1H, H1 (A)), 4.31 (br. s, 1H, H3 (B)), 4.19 (m, 1H, H5 (D)), 4.07 (m, 1H, H5 (B)), 4.01 (s, 3H, OCH_3 (Dau)), 3.97 (m, 3H, H3 (A), C7 (Dau))-CH_2CH_2), 3.89 (s, 3H, OCH_3 (C)), 3.84 (s, 4H, H3 (D), OCH_3 (C)), 3.76–3.73 (m, 5H, H4 (B), $H5_{ax}$ (B), $H5_{eq}$ (E), O7-CH_2CH_2), 3.70 (m, 1H, H5 (A)), 3.73–3.60 (m, 4H, OCH_2CH_2O-C1 (A)), 3.65 (t, $J = 9.5$ Hz, 1H, H4 (D)), 3.57 (s, 3H, OCH_3 (D)), 3.47 (t, $J = 8.7$ Hz, 2H, H2 (A), H3 (E)), 3.38 (br. s, 3H, OCH_3 (E)), 3.24 (d, $J = 18$ Hz, 1H, H10b (Dau)), 2.96 (d, $J = 18$ Hz, 1H, H10a (Dau)), 2.90–2.70 (br. m, 4H, $NHCH_2CH_3$, H4 (E)), 2.50 (m, 1H, H8b (Dau)), 2.43 (s, 3H, $C(O)CH_3$ (Dau)), 2.36 (s, 3H, CH_3 (C)), 2.36 (m, 1H, $H2_{eq}$ (E)), 2.32 (m, 1H, H4 (A)), 2.04 (m, 1H, $H2_{eq}$ (B)), 1.96 (m, 1H, H8a (Dau)), 1.78 (m, 1H, $H2_{ax}$ (B)), 1.62 (m, 1H, $H2_{ax}$ (E)), 1.41 (d, $J = 6.2$ Hz, 3H, H6 (B)), 1.31 (d, $J = 6.1$ Hz, 3H, H6 (A)), 1.30 (d, $J = 6.2$ Hz, 3H, H6 (D)), 1.11 (m, 3H, $NHCH_2CH_3$); IR ($CHCl_3$): $\tilde{\nu} = 3594$, 3469, 2930, 2856, 1718, 1677, 1619, 1580, 1460, 1416, 1402, 1354, 1321, 1287, 1239, 1071, 993, 965, 907, 825 cm^{-1}; HRMS (FAB): *m/z*: 1431.4094; $[M+H]^+$; calcd for $C_{62}H_{83}IN_2O_{26}S$: 1343.3550.

Received: June 10, 1996 [Z9225IE]
German version: *Angew. Chem.* **1996**, *108*, 2972–2975

Keywords: anthracyclines · carbohydrates · DNA cleavage · drug design · total syntheses

[1] a) W. J. Rost in *The Aminoglycoside Antibiotics: A Guide to Therapy* (Eds.: W. G. Barnes, G. R. Hodges), CRC Press, Boca Raton, FL, **1984**, p. 1; b) "Aminoglycoside Antibiotics": S. Umezawa, T. Tsuchiya in *Handbook of Experimental Pharmacology, Vol. 62* (Eds.: H. Umezawa, I. R. Hooper), Springer, New York, **1982**, p. 37; c) J. K. Aronson, *An Account of the Foxglove and its Medical Uses, 1785–1985*, Oxford, New York, **1985**.

[2] K. C. Nicolaou, W.-M. Dai, *Angew. Chem.* **1991**, *103*, 1453; *Angew. Chem. Int. Ed. Engl.* **1991**, *30*, 1387.

[3] a) M. D. Lee, T. S. Dunne, M. M. Siegel, C. C. Chang, G. O. Morton, D. B. Borders, *J. Am. Chem. Soc.* **1987**, *109*, 3464; b) M. D. Lee, T. S. Dunne, C. C. Chang, G. A. Ellestad, M. M. Siegel, G. O. Morton, W. J. McGahren, D. B. Borders, *ibid.* **1987**, *109*, 3466; c) M. D. Lee, G. A. Ellestad, D. B. Borders, *Acc. Chem. Res.* **1991**, *24*, 235; d) M. D. Lee, T. S. Dunne, C. C. Chang, M. M. Siegel, G. O. Morton, G. A. Ellestad, W. J. McGahren, D. B. Borders, *J. Am. Chem. Soc.* **1992**, *114*, 985; e) J. Golik, J. Clardy, G. Dubay, G. Groenewold, H. Kawaguchi, M. Konishi, B. Krishnan, H. Ohkuma, K.-i. Saitoh, T. W. Doyle, *ibid.* **1987**, *109*, 3461; f) J. Golik, G. Dubay, G. Groenewold, H. Kawaguchi, M. Konishi, B. Krishnan, H. Ohkuma, K.-i. Saitoh, T. W. Doyle, *ibid.* **1987**, *109*, 3462.

[4] a) J. Aiyar, S. J. Danishefsky, D. M. Crothers, *J. Am. Chem. Soc.* **1992**, *114*, 7552, and references therein; b) J. Aiyar, S. A. Hitchcock, D. Denhart, K. K. C. Liu, S. J. Danishefsky, D. M. Crothers, *Angew. Chem.* **1994**, *106*, 925; *Angew. Chem. Int. Ed. Engl.* **1994**, *33*, 855; c) J. Drak, N. Iwasawa, S. J. Danishefsky, D. M. Crothers, *Proc. Natl. Acad. Sci. USA* **1991**, *88*, 7464.

[5] a) K. C. Nicolaou, S.-C. Tsay, T. Suzuki, G. F. Joyce, *J. Am. Chem. Soc.* **1992**, *114*, 7555; b) L. G. Paloma, J. A. Smith, W. J. Chazin, K. C. Nicolaou, *ibid.* **1994**, *116*, 3697; c) T. Li, Z. Zeng, V. A. Estevez, K. U. Baldenius, K. C. Nicolaou, G. F. Joyce, *ibid.* **1994**, *116*, 3709.

[6] a) N. Zein, A. M. Sinha, W. J. McGahren, G. A. Ellestad, *Science* **1988**, *240*, 1198; b) N. Zein, M. Poncin, R. Nilakantan, G. A. Ellestad, *ibid.* **1989**, *244*, 697; c) S. Walker, R. Landovitz, W. D. Ding, G. A. Ellestad, D. Kahne, *Proc. Natl. Acad. Sci. USA* **1992**, *89*, 4608; d) D. Kahne, *Chem. Biol.* **1995**, *2*, 7, and references therein.

[7] a) S. C. Mah, C. A. Townsend, T. D. Tullius, *Biochemistry* **1994**, *33*, 614; b) S. C. Mab, M. A. Price, C. A. Townsend, T. D. Tullius, *Tetrahedron* **1994**, *50*, 1361.

[8] N. Ikemoto, R. A. Kumar, T.-T. Ling, G. A. Ellestad, S. J. Danishefsky, D. J. Patel, *Proc. Natl. Acad. Sci. USA* **1995**, *92*, 10506.

[9] N. Ikemoto, R. A. Kumar, P. C. Dedon, S. J. Danishefsky, D. J. Patel, *J. Am. Chem. Soc.* **1994**, *116*, 9387.

[10] a) F. Arcamone, S. Penco, *Gann Monogr. Cancer Res.* **1989**, *36*, 81; b) B. R. J. Abdella, J. Fisher, *Environ. Health Perspect.* **1985**, *64*, 3; c) F. Arcamone in *Doxorubicin Anticancer Antibiotics. Medicinal Chemistry Series of Monographs, Vol. 17* (Ed.: G. Stevens), Academic Press, New York, **1981**; d) F. Arcamone, G. Franceschi, P. Orezzi, G. Cassinelli, W. Barbieri, R. Mondelli, *J. Am. Chem. Soc.* **1964**, *86*, 5334; e) J. B. Chaires, N. Dattagupta, D. M. Crothers, *Biochemistry* **1982**, *21*, 3933; f) J. B. Chaires, K. R. Fox, J. E. Herrera, M. Britt, M. J. Waring, *ibid.* **1987**, *26*, 8227; g) D. P. Remeta, C. P. Mudd, R. L. Berger, K. J. Breslauer, *ibid.* **1993**, *32*, 5064; h) C. J. Roche, J. A. Thompson, D. M. Crothers, *ibid.* **1994**, *33*, 926; i) V. Berlin, W. A. Haseltine, *J. Biol. Chem.* **1981**, *256*, 4747; j) M. W. Van Dyke, R. P. Hertzberg, P. B. Dervan, *Proc. Natl. Acad. Sci. USA* **1982**, *79*, 5470; k) M. H. Moore, W. N. Hunter, B. L. d'Estaintot, O. Kennard, *J. Mol. Biol.* **1989**, *206*, 693; l) C. M. Nunn, L. van Mervelt, S. Zhang, M. H. Moore, O. Kennard, *ibid.* **1991**, *222*, 167.

[11] a) G. J. Quigley, A. H.-J. Wang, G. Ughetto, G. van der Marel, J. H. van Boom, A. Rich, *Proc. Natl. Acad. Sci. USA* **1980**, *77*, 7204; b) A. H.-J. Wang, G. Ughetto, G. J. Quigley, A. Rich, *Biochemistry* **1987**, *26*, 1152; c) C. A. Frederick, L. D. Williams, G. Ughetto, G. A. van der Marel, J. H. van Boom, A. Rich, A. H.-J. Wang, *ibid.* **1990**, *29*, 2538; d) Y.-G. Gao, Y.-C. Liaw, Y.-K. Li, G. A. van der Marel, J. H. van Boom, A. H.-J. Wang, *Proc. Natl. Acad. Sci. USA* **1991**, *88*, 4845; e) A. H.-J. Wang in *Molecular Aspects Anticancer Drug-DNA Interaction* (Eds.: S. Neidle, M. J. Waring), MacMillan, Basingstroke, UK, **1993**, p. 32.

[12] The name calichearubicin is derived from calicheamicin and daunorubicin. The name is also evocative of the ruby color of the compound.

[13] a) S. A. Hitchcock, M. Y. Chu-Moyer, S. H. Boyer, S. H. Olson, S. J. Danishefsky, *J. Am. Chem. Soc.* **1995**, *117*, 5750; b) S. A. Hitchcock, S. H. Boyer, M. Y. Chu-Moyer, S. H. Olson, S. J. Danishefsky, *Angew. Chem.* **1994**, *106*, 928; *Angew. Chem. Int. Ed. Engl.* **1994**, *33*, 858; c) R. L. Halcomb, S. H. Boyer, M. D. Wittman, S. H. Olson, D. J. Derhart, K. K. C. Liu, S. J. Danishefsky, *J. Am. Chem. Soc.* **1995**, *117*, 5720.

[14] R. R. Schmidt, *Angew. Chem.* **1986**, *98*, 213; *Angew. Chem. Int. Ed. Engl.* **1986**, *25*, 212.

[15] S. H. Boyer, Dissertation, Yale University, New Haven, CT, **1994**.

[16] G. A. Sulikowski, E. Turos, S. J. Danishefsky, G. M. Shulte, *J. Am. Chem. Soc.* **1991**, *113*, 1373.

[17] J. V. Jizba, P. Sedmera, J. Vokoun, H. Lipavska, M. Podojil, Z. Vanek, *Coll. Czech. Chem. Commun.* **1984**, *49*, 653.

[18] a) R. L. Halcomb, S. H. Boyer, S. J. Danishefsky, *Angew. Chem.* **1992**, *104*, 314; *Angew. Chem. Int. Ed. Engl.* **1992**, *31*, 338; b) K. C. Nicolaou, K. Ajito, H. Komatsu, B. M. Smith, T. Li, M. G. Egan, L. Gomez-Paloma, *ibid.* **1995**, *107*, 614 and **1995**, *34*, 576.

[19] E. J. Gabbay, D. Grier, R. E. Fingerle, R. Reimer, R. Levy, S. W. Pearce, W. D. Wilson, *Biochemistry* **1976**, *15*, 2062.

[20] A. Di Marco, F. Zunino, R. Silvestrini, C. Gambarucci, R. A. Gambetta, *Biochem. Pharmacol.* **1971**, *20*, 1323.

[21] Solutions of **6** and **7** (each 100 μM at start) were titrated with a solution of sonicated calf thymus DNA, and the resulting spectral profiles were measured. For each run, volume changes due to DNA additions were taken into account in the calculation of the [DNA]:[drug] ratio. DNA concentration is given in pairs of base pairs (pbp), as this unit represents the minimum structural motif required for intercalation (Table 1).

[22] a) R. P. Hertzberg, P. B. Dervan, *Biochemistry* **1984**, *23*, 3934; b) M. W. Van Dyke, P. B. Dervan, *Nucleic Acids Res.* **1983**, *11*, 5555; c) *Biochemistry* **1983**, *22*, 2373.

Total Synthesis of (−)-Epothilone A**

Aaron Balog, Dongfang Meng, Ted Kamenecka, Peter Bertinato, Dai-Shi Su, Erik J. Sorensen, and Samuel J. Danishefsky*

Epothilones A and B were isolated from the myxobacteria of the genus *Sorangium*. The full structures of these compounds, determined from an X-ray crystallographic analysis, were recently communicated by Höfle.[1] Interest in the total synthesis of the epothilones arises from several considerations. First, they contain substructural motifs that pose intrinsic problems for a total synthesis. Not uncommonly, solutions to novel structural challenges carry with them important lessons for organic chemistry, which transcend the particular goal under investigation. Moreover, the biological profiles of the epothilones warrant multidisciplinary scientific attention. As is well known by now, taxol is already a useful resource in chemotherapy against ovarian and breast cancers.[2] Furthermore, its range of applicability seems to be expanding under continuing clinical scrutiny. The mechanism of the cytotoxic action of taxol, at least at the in vitro level, involves stabilization of microtubule assemblies.[3] A series of complementary in vitro investigations with the epothilones indicated that they function by the same mechanism as the taxoids, apparently down to the binding sites to their protein target.[4] Moreover, the epothilones surpass taxol in terms of cytotoxicity and far surpass it as regards in vitro efficacy against drug-resistant cells. Since multiple drug resistance (MDR) is one of the serious limitations of taxol,[5] any agent that promises relief from this problem merits serious attention. Furthermore, formulatability of the epothilones is claimed to be more straightforward than is the case with taxol. Accordingly, we have undertaken the total synthesis of epothilones, focusing first on epothilone A (**1**). Herein we report for the first time the total synthesis of this target.

Carbons 9 through 11 insulate the chiral domains embracing carbons 3 through 8 on the acyl side of the macrolactone, and carbons 12 through 15 on the alkyl side. We reasoned from the outset that the prospects of transmitting stereochemical information from one of the segments to the other were bleak. Accordingly, it seemed more prudent to deal with the stereochemistry of each segment individually. In the acyl segment this required solution to both the relative and absolute configurations of the "polypropionate-like" network. In the alkyl segment, two possibilities presented themselves. In one instance, the C12–C13 epoxide would be included in the unit to be merged with the acyl-related substructure. In that case it would be necessary to secure the relative as well as absolute stereochemical relationships of carbons 15, 13, and 12. As matters transpired, we came to consider omitting the epoxide from the alkyl-side moiety undergoing coupling. This strategy would be feasible only if the epoxide could be introduced with acceptable stereocontrol after closure of the macrocycle.

In an earlier disclosure[6] we described the synthesis of compound **4**, which contains most of the requisite stereochemical information required for the acyl fragment. This intermediate was reached by a novel, oxidatively induced, solvolytic cleavage of the cyclopropanopyran **3**. We also described a construct containing the alkyl-side coupling partner embodying the absolute and relative stereochemistry at carbons 15, 13, and 12, which was not used in the studies described herein.[7]

Several potential connection sites attracted attention for the union of the alkyl and acyl domains. At some point an acylation would be required to establish an ester (or lactone) bond (see bold arrow *2*, Scheme 1). Furthermore, an aldol condensation seemed to be called for in fashioning a C2–C3 connection. Less obvious was the timing of this aldol step. It could be considered for the elongation of the C3–C9 construct to prepare it for acylation of the C-15 hydroxyl group. As matters developed, however, we employed a bolder possibility: the closure of the macrolide by a virtually unprecedented macroaldolization.[8] This risky but otherwise attractive option is implied by bold arrow *3*.

Considerable debate and experimentation attended the decision on the first union between the acyl and alkyl fragments (see bold arrow *1*). As alluded to in earlier publications,[6, 7] and as will be expanded upon in subsequent disclosures, significant resistance was encountered against proposed bond formation between carbons 9 and 10 or between carbons 10 and 11, for which the epoxide would be included in the alkyl coupling partner. Complications had arisen from unanticipated difficulties in fashioning acyl and alkyl reactants with the appropriate complementarity for merger across either of these bonds. We thus turned to the possibility of establishing the initial merger between carbons 11 and 12. This approach dictated deletion of the oxirane linkage from the O-alkyl coupling partner. After examination of several permutations, we settled upon generalized systems **5** and **6** to enter the first-stage coupling reaction. A de novo synthesis of a usable substrate corresponding to generalized system **5**, starting from **4**, would be necessary.

The steps leading from **4** to **11** are shown in Scheme 2. Protection of the future C-7 alcohol (see compound **7**) was followed by cleavage of the benzyl ether and oxidation to form aldehyde **8**. Elongation of the aldehyde to the terminal allyl-containing fragment **10** proceeded through enol ether **9** (mixture of *E* and *Z* geometrical isomers). Finally, the dithiane linkage was oxidatively cleaved under solvolytic trapping conditions[9] to give rise to specific coupling component **11**.

[*] Prof. S. J. Danishefsky,[+] Dr. A. Balog, D. Meng,[+] Dr. T. Kamenecka, Dr. P. Bertinato, Dr. D.-S. Su, Dr. E. J. Sorensen
Laboratory for Bioorganic Chemistry
Sloan-Kettering Institute for Cancer Research
1275 York Avenue, New York, NY 10021 (USA)
Fax: Int. code +(212)772-8691

[+] Other address:
Department of Chemistry, Columbia University
Havemeyer Hall, New York, NY 10027 (USA)

[**] This research was supported by the National Institutes of Health (grant number CA-28824). Postdoctoral fellowship support is gratefully acknowledged by E. J. S. (N. S. F., CHE-9504805), A. B. (N. I. H., CA-GM 72231), P. B. (N. I. H., CA 62948), T. K. (N. I. H., AI0-9355). We gratefully acknowledge Dr. George Sukenick (NMR Core Facility, Sloan-Kettering Institute) for NMR and mass spectral analyses. Professor Dr. G. Höfle of the Gesellschaft für Biotechnologische Forschung is gratefully acknowledged for providing natural epothilone A for comparative analysis. We also thank Professor Gunda Georg of the University of Kansas for bringing this problem to our attention.

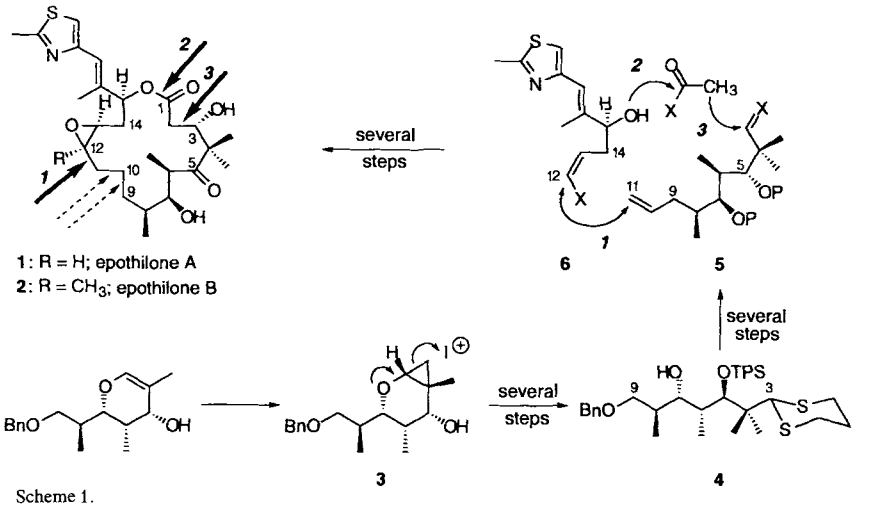

Scheme 1.

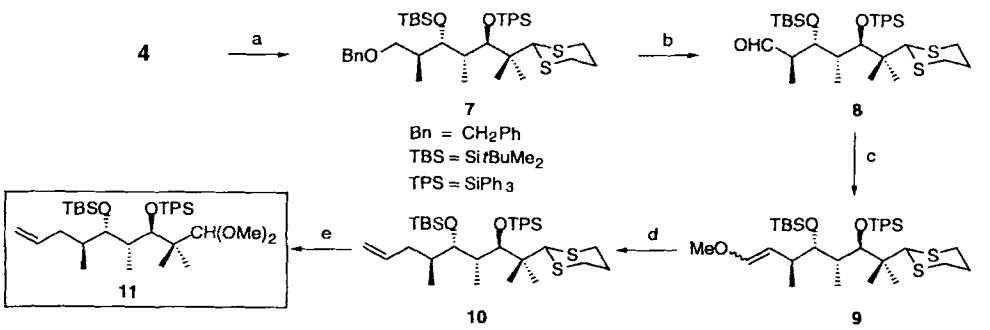

Scheme 2. a) *t*-BuMe$_2$OTf (Tf = trifluoromethanesulfonate), 2,6-lutidine, CH_2Cl_2, 98%; b) 1. 2,3-dichloro-5,6-dicyano-1,4-benzoquinone (DDQ), CH_2Cl_2/H_2O, 89%; 2. $(COCl)_2$, DMSO, CH_2Cl_2, $-78\,^{\circ}C$; then Et_3N, $-78\,^{\circ}C \rightarrow RT$, 90%; c) $MeOCH_2PPh_3Cl$, *t*-BuOK, THF, $0\,^{\circ}C \rightarrow RT$, 86%; d) 1. *p*-TsOH, dioxane/H_2O, $50\,^{\circ}C$, 99%; 2. CH_3PPh_3Br, sodium hexamethyldisilazide (NaHMDS), $PhCH_3$, $0\,^{\circ}C \rightarrow RT$, 76%; e) $PhI(OCOCF_3)_2$, MeOH/THF, RT, 0.25 h, 92%.

The synthesis of the alkyl fragment started with commercially available (*R*)-glycidol **12**, which was converted, via its THP derivative **13**, into alcohol **14**. After cleavage of the tetrahydropyran blocking group, the resultant alcohol was smoothly converted into the methyl ketone **15**, as shown. The latter underwent an Emmons-type homologation with phosphane oxide **16**.[7, 10] The resultant alkyne **17** was then converted, via compound **18**, into *Z*-iodoalkene **19**[11] (Scheme 3).

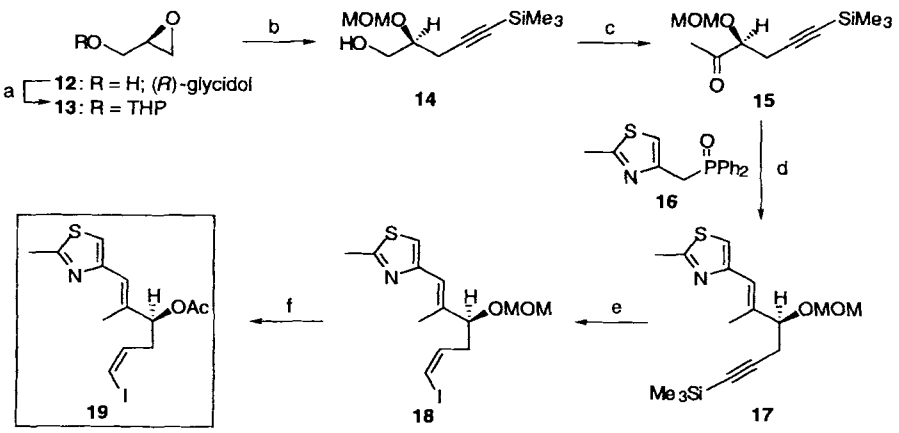

Scheme 3. a) Dihydropyran (DHP), pyridinium *p*-toluenesulfonate (PPTS), CH_2Cl_2, RT; b) 1. $Me_3SiCCLi$, $BF_3 \cdot OEt_2$, THF, $-78\,^{\circ}C$; 2. methoxymethyl chloride (MOMCl), iPr_2NEt, $Cl(CH_2)_2Cl$, $55\,^{\circ}C$; 3. PPTS, MeOH, RT; c) 1. $(COCl)_2$, DMSO, CH_2Cl_2, $-78\,^{\circ}C$, then Et_3N, $-78\,^{\circ}C \rightarrow RT$; 2. MeMgBr, Et_2O, $0\,^{\circ}C \rightarrow RT$; 3. tetra-*n*-propylammonium perruthenate (TPAP), *N*-methylmorpholine *N*-oxide (NMO), 4 Å mol. sieves, CH_2Cl_2, $0\,^{\circ}C \rightarrow RT$; d) **16**, *n*BuLi, THF, $-78\,^{\circ}C$, then **15**, THF, $-78\,^{\circ}C \rightarrow RT$; e) 1. *N*-iodosuccinimide, $AgNO_3$, $(CH_3)_2CO$; 2. Cy_2BH, Et_2O, AcOH; f) PhSH, $BF_3 \cdot OEt_2$, CH_2Cl_2, RT; 2. Ac_2O, Py, 4-dimethylaminopyridine (4-DMAP), CH_2Cl_2, RT.

The coupling of the two fragments, the all-critical first coupling, was achieved by a *B*-alkyl Suzuki carbon–carbon bond construction.[12] Hydroboration of the pre-acyl fragment **11** with 9-BBN furnished the mixed borane, which under the conditions indicated cross-coupled to iodoolefin **19** to give **20** in 71% yield. Upon cleavage of the acetal, aldehyde **21** was in hand.

With **21** we could explore the aggressive strategy of employing the methyl group of the C-1 bound acetoxy function as the nucleophilic component in a macroaldolization.[8] In the event, deprotonation was accomplished with potassium hexamethyldisilazide in THF at $-78\,^{\circ}C$. Remarkably, these conditions gave rise to a highly stereoselective macroaldolization, resulting in the formation of the C-3 (*S*)-alcohol **22** (Scheme 4). The heavy preponderance of **22** was favored when its precursor potassium aldolate was quenched at about $0\,^{\circ}C$. When the aldolate was protonated at lower temperature, higher amounts of the C-3 (*R*) compound were detected. In fact, under some treatments, the C-3 (*R*) epimer predominates. This matter remains to be fully sorted out. At present, we are able to generate highly favorable C-3 (*R*):C-3 (*S*) ratios if the quenching is performed on an analytical scale. In preparative-scale experiments, we can reliably obtain **22** and its C-3 epimer in a 6:1 ratio.

Having fashioned compound **22**, we could converge on our subgoal, desoxyepothilone (**23**). This objective was accomplished by selective removal of the triphenylsilyl (TPS) group in **22**, followed, sequentially, by selective silylation of the C-3 alcohol, oxidation of the C-5 alcohol, and, finally, fluoride-induced cleavage of the two silyl ethers.

Examination of a model based on the crystal structure of epothilone[1] suggested that the oxirane is disposed on the exterior face of the macrolide. In the event, oxidation of **23** was carried out with dimethyl dioxirane under the conditions shown. The major product of this reaction was (−)-epothilone A (**1**), whose identity was established by NMR and infrared spectroscopy, mass spectrometry, optical rotation, and chromatographic comparisons with authentic material kindly provided by Professor Höfle.[13]

While subject to further improvements, the synthesis in its present form, already provides us with workable amounts of epothilone A. More importantly, it provides routes to congeners not available from the natural product itself. The biological properties of some of these now accessible probe structures, as well as several of the chemical issues raised during the course of this synthesis, are receiving continuing attention.[14]

 © VCH Verlagsgesellschaft mbH, D-69451 Weinheim, 1996 0570-0833/96/3523-2802 $ 15.00+.25/0

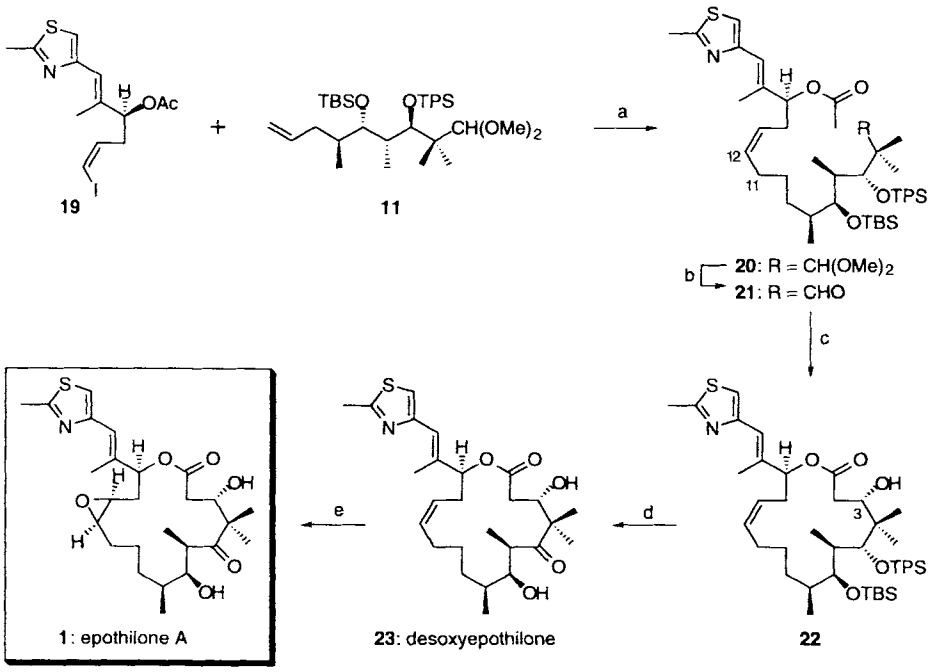

Scheme 4. a) **11**, 9-borabicyclo[3.3.1]nonane (9-BBN), THF, RT, then $PdCl_2(dppf)_2$, (dppf = 1,1'-bis(diphenylphosphino)ferrocene) $CsCO_3$, Ph_3As, H_2O, DMF, **19**, RT, 71%; b) TsOH, dioxane/H_2O, 50 °C; c) KHMDS, THF, −78 °C, 51%; d) 1. HF·Py, Py, THF, RT, 97%; 2. *t*BuMe$_2$SiOTf, 2,6-lutidine, CH_2Cl_2, −25 °C, 93%; 3. Dess–Martin periodinane, CH_2Cl_2, 87%; 4. HF·Py, THF, RT, 99%; e) dimethyl dioxirane, CH_2Cl_2, 0.5 h, −50 °C, 45% (≥20:1).

Received: October 17, 1996 [Z9663IE]
German version: *Angew. Chem.* **1996**, *108*, 2976–2978

Keywords: C–C coupling · cyclization · epothilone · natural products · synthesis methods

[1] G. Höfle, N. Bedorf, H. Steinmetz, D. Schomberg, K. Gerth, H. Reichenbach, *Angew. Chem.* **1996**, *108*, 1671; *Angew. Chem. Int. Ed. Engl.* **1996**, *35*, 1567.
[2] G. I. Georg, T. T. Chen, I. Ojima, D. M. Vyas, *Taxane Anticancer Agents*, American Cancer Society, San Diego, **1995**.
[3] P. B. Schiff, J. Fant, S. B. Horwitz, *Nature* **1979**, 277, 665.
[4] D. M. Bollag, P. A. McQueney, J. Zhu, O. Hensens, L. Koupal, J. Liesch, M. Goetz, E. Lazarides, C. M. Woods, *Cancer Res.* **1995**, 55, 2325.
[5] L. M. Landino, T. L. MacDonald in *The Chemistry and Pharmacology of Taxol and its Derivatives* (Ed.: V. Farin), Elsevier, New York, **1995**, p. 301.
[6] P. Bertinato, E. J. Sorensen, D. Meng, S. J. Danishefsky, *J. Org. Chem.*, **1996**, *61*, 8000–8001.
[7] D. Meng, E. J. Sorensen, P. Bertinato, S. J. Danishefsky, *J. Org. Chem.*, **1996**, *61*, 7998–7999.
[8] For a previous instance of a keto aldehyde macroaldolization, see C. M. Hayward, D. Yohannes, S. J. Danishefsky, *J. Am. Chem. Soc.* **1993**, *115*, 9345.
[9] G. Stork, K. Zhao, *Tetrahedron Lett.* **1989**, 30, 287.
[10] This Emmons coupling provided about an 8:1 mixture of olefin stereoisomers in favor of *trans*-**17**.
[11] E. J. Corey, J. R. Cashman, T. M. Eckrich, D. R. Corey, *J. Am. Chem. Soc.* **1985**, *107*, 713.
[12] a) N. Miyaura, T. Ishiyama, H. Sasaki, M. Ishi-Kawa, M. Satoh, A. Suzuki, *J. Am. Chem. Soc.* **1989**, *111*, 314; b) N. Miyaura, A. Suzuki, *Chem. Rev.* **1995**, *95*, 2457.
[13] In addition to epothilone A (**1**), small amounts of a diepoxide mixture, as well as traces of the diastereomeric *cis* C12–C13 monoepoxide (≥20:1) were detected.
[14] For alternative strategies toward the epothilones, see a) K. C. Nicolaou, Y. He, D. Vourloumis, H. Vallberg, Z. Yang, *Angew. Chem.* **1996**, *108*, 2554; *Angew. Chem. Int. Ed. Engl.* **1996**, *35*, 2399; b) D. Schinzer, A. Limberg, O. M. Böhm, *Chem. Eur. J.* **1996**, *2*, 4007.

A Molecularly Defined, Grafted Olefin Metathesis Catalyst from Tris(neopentyl)-nitridomolybdenum(VI)**

Wolfgang A. Herrmann,* Andreas W. Stumpf, Thomas Priermeier, Sandra Bogdanović, Veronique Dufaud, and Jean-Marie Basset

The development of immobilized of homogeneous catalysts by grafting to reactive surface structures is still far behind scientific and industrial demands.[1] While the mechanistic features of olefin metathesis have been elucidated in much detail,[2] only little is known on immobilized heterogeneous catalysts having well-defined surface structures.[3] We now report on the potential of alkylnitrido complexes as suitable precursors for surface-grafted imidoalkylidene species.

Tris(neopentyl)nitridomolybdenum(VI) (**1**) represents a linear coordination polymer in the solid state but reacts like a tetracoordinated monomer in solution.[4] This complex exhibits catalytic activity in the ring-opening metathesis polymerization of cyclic olefins such as norbornene at 60 °C ([mon.]/[Mo] = 200, 5 h, 20%). The instability of the nitridoneopentylidene complex [N≡Mo(CH*t*Bu)(CH$_2$*t*Bu)] presumably formed in situ is demonstrated by the immediate degradation by elimination of the neopentylidene coupling product 2,2,5,5-tetramethyl-3-hex-

[*] Prof. Dr. W. A. Herrmann, Dr. A. W. Stumpf, T. Priermeier, Dr. S. Bogdanović
Anorganisch-chemisches Institut der Technischen Universität München
Lichtenbergstrasse 4, D-85747 Garching (Germany)
Fax: Int. code + (89) 2891-3473
V. Dufaud, Prof. Dr. J.-M. Basset
Laboratoire de Chimie Organométallique de Surface
École Superieur Chimie, Physique, Electronique (CPE)
F-69626 Villeurbanne/Lyon (France)

[**] Multiple bonds between Main-Group Elements and Transition Metals, Part 159. This work was generously supported by the Deutsche Akademische Austauschdienst through a PROCOPE grant to the Munich and Lyon laboratories. Part 158: W. A. Herrmann, H.-D. Brauer, M. R. Geisberger, I. Hatzopoulos, *J. Organomet. Chem.* **1996**, in press.

 © VCH Verlagsgesellschaft mbH, D-69451 Weinheim, 1996 0570-0833/96/3523-2803 $ 15.00+.25/0

ene.[5] Cross-over experiments revealed an intermolecular mechanism for this decomposition reaction.[5] This fact and the reactivity profile of **1** toward organosilanols yielding imidotris(neopentyl)complexes[6] of type **2a** and **2b**, [Eqs. (a) and (b)] prompted the attempt to immobilize **1** on inorganic oxides.

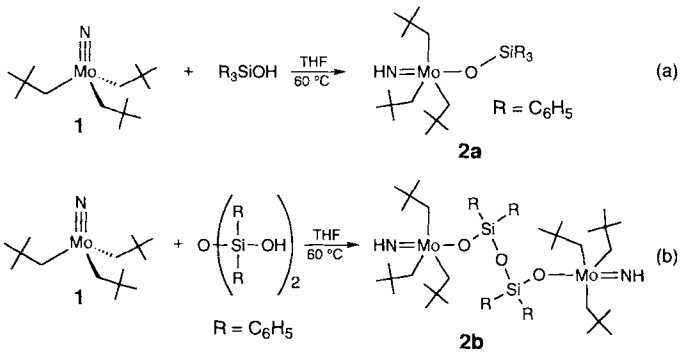

The oxyfunctionalization of **1** demonstrates that this molecule exhibits ideal prerequisites for surface grafting, both from the molecular structure (low-coordinate molybdenum) and the electronic structure (electron-deficient metal center). The formation of the siloxy-bridged, dinuclear imidomolybdenum complex **2b** reflects the stability of the metal–alkyl bonds toward a possible protolytic scission. This complex exhibits two nearly linear HN=MoO arrangements [average N-Mo-O angle 178.3(1)°] and trigonal-bipyramidal core geometries around the two metal centers (Fig. 1).[7]

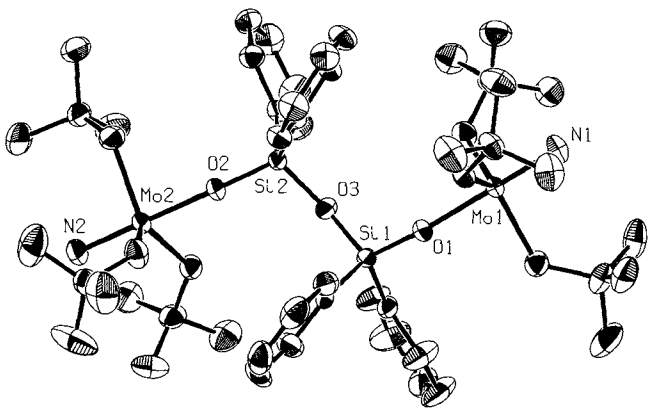

Fig. 1. Structure of the siloxy-bridged imidomolybdenum(VI) complex **2b** (PLATON representation). Hydrogen atoms are omitted for simplicity. Selected distances [Å] und angles [°]: Mo–N (av.): 1.727(3); Mo–O (av.): 1.988(2); Mo–C (av.): 2.124(5); Mo-N-H (av.): 179.2(1); Si1-O1-Mo1: 161.9(1); Si2-O2-Mo2: 156.8(1); Si2-O3-Si1: 143.7(1). Further details of the crystal structure investigation can be obtained from the Fachinformationszentrum Karlsruhe, Gesellschaft für Wissenschaftlich-Technische Information mbH, D-76344 Eggenstein-Leopoldshafen (Germany) on quoting the depository number CSD-405836.

When a sample of **1** is sublimed at 70 °C onto a silica disc in a vacuum,[8] the intensity of the $\tilde{\nu}$(SiOH) bands at 3745 cm^{-1} decreases strongly, while simultaneously bands at 3370 cm^{-1} for $\tilde{\nu}$(NH), in the range 3000–2850 cm^{-1} for $\tilde{\nu}$(CH), and in the range 1500–1300 cm^{-1} for δ(CH) grow gradually within about 15 h. When deuterated silica was used (>90% SiOD according to IR), a band at 2465 cm^{-1} appeared during treatment with **1** in place of the former absorption at 3370 cm^{-1}, proving the assignment of an imido moiety (=ND vs. =NH) formed by 1,2-addition of surface silanols across the nitridomolybdenum fragment in **1**. The evolution of neopentane during the surface reaction is indicative of a further reaction step. Labeling experiments with $N{\equiv}Mo(CD_2tBu)_3$ ([D]-**1**) yielded [D_3]neopentane but *no* [D_2]neopentane (GC/MS). This result gives strong evidence that the detachment of *one* hydrocarbon equivalent from the metal is a α-hydrogen abstraction step subsequent to the initial grafting process of Equation (c). The proposed molecular structure of the final grafting complex **4** is in agreement with the elemental analyses, which yield a Mo/N/C ratio of 1/1/10.

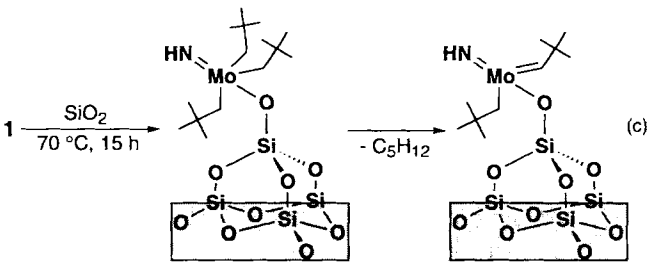

The ^{2}H NMR spectrum of **4** exhibits a single resonance at $\delta = 2.45$ attributable to the CD_2 group in the remaining neopentyl ligand. Similar chemical shifts in the structurally related molybdenum alkylidene complex [tBuNMo(CHtBu)(CH_2tBu)(OSiPh$_3$)] were reported by Osborn.[9] The ^{13}C NMR spectrum of **4** exhibits one resonance at $\delta = 32.9$, readily assignable to the CH_3 carbon atoms of the *tert*-butyl groups. The alkylidene carbon atom was not detectable; similar problems were reported by Weiss and Basset.[3] The proposed neopentylidene structure of **4** is, however, in full accord with the observed reactivity. For example, treatment with dry acetone at ambient temperature for 30 min gave the Wittig-type coupling product 2,4,4-trimethylpent-2-ene in *quantitative* yield.

The catalytic activity of the immobilized species **4** in olefin metathesis and ring-opening metathesis polymerization was compared with the homogeneous precursor compound **1**. The surface grafting of **1** on the partially dehydroxylated silica surface results in a strong enhancement of the catalytic activity as shown in Table 1.

For example, norbornene yields at ambient temperature the ROMP polymer at an olefin/molybdenum ratio of 300 with turnover frequencies beyond 3000 h^{-1}. In contrast, the molecular nitrido complex is completely inactive under these and related reaction conditions. The concept of organometallic surface catalysis experienced its breakthrough when metal alkyls based

Table 1. Catalytic activity of **1** and **4** in olefin metathesis ([mon.]/[Mo] = 300; T = 25 °C; CH_2Cl_2).

Complex	Monomer	Yield [%]	TOF [a]
$NMo(CH_2tBu)_3/SiO_2$ **4**	norbornene	85 [b]	3060
$NMo(CH_2tBu)_3/SiO_2$ **4**	*cis*-cyclooctene	74 [c]	1200
$NMo(CH_2tBu)_3/SiO_2$ **4**	*trans*-2-pentene	45	50 88 2800 [d]
$NMo(CH_2tBu)_3$ **1**	norbornene	0	–
$NMo(CH_2tBu)_3$ **1**	*cis*-cyclooctene	0	–
$NMo(CH_2tBu)_3$ **1**	*trans*-2-pentene	5	>10

[a] TOF = turnover frequency: mol(product)/[mol(catalyst) × h]. [b] M_n = 317000, PDI = 1.8. [c] M_n = 307000, PDI = 1.9. [d] T = 60 °C.

 © VCH Verlagsgesellschaft mbH, D-69451 Weinheim, 1996 0570-0833/96/3523-2804 $ 15.00+.25/0

on tantalum or zirconium were used as molecular precursors. In these cases, however, alkyl groups are detached during the grafting process as a consequence of protolysis.[9] In our case, all alkyl groups first remain at the metal since the acidic surface silanols attack the nitridomolybdenum moiety, whereas only in the second step an α-elimination occurs, yielding the corresponding alkylidene species. Further work in this area is in progress.

Received: May 27, 1996 [Z 8978 IE]
German version: *Angew. Chem.* **1996**, *108*, 2978–2980

Keywords: catalysis · complexes with nitrogen ligands · molybdenum compounds · polymerizations · ring-opening metatheses polymerizations

[1] *Applied Homogeneous Catalysis by Organometallic Complexes* (Eds.: B. Cornils, W. A. Herrmann), VCH, Weinheim, **1996**.
[2] a) K. J. Ivin, *Olefin Metathesis*, Academic Press, London **1983**. b) Recent review: J. Mol. in ref. [1], p. 318.
[3] a) K. Weiss, G. Lössel, *Angew. Chem.* **1989**, *101*, 75; *Angew. Chem. Int. Ed. Engl.* **1989**, *28*, 62. b) V. Dufaud, G. P. Niccolai, J. Thivolle-Cazat, J.-M. Basset, *J. Am. Chem. Soc.* **1995**, *117*, 4289.
[4] W. A. Herrmann, S. Bogdanovic, R. Poli, T. Priermeier, *J. Am. Chem. Soc.* **1994**, *116*, 4989.
[5] S. Bogdanovic, Ph.D. Thesis, Technische Universität München, **1994**.
[6] a) **2a**: **1** (1.0 mmol) and triphenylsilanol (1 mmol) were placed in a Schlenk tube under argon and dissolved in THF (30 mL). The reaction mixture was stirred at 60 °C for 48 h. Removal of the solvent under reduced pressure and extraction of the residue with *n*-hexane (5 mL) afforded **2a** as a white powder. Recrystallization from *n*-hexane at 0 °C gave 240 mg of **2a** as white crystals in 40% yield. Analysis: calcd (found): C 61.68 (61.30), H 8.36 (8.40), N 2.72 (2.74). Spectroscopic data: FT-IR (Nujol) $\tilde{\nu} = 3371\ cm^{-1}$: ν(N–H). ^1H NMR (400 MHz, C_6D_6, 25 °C): $\delta = 7.93$ (m, 6H), 7.22 (m, 9H), 2.24 (Mo-CH_2*t*Bu, s, 6H), 0.99 (Mo-$CH_2C(CH_3)_3$, s, 27H). ^{13}C NMR (100 MHz, C_6D_6, 25 °C): $\delta = 138.81$, 135.95, 129.50, 128.98, 84.94 (MoCH_2*t*Bu), 34.84 (Mo-$CH_2C(CH_3)_3$), 32.59 (MoC$H_2C(CH_3)_3$). ^{29}Si NMR (80 MHz, C_6D_6, 25 °C): $\delta = -19.5$. b) **2b**: **1** (1.0 mmol) and 1,1,3,3-tetraphenyldisiloxane-1,3-diol (0.5 mmol) were placed in a Schlenk tube under argon and dissolved in THF (30 mL). The reaction mixture was stirred at 60 °C for 4 h. Removal of the solvent under reduced pressure and extraction of the residue with *n*-hexane (10 mL) afforded **2b** as off-white crystals. Recrystallization from *n*-hexane at 0 °C gave 409 mg of **2b** as pale yellow crystals in 77% yield. Analysis: calcd (found): C 61.11 (61.30), H 8.36 (8.40), N 2.64 (2.74). Spectroscopic data: FT-IR (Nujol) $\tilde{\nu} = 3371\ cm^{-1}$: ν(N–H). ^1H NMR (400 MHz, C_6D_6, 25 °C): $\delta = 8.11$ (m, 8H), 7.27 (m, 12H), 2.16 (Mo-CH_2*t*Bu, s, 12H), 0.97 (Mo-$CH_2C(CH_3)_3$, s, 54H). ^{13}C NMR (100 MHz, C_6D_6, 25 °C): $\delta = 139.44$, 135.40, 129.37, 128.99, 128.01, 85.56 (Mo-CH_2*t*Bu), 34.95 (Mo-$CH_2C(CH_3)_3$), 32.58 (Mo-$CH_2C(CH_3)_3$). ^{29}Si NMR (80 MHz, C_6D_6, 25 °C): $\delta = -45.8$.
[7] Single crystals from *n*-hexane solution at 0 °C. Crystal data: $C_{54}H_{88}Mo_2N_2O_3Si_2$ (1061.4), monoclinic, space group $P2_1/c$ (no. 14); $a = 11.653(1)$, $b = 20.305(2)$, $c = 24.496(3)$ Å, $\beta = 97.15(1)°$, $Z = 4$, $V = 5751(1)$ Å^3, $\rho_{calcd} = 1.226\ g cm^{-3}$, $\mu = 5.2\ cm^{-1}$, $Mo_{K\alpha}$ radiation, −80 °C; Enraf-Nonius CAD4, ω scan, 10681 recorded reflections, of which 8929 with $I > 0$ were used in the refinement. The structure solution was achieved by direct methods. $R = 0.04$, $Rw = 0.032$, residual electron density $+0.44/-0.36\ e Å^{-3}$.
[8] Partially dehydroxylated silica was used for the grafting study (Degussa, 200 $m^2 g^{-1}$; pretreatment at 500 °C for 15 h under vacuum).
[9] J. Kress, J. A. Osborn, G. Schoettel in *Advances in Metal Carbene Chemistry* (Ed.: U. Schubert), Kluwer, Dordrecht, **1989**.
[10] J.-M. Basset in ref. [1], p. 624.

Chiral Heterocyclic Carbenes in Asymmetric Homogeneous Catalysis**

Wolfgang A. Herrmann,* Lukas J. Goossen, Christian Köcher, and Georg R. J. Artus

According to preliminary investigations, N-heterocyclic carbenes of the imidazole, pyrazole, and triazole type act as controlling ligands in organometallic homogeneous catalysis.[1, 2] The key advantage of these ligands appears to be that they do not dissociate from the metal centers, particularly in the case of electron-rich catalytically active metals like rhodium or palladium.[1] In contrast to the well-established phosphanes, an excess of ligand is not needed—an important criterion for future industrial applications. In this publication it is shown that *chiral* N-heterocyclic carbenes can be prepared conveniently; moreover, they form organometallic complexes for asymmetric homogeneous catalysis.

For the chiral imidazolium salts **1a,b** a ring closure synthesis starting from inexpensive materials was needed,[3] which can be applied broadly and which proceeds without racemization. The C_2-symmetric derivatives **1a,b** with chiral centers directly connected to the ligand core were obtained *in one step* and without racemization from chiral amines, glyoxal, and formaldehyde according to Equation (1). The identity of **1a** was confirmed by a crystal structure.[4] Deprotonation of the chiral imidazolium salts was accomplished quantitatively by a novel procedure[5] with sodium hydride in liquid ammonia at −33 °C.[6] No side reactions were observed.

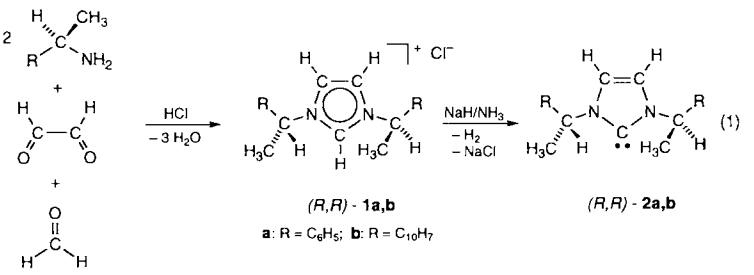

(1)

If the ring closure is performed with racemic amines the *meso*-isomers of **1a,b** and **2a,b** are formed as well (NMR). This confirms that the synthesis is free from racemization up to the step of the free carbenes **2a,b**. A possible configurational lability of **2a,b** because of the high acidity of the α-protons could not be excluded.

The large tendency of the N-heterocyclic carbenes toward complexation[7] was confirmed with these new chiral derivatives. For example, hexacarbonyltungsten reacts at 25 °C with the (*R,R*)-configurated carbenes **2a,b** (generated in situ) to form the chiral carbene complexes (*R,R*)-**4a,b** as shown in Equation (2). According to an X-ray structure analysis the naphthyl

[*] Prof. Dr. W. A. Herrmann, L. J. Goossen, C. Köcher, Dr. G. J. R. Artus
Anorganisch-chemisches Institut der Technischen Universität München
Lichtenbergstrasse 4, D-85747 Garching (Germany)
Fax: Int. code +(89)289-13473
e-mail: herrmann@arthur.anorg.chemie.tu-muenchen.de

[**] Heterocyclic Carbenes, Part 9. This work received generous support from the Deutsche Forschungsgemeinschaft, the Fonds der Chemischen Industrie (PhD scholarship to L.J.G.), the Bayerische Forschungsstiftung (Bayerischer Forschungsverbund Katalyse, FORKAT), and the Volkswagenstiftung. Part 8: W. A. Herrmann, M. Elison, O. Runte, G. R. J. Artus, *J. Organomet. Chem.* **1995**, *501*, C1–C4.

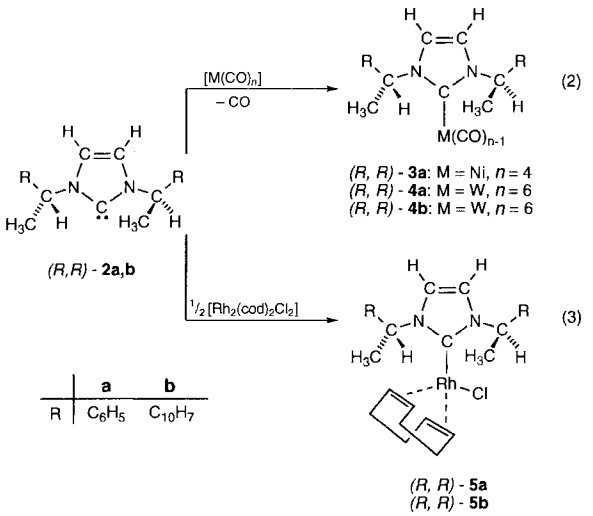

derivative **2b** contains two independent molecules in the asymmetric unit of the unit cell, which are distinguished by different conformations of the carbene ligand in relation to the $M(CO)_5$ fragment (Fig. 1).[8] The average carbene–tungsten distance C1–W1 is as long as expected (2.303 Å), and both the bond lengths and IR spectrum indicate that π backbonding is not significant with the N-heterocyclic ligand.[9] Starting from (*S*,*S*)-**1a** the nickel complex (*S*,*S*)-**3a** was synthesized in two steps.[10] The absolute configuration was confirmed by a crystal structure.[4]

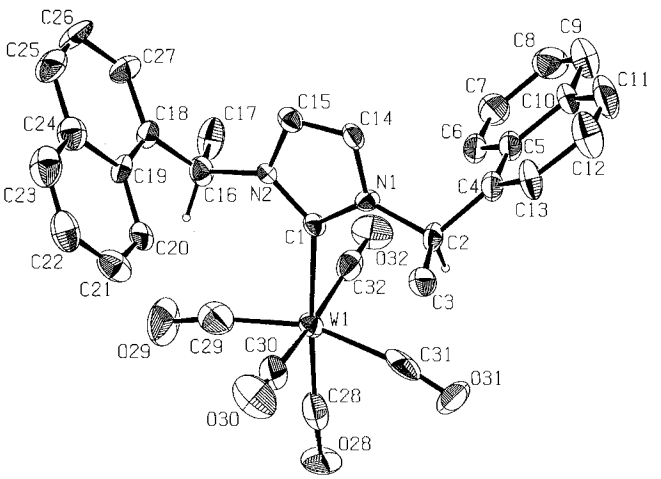

Fig. 1. Crystal structure (PLATON drawing) of one of the two independent molecules of the chiral tungsten complex (*R*,*R*)-**4b**. The thermal ellipsoides are drawn at the 50% probability level, and unimportant H atoms are omitted for clarity. Selected bond lengths [Å] and angles [°] (values in square brackets correspond to the second independent molecule in the unit cell): W1–C1 2.308(7), [2.298(7)] N1–C1 1.359(9), [1.36(1)] N1–C14 1.373(9), [1.349(9)] N2–C1 1.356(9) [1.37(1)], N2–C15 1.37(1) [1.36(1)], C14–C15 1.34(1) [1.33(1)]; C1-N1-C14 111.8(6) [112.9(6)], C1-N2-C15 111.0(6) [111.6(6)], N1-C1-N2 103.5(6) [101.9(6)], N1-C14-C15 106.0(6) [106.3(6)], N2-C15-C14 107(7) [107.3(6)].

The rhodium complexes **5a**,**b** were obtained according to Equation (3) in 88% yield.[11] They are stable in air both as solids and in solution, and their thermal stability is also remarkable (decomposition at 202 °C (**5a**) and 210 °C (**5b**)). When heated in solution they do not lose the heterocyclic carbene ligand even at temperatures higher than 100 °C (NMR study). Thus, the new complex type has excellent properties for an application in asymmetric synthesis. This was confirmed in the first tested application, the hydrosilylation of acetophenone according to Equation (4): With complex **5b** as a catalyst, almost quantitative conversions and optical inductions higher than 30% were achieved.

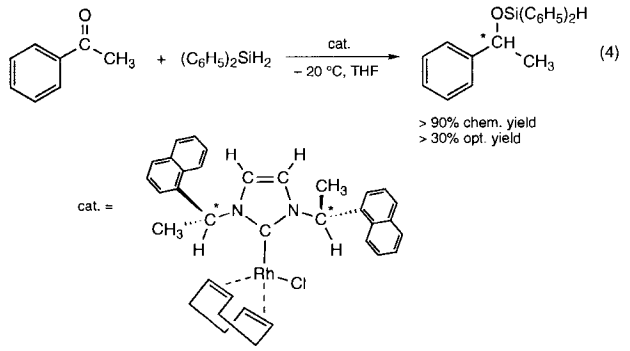

The complexes **5a**,**b** are active in hydrosilylation *without* an induction period and even at low temperatures (Fig. 2). The enantiomeric excesses are independent of the catalyst concentration as well as of the degree of conversion. All observations lead to the conclusion that the chiral N-heterocyclic carbenes remain bound to the metal center, in particular because a dissociated carbene ligand would not be stable under the conditions of the catalysis. The lifetime of the catalysts is remarkably high; even after reaction times of more than two weeks the catalysts showed no signs of decomposition.

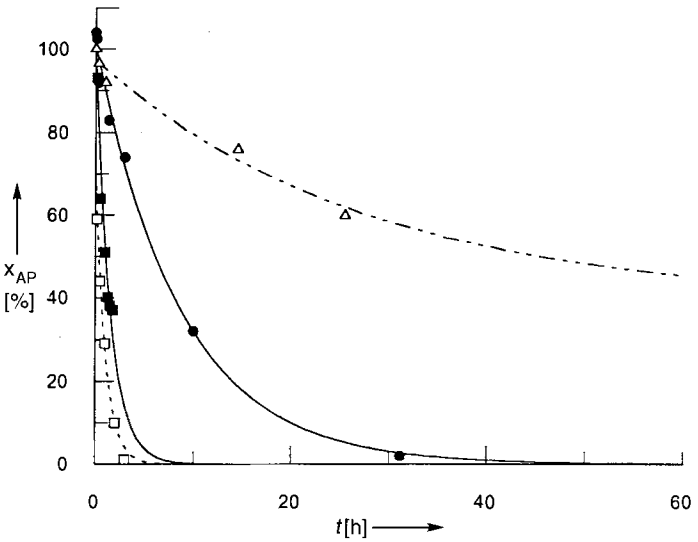

Fig. 2. Catalytic hydrosilylation of acetophenone: conversion vs. time. x_{AP} = acetophenone concentration. Conditions: ● −20 °C, 1% **5b**; □ 20 °C, 1% **5b**; ■ 0 °C, 1% **5b**; △ −20 °C, 0.1% **5b**.

These particular ligands were selected, because they do not contain any functional groups; decomposition products of the chiral ligands, for example the imiazolium salts **1a**,**b**, can therefore not coordinate to the catalytic center. All optical induction is lost if the catalyst is purposely degraded by addition of acid during the catalysis. A mixture of $[Rh_2(cod)_2Cl_2]$ and **1b** shows high activity in hydrosilylation; however, no enantiomeric enrichment results. Addition of **1b** alone also does not influence the optical induction of the catalysts **5a**,**b**. The optical induction is distinctly temperature-dependent and decreases at higher temperatures (Table 1). However, no significant solvent dependence could be observed.

 © VCH Verlagsgesellschaft mbH, D-69451 Weinheim, 1996 0570-0833/96/3523-2806 $ 15.00+.25/0 Angew. Chem. Int. Ed. Engl. 1996 35 No. 23/24

Table 1. Hydrosilylation of acetophenone with diphenylsilane in THF with **5b** as catalyst.

x (cat) [%]	T [°C]	t	Conv. [%]	ee [%]	TON
1	−20	1 d	90	26	90
0.2	−20	6 d	90	26	450
0.1	−20	12 d	90	26	900
1	−34	2 d	90	32	90
1	0	4 h	90	12	90
1	20	1 h	90	< 5	90
1 [a]	−20	24 h	90	26	90
0.1 [b]	−20	6 d	90	24	900
1	−20	7 h	60	26	60
1 [c]	−20	24 h	60	27	60

[a] Addition of 3 equiv **1b**. [b] Containing 5% $[Rh_2(cod)_2Cl_2]$. [c] Methyl naphthyl ketone instead of acetophenone.

Only chiral chelate complexes of rhodium lead to higher enantiomeric excesses in the catalytic hydrosilylation. For example, Rh/glucophinite yields 65% *ee*,[12] Rh/MPFA 49% *ee*,[13] and Rh/Pybox (without excess ligand) 83% *ee*.[14]

In spite of as yet unsatisfactory *ee* values, N-heterocyclic carbenes indeed appear to be controlling ligands well suitable for asymmetric homogeneous catalysis. Because the metal–carbon bond is very stable, no ligand excess is needed. The inexpensive synthesis and the structural variety of these types of ligands is another advantage. A significant improvement in the optical yields can be anticipated from further modified, donor-functionalized ligands.

Experimental Procedure

1a,b: A 500 mL round-bottomed flask was charged with (*R*)- or (*S*)-1-phenylethylamine (11.9 g, 0.10 mol) in toluene (100 mL). Under vigorous stirring and slight cooling paraformaldehyde (3.00 g, 0.10 mol) was added. After 30 min another equivalent of the amine was added at 0 °C. Under constant cooling 3.3 N HCl (30 mL, 0.10 mol) was slowly added. After removal of the cold bath 40% aqueous glyoxal solution was slowly added (14.5 mL, 0.10 mol). The mixture was stirred for 12 h at 35–40 °C. For workup diethyl ether (100 mL) and saturated Na_2CO_3 solution (50 mL) were added, the phases separated, and the aqueous layer washed with diethyl ether. After removal of the volatiles in vacuo the residue was taken up in CH_2Cl_2 (150 mL), dried over $MgSO_4$, and filtered. The solvent was then evaporated off, and the yellow residue was washed with diethyl ether, which transformed it into a light yellow extremely hygroscopic powder. Yield: 24.5 g (79%). The naphthyl derivative **1b** was prepared similarly from (*R*)-naphthylethylamine in 77% yield.

2a,b: The imidazolium salts **1a,b** (10.0 mmol) were deprotonated in a mixture of THF (20 mL) and ammonia (100 mL) at −33 °C with NaH (10.8 mmol). The starting materials were not completely soluble, but during the deprotonation a clear yellow solution was formed. After evaporation of the ammonia the volume was adjusted to 40 mL with THF. The 0.25 M solution obtained this way was used without further workup. NMR spectroscopic characterization (100 MHz, (THF/CD_3NO_2): δ[C(carbene)] = 211.2 (**2a**), 210.5 (**2b**).

3a,b: Hexacarbonyltungsten (880 mg, 2.5 mmol) or tetracarbonylnickel (426 mg, 2.5 mmol) were treated with solutions of the free carbenes **2a** or **2b** (2.5 mmol). After chromatography the residues were crystallized from methylene chloride. Compounds **3a** (629 g, 63%, colorless crystals) and **4a** (945 mg, 63%, yellow crystals) were obtained in good yield, and **4b** in moderate yield (525 mg, 29%, yellow crystals).

5a,b: $[Rh_2(cod)_2Cl_2]$ (200 mg, 0.40 mmol) in THF (5 mL) was treated with a freshly produced carbene solution (see **2**, 3.3 mL, 0.8 mmol). After 1 h the solvent was removed in vacuo, the residue taken up in CH_2Cl_2, and the resulting mixture filtered. Compounds **5a,b** were purified by precipitation from *n*-pentane/CH_2Cl_2 mixtures. Yield: 327 mg **5a** (79%) and 441 mg **5b** (71%) as yellow powders.

Typical catalytic hydrosilylation: A vial equipped with magnetic stirrer and septum was charged with (*R,R*)-**5b** (25 mg, 1 mol%), acetophenone (0.5 mL, 4.2 mmol), THF (1 mL), and di-*n*-butyl ether (100 mg as internal standard). The solution was cooled to −20 °C, and diphenylsilane (0.8 mL, 4.2 mmol) was added by syringe. Thereafter, methanol (1 mL) and a catalytic amount of *p*-tolylsulfonic acid were added to hydrolyze the silyl ether (20 min). The 1-phenylethanol was separated from the silyl ethers by kugelrohr distillation, and its purity was determined by NMR spectroscopy. The enantiomeric excesses were determined by gas chromatography (Lipodex A column, 80 °C isothermal).

Received: June 27, 1996 [Z 9260 IE]
German version: *Angew. Chem.* **1996**, *108*, 2980–2982

Keywords: asymmetric catalysis · carbene complexes · homogeneous catalysis · hydrosilylations · rhodium compounds

[1] W. A. Herrmann, M. Elison, J. Fischer, C. Köcher, G. R. J. Artus, *Angew. Chem.* **1995**, *107*, 2602–2605; *Angew. Chem. Int. Ed. Engl.* **1995**, *34*, 2371–2374.

[2] W. A. Herrmann, M. Elison, J. Fischer, C. Köcher, DE4447068 (Hoechst AG), **1994**; EP0719758, **1996**; DE4447067 (Hoechst AG), **1994**; EP0719753, **1996**; DE47066 (Hoechst AG), **1994**; EP0721953, **1996**.

[3] A. A. Griednev, I. M. Mihaltseva, *Synth. Commun.* **1994**, *24*, 1547–1555.

[4] W. A. Herrmann, L. J. Goossen, G. R. J. Artus, *Organometallics*, in print.

[5] W. A. Herrmann, C. Köcher, L. J. Goossen, G. R. J. Artus, *Chem. Eur. J.* **1996**, *2*, 1627–1636.

[6] (*S,S*)-**2a**: ^{13}C NMR (100 MHz, THF/CD_3NO_2): δ = 211.2 (C:), 144.3 (phenyl-*C*R), 127.1 (*p*-phenyl-*C*H), 126.6 (phenyl-*C*H), 117.8 (NCH=), 59.5 (NCH), 22.3 (CH_3). (*S,S*)-**2b**: ^{13}C NMR (400 MHz,$CDCl_3$): δ = 210.5 (C:), 134.4, 131.8, 129.3, 129.0, 126.9, 126.3, 125.9, 124.4, 124.3 (naphthyl), 118.7 (NC=), 56.4 (NCH), 22.2 (CH_3).

[7] a) K. Öfele, W. A. Herrmann, D. Mihalios, M. Elison, E. Herdtweck, E. Scherer, J. Mink, *J. Organomet. Chem.* **1993**, *459*, 177–184; b) M. Regitz, *Angew. Chem.* **1996**, *122*, 791–794; *Angew. Chem. Int. Ed. Engl.* **1996**, *35*, 725–728.

[8] Crystal structure analysis of **4b** ($C_{32}H_{24}N_2O_5W$), M_r = 700.39, yellow plate 0.05 × 0.15 × 0.15 mm^3, monoclinic, space group $P2_1$, a = 12.481(2), b = 12.349(1), c = 19.073(2) Å, b = 100.14(1)°, V = 2893.8 Å^3, Z = 4, ρ_{calcd} = 1.61 g cm^{-3}, μ = 41.2 cm^{-1}, T = −100.0(3) °C, measured with IPDS (STOE) with $Mo_{K\alpha}$ radiation, 240 pictures in the range $0° < \varphi < 360°$, $\Delta\varphi$ = 1.5°, 5 min exposure, distance between detector and crystal 80 mm, range $1.42° < \theta < 24.2°$; 32746 reflections measured, 7 beyond the dynamic region, 0 overlapping, 2690 systematic absences or reflections with negative intensity, 8569 independent; R_{merge} = 0.06, Lorentzian polarization and empirical absorption corrections performed with IPDS-Software, 7699 reflections with $I > 1.0\sigma(I)$ used for refinement, 720 parameters, 10.7 reflections per parameter, Flack parameter −0.02(1), Chebychev polynomial weighting, hydrogen atoms calculated, residual electron density 1.71 e Å^{-3} and −2.28 e Å^{-3}, GOF = 0.814, $R = \sum(||F_o| - |F_c||)/\sum|F_o| = 0.035$, $R_w = [\sum w(|F_o| - |F_c|)^2/\sum wF_o^2]^{1/2} = 0.040$. Several physically doubtful thermal displacement parameters were obtained from refinement of **4b**. Unsatisfactorily corrected absorption effects cannot be excluded as a reason. However, there is some evidence that **4b** is contaminated with a small amount of **4a**. The resulting unresolvable disorder in the crystal of **4b** may well cause meaningless displacement parameters. Crystallographic data (excluding structure factors) for the structure reported in this paper have been deposited with the Cambridge Crystallographic Data Centre as supplementary publication no. CCDC-179-122. Copies of the data can be obtained free of charge on application to The Director, CCDC, 12 Union Road, Cambridge CB2 1EZ, UK (fax: int. code +(1223) 336-033; e-mail: teched@chemcrys.cam.ac.uk).

[9] *Transition Metal Carbene Complexes* (Eds.: U. Schubert, H. Fischer, P. Hofmann, K. Weiss, K.-H. Dötz, F. R. Kreissl), VCH, Weinheim **1983**, p. 137–143.

[10] **3a**: ^{1}H NMR (400 MHz, $CDCl_3$): δ = 7.4–7.2 (overlapping multipletts, 10H, phenyl-H), 6.75 (s, 2H, HC=), 6.08 (q, ^3J(H,H) = 7 Hz, 2H, NCH), 1.73 (d, ^3J(H,H) = 7 Hz, 6H, CH_3); ^{13}C NMR (100 MHz, $CDCl_3$): δ = 197.8 (CO), 189.2 (CN_2), 141.0, 128.6, 127.7, 126.7 (Ph-C), 118.4 (NC=), 58.5 (NCH), 20.8 (CH_3); IR (THF) $\tilde{\nu}$(CO) = 2050, 1968 cm^{-1}. **4a**: ^{1}H NMR (400 MHz, C_6D_6): δ = 7.14–7.29 (m, 10H, Ph-H); 6.48 (q, ^3J(H,H) = 3 Hz, 2H, NC*H*), 6.28 (s, 2H, HC=), 1.55 (d, ^3J(H,H) = 6.5 Hz, 6H, CH_3); ^{13}C NMR (100 MHz, C_6D_6): δ = 200.9 (*trans*-CO), 198.5 (*cis*-CO), 180.3 (CN_2), 141.2 (*p*-PhC), 129.4 (PhC), 128.6 (Ph*C*R), 127.1 (PhC), 120.4 (=CH), 60.9 (CH), 21.7 (CH_3); IR (THF) $\tilde{\nu}$ = 2060, 1927 cm^{-1}.

[11] **5b**: ^{1}H NMR (400 MHz, $CDCl_3$): δ = 8.97 (d, ^3J(H,H) = 9 Hz, 1H, naphthyl-H), 8.58 (d, ^3J(H,H) = 9 Hz, 1H, naphthyl-H), 8.0–7.0 (m, 12H, naphthyl-H), 7.22 (q, ^3J(H,H) = 7 Hz, 2H, NCH), 7.01 (m, 2H, HC=), 4.8 (m, 2H, cod-CH), 4.19 (m, 1H, cod-CH), 3.39 (m, 1H, cod-CH), 2.5–1.0 (m, 8H, cod-CH_2), 2.03 (d, ^3J(H,H) = 7 Hz, 3H, CH_3), 1.84 (d, ^3J(H,H) = 7 Hz, 3H, CH_3); ^{13}C NMR (100 MHz, $CDCl_3$): δ = 183.5 (d, $^1J(^{103}Rh,C)$ = 51 Hz, CN_2), 141.0, 136.4, 133.8, 131.0, 130.1, 129.0, 128.8, 128.5, 127.7, 127.2, 126.7, 126.1, 125.3, 125.1, 124.9, 123.8, 123.7, 121.4 (naphthyl-C), 119.3 (NCH), 118.6 (NCH), 98.4 (d, $^1J(^{103}Rh,C)$ = 7 Hz, cod-CH), 97.6 (d, $^1J(^{103}Rh,C)$ = 7 Hz, cod-CH), 70.0 (d, $^1J(^{103}Rh,C)$ = 5 Hz, cod-CH), 66.5 (d, $^1J(^{103}Rh,C)$ = 5 Hz, cod-CH), 57.2 (NCH), 55.2 (NCH), 32.5, 32.0 (cod-CH_2), 29.2 (CH_3), 27.2 (CH_3), 23.1, 22.8 (cod-CH_2).

[12] T. H. Johnson, K. C. Klein, S. Thomen, *J. Mol. Catal.* **1981**, *12*, 37–40.

[13] I. Ojima, K. Hirai in Asymmetric Synthesis, *Vol. 5* (Ed. J. D. Morrison), Academic Press, **1985**, p. 103–113.

[14] H. Brunner, *Methoden der Organischen Chemie* (Houben–Weyl), 4th ed. 1952–, Vol. E 21, Thieme, Stuttgart, **1995**, p. 4074–4081.

 © VCH Verlagsgesellschaft mbH, D-69451 Weinheim, 1996 0570-0833/96/3523-2807 $ 15.00+.25/0

Supramolecular Host–Guest Compounds with Tripod–Metal Templates as Building Blocks at the Corners**

Susanne Mann, Gottfried Huttner,* Laszlo Zsolnai, and Katja Heinze

Dedicated to Professor Walter Siebert on the occasion of his 60th birthday

Tripod–metal templates tripodM^{n+} (tripod = $CH_3C(CH_2PPh_2)_3$) are stable units, which, depending on the metal center M and the charge n, can form strong bonds with a multitude of donors.[1–7] The coordination chemistry of these tripod–metal templates is established by the respective metal and its charge: tripod–cobalt(II) templates form, almost without exception,[4] five-coordinate complexes,[2] tripod–iron(II) templates form, likewise almost without exception,[3, 5] six-coordinate complexes, which adopt an idealized octahedral geometry.[4, 6, 7] These structure-determining properties have been detected and confirmed for many mononuclear complexes;[1–7] however, these templates have not been used for the specific construction of supramolecular units.[8] The fact that the tripod–iron(II) template binds relatively strongly to three additional ligands, and that the resulting bonds are at right angles to one another, suggests that these templates could be used for the construction of three-dimensional cage compounds. For cages of an appropriate size, counterions of matching symmetry could be incorporated into the framework of the host molecule. We report here on the synthesis of tetrahedral host–guest complexes, which are formed by molecular self-assembly according to this principle. According to Equation (a) six fumaronitrile ligands, four iron(II) ions, four tripod ligands, and one tetrafluoroborate ion react to give the tetrahedral host–guest complex **1a**.

$$4\,CH_3C(CH_2PPh_2)_3 + 4\,Fe(BF_4)_2 \cdot 6\,H_2O + 6\,NCC_2H_2CN \xrightarrow[20\,^\circ C]{[CH_2Cl_2/EtOH]} [\{(CH_3C(CH_2PPh_2)_3Fe)\}_4(NCC_2H_2CN)_6(BF_4)](BF_4)_7 \quad (a)$$

$$\mathbf{1a}(BF_4)_7$$

The BF_4^- salt of **1a** was characterized by a complete elemental analysis as well as by NMR spectroscopy and X-ray structure analysis.[9] The cationic unit of $\mathbf{1a}(BF_4)_7$, the host–guest complex **1a**, is shown in Figure 1.

This unit exhibits C_2 symmetry (twofold axis through the middle of the edges Fe1, Fe1A and Fe2, Fe2A, and the central BF_4^- ion); the symmetry of the core composed of the four iron centers that are located at the corners and the encapsulated BF_4^- ion is higher (Fig. 2). The B–F bonds of the encapsulated anion point towards the four iron centers located at the corners of the tetrahedron. The agreement between the symmetry of the guest molecule and that of the basic framework of the host molecule (Figs. 1 and 2) could be one of the reasons why 15 components, which exist isolated in solution, organize to give the molecular host–guest complex **1a**. Due to the width of the signals, the ^{19}F NMR spectra of the salt $\mathbf{1a}(BF_4)_7$ do not permit any clear differentiation between the encapsulated BF_4^- ion and the seven free BF_4^- ions at 25 °C; however, at −30 °C a clear splitting into two

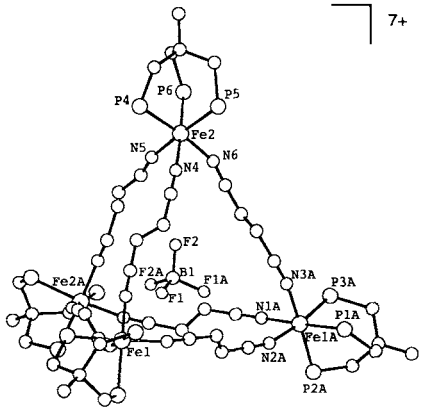

1a

Fig. 1. Crystal structure of the tetrahedral host–guest complex **1a** (the phenyl rings at the phosphorus atoms of the four tripod ligands are omitted for clarity, those atoms labeled with an A were generated by symmetry operation). Bond lengths [Å] and angles [°]: Fe–N 1.93–1.98, Fe–P 2.29–2.31, Fe1–F1 (Fe1A–F1A) 4.38, Fe2–F2 (Fe2A–F2A) 4.60, B1–F1 (B1–F1A) 1.47, B1–F2 (B1–F2A) 1.40; N-Fe-N 81.8–84.6, P-Fe-P 87.8–91.1.

sharp signals occurs ($\delta = -202.5$ and -197.0), the integrals of which are as expected in the ratio of 1:7.

The specific and rigid form of the fumaronitrile ligand is not responsible for the formation of the tetranuclear host molecule: succinonitrile, the saturated derivative of fumaronitrile, leads, under reaction conditions analogous to those used for the preparation of **1a**, to the host–guest complex **1b** [Eq. (b)].

Fig. 2. Schematic representation of the iron tetrahedron with encapsulated BF_4^- tetrahedron of compound **1a**.

$$4\,CH_3C(CH_2PPh_2)_3 + 4\,Fe(BF_4)_2 \cdot 6\,H_2O + 6\,NCC_2H_4CN \xrightarrow[20\,^\circ C]{[CH_2Cl_2/EtOH]} [\{(CH_3C(CH_2PPh_2)_3Fe)\}_4(NCC_2H_4CN)_4(BF_4)](BF_4)_7 \quad (b)$$

$$\mathbf{1b}(BF_4)_7$$

Despite the considerably higher flexibility of the saturated derivative in comparison to that of fumaronitrile, a rigid tetrahedral arrangement of the four iron centers with an encapsulated BF_4^- ion, whose position is fit to the symmetry, is likewise formed (Fig. 2). Spectroscopic and analytical data confirm the composition of **1b**. The BF_4^- salt of **1b** crystallizes isotypic to the salt of **1a**, the structure is therefore shown only for **1a**[10] (Fig. 1).

The high positive charge of **1a** (**1b**) is the reason why in each case four BF_4^- anions occur in associated form in the outer coordination sphere of the tetrahedra ($\mathbf{1a}(BF_4)_4^{3+}$, Fig. 3). These anions occupy positions above the centers of the four triangular faces of each tetrahedron. They are oriented in such a way that in each case three B–F bonds are directed towards the iron centers, which form the triangular faces.

The shortest Fe–F distances in each case lie between 4.76 and 5.55 Å

Fig. 3. Schematic representation of the iron tetrahedron with encapsulated BF_4^- ion and the four tetrahedron-face-capping BF_4^- ions of the compound **1a** (**1b**) (light: iron tetrahedron; dark: central BF_4^- ion as well as the four capping BF_4^- ions).

[*] Prof. Dr. G. Huttner, S. Mann, Dr. L. Zsolnai, K. Heinze
Anorganisch-chemisches Institut der Universität
Im Neuenheimer Feld 270, D-69120 Heidelberg (Germany)
Fax: Int. code +(6221)545707

[**] We thank Prof. D. Sellmann and Dr. M. Moll for the ^{19}F NMR spectroscopic measurements.

for the capping BF_4^- ions for **1a**, and between 4.68 and 5.57 Å for **1b**. They are significantly larger than the Fe–F distances of the BF_4^- ion encapsulated in the tetrahedron[10] (Fig. 1). The weaker coordination of the outer BF_4^- ions is apparent since, unlike the BF_4^- ion encapsulated in the tetrahedron, they can be rapidly exchanged for counterions in solution. In accordance with the comparatively isometric form of the associates $\mathbf{1a}(BF_4)_4^{3+}$ and $\mathbf{1b}(BF_4)_4^{3+}$, their crystal packing can be described to a good approximation as face-centered cubic[11] (Fig. 4).

Fig. 4. Space-filling representation of the associate $\mathbf{1b}(BF_4)_4^{3+}$ (light: host–guest complex **1b**, dark: tetrahedron-face-capping BF_4^- ions).

The remaining three BF_4^- ions per associate occupy the tetrahedral and octahedral holes of this idealized densest packing. In the larger octahedral holes they are distributed between two positions with 50% in each. According to NMR data, the packing present in the crystal is a result of the supramolecular organization of the building blocks.

The fact that the tetrahedral host–guest complexes **1** despite the different structure of the bifunctional bridging ligands are formed selectively in each case indicates the great variations possibile with the presented synthetic concept.

Experimental Procedure

A solution of 1,1,1-tris(diphenylphosphinomethyl)ethane [7] (624 mg, 1 mmol) in CH_2Cl_2 (20 mL) was added dropwise to a solution of $Fe(BF_4)_2 \cdot 6H_2O$ [12] (338 mg, 1 mmol) in EtOH (10 mL) and stirred. After the mixture had been stirred for 20 min at 20 °C, fumaronitrile (117 mg, 1.5 mmol) (in the case of **1a**) or succinonitrile (120 mg, 1.5 mmol) (in the case of **1b**) as a solid was added in one portion; the color did not change initially. After the mixture had been stirred for 15 h at 20 °C a slightly cloudy solution was formed (in the case of **1a** deep orange, in the case of **1b** red), which was concentrated to dryness. The residue was washed with Et_2O (3 × 20 mL) and subsequently dried under vacuum at 10^{-2} mbar. Crystals suitable for X-ray structure analysis were obtained by dissolving the microcrystalline powder in $CH_3NO_2 \cdot CH_2Cl_2$ (4:1) followed by gas-phase diffusion of Et_2O at room temperature.

1a: Yield: 92%; ^1H NMR: $\delta = 7.5-7.3$ (br., 120 H, H_{Ar}), 7.1 (br., 12 H, CN-CH), 2.9 (br., 24 H, CH_2-PPh_2), 1.95 (br., 12 H, CH_3-C); ^{31}P NMR: $\delta = 28.5$ (s); ^{13}C NMR: $\delta = 133.6$ (d, $^2J(CP_{trans}) = 10$ Hz, P-C_{ipso}), 133.2 (m, C_{ortho}), 131.9 (br., C_{para}), 130.1 (m, C_{meta}), 129.2 (m, C≡N), 122.8 (s, CH-C≡N), 37.3 (CH_3-C), 36.5 (CH_3-C), 31.0 (m, CH_2-P); ^{11}B NMR: $\delta = 0.25$ (s); ^{19}F NMR ($T = -30$ C): $\delta = -202.5$ (s, 28 F, BF_4 outer), −197.0 (s, 4 F, BF_4 inner); MS (FAB): m/z (%) = 699 (100, TripodFeF), 547 (66,Tripod-Ph), 1416 (6, $Tripod_2Fe_2F_3$-2); IR (CsI): $\tilde{\nu}$ [cm^{-1}] = 2254 (w, C≡N), 1437 (m), 1062 (s, br., B-F), 833 (w, P-C-alkyl), 742 (m), 696 (m), 520 (m); elemental analysis calculated for $C_{188}H_{168}P_{12}N_{12}Fe_4B_8F_{32}$: C 58.12, H 4.36, P 9.57, N 4.33, B 2.23, F 15.65, Fe 5.75; found: C 56.38, H 4.34, P 6.37, N 4.04, B 4.05, F 16.4, Fe 6.25.

1b: Yield: 85%; ^1H NMR: $\delta = 7.5-7.4$ (m, 120 H, H_{Ar}), 3.5 (br., 24 H, CN-CH_2), 2.8 (br., 24 H, CH_2-PPh_2), 1.9 (br., 12 H, CH_3-C); ^{31}P NMR: $\delta = 30.9$ (s); ^{13}C NMR: $\delta = 134.1$ (dd, $^1J(CP) \approx 13.1$, $^3J(CP_{trans}) = 25.5$ Hz, P-C_{ipso}), 133.4 (m, C_{ortho}), 131.7 (br., C_{para}), 129.9 (m, C_{meta}), 36.9 (m, CH_3-C), 36.5 (m, CH_3-C), 31.6 (m, CH_2-P), 17.1(s, CH_2-C≡N); ^{11}B NMR: $\delta = 0.21$ (s); ^{19}F NMR ($T = 23$ C): $\delta = -198.3$ (br.); ^{19}F NMR ($T = -30$ °C): $\delta = -201.4$ (s, BF_4 outer), −199.6 (s, BF_4 inner); MS (FAB): m/z (%) = 699 (100, TripodFeF), 547 (54, Tripod-Ph), 1417 (15, $Tripod_2Fe_2F_3$-1); IR (CsI): $\tilde{\nu}$ [cm^{-1}] = 1484 (m), 1436 (m), 1060 (s, br., B-F), 837 (m, P-C-Alkyl), 742 (m), 700 (m), 521(m); elemental analysis calculated for $C_{188}H_{180}P_{12}N_{12}Fe_4B_8F_{32}$: C 57.94, H 4.66, P 9.54, N 4.31, B 2.22, F 15.6, Fe 5.73; found: C 56.67, H 4.75, P 7.27, N 5.04, B 2.12, F 16.7, Fe 4.91.

Received: July 22, 1996 [Z.9358 IE]
German version: *Angew. Chem.* **1996**, *108*, 2983–2984

Keywords: cage compounds · host–guest chemistry · iron compounds · supramolecular chemistry · template syntheses

[1] H. A. Mayer, *Chem. Rev.* **1994**, *94*, 1239; M. Di Vaira, M. Sacconi, *Angew. Chem.* **1982**, *94*, 338; *Angew. Chem. Int. Ed. Engl.* **1982**, *21*, 330; M. Di Vaira, F. Mani, S. Moneti, M. Peruzzini, L. Sacconi, P. Stoppioni, *Inorg. Chem.* **1985**, *24*, 2230; C. Bianchini, C. Mealli, A. Meli, M. Sabat, P. Zanello, *J. Am. Chem. Soc.* **1987**, *109*, 185.

[2] M. Di Vaira, S. Midollini, L. Sacconi, *J. Am. Chem. Soc.* **1979**, *101*, 1757; C. Mealli, S. Midollini, L. Sacconi, *Inorg. Chem.* **1975**, *14*, 2513; A. Barth, G. Huttner, M. Fritz, L. Zsolnai, *Angew. Chem.* **1990**, *102*, 956; *Angew. Chem. Int. Ed. Engl.* **1990**, *29*, 929; S. Vogel, A. Barth, G. Huttner, L. Zsolnai, R. Kremer, *ibid.* **1991**, *103*, 325 and. **1991**, *30*, 303.

[3] C. A. Ghilardi, F. Laschi, S. Midollini, A. Orlandini, G. Scapacci, P. Zanello, *J. Chem. Soc. Dalton Trans.* **1995**, *4*, 531.

[4] P. Dapporto, S. Midollini, L. Sacconi, *Inorg. Chem* **1975**, *14*, 1643.

[5] V. Körner, A. Asam, G. Huttner, L. Zsolnai, M. Büchner, *Z. Naturforsch. B* **1994**, *49*, 1183.

[6] A. Asam, B. Janssen, G. Huttner, L. Zsolnai, O. Walter, *Z. Naturforsch. B* **1994**, *48*, 1707.

[7] A. Muth, O. Walter, G. Huttner, A. Asam, L. Zsolnai, C. Emmerich, *J. Organomet. Chem.* **1994**, *468*, 149.

[8] R. W. Saalfrank, R. Burak, A. Breit, D. Stalke, R. Herbst-Irmer, J. Daub, M. Porsch, E. Bill, M. Müther, A. X. Trautwein, *Angew. Chem.* **1994**, *106*, 1697; *Angew. Chem. Int. Ed. Engl.* **1994**, *33*, 1621; R. W. Saalfrank, *ibid.* **1995**, *107*, 1085 and **1995**, *34*, 993; B. Dietrich, *Pure Appl. Chem.* **1993**, *65*, 1457; M. Fujita, S. Nagao, K. Ogura, *J. Am. Chem. Soc.* **1995**, *117*, 1649; P. Baxter, J. M. Lehn, A. DeCian, J. Fischer, *Angew. Chem.* **1993**, *105*, 92; *Angew. Chem. Int. Ed. Engl.* **1993**, *32*, 69; K. Worm, F. P. Schmidtchen, A. Schier, A. Schäfer, M. Hesse, *ibid.* **1994**, *106*, 360, and **1994**, *33*, 327; F. P. Schmidtchen, *Nachr. Chem. Tech. Lab.* **1988**, *36*, 8; A. Müller, H. Reuter, S. Dillinger, *Angew. Chem.* **1995**, *107*, 2505; *Angew. Chem. Int. Ed. Engl.* **1995**, *34*, 2328; X. Yang, C. B. Knobler, M. F. Hawthrone, *ibid.* **1991**, *103*, 1519 and **1991**, *30*, 1507; M. Newcomb, J. H. Horner, M. T. Blanda, P. J. Squattrito, *J. Am. Chem. Soc.* **1989**, *111*, 6294; T. Beissel, R. E. Powers, K. N. Raymond, *Angew. Chem.* **1996**, *108*, 1166; *Angew. Chem. Int. Ed. Engl.* **1996**, *35*, 1084.

[9] **1a**·$[BF_4]_3$: $0.20 \times 0.30 \times 0.30$ mm; orthorhombic; space group *Aba*2; $Z = 4$; $a = 2766(1)$, $b = 3007(1)$, $c = 2908(2)$ pm; $V = 24190 \times 10^6$ pm^3; $\rho_{calcd} = 1.127$ g cm^{-3}; measurement range $2.7 \le 2\theta \le 54.0°$; 13481 measured reflections, of which 13481 were independent; 5583 observed ($I \ge 2\sigma(I)$); $R = 0.138$, $R_w = 0.434$, residual electron density 1.23×10^{-6} e pm^{-3}. **1b**·$(BF_4)_3$: $0.30 \times 0.30 \times 0.30$ mm; orthorhombic; space group *Aba*2; $Z = 4$; $a = 2743.2(6)$, $b = 2975(2)$, $c = 2866.9(8)$ pm; $V = 23396 \times 10^6$ pm^3; $\rho_{calcd} = 1.215$ g cm^{-3}; measurement range $4.1 \le 2\theta \le 47.0°$; 8751 measured reflections, of which 8751 independent; 6932 observed ($I \ge 2\sigma(I)$); $R = 0.094$; $R_w = 0.278$; residual electron density 1.21×10^{-6} e pm^{-3}. For **1a** and **1b**: Siemens(Nicolet Syntex) R3m/V Diffractometer, $Mo_{K\alpha}$, graphite monochromator. Lorentz and polarization factors; experimental absorption correction; ψ scan; direct methods; SHELXL93 [1], SHELXS-86 [2] (G M. Sheldrick, University Cambridge, **1976**); least squares method. Further details of the crystal structure investigations may be obtained from the Fachinformationszentrum Karlsruhe, D-76344 Eggenstein-Leopoldshafen (Germany), on quoting the depository numbers CSD-405687 (**1a**) and CSD-405686 (**1b**).

[10] Bond lengths [Å] and angles [°] for **1b** (cf. Fig. 1): Fe–N 1.91–1.97, Fe–P 2.25–2.29, Fe1–F1 (Fe1A–F1A) 4.27, Fe2–F2 (Fe2A–F2A) 4.66, B1–F1 (B1–F1A) 1.39, B1–F2 (B1–F2A) 1.40; N-Fe-N 81.7–85.2, P-Fe-P 88.4–91.0.

[11] An idealized orthorhombic face-centered unit cell is formed by the translation along the z axis by about 1/4 c.

[12] H. Funk, F. Binder, *Z. Anorg. Chem.* **1926**, *166*, 327.

 © VCH Verlagsgesellschaft mbH, D-69451 Weinheim, 1996 0570-0833/96/3523-2809 $ 15.00+.25/0

Smaller Substituents on Nitrogen Facilitate the Osmium-Catalyzed Asymmetric Aminohydroxylation**

Joachim Rudolph, Peter C. Sennhenn, Cornelis P. Vlaar, and K. Barry Sharpless*

Dedicated to Professor Henri B. Kagan

The β-hydroxyamino structural unit is a key motif in many biologically important molecules. It is difficult to imagine a more efficient means of creating this functionality than by direct addition of the two heteroatom substituents to an olefin, especially if this transformation could also be regio- and/or enantioselective when required. We recently reported the discovery of such a catalytic asymmetric aminohydroxylation (AA) reaction. On treatment with a chiral alkaloid ligand, catalytic osmium, Chloramine-T as the nitrogen source, and water as the oxygen source, olefins undergo enantioselective vicinal addition of a sulfonamido and a hydroxyl group.[1] A limited range of substrates was investigated and enantioselectivities of up to 82% were achieved.[2] These initial results clearly leave much room for improvement. Above all, higher enantioselectivities are needed and, when applicable, higher regioselectivities. Another goal is better chemoselectivity, which principally means suppressing formation of the vicinal diol, sometimes a significant by-product.

We report here on progress in all three selectivity categories by use of sulfonamide-derived chloramine salts with smaller organic substituents on the sulfur.[3] The best results to date (Scheme 1, Table 1) were obtained with the methanesulfonamide-derived chloramine salt **2** (Chloramine-M[4]). This reagent can be prepared separately and added as the stable anhydrous salt or it can be generated in situ.[5, 6] The in situ method is preferred for large-scale applications.

As shown in Scheme 1 for methyl *trans*-cinnamate (**1**), the procedure is identical to the original AA procedure with the exception that Chloramine-M replaces Chloramine-T. This substitution results in the across-the-board improvements seen in Table 1 (cf. Table 1 in ref. [1]), where, for the sake of comparison, the olefins examined are the same ones used in the original Chloramine-T-based work.[7] In addition, it was possible to obtain all the products in enantiomerically pure form by recrystallization, an approach that did not always succeed with the related Chloramine-T derived products.[1] A further advantage is that residual methanesulfonamide, a major by-product (due to the use of three equivalents of Chloramine-M) can be removed quantitatively from the desired product by simply washing the

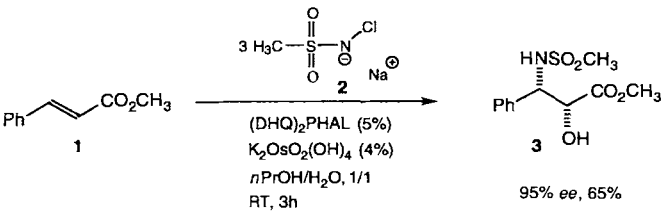

Scheme 1. AA process based on Chloramine-M. DHQ-H = dihydroquinine, PHAL = 1,3-phthalazinediyl, RT = room temperature.

Table 1. Catalytic asymmetric aminohydroxylation reaction with Chloramine-M as the nitrogen source.

Entry	Substrate	Product [a] $(DHQ)_2PHAL$	*ee* [%] [b] $(DHQD)_2PHAL$	Yield [%]	*t* [h]	M.p. [°C] [c]	$[\alpha]_D^{25}$ [c]
1 [d]	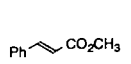	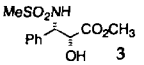 **3**	95 (99)*	95	65	3	150–152	+28.3
2 [e]	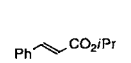	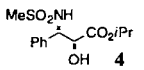 **4**	94 (99)*	95	65	3.5	97– 98	+26.2
3 [f]	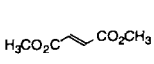	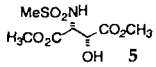 **5**	95 (99)*	94	76	2	91– 92	+16.8
4	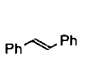	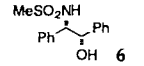 **6**	75 (99)	82	71	16	134–135	−6.9
5	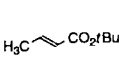	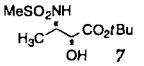 **7**	80 (99)	82	63	16	117–118	+8.1
6		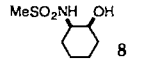 **8**	66 (99)	63	49	18	114–115	+18.8

[a] All reactions, except entry 3, were conducted in *n*PrOH/H_2O (1:1) in a room-temperature water bath. In all cases 4% $K_2OsO_2(OH)_4$ and 5% ligand were used. [b] Numbers in parentheses are *ee* values after recrystallization of the product from ethyl acetate/diethyl ether or ethyl acetate/hexane. (Asterisks mark cases in which the mother liquor is enantiomerically enriched, since the racemate crystallized preferentially.) [c] The melting points and optical rotations ($c = 1.0$ in 95% EtOH) refer to samples obtained by using $(DHQ)_2PHAL$ and which were subsequently recrystallized to enantiomeric purity. [d] Regioselectivity: 91:9. [e] Regioselectivity: 95:5. [f] CH_3CN/H_2O (1:1) was the solvent, and an additional 0.5 equiv of *tert*-butylhypochlorite was necessary to achieve these results. DHQ-H = dihydroquinine, DHQD-H = dihydroquinidine, PHAL = 1,3-phthalazinediyl.

[*] Prof. Dr. K. B. Sharpless, Dr. J. Rudolph, Dr. P. C. Sennhenn, Dr. C. P. Vlaar
Department of Chemistry, The Scripps Research Institute
10550 N. Torrey Pines Road, La Jolla, CA 92037 (USA)
Fax: Int. code + (619) 784-7562
e-mail: sharples@scripps.edu

[**] This research was supported by the National Institutes of Health (GM 28384), the National Science Foundation (CHE 9531152), and the W. M. Keck Foundation. J. R. is grateful for a NATO postdoctoral fellowship granted by the Deutsche Akademische Austauschdienst (DAAD); P. C. S. thanks the Deutsche Forschungsgemeinschaft (DFG), and C. P. V. thanks The Netherlands Organization for Scientific Research (NWO) for providing postdoctoral fellowships. We thank H.-T. Chang for many helpful discussions.

combined organic extracts with water. By contrast, removal of excess toluenesulfonamide often requires a tedious chromatographic separation. Methanesulfonamide was also easily removed by sublimation in vacuo.

A number of differences between the new and old systems are noteworthy: 1) Catalyst activity (i.e. turnover rate) is better in this new system. For example, in acetonitrile/water the AA process for isopropyl *trans*-cinnamate and Chloramine-T takes 3.5 hours to reach completion, while with Chloramine-M the reaction is complete in 40 minutes (side-by-side reactions in a water bath at room temperature). This rate increase is accompanied by significant increases in both enantioselectivity (from 60 to 89% *ee*) and regioselectivity (from 76:24 to 90:10). 2) The choice of solvent is a critical variable, and it can also be substrate dependent. In reactions with Chloramine-M, we found that *n*-propanol/water (1:1) generally gave better results than the acetonitrile/water system,[8] even though reactions in the former were slower (with isopropyl *trans*-cinnamate the reaction required 40 minutes in acetonitrile/water and 3.5 hours in *n*-propanol/water). Hence, the advantages of the *n*-propanol/water system are improved enantio-, regio-, and chemoselectivities but not rate. 3) A sensitive variable is temperature. Temperatures above 25 °C lead to a considerable increase in diol formation as well as a decline in selectivity. Therefore, use of a room-temperature water bath is usually adequate.[9] 4) Another significant difference between Chloramine-T and Chloramine-M in the AA process is the effect of the ligand on the rate. In the presence of the ligand, Chloramine-M generally reacts faster than Chloramine-T; in the absence of the ligand, Chloramine-T reacts faster. In fact, the ligand is required for the reaction of Chloramine-M to occur on a reasonable time scale. Thus this represents a clearcut example of the desirable phenomenon of ligand-accelerated catalysis.[10] By contrast, in the Chloramine-T system,[11] for most substrates, the ligand retards turnover (i.e. ligand-decelerated catalysis).

Scheme 2 shows our proposal for the key intermediate complexes involved in these catalytic systems. Like the AD process,[11] there is substantial evidence[12] that at least two catalytic cycles are operative in the AA system. The following discussion offers preliminary speculation on how the two cycles in Scheme 2 may explain some of the more important observations to date.

These initial investigations offer no decisive evidence as to why Chloramine-M is the superior reagent. However, experiments with other aliphatic and aromatic sulfonamide derivatives suggest that both electronic and steric factors play a role.[13] The steric demand of the organic substituent on the sulfonamide seems especially important. The smaller substituent (for example, methyl compared to *p*-tolyl) is thought to allow a better fit of the ensemble into the "binding pocket" of the catalyst in the transition state of the irreversible step (step a^1 in Scheme 2). However, effects on this irreversible step in the first cycle provide only part of the story, since the "direct"[14] effects of the ligand on selectivity are only possible when turnover occurs in the first cycle (Scheme 2). To whatever extent the ligand-independent second cycle intrudes, the ligand-mediated selectivity features are lost. Just like the *N*-morpholine-*N*-oxide (NMO) variants of the AD process,[15] these catalytic AA processes are conducted in homogeneous solution and therefore prone to the problems in the second cycle, where products are formed in a catalytic cycle not involving the ligand. Involvement of this cycle (a^2, h^2, o, repeat; Scheme 2) affords almost no enantio- or regioselectivity. In general, catalysis in the second cycle proceeds with much slower turnover rates, since the osmium(VI) bisazaglycolates (**IV**, Scheme 2) are often slow to hydrolyze (h^2), which is necessary before reoxidation (o) can occur.[12] There is considerable evidence that entry into the deleterious second cycle is suppressed by any factors that favor hydrolytic release of the glycolate or azaglycolate product from osmium. Since the methyl group is both smaller and less hydrophobic than the *p*-tolyl group, hydrolysis is expected to be easier in both cycles (steps h^1 and h^2), accounting for the faster catalysis rates. Of course, it is the suppression of the second cycle that is thought to account for most of the rate and selectivity advantages of the methyl over the *p*-tolyl substituent. This is not only because the second cycle is known to have devastating effects on both selectivity and turnover rate,[11] but also because once the second cycle is engaged, any enantio- and regioselectivity benefits that might accrue from better attractions in the catalyst binding pocket in the first cycle are irrelevant. Interestingly, the use of Chloramine-M seems to lead to faster hydrolysis of the azaglycolate complex (**III**, Scheme 2) *only* in the

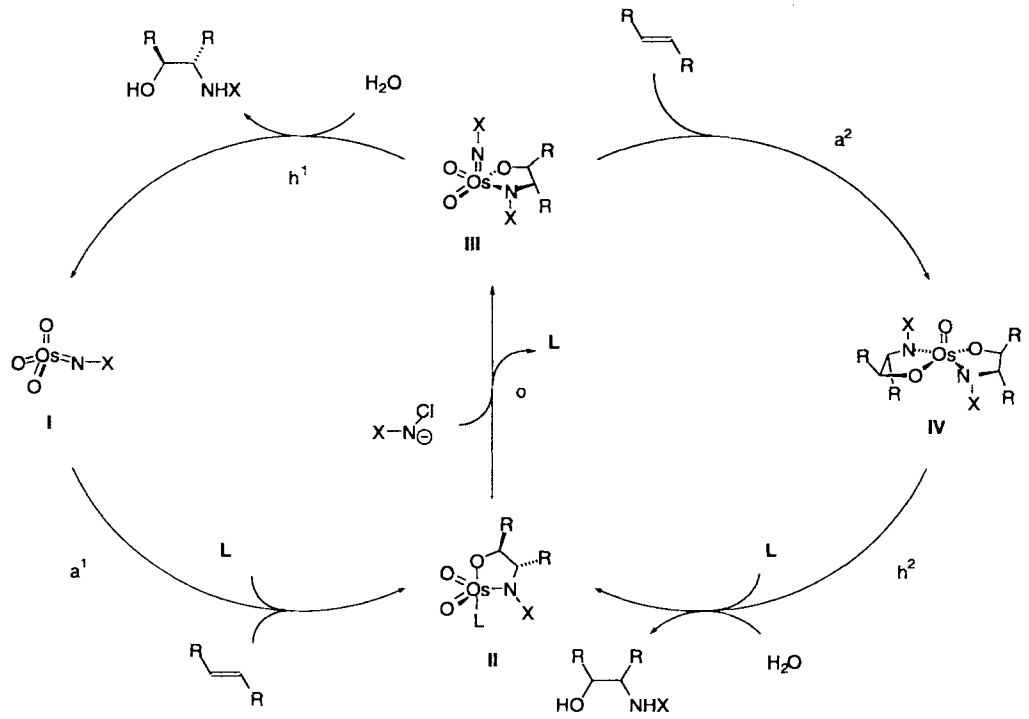

Scheme 2. Proposed mechanism for the AA reaction. Sequence of steps in the first catalytic cycle (left): 1) addition (a^1), 2) reoxidation (o), 3) hydrolysis (h^1); in the second catalytic cycle: 1) addition (a^2), hydrolysis (h^2), reoxidation (o). The first cycle proceeds with high enantioselectivity, the second with low enantioselectivity. L = ligand, X = CH_3SO_2.

presence of the ligand, since in the absence of ligand only very slow turnover is observed, underscoring again the stronger ligand dependence of the Chloramine-M system.

This work constitutes a major improvement in all the desirable selectivity features of the catalytic AA process, and taken together with a known procedure for the deprotection of methanesulfonamides,[16] can be used to prepare unprotected amino alcohols. However, this deprotection method (Red-Al, refluxing toluene) does not tolerate many functional groups, so that discovery of other effective nitrenoid sources with groups more easily removed from nitrogen remains an important goal. In this connection, we have found that the chloramine salt $Me_3SiCH_2CH_2SO_2NClNa$, derived from the easily deprotected "Weinreb sulfonamide",[3] gives results very similar to those obtained with Chloramine-M,[13] presumably because the organic substituent near the reaction zone is also "small".

In conclusion, this and a related study[13] provided the key insight that (at least for sulfonamide-derived chloramine salts) the AA process is better with the least sterically demanding substituents on sulfur. Appreciation of this trend was in part responsible for our decision to have another look at the old carbamate-based version of the catalytic aminohydroxylation process.[17] This was a fortuitous decision, since it led to the discovery of the highly effective carbamate-based AA process described in the following paper.[18]

Experimental Procedure

Chloramine-M (**2**): To a stirred solution of methanesulfonamide (4.81 g, 50 mmol) and sodium hydroxide (2.0 g, 50 mmol) in 40 mL of water was added slowly *tert*-butylhypochlorite (5.63 mL, 5.4 g, 50 mmol). The solution was stirred for 1 h and concentrated to dryness in vacuo. After one trituration with diethyl ether the pure salt sodium *N*-chloro,*N*-methanesulfonamide was obtained in almost quantitative yield (7.5 g). CH_3NSO_2NaCl (M_r = 151.54); elemental analysis: calcd. C 7.93, H 2.00, N 9.24, Na 15.17, Cl 23.39; found: C 8.03, H 2.08, N 9.24, Na 15.36, Cl 23.12. Recrystallization of the product from *tert*-butyl alcohol did not lead to any change in its reaction behavior. The in situ generation of Chloramine-M was accomplished with this same procedure except that the amount of water used was adjusted to equal the required water content for the AA process for which it is intended and, of course, the resulting solution was used directly in the reaction.

General procedure: All AA reactions included in Table 1 were carried out as in the following example, the preparation of **4** on the 1 mmol scale: A 20 mL scintillation vial equipped with a magnetic stirrer was charged with a solution of $MeSO_2NClNa$ (455 mg, 3.0 mmol, 3.0 equiv) in 7.5 mL of water, 7.5 mL of *n*PrOH, and $(DHQD)_2PHAL$ (40 mg, 0.05 mmol, 0.05 equiv). To the resulting stirred clear colorless solution was then added isopropyl *trans*-cinnamate (190 mg, 1.0 mmol), followed by $K_2OsO_2(OH)_4$ (14.8 mg, 0.04 mmol, 0.04 equiv). The reaction mixture turned green after several minutes and was stirred for 3.5 h, by which time the reaction mixture had turned a clear, light yellow. The presumed significance of the color change as an indication of the end point of the reaction was confirmed by a TLC analysis, which revealed that no olefin remained. (With dimethyl fumarate the green color was only observed when an additional 0.5 equiv *tert*-butyl hypochlorite was added. For the fumarate case, the extra *tert*-butyl hypochlorite also resulted in much better *ee* and yield.) The reaction was then quenched by addition of 10 mL of saturated aqueous Na_2SO_3 (this reductive quench is exothermic and cooling is needed for large-scale reactions). The added salt caused phase separation. The aqueous phase was separated and extracted with ethyl acetate (3 × 30 mL). The combined organic phases were dried over $MgSO_4$ and concentrated to afford the crude product (impurities were mainly methanesulfonamide and diol). For an accurate yield the crude product was purified by flash chromatography (SiO_2, 30% ethyl acetate/hexane) and afforded 195 mg (65%) crystalline aminohydroxylation product. In cases in which regioisomeric products can result, the yields are given for the mixture of the two regioisomers. In the particular case described, crystallization from ethyl acetate/hexane furnished the regio- and enantiomerically pure (>99% *ee*) *β*-hydroxyaminomethanesulfonamide **4** (isopropyl (2*R*,3*S*)-*N*-(methanesulfonyl)-3-amino-2-hydroxy-2-phenyl-propanoate).

In preparative-scale applications the workup and purification steps can be simplified. Since methanesulfonamide is insoluble in CH_2Cl_2 and diethyl ether but quite soluble in aqueous solution (even saturated brine solutions), it can be removed from the crude product by two aqueous extractions. Alternatively it can be sublimed in vacuo (0.1 mbar) from the crude material at 80 °C. Finally, it also precipitates from solutions in CH_2Cl_2 and CH_2Cl_2/hexane.

In the case of **5** (the AA product from dimethyl fumarate) extractive and chromatographic purification both failed (**5** is too water soluble). On the other hand, sublimation at 80 °C removed both the diol by-product and the excess methanesulfonamide, leaving pure **5** behind.

Methyl (2*R*,3*S*)-*N*-(methanesulfonyl)-3-amino-2-hydroxy-2-phenylpropanoate (**3**): $C_{11}H_{15}NO_5S$, M_w = 273.30; m.p. 150–152 °C; $[\alpha]_D^{25}$ = + 28.3 (*c* = 1.0 in EtOH/H_2O 95:5); ^1H NMR (400 MHz, CD_3CN): δ = 2.63 (s, 3H, SO_2CH_3), 3.75 (s, 3H, CO_2CH_3), 3.78 (s, 1H, OH), 4.36 (s, 1H, *CH*OH), 4.86 (dd, *J* = 3.2, 9.9 Hz, 1H, CHN), 6.08 (d, *J* = 9.9 Hz, 1H, NH), 7.30–7.43 (m, 5H, arom. H); ^{13}C NMR (100 MHz, CD_3CN): δ = 41.8 (SO_2CH_3), 53.0 (CN), 60.4 (COH), 75.3 (CO_2CH_3), 128.1, 128.7, 129.3, 139.6 (arom. C), 172.9 (C=O); Positive-ion FAB-MS: *m*/*z* (%): 272 $[M+Cs]^+$ (45); HPLC: Chiralcel AS, 210 nm, 30% *i*PrOH/hexane, 0.6 mL min^{-1}, 21.7 min (2*R*,3*S*)-**3**, 25.9 min (2*S*,3*R*)-**3**.

Isopropyl (2*R*,3*S*)-*N*-(methanesulfonyl)-3-amino-2-hydroxy-2-phenylpropanoate (**4**): $C_{13}H_{19}NO_5S$, M_w = 301.36; m.p. 97–98 °C; $[\alpha]_D^{25}$ = + 26.2 (*c* = 1.0 in EtOH/H_2O 95:5); ^1H NMR (CD_3CN, 400 MHz): δ = 1.23 (dd, *J* = 15.0, 6.3 Hz, 3H, *i*PrCH_3), 2.59 (s, 3H, SO_2CH_3), 3.73 (d, *J* = 5.2 Hz, 1H, OH), 4.26 (dd, *J* = 3.4, 5.2 Hz, 1H, *CH*OH), 4.83 (dd, *J* = 5.2, 9.7 Hz, 1H, CHN), 5.01 (sept, *J* = 6.3 Hz, 1H, *i*PrC*H*), 6.04 (d, *J* = 9.7 Hz, 1H, NH), 7.33–7.44 (m, 5H, arom. H); ^{13}C NMR (CD_3CN, 100 MHz) δ = 21.8 (*i*PrCH_3), 42.0 (SO_2CH_3), 60.7 (CN), 70.5 (*i*PrCH), 75.3 (COH), 128.3, 128.8, 129.3, 139.6 (arom. C), 172.0 (C=O); Positive-ion FAB-MS: *m*/*z* (%): 324 $[M+Na]^+$ (100); HPLC: Chiralcel AD, 210 nm, 30% *i*PrOH/hexane, 1 mL min^{-1}, 14.5 min (2*S*,3*R*)-**4**, 19.4 min (2*R*,3*S*)-**4**.

Dimethyl (1*R*,2*R*)-*N*-(methanesulfonyl)-3-amino-3-phenyl-2-hydroxysuccinate (**5**): $C_{13}H_{13}NO_7S$, M_w = 255.24; m.p. 91–92 °C; $[\alpha]_D^{25}$ = +16.8 (*c* = 1.0 in EtOH/H_2O 95:5); ^1H NMR (400 MHz, CD_3CN): δ = 2.90 (s, 3H, SO_2CH_3), 3.73 (s, 3H, CO_2CH_3), 3.76 (s, 3H, CO_2CH_3), 3.84 (d, *J* = 5.3 Hz, 1H, OH), 4.47 (d, *J* = 9.7 Hz, 1H, CHN), 4.69 (d, *J* = 5.3 Hz, 1H, CHO), 5.84 (d, *J* = 9.7 Hz, 1H, NH); ^{13}C NMR (100 MHz, CD_3CN): δ = 41.6 (SO_2CH_3), 53.1 (CO_2CH_3), 53.5 (CO_2CH_3), 59.6 (CN), 72.4 (CO); Positive-ion FAB-MS: *m*/*z* (%): 256 $[M+H]$ (100); HPLC: Chiralcel AD, 210 nm, 30% *i*PrOH/hexane, 1 mL min^{-1}, 9.4 min (1*S*,2*S*)-**5**, 12.6 min (1*R*,2*R*)-**5**.

(1*S*,2*S*)-*N*-(Methanesulfonyl)-2-amino-1,2-diphenylethanol (**6**): $C_{15}H_{17}NO_3S$, M_w = 291.37; m.p. 134–135 °C; $[\alpha]^{25}{}_D$ = − 6.9 (*c* = 1.0 in EtOH/H_2O 95:5); ^1H NMR (400 MHz, CD_3CN): δ = 2.39 (s, 3H, CH_3), 3.74 (d, *J* = 4.1 Hz, 1H, OH), 4.54 (dd, *J* = 7.9, 5.6 Hz, 1H, CHNH), 4.84 (dd, *J* = 5.6, 4.1 Hz, 1H, CHOH), 5.91 (d, *J* = 7.9 Hz, 1H, NH), 7.23–7.34 (m, 10H, arom. H); ^{13}C NMR (100 MHz, CD_3CN): δ = 41.2 (SO_2CH_3), 65.1 (CN), 77.0 (CO), 118.2, 127.6, 127.7, 128.3, 128.4, 128.5, 128.5, 128.9, 129.1, 129.1, 141.1, 142.5 (arom. C); Positive-ion FAB-MS: *m*/*z* (%): 314 $[M+Na]^+$ (18); HPLC: Chiralcel OD-H, 210 nm, 15% *i*PrOH/hexane, 0.9 mL min^{-1}, 10.0 min (1*R*,2*R*)-**6**, 21.7 min (1*S*,2*S*)-**6**.

(2*R*,3*S*)-*tert*-Butyl-*N*-(methanesulfonyl)-3-amino-2-hydroxybutanoate (**7**): $C_9H_{19}NO_5S$, M_w = 253.31; m.p. 117–118 °C; $[\alpha]_D^{25}$ = + 8.1 (*c* = 1.0 in EtOH/H_2O 95:5); ^1H NMR (400 MHz, CD_3CN): δ = 1.25 (d, *J* = 6.9 Hz, 3H, *CH*$_3$CHN), 1.46 (s, 9H, $(CH_3)C$), 2.90 (s, 3H, CH_3SO_2N), 3.45 (d, *J* = 5.2 Hz, 1H, OH), 3.81 (qdd, *J* = 9.4, 6.9, 2.7 Hz, 1H, NCH), 3.94 (dd, *J* = 5.2, 2.7 Hz, 1H, OCH), 5.15 (d, *J* = 9.4 Hz, 1H, NH); ^{13}C NMR (100 MHz, CD_3CN): δ = 18.8 (CH_3CHN), 28.1 ($(CH_3)_3C$), 42.2 (CH_3SO_2), 52.9 (CNH), 75.0 (COH), 83.3 ($(CH_3)_3C$), 172.5 (C=O); Positive-ion FAB-MS: *m*/*z* (%): 254 $[M+H]^+$ (29); HPLC (4-methoxybenzenesulfonyl ester of **7**): Chiralcel AS, 254 nm, 30% *i*PrOH/hexane, 1.0 mL min^{-1}, 21.5 min (2*S*, 3*R*)-**7**, 28.3 min (2*R*, 3*S*)-**7**.

(1*S*,2*R*)-*N*-(Methanesulfonyl)-2-amino-cyclohexanol (**8**): $C_7H_{15}NO_3S$, M_w = 193.26; m.p. 114–115 °C; $[\alpha]_D^{25}$ = +18.8 (*c* = 1.0 in EtOH/H_2O 95:5); ^1H NMR (400 MHz, CD_3CN): δ = 1.31–1.33 (m, 2H, CH_2), 1.50–1.66 (m, 6H, CH_2), 2.90 (s, 3H, CH_3), 2.92 (d, *J* = 4.5 Hz, 1H, OH), 3.31–3.34 (m, 1H, NCH), 3.80–3.83 (m, 1H, OCH), 5.14 (br. s, 1H, NH); ^{13}C NMR (100 MHz, CD_3CN): δ = 20.7, 24.1, 29.3, 32.2 (CH_2), 41.7 (SO_2CH_3), 56.3 (CN), 69.5 (CO); Positive-ion FAB-MS: *m*/*z* (%): 216 $[M+Na]^+$ (100); HPLC (benzoate of **8**): Chiralcel AD, 210 nm, 5% *i*PrOH/hexane, 1.0 mL min^{-1}, 18.9 min (1*R*,2*S*)-**8**, 21.3 min (1*S*,2*R*)-**8**.

Received: July 1, 1996 [Z9274IE]
German version: *Angew. Chem.* **1996**, *108*, 2991–2995

Keywords: amino alcohols · asymmetric aminohydroxylation · catalysis · chloramines · sulfonamides

[1] a) G. Li, H.-T. Chang, K. B. Sharpless, *Angew. Chem.* **1996**, *108*, 449–452; *Angew. Chem. Int. Ed. Engl.* **1996**, *35*, 451–454; b) G. Li, K. B. Sharpless, *Acta Chem. Scand.* **1996**, *50*, 649–651.

[2] Stopping the reaction after partial conversion usually leads to higher regio- and enantioselectivities. In addition, we have come across new substrates giving higher enantioselectivities in reactions with the Chloramine-T system since the original report appeared.

[3] Certain functionalized alkylsulfonamides have recently been found to be interesting candidates for deprotection: a) S. M. Weinreb, D. M. Demko, T. A. Lessen, J. P. Demers, *Tetrahedron Lett.* **1986**, *27*, 2099–2102; b) T. Fukuyama, personal communication.

[4] In analogy to the common names "Chloramine-T" for sodium *N*-chloro-*N*-toluenesulfonamide and "Chloramine-B" for sodium *N*-chloro-*N*-benzenesulfonamide, the trivial name "Chloramine-M" for the sodium *N*-chloro-*N*-methanesulfonamide seems appropiate.

[5] a) Chloramine-M is readily prepared from methanesulfonamide in water by addition of the stoichiometric amount of sodium hydroxide and *tert*-butylhypochlorite [5b]. This method is adapted from a procedure developed by Campbell et al. for the preparation of sodium *N*-chloro-*N*-carbamates [5c–e] and proved general for synthesis of both sodium *N*-chloro-*N*-aryl- and -alkylsulfonamides. Substitution of the recommended [5c–e] solvent methanol by water proved to be highly advantageous. b) *tert*-Butylhypochlorite is commercially available; for a simple preparative procedure see: M. J. Mintz, C. Walling, *Org. Synth. Coll. Vol. V*, **1983**, 183–187; c) M. M. Campbell, G. Johnson, *Chem. Rev.* **1978**, *78*, 65–79; d) E. Herranz, S. A. Biller, K. B. Sharpless, *J. Am. Chem. Soc.* **1978**, *100*, 3596–3598; e) E. Herranz, K. B. Sharpless, *J. Org. Chem.* **1978**, *43*, 2544–2548.

[6] Alkyl sulfonamide derived chloramine salts appear to have been little studied. In fact, we found only one earlier report on this class of compounds: F. E. Hardy, *J. Chem. Soc.* **1970**, 2087–2089.

[7] Only *tert*-butyl *trans*-crotonate and isopropyl *trans*-cinnamate did not appear in the first paper. The isopropyl *trans*-cinnamate is included here in addition to the methyl *trans*-cinnamate because it gave a considerably worse result when Chloramine-T in CH_3CN/H_2O was employed: regioselectivity: 76:24, *ee*: 60%).

[8] The *n*-propanol water solvent system was also shown to give better selectivities with Chloramine-T, although in some cases the reaction became too slow to be useful: A. Houri, K. B. Sharpless, unpublished results.

[9] Temperatures lower than 10 °C led to longer reaction times and problems with ligand solubility.

[10] D. J. Berrisford, C. Bolm, K. B. Sharpless, *Angew. Chem.* **1995**, *107*, 1159–1171; *Angew. Chem. Int. Ed. Engl.* **1995**, *34*, 1059–1070.

[11] Considerable evidence for the existence of a second cycle has been recognized and examined in the closely related catalytic asymmetric dihydroxylation process. For detailed discussion of problems in the second cycle in the AD process see: a) J. S. M. Wai, I. Markó, J. S. Svendsen, M. G. Finn, E. N. Jacobsen, K. B. Sharpless, *J. Am. Chem. Soc.* **1989**, *111*, 1123–1125; b) H. L. Kwong, C. Sorato, Y. Ogino, H. Chen, K. B. Sharpless, *Tetrahedron Lett.* **1990**, *31*, 2999–3002.

[12] H.-T. Chang, K. B. Sharpless, unpublished results.

[13] P. C. Sennhenn, J. Rudolph, C. P. Vlaar, M. Bruncko, S. Immel, H. C. Kolb, K. B. Sharpless, unpublished results.

[14] We believe that there are also "indirect" effects since the presence of the ligand dramatically shifts the **IV** – **II** equilibrium (step h^2) in favor of **II**; H.-T. Chang, K. B. Sharpless, unpublished results.

[15] H. C. Kolb, M. S. Van Nieuwenhze, K. B. Sharpless, *Chem. Rev.* **1994**, *94*, 2483–2547.

[16] a) E. H. Gold, E. Babad, *J. Org. Chem.* **1972**, *37*, 2208–2210. This method has recently been applied successfully by Seebach et al. for the deprotection of *N*-methanesulfonamides derived from δ-amino alcohols: b) D. J. Ramón, G. Guillena, D. Seebach, *Helv. Chim. Acta* **1996**, *79*, 875–894.

[17] K. B. Sharpless, A. O. Chong, K. Oshima, *J. Org. Chem.* **1976**, *41*, 177–179; see also [5d, e].

[18] G. Li, H. Angert, K. B. Sharpless, *Angew. Chem.* **1996**, *108*, 2995–2999; *Angew. Chem. Int. Ed. Engl.* **1996**, *35*, 2813–2817.

N-Halocarbamate Salts Lead to More Efficient Catalytic Asymmetric Aminohydroxylation**

Guigen Li, Hubert H. Angert, and K. Barry Sharpless*

Dedicated to Professor Koji Nakanishi

The recently discovered catalytic asymmetric aminohydroxylation (AA) process[1] has been easier to improve than anticipated. In the preceding paper, we described how substantial increases in enantio- and regioselectivity were achieved by replacing Chloramine-T (TsNClNa) with analogs bearing substituents smaller than the *p*-tolyl group (e.g. CH_3SO_2NClNa).[2] We report here that the process becomes even more effective when the chloramine salts of sulfonamides are replaced by those of alkyl carbamates. Application of the new procedure to 2-vinylnaphthalene (**1**) with BnOCONClNa as the oxidant and nitrogen source (Scheme 1) proceeds with exceptional enantioselectivity and regioselectivity (>10:1). In addition, in virtually all the entries in Tables 1 and 2 better selectivities were achieved than those realized in the sulfonamide-based procedures for the AA.[1–3] Also noteworthy is the increased scope, hinted at here by the very good results obtained with methyl acrylate and vinylnaphthalene **1** (Table 1, entries 4 and 7), which will be further documented soon.[4]

Styrene-type olefins such as **1** are conspicuously absent from the first sulfonamide-based AA reports[1, 2] for the simple reason that they were poor substrates. The reaction of styrene itself produced an approximately 2:1 mixture of regioisomers, 50–70% *ee* each, in low yield.[5] This was quite unexpected, since in terms of both turnover and enantioselectivity styrenes are by far the best substrates in the catalytic asymmetric dihydroxylation (AD) process.[6] However, even more surprising than the low selectivities were the abysmal rates. Styrenes, the fastest reacting AD substrates, were among the slowest reacting substrates in the sulfonamide-based AA reactions,[1, 2] and since the reactions were even slower when the ligand was added than when it was omitted, this is an example of ligand-decelerated catalysis.[6] By contrast, in this new carbamate-based process the reactions of all olefins studied to date are ligand-accelerated, as has been the universal experience in the AD process.[7]

In comparing Tables 1 and 2, it becomes clear that the ethyl carbamate series is superior to the benzyl carbamate series in terms of rate, enantioselectivity, regioselectivity, and yield. The effect of the smaller ethyl substituent may be analogous to that assumed on replacement of a methyl substituent for the *p*-tolyl substituent on the sulfonamide—suppression of the second cycle and better fit in the ligand binding pocket of the catalyst.[8] Despite the greater effectiveness of the ethyl reagent, the benzyl reagent will often be preferred because it can be cleaved easily by hydrogenolysis.

Since the other results in the tables need no comment, we now consider what general insight this new system offers for catalysis research. Such lessons are often more valuable than any particular catalytic process can ever be.

The original report on carbamate-based, osmium-catalyzed aminohydroxylation of olefins appeared in 1978,[9] two years after publication of the analogous sulfonamide-based process.[10] The latter process[10] was used many times over the past twenty years, especially in syntheses of amino sugars. The old carbamate version[9, 11] was used much less frequently, but it has the distinction of being a key step in the first synthesis of the *tert*-butoxycarbonyl (BOC) protected side chain analog of taxol, now known as Taxotere.[12]

Those familiar with the original, nonasymmetric, carbamate-based procedures will realize that the sodium *N*-chlorocarbamate salts were never used directly in the process, either by us or by others.[13] They were always first converted in situ to the corresponding silver or mercury salts. So why did we fail to discover earlier that the original sodium salts are superior to their silver and mercury analogs?[14] The answer is that far too little water was present, so we observed no turnover in the first few attempts to extend the effective process based on TsNClNa to one based on ROCONClNa. Scott Biller (then an undergraduate at MIT) came up with the idea of using the silver salt, which

[*] Prof. K. B. Sharpless, Dr. G. Li, Dr. H. H. Angert
Department of Chemistry, The Scripps Research Institute
10550 N. Torrey Pines Road, La Jolla, CA 92037 (USA)
Fax: Int. code +(619)784-7562
e-mail: sharpless@scripps.edu

[**] This research was supported by the National Institutes of Health (GM 28384), the National Science Foundation (CHE 9531152), and the W. M. Keck Foundation. We thank Dr. Pui Tong Ho for many helpful discussions. H. H. A. is grateful to the Deutsche Forschungsgemeinschaft (DFG) for providing a postdoctoral fellowship.

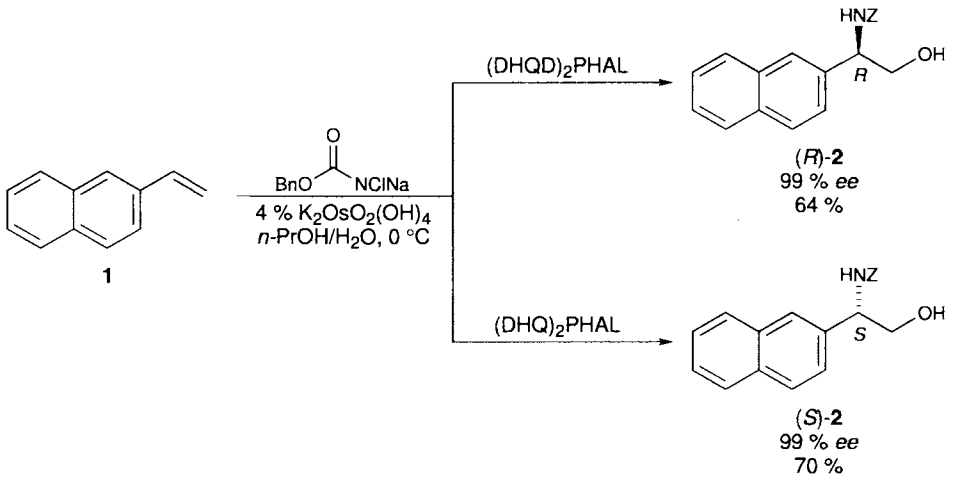

Scheme 1. AA reactions of 2-vinylnaphthalene (1) with benzyl carbamate. DHQD-H = dihydroquinidine, DHQ-H = dihydroquinine, PHAL = 1,3-phthalazinediyl, Z = benzyloxycarbonyl.

proved highly successful even under our water-starved conditions. No one ever tried the sodium salt again. Even if it had been tried, "no reaction" would have been the verdict unless a lot more water were present than described in any of the published procedures.

Following the encouraging results of the catalytic AA reaction with sulfonamides,[1, 2] we reexamined the carbamate-based catalytic aminohydroxylation process, primarily because carbamate protecting groups are easier to remove from nitrogen. Optimization of the AA procedure using $ArSO_2NClNa$ salts had led to the choice of cosolvent systems containing 50% water. The high water content is thought to speed the slow hydrolytic steps and thereby suppress involvement of the rate- and selectivity-damaging second cycle.[8] At this point, good fortune struck.

One of us (G. L.)—unaware that the standard carbamate process called for acetonitrile solvent with only a few equivalents of water and for the silver, not the sodium salt of the chloramine—ran the first experiment using 50% aqueous *n*-propyl alcohol as solvent, EtOCONClNa as the chloramine salt, $(DHQ)_2PHAL$ as the chiral ligand, and methyl cinnamate as the substrate. The result was spectacular (Table 2, entry 1). For even though the system was homogeneous, the reaction was almost free of the deleterious effects on selectivity that arise whenever second-cycle catalysis participates.[8] Recall that in all homogeneous versions of the AD, the second cycle always intrudes to some extent and can only be completely suppressed by using inconvenient two-phase systems.[6]

Further controls revealed which variables are crucial for maintaining the exceptional catalyst activity and selectivity of this new AA system.[16] The two most important factors are water concentration and the nature of the metal salt of the *N*-chlorocarbamate, and the two factors are linked. The interdependence is dramatic for the alkali metal salts of *N*-chlorocarbamates: from essentially no turnover with a few equivalents of water, to better and better reactivity as the percentage of solvent water increases. The effect of water concentration on reactivity in the silver *N*-chlorocarbamate system is, as expected, less dramatic. In any case, whatever the water concentration, in the system examined (stilbene, sodium or silver benzyl *N*-chlorocarbamate, $(DHQ)_2PHAL$, $K_2OsO_2(OH)_4$, CH_3CN, and H_2O),[16] reactions with the silver carbamate always gave lower yields, lower enantioselectivities, and more by-products than reactions with the sodium carbamate.

With this better catalytic asymmetric aminohydroxylation process now in hand, we and others are busy trying to map out its scope.[4] There may also be a message here of broader significance for catalyst-discovery research. As noted in the brief historical account, this trivially different, but successful, system was passed by long ago simply because we failed to examine the effect of water concentration with every change of chloramine salt. This joins the list of many important lessons in catalysis we have learned the hard way over the last 20 years. The common theme of these lessons is that catalytic cycles are sensitive to far too many reaction variables for even the best catalyst discovery endeavors to have a high success rate. Whether one is just trying to improve existing, but feeble catalysis, or prospecting for the first hint of a new catalytic transformation, unknown obstructions, usually interconnected in sinister ways, lie everywhere. Fast (automated) screening techniques, along with the chance discoveries they engender, would seem to offer the best chance of getting through such minefields quicker and more often. At present, it could be argued that attempts to discover new catalysts fail, because of the limited endurance of human researchers.

Finally, the significance of entry 7 in Table 1 will not be lost on chemists interested in the synthesis of unusual amino acids. This result opens a simple two-step route from vinyl arenes to enantiomerically pure aryl glycines of either *R* or *S* configuration.[17]

Experimental Procedure

General Procedure: Unless otherwise noted, all the carbamate AA reactions shown in Tables 1 and 2 were carried out on a 1 mmol scale as described here for methyl *trans*-cinnamate and the benzyl carbamate derived chloramine salt (Table 1, entry 1). Ethyl carbamate or *tert*-butyl carbamate can also be used in place of benzyl carbamate.

Benzyl carbamate (0.469 g, 3.10 mmol) was dissolved in 4 mL of *n*-propyl alcohol in a 20-mL scintillation vial equipped for magnetic stirring. To this stirred solution was added a freshly prepared solution of NaOH (NaOH (0.122 g, 3.05 mmol) in 7.5 mL of water), followed by a freshly prepared solution of *tert*-butyl hypochlorite (0.331 g, 3.05 mmol, ca. 0.35 mL) [18]. Then a solution of the ligand $(DHQ)_2PHAL$ (40 mg, 0.05 mmol, 5 mol%) in 3.5 mL of *n*-propyl alcohol was added. (It is important that the ligand be completely dissolved in the *n*-propyl alcohol before it is added; the DHQ analog is more readily soluble than the DHQD analog.) The reaction mixture should be homogeneous at this point. The vial was then immersed in a room-temperature water bath, and stirred for a few minutes. Then the olefin (*trans*-methyl cinnamate, 0.162 g, 1 mmol, 0.067 M) was added, followed by the osmium catalyst ($K_2OsO_2(OH)_4$, 14.7 mg, 0.04 mmol, 4 mol%). The reaction mixture was stirred for 40 min (the approximate reaction time is given for each entry in the tables), and the light green color of the solution gave way to light yellow at the end. After TLC analysis confirmed the absence of starting material, 7 mL of ethyl acetate was added and the phases were separated. The lower, aqueous phase was extracted with ethyl acetate (3 × 5 mL). The combined organic extracts were washed with water and brine, dried over $MgSO_4$, and concentrated to dryness to afford the crude product contaminated by some excess benzyl carbamate. Purification by flash chromatography (hexane/chloroform/methanol 6/4/1, v/v/v) provided (2*R*,3*S*)-**3** (0.204 g, 65% yield, 94% *ee*) as a colorless solid; m.p. 101–103 °C; $[\alpha]_D^{20} = +4.4$ ($c = 0.32$ in 95% EtOH).

Simplified procedures for cases in which the product crystallizes directly from the reaction mixture:

1) (*S*)-**2** (Table 1, entry 7): This is one of only three cases in which the reaction was conducted at 0 °C, but the procedure is otherwise identical (up to the generation of the chloramine salt) to the one used for methyl cinnamate. It then diverges as follows: The vial was immersed in a 0 °C icebath and 2-vinylnaphthalene (1) (0.154 g, 1 mmol) was added, followed by $K_2OsO_2(OH)_4$ (14.7 mg, 0.04 mmol,

Table 1. Results of AA reactions with BnOCONClNa.

Entry	Substrate	Product [a]	Config. [a]	*ee* [%] (DHQ)$_2$PHAL	*ee* [%] (DHQD)$_2$PHAL	Yield [%] [b]	*t* [h]
1	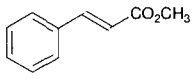	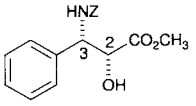 **3**	2*R*,3*S*	94	97	65	0.6
2	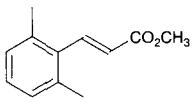	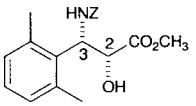 **4**	2*R*,3*S*	94	86	61	2.0
3 [c]	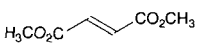	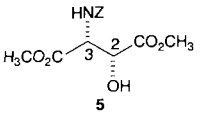 **5**	2*R*,3*R*	84	87	55	24
4 [c]	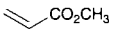	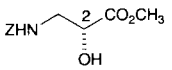 **6**	2*R*	84	87	89	0.8
5		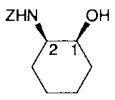 **7**	1*S*,2*R*	63	56	51	2.0
6 [d]	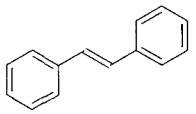	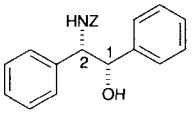 **8**	1*S*,2*S*	91	88	92	3.0
7 [d]	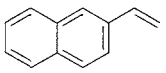	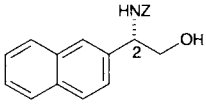 **2**	2*S*	99	99	70	3.0
8 [d]	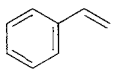	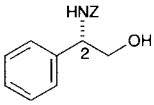 **9**	2*S*	93	90	60	1.5

[a] Major product from the reaction using (DHQ)$_2$PHAL. [b] Yields of the reactions using (DHQ)$_2$PHAL. [c] CH_3CN/H_2O was used as the solvent. [d] Reactions were performed at 0 °C.

4 mol%). The green homogeneous mixture was stirred at 0 °C for 3 h by which time it had transformed into an almost colorless slurry. A crystalline precipitate, which was nearly pure by HPLC and NMR, was removed by filtration. One wash with cold (ca. 5 °C) *n*PrOH/H_2O (1/1, 3 mL) yielded pure (*S*)-**2** (0.460 g, 70% yield, >99% *ee*). A small sample of this solid was dissolved in ethyl acetate and filtered through a small plug of silica gel; m.p. 133–134 °C; $[\alpha]_D^{20} = +50.9$ ($c = 0.32$ in 95% EtOH). (A practical note: Very similar results were realized in an otherwise identical experiment in which the solvent volume and the amounts of ligand and osmium were the same, but 2 mmol of olefin and 4 mmol of chloramine were used. One-half of the total amount of olefin was added at the beginning of the reaction. After that portion was consumed, the remainder was added and the reaction completed as usual.)

2) (1*S*,2*S*)-**8** (Table 1, entry 6): This procedure for stilbene is reminiscent of earlier AD [19] and AA [1] processes, which take advantage of the fact that both the stilbene and its oxidation product are insoluble in the medium. As in the preparation of **2**, workup consists of merely filtering the crude reaction mixture. The following procedure differs from that for **2** in that it is a straight sixfold scale-up and requires a 120-mL bottle. (Another small difference is that in addition to finishing as a slurry, the reaction mixture starts as a slurry.) However, since the reaction sequence is otherwise identical to that just described for **2** (even down to the reaction time of 3 h at 0 °C), the only new details describe the treatment of the product after its isolation from the reaction mixture. Filtration of the cold slurry provided the crude solid product which was washed once with cold (ca. 5 °C) *n*PrOH/H_2O (1/1, 12 mL) to give (1*S*,2*S*)-**8** (1.85 g, 92% yield, 91% *ee*, nearly pure by NMR and HPLC); m.p. 135–137 °C; $[\alpha]_D^{20} = -7.8$ ($c = 0.70$ in 95% EtOH). A single recrystallization from methanol raised the *ee* to >99%; m.p. 149–151 °C; $[\alpha]_D^{20} = -10.0$ ($c = 0.57$ in 95% EtOH).

Determination of enantiomeric excesses and optical rotations: Rotations were determined for the products in Tables 1 and 2 at the stated enantiomeric excesses obtained with the (DHQ)$_2$PHAL ligand unless otherwise indicated, and were measured in 95% EtOH.

3: Chiralcel OD-H, *i*PrOH/hexane (15/85), 0.60 mL min^{-1}; 16.9 min (2*S*,3*R*), 19.7 min (2*R*,3*S*); $[\alpha]_D^{20} = +4.4$ ($c = 0.32$).

4: Chiralcel AD, *i*PrOH/hexane (3/7), 0.60 mL min^{-1}, 10.4 min (2*S*,3*R*), 8.6 min (2*R*,3*S*); $[\alpha]_D^{20} = +8.75$ ($c = 0.13$).

5: Chiralcel AD, *i*PrOH/hexane (1/9), 0.80 mL min^{-1}, 40.7 min (2*S*,3*S*), 27.0 min (2*R*,3*R*); $[\alpha]_D^{20} = -5.4$ ($c = 1.2$; mother liquor after two recrystallizations from toluene).

6: Chiralcel OB, *i*PrOH/hexane (1/9), 0.70 mL min^{-1}, 54.7 min (2*R*), 68.9 min (2*S*); $[\alpha]_D^{20} = -17.6$ ($c = 0.80$).

7: Chiralcel AD, *i*PrOH/hexane (5/95), 0.60 mL min^{-1}, 44.2 min (1*S*,2*R*), 25.6 min (1*R*,2*S*); $[\alpha]_D^{20} = +19.8$ ($c = 1.5$).

8: Chiralcel OD-H, *i*PrOH/hexane (3/7), 0.70 mL min^{-1}, 10.7 min (1*S*,2*S*), 12.6 min (1*R*,2*R*); $[\alpha]_D^{20} = -7.8$ ($c = 0.57$).

Table 2. Results of AA reactions with EtOCONClNa.

Entry	Substrate	Product [a]	Config. [a]	*ee* [%] $(DHQ)_2PHAL$	$(DHQD)_2PHAL$	Yield [%] [b]	*t* [h]
1	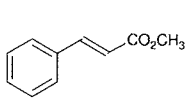	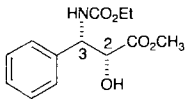 **10**	2*R*,3*S*	99	99	78	0.75
2 [c]	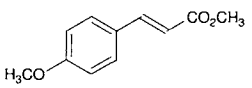	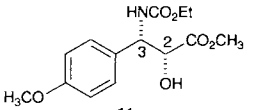 **11**	2*R*,3*S*	98	99	70	0.5
3 [c]	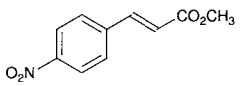	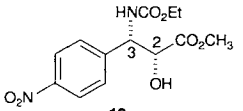 **12**	2*R*,3*S*	97	98	75	1.0
4	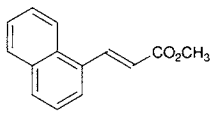	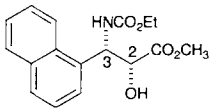 **13**	2*R*,3*S*	97	96	65	2.0

[a] Major product from the reaction using $(DHQ)_2PHAL$. [b] Yields of the reactions using $(DHQ)_2PHAL$. [c] CH_3CN/H_2O was used as the solvent.

2: Chiralcel AD, *i*PrOH/hexane (3/7), 0.70 mL min^{-1}, 9.7 min (2*S*), 13.8 min (2*R*); $[\alpha]_D^{20} = +50.9$ ($c = 0.32$).
9: Chiralcel AD, *i*PrOH/hexane (1/9), 0.70 mL min^{-1}, 18.8 min (2*S*), 27.0 min (2*R*); $[\alpha]_D^{20} = +30.0$ ($c = 0.55$).
10: Chiralcel OD-H, *i*PrOH/hexane (15/85), 0.60 mL min^{-1}; 11.6 min (2*S*,3*R*), 12.6 min (2*R*,3*S*); $[\alpha]_D^{20} = +2.78$ ($c = 0.90$).
11: Chiralcel AD, *i*PrOH/hexane (1/9), 0.70 mL min^{-1}, 30.3 min (2*S*,3*R*), 19.5 min (2*R*,3*S*); $[\alpha]_D^{20} = +17.9$ ($c = 0.43$).
12: Chiralcel AD, *i*PrOH/hexane (1/9), 1.0 mL min^{-1}, 40.1 min (2*S*,3*R*), 23.9 min (2*R*,3*S*); $[\alpha]_D^{20} = +16.5$ ($c = 0.67$).
13: Chiralcel AD, *i*PrOH/hexane (1/9), 1.0 mL min^{-1}, 26.2 min (2*R*,3*R*), 18.0 min (2*S*,3*S*); $[\alpha]_D^{20} = -38.2$ ($c = 0.10$).

Assignment of the absolute configurations: The methyl cinnamate derivative **3** was converted into an authentic sample of the methyl ester of the taxol side chain by hydrogenolysis (Pd/C) and subsequent Schotten–Baumann acylation [3] [HPLC: Chiralcel AD, 10% *i*PrOH/hexane (1/9), 1 mL min^{-1}, 19.1 min (2*R*,3*S*), 22.1 min (2*S*,3*R*)] [1]. The methyl 2′,6′-dimethylcinnamate derivative **4** was assumed to have the same configuration as the methyl cinnamate derivative **3**. The signs of the rotations for the Z-protected derivatives of the dimethyl fumarate derivative **5** and the methyl acrylate derivative **6** were compared to the literature values; (2*R*,3*R*)-**5**: $[\alpha]_D^{25} = -22.6$ ($c = 2.0$ in $CHCl_3$); (2*S*,3*S*)-**5**: $[\alpha]_D^{25} = +24.2$ ($c = 1.0$ in $CHCl_3$) [21]; (2*R*)-**6**: $[\alpha]_D^{20} = -17.7$ ($c = 1.3$ in CH_3OH); (2*S*)-**6**: $[\alpha]_D^{20} = +18.8$ ($c = 1.42$ in CH_3OH) [22]. Cyclohexene derivative **7** and *trans*-stilbene derivative **8** were correlated with authentic samples of their *p*-toluenesulfonamide analogs by hydrogenolysis (Pd/C), followed by *N*-tosylsulfonylation [HPLC for sulfonamide from **7**: Chiralcel OG, 15% *i*PrOH/hexane, 1 mL min^{-1}, 14.3 min (1*S*,2*R*), 17.6 min (1*R*,2*S*). HPLC for sulfonamide from **8**: Chiralcel OD-H, 15% *i*PrOH/hexane, 1 mL min^{-1}, 14.3 min (1*S*,2*R*), 17.6 min (1*R*,2*S*)]. Styrene derivative **9** was converted into (*S*)-(+)-2-phenylglycinol, $[\alpha]_D^{25} = +29.8$ ($c = 0.5$ in 1 N HCl), $[\alpha]_D^{25} = +33$ ($c = 0.75$ in 1 N HCl) (Aldrich). The $RuCl_3/H_5IO_6$ oxidation of **9** also provided the known N^{α}-(benzyloxycarbonyl)-L-phenylglycine. Vinylnaphthalene derivative **2** was assumed to have the same configuration as styrene derivative **9**. Methyl cinnamate derivative **10** was compared with a sample that was prepared from the known toluenesulfonamide analog [1,3]. Compounds **11**–**13** were assumed to have the same configuration as **10**.

Received: July 1, 1996 [Z92751E]
German version: *Angew. Chem.* **1996**, *108*, 2995–2999

Keywords: amino alcohols · asymmetric aminohydroxylation · carbamates · catalysis

[1] G. Li, H.-T. Chang, K. B. Sharpless, *Angew. Chem.* **1996**, *108*, 449–452; *Angew. Chem. Int. Ed. Engl.* **1996**, *35*, 451–454.
[2] K. B. Sharpless, J. Rudolph, P. C. Sennhenn, C. P. Vlaar, *Angew. Chem.* **1996**, *108*, 2991–2995; *Angew. Chem. Int. Ed. Engl.* **1996**, *35*, 2810–2813.
[3] G. Li, K. B. Sharpless, *Acta Chem. Scand.* **1996**, *50*, 649–651.
[4] K. B. Sharpless et al., unpublished results.
[5] H.-T. Chang, K. B. Sharpless, unpublished results.
[6] H. C. Kolb, M. S. VanNieuwenhze, K. B. Sharpless, *Chem. Rev.* **1994**, *94*, 2483–2547.
[7] D. J. Berrisford, C. Bolm, K. B. Sharpless, *Angew. Chem.* **1995**, *107*, 1159–1171; *Angew. Chem. Int. Ed. Engl.* **1995**, *34*, 1059–1070. With more hindered olefins in the original NMO-AD procedure and also in the two-phase ferricyanide procedure, the ligand may not noticeably increase the turnover rate, but to the best of our knowledge it does not slow it down either.
[8] See Scheme 2 in ref. [2]. In the present case X = COOR. This assumption is supported by our finding (not in tables) that methyl *trans*-cinnamate gives the BOC-protected product in only 78% *ee* when *tert*-BuOCONClNa is used as the oxidant (cf. 99% *ee* and 94% *ee* in Tables 1 and 2 for the reaction of the same substrate with the corresponding benzyl and ethyl carbamates (R = Bn and Et), respectively).
[9] E. Herranz, S. A. Biller, K. B. Sharpless, *J. Am. Chem. Soc.* **1978**, *100*, 3596–3598.
[10] K. B. Sharpless, A. O. Chong, K. Oshima, *J. Org. Chem.* **1976**, *41*, 177–179.
[11] a) E. Herranz, K. B. Sharpless, *J. Org. Chem.* **1980**, *45*, 2257–2259; b) *Org. Synth.* **1983**, *61*, 85–93; c) *ibid.* **1983**, *61*, 93–97.
[12] a) D. Guénard, F. Guéritte-Voegelein, P. Potier, *Acc. Chem. Res.* **1993**, *26*, 160–167; b) F. Guéritte-Voegelein, D. Guénard, F. Lavelle, M.-T. Le Goff, L. Mangatal, P. Potier, *J. Med. Chem.* **1991**, *34*, 992–998.
[13] The literature appears to be in error: M. M. Campbell, G. Johnson, *Chem. Rev.* **1978**, *78*, 65–79.
[14] In reexamining the results of the old experiments [9, 11] one sees that only trace amounts of water were used (2–4.5 equiv based on olefin (1% of total solvent)), probably due to concern that the $O_3Os{=}NCOOR$ species might hydrolyze to OsO_4 faster than it reacted with the olefin. In any case, it is frustrating to realize how very close, and on how many different occasions, one can come to the "right" conditions over years of experimenting, and still miss the target zone or zones within which the reaction conditions support useful, or at least detectable, catalytic turnover. – Metal-catalyzed redox processes are inherently multistep reactions, and the principal challenge in developing them is to find reaction conditions under which each of the steps can function at an acceptable rate. The search is guided above all by the knowledge that compromises are inevitable. A given set of reaction conditions can never be optimal for all the component reactions of the cycle. The slowest step constitutes the turnover-limiting step and defines the throughput (turnover rate) of the entire system [15]. In terms of the utility of a catalyst, the turnover rate (activity) is "not everything, it is the only thing" (paraphrased from a quote about the importance of winning, attributed to Vince Lombardi). – The complexity and interdependence of catalytic cycles means that "apparently" minor variations in the reaction conditions sometimes have major effects on the catalytic activity. This has certainly been the case for osmium-catalyzed oxidations of olefins, for which the maximum turnover rates (v_{max}) are virtually always identical with the rates for hydrolytic release of the chelated diol or amino alcohol product from the osmium coordination sphere. This is probably the least "interesting"

step in the entire sequence, but in catalysis every step in the cycle is by definition of equal importance.
[15] B. Bosnich, personal communication.
[16] G. Schlingloff, H. H. Angert, G. Li, K. B. Sharpless, unpublished results.
[17] The oxidation of the Z-protected amino alcohol from styrene (see Experimental Procedure) gave the Z-protected aryl glycine in roughly 80% yield and with no loss of enantiomeric purity. The scope of this two-step amino acid synthesis will be reported soon: K. L. Reddy, G. Li, K. B. Sharpless, unpublished results.
[18] We strongly recommend using *tert*-butyl hypochlorite that has been freshly prepared following the procedure described in M. J. Mintz, C. Walling, *Org. Synth. Coll. Vol. V* **1983**, 183–187. This material has proven reliable for up to two months if it is kept and dispensed under cold (at roughly 4 °C) and dry conditions. Some commercially obtained samples of *tert*-butyl hypochlorite have given substandard enantioselectivities and yields, probably because they were stored for longer periods at or above room temperature and/or not under dry conditions.
[19] Z.-M. Wang, K. B. Sharpless, *J. Org. Chem.* **1994**, *59*, 8302–8303.
[20] a) M. T. Nuñez, V. S. Martín, *J. Org. Chem.* **1990**, *55*, 1928–1932; b) P. H. Carlsen, T. Katsuki, V. S. Martín, K. B. Sharpless, *ibid.* **1981**, *46*, 3936–3938.
[21] S. Hanessian, B. Vanasse, *Can. J. Chem.* **1993**, *71*, 1401–1406.
[22] U. Schmidt, R. Meyer, V. Leitenberger, F. Stäbler, A. Lieberknecht, *Synthesis* **1991**, 409–413.

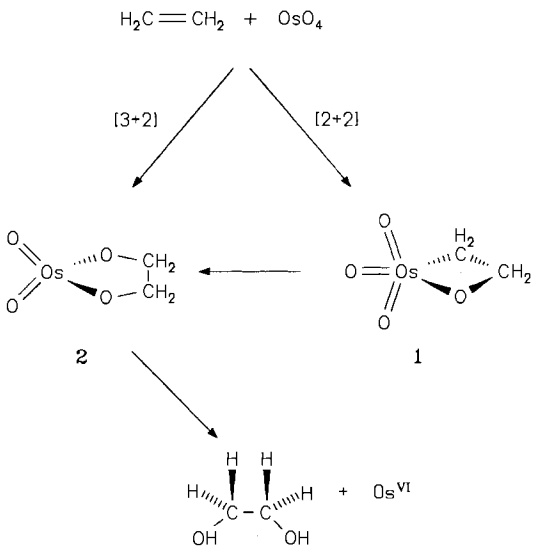

Scheme 1. Reaction course for the *cis*-dihydroxylation of olefins with OsO_4 as suggested by Sharpless.

Theory Rules Out a [2+2] Addition of Osmium Tetroxide to Olefins as Initial Step of the Dihydroxylation Reaction**

Ulrich Pidun, Christian Boehme, and Gernot Frenking*

The addition of OsO_4 to olefins yielding *cis*-diols has become an intensively investigated reaction in stereoselective synthesis since Sharpless developed the catalytic version of the reaction into a powerful method for highly enantioselective functionalization of olefins using cinchona alkaloids as ligands.[1] The transfer of the stereochemical information of the chiral ligand to the substrate was explained by Sharpless with a two-step mechanism for the addition reaction (Scheme 1), which should occur rather than a concerted [3 + 2] addition as originally proposed by Criegee.[2] It was suggested that the initial step of the reaction course is a [2 + 2] addition yielding the metallaoxetane **1**, which then rearranges to the cyclic ester **2**.[3] The barrier for the bond migration **1** → **2** must be very low, because intermediates of structure **1** have never been observed, whereas base adducts of **2** are well known.[4]

Strong support for a two-step mechanism of the osmylation reaction came from kinetic studies, which revealed a nonlinear correlation between the temperature and the enantioselectivity of the reaction.[5a] More recently kinetic studies of the addition of OsO_4 to various olefins both in the presence and the absence of a base (pyridine) have been carried out.[5b] In all cases the Eyring plots showed *two* linear regions. It follows that even the base-free osmylation appears to proceed by a two-step mechanism.

In a previous theoretical study at the QCISD(T)//HF level of theory we could show that the postulated intermediate **1** and the elusive base adduct **1**·NH_3 are indeed minima on the potential energy surfaces.[6] The metallaoxetane **1** was calculated to be 30.5 kcal mol^{-1} higher in energy than the osmate ester **2**. The reaction of ethylene with osmium tetroxide yielding **1** was predicted to be endothermic by +18.3 kcal mol^{-1}, while the [3+2] addition yielding **2** was calculated to be exothermic by −12.2 kcal mol^{-1}.[6] The activation barriers for the two reactions and for the rearrangement **1** → **2** were not given, however. In this paper we present the calculated transition states for the [2+2] and [3+2] additions of OsO_4 to C_2H_4 and for the rearrangement **1** → **2** using density functional theory (DFT)[7] in conjunction with a relativistic effective core potential (ECP) for osmium.[8] We also calculated the transition states for the base-catalyzed reaction using $OsO_4(NH_3)$ as model compound. The reaction energies and activation barriers for the base-free reaction are predicted at the CCSD(T) level of theory[9] with DFT optimized geometries. The nature of the transition states was analyzed by IRC (intrinsic reaction coordinate) calculations. The NH_3 complexed structures were studied only at the DFT level.[10]

Figure 1 shows the calculated geometries of the molecules and the transition states, optimized at B3LYP with basis set II.[10] The theoretically predicted Os–O distance for OsO_4 (1.716 Å) is in excellent agreement with the experimental value (1.711 Å).[11] The calculated geometry of the complex **2**·NH_3 is also in accord with the X-ray structure analyses of related cinchona alkaloid complexes of Os^{VI}.[12] The observed Os–N distances are 2.243(5) and 2.27(2) Å; the calculated value is 2.264 Å.

Figure 2 shows the calculated reaction profile for the base-free reaction. The theoretical reaction energy at CCSD(T)/II//B3LYP/II for the reaction $C_2H_4 + OsO_4 \rightarrow$ **1** is +11.1 kcal mol^{-1}, while the formation of **2** is exothermic (−21.2 kcal mol^{-1}). The [2+2] and [3+2] reactions are calculated to be thermodynamically slightly more favorable than determined in our previous work,[6] which is due to the different methods used in the two studies. The energy difference between **1** and **2** calculated here (32.3 kcal mol^{-1}) is very similar to our previous result (30.5 kcal mol^{-1}).[6]

The most important results of the present study are the activation barriers for the reactions. Figure 2 shows that the activation barrier at CCSD(T)/II[10] for the [2 + 2] addition yielding **1** is very high (44.7 kcal mol^{-1}). In contrast, the activation barrier for the [3 + 2] addition is much lower (9.6 kcal mol^{-1}). The

[*] Prof. Dr. G. Frenking, Dipl. Chem. U. Pidun, Dipl. Chem. C. Boehme
Fachbereich Chemie der Universität
Hans-Meerwein-Strasse, D-35032 Marburg (Germany)
Fax: Int. code +(6421)28-2189
e-mail: frenking@ps1515.chemie.uni-marburg.de.

[**] Theoretical Studies of Organometallic Compounds, Part 24. This work has been supported by the Deutsche Forschungsgemeinschaft (SFB 260, Graduiertenkolleg Metallorganische Chemie) and the Fonds der Chemischen Industrie. We thank Dr. P.-O. Norrby for helpful comments. Part 23: S. Dapprich, G. Frenking, *Organometallics* **1996**, *15*, 4547.

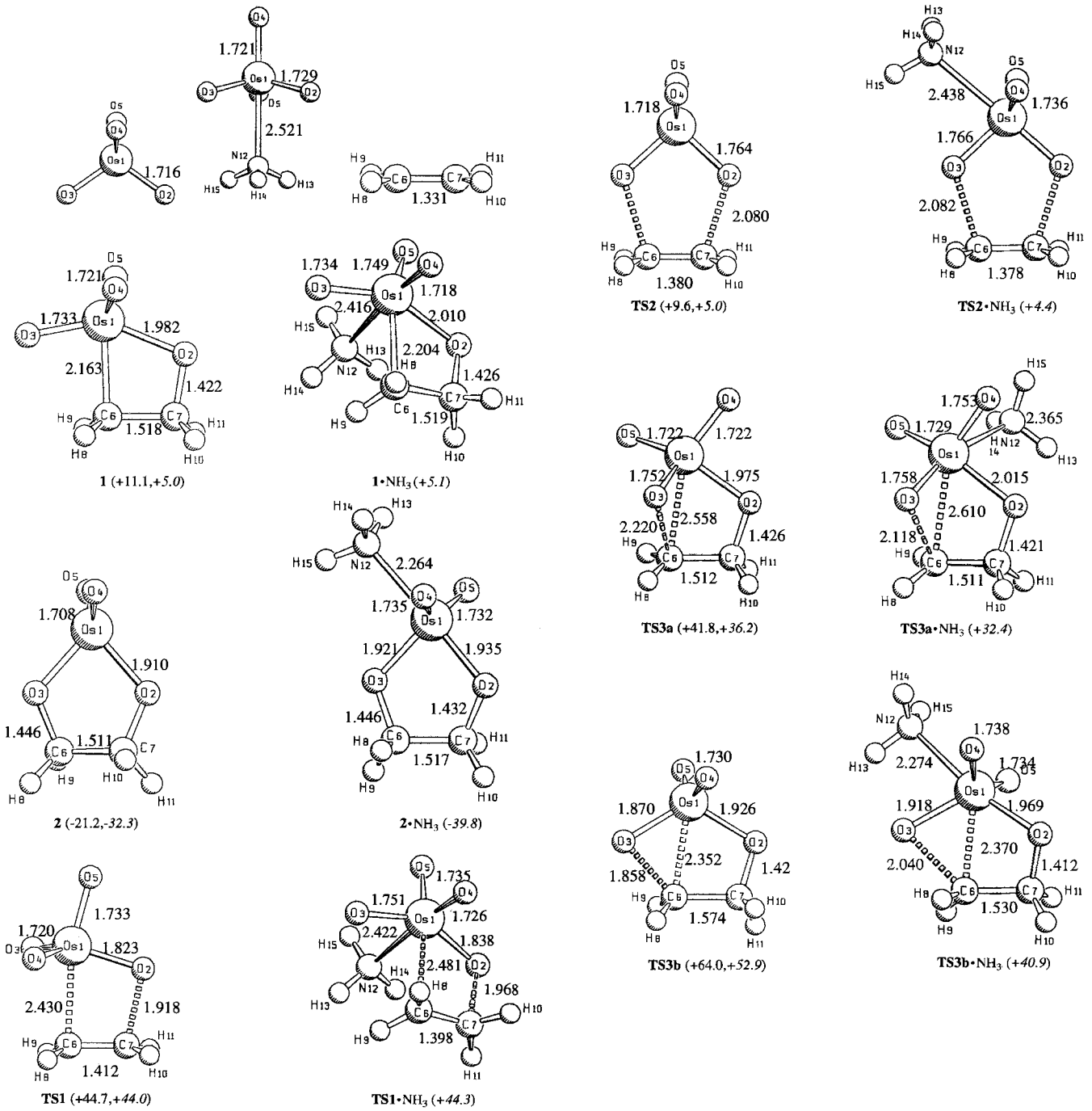

Fig. 1. Optimized geometries of energy minimum structures and transition states at B3LYP/II (distances in Å, energies in kcal mol^{-1} relative to that of the reactants ($OsO_4 + C_2H_4$ or $OsO_4(NH_3) + C_2H_4$) at CCSD(T)/II; values in italics refer to B3LYP/II energies).

energy differences change only slightly when zero-point energy contributions are considered. The energies at B3LYP give essentially the same reaction profile as the CCSD(T) values (Fig. 2). The large difference in the barrier heights for the two reactions does not agree with the suggestion that both mechanisms play a role in the course of the reaction, and that the dominance of one mechanism over the other depends on temperature.[5b] Such a scenario would require that the activation energies are much closer.

The calculations gave two transition states **TS3a** and **TS3b** for the rearrangement **1** → **2**. **TS3a** is the transition state along the reaction coordinate for the bond formation between C6 and the out-of-plane oxygen atom, whereas **TS3b** belongs to the bond formation between C6 and the in-plane oxygen atom (Fig. 1). **TS3a** is clearly lower in energy than **TS3b**. The barrier for the rearrangement **1** → **2** given by **TS3a** (41.8 kcal mol^{-1}) is still high, however, when compared with the activation barrier for the [3+2] addition given by **TS2** (9.6 kcal mol^{-1}). The theoretically predicted activation barriers for the base-free addition of OsO_4 to olefins (Fig. 2) rule out the competition between the stepwise [2+2] addition reaction and the [3+2] cycloaddition.

Does the reaction profile for the osmylation reaction in the presence of a base differ significantly from that of the base-free reaction? The answer is no! Figure 1 shows the optimized transition state structures **TS1**·NH_3 for the [2+2] addition and

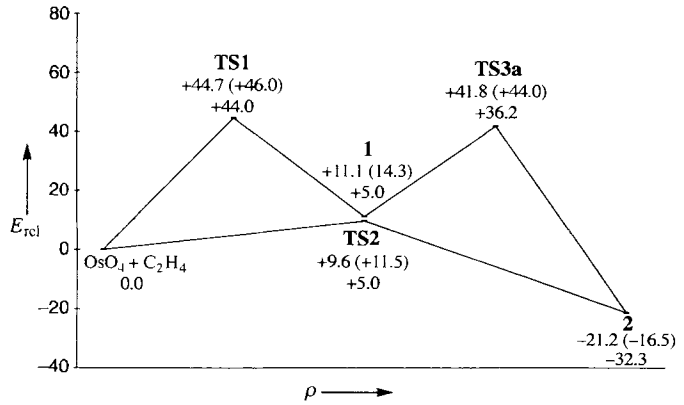

Fig. 2. Calculated reaction profile of the addition of OsO_4 to ethylene at CCSD(T)//B3LYP using basis sets as described in reference [10] (relative energies in kcal mol^{-1}; values in parentheses include ZPE contributions; values in italics refer to B3LYP energies).

TS2·NH_3 for the [3+2] addition of the $OsO_4(NH_3)$ adduct to C_2H_4. The activation barrier for the [3+2] addition in the presence of NH_3 is lower in energy (4.4 kcal mol^{-1} at B3LYP/II) than that of the base-free [3+2] reaction (5.0 kcal mol^{-1}). This is in agreement with the observed acceleration of the osmylation reaction by a base. The activation barrier for the [2+2] addition in the presence of NH_3 remains much higher than for the [3+2] reaction. Transition state **TS1**·NH_3 is energetically 44.3 kcal mol^{-1} (B3LYP/II) above the reactants and 39.9 kcal mol^{-1} higher in energy than **TS2**·NH_3. The calculated geometries of the transition states **TS1**·NH_3 and **TS2**·NH_3 are very similar to the geometries of **TS1** and **TS2**, respectively. The same holds true for the transition states of the rearrangement **TS3a**·NH_3 and **TS3b**·NH_3 relative to **TS3a** and **TS3b** (Fig. 1). The barrier height for the rearrangement **1** → **2** in the presence of NH_3 is slightly lower than without the base, but it still remains very high. The presence of a base therefore does not change the reaction profile of the osmylation reaction significantly. While the absolute values of the calculated activation barriers may change at different levels of theory, it is highly unlikely that the *relative* barrier heights for the concerted and stepwise reactions will change a lot.[13]

To make sure that the optimized transition states belong to the desired reaction courses, we calculated the intrinsic reaction coordinates (IRC)[14] starting from the transition state structures **TS1**, **TS2**, **TS3a**, and **TS3b** (Fig. 1). The results of the IRC calculations confirmed that **TS1** and **TS2** are the transition states for the [2+2] and [3+2] addition, respectively, and that **TS3a** and **TS3b** are transition states for the bond migration **1** → **2**. The high barriers for the [2+2] addition and for the bond migration **1** → **2** suggest that these reactions are symmetry forbidden, while the [3+2] addition is symmetry allowed. A previous frontier orbital study of the possible reaction mechanism by Jørgensen and Hoffmann did not conclusively discriminate between reaction paths via **1** and **2**, but arguments were given in favor of the [3+2] over the [2+2] addition.[15] The more quantitative results presented here indicate that the difference in the activation barriers is much higher than that deduced from the qualitative orbital diagrams. It is noteworthy that the geometry changes from **TS1** to **1** involve a rotation of the OsO_3 moiety about the Os–O2 axis (Fig. 1). In **TS1** an oxygen atom is *trans* to the incipient Os–C6 bond, whereas in **1** an oxygen is *trans* to the Os-O2 bond. The reaction path is clearly different from a least-motion path. This is a further hint that the reaction proceeds by an orbital-symmetry forbidden pathway.

While the results of the calculations show clearly that the [2+2] addition of OsO_4 to olefins can not compete energetically with the [3+2] addition, the calculations cannot explain the results of the kinetic studies of Sharpless et al.,[5] which indicate that two different mechanisms are operating in the ligand-free osmylation reaction. We want to point out, however, that an alternative mechanistic model for the enantioselective asymmetric dihydroxlation suggested by Corey assumes that the reaction proceeds by a [3+2] cycloaddition.[16] This model would be in better agreement with our calculations. Very recent experimental tests of the [3+2] and [2+2] pathways by means of $^{12}C/^{13}C$ kinetic isotope effects have shown that the [3+2] model is in accord with the experimental results, while the [2+2] model is not.[16d] The remaining puzzle concerns the interpretation and understanding of the kinetic measurements of Sharpless, which unequivocally show an inversion point in the Eyring diagram of the dihydroxylation.[5] A very recent kinetic study of Heller et al.[21] showed that a nonlinear temperature behavior of product ratios in selection processes may possibly be due to a distortion of the reactant equilibrium. Another explanation might be an intramolecular exchange between the diastereomeric substrate complexes, which has been determined for 7-membered chelates.[22] Further experimental studies appear necessary to clarify this point.

Although our previous theoretical study showed that the stepwise mechanism of the osmylation reaction by [2+2] addition might be possible, because the postulated metallaoxetane is indeed an intermediate that is not too high in energy,[6] the calculated activation barriers presented here and the experimentally observed kinetic isotope effects[16d] suggest that the reaction proceeds by a concerted [3 + 2] pathway as originally suggested by Criegee.[2]

Received: July 8, 1996 [Z93051E]
German version: *Angew. Chem.* **1996**, *108*, 3008–3011

Keywords: ab initio calculations · asymmetric dihydroxylation · reaction mechanisms

[1] R. A. Johnson, K. B. Sharpless in *Catalytic Asymmetric Synthesis* (Ed.: I. Ojima), VCH, New York, **1993**, pp. 227–272.

[2] R. Criegee, B. Marchand, H. Wannowius, *Justus Liebigs Ann. Chem.* **1942**, *550*, 99.

[3] a) S. G. Hentges, K. B. Sharpless, *J. Am. Chem. Soc.* **1980**, *102*, 4263; b) E. N. Jacobsen, I. Markó, W. S. Mungall, G. Schröder, K. B. Sharpless, *ibid.* **1988**, *110*, 1968.

[4] a) W. P. Griffith, C. J. Raub in *Gmelin Handbuch der Anorganischen Chemie, Osmium Suppl. Vol. 1* (Ed.: K. Swars), Springer, Heidelberg, **1980**, pp. 184–208; b) J. S. Svendson, I. Markó, E. N. Jacobsen, C. P. Rao, S. Bott, K. B. Sharpless, *J. Org. Chem.* **1989**, *54*, 2263; c) R. M. Pearlstein, B. K. Blackburn, W. M. Davis, K. B. Sharpless, *Angew. Chem.* **1990**, *102*, 710; *Angew. Chem. Int. Ed. Engl.* **1990**, *29*, 639.

[5] a) T. Göbel, K. B. Sharpless, *ibid.* **1993**, *105*, 1417 and **1993**, *32*, 1329; b) D. V. McGrath, A. Makita, K. B. Sharpless, in preparation. We thank Prof. Sharpless for a preprint.

[6] The calculations were carried out at the QCISD(T)//HF level using a pseudopotential for Os: A. Veldkamp, G. Frenking, *J. Am. Chem. Soc.* **1994**, *116*, 4937.

[7] *Density Functional Methods in Chemistry* (Eds.: J. Labanowski, J. Andzelm), Springer, Heidelberg, **1991**.

[8] P. J. Hay, W. R. Wadt, *J. Chem. Phys.* **1985**, *82*, 299.

[9] a) J. A. Pople, R. Krishnan, H. B. Schlegel, J. S. Binkley, *Int. J. Quantum Chem.* **1978**, *14*, 545; b) R. J. Bartlett, G. D. Purvis, *ibid.* **1978**, *14*, 561; c) G. D. Purvis, R. J. Bartlett, *J. Chem. Phys.* **1982**, *76*, 1910; d) *ibid.* **1987**, *86*, 7041; e) J. A. Pople, M. Head-Gordon, K. Raghavachari, *ibid.* **1987**, *87*, 5968.

[10] The program packages Gaussian 94 [17a] and ACESII [17b] have been used for the calculations. The geometries were optimized at the DFT level with the nonlocal hybrid functionals B3LYP of Becke [18]. A quasi-relativistic effective core potential (ECP) [8] for osmium (small core) with a (441/2111/21) basis set for the 16 valence and outer-core electrons in conjunction with a 6-31G(d) basis set for the other atoms was used. This is our standard basis set II [19]. The vibrational frequencies and the intrinsic reaction coordinates [14] were calculated at the same level of theory (B3LYP/II). Improved total energies of the base-free species were calculated at the CCSD(T) level [9] with the same basis

set II, except that for computational reasons an STO-3G basis set was employed for hydrogen. The accuracy of the CCSD(T) level of theory for calculating energies of transition metal compounds has been documented [19]. CCSD(T) calculations of the NH_3-complexed species could not be carried out for technical reasons (<2 GByte size limit for a single file). The accuracy of B3LYP calculations is also well known [20].

[11] A. Zalkin, D. H. Templeton, *Acta Crystallogr.* **1953**, *6*, 106.

[12] R. M. Pearlstein, B. K. Blackburn, W. M. Davis, K. B. Sharpless, *Angew. Chem.* **1990**, *102*, 710; *Angew. Chem. Int. Ed. Engl.* **1990**, *29*, 639.

[13] Similar results have been obtained in an independent theoretical study by Morokuma and co-workers. We thank Prof. Morokuma for sending us a preprint of his work: S. Dapprich, G. Ujaque, F. Maseras, A. Lledós, K. Morokuma, *J. Am. Chem. Soc.*, in press.

[14] a) K. Fukui, *Acc. Chem. Res.* **1981**, *14*, 363; b) C. Gonzalez, H. B. Schlegel, *J. Chem. Phys.* **1991**, *95*, 5853.

[15] K. A. Jørgensen, R. Hoffmann, *J. Am. Chem. Soc.* **1986**, *108*, 1867.

[16] a) E. J. Corey, A. Guzman-Perez, M. C. Noe, *J. Am. Chem. Soc.* **1994**, *116*, 12109; b) *ibid.* **1995**, *117*, 10805; c) E. J. Corey, M. C. Noe, *ibid.* **1996**, *118*, 319; d) E. J. Corey, M. C. Noe, M. J. Grogan, *Tetrahedron Lett.* **1996**, *37*, 4899.

[17] a) Gaussian 94: M. J. Frisch, G. W. Trucks, H. B. Schlegel, P. M. W. Gill, B. G. Johnson, M. A. Robb, J. R. Cheeseman, T. A. Keith, G. A. Petersson, J. A. Montgomery, K. Raghavachari, M. A. Al-Laham, V. G. Zakrzewski, J. V. Ortiz, J. B. Foresman, J. Cioslowski, B. B. Stefanov, A. Nanayakkara, M. Challacombe, C. Y. Peng, P. Y. Ayala, W. Chen, M. W. Wong, J. L. Andres, E. S. Replogle, R. Gomberts, R. L. Martin, D. J. Fox, J. S. Binkley, D. J. Defrees, J. Baker, J. J. P. Stewart, M. Head-Gordon, C. Gonzalez, J. A. Pople, Gaussian Inc., Pittsburgh, PA, **1995**; b) ACES II, an ab initio program system by J. F. Stanton, J. Gauss, J. D. Watts, W. J. Lauderdale, and R. J. Bartlett, University of Florida, Gainesville, FL, **1991**.

[18] a) A. D. Becke, *J. Chem. Phys.* **1993**, *98*, 5648; b) P. J. Stevens, F. J. Devlin, C. F. Chablowski, M. J. Frisch, *J. Phys. Chem.* **1994**, *98*, 11623.

[19] G. Frenking, I. Antes, M. Böhme, S. Dapprich, A. W. Ehlers, V. Jonas, A. Neuhaus, M. Otto, R. Stegmann, A. Veldkamp, S. F. Vyboishchikov in *Reviews in Computational Chemistry, Vol. 8* (Eds.: K. B. Lipkowitz, D. B. Boyd), VCH, New York, **1996**, pp. 63–144.

[20] a) A. Ricca, C. W. Bauschlicher, Jr., *Theor. Chim. Acta* **1995**, *92*, 123; b) O. Wiest, K. A. Black, K. N. Houk, *J. Am. Chem. Soc.* **1994**, *116*, 10336.

[21] a) D. Heller, H. Buschmann, H.-D. Scharf, *Angew. Chem.* **1996**, *108*, 1964; *Angew. Chem. Int. Ed. Engl.* **1996**, *35*, 1852; b) D. Heller (Rostock), personal communication to G. F.

[22] R. Kadyrov, T. Freier, D. Heller, M. Michalik, R. Selke, *J. Chem. Soc. Chem. Commun.* **1995**, 1745.

5-*exo* or 6-*endo*? Exploring Transition State Structures in Cyclizations of 4-Penten-1-oxyl Radicals**

Jens Hartung,* Ralf Stowasser, Daniel Vitt, and Gerhard Bringmann*

Dedicated to Professor Siegfried Hünig on the occasion of his 75th birthday

A recent study on stereoselective ring closures of substituted 4-penten-1-oxyl radicals indicates that transformations involving alkoxyl radicals may indeed be free radical reactions with notable synthetic utility.[1] Despite the high reactivity ($k^{exo} = (5 \pm 2) \times 10^8\ s^{-1}$) the 4-penten-1-oxyl radical **1a** cyclizes regioselectively; derivatives of **1a** even react stereoselectively. To uncover the origin of the high *exo* selectivity of the cyclization, the isoelectronic, all-carbon derivative **1b** of the 4-penten-1-oxyl radical **1a** has been the subject of several semiempirical and low-level ab initio calculations.[2] However, the prediction of radical selectivities in cyclization reactions remained a difficult task, because treatment of open-shell molecules with unrestricted Hartree–Fock (UHF) methods led in most of the cases to "spin contamination" in the transition states. To account for these problems and to obtain more reliable energy values in general, the computed heats of formation were often corrected by additional time-consuming configuration interaction calculations (CI calculations).[3]

Several new developments in the theoretical treatment of radical additions to olefins[3] sparked our interest in a more detailed description of the 5-*exo* (**1a** → **3a**) and the competitive 6-*endo* (**1a** → **5a**) cyclizations of the 4-penten-1-oxyl radical. We now

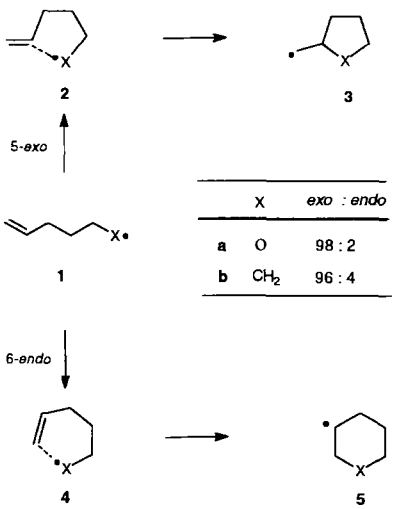

report on our results of semiempirical (AM1, PM3) and selected ab initio calculations (UHF/6-31G*, UQCISD/6-31G*//UHF/6-31G*, UHF/6-31+G*, UHF/6-311+G*) UBP/DZVP i.e. DFT[4]). We have included the 5-hexen-1-l radical (**1b**) in our studies, because according to our knowledge it had not been investigated by these methods previously.

All the methods used predict that the lowest energy transition structures **2** and **4** resemble cyclohexane chairs (Fig. 1).[5, 6] However, structures **2a** and **2b** are significantly flattened and more reminiscent of envelope conformations of the corresponding saturated five-membered ring compounds. The most important geometrical parameters, the distances between the radical center and the carbon atom C5 (r_1) and the second carbon C6 of the π-bond (r_2), the angle of attack (φ), and the torsion angles δ_1 and δ_2, which indicate the degree of rehybridization at C5 and C6 in the transition state, vary markedly depending on the computational method (Fig. 2, Table 1). The calculated relative heats of formation (ΔH_f) and corresponding expectation values of the respective spin operators $\hat{S}^2$ ($<\hat{S}^2>$ values) of the intermediates **1**–**5** are listed in Tables 2 and 3.

The data in Table 2 indicate that the semiempirical methods are not suitable for the description of the alkoxyl radical ring closures. Even considering the uncertainties of semiempirical methods, AM1 still predicts the formation of the thermodynamically favored 6-*endo* product **5a**, as judged by the differences in the enthalpies of activation $\Delta H^{\neq}_{exo} - \Delta H^{\neq}_{endo} = \Delta\Delta H^{\neq}$. PM3 does not lead to a clear-cut result.[7] However, the results of ab initio calculations are generally more satisfactory, and in some cases they are in excellent agreement with the experimental values.

[*] Dr. J. Hartung, Prof. Dr. G. Bringmann, Dipl.-Chem. R. Stowasser, Dipl.-Chem. D. Vitt
Institut für Organische Chemie der Universität
Am Hubland, D-97074 Würzburg (Germany)
Fax: Int. code +(931)888-4755
e-mail: hartung@chemie.uni-wuerzburg.de
bringman@chemie.uni-wuerzburg.de

[**] This work was supported by the Deutsche Forschungsgemeinschaft (SFB 347 "Selektive Reaktionen Metall-aktivierter Moleküle" and "Normalverfahren") and by the Fonds der Chemischen Industrie (fellowships for J. H. and R. S. as well as equipment). We thank Dipl.-Chem. Martin Stahl for helpful discussions.

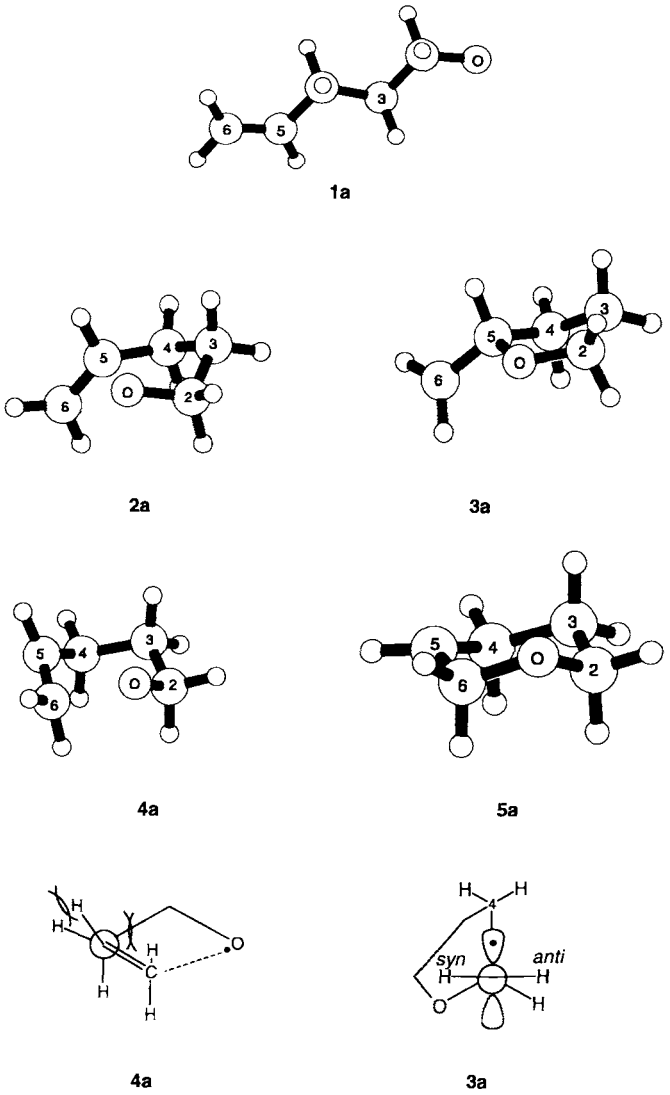

Fig. 1. Top: Computed structures (UHF/6-31G*) of radicals **1a**–**5a**. The structures **2a** and **4a** show the transition state structures of the 5-*exo* and 6-*endo* reactions, respectively. Bottom: The representation of the 5-*exo* product **3a** shows the coplanar arrangement of the unpaired electron and the C5–C4 bond of the heterocyclic ring (C4-C5-C6-H6*syn* = 83.08°, C4-C5-C6-H6*anti* = −83.14°) [5]. The Newman projection along the C5–C4 bond of the 6-*endo-trig* transition state structure **4a** indicates the torsional strain between the hydrogen atoms at C5 and the *syn* hydrogens bound at C4 and C6 [6].

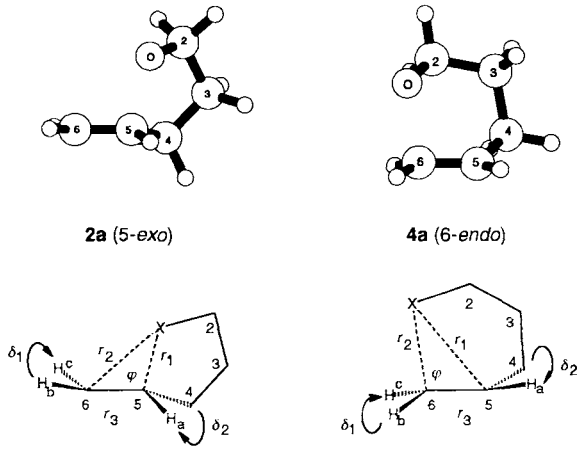

Fig. 2. Top: The calculated transition state structures for the 5-*exo* (**2a**) and 6-*endo* (**4a**) (UHF/6-31G*) cyclizations of the 4-penten-1-oxyl radical (**1a**). Bottom: Schematic representation of the geometric parameters used to describe the 5-*exo* and of the 6-*endo* transition state structures **2** and **4**. δ_1 corresponds to angle C5-C6-Hb-Hc, δ_2 angle C6-C5-C4-Ha, φ angle X-C5-C6 for the *exo* attack and X-C6-C5 for the *endo* approach of the radical.

Table 1. Parameters for describing the transition state structures for the 5-*exo* and 6-*endo* cyclizations of the 4-penten-1-oxyl (**1a**) and of the 5-hexenyl radical (**1b**) at different levels of theory.

Structure	Parameter	AM1	UHF/6-31G*	UBP/DZVP
2a	r_1 [Å]	2.027	1.907	2.168
	r_2 [Å]	2.506	2.637	2.723
	r_3 [Å]	1.369	1.403	1.374
	φ [°]	93.07	104.6	97.97
	δ_1 [°]	−176.2	−170.1	−176.4
	δ_2 [°]	169.1	150.5	169.0
3a	r_1 [Å]	2.482	2.562	2.566
	r_2 [Å]	2.057	1.925	2.189
	r_3 [Å]	1.366	1.398	1.367
	φ [°]	90.60	99.69	89.27
	δ_1 [°]	171.49	153.2	173.4
	δ_2 [°]	−170.69	−154.4	−167.8
2b	r_1 [Å]	2.102	2.186	2.324
	r_2 [Å]	2.681	2.963	2.954
	r_3 [Å]	1.377	1.393	1.376
	φ [°]	98.66	109.7	102.9
	δ_1 [°]	177.3	171.9	−169.8
	δ_2 [°]	−156.4	−149.7	161.7
3b	r_1 [Å]	2.643	2.818	2.893
	r_2 [Å]	2.141	2.260	2.441
	r_3 [Å]	1.373	1.384	1.363
	φ [°]	95.03	98.41	94.80
	δ_1 [°]	−162.8	−157.13	−170.6
	δ_2 [°]	172.5	158.4	162.4

The UHF/3-21G*-computed $\Delta\Delta H^{\neq}$ value is $-3.90\ kJ\,mol^{-1}$. When a larger basis set is used for the calculations (UHF/6-31G*), the difference in the activation enthalpies is even more pronounced ($\Delta\Delta H^{\neq} = -9.70\ kJ\,mol^{-1}$), which is in good agreement with the experimentally determined $\Delta\Delta G^{\neq}$ value of this reaction at 298 K ($-9.50\ kJ\,mol^{-1}$ [1, 8]). When the heats of formation of the UHF/6-31G*-optimized structures are corrected with UQCISD calculations, the $\Delta\Delta H^{\neq}$ value increases to $-4.75\ kJ\,mol^{-1}$. For the description of the 5-*exo* and the competitive 6-*endo* reaction, UQCISD/6-31//UHF/6-31G* corrections are inferior to calculations with a more flexible basis set (UHF/6-31+G*, $\Delta\Delta H^{\neq} = -7.30\ kJ\,mol^{-1}$). It is likely that the latter method better accounts for the diffuse electron distribution at the reacting centers and the double bond being attacked. However, computational studies on our structures using a triple-zeta basis set (UHF/6-311+G*) do not improve the $\Delta\Delta H^{\neq}$ values significantly in spite of prolonged computation time.[9] Density functional calculations (UBP/DZVP) are often faster to perform, and although the resulting calculated *exo*:*endo* ratio ($\Delta\Delta H^{\neq} = -5.59\ kJ\,mol^{-1}$) is lower than the experimental value, this method seems to be a useful alternative to the other ab initio methods (Table 2). Future studies will show whether this result is of general significance.

The results obtained for the cyclizations of the 5-hexenyl radical (Table 3) are qualitatively similar to the data for the reactions of the alkoxyl radical **1a**. The AM1 approximation predicts the formation of the 6-*endo* intermediate **5a** as the major product. However, the results from UHF/6-31G* calculations without corrections ($\Delta\Delta H^{\neq} = -8.75\ kJ\,mol^{-1}$) and with UQCISD/6-31G*//UHF/6-31G* corrections ($\Delta\Delta H^{\neq} =$

Table 2. Calculated energies [Hartree], relative heats of formation ΔH_f [kJ mol^{-1}], and $\langle \hat{S}^2 \rangle$ values for radicals **1a**–**5a** [a].

Method		**1a**	**3a**	**5a**	**2a** [b]	**4a** [c]
AM1	ΔH_f	129.9	43.0	≡0	190.8	184.1
	$\langle \hat{S}^2 \rangle$	0.756	0.763	0.763	0.918	0.908
PM3	ΔH_f	125.6	30.9	≡0	183.3	180.6
	$\langle \hat{S}^2 \rangle$	0.756	0.763	0.763	0.918	0.908
UHF/3-21G*//	E	−267.88544	−267.89248	−267.89501	−267.86609	−267.8637
UHF/3-21G*	ΔH_f	36.20	13.18	≡0	85.36	89.25
	$\langle \hat{S}^2 \rangle$	0.756	0.763	0.763	0.918	0.908
UHF/6-31G*//	E	−269.37272	−269.38341	−269.38795	−269.34655	−269.34361
UHF/6-31G*	ΔH_f	52.78	18.50	≡0	119.86	129.26
	$\langle \hat{S}^2 \rangle$	0.758	0.762	0.762	1.008	1.031
UQCISD/	E	−270.21856	−270.23823	−270.24585	−270.21034	−270.20759
6-31G*//	ΔH_f	84.47	26.59	≡0	104.39	109.14
UHF/6-31G*	$\langle \hat{S}^2 \rangle$	0.758	0.762	0.762	1.008	1.031
UHF/6-31+G*//	E	−269.38059	−269.38976	−269.39398	−269.35304	−269.34951
UHF/6-31+G*	ΔH_f	48.49	22.18	≡0	118.66	125.96
	$\langle \hat{S}^2 \rangle$	0.758	0.762	0.762	1.004	1.024
UHF/6-311+G*	E	−269.433201	−269.44129	−269.44602	−269.40456	−269.40170
	ΔH_f	44.82	25.70	≡0	120.02	125.69
	$\langle \hat{S}^2 \rangle$	0.759	0.763	0.763	1.003	1.023
UBP/DZVP	E	−271.14001	−271.15558	−271.16500	−271.13777	−271.13602
	ΔH_f	71.76	26.74	≡0	77.28	82.87
	$\langle \hat{S}^2 \rangle$	0.752	0.752	0.754	0.754	0.761

[a] The ΔH_f values from the AM1 and PM3 calculations are ZPVE corrected. All ab initio calculated ΔH_f values are ZPVE corrected, but not temperature corrected (1 Hartree = 2627.26 kJ mol^{-1}). [b] ΔH_{exo} = 60.9 kJ mol^{-1} (AM1), 57.7 kJ mol^{-1} (PM3), 49.2 kJ mol^{-1} (UHF 3-21G*//UHF 3-21G*), 67.08 kJ mol^{-1} (UHF/6-31G*//UHF/6-31G*), 19.92 kJ mol^{-1} (UQCISD/6-31G*//UHF/6-31G*), 70.17 kJ mol^{-1} (UHF/6-31+G*//UHF/6-31+G*), 75.20 kJ mol^{-1}, (UHF/6-311+G*//UHF/6-311+G*), 5.51 kJ mol^{-1} (UBP/DZVP). [c] ΔH_{endo} = 54.2 kJ mol^{-1} (AM1), 55.0 kJ mol^{-1} (PM3), 53.2 kJ mol^{-1} (UHF/3-21G*//UHF/3-21G*), 76.48 kJ mol^{-1} (UHF/6-31G*//UHF/6-31G*), 24.67 kJ mol^{-1} (UQCISD/6-31G*//UHF/6-31G*), 77.47 kJ mol^{-1} (UHF/6-31+G*//UHF/6-31+G*), 80.87 kJ mol^{-1} (UHF/6-311+G*//UHF/6-311+G*), 11.10 kJ mol^{-1} (UBP/DZVP).

Table 3. Calculated energies E [Hartree], relative heats of formation ΔH_f [kJ mol^{-1}], and $\langle \hat{S}^2 \rangle$ values for radicals **1b**–**5b** [a].

Method		**1b**	**3b**	**5b**	**2b** [b]	**4b** [c]
AM1	ΔH_f	138.1	42.3	≡0	176.6	171.6
	$\langle \hat{S}^2 \rangle$	0.762	0.762	0.763	0.957	0.960
UHF/6-31G*//	E	−233.54377	−233.56741	−233.57994	−233.52555	−233.52190
UHF/6-31G*	ΔH_f	110.25	39.24	≡0	157.26	166.01
	$\langle \hat{S}^2 \rangle$	0.762	0.762	0.763	1.017	1.048
UQCISD/	E	−234.36624	−234.39407	−234.40668	−234.35210	−234.34825
6-31G*//	ΔH_f	121.47	39.45	≡0	157.76	167.03
UHF/6-31G*	$\langle \hat{S}^2 \rangle$	0.762	0.762	0.763	1.017	1.048
UBP/DZVP	E	−235.21600	−235.23983	−235.25050	−235.20849	−235.20627
	ΔH_f	101.35	31.51	≡0	121.76	128.04
	$\langle \hat{S}^2 \rangle$	0.754	0.754	0.754	0.767	0.763

[a] The ΔH_f values from the AM1 calculations are ZPVE corrected. All ΔH_f values from ab initio calculations are ZPVE corrected, but not temperature corrected (1 Hartree = 2627.26 kJ mol^{-1}). [b] ΔH_{exo} = 38.5 kJ mol^{-1} (AM1), 47.01 kJ mol^{-1} (UHF/6-31G*//UHF/6-31G*), 36.29 kJ mol^{-1} (UQCISD/UHF/6-31G*//UHF/6-31G*), 20.41 kJ mol^{-1} (UBP/DZVP). [c] ΔH_{endo} = 33.50 kJ mol^{-1} (AM1), 55.76 kJ mol^{-1} (UHF/6-31G*//UHF/6-31G*), 45.56 kJ mol^{-1} (UQCISD/6-31G*//UHF/6-31G*), 26.69 kJ mol^{-1} (UBP/DZVP).

The ab initio procedures locate the transition state structures at different points on the potential energy surface. UHF/6-31G* calculations give a rather tight 5-*exo* transition state structure (r_1 = 1.907 Å), while UBP/DZVP computations set the reacting centers in the transition state 0.261 Å further apart. In general, the differences in r_1 (X–C5) for the 5-*exo* reaction and r_2 (X–C6) for the 6-*endo* reaction of alkoxyl radical **1a** are negligible, but the angle φ of attack is smaller in the *endo* approach of the incoming O-radical by 4.91° (UHF/6-31G*) and 8.70° (UBP/DZVP) than in the *exo* attack. The same angle φ is larger for the computed C-radical additions than for the alkoxyl radical cyclizations.

The intramolecular addition of the radical center (e.g. X = O in **2a**) to the C–C double bond causes a slight change in hybridization at C5 and at C6; in transition states **2** and **4** the torsion angles δ_1 = C5-C6-Hb-Hc and δ_2 = C6-C5-C4-Ha deviate significantly from 180°.[2c] The hydrogen atoms at the attacked carbon move slightly away from the oxygen atom, while the adjacent H atoms of the C–C double bond point towards the radical center (Fig. 2). These changes in geometry are of minor significance for the 5-*exo-trig* reaction (e.g. **1a** → **3a**). In the course of C–O bond formation the torsional strain between the *syn* hydrogens at C5 and at C6 is continuously minimized due to the transformation of the C–C double bond into a single bond and the resulting gain in rotational freedom of the *exo* methylene group. The product of the 5-*exo-trig* cyclization of the alkoxyl radical **1a** is the tetrahydrofurylmethyl radical **3a**, which shows a coplanar arrangement of the β-C–C bond and the radical center in the lowest energy conformer.[5a] In the course of the 6-*endo* reaction **1a** → **5a** the changes in δ_1 and in δ_2 described above lead to more severe torsional strain. The formation of the C–O bond is accompanied by a significant change in geometry at C5 and repulsive interactions due to the movement of H5 past the *syn* hydrogens at C4 and at C6 for the formation of the 6-*endo* product **5a**, which has an almost planar radical center C5[6a, 11] (Fig. 1, bottom). This torsional strain is possibly one of the reasons for the kinetic preference of the 5-*exo-trig* reaction of the 4-pentenoxyl radical **1a** and the isoelectronic 5-hexenyl radical **1b**.

The results of the theoretical treatment of the reactions of **1b** are slightly different from those of previous studies. The reacting centers are further apart in the 6-*endo* transition state structure than in the 5-*exo* transition state structure (UHF/6-31G*: Δr_1 = 0.074 Å; UBP/DZVP: Δr_1 = 0.117 Å), which could be caused by torsional strain in the reaction **1b** → **5b** as mentioned above. The large separation between the reacting centers in all transition states in UBP/DZVP calcula-

−9.27 kJ mol^{-1}) are in accord with the experimental value of $\Delta G^{\neq}$ (298 K) = −7.87 kJ mol^{-1}.[8, 10] The difference of the UBP/DZVP-computed relative heats of formation ($\Delta\Delta H^{\neq}$ = −6.80 kJ mol^{-1}) is even closer to the experimental value than in case of the 4-pentenoxyl radical reaction.

tions is significant, and future studies will show whether these findings are limited to the systems here or a general feature for density functional treatments of 5-hexenyl and related radical rearrangements.

In conclusion we have been able to draw a clear picture of the lowest energy transition state structures of the cyclizations of 4-penten-1-oxyl radical by ab initio methods. Semiempirical calculations are not suited for our calculations on open-shell molecules; however, computational studies on radicals **1**–**5** using UHF/6-31G* and UBP/DZVP methods provide results that are qualitatively and quantitatively in good agreement with the experimental findings.

Computational Methods

Semiempirical calculations were performed on an SGI IRIS INDIGO R4000/R4400 workstation with the program package VAMP 5.0/5.5 [12]. All other ab initio calculations were performed on a CRAY Y-MP/8-128 computer using the Gaussian 92 program [13] (Hartree–Fock approach) and DGauss 3.0 [14] (density functional approach). The UHF/6-31G*-minimized structures of radicals **1**, **3** and **5** were determined by using the default optimization algorithm as implemented in Gaussian 92. The DFT geometries of radicals **1**, **3** and **5**, were minimized by means of a Newton–Raphson/DFGS optimization technique using a unrestricted nonlocal SCF spin-density approach with the Becke–Perdew functional. A DZVP basis set was used and the electron density was fitted by means of a triple-zeta A1 set. The transition state geometries were optimized with the optimization algorithm by Baker (UHF) and the standard algorithm (DF) after full calculation of the hessian matrix. Force calculations were applied to characterize minima and transition structures by calculation of their normal vibrations.

Received: February 21, 1996
Revised: August 22, 1996 [Z 8846 IE]
German version: *Angew. Chem.* **1996**, *108*, 3056–3059

Keywords: ab initio calculations · cyclizations · density functional calculations · radicals

[1] J. Hartung, F. Gallou, *J. Org. Chem.* **1995**, *60*, 6706–6716.
[2] a) A. L. J. Beckwith, J. Zimmermann, *J. Org. Chem.* **1991**, *56*, 5791–5796; b) A. L. J. Beckwith, C. H. Schiesser, *Tetrahedron*, **1985**, 1, 3925–3941; c) D. C. Spellmeyer, K. N. Houk, *J. Org. Chem.* **1987**, *52*, 959–974; d) P. Bischof, *Helv. Chim Acta*, **1980**, *63*, 1434–1450; e) E. Canadell, J. Igual, *J. Chem. Soc. Perkin Trans. 2* **1985**, 1331–1338.
[3] M. W. Wong, L. Radom, *J. Phys. Chem.* **1995**, *99*, 8582–8588.
[4] The semiempirical calculations were carried out using unrestricted Hartree–Fock wave functions. The general term UHF in this communication refers to ab initio calculations. The following abbreviations have been used throughout the paper: DFT: density functional theory; DZVP: double-zeta valence split polarization; UBP: unrestricted Becke–Perdew; UQCISD: unrestricted quadric configuration interaction including singles and doubles substitutions.
[5] UHF/6-31G* geometries: a) Selected bond angles in **2a**: O-C2-C3 = 107.7°, C2-C3-C4 = 104.1°, C3-C4-C5 = 107.9°, C4-C5-C6 = 121.1°. Selected torsion angles in **2a**: O-C2-C3-C4 = − 48.55°, C2-C3-C4-C5 = 41.06°, C3-C4-C5-C6 = −131.7°. Selected bond angles in **3a**: O-C2-C3 = 106.5°, C2-C3-C4 = 101.8°, C3-C4-C5 = 101.4°, C4-C5-C6 = 115.7°. Selected torsion angles in **3a**: O-C2-C3-C4 = − 24.50°, C2-C3-C4-C5 = 35.61°, C3-C4-C5-C6 = −156.0°, H6*syn*-C6-C5-H5 = − 20.39°, H5-C5-C4-H4*syn* = − 44.61°; b) Selected bond angles in **2b**: C1-C2-C3 = 108.3°, C2-C3-C4 = 107.3°, C3-C4-C5 = 110.6°, C4-C5-C6 = 121.7°. Selected torsion angles in **2b**: C1-C2-C3-C4 = − 50.00°, C2-C3-C4-C5 = 50.07°, C3-C4-C5-C6 = −142.6°. Selected bond angles in **3b**: C1-C2-C3 = 105.8°, C2-C3-C4 = 105.8°, C3-C4-C5 = 104.4°, C4-C5-C6 = 114.9°. Selected torsion angles in **3b**: C1-C2-C3-C4 = − 0.05°, C2-C3-C4-C5 = 24.83°, C3-C4-C5-C6 = −165.1°
[6] UHF/6-31G* geometries: a) Selected bond angles in **4a**: O-C2-C3 = 113.6°, C2-C3-C4 = 111.2°, C3-C4-C5 = 108.4°, C4-C5-C6 = 118.2°. Selected torsion angles in **4a**: O-C2-C3-C4 = − 61.48°, C2-C3-C4-C5 = 53.28, C3-C4-C5-C6 = − 65.55°, H5-C5-C4-H4*syn* = − 32.78°, H6*syn*-C6-C5-H5 = 15.38°. Selected bond angles in **5a**: O-C2-C3 = 111.0°, C2-C3-C4 = 110.2°, C3-C4-C5 = 110.4°, C4-C5-C6 = 117.9°, H5-C5-C4 = 119.4°, C6-C5-H5 = 117.9°. Selected torsion angles in **5a**: O-C2-C3-C4 = − 58.56°, C2-C3-C4-C5 = 45.43°, C3-C4-C5-C6 = − 38.79°; b) Selected bond angles in **4b**: C1-C2-C3 = 114.5°, C2-C3-C4 = 113.5°, C3-C4-C5 = 110.5°, C4-C5-C6 = 119.7°. Selected torsion angles in **4b**: C1-C2-C3-C4 = − 64.33°, C2-C3-C4-C5 = 59.20, C3-C4-C5-C6 = −70.86°. Selected bond angles in **5b**: C1-C2-C3 = 111.3°, C2-C3-C4 = 111.5°, C3-C4-C5 = 111.7°, C4-C5-C6 = 118.5°. Selected torsion angles in **5b**: C1-C2-C3-C4 = − 57.28°, C2-C3-C4-C5 = 49.59°, C3-C4-C5-C6 = − 45.05°.
[7] a) MNDO treatment of the cyclizations **1a** → **3a** and **1a** → **5a** affords $\Delta H^{\pm}_{exo} - \Delta H^{\pm}_{endo} = \Delta\Delta H^{\pm} = -8.7\ kJ\,mol^{-1}$ (J. Hartung, R. Stowasser, D. Vitt, G. Bringmann, unpublished results). However, MNDO is generally not as well suited as AM1 [7b] or PM3 [7c] for the description of radical reactions, and this result will not be discussed further; b) M. J. S. Dewar, E. G. Zoebisch, E. F. Healy, J. J. P. Stewart, *J. Am. Chem. Soc.* **1985**, *107*, 3902–3909; c) J. J. P. Stewart, *J. Comput. Chem.* **1989**, *10*, 209–220.
[8] The entropy differences between the 5-*exo* and the 6-*endo* transition states structure are likely to be negligible [2c].
[9] UQCISD/6-31 + G*//UHF/6-31 + G* calculations for the treatment of alkoxyl radical cyclizations required extensive computer time without affording significantly better results than the UQCISD/6-31G*//UHF/6-31G* calculations. Thus, the former calculations were not further pursued.
[10] R. C. Lamb, P. W. Ayers, M. K. Toney, *J. Am. Chem. Soc.* **1963**, *85*, 3483–3486.
[11] W. Damm, B. Giese, J. Hartung, T. Hasskerl, K. N. Houk, O. Hüter, H. Zipse, *J. Am. Chem. Soc.* **1992**, *114*, 4067–4079.
[12] G. Rauhut, J. Chandrasekhar, A. Alex, B. Beck, W. Sauer, T. Clark, *VAMP 5.5*, avalible from Oxford Molecular Limited, The Magdalen Centre, Oxford Science Park, Sandford on Thames, Oxford OX4 4GA (UK).
[13] G. W. Trucks, M. Head-Gordon, P. M. W. Gill, M. W. Wong, J. B. Foresman, B. G. Johnson, H. B. Schlegel, M. A. Robb, E. S. Replogle, R. Gomperts, J. L. Andres, K. Raghavachari, J. S. Binkley, C. Gonzalez, R. L. Martin, D. J. Fox, D. J. Defrees, J. Baker, J. J. P. Stewart, J. A. Pople, Gaussian, Inc., Pittsburgh PA, USA, **1992**.
[14] J. Andzelm in *Density Functional Methods in Chemistry* (Eds.: J. Labanowski, J. Andzelm), Springer, New York, **1991**. DGauss is part of the UniChem program of Cray Research, Inc., Eagan, MN, USA.

Recognition of the Helical Sense of Polypeptides by a Chiral Metalloporphyrin Receptor**

Katsuaki Konishi, Shu-ichi Kimata, Kiyoko Yoshida, Masanobu Tanaka, and Takuzo Aida*

Recognition of the secondary structures of biologically important macromolecules by synthetic receptors is a fascinating and challenging goal in biomimetic and supramolecular chemistry. Although the recognition of DNA helices has been successful,[1] examples are very limited for the recognition of the secondary structures of polypeptides in solution.[2] Herein we report the first example of the recognition of the helical sense of poly(glutamic acid) (PGA)[3] by using a chiral metalloporphyrin receptor (**1a**) having an α,α′-xylylenediamide strap. We have found that **1a** is capable of enantioselectively binding amino acid derivatives by means of axial ligand exchange.[4]

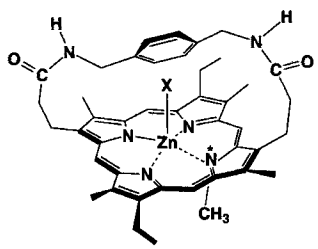

1a X = OAc
1b X = Cl

Poly(L-glutamic acid) (L-PGA) assumes a right-handed α-helical structure in aqueous CH_3OH or CH_3CN over a pH range of 3–8.[5] Addition of racemic

[*] Prof. T. Aida, Dr. K. Konishi, S. Kimata, K. Yoshida, M. Tanaka
Department of Chemistry and Biotechnology
Graduate School of Engineering, The University of Tokyo
Hongo, Bunkyo-ku, Tokyo 113 (Japan)
Fax: Int. code + (3) 5802-3363
e-mail: aida@chiral.t.u-tokyo.ac.jp

[**] This work was partly supported by Ministry of Education, Science, Sports, and Culture, Japan (Grant-in-Aid for Scientific Research No. 05234207). Compounds **1a,b** and **2a,b** were derived from mesoporphyrin II and etioporphyrin I with enantiotopic faces, respectively, and a stereogenic center at the alkylated nitrogen atom.

Table 1. Asymmetric binding of PGA with **1a** and **2a** [a].

Entry	Receptor	Medium	PGA		Product [d]	**1b** or **2b**
			P [b]	Conf. [c]	Yield [%] [e]	(*R*)/(*S*) (*ee*)[%] [f] [g]
1	**1a**	CH_3OH/H_2O (3/1, acidic)	186 L	α-helix	41	18.5/81.5(63)
2	**1a**	CH_3OH/H_2O (3/1, acidic)	84 L	α-helix	nd	32.5/67.5(35)
3	**1a**	CH_3CN/H_2O (3/1, acidic)	84 L	α-helix	nd	16.5/83.5(67)
4	**1a**	CH_3CN/H_2O (0.6/1, acidic)	84 L	α-helix	34	33.5/66.5(33)
5	**1a**	CH_3OH/H_2O (3/1, basic)	84 L	random coil	22	53.5/46.5(7)
6	**1a**	CH_3CN/H_2O (0.6/1, basic)	84 L	random coil	25	53.5/46.5(7)
7	**1a**	CH_3OH/H_2O (3/1, acidic)	68 D	α-helix	nd	71.0/29.0(42)
8	**2a**	CH_3CN/H_2O (0.6/1, acidic)	84 L	α-helix	21	54.5/45.5(9) [h]

[a] c_0(Receptor)/c_0(Glu) = 625/625 μM (40 mL solvent) at room temperature for 50 h. The apparent pH of the reaction mixture (indicated by a pH meter) was adjusted to either 4.1–5.2 (entries 1–4, 7, 8) or 11.0–11.7 (entries 5, 6) by addition of a few drops of CH_3CO_2H or 1 N aqueous NaOH. [b] *P* = degree of polymerization. [c] By CD spectroscopy (ref. [5]). [d] Precipitate was collected by centrifugation, washed with water, dried under vacuum, and weighed. nd = not determined. [e] From the weight of precipitate relative to sum of the weights of PGA and receptor. [f] *ee* [%] = $100 \times (|c(R) - c(S)|)/(c(R) + c(S))$. [g] From the CD intensity at 426 nm relative to that of the enantiomerically pure **1b** (ref. [4]). [h] By chiral HPLC (Chiralcel OD).

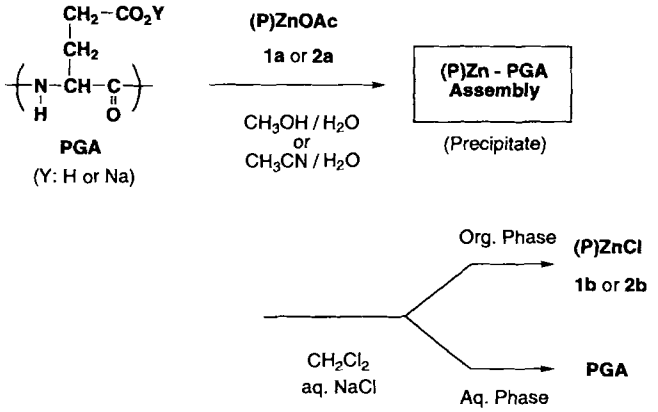

Scheme 1. Reaction of **1a** and **2a** with PGA.

1a (*rac*-**1a**) to an acidic solution of L-PGA gave an assembly, in which (*S*)-**1a** was enantioselectively incorporated (Scheme 1). For example, when *rac*-**1a** was mixed with L-PGA (degree of polymerization $P = 186$) in CH_3OH/water (3/1, v/v) (concentration of glutamic acid unit = 625 μM) at pH 4.6 and the resulting solution stirred for 50 h at room temperature,[6] a precipitate formed. Upon treatment of the precipitate with CH_2Cl_2/aqueous NaCl, the receptor was quantitatively extracted into the organic phase in the form of **1b**. The receptor thus recovered was highly enriched in the (*S*) enantiomer with an (*R*):(*S*) ratio of 18.5:81.5 (63% *ee*; entry 1, Table 1). As expected, mixing of a left-handed helical D-PGA ($P = 68$) with *rac*-**1a** under similar conditions resulted in preferential binding of the opposite receptor, (*R*)-**1a** [(*R*):(*S*) = 71:29) (entry 7). In sharp contrast, under basic conditions (pH 11.0)[6] where PGA assumes a randomly coiled conformation,[5] the binding was not enantioselective (entry 5). It should be mentioned that the complexation of (*R*)-**1a** with racemic *N*-*tert*-butoxycarbonylglutamic acid α-methyl ester or its sodium salt was not enantioselective.[7] Furthermore, a short-chain oligomer of L-glutamic acid ($P = 4$), whose secondary structure is labile,[8] did not undergo enantioselective complexation with *rac*-**1a** under acidic conditions. Thus, the enantioselectivity of the reaction of **1a** with α-helical PGA is induced by the helicity of the polypeptide chain rather than the chirality of the amino acid unit.

When L-PGA with a shorter helical chain ($P = 84$) was subjected to conditions similar to those in entry 1, a lower enantioselectivity resulted (entry 2). The polarity of the medium also affects the enantioselectivity: When the CH_3OH/H_2O solvent system in entry 2 was replaced by CH_3CN/H_2O, the enantioselectivity was much enhanced (entry 3). In contrast, it decreased when the proportion of water in the medium was increased (entry 4). However, even in CH_3CN/water (0.6/1, v/v), the binding was not enantioselective under basic conditions (randomly coiled L-PGA; entry 6).

When the concentration of **1a** was less than 50 μM in CH_3OH/water (3/1, v/v) at 20 °C, the reaction system was homogeneous and no precipitate formed. The reaction between **1a** and PGA was monitored quantitatively. Upon titration of (*R*)- or (*S*)-**1a** (10 μM) with L-PGA ($P = 84$) at pH 7.5, the Soret band of **1a** was observed to shift from 416.4 to 421.8 nm with a clear isosbestic point at 418.4 nm. According the circular dichroism (CD) profile, the L-PGA chain retains the right-handed α-helical structure. The changes in absorption for solutions of different starting concentrations c_0(Glu)/c_0(**1a**) were obviously different for (*R*)- and (*S*)-**1a** (Fig. 1). For example, at c_0(Glu)/c_0(**1a**) =

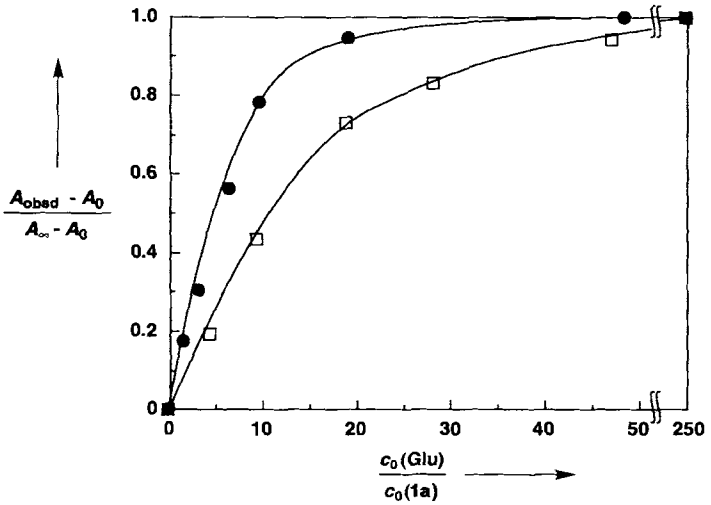

Fig. 1. Spectroscopic titration of (*R*)- (□) and (*S*)-**1a** (●) (c_0(**1a**) = 10 μM) at 20 °C with L-PGA in CH_3OH/water (3/1, v/v) at pH 7.5. Changes in absorption at 413 nm are plotted versus mole ratio of the glutamic acid unit to **1a** (c_0(Glu)/c_0(**1a**)). A_{obs} = observed absorption, A_0 = absorption of uncomplexed **1a**, A_∞ = absorption of complexed **1a**.

10, 74% of (*S*)-**1a** was complexed with L-PGA, whereas the extent of complexation was only 42% for (*R*)-**1a**. Fitting of the observed spectral changes for (*R*)- and (*S*)-**1a** to Equation (a)[9]

$$\text{(P)ZnOAc} + n\,\text{Glu} \underset{}{\overset{K_{ass}}{\rightleftharpoons}} \text{(P)ZnO}_2\text{C-(Glu)}_n + \text{AcOH} \qquad \text{(a)}$$

 © VCH Verlagsgesellschaft mbH, D-69451 Weinheim, 1996 0570-0833/96/3523-2824 $ 15.00+.25/0

showed that, in both cases, approximately two amino acid units participate in binding one receptor molecule. On the other hand, in agreement with the preferred helical sense (Table 1), the association constant (K_{ass}) evaluated for (*S*)-**1a** (3.0×10^3 M^{-1}) is much higher than that for (*R*)-**1a** (5.1×10^2 M^{-1}). These K_{ass} values were used to estimate the selectivity (*ee*) and $\Delta\Delta G$ of the reaction to be 71% and -1.0 kcal mol^{-1} K^{-1}, respectively.

In previous work on the enantioselective binding of *N*-benzyloxycarbonylamino acids with **1a**,[4] we have clearly shown the presence of electrostatic ($Zn^+ \cdots {}^-O_2C$) and hydrogen-bonding ($NH \cdots O{=}C$) interactions between the receptor and the substrates. In relation to this, the free base of **1** did not interact with PGA in CH_3OH/water (3/1, v/v), irrespective of the acidity of the medium. Furthermore, although chiral **2a**,[10] bearing no hydrogen-bonding "strap amide" functionalities, formed a precipitate when it was mixed with L-PGA ($P = 84$) under acidic conditions, the observed enantioselectivity was negligibly low (entry 8).

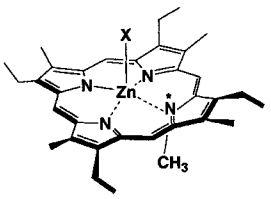

2a X = OAc
2b X = Cl

Finally, it is also worth noting that the enantiomers of **1a** could be used to separate right- and left-handed PGA chains. For example, addition of (*S*)-**1a**, under acidic conditions in CH_3CN/water (3/1, v/v), to an equimolar mixture of helical L-PGA ($P = 84$) and D-PGA ($P = 87$) at a ratio c(Glu):c(**1a**) of 2:1 gave a precipitate, which showed, after the removal of the receptor, a CD profile in water at pH 4.2 typical of the right-handed helix. Hydrolysis of this PGA[11] gave glutamic acid that was rich in the L enantiomer (L:D = 82:18). In sharp contrast, under basic conditions, randomly coiled L-PGA and D-PGA were not separable with (*S*)-**1a**.

In conclusion, we have demonstrated that **1** is the first chiral receptor capable of recognizing the helical sense of poly(glutamic acid) in solution. Stereo- and sequence-selective recognition of natural proteins with a tuned metalloporphyrin receptor is a subject worthy of further investigation.

Received: May 8, 1996
Revised version: September 11, 1996 [Z 9107 IE]
German version: *Angew. Chem.* **1996**, *108*, 3001–3003

Keywords: helices · molecular recognition · polypeptides · porphyrinoids

[1] Selected examples: a) J. K. Barton, *Science* **1986**, *233*, 727–734; b) R. E. McKinnie, J. D. Choi, J. W. Bell, E. J. Gibbs, R. F. Pasternack, *J. Inorg. Biochem.* **1988**, *32*, 207–224; c) M. Shionoya, E. Kimura, H. Hayashida, G. Petho, L. G. Marzilli, *Supramol. Chem.* **1993**, *2*, 173–176.

[2] Some receptors have been reported to induce the formation of α-helices or β-sheets by self-assembly: a) N. Voyer, D. Deschenes, J. Bernier, J. Roby, *J. Chem. Soc. Chem. Commun.* **1992**, 134–136; b) M. Tabet, V. Labroo, P. Sheppard, T. Sasaki, *J. Am. Chem. Soc.* **1993**, *115*, 3866–3868; c) J. Albert, S. Goodman, A. Hamilton, *ibid.* **1995**, *117*, 1143–1144; d) S. R. LaBrenz, J. W. Kelley, *ibid.* **1995**, *117*, 1655–1656.

[3] The interaction between achiral receptors and helical PGA has been extensively studied: a) E. R. Blout; L. Stryer, *J. Am. Chem. Soc.* **1961**, *83*, 1411–1418; b) M. Hatano, *Adv. Polym. Sci.* **1986**, *77*, 72–78; c) R. F. Pasternack, A. Gianneto, P. Pagano, E. J. Gibbs, *J. Am. Chem. Soc.* **1991**, *113*, 7799–7800; d) S. Ikeda, T. Nezu, G. Ebert, *Biopolymers*, **1991**, *31*, 1257-1263.

[4] K. Konishi, K. Yahara, H. Toshishige, T. Aida, S. Inoue, *J. Am. Chem. Soc.* **1994**, *116*, 1337–1344.

[5] The proportion of the helical form in solution was determined by circular dichroism (CD) spectroscopy. At pH 3–8 between 85 and 100% of L-PGA was in the helical form, as estimated from the CD intensities at 222 nm and based on the literature value in water: a) G. Holtzwarth, P. Doty, *J. Am. Chem. Soc.* **1965**, *87*, 218–228; b) M. L. Tiffany, S. Krimm, *Biopolymers* **1968**, *6*, 1379–1382.

[6] See footnote [a] in Table 1.

[7] The ^{1}H NMR spectrum of the reaction mixture in $CDCl_3$ showed two signals of diastereomeric protons in $ZnO_2CCH_2CH_2$ with comparable intensities ($\delta = -1.90$ [(*R*)-1/D-Glu], -1.58 [(*R*)-1/L-Glu]).

[8] E. J. Spek, Y. Gong, N. Kallenbach, *J. Am. Chem. Soc.* **1995**, *117*, 10773–10774.

[9] When *rac*-**1a** or (*S*)-**1a** was mixed with L-PGA in CD_3OD/D_2O (3/1, v/v), acetic acid ($\delta = 1.99$, CH_3) was generated at the expense of the axial acetate group ($\delta = -2.48$, CH_3), as confirmed by ^{1}H NMR spectroscopy.

[10] a) H. Kubo, T. Aida, S. Inoue, *J. Chem. Soc. Chem. Commun.* **1988**, 1015–1017; b) K. Konishi, T. Sugino, T. Aida, S. Inoue, *J. Am. Chem. Soc.* **1991**, *113*, 6487–6491.

[11] S. Moore, W. H. Stein, *J. Biol. Chem.* **1951**, 192, 663–666.

(Alkylidyne)tungsten Complexes Anchored to a Planar Tetraoxo Surface: Exhaustive Alkylation of a (Calixarene)tungsten Complex**

Luca Giannini, Euro Solari, Antonio Zanotti-Gerosa, Carlo Floriani,* Angiola Chiesi-Villa, and Corrado Rizzoli

The metal–alkylidyne group has had an extraordinary impact in organic synthesis and mainly in catalysis.[1] A variety of metal fragments have been used, and a significant preference has emerged for the Group VI metals bearing alkoxo groups as ancillary ligands, because of their reactivity and their use as catalysts.[2] In this context much attention has been devoted to coordination environments that can mimic an oxo surface.[3] In order to synthesize model compounds containing the metal–alkylidyne group anchored to an oxo-complex,[4, 5] we functionalized a metal–calix[4]arene complex, starting with the [*cis*-Cl_2W(cal)] (**1**, cal = calix[4]arene).[5c] During these investigations we observed the isomerization of **1** to the [*trans*-Cl_2W(cal)] (**2**), for which a selective synthesis is now available. This kind of isomerization is assisted by Lewis acids (WCl_6 excess, $AlCl_3$). Compound **2** has been identified both in solution (by NMR spectroscopy) and in the solid state (by X-ray analysis).

Alkylation of **1** (Scheme 1) with a metal alkylating agent in a 1:3 molar ratio cleanly forms the corresponding alkylidyne derivative. When lower metal/alkylating agent ratios were employed, a mixture of reduced and alkylated products (which are currently under investigation) were obtained. The reaction does not depend on the alkyl substituent and the nature of the alkylating agent. The solvent plays an important role both in the selection of the reaction path (elimination vs. reduction) and in the separation of Mg and Li halides. The reaction proceeds by a double α-elimination process, which seems impossible to stop at any earlier stage, that is, at the stage of alkyl or alkylidene derivatives.[6]

[*] Prof. Dr. C. Floriani, L. Giannini, Dr. E. Solari, Dr. A. Zanotti-Gerosa
Institut de Chimie Minérale et Analytique
Université de Lausanne
BCH 3307, CH-1015 Lausanne (Switzerland)
Fax: Int. code +(21)692-3905
Prof. Dr. A. Chiesi-Villa, Dr. C. Rizzoli
Dipartimento di Chimica, Università di Parma
Viale delle Scienze, I-43100 Parma (Italy)

[**] This work was supported by the Fonds National Suisse de la Recherche Scientifique (Grant. No. 20-40268.94) and Ciba–Geigy SA (Basel, Switzerland).

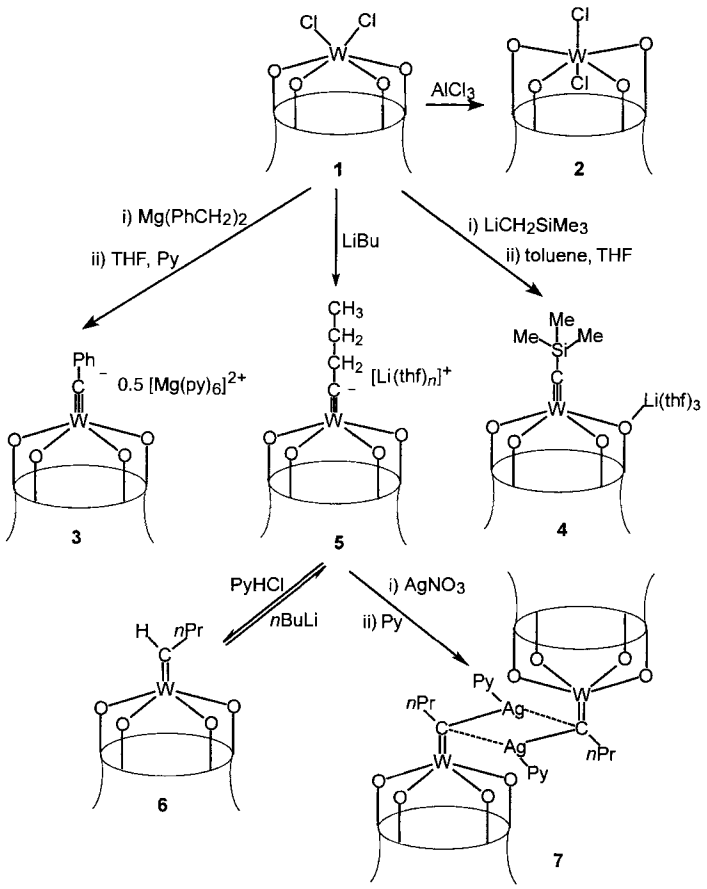

Scheme 1. Exhaustive alkylation of **1** leading to tungsten–alkylidyne derivatives.

Complexes **3**–**5** have been fully characterized; an X-ray analysis was performed on **3**[7] and **4**. The structure of **3** consists of a [PhC≡W(cal)] anion (Fig. 1) and the centrosymmetric cation

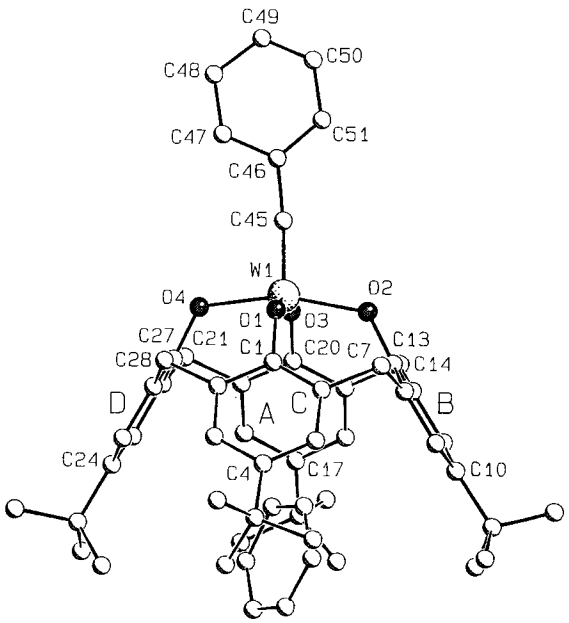

Fig. 1. Structure of the anion (SCHAKAL view) in complex **3**. Selected interatomic distances [Å]: W1–C45 1.722(7), W1–O1 2.000(5), W1–O2 1.995(5), W1–O3 1.957(5), W1–O4 1.987(5), C45–C46 1.449(11). Selected bond angles [°]: O3-W1-O4 88.5(2), O2-W1-O4 161.7(2), O2-W1-O3 88.3(2), O1-W1-O4 88.9(2), O1-W1-O3 160.1(2), O1-W1-O2 88.0(2), W1-C45-C46 173.8(7). For clarity only the E position is given for the disordered pyridine molecule.

$[MgPy_6]^{2+}$. Two additional molecules of pyridine are present, one as guest in the calix[4]arene cavity. The aromatic rings bonded to the O1, O2, O3, O4 oxygen atoms are labeled A, B, C, and D respectively. The tungsten atom exhibits square-pyramidal coordination with the four oxygen atoms of calixarene at the base and the C45 carbon atom of the phenylalkylidyne ligand at the apex. The W–C45 bond length [1.722(7) Å][8] has triple-bond character. The W–C45 bond forms an angle of 1.9(3)° with the normal to the planar O_4 core. Tungsten is displaced by 0.328(1) Å from this plane towards the C45 carbon. The W–O bond lengths, which fall in a rather narrow range, are longer than those in neutral [W(cal)] derivatives containing WCl_2,[5c] W=O,[5c] and $W(OAr)_2$[9] groups. The calix[4]arene unit is in a *cone* conformation as is usually found in square-pyramidal pentacoordinated metals.[5] The almost symmetrical conformation is indicated by the narrow range of the dihedral angles formed by the plane through the bridging methylene carbons C7, C14, C21, C28 (reference plane) and the aromatic rings [119.5(2)–125.1(2)°]. The reference plane is parallel to the O4 core [dihedral angle 1.3(1)°]. The guest pyridine molecule is disordered in two positions (E and F), which are rotated by about 30° and tilted by 13.1(11)° relative to each other. The molecular axis of the complex runs approximately through the midpoint of the C61–C66 bond for the E position (Fig. 1) and through the C66···C63 axis for the F position.[10]

Let us summarize some of the features of this novel class of tungsten–alkylidynes: 1) their synthesis is straightforward as alkylation is achieved under very mild conditions; 2) they occur in a rather rare and stable anionic form; 3) the bonding mode of the W≡CR fragment to a tetraalkoxo fragment renders the metal electronically saturated according to P. Hofmann's considerations;[11] 4) the O4 matrix binds so strongly to the metal that the reactivity of the W≡C group can be studied without disturbing from the ancillary ligand. This fourth feature suggests that this electron-rich alkylidyne fragment will be a particularly good candidate for electrophilic and oxidation reactions. We, for instance, observed the rather unique reversible protonation of the alkylidyne and deprotonation of the resulting alkylidene. Both occur without any rearrangement or protolysis of the ancillary ligand, as is usually the case.[12] Although the reaction is general for **3**–**5**, we report details for **5** only.

A synthetically useful derivatization of the anionic alkylidynes **3**–**5** is their metalation, which we performed with the carbophilic Ag^+. The reaction carried out on **5** with $AgNO_3$, followed by crystallization in pyridine, led to the silver–alkylidene complex **7** (Scheme 1). Such a formulation has been supported by an X-ray analysis on **7**. The W–C bond length supports the transformation of the alkylidyne into a metalated alkylidene [W=C, 1.835(7) vs. 1.722 in **3**]. Reaction of M≡C bonds with Cu^+ or Ag^+ normally lead to π interactions.[13] The reactions mentioned above show how the alkylidyne group anchored to a calixarene matrix undergoes some unprecedented and novel transformations.

Experimental Procedure

3: $Mg(PhCH_2)_2$ (23 mL, 0.67 N, 15.40 mmol) was added dropwise to suspension of $1 \cdot 3C_6H_6$ (5.81 g, 5.12 mmol) in THF (200 mL) at −30 °C. The resulting red solution was allowed to warm to room temperature and gave a yellow solid in a green solution. The solid was collected and then extracted with hot THF over 9 h (most of the solid was not soluble in THF). Bright yellow $[\{(cal)W{\equiv}CPh\}_2(thf)\{Mg(thf)_6\}_{0.5}]$ was left on the septum and then dried in vacuo (2.7 g, 42%). Elemental analysis calcd (found): C 66.05 (65.45), H 7.36 (7.70). ^{1}H NMR (400 MHz, $[D_5]$Py, 300 K): δ = 7.27 (s, 8H; ArH), 7.10 (m, 2H; ArH), 7.03 (m, 2H; ArH), 6.65 (m, 1H; ArH), 5.26 (d, J = 11.6 Hz, 4H; *endo*-CH_2), 3.62 (m, 16H; THF), 3.33 (d, J = 11.6 Hz, 4H; *exo*-CH_2), 1.59 (m, 16H; THF), 1.22 (s, 36H; *t*Bu). ^{13}C NMR ($[D_5]$Py, 300 K): δ = 267.9. The X-ray analysis of **3** was carried out on $[\{(cal)W{\equiv}CPh\}_2\{[MgPy_6]\}_{0.5}]$ recrystallized from pyridine.

 © VCH Verlagsgesellschaft mbH, D-69451 Weinheim, 1996 0570-0833/96/3523-2826 $ 15.00+.25/0 Angew. Chem. Int. Ed. Engl. 1996, 35, No. 23/24

4: $LiCH_2SiMe_3$ (1.57 g, 16.70 mmol) was dissolved in toluene (150 mL), cooled (−30 °C), and then **1**·3 C_6H_6 (6.28 g, 5.54 mmol) was added. The resulting red solution was allowed to warm to room temperature overnight. Yellow [{(cal)W≡$CSiMe_3$}Li]·C_7H_8·LiCl formed and was collected and dried in vacuo (2.76 g, 47%). Elemental analysis calcd (found): C 62.53 (62.26), H 6.68 (6.67). ^{1}H NMR (400 MHz, [D_5]Py, 300 K): δ = 7.20 (m, tol), 7.16 (s, 8H; ArH), 5.28 (d, J = 11.6 Hz, 4H; *endo*-CH_2), 3.26 (d, J = 11.6 Hz, 4H; *exo*-CH_2), 2.20 (s, 3H; tol), 1.16 (s, 36H; *t*Bu), 0.26 (s, 9H; $SiMe_3$). ^{13}C NMR ([D_5]Py, 300 K): δ = 308.1 (W≡$CSi(CH_3)_3$), 2.57 (-Si(CH_3)$_3$). Crystals suitable for an X-ray analysis were obtained from crystallization in THF/toluene; the solvated form [{(Cal)W≡C-$SiMe_3$}{Li(thf)$_3$}] (**4**), which does not contain LiCl, has been isolated.

5: BuLi (6.6 mL, 1.65 N, 10.89 mmol) was added dropwise to a suspension of **1**·3 C_6H_6 (4.08 g, 3.60 mmol) in toluene (80 mL) at −30 °C. The resulting red solution was allowed to warm to room temperature, and THF (50 mL) was added to the reaction mixture. Volatiles were removed in vacuo, and Et_2O (100 mL) was added to the residue. A white powder was removed by filtration, and THF (10 mL) was added to the resulting brown solution. Volatiles were removed in vacuo, *n*-hexane (30 mL) was added to the residue, and the greenish Li[(cal)$WCCH_2CH_2CH_3$]·LiCl·2THF·C_6H_{12} then collected and dried in vacuo (2.2 g, 53%). Elemental analysis calcd (found): C 64.00 (64.30), H 7.71 (8.13). ^{1}H NMR (400 MHz, [D_5]Py, 300 K): δ = 7.15 (s, 8H; ArH), 5.22 (d, J = 11.6 Hz, 4H; *endo*-CH_2), 4.08 (t, J = 6.6 Hz, 2H; $WCCH_2CH_2CH_3$), 3.62 (m, 8H; THF), 3.23 (d, J = 11.6 Hz, 4H; *exo*-CH_2), 1.80 (m, 2H; $WCCH_2CH_2CH_3$), 1.59 (m, 8H; THF), 1.46 (t, J = 7.2 Hz, 3H; $WCCH_2CH_2CH_3$), 1.16 (s, 36H; *t*Bu). ^{13}C NMR ([D_5]Py, 300 K): δ = 276.6 (WC(Pr), J_{CW} = 278 Hz), 48.3 ($WCCH_2CH_2CH_3$), 27.0 ($WCCH_2CH_2CH_3$), 14.5 ($WCCH_2CH_2CH_3$).

Protonation and deprotonation of **5**: PyHCl (0.22 g, 1.9 mmol) was added to a solution of **5** (2.2 g, 1.9 mmol) in Et_2O (100 mL), and the mixture stirred for 2 h. A white solid was filtered off, volatiles were removed in vacuo, and pentane was added to the residue. Compound **6** was then collected as a brown solid and dried in vacuo (0.97 g, 57%). ^{1}H NMR (400 MHz, C_6D_6, 300 K): δ = 10.0 (t, J = 7.5 Hz, 1H; WC(Pr)H), 7.07 (s, 8H; ArH), 5.47 (m, 2H; $WCCH_2CH_2CH_3$), 4.95 (d, J = 12.2 Hz, 4H; *endo*-CH_2), 3.24 (d, J = 12.2 Hz, 4H; *exo*-CH_2), 1.69 (m, 2H; $WCCH_2CH_2CH_3$), 1.15 (t, J = 7.2 Hz, 3H; $WCCH_2CH_2CH_3$), 1.08 (s, 36H; *t*Bu). ^{13}C NMR (C_6D_6, 300 K): δ = 272 (WC(Pr)H, J_{CW} = 180 Hz, J_{CH} = 142 Hz), 41.6 ($WCCH_2CH_2CH_3$), 29.5 ($WCCH_2CH_2CH_3$), 14.5 ($WCCH_2CH_2CH_3$). The reaction of **6** with a stoichiometric amount of BuLi (in toluene at −30 °C) leads to pure **5**, as determined by ^{1}H NMR spectroscopy.

7: $AgNO_3$ (0.3 g, 1.76 mmol) was added to a solution of **5** (1.97 g, 1.69 mmol) in THF (100 mL), and the mixture stirred overnight. Volatiles were removed in vacuo, and the residue was extracted with Et_2O (100 mL). The resulting deep red solution was kept at −25 °C over 24 h to yield [(cal)W=C(Ag)(*n*Pr)] as red needles (0.5 g, 30%). Elemental analysis calcd (found): C 58.13 (57.95), H 6.00 (6.03). ^{1}H NMR (400 MHz, [D_5]Py, 300 K): δ = 7.25 (s, 8H; ArH), 5.31 (d, J = 11.6 Hz, 4H; *endo*-CH_2), 4.74 (t, J = 6.8 Hz, 2H; $WCCH_2CH_2CH_3$), 3.35 (d, J = 11.6 Hz, 4H; *exo*-CH_2), 2.0 (m, 2H; $WCCH_2CH_2CH_3$), 1.41 (t, J = 7.4 Hz, 3H; $WCCH_2CH_2CH_3$), 1.19 (s, 36H; *t*Bu). ^{13}C NMR ([D_5]Py, 300 K): δ = 272 (WC(Pr)Ag), 50.0 ($WCCH_2CH_2CH_3$), 27.9 ($WCCH_2CH_2CH_3$), 14.6 ($WCCH_2CH_2CH_3$). The X-ray analysis was performed on the solid [(cal)W=C(Ag)(*n*Pr)] recrystallized from pyridine to give [7·2Py].

Received: June 27, 1996
Revised: September 13, 1996 [Z 9262 IE]
German version: *Angew. Chem.* **1996**, *108*, 3051–3053

Keywords: alkylidines · calixarenes · tungsten compounds

[1] a) H. Fischer, P. Hofmann, F. R. Kreissl, R. R. Schrock, U. Schubert, K. Weiss, *Carbyne Complexes*, VCH, Weinheim, Germany, **1988**; b) W. A. Nugent, J. M. Mayer, *Metal-Ligand Multiple Bonds*, Wiley, New York, **1988**; c) A. Mayr, C. M. Bastos, *Progr. Inorg. Chem.* **1992**, *40*, 1; d) A. Mayr, H Hoffmeister, *Adv. Organomet. Chem.* **1991**, *32*, 227.

[2] J. S. Murdzek, R. R. Schrock, *High oxidation State Alkylidyne Complexes*, Chapter 5 in ref. [1a], p. 165ff.

[3] K. Weiss, *Catalytic Reactions of Carbyne Complexes*, Chapter 6 in Ref. [1], p. 206.

[4] For metalation of calix[4]arene, see a) S. G. Bott, A. W. Coleman, J. L. Atwood, *J. Chem. Soc. Chem. Commun.* **1986**, 610–611; b) M. M. Olmstead, G. Sigel, H. Hope, X. Xu, P. P. Power, *J. Am. Chem. Soc.* **1985**, *107*, 8087–8091; c) G. E. Hofmeister, F. E. Kahn, S. F. Pedersen, *ibid.* **1989**, *111*, 2318–2319; d) G. E. Hofmeister, E. Alvarado, J. A. Leary, D. I. Yoon, S. F. Pedersen, *ibid.* **1990**, *112*, 8843–8851; e) B. M. Furphy, J. M. Harrowfield, D. L. Kepert, B. W. Skelton, A. H. White, F. R. Wilner, *Inorg. Chem.* **1987**, *26*, 4231–4236.

[5] a) F. Corazza, C. Floriani, A. Chiesi-Villa, C. Guastini, *J. Chem. Soc. Chem. Commun.* **1990**, 640–641; b) *ibid.* **1990**, 1083–1084; c) F. Corazza, C. Floriani, A. Chiesi-Villa, C. Rizzoli, *Inorg. Chem.* **1991**, *30*, 4465–4468; d) J. A. Acho, L. H. Doerrer, S. J. Lippard, *ibid.* **1995**, *34*, 2542–2556; e) J. A. Acho, T. Ren, J. W. Yun, S. J. Lippard, *ibid.* **1995**, *34*, 5226–5233.

[6] a) L. Li, M. Hung, Z. Xue, *J. Am. Chem. Soc.* **1995**, *117*, 12746–12750; b) R. R. Schrock, K.-Y Shih, D. A. Dobbs, W. M. Davis, *ibid.* **1995**, *117*, 6609–6610.

[7] Crystal structure analysis of **3**: $C_{51}H_{57}W·0.5C_{30}H_{30}MgN_6·2C_5H_5N$, M_r = 1325.5, monoclinic, space group $P2_1/c$, a = 22.038(3), b = 12.415(2), c = 25.171(3) Å, β = 98.74(1)°, V = 6806.9(17) Å^3, Z = 4, ρ_{calcd} = 1.293 g cm^{-3}, $F(000)$ = 2740, $Mo_{K\alpha}$ radiation (λ = 0.71069 Å, $\mu(Mo_{K\alpha})$ = 17.86 cm^{-1}. Crystal dimensions 0.20 × 0.25 × 0.38 mm. The structure was solved by the heavy atom method, and all non-H atoms except those affected by disorder were anisotropically refined. The guest pyridine molecule (C61–C66) and the pyridine solvent molecule of crystallization (N4, C91–C95) were affected by high thermal parameters indicating the presence of disorder. The best fit was found by splitting the atoms over two positions (A and B), which were isotropically refined with site occupation factors of 0.65 and 0.35, respectively, for both molecules. The nitrogen atom in the guest pyridine molecule could not be unambiguosly distinguished. During the refinement the disordered pyridine solvent molecule of crystallization was constrained to be a regular hexagon. All the hydrogen atoms except those related to the disordered pyridine molecules, which were ignored, were located from a difference Fourier map and introduced as fixed contributors in the last stage of refinement (U_{iso} = 0.08 Å^2). For 7981 unique observed reflections [$I > 2\sigma(I)$], collected at T = 295 K on a Rigaku AFC6S diffractometer ($6° < 2\theta < 50°$) and corrected for absorption, the final R is 0.053 ($wR2$ = 0.133). All calculations were carried out on a Quansan Personal Computer equipped with an Intel Pentium processor. Crystallographic data (excluding structure factors) for the structure reported in this paper have been deposited with the Cambridge Crystallographic Data Centre as supplementary publication no. CCDC-179-127. Copies of the data can be obtained free of charge on application to the Director, CCDC, 12 Union Road, Cambridge CB2 1EZ, UK (fax: int. code Int. +(1223)336-033; e-mail: teched@chemcrys.cam.ac.uk).

[8] a) F. A. Cotton, W. Schwotzer, E. S. Shamshoum, *Organometallics* **1984**, *3*, 1770; *J. Organomet. Chem.* **1985**, *296*, 55; b) U. Schubert, *Solid State Structure of Carbyne Complexes*, Chapter 2 in Ref. [1], p. 40.

[9] A. Zanotti-Gerosa, E. Solari, L. Giannini, C. Floriani, A. Chiesi-Villa, C. Rizzoli, *J. Chem. Soc. Chem. Commun.* **1996**, 119–120.

[10] No further discussion on the F position is possible due to its low occupancy. The shortest contact distances are between the C61A atom and the B ring of calixarene (range varying from 3.54(3) to 3.88(2) Å) as well as the C66A atom and the C ring (range varying from 3.75(3) to 3.90(2) Å).

[11] P. Hofmann, *Electronic Structures of Transition Metal Carbyne Complexes*, Chapter 3 in ref. [1a], p. 74.

[12] See ref. [2], p. 189–190.

[13] a) G. R. Clark, C. M. Cochrane, K. Marsden, W. R. Roper, L. J. Wright, *J. Organomet. Chem.* **1986**, *315*, 211–230. b) G. R. Clark, C. M. Cochrane, W. R. Roper, L. J. Wright, *ibid.* **1980**, *199*, C35–C38.

The First Stable Copper(III) Complex Containing Aliphatic Thiolates as Ligands: Structural and Spectroscopic Evidence for Cu^{II} and Cu^{III} Ions in Complexes with Square-Planar CuN_2S_2 Coordination Environments**

Jan Hanss and Hans-Jörg Krüger*

Dedicated to Professor Erwin Weiss on the occasion of his 70th birthday

The tremendous interest in copper(II) complexes containing thiolates as ligands has been inspired for the most part by the occurrence of such types of complexes in the mononuclear copper(II) sites of the electron transfer proteins plastocyanin and azurin, as well as in the dinuclear Cu_A-site of cytochrome-c oxidase.[1] The synthesis of suitable low molecular weight model complexes, however, has been thwarted by the intrinsic tendency of copper(II) thiolate complexes to suffer autoreduction of Cu^{II} by the coordinated thiolates with the concomitant formation of disulfides.[1a, 1e] Thus, the preparation of such complexes

[*] Dr. H.-J. Krüger, J. Hanss
Institut für Anorganische und Angewandte Chemie der Universität
Martin-Luther-King-Platz 6, D-20146 Hamburg (Germany)
Fax: Int. code +(40) 4123-2893

[**] This work was supported by the Deutsche Forschungsgemeinschaft.

is still quite a challenging task for synthetic chemists. Of the few sufficiently stable copper thiolate compounds that can be characterized structurally, most of them contain anionic sulfur centers that are bound to sp^2-hybridized carbon atoms.[2, 3]. The preparation of mononuclear complexes containing aliphatic thiolates has been unsuccessful in most cases, and those complexes prepared in situ have such short lifetimes in solution that any detailed investigation is impeded. In only three cases have the structures of such aliphatic thiolate complexes been determined.[1e, 3-5] The copper(II) ions in these complexes have tetrahedral (**1**),[1e, 3] square-planar (**2**),[4] or trigonal-bipyramidal coordination geometries (**3**).[5] Here we report on the synthesis,

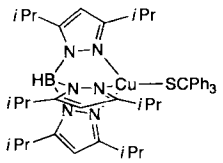

1

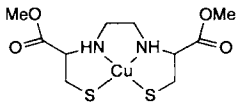

2

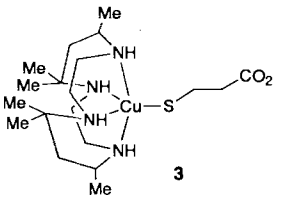

3

spectroscopic characterization, and structures of stable mononuclear complexes of aliphatic thiolates with square-planar Cu^{II} and Cu^{III} ions.

In analogy to the chemistry of copper(II) thiolates, nickel(II) thiolates are prone to form disulfides from coordinated thiolates upon oxidation.[6] Here, complexes containing both a nickel(III) ion and coordinated thiolates have been successfully prepared by utilizing ligands that provide nitrogen donor atoms from deprotonated amide functions in addition to the anionic sulfur donors of the thiolates.[7] This strategy was also employed in earlier works by Sugiura et al.,[8] who used peptides with SH groups that coordinate to copper(II) ions. In these complexes the coordination of thiolate was mainly inferred from ESR and electronic absorption spectroscopy on the copper(II) complexes and from NMR spectra of the copper(I) complexes; no X-ray structural evidence was given. We have synthesized the red copper(II) complex **4** from the bis-*S*-acetyl-derivative of the ligand *N*,*N*′-1,2-phenylenebis(2-mercapto-2-methylpropionamide) (H_4phmi) (Scheme 1).

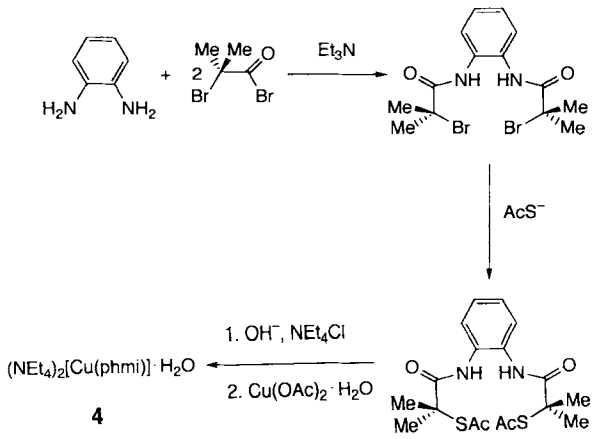

Scheme 1.

A structure determination of **4**[9] reveals that the copper ion is coordinated by two thiolates and two deprotonated amides. Some selected bond lengths and angles are listed in the legend of Figure 2. All non-hydrogen atoms, except those of the four methyl groups, are coplanar (maximum deviation: ± 0.129 Å). The average Cu–N bond length of 1.963 ± 0.001 Å is at the high end of the range commonly observed for square-planar copper(II) ions coordinated to deprotonated amides of acyclic ligands.[10] The average Cu–S bond length of 2.241 ± 0.003 Å is quite similar to that observed for square-planar **2**.[4]

The visible region of the electronic absorption spectrum of **4** comprises a band at 489 nm ($\varepsilon_M = 538\ M^{-1}\ cm^{-1}$) with a shoulder at 580 nm ($\varepsilon_M = 110\ M^{-1}\ cm^{-1}$). Both features are tentatively assigned to d–d transitions. The position and the intensities of these absorptions reveal that the square-planar geometry around the copper(II) ion is preserved in solution. The ESR spectrum (Fig. 1) of **4** in acetonitrile/toluene (1:4) solution displays a signal at $g_{iso} = 2.060$. The hyperfine and superhyperfine

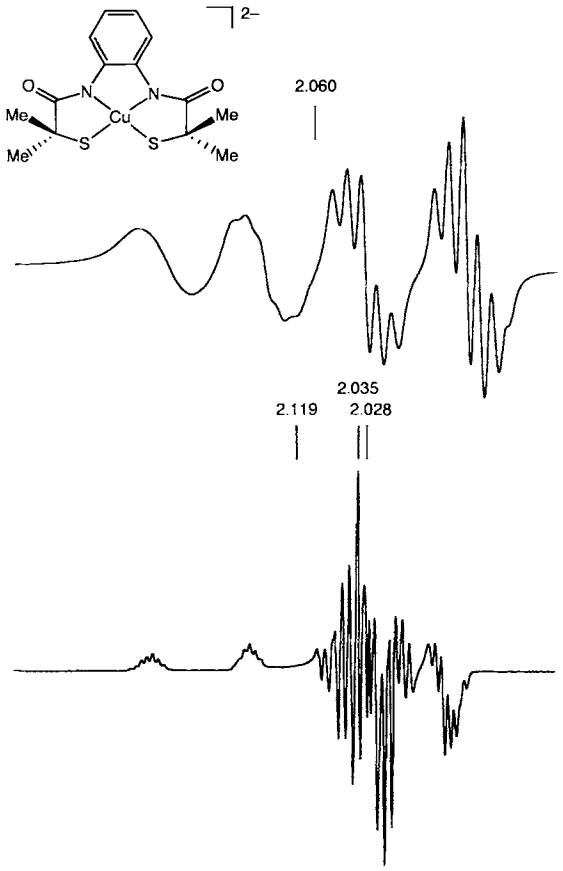

Fig. 1. X-Band EPR spectra of $(NEt_4)_2$[Cu(phmi)] · H_2O **4** in acetonitrile/toluene (v/v = 1:4) at room temperature (top) and as frozen glass in ethanol at 140 K (bottom).

coupling constants to the copper ion ($I = 1.5$) A^{Cu}_{iso} and to the two nitrogen atoms ($I = 1$) A^{N}_{iso} were determined to be 88.5×10^{-4} and $12.6 \times 10^{-4}\ cm^{-1}$, respectively. The powder spectrum of **4** in frozen ethanol solution consists of a nearly axial signal with a very distinct coupling pattern. Simulation[11] of the rather complex spectrum yielded $g_z = 2.119$, $g_y = 2.035$, and $g_x = 2.028$ as the best fit for the g-values, and $A^{Cu}_z = 195 \times 10^{-4}\ cm^{-1}$, $A^{Cu}_y = 35.2 \times 10^{-4}\ cm^{-1}$, $A^{Cu}_x = 36.8 \times 10^{-4}\ cm^{-1}$, $A^{N}_z = 12.3 \times 10^{-4}\ cm^{-1}$, $A^{N}_y = 15.1 \times 10^{-4}\ cm^{-1}$, and $A^{N}_x = 12.6 \times 10^{-4}\ cm^{-1}$ for the coupling constants. The

 © VCH Verlagsgesellschaft mbH, D-69451 Weinheim, 1996 0570-0833/96/3523-2828 $ 15.00+.25/0

ESR spectra of **4** demonstrate unambiguously that the metal center is a copper(II) ion rather than a copper(I) ion coordinated to a ligand radical, and that the unpaired electron resides in the d_{xy} orbital[12] of the metal ion.

In the cyclic voltammogram of the extremely oxygen-sensitive complex **4**, an oxidation takes place at -1.16 V vs. the ferrocene/ferrocenium (Fc/Fc^+) redox couple. The oxidative response displays all the characteristics for an electron transfer reaction that approaches electrochemical reversibility. Coulometric oxidation at -0.96 V vs. Fc/Fc^+ shows that one electron is transferred; upon re-reduction, 99% of the original copper(II) species is recovered. No reversible reduction is observed for **4**.

The oxidized species was prepared by bulk electrolysis of the copper(II) complex at -0.96 V vs. Fc/Fc^+ and isolated as greenish-yellow (PPh_4)[Cu(phmi)] (**5**). The crystal structure of **5** (Fig. 2)[9] ascribes a square-planar coordination geometry to

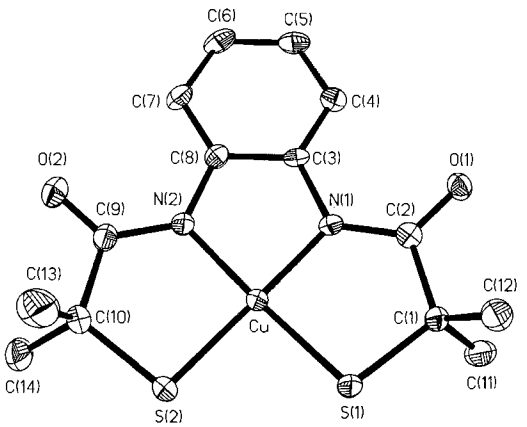

Fig. 2. Crystal structure of the $[Cu(phmi)]^-$ ion showing thermal ellipsoids at 50% probability and the atom numbering scheme. The complex anion $[Cu(phmi)]^{2-}$ has the same connectivity and coordination geometry. Selected distances [Å] and angles [°] in the $[Cu(phmi)]^-$ ion [in the $[Cu(phmi)]^{2-}$ ion]: Cu-S(1) 2.145(1) [2.2381(8)], Cu-S(2) 2.150(1) [2.243(1)], Cu-N(1) 1.863(3) [1.963(2)], Cu-N(2) 1.864(3) [1.962(2)], N(1)-C(2) 1.357(4) [1.329(3)], N(1)-C(3) 1.430(4) [1.425(3)], N(2)-C(9) 1.359(4) [1.332(3)], N(2)-C(8) 1.427(4) [1.419(3)], O(1)-C(2) 1.238(4) [1.252(4)], O(2)-C(9) 1.232(4) [1.247(3)], C(3)-C(4) 1.397(4) [1.400(4)], C(3)-C(8) 1.419(4) [1.424(4)], C(4)-C(5) 1.393(4) [1.396(4)], C(5)-C(6) 1.391(5) [1.381(4)], C(6)-C(7) 1.398(5) [1.399(4)], C(7)-C(8) 1.396(4) [1.400(4)]; S(1)-Cu-S(2) 92.11(4) [100.27(3)], S(1)-Cu-N(1) 90.36(8) [87.68(7)], S(1)-Cu-N(2) 176.24(8) [171.40(7)], S(2)-Cu-N(1) 174.93(8) [172.05(6)], S(2)-Cu-N(2) 90.24(8) [88.09(7)], N(1)-Cu-N(2) 87.52(11) [83.97(9)].

the copper ion. The most distinctive feature of the complex is the decrease of the Cu–N and Cu–S bond lengths from 1.963 and 2.241 Å in **4** to 1.864 ± 0.001 and 2.148 ± 0.003 Å in **5**, respectively. The C–C and C–N bond lengths of the phenylenediamide moiety in **5** are, within the 3σ criterion, the same as those in **4**. These findings clearly indicate that the oxidation is metal-centered and that the electron is removed from the strongly antibonding d_{xy} orbital,[12] thereby strengthening the Cu–N and Cu–S bonds in **5**. The Cu–N bond lengths are slightly longer than those observed in the other copper(III) complexes containing deprotonated amides as ligands.[13] Further, the average C–N and C–O bond lengths of the amide functions change from 1.331 ± 0.002 and 1.250 ± 0.003 Å in **4** to 1.358 ± 0.001 and 1.235 ± 0.003 Å in **5**, respectively.[14] This is interpreted to mean that, as a response to the higher positive charge on the metal ion in **5**, the partial double bond character of the C–N bond in the amide function is reduced in order to increase the negative charge on the nitrogen atom. As a consequence of the shorter distances between the metal and the donor atoms, the acyclic ligand can surround the metal ion more completely, as shown by the smaller S–Cu–S angle and S–S distance; despite the substantial decrease in the distance between the two sulfur atoms from 3.439 Å in **4** to 3.092 Å in **5**, no bonding interaction between the sulfur atoms exists.

As expected for a square-planar metal ion with a d^8 electron configuration, **5** is diamagnetic. A comparison of the NMR spectrum of **5** in deuterated acetonitrile [$\delta = 8.44$ (dd, 2H), 6.75 (dd, 2H), 1.46 (s, 12H)] with that of the nickel(II) complex $[Ni(phmi)]^{2-}$ [$\delta = 8.64$ (dd, 2H), 6.46 (dd, 2H), 1.23 (s, 12H)][15] and that of the copper(III) complex of the alcoholate analogue of $phmi^{4-}$ [$\delta = 7.85$ (dd, 2H), 6.75 (dd, 2H), 1.23 (s, 12H)][13b] is further indication that the ligand is not involved in the redox reaction.

All structural and spectroscopic results support the description of the metal ions as Cu^{II} in **4** and as Cu^{III} in **5**. The ligand itself is redox-inert. The oxidation potential of **4** is, to our knowledge, the lowest ever recorded for a true Cu^{III}/Cu^{II} redox couple. As in some Ni^{III}/Ni^{II} redox couples,[7a] the replacement of the thiolate donor functions in **4** by alcoholates raises the redox potential by 290 mV.[13b] Since the type of ligand donor sets in $phmi^{4-}$ are potentially available in nature in the form of cysteine-containing peptides, these results demonstrate that, in contrast to the previously stated opinion[1f] that "the Cu^{III} state is not a biologically relevant oxidation state" since "the redox potentials for the transition Cu^{III}/Cu^{II} are generally very high," the occurrence of Cu^{III} centers in natural systems cannot be dismissed as irrelevant.

Our investigation presents strong evidence that copper ions in high oxidation states are viable in the presence of aliphatic thiolates. For the first time, a copper(III) ion has been structurally characterized in a coordination environment consisting partly of thiolates. While the oxidation state of the metal ion in the complex $[Cu(tdt)_2]^-$[16] is ambiguous and thus the complex is better described as a copper(II) ion stabilized ligand radical,[16] the oxidation state of the copper ion in complexes **4** and **5** has been proven beyond doubt. However, one has to keep in mind that the stabilization of Cu^{II} and especially of Cu^{III} ions can only be accomplished here due to the presence of highly polarizable, anionic nitrogen donors. Deprotonated amides have been known to stabilize high oxidation states of copper,[13, 17] and it is only because these nitrogen donors are able to provide the electropositive copper ions in complexes **4** and **5** with sufficient electron density that autoreduction of the metal ion by the coordinated thiolates does not occur.

Experimental Procedure

4: Under strictly anaerobic conditions, a solution of *N,N'*-1,2-phenylenebis-(*S*-acetyl-2-mercapto-2-methylpropionamide) (200 mg, 0.5 mmol), KOH (140 mg, 2.5 mmol), and NEt_4Cl (166 mg, 1.0 mmol) in absolute ethanol (40 mL) was stirred for 0.5 h before a suspension of $Cu(OAc)_2 \cdot H_2O$ (99.8 mg, 0.5 mmol) in absolute ethanol (50 mL) was added. After the reaction mixture was heated at reflux for a short time, the solvent was completely removed in vacuo. The residue was treated with acetonitrile (30 mL) and the resulting red solution was filtered. Slow diffusion of ether into the acetonitrile solution afforded a red crystalline material which was collected, washed with ether, and dried in vacuo to yield analytically pure product (209 mg, 66% yield). Under vacuum the compound lost its crystal water molecule. Anal. calcd. for $C_{30}H_{56}CuN_4O_2S_2$: C 56.97, H 8.92, N 8.86; found: C 57.10, H 8.98, N 8.76. Absorption spectrum (acetonitrile): λ_{max} (ε_M) = 580 (sh, 110), 489 (538), 340 (sh, 3800), 310 (sh, 11000), 294 (23800), 285 (sh, 20900), 255 (sh, 23500), 247 (24100), 230 (25800) nm. The synthesis of $(PPh_4)_2$[Cu(phmi)] was achieved using PPh_4Cl following procedures similar to those described above.

5: A solution of $(PPh_4)_2$[Cu(phmi)] (286.8 mg, 273 mmol) in acetonitrile (10 mL) containing 0.05 M PPh_4Cl as supporting electrolyte was oxidized at -0.96 V vs. Fc/Fc^+ in an electrochemical cell placed in a glove box. The electrolysis was carried out at a platinum net electrode with a PAR Model 273A Potentiostat/Galvanostat controlled by the PAR Model 270 Research Electrochemistry Software. After the oxidation was complete, the electrolyte PPh_4Cl was precipitated by diffusion of

ether to the resulting solution. Removal of the solvent from the filtered solution yielded a greenish yellow solid, which was redissolved in acetone (10 mL) under air. Diffusion of ether to this solution afforded analytically pure product as greenish yellow crystals (164.9 mg, 85% yield). Anal. calcd. for $C_{38}H_{36}CuN_2O_2PS_2$: C 64.16, H 5.10, N 3.94; found: C 64.13, H 5.04, N 3.90. Absorption spectrum (acetonitrile): λ_{max} (ε_M) = 711 (218), 417 (6130), 295 (sh, 18900), 277 (32900), 245 (23000), 220 (22300) nm.

Received: March 5, 1996 [Z 8895 IE]
German version: *Angew. Chem.* **1996**, *108*, 2989–2991
Publication delayed on authors' request

Keywords: copper compounds · thiolate complexes

[1] a) H. Toftlund, J. Becher, P. H. Oleson, J. Z. Pedersen, *Isr. J. Chem.* **1985**, *25*, 56; b) E. T. Adman in *Metalloproteins Part 1* (Ed.: P. Harrison), Verlag Chemie, Weinheim, **1985**, p. 1; c) A. G. Sykes *Struct. Bonding* **1990**, *75*, 175; d) *Adv. Inorg. Chem.* **1991**, *36*, 377; e) N. Kitajima, *ibid.* **1992**, *39*, 1; f) W. Kaim, J. Rall, *Angew. Chem.* **1996**, *108*, 47; *Angew. Chem. Int. Ed. Engl.* **1996**, *35*, 60, and references therein.

[2] a) J. D. Forrester, A. Zalkin, D. H. Templeton, *Inorg. Chem.* **1964**, *3*, 1507; b) J. L. Hughey, T. G. Fawcett, S. M. Rudich, R. A. Lalancette, J. A. Potenza, H. J. Schugar, *J. Am. Chem. Soc.* **1979**, *101*, 2617; c) R. Cini, A. Cinquantini, P. Orioli, M. Sabat, *Cryst. Struct. Commun.* **1980**, *9*, 865; d) O. P. Anderson, C. M. Perkins, K. K. Brito, *Inorg. Chem.* **1983**, *22*, 1267; e) A. W. Addison, E. Sinn, *ibid.* **1983**, *22*, 1225; f) O. Anderson, J. Becher, H. Frydendahl, L. F. Taylor, H. Toftlund, *J. Chem. Soc. Chem. Commun.* **1986**, 699; g) M. Gullotti, L. Casella, A. Pintar, E. Suardi, P. Zanello, S. Mangani, *J. Chem. Soc. Dalton Trans.* **1989**, 1979.

[3] N. Kitajima, K. Fujisawa, M. Tanaka, Y. Moro-oka, *J. Am. Chem. Soc.* **1992**, *114*, 9232.

[4] P. K. Bharadwaj, J. A. Potenza, H. J. Schugar, *J. Am. Chem. Soc.* **1986**, *108*, 1351.

[5] E. John, P. K. Bharadwaj, J. A. Potenza, H. J. Schugar, *Inorg. Chem.* **1986**, *25*, 3065.

[6] H.-J. Krüger, R. H. Holm, *Inorg. Chem.* **1989**, *28*, 1148.

[7] H.-J. Krüger, R. H. Holm, *Inorg. Chem.* **1987**, *26*, 3645; b) H.-J. Krüger, G. Peng, R. H. Holm, *ibid.* **1991**, *30*, 734.

[8] a) Y. Sugiura, Y. Hirayama, H. Tanaka, K. Ishizu, *J. Am. Chem. Soc.* **1975**, *97*, 5577; b) Y. Sugiura, Y. Hirayama, *Inorg. Chem.* **1976**, *15*, 679; c) *J. Am. Chem. Soc.* **1977**, *99*, 1581; d) Y. Sugiura, *Inorg. Chem.* **1978**, *17*, 2177.

[9] Crystallographic data of **4**: orthorhombic space group $P2_12_12_1$, a = 10.788(2), b = 14.993(3), c = 21.324(10) Å, V = 3449(2) Å^3, Z = 4, ρ_{calcd} = 1.253 g cm^{-3}; T = 153 K; 5115 unique reflections (4516 reflections with $F_o > 4\sigma(F_o)$), $\mu(Mo_{K\alpha})$ = 7.89 cm^{-1}; 375 parameters; R = 0.0348 ($F_o > 4\sigma(F_o)$). – Crystallographic data of **5**: monoclinic space group $P2_1/n$, a = 14.225(2), b = 11.399(2), c = 21.109(7) Å, β = 98.94(2)°, V = 3381(1) Å^3, Z = 4, ρ_{calcd} = 1.397 g cm^{-3}; T = 153 K; 5983 unique reflections (4230 reflections with $F_o > 4\sigma(F_o)$), $\mu(Mo_{K\alpha})$ = 8.54 cm^{-1}; 418 parameters; R = 0.0410 ($F_o > 4\sigma(F_o)$). Further details of the crystal structure investigations are available on request from the Fachinformationszentrum Karlsruhe, D-76344 Eggenstein-Leopoldshafen (Germany), on quoting the depository numbers CSD-405708 (**4**) and CSD-405709 (**5**).

[10] The Cu–N(amidato) bond lengths in mononuclear square-planar complexes range from 1.867 to 1.996 Å, with a mean at 1.923 Å: Cambridge Structural Database 5.10, October **1995**.

[11] Program "EPR" 1.0, F. Neese, Diplomarbeit, Universität Konstanz (Germany), **1993**.

[12] The coordinate system is arranged in such a way that the z axis lies perpendicular to the CuN_2S_2 plane and the x axis dissects the S-M-S angle.

[13] a) L. L. Diaddario, W. R. Robinson, D. W. Margerum, *Inorg. Chem.* **1983**, *22*, 1021; b) F. C. Anson, T. J. Collins, T. G. Richmond, B. D. Santarsiero, J. E. Toth, B. G. R. T. Treco, *J. Am. Chem. Soc.* **1987**, *109*, 2974.

[14] Similar observations were also made with other divalent and trivalent metal ion complexes [15]; however, no water molecule was present in the crystal lattice. Therefore, the hydrogen bonding interaction between the water oxygen atom and the oxygen atom of the amide function can be discounted as the primary reason behind the elongation of the C–O bond length.

[15] J. Hanss, H.-J. Krüger, unpublished results.

[16] tdt = 3,4-toluenedithiolate(2–); D. T. Sawyer, G. S. Srivatsa, M. E. Bodini, W. P. Schaefer, R. M. Wing, *J. Am. Chem. Soc.* **1986**, *108*, 936.

[17] M. R. McDonald, W. M. Scheper, H. D. Lee, D. W. Margerum, *Inorg. Chem.* **1995**, *34*, 229, and references therein.

Formal Total Synthesis of (–)-Morphine by Cuprate Conjugate Addition

Johann Mulzer,* Gerd Dürner, and Dirk Trauner

Dedicated to Professor Wilhelm Fleischhacker on the occasion of his 65th birthday

The opium alkaloids (–)-morphine (**1**) and (–)-codeine (**2**) have long been challenges for natural product synthesis.[1] Remarkably, activity in this field has increased in recent years, as it has done with other "classical" alkaloids. The attraction of **1** and **2** results from their complex molecular architecture, which

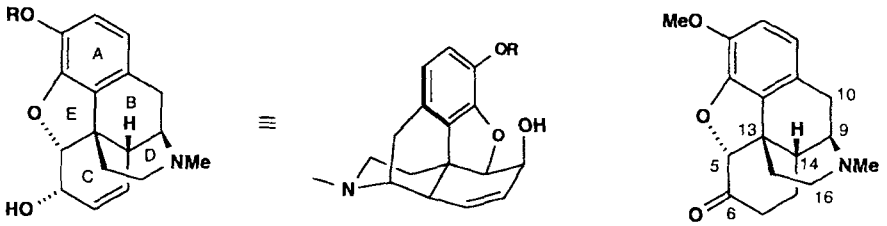

R = H (–)-morphine **1**
R = Me (–)-codeine **2**

(–)-dihydrocodeinone **3**

is due to a dense network of three carbocycles and two heterocycles containing five vicinal stereogenic carbons. One of these stereocenters (C13) is a quaternary benzylic carbon atom and therefore difficult to create.

In fact, the total syntheses of morphine published recently focus on the construction of this quaternary benzylic stereocenter, by employing either an intramolecular Heck reaction,[2a] a tandem radical cyclization,[2b] a Diels–Alder reaction,[2c] an intramolecular conjugate addition to a vinylsulfone,[2d] or an Eschenmoser–Claisen rearrangement[2e] as key reactions. However, one of the most efficient methods for the synthesis of quaternary centers, the 1,4-addition of cuprates,[3] has not yet been attempted in this context.

Our synthetic strategy was first to provide a functionalized phenanthrene derivative of type **5** with a correctly substituted aromatic ring A and then to employ the conjugate addition of a C_2-unit for the construction of the quaternary benzylic stereocenter.[4] Formal insertion of an NCH_3 group between C16 and C9 would then complete the morphinan ring system.

The readily available tetralone **4**[5] was converted by Robinson annulation into phenanthrenone **5**, which contains 14 of the 17 carbons and all three carbocycles of the morphinan skeleton. Phenanthrenone **5** was resolved on a preparative scale by chromatography on cellulose triacetate.[6] The undesired enantiomer could be racemized by treatment with base.

We next turned our attention to the key conjugate addition of a vinyl cuprate to **5**. Because of the high steric hindrance at the reaction center, activation by chlorotrimethylsilane (TMSCl) seemed to be necessary.[3, 7] However, the conditions described in the literature led to complex reaction mixtures, which contained only modest amounts of the desired silyl enol ether. As by-

[*] Prof. Dr. J. Mulzer, Dipl.-Chem. D. Trauner
Institut für Organische Chemie der Universität
Währingerstrasse 38, A-1090 Wien (Austria)
Fax: Int. code +(1)313672280
e-mail: mulzer@felix.orc.univie.ac.at
Dr. G. Dürner
Institut für Organische Chemie der Universität
Marie-Curie-Strasse 11, D-60439 Frankfurt am Main (Germany)

 © VCH Verlagsgesellschaft mbH, D-69451 Weinheim, 1996 0570-0833/96/3523-2830 $ 15.00+.25/0

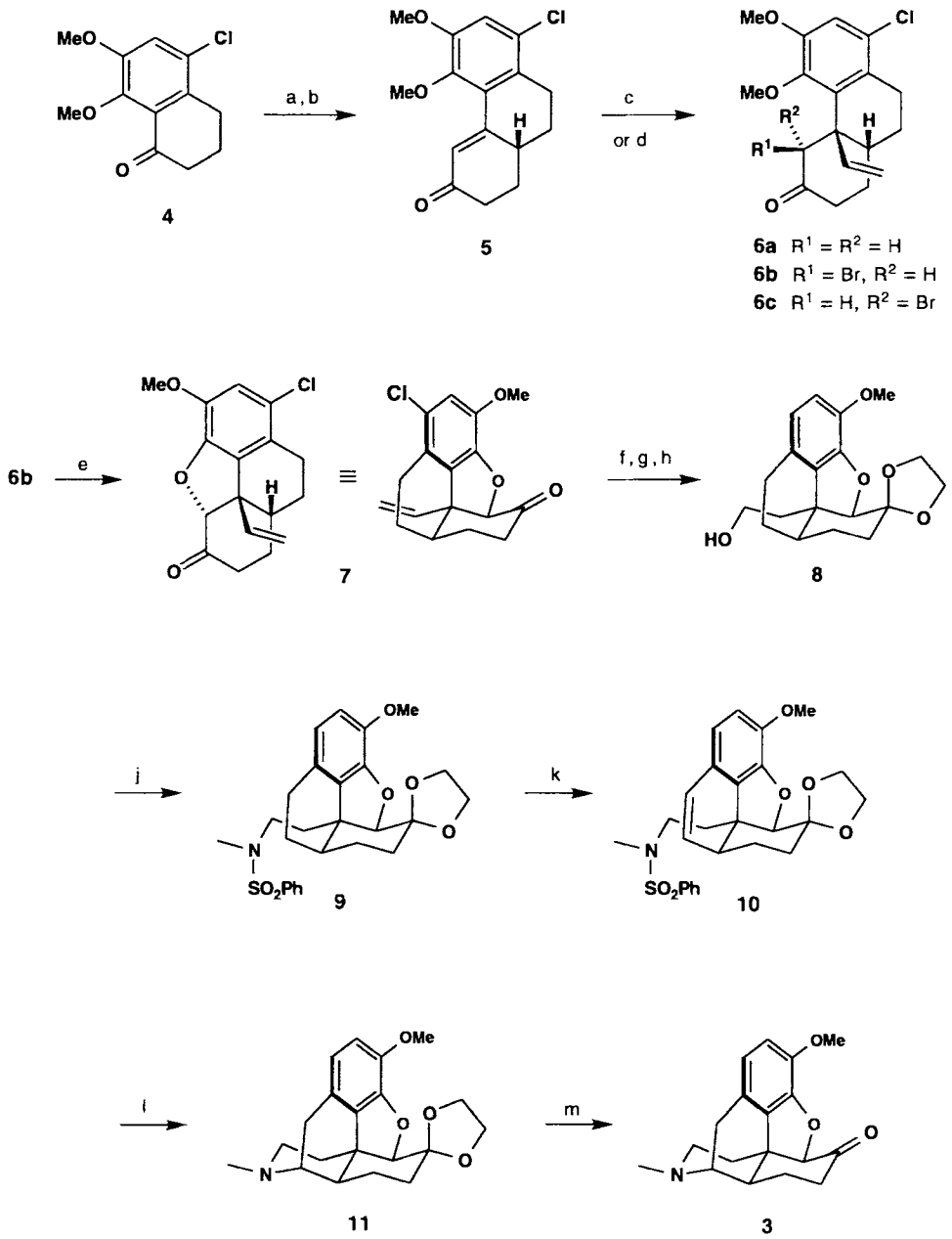

Scheme 1. a) HCOOMe, NaOMe, C_6H_6 (95%); b) 1. methyl vinyl ketone (MVK), Et_3N, MeOH; 2. KOH, dioxane, H_2O (77%); c) $(H_2C{=}CH)_2CuMgCl$, THF, $-78\,^{\circ}C \rightarrow 0\,^{\circ}C$ (91%); d) 1. $(H_2C{=}CH)_2CuMgCl$, THF, $-78\,^{\circ}C \rightarrow 0\,^{\circ}C$; 2. TMSCl, Et_3N, $0\,^{\circ}C \rightarrow 25\,^{\circ}C$; 3. NBS, THF, $-78\,^{\circ}C$ (84%); e) DMF, 140 °C (100%); f) TMSCl, $(CH_2OH)_2$, CH_2Cl_2 (92%); g) 1. $BH_3 \cdot Me_2S$, THF; 2. H_2O_2, OH^- (70%); h) Ra-Ni, MeOH, KOH (98%); j) $PhSO_2NHMe$, ADDP, Bu_3P (81%); k) NBS, $(PhCOO)_2$, CCl_4, reflux (65%); l) Li, NH_3, THF, *t*BuOH (79%); m) 3N HCl, 90 °C (95%).

product we isolated the C_2-symmetric, silylated pinacol **12**. We regard this as evidence that the cuprate conjugate addition follows a single electron transfer (SET) mechanism (Fig. 2).[8]

In contrast, the simple vinyl cuprate $(CH_2{=}CH)_2CuMgCl$[9] reacts with **5** in absence of chlorosilanes to afford ketone **6a** in

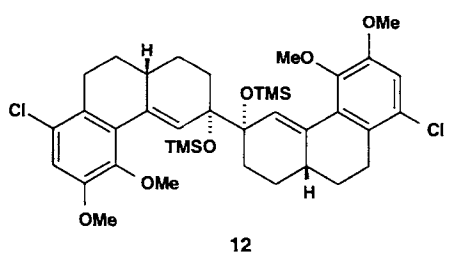

12

91% yield. The enolate existing after conjugate addition could be trapped quantitatively by subsequent addition of TMSCl. Treatment of the crude silyl enol ether with *N*-bromosuccinimide (NBS)[10] then furnished α-bromoketones **6b** and **6c** in a 3:1 ratio. Compounds **6a–c** display the correct relative configuration at C13 and C14 and contain all carbons of morphine apart from the N-methyl group.

The main isomer **6b** cyclized quantitatively to **7** on brief heating at 140 °C in DMF.[11] Ketone **6c** remained unchanged under these conditions. Ketalization of the carbonyl function of **7**,[12] hydroboration/oxidation of the vinyl residue, and subsequent dechlorination of the aromatic ring with Raney-nickel proceeded uneventfully. The resulting primary alcohol **8** was converted into secomorphinan **9** by a novel variant of the Mitsunobu reaction[13] involving *N*-methylbenzenesulfonamide, 1,1′-(azodicarbonyl)dipiperidine (ADDP), and tributylphosphane.

For the final bond formation between C9 and the nitrogen we used the piperidine ring closure described by Parker and Focas.[2b] Benzylic bromination of **9** with NBS, followed by spontanous thermal elimination of HBr[14] furnished styrene **10**, which underwent radical (or anionic) cyclization to yield morphinan **11** on reductive desulfonation with lithium in liquid ammonia. The benzenesulfonyl group performs a threefold task in the sequence leading from **8** to **11** (acidification of the NH bond for Mitsunobu reaction, protection against NBS, generation of a nitrogen radical) and is therefore more than a mere protective group. Acidic cleavage of ethylene ketal **11** finally yielded (−)-dihydrocodeinone (**3**), which can be efficiently converted into (−)-codeine und (−)-morphine.[15] Synthetic **3** was identical with an authentic sample according to conventional standards (^1H and ^{13}C NMR, IR, MS, TLC, $[\alpha]_D^{20}$, m.p.). Table 1 contains selected physical data of compounds **5**, **6b**, **7**, **9**, **10**, **11**, and **12**.

Our chirally economic[16] asymmetric total synthesis is linear, yet very short with 11 isolated steps (total yield: 11.5%) from tetralone **4** to dihydrocodeinone **3**.[17] Its stereochemical course is determined by the first stereogenic center at C14. Due to the curvature of phenanthrenone **5**, the vinyl group and the bromine atom preferentially add to the convex side of the molecule. The subsequent ring closures of both heterocycles by an S_N2 reaction in one case and a radical cyclization in the other are

 © VCH Verlagsgesellschaft mbH, D-69451 Weinheim, 1996 0570-0833/96/3523-2831 $ 15.00+.25/0

Table 1. Selected physical data of compounds **5**, **6b**, 7, **9**, **10**, **11**, and **12** [a].

5: colorless crystals, m.p. 113–115 °C; $[\alpha]_D^{20} = -245.1$ ($c = 2$, $CHCl_3$); ^1H NMR (270 MHz, $CDCl_3$): $\delta = 1.73$ (m_c, 1H), 1.83 (dddd, 1H, $J = 5.9, 8.5, 13.3, 19.1$ Hz), 2.03 (m_c, 1H), 2.24 (m_c, 1H), 2.40–2.62 (m, 3H), 2.72–2.84 (m, 1H), 2.92 (ddd, 1H, $J = 4.3, 5.5, 17.1$ Hz), 3.74 (s, 3H), 3.86 (s, 3H), 6.99 (s, 1H), 7.16 (d, 1H, $J = 2.1$ Hz); ^{13}C NMR (68 MHz, $CDCl_3$): $\delta = 26.99, 29.54, 29.73, 36.14, 36.53, 56.17, 60.05, 114.79, 127.66, 128.42, 128.51, 129.72, 147.82, 151.69, 154.54, 200.65$; correct elemental analysis for $C_{16}H_{17}ClO_3$

6b: colorless crystals, m.p. 102–104 °C; $[\alpha]_D^{20} = -1.2$, $[\alpha]_{436}^{20} = +33.7$ ($c = 2$, $CHCl_3$); ^1H NMR (250 MHz, $CDCl_3$): $\delta = 1.64-1.82$ (m, 2H), 1.94–2.16 (m, 3H), 2.61–2.75 (m, 3H), 3.14 (ddd, 1H, $J = 6.6, 10.7, 10.8$ Hz), 3.80 (s, 3H), 3.81 (s, 3H), 4.47 (dd, 1H, $J = 1.1, 17.2$ Hz), 5.21 (dd, 1H, $J = 1.1, 10.5$ Hz), 5.87 (s, 1H), 6.34 (dd, 1H, $J = 10.5, 17.2$ Hz), 6.93 (s, 1H); ^{13}C NMR (63 MHz, $CDCl_3$): $\delta = 22.56, 23.81, 24.88, 32.22, 34.58, 50.85, 55.87, 57.80, 60.32, 113.76, 116.78, 127.79, 128.67, 128.84, 142.24, 147.94, 151.29, 203.54$; correct elemental analysis for $C_{18}H_{20}BrClO_3$

7: colorless crystals, m.p. 178–179 °C; $[\alpha]_D^{20} = -35.7$ ($c = 2$, $CHCl_3$); ^1H NMR (250 MHz, $CDCl_3$): $\delta = 1.29$ (dq, 1H, $J = 4.9, 12.6$ Hz), 1.70–2.20 (m, 3H), 2.23–2.45 (m, 4H), 2.61 (ddd, 1H, $J = 0.9, 7.3, 18.0$ Hz), 3.82 (s, 3H), 4.52 (dd, 1H, $J = 0.7, 17.0$ Hz), 4.71 (s, 1H), 5.14 (dd, 1H, $J = 0.7, 10.2$ Hz), 5.97 (dd, 1H, $J = 10.2, 17$ Hz), 6.71 (s, 1H); ^{13}C NMR (63 MHz, $CDCl_3$): $\delta = 19.94, 22.91, 26.45, 36.10, 39.35, 55.19, 56.64, 91.73, 114.69, 117.12, 123.84, 125.03, 126.83, 141.76, 142.94, 145.58, 206.46$; correct elemental analysis for $C_{17}H_{17}ClO_3$

9: colorless crystals, m.p. 175 °C; $[\alpha]_D^{20} = -15.0$ ($c = 1$, $CHCl_3$); ^1H NMR (400 MHz, $CDCl_3$): $\delta = 1.29$ (m_c, 1H), 1.46–1.53 (m, 2H), 1.61 (m_c, 1H), 1.70–1.82 (m, 2H), 1.90 (ddd, 1H, $J = 5.2, 10.3, 15.1$ Hz), 2.03–2.16 (m, 2H), 2.54 (m_c, 1H), 2.68 (m_c, 1H), 2.70 (s, 3H), 2.88 (ddd, 1H, $J = 5.2, 10.5, 15.7$ Hz), 3.34 (ddd, 1H, $J = 5.6, 10.5, 16.1$ Hz), 3.75 (m_c, 1H), 3.84 (m_c, 1H), 3.85 (s, 3H), 3.94 (m_c, 1H), 4.17 (m_c, 1H), 4.59 (s, 1H), 6.60 (d, 1H, $J = 8.2$ Hz), 6.74 (d, 1H, $J = 8.2$ Hz), 7.48–7.58 (m, 3H), 7.72–7.74 (m, 2H); ^{13}C NMR (100 MHz, $CDCl_3$): $\delta = 21.05, 23.60, 23.89, 32.96, 34.51, 34.88, 37.03, 46.20, 46.53, 56.66, 64.85, 66.37, 93.37, 108.33, 113.87, 120.34, 125.39, 127.28, 129.04, 129.93, 132.48, 137.70, 141.91, 147.09$; correct elemental analysis for $C_{26}H_{31}NO_6S$

10: colorless crystals, m.p. 115–117 °C; $[\alpha]_D^{20} = -24.1$ ($c = 1$, $CHCl_3$); ^1H NMR (400 MHz, $CDCl_3$): $\delta = 1.24$ (dq, 1H, $J = 2.7, 12.8$ Hz), 1.38–1.62 (m, 2H), 1.66–1.93 (m, 3H), 2.43 (m_c, 1H), 2.62 (s, 3H), 2.86 (ddd, 1H, $J = 5.4, 10.7, 16.0$ Hz), 3.18 (ddd, 1H, $J = 5.4, 10.7, 16.0$ Hz), 3.66–3.90 (m, 2H), 3.87 (s, 3H), 4.00 (m_c, 1H), 4.20 (m_c, 1H), 4.69 (s, 1H), 5.79 (dd, 1H, $J = 5.7, 9.6$ Hz), 6.36 (d, 1H, $J = 0.8, 9.6$ Hz), 6.63 (d, 1H, $J = 4.1$ Hz), 6.71 (d, 1H, $J = 8.1$ Hz), 7.44–7.58 (m, 3H), 7.67–7.72 (m, 1H); ^{13}C NMR (100 MHz, $CDCl_3$): $\delta = 25.18, 31.31, 34.65, 36.47, 38.84, 45.25, 46.12, 56.27, 64.80, 66.42, 94.07, 108.01, 112.93, 117.55, 122.95, 123.05, 127.14, 128.87, 129.60, 132.30, 137.59, 143.78, 146.05$; correct elemental analysis for $C_{26}H_{29}NO_6S$

11: colorless crystals, m.p. 173–175 °C; $[\alpha]_D^{20} = -173.3$ ($c = 1$, $CHCl_3$); ^1H NMR (400 MHz, $CDCl_3$): $\delta = 1.16$ (dq, 1H, $J = 2.3, 12.8$ Hz), 1.50–1.56 (m, 2H), 1.64–1.71 (m, 2H), 1.88 (td, 1H, $J = 4.9, 12.3$ Hz), 2.19–2.24 (m, 2H), 2.36 (dd, 1H, $J = 5.4, 18.3$ Hz), 2.41 (s, 3H), 2.53 (dd, 1H, $J = 3.8, 12.2$ Hz), 3.00 (d, 1H, $J = 18.3$ Hz), 3.11 (dd, 1H, $J = 2.6, 5.4$ Hz), 3.79 (m_c, 1H), 3.87 (s, 3H), 3.88 (m_c, 1H), 4.11 (m_c, 1H), 4.18 (m_c, 1H), 4.48 (s, 1H), 6.62 (d, 1H, $J = 8.2$ Hz), 6.74 (d, 1H, $J = 8.2$ Hz); ^{13}C NMR (100 MHz, $CDCl_3$): $\delta = 20.03, 22.20, 33.22, 36.33, 42.37, 42.73, 43.45, 47.02, 56.43, 59.46, 64.77, 66.28, 94.24, 108.44, 113.40, 118.51, 126.18, 128.98, 142.07, 146.39$; correct elemental analysis for $C_{20}H_{25}NO_4$

12: colorless crystals, m.p. 157-159 °C; ^1H NMR (250 MHz, $CDCl_3$): $\delta = 0$ (s, 18H), 1.29–1.81 (m, 12H), 1.97 (m_c, 2H), 2.62 (m_c 4H), 3.68 (s, 6H), 3.72 (s, 6H), 6.73 (s, 2H), 6.88 (d, 2H, $J = 1.6$ Hz); ^{13}C NMR (63 MHz, $CDCl_3$): $\delta = 3.35, 26.62, 27.53, 29.57, 31.61, 34.82, 55.85, 60.50, 80.23, 111.63, 127.70, 129.43, 130.90, 131.08, 134.92, 146.51, 151.59$; correct elemental analysis for $C_{38}H_{52}Cl_2O_6Si_2$

[a] m_c = centered multiplet.

stereospecific. Accordingly, the synthesis does not require chiral assistance by the reagents. The number of mere protecting groups is reduced to one only (the C6 ethylene ketal).

Received: June 21, 1996 [Z9249IE]
German version: *Angew. Chem.* **1996**, *108*, 3046–3048

Keywords: cuprates · morphine alkaloids · total syntheses

[1] For excellent reviews of the total synthesis of morphine alkaloids see a) T. Hudlicky, G. Butora, S. P. Fearnley, A. G. Gum, M. R. Stabile in *Studies in Natural Products Chemistry, Vol. 18* (Ed.: Atta-ur-Rahman), Elsevier, Amsterdam, **1996**, p. 43; b) M. Maier in *Organic Synthesis Highlights II* (Ed.: H. Waldmann), VCH, Weinheim, **1995**, p. 357; c) G. Szántay, G. Dörnyei in *The Alkaloids, Vol. 45* (Eds.: G. A. Cordell, A. Brossi), Academic Press, New York, **1994**, p. 127.

[2] a) C. Y. Hong, N. Kado, L. E. Overman, *J. Am. Chem. Soc.* **1993**, *115*, 11028; b) K. A. Parker, D. Focas, *ibid.* **1992**, *114*, 9688; c) M. A. Tius, M. A. Kerr, *ibid.* **1992**, *114*, 5959; d) J. E. Toth, P. R. Hamann, P. L. Fuchs, *J. Org. Chem.* **1988**, 53, 4694; e) P. J. Parsons, C. S. Penkett, A. Shell, *Chem. Rev.* **1996**, *96*, 195.

[3] a) *Organocopper Reagents, A Practical Approach* (Ed.: R. K. Taylor), Oxford University Press, **1994**; b) B. H. Lipshutz in *Organometallics in Synthesis*, Chap.4 (Ed.: M. Schlosser), Wiley, Chichester, **1994**; c) B. H. Lipshutz, S. Sengupta, *Org. React.* **1992**, *41*, 135; d) P. Perlmutter, *Conjugate Addition Reactions in Organic Synthesis*, Pergamon, Oxford, **1992**.

[4] Alternatively, the Eschenmoser–Claisen and [2,3]–Wittig rearrangements were successfully applied. The two strategies could be pursued in parallel, since the conjugate addition is performed with an enone, which on reduction delivers the allylic alcohol necessary for a sigmatropic rearrangement.

[5] R. Ghosh, R. Robinson, *J. Chem. Soc.* **1944**, 506.

[6] Flash chromatography; cellulose triacetate from the company Merck (No. 16362); methanol as eluent; 0.5 g **5** per 200 g cellulose triacetate.

[7] E. Nakamura in ref. [3a]; b) S. Matsuzawa, Y. Horiguchi, E. Nakamura, I. Kuwajima, *Tetrahedron* **1989**, *45*, 349; c) E. J. Corey, N. W. Boaz, *Tetrahedron Lett.* **1985**, *26*, 6019.

[8] J. Mulzer, J. W. Bats, D. Trauner, *Synlett*, submitted.

[9] a) K. E. Harding, B. A. Clement, L. Moreno, J. Peter-Katalinic, *J. Org. Chem.* **1981**, *46*, 940; b) P. M. Wege, R. D. Clark, C. H. Heathcock, *ibid.* **1976**, *41*, 3144.

[10] a) M. Ihara, A. Katsumata, M. Egashira, S. Suzuki, Y. Tokunaga, K. Fukumoto, *J. Org. Chem.* **1995**, *60*, 5560; b) M. J. Chapdelaine, M. Hulce, *Org. React.* **1990**, *38*, 225.

[11] T. K. Kawabata, P. A. Grieco, H.-L. Sham, H. Kim, J. Y. Jaw, S. Tu, *J. Org. Chem.* **1987**, *52*, 3347.

[12] T. H. Chan, M. A. Brook, T. Chaly, *Synthesis* **1983**, 203.

[13] T. Tsunoda, Y. Yamamiya, S. Itô, *Tetrahedron Lett.* **1993**, *34*, 1639.

[14] T. Kametani, Y. Suzuki, T. Honda, *J. Chem. Soc. Perkin Trans. 1* **1986**, 1372.

[15] a) D. D. Weller, H. Rapoport, *J. Med. Chem.* **1976**, *19*, 1173; b) I. Ijima, J. Minamikawa, A. E. Jacobson, A. Brossi, K. C. Rice, *J. Org. Chem.* **1978**, *43*, 1463; c) K. C. Rice, *ibid.* **1980**, *45*, 3135.

[16] J. Mulzer in *Houben-Weyl, Methoden der Organischen Chemie, Vol. E21a*, Chap. A.2.1 (Eds.: G. Helmchen, R. W. Hoffmann, J. Mulzer, E. Schaumann), Thieme, Stuttgart **1995**, p. 91.

[17] Cf. ref. [2a]: 14 steps (6.5%); ref. [2b]: 13 steps (9.5%); ref. [12c]: 9 steps (29%).

Pyrazolate "Golden" Rings: Trinuclear Complexes That Form Columnar Mesophases at Room Temperature**

Joaquín Barberá, Anabel Elduque, Raquel Giménez, Luis A. Oro,* and José Luis Serrano*

The interest in supramolecular columnar organizations has continued to increase since these systems possess many of the properties required for photonics, electronics, and ionic transport.[1] The incorporation of metal atoms into mesogenic molecules has brought about a considerable expansion in the field of columnar liquid crystals[2] and has at the same time introduced new properties attributed to the metal atoms, such as color, ease of polarization, and paramagnetism. One of our research interests involves the preparation of mesogenic pyrazole derivatives. Our original aim was to prepare columnar phases, which show hydrogen-bonding interactions (Scheme 1, **A** and **B**). However,

[*] Prof. L. A. Oro, Dr. A. Elduque.
Dpto de Química Inorgánica, Facultad de Ciencias-ICMA
Universidad de Zaragoza-CSIC
E-50009 Zaragoza (Spain)
Fax: Int. code +(76)761143
e-mail: oro@msf.unizar.es

Prof. J. L. Serrano, Dr. J. Barberá, R. Giménez
Dpto de Química Orgánica, Facultad de Ciencias-ICMA
Universidad de Zaragoza-CSIC
E-50009 Zaragoza (Spain)
Fax: Int. code +(76)761209
e-mail: bros@msf.unizar.es

[**] This work was supported by the Comisión Interministerial de Ciencia y Tecnología (projects MAT93-0104 and MAT94-0717-CO2-01) and the Diputación General de Aragón (Research studentship to R. G.).

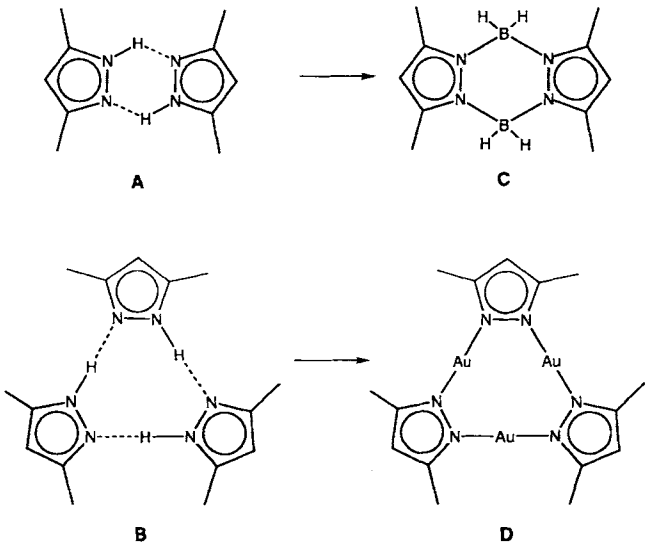

Scheme 1.

in the case of pyrazole derivatives, this objective failed,[3] and it was necessary to force the dimerization through the formation of covalent bonds like in **C**.[4]

As part of our ongoing investigations toward trimeric derivatives such as **B**, we decided to prepare new mesogenic gold compounds of type **D**, since the coinage metals are known to form trimers such as $[M(pz)]_3$ (pz = pyrazolate type ligands).[5] These complexes could present novel supramolecular structures and interesting reactivity.[5a, 6]

Several mesogenic complexes containing different ligands and metals have been described; however, no columnar structures with trinuclear complexes or gold atoms. Herein we report the first complex containing a trinuclear gold ring that exhibits a hexagonal columnar mesophase at room temperature.

The potassium salts of the non-mesogenic pyrazolate ligands derived from 3,5-*bis*-(3′,4′-*di*-*n*-decyloxyphenyl)pyrazole (**L1**) and 3-(3′,4′,5′-*tri*-*n*-decyloxyphenyl)-5-(3″,4″-*di*-*n*-decyloxyphenyl)pyrazole (**L2**) react with [AuCl(tht)], (tht = tetrahydrothiophene) to yield the trinuclear complexes **C1** and **C2**, respectively. The nuclearity of the complexes were confirmed by molecular weight determinations and mass spectrometric measurements. Related trinuclear gold pyrazolate compounds have been reported previously.[5]

Interestingly, complexes **C1** and **C2** form hexagonal columnar mesophases (Scheme 2), which were studied by optical microscopy, differential scanning calorimetry (DSC), and X-ray diffraction. The most important data obtained by these three techniques is summarized in Table 1. Compound **C1** melts at 59 °C to give the columnar phase, and clears at 64 °C. The freshly prepared compound **C2** shows the same mesophase at room temperature and becomes isotropic at 59 °C. During the transition of the isotropic liquid to the mesophase, a slight hysteresis was observed in the cooling process (ca. 9 and 4 K, respectively). In both cases the mesophase remains up to temperatures of

Table 1. Optical and thermal properties of the complexes **C1** and **C2** and X-ray parameters of the mesophases.

Compound	Mesomorphic properties [a]					**a** [b]
C1	C	59 (112.1) [c]	D_{hd}	64 (2.8)	I	32.4
		– [d]	D_{hd}	55 (2.2)	I	
C2	C	36 [e]	D_{hd}	59 (5.8)	I	31.7
		– [d]	D_{hd}	55 (4.8)	I	

[a] C, crystal phase; D_{hd}, disordered hexagonal columnar phase (disordered means that there is no periodicity along the columnar axis); I, isotropic phase; T [°C] (ΔH [kJ mol^{-1}]). Temperatures given for onset of transition. Heating and cooling scans at 10 K min^{-1}. [b] Intercolumnar parameter [Å]. [c] This transition only appears in the first heating. [d] Cooling scan, the D_{hd} phase remains unchangeable at −30 °C. [e] This transition only appears when the compound is heated for the first time, several weeks after it was obtained. The enthalpy could not be measured because the sample was not fully crystalline.

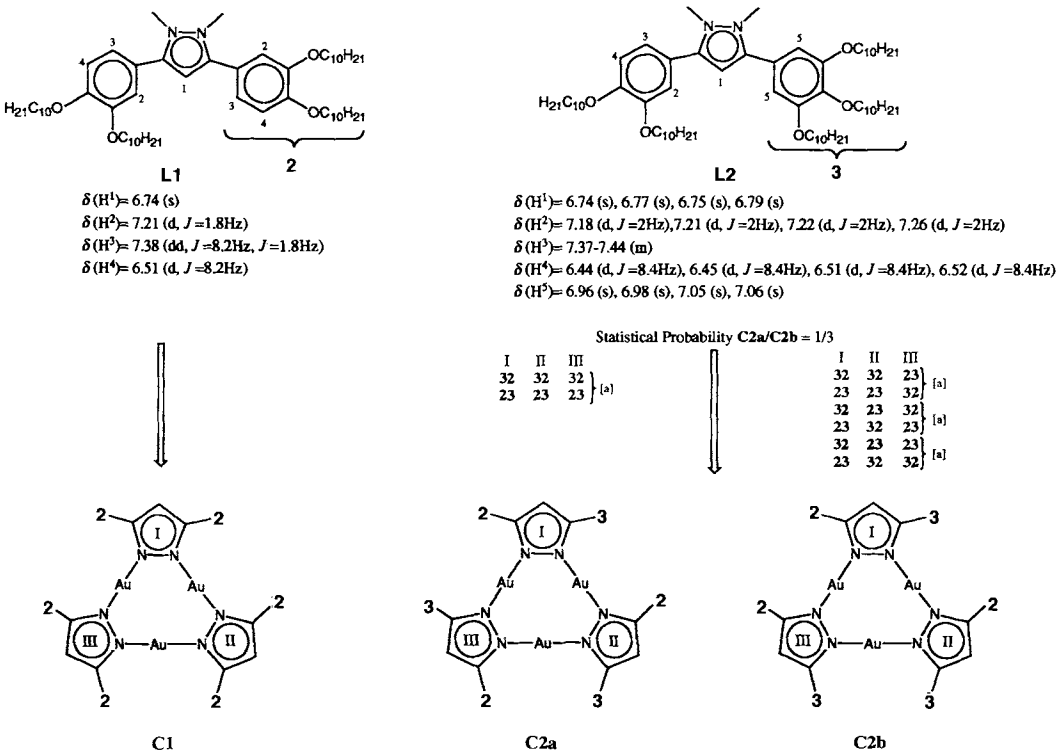

Scheme 2. Assignment of the ^{1}H NMR signals of the aromatic protons in the complexes **C1**, **C2a**, and **C2b**, and the statistical probability of isomers for compound **C2**. [a] Those products with these statistical probabilities are structurally equivalent.

 © VCH Verlagsgesellschaft mbH, D-69451 Weinheim, 1996 0570-0833/96/3523-2833 $ 15.00+.25/0

−30 °C. However, compound **C1** crystallizes after five or six hours at room temperature. On the other hand, compound **C2** remains in the hexagonal mesophase for several weeks before starting to crystallize very slowly.

The textures observed by optical microscopy under polarized light are fan-shaped (Fig. 1), which is typical for hexagonal columnar mesophases.

Fig. 1. Fan-shaped texture of the D_{hd} phase of compound **C1** at 20 °C between two crossed polarizers.

In order to obtain more information on the structures of the different phases exhibited by compounds **C1** and **C2**, the mesophase of both compounds and the solid crystalline phase of compound **C1** were analyzed at room temperature by X-ray diffraction. The solid phase of **C2** could not be studied because it was not fully crystallized. The X-ray diffraction patterns of the mesophase of both compounds display a set of sharp peaks in the small-angle region with reciprocal spacings in the ratio $1:\sqrt{3}:\sqrt{4}:\sqrt{7}$. These peaks are the (1 0), (1 1), (2 0), and (2 1) reflections of a two-dimensional hexagonal network with a lattice constant $a = 32.4$ Å for compound **C1** and $a = 31.7$ Å for compound **C2** (see Table 1). This agrees with a hexagonal columnar mesophase, in which the column axes are located at the nodes of the two-dimensional network and are oriented along the c axis. The absence of any other peaks in the diffraction pattern rules out the existence of periodicity along the columns. For this reason, no reflection is observed with the Miller index $l \neq 0$, and only a broad diffuse halo centered at 4.4 Å is found in the large-angle region; this is attributed to the averaged short-range correlations between stacked macrocycles and aliphatic chains.

The solid phase of compound **C1** yields a more complex X-ray pattern containing numerous peaks, which can be conveniently assigned to a three-dimensional C-centered orthorhombic network with cell parameters $a = 28.5$, $b = 66$, $c = 9.4$ Å. If the unit cell contains four molecules ($Z = 4$), a density of 1.17 g cm^{-3} is calculated for this structure. The area per molecule in this structure is $28.5 \times 66/2 = 940$ Å^2, and thus comparable with the area per molecule in the mesophase ($32.4 \times 32.4 \times \sqrt{3}/2 = 909$ Å^2. This, together with the fact that parameter c is much shorter than a and b suggests that the molecules also stack along the c axis in the solid state. As the unit cell is C-centered, two molecules are located at 0,0,0 and 1/2,1/2,0. If the other two molecules are located at $z = 1/2$, the stacking distance is $9.4/2 = 4.7$ Å, a typical intermolecular distance in disklike molecules.[7] A plausible explanation for the duplicity of parameter c is based on the single-crystal structure of the analogous gold complex without aliphatic chains, which was determined by Fackler et al.:[5c] There is a correlated organization in which close-stacked neighboring macrocycles are mutually rotated in such a way that the gold atoms of a molecule lie on top of the pyrazole rings of the lower neighbor, whereas the next nearest neighbor, situated at 9.4 Å along the c axis, has the same orientation. Unfortunately, all attempts to grow single crystals of compound **C1** have been unsuccesful.

If we compare the cell parameters, the transition from the crystalline to the liquid crystal phase in compound **C1** could be viewed as a distorsion of the *ab* plane (cf. Fig. 2), together with the loss of long-range periodical order along the direction of the c axis.

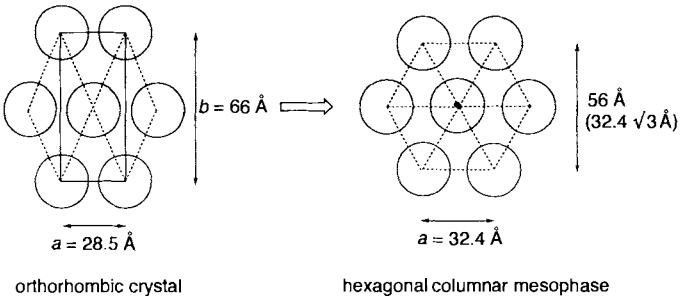

Fig. 2. Schematic diagram of the transition from the solid to the mesophase in the *ab* plane in compound **C1**; view along the c axis. The transition results in a lengthening of the orthorhombic lattice along the a axis and a shortening along the b axis; the ratio b/a becomes $\sqrt{3}$ (characteristic of a hexagonal structure).

The different mesogenic behavior of **C1** and **C2** could be explained based on their structural characteristics. The ^{1}H NMR spectrum of compound **C1** indicates the formation of only one isomer; a consequence of the free rotation of the aromatic rings around the C(pyrazole)–C(benzene) bond in solution. Only one type aromatic ring was detected. On the other hand, compound **C2**, which bears two different substituted aromatic rings on the pyrazolate groups, exhibits a more complicated ^{1}H NMR spectrum. Four signals were detected for each of the different hydrogen atoms of the pyrazolate core and the phenyl rings (Scheme 2). Curiously, the four signals have similar intensities. The spectra are consistent with the existence of two different geometrical isomers, **C2a** and **C2b**, in the ratio 1:3. Isomer **C2a** exhibits D_{3h} symmetry; this implies that the substituents **2** and **3** on the pyrazolate rings are magnetically equivalent. However, the pyrazolate substituents in isomer **C2b** are disposed asymmetrically, leading to three different possible geometrical arrangements (Scheme 2).

The existence of the two isomers in different proportions, hinders the interaction between the molecules. This interaction is necessary to obtain the crystal state, and thus compound **C2** remains as a mesophase at room temperature for a long time. On the other hand, compound **C1**, which is present in the form of one isomer and contains less aliphatic terminal chains, crystallizes more easily, melting at 59 °C and exists as a mesophase only in a narrow temperature range in the heating process.

Reactivity studies on these trinuclear compounds, aimed toward the formation of charge transfer complexes and the synthesis of new derivatives exhibiting D_{3h} symmetry (which are of interest for nonlinear optical applications) are currently in progress.

Experimental Procedure

All reactions were carried out under a N_2 atmosphere by using Schlenk techniques. The solvents were dried and freshly distilled. [AuCl(tht)] [8], **L1**, and **L2** were prepared by literature methods [3].

C1: A solution of K-**L1** (prepared in situ by reaction of a solution of **L1** (263 mg, 0.312 mmol) in acetone (20 mL) and KOH in methanol (1 mL, 0.309 M)) was added

dropwise to a suspension of [AuCl(tht)] (100 mg, 0.312 mmol) in acetone (10 mL). The reaction mixture was stirred for 5 h and the solvents were evaporated to dryness. Addition of hexane (10 mL) and filtration through Kieselguhr led to a colorless solution. Concentration of the solution to about 1 mL and addition of a mixture of ether (1 mL) and methanol (10 mL) gave a white solid which was separated by filtration, washed with methanol, and dried under vacuum. Compound **C1** was purified by column chromatography (hexane/dichloromethane 4/1) to give a white microcrystalline product. Yield: 40%. Elemental analysis for $C_{165}H_{273}N_6Au_3O_{12}$: calcd. (found) (%): C 63.44 (63.13), H 8.81 (8.69), N 2.69 (2.64); ^{1}H NMR (300 Hz, $CDCl_3$, 55 C): δ = 0.83–0.87 (m, 36H), 1.24–1.47 (m, 168H), 1.70–1.80 (m, 24H), 3.74 (t, J = 6.4 Hz, 12H), 3.92 (t, J = 6.4 Hz, 12H), 6.51 (d, J = 8.2 Hz, 6H, H4), 6.74 (s, 3H, H1), 7.21 (d, J = 1.8 Hz, 6H, H2), 7.38 (dd, J = 8.2 Hz, J = 1.8 Hz, 6H, H3); IR (nujol, NaCl pellet): ν (C=N and arC=C): 1607, 1589, 1528 and 1501 cm^{-1}; ν (C–O) = 1261 cm^{-1}; MS (FAB$^+$): m/z : 3123 ([M – 1]$^+$). M_r (calcd.) = 3124.0, M_r (found) = 3020.0.

C2: Compound **C2** was prepared analogously to **C1** starting from **L2** (312 mg, 0.312 mmol), KOH/MeOH (1 mL, 0.309 M), and [AuCl(tht)] (100 mg, 0.312 mmol), to give a colorless waxy product. Yield: 35%. Elemental analysis for $C_{195}H_{333}N_6Au_3O_{15}$: calc (found) (%): C 65.19 (65.42), H 9.34 (8.96), N 2.34 (2.37); ^{1}H NMR (300 MHz, $CDCl_3$, 55 °C): δ = 0.84–0.89 (m, 45H), 1.26–1.49 (m, 210H), 1.65–1.79 (m, 30H), 3.59-3.92 (4t, 30H), 6.44, 6.45, 6.51, 6.52 (4d, J = 8.4 Hz, 3H, H4), 6.74, 6.75, 6.77, 6.79 (4s, 3H, H1), 6.96, 6.98, 7.05, 7.06 (4s, 6H, H5), 7.18, 7.21, 7.22, and 7.26 (d, J = 2 Hz, 3H, H2), 7.37–7.44 (m, 3H, H3). IR (nujol, NaCl pellet): ν (C=N and arC=C): 1586, 1524, 1494 cm^{-1}; ν (C–O) = 1259, 1239 cm^{-1}; MS (FAB$^+$) m/z: 3593 (M^+); M_r (calcd.) = 3592.8, M_r (found) = 3432.8.

Received: June 17, 1996 [Z 9235 IE]
German version: *Angew. Chem.* **1996**, *108*, 3048–3051

Keywords: gold compounds · liquid crystals · metallomesogens

[1] a) B. Ros in *Metallomesogens. Synthesis, Properties and Applications* (Ed.: J. L. Serrano), VCH, Weinheim, **1996**, Chapt. 11; b) *Organic Materials for Photonics* (Ed.: G. Zerbi), North Holland, Amsterdam, **1993**; c) M. Matsumoto, H. Tachibana, T. Nakamura in *Organic Conductors: Fundamentals and Applications* (Ed.: J. P. Farges), Marcel Dekker, New York, **1994**, Chapt. 16; d) P. Di Marco, G. Giro, *ibid.* Chapt. 17; e) *Molecular Electronics Devices* (Ed.: F. L. Carter), Marcel Dekker, New York, **1982**.

[2] a) J. Barberá in *Metallomesogens. Synthesis, Properties and Applications* (Ed.: J. L. Serrano), VCH, Weinheim, **1996**, Chapt. 4; b) P. Espinet, M. A. Esteruelas, L. A. Oro, J. L. Serrano, E. Sola, *Coord. Chem. Rev.* **1992**, *117*, 2215; c) D. W. Bruce in *Inorganic Materials* (Eds.: D. W. Bruce, D. O'Hare), Wiley, New York, **1992**; d) A. M. Giroud-Godquin, P. M. Maitlis, *Angew. Chem.* **1991**, *103*, 370; *Angew. Chem. Int. Ed. Engl.* **1991**, *30*, 375.

[3] J. Barberá, C. Cativiela, J. L. Serrano, M. M. Zurbano, *Liq. Cryst.* **1992**, *11*, 887.

[4] J. Barberá, R. Giménez, J. L. Serrano, *Adv. Mater.* **1994**, *6*, 470.

[5] a) G. Minghetti, G. Banditelli, F. Bonati, *Inorg. Chem.* **1979**, *18*, 658; b) B. Bovio, F. Bonati, G. Banditelli, *Inorg. Chim. Acta* **1984**, *87*, 25; c) H. H. Murray, R. G. Raptis, J. P. Fackler, *Inorg. Chem.* **1988**, *27*, 26.

[6] a) F. Bonati, G. Minghetti, *J. Organomet. Chem.* **1973**, *60*, C43. b) R. G. Raptis, J. P. Fackler, *Inorg. Chem.* **1990**, *29*, 5003.

[7] A. M. Levelut, *J. Chim. Physique* **1983**, *80*, 149.

[8] R. Usón, A. Laguna, M. Laguna, *Inorg. Synth.* **1989**, *26*, 85.

Substrate-Directed Diastereoselective Hydroformylation of Methallylic Alcohols**

Bernhard Breit*

Structural units with two adjacent stereocenters are important targets in stereoselective synthesis. In the construction of such units it is often advantageous to start with a compound already containing a stereocenter and to generate the second stereocenter by substrate-directed asymmetric induction.[1] For synthetic efficiency the second step should lead to an extension of the carbon framework. The hydroformylation of methallylic alcohols meets these requirements.[2, 3] However, preliminary studies with free methallylic alcohols showed, that in contrast to the rhodium-catalyzed hydrogenation of 2-substituted allylic alcohols,[4] the hydroxyl functionality alone is not able to direct the reaction efficiently. Thus hydroformylation of the methallylic alcohol **1b** gave a 1:1 *syn/anti* mixture of the lactols **2**. The diastereomer ratio was determined after oxidation to the lactones **3** (Scheme 1).

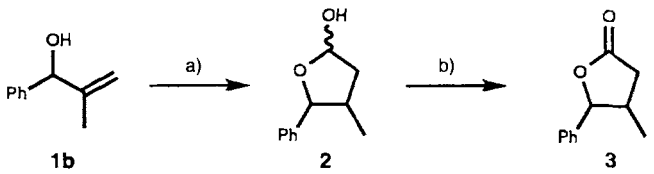

Scheme 1. a) 0.357 mol% $[Rh(CO)_2(acac)]$, 20 equiv PPh_3, 20 bar H_2/CO (1:1), toluene, 90 °C, 24 h, 83%; b) pyridinium chlorochromate, CH_2Cl_2, 20 °C, 16 h, 95%. For lactone **3**, *syn/anti* = 1:1. Hacac = acetyl acetone.

This experiment indicated that an effective directing metal-coordinating group is required and should meet several requirements. First, this functionality must be able to compete as a ligand with carbon monoxide, which is present in large excess. Simultaneously it must not coordinate irreversibly to the catalytically active transition metal center, because this would consume stoichiometric amounts of rhodium and catalysis would not be possible. One suitable ligand would be a triarylphosphane, because the rapid exchange of monodentate triarylphosphanes on rhodium complexes under hydroformylation conditions is documented.[5] Second, this coordinating group has to be introduced and removed readily, and should also be sufficiently stable against oxidation and hydrolysis. A ligand fulfilling all these requirements is the *ortho*-diphenylphosphinobenzoic acid (*o*-DPPBA), which is readily available from triphenylphosphane, sodium, and *ortho*-chlorobenzoic acid.[6] The corresponding methallylic *ortho*-diphenylphosphino benzoic esters **4a–i** can be obtained by esterification with dicyclohexylcarbodiimide in the presence of catalytic amounts of *N*,*N*-dimethylaminopyridine.[7]

In the catalytically active species in the hydroformylation the rhodium center is supposed to coordinate two P-donor ligands besides the olefin.[5] For that reason a second P-donor besides the coordinating *o*-DPPB unit becomes necessary. Such an ideal coligand should simultaneously stabilize the catalyst and enhance stereoselectivity of the reaction by increased steric interactions. Both might be achieved by using a sterically demanding π-acceptor ligand like triphenylphosphite.[8]

Hydroformylation of the methallylic *ortho*-diphenylphosphinobenzoates **4a–i** employing $[Rh(CO)_2(acac)]/P(OPh)_3$ as the catalyst system gave the *syn*-aldehydes **5a–i** as the major diastereomers usually in high yields and with mostly excellent diastereoselectivities (Scheme 2, Tables 1, 2). In particular, the reactions of methallylic alcohols with a branched substituent in the α-position, which is attached either by an sp^2- or sp^3-hybridized carbon atom, gave products with preparatively valuable diastereomeric ratios between 90:10 and 96:4 (entries 1–6, and 10). Only in the case of methallylic alcohols with primary alkyl substituents at the stereogenic center (entries 7 and 8) were the diastereoselectivities moderate. Evidently this α-substituent must exert a certain steric demand for differentiation of the two

[*] Dr. B. Breit
Fachbereich Chemie der Universität
Hans-Meerwein Strasse, D-35043 Marburg (Germany)
Fax: Int. code +(6421)28-8917
e-mail: breit@ps1515.chemie.uni-marburg.de

[**] This work was supported by the Fonds der Chemischen Industrie (Liebig fellowship for B. B.) and by the Deutsche Forschungsgemeinschaft (SFB 260). The author thanks Prof. R. W. Hoffmann for generous support as well as BASF und Degussa for gifts of chemicals.

Table 1. Results of diastereoselective hydroformylation of selected methallylic alcohol *o*-DPPB esters (**4** → **5**).

Entry	Methallylic alcohol **1**	Major diastereomer **5** [a]	Yield **5** [%] [b]	d.r. (*syn*:*anti*) [c]
1	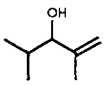 (±)-**1a**	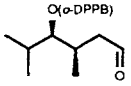 (±)-**5a**	97	96:4
2	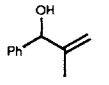 (±)-**1b**	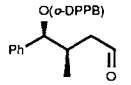 (±)-**5b**	99	92:8
3	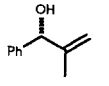 (+)-**1b**	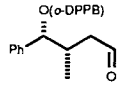 (+)-**5b**	98	92:8
4	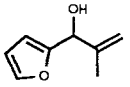 (±)-**1c**	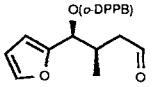 (±)-**5c**	63 [d]	93:7
5	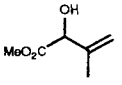 (±)-**1d**	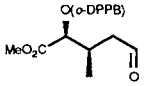 (±)-**5d**	80	90:10
6	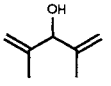 (±)-**1e**	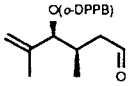 (±)-**5e**	90 [e]	96:4
7	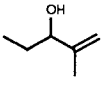 (±)-**1f**	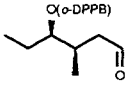 (±)-**5f**	83	73:27
8	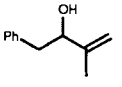 (±)-**1g**	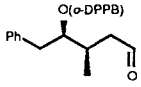 (±)-**5g**	75	80:20
9	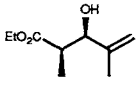 (±)-**1h**	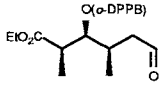 (±)-**5h**	98	81:19
10	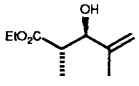 (±)-**1i**	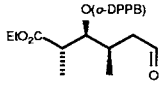 (±)-**5i**	82	94:6

[a] Hydroformylations of the corresponding *o*-DPPB-esters **4** have all been performed under identical reaction conditions employing the procedure described for **5a**. [b] After purification by column chromatography. [c] Determined from ^{1}H NMR spectra of the crude product. [d] Hydroformylation performed at 70 °C. [e] At 40% conversion.

diastereotopic faces of the olefin to be effective. The influence of a second stereocenter in the methallylic alcohol was investigated with the two diastereomeric substrates **1h** and **1i** (**4h** and **4i**, respectively). Hydroformylation led in both cases to the construction of stereotriades—a central structural unit of polyketide natural products—with excellent diastereoselectivity (*syn*/*anti*, 94:6) for **4i** (→ **5i**).[9] The *o*-DPPBA unit in **5b** was cleaved under alkaline hydrolysis to give in quantitative yields

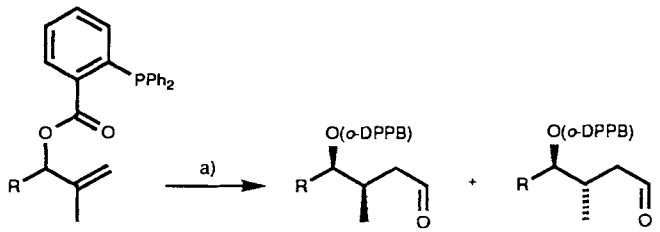

4a-i **5a-i**

Scheme 2. a) 0.7 mol% [$Rh(CO)_2(acac)$], 4 equiv $P(OPh)_3$, 20 bar H_2/CO (1:1), toluene, 90 °C, 24 h, 60–100%. For **5a–i**, *syn*/*anti* up to 96:4. *o*-DPPB = *ortho*-diphenylphosphinobenzoate.

Table 2. Selected physical data for **4a** and **5a**.

4a: colorless crystals, m.p. = 98–99 °C, ^{1}H NMR (300 MHz, $CDCl_3$): δ = 0.9 (d, ^3J(H,H) = 6.82 Hz, 3H, $CH(CH_3)_2$), 0.94 (d, ^3J(H,H) = 6.64 Hz, 3H, $CH(CH_3)_2$), 1.74 (s, 3H, CH_3), 2.0 (pseudo sext., J(H,H) = 6.83 Hz, $CH(CH_3)_2$), 4.92 (s, 1H, =CH_2), 4.99 (s, 1H, =CH_2), 5.18 (d, ^3J(H,H) = 7.48 Hz, OCH), 7.0 (m, 1H, Ar-H), 7.32–7.42 (m, 12H, Ar-H), 8.2 (m, 1H, Ar-H); ^{13}C NMR (75.469 MHz, $CDCl_3$): δ = 18.05, 18.52, 19.03, 29.87, 83.06, 114.08, 128.17, 128.39 (d, ^3J(C,P) = 7.1 Hz), 128.48 (d, ^4J(C,P) = 1.5 Hz), 130.43 (d, ^3J(C,P) = 2.3 Hz), 131.77, 133.84 (d, ^2J(C,P) = 20.7 Hz), 133.97 (d, ^2J(C,P) = 20.8 Hz), 134.34, 134.73 (d, ^2J(C,P) = 18.9 Hz), 138.14 (d, ^1J(C,P) = 12.5 Hz), 138.26 (d, ^1J(C,P) = 11.9 Hz), 140.75 (d, ^1J((C,P) = 27.9 Hz), 141.9, 165.78; ^{31}P NMR (161.978 MHz, CDCl): δ = − 4.3; elemental analysis calcd. for: $C_{26}H_{27}O_2P$: C 77.59, H 6.76; found.: C 77.32, H 6.8

syn-**5a**: colorless, viscous oil, ^{1}H NMR (300 MHz, $CDCl_3$): δ = 0.9 (d, ^3J(H,H) = 6.59 Hz, 3H, CH_3), (d, ^3J(H,H) = 6.84 Hz, 3H, $CH(CH_3)_2$), 0.98 (d, ^3J(H,H) = 6.77 Hz, 3H, $CH(CH_3)_2$), 1.94 (m, 1H, $CH(CH_3)_2$), 2.11 (ddd, ^2J(H,H) = 17.62 Hz, ^3J(H,H) = 8.26 and 1.76 Hz, 1H, CH_2), 2.30 (dd, ^2J(H,H) = 17.62 Hz, ^3J(H,H) = 5.33 Hz, 1H, CH_2), 2.52 (m, 1H, H at C2), 4.87 (dd, ^3J(H,H) = 8.89 and 3.25 Hz, 1H, CH), 7.02 (m, 1H, Ar-H), 7.22–7.47 (m, 12H, Ar-H), 8.2 (m, 1H, Ar-H), 9.57 (d, ^3J(H,H) = 0.73 Hz, CHO-*syn*) [9.68 (CHO-*anti*)]; ^{13}C NMR (75.469 MHz; $CDCl_3$): δ = 13.69, 19.15, 29.09, 29.83, 48.33, 82.07, 125.47, 128.62 (d, ^4J(C,P) = 2.1 Hz), 128.81 (d, ^3J(C,P) = 7.3 Hz), 130.72 (d, ^3J(C,P) = 1.7 Hz), 132.23, 133.85 (d, ^2J(C,P) = 18 Hz), 134.08 (d, ^2J(C,P) = 20.8 Hz), 134.28 (d, ^2J(C,P) = 21.1 Hz), 134.41, 166.62, 201.47 (CHO-*syn*) [202.03 (CHO-*anti*)]; ^{31}P NMR (161.978 MHz, $CDCl_3$): δ = − 3.1 (s); elemental analysis for: $C_{27}H_{29}O_3P$: C 74.98, H 6.76; found: C 74.91, H 6.90

the lactols **2** and the phosphinocarboxylic acid. Oxidation of the lactols **2** provided the known lactones *syn*-**3** und *anti*-**3**.[10]

Even though the *ortho*-diphenylphosphinobenzoate unit is an intrinsically coordinating functionality, this role was not yet proven as the basis for the observed diastereoselectivity. An experiment that could give further mechanistic insight is the hydroformylation of the methallylic benzoate **6**, which differs from **4b** only by the replacement of the phosphorus atom by a CH unit. Although benzoate function in **6** should have almost the same structural features as the *o*-DPPB unit in **4b**, **6** cannot be temporarily coordinated by the catalytically active transition metal center (Scheme 3).

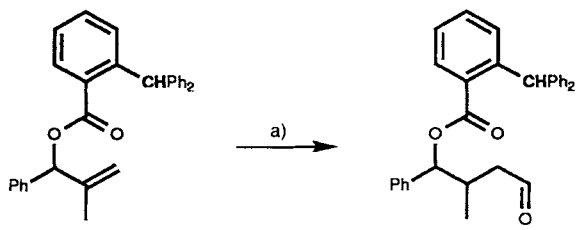

6 **7**

Scheme 3. a) 0.7 mol% [$Rh(CO)_2(acac)$], 4 equiv $P(OPh)_3$, 20 bar H_2/CO (1:1), toluene, 90 °C, 24 h, 60% conversion. For **7**, *syn*/*anti* = 1:1.

 © VCH Verlagsgesellschaft mbH, D-69451 Weinheim, 1996 0570-0833/96/3523-2836 $ 15.00+.25/0

The reaction conditions in hydroformylation experiment with **6** were identical to those employed in the experiment with **4b**. At 60% conversion the crude reaction mixture contained a 1:1 mixture of *syn*- and *anti*-**7**, in other words, no diastereoselectivity. In contrast, **4b** reacted quantitatively to give **5b** (*syn*/*anti*, 92:8). This experiment demonstrates that the presence of a sterically demanding substituent alone is not sufficient for diastereoselective hydroformylation of methallylic alcohols; however, a structurally and electronically well-suited functionality like the *o*-DPPB unit can serve as a coordinating and directing group and lead to synthetically useful diastereoselectivities in hydroformylation. The extension of this concept to other substrates and transition metal catalyzed reactions is currently under way.

Experimental Procedure

5a (entry 1 in Table 1): A solution of $[Rh(CO)_2(acac)]$ (0.9 mg, 3.5×10^{-3} mmol) in 3 mL of toluene at 20 °C (exclusion of air and moisture) was charged with $P(OPh)_3$ (4.5 mg, 1.4×10^{-2} mmol) and stirred for 15 min at 20 °C. Subsequently **4a** (201 mg, 0.5 mmol) was added and the resulting solution was cannulated into a stainless-steel autoclave, which had been evacuated and refilled with argon several times. The cannula was rinsed with additional toluene (2 mL). The autoclave was heated to 90 °C and then pressurized successively with carbon monoxide (10 bar) and hydrogen (10 bar). The reaction mixture was stirred at 90 °C for 24 h, then the autoclave was cooled rapidly to 20 °C. The reaction mixture was filtered through a small plug of silica gel with *tert*-butyl methyl ether (30 mL). After evaporation of the solvent in vacuo, the crude product was analyzed by NMR to determine the conversion (99%) and the diastereomer ratio (96:4). Subsequent column chromatography on silica (solvent: 1/9 *tert*-butyl methyl ether/petroleum ether) provided **5a** (210 mg, 97%) as a highly viscous oil.

Received: April 30, 1996
Revised version: June 26, 1996 [Z90841E]
German version: *Angew. Chem.* **1996**, *108*, 3021–3023

Keywords: asymmetric syntheses · catalysis · hydroformylations · rhodium compounds

[1] A. H. Hoveyda, D. A. Evans, G. C. Fu, *Chem. Rev.* **1993**, *93*, 1307–1370.
[2] For a review on hydroformylation see J. K. Stille in *Comprehensive Organic Synthesis, Vol. 4* (Eds.: B. M. Trost, I. Fleming), Pergamon, Oxford, **1991**, pp. 913–950.
[3] For substrate-directed diastereoselective hydroformylation of cyclic systems see a) S. D. Burke, J. E. Cobb, *Tetrahedron Lett.* **1986**, *27*, 4237–4240; b) W. R. Jackson, P. Perlmutter, E. E. Tasdelen, *J. Chem. Soc. Chem. Commun.* **1990**, 763–764.
[4] For a review see J. M. Brown, *Angew. Chem.* **1987**, *99*, 169–182; *Angew. Chem. Int. Ed. Engl.* **1987**, *26*, 190–203.
[5] J. M. Brown, A. G. Kent, *J. Chem. Soc. Perkin Trans. 2* **1987**, 1597–1607. A bidentate ligand would not be suited here; because of the chelate effect the binding constant would be too large.
[6] J. E. Hootes, T. B. Rauchfuss, D. A. Wrobleski, H. C. Knachel, *Inorg. Synth.* **1982**, *21*, 175–179.
[7] G. Höfle, W. Steglich, H. Vorbrüggen, *Angew. Chem.* **1978**, *17*, 602–615; *Angew. Chem. Int. Ed. Engl.* **1978**, *17*, 569–583.
[8] Without a coligand no reaction occurs and the catalyst decomposes. With triphenylphosphane as the coligand the reaction takes place, but the reactivity and diastereoselectivity are lower than when triphenylphosphite is used as a coligand.
[9] For a definition of stereotriades see R. W. Hoffmann, *Angew. Chem.* **1987**, *99*, 503–517; *Angew. Chem. Int. Ed. Engl.* **1987**, *26*, 489–503.
[10] J.-M. Fang, B.-C. Hong, L.-F. Liao, *J. Org. Chem.* **1987**, *52*, 855–861.

The Ca^{2+} Ion as a Cofactor for a Novel RNA-Cleaving Deoxyribozyme**

Dirk Faulhammer, and Michael Famulok*

The structure and reactivity of ribozymes and proteins depend on specific interactions of their monomers with each other, and in the end it is their primary sequence that determines their secondary and tertiary structure. However, the ionic strength of the buffer solution and the presence of certain divalent metal ions are often crucial for the formation of stable and active structures. This is particularly true for ribozymes,[1] for which Mg^{2+} or Mn^{2+} ions are commonly used as cofactors for catalysis. These ions are directly involved in the reaction by activating functional groups or water and cannot be substituted by other polycations. Therefore, ribozymes are a special class of metalloenzymes; no known ribozyme is active in the absence of divalent metal ions, which are thus essential for their chemistry. In principle, one can think of RNA as a scaffold for a site-specific reaction of the metal ion.

We wondered whether it might be possible to apply in vitro selection of combinatorial nucleic acid libraries to isolate a deoxyribozyme that cleaves an RNA substrate using a non-metal cofactor rather than divalent metal ions. As a promising candidate we chose the amino acid histidine, which plays a central role in the hydrolysis of RNA by ribonuclease A.[2] In the catalytic center of the enzyme the imidazole side chains of His12 and His119 form an acid–base pair and promote the hydrolysis of the phosphodiester bond. Free imidazole in solution is known to hydrolyze RNA by forming an acid–base pair.[3] Moreover, the catalytic center of ribonuclease A has been mimicked by model compounds.[4] Our experimental approach was based on the assumption that a histidine molecule would be complexed in the immediate proximity of the cleavage site and would form an acid–base pair with a free histidine molecule in solution. The nucleic acid would thus serve to position the imidazole residues in a suitable fashion and catalyze RNA cleavage.

The selection protocol was designed following a recent experiment by Breaker and Joyce which described the selection of Pb^{2+}- and Mg^{2+}-dependent DNA enzymes.[5] We constructed a library of single-stranded DNA with a complexity of roughly 5×10^{14} molecules. The 5′-end of the DNA was biotinylated and consisted of a constant region with a single ribonucleotide (rA) at position 28, which served as a defined cleavage site. This domain was followed by a randomized region of 74 nucleotides which carried a second constant primer-binding site at its 3′-end. The library prepared from synthetic DNA was amplified by the polymerase chain reaction (PCR); a second round of PCR was used to introduce the 5′-biotinylated region including the ribonucleotide cleavage site. The resulting double-stranded DNA pool was then immobilized on a streptavidin matrix. The non-biotinylated strand was removed by increasing the pH of the buffer, and the remaining immobilized library of single-stranded DNA was equilibrated and incubated with 20 mM histidine in buffered solution at pH 7.0 and 37 °C. The Mg^{2+} concentration of 0.5 mM was 40 times less than that of histidine,

[*] Priv.-Doz. Dr. M. Famulok, Dipl.-Chem. D. Faulhammer
Institut für Biochemie der Universität
Feodor-Lynen-Strasse 25, D-81377 München (Germany)
Fax: Int. code + (89) 74017-448
e-mail: famulok@lmb.uni-muenchen.de

[**] This work was supported by the Deutsche Forschungsgemeinschaft and the European Community (project no. Biot-CT93-0345). We thank E.-L. Winnacker for his support, and P. Burgstaller and H. Büning for helpful comments.

which was thought to result in a preference for the amino acid rather than the metal ion in cofactor selection (Scheme 1). To largely exclude the effect of heavy metals, the buffer also contained 20 μM EDTA. The eluted hydrolysis products were amplified as described above, and the enriched pool was subjected to subsequent selection cycles (Scheme 1). After seven cycles of selection and amplification, a marked increase in the rate of hydrolysis at the ribonucleotide position was observed. No activity was detected in a control experiment in which the ribonucleotide rA in the library was replaced by a deoxynucleotide. However, despite the large excess of histidine, the metal ion was selected as a cofactor, as shown in a control without histidine.[6]

After three additional cycles of selection/amplification, 44 clones were sequenced and could be divided into eight related classes, each of which contained individual sequences that differed only by point mutations or deletions (Table 1). Four classes showed homology within a 23 nucleotide region, which varied in location and sequence context from class to class. It could not be determined whether this homologous region is presented within a unique structural context (for example Watson–Crick helices or other structural elements). Thus, a common secondary structure was not found for these classes. Moreover, no homologies to a recently selected Mg^{2+}-dependent DNA enzyme were found.[5b]

Single clones from the different classes were chosen and tested for catalytic self-cleavage in solution under selection conditions, but in the absence of histidine. In addition, we tested the cleavage in the presence of other divalent metal ions (Mg^{2+}, Ca^{2+}, Ba^{2+}, Sr^{2+}, Pb^{2+}, Mn^{2+}, Zn^{2+}, Cd^{2+}). For clone Mg5 (Fig. 1), the extent of hydrolysis with 500 μM Ca^{2+} (63%) was significantly higher than with Mg^{2+} (25%). This result is remarkable not only because the selection had been performed in absence of Ca^{2+} ions but also because the pK_a von Mg^{2+} is considerably lower than that of Ca^{2+} (Table 2). On first glance this might argue against the direct participation of metal hydroxides, in contrast to the situation found, for example, for the hammerhead ribozyme.[7] However, Table 2 shows that for the other divalent metal ions the rates of hydrolysis follow the trend given by their pK_a values, as would be expected for the direct involvement of metal hydroxides. Furthermore, chemical modification analyses revealed no Mg^{2+}- or Ca^{2+}-dependent differences in the secondary structure of the DNA enzyme.

The catalytic efficiency of clone Mg5 strongly depends on the concentration of Mg^{2+} and Ca^{2+} ions. In both cases, the rate constants approach a saturation value with increasing metal ion concentration. Indeed, Figure 2a not only shows that the selection was performed at far below optimal concentration of the metal ion, but also that Ca^{2+} ions might promote the structure formation of this catalyst better than Mg^{2+} ions, because the saturation value is reached at a much lower concentration.

Based on the secondary structure of clone Mg5 (see Fig. 1), the unimolecular system was transferred into a bimolecular sys-

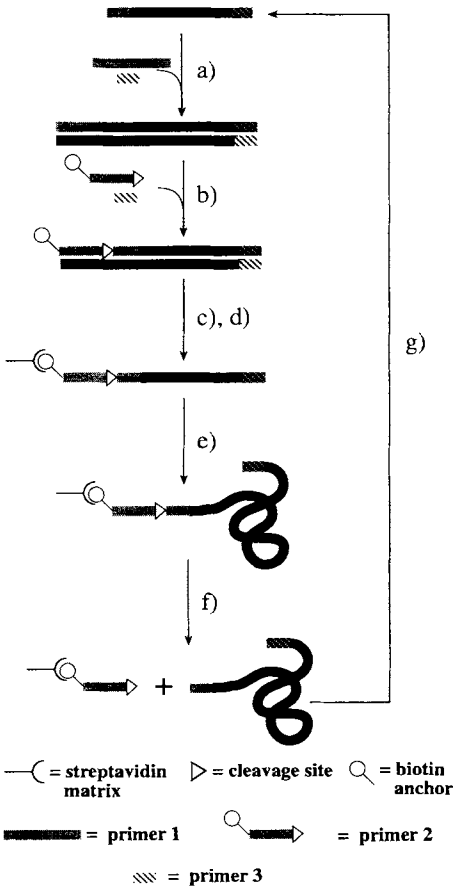

Scheme 1. Selection scheme; black strands: randomized region; gray and striped strands: constant regions (primer binding sites); ▽ in primer 2: rA position. a) In the first PCR the DNA library pool is amplified using primers **1** and **3**, whereas in the selection the eluted cleavage products are amplified (see Experimentel Procedure). b) In the second PCR with primers **2** and **3** the library is labeled with [α-^{32}P]-dCTP. c) Double-stranded DNA is dissolved in buffer containing 1 M NaCl and 50 mM 2-[4-(hydroxyethyl)piperazin-1-yl]ethanesulfonic acid (HEPES) (pH 7.4), loaded on 50–100 μL streptavidine agarose, and washed with the same buffer (5 × 500 μL). d) Single-stranded DNA is obtained by denaturing with 200 mM NaOH (5 × 500 μL). e) Single-stranded DNA is equilibrated by addition of 125 mM NaCl (5 × 500 μL), 125 mM KCl, 0.5 mM $MgCl_2$, 20 μM EDTA, and 50 mM NaH_2PO_4/Na_2HPO_4 (pH 7.0 at 37 °C). f) Single-stranded DNA is then incubated at 37 °C with the same buffer containing 50 mM histidine. Incubation time in rounds 1–8: 12 h, in rounds 9 and 10: 1 h. g) Eluted cleavage products were subjected to further cycles of selection and amplification.

Table 1. Sequence classes of the selected clones. Onla the randomized region with the constant primer binding sites is shown. The homologous regions found in four classes are highlighted in gray. Clone Mg5 belongs to class 2.

Classes	Sequences	No.
1	AAGCTCTCTCAGCGAGACGAAATAGGGAGTTAGCAGCACGAGGTTACACTTTTATCCTCTCCCAAAGTAGGGAC	19
2	AGCACGCATGACTTTGATGCCACGTAAAGTGAAAGAGCTGTTGATCTGTCAGCGACACGAAATGGTGATGCCCT	12
3	GGCATGTACCCAAGAAGGGGTGGAGCCGGCAGTGACCCCTGCGAGTAGGGAAGCCCAAGAACGAAGAGTTAAGC	5
4	ATGCTGTTGCTCTGTCAGCGGACACGAAATAGTGGGTCGCGATGCTGAATAATCACGGCGAAAGTGGTTGCCTA	3
5	CAGATGTGAAGTTAGAGCTTTGCCAGCnTCGTTAGTAGAGTCAGCGCACAGGGGAAGATTGTATGTCTATAG	2
6	TAGGAAGTAGGGACCTACAAGTTGTCATTGTAACTGAGTTCTGCCAGCTGsACGAAATAGTCAGGAGTTAG	1
7	CGTCATGCGAAAAGAATGGTGAGATTTGCCAGCsGTCGAGTAGTAGTCCAGGGAACATTGCCCGGGGGATT	1
8	AGAACGGTAGAGTGCNGGGGGTGCAGTTGAGCTTTGTCAGCsACACGAATAAGAGTCTCGTAGGATTCACCAAG	1

 © VCH Verlagsgesellschaft mbH, D-69451 Weinheim, 1996 0570-0833/96/3523-2838 $ 15.00+.25/0

Table 2. Self-cleavage of clone Mg5 in the presence of various divalent metal ions M^{2+} (0.5 mM). Yield of cleavage product and pK_a values [1b, 8] of the hydrated metal ions.

M^{2+}	Cleavage product [%] [a]	$pK_a([M(H_2O)_n]^{2+})$ [b]	M^{2+}	Cleavage product [%] [a]	$pK_a([M(H_2O)_n]^{2+})$ [b]
Pb^{2+}	91.3 ± 1.2	7.7	Mg^{2+}	24.8 ± 2.9	11.4
Zn^{2+}	89.0 ± 0.5	9.0	Ca^{2+}	62.9 ± 10.1	12.9
Cd^{2+}	81.1 ± 0.2	9.6	Sr^{2+}	8.8 ± 0.1	13.3
Mn^{2+}	76.2 ± 4.2	10.6	Ba^{2+}	4.4 ± 1.2	13.5
–	1.7 ± 0.2	–			

[a] The single-stranded clone Mg5 labeled at the 5'-end was incubated in the presence of the respective metal ion at 37 °C for 4 h with 125 mM NaCl, 125 mM KCl, 20 μM EDTA, and 50 mM MOPS/KOH (pH 7.0 at 37 °C). Cleavage products were separated on 10% PAGE and quantified with a phosphorimager. The tests were carried out twice. Absolute errors are given. [b] K_a is based on the equilibrium: $[M(H_2O)_n]^{2+} \rightleftharpoons [M(H_2O)_{n-1}(OH)]^{+} + H^{+}$. pK_a is thus a measure of the acidity of a water molecule coordinated to a metal ion (or the basity of a metal-coordinated hydroxide ion, which decreases with increasing pK_a). Therefore, $M(H_2O)_n^{2+}$ is cited instead of M^{2+}.

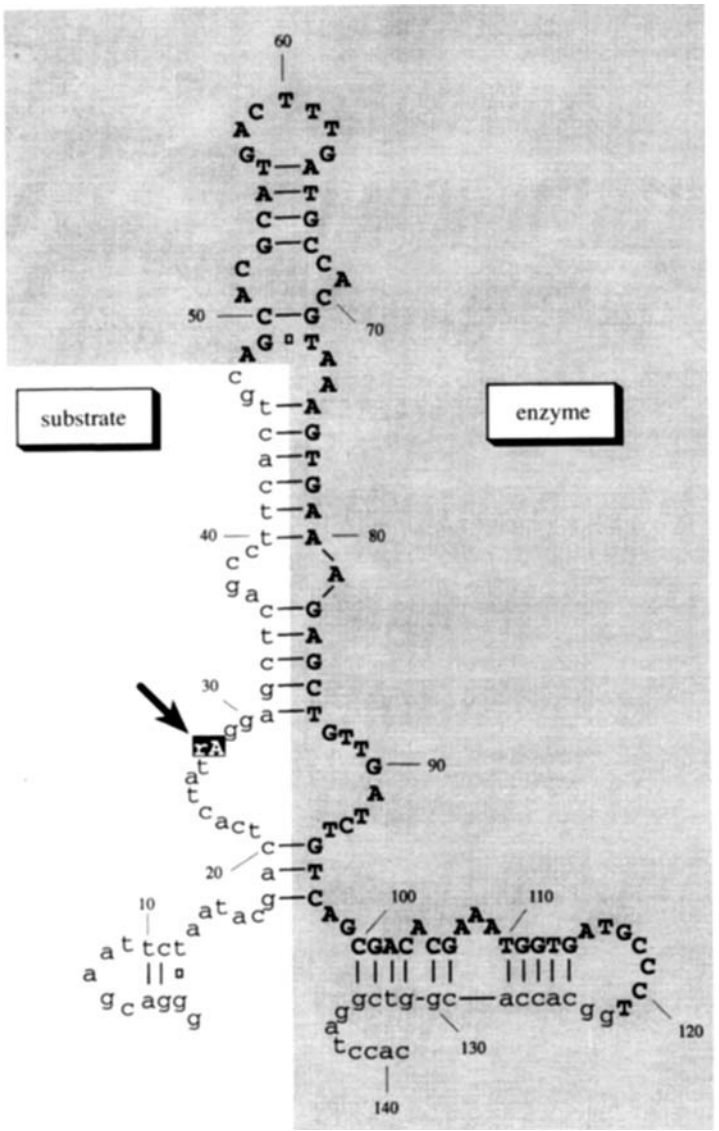

Fig. 1. a) Secondary structure of clone Mg5. The structure was proven by chemical modification analysis (data not shown). The 5'-primer binding site (in lowercase letters) is identical with the substrate. The defined rA cleavage site in this region is marked by an arrow. The enzyme consists of the randomized region (capital letters in boldface) and the primer binding site at the 3'-end (lowercase letters), both of which are printed on a gray background.

tem; the 47 nucleotide long, defined 5'-region with the rA cleavage site served as the substrate. The remaining 94 nucleotide enzyme contained the randomized region and the 3'-primer binding site. Like the intramolecular system, the cleavage efficiency of the intermolecular system was dependent on the concentrations of Mg^{2+} and Ca^{2+} ions (Fig. 2b). In analogy to similar catalyst systems,[9] the optimal metal ion concentration is much higher than in the intramolecular reaction. It is important to note, however, that in our system the values of the observed rate constants of the cleavage reaction are always lower with Mg^{2+} ions than with Ca^{2+} ions within the range of concentrations evaluated. When the pH of the buffer was increased while the other reaction conditions were left unchanged (10 mM Mg^{2+} or Ca^{2+}), the rate constants for the catalyzed hydrolysis increased (Fig. 3). This result clearly indicates the participitation of metal hydroxides in the reaction, particularly as an increase of the uncatalyzed hydrolysis under the same conditions could not be detected. Therefore, it seems reasonable to propose that catalysis in the presence of Ca^{2+} ions is more efficient owing to the more suitable positioning of this ion at the cleavage site, similar to special situations in the group I intron of *Tetrahymena*.[10] Alternatively, these results might indicate that the selection criterion is merely a favorable arrangement of the leaving group and the attacking nucleophile near the phosphodiester cleavage site[11] and that the divalent metal ion does not play any role initially. The metal ion could then serve as a Lewis acid or its hydroxide form could accelerate cleavage. It is known that Ca^{2+} ions can directly coordinate to ribose hydroxyl groups,[12] thereby contributing to the activation of the 2'-hydroxyl group of the sugar.

With substrate saturation, the intermolecular system shows the properties of a true enzyme–substrate complex (Table 3). At 10 mM concentration of the metal ion, the Michaelis–Menten constants K_M of the Mg^{2+}-dependent (5.7 μM) and the Ca^{2+}-dependent cleavage (6.4 μM) are on the same order of magnitude. The rate constants for Mg^{2+}- and Ca^{2+}-dependent cleavage ($k_{cat} = 0.01\ min^{-1}$ and $0.1\ min^{-1}$, respectively) differ significantly, by a factor of ten. However, in the Michaelis–Menten equation k_{cat} not only describes the rate of the chemical step but also that of the decomposition of the enzyme–product complex and other reaction parameters. So it still remains open to what extent the values of k_{cat} are influenced by the chemical step of the reaction—the hydrolysis of the phosphodiester bond. The mag-

Table 3. Michaelis–Menten parameters of the enzyme–substrate complex based on clone Mg5 (the same experimental conditions for both [a] and [b]).

M^{2+}	k_{cat} [min^{-1}]	K_M [μM]	k_{cat}/K_M [$M^{-1}\,min^{-1}$] [a]	$k_{cat}\,K_M$ [$M^{-1}\,min^{-1}$] [b]
Mg^{2+}	0.01	5.7	1.8×10^3	4.4×10^3
Ca^{2+}	0.1	6.4	1.6×10^4	3.4×10^4

[a] At substrate saturation; substrate concentrations: 0.1, 0.2, 0.5, 1, 2.5, 10, 20, and 50 μM; enzyme concentration: 0.1 μM. Both k_{cat} and K_M were determined by linearization in a Lineweaver–Burke plot. [b] Enzyme in excess over substrate. k_{cat}/K_M were determined at different enzyme concentrations (10, 20, 50, 100, 200, 500, and 1000 nM) and obtained by dividing pseudo-first order rate constants by the enzyme concentration. The calculated values were averaged for each metal ion. Substrate concentration: 1 nM.

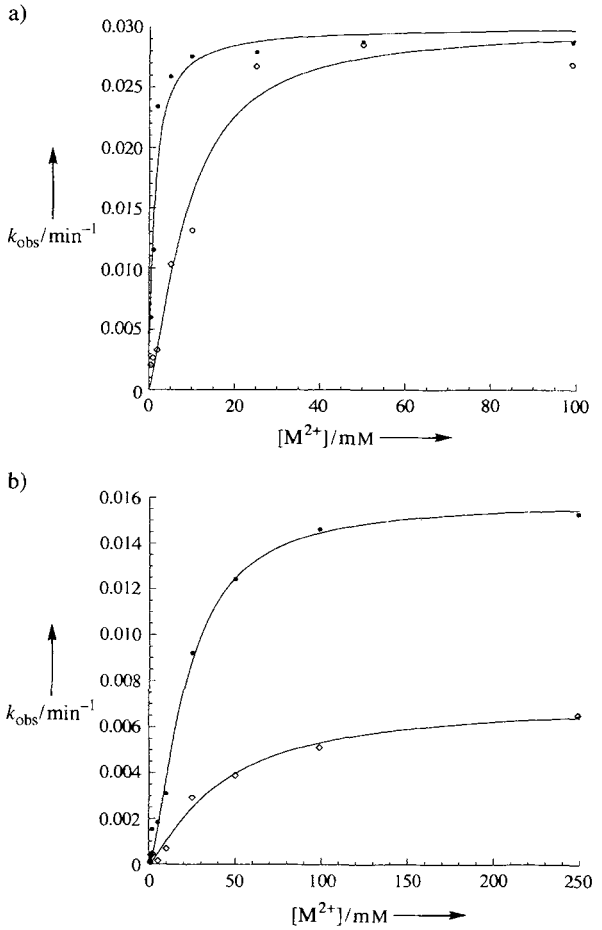

Fig. 2. Dependence of the cleavage activity on Mg^{2+} and Ca^{2+} concentrations: a) intramolecular reaction: clone Mg5 was amplified by PCR using primers **2a** and **3a** (see Experimental Procedure). 10 pmol of the purified PCR product was labeled at the 5'-end with [γ-^{32}P]-ATP (30 μCi) in 70 mM Tris-HCl (pH 7.6), 10 mM $MgCl_2$, and 5 mM dithiothretiol (DTT) using T4 polynucleotide kinase (NEB), and immobilized on streptavidin agarose. The labeled DNA strand was eluted by washing with 200 mM NaOH (300 μL) and precipitated with ethanol from 0.3 M NaOAc. After centrifugation and washing the DNA was resuspended in H_2O. Labeled single-stranded DNA with an activity of 150–200 cps was incubated at 37 °C with 250 mM NaCl, 250 mM KCl, 1 mM EDTA, 50 $\mu g mL^{-1}$ bovine serum albumin (BSA), 50 mM 2-(*N*-morpholino)propanesulfonic acid (MOPS)/KOH (pH 7.0 at 37 °C), and with 0.5, 1, 2, 5, 10, 25, 50, and 100 mM $MgCl_2$ ($\diamond$) or $CaCl_2$ ($\bullet$). Aliquots were taken after 0, 30, 60, 120, and 240 min, and the reaction was stopped by precipitation with ethanol. Hydrolysis products were separated on 10% polyacrylamide gel (PAGE) and quantified on a STORM 860 phosphorimager (Molecular Dynamics). Observed rate constants k_{obs} were determined by linear plots of the logarithm of substrate decay versus time. In the graph k_{obs} is plotted versus metal ion concentration. b) Intermolecular reaction: 1 nM substrate labeled at the 5'-end (prepared in analogy to a)) was incubated with 100 nM enzyme under the same conditions as described in a) with 0.5, 1, 2, 5, 10, 25, 50, 100, and 250 mM $MgCl_2$ ($\diamond$) and $CaCl_2$ ($\bullet$). Aliquots were taken after 0, 30, 60, 120, and 240 min, and the reaction was stopped by precipitation with ethanol. Analysis and quantification was as described in a). Observed rate constants k_{obs} were determined from the slope of the initial rates of substrate decay at the actual metal ion concentration. In the graph k_{obs} is plotted versus metal ion concentration.

nitudes of k_{cat}/K_M were confirmed by experiments under single-turnover conditions. Values were 4400 $M^{-1}min^{-1}$ (Mg^{2+}-dependent cleavage) and 34000 $M^{-1}min^{-1}$ (Ca^{2+}-dependent cleavage) (Table 3). Cleavage of a pure RNA substrate under the same reaction conditions was not observed.

The result of the selection described here is unexpected. Although the sequences of the selected library were not in contact with Ca^{2+} ions during the selection, cleavage with this cofactor is more efficient than with Mg^{2+} ions even though Mg^{2+} ions were present during selection, albeit in suboptimal concentrations, and even though the pK_a of Mg^{2+} is lower than that of Ca^{2+}. Despite the vast excess of histidine, the selected clones are histidine-independent. A possible explanation for this result might be that in a nucleic acid many more binding sites exist for metal ions than for non-metal cofactors. To select for cleavage induced by a non-metal cofactor it might therefore be more promising to use pools that contain a preformed binding pocket for the cofactor. In this way, the non-metal cofactor might be able to compete successfully against the high number of metal binding sites. Secondly, an amino acid might not be an optimal cofactor in such a system because of the electrostatic forces between the phosphate backbone of the nucleic acid and the negative charge of the α-carboxyl group. However, numerous in vitro selections for the binding of RNA or single-stranded DNA to various amino acids (for example arginine, citrulline, tryptophane, and even the hydrophobe valine) have demonstrated the ability of nucleic acids to recognize amino acids with high affinity and specificity.[13] It would be interesting to compare the results of the selection described here with those of a selection in which the cofactor is the uncharged imidazole or the positively charged histamine instead of the zwitterionic histidine.

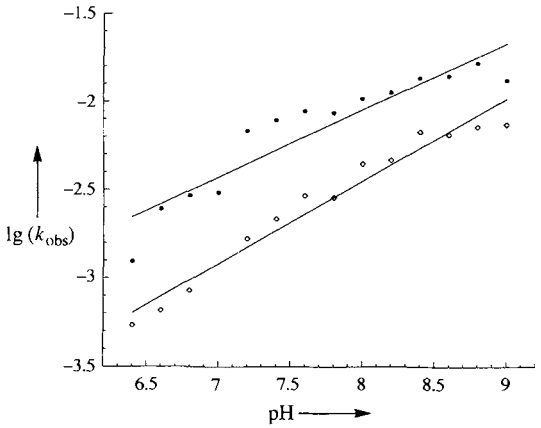

Fig. 3. Dependence of catalytic activity on pH: 1 nM substrate labeled at the 5'-end (see Fig. 2a) was incubated at 37 °C with 100 nM enzyme and 250 mM NaCl, 250 mM KCl, 1 mM EDTA, 50 $\mu g mL^{-1}$ BSA, and 50 mM buffer of the actual pH: 2-[*N*-morpholino]ethanesulfonic acid (MES)/KOH (pH 6.4, 6.6 at 37 °C), MOPS/KOH (pH 6.8, 7.0, 7.2, 7.4, 7.6, 7.8 at 37 °C), 3-[tris(hydroxymethyl)methylamino]-2-hydroxypropanesulfonic acid (TAPS)/KOH (pH 8.0, 8.2, 8.4, 8.6, 8.8, 9.0 at 37 °C). The incubation mixture contained 10 mM $MgCl_2$ ($\diamond$) or $CaCl_2$ ($\bullet$). Aliquots were taken after 0, 30, 60, 120, and 240 min, and the reaction was stopped by precipitation with ethanol (analysis and quantification as in Fig. 2a). Observed rate constants k_{obs} were determined from the slope of the initial rates of substrate decay at the actual metal ion concentration. In the graph $lg(k_{obs})$ is plotted versus pH.

Experimental Procedure

DNA library and oligonucleotides: The DNA library GGAGCTCAGC-CTTCACTGC—$(N)_{74}$—GGCACCACGGTCGGATCC (N = nucleotide), the oligonucleotides GGGACGAATTCTAATACGACTCACTATAGGAGCTCAGC-CTTCACTGC (**1**), biotin-GGGACGAATTCTAATACGACTCACTATrA (**2**), GTGGATCCGACCGTGGTGCC (**3**), and biotin-**3** (**3a**), and the DNA enzyme AGCACGCATGACTTTGATGCCACGTAAGTGAAAGAGCTGTTGATCTG-TCA GCGACACGAATGGTGATCCCTGGCACCACGGTCGGATCCAC were synthesized by solid-phase synthesis on a Millipore Expedite oligonucleotide synthesizer. The substrate 47 nucleotides long, GGGACGAATTCTAATACGACT-CACTATrAGGAGCTCAGCCTTCACTGC, was purchased from Eurogentec (Seraing, Belgium); oligonucleotide **2a** (same sequence as **2**, but lacking the biotin) was purchased from MWG Biotech (Ebersberg, Germany). The RNA substrate GGGACGAAUUCUAAUACGACUCACUAUAGGAGCUCAGCCUUCAC-UGC was transcribed in vitro from GCAGTGAAGGCTGAGCTCCTATAGT-GAGTCGTATTAGAATTCGTCCCTATAGTGAGTCGTATTAGAGCGC and GCGCTCTAATACGACTCACTATAGGGACGAATTC using T7 RNA polymerase.

Polymerase chain reaction (PCR): The library of random-sequence DNA was amplified by PCR (2 mL) with 800 pmol single-stranded DNA and 2 μM oligonucle-

otides **1** and **3** as primers, as well as 10 mM Tris-HCl (pH 8.3), 50 mM KCl, 1.5 mM $MgCl_2$, 0.03% polyoxyethylenesorbitan monolaurate (Tween 20), 0.001% gelatin, 200 μM of each dNTP, and 0.02 U μL^{-1} Taq DNA Polymerase, in five cycles at 94 °C for 1 min, 55 °C for 1 min, and 72 °C for 2 min. This PCR was followed by three cycles of PCR (20 mL) conducted under the same reaction conditions using 0.4 μM **2** and **3** as primers. Cycles of PCR were performed at 94 °C for 4 min, 55 °C for 7 min, and 72 °C for 7 min. During selection, eluted DNA was amplified first in 7–12 cycles of PCR (100 μL) using 0.2 μM **1** and **3**. Cycles of PCR were performed at 94 °C for 1 min, 55 °C for 1 min, and 72 °C for 2 min. A 10 μL sample of the reaction mixture was then subjected to 7–10 cycles of PCR (200 μL) with 1 μM **2** and **3**, and 10 μCi [α-^{32}P]-dCTP.

Received: July 17, 1996 [Z9339IE]
German version: *Angew. Chem.* **1996**, *108*, 2984–2988

Keywords: catalysis · DNA enzymes · in vitro selection · metalloenzymes · ribozymes

[1] a) S. C. Dahm, O. C. Uhlenbeck, *Biochemistry* **1991**, *30*, 9464; b) T. Pan, D. M. Long, O. C. Uhlenbeck in *The RNA-World* (Eds.: R. F. Gesteland, J. F. Atkins), Cold Spring Harbor Laboratory Press, New York, **1993**, p. 271; c) T. A. Steitz, J. A. Steitz, *Proc. Natl. Acad. Sci. USA* **1993**, *90*, 6498; d) L. G. Laing, T. C. Gluick, D. E. Draper, *J. Mol. Biol.* **1994**, *237*, 577; e) D. M. Long, F. J. LaRiviere, O. C. Uhlenbeck, *Biochemistry* **1995**, *34*, 14435; f) W. G. Scott, A. Klug, *Trends Biochem. Sci.* **1996**, *21*, 220.

[2] A. Wlodawer, R. Bott, L. Sjölin, *J. Biol. Chem.* **1982**, *257*, 1325.

[3] R. Breslow, *Acc. Chem. Res.* **1991**, *24*, 317; A. J. Kirby, R. E. Marriott, *J. Am. Chem. Soc.* **1995**, *117*, 833.

[4] M. A. Podyminogin, V. V. Vlassov, R. Giège, *Nucleic Acids Res.* **1993**, *21*, 5960.

[5] a) R. R. Breaker, G. F. Joyce, *Chem. Biol.* **1994**, *1*, 223; P. Burgstaller, M. Famulok, *Angew. Chem.* **1995**, *107*, 1303; *Angew. Chem. Int. Ed. Engl.* **1995**, *34*, 1189; b) R. R. Breaker, G. F. Joyce, *Chem. Biol.* **1995**, *2*, 655.

[6] A selection in which spermine replaced Mg^{2+} for stabilizing tertiary structures gave the same result.

[7] S. C. Dahm, W. B. Derrick, O. C. Uhlenbeck, *Biochemistry* **1993**, *32*, 13040.

[8] R. Rohatgi, D. P. Bartel, J. W. Szostak, *J. Am. Chem. Soc.* **1996**, *118*, 3332.

[9] S. E. Butcher, J. E. Heckman, J. M. Burke, *J. Biol. Chem.* **1995**, *270*, 29648.

[10] In the group I intron Ca^{2+} yields a different cleavage product than Mg^{2+} at pH 9 in the absence of a guanosine cofactor. a) B. Streicher, E. Westhof, R. Schroeder, *EMBO J.* **1996**, *15*, 2556; b) A variant of a group I intron in which Ca^{2+} can substitute for Mg^{2+} was isolated by in vitro evolution. N. Lehman, G. F. Joyce, *Nature* **1993**, *361*, 182.

[11] Situations of this kind were proven by a crystal structure of an RNA helix containing a single bulged adenosine residue. S. Portmann, S. Grimm, C. Workman, N. Usman, M. Egli, *Chem. Biol.* **1996**, *3*, 173.

[12] E. A. Brown, C. E. Bugg, *Acta Crystallogr. Sect. B* **1980**, *36*, 2597.

[13] a) M. Famulok, J. W. Szostak, *J. Am. Chem. Soc.* **1992**, *114*, 3990; b) G. J. Connell, M. Illangesekare, M. Yarus, *Biochemistry* **1993**, *32*, 5497; c) M. Famulok, *J. Am. Chem. Soc.* **1994**, *116*, 1698; d) I. Majerfeld, M. Yarus, *Nat. Struct. Biol.* **1994**, *1*, 267; e) K. Harada, A. D. Frankel, *EMBO J.* **1995**, *14*, 5798; f) A. Geiger, P. Burgstaller, H. von der Eltz, A. Roeder, M. Famulok, *Nucleic Acids Res.* **1996**, *24*, 1029; g) Y. Yang, M. Kochoyan, P. Burgstaller, E. Westhof, M. Famulok, *Science* **1996**, *274*, 1343.

A Planar [15]Metallacrown-5 That Selectively Binds the Uranyl Cation**

Ann J. Stemmler, Jeff W. Kampf, and Vincent L. Pecoraro*

One of the enduring legacies of the Cold War is the vast quantity of radioactive isotopes generated as a result of nuclear weapons development. Predictably, considerable current interest is focused on the sequestration of actinides as a means of safe waste disposal.[1] One criterion that must be satisfied in order for a molecule to be an effective agent for these purposes is that it selectively recognizes actinides. The specific recognition of ions often relies on the match between the architecture of the host molecule and the size and shape of the guest molecule.[2] Many organic ligands can bind actinides with high affinity.[3] However, while many examples exist of the preorganization of a macrocyclic compound to bind ions specifically,[4] few are selective for actinides in the presence of other hard ions such as Ca^{II}.[5, 6] We report here the rationale for the design of the first planar [15]metallacrown-5. This agent incorporates copper atoms in a macrocyclic ring and binds the uranyl ion in preference to Cu^{2+} and Ca^{2+}.

Metallacrowns are one class of molecular recognition agents that selectively bind cations or anions.[7–11] Their names are based on their similarity in structure and function to organic crown ethers. The first metallacrowns were synthesized with the ligand, salicylohydroxamic acid. This ligand binds a metal in a five-membered chelate ring with the hydroximate moiety and in a six-membered chelate ring with the iminophenolate moiety. These two chelate rings allow for a $[M-N-O]_n$ repeat unit that forms a cyclic structure orienting oxime oxygen donors toward the center of a cavity that is capable of binding cations. This synthetic strategy with salicylhydroximate (shi^{3-}) has been used to generate metallacryptate,[7b] [9]metallacrown-3,[9] [12]metallacrown-4,[7a, 7c, 7d, 7f, 10] and *nonplanar* [15]metallacrown-5[11] structural types. The metallacrowns are generally prepared in a one-step synthesis by stoichiometric addition of metal salt to the ligand in either DMF or methanol. The yield of crystalline product is usually between 60–90%.[7f]

The strategy we used to prepare an actinide-specific chelating agent required the synthesis of a ligand that forces five donor atoms into a plane while generating a cavity of sufficient size to accommodate a large, high-valent cation. Salicylohydroximate is poorly suited for this application, since the [15]metallacrown-5 isolated with this ligand contained a ring that wrapped around a central Mn^{2+} ion forming a three-dimensional cavity.[11] Salicylohydroxamic acid (H_3shi) is the perfect vehicle to achieve the 12-metallacrown-4 structural type, since the ligands are oriented at 90° angles to one another; however, it is not possible for higher denticity, planar rings to form with the shi^{3-} ligand. As shown in Figure 1, a ligand that enforces an angle of 108° is necessary in order to realize a planar, pentagonal ring. Picolinyl hydroximate, which forms two five-membered chelate rings, sat-

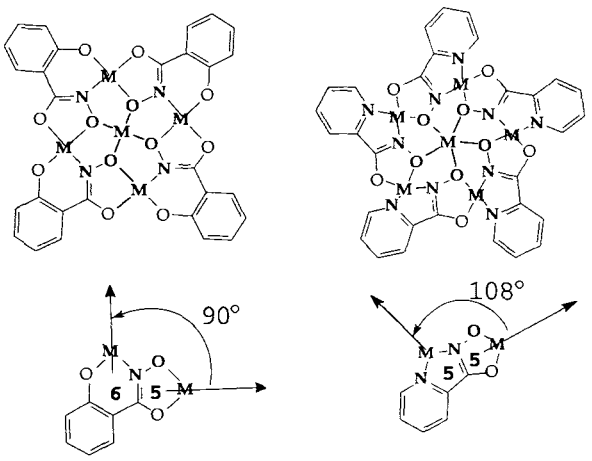

Fig. 1. Drawing of ligand/metal orientation in a [12]metallacrown-4 (12-MC-4) and a [15]metallacrown-5 (15-MC-5) complex. Bottom: the correspnding repeat units.

[*] Prof. V. L. Pecoraro, Dr. A. J. Stemmler, Dr. J. W. Kampf
Department of Chemistry
University of Michigan
Ann Arbor, MI 48109 (USA)
Fax: Int. code +(313)936-7628
e-mail: vlpeca umich.edu

[**] Note from the editor: According to IUPAC recommendations hydroxamic acid is retained as the name of a class, but the compounds are preferably named as *N*-hydroxy amides. The systematic name of the triply deprotonated ion salicylhydroximate (used throughout this communication) is thus *N*,2-dioxidobenzoyl amide.

isfies this requirement. A planar ring is realized with copper(II) as a ring metal, since it prefers square-planar coordination. Transition metal complexation by the central cavity of a [15]metallacrown-5 would be disfavored by the pentagonal coordination mode; however, there are several examples of the pentagonal-bipyramidal geometry for actinides.[4c]

The predicted, planar [15]metallacrown-5 structure was demonstrated with the facile synthesis[12] and subsequent crystal structure analysis of the uranyl complex **1** (Fig. 2).[13]

$[UO_2(15\text{-}MC_{Cu^{II}/N(pic)}\text{-}5)](NO_3)_2$ **1**

At the top of Figure 2 a top view of the molecule is illustrated; the metallacrown ring is outlined in bold. At the bottom is a side view of the molecule that shows the mostly planar structure of the [15]metallacrown-5. The slight deviations from planarity are due to solvent molecules, which are bound as fifth ligands to the copper ions and lead to a square-pyramidal geometry, thus buckling the ring slightly. Two nitrate ions are bound to two of the copper ions, and a DMF oxygen atom is bound to each of the other three copper ions. The uranyl ion resides in the plane of the five oxime oxygen donors.

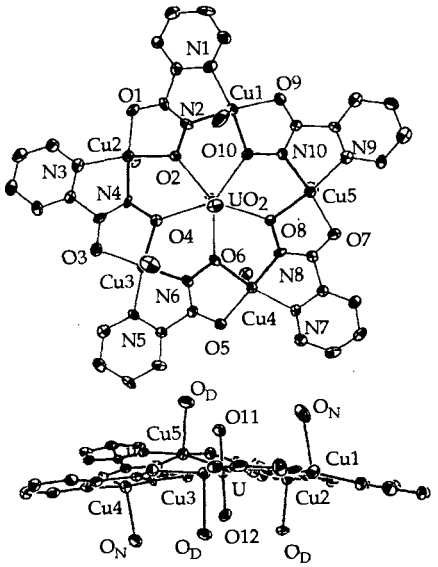

Fig. 2. Crystal structure of **1**. Top: full view. Bottom: side view. O_D = bound solvent (DMF), O_N = bound nitrate. Selected averaged bond lengths [Å] and angles [°]: U–O(11,12) 1.755(5), U–O(even) 2.402(5), Cu–O(even) 1.953(5), Cu–O(odd) 1.952(5), Cu–N(even) 1.924(6), Cu–N(odd) 2.002(6); O11-U-O12 179.2(3), O(11,12)-U-O(even) 90.0(2), O(even)-U-O(even, *cis*) 72.6(2).

Complex **1** retains its integrity in water. This conclusion is based upon mass spectral and NMR analyses. A clean electrospray ionization (ESI) mass spectrum is obtained in water with a base peak of the intact ion at *m/z* 634 ($[UO_2(15\text{-}MC_{Cu^{II}N(pic)}\text{-}5)]^{2+}$) and *m/z* 1329 ($[UO_2(NO_3)(15\text{-}MC_{Cu^{II}N(pic)}\text{-}5)]^{+}$). The four peaks from picoline protons are evident in the ^1H NMR spectrum at $\delta = +13.22, +40.97, +41.89$, and $+112$(br) in D_2O. The strong paramagnetic shift of the proton peaks can be attributed to the paramagnetism of the copper atoms. The UV/Vis spectrum of **1** in water has an absorption band at 614 nm ($\varepsilon = 397\,M^{-1}cm^{-1}$ per complex). The absorption varies linearly with the concentration of metallacrown, which demonstrates that the cluster does not decompose between 0.5 and 5 mM.

A similar metallacrown (**2**) was synthesized with calcium nitrate instead of uranyl nitrate. Complex **2** has an IR spectrum that closely resembles that of **1** except for the band at 920 cm^{-1}, which is assigned to the characteristic O=U=O stretch.[4b] It has two ESI-MS peaks, one at *m/z* 519 and one at *m/z* 1098 corresponding to $[Ca(15\text{-}MC_{Cu^{II}N(pic)}\text{-}5)]^{2+}$ and $[Ca(NO_3)(15\text{-}MC_{Cu^{II}N(pic)}\text{-}5)]^{+}\}$, respectively. The NMR spectrum showed peaks at $\delta = 10.92, 32.78, 31.79$, and 83(br) in D_2O. The UV/Vis spectrum also has a concentration-independent extinction coefficient ($\varepsilon = 420\,M^{-1}cm^{-1}$ per complex) at 569 nm. These data indicate that the basic [15]metallacrown-5 structure is retained with a different central cation.

Competition studies were undertaken to determine the selectivity of the planar [15]metallacrown-5 for these cations. NMR spectroscopy was used to monitor the addition of uranyl nitrate to **2** and calcium nitrate to **1**. After five days and a stoichiometric amount of uranyl nitrate, **2** is quantitatively converted into **1** in D_2O (Fig. 3). The reverse experiment showed no change in the NMR spectrum under the same conditions, or with a tenfold excess of Ca^{2+}, suggesting that the [15]metallacrown-5 thermodynamically prefers the uranyl ion over the calcium ion. Similarly, we have not found evidence for binding of Cu^{2+} ions in the central cavity, even when $U^{VI}O_2^{2+}$ or Ca^{II} are absent from the reaction mixture. In contrast, lanthanides can be sequestered by this metallacrown;[8] however, even these trivalent ions are displaced by UO_2^{2+} to form **1**.

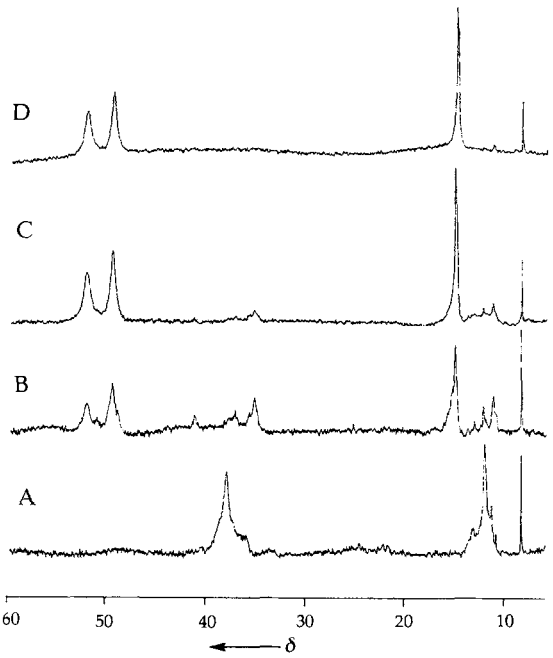

Fig. 3. ^1H NMR spectra of the conversion of **2** to **1** in D_2O. A: pure product **2**. B: **2** plus 1 equiv uranyl nitrate after 18 hours. C: same solution after 5 days. D: authentic sample of **1** dissolved in D_2O.

In summary, we have reported the preparation of a new class of molecules that can sequester UO_2^{2+} ion in aqueous solution. The [15]metallacrown-5 can be prepared in a one step synthesis with a 70% yield of crystalline product and is both stable and soluble in water. Furthermore, one can displace Ca^{2+} from the cavity of **2** with UO_2 to form **1** quantitatively. This synthetically simple and chemically stable molecule invites a new approach to sequestering actinides selectively.

Received: April 23, 1996 [Z9063IE]
German version: *Angew. Chem.* **1996**, *108*, 3011–3013

$[Ca(15\text{-}MC_{Cu^{II}N(pic)}\text{-}5)](NO_3)_2$ **2**

Keywords: crown compounds · metallacrown ethers · supramolecular chemistry · uranium compounds

[1] a) K. N. Raymond, W. L. Smith, F. L. Weitl, P. W. Durbin, S. Jones, K. Abu-Dari, S. R. Sofen, S. R. Cooper in *Lanthanide and Actinide Chemistry and Spectroscopy* (Ed.: N. M. Edelstein), *ACS Symp. Ser.* **1980**, *131*, 143; b) K. N. Raymond, G. E. Freeman, M. J. Kappel, *Inorg. Chim. Acta* **1984**, *94*, 193.
[2] a) J. M. Lehn, *Angew. Chem.* **1988**, *100*, 91; *Angew. Chem. Int. Ed. Engl.* **1988**, *27*, 89; b) D. J. Cram, *ibid.* **1986**, *98*, 1041 and **1986**, *25*, 1039.
[3] a) I. Tabushi, A. Yoshizawa, H. Mizuno, *J. Am. Chem. Soc.* **1985**, *107*, 4585; b) R. L. Lintvedt, W. E Lynch, J. K. Zehetmair, *Inorg. Chem.* **1990**, *29*, 3009–3013. c) D. E. Fenton, P. A. Vigato, *Chem. Soc. Rev.* **1988**, *17*, 69–90;
[4] a) T. S. Franczyk, K. R. Czerwinski, K. N. Raymond, *J. Am. Chem. Soc.* **1992**, *114*, 8138; b) M. Brighli, P. Fux, J. Lagrange, P. Lagrange, *Inorg. Chem.* **1985**, *24*, 80; c) A. Gül, Ö. Bekâroglu, *J. Chem. Soc. Dalton Trans.* **1983**, 2537; d) S. Can, Ö. Bekâroglu, *ibid.* **1988**, 2831.
[5] D. M. Roundhill, *Prog. Inorg. Chem.* **1995**, *43*, 571–574, and references therein.
[6] a) D. M. Rudevich, W. Stauthamer, W. Verboom, J. F. J. Engbersen, S. Harkema, D. Reinhoudt, *J. Am. Chem. Soc.* **1992**, *114*, 9671; b) A. K. Burrell, G. Hemmi, V. Lynch, J. L. Sessler, *ibid.* **1991**, *113*, 4690; c) J. L. Sessler, T. Mody, V. Lynch, *Inorg. Chem.* **1992**, *31*, 529.
[7] M. S. Lah, V. L. Pecoraro, *J. Am. Chem. Soc.* **1989**, *111*, 7258; b) M. S. Lah, B. R. Gibney, D. L. Tierney, J. E. Penner-Hahn, V. L. Pecoraro, *ibid.* **1993**, *115*, 5857; c) B. R. Gibney, H. Wang, J. W. Kampf, V. L. Pecoraro, *Inorg. Chem.*, in press; d) M. S. Lah, V. L. Pecoraro, *ibid.* **1991**, *30*, 878; e) A. J. Stemmler, J. W. Kampf, V. L. Pecoraro, *ibid.* **1995**, *34*, 2271; f) V. L. Pecoraro, A. J. Stemmler, B. P. Gibney, J. Bodwin, J. W. Kampf, H. Wang, *Prog. Inorg. Chem.*, in press.
[8] A. J. Stemmler, A. Barwinski, M. J. Baldwin, V. Young, Jr., V. L. Pecoraro, *J. Am. Chem. Soc.*, submitted.
[9] B. R. Gibney, A. J. Stemmler, S. Pilotek, J. W. Kampf, V. L. Pecoraro, *Inorg. Chem.* **1993**, *32*, 6008; b) V. L. Pecoraro, *Inorg. Chim. Acta* **1989**, *155*, 171; c) M. S. Lah, M. L. Kirk, W. Hatfield, V. L Pecoraro, *J. Chem. Soc. Chem. Commun.* **1989**, 1606.
[10] B. R. Gibney, J. W. Kampf, D. P. Kessissiglou, V. L. Pecoraro, *Inorg. Chem.* **1994**, *33*, 4840.
[11] D. P. Kessissoglou, J. W. Kampf, V. L. Pecoraro, *Polyhedron* **1994**, *13*, 1379–1391.
[12] This [15]metallacrown-5 was synthesized with $Cu(OAc)_2$ (0.40 g, 2 mmol) and picolinyl hydroxamic acid (0.27 g, 2 mmol) dissolved in dimethylformamide (DMF) followed by the addition of $UO_2(NO_3)_2$ (0.20 g, 0.4 mmol). A 69% yield of crystals of **1** was realized after vapor diffusion with ether. Compound **2** was synthesized by adding calcium nitrate (2.5 mmol) to a solution of $Cu(OAc)_2$ (2 mmol) and picolinyl hydroxamic acid (2 mmol) dissolved in DMF. A brown solid precipitated from solution after one week (47.5% yield). The brown precipitate turned green when dissolved in methanol or water.
[13] X-ray crystal structure determination of **1**: $C_{45}H_{55}Cu_5N_{17}O_{23}U$, $M_r = 1757.79$, triclinic, space group $P\bar{1}$ (no. 2), $a = 11.910(2)$, $b = 15.585(2)$, $c = 17.813(3)$, $\alpha = 85.780(10)$, $\beta = 70.490(10)°$, $\gamma = 71.980(10)°$, $V = 2962.1(8)$ Å^3, $Z = 2$; $\rho_{calcd} = 1.971$ g cm^{-3}; $2.55 < \theta < 24.99°$; crystal dimensions (mm), $0.18 \times 0.12 \times 0.10$; $Mo_{K\alpha}$ radiation $\lambda = 0.71073$ Å, $\mu = 45.80$ cm^{-1}; $T = 178(2)$ K; scan mode ω-2θ; Siemens R3 m/v diffractometer, equipped with LT-2. The structure was solved by direct methods and refined with the SHELXTL PLUS and SHELXL-93 program on a VAXStation 3500. Reflections collected 10412, 832 parameters used for the full-matrix, least-squares refinement on F^2, $R1 = 0.0889$, $wR2 = 0.0742$. Crystallographic data (excluding structure factors) for the structure reported in this paper have been deposited with the Cambridge Crystallographic Data Centre as supplementary publication no. CCDC-179-123. Copies of the data can be obtained free of charge on application to The Director, CCDC, 12 Union Road, Cambridge CB2 1EZ, UK (fax: int. code + (1223) 336-033; e-mail: teched@chemcrys.cam.ac.uk).

First Phenylene Polymers Linked by Sulfonium Groups

Eishun Tsuchida,* Kimihisa Yamamoto, Kenji Miyatake, and Yukio Nishimura

Arylsulfonium salts have been extensively used as photoactive cationic initiators[1–3] and for the photogeneration of protic acids in the area of lithographic resists (chemically amplified resists).[4] Polymeric sulfonium salts should also receive much attention as possible new materials. We were interested in whether the poly(phenylenesulfonium salt)s **1** could be synthesized even though the structure of the alternating phenylene rings and methylsulfonium groups is very simple and is estimated to be unstable due to the strong electron-withdrawing property of the sulfonium group. Until now, most known poly(arylenesulfonium salt)s, which were prepared by polymerization of methyl phenyl sulfoxide[5, 6] or by methylation or phenylation of poly(thiophenylene) (PPS) using methyl triflate or diphenyliodonium salts,[7] have a sulfonium substitution level below 50%.

We have already found and reported on the preparation of arylsulfonium salts with the sulfinate/acid system. For example, the reaction of sodium methanesulfinate with benzene (2:1 mol ratio) in trifluoromethanesulfonic acid gives methyldiphenylsulfonium trifluoromethanesulfonate in 92% yield.[8] This reaction should be applicable to the preparation of sulfonium-containing polymers. We report here on our successful preparation of a poly(methylsulfonio-1,4-phenylene salt) by the simple polymerization of benzene with sodium methanesulfinate in trifluoromethanesulfonic acid; the active electrophilic species in the polymerization is the dihydroxy(methyl)sulfonium cation.

Benzene was stirred with an equimolar amount of sodium methanesulfinate in trifluoromethanesulfonic acid under ambient conditions for 12 h (Scheme 1). A standard workup yielded

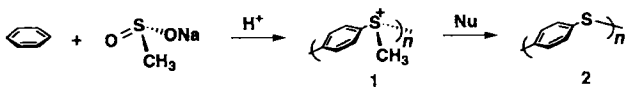

Scheme 1. Polymerization of benzene with sodium methanesulfinate in trifluoromethanesulfonic acid to yield **1** and **2**.

a white powder having the empirical formula $C_8H_7F_3O_3S_2$ in 42% yield.[9] A combination of NMR and IR spectra reveals the formation of poly(methylsulfonio-1,4-phenylene trifluoromethanesulfonate) (**1**). A singlet peak in range of aromatic phenyl protons is observed at $\delta = 8.30$ in the ^{1}H NMR spectrum (in CF_3COOD), which suggests that the phenylene units are symmetrically substituted at the 1- and 4-positions with electron-withdrawing groups. The peak is shifted to lower field due to the two sulfonium groups bound to the phenylene ring, and contrasts with the phenylene signals of the phenylene polymer with alternating sulfide and sulfonium groups, poly(methylsul-

[*] Prof. E. Tsuchida, Dr. K. Yamamoto, Dr. K. Miyatake, Dr. Y. Nishimura
Department of Polymer Chemistry
Advanced Research Institute for Science and Engineering
Waseda University, Tokyo 169 (Japan)
Fax: Int. code + (3) 3209-5522
e-mail: eishun@cfi.waseda.ac.jp

[**] This work was partially supported by the Ministry of Education, Science, Sports and Culture, Japan, (Grant-in-Aid for Scientific Research, Nos. 07651006 and 085410) and by the International Scientific Research Program, Joint Research No. 08044174, and funded by the Tokuyama Science Foundation.

 © VCH Verlagsgesellschaft mbH, D-69451 Weinheim, 1996 0570-0833/96/3523-2843 $ 15.00+.25/0

fonio-1,4-phenylenethio-1,4-phenylene trifluoromethanesulfonate), which appear as an AB quartet ($\delta = 7.34$, 7.32, 7.30, 7.28, in D_2SO_4).[5] The peak assigned to the methyl protons of **1** ($\delta = 3.85$) is also observed at lower field than that of poly(methylsulfonio-1,4-phenylenethio-1,4-phenylene trifluoromethanesulfonate) ($\delta = 3.12$). The two peaks at $\delta = 133.5$ and 134.6 in the ^{13}C NMR spectrum of **1**, which are assigned to aromatic carbons, further support the structure. The experimental and calculated chemical shifts were in very good agreement. Polymer **1** was also characterized by a COSY ^1H-^{13}C NMR spectrum (Fig. 1). The minor peaks at $\delta = 3.72$ and 7.62–7.88 in the ^1H NMR spectrum and at $\delta = 131.5$, 135.2, and 137.6 in the ^{13}C NMR spectrum are assigned to the end group of the polymer chain.[10] The degree of polymerization is estimated to be 15 based on the integration ratio in the ^1H NMR spectrum.

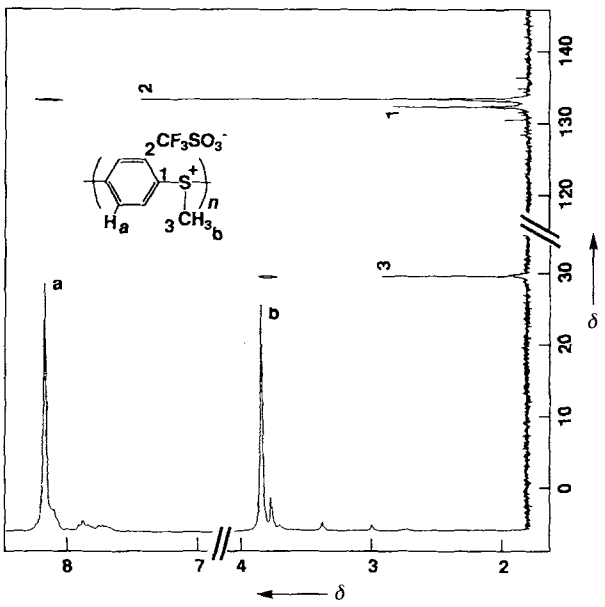

Fig. 1. COSY ^1H-^{13}C NMR spectrum of **1**.

The formation of the sulfonium bond was also confirmed by XPS investigations. The sulfur 2p core-level signals at 165.7 (S2p3/2) and 167.0 eV (S2p1/2) due to sulfonium are observed in the spectrum of **1**. The signals obviously differ from those of poly(thio-1,4-phenylene) (162.5 and 164.1 eV), which are assigned to the sulfide. The signals due to both sulfonium and sulfide groups are observed in the spectrum of poly(methylsulfonio-1,4-phenylenethio-1,4-phenylene trifluoromethanesulfonate). These results suggest that the polymer **1** consists of alternating methylsulfonium groups and 1,4-phenylene rings.

Polymer **1** is isolated as a white powder and is soluble in water, dimethyl sulfoxide (DMSO), trifluoroacetic acid, and sulfuric acid, however, it slowly demethylates in water and DMSO owing to the nucleophilic attack of the solvents. Compound **1** does not show any decomposition up to 135 °C in the solid state, and is stable in solution at up to 110 °C for over 12 h in trifluoromethanesulfonic acid, which was confirmed by thermogravimetric and ^1H NMR analyses. Polymer **1** can be quantitatively converted to poly(thio-1,4-phenylene) (PPS) (**2**) by demethylation using pyridine as a nucleophile. The IR spectrum of the resulting PPS is completely consistent with that of the previously reported PPS prepared by the polycondensation of *p*-dichlorobenzene with sodium sulfide. A single strong IR band at 820 cm^{-1} in the region of aromatic C–H out-of-plane bending supports the 1,4-linkage of the phenylene units in **2**. No absorption bands attributed to the methyl, sulfone, and sulfoxide groups are detected. High-temperature gel permeation chromatography analysis (210 °C, 1-chloronaphthalene) reveals the formation of PPS with a weight average molecular weight (M_w) of 2.7×10^3 (P_n (average degree of polymerization) = 25) and a number average molecular weight (M_n) of 1.9×10^3 ($P_n = 17$), which roughly agrees with the degree of polymerization determined from the ^1H NMR spectrum ($P_n = 15$). The melting temperature (T_m) of the PPS determined by differential scanning calorimetry (278 °C) is comparable to that of conventional PPS ($T_m = 282$ °C, $M_w = 18000$).

The sulfinate/acid polymerization system can be applied to other simple aromatic monomers. For example, the polymerization of *p*-xylene with sodium methanesulfinate produces poly(methylsulfonio-dimethylphenylene trifluoromethanesulfonate) (**5**) ($P_n = 10$) in 43% yield (Table 1). Polymer **5** is less hydrophilic than **1** because each phenyl ring has two methyl substituents. Consequently, **5** is soluble in acetone and acetonitrile but not in water. The electronic effect of two methyl substituents of **5** could also be confirmed by UV spectra; the λ_{max} of **5** (291 nm) is shifted bathochromically to compared to that of **1** (251 nm). Polymer **5** is consists mainly of 2,5-dimethyl-1,4-phenylene units; however, the splitting of the methyl and phenyl signals in the ^1H NMR spectrum indicates a small amount of the methylsulfonio-2,5-dimethyl-1,3-phenylene structure. Steric interactions between the methyl group and methylsulfonium group might explain why the molecular weight and the regularity of the 1,4-phenylene structure of **5** are lower than that of **1**. The polymerization of durene, which is more crowded than xylene or benzene, did not afford the corresponding sulfonium polymer. Arenes with a higher HOMO energy[11] than that of benzene (HOMO: −9.55 eV) are more effective for the polymerization. When diphenyl ether (HOMO: −9.27 eV) was polymerized with our system, the corresponding poly(sulfonium salt) **7** with a higher molecular weight ($P_n = 389$) was obtained. Diphenyl sulfide (HOMO = −9.31 eV), however, reacted to give the low molecular weight polymer **6** ($P_n = 16$) presumably due to side reactions such as the exchange[12] of the sulfide and the sulfonium species derived from sulfinic acid.

Table 1. Synthesis of poly(arylenesulfonium salt)s; the anions are trifluromethansulfonate ions in all cases.

Polymer		Yield [%]	P_n [a]	λ_{max} [nm]
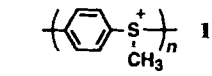	**1**	42	25	251
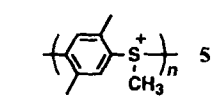	**5**	43	11	291
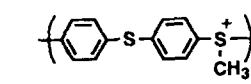	**6**	88	16	322
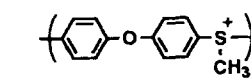	**7**	95	389	270

[a] Average degree of polymerization based on the M_w value determined by GPC.

We postulate that the polymerization proceeds by electrophilic aromatic substitution; the dihydroxy(methyl)sulfonium cation (**3**) formed by protonation of the oxygen atom of the sulfinyl group serves as the active species (Scheme 2).

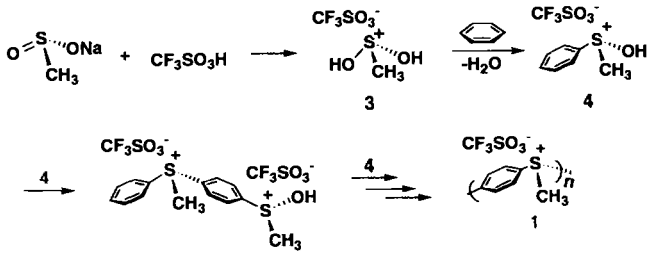

Scheme 2. Possible polymerization mechanism for the formation of **1**.

The formation of **3** requires a strong protic acid such as trifluoromethanesulfonic acid ($pK_a = -14.5$).[13] The sulfonium cation **3** reacts with a benzene unit to form a hydroxy(methyl)-phenylsulfonium cation (**4**), and successive electrophilic substitution results in the formation of poly(methylsulfonio-1,4-phenylene salt). It has not been clarified why electrophilic substitution of **4** occurs at the *para* position.[14] The electron-donating property of the lone pair of the sulfonium group through 3d–2p resonance might predominate over the electron-withdrawing effect in a strongly acidic media in analogy to electrophilic substitutions with aromatic sulfoxide.[15]

Experimental Procedure

1: (Typical polymerization procedure): To a solution of benzene (0.47 g, 6 mmol) in trifluoromethanesulfonic acid (5 mL) at 0 °C, was added anhydrous sodium methanesulfinate (0.41g, 4 mmol) slowly over 10 min. The mixture was stirred for 12 h at room temperature. The color of the reaction mixture gradually changed from pale yellow to orange. After the reaction, the mixture was poured into diethyl ether (200 mL) and a white powder precipitated. The precipitate was filtered and washed several times with diethyl ether and acetone, and then dried under high vacuum for 12 h to obtain **1** in 42% yield. Correct elemental analysis. ^{1}H NMR (400 MHz, CF_3COOD, 25 °C): $\delta = 3.85$ (s, 3H, CH_3), 8.30 (s, 4H, phenyl); ^{13}C NMR (100 MHz, CF_3COOD, 25 °C): $\delta = 28.9$ (s, CH_3, C1), 133.5 (s, phenyl, C2), 134.6 (s, phenyl, C3); IR (KBr): $\tilde{\nu}$ [cm^{-1}] = 3094 m, 3027 m, 2938 m, 1638 w, 1572 w, 1400 m, 1258 vs, 1159 s, 1032 s, 820 m, 639 s.

2: A solution of **1** (0.15 g) in pyridine (3 mL) was stirred at room temperature for several minutes until a white powder precipitated. The reaction mixture was stirred a further 30 min and then heated to 120 °C for 10 h. The reaction mixture was poured into 15% hydrochloric acid (200 mL), and the precipitate was washed several times with water, methanol, and chloroform. After drying under high vacuum for 12 h, a **2** was obtained as a white powder in 100% yield. Correct elemental analysis. IR (KBr): $\tilde{\nu}$ [cm^{-1}] = 2922 m, 2840 w, 1638 m, 1576 w, 1474 s, 1389 m, 1094 m, 1011 m, 820 s, 741 w, 691 vw.

5: As described for **1**, *p*-xylene and sodium methanesulfinate were polymerized. The usual workup gave **5** as a white powder in 43% yield. Correct elemental analysis. ^{1}H NMR (400 MHz, [D$_6$]acetone, 25 °C): $\delta = 2.24$–3.08 (m, 6H, CH_3), 3.87–4.00 (m, 3H, CH_3), 7.38–8.35 (m, 2H, phenyl); IR (KBr): $\tilde{\nu}$ [cm^{-1}] = 3023 w, 2932 w, 1709 w, 1636 m, 1451 m, 1260 vs, 1165 s, 1032 s, 880 w, 820 w, 640 s.

6: As described for **1**, diphenylsulfide and sodium methanesulfinate were polymerized. The usual workup gave a **6** as a white powder in 88% yield. Correct elemental analysis. ^{1}H NMR (400 MHz, [D$_6$]acetone, 25 °C): $\delta = 3.95$ (s, 3H, CH_3), 7.68–8.15 (m, 8H, phenyl); IR (KBr): $\tilde{\nu}$ [cm^{-1}] = 3086 w, 2930 w, 1570 m, 1478 m, 1260 vs, 1164 s, 1029 s, 818 w, 754 w, 639 s.

7: As described for **1**, diphenylether and sodium methanesulfinate were polymerized. The usual workup gave **7** as a white powder in 95% yield. Correct elemental analysis. ^{1}H NMR (400 MHz, CD_3CN, 25 °C): $\delta = 3.67$ (s, 3H, CH_3), 7.39, 7.42, 8.21, 8.23 (AB quartet, 8H, phenyl); ^{13}C NMR (400 MHz, CD_3CN, 25 °C): $\delta = 29.7$ (CH_3), 122.2, 122.5, 133.8, 161.6 (phenyl); IR (KBr): $\tilde{\nu}$ [cm^{-1}] = 3100 w, 2937 w, 1704 w, 1489 m, 1413 m, 1254 vs, 1168 s, 1035 s, 876 w, 856 w, 835 w, 640 s.

Received: June 10, 1996 [Z 9203 1E]
German version: *Angew. Chem.* **1996**, *108*, 3005–3008

Keywords: electrophilic substitutions · polymers · sulfur compounds · sulfinic acids · sulfonium ions

[1] J. V. Crivello, *Makromol. Chem. Macromol. Symp.* **1988**, *13/14*, 145.
[2] C. G. Willson, M. J. Bowden, *CHEMTECH* **1989**, *19*, 182.
[3] W. R. Watt, *UV Curing: Science and Technology, Vol. II*, Technology Marketing Corp., Norwalk, CT, **1985**, p. 247.
[4] K. E. Uhrich, E. Reichmanis, S. A. Heffner, J. M. Kometani, O. Nalamasu, *Chem. Mater.* **1994**, *6*, 287.
[5] K. Yamamoto, E. Shouji, H. Nishide, E. Tsuchida, *J. Am. Chem. Soc.* **1993**, *115*, 5819.
[6] E. Tsuchida, E. Shouji, K. Yamamoto, *Macromolecules* **1993**, *26*, 7144.
[7] B. M. Novak, E. Hagen, S. Hoff, A. Viswanathan, *Macromolecules* **1994**, *27*, 1985.
[8] K. Yamamoto, K. Miyatake, Y. Nishimura, E. Tsuchida, *Chem. Comm.* **1996**, 2101.
[9] The other product is the dimer of methyldiphenylsulfonium trifluoromethanesulfonate.
[10] Another small peak observed at $\delta = 3.39$ in ^{1}H NMR spectrum is attributed to methyl proton of methanol, which is formed by the reaction of methylsulfonium group with water.
[11] HOMO (highest occupied molecular orbital) energies were calculated by the semiempirical method PM3 (MOPAC Version 6.00) using the keyword subroutine ENPART. An optimized structure was obtained using the keyword subroutine PULAY. PM3 calculations were performed on a Fujitsu VP2200 super computer.
[12] E. Tsuchida, K. Yamamoto, H. Nishide, S. Yoshida, M. Jikei, *Macromolecules* **1990**, *23*, 2101.
[13] Actually, the reaction did not proceed in sulfuric acid ($pK_a = -11.9$) and methanesulfonic acid ($pK_a = -8.2$).
[14] Nitration of dimethylphenylsulfonium cation occurs preferentially at the *meta* position. See: a) H. M. Gilow, G. L. Walker, *J. Org. Chem.* **1967**, *32*, 2580; b) H. M. Gilow, M. De Shazo, W. C. Van Cheave, *J. Org. Chem.* **1971**, *36*, 1745.
[15] G. Leandri, A. Mangini, R. Posserini, *J. Chem. Soc.* **1952**, 1386.

Vinyl Glycosides in Oligosaccharide Synthesis: A Strategy for the Preparation of Trisaccharide Libraries Based on Latent-Active Glycosylation**

Geert-Jan Boons,* Barbra Heskamp, and Floris Hout

Glycoconjugates are involved in many different biological processes, and (oligo)saccharides may provide lead compounds for drug development.[1] Recently, the generation of "chemical libraries" by combinatorial chemistry methods has received considerable interest, since these libraries are potential sources of new leads for drug discovery.[2] Combinatorial chemistry has been developed mainly for the preparation of peptide, nucleic acid, and small-molecule libraries,[2] and only a very few reports deal with combinatorial carbohydrate chemistry.[3, 4] The development of combinatorial carbohydrate chemistry is complicated by several factors,[5] the most important being the number of functionalities and the polyvalent nature of carbohydrates and the lack of a general method for forming glycosidic linkages.[6]

Recently, a random glycosylation strategy was reported for the preparation of saccharide libraries.[4] Although this strategy avoids extensive protecting group manipulations, the resulting library is not well-defined and identification of an active com-

[*] Dr. G.-J. Boons, Dr. B. Heskamp, F. Hout
School of Chemistry, The University of Birmingham
Edgbaston, Birmingham B15 2TT (UK)
Fax: Int. code +(121)414-4403
e-mail: gjboons@chemwww.bham.ac.uk

[**] Vinyl Glycosides in Oligosaccharide Synthesis, Part 3. Part 2: ref. [7b]. Financial support for this project was provided by the BBSRC (Biotechnical and Biological Sciences Research Council.

pound from such a library may be troublesome. A key element for the successful construction of a well-defined carbohydrate-based library is a technique that enables the rapid generation of building blocks that can be assembled in a controlled and combinatorial fashion.[5] We report here an efficient method for the synthesis of trisaccharide libraries, which relies on a known latent-active glycosylation strategy[7] and meets the requirements discussed above.

As illustrated in Scheme 1, the efficiency of latent-active glycosylation is based on the possibility of preparing a glycosyl donor and acceptor from a common building block. For example, removal of the acetyl protecting group of compound **1**

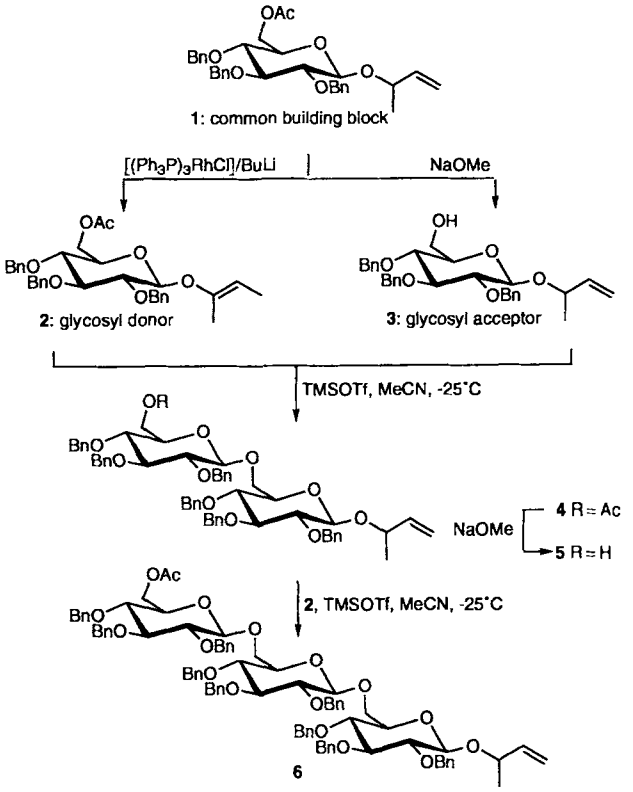

Scheme 1. TMSOTf = $Me_3SiOSO_2CF_3$.

gave glycosyl acceptor **3** and isomerization of the anomeric allyl ether function of **1** yielded the substituted vinyl glycosyl donor **2**. Glycosyl donor **2** was coupled with acceptor **3** in the presence of trimethylsilyl trifluoromethanesulfonate (TMSOTf) to give the β-linked dimer **4** in excellent yield (89%, $\alpha/\beta = 1/20$). Disaccharide **4** can be converted into a glycosyl acceptor by removing the acetyl protecting group and into a glycosyl donor by isomerizing the allyl moiety. These compounds can be used in oligosaccharide synthesis; for example, coupling of compound **5** with **2** gave trisaccharide **6**.

We envisaged that the allyl–vinyl glycosylation protocol would provide a powerful tool for the preparation of oligosaccharide libraries. For example, four allyl glycosyl building blocks ($B^{1\rightarrow4}$, e.g. **1**, see Schemes 1 and 2) can be converted into four vinyl glycosyl donors ($D^{1\rightarrow4}$, e.g. **2**) and four allyl glycosyl acceptors ($A^{1\rightarrow4}$, e.g. **3**). In individual glycosylations, each donor can be coupled with each acceptor to give 32 disaccharides as 16 mixtures of anomers ($D^{1\rightarrow4}A^{1\rightarrow4}$, e.g. **4**),[8] which can be purified and identified by conventional methods. Next, the disaccharides can be mixed; removal of the acetyl group of the saccharides will give a mixture of glycosyl acceptors. The

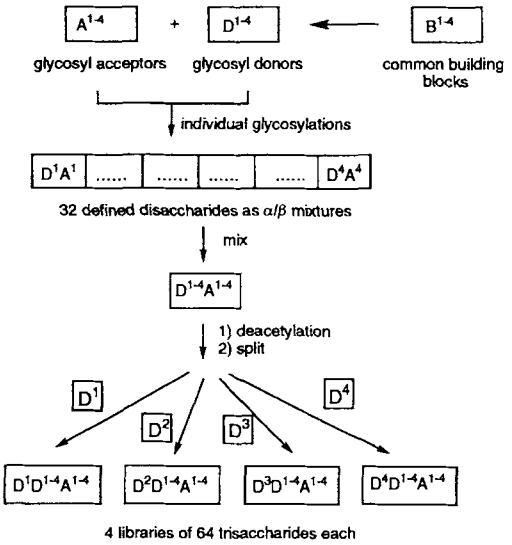

Scheme 2.

pool of compounds can be split, and in combinatorial steps each pool of glycosyl acceptors can be coupled with a particular glycosyl donor ($D^{1\rightarrow4}$), resulting in four libraries of 64 trisaccharides each ($D^1D^{1\rightarrow4}A^{1\rightarrow4}$, $D^2D^{1\rightarrow4}A^{1\rightarrow4}$, $D^3D^{1\rightarrow4}A^{1\rightarrow4}$, and $D^4D^{1\rightarrow4}A^{1\rightarrow4}$). Thus, in a minimum number of synthetic steps, four building blocks can in principle be converted into 256 trisaccharides. It should be noted that the reactions are performed in solution and since an excess of reagents is required, the libraries need to be purified. Size-exclusion chromatography is envisaged as the best means, since this purification method relies on the fact that all the saccharides in the library have very similar molecular weights. The purified libraries can be characterized by a combination of mass spectrometry[9] and monosaccharide composition analysis.[10] To verify the proposed strategy, a relatively small library of 20 trisaccharides[11] has been prepared.

In the first stage of the synthetic strategy, the allyl glycosyl building blocks **7a** and **10a** were converted into the vinyl glycosyl donors **7b** and **10b** by isomerization with [$(Ph_3P)_3$-RhCl]/BuLi[12] and the allyl glycosyl acceptors **7c**–**10c** were

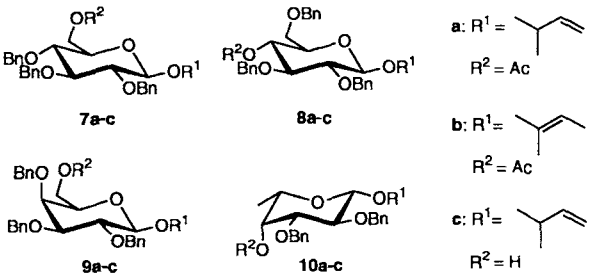

obtained by removal of the acetyl protecting group from compounds **7a**–**10a**. Subsequently, the disaccharides **11**–**15** were prepared by coupling the appropriate donors and acceptors. The glycosylation reactions were performed at room temperature in acetonitrile and promoted by a catalytic amount of TMSOTf. Under these conditions,[8] each disaccharide was obtained as a mixture of anomers ($\alpha/\beta \approx 1/1$, yields in excess of 70%). Next, samples from the five disaccharides (α/β mixtures) were combined (library **16**); removal of the acetyl protecting group gave a pool of disaccharide acceptors (library **17**) (Scheme 3). In a combinatorial fashion, the vinyl glycosyl donor

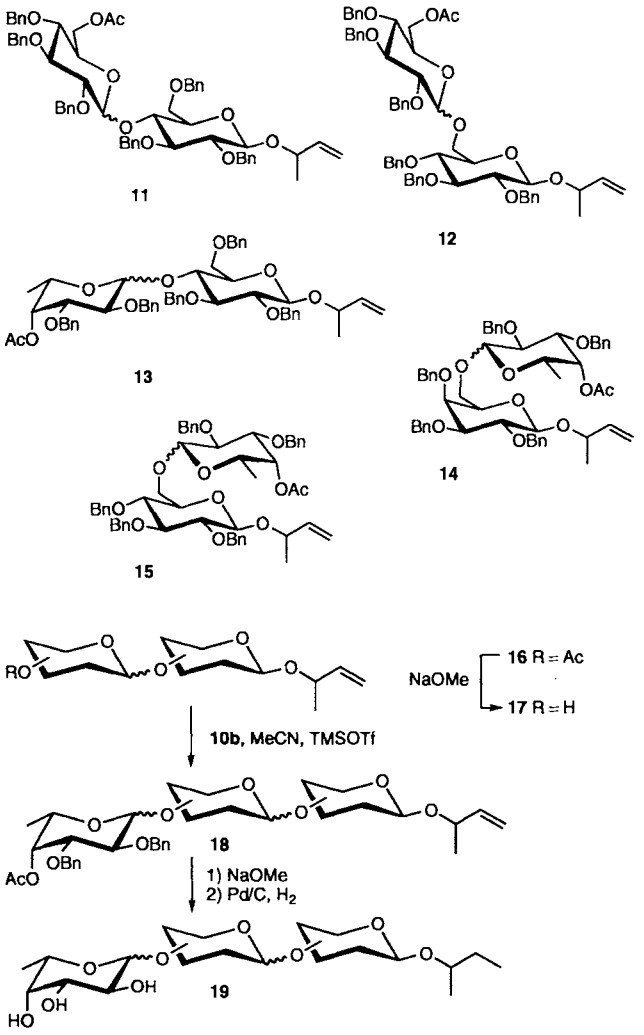

Scheme 3.

10b was coupled with the acceptor pool **17** to give a fully protected trisaccharide library of 20 different compounds (**18**). The reaction was performed under standard conditions using an excess of glycosyl donor (2 equiv). The fast atom bombardment (FAB) mass spectrum of the crude reaction mixture indicated that no disaccharides were present and that trisaccharides had formed.[13] Also a substantial amount of unreacted donor was detected. Library **18** was purified by LH-20 gel filtration column chromatography, and the FAB mass spectra of appropriate fractions showed the presence of only trisaccharides. Finally, the protecting groups were removed by treatment with base followed by hydrogenation over Pd/C to give library **19**.[14] Under these conditions, the allyl moieties at the reducing end of the saccharides were converted into isobutyl groups. Alternatively, the allyl moieties can be removed easily by isomerization and acid-mediated cleavage.

Since formation of the glycosidic bond is not equally successful in every case, additional quality control is required and therefore a monosaccharide compositional analysis was performed. Thus, a portion of the trisaccharide library was treated with aqueous trifluoracetic acid (2 M solution) at 100 °C for 4 h. Analysis of the resulting mixture of monosaccharides on a Dionex HPLC system with a PA1 column and pulsed amperometric detection (PAD)[15] showed that glucose, galactose, and fucose were present in approximately the required ratio.[16]

The strategy described here for the preparation of saccharide libraries is very efficient, and a small number of building blocks is employed to generate a relatively large number of trisaccharides. Furthermore, the difficult stereoselective formation of glycosides is avoided, and relatively "pure" mixtures of compounds have been obtained. These aspects are of particular importance when an active compound is present in the library. The structure of such a compound can be determined by a deconvolution approach, which has to proceed through iterative resyntheses.[2] The required sublibraries can be prepared efficiently from the previously synthesized mono- and disaccharides. In this respect, it is important to note that no general protocols for the sequencing of oligosaccharides are available. At present, the libraries described here are being screened, and the results obtained will be published in due course.

Received: June 17, 1996
Revised version: August 5, 1996 [Z9236IE]
German version: *Angew. Chem.* **1996**, *106*, 3053–3056

Keywords: combinatorial chemistry · compound libraries · glycosylations · oligosaccharides

[1] a) A. Varki, *Glycobiology*, **1993**, *3*, 97; b) R. A. Dwek, *Chem. Rev.* **1996**, *96*, 683.
[2] a) M. A. Gallop, R. W. Barrett, W. J. Dower, S. P. A. Fodor, E. M. Gordon, *J. Med. Chem.* **1994**, *37*, 1233; b) M. A. Gallop, R. W. Barrett, W. J. Dower, S. P. A. Fodor, E. M. Gordon, *Med. Chem.* **1994**, *37*, 1385; c) N. K. Terrett, M. Gardner, D. Gordon, R. J. Kobylecki, J. Steele, *Tetrahedron* **1995**, *51*, 8135.
[3] In this paper we use the term combinatorial carbohydrate chemistry to describe the combinatorial synthesis of oligosaccharides. Other authors have employed the same term for the preparation of modified monosaccharide libaries: M. Goebel, I. Ugi, *Tetrahedron Lett.* **1995**, *36*, 6043.
[4] O. Kanie, F. Barresi, Y. Ding, J. Labbe, A. Otter, L. S. Forsberg, B. Ernst, O. Hindsgaul, *Angew. Chem.* **1995**, *107*, 2912; *Angew. Chem. Int. Ed. Engl.* **1995**, *34*, 2720.
[5] M. J. Sofia, *Drugs Discovery Today* **1996**, *1*, 27.
[6] a) H. Paulsen, *Angew. Chem. 1982, 94*, 184; *Angew. Chem. Int. Ed. Engl.* **1982**, *21*, 155; b) R. R. Schmidt, *ibid.* **1986**, *98*, 213 and **1986**, *25*, 212; c) B. Fraser-Reid, U. E. Udodong, Z. Wu, H. Ottoson, J. R. Merritt, S. Rao, C. Roberts, R. Madsen, *Synlett*, **1992**, *12*, 927; d) P. Fugedi, P. J. Garegg, H. Löhn, T. Norberg, *Glycoconjugate J.* **1987**, *4*, 97; e) K. Toshima, K. Tatsuta, *Chem. Rev.* **1993**, *93* 1503; f) G. J. Boons, *Tetrahedron*, **1996**, *52*, 1095.
[7] a) G. J. Boons, S. Isles, *Tetrahedron Lett.* **1994**, *35*, 3593; b) G. J. Boons, S. Isles, *J. Org. Chem.* **1996**, 61, 4262–4271.
[8] When a glycosylation is performed in acetonitrile at low temperature mainly the β-anomer is obtained. a) J. Pougny P, Sinaÿ, *Tetrahedron Lett.* **1976**, 4073; b) R. U. Lemieux, R. M. Ratcliffe, *Can. J. Chem.*, **1979**, *57*, 1244; c) R. R. Schmidt, J. Michel, *J. Carbohydr. Chem.* **1985**, *1*, 441; d) A. J. Rattcliffe, B. Fraser-Reid, *J. Chem. Soc. Perkin Trans 1*, **1990**, 747; e) Y. D. Vankar, P. S. Vankar, M. Behrendt, R. R. Schmidt, *Tetrahedron Lett.* **1991**, *47*, 9985. This anomeric selectivity is lost when such a reaction is performed at ambient temperature. In individual glycosylations, the disaccharides **12**–**15** were fucosylated, and as expected, each glycosidic linkage was formed as a mixture of anomers. Apart from the data presented here, we have performed many other glycosylations under these conditions and in each case mixtures of anomers have been obtained (unpublished data).
[9] J. W. Metzger, K. H. Wiesmüller, V. Gnau, J. Brunjes, G. Jung, *Angew. Chem.* **1993**, *105*, 901; *Angew. Chem. Int. Ed. Engl.* **1993**, *32*, 894.
[10] M. R. Hardy, R. R. Towdend, Y. C. Lee, *Anal. Biochem.* **1988**, *170*, 54.
[11] The prepared library has a high fucose content and consists of trisaccharides with two different masses (see ref. [13]).
[12] G. J. Boons, S. Isles, A. Burton, *Chem Commun.* **1996**, 141.
[13] Peaks were observed at *m/z* 1221 and 1327 ($[M+Na]^+$), corresponding to trisaccharides with two and one fucose units, respectively. Peaks arising from the related disaccharides at *m/z* 872 and 978 were not detected.
[14] In the FAB mass spectrum the expected peaks were present at *m/z* 551 and 567 ($[M+Na]^+$).
[15] See Dionex technical note no. 20.
[16] Expected product ratios Fuc/Glc/Gal: 1.0/0.8/0.15; found: 1.0/0.9/0.2. The disaccharide library was prepared from equimolar amounts of disaccharides.

Unusual Regioselectivity in the Reaction of Allyl- or Allenylpropargyltitanium Compounds with Carbonyl Compounds: An Efficient Synthesis of Alkylidenecyclopropane Derivatives

Aleksandr Kasatkin and Fumie Sato*

Recently, we have developed a highly efficient and practical procedure for preparation of allyltitanium compounds by the reaction of allylic substrates, including carbonates, with [(η^2-propene)Ti(O*i*Pr)$_2$] (**1**), which is readily generated from [Ti(O*i*Pr)$_4$] and two equivalents of *i*PrMgBr.[1] Allyltitanium compounds, prepared in this way or by transmetalation using organolithium or -magnesium compounds,[2] react with aldehydes exclusively at the most substituted allylic carbon to afford the "branched" addition product **2** (Scheme 1). This regiochemistry can be explained by the preference of the primary titanium derivative **3** over the more congested intermediate **4** and its reaction with aldehydes through a six-membered transition state.[3] However, the substituent R^1 is a functional group containing a heteroatom that can strongly coordinate to titanium, the equilibrium may be shifted in favor of the more hindered regioisomer **4**, thus providing the "terminal" addition product **5** by the reaction with aldehydes.[4, 5]

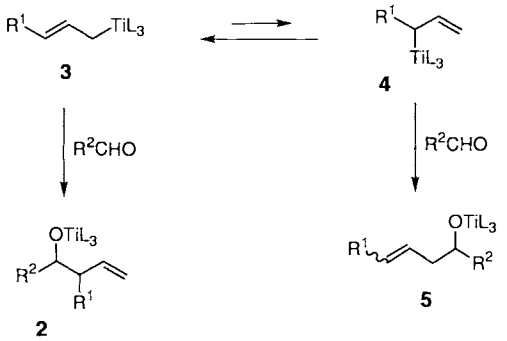

Scheme 1. Synthesis of **2** and **5**.

We postulated that ring strain might be another factor for controlling the equilibrium between **3** and **4**. Thus, we anticipated that the allyltitanium compound generated from **1** and the ethyl carbonate derivative (**6**) of 1-vinylcyclopropanol[6] would exist mostly as the tertiary titanium derivative **7** but not as the primary regioisomer **8** having the strained alkylidenecyclopropane fragment[8] (Scheme 2). The subsequent reaction with aldehydes, therefore, would result in alkylidenecyclopropanes **9** ("terminal" adducts), which are widely employed starting materials or intermediates in organic synthesis.[9]

Our assumption proved to be correct. The reaction of **1** with the carbonate **6** followed by treatment with EtCHO led to the alkylidenecyclopropane **9a** in high yield and the regioisomeric vinylcyclopropane **10a** in only 6% yield (Table 1, entry 1). Similar results were obtained when PhCHO and Me$_2$CO were used instead of EtCHO (**9** was the main product in both cases), although the regioselectivity was somewhat dependent on the nature of the carbonyl electrophile (entries 2 and 3).[10]

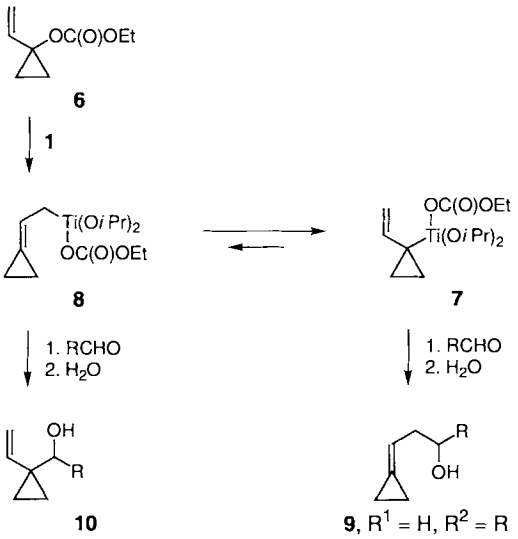

Scheme 2. Synthesis of **9** and **10**.

Table 1. Synthesis of **9**, **10**, **16**, and **17** [a].

Entry	Carbonate	Carbonyl cmpd.	Products, regioselectivity [%] [b]	Yield [%] [c]
1	**6**	EtCHO	**9a** (R^1 = H, R^2 = Et), 94; **10a**, 6	76
2	**6**	PhCHO	**9b** (R^1 = H, R^2 = Ph), 80; **10b**, 20	84
3	**6**	Me_2CO	**9c** (R^1 = R^2 = Me), >97	40
4	**11**	EtCHO	**12**, >97	65
5	**13a**	PhCHO	**16a** (R^1 = R^2 = Ph), 93; **17a**, 7	62
6	**13a**	EtCHO	**16b** (R^1 = Ph, R^2 = Et), >97	65
7	**13b**	EtCHO	**16c** (R^1 = Hex, R^2 = Et), >97	74
8	**13b**	CH_2O [d]	**16d** (R^1 = Hex, R^2 = H), >97	80
9	**13c**	EtCHO	**16e** (R^1 = Me_3Si, R^2 = Et), 74; **17e**, 26	45

[a] Titanium reagents were generated from 2.0 equiv [Ti(O*i*Pr)$_4$] and 4.0 equiv *i*PrMgCl in Et$_2$O at -40 to -45 °C (1 h); then 2.0 equiv carbonyl compound was added and the reaction mixture was stirred at -40 to -45 °C for 1 h. [b] According to ^{1}H NMR data of isolated regioisomeric mixtures. [c] Yields of isolated products based on starting carbonates. [d] Et$_2$O solution of monomeric CH_2O prepared by thermolysis of paraformaldehyde was used.

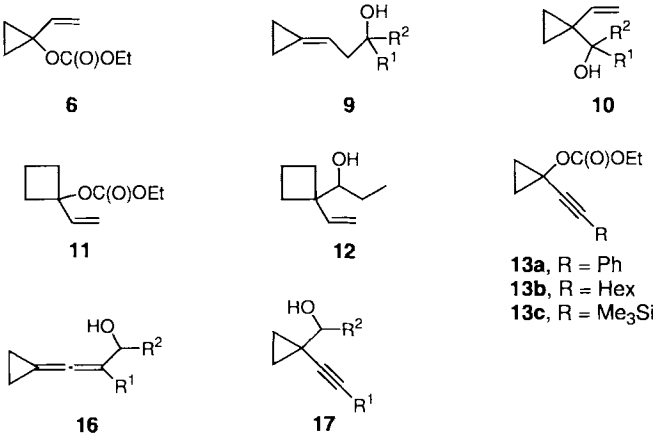

The fact that the reaction of **1** with ethyl 1-vinylcyclobutyl carbonate (**11**) (the carbonate derivative of vinylcyclobutanol), followed by treatment with EtCHO afforded exclusively the vinylcyclobutane **12** (the usual "branched" adduct) strongly demonstrates the principal role of the alkylidenecyclopropane

[*] Prof. Dr. F. Sato, Dr. A. Kasatkin[+]
Department of Biomolecular Engineering, Tokyo Institute of Technology
4259 Nagatsuta-cho, Midori-ku, Yokohama, Kanagawa 226 (Japan)
Fax: Int. code +(45)924-5826
e-mail: fsato@bio.titech.ac.jp
[+] On leave from the Institute of Organic Chemistry, Ufa Research Center, Russian Academy of Science.

strain in controlling the regiochemistry observed here (Table 1, entry 4).

The reaction of **1** with secondary or tertiary propargylic carbonates has been shown to provide allenyltitanium compounds which, in turn, react with aldehydes to give homopropargyl alcohols.[11] However, the results obtained by the reaction of **1** with **6** strongly suggested that the reaction with carbonate derivatives **13** of 1-alkynylcyclopropanols[6] would afford the propargyltitanium compounds **14** rather than the more strained allenyltitaniums **15** as shown in Scheme 3.[12] Thus, the subsequent treatment with aldehydes would give the allenic cyclopropanes **16**, which are of synthetic interest but are not readily available by other methods.[13] As expected, the reaction of **1** with the ethyl carbonate derivative **13a** of 1-(phenylethynyl)cyclopropanol followed by addition of PhCHO led primarily to the allenic cyclopropane **16a** with only 7% yield of the corresponding regioisomeric alkynylcyclopropane **17a** (Table 1, entry 5). Similarly, the treatment of the titanium reagents generated from the carbonates **13a–c** with EtCHO and/or CH_2O afforded **16** exclusively (entries 6–8) or predominantly (entry 9).[14]

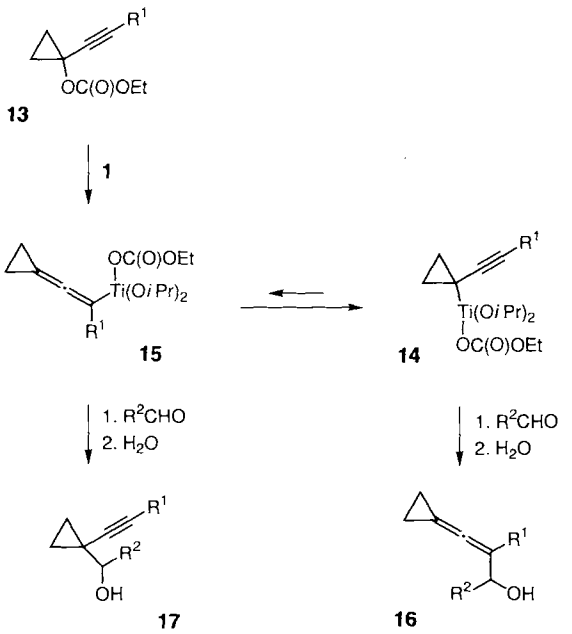

Scheme 3. Synthesis of **16** and **17**.

Experimental Procedure

The following procedure for preparation of **9a** and **10a** (entry 1 in Table 1) is representative: To a solution of $[Ti(OiPr)_4]$ (284 mg, 1.00 mmol) and **6** (156 mg, 0.50 mmol) in Et_2O (7.5 mL) was added dropwise *i*PrMgCl (1.35 mL, 1.48 M in Et_2O, 2.00 mmol) at −50 °C. The reaction mixture was stirred at −45 to −40 °C for 1 h, then EtCHO (58 mg, 1.00 mmol) was added. The reaction mixture was stirred for 1 h at −45 to −40 °C then hydrolyzed with a solution of water (1.2 mL) in THF (3.0 mL), warmed up to 20 °C, and stirred for 30 min. The organic layer was decanted and the white solid was washed thoroughly with ether. The combined organic layers were dried over $MgSO_4$ and concentrated under reduced pressure. After separation by column chromatography (silica gel, hexane: EtOAc = 5:1), a mixture of **9a** and **10a** (48 mg, 76% total yield) was isolated as a colorless oil. ^{1}H NMR (300 MHz, $CDCl_3$): **9a**: δ = 0.97 (t, J = 6.3 Hz, 3H), 1.09 (m, 2H), 1.43–1.70 (m, 4H), 2.22–2.48 (m, 2H), 3.67 (m, 1H), 5.80 (m, 1H); **10a**: δ = 0.62 (m, 2H), 2.95 (m, 1H), 4.96–5.03 (m, 2H), 6.13 (dd, J = 16.8, 10.2 Hz, 1H). ^{13}C NMR (75 MHz, $CDCl_3$): **9a**: δ = 1.93, 2.67, 9.91, 29.55, 39.31, 72.65, 114.25, 124.89; **10a**: δ = 11.02, 12.29, 27.90, 79.40, 113.57.

Received: June 10, 1996
Revised version: July 29, 1996 [Z9206IE]
German version: *Angew. Chem.* **1996**, *108*, 3024–3025

Keywords: cyclopropanes · propargyl compounds · titanium compounds

[1] A. Kasatkin, T. Nakagawa, S. Okamoto, F. Sato, *J. Am. Chem. Soc.* **1995**, *117*, 3881.
[2] M. T. Reetz, *Top. Curr. Chem.* **1982**, *106*, 1; D. Seebach, B. Weidmann, L. Widler, *Modern Synthetic Methods. Transition Metals in Organic Synthesis* (Ed. R. Scheffald), Otto Salle Verlag, Frankfurt, **1983**, pp. 217–354; M. T. Reetz, *Organotitanium Reagents in Organic Synthesis*, Springer, Heidelberg, **1986**.
[3] R. W. Hoffmann, *Angew. Chem.* **1982**, *94*, 569; *Angew. Chem. Int. Ed. Engl.* **1982**, *21*, 555; Y. Yamamoto, *Acc. Chem. Res.* **1987**, *20*, 243.
[4] R. Hanko, D. Hoppe, *Angew. Chem.* **1982**, *94*, 378; *Angew. Chem. Int. Ed. Engl.* **1982**, *21*, 372; B. Weidmann, D. Seebach, *ibid.* **1983**, *95*, 12 and **1983**, *22*, 31.
[5] P. K. Zubaidha, A. Kasatkin, F. Sato, *J. Chem. Soc. Chem. Commun.* **1996**, 197.
[6] 1-Vinyl- and 1-alkynylcyclopropanols were prepared by the reaction of 1-ethoxycyclopropanol with two equivalents of vinyl- and alkynylmagnesium bromides, respectively (see ref. [7]); the successive treatment of the tertiary alcohols with 1.1 equiv EtMgBr (Et_2O, 0 °C, 5 min) and 1.2 equiv EtOC(O)Cl (20 °C, 4 h) gave the carbonates **6** and **13** in 80–90% yield.
[7] J. R. Y. Salaun, *Top. Curr. Chem.* **1988**, *144*, 1.
[8] The ring strain of methylenecyclopropane is 14 kcal mol^{-1} higher than that of methylcyclopropane: A. Krief, *Top. Curr. Chem.* **1987**, *135*, 35.
[9] P. Binger, H. M. Buch, *Top. Curr. Chem.* **1987**, *135*, 77; T. Ohta, H. Takaya, *Comprehensive Organic Synthesis, Vol. 5* (Eds.: B. M. Trost, I. Fleming), Pergamon, Oxford, **1991**, p. 1188. See also: S. Bräse, S. Schömenauer, G. McGaffin, A. Stolle, A. de Meijere, *Chem. Eur. J.* **1996**, *2*, 545, and references therein.
[10] The related lithium derivatives prepared by the treatment of 1-alkenyl-1-methylseleno-cyclopropanes with BuLi exhibited low regioselectivity in the reaction with aldehydes: S. Halazy, A. Krief, *Tetrahedron Lett.* **1981**, *22*, 4341.
[11] T. Nakagawa, A. Kasatkin, F. Sato, *Tetrahedron Lett.* **1995**, *36*, 3207. See also: K. Furuta, M. Ishiguro, R. Haruta, N. Ikeda, H. Yamamoto, *Bull. Chem. Soc. Jpn* **1984**, *57*, 2768.
[12] It has been recently shown by using ^{13}C NMR spectroscopy that lithiated dicyclopropylacetylene exists exclusively as a propargyllithium (but not allenyllithium) compound: H. J. Reich, J. E. Holladay, *J. Am. Chem. Soc.* **1995**, *117*, 8470.
[13] To our knowledge, no general approach to compounds containing an 1-alkenylidenecyclopropane fragment has been developed so far. For a few examples of this type of compound prepared by using other methods, see: T. Liese, A. de Meijere, *Chem. Ber.* **1986**, *119*, 2995; J. Al-Dulayymi, M. S. Baird, *Tetrahedron Lett.* **1988**, *29*, 6147; K. Tanaka, K. Otsubo, K. Fuji, *Synlett* **1995**, 933.
[14] It is noteworthy that lithiated 1-ethoxy-2-(trimethylsilylethynyl)cyclopropane showed the opposite regioselectivity to afford only acetylenic addition products in the reaction with carbonyl compounds: H. C. Militzer, S. Schoemenauer, C. Otte, C. Puls, J. Hain, S. Braese, A. de Meijere, *Synthesis* **1993**, 998.

Diastereoselective Addition of *n*-Butyllithium to 2-Phenylpropanal: A Reassessment of the Solvent and Temperature Effects**

Gianfranco Cainelli,* Daria Giacomini,* P. Galletti, and A. Marini

The mechanism of asymmetric induction in reactions of α-chiral aldehydes and ketones has been a subject of continued speculation since Cram and Kopecky's seminal work.[1] Among several factors that have been recognized to influence the π-facial diastereoselectivity, the role of the solvent has hitherto been underestimated.

[*] Prof. Dr. G. Cainelli, Dr. D. Giacomini, P. Galletti, A. Marini
Dipartimento di Chimica "G. Ciamician"
Via Selmi 2, I-40126 Bologna (Italy)
Fax: Int. code + (51)25-9456
e-mail: cainelli@ciam01.ciam.unibo.it

[**] This work was supported by Ministero dell' Università e della Ricerca Scientifica e Tecnologica (MURST) (fondi 60%) and the University of Bologna (fund for selected topics). We thank Micaela Fabbri for performing the HPLC analysis.

Recently we demonstrated that in nucleophilic addition reactions to O-protected (2*S*)-lactal[2] and to its corresponding *N*-(trimethylsilyl)imine,[3] the diastereoselection was highly dependent on the nature of the solvent and on the temperature. In these α-oxy substrates, chelation was often invoked to account for the stereochemical outcome of the reactions with organometallic reagents; thus, the diastereoselection was often discussed in terms of a chelation versus a nonchelation mechanism.[4]

In the present investigation, in which we use racemic 2-phenylpropanal **1**[5] as the model aldehyde, we focus on the influence of the solvent and temperature on the π-facial diastereoselectivity. Compound **1** has been studied previously by Reetz et al.,[6] who highlighted the high Cram-selectivity of this substrate (90–94%) in reaction with *n*BuLi under standard conditions (THF, −78 °C), while a lower selectivity was observed when the reaction was carried out using *n*-pentane as solvent. We report here on a systematic study of the diastereofacial selectivity of **1** in reactions with *n*BuLi using hydrocarbons and ethers as solvents.

The addition reaction was performed by adding a stoichiometric amount of *n*BuLi (1.6 M solution in hexane) to **1** in different dry solvents. The reaction temperature was varied over a range between the melting and boiling point of the respective solvents (Scheme 1). The diastereomeric excess (*de*) of products

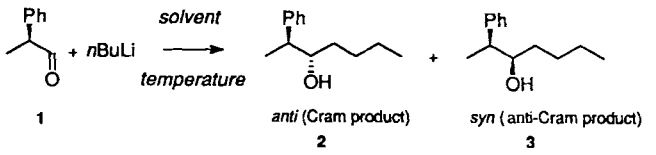

Scheme 1. Syntheses of **2** and **3**. Solvents: THF, *t*BuOMe, 1,4-dioxane, propane, *n*-pentane, *n*-hexane, *n*-octane, *n*-decane, *n*-dodecane, cyclohexane, cyclopentane.

2 and **3** in the crude reaction mixture was determined by HPLC analysis.[7] Results obtained with THF, *t*BuOMe, *p*-dioxane, and *n*-hexane are given in Table 1.

The temperature dependence of the *de* values was analyzed according to the modified Eyring equation [Eq. (a)],[8] where

$$\ln P = -(\Delta\Delta H^{*}/RT) + (\Delta\Delta S^{*}/R) \qquad (1)$$

$P = k(anti)/k'(syn) = I/I'$, k and k' are the overall rate constants, and I and I' are the chromatographic area [%] of **2** and **3**, respectively. The results are summarized in Figure 1.

At low temperature, THF exhibited the best diastereoselectivity, while reactions in *t*BuOMe and 1,4-dioxane gave lower *de* values. A continuous linear correlation between the ln (*anti*/*syn*) value and $1/T$ was observed in all ethers; in contrast, in reactions carried out in *n*-hexane we established an inversion temperature (T_{inv}).[9] A small amount (5%) of THF in *n*-hexane was sufficient to obtain results similar to those obtained in pure THF. This could be attributed to a direct (primary shell) THF–lithium interaction, where the donor solvent acts as ligand to the lithium coordination sphere.[10] The evidence of an inversion temperature for *n*-hexane prompted further investigation. The Eyring plots for a series of linear and cyclic hydrocarbons is shown in Figure 2. Each aldehyde–solvent combination showed two linear regions, and a characteristic inversion temperature was observed in each case.[11]

Interestingly, for linear hydrocarbons and their cyclic counterparts, the inversion point T_{inv} represents a cusp with an opposite orientation. The pattern is consistent with the chain length

Table 1. Influence of temperature and solvent on the diastereoselectivity of the nucleophilic addition of *n*-butyllithium to 2-phenylpropanal. The *de* values were determined by HPLC analysis.

Solvent	*T* [°C]	*de* [%]	*anti*/*syn*	Yield [%]
THF	−91	86	93:7	76
THF	−79	78	89:11	73
THF	−60	78	89:11	75
THF	−50	74	87:13	83
THF	−40	64	82:18	83
THF	−30	66	83:17	81
THF	−14	60	80:20	65
THF	2	46	73:27	80
*t*BuOMe	−86	82	91:9	78
*t*BuOMe	−69	82	91:9	60
*t*BuOMe	−60	74	87:13	76
*t*BuOMe	−40	70	85:15	73
*t*BuOMe	−31	70	85:15	60
*t*BuOMe	−15	66	83:17	96
*t*BuOMe	2	62	81:19	83
*t*BuOMe	23	56	78:22	78
*t*BuOMe	54	50	75:25	52
1,4-dioxane	15	52	76:24	68
1,4-dioxane	34	48	74:26	75
1,4-dioxane	54	44	72:28	78
1,4-dioxane	69	42	71:29	68
1,4-dioxane	79	38	69:31	65
n-hexane	−93	66	83:17	86
n-hexane	−80	66	83:17	96
n-hexane	−69	64	82:18	76
n-hexane	−60	64	82:18	96
n-hexane	−50	64	82:18	78
n-hexane	−32	60	80:20	86
n-hexane	−17	56	78:22	70
n-hexane	− 9	56	78:22	81
n-hexane	4	54	77:23	81
n-hexane	31	46	73:27	78
n-hexane	54	42	71:29	76

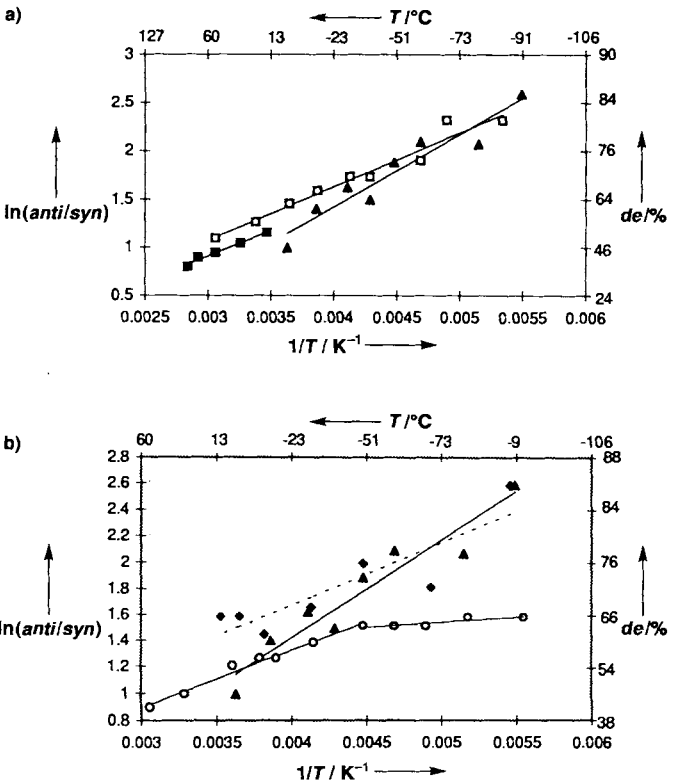

Fig. 1. Eyring plots for the diastereomeric excess obtained in the nucleophilic addition of *n*-butyllithium to **1** at various temperatures in a) THF (▲), *t*BuOMe (□), 1,4-dioxane (■), and b) in THF (▲), *n*-hexane (○), and THF/*n*-hexane (5/95, ◆).

 © VCH Verlagsgesellschaft mbH, D-69451 Weinheim, 1996 0570-0833/96/3523-2850 $ 15.00+.25/0

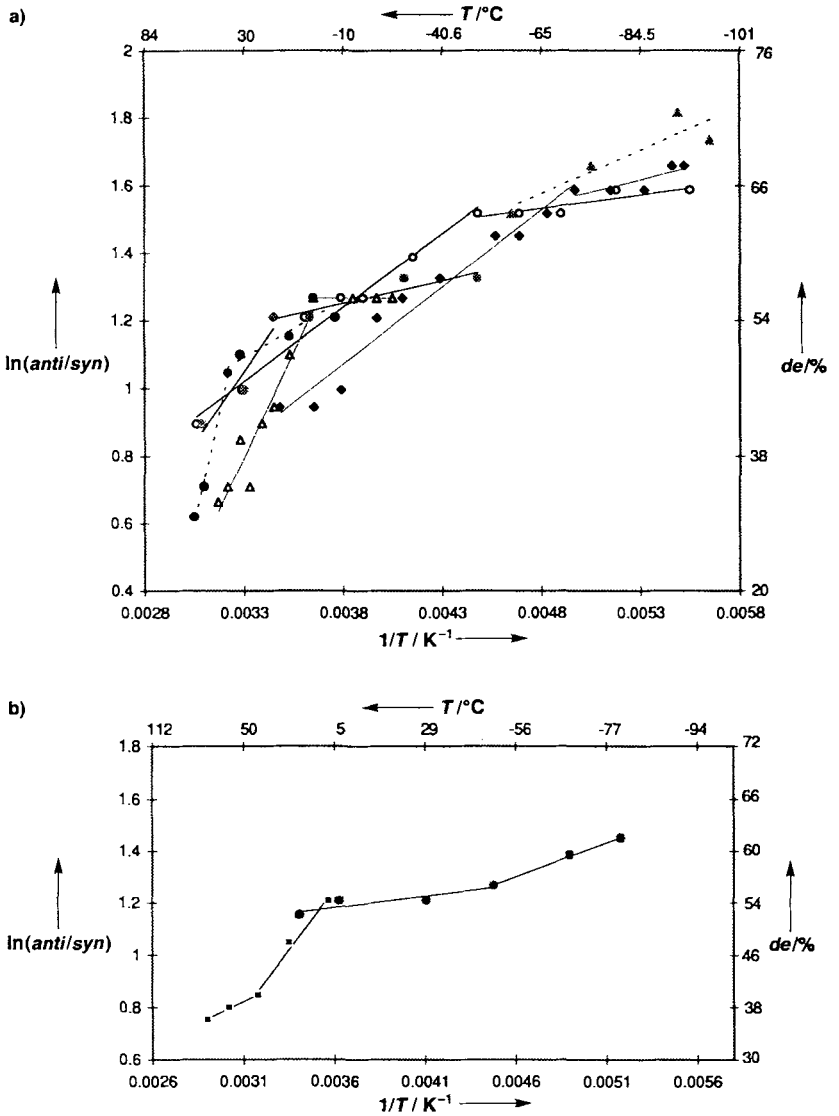

Fig. 2. Eyring plots for the diastereomeric excess obtained in the nucleophilic addition of *n*-butyllithium to **1** at various temperature a) in propane (△), *n*-pentane (◆), *n*-hexane (○), *n*-octane (○), *n*-decane (▲), *n*-dodecane (◆), and b) in cyclohexane (■), cyclopentane (○).

of the solvent: the longer the chain, the lower the diastereofacial selectivity; for example, the diastereofacial selectivity obtained with propane is better than that with *n*-dodecane. It appears that even though apolar aprotic solvents interact only slightly with the solute (since only the nonspecific directional, induction, and dispersion forces can operate) the diastereoselectivity could be doubled by using a solvent with a short chain length. To the best of our knowledge, this possibility has never been raised in the discussion of diastereofacial selectivity. In both temperature regions, the slopes of regression lines, which reflect the enthalpic contribution, are not very different. On the other hand, the differences in the intercepts ($\Delta\Delta S^{\ddagger}$) are significant. Thus, the chain length effect might be ascribed to entropic control over the selectivity of this type of organometallic addition.

Considerable attention has been paid to the significance of the difference $\delta\Delta\Delta H^{\ddagger} = \Delta\Delta H_1^{\ddagger} - \Delta\Delta H_2^{\ddagger}$ ($\Delta\Delta H_1^{\ddagger}$, $T > T_{inv}$ and $\Delta\Delta H_2^{\ddagger}$, $T < T_{inv}$). A plot of $\delta\Delta\Delta H^{\ddagger}$ against the corresponding entropy term $\delta\Delta\Delta H^{\ddagger}$ is linear for all the hydrocarbons measured. From the slope of this plot (Fig. 3) we can determine the isoinversion temperature $T_i = 299$ K (21 °C).

In contrast with our results with the *N*-(trimethylsilyl)imine of lactal,[3] we did not obtain an optimal value of the selectivity for the aldehyde **1** at a reaction temperature near to T_i, and moreover solvents with a T_{inv} value close to the T_i value, such as *n*-decane and *n*-dodecane, produced a lower diastereoselectivity.

The inversion temperatures for all the linear and cyclic hydrocarbon solvents examined ranged between 205 and 317 K, noteworthy is that the T_{inv} value for linear hydrocarbons increases as the chain length increases on going from *n*-pentane to *n*-dodecane (Table 2).[12]

Table 2. Melting points [K] of several solvents and inversion temperatures T_{inv} [K] for the reaction of **1** to give **2** and **3** in these solvents.

Solvent	M.p.	T_{inv}
n-pentane	143	205.3
n-hexane	178	227.8
cyclopentane	179	225.1
n-octane	216	287
n-decane	243	271.7
n-dodecane	261	309.6
cyclohexane	279.5	317

Assuming that the inversion temperature is a property of every substrate–solvent pair, all efforts to correlate T_{inv} with some classical solvent parameters, such as dielectric constant and viscosity, failed. Interestingly, we found an extrathermodynamic correlation between T_{inv} and the melting points of the linear and cyclic hydrocarbons; the resulting straight line has a correlation coefficient (r) of 0.96 (Fig. 4). This suggests a relationship between the inversion temperature and the phase modification that happens on melting. This could be consistent with the hypothesis that inversion points represent a transition between two "phases", which in the case of solutions could be represented by two different solvation states (a more ordered one in the low-temperature region) that have different k and k' values, and therefore different diastereoselectivity.

These results indicate the unexpected role the reaction solvent plays in determining the inversion temperature and confirms its peculiar influence on the diastereofacial selectivity.

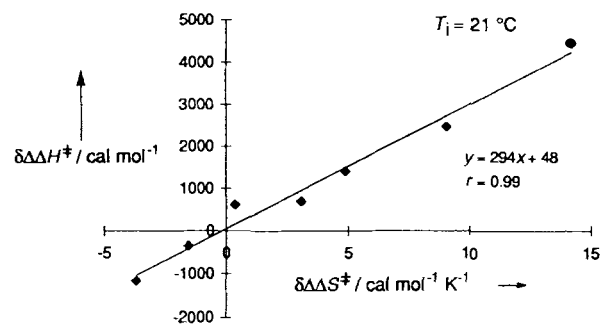

Fig. 3. $\delta\Delta\Delta H^{\ddagger}/\delta\Delta\Delta S^{\ddagger}$ plot for the determination of the isoinversion temperature T_{inv}

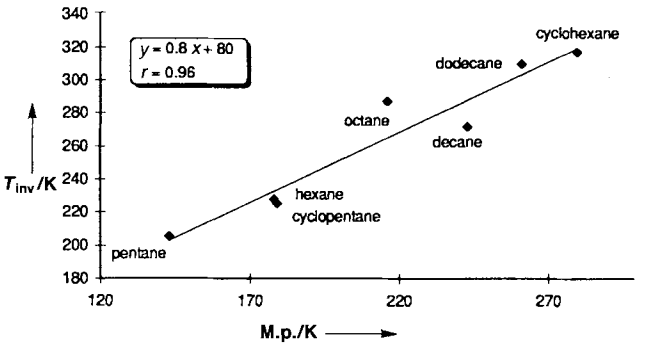

Fig. 4. Correlation between melting points and inversion temperature for hydrocarbons.

Experimental Procedure

In a typical experiment, **1** (0.268 g, 2 mmol) was dissolved in anhydrous solvent (20 mL) under inert atmosphere, and the solution cooled to the desired temperature; then *n*-butyllithium (2.2 mmol, 1.37 mL of a 1.6 M solution in *n*-hexane) was added. After the starting aldehyde had disappeared (GC-monitoring), the reaction was quenched at 0 °C with a saturated aqueous solution of NH_4Cl, extracted with CH_2Cl_2 (3 × 50 mL), and dried with $MgSO_4$. From HPLC analysis of the crude product the *anti*/*syn* ratio and the *de* value were obtained. Chromatography of the residue on a silica gel column gave the mixture of the two alcohols **2** and **3** so that the chemical yield could be calculated.

Received: June 27, 1996 [Z 9264 IE]
German version: *Angew. Chem.* **1996**, *108*, 3016–3019

Keywords: aldehydes · asymmetric synthesis · inversion temperature · nucleophilic additions · solvent effects

[1] D. J. Cram, K. R. Kopecky, *J. Am. Chem. Soc.* **1952**, *74*, 5828.
[2] G. Cainelli, D. Giacomini, F. Perciaccante, *Tetrahedron Asymmetry* **1994**, *5*, 1913.
[3] G. Cainelli, D. Giacomini, M. Walzl, *Angew. Chem.* **1995**, *107*, 2336; *Angew. Chem. Int. Ed. Engl.* **1995**, *34*, 2150.
[4] M. T. Reetz, *Angew. Chem.* **1984**, *96*, 542; *Angew. Chem. Int. Ed. Engl.* **1984**, *23*, 556.
[5] In testing diastereofacial selectivity, racemic aldehyde was employed. Only one enantiomeric form is arbitrarily shown.
[6] M. T. Reetz, S. Stanchev, H. Haning, *Tetrahedron* **1992**, *48*, 6813.
[7] The diastereoselectivity of the product formation is characterized by the *de* value of the *anti* adduct, which was determined by HPLC analysis of the crude product (column: Accubond OVS 5V, 25 × 4.6 cm, $T = 35$ °C, flow = 1.5 mL min^{-1}, eluent H_2O/CH_3CN from 10 to 100% of H_2O in 45 min).
[8] a) H. Eyring, *J. Phys. Chem.* **1935**, *3*, 107; b) S. Glasstone, K. J. Laidler, H. Eyring, *The Theory of Rate Processes*, McGraw-Hill, New York, **1941**, Chapter 4.
[9] For a review see: H. Buschmann, H.-D. Scharf, N. Hoffmann, P. Esser, *Angew. Chem.* **1991**, *103*, 480; *Angew. Chem. Int. Ed. Engl.* **1991**, *30*, 477. For recent papers see: K. J. Hale, J. H. Ridd, *J. Chem. Soc. Chem. Commun.* **1995**, 357; M. Palucki, P. J. Pospisil, W. Zhang, E. N. Jacobsen, *J. Am. Chem. Soc.* **1994**, *116*, 9333; J. Brunne, N. Hoffmann, H.-D. Scharf, *Tetrahedron* **1994**, *50*, 6819; T. Göbel, K. B. Sharpless, *Angew. Chem.* **1993**, *105*, 1417; *Angew. Chem. Int. Ed. Engl.* **1993**, *32*, 1329; J. Muzart, F. Hénin, J.-P. Pète, A. M'boungou-M'Passi, *Tetrahedron Asymmetry* **1993**, *4*, 2531; I. Tóth, I. Guo, B. E. Hanson, *Organometallics* **1993**, *12*, 477.
[10] See for instance: C. Reichardt, *Solvents and Solvent Effects in Organic Chemistry*, 2nd ed., VCH, Weinheim, **1990**.
[11] In our opinion, this behavior is quite general for diastereoselective reactions in solution. The absence of the inversion temperature was attributed either to a limited temperature range (the T_{inv} results lie outside the observable range) or to the fact that the two slopes of the linear correlations differ too little to appreciate the cusp.
[12] The plot of ln (*anti*/*syn*) against $1/T$ in propane did not reveal an inversion temperature because in this reaction the inversion temperature could have a lower value than the lowest reaction temperature we reached. In fact, in this solvent, at $T \leq -100$ °C, the starting aldehyde was quite insoluble and the conversion yield was very low.

Synthesis and Structure of the Metalated Zintl Ion $[Ge_9(\mu_{10}\text{-}Ge)Ni(PPh_3)]^{2-}$

Donna R. Gardner, James C. Fettinger, and Bryan W. Eichhorn*

Since the discovery[1, 2] and subsequent investigation[3–6] of the Group 14 Zintl ions, only a few transition metal derivatives of these unusual clusters have been detected. The only structurally characterized examples, the tin and lead [*closo*-$E_9Cr(CO)_3]^{4-}$ ions[7, 8] and the $[Sn_6\{Cr(CO)_5\}_6]^{2-}$ ion,[9] were made by two vastly different synthetic methods. Teixidor et al. characterized two Pt–E_9 species (E = Sn, Pb) by NMR spectroscopy;[10] however, little is known about their structures. Even though there are several structurally characterized naked germanide ions (Ge_9^{n-}, where $n = 2$, 3, or 4; Ge_{10}^{2n-}),[11–14] complexes of the germanide Zintl anion with transition metals have not previously been described. Herein we report the synthesis and characterization of [K([2.2.2]-cryptand)]$_2$[$Ge_9(\mu_{10}$-Ge)Ni(PPh_3)]·en (for [2.2.2]cryptand see [17], en = ethylenediamine), the first metalated germanide anion and only the second example of the rare *nido*-10 (iv + iv)[15] structure type.

The reaction of $[Ni(CO)_2(PPh_3)_2]$, K_4Ge_9,[16] and [2.2.2]cryptand[17] in ethylenediamine gives $[Ge_9(\mu_{10}$-Ge)-$Ni(PPh_3)]^{2-}$ (**1**) as the [K([2.2.2]cryptand)]$^+$ salt in low yields. The compound [K([2.2.2]cryptand)]$_2$(**1**)·en decomposes upon exposure to air and moisture. The dark brown crystals have been characterized by single-crystal X-ray diffraction, energy dispersive X-ray analysis (EDX), microanalysis, and ^{31}P NMR.

A single crystal X-ray diffraction study[18, 19] revealed two [K([2.2.2]cryptand)]$^+$ cations, an en solvent molecule, and the $[Ge_9(\mu_{10}$-Ge)Ni$(PPh_3)]^{2-}$ (**1**) anion. This anion displays no crystallographic symmetry, consists of nine surface Ge atoms, one interstitial Ge atom Ge(i), and an [Ni(PPh_3)] fragment (Fig. 1). The [Ni(PPh_3)] fragment has been incorporated into the anion framework as a vertex of the cluster. The two [K([2.2.2]-cryptand)]$^+$ cations are well separated from the anion and are not disordered. The en solvent molecule is not fully resolved due to local disorder. Two independent crystal studies were performed on crystals of independent syntheses and both studies gave the same results within experimental error.

The Ge–Ge bond distances for the surface Ge atoms range from 2.595(4) Å to 3.291(4) Å. These distances are similar to those of Ge–Ge contacts in other polygermanide clusters such as [K([2.2.2]cryptand)]$_3$[$P(C_6H_5)_3Ge_9$], where bonding Ge contacts vary from 2.53 Å to 3.27 Å.[11–14] The distances between the nearest neighbor surface Ge atoms and the Ni atom range from 2.364(3) Å to 2.381(3) Å; a longer contact exists between Ni(1) and Ge(2) of 3.307(3) Å. Excluding the longer contact, the Ni–Ge bond lengths are similar to other reported distances, for example, 2.36 Å (av) in $[Ni_9(\mu_4\text{-}GeEt)_6(CO)_8]$.[20–25] The contacts between the surface Ge atoms and the interstitial atom Ge(i) range from 2.355(3) Å to 2.446(3) Å (average 2.40 Å) and are slightly shorter than those in metallic germanium (2.44 Å).[26] The Ni–Ge(i) distance in **1** of 2.361 Å is significantly shorter than the Ni–Ge(i) contacts in the interstitial Ge clusters $[Ni_{12}Ge(CO)_{22}]^{2-}$ (average 2.49 and 2.69 Å) and $[Ni_{10}Ge(CO)_{20}]^{2-}$ (average 2.47 Å).[27] The shorter distance in **1**

[*] Prof. B. W. Eichhorn, D. R. Gardner, Dr. J. C. Fettinger
Department of Chemistry
University of Maryland
College Park, MD 20742 (USA)
Fax: Int. code +(301)314-9121
e-mail: b_eichhorn@umail.umd.edu

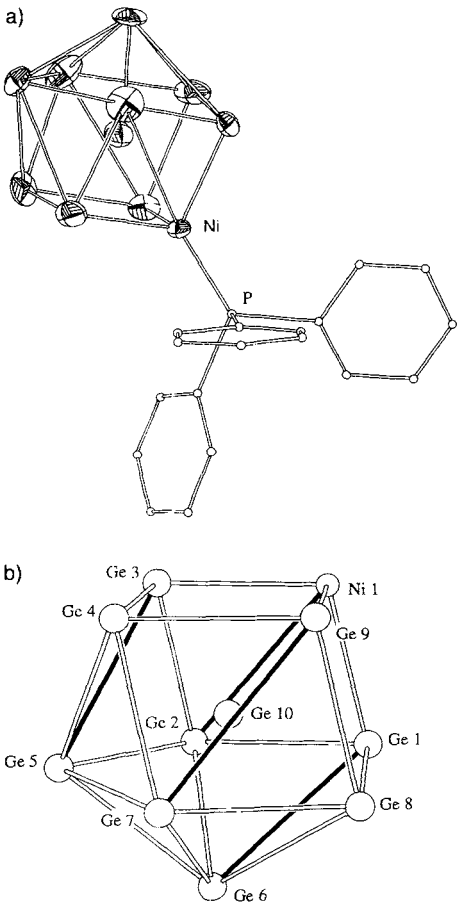

Fig. 1. a) ORTEP drawing of $[Ge_9(\mu_{10}\text{-}Ge)Ni(PPh_3)]^{2-}$ (**1**) (thermal ellipsoids are drawn at the 50% probability level). b) Ball-and-stick representation of cluster **1** emphasizing the cluster distortions and giving the atom numbering scheme. Darkened bonds represent long intracluster contacts. Pertinent bond lengths [Å] and angles [°] are: Ge1–Ge10 2.349(3), Ge2–Ge10 2.426(3), Ge3–Ge10 2.366(3), Ge4–Ge10 2.424(3), Ge5–Ge10 2.442(3), Ge6–Ge10 2.446(3), Ge7–Ge10 2.421(3), Ge8–Ge10 2.422(3), Ge9–Ge10 2.335(3), Ni1–Ge10 2.361(3), Ge1–Ni1 2.381(3), Ge2–Ni1 3.307(3), Ge3–Ni1 2.370(3), Ge4–Ni1 3.581(4), Ge8–Ni1 3.601(4), Ge9–Ni1 2.364(3), $Ge_{surface}$–$Ge_{surface}$ 2.74 (average) [included in the average are the longer contacts Ge1–Ge6 3.013(4), Ge3–Ge5 3.005(3), Ge7–Ge9 3.291(4)]; Ge1–Ge3 3.708(3), Ge1–Ge9 3.443(3), Ge2–Ge8 4.240(4), Ge3–Ge9 3.454(3), Ge4–Ge8 4.096(4); Ge3-Ge4-Ge9 82.68(10), Ge3-Ni1-Ge9 93.72(12), Ge4-Ge3-Ni1 92.22(12), Ge4-Ge9-Ni1 91.38(11), Ni1-Ge9-Ge8 92.21(12), Ni1-Ge1-Ge8 92.40(12), Ge9-Ni1-Ge1 93.04(12), Ge9-Ge8-Ge1 82.33(10).

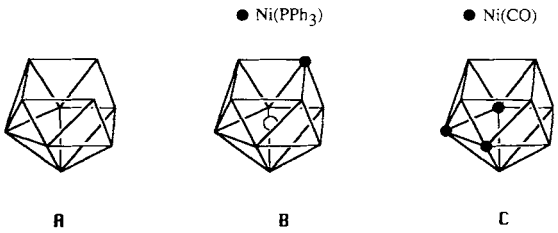

disparity in the interatomic distances between Ge atoms (average 2.74 Å) and those between Ge and Ni atoms (average 2.37 Å). It appears that the cluster compensates for the disparity by lengthening the contacts to the five coordinate Ge atoms (see Fig. 1b) while optimizing the Ge–Ni interactions.

In both the known *nido*-10 (iv+iv) structural types the [Ni–L] (L = CO or PPh_3) fragment occupies vertices on the surface of the cage but not in the same location. The three [Ni(CO)] fragments of the $[Sb_7Ni_3(CO)_3]^{3-}$ ion[33] (see **C**) occupy vertices on the pentagonal waist, whereas in the germanium complex, the $[Ni(PPh_3)]$ fragment occupies a vertex of one of the open square faces. Further investigations may elucidate new families of cluster structural types, which may only be accessible when derived from naked anions of heavier main group elements.

The solution dynamics of reaction mixtures containing polygermanide anions is clearly quite complicated. For example, the Ge_{10}^{2-} anion was isolated from ethylenediamine solutions of $KGe_{1.8}$ and [2.2.2]cryptand with tetrakis(triphenylphosphanyl)nickel(0).[13]

Experimental Procedure

K_4Ge_9 was prepared by fusing a stoichiometric ratio of the elements in a sealed, evacuated silica ampoule. Ethylenediamine was dried over CaH_2 and then distilled from K_4Sn_9. All manipulations were carried out under a dinitrogen atmosphere. In a dry box, K_4Ge_9 [16] (54 mg, 0.07 mmol), [2.2.2]cryptand (100 mg, 0.27 mmol), and $[Ni(CO)_2(PPh_3)_2]$ (84 mg, 0.14 mmol) were dissolved in 6 mL of ethylenediamine. The red-brown mixture was heated (35 °C < T < 45 °C) and stirred for about 15 min. The mixture was filtered and after 15 days well-formed brown crystals of $[K([2.2.2]cryptand)]_2$(**1**)·en could be isolated (22 mg; the exact yield could not be determined due to inconsistent microanalysis. Repeated microanalysis gave inconsistent and unsatisfactory results, presumably due to elemental Ge contaminants. The elemental analysis for Ni ranged from 0.95–4.45%; expected 3.03%.). EDX analysis on crystals showed presence of K, P, Ge, and Ni. In a $[D_7]$DMF solution, only free triphenylphosphane is observed in the ^{31}P NMR spectrum at room temperature.

Received: June 10, 1996 [Z92121E]
German version: *Angew. Chem.* **1996**, *108*, 3032–3033

Keywords: germanium compounds · Zintl compounds

than in the carbonyl clusters is consistent with the smaller cage size of **1**. The Ni–P contact of 2.121(6) Å is slightly shorter than most Ni–P distances for other zero-valent triphenyphosphanylnickel complexes (2.15–2.28 Å).[28–30]

If the interstitial Ge atom is considered a four-electron donor, the anion has 24 skeletal electrons which is indicative of a *nido* cluster in accordance with Wade's rules.[31] However, unlike the typical *nido*-10 (vi) cluster (for example, $B_{10}H_{14}$, $C_4B_6H_{10}$),[32] which has an open six-membered ring (**A**), anion **1** has two four-membered rings fused along a common bond between Ni(1) and Ge(9) (**B**, Fig. 1b). This structural type has been reported once before as the Zintl ion derivative $[Sb_7Ni_3(CO)_3]^{3-}$[33] (**C**) and was found to be a local minimum for geometries for carborane clusters.[34]

The cluster is significantly distorted from a *nido*-10 (iv+iv) idealized geometry. The $[Ni(PPh_3)]$ vertex of the cluster is pulled in towards the interstitial Ge atom and the Ge(3)–Ge(5), Ni(1)–Ge(2), Ge(9)–Ge(7), and Ge(1)–Ge(6) edges are elongated. The dominant factor for the distortion seems to be the

[1] A. Joannis, *Comp. Rend.* **1891**, *113*, 795.
[2] A. Joannis, *Comp. Rend.* **1892**, *114*, 585.
[3] H. G. von Schnering, *Angew. Chem.* **1981**, *93*, 44; *Angew. Chem. Int. Ed. Engl.* **1981**, *20*, 33.
[4] J. D. Corbett, *Chem. Rev.* **1985**, *85*, 383.
[5] W. L. Wilson, R. W. Rudolph, L. L. Lohr, R. C. Taylor, P. Pyykko, *Inorg. Chem.* **1986**, *25*, 1535.
[6] J. Campbell, D. A. Dixon, H. P. A. Mercier, G. J. Schrolbilgen, *Inorg. Chem.* **1995**, *34*, 5798.
[7] B. W. Eichhorn, R. C. Haushalter, W. T. Pennington, *J. Am. Chem. Soc.* **1988**, *110*, 8704.
[8] B. W. Eichhorn, R. C. Haushalter, *J. Chem. Soc. Chem. Commun.* **1990**, 937.
[9] B. Schiemenz, G. Huttner, *Angew. Chem.* **1993**, *105*, 295; *Angew. Chem. Int. Ed. Engl.* **1993**, *32*, 297.
[10] F. Teixidor, M. L. Leutkens, Jr., R. W. Rudolph, *J. Am. Chem. Soc.* **1983**, *105*, 149.
[11] V. Angilella, C. Belin, *J. Chem. Soc. Faraday Trans.* **1991**, *87*, 203.
[12] C. H. E. Belin, J. D. Corbett, A. Cisar, *J. Am. Chem. Soc.* **1977**, *99*, 7163.
[13] C. Belin, H. Mercier, V. Angilella, *New. J. Chem.* **1991**, *15*, 931.
[14] T. J. Fässler, M. Hunziker, *Inorg. Chem.* **1994**, *33*, 5380.

[15] R. E. Williams in *Electron Deficient Boron and Carbon Clusters* (Eds.: G. A. Olah, K. Wade, R. E. Williams), Wiley, New York, **1991**, p 11.
[16] K_4Ge_9 melt is of nominal composition.
[17] [2.2.2]cryptand is an abbreviation for 4,7,13,16,21,24-hexaoxa-1,10-diazabicyclo[8.8.8]hexacosane.
[18] Crystal data: Triclinic, space group $P\bar{1}$ (No. 2), $a = 12.863(2)$, $b = 13.036(2)$, $c = 23.559(3)$ Å; $\alpha = 96.439(12)$, $\beta = 104.775(13)$, $\gamma = 96.95(2)°$; $V = 3749.4(9)$ Å^3, $Z = 2$, $\rho_{calcd} = 1.717$ g cm^{-3}; $Mo_{K\alpha}$ radiation ($\lambda = 0.71073$ Å); $\mu(Mo_{K\alpha}) = 4.379$ mm^{-1}; $T = 153$ K; crystal dimensions $0.425 \times 0.25 \times 0.175$ mm. The data were collected on an Enraf-Nonius CAD-4 diffractometer with ω-2θ scans over the range $2.4 < \theta < 21.0$. Of the 8494 reflections collected, 8042 were unique, and 6192 were observed with $F_o > 4\sigma(F_o)$. Data were corrected for Lorentz and polarization factors (XCAD4) [19]. Absorption correction was semiemperical from psi-scans. Max./min. transmission = 0.9083/0.2824. The structure was solved by direct methods (XS). Restraints were implemented to refine the two [K([2.2.2]cryptand)]$^+$ ions (SAME and DELU). The structure was refined by full-matrix least squares against $|F^2|$ to $R = 0.1053$, $R_w = \{\Sigma[w(F_o^2 - F_c^2)^2]/\Sigma[w(F_o^2)^2]\}^{0.5} = 0.2369$ (unit weights) (6192 data) for 743 parameters and 336 restraints. The largest difference peak and hole are 1.656 and -1.394 e Å^{-3}. Further details of the crystal structure investigation may be obtained from the Fachinformations-zentrum Karlsruhe, D-76344 Eggenstein-Leopoldshafen (Germany), on quoting the depository number CSD-405587.
[19] G. Sheldrick, *Acta. Crystallogr. Sect. A* **1990**, *46*, 467.
[20] J. P. Zebrowski, R. K. Hayashi, A. Bjarnason, L. F. Dahl, *J. Am. Chem. Soc.* **1992**, *114*, 3121.
[21] M. Grenz, E. Hahn, W.-W. duMont, J. Pickardt, *Angew. Chem.* **1984**, *96*, 69; *Angew. Chem. Int. Ed. Engl.* **1984**, *23*, 61.
[22] W. A. Herrmann, M. Denk, J. Behm, W. Scherer, F.-R. Klingan, H. Bock, B. Solouki, M. Wagner, *Angew. Chem.* **1992**, *104*, 1489; *Angew. Chem. Int. Ed. Engl.* **1992**, *31*, 1485.
[23] H. Pohlmann, E. Weiss, *Chem. Ber.* **1988**, *121*, 1427.
[24] P. Gusbeth, H. Vahrenkamp, *Chem. Ber.* **1985**, *118*, 1746.
[25] L. V. Pankratov, V. I. Nevodchikov, L. N. Zakharov, M. N. Bochkarev, I. V. Zdanovich, V. N. Latyaeva, A. N. Lineva, A. S. Batsanov, Y. T. Struchkov, *J. Organometal. Chem.* **1992**, *429*, 13.
[26] *Gmelins Handbuch der anorganischen Chemie*, 8th ed., No. 45, supplementary volume, Verlag Chemie, Weinheim, 1958, p. 15.
[27] A. Ceriotti, F. Demartin, B. T. Heaton, P. Ingallina, G. Longoni, M. Manassero, M. Marchionna, N. Masciocchi, *J. Chem. Soc. Chem. Commun.* **1989**, 789.
[28] D. C. Moody, R. R. Ryan, *Inorg. Chem.* **1979**, *18*, 223.
[29] C. Krüger, Y.-H. Tsay, *Cryst. Struct. Commun.* **1974**, *3*, 455.
[30] P.-T. Cheng, C. D. Cook, C. H. Koo, S. C. Nyburg, M. T. Shiomi, *Acta. Crystallogr. Sect. B* **1971**, *27*, 1904.
[31] K. J. Wade, *Adv. Inorg. Chem. Radiochem.* **1976**, *18*, 1.
[32] N. N. Greenwood, A. Earnshaw, *Chemistry of the Elements*, Pergamon, Oxford, **1984**, p. 198–209.
[33] S. Charles, B. W. Eichhorn, S. G. Bott, *J. Am. Chem. Soc.* **1993**, *115*, 5837.
[34] S. Lee, *Inorg. Chem.* **1992**, *31*, 3063.

nent of such chemistry, the chemistry of halotellurato clusters of the early transition metals, especially Re, is undeveloped compared with that of halosulfato and haloselenato clusters. Yet the incipient chemistry of halotellurato clusters shows striking differences from that of the S and Se derivatives. For instance, there are unusual halotellurato ligands with no analogs in the S and Se systems. In these Te ligands, tellurium is predominantly in the oxidation state +II.[6, 7] Neutral $TeCl_2$ and $TeBr_2$ ligands are featured in the Re_6 cluster compounds $Re_6(\mu_3\text{-}Te)_6(\mu_3\text{-}Cl)_2(TeCl_2)_2Cl_4$ and $[Re_6(\mu_3\text{-}Te)_8(TeBr_2)_6]Br_2$.[8] However, halotellurium(IV) ligands, such as the $[TeCl_2]^{2+}$ ligand in $[Fe_2(CO)_6(Te_4)(TeCl_2)]$, are also known.[9] Here we present the synthesis and structures of two new solid-state compounds, $Re_6Te_{16}Cl_{18}$ and $Re_6Te_{16}Cl_6$, which contain $[Re_6Te_8]^{2+}$ octahedral clusters linked together by new tellurium and chlorotellurato ligands to form multidimensional structures.

$Re_6Te_{16}Cl_{18}$ may be thought of as $[(Re_6Te_8)(Te_8Cl_{18})]$ since it contains $[Re_6Te_8]^{2+}$ clusters and $[Te_8Cl_{18}]^{2-}$ ligands. The $[Re_6Te_8]^{2+}$ cluster consists of a Re^{III}–Re^{III}-bonded Re_6 octahedron inscribed in a cube by eight μ_3-Te^{2-} ligands. Re–Re bond lengths range from 2.674(2) to 2.691(2) Å and Re–μ_3-Te bond lengths from 2.669(2) to 2.699(2) Å. $[Re_6Te_8]^{2+}$ clusters have been previously observed in Re_6Te_{15} ($[(Re_6Te_8)(Te_7)]$),[10, 11] $[Re_6Te_8(TeBr_2)_6]Br_2$,[8] and the $[Re_6Te_8(CN)_6]^{4-}$ ion.[12] In addition to four μ_3-Te^{2-} ligands, each Re atom of the Re_6Te_8 core is coordinated by the previously unknown $[Te_8Cl_{18}]^{2-}$ chlorotellurato ligand through a Re–Te bond (2.638(2) Å). In turn, each $[Te_8Cl_{18}]^{2-}$ ligand chelates six $[Re_6Te_8]^{2+}$ clusters (Fig. 1);

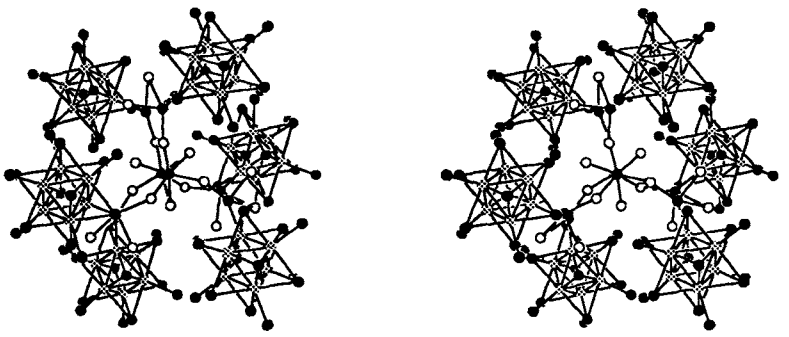

Fig. 1. Stereoview of the $[Te_8Cl_{18}]^{2-}$ ligand environment in $Re_6Te_{16}Cl_{18}$. Each ligand chelates six $[Re_6Te_8]^{2+}$ clusters, and each cluster is bound by an additional five ligands (not shown) through Te atoms (shown dangling). Re atoms are drawn as checkered spheres, Te atoms as solid spheres, and Cl atoms as hollow spheres.

Te_6, $[Te_8Cl_{18}]^{2-}$, and $[TeCl_3]^-$: New Tellurium and Chlorotellurato Ligands in the Re_6 Solid-State Cluster Compounds $Re_6Te_{16}Cl_{18}$ and $Re_6Te_{16}Cl_6$**

Yuri V. Mironov, Michael A. Pell, and James A. Ibers*

Dedicated to Professor Richard H. Holm

Re_6 octahedral clusters are important building blocks in the solid-state chemistry of Re-containing compounds.[1–5] Whereas halides and chalcogenides are an important component of such chemistry, the chemistry of halotellurato clusters of the early transition metals, especially Re, is undeveloped compared with that of halosulfato and haloselenato clusters. Yet the incipient chemistry of halotellurato clusters shows striking differences from that of the S and Se derivatives. For instance, there are unusual halotellurato ligands with no analogs in the S and Se systems. In these Te ligands, tellurium is predominantly in the oxidation state +II.[6, 7] Neutral $TeCl_2$ and $TeBr_2$ ligands are featured in the Re_6 cluster compounds $Re_6(\mu_3\text{-}Te)_6(\mu_3\text{-}Cl)_2(TeCl_2)_2Cl_4$ and $[Re_6(\mu_3\text{-}Te)_8(TeBr_2)_6]Br_2$.[8] However, halotellurium(IV) ligands, such as the $[TeCl_2]^{2+}$ ligand in $[Fe_2(CO)_6(Te_4)(TeCl_2)]$, are also known.[9] Here we present the synthesis and structures of two new solid-state compounds, $Re_6Te_{16}Cl_{18}$ and $Re_6Te_{16}Cl_6$, which contain $[Re_6Te_8]^{2+}$ octahedral clusters linked together by new tellurium and chlorotellurato ligands to form multidimensional structures.

$Re_6Te_{16}Cl_{18}$ may be thought of as $[(Re_6Te_8)(Te_8Cl_{18})]$ since it contains $[Re_6Te_8]^{2+}$ clusters and $[Te_8Cl_{18}]^{2-}$ ligands. The $[Re_6Te_8]^{2+}$ cluster consists of a Re^{III}–Re^{III}-bonded Re_6 octahedron inscribed in a cube by eight μ_3-Te^{2-} ligands. Re–Re bond lengths range from 2.674(2) to 2.691(2) Å and Re–μ_3-Te bond lengths from 2.669(2) to 2.699(2) Å. $[Re_6Te_8]^{2+}$ clusters have been previously observed in Re_6Te_{15} ($[(Re_6Te_8)(Te_7)]$),[10, 11] $[Re_6Te_8(TeBr_2)_6]Br_2$,[8] and the $[Re_6Te_8(CN)_6]^{4-}$ ion.[12] In addition to four μ_3-Te^{2-} ligands, each Re atom of the Re_6Te_8 core is coordinated by the previously unknown $[Te_8Cl_{18}]^{2-}$ chlorotellurato ligand through a Re–Te bond (2.638(2) Å). In turn, each $[Te_8Cl_{18}]^{2-}$ ligand chelates six $[Re_6Te_8]^{2+}$ clusters (Fig. 1); the ratio of $[Re_6Te_8]^{2+}$ clusters to $[Te_8Cl_{18}]^{2-}$ ligands is 1:1. The clusters and ligands are arranged in a nearly perfect rock-salt (NaCl) formation, similar to the arrangement of $[Re_6Te_8]^{2+}$ clusters and Te_7^{2-} ligands in Re_6Te_{15}. The structure of $Re_6Te_{16}Cl_{18}$ is thus three-dimensional. The $[Te_8Cl_{18}]^{2-}$ ligand can be described as consisting of two components. Component A is a central Te_2Cl_9 unit composed of a pair of face-sharing $TeCl_6$ octahedra, and component B comprises Te_2Cl_3 units that bridge A to two $[Re_6Te_8]^{2+}$ clusters (Fig. 2). There are three B units per A unit, and therefore six $[Re_6Te_8]^{2+}$ clusters are bridged to each A component (Fig. 3). In component A the Te–Te interatomic distance is 3.11(1) Å suggestive of a bonding interaction. The Te–μ_2-Cl bond length is 2.555(8) Å. Thus, component A may be formulated as $[Cl'_3TeCl_3TeCl'_3]$, where the two sets of Cl'_3 atoms join component A to component B; each B component bischelates an A component through one Cl atom per octahedron. Component B is a corner-sharing pair of $TeCl_2$

[*] Prof. J. A. Ibers, Y. V. Mironov, M. A. Pell
Department of Chemistry, Northwestern University
Evanston, IL 60208-3113 (USA)
Fax: Int. code +(847)491-2976
e-mail: ibers@chem.nwu.edu

[**] This research was sponsored by the U. S. National Science Foundation, Grant DMR91-14934.

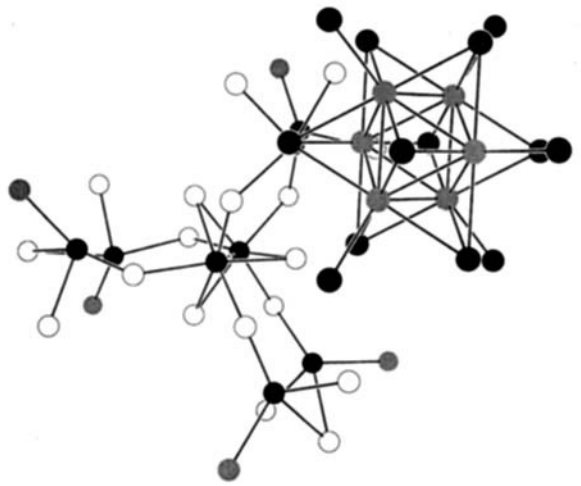

Fig. 2. View of a $[Te_8Cl_{18}]^{2-}$ ligand bound to a single $[Re_6Te_8]^{2+}$ cluster. Dangling Re atoms belong to other $[Re_6Te_8]^{2+}$ clusters, dangling Te atoms belong to other $[Te_8Cl_{18}]^{2-}$ ligands. Re atoms are drawn as checkered spheres, Te atoms as solid spheres, and Cl atoms as hollow spheres.

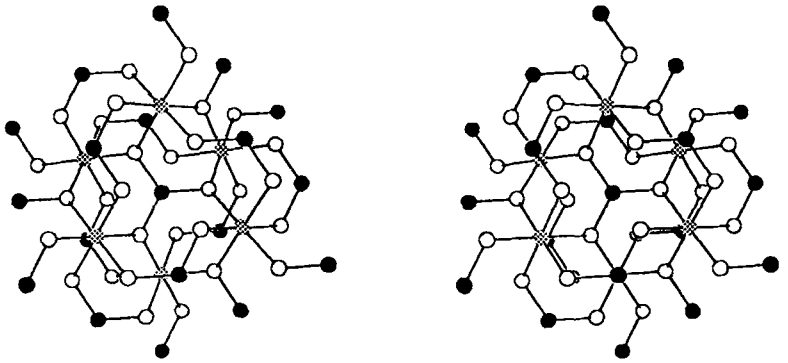

Fig. 3. Stereoview of the connectivity in $Re_6Te_{16}Cl_{18}$. Each $[Te_8Cl_{18}]^{2-}$ ligand is formed of a central A component (Te_2Cl_9) linked to three B components (Te_2Cl_3) through μ_2-Cl atoms. Each B component chelates two $[Re_6Te_8]^{2+}$ clusters. Thus $[Te_8Cl_{18}]^{2-}$ chelates a total of six clusters. A components are drawn as solid spheres, B components as hollow spheres, and Re_6Te_8 clusters as checkered spheres.

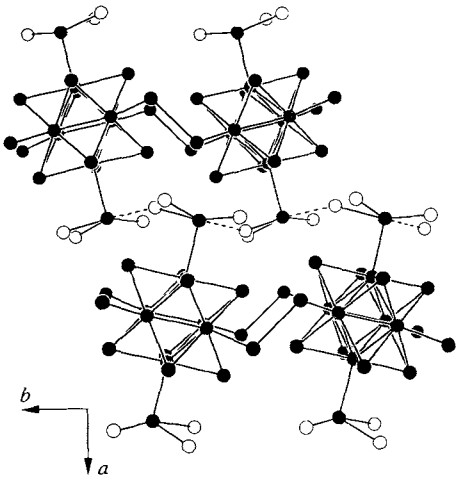

Fig. 4. Structure of $Re_6Te_{16}Cl_6$ viewed along [001].

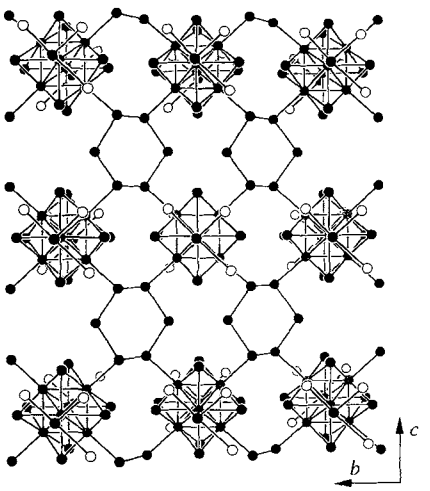

Fig. 5. Structure of $Re_6Te_{16}Cl_6$ viewed along [100].

units, Te_2Cl_3 or $(TeClCl_{1/2})_2$. The Te–Cl bond lengths in component B are 2.323(7) and 2.860(7) Å. Accordingly, we can write the $[Te_8Cl_{18}]^{2-}$ ligand as $[(Cl_3TeCl_3TeCl_3)((TeClCl_{1/2})_2)_3]^{2-}$, in which the Te centers are Te^{2+}.

$Re_6Te_{16}Cl_6$ may be thought of as $[(Re_6Te_8)(Te_6)(TeCl_3)_2]$, since it consists of $[Re_6Te_8]^{2+}$ clusters joined together by Te_6 and $[TeCl_3]^-$ ligands. The $[Re_6Te_8]^{2+}$ cluster core, which has a crystallographically imposed twofold axis, has bond lengths and angles similar to those observed in $Re_6Te_{16}Cl_{18}$. In $Re_6Te_{16}Cl_6$ two Re atoms at opposite vertices of the Re_6 octahedron are capped by $[TeCl_3]^-$ ligands (Fig. 4). The four remaining Re atoms are capped with neutral Te_6 ligands. The Te_6 ligands have a chair conformation with Te–Te bond lengths ranging from 2.762(4) to 2.899(5) Å. The neutral Te_6 species has not been previously observed, either as an isolated species or as a ligand. The neutral molecule S_6 has a chair conformation.[13] Known Te_6 species include $[Te_6I_2]^{2+}$, Te_6^{2+} (boat conformation),[14] and Te_6^{4+}.[15, 16] In the present structure each Te_6 chair chelates four $Re_6Te_8(TeCl_3)_2$ clusters (Re–Te = 2.697(3) and 2.707(3) Å) to create a two-dimensional network (Fig. 5). The four Re-bound Te atoms of the Te_6 chair are coplanar. The Te–Cl bond lengths in the $[TeCl_3]^-$ ligands are 2.387(8), 2.433(8), and 2.817(9) Å. The Cl atom that forms the longer Te–Cl bond interacts further with the Te^{2+} center of a $[TeCl_3]^-$ ligand from an adjacent layer, creating a square-planar geometry about the Te^{2+} center ($Cl_3Te\cdots Cl$ 3.028(9) Å, Cl-Te-Cl = 84.5(3)–101.0(2)°). A square-planar arrangement of Te^{2+} centers has also been observed in $Nb_2Te_8I_{12}$,[6] in which each Te atom of the $[Te_2I_6]^{2-}$ ligand resides in a square-planar environment. Whereas the $[TeI_3]^-$ ligand has been observed in $Mo_3Te_{10}I_{10}$,[7] no $[TeCl_3]^-$ ligands have been characterized previously.

The discovery of these remarkable new ligands is astonishing. Previous investigations in the $ReCl_5$/Te system yielded the isolated clusters $Re_6(\mu_3\text{-}Te)_6(\mu_3\text{-}Cl)_2(TeCl_2)_2Cl_4$[8] at similar reaction temperatures, and $Re_4Te_4(TeCl_2)_4Cl_8$[17] at lower reaction temperatures. The tremendous dependence of stoichiometry, ligand type, and structure dimensionality on reaction conditions in this system suggests that exciting new frontiers still exist in seemingly classical cluster halochalcogenide chemistry.

Experimental Procedure

$Re_6Te_{18}Cl_{16}$ and $Re_6Te_{16}Cl_6$ were obtained from the reaction of $ReCl_5$ and elemental Te in the ratio 1:3. The synthesis was carried out in an evacuated fused-silica tube heated at 450 °C for 1 d and then cooled at 4 K h^{-1} to promote crystal growth. The reaction mixture was washed with CH_3CN, and single crystals were collected and separated by their habits. The initial atomic composition of each compound was obtained from energy dispersive X-ray analysis (EDX).

X-ray structural analyses: $Re_6Te_{16}Cl_{18}$: black hexagonal plates, crystal dimensions $0.32 \times 0.30 \times 0.21 \times 0.046$ mm, trigonal, D_{3d}^6-$R\bar{3}c$, $Z = 6$, $a = 11.814(2)$, $c =$

54.46(1) Å, $V = 6583(2)$ Å^3 ($T = 113$ K), $\rho_{calcd} = 5.747$ g cm^{-3}, Picker diffractometer: $2\theta_{max} = 53.11°$, $Mo_{K\alpha}$, $\lambda(K_{\alpha 1}) = 0.7093$ Å, ω scan mode, 10788 reflections measured, 1537 independent reflections all of which were included in the refinement, data corrected for Lorentz-polarization effects and for absorption (analytical method), $\mu = 280$ cm^{-1}, min./max. trans. = 0.027/0.282, solution by direct methods [18], anisotropic refinement on F^2 by full-matrix least-squares [19], 62 parameters, $R_w(F^2) = 0.197$, $R_1 = 0.068$ for 1198 reflections having $F_o^2 > 2\sigma(F_o^2)$, residual electron density = 5.4 e Å^{-3}. $Re_6Te_{16}Cl_6$: dark red needlelike plates, crystal dimensions $0.010 \times 0.025 \times 0.133$ mm, orthorhombic D_2^3-$P2_12_12$, $Z = 2$, $a = 18.15(2)$, $b = 8.45(1)$, $c = 10.67(1)$ Å, $V = 1636(4)$ Å^3 ($T = 113$ K) $\rho_{calcd} = 6.845$ g cm^{-3}, Picker diffractometer: $2\theta_{max} = 51.98°$, $Mo_{K\alpha}$, $\lambda(K_{\alpha 1}) = 0.7093$ Å, θ-2θ scan mode, 8200 reflections measured, 3242 independent reflections all of which were included in the refinement, data corrected for Lorentz-polarization effects and for absorption (analytical method), $\mu = 366$ cm^{-1}, min./max. trans. = 0.200/0.394, solution by direct methods [18], anisotropic refinement on F^2 by full-matrix least-squares [19], 127 parameters, $R_w(F^2) = 0.104$, $R_1 = 0.047$ for 2276 reflections having $F_o^2 > 2\sigma(F_o^2)$, residual electron density = 3.2 e Å^{-3}. Further details of the crystal structure investigations may be obtained from the Fachinformationszentrum Karlsruhe, D-76344 Eggenstein-Leopoldshafen (Germany), on quoting the depository numbers CSD-405812 and CSD-405813.

Received: July 9, 1996 [Z 93161E]
German version: *Angew. Chem.* **1996**, *108*, 2999–3001

Keywords: clusters · rhenium compounds · structure elucidation · tellurium compounds

[1] A. Perrin, M. Sergent, *New J. Chem.* **1988**, *12*, 337–356.
[2] O. M. Yaghi, M. J. Scott, R. H. Holm, *Inorg. Chem.* **1992**, *31*, 4778–4784.
[3] J. R. Long, A. S. Williamson, R. H. Holm, *Angew. Chem.* **1995**, *107*, 248; *Angew. Chem. Int. Ed. Engl.* **1995**, *34*, 226–229.
[4] J.-C. Gabriel, K. Boubekeur, P. Batail, *Inorg. Chem.* **1993**, *32*, 2894–2900.
[5] J. R. Long, L. S. McCarty, R. H. Holm, *J. Am. Chem. Soc.* **1996**, *118*, 4603–4616.
[6] A. Leist, W. Tremel, *Angew. Chem.* **1993**, *105*, 1798–1799; *Angew. Chem. Int. Ed. Engl.* **1993**, *32*, 1751–1752.
[7] V. P. Fedin, H. Imoto, T. Saito, *J. Chem. Soc. Chem. Commun.* **1995**, 1559–1560.
[8] Y. V. Mironov, M. A. Pell, J. A. Ibers, *Inorg. Chem.* **1996**, *35*, 2709–2710.
[9] J. R. Eveland, K. H. Whitmire, *Angew. Chem.* **1996**, *108*, 841–843; *Angew. Chem. Int. Ed. Engl.* **1996**, *35*, 741–742.
[10] F. Klaiber, W. Petter, F. Hulliger, *J. Solid State Chem.* **1983**, *46*, 112–120.
[11] V. E. Fedorov, N. V. Podberezskaya, A. V. Mischenko, G. F. Khudorozko, I. P. Asanov, *Mater. Res. Bull.* **1986**, *21*, 1335–1342.
[12] Y. V. Mironov, J. A. Cody, T. E. Albrecht-Schmitt, J. A. Ibers, *J. Am. Chem. Soc.*, in press.
[13] J. Donohue, A. Caron, E. Goldish, *J. Am. Chem. Soc.* **1961**, *83*, 3748–3751.
[14] J. Beck, *Chem. Ber.* **1995**, *128*, 23–27.
[15] R. C. Burns, R. J. Gillespie, W.-C. Luk, D. R. Slim, *Inorg. Chem.* **1979**, *18*, 3086–3094.
[16] M. J. Collins, R. J. Gillespie, J. F. Sawyer, *Acta Crystallogr. Sect. C* **1988**, *44*, 405–409.
[17] Y. V. Mironov, T. E. Albrecht-Schmitt, J. A. Ibers, *Inorg. Chem.*, submitted.
[18] G. M. Sheldrick, in "*Crystallographic Computing 3*", (Eds.: G. M. Sheldrick, C. Krüger, R. Goddard), Oxford University Press, London, **1985**, pp. 175–189.
[19] G. M. Sheldrick, *J. Appl. Crystallogr.* **1996**, in press.

First Experimental Determination of the Ionization Potentials of Berkelium and Californium

Stefan Köhler, Nicole Erdmann, Martin Nunnemann, Günter Herrmann, Gerhard Huber, Jens Volker Kratz, Gerd Passler, and Norbert Trautmann*

The first ionization potential is a fundamental property of an element and is of great importance for many physical and chemical processes. Its accurate determination enables one to identify systematic trends in binding energies from element to element, and to draw conclusions on the electronic structure of atoms, since the first ionization potential is directly connected to the atomic spectrum: The energy levels can either be given as (negative) binding energies, where the ionization potential represents the energetic zero point, or as (positive) excitation energies. In this case the level energy E_n for $n \rightarrow \infty$ converges to the ionization potential.

Reliable information about the electronic structure of the heaviest elements is needed to be able to state whether the regularities of the Periodic Table of Elements are maintained up through these elements or whether they are disturbed.[1] The first ionization potential is a property that sensitively depends on relativistic effects, which are expected in the heaviest elements as a result of the relativistic mass increase of the inner electrons.[2] The precise determination of the first ionization potential of these elements can serve as a test of the predictions of relativistic multiconfiguration Dirac–Fock calculations.[3] Furthermore, the first ionization potential is an important quantity in the Born–Haber cycle.[4]

The most accurate ionization potentials have been obtained by laser spectroscopic methods. The first ionization potentials of the lanthanide elements as well as those of uranium and the lighter transuranium elements neptunium and plutonium have been determined very accurately from the convergence of long series of highly excited Rydberg states.[5–8] A large amount of data is required for a correct interpretation of the spectra, due to configuration-interactions. The determination of the first ionization potential of plutonium by Worden et al.[8] shows the limitations of the method: up to 2 g of radioactive ^{239}Pu had to be used.

We present here a method that allows the accurate determination of the first ionization potential with samples in the nanogram range (ca. 10^{12} atoms). This opens the possibility for determining ionization potentials of the heavier actinide elements which can be conveniently handled only in very small quantities because of their strong radioactivity, or are available only in limited amounts. With such small amounts we were able to confirm the first ionization potential of ^{239}Pu, and to measure for the first time those of americium and curium.[9]

The method is based on the determination of photoionization thresholds in the presence of an external static electric field. The required detection efficiency is obtained by using resonance ion-

[*] Dr. N. Trautmann, Dr. S. Köhler, Dipl.-Phys. N. Erdmann, Prof. Dr. G. Herrmann, Prof. Dr. J. V. Kratz
Institut für Kernchemie der Universität
Fritz-Strassmann-Weg 2, D-55128 Mainz (Germany)
Fax: Int. code + (6131)394-488
Dipl.-Phys. M. Nunnemann, Prof. Dr. G. Huber, Dr. G. Passler
Institut für Physik der Universität Mainz (Germany)

[**] This work was supported by the Bundesministerium für Umwelt, Naturschutz und Reaktorsicherheit, Bundesamt für Strahlenschutz, Bundesministerium für Bildung, Wissenschaft, Forschung und Technologie, Deutsche Forschungsgemeinschaft, and United States Department of Energy.

 © VCH Verlagsgesellschaft mbH, D-69451 Weinheim, 1996 0570-0833/96/3523-2856 $ 15.00+.25/0

ization mass spectrometry developed by our group for ultratrace analysis of actinide elements.[10] According to the classical saddle point model[11] the Coulomb potential of an atom changes in the presence of an external electric field; the potential is shifted to lower values with increasing field strength. The energetic position of the saddle point depends linearly on the square root of the electric field strength.[12] All levels of higher energy than the saddle point are field ionized. Therefore, the saddle point denotes the ionization threshold as a function of the electric field. Experimentally, a high-lying state is populated by two-step resonant laser excitation. Located in a known static electric field, the atom is then ionized by scanning across the threshold the wavelength of the laser for the ionizing step. This is shown in Figure 1 for berkelium; two different excitation schemes were used as an internal control of the method.

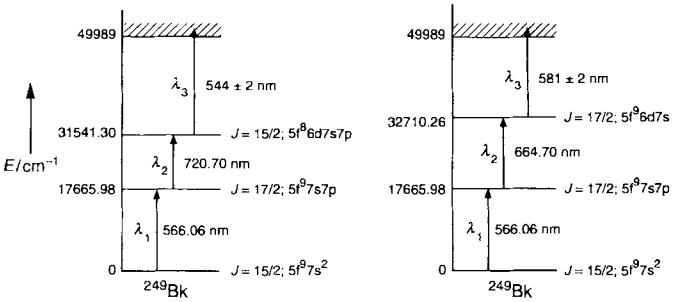

Fig. 1. Excitation schemes for berkelium as used in the determination of the first ionization potential by resonance ionization mass spectrometry. After a resonant two-step excitation (λ_1, λ_2) the wavelength λ_3 of the laser for the ionizing step is scanned across the ionization threshold W_{th}.

The ions produced are mass-selectively detected in a time-of-flight mass spectrometer. The ionization threshold is marked by the sudden increase of the intensity of the ion signal. Figure 2 illustrates for berkelium how the ionization threshold is shifted to lower values with increasing field strength. Only a very low

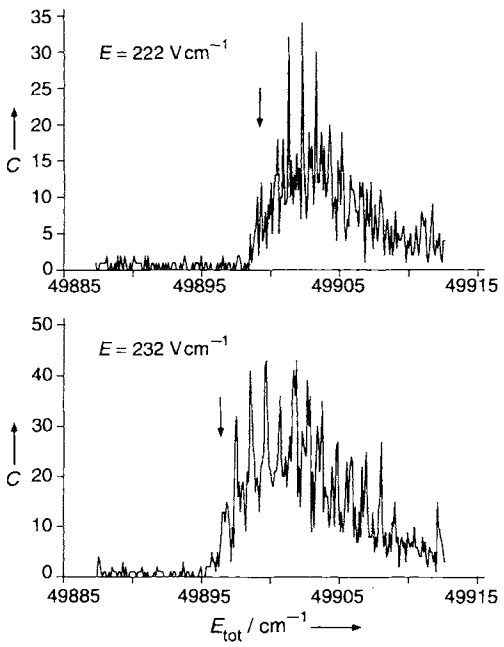

Fig. 2. Ionization thresholds (arrows) of berkelium for two different electric field strengths E in the interaction region of the atomic beam and the laser beams. Recorded is the number C of the ions as a function of the total photon energy E_{tot} of the three laser beams (λ_1, λ_2, λ_3, see Fig. 1).

background is present below the threshold which may be due to nonresonant multiphoton ionization. Hence, the increase of the ion signal at the threshold can be determined accurately. Beyond the threshold autoionizing Rydberg–Stark manifolds are observed. By measuring the ionization thresholds for various electric field strengths, the first ionization potential can be determined by extrapolation to zero field strength according to the saddle point model.[12] The precision of this method can be seen from Figure 3, which shows the data obtained for berkelium with two alternative excitation schemes. For berkelium as well as for californium the values fit perfectly the linear extrapolation to zero field strength by a least-squares fit.

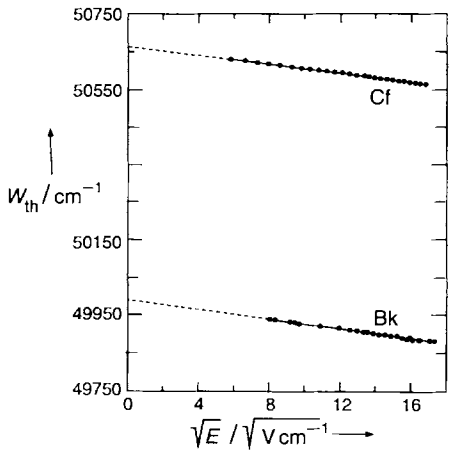

Fig. 3. Determination of the first ionization potentials of berkelium and californium. The measured ionization thresholds W_{th} of ^{249}Bk and ^{249}Cf are plotted versus the square root of the electric field strength E. Extrapolation to $E = 0$ gives the first ionization potential. Samples of 1×10^{12} atoms (0.4 ng) were used.

For the investigation of berkelium and californium three-step excitations were used starting from the atomic ground state. The excitation schemes were chosen taking into account the values for the first ionization potential predicted in the literature[13] from extrapolations of spectroscopic data (Table 1). Table 1 also gives the first ionization potentials I_{exp} obtained for ^{249}Bk ($T_{\frac{1}{2}}$ = 320 days) and ^{249}Cf ($T_{\frac{1}{2}}$ = 351 years); the corresponding values in cm^{-1} are 49989(2) and 50665(2), respectively.

Table. 1. First ionization potentials I of berkelium and californium determined by photoionization in an electric field. All wavelengths are given for vacuum. The values from the literature $I_{extr.}$ were extrapolated from spectral data [13].

Element	I[eV][a] (exp.)	$I_{extr.}$[eV] (extrapol.)	Excitation scheme λ_1[nm]	λ_2[nm]	λ_3[nm]
berkelium	6.1979(2)	6.229(25)	566.06	720.70	ca. 544
	6.1979(2)	6.229(25)	566.06	664.70	ca. 581
californium	6.2817(2)	6.298(25)	572.77	625.23	ca. 581

[a] The given 2σ errors of the first ionization potential result from the uncertainty of the ordinate of the least-squares fit.

The experimental values for the first ionization potentials of the actinide elements are between the extrapolated data[13] and those from Hartree–Fock calculations.[14] They follow the trend for binding energies of the s electrons determined by ab initio Hartree–Fock calculations for the ionization process 5f^{N}7s^2 → 5f^{N}7s. These binding energies are called the normalized ionization potentials I_n of the actinides. If the ground state dif-

fers from the configuration $5f^N7s^2$ due to population of the 6d shell, the values of the ionization potentials are corrected by the difference of the term energies. For berkelium and californium no correction is required. Hartree–Fock calculations predict that the normalized ionization potentials, when plotted against N, form two straight lines, changing the slope at americium (half-filled 5f shell) (Fig. 4). While the experimental data for the

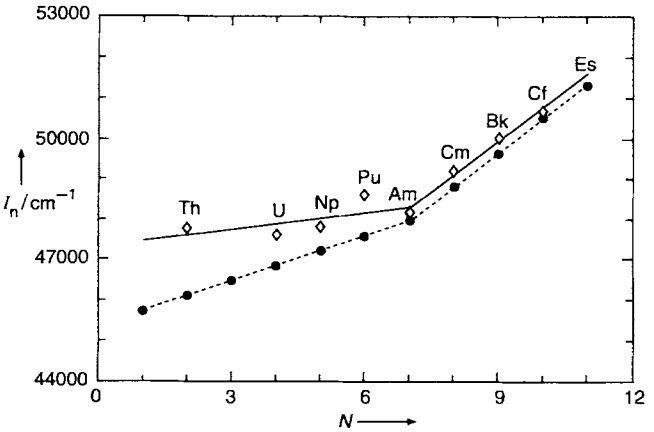

Fig. 4. Normalized first ionization potentials of the actinide elements for the ionization process $5f^N7s^2 \rightarrow 5f^N7s$ as a function of N. Plotted are the normalized experimental data (◇), this work and reference [9], and the theoretical values (●) obtained by Hartree–Fock calculations [14].

elements beyond americium agree very well with the assumption of a linear dependence, the lighter actinides show stronger deviations from the straight line. This may be due to the participation of 5f electrons in the ionization process. The determination of the still unknown first ionization potentials of protactinium and actinium is therefore of interest.

Experimental Procedure

Resonance ionization of the actinide elements required an atomic beam. This was achieved by resistive heating of a filament consisting of a thin tantalum foil, on which the element under investigation was electrochemically deposited as hydroxide, and covered with a titanium layer produced by sputtering. By heating such a filament the hydroxide was converted into the oxide, which was reduced to the metallic state during diffusion through the covering layer.

Three tunable dye lasers, which were pumped by two copper vapor lasers of high pulse repetition rate (6.5 kHz, 30 W, and 50 W average output power, 30 ns pulse duration), are used for optical excitation of the atoms. With the dye lasers a wavelength range from 520 nm to 850 nm can be covered; a conversion efficiency of up to 25% of the pump laser power can be achieved. The wavelengths were determined with a pulsed wavemeter. The dye laser beams were introduced with quartz fibers or prisms into the setup where they cross the atomic beam. The ions produced were accelerated by electric fields and detected with a multichannel plate detector after they had passed a field-free drift tube.

Received: July 26, 1996 [Z9385IE]
German version: *Angew. Chem.* **1996**, *108*, 3036–3038

Keywords: actinides · berkelium · californium · ionization potentials · laser spectroscopy

[1] P. Pyykkö, J. P. Desclaux, *Acc. Chem. Res.* **1979**, *12*, 276–281.
[2] P. Pyykkö, *Chem. Rev.* **1988**, *88*, 563–594.
[3] B. Fricke, E. Johnson, G. M. Rivera, *Radiochim. Acta* **1993**, *62*, 17–25.
[4] L. R. Morss, *J. Phys. Chem.* **1971**, *75*, 392–399.
[5] R. W. Solarz, C. A. May, L. R. Carlson, E. F. Worden, S. A. Johnson, J. A. Paisner, L. J. Radziemski, *Phys. Rev. A* **1976**, *14*, 1129–1136.
[6] E. F. Worden, R. W. Solarz, J. A. Paisner, J. G. Conway, *J. Opt. Soc. Am.* **1978**, *68*, 52–61.
[7] E. F. Worden, J. G. Conway, *J. Opt. Soc. Am.* **1979**, *69*, 733–738.
[8] E. F. Worden, L. R. Carlson, S. A. Johnson, J. A. Paisner, R. W. Solarz, *J. Opt. Soc. Am. B* **1993**, *10*, 1998–2005.
[9] R. Deissenberger, S. Köhler, F. Ames, K. Eberhardt, N. Erdmann, H. Funk, G. Herrmann, H.-J. Kluge, M. Nunnemann, G. Passler, J. Riegel, F. Scheerer, N. Trautmann, F.-J. Urban, *Angew. Chem.* **1995**, *107*, 891–893; *Angew. Chem. Int. Ed. Engl.* **1995**, *34*, 814–815.
[10] W. Ruster, F. Ames, H.-J. Kluge, E.-W. Otten, D. Rehklau, F. Scheerer, G. Herrmann, C. Mühleck, J. Riegel, H. Rimke, P. Sattelberger, N. Trautmann, *Nucl. Instrum. Meth. Phys. Res. Sect. A* **1989**, *281*, 547–558.
[11] B. H. Bransden, C. J. Joachain, *Physics of Atoms and Molecules*, Longman, London, **1984**, p. 227.
[12] In a constant external electric field E the excitation energy $W(r)$ of an atom with a highly excited electron is given by Equation (a), relative to its electronic

$$W(r) = I - \frac{Z_{eff}e^2}{4\pi\varepsilon_0 r} - eEr \qquad \text{(a)}$$

ground state in a one-dimensional approximation, where e is the electron charge, Z_{eff} the effective nuclear charge, ε_0 the dielectric constant of the vacuum, r the distance of the excited electron from the nucleus, and I the first ionization potential. The ionization threshold W_{th}, which is the maximum value of $W(r)$, results from Equation (b). Extrapolation to $E = 0$ leads to the first ionization potential.

$$W_{th}(E) = I - 2\sqrt{\frac{Z_{eff}e^3}{4\pi\varepsilon_0}}\sqrt{E} = I - const\sqrt{E} \qquad \text{(b)}$$

[13] J. Sugar, *J. Chem. Phys.* **1974**, *60*, 4103.
[14] K. Rajnak, B. W. Shore, *J. Opt. Soc. Am.* **1978**, *68*, 360–367.

From Pagodanes to Nonpentagonal (Homo)Dodecahedranes—The Undecacyclo-[10.10.0.0^{2,20}.0^{3,10}.0^{4,19}.0^{5,9}.0^{6,18}.0^{7,15}.0^{8,13}.0^{19,22}.0^{16,21}]docosane Cage**

Veeraraghava Sharma, Manfred Keller, Andreas Weiler, Dieter Hunkler, and Horst Prinzbach*

Dedicated to Professor Rolf Gleiter on the occasion of his 60th birthday

Pagodane and (seco)dodecahedrane cage structures[1] allowed the study of unusual electronic phenomena[2] and of unusual molecular species (for example, valence isomeric 4c/3e radical cations[3] and σ-bishomoaromatic 4c/2e dications[4]). For the quantification of the factors determining the transannular electronic interactions, additional model structures with well-defined molecular dimensions are sought. In the synthetic route presented here, pagodanes **A** are transformed into unsubstituted and into pairwise symmetrically functionalized bis(homo)dodecahedranes **C**. This strategy, which in principle is also applicable to hetero analogs, is characterized by twofold cyclization of bissecododecahedranes **B**, with transcaveally opposed C=X bonds and *anti*-positioned leaving groups L, and corresponds to, without any mechanistic implication, substitution by the relatively distant X groups.[5, 6]

[*] Prof. Dr. H. Prinzbach, Dr. V. Sharma, Dr. M. Keller, Dipl.-Chem. A. Weiler, Dr. D. Hunkler
Chemisches Laboratorium der Universität
Institut für Organische Chemie und Biochemie
Albertstrasse 21, D-79104 Freiburg (Germany)
Fax: Int. code +(761)203-5987

[**] This work was supported by the Deutsche Forschungsgemeinschaft, the Fonds der Chemischen Industrie, and BASF AG. We thank Dr. J. Wörth and C. Warth for MS measurements. V. S. thanks the Alexander-von-Humboldt-Stiftung for a fellowship.

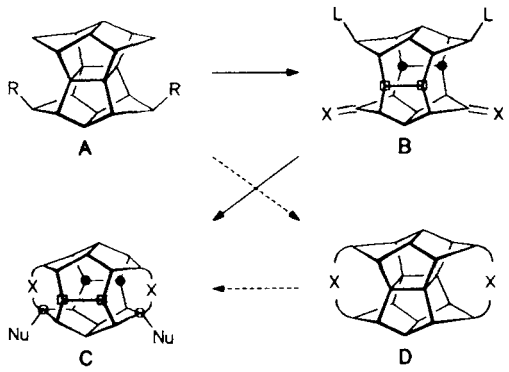

Based on the calculated energy and structure data (MM2)[7, 8] given in Scheme 1, the insertion of two methylene bridges into the pentagonal structures **1**–**3** has the following consequences:[8, 9] The molecular strain energy increases significantly for **1** → **4** (ΔE_{str} = 9.9 kcal mol^{-1}) and decreases significantly for **2** → **5** and even more for **3** → **6** (ΔE_{str} = −12.1 and −31.0 kcal mol^{-1}, respectively); the homologous cages are less "bulged" (e.g. Δd = −0.72 Å for **3** → **6**), the C=C bonds less "hyperstable", and the olefinic carbons much less but still significantly pyramidalized. From the comparison with the bismethano-bridged [1.1.1.1]pagodane **7** (**D**, X = CH_2) it is apparent that the alternative route **A** → **D** → **C** has no chance here.

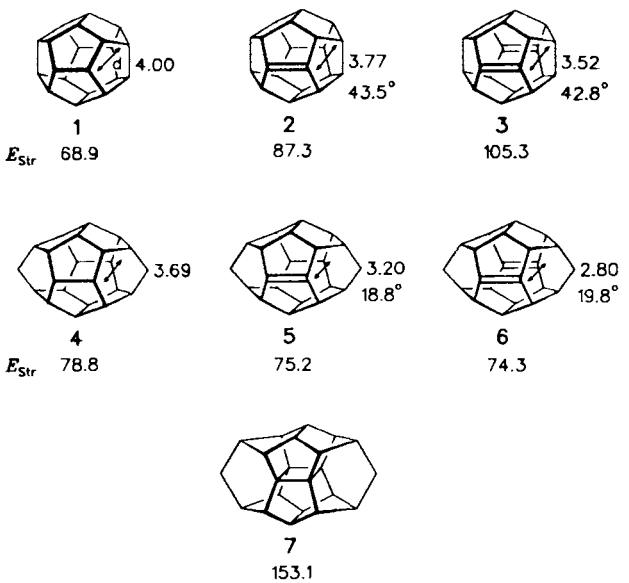

Scheme 1. Calculated (MM2) strain energies E_{Str} [kcal mol^{-1}]), distances d[Å], and angles Φ [°].

In the first examples of the route **A** → **B** → **C** presented in Schemes 2 and 3, 3,8-bis(methylene)bissecododecahedranes with *anti*-positioned Br nucleofugs (**10**, **13**, **16**) serve as the central intermediates **B**. The cyclizations at the exocyclic methylene C atoms (C-3′(8′)) must potentially compete with the formation of five-membered rings (through C-3(8)) to give pentagonal dodecahedranes. Chances were seen a priori to steer this competition by appropriate "timing" of the bond-breaking and -forming events. A comparable competition in electrophilic and radical additions to 3,7-bis(methylene)bicyclo[3.3.1]nonanes (formation of noradamantanes vs. adamantanes) has been extensively studied.[10]

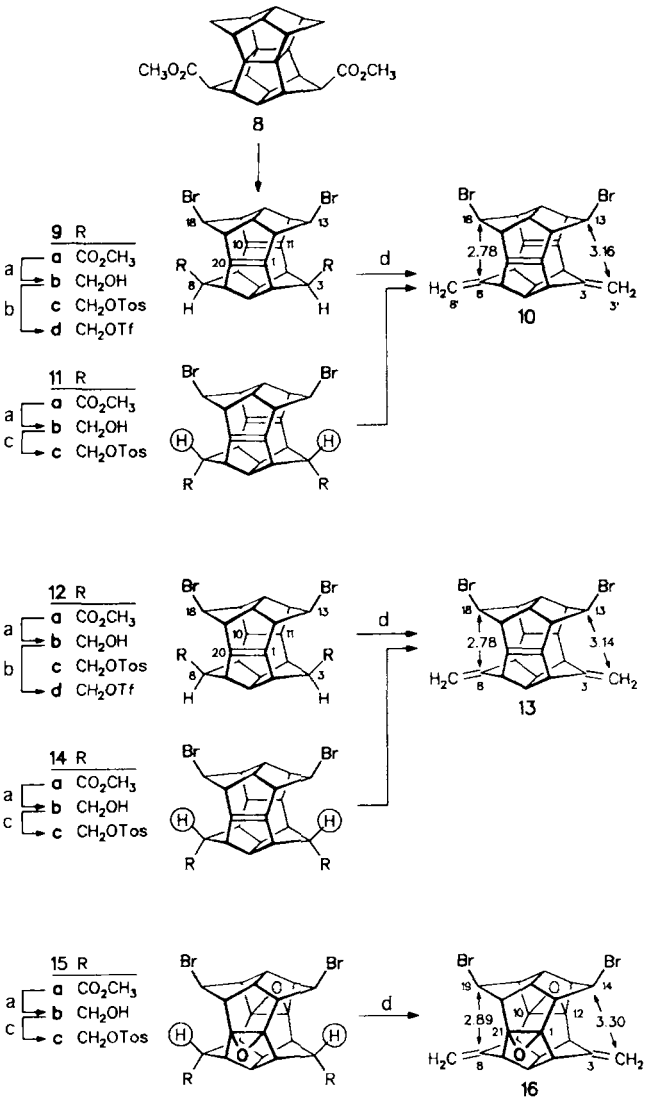

Scheme 2. a) DIBAH, CH_2Cl_2 (abs.), −78 °C, 3 h, 85%; b) Tf_2O, CH_2Cl_2 (abs.), pyridine (abs.), 0 °C → RT, 12 h, 60%; c) TosCl, pyridine (abs.), 50 °C, 24 h, 90%; d) "P2F" (6 equiv), benzene, RT, 1 h, 75–80%. DIBAH = diisobutylaluminum hydride, Tf = trifluoromethanesulfonyl, Tos = *p*-toluenesulfonyl.

Efficient protocols for the preparation of the precursors, the *syn,syn,anti,anti*- (**9a** and **12a**) and all-*anti*-dibromobissecodiesters (**11a**, **14a**, and **15a**), starting from the 4-*syn*,9-*syn*-diester **8** as a direct offshoot of the standard pagodane synthesis, have been described.[10, 11] We pursued two synthetic variants because of complications caused by the special structural situation in the lateral pockets of the bissecododecahedranes: *syn,syn*-Bistosylates **9c** and **12c**[13] are not accessible from the *syn,syn*-diols **9b** and **12b**; the accessible, sterically less encumbered bistriflates **9d** and **12d** reduce the strain through spontaneous β-eliminations to give **10** and **13**, respectively, in 60% yield. In the *anti,anti*-diols **11b**, **14b**, and **15b** twofold tosylation was unproblematic. Yet deprotonation in the effectively protected β-positions of the diesters **11c**, **14c** and **15c** was not possible with a variety of bases even under conditions leading to decomposition. The breakthrough came once again[12] by use of the small, very strong, and only weakly nucleophilic Schwesinger bases "P_2F" ("P_5F");[14] the colorless, crystalline dienes **10**, **13**, and **16** were obtained in 75–80% yield. The longer routes via **11a**, **14a**, and **15a** became the first choice also because of their better

accessibility (ca. 60% total yield based on **8**). Transcaveal 1,5-HBr eliminations as intrinsic alternatives to the β-eliminations (cf. the efficient base-catalyzed S_N2 cyclization of the diesters (**a**) to the corresponding pentagonal dodecahedranes[11]) do not play a significant role; there are indications that this competition only becomes detractive with better leaving groups as, for example, in the 13,18-diiodide corresponding to **11c**.

For the cyclizations of **10**, **13**, and **16** (**B** → **C**) to occur, steric as well as energetic aspects seem to require an effective interplay of C–Br bond breaking and transannular C–C bond forming events. For this problem a simple, though not yet optimal, and mechanistically still obscure solution was found (Scheme 3):

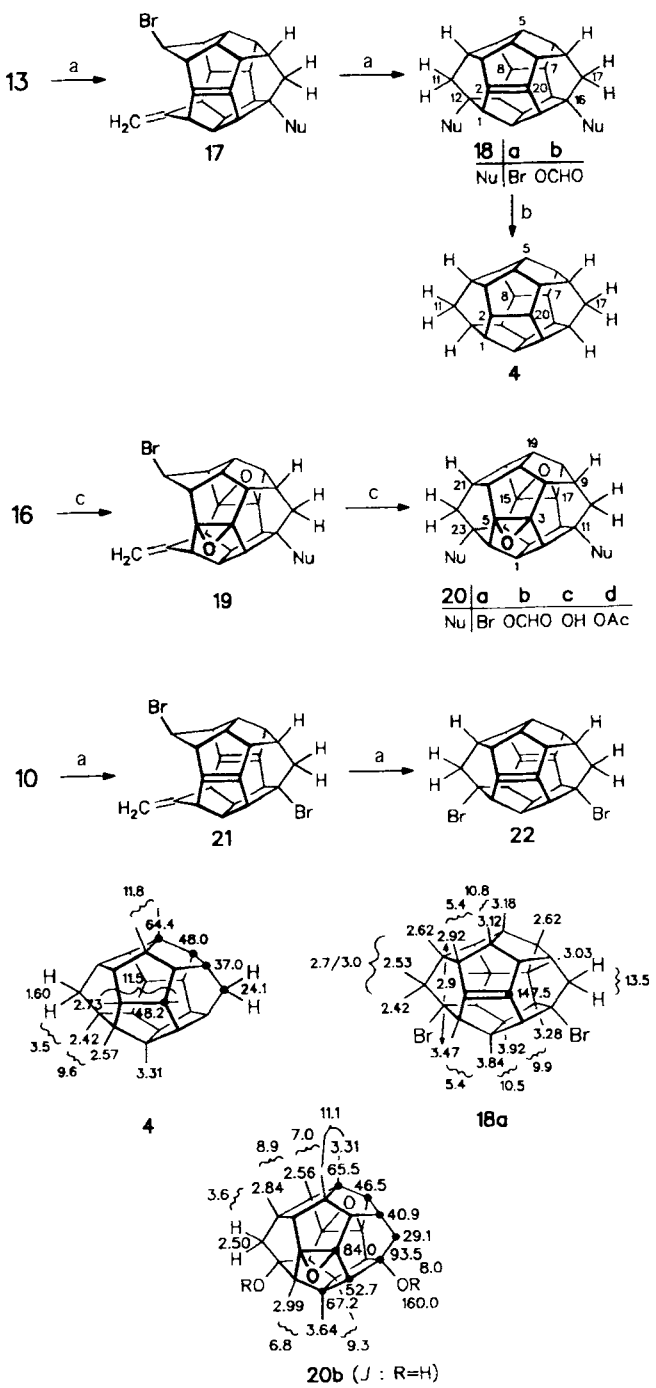

Scheme 3. a) KBr (10 equiv), DMF (abs.), 180 °C, 12 min; b) H_2, 10% Pd/C, methanol, RT, 1 h, >95%; c) analogous to a), 30 min.

When the degassed suspension of **13** and a large excess of KBr in DMF was heated at reflux until total conversion (TLC, ca. 12 min), the crude product isolated chromatographically in approximately 75% yield was practically uniform dibromo-bis(homo)dodecahedrene **18a** (and roughly 1% diformiate **18b**). Monitoring the reaction by TLC and ^{1}H NMR spectroscopy confirmed that the monocyclized **17a** was the only other monomeric component present in a low stationary concentration besides polymers; dodecahedranes resulting from bond formation between the less distant C3–C13 (C8–C18) positions would have been detected in small quantities (>2%). Obviously, within the analytical limits both cyclization steps were regiospecific.

The bis(homo)dodecahedrenes **18** ($\Phi \approx 19°$) are, as expected, much less reactive than their pentagonal analogs (e.g. **2**, $\Phi = 43.5°$[9]) and are relatively stable to air. Hydrogenation and twofold hydrogenolysis (Pd/C) of dibromide **18a** to give the $C_{22}H_{24}$ parent hydrocarbon **4** proceeded nearly quantitatively. The stability of the latter (m.p. >300 °C)—as in **1** the molecular strain (Scheme 1) is largely caused by H/H interactions—is mirrored in the mass spectrum: the molecular ion signal (*m/z*: 288) is by far the most intensive. The smaller molecular curvature of the "olefinic side" in the cages **18**—also compared with that in **2**—is manifested inter alia by the ^{13}C NMR shift of the olefinic C atoms (δ = 147.5 (**18**), 157.0 (**10**), 166.6 (**2**)) and by the vicinal H,H coupling constants, as determined by decoupling and simulation experiments (**18a**: e.g. $J_{1,22} = J_{3,4} = 5.4$, $J_{14,15} = 9.9$ Hz; **4**: $J_{1,12} = 9.6$, $J_{2,20} = 11.5$ Hz).

The diepoxide **16**, a "protected" form of diene **10**, reacts more slowly than **13** in the boiling DMF/KBr suspension—as was expected since the strain caused by the cyclization becomes larger with the increasing sp^3 character of the central C atoms (Scheme 1). After approximately 90% conversion (30 min) bromide **19a** (<5%), formiate **19b** (15%), and diformiate **20b** (42%) were isolated chromatographically (after longer reaction times the proportion of **20b** had decreased). The crystalline diformiate **20b** was transformed into diol **20c** by ammonolysis and additionally characterized as diacetate **20d**. According to the vicinal H,H coupling constants (e.g. $J_{1,24} = 6.8$, $J_{19,20} = 7.0$, $J_{20,21} = 8.9$ Hz), the curvature on the "epoxide sides" is larger than on the olefinic and smaller than on the saturated side of **18a**.

Cyclization of the tetraene **10** to give the "*syn*-periplanar" diene **22** of primary interest—the increase in strain is comparable to that for **13** → **18**—does not significantly affect the transannular π,π distance (2.75 → 2.80 Å, the calculated values are probably somewhat too small[6]). The consequently pronounced tendency in the starting compound and the product to undergo transannular additions[15] is considered to be (one) reason for the finding that the reaction of **10** under the conditions successfully used for **18** and **20** generated only traces of **21** and **22**, if any,[16] in complex product mixtures. If this complication cannot be overcome by changing the cyclization conditions, an approach to **22** via **20** is possible.

Crystallization of **4** from ethyl acetate provided small cubes suitable for an X-ray structural analysis.[17] In the crystal the molecule is situated on an inversion center. The structural details (Fig. 1), particularly the dimensions of the cavity, are in good agreement with the calculations. The C–C bond lengths range from 1.524 Å (C8–C9) to 1.556 Å (C3–C11), the C-C-C valence angles from 105.8° (C9-C7-C10) to 118.9° (C7-C6-C1); the cyclohexane rings of the bicyclo[3.3.1]nonane units are fixed as typical half-chairs. The symmetry-averaged H-C-C-H interplanar angles ($\alpha - \delta$) nicely correspond with the vicinal H,H coupling constants.

 © VCH Verlagsgesellschaft mbH, D-69451 Weinheim, 1996 0570-0833/96/3523-2860 $ 15.00+.25/0 Angew. Chem. Int. Ed. Engl. 1996 35 No. 23/24

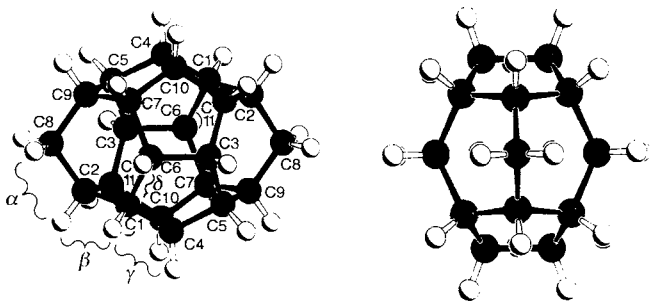

Fig. 1. X-ray crystal structure of **4** (front view, side view). Selected transcaveal distances [Å] and averaged interplanar angles [°]: C8–C8′ 6.106(2), C3–C6 3.737(1), C4···C10 4.213(1) (the atom numbers in the crystal structure do not correspond to those dictated by nomenclature [13]); α 60, β 28, γ 11, δ 2.

Remaining points to be clarified in view of the methodological problems noted for **10** and of further synthetic applications include the mechanistic ambiguities in the selective formation of dibromide **18a** and diformiate **20b**.

Received: July 3, 1996 [Z 9288 IE]
German version: *Angew. Chem.* **1996**, *108*, 3029–3031

Keywords: cage compounds · cyclizations · dodecahedranes

[1] a) H. Prinzbach, K. Weber, *Angew. Chem.* **1994**, *106*, 2329; *Angew. Chem. Int. Ed. Engl.* **1994**, *33*, 2239; b) W.-D. Fessner, H. Prinzbach in ref [1c], p. 353; c) *Cage Hydrocarbons* (Ed.: G. A. Olah), Wiley, New York, **1990**.

[2] H.-D. Martin, B. Mayer, K. Weber, H. Prinzbach, *Liebigs Ann.* **1995**, 2019; K. Weber, G. Lutz, L. Knothe, J. Mortensen, J. Heinze, H. Prinzbach, *J. Chem. Soc. Perkin Trans. 1* **1995**, 1991; H. Prinzbach, G. Gescheidt, H.-D. Martin, R. Herges, J. Heinze, G. K. S. Prakash, G. A. Olah, *Pure Appl. Chem.* **1995**, *67*, 673.

[3] A. D. Trifunac, D. W. Werst, R. Herges, H. Neumann, H. Prinzbach, M. Etzkorn, *J. Am. Chem. Soc.* **1996**, *118*, 9444; see also G. Gescheidt, R. Herges, H. Neumann, J. Heinze, M. Wollenweber, M. Etzkorn, H. Prinzbach, *Angew. Chem.* **1995**, *107*, 1109; *Angew. Chem. Int. Ed. Engl.* **1995**, *34*, 1016.

[4] G. A. Olah in ref. [1c], p. 103; G. K. S. Prakash, V. V. Krishnamurthy, R. Herges, R. Bau, H. Yuan, G. A. Olah, W.-D. Fessner, H. Prinzbach, *J. Am. Chem. Soc.* **1988**, *110*, 7764; R. Herges, P. von R. Schleyer, M. Schindler, W.-D. Fessner, *ibid.* **1991**, *113*, 3649; G. K. S. Prakash in *Stable Carbocation Chemistry* (Eds.: G. K. S. Prakash, P. von R. Schleyer), Wiley, New York, **1996**, in press.

[5] For the preparation of (aza)homododecahedranes by ring enlargement of the parent pentagonal skeleton see L. A. Paquette in ref. [1c], p. 313, and references therein. For oxahomododecahedranes see T. Voss, H. Prinzbach, *Tetrahedron Lett.* **1994**, *35*, 1535. Double ring enlargement of suitably 1,6-disubstituted dodecahedranes occurred without preferred direction and yielded complex mixtures of bishomododecahedranes: K. Scheumann, Dissertation, Universität Freiburg, **1993**.

[6] For unsaturated bislactones of type **C** (X = OCO, Nu = H) see R. Pinkos, J.-P. Melder, H. Fritz, H. Prinzbach, *Angew. Chem.* **1989**, *101*, 319; *Angew. Chem. Int. Ed. Engl.* **1989**, *28*, 310.

[7] N. L. Allinger, *J. Am. Chem. Soc.* **1977**, *99*, 8127; N. L. Allinger, H. L. Flanagan, *J. Comput. Chem.* **1983**, *4*, 399; O. Ermer, *Aspekte von Kraftfeldrechnungen*, Baur, München, **1981**; K. B. Lipkowitz, M. A. Peterson, *Chem. Rev.* **1993**, *93*, 4263, and references therein; W.-D. Fessner, B. A. R. C. Murty, P. R. Spurr, R. Pinkos, J.-P. Melder, H. Fritz, H. Prinzbach, *Chem. Ber.* **1992**, *125*, 1697.

[8] T. Voss, Dissertation, Universität Freiburg, **1995**.

[9] J.-P. Melder, K. Weber, A. Weiler, E. Sackers, H. Fritz, D. Hunkler, H. Prinzbach, *Res. Chem. Int.* **1996**, *22*, 667.

[10] H. Stetter, J. Gärtner, P. Tacke, *Chem. Ber.* **1968**, *98*, 3888; A. G. Yurchenko in ref. [1c], p. 155.

[11] R. Pinkos, J.-P. Melder, K. Weber, D. Hunkler, H. Prinzbach, *J. Am. Chem. Soc.* **1993**, *115*, 7173.

[12] M. Bertau, J. Leonhardt, A. Weiler, K. Weber, H. Prinzbach, *Chem. Eur. J.* **1996**, *2*, 570.

[13] The new compunds were fully characterized (^{1}H and ^{13}C NMR, IR, MS, elemental analysis). For nomenclature and numbering see the POLCYC programm (G. Rücker, C. Rücker, *Chimia*, **1990**, *44*, 116); e.g. **4**: undecacyclo[10.10.0.0^{2,20}.0^{3,10}.0^{4,19}.0^{5,9}.0^{6,18}.0^{7,15}.0^{8,13}.0^{19,22}.0^{16,21}]docosane; **18a**: 12,16-dibromoundecacyclo[10.10.0.0^{2,20}.0^{3,10}.0^{4,19}.0^{5,9}.0^{6,18}.0^{7,15}.0^{8,13}.0^{19,22}.0^{16,21}]docos-2(20)-ene; **20b**: 4,16-dioxatridecacyclo[11.11.0.0^{2,4}.0^{3,5}.0^{3,8}.0^{5,24}.0^{6,21}.0^{7,19}.0^{9,18}.0^{14,23}.0^{15,17}.0^{15,20}]tetracosane-11,23-diyl diformiate.

[14] R. Schwesinger, R. Link, G. Thiele, H. Rotter, D. Honert, H.-H. Limbach, F. Männle, *Angew. Chem.* **1991**, *103*, 1376; *Angew. Chem. Int. Ed. Engl.* **1991**, *30*, 1372; R. Schwesinger, H. Schlemper, C. Hasenfratz, J. Willaredt, T. Dambacher, T. Breuer, C. Ottaway, M. Fletschinger, J. Boele, H. Fritz, D. Putzas, H. W. Rotter, F. G. Bordwell, A. V. Satish, G.-Z. Ji, E.-M. Peters, K. Peters, H. G. von Schnering, L. Walz, *Liebigs Ann.* **1996**, 1055.

[15] B. A. R. C. Murty, R. Pinkos, P. R. Spurr, W.-D. Fessner, G. Lutz, H. Fritz, D. Hunkler, H. Prinzbach, *Chem. Ber.* **1992**, *125*, 1719; G. K. S. Prakash, W.-D. Fessner, G. A. Olah, G. Lutz, H. Prinzbach, *J. Am. Chem. Soc.* **1989**, *111*, 746.

[16] E. Quennet, Diplomarbeit, Universität Freiburg, **1996**.

[17] Crystal structure data of **4** ($C_{22}H_{24}$, M_r = 288.41): monoclinic, space group $C2/c$ (No. 15), a = 13.4664(4), b = 7.3744(1), c = 14.1556(4) Å, β = 100.217(2)°, V = 1383.45(6) Å^3, Z = 4, ρ_{calcd} = 1.385 g cm^{-3}; crystal dimensions: 0.40 × 0.26 × 0.26 mm^3, Enraf-Nonius CAD4 diffractometer, λ = 1.54178 Å, $Cu_{K\alpha}$ radiation, graphite monochromator, ω-2θ scan, 2749 collected reflections, 1389 independent reflections (R_{int} = 0.014), 1334 observed reflections ($I > 2\sigma(I)$), μ = 0.576 mm^{-1}, no absorption correction. The structure was solved by direct methods (SHELXS-86) and refined by full-matrix least-squares versus F^2 (SHELXL-93). The positions of hydrogen atoms were refined isotropically. 149 Parameters, R = 0.0453, R_w^2 = 0.1717, GOF = 1.716 (F^2), extinction coefficient: 0.008(2), largest difference peak: 0.299 e Å^{-3}. Further details of the crystal structure investigation may be obtained from the Fachinformationszentrum Karlsruhe, D-76344 Eggenstein-Leopoldshafen (Germany), on quoting the depository number CSD-404744.

Aggregation of Modified Zinc Chlorins in Nonpolar Solvents–Bacteriochlorophyll *c* Mimics with Interchanged Hydroxy and Carbonyl Functions**

Aldo Jesorka, Teodor Silviu Balaban, Alfred R. Holzwarth,* and Kurt Schaffner

In the self-assembly of the zinc chlorin **1** in nonpolar solvents (hexane solutions containing up to 1% v/v CH_2Cl_2), the central metal and the 3^1-hydroxy and 13^1-keto groups play an essential role in the formation of large aggregates.[1] We now provide evidence that the conditions for this aggregation tolerate an interchange of the hydroxy and carbonyl functions. Such an interchange does not sacrifice the capacity to self-assemble and form aggregates of the same type. This finding is not trivial, as it might seem at first sight, since experimental experience and molecular modeling have shown that the extent of self-assembly as well as the type and stability of the aggregates formed are subject to seemingly slight structural factors such as diastereoselective control by the configuration at C3^1 (e.g. in **2**[2]), steric crowding by substituents,[3] and the size of the ester side chain.[4] The functionally "inverse" zinc chlorins (**6a**-Zn and **6b**-Zn) thus access novel types of self-assembled aggregates.

The large aggregates of **1** possess a broad Q_y absorption band at 740 nm, which amounts to a large red shift of about 1820 cm^{-1} from the absorption of monomeric **1** (in solutions containing up to 5% v/v CH_3OH). The absorption is reminis-

[*] Prof. Dr. A. R. Holzwarth, Dipl.-Chem. A. Jesorka, Dr. T. S. Balaban, Prof. Dr. K. Schaffner
Max-Planck-Institut für Strahlenchemie
Postfach 10 13 65, D-45413 Mülheim an der Ruhr (Germany)
Fax: Int. code +(208) 306-3952
e-mail: holzwarth@mpi-muelheim.mpg.de

[**] We thank Dr. D. Müller, Ruhr-Universität Bochum, for FAB high-resolution mass spectra and M. Trinoga, J. Bitter and K. Sand for experimental assistance.

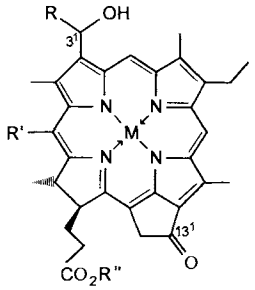

Scheme 1. Zinc chlorin model compounds:
1 R = R′ = H, R″ = CH_3, M = Zn
2 R = R″ = CH_3, R′ = H, M = Zn [1, 2]
3 R = R′ = CH_3, R″ = $C_{18}H_{37}$, M = Mg (BChl c_s, stearyl ester)

cent[5] of that of bacteriochlorophyll (BChl) *c* (e.g. **3**), *d*, and *e* aggregates, which function as antenna pigments in the light-harvesting chlorosomes of green photosynthetic bacteria.[6–8] The aggregates of **1**–**3** and related compounds, when formed in nonpolar solvents, possess comparable supramolecular structures based on cooperative interaction within a bonding network, which has been proposed on compelling molecular modeling[3b] and spectroscopic[6b, 7b, 9] data, and which is exemplified by the building block shown in Figure 1. The in vitro

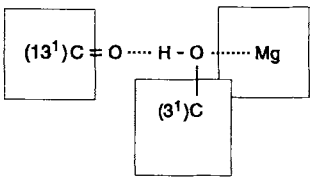

Fig. 1. Schematic representation of the central building block formed by a bonding network interconnecting three BChl *c* molecules (rectangles): the 3¹-hydroxy group of one BChl is bound to the magnesium of a second through oxygen ligation and simultaneously to the 13¹-keto group of a third BChl by hydrogen bonding [13].

aggregates possess tubular inverted micelle structures, the diameters of which Katz and co-workers[10, 11] found by neutron small-angle scattering to be very close to those determined by electron microscopy for the BChl *c*, *d*, and *e* rods in the interior of chlorosomes.[12]

Compounds **6a**-Zn and **6b**-Zn were prepared from methyl pyropheophorbide *a* (**4**-2H)[16] by $NaBH_4$ reduction to a 1:1 mixture of the (13¹*R*)- and (13¹*S*)-configurated diastereoisomeric alcohols (**5a**-2H and **5b**-ZH, respectively), vinyl cleavage with $OsO_4/NaIO_4$[17] to **6a**-2H and **6b**-2H, and metalation to **6a**-Zn and **6b**-Zn. The resulting diastereoisomers were separated by HPLC, and the configurations at C13¹ were assigned by ^{1}H NMR NOE difference spectra based on correlation with the fixed (*S*) configuration at C17.[18, 19]

When the solution of an equimolar mixture of **6a**-Zn and **6b**-Zn in dry CH_2Cl_2 was diluted with 99 parts of hexane, a broad Q_y maximum appeared at 738 nm (Fig. 2), red-shifted by 1760 cm^{-1} from the sharp 653 nm Q_y band of the monomers.[20]

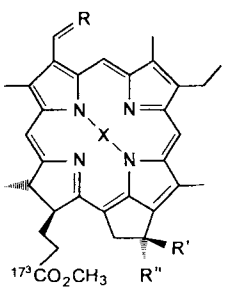

	C13¹ config.	R	R′	R″
4-X	-	CH_2		-O-
5a-X	(*R*)	CH_2	H	OH
5b-X	(*S*)	CH_2	OH	H
6a-X	(*R*)	O	H	OH
6b-X	(*S*)	O	OH	H
7a-X	(*R*)	O	H	$OCOCH_3$
7b-X	(*S*)	O	$OCOCH_3$	H

X = 2H, Zn

Scheme 2. "Inverse" chlorin compounds **4**–**7**.

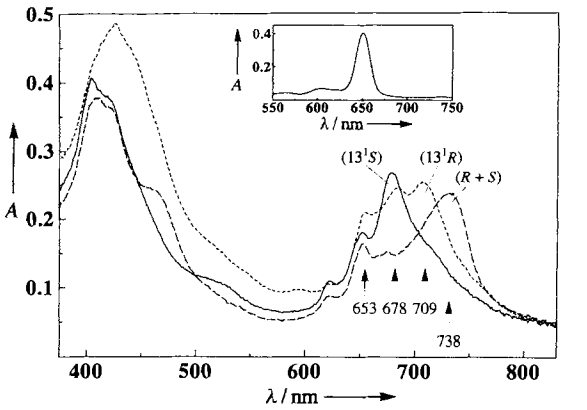

Fig. 2. UV/Vis absorption spectra of **6a**-Zn [(13¹*R*) ----], **6b**-Zn [(13¹*S*) ——], and a 1:1 epimer mixture of **6a**-Zn and **6b**-Zn [(13¹*R* + 13¹*S*) – – –]. All sample solutions (CH_2Cl_2/hexane, 1/99, v/v) were prepared by diluting concentrated CH_2Cl_2 solutions with *n*-hexane. Inset: Spectrum of the epimer mixture in CH_2Cl_2/hexane/methanol 1/99/5, v/v/v showing deaggregation after methanol addition. Spectra not corrected for scattering.

In conjunction with FT-IR data[21] recorded for the same solutions (for example, a 1640 cm^{-1} band for the hydrogen-bonded aldehyde), this aggregation can be assigned to the bonding network depicted in Figure 3, which is analogous to that elucidated

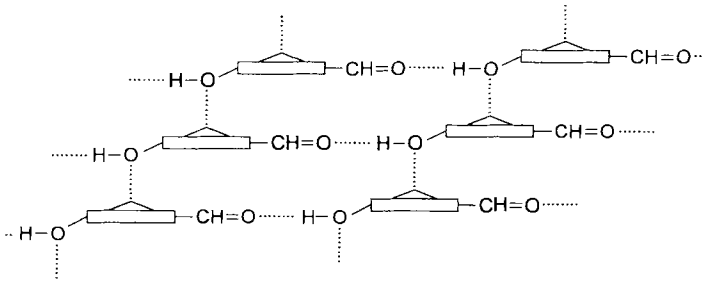

Fig. 3. Proposed bonding network for the large aggregate formed by **6a**-Zn and **6b**-Zn in *n*-hexane (absorption at λ_{max} = 738 nm), based on the building block as defined in Fig. 1; △: central zinc atom.

for BChl *c* and model compounds.[3b, 9] Thus both "normal" and "inverted" compounds lead to basically the same relative orientation of the chlorin rings. Aggregation of **6a**-Zn is subject to diastereoselective control, and clearly more so than the aggregation of **2** and **3**.[2, 9b] The absorption spectra of the separate (*R*) and (*S*) epimers under identical conditions show that monomers (λ_{max} 653 nm) and dimers (λ_{max} 678 nm) are the major components, but contribute a distinctly minor part of the composite absorption of the epimer mixture. Small oligomers absorbing around 708 nm are present in all three samples, which has been ascertained by Gaussian deconvolution. In the spectra of the separate epimers a minor longer wavelength absorption, attributable to large aggregates as in the (*R* + *S*) mixture, is observed for the (13¹*R*) epimer and for the (13¹*S*) epimer at higher concentrations.[22]

The epimer mixture affords more of the strongly red-shifted aggregate than the epimers separately. A rationalization of this observation cannot be offered at present. We should note, however, that in **1**–**3** configurational and conformational isomerism is restricted to the C3 substituent, whereas the constitution of **6a** and **6b** includes conformational isomerism of the C3 substituent and two configurations at C13¹. Cooperative self-

 © VCH Verlagsgesellschaft mbH, D-69451 Weinheim, 1996 0570-0833/96/3523-2862 $ 15.00+.25/0 Angew. Chem. Int. Ed. Engl. 1996, 35, No. 23/24

assembly[15] to large aggregates (Fig. 3) may involve selective stereocombinations that suffice to exert diastereoselective controls.

Addition of methanol, (which competes for ligation with zinc), to solutions of **6a**-Zn, **6b**-Zn, and (**6a**-Zn + **6b**-Zn) disintegrated all aggregates and formed homogeneous solutions of monomer (λ_{max} = 653 nm, see inset in Figure 2).

Neither **5a**-Zn/**5b**-Zn nor **7a**-Zn/**7b**-Zn in which one of the functional groups at either C3[1] or C13[1] is derivatized, exhibited any red shift in absorption in the wavelength region above 653 nm upon dilution of their CH_2Cl_2 solutions with hexane. This is in accordance with an earlier observation by Smith et al.[8] and confirms the binding roles of the 3[1]-aldehyde and the 13[1]-hydroxy groups (Fig. 1), as postulated previously for the original arrangement of the functions in **1**–**3**.[23] Furthermore, it provides independent evidence (in addition to FT-IR[21]) against the postulates that the C13[1] ketone[14c] and the C17[3] ester[14i] carbonyl groups coordinate directly with magnesium in BChl *c* aggregation.

Based on the structural conditions for the formation of chlorosomal type aggregates, as now defined by the two classes of metallochlorins (**1**–**3** and **6a**-Zn/**6b**-Zn) it should be possible to synthesize different macrocycles capable of similar self-assembly, and using them to design photoactive functional units by coupling to appropriate energy traps.[24]

Received: July 25, 1996 [Z 9383 IE]
German version: *Angew. Chem.* **1996**, *108*, 3019–3021

Keywords: aggregates · chlorins · chlorosomes · self-assembly

[1] H. Tamiaki, A. R. H. Holzwarth, K. Schaffner, *J. Photochem. Photobiol. B Biol.* **1992**, *15*, 355–360; H. Amakawa, Y. Shimono, R. Tanikaga, A. R. Holzwarth, K. Schaffner, *Photochem. Photobiol.* **1996**, *63*, 92–99.

[2] a) H. Tamiaki, S. Takeuchi, R. Tanikaga, S. T. Balaban, A. R. Holzwarth, K. Schaffner, *Chem. Lett.* **1994**, 401–402; b) T. S. Balaban, H. Tamiaki, A. R. Holzwarth, K. Schaffner, unpublished results.

[3] a) K. M. Smith, D. A. Goff, J. Fajer, K. M. Barkigia, *J. Am. Chem. Soc.* **1983**, *105*, 1674–1676; b) A. R. Holzwarth, K. Schaffner, *Photosynth. Res.* **1994**, *41*, 225–233.

[4] H. Tamiaki, S. Miyata, Y. Kureishi, R. Tanikaga, *Tetrahedron* **1996**, *52*, 12421–12432.

[5] For analogies between magnesium and zinc chlorins, see Ref. [8].

[6] a) M. I. Bystrova, I. N. Mal'gosheva, A. A. Krasnovskii, *Mol. Biol. Engl. Transl.* **1979**, *13*, 440–451; b) A. R. Holzwarth, K. Griebenow, K. Schaffner, *J. Photochem. Photobiol. A Chem.* **1992**, *65*, 61–71, and references therein.

[7] a) Recent reviews: R. E. Blankenship, J. M. Olson, M. Miller in *Anoxygenic Photosynthetic Bacteria* (Eds.: R. E. Blankenship, M. T. Madigan, C. E. Bauer), Kluwer, Dordrecht, **1995**, pp. 399–435; b) see also T. S. Balaban, A. R. Holzwarth, K. Schaffner, G.-J. Boender, H. J. M. de Groot, *Biochemistry* **1995**, *34*, 15259–15266, and references therein.

[8] K. M. Smith, L. A. Kehres, J. Fajer, *J. Am. Chem. Soc.* **1983**, *105*, 1387–1389.

[9] a) P. Hildebrandt, H. Tamiaki, A. R. Holzwarth, K. Schaffner, *J. Phys. Chem.* **1994**, *98*, 2192–2197; b) J. Chiefari, F. Fages, K. Griebenow, N. Griebenow, T. S. Balaban, A. R. Holzwarth, K. Schaffner, *ibid.* **1995**, 1357–1365.

[10] a) D. L. Worcester, T. J. Michalski, J. J. Katz, *Proc. Natl. Acad. Sci. USA* **1986**, *83*, 3791–3795; b) D. L. Worcester, T. J. Michalski, M. K. Bowman, J. J. Katz, *Mat. Res. Soc. Symp. Proc.* **1990**, *174*, 157–161.

[11] The formation of tubular inverted micelles from chlorophyll *a*, which possesses a 3-vinyl instead of a 3-(1-hydroxyethyl) group, is mediated by water molecules [10], as ascertained in X-ray structure analyses by H. C. Chow, R. Serlin, C. E. Strouse, *J. Am. Chem. Soc.* **1975**, *97*, 7230–7237; R. Serlin, H. C. Chow, C. E. Strouse, *ibid.* **1975**, *97*, 7237–7242; C. Kratky, J. D. Dunitz, *Acta Crystallogr. Sect. B* **1975**, *31*, 1586–1589.

[12] L. A. Staehelin, J. R. Golecki, R. C. Fuller, G. Drews, *Arch. Mikrobiol.* **1978**, *119*, 269–277.

[13] The bonding in Fig. 1 is an extension of the model initially advocated by Smith et al. [8]. None of numerous other proposals [10a, 14] of the organization of such aggregates has been found by molecular modeling [3b, 15] to afford tubular arrangements of appropriate diameters.

[14] a) D. C. Brune, T. Nozawa, R. E. Blankenship, *Biochemistry* **1987**, *26*, 8644–8652; b) D. C. Brune, G. H. King, R. E. Blankenship in *Photosynthetic Lightharvesting Systems* (Eds.: H. Scheer, S. Schneider), Walter de Gruyter, Berlin, **1988**, pp. 141–151; c) M. Lutz, G. van Brakel in *Green Photosynthetic Bacteria* (Eds.: J. M. Olson, J. G. Ormerod, J. Amesz, E. Stackebrandt, H. G. Trüper), Plenum, New York, **1988**, pp. 23–34; d) T. Nozawa, M. Suzuki, S. Kanno, S. Shirai, *Chem. Lett.* **1990**, 1805–1808; e) T. Nozawa, M. Suzuki, K. Ohtomo, Y. Morishita, H. Konomi, M. T. Madigan, *ibid.* **1991**, 164; f) K. Uehara, J. M. Olson, *Photosynth. Res.* **1992**, *33*, 251–257; g) K. Matsuura, M. Hirota, K. Shimada, M. Mimuro, *Photochem. Photobiol.* **1993**, *57*, 92–97; h) T. Nozawa, K. Ohtomo, M. Suzuki, M. Morishita, M. T. Madigan, *Bull. Chem. Soc. Jpn.* **1993**, *66*, 231; i) H. Sato, K. Uehara, T. Ishii, Y. Ozaki, *Biochemistry* **1995**, *34*, 7854–7860; j) T. Oba, T. Watanabe, M. Mimuro, M. Kobayashi, S. Yoshida, *Photochem. Photobiol.* **1996**, *63*, 639–648.

[15] T. S. Balaban, A. R. Holzwarth, K. Schaffner, unpublished results.

[16] K. M. Smith, D. J. Simpson, *J. Am. Chem. Soc.* **1985**, *107*, 4946–4954.

[17] H. Tamiaki, M. Amakawa, Y. Shimono, R. Tanikaga, A. R. Holzwarth, K. Schaffner, *Photochem. Photobiol.* **1996**, *63*, 92–99.

[18] H. Scheer in *Chlorophylls* (Ed.: H. Scheer), CRC Press, Boca Raton, FL, **1991**, p. 4.

[19] Satisfactory analytical data have been obtained for all new compounds.

[20] After elution with aqueous methanol from the HPLC column and evaporation of the solvents, a sharp blue-shifted peak at 622 nm is visible in the dichloromethane solutions of **6a**-Zn diluted with hexane. This peak is removed after washing with brine a dichloromethane extract of **6a**-Zn. We tentatively assign this peak to a methanol-bridged dimeric species.

[21] For **6a**-Zn and **6b**-Zn in dichloromethane solution the ester C=O band is at 1733 cm^{-1}, that of the aldehyde at 1664 cm^{-1}, and a chlorin mode at 1606 cm^{-1}. Upon addition of methanol the ester C=O band remains unshifted, whereas the aldehyde C=O appears at 1657 ± 2 cm^{-1}, probably due to hydrogen bonding to methanol. When dichloromethane solutions are diluted with hexane, the ester C=O band is slightly shifted to larger wavenumbers (1738 cm^{-1}), whereas the aldehyde carbonyl band is strongly shifted to lower frequencies [broad band at 1640 cm^{-1} for the more soluble (13[1]*S*) epimer]. This is reminiscent of the strongly down-shifted 13[1]-carbonyl vibration in BChl *c* aggregates and chlorosomes [9b]. We correspondingly assign this latter band to the aldehyde carbonyl group strongly hydrogen-bonded to a hydroxy group, which simultaneously coordinates with a zinc atom.

[22] The proportion of red-shifted oligomers is slightly greater on aggregation in pentane than for that in hexane and heptane. Furthermore, the amount is also determined by the concentration of the CH_2Cl_2 stock solution: the higher this concentration, the more aggregated species are formed, as is expected from a cooperative process for the self-assembly. This has been shown for BChl *c* oligomers (predominantly tetramers; cooperativity of 3.6) [15].

[23] Solutions of **5a**-Zn and **5b**-Zn in hexane tend to form deposits upon standing, albeit without a red shift in absorption of the supernatant.

[24] For a first example of a functional unit based on the self-organized assembly of zinc chlorins coupled to a metal-free bacteriochlorin as energy acceptor: H. Tamiaki, T. Miyatake, R. Tanikaga, A. R. Holzwarth, K. Schaffner, *Angew. Chem.* **1996**, *108*, 810–812; *Angew. Chem. Int. Ed. Engl.* **1996**, *35*, 772–774.

New Imido-Bridged Transition Metal Clusters: $[(C_5H_5)_4Ti_4(NSnMe_3)_4]$, $[Co_{11}(PPh_3)_3(NPh)_{12}]$, $[Ni_{11}Br_6(NtBu)_8]$, and $[Li(thf)_4]_4[Cu_{24}(NPh)_{14}]$**

Andrea Decker, Dieter Fenske,* and Klaus Maczek

Dedicated to Professor Rudolf Taube on the occasion of his 65th birthday

Transition metal compounds with nitrogen-containing ligands usually form, with few exceptions, mononuclear compounds.[1–3] Recently Dehnicke et al, for example, described the synthesis of N-containing cluster compounds such as $[Cu_4(NPMe_3)_3(O_2CCH_3)_5]$, $[Cu_6Cl_6(NPMe_3)_4]^+$, and $[Cu_6Br_6(NPMe_3)_4]^+$,[4–6] in which the phosphane imine groups act as bridging ligands. These compounds were the first N-bridged clusters of electron-rich transition metals to be synthesized.

[*] Prof. Dr. D. Fenske, Dr. A. Decker, Dr. K. Maczek
Institut für Anorganische Chemie der Universität
Engesserstrasse, Geb.-Nr. 30.45, D-76128 Karlsruhe (Germany)
Telefax: Int. code +(721)661921

[**] This work was supported by the Deutsche Forschungsgemeinschaft.

Herein we report that imido-bridged transition metal clusters can also be synthesized. The synthetic strategy is based on the reaction of chlorotransition metal phosphane complexes with stannylamines; the elimination of trimethylchlorostannane leads to the formation of nitrogen-bridged clusters.

The Ti_4 cluster **1** can be isolated as brown crystals in a low yield (20%) from the reaction of $[CpTiCl_2(PEt_3)_2]$ ($Cp = C_5H_5$) with tris(trimethylstannyl)amine [Eq. (a)].

$$[CpTiCl_2(PEt_3)_2] \xrightarrow{N(SnMe_3)_3} [Cp_4Ti_4(\mu_3\text{-}NSnMe_3)_4] \quad (a)$$

1

The results of the single-crystal X-ray structure analysis of **1** are shown in Figure 1.[9] Compound **1** consists of a Ti_4N_4 cluster with a heterocubane structure, in which the titanium atoms

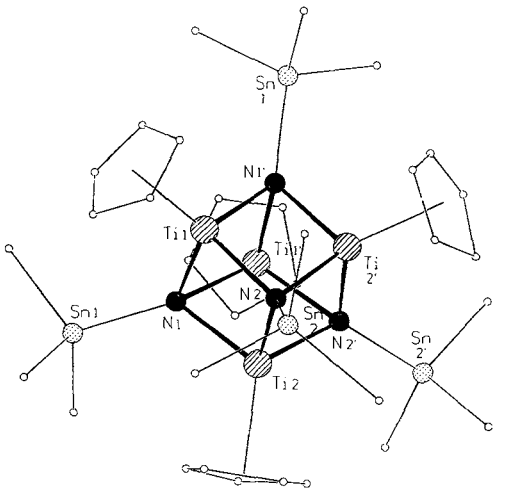

Fig. 1. Molecular structure of **1**. Hydrogen atoms have been omitted for clarity. Selected bond lengths [pm] and angles [°]: Ti1–Ti1′ 277.9(4), Ti1–Ti2′ 268.6(3), Ti2–Ti2′ 277.3(3), Ti1–Ti2 278.5(3), Ti1–N1 197.0(9), Ti1–N1′ 205.8(9), Ti1–N2 206.4(8), Ti2–N2 195.0(8), Ti2–N2′ 203.2(8); N1-Ti1-N2 91.2(3), N1′-Ti1-N2 97.4(3), Ti2-Ti1-Ti1′ 57.72(8), Ti2-Ti1-Ti2′ 60.86(8).

are each coordinated to an η_5-Cp ligand, and the N atoms are bound to $SnMe_3$ groups. Within the four-membered rings of the cubane framework, the Ti-N-Ti and the N-Ti-N angles lie between 87.2–88.2° and 91.1–92.3°, respectively. The Ti atoms in **1** are all formally in the oxidation state +III. Surprisingly this complex shows diamagnetic behavior. This must be a result of coupling between the d^1 spin centers.[8] Compound **1** has 52 valence electrons (VE) and therefore 8 VE less than expected for a M_4 cluster with a tetrahedral structure.[7a] However, **1** is isoelectronic with $[MXNPEt_3]_4$ (X = Cl, I), in which M_4N_4 heterocubane structures are also found.[7b]

On the other hand there are many heterocubane clusters for which the noble gas rule (60 VE) is exceeded or not met. Extended Hückel calculations show that a M_4 tetrahedral cluster with 52 VE should possess D_{2d} symmetry with four longer and two shorter M–M bonds.[8a] This is indeed found to be true for **1**, which has two short Ti–Ti bonds (268.3(3) pm) and four longer Ti–Ti bonds (277.2–278.5(3) pm). Other titanium clusters with the same number of valence electrons have already been reported. Examples include $[Cp_4Ti_4Te_4]$ and $[Cp'_4Ti_4S_4]$ ($Cp' = i\text{PrC}_5H_4$),[8a] in which the Ti–Ti distances are significantly longer (292.7–300.8 and 314.5–321.4 pm, respectively). $[Cp^*_4Ti_4N_4]$ ($Cp^* = C_5Me_5$) is another compound with a Ti_4N_4 structural unit that has recently been reported;[8b] however, in contrast to **1**, this compound contains an undistorted Ti_4 tetrahedron (Ti–Ti 278.8 pm).

Since **1** contains four $SnMe_3$ ligands, there are four reactive N–Sn bonds, which are potential centers for further reaction to form links between Ti_4N_4 heterocubane units. However, reactions with transition metal and main group element halide compounds have so far proved unsuccessful.

The reaction of $PhN(SnMe_3)_2$ with $[CoCl_2(PPh_3)_2]$ led to dark green crystals of **2** [Eq. (b)], which tend to decompose very quickly. The central metal framework in **2** consists of a planar

$$[CoCl_2(PPh_3)_2] \xrightarrow{PhN(SnMe_3)_2} [Co_{11}(PPh_3)_3(\mu_2\text{-}NPh)_6(\mu_3\text{-}NPh)_6] \quad (b)$$

2

Co_6 ring that is formed from the atoms Co1, Co3, Co4, Co6, Co7, and Co9 (Fig. 2). Single Co atoms lie above and below the Co_6 plane lie at distances of 118.6 pm (Co10) and 121 pm

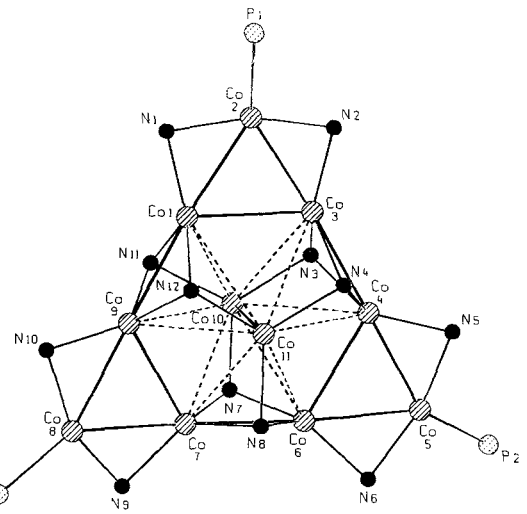

Fig. 2. Molecular structure of **2** (C and H atoms omitted). Selected bond lengths [pm]: Co1–Co2 242.9(3), Co1–Co3 258.4(3), Co1–Co9 248.2(3), Co1–Co10 272.4(3), Co1–Co11 287.2(3), Co2–Co3 243.7(3), Co3–Co4 247.3(3), Co3–Co10 279.0(4), Co3–Co11 282.5(3), Co4–Co5 242.0(3), Co4–Co6 255.9(3), Co4–Co10 279.5(3), Co4–Co11 271.5(3), Co5–Co6 243.7(3), Co6–Co7 246.0(3), Co6–Co10 280.9(2), Co6–Co11 275.3(2), Co7–Co8 243.6(3), Co7–Co9 249.6(3), Co7–Co10 275.9(3), Co7–Co11 277.4(3), Co8–Co9 245.4(3), Co9–Co10 276.9(2), Co9–Co11 276.8(3), Co10–Co11 239.8(3), Co–P 220.7–221.3(5), μ_2-N–Co 175.4–178.3(10) μ_3-N–Co 186.1–191.8(10)

(Co11), respectively. In addition, three alternate edges of the Co_6 ring are μ_2-bridged by Co atoms (Co2, Co5, and Co8). The distances between the Co ring atoms and the μ_2-bridging Co atoms, which lie in the plane of the ring, range between 242.9 and 245.4(3) pm. Within the Co_6 ring, the Co3–Co4, Co6–Co7, and Co1–Co9 bonds are significantly shorter (246.0–248.2(3) pm) than the Co4–Co6, Co7–Co9, and Co1–Co3 bonds (249.6–258.4(3) pm). In contrast, the bond lengths to the apical Co atoms in the Co_6 ring range from 271.5(3) to 287.2(3) pm. The Co10–Co11 bond length (239.8(3) pm) is conspicuously short. N3, N7, and N11 and N4, N7, and N12 form the triangular faces of an almost undistorted trigonal prism. Co10 and Co11 lie only 20 pm below the mean planes defined by these nitrogen atoms, which is a consequence of the short bond length between these two Co atoms. This unusual, distorted trigonal-planar coordination of Co10 and Co11 ($\sum$ N-Co-N: Co10: 358.5°; Co11: 357.0°) is a result of the steric shielding of the nitrogen-bound phenyl groups. The cluster framework of **2** is also sterically shielded by the terminally bound triphenylphosphane ligands at Co2, Co5, and Co8, as

well as by twelve phenylimido groups. These phenylimido groups bind in two ways: there are six μ_2-imido bridges (N1, N2, N3, N6, N9, and N10) between the Co atoms in the periphery of the cluster (Co-μ_2-N 175.4–178.3(10) pm) and six μ_3-imido groups (N3, N4, N7, N8, N11, and N12) that form bridges between the two apical Co atoms (Co10 and Co11) and the Co atoms in the Co_6 ring (Co-μ_3-N 186.1–191.8(10) pm).

Compound **2** contains a Co_{11} cluster, which possesses an overall charge of +24. Evidently, we are dealing with a mixed-valent cluster. A possible charge distribution would be nine Co^{2+} and two Co^{3+} ions. In agreement with this proposal, **2** is paramagnetic. Taking the coordination of the Co atoms into consideration, it is conceivable that the Co^{3+} ions can be assigned to Co10 and Co11.

The low reactivity of the amine derivative in the reaction of the stannylamine with transition metal halide complexes proved to be problematic. Therefore, we investigated whether the use of the significantly more reactive lithium amide would provide a pathway to the formation of imido-bridged clusters of the d^9 and d^{10} transition metals.

In the previously known nitrogen-bridged compounds of nickel, the Ni_3 cluster is the dominant structure motif.[8a, 10, 11] The reaction of $[NiBr_2(dme)]$ with *t*BuNHLi afforded the Ni_{11} cluster **3** [Eq. (c)].

$$[NiBr_2(dme)] \xrightarrow{t\text{BuNHLi}} \underset{\mathbf{3}}{[Ni_{11}Br_6(\mu_3\text{-N}t\text{Bu})_8]} \quad (c)$$

The main building blocks of **3** consist of two square pyramids of Ni atoms (Ni1–Ni5, Ni6–Ni10) (Fig. 3). The apical Ni atoms (Ni1 and Ni10) are coordinated to terminal bromo ligands (Br1, Br2; Ni–Br 236.5–238.0 pm). The Ni–Ni distances within the Ni_5 unit lie in the range 245.8(2)–259.2(13) pm, and can be described as bonding interactions.[8a] The two Ni pyramids are linked in several ways. Ni11 acts as a bridge bridge between Ni3 and Ni8, and the Ni–Ni distances are 240.2(2) pm. This distance is typical for a Ni–Ni bond.[8, 10, 11] There is a further metal–metal contact between the two Ni_5 pyramids from Ni5 to Ni6 (230.5(2) pm).

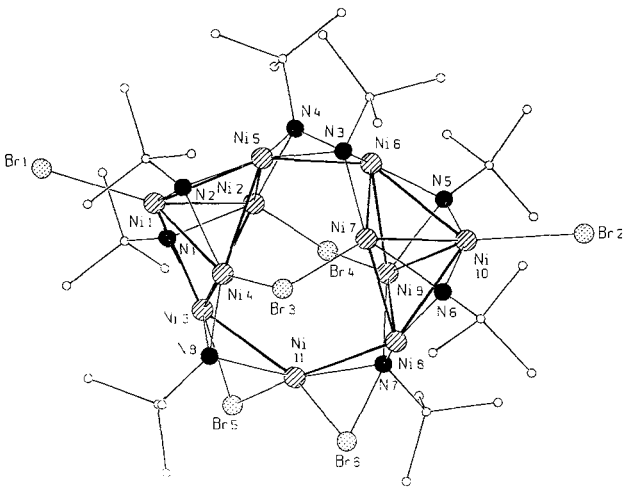

Fig. 3. Molecular structure of **3** (H atoms omitted). Selected bond lengths [pm]: Ni1–Ni 245.7–253.3(2), Ni2–Ni3 247.9(2), Ni3–Ni4 249.4(1), Ni2–Ni5 257.2(2), Ni4–Ni5 255.4(1), Ni5–Ni6 230.5(2), Ni3–Ni11 240.0(2), Ni8–Ni11 240.2(2), Ni10–Ni 245.8–253.2(2), Ni6–Ni7 259.2(1), Ni7–Ni8 247.4(1), Ni8–Ni9 249.2(2), Ni6–Ni9 254.3(1), N1–Ni 185.3–188.5(6), N2–Ni 184.9–185.2(5), N3–Ni 187.1–190.8(6), N4–Ni 186.6–190.5(7), N5–Ni 185.5–191.4(6), N6–Ni 183.7–188.5(6), N7–Ni 184.5–192.7(6), N8–Ni 184.9–193.7(6), Ni1–Br1 238.0(2), Ni10–Br2 236.5(2), Ni–Br3 236.3–238.3(2), Ni–Br4 235.9–238.5(2), Ni–Br5 240.0–251.1(1), Ni–Br6 239.8–252.2(1).

Apart from the metal–metal interactions, the two Ni_5 pyramids are also connected by four μ_2-bromo bridges (Br3–Br6) between Ni3–Ni11, Ni8–Ni11, Ni2–Ni9, and Ni4–Ni7 (Ni–Br 236.3(1)–240.9(1) pm). Irrespective of this there are eight μ_3-*tert*-butylimido groups in **3**; the Ni–N bond lengths range from 184.9(7) pm to 194.2(7) pm. The six Br^- and eight $Nt Bu^{2-}$ ligands lead to a formal oxidation state of +II for all nickel atoms.

The reaction of CuBr with $PhNLi_2$ affords the copper cluster **4** with NPh bridging ligands [Eq. (d)].[12] It is an orange colored

$$CuBr \xrightarrow{PhNLi_2} \underset{\mathbf{4}}{[Li(thf)_4]_4[Cu_{24}(\mu_3\text{-NPh})_8(\mu_4\text{-NPh})_6]} \quad (d)$$

ionic compound, which consists of four $[Li(thf)_4]^+$ ions and one $[Cu_{24}(NPh)_{14}]^{4-}$ ion. Correspondingly, all Cu atoms are in the oxidation state +I. The structure of the cluster anion (without C atoms) with $\bar{1}$ symmetry is shown in Figure 4. The metal

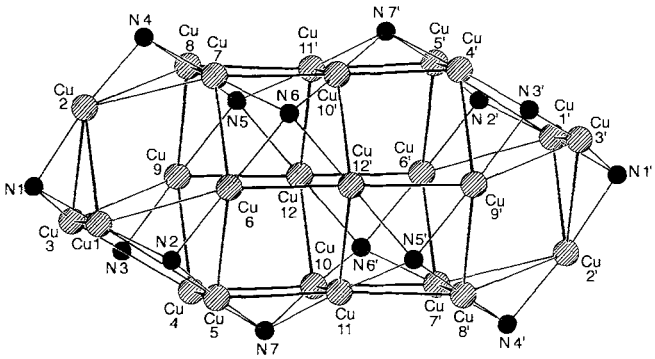

Fig. 4. Structure of the $Cu_{24}N_{14}$ cluster of **4**. Selected bond lengths [pm]: Cu1–Cu2 265.2, Cu1–Cu3 270.9, Cu2–Cu3 272.1, Cu4–Cu5 258.5, Cu5–Cu6 258.4 Cu6–Cu7 255.1, Cu7–Cu8 257.1, Cu8–Cu9 258.9, Cu4–Cu9 261.5, Cu10–Cu11 250.4, Cu10–Cu12 252.8, Cu11–Cu12 252.0, Cu1–Cu6 281.3, Cu2–Cu7 278.8, Cu2–Cu8 285.3, Cu3–Cu9 281.9, Cu3–Cu7 281.4, Cu4–Cu10 249.5, Cu5–Cu11 251.6, Cu6–Cu12′ 250.6, Cu7–Cu10′ 251.0, Cu8–Cu11′ 251.7, Cu9–Cu12 248.9, N1–Cu 186.3–189.2, N2–Cu 185.7–188.6, N3–Cu 184.2–189.2, N4–Cu 185.9–189.3, N5–Cu 193.3–196.7, N6–Cu 193.3–194.9, N7–Cu 193.0–195.5.

framework of **4** is formed from three planar Cu_6 rings (Cu4–Cu9, Cu10–Cu12, and Cu10′–Cu12′, Cu4′–Cu9′) and two Cu_3 rings (Cu1–Cu3, Cu1′–Cu3′). These rings lie parallel to one another with the two three-membered rings at either end. Thus, a Cu_{24} polyhedron is formed comprising Cu_3 and Cu_4 faces. The Cu_3 faces are bridged by μ_3-phenylimido groups (N1–N4, N1′–N4′) and half of the Cu_4 faces by μ_4-phenylimido groups (N5–N7, N5′–N7′). All the Cu atoms, as is usual for Cu^I ions, are approximately linearly coordinated by the N atoms of the NPh ligands (N-Cu-N 171.3–178.0°). The difference in the degree of bridging is also evident from the bond lengths. Thus, the Cu–μ_3-N bond lengths are 184.2(5) and 189.3(6) pm, while, as expected, the Cu–μ_4-N bond lengths are longer (193.0(6) and 196.7(6) pm). The Cu–Cu distances lie between 248.9(1) and 285.3(1) pm. Notably, the bond lengths of the Cu_3 rings, 265.2–272.2 pm are significantly longer than those found in the Cu_6 rings. The ring formed from Cu4–Cu9 contains Cu–Cu distances of between 257.1 and 261.5 pm. In comparison, the six-membered ring containing the atoms Cu10–Cu12 and Cu10′–Cu12′ has much shorter Cu–Cu contacts (250.3–252.8 pm). The interactions between the Cu atoms of the Cu_3 ring and between the Cu_3 ring (Cu1–Cu3) and the Cu_6 ring (Cu4–Cu9) are weak (Cu–Cu 278.9–285.3 pm). In

contrast the distances between the Cu_6 rings are significantly shorter (Cu–Cu 248.9–252.9 pm). In this respect, it is more meaningful to describe the structure of the cluster as a hexagonal prism derived from 18 Cu atoms that is linked to two Cu_3 clusters through μ_3-bridging NPh ligands. The construction principle of parallel hexagonal and triangular layers is observed in other Cu clusters such as $[Cu_{12}(PPh)_6(PPh_3)_6]$ and $[Cu_{12}S_6(PEt_3)_8]$.[12] Therefore one could describe the skeleton of **4** as a $[Cu_{12}E_6]$ structure fragment that has been extended by the insertion of two Cu_6 layers.

In contrast to other main group element bridged Cu clusters, the Cu framework in **4** is not shielded by terminal ligands coordinated to copper, but by the phenyl groups of the imido bridging ligands (Fig. 5). No definite statement can be made about

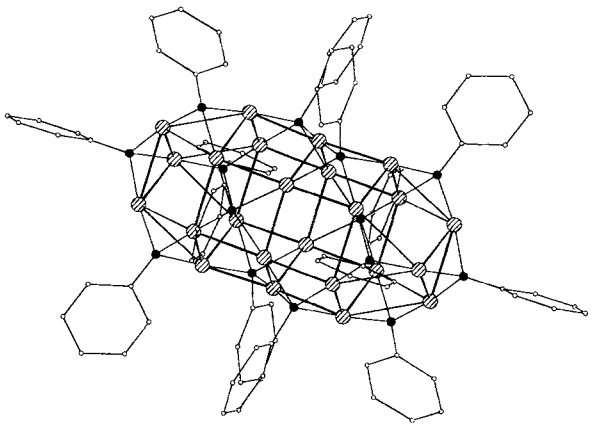

Fig. 5. Molecular structure of **4** (H atoms omitted). Cu atoms are shown striped and N atoms in black.

the results that have been obtained from preliminary reactions of AgCl with $PhNLi_2$. Interestingly, however, dark red solutions are formed, from which it has not yet been possible to isolate a crystalline product. If the solvent is evaporated, a red powder is afforded, the IR spectrum of which is very similar to that of **4**.

Experimental Procedure

1: PEt_3 (0.45 mL, 6 mmol) was added to a suspension of $[CpTiCl_2)_x]$ in toluene (30 mL). The solution became clear. To this tris(trimethylstannyl)amine (1 mL, 3 mmol) was added, and the mixture was stirred at room temperature to give a dark brown solution. The solvent was removed by evaporation and the residue redissolved in hexane and filtered, and the filtrate kept at −25 °C. Crystals of **1** (yield 20%) were isolated after a few days.

2: To a solution of $[CoCl_2(PPh_3)_2]$ (4.1 g, 6.26 mmol) in DME (100 mL), bis(trimethylstannyl)phenylamine (1.75 mL, 6.28 mmol) was added. The reaction mixture was heated to reflux for several days, which led to a black-brown solution. Dark green crystals of **2** (yield 40%) were obtained after several days at −25 °C.

3: To a suspension of $[NiBr_2(dme)]$ (2.75 g, 6.9 mmol) in THF (100 mL) at −78 °C, *t*BuNLiH (0.65 g, 8.3 mmol) was added. The reaction solution darkened at about −40 °C. The reaction mixture was allowed to warm to room temperature, and the solvent was removed by evaporation. The black residue was then stirred in a mixture of hexane/toluene (2:1). Some of the residue dissolved, and black rodlike crystals of **3** (yield 60%) were obtained from this fraction after reduction of the solvent.

4: To a suspension of CuBr (2.67 g, 18.6 mmol) in THF (100 mL), Bu_2NH (3.12 mL, 18.6 mmol) was added. The resulting clear solution was cooled in an ice bath, and $PhNLi_2$ (1.95 g, 18.6 mmol) was added slowly. Orange crystals of **4** (yield 80%) were formed from the red brown solution after several days at room temperature.

Received: July 8, 1996 [Z9303IE]
German version: *Angew. Chem.* **1996**, *108*, 3025–3028

Keywords: clusters · imido ligands · transition metal compounds

[1] W. Nugent, B. L. Haymore, *Coord. Chem. Rev.* **1980**, *31*, 123.
[2] D. E. Wigley, *Prog. Inorg. Chem.* **1994**, *42*, 239.
[3] M. Lappert, P. P. Power, A. Sanger, *Metal and Metalloid Amides*, Wiley, New York, **1980**.
[4] K. Dehnicke, D. Fenske, C. Friebel, R. Meyer zu Köcker, J. Pebler, *Z. Anorg. Allg. Chem.* **1995**, *621*, 1311.
[5] A. Behrendt, K. Dehnicke, D. Fenske, R. Meyer zu Köcker, *Z. Naturforsch. B* **1994**, *49*, 301.
[6] K. Dehnicke, D. Fenske, R. Meyer zu Köcker, *Z. Naturforsch. B* **1994**, *49*, 987
[7] a) G. L. Simon, L. F. Dahl, *J. Am. Chem. Soc.* **1973**, *95*, 2164; H. J. Mai, H. C. Kang, S. Wocadlo, W. Massa, K. Dehnicke, *Z. Anorg. Allg. Chem.*, **1995**, *621*, 1963; b) H. J. Mai, R. Meyer zu Köcker, S. Wocadlo, W. Massa, K. Dehnicke, *Angew. Chem.* **1995**, *107*, 1349; *Angew. Chem. Int. Ed. Engl.* **1995**, *34*, 1235
[8] a) F. Bottomley, F. Grein, *Inorg. Chem.* **1982**, *21*, 4170; J. D. Darkwa, J. R. Lockemeyer, P. D. W. Boyd, T. B. Rauchfuss, A. L. Rheingold, *J. Am. Chem. Soc.* **1988**, *110*, 141; A. Grissinger, Dissertation, Universität Karlsruhe **1991**; b) P. Gomez-Sal, A. Martin, M. Mena, C. Yélamos, *J. Chem. Soc. Chem. Commun.* **1995**, 2185.
[9] X-ray crystal structure analysis: Stoe-STADI IV and Stoe-IPDS diffractometer, ($Mo_{K\alpha}$ radiation); data collection and refinement (SHELX-76, SHELXS-86 and SHELXL-93): **1**: The compound crystallizes with two molecules of hexane per formula unit; monoclinic, space group $C2/c$ (no. 15); lattice constants (230 K): $a = 20.925(13)$, $b = 11.327(8)$, $c = 23.472(19)$ Å, $\beta = 97.84(5)°$, $V = 5511.27$ Å^3; $Z = 4$; $\mu(Mo_{K\alpha}) = 23.6$ cm^{-1}; $2\theta_{max} = 54°$; 7952 reflections measured of which 5498 were independent; max. residual electron density 1.87 e Å^{-3}; 129 parameters (Sn, Ti, N, and C atoms of the methyl groups anisotropic, C atoms of the Cp groups disordered); $R_1 = 0.084$; $R_w = 0.076$. **2**: The compound crystallizes with five dimethoxyethane molecules per formula unit; triclinic, space group $P\bar{1}$ (no. 2); lattice constants (160 K): $a = 15.893(8)$, $b = 19.986(16)$, $c = 24.739(13)$ Å, $\alpha = 97.63(4)$, $\beta = 102.54(3)$, $\gamma = 107.43(3)°$, $V = 7151.39$ Å^3; $Z = 2$; $\mu(Mo_{K\alpha}) = 13.2$ cm^{-1}; $2\theta_{max} = 48°$; 23630 reflections measured of which 20385 were independent; max. residual electron density 1.56 e Å^{-3}; 1479 parameters (Co, P, N, and C atoms of the phenyl groups anisotropic. The H atoms were calculated in idealized positions); $R_1 = 0.081$; $R_w = 0.076$. **3**: The compound crystallizes with two dimethoxyethane molecules and one toluene molecule per formula unit; monoclinic, space group $C2/c$ (no. 15); lattice constants (200 K): $a = 24.547(3)$, $b = 11.942(1)$, $c = 48.483(7)$ Å, $\beta = 94.079(10)°$, $V = 14176.23(2)$ Å^3; $Z = 8$; $\mu(Mo_{K\alpha}) = 62.8$ cm^{-1}; $2\theta_{max} = 50°$; 18916 reflections measured of which 10127 were independent; max. residual electron density 1.27 e Å^{-3}; 613 parameters (Ni, Br, N, and C atoms of the cluster molecule anisotropic. The H atoms were calculated in idealized positions.); $R_1 = 0.084$; $wR_2 = 0.192$. **4**: The compound crystallizes with two THF molecules per formula unit; monoclinic, space group $P2_1/n$ (no. 14); lattice constants (190 K): $a = 19.474(4)$, $b = 19841(5)$, $c = 26.343(6)$ Å, $\beta = 94.02(2)°$, $V = 10154(4)$ Å^3; $Z = 2$; $\mu(Mo_{K\alpha}) = 27.84$ cm^{-1}, $2\theta_{max} = 52°$; 44927 reflections measured of which 17871 were independent; max. residual electron density 0.72 e Å^{-3}; 790 parameters (Cu, N, and C atoms of the phenyl groups anisotropic. The H atoms were calculated in idealized positions); $R_1 = 0.067$; $wR_2 = 0.184$. Further details of the crystal structure investigations may be obtained from the Fachinformationszentrum Karlsruhe, 76344 Eggenstein-Leopoldshafen (Germany) on quoting the depository numbers CSD-405340, CSD-405341, CSD-405342, and CSD-405343.
[10] H. F. Klein, S. Haller, H. König, *J. Am. Chem. Soc.* **1991**, *113*, 4673.
[11] a) S. Otsuka, A. Nakamura, T. Yoshida, *Inorg. Chem.* **1968**, *7*, 261; b) J. Müller, *Chem. Ber.* **1973**, *106*, 1122.
[12] D. Fenske, J. Ohmer, J. Hachgenei, K. Merzweiler, *Angew. Chem.* **1988**, *100*, 1300; *Angew. Chem. Int. Ed. Engl.* **1988**, *27*, 1277; A. Eichhöfer, D. Fenske, W. Holstein, *ibid.* **1993**, *105*, 257 and **1993**, *32*, 1277; H. Krautscheid, D. Fenske, G. Baum, M. Semmelmann, *ibid.* **1993**, *105*, 1364 and **1993**, *32*, 1302; D. Fenske, J. Steck, *ibid.* **1993**, *105*, 254 and **1993**, *32*, 238; S. Dehnen, D. Fenske, *ibid.* **1994**, *106*, 2369 and **1994**, *33*, 2287; D. Fenske, W. Holstein, *ibid.* **1994**, *106*, 1311 and **1994**, *33*, 1290.

Monitoring the Reaction Progress in Combinatorial Chemistry: ^{1}H MAS NMR Investigations on Single Macro Beads in the Suspended State

Matthias Pursch, Götz Schlotterbeck, Li-Hong Tseng, Klaus Albert,* and Wolfgang Rapp

Dedicated to Professor E. Bayer on the occasion of his 70th birthday

Since R. B. Merrifield[1] introduced the synthesis of peptides on an insoluble polymeric support, solid-phase synthesis has become a major tool in many areas of organic chemistry and is continuously being improved. In recent years, organic chemistry on the solid support is facing a rapid growth and is being applied widely in many fields.[2] By the use of combinatorial methods, hundreds to thousands of compounds are prepared in parallel and mostly with automated work-stations. These combinatorial methods are poised to gain importance in discovering new lead structures in drug research and development.[3, 4] Already high throughput assays allow testing hundreds of compounds per day. As testing methods improve further, a higher throughput of compounds will be possible, which makes a higher throughput in synthesis mandatory. This is only possible by further optimization and miniaturization of organic synthesis incorporating combinatorial aspects.

We have developed a system that allows both the search for new drugs and the optimization of chemical reactions on a solid support in a miniaturized fashion on a nanomolar scale.[5–7] In solid-phase synthesis the polymeric support represents the reaction unit. This reaction unit (represented by the amount of resin employed) is divided into discrete small segments. Each single resin particle thus is a micro reaction unit.

The common resins used today for synthesis have particle sizes of 40–130 μm. The loading of each individual particle with reactive functional groups is in the order of 10–300 pmol per bead. Often, this loading is too low for sequential cleavage and subsequent characterization of the compound synthesized on the bead. We have therefore developed macro beads with particle sizes of 400–750 μm based on resins with long, flexible tentacles as tethers.[8] These are characterized as grafted polystyrene–polyoxyethylene copolymers. The capacity of the individual beads, depending on the particle size, is in the order of 10–65 nmol per bead. This thousandfold scaleup of the amount of substance per bead enables reactions to be performed and monitored on single beads and products to be investigated on the supports. The macro beads thus become micro reactors. A further big advantage in the reduction of the reaction space is that only small amounts of solvents are required. With a millimole of organic building blocks it is possible to perform 200–500 reactions. In the combinatorial approach where hundreds of reactions are carried out in parallel, the available resources can now be used more efficiently.

The fast and exact characterization of building blocks on a polymeric support presents a challenge for analytical methods. FT-IR/Raman spectroscopy, MALDI-TOF mass spectrometry, as well as ^{1}H and ^{13}C NMR spectroscopy in suspended state (gel-phase NMR) are some important tools for structural elucidation. In ^{1}H NMR spectra the broadness of the lines (in the order of at least 50–100 Hz) prevents an exact structural elucidation; ^{13}C NMR spectra in suspension exhibit small line widths due to reduced dipolar couplings and an increased dispersion of the chemical shift,[9–11] but the low sensitivity of the ^{13}C nucleus causes long measuring times.

The recently introduced ^{1}H MAS NMR spectroscopy (MAS = Magic Angle Spinning) of resins in suspension revealed that a very good resolution of the NMR signals is achievable.[12–17] Under fast sample spinning at the magic angle, differences in susceptibility within the sample as well as dipolar couplings are eliminated, while *J*-couplings are maintained. This leads to a resolution close to that obtained in liquid NMR spectroscopy.

On such a miniaturized system—a single macro bead—hydantoins were prepared in parallel by combinatorial methods. Each step in synthesis was followed by high-resolution ^{1}H MAS NMR spectroscopy. We took a single bead that was swollen in a solvent (for example, [D_6]DMSO or $CDCl_3$), fixed it into an insert, and placed it in a standard 4 mm solid-state NMR rotor (Fig. 1). The detection volume, depending on the size of the bead, is in the nanoliter region (200–400 nL). A commercially available CP/MAS (solid-state) NMR probe was used to perform the high-resolution MAS NMR measurements.

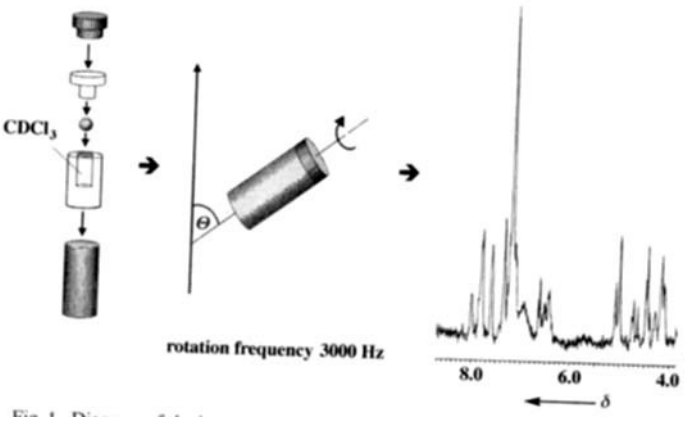

Fig. 1. Diagram of the instrumentation to record high-resolution ^{1}H MAS NMR spectra of individual resin particles in suspension. The ^{1}H NMR spectrum (on the right) is a except from Figure 2c.

The high-resolution ^{1}H MAS NMR spectra of the reaction sequence are shown in Figure 2. It takes only 6–8 minutes to record such a spectrum with 128–160 scans. Since the long polyoxyethylene spacer of the resin makes the organic building blocks attached to the bead very mobile, the line widths of the ^{1}H NMR signals are in the order of 5–8 Hz. Consequently, each reaction step can be monitored on a single macro bead. The main ^{1}H NMR signal of the OCH_2CH_2 units appears at $\delta = 3.5$. With every subsequent synthesis step, new characteristic peaks are observable, which allow an exact structural assignment (Fig. 2). The binding of an acid-sensitive linker (AC linker) to the polymeric support (Fig. 2a) is indicated in the ^{1}H MAS NMR spectrum by additional peaks in the aromatic region ($\delta = 6–7.5$) and signals from the CH_2O and the methoxy group (at $\delta = 4.8$ and 3.75, respectively; Fig. 2b). In the next step, phenylalanin–Fmoc is bound to the supported linker. The proton signals of the Fmoc unit are clearly visible in the aromatic region (Fig. 2c). Then Fmoc is cleaved, and the activated resin treated with *n*-propylisocyanate. Again, the intensity of the peaks in the aromatic region decreases, and additional signals in

[*] Priv.-Doz. Dr. K. Albert, Dipl.-Chem. M. Pursch, Dipl.-Chem. G. Schlotterbeck, L.-H. Tseng
Institut für Organische Chemie der Universität
Auf der Morgenstelle 18, D-72076 Tübingen (Germany)
Fax: Int. code +7071/295246
e-mail: klaus.albert@uni-tuebingen.de
Dr. W. Rapp
Rapp Polymere GmbH, Tübingen (Germany)

 © VCH Verlagsgesellschaft mbH, D-69451 Weinheim, 1996 0570-0833/96/3523-2867 $ 15.00+.25/0

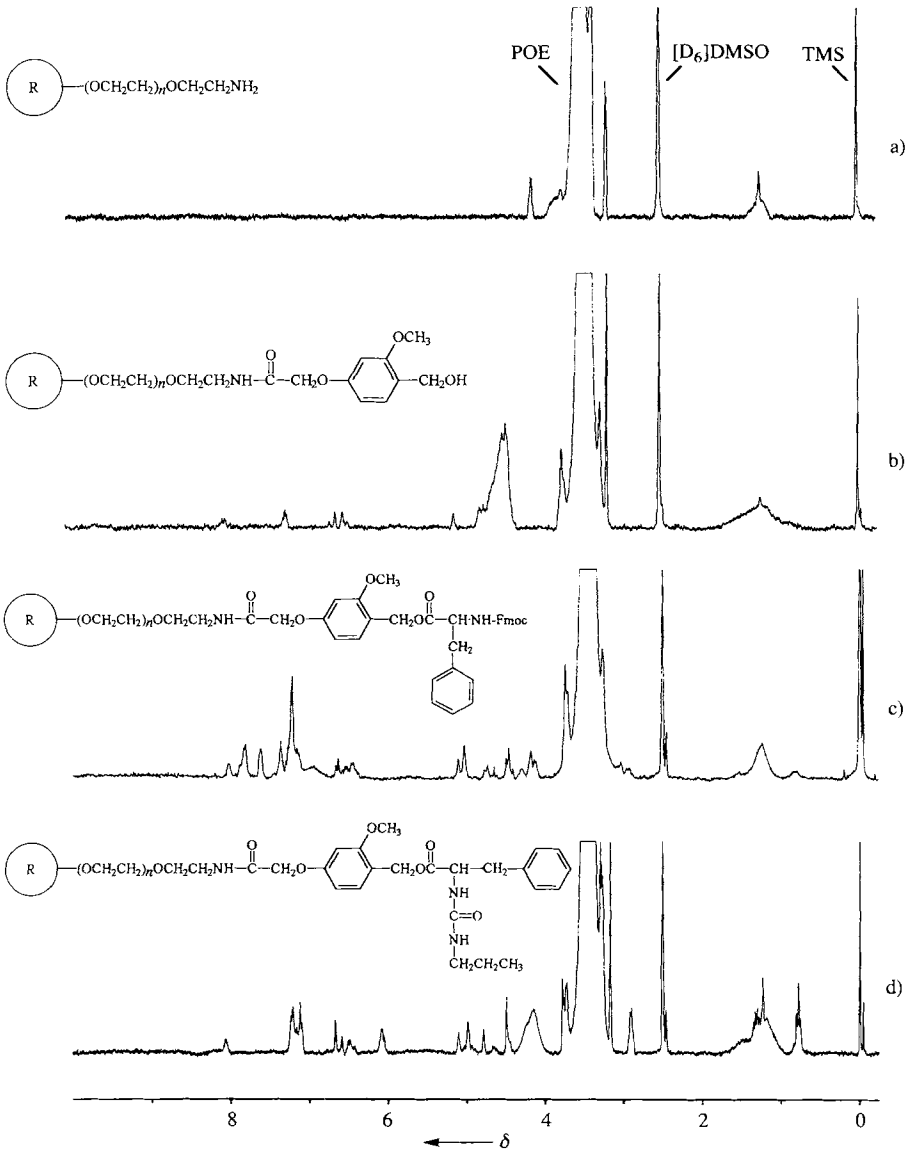

Fig. 2. ^{1}H MAS NMR spectra of a suspension of individual resin particles in the hydantoin reaction sequence: spectra of the support-bound polyoxyethylene spacer (POE, see a) (a), with acid-labile linker (b), after treatment with phenylalanine–Fmoc (c), and after scission of the Fmoc group and treatment with isocyanate (d).

Table 1. Assignment of the signals with the aid of the ^{1}H MAS NMR spectrum of a hydantoin precursor (Fig. 2d).

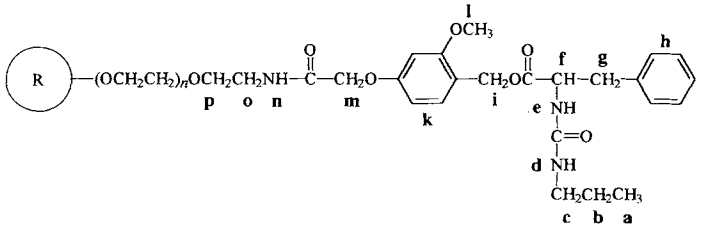

Position	Functional group	δ	Position	Functional group	δ
a	CH_3	0.75	i	CH_2O	5.1
b	CH_2	1.2	k	H_{ar}	6.5, 6.6, 7.2
c	CH_2	2.9	l	OCH_3	3.75
d	CONH	6.0	m	CH_2O	4.8
e	NHCO	6.1	n	CONH	8.05
f	OCOCH	4.5	o	CH_2NH	3.15
g	CHz	3.5	p	OCH_2CH_2	3.3
h	H_{ar}	7.1			

the aliphatic region appear (Fig. 2d). The high resolution of the ^{1}H NMR signals is particularly remarkable; in the last spectum of a hydantoin precursor even the scalar couplings of the terminal *n*-propyl group are visible. The exact signal assignment is shown in Table 1. As can be seen from the NMR spectra of the reaction sequence, monitoring of syntheses on a single macro bead is possible within a short time (approximately 6 min per spectrum). Thus, time-consuming cleavage and isolation processes are no longer needed.

The polystyrene backbone of the grafted copolymer in [D_6]DMSO has (in contrast to $CDCl_3$) only a limited swelling capability. Extremely broad NMR signals result from very short T_2^* relaxation times, and in the ^{1}H MAS NMR spectra (Fig. 2) no polystyrene signals appear. The influence of various solvents on the line widths of the ^{1}H MAS NMR spectra of dissimilar resins has been thoroughly discussed recently.[15, 16]

In addition to the direct monitoring of syntheses on the resin, two-dimensional NMR techniques are crucial for structural investigations. Figure 3 shows an example of a 2D suspension MAS NMR spectrum (H,H-COSY), which was recorded in an acceptable measuring time of 40 minutes. The cross-peaks indicate that the *n*-propyl group is bound to the resin. It may be a general advantage to make use of an *n*-propyl group as a label for synthesis, for it is easily characterized by NMR spectroscopy and gives information about the success of the synthesis.

The ^{1}H MAS NMR spectroscopy in the nanoliter scale proves to be a fast and efficient tool in monitoring chemical reactions in combinatorial chemisty, even if only a single micro reactor is the analyte.

Experimental Procedure

The micro reactors were loaded with different amino acids (Fmoc-protected), which were bound to the resin on the acid-labile anchor 3-methoxy-4-hydroxymethylphenoxyacetic acid. Further reactions were performed in glass capillaries, 100 mm in length and 2.6 mm in diameter. The top end of the capillaries was open, and the bottom end contained a glass frit. One to four single beads loaded with amino acids were put into the glass capillaries. The loading was quantified by UV spectroscopy after the Fmoc protective unit had been cleaved with piperidine. After thorough washing out of the protective group, the micro reactors each were treated in the capillaries with 25 μL of a 1 M isocyanate solution. This corresponds to between a hundredfold and a thousandfold excess of reagent. After three hours the beads were washed in the capillaries to remove the excessive isocyanate.

NMR parameters: Bruker ASX-300 spectrometer, 4 mm CP/MAS probe, sample spinning (MAS) at 3000 Hz, 128–160 transients per FID, 60° pulse angle, delay time 1.5 s, time domain 16 K data points (TD) with a spectral width of (SW) 3800 Hz, acquisition time 1.1 s.

COSY 45: 16 transients per FID, time domain 2 K data points (TD2) with spectral width (SW2) of 4300 Hz, 128 increments (TD1), acquisition time 127 ms. Zerofilling in t_1 to 1 K data points, multiplication with a sine function along the F1 and F2 directions.

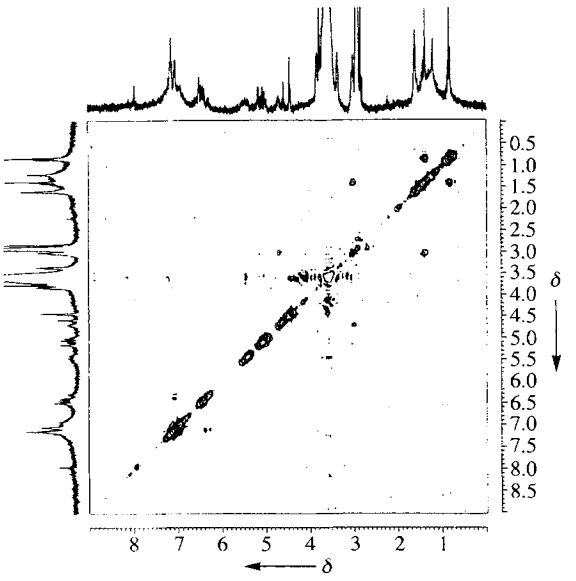

Fig. 3. 2D MAS NMR spectrum (COSY 45) of a hydantoin precursor on a bead in suspension.

For the acquisition of the 1D NMR spectra (in [D$_6$]DMSO), the deuterium lock of the available lock channel was used. The lock signal was detected by the heteronuclear transmitter coil. The COSY45 spectrum was acquired in $CDCl_3$, but due to the limited solvent volume the lock signal was too low.

Received: May 29, 1996 [Z 9163 IE]
German version: *Angew. Chem.* **1996**, *108*, 3034–3036

Keywords: combinatorial chemistry · solid-phase synthesis · NMR spectroscopy

[1] R. B. Merrifield, *J. Am. Chem. Soc.* **1963**, *85*, 2149.
[2] J. S. Früchtel, G. Jung, *Angew. Chem.* **1996**, *108*, 19; *Angew. Chem. Int. Ed. Engl.* **1996**, *35*, 17.
[3] M. C. Desai, R. N. Zuckermann, W. H. Moos, *Drug Dev. Res.* **1994**, *33*, 174.
[4] M. A. Gallop, R. W. Barrett, W. J. Dower, S. P. A. Fodor, E. M. Gordon, *J. Med. Chem.* **1994**, *37*, 1233.
[5] W. Rapp, K. H. Wiesmüller, B. Fleckenstein, V. Gnau, G. Jung in *Peptides 1994* (Ed.: H. L. S. Maia), Escom, Leiden, **1995**, p. 87.
[6] W. Rapp in *Peptides, Chemistry, Structure and Biology, Proceedings of the 13th American Peptide Symposium* (Eds.: T. P. Kaumaya, R. S. Hodges), Escom, Leiden, **1995**, p. 313.
[7] W. Rapp in *Innovations and Perspectives in Solid-Phase Synthesis and Related Technologies, Collected Papers, 4th International Symposium* (Ed.: R. Epton), Mayflower, Edinburgh, **1995**, in press.
[8] Tentacel Polymers are available under the name TentaGel from the firm Rapp Polymere GmbH.
[9] W. Schoknecht, K. Albert, G. Jung, E. Bayer, *Liebigs. Ann. Chem.* **1982**, 1514.
[10] K. Albert, B. Evers, E. Bayer, *J. Magn. Reson.* **1985**, *62*, 428.
[11] E. Bayer, K. Albert, H. Willisch, W. Rapp, B. Hemmasi, *Macromolecules* **1990**, *23*, 1937.
[12] W. L. Fitch, G. Detre, C. P. Holmes, J. N. Shoolery, P. A. Keifer, *J. Org. Chem.* **1994**, *59*, 7955.
[13] R. C. Anderson, M. A. Jarema, M. J. Shapiro, J. P. Stokes, M. Ziliox, *J. Org. Chem.* **1995**, *60*, 2650.
[14] R. C. Anderson, J. P. Stokes, M. Shapiro, *Tetrahedron Lett.* **1995**, *36*, 5311.
[15] P. A. Keifer, L. Baltusis, D. M. Rice, A. A. Tymiak, J. N. Shoolery, *J. Magn. Reson.* **1996**, *119*, 65.
[16] P. A. Keifer, *J. Org. Chem.* **1996**, *61*, 1558.
[17] S. K. Sarkar, R. S. Garigipati, J. L. Adams, P. A. Keifer, *J. Am. Chem. Soc.* **1996**, *118*, 2305.

A Layer Silicate: Synthesis and Structure of the Zeolite Precursor RUB-15—$[N(CH_3)_4]_8[Si_{24}O_{52}(OH)_4]\cdot 20H_2O$**

Uwe Oberhagemann, Parwis Bayat, Bernd Marler, Hermann Gies,* and Jordi Rius

The investigation of the synthesis mechanisms and the tailored synthesis of zeolites are areas of current interest in preparative inorganic chemistry. In the 1970s and 1980s many attempts were made to identify precursors in silicate solutions that would condense in the crystallization process to give the different zeolite structure types.[1, 2] In the 1990s the structure-directing potential of template molecules[3–5] and self-organizing template/silicate systems were seen as the key for the crystallization of micro- and mesoporous tectosilicate structures.[6–8] We present herein a crystalline zeolite precursor, RUB-15, which was obtained in mild hydrothermal syntheses by using tetramethylammonium cations as templates.

The crystalline layer silicate with the codename RUB-15 was synthesized from aqueous tetramethylammonium silicate solutions in the temperature range from 120 to 140 °C. Thermogravimetric analysis of the compound revealed the proportion of volatile components in the structure to be about 39%. ^{29}Si and ^{13}C solid-state MAS NMR investigations showed that the silicate layer is composed of Q^3- ($\delta = -101$) and Q^4-connected silicon ($\delta = -108$) in the ratio of 2:1 and that tetramethylammonium (TMA) ions ($\delta = 56.4$) are present as counterions. The X-ray powder diagram was indexed in the orthorhombic system with lattice constants $a = 27.92$, $b = 8.41$, and $c = 11.52$ Å. The evaluation of the systematic absences restricted the space group symmetry to *Ibam* and *Iba*2. The Rietveld analysis of the structure (see below) revealed that RUB-15 has the symmetry *Iba2*.

Crystalline silicate structures of low density such as RUB-15 are often microcrystalline powders of poor crystallinity. In addition, the scattering power of the material is low. Depending on the complexity of the structure, X-ray reflections can only be indexed unambiguously to *d*-spacings of about 2 Å ($2\theta = 45°$ for $\lambda = 1.5406$ Å). In the case of RUB-15, scattering information up to a resolution of about 2.0 Å could be used for the structure determination. This resolution is sufficient to clearly distinguish between neighboring [SiO_4] units in the electron density maps.

The crystal structure of RUB-15 was solved from integral intensities of unambiguously indexed reflections by direct methods by using a modified tangent formula.[9] The structure of the silicate layer was obtained directly from the direct method solution and geometrically optimized for the remaining structural analysis by distance least squares procedure (DLS). In the subsequent Rietveld analysis[10] this model of the partial structure was initially kept invariant and used to determine the phases for difference-Fourier calculations. All the X-ray powder data up to an angle of 65° 2θ was then included for the refine-

[*] Prof. Dr. H. Gies, Dipl.-Min. U. Oberhagemann, Dipl.-Min. P. Bayat, Dr. B. Marler
Institut für Mineralogie der Universität
D-44780 Bochum (Germany)
Fax: Int. code +(234)709-4433
Dr. J. Rius
Institut de Ciència de Materials de Barcelona, Bellaterra, Catalunya (Spain)

[**] H. G. acknowledges financial support for parts of the program by the Deutsche Forschungsgemeinschaft (Gi 139-13/1). J. R. thanks the Spanish Dirección General de Investigación Científica y Técnica (DGICYT) for financing the cooperation (accion intergrada hispano-alemana).

ment. These calculations gave the locations of the TMA ions, and their subsequent refinement in the structure revealed the hydrate water which was then successfully included into the Rietveld analysis. The results of the structure refinement are summarized in Table 1. A comparison of the experimental and calculated powder pattern after the final refinement is given in Figure 1.

Table 1. Summary of the measurement parameters and results of the Rietveld analysis.

diffractometer	Siemens D5000 with 6° PSD
wavelength [Å]	1.5406
2θ range [° 2θ]	5–65
step width [° 2θ]	0.00776
no. of observations	7133
no. of reflections	260
no. of soft restraints	45
no. of structural variables	57
no. of profile parameters	6
profile width used in the refinement	10 × FWHM
space group symmetry	*Iba*2
lattice parameters	
a_0 [Å]	27.905(6)
b_0 [Å]	8.408(1)
c_0 [Å]	11.518(2)
FWHM at 20.0° [° 2θ]	0.115
R_F	0.086
R_{wp}	0.114
R_{exp}	0.089
weighting factor for soft restraints	10

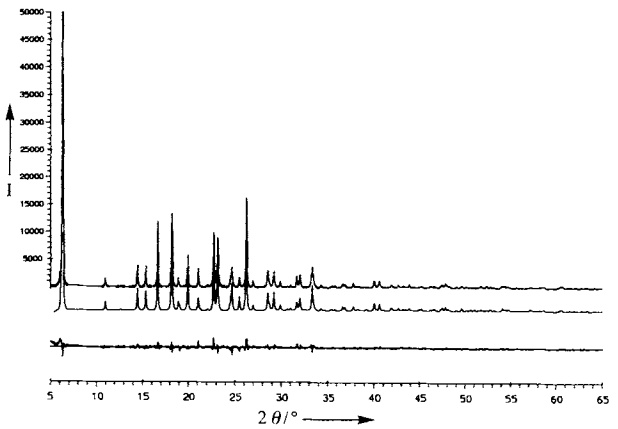

Fig. 1. The observed and calculated X-ray powder diagram of RUB-15 as well as its difference after the completion of the Rietveld analysis. I = intensity in arbitrary units.

In agreement with the results of the ^{29}Si solid-state MAS NMR spectroscopic investigation, the silicate layer is built from three-connected [SiO_3OH] ([SiO_3O^-]) and four-connected [SiO_4] tetrahedral units in the ratio of 2:1 (Fig. 2). The layer shows hemihedral cavities, which are formed from two six-rings and two four-rings, and which are similar to one half of the sodalite cage. Each cavity contains a TMA ion—with one methyl group pointing inwards—leading to an ideal space-filling arrangement. This arrangement is supported by the chemical shift of the ^{13}C NMR signal of the methyl carbon atoms ($\delta = 56.4$), which lies between the values for the TMA ions in the β-cages of the zeolite faujasite ($\delta = 56.7$) and that for the free TMA ion ($\delta = 56.0$).[11] Hydrate water molecules and hydroxide ions terminate the silicate layer by building a hydrogen bonding network together with the terminal oxygen atoms of the silicate layer. In this way the TMA ion is completely embedded in the silicate–hydrate layer (Fig. 3).

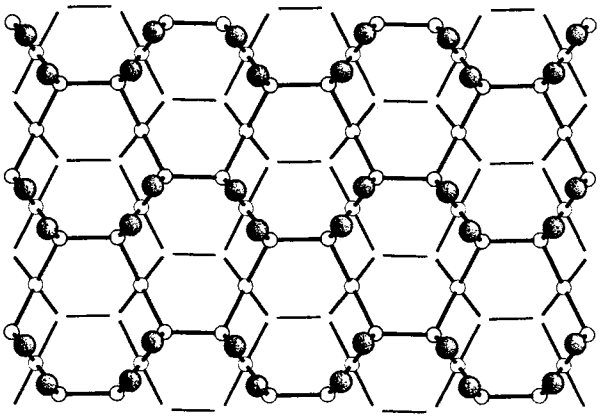

Fig. 2. Schematic view of a section of the silicate layer of RUB-15 including the terminal OH groups (projection along [100]). The Si atoms are located at the nodes of the network; the O atoms are located close to the midpoint between two Si atoms. Shaded spheres are OH groups.

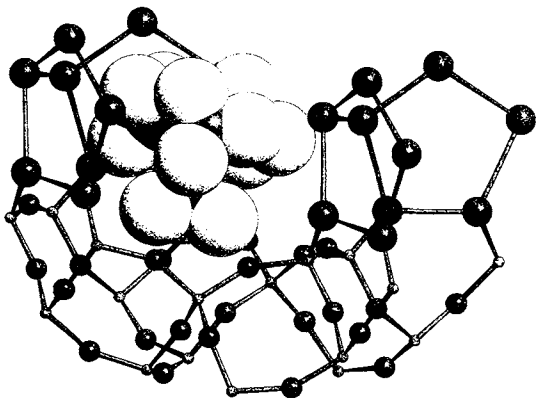

Fig. 3. The TMA ion embedded inside the hydrated silicate layer. The TMA ion is shown as a space-filling model. Small, medium, and large spheres represent Si, O, and OH and H_2O, respectively.

The silicate–hydrate layer is connected to neighboring layers through additional hydrogen-bonded water molecules. Only the oxygen atoms of these molecules have been localized in the structure analysis; they are tetrahedrally coordinated to four neighboring oxygen atoms at distances typical for O-H···O hydrogen bonds (d(O–O) = 2.5–2.9 Å) (Fig. 4 top). The arrangement is only a time- and space-averaged model of the water molecule, which cannot be resolved in the diffraction experiment. For similar reasons the position of the hydrogen atoms cannot be determined because of their very low scattering power. The positive charge of the TMA ion is balanced by the negative charge that is delocalized over the hydrogen bonding system composed of water molecules, hydroxide ions, and terminal silanol groups.

Thus, the structure of RUB-15 is a three-dimensional bonding network consisting of layerlike silicate ions and water molecules or hydroxide ions. The stacking of the silicate layers occurs along the a axis of the unit cell and takes into account the body-centred symmetry. A vacancy located in the center of a group of four TMA ions exist between neighboring silicate layers in the structure. This vacancy is big enough for an additional water molecule (Fig. 4 bottom). Interestingly, the occupation of this vacancy with a water molecule would lead to a hydrate layer, which is topologically equivalent to the silicate layer, and this, in turn, would create a mixed-layer silica–water tetrahedral network. However, our refinement calculations clearly reveal that this water molecule is not present and that a

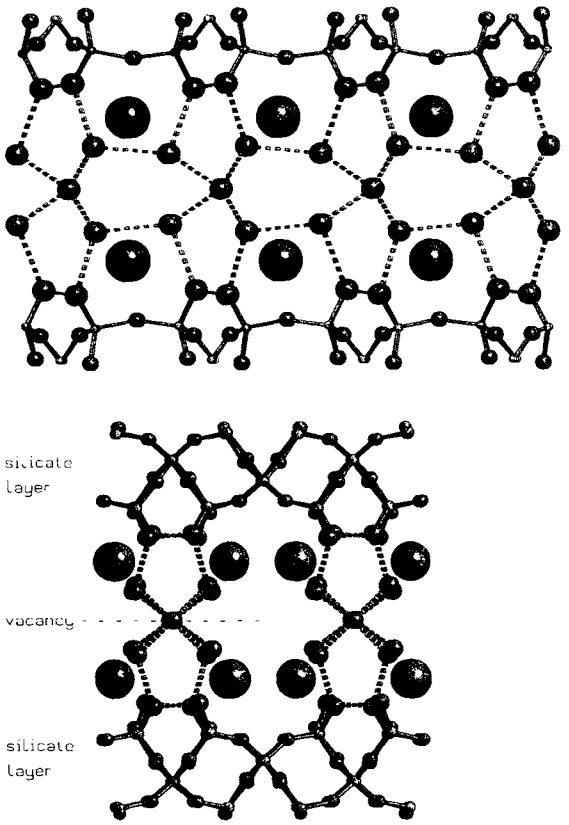

Fig. 4. Hydrogen bonding system in RUB-15: dashed lines are the hydrogen bonds, solid lines are Si–O bonds. Top: Projection along [010], bottom: Projection along [001]. Spheres in order of increasing size represent Si, O, OH and H_2O, and TMA, respectively.

narrow, channel-like void occurs in the structure (Fig. 4 bottom). The structure refinement shows the composition of the unit cell of RUB-15 to be $[N(CH_3)_4]_8[Si_{24}O_{52}(OH)_4]\cdot 20H_2O$.

The layer silicate RUB-15 belongs to the series of inclusion compounds of different composition formed with the TMA ion. The TMA ion is a very effective template cation that yields clathrate-type inclusion compounds in the presence of network-forming molecules and ions (H_2O, $[SiO_4]^{4-}$, $[AlO_4]^{5-}$, $[PO_4]^{3-}$). The structure-directing potential of the TMA ion is demonstrated in Table 2, which shows a selection of clathrate inclusion compounds that have been synthesized in the presence the TMA ion, and that contain TMA as an essential component. In the examples given the TMA ion occupies cagelike voids, which are formed by water molecules, by $[SiO_4]$ tetrahedra, or by different combinations (for example H_2O+$[SiO_4]$ tetrahedra; $[AlO_4]$ and $[PO_4]$ tetrahedra).

Whereas in the TMA + H_2O system only materials with three-dimensional four-connected water frameworks are formed, the addition of SiO_2 leads to TMA–silicate hydrates at room temperature for high concentrations of silica and TMA. Structure analyses revealed that in TMA–silicate hydrates the silicate ions (cubic octamer) together with the hydrate water build a three-dimensional hydrogen bonding network that occludes the TMA ions in cagelike voids.[14]

Furthermore, in the TMA + H_2O + SiO_2 system the synthesis temperature has a decisive influence on the extent of the condensation of the silicate ion. RUB-15, which was obtained at higher temperatures but under otherwise identical synthesis conditions to those used for the room temperature silicate hydrate, contains a two-dimensional silicate ion. This contributes higher bonding energies to the total lattice energy and thus to the higher thermal stability. At the same time, the contributions from the weak hydrogen bonds to the lattice energy decreases. In this case, the TMA ion also occupies cagelike voids, which consist of silicate sodalite semicages and additional water molecules.

From the crystal structure analysis of TMA–sodalite[16] it is known that the TMA ion fills the cage ideally; therefore, the cage with the TMA ion could be regarded as a typical host–guest pair. In analogy to the situation in the TMA–sodalite, the TMA ion in the layer silicate structure of RUB-15 has a template effect on the formation and stabilization of the silicate layer.

A further increase of the synthesis temperature in the TMA + H_2O + SiO_2 system gives the clathrasil Dodecasil 3C, which is the silica analogue of the clathrate hydrate of type II. Thus, RUB-15 could be regarded as a link in the series group-silicate hydrates - layer-silicate hydrates - framework silicates, further illustrating the close relationship between crystalline and non-crystalline compounds of water and silica.[21]

The platelike morphology of RUB-15 crystals suggests that crystal growth is fast at the edge of the silicate layer, but slow perpendicular to the silicate layer; that is, the rate of nucleation of a new layer is slower than the ongoing growth of the unit. The rapid sorption of the TMA ions onto the silicate layer might further stabilize the phase boundary. At the same time these cations serve as a nucleation seed for the new silicate unit.

Sodium layer silicates in their ion-exchanged H-form are useful materials[22] for heterogeneous catalysis because of their acidity and they also serve as ion exchanger in detergent formulations. For instance, the sodium layer silicate kanemite was introduced as a water softener in washing powders a few years ago.[23] Likewise, there are many examples that describe the catalytic properties of layer silicates. As RUB-15 is closely related to the family of sodium layer silicates, similar properties are expected. The presence of acid centers at the surface close to the sodalite half-cavities is of particular interest, since it might lead to form-selective catalysis on the outer surface of the silicate.

Recently two layer silicate structures have been described that are potential zeolite precursors.[24, 25] Careful heating of the

Table 2. Comparison of selected structures synthesized with tetramethylammonium ions at different synthesis temperatures.

Synthesis system	TMA + H_2O	TMA + H_2O + SiO_2	TMA + H_2O + SiO_2 + Al_2O_3	TMA + H_2O + P_2O_5 + Al_2O_3
synthesis temperatur				
low (≈ 20 °C)	clathrate hydrates [12, 13]	silicate hydrates [14] *group silicates*	–	–
medium (≈ 130 °C)	–	**RUB-15** **layer silicate**	sodalite [16] gismondine [17] *porous framework silicates*	$AlPO_4$-20 (sodalite) [19] *porous framework aluminophosphate*
high (≈ 180 °C)	–	Dodecasil 3C [15] *porous framework silica*	NU-1 [18] *porous framework silicate*	$AlPO_4$-12-TAMU [20] *porous framework aluminophosphate*

materials causes the condensation of the silicate layers, giving the zeolite structures MCM-22 and ferrierite. Similar behavior can also be expected for RUB-15, since the silicate layer terminated with silanol groups should be the perfect subunit for the formation of the silica framework of the zeolite sodalite.

Experimental Procedure

RUB-15 crystallized from a reaction mixture with the following composition: SiO_2:TMAOH:H_2O = 1.00:0.75:55.52. The solution was filled in Teflon-lined autoclaves (60% filling factor) and kept in an oven at a temperature between 120 and 140 °C for about four weeks. The reaction product was filtered, washed with distilled water, dried at 80 °C, and subsequently identified by X-ray powder diffraction.

Received: June 7, 1996 [Z 9198 IE]
German version: *Angew. Chem.* **1996**, *108*, 3041–3044

Keywords: silicon compounds · solid-state structures · zeolites

[1] R. A. van Santen, J. Keijsper, G. Ooms, A. G. T. G. Kortbeek in *New Developements in Zeolites Science and Technology*, (Eds.: Y. Murakami, A. Iijima, J. W. Ward) Elsevier, Amsterdam, **1986**, pp. 169–175.
[2] C. T. G. Knight, *Zeolites* **1990** *10*, 140–144.
[3] H. Gies, B. Marler, *Zeolites* **1992**, *12*, 42–49.
[4] K. R. Franklin, B. M. Lowe in *Zeolites: Facts, Figures, Future, Studies in Surface Science and Catalysis, Vol. 49A* (Eds.: P. A. Jacobs R. A. van Santen), Elsevier, Amsterdam, **1989**, pp. 179–188.
[5] A. Moini, K. D. Schmitt, E. W. Valyocsik, R. F. Polomski, *Zeolites* **1994**, *14*, 504–511.
[6] J. S. Beck, J. C. Vartuli, W. J. Roth, M. E. Leonowicz, C. T. Kresge, K. D. Schmitt, C. T.-W. Chu, D. H. Olson, E. W. Sheppard, S. B. McCulen, J. B. Higgins, J. L. Schlenker, *J. Am. Chem. Soc* **1992**, *114*, 10834–10842.
[7] C.-Y. Chen, S. L. Burkett, H.-X. Li, M. E. Davis, *Microporous Mater.* **1993**, *2*, 27–34.
[8] A. Monnier, F. Schüth, Q. Huo, D. Kumar, D. Magrolese, R. S. Maxwell, G. D. Stucky, M. Krishnamurty, P. Petroff, A. Firouzi, M. Janicke, B. F. Chmelka, *Science* **1993**, *261*, 1299–1303.
[9] J. Rius, J. Sane, C. Miravitlles, H. Gies, B. Marler, U. Oberhagemann, *Acta Crystallogr. Sect. A* **1995**, *51*, 840–845. Further details of the crystal structure investigation may be obtained from the Fachinformationszentrum Karlsruhe, D-76344 Eggenstein-Leopoldshafen (Germany), on quoting the depository number CSD-405713.
[10] C. Baerlocher, X-ray Rietveld System XRS-82, Institut für Kristallographie und Petrographie, ETH Zürich, Switzerland, **1991**.
[11] S. Hayashi, K. Susuki, S. Shin, K. Hayamizu, O. Yamamoto, *Chem. Phys. Lett.* **1985**, *113*, 368–371.
[12] R. K. McMullen, T. C. W. Mak, G. A. Jeffrey, *J. Chem. Phys.* **1966**, *44*, 2338–2345.
[13] D. Mootz, R. Seidel, *J. Inclusion Phenom. Mol. Recognit. Chem.* **990**, *8*, 139–157.
[14] a) Y. I. Smolin, Y. F. Shepelev, R. Pomes, D. Hoebbel, W. Wieker, *Sov. Phys. Crystallogr. (Engl. Transl.)* **1979**, *24*, 19–23; b) M. Wiebcke, *J. Chem. Soc. Chem. Commun.* **1991**, 1507–1508; c) M. Wiebcke, D. Hoebbel, *J. Chem. Soc. Dalton Trans.* **1992**, 2451–2455; d) M. Wiebcke, M. Grube, H. Koller, G. Engelhardt, J. Felsche, *Microporous Mater.* **1993**, *2*, 55–63.
[15] J. Patarin, ENSC de Mulhouse, Mulhouse, France, personal communication.
[16] C. Baerlocher, W. M. Meier, *Helv. Chim. Acta* **1969**, *52*, 1853–1860.
[17] C. Baerlocher, W. M. Meier, *Helv. Chim. Acta* **1970**, *53*, 1285–1293.
[18] G. Bellussi, R. Millini, A. Carati, G. Maddinelli, A. Gervasini, *Zeolites* **1990**, *10*, 642–649.
[19] S. T. Wilson in *Introduction to Zeolites Science and Practice, Studies in Surface Science and Catalysis, Vol. 58*, (Eds.: H. van Bekkum, E. M. Flanigen, J. C. Jansen) Elsevier, Amsterdam, **1991**, pp. 137–151.
[20] P. R. Rudolf, C. Sadarriaga-Molina, A. Clearfield, *J. Chem. Phys.* **1986**, *90*, 6122–6125.
[21] F. Liebau in *The Physics and Technology of Amorphous SiO_2* (Eds.: R. A. B. Devine), Plenum Press, New York, **1988**, p. 15.
[22] J. Cornier, J.-M. Popa, M. Gubelmann, *L'actualité chimique* **1992**, 405–414.
[23] J. Himmrich, W. Gohla *Seifen, Oele, Fette, Wachse* **1994**, *120*(13), 784, 787, 790, 792.
[24] R. Millini, G. Perego, W. O. Parker Jr., G. Bellussi, L. Carluccio, *Microporous Mater.* **1995**, *4*, 221–230.
[25] L. Schreyeck, P. Caullet, J. C. Mougenel, J.-L. Guth, B. Marler, *J. Chem. Soc. Chem. Commun.*, **1995**, 2187–2188.

Synthesis and Characterization of the Stable Dicarbonyl(cyclopentadienyl)iron Radical $[(C_5R_5)Fe(CO)_2]$ (R = $CHMe_2$)**

Helmut Sitzmann,* Thomas Dezember, Wolfgang Kaim, Frank Baumann, Dietmar Stalke, Joerg Kärcher, Elmar Dormann, Hubert Winter, Christoph Wachter, and Marc Kelemen

Dedicated to Professor Max Herberhold on the occasion of his 60th birthday

Thermally labile cyclopentadienyliron halide solvates of the type $[CpFe(X)(thf)_2]$ (X = Cl, Br), which can be obtained in solution under mild conditions, have been known for a long time. As reactive intermediates they are of interest[2c] for the synthesis of triple-decker sandwich complexes,[1] ferrocenes with different ring ligands,[2] and half-sandwich complexes.[2a, 3] When the stabilizing donor ligands are removed, the remaining cyclopentadienyliron(II) chloride decomposes by dismutation, as has been demonstrated recently for the chelate complex $[(C_5Me_5)Fe(Me_2NC_2H_4NMe_2)Cl]$.[4] We report here on the characterization of isolable cyclopentadienyliron(II) halides and of the dicarbonyl(pentaisopropylcyclopentadienyl)iron(I) radical.

Treatment of $[FeBr_2(dme)]$[2a] in tetrahydrofuran with one equivalent of tetra-[5a] or pentaisopropylcyclopentadienide,[5b] led in each case to a dark green solution, the color of which became lighter on evaporation of the solvent. Crystalline, orange-red, extremely air-sensitive products are isolated, which can be stored under inert gas at room temperature (Scheme 1).

We postulate a dimeric structure with bridging bromo ligands for complexes **1** and **2**. A monomeric structure is very unlikely because of the number of valence electrons (14) and the low coordination number of the [CpFeX]-type fragment, and higher nuclearity complexes are not considered because of the extremely bulky five-membered ring ligands. The magnetic properties of complexes **1** and **2** (see below) support this hypothesis (pentamethylcyclopentadienylruthenium chloride is tetrameric and diamagnetic[6]). The strongest argument is supplied by the analogous cyclopentadienyl halides $[\{(C_5R_4H)MX\}_2]$ (R = $CHMe_2$, M = Co,[7a] Ni[7b]), for which a dimeric structure with bridging halide ligands has been confirmed by X-ray crystallography. Complexes **1** and **2** are readily soluble in all common solvents; in acetonitrile a reversible color change to dark violet occurs, in tetrahydrofuran one to dark green. This feature presumably arises from the formation of mononuclear complexes $[(C_5R_4R')Fe(L)_2Br]$ (R = $CHMe_2$, R' = H, $CHMe_2$, L = thf, MeCN) with two loosely coordinated donor molecules.

[*] Dr. H. Sitzmann, Dipl.-Chem. T. Dezember
FB Chemie der Universität
Erwin-Schrödinger-Strasse, D-67663 Kaiserslautern (Germany)
Fax: Int. code +(631)205-2187
e-mail: sitzmann@rhrk.uni-kl.de
Prof. Dr. W. Kaim, Dipl.-Chem. F. Baumann
Institut für Anorganische Chemie der Universität Stuttgart (Germany)
Prof. Dr. D. Stalke
Institut für Anorganische Chemie der Universität Würzburg (Germany)
Dipl.-Chem. J. Kärcher
Institut für Anorganische Chemie der Universität Göttingen (Germany)
Prof. Dr. E. Dormann, Dr. H. Winter, Dipl.-Phys. C. Wachter, Dipl. Phys. M. Kelemen
Physikalisches Institut der Universität Karlsruhe (Germany)

[**] High-Spin Cyclopentadienyl Complexes, Part 1. This work was supported by Fonds der Chemischen Industrie. H. S. is grateful to Prof. Dr. O. J. Scherer, Kaiserslautern, for his generous support, and to Prof. Dr. R. Gleiter, Heidelberg, for recording photoelectron spectra.

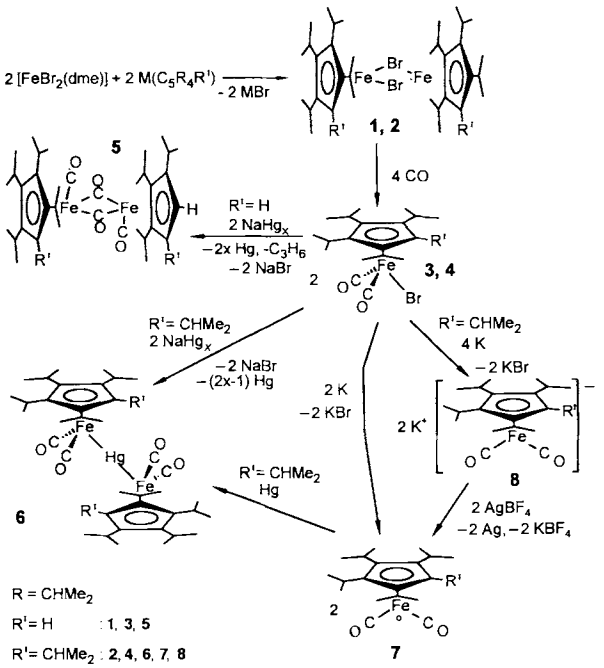

Scheme 1. Synthesis of compounds **1**–**8**.

Magnetic susceptibility measurements of **1** in the solid state gave good agreement with the Curie–Weiss law above 125 K (Fig. 1). The effective magnetic moment is 5.15 μ_B and corresponds to a high-spin Fe^{2+} ion (highly unusual for cyclopentadienyliron(II) complexes) with four unpaired electrons and parallel spin coupling of the two d^6-Fe^{2+} centers within one dimer;

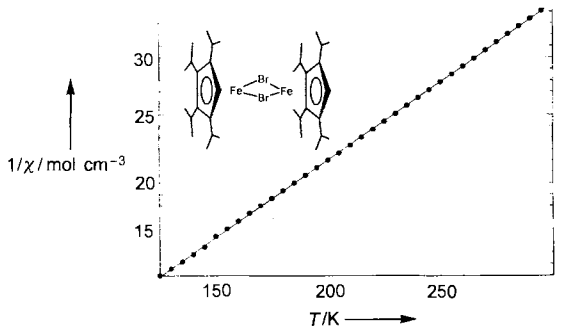

Fig. 1. Reciprocal of the molar magnetic susceptibility of **1** in the solid state as a function of absolute temperature.

the Weiss constant Θ is 45.5 K. The plot of χT (molar magnetic susceptibility × absolute temperature) against the absolute temperature (Fig. 2) shows a steep rise at low temperatures, reaches a maximum dependent on the strength of the magnetic field, and drops away again at very low temperature. This behavior corresponds to parallel spin coupling within the dimers together with absence of long-range magnetic ordering within the crystal.

The ^{1}H NMR spectrum of **1**, which extends from $\delta = 102$ to $\delta = -110.9$ (298 K, C_6D_6), is characterized by very strong broadening and a temperature-dependent shift of the resonance signals. It has not been possible to assign the signals. Dimers **1** and **2** take up carbon monoxide under mild conditions, leading to high yields of the bromo(dicarbonyl)iron complexes **3** and **4**, respectively (see Scheme 1). Reduction of the tetraisopropylcyclopentadienyl derivative **3** with sodium amalgam afforded

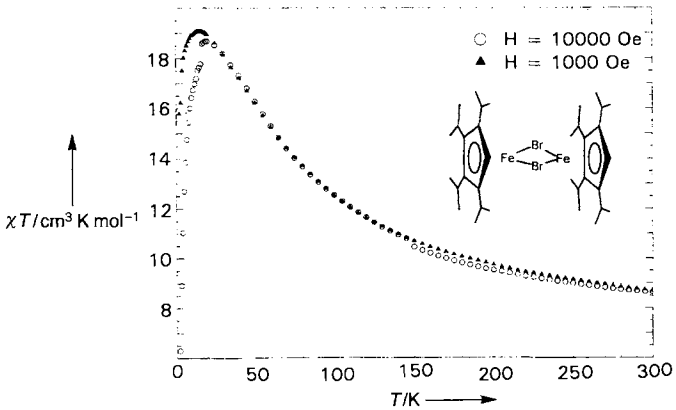

Fig. 2. Product of the molar magnetic susceptibility and the absolute temperature as a function of absolute temperature for complex **1**.

the dimer **5**, which contains one tetra- and one triisopropylcyclopentadienyl ring; the latter is formed by regiospecific propene elimination (Scheme 1).

Precedence for spontaneous diversification of two alkylated cyclopentadienyl ligands lies in the selective formation of $[(C_5R_4H)(C_5R_3H_2)BiCl]$ ($R = CHMe_2$) from $BiCl_3$ and two equivalents of tetraisopropylcyclopentadienide; a reaction that was studied with labeling experiments.[9] That compound **5** does not undergo redistribution of the two different "molecule halves" at room temperature, at least for a period of about an hour, can be deduced from ^{13}C NMR spectra (Fig. 3). ^{1}H NMR spectra of **5** show two superimposed ring CH signals, four septets (two of which are superimposed) and seven doublets with a ratio of integrals 1:2:2:2:1:2:6:6:6:6:6:6:6; as expected one singlet for one ring-H atom, two septets of equal intensity for

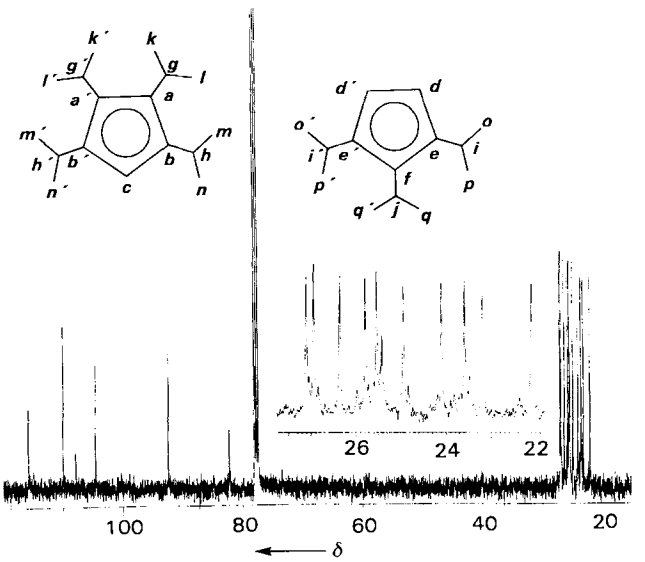

Fig. 3. ^{13}C NMR spectra of **5** showing the region for the alkyl-C and ring-C atoms. Three ring carbon signals, each (*a*–*c* and *d*–*f*) with an intensity ratio 2:2:1, are expected for the two different five-membered rings of **5**. This corresponds exactly to the six signals observed beween $\delta = 80$ and $\delta = 120$. Analogously, four signals with intensity ratio 2:2:2:1 are expected (positions *g*–*j*) for the methine C atoms. The seven pairs of enantiotopic methyl groups (*kk'*, *ll'*, *mm'*, *nn'*, *oo'*, *pp'*, *qq'*) correspond to three pairs of symmetry-equivalent isopropyl groups, each with two diastereotopic methyl positions (*kl* for instance), and one isopropyl group with two enantiotopic methyl positions (*qq'*). Therefore one expects seven signals of intensity ratio 2:2:2:2:2:2:2 for the 14 methyl groups. As expected eleven signals are observed for methine- and methyl-carbon atoms, of which ten signals represent two carbon atoms each and the eleventh signal represents one carbon atom. The signal of highest intensity arises from the solvent $CDCl_3$.

four methine-H atoms of two pairs of isopropyl groups, and four doublets of equal intensity for the total of eight methyl groups (because each pair of symmetry-equivalent isopropyl groups has two diastereotopic methyl positions) are assigned to the tetraisopropylcyclopentadienyl ring. One singlet for two ring-H atoms, two septets (1:2) for three methine-H atoms, two doublets (6:6) for the diastereotopic methyl positions of the two symmetry-equivalent isopropyl groups, and one more doublet for the two enantiotopic methyl positions of the remaining isopropyl group (cf. Fig. 3; for confirmation of the diastereotopic methyl positions of isopropylcyclopentadienyl ligands bound to iron by selective decoupling experiments see reference [5a]) are assigned to the triisopropylcyclopentadienyl ligand. In contrast, the reduction of **4** with sodium amalgam gave only the mercury compound **6** (Scheme 1).[10] Reduction of **4** with two equivalents of potassium afforded the potassium salt of dicarbonyl(pentaisopropylcyclopentadienyl)ferrate(0) (**8**), and subsequent oxidation with one equivalent of silver tetrafluoroborate, or by reduction of **4** with one equivalent of potassium gave a dark green solution for which no IR absorptions are observed in the bridging carbonyl region. The signals observed correspond to the IR bands of the unstable dicarbonyl(pentamethylcyclopentadienyl)iron radical obtained from irradiation experiments,[11] and prove that the dicarbonyl(pentaisopropylcyclopentadienyl) iron radical **7** practically does not dimerize at all in solution (Scheme 1). Measurement of the magnetic susceptibility in solution by using the method employed by Evans[12] gave a magnetic moment of 1.7 μ_B. EPR spectra support the above-mentioned results. Compound **7** is also monomeric in frozen toluene solution ($g_\perp = 2.1215$; $g_\parallel = 2.1534$). The recently investigated pentaphenylcyclopentadienyl derivative shows in addition to the IR bands of the dimer two low intensity absorptions for the monomeric radical, which, however, could not be detected by EPR spectroscopy.[13] A low first ionization energy of 6.88 eV was observed in the photoelectron spectra of **7**. Compound **7** is an olive green powder and could be obtained as compact, completely non-transparent crystals with metallic luster. The crystal structure analysis of **7**[14] shows a carbonyl-bridged dimer with planar cyclopentadienyl rings inclined towards the Fe–Fe axis by 54.6° (Fig. 4).

The Fe–Fe distance (2.60 Å) is somewhat longer than that found in other derivatives (2.49–2.57 Å[15a]) or the sum of the covalent radii of two Fe atoms (2.50 Å[15b]), and significantly less than the Fe–Fe distance (3.138(3) Å) in $[\{(\eta^3\text{-}C_3H_5)\text{-}Fe(CO)_3\}_2]$.[15c] Complete dissociation of **7** in solution confirms that the distance between the two carbonyl-bridged Fe atoms in the crystal does not not allow any conclusions to be drawn on the Fe–Fe bond order. A determination of the electron density by using the X–N method afforded no indication of bond electrons between the Fe atoms also in the case of the C_5H_5 derivative,[16] and is in accordance with MO calculations.[17]

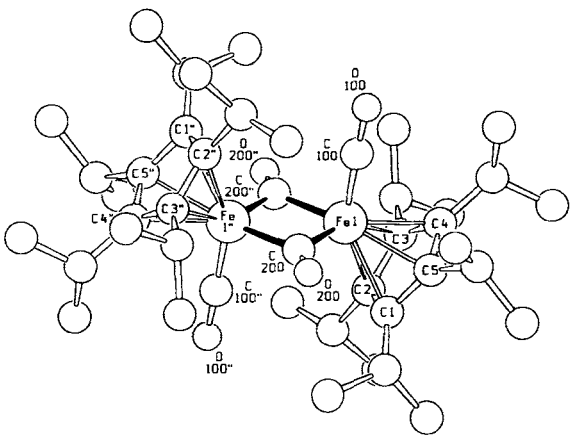

Fig. 4. Crystal structure of **4**. Selected bond lengths [Å] and angles [°]: Fe1–Fe1'' 2.600(2), Fe1–C100 1.725(6), Fe1–C200 1.931(5), C100–O100 1.157(7), C200–O200 1.169(6), Fe1–C1 2.188(5), Fe1–C2 2.198(5), Fe1–C3 2.154(5), Fe1–C4 2.149(5), Fe1–C5 2.150(5), Fe1–Cp(centroid) 1.80; Fe1-C200-Fe1'' 84.4(2), C200-Fe1-C200'' 95.6(2), C100-Fe1-Fe1'' 92.8(2). Only one of the two possible orientations of the pentaisopropylcyclopentadienyl "paddle wheel" in the crystal is shown.

The dicarbonyl radical **7** reacts smoothly in solution with elemental mercury at room temperature to give the yellow mercury compound **6** (see Scheme 1).

In contrast to all other cyclopentadienyl derivatives studied so far, the steric and electronic properties of the pentaisopropylcyclopentadienyl ligand cause the dissociation of complexes of the type $[(Cp^R{}_2Fe_2(CO)_4]$ in solution, leading to the formation of the monomeric radicals of the type $[(Cp^R)Fe(CO)_2]$ with 17 valence electrons. Since **7** exists practically completely as a monomeric radical in solution, interesting prospects for possible follow-up reactions emerge.

Experimental Procedure

1 (**2** was synthesized analogously): $[FeBr_2(dme)]$ (7.23 g, 27.7 mmol) was suspended in DME (100 mL) at −30 °C and treated dropwise with a solution of sodium tetraisopropylcyclopentadienide (6.96 g, 27.1 mmol) in DME (75 mL). After the mixture had been stirred for 2 h, the solvent was evaporated in vacuo, and the residue was taken up in petroleum ether (120 mL). The centrifuged, red-brown solution was evaporated to dryness, and the residue was taken up in pentane (100 mL). After the solution had been centrifuged again, the volume of the solvent was reduced by half. Dimer **1** crystallized at −30 °C from this solution in 33.5% yield (3.35 g, 4.54 mmol). ^{1}H NMR (400 MHz, C_6D_6, external TMS): δ = 94.07, 86.84, 20.89, −82.29.

3: **1** (0.573 g, 0.76 mmol) in diethyl ether (50 mL) was stirred under a CO atmosphere (1 bar) for 1 h at −78 °C, and then a further 12 h at room temperature. The dark red-brown solution was evaporated in vacuo, the crude product taken up in pentane/dichloromethane (3:1), and centrifuged. Red-brown, shiny crystals of **3** (0.404 g, 0.95 mmol, 66%; m.p. 112–115 °C (decomp)) were obtained at −35 °C. ^{1}H NMR (400 MHz, $CDCl_3$, ext. TMS): δ = 4.68 (s, 1H, ring-H), 2.85 (sept, br, 2H, C*H*Me$_2$), 2.73 (sept, br, 2H, C*H*Me$_2$), 1.37 (d, br, 12H, CH$_3$), 1.21 (d, br, 12H, CH$_3$). ^{13}C{^{1}H} NMR (100 MHz, $CDCl_3$, ext. TMS): δ = 214.5 (2C, CO), 109.1 (2C, ring-CCHMe$_2$), 106.5 (2C, ring-*C*CHMe$_2$), 77.6 (1C, ring-*C*H), 25,2. 25.0, 23.8, 23.3, 22.9 (alkyl C atoms; the signal at δ = 25.2 is particularly intense because of superimposition of two alkyl C signals); IR (toluene): $\tilde{\nu}$[cm^{-1}] = 2024 (s), 1977 (s) (CO).

4: A solution of $LiC_5(CHMe_2)_5$ (5.48 g, 15.4 mmol) in DME (80 mL) was added dropwise over 90 min to a suspension of $[FeBr_2(dme)]$ (4.82 g, 15.8 mmol) in DME (40 mL) at −30 °C, and stirred for a further 30 min at that temperature. The mixture was then stirred under a CO atmosphere for 30 min at −30 °C and allowed to warm slowly to room temperature, while from time to time the consumed CO was replenished. Workup as described for **3** gave **4** (5.02 g, 10.7 mmol, 70%) as a red-brown product that decomposed above 120 °C. ^{13}C NMR (100 MHz, $CDCl_3$, ext. TMS): δ = 215.7 (s, 2C, CO) 107.7 (s, br, 5C, ring-C), 25.9 (d, ^1J(CH) = 127 Hz, 5C, *C*HMe$_2$), 24.5 (q, ^{1}J(CH) = 126 Hz, 10C, *C*H$_3$); IR (toluene): $\tilde{\nu}$[cm^{-1}] = 2021 (vs), 1974 (s) (CO).

5: A solution of **3** (0.457 g, 1.08 mmol) in THF (20 mL) was stirred with potassium (0.045 g, 1.15 mmol) at room temperature for 20 h, then the solution was evaporated to dryness in vacuo. Extraction with diethyl ether (10 mL), reduction in volume to 5–6 mL, and cooling of the solution to −30 °C gave **5** (0.106 g, 0.163 mmol, 30%) as a red-violet, microcrystalline product that decomposed above 120 °C. ^{1}H NMR (400 MHz, C_6D_6): δ = 4.34 (2s, superimposed, 3H, ring-H), 3.15 (sept, 2H, C*H*Me$_2$), 2.78 (2 sept, superimposed, 3H, C*H*Me$_2$), 2.70 (sept, 2H, C*H*Me$_2$), 1.62 (d, ^3J = 7.1 Hz, 6H, CH$_3$), 1.36 (d, ^3J = 6.6 Hz, 6H, CH$_3$), 1.32 (d, ^3J = 7.1 Hz, 6H, CH$_3$), 1.21 (d, ^3J = 6.7 Hz, 6H, CH$_3$), 1.15 (d, ^3J = 6.8 Hz, 6H, CH$_3$), 1.05 (d, ^3J = 6.7 Hz, 6H, CH$_3$), 0.92 (d, ^3J = 6.7 Hz, 6H, CH$_3$); ^{13}C NMR (100 MHz, C_6D_6): δ = 215.1 (s, 2C, CO), 214.4 (s, 2C, CO), 115.7 (s, 2C, ring-*C*-CHMe$_2$), 109.9 (s, 2C, ring-*C*-CHMe$_2$), 107.9 (s, 1C, ring-*C*-CHMe$_2$), 104.6 (s, 2C, ring-*C*-CHMe$_2$), 92.4 (d, ^1J(C,H) = 165 Hz, 2C, ring-*C*H), 82.3 (d, ^1J(C,H) = 172 Hz, 1C, ring-*C*H), 27.1, 26.9, 26.4, 25.8, 25.5, 25.4, 24.9, 24.1, 23.6, 23.2, 22.1 (methine- and methyl-C-atoms, superimposed). IR (nujol): $\tilde{\nu}$[cm^{-1}] = 1924 (s), 1757 (s), (CO).

6: A solution of **7** was stirred with an excess of mercury to give **6** as a yellow, almost insoluble powder in nearly quantitative yield. IR (nujol): $\tilde{\nu}$[cm^{-1}] = 1932 (s), 1894 (s), (CO).

7: A solution of **4** (679 mg, 1.45 mmol) in THF (20 mL) was stirred with finely divided potassium (115 mg, 2.90 mmol) for 20 h at room temperature. The solvent was removed in vacuo and the residue was washed with pentane (3 × 10 mL). Yield:

441 mg (0.90 mmol, 62%) orange-red potassium salt **8**. IR (nujol): $\tilde{\nu}$[cm^{-1}] = 1820 (s, br), 1807 (s, br), 1722 (s, br) [18]. Compound **8** (500 mg, 1.17 mmol) and silver tetrafluoroborate (228 mg, 1.17 mmol) were mixed at -30 °C with precooled THF. The reaction mixture was allowed to warm to room temperature and stirred for 1 h. The dark green solution was filtered over Celite and evaporated to dryness. Compound **7** (409 mg, 1.06 mmol, 90%) was obtained as an olive-green powder that sublimed at 10^{-2} mbar above 70 °C. ^{1}H NMR (400 MHz, 343 K, C_6D_6): δ = 8.67 (br, 15H, CH_3, presumably proximal), 6.51 (br, 5H, CH), 4.50 (br, 15H, CH_3, presumably distal). IR (toluene): $\tilde{\nu}$[cm^{-1}] = 1975 (s), 1901 (s); IR (KBr): $\tilde{\nu}$[cm^{-1}] = 1916 (vs), 1759 (s, br). Crystals suitable for X-ray diffraction were obtained from petroleum ether at -30 °C.

Received: May 17, 1996 [Z9125IE]
German version: *Angew. Chem.* **1996**, *108*, 3013–3016

Keywords: cyclopentadienyl complexes · high-spin complexes · iron compounds · radicals

[1] M Stephan, P. Müller, U. Zenneck, H. Pritzkow, W. Siebert, R. N. Grimes, *Inorg. Chem.* **1995**, *34*, 2058–2067.
[2] a) U. Kölle, B. Fuss, F. Khouzami, J. Gersdorf, *J. Organomet. Chem.* **1985**, *290*, 77–83; b) J. Okuda, E. Herdtweck, *Chem. Ber.* **1988**, *121*, 1899–1905; c) R. Poli, *Chem. Rev.* **1991**, *91*, 509–551.
[3] J. Okuda, *Chem. Ber.* **1989**, *122*, 1259–1260.
[4] K. Jonas, P. Klusmann, R. Goddard, *Z. Naturforsch. B* **1995**, *50*, 394–404.
[5] a) H. Sitzmann, *J. Organomet. Chem.* **1988**, *354*, 203–214; b) H. Sitzmann, *Z. Naturforsch. B* **1989**, *44*, 1293–1297.
[6] P. J. Fagan, M. D. Ward, J. V. Caspar, J. C. Calabrese, P. J. Krusic, *J. Am. Chem. Soc.* **1988**, *110*, 2981–2983.
[7] a) H. Sitzmann, Y. Ehleiter, G. Wolmershäuser, unpublished results; b) H. Sitzmann, G. Wolmershäuser, unpublished results.
[8] To our knowledge, cyclopentadienyl complexes with high-spin electron configuration are known only with manganese: a) C. G. Howard, G. S. Girolami, G. Wilkinson, M. Thornton-Pett, M. B. Hursthouse, *J. Am. Chem. Soc.* **1984**, *106*, 2033–2040; b) J. Heck, W. Massa, P. Weinig, *Angew. Chem.* **1984**, *96*, 699–700; *Angew. Chem. Int. Ed. Engl.* **1984**, *23*, 722–723; c) N. Hebendanz, F. H. Köhler, G. Müller, J. Riede, *ibid.* **1986**, *108*, 3281–3289; d) an excellent review article on open shell transition metal complexes is given by R. Poli, *Chem. Rev.* **1996**, *96*, 2135–2204.
[9] H. Sitzmann, G. Wolmershäuser, *Chem. Ber.* **1994**, *127*, 1335–1342.
[10] Complexes of this type have been known for a long time: E. O. Fischer, W. Hafner, H. O. Stahl, *Z. Anorg. Allg. Chem.* **1955**, *282*, 47.
[11] B. D. Moore, M. Poliakoff, J. J. Turner, *J. Am. Chem. Soc.* **1986**, *108*, 1819–1822.
[12] D. F. Evans, *J. Chem. Soc.* **1959**, 2003–2007.
[13] I. Kuksis, M. C. Baird, *Organometallics* **1994**, *13*, 1551–1553.
[14] X-ray crystal structure data for **7**: $C_{22}H_{35}FeO_2$: T = 193 K, triclinic space group $P\bar{1}$, a = 1.0392(2), b = 1.0489(2), c = 1.0536(2) Å, α = 105.44(3), β = 106.30(3), γ = 101.22(3)°, V = 1016.5(4) Å^3, Z = 2, $\rho_{calcd.}$ = 1.265 g cm^{-1}, $F(000)$ = 418, λ = 71.073 pm, $\mu(Mo_{K\alpha})$ = 0.754 mm^{-1}. Data were collected on a Stoe-Siemens-AED-diffractometer. Intensities were measured on a rapidly cooled crystal (0.3 × 0.1 × 0.05 mm) in an oil drop [19] with $2\theta/\omega$ scans in the range $8° \le 2\theta \le 45°$. Of 2660 collected reflections, 2660 were independent and 2659 were used in refinement of 296 parameters (84 restraints); maximum and minimum of the difference fourier map 0.534 and 0.477 e Å^{-3}, $R1$ [$F > 2\sigma(F)$] = 0.0595, wR2 (all data) = 0.1281, $R1 = \sum||F_o| - |F_c||/\sum|F_o|$ and $wR2 = (\sum W(F_o^2 - F_c^2)^2/\sum W(F_o^2)^2)^{0.5}$. The structure was solved with direct methods (SHELXS92) [20] and refined by full-matrix least squares on F^2 (SHELXL-93) [21]. Hydrogen atoms were refined by using a riding model. Crystallographic data (excluding structure factors) for the structure reported in this paper have been deposited with the Cambridge Crystallographic Data Centre as supplementary publication no. CCDC-179-121. Copies of the data can be obtained free of charge on application to The Director, CCDC, 12 Union Road, Cambridge CB2 1EZ, UK (fax: Int. code + (1223) 336-033; e-mail: teched@chemcrys.cam.ac.uk).
[15] a) E. D. Jemmis, A. R. Pinhas, R. Hoffmann, *J. Am. Chem. Soc.* **1980**, *102*, 2576–2585 and references therein; b) L. F. Dahl, E. R. de Gil, R. D. Feltham, *J. Am. Chem. Soc.* **1969**, *91*, 1653–1664; c) C. F. Putnik, J. J. Welter, G. D. Stucky, M. J. D'Aniello, Jr., B. A. Sosinsky, J. F. Kirner, E. L. Muetterties, *ibid.* **1978**, *100*, 4107–4116.
[16] A. Mitschler, B. Rees, M. S. Lehmann, *J. Am. Chem. Soc.* **1978**, *100*, 3390–3397.
[17] M. V. Andreocci, M. Bossa, C. Cauletti, R. Paolesse, G. Ortaggi, T. Vondrak, M. N. Piancastelli, M. Casarin, M. Dal Colle, G. Granozzi, *J. Organomet. Chem.* **1989**, *366*, 343–355.
[18] The observation of three bands in IR spectra of **8** could possibly be due to the occurence of two different pentaisopropylcyclopentadienyl ring conformations, cf. H. Sitzmann, *Chem. Ber.* **1990**, *123*, 2311–2315.
[19] T. Kottke, D. Stalke, *J. Appl. Crystallogr.* **1993**, *26*, 615.
[20] G. M. Sheldrick, *Acta Crystallogr. Sect. A* **1990**, *46*, 467.
[21] G. M. Sheldrick, SHELXL-93, program for crystal structure refinement, Göttingen, **1993**.

$[As_2(AlCp^*)_3]$—A Compound with a Polyhedral As_2Al_3 Framework**

Carsten K. F. von Hänisch, Christoph Üffing, Markus A. Junker, Achim Ecker, Boris O. Kneisel, and Hansgeorg Schnöckel*

Since the first report on the synthesis[1] of $[(Cp^*Al)_4]$ (Cp^* = pentamethylcyclopentadienyl, C_5Me_5), this versatile reagent has been used for the synthesis of new organoaluminum compounds. For example, reaction with selenium or tellurium provided heterocubane analogues,[2] while that with P_4 led to a compound containing $[P_4(AlCp^*)_6]$ units.[3] These do not have the expected adamantane-like structure with AlCp*-bridged P_4 tetrahedra; instead, they are made up of two face-sharing heterocubanes, each of which lacks one phosphorus atom (see Fig. 2). Halving this molecule would lead to $[P_2(AlCp^*)_3]$, for which a trigonal-bipyramidal structure is expected. Although no geometric parameters could be obtained, a similar structure has been proposed by Roesky et al. for the analogous $[Sb_2(AlCp^*)_3]$ on the basis of preliminary X-ray structure studies.[4] We report here on the analogous arsenic compound $[As_2(AlCp^*)_3]$ (**1**), which, according to X-ray structure analysis, exists as a heteropolyhedron with a trigonal-bipyramidal structure (Fig. 1).

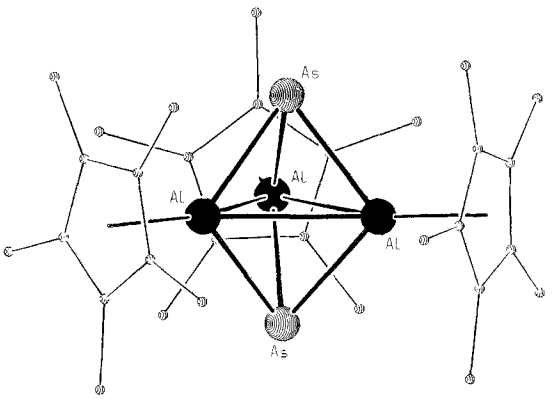

Fig. 1. Molecular structure of $As_2(AlCp^*)_3$ (**1**) in the crystal (hydrogen atoms are not shown).

When $[(Cp^*Al)_4]$ is heated with $[(t\text{BuAs})_4]$ in toluene, **1** is formed together with 2-methylpropane and isobutene. During the reaction, the solution slowly changes color from yellow to orange. After filtration, concentration of the solution, and cooling to -25 °C, **1** can be isolated as yellow crystals. The X-ray crystal structure analysis[5] showed that **1** has an As_2Al_3 framework with approximate D_{3h} symmetry (Fig. 1). The As–Al bond (248 pm) is shorter than that in the organometallic compounds reported so far (249–257 pm).[6]

This shortening of the As–Al bond in **1** is understandable since both arsenic and aluminum have the (higher) coordination number four in all the other known As–Al compounds.[7] However, $(Mes^*AlAsPh)_3$ (Mes^* = 2,4,6-$(t\text{Bu})_3C_6H_2$) was recently

[*] Prof. Dr. H. Schnöckel, C. K. F. von Hänisch, C. Üffing, M. A. Junker, A. Ecker, B. O. Kneisel
Institut für Anorganische Chemie der Universität
Engesserstrasse, Geb.-Nr. 30.45, D-76131 Karlsruhe (Germany)
Fax: Int. code + (721) 608-4854
e-mail: hg@achpc9.chemie.uni.karlsruhe.de

[**] This work was supported by the Deutsche Forschungsgemeinschaft and the Fonds der Chemischen Industrie. We thank Dr. R. Köppe for the helpful discussions on the quantum chemical results.

reported, in which both the As and the Al atoms are three coordinate. Consequently, an especially short As–Al bond length of 243 pm is present.[9] The lower coordination number is also responsible for the shorter As–Al bonds in the Zintl anions $[Al_2As_4]^{6-}$ (terminal: 233–235 pm, bridging: 243–245 pm).[10]

The Al–Al distances in **1** (283 pm) are only slightly longer than those, for example, in R_2AlAlR_2 ($R = CH(SiMe_3)_2$, 266 pm)[11] and $[(Cp^*Al)_4]$ (277 pm),[1] indicating the presence of Al–Al bonding. However, in the case of **1**, there are only twelve electrons available for the nine bonds of the As_2Al_3 framework; thus, there is an electron deficient situation, such that the bonding in the As_2Al_3 polyhedron is similar to that in *closo*-boranes.

In contrast to As_2Al_3, the analogous P_2B_3 framework in $P_2[BN(iPr)_2]_3$ (**2**) shows classical two-electron–two-center (2e2c) bonding and, due to the stronger B–N backbonding, only weak B–B interactions.[12] This is supported by the B–B bond lengths (223 pm), which are about 30% longer than a normal B–B single bond (B_2Cl_4: 175 pm),[13] and could further be confirmed by our quantum chemical calculations.[14] Since our calculations are basically in agreement with the recently published results for $[(BX)_n(Y)_2]$ molecules,[15] we will avoid a detailed description of the results here, and only those points that are decisive for the interpretation of the bonding in **1** will be presented.

SCF calculations on the model compound $P_2(BNH_2)_3$[16] confirmed the experimentally observed weak B–B interactions: $d(B–B) = 222$ pm (as in **2**). The extremely long B–B bond length indicates that the bonding can be described solely with 2e2c B–P bonding. Substitution of the NH_2 groups with hydrogen atoms, for which backbonding is no longer possible, results in a shortening of the B–B bond length by 25 pm to 197 pm. This bonding is now better described as a 2e3c interaction (such as that in a *closo*-polyhedron).

According to quantum chemical calculations, the situation in the analogous AlP compound $[P_2(AlH)_3]$ (**3**) is not so clear, since due to the reduced stability of the monomer, owing to the multicenter bonding, the dimer $[P_4(AlH)_6]$ (**4**) must also be considered. Recently, a compound with a P_4Al_6 framework was detected experimentally in the reaction of P_4 with $[(Cp^*Al)_4]$. Two isomers, **4a** (T_d) and **4b** (C_{2h}), are conceivable for this dimeric compound (Fig. 2), although quantum chemical calculations indicate that the T_d structure (**4a**) should be slightly higher in energy.[3]

The calculations reveal that the dimerization of **3** to give the less stable **4a** is strongly exothermic (-184 kJ mol^{-1}).[17] This result is in agreement with the experimental finding that no monomer with the trigonal-bipyramidal structure of **3** has yet been found.

Substitution of phosphorus with arsenic apparently leads to a change in the bonding: only the monomeric unit $[As_2(AlCp^*)_3]$ (**1**) can be detected. Initially, we attributed this to a stabilization by electron delocalization in the As_2Al_3 framework, similar to the Wade description of *closo*-boranes; however, quantum chemical calculations for the H-substituted parent compound $[As_2(AlH)_3]$ (**1a**) and its dimer $[As_4(AlH)_6]$ (**5**) with an adamantane structure show that the dimerization energy (-144 kJ mol^{-1}) is decidedly negative.[18] In order to understand the bonding in monomeric $[As_2(AlR)_3]$ compounds, we have carried out SCF calculations for molecules with R = H, Cl, NH_2, and Cp (**1a–d**).

For the compounds **1a–d** we were able to assign five or six of the highest occupied MOs to the framework electron system, for example, for **1a**: $9a'' = -0.298$, $6e'' = -0.330$, $10e' = -0.383$ a.u. The missing a_1 MO is 0.05 a.u. lower in energy than the fifth bonding MO. However, for **1c** and **1d** there are still two to three MOs, which are higher in energy than the lowest lying a_1 MO of the As_2Al_3 framework and can be assigned to AlR bonding as well as to the lone pairs of electrons on the nitrogen atoms. In all cases, the MOs assigned to lone pairs of electrons on As are separated from the framework electron system by a lowering in energy of 0.18–0.25 a.u. (depending on the substituent). The minimal changes in the electronic structures[19] of **1a–d** indicate similar geometric bonding situations, and the Al–Al bond lengths are barely influenced: 279 (**1a**), 277 (**1b**), 280 (**1c**), and 293 pm (**1d**). The particularly long Al–Al bond lengths on Cp substitution (**1d**) were expected based on earlier results for $[(Cp^*Al)_4]$.

The population analysis for **1a–d** also confirms a clear electron delocalization and, consequently, *closo*-compounds. Therefore, the shared electron number (SEN) values[20] of approximately 0.2 for the Al–Al interaction are expectedly low;[21] however, substantial three-center Al–As–Al population does take place.[22] The partial charges based on the Roby–Davidson population analysis for Al and As vary, according to substituent, from +0.3 to +0.45 and −0.3 to −0.45, respectively.

Based on these experimental and quantum chemical investigations of **1**, its derivatives, and other homologous compounds, it can be concluded that the heavy main group elements can also form heteropolyhedral compounds of the *closo*-borane type. However, the extent of multicenter bonding is significantly lower for molecules with a P_2Al_3 framework and trigonal-bipyramidal structure than for the analogous boron compounds.

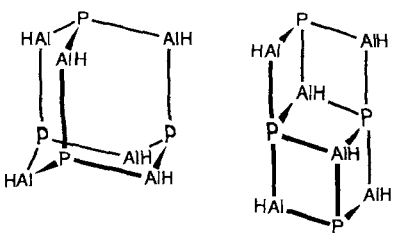

Fig. 2. Structural isomers of $P_4(AlH)_6$: **4a** (left) and **4b** (right).

Experimental Procedure

^{1}H NMR spectra were recorded at room temperature with a Bruker AC250 spectrometer (solvent: C_6D_6, $\delta(C_6D_5H) = 7.16$).

$[(t\text{BuAs})_4]$ [23] (40 mg, 0.077 mmol) was dissolved in toluene (8 mL) and added to $[(Cp^*Al)_4]$ (50 mg, 0.077 mmol) at room temperature. The clear, light yellow solution was tempered alternately at 60°C and 115°C and then cooled to room temperature, leading to an intensification of the color. Filtration and concentration of the solution in vacuo provided an orange solution, from which yellow crystals of **1** were obtained at −25°C. The ^{1}H NMR spectra of the reaction mixture show signals that can be assigned to the starting material as well as isobutene, Cp*H, and 2-methylpropane. A signal, which is shifted downfield by 0.04 with respect to the $[(Cp^*Al)_4]$ signal ($\delta = 1.94$), became more intense at the expense of the $[(Cp^*Al)_4]$ signal and is assigned to compound **1**. No signals could be detected by ^{27}Al NMR spectroscopy. Under high vacuum conditions **1** can be evaporated at about 160°C without decomposition. Mass spectrometry shows 1^+ to be the molecular ion peak at 180°C. MS (EI, 70 eV, 180°C): *m/z* (%): 636 (100, M^+), 501 (10), 474 (18), 399 (4), 324 (15), 162 (27), 121 (14).

Received: June 24, 1996 [Z92671E]
German version: *Angew. Chem.* **1996**, *108*, 3003–3004

Keywords: aluminum compounds · arsenic compounds · clusters

[1] C. Dohmeier, C. Robl, M. Tacke, H. Schnöckel, *Angew. Chem.* **1991**, *103*, 594–595; *Angew. Chem. Int. Ed. Engl.* **1991**, *30*, 564–565.
[2] S. Schulz, H. W. Roesky, H. J. Koch, G. M. Sheldrick, D. Stalke, A. Kuhn, *Angew. Chem.* **1993**, *105*, 1828–1830; *Angew. Chem. Int. Ed. Engl.* **1993**, *32*, 1729–1731.

[3] C. Dohmeier, H. Schnöckel, C. Robl, U. Schneider, R. Ahlrichs, *Angew. Chem.* **1994**, *106*, 225–227; *Angew. Chem. Int. Ed. Engl.* **1994**, *33*, 199–200.

[4] S. Schulz, T. Schoop, H. W. Roesky, L. Häming, A. Steiner, R. Herbst-Irmer, *Angew. Chem.* **1995**, *107*, 1015–1016; *Angew. Chem. Int. Ed. Engl.* **1995**, *34*, 919–920.

[5] Crystal structure analysis of **1**: $C_{37}H_{53}Al_3As_2$: $\{(As_2(AlCp^*)_3 \cdot C_7H_8\}$: $M_r = 728.57$; crystal dimensions: $0.2 \times 0.2 \times 0.2$ mm; $T = 200$ K; $a = 20.951(6)$, $b = 10.973(9)$, $c = 16.770(8)$ Å, $\beta = 103.30(5)^\circ$, $V = 3751.7(3)$ Å^3, $Z = 4$, monoclinic, space group $C2/c$, $\rho_{calc} = 1.290$ g cm^{-3}, $\mu(Mo_{K\alpha}) = 1.875$ mm^{-1}; ω scan mode ($\Delta\omega = 1.1^\circ$), $3^\circ \leq 2\theta \leq 45^\circ$, 5072 reflections were measured on a four-circle diffractometer (STOE STADI4)($Mo_{K\alpha}$, $\lambda = 0.71073$ Å, graphite monochromator), 2443 independent reflections ($R_{int} = 0.0365$), structure solution with direct methods (SHELXS-86 [24]), 1766 reflections with $F > 4\sigma(F)$ for full-matrix refinement of 263 parameters by the method of least squares against $|F^2|$ (SHELXS-93 [25]), H atoms with fixed isotropic U according to the riding model; weighting scheme: $w^{-1} = \sigma^2 F_o^2 + (0.0421P)^2$, where $P = (F_o^2 + 2F_c^2)/3$; $R1$ ($F > 4\sigma(F)$): 0.0365, weighted R value (all data): $wR2 = 0.1085$, remaining electron density: max. 0.454, min. -0.252 e Å^{-3}. Crystallographic data (excluding structure factors) for the structure(s) reported in this paper have been deposited with the Cambridge Crystallographic Data Centre as supplementary publication no. CCDC-179-118. Copies of the data can be obtained free of charge on application to The Director, CCDC, 12 Union Road, Cambridge CB2 1EZ, UK (fax: Int. code +(1223) 336-033; e-mail: teched@chemcrys.cam.ac.uk).

[6] a) N. A. Bailey, P. H. Bird, M. G. H. Wallbridge, *Inorg. Chem.* **1968**, *7*, 1575–1581; b) D. E. Heaton, R. A. Jones, K. B. Kidd, A. H. Cowley, C. M. Nunn, *Polyhedron* **1988**, *7*, 1901–1908; c) R. L. Wells, A. T. McPhail, T.M. Speer, *Eur. J. Solid State Inorg. Chem.* **1992**, *29*, 63–79; d) R. L. Wells, A. T. McPhail, T. M. Speer, *Organometallics* **1992**, *11*, 960–963; e) J. A. Laske Cooke, R. L. Wells, P. S. White, *ibid.* **1995**, *14*, 3562–3565; f) J. A. Laske Cooke, A. P. Purdy, R. L. Wells, P. S. White, *ibid.* **1996**, *15*, 84–90.

[7] In this view, for aluminum only the electronegative ligands, but not the bonding to other Al atoms (as in **1**), has been taken into account. A compound with a particularly short As–Al bond length of 246 pm, despite having four-coordinate As and Al atoms, is $(Me_3Si)_3As \cdot AlCl_3$ [8].

[8] R. L. Wells, C. G. Pitt, A. T. McPhail, A. P. Purdy, R. B. Shafieezad, R. B. Hallock, *Mater. Res. Soc. Sym. Proc.* **1989**, *131*, 45.

[9] R. J. Wehmschulte, P. P. Power, *J. Am. Chem. Soc.* **1996**, *118*, 791–797.

[10] M. Somer, D. Thiery, K. Peters, L. Walz, M. Hartweg, T. Popp, H. G. von Schnering, *Z. Naturforsch. B* **1991**, *46*, 789–794.

[11] W. Uhl, *Z. Naturforsch. B* **1988**, *43*, 1113–1118.

[12] G. L. Wood, E. N. Duesler, C. K. Narula, R. T. Paine, H. Nöth, *J. Chem. Soc. Chem. Commun.* **1987**, 496–498.

[13] M. Atoji, W. N. Lipscomb, P. J. Wheatley, *J. Chem. Phys.* **1955**, *23*, 1176; M. Atoji, P. J. Wheatley, W. N. Lipscomb, *ibid.* **1957**, *27*, 196–199; R. R. Ryan, K. Hedberg, *ibid.* **1969**, *50*, 4986–4995.

[14] Method of calculation: HF-SCF, TURBOMOLE (R. Ahlrichs, M. Bär, M. Häser, H. Horn, C. Kölmel, *Chem. Phys. Lett.* **1989**, *162*, 165.). Standard basis sets from the TURBOMOLE library: H: TZP (5s)/[3s] {311} + (1p), $\eta_p = 0.8$; B: TZP (10s6p)/[6s3p] {511111/411} + (1d), $\eta_d = 0.5$; C: TZP (7s4p)/[3s2p] {511 31} + (1d), $\eta_d = 0.8$; N: TZP (10s6p)/[6s3p] {511111/411} + (1d), $\eta_d = 1.0$; Al: TZP (12s9p)/[7s5p] {5121111/51111} + (1d), $\eta_d = 0.3$; P: TZP (12s9p)/[7s5p] {5121111/51111} + (1d), $\eta_d = 0.45$; Cl: TZP (12s9p)/[7s5p] {5121111 51111} + (1d), $\eta_d = 0.65$; As: TZVP (17s13p6d)/[6s5p2d] {842111/64111 51} + (1d), $\eta_d = 0.293$.

[15] J. K. Burdett, O. Eisenstein, *J. Am. Chem. Soc.* **1995**, *117*, 11939–11945.

[16] 1 a.u. ≙ 1 Hartree ≙ 2625.5 kJ mol^{-1}: $P_2(BNH_2)_3$: D_{3h} symmetry; energy (total): -922.606859 a.u.; bond lengths [pm]: P–P: 307.8, B–B: 221.9, P–B 196.0, B–N 139.2, N–H 99.3. $P_2(BH)_3$: D_{3h} symmetry: energy (total): -757.290877 a.u.; bond lengths [pm]: B–H 118.1 pm, P–B 191.5, B–B 197.5, P–P 307.8 pm.

[17] $P_2(AlH)_3$ (**3**): D_{3h} symmetry; energy (total): -1409.079110 a.u.; bond lengths [pm]: A H 156.9, P–Al 236.3, Al–Al 272.8. $P_4(AlH)_6$ (**4a**): T_d symmetry; energy (total): -2018.228374 a.u.; bond lengths [pm] and angles [°]: Al–H 157.6, P–Al 233.6; Al-P-Al 98.5, P-Al-P 128.5; dimerization energy: -184.2 kJ mol^{-1}. $P_8(AlH)_6$ (**4b**): C_{2h} symmetry: see ref. [3]

[18] The formation of the monomer $As_2(AlCp^*)_3$ (**1**), which is unstable with respect to the dimer, must therefore be kinetically controlled and thus be possible by using (tBuAs)$_4$ instead of As_4. $As_2(AlH)_3$ (**1a**): D_{3h} symmetry; energy (total): -5196.017199 a.u.; bond lengths [pm] and angles [°]: As–As 373.2, Al–H 157.1, As–Al 246.6, Al–Al 279.2; As-Al-As 98.4. $As_8(AlH)_6$ (**5**): T_d symmetry; energy (total): -10392.088140 a.u.; bond lengths [pm] and angles [°]: Al–H 157.8, As–Al 243.8, Al-As-Al 97.12, As-Al-As 130.62; dimerization energy: -144.2 kJ mol^{-1}.

[19] Energy of the highest filled MOs (a.u.), bond lengths [pm] and angles [°]: **1a** (D_{3h}): $9a_2'' = -0.298$; $6e'' = -0.330$; $10e' = -0.383$; $12a_1' = -0.440$. **1b** (D_{3h}): $11a_2'' = -0.322$; $8e'' = -0.348$; $16e' = 0.431$; $16a_1' = -0.473$. As–As 374.1, As–Al 246.3, Al–Al 277.5, Al–Cl 209.7, As-Al-As 98.8. **1c** (D_{3h}): $10a_2'' = -0.282$; $7e'' = -0.313$; $2a_2' = -0.408$; $12e' = -0.420$; $14a_1' = -0.432$. As–As 372.7, As–Al 246.8, Al–Al 280.3, Al–N 176.6, As-Al-As 98.1, As-Al-N 131.0, H-N-H 110.6. **1d** (C_{3v}): $31a_1 = -0.240$; $33e = -0.249$; $32e = -0.332$; $30a_1 = -0.347$; $8a_2 = -0.348$; $31e = -0.370$; $30e = -0.385$; $29a_1 = -0.394$. As–As 366.0, As–Al 249.1, Al–Al 292.6, Al–C 229.1, 233.0, 228.5; As-Al-As 94.6.

[20] R. Heinzmann, R. Ahlrichs, *Theor. Chim. Acta* **1976**, *42*, 33–45; R. Ahlrichs, C. Ehrhardt, *Chem. unserer Zeit* **1985**, *19*, 120–124.

[21] **1a**: 0.23; **1b**: 0.16; **1c**: 0.21; **1d**: 0.27.

[22] **1a**: 0.11; **1b**: 0.08; **1c**: 0.11; **1d**: 0.13.

[23] A. Tzschach, V. Kiesel, *J. Prakt. Chem.* **1971**, *313*, 259; reduction with magnesium instead of sodium.

[24] G. M. Sheldrick, *Acta Crystallogr. Sect. A* **1990**, *46*, 467–473.

[25] G. M. Sheldrick, SHELXL-93, *J. Appl. Crystallogr.*, submitted.

Functionalized Organoimidorhenium(v) Complexes as Potential Radiopharmaceuticals: Syntheses of Glycine Derivatives and the Structure Determination of a Rhenium Analogue of Chlorambucil**

Jeffrey B. Arterburn,* Ian M. Fogarty, Keith A. Hall, Kevin C. Ott, and Jeffrey C. Bryan

Metal-based pharmaceuticals play a prominent role in modern medicine, and new combinations of metals with biologically relevant organic molecules offer versatility in drug design for many potential applications.[1] The coordination chemistry of the metal may be essential, as is the case with cisplatin and related derivatives,[2] while other applications may be based on the existence of radioisotopes of the metal (for example, radioimaging and radiotherapy). In the latter context, diagnostic imaging with ^{99m}Tc complexes has become a routine medical procedure, and current research has focused on finding radiopharmaceuticals that bind selectively to organs or cells.[3] Complexes containing radioisotopes of rhenium (^{186}Re and ^{188}Re) are equally suitable for imaging and radiotherapy of certain cancers.[4]

The linkage used in a metal bioconjugate determines its ease of synthesis, stability, and biological activity of the complex. Multihapto chelating ligands are the most thoroughly investigated ligand class for metal-based drugs, because of favorable complexation kinetics and chelate stability.[5] However, chelating ligands may adversely affect the solubility or lipophilicity characteristics of the complexes, influence target tissue selectivity, and can potentially modify receptor binding. To circumvent these problems, we decided to explore the use of a multiply bonded organoimide linkage (M≡N–biomolecule) that can be easily synthesized for a stable, covalent connection between a metal and a biologically relevant organic molecule as an alternative to chelating linkages.[6, 7] For the purposes of radiopharmaceutical design, ancillary organoimide ligands functionalized with a carboxylic acid would provide a convenient site for the

[*] Prof. Dr. J. B. Arterburn, I. M. Fogarty
Department of Chemistry and Biochemistry
New Mexico State University
Box 30001/3C, Las Cruces, NM 88003 (USA)
Fax: Int. code +(505)646-2549
Dr. K. A. Hall, Dr. K. C. Ott
CST Division, Los Alamos National Laboratory (USA)
Dr. J. C. Bryan
CS Group, Oak Ridge National Laboratory (USA)

[**] J. B. A. thanks the Donors of the Petroleum Research Fund; K. A. H and K. C. O thank the Department of Energy OHER and Dr. Russ Knapp of ORNL for providing the ^{188}W/^{188}Re generator.

conjugation of biomolecules and permit fine tuning of desirable properties by varying labile ligands in the coordination sphere, an option unavailable to chelates. Here we report the syntheses of a new class of potential metal-pharmaceuticals, a ^{188}Re organoimido analogue of the anti-cancer drug chlorambucil,[8] and its X-ray crystal structure determination, as well as of functionalized imidorhenium complexes containing the amino acid glycine, demonstrating the stability of the imido group in the presence of carboxylic acid, ester, and amide groups.

The oxorhenium(v) complex **1**[9] reacts rapidly with simple, functionalized *N*-acetylarylhydrazine[10] and triphenylphosphane in a refluxing 1:1 mixture of toluene and 2-propanol to give the green, air-stable organoimido complexes **2** and **3** in high yields (≥85%) (Scheme 1). No precautions against air or adventitious water in the reagents were required. The $^{31}P\{^1H\}$ NMR spectra for the complexes are particularly diagnostic and show a characteristic single resonance at about $\delta = -20$ to -22 for the equivalent *trans* phosphane ligands. The FT-IR spectra of the glycine derivatives **2** and chlorambucil analogues **3** display absorptions assigned to the carbonyl groups in the acids, esters, and amides, as well as a strong absorption for the ligated phosphane ligands. Complexes **3** have also been characterized by HPLC.[11]

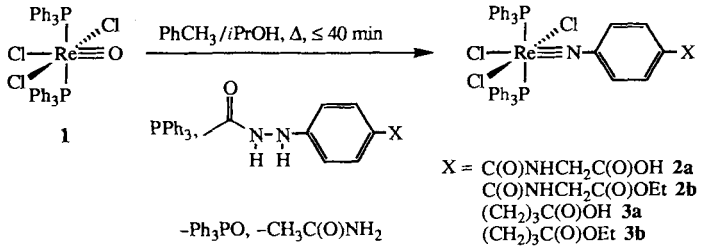

Scheme 1. Synthesis of functionalized arylimidorhenium(v) complexes from **1**.

To test the viability of this route for radiopharmaceutical syntheses we synthesized complex **3b** labeled with carrier-free ^{188}Re. A CH_2Cl_2 solution containing the ^{188}Re labeled oxo complex **1***[12] reacted with acetylhydrazine (in excess) and PPh_3 to produce **3b*** as determined by HPLC with radiometric detection. The reaction proceeded smoothly at room temperature to produce **3b*** in quantitative radiochemical yields.

Complex **3b** was recrystallized by slow diffusion of ethanol into a dichloromethane solution, and produced crystals suitable for X-ray diffraction.[13] The structure of the complex (Fig. 1) consists of an octahedral arrangement of *mer*-oriented chloride ligands, the *trans*-triphenylphosphane ligands, and the imide ligand. The ligand arrangement around the rhenium is consistent with the spectroscopic data for complex **3b** in solution and similar to that of previously reported phenylimido complexes.[14] The Re–N bond length of 1.713(4) Å and the Re-N-C1 bond angle of 179.0(3)° are typical of rhenium(v) monoimido complexes (1.69–1.75 Å, 156–180°).[7, 16] The Re–Cl and Re–P distances are similar to those reported for the closely related $[Re(NPh)Cl_3(PPh_3)_2]$.[15]

Though organoimide ligands are ubiquitous in the chemistry of transition metals in their higher oxidation states, there are surprisingly very few examples where the alkyl or aryl group has itself been functionalized.[7] To our knowledge, complexes **2a** and **3a** represent the first examples in which an organoimide ligand and free carboxylic acid groups are present within the same molecule. The efficient Re–N π bonding[16] in these

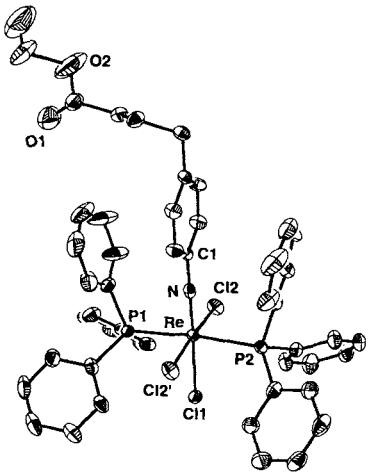

Fig. 1. ORTEP representation of the crystal structure of **3b** (50% thermal ellipsoids). Hydrogen atoms and one set of the pairs of disordered atoms are omitted for clarity [13]. Relevant distances [Å] and angles [°]: Re–N 1.713(4), Re–Cl1 2.447(1), Re–Cl2 2.412(1), Re–P1 2.485(1), Re–P2 2.488(1), Re-N-C1 179.0(3), P1-Re-P2 174.5(1), Cl2-Re-Cl2' 176.9(1), Cl1-Re-N 178.9(1), Cl1-Re-P1 87.0(1), Cl1-Re-P2 87.5(1), Cl1-Re-Cl2 89.0(1).

complexes results in the weak basicity/nucleophilicity of the nitrogen atom and imparts stability to the complexes against hydrolysis in protic media.[11] The solubility, charge, and size of these and related complexes can be modified by making appropriate ligand substitutions without compromising the imido linkage.[7] Since flexibility is important for radiopharmaceutical design, where biodistribution and high receptor specificity are both necessary requirements, this capability is a distinct advantage of the multiply bonded organoimide ligand over chelating linkages.[17]

In conclusion, the use of a covalent organoimido–metal bioconjugate represents a new and potentially powerful methodology in radiopharmaceutical design. The imido-forming reactions proceed readily under mild conditions and are compatible with unprotected carboxylic acids, esters, and amides. They give stable imido complexes and can be adapted to high-yield syntheses utilizing ^{188}Re. The extension of this chemistry to other rhenium organoimido complexes containing biologically relevant organic substrates, and an investigation of the biological stability and potential anticancer activity of the complex **3a** as a bifunctional analogue of chlorambucil[8] with electrophilic DNA crosslinking capability are currently in progress.

Experimental Procedure

Complexes **2** and **3** were prepared by refluxing **1** (716 mg, 0.86 mmol), PPh_3 (451 mg, 1.72 mmol), and the appropriate acetylhydrazine [18] (0.86 mmol) in toluene/2-propanol (60 mL each) for 40 min. The solutions were then concentrated to 5 mL in vacuo, and the products precipitated by the addition of 1:1 ether:hexane (60 mL total). The green solids were filtered, washed with ethanol, and dried in vacuo. Complexes **2a** and **3a** were recrystallized by slow evaporation of a benzene solution, while **2b** and **3b** were recrystallized by slow diffusion of ethanol into dichloromethane solutions of the complexes. $^{31}P\{^1H\}$ NMR spectra were obtained at 161.9 MHz, $CDCl_3$, 22 °C, referenced to an internal capillary containing H_3PO_4 ($\delta = 0$). **2a**: Yield 738 mg, 85%. $^{31}P\{^1H\}$ NMR: $\delta = -21.7$ (s); IR (KBr): $\tilde{\nu} = 3396$ (O–H), 1732 (C=O), 1668 (C=O), 1092 cm^{-1} (P–C). Elemental analysis calcd. for $C_{45}H_{38}Cl_3N_2O_3P_2Re$: C 53.57, H 3.79, N 2.78; found: C 53.63, H 3.84, N 2.85. **2b**: Yield 776 mg, 87%. $^{31}P\{^1H\}$ NMR: $\delta = -22.0$ (s); IR (KBr): $\tilde{\nu} = 1748$ (C=O), 1664 (C=O), 1092 cm^{-1} (P–C). Elemental analysis calcd. for $C_{47}H_{42}Cl_3N_2O_3P_2Re$: C 54.42, H 4.08, N 2.70; found: C 54.05, H 4.04, N 2.46. **3a**: Yield 735 mg, 86%. $^{31}P\{^1H\}$ NMR: $\delta = -19.6$ (s); IR (KBr): $\tilde{\nu} = 3436$ (O–H), 1704 (C=O), 1092 cm^{-1} (P–C); HPLC (9:1 MeCN:H_2O; Waters C8, 60 Å, 4 μm, 3.9 × 150 mm column): 1.77 min. Elemental analysis calcd. for $C_{46}H_{41}Cl_3NO_2P_2Re$: C 55.56, H 4.16, N 1.41; found: C 55.52, H 4.39, N 1.04. **3b**: Yield 800 mg, 91%. $^{31}P\{^1H\}$ NMR: $\delta = -19.6$ (s); IR (KBr): $\tilde{\nu} = 1728$ (C=O), 1092 (P–C);

 © VCH Verlagsgesellschaft mbH, D-69451 Weinheim, 1996 0570-0833/96/3523-2878 $ 15.00+.25/0

HPLC (9:1 MeCN:H_2O; Waters C8, 60 Å, 4 μm, 3.9 × 150 mm column): 2.45 min. Elemental analysis calcd. for $C_{48}H_{45}Cl_3NO_2P_2Re$: C 56.39, H 4.44, N 1.37; found: C 56.38, H 4.51, N 1.32.

Received: April 29, 1996
Revised: August 12, 1996 [Z 9080 IE]
German version: *Angew. Chem.* **1996**, *108*, 3039–3040

Keywords: Complexes with nitrogen ligands · radiopharmaceuticals · rhenium compounds

[1] P. J. Sadler, *Adv. Inorg. Chem.* **1991**, *36*, 1; P. Kopfmaier, *Eur. J. Clin. Pharmacol.* **1994**, *47*, 1.
[2] P. Kopfmaier, T. Klapotke, *Cancer Chemother. Pharmacol.* **1992**, *29*, 361; S. U. Dunham, S. J. Lippard, *J. Am. Chem. Soc.* **1995**, *117*, 10702.
[3] S. Jurisson, D. Berning, W. Jia, D. Ma, *Chem. Rev.* **1993**, *93*, 1137; *Technetium and Rhenium in Chemistry and Nuclear Medicine, Vol. 4* (Eds.: M. Nicolini, G. Bandoli, U. Mazzi), SGE Ditoriali, Padova, Italy, **1995**.
[4] K. Hashimoto, K. Yoshihara in *Top. Curr. Chem., Vol. 176* (Eds.: J. D. Dunitz, K. Hafner, S. Ito, J.-M. Lehn, K. N. Raymond, C. W. Rees, J. Thiem, F. Vogtle), Springer, Berlin, **1996**, p. 275. ^{188}Re has a 2.12 Mev β^-, 155 kev γ; ^{186}Re has a 1.07 Mev β^-, 137 kev γ; C. M. Lederer, J. M. Hollander, I. Perlman, *Table of Isotopes*, Wiley, New York, **1967**, p. 110.
[5] J. P. O'Neil, S. R. Wilson, J. A. Katzenellenbogen, *Inorg. Chem.* **1994**, *33*, 319.
[6] Recent review of related ^{99m}Tc-bioconjugates: W. C. Eckelman, *Eur. J. Nucl. Med.* **1995**, *22*, 249, and references therein.
[7] Recent review on metal imido chemistry: D. E. Wigley, *Prog. Inorg. Chem.* **1994**, *42*, 239; recently reported functionalized imide ligands: M. T. Ahmet, B. Coutinho, J. R. Dilworth, J. R. Miller, S. J. Parrott, Y. Zheng, M. Harman, M. B. Hursthouse, A. Malik, *J. Chem. Soc. Dalton Trans.* **1995**, 3041; S. Ritter, U. Abram, *Inorg. Chim. Acta* **1995**, *231*, 245; P. L. Hill, G. P. A. Yap, A. L. Rheingold, E. A. Maatta, *J. Chem. Soc. Chem. Commun.* **1995**, 737.
[8] The aromatic, nitrogen-containing, mustard chlorambucil $(ClCH_2CH_2)_2NC_6H_4CH_2CH_2CH_2CO_2H$ is a clinically important chemotherapeutic agent capable of cross-linking duplex DNA; see for example, P. M. Cullis, L. Merson-Davies, R. Weaver, *J. Am. Chem. Soc.* **1995**, *117*, 8033. The organic portion of $(PPh_3)_2Cl_3ReNC_6H_4CH_2CH_2CH_2CO_2H$ (**3a**) is structurally analogous, and similar cross-linking chemistry may be possible by ligand substitution at Re^V.
[9] N. P. Johnson, C. J. L. Lock, G. Wilkinson, *Inorg. Synth.* **1967**, *9*, 145.
[10] Phenylimido complexes have been prepared previously from 1-acetyl-2-phenylhydrazine: J. Chatt, J. R. Dilworth, G. L. Leigh, *J. Chem. Soc. A* **1970**, 2239; T. Nicholson, J. Cook, A. Davison, A. G. Jones, *Inorg. Chim. Acta* **1994**, *218*, 97; F. D. Rochon, R. Melanson, P. C. Kong, *Inorg. Chem.* **1995**, *34*, 2273.
[11] The imido complexes **3** were chromatographed by HPLC on a reverse-phase column (C8 on silica) with gradient elution (acetonitrile:water from 80:20 to 95:5) without detectable decomposition or hydrolysis.
[12] E. Lisic, S. Mirzadeh, F. Knapp, *J. Labelled Compd. Radiopharm.* **1993**, *33*, 65.
[13] $ReC_{48}H_{45}Cl_3NO_2P_2$ **3b**, $M = 1022.3$, monoclinic, $P2_1/m$, $Z = 2$, $a = 12.550(2)$, $b = 13.6426(8)$, $c = 12.586(2)$ Å, $\beta = 91.380(8)°$, $V = 2154.2(5)$ Å^3, $\rho_{calcd.} = 1.576$ g cm^{-3}, $T = -100$ °C; the structure was solved by direct methods and expanded with Fourier techniques. The Re, P, Cl1, N, and several carbon atoms lie on a crystallographic mirror plane. The methylene carbon atoms of the phenyl(ethylbutanoate) group, which all lie close to this mirror plane, are disordered and were therefore refined at half-occupancy. All non-hydrogen atoms were refined anisotropically. Hydrogen atoms were included, but not refined. Final refinement on $|F|$, with 296 variables and 3547 independent reflections ($F > 4\sigma_F$) gave an unweighted residual $R = 0.0275$, $R_w = 0.0370$ and a GOF = 1.04. Crystallographic data (excluding structure factors) for the structure reported in this paper have been deposited with the Cambridge Crystallographic Data Centre as supplementary publication no. CCDC-179-125. Copies of the data can be obtained free of charge on application to The Director, CCDC, 12 Union Road, Cambridge CB21EZ, UK (fax: int. code +(1223)336-033; e-mail: teched@chemcrys.cam.ac.uk).
[14] G. V. Goeden, B. L. Haymore, *Inorg. Chem.* **1983**, *22*, 157.
[15] E. Forsellini, U. Casellato, R. Graziani, M. C. Carletti, L. Magon, *Acta Crystallogr. C* **1984**, *40*, 1795; U. Wittern, J. Strahle, U. Abram, *Z. Naturforsch. B* **1995**, *50*, 997.
[16] W. A. Nugent, J. M. Mayer, *Metal–Ligand Multiple Bonds*; Wiley, New York, **1988**.
[17] J. P. O'Neil, K. E. Carlson, C. J. Anderson, M. J. Welch, J. A. Katzenellenbogen, *Bioconjugate Chem.* **1994**, *5*, 182.
[18] The arylhydrazines were prepared by reduction of the diazonium salts: G. H. Coleman in *Organic Syntheses Collective, Vol. 1*, 2nd ed. (Eds.: H. Gilman, A. H. Blatt), Wiley, London, **1948**, p. 442.

Solvent-Dependent C–N Bond Lengths in a Protonated Orthoamide**

Randolf D. Köhn,* Guido Seifert, and Gabriele Kociok-Köhn

In the early 1970s a new kind of isomerism, in which two isomers differ only in their bond lengths, was proposed by Chatt et al. based on X-ray structure analyses on transition metal complexes,[1] and by Hoffmann et al. based on theoretical studies.[2] The "bond stretch isomers" established to date by crystallography have been critically reviewed by Parkin,[3] and errors were found in most (if not all) interpretations of the X-ray data. This failure to conclusively prove bond stretch isomerism in these complexes, cast doubts on the existence of this type of isomerism.[1]

However, the early theoretical studies indicated the possible existence of bond stretch isomers in organic compounds Scheme 1).[4] The opposing effects of bond energy and ring strain lead to two very different minima; the corresponding isomers differ in their dominant electron configuration (σ and σ^*).

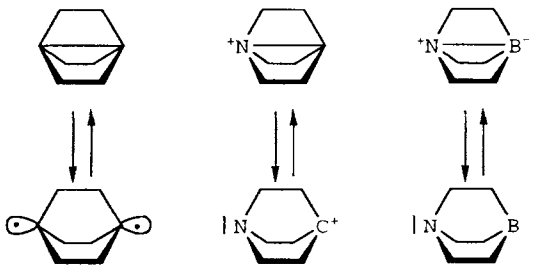

Scheme 1. Theoretically well studied bond stretch isomers in organic compounds.

Based on the difference in polarity, a solvent dependence of the equilibrium between the two isomers was predicted; however, none of the proposed molecules could be prepared because of experimental difficulties and thus the bond stretch isomerism could not be confirmed.

We have tried to prepare complexes from VCl_3 or $FeCl_3$ and the orthoamide **1** analogous to those with $CuCl_2$.[5] However, crystallization of the crude products from CH_2Cl_2/toluene over several weeks resulted in colorless crystals of $\mathbf{2}^+Cl^-$[6] and yel-

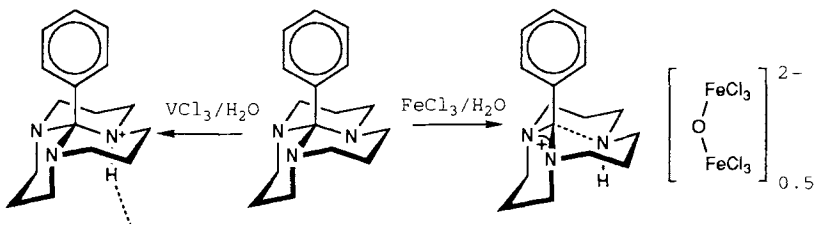

[*] Dr. R. D. Köhn, G. Seifert
Institut für Anorganische und Analytische Chemie der Technische Universität
Strasse des 17. Juni 135, D-10623 Berlin (Germany)
Fax: Int. code +(30)314-22168
e-mail: kociok@wap0203.chem.tu-berlin.de
Dr. G. Kociok-Köhn
Institut für Anorganische und Allgemeine Chemie der Humboldt-Universität
Hessische Strasse 1–2, D-10115 Berlin (Germany)

[**] This work was supported by the Deutsche Forschungsgemeinschaft and by the Fonds der Chemischen Industrie. R. D. K thanks the Deutsche Forschungsgemeinschaft for a habilitation fellowship and Prof. H. Schumann for support of this work.

lowish crystals of $(3^+)_2[Fe_2Cl_6O]^{2-}$,[7] respectively. These compounds are adducts of **1** with acids that were probably formed from moisture that found its way into the reaction mixture.

In the case of $FeCl_3$, the large and weakly coordinating anion $[Fe_2Cl_6O]^{2-}$ was formed, while the hydrogen-bond-forming Cl^- ion resulted from the reaction with VCl_3. Depending on the interaction with the anion, the ammonium cation 2^+ (Fig. 1) or the amidinium cation 3^+ (Fig. 2) with nearly broken N–C bond

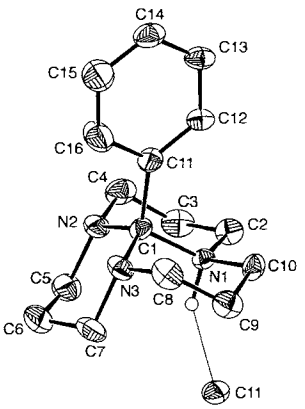

Fig. 1. Structure of 2^+Cl^- in the crystal; selected bond lengths [pm] and angles [°]: C1–N1 159.2(6), C1–N2 143.6(6); N2-C1-N3 113.0(4), N1-C1-C11 112.5(4).

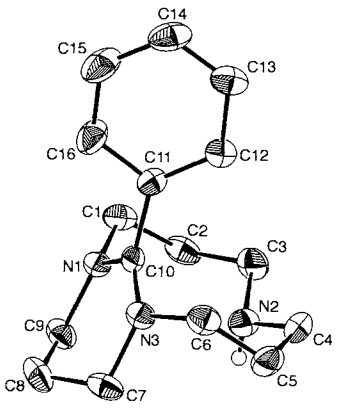

Fig. 2. Structure of the cation 3^+ in the crystal of $(3^+)_2[Fe_2OCl_6]^{2-}$; selected bond lengths [pm] and angles [°]: C2–N10 269(1), C10–N1 133.3(8); N1-C10-N3 123.2(3), N1-C10-C11 115.7(4).

was formed. IR and NMR studies on a similar orthoamide (with a H atom instead of a Ph group) prepared by Wuest et al.[8] revealed that cations analogous to 2^+ and 3^+ can be obtained by protonation depending on the anion and that they are in a fast equilibrium. In 1967 a comparable compound with solvent-dependent C–N bond length was observed, although only in solution, by UV/Vis spectroscopy.[9]

The two cations 2^+ and 3^+ (Fig. 3) are nearly superimposable; however, they differ in one C–N bond and thus in the position of the phenyl group. This situation appears to be similar to the theoretical bond stretch isomers in Scheme 1. The central C–N bond in **1**, which is already extended due to a twofold anomeric effect and some ring strain (155.1(5) pm[5]), is elongated to 159.2(6) pm in 2^+ and to 269(1) pm in 3^+. Thus, both distances are longer than regular C–N bond lengths (147 pm) and shorter than the sum of the van der Waals radii (320 pm).[10] The cation 3^+ is apparently favored when no hydrogen bond is formed to the anion; in contrast, 2^+ is favored by a hydrogen bond between the chloride ion and the NH group. Such a hydrogen bond should also be accessible by a suitable solvent with hydrogen bond acceptor properties. Thus, $(3^+)_2[Fe_2OCl_6]^{2-}$ might close the C–N bond to form the cation 2^+ in polar solvents. In such a case $(3^+)_2[Fe_2OCl_6]^{2-}$ would exist as solvent-dependent isomers with different bond lengths for the same anion. The accidental formation of $(3^+)_2[Fe_2OCl_6]^{2-}$, its probable low solubility in nonpolar solvents, and the paramagnetism of the anion forced us to change to the more suitable anion $[B(3,5\text{-}C_6H_3(CF_3)_2)_4]^-$ (TFPB$^-$), which is a diamagnetic, weakly coordinating anion with higher solubility.

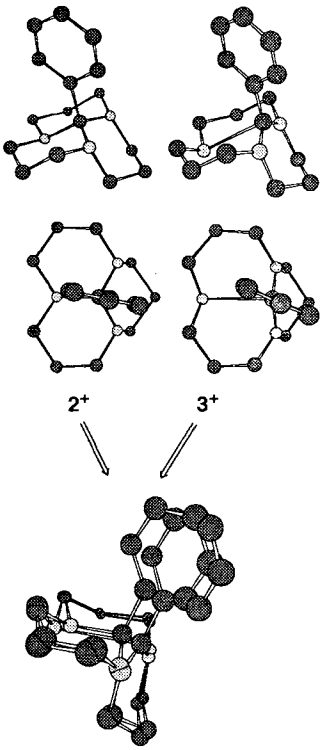

Fig. 3. Superposition of the cations 2^+ (from 2^+Cl^-) and 3^+ (from $(3^+)_2[Fe_2OCl_6]^{2-}$).

Compound **1** reacts with $[H(OEt_2)_2]$TFPB in CH_2Cl_2 to yield 3^+TFPB$^-$, which is soluble in $CDCl_3$ and CD_2Cl_2 without reformation of the C–N bond. The formation of the amidinium ion was evident from a ^{13}C NMR signal at $\delta = 173.6$. Contrary to the cation investigated by Wuest et al.,[8] the ^1H NMR spectrum of the amidinium ion shows no dynamic exchange. The well-resolved spectrum shows all expected signals for the protons in the three six-membered rings in chair conformation with C_s symmetry; these signals were assigned by $^1H,^1H$-COSY NMR spectroscopy. The coupling patterns feature large J_{gem} and J_{ax-ax} ($J \approx 13$ Hz) coupling constants, including coupling to the amine proton, and show that the conformation of the ten-membered ring is fixed by the weak C^+–N interaction. The chemical shift of the NH protons of $\delta = 0.82$ and the down field shift of the protons adjacent to the amidinium cation confirm the presence of the cation 3^+. The IR spectrum of the solid also indicates the presence of cation 3^+; no ammonium absorption band (<2800 cm^{-1}) is present, but an amine absorption band appears at 3345 cm^{-1}. The ^1H NMR spectra in more polar solvents such as CD_3CN and [D$_6$]DMSO look completely different. The signal for the amine proton at $\delta = 0.8$ is replaced by one for an ammonium proton at $\delta = 8.8$ (in [D$_6$]DMSO). The signals for the propylene bridge are only broad signal groups; the average signal for the protons adjacent to the nitrogen atoms is shifted considerably less down field than that in 3^+. This indicates the absence of the amidinium group. Moreover, no signal for an amidinium C atom was found in the ^{13}C NMR spectrum. Thus, the cation 2^+ exists in these more polar solvents. Removal of the sol-

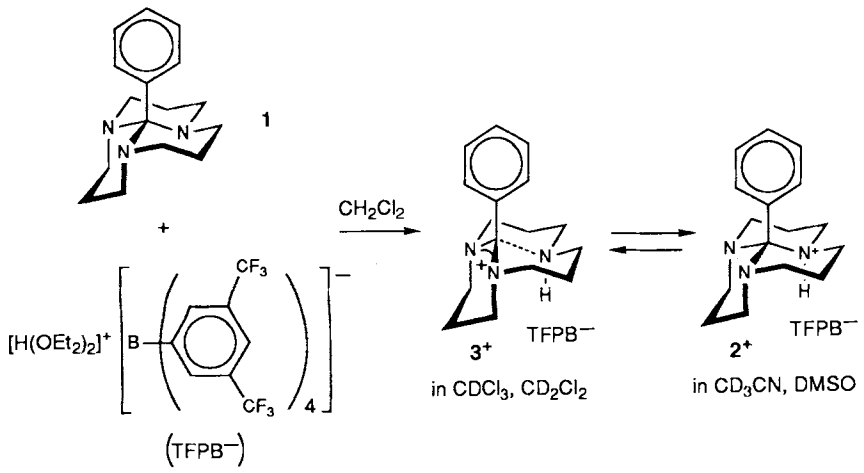

vent in vacuo and dissolution in $CDCl_3$ regenerates the cation 3^+; therefore, 2^+ and 3^+ can be interconverted depending on the solvent. In DMSO, besides 2^+ approximately 30% of the unprotonated compound **1** and probably H_3O^+ (from water in the DMSO) were observed. The same signals for 2^+ are obtained when 20% [D_6]DMSO are added to a solution of 3^+TFPB^- in $CDCl_3$.

In summary, X-ray crystal structure analysis has revealed very different C–N bond lengths in the isomeric cations 2^+ and 3^+ with two different anions. NMR spectroscopy of compound 3^+TFPB^- has shown that the two isomeric cations can be interconverted depending on the polarity of the solvent; thus, 3^+TFPB^- is a possible candidate for bond stretch isomerism.[11]

Experimental Procedure

3^+TFPB^-: CH_2Cl_2 (2 mL) was condensed to **1** [5] (41 mg, 0.16 mmol) and $[H(OEt_2)_2]TFPB$ [12] (156 mg, 0.15 mmol). After the mixture had been stirred for 10 minutes, the solvent was removed in vacuo. The colorless residue was washed with hexanes (4 mL) and dried in vacuo (124 mg, 74%, m.p. 158–159 °C). Elemental analysis: found (calcd.) (M_r = 1121.61): C 50.25 (51.40), H 3.46 (3.24), N 3.71 (3.75)%; ^{1}H NMR (400 MHz, $CDCl_3$, TMS ext.): δ = 7.70 (m, 9H, Ph + *p*-TFPB), 7.54 (s, 8H, *m*-TFPB), 3.83 (t [13], 2H, H1/6_{ax} [14]), 3.59 (t, 2H, H7/9_{ax}), 3.30 (d, 2H, H3/4_{eq}), 3.23 (d, 2H, H7/9_{eq}), 3.11 (d, 2H, H1/6_{eq}), 3.78 (q, 2H, H3/4_{ax}), 2.25 (t, 1H, H8_{ax}), 2.20 (d, 1H, H8_{eq}), 2.00 (q, 2H, H2/5_{ax}), 1.43 (d, 2H, H2/5_{eq}), 0.82 (br, 1H, N*H*) (similar in CD_2Cl_2); $^{13}C\{^1H\}$ NMR (100 MHz, CD_2Cl_2, TMS ext.): δ = 173.6 (C10), 162.1 (q, J(C,B) = 148 Hz, *ipso*-TFPB), 135.2 (*o*-TFPB), 132.1 (*m*-Ph), 130.9 (*ipso*-Ph), 130.2 (*o*, *p*-Ph), 129.6 (q, J(C,F) = 37 Hz, *m*-TFPB), 125.0 (q, J(C,F) = 267 Hz, CF_3), 117.8 (sept, J(C,F) = 4 Hz, *p*-TFPB), 48.7 (C1/6 + C7/9), 46.1 (C3/4), 26.8 (C2/5), 20.4 (C8) (similar in $CDCl_3$); IR (KBr): $\tilde{\nu}$ = 3345 (N–H), 1599 cm^{-1} (Ph, NCN^+).

2^+TFPB^- was formed by dissolving 3^+TFPB^- in acetonitrile or DMSO: ^{1}H NMR (400 MHz, CD_3CN, TMS ext.): δ = 7.66 (s, 12H, TFPB), 7.70 (m, 2H, *m*-Ph), 7.55 (m, 3H, *o*, *p*-Ph), 3.62 (br, 2H), 2.9–3.2 (br m, 10H), 2.2 (br, 4H), 1.45 (br, 2H) (similar in [D_6]DMSO + 8.8 (br, 1H, N*H*) + signals for **1** [5]); $^{13}C\{^1H\}$ NMR (50 MHz, CD_3CN, TMS ext.): δ = 162.6 (q, J(C,B) = 150 Hz, *ipso*-TFPB), 135.7 (*o*-TFPB), 131.6 (*ipso*-Ph), 131.1 (*o*, *p*-Ph), 129.9 (q, J(C,F) = 32 Hz, *m*-TFPB), 129.8 (*m*-Ph), 125.5 (q, J(C,F) = 272 Hz, CF_3), 118.7 (sept, J(C,F) = 4 Hz, *p*-TFPB), 49 (CCN), 23.5 (*C*CN).

Received: August 1, 1996 [Z9408IE]
German version: *Angew. Chem.* **1996**, *108*, 3044–3046

Keywords: bond stretch isomerism · isomerism · nitrogen compounds · solvent effects

[1] a) J. Chatt, L. Manjlivovic'-Muir, K. Muir, *Chem. Commun.* **1971**, 655–656; J. M. Mayer, *Angew. Chem.* **1992**, *104*, 293–295; *Angew. Chem. Int. Ed. Engl.* **1992**, *31*, 286–288; and references therein.
[2] W.-D. Stohrer, R. Hoffmann, *J. Am. Chem. Soc.* **1972**, *94*, 1661–1668.
[3] G. Parkin, *Chem. Rev.* **1993**, *93*, 887–911.
[4] W.-D. Stohrer, R. Hoffmann, *J. Am. Chem. Soc.* **1972**, *94*, 779–786; M. D. Newton, J. M. Schulmann, *ibid.* **1972**, *94*, 4391–4392; J. J. Dannenberg, T. M. Prociv, *J. Chem. Soc. Chem. Commun.* **1973**, 291.
[5] R. D. Köhn, G. Seifert, G. Kociok-Köhn, *Chem. Ber.* **1996**, *129*, 21–24.
[6] X-ray crystal structure determinations: Data collection was carried out on a CAD4-Enraf-Nonius diffractometer ($Mo_{K\alpha}$ = 0.71069 Å) in the ω-2θ scan mode. The structures were solved and refined with SHELXS-86 and SHELXL-93. Non-hydrogen atoms were refined anisotropically, whereas the hydrogen atoms were placed in idealized positions and refined by using a riding model. X-ray structure analysis of 2^+Cl^-: $C_{16}H_{24}N_3Cl$, trigonal, space group $R\bar{3}$ (no. 148), a = 15.549(4) Å, α = 113.66(2)°, V = 2340.4(9) Å^3, Z = 6, ρ_{calcd} = 1.251 Mg m^{-3}, $\mu(Mo_{K\alpha})$ = 0.240 mm^{-1}, $F(000)$ = 948. T = 163 K, crystal dimensions: 0.8 × 0.8 × 0.5 mm, $6° \le 3\theta \le 50°$ ($-18 \le h \le 12$, $-8 \le k \le 11$, $-11 \le l \le 15$); 1848 data collected, of which 1287 were unique and 1256 with $I > 2\sigma(I)$, 185 parameters, min./max residual electron density −0.71/0.74 e Å^{-3}. The refinement converged at R = 0.0637; $wR(F^2)$ = 0.1765, GOF = 1.057 (SHELXL-93). The hydrogen atom H1 bound to the nitrogen atom N1 was located in the differential map and refined isotropically [7b].
[7] a) X-ray structure analysis of $(3^+)_2[Fe_2Cl_6O]^{2-}$: $C_{32}H_{48}N_6Cl_6Fe_2O$, monoclinic, space group $P2_1/c$ (no. 14), a = 14.910(6), b = 16.747(9), c = 15.512(7) Å, β = 100.12(4)°, V = 3813(3) Å^3, Z = 4, ρ_{calcd} = 1.493 Mg m^{-3}, $\mu(Mo_{K\alpha})$ = 1.194 mm^{-1}, $F(000)$ = 1776, T = 166 K, crystal dimensions: 0.18 × 0.35 × 0.55 mm, $3° \le 2\theta \le 46°$ ($-16 \le h \le 16$, $0 \le k \le 18$, $0 \le l \le 16$); 5989 collected data, of which 4406 were unique and 4392 with $I > 4\sigma(I)$; empirical absorption correction DIFABS (min. 0.688, max. 1.116). Residual electron density min/max −0.39/0.65 e Å^{-3}. Refinement of the 431 parameters by full-matrix least-squares resulted in R = 0.0409; $wR(F^2)$ = 0.1057, GOF = 1.017 (SHELXL-93). The hydrogen atoms H2 and H5 bound to the nitrogen atoms N2 and N5, respectively, were located in the difference map and refined isotropically. b) Further details of the crystal structure investigations may be obtained from the Fachinformationszentrum Karlsruhe, D-76344 Eggenstein-Leopoldshafen, on quoting the depository numbers CSD-405863 for 2^+Cl^- and CSD-405864 for $(3^+)_2[Fe_2OCl_6]^{2-}$).
[8] J. M. Erhardt, J. D. Wuest, *J. Am. Chem. Soc.* **1980**, *102*, 6363–6364.
[9] L. J. Dolby, G. W. Gribble, *J. Org. Chem.* **1967**, *32*, 1391–1398.
[10] J. E. Huheey, *Inorganic Chemistry*, 3rd ed., Harper & Row, New York, **1983**.
[11] A theoretical study by W.-D. Stohrer et al. of the electron configuration along the C–N bond is in progress.
[12] M. Brookhart, B. Grant, A. F. Volpe, Jr., *Organometallics*, **1992**, *11*, 3920–3922.
[13] Apparent coupling scheme with J < 13 Hz, additional couplings with J < 4 Hz are observed.
[14] Assignment according to ^{1}H,^{1}H-COSY; the position number is derived from the corresponding carbon atom in Figure 2.

Corrigenda

In the communication "Wittig Olefination of Lactones" by M. Lakhrissi and Y. Chapleur (*Angew. Chem. Int. Ed. Engl.* **1996**, *35*, 750–752) the COOEt group in formula **II** should be a COOMe group. Furthermore in the *Experimental Procedure* the ^{1}H NMR signal of **3** at δ = 5.12 should be assigned to H-2 and not to H-4.

In the communication "Microporous Mixed Oxides—Catalysts with Tunable Surface Polarity" by S. Klein and W. F. Maier (*Angew. Chem. Int. Ed. Engl.* **1996**, *35*, 2230–2233) the reference to equation (a) and the equation itself has been omitted from the third paragraph. Immediately after the citation [5] the sentence should read: This synthesis concept has now been expanded to include the preparation of microporous mixed oxides, where the number of Si atoms carrying a covalently bound alkyl group is freely variable [Eq. (a)].

$$(RO)_4Si + x(R'O)_nM + yH_3C{-}Si(OR)_3 \xrightarrow[-ROH]{H_2O/H^+} SiO_2(MO_{n/2})_x(H_3C{-}SiO_{1.5})_y \quad (a)$$

 © VCH Verlagsgesellschaft mbH, D-69451 Weinheim, 1996 0570-0833/96/3523-2881 $ 15.00+.25/0